68/1

NEWARK PUBLIC LIBRARY

MAR 1 1982

U.S. GOVT. PUBS
DEPOSITORY 376

JNCI

Journal of the National
Cancer Institute

January 1982
Volume 68
Number 1

JNCI Journal of the National Cancer Institute Volume 68 Number 1 pp. 1-175 Jan. 1982

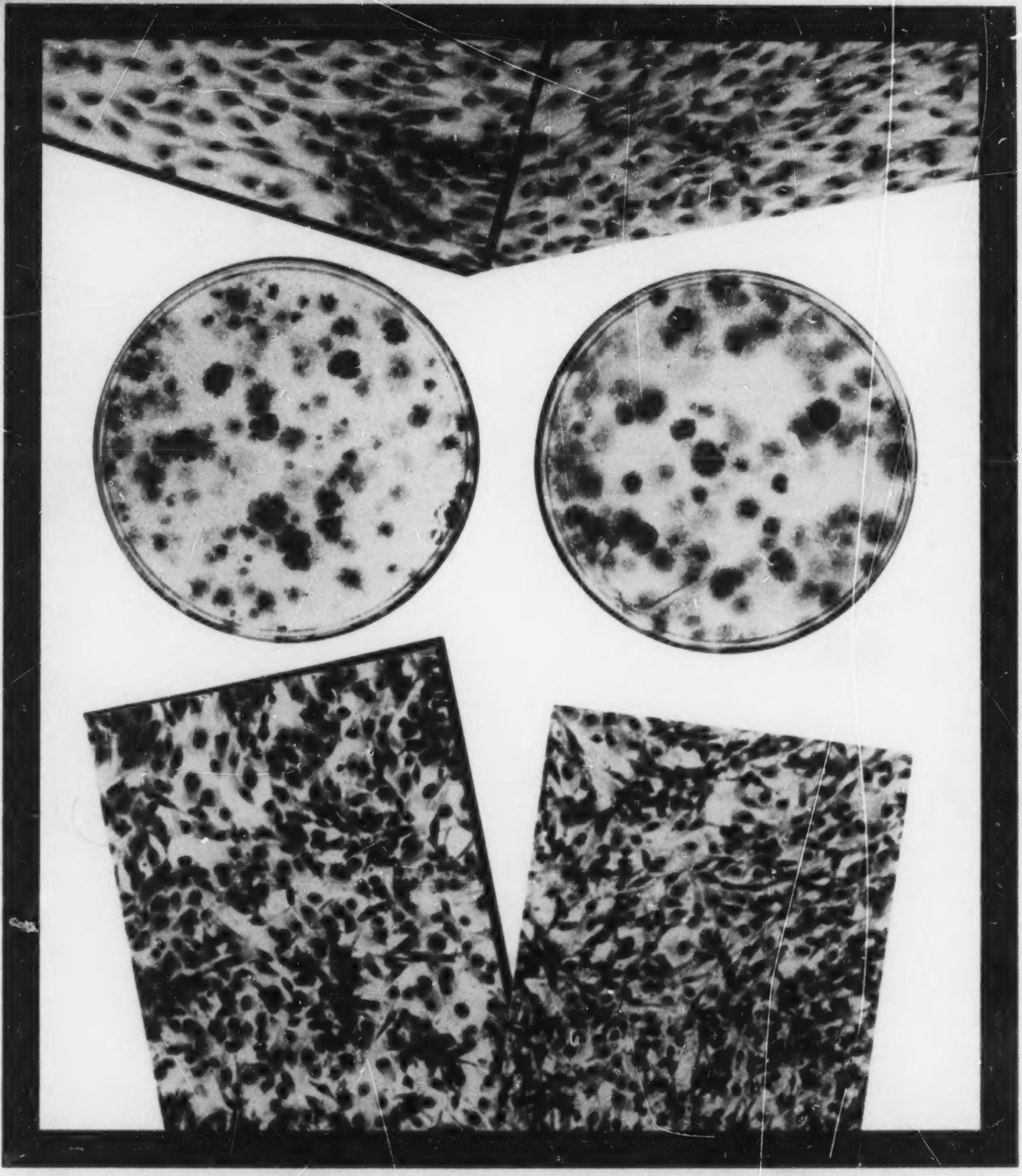

U.S. DEPARTMENT OF HEALTH AND HUMAN SERVICES Public Health Service National Institutes of Health

HE 20. 3161:

The cover shows petri dishes containing control (acetone-treated) Syrian hamster cells grown in the presence of feeder cells (*left*) or endothelial cell growth supplement (*right*). The peripheral areas show the detail of control cells (*top*) or benzo[*a*]pyrene-treated cells (*bottom*) (*see* paper by Evans and DiPaolo on pages 127-131).

JNCI

Journal of the National
Cancer Institute

January 1982
Volume 68
Number 1

THE JOURNAL of the National Cancer Institute solicits manuscripts on original observations in laboratory and clinical research from all scientists. A manuscript is considered for publication with the understanding that it has not been published previously and is submitted exclusively to the Journal. Opinions expressed by the authors are not necessarily those of the publisher or its editors.

THE JOURNAL is published monthly (two volumes a year). The Secretary of Health and Human Services has determined that the publication of this periodical is necessary in the transaction of the public business required by law of this Department.

A MONOGRAPH SERIES covering proceedings of scientific meetings pertaining to cancer is also published. These books may be purchased from the Superintendent of Documents. Series subscriptions are not available and monographs are not included in a subscription to the Journal.

THE JOURNAL is for sale by the Superintendent of Documents, U.S. Government Printing Office, Washington, D.C. 20402. Price per copy, $6.00. Subscription price for two volumes per year in the United States, $65.00; foreign, $81.25. Payment is required in advance, and check or money order should be made payable to the Superintendent of Documents.

All inquiries regarding purchase of subscriptions or depository library distribution, including inquiries about missing issues and change of address, should be addressed to the Government Printing Office. The Government Printing Office requires payment in advance on all orders. Inquiries regarding missing issues or change of address for official subscriptions should be addressed to the Editorial Office, Room 850, Westwood Building, 5333 Westbard Avenue, Bethesda, Md. 20016.

VINCENT T. DEVITA, JR., *Director, National Cancer Institute*

BOARD OF EDITORS

ELIZABETH K. WEISBURGER, *Acting Editor in Chief*

STUART A. AARONSON, *Associate Editor*

MARY A. FINK, *Associate Editor*

JANET W. HARTLEY, *Associate Editor*

DONALD HENSON, *Associate Editor*

RONALD B. HERBERMAN, *Associate Editor*

GEORGE S. JOHNSON, *Associate Editor*

KURT W. KOHN, *Associate Editor*

ARTHUR S. LEVINE, *Associate Editor*

JOHN J. MULVIHILL, *Associate Editor*

ALAN S. RABSON, *Associate Editor*

RICHARD M. SIMON, *Associate Editor*

EDITORIAL STAFF

EDWIN A. HAUGH, *Managing Editor*

PAMELA T. ALLEN, *Assistant Managing Editor*

FLORENCE I. GREGORIC, *Monograph Editor*

Editors: DOROTHY D. KATZ, MERCEDES B. LA CHARITY, I. AGNES REVESZ, JOAN O'BRIEN RODRIGUEZ, CONSTANCE R. STONESTREET, and ANNA B. WITTIG

JNCI (NIH Publication No. 82-13)

U.S. DEPARTMENT OF HEALTH AND HUMAN SERVICES Public Health Service National Institutes of Health

Instructions to Authors

Text: Send one original and two copies. **Text-figures** (graphs, charts, and line drawings): Send one original and two copies. **Figures** (photomicrographs and photographs): Send three original glossy prints, unmounted. **Tables:** Send tabular material in typewritten form; do not submit tables as glossy prints to be photographed. The entire manuscript including footnotes, legends, and references must be typed double spaced. Single-spaced portions of a manuscript will be returned to the author for retyping. The mailing address is: Journal of the National Cancer Institute, Westwood Building, Room 850, 5333 Westbard Avenue, Bethesda, Maryland 20016.

Manuscripts should be accompanied by a covering letter from the author responsible for correspondence about the manuscript. The covering letter should contain a statement that the manuscript has been seen and approved by all authors and that all persons listed as authors have made significant (not merely administrative, technical, or supervisory) contributions to the content of the paper. The letter should also state that the manuscript or substantial portions thereof have not been previously published nor are they under consideration for publication in another journal.

Data too extensive for inclusion in a manuscript, but which may be of interest to other investigators, may be deposited with the National Auxiliary Publications Service (NAPS), c/o Microfiche Publications, P.O. Box 3513, Grand Central Station, New York, New York 10017. Authors using the NAPS facilities should indicate in a footnote how their additional data may be obtained.

Approximately one-half of all manuscripts submitted to the Journal are accepted for publication. Publication of manuscripts is contingent on transfer of copyright to the Journal. Forms for this purpose will be sent to authors when a manuscript has been approved for publication. All material published in the Journal is in the public domain; therefore, permission to reproduce any portions is not necessary. As a matter of courtesy, communication should be made to the author(s) concerned.

TITLE: Be brief (no more than 14 words, if possible), but for indexing purposes include all key words. The annual subject index is prepared directly from the titles. Titles that form complete sentences are not acceptable. Do not use abbreviations or chemical formulas in titles.

BYLINE: Supply the complete first name, middle initial, and last name of each author. Avoid use of nicknames. Academic degree is optional; however, if a degree is provided for one author, it should be provided for all authors on a manuscript. Include the name of the institution, address, and zip code for each author. Indicate address for reprint requests in a footnote on the byline.

ACKNOWLEDGMENTS: Financial aid in support of research should be recognized in a footnote. Aid in technical fields, animal care, photography, stenography, and other areas may be mentioned in a separate footnote. Indicate the title (Dr., Mr., Mrs., Miss, Ms.) and affiliation of each person acknowledged.

ABSTRACT: Provide an abstract, 150 words or less, on a separate page. The abstract should describe only *results* of the work being reported. Speculation, historical background, or reference to published works will be deleted from abstracts. Any inbred strains, outbred stocks, cell lines, or other living materials used in the work should be noted in the abstract.

TEXT: Avoid the use of laboratory jargon and abbreviations not in common usage. When possible, refrain from the use of abbreviations that form words (exceptions are PAGE, ALL). Whenever possible, write mathematical equations and chemical formulas on a single line; submit complicated chemical structures as artwork. Avoid repetition of data in the text when it is presented in tables or text-figures.

Use the following style sources: Webster's *Third New International Dictionary* and Dorland's *Illustrated Medical Dictionary* (25th ed) for spelling; *Council of Biology Editors Style Manual* (4th ed) for scientific abbreviations and symbols; *Government Printing Office Style Manual* for other abbreviations and symbols, punctuation, and hyphenation; *Collected Tentative Rules & Recommendations of the Commission on Biochemical Nomenclature IUPAC-IUB* (2d ed) for abbreviations of chemical substances; *Enzyme Nomenclature*, recommendations (1972) of the IUPAC-IUB for recommended names of enzymes and information on nomenclature of isoenzymes; *The Merck Index* (9th ed) for chemical compounds; "Standardized Nomenclature for Inbred Strains of Mice: Seventh Listing" by Joan Staats (Cancer Res 1980;40:2083-2128) for inbred mouse strains; "Standardized Nomenclature for Inbred Strains of Rats: Fourth Listing" by Joan Staats and Michael Festing (Transplantation 1973;16:221-245) for designations of inbred rat strains; *Animals for Research* (9th ed) prepared by the Institute of Laboratory Animal Resources, National Academy of Sciences, for designations of laboratory animal stocks and strains.

TABLES: Submit tabular material typed double spaced on a separate page. Computer print-outs of tables are acceptable only if they are double spaced and with satisfactory title, column headings, legends, and other textual material. Provide headings for all columns of a table and indicate units of measurement where applicable.

TEXT-FIGURES: Refer to graphs, charts, and line drawings as text-figures. Make the abbreviations on text-figures identical to the abbreviations used in the text and legends. Symbols and lettering should be large enough to be legible if reduced. Glossy prints or original drawings in black ink are acceptable; orient vertically instead of horizontally.

FIGURES: Refer to photomicrographs and photographs as figures. Figures and their legends should fit a 7.5- by 9-inch dimension. Calculate that nine typewritten lines of legend will require 1 inch of vertical space. Type figure legends on a separate sheet and identify in the legend any lettering used on the figure. Trim photographs to show only important areas. Do not number face of photographs; use the back or overlay to indicate the top and number of each. Printed indicators may be included on photographs; do not use hand-drawn indicators. *Insert internal scale markers on all photomicrographs.* Color photographs must be grouped as a single plate. For color reproduction, submit both color transparencies and high-quality black and white reproductions. The need for color must be documented before it will be considered.

REFERENCES: Use any recent issue of the Journal as a style guide for reference lists. Number references in order of citation in both text and reference list. For periodicals, provide author(s), title of paper, journal, year, volume, and first and last page numbers. For books, give the author(s), title, name(s) of editor(s), location and name of publisher, year, pertinent chapter or section title, and page numbers. Follow *Index Medicus* for punctuation and abbreviations. Citations of papers in preparation or submitted for publication, unpublished observations, and personal communications should be noted parenthetically in the text. Do *not* include them in the reference list. The accuracy of all references is the responsibility of the authors and not of the editorial staff.

LETTERS TO THE EDITOR should pertain to recent articles in the Journal and should not contain new data unless relevant to the discussion of a particular paper. The authors addressed will be invited to reply to comments before correspondence is published. Letters will be edited by the Staff, subject to contributor approval.

FURTHER DETAILS on the preparation of manuscripts are set forth in the document "Uniform Requirements for Manuscripts Submitted to Biomedical Journals" prepared by the International Steering Committee of medical editors (*see* Am Rev Respir Dis 1979;119:3-10/ Ann Intern Med 1979;90:95-99/ Br Med J 1979;1:532-535/ or Lancet 1979;1:428-430).

UNITED STATES GOVERNMENT PRINTING OFFICE, WASHINGTON, D.C.: 1982

Table of Contents

Vol. 68, No. 1——January 1982

1 Howard Bancroft Andervont, *D.Sc.*—A Tribute

Investigations on Man

3	Neoplasms following childhood radium irradiation of the nasopharynx	*Dale P. Sandler, George W. Comstock, Genevieve M. Matanoski*
9	Epithelial dysplasia in nipple aspirates of breast fluid: Association with family history and other breast cancer risk factors	*Nicholas L. Petrakis, Virginia L. Ernster, Eileen B. King, Susan T. Sacks*
15	Successful transplantation of a human leukemia cell into nude mice: Conditions optimizing graft acceptance	*H. W. (Löms) Ziegler, Glauco Frizzera, Fritz H. Bach*
19	Enhanced expression of melanoma-associated antigens and β_2-microglobulin on cultured human melanoma cells by interferon	*Shuen-Kuei Liao, Pak C. Kwong, Mohammed Khosravi, Peter B. Dent*
27	In vitro reversal of depressed T-lymphocyte function in the peripheral blood of brain tumor patients	*Gary W. Wood, Robert A. Morantz*
35	Human adherent cell contact-mediated modulation of normal myeloid colony formation	*Gary Spitzer, Dharmvir S. Verma, Miloslav Beran, Axel R. Zander, Kenneth B. McCredie, Karel A. Dicke*
43	Pathology panel for lymphoma clinical studies: A comprehensive analysis of cases accumulated since its inception	*Hun Kim, Ronald J. Zelman. Michael A. Fox, John M. Bennett, Costan W. Berard, James J. Butler, Gerald E. Byrne, Jr., Ronald F. Dorfman, Robert J. Hartsock, Robert J. Lukes, Risa B. Mann, Richard S. Neiman, John W. Rebuck, William W. Sheehan, Daina Variakojis, John F. Wilson, Henry Rappaport*
69	Maximizing differences in the concanavalin A-induced blastogenic responses of lymphocytes from breast cancer patients and controls by the use of α-methyl-D-mannoside	*John A. Distasio, David A. Cheresh, Russell J. Schilder, Charles L. Vogel, Michael A. Silverman, Diana M. Lopez*
75	Value of plasma α-1-acid glycoprotein assay in the detection of human colorectal cancer: Comparison with carcinoembryonic antigen	*Clement Y-T. Chu, Lilian T-Y. Lai, Hari P. Pokala*

81	Various isozyme gene expression patterns among human colorectal adenocarcinoma cell lines and tissues	*Lynne P. Rutzky, Michael J. Siciliano*
91	Coffee drinking and cancer of the lower urinary tract	*Alan S. Morrison, Julie E. Buring, Wendy G. Verhoek, Kunio Aoki, Ian Leck, Yoshiyuki Ohno, Koji Obata*
95	Noncontraceptive estrogen use and the occurrence of ovarian cancer	*Noel S. Weiss, J. Lynn Lyon, Sarala Krishnamurthy, Scott E. Dietert, Jonathan M. Liff, Janel R. Daling*
99	Multiple marker evaluation in human prostate cancer with the use of tissue-specific antigens	*M. Kuriyama, M. C. Wang, C. L. Lee, C. S. Killian, L. D. Papsidero, H. Inaji, R. M. Loor, M. F. Lin, T. Nishiura, N. H. Slack, G. P. Murphy, T. M. Chu*
107	Environmental factors in the etiology of rhabdomyosarcoma in childhood	*Seymour Grufferman, Helen H. Wang, Elizabeth R. DeLong, Sue Y. S. Kimm, Elizabeth S. Delzell, John M. Falletta*
115	Anticancer drugs: Effect on the cloning of Raji lymphoma cells in soft agar	*Pao-Chen Wu, Robert F. Ozols, Masakazu Hatanaka, Charles W. Boone*

Investigations on Nonhuman Systems

123	Antitumor activity of picolinic acid in CBA/J mice	*Susan W. C. Leuthauser, Larry W. Oberley, Terry D. Oberley*
127	Equivalency of endothelial cell growth supplement to irradiated feeder cells in carcinogen-induced morphologic transformation of Syrian hamster embryo cells	*Charles H. Evans, Joseph A. DiPaolo*
133	Effect of thymectomy on development of Lucké renal adenocarcinomas in virus-infected leopard frog tadpoles	*Louise A. Rollins-Smith, Nicholas Cohen*
139	Studies on the antitumor activities of pyrimidinone-interferon inducers. I. Effect against artificial and spontaneous lung metastases of murine tumors	*Luka Milas, Evan M. Hersh, Dale A. Stringfellow, Nancy Hunter*
147	Rat mammary tumor classification: Notes on comparative aspects	*Dymitr Komitowski, Bernard Sass, Walter Laub*
157	Induction of nasal tumors in rats exposed to hexamethylphosphoramide by inhalation	*Ki P. Lee, Henry J. Trochimowicz*

Meeting Highlights

173	Host factors in human carcinogenesis	*John J. Mulvihill*

Announcements

175 Sixteenth Annual Clinical Symposium

175 Thirty-Second Annual Conference of The National Council on the Aging, Inc.

175 Oncology Update 1982

175 North American Society for Cardiac Radiology—1982 Postgraduate Course

175 Second Annual Washington Imaging Conference

175 Fourth Annual Course in Flow Cytometry

175 Educational Video Cassettes

blank page

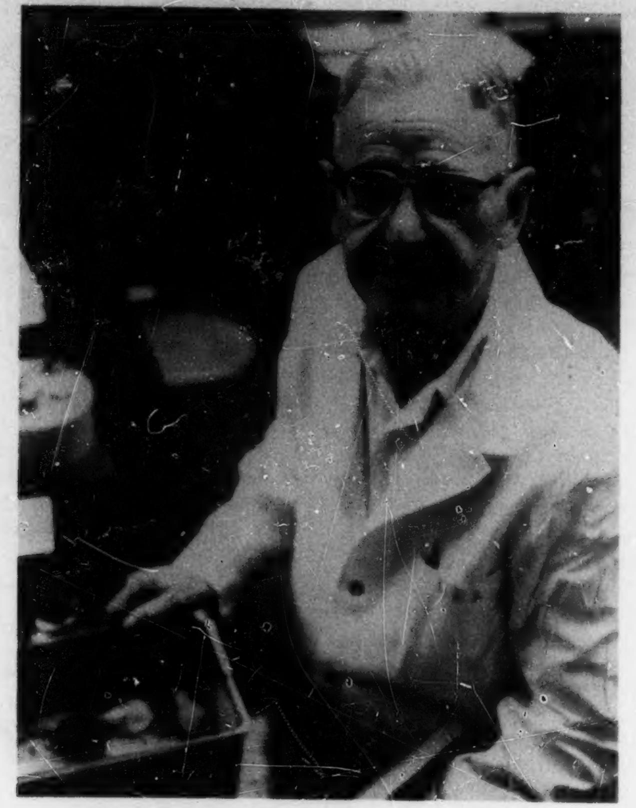

Howard B. Andervont, *D.Sc.*—A Tribute

Dr. Howard Bancroft Andervont, who died on March 11, 1981,[1] at the age of 83, served as Scientific Editor of the *Journal of the National Cancer Institute* from 1961 until his retirement from the Public Health Service in 1968. Dr. Andervont's association with the National Cancer Institute (NCI) had its beginnings in 1930 when he became the first professional staff member of the Office of Cancer Investigations in Cambridge, Massachusetts.[2] This group later became part of NCI and moved from Cambridge to Bethesda, Maryland, in 1939. His research work at NCI included significant contributions to the study of induced and spontaneous tumors in mice and the role of environment in the occurrence of breast cancer in mice. He pioneered the use of inbred animals for such studies.[3] When the NCI underwent a major reorganization in 1947, Dr. Andervont was named to head the Biology Section. This position later became Chief of the Laboratory of Biology, a post he held until 1961 when he became Editor of the *Journal of the National Cancer Institute*. He was active in many scientific societies and he served on numerous committees. In 1955 he was president of the American Association for Cancer Research.

In recognition of his important contributions to cancer biology and his editorial accomplishments, the Board of Editors of JNCI pays tribute to Howard B. Andervont, *D.Sc.*

---

[1] Obituary—Howard Bancroft Andervont. JNCI 1981; 67:1.

[2] SHIMKIN MB. Howard B. Andervont: An appreciation, J Natl Cancer Inst 1968; 40:xiii–xv.

[3] ———. As memory serves—an informal history of the National Cancer Institute. 1937–57. J Natl Cancer Inst 1977; 59:559–600.

blank page

Neoplasms Following Childhood Radium Irradiation of the Nasopharynx [1,2,3]

Dale P. Sandler, [4] **George W. Comstock,** [5,6] *and* **Genevieve M. Matanoski** [5,7]

ABSTRACT—Eighteen to 35 years after admission to a clinic for the prevention of deafness, no increased overall cancer risk could be detected among 904 persons who had been treated with nasopharyngeal radium irradiation when compared with the risk among 2,021 persons who were either treated surgically or not treated at all, although there were differences at specific sites. An increased risk of developing both benign and malignant head and neck tumors was found among irradiated persons. Whereas no one head and neck site showed a statistically significant excess, a slight excess of brain cancer occurred 15-20 years after radium treatment. No increase in thyroid cancer risk was observed, a result possibly attributable to the low radiation doses to this organ and the relatively small population irradiated.—JNCI 1982; 68:3-8.

Previous studies of populations treated with head and neck irradiation have demonstrated a link between head and neck irradiation and cancer, particularly for thyroid cancer at doses to the thyroid gland in the range of 100-1,000, rad (*1-6*). In addition to thyroid cancer, increased rates of leukemia (*2, 7, 8*), benign and malignant salivary gland tumors (*2, 4, 7*), benign and malignant brain tumors (*7-9*), other malignant neoplasms (*6-8, 10*), and benign thyroid tumors (*2, 8, 10, 11*) have been reported following head and neck X-ray irradiation.

The evidence that radiation doses lower than 20 rad are carcinogenic is less conclusive than for larger doses. Whereas Modan et al. (*7*) and Ron and Modan (*11*) demonstrated a fourfold to fivefold thyroid cancer risk following doses of 9 rad to the thyroid from treatment of tinea capitis, Shore et al. (*8*) found no increased thyroid cancer risk after similar treatment. Other suggestive evidence of increased thyroid cancer risk at doses as low as 20 rad includes the occurrence of one or two cancers in irradiated populations when none were expected (*9, 10*).

Screening programs for detection of thyroid cancer among irradiated persons (*12-14*) confirm a thyroid cancer risk and demonstrate a risk for benign thyroid tumors. In these analyses, the lack of appropriate comparison groups studied with equal care for occult thyroid tumors may have led to an overestimation of the thyroid cancer risk (*15, 16*). This situation may also be true for questionnaire surveys of irradiated populations, especially those studies in which the population has been resurveyed three or four times. The increasing ratio of benign to malignant tumors reported for these radiation-exposed populations on successive examination is consistent with more extensive case finding for subsequent surveys (*2, 8*).

The present study affords an opportunity to examine the possible effects of low-dose irradiation in a population that had no prior screening for such effects. Study subjects were treated during childhood with radium irradiation of the nasopharynx. The treatment, which reduced the size of the adenoids, was delivered to reduce the frequency of ear, nose, and throat infections and prevent the mild hearing loss associated with adenoid hypertrophy (*17*). The radium treatment involved inserting radium-containing applicators into the nasopharynx, where the resulting radiation dose was greatest. Other nearby sites, such as the brain and pituitary gland, also received some exposure. Unlike many of the other types of head and neck irradiation that have been studied, most radiation doses to the thyroid gland were lower than 20 rad.

METHODS

Study population and follow-up.—The study population consists of 2,925 persons from Washington County, Maryland, who were seen between 1943 and 1960 at a clinic established to prevent deafness among children. The population includes all persons who were first seen prior to 1960 and had become 21 years of age or had stopped coming to the clinic by 1978. Of the eligible study cohort of 2,925 persons, 904 (31%) had been treated with nasopharyngeal radium irradiation. The remaining 2,021 were treated with tonsil and

---

ABBREVIATION USED: RR = relative risk(s).

---

[1] Received September 10, 1980; revised July 27, 1981; accepted August 7, 1981.

[2] Supported by Food and Drug Administration research grant 1-R01-FD00977 from the Bureau of Radiological Health and by Public Health Service (PHS) grant CA24758 from the National Cancer Institute.

[3] Research procedures were in accord with the ethical standards of the Committee on Human Volunteers, The Johns Hopkins University School of Hygiene and Public Health.

[4] Biometry Branch, Epidemiology Program, National Institute of Environmental Health Sciences, National Institutes of Health, PHS, U.S. Department of Health and Human Services, P.O. Box 12233, Research Triangle Park, N.C. 27709.

[5] Department of Epidemiology, School of Hygiene and Public Health, The Johns Hopkins University, 615 North Wolfe St., Baltimore, Md. 21205.

[6] Recipient of PHS Career Development Award 5-K06-HL21670-18 from the National Heart, Lung, and Blood Institute.

[7] We thank the staffs of the Johns Hopkins Training Center for Public Health Research and of the Washington County (Maryland) Health Department for their assistance.

adenoid surgery or were given other treatment to relieve their symptoms.

The entire cohort was traced through a special county census that had been conducted in 1963 and again in 1975 (*18*), through telephone books and city directories, through departments of motor vehicles in Maryland and neighboring states, and through obituaries and death certificates. Other information used in tracing procedures included names of parents, names of siblings also seen at the Washington County Health Department clinics, address at time of visits to the clinic, and school attended.

Each traced individual was mailed an explanatory letter and a questionnaire for self completion. At the request of the Washington County Health Department, persons who had been irradiated were so notified. The questionnaires, however, were identical for the groups exposed and not exposed to radiation. Four main areas were emphasized: radiation exposure, tumor history, conditions potentially relating to pituitary gland function, and difficulty with hearing.

The first questionnaire mailing was followed by a second mailing to initial nonrespondents. Persons who did not return a questionnaire were contacted by an interviewer who obtained the questionnaire data over the telephone. Interviewers were not informed of the exposure status of study subjects. Nonrespondents living in Washington County were visited at home when telephone interviews were not possible.

To determine cause of death, death certificates were obtained for persons known to have died. Questionnaire reports of tumors, "lumps," or "growths" were followed up with requests to hospitals and physicians for pathology reports and diagnostic summaries, which were obtained for 80% of all hospitalizations for which the reported cause seemed in any way to be related to malignant or benign tumors. Financial restrictions precluded any review of pathology specimens.

To minimize reporting bias that might result from notification to the group about their past irradiation and from suggestions that they be examined, only illnesses diagnosed prior to the date of the first study letter were included in the analysis. For a subsample of the population who remained in Washington County, reported hospitalizations were compared with those gleaned from Washington County Hospital diagnostic indices and from the Washington County hospital-based tumor registry. There was no indication of over-reporting or under-reporting of hospitalizations for either group.

Radiation exposure and dosimetry.—When irradiation to the adenoids was recommended, a radium applicator, containing 50 mg of radium salt in a 15-mm length chamber screened with 0.3-mm monel metal, a nickel alloy, was inserted into each nostril. When in place, the radium chamber extended from the eustachian tube orifice back to the posterior nasopharyngeal wall, as close to the adenoids as possible. The monel metal filter allowed both β- and γ-rays to reach the surrounding tissues. The applicators were left in place an average of 12 minutes. Treatments were generally given three times at 2-week intervals. Occasionally, a treatment series was repeated after approximately 6 months (*19*).

The radiation doses at various distances from the applicators are listed in table 1. These doses were estimated with the use of a method that takes into account the varying energies and absorption fractions of the different products of radium decay and known properties of the radium applicators (*20*). The radiation dose is high at 1 cm, the area immediately surrounding the applicators, and drops off quickly as the distance from the applicators increases.

The distances from different tissues to the applicators are a function of the age and size of each individual at the time of treatment and the exact positioning of the applicators. These measurements were not available for the study population, but estimates of different tissue doses have been made by calculations for "average individuals" in each age group. Measurements were taken from skull films of individuals who were between 2 and 16 years old but were not in the study population. Distances from the radium applicators in the nasopharynx to the thyroid, pituitary, and salivary glands are shown in table 2. These measurements were in agreement with adenoid-thyroid distances reported by Hazen (*4*) for individuals between ages 4 and 17 years. Whereas the nasopharynx and eustachian tube orifices received approximately 700 rad, the pituitary gland and lower portion of the brain received approximately 78 rad from the standard three treatment series. In most instances, the thyroid gland was 6 to 12 cm from the applicators in the nasopharynx and received exposures ranging from less than 5 to 20 rad. The distribution of study subjects by age at first treatment and total number of treatments given are shown in table 3.

Data analysis.—Cancer incidence rates were based on person-years of observation. For persons with cancer, time at risk extended from the date of first treatment to the date of diagnosis of first cancer occurrence (or date of death if the information was obtained only from a death certificate). For persons without cancer, time at risk extended to the last date of observation.

The incidence rates for benign tumors and skin cancers were calculated only on the basis of the

TABLE 1.—*Estimated radiation doses for standard radium therapy*[a]

Distance, cm	Dose, rad
1	723
2	177
3	78
4	44
5	26
6	19
8	9
10	7
12	4

[a] Three 12-min treatments.

TABLE 2.—*Approximate distances from radium applicators to different anatomic sites*

Age, yr	Distance, cm, to:		
	Thyroid gland	Pituitary gland	Salivary glands
≤3	4–5	2–3	5–6
4	5–6	2–3	5–6
5	6–7	2–3	5–6
6	7–8	2–3	6–7
7	7–8	2–3	6–7
8	8–9	2–3	6–7
9	8–9	2–3	6–7
10	9–10	3–4	7–8
11	10–11	3–4	7–8
12	11–12	3–4	7–8
≥13	12–13	3–4	7–8

experience of individuals who completed a questionnaire. Incidence rates of cancers of sites other than skin were calculated on the basis of experience of all located individuals.

Standardized incidence ratios were used to adjust the crude cancer incidence rates for differences in ages and years of follow-up between subgroups exposed and not exposed to radiation. An indirect adjustment procedure that used an internal standard was used. We computed the standardized incidence ratios by using a multiplicative log-linear model described by Breslow and Day (*21*) and by using a computer program developed by Tonascia (*22*). With this program, maximum likelihood estimates of the ratio of the number of observed events in the groups exposed and not exposed to radiation to that expected on the basis of pooled standard rates adjusted by age/year for the entire study population were calculated. The ratio of the calculated standardized incidence ratios for the irradiated and nonirradiated subgroups provides a maximum likelihood estimate of the RR of that outcome. Confidence intervals were placed on the observed RR (ratios of two Poisson parameters) with the use of a method described by Ederer and Mantel (*23*) and modified by Hamman (*24*) in cases where age/year adjustment altered the observed RR.

RESULTS

Ninety percent of the study population was either located (87%) or determined to be dead (3%) (table 4). Tracing efforts were equally successful for persons exposed and not exposed to radiation. Located individuals were similar to those not located with respect to age at first clinic visit, year of birth, sex, race, reason for clinic visit, and examination findings.

Of 2,135 study subjects who were located alive, 84% completed a questionnaire either by mail, telephone, or home interview. Questionnaires were completed by mail for 60% of the respondents and by interview for 40%. A slightly greater proportion of the irradiated group completed a questionnaire (86%) than did the nonirradiated group (83%) (table 4).

Study subjects exposed and not exposed to radiation were not substantially different in mean age at start of follow-up, average length of follow-up, race, or sex (table 5). Irradiated and nonirradiated study subjects were also compared with regard to a number of clinical parameters at the first clinic visit. The 2 groups did not differ by family history of deafness, hearing loss at clinic visit, or frequency of colds. Radiation-exposed individuals, however, were more likely than others to have had a prior tonsillectomy and to have had frequent ear infections.

Tumor Incidence

The tumor incidence for exposed and nonexposed subjects is compared in table 6. The RR, adjusted for differences in age at entry into the study and in number of years of follow-up, are also shown.

There were no differences in the overall incidence of malignant neoplasms (RR = 1.1) or benign neoplasms (RR = 1.0), but there was a statistically significant overall excess of malignant neoplasms of the head and neck among exposed subjects. This excess was accounted for mainly by three brain tumor deaths for subjects exposed to radiation. The other malignant tumor was an undifferentiated anaplastic cancer of the soft palate. The RR of 1.6 for benign neoplasms of the head and neck was not statistically significant, but when combined with malignant neoplasms, the twofold increase in all head and neck neoplasms was statistically significant.

Thyroid cancer was not reported by either irradiated or nonirradiated individuals. There was, however, a

TABLE 3.—*Age at first treatment and number of treatments obtained for 904 individuals exposed to radiation*

Age at first treatment, yr	No. of persons given:				Total No. treated
	One or two treatments	Three treatments, one full series	Four or five treatments	Six treatments	
0–4	12	57	6	12	87
5–9	37	373	38	61	509
10–14	21	192	13	30	256
≥15	9	37	4	2	52
Total	79	659	61	105	904

TABLE 4.—*Success of efforts to trace study population and response rates for subjects exposed and not exposed to radiation*

Status	No. exposed to radiation (%)	No. not exposed to radiation (%)
Total population	904 (100.0)	2,021 (100.0)
Not located	96 (10.6)	202 (10.0)
Deceased	35 (3.9)	48 (2.4)
Located	773 (85.5)	1,771 (87.6)
Respondents	667 (86.3)	1,468 (82.9)
Nonrespondents	106 (13.7)	303 (17.1)

TABLE 5.—*Comparison of study subjects exposed and not exposed to radiation*

Parameter	Exposed to radiation	Not exposed to radiation
Mean age at start of follow-up, yr	8.8±0.18[a]	9.2±0.11[a]
Median date at start of follow-up	Sept. 1951	Dec. 1952
Mean age when lost to follow-up, yr	33.9±0.31[a]	32.8±0.20[a]
Average yr of follow-up	24.9±8.09[a]	23.4±7.29[a]
Percent male	56.1	52.9
Percent white	98.0	97.0
No. of subjects	904	2,021
Person-yr of follow-up	22,544	47,293
Peraon-yr of follow-up—questionnaire respondents only	18,500	37,600

[a] Values are means±SD.

twofold increase in the risk (not statistically significant) of benign thyroid neoplasms. There was an increased risk of neoplasms of the lymphatic and hematopoietic tissue (RR=1.7) and a decreased risk of breast cancer (RR=0), but neither risk was statistically significant.

Analyses were repeated separately for each sex. No additional differences of any consequences were observed.

Relationship of Radium Dose to Tumor Incidence

The average number of radium treatments given the exposed group and the average treatment age are shown in table 7. The number of treatments given persons who developed head and neck tumors did not differ from that of the irradiated group as a whole. Radiation-exposed individuals who developed head and neck tumors did not receive greater irradiation (mg-hr) than did other radiation-exposed subjects. In fact, because they were older at first radiation exposure, the radiation dose to the lower portion of the brain for the 3 persons who died from brain tumors approximated 44-78 rad, which was lower than the dose for the remaining radiation-exposed persons. Those who developed benign thyroid tumors had radiation doses to the thyroid gland between 6.5 and 9.3 rad.

DISCUSSION

An increased risk of developing tumors of the head and neck has previously been demonstrated for persons who were given X-ray treatment for benign head and neck disorders. Thyroid tumors have most often been reported, possibly due to the types of irradiation treatments that have been studied. The treatments for enlarged thymus glands, enlarged tonsils and adenoids, and hemangiomas of the head and neck usually in-

TABLE 6.—*Comparison of tumor incidence in study subjects exposed and not exposed to radiation*

Type of neoplasm	No. exposed to radiation (rate/100,000)	No. not exposed to radiation (rate/100,000)	Adjusted RR[a]
Total malignant neoplasms	23 (102.6)	46 (97.8)	1.06 (0.61–1.77)
Malignant neoplasms of head and neck (excluding skin)	4 (17.8)	0 (0.0)	Inf (1.39–inf)
Brain	3 (13.3)	0 (0.0)	Inf (0.87–inf)
Lymphatic and hematopoietic tissue	3 (13.3)	4 (8.5)	1.69 (0.23–9.30)
Breast	0 (0.0)	5 (22.4)	0.00 (0–2.46)
Skin cancer of head and neck	4 (21.6)	5 (13.3)	1.59 (0.32–7.56)
Total benign neoplasms	98 (551.0)	196 (539.6)	0.99 (0.80–1.33)
Benign neoplasms of head and neck	19 (103.1)	23 (61.4)	1.67 (0.86–3.22)
Benign neoplasms of head and neck (excluding thyroid gland)	16 (86.8)	20 (53.4)	1.59 (0.79–3.30)
Thyroid gland	3 (16.2)	3 (8.0)	2.01 (0.26–15.17)
Total malignant and benign neoplasms of head and neck	23 (102.5)	23 (48.9)	2.08 (1.12–3.91)

[a] Adjusted for differences in age at entry into the study and yr of follow-up. *Numbers in parentheses* are 95% confidence limits on adjusted RR; inf=infinite No.

TABLE 7.—*Average number of treatments, treatment dose, and median age at first exposure to radiation for individuals with selected neoplasms*

Neoplasm	No.	No. of treatments	Dose, mg–hr	Median age at exposure, yr	Dose to site, rad
Malignant neoplasms of head and neck	4	2.63	46.50	11	4–723
Brain cancer	3	3.00	56.00	11	44–78
Benign neoplasms of head and neck, excluding thyroid gland	16	3.53	71.19	9	7–723
Benign neoplasms of the thyroid gland	3	3.13	62.50	9	6–9
Total radiation-exposed subjects					

cluded the thyroid gland in the radiation ports. The resulting radiation doses to the thyroid gland were generally in excess of 100 rad, and thyroid tumorigenesis has been most convincingly demonstrated at or above this level.

Many of the studies of persons with head and neck irradiation that have appeared in the literature have relied on population cancer rates (*5, 7, 9*) or cancer rates among siblings (*2, 4, 7*) for statistical comparison. One potential shortcoming of studies of groups exposed to radiation for treatment of some medical condition is that the medical condition itself may be related to later cancer risk. Furthermore, for certain tumors with a familial component, cancer risk from irradiation could be underestimated when sibling controls are used. In the present study the radiation-exposed group and comparison group consisted of persons who were seen at the same clinic for similar reasons. The 2 groups were also similar for a variety of economic, medical, and ethnic factors. The possibility that individuals who did not receive radiation exposure might have a cancer risk different from those who were treated cannot be ruled out. However, this possibility is less likely to be so than with a general population comparison.

The size of the radiation-exposed population in this study is inadequate to detect with reasonable power small increases in cancer risk at specific sites. However, large populations of radiation-exposed individuals are not easily identified. Nonetheless, consistency of suggestive findings in different populations may be sufficient to establish the presence of a disease risk. In addition, whereas the existence of no effect can never be proved, it is possible, by use of data from smaller studies, to define limits of disease risk. The overall increased incidence of benign and malignant head and neck tumors among irradiated subjects in the present study is consistent with what has been found in other populations.

In this study, by far the greatest radiation dose was to the nasopharynx and eustachian tube orifices. The applicators probably placed the radium source no more than 2-4 cm from the pituitary fossa. The nasal passages, sinuses, larynx, pharynx, and salivary glands generally were within 8 cm of the applicators and were thus likely to have received radiation doses that were greater than 10 rad. The thyroid gland, which was further from the applicators, received doses that most often ranged from 20 to 5 rad or fewer.

The one cancer site that did appear to be in excess among the irradiated subjects in this study was the brain. A possible etiologic role of radiation in the development of brain tumors has been demonstrated by others (*4, 7-9*). The most convincing evidence has come from studies of persons irradiated for tinea capitis (*7, 8*), for whom brain doses were estimated to have been between 140 and 150 rad at the surface and 50 rad at the pituitary fossa. In this study, the average pituitary dose following nasopharyngeal radium irradiation was between 44 and 177 rad. Brain doses were likely lower than this, being higher centrally and caudally and lower at the cortex. Two of the tumors were astrocytomas; autopsy information was not available for the third tumor. Irradiation-related brain tumors are often meningiomas (*7, 25*), perhaps because most radiation sources deliver the highest doses to the surface of the brain. However, 2 of the 6 tumors reported by Shore et al. (*8*) were astrocytomas.

The crude cumulative brain tumor incidence rate for radiation-exposed subjects in our population was 3.7 per 1,000 individuals, which is higher than that reported at 1.4 by Modan et al. (7) or at 2.8 by Shore et al. (*8*). The 3 tumors we found were all diagnosed between 15 and 20 years after treatment, which is consistent with the latent interval reported by Modan et al. (7) and Shore et al. (*8*). The average age at treatment of individuals with brain tumors was 11 years old, and all 3 patients received only the standard number of radium treatments.

Only 1 other malignant head and neck tumor was reported for study subjects. This was a cancer of the soft palate in an individual who received 10-20 rad to the soft palate.

Although no thyroid cancer was observed in the present study, the possibility that thyroid doses as low as these might be carcinogenic cannot be ruled out, because the study sample size was too small to detect less than an eightfold cancer risk with 80% power. Furthermore, the use of a questionnaire rather than an examination to determine tumor incidence reduced the likelihood of finding tumors that might exist.

Although the incidence of thyroid cancer in this population may have been underestimated, it is also possible that other studies have overestimated the risk because of preferential case finding (*15, 16*). For the present study, prior knowledge of radiation exposure and effects is not likely to have led irradiated individuals to preferentially seek medical care. Radiation-exposed individuals did not often associate the radium treatments with radiation, because no X-rays were used. Although 60% of radiation-exposed individuals reported knowing they had received treatments (as did 4% of the group not exposed to radiation), only 12% of the irradiated group reported asking a physician about radiation exposure. Furthermore, only 7% of irradiated subjects and 4% of nonirradiated subjects reported having thyroid scans.

Although we reported the incidence of benign thyroid nodules in the irradiated group to be twice that in the nonirradiated group, this finding could easily have occurred by chance. An increased risk of developing thyroid adenomas has been reported for irradiated individuals (*8, 11*). None of the thyroid nodules we report have been classified as adenomas, but because we did not review pathology specimens, we cannot be sure that none of the nodules were true adenomas.

If the slight increase in benign thyroid tumors in the radiation-exposed group is not due to chance, it may be related to thyroid irradiation, or it might also be due to pituitary irradiation. As in the populations irradiated for tinea capitis (*7, 8*) and in other populations for whom increased thyroid tumor risks have been confirmed (*4, 26*), the individuals in our study population received substantial doses of radiation to the pituitary gland along with lesser doses to the thyroid gland. Pituitary irradiation is thought to increase production of thyroid-stimulating hormones (*4, 27*) and excessive thyroid stimulation may play a role in the development of benign thyroid tumors in addition to that played by minimal radiation doses to the thyroid gland.

The absence of breast cancer among the radiation-exposed women when five cases were reported for the nonirradiated group is interesting in view of the fact that the questionnaire was designed to detect abnormalities that might be related to pituitary function. A decreased incidence of breast cancer has also been reported for one other population that received substantial pituitary exposure from nasopharyngeal radium treatments (*4*).

ADDENDUM

After completion of the survey, one malignant thyroid tumor was reported by an individual exposed to radiation. This indicates that a thyroid cancer risk might be demonstrated with longer follow-up. However, this could also reflect increased medical surveillance following notification of irradiation.

REFERENCES

(*1*) Pifer JW, Toyooka ET, Murray RW, Ames WR, Hempelmann LH. Neoplasms in children treated with X rays for thymic enlargement. I. Neoplasms and mortality. J Natl Cancer Inst 1963; 31:1333-1356.

(*2*) Hempelmann LH, Hall WJ, Phillips M, Cooper RA, Ames WR. Neoplasms in persons treated with X-rays in infancy: Fourth survey in 20 years. J Natl Cancer Inst 1975; 55:519-530.

(*3*) Shore RE, Woodard ED, Pasternak BS, Hempelmann LH. Radiation and host factors in human thyroid tumors following thymus irradiation. Health Phys 1980; 38:451-465.

(*4*) Hazen RW, Pifer JW, Toyooka ET, Livingood J, Hempelmann LH. Neoplasms following irradiation of the head. Cancer Res 1966; 26:305-311.

(*5*) Hanford JM, Quimby EH, Frantz VK. Cancer arising many years after radiation therapy. JAMA 1962; 181:132-138.

(*6*) Saenger EL, Silverman FN, Sterling TD, Turner ME. Neoplasia following therapeutic irradiation for benign conditions in childhood. Radiology 1960; 74:889-901.

(*7*) Modan B, Baidatz D, Mart H, Steinitz R, Levin SG. Radiation induced head and neck tumours. Lancet 1974; 1:277-279.

(*8*) Shore RE, Albert RE, Pasternack BS. Follow-up study of patients treated by x-ray epilation for tinea capitis. Arch Environ Health 1976; 31:17-24.

(*9*) Pifer JW, Hempelmann LH, Dodge HJ, Hodges II. Neoplasms in the Ann Arbor series of thymus-irradiated children; a second survey. Am J Roentgenol 1968; 103:13-18.

(*10*) Janower ML, Miettinen OS. Neoplasms after childhood irradiation of the thymus gland. JAMA 1971; 215:753-756.

(*11*) Ron E, Modan B. Benign and malignant thyroid neoplasms after childhood irradiation for tinea capitis. JNCI 1980; 65:7-11.

(*12*) Murphy ED, Scanlon EF, Swelstad JA. A community hospital thyroid recall clinic for irradiated patients. In: deGroot LJ, ed. Radiation associated thyroid carcinoma. New York: Grune, 1977:35.

(*13*) DiGuilio W, Douglas R, Fink-Bennett D, et al. Results of screening patients with prior irradiation to the head and neck in five Detroit area hospitals. In: deGroot LJ, ed. Radiation associated thyroid carcinoma. New York: Grune, 1977:33.

(*14*) Schneider AB, Favus MJ, Stachura ME, Arnold J, Arnold MJ, Frohman LA. Incidence, prevalence and characteristics of radiation-induced thyroid tumors. Am J Med 1978; 64:243-252.

(*15*) Royce PG, MacKay BR, DiSabella PM. Value of post-irradiation screening for thyroid nodules. A controlled study of recalled patients. JAMA 1979; 242:2675-2678.

(*16*) Utiger RD. Editorial. JAMA 1979; 242:2702.

(*17*) Crowe SJ. Irradiation of the nasopharynx (Wherry memorial lecture). Trans Am Acad Ophthalmol 1946; 51:29-35.

(*18*) Comstocx GW, Abbey H, Lundin FE. The nonofficial census as a basic tool for epidemiologic observations in Washington County, Maryland. In: Kessler II, and Levin ML, eds. The community as an epidemiologic laboratory. Baltimore: Johns Hopkins Press, 1970:73-99.

(*19*) Proctor DF, Willard WR. Washington County (Maryland) program for the prevention of deafness in children. Arch Otolaryngol 1946; 43:462-472.

(*20*) Brownell GL, Ellett WH, Reddy AR. Absorbed fractions for photon dosimetry. J Nucl Med 1968; suppl 1:29-39.

(*21*) Breslow NE, Day NE. Indirect standardization and multiplicative models for rates with reference to the age adjustment of cancer incidence and relative frequency data. J Chronic Dis 1975; 28:289-303.

(*22*) Tonascia J. Computer program for the calculation of standardized mortality ratios using the method of Breslow and Day. Baltimore: The Johns Hopkins University School of Hygiene and Public Health, 1979.

(*23*) Ederer F, Mantel N. Confidence limits on the ratio of two Poisson variables. Am J Epidemiol 1974; 100:165-167.

(*24*) Hamman R. Cause specific mortality rates among old order Amish. Doctoral thesis. Baltimore: The Johns Hopkins University School of Hygiene and Public Health, 1978.

(*25*) Waga S, Handa H. Radiation-induced meningioma with review of the literature. Surg Neurol 1967; 5:215-219.

(*26*) Toyooka ET, Pifer JW, Crump SL, Dutton AM, Hempelmann LH. Neoplasms in children treated with X rays for thymic enlargement. II. Tumor incidence as a function of radiation factors. J Natl Cancer Inst 1963; 31:1357-1377.

(*27*) Shalet SM, Beardwell CG, MacFarlane IA, Morris Jones PH, Pearson D. Endocrine morbidity in adults treated with cerebral irradiation for brain tumors during childhood. Acta Endocrinol (Copenh) 1967; 84:673-680.

Epithelial Dysplasia in Nipple Aspirates of Breast Fluid: Association With Family History and Other Breast Cancer Risk Factors [1,2,3]

Nicholas L. Petrakis, [4,5] **Virginia L. Ernster,** [4] **Eileen B. King,** [4] *and* **Susan T. Sacks** [4,6]

ABSTRACT—Because of the strong association of epithelial dysplasia and breast cancer, the extent to which dysplasia of breast fluid epithelial cells obtained by nipple aspiration is associated with breast cancer risk factors was investigated. A significantly higher proportion of women who had a first-degree family history of breast cancer had dysplastic cells in breast fluid than women who had no such history. When family history status was correlated with various breast cancer risk factors, higher proportions of women with dysplasia were found among those who had a first degree family history of breast cancer and for whom certain other risk factors were present, which suggested additive and synergistic effects of these factors on breast epithelium. Breast epithelia of women with a first-degree family history of breast cancer may be more prone to abnormal differentiation in response to environmentally conditioned risk factors.—JNCI 1982; 68:9–13.

Breast gland epithelial alterations and abnormalities (hyperplasia, atypical hyperplasia, dysplasia, and carcinoma in situ) have been identified in breast tissue associated with carcinoma and appear to reflect a sequence of histopathologic events antedating frank cancer (*1, 2*). Breast fluid contains epithelial cells that are desquamated from the epithelial lining of the ductal-lobular system of the breast. Beginning in 1958, investigators have reported the occurrence of abnormal epithelial cells in nipple aspirates of breast fluid (*3–7*). Studies correlating breast fluid cytology with breast histopathology have shown that atypical hyperplastic epithelial (dysplastic) cells in nipple aspirates are shed from ductal-lobular epithelium and that this cytologic abnormality is associated with the presence of cancer (*6–8*). In a recent analysis of breast fluid from 3,208 women, cytologic dysplasia was present in 13.9% of asymptomatic women, in 19.5% of women whose tissue biopsy indicated benign disease, and in 58.6% of breast cancer patients (*9, 10*). Because of the strong association of dysplasia with breast cancer, we investigated the extent to which dysplasia of breast fluid epithelial cells was associated with breast cancer risk factors.

It has been known for many years that breast cancer has a familial component. Women whose first-degree relatives (mother, sister, or daughter) had breast cancer have a twofold to threefold increased lifetime risk of developing the disease, and they are even more at risk if the familial cancer was premenopausal rather than postmenopausal (*11*). An allele that increases susceptibility to breast cancer in certain very high-risk families, apparently linked to the polymorphic glutamate-pyruvate transaminase locus on chromosome 10, has been reported (*12*). How such a "susceptibility gene" might function to predispose to breast cancer is unknown, but the finding strengthens the likelihood that genetically determined susceptibility to breast cancer may exist in the general population.

An obvious site for the detection of such a genetic influence might be the breast epithelium itself. We present a preliminary analysis of the possible effect that risk factors have on breast epithelial cytology in terms of the classic nature-nurture model, whereby "genes plus environment equals phenotype." In this model the phenotype (cytologic dysplasia) results from a combination of "genetic" susceptibility (a first-degree family history of breast cancer) and "environmentally influenced" factors (other possible breast cancer risk factors). The model, obviously, is an oversimplification because environmental factors may play a role in family history, and genetics may influence reproductive and other so-called environmental characteristics.

MATERIALS AND METHODS

The women for this study were volunteers examined at the Hospitals and Clinics of California, San Francisco; the Breast Screening Center of Northern California, Oakland, Calif.; and other community health and screening centers. All women completed a questionnaire on their demographic, clinical, marital, reproductive, and other characteristics. A specially trained nurse or a physician examined their breasts. Clinical evaluation of breast status was recorded as normal or as clinical gross fibrocystic disease. Women who had had cancer were excluded from this report. Aspiration of fluid was attempted from both breasts by a breast pump technique consisting of a modification of the Sartorius suction cup device which is placed over the nipple and is attached to a 10-ml syringe (*4, 13*). Retraction of the syringe creates a negative pressure in

---

[1] Received September 19, 1980; revised August 4, 1981; accepted August 13, 1981.

[2] Supported in part by Public Health Service grant P01CA-13556-10 from the National Cancer Institute.

[3] Research procedures were in accord with the Committee on Human Research, University of California, San Francisco.

[4] Department of Epidemiology and International Health, University of California, San Francisco, Calif. 94143.

[5] *Address reprint requests to* Dr. Petrakis, c/o Editor, Department of Epidemiology and International Health, 1699 HSW, University of California, San Francisco, Calif. 94143.

[6] We thank Ms. Diana Barrett, Ms. Karen Chew, Ms. Lois Kromhout, Ms. Lynn Mason, and Ms. Rei Miike for their technical assistance.

the cup, yielding fluid that is collected in capillary tubes. The methods used in the preparation of the breast fluid for cytologic examination have been described previously (*6, 7*).

The breast fluid specimens were classified cytologically into 2 groups: *a*) normal or showing benign hyperplasia and *b*) showing dysplasia, with various degrees of atypia (figs. 1A–D). The dysplasia group with the significant breast epithelial abnormality is characterized by groups of epithelial cells and single cells that show overall nuclear enlargement, variation in nuclear size, chromatin pattern and nucleolar prominence.[7]

In our analysis, we included only women from whom satisfactory bilateral fluid samples were obtained for cytologic examination. An independent analysis of unilateral samples revealed results similar to those obtained with bilateral samples. The criterion for a satisfactory smear was the presence of colostrum (foam) cells indicating that a breast fluid sample had been obtained. The analysis was limited to white women under age 50, in view of our previous findings and those of others that secretory patterns vary by race and age (*13, 14*). Breast fluid can be obtained from about 70% of white women between 30 and 50 years of age. The percentage drops sharply in older women, making secretors over age 50 much less representative of their age group than younger secretors. Inasmuch as family history of breast cancer is thought to be a more significant factor in breast cancers that develop earlier in life than in those that occur later in life, the under-50 age group seemed the most plausible one for our inquiry. Our final study population comprised over 1,100 white women under age 50, of whom 15.3% were found to have cytologic dysplasia in one or both breast fluid samples.

A number of breast cancer risk factors were compared between women with dysplasia (cases) and women with normal nipple aspirates (controls), including age at menarche, parity, age at first pregnancy, nursing history, gross fibrocystic disease as diagnosed by physical examination, use of oral contraceptives and menopausal estrogens, and first-degree family history of breast cancer.

Gross fibrocystic disease status was based solely on physical examination by physicians and by trained and experienced nurses using standard criteria. While some differences in this diagnosis would be expected among examiners, it is likely that most would agree on the presence of gross fibrocystic disease. Gross fibrocystic disease is prevalent among white U.S. women, but only a small proportion of biopsy specimens are taken from women with this disease. The women in our study consist of the group with clinical evidence of fibrocystic disease who at the time of examination did not warrant surgical intervention. Other findings indicate that even greater proportions of women have microscopic evidence of fibrocystic disease (*15*).

Analytic methods were those standard to case-control studies, including estimation of the relative risk of cytologic dysplasia associated with various factors by means of the odds ratio and its 90% confidence intervals. The data were adjusted for age by the method of Mantel and Haenszel (*16*).

We investigated the following hypotheses: A) The risk factors for breast cancer are associated with epithelial dysplasia in breast nipple aspirates. B) The relation between family history of breast cancer and dysplasia holds when other variables are controlled. C) First-degree family history of breast cancer and fibrocystic disease interact to increase risk of cytologic dysplasia in breast fluid.

RESULTS

Hypothesis A.—Table 1 shows the estimated risk ratio and 90% confidence limits (age-adjusted) of cytologic dysplasia for several major factors thought to influence risk of breast cancer as well as for the minor factors (i.e., use of oral contraceptives and menopausal estrogens). Only family history of breast cancer was found to be positively associated with cytologic dysplasia; clinically palpable fibrocystic disease was of borderline significance. Early menarche, nulliparity,

TABLE 1.—*Cytologic dysplasia in nipple aspirates associated with breast cancer risk factors*[a]

Risk factors	Odds ratio	90% confidence interval
Menarch: ≤12 vs. ≥13 yr of age	0.94	0.71–1.25
Parity: nulliparous vs. parous	1.04	0.72–1.50
Age at first pregnancy: ≥26 vs. ≤25 yr of age	1.26	0.90–1.80
Nursing: never vs. ever	0.71	0.52–0.98[b]
Clinical fibrocystic disease: present vs. absent	1.21	0.89–1.63
Family history of breast cancer (first degree): positive vs. negative	1.60	1.10–2.32[b]
Oral contraceptive use: ever vs. never	1.21	0.88–1.68
Menopausal estrogen use: ever vs. never	0.72	0.51–0.96[b]

[a] In white women <50 yr old (age adjusted).

[b] Mantel-Haenszel estimates of odds ratios, adjusted over categories of age in decades. In all comparisons, the referrent category was women who were at lower risk for a particular risk factor. The 90% confidence interval does not overlap 1.00.

---

[7] Lesions intermediate between benign and malignant disease have been called by a variety of terms. "Dysplasia" is the widely accepted term for describing such lesions of the uterine cervix. In the past, mammary dysplasia has meant any one or a combination of breast lesions in a broad spectrum of benign breast disease. We use the term "dysplasia" to describe epithelial atypia (of varying degrees of severity) of nipple secretion specimens and of breast tissue from biopsy or mastectomy. Although we subclassify the dysplasia of breast duct epithelium as mild, moderate, or severe, the results of subclassification will not be discussed here. In previous reports (*6–8*), we used the term "dysplasia" to describe severe atypia and "atypical hyperplasia" for lesser degrees of breast duct epithelial abnormality. Here the categories "atypical hyperplasia" and "dysplasia" are lumped together as "dysplasia."

age at first pregnancy, or oral contraceptive use showed no significant relation to abnormal breast fluid cytology. Never having nursed and using menopausal estrogen were negatively associated with cytologic dysplasia. The positive association of cytologic dysplasia with family history of breast cancer directed our attention to the genetic susceptibility model and gave impetus to the remaining analyses.

Hypothesis B.—We calculated the relative risk of dysplasia associated with a positive first-degree family history of breast cancer across subgroups of women differing with respect to the variables in table 1. Information on family history was available for 1,133 women, of whom 141 (12.4%) had a first-degree family history of breast cancer (table 2). Across strata, with one exception, family history of breast cancer was consistently associated with an increased risk of cytologic dysplasia, although the finding did not always attain statistical significance. When such variables as age at first pregnancy or clinical fibrocystic disease were controlled, the positive association between family history of breast cancer and cytologic dysplasia was maintained.

Hypothesis C.—Because family history of breast cancer and gross fibrocystic breast disease are important risk factors for both cytologic dysplasia and breast cancer, we wanted to know whether the combination of both factors increased risk of dysplasia beyond that observed when only one factor was present. That is, do first-degree family history of breast cancer and fibrocystic disease interact to increase risk of cytologic dysplasia in breast fluid?

TABLE 2.—*Cytologic dysplasia in nipple aspirates associated with positive family history of breast cancer, controlling for selected variables*[a]

Variable	No. of women	Odds ratio	90% confidence interval
Age, yr, at menarche			
≤12	67	1.40	0.79–2.48
≥13	566	1.90	1.14–3.15[b]
Parity			
Nulliparous	235	0.73	0.25–2.11
Parous	784	1.65	1.06–2.55[b]
Age, yr, at first pregnancy			
≤25	607	1.47	0.87–2.56
≥26	229	2.26	1.20–4.65[b]
Nursing history			
Never	403	2.68	1.46–4.85[b]
Ever	492	1.35	0.77–2.35
Clinical fibrocystic disease			
Absent	318	1.38	0.69–2.73
Present	810	1.63	1.04–2.58[b]
Oral contraceptive use			
Ever	760	1.17	0.73–1.91
Never	344	3.55	1.90–6.66[b]
Menopausal estrogen use			
Ever	414	2.23	1.24–4.03[b]
Never	636	1.47	0.89–2.38

[a] In white women <50 yr old (age adjusted).

[b] 90% confidence interval does not overlap 1.00.

TABLE 3.—*Cytologic dysplasia in breast nipple aspirates associated with family history and fibrocystic disease*[a]

Family history[b]	Clinical fibrocystic disease[b]	Odds ratio	90% confidence interval
–	–	1.00	
–	+	1.29	0.99–1.72
+	–	1.63	1.04–2.58[c]
+	+	1.91	1.09–3.25[c]

[a] In white women <50 yr old (age adjusted).

[b] –, absent; +, present.

[c] 90% confidence interval does not overlap 1.00.

We set at 1.00 the risk of dysplasia when neither a positive family history of breast cancer nor clinically palpable fibrocystic disease was present. We then calculated the odds ratios of dysplasia for women with fibrocystic disease alone, for those with a family history of breast cancer alone, and for those with both factors present. Table 3 shows an elevated risk in the presence of either factor alone (1.29 and 1.63); the risk was increased (to 1.91) in women who had both a family history of breast cancer and gross clinical fibrocystic disease. From these data one might conclude that family history of breast cancer and gross fibrocystic disease act additively to increase risk of dysplasia of epithelial cells in breast fluid aspirates.

DISCUSSION

Our findings indicate that among white women under 50 years of age *a*) dysplasia of epithelial cells in breast fluid aspirates is likely to be associated with a first-degree family history of breast cancer; *b*) the relationship holds if we control for other risk factors; and *c*) the relationship is strengthened in the presence of gross fibrocystic disease.

The outcome of interest in our study was breast fluid epithelial dysplasia, not breast cancer. Histopathologic studies are inconsistent that seek to determine whether atypical epithelial proliferation in benign breast lesions is associated with breast cancer (*17-20*), but, clearly, only a small proportion of women who undergo breast biopsy eventually develop breast cancer. Conversely, it would not be expected that all women having epithelial dysplasia in nipple aspirates would develop breast cancer. Instead, it seems more likely that epithelial dysplasia represents the response of the breast epithelium to a variety of chemical and endocrine influences. Changes in breast fluid cytology may be analogous to those found in Papanicolaou smears of the cervix in which dysplastic epithelium undergoes regression, persists for prolonged periods, or, in relatively rare instances, progresses to carcinoma in situ. Our criteria for the cells of dysplasia adhere to a definition of abnormal cells with conventional histopathologic criteria that have included a broad spectrum of benign breast diseases with or without duct epithelial atypia. Thus risk factors for dysplasia of breast fluid epithelial cells and breast cancer would not necessarily be expected to be identical. Not all women yield breast fluid when aspiration is attempted, and about one-fifth of fluid samples obtained are unsatisfactory for cytologic analysis. To the extent that breast epithelia of nonsecretors or scant secretors might not be similar to those of secretors, our findings may not be applicable to the entire population of white women under age 50.

Our findings strongly indicate that women with a family history of breast cancer and fibrocystic disease have a significantly greater risk of epithelial dysplasia in breast fluid, which suggests several areas for future investigation. The elevated odds ratios found in women with a positive family history of breast cancer when controlled for other risk factors need further study. We have demonstrated that the breast epithelia are in contact through metabolic and secretory mechanisms with exogenously and endogenously derived chemicals, including mutagenic and carcinogenic substances (*21–24*). We have detected in breast fluids substances giving positive Ames tests and, recently, cholesterol epoxides in a significant number of women. Cholesterol epoxides have been reported to be potent transforming substances, to damage chromosomes, to stimulate DNA repair in vitro, and to be carcinogenic in animals (*25–28*). The secretion of toxic and possibly carcinogenic substances by the breast might cause detectable morphologic changes in breast epithelium. These and other substances might exert greater effects on genetically susceptible epithelia of women with a family history of breast cancer, especially in the presence of fibrocystic disease. Future studies will attempt to determine whether the presence of such substances is related to the occurrence of epithelial dysplasia reported here.

REFERENCES

(*1*) Black MM, Chabon AB. In situ carcinoma of the breast. Pathobiol Annu 1969; 4:185–210.

(*2*) Wellings SR, Jensen HM, Marcum RG. An atlas of subgross pathology of the human breast with special reference to possible precancerous lesions. J Natl Cancer Inst 1975; 55: 231–273.

(*3*) Papanicolaou GB. Exfoliative cytology of the human mammary gland and its value in the diagnosis of cancer and other diseases of the breast. Cancer 1958; 11:377–409.

(*4*) Sartorius OW, Smith HS, Morris P, Benedict D, Friesen L. Cytologic evaluation of breast fluid in the detection of breast disease. J Natl Cancer Inst 1977; 59:1073–1080.

(*5*) Buehring GC. Screening for breast atypias using exfoliative cytology. Cancer 1979; 43:1788–1799.

(*6*) King EB, Barrett DL, King M-C, Petrakis NL. Cellular composition of the nipple aspirate specimen of breast fluid. I. The benign cells. Am J Clin Pathol 1975; 64:728–738.

(*7*) King EB, Barrett DL, Petrakis NL. Cellular composition of the nipple aspirate specimen of breast fluid. II. Abnormal findings. Am J Clin Pathol 1975; 64:739–748.

(*8*) King EB, Zimmerman AL, Barrett DL, Petrakis NL, King M-C. Cytopathology of abnormal mammary duct epithelium. In: Nieburgs HE, ed. Prevention and detection of cancer. Part II. Detection. Vol 2. Cancer detection in specifi es. New York: Marcel-Dekker, 1980:1831–1845.

(*9*) King EB, Chew K, Barrett DL, Ernster VL, Petrakis NL. Abnormal nipple aspirate cytology and proliferative changes in benign breast disease (Abstract). In: Proceedings of the 28th annual meeting of the American Society of Cytology, Boston, Mass., Nov. 4–8, 1980.

(*10*) King EB, Chew K, Ernster VL, Barrett DL, Petrakis NL. Abnormal nipple aspirate cytology and proliferative changes associated with malignant breast disease. In: Proceedings of the 29th Annual Meeting of the American Society of Cytology, St. Louis, Mo., 1981. Abstract. In press.

(*11*) Anderson DE. Breast cancer in families. Cancer 1977; 40:1855–1860.

(*12*) King M-C, Go RC, Elston RC, Lynch HT, Petrakis NL. Allele increasing susceptibility to human breast cancer may be linked to the glutamate-pyruvate transaminase locus. Science 1980; 208:406–408.

(*13*) Petrakis NL, Mason L, Lee R, Sugimoto B, Pawson S, Catchpool F. Association of race, age, menopausal status, and cerumen type with breast fluid secretion in nonlactating women, as determined by nipple aspiration. J Natl Cancer Inst 1975; 54:829–834.

(*14*) Petrakis NL, Ernster VL, Sacks ST, et al. Epidemiology of breast fluid secretion: Association with breast cancer risk factors and cerumen type. JNCI 1981; 67:277–284.

(*15*) Frantz VK, Pickren JW, Melcher GW, Auchincloss H Jr. Incidence of chronic cystic disease in so-called "normal breasts." Cancer 1951; 4:762–783.

(*16*) Mantel N, Haenszel W. Statistical aspects of the analysis of data from retrospective studies of disease. J Natl Cancer Inst 1959; 22:719–748.

(*17*) Black MM, Barclay TH, Cutler SJ, Hankey BF, Asire AJ. Association of atypical characteristics of benign breast lesions with subsequent risk of breast cancer. Cancer 1972; 29:338–343.

(*18*) Page DL, Vander Zwaag R, Rogers LW, Williams LT, Walker WE, Hartmann WH. Relation between component parts of fibrocystic disease complex and breast cancer. JNCI 1978; 61:1055–1063.

(*19*) Hutchinson WB, Thomas DB, Hamlin WB, Roth GJ, Peterson AV, Williams B. Risk of breast cancer in women with benign breast disease. JNCI 1980; 65:13–20.

(*20*) Kodlin D, Winger EE, Morgenstern NL, Chen U. Chronic mastopathy and breast cancer. A follow-up study. Cancer 1977; 39:2603–2607.

(*21*) Petrakis NL, Gruenke LD, Beelen TC, Craig JC, Castagnoli N. Nicotine in breast fluid of nonlactating women. Science 1978; 199:303–305.

(*22*) Petrakis NL, Maack CA, Lee RE, Lyon M. Mutagenic activity in nipple aspirates of human breast fluid. Cancer Res 1980; 40:188–189.

(*23*) Petrakis NL, Gruenke LD, Craig JC. Cholesterol and cholesterol epoxides in nipple aspirates of human breast fluid. Cancer Res 1981; 41:2563–2565.

(*24*) Petrakis NL. Epidemiologic studies of mutagenicity of breast fluids—relevance to breast cancer risk. Banbury report 8: Hormones and breast cancer. Cold Spring Harbor, N.Y.: Cold Spring Harbor Laboratory, 1981:243–255.

(*25*) Kelsey MI, Pienta RF. Transformation of hamster embryo cells by cholesterol-alpha-epoxide and lithocholic acid. Cancer Lett 1979; 6:143–149.

(*26*) Parsons PG, Goss P. Chromosome damage and DNA repair induced in human fibroblasts by UV and cholesterol oxide. Aust J Exp Biol Med Sci 1978; 56:287–296.

(*27*) Hieger I. Carcinogenic activity of lipoid substances. Br J Cancer 1949; 3:123–139.

(*28*) Bischoff F. Carcinogenic effects of steroids. Adv Lipid Res 1969; 7:165–244.

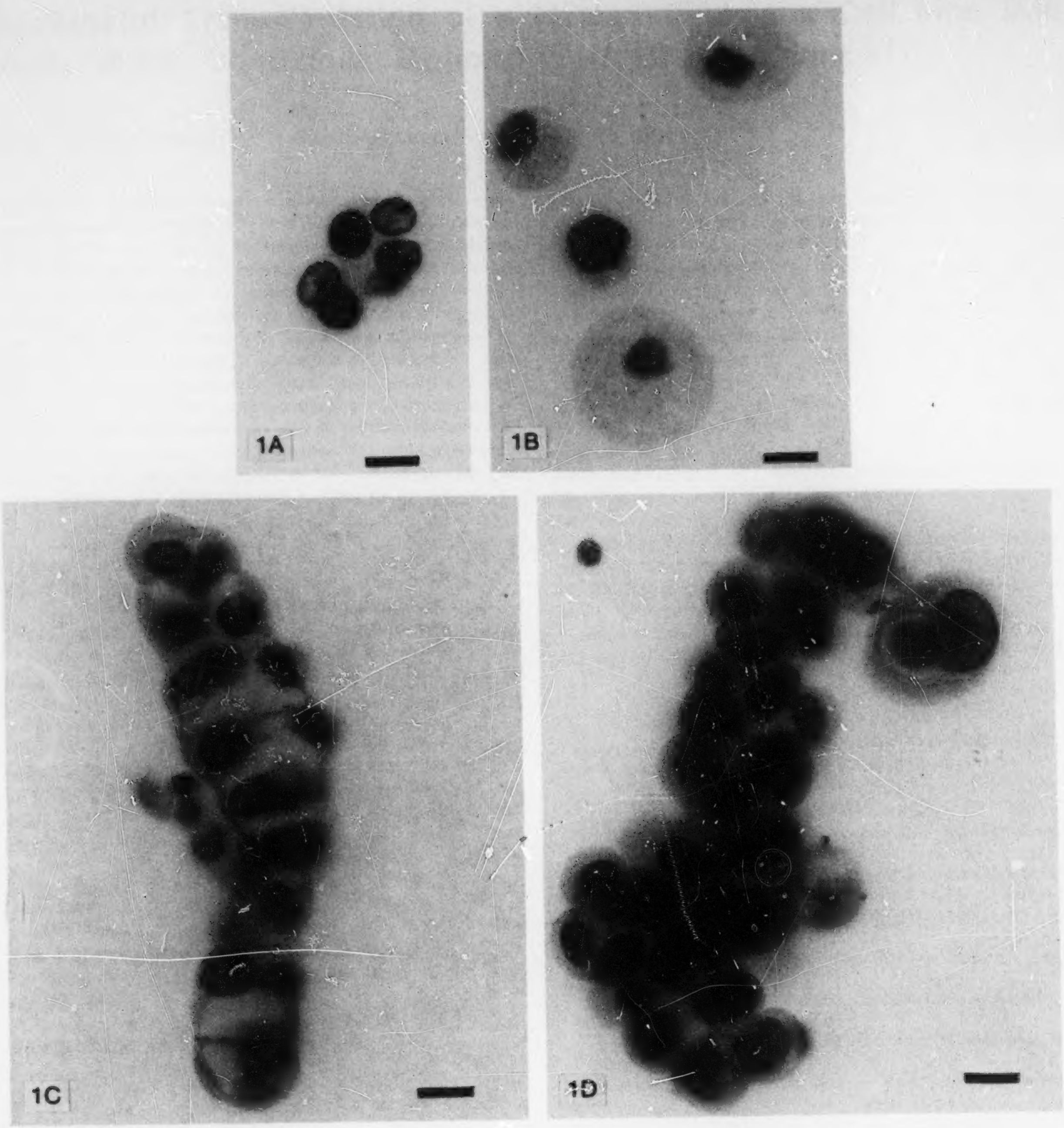

FIGURE 1.—A) Normal well-preserved duct cells have uniform oval nuclei with a finely granular chromatin pattern. B) Single cell suggesting dysplasia has a markedly enlarged nucleus and an increase in the nuclear:cytoplasmic ratio. *Note* uniform, coarse granularity of the chromatin pattern and irregular nuclear contour. C) Cells suggesting hyperplasia are slightly enlarged but remain fairly uniform. Chromatin is finely granular and evenly distributed. D) Cells suggesting atypical hyperplasia vary in nuclear size and shape, finely and coarsely granular chromatin, and prominent nucleoli. *Bars*=10 μm. × 250

blank page

Successful Transplantation of a Human Leukemia Cell Line Into Nude Mice: Conditions Optimizing Graft Acceptance[1,2,3,4]

H. W. (Löms) Ziegler,[5,6,7] **Glauco Frizzera,**[6] *and* **Fritz H. Bach**[5,6,8,9,10]

ABSTRACT—Conditions were determined for successful subcutaneous tumor development of MOLT-4 human T-cell leukemia cells in BALB/c nude (*nu/nu*) female mice. MOLT-4 cells injected alone at one site resulted in tumors in none of 21 mice, whereas MOLT-4 cells injected with X-irradiated human fibrosarcoma cells (HT-1080) at another site resulted in tumors in 5 of 21 mice. When X-irradiated three times with 200 rad over a 3-week period and then inoculated with MOLT-4 cells and X-irradiated HT-1080 cells, 19 of 25 mice developed tumors, which indicated that a combination of X-irradiation of the recipients and inoculation of an admixture of the leukemia cells with X-irradiated fibrosarcoma cells markedly increases tumor incidence. The cells growing in the tumors had the characteristics of MOLT-4, as assessed by marker studies and histology.—JNCI 1982; 68:15-18.

Many human solid tumors grow readily after transplantation into nude mice; this in vivo model has been used to assess the susceptibility of malignant cells to chemotherapy, radiotherapy, or immunotherapy (*1*). Growth of human leukemia cells following transplantation into nude mice is less successful; after sc injection into nude mice, only a few cell lines and a few fresh leukemia cells from patients have been reported to grow (*2, 3*). At least two reasons may account for this low success rate. 1) In contrast to solid tumors, leukemias usually grow by infiltrating the local tissue; no nodules thus form at the injection site, which may be due to the lack of the AGF (*4*). 2) Nude mice have high NK activity, and leukemia cells can be susceptible to natural killing even in xenogeneic combinations (*5*). In this report we show that MOLT-4 leukemia cells grow into palpable tumors when these cells are inoculated together with X-irradiated human fibrosarcoma cells into nude mice that have been preirradiated.

MATERIALS AND METHODS

Mice.—BALB/c nude (*nu/nu*) female mice 5-6 weeks old were obtained from Harlan Industries, Madison, Wis. They were kept under sterile conditions in cages with filter bonnets in a laminar flow unit (Lab Products, Rochelle Park, N.J.) and were fed Teklad L-485 sterilized mouse diet and distilled water plus antibiotics and vitamins. For irradiation, mice were placed in 50-ml sterile plastic tubes within their cages and then exposed to 200 rad once a week for 3 weeks.

Cell lines.—The human T-cell leukemia line MOLT-4, established by Minowada et al. (*6*), was grown in suspension culture in RPMI-1640 medium (KC Biologicals, Lenexa, Kans.) supplemented with 5% heat-inactivated FCS. Cells to be injected were taken from culture during the log phase of growth. HT-1080, a human fibrosarcoma cell line established by Rasheed et al. (*7*), was grown in monolayer culture in RPMI-1640 medium containing 5% FCS. HT-1080 cells were stored in liquid nitrogen and were thawed and X-irradiated with 6,000 rad before inoculation into mice.

Injection of tumor cells.—Each mouse received two sc injections, one into each anterolateral side of the thorax. One injection consisted of MOLT-4 cells alone (2×10^4, 2×10^5, or 2×10^6 in 0.2 ml); the other injection consisted of the same numbers of MOLT-4 cells and 2×10^6 X-irradiated (6,000 rad) HT-1080 cells in a total volume of 0.2 ml. Control mice given injections of only X-irradiated HT-1080 cells developed no tumors. We followed local tumor growth by measuring two perpendicular diameters.

Histology.—Five to 6 weeks after tumor cell inoculation, all mice were killed and tissue samples were fixed in B5 fixative (*8*), embedded in paraffin, and stained with hematoxylin and eosin.

Marker studies.—Two T-cell markers were used to determine whether the tumors were comprised of the

---

ABBREVIATIONS USED: AGF=angiogenesis factor; FCS=fetal calf serum; NK=natural killer; SRBC=sheep red blood cells.

---

[1] Received September 29, 1980; revised July 20, 1981; accepted August 13, 1981.

[2] Supported by Public Health Service (PHS) grants R01AI-15588 and R01AI-17687 from the National Institute of Allergy and Infectious Diseases and by PHS grants R01CA-27826 and CA-19527 from the National Cancer Institute.

[3] Paper No. 250 from the Immunobiology Research Center, University of Minnesota.

[4] Animals were maintained under the guidelines set forth by the University of Minnesota.

[5] Immunobiology Research Center, University of Minnesota, Minneapolis, Minn. 55455.

[6] Department of Laboratory Medicine and Pathology, University of Minnesota.

[7] *Present address:* Institute for Immunology, University of Munich, Schillerstrasse 42, 8 Munich 2, Federal Republic of Germany.

[8] Department of Surgery, University of Minnesota.

[9] *Address reprint requests to* Dr. Bach *at* Immunobiology Research Center, Box 724 May Memorial Building, University of Minnesota, Minneapolis, Minn. 55455.

[10] We thank Mr. Michael Allison (University of Minnesota) for his expert handling of the animals; all members of the Research Animal Resources at the University of Minnesota for their support; Dr. T. LeBien (University of Minnesota) for the MOLT-4 cell line; Dr. L. Furcht (University of Minnesota) for the HT-1080 cell line; Ms. Sandy Johnson (University of Minnesota) for her excellent histologic work; and Dr. Judah Folkmann (Harvard University Medical School) for helpful discussions.

MOLT-4 T-cell leukemia cells. 1) Acid phosphatase staining of imprints from the tumors and of smears from the MOLT-4 tissue culture cell line was done according to the technique of Li et al. (*9*). 2) Single cell suspensions of the tumors were rosetted with SRBC that were treated with *S*-(2-aminoethyl)isothiuronium bromide hydrobromide (AET) as previously described (*10*). Tumor cells with three or more SRBC attached were considered to have formed rosettes.

Statistical analysis.—Tumor incidences were statistically compared with the use of Fisher's exact probability test (*11*).

RESULTS AND DISCUSSION

Inoculation of MOLT-4 leukemia cells alone into nude mice failed to produce tumors in any of 21 recipients. In contrast, a combination of an admixture of MOLT-4 cells with X-irradiated HT-1080 fibrosarcoma cells and X-irradiation of the recipients resulted in tumor development in most nude mice.

The incidence of detectable tumors that developed in mice following inoculation of MOLT-4 cells with X-irradiated (6,000 rad) HT-1080 cells is shown in table 1. In experiment I, terminated 5 weeks after injection of the tumor cells, 2 of 10 mice that had not been X-irradiated developed tumors, whereas 12 of 13 mice that had been X-irradiated with 200 rad at weekly intervals three times before tumor cell inoculation developed tumors. In experiment II, terminated after 6 weeks, 3 of 11 unirradiated mice given injections of MOLT-4 cells plus X-irradiated HT-1080 cells developed tumors, whereas 7 of 12 preirradiated recipients developed tumors. Control mice inoculated with X-irradiated HT-1080 cells alone did not develop tumors. The data from both experiments reveal that the frequency of palpable tumors increased modestly when the MOLT-4 cells were injected with X-irradiated HT-1080 cells as compared to when these cells were injected alone in unirradiated mice (5/21 vs. 0/21, $p<0.01$). The frequency of tumor development in mice inoculated with MOLT-4 cells plus X-irradiated HT-1080 cells was much higher when the recipient mice were preirradiated (5/21 vs. 19/25, $P<0.001$).

Tumors were first detectable 2-3 weeks after transplantation. The sizes of the tumors at the time the mice were killed ranged from 2×2 mm to 17×18 mm with an overall range of 9 mm in diameter in both experiments. The soft tumor was evenly round with a lens shape on the cut sections. The central portion of the tumor often showed a core of fibrous trabeculae, containing capillaries. Small areas of necrosis were often seen in the peripheral portion of the tumor nodule. The predominant cells were lymphoid with fine chromatin and nonconspicuous nucleoli, characteristic of lymphoblastic lymphomas and leukemias (fig. 1). Intermixed with the lymphoid cells were very few large cells (*see arrow* on fig. 1) with abundant eosinophilic cytoplasm always associated with fibrous trabeculae. These cells resembled HT-1080 tumor cells and were probably residual X-irradiated HT-1080 cells that did not proliferate in vivo, since no aggregates of these cells were visible in tumor sections. Further evidence that the tumors which grew were comprised predominantly of the MOLT-4 T-cell leukemia cells derived from the two marker studies. First, acid phosphatase staining revealed polar cytoplasmic staining of the cells from both the subcutaneous tumors and the MOLT-4 cell line. Second, the percentages of cells forming rosettes with SRBC (±SD) were 90±10 in the preparations from 5 separate tumors and 62±5 in 2 samples from the MOLT-4 tissue culture line. HT-1080 fibrosarcoma cells do not form rosettes.

All nude mice from experiment I were examined for evidence of MOLT-4 metastases. No malignant cells were found in any histologic sections of the draining and distant lymph nodes, spleen, bone marrow, pancreas, liver, kidneys, lungs, mediastinum, heart, and brain. Thus, apparently, MOLT-4 cells remain localized and develop into tumors; however, we cannot rule out the possibility that some MOLT-4 cells metastasize but are eliminated before tumor establishment.

The previously reported low success rate for subcutaneous transplantation into nude mice of human

TABLE 1.—*Growth of MOLT-4 leukemia cell-induced tumors in unirradiated versus X-irradiated mice inoculated with MOLT-4 cells and X-irradiated HT-1080 fibrosarcoma cells*[a]

Expt No.	Tumor incidence in[b]					
	Unirradiated mice given			X-irradiated mice given		
	2×10^4 MOLT-4 cells	2×10^5 MOLT-4 cells	2×10^6 MOLT-4 cells	2×10^4 MOLT-4 cells	2×10^5 MOLT-4 cells	2×10^6 MOLT-4 cells
I	0/4	1/2	1/4	4/4	5/5	3/4
II	1/4	2/4	0/3	3/4	1/4	3/4
I + II	1/8	3/6	1/7	7/8	6/9	6/8
Total tumor incidence (I + II)		5/21			19/25	

[a] Unirradiated mice or mice X-irradiated with 200 rad three times at weekly intervals were inoculated with the designated No. of MOLT-4 cells together with 2×10^6 X-irradiated (6,000 rad) HT-1080 cells. The same mice were given injections at a distant site with the same No. of MOLT-4 cells alone, and no tumors developed.

[b] Results are expressed as No. of mice with tumors/total No. of mice given MOLT-4 cell injections.

leukemia cell lines or fresh leukemia cells from patients (*2, 3*) might be explained by the fact that leukemia cells produce relatively little AGF as compared with solid tumors (*4*) or by the elimination of circulating leukemia cells by NK cells. Although reports (*2, 3*) have indicated that MOLT-4 leukemia cells can grow sc when many cells are injected, we failed to detect any tumors in 21 mice inoculated with low numbers of MOLT-4 cells alone. On the basis of the observation that X-irradiated cells from solid tumors continue to produce AGF for several weeks (*12*), one explanation for the finding that the X-irradiated HT-1080 fibrosarcoma cells allow MOLT-4 cells to establish as tumors may be that the HT-1080 cells produce AGF; the appearance of large MOLT-4 cell-induced nodules with good vascularization and little necrosis at least supports this contention. A second explanation for this finding is that the fibrosarcoma cells may produce growth factors enabling establishment of MOLT-4 cell-induced tumors. A third explanation is that the fibrosarcoma cells may by some mechanism halt migration of the leukemia cells, thereby decreasing the chance that the leukemia cells would be eliminated by NK cells.

Watanabe et al. (*13*) reported that irradiation of nude mice with 500 rad enabled the growth of iv injected tumor cell lines. Since nude mice have high NK cell activity (*14*) and since many T-cell leukemia cells, including MOLT-4, are sensitive targets for NK cells (*15*), the decrease in NK cell activity occurring after X-irradiation (*16*) might explain the increased tumor frequency. In preliminary experiments we found that spleen cells from unirradiated nude mice caused significant lysis of MOLT-4 cells, whereas spleen cells obtained from mice 1 week after the last of 3 doses of 200 rad of X-irradiation mediated no detectable NK activity against the MOLT-4 target cells.

In summary, our results show that MOLT-4 leukemia cells when inoculated alone did not grow in nude mice, but the incidence of tumor development by these leukemia cells was dramatically increased when the leukemia cells were admixed with X-irradiated fibrosarcoma cells and when the mice were X-irradiated before tumor cell injection. Initial results with freshly isolated human leukemia cells that have not been adapted to tissue culture are encouraging in that it appears that the conditions used in this study to allow establishment of MOLT-4 cell-induced tumors also allow growth of at least some patients' fresh leukemia cells in nude mice. Further studies are required, however, before we can generalize that many, or most, patients' leukemia cells can be established as tumors in nude mice by the procedure we have described.

Although human leukemia is usually characterized by the infiltrative growth of malignant cells in bone marrow and parenchymal organs, growth of leukemias as solid masses is rare (*17*). The growth of human leukemia cells as localized nodules in mice, while not mimicking the disease in humans, may allow assessment of tumor progression and regression by direct measurement of the tumors without invasive techniques; thus it may be a useful model in which to study the effects of various therapeutic modalities on human leukemia, as has been done with human solid tumors (*1, 18*).

REFERENCES

(*1*) GIOVANELLA BC, STEHLIN JS, WILLIAMS LJ, LEE SS, SHEPARD RC. Heterotransplantation of human cancers into nude mice. A model system for human cancer chemotherapy. Cancer 1978; 42:2269-2281.

(*2*) KUGA N, YOSHIDA K, SEIDO T, et al. Heterotransplantation of cultured human cancer cells and human cancer tissues into nude mice. Gan 1975; 66:547-560.

(*3*) NILSSON K, GIOVANELLA BC, STEHLIN JS, KLEIN G. Tumorigenicity of human hematopoietic cell lines in athymic nude mice. Int J Cancer 1977; 19:337-344.

(*4*) BREM S, COTRAN R, FOLKMAN J. Tumor angiogenesis: A quantitative method for histologic grading. J Natl Cancer Inst 1972; 48:347-356.

(*5*) RODER JC, AHRLUND-RICHTER L, JONDAL M. Target-effector interaction in the human and murine natural killer system. Specificity and xenogeneic reactivity of the solubilized natural killer-target structure complex and its loss in a somatic cell hybrid. J Exp Med 1979; 150:471-481.

(*6*) MINOWADA J, OHNUMA T, MOORE GE. *Brief communication:* Rosette-forming human lymphoid cell lines. I. Establishment and evidence for origin of thymus-derived lymphocytes. J Natl Cancer Inst 1972; 49:891-895.

(*7*) RASHEED S, NELSON-REES WA, TOTH EM, ARNSTEIN P, GARDNER MB. Characterization of a newly derived human sarcoma cell line (HT-1080). Cancer 1974; 33:1027-1033.

(*8*) LILLIE RD. Histopathologic technique and practical histochemistry. 3d ed. New York: McGraw-Hill, 1965.

(*9*) LI CY, YAM LT, LAM KW. Acid phosphatase isoenzyme in human leukocytes in normal and pathological conditions. J Histochem Cytochem 1970; 18:473-481.

(*10*) KAY NE, JOHNSON JD, STANEK R, DOUGLAS SD. T-cell subpopulations in chronic lymphocytic leukemia: Abnormalities in distribution and in in vitro receptor maturation. Blood 1979; 54:540-544.

(*11*) SIEGEL S. Nonparametric statistics for the behavioral sciences. New York, Toronto, and London: McGraw-Hill, 1956.

(*12*) AUERBACH R, ARENSMAN R, KUBAI L, FOLKMAN J. Tumor-induced angiogenesis: Lack of inhibition by irradiation. Int J Cancer 1975; 15:241-245.

(*13*) WATANABE S, SHIMOSATO Y, KAMEYA T, et al. Leukemic distribution of a human acute lymphocytic leukemia cell line (Ichikawa strain) in nude mice conditioned with whole-body irradiation. Cancer Res 1978; 38:3494-3498.

(*14*) HERBERMAN RB, ed. Natural cell-mediated immunity against tumors. New York: Academic Press, 1980.

(*15*) ONO A, AMOS DB, KOREN HS. Selective cellular natural killing against leukaemic T cells and thymus. Nature 1977; 266: 546-548.

(*16*) CUDKOWICZ G, HOCHMAN PS. Do natural killer cells engage in regulated reactions against self to ensure homostasis? Immunol Rev 1979; 44:13-41.

(*17*) KRAUSE JR. Granulocytic sarcoma preceding acute leukemia. Cancer 1979; 44:1017-1021.

(*18*) LATIF ZA, LOZZIO BB, WUST CJ, KRAUSS S, AGGIO MC, LOZZIO CB. Evaluation of drug-antibody conjugates in the treatment of human myelosarcomas transplanted in nude mice. Cancer 1980; 45:1326-1333.

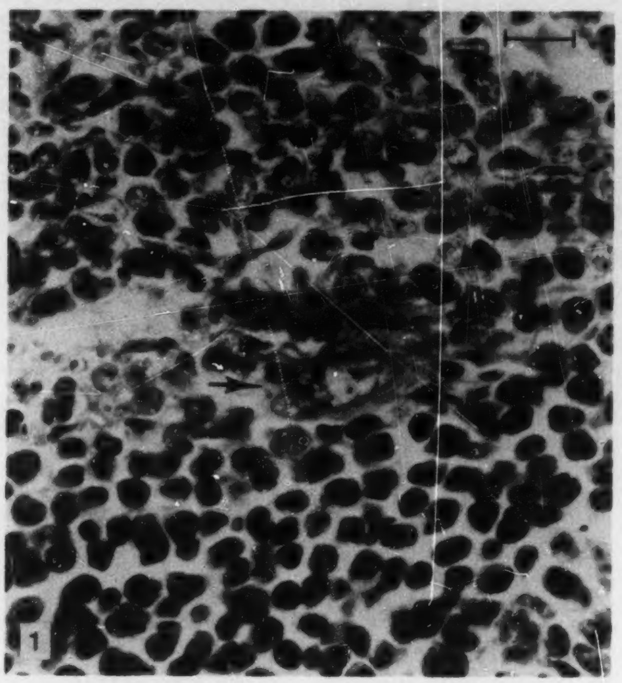

FIGURE 1.—Central area of a tumor that developed in a preirradiated mouse inoculated sc with MOLT-4 cells and X-irradiated (6,000 rad) HT-1080 fibrosarcoma cells. Tumor cells were predominantly lymphoid, characteristic of MOLT-4 leukemia cells, with the exception of a rare residual X-irradiated HT-1080 cell (*arrow*). Hematoxylin and eosin. *Bar*=16 µm. × 640

Enhanced Expression of Melanoma-Associated Antigens and β_2-Microglobulin on Cultured Human Melanoma Cells by Interferon[1,2]

Shuen-Kuei Liao,[3,4] Pak C. Kwong,[3] Mohammed Khosravi,[3] *and* Peter B. Dent[3,5]

ABSTRACT—The effect of human leukocyte interferon (IFN) on the in vitro growth and expression of melanoma-associated antigens (MAA), β_2-microglobulin (β_2m) and HLA-DR antigen on cultured human melanoma cells was studied. Exposure of melanoma cells to IFN for 64 hours resulted in a dose-dependent inhibition of growth with 46% reduction in cell number at 10^3 U IFN/ml and 74% reduction at 10^5 U/ml. Quantitative absorption experiments in the mixed hemadsorption assay determined that the expression of MAA and β_2m on treated cells was enhanced at 10^2–10^5 U IFN/ml, twofold to fivefold for MAA and fivefold to twelvefold for β_2m. No change was seen in HLA-DR antigen expression. The IFN-induced enhancement of MAA and β_2m could be detected as early as after 16 hours and a maximum expression was reached at 96 hours after IFN exposure. The IFN-induced enhancement of MAA and β_2m on melanoma cells was reversible. Studies with melanoma cells grown in stationary phase and serum-deprived conditions indicated that IFN-induced augmentation of MAA and β_2m did not require cell proliferation. The data suggest that the effect of IFN on antigen expression is independent of its effect on cell growth. Further studies are needed to fully elucidate the mechanism.—JNCI 1982; 68:19-25.

The antiviral agent IFN, thought to be of questionable clinical usefulness for years, has recently shown great promise in the treatment of neoplastic diseases (*1-3*). This substance exhibits a variety of biological effects, which include inhibition of cell proliferation (*4-7*), elevation of cellular enzyme activity (*8*), increase in phagocytosis (*9*), regulation of immune responses (*10-15*), and antitumor effects in experimental animals and man (*16-18*). IFN has also been shown to increase the expression in vitro of a number of cell surface antigens, such as antigens on mouse leukemia cells (*10*), and HLA antigens and β_2m on human lymphoid cells (*19-21*). We have recently described common MAA on cultured and fresh melanoma cells detected by nonhuman primate antisera (*22*). In this report we have shown that human leukocyte IFN enhances the expression of MAA and β_2m on the surface of cultured human melanoma cells as much as fifteenfold to twentyfold. The effect is not due simply to growth inhibition and is reversible upon removal of IFN from the medium.

MATERIALS AND METHODS

IFN.—Human leukocyte IFN, lot P-IF (*23*), was supplied by Dr. K. Cantell, Central Public Health Laboratory, Helsinki, Finland. The titer of this partially purified IFN preparation was 6×10^6 reference U/ml, the specific activity was 4×10^6 reference U/mg of protein. In this paper in referring to the biologically active material as IFN, we recognize the fact that the term refers to a family of different molecules with related properties.

Cells and culture.—Two cell lines, CaCL 73-36 and Daudi, were used. The melanoma line, CaCL 73-36 (*24*), established in our laboratory has been shown to express MAA and HLA-DR antigen as revealed by monkey anti-MAA (*22*) and rabbit-anti-HLA-DR antibodies (Liao S-K, Jerry LM: Unpublished observation). CaCL 73-36 is known to express HLA-A10 on the surface membrane as determined by absorption analysis with HLA-A10 specific alloantibody (*25*). The Daudi lymphoblastoid cell line (*26*), known to be devoid of β_2m and HLA antigens, was obtained from Dr. J. Minowada, Roswell Park Memorial Institute, Buffalo, N.Y.

Melanoma cell line was maintained in monolayer culture in EMEM supplemented with 10% heat-inactivated FCS. The Daudi cells were grown in suspension in RPMI-1640 medium containing 10% FCS. The cultures were incubated at 37°C in a 100% humidified atmosphere of 5% CO_2 and 95% air.

Growth curves.—We seeded 75-cm^2 culture flasks (Falcon Plastics, Los Angeles, Calif.) with 2×10^6 cells in 20 ml EMEM containing 10% FCS. All flasks were incubated at 37°C for up to 7 days without change of medium. Four duplicate flasks were removed from the

---

ABBREVIATIONS USED: AI = absorption index; β_2m = β_2-microglobulin; EMEM = Eagle's minimum essential medium; FCS = fetal calf serum; HLA-DR = human leukocyte antigen system, DR locus; IFN = interferon; MAA = melanoma-associated antigens; SRBC = sheep red blood cells.

---

[1] Received October 8, 1980; revised June 9, 1981; accepted July 21, 1981.

[2] Supported by grants from the Medical Research Council of Canada and from the Ontario Cancer Treatment and Research Foundation.

[3] Department of Pathology and Department of Pediatrics, McMaster University, Health Sciences Centre, 1200 Main St. West, Hamilton, Ontario L8N 3Z5, Canada, and the Ontario Cancer Treatment and Research Foundation, Hamilton Clinic, Hamilton, Ontario L8V 1C3, Canada.

[4] Associate of the Ontario Cancer Treatment and Research Foundation.

[5] We thank Miss Patricia Chmielewski for expert technical assistance and Mrs. Janice Giles for secretarial assistance.

incubator every 24 hours. They were rinsed with 0.02% EDTA solution, then trypsinized, and the released cells were counted in a hemacytometer. The results were expressed as the total number of cells per culture.

Antisera.—Anti-CaCL 73-36 raised in an African green monkey (*Cercopithecus aethiops*) by immunizing with the human melanoma line CaCL 73-36, was absorbed with human AB erythrocytes, peripheral blood leukocytes and cells of the oral carcinoma line (KB) to render it melanoma specific (*22*). Anti-β_2m, provided by Dr. J. Gauldie, McMaster University, was raised by immunizing a rabbit with purified human β_2m prepared and donated by Dr. M.D. Poulik, William Beaumont Hospital, Royal Oak, Mich. The immunizing material gave a single precipitating line with the anti-β_2m antiserum but did not react with preimmune serum in Ouchterlony gel diffusion. The anti-β_2m failed to react with the Daudi line but its reactivity was completely removed by four of four B-lymphoid lines as revealed by quantitative absorption analysis. Anti-HLA-DR was supplied by Dr. L.M. Jerry, University of Calgary, Calgary, Canada. This antiserum was produced by immunizing a rabbit with purified human B-lymphocyte glycoprotein and preabsorbed with T-lymphoid cells (Jurkat). The production and immunochemical characterization of this antiserum have been previously described (*27*).

Mixed hemadsorption assay.—This assay was performed as previously described (*25*). The source of sensitizing antisera used in the indicator system depends on the species of origin of the antibody to be detected and the dilution of each antiserum used was previously described (*28*). SRBC sensitized with rabbit or monkey anti-SRBC antiserum, followed by a second sensitization with sheep anti-rabbit IgG or sheep anti-human IgG, are effective for the detection of rabbit or monkey, (human) antibodies, respectively. Monkey and human reagents can be used interchangeably because of the antigenic cross-reactivity of their immunoglobulins.

Quantitative absorption technique.—To quantitate changes in cell surface antigen content, we followed the principles previously reported by Boyse et al. (*29*). The quantitative absorption test was done with the use of a concentration of antiserum, two doubling dilutions higher than that which gave 50% positivity in antibody titration. Antiserum in 100-μl aliquots was absorbed with increasing numbers of treated or untreated cells by gentle rotation of the microtubes containing cells and serum at room temperature for 1 hour. The microtubes were subsequently kept at 4°C overnight. Sera were collected by centrifugation at 3,000×g for 3 minutes in a microcentrifuge (model 59, Fisher Scientific, Montreal, Canada). Absorbed and unabsorbed sera were then assayed by mixed hemadsorption with use of the appropriate reference cell line.

The percentage of inhibition of antiserum reactivity relative to the unabsorbed antiserum control was plotted on an arithmetic scale against the number of cells used for absorption on a logarithmic scale. The number of cells required for 50% inhibition of binding activity by antiserum (AD_{50}) was calculated from the inhibition curve. The absorptive capacity of the IFN-treated group was expressed in relation to the untreated control group by means of the formula: AI = AD_{50} of untreated group/AD_{50} of treated group.

RESULTS

Effect of Different Concentrations of IFN on In Vitro Growth and Surface Antigen Expression

Table 1 shows the effect of various IFN concentrations on melanoma cells grown for a period of 64 hours. Treatment of the CaCL 73-36 melanoma cells with IFN resulted in a dose-dependent growth inhibition, with a 45.5% reduction in cell number at 10^3 U IFN/ml and 73.6% reduction at 10^5 U IFN/ml, compared to the untreated control cells. Expression of MAA and β_2m on the treated cells was enhanced at all IFN concentrations, 1.7- to 4.8-fold for MAA and 4.6- to 12.4-fold for β_2m. No enhancement of HLA-DR expression was observed following IFN exposure for 64 hours (table 1) or for 168 hours (stationary phase, data not shown).

Since there was a diminution in the rate of increase of antigen expression as well as cell growth with IFN concentrations higher than 10^3 U/ml, in subsequent experiments 10^3 U/ml was employed.

In text-figure 1 results of a representative experiment show the effect of 10^3 U IFN/ml on the growth curve of melanoma cells over a 7-day culture period. There was an initial prolongation of the lag phase, but by day 4 the IFN-treated cells reached a saturation density equal to that of the untreated cells. Over the next 24 hours a 50% decrease in cell numbers occurred in the IFN-treated cultures due to detachment of dead cells as determined by trypan blue dye exclusion test.

No differences could be detected in the cellular morphology between control and IFN-treated melanoma cells by light microscopy. This melanoma cell line is grossly amelanotic, and no obvious pigmenta-

TABLE 1.—*Effect of various concentrations of IFN in medium on cell growth and expression of surface MAA, β_2m and HLA-DR antigens on human melanoma cells as determined by quantitative absorption analysis*

IFN concentration, U/ml	No. of cells/culture[a] $\times 10^{-6}$, (% reduction)[b]	MAA		β_2m		HLA-DR	
		AD_{50}	AI[c]	AD_{50}	AI[c]	AD_{50}	AI[c]
0	11.0	19.5×10^4		27.4×10^4		6.9×10^4	
10^2	10.9 (0.9)	11.5×10^4	1.7	6.1×10^4	4.6	7.1×10^4	0.97
10^3	6.0 (45.5)	5.0×10^4	3.9	2.8×10^4	9.8	7.0×10^4	0.99
10^4	4.7 (57.3)	4.5×10^4	4.3	2.4×10^4	11.4	6.7×10^4	1.00
10^5	2.9 (73.6)	4.1×10^4	4.8	2.2×10^4	12.4	6.8×10^4	1.00

[a] 2×10^6 cells/75-cm^2 flask were plated in duplicate for each group and allowed to grow for 64 hr.

[b] Percent reduction in cell number relative to untreated control.

[c] AI = AD_{50} of untreated control/AD_{50} of treated group.

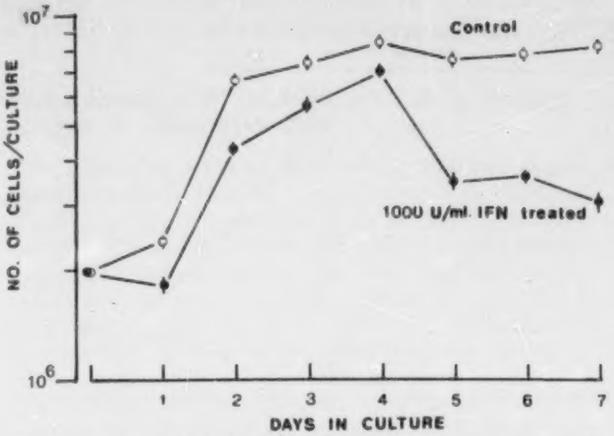

TEXT-FIGURE 1.—Effect of 10^3 U IFN/ml on the growth of CaCL 73-36 melanoma cells. *Note* that the cultures were not fed nor was fresh IFN added at any point except at the beginning of culture. *Each point* represents the mean of four culture flask ± SE.

tion was induced by IFN treatment as judged by the color of the cell pellets.

Kinetics of Enhancement by IFN of MAA and β^2m Expression

A time course study was performed to determine the effect of 10^3 U IFN/ml on the expression of MAA. The expression of MAA on melanoma cells at different times after the initiation of culture was determined by quantitative absorption experiments with the use of an anti-MAA antibody. Results of a representative experiment (text-fig. 2) show that AI for the IFN-treated groups at 16, 64, 96, and 168 hours are 1.5, 3.5, 15.0, and 5.4, respectively. It is clear that an increase in MAA expression could be detected as early as 16 hours after IFN-exposure, and maximal expression of MAA on the treated cells was reached at 96 hours. The untreated melanoma cells did not change in their MAA expression during the culture period from 16 through 168 hours.

Text-figure 3 shows the effect of IFN on β_2m expression by the melanoma cells in the same time course experiment described above. Enhanced expression of β_2m was first detectable at 16 hours and the AI value was 3.1. The AI progressively rose to a maximum of 20.0 at 96 hours and declined to 14.3 at 168 hours. No changes were seen in β_2m expression on the untreated cells over the 168-hour culture period.

Reversibility of IFN-Induced Enhancement of Antigen Expression

To determine whether the effect of IFN treatment on MAA and β_2m expression was reversible, the following

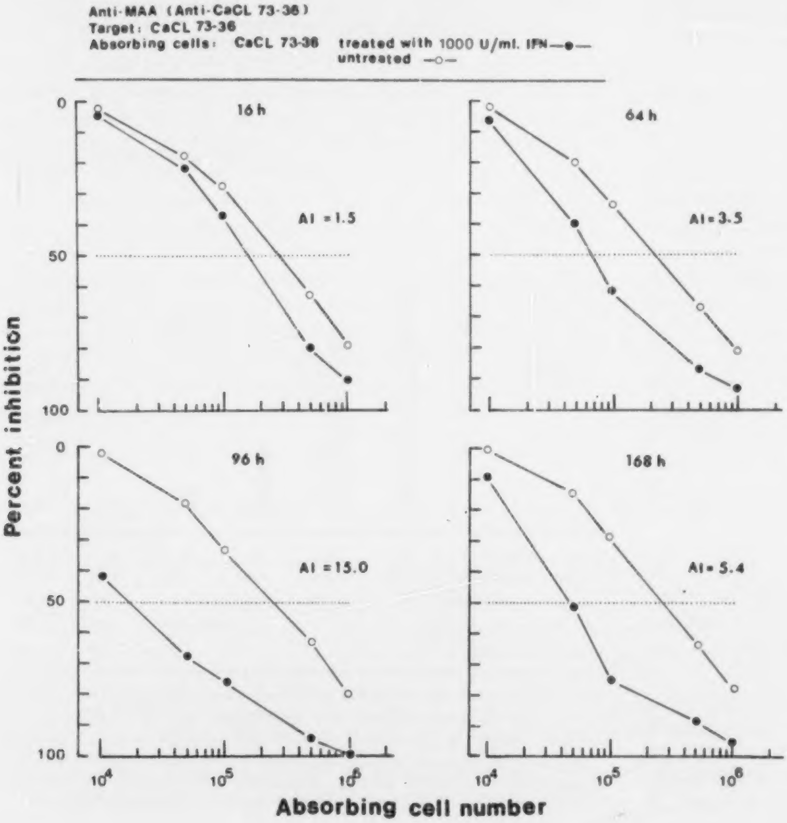

TEXT-FIGURE 2.—Kinetics of enhanced MAA expression by IFN-treated melanoma cells as determined by quantitative absorption. 2×10^6 cells were cultured in 75-cm² flasks in 20 ml medium.

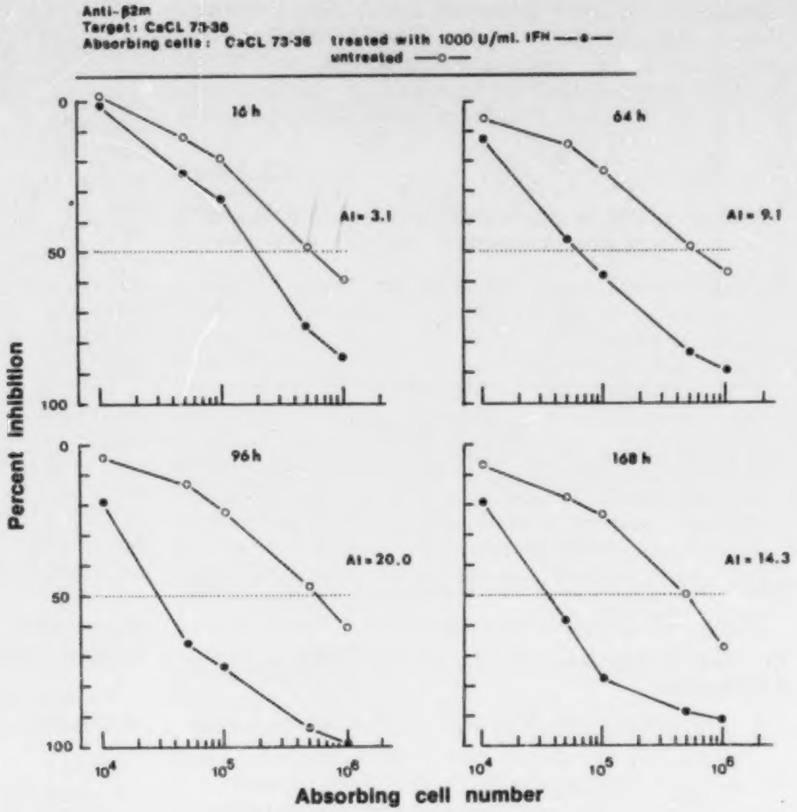

TEXT-FIGURE 3.—Kinetics of enhanced β_2m expression by IFN-treated melanoma cells as determined by quantitative absorption. 2×10^6 cells were cultured in 75-cm^2 flasks in 20 ml medium.

experiment was performed (text-fig. 4). Melanoma cells were grown in medium containing 10^3 U IFN/ml for 96 hours and then divided into 5 groups: Group 1) cultures were terminated at this point; Group 2) cultures were allowed to continue for a further 48 hours after replacement of medium with fresh medium containing 10^3 U IFN/ml; Group 3) cultures were allowed to continue for a further 48 hours after replacement of medium with fresh medium without IFN; Group 4) cultures were allowed to continue for a further 96 hours after replacement of medium with fresh medium without IFN; Group 5) cultures were allowed to continue for a further 144 hours after replacement of medium with fresh medium without IFN. In a sixth group, melanoma cells were initially grown in medium without IFN for 96 hours and then allowed to continue for a further 144 hours after replacement of medium with fresh medium without IFN. In a last group, melanoma cells were grown in medium without IFN for 96 hours. The cells harvested from each group were analyzed by quantitative absorption with anti-MAA and anti-β_2m antibodies for surface antigen content.

Relative antigen content of melanoma cells in groups 1 to 6 was determined by AI value, which was obtained by dividing AD$_{50}$ of the last group (cells grown for 96 hours in IFN-free medium) by AD$_{50}$ of each experimental group. As can be seen in text-figure 4, removal of IFN from the culture medium (groups 3, 4, and 5) resulted in significant reduction in MAA and β_2m expression as compared to group 1 or 2. After 144 hours of incubation in IFN-free medium, the antigen

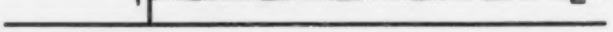

Experimental group	1	2	3	4	5	6
1st 96 hr of incubation	+ IFN	+ IFN	+ IFN	+ IFN	+IFN	− IFN
2nd 48 hr of incubation		+ IFN	− IFN	− IFN	−IFN	− IFN
3rd 48 hr of incubation				− IFN	−IFN	− IFN
4th 48 hr of incubation					−IFN	− IFN

TEXT-FIGURE 4.—Reversibility of IFN-induced enhancement of MAA and β_2m antigen expression on melanoma cells 2×10^6 cells/75-cm^2 flask plated in quadruplicate for each group. Relative antigen content of each group was reflected by AI value, which was expressed in relation to the melanoma cells grown in medium without IFN for 96 hr. *See* text for experimental details.

level was reduced to the basal content of the antigens expressed on the untreated melanoma cells.

Enhancement by IFN of MAA and β_2m in Stationary Cultures of Melanoma Cells

To determine whether IFN would enhance expression of MAA and β_2m by melanoma cells in stationary cultures, we grew melanoma cells in EMEM containing 10% FCS for 96 hours, by which time stationary phase was reached (text-fig. 1). This was followed by replacement of spent medium with serum-free EMEM and further incubation for 72 hours. At this point two experimental groups were established: In group 1, cultures were allowed to continue for a further 64 hours with or without addition of 10^3 U IFN/ml after replacement of exhausted medium with fresh, but serum-deprived medium; In group 2, cultures were allowed to continue for a further 64 hours with and without addition of 10^3 U IFN/ml after replacement of exhausted medium with fresh medium containing 10% FCS. The harvested cells from each group were used for quantitative absorption with anti-MAA and anti-β_2m antibodies for determination of antigen content. As can be seen in table 2, the expression of MAA and β_2m by stationary phase melanoma cells was enhanced by IFN treatment. The addition of FCS during the period of IFN exposure was not necessary for the enhancement, although the degree of β_2m expression appeared greater in the presence of added FCS. These data suggest that enhancement of expression of these two antigens by IFN does not require cell growth.

Control Experiments

To exclude the possibility that IFN nonspecifically induces neoantigens or promotes expression of cryptic antigens, Daudi lymphoid cells known to be free of MAA and β_2m were incubated with and without IFN for 64 and 96 hours. When the cells were tested for expression of these two antigens by quantitative absorption with anti-MAA and anti-β_2m antibodies, reduction of antibody reactivity was not seen in either instance (data not shown).

DISCUSSION

In this study we demonstrated that human leukocyte IFN enhances the expression of MAA and β_2m in cultured human melanoma cells. Previous studies have documented increased expression of β_2m (*19, 21*) and histocompatibility antigens (*10, 19, 20, 30-33*) on both murine and human lymphoid cells; however, this is the first demonstration of a similar phenomenon on nonlymphoid tumor cells. The effect is more marked with β_2m, although the qualitative aspects of enhanced MAA and β_2m expression are similar, such as dose response, kinetics and reversibility. We have shown that there is a dose-dependent enhancement of MAA and β_2m by IFN and that the effect can be detected as early as 16 hours after addition of IFN to the cultures. The enhancement is maximal at 96 hours and then declines somewhat by 168 hours. This decline could be due to depletion of IFN in the medium inasmuch as an addition of fresh IFN at 96 hours appears to sustain the effect (table 2). Alternatively or additionally, antigen-rich cells may selectively detach from the culture flask as can be seen by the decrease in cell numbers observed after 96 hours. The specificity of the effect can be seen from the absence of concomitant enhancement of HLA-DR expression and the lack of appearance of β_2m or MAA on Daudi cells which normally do not express the antigens.

The enhancing effect of IFN on antigen expression by melanoma cells was also seen on two additional melanoma cell lines and is therefore not a unique finding for the CaCL 73-36 cell line. We are currently examining a panel of melanoma cell lines representative of a spectrum of MAA expression to explore the relationship of the degree of IFN-induced enhancement to the basal antigen concentration. Using hybridoma antibodies, we have recently described a common fetal neuroectodermal antigen of melanoma, neuroblastoma, retinoblastoma, glioma, and fetal brain cells (*34*). IFN treatment induces a fourfold enhancement of the expression of this antigen on melanoma cells (data not shown).

Although we have not determined the exact mechanism of action of IFN in antigen enhancement, we have considered the possibility that IFN selectively suppresses the proliferation of cells that are antigen-

TABLE 2.—*IFN-induced enhancement of expression of MAA and β_2m in stationary cultures of melanoma cells*

Group	Culture condition[a]	No. of cells/culture $\times 10^{-6}$ at termination of culture[b]		MAA			β_2m		
				AD$_{50}$		AI	AD$_{50}$		AI
		+IFN	−IFN	+IFN	−IFN		+IFN	−IFN	
1	Serum deprived	13.1	14.3	3.4×10^4	7.4×10^4	2.2	1.6×10^4	9.0×10^4	5.6
2	Control, 10% FCS	18.1	18.3	3.4×10^4	7.6×10^4	2.2	1.4×10^4	$1.2\ \times10^5$	8.6

[a] 2×10^6 CaCL 73-36 cells/75-cm^2 flask seeded in quadruplicates for each group. *See* text for experimental detail.
[b] No detached cells observed at the termination of culture.

deficient, permitting the outgrowth of a population of antigen-rich cells. This is, however, unlikely because enhanced antigen expression occurs in cells that are not growing (table 2), as well as in cells that are in lag phase of growth (text-figs. 1 and 2). The fact that enhancement is reversible argues against selective population deletion. Finally analysis of IFN-treated human lymphoid cells for β_2m expression using the fluorescence activated cell sorter showed a homogeneous alteration of distribution of staining intensity rather than the appearance of two cell populations (*19*). A similar result was obtained with the expression of H-2 antigens on IFN-treated murine lymphoma cells (*35*). We conclude, therefore, that elimination of an antigen-deficient population of cells does not explain the phenomenon. Alternatively, IFN treatment may result in a decreased turnover of cell surface antigens and/or stimulation of antigen synthesis.

The observations of Chang et al. (*36, 37*) suggest that the changes observed in IFN-treated cell membranes are general changes; however, there is a definite selectivity in what sorts of antigen show enhanced expression. Histocompatibility antigens (*19, 20, 30–32*), β_2m (*19, 21*) and MAA are enhanced whereas HLA-DR (*20, 21, 29*) Thy-1 (*31*), human T-antigen (*19*), surface IgG and IgM (*19, 30*) and Fc receptor (*30*) expression are not affected. It is not immediately clear what property or characteristic of a surface antigen determines its enhanceability by IFN. Nevertheless, it is of interest that none of the nonenhanced structures are β_2m related while HLA and H-2 antigens are β_2m associated. We (*38*) and others (*39, 40*) have evidence suggesting an association of β_2m with MAA, although there is also evidence to the contrary (*41, 42*).

We conclude that growth inhibition alone does not account for enhanced antigen expression since the enhancement was seen in cells that were fully confluent and serum starved (table 2). A similar conclusion regarding the independence of antigen enhancement and cellular proliferation was reached by Killander et al. (*35*) who performed simultaneous single cell analysis of H-2 antigen expression, DNA content, dry cell mass, and [^{3}H]thymidine uptake of IFN-treated leukemia cells.

Finally, it is tempting to speculate that enhancement of tumor antigenicity by IFN may be an important mechanism to explain the antitumor effects of IFN (*3, 16*). One could envisage that IFN-treated antigen-enriched cells might be more immunogenic and, at the same time, more susceptible to immune attack.

REFERENCES

(*1*) Strander H. Anti-tumor effects of interferon and its possible use as an antineoplastic agent in man. Tex Rep Biol Med 1977; 35:429–435.

(*2*) Borden EC. Interferons: Rationale for clinical trials in neoplastic disease. Ann Intern Med 1979; 91:472–497.

(*3*) Krim M. Towards tumor therapy with interferons, part II. Interferons: In vivo effects. Blood 1980; 55:875–884.

(*4*) Lindahl-Magnusson P, Leary P, Gresser I. Interferon inhibits DNA synthesis induced in mouse lymphocyte suspensions by phytohemagglutinin or by allogeneic cells. Nature [New Biol] 1972; 237:120–121.

(*5*) Stewart WE II, Gresser I, Tovey MG, Branden MT, Le Goff S. Identification of the cell multiplication inhibitory factors in interferon preparations as interferon. Nature 1976; 262:300–302.

(*6*) Glasgow LA, Crane JL Jr, Kern ER. Antitumor activity of interferon against murine osteogenic sarcoma cells in vitro. J Natl Cancer Inst 1978; 60:659–666.

(*7*) Creasy AA, Bartholomew JC, Merigan TC. Role of G_0-G_1 arrest in the inhibition of tumor cell growth by interferon. Proc Natl Acad Sci USA 1980; 77:1471–1475.

(*8*) Wood JN, Hovanessian AG. Interferon enhances 2-5A synthetase in embryonal carcinoma cells. Nature 1979; 282:74–76.

(*9*) Huang E, Donahue RM, Gordon FB, Dressler HR. Enhancement of phagocytosis by interferon-containing preparations. Infect Immun 1971; 4:581–588.

(*10*) Lindahl P, Leary P, Gresser I. Enhancement by interferon of the expression of surface antigens on murine leukemia L1210 cells. Proc Natl Acad Sci USA 1972; 69:721–725.

(*11*) DeMaeyer E, DeMaeyer-Guignard J, Vandeputte M. Inhibition by interferon of delayed-type hypersensitivity in the mouse. Proc Natl Acad Sci USA 1975; 72:1753–1758.

(*12*) Heron I, Berg K, Cantell K. Regulatory effect of interferon on T cells in vitro. J Immunol 1976; 117:1371–1373.

(*13*) Johnson JM, Staton GJ, Baron S. Relative ability of mitogens to stimulate production of interferon by lymphoid cells and to induce suppression of the in vitro immune response. Proc Soc Exp Biol Med 1977; 154:138–141.

(*14*) Trinchieri G, Santoli D. Antiviral activity induced by culturing lymphocytes with tumor-derived or virus-transformed cells. Enhancement of human natural killer cell activity by interferon and antagonistic inhibition of susceptibility of target cells to lysis. J Exp Med 1978; 147:1314–1333.

(*15*) Heron I, Berg K. The actions of interferon are potentiated at elevated temperature. Nature 1978; 274:508–510.

(*16*) Gresser I, Tovey MG. Antitumor effects of interferon. Biochem Biophys Acta 1978; 516:231–247.

(*17*) Strander H, Cantell K, Ingimarsson S, Jakobson Å, Nilsonne U, Söderberg G. Interferon treatment of osteogenic sarcoma: A clinical trial. In: Chirigos MA, ed. Modulation of host immune resistance in the prevention or treatment of induced neoplasias. Fogarty International Center Proceedings. Washington, D.C.: U.S. Govt Print. Off, 1977; 28:377–381.

(*18*) Ratner L, Nordlund JJ, Lengyel P. Interferon as an inhibitor of cell growth: Studies with mouse melanoma cells. Proc Soc Exp Biol Med 1980; 163:267–272.

(*19*) Heron I, Hokland M, Berg K. Enhanced expression of β_2-microglobulin and HLA antigens on human lymphoid cells by interferon. Proc Natl Acad Sci USA 1978; 75:6215–6219.

(*20*) Attallah AM, Strong DM. Differential effects of interferon on the MHC expression of HLA without effect on Ia. Int Arch Allergy Appl Immunol 1979; 60:101–105.

(*21*) Fellous M, Kamoun M, Gresser I, Bono R. Enhanced expression of HLA antigens and beta 2 microglobulin on interferon-treated human lymphoid cells. Eur J Immunol 1979; 9:446–449.

(*22*) Liao SK, Kwong PC, Thompson JC, Dent PB. Spectrum of melanoma antigens on cultured human malignant melanoma cells as detected by monkey antibodies. Cancer Res 1979; 39:183–192.

(*23*) Cantell K. Towards the clinical use of interferon. Endeavour 1978; 2:27–30.

(*24*) Liao SK, Dent PB, McCulloch PB. Characterization of human malignant melanoma cell lines. I. Morphology and growth characteristics in culture. J Natl Cancer Inst 1975; 54:1037–1044.

(*25*) Liao SK, Khosravi M, Kwong PC, Singal DP, Dent PB. Miniaturization makes mixed hemadsorption assays more sensitive, reliable and economic. Immunol Lett 1980; 2:123–127.

(*26*) Klein E, Klein G, Nadkarni JJ, Wigzell H, Clifford P. Surface IgM-kappa specificity on a Burkitt lymphoma cell in vivo and in derived culture lines. Cancer Res 1968; 28:1300–1310.

(*27*) Sullivan AK, Jerry LM, Ikeman RL, Maccari RJ, Lithi H, Sylvester C. Isolation of a human B lymphocyte membrane protein with Ia-like properties. Can J Biochem 1979; 57:21-23.

(28) Liao SK, Rahman AF, Kwong PC, Dent PB. A simple microassay for detection of antibodies to fetal calf serum and related antigens and its application to the serological definition of human tumor antigens. J Immunol Methods 1979; 27:111-125.

(29) Boyse EA, Miyazawa M, Aoki T, Old LJ. Ly-A and Ly-B: Two systems of lymphocyte isoantigens in the mouse. Proc R Soc Lond [Biol] 1968; 170:175-193.

(30) Vignaux F, Gresser I. Differential effects of interferon on the expression of H-2K, H-2D and Ia antigens on mouse lymphocytes. J Immunol 1977; 118:721-723.

(31) Lindahl P, Leary P, Gresser I. Enhancement by interferon of the expression of surface antigens on murine leukemia L1210 cells. Proc Natl Acad Sci USA 1973; 70:2785-2788.

(32) ———. Enhancement of the expression of histocompatibility antigens of mouse lymphoid cells by interferon in vitro. Eur J Immunol 1974; 4:779-784.

(33) Lindahl P, Gresser I, Leary P, Torey M. Interferon treatment of mice: Enhanced expression of histocompatibility antigens on lymphoid cells. Proc Natl Acad Sci USA 1976; 73: 1284-1287.

(34) Liao SK, Clarke BJ, Kwong PC, Brickenden A, Gallie BL, Dent PB. Common neuroectodermal antigens on human melanoma, neuroblastoma, retinoblastoma, glioblastoma and fetal brain revealed by hybridoma antibodies raised against melanoma cells. Eur J Immunol 1981; 11:450-454.

(35) Killander D, Lindahl P, Lundin L, Leary P, Gresser I. Relationship between the enhanced expression of histocompatibility antigens on interferon-treated L1210 cells and their position in the cell cycle. Eur J Immunol 1976; 6:56-59.

(36) Chang EH, Mims SJ, Triche TJ, Friedman RM. Interferon inhibits mouse leukemia virus release: An electron microscope study. J Gen Virol 1977; 34:363-367.

(37) Chang EH, Jay FT, Friedman RM. Physical, morphological and biochemical alterations in the membrane of AKR mouse cells after interferon treatment. Natl Acad Sci USA 1978; 75: 1859-1863.

(38) Khoskavi M, Liao SK, Thomson DM, Dent PB. Relationship of melanoma-associated antigens (MAA) to $\beta 2$ microglobulin ($\beta 2$M) and HLA antigen in materials shed by cultured human melanoma cells. Proc Am Assoc Cancer Res 1981; 22:292.

(39) Thomson DM, Raunch JE, Weatherhead JC, et al. Isolation of human tumour-specific antigens associated with beta2 microglobulin. Br J Cancer 1978; 37:753-775.

(40) Malley A, Burger DR, Vandenbark AA, et al. Association of melanoma tumor antigen activity with β_2-microglobulin. Cancer Res 1979; 39:619-623.

(41) McCabe RP, Ferrone S, Pellegrino MA, Kerr DH, Holmes EC, Reisfeld RA. Purification and immunologic evaluation of human melanoma-associated antigens. J Natl Cancer Inst 1978; 60:773-777.

(42) Carey TE, Lloyd KO, Takahashi T, Travassos LR, Old LJ. AU cell surface-antigen of human malignant melanoma: Solubilization and partial characterization. Proc Natl Acad Sci USA 1979; 76:2898-2902.

blank page

In Vitro Reversal of Depressed T-Lymphocyte Function in the Peripheral Blood of Brain Tumor Patients[1, 2]

Gary W. Wood[3] *and* **Robert A. Morantz**[4]

ABSTRACT—Peripheral blood mononuclear cells from some brain tumor patients exhibited depressed T-lymphocyte responses to the polyclonal mitogen phytohemagglutinin (PHA). These responses, initially depressed, were restored to near normal by a 24-hour preculture in growth medium. The effect of preculture was mimicked by mild trypsinization before addition of PHA. In addition, cells treated with deaggregated antihuman IgG resulted in greatly reduced responses to mitogen by mononuclear cells from all brain tumor patients. Anti-IgG had no effect if cells were precultured for 24 hours. The results suggest that, in brain tumor patients, depressed immune function associated with tumor progression was caused by suppressor cells which were activated by humoral factors that express IgG antigenic determinants.—JNCI 1982; 68:27-33.

Depressed peripheral T-lymphocyte function in patients with cancers is well established. In general, the existence and magnitude of depressed responses correlate well with advanced disease (*1*). That observation indicates that immunodepression is secondary to interaction between tumor and host. Although the precise role of tumor immunity in limiting or promoting tumor spread is unknown, there is considerable evidence that progressive tumor growth is linked to the functional integrity of the immune system.

A high proportion of patients with tumors of the CNS exhibit compromised peripheral immune function (*2-4*). Because these patients present initially in a depressed functional state, they serve as an excellent model system for studying responsible mechanisms. Early studies of CNS tumor patients' cells demonstrated that depressed function was at least partially produced by a serum factor that co-purified with IgG (*2, 3*). The mechanism whereby such serum factors may be functioning remains to be elucidated. The situation is further complicated by the observation that a high proportion of CNS patients exhibit depressed T-cell function in the absence of autologous serum, a suggestion that nonhumoral suppressor factors are present [Wood GW, Morantz RA: Unpublished observations, (*2*)]. The possibility has been considered that CNS tumor patients may also have high levels of circulating suppressor cells.

Several recent studies have demonstrated that peripheral blood monocytes can function as suppressor cells in cancer patients (*5-7*). Therefore, a previous study (Wood GW, Morantz RA: Submitted for publication) was undertaken in this laboratory to determine if monocytes were exerting suppressor function in CNS tumor patients. We established that in most patients immune depression was related to monocytosis and that monocytes functioned as suppressors. Nevertheless, all depressed function was not due to monocyte activity (Wood GW, Morantz RA: Unpublished observations). At least two mechanisms appear to be involved, one humoral and the other cellular, although other possibilities have yet to be evaluated.

The present study was designed to probe the possibility that a unified theory might explain the previous results. Many of the findings can be explained by postulating that circulating suppressor factors function by activating suppressor cells rather than by directly inhibiting T-lymphocyte differentiation. Thus suppression would occur in vitro in the presence of humoral factors but could also occur when such factors were not included in the culture system. This last effect would be observed if suppressor cells remained activated for significant periods of time in vitro or if a sufficiently high concentration of suppressor factors remained bound to the cells when they were removed from the in vivo milieu. Thus factor-induced suppression could be maintained in vitro in the absence of autologous serum. Such a possibility is supported by the observation that depressed T-cell responses can be reversed by extensively washing the cells or by culturing the cells for 24-48 hours before adding the mitogen (*8-11*). Thus removal of the in vivo adsorbed suppressor factors from the surface of cells appears to result in enhanced responses (*8-11*). Further support for the theorized mechanism is provided by the fact that antigen-antibody complexes, which function as blocking factors, have been eluted from peripheral blood leukocytes of cancer patients (*12*). If the cells to which suppressor factors were adsorbed include monocytes, then the possibility of a common mechanism is increased, because monocytes are the major circulating suppressor cells that have been described in cancer patients.

ABBREVIATIONS USED: CNS=central nervous system; FBS=fetal bovine serum; HBSS=Hanks' balanced salt solution; [^{3}H]dThd=tritiated thymidine; MEM=minimum essential medium; PHA=phytohemagglutinin.

---

[1] Received October 28, 1980; revised July 24, 1981; accepted August 20, 1981.

[2] Research procedures were in accord with the ethical standards of the Human Subjects Committee of the University of Kansas Medical Center.

[3] Department of Pathology, University of Kansas Medical Center, 39th and Rainbow Blvd., Kansas City, Kans. 66103.

[4] Department of Surgery, University of Kansas Medical Center.

MATERIALS AND METHODS

Patients.—Of 47 patients with CNS tumors, 8 had glioblastomas, 7 had astrocytomas, 4 had meningiomas, 2 had oligodendrogliomas, 14 had an assortment of other primary tumors of the CNS, and 12 had tumors metastatic to the brain from other sites. All patients were studied before their tumors were surgically removed and were receiving neither radiotherapy nor chemotherapy. Healthy adults were included as controls for the separation procedures, cell enumerations, and T-cell function studies.

Mononuclear cell isolation.—Peripheral venous blood was drawn into Vacutainer tubes containing 250 U of preservative-free heparin. Mononuclear cells were isolated by Ficoll-Hypaque density gradient sedimentation, washed twice with HBSS, and suspended in Eagle's MEM supplemented with 15% FBS, 100 μg streptomycin/ml, and 100 U penicillin/ml. Cell populations obtained were evaluated without further modification.

Monocyte depletion.—Mononuclear phagocytes were selectively removed from mononuclear cell suspensions by glass adherence. After 3 ml of growth medium containing $3\text{-}5\times10^6$ cells/ml were added to sterile glass slides, the cells were allowed to adhere for 30 minutes at 37°C. Nonadherent cells were washed from the slides with HBSS and readhered under identical conditions. The final population of nonadherent cells was counted, cytocentrifuged, and stained with Wright's agent. The effectiveness of adherent cell removal was determined by counting the percentage of morphologically identifiable monocytes.

Mitogen stimulation.—A suspension of 5×10^4 mononuclear cells in 0.2 ml of MEM plus 15% FBS was added to each well of a Linbro 96-well flat-bottomed Disposotray. PHA-M (GIBCO, Grand Island, N.Y.) at three concentrations (1, 5, and 10 μl of stock PHA-M/ml) was added to each well. Six replicates were performed for each mitogen concentration as well as for the cell control. Cells were cultured in 5% CO_2 in a humidified incubator at 37°C. After a 72-hour incubation, 12.5 μCi of [^{3}H]dThd was added to each well and the culture was continued for 18 hours. Samples were harvested on glass-fiber filters with an automated cell harvester, solubilized, and counted in a Mark III beta-scintillation counter.

Preculture.—Cells were added to wells as described above, but mitogen was omitted. Plates containing cells in growth medium were incubated under the described culture conditions for 24 hours. Mitogen was added to unchanged medium. The cultures were continued for the prescribed post-mitogen period, i.e., 72 hours in the presence of PHA-M and an additional 18 hours with [^{3}H]dThd as described above.

Enzyme treatment.—From density gradient sedimentation, 5×10^6 mononuclear cells were obtained and washed as described, were suspended in 5 ml of 0.25% trypsin, and were incubated for 15 minutes at 37°C and washed twice with HBSS. Trypsinized cells were then tested for mitogen responsiveness as described above.

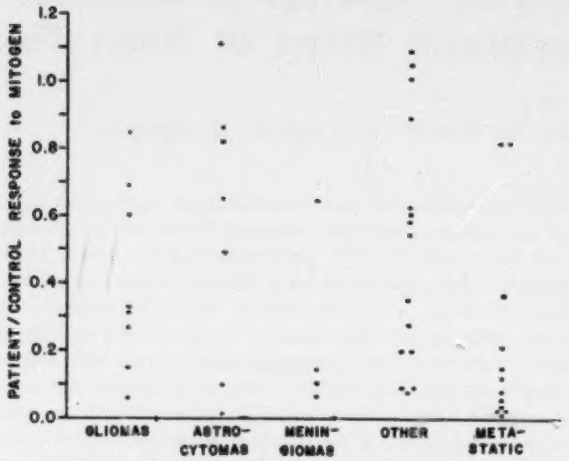

TEXT-FIGURE 1.—Mitogenic responses to PHA by T-lymphocytes from CNS tumor patients. Data are presented as ratios of maximum patient responses to maximum control responses.

Statistics.—Because all analyses involved demonstration of differences between paired samples, Student's *t*-test was used to determine significance.

RESULTS

Depressed mitogen responsiveness.—More than 50% of mononuclear cell samples from CNS tumor patients exhibited depressed T-lymphocyte mitogen responsiveness (text-fig. 1). Depressed responses were identified by comparison of the maximum response of the patient's mononuclear cells to the maximum response of a healthy individual's mononuclear cells on the same day. The values were expressed as ratios (the maximum mean patient response divided by the maximum mean control response). We have arbitrarily defined depressed responses as those producing a ratio of 0.5 or less. The normal response range from this laboratory has been reported previously (*13*).

Effect of preculture on normal mitogen responses of mononuclear cells.—The present experiments were designed to determine whether depressed mitogen responses could be reversed by a 24-hour preculture. Precultured control cells previously showed enhanced mitogen responsiveness (*14*), and similar results were obtained in the present study. A 24-hour preculture generally produced a significantly enhanced [^{3}H]dThd uptake (table 1, $P<0.005$).

Although the apparent effect of preculture was an overall increase in responsiveness, there was some concern that preculture simply altered the response profile. Maximum mitogen response was usually observed after 72-96 hours of culture, but evaluation of the possibility that artifacts were induced by preculture was needed. We found that peak responses to PHA for control cells occurred between 72 and 96 hours; peak responses for 24-hour precultured cells also occurred at 72-96 hours. Although there was no significant shift of the response peak, enhanced responsiveness produced

TABLE 1.—*Mononuclear leukocytes from healthy individuals: Effect of preculture on PHA responses*

Mononuclear cell response to PHA, cpm ± SD		Ratio of without to with
Without preculture[a]	With preculture[b]	
20,962±3,651	35,138±7,684	1.7
40,497±2,974	57,419±4,115	1.4
37,488±3,734	52,363±8,603	1.4
61,476±6,575	71,819±8,490	1.2
66,369±7,318	74,771±5,755	1.1
34,197±4,053	52,556±5,355	1.5
85,447±6,450	122,970±22,553	1.5
70,912±7,190	109,120±8,296	1.5
56,126±3,719	85,739±6,394	1.5
39,724±4,744	52,946±9,734	1.3
Mean		1.4

[a] Mononuclear cells were precultured for 24 hr at 37°C in the absence of mitogen.

[b] Cells were cultured for 72 hr in the presence of PHA. [^{3}H]dThd was added and responses were measured after 18 hr. Only maximum responses are listed.

TABLE 2.—*Mononuclear leukocytes from CNS tumor patients with nondepressed mitogen responses: Effect of preculture on PHA responses*

Mononuclear cell response to PHA, cpm ± SD		Ratio of without to with
Without preculture[a]	With preculture[b]	
21,889±1,018	35,128±7,684	1.6
33,461±4,350	40,454±10,698	1.2
63,515±2,391	35,635±7,261	0.6
32,221±8,650	38,750±4,847	1.2
37,620±17,805	65,466±12,323	1.7
39,641±3,206	76,331±4,275	1.9
25,136±5,129	32,386±2,099	1.3
30,054±4,216	66,304±6,487	2.2
15,682±4,567	14,601±2,576	0.9
28,757±4,601	67,847±14,243	2.4
15,027±2,785	20,081±51,484	1.3
Mean		1.5

[a] Mononuclear cells were precultured for 24 hr at 37°C in the absence of mitogen.

[b] Cells were cultured for 72 hr in the presence of PHA. [^{3}H]dThd was added and responses were measured after 18 hr. Only maximum responses are listed.

by preculture was frequently greater after 48 hours than after 72 or 96 hours of culture.

We were also concerned that preculture could shift the mitogen concentration optimum. Extensive titration of mitogen demonstrated that lower or higher PHA concentrations consistently resulted in reduced responses, i.e., optimum mitogen concentrations were used throughout the study. Therefore, preculture appeared to produce an objective increase in mitogen responses of mononuclear cells from healthy individuals.

Effect of preculture on mitogen responses of patients' mononuclear cells.—Patient responses to PHA were divided: Some responses were normal and some were depressed. Patients whose responses were defined as depressed gave a maximum response that was less than 50% of the maximum response of control cells. The effect of preculture on cells from patients in the nondepressed group is summarized in table 2. As was seen with control cells, preculture produced a consistent increase in responsiveness ($P<0.05$). The mean increase for this group of patients was nearly identical to that of the control cells. However, the variance was greater. Responses were suppressed in 2 patients and were more than doubled in another 2. These results suggest that some of the patients in the group with arbitrarily defined "normal" responses actually had moderately depressed T-lymphocyte function. The major value of the studies of the effects of preculture on normal responses was to demonstrate that preculture had no apparent negative effects on mononuclear cells and that enhancement of nondepressed responses was minimal.

The effect of preculture on cells from CNS tumor patients with depressed responses to mitogen also is presented in table 3. In each case there was a highly significant ($P<0.0005$) enhancement of mitogen responsiveness subsequent to preculture. Responses were at least doubled in all cases, bringing more than one-half of them within the normal range. Although responses that initially had been severely depressed were enhanced by preculture, they remained subnormal.

The possibility was considered that the depressed responses observed were an artifact of the culture system. Perhaps cells from these patients exhibited maximum proliferation within a different time frame. However, we found that depressed responses were observed whether cultures were terminated after 24, 48, 72, 96, or 120 hours; maximum response was again obtained between 72 and 96 hours.

TABLE 3.—*Mononuclear leukocytes from CNS tumor patients with depressed mitogen responses: Effect of preculture on PHA responses*

Mononuclear cell response to PHA, cpm ± SD		Ratio of without to with
Without preculture[a]	With preculture[b]	
8,503±3,467	30,988±4,134	3.6
4,079±1,292	15,384±6,038	3.8
8,856±1,134	22,419±3,756	2.5
6,858±1,541	23,947±4,359	3.5
6,898±1,074	13,792±3,977	2.0
11,634±6,814	30,193±2,511	2.6
2,827±915	8,764±2,511	3.1
1,008±522	6,639±1,351	6.6
1,996±376	10,770±1,809	5.4
5,677±1,775	27,663±1,073	4.9
10,595±870	31,794±2,531	3.0
15,980±3,175	39,639±6,703	2.5
22,725±5,429	66,074±7,423	2.9
Mean		3.6

[a] Mononuclear cells were precultured for 24 hr at 37°C in the absence of mitogen.

[b] Cells were cultured for 72 hr in the presence of PHA. [^{3}H]dThd was added and responses were measured after 18 hr. Only maximum responses are listed.

Comparison of the effects of preculture and adherent cell removal.—In previous studies (*5-8*), the possibility was explored that monocytes functioned as suppressor cells. We observed that T-cell dysfunction could be partially reversed by removal of adherent cells (Wood GW, Morantz RA: Unpublished observations). We therefore evaluated the relative benefits of preculture and adherent cell removal by manipulating the adherent fraction of mononuclear cells from several patients, and we present the data in table 4. In all cases, preculture reversed the depressed lymphocyte function, whereas adherent cell removal was not always effective. In table 4, the patients are divided into 2 groups, one in which adherent cell removal resulted in significantly improved responses ($P<0.05$) to PHA, and the other in which the responses were not enhanced. In fact, the responses were depressed further. The effect of preculture on these 2 groups was highly significant ($P<0.005$). These experiments do not establish whether common or different mechanisms were involved. However, when total reversal of the functional defect was obtained by preculture, adherent cell removal sometimes also produced partial reversal, suggesting that the two events may be related.

Effect of trypsinization on mononuclear cell mitogen responsiveness.—If one of the possible effects of preculture is to allow either the death or the destruction of suppressor cells, then it should not be possible to reconstitute T-cell function by stripping proteins from the cell membrane immediately before culture. To test this hypothesis, we briefly exposed mononuclear cells to trypsin, then cultured the treated cells in the presence of mitogen. The results obtained for cells from healthy individuals and from CNS tumor patients with nondepressed responses are summarized in table 5. Treatment of normal cells with trypsin did not appreciably affect responsiveness to mitogen; the cells were viable and apparently capable of interacting with mitogen. In contrast, when cells from patients with depressed responses were similarly treated, a significant ($P<0.05$) augmentation of responses was observed (table 6). Trypsinization and preculture had similar effects on mitogenic responses. These results suggest that a major proportion of depressed T-lymphocyte function in brain tumor patients was produced by a cell surface-associated factor.

TABLE 4.—*Mononuclear leukocytes from CNS tumor patients: Ability of monocyte depletion and preculture to reconstitute depressed PHA responses*[a]

Mononuclear cell response to PHA, cpm ± SD			Ratio of untreated to:	
Untreated	Adherent cell depleted	Precultured	Depleted	Precultured
4,079±1,292	7,944±1,064	15,384±6,038	1.9	3.8
6,858±1,134	10,615±5,513	13,782±3,977	1.5	2.0
2,110±607	3,741±1,915	10,770±1,807	1.8	5.4
5,677±1,775	16,824±4,003	27,166±1,073	3.0	4.9
15,980±3,175	26,802±4,372	39,639±6,703	1.7	2.5
Mean			2.0	3.7
1,008±522	258±181	6,639±1,351	0.3	6.6
6,556±1,134	2,364±438	22,419±3,756	0.3	2.5
11,634±6,814	534±211	30,193±2,511	0.1	2.6
10,595±870	4,535±1,436	31,794±2,531	0.4	3.0
Mean			0.3	3.7

[a] The 9 patients listed in this table are divided into 2 groups: The upper group of 5 is that in which adherent cell depletion resulted in increased mitogen responsiveness; the lower group of 4 is that in which adherent cell depletion had no effect.

TABLE 5.—*Mononuclear leukocytes from healthy individuals and CNS tumor patients with nondepressed mitogen responses: Effect of trypsinization on PHA responses*

Subjects	Mononuclear cell response to PHA, cpm ± SD		Ratio of untreated to trypsinized
	Untreated	Trypsinized[a]	
Healthy individuals	34,197±4,053	47,331±6,596	1.4
	85,447±6,450	86,769±10,856	1.0
	70,912±7,190	82,450±7,630	1.2
	56,126±3,719	69,971±3,126	1.3
	39,969±9,072	44,404±6,084	1.1
	39,724±4,744	29,016±4,725	0.7
	75,780±3,422	68,018±8,004	0.9
	48,885±7,496	57,826±4,071	1.2
	19,121±3,246	16,919±2,451	0.9
Mean			1.1
CNS tumor patients	37,620±17,805	61,665±20,104	1.6
	39,641±3,206	69,971±3,126	1.8
	42,079±1,723	20,626±6,019	0.5
	25,136±5,129	20,293±1,350	0.8
	47,307±4,482	45,969±7,715	1.0
	30,054±216	29,997±1,340	1.3
	19,164±3,907	25,213±2,966	1.3
Mean			1.2

[a] After a 15-min incubation at 37°C in 0.25% trypsin, mononuclear cells were washed and cultured with PHA.

Effect of rabbit anti-human IgG on mitogen responses.—Previous studies of depressed T-cell function in brain tumor patients have implicated IgG as a humoral suppressor factor (*2, 3*). The suppressive IgG could theoretically be in several forms which include antigen-antibody complexes, antilymphocyte antibodies, and immunoglobulin fragments. Because previous experiments suggested that membrane-associated factors were responsible for T-cell dysfunction and because circulating IgG-associated factors are known to have immunosuppressive effects in brain tumor patients, the important determination was whether some part of the membrane-associated events might be related to IgG. We theorized that if membrane-associated IgG was causing the suppression, then introduction of specific anti-IgG to the culture system might enhance the effect. In fact, each time anti-IgG was either bound to cells before culture or added to the cultured cells, depressed responses were further depressed (data not shown). Anti-IgG not only futher depressed already depressed responses but also produced a profound suppression of responses by cells from patients with

TABLE 6.—*Mononuclear leukocytes from CNS patients with depressed mitogen responses: Effect of trypsinization and preculture on PHA responses*

Mononuclear cell response to PHA, cpm ± SD			Ratio of untreated to:	
Untreated	Trypsinized[a]	Preincubated[b]	Trypsinized	Preincubated[b]
6,858±1,541	58,106±5,862	23,947±4,847	8.5	3.5
11,634±6,814	29,004±5,404	30,193±6,122	2.5	2.6
1,536±857	14,658±5,690	ND	9.5	ND
5,677±1,775	27,581±2,876	27,663±1,073	4.9	4.9

[a] After a 15-min incubation at 37°C in 0.25% trypsin, mononuclear cells were washed and cultured with PHA.
[b] ND=not done.

initially normal responses (table 7). The effect of anti-IgG on PHA responses of cells from healthy individuals was not specifically suppressed. Normal rabbit serum sometimes suppressed responses, but not to the degree that the rabbit anti-human IgG did.

The effect of anti-IgG on precultured cells also was tested. The results in table 8 clearly demonstrate that, whereas reacting cells with anti-IgG before preculture caused suppression of mitogenesis, the combination of anti-IgG with preculture had no comparable effect.

DISCUSSION

Progression of tumors is thought to be facilitated by blocking factors, possibly antigen-antibody complexes, which interfere with cell-mediated cytotoxicity by as yet undefined mechanisms (*15*). Although most experimentation has focused on specific blocking of T-cell-mediated tumor cell destruction, Gorczynski et al. (*16*) have also suggested that antigen-antibody complexes may have a nonspecific immunoregulatory role. It is known that "blocking factors" eluted from tumors function nonspecifically as well as specifically (*17*). Despite these observations, few attempts have been made to link blocking phenomena with the generalized nonspecific immune depression that often is seen in association with neoplasia. Similarly and interestingly, brain tumor patients have circulating factors that are IgG in nature, i.e., either antibody or antigen-antibody complexes, which nonspecifically suppress immune function (*2, 3*), and they have blocking factors that inhibit T-cell-mediated cytotoxicity (*18*).

The present study was based on the assumption that depressed responses to T-lymphocyte mitogens, which are seen with mononuclear cells from brain tumor patients, are real phenomena and was designed to explore possible mechanisms. Our culture conditions did not include autologous serum so that initially we could evaluate the possible presence of suppressor cells. Extensive studies established that most patients with depressed responses exhibited evidence for the presence of suppressor cells, principally monocytes (Wood GW, Morantz RA: Unpublished observations). Those observations were essentially confirmatory of previous studies

TABLE 7.—*Mononuclear cells from healthy individuals and CNS tumor patients: Effect of rabbit anti-human IgG (γ-chain specific) on mitogen responses*

Subjects	Mononuclear cell response to PHA, cpm ± SD[a]			Ratio of after anti-IgG to:	
	Before anti-IgG	After normal rabbit serum[b]	After anti-IgG	After normal rabbit serum	Before anti-IgG
Healthy individuals	39,324±4,744	ND	22,871±1,749	ND	1.7
	75,780±3,722	ND	47,603±5,303	ND	1.6
	17,269±3,076	10,203±1,463	8,489±334	1.7	2.0
	28,552±1,268	23,463±1,956	24,085±890	1.2	1.2
Mean				1.5	1.6
Brain tumor patients	42,079±1,723	ND	8,954±3,628	ND	4.7
	25,136±5,129	ND	4,289±339	ND	5.9
	47,407±4,482	ND	1,982±743	ND	23.3
	30,054±4,216	37,475±10,140	6,072±258	0.8	5.0
	19,167±3,906	16,520±4,305	1,727±1,920	1.2	11.1
	15,027±2,785	7,437±622	2,555±622	2.0	5.9
Mean				1.3	9.4

[a] After a 30-min incubation with rabbit anti-human IgG (1:10) or normal rabbit serum, mononuclear cells were washed and cultured with PHA.
[b] ND=not done.

TABLE 8.—*Mononuclear leukocytes from CNS tumor patients: Effect of rabbit anti-human IgG (γ-chain specific) and preculture on mitogen responses*[a]

Precultured	Patient	Mononuclear cell response to PHA, cpm ± SD		
		Medium alone	Anti-IgG	Normal rabbit serum
No	A	15,027±2,785	2,555±622	7,437±1,058
	B	16,863±2,309	2,574±473	16,694±2,458
	C	3,822±702	384±107	2,927±567
Yes	A	20,081±5,484	18,509±1,373	24,469±4,221
	B	23,461±4,542	19,433±3,543	27,601±437
	C	5,340±1,834	5,508±266	11,872±2,911

[a] Either before or after mononuclear cells were precultured for 24 hr, 10 μl of deaggregated rabbit anti-human IgG (1:10) or normal rabbit serum was added to each culture.

demonstrating monocyte suppressors in patients with various types of cancer. Representative results are included here. The importance is that, although responses to mitogen were improved by removal of adherent cells, responses rarely returned to normal. Moreover, our preculture and trypsinization results strongly suggest an even more complex situation. Both preculture of mononuclear cells for 24 hours and trypsinization of mononuclear cells for 15 minutes generally produced an almost complete reconstitution of T-cell function, at least as determined by responsiveness to a polyclonal mitogen.

These results are important for three reasons. First, they establish that depressed T-cell function is a real rather than a statistical phenomenon. That is, relatively trivial manipulations of the cells allow them to respond in the normal range. The responses weren't low just because the control for that day happened to give a high response or just because the number of T-cells present was too low. Second, the results suggest that some type of control mechanism is involved rather than an inherent T-cell defect. Third, the return of responsiveness with preculture could be explained by loss of suppressor cells, but the trypsinization results suggest that some alternative explanation must be sought. The results of trypsinization are difficult to explain in any other way than by removal of cell-associated factors. Viability was not lost during trypsinization, and trypsinization had no appreciable effect on normal cells. This interpretation is totally consistent with previous observations that brain tumor patients have circulating soluble suppressor factors (*2, 3*). Moreover, the results are consistent with previous reports in humans and experimental animals which demonstrated that extensive washing (*8*), preculture (*9, 10*), or trypsinization (*11*) of cells could bring about enhanced immune responsiveness. Of course, all of these observations only demonstrate that if there are humoral immunosuppressive factors their ultimate effect must be on or through cells. It does not tell us what cell types are affected.

There are two major explanations for the immunodepression: suppressor cells and soluble immunoregulatory factors. The results of the present study clearly demonstrate that suppressor cells and suppressor factors coexist in the same patient. One might be able to explain this by saying that each independently contributes to the depression. However, as was mentioned earlier, humoral factors must either act directly on the T-cells or act indirectly through accessory cells. Because suppressor cells clearly were present, but depression often was completely reversed by removal of cell-associated factors, we hypothesize that the circulating factors act by stimulating suppressor cells, i.e., there is no inherent suppressor cell defect. However, the results of the present study do not prove that this is the situation. The alternative that the factors act directly on T-cells remains viable.

The precise nature of the humoral factors involved is an open question. Clearly, the fact that previous studies demonstrated IgG suppressor factors would suggest antibodies or antigen-antibody complexes as prime candidates. Moreover, a previous study in which peripheral blood cells from patients with differnt types of cancer were used also implicated membrane-associated antigen-antibody complexes in the depression (*13*). Those results are further supported by the preliminary results obtained in the present study. Highly specific anti-IgG consistently produced profound depression of responses to PHA. Although some depression was produced also by normal rabbit serum, it was not comparable. The fact that the inhibitory effect of anti-IgG is lost subsequent to preincubation clearly supports the concept that a surface-associated IgG factor is associated with the suppression.

The results of the present study support the idea that tumor-associated nonspecific T-lymphocyte dysfunction is produced by membrane-associated suppressor factors, which appear to be IgG in nature. Clearly, much more work must be done before the nature of these factors and the cells to which they are adsorbed has been established. However, our results are consistent with previous observations that antigen-antibody complexes are capable of inducing profound immunosuppression through an Fc-dependent mechanism. This mechanism would explain the reversal of immunodepression by washing, trypsinization, or preculture (endocytosis or shedding of surface-associated Ig) and would explain the enhanced depression induced by anti-IgG. The model that appears most consistent with the various observations is that circulating, soluble antigen-antibody complexes bind to the surfaces of Fc receptor-positive cells, including monocytes, which are induced to suppress the T-cell responses. Again, we emphasize that the present results do not prove this mechanism; they only suggest that further work is necessary.

REFERENCES

(*1*) MEKORI T, SHER S, ROBINSON E. Suppression of the mitogenic response to phytohemagglutinin in malignant neoplasia: Correlation with clinical stage and therapy. J Natl Cancer Inst

1974; 52:9-12.

(*2*) Brooks WA, Netsky MG, Normansell DB, Horowitz DA. Depressed cell-mediated immunity in patients with primary intracranial tumors. J Exp Med 1972; 136:1631-1637.

(*3*) Young HR, Sakala R, Kaplan AM. Inhibition of cell-mediated immunity in patients with brain tumors. Surg Neurol 1976; 5: 19-23.

(*4*) Mahaley MS, Brooks WH, Rozmann TL, Bigner DD, Dudka L, Richardson S. Immunobiology of primary intracranial tumors: Studies of the cellular and humoral general immune competence of brain tumor patients. J Neurosurg 1977; 46: 467-476.

(*5*) Zembala M, Mytar B, Popiela T, Asherson GL. Depressed in vitro peripheral blood lymphocyte response to mitogens in cancer patients: The role of suppressor cells. Int J Cancer 1977; 19:605-613.

(*6*) Jerrells TR, Dean JH, Richardson GL, McCoy JL, Herberman RB. Role of suppressor cells in depression of in vitro lymphoproliferative responses of lung cancer and breast cancer patients. JNCI 1978; 61:1001-1009.

(*7*) Quan PC, Burtin P. Demonstration of nonspecific suppressor cells in the peripheral lymphocytes of cancer patients. Cancer Res 1978; 38:288-296.

(*8*) Mannick JA, Constantian J, Peidridge L, Saporoschetz I, Badger A. Improvement of phytohemagglutinin responsiveness of lymphocytes from cancer patients after washing in vitro. Cancer Res 1977; 37:3066-3070.

(*9*) Rambotti P, Velardi A, Spinozzi F, Falini B, Martelli MD. Study of cellular immunity in patients with Hodgkin's disease: Modification induced by incubation of lymphocytes with fetal calf serum and serum from a Hodgkin's disease patient. Boll Ist Sieroter Milan 1979; 58:90-99.

(*10*) Laux D, Lausch RN. Reversal of tumor-mediated suppression of immune reactivity by in vitro incubation of spleen cells. J Immunol 1974; 112:1900-1908.

(*11*) Blasecki JW, Tevethia SS. Restoration of specific immunity against SV40 tumor-specific transplantation antigen to lymphoid cells from tumor-bearing mice. Int J Cancer 1975; 16: 275-283.

(*12*) Hattler BG, Soehnlen B. Inhibition of tumor-induced lymphocyte blastogenesis by a factor or factors associated with peripheral leukocytes. Science 1974; 184:1374-1375.

(*13*) Wood GW, Neff JE, Stephens R. Relationship between monocytosis and T-lymphocyte function in human cancer. JNCI 1979; 63:587-592.

(*14*) Bresnihan B, Josin HB. Suppressor function of peripheral blood mononuclear cells in normal individuals and in patients with systemic lupus erythematosus. J Clin Invest 1977; 59:106-116.

(*15*) Hellström KE, Hellström I, Nepom JT. Specific blocking factors. Are they important? Biochim Biophys Acta 1977; 473: 121-148.

(*16*) Gorczynski RM, Kilburn DG, Knight RA, Norbury C, Parker D. Nonspecific and specific immunosuppression in tumour-bearing mice by soluble immune complexes. Nature 1975; 254:141-143.

(*17*) Hellström KE, Hellström I. Enhancement of tumor outgrowth by tumor-associated blocking factors. Int J Cancer 1979; 23:366-373.

(*18*) Levy NL. Cell-mediated cytotoxicity and serum-mediated blocking: Evidence that their associated determinants on human tumor cells are different. J Immunol 1978; 121:916-922.

blank page

Human Adherent Cell Contact-Mediated Modulation of Normal Myeloid Colony Formation[1,2,3]

Gary Spitzer,[4,5] **Dharmvir S. Verma,**[4] **Miloslav Beran,**[6] **Axel R. Zander,**[4]
Kenneth B. McCredie,[4] *and* **Karel A. Dicke**[4]

ABSTRACT—The effects of coincubation of normal nonadherent bone marrow cells on adherent monolayers created from human peripheral blood mononuclear cells or marrow cells were investigated. Nonadherent marrow cells were coincubated for 4 hours with peripheral blood adherent cells at ratios of adherent cells to marrow cells of 2:1 to 5:1. This coincubation suppressed subsequent neutrophilic agar colony growth but not eosinophilic growth. Further studies suggested that this suppression was a cell-cell-mediated process and not secondary to soluble factors. However, coincubation on marrow adherent cells caused increased neutrophilic colony recovery. The possible in vivo relevance is discussed.—JNCI 1982; 68:35–42.

Adherent cells, probably monocytes, have been reported to have many regulatory influences on the clonal growth of human hematopoietic progenitor cells. Monocytes incorporated into agar cultures have been shown to have both stimulatory effects on myeloid CFU-C secondary to CSA release and inhibitory effects when in high numbers secondary to PGE_2 release (*1–3*). Monocytes from peripheral blood have been reported to inhibit erythroid colony growth (*4*), but those from bone marrow stimulate such growth (*5*). We have described inhibitory effects of bone marrow adherent cells from leukemia marrow on leukemia growth (*6*). However, those experiments incorporated adherent cells in differing numbers directly into the agar, an experimental situation in which cells are relatively immobilized and which does not allow significant cell-cell contact.

More recently, we demonstrated that peripheral blood cells from normal donors could inhibit leukemia clonogenic cells (*7*). This inhibition required only brief cell-cell contact and could not be reproduced by the same number of cells when incorporated into agar but separated from the marrow target. We next investigated the question of whether such inhibition was specific to leukemia clonogenic cells. This article describes experiments showing similar inhibition of normal GM-CFC by peripheral blood adherent cells. The possible in vivo relevance to hematopoietic control and the microenvironment is discussed.

MATERIALS AND METHODS

Acquisition of specimen.—Peripheral blood, a source of $M\phi$, was obtained by venipuncture from normal human volunteers. The marrow cells used were obtained by posterior iliac crest puncture from lung cancer patients under local anesthesia and without any hematologic abnormalities. Before acquiring any specimens for experimentation, we obtained a signed written consent from each patient as required by the Surveillance Committee on Human Experimentation at The University of Texas System Cancer Center, M. D. Anderson Hospital and Tumor Institute. The specimens were collected in polystyrene tubes (Corning Glass Works, Corning, N.Y.) containing 0.3-ml preservative-free heparin (100 U/ml) in 1.7 ml PBS.

Cell separation procedures.—T-lymphocytes: To obtain mononuclear cells, we diluted peripheral blood in an equal volume of α-MEM plus 15% FCS and centrifuged the mixture at 400×g for 35 minutes over Ficoll-Hypaque columns (density, 1.077 g/ml) in 15-ml plastic tubes. To separate T-cells, we used a modification of the method described by Weiner et al. (*8*) in which a 1-ml 5% sheep erythrocyte suspension was incubated for 1 hour at 37°C in a neuraminidase solution at a final concentration of 17 U/ml and then washed three times with α-MEM. Subsequently, the mononuclear cells or low-density nonadherent marrow cells were incubated with NE as described (*8*), and the NE rosettes were pelleted by centrifugation over a Ficoll-Hypaque column (density, 1.080 g/ml). The NE in the pellet were lysed with Tris buffer, and the remaining cells were subjected to carbonyl iron phagocytosis and plastic adherence procedures to remove contaminating phagocytic and adherent cell populations. This preparation contained 99% rosetting cells.

ABBREVIATIONS USED: CFU-C = colony-forming unit(s)—culture; CSA = colony-stimulating activity; FCS = fetal calf serum; GM-CFC = granulocyte-macrophage colony-forming cells; HPCM = human placental conditioned medium; $M\phi$ = monocyte-macrophage; α-MEM = alpha modification of minimum essential medium; NE = neuraminidase-treated erythrocyte(s); PBS = phosphate-buffered saline; PGE_2 = prostaglandin.

---

[1] Received February 19, 1981; revised August 3, 1981; accepted August 28, 1981.

[2] Supported in part by Public Health Service grants CA-28153 and CA-14528 from the National Cancer Institute.

[3] Research procedures were in accord with the ethical standards of the Surveillance Committee on Human Experimentation, The University of Texas System Cancer Center.

[4] Department of Developmental Therapeutics, The University of Texas System Cancer Center, M. D. Anderson Hospital and Tumor Institute, 6723 Bertner Ave., Houston, Tex. 77030.

[5] Scholar of the Leukemia Society of America, Inc.

[6] Department of Hematology/Med. 2, Karolinska Hospital, 10401 Stockholm, Sweden.

The T-cell-depleted population contained 1% or less T-cells.

Mϕ: Mononuclear cells in a 2-ml total volume ($2\text{-}4\times10^6$/ml), in some cases T-cell depleted, were subjected to active adherence by incubation for 3 hours in α-MEM in the presence of 20% FCS at 37°C in a 5% CO_2 atmosphere. Subsequently, the nonadherent cells contained in the supernatant were aspirated and the dishes were washed twice with α-MEM plus 15% FCS. We determined the number of adherent cells remaining in the dish by subtracting the number of nonadherent cells per dish (the total number of nucleated cells in the supernatant and washes) from the total number of cells per dish subjected to the adherence procedure. This number of remaining adherent cells correlated with the predicted number of adherent cells based on the percentage of latex-phagocytosing cells in the interface cells.

Low-density nonadherent marrow cells: Low-density nonadherent bone marrow cells for coincubation assays were obtained as described elsewhere (*9*). Low-density cells (<1.078 g/ml) obtained by Ficoll-Hypaque gradient centrifugation were subjected to the plastic adherence procedure described above. Subsequently, the nonadherent cells were aspirated, washed once, and resuspended in α-MEM plus 15% FCS at a cell concentration of approximately 10^6/ml.

Coincubation of nonadherent normal marrow cells with the adherent monolayer: Low-density nonadherent human bone marrow cells were added in varying numbers to petri dishes with (coincubation) and without (control) normal peripheral blood adherent cells. After the number of adherent cells was calculated, marrow cells were then added to achieve ratios of 0.5:1, 2:1, 3:1, or 5:1 adherent normal cells to nonadherent target cells. Controls contained the same number of nonadherent marrow cells. With low numbers of nonadherent normal cells (higher adherent to nonadherent ratios), two to four identical cultures were established to later retrieve adequate nonadherent cells. Cells were then allowed to coincubate, usually for 4 hours but sometimes for 15 hours. We then extracted nonadherent cells by rinsing the petri dish several times with the supernatant using a Pasteur pipette and washing the dish once with 2 ml α-MEM. The cells were then centrifuged and resuspended to a final volume of 0.5 or 1 ml in α-MEM. Cell recoveries at the end of the 4-hour incubation were equivalent to the number of nonadherent cells, suggesting that target cells were not lost by adherence and that adherent cells did not lose their adherence during coincubation. Target cells were also 100% viable as assessed by trypan blue and contained 2% or less latex-positive cells. Nonadherent target cells incubated in the same way were pooled and cultured. Identical volumes were cultured from coincubation and control experiments and were equivalent to a volume that should contain 1×10^5 cells, if one assumes that the cell counts did not change during the 4-hour culture periods. This procedure eliminated any error in a repeated cell count and also allowed comparisons of 15-hour incubations in which cell counts varied between coincubation and control experiments.

To exclude any entrapment of CFU-C in the monolayers, we included the following controls: The monolayers were overlaid with 0.3% agar α-MEM and HPCM and scored for colony formation 7-14 days later. To eliminate the possibility that PGE_2 secretion prevented the detection of CFU-C, we removed monolayers with PBS-EDTA lidocaine solution and cultured the monolayers in an upper agar layer at 1×10^5 cells with or without 10^{-6} *M* indomethacin and with HPCM in the underlayer. Exposure of nonadherent marrow to PBS-EDTA lidocaine was not associated with loss of GM-CFC, eliminating a possible toxic effect. The GM-CFC entrapment was reexpressed as the number of colonies per 1×10^5 previously coincubated marrow cells. For instance, if four colonies were recovered from 1×10^5 adherent cells in a coincubation experiment performed at a ratio of 0.5:1 adherent to nonadherent cells, these colonies would be derived from 2×10^5 nonadherent cells. The number from 1×10^5 nonadherent cells would equal two. For the determination of the number of CFU-C not retrieved from control cultures, the dishes were treated identically, the suspensions were pelleted, media were removed, and the minute number of cells were resuspended with agar α-MEM and cultured on three plates. The total number of colonies on all three plates would be derived from the total nonadherent cells in the cultures.

Entrapped CFU-C derived from these calculations were identical to those derived from a colony incidence when monolayers from coincubations or the bottom of the dishes from control incubations were overlaid with agar α-MEM and HPCM. With the overlayer experimental approach, the colonies would be derived from all the incubated nonadherent cells, approximately 1.2×10^6 in a 0.5:1 coincubation or 3×10^5 in a 2:1 coincubation. A general schema of this experimental approach is given in text-figure 1.

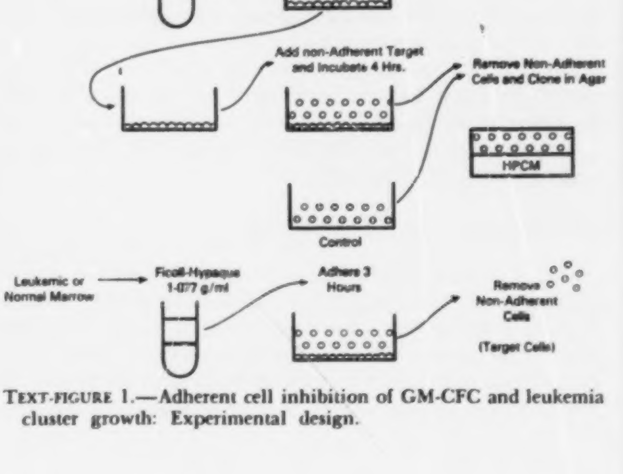
Normal Blood
Ficoll-Hypaque 1·077 g/ml
Adhere 3 Hours
Remove Non-Adherent Cells
Add non-Adherent Target and Incubate 4 Hrs.
Remove Non-Adherent Cells and Clone in Agar
HPCM
Control
Leukemic or Normal Marrow
Ficoll-Hypaque 1·077 g/ml
Adhere 3 Hours
Remove Non-Adherent Cells
(Target Cells)

TEXT-FIGURE 1.—Adherent cell inhibition of GM-CFC and leukemia cluster growth: Experimental design.

Culture procedure.—The culture procedure was described previously (*10*). The marrow preparations were cultured in equal volumes of double-strength α-MEM with 30% FCS and 0.6% agar (Bacto-agar; Difco Laboratories, Detroit, Mich.), giving a final concentration of 0.3% agar with single-strength α-MEM and 15% FCS. For all cultures, 0.1-0.3 ml of HPCM was used as a source of colony-stimulating factor in underlayers of 0.5% agar and α-MEM with 15% FCS. All cultures were plated in triplicate and incubated for 7-14 days in a fully humidified atmosphere of 7% CO_2 and air at 37°C.

Culture scoring.—Cultures were scored on days 7-14 with an Olympus dissecting microscope at × 25-40. They were analyzed for total number of colonies (aggregates of ≥40 cells) per plate. The final incidence was the mean colony incidence from each plate. Individual colonies were picked up with a Unopette pipette (Becton, Dickinson & Co., Rutherford, N.J.) and fixed on egg-albumin-smeared microscopic slides that were etched in small squares on the back by a diamond pencil (1 colony/square) (*11*). After the colonies were dried, they were stained for 2 hours with Luxol fast blue MBS (Hartman-Leddon Co., Philadelphia, Pa.). Subsequently, the slides were rinsed and kept in distilled water for another 2 hours and then counterstained with Harris' hematoxylin for 2 minutes. The staining solution consisted of 0.1 g Luxol fast blue in 100 ml of 70% alcohol saturated with urea. The percentage of each morphologic type of colony presented is based on examination of 50 colonies or more per observation.

Statistics.—Differences between the results of experiments were examined with the use of a two-sample Student's *t*-test. All comparisons were two-sided.

RESULTS

Text-figure 2 shows an initial experiment in which peripheral blood cells from one donor were coincubated with nonadherent bone marrow cells from the same person (autologous mix) and a second experiment with the peripheral blood and bone marow cells from unrelated donors (allogeneic mix). Suppression of CFU-C occurred in cultures with adherent cells and was present at lower ratios of adherent cells to marrow cells (0.5:1) with the autologous combination than with the allogeneic combination. When suppression occurred, colonies fell to 12.5 or less/10^5 light-density nonadherent human cells. However, these adherent cells were stimulatory to CFU-C when placed on the bottom of the petri dish and separated from the nonadherent marrow target by an agar layer (text-fig. 3). Here all cultures contained 25 colonies or more. Furthermore, all cultures containing adherent cell underlayers had more colonies than the target marrow cultured with HPCM alone.

Conditioned media were also harvested after coincubation. Incubating fresh nonadherent marrow cells for 4-15 hours in liquid culture with these conditioned media at 10-100% (vol/vol) did not lower subsequent CFU-C recovery (data not shown).

Text-figure 4 shows the cumulative data from these experiments and the next group of experiments performed. CFU-C were suppressed in 5 of 7 of these experiments at ratios of 2:1 or greater adherent cells to nonadherent normal marrow cells. However, at higher marrow cell numbers (lower ratios of adherent cells to marrow cells), the results were variable, with stimulation occurring in three of seven experiments. Because inhibition occurred more regularly at lower marrow cell numbers, later experiments were performed at

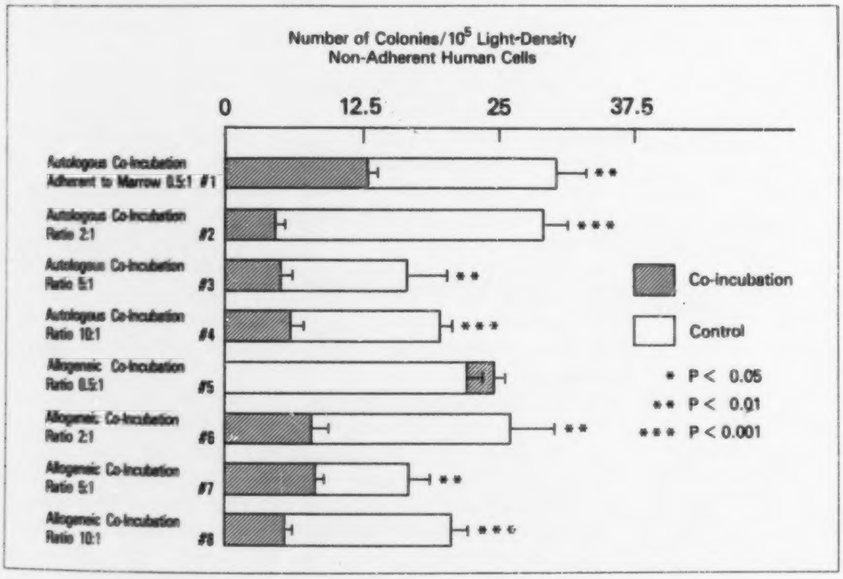

TEXT-FIGURE 2.—Adherent cell inhibition of CFU-C: Autologous combinations also suppress. Peripheral blood adherent cell layers were prepared from 1 donor. Nonadherent bone marrow from the same donor (autologous) or from an unrelated donor (allogeneic) was cultured at various concentrations for 4 hr with or without an adherent layer before removal and culture in agar for assay of CFU-C. Results are means ± SEM of triplicate cultures.

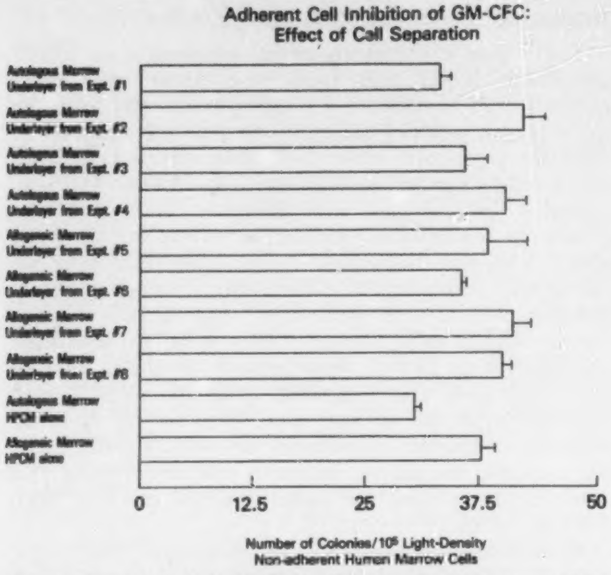

TEXT-FIGURE 3.—Peripheral blood adherent cells when separated by agar from nonadherent marrow target do not suppress. The same adherent layers (6×10^5 cells) used for coincubation expts 1-8 in text-fig. 1 were overlaid with 0.5% agar after coincubation, and the cells recovered from the equivalent control cultures were cultured at a volume equivalent to 1×10^5 nucleated cells in an upper layer. Comparison with control cultures in text-fig. 1 shows the lack of inhibition. Nonadherent bone marrow cells cultured directly into agar are also shown for comparison. Results are means ± SEM of triplicate cultures.

ratios of 3:1 and 5:1. We have now performed 20 experiments and have seen suppression in allogeneic mixes in 16. Suppression was absent when the percentage of adherent cells was low (≤10%), and the monolayers so formed were nowhere near confluence.

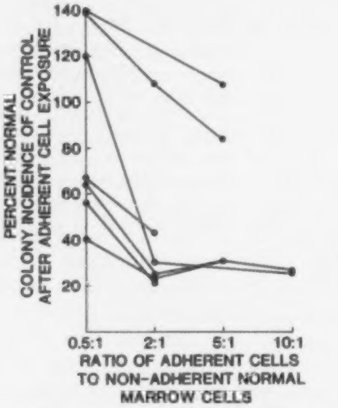

TEXT-FIGURE 4.—Adherent cell modulation of CFU-C growth: Effect of the ratio of adherent to nonadherent marrow cells. Nonadherent marrow cells were cultured in liquid with or without adherent cell underlayers created by adherence at two cell concentrations. CFU-C incidence of nonadherent marrow without prior culture is also given for comparison of CFU-C survival in liquid culture. Results are the means ± SEM of triplicate cultures.

Approximately 50% of these experiments were performed with the inclusion of 10^{-6} *M* indomethacin in liquid, solid, and both phases, and no differences in the results were seen.

Monolayers harvested from these coincubations and plated in agar with or without 10^{-6} *M* indomethacin did not contain more than 2 CFU-C/10^5 previously coincubated nonadherent bone marrow cells. This number was usually equivalent to the number of adherent CFU-C recovered from control petri dishes incubated for 4 hours with nonadherent marrow. Because sparse monolayers were sometimes associated with no inhibition, monolayers were also prepared for the next set of experiments at concentrations of 4×10^6/ml and 2×10^6/ml.

Inhibition was demonstrated with 15-hour coincubation as well as with 4-hour coincubation, but, as shown in text figure 5, was not enhanced by prolonged coincubation. Inhibition was also seen when cultures were scored at day 14, suggesting that these results were not related to a growth delay (text-fig. 6). However, morphologic examination of the colonies showed that suppression was specific. Neutrophilic colonies were markedly suppressed, whereas eosinophilic colonies were not, and there were too few data to delineate the relative sensitivity of granulocyte-macrophage or macrophage CFU-C (table 1). Differences were not associated with increased cluster growth in coincubation experiments. Both colonies and clusters were inhibited equally.

These results seemed reminiscent of the in vivo situation. In blood, neutrophilic colonies do not circulate much and circulating CFU-C are predominantly eosinophilic (*11*).

Therefore, we reasoned that if what we had shown was physiologically relevant, adherent cells from marrow should not suppress GM-CFC, inasmuch as these CFU-C are abundant in marrow. Also these experiments would serve as a control to show that adherent monolayers from other sources in general did not suppress CFU-C growth.

Text-figure 7 is representative of four other experiments. When coincubated on monolayers from marrow, CFU-C scored at day 7 (neutrophilic) showed significantly enhanced recovery. Moreover, the differences at day 14, when eosinophilic colonies were more pronounced, were not significant; if anything, they favored a slight increase in the controls (table 2). Adherent monolayers from marrow contained 0-2 CFU-C/10^5 nucleated cells. However, after coincubation CFU-C were recovered from these monolayers in greater numbers—a finding not observed with peripheral blood adherent cells.

To delineate further the nature of the peripheral blood adherent cells responsible for this inhibition and to be sure that the inhibition did not require T-lymphocyte interaction, we also did experiments with T-cell-depleted nonadherent marrow targets and adherent layers formed after T-cell removal (table 3). Addition of increasing numbers of T-cells induced extra

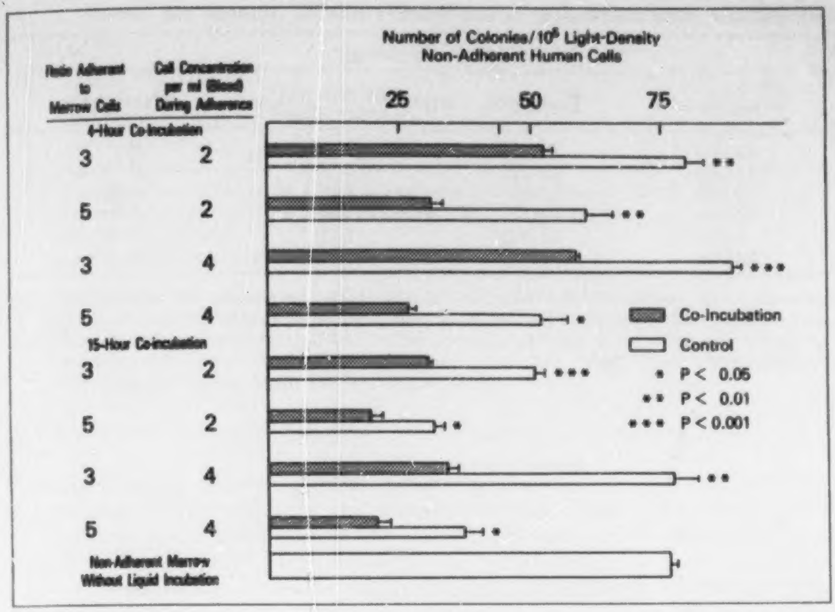

TEXT-FIGURE 5.—Adherent cell modulation of CFU-C growth: Effect of more prolonged cell contact. In addition, the effect of preparation of denser monolayers was studied by the incubation during adherence of 4×10^6 cells/ml. Results are the means ± SEM of triplicate cultures.

colony-forming cells from the controls, which was probably secondary to lymphoid CSA release synergizing with HPCM. The doses of HPCM used in all experiments were at plateau dose-responsive levels. Suppression was still seen, regardless of whether adherent monolayers were formed before or after T-cell removal. Adding T-cells again did not increase the suppression.

DISCUSSION

These experiments examine for the first time the short-term effects of cell-cell interactions between adherent cells and CFU-C progenitor cells. The results appear compatible with what happens in vivo, where predominantly eosinophilic progenitor cells circulate (*11*, *12*). The relative absence of GM-CFC in the

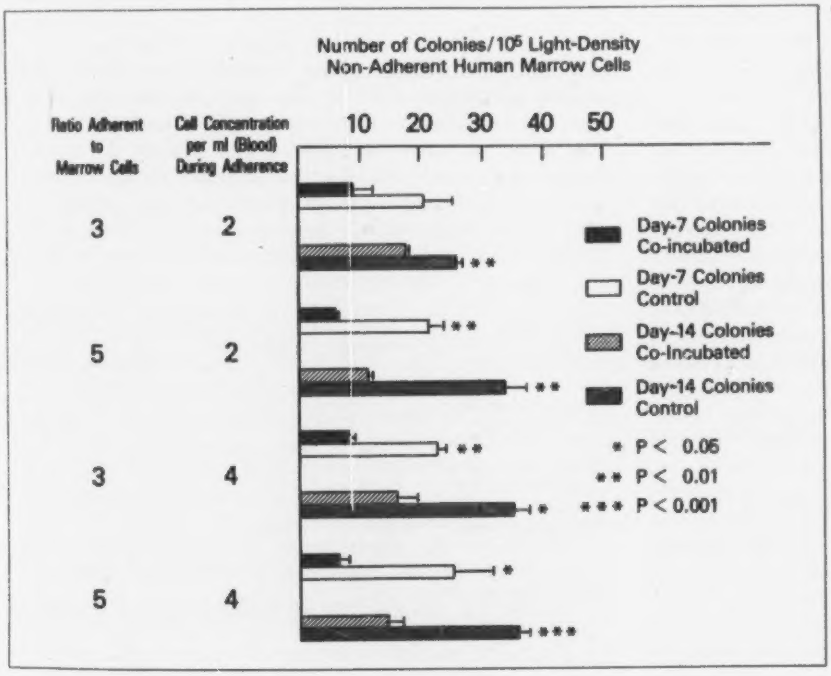

TEXT-FIGURE 6.—Adherent cell modulation of day-7 and day-14 CFU-C growth. As in text-fig. 5, inhibition was compared between monolayers prepared from the incubation of 2 and 4×10^6 cells/ml. Results are the means ± SEM of triplicate cultures.

TABLE 1.—*Suppression of granulocytic colonies from nonadherent human marrow cells by adherent cell contact*

Expt No. and procedure	Day of analysis	Colony morphology[a]			
		Granulocyte	Eosinophil	Granulocyte–macrophage	Macrophage
1. Coincubation	9	35 (45)	35 (45)	8 (10)	0
Control		112 (78)	31 (22)	0	0
2. Coincubation	14	3 (19)	11 (67)	2 (12)	1 (2)
Control		19 (48)	11 (28)	7 (19)	2 (5)
3. Coincubation	10	5 (20)	15 (57)	2 (8)	4 (15)
Control		26 (49)	20 (38)	7 (13)	0

[a] Results are absolute No. of colonies/standard volume of culture (%). *See* "Materials and Methods" for details. All colonies from the three plates of any individual experiment were harvested. The minimum No. analyzed was 51 colonies in the coincubation of expt 2, the total No. and percentage of each individual colony were calculated, and the absolute No. of any individual colony type was divided by 3 to express the No. on an individual culture dish.

TEXT-FIGURE 7.—Marrow adherent cell modulation of CFU-C growth. Nonadherent marrow cells were cultured in liquids of various concentrations with or without adherent underlayers derived from marrow. In contrast to peripheral blood adherent underlayers, marrow underlayers improved day-7 CFU-C survival. Also, significant numbers of CFU-C were detected within the adherent underlayers.

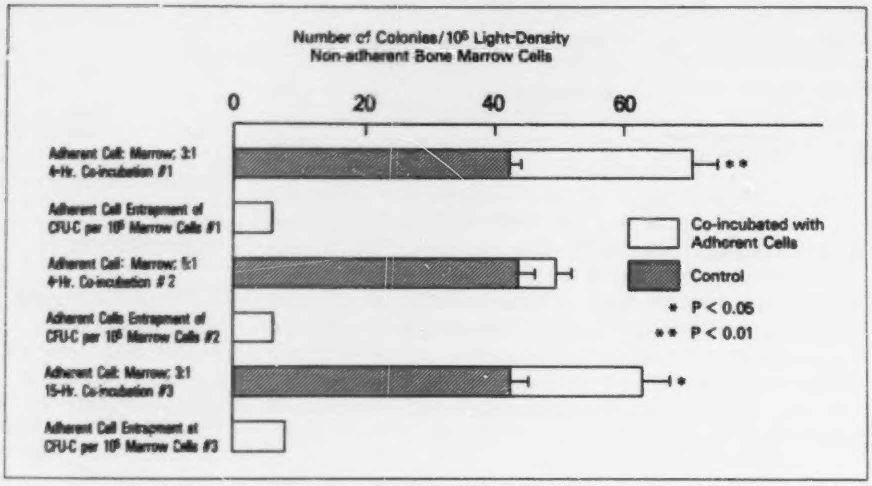

circulation may be related to inhibition of their growth by circulating adherent cells.

For inhibition to occur, there must be favorable ratios of adherent cells to marrow cells. One of the many possible explanations is that too high a number of marrow cells may block interactions between adherent cells and CFU-C. The question arises whether such ratios or circumstances exist in peripheral blood. In vivo cells are mobile, and the chance of interaction would be greatly magnified. Possibly, these interactions occur primarily at the vessel wall, where monocytes may be concentrated by margination. Lastly, a possible competition or blocking of a monocyte receptor for CFU-C by peripheral blood cells may not be as effective as that of cells such as promyelocytes and myelocytes in a nonadherent marrow fraction.

A number of potential technical artifacts to explain these results were eliminated. First, loss of CFU-C was not related to viable entrapment in the monolayer. Monolayers that were removed and cultured did not contain more than 2 CFU-C/10^5 previously coincubated marrow cells. Certainly, this amount was not sufficient to explain the gross differences between results in coincubation and control experiments. This failure to recover CFU-C does not exclude the possibility that CFU-C were entrapped within the monolayers. Some may have been, and failure to recover them may have been due to the fact that they were rendered nonviable. This probable entrapment of CFU-C is suggested by the fact that we can routinely recover CFU-C in considerable numbers from marrow

TABLE 2.—*Day-14 colonies after coincubation on marrow adherent underlayers*

Experimental procedure	Colonies[a]	Colony morphology[b]		
		Granulocyte	Granulocyte–macrophage	Eosinophil
3:1 coincubation	64±1	22 (34)	12 (19)	30 (47)
Control	77±6	21 (28)	19 (25)	34 (44)[c]
Adherent layer	5±1	(32)	(37)	(38)

[a] Results are means ± SEM of colonies/volume of culture with 1×10^5 marrow cells.

[b] Results are absolute No. of colonies/standard volume of culture (%).

[c] Two pure monocytic colonies.

TABLE 3.—*Effect of T-cells on adherent cell inhibition of GM-CFC*[a]

Nature of adherent layer	Nature of nonadherent target[b]			
	Non-ad BM, T-cell depleted alone	Non-ad BM + T-cells,[c] 1:1	Non-ad BM + T-cells, 1:2	Non-ad BM + T-cells, 1:5
Adherent cells derived from WMC; 2:1 adherent cells to Non-ad BM	13±1[d]	15±3[e]	18±4[d]	23±1[d]
Adherent cells derived from T-cell-depleted WMC; 2:1 adherent cells to Non-ad BM	11±2[d]	15±1[e]	22±1[d]	19±1[d]
Nonadherent cells, control	32±2	38±6	63±3	71±2

[a] WMC = whole mononuclear cells; Non-ad BM = nonadherent bone marrow.

[b] Results are means ± SD of triplicate cultures/1×10^5 bone marrow cells.

[c] No. of Non-ad cells was kept constant, while the No. of T-cells varied.

[d] Significantly lower (two-sided, two-sample Student's *t*-test) than the control, $P<0.001$.

[e] Significantly lower than the control, $P<0.005$.

adherent layers. Second, this inhibition was not due to monocytes lifting off from the monolayers and being transferred to the solid cultures. If sufficient monocytes were loosened when we retrieved the nonadherent target, suppression could be mediated by PGE_2 secretion during agar culture. This was a possibility that we had to rule out because PGE_2 can preferentially suppress noneosinophilic colonies (*3, 13*). However, after most coincubation experiments we had less than 2% latex-positive cells. Cell recoveries were close to 100%, and the inclusion of indomethacin at 10^{-6} *M* in liquid, solid, or both phases made no difference to the inhibition. Finally, these same monolayers, when overlaid with agar and separated from the target by an underlayer, enhanced CFU-C growth. This observation would suggest that if there was some transference of monocytes, it would have a positive influence on growth.

The information from the above-mentioned experiment and the fact that media harvested from these coincubation experiments did not suppress CFU-C growth argue strongly against a soluble factor mechanism. It would be unusual to generate significant factors within 4 hours that could be detected by tests in agar culture. This failure to detect an inhibitory factor from these media does not totally rule out a short-range, locally concentrated factor.

As a further control to rule out the possibility that poor CFU-C recovery was related to differing numbers of cells in liquid culture in coincubation and control experiments, we prepared adherent cells from a different source, human bone marrow. In this situation, recovery of day-7 CFU-C (neutrophilic) was greater in coincubation experiments, with no significant difference at day 14. Adherent cells from marrow are certainly contaminated with peripheral blood, but the composition of monocytes is lower than that of adherent monolayers prepared from blood (*6, 9*). Monocytes usually comprise 60% or less of the adherent layer. These monocytes may be derived from both blood and marrow. Other cells in these monolayers include metamyelocytes, some juvenile polymorphs, myelocytes, and lymphoid cells. Why monolayers created from marrow are more favorable to GM-CFC proliferation will be investigated. Some have suggested that marrow monocytes or macrophages are a different subset from peripheral blood monocytes or macrophages with consequent different actions on hematopoiesis (*5*). Another proposal is that other cells within the adherent layer modify the action of the monolayer. This proposal could explain the variability in inhibition when higher marrow numbers are used in coincubation experiments with peripheral blood adherent cells.

We chose to use freshly derived adherent cells rather than to create monolayers from tissue culture-derived macrophages. We thought this approach would better mimic the in vivo situation. As with leukemia cluster inhibition demonstrated previously (*7*), normal GM-CFC inhibition appears unlikely to be a cytostatic phenomenon. The mechanism behind the CFU-C loss remains to be elucidated. Whether this is classical cytotoxicity, as shown by macrophages or human monocytes toward tumor cell lines (*14-18*), can be resolved only by an experiment in which we radioactively label purer populations of CFU-C.

It has been postulated that different differentiation tendencies in different organs, (e.g., myelopoiesis in marrow, erythropoiesis in spleen, and lymphopoiesis within the lymph node) are determined by different microenvironments (*19-25*). These inductive microenvironments are thought to be related to different fibroblast populations (*22, 23*). However, different directions of differentiation conceivably could be due to negative or positive controls exerted by other adherent cells within different organs. This adherent population is highly likely to consist predominantly of monocytes or macrophages. These cell populations are known to interact by a cell-to-cell contact mechanism with lymphocytes and, as a consequence, to regulate lymphopoiesis (*26*). Alternatively, any of these phenomena may be simply mechanisms to limit hematopoiesis to the marrow, where it may be finally regulated. At the same time, soluble factors from these cells may enhance hematopoiesis, a long-range regulatory mechanism, which thus would allow tissue invasion by microorganisms to be recognized and translated into increased marrow hematopoiesis.

REFERENCES

(*1*) Kurland J, Moore MA. The regulatory role of the macrophage in normal and neoplastic hematopoiesis. In: Baum SJ, Ledney GD, eds. Experimental hematology today. Baltimore: Springer-Verlag, 1977:51-62.

(*2*) Kurland JI, Broxmeyer HE, Pelus LM, Bockman RS, Moore MA. Role for monocyte macrophage derived colony stimulating factor and prostaglandin E in the positive and negative feedback control of myeloid stem cell proliferation. Blood 1978; 52:388-407.

(*3*) Pelus LM, Broxmeyer HE, Kurland JI, Moore MA. Regulation of macrophage and granulocyte proliferation. J Exp Med 1979; 150:277-292.

(*4*) Rinehart JJ, Zanjani ZD, Nomdedeu B, Gormus BT, Kaplan ME. Cell-cell interaction in erythropoiesis: Role of human monocytes. J Clin Invest 1978; 62:979-986.

(*5*) Gordon LI, Miller WJ, Branda RF, Zanjani ED, Jacobs HS. Regulation of erythroid colony formation by bone marrow macrophages. Blood 1980; 55:1047-1050.

(*6*) Spitzer G, Verma DS, Zander AR, et al. Adherent cell-mediated inhibition of human leukemic myelopoiesis. Exp Hematol 1980; 8:1146-1156.

(*7*) Spitzer G, Verma DS, Beran M, Zander AR, Dicke KA, McCredie KB. Adherent cell inhibition of human leukemic in vitro agar clonal growth by short term cell-cell contact. Blood 1981; 57:71-74.

(*8*) Weiner MS, Bianco J, Nussenzwerg J. Enhanced binding of neuraminidase sheep erythrocytes to human T lymphocytes. Blood 1973; 42:939-946.

(*9*) Verma DS, Spitzer G, Dicke KA, Zander AR, Vellekoop L, Beran M. Myelopoietic enhancement by immunoadjuvants: In vitro studies for their rational use in neutropenic patients. Exp Hematol 1979; 7 (suppl 5):228-245.

(*10*) Spitzer G, Verma DS, Dicke KA, Smith T, McCredie KB. Subgroups of oligoleukemia as identified by in vitro agar culture. Leuk Res 1979; 3:29-39.

(*11*) Verma DS, Spitzer G, Zander AR, Fisher R, McCredie KB, Dicke KA. The myeloid progenitor cell: A parallel study of subpopulations in human marrow and peripheral blood. Exp Hematol 1980; 8:32-43.

(*12*) Chervenick PA, Boggs DR. In vitro growth of granulocytic and mononuclear cell colonies from blood of normal individuals. Blood 1971; 37:131-135.

(*13*) Williams N. Preferential inhibition of murine macrophage colony formation by prostaglandin E. Blood 1979; 53:1089-1094.

(*14*) Hibbs JB, Chapman HA, Weinberg BJ. The macrophage as an antineoplastic surveillance cell: Biological perspectives. J Reticuloendothel Soc 1978; 24:549-570.

(*15*) Horwitz DA, Knight N, Temple A, Allison AC. Spontaneous and induced cytotoxic properties of human adherent mononuclear cells. Immunology 1979; 36:225-228.

(*16*) Montavani A, Jerrels TR, Dean JH, Herberman RB. Cytolytic and cytostatic activity on tumor cells of circulating human monocytes. Int J Cancer 1979; 23:18-22.

(*17*) Montavani A, Tagliabue A, Dean JH, Jerrels TR, Herberman RB. Cytolytic activity of circulating human monocytes on transformed and untransformed fibroblasts. Int J Cancer 1979; 23:23-28.

(*18*) Rinehart JJ, Lange P, Gormus BP, Kaplan ME. Human monocyte-induced tumor cell cytotoxicity. Blood 1978; 52:211-218.

(*19*) Curry JL, Trentin JJ. Hemopoietic spleen colony studies: Growth and differentiation. Blood 1967; 15:395-413.

(*20*) Wolf NS, Trentin JJ. Hemopoietic colony studies. V. Effect of hemopoietic organ stroma in differentiation of pluripotent stem cells. J Exp Med 1967; 127:205-214.

(*21*) Trentin JJ. Influence of hematopoietic organ stroma (hematopoietic inductive microenvironments) in stem cell differentiation. In: Gordon AS, ed. Regulation of hematopoiesis. New York: Appelton-Century-Crofts, 1970:161-186.

(*22*) Friedenstein AJ, Chailakhyan RK, Latsinik NV, Panasyuk AF, Keiliss-Berek IV. Stromal cells responsible for transferring the microenvironment of the hemopoietic tissue. Cloning in vitro and retransplantation in vivo. Transplantation 1974; 17:331-340.

(*23*) Friedenstein AJ, Gorskaja UF, Kulagina NN. Fibroblast precursors in normal and irradiated mouse hematopoietic organs. Exp Hematol 1976; 4:267-274.

(*24*) Tavassolii M. Studies on hemopoietic microenvironments. Exp Hematol 1975; 3:213-226.

(*25*) Boggs DR. The hematopoietic microenvironment. N Engl J Med 1980; 302:1359-1360.

(*26*) Rosenthal AS, Thomas-Black J, Ellner JJ, Greineder DK, Lipsky PE. Macrophage function in antigen recognition by T lymphocytes. In: Wilson DS, ed. Immunobiology of the macrophages. New York: Academic Press, 1976:131-160.

Pathology Panel for Lymphoma Clinical Studies: A Comprehensive Analysis of Cases Accumulated Since Its Inception[1,2]

Hun Kim, *M.D.,*[3] **Ronald J. Zelman,** *M.S.,*[4] **Michael A. Fox,** *Ph.D.,*[5] **John M. Bennett,** *M.D.,*[6] **Costan W. Berard,** *M.D.,*[7] **James J. Butler,** *M.D.,*[8] **Gerald E. Byrne, Jr.,** *M.D.,*[9] **Ronald F. Dorfman,** *M.D.,*[10] **Robert J. Hartsock,** *M.D.,*[11] **Robert J. Lukes,** *M.D.,*[12] **Risa B. Mann** *M.D.,*[13] **Richard S. Neiman,** *M.D.,*[14] **John W. Rebuck,** *M.D., Ph.D.,*[15] **William W. Sheehan,** *M.D.,*[16] **Daina Variakojis,** *M.D.,*[17] **John F. Wilson,** *M.D.,*[18] *and* **Henry Rappaport,** *M.D.*[3,19,20]

ABSTRACT—This report presents a detailed analysis of 8,915 cases of malignant lymphomas accumulated since the inception of the Pathology Panel and Repository Centers for Lymphoma Clinical Studies in 1967. Of 8,915 cases 3,105, 34.8%, were classified as Hodgkin's disease (HD) and 5,061 cases, 56.8%, were classified as non-Hodgkin's lymphoma (NL) according to the final diagnosis. In HD, nodular sclerosis was the most common type (1,730/3,105 cases, or 55.7%), followed in order of frequency by mixed cell type (865/3,105, 27.9%), lymphocyte depletion type (224/3,105, 7.2%), and lymphocyte predominance type (94/3,105, 3%). Children showed a higher incidence of the lymphocyte predominance (16/129, 12.4%) and nodular sclerosis (76/129, 58.9%) categories. In cases having the diagnosis and classification of HD provided by the contributors 51.6% (1,523/2,953) were confirmed by final diagnoses. The nodular sclerosis subtype was the most reproducible category of disease, and was confirmed in 83.8% of the cases (912/1,088). The category of HD most difficult to reproduce proved to be the lymphocyte predominance subtype, in which the concurrence by the panel was only 23.3% (41/176). Major disagreements between the contributors and the panel on the diagnosis and subclassification of HD occurred in 16.7% (494/2,953) of the cases. When the diagnoses of the Regional Center, composed of member(s) of the panel serving cooperative groups, and the final diagnoses were compared, the incidence of complete agreement in the classification of HD was appreciably higher (2,747/3,080, 89.2%) than when the diagnoses and classification of HD provided by the contributors were compared with the final diagnoses (1,523/2,953, 51.6%). However, the experts also had difficulties with the lymphocyte predominance category, with an agreement incidence of 73% (79/108). The major disagreement in the classification of HD between the diagnosis of the Regional Center and the final diagnosis was 3.8% (118/3,080). In NL, poorly differentiated lymphocytic lymphoma showing varying degrees of nodularity had the highest incidence (1,284/5,061, 25.4%); diffuse histiocytic lymphoma was next highest (1,248/5,061, 24.7%), followed by diffuse poorly differentiated lymphocytic type (467/5,061, 9.2%). However, lymphoblastic lymphoma became the third or fourth most common form of NL in the years 1977–79 after it was identified and separated from diffuse poorly differentiated lymphocytic lymphoma. We believe that this is related in part to the participation of Children's Cancer Study Group during this time period. The incidence of agreement for NL was less than that for HD. The contributor's diagnosis was verified with regard to both pattern and cytology in 48.6% (1,674/3,441) of NL cases. Nodular poorly differentiated lymphocytic lymphoma and diffuse histiocytic lymphoma, representing 50% (2,532/5,061) of all NL cases, were confirmed most often by the Panel in 80.4% (518/644) and 71.9% (590/821) of the cases, respectively. Diagnoses of the contributors were confirmed in less than 35% of the cases in the following categories: nodular well-differentiated lymphocytic lymphoma, nodular histiocytic lymphoma, diffuse poorly differentiated lymphocytic lymphoma, diffuse mixed-cell lymphoma, lymphocytic lymphoma of the intermediate degree of differentiation, and undifferentiated malignant lymphoma. Major disagreements were higher with regard to NL cases (1,143/4,190, 27.3%) than to HD cases (494/2,953, 16.7%). The agreement of the final diagnosis with the Regional Center diagnosis for nodular poorly differentiated lymphocytic lymphoma was 95%, and for diffuse histiocytic lymphoma, 89%. Major disagreements between the Regional Center's diagnosis and the final diagnosis (435/4,993, 8.7%) were also significantly less than major disagreements between contributor's and final diagnosis. With regard to correct pattern recognition, the contributors were more often correct in the diagnosis of nodular or nodular and diffuse NL (86.3%) than in that of diffuse NL (74.6%). This analysis shows *a*) that difficulties in the diagnosis and classification of malignant lymphomas by the contributors persist, *b*) that the disagreement resulting from this difficulty can be lessened when reviewed by an experienced hematopathologist, and *c*) that it can be further

---

[1] Received February 20, 1981; accepted August 7, 1981.

[2] Supported by Public Health Service grant R01CA-18044 from the National Cancer Institute.

[3] Department of Anatomic Pathology, City of Hope National Medical Center, Duarte, Calif.

[4] Data Processing Department, City of Hope National Medical Center, Duarte, Calif.

[5] Hospital Computing Facility and the Cancer Center, University of California at Los Angeles, Los Angeles, Calif.

[6] Cancer Center of the University of Rochester Medical Center, Rochester, N.Y.

[7] St. Jude Children's Research Hospital, Memphis, Tenn.

[8] M. D. Anderson Hospital and Tumor Institute, Houston, Tex.

[9] University of Miami, Miami, Fla.

[10] Stanford University Medical Center, Stanford, Calif.

[11] Allegheny General Hospital, Pittsburgh, Pa.

[12] University of Southern California School of Medicine, Los Angeles, Calif.

[13] Johns Hopkins Hospital, Baltimore, Md.

[14] Mallory Institute of Pathology, Boston, Mass.

[15] Henry Ford Hospital, Detroit, Mich.

[16] University of Texas, Dallas, Tex.

[17] University of Chicago, Chicago, Ill.

[18] Primary Children's Medical Center, Salt Lake City, Utah.

[19] *Address reprint requests to* Dr. Henry Rappaport, City of Hope National Medical Center, Duarte, Calif. 91010.

[20] We thank Mrs. Maryalice Miller, Mrs. Mary Rose Wiedrich, and Mrs. Sharon Wilson for secretarial assistance.

reduced through a central review process by a panel of experts.—JNCI 1982; 68:43-67.

The Lymphoma Task Force was organized under the auspices of the National Cancer Institute in 1964 to bring together a group of investigators whose primary interest was in malignant lymphomas. The goal was to achieve a multidisciplinary and multi-institutional approach to the management of malignant lymphoma. Difficulties in the classification of malignant lymphomas made it desirable to establish a pathology reference and repository center for lymphoma clinical studies. Clinicians of the cooperative study groups took the initiative to create such a center in 1967 (*1*). In the same year, the Pathology Panel and Repository Center actually started to receive slides from patients entered in protocol studies of the various cooperative study groups. The primary purpose was to provide these groups with confirmation or revision of the original diagnosis by a panel of experts who were recognized as having special expertise in hematopathology. Initially, they were selected to membership of the Pathology Panel on the basis of their scientific and professional achievements without regard to their affiliation with study groups. These pathologists were in charge of Regional Centers serving at least one cooperative study group. In addition, a clinician-hematologist with expertise in the various therapeutic programs was appointed to the panel. Currently, all regional pathology centers are headed by the chairmen of the lymphoma pathology subcommittees of each cooperative study group.

The Chairman and the Executive Secretary of the Panel perform the functions of the Repository Center. They are also the principal and co-principal investigators of the NCI grant that provides financial support for the Pathology Panel and Repository Center for Lymphoma Clinical Studies.

Every protocol case was reviewed independently by the Regional Centers and Repository Center. When diagnoses of the Regional Centers and Repository Center differed, the cases were presented to the annual meeting of the entire panel. The main functions of the panel were: *a*) resolution of diagnostic disagreements between the Repository Center and Regional Centers, and *b*) identification of problems in the diagnosis and classification of malignant lymphomas. The creation of the Pathology Panel and Repository Center for Lymphoma Clinical Studies was the first effort of this kind by pathologists to organize themselves in a categorical discipline of pathology. The dual purpose was: *a*) to offer their skills and expertise to their clinical colleagues to confirm or to revise the diagnosis of record, thus to provide a uniform histopathologic review of all cooperative group lymphoma cases, as well as to allow for more valid comparison of therapeutic response and survival data, and *b*) to form a cohesive group that would be available for advice and counsel in areas pertaining to histologic diagnosis and classification of malignant lymphomas and allied diseases. The organization was unique in that it incorporated a central review process in addition to the review by experts at the regional level.

This report covers the period from 1967, when the Pathology Panel and Repository Center for Lymphoma Clinical Studies was created, through the end of

TABLE 1.—*Panel members, study group assignments, and periods of appointment*

Repository Center		
Henry Rappaport, *M.D.*	Principal Investigator	1967–present
Daina Variakojis, *M.D.*	Co-Investigator and Executive Secretary	1967–74
Hun Kim, *M.D.*	Co-Investigator and Executive Secretary	1975–present
Regional Centers and Consultants		
John M. Bennett, *M.D.*	Consultant in clinical hematology	1967–present
Costan W. Berard, *M.D.*	Eastern Cooperative Oncology Group (ECOG)	1967–79
	Consultant in hematopathology	1979–present
James J. Butler, *M.D.*	Southwestern Oncology Group (SWOG)	1967–78
	Consultant in hematopathology	1978–present
Gerald E. Byrne, Jr., *M.D.*	SWOG	1975–present
	Southeastern Cooperative Cancer Study Group (SEG)	1975–77
	SEG	1979–present
Ronald F. Dorfman, *M.R.C.*	SEG	1967–79
	Consultant in hematopathology	1979–present
Edgar G. Harrison, *M.D.*	SEG	1974–75
Robert J. Hartsock, *M.D.*	ECOG	1974–78
	SWOG	1978–present
Philip H. Lieberman, *M.D.*	ECOG	1967–69
Robert J. Lukes, *M.D.*	Western Cancer Study Group (WSG)	1967–75
	Consultant in hematopathology	1975–78
Risa B. Mann, *M.D.*	ECOG	1979–present
Richard S. Neiman, *M.D.*	ECOG	1978–present
John W. Rebuck, *M.D., Ph.D.*	SWOG	1967–present
William W. Sheehan, *M.D.*	WSG	1975–76
	SEG	1975–78
	SWOG	1978–present
	Intergroup Hodgkin's Disease in Children	1978–present
	Children's Cancer Study Group (CCSG)	1978–present
Louis B. Thomas, *M.D.*	ECOG	1967–70
John F. Wilson, *M.D.*	CCSG	1978–present
Daina Variakojis, *M.D.*	Cancer and Leukemia Group B	1967–present

February 1980. In this report our purpose is to present a detailed analysis of 8,915 cases accumulated since the inception of the panel and to identify areas of difficulty in the diagnosis and classification of malignant lymphomas by pathologists.

MATERIALS AND METHODS

Case entry and review procedure.—When a clinical investigator entered a new patient in the study, the contributing pathologist was asked to forward pretreatment diagnostic material (stained and/or unstained sections and/or paraffin blocks with corresponding pathology report) to the study group operations office. Histologic material obtained by the group office was then forwarded to the member of the Pathology Panel at the Regional Center, assigned to that study group. The panel members, their assignments, and their periods of appointment are shown in table 1. These panel members, representing the Regional Centers, rendered their diagnostic interpretation and recorded both their own and the contributing pathologist's opinion (entry diagnosis) on the same report. The report was then sent to the group office, where it was filed with the on-study card, and to the principal investigator of the study group, who was responsible for the care of the patient. The Repository Center also received the report along with histologic material. Electron microscopy and special histochemical and cytochemical stains were performed at the Repository Center for further study of selected cases where such studies were indicated and feasible. All slides submitted to the Repository Center were reviewed, and a diagnosis was rendered. When there was agreement between the Regional Center and Repository Center, it was recorded. If the opinion of the Repository Center did not agree with the diagnosis of the Regional Center, or the Regional Center did not wish to accept the opinion of the Repository Center, the case was submitted to the entire Pathology Panel at its annual meeting to seek consensus. When the diagnosis of the Regional Center was modified by the Repository Center or by the Panel, a final corrected report was forwarded to the originating cooperative group operations office. The term *final diagnosis* will be used in this paper to refer to either the diagnosis agreed upon by both Regional Center and Repository Center or, when such an agreement could not be reached, the consensus diagnosis of the panel.

Pathology Report Form for Lymphoma Clinical Studies.—The Rye classification (modified Lukes-Butler classification (*2*) and modified Rappaport classification (*3, 4*) were employed. In accordance with changes in concepts and terminology of non-Hodgkin's lymphomas, however, the Pathology Report Form for Lymphoma Clinical Studies was changed four times (text-fig. 1) during this period. The computer codes were incorporated in the last report form. Table 2

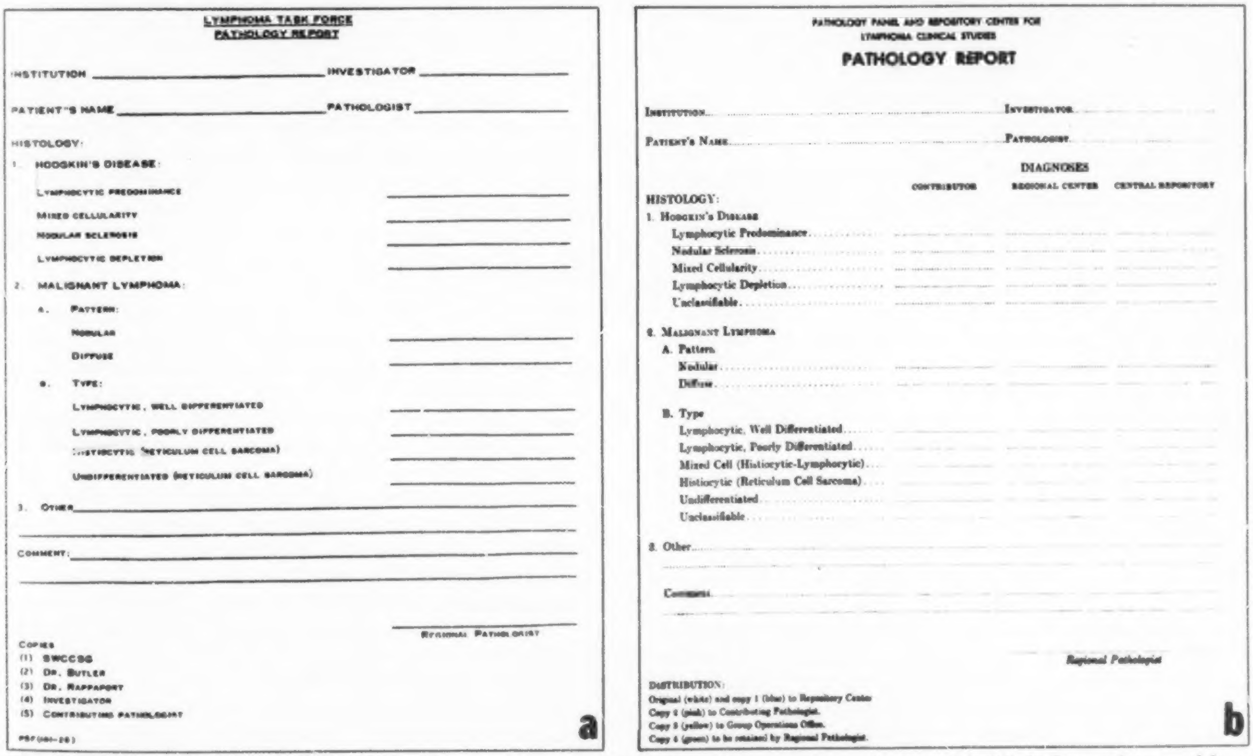

LYMPHOMA TASK FORCE
PATHOLOGY REPORT

INSTITUTION ________ INVESTIGATOR ________

PATIENT'S NAME ________ PATHOLOGIST ________

HISTOLOGY:

1. HODGKIN'S DISEASE:
   - LYMPHOCYTIC PREDOMINANCE ________
   - MIXED CELLULARITY ________
   - NODULAR SCLEROSIS ________
   - LYMPHOCYTIC DEPLETION ________
2. MALIGNANT LYMPHOMA:
   - A. PATTERN:
     - NODULAR ________
     - DIFFUSE ________
   - B. TYPE:
     - LYMPHOCYTIC, WELL DIFFERENTIATED ________
     - LYMPHOCYTIC, POORLY DIFFERENTIATED ________
     - HISTIOCYTIC (RETICULUM CELL SARCOMA) ________
     - UNDIFFERENTIATED (RETICULUM CELL SARCOMA) ________
3. OTHER ________

COMMENT: ________

____
REGIONAL PATHOLOGIST

COPIES
(1) SWCCSG
(2) DR. BUTLER
(3) DR. RAPPAPORT
(4) INVESTIGATOR
(5) CONTRIBUTING PATHOLOGIST

PSF(001-28)

PATHOLOGY PANEL AND REPOSITORY CENTER FOR
LYMPHOMA CLINICAL STUDIES
PATHOLOGY REPORT

INSTITUTION........ INVESTIGATOR........

PATIENT'S NAME........ PATHOLOGIST........

	DIAGNOSES		
	CONTRIBUTOR	REGIONAL CENTER	CENTRAL REPOSITORY
HISTOLOGY:			
1. Hodgkin's Disease			
Lymphocytic Predominance			
Nodular Sclerosis			
Mixed Cellularity			
Lymphocytic Depletion			
Unclassifiable			
2. Malignant Lymphoma			
A. Pattern			
Nodular			
Diffuse			
B. Type			
Lymphocytic, Well Differentiated			
Lymphocytic, Poorly Differentiated			
Mixed Cell (Histiocytic-Lymphocytic)			
Histiocytic (Reticulum Cell Sarcoma)			
Undifferentiated			
Unclassifiable			

3. Other........

Comments........

Regional Pathologist

DISTRIBUTION:
Original (white) and copy 1 (blue) to Repository Center
Copy 2 (pink) to Contributing Pathologist.
Copy 3 (yellow) to Group Operations Office.
Copy 4 (green) to be retained by Regional Pathologist.

TEXT-FIGURE 1.—Pathology report form for lymphoma clinical studies. a) Report form used from 1967 to mid-1968. b) Report form used from mid-1968 to 1977.

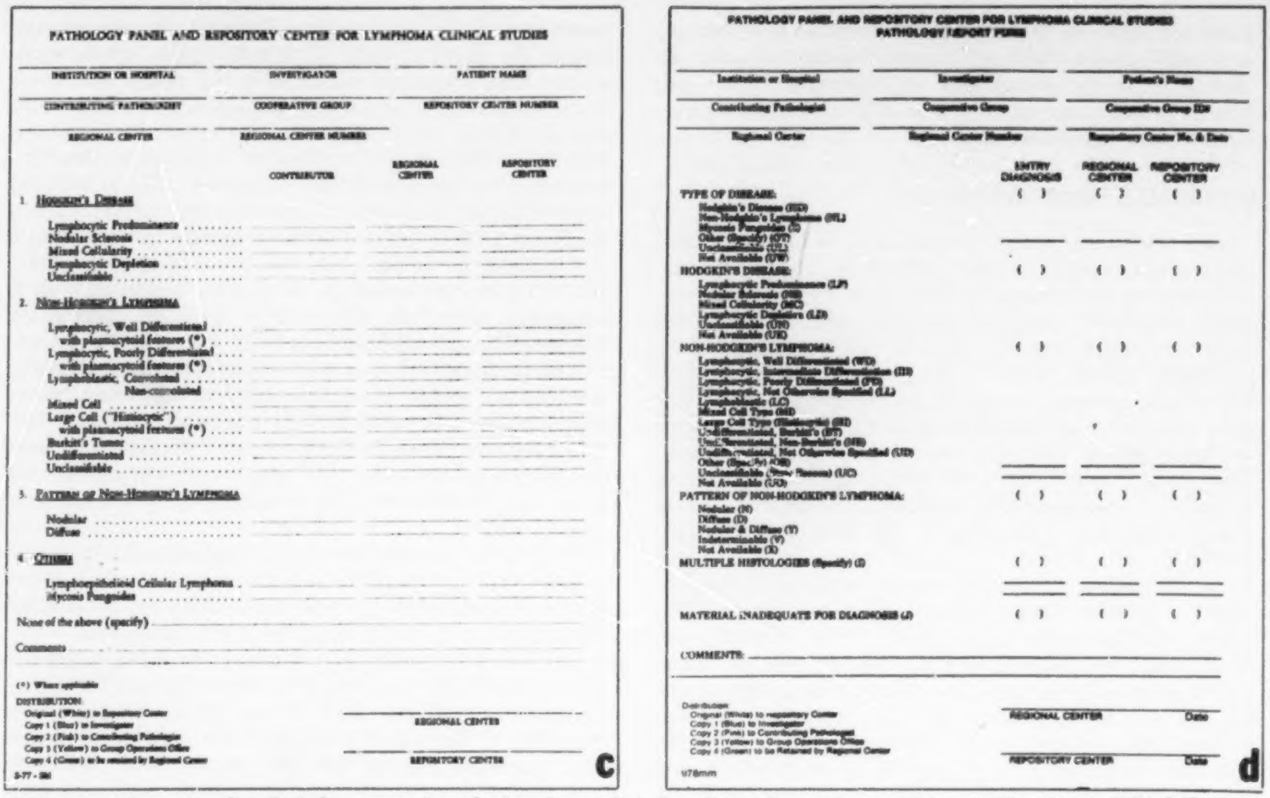

PATHOLOGY PANEL AND REPOSITORY CENTER FOR LYMPHOMA CLINICAL STUDIES

INSTITUTION OR HOSPITAL ____ INVESTIGATOR ____ PATIENT NAME ____
CONTRIBUTING PATHOLOGIST ____ COOPERATIVE GROUP ____ REPOSITORY CENTER NUMBER ____
REGIONAL CENTER ____ REGIONAL CENTER NUMBER ____

	CONTRIBUTOR	REGIONAL CENTER	REPOSITORY CENTER
1. Hodgkin's Disease			
Lymphocytic Predominance			
Nodular Sclerosis			
Mixed Cellularity			
Lymphocytic Depletion			
Unclassifiable			
2. Non-Hodgkin's Lymphoma			
Lymphocytic, Well Differentiated			
with plasmacytoid features (*)			
Lymphocytic, Poorly Differentiated			
with plasmacytoid features (*)			
Lymphoblastic, Convoluted			
Non-convoluted			
Mixed Cell			
Large Cell ("Histiocytic")			
with plasmacytoid features (*)			
Burkitt's Tumor			
Undifferentiated			
Unclassifiable			
3. Pattern of Non-Hodgkin's Lymphoma			
Nodular			
Diffuse			
4. Others			
Lymphoepithelioid Cellular Lymphoma			
Mycosis Fungoides			

None of the above (specify) ____

Comments ____

(*) Where applicable

DISTRIBUTION
Original (White) to Repository Center
Copy 1 (Blue) to Investigator
Copy 2 (Pink) to Contributing Pathologist
Copy 3 (Yellow) to Group Operations Office
Copy 4 (Green) to be retained by Regional Center

____ REGIONAL CENTER
____ REPOSITORY CENTER

8-77 - 8M

c

PATHOLOGY PANEL AND REPOSITORY CENTER FOR LYMPHOMA CLINICAL STUDIES
PATHOLOGY REPORT FORM

Institution or Hospital ____ Investigator ____ Patient's Name ____
Contributing Pathologist ____ Cooperative Group ____ Cooperative Group ID# ____
Regional Center ____ Regional Center Number ____ Repository Center No. & Date ____

	ENTRY DIAGNOSIS	REGIONAL CENTER	REPOSITORY CENTER
TYPE OF DISEASE:	( )	( )	( )
Hodgkin's Disease (HD)			
Non-Hodgkin's Lymphoma (NL)			
Mycosis Fungoides (F)			
Other (Specify) (OT)	____	____	____
Unclassifiable (UL)			
Not Available (UW)			
HODGKIN'S DISEASE:	( )	( )	( )
Lymphocytic Predominance (LP)			
Nodular Sclerosis (NS)			
Mixed Cellularity (MC)			
Lymphocytic Depletion (LD)			
Unclassifiable (UN)			
Not Available (UK)			
NON-HODGKIN'S LYMPHOMA:	( )	( )	( )
Lymphocytic, Well Differentiated (WD)			
Lymphocytic, Intermediate Differentiation (ID)			
Lymphocytic, Poorly Differentiated (PD)			
Lymphocytic, Not Otherwise Specified (LL)			
Lymphoblastic (LC)			
Mixed Cell Type (MD)			
Large Cell Type (Histiocytic) (HI)			
Undifferentiated, Burkitt's (BT)			
Undifferentiated, Non-Burkitt's (NB)			
Undifferentiated, Not Otherwise Specified (UD)			
Other (Specify) (OB)	____	____	____
Unclassifiable (State Reason) (UC)	____	____	____
Not Available (UO)			
PATTERN OF NON-HODGKIN'S LYMPHOMA:	( )	( )	( )
Nodular (N)			
Diffuse (D)			
Nodular & Diffuse (Y)			
Indeterminable (V)			
Not Available (X)			
MULTIPLE HISTOLOGIES (Specify) (Z)	( )	( )	( )
	____ ____	____ ____	____ ____
MATERIAL INADEQUATE FOR DIAGNOSIS (J)	( )	( )	( )

COMMENTS: ____

Distribution:
Original (White) to Repository Center
Copy 1 (Blue) to Investigator
Copy 2 (Pink) to Contributing Pathologist
Copy 3 (Yellow) to Group Operations Office
Copy 4 (Green) to be Retained by Regional Center

REGIONAL CENTER ____ Date
REPOSITORY CENTER ____ Date

978mm

d

TEXT-FIGURE 1 (continued).—Pathology report form for lymphoma clinical studies. c) Report form used from 1977 to August 1978. d) Current report form, used since September 1978.

shows a complete list of code symbols for diagnosis, as used by the Repository Center, Regional Centers, and Study Groups.

Explanation of code symbols.—The code symbols for diagnosis are the same as those used for the current Pathology Report Form for Lymphoma Clinical Studies, and most are self-explanatory. The codes HD and UK are essentially the same; they were used for those cases that were diagnosed as Hodgkin's disease but for which a subclassification was lacking for unknown reasons. The same is true for the codes NL and UO for non-Hodgkin's lymphoma. The codes UN and UC were used for cases of Hodgkin's disease and non-Hodgkin's lymphoma, respectively, that were specifically stated to be unclassifiable. The code UL pertains to cases that were either not diagnosable with certainty as malignant tumors, or when they were diagnosable as such, could not be further classified. Cases received at the Repository Center without diagnosis were assigned the code UW. The code OT refers to cases of miscellaneous categories, which include benign lymphoid proliferation, nonlymphomatous hematopoietic malignancies, carcinoma, sarcoma, malignant histiocytosis, angioimmunoblastic lymphadenopathy, mycosis fungoides, lymphoepithelioid cellular lymphoma, composite lymphoma, malignant tumor (not otherwise specified), and others.

Case material.—Since the creation of the Pathology Panel and Repository Center, a total of 8,915 cases have been reviewed as of February 28, 1980. Detailed analyses of these cases and their discussion are presented below.

ANALYSIS OF DATA

The results of the analyses are shown in tables 3-18.

Case distribution according to histology and study group by Regional Center diagnosis and final diagnosis (table 3).—Of 8,915 cases, 3,080 (34.5%) were classified by Regional Centers as HD, 5,039 (56.5%) as NL, and 796 as miscellaneous categories. Final diagnoses are shown *in parentheses* for comparison. The overall difference between the diagnoses of each study group and the final diagnoses is relatively small. Further comparisons between the two are shown in tables 8 and 9 for HD, and in tables 12 and 13 for NL.

Composition of HD case material: According to the Regional Center diagnoses, HD comprised 20.3% (42/207) for Children's Cancer Study Group (CCSG) to 44.2% (729/1,648) for Southeastern Cooperative Cancer Study Group (SEG) of all cases treated by each group. Intergroup Hodgkin's Disease in Children (IHDC) treated only HD patients. Table 3 shows that IHDC and CCSG, both of which manage pediatric age

TABLE 2.—*Code symbols for diagnosis*

Type of disease:	
HD	Hodgkin's disease, not otherwise specified (NOS)
NL	Non-Hodgkin's lymphoma
OT	Other miscellaneous categories
UL	Unclassifiable
UW	Not available
Hodgkin's disease:	
LP	Lymphocytic predominance
NS	Nodular sclerosis
MC	Mixed cellularity
LD	Lymphocytic depletion
UN	Unclassifiable
UK	Classification not available
Non-Hodgkin's lymphoma:	
WD	Lymphocytic, well differentiated
ID	Lymphocytic, intermediate differentiation
PD	Lymphocytic, poorly differentiated
LL	Lymphocytic, not otherwise specified
LC	Lymphoblastic
MI	Mixed-cell type
HI	Large-cell (histiocytic)
BT	Undifferentiated, Burkitt's type
NB	Undifferentiated, non-Burkitt's type
UD	Undifferentiated, not otherwise specified
OR	Other
UC	Unclassifiable
UO	Classification not available
Pattern of non-Hodgkin's lymphoma:	
N	Nodular
D	Diffuse
V	Indeterminable
Y	Nodular and diffuse
X	Not available

groups, have a high incidence of LP (11.4% and 11.9%, respectively, compared with the national average of 3.5%) and NS (60.2% and 61.9%, respectively, compared with the national average of 55.6%). Conversely, LD is much rarer in children. The relative proportion of LP, NS, MC, and LD is similar in different study groups, although some variations are present for LP and LD.

Composition of NL case material: NL comprised 45% (509/1,132) for Cancer and Leukemia Group B (CALGB) to 71% (147/207) for CCSG according to the Regional Center diagnoses. The ratios for NL to HD are highest for CCSG (3.5:1) and Eastern Cooperative Oncology Group (ECOG) (3:1). Table 3 also shows *a*) the rarity of nodular lymphoma and *b*) the high incidence of LC, BT, NB, and UD (combined total of 122/147, 83%) in the pediatric age group. The ratio of PDN+PDY to MIN+MIY varied from 2:1 Western Cancer Study Group (WSG) to 3.9:1 at the Southwestern Oncology Group (SWOG). These variations imply that the therapeutic results for PDN versus MIN obtained by different study groups cannot be compared since the criteria for diagnosis of PD and MI may be different for different Regional Centers.

Case distribution according to final diagnosis and diagnoses of contributor, Regional Center, and Repository Center (table 4).—According to the final diagnosis, 34.8% (3,105/8,915) of cases were classified as HD, 56.8% (5,061/8,915) as NL, and the remainder as miscellaneous categories. The relative percentage of each histologic subgroup is shown in the table. PD showing varying degrees of nodularity (PDN+PDY) is the most common diagnosis (1,284/5,061, 25.4%); the second in frequency is HID (1,248/5,061, 24.7%). There were 715 cases of miscellaneous categories of which 113 (1.3%) of the cases were considered to be nonneoplastic lesions according to final diagnosis.

Table 4 shows that the differences between the contributor's diagnosis and final diagnosis are much greater than the differences between diagnoses by the Regional Center, Repository Center, and final diagnosis, respectively. Histologic subtypes for which greatest differences were evident are indicated. Further details of the disagreement between the contributor's diagnosis and the final diagnosis are shown in tables 6 and 7 for HD, and in tables 10 and 11 for NL.

Case distribution according to final diagnosis and year (table 5).—This table shows the yearly trend as well as variations for each of the histologic categories. For example, the incidence of PDD decreased as the number of cases of LC (*5*) increased, which demonstrates the fact that most of the LC had been classified as PDD prior to its recognition. LC has become the third or fourth most common type of NL after PDN+PDY, HID, and MIN+MIY in the years 1978-79. The participation of CCSG during this time period is believed to be responsible for the increase of LC cases in addition to the ability to recognize LC as an entity. LC outnumbered PDD in the ratio of 1.7:1 (61:36) in 1978, and by 1.4:1 (49:34) in 1979. In HD, the relative incidence of LD has dropped from 4.9% of all cases submitted (13.5% of all HD) in the year 1969 to 1.4% (4.1% of all HD) in 1979. There are yearly variations for other subgroups of HD as well.

Comparison of contributor's diagnosis with final diagnosis in HD (final/contributor's) (table 6).—Cases diagnosed as HD and UK were combined as HD in tables 6-9. The following observations can be made on table 6.

1) Agreement	1,523/2,953 (51.6%)
2) Major disagreement	
a. Diagnosis changed to NL	249/2,953 (8.4%)
b. Diagnosis changed to OT[21]	127/2,953 (4.3%)
c. Good-risk diagnosis (LP, NS, or MC)[22] was changed to poor-risk diagnosis (LD)	69/2,242 (3%)
d. Poor-risk diagnosis was changed to good-risk diagnosis	49/205 (23.9%)
Total major disagreement	494/2,953 (16.7%)

---

[21] *See* table 6 for details.

[22] Inclusion of MC under good risk diagnosis is based on survival data in recently reported series of HD treatment (*6, 7*).

TABLE 3.—*Case distribution according to histology and study group by regional center diagnosis and final diagnosis*[a]

Histology	NA[b]	ECOG	CALGB	SEG	SWOG	IHDC	CCSG	WSG	Totals
UL	0 (0)	2 (1)	6 (3)	2 (1)	2 (1)	0 (0)	2 (1)	0 (0)	14 (7)
UW	2 (0)	10 (4)	126 (0)	10 (12)	16 (10)	0 (0)	1 (0)	3 (1)	168 (27)
HD	1 (0)	5 (3)	12 (3)	7 (9)	4 (4)	1 (1)	0 (0)	2 (3)	32 (23)
LP	1 (1)	20 (20)	19 (15)	17 (10)	34 (30)	10 (10)	5 (6)	2 (2)	108 (94)
NS	1 (0)	276 (284)	225 (240)	417 (396)	666 (679)	53 (51)	26 (25)	50 (55)	1,714 (1,730)
MC	1 (1)	154 (144)	123 (133)	187 (204)	357 (328)	20 (22)	11 (10)	28 (23)	881 (865)
LD	0 (1)	50 (44)	45 (40)	55 (60)	65 (64)	1 (1)	0 (0)	13 (14)	229 (224)
UN	0 (0)	20 (24)	12 (46)	40 (44)	30 (44)	3 (3)	0 (0)	5 (8)	110 (169)
UK	0 (0)	0 (0)	0 (0)	6 (0)	0 (0)	0 (0)	0 (0)	0 (0)	6 (0)
NLN	0 (0)	2 (4)	1 (1)	0 (1)	0 (0)	0 (0)	0 (0)	1 (0)	4 (6)
NLD	0 (0)	5 (2)	3 (1)	2 (0)	4 (1)	0 (0)	0 (0)	0 (0)	14 (4)
NLY	0 (0)	0 (0)	0 (0)	0 (0)	1 (0)	0 (0)	0 (0)	0 (0)	1 (0)
NLX	0 (0)	13 (3)	3 (1)	4 (2)	5 (5)	0 (0)	0 (0)	2 (3)	27 (14)
WDN	0 (0)	3 (3)	2 (1)	1 (1)	5 (2)	0 (0)	0 (0)	1 (0)	12 (7)
WDD	0 (0)	113 (113)	13 (18)	37 (39)	103 (110)	0 (0)	0 (0)	12 (12)	278 (292)
WDY	0 (0)	4 (2)	0 (0)	1 (1)	2 (2)	0 (0)	0 (0)	0 (1)	7 (6)
WDX	0 (0)	13 (8)	10 (4)	2 (4)	9 (14)	0 (0)	0 (0)	2 (1)	36 (31)
WDV	0 (0)	0 (0)	0 (0)	0 (1)	1 (1)	0 (0)	0 (0)	0 (0)	1 (2)
IDN	0 (0)	2 (1)	0 (1)	2 (0)	2 (1)	0 (0)	0 (0)	0 (0)	6 (3)
IDD	0 (0)	13 (8)	2 (4)	2 (1)	23 (6)	0 (0)	0 (0)	2 (1)	42 (20)
IDY	0 (0)	3 (3)	0 (0)	4 (1)	1 (2)	0 (0)	0 (0)	0 (0)	8 (6)
IDX	0 (0)	4 (5)	4 (4)	1 (1)	5 (5)	0 (0)	0 (0)	0 (1)	14 (16)
PDN	0 (2)	368 (381)	87 (102)	116 (114)	402 (382)	0 (0)	0 (0)	44 (46)	1,017 (1,027)
PDD	0 (0)	205 (187)	51 (60)	86 (87)	107 (100)	0 (0)	2 (2)	28 (31)	479 (467)
PDY	0 (0)	66 (78)	27 (29)	31 (44)	78 (102)	0 (0)	0 (0)	0 (4)	202 (257)
PDX	0 (0)	23 (31)	20 (17)	4 (6)	20 (24)	0 (0)	0 (0)	4 (4)	71 (82)
PDV	0 (0)	1 (1)	0 (2)	2 (1)	0 (0)	0 (0)	0 (0)	0 (0)	3 (4)
LLN	1 (0)	0 (0)	0 (0)	0 (0)	0 (0)	0 (0)	0 (0)	0 (0)	1 (0)
LLD	0 (0)	2 (3)	0 (0)	0 (0)	0 (4)	0 (0)	0 (0)	0 (0)	2 (7)
LCD	0 (0)	14 (13)	5 (9)	3 (4)	73 (70)	0 (0)	31 (37)	0 (0)	126 (133)
LCY	0 (0)	0 (0)	0 (0)	0 (0)	1 (0)	0 (0)	0 (0)	0 (0)	1 (0)
LCX	1 (0)	0 (2)	7 (3)	3 (3)	11 (11)	0 (0)	14 (5)	0 (0)	36 (24)
LCV	0 (0)	0 (0)	0 (0)	0 (0)	1 (2)	0 (0)	0 (0)	0 (0)	1 (2)
MIN	0 (1)	110 (87)	29 (28)	57 (50)	105 (94)	0 (0)	1 (1)	21 (20)	323 (281)
MID	0 (0)	90 (62)	22 (20)	47 (34)	49 (46)	0 (0)	0 (1)	14 (7)	222 (170)
MIY	0 (0)	52 (59)	18 (17)	12 (15)	19 (30)	0 (0)	0 (0)	1 (2)	102 (123)
MIX	0 (0)	9 (12)	14 (5)	8 (2)	12 (18)	1 (0)	0 (0)	4 (5)	48 (42)
MIV	0 (0)	0 (0)	2 (1)	0 (0)	0 (1)	0 (0)	0 (0)	0 (0)	2 (2)
HIN	0 (0)	19 (13)	6 (9)	20 (15)	45 (29)	0 (0)	0 (0)	3 (3)	93 (69)
HID	0 (0)	281 (293)	95 (144)	261 (256)	533 (498)	0 (0)	13 (21)	40 (36)	1,223 (1,248)
HIY	0 (0)	25 (32)	6 (14)	23 (25)	34 (50)	0 (0)	1 (1)	1 (1)	90 (123)
HIX	0 (0)	38 (41)	72 (36)	28 (39)	73 (76)	0 (0)	6 (0)	5 (14)	222 (206)
HIV	0 (0)	1 (2)	0 (0)	0 (0)	4 (5)	0 (0)	0 (1)	0 (0)	5 (8)
BTD	0 (0)	0 (0)	0 (0)	1 (1)	10 (10)	0 (0)	31 (28)	0 (0)	42 (39)
BTY	0 (0)	0 (0)	0 (0)	0 (0)	0 (0)	0 (0)	2 (3)	0 (0)	2 (3)
BTX	0 (0)	0 (0)	0 (0)	0 (0)	3 (2)	0 (0)	6 (6)	0 (1)	9 (9)
NBD	0 (0)	5 (5)	0 (0)	1 (1)	3 (4)	0 (0)	10 (12)	0 (0)	19 (22)
NBY	0 (0)	0 (0)	0 (0)	0 (0)	1 (0)	0 (0)	2 (2)	0 (0)	3 (2)
NBX	0 (0)	0 (0)	0 (0)	2 (0)	0 (0)	0 (0)	3 (0)	0 (0)	5 (0)
UDD	0 (0)	19 (10)	1 (6)	11 (7)	22 (18)	1 (1)	14 (19)	3 (0)	71 (61)
UDY	0 (0)	1 (0)	0 (0)	0 (0)	0 (1)	0 (0)	0 (0)	0 (0)	1 (1)
UDX	0 (0)	6 (8)	0 (0)	0 (1)	11 (11)	0 (0)	9 (4)	2 (2)	28 (26)
ORD	0 (0)	1 (0)	0 (0)	0 (0)	0 (0)	0 (0)	0 (0)	1 (0)	2 (0)
ORX	0 (0)	0 (0)	0 (0)	0 (0)	1 (0)	0 (0)	0 (0)	0 (0)	1 (0)
UCN	0 (0)	2 (4)	0 (0)	1 (2)	1 (1)	0 (0)	0 (0)	0 (0)	4 (7)
UCD	0 (0)	19 (14)	3 (11)	12 (9)	17 (24)	0 (0)	1 (3)	5 (5)	57 (66)
UCY	0 (0)	1 (1)	0 (0)	0 (2)	0 (2)	0 (0)	0 (0)	0 (0)	1 (5)
UCX	0 (0)	24 (30)	5 (18)	13 (27)	22 (45)	0 (0)	1 (3)	6 (7)	71 (130)
UCV	0 (0)	1 (3)	0 (1)	1 (2)	1 (1)	0 (0)	0 (0)	0 (0)	3 (7)
UOD	0 (0)	0 (0)	0 (1)	0 (0)	0 (0)	0 (0)	0 (0)	0 (0)	0 (1)
UOX	0 (0)	0 (0)	1 (0)	0 (0)	0 (0)	0 (0)	0 (0)	0 (0)	1 (0)
OT	14 (16)	124 (171)	55 (84)	108 (113)	247 (271)	1 (2)	15 (16)	50 (42)	614 (715)
Total	22 (22)	2,219 (2,219)	1.132 (1,132)	1,648 (1,648)	3,241 (3,241)	91 (91)	207 (207)	355 (355)	8,915 (8,915)

[a] *See* table 2 for code symbols. Final diagnoses are *in parentheses.*
[b] Study groups could not be identified or assigned.

TABLE 4.—*Case distribution according to final diagnosis and diagnoses of contributor, Regional Center, and Repository Center*

Histologic subtype[a]	Diagnosis of				[% of all cases][b]	(% of HD or NL cases)[b]
	Contributor	Regional center	Repository center	Final		
UL	7	14	8	7		
UW	1,287	168	36	27		
HD	359	22	22	23		
LP[c]	176	108	92	94	[1.05]	(3)
NS[c]	1,088	1,714	1,738	1,730	[19.4]	(55.7)
MC	978	881	871	865	[9.7]	(27.9)
LD	205	229	234	224	[2.51]	(7.2)
UN	137	110	176	168	[1.9]	(5.4)
UK	10	6	0	0		
NLN	66	4	3	6		
NLD	31	14	4	4		
NLY	1	1	0	0		
NLX	221	27	11	14		
WDN[c]	158	12	8	7		
WDD	254	278	300	292	[3.27]	
WDY	6	7	7	6		
WDX	65	36	29	31		
WDV	0	1	2	2		
IDN	8	6	4	3		
IDD[c]	14	42	19	20		
IDY	1	8	6	6		
IDX	6	14	15	16		
PDN[c]	644	1,017	1,028	1,027	[11.52]	(20.3)
PDD[c]	682	479	472	467	[5.24]	(9.2)
PDY[c]	56	202	259	257	[2.88]	(5.1)
PDX	129	71	73	82		
PDV	1	3	4	4		
LLN	2	1	0	0		
LLD	2	2	7	7		
LLX	1	0	0	0		
LCN	2	0	0	0		
LCD[c]	56	126	137	133	[1.49]	(2.6)
LCY	1	1	0	0		
LCX	23	36	21	24		
LCV	1	1	2	2		
MIN[c]	232	323	284	281	[3.15]	(5.6)
MID	249	222	158	170	[1.91]	(3.4)
MIY[c]	25	102	128	123	[1.38]	(2.4)
MIX	79	48	34	42		
MIV	1	2	2	2		
HIN	105	93	71	69	[0.77]	
HID[c]	821	1,223	1,253	1,248	[14]	(24.7)
HIY[c]	17	90	121	123	[1.38]	(2.4)
HIX	337	222	211	206	[2.3]	(4.1)
HIV	3	5	9	8		
BTD	32	42	40	39	[0.44]	
BTY	1	2	4	3		
BTX	13	9	10	9		
BTV	1	0	0	0		
NBD	14	19	22	22		
NBY	1	3	2	2		
NBX	2	5	0	0		
UDN	4	0	0	0		
UDD	54	71	53	61		
UDY	0	1	1	1		
UDX	16	28	26	26		
ORD	0	2	0	0		
ORX	0	1	0	0		
UCN	2	4	6	7		
UCD	16	57	77	66		
UCY	0	1	5	5		
UCX	40	71	130	130		
UCV	1	3	6	7		
UON	6	0	0	0		
UOD	2	0	1	1		
UOY	1	0	0	0		
UOX	3	1	0	0		
OT	159	614	613	715		
Totals	8,915	8,915	8,915	8,915		

[a] *See* table 2 for code symbols.
[b] Percentages according to final diagnosis.
[c] Histologic subtypes for which greatest differences in diagnoses were found between the sources of diagnoses.

3) Other findings
   a. Contributors had the greatest difficulty in correctly recognizing LP. Their diagnoses are confirmed in only 23.3% of the cases they submitted as LP.
   b. Most (83.8%) of the contributors' diagnoses of NS proved to be NS.
   c. 28.6% (280/978) of the contributors' diagnoses of MC were changed to NS, whereas only 6.4% (70/1,088) of their NS diagnoses were changed to MC.
   d. It is difficult to distinguish between LD and HI, 16.6% (34/205) of contributors' diagnoses of LD were changed to HI.

Comparison of final diagnosis with contributor's diagnosis of HD (contributor's/final) (table 7).—This table shows:

1) Agreement (excluding 461 cases without contributor's diagnosis)	1,523/2,644 (58.2%)
2) Major disagreement	
a. Contributor's diagnosis was NL	63/2,644 (2.4%)
b. Contributor's diagnosis was among OT	6/2,644 (0.2%)
c. A final good-risk diagnosis (LP, NS, or MC) was considered to be a poor-risk diagnosis (LD) by contributors	49/2,294 (2.1%)
d. A final poor-risk diagnosis	69/191[23] (36.6%)

---

[23] Of the 224 cases with a final diagnosis of LD, the contributor's diagnosis was unavailable in 33 cases.

TABLE 5.—*Case distribution according to final diagnosis and year*[a]

Histologic subtype	No. of cases in:														Total No. of cases
	1967	1968	1969	1970	1971	1972	1973	1974	1975	1976	1977	1978	1979	1980	
UL	0	0	0	0	0	0	0	0	0	0	0	0	6	1	7
UW	0	2	14	1	0	0	1	0	4	2	3	0	0	0	27
HD	0	1	2	1	1	2	8	5	1	0	1	1	0	0	23
LP	1	3	4	3	1	5	7	7	5	7	15	12	23	1	94
NS	0	7	50	100	43	137	131	148	218	252	199	232	186	27	1,730
MC	1	13	20	37	29	68	81	79	103	99	116	92	118	9	865
LD	1	2	12	18	11	27	22	20	29	25	21	20	15	1	224
UN	0	0	1	7	7	19	13	16	9	28	28	16	20	5	169
NL	0	0	1	2	0	0	3	6	2	3	6	1	0	0	24
WDN	0	1	0	0	2	1	0	0	0	0	1	0	1	1	7
WDD	0	0	1	1	1	14	20	31	48	42	45	47	36	6	292
WDY	0	0	0	0	0	0	0	1	1	1	0	1	2	0	6
WDX	0	0	6	6	0	5	1	6	4	1	1	1	0	0	31
WDV	0	0	0	0	0	0	1	0	0	0	0	0	1	0	2
IDN	0	0	0	0	1	0	0	1	0	0	0	0	1	0	3
IDD	0	0	0	0	0	1	1	3	0	4	1	5	5	0	20
IDY	0	0	0	0	0	1	2	0	1	1	1	0	0	0	6
IDX	0	0	2	1	1	4	2	1	3	2	0	0	0	0	16
PDN	2	1	21	23	26	52	87	117	149	156	134	136	114	9	1,027
PDD	0	0	4	19	9	33	57	110	72	56	34	36	34	3	467
PDY	0	0	1	2	3	5	11	45	49	26	37	31	41	6	257
PDX	0	1	11	5	7	11	18	14	5	1	7	2	0	0	82
PDV	0	0	0	0	0	0	1	1	0	0	0	0	2	0	4
LLD	0	0	0	0	0	0	0	0	0	0	0	0	7	0	7
LCD	0	0	0	0	0	0	1	0	2	4	23	53	46	4	133
LCY	0	0	0	0	0	0	0	0	1	3	9	8	2	1	24
LCX	0	0	0	0	0	0	0	0	0	0	0	0	1	1	2
MIN	1	1	5	8	7	32	32	37	40	32	28	27	30	1	281
MID	0	0	0	1	1	6	14	45	20	11	26	19	23	4	170
MIY	0	0	0	2	1	3	13	10	20	16	16	13	28	1	123
MIX	0	0	9	3	1	7	10	5	1	2	3	1	0	0	42
MIV	0	0	0	0	0	0	0	0	0	0	0	0	2	0	2
HIN	0	0	3	1	2	6	6	8	12	7	10	7	7	0	69
HID	0	1	21	25	20	60	98	142	177	172	183	165	162	22	1,248
HIY	0	0	1	2	1	4	5	14	13	20	29	17	16	1	123
HIX	0	3	21	24	32	32	27	26	16	7	12	4	2	0	206
HIV	0	0	0	0	0	0	0	0	0	1	1	2	4	0	8
BTD	0	0	0	0	0	0	0	0	0	0	2	11	22	4	39
BTY	0	0	0	0	0	0	0	0	0	0	0	1	2	0	3
BTX	0	0	0	0	0	0	0	1	0	0	2	2	4	0	9
NBD	0	0	0	0	0	0	0	0	0	0	1	1	16	4	22
NBY	0	0	0	0	0	0	0	0	0	0	0	0	2	0	2
UDD	0	0	0	0	1	1	2	2	9	8	8	21	8	1	61
UDY	0	0	0	0	0	0	0	0	0	0	0	1	0	0	1
UDX	0	0	1	1	4	6	5	2	2	0	4	1	0	0	26
UCN	0	0	0	1	1	1	0	1	1	0	0	0	2	0	7
UCD	0	0	0	1	0	1	7	6	4	2	6	18	18	3	66
UCY	0	0	0	0	0	0	1	0	1	0	1	0	2	0	5
UCX	0	0	3	12	11	21	11	18	12	10	14	8	10	0	130
UCV	0	0	0	0	0	0	0	0	0	0	0	3	4	0	7
UOD	0	0	0	0	0	0	0	0	0	0	0	0	1	0	1
OT	3	6	32	63	29	57	53	72	74	78	71	91	70	16	715
Total	9	42	246	370	253	622	752	1,000	1,108	1,079	1,099	1,107	1,096	132	8,915

[a] *See* table 2 for code symbols.

was considered to be a good-risk diagnosis by contributors

Total major disagreement 187/2,644 (7%)

3) Other findings

a. Although 83.8% of the contributors' diagnoses of NS was confirmed, contributors

TABLE 6.—*Hodgkin's disease: Comparison of contributor's diagnosis with final diagnosis*[a]

Contributor's diagnosis	Final diagnosis[b]																
	UL or UW (2)	HD (2,575)						NL (249)								Miscellaneous (127) OT	Totals [% of grand total]
		HD	LP	NS	MC	LD	UN	WD	ID	PD	LC	MI	HI	UD	UC		
HD	1	4 (1.1%)	4	163	83	18	17	0	0	9	0	7	28	0	9	26	369 [12.5]
LP	0	0	**41** **(23.3%)**	37	47	1	4	4	1	12	1	4	3	0	5	16	176 [6]
NS	1	3	8	**912** **(83.8%)**	70	10	38	0	0	5	0	9	7	0	1	24	1,088 [36.8]
MC	0	6	6	280	**465** **(47.5%)**	58	53	2	1	8	1	23	29	1	12	33	978 [33.1]
LD	0	0	0	32	17	**84** **(41%)**	7	0	0	3	0	10	34	0	5	13	205 [6.9]
UN	0	1	0	44	33	12	17 (12.4%)	0	0	2	0	3	6	1	3	15	137 [4.6]
Totals	2	14	59	1,468	715	183	136	6	2	29	2	56	107	2	35	127	2,953 [100]

[a] For code symbols, *see* table 2.
[b] *Values in parentheses* are No. of cases. *Bold face values* represent agreement for each histologic subtype when compared with final diagnosis.

identified only 61.3% (912/1,487) of all NS cases. 18.8% (280/1,487) of NS was classified as MC.

b. 30.4% (58/191[23]) of LD was considered to be MC by contributors.

Comparison of Regional Center's diagnosis with final diagnosis of HD (final/Regional) (table 8).—This table can be summarized as follows:

1) Agreement 2,747/3,080 (89.2%)
2) Major disagreement
  a. Diagnosis changed to NL 42/3,080 (1.4%)
  b. Diagnosis changed to OT 37/3,080 (1.2%)
  c. Good-risk diagnosis (LP, NS, MC) was changed to poor-risk diagnosis (LD) 15/2,703 (0.6%)
  d. Poor-risk diagnosis was changed to good-risk diagnosis 24/229 (10.5%)
    Total major disagreement 118/3,080 (3.8%)
3) Other findings:
  a. LP has the lowest agreement rate (73%).
  b. Disagreement rate is significantly less than for the results shown in table 6.

Comparison of final diagnosis with Regional Center's diagnosis of HD (Regional/final) (table 9).—This table shows:

1) Agreement 2,747/3,105 (88.5%)
2) Major disagreement
  a. Regional Center's diagnosis was NL 35/3,105 (1.1%)

TABLE 7.—*Hodgkin's disease: Comparison of final diagnosis with contributor's diagnosis*[a]

Final diagnosis	Contributor's diagnosis[b]															
	NA (461)	HD (2,575)						NL (63)							Miscellaneous (6) OT	Totals [% of grand total]
		HD	LP	NS	MC	LD	UN	WD	PD	LC	MI	HI	UC	UO		
HD	8	4 (26.7%)	0	3	6	0	1	0	0	0	0	0	1	0	0	23 [0.7]
LP	19	4	**41** **(54.7%)**	8	6	0	0	7	3	0	1	2	0	2	1	94 [3]
NS	243	163	37	**912** **(61.3%)**	280	32	44	3	1	0	6	4	2	2	1	1,730 [55.7]
MC	133	83	47	70	**465** **(63.5%)**	17	33	1	3	0	5	2	2	3	1	865 [27.9]
LD	33	18	1	10	58	**84** **(44%)**	12	0	1	0	0	6	1	0	0	224 [7.2]
UN	25	17	4	38	53	7	17 (11.8%)	0	3	1	0	1	0	0	3	169 [5.4]
Totals	461	289	130	1,041	868	140	107	11	11	1	12	15	6	7	6	3,105 [100]

[a] For code symbols *see* table 2. NA = type of disease unclassifiable or classification not available.
[b] *Values in parentheses* are No. of cases. *Bold face values* represent agreement for each histologic subtype. NA cases were not included in calculation.

TABLE 8.—*Hodgkin's disease: Comparison of Regional Center's diagnosis with final diagnosis*[a]

Regional Center's diagnosis	Final diagnosis[b] UL	UW (11)	HD (2,990) HD	LP	NS	MC	LD	UN	NL (42) NL	WD	PD	LC	MI	HI	UD	UC	Miscellaneous (37) OT	Totals [% of grand total]
HD	0	1	**14 (43.8%)**	0	7	4	3	4	1	0	0	0	1	0	0	1	2	38 [1.2]
LP	0	0	0	**79 (73%)**	7	12	1	2	0	1	1	0	0	0	0	1	4	108 [3.5]
NS	0	7	3	3	**1,616 (94.3%)**	36	4	27	0	0	0	0	3	2	0	1	12	1,714 [55.6]
MC	0	1	3	1	46	**768 (87.2%)**	10	26	0	0	1	1	6	3	0	3	12	881 [28.6]
LD	0	1	0	1	15	8	**186 (81.2%)**	4	0	0	0	0	2	8	1	0	3	229 [7.4]
UN	1	0	0	1	4	6	5	**84 (76.4%)**	0	0	2	0	0	2	0	1	4	110 [3.6]
Total	1	10	20	85	1,695	834	209	147	1	1	4	1	12	15	1	7	37	3,080 [100]

[a] For code symbols, *see* table 2.

[b] *Values in parentheses* are No. of cases. *Bold face values* represent agreement for each histologic subtype when compared with final diagnosis.

b. Regional Center's diagnosis was among OT — 17/3,105 (0.5%)

c. A final good-risk diagnosis (LP, NS, or MC) was considered to be a poor-risk diagnosis (LD) by the Regional Center — 24/2,689 (0.9%)

d. A final poor-risk diagnosis was considered to be a good-risk diagnosis by the Regional Center — 15/224 (6.7%)

Total major disagreement — 91/3,105 (2.9%)

3) Others

LP has the lowest agreement rate (60.9%).

Comparison of contributor's diagnosis with final diagnosis of NL (final/contributor's) (table 10).—In the comparison of the diagnoses for NL shown in tables 10-13, four quadrants of each square were utilized to specify different pattern designations as follows: upper left quadrant—nodular, upper right quadrant—nodular and diffuse, lower left quadrant—diffuse, lower right quadrant—pattern not available or indeterminable. In analyses for tables 10-13, a designation of nodular versus nodular and diffuse was considered a disagreement when complete agreement was computed. The findings of table 10 can be summarized as follows:

1) Complete agreement for both cytologic type and pattern (excluding cases without cytologic and/or pattern designation) — 1,674/3,441 (48.6%)

2) Major disagreement

a. Diagnosis changed to HD — 57/4,190 (1.4%)

TABLE 9.—*Hodgkin's disease: Comparison of final diagnosis with Regional Center's diagnosis*

Final diagnosis	Regional Center's diagnosis[b] UL	UW (63)	HD (2,990) HD	LP	NS	MC	LD	UN	NL (35) NL	WD	PD	LC	MI	HI	UD	UC	Miscellaneous (17) OT	Totals [% of grand total]
HD	0	1	**14 (60.9%)**	0	3	3	0	0	0	0	0	0	0	0	0	0	2	23 [0.7]
LP	0	1	0	**79 (84%)**	3	1	1	1	0	2	1	0	1	0	0	3	1	94 [3]
NS	1	26	7	7	**1,616 (93.4%)**	46	15	4	0	0	1	0	2	3	0	1	1	1,730 [55.7]
MC	1	17	4	12	36	**768 (88.8%)**	8	6	0	0	3	0	3	0	0	1	6	865 [27.9]
LD	0	6	3	1	4	10	**186 (83%)**	5	0	0	0	0	1	7	0	1	0	224 [7.2]
UN	0	10	4	2	27	26	4	**84 (49.7%)**	1	0	0	1	1	0	1	1	7	169 [5.4]
Totals	2	61	32	101	1,689	854	214	100	1	2	5	1	8	10	1	7	17	3,105 [100]

[a] For code symbols, *see* table 2.

[b] *Values in parentheses* are No. of cases. *Bold face values* represent agreement for each histologic subtype.

TABLE 10 (part I).—*Non-Hodgkin's lymphoma: Comparison of contributor's diagnosis with final diagnosis (final/contributor's)*

N	Y
D	X

FINAL DIAGNOSIS

CONTRIBUTOR'S DIAGNOSIS

	WD		ID		PD		LL		LC		MI		HI		BT		NB		UD		UC		UO		Subtotal		HD	OT	Total
WDN	5				102	7					15	1	1	2							1				124	10	5	2	158
	3	1	1	1	6	2			1															2	11	6			
WDD				3	21	16					2	1		2											23	22	5	14	254
	110	4	3	1	51	4	1		3		1	1	3	1							4	3			176	14			
WDY					1	2					1														2	2		1	6
									1																1				
WDX	1	1			7	3					2		1												11	4	1	5	65
	10	8		3	13	3	1		1			1	1	1							1	1			27	17			
IDN			1		4						2														7				8
	1																								1				
IDD						1																				1			14
	6		2		4				1																13				
IDY				1																						1			1
IDX																													6
	1	1	1	1																	1	1			3	3			
PDN		2	1		468	50					50		5	6							1	1			525	59	2	14	644
	6		1		7	6			1		5		7								2	6		3	29	15			
PDD					28	59					4	8	1	6								1		2	33	76	8	33	682
	81	1	4	1	216	5	2		46	3	22	1	96	2	4		7		8	2	15	14		2	501	31			
PDY		1			8	28						4		4											8	37		1	56
	1				4						3		1									1			9	1			
PDX					15	4					4	1		1											19	6	1	8	130
	7	2		2	22	9			6	5	2	3	10	8			1		2	8	1	4		4	51	45			
LLN					1	1																			1	1			2
LLD																													2
									1								1								2				
LLX																												1	1
LCN					1						1														2				2
LCD					1													2							1	2	1	2	56
					1				40	1			2		2				2			1		1	47	3			
LCY																													1
										1																1			
LCX																												4	24
						1			8	6			1	1	1			2							10	10			
MIN					70	7					85	23	9	4							3				167	34	5	9	232
					3	1					3	3	6											1	12	5			
MID					5	9					6	15	3	7								1			14	32	2	28	249
	12	1			17	2			4		47	2	64	2					1	1	9	7		4	154	19			
MIY					3	2					3	8		2											6	12		3	25
											1		2									1			3	1			
MIX					10	1					12	5													22	6	5	7	80
	1		1		4	2					10	4	13	2								1		2	29	11			

TABLE 10 (part II).—*Non-Hodgkin's lymphoma: Comparison of contributor's diagnosis with final diagnosis (final/contributor's)*

N	Y
D	X

FINAL DIAGNOSIS

CONTRIBUTOR'S DIAGNOSIS

	WD		ID		PD		LL		LC		MI		HI		BT		NB		UD		UC		UO		Subtotal		HD	OT	Total
HIN					12	2					20	4	21	13							2				55	19	3	2	105
											1		17	4								2		2	18	8			
HID					1	1					3	6	6	28						1	1	1			11	37	7	54	821
	3		1		12		1		1		21	2	530	35	1		4		4		10	14		13	648	64			
HIY						1						2		9												12		1	17
													4												4				
HIX					15	1					5	7	6	5											26	13	5	61	340
		1			3	5			2		4	4	125	67					1	1	1	16		5	136	99			
BTD																1										1			32
									2				1		19	2	1		5		1				29	2			
BTY																1										1			1
BTX																1										1			14
													1		5	4				2	1				7	6			
NBD																													14
													2		5		6		1						14				
NBY																													1
																1										1			
NBX																													2
													1				1								2				
UDN					2						1														3				4
																			1						1				
UDD						1					1			1											1	2		2	54
	1				8				1		2		11		2	2	1		17	1	3				46	3			
UDX																												2	16
					1	1			1	2			4						2		2	1			10	4			
UCN																													2
					1																	1			1	1			
UCD					1																				1		1	3	16
	1				2						1		1						3		2	1			10	1			
UCX					3									1											3	1	5	8	41
					1	2					2		9	1							1	7		1	13	11			
UON					4						1														5				6
													1												1				
UOD																											1		2
											1														1				
UOY																													1
					1																				1				
UOX					1																				1				3
									1														1		2				
Sub-	6	4	2	4	784	196					218	85	53	91		3		2		1	8	4		2	1071	392			
total	244	19	14	9	377	43	5		121	18	126	21	973	124	39	9	22	2	47	15	54	82	1	40	2023	382			
Total	273		29		1400		5		139		450		1241		51		26		63		148		43		3868		57	265	4190

b. Diagnosis changed to OT	265/4,190 (6.3%)
c. Nodular or nodular and diffuse pattern designation changed to diffuse	92/1,272 (7.2%)
d. Diffuse pattern designation changed to nodular or nodular and diffuse	257/2,196 (11.8%)
e. Good-risk diagnosis (all WD, all ID, PDN, PDY, MIN, and MIY) changed to poor-risk diagnosis (PDD, all LC, MID, all HI, all BT, all NB, and all UD	167/1,469 (11.4%)
f. Poor-risk diagnosis changed to good-risk diagnosis	305/2,435 (12.7%)
Total major disagreement	1,143/4,190 (27.3%)
3) Others	
a. Contributor's WDN changed to PDN or MIN	117/158 (74%)
b. Contributor's PDN confirmed	468/644 (72.7%)
c. Contributor's HID confirmed	590/821 (71.9%)

Comparison of final diagnosis with contributor's diagnosis of NL (contributor's/final) (table 11).—

1) Complete agreement for both cytologic type and pattern, excluding cases without designation of cytology and/or pattern	1,674/4,367 (38.3%)
2) Major disagreement	
a. Contributor's diagnosis was HD	246/5,037 (4.9%)
b. Contributor's diagnosis was among OT	704/5,037 (14.0%)
c. Nodular or nodular and diffuse lymphoma was considered by contributors to be diffuse lymphoma	262/1,920 (13.6%)
d. Diffuse lymphoma was considered by contributors to be nodular and diffuse lymphoma	91/2,525 (3.6%)
e. Good-risk categories (all WD, all ID, PDN, PDY, MIN, and MIY) were considered to be poor-risk categories (PDD, all LC, MID, all HI, all BT, all NB, and all UD) by contributors	325/2,071 (15.7%)
f. Poor-risk categories were considered to be good-risk categories by contributors	162/2,613 (6.2%)
Total major disagreement	1,790/5,037 (35.5%)

Comparison of Regional Center's diagnosis with final diagnosis of NL (final/Regional) (table 12).—

1) Complete agreement for both cytologic type and pattern, excluding cases without designation of cytology and/or pattern	3,612/4,372 (82.6%)
2) Major disagreement	
a. Diagnosis changed to HD	34/4,993 (0.7%)
b. Diagnosis changed to OT	125/4,993 (2.5%)
c. Nodular or nodular and diffuse designation changed to diffuse	44/1,873 (2.3%)
d. Diffuse designation changed to nodular or nodular and diffuse	94/2,563 (3.7%)
e. Good-risk diagnosis (all WD, all ID, PDN, PDY, MIN, and MIY) changed to poor-risk diagnosis (PDD, all LC, MID, all HI, all BT, all NB, and all UD)	58/2,048 (2.8%)
f. Poor-risk diagnosis changed to good-risk diagnosis	80/2,678 (3%)
Total major disagreement	435/4,993 (8.7%)

Comparison of final diagnosis with Regional Center's diagnosis of NL (Regional/final) (table 13).—

1) Complete agreement for both cytologic type and pattern, excluding cases without designation of cytology and/or pattern	3,612/4,367 (82.7%)
2) Major disagreement	
a. Regional Center's diagnosis was HD	41/5,037 (0.8%)
b. Regional Center's diagnosis was among OT	174/5,037 (3.5%)
c. Nodular or nodular and diffuse lymphoma was considered to be diffuse lymphoma by Regional Center	90/1,920 (4.7%)
d. Diffuse lymphoma was considered to be nodular or nodular and diffuse lymphoma by Regional Center	45/2,526 (1.8%)
e. Good-risk categories (all WD, all ID, PDN, PDY, MIN, and MIY) were considered to be poor-risk categories (PDD, all LC, MID, all HI, all BT, all NB, and all UD) by Regional Center	84/2,071 (4.1%)
f. Poor-risk categories were considered to be good-risk categories by Regional Center	47/2,518 (1.9%)
Total major disagreement	481/5,037 (9.5%)

Comparison of contributor's diagnosis with final diagnosis of nodular, or nodular and diffuse NL (final/contributor's) (table 14).—This table shows the degree of confirmation of the pattern designated by contributors for those cases interpreted by them as either nodular or nodular and diffuse NL. "No agreement" means that the final diagnosis was something other than NL; "agree on NL only" means that the final diagnosis was NL, but both pattern and cytologic classification were different from those of the contributors; and "total agreement" means that the final diagnosis was identical to that of the contributors for both pattern and cytology. A correct pattern designa-

TABLE 11 (part I).—*Non-Hodgkin's lymphoma: Comparison of final diagnosis with contributor's diagnosis (contributor's/final)*

N	Y
D	X

CONTRIBUTOR'S DIAGNOSIS

FINAL DIAGNOSIS

	WD		ID		PD		LL		LC		MI		HI		BT		NB		UD		UC		UO		Subtotal		HD	OT	Total
WDN	5																								5			1	7
		1																								1			
WDD	3		1		6	1															3				13	1	5	27	292
	110	10	6	1	81	7					12	1	3						1		1	13			214	32			
WDY					2	1																			2	1	1	1	6
		1																								1			
WDX	1																								1			9	33
	4	8		1	1	2					1			1								5			6	17			
IDN			1		1																				2		1		3
IDD	1				1																				2			2	20
	3		2	1	4							1	1										2	2	12	4			
IDY				1																						1			6
	3																							2	3	2			
IDX	1																								1		1	5	16
	1	3		1	1	2																		1	2	7			
PDN	102	1	4		468	8	1		1		70	3	12						2		40		4		704	12	24	135	1027
	21	7			28	15			1		5	10	1	15							4	44		1	60	92			
PDD	6				7	4					3										2			1	18	5	5	55	467
	51	13	4		216	22			1		17	4	12	3					8	1	8	24			317	67			
PDY	7	2			50	28	1				7	2	2	1							2	1			69	34	7	36	257
	16	3	1		59	4					9	1	1	1					1		2	13			89	22			
PDX	2				6						1														9		3	26	86
	4	3			5	9				1	2	2		5						1	2	14			13	35			
LLD																												2	7
	1	1			2								1												4	1			
LCD	1	1			1																				2	1		10	133
	3	1	1		46	6	1		40	8	4		1	2	2				1	1		2		1	99	21			
LCX										1																1	2	4	26
					3	5			1	6		1								2		1			4	15			
MIN	15	1	2		50				1		85	3	20						1		12		1		187	4	10	30	281
	2	2			4	4					6	12	3	5					1		1	4			17	27			
MID						3					3	1	1												4	4	25	15	170
	1				22	2					47	10	21	4					2		3	5	1		97	21			
MIY	1				5	4					23	8	4	2							2				35	14	11	12	123
	1				8	1					15	5	6	7							1	7			31	20			

tion (total pattern agreement) consists of the sum of the percentages of agreement on pattern only and of total agreement. For the purpose of computing the agreement percentage for the pattern designation of NL in tables 14-17, we considered N versus Y as agreement, whereas D versus N or Y was considered a disagreement. Table 14 shows that:

1) When contributors diagnosed nodular or nodular and diffuse NL, their pattern designation was confirmed in 86.3% of the cases.

TABLE 11 (part II).—*Non-Hodgkin's lymphoma: Comparison of final diagnosis with contributor's diagnosis (contributor's/final)*

N	Y
D	X

CONTRIBUTOR'S DIAGNOSIS

FINAL DIAGNOSIS

	WD		ID		PD		LL		LC		MI		HI		BT		NB		UD		UC		UO		Subtotal		HD	OT	Total
MIX											3										1				4		6	12	44
	1	1			1	3					2	4	2	4								4			6	16			
HIN	1				5						9		21								1				37		1	12	69
		1			1						3		6	6								2			10	9			
HID					7	1					6	2	17	4									1		31	7	75	171	1248
	3	1			96	10			2	1	64	13	590	125	1	1	2	1	11	4	6	32		1	775	189			
HIY	2				6	4					4	2	13	9											25	15	4	25	123
	2				6	2					7		28	5					1			3			44	10			
HIX													4												4		27	55	214
	1	1			2	7				1	2	2	35	67							1	9			41	87			
BTD																													39
					4				2	1			1		19	5	5		2						33	6			
BTY																1										1			3
															1	1									1	1			
BTX																		1								1			9
															2	4			2						4	4			
NBD																													22
					7	1	1						4		1		6	1	1						20	2			
NBY																													2
									2																2				
UDD																			1						1			8	61
					8	2			2	2	1		4	1	5		1		17	2	3	4			41	11			
UDY																													1
													1												1				
UDX																											2	4	26
					2	8					1			1		2			1			5			4	16			
UCN											1		2												3		1	1	7
													1									1			1	1			
UCD					2																				2		2	11	66
	3			1	14						9		10	1	1	1			3	2	2	4			42	9			
UCY					1																				1			1	5
					1						1		1												3				
UCX					4	1						1	2								1				7	2	29	28	137
	3	1		1	14	4			1		7	1	13	12						1	1	12			39	32			
UO																													1
																								1		1			
Sub-total	148	5	8	1	622	55	2		2	1	215	22	98	16		1		1	4		64	1	6	1	1169	104			
	234	58	14	6	636	116	2		52	20	215	67	746	265	32	16	14	2	52	14	35	208	3	9	2035	779			
Total	445		29		1429		4		75		519		1125		47		17		70		308		19		4087		246	704	5037

TABLE 12 (part I).—*Non-Hodgkin's lymphoma: Comparison of Regional Center's diagnosis with final diagnosis (final/Regional)*

N	Y
D	X

FINAL DIAGNOSIS

REGIONAL DIAGNOSIS

	WD		ID		PD		LL		LC		MI		HI		BT		NB		UD		OR		UC		UO		Subtotal		HD	OT	Total
WDN	5				2						1																8				12
	1					2																				1	1	3			
WDD				1		1																						2	1	6	278
	236	6	1	3	12	1	3		1	2													3	1			256	13			
WDY		3		1		1																						5			7
		1	1																								1	1			
WDX					2																						2		1	2	37
	8	17		1	1	4	1																				10	22			
IDN			1		5																						6				6
IDD						3																						3			42
	18		12	2	4	1			1															1			35	4			
IDY				2		2																		1				5		1	8
	2																										2				
IDX				1																								1		1	14
		3	3	4		1							1														4	8			
PDN	1	1	1		928	38					6	2	1														937	41	2	4	1017
	1				7	8					1	3	3										1	2		7	13	20			
PDD					6	23						3														1	6	27	2	10	479
	12	2	1		376	8	1		5	2	2	2	7	2					2	1			2	7		2	408	26			
PDY				1	12	172						5															12	178		2	202
	1		1	2	4							1												1			6	4			
PDX					6						1																7		1	8	74
				1	8	34			1		3	2	1	3						1				1		3	13	45			
LLN					1																						1				1
LLD																															2
							2																				2				
LCD														1														1	1	3	126
					5	1			104	2	1		2				1		2				2	1			117	4			
LCY																															1
										1																		1			
LCX											1																1			1	37
						1			16	17														1			16	19			
MIN					29	5					251	10	5	3									2				287	18	1	3	323
					1						2	6	2											1		2	5	9			
MID						3						13		1									2				2	17	3	11	222
					11	1					136	3	16	3					2	1			2	11	1	2	168	21			
MIY					3	5					3	78		1													6	84		3	102
					2				1		1	1		1										2		1	4	5			
MIX		1			2						1	1															3	2	4	5	50
		1				3					8	16	1	1										5		1	9	27			

2) There were no significant yearly differences, although the total agreement rate has improved with time.

Comparison of final diagnosis with contributor's diagnosis of nodular or nodular and diffuse NL (contributor's/final) (table 15).—Definitions for each column of figures in this table are the same as for table 14. This table shows:

1) Contributors designated the nodular pattern correctly in 60.3% of nodular or nodular and diffuse lymphomas. This means that contributors failed to designate nodu-

TABLE 12 (part II).—*Non-Hodgkin's lymphoma: Comparison of Regional Center's diagnosis with final diagnosis (final/Regional)*

N	Y
D	X

FINAL DIAGNOSIS

REGIONAL DIAGNOSIS	WD		ID		PD		LL		LC		MI		HI		BT		NB		UD		OR		UC		UO		Subtotal		HD	OT	Total
HIN					2						9		54	16									1				66	16		1	93
						2							5	2										1			5	5			
HID					1						1	2		22									7	1			9	25	6	24	1223
	1				3	1			5		1	1	1089	33	1		1		2					9		12	1103	56			
HIY												3	3	70						1			1	1			4	75			90
													5	4										1		1	5	6			
HIX					1						1		4	7													6	7	4	14	227
						1			1				59	123					2				4	6			66	130			
BTD																															42
															34	2	2		3				1				40	2			
BTY																2												2			2
BTX																1												1			9
															3	2	1		1				1				6	2			
NBD																															19
													3		1		15										19				
NBY																		2										2			3
																1												1			
NBX																															5
													3				2										5				
UDD														1														1	1	2	71
	1				4				1				6	2		2			40	5			1	5			53	14			
UDY					1																						1				1
UDX																														3	28
						1								1		2			4	15				1		1	4	21			
ORD														1														1		1	2
ORX																															1
													1														1				
UCN					1																		3				4				4
UCD																													1	12	57
					2				1		3			1									27	8		2	33	11			
UCY					1																						1				1
UCX					1																		1				2		6	8	74
					1	1							2	4						1			6	42		1	9	49			
UOX																															1
						1																						1			
Sub-total	6	5	2	6	1004	253					275	117	67	123		3		2		1			17	3		1	1371	514			
	281	30	19	13	445	72	7		133	24	158	35	1206	180	39	9	22		58	24			50	107	1	36	2419	530			
Total	322		40		1774		7		157		585		1576		51		24		83				177		38		4834		34	125	4993

TABLE 13 (part I).—*Non-Hodgkin's lymphoma: Comparison of final diagnosis with Regional Center's diagnosis (Regional/final)*

N	Y
D	X

REGIONAL DIAGNOSIS

FINAL DIAGNOSIS	WD		ID		PD		LL		LC		MI		HI		BT		NB		UD		UC		UO		OR		Subtotal		HD	OT	Total
WDN	5				1																						6			1	7
WDD				2	1	1																1					1	4	1	9	292
	236	8	18		12								1						1		1						269	8			
WDY		3			1																						1	3			6
	1											1															1	1			
WDX		1																										1		2	33
	6	17		3	2							1										1					8	22			
IDN			1		1																						2			1	3
IDD		1				1																						2			20
	1		12	3	1																	1					14	4			
IDY		1		2		1																						4			6
	1			1																							1	1			
IDX						2																						2		2	16
	3	1	2	4		1																1					5	7			
PDN	2		5		928	12	1				29	3	2							1	1	1					968	17		21	1027
		2			6	6						2	1	1								3					7	14			
PDD					7	4					1	2															8	6	4	17	467
	12	1	4		376	8			5		11		7						4		3	1					422	10			
PDY		1		2	38	172					5	5															43	180		4	257
	1		3		23						3																30				
PDX	2				8								2								1						13			10	86
	1	4	1	1	8	34			1	1	1	3	1	1						1	1	3		1			14	49			
LLD																															7
	3	1			1		2																				6	1			
LCD												1																1			133
	1		1		5	1			104	16			1	1					1		1						114	18			
LCX										1																		1	1	1	26
	2				2				2	17																	6	17			
MIN	1				6						251	3	9														267	3	1	5	281
						1				1		1	1	1													1	4			
MID					1						2	1															3	1	6	6	170
					2	3			1		136	8	1							3							143	11			
MIY					2	5					10	78		3													12	86	1	4	123
					3						13	1	2							1							19	1			

larity in a significant percentage of cases; however, when nodularity was designated, it was usually confirmed (86.3%).

2) There has been a yearly trend of improvement from 1972 to 1979 in designation of nodularity (45.7% to 75.4%) and in total agreement (19% to 50.8%).

Comparison of contributor's diagnosis with final diagnosis of diffuse NL (final/contributor's) (table 16).—The definitions for each column of figures in this table are the same as for table 14. This table shows:

1) When contributors classified NL as diffuse, they were confirmed in 74.6% of the cases; this percentage is not as

TABLE 13 (part II).—*Non-Hodgkin's lymphoma: Comparison of final diagnosis with Regional Center's diagnosis (Regional/final)*

N	Y
D	X

REGIONAL DIAGNOSIS

FINAL DIAGNOSIS

	WD		ID		PD		LL		LC		MI		HI		BT		NB		UD		UC		UO		OR		Subtotal		HD	OT	Total
MIX					3	1					6	1															9	2	4	4	44
					2	2					3	16	1								1						6	19			
HIN					1						5		54	3						1							61	3		1	69
														4														4			
HID					3						2		5	5			3										13	5	7	25	1248
				1	7	1			2		16	1	1089	59				3	6		3	6		3		1	1123	75			
HIV											3	1	16	70													19	71			123
									1		1		22	7					1						1		26	7			
HIX												1	2	4													2	5	8	24	214
					2	3					3	1	33	123					2	1	1	4		2			41	134			
BTD																															39
													1		34	3	1										36	3			
BTY																2												2			3
																1												1			
BTX																		1										1			9
															2	2			2	2							4	4			
NBD																															22
									1				1		2	1	15	2									19	3			
NBY																		2										2			2
UDD																													1	2	61
					2				2		2		2	2	3	1			40	4							51	7			
UDY														1														1			1
UDX																														2	26
					1	1					1								5	15		1					7	17			
UCN														1														1		1	7
											1										3	1					4	1			
UCD					1																						1			7	66
	3				2				2		2		7	4	1	1			1		28	6		1			46	12			
UCY				1										1														2		2	5
													1														1				
UCX					1						1	2		1													2	3	7	23	137
	1		1		7	1			1	1	10	5	8	6					4	1	8	45		3			40	62			
UOD																															1
											1																1				
Sub-total	10	7	6	7	1003	199	1			1	315	98	90	89		2	3	3		1	3	2					1431	409			
	272	34	42	13	464	62	2		122	36	204	40	1180	209	42	9	16	5	67	24	53	74		10	1	1	2465	517			
Total	323		68		1728		3		159		657		1568		53		27		92		132		10		2		4822		41	174	5037

TABLE 14.—*Nodular or nodular and diffuse non-Hodgkin's lymphoma: Comparison of contributor's diagnosis with final diagnosis*

Year	Contributor's diagnosis vs. final diagnosis, No. of cases (%)					
	No agreement	Agree on NL only	Agree on pattern only[a]	Agree on cytology only	Total agreement	Totals
1968	1	0	0	0	0	1
1969	0	3	1	0	0	4
1970	4	1	10	0	1	16
1971	2	2	5	0	9	18
1972	3	3	28 (50.9)	1	20 (36.4)	55
1973	2	2	41 (45.6)	4	41 (45.6)	90
1974	2	5	48 (32.2)	13	81 (54.4)	149
1975	8	9	75 (37.5)	7	101 (50.5)	200
1976	8	2	69 (40.8)	5	85 (50.3)	169
1977	10	9	54 (27.6)	9	114 (58.2)	196
1978	10	13	40 (19.9)	4	134 (66.7)	201
1979	9	15	58 (26.4)	12	126 (57.3)	220
1980	3	0	4 (20.0)	1	12 (60.0)	20
Totals	62 (4.6)	64 (4.8)	433 (32.3)	56 (4.2)	724 (54.0)	1,339 (100.0)

[a] Nodular vs. nodular and diffuse pattern descriptions were considered agreement.

TABLE 15.—*Nodular or nodular and diffuse non-Hodgkin's lymphoma: Comparison of final diagnosis with contributor's diagnosis*

Year	Final diagnosis vs. contributor's diagnosis, No. of cases (%)					
	No agreement	Agree on NL only	Agree on pattern only[a]	Agree on cytology only	Total agreement	Totals
1967	3	0	0	0	0	3
1968	3	0	0	0	0	3
1969	22	6	1	2	0	31
1970	18	7	10	3	1	39
1971	12	16	5	2	9	44
1972	17	25	28 (26.7)	15	20 (19.0)	105
1973	28	35	41 (25.8)	14	41 (25.8)	159
1974	49	39	48 (20.5)	17	81 (34.6)	234
1975	37	43	75 (26.1)	31	101 (35.2)	287
1976	62	25	69 (26.5)	19	85 (32.7)	260
1977	35	27	54 (70.8)	29	114 (44.0)	259
1978	16	16	42 (17.9)	27	134 (57.0)	235
1979	13	16	61 (24.6)	32	126 (50.8)	248
1980	0	1	4 (21.0)	2	12 (63.2)	19
Totals	315 (16.4)	256 (13.3)	438 (22.7)	193 (10.0)	724 (37.6)	1,926 (100.0)

[a] Nodular vs. nodular and diffuse pattern designations were considered agreement.

TABLE 16.—*Diffuse non-Hodgkin's lymphoma: Comparison of contributor's diagnosis with final diagnosis*

Year	Contributor's diagnosis vs. final diagnosis, No. of cases (%)					
	No agreement	Agree on NL only	Agree on pattern only[a]	Agree on cytology only	Total agreement	Totals
1969	0	0	0	1	1	2
1970	2	2	2	2	1	9
1971	1	2	1	2	6	12
1972	2	12	8 (10.4)	15	40 (51.9)	77
1973	10	21	42 (24.7)	15	82 (48.2)	170
1974	23	25	62 (22.7)	23	140 (51.3)	273
1975	19	30	65 (22.0)	29	152 (51.5)	295
1976	38	24	80 (28.2)	17	125 (44.0)	284
1977	34	31	106 (32.2)	31	127 (38.6)	329
1978	30	21	123 (33.4)	28	166 (45.1)	368
1979	21	19	109 (30.4)	29	181 (50.4)	359
1980	4	0	14 (28.6)	2	29 (59.2)	49
Totals	184 (8.3)	187 (8.4)	612 (27.5)	194 (8.7)	1,050 (47.1)	2,227 (100.0)

[a] Nodular vs. nodular and diffuse pattern designations were considered agreement.

TABLE 17.—*Diffuse non-Hodgkin's lymphoma: Comparison of final diagnosis with contributor's diagnosis*

Year	Final diagnosis vs. contributor's diagnosis, No. of cases (%)					
	No agreement	Agree on NL only	Agree on pattern only[a]	Agree on cytology only	Total agreement	Totals
1968	1	0	0	0	0	1
1969	20	1	0	4	1	26
1970	14	14	2	16	1	47
1971	12	6	1	7	6	32
1972	16	25	8 (6.9)	27	40 (34.5)	116
1973	37	18	42 (21.0)	21	82 (41.0)	200
1974	66	35	63 (18.4)	38	140 (40.9)	342
1975	58	36	65 (19.6)	21	152 (45.8)	332
1976	71	12	80 (26.8)	11	125 (41.8)	299
1977	56	20	106 (32.1)	21	127 (38.5)	330
1978	34	28	123 (32.7)	25	166 (44.1)	376
1979	27	27	110 (29.1)	33	181 (47.9)	378
1980	3	3	14 (27.5)	2	29 (56.9)	51
Totals	415 (16.4)	225 (8.9)	614 (24.3)	226 (8.9)	1,050 (41.5)	2,530 (100.0)

[a] Diffuse vs. nodular and diffuse pattern designations were considered disagreement.

high as that obtained when they classified cases as nodular or nodular and diffuse NL (86.3%).

2) An improvement in designation diffuse pattern from 62.3% in 1972 to 80.8% in 1979 was noted.

Comparison of final diagnosis with contributor's diagnosis of diffuse NL (contributor's/final) (table 17).—The definition for each column of figures in this table is same as for table 14. This table shows that:

1) In diffuse NL, the contributor's pattern designation was confirmed in 65.8% of cases.
2) There has been an improvement in:
    a. Correct pattern designation from 41.4% in 1972 to 77% in 1979.
    b. Total agreement from 34.5% in 1972 to 47.9% in 1979.

The percentages of agreement for the subtypes of HD and NL are summarized in tables 18 and 19, respectively.

Agreement in percents for different histologic subtypes of HD when diagnoses of contributors and Regional Center are compared with final diagnosis (table 18).—This table shows that:

1) NS is the most reproducible (61.3% to 94.3% incidence of agreement) and LP is the least reproducible category (23.3% to 84% incidence of agreement).
2) When contributors mistakenly designated as NS cases not confirmed as such by the final diagnosis, these cases were most likely to have been classified as MC, as shown in table 8.
3) There is a significant difference in percent agreements between contributor's versus final diagnosis and Regional Center's versus final diagnosis.

Agreement in percents for different histologic subtypes of NL when diagnoses of contributor and Regional Center are compared with final diagnosis (table 19).—This table shows that:

1) PDN and HID, the two most common subcategories of NL, are the most reproducible with an incidence of agreement ranging from 46.3 to 95% for PDN and from 47.3 to 89% for HID.
2) MID and PDD are the least reproducible among the major categories. The incidence of agreement ranges from 18.9 to 80% for MID and from 31.7 to 80.5% for PDD.

TABLE 18.—*Agreement for different histologic subtypes of Hodgkin's disease when diagnoses of contributor and Regional Center are compared with final diagnosis*[a]

Histologic subtype	Comparison of No. of cases diagnosed							
	Final/contributor[b]		Contributor/final[c]		Final/Regional Center[d]		Regional Center/final[e]	
	No.	%	No.	%	No.	%	No.	%
LP	41/176	23.3	41/75	54.7	79/108	73.0	79/94	84.0
NS	912/1,088	83.8	912/1,487	61.3	1,616/1,714	94.3	1,616/1,730	93.4
MC	465/978	47.5	465/732	63.5	768/881	87.2	768/865	88.8
LD	84/205	41.0	84/191	44.0	186/229	81.2	186/224	83.0
All HD	1,523/2,953	51.6	1,523/2,644	58.2	2,747/3,080	89.2	2,747/3,105	88.5

[a] Comparisons exclude all cases without diagnosis by contributors.
[b] Based on data from table 6.
[c] Based on data from table 7.
[d] Based on data from table 8.
[e] Based on data from table 9.

TABLE 19.—*Agreement for different histologic subtypes of non-Hodgkin's lymphoma when diagnoses of contributor and Regional Center are compared with final diagnosis*[a]

Histologic subtype	Final/contributor[b]		Contributor/final[c]		Final/Regional Center[d]		Regional Center/final[e]	
	No.	%	No.	%	No.	%	No.	%
WDN	5/158	3.2	5/7	71.4	5/12	41.7	5/7	71.4
WDD	110/254	43.3	110/292	37.7	236/278	84.9	236/292	80.8
All ID[f]	6/29	20.7	6/45	13.3	24/56	42.9	24/45	55.6
PDN	518/644	80.4	476/1,027	46.3	966/1,017	95.0	940/1,027	91.5
PDD	216/682	31.7	216/467	46.3	376/479	78.5	376/467	80.5
PDY	36/56	64.3	78/257	30.4	184/202	91.0	210/257	81.7
All LC[f]	56/82	68.3	56/159	35.2	140/164	85.4	140/159	88.0
MIN	108/232	46.6	88/281	31.3	261/323	80.8	254/281	90.4
MID	47/249	18.9	47/170	27.6	136/222	61.3	136/170	80.0
MIY	11/25	44.0	31/123	25.2	81/102	79.4	88/123	71.5
HIN	34/105	32.4	21/69	30.4	70/93	75.3	57/69	82.6
HID	590/821	71.9	590/1,248	47.3	1,089/1,223	89.0	1,089/1,248	87.3
HIY	9/17	52.9	22/123	17.9	73/90	81.1	86/123	69.9
All BT[f]	33/47	70.2	33/51	64.7	44/53	83.0	44/51	86.3
All NB[f]	7/17	41.2	7/24	29.2	19/27	70.4	19/24	79.2
All UD[f]	21/74	28.4	21/88	23.9	64/100	64.0	64/88	72.7
All NL[g]	1,674/3,441	48.6	1,674/4,367	38.3	3,612/4,372	82.6	3,612/4,367	82.7

[a] N vs. Y pattern designation was considered agreement for categories WD, PD, MI, and HI.

[b] Based on data from table 10.

[c] Based on data from table 11.

[d] Based on data from table 12.

[e] Based on data from table 13.

[f] For this table, differences in pattern designation were not considered as disagreement in categories ID, LC, BT, NB, and UD since these are almost always diffuse.

[g] There are some questions whether N vs. Y designation represents true disagreement in the PD category. Some of the panel members do not consider the use of Y as a separate subcategory worthy of a special designation. However, in the analysis pertaining to "all NL" (last line of table) we have chosen to consider as disagreement every diagnostic designation that does not represent a complete agreement.

3) There is a significant difference in percent agreement between contributor's versus final diagnosis and Regional Center's versus final diagnosis.

Reproducibility of classification in HD and NL (table 20).—This table summarizes some of the findings mentioned above. The analysis confirms that *a*) difficulties persist in the diagnosis and classification of malignant lymphomas by contributors, *b*) the resulting disagreements in diagnosis can be lessened by a review by an experienced hematopathologist (Regional Center) and that *c*) disagreements can be further reduced by a central review process done by a panel of experts. It also reveals that reproducibility of diagnosis and classification for HD is better overall than for NL.

DISCUSSION

The importance of accurate diagnosis and classification of malignant neoplasms of the immune system is universally accepted. It is particularly important for the evaluation of clinical trials in which the histologic diagnosis plays an important role in the selection of an appropriate mode of therapy (*8*). Review of the histologic material by a pathologist is, in most instances, an initial step in the entry of patients into any of the protocols for clinical trial studies. This review process ensures not only that a correct diagnosis has been established but also that a patient population within a histologic subtype is homogeneous for evaluation and comparison of clinical results. It also identifies problems in diagnosis and classification that are not appreciated by pathologists who have limited exposure to such case material. It is, therefore, not surprising that the papers by Jones et al. (*9*) and Russell (*10*), in particular, emphasize the need of having the histopathologic material of all cases entered in major protocol studies reviewed by someone other than the original pathologist. It has also been recognized that accuracy of diagnosis and consistency in classification can be achieved better by a panel of experts than by individual pathologists with different degrees of expertise (*11*).

The creation of the Pathology Panel and Repository Center in 1967 (*1*) afforded the opportunity for two independent and separate review processes by a panel of expert hematopathologists in the clinical study of malignant lymphomas. This study, based on 8,915 cases accumulated since its inception, shows disagree-

TABLE 20.—*Reproducibility of classification in HD and NL*

Extent of agreement	Diagnosis	Final/contributor, %	Contributor/final, %	Final/Regional Center, %	Regional Center/final, %
Complete agreement	HD NL	48.6 51.6	38.3 58.2	82.6 89.2	82.7 88.5
Major disagreement	HD NL	27.3 16.7	35.5 7	8.7 3.8	9.5 2.9

ment on diagnosis and classification between contributors and experts and, to a lesser extent, among experts themselves, thus confirming the need for such a review process, as expressed by other investigators.

Of the total 8,915 cases, 3,105 (34.8%) were classified as HD and 5,061 (56.8%) as NL according to the final diagnosis (table 4).

In the HD group, NS was the most common type (1,730/3,105, 55.7%), although the incidence was not as high as reported in some series at individual institutions (*6, 12*). The relatively high number of unclassified cases (92/3,105, 6.2%) is, in part, attributable to the submission of histologic sections of either extranodal tissue or spleen only, without initial diagnostic biopsy. The most likely explanation for the different proportion of HD, which ranged from 20.3% to 44.2% of all cases in different study groups, was the level of activity of active protocols in the groups during the period under study (table 3).

The variation, however, in the incidence of each subtype of HD should be a true reflection of the study groups' patient populations since the same histologic criteria were utilized for all study group cases (table 3). It is of particular interest that pediatric patients with HD have higher incidences of LP and NS than do patients of all age groups with HD; this finding is based on cases submitted by IHDC and CCSG from trials limited to children. Reproducibility of classifying HD can be considered in different ways and levels of expertise. If one looks at the contributor's classification of HD and compares it with the final diagnosis (table 6), the agreement rate was 51.6% (1,523/2,953). NS was the most reproducible subtype and was confirmed in 83.8% of cases (912/1,088). Conversely, contributors designated only 61.3% (912/1,487) of all NS correctly, because they classified a considerable percentage of NS as MC. This misclassification may be due to their unawareness of the Ann Arbor criteria, (*13*) according to which all cases of HD should be classified as NS even if histologic features for NS can be identified only in focal areas. The diagnostically least reproducible category of HD proved to be LP, which was confirmed only in 23.3% (41/176). Most of the cases classified by the contributors as LP were changed to NS or MC. When one examines all cases of HD confirmed by the panel, the overall accuracy of the contributors' classification remains similar (1,523/2,644, 58.2%), but the LD category shows the lowest percentage of agreement because, in a significant number of cases, LD was considered by the contributors to be MC.

Of great importance are the cases listed under "major disagreement" in the above analysis of data. Such major disagreements occurred between contributors and the panel in 16.7% of the HD cases (494/2,953). Some misinterpretation or disagreement on the classification of malignant lymphoma is unavoidable even among experts. This fact is shown in tables 8 and 9, which compare the classification of the Regional Centers with that of the final diagnosis for HD. Although the incidence of complete agreement among panel members if appreciably higher, experts also have difficulties in the same areas. For example, the disagreement rate between the Regional Center diagnosis and final diagnosis with respect to LP and LD was also higher than that for NS and MC. NS was again the most reproducible classification, with an agreement rate of more than 93%. The agreements for different histologic subtypes of HD, when diagnoses of contributors and Regional Centers are compared with the final diagnosis, are summarized in table 18, expressed in percentages.

The NL comprised from 45% (509/1,132) for CALGB to 71% (147/207) for CCSG (table 3). Among the NL, PDN+PDY had the highest incidence (1,284/5,061, 25.4%); HID was next (1,248/5,061, 24.7%), followed by PDD (467/5,061, 9.2%). However, if lymphoblastic lymphoma (LC) is excluded from PDD, as is done in table 5, LC becomes the third or fourth most common form of NL in the years 1977–1979. It is not certain how much of the difference in the ratio of PDN+PDY to MIN+MIY among the different Regional Centers reflects a true difference in their incidence or a difference in the histologic criteria used. It is certain, however, that the different Regional Centers employ different criteria for classifying PDN or PDY versus MIN or MIY since, for example, the ratio for the ECOG cases changed from 3.9:1 to 8.5:1 with the change of the head of the Regional Center. This variation in the ratio of PDN+PDY versus MIN+MIY still exists even when the ratio is calculated according to the final diagnosis. This is due to the difficulty of establishing generally acceptable objective criteria for the distinction between these two subtypes short of actual counting of large and small cells. Hence, the Repository Center is reluctant to disagree with Regional Centers on this particular problem of classification. This may explain the different therapeutic results reported by different investigators when one compares the PDN+PDY and MIN+MIY groups (*14–16*).

The CCSG data shown in table 3 reaffirm the extreme rarity of nodular lymphomas in the pediatric age group. As expected, LC, BT, NB and UD accounted for the majority of the pediatric NL (122/147, 83%). Since their distinction is based on morphologic differences which are quite subtle even in histologic sections of the best possible technical quality, the high incidence of LC, BT, NB and UD makes it especially challenging to classify children's NL with the greatest possible precision.

With regard to the percentages of complete agreement, the results for NL are less favorable than those for HD. The contributor's diagnosis was verified as to both pattern and cytology in only 48.6% (1,674/3,441) of cases (table 10). In WDN, ID, PDD, MID, HIN and UD, the diagnoses of contributors were confirmed in less than 35% of the cases (table 19). In most instances, WDN was changed to PDN. When the comparison of reproducibility in NL was based on final diagnosis, the incidence of correct identification by the contributors of both pattern and cytology was even lower (1,674/

4,367, 38.3%) (tables 10 and 19). Major disagreements occurred with a higher percentage in NL (1,143/4,190), 27.3%) than in HD (494/2,953, 16.7%). Included among the major disagreements were NL versus HD, pattern disagreements, and good risk diagnosis versus poor risk diagnosis.

On the other hand, PDN and HID were confirmed most often by the panel (518/644, 80.4%, for PDN and 590/821, 71.9%, for HID) (table 19). This is significant inasmuch as PDN and HID combined represent 50% (2,532/5,061) of all NL. Among the experts, the agreement rates for PDN and HID were 95% and 89%, respectively. With the exception of WDN, ID, MID and UD, all categories showed agreement in more than 70% of the cases (tables 12 and 19). Major disagreement was also significantly less than when contributors' and Regional Center's diagnoses were compared. Nevertheless, major disagreements constituted 8.7% (table 12) to 9.5% (table 13), depending on how the diagnoses were compared. As far as correct pattern designation is concerned, contributors' diagnoses were more often confirmed in nodular or nodular and diffuse NL (86.3% agreement) than in diffuse NL (74.6% agreement). Tables 14 and 15 also indicate that the contributors fail to designate nodularity in a significant proportion of nodular NL (39.7%), although, when they classified NL as nodular, they usually were confirmed (86.3%). Tables 14-17, in which reproducibility of opinions on NL pattern and/or cytology is analyzed, show trends toward gradual improvement in the designation of pattern and/or cytologic subcategories. Whether this trend for improvement is due to an educational effort by the Pathology Panel and Repository Center for Lymphoma Clinical Studies is difficult to prove.

In summary, this comprehensive analysis shows that difficulties persist in the diagnosis and classification of malignant lymphomas by contributors. It confirms the findings of other studies based on some of the ECOG (*17*) and SWOG (*9*) material included in this study and on other case material (*18*). The resulting disagreements can be lessened appreciably by the review of a panel of experts. Our analysis reveals, in addition, that the same difficulties of diagnosis and classification exist, although to a lesser extent, among the experts themselves. The disagreement can be reduced further by a central review process aimed at a consensus for each case on which disagreement exists (table 20). This has been achieved by a process of reconciling differences in diagnosis and classification either by correspondence or during the annual meeting of all panel members.

REFERENCES

(*1*) DeVita VT, Rappaport H, Frei E. Announcement of formation of: The Lymphoma Task Force and Pathology Reference Center. Cancer 1968; 22:1087-1088.

(*2*) Lukes RJ, Butler JJ. The pathology and nomenclature of Hodgkin's disease. Cancer Res 1966; 26:1063-1081.

(*3*) Mann RB, Jaffe ES, Berard CW. Malignant lymphomas—a conceptual understanding of morphologic diversity. Am J Pathol 1979; 94:103-192.

(*4*) Nathwani BN. A critical analysis of the classifications of non-Hodgkin's lymphomas. Cancer 1979; 44:347-384.

(*5*) Nathwani BN, Kim H, Rappaport H. Malignant lymphoma, lymphoblastic. Cancer 1976; 38:964-983.

(*6*) Kaplan HS. Hodgkin's disease and other human malignant lymphomas: advances and prospects. G.H.A. Clowes Memorial Lecture. Cancer Res 1976; 36:3863-3878.

(*7*) Kaplan HS. Hodgkin's disease: Unfolding concepts concerning the nature, management and prognosis. Cancer 1980; 45:2439-2474.

(*8*) Coltman CA, Gams RA, Glick JH, Jenkin RD. Lymphoma. In: Hoogstraten B, ed. Cancer research. Impact of the cooperative groups. New York: Masson Publishing USA, Inc., 1980:39-84.

(*9*) Jones SE, Butler JJ, Byrne GE Jr, Coltman CA Jr, Moon TE. Histopathologic review of lymphoma cases from the Southwest Oncology Group. Cancer 1977; 39:1071-1076.

(*10*) Russell WO. The pathologic diagnosis of cancer—a crescendo of importance in current and future therapies. Ward Burdick Award Lecture. Am J Clin Pathol 1980; 73:3-11.

(*11*) Coppleson LW, Factor RM, Strum SB, Graff PW, Rappaport H. Observer disagreement in the classification and histology of Hodgkin's disease. J Natl Cancer Inst 1970; 45: 731-740.

(*12*) Dorfman RF. Relationship of histology to site in Hodgkin's disease. Cancer Res 1971; 31:1786-1793.

(*13*) Lukes RJ. Criteria for involvement of lymph node, bone marrow, spleen and liver in Hodgkin's disease. Cancer Res 1971; 31:1755-1767.

(*14*) Anderson T, Bender RA, Fisher RI, et al. Combination chemotherapy in non-Hodgkin's lymphoma: Results of long-term follow up. Cancer Treat Rep 1977; 61:1057-1066.

(*15*) Ezdinli EZ, Costello WG, Icli F, et al. Nodular mixed lymphocytic-histiocytic lymphoma (NM). Response and survival. Cancer 1980; 45:261-267.

(*16*) Jones SE, Fuks Z, Bull M, et al. Non-Hodgkin's lymphomas. IV. Clinicopathologic correlation in 405 cases. Cancer 1973; 31:806-823.

(*17*) Ezdinli EZ, Costello W, Wasser LP, et al. Eastern Cooperative Oncology Group experience with the Rappaport classification of non-Hodgkin's lymphomas. Cancer 1979; 43:544-550.

(*18*) Byrne GE Jr. Rappaport classification of non-Hodgkin's lymphoma: Histologic features and clinical significance. Cancer Treat Rep 1977; 61:935-944.

APPENDIX: LIST OF MEMBERS OF THE PATHOLOGY PANEL FOR LYMPHOMA CLINICAL STUDIES

Hun Kim, *M.D.*
Pathologist
Department of Anatomic Pathology
City of Hope National Medical Center
Duarte, California
and
Associate Adjunct Professor
Department of Pathology
University of California, Irvine
Medical Center
College of Medicine
Orange, California

John M. Bennett, *M.D.*[24]
Professor of Oncology in Medicine
Cancer Center of the University of Rochester Medical Center
Rochester, New York

Costan W. Berard, *M.D.*[24]
St. Jude Children's Hospital
Memphis, Tennessee

James J. Butler, *M.D.*[24]
M. D. Anderson Hospital and Tumor Institute
Houston, Texas

Gerald E. Byrne, Jr., *M.D.*[25]
University of Miami
Miami, Florida

Ronald E. Dorfman, *M.D.*[24]
Stanford University Medical Center
Stanford, California

Robert J. Hartsock, *M.D.*[25]
Allegheny General Hospital
Pittsburgh, Pennsylvania

Robert J. Lukes, *M.D.*[24]
University of Southern California School of Medicine
Los Angeles, California

Risa B. Mann, *M.D.*[25]
Johns Hopkins Hospital
Baltimore, Maryland

Richard S. Neiman, *M.D.*[25]
Mallory Institute of Pathology
Boston, Massachusetts

John W. Rebuck, *M.D., Ph.D.*[25]
Henry Ford Hospital
Detroit, Michigan

William W. Sheehan, *M.D.*[25]
University of Texas
Dallas, Texas

Daina Variakojis, *M.D.*[25]
University of Chicago
Chicago, Illinois

John F. Wilson, *M.D.*[25]
Primary Children's Medical Center
Salt Lake City, Utah

Henry Rappaport, *M.D.*
Chairman
Department of Anatomic Pathology
City of Hope National Medical Center
Duarte, California

---

[24] Consultant to the Pathology Panel for Lymphoma Clinical Studies.

[25] Member of the Panel and Regional Center Head of the Cooperative Study Group.

blank page

Maximizing Differences in the Concanavalin A-Induced Blastogenic Responses of Lymphocytes From Breast Cancer Patients and Controls by the Use of α-Methyl-D-mannoside [1,2,3]

John A. Distasio, [4] **David A. Cheresh,** [4] **Russell J. Schilder,** [4] **Charles L. Vogel,** [5]
Michael A. Silverman, [5,6] *and* **Diana M. Lopez** [4,7]

ABSTRACT—In an attempt to magnify differences in the immune responses of potentially immunosuppressed cancer patients and normal controls, an assessment was made on the effects of the competitive inhibitor α-methyl-D-mannoside on the concanavalin A (Con A)-induced blastogenic responses of lymphocytes from each of these populations. Lymphocytes from breast cancer patients with metastatic disease were significantly deficient in their capability to undergo blast transformation regardless of whether the monosaccharide inhibitor was added to the assay cultures. In contrast, lymphocytes from breast cancer patients who did not display metastatic disease were capable of normal blastogenic responses to Con A. The addition of α-methyl-D-mannoside to lymphocyte cultures caused a significantly greater inhibition of the blastogenic responses of these patients' cells as compared to cells of normal controls. Thus the monosaccharide seems to serve as a useful reagent for optimizing differences between lymphocyte blastogenic responses of normal donors and those of immunodepressed donors. The results suggest that lymphocytes from breast cancer patients without clinically evident metastases possess some modification of their cell membrane. One possibility discussed was that the number or distribution of receptors for Con A on the membrane of lymphocytes of these patients is deficient.—JNCI 1982; 68:69–74.

Evaluation of the immune status of cancer patients has been the subject of many studies (*1–6*). When assaying for cytotoxic responses, blastogenic transformation, delayed-type hypersensitivity reactions, and lymphokine production, some investigators have demonstrated reduced immunocompetence in these patients. In these studies, the cancer patient populations were usually heterogeneous, consisting of patients with advanced disease as well as those with no evidence of metastases. It has been much more difficult to show that cancer patients with early-stage disease are immunosuppressed.

Most investigations of immunocompetence have been performed with the use of optimal assay conditions in an attempt to maximize differences between normal donors and immunosuppressed patients. Fitzgerald (*7*) has demonstrated that by titrating the PHA dose used in a blastogenic assay, it was possible to maximize the difference in response between lymphoid cells from normal donors and those from an immunosuppressed patient with ataxia telangiectasia. In a more recent study, Bernhard et al. (*8*) reported on the effects of varying mitogen concentration and incubation time on the blastogenic responses of lymphocytes from normal donors and cancer patients. Significant differences between the two populations could be maximized when the blastogenic assay was performed with suboptimal concentrations of PHA-M and suboptimal incubation times. For Con A, maximal differences were obtained with optimal concentrations of mitogen and suboptimal incubation times. These investigators (*8*) were able to conclude that modification of assay conditions was useful in distinguishing between the blastogenic responses of normal donors and potentially immunodepressed donors.

Several other studies have been reported demonstrating that assays of immunocompetence performed under suboptimal conditions can be used to detect differences in the immunocompetence of normal individuals and cancer patients. West et al. (*9*) demonstrated that when the rosette assay between T-lymphocytes and sheep red blood cells was performed at elevated temperatures (high-affinity rosette assay), the proportion of RFC of normal adults differed significantly from that of patients with cancer. Specifically, when the assay was done at 20°C, 80% of the cancer

---

ABBREVIATIONS USED: Con A = concanavalin A; FCS = fetal calf serum; LSM = Lymphocyte Separation Medium; PHA = phytohemagglutinin; RFC = rosette-forming cells.

---

[1] Received February 20, 1981; accepted August 20, 1981.

[2] Supported by grant IN-51S from the American Cancer Society and by grants from the United Way and the Women's Cancer Association of the University of Miami.

[3] Research procedures were in accord with the ethical standards of the Human Assurance Committee, University of Miami School of Medicine.

[4] Department of Microbiology D4-4, University of Miami School of Medicine, P.O. Box 016960, Miami, Fla. 33101.

[5] Department of Oncology, University of Miami School of Medicine.

[6] *Present address:* 1399 S.W. 1st Ave., Suite 200, Miami, Fla. 33101.

[7] We thank Dr. Marc Saltzman and Dr. Julio Garcia (Miami) for providing some of the blood samples to perform these studies; Ms. Ileana Zapatero and Ms. Anna Salazar (University of Miami) who worked on this project as undergraduate research assistants; Ms. Dawn East, Ms. Chris Kahl, Ms. Darlene Padgett, and Ms. Margaret Szaro (University of Miami Hospitals and Clinics) for identifying suitable patients for our study, confirming clinical characteristics of patients, and blood drawing; Ms. Susan Hilsenbeck (Comprehensive Cancer Center for the State of Florida) for performing the statistical analyses; and Dr. Robert Duncan (University of Miami School of Medicine) for his helpful comments.

patients had normal levels of RFC, whereas when it was done at 29°C, 41 of 50 patients had significantly depressed proportions of RFC. Using this same assay, Quan and Burtin (*10*) obtained similar results. Moroz and co-workers (*11*) showed that cancer patients' peripheral blood mononuclear cells incubated in the presence of autologous serum had a reduction in RFC by as much as 20% compared to the RFC found among cells incubated in the presence of FCS. Ferritin bound to the surfaces of the cells was shown to be responsible for this reduction. When the same mononuclear cells were preincubated in FCS to remove ferritin, the patients' lymphocytes exhibited increased [^{3}H]thymidine incorporation after stimulation with mitomycin C-treated allogeneic lymphocytes. No increase was observed with lymphocytes from normal donors after cells were preincubated in FCS.

These studies support the concept that some modification of the cell membrane may exist on lymphocytes from cancer patients. The effects of this putative membrane alteration, however, could be observed only by use of suboptimal assay conditions to magnify these differences. Early events in lymphocyte activation appear to involve binding of lectin (e.g., Con A) followed by passive receptor movement resulting in cross-linking of receptor-lectin complexes (*12-14*). Titration of mitogens in blastogenic assays could be useful in the establishment of a concentration that would accentuate modifications in lectin binding. The results of the study by Bernhard et al. (*8*) as presented above may demonstrate this phenomenon. Receptor cross-linking has been shown to be highly dependent on lectin valence (*14-16*). To investigate changes in the capacity of receptor cross-linking that may ultimately affect activation of lymphocytes, one may find it useful to incorporate in the blastogenic assay mixture an agent that has the ability to alter mitogen valence. To explore this possibility, we examined the effects of the monosaccharide α-methyl-D-mannoside on Con A-induced blastogenesis. This sugar acts as a competitive inhibitor for Con A and thus limits the available number of lectin molecules for binding to membrane receptors. More importantly, the sugar binds to one or more of the four available sites on the Con A molecule (*17*) and effectively alters its valence. For our studies, we examined the effects of incorporating α-methyl-D-mannoside in lymphocyte cultures stimulated with Con A. We used a well-defined human breast cancer system in an attempt to avoid such variables as age of donors, effects of cytotoxic drug treatment, and effects of radiation. Our results confirm that suboptimal assay conditions as described by Bernhard et al. (*8*) magnify differences in the Con A-induced blastogenic responses of normal donors and breast cancer patients with metastatic disease, but not in those of patients without clinical evidence of metastases. The addition of α-methyl-D-mannoside to the assay, however, can accentuate differences in the blastogenic responses of lymphocytes from patients without clinical evidence of metastases and from normal controls.

MATERIALS AND METHODS

Patient population.—Before entry into this study, 33 women with breast cancer underwent the following staging procedures: complete medical history, physical examination, and blood and platelet counts; liver function tests; plasma carcinoembryonic antigen assay; chest X-ray; liver and bone radionuclide scans; and confirmatory bone X-rays of bone scan-positive areas. The patients were divided into two subpopulations. The first group consisted of patients with a recent mastectomy for stage II or III breast cancer and positive axillary nodes but no clinical evidence of distant disease. The second group consisted of patients with documented local, regional, or distant metastatic disease. This group was further subdivided into patients with no prior systemic therapy for cancer or none within the preceding year and patients who were treated with cytotoxic chemotherapy 1-6 months previously. Excluded from the study were patients who had received radiation therapy and patients with a history of diabetes mellitus, alcoholism, or any other chronic condition. It took approximately 1½ years to obtain enough patients to perform these studies. The group of women with no clinical evidence of distant metastatic disease consisted of 12 patients with a mean age of 53.3 years (range, 31-75 yr). The group with metastatic disease and no prior systemic therapy for at least 1 year consisted of 13 patients with a mean age of 57.5 years (range, 45-72 yr). The group with metastatic disease and prior cytotoxic chemotherapy 1-6 months before sampling consisted of 8 patients with a mean age of 62.0 years (range, 37-78 yr). For those patients without clinical evidence of metastatic disease, blood was obtained within 2 months of mastectomy. For those patients with metastatic disease, blood was obtained just before systemic therapy. Twenty-eight women with a mean age of 47.0 years (range, 25-73 yr) served as controls. These controls were selected from volunteers in the community who did not have an affiliation with the hospital community or prior history of cancer, who were free of disease, and who were not taking any drugs at that time. Information concerning each patient's stage of disease was withheld from those individuals performing the blastogenic assays until completion of the study.

Isolation of mononuclear cells.—Blood was obtained by venipuncture with the use of syringes containing sufficient heparin (The Upjohn Co., Kalamazoo, Mich.) to yield a final concentration of 100 U/ml of blood. Blood was diluted with an equal volume of sterile saline. Mononuclear cells were isolated by discontinuous density gradient centrifugation (*18*) with the use of LSM (Litton Bionetics Inc., Kensington, Md.). Diluted blood (20 ml) was layered over 15 ml of LSM. The gradients were spun at 400×g for 40 minutes at 19°C. Mononuclear cells were recovered from the interface and washed three times with RPMI-1640 growth medium (GIBCO, Grand Island, N.Y.) supplemented with 10% FCS, 100 U penicillin/ml, and 50 μg streptomycin/ml (Associated Biomedic Systems, Inc., Buffalo, N.Y.). Washed cells were pelleted by centrifugation for 10 minutes at 10°C.

Blastogenesis assay.—Cultures were set up in six replicates with the use of #3040 microtiter plates (Falcon Plastics, Los Angeles, Calif.). To each well was added 0.01 ml of Con A (Calbiochem-Behring Corp., Los Angeles) to yield a final concentration of 5 μg/ml and 0.01 ml of a solution of α-methyl-D-mannoside (GIBCO) to yield a final concentration of 0.875–56.0 mg/ml. To those cultures containing PHA-P (isolated from *Phaseolus vulgaris;* Difco Laboratories, Detroit, Mich.), 0.01 ml was added to yield a final concentration of 6.25 μg/ml. The monosaccharide solutions were sterilized by passage through a Swinnex assembly filter (Millipore Corp., Bedford, Mass.) containing a membrane with a pore size of 0.22 μm. Control cultures contained growth medium instead of mitogen, sugar, or both. Plates were sequentially incubated at room temperature for 15 minutes and at 37°C for 15 minutes. Then 0.18 ml of culture medium containing 1×10^5 mononuclear cells was added to each well. Cultures were incubated for 72 hours in a 5% CO_2, humidified atmosphere. Eighteen hours before being harvested, cultures were pulsed with 0.01 ml of [^{3}H]thymidine solution (50 μCi/ml). Harvesting was facilitated by a Skatron cell harvester (Flow Laboratories, Inc., Rockville, Md.). Cells were collected on #78-105-05 glass fiber filter paper (Flow Laboratories, Inc.) and lysed with water. Filter paper disks containing [^{3}H]DNA were placed in polyethylene vials with 5 ml of a scintillation cocktail of toluene containing 5 g 2,5-diphenyloxazole/liter and 0.2 g 2-(5-phenyloxazoly)-benzene/liter (Yorktown, Inc., Hackensack, N.J.). Vials were enumerated in a Tricarb scintillation counter (model 3330; Packard Instrument Co., La Grange, Ill.).

Only lymphocytes from patients with metastatic disease (untreated for >1 yr) were used in the studies to determine the concentrations of Con A and α-methyl-D-mannoside that would optimize differences between the blastogenic responses of lymphocytes from patients and normal controls. These patients were chosen, since most likely they would be immunodeficient. For each of these experiments, 5 patients and 5 normal controls were used.

Data are presented as the cpm of experimental cultures with Con A minus the cpm of control cultures without Con A. When experimental cultures contained sugar, so did the control cultures at the same concentration. The control cultures never had more than 1,000 cpm. Results were analyzed by computer with the use of the square root transformation of the data in a two-way analysis of variance. Data were considered significantly different at a value of $P<0.05$.

RESULTS

Con A blastogenic responses of lymphocytes from normal human donors and breast cancer patients.—The Con A blastogenic responses of lymphocytes from normal human donors and breast cancer patients with metastatic disease are compared in text-figure 1. The optimal responses for both groups were obtained at 5 μg Con A/ml. This same concentration of Con A resulted in maximal differences between the two populations of lymphocytes. All subsequent experiments were performed with 5 μg Con A/ml. A two-way analysis of variance with the square root-transformed data indicated that the blastogenic responses of the lymphocytes from normal donors and cancer patients were significantly different at concentrations of Con A ranging from 1.5 to 12 μg/ml.

Con A blastogenic responses of lymphocytes from normal human donors and breast cancer patients in the presence of α-methyl-D-mannoside.—The results of the con A-induced blastogenesis of lymphocytes from normal human donors and breast cancer patients with metastatic disease in the presence of α-methyl-D-mannoside are presented in text-figure 2. The blastogenic responses of lymphocytes from both groups were inhibited by the monosaccharide in a dose-dependent manner. The blastogenic responses of lymphocytes from the breast cancer patients, however, were more inhibited than were those of lymphocytes from normal donors at each of the concentrations of α-methyl-D-mannoside tested. Maximal discrimination between the two populations of lymphocytes was obtained at 3.5 mg/ml of the sugar.

Specificity of inhibition of the blastogenic response by α-methyl-D-mannoside.—The specificity of inhibition by α-methyl-D-mannoside of the blastogenic responses of lymphocytes from normal human donors and breast cancer patients with metastatic disease was examined. As much as 14 mg monosaccharide/ml did

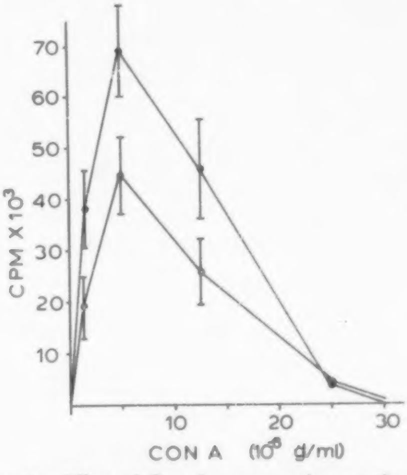

TEXT-FIGURE 1.—Effect of Con A concentration on the blastogenic response of lymphocytes from normal donors and breast cancer patients. For experimental details, *see* "Materials and Methods." ●, blastogenic responses of lymphocytes from normal donors; ○, blastogenic responses of lymphocytes from patients with metastatic disease and untreated for at least 1 yr. *Each point* represents the mean cpm, and *bars* indicate the standard error.

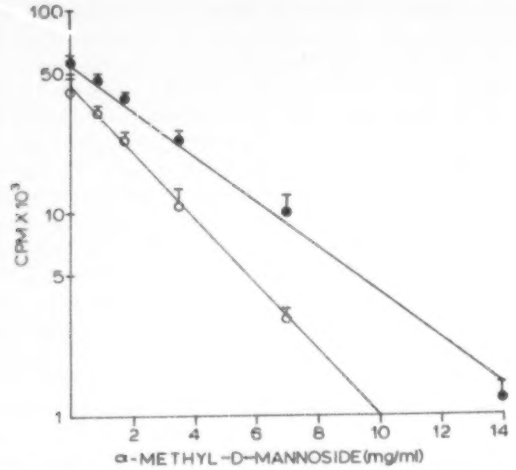

TEXT-FIGURE 2.—Effect of α-methyl-D-mannoside concentration on the blastogenic responses of lymphocytes from normal donors and breast cancer patients. Con A was used at a final concentration of 5.0 μg/ml of culture. For other experimental details, *see* "Materials and Methods." ●, blastogenic responses of lymphocytes from normal donors; ○, blastogenic responses of lymphocytes from patients with metastatic disease and untreated for at least 1 yr. *Each point* represents the mean cpm, and *bars* indicate the standard error.

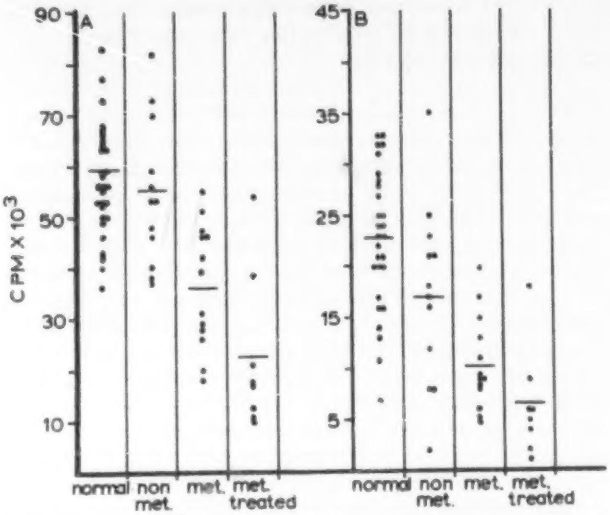

TEXT-FIGURE 3.—Effects of α-methyl-D-mannoside on the blastogenic responses of lymphocytes from normal donors and various groups of breast cancer patients. A) The individual blastogenic response when Con A was added to the culture and α-methyl-D-mannoside was omitted. B) The individual blastogenic response when Con A and α-methyl-D-mannoside were added to the culture. Con A was used at 5.0 μg/ml and α-methyl-D-mannoside at 3.5 mg/ml. For other experimental details, *see* "Materials and Methods." The abbreviations used were: non met., patients with no clinical evidence of metastases; met., patients with metastatic disease and untreated for at least 1 yr; met. treated, patients having metastatic disease and receiving cytotoxic chemotherapy within 1-6 mo of being tested.

not inhibit PHA-P-induced blastogenesis of lymphocytes from normal donors or from breast cancer patients (table 1), whereas it effectively inhibited Con A-induced blastogenesis. At higher concentrations of α-methyl-D-mannoside, inhibition did not seem to be specific, since PHA-P and Con A-induced blastogenesis were inhibited.

Inhibition of Con A-induced blastogenesis of breast cancer patients' lymphocytes by α-methyl-D-mannoside.—The Con A-induced blastogenic responses of lymphocytes from normal human donors and various breast cancer patients were determined in a replicate series of experiments with or without α-methyl-D-mannoside (text-fig. 3, table 2). The monosaccharide caused a greater inhibition in the blastogenic responses of lymphocytes from each of the patient groups as compared to lymphocytes from normal donors. Using the square root-transformed data in a two-way analysis of variance, we found a significant difference between the responses of normal lymphocytes and metastatic breast cancer patients' lymphocytes with or without the addition of sugar. This observation was true for patients with metastatic breast cancer who were not on any therapeutic regimen for more than 1 year and for those who were treated between 1 and 6 months before the experiments. In contrast, no significant difference was observed between the Con A-induced blastogenic responses of lymphocytes from normal donors and breast cancer patients without detectable metastases unless 3.5 mg α-methyl-D-mannoside/ml was added to the assay mixture.

TABLE 1.—*Specificity of inhibition of Con A-induced blastogenesis by α-methyl-D-mannoside*[a]

α-Methyl-D-mannoside, mg/ml	Normal donors[b]		Breast cancer patients[b]	
	PHA-P, cpm	Con A, cpm	PHA-P, cpm	Con A, cpm
0	69,875±4,433	57,014±4,272	44,768±9,624	40,745±6,073
0.875	72,866±5,990	46,083±3,592	48,969±6,548	31,989±5,177
1.75	71,266±6,924	37,843±2,372	51,406±6,180	23,530±4,615
3.5	70,847±7,303	23,248±2,507	44,473±4,828	11,095±2,527
7.0	76,666±7,504	10,124±2,044	56,292±8,704	3,080±676
14.0	85,406±7,276	1,232±281	56,991±10,191	661±277

[a] For experimental details, *see* "Materials and Methods."
[b] Results are expressed as mean cpm ± SE.

TABLE 2.—*Comparison of the percent inhibition of α-methyl-D-mannoside of the Con A-induced blastogenic responses of lymphocytes from normal donors and breast cancer patients*[a]

Donors[b]	Con A, cpm[c]	Con A and α-methyl-D-mannoside, cpm[c]
Normal	58,778±2,644	22,653±1,307
non met.	54,580±4,126 (92.9)	17,217±2,596[d] (76.0)
met.	35,972±3,521[d,e] (61.2)	10,392±1,312[d] (45.9)
met. treated	22,576±5,518[d] (38.4)	6,505±1,868[d] (28.7)

[a] For experimental details, *see* "Materials and Methods."

[b] non met., patients with no clinical evidence of metastases; met., patients with metastatic disease and untreated for at least 1 yr; met. treated, patients having metastatic disease and receiving cytotoxic chemotherapy within 1–6 mo of being tested.

[c] Results are expressed as mean cpm ± SE. *Numbers in parentheses* are percents of the control.

[d] The groups were statistically different at a value of $P<0.05$.

[e] For statistical analysis the square root-transformed cpm of the patients were compared to the transformed cpm of the normal controls.

DISCUSSION

Various assays have been used to assess the immunocompetence of cancer patients (*1–6*). These studies have demonstrated that cancer patients with metastatic disease usually have suppressed immune responses. Partly due to the inherent variability of the immune responses of humans (*19*), it has been more difficult, however, to demonstrate that patients with earlier stages of disease have impaired immunocompetence. In most studies the assays have been performed under optimal conditions to measure immune responsiveness. More recently, investigators have attempted to vary assay conditions to maximize differences between normal donors and cancer patients (*8–11*). In most of these studies the cancer population consisted of groups of patients who were not homogeneous with regard to the type of cancer they had or the stage of the disease. Using suboptimal incubation times and mitogen concentrations, Bernhard et al. (*8*) were able to maximize differences between the blastogenic responses of lymphocytes from controls and cancer patients hospitalized for primary cancer surgery. No statistical difference was obtained when the assays were performed under optimal conditions. The authors were unable, however, to conclude that the patients' lymphocytes were deficient in their blastogenic responses, since the difference in mean age between the normal donors and cancer patients was 24 years. Catalona et al. (*20*) showed that increasing age correlates with decreasing lymphocyte blastogenic response. Bernhard et al. (*8*) concluded that suboptimal assay conditions were useful in magnifying differences in the blastogenic responses of normal and immunodepressed donors.

Using optimal concentrations of Con A and suboptimal incubation times as established by Bernhard et al. (*8*), we were able to demonstrate that the lymphocytes from breast cancer patients with metastatic disease had significantly reduced blastogenic responses as compared to those found with lymphocytes from normal donors. Breast cancer patients without clinical evidence of metastases did not display such an immunodepression. Using the competitive inhibitor α-methyl-D-mannoside and suboptimal incubation times (*8*), we were able to demonstrate a statistically significant difference between the Con A-induced blastogenic responses of lymphocytes from normal human donors and breast cancers without clinical evidence of metastatic disease. Our results are not likely due to differences in age between the population groups, since the mean age of the cancer patients was 53 years and the mean age of the normal donors was 47 years. Thus the use of the competitive inhibitor α-methyl-D-mannoside in Con A-induced blastogenic assays serves as a sensitive method of magnifying differences in lymphocyte responses of normal donors and those of cancer patients who are potentially immunosuppressed.

We have several hypotheses to explain our observation that α-methyl-D-mannoside causes a greater inhibition of Con A-induced blastogenesis of breast cancer patients' lymphocytes than that of lymphocytes of normal donors. One explanation is that the receptor(s) for Con A are modified on the surfaces of lymphocytes from breast cancer patients. This modification may be a change in the average number of Con A receptors per cell, a change in the average affinity of the receptors, or a change in the number of cells bearing Con A receptors. Since lymphocytes from patients without clinical evidence of metastatic disease do not display decreased blastogenic responses when α-methyl-D-mannoside is omitted from the assay mixture, it is difficult to envisage that lymphocytes from these patients have a reduced number of receptors per cell or number of cells bearing receptors. In addition, less than 15% of mitogen receptors must be bound to mitogen to trigger blastogenesis (*21*). Thus it seems that a large change in the number of receptors per cell would have to exist for a significant reduction in the blastogenic response to occur. Moreover, in preliminary experiments with ^{125}I-labeled Con A, we have demonstrated that the average number of mitogen receptors and the average affinity for lectin are the same on lymphocytes from normal donors and breast cancer patients with metastatic disease.

Alternatively, Con A receptors may be redistributed on the membranes of lymphocytes from the breast cancer patient. While this redistribution has been documented for transformed cells (*22*) and for lymphoid tumors (*23*), it has not been demonstrated for any nonlymphoid cancers. Such a change could be the result of a serum factor binding to the membrane, altering membrane fluidity, and/or preventing cross-linking of ligand-receptor complexes, which might ultimately lead to an inhibition of the triggering mechanism of blastogenesis (*24, 25*). Dunlap et al. (*26*) showed that depression of Con A-induced blastogenesis occurs in cats bearing feline leukemia virus-induced lymphomas and correlated this depression to a decreased capability for Con A receptors to cap. This group of investigators (*27*) has also shown that the p15 protein of feline leukemia virus can similarly inhibit Con A receptor capping on normal human lymphocytes. We are presently examining properties of lymphoid membranes and serum factors from breast cancer patients to explain the decreased Con A-induced blastogenic responses of their lymphocytes in the presence of α-methyl-D-mannoside.

REFERENCES

(*1*) Jeejeebhoy HF. Immunological studies of women with primary breast cancer. Int J Cancer 1975; 15:867-878.

(*2*) Wanebo JH, Thaler HT, Hansen JA, et al. Immunologic reactivity in patients with primary operable breast cancer. Cancer 1978; 41:84-94.

(*3*) Nemoto T, Han T, Minowada J, Angkur V, Chamberlain A, Dao TL. Cell-mediated immune status of breast cancer patients: Evaluation by skin tests, lymphocyte stimulation, and counts of rosette-forming cells. J Natl Cancer Inst 1974; 53: 641-645.

(*4*) Stein JA, Adler A, Efraim SB, Maor H. Immunocompetence, immunosuppression and human breast cancer. Cancer 1976; 38:1171-1187.

(*5*) Dean JR, Connor R, Herberman RB, Silva J, McCoy JL, Oldham RK. The relative proliferation index as a more sensitive parameter for evaluating lymphoproliferative responses of cancer patients to mitogens and alloantigens. Int J Cancer 1977; 20:359-370.

(*6*) Rees JC, Rossio JL, Wilson HE, Minton JP, Dodd MC. Cellular immunity in neoplasia: Antigen and mitogen responses in patients with bronchiogenic carcinoma. Cancer 1975; 36: 2010-2015.

(*7*) Fitzgerald MG. The establishment of a normal human population dose-response curve for lymphocytes cultured with PHA (phytohaemagglutinin). Clin Exp Immunol 1971; 8:421-425.

(*8*) Bernhard MI, Pace RC, Unger SW, Wanebo HJ. The influence of incubation time and mitogen concentration on lymphocyte blastogenic response: Determination of conditions that maximize population differences. J Immunol 1980; 124: 964-968.

(*9*) West WH, Sienknecht CW, Townes AS, Herberman RB. Performance of a rosette assay between lymphocytes and sheep erythrocytes at elevated temperatures to study patients with cancer and other diseases. Clin Immunol Immunopathol 1976; 5:60-66.

(*10*) Quan PC, Burtin P. E-rosette-forming cells at 29°C: An assay for the evaluation of the immune status of cancer patients. Br J Cancer 1978; 38:606-611.

(*11*) Moroz C, Kupfer B, Giler S. Circulating T cell subset with a reversible E-rosette capacity in breast cancer and its role in cell mediated immunity. In: Quastel MR, ed. Twelfth international leukocyte culture conference. New York: Academic Press, 1979:869-876.

(*12*) Ashman RF. Membrane defects in the tolerant B cell. II. Mechanism of capping failure and reversal by antigen exposure. Cell Immunol 1979; 44:329-342.

(*13*) Nichols WS, Dunlap JO, Hebebrand LC, Mathes LE, Olsen RG. Feline lymphocytes: Observations on surface membrane concanavalin A receptor mobility. Am J Vet Res 1979; 40: 959-961.

(*14*) Greaves M, Janossy G. Elicitation of selective T and B lymphocyte responses by cell surface binding ligands. Transplant Rev 1972; 11:87-130.

(*15*) Edelman GM. Surface modulation in cell recognition and cell growth. Some new hypotheses on phenotypic alteration and transmembranous control of cell surface receptors. Science 1976; 192:218-226.

(*16*) Fraser AR, Hemperly JJ, Wang JL, Edelman GM. Monovalent derivatives of concanavalin A. Proc Natl Acad Sci USA 1976; 73:790-794.

(*17*) So LL, Goldstein IJ. Protein-carbohydrate interaction. XX. On the number of combining sites on concanavalin A, the phytohemagglutinin of the jack bean. Biochim Biophys Acta 1968; 165:398-404.

(*18*) Bøyum A. Separation of leucocytes from blood and bone marrow. Scand J Clin Lab Invest 1968; 21:9-29.

(*19*) Faguet GB. Lymphocyte responsiveness to phytohemagglutinin (PHA): Quantitative aspects and reproducibility. J Reticuloendothel Soc 1974; 16:114-121.

(*20*) Catalona WJ, Sample WF, Chretien PB. Lymphocyte reactivity in cancer patients: Correlation with tumor histology and clinical stage. Cancer 1973; 31:65-71.

(*21*) Faguet GB. Mechanisms of lymphocyte activation. II. Negative cooperativity in the binding of phytohemagglutinin (PHA) to its lymphocyte receptors. In: Eijsvoogel VP, Roos D, Zeijlemaker P, eds. Leukocyte membrane determinants regulating immune reactivity. New York: Academic Press, 1976:65-72.

(*22*) Nicolsen GL. Differences in topology of normal and tumor cell membranes shown by different surface distributions of ferritin-conjugated concanavalin A. Nature [New Biol] 1971; 233: 244-246.

(*23*) Ben-Bassat H, Goldblum N, Mitrani S, Klein G, Jahansson B. Concanavalin A receptors on the surface membrane of lymphocytes from patients with African Burkitt's lymphoma and lymphoma cell lines. Int J Cancer 1976; 17:448-454.

(*24*) Fanger MW, Hart DA, Wells JV, Nisonoff A. Requirement for cross-linkage in the stimulation of transformation of rabbit peripheral lymphocytes by antiglobulin reagents. J Immunol 1970; 105:1484-1492.

(*25*) Edelman GM, Yahara I, Wang JL. Receptor mobility and receptor-cytoplasmic interactions in lymphocytes. Proc Natl Acad Sci USA 1973; 70:1442-1446.

(*26*) Dunlap JE, Nichols WS, Hebebrand LC, Mathes LE, Olsen RG. Mobility of lymphocyte surface membrane concanavalin A receptors of normal and feline leukemia virus-infected viremic felines. Cancer Res 1979; 39:956-958.

(*27*) Hebebrand LC, Olsen RG, Mathes LE, Nichols WS. Inhibition of human lymphocyte mitogen and antigen response by a 15,000-dalton protein from feline leukemia virus. Cancer Res 1979; 39:443-447.

Value of Plasma α-1-Acid Glycoprotein Assay in the Detection of Human Colorectal Cancer: Comparison with Carcinoembryonic Antigen[1,2]

Clement Y-T. Chu, *M.D.,*[3] **Lilian T-Y, Lai,** *M.S.,*[3] *and* **Hari P. Pokala,** *M.D.*[3,4]

ABSTRACT—Plasma specimens assessed for carcinoembryonic antigen (CEA) in the clinical laboratory for the detection of colorectal cancer were simultaneously assayed in our laboratory for α-1-acid glycoprotein (α_1AG), by means of a solid-phase enzyme-linked immunosorbent assay we developed. In 28 patients with colorectal cancer of Dukes A, B, and C classes, elevated levels of α_1AG were seen in 12 and of CEA in 8. In 44 patients with distant metastasis (Dukes D lesions), elevated plasma levels of α_1AG were seen in 29 and of CEA in 34. No statistical differences in the detection rate were found among these markers in these 2 groups of patients. In 33 cases of nonneoplastic disease involving the large bowel, elevated plasma levels of α_1AG were seen in 6, and elevated CEA levels were seen in 7. There was no statistical difference of false positive rates among these two markers. Elevated plasma levels of either CEA or α_1AG were found in 57 cases of colorectal cancer. This preliminary study suggests that the sensitivity of the plasma α_1AG assay is similar to that of the CEA assay in the detection of colorectal cancer. The combination of these two assays increases the detection rate of colorectal cancer significantly.—JNCI 1982; 68:75–79.

α_1AG is a low molecular weight (approximately 40,000) plasma glycoprotein containing 45% carbohydrate in the moiety (*1*). It has been isolated from the plasma in pure form (*2-4*). The structure of its carbohydrate portion and amino acid sequence have been elucidated (*5, 6*). The function of this protein in pathophysiological states is not yet completely known, but recent studies have suggested that it may participate in the modulation of the immunologic response (*7, 8*).

Several studies of changes in plasma levels of α_1AG have been reported (*9-11*). Recently, attention has gradually shifted to the elevation of plasma α_1AG in neoplastic diseases (*12-16*). A preliminary study on the plasma levels of α_1AG in colorectal cancer has been reported by our group previously in abstract form (*17*). In the present study we evaluate the use of plasma α_1AG assay in the detection of colorectal cancer in symptomatic patients and compare its value with that of CEA.

MATERIALS AND METHODS

Aliquots of plasma specimens sent by physicians for CEA assays were obtained from the Clinical Chemistry Department of the Harper-Grace Hospital and were assayed for α_1AG. The clinical records were reviewed without knowledge of results of α_1AG assay. The diagnosis of colorectal cancer in all cases was established histologically. All patients in whom cancer was excluded had complete clinical studies including thorough physical examination, roentgenological study, radioisotope scanning, and in some instances, endoscopic procedures. In those patients in whom cancer was excluded, the major diagnosis was taken as the "diagnosis." There were 72 cases of colorectal cancer studied, including 28 cases with Dukes A, B, and C lesions. Blood samples of these patients were obtained before resection. Another 44 patients, designated as the Dukes D group, had cancer that extended beyond the bowel wall and invaded the contiguous organs or had distant metastases. Blood samples of these 44 patients were taken at least 1 month after the exploratory operations, or after cessation of chemotherapy for more than 1 month and radiation for 3 months. Among the specimens studied, 33 were ultimately proven to be obtained from patients with nonneoplastic diseases involving the large bowel.

A solid-phase enzyme-linked immunosorbent assay developed in this laboratory (*18*) was used to assay plasma α_1AG. In measuring plasma α_1AG levels of 62 normal healthy individuals (aged 18–61), with the exclusion of females who were on oral contraceptives or estrogen compounds, a value of 0.67 ± 0.20 mg/ml (means±SD) was obtained. Since α_1AG values were distributed in the Gaussian fashion (text-fig. 1), the normal range of plasma α_1AG for the healthy population was estimated as 0.27–1.07 mg/ml (mean±2SD). Plasma α_1AG level exceeding 1.07 mg/ml was considered as elevated. This assay has an intra-assay coefficient of variation under 6% and interassay coefficient of variation under 8%.

The CEA assay was performed by the Clinical

ABBREVIATIONS USED: α_1AG = α-1-acid glycoprotein; CEA = carcinoembryonic antigen.

---

[1] Received March 23, 1981; accepted August 28, 1981.

[2] Supported by a grant from the Skillman Foundation of Detroit, Mich.

[3] Department of Medicine, Wayne State University of Harper-Grace Hospital, 3990 John R., Detroit, Mich. 48201.

[4] We thank Dr. George Fisher and his colleagues in the Clinical Chemistry Department of Harper-Grace Hospital for performing the CEA assay and Ms. Cindy Sulad for the preparation of the manuscript.

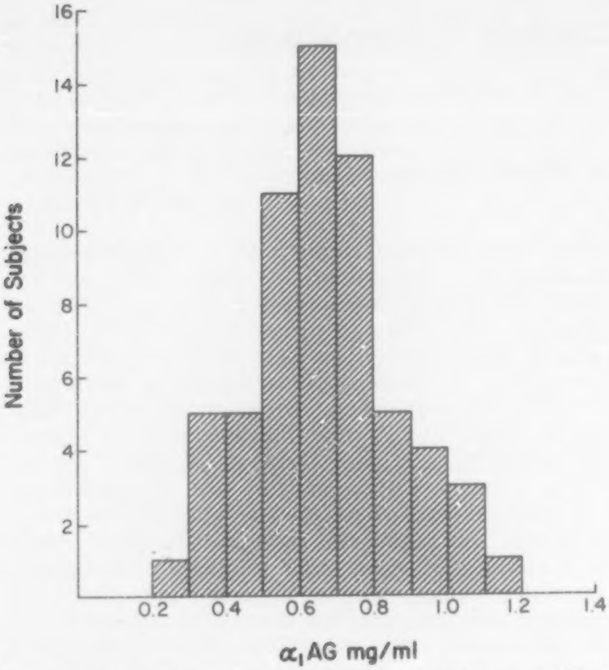

TEXT-FIGURE 1.—Distribution of plasma α_1AG values in healthy subjects.

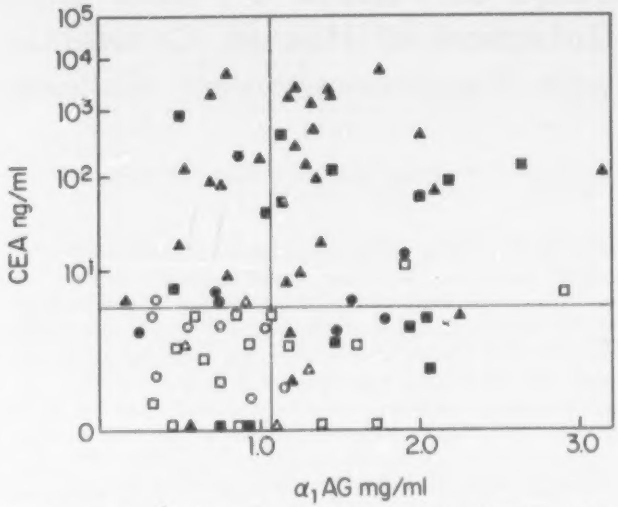

TEXT-FIGURE 2.—Plasma levels of α_1AG and CEA in 8 patients with benign colon polyps, ○, and in 72 patients with colon cancer at different patologic stages. — Dukes classification: A, △; B, □; C, ●. Liver metastasis, ▲; distal metastasis without liver metastasis, ■.

Chemistry Department of the Harper-Grace Hospital using the CEA kits® (Hoffmann-La Roche Inc., Nutley, N.J.) and the assay procedure suggested by the manufacturer (Hansen's Z-gel assay). The upper normal limit was set at 5 ng/ml since 95% of the healthy individuals of the general population have plasma CEA below this level (*19*), and this cut-off point was considered to be appropriate by many investigators (*20-24*).

Analysis of variance and multiple comparison tests were performed with the use of a Hewlett-Packard HP97 calculator and programmed tapes, the rest of the statistical tests were done by standard statistical methods.

RESULTS

The distribution of elevated plasma α_1AG and CEA values in colorectal cancer patients is shown in text-figure 2. Among the 72 patients, elevated plasma levels of both α_1AG and CEA were seen in 26, elevated plasma levels of α_1AG alone in 15, and of CEA alone in 16. There were no statistical differences between the detection rates in α_1AG (41/72) and CEA (42/72). In 16 cases plasma levels of neither α_1AG or CEA were elevated.

The frequency of elevated plasma levels of α_1AG or CEA in colorectal cancer patients with different pathologic stages are shown in table 1. In the potentially curable Dukes A, B, and C lesions, elevated plasma levels of α_1AG alone were seen in 8 of 28 cases and CEA alone in 4 of 28. In patients with Dukes D lesion, elevated plasma levels of α_1AG alone were seen in 7 of 44 cases and CEA alone in 12 of 44 cases. There was no statistically significant difference among the positive rates of α_1AG and CEA in the potentially curable lesions ($P>0.317$) or in Dukes D lesion ($P>0.317$), analyzed by the McNemar test. Mean values of α_1AG and CEA in different pathologic stages are shown in table 2. Analysis of variance revealed that there was no statistically significant difference among mean values of α_1AG in the different pathologic stages. However, the difference became apparent when the mean value of α_1AG from normal control group was added ($F=12.40$, significant at the $P<0.01$ level). Multiple comparison tests revealed that mean plasma values of patients with Dukes B, C, and D lesions were significantly different from that of a normal healthy control group (table 3).

Correlations of plasma levels of α_1AG and CEA are

TABLE 1.—*Frequency of elevated plasma levels of α_1AG and CEA in colorectal cancer of different pathologic stages*

Dukes classification	No. of patients	Patients with elevated plasma level		
		α_1AG alone	CEA alone	α_1AG and CEA
A	4	2	1	0
B	16	4	0	2
C	8	2	3	2
D, liver (−)[a]	15	4	3	6
D, liver (+)[b]	29	3	9	16
Total	72	15	16	26

[a] Without liver metastasis.
[b] With liver metastasis.

TABLE 2.—*Mean values of plasma α_1AG and CEA in different pathologic stages of colorectal cancer*

Dukes classification	No. of patients	Plasma level, mean ± SD	
		α_1AG, mg/ml	CEA, ng/ml
A	4	0.96±0.33	2.58±2.24
B	16	1.11±0.67	3.11±2.69
C	8	1.13±0.55	29.25±65.04
D	44	1.28±0.62	562.03±1,169.70
Normal	62	0.67±0.20	Not available

TABLE 4.—*Correlations of plasma levels of α'AG and CEA[a] in different pathologic stages of colorectal cancer*

Dukes stage	No. of patients	*t*-value	*P*
A, B, C	28	−0.17	>0.05
D, liver (+)[b]	29	0.01	>0.05
D, liver (−)[c]	15	0.01	>0.05
Total D	44	0.003	>0.05

[a] Plasma CEA levels had logarithmic transformation.

[b] With liver metastasis.

[c] Without liver metastasis.

shown in table 4. There was no correlation of plasma levels of α_1AG and CEA in either of the Dukes A, B, C, or D groups, regardless of the presence or absence of liver metastasis in group D.

Among 44 patients with Dukes D lesions, 29 had liver metastasis detected by radioisotope scanning and 15 had no liver metastasis. Plasma α_1AG levels among these 2 subgroups were not statistically different, plasma CEA levels however, were significantly different (table 5).

Frequency of false-positive tests of α_1AG and CEA in nonneoplastic colorectal diseases are shown in table 6. Plasma specimens of 33 symptomatic patients in whom colorectal cancer could not be completely ruled our clinically, were assayed for CEA, and the final diagnosis was nonneoplastic colorectal disease. Among these 33 cases elevated plasma levels of CEA alone were found in 5 and of α_1AG in 4 (table 6). The difference was not statistically significant.

The accuracy of the plasma α_1AG and CEA assays to discriminate between colorectal cancer and nonneoplastic colorectal diseases was statistically evaluated by the chi-square test with Yate's correction for small member samples. We obtained almost identical results with the α_1AG and the CEA assays (tables 7, 8). The discrimination of cancer and nonneoplastic diseases in both assays all reach highly significant levels ($P<0.001$).

When plasma α_1AG assay is performed in addition to CEA assay, the sensitivity of detecting colorectal cancer increases significantly without an increase in the number of misclassifications (table 9).

DISCUSSION

Early studies on the changes of α_1AG level in the plasma in various pathologic conditions stressed the changes seen in acute inflammation and severe surgical trauma. Hence, α_1AG was classified as one of the "acute phase proteins." The potential of using α_1AG in cancer diagnosis was apparently overlooked. In the evaluation of the diagnostic potential of plasma α_1AG assay in cancer, we chose colorectal cancer as the model because colorectal cancer has been the subject of intensive research in the tumor marker studies. We also elected to assay CEA concomitantly for comparison, since the CEA assay had been used extensively in the detection of colorectal cancer. The results suggest that plasma α_1AG assay has a sensitivity similar to that of CEA in the detection of colorectal cancer (table 1). This is true regardless of whether the cancer is an operable Dukes A, B, or C lesion, or an inoperable Dukes D lesion. Mean plasma α_1AG levels increase gradually with the progression of the pathologic stages (table 2). Although simultaneously elevated plasma levels of α_1AG and CEA are frequently seen among patients, α_1AG appears to be a marker independent of CEA (table 4). The actual plasma levels of CEA in Dukes D lesions with liver metastasis were higher than in those without hepatic metastasis, even though the percentage of patients who had elevated levels of CEA did not change (table 5). However, hepatic metastasis does not cause an augmented elevation of plasma α_1AG level in colorectal cancer patients in spite of the fact that α_1AG is synthesized by the liver.

To evaluate a test in detecting colorectal cancer from symptomatic patients, false-positive tests that occur in some nonneoplastic colorectal diseases must be taken into account. In this series, 33 patients who presented with rectal bleeding, constipation, roentgenographic polypoid lesions and stenosis mimicking colorectal cancer, were ultimately proven to be suffering from

TABLE 3.—*Multiple comparison tests of the mean values of plasma α'AG among healthy control subjects and colorectal cancer patients in different pathologic stages*

Controls compared to cancer patients with Dukes classification:	Degree of freedom	*t*-value	*P*
A	64	1.74	>0.05
B	76	2.60	<0.02[a]
C	68	2.35	<0.025[a]
D	104	6.23	<0.001[a]

[a] Statistically significant.

TABLE 5.—*Plasma levels of α'AG and CEA in Dukes D lesion with or without liver metastasis*

Marker	Degree of freedom	*t*-value	*P*
α_1AG	42	1.2214	>0.2
CEA	42	2.48	<0.02[a]

[a] Statistically significant.

TABLE 6.—*Frequency of elevated plasma levels of α_1AG and CEA in nonneoplastic colorectal diseases*

Diagnosis	No. of patients	Patients with elevated plasma level		
		CEA alone	α_1AG alone	CEA and α_1AG
Benign colonic polyp	8	1	1	0
Diverticulosis	8	3	0	0
Diverticulitis	2	0	1	1
Hemorrhoid	3	1	1[a]	0
Chronic inflammatory bowel disease	11	0	1	1
Radiation proctitis	1	0	0	0
Total	33	5	4	2

[a] With acute thrombosis.

TABLE 7.—*Chi-square analyses[a] comparing colorectal cancer to nonneoplastic disease based on the results of plasma α_1AG assay*

Test results	No. of patients with:	
	Colorectal cancer	Nonneoplastic disease
Positive	41	6
Negative	31	27

[a] $\chi^2=12.23$; $P<0.001$; sensitivity = 0.57; specificity = 0.82; misclassified cases = 0.35.

TABLE 8.—*Chi-square analyses[a] comparing colorectal cancer to nonneoplastic disease based on the results of plasma CEA assay*

Test results	No. of patients with:	
	Colorectal cancer	Nonneoplastic disease
Positive	42	7
Negative	30	26

[a] $\chi^2=11.31$; $P<0.001$; sensitivity = 0.58; specificity = 0.79; misclassified cases = 0.35.

TABLE 9.—*Chi-square analyses[a] comparing colorectal cancer to nonneoplastic diseases based on a positive result of plasma α_1AG Assay or CEA Assay*

Test results	No. of patients with:	
	Colorectal cancer	Nonneoplastic disease
Positive	57	11
Negative	15	22

[a] $\chi^2=18.87$; $P<0.001$; sensitivity = 0.79; specificity = 0.67; misclassified cases = 0.25.

nonneoplastic diseases. In this group false-positive tests for CEA were seen in 7 of 33 patients (21%), and α_1AG in 6 of 33 (18%). With the true-positive and false-positive tests in mind, results were analyzed by the chi-square test. It was found that the abilities of these 2 assays in discriminating colorectal cancers and nonneoplastic diseases were very high, $P<0.001$ for both (tables 7 and 8). These results suggest that both α_1AG and CEA assay can be used effectively to detect colorectal cancer in symptomatic patients.

On the basis of observations of multiple tumor markers produced by tumor cells, simultaneous assays of several markers to achieve a greater sensitivity in tumor detection have been recently proposed (*25-27*). Whether a combination of two or more markers brings an improvement in the sensitivity and specificity of cancer detection requires careful study. In this study, we have shown that if both α_1AG and CEA assays are performed, the detection rate of colorectal cancer increases from 58 to 79% ($P<0.01$). Although the specificity will drop from 79 to 67%, the difference is not significant ($P>0.10$). The overall result of this combination is that the sensitivity in cancer detection increases significantly and yet the percentage of misclassified cases does not increase significantly (table 9).

Since there are no correlations of plasma α_1AG and CEA levels in any of the pathologic stages (table 4), plasma levels of α_1AG and CEA represent different parameters. Because of this, the combination of these two assays is not redundant.

In recent years, the major applications of tumor marker assays have been in monitoring the response of tumor to chemotherapy and in detecting early recurrences after tumor resection (*28-31*). Since the combinations of plasma α_1AG and CEA assay increase the detection rate of localized, Dukes A, B, and C, colorectal cancers from 29 to 57% ($P<0.046$), it seems logical to use this combination in the detection of recurrence after tumor resection. Our recent studies also suggested that changes of plasma α_1AG levels correlated well with responses to chemotherapy in cancers of the head and neck (*32*) as well as in metastatic cancer of the stomach (Chu CY-T, Rashid S, Lai LT-Y: Unpublished observation). The study of using serial plasma α_1AG measurements to monitor the response of colorectal cancer to chemotherapy seems warranted.

REFERENCES

(*1*) SCHMID K. α_1-Acid glycoprotein. In: Putnam FW, ed. The plasma proteins. Vol 1. New York: Academic Press, 1975:183-228.

(*2*) WEIMER HE, MEHL JW, WINZLER RJ. Studies on the mucoproteins of human plasma; isolation and characterization of a homogeneous mucoprotein. J Biol Chem 1950; 185:561-568.

(*3*) SCHMID K. Preparation and properties of serum and plasma proteins. XXIX. Separation from human plasma of polysaccharides, peptides, and protein of low molecular weight. Crystallization of an acid glycoprotein. J Am Chem Soc 1953; 75:60-68.

(*4*) HAO Y-L, WICKERHAUSER M. Development of large-scale fractionation methods. IV. A simple method for the large-scale preparations of alpha$_1$-acid glycoprotein. Biochem Biophys Acta 1973; 322:99-108.

(*5*) SCHWARZMANN GO, HATCHER VB, JEANLOZ RW. Purification and structural elucidation of several carbohydrate side chains from alpha-1-acid glycoproteins. J Biol Chem 1978; 253:6983-6987.

(*6*) SCHMID K. Structure of α_1-acid glycoprotein. The complete amino acid sequence, multiple amino acid substitutions, and homology with immunoglobulins. Biochemistry 1973; 12: 2711–2724.

(*7*) Chiu KM, Mortensen RF, Osmand AP, Gewurz M. Interactions of alpha-1-acid glycoprotein with the immune system. Immunology 1977; 32:997–1005.

(*8*) Bennett M, Schmid K. Immunosupression by human plasma α_1-acid glycoprotein: Importance of the carbohydrate moiety. Proc Natl Acad Sci USA 1980; 77:6109–6113.

(*9*) Easton EA, Hardwicke J, Whitehead PH. The estimation of two alpha-1-glycoproteins (orosomucoid and another alpha-1-acid glycoprotein) in health and disease. J Clin Pathol 1962; 15:585–590.

(*10*) Crockson RA, Payne CJ, Ratcliff AP, Soothill JF. The sequence of acute phase reactive proteins following surgical trauma. Clin Chim Acta 1966; 14:435–441.

(*11*) Werner M. Serum protein changes during the acute phase reaction. Clin Chim Acta 1969; 25:299–305.

(*12*) Snyder S, Ashwell G. Quantitation of specific serum glycoproteins in malignancy. Clin Chim Acta 1971; 34:449–455.

(*13*) Rudman D, Treadwell P, Vogler WR, et al. Abnormal orosomucoid in the plasma of patients with neoplastic disease. Cancer Res 1972; 32:1951–1959.

(*14*) Ward AM, Cooper EH, Turner R, Anderson JA, Nevilla AM. Acute-phase reactant protein profiles: An aid to monitoring large bowel cancer by carcinoembryonic antigen and serum enzymes. Br J Cancer 1977; 35:170–178.

(*15*) Hollinshead HC, Chuang CY, Cooper EH, Catalona WJ. Interrelationship of pre-albumin and α_1-acid glycoprotein in cancer sera. Cancer 1977; 40:2993–2998.

(*16*) Wolf GT, Chretien PB, Elias EG, et al. Serum glycoproteins in head and neck squamous carcinoma. Am J Surg 1979; 138:489–500.

(*17*) Chu CY-T, Wang H-P. Plasma α_1-acid glycoprotein levels in colorectal cancers. Gastroenterology 1979; 76:1114.

(*18*) Wang H-P, Chu CY-T. A solid-phase enzyme-linked immunosorbent assay for the quantitation of human plasma α_1-acid glycoprotein. Clin Chem 1979; 25:546–549.

(*19*) Hansen HJ, Snyder JJ, Miller E, et al. Carcinoembryonic antigen (CEA) assay: A laboratory adjunct in the diagnosis and management of cancer. Hum Pathol 1974; 5:139–147.

(*20*) Concannon JP, Dalbow MM, Lieber GA, Blake KE, Weil CS, Cooper JW. The carcinoembryonic antigen assay in bronchogenic carcinoma. Cancer 1974; 34:184–192.

(*21*) Go VL. Carcinoembryonic antigen clinical application. Cancer 1974; suppl 37:184–192.

(*22*) Silverman NA, Alexander JC, Chretian PB. Carcinoembryonic antigen levels in head and neck cancer. Cancer 1976; 37: 2104–2111.

(*23*) Bender RA, Weintraub BD, Rosen SW. Prospective evaluation of two tumor-associated proteins in pancreatic adenocarcinoma. Cancer 1979; 43:591–595.

(*24*) Brooks WS, Hersh T, Hall EC, Moore C. Carcinoembryonic antigen as a diagnostic adjunct in cancer of the gastrointestinal tract. In: Lehmann F-G, ed. Carcino-embryonic proteins. Vol I. Amsterdam: Elsevier/North-Holland, 1979:41–49.

(*25*) Rees LH, Bloomfield GA, Rees GM. Multiple hormones in a bronchial tumor. J Clin Endocrinol Metab 1974; 38:1090–1097.

(*26*) Neville AM, Cooper EH. Biochemical monitoring of cancer: A review. Ann Clin Biochem 1976; 13:283–305.

(*27*) McIntire KR. Use of multiple immunoassays for circulating tumor markers. In: Herberman R, McIntire KR, eds. Immunodiagnosis of cancer. Vol I. New York: Marcel Dekker, 1979: 521–538.

(*28*) Al-Sarraf M, Baker L, Talley R, Kithier K, Vaitkevicius VK. The value of serial carcinoembryonic antigen in predicting response rate and survival of patients with gastrointestinal cancer treated with chemotherapy. Cancer 1979; 44:1222–1225.

(*29*) Mach JP, Jaeger P, Bertholet MM, Ruegsegger C-H, Lorsi RM, Pettavel J. Detection of recurrence of large-bowel carcinoma by radioimmunoassay of circulating carcinoembryonic antigen. Lancet 1974; 2:535–540.

(*30*) Herrera MH, Chu TM, Holvoke ED. Carcinoembryonic antigen as a prognostic and monitoring test in clinically complete resection of colorectal carcinoma. Ann Surg 1976; 183:5–9.

(*31*) Martin EW, James KK, Hurtubise PE, Catalano P, Minton JP. The use of carcinoembryonic antigen as an early indicator for gastrointestinal recurrence and second-look procedure. Cancer 1977; 34:440–446.

(*32*) Al-Sarraf M, Chu CY-T, Lai LT, et al. Multiple tumor markers in monitoring patients with epidermoid cancer of the head and neck. (Abstr) Proc Am Assoc Cancer Res 1981; 22:285.

blank page

Various Isozyme Gene Expression Patterns Among Human Colorectal Adenocarcinoma Cell Lines and Tissues[1,2,3]

Lynne P. Rutzky[4] *and* **Michael J. Siciliano**[5]

ABSTRACT—Seven tissue-specific isozymes—lactate dehydrogenases A and B (LDHA and LDHB), esterases B2 and A4 (ESB2 and ESA4), creatine kinase B (CKB), and red blood cell and tissue forms of adenosine deaminases (ADA)—were examined in the human adenocarcinoma cell line LS174T and its subclones grown under a wide variety of conditions. Strong expressions of ESB2, ESA4, and CKB were stable in all material studied, as was a greater expression of LDHA than of LDHB. ADA isozyme expression varied with culture conditions. Identical expression of the five stable isozymes was observed in six surgical specimens of normal bowel mucosa, while cell lines derived from normal mucosa varied in the expression of these isozymes. An additional 23 colorectal cell lines, derived from primary or metastatic adenocarcinomas in different stages of invasiveness and differentiation from 18 individuals, were verified as to their origin by genetic signature analysis and similarly studied for isozyme expression. These lines had different, yet stable, gene expression patterns similar to differences observed among six adenocarcinoma surgical specimens. These differences could not be related to the number of passages that the cell lines were in culture nor to the stages of the tumors at the time that the cell lines were initiated or surgical samples tested. Gene expression patterns in adenocarcinomas differed, these differences might have been due to the origin of colorectal adenocarcinomas from different cell types within a heterogeneous mucosa, and tne colorectal cell lines studied represented appropriate models for colon cancer.—JNCI 1982; 68:81-90.

Until recently, the difficulties encountered in studying viable colon cancer tissue such as heterogeneous populations, microbial contamination, necrosis, and insufficient viable cells impeded an understanding of its biology and possible treatment. Cultured cell lines ameliorate many of the problems. Although human colon tumors have been refractory to in vitro propagation, several cell lines (*1-7*) are now available for investigation of the unique biological, biochemical, and immunological properties of the disease.

To be relevant and useful, cell lines must be continuously evaluated for genetic integrity and maintenance of stable neoplastic properties. During the last 5 years, one set of cell lines, LS180 and its trypsinized variant LS174T (*6*), have been monitored for growth properties, carcinoembryonic antigen production (*8-10*), and karyology (*11*).

In the present study, we examined 24 colorectal tumor cell lines derived from 18 individuals for 13 electrophoretically polymorphic loci to establish their genetic signatures (*12-14*) and to verify their independent genetic origin and freedom from HeLa contamination (*15*). LS174T (our reference line) and its subclones were studied for the expression of seven tissue-specific isozymes after growth under a variety of conditions. Five isozymes were found to be stably expressed in the line and all its subclones. The expression of these isozyme loci was then compared to other colorectal tumor lines, cell lines derived from normal bowel mucosa, and six paired normal bowel and colon adenocarcinoma surgical specimens. Results indicate that the patterns of gene expression in LS174T and certain other tumor lines reflect those of normal bowel mucosa. Other colorectal tumor cell lines may have different, yet stable, patterns, which were also observed among the six adenocarcinoma surgical specimens. These differences could not be related to the number of passages the cell lines were cultured nor to the differentiated or disseminated state of the tumors the time that cell lines were initiated or surgical samples were studied. The possibility that different expressional patterns are due to the origin of colon adenocarcinomas from one of several cell types within a heterogeneous mucosa is discussed.

MATERIALS AND METHODS

Cell cultures.—Cell lines LS180 and LS174T were established in our laboratory from a moderately well-differentiated primary human colon adenocarcinoma

---

ABBREVIATIONS USED: ACP = acid phosphatase; ACP1 = ACP-1; ADA = adenosine deaminase(s); ADAR = ADA, red blood cell form; ADAt = ADA, tissue form; AK = adenylate kinase; CK = creatine kinase; CKB = CK, brain form; EMEM = Eagle's minimum essential medium; ES = esterase(s); ESA4 = ES-A4; ESB2 = ES-B2; ESD = ES-D; FBS = fetal bovine serum; GLO = glyoxalase; GOT = glutamic-oxaloacetic transaminase; G6PD = glucose-6-phosphate dehydrogenase; LDH = lactate dehydrogenase(s); LDHA = LDH-A; LDHB = LDH-B; ME = malic enzyme; PEP = peptidases; PGD = phosphogluconate dehydrogenase; PGM = phosphoglucomutases; TC = tissue culture passage level(s); TCF = tissue conversion factor.

---

[1] Received March 26, 1981; accepted August 13, 1981.

[2] Supported in part by Public Health Service (PHS) grants CA23871 and CA22370 from the National Cancer Institute, by PHS grant ES01287 from the National Institute of Environmental Health Sciences, and by a gift from the Kleberg Foundation.

[3] Animals were maintained under the guidelines of the University of Texas.

[4] Departments of Surgery and Biochemistry and Molecular Biology, The University of Texas Medical School at Houston, Houston, Tex. 77030.

[5] Department of Genetics, The University of Texas System Cancer Center, M. D. Anderson Hospital and Tumor Institute, Houston, Tex. 77030.

tumor (*6, 11*). LS174T cells were routinely subcultured with 0.1% trypsin (GIBCO, Grand Island, N.Y.) diluted in 0.02% Versene; LS180 cultures were mechanically subcultured with a rubber policeman and have never been exposed to exogenous proteolytic enzymes. Monolayer cultures were grown in EMEM with Hanks' salts supplemented with nonessential amino acids (Eagle's), 10% heat-inactivated (56°C, 30 min) FBS (Sterile Systems, Logan, Utah), 2 m*M* L-glutamine, 50 μg streptomycin/ml and 50 U penicillin/ml. The cells were incubated at 37°C in an atmosphere of 95% air, 5% CO_2, and 95% humidity. The cell lines were mycoplasma-free as determined by transmission and scanning electron microscopy, by the absence of cytoplasmic fluorescence with Hoechst Bisbenzimid H 33258 dye (American Hoechst Corp., North Somerville, N.J.) (*16*), and by negligible arginine deiminase activity (*17*).

Normal bowel cells, NB(LS174T), NB-V, NB-M, and NB(LS123), were derived from the large bowel mucosa dissected at sites distinct from the tumor masses in 4 adult patients. NB(LS174T), LS180, and LS174T were derived from the same patient. Trypsin dissociation of the normal bowel tissue yielded a mixed population of cells, which became predominantly fibroblastic with prolonged subculture. The cells were cultured in the medium noted above. An average of 17 serial subcultivations was achieved with NB(LS174T) cultures before they senesced (*18*). The cells were predominately diploid throughout subcultivation (*11*). Two cell cultures Hs00764Int and Hs0677Int, derived from human fetal intestinal tissue were obtained from Dr. W. Nelson-Rees (University of California Naval Biosciences Laboratory, Berkeley, Calif.). The Hs cell cultures were produced with support from the Viral Oncology Program, National Cancer Institute, under the auspices of the Office of Naval Research and the Regents of the University of California.

Twelve independently derived colorectal carcinoma cell lines of primary or metastatic origin were provided by Col. A. Leibovitz, formerly of the Scott and White Clinic, Temple, Tex. The cultures were sent to us as lysed homogenates, and all are designated with SW-prefixes: 48, 403, 742, 802, 837, 948, 1116, 1222, 1345, 1398, 1417, and 1463. HT-29, an established human colon tumor cell line, was provided by Dr. Jørgen Fogh (Sloan-Kettering Institute for Cancer Research, Rye, N.Y.). HeLa was supplied by Dr. J. Clarkson, The University of Texas System Cancer Center, Science Park, Smithville, Tex. Cell lines LS123 and NB(LS123) were established in our laboratory in 1974 from 1 patient's human colon adenocarcinoma and normal large bowel mucosa, respectively. Genetic signature analysis revealed that LS123 and NB(LS123) were identical and distinct from the LS180 and LS174T cell lines (*11*). Two human colon tumor cell cultures, COLO 205 (*5*) and COLO 399, and frozen cell pellets of COLO 206, COLO 320, COLO 321, COLO 394, COLO 396, and COLO 463 were supplied by Dr. G. E. Moore, Denver General Hospital, Denver, Colo.

Cloning.—LS174T cells at TC 10, 11, 13.6, and 80.4 were cloned by two methods. The cells were placed into 60-mm petri dishes (Falcon Plastics, Oxnard, Calif.) treated with poly-D-lysine (*19*). Glass cloning rings were used to isolate single cells. Clones 10-1, 10-2, 10-3, 10-4, 9-1, 9-2, and 8-1 were subcultured and frozen in liquid nitrogen. Clones 3-5 and 6-6 were isolated by similar procedures by Dr. I. Tribbe (Abbott Laboratories, North Chicago, Ill.). Some clones were isolated by seeding cells on sterile precleaned, broken glass cover slips. After overnight incubation, glass fragments with one adherent cell were transferred to MicroTest II wells (Falcon Plastics), monitored for growth, and subcultured . Subclones of clones 3-5, 6-6, 10-1, and 10-4 were isolated in either 0.3% soft Noble agar (Difco Laboratories, Detroit, Mich.) or agarose (SeaKem; FMC Corp., Marine Colloids Division, Springfield, N.J.), according to the procedures of Macpherson and Montagnier (*20*).

Tumorigenicity studies.—Ten million cells of LS174T, LS180, or of clones 3-5, 6-6, 10-2, 10-3, or 10-4 were inoculated sc in 4 nude mice (*nu/nu* Swiss mice) by the methods of Giovanella and Stehlin (*21*). Tumors were measured weekly for at least 120 days. Animals were killed, tumors were removed, and portions of the tissue were dissected and processed for histologic examination, tissue culture, and isozyme analysis. In every instance, the tumor cells outgrew the mouse stromal cells in culture, and the tumor cell types could be identified by morphology and isozymes. The tumors were either trypsin or mechanically dissociated and cultured in either EMEM or L-15 medium containing 10% heat-inactivated FBS. After four to eight serial passages, the cell cultures were examined for isozyme profiles.

Surgical specimens.—Six pairs of autochthonous human bowel tumor and normal bowel mucosa specimens and one unpaired normal bowel mucosa specimen were examined for gene expression. The tissues were held at −20°C until they were processed. The tumor and normal mucosa were dissected away from the underlying stromal tissue and processed for isozyme analysis as noted below.

Isozyme analysis.—A pellet (0.1-0.2 ml) of cells or 0.5 g of tissue was placed in two volumes of homogenizing medium [0.01 *M* Tris-HCl (pH 7.5), 1 m*M* 2-mercaptoethanol, 1 m*M* EDTA], disrupted with a Dounce homogenizer at 4°C, and centrifuged (10,000×*g*, 45 min). Supernatants were stored at −70°C for less than 2 months (a temperature and time that preserve the activity of most enzymes). After thawing, supernatants were recentrifuged and subjected simultaneously to starch gel electrophoresis as generally described by Siciliano and Shaw (*22*). Four different buffer systems were used: 1) electrode consisting of 0.5 *M* Tris, 0.16 *M* EDTA, and 0.65 *M* borate (pH 8.0), and a gel consisting of 60 ml electrode buffer diluted to 600 ml with water with 20 mg NADP added after degassing; 2) an electrode consisting of 0.13 *M* Tris and 0.43 *M* citrate (pH 7.0), and a gel consisting of 40 ml of electrode buffer diluted to 600 ml with water; 3) an electrode consisting of 0.1 *M* Tris, 0.1 *M* maleic acid, 0.1 *M* EDTA, and 0.01 *M* $MgCl_2$ (pH 7.4), and a gel consisting of a 1:15 dilution of electrode buffer; and 4) an electrode consisting of 0.02 *M* Na_2HPO_4 and 0.046 *M* KH_2PO_4 (pH 6.5), and a gel consisting of a 1:10 dilution of electrode buffer. We swirled two Pasteur pipette drops of 2-mercaptoethanol into molten gels to restrict oxidation and secondary isozyme band formation during electrophoresis before we degassed the gels.

The isozymes and allozymes of the following enzymes were resolved on the following buffer systems: buffer system 1—CK, ME, PEP, PGD, G6PD, GOT, and ES; buffer system 2—ES, ADA, AK, GLO, and LDH; buffer system 3—PGM; and buffer system 4—ACP.

After electrophoresis, gels were sliced into as many as seven slabs, and on each slab an enzyme was identified from its histochemical stain. Recipes for enzyme stains have been described (*22, 23*). After being stained, gel slices were photographed (35-mm film) and discarded.

RESULTS

Genetic Signatures

Allozyme phenotypes of 13 polymorphic enzyme loci were studied in cell lines derived from colorectal adenocarcinomas and in lines derived from nonmalignant adult and fetal bowel mucosa (table 1). Examples of these phenotypes (except ACP) as resolved in this laboratory are published (*14*). ACP phenotypes are demonstrated in figure 1. Presence of the B-phenotype for *G6PD* in all cell lines indicates that they are free of HeLa cell contamination (*15, 25*). All SW samples were sent to us as lysed homogenates. With the exceptions of SW-742 and SW-802, the SW lines had different genetic signatures for the enzymes studied, indicating that they were derived from different individuals and are therefore of independent genetic origin and not cross contaminated. SW-742 and SW-802 have identical phenotypes for the 11 loci for which they were both examined. The probability is 0.042 of encountering

TABLE 1.—*Human colorectal malignant and nonmalignant cell lines: Genetic signatures*

Cell lines	Phenotypes of informative loci[a]									P[b]
	ACP	*AK1*	*ADAR*	*ESD*	*GLO*	*PGD*	*PGM1*	*PGM3*	*ME2*	
Malignant										
SW-48	a,b	1	NR	1	1, 2	a	1	1, 2	1	0.015
SW-403	a,b	1	NR	1	1, 2	a	1	1, 2	1, 2	0.016
SW-742	b	1	NR	1	1, 2	a	1	1	NR	0.042
SW-802	b	1	1	1	1, 2	a	1	1	NR	0.037
SW-837	b	1	1	1	1	a	1	1	1, 2	0.007
SW-948	b	NR	NR	1	2	a	1, 2	1, 2	1, 2	0.007
SW-1116	b	NR	NR	1	1, 2	a	1	1, 2	1, 2	0.017
SW-1222	b	NR	NR	1	2	a	1, 2	1	1	0.008
SW-1345	b	1	NR	1	2	a	1, 2	1	1, 2	0.008
SW-1398	a,b	1	1, 2	1	2	a	2	1, 2	1, 2	0.1×10^{-4}
SW-1417	NR	1	1	1	1	a	1	1	1	0.006
SW-1463	b	1, 2	NR	1	2	a	2	1, 2	1	0.8×10^{-4}
COLO 205	b	1	NR	1, 2	1, 2	a	1, 2	NR	2	5.5×10^{-4}
COLO 206	b	1	1	1, 2	1, 2	a	1, 2	NR	2	5.5×10^{-4}
COLO 320	a,b	1, 2	1	1	2	a	1	NR	2	2.3×10^{-4}
COLO 321	a,b	1, 2	NR	1	2	a	1	NR	2	2.6×10^{-4}
COLO 394	b	1	NR	1	2	a	1, 2	NR	1, 2	0.015
COLO 396	b	1	1	1	2	a	1, 2	NR	1, 2	0.013
COLO 399	b	1	1	1	2	a	1, 2	NR	1, 2	0.013
COLO 463	b	1	1	1	2	a	1, 2	NR	1, 2	0.013
HT-29	a,b	1	NR	1	1, 2	a	1, 2	1, 2	1	0.008
LS123	b	1	1	1	1	a	1	1, 2	1	0.004
LS174T	a,b	1	1	1	2	a	1	2	2	1.4×10^{-4}
LS180	a,b	1	1	1	2	a	1	2	2	1.4×10^{-4}
Nonmalignant										
NB(LS174T)	a,b	1	1	1	2	a	1	2	2	1.4×10^{-4}
NB(LS123)	b	1	NR	1	1	a	1	1, 2	1	0.005
NB-M	b	1	NR	1	1, 2	a	1	1	NR	0.042
NB-V	NR	1	NR	1, 2	1, 2	a,c	1	1	1, 2	5.5×10^{-4}
Hs0677Int	b	1	1	1, 2	2	a	1	1, 2	NR	0.004
Hs0074Int	b	1	1	1, 2	1	a	1	2	NR	3.3×10^{-4}

[a] The G6PD B phenotype was present in all cell lines, indicating their freedom from HeLa cell contamination (*15, 25*). Other polymorphic loci studied in each cell line, which are part of the cell line's genetic signature but which were uninformative in sorting out the cell lines because all lines had only the most common phenotype, were *GOT2, PEPA*, and *PEPC*. NR=not read. Phenotypes for *ADAR* were often not read because of either the lack of expression of the *ADA* locus or the production of ADA TCF, which obscured the electrophoretic typing of ADA (*26*). Phenotypes not read for other loci were not resolved from the material received for analysis.

[b] Probability of encountering the genetic signature of the cell line in human Caucasian population was calculated as the product of the frequencies of each phenotype at each locus (*14*).

this genetic signature by chance for the 11 loci in a Caucasian individual. For 12 lines of independent origin established in the same laboratory, the probability is 0.08 of finding two lines with the same genetic signature as that in SW-742 and SW-802 [for basis of these calculations, *see* (*14*)]. Since this is not too improbable (<0.05), these lines will be considered to be of independent origin in this report.

The eight COLO tumor lines carried in this laboratory were derived from 3 individuals. COLO 205 and COLO 206 were established from ascites cells sampled 2 weeks apart from the same individual; COLO 320 and COLO 321 were established from the same primary lesion of a second individual; COLO 394, COLO 396, COLO 399, and COLO 463 were established from one metastasis to the same iliac lymph node of a 3d individual. Genetic signature analyses confirm the independent origin of the 3 groups of cell lines. The five LS lines carried in this laboratory were derived from 2 individuals—LS123 and NB(LS123) were established from 1 person's primary adenocarcinoma and normal bowel mucosa, respectively; LS174T and LS180 were established from the primary colon adenocarcinoma, and NB(LS174T) was derived from the normal bowel mucosa of a 2d individual. Genetic signature analyses confirm the independent origin of these 2 groups of cell lines and their independence from the 3 COLO groups. The genetic signature analyses indicate that the remaining cell lines carried in this laboratory (HT-29, NB-M, NB-V, Hs0677Int, and Hs0074Int) are genetically independent of each other and the COLO and LS groups. As expected, cell lines derived from the same individual have identical genetic signatures (*11*).

The validity of these conclusions is further supported by the fact that the phenotype frequencies at each locus for all the cell lines derived from different individuals are not significantly different than the frequencies in the human Caucasian population.

Expression of Tissue-Specific Loci in Colon Tumor Cells and Their Subclones Grown Under Different Conditions

Seven isozyme loci (*LDHA, LDHB, ESB2, ESA4, CKB, ADAR*, and *ADAt*), which are variably expressed in different tissues, were examined in the reference colon tumor cell lines, LS174T and LS180. LS174T and LS180 expressed greater amounts of LDHA than of LDHB and had as much ESB2, ESA4, and CKB activity as did any cell line or human tissue studied in this laboratory (*see* figs. 2A and 2B, 3A-3C for examples). Six surgical specimens of nonmalignant human colon mucosal cells had the same pattern of isozyme expression. Identical gene expression patterns were observed in LS174T cells *a*) studied from TC 6-73, *b*) cultured in FBS-supplemented EMEM, Ham's medium F12, galactose-containing L-15 medium, or peptone-containing serum-free medium (*9*), *c*) harvested by trypsin or mechanical scraping (LS180), *d*) cultured on dishes or in a perfused hollow fiber culture system (*10*), and *e*) grown as tumors in nude mice or in cell cultures reinitiated from the mouse tumors after their trypsin disassociation. The expression of these loci was also the same in nine soft agar subclones of LS174T, nine plated subclones, 5 solid tumors produced in nude mice from five subclones, and in five subclones recultured after passage through nude mice. Therefore, the expression of these loci in LS174T is stable, homogeneous, and consistent with the colon mucosal origin of the cells.

The same cannot be said for ADA expression in the cell lines. Forms of ADA in LS174T cells varied in their expression under different culture conditions. The ADA structural locus is located on human chromosome 20 (*33*), is expressed variably in different tissues (*34-36*), and specifies the production of a low-molecular-weight enzymatic subunit that is responsible for the total ADA activity in cells (*26*). A second locus in human cells is active in certain tissues and produces a high-molecular-weight protein (TCF). Binding of TCF to the enzymatic subunit produces an electrophoretically slower form of the enzyme (*26*). When the structural *ADA* locus is active and TCF is not produced, the fast-migrating form of ADA (ADAR) is seen. Depending on the amount of TCF produced in cells, all or some of the ADA will appear as the slower migrating form (ADAt, *see* fig. 3B). LS174T and subclones, LS180 cells, and normal colon mucosal tissue produce ADAt. Insufficient TCF was produced to bind all the ADAR in all nude mouse solid tumors of LS cells and in one of four instances of LS cells grown in the hollow fiber system; consequently both isozymes appeared on the gels.

Isozyme Loci Expression

Various Colorectal Cell Lines Derived From Material in Different Malignant Stages

Data on isozyme expression in a series of colorectal cell lines derived from material of various malignant stages are listed in table 2. Only SW-742 and SW-1345 possessed the same isozyme pattern seen stably and homogeneously expressed in LS174T and LS180 tumor cells (LDHA > LDHB; ESB2, ESA4, and CKB were +++). While SW-742, like LS174T and LS180, was derived from a moderately invasive (Dukes B_2) and a relatively undifferentiated (Broders 2) colon adenocarcinoma, SW-1345 was derived from a more malignant rectal adenocarcinoma. Two other lines, SW-1116 and SW-1398, were derived from primary lesions of similar source and class as LS174T, but they had no detectable CKB activity. Lack of CKB expression cannot be accounted for by difference in the length of time in culture of SW-1116 and SW-1398. TC at which they were examined (TC 36 and 30, respectively) were neither higher than those for SW-742 and SW-1345 (TC 34 and 47) nor beyond the number of TC for which LS174T showed stable expression (TC 6-73).

TABLE 2.—*Human colorectal malignant and nonmalignant cell lines: Isozyme expression*

Cell lines	Isozyme activity[a]						TC tested[b]	Tissue		
	LDH	ESB2	ESA4	CKB	ADAt	ADAR		Source (metastases)[c]	Class[d]	
									Broders	Dukes
Malignant										
SW-48	A=B	–	+++	–	+++	–	57	*C*	4	C_2
SW-403	A>B	+++	+++	++	+	–	89	*C*	3	C_1
SW-742	A>B	+++	+++	+++	+++	–	34	*C*	2	B_2
SW-802	A>B	+	–	–	++	+++	15	*C*	1	B_1
SW-837	A>B	++	+	++	–	+++	45	*R*	4	C_2
SW-948	A>B	++	+++	+++	++	–	57	*C*	3	C_1
SW-1116	A>B	+++	++	–	+++	–	36	*C*	2	B_2
SW-1222	A<B	++	++	+++	–	+	39	*C*	3	C_2
SW-1345	A<B	+++	+++	+++	++	–	47	*R*	3	C_2
SW-1398	A>B	+++	+++	–	+++	–	30	*C*	2	B_2
SW-1417	A>B	++	++	–	+++	+	18	*C*	3	C_2
SW-1463	A>B	+++	+++	–	–	–	43	*R*	3	C_2
COLO 205	A	–	–	–	–	–	744	C (A)	3	D
COLO 206	A	–	–	–	–	+++	564	C (A)	3	D
COLO 320	A>B	–	–	+++	–	+++	144	*C*	2	C_2
COLO 321	A>B	–	–	+++	++	–	276	*C*	2	C_2
COLO 394	A>B	+	–	–	++	–	144	C (N)	3	D
COLO 396	A>B	+	–	–	–	+++	160	C (N)	3	D
COLO 399	A>B	+	–	–	–	+++	172	C (N)	3	D
COLO 463	A>B	+	–	–	–	+	150	C (N)	3	D
HT-29	A>B	–	–	+++	–	–	191	*C*	ND	ND
LS123	A>B	–	+	–	–	+++	23–214	*C*	ND	B
LS174T	A>B	+++	+++	+++	+++	–	6–73	*C*	2	B
LS180	A>B	+++	+++	+++	+++	–	12–70	*C*	2	B
Nonmalignant										
NB(LS174T)	A>B	–	–	+	–	+++	17	C	—	—
NB(LS123)	A>B	–	++	++	+++	–	8	C	—	—
NB-M	A>B	–	++	+	+	–	22	C	—	—
NB-V	A>B	+	+++	+	++	–	15	C	—	—
Hs0677Int	A>B	–	–	+	–	+	24	FI	—	—
Hs0074Int	A>B	–	–	+	–	+	32	FI	—	—

[a] Activity was judged by intensity of histochemical staining of the gene product on starch gels after electrophoresis of cleared homogenate containing ≈10 mg protein/ml. +++ = greatest intensity observed in this laboratory; – = invisible gene product; + = barely visible gene product; and ++ = intermediate (between + and +++) intensity. For LDH activity, products of the *A* and *B* genes were compared as judged by skewing of the five banded LDH patterns in the direction of the *A* or the *B* gene product. Examples are shown in figs. 2 and 3.

[b] Only the earliest and latest passages tested are listed when several passages of a line were examined inasmuch as they all gave the same results.

[c] Malignant lines were derived from either colon (C) or rectal (R) adenocarcinomas; nonmalignant lines were derived from adult colon (C) or fetal intestine (FI) mucosal tissue. If the source of the line was the primary tumor, the source is *italicized;* ascites (A) and iliac node (N) indicate metastatic source.

[d] Broders class indicates percent of undifferentiated cells in the malignant tissue source (*37*): 1, ≈25%; 2, ≈50%; 3, ≈75%; and 4, ≈100%. Dukes class indicates extent of lesion invasion of the malignant tissue source (*38*): A, mucosa and submucosa; B, muscularis; B_1, into muscularis; B_2, muscularis penetrated; C, intestinal wall; C_1, limited to intestinal wall; C_2, extended through all layers with posterior node involvement; D, extent of metastasis includes other organs. ND = no data; — = not applicable.

In addition to CKB, activities of LDHA versus LDHB, and of ESB2 and ESA4 also varied among the colorectal tumor cell lines. Once again, no correlation was observed between isozyme expression and *a*) invasiveness or differentiation of the original tumor tissue, *b*) time in culture, *c*) colon or rectum tumor site, or *d*) derivation from primary or metastatic lesions. LDHA activity was not greater than was LDHA in SW-48, SW-1222, or SW-1345. All three lines were derived from rather malignant adenocarcinomas of both the colon and rectum. SW-837, SW-1417, SW-1463, and all eight COLO lines were derived from tumors at least as invasive as SW-48, SW-1222, and SW-1345 and had LDHA activity greater than that of LDHB. ESB2 was not expressed (–) or only weakly expressed (+) in several lines of a more malignant origin (SW-48 and the COLO series). However, ESB2 was well expressed (++) in SW-837 which was equivalent in TC and malignant nature to SW-48. Also, ESB2 was absent or only weakly expressed in SW-802 and LS123T—two lines originated from less invasive and differentiated tumors (both) or studied at a wide range of passage levels (LS123T). Similarly, weak or nonexistent ESA4 activity could not be related to the malignant status of the tumor source or the passage level of the cultured cells.

Stability of expression of the loci for the above-mentioned isozymes in the LS174T and LS180 cells grown under a wide variety of conditions is important in evaluating different expressional patterns observed in the other colorectal cell lines. Further evidence for the stability of expression of LDHA, LDHB, ESB2, ESA4, and CKB in the lines is provided by the data from the COLO cells. COLO 205 and COLO 206 were both establisned from 1 individual's ascites metastasis, obtained 2 weeks apart. The cell lines were maintained as separate cultures for 792 and 564 serial passages, respectively. Expressional patterns for the five stable isozymes were identical and included a unique pattern for LDH (fig. 3C). Similarly, COLO 320 and COLO 321 were derived from the same colon primary tumor and maintained separately. These cell lines have the same expressional pattern which differs from the COLO 205-COLO 206 set. The COLO 394, COLO 396, COLO 399, and COLO 463 lines were established from one iliac node metastasis and were carried in vitro separately. All four of these lines have the same expression patterns which differ from the other two COLO sets.

The inconsistency of the expression of the ADA isozymes observed in the LS174T and LS180 cells is also seen in the COLO sets. COLO 205 is essentially deficient in ADA expression, whereas COLO 206 is +++ for ADAR. Patterns of ADAt and ADAR expressions are reversed in COLO 320 and COLO 321, whereas the COLO 394-COLO 396-COLO 399-COLO 463 set displays several levels of ADA activity. Clearly, the ADA isozymes are not reliable markers for gene expression patterns in these cell lines.

Normal Colon Mucosa-Colon Adenocarcinoma Surgical Samples

The differences in expressions of the loci stably expressed in the colon tumor cell lines of independent origin suggest that these loci might be expressed differently either in the colon mucosae of different individuals or in adenocarcinomas that develop in different individuals. The data on isozyme expression for paired normal colon mucosa and adenocarcinoma surgical samples from 6 patients are shown in table 3. All of the normal colon mucosal samples were identical for every isozyme studied. Colon adenocarcinoma biopsy specimens had isozyme expressions that reflected the spectrum seen among the colorectal tumor cell lines.

Cell Lines Derived From Nonmalignant Colorectal Mucosa

General expressional patterns for cell lines derived from nonmalignant colorectal mucosae (table 2) are inconsistent with the patterns observed in normal bowel mucosa surgical samples (cf. with data in table 3). The only similarity of these lines with normal bowel mucosa is the greater expression of LDHA than of LDHB. However, with certain exceptions, e.g., SW-48, SW-948, and SW-1116 (this report) and choriocarcinoma cell lines (*36*), LDHA activity is usually greater than LDHB activity in mammalian cell lines. Lines derived from normal bowel mucosa and colon adenocarcinoma of the same patient have different expressional patterns [cf. paired NB(LS174T) with LS174T and NB(LS123) with LS123 (table 2)].

DISCUSSION

Cell Line Verification

The genetic signature analysis has been essential in determining the origin and integrity of cell lines maintained in the laboratory (*12-14*). Since gene expression patterns may differ in two cell lines derived from the same individual [cf. LS174T with NB(LS174T) and LS123 with NB(LS123), table 2], isozymes coded by multiple loci are less useful in that regard. The use of ADA expression for monitoring cell line contamination (*12*) is inappropriate, since we have shown that ADA

TABLE 3.—*Normal colon mucosa and adenocarcinoma:*[a] *Isozyme expression*

Patient No.	Isozyme activity[a]					Tumor class[b]	
	ESB2	ESA4	CKB	ADAt	ADAR	Broders	Dukes
Normal mucosa							
1	+++	+++	+++	++	–	—	—
2	+++	+++	+++	++	–	—	—
3	+++	+++	+++	++	–	—	—
4	+++	+++	+++	++	–	—	—
5	+++	+++	+++	++	–	—	—
6	+++	+++	+++	++	–	—	—
Adenocarcinoma							
1	+++	+++	–	++	++	1	B
2	+++	+++	+++	+++	–	2	B
3	+++	+++	+++	++	++	2	C
4	+	+	+++	–	–	4	A
5	–	+++	–	+++	–	4	C
6	+	–	+++	+	++	2	B

[a] Six paired surgical specimens were used, all of which had a greater expression of LDHA than of LDHB.
[b] — = not applicable. *See* fn *d*, table 2, for definition of terms.

isozyme expression varies considerably with culture conditions. Incorporation of ADAR phenotypes in the genetic signature is appropriate, when expressed, since it and other allozymatic markers have proven stable in cultured cells (*13*, *25*), varying only at mutational frequencies in isolated subclones (*39*, *40*).

Our conclusion that SW-742 and SW-802 have independent origins, even though they have the same genetic signature ($P=0.08$) appears justified because of their different expressions of ESB2, ESA4, and CKB, which we have shown to be stably expressed in the colorectal adenocarcinoma cell lines through the TC at which SW-742 and SW-802 were examined.

Isozyme Expression

Five tissue-specific isozymes maintain stable expression in colorectal tumor cell lines through a wide range of serial passages and culture conditions and in multiple cell lines from the same tissue sample. A range of expressional patterns for these loci occurs in lines of independent origin and in colon adenocarcinoma surgical samples. We conclude from these observations that colorectal adenocarcinomas differ from one another in their gene expression characteristics. When one considers the facts that these isozyme loci have been shown to be under both stage and tissue-specific regulation [*see* review (*41*)] and that cell lines lacking their expression have been shown to contain the chromosomes known to bear the structural loci (*5*), the differences in gene expression characteristics are viewed as having a regulatory rather than structural basis. Colorectal adenocarcinoma cell lines reflect the diversity in isozyme expression in tumors and represent important and useful models for the disease.

The question of whether the gene expression pattern in a tumor cell line reflects the pattern in the solid tumor from which it was derived or represents a subpopulation of cells selected by culture from the tumor cannot be answered at this time. Experiments are in progress to compare the expressional patterns in solid tumors with those of lines and soft-agar clones established directly from them (*42*). We emphasize caution in this area because we observed different expressional patterns among cell lines derived from normal bowel mucosa while several surgical mucosal samples exhibited identical gene expression patterns. These results also indicate that the normal bowel cell lines studied are not adequate models for normal bowel mucosa.

Recent studies have shown that solid tumors and tumor cell lines are composed of subpopulations that are heterogeneous with regard to metastatic potential (*43*, *44*), responses to chemotherapeutic agents (*45–47*), growth rate and differentiation (*48*), karyology (*49*), and antigenic composition (*50–52*). Our results suggest that the gene expression patterns of colorectal adenocarcinoma cell lines may be the same as patterns of the original tumors, and individual colorectal tumors may not be extensively heterogeneous for these properties. This suggestion is supported by the observation that CKB activity was not detectable in two tumor biopsy specimens (from patients #1 and #5; table 3). Dilution experiments (data not shown) indicate that as little as 5% of full CKB cellular activity can be detected on starch gels after electrophoresis. It would appear, therefore, that if some cells in the tumors were producing high levels of CKB activity, they probably represent less than 5% of the tumor population.

Other indirect evidence that the gene expression patterns of the tumor cell lines may actually represent the isozymes in the original tumors is the inability to correlate expressional differences with the TC in culture. Also, similar patterns were observed for the stable isozymes when independent tumor cell lines were compared with colon adenocarcinoma surgical samples. For example, similar gene expression was observed for *a*) SW-1116, SW-1398, SW-1417, and SW-1463 and the surgical specimen from patient #1; *b*) SW-403, SW-742, SW-948, and LS174T and the surgical specimens from patients #2 and #3; *c*) COLO 320, COLO 321, and HT-29 and the surgical specimens from patients #4 and #6; and *d*) SW-48 and the surgical sample from patient #5. While our data are conclusive for the tumor-to-tumor variations in gene expression, preliminary data and speculation indicate that cell-to-cell variations for isozyme expression with these tumors may be minimal.

No correlation was observed between isozyme gene expressions in the tumor cell lines and either the extent of invasion (Dukes classification) or the level of differentiation (Broders grade). Thus development of tumors from specific cell types originally present in normal bowel mucosa may be more important in isozyme gene expression differences than changes in expression to fetal forms of isozymes (*53*). Such a phenomenon would also account for the tumor-to-tumor variations observed in the expressional patterns. Further experiments are needed to understand these basic biological characteristics of colorectal cancer, which may be useful in biochemical classification of colorectal tumor subtypes, in the design of therapy modes, and in management of colon cancer.

REFERENCES

(*1*) Drewinko B, Romsdahl MM, Yang LY, Ahern MJ, Trujillo JM. Establishment of a human carcinoembryonic antigen-producing cell line. Cancer Res 1976; 36:467–475.

(*2*) Leibovitz A, Stinson JC, McCombs WB III, McCoy CE, Mazur KC, Mabry ND. Classification of human colorectal adenocarcinoma cell lines. Cancer Res 1976; 36:4562–4569.

(*3*) Noguchi P, Wallace R, Johnson J, et al. Characterization of WiDr: A human colon carcinoma cell line. In Vitro 1979; 15: 401–408.

(*4*) Quinn LA, Moore GE, Morgan RT, Woods LK. Cell lines from human colon carcinoma with unusual cell products, double minutes, and homogeneously staining regions. Cancer Res 1979; 39:4914–4924.

(*5*) Semple TU, Quinn LA, Woods LK, Moore GE. Tumor and lymphoid cell lines from a patient with carcinoma of the colon for a cytotoxicity model. Cancer Res 1978; 38:1345–1355.

(6) Tom BH, Rutzky LP, Jakstys MM, Oyasu R, Kaye CI, Kahan BD. Human colonic adenocarcinoma cells. I. Establishment and description of a new line. In Vitro 1976; 12:180-191.

(7) Tompkins WA, Watrach AM, Schmale JD, Schultz RM, Harris JA. Cultural and antigenic properties of newly established cell strains derived from adenocarcinomas of the human colon and rectum. J Natl Cancer Inst 1974; 52:1101-1110.

(8) Tom BH, Rutzky LP, Oyasu R, Tomita JT, Goldenberg DM, Kahan BD. *Brief communication:* Human colon adenocarcinoma cells. II. Tumorigenic and organoid expression in vivo and *in* vitro. J Natl Cancer Inst 1977; 58:1507-1512.

(9) Kahan BD. Rutzky LP, LeGrue SJ, Tom BH. Molecular approaches to human colon cancer. Methods Cancer Res 1979; 18:197-275.

(10) Rutzky LP, Tomita JT, Calenoff MA, Kahan BD. Human colon adenocarcinoma cells. III. In vitro organoid expression and carcinoembryonic antigen kinetics in hollow fiber culture. JNCI 1979; 63:893-902.

(11) Rutzky LP, Kaye CI, Siciliano MJ, Chao M, Kahan BD. Longitudinal karyotype and genetic signature analysis of cultured human adenocarcinoma cell lines LS180 and LS174T. Cancer Res 1980; 40:1443-1448.

(12) O'Brien SJ, Kleiner G, Olsen R, Shannon JE. Enzyme polymorphisms as genetic signatures in human cell cultures. Science 1977; 195:1345-1348.

(13) Povey S, Hopkinson DA, Harris H, Franks LM. Characterisation of human cell lines and differentiation from HeLa by enzyme typing. Nature 1976; 264:60-63.

(14) Siciliano MJ, Barker PE, Cailleau R. Mutually exclusive genetic signatures of human breast tumor cell lines with a common chromosomal marker. Cancer Res 1979; 39:919-922.

(15) Gartler SM. Apparent HeLa cell contamination of human heteroploid cell lines. Nature 1968; 217:750-751.

(16) Chen TR. Microscopic demonstration of mycoplasma contamination in cell cultures and cell culture media. Procedure 75361, Tissue Culture Association Manual 1975; 1:229-232.

(17) Barile MF, Schimke RT. A rapid chemical method for detecting PPLO contamination of tissue cell cultures. Proc Soc Exp Biol Med 1963; 114:676-679.

(18) Hayflick L, Moorhead PS. The serial cultivation of human diploid cell strains. Exp Cell Res 1961; 25:585-621.

(19) McKeehan WL, Ham RG. Stimulation of clonal growth of normal fibroblasts with substrata coated with basic polymers. J Cell Biol 1976; 71:727-734.

(20) Macpherson I, Montagnier L. Agar suspension culture for the selective assay of cells transformed by polyoma virus. Virology 1964; 23:291-294.

(21) Giovanella BC, Stehlin JS. Heterotransplantation of human malignant tumors in "nude" thymusless mice. I. Breeding and maintenance of "nude" mice. J Natl Cancer Inst 1973; 51:615-619.

(22) Siciliano MJ, Shaw CR. Separation and visualization of enzymes on gels in chromatographic and electrophoretic techniques. Vol 2. 4th ed. London: Heinemann, 1976:185-209.

(23) Harris H, Hopkinson DA. Handbook of enzyme electrophoresis in human genetics. Oxford: Elsevier/North-Holland, 1976.

(24) Luffman JE, Harris H. A comparison of some properties of human red cell acid phosphatase in different phenotypes. Ann Hum Genet 1967; 30:387-401.

(25) Auersperg N, Gartler SM. Isoenzyme stability in human heteroploid cell lines. Exp Cell Res 1970; 61:465-467.

(26) Hirschhorn R, Levytska V, Pollara B, Meuwissen HJ. Evidence for control of several different tissue-specific isozymes of adenosine deaminase by a single genetic locus. Nature [New Biol] 1973; 246:200-202.

(27) Coates PM, Mestriner MA, Hopkinson DA. A preliminary genetic interpretation of the esterase isozymes of human tissues. Ann Hum Genet 1975; 39:1-20.

(28) Hopkinson DA, Mestriner MA, Cortner J, Harris H. Esterase D: A new human polymorphism. Ann Hum Genet 1973; 37:119-137.

(29) Sparkes RS, Sparkes MC, Wilson MG, et al. Regional assignment of genes for human esterase D and retinoblastoma to chromosome band 13q14. Science 1980; 208:1042-1044.

(30) Dawson DM, Eppenberger HM, Eppenberger ME. Multiple molecular forms of creatine kinases. Ann NY Acad Sci 1968; 151:616-626.

(31) Jockers E, Wrentou EJ, Pfleiderer G. Quantitation of creatine kinase isoenzymes in human tissues and sera by an immunological method. Clin Chim Acta 1975; 58:223-232.

(32) Markert CL. Lactate dehydrogenase isozymes: Dissociation and recombination of subunits. Science 1963; 140:1329-1330.

(33) Tischfield JA, Creagan RP, Nichols EA, Ruddle FH. Assignment of a gene for adenosine deaminase to human chromosome 20. Hum Hered 1974; 24:1-11.

(34) Hayashi TT. Studies on placental metabolism. Purine nucleotide catabolism in early placenta. Am J Obstet Gynecol 1965; 93:266-268.

(35) Lee PC. Developmental changes of adenosine deaminase, xanthine oxidase, and uricase in mouse tissues. Dev Biol 1973; 31:227-233.

(36) Siciliano MJ, Bordelon-Riser ME, Freedman RS, Kohler PO. A human trophoblastic isozyme (lactate dehydrogenase-Z) associated with choriocarcinoma. Cancer Res 1980; 40:283-287.

(37) Broders AC. The grading of carcinoma. Minn Med 1925; 8:726-730.

(38) Dukes CE. Classification of cancer of the rectum. J Pathol Bacteriol 1932; 35:323-332.

(39) Povey S, Gardiner SE, Watson B, et al. Genetic studies on human lymphoblastoid lines: Isozyme analysis on cell lines from forty-one different individuals and on mutants produced following exposure to chemical mutagen. Ann Hum Genet 1973; 36:247-266.

(40) Siciliano MJ, Siciliano J, Humphrey RM. Electrophoretic shift mutants in Chinese hamster ovary cells: Evidence for genetic diploidy. Proc Natl Acad Sci USA 1978; 75:1919-1923.

(41) Edwards YH, Hopkinson DA. Developmental changes in the electrophoretic patterns of human enzymes and other proteins. Isozymes 1977; 1:19-78.

(42) Laboisse CL, Augeron C, Potet F. Growth and differentiation of human gastrointestinal adenocarcinoma stem cells in soft agarose. Cancer Res 1981; 41:310-315.

(43) Fidler IJ. Selection of successive tumour lines for metastasis. Nature [New Biol] 1973; 242:148-149.

(44) Fidler IJ, Kripke ML. Metastasis results from pre-existing variant cells within a malignant tumor. Science 1977; 197:893-895.

(45) Barranco SC, Ho DH, Drewinko B, Romsdahl MM, Humphrey RM. Differential sensitivities of human melanoma cells grown in vitro to arabinosylcytosine. Cancer Res 1972; 32:2733-2736.

(46) Barranco SC, Drewinko B, Humphrey RM. Differential response by human melanoma cells to 1,3-bis-(2-chloroethyl)-1-nitrosourea and bleomycin. Mutat Res 1973; 19:277-280.

(47) Heppner GH, Dexter DL, DeNucci T, Miller FR, Calabresi P. Heterogeneity in drug sensitivity among tumor cell subpopulations of a single mammary tumor. Cancer Res 1978; 38:3758-3763.

(48) Gray JM, Pierce GB. Relationship between growth rate and differentiation of melanoma in vivo. J Natl Cancer Inst 1964; 32:1201-1211.

(49) Mittelman F, Mark J, Levan G, Levan A. Tumor etiology and chromosome pattern. Science 1972; 176:1340-1341.

(50) DeBaetselier P, Katzav S, Gorelik E, Feldman M, Segal S. Differential expression of *H-2* gene products in tumour cells is associated with their metastatogenic properties. Nature 1980; 288:179-181.

(51) Prehn RT. Analysis of antigenic heterogeneity within individual 3-methylcholanthrene-induced mouse sarcomas. J Natl Cancer Inst 1970; 45:1039-1045.

(52) Primm MV, Baldwin RW. Antigenic differences between primary methylcholanthrene-induced rat sarcomas and post-surgical reoccurrences. Int J Cancer 1977; 20:37-45.

(53) Weinhouse S. New dimensions in the biology of cancer. Cancer 1980; 45:2975-2980.

Figures 1-3.—Zymograms of representative isozymes studied. Origins are marked "o" at the *right*; anodes are toward the top, cathodes toward the bottom.

Figure 1.—ACP1. Positions of the products of the *a* allele (single cathodal band) and *b* allele (double anodal bands) are indicated to the *left*. These are the expected positions of these gene products after electrophoresis on a pH 6.5 phosphate buffer system lacking citrate (*24*). Both *a,b* and *a* phenotypes are readily distinguishable.

Figure 2.—ES run on the Tris-citrate, pH 7 system and stained with methyl umbelliferyl acetate (fig. 2A) and on the Tris-Versene-borate, pH 8 system stained with a diazonium salt (fig. 2B). Positions of the ES isozymes under study are indicated to the *left* of each figure and are consistent with the findings of Coates et al. (*27*). Sample order on both gels is 1: COLO 320; 2: Hs0677Int; 3: Hs0074Int; 4: LS174T; 5, 6: two subclones of LS174T re-established in culture after forming solid tumors in nude mice; and 7: LS123. ESD phenotypes are part of the genetic signature analysis since they are polymorphic (*28*) and constitutively expressed in all tissues and cell lines studied (*29*). ESB2 and ESA4 are differentially expressed in different human tissues (*27*) and are seen on these gels only in LS174T and its subclones after passage through nude mice.

Figure 3.—Isozymes after electrophoresis and histochemical staining of 1: LS174T grown in the perfused hollow fiber system; 2: COLO 205; 3: COLO 396; and 4-6: three subclones of LS174T. 3A) Fast-migrating CKB is expressed in several different human tissues (*30, 31*). It is clearly expressed in the LS174T line and its subclones and is absent in COLO 205 and COLO 396. The more slowly migrating zones are AK activity, which also stain but are not well resolved on this buffer system. 3B) ADAR and ADAt are indicated on the *left*. These ADA isozymes are expressed in different tissues, as described in the text. Nearly all the ADA of LS174T cells is ADAt, whereas it is ADAR in both COLO lines due to their lack of TCF expression (*26*). 3C) Five common forms of LDH are the result of the two differentially expressed genetic loci *A* and *B* (*32*). The five are electrophoretically separable tetramers. Positions of the A and B homotetramers are indicated on the *left*. A slightly greater expression of LDHA than of LDHB is indicated in most of the cell lines by a greater staining intensity of the more cathodally positioned isozymes. COLO 205 is remarkable due to its exclusive expression of LDHA.

1

2A

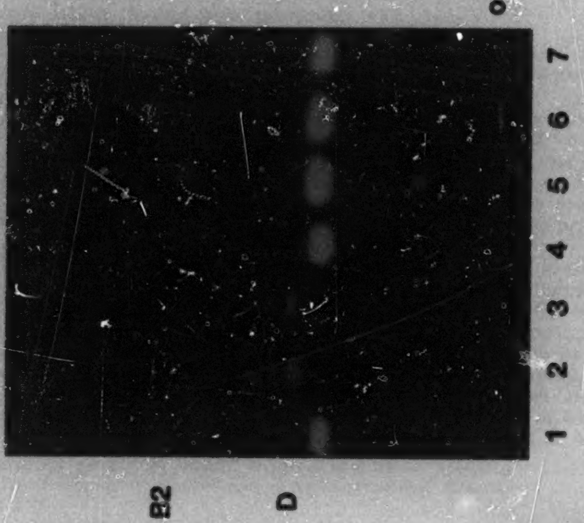
o
7
6
5
4
3
2
1
B2
D

2B

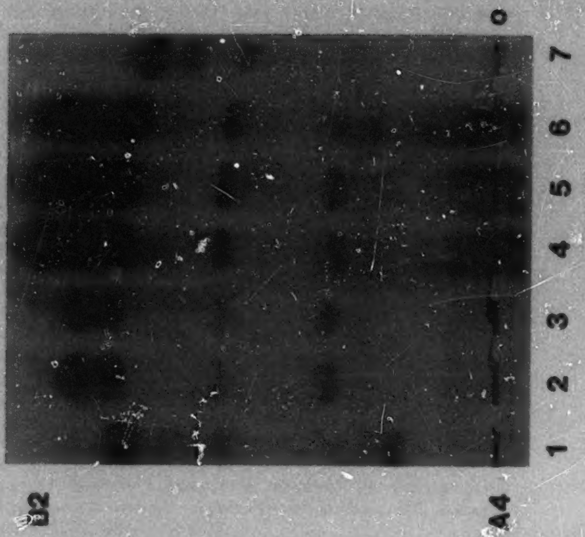
o
7
6
5
4
3
2
1
B2
A4

3A

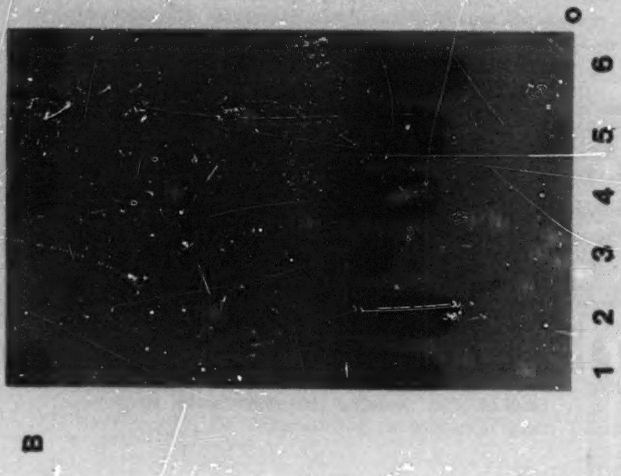

3B

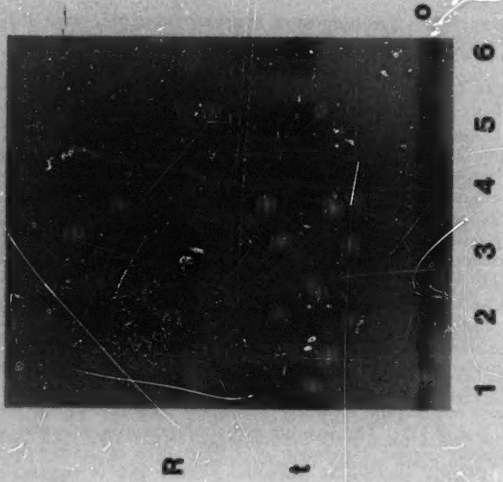

3C

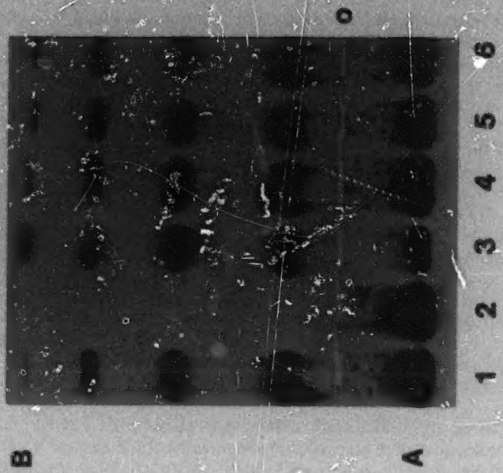

Coffee Drinking and Cancer of the Lower Urinary Tract[1,2,3]

Alan S. Morrison, *M.D.*,[4] **Julie E. Buring**, *M.S.*,[4] **Wendy G. Verhoek**, *M.S.*,[5] **Kunio Aoki**, *M.D.*,[6] **Ian Leck**, *M.B.*, *Ph.D.*,[5,7] **Yoshiyuki Ohno**, *M.D.*,[6] *and* **Koji Obata**, *M.D.*[8,9]

ABSTRACT—The relation of coffee drinking to the incidence rate of cancer of the lower urinary tract ("bladder cancer") was evaluated. Broadly based series of cases and series of controls drawn from the general population of each area were assembled and interviewed in Boston, Massachusetts (587 cases, 528 controls), Manchester, England (541 cases, 725 controls), and Nagoya, Japan (289 cases, 586 controls). Compared to drinkers of an average of less than 1 cup of coffee per day, those who drank more had a relative risk of bladder cancer estimated as 1.0 (0.8-1.2, 95% confidence interval). With adjustment for cigarette smoking habits, only small and irregular changes in risk were seen with increasing frequency of coffee consumption. Duration of coffee drinking showed little relation to risk of bladder cancer. Apparent associations of coffee drinking and bladder cancer may be due to incomplete control of the effect of cigarette smoking. If there is a true association of coffee drinking and bladder cancer it is likely to be weak.—JNCI 1982; 68:91-94.

A positive association between coffee drinking and cancer of the lower urinary tract has been suspected for nearly a decade (*1*). Additional studies also suggest an association but the question of whether there is a causal link has not been resolved (*2-8*). Here we present data from an international collaborative case-control study of the relation of coffee drinking to the incidence of cancer of the lower urinary tract.

METHODS

The study was done in three areas: The Boston, Massachusetts, Standard Metropolitan Statistical Area; six contiguous health districts in greater Manchester, United Kingdom (Central and South Manchester, Oldham, Stockport, Tameside, and Trafford); and Nagoya, Japan, and ten of its surrounding cities and towns. An attempt was made to assemble a complete series of incident cases in each area during a defined study period, which was March 1976 through May 1977 in Boston, October 1976 through September 1978 in Manchester, and January 1976 through December 1978 in Nagoya. To be eligible a person had to have had an initial diagnosis of a primary neoplasm of the lower urinary tract (bladder, ureter, renal pelvis, or urethra) during the study period and to be at least 21 years old and a resident of the study area at the time of diagnosis. Persons over 89 years old at the time of diagnosis were not eligible for interview.

Case identification was accomplished primarily through hospitals. Tumors throughout the histologic spectrum from papilloma to invasive neoplasia were included. For brevity, the term "bladder cancer" is used as a synonym for neoplasms of the lower urinary tract (*9*). The number of identified patients less than 90 years old was 741 in Boston, 577 in Manchester, and 348 in Nagoya. Of these patients, 95% had bladder tumors and 83% were specified as having squamous or transitional cell carcinomas.

Controls were selected by random sampling procedures from electoral registers for each study area. Each of these registers is updated annually and is believed to contain a nearly complete list of adult residents. Sampling methods were designed so that each control series would have an age and sex distribution similar to that of the respective series of cases. The number of controls was 677 in Boston, 817 in Manchester, and 735 in Nagoya.

The specific methods of identification of the subjects in Boston have been described (*9*). Cases and controls were selected in Manchester and Nagoya as follows: In Manchester, periodic searches for cases were made with the use of pathology log books or reports on all surgical specimens at nine of the ten hospitals with pathology departments in the study area. The discharge summaries received by the North Western Regional Health Authority for all ten hospitals also were searched, as were the records of the North Western

---

[1] Received April 3, 1981; accepted August 18, 1981.

[2] Supported by Public Health Service grant R26CA-18660 from the National Cancer Institute through the National Bladder Cancer Project, and by a research grant from the North Western Regional Health Authority, England.

[3] Research procedures were in accord with the ethical standards of the Committee on the Use of Human Subjects in Research, Harvard School of Public Health.

[4] Department of Epidemiology, Harvard University, School of Public Health, 677 Huntington Ave., Boston, Mass. 02115.

[5] Department of Community Medicine, University of Manchester, and the Department of Epidemiology and Social Research, University Hospital of South Manchester, Manchester, England.

[6] Department of Preventive Medicine, Nagoya University School of Medicine, Nagoya, Japan.

[7] Department of Oncology, University of Manchester, Manchester, England.

[8] Department of Urology, First Red Cross Hospital, Nagoya, Japan.

[9] We thank the many urologists, pathologists, and other physicians, hospital administrators, and staff members of the medical records and pathology departments whose cooperation made this study possible. We also thank the following people who made important contributions to the data collection and processing: N. Benotti, R. Bruno, D. Dysert, M. Fegreus, R. Halpert, D. Helvarg, L. Jewler, L. Mayer, M. Siskind, M. Smith, A. Travis, and R. Udin-Boston; Y. Chubb, M. Clipson, J. Forshaw, S. Hunton, F. Kelly, P. Murray, H. Peterson, L. Sutcliffe, M. Wade, M. Wilkinson, and C. Yeardley-Manchester; S. Hayakawa, H. Igami, Y. Kato, T. Mori, and T. Sakurai-Nagoya.

best copy available

Regional Cancer Registry, where all cases in residents of the study area should have been registered regardless of their place of treatment. Controls were selected from the 1977 and 1978 electoral rolls for the cities and towns surveyed. Because these rolls do not indicate residents' ages, it was impossible to select directly a series of controls with the desired age distribution. Therefore, the selection of the controls was done in two phases. Initially, six names were sampled for each of the first 464 cases identified, with matching by sex but not by place of residence. An attempt was made to determine the dates of birth of the 2,784 people identified. In most instances the information was obtained by interview of the subject or a household member; otherwise, the Family Practitioner Committee for the relevant area was asked. (Each Family Practitioner Committee keeps records of all residents of its area who have registered for general medical care within the National Health Service.) Of the 2,745 potential controls for whom the dates of birth were learned, 817 then were subsampled, with a probability based on present age, as eligible for interview.

In Nagoya, virtually all patients with urinary tract tumors are referred for definitive diagnosis and treatment to hospitals with staff urologists (Obata K: Unpublished data). There were 19 such hospitals in the study area. The responsible urologist in each of these hospitals reported all patients with tumors of the lower urinary tract to the project staff. The selection of controls was based on the 1976, 1977, and 1978 electoral registers for the communities that comprised the study area. The case and control series were similar with respect to residence in Nagoya City versus one of the surrounding communities but were not matched more closely on residence within these broad areas.

As many eligible subjects as possible were interviewed. If a subject was too ill for interview, could not be contacted, or had died, an attempt was made to interview a proxy (i.e., a relative or friend familiar with the subject's background and habits). Interviews were obtained for 597 patients (81% of the total eligible) and 544 controls (80%) in Boston, 555 patients (96%) and 735 controls (90%) in Manchester, and 293 patients (84%) and 589 controls (80%) in Nagoya. In general, interviews were done at subjects' homes. The major exception occurred in Nagoya, where 87 patients were interviewed as inpatients and 107 were interviewed during an outpatient visit. In Manchester, 54 patients were interviewed as inpatients at the request of the responsible physician. In all three study areas, some subjects were interviewed at another location, such as a place of employment, or by telephone.

To the extent compatible with differences in language and customs, the interview schedule was standardized among the study centers. Questions were included on many known or suspected causes of bladder cancer (*9*). With respect to coffee consumption, subjects were asked whether they had ever drunk coffee. Those who had were asked the amount they had drunk on the average, when they began drinking coffee, the period in which they were drinking the most coffee and how much that was, what their current consumption of coffee was, and, if they had stopped drinking coffee, when. Those whose current consumption of coffee was at least 2 cups per week were questioned in detail about the amount of coffee consumed according to type (ground and brewed or instant; in Boston and Nagoya, use of regular or decaffeinated coffee as well). Current consumption was defined as consumption 1 year before interview or in the calendar year before diagnosis for patients interviewed more than a year after diagnosis.

Results are given primarily in terms of the "relative risk," an estimate of the ratio of the bladder cancer incidence rate among drinkers of a specified amount of coffee compared to persons drinking less than 1 cup per day. Trends in relative risk were similar for three measures of the frequency of coffee drinking—average, current, and maximum. Therefore, this presentation focuses on the average frequency. Relative risks presented are simultaneous maximum likelihood estimates (*10*). Variables controlled are indicated in context and included age (<65, 65-74, and ≥ 75 yr), sex, study area, and cigarette smoking habit (never smoked, ex-smoker, or current smoker of <1, 1, 2, or ≥ 3 packs/day). Occupational history (*9*) was not controlled, since adjustment for this variable (in men) had no effect on the respective relative risk estimates. The analysis was restricted to subjects for whom both coffee drinking and cigarette smoking habits were known.

RESULTS

Compared to subjects who drank an average of less than 1 cup of coffee per day, those who drank more had a relative risk estimated as 1.0 (0.8-1.2, 95% confidence interval), with adjustment for age, sex, study area, and cigarette smoking. In subjects who never had smoked cigarettes, the relative risk (adjusted for age, sex, and study area) was estimated as 1.0.

The distributions of cases and controls according to average daily coffee consumption are given in tables 1-3. Generally, the distributions of coffee consumption were similar between cases and controls, and the differences present do not appear to follow a regular pattern. However, there was a moderate excess of cases compared to controls among both men and women in Boston who drank 6 or more cups per day.

With age and cigarette smoking controlled, a regular increase in relative risk with increasing coffee consumption was not apparent in any of the study areas. Most of the relative risk estimates were close to 1. The highest relative risk observed, 1.9, was that for men in Nagoya who drank 5 or more cups of coffee per day. However, this estimate was based on only 13 heavily exposed subjects.

In Manchester and Nagoya, there were substantial numbers of subjects who consumed small amounts of coffee, less than a cup per day but at least a cup per year. At these low levels of consumption, no regular

TABLE 1.—*Percentage distribution of cases and controls and relative risk of bladder cancer according to average frequency of coffee drinking by sex in Boston*

Sex	Study group	No. of cups of coffee/day							No. of subjects
		<1	1	2	3	4	5	≥6	
Males	Cases, %	5.4	23.2	22.5	19.4	9.7	4.5	15.4	423
	Controls, %	5.9	25.4	28.5	19.5	9.0	3.9	7.7	389
	Relative risk[a] ...	1	0.8	0.7	0.9	0.8	0.8	1.5	
Females	Cases, %	12.2	25.0	18.9	20.7	7.9	5.5	9.8	164
	Controls, %	12.2	36.0	23.0	11.5	7.2	5.8	4.3	139
	Relative risk[a] ...	1	0.8	0.6	1.7	0.9	0.7	1.0	

[a] Adjusted for age and cigarette smoking.

pattern of increasing relative risk in relation to increasing intake was apparent.

The relation of coffee drinking and bladder cancer was similar for ground versus instant coffee. No large or regular changes in relative risk were associated with increasing duration of coffee drinking.

Telephone interviews, interviews with proxies, and interviews rated "unreliable" by the interviewer were considered to have yielded relatively poor information. In this category there were 130 cases and 117 controls in Boston, 113 cases and 68 controls in Manchester, and 31 cases and 89 controls in Nagoya. With these cases excluded, the relative risk of bladder cancer among drinkers of a cup or more of coffee per day was virtually unchanged.

DISCUSSION

The results of the present study indicate that coffee drinking confers little or no risk of bladder cancer. People who drank an average of a cup or more of coffee per day had a risk similar to that of people who drank less. There was little evidence of an increase in risk with increasing coffee consumption. Other aspects of coffee consumption such as duration of use or type of coffee used also showed little relation to risk of bladder cancer.

A number of previous studies of coffee drinking and bladder cancer have been done in the United States. In a study in the Boston area, Cole (*1*) reported relative risks of 1.3 in men and 2.5 in women for drinkers of 1 or more cups of coffee per day compared to those who drank less. A positive association also was observed in another study that was limited to women in the Boston area (*2*). Fraumeni et al. (*3*) reported relative risks of 2.0 in men and 1.2 in women for drinkers of coffee relative to nondrinkers. Bross and Tidings (*4*) reported a weak positive assocition for men and a weak inverse one for women. Wynder and Goldsmith (*5*) found positive associations in both men and women; the relative risk appeared slightly higher for men. Mettlin and Graham (*6*) reported a positive association between coffee drinking and bladder cancer in men, but little relation in women. Two case-control studies have been reported from Canada. Morgan and Jain (*7*) observed little relation of coffee drinking and bladder cancer in either men or women. Howe et al. (*8*) observed a positive association among men but not among women.

On the basis of the essentially "negative" results of the present study and the low and inconsistent relative risks observed previously, it appears that if there is a relation between coffee drinking and bladder cancer, it is weak. Moreover, we believe that the positive associations reported may have been in part the result of incomplete control of the effect of cigarette smoking.

Cigarette smoking is an important risk factor for bladder cancer, and smoking is correlated strongly with coffee drinking. Therefore, the cigarette smoking habits of subjects should be controlled in an analysis of coffee drinking and bladder cancer. In each of the studies cited except one (*7*), some adjustment for smoking was made. However, smoking might not have been con-

TABLE 2.—*Percentage distribution of cases and controls and relative risk of bladder cancer according to average frequency of coffee drinking by sex in Manchester*

Sex	Study group	No. of cups of coffee/day					No. of subjects
		<1	1	2	3–4	≥5	
Males	Cases, %	57.8	21.9	10.3	6.9	3.1	389
	Controls, %	56.8	19.3	12.1	8.0	3.7	486
	Relative risk[a] .	1	1.1	0.9	0.9	0.8	
Females	Cases, %	52.0	30.3	5.3	9.2	3.3	152
	Controls, %	47.3	22.6	15.9	10.5	3.8	239
	Relative risk[a] .	1	1.4	0.4	1.2	1.0	

[a] Adjusted for age and cigarette smoking.

TABLE 3.—*Percentage distribution of cases and controls and relative risk of bladder cancer according to average frequency of coffee drinking by sex in Nagoya*

Sex	Study group	No. of cups of coffee/day					No. of subjects
		<1	1	2	3–4	≥5	
Males	Cases, %	51.8	19.2	17.0	8.9	3.1	224
	Controls, %	56.6	21.6	13.4	6.8	1.6	440
	Relative risk[a] .	1	1.0	1.2	1.3	1.9	
Females	Cases, %	80.0	16.9		3.1[b]		65
	Controls, %	81.5	12.3		6.2[b]		146
	Relative risk[a] .	1	0.7		0.7[b]		

[a] Adjusted for age and cigarette smoking.
[b] Value pertains to drinkers of ≥2 cups of coffee/day.

trolled completely due to use of an insufficient number of smoking strata in the analysis (*11*). Given a limited amount of data, the degree of stratification necessary for adequate control of smoking might not be feasible. Several investigators (*2, 4–6*) have used from two to four smoking strata. In contrast, estimates in the present study summarize the coffee-bladder cancer relation over six categories of smoking.

Incomplete control of smoking also might be a consequence of random inaccuracies in the smoking histories available. If the smoking history is unreliable, it will fail to reflect fully the hazard of smoking and its association with coffee drinking, so that complete control of the effect of smoking will not be obtained (*12*). An apparent relation of coffee drinking and bladder cancer could stem from this source, which is not related to response bias.

The conditions that could lead to distortion of the coffee-bladder cancer relation by smoking appear to be especially marked in the United States. The extent of such distortion would depend in part on the disparity in smoking habits between drinkers of large and of small amounts of coffee. In the male control series in the Boston center of the present study, the proportion of heavy smokers (≥2 packs/day) was six times greater among drinkers of 5 or more cups of coffee per day than among drinkers of less than 2 cups per day. In contrast, the proportion of heavy smokers was only about twice as high among drinkers of large amounts compared to small amounts of coffee in Manchester and Nagoya. The distortion related to cigarette smoking also would depend on the actual proportion of heavy smokers among drinkers of large amounts of coffee. This proportion was about twice as high in Boston as in Manchester or Nagoya.

Finally, cigarette smoking is more prevalent in men than in women. Therefore, a secondary association of coffee drinking and bladder cancer might be expected to be stronger in men. Most studies have, in fact, found a stronger positive association in men than in women.

REFERENCES

(*1*) COLE P. Coffee drinking and cancer of the lower urinary tract. Lancet 1971; 1:1335–1337.

(*2*) SIMON D, YEN S, COLE P. Coffee drinking and cancer of the lower urinary tract. J Natl Cancer Inst 1975; 54:587–591.

(*3*) FRAUMENI JF JR, SCOTTO J, DUNHAM LF. Coffee drinking and bladder cancer. Lancet 1971; 2:1204.

(*4*) BROSS ID, TIDINGS J. Another look at coffee drinking and cancer of the urinary bladder. Prev Med 1973; 2:445–451.

(*5*) WYNDER EL, GOLDSMITH R. The epidemiology of bladder cancer. A second look. Cancer 1977; 40:1246–1268.

(*6*) METTLIN C, GRAHAM S. Dietary risk factors in human bladder cancer. Am J Epidemiol 1979; 110:255–263.

(*7*) MORGAN RW, JAIN MG. Bladder cancer: Smoking, beverages and artificial sweeteners. Can Med Assoc J 1974; 111:1067–1070.

(*8*) HOWE GR, BURCH JD, MILLER AB, et al. Tobacco use, occupation, coffee, various nutrients, and bladder cancer. JNCI 1980; 64:701–713.

(*9*) MORRISON AS, BURING J. Artificial sweeteners and cancer of the lower urinary tract. N Engl J Med 1980; 302:537–541.

(*10*) BISHOP YM, FIENBERG SE, HOLLAND PW. Discrete multivariate analysis. Cambridge, Mass.: MIT Press, 1975.

(*11*) COCHRAN WG, RUBIN DB. Controlling bias in observational studies: A review. Sankhyā. Indian J Stat 1973; A35(4):417–446.

(*12*) GREENLAND S. The effect of misclassification in the presence of covariates. Am J Epidemiol 1980; 112:564–569.

Noncontraceptive Estrogen Use and the Occurrence of Ovarian Cancer [1,2,3]

Noel S. Weiss, *M.D., Dr.P.H.*, [4,5,6] **Joseph L. Lyon**, *M.D., M.P.H.*, [7] **Sarala Krishnamurthy**, *M.B.B.S., M.D.*, [5] **Scott E. Dietert**, *M.D.*, [5] **Jonathan M. Liff**, *M.S.*, [5] *and* **Janet R. Daling**, *Ph.D.* [4,5]

ABSTRACT—Female residents of six counties in Washington and Utah in whom ovarian cancer was diagnosed during 1975–79 were interviewed concerning prior use of noncontraceptive estrogens. Interviews with a random sample of women drawn from these counties were obtained for comparison. Taken as a whole, women with epithelial ovarian tumors reported estrogen use for 1 year or more somewhat more often than did controls [relative risk (RR) = 1.3, 95% confidence interval (CI) = 0.9–1.8]. The proportion of women who had used estrogens varied according to the histology of their tumor; notably, of 17 women with endometrioid tumors, 12 had used estrogens (RR = 3.1, 95% CI = 1.0–9.8). The excess risk of endometrioid carcinoma related to estrogen use was not further increased when these hormones were taken for long durations, in high doses, or proximate to the time of diagnosis. Neither was there any evidence of increased risk from estrogen use in the small group of women with clear cell tumors, a histologic tumor type believed to be closely related to endometrioid carcinoma. Thus the observed association between menopausal estrogen use and the occurrence of ovarian endometrioid tumors should be interpreted cautiously until the results of additional studies are available.—JNCI 1982; 68:95–98.

The patterns of occurrence of malignant tumors of the ovary, endometrium, and breast have a number of common features. The incidence of each tumor type tends to be higher in Western than in Eastern cultures and, within the West, higher in white women than in nonwhites (*1*). Though their incidence rises rapidly during late reproductive life, after that time it fails to show the age-related exponential increase that is characteristic of many other tumors (*1*). Ovarian, endometrial, and breast cancer are all less common among women who have borne children than among nulliparous women (*2–5*). Thus it is likely that these 3 neoplasms share one or more etiologies. Since use of noncontraceptive estrogens is a strong risk factor for endometrial cancer (*6*), and possibly a weaker one for breast cancer as well (*7–9*), we conducted a study to determine what, if any, role estrogens play in the genesis of ovarian cancer.

METHODS

With the assistance of population-based cancer reporting systems, we identified all white females ages 50–74 years with ovarian cancer who were *a*) residents of King and Pierce Counties (Washington) and diagnosed during 1976–79, and *b*) residents of Salt Lake, Weber, Utah, and Davis Counties (Utah) and diagnosed during 1975–77. Using the original pathologists' diagnoses as a criterion, we excluded tumors of sex cord-stromal or germ cell origin; this left only women bearing "epithelial" tumors. In the Washington counties only, 22 women with "borderline" tumors (i.e., lesions that lacked stromal invasion but had an otherwise malignant appearance) were identified by the reporting system. Because of the potential of borderline tumors for metastasis, these women were included in the analysis.

Between 1 and 18 months after diagnosis, each woman was approached through her physician for an interview at home. The response status of the women with cancer is shown in table 1. Of those who were not interviewed, about two-thirds had died before or during our efforts to contact them. The interview itself covered the woman's menstrual and reproductive history, with particular attention to the use of contraceptive and noncontraceptive estrogens. In an effort to aid recall, we used a color display of commonly used estrogen preparations.

To identify and interview women against whom the patients with cancer could be compared, we did household surveys in both areas. In the Washington counties, this was accomplished by standard area sampling methods in 1976, 1977, and 1979 (*10*). In Utah in 1977, a systematic sample of telephone numbers was selected from the directories serving the four counties. The final two digits were replaced with a number chosen at random, and each resulting telephone number was dialed up to six times. If a household was reached, we sought to obtain a census; this was possible for 91% of households. If a women resided there who was 35–75 years of age, we sought to interview her at home.

The average interval from the diagnosis of ovarian cancer until the study interview was nearly 1 year.

ABBREVIATION USED: RR = relative risk.

---

[1] Received April 3, 1981; accepted September 29, 1981.

[2] Supported in part by Public Health Service grants R01CA-18764 and 1-K04CA-00048 from the National Cancer Institute.

[3] Research procedures were in accord with the ethical standards of the Human Subjects Review Committee, Fred Hutchinson Cancer Research Center.

[4] Fred Hutchinson Cancer Research Center, 1124 Columbia St., Seattle, Wash. 98104.

[5] University of Washington, Seattle, Wash. 98195.

[6] *Address reprint requests to* Dr. Weiss at the Fred Hutchinson Cancer Research Center.

[7] University of Utah, Salt Lake City, Utah 84112.

TABLE 1.—*Response status of women with ovarian tumors*

Cases[a]	No. of subjects
Washington counties, diagnosed 1976–79	298
Women for whom no interview was obtained (physician or patient refused interview, moved, or died)	129
Subjects interviewed	169
Utah counties, diagnosed 1975–77	74
Women for whom no interview was obtained	36
Subjects interviewed	38
Total No. of subjects interviewed	207

[a] White women ages 50–74 yr had epithelial ovarian tumors.

Thus only those control subjects ages 51–75 at the time of interview are included in the analysis, so as to conform more closely to the age range of the women with cancer. Information on estrogen use among controls during the year before interview was deleted to parallel the deletion of information on cases after diagnosis. We also excluded potential controls who reported having undergone a bilateral oophorectomy more than 1 year before interview. The selection of controls is summarized in table 2.

The proportion of women reporting use of noncontraceptive estrogens (defined as use for ≥1 yr) varied little during the course of the study. In the Washington counties, for example, the proportion of users among controls interviewed in 1976, 1977, and 1979 was 45.0, 47.5, and 44.4%, respectively. Variables that did correlate with estrogen use were age, hysterectomy status, and income (median family income of census tract of residence). Since the distribution of income level was similar in women with and without ovarian cancer, our case-control comparisons regarding history of estrogen use are standardized only for age (50–54, 55–64, and 65–74 yr), presence of a uterus, and state of residence (Washington or Utah).

TABLE 2.—*Response status of potential control subjects*

Controls	No. of subjects
Washington Counties[a]	1,271
Subjects excluded	
No interview obtained	99
<51 yr of age	463
Nonwhite women	43
Bilateral oophorectomy ≥1 yr before interview	116
Subjects interviewed	550
Utah Counties	111
Subjects excluded	
No interview obtained	12
<51 yr of age	28
Bilateral oophorectomy ≥1 yr before interview	8
Subjects interviewed	63
Total No. of subjects interviewed	613

[a] Women ages 36–74 yr were identified in three sample surveys.

[b] White women ages 36–75 yr were identified in the 1977 survey.

This study directly measured the relative proportion of estrogen users and nonusers among patients and controls, i.e., the relative odds of estrogen use. Because the incidence in users relative to nonusers (i.e., RR) is accurately estimated by the relative odds, and because it has greater intuitive meaning, the results will be expressed in these terms.

RESULTS

As a group, women with epithelial ovarian tumors reported taking estrogens (for ≥1 yr) to a somewhat greater extent than did control women (table 3). The small group of women diagnosed as having endometrioid tumors was responsible for a part of this excess; 12 of the 17 women in the group had taken estrogens, giving an RR of 3.1 ($P=0.05$). Among women diagnosed as having one of the other histologic tumor types, women with serous tumors had used estrogens more than had controls ($RR=1.6$; $P=0.07$), whereas those with mucinous tumors had used them less often ($RR=0.7$; $P=0.27$).

The estrogen-endometrioid tumor association was present in both states (8 of 13 Washington patients and 4 of 4 Utah patients had used estrogens for ≥1 yr) and was present whether or not the women retained her uterus and whether or not she had given birth to a child. The association was not further strengthened when only long durations or higher doses of estrogen use were considered, because patients and controls who reported taking estrogens had similar patterns of doing so (table 4). The small excess risk observed for all histologic tumor types combined also was not influenced further by the duration (54 cases observed with duration >5 yr, 52.3 expected on the basis of controls who were users), amount, or timing of estrogen use. In contrast to the findings of an earlier study

TABLE 3.—*Use of noncontraceptive estrogens among women with various histologic types of ovarian cancer and among controls*

Histologic type	Estrogen users, %[a] No. of patients	RR[b]	95% confidence interval[c]
All cases[d]	49.8 (205)	1.3	0.9–1.8
Serous	54.2 (72)	1.6	1.0–2.6
Mucinous	34.4 (32)	0.7	0.3–1.4
Endometrioid[e]	70.6 (17)	3.1	1.0–9.8
Other epithelial[f]	47.6 (84)	1.3	0.9–2.3
Controls	44.2 (611)	—	—

[a] Users for ≥1 yr.

[b] Relative to risk of 1.0 in estrogen nonusers and users of <1 yr. Standardized for age, hysterectomy status, and state of residence (Washington, Utah) by the method of Mantel and Haenszel (*11*).

[c] Approximate, according to the method of Miettinen (*12*).

[d] Epithelial tumors only; excludes tumors of germ cell or sex cord-stromal origin.

[e] Includes one case each of "adenocarcinoma with squamous metaplasia" and "adenosquamous" cancer.

[f] Primarily tumors labeled as "papillary," "adenocarcinoma," or "carcinoma" without further specification.

TABLE 4.—*Pattern of noncontraceptive estrogen use among women with endometrioid tumors*

Pattern of use	No. of estrogen users	
	Observed[a]	Expected[b]
Total duration >5 yr	7	6.5
First use >5 yr before diagnosis	9	8.5
Use during year before diagnosis	6	8.1
Average daily dose >1.0 mg	9	8.4
Ever used diethylstilbestrol	0	1.0

[a] No. = 12.

[b] Based on the experience of those control subjects who used noncontraceptive estrogens, standardized for age and state of residence.

(*13*), use of diethylstilbestrol was related neither to the occurrence of all epithelial types (observed:expected = 3:5.4) nor to that of endometrioid tumors (observed:expected = 0:1.0). We interviewed eight women who had clear cell tumors, a tumor type believed to be histogenetically related to endometrioid tumors (*14*); only 2 of the 8 reported having used estrogens (RR = 0.5; $P = 0.4$).

The entity "endometrioid" carcinoma has been included for less than 20 years in widely recognized schemes for classification of ovarian tumors. Thus we were concerned as to the accuracy of the diagnoses of this histologic type of tumor which were made in individual hospital laboratories and which had not been reviewed by standard criteria. Because of this concern, we procured the original slides of the 13 tumors for the Washington cases labeled as endometrioid. Two of us (S. K. and S. D.) reviewed these slides along with those from tumors of 10 estrogen users and 10 estrogen nonusers selected at random from the other Washington cases; the reviewers had no knowledge of the original diagnosis or the history of estrogen consumption. The criteria used to classify tumors as endometrioid were those of Long and Taylor (*15*) and of Serov et al. (*16*). The histology of an ovarian tumor often is not homogeneous, so, though we classified each one according to its major component, the presence of endometrioid characteristics as a minor component was specified as well. The results of our review are shown in table 5. The original diagnosis of endometrioid carcinoma was confirmed in 10 of 13 cases, and an endometrioid pattern present to a minor degree was observed in the remaining 3. Estrogens had been used in 7 of the 10 confirmed cases and in 1 of the 3 cases with a minor endometrioid component. The agreement of the review diagnosis with the original diagnosis of "nonendometrioid" carcinoma varied according to whether the patient had previously used estrogens: In the absence of exogenous estrogen exposure, the degree of correspondence was high, whereas in tumors of 5 of the 10 women with a history of estrogen use, at least a minor degree of endometrioid features was exhibited.

TABLE 5.—*Results of histologic review of slides from cases of ovarian cancer in western Washington*[a]

Original diagnosis	Diagnosis from slide review			
		Other epithelial		
	Endometrioid	Endometrioid component present	Endometrioid component absent	Total
Endometrioid	10	3	0	13
Other epithelial				
History of estrogen use	2	3	5	10
No history of estrogen use	1	0	9	10

[a] *See* text for criteria for selection of case groups.

DISCUSSION

Several features of the association found here between the use of noncontraceptive estrogens and the incidence of ovarian endometrioid tumors suggest that the association may be real. The estimated risk to users relative to nonusers is high ($\approx$3), and the diagnoses upon which this estimate is based appear accurate. In several areas of the United States, the *reported* incidence of endometrioid tumors increased during the early 1970's (*17*) in parallel with the increasing use of noncontraceptive estrogens. (However, since acceptance among pathologists of endometrioid tumors as a histologic entity was also growing during this period, the *true* increase in incidence was undoubtedly smaller than that reported). Also, as their name suggests, these lesions are similar in appearance to carcinoma of the endometrium, a tumor whose relationship to exogenous estrogens has been well documented (*6*).

Nonetheless, some aspects of this study require caution when the results are interpreted. First, a sizable fraction (44%) of the women with cancer who were eligible to take part in the study were not interviewed, the primary reasons for noninterview being death and terminal illness. While this degree of nonresponse could bias the risk estimates in either direction, it is more likely to have forced them higher: Estrogen users were possibly diagnosed earlier in the course of their disease than were nonusers (estrogen users were likely to have received regular gynecologic examinations), and so it is possible that a disproportionately high percentage of estrogen-using patients were able to provide an interview. However, while the small excess risk for nonendometrioid epithelial tumors might to some extent be explained by this bias, it is not likely to account for the association between estrogen use and endometrioid tumors: The magnitude of that association was much stronger, and the proportion of women with endometrioid carcinoma who were not interviewed was lower (5/22 = 23%).

Second, at least some inaccuracy was likely in the interview information on oophorectomy status which served as the basis for exclusion of individual control subjects. *a*) Some potential controls who claimed that both ovaries had been removed, in truth, had one or both retained, but nonetheless were excluded from the analysis. *b*) Contrariwise, some women who believed that one or both of their ovaries were present, in truth, had no ovarian tissue left, and yet were included as control subjects. Because having undergone a bilateral oophorectomy is a strong predictor of having used estrogens, an artificially positive association of estrogen use and ovarian cancer could have resulted if errors of type *a*) above exceeded those of type *b*). However, since self-reported oophorectomy status has been found to correspond closely to information obtained from the women's hospital records at the time of surgery (*18*), the magnitude of any bias of this sort is likely to have been small.

Third, though the incidence of endometrial cancer increases steadily with increasing duration of noncontraceptive estrogen use (at least through the first 10-15 yr of use) (*19*), we did not find such increases to be true for ovarian endometrioid tumors (table 4). Finally, there was no evidence for the association of estrogen use and the incidence of ovarian clear cell tumors, the histologic type thought to be closely related to endometrioid tumors in terms of histogenesis.

Even if the use of menopausal estrogens were truly associated with the incidence of ovarian endometrioid tumors, it is conceivable that the overall incidence of ovarian tumors in estrogen users is not altered. For example, it is possible that, in response to the presence of exogenous estrogens, epithelial ovarian tumors that arise through other etiologic pathways are stimulated to exhibit a glandular (endometrioid) component. Or, if some ovarian tumors begin as highly differentiated lesions and over time become increasingly less differentiated, then the estrogen user, who may have her cancer diagnosed more promptly than the nonuser, will tend to have a more highly differentiated tumor (e.g., endometrioid) at diagnosis.

However, for either or both of the above hypotheses to fully explain the estrogen-endometrioid tumor association, the risk to estrogen users relative to that of nonusers for ovarian epithelial tumors *other than* endometrioid must be less than 1.0: Each hypothesis provides for no excess cases of ovarian cancer as a result of estrogen use, so that the excess "risk" seen for endometrioid tumors must be balanced by a deficit in risk for the others. Except for the relatively small group of women with mucinous tumors, no indication of such a deficit was present in our data.

We believe that another, more plausible, explanation for the observations is that estrogen use does lead to an increased incidence of endometrioid tumors but not of other ovarian epithelial tumors, and that the excess risk for the latter group is due to the inclusion of endometrioid tumors not recognized as such (*see* table 5). Nonetheless, the data we have presented here in support of this interpretation are far from definitive. A larger case-control study, with a histologic review of a larger proportion of the cases, will be needed before much faith can be put in any of these interpretations.

REFERENCES

(*1*) Waterhouse JA, Muir C, Correa P, Powell J, eds. Cancer incidence in five continents. Vol 3. Lyon: IARC, 1976.

(*2*) Joly DJ, Lilienfeld AM, Diamond EL, Bross ID. An epidemiologic study of the relationship of reproductive experience to cancer of the ovary. Am J Epidemiol 1974; 99:190-209.

(*3*) Newhouse ML, Pearson RM, Fullerton JM, Boesen EA, Shannon HS. A case control study of carcinoma of the ovary. Br J Prev Soc Med 1977; 31:148-153.

(*4*) Elwood JM, Cole P, Rothman KJ, Kaplan SD. Epidemiology of endometrial cancer. J Natl Cancer Inst 1977; 59:1055-1060.

(*5*) MacMahon B, Cole P, Lin TM, et al. Age at first birth and breast cancer risk. Bull WHO 1970; 43:209-221.

(*6*) Weiss NS. Noncontraceptive estrogens and abnormalities of endometrial proliferation. Ann Intern Med 1978; 88:410-412.

(*7*) Hoover R, Gray LA, Cole P, MacMahon B. Menopausal estrogens and breast cancer. N Engl J Med 1976; 295:401-405.

(*8*) Ross RK, Paganini-Hill A, Gerkins VR, et al. A case-control study of menopausal estrogen therapy and breast cancer. JAMA 1980; 243:1635-1639.

(*9*) Jick H, Walker AM, Watkins RN, et al. Replacement estrogens and breast cancer. Am J Epidemiol 1980; 112:586-594.

(*10*) Koepsell TD, Weiss NS, Thompson DJ, Martin DP. Prevalence of prior hysterectomy in the Seattle-Tacoma area. Am J Public Health 1980; 70:40-47.

(*11*) Mantel N, Haenszel W. Statistical aspects of the analysis of data from retrospective studies of disease. J Natl Cancer Inst 1959; 22:719-748.

(*12*) Miettinen O. Estimability and estimation in case-referent studies. Am J Epidemiol 1976; 103:226-235.

(*13*) Hoover R, Gray LA, Fraumeni JF Jr. Stilbestrol and the risk of ovarian cancer. Lancet 1977; 2:533-534.

(*14*) Scully RE. Recent progress in ovarian carcinoma. Hum Pathol 1979; 1:73-98.

(*15*) Long ME, Taylor HC. Endometrioid carcinoma of the ovary. Am J Obstet Gynecol 1964; 90:935-950.

(*16*) Serov SF, Scully RE, Sobin LH. International histological classification of tumors, No. 9. Histological typing of ovarian tumors. Geneva: WHO, 1973.

(*17*) Weiss NS. Exogenous estrogens and the incidence of neoplasms in tissues of müllerian origin. In: Hiatt HH, Watson JD, Winsten JA, eds. The origins of human cancer. Cold Spring Harbor conference on cell proliferation. Vol 4. New York: Cold Spring Harbor Laboratory, 1977:413-422.

(*18*) Brinton LA, Hoover RN, Szklo M, Fraumeni JF Jr. Menopausal estrogen use and risk of breast cancer. Cancer 1981; 47:2517-2522.

(*19*) Weiss NS, Szekely DR, English DR, Schweid AI. Endometrial cancer in relation to patterns of menopausal estrogen use. JAMA 1979; 242:261-264.

Multiple Marker Evaluation in Human Prostate Cancer With the Use of Tissue-Specific Antigens[1, 2, 3]

M. Kuriyama,[4] M. C. Wang,[4] C. L. Lee,[4] C. S. Killian,[4] L. D. Papsidero,[4] H. Inaji,[4] R. M. Loor,[4] M. F. Lin,[4] T. Nishiura,[5] N. H. Slack,[6] G. P. Murphy,[6] *and* T. M. Chu[4,7,8]

ABSTRACT—Serum prostate-specific antigen and prostatic acid phosphatase were simultaneously evaluated in 22 healthy males, 29 patients with benign prostatic hypertrophy, and 192 patients with prostate cancers at various stages as well as in 30 patients with cancers other than prostate cancer. Both markers were quantitated by specific sandwich-type, enzyme-linked, immunocorbent assays with the use of specific antiserum reagents. Serum assays revealed a discordance between these two markers; thus expressions of these two biochemically and immunologically distinct prostate-specific proteins may reflect different aspects in the biology of prostate cancer. A combination test with the use of 7.5 ng of prostate antigen and 15.5 ng of prostatic acid phosphatase/ml of serum, respectively, as cutoff values resulted in a positive detection rate of 58% for prostate cancers of stages A (7/12) and B (21/36) each, 68% for prostate cancer of stage C (19/28), 92% for prostate cancer of stage D (108/118), and only 10% for benign prostatic hypertrophy (3/29). None of 52 other cancers or healthy controls was registered as positive. This study demonstrates that a multiple marker test of tissue-specific antigens can be of an additive value in the immunodiagnosis of cancer and may be a logical and effective approach at this time, in light of the unavailability of human tumor-specific markers.—JNCI 1982; 68:99–105.

Assay of acid phosphatase activity (EC 3.1.3.2) has been used as an aid in the diagnosis of prostate cancer, since Gutman et al. (*1*) in 1936 reported an association between elevated serum acid phosphatase and metastatic prostate cancer. Recently, several immunochemical procedures have been developed for quantitation of serum PAP (*2–8*). By these immunoassays with antisera specific to PAP, various results with regard to the detection of elevated serum PAP in prostate cancer have been reported.

This laboratory reported 2 years ago the identification and purification of a new antigen, PA (*9*). By an immunocytochemical technique, PA has been shown to be localized in the cytoplasm of prostatic ductal cells (*10*). Human prostate tumor cells in vitro and in vivo also express this antigen (*11*). Circulating PA in patients with prostate cancer has been shown to be biochemically similar and immunologically identical to that of prostate tissue (*12*). Further, a sensitive sandwich-type ELISA has been developed for quantitation of PA (*13*). PA was not detectable in sera from healthy females or from female cancer patients. Sera from male patients with cancers other than prostate cancer contained a range of PA similar to that of healthy males. However, patients with prostate cancer had significantly elevated levels of serum PA. Since PA is biochemically and immunologically distinct from PAP (*9, 11*), the expressions of these two prostate-specific proteins may be unique parameters in combination tests for serologic detection of prostate cancer. The data may provide useful information for the design of multiple marker studies for cancer. Also, new potential uses of tissue- or organ-specific antigens, rather than tumor-specific antigens, may be realized in the immunodiagnosis of cancer. This report describes our initial evaluation on the simultaneous measurements by two ELISA procedures of serum PA and PAP in prostate cancer.

ABBREVIATIONS USED: BPH=benign prostatic hypertrophy; BSA=bovine serum albumin; ELISA=enzyme-linked immunosorbent assay; HRP=horseradish peroxidase; PA=human prostate-specific antigen; PAP=human prostatic acid phosphatase; PBS=phosphate-buffered saline [0.01 M NaH_2PO_4–0.01 M Na_2HPO_4–0.154 M NaCl (pH 7.1)]; pI=isoelectric point(s).

---

[1] Received April 24, 1981; accepted August 20, 1981.

[2] Supported in part by Public Health Service grants CA-15437, CA-15126, and CA-23990 from the National Cancer Institute.

[3] Research procedures were in accord with the ethical standards of the Human Experimentation Committee, Roswell Park Memorial Institute.

[4] Department of Diagnostic Immunology Research and Biochemistry, Roswell Park Memorial Institute, 666 Elm St., Buffalo, N.Y. 14263.

[5] Department of Urology, Gifu University School of Medicine, Gifu, Japan.

[6] National Prostatic Cancer Project, Roswell Park Memorial Institute. Other investigators include: Dr. D. Johnson, M. D. Anderson Hospital and Tumor Institute, Houston, Tex.; Dr. S. A. Leoning, University of Iowa Hospitals and Clinics, Iowa City, Iowa; Dr. R. P. Gibbons, The Mason Clinic, Seattle, Wash.; Dr. G. R. Prout, Massachusetts General Hospital, Boston, Mass.; Dr. W. W. Scott, The Johns Hopkins University Hospital, Baltimore, Md.; Dr. M. Soloway, University of Tennessee, Memphis, Tenn.; Dr. J. D. Schmidt, University of California at San Diego, San Diego, Calif.; Dr. S. Bergman, Tulane Medical Center, New Orleans, La.; Dr. J. M. Pierce, Hutzel Hospital/Wayne State University, Detroit, Mich.; Dr. F. Scardino, Baylor University, Houston, Tex.; Dr. M. McLeod, Walter Reed Army Medical Center, Washington, D.C.; Dr. C. McKiel, Rush-Presbyterian–St. Luke's Medical Center, Chicago, Ill.; Dr. J deKernion, University of California at Los Angeles, Los Angeles, Calif.; Dr. S. Beckley, Roswell Park Memorial Institute; and Dr. E. J. Pontes, Roswell Park Memorial Institute, formerly at Hutzel Hospital/Wayne State University.

[7] *Address reprint requests to* Dr. Chu.

[8] We acknowledge the valuable secretarial assistance of Ms. J. Ogledzinski and Ms. S. Witalis.

MATERIALS AND METHODS

Materials.—HRP (EC 1.11.1.7: type VI, RZ3.2, lot #59C-9760), 2,4-dinitrofluorobenzene, sodium borohydride, *o*-dianisidine, poly-L-lysine succinate, and BSA were purchased from Sigma Chemical Co., St. Louis, Mo. Sodium metaperiodate and monoethanolamine were obtained from Fisher Scientific Co., Fair Lawn, N.J. Sephadex G-200 was the product of Pharmacia Fine Chemicals, Piscataway, N.J.

Normal human sera were collected from apparently healthy volunteers 24-65 years old. Serum specimens from patients with histologically confirmed prostate cancers and BPH were received from the National Prostatic Cancer Project's Serum Bank and Gifu University School of Medicine, respectively. Prostate cancers were staged by investigators of the National Prostatic Cancer Project (*14*). All patients had active disease, although some patients were receiving treatment. Most patients with stages A, B, and C cancer had had no treatment. All patients with advanced stage D were refractory to hormone or radiation therapy and had not yet been given chemotherapy. Sera from patients with other cancers were obtained from Roswell Park Memorial Institute; all of these patients had metastatic cancer. Specimens were stored at −85°C until used.

Immunologic reagents.— Preparation of purified PA and PAP and production of specific anti-PA and anti-PAP antisera in the goat were reported previously (*3, 6, 9, 12*). The IgG fraction of goat immune sera was prepared by ammonium sulfate precipitation and Sephadex G-200 gel filtration (*13*). The IgG fraction from goat normal serum was isolated in the same manner. Coupling of HRP to anti-PA IgG and anti-PAP IgG was described previously (*13*).

Coating of anti-PAP to tube.—Coating of anti-PAP IgG to a polystyrene tube (12×75 mm) was done by the procedure of Kelsoe and Weller (*15*). Each tube was incubated first with 200 µl of solution containing 0.25 mg of poly-L-lysine succinate/ml for 15 minutes at room temperature. The tube was washed three times with 1 ml of PBS, after which 200 µl of anti-PAP IgG or normal goat IgG in 0.01 *M* carbonate buffer (pH 9.6; 50 µg/ml or 25 µg/ml) was added to each tube and each tube was incubated at 37°C for 24 hours. Then 1 ml of 1% BSA in PBS was added to the tube to saturate any uncoated sites. After 3 hours of incubation at 37°C, the antibody-coated tube was stored at 4°C until used.

Quantitation of PAP.—Purified PAP or a diluted serum sample (200 µl) was incubated in an anti-PAP-coated tube for 3 hours at 37°C. To each tube was added 1 ml of washing buffer (PBS containing 1% BSA and 0.01 *M* EDTA:Na salt). After gently whirling in a vortex, 1 ml of the solution was removed. This washing step was repeated three times. HRP-labeled anti-PAP IgG (100 µl) was then added, and the tube was incubated for another 3 hours at 37°C, which resulted in the formation of anti-PAP IgG:PAP:anti-PAP IgG-HRP. After the tube was washed three times, the peroxidase activity of the complex was then quantitated as described previously at 403 nm (A_{403}) (*13*). The percentage bound was calculated from $[(B-Bo)/(B_t-Bo)]\times100$, where $B=A_{403}$ of the sample, $B_t=A_{403}$ of maximum, and $Bo=A_{403}$ of the blank. Each assay was performed in duplicate with two controls, one blank (without sample) and the other containing purified PAP at a concentration of 10 µg/ml for the maximal binding. The quantity of PAP in the specimen was determined from a standard curve constructed in an identical manner with the use of various concentrations of purified PAP.

The reproducibility of this procedure was evaluated by the determination of the coefficients of variation between assays (i.e., two samples containing different concentrations of PAP were assayed in 10 separate experiments) and by the determination of the variation within assays (i.e., two other samples with different PAP levels were analyzed in a series of 10 assays each) (*13*).

Nonspecific adsorption of the tube-coated anti-PAP IgG.—A total of 27 normal male sera were tested for nonspecific adsorption to the insolubilized antibody with the use of goat normal IgG coated to the tube.

Quantitation of PA.—Serum PA levels were determined by the ELISA procedure as reported recently (*13*); by this procedure, anti-PA IgG was conjugated to a solid-phase support, CNBr-activated Sepharose 4B. After incubation of the specimen with Sepharose 4B-anti-PA, the resulting Sepharose-anti-PA:PA was further reacted with anti-PA-HRP. The HRP in the sandwich-type Sepharose 4B-anti-PA:PA:anti-PA-HRP was then quantitated and used as a parameter for serum PA concentration.

RESULTS

ELISA of PAP

The newly developed, tube-supported, sandwich-type ELISA of PAP, as performed by the experimental protocol described, yielded a working range of 1.0-100 ng of PAP/ml of serum sample (text-fig. 1). Quality-control data of within-assay variation (two levels of PAP, 6.5 and 35, and 10 assays each) and between-assay variation (two levels of PAP, 2.6 and 51, and 10 assays each) revealed an overall mean coefficient of variation of 4.3% (ranging from 3.2 to 5.7%), indicating that this new enzyme immunoassay for PAP was a reproducible procedure. With the use of a tube coated with goat preimmune IgG, rather than with goat immune anti-PAP IgG, 27 serum specimens of healthy males were shown to have levels of nonspecific binding from 15 to 19% (mean, 17.4%). The ranges represented approximate values of 1.0 ng or less, the sensitivity limit of this ELISA (text-fig. 1). Therefore, the PAP assay was performed without the simultaneous use of a control, e.g., a preimmune goat IgG-coated tube.

In addition, sera from a group of 27 apparently

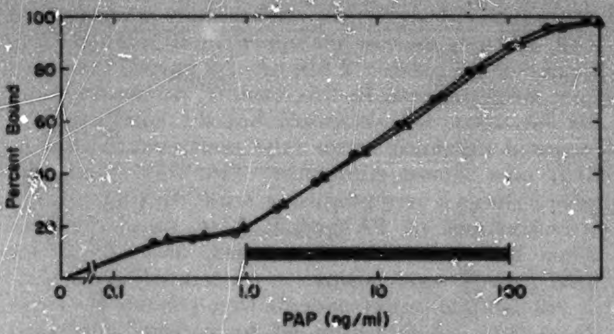

TEXT-FIGURE 1.—Standard calibration curve of PAP as determined by the ELISA with the use of a hundredfold-diluted HRP-anti-PAP IgG and 10 μg of anti-PAP IgG applied to a polystyrene tube. ●, purified PAP; ▲, serum containing 480 ng PAP/ml as standard. *Horizontal bar* indicates the working range of this ELISA. Percent bound was calculated by the formula $[(B-Bo)/(B_t-Bo)]\times 100$, where $B = A_{405}$ of the sample, $B_t = A_{405}$ of the maximum, and $Bo = A_{405}$ of the blank as indicated in the text.

healthy normal male controls were shown by this ELISA to have PAP levels ranging from less than 1.0 to 13 ng/ml with a mean plus or minus standard deviation of 4.4±3.7. For statistical analysis, an upper cutoff point for the normal range was, therefore, calculated as 15.5 ng PAP/ml of serum (mean + 3 SD).

Single Assay of PAP

Serum PAP values in patients with prostate cancers, BPH, and other cancers are shown in table 1. Thirty male patients with cancers of the lung, pancreas, and colon-rectum (10 each) showed a range of serum PAP similar to that seen in 27 healthy males, as did 29 patients with BPH. A significantly higher mean serum PAP value, however, was obtained from patients with all clinical stages of prostate cancers. The mean of serum PAP in 12 patients with stage A prostate cancer, 15.5 ng/ml, was equal to the upper cutoff point for the range in 27 healthy males. In addition, the mean serum PAP increased with increasing disease stage. Serum PAP levels were elevated in 33% of stage A, 42% of stage B, 64% of stage C, and 73% of stage D prostate cancer patients. Text-figure 2 shows a scattergram of the data presented in table 1 for males.

This study also included serum "PAP" values from 10 healthy female controls and 19 female cancer patients. As table 1 shows, all mean values were less than 1.5, representing circulating acid phosphatase of nonprostate origin or other proteins that may react nonspecifically with goat anti-PAP serum by the ELISA procedure, although anti-PAP serum used in the assay previously has been shown by immunoprecipitation and immunocytochemical techniques to be specific to acid phosphatase of prostate origin.

Single Assay of PA

The PA assay also was performed in serum specimens at the time that PAP levels were determined. For statistical analysis, an upper cutoff value also was calculated from the means + 3 SD of healthy controls, which yielded a value of 2.5 ng PA/ml of serum. As reported previously, the sensitivity of our ELISA of PA was 0.10 ng/ml, and sera of all females, either healthy controls or cancer patients, contained PA less than 0.10 ng/ml (as further demonstrated in the 29 specimens assayed in this study). Again, with one exception, male patients with cancers other than prostate cancer had serum PA values of less than 2.5 ng/ml. Although 41% (12/29) of the BPH patients exhibited elevated serum PA levels, more prostate cancer patients [67% (8/12) with stage A cancer, 69% (25/36) with stage B, 79% (22/28) with stage C, and 83% (96/116) with stage D] demonstrated an elevated PA with a higher mean value

TABLE 1.—*Serum PAP level by ELISA in various diseases*

Groups	No. of persons examined	Serum PAP, ng/ml						
		Male				Female		
		No. of males	Range	Mean ± SD	>15.5 (%)	No. of females	Range	Mean ± SD
Healthy subjects	37	27	<1.0–13	4.4±3.7	0	10	<1.0–2.4	1.3±0.6
Patients with cancers other than prostate cancer[a]	49	30	<1.0–12	4.2±3.2	0	19	<1.0–3.6	1.4±0.7
Lung cancer	15	10	1.0–12	4.4±3.3	0	5	<1.0–2.3	1.5±0.6
Breast cancer	5					5	<1.0–2.2	1.3±0.5
Pancreatic cancer	14	10	1.0–11	4.0±2.8	0	4	<1.0–3.6	1.5±1.2
Colorectal cancer	15	10	<1.0–9.9	4.3±3.4	0	5	<1.0–2.2	1.4±0.5
Patients with BPH	29	29	<1.0–18	6.0±4.8	2 (7)			
Patients with prostate cancers of[b]								
Stage A	12	12	5.3–48	15.5±10.9	4 (33)			
Stage B	36	36	5.0–55	15.9±9.4	15 (42)			
Stage C	28	28	8.4–110	26.0±21.4	18 (64)			
Stage D	116	116	4.7–480	65.3±86.1	85 (73)			

[a] All with metastatic cancer.

[b] All with disease present. Most patients with stages A, B, and C cancers had not yet been treated. All patients with stage D cancer were refractory to hormone or radiation therapy and had not yet received chemotherapy.

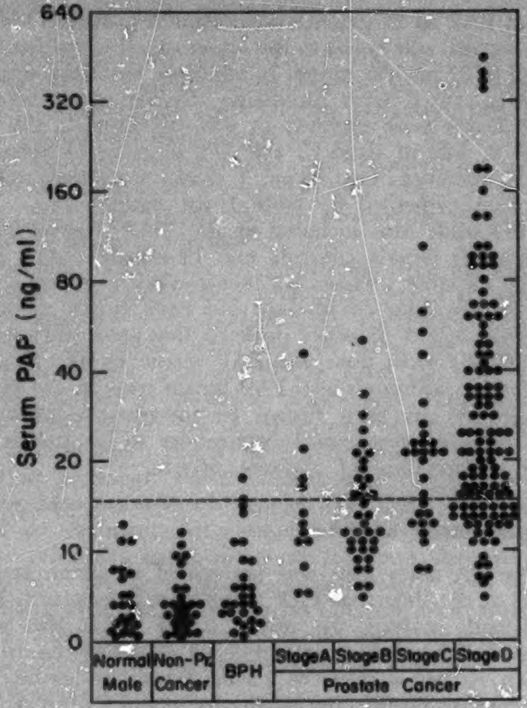

TEXT-FIGURE 2.—Serum PAP levels in healthy male controls (Normal Male), male patients with cancers other than prostate cancer (Non-pr. Cancer), patients with BPH, and patients with prostate cancers of various stages. *Broken horizontal line* shows a PAP level of 15.5 ng/ml, the upper limit of the normal range (mean + 3 SD).

(text-fig. 3). In comparison to the PAP assay, the PA assay registered positive values more often in the BPH patients.

Multiple Assays of PA and PAP

Among 22 healthy male controls, 29 BPH patients, 192 prostate cancer patients, and 30 males with other cancers, assays of both PA and PAP were performed simultaneously. The elevation of either PA or PAP levels was then determined. Overall, 64 and 79% of 192 patients with prostate cancers had elevated PAP and PA levels, respectively. As already noted, an elevated PA also was shown in a higher percentage of the patient population. It was found in 67% of the patients with stage A prostate cancer, 69% with stage B, 79% with stage C, 83% with stage D, and in 41% of the patients with BPH. In comparison with the elevations in PA levels, the levels of PAP were elevated in 34, 41, 64, and 74% of the patients with stages A, B, C, and D prostate cancers, respectively, and in 7% of the patients with BPH. For both assays, 83% of the patients with stage A cancer to 94% of the patients with stage D were shown to have elevated PA and/or PAP values, although 48% of the patients with BPH also registered as positive in either PA or PAP assay.

In practice, for multiple marker study using PA and PAP, one may increase the upper cutoff point of PA to a value of the mean + 2 SD, i.e., 7.5 ng/ml, calculated from BPH patients. In this manner, the sensitivity of the PA assay was decreased, but the specificity was increased inasmuch as the false positives presented by BPH were almost eliminated. With this adjustment, table 2 shows a very promising result for simultaneous determinations of PA and PAP in prostate cancer. When both assays were combined, only 10% of the BPH patients were positive in the test. Also, 153 (79%) of 192 prostate cancer patients were positive for either PA or PAP, ranging from 58% for patients with stages A and B each, to 68% for patients with stage C, to 92% for patients with stage D; a significant number (53) of the patients were positive with both assays. Furthermore, patients with other cancers or healthy controls registered no positive assay. Therefore, these results as derived from two prostate tissue antigens that were measured simultaneously clearly demonstrated an additive value.

DISCUSSION

Data obtained from simultaneous assays of two prostate-specific markers, PA and PAP, have been presented. Serum PA is quantitated by an established solid-phase sandwich-type (Sepharose 4B-anti-PA:PA: anti-PA-HRP) ELISA (*13*), whereas PAP is measured

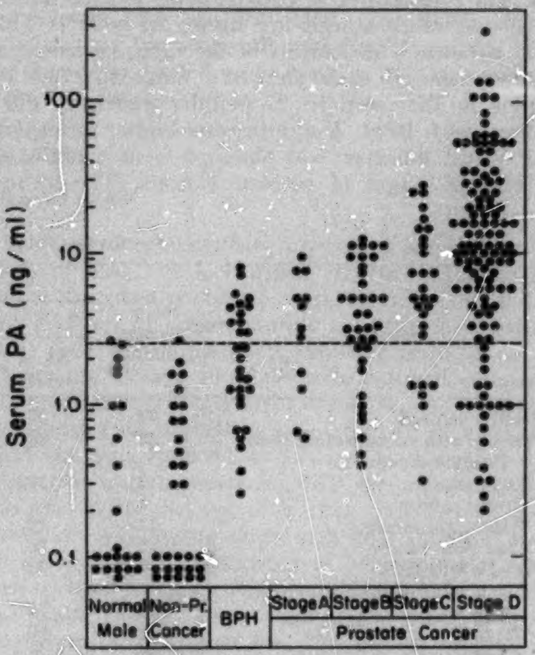

TEXT-FIGURE 3.—Serum PA levels in healthy male controls, male patients with cancers other than prostate cancer (Non-Pr. Cancer), patients with BPH, and patients with prostate cancers of various stages. *Broken horizontal line* indicates a PA level of 2.5 ng/ml, the upper limit of the normal range (mean + 3 SD).

TABLE 2.—*Simultaneous assay of serum PA and PAP*

Groups	No. of persons examined	Assay results[a]			
		PAP (−) and PA (−)	PAP (−) and PA (+)	PAP (+) and PA (−)	PAP (+) and PA (+)
Healthy males	22	22 (100)	0 (0)	0 (0)	0 (0)
Patients with cancers other than prostate cancers[b]	30	30 (100)	0 (0)	0 (0)	0 (0)
BPH patients	29	26 (90)	1 (3)	2 (7)	0 (0)
Patients with prostate cancers of[c]	192	39 (20)	31 (16)	56 (29)	66 (34)
Stage A	12	5 (42)	3 (25)	4 (33)	0 (0)
Stage B	36	15 (42)	6 (17)	11 (31)	4 (11)
Stage C	28	9 (32)	1 (4)	9 (32)	9 (32)
Stage D	116	10 (8)	21 (18)	32 (28)	53 (46)

[a] Results are expressed as No. of individuals in each category (%). PAP, <15.5 ng/ml (−) or >15.5 ng/ml (+); 15.5=mean + 3 SD of normal values. PA, <7.5 ng/ml (−) or >7.5 ng/ml (+); 7.5=mean + 2 SD of BPH values.

[b] All with metastatic cancer.

[c] All with disease present. Most patients with stages A, B, and C cancers had not yet been treated. All patients with stage D cancer were refractory to hormons or radiation therapy and had not yet received chemotherapy.

by a newly reported, tube-supported, sandwich-type (tube-anti-PAP:PAP:anti-PAP-HRP) ELISA. The ELISA of PAP detects an antigenic protein of the enzyme, unlike our several other immunochemical procedures, such as counterimmunoelectrophoresis (*3, 8*), fluorescent immunoassay (*4*), immunoadsorbent assay (*6*), and the double-antibody immunoenzyme assay of Choe et al. (*5*), which detect both antigenic sites and the hydrolytic activity of the enzyme. In this ELISA of PAP, the HRP activity of the final conjugate, tube-anti-PAP:PAP:anti-PAP-HRP, is measured and serves as an index for quantitation of PAP. This assay detects more elevated serum PAP in the early stage of prostate cancer than does the counterimmunoelectrophoresis technique (*3, 8*) but reveals a similar detection rate as the fluorescent immunoassay (*4*) or the immunoadsorbent assay (*6*).

Both PA and PAP are proteins of human prostate-specific origin (*3, 9*). Biochemically, PA is a glycoprotein of molecular weight 33,000 with a pI of 6.9, whereas PAP is a larger, 100,000, glycoprotein with multiple pI ranging from 4.2 to 5.5 (*3, 9, 16*). Immunologically, PA and PAP are two distinct antigen moieties; i.e., antisera possess specific reactivity against their respective antigens and demonstrate no cross-reactivity with each other (*12*). PA is not a subunit or a related peptide of PAP, because both proteins exhibit different amino acid compositions and peptide mapping (*17*). As text-figure 4 shows, different levels of PA and PAP are expressed by patients with prostate cancer; i.e., in some patients PAP levels are in the normal range, while PA levels are elevated. Further, although not prostate tumor-specific, PA and PAP have been shown to be promising markers in the detection of prostate cancer; they may reflect different aspects of neoplastic transformation in prostate cancer. These observations are the rationale for this study.

In evaluating the possible role of serum PA and PAP assays in the immunodiagnosis of prostate cancer, we have used the conventional mean + 3 SD of male controls as the upper normal limits for serum PA and PAP values. Under these criteria, each assay alone detected an elevation of PAP and PA in 64 and 79% of prostate cancer patients, respectively. None of the healthy males and 7% of the BPH patients had an elevated PAP, whereas 9% of the healthy males, 3% of the patients with cancers other than prostate cancer, and 41% of the BPH patients demonstrated an elevated PA value. In the combination test, these individuals also registered positive assay values. However, in pros-

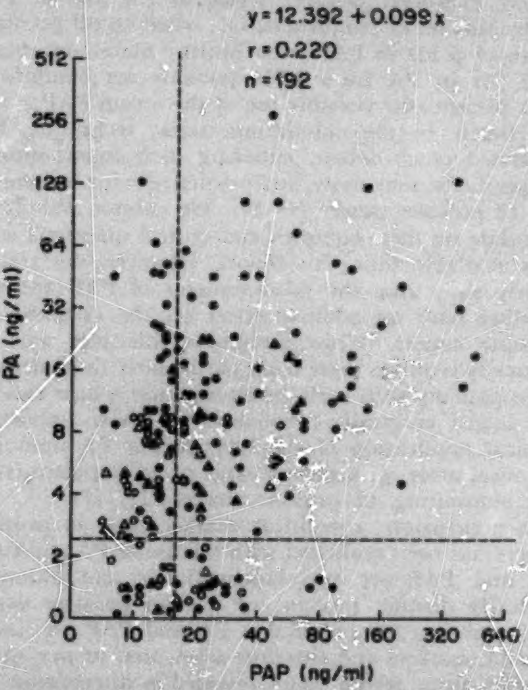

TEXT-FIGURE 4.—Simultaneous assays of serum PA and PAP in 192 randomly selected prostate cancer patients. *Two broken lines* indicate the upper normal limits of serum PA and PAP. △, stage A; ○, stage B; ▲, stage C; ●, stage D. y, PA; x, PAP. r=correlation coefficient; n=number.

tate cancer, a combination of these two assays increased the positive detection rate of PA and/or PAP to 83% for the patients with stage A prostate cancer, 89% for the patients with stages B and C, and 94% for the patients with stage D. The PA assay alone and the PAP assay alone gave respective rates of 57, 69, 79, and 80% and 33, 42, 64, and 73% for patients with stages A, B, C, and D prostate cancers. An elevated PA level still was detected in 41% of the BPH patients as indicated.

As already indicated, one advantage of a combination test with the use of prostate-specific markers is the increase in the sensitivity of detection of an elevation of either marker in prostate cancer. It is of concern that 41% of the BPH patients exhibited an elevated PA. Another obvious advantage in the use of a combination test is that adjustment can be made of various cutoff points for each marker assay and comparisons can be done of the sensitivity and specificity of the combined test. In this study, the cutoff of PA is calculated as the level of the mean + 2 SD for BPH, 7.5 ng/ml, and used for analysis of combined PA and PAP assays. Comparison of the sensitivity and specificity of the combination test results in an impressive figure, as shown in table 2; 58% each of the patients with stages A and B prostate cancers, 68% of the patients with stage C, and 92% of the patients with stage D prostate cancers (overall, 80%) and only 10% of the patients with BPH demonstrated positive PA and/or PAP levels. In addition, no healthy control or patients with cancers other than prostate cancer exhibited positive levels of PA and/or PAP under this set of parameters, i.e., when cutoff points of means + 3 SD in PAP from healthy males and means + 2 SD in PA from BPH patients are combined.

At present, the possible use of the serum PAP assay, specifically by the radioimmunoassay technique, has generated much debate, entailing such considerations as specificity, sensitivity, and predictive value for screening of prostate cancer (*18-20*). We cannot address or speculate on these complex and critical questions with data available from this report. However, our results clearly show that the measurements of PAP and PA together have an additive effect on the diagnosis of prostate cancer. What usefulness this fact will be clinically requires more data, particularly those derived from patients with early prostate cancer whose cancers are staged surgically. Probably, the most important clinical application of the PAP and/or PA immunochemical assay at its present stage of development is for the monitoring of prostate cancer (*21, 22*).

In conclusion, a multiple marker assay in prostate cancer has been evaluated with the use of PA and PAP. PA and PAP are two biochemically and immunologically distinct proteins of human prostate tissue. Although not tumor-specific, PA and PAP are tissue-specific markers and therefore were used in our study. Results from serum assay revealed a discordance between the PA and PAP values, which thus suggested that the expressions of these two markers reflect different aspects of the biology of prostate cancer. Combination tests with different and selected values of PA and PAP levels produced very encouraging results. This study demonstrates that a combination test of tissue-specific markers can result in additive clinical value in the immunodiagnosis of cancer and should be a logical avenue for serious consideration at this time in light of the absence of human tumor-specific markers.

REFERENCES

(*1*) Gutman EB, Sproul EB, Gutman AB. Significance of increased phosphatase activity of bone at site of osteoplastic metastasis secondary to carcinoma of prostate gland. Am J Cancer 1936; 28:485–495.

(*2*) Foti AG, Herschman H, Cooper JF. A solid-phase radioimmunoassay for human prostatic acid phosphatase. Cancer Res 1975; 35:2446–2452.

(*3*) Chu TM, Wang MC, Scott WW, et al. Immunochemical detection of serum prostatic acid phosphatase. Methodology and clinical evaluation. Invest Urol 1978; 15:319–322.

(*4*) Lee CL, Wang MC, Murphy GP, Chu TM. A solid-phase fluorescent immunoassay for human prostatic acid phosphatase. Cancer Res 1978; 38:2871–2878.

(*5*) Choe BK, Pontes JE, Dong MK, Rose NR. Double antibody immunoenzyme assay for human prostatic acid phosphatase. Clin Chem 1980; 26:1854–1858.

(*6*) Lee CL, Killian CS, Murphy GP, Chu TM. A solid-phase immunoadsorbent assay for serum prostatic acid phosphatase. Clin Chim Acta 1980; 101:209–216.

(*7*) Vihko P, Sagant E, Janne O, Peltonen L, Vihko R. Serum prostate-specific acid phosphatase: Development and validation of a specific radioimmunoassay. Clin Chem 1978; 24: 1915–1919.

(*8*) Killian CS, Vargas FP, Lee CL, et al. Quantitative counterimmunoelectrophoresis assay for prostatic acid phosphatase. Invest Urol 1980; 18:219–224.

(*9*) Wang MC, Valenzuela LA, Murphy GP, Chu TM. Purification of a human prostate specific antigen. Invest Urol 1979; 17:159–163.

(*10*) Nadji M, Tabei SZ, Castro A, et al. Prostatic specific antigen: An immunohistologic marker for prostatic neoplasm. Cancer 1981; 48:1229–1232.

(*11*) Papsidero LD, Kuriyama M, Wang MC, et al. Prostate antigen: A marker for human prostate epithelial cells. JNCI 1981; 66:37–42.

(*12*) Papsidero LD, Wang MC, Valenzuela LA, Murphy GP, Chu TM. A prostatic antigen in sera of prostatic cancer patients. Cancer Res 1980; 40:2428–2432.

(*13*) Kuriyama M, Wang MC, Papsidero LD, et al. Quantitation of prostate-specific antigen in serum by a sensitive enzyme immunoassay. Cancer Res 1980; 40:4658–4662.

(*14*) Whitmore WF Jr. The rationale and results of ablative surgery for prostatic cancer. Cancer 1963; 16:1119–1132.

(*15*) Kelsoe GH, Weller TH. Immunodiagnosis of infection with *Schistosoma mansoni*: Enzyme-linked immunosorbent assay for detection of antibody to circulating antigen. Proc Natl Acad Sci USA 1978; 75:5715–5717.

(*16*) Chu TM, Wang MC, Valenzuela LA, Merrin C, Murphy GP. Isoenzymes of prostatic acid phosphatase. Oncology 1978; 35: 198–200.

(*17*) Wang MC, Kuriyama M, Loor RM, Li SC, Chu TM. Biochemical characterization of human prostate-specific antigen. Fed Proc 1981; 40:1564.

(*18*) Foti AG, Cooper JF, Herschman H, Malvaez RR. Detection of prostate cancer by solid phase radioimmunoassay of serum prostatic acid phosphatase. N Engl J Med 1977; 297:1357–1359.

(*19*) Watson RA, Tang DB. The predictive value of prostatic acid phosphatase as a screening test for prostatic cancer. N Engl J Med 1980; 303:497–499.

(20) Lindholm GR, Stirton MS, Liedtke RJ, Batjer JD. Prostatic acid phosphatase by radioimmunoassay. JAMA 1980; 244: 2071-2073.

(21) Killian CS, Vargas FP, Slack NH, Murphy GP, Chu TM. Prostatic-specific acid phosphatase versus acid phosphatase in monitoring patients with prostate cancer. Clin Chem 1981; 27: 1064.

(22) Kuriyama M, Wang MC, Lee CL, et al. Use of human prostate-specific antigen in monitoring prostate cancer. Cancer Res 1981; 41:3874-3876.

Environmental Factors in the Etiology of Rhabdomyosarcoma in Childhood[1,2,3]

Seymour Grufferman, *M.D.*,[4,5,6,7] **Helen H. Wang**, *M.D.*,[5,8] **Elizabeth R. DeLong**, *Ph.D.*[5,8]
Sue Y. S. Kimm, *M. D.*,[4,5,9] **Elizabeth S. Delzell**, *D.Sc.*,[5,8] *and* **John M. Falletta**, *M.D.*[4,5,10]

ABSTRACT—In a case-control study of childhood rhabdomyosarcoma (RMS), families of 33 cases and 99 controls were interviewed. A relative risk (RR) of 3.9 was found associated with fathers' (but not mothers') cigarette smoking ($P=0.003$). Cases had had fewer immunizations than controls, particularly smallpox vaccination (RR=0.2; $P=0.001$), and conversely had more preventable infections. An RR of 3.2 ($P=0.03$) was found associated with exposure to chemicals and an RR of 3.7 ($P=0.004$) was found associated with diets that included organ meats. Mothers of cases were more likely to be over age 30 years at subject's birth, to have used antibiotics preceding or during pregnancy, and to have had an overdue and/or assisted delivery. Other findings suggest that low socioeconomic status is associated with an increased risk of RMS. These aggregate findings imply that environmental factors may play an important role in the etiology of childhood RMS.—JNCI 1982; 68:107–113.

RMS is the sixth most common cancer of childhood with an annual incidence of about 4 cases per million children (*1, 2*). Little is known about its epidemiologic features, and there are few etiologic hypotheses for this rare disease. Previous epidemiologic studies, based on mortality statistics and case series, indicate the following: Males are more susceptible than females, with whites being more susceptible than blacks; the peak incidence is at about ages 3–4 years; relatives of patients are at markedly increased risk of RMS; and there appears to be familial aggregation of RMS with other soft tissue sarcomas and breast cancer (*3–5*). In this first case-control study of childhood RMS we evaluated possible etiologic factors.

SUBJECTS AND METHODS

We attempted to identify all incident cases of childhood RMS in NC residents during the period 1967–76. Diagnostic indexes, tumor registries, and pathology logs were searched at 141 of the 150 nonpsychiatric hospitals in NC that admit children and at three major referral hospitals in two adjacent states. The nine nonparticipating institutions were military hospitals, which usually referred their pediatric oncology patients to in-state civilian hospitals for care. A total of 37 cases was identified, and the subjects were 0–14 years of age; all but 1 were diagnosed at an NC hospital. We also searched the NC State Tumor Registry and oncology records at the (then) three NC medical schools but found no additional cases. To be eligible for study, a patient ("case") had to have been born in NC and reside there at the time of a histopathologically confirmed diagnosis. Because birth certificates served as our means of selecting controls, cases also had to have a birth certificate on file with the NC Department of Human Resources. Four of the 37 cases were excluded: Two had been born out of state; 1 had been adopted (hence her birth certificate was not publicly listed), and another, although born in NC, had no birth certificate on file. For each of the 33 resulting cases, 3 controls of the same age (±2 mo), sex, and race were randomly selected from NC birth certificates. We excluded subjects who had been adopted, who had died during the neonatal period, or who had been born to parents serving in the military.

Recent addresses for case families were obtained in most instances from their physicians and from medical records. Current addresses for the parents of controls were obtained by a variety of means. The first resource was a library of telephone and city directories from which we tried to match an address with that on the birth certificate. Where necessary, we next searched driver's license and motor vehicle registries. In some instances it was possible to trace parents through the physician listed on the birth certificate. Our last resort was to visit the town of last known address and make inquiries of neighbors and at the post office.

Abbreviations used: NC=North Carolina; RMS=rhabdomyosarcoma; RR=relative risk(s); SES=socioeconomic status.

---

[1] Received May 13, 1981; accepted September 10, 1981.

[2] Supported by Public Health Service grant R01CA-21244 from the National Cancer Institute.

[3] Presented in part at the Society for Epidemiologic Research Meeting, Minneapolis, Minn., June 18, 1980.

[4] Department of Pediatrics, Duke University Medical Center, Durham, N.C. 27710.

[5] Duke University Comprehensive Cancer Center, Duke University Medical Center.

[6] Recipient of a Preventive Oncology Academic Award (K07CA-00726) from the National Cancer Institute.

[7] *Address reprint requests to* Dr. Grufferman *at* P.O. Box 2953, Duke University Medical Center.

[8] Department of Community and Family Medicine, Duke University Medical Center.

[9] Recipient of a Preventive Cardiology Academic Award (K07HL-00633) from the National Heart, Lung, and Blood Institute.

[10] We thank the hospitals of North Carolina for their generous assistance; the Vital Records Branch of the North Carolina Department of Human Resources for providing us with controls; and Ms. M. Griffin, Ms. J. McMillan, Ms. J. Wood, and Ms. K. Baker for their long hours on North Carolina's highways and byways to interview our subjects.

We were thus able to trace all 33 cases. Of the 99 controls first selected, only 70 were found and interviewed; 9 were located but refused to participate, and the other 20 were untraceable. These 29 controls were then replaced by children whose birth certificates were selected by the same methods described above. Twenty-three of these replacements were located and interviewed; 1 more was located but refused to participate, and the other 5 could not be found. A second replacement was chosen for these 6 controls by the same methods. Five of the 6 second-round replacements were interviewed, and 1 refused to cooperate. This control was replaced by a third-round selection.

Using the information on birth certificates, we assessed bias potentially introduced by our loss and replacement of original controls. First, we compared the participating original (first-round) controls with all of the lost and nonparticipating ones and found similar distributions of sex, race, date of birth, extent of parents' education, parents' age at birth of subject, region of residence, duration of pregnancy, and father's occupation (table 1). This finding indicates that the lost and nonparticipating controls were quite similar to the participating first-round controls. Second, we compared the lost and nonparticipating controls with their replacements. As shown in table 1, the only major difference between these 2 groups was in the area of father's occupation. Fewer replacement controls had fathers with professional or managerial occupations, and replacements had more prenatal visits.

Since our evaluation of potential bias was based on birth certificate information, we assessed the reliability of this information by checking it against our interview data. The correlation between fathers' occupations (in terms of "professional and managerial" vs. "other") from the two sources was 0.83. Similarly, the correlation coefficient for years of fathers' education was 0.58 and for years of mothers' education, 0.68.

After case and control families had been located, they were invited by letter to participate in a "study of child health." Interviews were then arranged by telephone call or home visit if the family had no telephone. A standard questionnaire was administered by trained interviewers. The mean duration of interviews for cases was 70.5 minutes and that for controls, 65.1 minutes. All but eight interviews were conducted in the subjects' homes. Three took place at the mothers' place of employment (1 case and 2 control mothers) and one at Duke University Medical Center (a case); four were done by telephone because the families had moved out of NC (2 cases and 2 controls). The informant in all but two instances was the subject's parent, usually the mother (91% of cases and 92% of controls).

In our analyses, we estimated RR and 95% confidence intervals by using both matched and unmatched methods (*6–8*). Since results from both analyses were similar (the differences being <10%), only the unmatched results are presented. Since the purpose of our study was to generate hypotheses for later confirmation, we made no effort to adjust for the multiple testing situation in which we examined numerous potential risk factors. Even if none of the factors examined were related to risk of RMS, an analysis such as this would be expected to generate *P*-values of less than 0.05 for 5 of every 100 variables. Thus for those variables that we have found to be significant, the actual significance level may be greater than our stated *P*-value.

RESULTS

SES.—The first group of variables examined were correlates of SES (table 2). We found the estimated RR associated with mothers' education beyond high school to be 0.3 ($P=0.04$); that for fathers was 0.5 ($P=0.13$). Similarly, the RR associated with mothers' having professional or managerial occupations was 0.4 and that for fathers was 0.5. The RR associated with annual family income of $10,000 or more was 0.5 ($P=0.09$). Whereas only one of these variables reached statistical significance at the 0.05 level, all RR were markedly low and deviated in the same direction from unity. This confluence of findings suggests that low SES is a risk marker for RMS.

Family medical history.—A second group of ques-

TABLE 1.—*Comparison of birth certificate information: Participating, lost and nonparticipating, and replacement controls*

Birth certificate information	Participating original controls[a]	Lost and non-participating controls[b]	Replacement controls[c]
Percentage of fathers with professional or managerial occupations	28	27	11
Mean years of fathers' education	11.6	10.5	12.0
Mean years of mothers' education	11.5	11.7	11.2
Mean age of fathers at subjects' birth	26.6	28.1	28.2
Mean age of mothers at subjects' birth	24.1	25.0	25.4
Percentage of married mothers	100	100	100
Percentage of mothers attended by physician at delivery	96	96	100
Mean gestational period, wk	38.5	38.4	39.1
Mean No. of prenatal visits	10.1	8.7	10.3

[a] No. = 70.

[b] No. = 36

[c] No. = 29.

TABLE 2.—*Childhood RMS risk factors: Socioeconomic indicators*

Risk factors	No. of cases (%)	No. of controls (%)	RR	95% confidence interval
Mothers with ≥13 yr of education	4 (13)	31 (32)	0.3	0.1–0.9
Fathers with ≥13 yr of education	6 (19)	31 (33)	0.5	0.2–1.3
Mothers with professional or managerial occupations	3 (14)	18 (29)	0.4	0.1–1.6
Fathers with professional or managerial occupations	6 (21)	29 (34)	0.5	0.2–1.5
No. of families with annual income of $10,000 or more	14 (44)	59 (61)	0.5	0.2–1.1

tions dealt with family history of disease (table 3). The estimated RR for cancer in relatives of cases versus controls was 2.3 ($P=0.08$). However, when restricted to first-degree relatives—where recall would be more complete for both cases and controls—there was little difference in history of cancer between case and control families (RR=0.7). Thus there was probably "selective recall" bias wherein case families are more apt to remember cancer in remote relatives.

We found an association of RMS with family history of asthma or allergies (RR=2.5; $P=0.03$). When we restricted this analysis to first-degree relatives only, we found little change. Thus this finding is probably not subject to selective recall. Despite the more frequent history of asthma and allergies in case families, the RR for relatives' having received "allergy shots" was 0.4; however, this finding was not close to being statistically significant. Perhaps related to the asthma and allergies finding was our finding of an RR of 1.9 associated with a family history of frequent or serious infections. We also found an association with family history of anemia (RR=2.1).

Gestational and delivery factors.—Several gestational and perinatal factors appeared to be associated with RMS (table 4). Mothers' use of antibiotics within 1 year preceding or during the subjects' gestation conferred an RR of 2.7 ($P=0.03$). Additionally, the RR associated with mothers' being over 30 years of age at the time of delivery was 2.6 ($P=0.06$). The RR associated with overdue versus normal delivery was 2.8 ($P=0.03$); that associated with premature delivery was 0.6. Forceps or cesarean section delivery conferred an RR of 2.4 ($P=0.10$). Thus the age of the mother, the length of her pregnancy, "assisted delivery," and gestational use of antibiotics may be risk markers for RMS. The RR for radiographic examination during pregnancy in case mothers versus control mothers was 0.5.

Neonatal history.—The RR associated with a history of neonatal jaundice was 0.3; that associated with neonatal conditions requiring medical treatment was 0.4 (table 5). However, the occurrence of neonatal problems was infrequent in cases and controls and none of the associations in this category was statistically significant at the 0.05 level.

Environmental exposures.—We also examined several environmental exposures (table 6). We found an RR of 3.2 associated with exposure to chemicals other than pesticides and rodenticides. This category includes exposures to such substances as solvents, paints, acids, bleaches, fertilizers, and gasoline. The only substances to which more than 1 case was exposed were chemical fertilizers. Three cases (9%) and 1 control (1%) had been exposed to fertilizers, yielding an RR of 10.0 (1.5–68, 95% confidence interval). Some of the cases had more than one type of chemical exposure. Similarly, living near a factory that emitted chemical pollution conferred an RR of 3.3 ($P=0.24$).

Diet.—The estimate of RR associated with the eating of organ meats (e.g., liver, brain, and tongue) was 3.7 ($P=0.004$) (table 7). Case families also used less animal fat (lard) in cooking than did control families (RR=0.4). No other dietary factors appeared remarkably associated.

Immunization history.—Cases had received far fewer routine childhood immunizations than had controls (table 8). The RR for smallpox vaccination was 0.2 ($P=0.001$), for measles-mumps-rubella immunization 0.3, and for diphtheria-pertussis-tetanus immunization 0.7. We assessed the RR associated with overall immunization status in terms of "any immunizations" versus "no immunizations" and obtained an estimate of 0.7. We did not include the estimate of RR for poliomyelitis immunization because one of the cells in the related fourfold table contained a zero value. All 33 cases and 96 of 98 controls had received this immunization (RR=0). In general, the RR deviated most from unity for those immunizations that might have a greater discretionary component on the part of the family (i.e., immunizations given latest in infancy).

Past medical history.—We found an RR of 4.1 (exact

TABLE 3.—*Childhood RMS risk factors: Family medical history*

Family history of	No. of cases (%)	No. of controls (%)	RR	95% confidence interval
"Hereditary diseases"	17 (53)	53 (54)	1.0	0.4–2.2
Congenital birth defects	14 (42)	34 (34)	1.4	0.6–3.2
Cancer (all relatives)	26 (79)	61 (62)	2.3	0.9–5.8
Cancer (in parents or siblings only)	2 (6)	8 (8)	0.7	0.1–3.6
Heart disease	30 (91)	87 (88)	1.4	0.4–5.2
Frequent and/or serious infections	14 (42)	28 (28)	1.9	0.8–4.2
Asthma or allergies (all relatives)	23 (70)	47 (47)	2.5	1.1–5.8
Asthma or allergies (in parents or siblings only)	12 (36)	21 (21)	2.1	0.9–5.0
Any relative receiving "allergy shots"	3 (9)	20 (21)	0.4	0.1–1.3
Psychiatric and/or neurologic disease	14 (42)	34 (35)	1.4	0.6–3.1
Anemia	7 (21)	11 (11)	2.1	0.8–6.0
Death of subject's sibling	4 (12)	8 (8)	1.5	0.4–5.3

TABLE 4.—*Childhood RMS risk factors: Gestational and parturitional histories*

Risk factors	No. of cases (%)	No. of controls (%)	RR	95% confidence interval
Mother's prior miscarriage	6 (19)	10 (11)	1.9	0.6–6.2
Mother's illness during pregnancy with subject	24 (73)	[illegible] (74)	1.0	0.4–2.3
Mother's cigarette smoking during pregnancy	9 (28)	27 (28)	1.0	0.4–2.4
Mother's consumption of alcohol during pregnancy	4 (13)	16 (17)	0.7	0.2–2.4
Radiographic examination during pregnancy	2 (6)	11 (12)	0.5	0.1–2.4
Weight gain during pregnancy (>11.3 vs. ≤11.3 kg)	10 (34)	32 (36)	0.9	0.4–2.2
Medications used by mother during and/or 1 yr prior to pregnancy:				
Aspirin	3 (72)	64 (70)	1.1	0.5–2.7
Antibiotics	13 (43)	19 (22)	2.7	1.1–6.3
Pain or cold remedies	10 (34)	28 (32)	1.1	0.5–2.7
Tranquilizers	2 (7)	5 (5)	1.3	0.2–6.9
Oral contraceptives or other birth control methods	8 (25)	23 (24)	1.0	0.4–2.6
Drugs for menstrual disorders or infertility	2 (6)	5 (5)	1.2	0.2–6.4
Length of pregnancy:				
Premature delivery (vs. normal)	4 (18)	19 (24)	0.7	0.2–1.8
Overdue delivery (vs. normal)	10 (36)	13 (18)	2.6	1.1–7.1
Length of labor (>10 hr vs. ≤10 hr)	10 (36)	25 (27)	1.5	0.6–3.7
Mother's age at subject's birth (>30 vs. ≤30 yr)	9 (27)	12 (13)	2.6	1.0–6.8
Type of delivery (forceps or cesarean vs. other)	8 (24)	11 (12)	2.4	0.9–6.6
Place of delivery (hospital vs. home)	31 (94)	93 (94)	1.0	0.2–5.2

TABLE 5.—*Childhood RMS risk factors: Neonatal history*

Risk factors	No. of cases (%)	No. of controls (%)	RR	95% confidence interval
Birth weight (>3.4 vs. ≤3.4 kg)	14 (44)	40 (42)	0.9	0.5–2.4
Birth length (>50 vs. ≤50 cm)	7 (35)	21 (46)	0.6	0.2–1.8
Congenital malformations	8 (24)	18 (19)	1.4	0.5–3.5
Circumcision (males)	19 (83)	53 (89)	0.6	0.2–2.2
Conditions requiring medical treatment	2 (6)	12 (13)	0.4	0.1–2.0
Newborn infections	1 (3)	4 (4)	0.7	0.1–6.5
Jaundice	1 (3)	8 (8)	0.3	0.04–2.6
Diarrhea and/or unusual vomiting	2 (6)	8 (9)	0.7	0.1–3.4
Feeding problems	1 (3)	5 (5)	0.6	0.1–4.8

P=0.05) associated with prior history of whooping cough and of 4.3 for impetigo (exact *P*=0.07) (table 8). There was also an increased history of measles (RR=2.0) and of asthma (RR=2.3) in cases. However, there was no association between RMS and history of infectious diseases for which no immunizations are available, such as otitis media or chickenpox (RR=0.9 for both). The RR associated with scarlet fever was 0.5.

Miscellaneous factors.—Table 9 summarizes our evaluation of a number of miscellaneous potential risk factors. Fathers who were ever-smokers (relative to those who were never-smokers) conferred an RR of 3.9 (*P*=0.003). This finding was in contrast to the findings of an RR of 0.8 for children of mothers who were ever-smokers and of 1.0 for children of mothers who smoked cigarettes during their pregnancy.

TABLE 6.—*Childhood RMS risk factors: Childhood environment*

Risk factors	No. of cases (%)	No. of controls (%)	RR	95% confidence interval
No. of people dwelling in home (>5 vs. ≤5)	4 (12)	15 (15)	0.8	0.2–2.5
No. of rooms in homes (≤5 vs. >5)	21 (64)	53 (55)	1.5	0.6–3.3
Sharing of bedroom by subject	25 (78)	74 (75)	1.2	0.5–3.1
Any pet animals	27 (82)	85 (86)	1.7	0.3–2.1
Dogs	24 (75)	75 (77)	0.9	0.3–2.2
Cats	16 (50)	41 (42)	1.4	0.6–3.0
Indoor plumbing	27 (82)	74 (76)	1.5	0.5–4.0
Water source (city or town water vs. other)	13 (39)	36 (36)	1.1	0.5–2.6
Pesticide exposure	3 (9)	6 (6)	1.5	0.4–6.5
Rodenticide exposure	1 (3)	3 (3)	1.0	0.1–9.9
Other chemical exposures	7 (22)	8 (8)	3.2	1.1–9.2
Any exposure to pollution from factories or plants	6 (19)	11 (11)	1.9	0.6–5.6
Exposure to chemicals from factories	2 (6)	2 (2)	3.3	0.5–22
Exposure to fumes from factories	3 (10)	9 (9)	1.0	0.3–4.2
Exposure to dust from factories	1 (3)	3 (3)	1.0	0.1–10.5
Exposure to waste from factories	2 (6)	5 (5)	1.2	0.2–6.8
Subject's travel abroad	2 (6)	5 (5)	1.2	0.2–6.6
Exposure to playmate who had cancer	1 (3)	2 (2)	1.5	0.1–17

TABLE 7.—*Childhood RMS risk factors: Diet*

Risk factors	No. of cases (%)	No. of controls (%)	RR	95% confidence interval
Subject's egg consumption (>4 vs. ≤4/wk)	12 (41)	35 (36)	1.3	0.5–2.9
Use of butter vs. margarine	2 (6)	6 (6)	1.0	0.2–5.4
Family's use of animal fat vs. vegetable oil in cooking	2 (6)	13 (15)	0.4	0.1–2.0
Formula vs. breast feeding in infancy	23 (72)	61 (63)	1.5	0.6–3.6
Daily milk consumption (>0.95 vs. ≤0.95 liter)	5 (17)	19 (20)	0.8	0.3–2.3
Use of whole vs. other milk	22 (73)	71 (75)	0.9	0.4–2.4
Luncheon meat consumption (>4 vs. ≤4 times/mo)	17 (55)	47 (50)	0.8	0.4–1.9
Hotdog consumption (>4 (vs. ≤4 times/mo)	11 (34)	29 (31)	1.2	0.5–2.8
Ham consumption (>4 vs. ≤4 times/mo)	3 (10)	8 (9)	1.1	0.3–4.5
Bacon consumption (>4 vs. ≤4 times/mo)	20 (63)	48 (52)	1.5	0.7–3.5
Sausage consumption (>4 vs. ≤4 times/mo)	13 (41)	37 (40)	1.0	0.4–2.3
Organ meat consumption	21 (70)	37 (39)	3.7	1.5–8.3
Frequency of family's purchase of 1 pound of salt (once/mo or more vs. other)	11 (35)	33 (34)	1.1	0.4–2.5
Subject's use of salt at table (yes vs. no)	19 (59)	48 (52)	1.4	0.6–3.1
Subject's use of food substitutes	5 (16)	18 (18)	0.8	0.3–2.4
Family's use of diet foods or beverages	2 (6)	6 (6)	1.0	0.2–5.2
Family's use of saccharin	7 (22)	15 (16)	1.5	0.6–4.1
Family consumption of meats:				
Beef (>2 vs. ≤2 times/wk)	16 (50)	53 (54)	0.9	0.4–1.9
Pork (>2 vs. ≤2 times/wk)	9 (28)	19 (20)	1.6	0.6–4.0
Chicken (>2 vs. ≤2 times/wk)	7 (22)	17 (17)	1.4	0.5–3.6
Fish (>2 vs. ≤2 times/wk)	4 (13)	16 (16)	0.7	0.2–2.4

Assessment of confounding by SES.—Because we were concerned that some of our findings might be confounded by SES, we controlled for family income and fathers' education and occupation in a matched logistic regression analysis of fathers' cigarette smoking and of smallpox vaccination status. In the analysis of fathers' smoking, we obtained an adjusted RR of 2.8 ($P=0.07$). In the analysis of smallpox vaccination, we obtained an adjusted RR of 0.2 ($P=0.009$). Due to incomplete data, the number of subjects included in these analyses was smaller than that in the univariate analyses.

TABLE 8.—*Childhood RMS risk factors: Subject's medical history*

Risk factors	No. of cases (%)	No. of controls (%)	RR	95% confidence interval
Smallpox vaccination	21 (66)	88 (90)	0.2	0.1–0.6
Measles–mumps–rubella immunization	29 (91)	93 (97)	0.3	0.1–1.5
Diphtheria–tetanus–pertussis immunization	32 (97)	96 (98)	0.7	0.1–7.6
Overall immunization status (ever vs. never)	32 (97)	96 (98)	0.7	0.1–7.6
Measles	14 (42)	25 (27)	2.0	0.9–4.6
Mumps	13 (39)	33 (34)	1.3	0.6–2.9
Rubella	5 (16)	21 (23)	0.6	0.2–1.8
Pertussis	5 (15)	4 (4)	4.1	1.1–15
Chickenpox	23 (70)	70 (73)	0.8	0.4–2.0
Scarlet fever	1 (3)	6 (6)	0.5	0.1–3.9
Hepatitis	1 (3)	5 (5)	0.6	0.1–5.0
Pneumonia	2 (6)	8 (8)	0.7	0.2–3.6
"Strep throat"	10 (30)	28 (29)	1.1	0.4–2.5
Otitis media	10 (30)	31 (32)	0.9	0.4–2.2
Impetigo	4 (12)	3 (3)	4.3	1.0–18
Warts	5 (15)	12 (14)	1.2	0.4–3.6
Asthma	3 (9)	4 (4)	2.3	0.5–11

DISCUSSION

This study uncovered a number of potential risk factors for RMS. First, we found a confluence of associations with variables related to SES. We found that both mothers and fathers of cases had received less education than control parents, that case parents' occupations tended to be of a lower income and prestige level, and that total family income for cases was lower than that for controls. Whereas only mothers'

TABLE 9.—*Childhood RMS risk factors: Miscellaneous factors*

Risk factors[a]	No. of cases (%)	No. of controls (%)	RR	95% confidence interval
Fathers who smoke cigarettes (ever)	23 (77)	40 (46)	3.9	1.5–9.6
Mothers who smoke cigarettes (ever)	8 (26)	29 (31)	0.8	0.3–2.0
Religion (Protestant vs. other)	26 (81)	68 (81)	1.0	0.4–2.9
Birth order (first vs. other)	13 (39)	41 (41)	0.9	0.4–2.1
No. of children in sibship (>5 vs. ≤5)	7 (21)	14 (14)	1.6	0.6–4.5
Father's age at subject's birth (>30 vs. ≤30 yr)	7 (22)	25 (26)	0.8	0.3–2.0
Marital status of mother (married vs. other)	23 (70)	73 (75)	0.8	0.3–1.8
Current residence (in town of ≥5,000 vs. <5,000)	20 (61)	61 (63)	0.9	0.4–2.0
Farm residence (ever vs. never)	2 (6)	6 (6)	1.0	0.2–5.2
Current residence (outside an SMSA vs. in an SMSA)	23 (70)	62 (64)	1.3	0.6–3.0

[a] SMSA = standard metropolitan statistical area.

educational level showed a statistically significant association with RMS and family income was at the margin of statistical significance, all of these factors, in the aggregate, suggested that low SES is a risk marker for RMS. Our characterization of lost and nonparticipating controls and comparisons with participating controls suggested that if our selection and location procedures introduced any SES bias, it was of a conservative nature.

Other studies that examined childhood cancer risk in relation to social class have dealt primarily with leukemia. Stewart et al. (*9*) found no association between social class (as indexed by father's occupation alone) and the risk of leukemia or of all childhood cancers. Fasal and co-workers (*10*), using birth and death certificates of children who died of leukemia, found a small but statistically significant increase in leukemia risk for children of high social class ($RR=1.33$; $\chi^2_1=4.58$), with social class defined by fathers' occupation. Although prior studies have found no or weak associations between social class and childhood cancer risk, these studies have been limited by having minimal data available for the classification of families' social class.

Perhaps our most salient finding is the strong association between RMS and fathers' cigarette smoking. This finding has two possible explanations. First, a direct carcinogenic effect may be introduced either in a prezygotic manner or by passive inhalation of cigarette smoke by the patients. In support of a direct effect are two studies suggesting a mutagenic effect of fathers' cigarette smoking. Evans and co-workers (*11*) found morphologic sperm abnormalities in cigarette smokers, and Mau and Netter (*12*) showed a twofold increase in the occurrence of severe malformations in children of fathers who were heavy cigarette smokers. The second interpretation relates to SES. Wynder and Hoffmann (*13*) showed that cigarette smoking is inversely related to educational level among men but not among women. Thus the positive finding for fathers but not for mothers may relate to our observation that low SES may be a marker of increased RMS risk. However, the results of our matched logistic regression analysis suggest that this is not a likely explanation. We believe the first hypothesis deserves further consideration.

Most of the numerous studies of mothers' cigarette smoking and risk of malformation in their offspring have shown no or weakly positive associations. The U.S. Surgeon General's 1979 Report on Smoking and Health (*14*) concluded: "There is no convincing evidence that maternal smoking increases the incidence of congenital malformations. Results of published studies, reviewed in the 1973 report (*15*), show relative risks for smokers versus nonsmokers ranging from 0.31 to 1.55." Thus if Mau and Netter's findings (*12*) prove valid, our observation of a possible association between fathers' (but not mothers') cigarette smoking and risk of RMS appears even more worthy of further study.

Several studies have directly examined cancer risk of children in relation to their parents' smoking status (*9, 16–18*). All have shown little or no association between mothers' smoking and cancer risk in their offspring and therefore are consistent with our findings. We found only one study that evaluated the association between fathers' smoking and risk of cancer among their children. Stewart et al. (*9*) found that fathers of children with leukemia were only slightly more apt to be smokers than those of control children, but the authors point out that their analysis was crude.

We found internal consistency in our study when we examined immunization status and history of infectious diseases. Cases had received remarkably fewer immunizations than had controls and, conversely, they had contracted more of those diseases preventable by immunization. The association of RMS with impetigo, a disease associated with poor hygiene, was also interesting. Our finding of an association with history of pertussis is similar to an observation made by Bross and Natarajan (*19*) in a study of children with leukemia. These investigators found a twofold increase in leukemia risk for children with a history of antecedent bacterial infection (defined as "pneumonia, whooping cough, or dysentery").

Our findings of fewer immunizations in cases are similar to those in Neumann's study (*20*) of children dying of cancer in Baden-Württemberg, Federal Republic of Germany. Neumann found statistically significantly less diphtheria immunization in case children than matched controls ($RR=0.25$). His cases had less tetanus ($RR=0.46$), poliomyelitis ($RR=0.75$), and BCG ($RR=0.69$) immunizations but more smallpox vaccination ($RR=1.28$) than did his controls, though these differences were not statistically significant. All of his findings are consistent with ours except for those with regard to smallpox vaccination. This would suggest that the specific immunizations are not themselves risk factors, but that immunization status per se is a risk marker for childhood cases.

We found a notable association with exposure to chemicals and chemical pollution. Cases also appeared to have eaten more organ meats than did controls and somewhat more pork ($RR=1.6$). The increased consumption of organ meat and pork may be interrelated in that NC farmers (and rural families) who slaughter their own pigs will usually utilize all organ and "variety" meats.

We found associations between RMS and several gestational and parturitional factors. These include a positive association with an overdue delivery and, conversely, a negative association with premature delivery of the propositus. Additionally, use of forceps and cesarean section in the delivery of subjects and use of antibiotics by mothers during the year and 9 months preceding the birth of their children appear to be risk markers of RMS. We found an interesting association with mothers' age at birth of subjects. Similar observations were made in earlier studies, which showed that mothers of children with leukemia were significantly older than mothers of controls (*9, 16, 21*). One of these studies (*9*) showed that the increased risk of leukemia with increasing maternal age was independent of the occurrence of Down's syndrome. Another study showed a "consistent, although not statistically significant, trend toward increasing rates with increasing maternal age" for all childhood cancers (*21*).

The findings of an association with history of asthma and allergies in families and of an RR of 2.3 for history of asthma in subjects suggest that immunologic factors play a role in the etiology of RMS. Bross and Natarajan (*19*), in their case-control study of childhood leukemia, similarly found a threefold increase in risk associated with subjects' history of antecedent allergic diseases (asthma and hives). Manning and Carroll (*16*) showed similar results more than 20 years ago. They also found a statistically significant association between risk of childhood leukemia (and lymphoma) and mothers' history of having had allergic diseases. However, there was no increased history of allergies for children with other cancers or their mothers.

In summary, we have found a number of potential risk factors for childhood RMS. We found immunization status, fathers' cigarette smoking, diet, chemical exposures, mothers' age, gestational factors, asthma, and SES to be associated with RMS. In particular, we believe that the association with fathers' smoking is deserving of further evaluation. The aggregate of our findings implies that environmental factors may play an important role in the etiology of childhood RMS. We must, however, caution that this is the first case-control study of this rare cancer and that our study size was small. Further investigation is needed to confirm our findings in another setting.

We believe that the issue of environmental factors in the etiology of childhood cancers has not been explored adequately. The relatively short latent periods between potential etiologic exposures and disease manifestation in children provide unique opportunities for the study of environmental factors. Similar case-control studies of other childhood cancers might provide important new etiologic leads.

REFERENCES

(*1*) YOUNG JL JR, MILLER RW. Incidence of malignant tumors in U.S. children. J Pediatr 1975; 86:254-258.

(*2*) JONES PM. Cancer in children. Practitioner 1979; 222:221-228.

(*3*) LI FP, FRAUMENI JF JR. Rhabdomyosarcoma in children: Epidemiologic study and identification of a familial cancer syndrome. J Natl Cancer Inst 1969; 43:1365-1373.

(*4*) MILLER RW, DALAGER NA. Fatal rhabdomyosarcoma among children in the United States, 1960-69. Cancer 1974; 34:1897-1900.

(*5*) LI FP, FRAUMENI JF JR. Soft-tissue sarcomas, breast cancer, and other neoplasms. A familial syndrome? Ann Intern Med 1969; 71:747-752.

(*6*) MIETTINEN OS. Estimability and estimation in case-referent studies. Am J Epidemiol 1976; 103:226-235.

(*7*) ———. Simple interval-estimation of risk ratios. Am J Epidemiol 1974; 100:515-516.

(*8*) ———. Estimation of relative risk from individually matched series. Biometrics 1970; 26:75-86.

(*9*) STEWART A, WEBB J, HEWITT D. A survey of childhood malignancies. Br Med J 1958; 1:1495-1508.

(*10*) FASAL E, JACKSON EW, KLAUBER MR. Birth characteristics and leukemia in childhood. J Natl Cancer Inst 1971; 47:501-509.

(*11*) EVANS HJ, FLETCHER J, TORRANCE M, HARGREAVE TB. Sperm abnormalities and cigarette smoking. Lancet 1981; 1:627-629.

(*12*) MAU G, NETTER P. Die Auswirkungen des väterlichen Zigarettenkonsums auf die perinatale Sterblichkeit und die Missbildungshaufigkeit. Dtsch Med Wochenschr 1974; 99:1113-1118.

(*13*) WYNDER EL, HOFFMANN D. Tobacco and health. A societal challenge. N Engl J Med 1979; 300:894-903.

(*14*) U.S. Public Health Service. Smoking and health. A report of the Surgeon General. Washington, D.C.: U.S. Govt Print Off, 1979, part 8:39 [DHEW publication No. (PHS)79-50066].

(*15*) U.S. Public Health Service. The health consequences of smoking. A report of the Surgeon General. Washington, D.C.: U.S. Govt Print Off, 1973:136-137 [DHEW publication No. (HSM) 73-8704].

(*16*) MANNING MD, CARROLL BE. Some epidemiologic aspects of leukemia in children. J Natl Cancer Inst 1957; 19:1087-1094.

(*17*) NEUTEL CI, BUCK C. Effect of smoking during pregnancy on the risk of cancer in children. J Natl Cancer Inst 1971; 47:59-63.

(*18*) GOLD E, GORDIS L, TONASCIA J, SZKLO M. Risk factors for brain tumors in children. Am J Epidemiol 1979; 109:309-319.

(*19*) BROSS ID, NATARAJAN N. Leukemia from low-level radiation. Identification of susceptible children. N Engl J Med 1972; 287:107-110.

(*20*) NEUMANN G. Zusammenhang zwischen Schutzimpfungen und bösartigen Neubildungen im Kindesalter? Med Klin 1980; 75:72-75.

(*21*) MACMAHON B, NEWILL VA. Birth characteristics of children dying of malignant neoplasms. J Natl Cancer Inst 1962; 28:231-244.

Anticancer Drugs: Effect on the Cloning of Raji Lymphoma Cells in Soft Agar[1]

Pao-Chen Wu,[2,3] **Robert F. Ozols,**[4,5] **Masakazu Hatanaka,**[2,6] *and* **Charles W. Boone**[2,7]

ABSTRACT—The effect of 11 anticancer drugs on the ability of Raji lymphoma cells to form colonies in soft agar was determined with the use of both a 1-hour and a continuous drug exposure. Three distinct patterns of drug sensitivities were observed: *a*) Dactinomycin, adriamycin, bleomycin, mitomycin C, vincristine, and *cis*-platinum II all produced a dose-dependent reduction in colony formation following a 1-hour exposure, which was further augmented by a continuous exposure to the drugs; *b*) the antimetabolites (methotrexate, β-cytosine arabinoside, and 5-fluorouracil) and pentamethylmelamine had no suppressive effects on colony formation with a 1-hour exposure, but they produced marked cytotoxicity with continuous drug exposure; and *c*) L-phenylalanine mustard had the same degree of colony suppression with both a 1-hour and a continuous drug exposure. Preincubation of Raji cells with an enzyme mixture (DNase + pronase + collagenase) did not alter the degree of colony suppression observed with the anticancer drugs. These results indicate that continuous drug exposure should be compared to a 1-hour drug incubation to determine in vitro drug sensitivities of fresh human tumors in the soft agar clonogenic assay, because the 1-hour drug exposure may not identify certain drugs that are potentially clinically active.—JNCI 1982; 68:115–121.

The growth of tumor colonies in soft agar from primary human tumor explants was initially described by Hamburger and Salmon (*1, 2*) and recently confirmed by other investigators (*3–5*). The human tumor clonogenic assay provides a technique to study the growth of human tumors in vitro and to determine the chemotherapeutic drug sensitivity of a particular tumor. Preliminary results indicate that the assay is 90–95% accurate in predicting clinical resistance and 60–65% accurate in predicting a clinical response (*6, 7*). Furthermore, the assay is of potential importance as a screening test for new antitumor agents (*8*). General applicability of the system has been limited in part by the lack of sufficient colony formation from most specimens to perform multiple drug sensitivities (*9, 10*).

In an effort to improve upon the mechanical disaggregation of tumors, enzymatic digestions with the use of single or multiple enzyme mixtures are under active investigation (*11, 12*). A potential concern regarding the use of proteolytic enzymes has been the possibility that these enzymes will disrupt membrane proteins of tumor cells and consequently alter the pattern of chemotherapy sensitivity. Observations regarding drug sensitivities and ways to improve the cloning efficiencies in an established human tumor cell line may have direct relevance to the soft agar cloning of fresh human tumors.

In this study we examined the effect of 11 anticancer drugs on colony formation in soft agar of Raji cells by means of both a 1-hour and a continuous exposure to various concentrations of drugs. Additionally, using the clonogenic assay, we examined the effect of preincubation of Raji cells with pronase, collagenase, and DNase on the patterns of drug sensitivity.

The Raji cell culture line of Burkitt's lymphoma, in which the chemotherapy sensitivity has not been previously reported in the soft agar assay, was chosen for the following reasons: *a*) The Raji cell line retains most of the morphologic characteristics of the original tumor even after numerous passages in defined media (*13*). *b*) The analysis of cytogenetic, HLA, and viral antigenic expressions indicated no demonstrable difference between early and late passages of cell line (Hatanaka M, Hampar B: Unpublished data). *c*) The Raji cell line is derived from an untreated patient with Burkitt's lymphoma and thus is potentially useful for the in vitro screening of new anticancer drugs.

MATERIALS AND METHODS

Tumor cells.—The Raji cell line was obtained from Dr. Berge Hampar, NCI. The cells were cultured in McCoy's 5-A medium with 10% FCS (GIBCO, Grand Island, N.Y.) in a 5% carbon dioxide incubator at 37°C.

ABBREVIATIONS USED: Act-D = actinomycin D (dactinomycin); ADR = adriamycin; Ara-C = β-cytosine arabinoside; BLEO = bleomycin; CMRL-1066 = Connaught Medical Research Laboratory medium 1066; C×T = concentration times time product; FCS = fetal calf serum; FUra = 5-fluorouracil; L-PAM = L-phenylalanine mustard; Mit-C = mitomycin C; MTX = methotrexate; NCI = National Cancer Institute; PENTA = pentamethylmelamine; PLAT = *cis*-platinum II; VCR = vincristine.

---

[1] Received May 19, 1981; accepted October 2, 1981.

[2] Laboratory of Viral Carcinogenesis, Division of Cancer Cause and Prevention, National Cancer Institute, National Institutes of Health, Public Health Service, U.S. Department of Health and Human Services, Bethesda, Md. 20205.

[3] *Present address:* Department of Obstetrics and Gynecology, Capital Hospital, Chinese Academy of Medical Science, Peking, China.

[4] Medicine Branch, Division of Cancer Treatment, National Cancer Institute.

[5] *Address reprint requests to* Dr. Ozols at the Medicine Branch, Bldg. 10, Room 12N226, National Cancer Institute, National Institutes of Health, 9000 Rockville Pike, Bethesda, Md. 20205.

[6] *Present address:* Department of Serology and Immunology, Institute of Virus Research, Kyoto University, Kyoto, Japan.

[7] *Present address:* Laboratory of Pathology, Al Hada Hospital, P.O. Box 1347, Kingdom of Saudi Arabia.

Cells were diluted 1:30 (vol/vol) with fresh medium at 10- to 12-day intervals. The cells were used for drug sensitivity studies between the 7th and 10th days following passage at which time the concentration was 0.8-1.5×10^6 cells/ml.

Soft agar cultures.—The culture system for the cloning of Raji cells in a double-layer agar system was the same as that previously reported for the growth of human ovarian cancer cells (*4, 14*). This system is similar to that reported initially by Hamburger and Salmon (*1, 2*), with the exception that feeder cells were not used in the underlayers and 2-mercaptoethanol was not added to the upper layers. All cultures were performed in 35-mm petri dishes. The underlayer consisted of 1.0 ml of McCoy's 5-A medium, 10% FCS, other nutrients (*1, 2*), and 0.5% agar. The upper layer in which the tumor cells were added consisted of 1.0 ml of CMRL-1066 medium with 15% horse serum (both from GIBCO), other nutrients (*1, 2*), and 0.3% agar.

Drugs.—A total of 11 anticancer drugs were examined for their effect on colony formation by Raji cells. The drugs included examples from each of the major clinically useful drug categories: alkylating agents (L-PAM); antimetabolites (MTX, FUra, and Ara-C); antibiotics (ADR, BLEO, Mit-C, and Act-D): and vinca alkaloids (VCR) as well as drugs whose mechanism of action has not been fully elucidated (PLAT and PENTA). All drugs were obtained from the Investigational Drug Branch, NCI. Stock solutions of all drugs were prepared and aliquots frozen at −20°C and diluted prior to use.

Drug sensitivity studies.—The method for determination of drug sensitivities by means of the clonogenic assay has been previously described by investigators at the University of Arizona Cancer Center (*6, 7*). Each of the drugs was tested at a minimum of three different dose levels, including a concentration at the peak plasma level achievable in patients receiving conventional drug doses. In addition, the effect on colony formation following exposure to a drug at the C×T as calculated by Alberts and Chen (*15*) was determined because this may more accurately reflect the pharmacologic disposition of the drug than the peak plasma level. The effect on colony formation was determined by the use of both a 1-hour drug exposure and a continuous exposure to the drug during the entire growth period in agar. One-hour exposure: From 3 to 8×10^3 Raji cells in 1.5 ml of McCoy's 5-A medium with 10% FCS were incubated for 1 hour at 37°C in the presence of the drugs at varying concentrations. The cells were washed twice with drug-free media, and the cell concentration was adjusted to 6×10^3 cells/ml. To 0.5 ml of the cells were added 2.2 ml of enriched CMRL-1066 and 0.3 ml of molten 3% agar. After mixing, the cells were plated in triplicate and incubated as described above.

Continuous exposure: The cell concentration was adjusted to 6×10^3 cells/ml in McCoy's 5-A medium with 10% FCS. To 0.5 ml of the cell suspension were added 1.9 ml of enriched CMRL-1066, 0.3 ml of the drugs at various concentrations, and 0.3 ml of 3% agar. The cells were plated and cultured as described above.

Examination of cultures.—Cultures were examined with an inverted phase microscope. Aggregates of 30 cells or more were counted as colonies. Colony counting was performed after 7, 10, and 14 days of incubation. For drug-treated plates, the results are expressed as the mean percent survival (± SE) of colonies compared with that of untreated controls.

Incubation of Raji cells with enzymes.—A 1-ml suspension of cells containing 3-8×10^5 cells was centrifuged, and the supernatant was discarded. The pellet was resuspended in 1.0 ml of an enzyme mixture at a final concentration of 0.02% collagenase (215 U/ml; Sigma Chemical Co., St. Louis, Mo.), 0.02% DNase (1,775 Kunitz U/ml; Sigma Chemical Co.), and 0.05% pronase (4.4 U/mg; Sigma Chemical Co.) (*11*) in McCoy's 5-A medium without FCS. The cells were incubated for 1 hour at 37°C and washed twice with McCoy's 5-A medium with added FCS. The cells were resuspended in 1.5 ml of McCoy's 5-A medium and exposed to drugs for 1 hour as described above. Raji cells that were not incubated with the enzyme mixture were exposed to the same drugs in parallel with the enzyme-incubated cells.

RESULTS

Growth of Raji Cells in Soft Agar

Raji cell doublings were observed by the 2d or 3d day after plating. Between days 2 and 5, when cell counts in aggregates could be determined, the doubling time was approximately 24 hours. By day 15 of growth the diameters of the colonies remained essentially unchanged. The mean plating efficiency of 59 control samples was 29.8±1.39% (SE), and there was a linear relationship between the number of cells plated over a range of 10^2 to 3×10^4 cells and the number of colonies.

Drug Sensitivity Testing

One-Hour Exposure

The effects of a 1-hour exposure to anticancer agents on colony formation of Raji cells are summarized in table 1, and representative dose-response curves for the different classes of drugs are presented in text-figure 1. Colony suppression was observed with the antibiotics, the vinca alkaloid, PLAT, and the alkylating agent L-PAM. In contrast, no colony suppression was observed with either PENTA or any of the antimetabolites under the standard conditions for a 1-hour exposure.

All the antibiotics demonstrated a linear dose-response effect on colony formation. ADR was the most active antibiotic tested; a 1-hour exposure at 0.025 µg/ml (equivalent to 2% of the achievable C×T) produced a 90% suppression of colony formation. In contrast, BLEO produced only a 30% suppression at a dose corresponding to the C×T level. Act-D and Mit-C had intermediate suppressive effects with an 82 and a

TABLE 1.—*Effect of anticancer drugs on colony formation: 1-hr drug exposure*[a]

Drug	Dose, µg/ml	Percent colony survival ± SE
ADR	0.005	70±6
	0.01	47±3
	0.025	8±1
	0.05	0
BLEO	2.5	72±5
	5.0	60±5
	10	40±5
	20	25±4
Act-D	0.05	81±7
	0.1	35±5
	0.25	8±2
	0.5	0
Mit-C	0.05	97±5
	0.2	62±10
	0.5	32±3
	1.0	7±1
MTX	1.0	99±1
	5.0	97±7
	10.0	94±3
FUra	5.0	91±4
	10.0	101±2
	25.0	97±6
Ara-C	0.5	101±7
	2.5	90±9
	10.0	105±8
	25.0	105±4
L-PAM	0.05	93±2
	0.25	28±2
	0.5	8±2
PENTA	5.0	112±8
	10	123±8
	25	102±16
	50	115±9
VCR	0.01	60±3
	0.05	28±2
	0.075	14±2
	0.1	9±3
PLAT	0.2	90±5
	0.5	65±5
	1.0	40±4
	2.0	8±1

[a] Drugs were incubated with Raji cells for 1 hr, and the effect on colony formation was compared to colony formation of untreated controls.

91% reduction, respectively, in colony formation at the C×T level. VCR, PLAT, and L-PAM had quantitatively similar dose-response curves as those for the antibiotics. VCR and PLAT both produced an 80% suppression of colony formation at the C×T level, whereas L-PAM produced a similar degree of suppression at only 20% of the C×T dose level.

The antimetabolites, conversely, had no effect on colony formation under these conditions even at dose levels 1.5–2.0 times greater than the achievable C×T level. PENTA also had no suppressive effects on colony formation following a 1-hour exposure even at a concentration of 50 µg/ml.

Continuous Exposure

The effect of continuous drug exposure during the 14-day incubation period on colony formation was compared to the suppression produced by a 1-hour drug exposure. The C×T for continuous drug exposure, even at the lower doses, was greater than the C×T for a 1-hour exposure at the highest doses used in the short-term incubations due to the markedly longer incubation period. Three patterns of drug sensitivity were observed (table 2): *a*) increased colony suppression with continuous exposure, *b*) colony suppression observed only with continuous drug exposure, and *c*) the same degree of suppression with either a 1-hour exposure or continuous exposure.

Six drugs that produced colony suppression with a 1-hour incubation produced a further suppression with continuous drug exposure. Included in this group were the four antibiotics, VCR, and PLAT. The increase in suppression with continuous drug exposure was most marked with Act-D, BLEO, and Mit-C. A 1-hour exposure to Act-D at 0.05 µg/ml produced a 20% reduction in colony formation, whereas continuous exposure at a concentration of only 0.001 µg/ml resulted in complete suppression of colony formation. With BLEO, a 1-hour exposure at 20 µg/ml produced the same degree of suppression (25% colony survival) as did continuous exposure at 0.1 µg/ml. With Mit-C a similar degree of suppression (31 and 21% colony survival) was observed with a 1-hour exposure at 0.5 µg/ml and with continuous exposure at 0.01 µg/ml.

Four drugs, the antimetabolites MTX, FUra, and Ara-C as well as PENTA, produced no suppression of colony formation following a 1-hour exposure but did have significant colony reduction with continuous exposure. The difference in colony formation between a 1-hour exposure and a continuous drug exposure was most marked with MTX and Ara-C. With MTX, a 1-hour exposure at 10 µg/ml had no effect on colony formation, whereas continuous exposure to 0.1 µg/ml produced complete suppression of colony formation. A 1-hour exposure to Ara-C at 25 µg/ml produced no effect on colony formation, whereas continuous exposure at 0.5 µg/ml produced complete suppression.

PENTA produced a dose-dependent reduction in colony formation with continuous exposure, whereas no effect was observed with a 1-hour exposure. Continuous exposure at 50 µg/ml resulted in 5% colony survival; this same dose was ineffective with a 1-hour exposure.

The third type of effect comparing 1-hour and continuous drug exposure was observed with only one of the tested drugs. L-PAM had the same degree of suppression with both a 1-hour exposure and continuous exposure.

Effect of Preincubation With Enzymes on Colony Formation and Drug Sensitivity

Text-figure 2 demonstrates the relationship between the length of incubation of Raji cells with the enzyme mixture and the subsequent ability of the cells to form colonies in soft agar. A 30-minute incubation produced

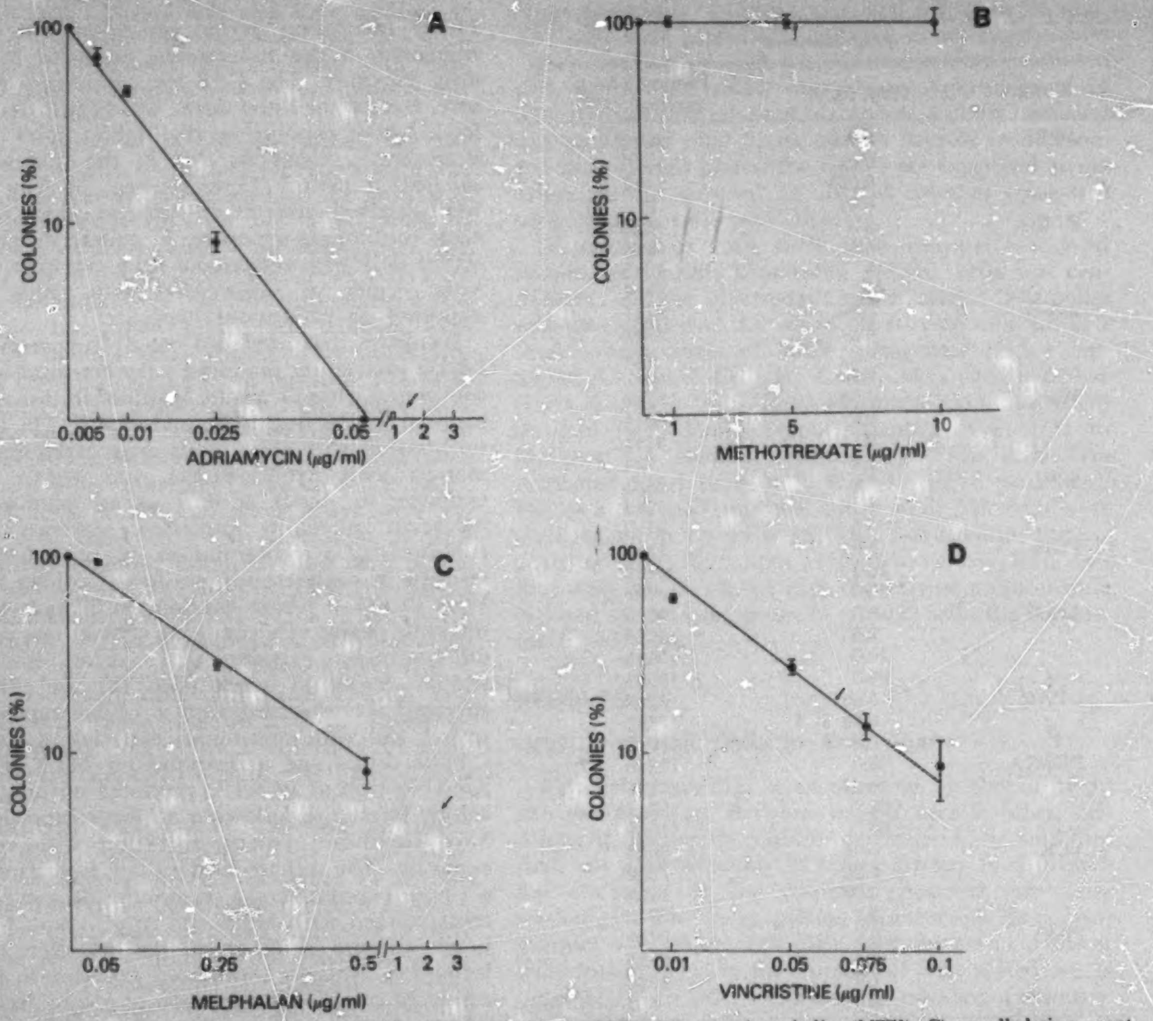

TEXT-FIGURE 1.—Effect of representative anticancer agents: A) an antibiotic (ADR); B) an antimetabolite (MTX); C) an alkylating agent [L-PAM (melphalan)]; and D) a vinca alkaloid (VCR) on survival of colony-forming cells following a 1-hr exposure at the concentrations given on the *abscissa*. Results are expressed as the mean (± SE) percent survivals of untreated controls. *Arrows* indicate clinically achievable C×T levels.

a 16% increase in colony formation compared to cells that were not exposed to digestive enzymes. However, after a 1-hour incubation, the colony formation had decreased to 74% of control, and by 2 hours there was only a 29% survival of colony-forming cells. Raji cells do not proliferate in serum-free medium, and the marked decrease in colony formation observed with a 2-hour incubation with enzymes in a serum-free medium may reflect the absence of required nutrients.

The effect of a 1-hour enzyme incubation on the subsequent pattern of anticancer drug sensitivity is summarized in table 3. Preincubation of the cells with enzymes did not appreciably alter the dose-response curves to six drugs that were tested with the use of 1-hour drug exposure.

DISCUSSION

The Raji lymphoma cell line is a suitable model system in which to study the effects of anticancer drugs on the ability of tumor cells to form colonies in soft agar. Observations made regarding drug sensitivities of Raji cells may have applicability in the optimization of the conditions currently used to determine drug sensitivities of fresh human tumors cloned in agar. The results of the present study demonstrate that the length of drug exposure can be an important determinant of a drug's cytotoxicity as measured by the effect on colony formation. Furthermore, the results also suggest that established human tumor cell lines may be useful for the screening of new anticancer drugs. If it can be

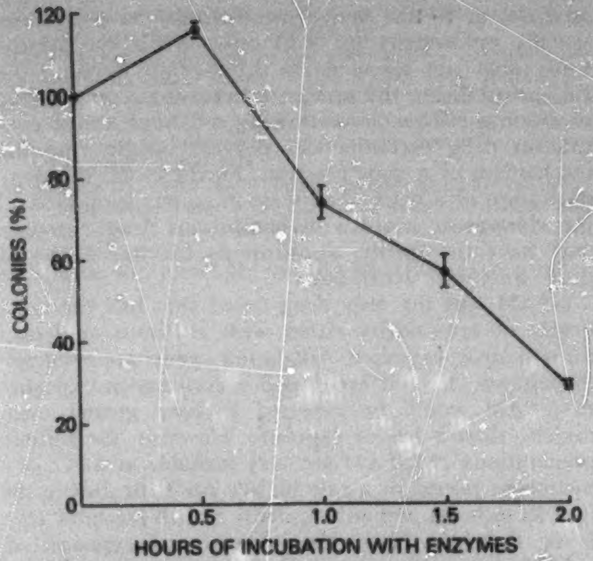

TEXT-FIGURE 2.—Effect on colony formation of Raji cells incubated with an enzyme mixture consisting of 0.02% collagenase, 0.02% DNase, and 0.05% pronase. Results are the mean (± SE) percent survivals of untreated controls.

determined that established cell lines retain the same drug sensitivity spectrum as that present in the original tumor when measured by the clonogenic assay, then for new drug screening, the higher efficiency of cell lines and the ability to culture large volumes of cells would make cell lines preferable to fresh tumor explants, which frequently may not produce sufficient colonies for a large drug-screening program.

The Raji cell line has a high cloning efficiency (30%) in soft agar under the same conditions currently in use for the human tumor clonogenic assay. In that regard, the Raji cell line is different from solid human tumors that have a cloning efficiency usually between 0.001 and 0.1% (*2, 4, 10*). The patterns of drug sensitivity observed with the Raji cell line therefore may be different than those observed in the human tumor stem cell assay. In addition, the Raji cells grow in suspension and are readily separated into single cells. In contrast, epithelial tumor cells are frequently tightly connected, and enzymatic incubation of Raji cells and epithelial tumor cells may produce different effects on cell membranes and subsequent drug sensitivities. In addition, tumor biopsy specimens contain a heterogeneous population of cells compared to homogeneous Raji cells in culture, and an enzyme incubation may produce differing effects on the various cells present in fresh tumor specimens. Accordingly, the observations made regarding the effect of enzymes on chemotherapy sensitivity and the effect of the length of incubation on the pattern of drug sensitivity in Raji cells need to be confirmed in the human tumor stem cell assay with fresh tumor specimens.

With a 1-hour drug exposure, dose-response relationships were observed with seven of the drugs tested including all the antibiotics, the alkylating agents, and VCR. Four drugs, all the antimetabolites plus PENTA, had no effect on colony formation following a 1-hour drug exposure. However, with continuous exposure to the drugs, the antimetabolites produced a marked suppression of colony formation. MTX produced a complete suppression of colony formation even at a concentration of 0.1 μg/ml compared to no suppression at a concentration of 10 μg/ml and a 1-hour drug exposure. The fact that no dose-response relationships were observed with continuous exposure to the antimetabolites indicates that all the doses used in the continuous-exposure studies produced a C×T that was cytotoxic. The marked differences in MTX cytotoxicity observed with a 1-hour and continuous drug exposures

TABLE 2.—*Effect of anticancer drugs on colony formation: 1-hr exposure versus continuous exposure*[a]

Patterns of colony suppression and drug	Dose, μg/ml	Percent colony survival ± SE
Increased suppression with continuous exposure		
ADR	0.0002	92±3
	0.001	69±1
	0.005	0
BLEO	0.1	26±1
	0.5	12±1
	2.5	0
Act-D	0.001	0
	0.01	0
	0.05	0
Mit-C	0.01	21±1
	0.1	0
	0.5	0
PLAT	0.02	61±2
	0.2	55±2
	0.5	6±1
VCR	0.0001	7±1
	0.001	0
	0.01	0
Suppression only with continuous exposure		
FUra	1.0	38±3
	5.0	0
	10.0	0
MTX	0.1	0
	1.0	0
	5.0	0
Ara-C	0.1	25±2
	0.5	0
	2.5	0
PENTA	1.0	73±2
	10.0	58±1
	50.0	5±1
Suppression not affected by length of exposure		
L-PAM	0.01	75±4
	0.25	49±5
	0.5	21±1

[a] Raji cells were incubated in soft agar culture system, as described in "Materials and Methods," to which was added the anticancer drug. Colony formation after 14 days in the drug-containing cultures was compared to that of untreated controls.

TABLE 3.—*Effect of pretreatment of Raji cells with collagenase, DNase, and pronase on anticancer drug sensitivity in soft agar*[a]

Drug	Dose, μg/ml	Percent colony survival ± SE	
		Without enzyme pretreatment	Enzymatically pretreated
ADR	0.005	90±1	84±3
	0.01	60±1	61±4
	0.025	38±2	42±3
Mit-C	0.1	74±2	75±1
	0.5	22±4	17±4
	1.0	5±1	5±1
MTX	1.0	110±2	103+3
	5.0	97±1	103±2
	10.0	89±1	103±1
L-PAM	0.05	81±3	82±2
	0.25	56±4	60±2
	0.5	21±1	31±2
VCR	0.01	57±1	52±3
	0.05	16±1	24±1
	0.1	9±1	10±1
PLAT	0.4	75±5	74±5
	1.0	51±3	64±2
	2.0	27±3	34±2

[a] Raji cells were incubated with an enzyme mixture of collagenase (0.02%), DNase (0.02%), and pronase (0.05%) for 1 hr followed by a 1-hr drug exposure.

may be the result of the following factors: *a*) MTX is an S-phase-specific drug, and its cytotoxic effects, which are due to the inhibition of dihydrofolate reductase, will be observed only with prolonged exposure to cells as they go through the cell cycle. *b*) MTX enters cells by a rapid carrier-mediated, active transport system and is also extruded by an active efflux mechanism that is most effective in an MTX-free environment. *c*) Folates present in calf serum used in the media may have overcome the effects of a 1-hour exposure to MTX but were not present in sufficient quantity to overcome the cytotoxic effects of continuous exposure. *d*) The active form of intracellular MTX may be polyglutamate derivatives. In cultured human breast cancer cells after 24 hours of incubation, 70% of the intracellular MTX exists as polyglutamates (*16*). Removal of extracellular MTX will favor efflux of the drug instead of formation of polyglutamates.

In a similar manner, the lack of colony suppression observed with a 1-hour drug exposure, compared to continuous incubation of the antimetabolites FUra and Ara-C, is likely to be predominantly due to the S-phase-specific cytotoxic nature of these drugs, although other factors such as intracellular metabolism may also require prolonged exposure to enhance cytotoxicity (*17*).

Neither the mechanism of action nor the nature of the cytotoxic metabolites of the S-triazines hexamethylmelamine and PENTA has been fully determined (*18, 19*). The marked difference in cloning efficiency of Raji cells following a 1-hour or a continuous drug exposure with PENTA suggests that *a*) the Raji lymphoma cell line can slowly metabolize PENTA to an active intermediate, or *b*) the active metabolite(s) have S-phase-specific cytotoxicity for Raji cells. While the present study does not allow us to differentiate between the two possibilities, the results indicate that comparisons of cloning efficiencies following a 1-hour and a continuous drug exposure can provide insight into the mechanism of a drug's action. Furthermore, the demonstration of a marked decrease in colony formation in the clonogenic assay with continuous drug exposure may have therapeutic applications for the design of drug treatment schedules.

L-PAM was the only drug tested that had the same degree of cytotoxicity either with a 1-hour or a continuous drug exposure. Alkylating agents are cytotoxic throughout the cell cycle, and a continuous exposure to L-PAM would be expected to have greater cytotoxicity than a 1-hour exposure. However, the soluble preparations of L-PAM are very unstable at 37°C, and hydrolysis occurs at a rate of 50% per hour during the first 30 minutes and subsequently at 30% per hour (*20*). It is therefore likely that continuous exposure to L-PAM did not produce any further increase in the cytotoxicity of a 1-hour exposure due to a rapid degradation to an inactive form of the drug.

REFERENCES

(*1*) HAMBURGER AW, SALMON SE. Primary bioassay of human tumor stem cells. Science 1977; 197:461-463.

(*2*) ———. Primary bioassay of human myeloma stem cells. J Clin Invest 1977; 60:846-854.

(*3*) VON HOFF DD, HARRIS GJ, JOHNSON G, GLAUBIGER D. Initial experience with the human stem cell assay system. In: Salmon SE, ed. Cloning of human tumor stem cells. New York: Liss, 1980:113-126.

(*4*) OZOLS RF, WILLSON JK, GROTZINGER K, YOUNG RC. Cloning of human ovarian cancer cells in soft agar from malignant effusion and peritoneal washings. Cancer Res 1980; 40:2743-2747.

(*5*) CARNEY DN, GAZDAR AF, MINNA JD. Positive correlation between histological tumor involvement and generation of tumor cells in agarose in specimens taken directly from patients with small-cell carcinoma of the lung. Cancer Res 1980; 40:1820-1823.

(*6*) SALMON SE, HAMBURGER AW, SOEHNLEN B, DURIE BG, ALBERTS DS, MOON TE. Quantitation of differential sensitivity of human tumor stem cells to anticancer drugs. N Engl J Med 1978; 298:1321-1327.

(*7*) ALBERTS DS, SALMON SE, CHEN HS, et al. In vitro clonogenic assay for predicting response of ovarian cancer to chemotherapy. Lancet 1980; 2:340-342.

(*8*) SALMON SE. Application of the human tumor stem cell assay to new drug evaluation and screening. In: Salmon SE, ed. Cloning of human tumor stem cells. New York: Liss, 1980: 291-314.

(*9*) RUPNIAK HT, HILL BT. The poor cloning ability in agar of biopsies of primary tumors. Cell Biol Int Rep 1980; 4:479-486.

(*10*) VON HOFF DD, CASPER J, BRADLEY E, SANDBACH J, JONES D, MAKUCH R. Association between human tumor colony-forming assay results and response of an individual patient's tumor to chemotherapy. Am J Med 1981; 70:1027-1032.

(*11*) PAVELIC ZP, SLOCUM HK, RUSTUM YM, CREAVEN PJ, KARAKOUSIS C, TAKITA H. Colony growth in soft agar of human melanoma, sarcoma, and lung carcinoma cells disaggregated by mechanical and enzymatic methods. Cancer Res 1980; 40: 2160-2163.

(*12*) ROSENBLUM ML. Chemosensitivity testing for human brain tumors. In: Salmon SE, ed. Cloning of human tumor stem cells. New York: Liss, 1980:259-276.

(*13*) Pulvertaft RJ. A study of malignant tumour in Nigeria by short-term tissue culture. J Clin Pathol 1965; 18:261-271.

(*14*) Ozols RF, Willson JK, Weltz MD, Grotzinger KR, Myers CE, Young RC. Inhibition of human ovarian cancer colony formation by adriamycin and its major metabolites. Cancer Res 1980; 40:4109-4112.

(*15*) Alberts DS, Chen HS. Tabular summary of pharmacokinetic parameters relevant to in vitro drug assay. In: Salmon SE, ed. Cloning of human tumor stem cells. New York: Liss, 1978:351-359.

(*16*) Schilsky RL, Bailey BD, Chabner BA. Methotrexate polyglutamate synthesis by cultured human breast cancer cells. Proc Natl Acad Sci USA 1980; 77:2919-2922.

(*17*) Maybaum J, Ullman B, Mandel HG, Day JL, Sadee W. Regulation of RNA- and DNA-directed actions of 5-fluoropyrimidines in mouse T-lymphoma (S-49) cells. Cancer Res 1980; 40:4209-4215.

(*18*) Metz ML, Winters DW. Utilization of metabolic activation for in vitro screening of potential antineoplastic agents. Cancer Treat Rep 1979; 63:1795-1801.

(*19*) Rutty CJ, Connors TA. In vitro studies with hexamethylmelamine. Biochem Pharmacol 1977; 26:2385-2391.

(*20*) Furner RL, Brown RK. L-Phenylalanine mustard (L-PAM): The first 25 years. Cancer Treat Rep 1980; 64:559-574.

blank page

Antitumor Activity of Picolinic Acid in CBA/J Mice[1, 2, 3]

Susan W. C. Leuthauser,[4] **Larry W. Oberley,**[4, 5] *and* **Terry D. Oberley**[6, 7]

ABSTRACT—The growth of a solid tumor induced by im implantation of Ehrlich ascites tumor cells in inbred CBA/J mice was retarded by treatment with an iron chelator, picolinic acid (PLA). Survival of the mice was also significantly increased after PLA treatment. However, the iron chelator deferoxamine had no such effects; tumor growth was slightly enhanced, and survival was decreased.—JNCI 1982; 68:123-126.

A nicotinic acid analog, PLA (NSC-171), is a metabolite of tryptophan (*1*). The function of this naturally occurring bidentate metal chelator (*2*) is still unknown. PLA has been found to facilitate the absorption of zinc from the intestine (*3*) and the binding of Fe^{3+} and Zn^{2+} (*4*). In the presence of PLA, spore formation by *Bacillus subtilis* and growth of *Escherichia coli* were inhibited (*5, 6*). NRK cells were reversibly arrested at the G_1 stage of the cell cycle when PLA was added to the culture media (*4, 7-9*). Growth of transformed NRK cells was also arrested by PLA. However, this G_1 block was not reversible in transformed NRK cells (*10, 11*). Upon removal of this block the transformed cells progressed through S- and G_2 phases and then died. Fernandez-Pol (*4*) and Fernandez-Pol and Johnson (*10*) proposed that this differential response may involve NAD metabolism, cyclic AMP interference, or the differences in trace metal requirement between normal and transformed cells. Analogs of PLA have been shown to inhibit tumor growth in vivo (*12-14*). PLA has been tested in a variety of rodent experimental tumor systems (*15*). No antitumor effect was observed when PLA was administered ip. This study is designed to investigate the effect of PLA on the growth of a solid tumor.

MATERIALS AND METHODS

Ehrlich ascites tumor cells were maintained intraperitoneally in inbred adult female CBA/J mice (The Jackson Laboratory, Bar Harbor, Maine) by weekly transfers into new hosts. Solid tumors were induced by im inoculation of 5×10^6 cells into the right flanks of 8- to 12-week-old CBA/J female mice. Cell counts were done with a Coulter Model B cell counter. Mice implanted with Ehrlich cells subsequently developed solid tumors at the injection sites. Diameters of the tumor-bearing legs were determined with a vernier caliper by two-dimension measurements of the affected limbs.

The mean and standard error of the limb size in each treatment group were determined. There were 24 mice in each group. Significance of the difference between the 2 treatment groups was determined by Student's *t*-test. Survival times of these tumor-bearing mice were also used as an end point for the effectiveness of the treatment. Survival curves were analyzed by Mantel-Cox's Generalized Savage Test.

PLA (α-picolinic acid) was purchased from Sigma Chemical Co., St. Louis, Mo.; DFO (Desferal) was obtained from Ciba-Geigy Corp., Summit, N.J. In preliminary studies, 5 mice/group were given doses of 1, 2.5, or 5 mg PLA/0.1 ml saline daily for 5 consecutive days. For the PLA survival studies, a standard dose of 2.5 mg PLA/0.1 ml saline or saline alone was given to 24 mice in each treatment group. Tumor-bearing mice were PLA treated with 5 daily doses or a total of 10 doses (on days 0, 2, 4, 7, 9, 11, 14, 16, 18, and 21). The first dose was given at the same site and immediately after inoculation of cells. In addition to the PLA-treated groups, treatment groups included mice given saline or 2.5 or 5 mg DFO daily for 5 days. Each of these 3 groups also had 5 mice.

RESULTS

A dose-response study (text-fig. 1) showed that 1 mg PLA/day for 5 days produced a 29% reduction in the diameter of the tumor-bearing leg by day 10. However, when the daily dose was increased to 2.5 mg, the reduction in the diameter of the tumor-bearing leg was increased from 29% to 40% ($P<0.001$, compared to saline-treated controls). Additional increases in the daily dose of PLA caused little further reduction in the size of the tumor-bearing leg, but at these doses, kidney damage occurred (Oberley TD: Manuscript in preparation). Therefore, the dose chosen for this study was 2.5 mg.

ABBREVIATIONS USED: DFO = deferoxamine; NRK = normal rat kidney; PLA = picolinic acid.

---

[1] Received February 6, 1981; revised July 15, 1981; accepted September 1, 1981.

[2] Supported by Public Health Service grant 5T32CA-09125-05 from the National Cancer Institute and by the Cancer Research Fund, Cancer Center, University of Iowa.

[3] Animals were maintained under the guidelines of The University of Iowa.

[4] Radiation Research Laboratory, 14 Medical Laboratories, University of Iowa, Iowa City, Iowa 52242.

[5] *Address reprint requests to* Professor L. W. Oberley.

[6] Department of Pathology, 470 North Charter St., University of Wisconsin, Madison, Wis. 53706.

[7] We thank the following people at The University of Iowa: Mr. Loren Schutt and Mr. John Pirro (Radiation Research Laboratory) for providing technical assistance, Dr. Robert Woolson (Department of Preventive Medicine) for assisting us in performing the statistical analysis, and Mrs. Susan Barnett (Radiation Research Laboratory) for typing the manuscript.

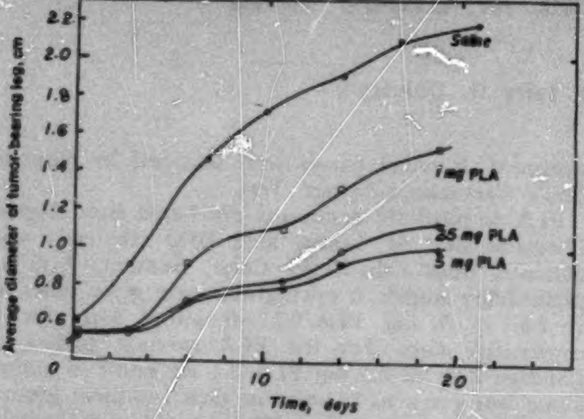

TEXT-FIGURE 1.—Response of Ehrlich ascites tumor in CBA/J mice to various doses of PLA. Diameters of tumor-bearing legs were measured as a function of time after 5 consecutive daily doses of saline or PLA. There are 5 mice in each treatment group.

Text-figure 2 shows the change in tumor-bearing leg diameters as a function of time after implantation. The various groups received different treatments. The control group received 5 daily doses of 0.1 ml of saline im. When 5 doses of 2.5 mg PLA were administered, a 25% reduction in the tumor-bearing leg diameter was observed by day 31 (27 days after the last treatment). When 10 doses of 2.5 mg PLA were given in a period of 22 days (on days 0, 2, 4, 7, 9, 11, 14, 16, 18, and 21), the reduction in the tumor-bearing limb diameter was unchanged by this additional treatment.

The antitumor activity of another iron chelator, DFO, was also tested in this tumor system. This compound is used clinically to treat iron poisoning; the maximum recommended im dose for adults is 6 g/day. When 2.5 or 5 mg of DFO (1.5 and 3 times the maximum recommended human dose) was given to these tumor-bearing mice daily for 5 days, no significant reduction in the tumor-bearing leg diameter was observed, as compared to the control; in contrast, growth of the tumor was slightly enhanced by DFO treatment, and the treated animals died faster than did the controls.

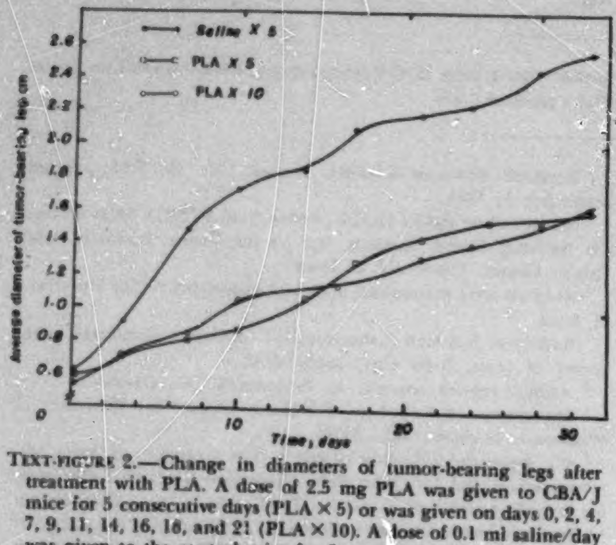

TEXT-FIGURE 2.—Change in diameters of tumor-bearing legs after treatment with PLA. A dose of 2.5 mg PLA was given to CBA/J mice for 5 consecutive days (PLA × 5) or was given on days 0, 2, 4, 7, 9, 11, 14, 16, 18, and 21 (PLA × 10). A dose of 0.1 ml saline/day was given to the control mice for 5 consecutive days (Saline × 5). There are 24 mice in each treatment group.

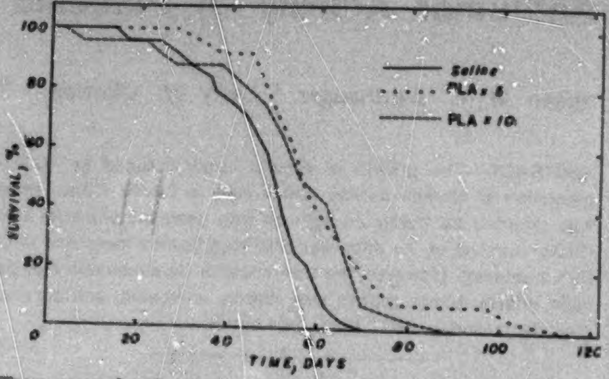

TEXT-FIGURE 3.—Survival of PLA- or saline-treated tumor-bearing CBA/J mice at the same dose schedules as in text-fig. 2. There are 24 mice in each treatment group.

Survival of the PLA-treated tumor-bearing mice was significantly increased. Text-figure 3 and table 1 show that the mean survival was increased from 49 to 62 days, or 127% that of the control ($P=0.001$), for the group receiving 5 doses and to 56 days, or 114% of the control ($P=0.01$), for the group receiving 10 doses. Median survival of both treatment groups was increased from 51 to 56 days, 110% that of control. Median survival data between the 2 PLA-treated groups remained the same, a further indication that additional PLA had no positive effect on the animals as was true for tumor size reduction.

No significant weight loss was observed in PLA-treated mice as compared to the saline-injected controls, suggesting that 1 group had not eaten less than had the other. The most significant change between the saline-treated and PLA-treated animals was the difference in maximum survival which, as shown in table 1, was increased from 70 to at least 112 days in the group receiving 5 doses (160% of the control) and from 70 to 89 days in the group receiving 10 daily

TABLE 1.—*Summary of survival data for CBA/J mice*

Treatment group, No. of doses[a]	Survival, days		
	Mean ± SE	Median	Maximum
Saline	49±3	51	70
PLA, 5	62±6	56	112[b]
PLA, 10	56±5	56	89

[a] *See* "Materials and Methods" for dose schedules.
[b] Experiment was terminated.

doses (127% of control). Thus, although the change in mean or median survival was not impressive, the change in maximum survival was quite substantial, which indicates an increase in longer term survivors. One mouse in the PLA-treated group appeared tumor-free at 112 days, at which time the experiment was terminated.

Autopsies on all tumor-bearing mice revealed that massive lung metastasis was invariably the cause of death. Kidney necrosis was observed in some of the PLA-treated mice. The effect of PLA on the kidneys of normal nontumorous mice will be reported elsewhere (Oberley TD: Manuscript in preparation).

DISCUSSION

Our results indicated that PLA has a positive antitumor activity in this experimental tumor model. PLA-treated mice had significantly slower increases in tumor size. The increases in mean and median survivals were not impressive, but the increase in maximum survival was substantial. Since the PLA-treated mice showed no weight difference when compared with the control group, it is unlikely (although not definitely proved) that the effects are due to reduced food intake and subsequent weight loss. These results contrast with those of previous studies in which PLA was ineffective in several rodent tumor systems when either tumor size or animal survival was used as a therapeutic indicator (*15*). One possible difference between our study and the previous ones is that we used im rather than ip injections. When given ip, PLA is rapidly excreted into the urine, with a half-life of 6 hours (*1*). PLA is probably excreted more slowly with the im injection used in this study.

The mechanism of action for the arrest of NRK cells by PLA in G_1 remains unknown. Fernandez-Pol and co-workers (*4, 10, 11*) proposed alteration of cyclic AMP metabolism, NAD metabolism, or chelation of Fe^{3+}-Zn^{2+} as possible modes of action. Reduced tumor growth could be due to the inhibition or retardation of the cell proliferation process or to the reduction in the number of cycling cells. Text-figure 2 shows that the growth rates of the tumors from the saline-treated and the PLA-treated mice were very similar after the initial period during treatment. Since the slopes of the growth curves remained unchanged, the number of viable cycling cells was most likely reduced after PLA treatment.

Fernandez-Pol and co-workers have proposed that deprivation of iron might be responsible for tumor cell toxicity. If this were true, why does PLA have such a marked effect on tumor cell growth whereas twice as much DFO has none? There are several possibilities why DFO was not effective. DFO may have been excreted much more rapidly than was PLA, or it could have other toxic side effects. We tested DFO at three times the maximum recommended human dose, but it is possible that this dose is still not high enough in mice. Although this possibility seems unlikely, DFO might have the same effect as PLA has at a much higher dose.

Lastly, the cytotoxicity of PLA may involve generation of hydroxyl radicals via the Fenton reaction (*16*). Generation of ·OH in an aqueous solution in the presence of PLA, Fe^{2+}, H_2O_2, and superoxide was detected by the electron spin resonance technique (Buettner GR, Oberley LW: Unpublished observation). DFO has been shown to be a powerful inhibitor of ·OH generation (*17*). Possibly, the difference in the response of the tumor to PLA and DFO is due to the ability of these agents to generate ·OH. In this tumor model, the activity of a superoxide scavenger, superoxide dismutase, is depressed (*18*). Since catalase and glutathione peroxidase activities are also reduced in tumors, such depletion in protective enzymes may lead lead to a surplus of O_2^- and H_2O_2; with the availability of PLA-Fe complexes, the toxic ·OH could be produced readily. Obviously, further studies are needed to confirm this hypothesis.

REFERENCES

(*1*) Mehler AH, May EL. Studies with carboxyl-labeled 3-hydroxyanthranilic and picolinic acids in vivo and in vitro. J Biol Chem 1956; 223:449–455.

(*2*) Chemical Society. Stability constants of metal ion complexes. Special Publ. No. 6. London: Chemical Society, 1964.

(*3*) Evans GW, Johnson PE. Characterization and quantitation of a zinc-binding ligand in human milk. Pediatr Res 1980; 14: 876–880.

(*4*) Fernandez-Pol JA. Transition metal ions induce cell growth in NRK cells synchronized in G_1 by picolinic acid. Biochem Biophys Res Commun 1977; 76:413–419.

(*5*) Fortnagel P, Freese E. Inhibition of aconitase by chelation of transition metals causing inhibition of sporulation in *Bacillus subtilis*. J Biol Chem 1968; 243:5289–5295.

(*6*) Collins JJ, Adler CR, Fernandez-Pol JA, Court D, Johnson GS. Transient growth inhibition of *Escherichia coli* K-12 by iron chelators: "In vivo" inhibition of ribonucleic acid synthesis. J Bacteriol 1979; 138:923–932.

(*7*) Johnson GS, Fernandez-Pol JA. NRK cells synchronized in G_1 by picolinic acid are super-sensitive to prostaglandin E_1 stimulation. FEBS Lett 1977; 74:201–204.

(*8*) Fernandez-Pol JA. Iron: Possible cause of the G_1 arrest induced in NRK cells by picolinic acid. Biochem Biophys Res Commun 1977; 78:136–143.

(*9*) Fernandez-Pol JA, Klos D, Donati RM. Iron transport in NRK cells synchronized in G_1 by picolinic acid. Cell Biol Int Rep 1978; 2:433–439.

(*10*) Fernandez-Pol JA, Johnson GS. Selective toxicity induced by picolinic acid in simian virus 40-transformed cells in tissue culture. Cancer Res 1977 37:4276–4279.

(*11*) Fernandez-Pol JA, Bond VH Jr, Johnson GS. Control of growth by picolinic acid: Differential response of normal and transformed cells. Proc Natl Acad Sci USA 1977; 74:2889–2893.

(*12*) Mishra LC, Mead JA. Physiological disposition of 1-acetyl-2-picolinoylhydrazine (NSC 68626) in rats bearing Walker carcinosarcoma 256. Cancer Res 1973; 33:2393–2397.

(*13*) Olson KB, Horton J, Pratt KL, et al. 1-Acetyl-2-picolinoylhydrazine (NSC-68626) in the treatment of advanced cancer. Cancer Chemother Rep 1969; 53 (pt. 1):291–296.

(*14*) Bradley RL, Shoemaker JP, Hickman RV Jr. Treatment of experimental mammary adenocarcinoma with herbicides. Cancer Chemother Rep 1974; 58 (pt. 1):745–748.

(*15*) Developmental Therapeutics Program, Division of Cancer Treatment, National Cancer Institute. Screening data summary: Synthetic products (NSC-171). Bethesda, Md.: Natl Inst Health, 1980.

(16) BUETTNER GR, OBERLEY LW, LEUTHAUSER SW. The effect of iron on the distribution of superoxide and hydroxyl radicals as seen by spin trapping and on the superoxide dismutase assay. Photochem Photobiol 1978; 28:661-668.

(17) GUTTERIDGE JM, RICHMOND R, HALLIWELL B. Inhibition of the iron-catalyzed formation of hydroxyl radicals from superoxide and of lipid peroxidation by desferrioxamine. Biochem J 1979; 184:469-472.

(18) LEUTHAUSER SW, OBERLEY LW, OBERLEY TD, SORENSON JR, RAMAKRISHNA K. Antitumor effect of a copper coordination compound with superoxide dismutase-like activity. JNCI 1981; 66:1077-1081.

Equivalency of Endothelial Cell Growth Supplement to Irradiated Feeder Cells in Carcinogen-Induced Morphologic Transformation of Syrian Hamster Embryo Cells[1]

Charles H. Evans[2] *and* **Joseph A. DiPaolo**[2,3]

ABSTRACT—Endothelial cell growth supplement (ECGS), an extract of bovine neural tissue with growth-promoting properties for human endothelial and epithelial cells and for mouse BALB/c fibroblast-like cells, can be substituted for feeder cells in a quantitative 7-day Syrian hamster embryo cell colony in vitro model of carcinogenesis. Inclusion of 50 or 100 μg ECGS/ml medium throughout the 7-day growth period produced results equal to those obtained with feeder cells. The frequency and morphology of normal fibroblast colonies and carcinogen-induced morphologically transformed cell colony growth in the presence of ECGS were similar to those in the presence of feeder cells. A positive dose-response relationship in transformation by benzo[a]pyrene occurred. The frequency of transformed colonies following UV irradiation and treatment of the cells with the cocarcinogenic tumor promoter 12-*O*-tetradecanoylphorbol 13-acetate was greatly augmented, and lymphotoxin, a lymphokine with anticarcinogenic activity, reduced transformation. Thus ECGS can substitute for feeder cells in supporting in vitro transformation and eliminates a potential complex source of variability for studies where interaction(s) with feeder cells are a consideration. The mechanics of this model system was simplified, and its versatility for the study of physiologic, carcinogenic, and other pathophysiologic processes was broadened.—JNCI 1982; 68: 127–131.

Carcinogen-induced morphologic transformation of early passage Syrian HEF strains in the conventional 7-day quantitative cell colony assay of carcinogenesis has been dependent upon the inclusion of X-irradiated feeder cells or conditioned medium to facilitate the growth of a relatively small number of cells seeded for colony formation in the study of carcinogenesis, cocarcinogenesis, and anticarcinogenesis (*1–3*). In addition to the logistic complexity and/or inconvenience of access to an irradiation source or of preparation of conditioned medium, both feeder cells and conditioned medium introduce potential additional variables and sources of positive or negative interaction(s) in each experiment. For example, feeder cells or conditioned medium have the potential to provide crossfeeding and other metabolic and/or inactivating or interfering effect(s) in the study of multiple interactions (*4–6*). For investigations where such interactions are undesirable or not permissible, it would be advantageous to have a nonliving and more constant substitute for feeder cells or conditioned medium.

A variety of growth factors, including FGF, epidermal growth factor, neural growth factor, platelet-derived growth factor, fibronectin, and ECGS, have been shown to enhance the growth of various cells (*7, 8*). Some of these growth factors or supplements hold promise as substitutes for the complex and frequently unknown variables resident in serum, feeder cells, and the plethora of ingredients in the manifold cell culture models developed for the study of normal and pathophysiologic conditions. For example, human endothelial cells produce a factor(s) that can replace the feeder cells in the growth of hybridoma cells for monoclonal antibody production (*9*). These human endothelial cell factors, however, are not commercially available, and their activities for other cells are unknown. Crude bovine brain extracts prepared at pH 8.5 contain potent mitogenic factor(s) for myoblasts, and the extracts may be useful for cloning cells or for accelerating the growth of slowly dividing cells (*10*). ECGS, a commercially available extract of bovine neural tissue, promotes the growth of human endothelial and epithelial cells and stimulates the growth of mouse Balb/3T3 cells (*11, 12*). This investigation demonstrates that ECGS can substitute for the feeder cells in the Syrian HEF colony in vitro model of carcinogenesis.

MATERIALS AND METHODS

Substitution of ECGS for feeder cells was studied in the HEF in vitro model of carcinogenesis in which the frequency of carcinogen-induced morphologic transformation is quantifiable and indicative of the cells' neoplastic potential (*1*). In each transformation experiment, secondary cultures of HEF, originally obtained from 12-day gestation fetuses of a single hamster and stored in liquid nitrogen as trypsinates of cell pools prior to any growth, were cultured and treated with carcinogens (*13*). Cell pools from three dams were utilized.

Tissue culture dishes (100 mm in diameter) were seeded with 10^7 freshly thawed cells in 10 ml DMEM

ABBREVIATIONS USED: BP = benzo[a]pyrene; DMEM = Dulbecco's modified Eagle's minimum essential medium; ECGS = endothelial cell growth supplement; FBS = fetal bovine serum; FGF = fibroblast growth factor; HEF = hamster embryo fibroblast(s); TPA = 12-*O*-tetradecanoylphorbol 13-acetate.

---

[1] Received April 10, 1981; accepted August 28, 1981.

[2] Laboratory of Biology, Division of Cancer Cause and Prevention, National Cancer Institute, Public Health Service, U.S. Department of Health and Human Services, Bethesda, Md. 20205.

[3] We thank Mr. Anthony J. DeMarinis and Mr. David J. Engle for their technical assistance.

containing 3×10^{-6} *M* thymidine, 3×10^{-5} *M* hypoxanthine, and 10% FBS (medium) but no antibiotics, and the cells were grown at 37°C in a 10% CO_2 water-saturated atmosphere of PHARM-AIR (Pall Trinity Micro Corp., Cortland, N.Y.) purified compressed air (*14*). Three lots of serum (#R6, R8, and 33K) were included in the study. Three days after removal from nitrogen and culture, the cells were trypsinized and 100-mm dishes were seeded with 2×10^6 cells in 10 ml medium. After 48 hours the cells were trypsinized, and 300 cells with 6×10^4 X-irradiated sister culture cells for a feeder layer were seeded per 60-mm dish in 4 ml medium. Feeder cells were prepared by removal of 5 ml of medium from a 2-day secondary culture of cells and delivery of 2,000 R of 100-kV peak X-rays from a Torex model 120 X-irradiator (Torr X-Ray Corp., Van Nuys, Calif.) immediately prior to plating. Nonirradiated cells were suspended in medium alone or with ECGS-containing medium for comparison of growth and transformation to cells cocultivated with feeder cells. Three lots (#797-8, 1084-9, and 1076-591) of ECGS were purchased (Collaborative Research, Inc., Waltham, Mass.) and stored at −20°C until dissolved in sterile Milli-Q deionized water, Dulbecco's phosphate-buffered saline, or medium without serum immediately prior to addition to the cells. ECGS lots #797-8, 1084-9, and 1076-591 had been stored for 2 years, 1 month, and 4 months, respectively, before use.

Twenty-four hours after cells were seeded, another 4 ml of medium containing BP and an appropriate additional ECGS to maintain the initial ECGS concentration were added or the medium was removed, the cells irradiated with 254 nm UV light, and the dishes refed with 8 ml of medium with or without ECGS. TPA (Vega Biochemicals, Tucson, Ariz.) was added 48 hours after UV irradiation as described for TPA enhancement of *N*-methyl-*N'*-nitro-*N*-nitrosoguanidine transformation (*15*). Lymphotoxin, a lymphokine with antitransforming activity for HEF, was prepared, concentrated, and equilibrated with phosphate-buffered saline (pH 7.4) by diafiltration on Amicon YM10 membranes (Amicon Corp., Danvers, Mass.), and added to the cells 48 hours after BP treatment (*3*). Six dishes were treated with each concentration of carcinogen, ECGS, or other chemical in each experiment. Six days after carcinogen treatment, the dishes were stained and the cell colonies examined for morphologic transformation, a random piled up layering of spindle-shaped fibroblasts not observed in noncarcinogen-treated cultures that correlates with the ability of the cells to grow as tumors in vivo (*1*).

RESULTS

The inclusion of ECGS in the culture medium in place of X-irradiated feeder cells resulted in equivalent growth and carcinogen-induced morphologic transformation of Syrian HEF (fig. 1). At a concentration of 50 or 100 μg ECGS/ml medium, colony formation and transformation frequencies were similar to those observed in the presence of feeder cells (table 1). The growth of control (solvent treated) cells in the presence of 50 μg ECGS/ml culture medium was also equivalent to growth with feeder cells (table 2). Similar results were obtained with each of three lots of serum, with three lots of ECGS, and with three pools of HEF.

TABLE 1.—*Substitution of ECGS for feeder cells in the BP induction of morphologic transformation of Syrian HEF*[a]

Culture medium supplement	Colony formation, %	Transformed colonies/dish
ECGS, μg/ml medium		
0	10.8±0.4	0.2±0.1
5	11.2±0.8	0.8±0.1
10	15.4±0.4	0.7±0.1
25	14.3±0.7	0.8±0.2
50	16.3±0.6	1.8±0.1
100	15.7±1.0	2.0±0.2
Feeder cell layer	13.2±0.7	1.2±0.1

[a] Three hundred HEF (pool F80-5) in 4 ml DMEM–10% FBS (lot #R8) medium containing ECGS (lot #1084-9) at the indicated concentrations or 6×10^4 X-irradiated HEF for feeder were seeded per 60-mm tissue culture dish. One day later, 4 ml of additional medium containing 5.0 μg BP/ml was added. Colonies (>2 mm) were enumerated and examined for morphologic transformation 7 days after seeding. Results are means±1 SE.

In the presence of ECGS the frequency of morphologic transformation increased with increased carcinogen concentration as previously established by use of feeder cells (table 3). ECGS also supported TPA enhancement of the transformation induced by UV irradiation and the inhibition of transformation by lymphotoxin to an extent similar to that observed in the presence of feeder cells (table 3).

TABLE 2.—*Comparison of medium alone, X-irradiated feeder cells, or ECGS in BP induction of morphologic transformation of Syrian HEF*[a]

Chemical treatment	Medium alone		Feeder cells		ECGS	
	CF	T/D	CF	T/D	CF	T/D
Expt 1						
BP	10.3±0.7	0.7±0.1	13.1±0.5	2.5±0.1	17.9±0.4	1.8±0.1
Solvent (alone)	14.0±0.5	0±0	21.4±0.7	0±0	20.8±0.8	0±0
Expt 2						
BP	10.8±0.4	0.2±0.1	13.2±0.9	1.2±0.2	14.1±0.4	1.8±0.6
Solvent (alone)	12.4±0.6	0±0	19.1±1.0	0±0	16.9±0.6	0±0

[a] Three hundred HEF (pool F80-5) in 4 ml DMEM–10% FBS (lot #R6) medium containing 50 μg ECGS (lot #797-8)/ml, 6×10^4 X-irradiated HEF for feeder, or neither one were seeded per 60-mm tissue culture dish. One day later, 4 ml of additional medium containing 5.0 μg BP/ml or solvent only were added. BP was initially dissolved in acetone, and the final solvent concentration in the dish was 0.04%. Colonies were enumerated and examined for morphologic transformation 7 days after seeding. Mean values±1 SE are presented of the percent colony formation (CF) and the number of transformed colonies/dish (T/D).

TABLE 3.—*Equivalency of ECGS with feeder cells in carcinogen and cocarcinogen-induced morphologic transformation of Syrian HEF*

Treatment[a]	Transformed colonies/dish	
	Usual response in the presence of feeder cells[b]	With ECGS substituted for feeder cells
BP, 0 μg/ml	0	0
BP, 1 μg/ml	1.3–2.0	0.9±0.3
BP, 2.5 μg/ml	2.2–3.1	1.7±0.3
BP, 5.0 μg/ml	2.2–4.2	2.7±0.5
UV irradiation, 3.0 J/m^2	0.1–1.6	0.1±0.1
UV irradiation, 3.0 J/m^2, plus TPA, 50 ng/ml	15- to 20-fold increase	1.3±0.4
TPA (alone), 50 ng/ml	0	0
BP, 2.5 μg/ml	2.2–3.1	1.7±0.4
BP, 2.5 μg/ml, plus lymphotoxin, 12.5 U/ml	50–100% inhibition	0.8±0.2
Lymphotoxin (alone), 12.5 U/ml	0	0

[a] HEF were seeded and treated 1 day later with carcinogen as described in table 2. TPA when added was done so 2 days after UV irradiation. Lymphotoxin when added was done so 2 days after BP. The FBS used in these expts was lot #32K, and the ECGS was lot #1076-591. Two pools of cells were used: F80-35 for the BP and F79-32 for the UV treatments.

[b] For BP, *see* (*3*), (*13*), (*14*), and (*16*); for UV irradiation, *see* (*3*), (*13*), (*16*), and (*17*); for TPA enhancement, *see* (*18*); and for lymphotoxin inhibition, *see* (*3*). UV irradiation transformation is particularly dependent upon the lot of FBS, frequently requiring 15 or 20% FBS to obtain the higher transformation frequencies within the indicated range. All expts in the present investigation were performed with the use of 10% FBS.

DISCUSSION

The current results demonstrate that ECGS can replace feeder cells in quantitative in vitro studies of carcinogenesis with the use of HEF. This will facilitate investigations where questions of potential feeder cell cooperation, inhibition, or other effects are entertained. Substitution of ECGS for the feeder cells also allows investigators without access to an X-ray source to consider the use of this model system in their laboratories.

The observation that 50–100 μg ECGS/ml medium produces results equivalent to those in the presence of feeder cells is similar to the report that 100 μg ECGS/ml is optimal for the proliferation and differentiation of normal human bronchial epithelial cells in culture (*11*). Additional optimal concentrations may be found for other cells inasmuch as up to 300 μg ECGS/ml has been reported to be stimulatory for human endothelial and Balb/3T3 cell growth (*12*). For HEF transformation, however, it appears that 50 or 100 μg ECGS/ml yields results equivalent to the results by use of the standard number of feeder cells in the colony assay for carcinogen-induced morphologic transformation of HEF. The results suggest that the supportive role of feeder cells and conditioned medium may be due to the production of growth factors similar to, if not identical to, those in ECGS. The growth factors in ECGS have been partially defined and include FGF and other mitogenic and growth-promoting activities (*12, 19*). Because the components in ECGS are isolated, it will be of interest to determine which support cell colony formation (cell proliferation) and morphologic transformation as well as to establish the relationship of ECGS to the growth factors isolated from other tissues.

REFERENCES

(*1*) DiPaolo JA, Nelson RL, Donovan PJ. Morphological characteristics of Syrian hamster cells transformed in vitro by carcinogenic polycyclic hydrocarbons. Cancer Res 1971; 31:1118–1127.

(*2*) Huberman E, Donovan PJ, DiPaolo JA. Mutation and transformation of cultured mammalian cells by *N*-acetoxy-*N*-2-fluorenylacetamide. J Natl Cancer Inst 1972; 48:837–842.

(*3*) Evans CH, DiPaolo JA. Lymphotoxin: An anticarcinogenic lymphokine as measured by inhibition of chemical carcinogen or ultraviolet-irradiation-induced transformation of Syrian hamster cells. Int J Cancer 1981; 27:45–49.

(*4*) Marquardt H, Heidelberger C. Influence of "feeder cells" and inducers and inhibitors of microsomal mixed-function oxidases on hydrocarbon-induced malignant transformation of cells derived from C3H mouse prostate. Cancer Res 1972; 32:721–725.

(*5*) Graves JA. Use of enzyme-deficient cell lines as feeder layers. In Vitro 1978; 14:506–509.

(*6*) Nishi Y, Mori M, Inui N. Chromosome aberrations induced by benzo[*a*]pyrene in a feeder cell-mediated assay. Toxicol Lett 1979; 4:275–279.

(*7*) Gospodarowicz D, Moran DS. Growth factors in mammalian cell culture. Ann Rev Biochem 1976; 45:531–538.

(*8*) Ross R, Vogel A. The platlet-derived growth factor. Cell 1978; 14:203–210.

(*9*) Astaldi GC, Janssen MC, Lansdorp P, Willems C, Zeijlemaker WP, Oosterhof F. Human endothelial culture supernatant (HECS): A growth factor for hybridomas. J Immunol 1980; 125:1411–1414.

(*10*) Gospodarowicz D, Weseman J, Moran J. Presence in brain of a mitogenic agent promoting proliferation of myoblasts in low density culture. Nature 1975; 256:216–219.

(*11*) Haugen A, McClendon I, Trump BF, Stoner GD, Harris CC. Influence of growth factors on proliferation and differentiation of normal human bronchial epithelial cells. Proc Am Assoc Cancer Res 1980; 21:91.

(*12*) Anonymous. Technical bulletin. Endothelial cell growth supplement (ECGS). Waltham, Mass.: Collaborative Research, Inc., 1979.

(*13*) DiPaolo JA. Quantitative in vitro transformation of Syrian golden hamster embryo cells with the use of frozen stored cells. JNCI 1980; 64:1485–1489.

(*14*) Evans CH, Greiner JW. Corticosteroid prevention of carcinogenesis in benzo[*a*]pyrene or ultraviolet irradiation treated Syrian hamster cells in vitro. Cancer Lett 1981; 12:23–27.

(*15*) Popescu NC, Amsbaugh SC, DiPaolo JA. Enhancement of *N*-methyl-*N'*-nitro-*N*-nitrosoguanidine transformation of Syrian hamster cells by a phorbol diester is independent of sister chromatid exchanges and chromosome aberrations. Proc Natl Acad Sci USA 1980; 77:7282–7286.

(*16*) DiPaolo JA, DeMarinis AJ, Doniger J. Asbestos and benzo(*a*)-

pyrene synergism in the transformation of Syrian hamster embryo cells. J Environ Pathol Toxicol. In press.

(*17*) DONIGER J, DIPAOLO JA. Excision and postreplication DNA repair capacities, enhanced transformation, and survival of Syrian hamster embryo cells irradiated by ultraviolet light. Cancer Res 1980; 40:582-587.

(*18*) DIPAOLO JA, DEMARINIS AJ, EVANS CH, DONIGER J. Expression of initiated and promoted stages of irradiation carcinogenesis in vitro. Cancer Lett. In press.

(*19*) MACIAG T, CERUNDOLO J, ILSLEY S, KELLEY P, FORAND R. Identification and partial characterization of a human endothelial cell growth factor. Fed Proc 1979; 38:634.

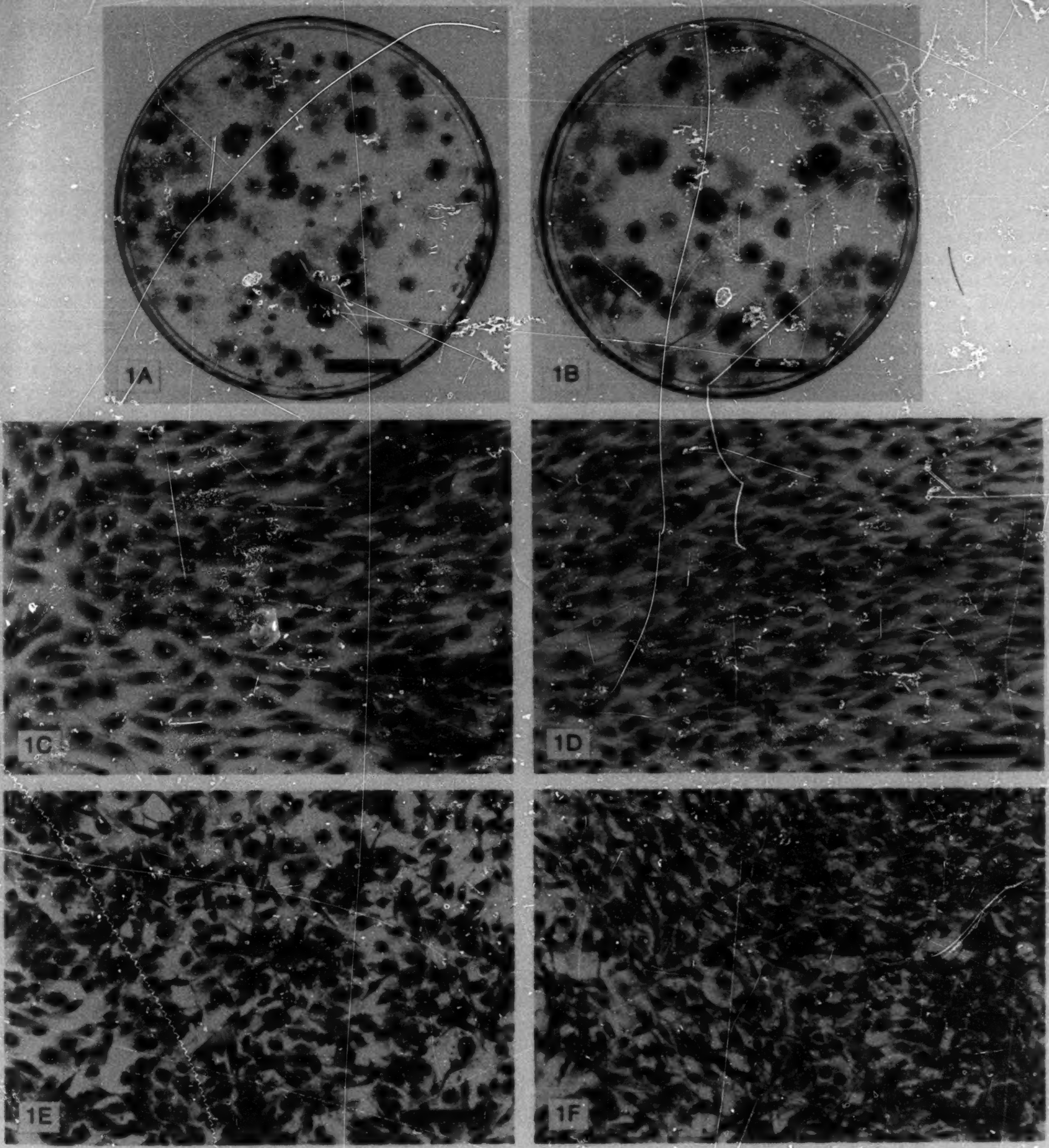

FIGURE 1.—Comparison of Giemsa-stained control and carcinogen-treated Syrian HEF grown in the presence of feeder cells or ECGS. Colonies of acetone-treated cells grown with feeder (A) or ECGS (B). *Bar*=1 cm. × 1. Periphery of colonies of acetone-treated cells with feeder (C) or ECGS (D) and BP morphologically transformed cells with feeder (E) or ECGS (F). *Bar*=50 μ. × 300

blank page

Effect of Thymectomy on Development of Lucké Renal Adenocarcinomas in Virus-Infected Leopard Frog Tadpoles[1, 2, 3]

Louise A. Rollins-Smith[4] *and* **Nicholas Cohen**[4, 5]

ABSTRACT—Thymectomy of very young leopard frog (*Rana pipiens*) larvae dramatically reduced in vitro lymphocyte responses to the mitogen phytohemagglutinin-P and prolonged survival of Lucké tumor alloimplants. However, tumor incidence in premetamorphic or metamorphosing frogs that had received injections as embryos of Lucké tumor herpesvirus (LTHV) was the same in thymectomized and normal immunocompetent animals. This result suggests that T-cell-mediated cytotoxicity does not prevent development of Lucké tumors in immunocompetent larvae and that if tumor-specific transplantation antigens appear, they may induce tolerance rather than destructive immunity in normal LTHV-infected larvae.—JNCI 1982; 68:133-138.

The Lucké renal adenocarcinoma of northern leopard frogs, *Rana pipiens,* provides an interesting model for the study of the development of cancer. The causative agent of the tumor is LTHV (*1, 2*). Among herpesvirus-related cancers, the Lucké tumor is unique because the tumorigenic phase of virus infection is distinctly separable from the virus-replicating phase; i.e., tumorigenesis occurs in the summer or under warm laboratory conditions, whereas virus replication occurs only in the winter or under cold (<9°C) laboratory conditions (*3-6*).

It has long been known that embryos and larvae of leopard frogs support growth of Lucké tumors better than do adults. Lucké (*7*) and Lucké and Schlumberger (*8*) showed that tumor allografts do not grow in the coelom, intramuscular space, or dorsal lymph sac of adults. These allografts survive only in the relatively "privileged" space of the anterior eye chamber (*9*). However, implanting tumor allografts in the dorsal tail fin of young larvae, Briggs (*10*) reported that nearly half showed "significant growth" at this site. Similarly, LTHV injected into adults does not seem to induce an incidence of primary tumors higher than that developing in uninoculated animals (*11*). However, LTHV injected into embryos does result in the development of a high proportion of tumors in late-stage larvae and metamorphosing juveniles (*12*). It has been generally assumed that the relative ease of transplantation or induction of tumors in embryonic and larval frogs may be due to a lack of "maturity" of the immune system. Surprisingly, few studies have been designed to examine this assumption. Since thymus-derived cells (T-cells) are generally thought to play some role in the maintenance or rejection of virus-induced tumors, an evaluation of tumor induction in virus-inoculated frogs that were tx during early larval life seemed a logical initial step in the determination of whether the immune response does play a role in the development of tumors in young frogs.

MATERIALS AND METHODS

Frogs.—Eggs were obtained from gravid female *R. pipiens* by the induction of ovulation according to standard methods (*13, 14*). We obtained sperm by mincing the testes from a mature male in several milliliters of 10% Ringer's solution (*13*). Embryos resulting from in vitro fertilization were reared at room temperatures (18-22°C) until they reached the appropriate stage for virus injection [stages 19-20 of Shumway (*15*)] or thymectomy [stages I-III of Taylor and Kollros (*16*)]. All larvae were reared in 4-liter containers (10 larvae/container). Their water was changed and they were fed boiled lettuce three times weekly.

Virus injections.—Two tumor-bearing frogs were held at 8°C for 4 to 5 months. Eosinophilic nuclear inclusions in a sectioned and stained tumor fragment confirmed the presence of viruses (*17*). A virus-containing mitochondrial fraction was prepared from each cold tumor according to the method of Tweedell (*12*). The mitochondrial precipitates from a 2.7-g tumor and a 1.8-g tumor were diluted in 13.5 ml and 9.0 ml, respectively, of 0.02 *M* phosphate buffer (pH 7.3) containing 0.24 *M* sucrose (PBS) (*12*) and stored at −70°C until used. Approximately 0.5-1 μl of the virus preparation, at full strength or at 1/10 and 1/100 dilutions in PBS, was injected into the left pronephric region of Shumway stages 17-20 embryos. A fine glass needle attached to a 100-μl Hamilton syringe was used. Each aliquot of virus preparation was kept on ice during the injection procedure and was used for no more than 3 hours.

Thymectomy.—The bilateral thymuses, which lie slightly caudal and ventral to the eye capsule, were

---

ABBREVIATIONS USED: LTHV = Lucké tumor herpesvirus; PBS = phosphate-buffered sucrose; PHA = phytohemagglutinin-P; TSTA = tumor-specific transplantation antigens; tx = thymectomized.

---

[1] Received April 16, 1981; accepted August 13, 1981.

[2] Supported by American Cancer Society Institutional Research grant IN-18 and by Public Health Service (PHS) grant F32-CA06375 (to L. R.-S.) from the National Cancer Institute and by PHS grant HD07901 (to N. C.) from the National Institute of Child Health and Human Development.

[3] Animals were maintained under the guidelines set forth by the University of Rochester.

[4] Department of Microbiology, Division of Immunology, The University of Rochester Medical Center, School of Medicine and Dentistry, 601 Elmwood Ave., Rochester, N.Y. 14642.

[5] We acknowledge the excellent animal care given by Ms. Deborah Sussman and Mr. Raphael Melendez of the University of Rochester.

exposed, loosened with fine glass needles, and removed in fragments by suction with a fine glass micropipette at stage I, II, or III of Taylor and Kollros.

Assessment of tumor development.—In one experiment involving a weakly oncogenic virus preparation, virus-injected embryos were reared through metamorphosis until 6 months of age post fertilization. At that time, the surviving frogs were killed and examined with a dissecting microscope for tumors in the region of the mesonephros or pronephros. (When the pronephros becomes tumorous in larval life, it persists through metamorphosis.) All larvae that died before metamorphosis were also examined for tumor development. Tumor incidence was recorded only for those frogs that survived more than 2 months post fertilization. In a second experiment involving a strongly oncogenic virus preparation, all virus-injected embryos were killed at 2 months post fertilization and examined for tumors.

Assessment of effectiveness of thymectomy.—Nearly all larvae and metamorphosing juveniles were checked for a regenerated thymus at the time of death. Blood lymphocytes from some tx larvae that had not been given injections of virus were cultured with the T-cell mitogen PHA and their responses compared with those of cells from normal intact larvae of the same age and relative stages. For in vitro lymphocyte studies, blood was drawn by cardiac puncture from anesthetized larvae at 1 month post thymectomy. The blood was mixed with about 100 μl of Leibovitz (L-15) culture medium (GIBCO, Grand Island, N.Y.) diluted to amphibian tonicity (*18*). The diluted blood was then layered on Ficoll-Hypaque (approximate density, 1.090) (*19*) in UV irradiation-sterilized 400-μl-capacity plastic microfuge tubes and centrifuged at low speed ($\approx 500 \times g$) for 5 minutes in a Beckman microfuge. The mononuclear cells were drawn off, washed once, and cultured at a density of 5×10^4 small lymphocytes/ml in Linbro 96-well U-bottom microtiter plates (Flow Laboratories, Inc., McLean, Va). Each well contained 200 μl of L-15 culture medium supplemented with 100 U penicillin/ml, 100 μg streptomycin/ml, 1.25×10^{-2} *M* HEPES[6] buffer, 1×10^{-2} *M* sodium bicarbonate, 5×10^{-5} *M* 2-mercaptoethanol, and 1% heat-inactivated fetal calf serum (GIBCO) (*18*). The cultures were assayed for mitogen-induced DNA synthesis according to published procedures (*18, 20*). The final concentration of PHA (Difco Laboratories, Detroit, Mich.) was 8 or 10 μg/ml. Cultures were incubated in Mishell-Dutton boxes (Norbo Machine, Huron, S.Dak.) at 26°C for 3 days and gassed with 5% CO_2-95% air every 24 hours. Before being harvested with a precipitator (Otto Hiller Co., Madison, Wis.), the cells were exposed to tritiated thymidine (10 μCi/ml; sp act = 2 Ci/mmol; obtained from New England Nuclear Corp., Boston, Mass.) for 8 hours. For each larva tested, an average of background cpm for cells cultured in medium alone, an average of stimulated cpm for cells cultured with mitogen, and a stimulation index (stimulated counts/background counts) were computed. Usually, two or three replicate wells with lymphocytes alone and lymphocytes plus mitogen were plated. However, paucity of cells (especially in tx animals) sometimes limited us to one well that contained control cells and one that contained mitogen-treated cells per tadpole. The mean cpm for all the individual tadpoles were then averaged to determine the mean background counts and mean stimulated counts for the population of larvae.

Tumor allograft implantation.—Larvae, tx at stage I or II of Taylor and Kollros, and unoperated controls were allowed to develop to stage III or IV (20-35 mm in length). They were than implanted with approximately 1 mg of freshly excised Lucké tumor that had been previously cultured in the anterior eye chamber of an adult frog (*9*). Tumors were implanted into a pocket in the dorsal tail fin according to the method of Briggs (*10*). Tumor implants were examined at frequent intervals with a dissecting microscope.

RESULTS

The incidence of tumors and premalignant lesions developing in normal and tx frogs that had been inoculated as embryos with LTHV was not significantly different regardless of the relative oncogenicity of the virus preparation or the dilution injected (table 1). There were no striking size differences in the tumors observed in tx frogs compared to intact controls. In both groups, premalignant cystic lesions were usually detected at 2 months. They were small, usually vesicular, growths within an otherwise normal kidney. At later times, either solid tumors or premalignant vesicles converting to solid tumors were observed. No metastases were ever observed in either the tx or intact group.

To determine whether thymectomy results in an earlier onset of tumor development, we regrouped the data from experiment 1 such that the incidence of tumors developing in an approximately 2-month period

TABLE 1.—*Tumors and premalignant lesions observed between 2 and 6 months of age in normal and tx frogs inoculated as embryos with LTHV*

Expt No.	Dilution of virus preparation[a]	Incidence of tumors developing in[b]	
		Normal frogs	tx frogs
1	Full strength	10/44 (22.7)	8/44 (18.2)
	10^{-1}	3/28 (10.7)	2/20 (10.0)
	10^{-2}	0/8 (0.0)	0/31 (0.0)
2	Full strength	22/23 (95.6)	11/11 (100.0)
	10^{-1}	3/6 (50.0)	5/12 (41.6)
	10^{-2}	3/9 (33.3)	—[c]

[a] Different virus preparations were used in expts 1 and 2. See "Materials and Methods" for details of virus preparations.
[b] No. of frogs with tumors/total No. of frogs (%).
[c] — = not done.

---

[6] 4-(2-Hydroxyethyl)-1-piperazine ethanesulfonic acid.

in normal and tx larvae that died before metamorphosis was compared with that developing in frogs that died during and after metamorphosis (a period of ≈2 mo) (table 2). The data in table 2 clearly show that most tumors were observed in both normal and tx frogs during and after metamorphosis. Further, tumor incidence did not differ significantly between normal and tx frogs in either the premetamorphic or postmetamorphic period for any virus dilution tested. In experiment 2 (table 1), all virus-injected larvae were killed 2 months after injection. Both intact and tx frogs were at early larval stages (IV–IX of Taylor and Kollros) (*16*). If thymectomy results in an earlier onset of tumor development, one would expect a higher incidence of tumors in these young tx frogs. Instead, we observed that the incidence of tumors was the same in intact and tx frogs. Thus the time of onset of tumor development seems to be related to the relative oncogenicity of the virus preparation used and does not seem to be affected by thymectomy.

Because there seems to be no difference in tumor incidence between normal and tx frogs, it is important to know the effectiveness of the thymectomy procedure. In experiment 1, most of the virus-inoculated tx frogs were examined under the dissecting microscope at the time of death for the presence of a regenerated thymus. Of 85 frogs autopsied, 75 (88.2%) had no trace of regenerated tissue. The others had less than one-fourth of the normal amount of thymus tissue. Thus the data from experiment 1 include data gathered from a few frogs that had a small amount of regenerated thymus tissue. These data are included because the frogs in question had severely impaired T-cell functions throughout most of the period of study, as evidenced by their diminished in vitro responses to the T-cell mitogen PHA (*see* below). In experiment 2, all virus-inoculated tx frogs were examined for regenerated thymus tissue at the time of death. About 66% were free of regenerated tissue. Those with evidence of thymus regeneration were excluded.

To determine to what extent early thymectomy impairs classical T-cell responses in this species, we studied PHA-induced lymphocyte proliferation in vitro and allograft rejection in vivo in normal and tx frogs. When tested at 1 month post thymectomy, lymphocytes from intact larvae responded significantly to PHA (average stimulated cpm about eight times background). Lymphocytes from tx larvae did not respond (text-fig. 1). Stimulation indices for cells from intact larvae ranged from 0.1 to 23.3 (median, 6.8). Stimulation indices for cells from tx larvae ranged from 0.6 to 3.9 (median, 0.9). At autopsy, all tx larvae included in these determinations were completely devoid of regenerated thymus tissue. Cells from animals with less than one-fourth of normal thymus tissue also responded poorly to PHA.

TABLE 2.—*Tumors observed between 2 and 6 months of age in larvae that died before metamorphosis compared to those observed in metamorphosing juveniles that survived*

Dilution of virus preparation[a]	Incidence of tumors developing in[b]			
	Premetamorphic frogs		Metamorphosing frogs	
	Normal	tx	Normal	tx
Full strength	4/27 (14.8)	4/29 (13.8)	6/17 (35.3)	4/19 (26.7)
10^{-1}	1/20 (5.0)	2/18 (11.1)	2/8 (25.0)	0/9 (0.0)

[a] *See* "Materials and Methods" for details of virus preparations.

[b] No. of frogs with tumors/total No. of frogs (%).

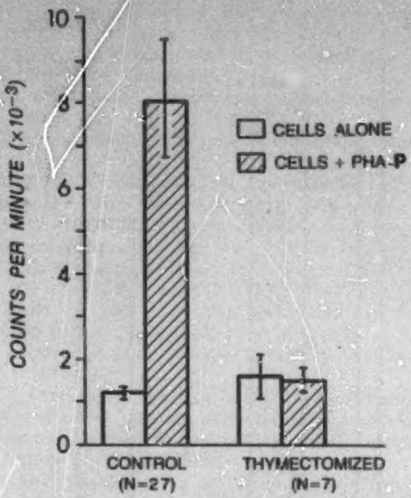

TEXT-FIGURE 1.—Average PHA responses of lymphocytes from intact control and tx larvae 1 mo post thymectomy (mean ± SE).

The ability of tx larvae to reject Lucké tumor allografts in the dorsal tail fin was also diminished relative to that of age-matched intact controls (text-fig. 2). Greater than 90% of intact larvae had rejected a tumor allograft before 40 days, whereas only about 50% of tx larvae had rejected their grafts by that time. Among those larvae that rejected their grafts, all had some degree of thymic regeneration at autopsy. This was an early experiment when we were still developing the technique of thymectomy. The effectiveness of the thymectomy procedure was greatly improved in subsequent experiments.

DISCUSSION

Complete thymectomy early in larval life effectively impairs both in vivo and in vitro responses that are attributed to T-cells in another anuran species (*21*) as well as in mammals. Thymectomy, however, had no effect on the incidence of tumors developing in virus-inoculated tadpoles. Thus normal intact larvae appear to be no better able to prevent tumor development than immunologically impaired larvae. Since the LTHV does not replicate at the temperatures at which frog larvae are reared (18–22°C), any destructive immune response would have to be directed against tumor-specific antigens and not against virus particles themselves. Nothing is known about the activity of the viral

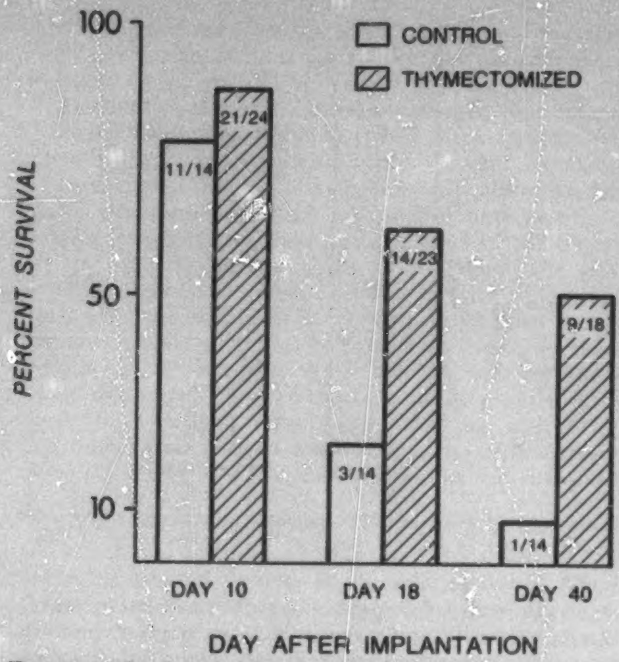

TEXT-FIGURE 2.—Percent survival of tumor allografts in normal and tx larvae. *Numbers inside bars* indicate No. of tumor implants surviving/tadpoles implanted.

genome in LTHV-infected cells until tumors develop. Presumably, there is no expression of viral products. However, the viral genome in tumor cells clearly is not silent. Virus-specific messenger RNA is synthesized in both warm-temperature-phase and cold-temperature-phase tumors (*22*). Similarly, virus-associated membrane antigens have been detected on both cold-temperature-phase and warm-temperature-phase tumors (*23*). Whether these virus-associated antigens behave as TSTA is not yet known. By analogy with other virus-induced tumors (*24-26*), the Lucké tumor would be expected to be immunogenic and to elicit, in an immunocompetent host, cytotoxic effector T-cells directed against the virus-associated antigens. Thus we would expect a higher incidence of tumors in tx individuals if the cytotoxic T-cell system were important in controlling tumorigenesis.

The Lucké tumor developing in immunocompetent tadpoles, then, is paradoxical. Although it probably expresses TSTA, immunocompetent tadpoles and metamorphosing frogs are no better able to prevent tumor development than are their immunologically impaired siblings. Perhaps, at a high virus dose, the immune system of competent hosts is overwhelmed. If so, one would expect that at lower virus doses, there would be significantly fewer tumors in normal hosts compared to tx hosts. The most oncogenic virus preparation that we used induced tumors in about 95-100% of virus-inoculated frogs. Neither at full strength nor at a 10^{-1} dilution was there a significant difference in the incidence of tumors developing in intact frogs compared to tx frogs (table 1, expt 2). Comparable results were seen with a second virus preparation of weaker oncogenicity. At full strength, this preparation induced tumors in about 20% of hosts regardless of whether they were intact or tx. Even at a 10^{-1} or 10^{-2} dilution, the incidence of tumors was not significantly different in normal frogs compared to tx frogs (table 1, expt 1).

Survival of immunogenic tumors such as those that are virus induced probably depends on a balance between antitumor responsiveness and protumor immunosuppression (*27*). In the frog tadpole the net effect of such opposing immune responses may favor suppression. There is considerable evidence from research with another anuran amphibian, the South African clawed frog (*Xenopus laevis*), that the entire larval period, like the neonatal period in mice (*28*), is a time in which specific tolerance to alloantigens is much more easily induced than in the adult postmetamorphic period (*29*). Prolonged or indefinite acceptance of skin grafts differing by major as well as minor histocompatibility antigens occurs at high frequency before (*29*) and during metamorphosis but not afterward (*30, 31*). In *R. pipiens* we have also shown that tolerance to self or to allogeneic eye implants in embryonically enucleated tadpoles frequently occurs (*32*). Thus the high incidence of tumors in premetamorphic and metamorphosing *R. pipiens* may be due to an enhanced capacity to become tolerant to TSTA during this developmental period. As a more formal statement of this hypothesis, virus-inoculated and immunocompetent frogs may have a high incidence of tumors because they become tolerant to TSTA, whereas tx frogs have a high incidence of tumors because they are unable to develop cytotoxic effector cells.

This hypothetical explanation of the data allows several predictions. One might predict that frogs with latent virus, due to embryonic infection, would develop some tumors in larval or perimetamorphic life and then few tumors in postmetamorphic life (until old age interfered with immune competence). A long-term study documenting tumor incidence at regular intervals over several years in embryonically infected frogs has yet to be done, but records of tumor incidence in field-collected and laboratory-held frogs suggest that among adults, tumors are never observed in young frogs but occur frequently in large and presumably older animals (*12, 33*). Tumors developing in premetamorphic tadpoles would presumably result in early death of these frogs.

Our hypothesis would also predict that adult frogs with latent virus would develop more tumors if they were experimentally made tolerant to tumor antigens. Perhaps this may explain the increased incidence of primary tumors in laboratory-held frogs that have been implanted with allogenic Lucké tumor in the anterior eye chamber [(*34*); Rollins-Smith L: Unpublished observations]. Recently, this site has been demonstrated to be a favorable route for induction of tolerance to alloantigens (*35*).

Alternative explanations for our data must include the possibilities that the Lucké tumor is not immunogenic and/or that immune surveillance is irrelevant to tumor survival (*36, 37*). The argument had been made that most tumors begin as small clones and that the early response to a small inoculum of immunogenic cells may lead to stimulation of tumor growth rather than to rejection (*36*). If an early thymic-dependent immune response to a small Lucké tumor is important for tumor promotion, we should have observed a decreased incidence of primary kidney tumors in tx frogs. In fact, the incidence of tumors was the same in normal frogs and tx, virus-infected frogs (tables 1, 2). Mechanisms other than T-cell cytotoxicity, such as natural killer cells or activated macrophages, may be important in the regulation of tumor growth. Little is known about the existence or effectiveness of these cellular effector mechanisms in frogs. Our study addresses only the question of whether T-cell-dependent mechanisms are effective in preventing tumor development; apparently, in these young frogs they are not.

In summary, no increased or decreased incidence of tumors in virus-infected tadpoles was observed as a function of thymectomy. We favor the hypothesis that in postmetamorphic frogs, cytotoxic T-cells, specific for virus-associated tumor antigens, may regulate the development of tumors. As yet, the existence of cytotoxic T-cells specific for Lucké tumor antigens has not been demonstrated. We suggest that tumors may develop at high frequency in normal and tx tadpoles because neither can generate cytotoxic T-cells directed at tumor-specific antigens. The tx frog lacks the thymus-derived progenitors necessary for cytotoxic responses, whereas the normal frog may have very active suppressor mechanisms that prevent their emergence.

REFERENCES

(*1*) McKinnell RG. The Lucké frog kidney tumor and its herpesviruses. Am Zool 1973; 13:97-114.

(*2*) Naegele RF, Granoff A, Darlington RW. The presence of the Lucké herpesvirus genome in induced tadpole tumors and its oncogenicity: Koch-Henle postulates fulfilled. Proc Natl Acad Sci USA 1974; 71:830-834.

(*3*) McKinnell RG, Ellis VL, Dapkus DC, Steven LM Jr. Early replication of herpesviruses in naturally occurring frog tumors. Cancer Res 1972; 32:1729-1733.

(*4*) Breidenbach GP, Skinner MS, Wallace JM, Mizell M. In vitro induction of a herpes-type virus in "summer-phase" Lucké tumor explants. J Virol 1971; 7:679-682.

(*5*) Morek DM. An organ culture study of frog renal tumor and its effects on normal frog kidney in vitro. Oncology 1973; 28:536-552.

(*6*) Mizell M, Stackpole CW, Halparen S. Herpes-type virus recovery from "virus-free" frog kidney tumors. Proc Soc Exp Biol Med 1968; 127:808-814.

(*7*) Lucké B. Carcinoma in the leopard frog: Its probable causation by a virus. J Exp Med 1938; 68:457-468.

(*8*) Lucké B, Schlumberger H. The manner of growth of frog carcinoma, studied by direct microscopic examination of living intraocular transplants. J Exp Med 1939; 70:257-268.

(*9*) Rollins LA, McKinnell RG. The influence of glucocorticoids on survival and growth of allografted tumors in the anterior eye chamber of leopard frogs. Dev Comp Immunol 1980; 4:283-294.

(*10*) Briggs R. Transplantation of kidney carcinoma from adult frogs to tadpoles. Cancer Res 1942; 2:309-323.

(*11*) Rafferty KA Jr. Kidney tumors of the leopard frog: A review. Cancer Res 1964; 24:169-185.

(*12*) Tweedell KS. Induced oncogenesis in developing frog kidney cells. Cancer Res 1967; 27:2042-2052.

(*13*) Rugh R. Experimental embryology. Minneapolis: Burgess, 1962:1-501.

(*14*) McKinnell RG. Cloning. Nuclear transplantation in amphibia. Minneapolis: Univ Minnesota Press, 1978:1-319.

(*15*) Shumway W. Stages in the normal development of *Rana pipiens*. I. External form. Anat Rec 1940; 78:139-147.

(*16*) Taylor AC, Kollros JJ. Stages in the normal development of *Rana pipiens* larvae. Anat Rec 1946; 94:7-23.

(*17*) Fawcett DW. Electron microscope observations on intracellular virus-like particles associated with the cells of the Lucké renal adenocarcinoma. J Biophys Biochem Cytol 1956; 2:725-742.

(*18*) Green N, Cohen N. Phylogeny of immunocompetent cells. III. Mitogen response characteristics of lymphocyte subpopulations from normal and thymectomized frogs (*Xenopus laevis*). Cell Immunol 1979; 48:59-70.

(*19*) Weiss N, Du Pasquier L. Factors affecting the reactivity of amphibian lymphocytes in a miniaturized technique of the mixed lymphocyte culture. J Immunol Methods 1973; 3:273-286.

(*20*) Goldstine SN, Collins NH, Cohen N. Mitogens as probes of lymphocyte heterogeneity in anuran amphibians. Adv Exp Med Biol 1975; 64:343-351.

(*21*) Cohen N, Turpen JB. Experimental analysis of lymphocyte ontogeny and differentiation in an amphibian model system. In: Gelfand EW, Dosh HO, eds. The biological basis for immunodeficiency. New York: Raven Press, 1979:25-37.

(*22*) Collard W, Thornton H, Mizell M, Green M. Virus-free adenocarcinoma of the frog (summer phase tumor) transcribes Lucké tumor herpesvirus-specific RNA. Science 1973; 181:448-449.

(*23*) Naegele RF, Granoff A. Viruses and renal carcinoma of *Rana pipiens*. XV. The presence of virus-associated membrane antigen(s) of Lucké tumor cells. Int J Cancer 1977; 19:414-418.

(*24*) Payne LN, Powell PC, Rennie MC, Ross LJ. Studies on the mechanism of vaccinal immunity to Marek's disease. Comp Immunol Microbiol Infect Dis 1978; 1:31-36.

(*25*) Klein G, Klein E. Immune surveillance against virus-induced tumors and nonrejectability of spontaneous tumors: Contrasting consequences of host versus tumor evolution. Proc Natl Acad Sci USA 1977; 74:2121-2125.

(*26*) Sjögren HO. Transplantation methods as a tool for detection of tumor-specific antigens. Prog Exp Tumor Res 1965; 6:289-322.

(*27*) Fernandez-Cruz E, Woda BA, Feldman JD. Elimination of syngeneic sarcomas in rats by a subset of T lymphocytes. J Exp Med 1980; 152:823-841.

(*28*) Billingham RE, Brent L. Quantitative studies on tissue transplantation immunity. IV. Induction of tolerance in newborn mice and studies on the phenomenon of runt disease. Philos Trans R Soc London [Biol] 1959; 242:439-477.

(*29*) DiMarzo S, Cohen N. An in vivo study of the ontogeny of alloreactivity in the frog, *Xenopus laevis*. Immunology. In press.

(*30*) Barlow E, DiMarzo S, Cohen N. Prolonged survival of MHC disparate skin allografts transplanted to the metamorphosing frog, *Xenopus laevis*. Transplantation 1981; 32:51-57.

(*31*) Cohen N, DiMarzo S, Hailparn-Barlow E. Induction of tolerance to alloantigens of the major histocompatibility complex in the metamorphosing frog, *Xenopus laevis*. In: Manning MJ, ed. The phylogeny of immunological memory. Amsterdam: Elsevier/North-Holland, 1980:225-231.

(*32*) Rollins LA, Cohen N. On tadpoles, transplantation, and tolerance. In: Horton JD, ed. Development and differentiation of vertebrate lymphocytes. Amsterdam: Elsevier/North-Holland, 1980:203-214.

(*33*) Rafferty KA Jr. Age and environmental temperature as factors influencing development of kidney tumors in uninoculated frogs. J Natl Cancer Inst 1962; 29:253-265.

(34) LUCKÉ B. Kidney carcinoma in the leopard frog: A virus tumor. Ann NY Acad Sci 1952; 54:1093-1109.

(35) STREILEIN JW, NIEDERKORN JY, SHADDUCK JA. Systemic immune unresponsiveness induced in adult mice by anterior chamber presentation of minor histocompatibility antigens. J Exp Med 1980; 152:1121-1125.

(36) STUTMAN O. Immunodepression and malignancy. Adv Cancer Res 1975; 22:261-422.

(37) PREHN RT. Do tumors grow because of the immune response of the host? Transplant Rev 1976; 28:34-42.

11

Studies on the Antitumor Activities of Pyrimidinone-Interferon Inducers. I. Effect Against Artificial and Spontaneous Lung Metastases of Murine Tumors [1, 2, 3]

Luka Milas, [4] Evan M. Hersh, [5] Dale A. Stringfellow, [6] *and* Nancy Hunter [4, 7]

ABSTRACT—Since pyrimidinone compounds induce interferon production in several animal species and have potent antivirus activities, it appeared important to determine whether these compounds could also induce antitumor activities in their recipients. Pyrimidinone compounds 2-amino-5-bromo-6-methyl-4-pyrimidinone (ABMP), 2-amino-5-bromo-6-phenyl-4-pyrimidinone (ABPP), and 2-amino-5-iodo-6-phenyl-4-pyrimidinone (AIPP) were studied for their activities against artificial lung metastases of the weakly immunogenic spontaneous fibrosarcoma NFSa, the moderately immunogenic spontaneous mammary carcinoma MCa-K, and the strongly immunogenic 3-methylcholanthrene-induced fibrosarcoma FSa syngeneic to inbred C3Hf/Kam mice. In addition, the therapeutic efficacy of ABPP and AIPP was also determined against spontaneous lung metastases of NFSa. ABPP and AIPP given ip at 250 mg/kg for 2 or 3 consecutive days before or after iv inoculation of NFSa, FSa, or MCa-K cells greatly reduced the number of tumor nodules developed in the lungs. ABMP, however, was considerably less effective. ABPP and AIPP were also effective in therapy of spontaneous lung metastases of NFSa, especially when these compounds were given before surgical removal of the primary tumor. Neither ABPP nor AIPP was effective against tumor nodules growing in whole-body irradiated (WBI) mice, but both protected mice against enhancement of lung metastasis formation induced by exposure to whole-body irradiation. ABPP was more effective than AIPP in inducing production of interferon in normal mice. When treated with ABPP, WBI mice, however, were unable to produce interferon. These results show that 6-phenyl-pyrimidinone compounds induce strong antitumor activities in mice, which correlated with neither tumor immunogenicity nor the ability of these agents to induce interferon, but which depended on the immune status of the tumor host.—JNCI 1982; 68:139–145.

Since their discovery in 1957 (*1*), interferons have been known for their antivirus properties. Recently, interferons also have become known for their antitumor activities, and these effects have been demonstrated against many experimental tumors and against several human tumors, including osteosarcoma, breast carcinoma, and tumors of the lymphohematopoietic system (*2*). Biologic activities of interferons are many, such as inhibition of virus replication, inhibition of cell proliferation, and modulation of the immune response, and they all are likely to participate in the exertion of the interferon-induced antitumor effect (*3*). Tumor cells treated with interferons have exhibited a reduced growth in vitro and a reduced potential to form tumors upon transplantation into animals (*3*). By modulating many immune reactions (*2*), interferons can modulate or initiate antitumor resistance mechanisms. They have enhanced specific lymphocyte cytotoxicity against tumor cells (*4*), activated macrophages (*5*), and augmented activity of NK and killer cells (*6*).

There are two approaches to interferon tumor therapy: *a*) administration of exogenous interferon and *b*) administration of interferon inducers to stimulate host cells to produce interferon. Since the production of interferons is limited and costly and their application is restricted by their "species-specific" activity, there is an increasing interest in the identification and development of compounds that could be used for stimulating host cells to produce their own interferons. A wide variety of natural and synthetic agents, including bacteria and their product(s), a double-stranded polyribonucleic acid (polyinosinic-polycytidylic acid), and pyran copolymer, are known for their ability to induce interferons (*3*). More recently, several pyrimidinone compounds have been identified as potent interferon inducers in several animal species and in cultured human tissues (*7, 8*). These compounds exert strong antivirus activities and modulate different immunologic reactions (*7*). Also, it was recently reported that pyrimidinone compounds can restrict the growth of B16 melanoma cells transplanted into the peritoneal

---

ABBREVIATIONS USED: ABMP = 2-amino-5-bromo-6-methyl-4-pyrimidinone; ABPP = 2-amino-5-bromo-6-phenyl-4-pyrimidinone; AIPP = 2-amino-5-iodo-6-phenyl-4-pyrimidinone; BRM = biologic response modifiers; NK = natural killer; WBI = whole-body irradiated (irradiation).

---

[1] Received May 7, 1981; accepted August 20, 1981.

[2] Supported in part by Public Health Service grant CA06294 from the National Cancer Institute.

[3] Animals were maintained in facilities approved by the American Association for Accreditation of Laboratory Animal Care and in accordance with current regulations and standards of the U.S. Department of Agriculture and of the National Institutes of Health, U.S. Department of Health and Human Services.

[4] Department of Experimental Radiotherapy, The University of Texas System Cancer Center, M. D. Anderson Hospital and Tumor Institute, 6723 Bertner Ave., Houston, Tex. 77030.

[5] Department of Developmental Therapeutics, The University of Texas System Cancer Center, M. D. Anderson Hospital and Tumor Institute.

[6] Experimental Biology Research, The Upjohn Company, Kalamazoo, Mich. 49001.

[7] We are grateful to Ms. Debra Palmatary and her staff (M. D. Anderson Hospital and Tumor Institute) for the supply and care of the mice used in these experiments. We also thank Ms. Rozanne Goddard for her assistance in the preparation of this manuscript.

cavities of mice (*8*). These observations suggest that pyrimidinones may be effective in the treatment of malignant tumors, and further experiments on the antitumor effect of pyrimidinone compounds were warranted.

Here we report studies that show that two 6-phenyl pyrimidinones, ABPP and AIPP, induce antitumor activity against pulmonary tumor growths of 3 murine tumors that vary in their immunogenicity and metastatic properties.

MATERIALS AND METHODS

Mice.—Inbred C3Hf/Kam mice of both sexes that had been bred and maintained in the specific-pathogen-free mouse colony of the Department of Experimental Radiotherapy, The University of Texas System Cancer Center, M. D. Anderson Hospital and Tumor Institute, were used. They were 11-14 weeks old at the beginning of the experiments. Within each experiment, the mice were of the same sex and were housed 4-7/cage.

Tumors.—Experiments were performed with 3 transplantable tumors, all syngeneic to C3Hf/Kam mice: spontaneous fibrosarcoma NFSa, 3-methylcholanthrene-induced fibrosarcoma FSa, and spontaneous mammary carcinoma MCa-K. These tumors vary in immunogenicity and metastatic capacity. Most experiments were performed with NFSa, which is a poorly immunogenic tumor as determined by the ability of specifically sensitized mice to influence the take of NFSa cells injected either iv or sc (*9*). Most mice bearing this tumor in the leg develop lung metastases after amputation of legs bearing tumors of approximately 10 mm in diameter (*9*). When used in these experiments, NFSa was in isotransplant generation 12.

FSa is a relatively strongly immunogenic tumor as determined by the same methods used for the estimation of the immunogenicity of NFSa (*10, 11*). A large proportion of mice dying of subcutaneous FSa have metastases in the lungs (*12*). However, mice rarely develop metastases if the primary tumor is removed (*13*). When used in this study, this tumor was in isotransplant generation 6.

The MCa-K tumor is moderately immunogenic as determined by the lung colony assay (*14*). This tumor is, however, of a highly metastasizing propensity: Most animals whose tumors of about 10 mm in diameter are surgically removed develop numerous pulmonary metastases in the lungs (*15*). In these experiments we used isotransplants of generation 7.

Single cell suspensions from fibrosarcomas were prepared by trypsin digestion of nonnecrotic tumor tissue (*11*). Viability of the cells was more than 95% as assessed by trypan blue dye exclusion and phase-contrast microscopy. Single cell suspensions of cells from MCa-K were prepared by a mechanical method (*14*). The viability of cells was approximately 60%.

All experiments, with the exception of the spontaneous metastasis experiment, were performed with the use of the lung colony assay. To produce artificial pulmonary metastases, we suspended 10^5-2.5×10^5 NFSa cells, 2×10^5 FSa cells, or 2×10^5 MCa-K cells in 0.5 ml Hsu's medium and injected these cells iv into groups of 6-10 mice. Fourteen days after inoculation of NFSa and FSa cells and 28 days after inoculation of MCa-K cells, the mice were killed, their lungs removed, and the lung lobes separated and fixed in Bouin's solution. Colonies of tumor cells (metastases) appeared as white, round nodules on the surface of the yellowish lung and were counted with the naked eye.

Studies of spontaneous metastases involved only NFSa. Mice were given injections of 5×10^5 cells in muscles of the right thigh. The resulting tumors were removed by surgery (*15*) when they had grown to about 12 mm in diameter, and 24 days later the mice were killed and their lungs inspected for the presence of metastases as described above.

Pyrimidinone compounds.—Three pyrimidinone compounds were used: ABPP, ABMP, and AIPP, synthesized by Dr. W. Wierenga and Dr. H. I. Skulnick (The Upjohn Co.). The first two compounds were reported to be potent interferon inducers, and the third was a weak interferon inducer (*7*). The compounds were administered ip in 0.3 ml of 1% carboxymethyl cellulose sodium (vehicle). Because of their poor solubility, these compounds were ground together with vehicle in a tissue grinder to achieve a uniform suspension. In most experiments the dose per injection was 250 mg/kg body weight given in two to six injections. In one experiment a single dose of ABPP and AIPP ranging between 62.5 and 1,000 mg/kg was used.

Interferon assays.—Interferon levels were determined in the sera and in 10% supernatants of homogenized spleen, thymus, and lung from mice treated with ABPP or AIPP 6 or 24 hours earlier. Each group consisted of 4 mice. To obtain 10% supernatants, we weighed and mixed the above tissues with Eagle's minimum essential medium in a 1:9 ratio. Each sample was homogenized with a Polytron tissue homogenizer and centrifuged at 2,200 rpm for 20 minutes. The supernatants were removed and refrigerated at −11°C. Serum was prepared by a method described elsewhere (*11*). A standard vesicular stomatitis plaque-reduction assay was performed on murine L929 cells (*7*). To standardize results, we included the international murine interferon standard (G002-904-511), which had a mean titer of 6,200 U/ml compared with its accepted titer of 6,800 U/ml.

WBI.—Mice were exposed to 650 rad WBI with gamma rays. During irradiation from a single-source ^{137}Cs irradiator with a dose rate of 238 rad/minute, groups of 5 mice without anesthesia were restrained in Lucite containers.

Statistical analysis.—The results were evaluated by the nonparametric Mann-Whitney *U* test or by the chi-square test. Differences between the groups were considered significant if the *P*-value of comparison was 0.05 or smaller.

RESULTS

Effect of ABPP, AIPP, and ABMP on artificial lung metastases of NFSa, FSa, and MCa-K.—Mice were given injections iv of 2.5×10^5 NFSa, 2×10^5 FSa, or 2×10^5 MCa-K cells. They were also treated with ABPP, AIPP, or ABMP given ip once a day for 2 or 3 consecutive days before, after, or before and after tumor cell injection. The number of NFSa and FSa tumor nodules was determined at day 14, and the number of MCa-K tumor nodules was determined at day 28 following tumor cell injection (table 1). If injected into mice before tumor cell injection, ABPP and AIPP were effective against all 3 tumors, as shown by a great reduction in the number of metastases. When administed after tumor cell injection, these drugs were effective against NFSa and FSa but not against MCa-K tumor nodules. This activity against NFSa and FSa was less profound than that produced by the drugs given prior to tumor cell injection. Also, two injections of ABPP and AIPP given at days 2 and 7 after injection of NFSa cells caused no reduction in the number of lung colonies. The activity of ABMP was investigated against FSa and NFSa. The number of nodules of FSa was reduced only if ABMP was given before tumor cells. No antitumor activity of ABMP was observed against NFSa; in contrast, certain schedules of ABMP administration even enhanced formation of metastases. However, treatment with ABMP was toxic, because 9 of 35 mice died within 1-9 days after treatment with ABMP. Because of its toxicity and lack of appreciable antitumor activity, ABMP was not used in further experiments.

Since none of the pyrimidinone compounds were effective when given at days 2 and 7 after tumor cell injection, it was important to determine whether the activities of these compounds depend on the dose delivered to mice. Mice received injections iv of 2×10^5 NFSa cells, and 2 days later they received injections ip of ABPP or AIPP in doses ranging from 62.5 to 1,000 mg/kg body weight. The number of lung metastases was determined 14 days after tumor cell injection and is presented in table 2. Single doses of ABPP and AIPP, up to 250 mg/kg, did not significantly reduce the number of colonies. Higher doses, however, did.

Effect of ABPP and AIPP against spontaneous metastases of NFSa.—A high percentage of mice having NFSa tumors in the leg develop metastases in the lungs (*9, 16*). Using this tumor, we investigated whether ABPP and AIPP produce an antimetastatic effect. Primary tumors were induced by injections of 5×10^5 NFSa cells into muscles of the right thighs of mice. Thirteen days later when tumors grew to about 12 mm in diameter, they were surgically removed. Groups of mice received 250 mg ABPP or AIPP/kg ip every day for 2 or 4 days within 5 days prior to surgery or two, four, or six injections of these compounds at different schedules within 14 days after surgery (table 3). Twenty-four days after primary tumors had been removed, mice were killed and their lungs were inspected for the presence of metastases. Of 12 mice, 10 (83%) treated by surgery alone had metastases in the lungs. ABPP and AIPP reduced the incidence of metastases to 39% (30/77) and to 34% (25/73), respectively. Preoperative application of ABPP and AIPP was more effective than postoperative application. Nine percent of the

TABLE 1.—*Effect of ABPP, AIPP, and ABMP on NFSa, FSa, and MCa-K tumor nodules in the lungs of C3Hf/Kam mice*

Treatment[a]	No. of lung metastases of:								
	NFSa			FSa			MCa-K		
	Mean ± SE	Range	P[b]	Mean ± SE	Range	P[b]	Mean ± SE	Range	P[b]
No treatment	68.7±7.5	34–98		47.0±8.5	14–85		104±25.0	10–175	
ABPP on days −4, −3, and −2	1.1±0.3	0–2	<0.001	0.7±0.4	0–2	<0.001	14.7±2.9	1–25	<0.01
ABPP on days −1, 0, and 1	43.6±8.8	15–75	<0.02	3.3±0.9	0–7	<0.001	2.4±0.7	0–6	<0.001
ABPP on days 2, 3, and 4	45.0±6.2	17–70	<0.05	16.4±3.7	6–33	<0.01	76.2±21.8	2–142	NS
ABPP on days −3 and 4	1.7±0.8	0–5	<0.01						
ABPP on days 2 and 7	86.3±11.1	48–119	NS						
AIPP on days −4, −3, and −2	1.0±0.5	0–3	<0.001	0.1±0.1	0–1	<0.001	18.0±3.3	4–30	<0.001
AIPP on days −1, 0, and 1	33.6±9.9	1–81	<0.02	2.4±0.5	1–4	<0.001	9.9±3.0	3–26	<0.001
AIPP on days 2, 3, and 4	30.6±8.6	0–58	<0.01	27.3±8.0	1–62	NS	140.0±9.0	105–178	NS
AIPP on days −3 and 4	7.6±1.3	4–14	<0.001						
AIPP on days 2 and 7	68.6±9.6	27–96	NS						
ABMP on days −4, −3, and −2	23, 64, 153[c]		NS	12.4±3.4	1–20	<0.01			
ABMP on days −1, 0, and 1	161.8±13.5	121–196	<0.001	32.8±8.8	2–59	NS			
ABMP on days 2, 3, and 4	76.2±15.2	48–121	NS	46.0±11.6	14–72	NS			
ABMP on days −3 and 4	105.2±17.8	65–155	NS						
ABMP on days 2 and 7	105.6±9.2	71–137	<0.01						

[a] ABPP, AIPP, and ABMP were given ip in the dose of 250 mg/kg/injection. Day 0 designates the time of iv injection of tumor cells. Mice received injections of 2.5×10^5 NFSa, 2×10^5 FSa, or 2×10^5 MCa-K cells. The No. of NFSa and FSa tumor nodules was determined at day 14; the No. of MCa-K tumor nodules was determined at day 28 following tumor cell injection.

[b] Determined by the Mann-Whitney *U* nonparametric test. NS=not significant.

[c] Individual data.

TABLE 2.—*Effect of a single injection of different doses of ABPP or AIPP on the number of NFSa tumor nodules in the lungs of C3Hf/Kam mice*

Dose of ABPP and AIPP, mg/kg[a]	No. of lung metastases in:[b]		
	Controls	ABPP-treated mice	AIPP-treated mice
None	130.2±8.2		
62.5		105.8±16.3 (NS)	113.0±19.2 (NS)
125.0		115.6±4.5 (NS)	124.9±15.5 (NS)
250.0		124.3±13.4 (NS)	108.9±9.8 (NS)
500.0		96.7±13.8 (=0.05)	99.9±9.9 (<0.05)
1,000.0		90.5±10.0 (<0.005)	107.5±10.6 (<0.05)

[a] ABPP or AIPP was injected ip into mice that received iv injections of 2×10^5 NFSa cells 2 days earlier. The No. of tumor nodules in the lung was determined 14 days after iv injection of tumor cells.

[b] Values are means ± SE. *Numbers in parentheses* are *P*-values determined by the Mann-Whitney *U* test. NS=not significant.

mice (3/35) developed metastases if ABPP was given prior to surgery, and 64% of the mice (27/42) had metastases if ABPP was given postoperatively. The incidence of metastases was 17% (5/30) and 47% (20/43) in mice that received AIPP preoperatively and postoperatively, respectively.

Antitumor effect of ABPP and AIPP in WBI mice.—In this experiment we tested whether ABPP and AIPP can exert antitumor activity in immunosuppressed mice. Mice were exposed to 650 rad of gamma rays, and 1 day later they were given injections of 10^5 NFSa cells. ABPP or AIPP was given at days 3 and 2 before or at 3 and 4 days after WBI. The number of lung colonies was determined 14 days after tumor cell injection (table 4). Radiation alone increased the number of lung metastases from 15.0±2.5 in normal mice to 92.0±12.8. Neither ABPP nor AIPP elicited antitumor responses in WBI mice by a detectable reduction in the number of lung colonies. However, when given before radiation, these compounds were able to reduce the metastasis-promoting effect of WBI.

Production of interferon in normal and WBI mice treated with ABPP and AIPP.—The ability of normal and WBI mice to produce interferon following treatment with ABPP or AIPP was determined. WBI with 650 rad was delivered 2 days before treatment of mice with ABPP. Interferon levels were determined in the serum and in supernatants of spleen, thymus, and lung tissue extracts 6 and 24 hours after a single injection or after two injections of ABPP or AIPP given 1 day apart. Results presented in table 5 show that one and two injections of ABPP induced significant production of interferon in normal mice. Levels of interferon were higher in the serum and thymus than in the spleen and lung. Interferon levels in the serum were higher after one injection than after two injections of ABPP. The levels were high at 6 hours after ABPP injections, but in all tested organs they returned to the normal value in 24 hours. At that time, however, a significant level of interferon was still present in the serum. AIPP induced appreciable amounts of interferon only after two injections, but its activity in this respect was far below that of ABPP. In contrast to the high interferon-producing potency of ABPP in normal mice, ABPP was an inefficient interferon inducer in WBI mice.

DISCUSSION

Our results indicate that all three pyrimidinone compounds are capable of inducing antitumor activity in mice, but the magnitude of their effects varies. ABPP and AIPP are similarly effective and far superior to the activity produced by treatment with ABMP. ABMP was not effective in reducing lung metastases of NFSa, but it reduced the number of lung nodules of FSa only if it was given before iv injection of tumor cells. Therefore, this compound does not seem promising as an immunotherapeutic agent. ABPP and AIPP are more effective when given before rather than after tumor cell injection, a common observation in studies with BRM (*17, 18*). It appears that to achieve appreciable antitumor effect, ABPP or AIPP when given after tumor cells should be given more than one or two times (tables 1, 2). Three injections were quite effective against NFSa and FSa, but they were not effective against MCa-K. Recently, Stringfellow (*8*) reported that

TABLE 3.—*Effect of ABPP and AIPP on spontaneous pulmonary metastases of NFSa in C3Hf/Kam mice*

Treatment with ABPP or AIPP, 250 mg/kg ip[a]	Proportion of mice with metastases at 24 days after amputation of the primary tumor[b]		P^c
None (surgery alone on day 0)	10/12 (83)		
ABPP on days −5 and −4	0/12	3/35 (9)	<0.0005
ABPP on days −5, −4, −1, and 0 (−3 hr)	0/12		
ABPP on days −1 and 0 (−3 hr)	3/11 (27)		
ABPP on days 2 and 3	3/12 (25)	27/42 (64)	NS
ABPP on days 6 and 7	7/9 (78)		
ABPP on days 2, 3, 6, and 7	10/11 (91)		
ABPP on days 2, 3, 6, 7, 13, and 14	7/10 (70)		
AIPP on days −5 and −4	1/10 (10)	5/30 (17)	<0.0005
AIPP on days −5, −4, −1, and 0 (−3 hr)	2/9 (22)		
AIPP on days −1 and 0 (−3 hr)	2/11 (18)		
AIPP on days 2 and 3	6/12 (50)	20/43 (47)	<0.025
AIPP on days 6 and 7	6/10 (60)		
AIPP on days 2, 3, 6, and 7	4/10 (40)		
AIPP on days 2, 3, 6, 7, 13, and 14	4/11 (36)		

[a] Primary tumors were generated by injection of 5×10^5 NFSa cells into muscles of the right hind thighs of mice and were surgically removed 13 days later when they reached ~12 mm in diameter.

[b] No. of mice with metastases/total No. of mice. *Numbers in parentheses* are the percentages of mice with metastases.

[c] *P*-values were determined by the chi-square test. NS=not significant.

TABLE 4.—*Effect of WBI on the antitumor activity of ABPP or AIPP*[a]

Treatment of mice with ABPP or AIPP, 250 mg/kg ip	Lung colonies in:					
	Normal mice			Mice treated with WBI		
	Mean ± SE	Range	P[b]	Mean ± SE	Range	P[b]
No treatment	15.0±2.5	4-23		92.0±12.8	59-137	
ABPP on days −4 and −3	3.3±2.3	0-17	<0.01	23.5±5.8	6-59	<0.002
ABPP on days 2 and 3	9.3±1.4	4-14	<0.05	91.4±10.8	55-138	NS
AIPP on days −4 and −3	3.1±0.5	0-5	<0.002	38.3±4.9	21-58	=0.001
AIPP on days 2 and 3	8.2±2.3	1-14	NS	115.7±11.5	84-171	NS

[a] On day 0, mice were given injections of 10^5 NFSa cells, and 14 days later they were killed for determination of the No. of tumor nodules in the lung. Mice were irradiated with 650 rad WBI on day −1.

[b] Determined by the Mann-Whitney *U* nonparametric test. NS = not significant.

ABPP, ABMP, and AIPP prolonged the survival of mice bearing B16 melanoma in the peritoneal cavity.

ABPP and AIPP reduced the incidence of spontaneous metastases of NFSa, especially when these compounds were applied to mice before surgical removal of primary tumors. The superiority of preoperative administration over that of postoperative administration is in agreement with our earlier observations of a similar effect produced by treatment with *Corynebacterium parvum* (*15*) and the MVE-2 fraction of pyran copolymer (*16*). The reasons for a better antimetastatic effect of preoperative application of ABPP and AIPP are not clear, but the following may be taken into account. Metastatic foci in the lung are composed of fewer cells at the time of preoperative application than at the time of postoperative application of pyrimidinone interferon inducers, and therefore these foci would be expected to be eliminated more easily by augmented antitumor resistance mechanisms. Also, in the preoperative situation, antitumor resistance mechanisms, initiated or augmented by ABPP or AIPP, most likely act not only against already established metastases but also against tumor cells prior to their establishment in the lung. Recently, Hanna and Fidler (*19*) observed that NK cells were effective in destroying tumor cells within the circulation, but they had only a limited inhibitory effect on established micrometastases. This may also be a major reason for the better prophylactic than therapeutic activities of ABPP and AIPP in experiments with artificial lung metastases. Depression of the immune system caused by surgical trauma may be an additional factor responsible for the less effective antimetastatic effect of postoperative application of ABPP and AIPP. Studies with WBI animals (table 4) showed that immunodepressed animals would be expected to respond to these agents less well than normal animals. BRM-augmented radiocurability of tumors exposed to local tumor irradiation is found to be ex-

TABLE 5.—*Serum and organ interferon levels in C3Hf/Kam mice, normal, WBI, or tumor bearing, after treatment with ABPP or AIPP*

Mice[a]	Hours after treatment with ABPP or AIPP inducers when interferon levels were determined	Interferon levels, U/ml in[b]			
		Serum	Spleen	Thymus	Lung
Normal mice		<10	<10	<10	<10
Normal mice plus ABPP (single injection)	6	850	100	400	100
	24	400	<10	<10	<10
Normal mice plus ABPP (two injections)	6	300	100	350	80
	24	60	<10	<10	<10
Normal mice plus AIPP (single injection)	6	<10	<10	<10	<10
	24	90	<10	<10	<10
Normal mice plus AIPP (two injections)	6	450	90	50	65
	24	100	<10	<10	<10
NFSa-bearing mice		<10	<10	<10	<10
NFSa-bearing mice plus ABPP (single injection)	6	400	80	450	<10
	24	380	100	<10	<10
WBI mice		16	<10	<10	<10
WBI mice plus ABPP (single injection)	6	<10	<10	<10	<10
	24	<10	<10	22	<10

[a] In normal mice ABPP and AIPP were given ip at a dose of 250 mg/kg once or twice with a 1-day interval between two injections. In tumor-bearing mice, 250 mg/kg was given 2 days after iv injection of 2×10^5 NFSa cells. WBI was achieved by 650 rad 2 days before treatment with ABPP.

[b] Determination of interferon levels described in the text. A level of <10 U/ml is the lowest detectable level, since samples were not assayed at dilutions lower than 1:10.

pressed more profoundly if BRM are applied before rather than after tumor radiation (*12, 20*). Therefore, the present observations (table 3) with those already reported (*12, 15, 16, 20*) suggest that it may be justifiable for the clinician to consider applying immunotherapeutic agents before the primary tumor is surgically removed or exposed to radiotherapy.

Three aspects of antitumor activity of pyrimidinone compounds were investigated in this study: *a*) efficacy against tumors that vary in their immunogenicity; *b*) dependency of antitumor activity on the immunocompetence of mice; and *c*) dependency of antitumor activity on the interferon-inducing potency of these agents.

To induce the immunosuppression state, we exposed mice to sublethal WBI. This procedure commonly facilitates tumor take by both suppression of antitumor resistance responses (*21*) and through nonimmunologic effects (*22*). WBI increased the number of lung colonies in the present study, and this increase was not affected by ABPP or AIPP when given 3 days following radiation. Also, in contrast to normal mice, WBI mice did not produce interferon when treated with ABPP. Stringfellow et al. (*7*) reported earlier that production of interferon by mice exposed to pyrimidinone compounds depended on the presence of radiosensitive but not cortisone-sensitive cells. It follows, therefore, that WBI compromised the system responsible for mounting antitumor responses. As mentioned in the introduction, pyrimidinone compounds activate macrophages and potentiate NK cell activity, and these cells are considered to play an important role in tumor rejection (*17, 18, 23*). It is likely, then, that antitumor activity observed in this study may be a result of such activity of pyrimidinone compounds. It is known that the antitumor activities of activated macrophages are resistant to ionizing radiation (*21, 24, 25*), but activation of macrophages is difficult to achieve in mice exposed to WBI. This fact may explain why treatment of mice with ABPP or AIPP can protect to a significant degree against enhancement of lung metastases produced by WBI delivered to mice following treatment with pyrimidinone compounds (table 4). The effect of ionizing radiation on NK cell activity is less defined than the effect of radiation on macrophages. Spleen cells derived from mice exposed to 1,100 rad (*26*) or 100-900 rad (*27*) WBI 1 day earlier exhibited no decrease in NK cell cytotoxicity. Hochman et al. (*28*) observed that the NK activity of spleen cells from mice given 700 rad of whole-body gamma rays persisted at the level of the NK activity of spleen cells from unirradiated mice for 12 days after radiation. Thereafter, the activity of NK cells temporarily declined, and the authors' conclusion was that NK progenitor cells, but not mature NK cells, are sensitive to ionizing radiation. More recently, Djeu et al. (*29*) reported that X-irradiation with doses of 300-1,200 rad inhibited NK cells when the activity of these cells was assayed 1 day after radiation. The extent of radiosensitivity of NK cells greatly depended on the mouse strain used. However, in vitro irradiation of spleen cells did not influence the cytotoxicity of NK cells. Also, an interferon inducer, polyinosinic-polycytidylic acid, was able to augment NK activity in mice exposed to 300-900 rad WBI 4-6 hours earlier. These observations led Djeu et al. (*29*) to conclude that precursor NK cells and lytic activity of NK cells exposed in vitro to radiation are radioresistant and that only active NK cells are radiosensitive following exposure of animals to radiation. Therefore, if NK cells participated in the antitumor resistance produced by ABPP and AIPP, the inability of these agents to mount an antitumor response in WBI mice might be explained on the basis that NK cells in our mice were sensitive to radiation. If, however, NK cells of our mice were not sensitive to radiation, their activity could not become augmented in WBI mice simply because radiation abrogated the ability of mice to produce interferon in response to treatment with ABPP and AIPP (table 5), and therefore a factor (interferon) that was needed for augmentation of NK cells was lacking.

Pyrimidinone compounds induce production of interferon (table 5), which can inhibit proliferation of tumor cells both by direct action on tumor cells and by stimulation of the antitumor responses of the host (*2*). Our data demonstrate the lack of correlation between the antitumor activities of pyrimidinone compounds and their ability to induce production of interferon. ABPP is a more potent interferon inducer than AIPP, yet both exhibit antitumor activities of similar magnitudes. Stringfellow et al. (*7*) reported that ABMP is as effective as ABPP in interferon-inducing capacity. However, ABMP is the least effective of the three pyrimidinone compounds tested in reducing the number of tumor nodules in the lung. The kinetics of interferon production are not the same for ABPP and AIPP. Whereas only one injection of ABPP is sufficient to produce high serum levels of interferon, two injections of AIPP are required to achieve any appreciable level of interferon in the serum. The relevance of this phenomenon to the antitumor activities of ABPP and AIPP remains to be established. We are presently performing experiments to establish whether sera from ABPP-treated and AIPP-treated animals, which contain different amounts of interferon, differ in their ability to transfer antimetastatic activity to normal mice.

It also appears that the activities of ABPP and AIPP did not depend on tumor immunogenicity. Both poorly and highly immunogenic fibrosarcomas were similarly affected, whereas moderately immunogenic MCa-K was less sensitive. If antitumor resistance mechanisms were involved in the activities of ABPP and AIPP, our observations suggest that they are likely to be mainly immunologically nonspecific.

Using the same animal models, we recently reported that the MVE-2 fraction of pyran copolymer, which is also a potent inducer of interferon, had an antitumor activity of similar magnitude to the antitumor activities reported here for pyrimidinones (*16*). For example, when given preoperatively, MVE-2 reduced the incidence of NFSa spontaneous metastases by 93%, and when given postoperatively, by 27%. Data presented in table 3 show that ABPP and AIPP when given before surgery of the primary tumor reduced spontaneous metastases of the same tumor by 89 and 80%, respectively, and when given after surgery, by 25 and 43%, respectively. However, the number of injections, dose, and time of injection in relation to the surgical treatment were different in studies with MVE-2 and in the present studies with ABPP and AIPP.

In conclusion, our results provide information that pyrimidinone compounds ABPP and AIPP exert an appreciable activity against both artificial and spontaneous tumor metastases in mice. The antitumor effect is dose-responsive. The activity was achieved in normal mice but not in WBI mice, was independent of tumor immunogenicity, and did not correlate with the potency of these compounds to induce production of interferon.

REFERENCES

(1) Isaacs A, Lindenmann J. Virus interference. I. The interferon. Proc R Soc Lond [Biol] 1957; 147:258-267.

(2) Krim M. Towards tumor therapy with interferons. Part II. Interferons: In vivo effects. Blood 1980; 55:875-884.

(3) ———. Towards tumor therapy with interferons. Part I. Interferons: Production and properties. Blood 1980; 55:711-721.

(4) Lindahl P, Leary P, Gresser I. Enhancement of interferon of the specific cytotoxicity of sensitized lymphocytes. Proc Natl Acad Sci USA 1972; 69:721-725.

(5) Schultz RM, Chirigos MA, Heine VI. Functional and morphologic characteristics of interferon-treated macrophages. Cell Immunol 1978; 35:84-91.

(6) Herberman R, Ortaldo J, Bonnard G. Augmentation by interferon of human natural and antibody-dependent cell-mediated cytotoxicity. Nature 1979; 277:221-223.

(7) Stringfellow DA, Vanderberg HC, Weed SD. Interferon induction by 5-halo-6-phenyl pyrimidinones. J Interferon Res 1980; 1:1-14.

(8) Stringfellow DA. 6-Aryl pyrimidinoles: Interferon inducers-immunomodulators antiviral and antineoplastic agents. In: Hersh E, Chirigos M, eds. Augmenting agents in cancer therapy. New York: Raven Press, 1980:215-229.

(9) Ando K, Hunter N, Peters LJ. Immunologically nonspecific enhancement of artificial lung metastases in tumor-bearing mice. Cancer Immunol Immunother 1979; 6:151-156.

(10) Suit HD, Kastelan A. Immunologic status of host and response of a methylcholanthrene-induced sarcoma to local X-irradiation. Cancer 1970; 26:232-238.

(11) Milas L, Hunter N, Mason K, Withers HR. Immunological resistance to pulmonary metastases in C3Hf/Bu mice bearing syngeneic fibrosarcoma of different sizes. Cancer Res 1974; 34: 61-71.

(12) Milas L, Hunter N, Stone HB, Withers HR. *Corynebacterium parvum:* Effect on radiocurability of murine tumors. Cancer Immunol Immunother 1978; 5:109-117.

(13) Stone HB, Peters LJ, Milas L. Effect of host immune capability on radiocurability and subsequent transplantability of a murine fibrosarcoma, JNCI 1979; 63:1229-1235.

(14) Milas L, Hunter N, Bašić I, Mason K, Grdina DJ, Withers HR. Nonspecific immunotherapy of murine solid tumors with *Corynebacterium granulosum*. J Natl Cancer Inst 1975; 54:895-902.

(15) Milas L, Mason K, Withers HR. Therapy of spontaneous pulmonary metastases of a murine mammary carcinoma with anaerobic corynebacteria. Cancer Immunol Immunother 1976; 1:233-237.

(16) Milas L, Hersh EM, Hunter N. Therapy of artificial and spontaneous metastases of murine tumors with MVE-2. Cancer Res 1981; 41:2378-2385.

(17) Pimm MV, Baldwin RW. Antigenic differences between primary methylcholanthrene-induced rat sarcomas and post-surgical recurrences. Int J Cancer 1977; 20:37-43.

(18) Milas L, Scott MT. Antitumor activity of *Corynebacterium parvum*. Adv Cancer Res 1978; 26:257-306.

(19) Hanna N, Fidler IJ. Role of natural killer cells in the destruction of circulating tumor emboli. JNCI 1980; 65:801-809.

(20) Suit HD, Sedlacek R, Wagner M, Orsi L, Silobrcic V, Rothman K. Effect of *Corynebacterium parvum* on the response to irradiation of a C3H fibrosarcoma. Cancer Res 1976; 36: 1305-1314.

(21) Anderson R, Warner N. Ionizing radiation and the immune response. Adv Immunol 1976; 24:215-335.

(22) Peters LJ. Enhancement of syngeneic murine tumour transplantability by whole-body irradiation—a nonimmunological phenomenon. Br J Cancer 1975; 31:293-300.

(23) Herberman RB, Holden HT. Natural cell-mediated immunity. Adv Cancer Res 1978; 27:305-330.

(24) Bašić I, Milas L, Grdina DJ, Withers HR. In vitro destruction of tumor cells by macrophages from mice treated with *Corynebacterium granulosum*. J Natl Cancer Inst 1975; 55:589-596.

(25) Milas L, Hunter N, Bašić I, Withers HR. Protection by *Corynebacterium granulosum* against radiation-induced enhancement of artificial pulmonary metastases of a murine fibrosarcoma. J Natl Cancer Inst 1974; 52:1875-1880.

(26) Lotzova E, Savary CA. Possible involvement of natural killer cells in bone marrow graft rejection. Biomedicine 1977; 27: 341-344.

(27) Kiessling R, Hochman PS, Haller O, Shearer GM, Wigzell H, Cudkowicz G. Evidence for a similar or common mechanism for natural killer cell activity and resistance to hemopoietic grafts. Eur J Immunol 1977; 7:655-663.

(28) Hochman PS, Cudkowicz G, Dausset J. Decline of natural killer cell activity in sublethally irradiated mice. JNCI 1978; 61:265-268.

(29) Djeu JY, Heinbaugh JA, Vieira WD, Holden HT, Herberman RB. The effect of immunopharmacological agents on mouse natural cell-mediated cytotoxicity and on its augmentation by poly I:C. Immunopharmacology 1979; 1:231-244.

blank page

Rat Mammary Tumor Classification: Notes on Comparative Aspects[1, 2]

Dymitr Komitowski,[3] Bernard Sass,[4, 5] *and* Walter Laub[3]

ABSTRACT—Mammary tumors (170 spontaneous and 1,613 induced with 7,12-dimethylbenz[*a*]anthracene) in inbred SD rats were classified histologically. The neoplasms were divided into three main categories: fibroepithelial, epithelial, and connective tissue. In the fibroepithelial category, compound tumors showing a wide range of histologic structures with variation in the arrangement of both epithelial and connective tissue elements that differ among lobules occurred in 44 (25.9%) spontaneous and 1,027 (63.7%) induced neoplasms, whereas fibroadenomas occurred in 41 (24.1%) untreated and 175 (10.9%) treated rats. Uncommon fissured tumors were found in 1 (0.7%) untreated and 6 (0.4%) treated animals, whereas carcinosarcomas were found in only 10 untreated animals. In the epithelial category, tubular adenomas occurred in 48 (28.2%) untreated and 164 (10.2%) treated animals. Cystadenomas, duct papillomas, intraductal carcinomas, and anaplastic carcinomas were found less frequently. Adenoacanthomas occurred in only 12 (0.8%) of the treated animals. Among tumors with a fibrous component only, fibromas occurred in 22 (13%) untreated and 97 (6.0%) treated animals. Fibrosarcomas were less frequent, occurring in 4 untreated (2.4%) and 54 (3.4%) treated animals.—JNCI 1982; 68:147–156.

Numerous attempts have been made to classify rat mammary tumors since the earliest report of their occurrence by McCoy (*1*). Bullock and colleagues (*2–4*) published early descriptions and attempts at classification of spontaneous mammary neoplasms. More recently, Thompson et al. (*5*), Crain (*6*), and Burek and Hollander (*7*) studied incidence patterns of spontaneously occurring neoplasms, including mammary neoplasms, in various rat strains and attempted to classify these neoplasms. The morphology of chemically induced neoplasms has been studied by Dunning et al. (*8*), Young et al. (*9*), Middleton (*10*), and Archer and Orlando (*11*). As yet, no one classification has been generally accepted because there are great variations in morphology not only among these tumors but also among components of a single tumor. Mammary tumors of rats also differ morphologically and biologically from those of other animals and humans, although histologically there is some superficial resemblance. The unique morphology of these tumors must be considered when one is classifying them for the purposes of experimental pathology. Uniform pathologic nomenclature and clearly defined criteria for classification are lacking.

Spontaneous and induced neoplasms of rat mammary glands have been used as experimental models for human breast tumors, particularly in studies of chemotherapy of such tumors. The implication is that both types of neoplasms are morphologically and biologically similar. To analyze similarities between morphologic forms of mammary gland tumors in rats and those in humans, one must introduce appropriate classifications. One report provides a classification of rat mammary tumors based on histologic criteria and terminology corresponding to those used for human breast neoplasms (*12*). Our classification of rat mammary tumors is based on two general, albeit opposite, concepts: 1) Unique histologic forms characteristic for the rat should be distinguished; 2) terminology and criteria for typing should permit comparison between tumors of humans and those of other animals.

A large number of rat mammary tumors, accessed at the Division of Histodiagnostic and Pathomorphological Documentation, the German Cancer Research Center, were used for this study.

MATERIALS AND METHODS

Tumors.—More than 2,500 tumors of the mammary gland obtained from different rat strains in our collection served as a basis for this study. Of the total, 1,783 mammary tumors (170 spontaneous and 1,613 induced) from female inbred SD rats were examined by stepwise serial sectioning of several slices from each tumor. The tumors were obtained from 1,494 rats (552 control and 942 treated). The rats with spontaneous tumors comprised 31% of the control animals. Most of the animals (80% control and 60% treated) developed only one tumor. Eighty induced tumors were obtained from in-house experiments, conducted by the senior author, in which 80 conventionally reared, 6-month-old female inbred SD rats obtained from in-house stock were used. The rats were housed in pairs in plastic cages and were fed a mixed diet (Altromin 1324) and received water ad libitum. The rats were then divided into groups of 20 each and were given 7,12-dimethylbenz[*a*]anthracene (The Upjohn Co., Kalamazoo, Mich.) either by iv injection at 25 mg/kg, by sc injection at 1 mg/kg, or by gavage at 10 mg/kg.

Histologic examination.—Animals were killed by cervical dislocation, and a complete necropsy was

---

[1] Received May 11, 1981; accepted September 18, 1981.

[2] Animals were maintained under the guidelines set forth by the German Cancer Research Center.

[3] Division of Histodiagnostic and Pathomorphological Documentation, Institute of Experimental Pathology, German Cancer Research Center, 6900 Heidelberg, Federal Republic of Germany.

[4] Registry of Experimental Cancers, Division of Cancer Cause and Prevention, National Cancer Institute, National Institutes of Health, Public Health Service, U.S. Department of Health and Human Services, Bethesda, Md. 20205.

[5] *Address reprint requests to* Dr. Sass.

blank page

Rat Mammary Tumor Classification: Notes on Comparative Aspects[1,2]

Dymitr Komitowski,[3] Bernard Sass,[4,5] *and* Walter Laub[3]

ABSTRACT—Mammary tumors (170 spontaneous and 1,613 induced with 7,12-dimethylbenz[*a*]anthracene) in inbred SD rats were classified histologically. The neoplasms were divided into three main categories: fibroepithelial, epithelial, and connective tissue. In the fibroepithelial category, compound tumors showing a wide range of histologic structures with variation in the arrangement of both epithelial and connective tissue elements that differ among lobules occurred in 44 (25.9%) spontaneous and 1,027 (63.7%) induced neoplasms, whereas fibroadenomas occurred in 41 (24.1%) untreated and 175 (10.9%) treated rats. Uncommon fissured tumors were found in 1 (0.7%) untreated and 6 (0.4%) treated animals, whereas carcinosarcomas were found in only 10 untreated animals. In the epithelial category, tubular adenomas occurred in 48 (28.2%) untreated and 164 (10.2%) treated animals. Cystadenomas, duct papillomas, intraductal carcinomas, and anaplastic carcinomas were found less frequently. Adenoacanthomas occurred in only 12 (0.8%) of the treated animals. Among tumors with a fibrous component only, fibromas occurred in 22 (13%) untreated and 97 (6.0%) treated animals. Fibrosarcomas were less frequent, occurring in 4 untreated (2.4%) and 54 (3.4%) treated animals.—JNCI 1982; 68:147–156.

Numerous attempts have been made to classify rat mammary tumors since the earliest report of their occurrence by McCoy (*1*). Bullock and colleagues (*2–4*) published early descriptions and attempts at classification of spontaneous mammary neoplasms. More recently, Thompson et al. (*5*), Crain (*6*), and Burek and Hollander (*7*) studied incidence patterns of spontaneously occurring neoplasms, including mammary neoplasms, in various rat strains and attempted to classify these neoplasms. The morphology of chemically induced neoplasms has been studied by Dunning et al. (*8*), Young et al. (*9*), Middleton (*10*), and Archer and Orlando (*11*). As yet, no one classification has been generally accepted because there are great variations in morphology not only among these tumors but also among components of a single tumor. Mammary tumors of rats also differ morphologically and biologically from those of other animals and humans, although histologically there is some superficial resemblance. The unique morphology of these tumors must be considered when one is classifying them for the purposes of experimental pathology. Uniform pathologic nomenclature and clearly defined criteria for classification are lacking.

Spontaneous and induced neoplasms of rat mammary glands have been used as experimental models for human breast tumors, particularly in studies of chemotherapy of such tumors. The implication is that both types of neoplasms are morphologically and biologically similar. To analyze similarities between morphologic forms of mammary gland tumors in rats and those in humans, one must introduce appropriate classifications. One report provides a classification of rat mammary tumors based on histologic criteria and terminology corresponding to those used for human breast neoplasms (*12*). Our classification of rat mammary tumors is based on two general, albeit opposite, concepts: 1) Unique histologic forms characteristic for the rat should be distinguished; 2) terminology and criteria for typing should permit comparison between tumors of humans and those of other animals.

A large number of rat mammary tumors, accessed at the Division of Histodiagnostic and Pathomorphological Documentation, the German Cancer Research Center, were used for this study.

MATERIALS AND METHODS

Tumors.—More than 2,500 tumors of the mammary gland obtained from different rat strains in our collection served as a basis for this study. Of the total, 1,783 mammary tumors (170 spontaneous and 1,613 induced) from female inbred SD rats were examined by stepwise serial sectioning of several slices from each tumor. The tumors were obtained from 1,494 rats (552 control and 942 treated). The rats with spontaneous tumors comprised 31% of the control animals. Most of the animals (80% control and 60% treated) developed only one tumor. Eighty induced tumors were obtained from in-house experiments, conducted by the senior author, in which 80 conventionally reared, 6-month-old female inbred SD rats obtained from in-house stock were used. The rats were housed in pairs in plastic cages and were fed a mixed diet (Altromin 1324) and received water ad libitum. The rats were then divided into groups of 20 each and were given 7,12-dimethylbenz[*a*]anthracene (The Upjohn Co., Kalamazoo, Mich.) either by iv injection at 25 mg/kg, by sc injection at 1 mg/kg, or by gavage at 10 mg/kg.

Histologic examination.—Animals were killed by cervical dislocation, and a complete necropsy was

---

[1] Received May 11, 1981; accepted September 18, 1981.

[2] Animals were maintained under the guidelines set forth by the German Cancer Research Center.

[3] Division of Histodiagnostic and Pathomorphological Documentation, Institute of Experimental Pathology, German Cancer Research Center, 6900 Heidelberg, Federal Republic of Germany.

[4] Registry of Experimental Cancers, Division of Cancer Cause and Prevention, National Cancer Institute, National Institutes of Health, Public Health Service, U.S. Department of Health and Human Services, Bethesda, Md. 20205.

[5] *Address reprint requests to* Dr. Sass.

performed. All mammary tumors were removed and cut into slices of approximately 5×10 mm. In addition to slices of mammary tumors and those from organs with gross evidence of metastasis, slices of liver, lung, spleen, kidney, adrenal gland, and brain were collected. The tissue samples were fixed in 10% neutral buffered Formalin (24 hr at 4°C) and embedded in Paraplast; they were sectioned at 4 µm and routinely stained with hematoxylin and eosin. Special stains were used. Van Giesson and Masson-Goldner's stains were used for collagen fibers. Orcein was used for elastic fibers. The impregnation technique of Gomori was used for the argyrophilic fibers, and a periodic acid-Schiff reaction, according to the method of McManus (*13*), was used for staining neutral mucopolysaccharides and basement membrane.

RESULTS

The histologic appearance of rat mammary tumors is related to the extent and distribution of the main structural components—fibrous stroma and duct epithelium. According to these criteria, the most prevalent types were fibroepithelial tumors, epithelial tumors, and fibrous tumors.

Fibroepithelial tumors assume a lobular growth pattern and are characterized by outgrowth of both the duct epithelium and the intralobular connective tissue.

The epithelial tumors are neoplasms with accentuated growth of the epithelium. Fibrous stroma, often abundant, appears as bands of dense collagen bundles between the compactly arranged epithelial formations.

Fibrous tumors have the growth pattern of connective tissue neoplasms. Structures resembling normal or atrophic ducts occasionally can be seen between the loosely textured connective tissue fibers.

The histologic criteria used to determine in which main groups individual tumor forms belonged were: uniformity of growth pattern, relationship between stroma and epithelium, gland and tubule formation, cell type, regularity of nuclei, mitosis, and invasiveness.

The following is a proposed classification of rat mammary tumors:

I. Fibroepithelial tumors
  A. Fibroadenomas
    1. Tubular or acinar
    2. Sclerosing
    3. Proliferating
    4. Fissured
  B. Compound tumors
  C. Carcinosarcomas
  D. Lobular carcinomas
II. Epithelial tumors
  A. Tubular (simple) adenomas
  B. Cystadenomas
  C. Anaplastic adenocarcinomas
    1. Small cell type
    2. Glomerate type
  D. Squamous cell tumors
    1. Squamous cell carcinomas
    2. Adenoacanthomas
III. Tumors composed wholly of fibrous tissue
  A. Fibromas
  B. Fibrosarcomas

The distribution of different histologic types among the 1,783 mammary tumors is shown in table 1. The incidence of spontaneous and induced tumors is given separately. Table 1 also presents the number and percent incidence of metastases in the different groups. All metastases were localized in the lungs and were observed by gross examination and confirmed histologically.

Fibroepithelial Tumors

Fibroepithelial tumors are the most frequently occurring type of mammary gland neoplasia in rats.

TABLE 1.—*Incidence of the different types of mammary tumors registered in the Division of Histodiagnostic and Pathomorphological Documentation, German Cancer Research Center*

Tumor classification	Spontaneous tumors		Induced tumors		Total tumors		Metastases	
	No.	Percent	No.	Percent	No.	Percent	No.	Percent
I. Fibroepithelial tumors								
A. Fibroadenomas	41	24.1	175	10.9	216	12.1	0	
B. Compound tumors	44	25.9	1,027	63.7	1,071	60.1	6	0.6
C. Carcinosarcomas	0	0	10	0.6	10	0.6	2	20.0
D. Lobular carcinomas	2	1.2	17	1.1	19	1.1	0	
II. Epithelial tumors								
A. Tubular (simple) adenomas	48	28.2	164	10.2	212	11.9	0	
B. Cystadenomas	8	4.7	30	1.9	38	2.1	0	
C. Anaplastic adenocarcinomas	1	0.6	27	1.7	28	1.6	10	36.0
D. Adenoacanthomas	0	0	12	0.8	12	0.7	2	16.7
III. Tumors composed wholly of fibrous tissue								
A. Fibromas	22	13.0	97	6.0	119	6.7	0	
B. Fibrosarcomas	4	2.4	54	3.4	58	3.3	1	1.8
	170		1,613		1,783		21	

Proliferation of both tubular epithelium and fibrous stroma and a lobular pattern of growth are distinguishing features of these tumors. Histologic appearance is characterized by more or less regular distribution of the epithelial structures throughout the excessive connective tissue stroma. Epithelial and fibrous components vary greatly in their proportions, structural relationships, and degree of differentiation in different tumors. On the basis of these criteria and the biologic features of tumors, different morphologic forms may be distinguished: fibroadenomas, compound tumors, carcinosarcomas, and lobular carcinomas.

Fibroadenomas

Fibroadenomas are the second most common spontaneous neoplasm of the rat mammary gland. Histologically, they reveal a characteristic pattern created by the appearance of tubules lined by a single layer of epithelium in an abundant fibrous stroma showing peritubular arrangement of the fibers. The epithelial and fibrous components of fibroadenomas vary in their morphologic features. Accordingly, four subtypes of fibroadenomas can be distinguished: tubular (acinar), sclerosing, proliferating, and fissured. Foulds (*14*) has reviewed the morphology of primary and transplanted fibroadenomas. These tumors are transplantable, although they grow very slowly. When these tumors are transplanted into young female rats, epithelial elements predominate, whereas in older females lipid or cartilage is abundant. If these tumors are transplanted into male rats, fibrosarcoma elements predominate. Thus fibroadenomas are hormone-dependent tumors.

Acinar fibroadenomas (fig. 4) are neoplasias in which epithelium is organized in single, well-formed acini separated by concentrically arranged loose-textured connective tissue fibers. The epithelium lining the acini consists of two layers and appears to be identical to that of normal mammary glands. The epithelial cells may contain cytoplasmic vacuoles as a result of secretory activity.

Sclerosing fibroadenomas (fig. 5) reveal extensive fibrosis. Stromal connective tissue is dense with abundant collagen fibers and acellular and hyalinized areas. These tumors often contain an increased number of mast cells. The duct epithelium is flat, sometimes apparently atrophic.

Proliferating fibroadenomas (fig. 6) exhibit morphologic evidence of an increase in growth potency of epithelium lining tubular structures. In comparison with other subtypes of fibroadenomas, the neoplastic tubular structures are elongated and irregular. The epithelium consisting of columnar or cuboidal cells with prominent nuclei is multilayered with focal budlike outgrowths.

Fissured fibroadenomas (fig. 7) are composed of epithelium arranged in slitlike gland spaces and of fibrous stroma forming polypoid structures. The epithelium varies in its appearance from one region to another. It may be found in one layer or multiple layers or even may be absent in some places. The bulky lobulated masses of the stroma exhibit cysts, myxomatous changes, and highly cellular and hyalinized areas.

Compound Tumors

Compound tumors are distinctive types of neoplasms of the rat mammary gland and the most frequently observed experimentally induced mammary tumors. These tumors have a lobular growth pattern and complex morphology in which a wide range of structures can be recognized—from well-organized tubules to cystic and pseudopapillary formations to solid, highly cellular foci. The general histologic pattern is tubulopapillary and is obviously a result of ingrowth of glandular epithelium into the dilated cystlike ducts (fig. 1).

Proliferating epithelium forms secondary structures of glandular, cribriform, lacelike, or arborescent appearance that fill the cystic spaces (fig. 2). Characteristically, the epithelium lining these structures is arranged in layers consisting of two types of cells: *a*) intensely eosinophilic columnar cells with dense nuclei of the innermost layer delineating the lumen and *b*) pale, polygonal, or round cells with lightly stained nuclei situated in the more peripheral layers (fig. 3). The cells of both types and especially those from peripheral layers contain many cytoplasmic vacuoles. The highly cellular solid foci are comprised of pale cells. The fibrous stroma shows differences in the cellularity and density of the fibers in different areas. Typical are the myxomatous changes. The compound tumors may be well differentiated and circumscribed or anaplastic and infiltrating.

No direct relationship between the degree of histologic differentiation and infiltrating growth or even metastases can be found. Therefore, the designation of benign or malignant is arbitrary. Compound tumors must be clearly distinguished from different subtypes of fibroadenomas and from the lobular carcinoma. Histologic criteria indicative of compound tumors are lobular growth pattern, variability of the histologic structure with areas of different histomorphology within the same tumor (including tubular, papillary, or solid formations), two types of epithelium, and myxomatous changes in the stroma.

Carcinosarcomas

Carcinosarcomas (fig. 9) are rare tumors of the rat mammary gland. In our collection we found few tumors (0.6% of all tumors) with apparently concomitant malignant growth of tubular epithelium and connective tissue. These tumors invade neighboring tissue and occasionally metastasize.

Lobular Carcinomas

Although most fibroepithelial mammary tumors of rats may show lobular patterns of growth, we believe that the lobular carcinoma (fig. 8) is a distinct tumor type. Lobular carcinoma apparently arises from the proliferating epithelium of the terminal ducts that fills and distends their lumina. The duct epithelium forms glandular or cribriform structures separated by a delicate fibrous stroma. The secondary lumina of these structures often contain eosinophilic secretory material. The intralobular stroma often contains a significant number of mast cells usually appearing in groups. Frequently, the stroma reveals myxomatous changes. In contrast, the perilobular stroma separating the individual lobules is composed of broad connective tissue bundles infiltrated diffusely by lymphocytes and mast cells.

Distinguishing features of lobular carcinoma are the lobular pattern, the glandular epithelial structures supported by typical connective tissue stroma, and the inconspicuous papillary formations.

Epithelial Tumors

A fibrous component is an integral part of all mammary tumors of rats. There are, however, tumor types that exhibit the basic growth pattern of glandular epithelial neoplasms. The individual tumor types in this group are: tubular (simple) adenomas, cystadenomas, anaplastic adenocarcinomas, and squamous cell tumors.

Tubular (Simple) Adenomas

Tubular adenoma is composed of compactly arranged tubular structures surrounded by delicate connective tissue fibers (fig. 10). The duct epithelium consists of large, pale, vacuolated cells that fill the lumen (fig. 11). The lobules of tumor tissue are surrounded partly by fibrous tissue.

Cystadenomas

Although cyst formation can be encountered in almost all rat mammary tumors, cystadenomas have distinctive histologic features. The tumors have a multicystic pattern with papillary projections that extend into the cystic spaces. The lining epithelium is cuboidal with basophilic cytoplasm and is arranged as fungiform aggregates of cells (fig. 12). Cystadenomas have calcific bodies.

Anaplastic Adenocarcinomas

Anaplastic adenocarcinoma is a common name for highly cellular infiltrating mammary neoplasms. The tumors are composed of pleomorphic cells arranged in various configurations. Large cell carcinomas with alveolar pattern and round cell, diffusely growing tumors can be recognized. Most of the anaplastic adenocarcinomas can be considered as more anaplastic compound tumors. Two histologic types of anaplastic adenocarcinomas of the rat mammary gland require special mention: small cell type and glomerate type.

The small cell type is the most characteristic form of anaplastic adenocarcinoma of the rat mammary gland and consists of small epithelium-like cells usually assembled into alveoli, giving rise to nests of cells or poorly defined glands and sheetlike formations of tumor cells that demonstrate marked loss of polarity (fig. 13). In our studies the small cell adenocarcinoma was the most malignant, on the basis of its ability to metastasize. Glomerate anaplastic adenocarcinomas have structures resembling abortive renal glomeruli and elongated cordlike tubules. The cells are arranged in compact nests or in tortuous ribbons and whorls in which several concentric layers can be recognized (fig. 14). One of these layers consists usually of darker cells having intensely stained nuclei lying close together and lining narrow tubules.

Squamous Cell Tumors

Although different histologic types of rat mammary tumors exhibit varying degrees of squamous metaplasia, pure squamous cell tumors are rare. On the basis of the extent of squamous metaplasia and tubular structure, two histologic forms can be distinguished: squamous cell carcinoma and adenoacanthoma.

Adenoacanthoma (adenosquamous carcinoma) consists of neoplastic epithelial cells arranged as acini and varying degrees of keratin pearl formation (fig. 15). Adenoacanthomas also occur in mice (*15, 16*).

Epithelial pearls were found also in tumors that appeared as anaplastic adenocarcinomas.

Tumors Composed Wholly of Fibrous Tissue

Large areas of fibrous connective tissue can be seen in different rat mammary tumors. In some instances, however, the extent and histologic features of the neoplastic connective tissue can assume the growth pattern of true fibromas (fig. 16) or fibrosarcomas. Characteristics of benign fibrous tumors and some well-differentiated fibrosarcomas of rat mammary gland that distinguish these tumors from fibrosarcomas of other sites are the fine-textured fibers, the tendency to form concentric whorls, and the abundance of mast cells.

DISCUSSION

Mammary tumors of rats reveal features characteristic of this species as compared with mammary gland neoplasms of other animals and humans. Human breast neoplasms are characterized by neoplastic growth of duct epithelium. Three stages of development can be distinguished: intraductal precancerous proliferation, intraductal noninfiltrating carcinomas, and extraductal infiltrating carcinomas.

All known classifications of human breast tumors indicate their genesis from duct epithelium and reflect their specific morphology distinguishing a variety of epithelial neoplasias; however, Wellings et al. (*17*) believe that human breast tumors originate in the terminal ductal-lobular unit. Such classifications, however, are inadequate for fibroepithelial tumors of the rat mammary gland in which both epithelial and fibrous components proliferate. This is also true for the existing classifications of rat mammary tumors based on the classification of human breast tumors. The major morphologic feature of rat mammary tumors differentiating them from human breast tumors is the great diversity of histologic appearances in different regions of one tumor in the rat. These features necessitate the introduction of different terminology for the classification of rat mammary tumors. We propose the term "compound tumors" for lesions that, despite complex morphology, are histologically quite distinct from all other forms of rat mammary tumors. Compound tumors have some features in common with fibroadenomas and are often composed in part of fibroadenomas. Compound tumors differ from fibroadenomas by their basic growth pattern of epithelial and fibrous components. Typical fibroadenomas are defined by the proportion of epithelium and connective tissue stroma and structural relationship. Histologically, they reveal single, epithelium-lined ducts dispersed between abundant stroma showing concentric periductal arrangement of the fibers. The duct epithelium proliferates to form new tubular branches. The epithelial cells lining the ducts, although occasionally exhibiting multilayered arrangements of solid clumps (proliferating and fissured fibroadenomas), resemble those in normal mammary tissue. The compound tumors are characterized by multilayered epithelium with two distinct cell types and by the coexistence of tubular, cystic, papillary, and solid formations. Proportions and structural relationships between the fibrous stroma and epithelium in compound tumors vary greatly and cannot be clearly defined. In contrast to fibroadenomas that are benign and exhibit expansive growth, compound tumors as pathologic entities include both benign and malignant elements. In our study, we observed compound tumors that metastasized but did not have the cell and nuclear pleomorphism indicative of cancer. The designation of fibroadenomas as benign or malignant is contradictory, since these neoplasms grow expansively and are transplantable. In addition, the term "compound tumor" implies neoplastic growths with complex morphology that fail to reveal definite histologic criteria for the differentiation of benign from malignant forms. Our preliminary histochemical and electron microscopic studies suggest that the morphogenesis of the compound tumors is a result of specific interactions between connective tissue stroma, ductular epithelium, and myoepithelial cells (Komitowski D: Unpublished data). The role of myoepithelial cells in the morphogenesis of rat mammary tumors, although postulated (*18, 19*), has not yet been proved. This is true also for mast cells that are a conspicuous cellular element of the connective tissue stroma of different rat mammary neoplasias, such as fibroadenomas, lobular carcinomas, compound tumors, or fibromas. In our studies, the number of the mast cells and the process of desmoplasia in the tumors are correlated. Therefore, mast cells are most prominent in sclerosing fibroadenomas as compared with other forms of fibroadenomas. The occurrence of mast cells in rat fibroadenomas has also been reported by others (*12*) but has not been explained. Because the mammary tumors of rats typically exhibit extensive fibrosis, the question of whether mast cells are a result of, or a possible contributing factor to, fibrosis may be an area for further investigations. Our studies indicate that fibroplasia is a process in which both basic types of connective tissue of rat mammary gland, interlobular and intralobular, evolve differently. Epithelial and fibrous tumor forms show proliferation of interlobular connective tissue, whereas fibroepithelial tumors show proliferation of the intralobular connective tissue. These types of connective tissue differ morphologically and functionally. Because the intralobular connective tissue changes under the influence of hormones, it may be suggested that hormones are important also in the morphogenesis of rat mammary tumors. This influence is also supported by the fact that most tumors show secretory activity.

Lobular carcinomas occur in both humans and rats. The lobular carcinoma of the human breast is a distinctive anatomic entity composed of small cells associated with a poor prognosis. The lobular carcinoma of the rat mammary gland resembles the lobular carcinoma of the human breast only with regard to its overall architecture. In both tumors, the lobular architecture is preserved. Further studies are needed to trace the development of lobular carcinoma in the rat.

Fibroadenoma of the rat mammary gland is the tumor type that most resembles its counterpart in humans, although carcinosarcoma and tubular adenoma are also morphologically similar in the two species.

Some of the neoplasms of the rat mammary gland are histologically similar to those in mice. Mammary tumors of mice have been investigated intensively and have been well characterized histologically. According to Dunn (*15*), these tumors reveal a basic acinar structure. The basic structure of rat mammary tumors is tubulopapillary. In our opinion, only a few histologic forms of these tumors can be compared with those in mice. This is true for cystic adenomas, which assume features similar to so-called "lacelike" or adenocarcinoma type L of mice initially described in strains DD and (C3H × Y)F_1. Corresponding to the fissured tumors of rats is a type Y mammary tumor of mice described in strain C3H-A^{vy} (*16*). As compared with those in rats, fissured tumors in mice show more tubular structures lined by cuboidal epithelium and branching at acute angles. Simple adenomas in rats may be compared with so-called "type C" tumor in mice. However it is unclear whether this type occurs only in old animals, as in the mouse, and whether it is a reaction to an atrophic process in the mammary

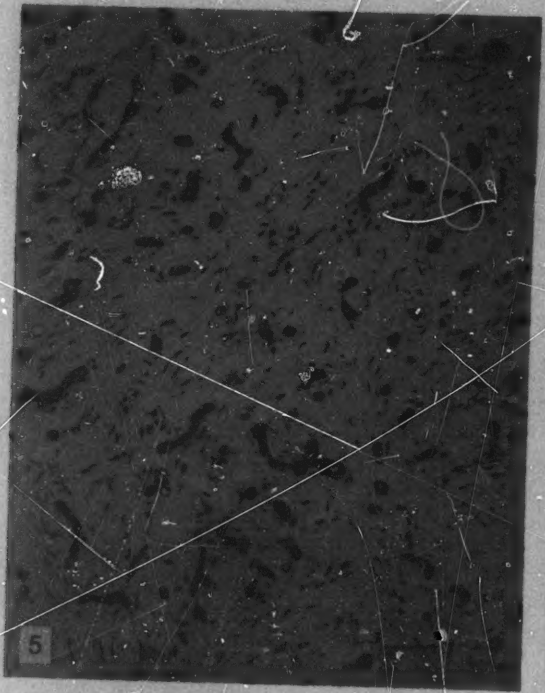

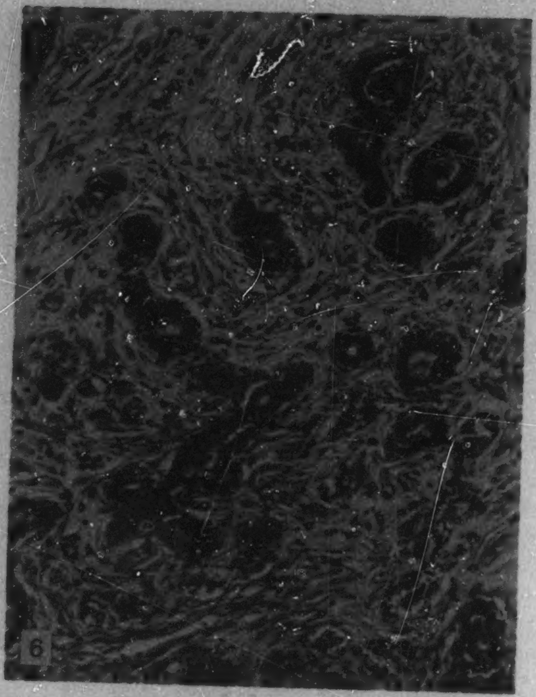

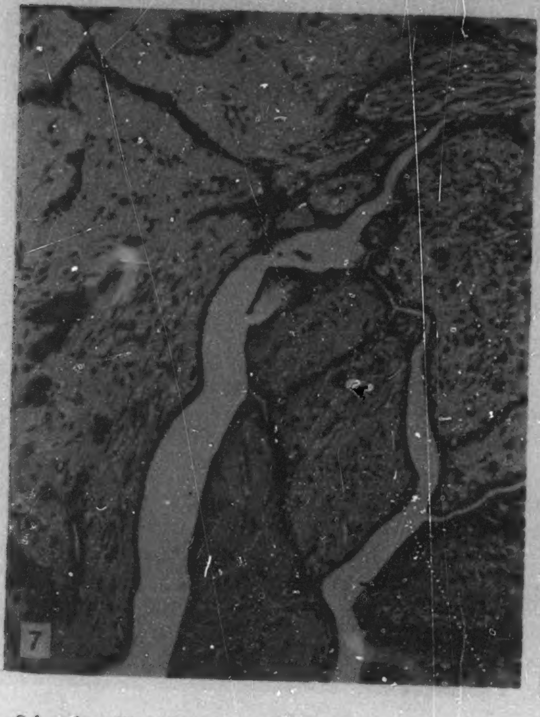

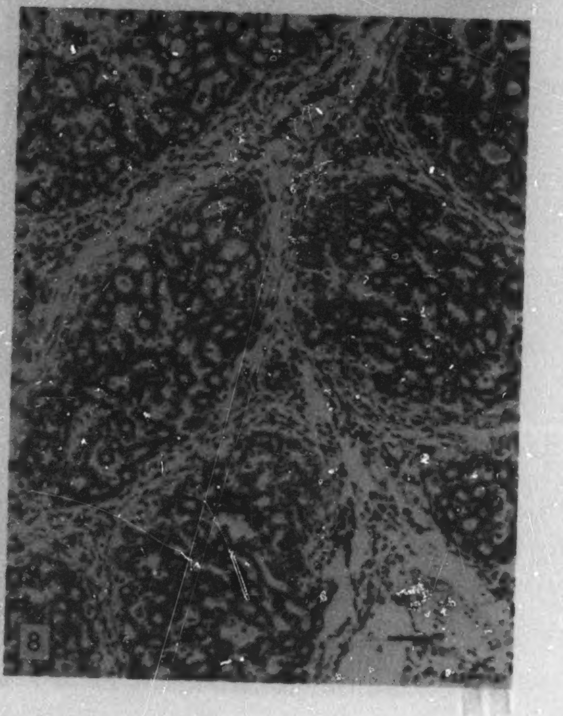

FIGURE 5.—Sclerosing fibroadenoma with prominent fibrous component. *Bar*=50 μm. × 140

FIGURE 6.—Proliferating fibroadenoma. *Note* elongated and distended tubular structure and large epithelial cells. *Bar*=50 μm. × 140

FIGURE 7.—Fissured fibroadenoma. *Note* slitlike spaces lined by epithelium. *Bar*=50 μm. × 140

FIGURE 8.—Lobular carcinoma with conspicuous lobular pattern and fibroepithelial tubular structures. *Bar*=50 μm. × 140

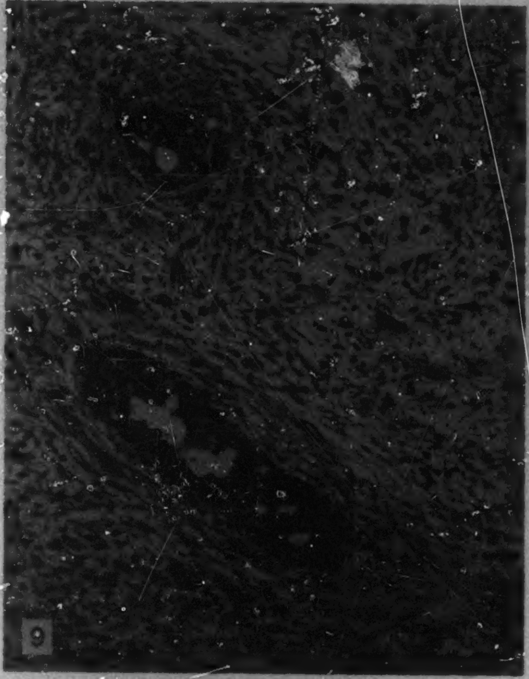

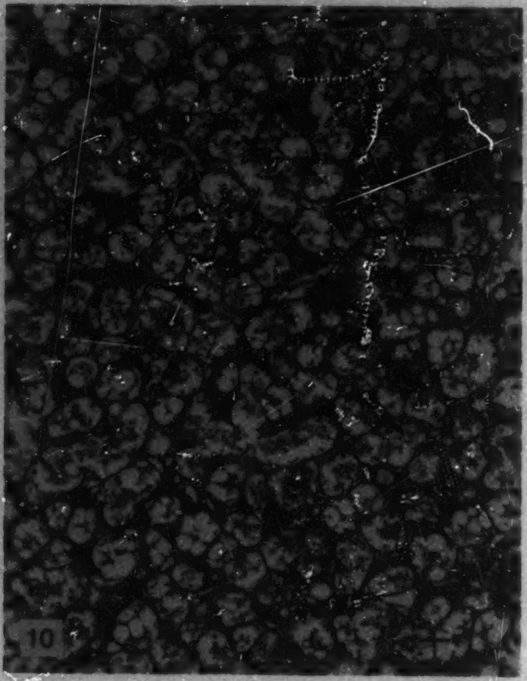

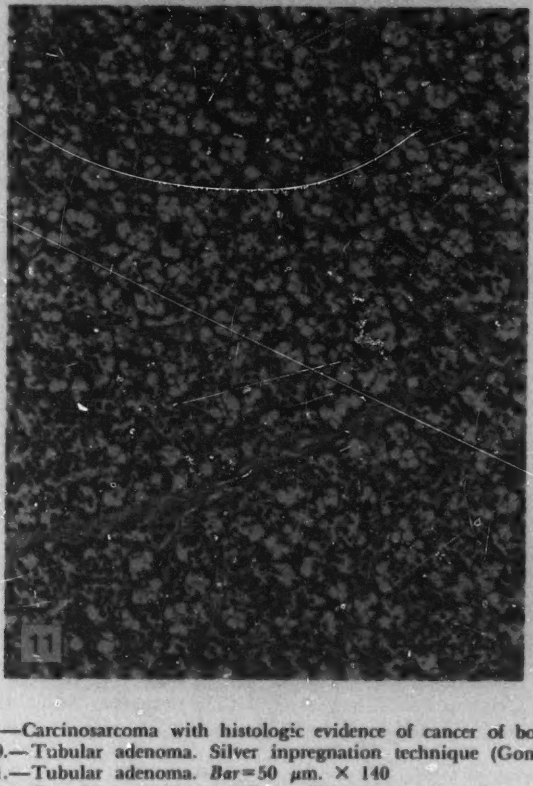

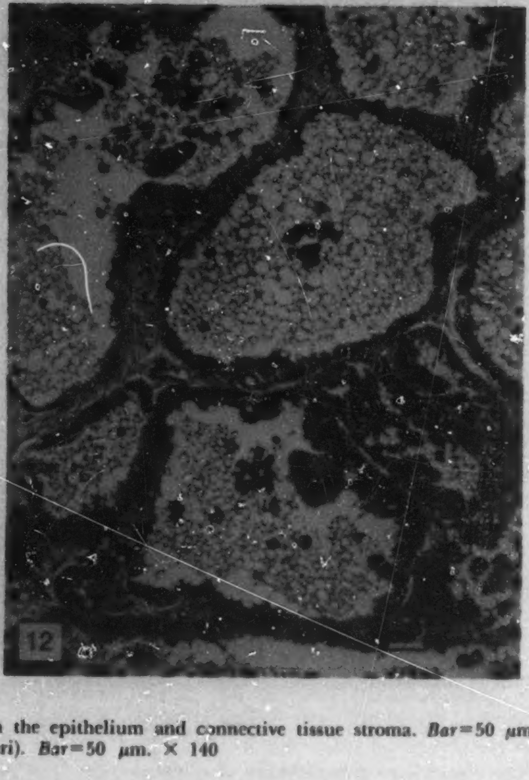

FIGURE 9.—Carcinosarcoma with histologic evidence of cancer of both the epithelium and connective tissue stroma. *Bar*=50 μm. × 140
FIGURE 10.—Tubular adenoma. Silver inpregnation technique (Gomori). *Bar*=50 μm. × 140
FIGURE 11.—Tubular adenoma. *Bar*=50 μm. × 140
FIGURE 12.—Cystadenoma. *Note* small papillary ingrowth and desquamated epithelial cells. *Bar*=50 μm. × 140

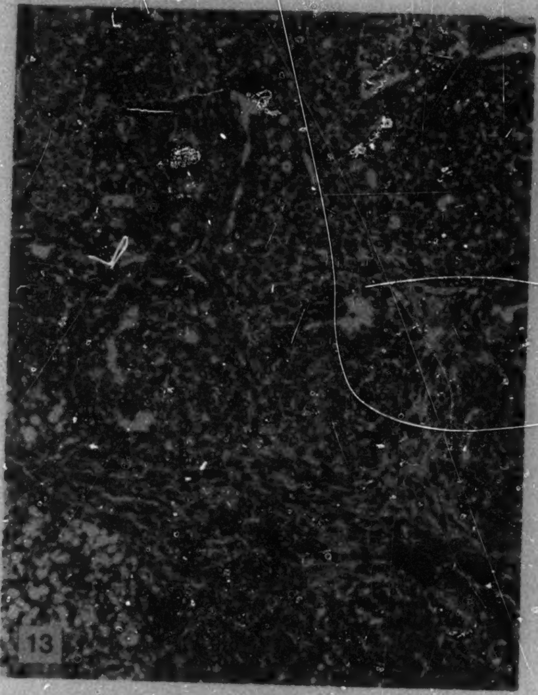

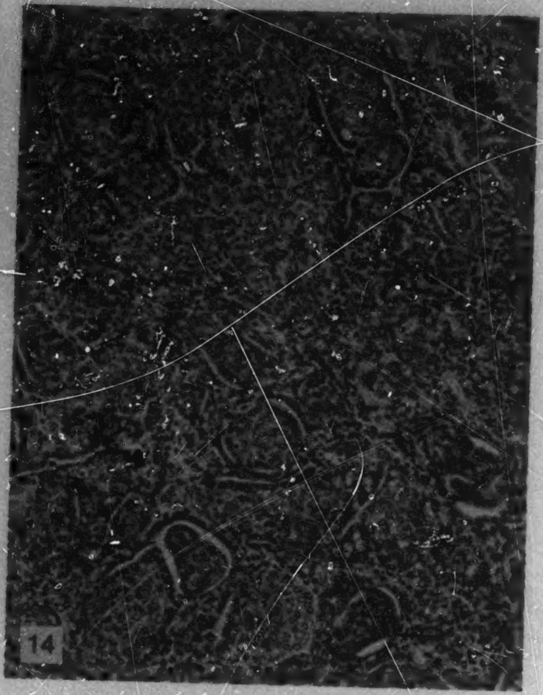

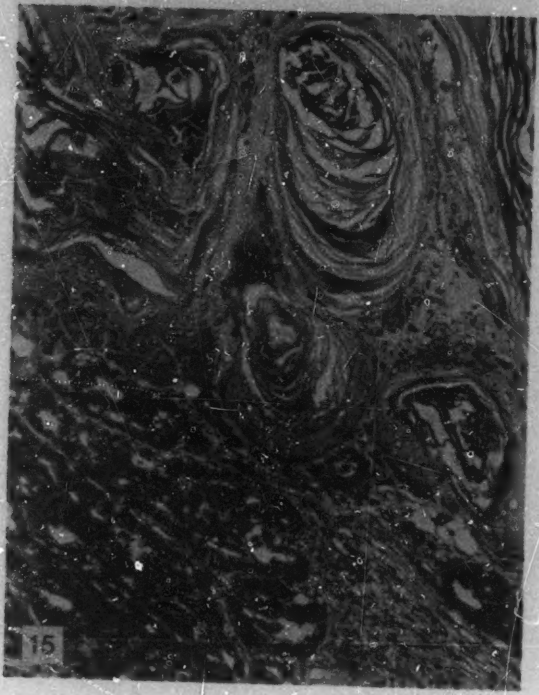

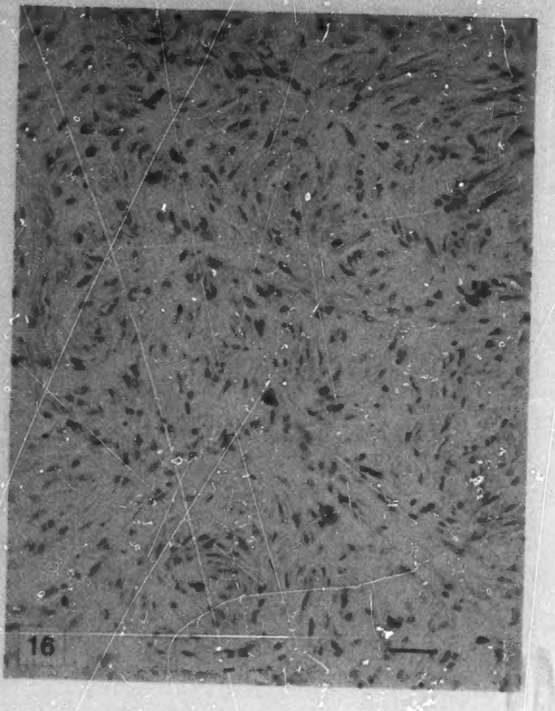

FIGURE 13.—Anaplastic adenocarcinoma of small cell type with nests and sheets of epithelial cells. Area of necrosis, *upper left*. *Bar*=50 µm. × 140

FIGURE 14.—Anaplastic adenocarcinoma of glomerate type. *Note* pronounced glomerate structure and narrow cordlike tubules. *Bar*=50 µm. × 140

FIGURE 15.—Adenoacanthoma with neoplastic acini and keratin pearl formation. *Bar*=50 µm. × 140

FIGURE 16.—Fibroma showing tendency for concentric arrangement of fibers. *Note* numerous mast cells with intensely stained cytoplasm. *Bar*=50 µm. × 140

Induction of Nasal Tumors in Rats Exposed to Hexamethylphosphoramide by Inhalation[1]

Ki P. Lee, *D.V.M., Ph.D.,*[2] *and* **Henry J. Trochimowicz,** *D.Sc.*[2,3]

ABSTRACT—Charles River-CD Sprague-Dawley rats in 4 equal groups of 240 each were exposed to 4,000, 400, 50, and 0 ppb of hexamethylphosphoramide (HMPA) vapor for 9 to 24 months. In an additional study, 4 equal groups of 200 rats were similarly exposed to 100, 50, 10, and 0 ppb HMPA vapor. Nasal tumors were first detected after approximately 7 months exposure at 4,000 and 400 ppb, after 9 months at 100 ppb, and 12 months at 50 ppb. No HMPA-related lesions were found at 10 ppb. Tumor incidence was 83% at 4,000 ppb exposure, 82% at 400 ppb, 38% at 100 ppb, and 20% at 50 ppb after 24 months of exposure. Most tumors developed from the squamous, respiratory epithelium and nasal gland both of which showed squamous metaplasia or dysplasia in the anterior nasal cavity. Exposure concentrations correlated with tumor induction and latency but not with tumor types. Of a total of 473 nasal tumors, epidermoid carcinoma was predominant (71.9%), followed by adenoid squamous carcinoma (15%), papilloma (8.2%), transitional (respiratory epithelial) carcinoma (1.9%), adenocarcinoma (1.3%), and undifferentiated tumor (1.1%), (mixed) pleomorphic tumor (0.4%), and adenomatous polyp (0.2%). Most tumors developed in the anterior nasal cavity (59.1%), then progressed to the posterior nasal cavity (40.9%). Only 0.4% of the tumors involved the posterior nasal cavity alone. Tumors invaded the nasal bone (47.5%) and brain (1.1%), or metastasized to the lung (1.5%) and cervical lymph nodes (1.1%). Malignancy of the epidermoid carcinoma was correlated to the cellular differentiation and degree of keratinization.—JNCI 1982; 68:157–171.

HMPA has been extensively used as a solvent in research laboratories. It has a wide range of uses in industry as a solvent for polymers, as a polymerization catalyst, as a stabilizer against thermal degradation in polystyrene, as an additive to polyvinyl and polyolefin resins, and as a protective agent against degradation by UV light (*1*, *2*). HMPA was one of the first nonalkylating compounds used for the sterilization of male insects (*3*). Because of its low acute toxicity, chemical stability, and solubility in most polar and nonpolar solvents, it has been tested widely as a chemosterilant for insects and other organisms (*4–6*).

HMPA was reported to induce dominant lethality in male mice (*7*). In contrast, no reproducible dominant lethality was seen in mice by other researchers (*8*). HMPA produced mutagenic effects in fruit flies (*9*), whereas studies of the effects of HMPA on human (*10*) and mouse chromosomes (*11*) showed no chromosomal aberrations. HMPA is known to cause a variety of toxic effects on laboratory animals after oral administration such as kidney damage (*12*), severe bronchopneumonia with bronchiectasis and squamous metaplasia (*13–15*), and testicular atrophy (*16*, *17*). Oral administration of HMPA produced synergistic effects on *Mycoplasma pulmonis* and markedly enhanced the incidence of murine pneumonia and rhinitis (*15*). Since the chronic inhalation toxicity of HMPA was unknown, we conducted a series of experiments to determine the toxic effects and carcinogenic potential of HMPA by inhalation.

MATERIALS AND METHODS

Exposure apparatus.—HMPA was delivered by syringe drive into a stainless steel tube extending through a preheated vapor generating furnace. Vapors from the furnace were carried to a 1-liter flask by houseline air at a rate of approximately 20 liters/minute and diluted to 28 liters of air/minute. The mixture then flowed into a delivery line carrying make-up air for the chamber. Make-up air consisted of a 2- to 5-m^3/minute flow of cooled room air, as a final dilution, to achieve the desired atmospheric concentration in a 5-cubic foot chamber. Chamber air temperature was always maintained below 30°C. To monitor chamber atmospheres for HMPA, a minimum of six samples were taken during each 6-hour exposure. To analyze HMPA levels, 4–40 liters of chamber air was drawn through a midget impinger containing deionized water. The solution from the impinger was diluted to a standard volume and analyzed by a wet chemistry method.

Experimental design.—In experiment I a total of 960 young adult outbred Charles River-CD Sprague-Dawley-derived rats was divided into 8 equal groups of 120 males and 120 females. Group 1 male and group 2 female rats were exposed to air and served as controls. In group 3, 60 of the 120 males and in group 4, 60 of the 120 females were exposed to HMPA at a concentration of 50 ppm for 1 year and were placed in holding rooms. The remaining 60 males and 60 females were exposed continuously for 2 years. Group 5 males and group 6 females were exposed to HMPA at a concentration of 400 ppb for 10 months. Group 7

ABBREVIATIONS USED: HMPA = hexamethylphosphoramide; H & E = hematoxylin and eosin; PAS = periodic acid-Schiff.

---

[1] Received June 2, 1981; accepted August 19, 1981.

[2] Haskell Laboratory for Toxicology and Industrial Medicine, E. I. du Pont de Nemours and Company, Inc., Elkton Road, Newark, Del. 19711.

[3] We thank our colleagues in the Pathology Division for technical assistance, Mr. J. W. Sarver for conducting the inhalation exposure, Dr. C. F. Reinhardt for criticism in the preparation of the manuscript, and Miss V. L. McCall for typing the manuscript.

males and group 8 females were exposed at a concentration of 4,000 ppb for 9 months. After 3 months exposure necropsy was performed on 18 rats from each group. In the first 4 groups 6 and 20 rats were killed after 8- and 12-months exposure, respectively. The remaining rats in all groups were killed after a 2-year exposure.

In experiment II 800 young adult Charles River-CD Sprague-Dawley-derived rats were divided into 8 equal groups of 100 males and 100 females. Group 1-A males and group 2-A females were exposed to air and used as controls. Group 3-A male and group 4-A female rats were exposed to HMPA at 50 ppb for 2 years. Group 9 male and group 10 female rats were exposed to HMPA at a concentration of 10 ppb for 2 years. In group 11, 50 of the 100 males and in group 12, 50 of the 100 females were exposed to HMPA at a concentration of 100 ppb for 6 months. The remaining 50 males and 50 females were exposed continuously for 13 months. In groups 3-A male and 4-A female, 20 rats each were killed after a 1-year exposure. All rats were killed at the end of 2-years exposure, and subjected to microscopic examination except group 3-A male and group 4-A female rats. The lungs and tracheas, the thyroid-, pituitary-, and adrenal glands, the testes, and the kidneys were fixed in Bouin's solution; all remaining organs and tissues were fixed in 10% Formalin solution. The noses were fixed in Bouin's solution, decalcified, and three coronal sections from each anterior nasal cavity and two coronal sections from the posterior nasal cavity were prepared for light microscopy. The sections were stained either by H & E, or PAS method, Alcian blue, or by modified trichrome stain.

RESULTS

Tumor Induction

The incidence of nasal tumors is summarized in table [illegible] and shown in text-figure 1. Dose-dependence was observed with tumor incidence and latent period but not with tumor types or malignancy. Higher exposure concentrations produced more tumors with a shorter latent period. Nasal tumors were first detected after 7 months of exposure at 400 ppb and 4,000 ppb, after 9 months at 100 ppb, and after 12 months at 50 ppb. There were no remarkable differences in the tumor incidence, latency, or malignancy between male and female rats. Nasal tumor incidence was 83.3% at 4,000 ppb after 9-months exposure, 82.1% at 400 ppb after 10-months exposure, 19% at 100 ppb after 6-months exposure, 56% at 100 ppb after 13-months exposure, 15.7% at 50 ppb after 12-months exposure, and 25.7% at 50 ppb after 24-months exposure (table 2). A striking finding was that no marked differences in tumor incidence and latency occurred between the 400 and 4,000 ppb exposure levels despite the factor 10 difference in concentration. Fifty percent of the nasal tumors occurred within 10 months at 4,000 ppb exposure, within 12 months at 400 ppb, within 17 months at 100 ppb, and within 21 months at 50 ppb. Cessation of exposure after 1 year at 50 ppb and 6 months at 100 ppb did not completely disrupt tumorigenesis but markedly reduced tumor induction and increased tumor latency (table 2).

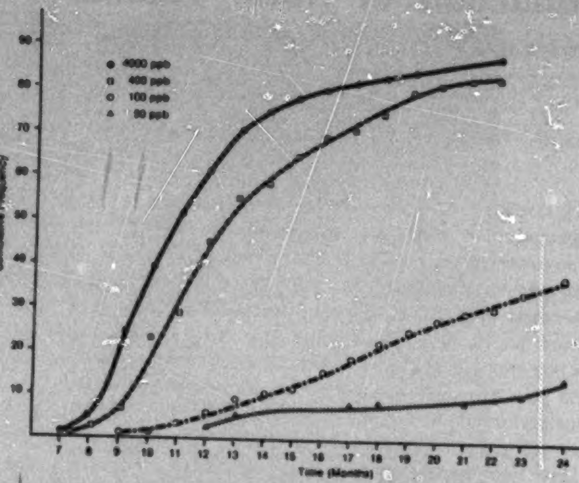

TEXT-FIGURE 1.—HMPA exposure concentrations are correlated with tumor induction. Higher exposure concentrations produced more tumors with shorter latent period. The curves for cumulative frequency of tumor induction at 400 and 4,000 ppb rise steeply up to 13 mo and gradually taper off, while the curves for 100 and 50 ppb rise gradually throughout the 24 mo.

Gross Pathology

In the early stages of tumor development, tiny tumor nodules were often seen at the nasoturbinals and nasal septum in the anterior nasal cavity (fig. 3), but not in the maxillary turbinates or in the ethmoturbinates. The tumor extended toward the posterior nasal cavity and invaded the ethmoturbinates (fig. 4) and occasionally the olfactory bulb of the brain (fig. 5). At the same time, the tumor expanded toward the dorsal nasal bone and bulged out after extensive destruction of the nasal bone (fig. 1). The nasal cavity was almost obstructed by the tumor and its internal structure was obliterated (figs. 2, 4). The gross findings of keratinized epidermoid carcinoma were characterized by tiny papillary projections and accumulation of pale yellow, friable, cheesy material, which was identified as the keratin material under microscopic examination (fig. 4). The cut surface of adenoid squamous carcinomas (fig. 2) and undifferentiated epidermoid carcinomas appeared smooth, moist, pale, and fleshy.

Histopathology

The nasal respiratory epithelium revealed acute inflammation, goblet cell hyperplasia, epithelial degeneration and desquamation, squamous metaplasia, and dysplasia (fig. 8). The dysplastic epithelium revealed loss of polarity, nuclear hyperchromatism, and mitotic activity. The acinar cells of subepithelial gland showed

TABLE 1.—*Incidence of nasal tumor and tumor types of rats exposed to HMPA*

Parameter												No. of tumor type/ No. of total tumors (%)
Group	1, 2	1-A, 2-A	9, 10	3, 4		11, 12		5, 6		7, 8		
Exposure concentration, ppb	0	0	10	50		100		400		4,000		
No. of rats examined	196	200	200	194		200		219		215		
Tumor incidence (%)												
Tumor type												
Papilloma, squamous cell	0	0	0	9	(4.6)	6	(3.0)	13	(5.9)	11	(5.1)	39/473 (8.2)
Adenomatoid polyp	0	0	0	0		1	(0.5)	0		0		1/473 (0.2)
Epidermoid carcinoma	0	0	0	24	(12.4)	59	(29.5)	137	(62.6)	120	(55.8)	340/473 (71.9)
Adenoid squamous carcinoma	0	0	0	4	(2.1)	5	(2.5)	21	(9.6)	41	(19.1)	71/473 (15.0)
Adenocarcinoma	0	0	0	1	(0.5)	1	(0.5)	2	(0.9)	2	(0.9)	6/473 (1.3)
Transitional carcinoma	0	0	0	1	(0.5)	1	(0.5)	3	(1.4)	4	(1.9)	9/473 (1.9)
Undifferentiated carcinoma	0	0	0	0		2	(1.0)	2		1	(0.5)	5/473 (1.1)
Mixed tumors	0	0	0	0		0		2	(0.9)			2/473 (0.4)
Total tumors/group				39/194 (20.1)		75/200 (37.5)		180/219 (82.1)		179/215 (83.3)		

hyperplasia and keratinized squamous metaplasia, which conglomerated with the squamous metaplasia developed from the epithelium. Pathologic lesions were often confined to the respiratory epithelia in the anterior nasal cavity and occasionally occurred in the ethmoturbinates of the posterior nasal cavity. The most striking finding was a massive accumulation of keratin material on the metaplastic respiratory epithelium in the anterior nasal cavity. The olfactory epithelium of the ethmoturbinates often showed squamous metaplasia with acute inflammatory reaction when malignant tumors were present in the anterior nasal cavity.

Typing of Nasal Tumors

Multiple sections of a nasal tumor often revealed mixtures of tumor cells originating from the glandular and epithelial cells. Also, there were mixtures of benign, malignant, and other types of tumors. Tumor typing was determined by the predominant malignant tumor cells when there were more than two different types of tumor cells in the sections. When tumors showed both benign and malignant tumor cells, the tumors were classified by malignant cells. Squamous cell papillomas were mostly exophytic. Inverted endophytic papilloma was relatively rare. Most squamous cell papillomas revealed marked hyperkeratosis, and there was no evidence of tumor invasion beyond the basement membrane (fig. 9). Adenomatous polyps were occasionally found with adenoid squamous carcinomas. The tumor growth was manifested by either invagination or projection with columnar or glandular epithelial lining (fig. 10). The basal membrane was intact with no evidence of tumor invasion into the submucosal layer. Adenocarcinomas (fig. 12) revealed tubular and acinar appearance with anaplasia and invasion. Epidermoid carcinomas were composed of squamous cells showing various degrees of differentiation and pleomorphism. Adenoid squamous carcinomas revealed glandular and and epidermoid structures (figs. 13, 14). The ratio of squamous to glandular cells varied, but in most cases squamous cells were predominant. Tumor cells formed duct-like structures containing PAS-Alcian blue-positive mucoid material. Most tumors were interspersed with cystic spaces forming a cribriform or lace-like pattern and were compatible with the adenoid cystic carcinoma in humans. Transitional papilloma (respiratory epithelial papilloma) consisted of the respiratory epithelial cells, and the basement membrane was intact and continuous with that of the remainder of the normal respiratory epithelium (fig. 11). Transitional carcinoma (respiratory epithelial carcinoma) was invasive and formed ribbon-like bands, and in many areas the tumor revealed intact basement

TABLE 2.—*Summary of nasal tumor incidence in rats exposed to HMPA for different exposure periods*

Group	Exposure concentration, ppb	No. of exposure months	Total No. of rats	Post-exposure month																			Total No. of tumors/ No. of animals examined (%)
				0	1	2	3	4	5	6	7	8	9	10	11	12	13	14	15	16	17	18	
3, 4	50	12	97		1				2	1	1	5	1			1	3						15/95 (15.7)
	50	24	97	19	5																		24/95 (25.7)
11, 12	100	6	100				1			3	1		1	3	2	2	1	2	1			2	19/99 (19)
	100	13	100	7	3	2	7	3	6	3	9	3	2	5	5	1							56/100 (56)

membrane (fig. 16). Pleomorphic (mixed) tumors consisted of glandular, epidermoid, chondroid (fig. 17), or osteoid strucutres (fig. 18). One mixed tumor showing chondroid tissue metastasized to the lung and the cervical lymph nodes (fig. 21). It was difficult to determine the origin of undifferentiated tumors (fig. 19).

Incidence of Tumor Types and Anatomic Sites

Tables 1 and 3 show the incidence of nasal tumor, tumor types, anatomic location of the tumors, tumor invasion, and metastasis. Of a total of 473 nasal tumors, the predominant tumor type was epidermoid carcinoma (71.9%), followed by adenoid squamous carcinoma (15%), squamous cell papilloma (8.2%), transitional carcinoma (1.9%), adenocarcinoma (1.3%), undifferentiated tumor (1.1%), mixed tumor (0.4%), and adenomatous polyp (0.2%). Transitional papillomas occurred with transitional carcinomas. The frequency distribution of the tumor types was similar in all exposed groups and was not related to the exposure concentrations. The incidence of nasal tumors in the anterior nasal cavity was 59%. Only 0.4% of the primary tumors was found in the ethmoturbinals of the posterior nasal cavity. The anterior and posterior nasal cavities contained 41% of the tumors. Most benign tumors were confined to the anterior nasal cavity. The nasal bone was invaded by 48% of all nasal tumors; epidermoid carcinoma incidence in this group was 52.9%, adenoid squamous carcinoma, 52.1%, adenocarcinoma, 33.3%, transitional carcinoma, 11.1%, undifferentiated tumor, 80%, and mixed tumor, 100%. Tumor invasion of the brain (figs. 5, 20) occurred in 1.1% of the total nasal tumors, in 4 of 340 epidermoid carcinomas (1.2%), and in 1 of 71 adenoid squamous carcinomas (1.4%). Tumor metastasis to the lung (figs. 7, 23) was seen in 1.5% of all nasal tumors, in 4 of 340 epidermoid carcinomas (1.2%), and 3 of 71 adenoid squamous carcinomas (4.2%). Of all nasal tumors, 1.1% metastasized to the cervical lymph nodes (figs. 6, 21, 22); 5 of 340 epidermoid carcinomas (1.5%) metastasized to the cervical lymph nodes.

Malignancy of Epidermoid Carcinoma

The epidermoid carcinomas were divided into four grades on the basis of cellular differentiation and degree of keratinization. In grade 1, more than 75% of the tumor cells were differentiated, in grade 2, more than 50% were differentiated, in grade 3, more than 25%, and in grade 4, less than 25%. Grade 1 epidermoid carcinoma consisted mainly of mature squamous cells with intercellular bridges and numerous horn pearls (figs. 15, 24). The tumor still showed some areas of intact basal layer and disorganized basal layer with tumor cell invasion of the submucosa. In grade 2 epidermoid carcinoma, a fairly large number of squamous cells were atypical and keratinization was much less evident than in grade 1. The invading tumor cells were poorly demarcated from the surrounding tissue (fig. 25). Grade 3 epidermoid carcinoma revealed minimal keratinization and the large typical horn pearls almost disappeared. The majority of tumor cells were atypical with a few intercellular bridges and conspicuous mitotic figures (fig. 26). In grade 4, nearly all tumor cells consisted of atypical spindle shaped cells and lacked intercellular bridges and keratinization. The tumors resembled fibrosarcoma, although some areas still showed tiny foci of squamous cells (fig. 27).

Tables 4 and 5 show the incidence of graded epidermoid carcinoma, anatomic location, and tumor invasion to the nasal bone. There were no significant differences in the incidence of graded epidermoid carcinoma among the exposed groups and tumor differentiations were not related to exposure concentrations. Most of the epidermoid carcinomas were well-differentiated and the incidence was 79.4% in grade 1, 11.2% in grade 2, 5.2% in grade 3, and 4.1% in grade 4. The tumor invasion of the nasal bone was clearly related to tumor grades: 46.7% of grade 1, 68.4% of

TABLE 3.—*Anatomic sites of nasal tumor, incidence of nasal bone destruction, and metastasis in rats exposed to HMPA*

Tumor types	Incidence/No. of rats (%)						
	Anatomic location			Tumor invasion		Tumor metastasis	
	Nasal septum, nasoturbinates	Ethmoturbinates	Nasoturbinate, ethmoturbinates	Nasal bone/ tumor type	Brain	Lung	Cervical lymph nodes
Papilloma, squamous cell	37/39 (94.9)		2/39 (5.1)	0/39			
Adenomatous polyp	1/1 (100)						
Epidermoid carcinoma	194/340 (56.61)	2/340 (0.6)	144/340 (42.4)	180/340 (52.9)	4/340 (1.2)	4/340 (1.2)	5/340 (1.5)
Adenoid squamous carcinoma	36/71 (50.7)		35/71 (49.2)	37/71 (52.1)	1/71 (1.4)	3/71 (4.2)	
Adenocarcinoma	3/6 (50)		3/6 (50)	2/6 (33.3)			
Transitional carcinoma	5/9 (55.6)		4/9 (44.5)	1/9 (11.1)			
Undifferentiated carcinoma	3/5 (60)		2/5 (40)	4/5 (80.0)			
Mixed tumors	1/2 (50)		1/2 (50)	2/2 (100)			
Total	279/473 (59.1)	2/473 (0.4)	193/473 (40.9)	224/473 (47.5)	5/473 (1.1)	7/473 (1.5)	5/472 (1.1)

TABLE 4.—*Incidence of epidermoid carcinoma with grades*

Grade of epidermoid carcinoma	Group, exposure concentration, tumor incidence (%)							Total
	1, 2	1-A, 2-A	9, 10	3, 4	11, 12	5, 6	6, 7	
	0	0	0	50 ppb	100 ppb	400 ppb	4,000 ppb	
I	0	0	0	20/24 (83.3)	45/59 (76.3)	106/137 (77.4)	99/120 (82.5)	270/340 (79.4)
II	0	0	0	3/24 (12.5)	7/59 (11.8)	17/137 (12.4)	11/120 (9.2)	38/340 (11.2)
III	0	0	0	1/24 (4.1)	2/59 (3.3)	10/137 (7.2)	5/120 (4.2)	18/340 (5.2)
IV	0	0	0	0/24	5/59 (8.4)	4/137 (2.9)	5/120 (4.2)	14/340 (4.1)

TABLE 5.—*Anatomical location and incidences of nasal bone destruction in a total of 340 graded epidermoid carcinomas*

Tumor grade	Incidence of nasal bone destruction/No. of epidermoid carcinomas (%) at:			Destruction of nasal bone/graded epidermoid carcinoma (%)
	Nasoturbinates, nasal septum	Ethmoturbinate	Nasoturbinates, ethmoturbinate	
I	168/270 (62.2)	2/270 (0.7)	100/270 (37.0)	126/270 (46.7)
II	18/38 (47.3)	0	20/38 (52.6)	26/38 (68.4)
III	4/18 (22.2)	0	14/18 (77.7)	14/18 (77.7)
IV	4/14 (28.5)	0	10/14 (71.4)	14/14 (100.0)
Total	194/340 (57.0)	2/340 (0.58)	144/340 (42.4)	180/340 (52.9)

grade 2, 77.7% of grade 3, and 100% of grade 4 tumors invaded the nasal bone. Also, tumor grades were related to the extensiveness of tumor involvement in the nasal cavity. Tumor invasion in both the anterior and posterior nasal cavity was 37.0% in grade 1, 52.6% in grade 2, 77.7% in grade 3, and 71.4% in grade 4.

DISCUSSION

Nasopharyngeal cancer in humans is a rare cancer in most countries of the world; however, it is a significant cancer problem in East and Southeast Asia. The incidence of nasopharyngeal cancer among Chinese and some Southeast Asian peoples is 10–50 times higher than in the rest of the world. Nasal tumors resulting from occupational exposure have been reported in workers at nickel refineries (*18–20*) and in the furniture (*21, 22*) and shoe industries (*23, 24*). The nasal tumors observed in the furniture industry were mostly adenocarcinomas, while a variety of tumor types were found in shoe factory workers. Tumors in the nickel refinery workers developed predominently in the ethmoid region of the nasal cavity (*22*).

The tumor type, anatomical location, invasiveness, and metastases in the nasal tumors induced by HMPA were similar to those seen in human nasal tumors (*29–40*). These microscopically detected small tumors were exclusively in the anterior region of the nasal cavity, especially in the nasoturbinals and nasal septum. The nasal tumors arose mostly from respiratory epithelium of the anterior nasal cavity and subsequently extended toward the posterior region involving the ethmoturbinals. HMPA-exposure concentrations correlated with carcinogenicity and latency of tumors at the levels of 50, 100, and 400 ppb but there was no remarkable correlation between 400 and 4,000 ppb. We observed that the carcinogenicity and latency are dose-related up to a certain upper threshold for HMPA carcinogenicity, but beyond that limit the dose-response relationship decreases. The decrease in dose-related carcinogenicity is possibly caused by an almost complete saturation of cell receptor sites by HMPA molecules and the subsequent decline in HMPA-reactivity at the receptors. Dose-related carcinogenicity was described for various chemical carcinogens including polycyclic aromatic hydrocarbons, aromatic amine derivatives, alkylating drugs, and alkylnitrosamines (*37*). However, the total cumulative dose necessary for carcinogenesis with small daily doses was smaller than the single dose required to produce an equivalent response (*38, 39*).

A large number of nitrosamine compounds have been known to cause cancers of the nasal cavity in laboratory animals. Diethylnitrosamine produced squamous cell carcinomas, adenocarcinomas, and olfactory neuroepitheliomas in hamsters (*40*). Subsequently, many investigators have reported that squamous cell carcinomas, adenocarcinomas, and esthesioneuroepitheliomas were induced by a wide variety of nitrosamines (*41*). Carcinomas originating from the olfactor epithelium in the posterior nasal cavity were induced in hamsters by nitroso-compounds (*42*). The adenocarcinomas and undifferentiated carcinomas were mostly induced in the posterior region of the nasal cavity in hamsters by subcutaneous injection with methyl-*n*-propylnitrosamine (*43*) or by intratracheal instillation with dimethylnitrosamine (*40*). The anatomic sites and tumor types produced by nitroso-compounds differ from those of HMPA-induced nasal tumors. A striking trait of nitroso-compounds is their strong organotropism for certain target organs which resulted in tumors in more than one organ by subcutaneous injection or oral administration. In contrast, there was no carcinogenic effect in the rats fed HMPA for 2 years (*44*). The animal experiments suggest that nitrosoamines not only have a local carcinogenic effect but are also transported in the bloodstream to the nasal cavity where they are excreted or metabolized into carcinogens. The administration of large doses of nitroso-compounds produced high multiplicity of neoplasms with short survival times and tumor latency (*45–48*). The low dose of di-*n*-propylnitrosoamine produced mostly benign epidermoid-, or mucoepidermoid tumors and polyps, whereas the highest dose also induced carcinomas in the posterior region of nasoturbinals and ethmoturbinals (*49*). In contrast, there were no remarkable differences in tumor types between the low and high dose groups of rats exposed to HMPA.

The following industrial chemicals have been known to cause nasal tumors in experimental animals: phenyl glycidyl ether (*50*), 1,4-dichlorobutene-2 (*51*), 1,2-dibromo-3-chloropropane (*52*), dimethylcarbamoyl chloride (*53*), epichlorohydrin (*54*), chloromethyl methylether (*55*), bis(chloromethyl)ether (*56*), hydrogen chloride and formaldehyde (*57, 58*), 1,4-dioxane (*59, 60*), dimethyl sulfate (*61*), quinoxaline 1,4-dioxide (*62*), and 1,2-dibromoethane (*63*). An important question to consider is how to extrapolate the HMPA-produced nasal tumors of rats to humans. In spite of many years of occupational or environmental exposure of man to some of these chemicals, we found no epidemiological studies indicating potential carcinogenic hazard to man by those industrial chemicals that are specific in causing only nasal tumors in animals. Human risk in HMPA-exposure can be better assessed by conducting extensive epidemiological studies in man. Workers exposed to chloromethyl methyl ether were shown to have an eight times higher than expected incidence of lung cancers and tumors, mainly of the oat cell type (*64*). Other studies have implicated lung cancers as the cause of death in workers exposed to bis(chloromethyl)-ether (*65, 66*). However, these two industrial chemicals have produced not only nasal tumors but also lung cancers in experimental animals.

Remarkable organotropism and carcinogenic effect on the nasal cavity were found in rats administered 1,4-dioxane in drinking water (*39, 40*) or by sc injection of dimethyl sulfate (*61*). Squamous cell carcinomas were induced mainly in the anterior nasal cavity of the animals exposed to phenyl glycidyl ether, 1,4-dichlorobutene-2, formaldehyde, 1,4-dioxane, and epichlorohydrin, whereas 1,2-dibromoethane produced predominantly adenomatous polyps and adenocarcinomas. In contrast, chloromethyl methyl ether and bis(chloromethyl) ether induced neurogenic carcinoma, mainly esthesioneuroepitheliomas in the posterior nasal cavity.

The toxic effects of HMPA-inhalation were sharply limited to the upper respiratory air passages, decreasing markedly in lower air passages without any effects on alveolar walls. Generally, the sites of toxic effects from most gases and fumes are dependent upon their water solubility and irritability. Highly water soluble substances (ammonia and hydrogen chloride) are absorbed into the mucous membrane contacted first, specifically in the nose and upper respiratory passages. In contrast, slightly water soluble substances (oxides of nitrogen, chlorine and phosgene) exert their toxic effects throughout the lower respiratory tracts and alveolar walls. Since HMPA is water soluble, its inhaled vapor appears to be absorbed mostly at the respiratory epithelium of the anterior nasal cavity, failing to provoke tissue response in the lower respiratory passages and alveoli.

In comparison with the nasal cavity of humans, the entrance and the exit of the nasal cavity of the rat are narrower, the nasal cavity is markedly longer, and the Jacobson's organ is larger. Another peculiarity of the rat is broad communication between the right and left nasal airway through the nasal septum at the posterior nasal cavity. The ethmoturbinates of the rat form complicated interdigitated structures that easily block drainage of inflammatory exudate and air passage. After exposure to HMPA, the interspaces between the ethmoturbinates were packed with inflammatory exudate when the anterior nasal cavity was occupied by the tumor mass. There are marked differences in patterns of respiration between the rat and man. The rat is an obligatory nose breather, and has a greater surface area-to-volume ratio of the upper respiratory tract than man (*67*). Because of these physioanatomical differences, the nasal cavity of the rat may be more susceptible to irritants and may develop more severe pathological changes than man when exposed to equal concentrations per body weight of irritants for equal amounts of time.

Compared to man, the rat has an approximately eight times higher pulmonary ventilation rate in terms of liters of air per minute per kilogram body weight. Therefore, rats can receive a higher net effective dose of HMPA for any given concentration and duration of exposure. Air flow patterns during respiration in rats permit incoming and outgoing air to directly contact the anterior-ventral region of the nasal cavity (*18*). Due to this unique air flow pattern, HMPA vapors are in constant contact with the anterior-ventral region of the nasal cavity during exposure. Inflammation and squamous metaplasia or dysplasia were often observed with nasal tumors in the respiratory epithelium of the rat's anterior-ventral nasal cavity. The fact that the epithelial surface of the nasoturbinals is larger than that of the maxilloturbinals should explain the higher incidence of nasal tumors in the nasoturbinates. The destruction of ventral nasal bones by tumor invasion is related to the preponderance of the nasal tumors in the nasoturbinates.

REFERENCES

(*1*) National Institute for Occupational Safety and Health. Background information on hexamethylphosphoric triamide. Rockville, Md.: U.S. Department of Health, Education, and Welfare. 1975.

(*2*) ROBERT L. Proprietes et emploi de l'hexaméthylphosphorotriamide. Chim Ind Gén Chim 1967; 97:337–345.

(*3*) CHANG SC, TERRY PH, BORKOVEC AB. Insect chemosterilants with low toxicity for mammals. Science 1964; 144:57-58.

(4) Jackson H, Craig AW. Antifertility action and metabolism of hexamethylphosphoramide. Nature 1966; 212:86-87.

(5) Jackson H, Davies P, Bock M. Chemosterilization of *Schistosoma mansoni*. Nature 1968; 218:977.

(6) LaBrecque GC, Meifert DW. Control of house flies (*Diptera: Muscidae*) in poultry houses with chemosterilants. J Med Entom 1966; 3:323-326.

(7) Srám RJ, Beneš V, Zudová Z. Induction of dominant lethals in mice by TEPA and HEMPA. Folia Biol (Praha) 1970; 16:407-415.

(8) Epstein AS, Arnold E, Andrea J, Bass W, Bishop Y. Detection of chemical mutagens by the dominant lethal assay in the mouse. Toxicol Appl Pharmacol 1972; 23:288-325.

(9) Beneš V, Srám RJ. Mutagenic activity of some pesticides in *Drosophila melanogaster*. Ind. Med Surg 1969; 38:442-444.

(10) Chang TH, Klassen W. Comparative effects on tretamine, tepa, aphlate and their structural analogs on human chromosomes in vitro. Chromosoma 1968; 24:314-323.

(11) Manna GK, Das PK. Effect of two chemosterilants aphola and hempa on the bone-marrow chromosomes of mice. Can J Genet Cytol 1973; 15:451-459.

(12) Shott LD, Borkovec AB, Knapp WA. Toxicology of hexamethylphosphoric triamide in rats and rabbits. Toxicol Appl Pharmacol 1971; 18:499-506.

(13) Kimbrough RD, Gaines TB. Toxicity of hexamethylphosphoramide in rats. Nature 1966; 211:146-147.

(14) Kimbrough RD, Sedlak VA. Lung morphology in rats treated with hexamethylphosphoramide. Toxicol Appl Pharmacol 1968; 12:60-67.

(15) Overcash RG, Lindsey JR, Cassell GH, Baker HJ. Enhancement of natural and experimental respiratory mycoplasmosis in rats by hexamethylphosphoramide. Am J Pathol 1976; 82: 171-186.

(16) Jackson H, Jones AR, Cooper ER. Effects of hexamethylphosphoramide on rat spermatogenesis and fertility. J Reprod Fertil 1969; 20:263-269.

(17) Sherman M, Herrick RR. Acute toxicity of five insect chemosterilants, hemel, hempa, tepa, metepa, and methotrexate, for cockerels. Toxicol Appl Pharmacol 1970; 16:100-107.

(18) Ballenger JJ. Disease of the nose, throat and ear. Philadelphia: Lea & Febiger, 1969.

(19) Konetzke GW. The carcinogenic action of arsenic and nickel. Arch Geschwulstforsch 1969; 44:16-22.

(20) Pedersen E, Hogetviet AC, Andersen A. Cancer of respiratory organs among workers at a nickel refinery in Norway. Int J Cancer 1973; 12:32-41.

(21) Mosbech J, Acheson ED. Nasal cancer in furniture makers in Denmark. Dan Med Bull 1971; 19:34-35.

(22) Formbeur JP. Recent cases of ethmoid-maxillary tumors in wood-workers. Arch Mal Prof Med Trav Secur Soc 1972; 33: 453-455.

(23) Hadfield EH. Cancer hazard from wood dust and in the boot and shoe industry. Ann Occup Hyg 1972; 15:39-41.

(24) Acheson ED. Nasal cancer in the furniture and boot and shoe manufacturing industries. Prev Med 1976; 5:295-315.

(25) Batsakis JG. Tumors of the head and neck. Clinical and pathological considerations. Baltimore: Williams & Wilkins, 1974: 112-122.

(26) Badib AO, Kurohara SS, Webster JH, Shedd DP. Treatment of cancer of the nasal cavity. Am J Roentgenol Radium Ther Nucl Med 1969; 106:824-830.

(27) Fletcher GH, Chau PM. Paranasal sinuses and nasal cavity. In: McComb WS, Fletcher GH, eds. Cancer of the head and neck. Baltimore: Williams & Wilkins, 1967.

(28) Deutsch HJ. Carcinoma of the nasal septum: Report of a case and review of the literature. Ann Otol Rhinol Laryngol 1966; 75:1049-1057.

(29) Larsson LG, Martensson G. Maxillary antral cancers. JAMA 1972; 219:342-345.

(30) Hara JH. Malignant tumors of the paranasal sinuses. West J Surg 1955; 63:348-354.

(31) Fitz-Hugh GS, Gorman JB. Cancer of the nasal accessory sinuses. South Med J 1960; 53:155-161.

(32) Osborn DA, Winston P. Carcinoma of the paranasal sinuses. J Laryngol 1961; 75:387-405.

(33) Weaver DF. Low grade cancer of the ethmoid sinus. Laryngoscope 1959; 69:284-296.

(34) Marchetta FC, Sako K, Mattick WL, Stinziano GD. Squamous cell carcinoma of the maxillary antrum. Am J Surg 1969; 118:805-807.

(35) Windeyer BW. Malignant tumours of the upper jaw. Br J Radiol 1943; 16:362-366.

(36) Chaudhry AP, Gorlin RJ, Mosser DG. Carcinoma of the antrum: A clinical and histopathologic study. Oral Surg 1960; 13:269-281.

(37) Arcos JC, Argus MF. Molecular geometry and carcinogenic activity of aromatic compounds. New perspectives. Adv Cancer Res 1968; 11:305-471.

(38) Weisburger JH. Chemical carcinogenesis. In: Casarett LJ, Doull J, eds. Toxicology. New York and Toronto: MacMillan,

(39) Schramel P. Comments on the question of threshold values for chemical carcinogens. In: Minutes of the meeting on scientific basis for establishment of threshold levels and dose response relationships of carcinogens. Vienna: International Atomic Energy Agency, December 2-3, 1975.

(40) Herrold KM, Dunham LJ. Induction of tumors in the Syrian hamsters with diethylnitrosamine (*N*-nitrosodiethylamine). Cancer Res 1963; 23:773-777.

(41) Thomas C. Zur Morphologie der Nasenhöhlentumoren bei der Ratte. Z Krebsforsch 1965; 67:1-10.

(42) Pour P, Cardesa A, Althoff J, Mohr U. Tumorigenesis in the nasal olfactory region of Syrian golden hamsters as a result of di-*n*-propylnitrosamine and related compounds. Cancer Res 1974; 34:16-26.

(43) Pour P, Krüger FW, Cardesa A, Althoff J, Mohr U. Tumorigenicity of methyl-*n*-propylnitrosamine in Syrian golden hamsters. J Natl Cancer Inst 1974; 52:457-462.

(44) Kimbrough RD, Gaines TB. The chronic toxicity of hexamethylphosphoramide in rats. Bull Environ Contam Toxicol 1973; 10:225-226.

(45) Herrold KM. Effect of route of administration of the carcinogenic action of diethylnitrosamine (*N*-nitrosodiethylamine). Br J Cancer 1964; 18:763-767.

(46) Montesano R, Saffiotti U. Carcinogenic response of the respiratory tract of Syrian golden hamsters to different doses of diethylnitrosamine. Cancer Res 1968; 28:2197-2210.

(47) Althoff J, Krüger FW, Mohr U, Schmahl D. Dibutylnitrosamine carcinogenesis in Syrian golden and Chinese hamsters. Proc Soc Exp Biol Med 1971; 136:168-173.

(48) Althoff J, Cardesa A, Pour P, Mohr U. Carcinogenic effect of *N*-nitrosohexamethylenimine in Syrian golden hamsters. J Natl Cancer Inst 1973; 50:323-329.

(49) Pour P, Krüger FW, Cardesa A, Althoff J, Mohr U. Carcinogenic effect of di-*n*-propylnitrosamine in Syrian hamsters. J Natl Cancer Inst 1973; 51:1019-1027.

(50) Chemical Regulation Reporter. Phenylglycidyl ether. 1979; 3(31): 1336.

(51) ———. Dichlorobutene. 1979; 3(31):1324.

(52) Reznik G, Reznik-Schüller H, Ward JM, Stinson SF. Morphology of nasal-cavity tumours in rats after chronic inhalation of 1,2-dibromo-3-chloropropane. Br J Cancer 1980; 42: 772-781.

(53) National Institute for Occupational Safety and Health. Current Intelligence. Dimethylcarbamoyl chloride. Bulletin No. 11, July 1976.

(54) ———. Current Intelligence. Epichlorohydrin. Bulletin No. 30, 1978.

(55) Laskin S, Drew RT, Cappiello V, Kuschner M, Nelson N. Inhalation carcinogenicity of alpha halo ethers. II. Chronic inhalation studies with chloromethyl ether. Arch Environ Health 1975; 30:70-72.

(56) Kuschner M, Laskin S, Drew RT, Cappiello V, Nelson N. Inhalation carcinogenicity of alpha halo ethers. III. Lifetime and limited period inhalation studies with bis(chloromethyl) ether at 0.1 ppm. Arch Environ Health 1975; 30:73-77.

(57) Sellakumar AR, Albert RE, Rusch GM, Katz GV, Nelson N, Kuschner M. Inhalation carcinogenicity of formaldehyde and hydrogen chloride in rats. Proc Am Assoc Cancer Res 1980; 21:106.

(58) Swenberg JA, Kerns WD, Mitchell RI, Gralla EJ, Pavkov KL. Induction of squamous cell carcinomas of the rats' nasal cavity by inhalation exposure to formaldehyde vapor. Cancer Res 1980; 40:3398-3401.

(59) Hoch-Ligeti C, Argus MF, Arcos JC. Induction of carcinomas in the nasal cavity of rats by dioxane. Br J Cancer 1970; 24: 164-170.

(60) Kociba RJ, McCollister SB, Park C, Torkelson TR. 1,4-Dioxane. I. Results of a two-year ingestion study in rats. Toxicol Appl Pharmacol 1974; 30:275-286.

(61) Druckrey H, Kruse H, Preussmann R, Ivankovic S, Landshutz C. Cancerogene alkylierende Substanzen. 3. Alkyl-halogenide, -sulfate, -sulfonate und ringgespannte Heterocyclen. Z Krebsforsch 1970; 74:241-273.

(62) Tucker MJ. Carcinogenic action of quinoxaline 1,4-dioxide in rats. J Natl Cancer Inst 1975; 55:137-145.

(63) National Institutes of Health, U.S. Department of Health and Human Services. Bioassay of 1,2-dibromoethane for possible carcinogenicity (inhalation study). Washington, D.C.: [DHHS publication No. (NIH)80-1766].

(64) Figueroa GW, Raszkowski R, Weiss W. Lung cancer in chloromethyl methyl ether workers. N Engl J Med 1973; 288: 1094-1096.

(65) Fishbein G, ed. Occupational Safety and Health Letter, March 22, 1972; 2:1.

(66) Sakabe H. Lung cancer due to exposure to bis(chloromethyl)-ether. Ind Health 1973; 11:145-148.

(67) Hatch TF, Gross P. Experimental studies on deposition of inhaled aerosols. In: Pulmonary deposition and retention of inhaled aerosols. New York: Academic Press, 1964:45-68.

Figure 1.—Dorsal surface of the nose is rounded due to bulging nasal tumor on the nasal bone.

Figure 2.—Cut surface of the nasal tumor shown in fig. 1. Architecture of nasal cavity is extensively obliterated by the tumor and the ethmoturbinates (E) are replaced with tumor extending from the anterior nasal cavity. (T) tongue, (C) cranial cavity, (h) hard palate.

Figure 3.—Sagittal section of the nasal cavity shows papillary tumor growth (P) in the nasoturbinate and nasal septum (S) at the anterior nasal cavity. (T) incisor tooth.

Figure 4.—Serial cross-section of the nasal cavity illustrates the tumor (*asterisks*) in the right nasal cavity throughout anterior and posterior region. Nasoturbinate and ethmoturbinate are almost completely obliterated by the tumor.

Figure 5.—Olfactory bulb and anterior region of brain are replaced with the invading nasal tumor (T) from the ethmoturbinate in the posterior nasal cavity.

Figure 6.—Markedly enlarged cervical lymph node (L), due to metastatic tumor from the nasal cavity. (S) salivary gland.

Figure 7.—Numerous metastatic tumor nodules (*arrows*) in lung, varying in size in the pleural surface.

Figure 8.—Squamous metaplasia (S), dysplasia (D), and normal respiratory epithelium (E) in the nasoturbinate. *Note* diffuse dense infiltration of acute inflammatory cells in the nasoturbinate and acute inflammatory exudate in the nasal cavity. H & E. × 100

Figure 9.—Squamous cell papilloma. *Note* long papillary projections (P) of epidermoid cells with massive keratin (K) accumulation. The basement membrane (*arrows*) is intact with no evidence of tumor invasion into the submucosa. H & E. × 100

Figure 10.—Adenomatous polyp. Polypoid protrusion consists of glandular structure showing cystic acini filled with eosinophilic secretion (S). H & E. × 100

Figure 11.—Transitional papilloma (respiratory epithelial papilloma) consists of columnar respiratory epithelium (E). *Note* a folded junction (*arrow*) between normal ciliated respiratory epithelium (R) and papillary projection. H & E. × 250

Figure 12.—Nasal bone (B) is invaded by adenocarcinoma showing acinar structure with eosinophilic secretion (S). H & E. × 250

Figure 13.—Adenoid squamous carcinoma shows a mixture of epidermoid (*large arrows*) and glandular structures showing acini with secreting material (*small arrows*). H & E. × 250

Figure 14.—Adenoid squamous carcinoma with PAS-positive secretion in the glandular acini (*arrows*) under intact respiratory epithelium (E). Adjacent epithelium shows epidermoid carcinoma (C). PAS. × 250

Figure 15.—Cross section of the anterior nasal cavity shows large epidermoid carcinoma bulged out on the destroyed nasal bone. *Note* the tumor involvement in the nasoturbinate (N). (B) nasal bone, (S) nasal septum, (M) maxilloturbinate, (P) pulp of incisor tooth, (J) Jacobson's organ, and (L) nasolacrimal duct. H & E. × 6.2

Figure 16.—Transitional carcinoma (respiratory epithelial carcinoma) consists of anaplastic respiratory epithelial cells with numerous mitotic figures (*arrows*). H & E. × 250

Figure 17.—Pleomorphic tumor (mixed tumor) shows the anaplastic chondroid (C) and epidermoid (E) cells. The chondrocytes reveal irregular sizes and shapes and disorderly cellular arrangement. H & E. × 250

Figure 18.—Pleomorphic tumor (mixed tumor) reveals numerous giant cells (*arrows*), osteoid (O) and undifferentiated spindle-shaped squamous cells (S). H & E. × 100

Figure 19.—Undifferentiated tumor shows large, anaplastic, bizarre giant cells H & E. × 250

Figure 20.—Epidermoid carcinoma (E) invading the olfactory bulb (O). *Note* absence of keratinization in the tumor cells showing intercellular spaces, hyperchromatic nuclei, and distinct nucleoli. H & E. × 250

Figure 21.—Metastatic pleomorphic tumor (mixed tumor) in the cervical lymph node. *Note* chondroid (C) tissue showing irregularly arranged chondrocytes in the lymphoid tissue (L). H & E. × 250

Figure 22.—Metastatic epidermoid carcinoma in the cervical lymph node. Cystic spaces (S) are filled with laminated keratin, denuded cells, and cellular debris. Wall of cysts is lined with well-differentiated epidermoid cells. (L) lymphoid tissue. H & E. × 100

Figure 23.—Metastatic epidermoid carcinoma in the lung. Tumor (T) compresses adjacent alveolar walls and forms slit-like air spaces. (A) alveolar air space. H & E. × 100

Figure 24.—Epidermoid carcinoma, grade 1. Tumor cells consist of mature squamous cells showing intercellular spaces with bridges, marked keratinization, keratin pearls (P), and disrupted basement membrane. H & E. × 450

Figure 25.—Epidermoid carcinoma, grade 2. Large number of squamous cells are atypical and disorganized (*arrows*) with acute inflammatory cell infiltration. Squamous cells show clear intercellular spaces with bridges (*slender arrow*) and scanty keratinization (K). H & E. × 450

Figure 26.—Epidermoid carcinoma, grade 3. The tumor consists of admixture of epidermoid cells (E) and spindle-shaped cells (S) with mitotic figures (*small arrows*). *Note* transition (*large arrows*) from epidermoid to spindle cells. H & E. × 450

Figure 27.—Epidermoid carcinoma, grade 4. Majority of tumor cells are spindle-shaped cells with hyperchromatic nuclei and numerous mitotic figures (*arrows*) resembling fibrosarcoma. H & E. × 450

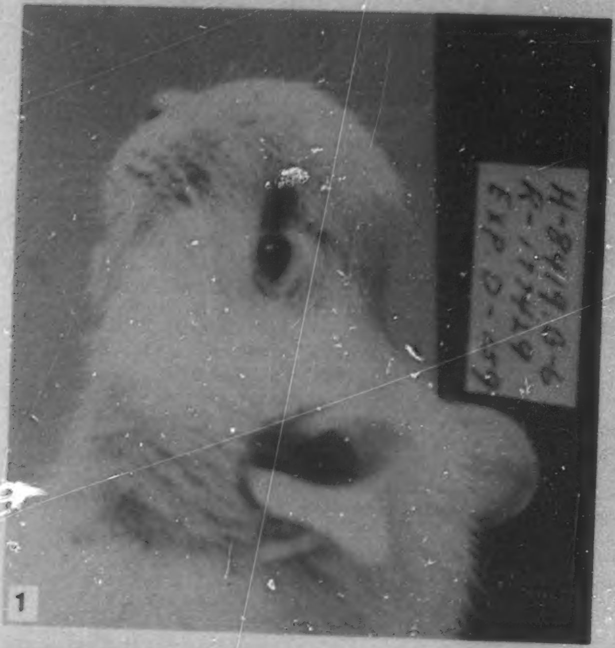
H-84113-6-a
R-17429
EXP 0-259
1

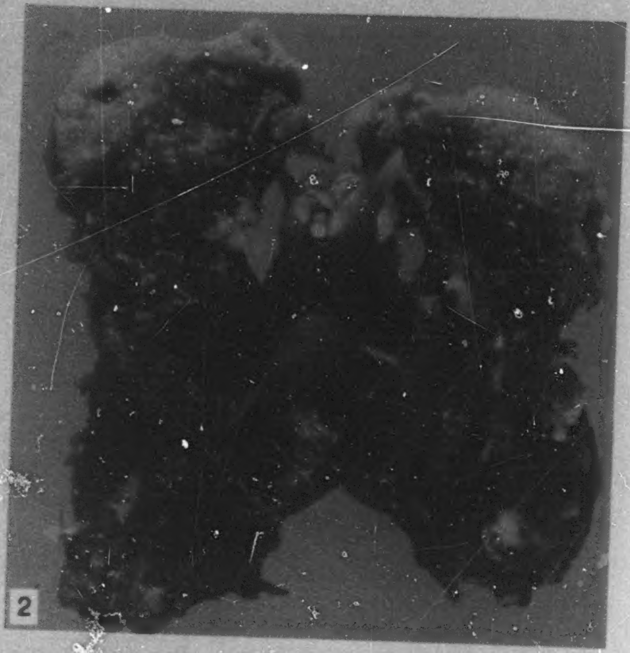
2

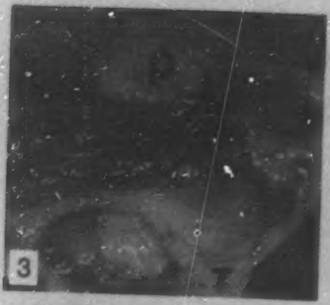
3

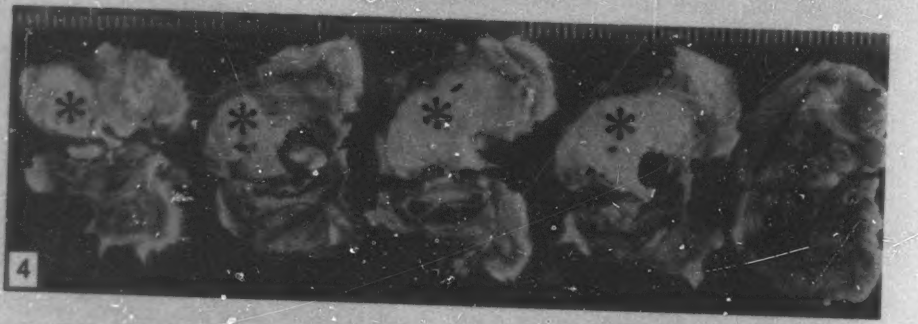
*
*
*
*
4

5

6

7

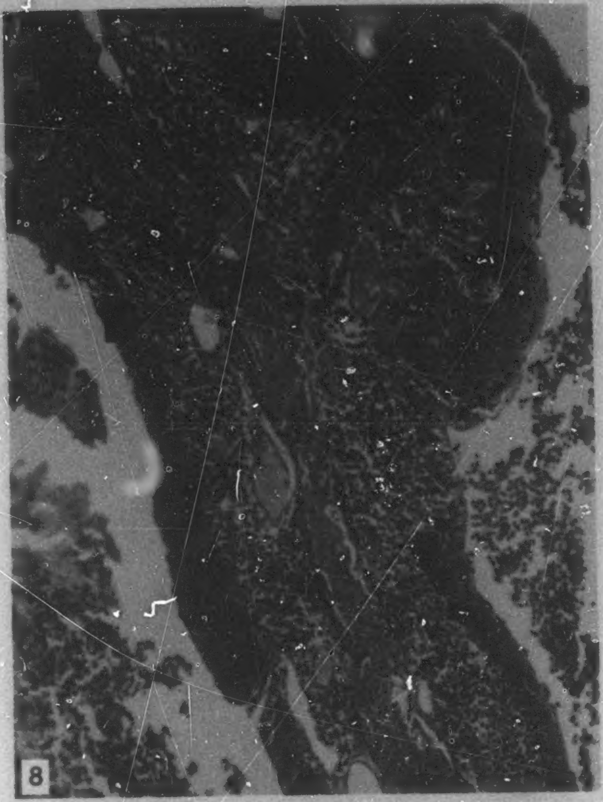

8

9

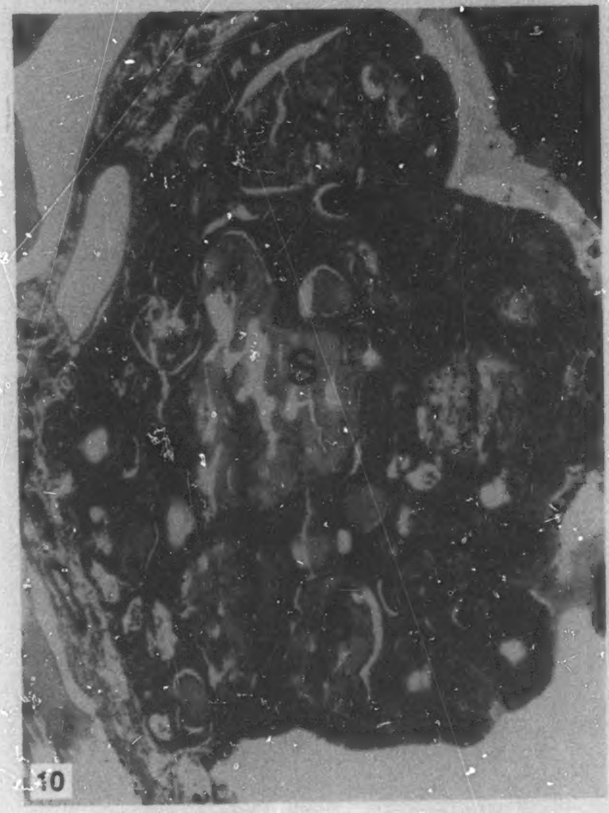

10

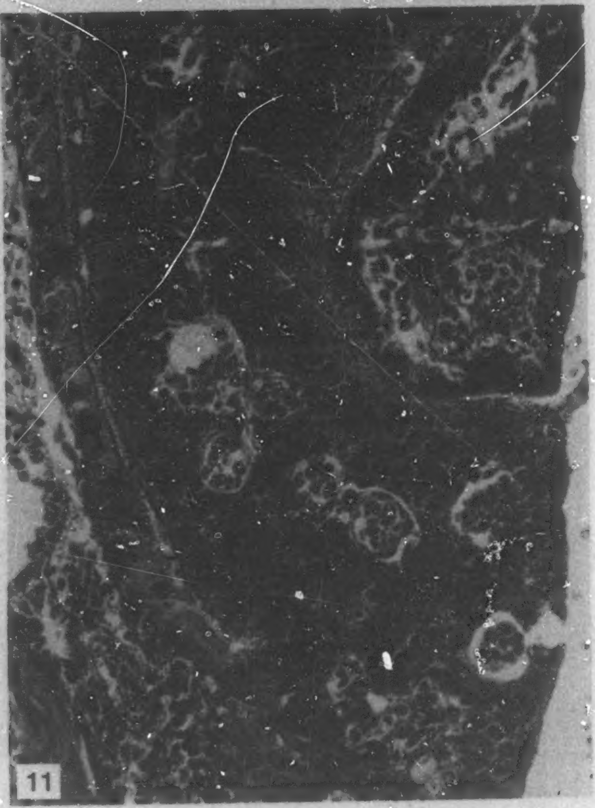

11

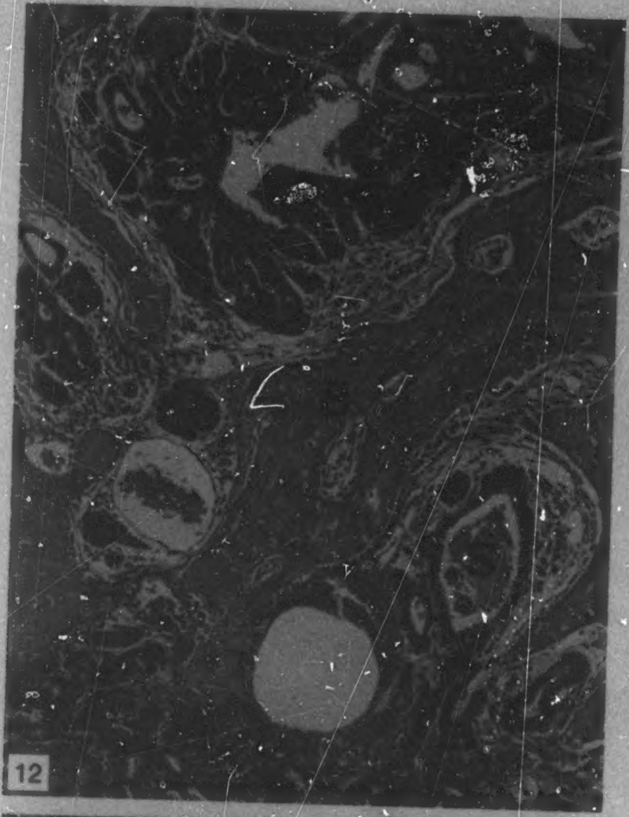

12

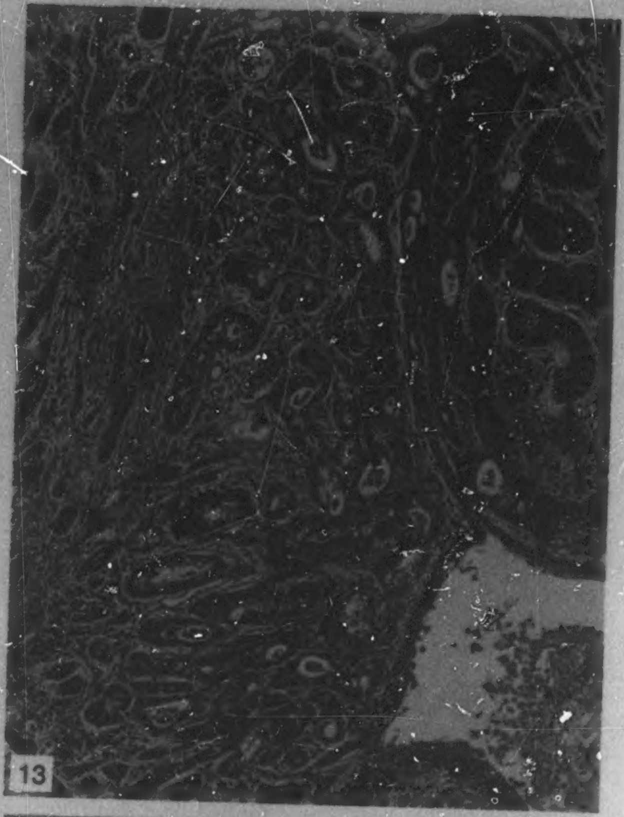

13

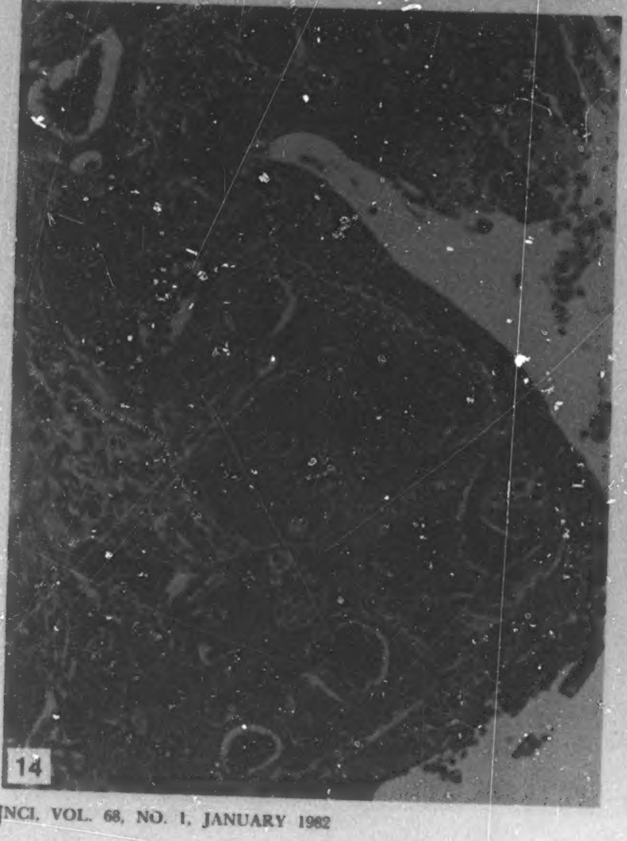

14

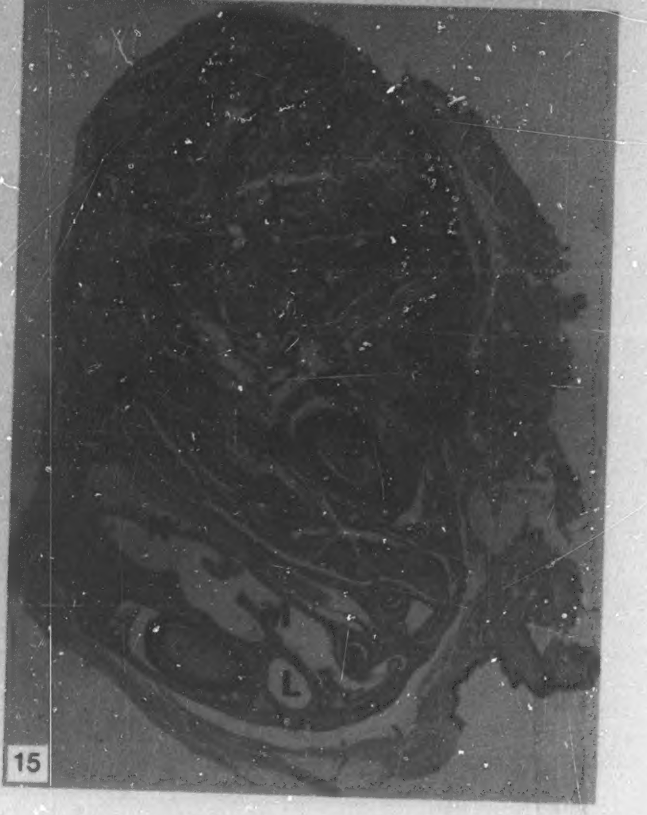

15

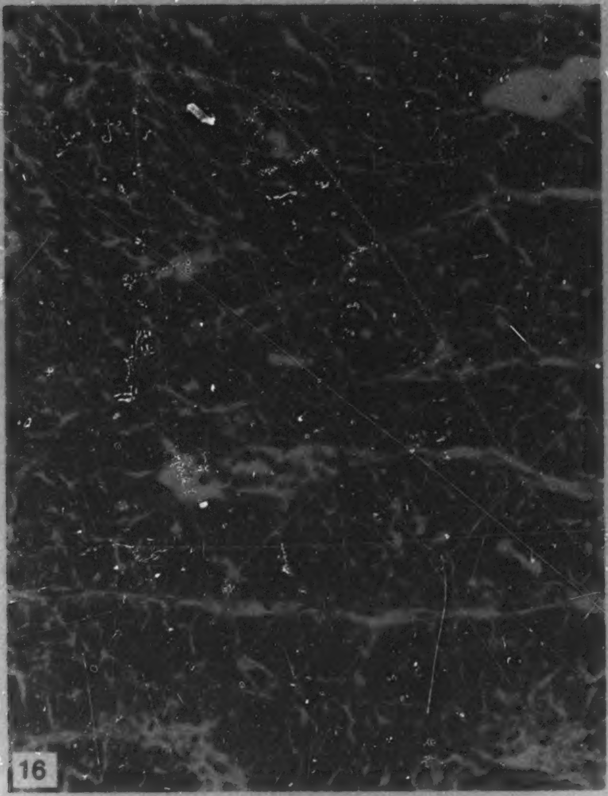

16

17

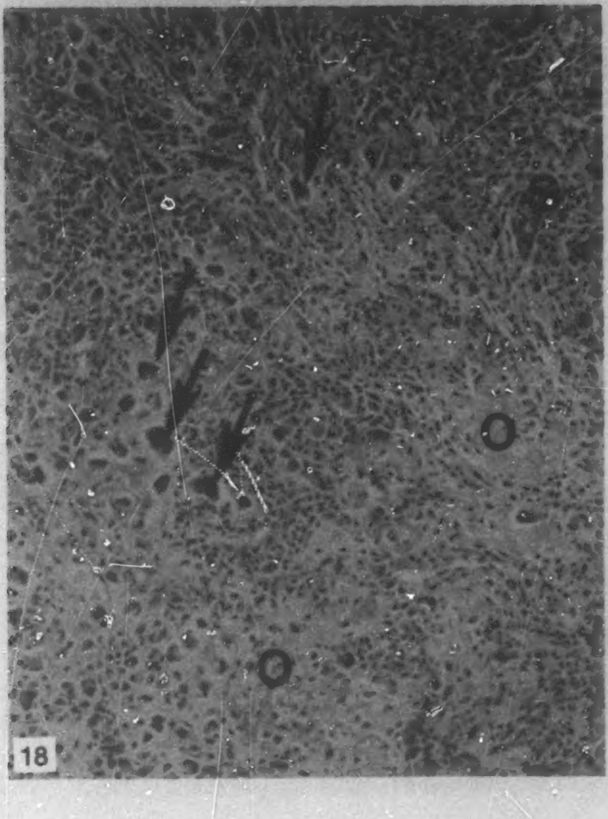

18

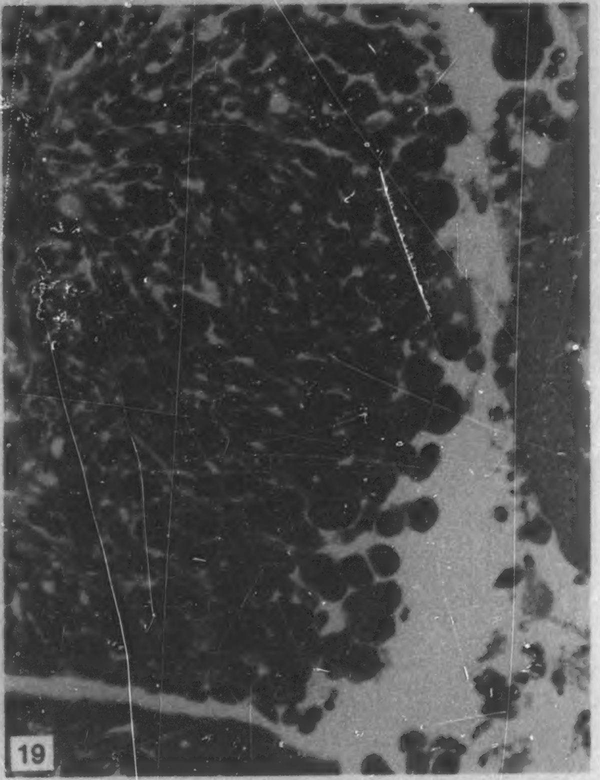

19

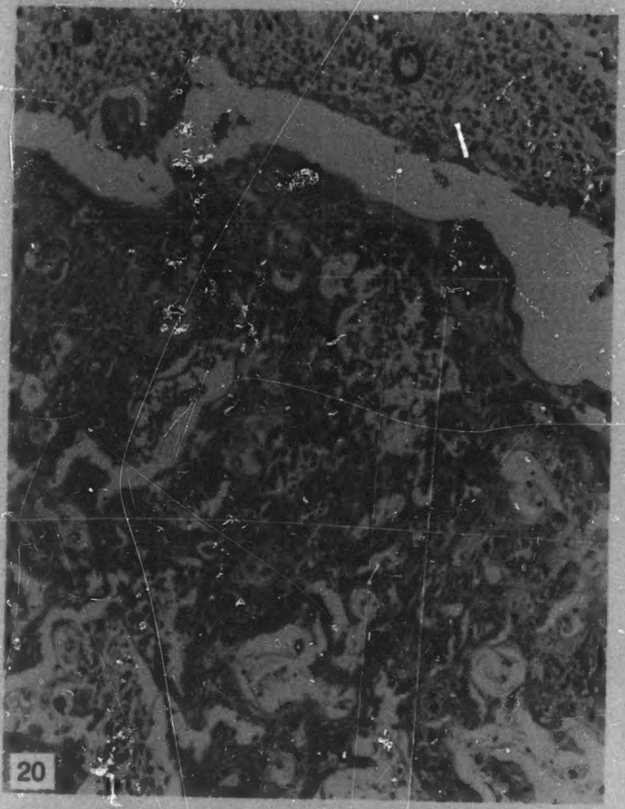

20

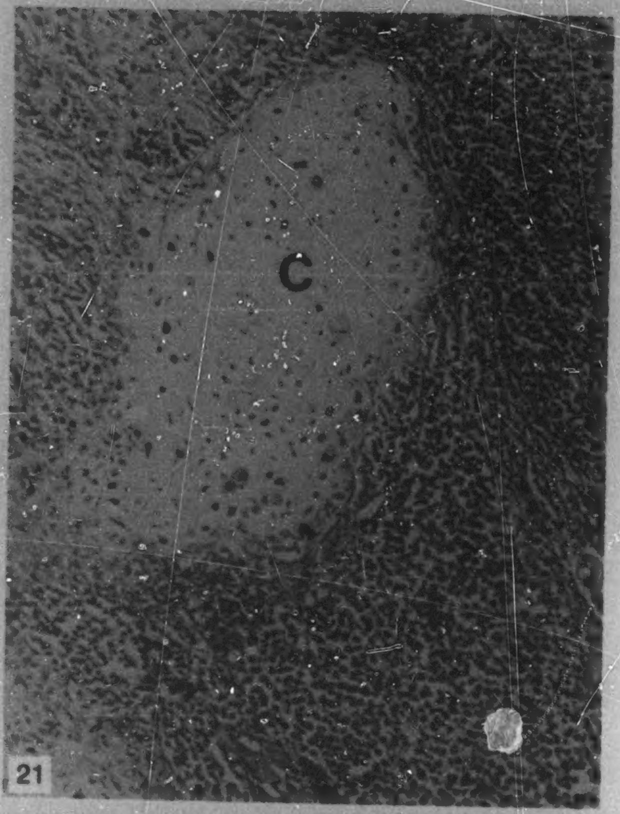

21

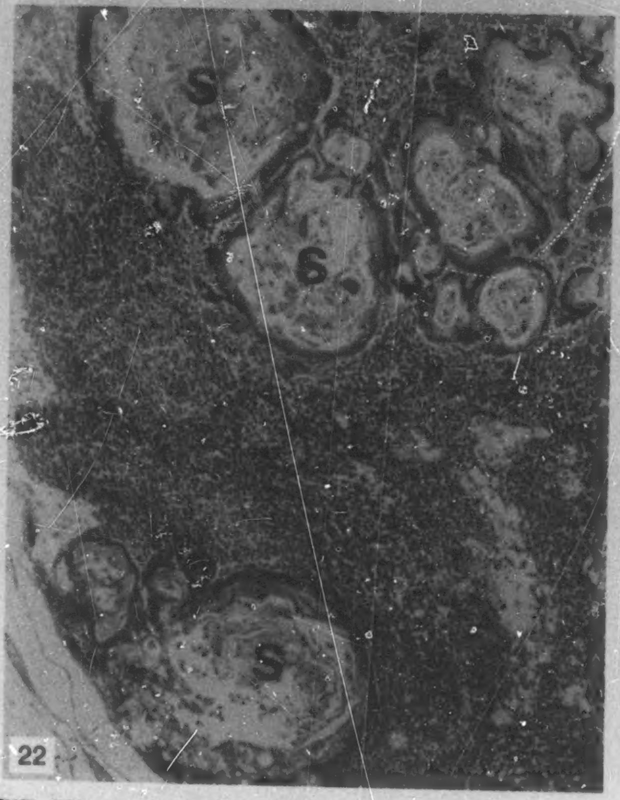

22

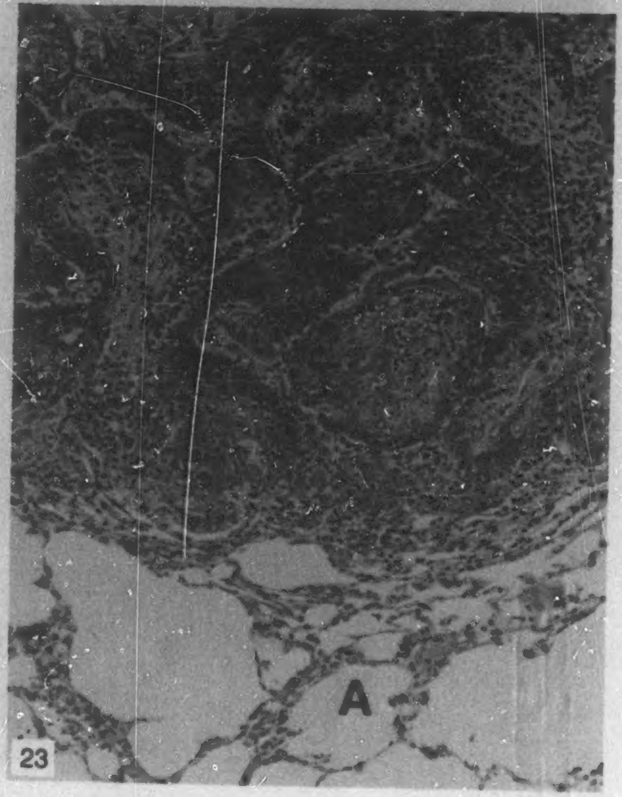

23

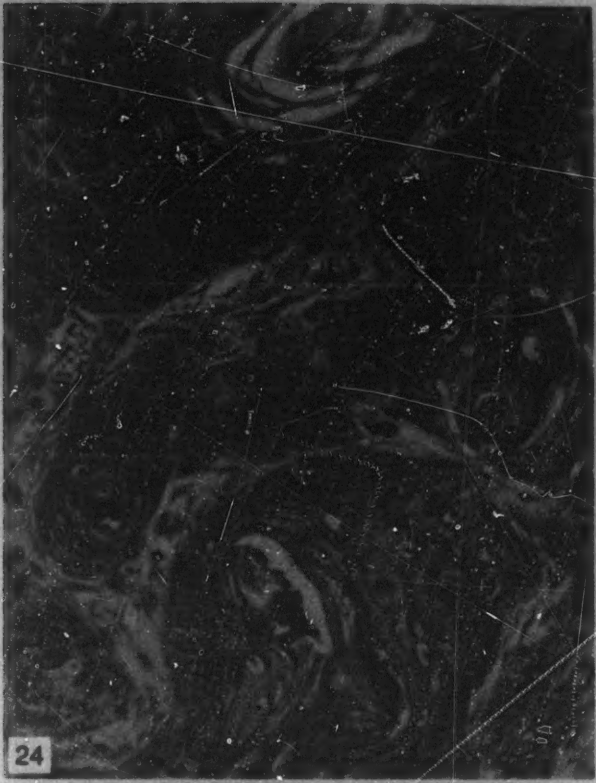
24

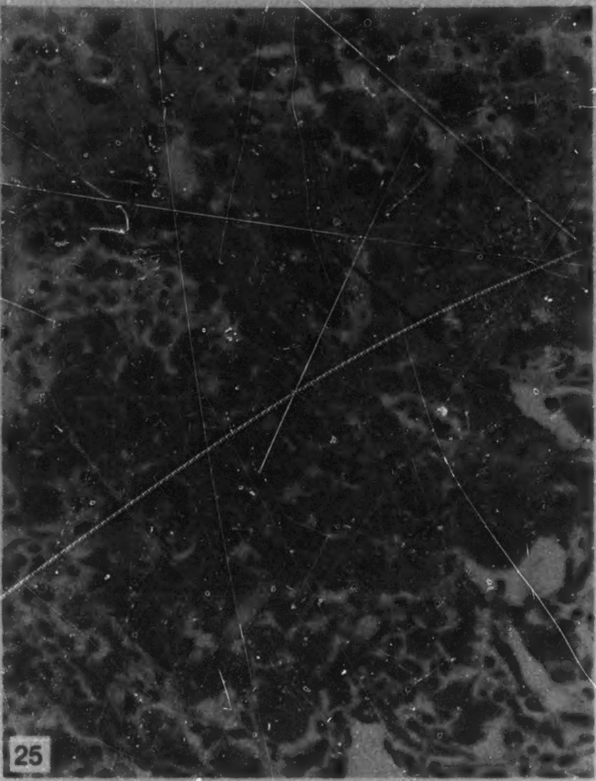
25

26

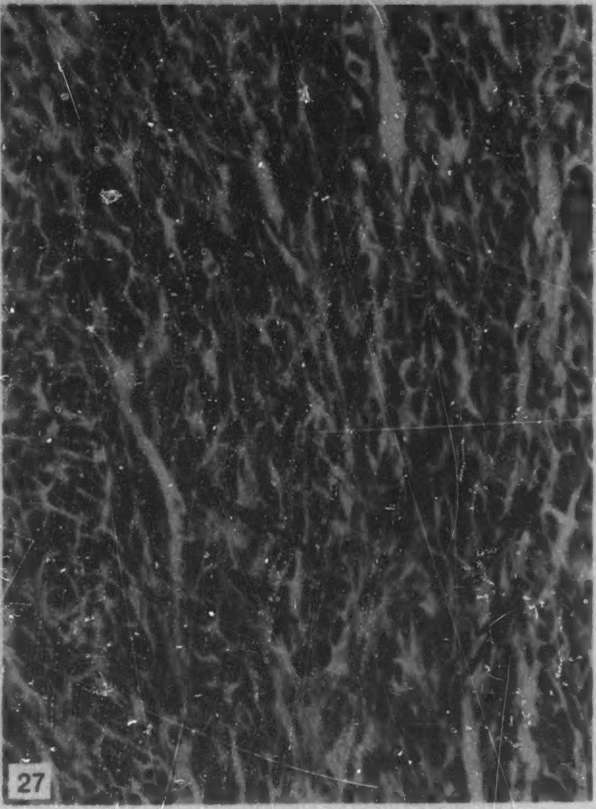
27

blank page

Meeting Highlights

Host Factors in Human Carcinogenesis[1]

"You can leave benzo[*a*]pyrene in a test tube forever, and it will never cause cancer," was the gist of a remark from the floor during the Symposium. Also, since only one out of every seven smokers gets lung cancer, more than cigarette smoking must be involved. These observations help explain why the International Agency for Research on Cancer, which has long focused on environmental factors as the cause of most human cancers, convened some 100 scientists to discuss host factors. The effect of even the most powerful carcinogen is likely modified and modulated by host factors. Invited participants (two laboratory scientists for each clinician or epidemiologist) stumbled repeatedly over the scope of the term "host factors." Some drew a line at DNA (i.e., purely genetic), and others at the mouth, nose, skin, and other body portals to the environment. Should internal estrogens be considered as host factors but not medicinal steroids? Where should nutrition be placed? To resolve the dilemma, several discussants preferred the classic dichotomy of Sir Francis Galton, the father of human genetics: genes and environment.

Introductory overviews gave evidence of host factors as seen by epidemiology (e.g., relating breast cancer to body form, reproductive status, and hormone levels), by laboratory experimentation (showing multiple interactions among such factors as DNA, exogenous chemicals, and membrane receptors), and by clinical medicine (observing peculiar occurrences of cancer that demonstrate gene-environment interaction).

The session on genetics indicated that each technical advance in visualizing human chromosomes strengthens the 1914 hypothesis of Boveri that cancer is related to chromosomal imbalance. For example, the prophase staining method (which now distinguishes 1,000 bands, in contrast to the 250 bands distinguished by standard techniques) revealed a small deletion in the short arm of chromosome 11 in patients with the Miller syndrome of aniridia-Wilms' tumor. Still, best techniques lack the power to locate individual cancer genes. When methods emerge, karyotyping solid tumors should be as useful as are the present prognostic and etiologic insights gained for the lymphoproliferative cancers. For example, many potential determinants of Burkitt's lymphoma besides the Epstein-Barr virus and malaria became suspect when it was shown that chromosome 14 has the gene for nucleoside phosphorylase near the break point at which translocation often occurs in Burkitt's lymphoma. In this connection, deletion of DNA sequences was noted to be a normal phenomenon in the synthesis of specific immunoglobulins with sometimes sloppy deletion and insertion of genetic material. The story begins to resemble the emerging principles of the action of retrovirus in murine and avian carcinogenesis.

The intense efforts in the pursuit of the elusive human cancer virus led to nucleic acid chemical techniques that dissect the genetic material better than the best chromosome banding methods. The present view is that long ago viral DNA sequences became integrated into human genes and may now mediate the initiation of cancer when they are transcribed at an inappropriate time in the cell cycle. Such transcription may be stimulated by genes transposed as a result of a chemical or physical agent. R. Weiss claimed, "Viruses may be considered endogenous host factors," supporting I. B. Weinstein's earlier remark, "Today's environmental factors are tomorrow's host factors."

Similar progress has occurred in explaining the relations between mutagens, carcinogens, and the mechanisms for repairing DNA as measured by in vitro studies of radiosensitivity of cells from patients at risk for cancer or with unusual reactions to radiation. The story is best shown by two autosomal recessive genetic conditions, xeroderma pigmentosum and ataxia-telangiectasia, and continues to develop as other disorders are studied. The insights, of course, are not limited to radiation carcinogenesis but include chemicals that mimic the action of photons.

The hunt for an RNA human cancer virus took a fruitful but unexpected turn. In contrast, evidence of a significant etiologic role of hepatitis B virus in the origins of hepatocellular carcinoma continues to mount in the model of a classic infectious disease. Since only 5% of hepatitis B virus carriers get liver cancer, additional factors must operate (such as exposure to aflatoxins and other hepatotoxins, early age of infection, or genetic predisposition). No one factor seems sufficient; several must act together.

If defects of DNA or gene action can be considered as initiators of cancer, surely host factors remain that could be considered promoters in modifying the clinical expression of cancer. Possibilities include genetically modulated variations in nutrition, hormones, and immunologic function. For example, exogenous estrogens seem to set up tissues for initiation and may help the action of other carcinogens, but they never seem to be initiators.

Another session was devoted to inborn variation and genetic differences in response to environmental agents (carcinogens), a field that could be termed "ecogenetics." The best examples in humans concern variations in drug metabolism—pharmacogenetics—exemplified by the recent finding of a probable excess of rapid metabolizers of debrisoquine among cancer patients in Ibadan. Further studies of drug metabolism in monozygous twins show differences resulting from surprisingly subtle environmental factors that are poorly recognized, such as interaction with other drugs, time since last meal, and antecedent or concurrent disease. The major point remains that the same genetically determined enzyme systems that metabolize drugs handle chemical carcinogens. Despite detailed knowledge of the homologous *Ah* locus in the mouse, the great expectation that aryl hydrocarbon hydroxylase inducibility would predispose some people to tobacco-associated cancer has not been substantiated. Contrary to the hope of epidemiologists, laboratory scientists at the meeting left little doubt that the complexities of monooxygenases are now poorly understood.

---

[1] The International Agency for Research on Cancer organized the Symposium, held in Cape Sounion, Greece, June 8-11, 1981.

[2] ARMSTRONG BK, BARTSCH H, eds. Host factors in human carcinogenesis. IARC Sci Publ No. 39. Lyon: IARC, 1981.

Just before a summarizing session, a potpourri of new approaches to the study of host factors in cancer was given. Immunologic and mass spectrophotometric assays, in part with the use of monoclonal antibodies, blend the high technology of several disciplines to achieve a sensitivity of detecting one molecule of DNA-carcinogen adduct per cell; such precision makes biologic interpretation a problematic task. Assays with the use of organ explants, cell transformation, and mutagenicity are continually being refined. Finally, exploring the biology of preneoplastic states should provide insights into anatomic and physiologic correlates of carcinogenesis and, perhaps, be of immediate use in prevention; e.g., abnormal sugar metabolites are found in intestinal metaplasia of the gastric epithelium in patients at high risk for stomach cancer.

Despite an idyllic setting, it was not clear that many lasting romances had been made between laboratory approaches studying DNA and clinical-epidemiologic strategies with populations. This perspective may change during the gestational period for the anticipated publication of the proceedings by the International Agency for Research on Cancer.[2]

John J. Mulvihill, M.D.
Clinical Epidemiology Branch
Division of Cancer Cause and Prevention
National Cancer Institute
National Institutes of Health
Public Health Service
U.S. Department of Health and Human Services
Bethesda, Maryland 20205

Announcements

The Journal will publish notices of major meetings dealing with cancer. Submission of notices 6 months in advance is requested to permit timely publication.

Sixteenth Annual Clinical Symposium

St. Jude Children's Research Hospital will hold its Sixteenth Annual Clinical Symposium in Memphis, Tennessee, on February 26-27, 1982. The symposium will be concerned with current results in the treatment of children with cancer and leukemia. Emphasis will be given to diagnosis and treatment programs for primary disease, and the care of complications. There will be discussions of various aspects of supportive care as an essential adjunct to chemotherapy regimens.

There are no registration or other fees for this symposium. Physicians may register by writing to: Associate Director for Clinical Research, St. Jude Children's Research Hospital, Box 318, Memphis, Tennessee 38101.

Thirty-Second Annual Conference of The National Council on the Aging, Inc.

"The 'American Dream'—Assessing the Status of Older Americans" will be the topic of this conference to be held at the Sheraton Washington in Washington, D.C., on March 31-April 3, 1982. Conference participants will focus their attention on the following areas: achieving economic security, assuring quality of life, and creating responsive services.

For further information contact the Conference Department, The National Council on the Aging, Inc., West Wing 100, 600 Maryland Avenue, S.W., Washington, D.C. 20024 (telephone: 202-479-1200).

Oncology Update 1982

The Northridge Hospital Medical Center will sponsor this symposium to be held at the Biltmore Hotel, Los Angeles, California, on April 3, 1982. The symposium will focus on the latest developments in cancer treatment and research including alternatives in primary management of breast carcinoma, emotional and psychological factors that have impact on the lives of cancer patients, results now achieved with newer chemotherapeutic agents, and the role of highly specific antibodies in the management of the cancer patient.

For reservations or further information please contact Ms. Sandra Rossen, Northridge Hospital Medical Center, Medical Education Department, 18300 Roscoe Boulevard, Northridge, California 91328 (telephone: 213-885-5311).

North American Society for Cardiac Radiology—1982 Postgraduate Course

"Cardiac Interventional Techniques and Diagnostic Imaging" is the subject of this course to be held at the Barbizon Plaza Hotel, New York, New York, on April 5-6, 1982. The subject fields to be covered are digital subtraction angiography, nuclear magnetic resonance, echocardiography, radionuclide studies, and interventional measures and techniques, e.g., shunts, ergonovine, PTCA, and PTA. Attention will be directed to pathophysiologic conditions such as congenital and acquired heart disease, fibrinolysis, venous hypertension, valvular heart disease, and diagnostic imaging.

For additional information contact Dr. Thomas A. Sos, Program Chairman, c/o Educational Resources Associates, Inc., 209 Harvard Street, Suite 500, Brookline, Massachusetts 02146 (telephone: 617-738-8859/8861).

Second Annual Washington Imaging Conference

The Department of Radiology of The Alexandria Hospital and the American College of Radiology will sponsor this conference to be held at the Washington Marriott Hotel, Washington, D.C., on May 2-7, 1982. "Recent Advances in Computed Tomography and Digital Imaging" will be the subject of the conference, and topics will include computed tomography of the abdomen, chest, pelvis, and spine, and digital angiography.

For further information please contact: Miss Susan Ferraro, Department of Radiology, The Alexandria Hospital, 4320 Seminary Road, Alexandria, Virginia 22304 (telephone: 703-379-3102).

Fourth Annual Course in Flow Cytometry

"Applications in Cell Biology" is the title of this course to be presented by the University of Rochester School of Medicine and the Department of Pathology and Cancer Center, at the University of Rochester, Rochester, New York on May 24-28, 1982. Lectures will include instrumentation description, cytochemistry, immunological analysis, and cell cycle analysis.

For additional information please contact Dr. Paul K. Horan, Course Director, Department of Pathology, Box 626, University of Rochester Medical Center, 601 Elmwood Avenue, Rochester, New York 14642 (telephone: 716-275-5516).

Educational Video Cassettes

To help health professionals recognize and manage patients at increased risk of melanoma, NCI investigator Dr. Mark H. Greene and his colleagues have developed a series of educational video cassettes. These materials illustrate the unique clinical and histologic characteristics of dysplastic nevi, the recognition of early melanoma, the melanoma warning signals, principles of skin examination, ways to minimize sunlight exposure, and recommendations for daily health care.

For additional information on obtaining educational video cassettes and written information on the prevention and early detection of malignant melanoma in persons at high risk, please contact: The National Cancer Institute, Office of Cancer Communications, Building 31, Room 10A18, Bethesda, Maryland 20205 (telephone: 301-496-6641).

★U.S. GOVERNMENT PRINTING OFFICE: 1982-311-216/24

JNCI Journal of the National Cancer Institute Volume 68 Number 2 pp 177-341 Feb

JNCI (NIH Publication No. 82-13)

68/2

JNCI

Journal of the National Cancer Institute

February 1982
Volume 68
Number 2

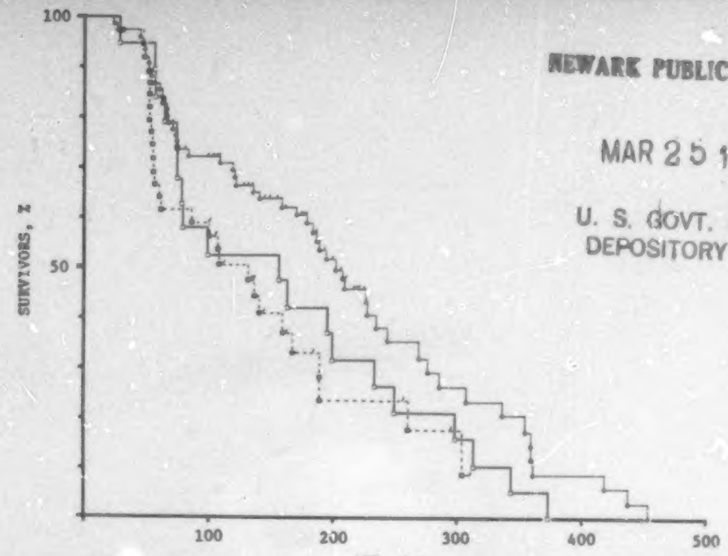

NEWARK PUBLIC LIBRARY
MAR 25 1982
U. S. GOVT. PUBS.
DEPOSITORY 376

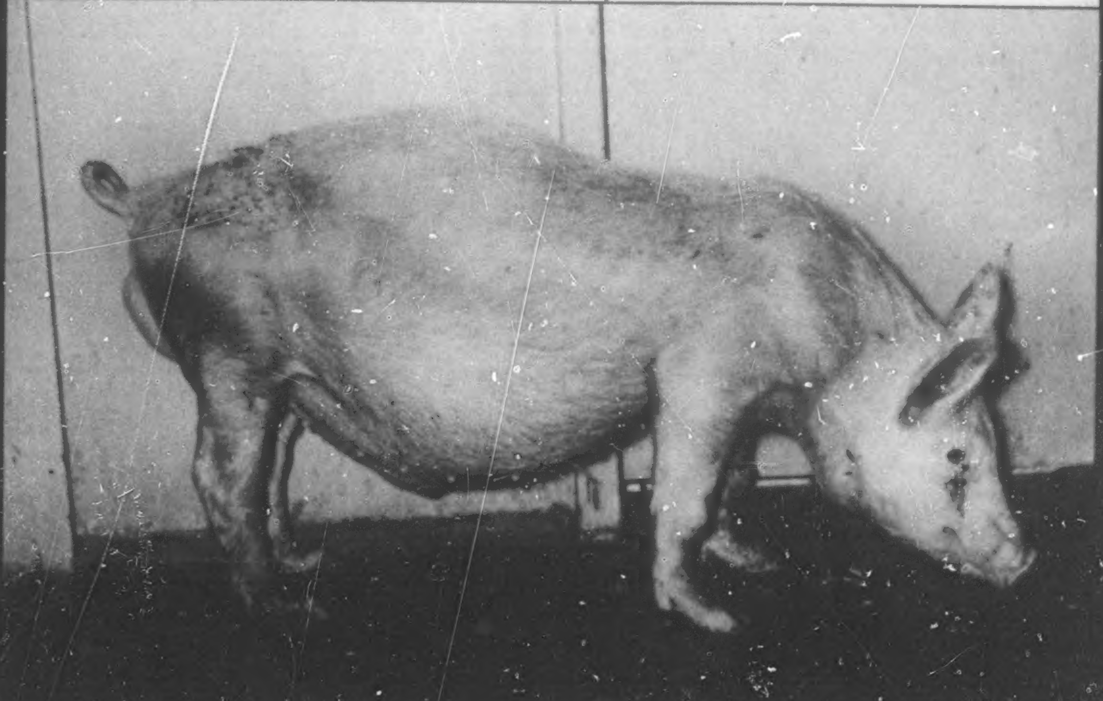

U.S. DEPARTMENT OF HEALTH AND HUMAN SERVICES Public Health Service National Institutes of Health

HE 20. 3161:

This month's cover (*top*) shows the overall survival curves based on age at death of three sex categories of pigs with untreated lymphosarcoma: females, entire males, and castrated males. The photograph (*bottom*) is of a 10-month-old male pig affected by hereditary porcine lymphosarcoma. The pendulous abdomen and arched spine were caused by gross enlargement of visceral lymph nodes and of the spleen (*see* article by McTaggart, Imlah, and Head on pages 239–248).

JNCI Journal of the National Cancer Institute

February 1982
Volume 68
Number 2

THE JOURNAL of the National Cancer Institute solicits manuscripts on original observations in laboratory and clinical research from all scientists. A manuscript is considered for publication with the understanding that it has not been published previously and is submitted exclusively to the Journal. Opinions expressed by the authors are not necessarily those of the publisher or its editors.

THE JOURNAL is published monthly (two volumes a year). The Secretary of Health and Human Services has determined that the publication of this periodical is necessary in the transaction of the public business required by law of this Department.

A MONOGRAPH SERIES covering proceedings of scientific meetings pertaining to cancer is also published. These books may be purchased from the Superintendent of Documents. Series subscriptions are not available and monographs are not included in a subscription to the Journal.

THE JOURNAL is for sale by the Superintendent of Documents, U.S. Government Printing Office, Washington, D.C. 20402. Price per copy, $6.00. Subscription price for two volumes per year in the United States, $65.00; foreign, $81.25. Payment is required in advance, and check or money order should be made payable to the Superintendent of Documents.

All inquiries regarding purchase of subscriptions or depository library distribution, including inquiries about missing issues and change of address, should be addressed to the Government Printing Office. The Government Printing Office requires payment in advance on all orders. Inquiries regarding missing issues or change of address for official subscriptions should be addressed to the Editorial Office, Room 850, Westwood Building, 5333 Westbard Avenue, Bethesda, Md. 20016.

VINCENT T. DEVITA, JR., *Director, National Cancer Institute*

BOARD OF EDITORS

ELIZABETH K. WEISBURGER, *Acting Editor in Chief*
STUART A. AARONSON, *Associate Editor*
MARY A. FINK, *Associate Editor*
JANET W. HARTLEY, *Associate Editor*
DONALD HENSON, *Associate Editor*
RONALD B. HERBERMAN, *Associate Editor*
GEORGE S. JOHNSON, *Associate Editor*
KURT W. KOHN, *Associate Editor*
ARTHUR S. LEVINE, *Associate Editor*
JOHN J. MULVIHILL, *Associate Editor*
ALAN S. RABSON, *Associate Editor*
RICHARD M. SIMON, *Associate Editor*

EDITORIAL STAFF

EDWIN A. HAUGH, *Managing Editor*
PAMELA T. ALLEN, *Assistant Managing Editor*
FLORENCE I. GREGORIC, *Monograph Editor*
Editors: DOROTHY D. KATZ, MERCEDES B. LA CHARITY,
I. AGNES REVESZ, JOAN O'BRIEN RODRIGUEZ,
CONSTANCE R. STONESTREET, and ANNA B. WITTIG

JNCI (NIH Publication No. 82-13)

U.S. DEPARTMENT OF HEALTH AND HUMAN SERVICES Public Health Service National Institutes of Health

Instructions to Authors

Text: Send one original and two copies. **Text-figures** (graphs, charts, and line drawings): Send one original and two copies. **Figures** (photomicrographs and photographs): Send three original glossy prints, unmounted. **Tables:** Send tabular material in typewritten form; do not submit tables as glossy prints to be photographed. The entire manuscript including footnotes, legends, and references must be typed double spaced. Single-spaced portions of a manuscript will be returned to the author for retyping. The mailing address is: Journal of the National Cancer Institute, Westwood Building, Room 850, 5333 Westbard Avenue, Bethesda, Maryland 20016.

Manuscripts should be accompanied by a covering letter from the author responsible for correspondence about the manuscript. The covering letter should contain a statement that the manuscript has been seen and approved by all authors and that all persons listed as authors have made significant (not merely administrative, technical, or supervisory) contributions to the content of the paper. The letter should also state that the manuscript or substantial portions thereof have not been previously published nor are they under consideration for publication in another journal.

Data too extensive for inclusion in a manuscript, but which may be of interest to other investigators, may be deposited with the National Auxiliary Publications Service (NAPS), c/o Microfiche Publications, P.O. Box 3513, Grand Central Station, New York, New York 10017. Authors using the NAPS facilities should indicate in a footnote how their additional data may be obtained.

TITLE: Be brief (no more than 14 words, if possible), but for indexing purposes include all key words. The annual subject index is prepared directly from the titles. Titles that form complete sentences are not acceptable. Do not use abbreviations or chemical formulas in titles.

BYLINE: Supply the complete first name, middle initial, and last name of each author. Avoid use of nicknames. Academic degree is optional; however, if a degree is provided for one author, it should be provided for all authors on a manuscript. Include the name of the institution, address, and zip code for each author. Indicate address for reprint requests in a footnote on the byline.

ACKNOWLEDGMENTS: Financial aid in support of research should be recognized in a footnote. Aid in technical fields, animal care, photography, stenography, and other areas may be mentioned in a separate footnote. Indicate the title (Dr., Mr., Mrs., Miss, Ms.) and affiliation of each person acknowledged.

ABSTRACT: Provide an abstract, 150 words or less, on a separate page. The abstract should describe only *results* of the work being reported. Speculation, historical background, or reference to published works will be deleted from abstracts. Any inbred strains, noninbred stocks, cell lines, or other living materials used in the work should be noted in the abstract.

TEXT: Avoid the use of laboratory jargon and abbreviations not in common usage. When possible, refrain from the use of abbreviations that form words (exceptions are PAGE, ALL). Whenever possible, write mathematical equations and chemical formulas on a single line; submit complicated chemical structures as artwork. Avoid repetition of data in the text when it is presented in tables or text-figures.

Use the following style sources: Webster's *Third New International Dictionary* and Dorland's *Illustrated Medical Dictionary* (25th ed) for spelling; *Council of Biology Editors Style Manual* (4th ed) for scientific abbreviations and symbols: *Government Printing Office Style Manual* for other abbreviations and symbols, punctuation, and hyphenation; *Biochemical Nomenclature and Related Documents* (IUB, 1978) for abbreviations of chemical substances; *Enzyme Nomenclature*, recommendations (1978) of the IUB for recommended names of enzymes and information on nomenclature of isozymes; *The Merck Index* (9th ed) for chemical compounds; "Standard Nomenclature for Inbred Strains of Mice: Seventh Listing" by Joan Staats (Cancer Res 1980;40:2083-2128) for inbred mouse strains; "Standardized Nomenclature for Inbred Strains of Rats: Fourth Listing" by Joan Staats and Michael Festing (Transplantation 1973;16:221-245) for designations of inbred rat strains; *Animals for Research* (9th ed) prepared by the Institute of Laboratory Animal Resources, National Academy of Sciences, for designations of laboratory animal stocks and strains.

TABLES: Submit tabular material typed double spaced on a separate page. Computer print-outs of tables are acceptable only if they are double spaced and with satisfactory title, column headings, legends and other textual material. Provide headings for all columns of a table and indicate units of measurement where applicable.

TEXT-FIGURES: Refer to graphs, charts, and line drawings as text-figures. Make the abbreviations on text-figures identical to the abbreviations used in the text and legends. Symbols and lettering should be large enough to be legible if reduced. Glossy prints or original drawings in black ink are acceptable; orient vertically instead of horizontally.

FIGURES: Refer to photomicrographs and photographs as figures. Figures and their legends should fit a 7.5- by 9-inch dimension. Calculate that nine typewritten lines of legend will require 1 inch of vertical space. Type figure legends on a separate sheet and identify in the legend any lettering used on the figure. Trim photographs to show only important areas. Do not number face of photographs; use the back or overlay to indicate the top and number of each. Printed indicators may be included on photographs; do not use hand-drawn indicators. *Insert internal scale markers on all photomicrographs.* Color photographs must be grouped as a single plate. For color reproduction, submit both color transparencies and high-quality black and white reproductions. The need for color must be documented before it will be considered.

REFERENCES: Use any recent issue of the Journal as a style guide for reference lists. Number references in order of citation in both text and reference list. For periodicals, provide author(s), title of paper, journal, year, volume, and first and last page numbers. For books, give the author(s), title, name(s) of editor(s), location and name of publisher, year, pertinent chapter or section title, and page numbers. Follow *Index Medicus* for punctuation and abbreviations. Citations of papers in preparation or submitted for publication, unpublished observations, and personal communications should be noted parenthetically in the text. Do *not* include them in the reference list. The accuracy of all references is the responsibility of the authors and not of the editorial staff.

LETTERS TO THE EDITOR should pertain to recent articles in the Journal and should not contain new data unless relevant to the discussion of a particular paper. The authors addressed will be invited to reply to comments before correspondence is published. Letters will be edited by the Staff, subject to contributor approval.

FURTHER DETAILS on the preparation of manuscripts are set forth in the document "Uniform Requirements for Manuscripts Submitted to Biomedical Journals" prepared by the International Steering Committee of medical editors (*see* Am Rev Respir Dis 1979;119:3-10/Ann Intern Med 1979;90:95-99/Br Med J 1979;1:532-535/Lancet 1979;1:428-430).

UNITED STATES GOVERNMENT PRINTING OFFICE, WASHINGTON, D.C.: 1982

Table of Contents

Vol. 68, No. 2——February 1982

177 Obituary——Herbert Joseph Rapp *Tibor Borsos*

Investigations on Man

179 Human lymphoma-lymphoma hybrids and lymphoma-leukemia hybrids. I. Isolation, characterization, cell surface markers, and B-cell markers *Jesper Zeuthen, George Klein, Rosalie Ber, Giuseppe Masucci, Susanne Bisballe, Susan Povey, Paul Terasaki, Peter Ralph*

197 Human lymphoma-lymphoma hybrids and lymphoma-leukemia hybrids. II. Epstein-Barr virus induction patterns *George Klein, Jesper Zeuthen, Rosalie Ber, Ingemar Ernberg*

203 Ganglioside patterns: New biochemical markers for human hematopoietic cell lines *Günter Rosenfelder, Andreas Ziegler, Peter Wernet, Dietmar G. Braun*

211 Risk factors for breast cancer in women in northern Alberta, Canada, as related to age at diagnosis *Jay H. Lubin, Patricia E. Burns, William J. Blot, Alan W. Lees, Carol May, Linda E. Morris, Joseph F. Fraumeni, Jr.*

219 Cancer incidence in the Republic of Panama, 1974–78 *William C. Reeves, Plinio F. Valdés, María M. Brenes, Rosa C. de Britton, Claire F. B. Joplin*

227 Phase I–Phase II trial of *N*-phosphonacetyl-L-aspartic acid given by intravenous infusion and 5-fluorouracil given by bolus injection *Charles Erlichman, Ross C. Donehower, James L. Speyer, Ray Klecker, Bruce A. Chabner*

233 Phytohemagglutinin or pokeweed mitogen induction of in vitro colony formation by T-cells from patients with chronic lymphocytic leukemia *Vito Pistoia, Arcangelo Nocera, Riccardo Ghio, Paola Minale, Manlio Ferrarini*

Investigations on Nonhuman Systems

239 Causes of death and sex differences in survival times of pigs with untreated hereditary lymphosarcoma (leukemia) *H. S. McTaggart, P. Imlah, K. W. Head*

249 Calorie restriction: Effect on growth of human tumors heterotransplanted in nude mice *Beppino C. Giovanella, Randall C. Shepard, John S. Stehlin, John M. Venditti, Betty J. Abbott*

259 Resting state depth and saturation density as modulated by tumor promoters and culture conditions: Relationship to chemical transformation in C3H/10T½ cells *David Miska, H. Bruce Bosmann*

267	Vasopressin: Action in WRK-1 rat mammary tumor cells	*M. E. Monaco, P. H. Kohn, W. R. Kidwell, J. S. Strobl, M. E. Lippman*
271	Cholangiocellular carcinomas induced in Syrian golden hamsters administered aflatoxin B_1 in large doses	*Michael R. Moore, Henry C. Pitot, Elizabeth C. Miller, James A. Miller*
279	L-Histidinol protection against cytotoxic action of cytosine arabinoside and 5-fluorouracil in cultured mouse spleen cells	*Robert C. Warrington, Wei D. Fang*
287	Murine lymphoma L5178Y cells resistant to purine antagonists: Differences in cross-resistance to thioguanine–platinum(II) and selenoguanine–platinum(II)	*Fumihiko Kanzawa, Mitsuaki Maeda, Takuma Sasaki, Akio Hoshi, Kazuo Kuretani*
293	Production of kidney tumors in rats with low dose of dimethylnitrosamine after partial hepatectomy	*Ritva P. Evarts, Carolyn A. Brown, Mostafa Hassan Mostafa*
299	Inhibition of iodinated nerve growth factor binding by the suspected tumor promoters saccharin and cyclamate	*Douglas N. Ishii*
305	Granulopoiesis longevity in continuous bone marrow cultures and factor-dependent cell line generation: Significant variation among 28 inbred mouse strains and outbred stocks	*Mary Ann Sakakeeny, Joel S. Greenberger*
319	Effects of dietary lipids on lactogenic hormone receptor binding in rat mammary tumors	*William T. Cave, Jr., Marsha J. Erickson-Lucas*
325	Lipopolysaccharide and pristane-induced peritoneal exudate requirements for plasma tumor cell colony formation	*Micsunica Platica, Catherine Bojko, Radu Clincea, Vincent Hollander*
329	Plasminogen activator, fibronectin, lymphotoxin sensitivity, and natural skin reactivity relationships to guinea pig cell tumorigenicity	*Richard P. McCabe, Charles H. Evans*

Meeting Highlights

337	Kaposi's sarcoma in homosexual men	*John L. Ziegler*
338	Monoclonal antibodies and breast cancer	*Marianne L. Egan, Donald E. Henson*

Announcements

341 National Toxicology Program Conference

341 Latest NCI Monographs Published

341 Other Monographs Available

Herbert Joseph Rapp

1923-1981

Dr. Herbert J. Rapp, Chief of the Laboratory of Immunobiology of the National Cancer Institute for the past 15 years, died on September 25, 1981. His untimely passing represents a great loss to science, to his family, and to his friends and colleagues.

Herb was born in Philadelphia on January 15, 1923; during the Great Depression his family moved to Ocean City, Maryland, where he finished his high school studies. He entered engineering school at The Johns Hopkins University in Baltimore; the Second World War interrupted this course of study, and for the duration of 1943–1946 he served in the U.S. Navy Hospital Corps, primarily at the Naval Hospital in Bethesda. After his discharge from the services, Herb turned away from engineering and studied biological sciences, with a strong stress on chemistry and his beloved subject, mathematics. The year 1948 was a crucial one for Herb: He married the former Marion Wasserman and got a job as a clinical laboratory technician at The Johns Hopkins Hospital; both of these events were to shape his life permanently. The marriage produced four children, Barbara, Margaret, Brian, and Frances, who were his pride and joy to the end of his days. The Hopkins job led him to Manfred M. Mayer, the newly arrived "Wizard of Complement" at the Department of Microbiology at the School of Hygiene and Public Health, who hired Herb as a technician and then kept him on as a graduate student until he obtained his M.Sc. in 1953 and his Sc.D. in 1955.

Herb's contributions to science are numerous and span a wide range of subjects. The title of his doctoral dissertation reveals his love for mathematics: "A Mathematical Theory and Analysis of Immune Hemolysis." His ability to apply mathematical analysis to complex problems never left him. His work at Hopkins was taken up by research on complement, and his two major contributions in that field left a permanent legacy: the quantitation of the activity of complement and its components on a sound theoretical basis and the separation of the components of complement by modern physicochemical methods. The result of these two approaches was the discovery that the then recognized third component comprised at least three distinct entities. Herb's work truly laid the foundation of the modern era of complement research.

In 1962 Herb was invited to head the Immunology Section of the Diagnostic Research Branch of the National Cancer Institute. He continued his work on complement but he felt driven to develop new approaches to the immunology of cancer. By inducing hepatomas in inbred guinea pigs with nitrosamines, he developed transplantable ascitic forms of these tumors appropriate for immunologic studies. Among these tumor lines was the famous line-10, which served for many of the pioneering studies by Herb and his many associates. His studies on the intralesional therapy of transplanted hepatomas with BCG, which showed that not only the primary but also lymph node metastases could be eradicated by this treatment, are now considered to be classic and have led to promising clinical trials in humans. His search for better models for immunotherapy of cancer led Herb to the application of nonliving BCG vaccines to naturally occurring carcinomas of large animals and, in the case of bovine ocular carcinoma, to spectacular results. He was in the midst of these studies when his life came to a tragic end.

During his career at the National Cancer Institute, Herb served on many committees where his insights into complex problems were often appreciated; he received the Superior Service Award of the National Institutes of Health in 1973; and for many years he served on the editorial boards of several journals including *Immunochemistry* (1969–72) and the *Journal of the National Cancer Institute* (1967–68).

Herb's greatest legacy survives in the colleagues who worked with him and in the younger associates who were trained by him. He taught them the importance of strict quantitation, of paying attention to the smallest detail, and of being supercritical of one's own work.

Many of us who knew Herb well and shared his working hours were also enriched by sharing many of his hours outside the laboratory. Strict adherence to time schedules led to the 11 a.m. exodus to the lunch table, where the conversation was free flowing, witty, and full of puns and jokes regardless of whether the discussion concerned science, politics, literature, his beloved music, or his other great loves: the ocean and fishing. While he could be generous with his wit and praise, he could be also a severe but just critic of the foibles of others as well as his own. Herb's death left us all poorer and we will miss him every day of our lives. Yet a small consolation remains: we were allowed to know him and be part of his life.

Tibor Borsos, *Sc.D.*
Chief, Humoral Immunity Section
Laboratory of Immunobiology
National Cancer Institute
Bethesda, Maryland 20205

blank page

Human Lymphoma–Lymphoma Hybrids and Lymphoma–Leukemia Hybrids. I. Isolation, Characterization, Cell Surface Markers, and B-Cell Markers[1,2,3]

Jesper Zeuthen,[4] **George Klein,**[5] **Rosalie Ber,**[6] **Giuseppe Masucci,**[5] **Susanne Bisballe,**[4] **Susan Povey,**[7] **Paul Terasaki,**[8] *and* **Peter Ralph**[9,10]

ABSTRACT—Four new somatic cell hybrids were obtained by fusion of various Burkitt's lymphoma (BL)-derived cell lines that had different selective markers: Raji–P3HR-1, Daudi–Raji, and a P3HR-1–P3HR-1 "autohybrid" derived from two P3HR-1 sublines. In addition, a hybrid was obtained between the Daudi (BL) line and the human leukemia cell line K562. The hybrids were extensively characterized by means of chromosome, isozyme, and HLA surface markers. The phenotypic differences between the parent cell lines allowed some conclusions with respect to the expression of latent Epstein-Barr virus (EBV) genomes, C3 and EBV receptors, and of immunoglobulin and beta 2-microglobulin–HLA expression as well as the influence of the leukemia cell (K562) genome on B-cell properties in the Daudi–K562 hybrid. B-cell and differentiated markers of these hybrids were characterized. High-level expression dominated for the marker C3 and EBV receptors, which showed a good correlation coefficient of 0.84, as was true for Fc receptors and surface immunoglobulin. The Daudi–K562 hybrid showed loss of all B-cell markers but retention of the leukemia cell markers (e.g., hemoglobin synthesis).—JNCI 1982; 68:179–195.

When two human lymphoid cell lines of B-cell derivation are hybridized, a variety of B-cell markers (e.g., Fc, C3, and EBV receptors) show an autonomous, codominant pattern of expression as a rule, while some other markers (e.g., sIg) appear to be subject to more complex regulatory mechanisms (*1–3*). The derived hybrid cells might resemble either the more or less marker-expressing parental cell. The expression of differentiated functions can in contrast be completely autonomous in hybrids between closely related BL cell lines, in which two Ig light chains are coexpressed in approximately the same proportion as those produced by the original parental cells (*4*).

When BL-derived cells are fused with cells of other differentiation lineages, such as with epithelial cells or fibroblasts, the B-cell markers are extinguished in the fused cells (*5, 6*). This behavior is similar to what is known for most differentiation markers in various hybrid combinations in which differentiation programs are mutually exclusive and in which highly differentiated (or "luxury") functions are usually lost after hybridization (*7, 8*). An additional factor of importance for the expression of differentiation functions appears to be cell shape, which must be compatible with the expression of a certain program of differentiation (*9*). In hybrids between BL-derived cell lines, various levels of expression ranging from complete coexpression (*4*) to variable quantitative effects on the expression of various B-cell markers may be observed. These effects presumably reflect subtle differences in the differentiation programs involved. In a previous study of a hybrid of the BL-derived cell line P3HR-1 with the CML-derived K562 human leukemia cell

---

ABBREVIATIONS USED: AI=absorption index; β_2m=beta 2-microglobulin; BL=Burkitt's lymphoma; BrdUrd=5-bromo-2'-deoxyuridine; BrdUrd^r=BrdUrd-resistant; CAP=chloramphenicol; CAP^r=CAP-resistant; CMIF=complement membrane immunofluorescence; CML=chronic myeloid leukemia; EA=erythrocyte-antibody; EAC=erythrocyte-antibody-complement; EBV=Epstein-Barr virus; EMS=ethyl methanesulfonate; FACS=fluorescence-activated cell sorter; FCS=fetal calf serum; FITC=fluorescein isothiocyanate; HAT medium=hypoxanthine, aminopterin, and thymidine medium; HPRT=hypoxanthine guanine phosphoribosyl transferase; HPRT$^-$=HPRT-negative; Ig=immunoglobulin(s); ME1=soluble malic enzyme; NK=natural killer; ouab=ouabain; ouab^r=ouab-resistant; Ph^1=Philadelphia chromosome; r=correlation coefficient; RBC=red blood cells; sIg=surface Ig; TG=thioguanine; TG^r=TG-resistant; TK=thymidine kinase; TK$^-$=TK-negative.

---

[1] Received September 23, 1980; revised August 4, 1981; accepted September 8, 1981.

[2] Supported in part by Public Health Service (PHS) contract N01CP-33316 from the Division of Cancer Cause and Prevention, National Cancer Institute (NCI); by PHS grants 5-R01CA-14054-05 and 5-R01CA-24300 from NCI; by the Swedish Cancer Society; by research grant 31/79 from the Danish Cancer Society; by grants 511-15354 and 511-10128 from the Danish Natural Science Research Council; by funds provided by the International Cancer Research Data Bank Programme (to R. B.) from NCI; and by PHS contract N01CO-65341 (to R. B.) from the Office of the Director, NCI.

[3] Paper VII of a series on somatic cell hybrids derived from Burkitt's lymphoma cells.

[4] Institute of Human Genetics, The Bartholin Building, University of Aarhus, DK-8000 Aarhus C, Denmark.

[5] Department of Tumor Biology, Karolinska Institutet, S-104 01 Stockholm 60, Sweden.

[6] Technion- Israel Institute of Technology, Faculty of Medicine, P.O. Box 9649, Haifa, Israel.

[7] MRC Human Biochemical Genetics Unit, The Galton Laboratory, University College, Wolfson House, 4 Stephenson Way, London NW1 2HE, England.

[8] Department of Surgery, School of Medicine, The Center for the Health Sciences, University of California at Los Angeles, Los Angeles, Calif. 90024.

[9] Sloan-Kettering Institute for Cancer Research, Donald S. Walker Laboratory, Rye, N.Y. 10580.

[10] We are grateful to Mr. Gunnar Klein for assistance with computer programming and to Ms. Kerstin Falk, Ms. Barbro Ehling, Ms. Agneta Manneborg, Ms. Bente Hauge Jensen, Mr. Steve Jeremiah, and Ms. Mary Wyn Evans for valuable technical assistance.

line, the markers of the K562 cell line were observed to dominate in this particular hybrid combination; one putative marker of B-cell differentiation, inducibility for EBV viral cycle antigens, was completely extinguished in this hybrid combination (*10*). This is of interest since K562 cells, reportedly established from a CML patient in blast crisis (*11*), would be assumed to share a common stem cell origin with human B-cells (*12*).

In the present report, we characterize five new somatic cell hybrids, four formed by fusion of BL-derived B-cell lines and one formed between the K562 cell line and a BL-derived line (Daudi), and present an analysis of their surface- and differentiation-related marker properties. An accompanying paper will report on the expression of EBV antigens in this hybrid panel (*13*).

MATERIALS AND METHODS

Cell lines.—The P3HR-1 line was derived from the established Jijoye cell line (*14*). The K562 cell line was derived from a CML patient in blast crisis (*11*) and contained an r(22) marker chromosome (*15*) derived from the original Ph^1 marker (*16*). The TG^r, $HPRT^-$ derivative of Daudi, DIT, previously described (*17*), was routinely grown in the presence of 50 µg TG/ml. The Raji TK^- subline RUD (*18*) was received from Dr. Berge Hampar (NCI Frederick Cancer Research Facility, Frederick, Md.) and grown routinely in the presence of 40 µg BrdUrd/ml. The two $ouab^r$ and TG^r sublines of P3HR-1 and Daudi, PUT and DUT, respectively, were derived from the $ouab^r$ sublines (*19*) by selection for resistance to TG at 50 µg TG/ml. The PUT subline has been described in more detail elsewhere (*10*). The CAP^r and TG^r subline of P3HR-1 was obtained after P3HR-1 was treated with 200 µg of the mutagen EMS/ml for 24 hours; then the TG concentration was increased stepwise to 50 µg TG/ml, and without further EMS exposure, treatment with 1,000 µg CAP/ml resulted in a doubly resistant (50 µg TG/ml, 1,000 µg CAP/ml) subline of P3HR-1, PICAT. P3HR-1 and RUD expired on 100 µg CAP/ml; K562 and RUD expired on 0.1 µ*M* ouab; all TG^r and $BrdUrd^r$ sublines expired on HAT medium. All lines were maintained in RPMI-1640 medium supplemented with 8% FCS and antibiotics (100 IU penicillin/ml, 50 µg streptomycin/ml), with additional supplements as mentioned above.

Cell hybridization.—All hybrids were obtained from cells fused with UV-inactivated Sendai virus, as described (*10*). After 24 hours, the medium was exchanged for HAT medium. For the fusions with PUT and DUT, the HAT medium was supplemented with 1 µ*M* ouab, which was later increased to 10 µ*M*. For the fusions with PICAT, the HAT medium was supplemented with 500 µg CAP/ml. Living cells were separated from dead cells during the hybrid selections by the Ficoll-Isopaque procedure (*20*). Vigorous hybrid growth commenced after 3–4 weeks, after which the first karyotyping was performed.

Chromosome analysis.—Cultures were harvested 1–2 days after subculture, following treatment with Colcemid. Cells were treated with 0.56% KCl for 8 minutes at room temperature, fixed three times, and spread on object slides. Preparations were stained with quinacrine mustard (*21*). For enumeration and more detailed analysis, the metaphases were photographed with a Zeiss photomicroscope that was equipped for fluorescence microscopy with an HB200 mercury light source, a KP500 excitation filter, an LP520 barrier filter, and an FT510 dichroic mirror. Photographic negatives were analyzed by projection (× 4,200), and karyotypes were compiled from photographic enlargements (× 2,400) and arranged according to the Paris Conference (*22*). The description of karyotypes follows the International System for Human Cytogenetic Nomenclature (*23*).

Isozyme analysis.—Cell pellets from parental cell lines and hybrid cells, each pellet containing about 10^7 cells, were used for enzyme analyses. Cells were lysed by freezing and thawing twice in a volume of distilled water approximately equal to that of the cell pellet. The resulting extract was subjected to horizontal starch gel electrophoresis and subsequent enzyme detection by the use of routine methods (*24*).

Cytotoxicity and absorption tests.—The assay for β_2m was by the cytotoxic absorption experiments as described in a previous study (*25*).

Quantitative immunofluorescence.—Cells were washed twice in medium and incubated with FITC-labeled rabbit anti-human β_2m (diluted 1:100; in some experiments, the reagent was Daudi absorbed and used at 1:16), with FITC-labeled rabbit anti-human Ig (1:20), anti-11 IgM (1:15), or with anti-11 κ-chains (1:10) (DAKO-immunoglobulins Ltd., Copenhagen, Denmark) for 30 minutes at 4°C, washed twice, and analyzed in a FACS (FACS III; Becton, Dickinson Electronics Lab., Mountain View, Calif.). CMIF staining was performed as described (*26*). This procedure leads to C3 activation by the cells with subsequent binding of activated C3 to preformed receptors (*27*). After this treatment, the cells were washed twice and similarly analyzed in the FACS III. The results were analyzed by a computer program (Klein, Gunnar: Unpublished program). To correct for nonspecific fluorescence, we defined a "cut level" to include 95% of negative control cells. The results were calculated as the following expressions of relative fluorescence of the cells analyzed: Mean = mean of all determinations/mean of values above cut level, percent positive cells = cells above cut level, and total fluorescence index = arbitrary value representing the area corresponding to cells above cut level.

HLA antigens.—Standard microlymphocyte cytotoxicity was used to determine the HLA antigens of the cells studied. The complement used for the hybrids and their parental lines was absorbed with 40×10^6 pooled lymphoblastoid cells/ml. High-titer HLA antisera diluted to a minimum of 4 cytotoxic U were absorbed with 100 and 20×10^6 cells/ml of antiserum during a 1 hour incubation at 4°C. The cell suspensions were centrifuged, and titrations (double dilutions) of the supernatants were tested for cytotoxicity with lymphocytes positive for the relevant HLA antigen. HLA antisera negative for the cells used for absorption served as the specificity controls. The absorptions were considered positive when the titer of the absorbed antiserum was reduced twofold compared to unabsorbed antisera, after the values for the nonspecific absorption controls were subtracted.

Rosette tests.—For C3 receptors, EAC rosettes were detected as described (*28*). For Fc receptors, sheep RBC were sensitized with rabbit IgG, as described (*29*). For sIg, *Staphylococcus aureus* protein A-coupled RBC rosettes were detected by polyvalent rabbit anti-human Ig. For Ia-like antigens, *S. aureus* protein A-coupled RBC rosettes were detected by rabbit anti-human Ia (Alpha Gamma Laboratories, Sierra Madre, Calif.). Target cells that bound at least three erythrocytes were scored positive in all rosette tests. Cell lines were scored negative when less than 3% formed rosettes.

EBV receptors.—EBV receptors were measured by a modification of the bioassay of Sairenji and Hinuma (*30*), as described in (*31*). An EBV-containing P3HR-1 cell supernatant was used as the virus source in a final dilution of 1:5; the unabsorbed supernatant induced 10–15% early antigen in Raji cells after 48 hours. After absorption with graded numbers of parental and hybrid cells, the residual supernatant was tested for its ability to induce early antigen in Raji cells after 48 hours. Standard EBV receptor-positive (Raji) and EBV receptor-negative (YAC-1) controls were included in each test. The AI was calculated as follows: AI = (maximum percent early antigen induced by unabsorbed control cells−maximum percent early antigen induced by absorbed test cells)/maximum percent early antigen induced by unabsorbed control cells.

Other markers.—*β*-Glucuronidase was assayed in 1% Nonidet P40 cell lysates in which phenolphthalein glucuronic acid was used as a substrate (kit No. 325; Sigma Chemical Co., St. Louis, Mo.). Cell culture supernatants contained less than 0.1 U *β*-glucuronidase/ml at 10^6 cells/ml. Lysozyme was determined turbidimetrically (*32*) and expressed as microgram equivalents of egg lysozyme per 10^6 cells/ml in 24-hour culture supernatants. Extracts contained less than 0.01 µg lysozyme/10^6 cells.

Incorporation of ^{59}Fe by whole cells, as assayed in extracted heme, was determined after incubation of 10-ml cultures with ^{59}Fe (ferrous citrate: 10 µCi/ml, 13.93 µCi/ng; New England Nuclear Corp., Boston, Mass.). Cultures were seeded at 5×10^4 cells/ml and analyzed at day 6. The counts in whole cells and in methyl ethyl ketone-extracted heme, after cleavage of hemoglobin into heme plus globin, was determined by a scintillation counter and expressed as picomoles ^{59}Fe incorporated per 10^5 cells (*33*). Percentages of hemoglobin-positive cells were estimated from cell slides stained with benzidine (*34*).

RESULTS

Derivation of Variant and Hybrid Cells

The five new somatic cell hybrids characterized in the present paper were isolated after fusion of the parental cells, which was induced by UV-inactivated Sendai virus. To facilitate the designation of the hybrid cells, we used the following *abbreviated designations* for the parental cells and their hybrids: The BrdUrd^r, TK$^-$ subline of Raji was designated RUD (*18*). The TG^r, HPRT$^-$ subline of Daudi was designated DIT (*17*). The ouab^r and TG^r (HPRT$^-$) subline of P3HR-1 was designated PUT (*10*). Cell lines lacking selective markers were K562 (*11*) (designated KO) and P3HR-1 (*14*) (designated PO). New variant sublines isolated in the course of the present study were the CAP^r and TG^r (HPRT$^-$) subline of P3HR-1 (designated PICAT) and the ouab^r and TG^r (HPRT$^-$) subline of Daudi (designated DUT).

The double variants containing one recessive (HPRT$^-$) and one dominant (ouab^r or CAP^r) marker permitted the isolation of hybrids from other cell lines carrying no such selective markers when grown in HAT medium supplemented with either ouab or CAP. We used this approach to isolate the DUT × K562 (DUTKO-1) and PICAT × P3HR-1 (PICATPO-1) hybrids. The double variants PUT and PICAT were hybridized with RUD, and double-selective systems (HAT medium with either ouab or CAP) were used to isolate the RUDPUT-2 and RUDPICAT-1 hybrids. In addition, a new Daudi–Raji hybrid was isolated when the standard HAT-medium selection process was used (DIT × RUD = DITRUD-1). The derivation of these somatic cell hybrids is summarized in table 1.

Chromosomal Characterization

RUDPUT-2 and RUDPICAT-1 Hybrids

The RUD parental cell line carried a number of specific markers. Three characteristic markers (4q+, 11q+, and 14q+) were derived from the t(8;14) translocation in BL

TABLE 1.—*Derivation of parental and hybrid cells*

Parental cells				Hybrid cells	Selection method
Cell line (derivation)	Markers (drug resistance)	Designation	Reference		
Raji (BL)	TK$^-$ (BrdUrd^r)	RUD	(*26*)	RUDPUT-2	HAT medium + ouab
P3HR-1 (BL)	ouab^{r}HPRT$^-$ (TG^r)	PUT	(*10*)		
Raji (BL)	TK$^-$ (BrdUrd^r)	RUD	(*26*)	RUDPICAT-1	HAT medium + CAP
P3HR-1 (BL)	CAP^{r}HPRT$^-$ (TG^r)	PICAT	This article		
Daudi (BL)	HRPT$^-$ (TG^r)	DIT	(*25*)	DITRUD-1	HAT medium
Raji (BL)	TK$^-$ (BrdUrd^r)	RUD	(*26*)		
Daudi (BL)	ouab^{r}HPRT$^-$ (TG^r)	DUT	This article	DUTKO-1	HAT medium + ouab
K562 (CML)	None	KO	(*11*)		
P3HR-1 (BL)	CAP^{r}HPRT$^-$ (TG^r)	PICAT	This article	PICATPO-1	HAT medium + CAP
P3HR-1[a] (BL)	None	PO	(*22*)		

[a] P3HR-1 was derived from the cell line Jijoye.

cells, which included Raji (*35*). These markers have also been found in other Raji sublines (*36*). In addition, the RUD line carried two translocation chromosomes in which chromosome 17 was involved. RUD translocations were designated as t(17;?)(q25;?) and t(17;?)(q24;?). The karyotype of RUD can thus be described as 46,XY,4q+,11q+, 14q+,t(17;?)(q25;?),t(17;?)(q24;?).

The karyotype of PUT was similar to that previously described (*10*), with the karyotype 48,XY,+large metacentric chromosome,+small metacentric chromosome,14q+. The karyotype of the PICAT subline indicated two types of cells with different karyotypes and containing a small metacentric marker (similar to the corresponding marker in PUT), a submetacentric marker, and a new characteristic isochromosome of the short arm of X, i(Xp). In approximately 60% of the cells, an additional marker presumably derived from the i(Xp) appeared, resulting in an increase in chromosome number from 48 to 49. The karyotype of the population of PICAT cells may therefore be represented as 48,Y,i(Xp),+small metacentric chromosome,+submetacentric chromosome/49,Y,i(Xp),?i(Xp),+small metacentric chromosome,+submetacentric chromosome.

The RUDPUT-2 hybrid cells, isolated approximately 1 month after fusion of the parental cells, had a modal chromosome number of 94, which was expected from the summation of the parental RUD and PUT modal chromosome numbers (46+48=94). The markers of the two parents were represented in very high frequency in the metaphases analyzed (table 2). Two characteristic new markers, 13q+ and Yp+, were present in all RUDPUT-2 hybrid metaphases. Some metaphases appeared to have lost the small metacentric marker of PUT. A representative karyotype of RUDPUT-2 is shown in figure 1. The karyotype can be represented as 94,XXY,Yp+,+large metacentric chromosome,+small metacentric chromosome,4q+,11q+,13q+, 14q+,14q+,t(17;?)(q25;?),t(17;?)(q24;?).

The RUDPICAT-1 hybrid cells were similarly isolated about 1 month after fusion of RUD with PICAT. The RUDPICAT-1 hybrid cells had a modal chromosome number of 94, which was similar to that of RUDPUT-1, but a few cells with 95 chromosomes were also found. Most hybrid cells appeared to be derived from the fusion of RUD with PICAT cells containing 48 chromosomes, and the modal number of 94 chromosomes in RUDPICAT-1 therefore corresponded to what is expected from the summation of the parental chromosome numbers (46+48=94). The markers of RUD were recognized in most metaphases, though the RUD-derived 14q+ marker was lost in most metaphases. A lower proportion of PICAT markers was recognized in the RUDPICAT-1 hybrid metaphases, and

TABLE 2.—*Chromosome markers in metaphase karyotypes of parent and hybrid cells*

Hybrid cells	Cells tested (No. of metaphases)	Presence of marker, % of metaphases[a]												
										New				
		4q+	11q+	14q+	17q+[b]	17q+[c]	14q+	LMC	SMC	13q+	Yp+			
RUDPUT-2 and RUDPICAT-1	RUD (26)	100	89	74	100	96								
	PUT (13)						100	100	100					
	RUDPUT-2 (12)	100	77	100	100	100	92	100	62	100	100			
							i(Xp)	?i(Xp)	SMC	subMC	New, +16			
	PICAT (28)						65	38	8	33				
	RUDPICAT-1 (17)	80	71	19	95	90	95	0	0	1	5			
							15q−[d]	14q+						
DITRUD-1	DIT (14)						100	100						
	RUD (26)	100	89	74	100	96								
	DITRUD-1 (20)	85	85	80, 40[e]	95	5	75	80, 40[e]						
													New	
		+7	3q+	15q−[d]	14q+	del(3)(p11)	del(9)(p11)+9(p11)	15q−	18q+	r(22)	del(X)(p21)	SMC	LsubMC	LsubMC
DUTKO-1	DUT (14)	93	93	100	93	100	100	100	100	100	43	50		
	KO[f] (14)					100	100	100	100	100	43	50		
	DUTKO-1 (21)	0	0	81	76	38	52	62	90	62	5	48	24	14
		i(Xp)	?i(Xp)	SMC	subMC	14q+	+11	14q+	LMC	2LMC				
PICATPO-1	PICAT (28)	65	38	8	33	8								
	PO[g] (22)						100	76	54	14				
	PICATPO-1 (12)	92	8	0	75	75, 17[e]	50	75	75, 17[e]	0				

[a] LMC=large metacentric chromosome; LsubMC=large submetacentric chromosome; SMC=small metacentric chromosome; subMC=submetacentric chromosome.

[b] t(17;?)(q25;?).

[c] t(17;?)(q24;?).

[d] del(15)(q14q21).

[e] Metaphases had *two* 14q+ markers identified.

[f] Cell line is K562 lacking selective markers.

[g] Cell line is P3HR-1 lacking selective markers.

two PICAT markers, ?i(Xp) and a small metacentric marker, were not found in any of the metaphases analyzed (table 2). In a small fraction of metaphases, an additional chromosome 16 was present. A representative karyotype of RUDPICAT-1 is shown in figure 1. The karyotype can be represented as 94,XYY,i(Xp),+submetacentric chromosome,+16,4q+,11q+,14q+,t(17;?)(q25;?),t(17;?)(q24;?).

DITRUD-1 Hybrid

The karyotype of DIT (Daudi-TG) was found to be identical to that previously published (*17*): 46,XY,14q+, del(15)(q14q21). The 14q+ marker, presumably derived from the BL t(8;14) translocation, was found in 100% of the cells analyzed. The specific interstitial deletion of one chromosome 15, del(15)(q14q21), was also found in other Daudi cell lines, also completely deficient in β_2m production (*37*). The standard locus for β_2m was assigned to the affected region of chromosome 15 (*38–40*).

The DITRUD-1 hybrid contained markers from both of its parents, DIT and RUD. Several months after selection, it had a modal chromosome number of 92, as expected from the summation of the parental cell modal number (46+46=92). The markers of the two parents were represented in the hybrid metaphases, as described in table 2. A few additional new markers were observed in some metaphases like the one illustrated in figure 2, in which the karyotype was 91,XXYY,+submetacentric chromosome,+acrocentric chromosome,−14,−16,−17,t(i(1q);?)(q36;?),4q+,11q+,14q+,14q+,del(15)(q14q21),t(17;?)(q24;?),t(17;?)(q25;?).

DUTKO-1 Hybrid

The karyotype of K562 (a cloned subline) was identical with that previously described (*10*) [69,XXX,+7,+9(p11),+small metacentric chromosome,−13,−17,−21,del(X)(p21), del(3)(p11),del(9)(p11),15q−, 18q+,r(22)], with loss of one chromosome 21 as the only difference from cultures studied 5 years ago (*15*). The karyotype of DUT was 47,XY,+7, 3q+,14q+,del(15)(q14q21). A deviation from the typical minimal deviation karyotype of Daudi was observed in this case. The gain of an extra chromosome 7, as found here, is a common observation during long-term cultivation of diploid lymphoblastoid cell lines.

The modal chromosome number of DUTKO-1 hybrid was 113, as determined several months after its selection. This is only two chromosomes less than the expected number (46+69=115). The marker chromosomes are indicated in table 2. In addition to the parental markers, two new submetacentric markers appeared in the DUTKO-1 hybrid. A representative karyotype is shown in figure 3: 113,XXXY,del(X)(p21),+2,+7,+small metacentric chromosome,+submetacentric chromosome,+large submetacentric chromosome,−4,−6,−6,−13,−17,−18,−21,−22,del(3)(p11),csb(9)(p11),del(9)(p11),15q−,18q+,r(22),14q+,del(15)(q14q21).

PICATPO-1 Hybrid

A P3HR-1 subline was hybridized with the PICAT variant, also derived from the parental P3HR-1 line, and therefore should represent a hybrid formed by the fusion of two P3HR-1 sublines. The parental, unmarked P3HR-1 subline (PO) used for hybridization was of the karyotype 48,XY,+11,+large metacentric chromosome,14q+. The karyotype of PICAT was identical to that described previously [48,Y,i(Xp),+small metacentric chromosome,+submetacentric chromosome/49,Y,i(Xp),?i(Xp),+small metacentric chromosome,+submetacentric chromosome]. The 14q+ marker was scored in only a low percentage of metaphases from PICAT, even in metaphases with quality good enough to discount the lack of detection for technical reasons; we therefore suggest that part of the population lost its 14q+ marker during cultivation.

Inasmuch as the two P3HR-1 sublines showed identical isozyme profiles, the detailed chromosomal characterization was particularly important for the characterization of the PICATPO-1 hybrid, because tetraploid cells arise rather frequently in cultures of BL cells. The PICATPO-1 hybrid cells, isolated approximately 1 month after fusion, had a modal chromosome number of 96, as expected (48+48=96); however, some cells corresponding to the karyotype indicated in figure 4 had 97 chromosomes. The karyotype (fig. 4) is 97,XYY,i(Xp),?i(Xp),+11,+small metacentric chromosome,+submetacentric chromosome,+large metacentric chromosome,14q+. Most metaphases contained only one 14q+ marker chromosome, in agreement with the apparent loss of this marker in most metaphases of the PICAT parent. The presence of the PICAT-derived markers [i(Xp),?i(Xp), small metacentric chromosome,submetacentric chromosome] in addition to the PO markers (+11,large metacentric chromosome) identifies the PICATPO-1 line as a true hybrid (table 2).

Isozyme Analyses

The parental and hybrid lines were tested for a number of marker enzymes previously found useful in cell identification (*41*) as well as for some additional enzymes (table 3). For the RUDPUT-2 and RUDPICAT-1 hybrids, four loci were informative: that for phosphoglucomutase 3 (*PGM3*), for glyoxalase I (*GLO*), for adenine phosphoribosyltransferase (*APRT*), and for peptidase A (*PEPA*). Glyoxalase I, a dimeric enzyme, provided good confirmation of the hybrid origin of the cells since RUD was type 2 and the P3HR-1 sublines were type 1 (table 3). DITRUD-1 was confirmed to be a hybrid by two informative loci: that for glucose-6-phosphate dehydrogenase (*G6PD*) and that for phosphoglucomutase 3 (*PGM3*). In addition, the parents of DITRUD-1 were abnormal in respect to expression of lysosomal hexosaminidases A and B [*HEXA* and *HEXB* (*42*)], and these defects were not complemented in the hybrid (table 3). For DUTKO-1 the following loci were informative: *PGM3*, *G6PD*, and that for phosphoglucomutase 1, *PGM1*, where the deficiency of K562 was complemented (table 3).

ME1 was absent in all BL cell lines tested but was present in K562; this enzyme was also expressed by DUTKO-1 (table 3). Further studies (*43*) indicate that this particular enzyme deficiency is a marker for the differentiation of malignant lymphoma and leukemia cells.

best copy available

TABLE 3.—*Isozyme characterization of parent and hybrid cells*[a]

Locus	Chromosome	K562	RUD	P3HR-1	PUT	PICAT	Daudi	RUDPUT-2	RUDPICAT-1	DITRUD-1	DUTKO-1
PGM1	1	0[b]	1	1	1	1	1	1	1	1	1, weak
PGM3	6	1	1	2	2	2	2	2[c]	2	2-1 (2>1)	2-1 (1>2)
GOT2	16	2-1	1	1	1	1	1	x-1 (1>x)	1	1	1
APRT	16	1	1	x-1	x-1	x-1	1	2-1 (1>2)	x-1 (1>x)	1	1
PEPA	18	1	1	2-1	2-1 (2>1)	2-1	1	B	2-1	1	1
G6PD	X	B	B	B	B	B	A	0	B	A-B	A-B
ME1	6	Strong	0	0	0	0	0	NT	NT	NT	Weak
HEXA, HEXB	15 and 5	NT	Fast	NT	NT	NT	0		NT	Weak	NT
GLO	6	2	2	1	1	1	2	2-1	2-1	NT	2

[a] By starch gel electrophoresis, 0=absent, 1=type 1, and 2=type 2. For APRT, x=variant; for G6PD, A=type A and B=type B. NT=not tested.

[b] A trace of enzyme was possibly present.

[c] Activity was very weak; cells could possibly have a trace of phosphoglucomutase 3-1.

Absorption Experiments

Rabbit anti-human β_2m antiserum, diluted 1:20, gave a cytotoxicity index between 0.80 and 0.95 against target P3HR-1 cells in various experiments. Text-figure 1 shows the results of absorptions performed with intact living cells and the corresponding absorptions made with lysates from frozen–thawed cells.

The β_2m-negative Daudi line absorbed no anti-β_2m in contrast to the positive control Raji cell line. The DITRUD-1 hybrid absorbed more than Raji, showing that the lack of β_2m is complemented after fusion of Daudi with Raji. Similar results were found with frozen–thawed cells. Living DUTKO-1 hybrid cells and their K562 parent absorbed anti-β_2m weakly. The corresponding experiment with frozen–thawed cells gave weak absorption for K562 and a somewhat increased absorption with DUTKO-1. The intermediate concentrations of β_2m of P3HR-1 found here correspond to the concentrations in the two sublines PUT and PICAT. The expression of β_2m by the DUTKO-1 hybrid was similar to that previously observed for the P3HR-1–K562 (PUTKO-1) hybrid (*10*).

Quantitative Immunofluorescence

Immunofluorescence staining of living cells was performed with an FITC-conjugated rabbit anti-human β_2m antiserum diluted 1:100. The membrane immunofluorescence-stained cells were analyzed in flow fluorimetry in a FACS cell sorter, and the distributions of fluorescence intensity were evaluated and plotted by means of a computer program. We defined our parameters in "Materials and Methods."

An example of this analysis performed on Daudi cells is given in text-figure 2. The DITRUD-1 hybrid showed complete expression of β_2m (text-fig. 2). A slight increase in fluorescence intensity was noted in the measurements on DUTKO-1 and its parents in the standard immunofluorescence analysis. However, it was not possible from these results to evaluate whether the increase was due to nonspecific fluorescence. For more precise estimation of DUTKO-1 β_2m expression, the immunofluorescence analysis was repeated with a less dilute (1:16) Daudi-absorbed rabbit anti-human β_2m reagent. In this series of experiments, the DUTKO-1 hybrid had markedly increased β_2m fluorescence compared to that of the two parental cell lines. The results from the quantitative analyses for β_2m are summarized in table 4.

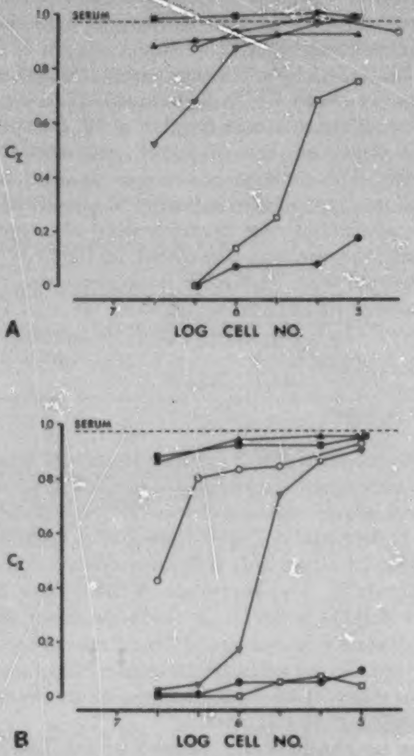

TEXT-FIGURE 1.—Quantitative absorption for β_2m with A) intact living cells and B) frozen–thawed cells. Rabbit anti-human β_2m serum was used at a dilution of 1:20. The cytotoxicity index (C_I) of the unabsorbed serum is indicated by ----. ▲=K562 (KO); ○=DUTKO-1; ■=Daudi; ▽=P3HR-1; □=Raji; ●=DITRUD-1.

A similar analysis was done for sIg expression. An example of the results for the DITRUD-1 hybrid is given in text-figure 3. The Daudi and Raji parental cells expressed very different levels of sIg (IgM κ-chain): Daudi expressed very high levels while Raji was almost negative. The DITRUD-

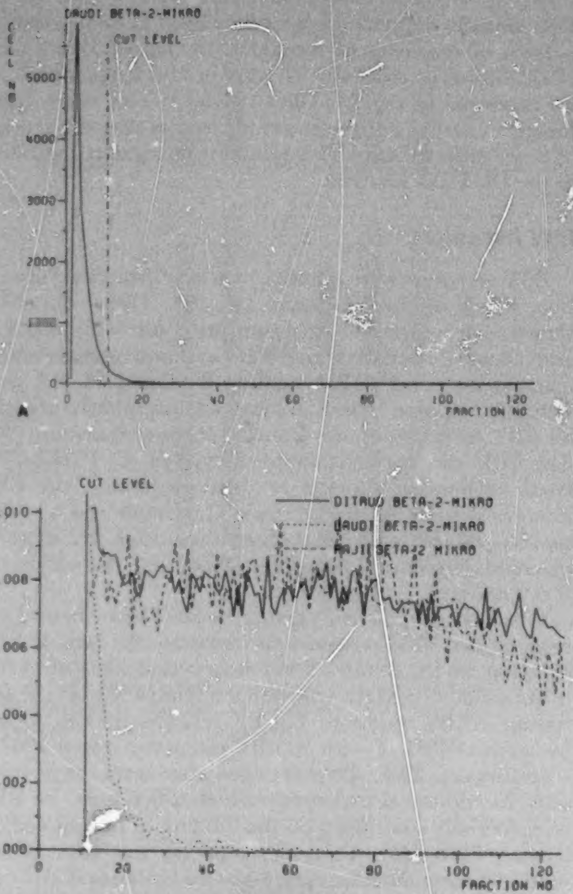

TEXT-FIGURE 2.—Quantitative immunofluorescence analysis of cells stained for surface β_2m (BETA-2-MIKRO) with an FITC-conjugated rabbit anti-human β_2m serum at a dilution of 1:100 and analyzed in the FACS. A) Analysis of β_2m-negative Daudi cells. The cut level, which includes 95% of the known negative cells, is indicated by ----. B) Analysis of the DITRUD-1 hybrid (DITRUD) and its two parents (RAJI and DAUDI). The Raji parents are β_2m-positive, as is the equally positive hybrid.

1 hybrid expressed intermediate sIg fluorescence as compared to the highly positive Daudi cell line. The DUTKO-1 hybrid showed an absolute suppression of sIgM, indicating extinction of this B-cell marker. The two Raji–P3HR-1 hybrids (RUDPUT-2 and RUDPICAT-1) were also analyzed for sIg; here, the relatively stronger expression of P3HR-1 dominated in the hybrids. The results of analyses of sIg expression are summarized in table 4.

HLA Antigens

The presence of HLA antigens was analyzed by complement-mediated cytotoxicity by the use of 1980 Workshop antisera (*44*). The P3HR-1 sublines PUT and PICAT were HLA-positive (A3;B17,w4;Cw4), although the detection of the third locus antigen (Cw4) was doubtful in PICAT. The RUD parent was positive for HLA-A3; Bw6;Cw3,w4. No HLA-A,B,C antigens were found on the DUT parental line in accordance with our previous data for Daudi cells (*25, 45*). The K562 cell line was negative for HLA-A,B,C and Ia-like antigens in accordance with previous results (*10*). The results of HLA typing of the parental cells and hybrids are summarized in table 5.

Since the DITRUD-1 hybrid was observed to express normal levels of β_2m, we assumed, analogous to our previous results showing complementation of the β_2m deficiency of Daudi cells and leading to re-expression of "hidden" HLA specificities in hybrids (*25, 45*), that this situation would be true also for the DITRUD-1 hybrid. The DITRUD-1 hybrid carried all the specificities except Cw4 of RUD; in addition the following new specificities were re-expressed: A26 (part of A10);B17,w4. No HLA antigen specificities were detected on DUTKO-1 and either of its two parents (DUT and K562) when standard cytotoxicity was measured.

Since the PUTKO-1 hybrid (*10*) was observed to express very low, subcytotoxic concentrations of the P3HR-1-derived specificity HLA-A3 by the relatively more sensitive absorption test, this test was used in an attempt to detect a low level of re-expression of the Daudi-derived hidden HLA specificities A26 and B17. An anti-B17 serum was absorbed by DUTKO-1 cells at 100×10^6 cells/ml, but at 20×10^6 cells/ml, absorption was doubtful. Anti-A26 serum and anti-B12 serum (anti-B12 was used as a specificity control) were not absorbed at either of the two cell concentrations. These results indicate that the observed complementation with respect to β_2m expression leads to re-expression of HLA.

TABLE 4.—*Quantitative immunofluorescence of surface β_2m and Ig*

Cells tested	Surface globulin	Parameters			
		Cut level	Mean[a]	Percent positive cells	Total fluorescence index
DITRUD-1[b]	β_2m	11	55.6	87.7	48.8
Raji	β_2m	11	55.0	85.0	46.8
Daudi	β_2m	11	9.4	6.5	0.6
DUTKO-1[b]	β_2m	20	22.7	41.6	9.44
K562	β_2m	20	18.1	31.8	5.76
Daudi	β_2m	20	14.5	23.7	3.44
DUTKO-1[c]	β_2m	49	*81.7*	40.9	33.4
K562	β_2m	49	*72.7*	16.4	11.9
Daudi	β_2m	49	*81.0*	4.9	4.0
DITRUD-1[d]	IgM	11	20.1	68.7	13.8
Raji	IgM	11	13.2	3.9	0.52
Daudi	IgM	11	21.7	79.5	17.3
DITRUD-1[e]	κ-chains	11	23.5	70.9	16.7
Raji	κ-chains	11	15.0	2.0	0.3
Daudi	κ-chains	11	41.5	82.9	34.2
8A[d]	IgM	17	10.2	16.1	1.64
Raji	IgM	17	6.0	4.8	0.29
Daudi	IgM	17	29.4	60.7	17.9
RUDPUT-2[f]	Ig	14	*29.5*	26.8	7.9
Raji	Ig	14	*24.2*	2.9	0.7
PUT	Ig	14	*27.8*	4.5	1.3
RUDPICAT-1[f]	Ig	14	*30.1*	16.0	4.8
Raji	Ig	14	*24.2*	2.9	0.7
PICAT	Ig	14	*38.8*	10.7	4.1

[a] Mean is of all values; *italicized* mean is the mean of values that exceeds the cut level (arbitrary units).

[b] Cells were tested with anti-β_2m at 1:100.

[c] Cells were tested with Daudi-adsorbed anti-β_2m at 1:16.

[d] Cells were tested with anti-IgM at 1:15.

[e] Cells were tested with anti-κ at 1:10.

[f] Cells were tested with anti-Ig at 1:20.

The reason that only one specificity (that of B17) was found to be re-expressed could be that this particular specificity competes more efficiently for the very limited amounts of β_2m available on the cell surface than does A26.

The DUTKO-1 hybrid and its two parents were also analyzed by the use of typing sera against Ia-like (HLA-DR) antigens for cytotoxicity. While DUT showed a similar pattern of reactivity as compared to that of Daudi, and K562 showed no reactivity whatsoever, this Ia reactivity was *not* expressed in the DUTKO-1 hybrid. This result (confirmed by Ia-like antigen rosetting) argues that this marker of B-cell differentiation, in addition to sIg, was extinguished in the DUTKO-1 hybrid.

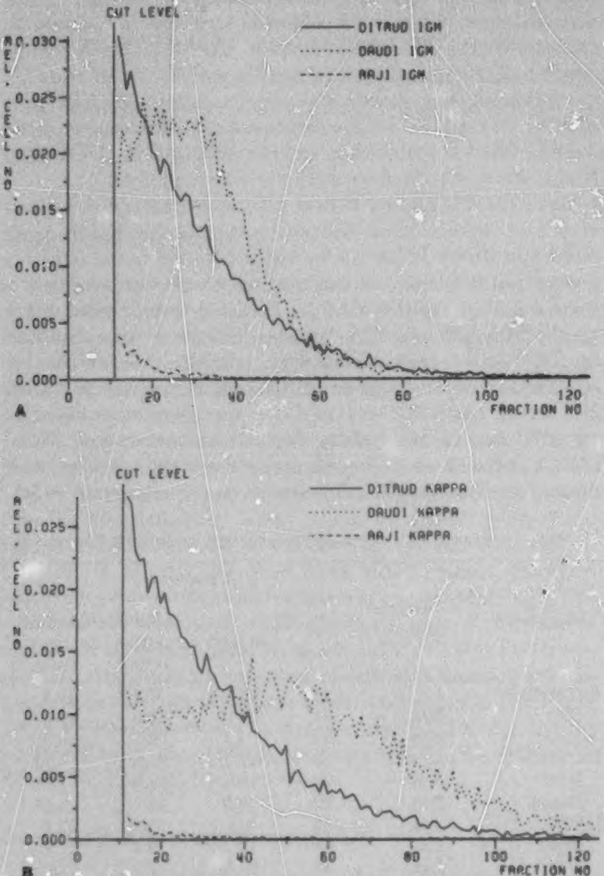

TEXT-FIGURE 3.—Quantitative immunofluorescence analysis of cells stained for sIg and analyzed in the FACS. The DITRUD-1 hybrid (DITRUD) and its two parents (RAJI and DAUDI) were stained for A) sIgM (IGM) with FITC-conjugated rabbit anti-human IgM at a dilution of 1:15 and for B) κ-chains (KAPPA) with FITC-conjugated anti-human κ-chains at a dilution of 1:10. The cut level excludes 95% of Raji cells.

EBV Receptors

EBV receptors were assessed by a modified virus absorption, infectious virus bioassay (*30, 31*). These results are shown in text-figure 4. As shown previously (25), the Raji and Daudi lines had a high EBV-receptor concentration, whereas the two P3HR-1 sublines PUT and PICAT were virtually negative. The K562 line was completely negative for EBV receptors, as also found in our previous study (*10*). The EBV receptor-negative phenotype of the P3HR-1-derived sublines in contrast to their progenitor, the EBV receptor-positive BL line Jijoye (*14*), is explained by selection in culture; whereas the negativity of K562 must be regarded as a natural property of K562 cells, which are not B-cell derived.

Like its negative K562 parent, the DUTKO-1 hybrid was negative for EBV receptors. In contrast, the lack of EBV receptors in PUT and PICAT was complemented by hybridization with RUD, which had a relatively high concentration of EBV receptors. The PICATPO-1 hybrid, derived by fusion of PICAT with an EBV receptor-negative P3HR-1 subline, was EBV receptor-negative, as were the parental cells. In additional experiments, a modified assay for EBV receptors was used based on the binding of [^{3}H]thymidine-labeled EBV (*46*). This very sensitive test gave similar results to those of the standard absorption assay.

Complement Receptors

For CMIF staining of C3, target cells were exposed to human complement (from EBV-negative donor serum) and were then stained with FITC-conjugated anti-human C3 (*26*). The data from the combined CMF and EAC analyses of the parent and hybrid cells are shown in table 6.

In contrast to the Raji and Daudi cell lines, which were highly positive for C3 receptors, P3HR-1 and its sublines PUT and PICAT were virtually negative. The three hybrids RUDPUT-2, RUDPICAT-1, and DITRUD-1 were intermediate between their parents. PICATPO-1 was higher

TABLE 5.—*HLA specificities detected by complement-mediated cytotoxicity*[a]

Parental cells	HLA antigens present			Hybrid cells	HLA antigens present		
	A	B	C		A	B	C
RUD	A3	4b	Cw3,w4	RUDPUT-2	A3	B17,w4,w6	Cw3?,w4
PUT	A3	B17,w4	Cw4				
RUD	A3	w6	Cw3,w4	RUDPICAT-1	A3	B17,w4,w6	Cw3,w4
PICAT	A3	B17,w4	Cw4?				
DIT	–	–	–	DITRUD-1	A3,26	B17,w4,w6	Cw3
RUD	A3	w6	Cw3,w4				
DUT	–	–	–	DUTKO-1	–	±	–
KO	–	–	–				

[a] –=negative reaction; ±=weak reaction for HLA-B17 in absorption.

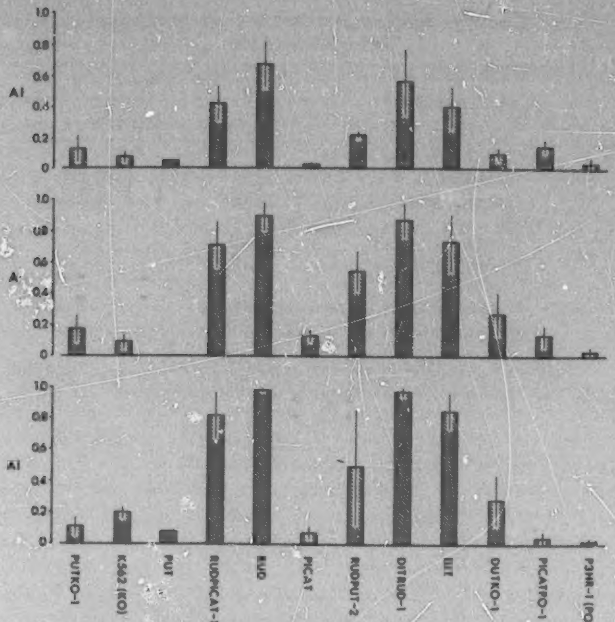

TEXT-FIGURE 4.—Determination of EBV receptor concentrations on parent and hybrid cell lines by the virus absorption, infectious virus bioassay of Sairenji and Hinuma (*30*), as modified in (*31*). AI is indicated at three concentrations of cells used for absorption: 1×10^6 (*upper panel*), 5×10^6 (*middle panel*), and 10×10^6 (*lower panel*).

TABLE 6.—*Detection of complement (C3) receptors on parent and hybrid cells*

Cells tested	CMIF[a] Visual, % positive[b]	CMIF[a] Total fluorescence index[c]	EAC, %
RUD	100	39.6	90
P3HR-1	0	2.1	0
PUT	0	4.0	0
PICAT	0	1.7	0
DIT	100	NT	89
K562	0	NT	6
RUDPUT-2	48	7.7	47
RUDPICAT-1	37	16.8	41
PICATPO-1	NT	5.7	34
DITRUD-1	NT	NT	48
DUTKO-1	TR	NT	25
PUTKO-1	TR	NT	12

[a] NT=not tested; TR=all cells showed a trace of positive reactivity.

[b] Percentages were determined by fluorescence microscopy.

[c] Arbitrary values were derived from quantitative analysis in the FACS.

than both parents, as judged from EAC rosetting. K562, DUTKO-1, and PUTKO-1 were weakly stained in the CMIF reaction and also gave a low frequency of EAC rosettes.

A close steric relationship has been established between the EBV and C3 receptors (*26, 47*). In the present data, there is a strong correlation between these parameters, as estimated by EBV absorption and by EAC rosetting. The plot of percent EAC rosettes against the EBV AI for the various cell lines and hybrids (text-fig. 5) shows a good correlation (r=0.84).

Rosette Tests for Surface Markers

Table 7 summarizes results for Fc receptors detected by EA rosettes (rabbit IgG antibody-coated sheep RBC), for sIg detected by *S. aureus* protein A-coupled RBC rosettes (polyvalent anti-human Ig), and for Ia-like (DR) antigens detected by *S. aureus* protein A-coupled RBC rosettes (rabbit anti-human Ia reagent).

The K562 cell line was characterized by a high percentage of EA rosette-positive cells, confirming previous results (*15*). In spite of the presence of Fc receptors, K562 was not capable of phagocytosing or lysing antibody-coated cells. RUD, DUT, P3HR-1, and its two sublines PUT and PICAT were negative for Fc receptors. Fc receptors were clearly amplified in the hybrids RUDPUT-2, RUDPICAT-1, and PICATPO-1, since these were all positive in the rosette tests (30% rosettes) compared to their respective parental lines. The DUTKO-1 line resembled its parental K562 line.

K562 was negative for B-cell markers like sIg and Ia-like (DR) antigens. The DUT line expressed high levels of sIg (IgM) and Ia-like antigen. Both of these markers were completely extinguished in the DUTKO-1 and PUTKO-1 hybrids. The Raji subline RUD showed a low but definite sIg expression in the rosette test and also showed a high level of Ia. The results for the various P3HR-1 sublines varied. PUT was negative for sIg, whereas P3HR-1 and PICAT both contained 16–17% positive cells. The PICATPO-1 cell line showed a surprisingly strong expression of Ia compared to that of its parents.

The RUDPUT-2 and RUDPICAT-1 hybrids exhibited dominance of the high levels of Ia expression characteristic of RUD, but the low levels of sIg expressed were similar to those of the parent cells. For DITRUD-1, the rosette tests confirmed the dominance of sIg expression observed previ-

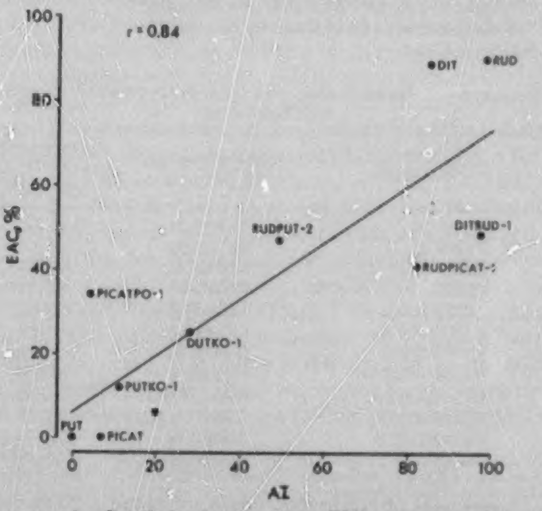

TEXT-FIGURE 5.—Correlation between mean EBV receptor concentration (expressed by AI for 10×10^6 cells) and C3 receptors (determined as percent EAC rosettes) in the present panel of hybrid and parental cells. r=0.84, P<0.01.

ously. Ia-like antigens were expressed at levels similar to the high levels characteristic of the RUD parent.

Markers of Myeloid and Erythroid Differentiation

K562 contained high levels of β-glucuronidase and secreted lysozyme at high levels (table 8), as would be expected for cells related to the myeloid or monocytoid lineage. In contrast to the other BL lines tested here, the Daudi-derived DUT line expressed high levels of β-glucuronidase. None of the BL lines tested secreted lysozyme. The DUTKO-1 and PUTKO-1 hybrids had high levels of β-glucuronidase and secreted lysozyme, indicating dominance of the K562 phenotype (table 8).

K562 shows several of the properties of erythroid cells (48–52). One property is induction of hemoglobin synthesis by the inducer hemin (*50*). We compared K562, DUT, and the DUTKO-1 hybrid with respect to the levels of ^{59}Fe incorporated into extracted heme in the presence or absence of hemin, as well as compared the induction of benzidine-positive cells in the presence of this inducer. The ^{59}Fe incorporated into the extracted heme was significantly higher in K562 than in DUT. In the presence of hemin, the levels for K562 were increased more than twice. The DUTKO-1 hybrid had approximately twice the amounts of ^{59}Fe incorporated into heme as did K562, and this level was further increased after hemin induction (table 9). Similar results were obtained for the PUTKO-1 hybrid. Benzidine-positive cells appeared after 1 day and increased to about 90% after 5 days in the presence of hemin (text-fig. 6) in cultures of K562 and DUTKO-1. The PUTKO-1 hybrid gave similar results.

TABLE 7.—*Rosette tests for surface markers on parent and hybrid cells*

Cells tested	Receptor-positive cells,[a] %		
	Fc[b]	sIg	Ia
K562	64	0	0
P3HR-1	0	17	7
PUT	0	0	50
PICAT	0	16	27
DUT	48	96	94
RUD	0	5	70
RUDPUT-2	20	12	72
RUDPICAT-1	11	8	60
DITRUD-1	30	47	65
PICATPO-1	17	NT[c]	73
DUTKO-1	82	0	0
PUTKO-1	76	0	0

[a] For procedures, see "Materials and Methods."

[b] Fc receptors were quantitated by EA rosettes.

[c] NT=not tested.

TABLE 8.—*β-Glucuronidase and lysozyme production by parent and hybrid cells*

Cells tested	β-Glucuronidase,[a] U/10^6 cells	Lysozyme secreted,[b] U/10^6 cells/24 hr
K562	1.85±0.34	0.24±0.03
P3HR-1	0.11±0.02	<0.03
PUT	0.08±0.02	<0.03
PICAT	0.05±0.01	<0.03
DUT	1.90±0.28	<0.03
RUD	0.18±0.01	<0.03
RUDPUT-2	0.40±0.04	<0.03
RUDPICAT-1	0.22±0.01	<0.03
DITRUD-1	0.34±0.04	<0.03
PICATPO-1	0.08±0.01	<0.03
DUTKO-1	0.98±0.12	0.32±0.03
PUTKO-1	0.77±0.11	0.19±0.02

[a] Assays were of cell lysates. Values are means ± SEM. Culture supernatants contained 10^6 cells/ml.

[b] Assays were of 24-hr culture supernatants. Values are means ± SEM, expressed as microgram equivalents of egg lysozyme/10^6 cells/ml. Extracts contained <0.01 U/10^6 cells.

TABLE 9.—*Incorporation of ^{59}Fe in whole cells and into extracted heme*

Cells tested	^{59}Fe content[a]	
	Whole cells	Extracted heme
DUT		
Untreated	10.15	0.032
Hemin treated	19.11	0.026
K562		
Untreated	27.52	0.23
Hemin treated	87.10	0.45
DUTKO-1		
Untreated	46.49	0.46
Hemin treated	178.81	0.95

[a] Content was measured on day 6 as picomoles ^{59}Fe incorporated/10^5 cells that had been seeded without or with 0.1 m*M* hemin.

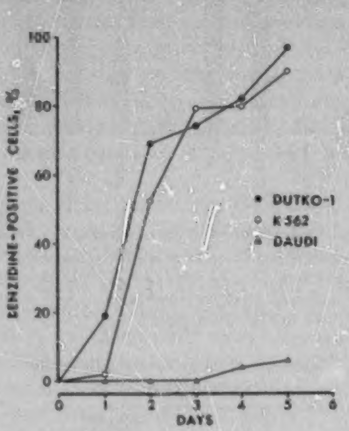

TEXT-FIGURE 6.—Induction of benzidine-positive cells in the presence of 0.1 m*M* hemin.

DISCUSSION

Previous work with hybrids between human hematopoietic cells (*1–6, 10, 15, 17*) has demonstrated a relatively high degree of stability for such hybrids with respect to chromosome, isozyme, and phenotype markers. This agrees with the evidence presented in this paper and argues well for the use of such hybrids in studies in which differentiation-related mechanisms of hybrid cells are examined, which at present is one of the few ways by which such an analysis can be achieved. A more analytical approach would be the use of hybrids of this type for targeted selection experiments against single phenotypic traits when the fate of additional markers are followed.

The results presented here extend and complement our previous studies (*1–6, 10, 15, 17*). Similarly, as in our previous work, we could unequivocally identify hybrids by the chromosome marker analysis described here. In one situation, that of the "autohybrid" (PICATPO-1) formed by the fusion of two P3HR-1 sublines, this approach was found useful for hybrid identification in a situation when other means of identification (e.g., HLA, isozymes) would have been uninformative.

As expected, HLA was coexpressed in the hybrids examined. Two hybrids are of special interest as regards HLA expression: The characteristic lack of β_2m in the Daudi line (*25, 37*) was fully complemented in the Daudi–Raji (DITRUD-1) hybrid, with resulting re-expression of new HLA-A,B specificities (A26 and B17), thus confirming previous data (*25, 45*). As shown previously (*37*), the K562 cell line was deficient in membrane-expressed β_2m but did contain intracellular β_2m. This membrane defect of K562 has been previously observed to be partially dominant in the P3HR-1-K562 hybrid PUTKO-1 (*10*), since only one P3HR-1-derived specificity (HLA-A3) was detected in low amounts on the surface of this hybrid line. The hybrid between Daudi and K562 (DUTKO-1) described here is therefore derived from two phenotypically different β_2m-deficient lines, and genetic complementation could be expected, as demonstrated here by the re-expression of low amounts of the Daudi-derived specificity HLA-B17.

Isozymes were also coexpressed in the hybrid lines in confirmation of their hybrid derivation. In the present and additional studies (*43*), the enzyme *ME1* was found to be absent from all BL-derived cell lines and their hybrids as well as from other cells of lymphoreticular, malignant origin. The parent K562 cell line and its two hybrid lines generated with BL cells expressed *ME1*, in line with the dominance of the K562 phenotype in these hybrids. That this effect could be related to the more primitive phenotype of K562 is suggested by the observation that human *ME1* is re-expressed in hybrids of BL cells with a murine teratocarcinoma cell line (*43*).

The expression of sIg in the hybrids between BL cells studied here suggests that strong expression of sIg is uninfluenced by fusion of highly sIg-positive cells with cells having low or undetectable expression of sIg. The Daudi line (as well as its two sublines DUT and DIT) is characterized by very high amounts of surface IgM κ-chain shown to be fully expressed in a Daudi–P3HR-1 hybrid (*17*). This observation would be in line with the autonomous expression of sIg indicated by the amount of and class of light chains expressed on the surface of Raji–Namalwa cell hybrids (*4*). A previously isolated Daudi–Raji hybrid, 8A (*53*), gave only low expression of sIgM (*25*), in marked contrast to the Daudi–Raji hybrid DITRUD-1 described here. A likely explanation for this difference is the different methods by which these hybrids were selected: The first (8A) hybrid was isolated from an adherent HPRT$^-$ Raji derivative and normal Daudi parent cells when hybrids were selected for adherent growth in HAT medium, whereas the second (DITRUD-1) hybrid was selected by standard HAT-medium selection methods from cells in suspension. Since expression of differentiated phenotypes can be related to cell shape (*9*), it is possible that the exceptional result in our previous study (*25*) could be caused by the selection of adherent cells (*53*).

In contrast to the hybrids between BL cells, the hybrid derived by fusion of Daudi and the K562 line showed complete loss of detectable sIg. The Daudi–K562 hybrid showed absence of EBV receptors, as did K562, but showed a very high level of Fc receptors, also similar to K562. Furthermore, in the other BL–BL hybrids, the levels of Fc receptors characteristic of the more highly expressing parent dominated, with the exception of the Daudi–Raji (DITRUD-1) hybrid. The two P3HR-1 sublines (PUT and PICAT) showed absence of EBV receptors in contrast to the parental P3HR-1. Such selection for absence of EBV receptors in cultures of EBV-producing cell lines has been observed previously and is thought to be caused by the selection of cells that are resistant to superinfection by EBV which has been released into the culture medium (*31*). The expression of EBV receptors was fully restored in the two Raji–P3HR-1 hybrids (RUDPUT-2 and RUDPICAT-1), while the P3HR-1–P3HR-1 autohybrid (PICATPO-1) showed the same lack of EBV receptors as the two parents. The expression of C3 receptors in the hybrids paralleled the expression of EBV receptors, and their expression showed a strong correlation (r=0.84).

Rosetting for Ia-like antigens indicated Ia-like expression in all BL lines and their hybrids. The expression was rather low in Daudi, which could be compatible with their continuing differentiation into plasma cells. Ia expression was similar to the high level of Raji in the Daudi–Raji (DITRUD-1) hybrid. As was their K562 parent, both the DUTKO-1 and PUTKO-1 hybrids were negative for Ia, indicating suppression of this B-cell character in these hybrids.

Whereas B-cell markers were suppressed, leukemia and erythroid cell markers were fully expressed in the DUTKO-1 and PUTKO-1 hybrids. Similar to their parental K562 line, both hybrids could be induced for hemoglobin production by treatment with hemin. K562 synthesizes embryonic hemoglobins in response to hemin induction (*49*). The patterns of embryonic hemoglobin production in the hybrids was observed to differ from the parent K562 line: DUTKO-1 produced excess γ- and δ-chains, whereas PUTKO-1 produced excess ε-chains (*54*). It is not now known whether these changes could be due to activation of globin genes contributed by the B-cell genome, similar to the recent example in murine teratocarcinoma–Friend cell hybrids (*55*). Both DUTKO-1 and PUTKO-1 contained high basal and induced levels of heme, as assessed by ^{59}Fe incorporation. K562 expressed high levels of the myeloid–monocytoid lineage-related enzymes β-glucuronidase and lysozyme, which were also expressed in the DUTKO-1 and PUTKO-1 hybrids.

In summary, these findings on DUTKO-1 and PUTKO-1 indicate loss of B-cell markers but retention of the erythroid–leukemia cell markers characteristic of the parental K562. In contrast to these findings, the recently isolated hybrid line between P3HR-1 and the more highly differentiated promyelocytic line HL-60 (*52*) showed the reverse, i.e., retention of B-cell markers but loss of the myeloid markers characteristic of the leukemic parent (*56*). Such findings indicate that the programs of differentiation of BL cells and of leukemia cells are not compatible in the sense that markers of both parents can be coexpressed in hybrid cells, in spite of the suggestion that B-cells and leukemia cells have a common stem cell origin (*12*). That loss of B-cell markers was observed in the hybrids with K562 and the reverse pattern was observed in hybrids with HL-60 could possibly reflect the variable differentiation between the two parent leukemia cell lines.

The present series of hybrids was also used to analyze the patterns of spontaneous and induced EBV antigens, which will be discussed in the following paper (*13*). As in other studies, spontaneous production and inducibility were found to vary in parallel, with the more productive status being dominant in the hybrid. In contrast to the previously studied "allohybrids," the autohybrid of a high and a low virus producer P3HR-1 subline (PICATPO-1) showed a dominant switch-off of the viral cycle. In DUTKO-1, the viral cycle could be induced, in contrast to PUTKO-1 in which it was completely suppressed.

As mentioned, the relatively high chromosomal and phenotypic stability of hybrids like the ones described here between various human hematopoietic cell lines offers the possibility of selection experiments against single phenotypic traits when the fate of additional markers is followed. A particularly interesting property of the K562 line is its high sensitivity to NK cells (*57*), which is exhibited by both PUTKO-1 (*58*) and DUTKO-1 (Masucci G: Unpublished results) as well as by other "primitive" cells such as murine teratocarcinoma cells (*59*). The two hybrids have been selected for NK resistance by in vitro selections, and stable NK-resistant variants have been obtained. This offers the opportunity to correlate the loss of NK sensitivity with other phenotypic markers of these cells.

REFERENCES

(*1*) Zeuthen J, Klein G. B-cell and Epstein-Barr virus (EBV) associated functions in human cells and hybrids. In: Celis JE, Graessmann A, Loyter A, eds. Transfer of cell constituents into eukaryotic cells. New York: Plenum, 1980:235–273.

(*2*) Klein G, Clements G, Zeuthen J, Westman A. Somatic cell hybrids between human lymphoma lines. II. Spontaneous and induced patterns of the Epstein-Barr virus (EBV) cycle. Int J Cancer 1976; 17:715–724.

(*3*) Nyormoi O, Klein G, Adams A, Dombos L. Sensitivity to EBV superinfection and IUdR inducibility of hybrid cells formed between a sensitive and a relatively resistant Burkitt lymphoma cell line. Int J Cancer 1973; 12:396–408.

(*4*) Rosén A, Clements G, Klein G, Zeuthen J. Double immunoglobulin production in cloned somatic cell hybrids between two human lymphoid cell lines. Cell 1977; 11:139–147.

(*5*) Klein G, Wiener F, Zech L, zur Hausen H, Reedman B. Segregation of the EBV-determined nuclear antigen (EBNA) in somatic cell hybrids derived from the fusion of a mouse fibroblast and a human Burkitt lymphoma line. Int J Cancer 1974; 24:54–64.

(*6*) Spira J, Povey S, Wiener F, Klein G, Andersson-Anvret M. Chromosome banding, isoenzyme studies and determination of Epstein-Barr virus DNA content on human Burkitt lymphoma/mouse hybrids. Int J Cancer 1977; 20:849–853.

(*7*) Fougere C, Weiss MC. Phenotypic exclusion in mouse melanoma-rat hepatoma hybrids: Pigment and albumin production are not reexpressed simultaneously. Cell 1978; 15:843–854.

(*8*) Ringertz NR, Savage RE. Cell hybrids. New York: Academic Press, 1976.

(*9*) Allan M, Harrison P. Co-expression of differentiation markers in hybrids between Friend cells and lymphoid cells and the influence of the cell shape. Cell 1980; 19:437–447.

(*10*) Klein G, Zeuthen J, Eriksson I, et al. Hybridization of a myeloid leukemia-derived human cell line (K562) with a human Burkitt's lymphoma line (P3HR-1). JNCI 1980; 64:725–738.

(*11*) Lozzio CB, Lozzio BB. *Brief communication:* Cytotoxicity of a factor isolated from human spleen. JNCI 1973; 50:535–538.

(*12*) Fialkow PJ, Denman AM, Jacobson RJ, Lowenthal MN. Chronic myelocytic leukemia. Origin of some lymphocytes from leukemic stem cells. J Clin Invest 1978; 62:815–823.

(*13*) Klein G, Zeuthen J, Ber R, Ernberg I. Human lymphoma–lymphoma hybrids and lymphoma–leukemia hybrids. II. Epstein-Barr virus-induction patterns. JNCI 1982; 68:197–202.

(*14*) Hinuma Y, Grace JT Jr. Cloning of immunoglobulin-producing human leukemic and lymphoma cells in long-term cultures. Proc Soc Exp Biol Med 1967; 124:107–111.

(*15*) Klein E, Ben-Bassat H, Neumann H, et al. Properties of the K562 cell line, derived from a patient with chronic myeloid leukemia. Int J Cancer 1976; 18:421–431.

(*16*) Lozzio CB, Lozzio BB. Human chronic myelogenous leukemia cell line with positive Philadelphia chromosome. Blood 1975; 45:321–334.

(*17*) Ber R, Klein G, Moar M, et al. Somatic cell hybrids between human lymphoma cell lines. IV. Establishment and characterization of a P3HR-1/Daudi hybrid. Int J Cancer 1978; 21:707–719.

(*18*) Hampar B, Derge JG, Martos LM, Walker JL. Synthesis of Epstein-Barr virus after activation of the viral genome in a "virus-negative" human lymphoblastoid cell (Raji) made resistant to 5-bromodeoxyuridine (thymidine kinase–virus antigen–immunofluoresence–herpesvirus fingerprints). Proc Natl Acad Sci USA 1972; 69:78–82.

(*19*) Ber R, Eriksson I. Isolation of ouabain-resistant human lymphoblastoid cell lines by multi-step selection. Mutat Res 1979; 61:411–414.

(*20*) Böyum A. Separation of white blood cells. Nature 1964; 204:793–794.

(*21*) Caspersson T, Zech L, Johansson C, Modest EJ. Identification of human chromosomes by DNA-binding fluorescent agents. Chromosoma 1970; 30:215–227.

(*22*) Paris Conference (1971). Standardization in human cytogenetics. Birth defects: Original article series. Vol VIII. No. 7. New York: The National Foundation, 1972–Cytogenetics 1972; 11:313–362.

(*23*) Standing Committee on Human Cytogenetic Nomenclature. An international system for human cytogenetic nomenclature (1978). Birth defects: Original article series. Vol XIV. No. 8. New York: The National Foundation, 1978–Cytogenet Cell Genet 1978; 21: 309–406.

(*24*) Harris H, Hopkinson DA. Handbook of enzyme electrophoresis in human genetics. Amsterdam: Elsevier/North-Holland, 1976.

(*25*) Klein G, Terasaki P, Billing R, et al. Somatic cell hybrids between human lymphoma lines. III. Surface markers. Int J Cancer 1977; 19:66–76.

(*26*) Yefenof E, Klein G, Jondal M, Oldstone MB. Surface markers on human B- and T-lymphocytes. IX. Two-color immunofluorescence studies on the association between EBV receptors and complement receptors on the surface of lymphoid cell lines. Int J Cancer 1976; 17:693–700.

(*27*) Yefenof E, Klein G, Kvarnung K. Relationship between complement activation, complement binding, and EBV absorption by human hematopoietic cell lines. Cell Immunol 1977; 31:225–233.

(*28*) Jondal M. Surface markers on human B and T lymphocytes. IV. Distribution of surface markers on resting and blast-transformed lymphocytes. Scand J Immunol 1974; 3:739–747.

(*29*) Hallberg T, Gurner BW, Coombs RR. Opsonic adherence of sensitized ox red cells to human lymphocytes as measured by rosette formation. Int Arch Allergy Appl Immunol 1973; 44:500–513.

(*30*) Sairenji T, Hinuma Y. Modes of Epstein-Barr virus infection in human floating cell lines. Gan 1973; 64:583–590.

(*31*) Klein G, Yefenof E, Falk K, Westman A. Relationship between Epstein-Barr virus (EBV) production and the loss of the EBV receptor/complement receptor complex in a series of sublines derived from the same original Burkitt's lymphoma. Int J Cancer

1978; 21:532–560.

(32) Ralph P, Moore MA, Nilsson K. Lysozyme synthesis by established human and murine histiocytic lymphoma cell lines. J Exp Med 1976; 143:1528–1533.

(33) Friend C, Scher W, Holland JG, Sato T. Hemoglobin synthesis in murine virus-induced leukemic cells in vitro. 2. Stimulation of erythroid differentiation by dimethyl sulfoxide. Proc Natl Acad Sci USA 1971; 68:378–382.

(34) Lillie RB, Fulmer HM. Histopathologic technic and practical histochemistry. 4th ed. New York: McGraw-Hill, 1976.

(35) Manolov G, Manolova Y. Marker band in one chromosome 14 from Burkitt lymphomas. Nature 1972; 237:33–34.

(36) Zech L, Haglund U, Nilsson K, Klein G. Characteristic chromosomal abnormalities in biopsies and lymphoid cell lines from patients with Burkitt and non-Burkitt lymphomas. Int J Cancer 1976; 17:47–56.

(37) Zeuthen J, Friedrich U, Rosén A, Klein E. Structural abnormalities in chromosome 15 in cell lines with reduced expression of beta-2 microglobulin. Immunogenetics 1977; 4:567–580.

(38) Goodfellow PN, Jones EA, Van Heyningen V, et al. The beta2-microglobulin gene is on chromosome 15 and not in the HL-A region. Nature 1975; 254:267–269.

(39) Oliver N, Francke U, Pellegrino MA. Regional assignment of genes for mannose phosphate isomerase, pyruvate kinase-3, and beta2-microglobulin expression on human chromosome 15 by hybridization of cells from a t(15;22)(q14;q13.3) translocation carrier. Cytogenet Cell Genet 1978; 22:506–510.

(40) Pajunen L, Solomon E, Burgess S, et al. Regional mapping of chromosome 15. Cytogenet Cell Genet 1978; 22:511–512.

(41) Povey S, Hopkinson DA, Harris H, Franks LM. Characterization of human cell lines and differentiation from HeLa by enzyme typing. Nature 1976; 264:60–63.

(42) Swallow DM, Gardiner SE, Harris H, Arthur E, Steel CM, Evans HJ. Lysosomal enzymes in human lymphoblastoid lines: Unusual characteristics of RAJI and DAUDI. Ann Hum Genet 1977; 41:9–16.

(43) Povey S, Jeremiah S, Arthur E, et al. Deficiency of malic enzyme: A possible marker for malignancy in lymphoid cells. Ann Hum Genet 1981; 45:237–252.

(44) Terasaki PI, ed. Histocompatibility testing 1980. Los Angeles: UCLA Tissue Typing Laboratory, 1980.

(45) Fellous M, Kamoun M, Wiels J, et al. Induction of HLA expression in Daudi cells after cell fusion. Immunogenetics 1977; 5:423–436.

(46) Wells A, Koide N, Klein G. Difference in viral binding between two Epstein-Barr virus substrains to a spectrum of receptor-positive target cells. Int J Cancer 1981; 27:303–309.

(47) Jondal M, Klein G, Oldstone M, et al. Surface markers on human B- and T-lymphocytes. VIII. Association between complement and Epstein-Barr virus (EBV) receptors on human lymphoid cells. Scand J Immunol 1976; 5:401–410.

(48) Andersson LC, Nilsson K, Gahmberg CG. K562, a human erythroleukemic cell line. Int J Cancer 1979; 23:143–147.

(49) Andersson LC, Jokinen M, Gahmberg CG. Induction of erythroid differentiation in the human leukaemia cell line K562. Nature 1979; 278:364–365.

(50) Rutherford TR, Clegg JB, Weatherall DJ. K562 human leukaemic cells synthesise embryonic haemoglobin in response to haemin. Nature 1979; 280:164–165.

(51) Fukuda M. K562 human leukaemic cells express fetal type (i) antigen on different glycoproteins from circulating erythrocytes. Nature 1980; 285:405–407.

(52) Koeffler HP, Golde DW. Human myeloid leukemia cell lines: A review. Blood 1980; 56:344–350.

(53) Clements GB, Klein G, Zeuthen J, Povey S. The selection of somatic cell hybrids between human lymphoma cell lines. Somatic Cell Genet 1976; 2:309–324.

(54) Rutherford T, Clegg JB, Higgs DR, Jones RW, Thompson J, Weatherall DJ. Embryonic erythroid differentiation in the human leukemic cell line K562. Proc Natl Acad Sci USA 1980; 78:348–352.

(55) McBurney M, Craig J, Stedman D, Featherstone M. Expression of globin genes in teratocarcinoma–Friend cell hybrids. Exp Cell Res 1981; 131:277–282.

(56) Koeffler HP, Sparkes RS, Billings R, Klein G. Somatic cell hybrid analyses of hematopoietic differentiation. J Exp Med. In press.

(57) Saksela E, Timonen T, Ranki A, Häyry P. Morphological and functional characterization of isolated effector cells responsible for human natural killer activity to fetal fibroblasts and to cultured cell line targets. Immunol Rev 1979; 44:71–123.

(58) Åhrlund-Richter L, Klein E, Masucci G. Somatic hybrids between a high NK-sensitive lymphoid (YACIR) and several low sensitive sarcoma or L-cell-derived mouse lines exhibit low sensitivity. Somatic Cell Genet 1980; 6:89–99.

(59) Stern P, Gidlund M, Örn A, Wigzell H. Natural killer cells mediate lysis of embryonal carcinoma cells lacking MHC. Nature 1980; 285:341–342.

Figure 1.—A) Karyogram of RUDPUT-2 hybrid. Marker chromosomes originating from RUD (parental) are indicated by *white arrowheads*; from PUT (parental), by *black arrowheads*; and new markers in the hybrid, by •. The karyotype shown is 94,XXY,Yp+,+large metacentric chromosome,+small metacentric chromosome,4q+,11q+,13q+,14q+,14q+,t(17;?)(q25;?),t(17;?)(q24;?). The loss of one chromosome 18 is an artifact. B) Karyogram of RUDPICAT-1 hybrid. Marker chromosomes originating from RUD (parental) are indicated by *white arrowheads*; from PICAT (parental), by *black arrowheads*; and new markers in the hybrid, by •. The karyotype shown is 94,XYY,i(Xp),+submetacentric chromosome,+16,4q+,11q+,14q+,t(17;?)(q25;?),t(17;?)(q24;?).

Figure 2.—Karyogram of DITRUD-1 hybrid. Marker chromosomes originating from DIT (parental) are indicated by *black arrowheads*; from RUD (parental), by *white arrowheads*; and new markers in the hybrid, by •. The karyotype shown is 91,XXYY,+submetacentric chromosome,+acrocentric chromosome,−14,−16,−17,t(i(1q);?)(q36;?),4q+,11q+,14q+,14q+,del(15)(q14q21),t(17;?)(q24;?),t(17;?)(q25;?).

Figure 3.—Karyogram of DUTKO-1 hybrid. Marker chromosomes originating from DUT (parental) are indicated by *white arrowhead*; from K562 (KO parental), by *black arrowheads*; and new markers in the hybrid, by •. The karotype of the K562 (KO) line used for hybridization was identical to that previously published (*10*) [69,XXX,+7,+9(p11),+small metacentric chromosome,−13,−17,−21,del(X)(p21),del(3)(p11),del(9)(p11),15q−,18q+,r(22)] and is not shown here. The r(22) marker presumably is derived from the original Ph^1 marker of K562. The karyotype shown is 113,XXXY,del(X)(p21),+2,+7,+small metacentric chromosome,+submetacentric chromosome,+large submetacentric chromosome,−4,−6,−6,−13,−17,−18,−21,−22,del(3)(p11),csb(9)(p11),del(9)(p11),15q−,18q+,r(22),14q+,del(15)(q14q21).

Figure 4.—Karyogram of PICATPO-1 hybrid. Marker chromosomes originating from PICAT (parental) are indicated by *black arrowheads* and from P3HR-1 (PO parental), by *white arrowheads*. The karyotype shown is 97,XYY,i(Xp),?i(Xp),+11,+small metacentric chromosome,+submetacentric chromosome,+large metacentric chromosome,14q+.

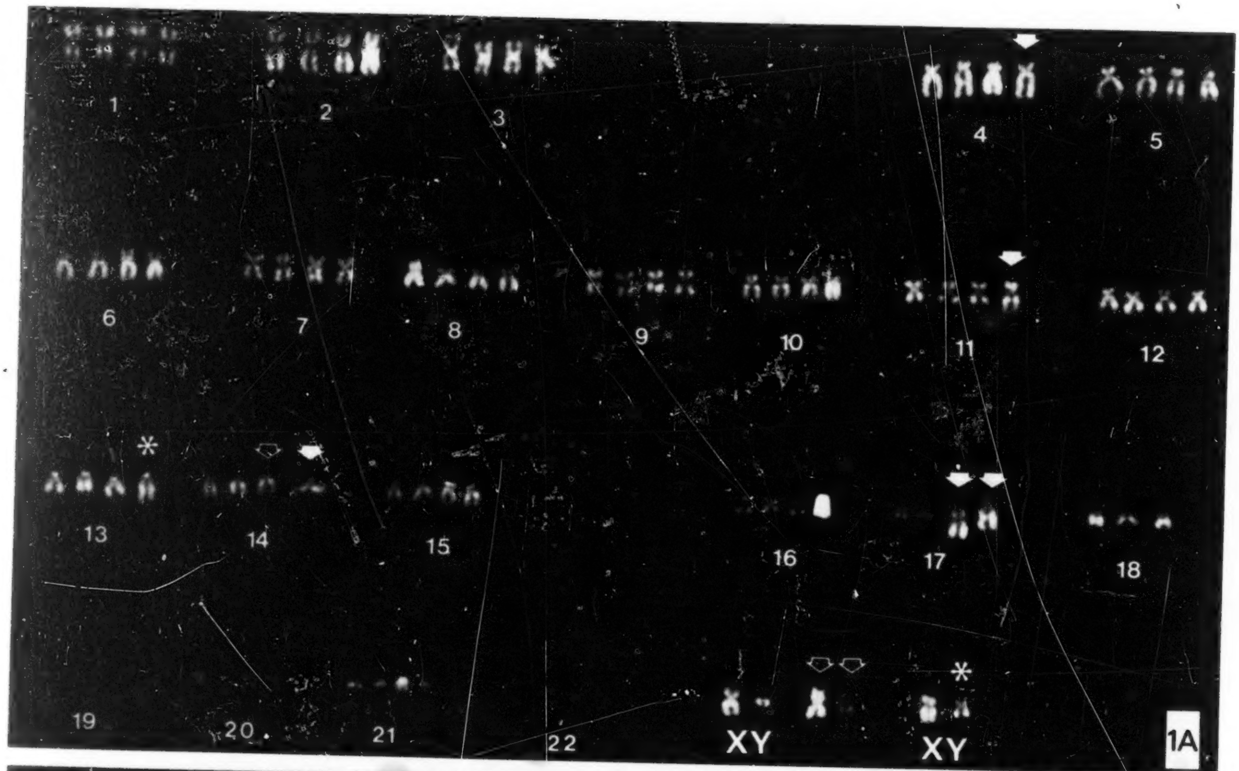
1
2
3
4
5
6
7
8
9
10
11
12
*
13
14
15
16
17
18
*
19
20
21
22
XY
XY

1A

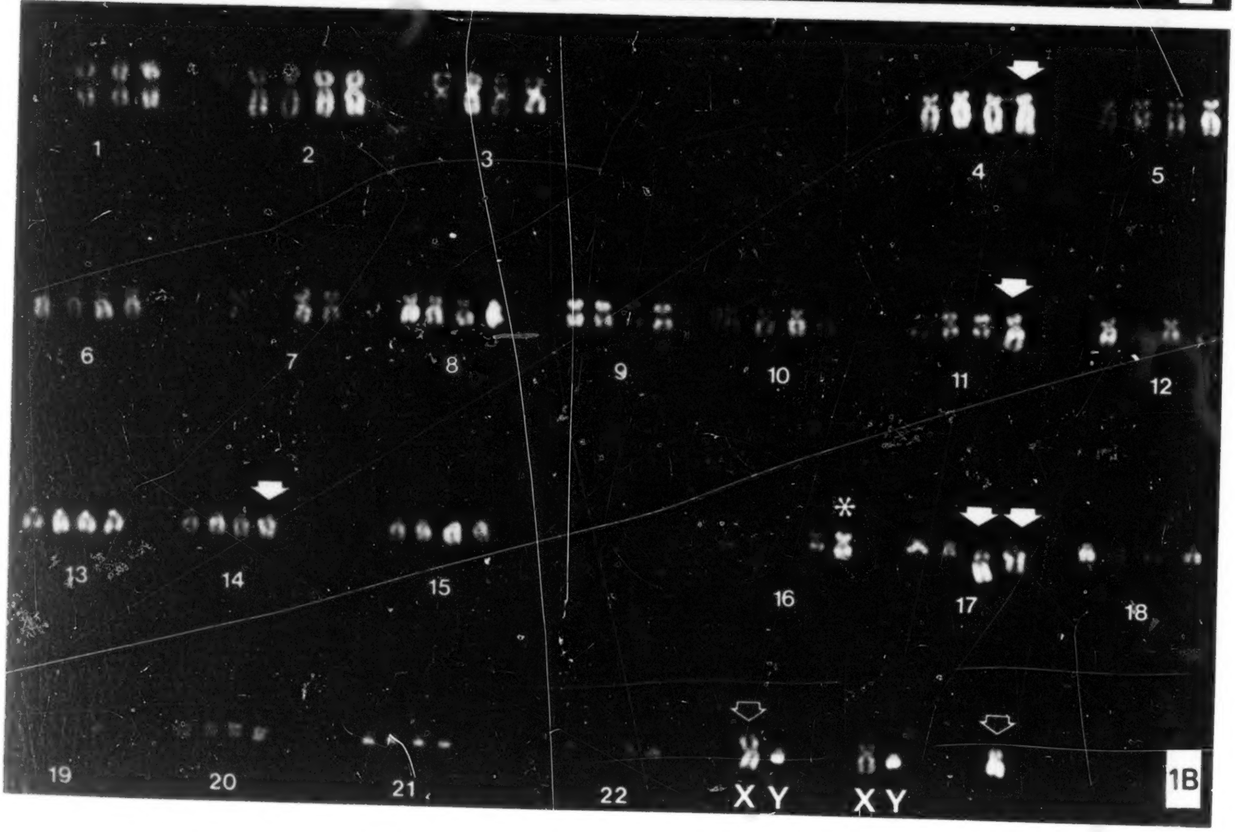
1
2
3
4
5
6
7
8
9
10
11
12
13
14
15
*
16
17
18
19
20
21
22
X Y
X Y

1B

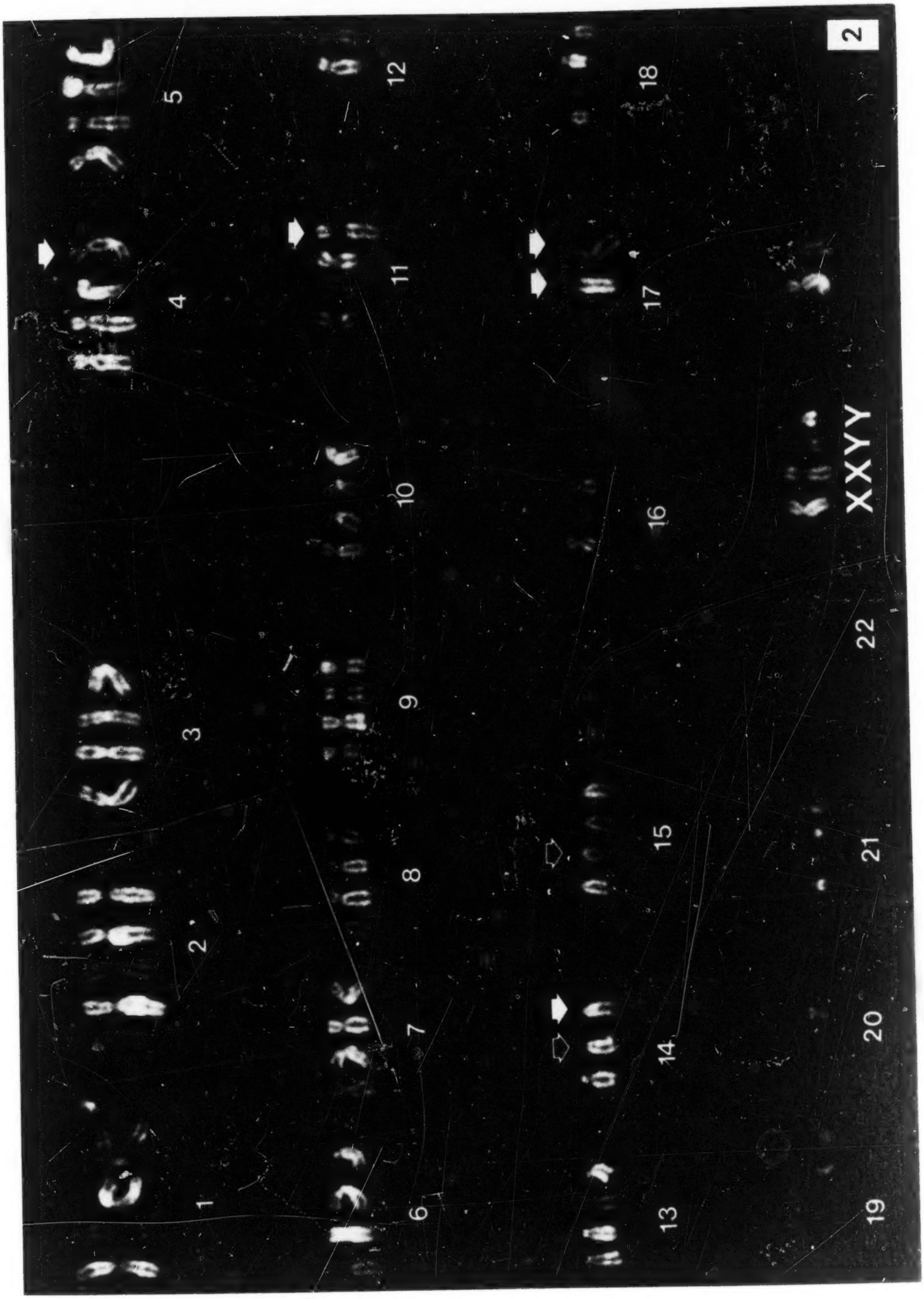
2
1
2
3
4
5
6
7
8
9
10
11
12
13
14
15
16
17
18
19
20
21
22
XXYY

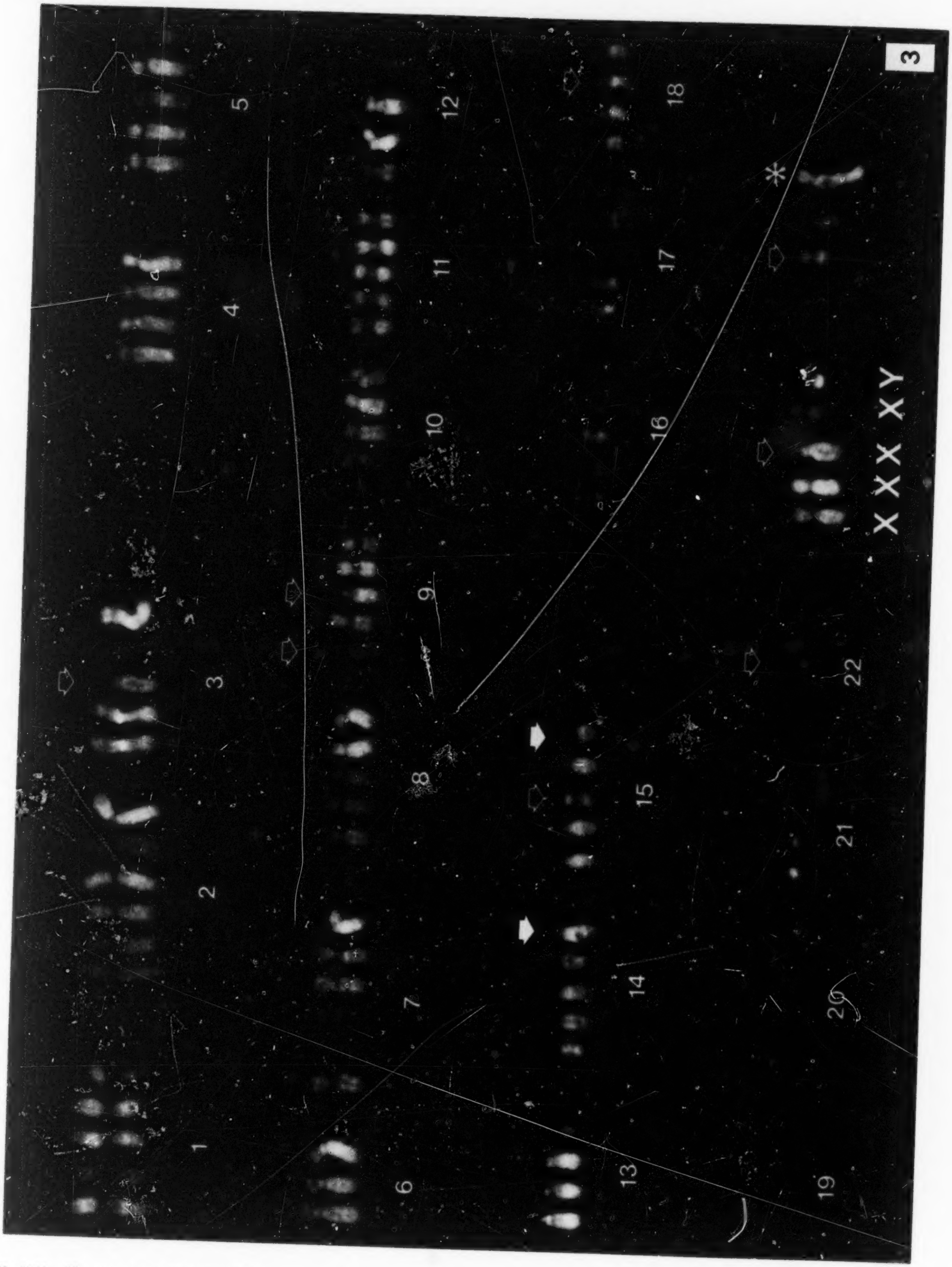
3
1
2
3
4
5
6
7
8
9
10
11
12
13
14
15
16
17
18
19
20
21
22
XX XX XY
*

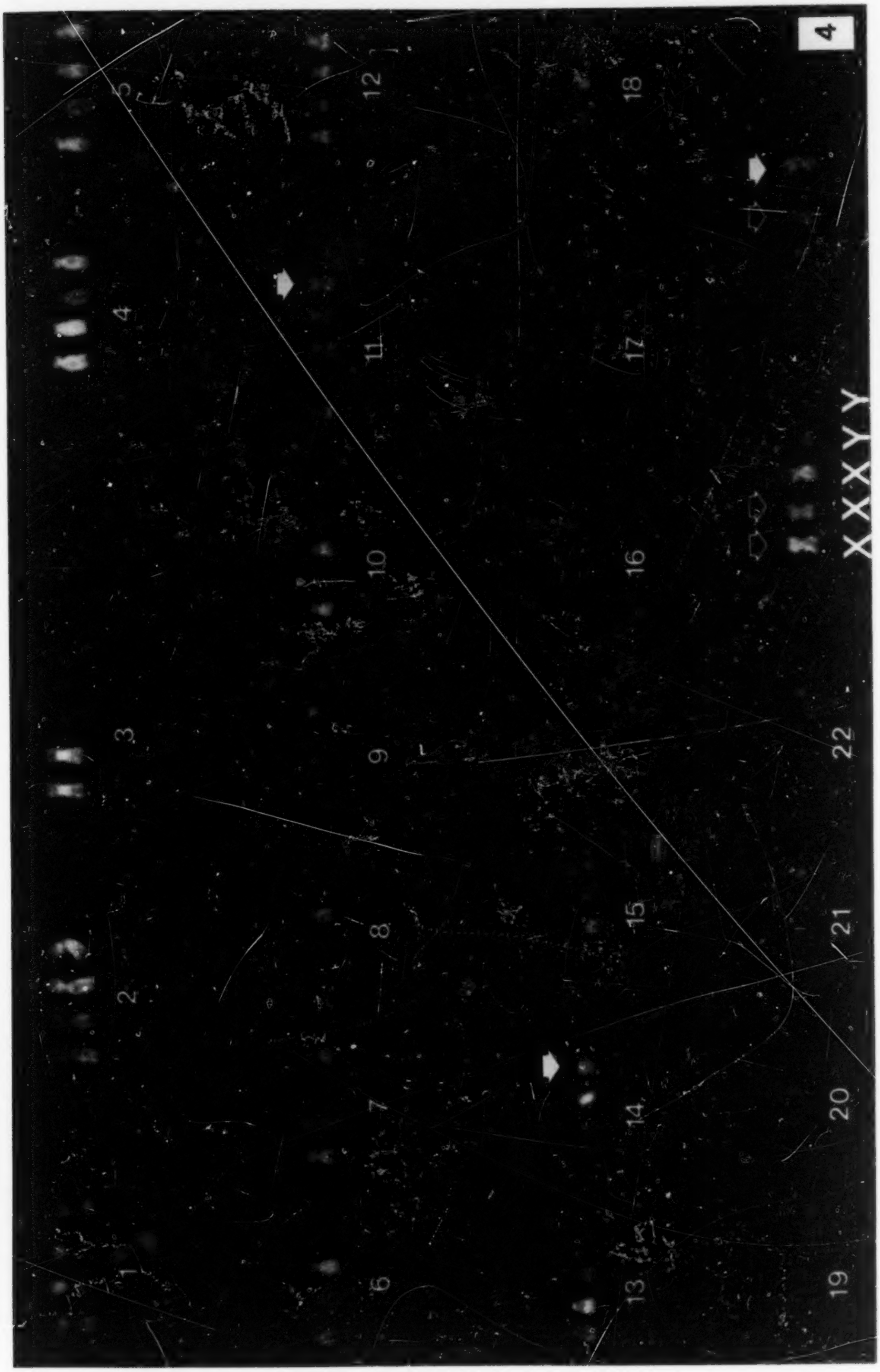
4
1
2
3
4
5
6
7
8
9
10
11
12
13
14
15
16
17
18
19
20
21
22
XXXYY

blank page

Human Lymphoma-Lymphoma Hybrids and Lymphoma-Leukemia Hybrids. II. Epstein-Barr Virus Induction Patterns [1,2,3]

George Klein,[4] Jesper Zeuthen,[5] Rosalie Ber,[6] *and* Ingemar Ernberg[4]

ABSTRACT—In addition to the spontaneous expression of markers of the early and late phases of the viral cycle [Epstein-Barr virus (EBV), early viral cycle antigens (EA), and viral capsid antigen (VCA)] by a panel of hybrid cell lines derived by fusion of human hematopoietic cell lines, the induction of these markers by three chemical inducers [5-iodo-2′-deoxyuridine, the tumor promoter 12-*O*-tetradecanoylphorbol 13-acetate (TPA), and sodium butyrate] were analyzed. A variant of the prototype producer of lytic EBV, P3HR-1 (PICAT) was observed to show consistent low spontaneous and induced production of EA and VCA as compared to the P3HR-1 line from which it was derived. An "autohybrid" (PICATPO-1) between these two lines showed a low production of VCA. Hybrids between Raji and P3HR-1 sublines (RUDPICAT-1 and RUDPUT-2) showed reduced expression of EBV antigens. Both hybrids were capable of VCA expression, in contrast to the Raji parent that expressed EA but not VCA. A new Raji-Daudi hybrid (DITRUD-1) expressed spontaneous and induced EA and VCA at levels intermediate between its two parents. A different type of hybrid was derived from a Daudi subline and the K562 leukemia cell line (DUTKO-1) and was found to be capable of spontaneous as well as induced EA and VCA expression. Both DUTKO-1 and DITRUD-1 were similar to Daudi in their induction profile in respect to a very low response to TPA.—JNCI 1982; 68:197–202.

In previous studies on the expression of EBV viral cycle antigens (EA and VCA) in somatic hybrids, we have examined hybrids derived from the fusion of two EBV-positive BL lines (*1–4*) or an EBV-positive and an EBV-negative BL line (*2*), or an EBV-positive BL line and the human leukemia line K562 (*5*). In hybrids between two BL cell lines, EBV-producer status (EA and VCA expression) dominated over nonproducer status, whereas the BL-K562 (P3HR-1-K562=PUTKO-1) hybrid was an absolute nonproducer (*5*). This result is in marked contrast to the expression of EA and VCA in studies when EBV in high multiplicity was transferred by bypassing the membrane barrier into receptor-negative cells of other lineages (*6, 7*). In cells carrying latent EBV genomes, the viral cycle can be induced by a variety of inducers, such as 5-bromo-2′-deoxyuridine (*8*), IdUrd (*9*), sodium butyrate (*10*), the tumor-promoting phorbol ester TPA (*11*), and anti-IgM (*12*).

A similar suppression of virus-producer status as that observed in the P3HR-1-K562 hybrid (*5*) has been previously observed after the hybridization of BL cells with murine or human fibroblasts (*13, 14*). Fusion with epithelial cells led, contrariwise, to more permissive hybrids (*14*). Inducible producer status, mainly studied after IdUrd treatment of hybrid cells, showed essentially similar patterns as spontaneous producer status (*1–5*).

This analysis, based on the interaction of two cell phenotypes in a common hybrid, provides an opportunity to analyze controls that regulate the latency of EBV versus the spontaneous switch on of the viral cycle as well as viral induction by inducing agents. We here examine a series of newly established hybrid lines, described and characterized in the preceding paper (*15*), and morever extend the induction studies to include, in addition to IdUrd, two additional inducers (sodium butyrate and TPA).

MATERIALS AND METHODS

Cell lines.—All lines were maintained in RPMI-1640 medium supplemented with 8% fetal calf serum and antibiotics (100 IU penicillin/ml, 50 μg streptomycin/ml), with additional supplements as described (*15*). The following hybrids and parental cells were used: The hybrid PICATPO-1 was derived from fusion of a CAP^r and TG^r variant of P3HR-1 (PICAT) with a P3HR-1 cell line lacking selective markers (PO). The hybrids RUDPUT-2 and RUDPICAT-1 were derived by fusion of Raji TK^- (RUD) with the $ouab^r$ and TG^r variant of P3HR-1 (PUT) and with the CAP^r and TG^r PICAT variant derived from P3HR-1, respectively. The hybrid DITRUD-1 was derived from fusion of TG^r Daudi (DIT) with Raji TK^- (RUD). The hybrid DUTKO-1 was derived from a $ouab^r$ and TG^r Daudi (DUT) and K562 (KO). Further details are given in (*15*).

Immunofluorescence.—EBV antigen tests were performed on

ABBREVIATIONS USED: BL=Burkitt's lymphoma; CAP^r=chloramphenicol-resistant; EA=early antigens; EBNA=Epstein-Barr virus-associated nuclear antigen; EBV=Epstein-Barr virus; IdUrd=5-iodo-2′-deoxyuridine; $ouab^r$=ouabain-resistant; TG^r=thioguanine-resistant; TK^-=thymidine kinase-negative; TPA=12-*O*-tetradecanoylphorbol 13-acetate; VCA=viral capsid antigens.

---

[1] Received October 22, 1980; revised August 4, 1981; accepted September 8, 1981.

[2] Supported in part by Public Health Service (PHS) grant 5-R01CA-14054-05 from the National Cancer Institute, by the Swedish Cancer Society, by research grant 31/79 from the Danish Cancer Society, and by grants 511-15354 and 511-10128 from the Danish Natural Science Research Council.

[3] Paper VIII of a series on somatic cell hybrids derived from Burkitt's lymphoma cells.

[4] Department of Tumor Biology, Karolinska Institutet, S-104 01 Stockholm 60, Sweden.

[5] Institute of Human Genetics, The Bartholin Building, University of Aarhus, DK-8000 Aarhus C, Denmark.

[6] Technion-Israel Institute of Technology, Faculty of Medicine, P.O. Box 9649, Haifa, Israel.

acetone-fixed smears. The EBV-determined nuclear antigen EBNA was stained by anticomplement immunofluorescence (*16*). We identified EA-positive cells by direct fluorescence (*17*) using the F_1 Esther conjugate at a 1:40 dilution. We stained VCA-positive cells by indirect fluorescence (*18*) using anti-VCA-positive, anti-EA-negative serum from a healthy donor (MBF) at a dilution of 1:10, followed by an anti-Fc (*8*) conjugate (Hyland Laboratories, Los Angeles, Calif.) at a dilution of 1:20.

EBV induction experiments.—The hybrids and parental cells were exposed to 25 μg IdUrd/ml (*9*), 3 mg sodium butyrate/ml (*10*), or 10 ng TPA/ml (*11*) and harvested after 3, 6, or 6 days, respectively. The frequency of EA- and VCA-positive cells was estimated by counting 1,000 cells in each smear. Four or five tests were performed with each cell-inducer combination.

RESULTS

PICATPO-1 (P3HR-1–P3HR-1 "Autohybrid")

The P3HR-1 line is often regarded as a prototype EBV-producer line. P3HR-1 virus has lost its transforming ability but is capable of lytic infection. The other prototype EBV producer, B95-8, produces a transforming virus incapable of lytic infection. Unlike B95-8, P3HR-1 cells have the tendency to "switch off" the viral cycle on prolonged propagation, which reduces the expression of surface receptors for EBV (*19*). These changes probably reflect strong internal selection in culture for reduced EBV production as well as reduced adsorption-infection by lytic, superinfecting virus.

The CAP^r and TG^r PICAT variant of P3HR-1 showed a consistently lower spontaneous expression of EA and VCA than did the P3HR-1 line from which it was derived by several cycles of selection (text-fig. 1). The same difference was found for induced expression, for the P3HR-1 line was considerably more inducible, in particular by TPA, than was the variant PICAT line. The autohybrid PICATPO-1 formed by fusion of these two lines was less inducible than either of its parents, and its spontaneous producer status resembled that of the low-producer PICAT; however, TPA inducibility was similar for PICAT and the PICATPO-1 hybrid. The dominance of the low-producer, low-inducibility status in PICATPO-1 suggested that the control mechanisms responsible for the emergence of the low-producer variants might be of a negative, trans-acting nature.

A variable proportion of EA-positive cells proceeded to VCA synthesis. This was expected since P3HR-1 cells did not have an internal block to VCA production.

RUDPICAT-1 and RUDPUT-2 (Raji–P3HR-1 Hybrids)

The Raji line is the prototype "abortive producer" cell line; i.e., EA can be induced but the viral cycle does not proceed further to viral DNA replication and VCA synthesis (*1–3, 9*). As expected, the Raji TK^- (RUD) parent was noninducible for EA expression by IdUrd in contrast to the other two inducers TPA and sodium butyrate, which induced EA at a low level (text-fig. 2). Compared to the P3HR-1-derived PICAT and PUT parental cells, both the RUDPICAT-1 and RUDPUT-2 hybrids showed a reduced inducibility but to different extents. The inducibility of the RUDPICAT-1 line was not strongly reduced compared to the highly inducible PICAT parent, whereas the inducibility of RUDPUT-2 was almost as low as that of the slightly inducible Raji TK^- (RUD) line.

The block between EA and VCA expression in Raji cells was lifted in both hybrids. The "recessiveness" of this barrier is interesting: It leads support to the idea that Raji was defective with respect to either EBV-DNA or cellular factors necessary for viral DNA replication and/or production of VCA. Note that the RUDPUT-2 hybrid also could produce VCA, in spite of its low Raji-like EA inducibility.

DITRUD-1 (Raji–Daudi Hybrid)

In contrast to Raji, the Daudi line was a producer line capable of EA and VCA expression (text-fig. 3). The Daudi parent showed a relatively low response to TPA, in contrast to its good inducibility with either IdUrd or sodium buty-

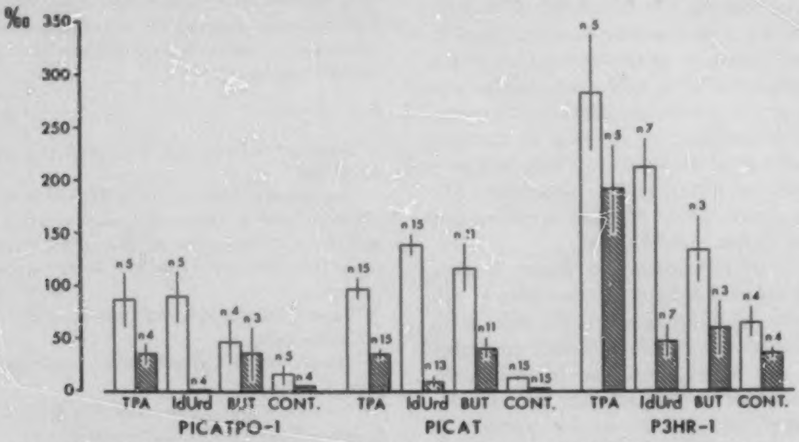

TEXT-FIGURE 1.—Induction of EA (*open columns*) and VCA (*shaded columns*) in PICATPO-1, an autohybrid from two parental P3HR-1 sublines—PICAT and P3HR-1, respectively. Untreated control (CONT.) cells and cells induced by TPA, IdUrd, and sodium butyrate (BUT) are compared. Staples indicate the range for SE; *n*=No. of tests performed.

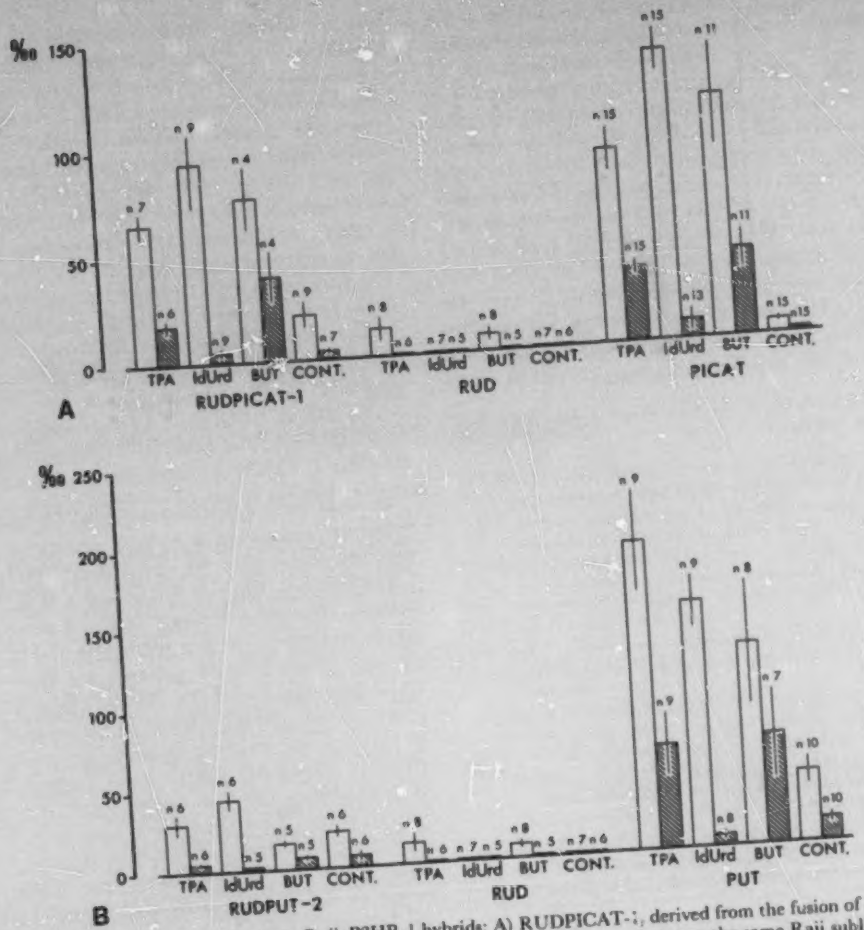

TEXT-FIGURE 2.—Inducibility and producer status of two Raji–P3HR-1 hybrids: A) RUDPICAT-1, derived from the fusion of a TK⁻ Raji subline (RUD) and a CAP^r and TG^r subline (PICAT) of P3HR-1, and B) RUDPUT-2, derived from the cross between the same Raji subline and the ouab^r and TG^r subline of P3HR-1 (PUT). Symbols and abbreviations are as in text-fig. 1.

rate. This considerable difference between the effects of the three chemical inducers was unique among many EBV-positive cell lines that were tested for their inducibility with IdUrd, TPA, and sodium butyrate (results not shown).

The low inducibility by TPA was not compensated in the DITRUD-1 hybrid, which behaved similarly to the Daudi parent. With IdUrd, DITRUD-1 was inducible at an intermediate level between its two parents. The response to sodium butyrate was a further example of the different activities of the three inducers: It was high in Daudi but low (at a level similar to Raji) in the DITRUD-1 hybrid. VCA expression was low in the DITRUD-1 hybrid, but it did occur at a low level similar to that of Daudi in cultures treated with TPA or IdUrd.

The relatively high level of expression of viral cycle antigens in the DITRUD-1 hybrid was somewhat different from our previous results for another Raji–Daudi hybrid, 8A (*2*), which was selected for an adherent phenotype. In 8A, spontaneous and IdUrd-induced EA production was low, corresponding to the level of its Raji parent. This difference corresponded to the observation of a more Daudi-like phenotype of DITRUD-1, even in regard to surface marker expression (*15*).

DUTKO-1 (Daudi–K562 Hybrid)

The ouab^r and TG^r subline of Daudi (DUT) expressed somewhat less EA and VCA spontaneously as well as when induced, as compared to its parent Daudi line (text-fig. 4). The EBV-negative K562 line was negative in all EBV antigen tests, as expected (results not shown). Similar to the normal Daudi line, the DUT line was highly inducible by IdUrd but not by TPA; however, DUT responded much less to sodium butyrate than did the normal Daudi line. Another difference was that DUT was virtually negative for VCA inducibility and spontaneous EA production when compared to those of the normal Daudi line. The DUTKO-1 hybrid was clearly inducible by all three inducers and also showed spontaneous expression of viral cycle antigens. The induced levels were comparable or slightly lower than those for the DUT parent. This result is in marked contrast to a previously examined hybrid between K562 and P3HR-1

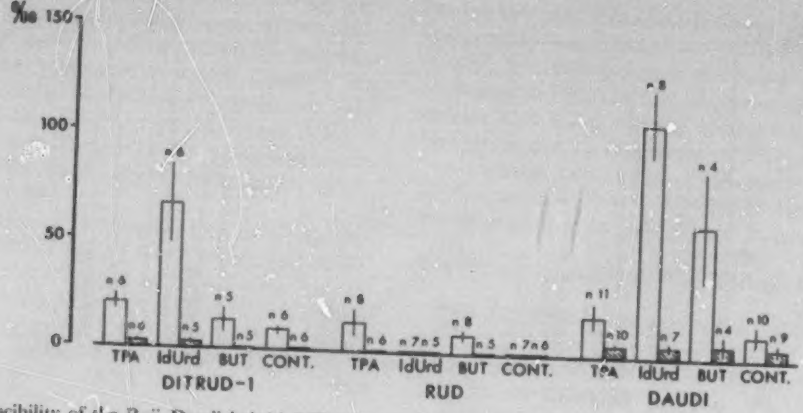

TEXT-FIGURE 3.—EBV inducibility of the Raji-Daudi hybrid DITRUD-1, as compared with the RUD and the Daudi (TG^{r}) parents. Symbols and abbreviations are as in text-fig. 1.

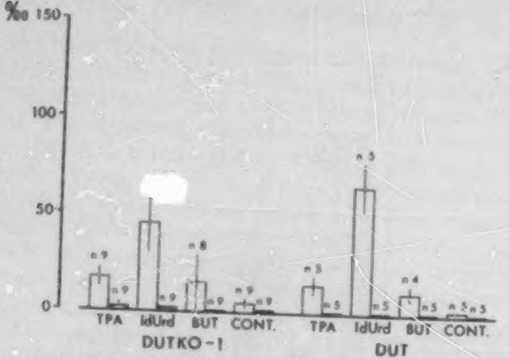

TEXT-FIGURE 4.—Inducibility of the Daudi-K562 hybrid DUTKO-1, as compared with the ouab^{r} and TG^{r} Daudi subline parent DUT. K562 is an EBV-negative line. Symbols and abbreviations are as in text-fig. 1.

(PUTKO-1) in which a totally eclipsed expression of viral cycle antigens was observed with all of the three inducing agents discussed here (*5*). The two hybrids, however, carry different numbers of EBV genomes: PUTKO-1 carries about 22; DUTKO-1, about 84 (*20*).

DISCUSSION

Somatic hybrids derived from the fusion of EBV-positive human lymphoma lines with each other or with cell lines of other derivations are useful for defining some of the control mechanisms involved in the maintenance of EBV latency. In our previous studies, the hybrid formed by fusion of two B-cell-derived lines usually expressed the more permissive parental condition, i.e., spontaneous production and inducibility of the respective parent; whereas B-cell lines fused with cells of certain other lineages, such as the erythroleukemia line K562 or with fibroblasts, produced hybrids with more or less completely eclipsed inducibility and producer status (*1–5, 13*).

In the present study, these conclusions were re-examined on a newly established series of hybrids described in the preceding paper (*15*). In addition to the previously tested inducer IdUrd, we have tested two other inducers: the tumor-promoting agent TPA and sodium butyrate.

Several new conclusions could be drawn. For the first time, we examined a hybrid produced by fusion of two sublines of the same BL cell line (P3HR-1) (the PICATPO-1 autohybrid). One of the sublines (PICAT), a CAP^{r}, TG^{r} variant, showed a strongly reduced productivity–inducibility as compared to the wild-type P3HR-1 line, its fusion partner. Nonproducer variants are known to arise during serial propagation of the P3HR-1 line. The fact that serial propagation regularly leads to the loss of virus production in this cell line suggests that the nonproducing cells have a selective advantage. Our results suggest that the switch-off of inducibility may be under negative, perhaps repressor-type control. This conclusion contrasts with our previous studies on the fusion of two (producer vs. nonproducer) BL lines when the opposite was seen. Clearly, the producer versus nonproducer status of different hybrids depends on the interaction of the stably established regulatory mechanisms confronted with each other in a given hybrid.

This point is further illustrated when the two independently derived Raji-P3HR-1 hybrids RUDPICAT-1 and RUDPUT-2 are compared. They were derived from the fusion of the same two BL lines, although different variant sublines with different phenotypes of P3HR-1 were used. The inducibility patterns of the two hybrids were quite different. These results indicate that even sublines of cells might differ markedly with respect to such regulatory mechanisms.

An additional point is illustrated when the DITRUD-1 hybrid in the present study was compared with an additional independently derived Daudi-Raji hybrid, 8A (*2*). While phenotypic characteristics of Raji dominated in 8A with regard to both surface immunoglobulin and EBV inducibility, DITRUD-1 resembled Daudi with regard to both properties.

The dominance of the characteristics of one parent with regard to surface and other phenotypic markers does not fully explain the inducibility patterns, however. This is made particularly clear by the Daudi-K562 (DUTKO-1) hybrid of the present study. We previously examined a P3HR-1-K562 hybrid, PUTKO-1 (*5*), in which the K562 phenotype dominated with respect to each parameter studied. B-cell markers were suppressed while the characteristic erythroid differentiation, high natural killer sensitivity, and surface receptors of K562 were expressed (*5*). DUTKO-1 has a very similar phenotype to that of PUTKO-1, as shown in the preceding paper (*15*). Both hybrids are 100% EBNA-positive and have multiple EBV genomes. However, PUTKO-1 is completely noninducible by all three agents studied, whereas DUTKO-1 is inducible by all. The two hybrids, however, differ in their average EBV genome copy number: PUTKO-1 carries 22 EBV genome equivalents while DUTKO-1 has 84 (*20*). In spite of the fact that IdUrd fails to induce viral antigen synthesis in PUTKO-1 cells (*5*), viral transcription has been shown to increase from 10 to 25% after IdUrd induction (*20*). In DUTKO-1 cells, IdUrd induced viral transcription from more than 40% of the EBV DNA, whereas TPA had no significant effect. RNA extracted from the polyribosomes of PUTKO-1 or DUTKO-1 cells contained only about 20% of the viral RNA sequences found in whole-cell extracts, whereas for P3HR-1 cells all the viral RNA transcripts could be found in polyribosomes (*20*).

These findings suggest the presence of additional translation control mechanisms that permit only certain viral RNA sequences to be associated with polyribosomes that might contribute to regulation of the expression of EBV antigens in the two BL-K562 hybrids. This suggests that two opposing forces are at work. The K562 genome tends to suppress all B-cell-associated characteristics, including the ability to produce EBV antigens. This control can be overridden, however, if a sufficient number of viral genomes is present. Since the ability to keep the viral cycle appears to be a B-cell-dependent characteristic, it is conceivable that the virus utilizes some differentiated phenotypic property of the B-cell to assure its latency, probably in a repressor-like fashion. If this control is of limited power, it will be overridden by an excessive number of viral genomes.

So far in this discussion, "induction" was used to mean the "point of no return," as signaled by the appearance of EA. In certain cells (prototype: Raji) the EBV cycle is hampered by a second carrier—between EA and replicative viral DNA (positive in subsequent VCA) synthesis. In the present study, this barrier was absent in both Raji-P3HR-1 hybrids and in the Daudi-Raji hybrid. This agrees with our previous findings and suggests that the Raji cell may be deficient in some component required for entry into the late part of the cycle.

This defect could be either viral or cellular. Since both Raji parents in the present series of hybrids carry endogenous EBV genomes, the present results only allow the conclusion that whatever the defect in Raji, it does not seem to be caused by negative, trans-acting factors that affect the expression of the viral genome. Further studies (results not shown) on a previously derived hybrid between Raji and the EBV-negative lymphoma line BJAB (*2*), have clearly indicated that, while EA production is even amplified in this hybrid after treatment with any of the three inducers used here, there is absolutely no production of VCA; i.e., the block between EA and VCA production is not lifted, suggesting that the abortive producer phenotype of Raji is caused by a deficient viral genome and not by a defective cellular mechanism. Recent analyses of the structure of Raji EBV DNA have shown that the Raji EBV genome is indeed defective since it contains two deleted sequences (Bornkamm G: Personal communication).

The three inducing agents (TPA, IdUrd, and sodium butyrate) acted largely in parallel but with some notable exceptions. The Daudi line did not respond well to TPA in contrast to its good inducibility with IdUrd and sodium butyrate. This difference was also observed in the hybrids of Daudi with other lines (DITRUD-1, DUTKO-1). In the Daudi-Raji (DITRUD-1) hybrid, there was also a dissociation between the IdUrd and sodium butyrate induction patterns. This phenomenon suggests that while the three agents may act similarly in most cells, the agents do not show the same activity with all cells, perhaps due to differences in the entry or processing of the drugs.

REFERENCES

(*1*) Nyormoi O, Klein G, Adams A, Dombos L. Sensitivity to EBV superinfection and IUdR inducibility of hybrid cells formed between a sensitive and a relatively resistant Burkitt lymphoma cell line. Int J Cancer 1973; 12:396–408.

(*2*) Klein G, Clements G, Zeuthen J, Westman A. Somatic cell hybrids between human lymphoma lines. II. Spontaneous and induced patterns of the Epstein-Barr virus (EBV) cycle. Int J Cancer 1976; 17:715–724.

(*3*) ———. Spontaneous and induced patterns of the Epstein-Barr virus (EBV) cycle in a new set of somatic cell hybrids. Cancer Lett 1977; 3:91–98.

(*4*) Ber R, Klein G, Moar M, et al. Somatic cell hybrids between human lymphoma lines. IV. Establishment and characterization of a P3HR-1/Daudi hybrid. Int J Cancer 1978; 21:707–719.

(*5*) Klein G, Zeuthen J, Eriksson I, et al. Hybridization of a myeloid leukemia-derived human cell line (K562) with a human Burkitt's lymphoma line (P3HR-1) JNCI 1980; 64:725–738.

(*6*) Graessman A, Wolf H, Bornkamm GW. Expression of Epstein-Barr virus genes in different cell types after microinjection of viral DNA. Proc Natl Acad Sci USA 1980; 77:433–436.

(*7*) Volsky DJ, Shapiro IM, Klein G. Transfer of Epstein-Barr virus (EBV) receptors to receptor negative cells permits virus penetration and antigen expression. Proc Natl Acad Sci USA 1980; 77:5453–5457.

(*8*) Hampar B, Derge JC, Martos LM, Walker JI. Synthesis of Epstein-Barr virus after activation of the viral genome in a virus negative human lymphoblastoid cell (Raji) made resistant to 5-bromodeoxyuridine. Proc Natl Acad Sci USA 1972; 69:78–82.

(*9*) Klein G, Dombos L. Relationship between the sensitivity of EBV-carrying lymphoblastoid lines to superinfection and the inducibility of the resident viral genome. Int J Cancer 1973; 11:327–337.

(*10*) Luka J, Källin B, Klein G. Induction of the Epstein-Barr (EBV) cycle in latently infected cells by *n*-butyrate. Virology 1979; 94:228–231.

(*11*) zur Hausen H, O'Neill FJ, Freese UK. Persisting oncogenic herpesvirus induced by the tumour promoter TPA. Nature 1978; 272:373–375.

(*12*) Tovey MG, Lenoir G, Begon-Lours J. Activation of latent Epstein-Barr virus by antibody to human IgM. Nature 1978; 276:270–272.

(*13*) Klein G, Wiener F, Zech L, zur Hausen H, Reedman B. Segregation of the EBV-determined nuclear antigen (EBNA) in somatic cell hybrids derived from the fusion of a mouse fibroblast and a human Burkitt lymphoma line. Int J Cancer 1974; 14:54–64.

(*14*) Glaser R, Nonoyama M, Whiteman M, Forcino T. Studies on an epithelial/Burkitt hybrid cell line with one EBV genome equivalent per cell. Virology 1979; 98:272–274.

(*15*) Zeuthen J, Klein G, Ber R, et al. Human lymphoma–lymphoma hybrids and lymphoma–leukemia hybrids. I. Isolation, characterization, cell surface markers, and B-cell markers. JNCI 1982; 68:179–195.

(*16*) Reedman BM, Klein G. Cellular localization of an Epstein-Barr virus

(EBV)-associated complement-fixing antigen in producer and nonproducer lymphoblastoid cell lines. Int J Cancer 1973; 11:499-520.

(17) Klein G, Gergely L, Goldstein G, Two-colour immunofluorescence studies on EBV-determined antigens. Clin Exp Immunol 1971; 8: 593-602.

(18) Henle G, Henle W. Immunofluorescence in cells derived from Burkitt's lymphoma. J Bacteriol 1966; 91:1248-1256.

(19) Klein G, Yefenof E, Falk K, Westman A. Relationship between Epstein-Barr virus (EBV)-production and the loss of the EBV-receptor/complement receptor complex in a series of sublines derived from the same original Burkitt's lymphoma. Int J Cancer 1978; 21:552-560.

(20) Lau R, Nonoyama M, Klein G. Somatic cell hybrids between human lymphoma and human myeloid leukemia cells. I. Induction of resident viral genome transcription and viral antigen formation by IUdR and TPA. Virology 1981; 110:259-269.

Ganglioside Patterns: New Biochemical Markers for Human Hematopoietic Cell Lines[1]

Günter Rosenfelder,[2] Andreas Ziegler,[3] Peter Wernet,[3] *and* Dietmar G. Braun[2,4]

ABSTRACT—The ganglioside patterns from a representative collection of 20 human B-cell, T-cell, null cell, myeloid cell, and early erythroid cell lines were determined. Radioactive sugar-labeled gangliosides from cultured cells were extracted, analyzed, and quantitated by high-performance thin-layer chromatography (HPTLC) and high-pressure liquid chromatography, essentially according to the polarity of the oligosaccharide chain. The ganglioside labeling patterns of the human cell lines were in some cases extremely complex, since more than 100 components could be separated upon two-dimensional HPTLC, e.g., in the case of a promyelocytic cell line. Each type of cell showed a characteristic pattern: Null cell lines were much less complex than T-cell lines, and myeloid and erythroid lines exhibited characteristic patterns as well. Although clearly distinguishable from all other cell lines, the B-cell lines showed a high degree of heterogeneity. Therefore, gangliosides can be expected to serve as additional markers to establish the origin of a cell line or to classify pathologic cell populations.—JNCI 1982; 68:203–209.

Considerable effort has been devoted to the serologic, biochemical, genetic, and functional characterization of human hematopoietic cell lines, since several of these are believed to be the in vitro correlates of cell types responsible for a variety of hematologic disorders. Analyses of chromosomal abnormalities (*1, 2*), morphologic and cytochemical characteristics (*3*), surface glycoprotein patterns (*4–8*), serologic markers (*9–12*), and functional attributes (*12–14*) have already established some differences among these cell lines. The recent finding that GSL are highly characteristic moieties of murine lymphoblastoid tumor cell lines (*15*) prompted us to perform similar analyses on a representative panel of human hematopoietic cell lines for the identification of new differentiation markers. The chromatographic analysis of radioactively labeled gangliosides from these lines revealed patterns that appear suitable for classification purposes.

MATERIALS AND METHODS

Cell lines.—The human cell lines used and some selected markers are given in table 1. ERL proliferated from a cultured paraaortic lymph node of a patient with testicular teratocarcinoma; it was supplied by Dr. R. Löwer and Dr. R. Kurth of the Medical University Clinic. BRW was obtained from Dr. I. Doxiadis, University of Munich, Munich, F.R.G., and was originally derived from a patient with an unclassified leukemia. SH00 and SH02 lines were established by EBV transformation of lymphocytes from umbilical cord blood (Schulte-Holthausen H: Unpublished results) and were obtained from Dr. Kurth. The K562 cell line was established from a patient with chronic myeloid leukemia in terminal blastic crisis (*16*), and it has characteristics of early erythroid cells (*17*). The origin and some properties of the following lines have already been described (*18*): KR3598, Priess (*19*), and Bri-8 (*20*) are EBV-transformed normal B-cells, while DAUDI (*21*), Raji (*22*), NC37 (*23*), BJAB (*24*), and EB3 (*25*) are derived from patients with Burkitt's lymphoma. MOLT-4 (*26*), JM1 (*27*), CCRF-CEM (*28*), and CCRF-HSB-2 (*29*) are cell lines derived from patients with acute lymphoblastic leukemia of the T-cell type; KM3 (*29*) and Reh (*30*) have been classified as null lymphoid cells because they lack the classical markers of B-cells and T-cells. Finally, the cell line HL-60 (*31*) bears characteristics of promyelocytes.

With the exception of JM1, all cell lines were grown in Dulbecco's modification of Eagle's minimum essential medium (Boehringer, Mannheim, F.R.G.) supplemented with 10% fetal calf serum (Seromed, Munich, F.R.G.), 2 m*M* glutamine, 200 U penicillin/ml, and 200 µg streptomycin/ml. JM1 was cultured in RPMI-1640 medium containing 25 m*M* HEPES[5] buffer (Gibco-Biocult, Glasgow, Scotland); the other ingredients were prepared as above.

Radioactive incorporations and isolation of gangliosides.[6]—Cells were radioactively labeled in 50 ml growth medium supplemented with 0.5 µCi D-[1-^{14}C]galactose/ml (sp act 60 mCi/mmol) and 0.5 µCi D-[1-^{14}C]glucosamine hydrochloride/ml (sp act, 57.8 mCi/mmol) (both from Amersham-Buchler, Braunschweig, F.R.G.). Cells were seeded at a concentration

---

ABBREVIATIONS USED: cALL=common form of acute lymphoblastic leukemia; EBV=Epstein-Barr virus; F.R.G.=Federal Republic of Germany; GSL=glycosphingolipid(s); HPLC=high-pressure liquid chromatography; HPTLC=high-performance thin-layer chromatography.

---

[1] Received March 3, 1981; revised August 18, 1981; accepted September 8, 1981.

[2] Pharmaceuticals Research Laboratories, CIBA-GEIGY Limited, CH-4002 Basel, Switzerland.

[3] Immunology Laboratory, Medical University Clinic, D-7400 Tübingen, Federal Republic of Germany.

[4] The skillful assistance of Mrs. A. Bordmann is gratefully acknowledged. We thank Ms. A. Hirschi and Ms. V. Forster for competent secretarial work.

[5] 4-(2-Hydroxyethyl)-1-piperazine ethanesulfonic acid.

[6] Abbreviations of gangliosides G_{M1}, G_{M2}, G_{M3}, and G_{D1a} are according to the nomenclature given in the *Recommendations of the Commission on Biochemical Nomenclature IUPAC-IUB* (1976). G=ganglioside, M=monosialo, and D=disialo. *Arabic numbers* indicate sequence of migration in thin-layer chromatograms.

of 2.5×10^5/ml or 5×10^5/ml. In most cases, incorporations were terminated after 48 hours, but cell lines Reh, KM3, JM1, and KR3598 were grown for longer periods up to 116 hours (KM3). About 5×10^7 cells were finally harvested by centrifugation, washed twice with phosphate-buffered saline (pH 7.3), and repeatedly extracted with chloroform:methanol (2:1 and 1:1, vol/vol). The ganglioside fraction was separated from the other lipids by a modified Folch partition and subsequent DEAE-Sepharose chromatography of the dialyzed upper phases (*15, 32*).

Chromatographic analysis of gangliosides.—An aliquot of the ganglioside fraction (10^4 cpm) obtained from the cell lines was analyzed on the basis of polarity on Merck silica gel HPTLC plates. Plates were developed in a solvent system of chloroform:methanol:water (55:45:10, vol/vol/vol, containing 1 m*M* $CaCl_2$). For two-dimensional HPTLC analyses, plates were developed for the first dimension as above, then dried and chromatographed for the second dimension with the use of chloroform:methanol:2.5 *M* NH_4OH (60:35:8, vol/vol/vol, containing 1 m*M* $CaCl_2$). Dried chromatograms were autoradiographed on Kodak RP Royal X-Omat X-ray films for 6 days. For comparison, CBA/J mouse brain gangliosides were applied as cold standards and subsequently stained with resorcinol (*33*).

HPLC analyses of the ganglioside fractions ($2-3\times10^4$ cpm) were performed on two Zorbax Sil columns in series (250×4.6 mm; E. I. du Pont de Nemours, Wilmington, Del.) with the use of two Altex model 110 pumps (Altex Scientific Inc., Berkeley, Calif.), a model 7120 injector with a 20-μl sample loop (Rheodyne, Berkeley, Calif.), a model LB 503 radioactivity flow-through monitor (Berthold Laboratories, Wildbad, F.R.G.) with a 200-μl flow cell containing glass scintillator beads, and a four-channel model 314 recorder (W+W Electronics, Basel, Switzerland). One pump provided a constant flow (0.45 ml/min) of chloroform:methanol:water:formic acid (60:35:4:1, vol/vol/vol/vol) through the columns, whereas the second pump provided a constant flow (0.05 ml/min) of the alkaline detergent Extran (E. Merck A.G., Darmstadt, F.R.G.) in water (5% vol/vol) into the main stream from the columns to the radioactivity monitor. The addition of Extran avoided memory effects caused by nonspecific absorption of gangliosides to glass by permanently "rinsing" the glass scintillator beads. Although in-line detection proved indispensable for optimization of separation conditions, accurate quantitation by means of the radioactivity monitor proved to be problematic due to high background signal noise and solvent quenching. Hence 1-ml fractions were collected, the organic solvent was evaporated under a gentle stream of air, and the radioactivity was counted in an Aquasol scintillator with the use of an Intertechnique liquid scintillation counter (model SL 4000; Nucletron SA, Lausanne, Switzerland).

RESULTS

The incorporation of ^{14}C-labeled sugars as label into dividing leukocytes has greatly facilitated the qualitative and quantitative analyses of GSL (*15, 34, 35*). Although incorporation of [^{14}C]galactose and [^{14}C]glucosamine into the ganglioside fraction varied considerably from cell line to cell line in this study, radioactivity of this fraction generally accounted for about 90% of that incorporated into total GSL (table 1).

Isolated gangliosides were analyzed either by HPTLC or,

TABLE 1.—*Human hematopoietic cell lines: Expression of selected cell surface antigens and incorporated ^{14}C-labeled sugars into GSL*

Cell line		Antigens[a]						
Type	Designation	HLA-A, HLA-B, HLA-C	HLA-DR	HTA1[b]	cALL	Surface immunoglobulin	Erythrocyte rosettes	Incorporation: cpm in ganglioside fraction[c]
B-cell	DAUDI	−	+	−	+	+	−	309,206
	Raji	+	+	−	+	+	−	228,170
	NC37	+	+	−	NT	+	−	101,370
	BJAB	+	+	−	NT	+	−	105,130
	EB3	+	+	−	NT	+	−	293,152
	KR3598	+	+	−	NT	+	−	123,809
	Priess	+	+	−	NT	+	−	102,481
	Bri-8	+	+	−	NT	+	−	464,291
	ERL	+	+	−	−	+	−	571,509
	BRW	+	+	−	−	−	−	849,257
	SH00	+	+	−	NT	NT	−	320,061
	SH02	+	+	−	NT	+	−	228,170
T-cell	MOLT-4	+	−	+	−	−	+	208,652
	JM1	+	−	+	−	−	+	140,540
	CCRF-CEM	+	−	+	−	−	+	65,280
	CCRF-HSB-2	+	−	−	−	−	+	210,585
Null cell	Reh	+	+	−	+	−	−	261,169
	KM3	+	+	−	+	−	−	[illegible]21,684
Promyelocytic	HL-60	+	−	−	−	−	−	161,061
Fetal erythroid	K562	+[d]	−	−	−	−	−	794,301

[a] (*20, 39*); Ziegler A: Unpublished results. Absence (−) or presence (+) was determined by radioactive binding (*20*) and immunofluorescence tests (*42*). K562 has a considerably reduced expression of HLA-A, HLA-B, and HLA-C antigens. NT = not tested.

[b] Human thymus antigen 1 (*41*).

[c] Obtained from 6×10^7 cells.

[d] Ziegler A: Submitted for publication.

for the quantitation of radioactive bands, by HPLC. HPLC proved less laborious and more reliable than the one used previously (*15*), where zones of radioactivity had been scraped off the silica plates before counting. Patterns of gangliosides from 12 selected lines and quantitation of the predominant bands from these lines are depicted in figures 1 and 2. A characteristic of all human as opposed to murine T-cell and B-cell lines tested was the presence of a double band in the ganglioside G_{M3} range. Furthermore, a distinct difference between lymphoid and other human hematopoietic cell lines became apparent: In B-cells, T-cells, and null cells, this double band (with the exception of triple bands in the G_{M3} range in KR3598 cells described below) contained between 52 and 85% of the radioactivity present in all gangliosides; this finding contrasted with the findings with the promyelocytic line HL-60 and the erythroid precursor line K562, in which these two components account for only 30–40% of the total cpm of the ganglioside fraction.

The ganglioside fraction of B-cell lines showed considerable heterogeneity (fig. 1). The patterns with the least complexity were those of Priess and ERL, two lines with totally different origins. The umbilical cord blood lines SH00 and SH02 (not shown) yielded the simplest patterns, consisting of virtually only the double band in the G_{M3} range. KR3598 was distinguishable from all other cell lines by a strong band (accounting for 20% of the total radioactivity) with a slightly higher retardation factor value than that of the double band in the G_{M3} range. The banding patterns of Bri-8 and BRW were quite similar in spite of clear-cut quantitative differences. Again, the origin of these lines was entirely distinct. The most pronounced difference among the B-cell lines was found when the Burkitt's lymphoma line DAUDI was compared with all other B-cell lines. The other Burkitt's lymphoma lines Raji, NC37 [apparently a subline of Raji (*23*)], BJAB, and EB3 (patterns not shown) resembled DAUDI.

GSL patterns were established for four T-cell lines: MOLT-4, JM1 (fig. 2), CCRF-CEM, and CCRF-HSB-2 (not shown). Despite quantitative differences, the banding patterns were more similar to each other than were the patterns of any of the other cell lines tested. In particular, a strongly labeled doublet in the G_{D1a} position appeared to be a characteristic of the T-cell lines (fig. 2).

Easily distinguishable from all other lines by their gangliosides, the non-T-cell, non-B-cell lines Reh and KM3 each exhibited two distinct bands in the G_{M2} range of about equal intensity. In addition to null cells, both bands appeared to be present only in the promyelocytic cell line HL-60 as part of an extremely complex pattern, which was, irrespective of several overlaps, entirely different from that of all other lines examined (fig. 2).

Finally, the erythroid precursor cell line K562 also exhibited a complex ganglioside pattern with a large number of bands. Although distinct from all other cell lines tested, there appeared to be a definite relationship with T-cell lines, whose bands in the G_{1Da} range were also present in K562; the same held true for bands in the G_{M2} region. The only clear-cut qualitative difference appeared to be a doublet in the G_{M2} range: Both T-cell lines possessed only one band at the retardation factor position of the K562 doublet. The slower migrating component of this doublet may have been identical with the faster moving band from the G_{M2} range of Reh and KM3.

The possibility that ganglioside patterns could be even more complex than suggested by the results presented above was examined by two-dimensional HPTLC. The cell lines MOLT-4, Bri-8, KM3, and HL-60 may serve as examples (fig. 3). Under these conditions even the restricted null cell pattern of KM3 consisted of an amazing number of spots. Two-dimensional HPTLC resolved single bands into two to three and sometimes more components. The two-dimensional chromatograms of cell lines with complex GSL patterns already after one-dimensional chromatography (such as MOLT-4 or HL-60) are good examples of the resolving power of this method.

DISCUSSION

Conventional procedures of cell classification were of considerable benefit when serologically defined surface and cytoplasmic markers became available. However, the cALL antigen for acute lymphoblastic leukemia cells has recently been found on a variety of B-cell and T-cell lines (*36, 37*). Hence there is a clear-cut need for additional markers identifying the origin of normal cells and of pathologic (e.g., leukemia and lymphoma) cell populations by other than established markers. GSL have proved to be valuable markers for certain murine cell lines (*15*); their analysis was therefore extended to human hematopoietic cells with the hope of establishing an alternative system of differentiation markers.

The ganglioside patterns depicted in figures 1 and 2 appear to be unrelated to the human cell surface antigens listed in table 1. This may not be too surprising because all these antigens are proteins, although, possibly, a particular GSL in the cell membrane could be a consequence of the non-expression of other antigens. Probably the most interesting aspect of the results given in this article is the possibility of defining ganglioside patterns characteristic of particular types of human cells. The most obvious case is that of the non-T-cell, non-B-cell lines KM3 and Reh, whose banding patterns, though virtually indistinguishable, are entirely distinct from those of all other cell lines investigated.

The B-cell lines analyzed exhibited a remarkable degree of heterogeneity in their GSL patterns. It is unlikely that the complex patterns of DAUDI and of the other cell lines derived from Burkitt's lymphoma are due to the absence of HLA-A, HLA-B, and HLA-C antigens, since the GSL patterns from the other Burkitt's lymphoma lines expressing these antigens were closely similar to those from DAUDI. The in vitro EBV-transformed lines and B-cell lines of other origins gave relatively simple GSL patterns, the most simple being those of unbilical cord blood lines. It thus appears that an analysis of gangliosides could lead to a subdivision of B-cell lines into Burkitt's lymphoma-derived lines and cells from other origins. An analysis with the use of monoclonal antibodies (Ziegler A: Submitted for publication) supports this conclusion.

The T-cell GSL patterns established here are considerably more complex than the B-cell GSL patterns (with the exception of DAUDI), and they bear remarkably little resemblance to the patterns of the B-cell lines. Several bands appear to be shared among T-cells, the promyelocytic cell line HL-60, and the chronic myeloid leukemia-derived cell line K562. This finding may indicate a closer relationship between myeloid cells and T-lymphocytes than was previously postulated. Although it cannot be decided on the basis of these data whether the divergence between T-cells and B-cells occurs earlier in hematopoiesis than that between T-lymphocytes and myeloid cells, the frequent occurrence of leukemia cells bearing characteristics of both myeloid and T-cells (*38*, *39*) points to the same direction, i.e., that myeloid cells and T-cells are closely related.

The reasons for the complexity of ganglioside patterns exhibited by human hematopoietic cell lines are unknown. The many GSL spots seen after two-dimensional chromatography in cell lines arrested at different stages of hematopoiesis must be a consequence of regulatory events during differentiation, since the GSL content of cell surfaces depends on the activity of sugar- and acyl-transferases, hydrolases, and various other enzyme systems. On what level these regulatory control mechanisms are exerted, (transcriptional, translational, or post-translational) cannot be decided at this stage, but there are a number of ways to approach these questions [*see*, e.g., (*40*)]. Although it appears to be unsuitable for routine work in its present form, the establishment of ganglioside patterns may be complementary in all those cases in which conventional analytic approaches have failed to indicate the origin of a cell line or a pathologic cell population, as in the case of the Sternberg-Reed cell (*2*).

REFERENCES

(*1*) Rowley JD. A new consistent chromosomal abnormality in chronic myelogenous leukaemia identified by quinacrine fluorescence and Giemsa staining. Nature 1973; 243:290–293.

(*2*) Schaadt M, Diehl V, Stein H, Fonatsch C, Kirchner HH. Two neoplastic cell lines with unique features derived from Hodgkin's disease. Int J Cancer. In press.

(*3*) McDonald GA, Dodds TC, Cruickshank B. Atlas of hematology. Edinburgh, London, and New York: Churchill-Livingstone, 1978.

(*4*) Warner NL. Membrane immunoglobulins and antigen receptors on B and T lymphocytes. Adv Immunol 1974; 19:67–216.

(*5*) Trowbridge IS, Hyman R, Mazauskas C. Surface molecules of cultured human lymphoid cells. Eur J Immunol 1976; 6:777–782.

(*6*) Andersson L, Gahmberg CG, Nilsson K, Wigzell H. Surface glycoprotein patterns of normal and malignant human lymphoid cells. I. T cells and leukemic T cell lines. Int J Cancer 1977; 20:702–707.

(*7*) Nilsson K, Andersson L, Gahmberg CG, Wigzell H. Surface glycoprotein patterns of normal and malignant human lymphoid cell lines. II. B cells, B blasts, and Epstein-Barr virus (EBV)-positive and negative B lymphoid cell lines. Int J Cancer 1977; 20:708–716.

(*8*) Wang CH, Fu SM, Kunkel HG. Isolation and immunological characterization of a major surface glycoprotein (Gp54) preferentially expressed on certain human B cells. J Exp Med 1979; 149:1424–1437.

(*9*) Balch CM, Dougherty PA, Volger LB, Ades EW, Ferrone S. A new B cell differentiation antigen (BDA) on normal and leukemic human B lymphocytes that is distinct from known DR (Ia-like) antigens. J Immunol 1978; 121:2322–2328.

(*10*) Barnstable CJ, Bodmer WF, Brown G, et al. Production of monoclonal antibodies to group A erythrocytes, HLA and other human cell surface antigens—new tools for genetic analysis. Cell 1978; 14: 9–20.

(*11*) Evans RL, Breard JM, Lazarus H, Schlossman SF, Chess L. Detection, isolation, and functional characterization of two human T-cell subclasses bearing unique differentiation antigens. J Exp Med 1977; 145:221–233.

(*12*) Reinherz EL, Schlossman SF. The differentiation and function of human T lymphocytes. Cell 1980; 19:821–827.

(*13*) Reinherz EL, Hussey RE, Schlossman SF. A monoclonal antibody blocking human T cell function. Eur J Immunol 1980; 10:758–762.

(*14*) Reisner Y, Biniaminov M, Rosental E, Sharon N, Ramot B. Interaction of peanut agglutinin with normal human lymphocytes and with leukemic cells. Proc Natl Acad Sci USA 1979; 76:447–451.

(*15*) Rosenfelder G, Herbst H, Braun DG. Glycolipids as markers of murine T and B lymphoblastoid tumour cell lines. FEBS Lett 1980; 114:213–218.

(*16*) Lozzio CB, Lozzio BB. Human chronic myelogenous leukemia cell line with positive Philadelphia chromosome. Blood 1975; 45:321–334.

(*17*) Benz EJ, Murnane MJ, Tonkonow BL, et al. Embryonic–fetal erythroid characteristics of a human leukemic cell line. Proc Natl Acad Sci USA 1980; 77:3509–3513.

(*18*) Heinrichs H, Wernet P, Ziegler A. Expression of major histocompatibility antigens on human thymocytes studied using monoclonal antibodies. Immunogenetics 1980; 11:629–635.

(*19*) Baron D, Thomsen M, Staub-Nielsen L, Wernet P, Svejgaard A. The comparison between normal and Epstein-Barr virus-transformed homozygous typing cells and their use for MLC, PLT and serological detection of human Ia-type alloantigens. Tissue Antigens 1979; 13:1–10.

(*20*) Snary D, Goodfellow P, Hayman MJ, Bodmer WF, Crumpton MJ. Subcellular separation and molecular nature of human histocompatibility antigens (HL-A). Nature 1974; 247:457–461.

(*21*) Klein E, Klein G, Nadkarni JS, Nadkarni JJ, Wigzell H, Clifford P. Surface IgM-κ specificity on a Burkitt lymphoma cell in vivo and in derived culture lines. Cancer Res 1968; 28:1300–1310.

(*22*) Epstein MA, Achong BG, Barr YM, Zajac B, Henle G, Henle W. Morphological and virological investigations on cultured Burkitt tumor lymphoblasts (strain Raji). J Natl Cancer Inst 1966; 37:547–559.

(*23*) Cho MS, Freesen KO, Zur Hausen H. Multiplicity-dependent biological and biochemical properties of Epstein-Barr virus (EBV) rescued from non-producer lines after superinfection with P3HR-1 EBV. Int J Cancer 1980; 26:357–363.

(*24*) Menezes J, Leibold W, Klein G, Clements G. Establishment and characterization of an Epstein-Barr virus (EBV)-negative lymphoblastoid B cell line (BJAB) from an exceptional EBV-genome-negative African Burkitt's lymphoma. Biomedicine 1975; 22:276–284.

(*25*) Epstein MA, Barr YM, Achong BG. Studies with Burkitt's lymphoma. Wistar Inst Symp Monogr 1965; 4:69–82.

(*26*) Minowada J, Ohnuma T, Moore GE. *Brief communication*: Rosette-forming human lymphoid cell lines. I. Establishment and evidence for origin of thymus-derived lymphocytes. J Natl Cancer Inst 1972; 49:891–895.

(*27*) Schneider U, Schwenk H-U, Bornkamm G. Characterization of EBV-genome negative "null" and "T" cell lines derived from children with acute lymphoblastic leukemia and leukemic transformed non-Hodgkin lymphoma. Int J Cancer 1977; 19:621–626.

(*28*) Foley GE, Lazarus H, Farber S, Uzman BG, Boone BA, McCarthy RE. Continuous culture of human lymphoblasts from peripheral blood of a child with acute leukemia. Cancer 1965; 18:522–529.

(*29*) Adams RA, Pothier L, Flowers A, Lazarus H, Farber S, Foley GE. The question of stem lines in human acute leukemia. Comparison of cells isolated in vitro and in vivo from a patient with acute lymphoblastic leukemia. Exp Cell Res 1970; 62:5–10.

(*30*) Rosenfeld C, Goutner A, Choquet C, et al. Phenotypic characterization of a unique non-T, non-B acute lymphoblastic leukaemia cell line. Nature 1977; 267:841–843.

(*31*) Gallagher R, Collins S, Trujillo J, et al. Characterization of the continuous, differentiating myeloid cell line (HL-60) from a patient with acute promyelocytic leukemia. Blood 1979; 54:713–733.

(*32*) Saito T, Hakomori S. Quantitative isolation of total glycosphingolipids from animal cells. J Lipid Res 1971; 12:257–259.

(*33*) Laine RA, Stellner K, Hakomori S. Isolation and characterization of membrane glycosphingolipids. In: Korn ED, ed. Methods in membrane biology. Vol 2. London and New York: Plenum, 1974: 205–243.

(34) Iwamori M, Nagai Y. A new chromatographic approach to the resolution of individual gangliosides. Biochim Biophys Acta 1978; 528:257–267.

(35) Rosenfelder G, Van Eijk RV, Muehlradt PF. Metabolic carbohydrate labelling of glycolipids from mouse splenocytes. Eur J Biochem 1979; 97:229–237.

(36) Greaves MF, Brown G, Rapson NT, Lister TA. Antiserum to acute lymphoblastic leukemia cells. Clin Immunol Immunopathol 1975; 4:67–84.

(37) Chechik BE, Minowada J. Quantitation of human thymus-leukemia-associated antigen in established hematopoietic cell lines by radioimmunoassay. JNCI 1979; 63:609–614.

(38) Takagi S, Morita R, Morita T, et al. Peroxidase-positive acute leukemia with T-cell markers. Blut 1980; 41:397–398.

(39) Ziegler A. Monoclonal antibodies as tools in hematology. Blut 1980; 41:1–10.

(40) Trowbridge IS, Hyman R, Mazauskas C. The synthesis and properties of T25 glycoprotein in Thy-1-negative mutant lymphoma cell. Cell 1978; 14:21–32.

(41) McMichael AJ, Pilch JR, Galfre G, Mason DY, Fabre JW, Milstein C. A human thymocyte antigen defined by a hybrid myeloma monoclonal antibody. Eur J Immunol 1979; 9:205–210.

(42) Uchanska-Ziegler B, Wernet P, Ziegler A. Rapid preparation of multiple cell samples for immunofluorescence analysis using microtiter plates. J Immunol 1980; 39:85–93.

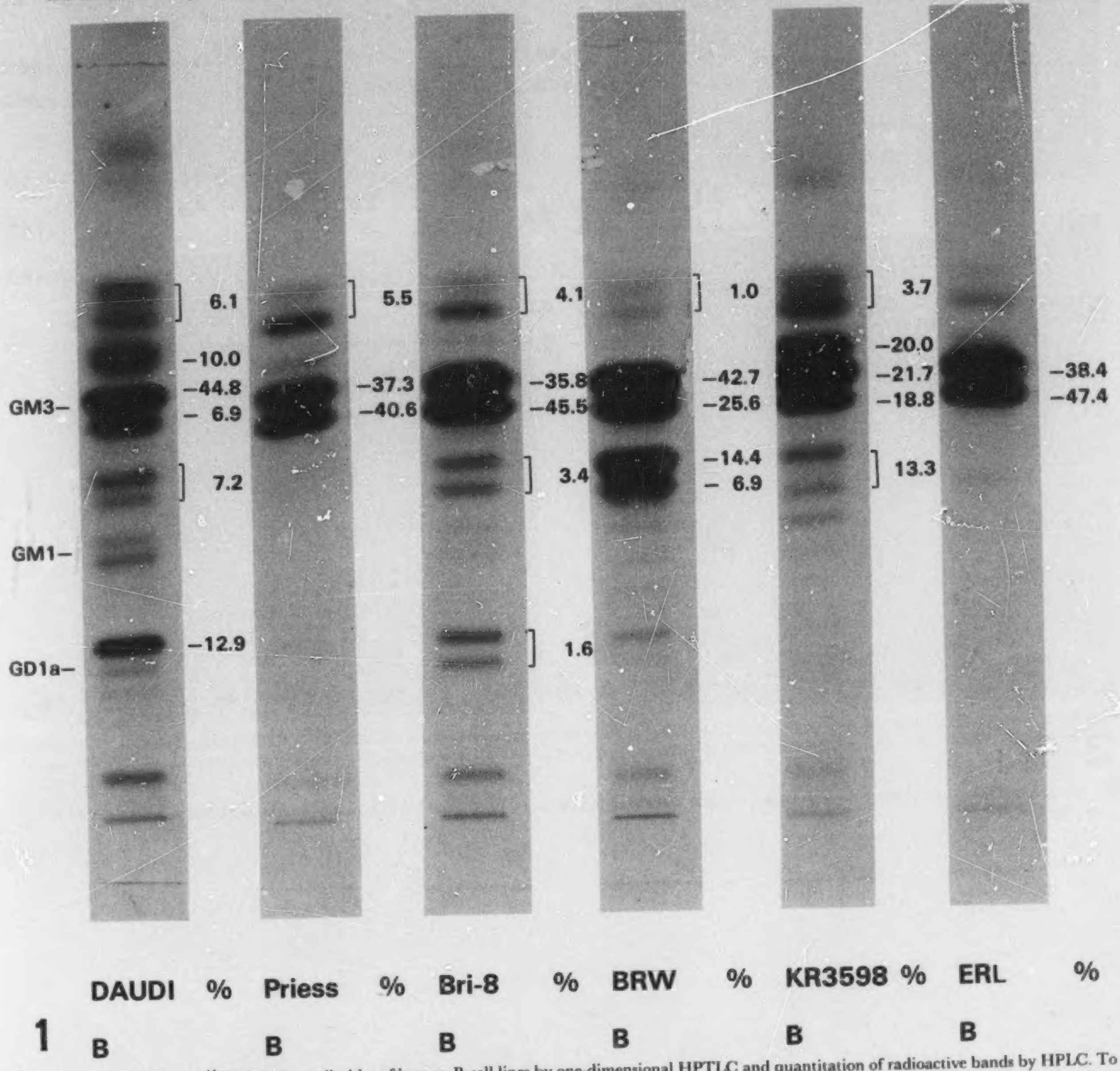

Figure 1.—Separation of ^{14}C-labeled gangliosides of human B-cell lines by one-dimensional HPTLC and quantitation of radioactive bands by HPLC. To every HPTLC, 10,000 cpm of gangliosides was applied. The migration behavior of human brain gangliosides is marked at the margin. Percentages given between HPTLC lanes relate to the total radioactivity (cpm) present in 100 fractions collected from the HPLC column.

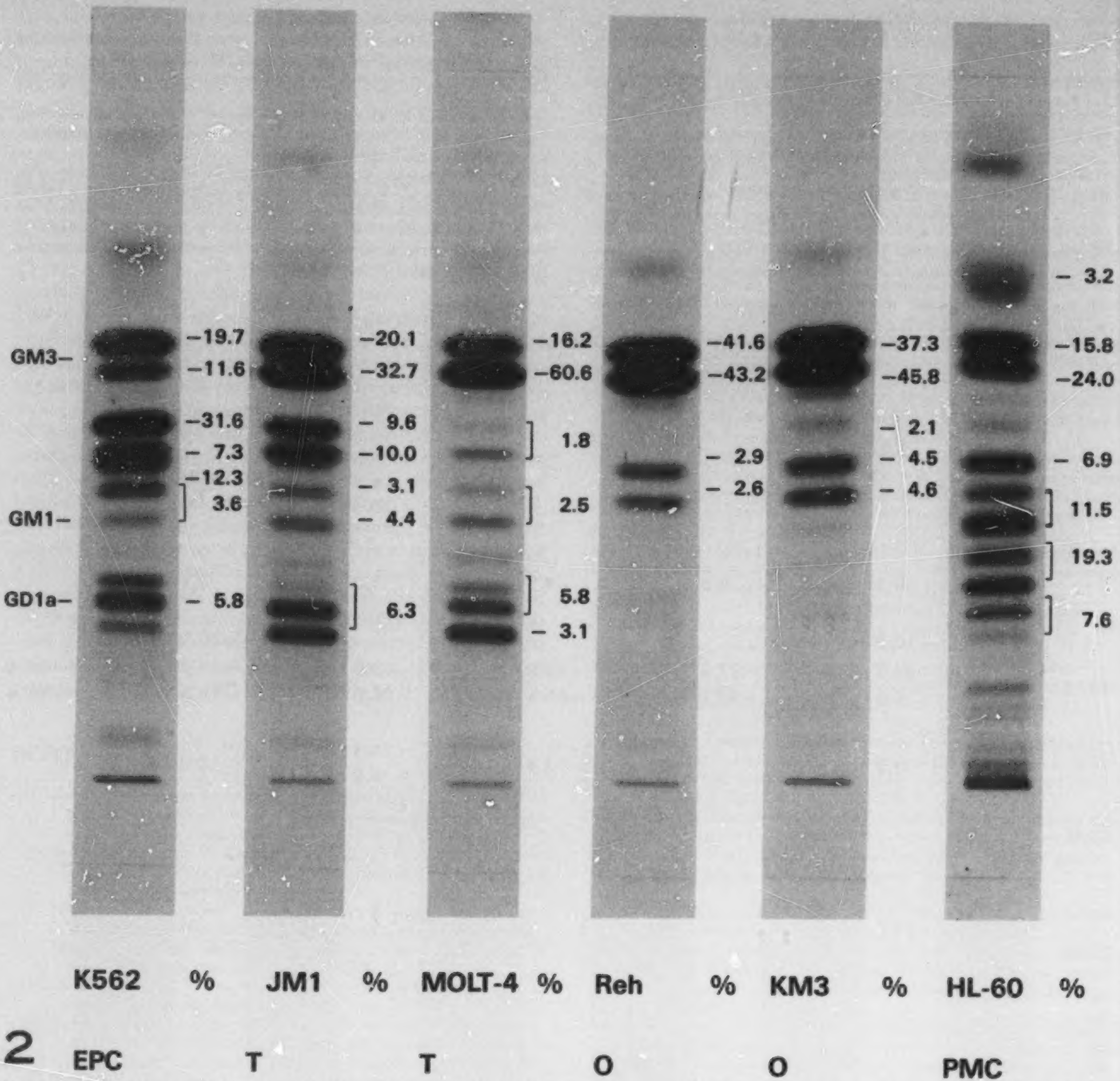

2

FIGURE 2.—Separation of ^{14}C-labeled gangliosides of human non-B-cell lines by one-dimensional HPTLC and quantitation of radioactive bands by HPLC. *See* fig. 1 legend.

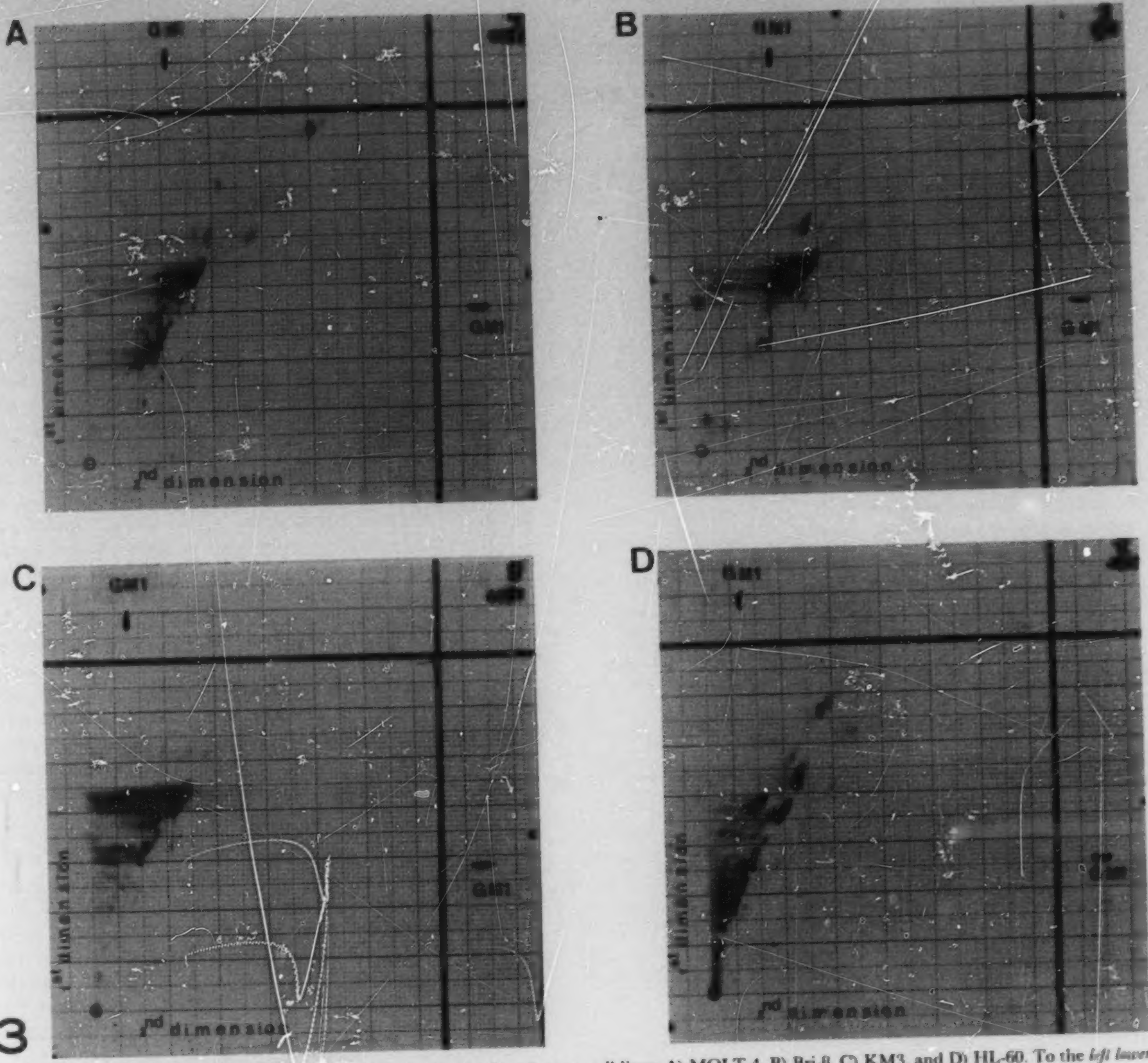

FIGURE 3.—Two-dimensional HPTLC of ^{14}C-labeled gangliosides from human cell lines: A) MOLT-4, B) Bri-8, C) KM3, and D) HL-60. To the *left lower corner* of every HPTLC plate, 20,000 cpm of gangliosides was applied. Human brain ganglioside G_{M1} as a standard was visualized by resorcinol staining.

blank page

Risk Factors for Breast Cancer in Women in Northern Alberta, Canada, as Related to Age at Diagnosis[1,2]

Jay H. Lubin,[3] Patricia E. Burns,[4] William J. Blot,[3] Alan W. Lees,[4] Carol May,[4] Linda E. Morris,[3] *and* Joseph F. Fraumeni, Jr.[3,5]

ABSTRACT—A population-based case–control study involving interviews with 577 female breast cancer patients and 826 controls in northern Alberta, Canada, revealed that some determinants of breast cancer varied according to age. Among women under age 45, risk factors included a younger age at menarche, late age at last birth, high parity, and recent use of oral contraceptives. At older ages risk was related to natural as opposed to surgical menopause, late age at first birth, low parity, late age at natural menopause, and tonsillectomy. At all ages there was an increased risk of breast cancer associated with difficulty in conceiving, benign breast disease, not having breast fed, and a history of breast cancer among mothers or sisters. For some variables the age differences were pronounced; the combination of low parity and late age at first birth was associated with a sevenfold increase in breast cancer risk at ages 55–80 but a slight decrease at ages under 45. The effect of tonsillectomy steadily increased with age and represents a new lead, but certain features of the data suggest that the link to oral contraceptives among younger women and the inverse relation to breast feeding at all ages may not be causal. Even though design limitations (cases interviewed in a different setting from controls) appeared not to influence conclusions, the results may have been subjected to interview bias and thus should be interpreted cautiously.—JNCI 1982; 68:211–217.

The causes of breast cancer among postmenopausal women may differ from those among premenopausal women (*1–6*). Taking advantage of a comprehensive reporting system in northern Alberta, Canada, in which virtually all women with breast cancer diagnosed during 1976–77 were identified and interviewed, we conducted a case–control study to evaluate differences in risk factors according to age at diagnosis.

MATERIALS AND METHODS

Breast cancer cases were drawn from the breast cancer registry (*7*) operated in conjunction with the Alberta Cancer Registry (*8*). The case group consisted of 631 women with breast cancer reported in northern Alberta during the 2-year period 1976–77. These women constitute all cases, since cancer registration is mandatory. Upon referral to diagnostic breast clinics held at the Cross Cancer Institute, 565 breast cancer patients were interviewed by two trained nurses, using a questionnaire designed to obtain information on descriptive variables and potential risk factors for breast cancer.

An age-stratified random sample, selected from social insurance files covering the entire population, of 1,268 women living in northern Alberta as of May 1978 was identified to act as a control group. The files of these women were checked against the cancer registry files to eliminate and replace those registered with breast cancer. Because of the small number of young patients with breast cancer, a greater percentage of young controls was selected to increase the power of detecting risk factors associated with early onset of disease. The resultant powers to detect a fixed level of risk were similar within our defined age categories. The same questions asked by the nurses interviewing cases, some modified slightly to adjust for a different interview setting, were asked of the controls in their homes by trained interviewers during the fall of 1978. Nearly all questions required an answer in closed form (e.g., yes or no or a response in one of but a few categories). Of the control women, 352 were not interviewed because of refusal to participate (109), incompetence (13), death (4), language difficulty (26), departure from the survey area (71), inability to locate (78), unavailability (36), and other reasons (15). Nine were interviewed but later excluded because of a previously diagnosed breast cancer. Thus a total of 907 apparently breast cancer-free women from the general population was available for comparison.

The analyses were restricted to the 577 cases and 826 controls aged 30–80 and were aimed at the examination of risk factors according to age at diagnosis for cases or age in January 1977 for controls. Age groups were selected as 30–44, 45–54, 55–64, and 65–80 years. Estimates of RR were calculated for various factors within each age stratum. The method of Gart (*9*) was used to estimate summary RR over age, when appropriate, or other strata and to obtain CI. Tests for linear trends for variables with multiple exposure

---

ABBREVIATIONS USED: CI=confidence intervals; OC=oral contraceptive(s); RR=relative risk(s).

---

[1] Received April 8, 1981; revised October 13, 1981; accepted October 19, 1981.

[2] Partially supported by the Medical Services Research Foundation of Alberta and the Alberta Heritage Savings and Trust Fund.

[3] Environmental Epidemiology Branch, Division of Cancer Cause and Prevention, National Cancer Institute, National Institutes of Health, Public Health Service, U.S. Department of Health and Human Services, Bethesda, Md. 20205.

[4] Cross Cancer Institute, 11560 University Ave., Edmonton, Alberta, T6G 1Z2 Canada.

[5] We acknowledge the advice and assistance of Dr. Louise Brinton, Dr. Michael Grace, Dr. Gerry Hill, Dr. Robert Hoover, Ms. Lucille Birkett, Ms. Leslie Gaudette, Ms. Mary Hurlburt, Ms. Heather Jenkins, and Ms. Peggy Kirdeikis. We thank Mrs. Theresa McKinney for manuscript preparation.

categories were done with the use of the Mantel extension procedure (*10*). The number of cases and controls used in the analyses of different factors varied slightly as a result of incomplete information on some variables.

To examine simultaneously several risk factors and to test interactions with age at diagnosis, we analyzed the data by using a binary logistic model for disease incidence (*11–13*). For these analyses only the 386 cases and 585 controls with data values for all variables considered were used. Although a rather large proportion of subjects was excluded (34% of cases and 29% of controls), results from the logistic analyses closely paralleled those from the crude and stratified analyses. A core set of variables related to disease status was defined and included in all models so as to adjust for potential confounding. This core set included variables for the four age strata, an additional linear age variable within the strata, religion (one variable indicating if Protestant and one if Catholic), and the occurrence (yes or no) of a previous biopsy for benign breast disease. When a potential risk factor was considered, the model included the core set, other potentially confounding variables (where appropriate), and the factor of interest. Tests of significance for various factors were done with the use of a likelihood ratio procedure.

RESULTS

General.—Table 1 summarizes some demographic characteristics for cases and controls. Although the sampling procedures specified a larger proportion of young controls, the mean ages of cases and controls were similar within the broad age strata. Most individuals were born in Canada, but for all ages, the proportion was higher for cases, while the proportion of Asian-born individuals was higher for controls. A higher proportion of cases was Protestant, but there were no significant differences according to level of education.

TABLE 1.—*Demographic and education variables for 577 cases and 826 controls*

Variable	Cases		Controls	
	Mean	Percent	Mean	Percent
Age, yr, at interview				
30–44	38.8	17.5	38.3	36.9
45–54	49.9	29.2	49.3	35.4
55–64	59.3	27.3	58.8	15.1
65–80	71.0	26.1	71.4	12.6
Years of education[a]				
≥13		28.9		27.8
9–12		40.2		41.5
0–8		31.0		30.7
Country of birth[b]				
Canada		70.1		63.3
North or Central Europe		8.0		9.8
United Kingdom or Ireland		7.8		10.5
United States		4.6		2.6
Asia or Pacific Islands		.6		5.6
Other		8.8		8.2
Religion[c]				
Catholic		21.7		27.2
Greek Orthodox		2.9		4.1
Protestant		64.4		53.5
Mennonite		.5		.9
Other		10.5		14.6

[a] Adjusted for age.

[b] Age-adjusted case-control difference, $P<0.001$.

[c] Age-adjusted case-control difference, $P=0.002$.

Table 2 presents the RR of breast cancer, according to age of diagnosis, associated with various risk factors examined in this survey. The number of cases and controls upon which the RR are based are given in table 3.

Age at menarche.—As shown in table 2, late age at menarche was associated with a decreased risk of breast cancer. The protective effect, however, was more pronounced in the youngest age stratum.

Age at first birth and parity.—There were linear trends of increased risk with late age at first birth compared to first birth before age 20 in each of the three oldest age strata. Similarly, increased risks were linked to low parity at older ages. At ages 30–44, however, the pattern in risk with low parity was reversed, while no significant effect with age at first birth was seen.

Table 4 shows that there were separate effects of both variables at the older ages. Among older women there was some evidence of interaction between the two variables, as the effect of low parity tended to be more pronounced among those with early age at first birth. [RR estimates for high (>3) and low (1–3) parity, if we summarize over the three oldest age groups, were, respectively, 1.0 and 2.8 (1.1, 7.0), 2.6 (1.4, 4.9) and 3.6 (1.9, 6.7), and 4.5 (2.2, 9.3) and 5.1 (2.8, 9.3) among women with a first birth at ages <20, 20–24, and ≥25, respectively, with an estimate of 6.1 (3.1, 11.6) for nulliparous women. All estimates were computed relative to women of high parity and early age (<20) at first birth]. At ages 30–44, after adjustment for parity, there was little or no trend with age at first birth. There remained, however, a significantly increased risk associated with high, rather than low, parity [RR=1.8 with 95% CI (1.1, 3.1) for women with parity >3 compared to those with parity ≤3 after adjustment for age at first birth].

Considering only parous women, we used a logistic model to analyze simultaneously age at first birth and parity and the interactions of these variables with each other and with age at diagnosis, while we controlled for the core set, use of OC and age at menarche. For the interaction effects, age at first birth and age were dichotomized (≥20 vs. <20 and ≥45 vs. <45, respectively). The risk associated with age at first birth significantly varied by age (with the effect limited to older ages) ($P=0.02$) but did not vary by parity category ($P=0.71$). Although much of the overall influence of parity was accounted for by age at first birth, the logistic analysis showed an interaction of this variable with age ($P=0.03$), even after we adjusted for the interaction between age at first birth and age ($P=0.12$).

Age at last birth.—For parous women, there was a slightly increased risk associated with an older age (≥35) at last birth within each age stratum and a linear trend at ages 30–44 (table 2). The previously described excess risk associated with high (<3) parity in the youngest age group was strongest among women whose last birth occurred after age 35. When we simultaneously controlled for parity, age at first birth, age at menarche, and the core set, the RR estimate from the logistic model was 1.7 (1.2, 2.4) for last birth over

TABLE 2.—*RR of breast cancer associated with selected variables according to age at diagnosis*

Variable	Age, yr, at diagnosis				Age adjusted
	30–44	45–54	55–64	65–80	
Age, yr, at menarche					
≥15	1.0	1.0	1.0	1.0	1.0
14	2.0	0.8	1.0	1.5	1.2
13	3.2	1.2	1.7	1.8	1.7
12	3.7	0.9	1.4	0.9	1.3
≤11	1.5	1.2	0.9	4.8	1.3
Age, yr, at first birth					
<20	1.0	1.0	1.0^a	1.0^b	1.0^b
20–24	1.0	1.7	3.2	2.4	1.7
≥25	0.7	2.1	3.7	5.7	2.0
Nulliparous	0.6	4.4	3.6	4.9	2.5
Parity					
>3	1.0^a	1.0^b	1.0	1.0^b	1.0^b
1–3	0.6	1.4	1.7	2.0	1.3
0	0.5	3.1	1.5	2.6	1.7
Age, yr, at last birth					
<25	1.0^a	1.0	1.0	1.0	1.0^a
25–34	1.2	0.9	0.7	0.4	0.9
≥35	1.8	1.1	1.3	1.3	1.4
Breast feeding ≥2 wk					
No	1.0	1.0	1.0^a	1.0	1.0^b
Yes	0.6	0.6	0.5	0.7	0.6
Spontaneous abortions					
0	1.0	1.0	1.0	1.0	1.0
1	1.0	1.3	0.6	1.0	1.0
≥2	0.9	0.9	0.9	0.7	0.8
Difficulty in conceiving					
No	1.0	1.0^b	1.0	1.0^a	1.0^b
Yes	1.4	2.1	1.5	2.5	1.8
Use of OC					
Never	1.0	1.0	1.0	—	1.0
Former	1.2	0.7	1.0	—	0.9
Recent	2.7^a	0.9	—	—	1.7
Menopausal status					
Premenopause	1.0	1.8^a	—	—	2.1^a
Post-natural menopause	—	1.0	1.0	1.0	1.0
Post-surgical menopause	0.6	0.2^b	0.8	0.6	0.6^a
Age, yr, of natural menopause					
<45	—	1.0	1.0^b	1.0^a	1.0^a
45–49	—	0.8	2.3	1.8	1.6
≥50	—	0.6	3.2	2.4	1.9
Breast cancer in mother					
No	1.0	1.0^a	1.0	1.0	1.0^b
Yes	2.4	2.5	1.5	2.5	2.2
Breast cancer in sister					
No	1.0	1.0^a	1.0	1.0	1.0^b
Yes	2.6	2.6	2.0	1.7	2.3
Previous benign biopsy specimen					
No	1.0	1.0^b	1.0^a	1.0	1.0^b
Yes	2.1	2.5	2.6	1.3	2.2
Diabetes					
No	1.0	1.0	1.0	1.0	1.0
Yes	—	0.4	0.6	0.7	0.6
Tonsillectomy					
No	1.0	1.0	1.0^a	1.0^a	1.0^b
Yes	1.0	1.2	1.9	2.3	1.4

[a] $P<0.05$ in test for linear trend or in test for significance relative to base-line category.

[b] $P<0.01$ in test for linear trend or in test for significance relative to base-line category.

age 35 relative to less than age 25. The RR was highest for the youngest age group, but differences by age were not significant. Results were similar when the analyses were restricted to those women having at least two births.

Breast feeding.—Among parous women, fewer of the cases than controls in each age group breast fed for 2 or more consecutive weeks. The overall RR estimate, after adjustment for age, age at first birth, and parity, was 0.6 (0.5, 0.8). Although the "protective" effect seemed independent of age at first birth and parity, no trend was seen with length of breast feeding. The effect of having breast fed was also significant (P=0.01) in the logistic analysis when we controlled for the core set, age at menarche, parity, and age at first birth.

Abortions and difficulty in conceiving.—No significant association between breast cancer and spontaneous abortions was seen, although slightly fewer of the cases reported 2 or more abortions.

Women were asked if they had difficulty in conceiving that was not due to their partner. For nulliparous women, 17 (46%) of 37 cases and 22 (28%) of 80 controls reported some difficulty. The age-adjusted RR associated with difficulty in conceiving with 95% CI was 2.6 (1.0, 6.6). For parous women, 61 (16%) of 379 cases and 68 (10%) of 680 controls experienced some problems in conceiving. The RR adjusted for age and age at first birth was 1.8 (1.1, 2.9). Using a logistic model in which we controlled for the core set, age at menarche, parity, and age at first birth, we found that difficulty in conceiving had a highly significant (P=0.002) effect with an RR estimate of 1.7 and no significant variation by age.

OC use.—A recent user of OC was defined as an individual having taken them within 1 year of diagnosis (for cases) or within 1 year of January 1977 (for controls). As shown in table 2, there was an increased risk associated with recent use in the age stratum 30–44. No clear trend emerged with length of OC use, however. At ages 30–44 the RR estimates were 1.3 for 1–4 years of use and 1.2 for 5 or more years of use. Among the small number of women aged 30–44 using OC for menstrual problems [10 cases (10%) and 17 controls (5%)], an increase in risk was suggested [RR=2.2 with 95% CI (0.8, 5.9)].

Menopausal status.—Menopausal status was categorized as premenopause, perimenopause, post-natural menopause, or post-surgical menopause. Perimenopausal women were excluded from analyses because of small numbers and the difficulty in obtaining an accurate determination of menopausal status. Women having a hysterectomy prior to experiencing symptoms of a natural menopause were classified as post-surgical menopause if both ovaries were removed. If neither or only one ovary had been removed or if women were uncertain as to their status, they were categorized as post-natural menopause if aged 60 or over and as unknown if under 60. Women having a hysterectomy following a natural menopause were classified as post-natural menopause. Table 2 shows that the RR of breast cancer for premenopausal women was higher than that for post-natural

TABLE 3.—*Numbers of breast cancer cases (D_1) and controls (D_0) for selected variables according to age at diagnosis*

Variable	Age, yr, at diagnosis							
	30–44		45–54		55–64		65–80	
	D_1	D_0	D_1	D_0	D_1	D_0	D_1	D_0
Age, yr, at menarche								
≥15	8	56	34	58	31	30	35	28
14	16	57	31	65	29	27	43	23
13	36	81	50	74	52	29	35	17
12	28	55	32	62	31	21	16	15
≤11	11	53	22	31	15	17	12	2
Age, yr, at first birth								
<20	21	57	10	34	5	13	12	25
20–24	46	120	65	128	58	47	44	39
≥25	16	64	45	81	54	38	52	19
Nulliparous	7	31	30	23	22	16	21	9
Parity								
>3	39	79	51	122	46	50	44	49
1–3	55	188	85	141	90	59	79	43
0	7	31	30	23	22	16	21	9
Age, yr, at last birth								
<25	10	35	10	20	9	7	6	5
25–34	59	178	69	149	49	55	45	43
≥35	14	28	45	75	60	36	59	37
Breast feeding								
No	39	83	46	65	56	26	25	13
Yes	57	191	92	204	81	83	103	82
Spontaneous abortions								
0	71	209	109	197	113	80	111	75
1	21	63	41	58	21	25	23	15
≥2	10	33	18	37	24	20	14	14
Difficulty in conceiving								
No	67	234	86	233	93	101	92	84
Yes	14	36	26	33	19	14	19	7
Use of OC								
Never	25	89	113	174	138	110	150	104
Former	62	183	46	97	18	14	—	—
Recent	15	20	9	15	1	0	—	—
Menopausal status								
Premenopause	88	228	62	58	2	0	0	0
Post-natural menopause	0	9	47	81	129	86	136	84
Post-surgical menopause	2	8	6	26	12	10	9	9
Age, yr, at natural menopause								
<45	0	9	10	13	9	16	16	19
45–49	—	—	23	36	34	26	29	19
≥50	—	—	14	32	73	41	72	35
Breast cancer in mother								
No	92	288	152	274	142	117	136	96
Yes	7	9	14	10	9	5	7	2
Breast cancer in sister								
No	76	232	124	223	123	103	115	86
Yes	6	7	16	11	10	4	14	6
Previous benign biopsy specimen								
No	90	285	129	260	137	118	134	95
Yes	13	20	39	32	21	7	15	8
Tonsillectomy								
No	46	142	71	143	72	77	83	78
Yes	54	163	90	148	82	48	60	25
Diabetes								
No	102	299	168	284	151	115	131	90
Yes	0	6	2	8	8	10	13	13

menopausal women, which in turn was higher than that for post-surgical menopausal women. These results were unchanged when we controlled for the use of menopausal hormones. Table 2 also shows, among women with natural menopause, a significant linear trend of increased risk with later age at natural menopause in the two oldest age strata. The reverse trend in the age stratum 45–54 was not significant.

The statements of breast cancer patients relating to a previous hysterectomy and/or oophorectomy were checked for accuracy by a review of their medical records. This review showed that 89% knew the type of surgery and the number of ovaries removed; among bilateral oophorectorized women, only 5% were misclassified.

Family history of cancer.—Risks were elevated in women having a mother or any sister with breast cancer, with RR among women under age 55 slightly higher. The age-adjusted RR were 2.2 (1.3, 3.8) and 2.3 (1.4, 3.8) associated with breast cancer in the mother or a sister, respectively. The effect was not influenced by menopausal status, and no significant variation with age was seen in the logistic analysis. Similar estimates were obtained for a history of a mother or any sister with breast cancer when calculations were limited to women with and without a previous benign breast biopsy. A history of cancer other than breast cancer in the mother or any sister did not affect the risk of breast cancer (RR of 1.1 and 1.0, respectively).

Previous breast biopsy.—A positive association was seen between breast cancer risk and a previous biopsy for benign breast disease. There was little variation by age, the age-adjusted RR being 2.2 (1.6, 3.1), but the risk estimates varied according to age at menarche (being higher among women with late menarche), parity (being higher among women of low parity), and menopausal status (being higher among postmenopausal women). The association was not influenced by the use of OC.

Diabetes.—There were 23 (5%) cases and 31 (6%) controls who had diabetes. The age-adjusted RR estimate was 0.6 (0.4, 1.1) with no significant differences between the age strata.

Tonsillectomy.—The RR of breast cancer was elevated among women with a history of tonsillectomy. The RR increased steadily with age, exceeding twofold among women over 65 [RR=2.3 with 95% CI (1.3, 3.9)]. The risk estimates with the use of a logistic model in which we controlled for the core set, age at menarche, and parity showed a significant (P=0.05) overall excess and a similar trend with age.

Other variables.—No association with risk of breast cancer was found for mother's age at the subject's birth, breast size (as estimated from brassiere size), or previous appendectomy.

DISCUSSION

This population-based survey in an area where incidence is high at all ages revealed that the determinants of breast

TABLE 4.—*RR of breast cancer associated with age at first term birth and parity according to age at diagnosis*

Parity	Age, yr, at first birth	Age, yr, at diagnosis											
		30–44			45–54			55–64			65–80		
		Case	Control	RR	Case	Control	RR	Case	Control	RR	Case	Control	RR
Nulliparous		7	31	0.4	30	23	5.9	22	16	5.5	21	9	6.7
1–3	≥25	20	69	0.6	43	63	3.1	49	34	5.8	51	19	7.7
	20–24	29	90	0.6	39	70	2.4	38	22	6.9	22	18	3.5
	<20	6	29	0.4	4	8	2.3	3	3	4.0	6	6	2.9
>3	≥25	5	10	1.0	17	31	2.5	19	9	8.4	11	5	6.3
	20–24	19	40	0.9	28	64	2.0	24	29	3.3	26	24	3.1
	<20	15	29	1.0	6	27	1.0	3	12	1.0	7	20	1.0

cancer may differ between younger and older women. Certain factors were linked to increased risk at all ages, but others (including low parity and late age at first birth) seemed to affect only older women, while still others were primarily related to risk at younger ages. The differences with respect to age were often substantial. The risk of breast cancer among women with late (≥25) age at first birth and low (≤3) parity exceeded that among women with early (<20) age at first birth and high (>3) parity by sevenfold at older ages, whereas a slight deficit was observed among women under 45 years. There was a more than 50% reduction in the risk of breast cancer at ages 55–80 for women with early natural menopause, but an increased risk was not seen at ages 45–54 (suggesting a "lag" in the protective effect of early menopause). Some of the interactive effects observed may be chance findings due to the multiple comparisons made, but taken together the data on the variables studied revealed a combination of independent influences and complex interrelationships that often varied by age. The identification and quantification of these interactions may help in providing clues to the intricate causal pathways leading to the development of breast cancer.

Several new associations were found in this study. Breast cancer was linked to tonsillectomy, with the strength of the association increasing steadily with age and exceeding twofold among women over age 65. The finding is of concern in view of the rising frequency of this surgical procedure during the mid-1900's and raises an hypothesis worthy of testing in other settings. Also provocative is the increased risk associated with recent use of OC among women aged 30–44. There were, however, no concomitant excess among the smaller number of recent users at older ages, no significant increase associated with past use, and no trend with duration of use, suggesting that the association may be noncausal. Furthermore the different interview settings, with cases interviewed in clinics by nurses and controls interviewed in their homes by professional survey personnel, may have affected response to questions of a sensitive nature, such as birth control use (potential biases of this sort are discussed further below). Although case–control and cohort studies have generally revealed no overall association between breast cancer and OC use (*14*), recent observations raise concern. A record-linkage survey reported large (over fourfold) excesses among current OC users for premenopausal women aged 46–55 but not for women aged 31–45 (*15*); a case–control study of breast cancer in women under age 33 showed a twofold excess risk among those who had used OC for more than 4 years before their first full-term pregnancy (*16*); a cohort study of OC users in Great Britain noted a nonsignificant increase in risk of nearly threefold in women under age 35 (*17*).

Another new finding was the twofold significantly increased risk associated with high parity at ages 30–44, which was independent of other risk factors such as age at first birth. This finding contrasts with the decreased risk with high parity often reported in the literature and also observed in our population of women aged 45–80. The association at younger ages was even stronger when the last birth occurred after age 35 and parallels that seen in mortality statistics (*18*), with higher death rates among fertile women than single or infertile women under age 35 but lower rates among fertile women at older ages. The reversal suggests that while high parity may in the long term protect against breast cancer, factors associated with the greater number and lateness of births may promote the risk of breast cancer during the childbearing ages.

Most results from this survey are consistent with the consensus of those reported elsewhere (*19–21*). Of note is the pattern of increasing risk with later age at first birth, at older but not younger ages at diagnosis, similar to the pattern observed in another Canadian population (*5*), although the effect seemed limited to younger ages in two case–control surveys in the United States (*3, 6*). Most studies of breast cancer, however, are comprised mainly of older (≥50 yr of age) women and clearly show an increase in risk with late age at first birth (*19–21*). Familial clustering of breast cancer has been documented at all ages but is thought to differentially affect younger women (*22*); our data tend to follow this pattern, with increased risks seen in individuals for whom either a mother or sister had breast cancer. A surprising result was an apparent protective effect of breast feeding in all age strata, independent of age at first birth and parity. Some studies have suggested that prolonged lactation (>17 mo) may have a protective effect against breast cancer (*23*), but MacMahon et al. (*24*) and others have shown no consistent relationship between breast cancer and breast feeding. The associaton in our study may not be causal, since no trend with length of breast feeding was observed. The association with benign breast disease (indicated by a previous benign biopsy) was consistent across age groups, but further analyses of the link were precluded in our study because of lack of information on the timing and characteristics of the benign breast diseases.

Of concern to us in this study were the possible biases introduced by the different interview procedures for cases and controls and by the higher percentage of nonresponders among the controls. The different interview settings could influence responses to less objective questions and questions with more of a medical orientation (such as those concerning difficulty in conceiving and spontaneous abortions) but would seem unlikely to affect "hard" data (such as the age at birth of first child, number of children, history of tonsillectomy, and most other questions asked in the interview). The different times of interview, with cases being interviewed throughout 1976 and 1977 and controls in the fall of 1978, could result in differences for exposures that have changed rapidly over time. Few variables in our study, however, fall in this category, except possibly for the use of OC, since practices have fluctuated during the 1970's.

We were able to make some internal evaluation of potential interviewer differences by comparing responses for 45 breast cancer patients, who were not interviewed in the clinic for a variety of reasons but in their homes in the same manner as controls, with responses for the 565 patients interviewed in the clinics. The 45 patients are not necessarily a random selection of the incident cases and comprise a somewhat higher percentage of older patients than the clinic-interviewed series. Comparison of the questionnaire responses, however, generally revealed concordance. There were no significant differences except for country of birth (more home-interviewed cases were born in Canada or the United States, $P=0.08$) and age at first birth (the mean ages were the same, but clinic-interviewed cases had a lower age at first birth for the oldest age strata and a higher age at first birth for the youngest strata, $P=0.08$). The 2 groups of cases were of sufficient sample size to generally (depending on the frequency of the "exposure") detect differences between them on the order of 2.5-fold with reasonably high power ($>80\%$).

To assess the representativeness of the interviewed control sample, we compared certain characteristics of this group with population statistics taken from the 1971 Canadian census (*25*, *26*). Differences between the control sample and census data covering northern Alberta (census divisions 7–15) with respect to the percentage in any religious group were small ($<3\%$). Census data for parity were available for only the Prairie Provinces (Alberta, Saskatchewan, and Manitoba). The control sample differed from the census data primarily in the youngest age group, in which controls had generally lower parity (27% had parity >3 compared to 37% in the population statistics). This fact could account in part for the excess risk associated wtih high parity at younger ages but may also be simply a reflection of urban–rural differences (northern Alberta being more urban than the Prairie Provinces as a whole) and possibly changes in childbearing practices between 1971 and 1978.

We also made renewed attempts to interview the 238 of the 352 nonresponders (i.e., the 352 women selected in the original control target sample who were not interviewed) available for recontact. After current addresses were obtained, a brief questionnaire was mailed in January 1980. If the questionnaire was not returned, telephone contact and interview were attempted. There were 59 completed interviews; a total of 140 women could not be relocated, 31 refused, 4 were deceased, and 4 could not be interviewed for other reasons. Questions were asked of the nonresponders on year of birth, years in primary, secondary, university, and/or other school, country of birth, age at menarche, type of and age at menopause, age at first and last birth, parity, occurrence of a previous breast biopsy, and difficulty in conceiving. There were no significant differences between the responders and the 907 controls for any of these variables. None of the interviewed nonresponders had breast cancer.

In summary, there were certain limitations inherent in this case–control study of breast cancer that may have affected some of the comparisons made. Their influences on the majority of variables, however, seem likely to be small and cannot account for the marked effect of age at diagnosis on the risk associated with several variables, especially reproductive factors. The data are generally consistent with other observations suggesting a varying set of determinants of breast cancer affecting younger and older women (*1–6*), even though some risk factors are common to all age groups. In further etiologic studies of breast cancer, analyses by age group should help delineate factors and provide insights into multicausal and multistage mechanisms.

REFERENCES

(*1*) Blot WJ, Fraumeni JF Jr., Stone BJ. Geographic patterns of breast cancer in the United States. J Natl Cancer Inst 1977; 59:1407–1411.

(*2*) Choi NW, Howe GR, Miller AB, et al. An epidemiologic study of breast cancer. Am J Epidemiol 1978; 107:510–521.

(*3*) Craig TJ, Comstock GW, Geiser PB. Epidemiologic comparison of breast cancer patients with early and late onset of malignancy and general population controls. J Natl Cancer Inst 1974; 53:1577–1581.

(*4*) Henderson BE, Powell D, Rosario I, et al. An epidemiologic study of breast cancer. J Natl Cancer Inst 1974; 53:609–614

(*5*) Stavraky K, Emmons S. Breast cancer in premenopausal and postmenopausal women. J Natl Cancer Inst 1974; 53:647–654.

(*6*) Wynder EL, MacCornack FA, Stellman SD. The epidemiology of breast cancer in 785 United States caucasian women. Cancer 1978; 41:2341–2345.

(*7*) Burns PE, Kredentser J, Grace M, Hanson J. Breast cancer in northern Alberta: A pilot study in computerized registration. Can Med Assoc J 1974; 116:1131–1134.

(*8*) Honeyman KA, Taylor RD, Gaudette L, Grace M. A systems design for surveillance of a chronic disease: A computerized cancer registry. Med Inf (Lond) 1977; 2:269–277.

(*9*) Gart JJ. Point and interval estimation of the common odds ratio in the combination of 2 × 2 tables with fixed marginals. Biometrika 1970; 57:471–475.

(*10*) Mantel N. Chi-square tests with one degree of freedom: Extension of the Mantel-Haenszel procedure. J Am Stat Assoc 1963; 59:690–700.

(*11*) Lubin JH. The development and examination of some regression methodologies for case–control studies. Ph.D. dissertation. Seattle: University of Washington, 1979.

(*12*) Prentice RL, Breslow NE. Retrospective studies and failure time models. Biometrika 1978; 65:167–180.

(*13*) Prentice RL, Pyke R. Logistic disease incidence models and case control studies. Biometrika 1979; 66:408–412.

(*14*) Editorial: Breast cancer and the pill—a muted reassurance. Br Med J 1981; 1:2075–2076.

(*15*) Jick H, Walker AM, Watkins RN, D'Ewart DC, Rothman KJ. Oral contraceptives and breast cancer. Am J Epidemiol 1980; 112:

577–585.

(*16*) Pike ML, Henderson BF, Casagrande JT, Rosario I, Gray GE. Oral contraceptive use and early abortion as risk factors for breast cancer in young women. Br J Cancer 1981; 43:72–76.

(*17*) Royal College of General Practicioners. Breast cancer and oral contraceptives: Findings in Royal College of General Practicioners study. Br Med J 1981; 1:2089–2093.

(*18*) Lilienfeld AM. The epidemiology of breast cancer. Cancer Res 1963; 23:1503–1513.

(*19*) Miller AB, Bulbrook RD. The epidemiology and etiology of breast cancer. N Engl J Med 1980; 303:1246–1248.

(*20*) Kelsey JL. A review of the epidemiology of human breast cancer. Epidemiol Rev 1979; 1:74–109.

(*21*) MacMahon B, Cole P, Brown J. Etiology of human breast cancer: A review. J Natl Cancer Inst 1973; 50:21–42.

(*22*) Anderson DE. Familial and genetic predisposition. In: Stoll BA, ed. Risk factors in breast cancer. Chicago: Heinemann Medical Books Publ, 1976:17.

(*23*) Levin ML, Sheene PR, Graham S, et al. Lactation and menstrual function as related to cancer of the breast. Am J Public Health 1964; 54:580.

(*24*) MacMahon B, Lin T, Lowe CR, et al. Lactation and cancer of the breast. A summary of an international study. Bull WHO 1970; 42: 185.

(*25*) 1971 Census of Canada: Population-religious denominations. Publication No. 92–724. Ottawa, Ontario: Ministry of Supply and Services, 1971.

(*26*) 1971 Census of Canada: Characteristics of women ever married by number of children born. Publication No. 92–751. Ottawa, Ontario: Ministry of Supply and Services, 1971.

blank page

Cancer Incidence in the Republic of Panama, 1974–78[1,2]

William C. Reeves,[3,4] Plinio F. Valdés,[5] María M. Brenes,[3] Rosa C. de Britton,[5] *and* Claire F. B. Joplin[3,6]

ABSTRACT—Data were examined from the Panama National Cancer Register, which was created by the Panamanian National Oncology Institute in 1974 to record data on all histopathologically diagnosed cancers in the Republic. Age- and sex-specific incidence rates were summarized for all cancers registered between 1974 and 1978. The age-adjusted incidences of invasive cervical cancer (37.8/100,000 population), penis cancer (1.9/100,000), and oral cancer (male, 3.2/100,000; female, 3.7/100,000) were among the highest in the world. In addition, both male and female genital cancers were clustered in rural Herrera Province (age-adjusted incidence: cervix, 84.7; and penis, 4.3).—JNCI 1982; 68:219–225.

Tropical countries have historically devoted most of their health resources to the fight against infectious diseases. In countries such as Panama, with rapidly improving environmental and health standards, infectious diseases remain the principal cause of morbidity but not of mortality. In Panama, along with the population's increasing life-span, noninfectious chronic diseases are emerging as major health problems, as reflected in the documented cause-specific mortality rates. Cancer has been among the three principal causes of death since 1968 (*1*). The National Oncology Institute of Panama initiated a National Cancer Register in 1974 to document and quantify cancer incidence. This paper reports results gathered during the Registry's first 5 years.

METHODS

Beginning in 1974, the Panama National Cancer Register recorded all histologically diagnosed cancers. The secretary of the Registry routinely visited each certified pathologist in Panama and reviewed all histopathology reports. We made no attempt to register individuals with only clinically diagnosed malignancy nor have we included people certified as dying of cancer, but without histopathologic evidence. For each newly diagnosed cancer we recorded the patient's name, age, sex, hospital or clinic chart number, as well as the date of diagnosis, anatomic site and type of cancer coded according to ICD-9 (*2*), and town where the tissue specimen was obtained (this allowed a crude estimation of residence). Register data was maintained on a General Automation SPC 16/65 minicomputer system with the use of the Conversational Computer Statistical System (*3*). Duplicate registration was monitored by checking the patient's name and hospital or clinic chart number. When necessary, specific charts were retrieved to verify information.

We obtained 1974–78 population data from the Census Bureau, Contraloria General de Panama. Panama maintains an extremely accurate and current census. A complete national census was taken in 1970; a second census in 1975 counted the voting population for the Canal Treaty ratification; a third census in 1978 documented the voting population to elect the House of Representatives; the fourth complete census in 10 years occurred in May 1980. Activities throughout the entire country ceased on census day and people were required to remain at home until enumerated. The Government made particular effort to completely tabulate the rural population. To compare Panama's cancer incidence rates with data reported by other countries, we adjusted the age to the standard world population (*4*). We used the Mantel-Haenszel method (*5*) to contrast age-specific interprovince incidence rates.

Cancer data from Darien Province or Comarca de San Bias are not reported. These areas are extremely isolated and have limited health care facilities. Data from Chiriqui and Bocas del Toro Provinces were combined.

RESULTS

The Republic of Panama is a rapidly developing tropical Latin American Country located 7° north of the equator. At the chronological midpoint of this report in 1976, the population of Panama was estimated as 1,718,700; with its 77,082-km^2 surface area, Panama had an overall population density of 24.9 persons/km^2.

Panama's public health system operated clinics and hospitals in each province (*1*). In 1976 there were 7.9 physicians per 10,000 population. This ratio ranged from 19.3 per 10,000 in the capital city to 2.7 per 10,000 in the most remote province. In 1976 Panama had 330 health care centers (30 hospital medical centers, 12 hospitals, and 288 health centers with outpatient clinics) or 1.9 health care centers per 10,000 inhabitants. Panama's cause-specific mortality rates reflected her excellent health care delivery sys-

---

ABBREVIATIONS USED: IARC=International Agency for Research on Cancer; ICD=International Classification of Diseases.

---

[1] Received April 15, 1981; accepted September 25, 1981.

[2] Supported in part by the Public Health Service grant 1 R01CA-25419-01 by the National Cancer Institute.

[3] Department of Epidemiology, Gorgas Memorial Laboratory, Apt. 6991, Panama 5, Panama.

[4] *Address reprint requests to* Dr. Reeves at Gorgas Memorial Laboratory, P.O. Box 935, APO Miami, Fla. 34002.

[5] Instituto Oncológico Nacional, Apt. 6-108, El Dorado-Panama, Panama.

[6] We acknowledge gratefully the valuable assistance given by Ms. Maritza Ramos, Ms. Ester Preciado, Ms. Nicky Angelkos, and Ms. Monserrat Adames of the Gorgas Memorial Laboratory, and Ms. Myrna Fitzgerald of the National Cancer Registry of Panama.

tem; ischemic heart disease, cancer, accidents-suicide-homicide, and stroke have constituted the principal causes of death since 1968 (*1*).

The average annual male and female age-specific incidence rates for all cancers registered during the period 1974–78 are shown in tables 1 and 2. Invasive cervical cancer was the most frequently diagnosed malignancy and accounted for 33% of female cancers. In addition, Panama's invasive cervical cancer incidence rate was higher than that in most of the countries in the World Health Organization and IARC registry programs (table 3) (*6*). Penis cancer also had a unusually high incidence compared to that of other areas (table 4).

Panama's cervical cancer incidence varied by province (text-fig. 1). Women living in Herrera Province had a risk of invasive cervical cancer 1.6 times that of women from Panama Province and 4.5 times more than the combined remaining provinces (overall rate 18.8 cases per 100,000). These relative risks remained constant between 1974 and 1978. Herrera had significantly greater in situ and invasive cervical cancer incidence rates than Panama Province ($P<.001$) and both diseases were significantly more frequent in Panama Province than in the combined other provinces ($P<.001$) (tables 5 and 6).

Penile cancer incidence also varied by province (text-fig. 2). Men from Herrera had a 1.7 times greater penile cancer incidence than that of males diagnosed in Panama Province and 3.4 times the risk of men in the combined other provinces (1.27 per 100,000). Since only 52 such cancers occurred during the study, differences in annual incidence were not apparent.

In addition to having a high overall rate, women from

TABLE 1.—*Male cancer incidence rates, Republic of Panama, 1974–78*

Site	No. of total cases		Average annual incidence per 100,000 by age group, yr												Crude rate[a]	Standardized rate[b]	ICD code
	All ages	Unknown age	0-	10-	15-	20-	25-	30-	35-	40-	45-	50-	55-	60+			
Lip, vermilion border	2	1	0.0	0.0	0.0	0.0	0.3	0.0	0.0	0.0	0.6	0.0	0.0	0.0	0.1	1.1	140
Tongue	26	2	0.0	0.0	0.0	0.0	0.0	0.0	0.4	0.0	0.0	1.3	2.5	8.1	0.6	1.1	141
Salivary gland	25	2	0.1	0.0	0.0	0.8	0.7	0.4	0.4	1.1	0.6	2.0	0.8	4.1	0.6	0.9	142
Mouth	80	4	0.0	0.0	0.0	0.0	0.7	0.8	0.4	2.6	1.8	4.0	9.0	20.3	1.9	3.1	143–145
Oropharynx	17	2	0.0	0.0	0.0	0.0	0.0	0.0	0.0	0.0	1.2	0.7	0.8	5.3	0.4	0.7	146
Nasopharynx	17	1	0.0	0.0	0.0	0.3	0.0	1.2	1.0	2.1	1.2	1.3	0.8	0.8	0.4	0.5	147
Hypopharynx	8	0	0.0	0.0	0.0	0.0	0.0	0.0	0.0	0.5	0.6	0.0	0.0	2.4	0.2	0.3	148
Esophagus	48	1	0.0	0.0	0.0	0.0	0.0	0.4	0.0	1.6	1.2	3.3	2.5	13.8	1.1	2.0	150
Stomach	270	12	0.0	0.0	0.0	0.5	1.3	3.2	3.6	6.3	13.6	28.1	27.1	56.0	6.5	10.4	151
Small intestine	4	1	0.0	0.0	0.0	0.3	0.0	0.0	0.0	0.0	0.0	0.7	0.0	0.8	0.1	0.1	152
Colon	44	6	0.0	0.0	0.0	0.0	0.0	0.0	0.4	1.6	1.8	3.3	4.9	10.6	1.2	1.8	153
Rectum	83	6	0.0	0.0	0.0	0.5	0.7	0.4	1.0	0.5	2.4	7.4	11.5	18.7	2.0	3.2	154
Liver	54	4	0.0	0.0	0.0	0.0	0.7	0.4	1.3	1.6	0.6	2.7	9.0	11.8	1.3	2.1	155
Gallbladder	24	2	0.0	0.0	0.0	0.0	0.0	0.0	0.4	0.0	1.2	0.7	4.1	6.1	0.6	1.0	156
Pancreas	15	1	0.0	0.0	0.0	0.0	0.0	0.4	0.0	0.0	0.6	2.0	1.6	3.2	0.4	0.6	157
Nose, sinuses	8	1	0.0	0.0	0.0	0.0	0.0	0.0	0.0	1.1	0.6	0.0	0.8	1.6	0.2	0.3	160
Larynx	67	7	0.0	0.0	0.0	0.0	0.0	0.0	1.0	0.5	3.6	2.7	9.9	17.0	1.7	2.7	161
Bronchus, trachea, lung	128	15	0.0	0.0	0.0	0.0	0.0	0.0	1.8	2.6	5.3	12.0	20.5	27.2	3.3	5.0	162
Bone	32	2	0.2	0.9	0.9	1.1	1.0	1.2	0.4	1.1	1.8	0.7	1.6	0.8	0.8	0.8	170
Connective tissue	68	1	0.2	0.8	0.0	1.1	1.6	2.0	1.3	2.1	4.1	4.7	2.5	9.3	1.6	2.3	171
Melanoma of skin	23	3	0.0	0.0	0.0	0.5	0.0	0.0	0.9	2.1	0.0	0.0	2.5	4.9	0.6	0.9	172
Other skin	433	67	0.0	0.2	0.0	1.1	2.0	3.6	10.2	8.9	15.4	33.4	38.6	101.4	11.5	16.9	173
Prostate	333	24	0.0	0.0	0.0	0.0	0.0	0.0	0.0	1.1	1.2	6.0	20.5	119.7	8.2	14.4	185
Testis	13	0	1.0	0.2	0.7	0.3	0.7	0.8	0.0	0.0	0.0	0.7	0.0	0.4	0.3	0.3	186
Penis	51	1	0.0	0.0	0.0	0.5	0.0	1.2	0.0	2.1	5.3	2.7	3.3	10.1	1.2	1.9	187
Bladder	59	9	0.0	0.0	0.0	0.3	0.0	0.0	1.3	1.1	1.2	2.7	4.1	17.0	1.6	2.4	188
Other urinary	28	4	0.4	0.0	0.0	0.0	0.0	0.4	0.4	2.1	1.2	2.0	0.8	4.5	0.7	1.0	189
Eye	20	0	0.5	0.2	0.0	0.0	0.0	0.0	0.0	1.6	0.0	0.7	1.6	2.4	0.5	0.6	190
Brain, nervous system	48	4	0.5	0.2	0.9	1.1	1.3	1.2	2.2	0.0	1.2	2.0	3.3	4.5	1.2	1.4	191–192
Thyroid	17	1	0.1	0.0	0.0	0.3	0.0	0.8	2.2	0.0	1.8	0.0	1.6	1.2	0.4	0.5	193
Other endocrine	6	1	0.0	0.0	0.0	0.0	0.3	0.0	0.4	0.5	0.0	0.7	0.0	0.0	0.2	0.2	194
Lymphosarcoma	45	1	0.3	0.4	0.9	0.3	1.0	0.8	0.4	2.1	0.6	2.7	0.8	7.3	1.1	1.5	200
Hodgkin's lymphoma	43	4	0.7	0.8	1.2	1.1	1.6	1.2	0.0	0.5	0.6	0.7	2.5	2.4	1.1	1.1	201
Other reticuloses	26	4	0.1	0.2	0.5	0.3	0.3	0.4	0.9	0.5	0.6	1.3	2.5	4.1	0.7	0.9	202
Multiple myeloma	9	4	0.0	0.0	0.0	0.0	0.0	0.0	0.0	0.0	0.0	0.7	0.8	2.8	0.3	0.4	203
Other and unspecified	114	17	0.1	0.4	0.0	0.3	1.0	2.0	0.9	0.5	2.9	6.7	11.5	26.4	3.0	4.4	149, 158, 159, 163, 195, 196, 199
All sites	2,288	215	3.3	4.1	5.3	10.4	15.0	22.7	33.3	48.2	77.5	140.9	205.4	530.1	57.7	89.0	

[a] Average total annual incidence per 100,000 population.

[b] Incidence per 100,000 population adjusted to standard world population.

Herrera developed invasive cervical cancer at an unusually young age (table 5). The Herrera invasive cervical cancer incidence among 20–39-year-old women was several times greater than that for the rest of the country. The age distribution of in situ carcinoma was similar throughout Panama (table 6), and women younger than 50 years were involved. Penis cancer mainly involved older men, and age-specific incidence rates were similar throughout the country.

DISCUSSION

The Panama National Cancer Register had two limitations. First, because it enumerated only histologically diagnosed disease, true cancer incidence was underestimated. However, limiting registration to confirmed diagnoses eliminated local variation in clinical diagnostic criteria. Histologic standards were constant because most biopsies were

TABLE 2.—*Female cancer incidence rates, Republic of Panama, 1974–78*

Site	No. of total cases		Average annual incidence per 100,000 by age group, yr															ICD code
	All ages	Unknown age	0-	10-	15-	20-	25-	30-	35-	40-	45-	50-	55-	60+	Crude rate[a]	Standardized rate[b]	
Lip, vermilion border	1	0	0.0	0.0	0.0	0.0	0.0	0.0	0.0	0.0	0.0	0.8	0.0	0.0	0.0	0.0	140
Tongue	21	1	0.0	0.0	0.0	0.0	0.3	0.6	0.0	0.0	0.0	0.8	0.0	7.9	0.5	0.9	141
Salivary gland	16	1	0.0	0.0	0.0	0.3	0.0	0.0	0.9	0.6	2.6	3.0	1.9	0.8	0.4	0.6	142
Mouth	84	7	0.0	0.0	0.0	0.0	0.0	0.4	0.5	0.6	2.0	3.8	3.7	23.5	2.2	3.7	143–145
Oropharynx	9	0	0.0	0.0	0.0	0.0	0.0	0.0	0.0	0.0	0.0	1.5	0.9	2.5	0.2	0.4	146
Nasopharynx	6	2	0.0	0.0	0.0	0.3	0.0	0.0	0.5	0.0	0.0	0.8	1.9	0.4	0.2	0.2	147
Hypopharynx	2	0	0.0	0.0	0.0	0.0	0.0	0.0	0.0	0.0	0.0	0.0	0.0	0.8	0.1	0.1	148
Esophagus	30	2	0.0	0.0	0.0	0.0	0.3	0.0	0.0	0.6	2.6	4.5	0.9	7.0	0.8	1.3	150
Stomach	153	7	0.0	0.0	0.0	0.8	0.7	1.6	4.2	6.8	7.8	9.8	20.5	31.4	3.8	6.1	151
Small intestine	4	0	0.0	0.0	0.0	0.0	0.0	0.0	0.0	0.0	0.7	0.0	0.0	1.2	0.1	0.2	152
Colon	63	5	0.0	0.2	0.2	0.8	0.3	1.6	1.4	2.3	2.0	3.8	4.7	13.6	1.6	2.4	153
Rectum	76	9	0.0	0.0	0.0	0.0	0.7	0.4	0.5	2.3	4.6	7.6	13.1	15.3	2.0	3.1	154
Liver	36	5	0.0	0.0	0.0	0.3	0.0	0.8	1.4	1.1	2.6	0.0	5.6	7.4	1.0	1.4	155
Gallbladder	42	4	0.0	0.0	0.0	0.0	0.0	0.4	0.9	0.0	1.3	0.8	7.5	11.6	1.1	1.8	156
Pancreas	9	1	0.0	0.0	0.0	0.0	0.0	0.0	0.0	1.1	0.7	0.0	0.9	2.1	0.2	0.4	157
Nose, sinuses	8	2	0.0	0.0	0.0	0.0	0.0	0.0	0.0	0.0	0.7	0.8	2.8	1.2	0.2	0.3	160
Larynx	20	2	0.0	0.0	0.0	0.0	0.3	0.4	0.0	0.6	1.3	1.5	3.7	3.7	0.5	0.8	161
Trachea, bronchus, lung	47	3	0.0	0.0	0.2	0.5	0.3	0.0	0.9	0.0	2.0	3.8	9.3	9.6	1.2	1.9	162
Bone	22	0	0.3	0.4	1.1	0.8	0.0	0.0	0.5	0.6	0.7	1.5	0.0	1.2	0.5	0.6	170
Connective tissue	55	10	0.2	0.6	0.9	0.8	1.0	2.4	1.9	1.7	3.9	3.0	2.8	5.4	1.5	1.8	171
Melanoma of skin	20	0	0.0	0.2	0.0	0.3	0.3	0.4	0.0	0.0	0.0	3.0	2.8	3.7	0.5	0.8	172
Other skin	364	59	0.0	0.0	0.2	0.5	2.6	4.1	10.2	11.3	19.6	27.9	35.5	80.9	10.0	14.7	173
Breast	382	34	0.0	0.0	0.2	0.8	3.9	9.8	16.6	22.6	33.3	34.7	39.2	52.5	9.8	14.4	174
Cervix uteri[c]	1,069	62	0.0	0.0	0.5	6.1	22.6	46.8	60.1	75.2	86.2	94.4	86.8	102.0	26.7	37.8	180
Placenta	18	1	0.0	0.0	0.7	1.1	2.0	0.0	0.9	0.0	1.3	0.8	0.0	0.0	0.5	0.5	181
Corpus uteri	104	4	0.0	0.0	0.0	1.1	0.7	2.0	2.3	2.8	3.3	6.0	14.0	22.7	2.6	4.1	182
Ovary	91	5	0.0	0.8	1.1	0.5	1.0	2.4	3.2	7.9	4.6	15.1	6.5	6.6	2.3	3.1	183
Other female genital	61	6	0.0	0.0	0.0	0.3	0.0	0.8	2.3	2.8	5.2	2.3	7.5	12.0	1.6	2.4	184
Bladder	29	7	0.0	0.0	0.0	0.0	0.0	0.0	0.0	0.0	0.7	1.5	4.7	8.7	0.9	1.3	188
Other urinary	27	4	0.5	0.2	0.0	0.0	0.3	0.0	0.9	2.3	0.7	0.8	1.9	5.7	0.7	0.9	189
Eye	6	5	0.1	0.0	0.0	0.0	0.0	0.0	0.0	0.6	0.0	0.8	0.0	1.2	0.3	0.2	190
Brain, nervous system	28	6	0.2	0.4	0.2	0.3	0.7	0.4	0.9	1.1	3.3	3.0	1.9	1.7	0.8	0.9	191–192
Thyroid	53	6	0.1	0.2	0.0	1.1	2.9	2.9	1.9	5.1	5.2	0.8	1.9	2.9	1.4	1.7	193
Other endocrine	5	0	0.0	0.2	0.0	0.0	0.0	0.0	0.9	0.6	0.7	0.0	0.0	0.0	0.1	0.2	194
Lymphosarcoma	31	3	0.1	0.4	0.0	0.0	0.3	0.0	0.9	0.0	1.3	3.8	2.8	6.2	0.8	1.2	200
Hodgkin's lymphoma	25	0	0.2	0.2	0.5	1.3	0.3	0.8	0.9	0.0	0.0	0.8	2.8	2.5	0.6	0.8	201
Other reticuloses	21	2	0.0	0.0	0.2	0.5	0.0	0.0	0.5	1.1	2.0	2.3	0.9	3.3	0.5	0.8	202
Multiple myeloma	5	3	0.0	0.0	0.0	0.0	0.0	0.0	0.0	0.0	0.0	1.5	0.0	1.2	0.2	0.2	203
Other and unspecified	141	14	0.1	0.6	0.5	1.1	2.0	2.0	2.8	2.8	6.5	11.3	14.0	18.6	2.7	3.8	149, 158, 159, 163, 195, 196, 199
All sites	3,184	282	1.7	4.3	1.4	18.7	43.8	80.6	117.8	156.0	209.1	255.3	294.0	481.9	81.6	121.5	
All sites except 180	2,115	220	1.7	4.3	5.9	12.7	21.2	33.8	57.7	80.8	122.8	160.9	207.2	379.9	54.2	80.7	

[a] Average total annual incidence per 100,000 population.

[b] Incidence per 100,000 population adjusted to standard world population.

[c] Includes only invasive cervical cancer.

evaluated at two major hospitals. Therefore, we are confident that unusually high observed rates accurately reflected the real situation. The second limitation was lack of epidemiologic data, such as race, occupation, residence, and birthplace, and follow-up. Most importantly, residence was estimated on the basis of the province the biopsy came from. However, since many people travel to Panama Province for diagnosis and treatment, cancer incidence there was overestimated.

Cancers of the uterine cervix and penis occurred at high incidence rates. Cancers of the mouth (ICD codes 143–145) also had extremely high age-adjusted rates: female oral cancer incidence 3.7 per 100,000 population, was third in the world after Singapore (Indians 16.9/100,000) and Bombay (5.4/100,000), while the male rate of 3.2 per 100,000 was only exceeded by 16 of the 80 IARC Registers (*6*).

None of the other frequently occurring Panamanian cancers presented striking epidemiologic differences when compared to areas that collaborate in the IARC Cancer Registry Program (*6*). In most instances, the standardized Panamanian cancer incidence rates were slightly lower than those reported from other Latin American and Caribbean populations.

TABLE 3.—*Age standardized cervix uteri cancer rates from selected registries*[a]

Registry	Incidence rate/100,000 population 0 10 20 30 40 50 60 70
Colombia: Cali	(62.8)
Brazil: Recife	(58.1)
Jamaica: Kingston	(51.0)
Panama	(37.8)
Africa: Bulawago	(28.4)
Brazil: São Paulo	(27.5)
Bay Area: black	(25.8)
Puerto Rico	(25.6)
India: Bombay	(23.2)
Nigeria: Ibadan	(21.6)
New Mexico: Spanish	(21.5)
Cuba	(19.5)
Singapore: Chinese	(18.6)
British Columbia	(18.4)
Norway	(18.1)
Sweden	(17.7)
Japan: Osaka	(16.2)
United Kingdom: Birmingham	(12.6)
Bay Area: white	(12.1)
New Mexico: white	(11.3)
Israel	(4.5)

[a] *Rules* represent graphic comparisons of incidence rates. *Values in parentheses* are actual incidence rates.

TABLE 4.—*Age standardized penis cancer rates from selected registries*[a]

Registry	Incidence rate/100,000 population 0 1 2 3 4 5 6 7
Brazil: Recife	(6.8)
Africa: Bulawago	(6.6)
Jamaica: Kingston	(6.4)
Puerto Rico	(4.6)
Brazil: São Paulo	(2.9)
Colombia: Cali	(2.0)
Panama	(1.9)
India: Bombay	(1.9)
Bay Area: black	(1.5)
Cuba	(1.4)
New Mexico: Spanish	(1.4)
Singapore: Chinese	(1.2)
New Mexico: white	(0.8)
British Columbia	(0.8)
Sweden	(0.8)
United Kingdom: Birmingham	(0.8)
Bay Area: white	(0.7)
Norway	(0.6)
Japan: Osaka	(0.5)
Nigeria: Ibadan	(0.2)
Israel	(0.1)

[a] *Rules* represent graphic comparisons of incidence rates. *Values in parentheses* are actual incidence rates.

Cervical cancer not only constituted the most frequently diagnosed malignancy in Panama, but its age-adjusted incidence ranked among the highest reported in the world. This fits into the worldwide epidemiologic picture of cervical cancer. Cervical cancer mortality rates have steadily decreased in industrialized countries (*7*) and concurrently increased in developing countries (*8*). Currently the Caribbean area of Latin America has the highest documented cervical cancer incidence among the developing countries (*9–12*). The three areas reporting a higher cervical cancer incidence than Panama (Cali, Colombia; Recife, Brazil; Kingston, Jamaica) have many cultural and ethnic similarities to Panama.

Significant differences between interprovince cervical

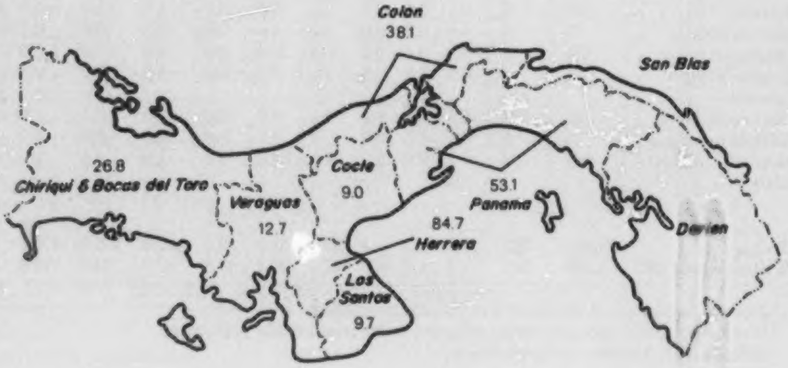

TEXT-FIGURE 1.—Invasive cervical cancer incidence in Panama, by province, age adjusted to standard world population.

cancer incidence rates also existed. Women from Herrera had 1.6 times the risk of developing invasive cervical carcinoma compared to women from Panama Province, and a 4.5-times greater risk than that of women from the combined other Provinces. No area in the world has documented a higher cervical cancer incidence than Herrera, and we know

TABLE 5.—*Summary of province and age-specific average annual incidence/100,000 of invasive cervical carcinoma, Panama 1974–78*

Age, yr	Incidence rate by province							Combined incidence, except Panama and Herrera
	Cocle	Colon	Chiriqui and Bocas del Toro	Herrera	Los Santos	Panama	Veraguas	
15–19	0.0	2.5	0.0	5.4	0.0	0.0	0.0	0.5
20–24	0.0	2.9	9.1	18.3	0.0	6.8	0.0	4.0
25–29	4.6	27.2	13.4	154.1	0.0	20.8	3.7	11.5
30–34	33.6	26.5	16.1	92.7	20.2	71.4	4.5	19.0
35–39	31.6	61.8	41.2	196.5	0.0	75.5	9.6	33.6
40–44	8.4	48.0	70.7	126.9	25.2	102.6	26.2	44.2
45–49	17.4	40.6	44.2	216.1	44.2	117.5	68.8	52.0
50–54	20.1	13.9	88.2	252.1	52.2	133.4	9.0	42.2
55–59	10.2	51.5	51.6	79.4	0.0	136.0	33.2	35.2
60+	16.3	70.4	74.8	151.7	15.6	152.2	37.3	51.6
Age adjusted[a]	9.0	38.1	26.8	84.7	9.7	53.1	12.7	18.8
Total No. of cases								
All ages	21	69	130	127	12	744	28	260
Unknown age	0	1	8	9	0	42	1	10

[a] Average annual incidence per 100,000 adjusted to standard world population.

TABLE 6.—*Summary of province and age-specific average annual incidence/100,000 of in situ cervical carcinoma, Panama 1974–78*

Age, yr	Incidence rate by province							Combined incidence, except Panama and Herrera
	Cocle	Colon	Chiriqui and Bocas del Toro	Herrera	Los Santos	Panama	Veraguas	
15–19	0.0	0.0	0.0	0.0	0.0	2.8	0.0	0.0
20–24	0.0	17.2	1.5	79.2	0.0	27.2	0.0	4.0
25–29	4.6	31.1	38.4	259.1	63.6	89.1	3.7	27.3
30–34	16.8	22.1	66.8	303.3	50.8	142.8	18.0	39.7
35–39	18.9	41.2	72.2	255.4	10.6	137.9	24.1	43.1
40–44	25.2	36.0	20.2	265.3	25.2	110.9	6.5	22.1
45–49	8.7	33.8	40.2	28.8	0.0	92.9	7.3	23.8
50–54	20.1	13.9	24.5	151.3	17.4	50.8	18.1	19.5
55–59	0.0	34.3	45.2	0.0	19.4	47.9	11.1	25.4
60+	5.4	3.7	10.7	75.8	0.0	34.3	0.0	5.2
Age adjusted[a]	6.1	14.3	19.4	94.1	11.9	46.9	5.0	12.8
Total No. of cases								
All ages	15	47	115	157	19	790	18	214
Unknown age	1	2	5	3	1	40	3	12

[a] Average annual incidence per 100,000 adjusted to standard world population.

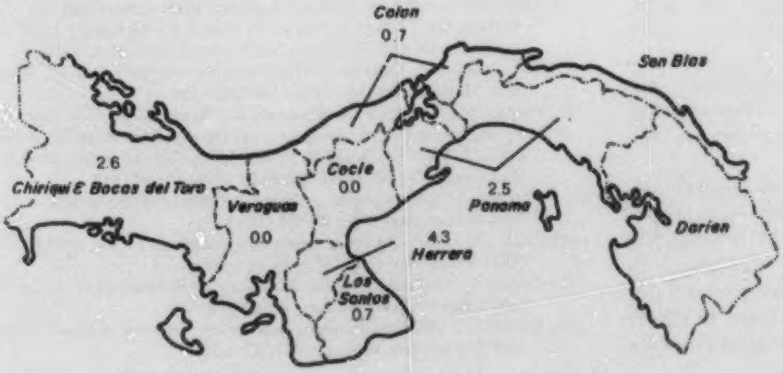

TEXT-FIGURE 2.—Penis cancer incidence in Panama, by province, age adjusted to standard world population.

that the histopathologically based Panama National Cancer Register not only underenumerated the actual number of cases but also was biased to classify many women from Herrera as residents of Panama Province.

Cancer of the penis also presented an extremely high incidence in Panama between 1974 and 1978 and was clustered in Herrera Province. Although rare in most of the world, cancer of the penis constitutes a public health problem in several developing countries of South America and the Caribbean (*6, 13*).

A relationship between carcinoma of the cervix and that of the penis was suggested by data from Puerto Rico (*14*) but has not been verified in other studies (*15, 16*). Some investigators (*17, 18*) have hypothesized a relationship between "high risk males" and cervical cancer, and this may be related to the occurrence of penile cancer. However, cancer of the penis and perhaps of the cervix may reflect other factors such as general hygiene.

We have evaluated several possible confounding factors but none of them seemed to account for this provincial clustering. Errors in enumerating the denominator, the population at risk, do not account for our findings. As stated previously, the Republic of Panama maintains an extremely complete and current census. The government has a special interest in delineating the rural population, which is stable and has not been affected by large-scale immigration. In addition, we eliminated Panama's two isolated undeveloped provinces from our analysis.

Similarly, the high invasive cervical cancer rate observed in Herrera was not due to bias in interpreting the tissue specimens. Since only Panama, Colon, and Chiriqui Provinces had pathology laboratory services between 1974 and 1978 (*19*), all histologic material from Herrera and the other outlying provinces was sent to Panama City and was evaluated (irrespective of origin) at either Santo Tomas or Seguro Social Hospital. Both hospitals have active pathology residency programs and maintain frequent interchange with pathologists at major U.S., South American, and European medical schools. The higher cancer incidence rates attributed to Panama Province were due to the many patients who were referred to hospitals in the capital for diagnosis and treatment.

Finally, differences in medical care could not have accounted for the extremely high rates of cervix and penis cancer seen in Herrera. Herrera was similar to other rural provinces with respect to physicians' services: physician-to-population ratio, availability of primary health care facilities, and overall patient utilization of such facilities (*19*). Moreover, if an unusually high awareness of cancer as a problem had prevailed, or an exceptionally aggressive group of gynecologists had worked in Herrera, the rates of other cancers should have been high also, but this was not the case (table 7).

Women living in Herrera were more likely to have Papanicolaou's (Pap) smears than women from other provinces. Between 1974 and 1978, an average of 9.9 per 100 Herrera women over 20 years of age had a Pap smear as contrasted to 6.4 per 100 in Panama Province and 4.6 per 100 in the combined other provinces. The extent to which Herrera's more intensive Pap smear program accounted for the increased invasive cervical cancer incidence cannot be estimated using currently available data (*20*).

Table 7.—*Incidence per 100,000 adjusted to the standard world population of the most common cancers in males and females, Panama 1974–78*

Site	Males			Females		
	Entire country	Herrera province	Panama province	Entire country	Herrera province	Panama province
Skin	16.9	11.5	26.8	14.7	13.2	23.5
Breast	—	—	—	14.4	5.5	24.8
Prostate	14.4	6.5	25.8	—	—	—
Stomach	10.4	9.4	17.2	6.1	5.2	10.3
Corpus uteri	—	—	—	4.1	1.7	6.7
Ovary	—	—	—	3.1	2.1	5.3
Other female genitals	—	—	—	2.4	3.1	3.8

Herrera also demonstrated a unique age-specific cervical cancer profile. Herrera women between 20 and 39 years of age had a disproportionately high invasive cervical cancer risk. In the remainder of Panama, and the rest of the world, women older than 40 manifest the highest rates. This may imply that young women from Herrera were exposed to unique risk factors (*21, 22*). An understanding of these risk factors would not only contribute to the basic epidemiology of cervical cancer but would also allow development of effective local cancer prevention programs.

To explore this problem in more detail, we are currently updating the histologic National Cancer Registry to an expanded internationally standardized format similar to that recommended by the IARC (*23*). This will include the cancers diagnosed clinically as well as histologically, and contain informations such as birthplace, town of residence, racial–ethnic group, occupation–socioeconomic status, and obstetric–gynecologic history.

REFERENCES

(*1*) Dirección de Estadísticas y Censo. Panamá en Cifras: Años 1974 a 1978. Panama: Contraloria General de la República, 1979.

(*2*) The International Classification of Diseases, 9th revision, clinical modification. Ann Arbor, Mich: Edwards Brothers, 1978.

(*3*) Kronmal RA, Bender L, Montenase J. A conversational statistical system for medical records. J R Stat Soc [Ser C] 1970; 19:82-92.

(*4*) Doll R. Comparison between registries, age standardized rates. In: Waterhouse J, Muir C, Correa P, Powell J. eds. Cancer incidence in five continents. Vol III. IARC Sci Publ 1976; 15:453-459.

(*5*) Snedecor GW, Cochran WG. Statistical methods. 6th ed. Ames, Iowa; Iowa State Univ Press, 1967:253-256.

(*6*) International Agency for Research on Cancer Table 9.5. Incidence by site and sex for each registry, age standardized rates. In: Waterhouse J, Muir C, Correa P, Powell J, eds. Cancer incidence in five continents. Vol III. IARC Sci Publ 1976; 15:486-535.

(*7*) Persaud V. Geographical pathology of cancer of the uterine cervix. Trop Geogr Med 1977; 29:335-345.

(*8*) Hill GB. Mortality from malignant neoplasm of the uterus since 1950. WHO Stat Rep 1975; 28:323-338.

(*9*) Caorsi I, Norambuena ML. El cáncer cervicouterino en el Sur de Chile. Bol Of Sanit Panam 1976; 80:68-77.

(*10*) Henderson BE. Epidemiology and cancer registries of Pacific basin. Natl Cancer Inst Monogr 1977; 47:1-182.

(11) Madrigal LM, Assal NE, Anderson PS. Cáncer de los organos de la reproducción en Costa Rica. Bol Of Sanit Panam 1976; 81:345–354.

(12) Rapp F. Herpesviruses and cancer. Adv Cancer Res 1974; 19:265–302.

(13) Muir CS, Nectoux J. Epidemiology of cancer of the testis and penis. Natl Cancer Inst Monogr 1979; 53:157–164.

(14) Martinez I. Relationship of squamous cell carcinoma of the cervix uteri to squamous cell carcinoma of the penis among Puerto Rican women married to men with penile carcinoma. Cancer 1969; 24: 777–780.

(15) Smith PG, Kinlen LJ, White GC, Adelstein AM, Fox AL. Carcinoma of penis and cervix. Lancet 1980; 2:417.

(16) Macgregor JE, Innes G. Carcinoma of penis and cervix. Lancet 1980; 1:1246–1247.

(17) Kessler II. Human cervical cancer as a venereal disease. Cancer Res 1976; 36:783–791.

(18) Singer A, Reid BL, Coppleson M. Hypothesis-role of a high risk male in etiology of cervical carcinoma-correlation of epidemiology and molecular biology. Am J Obstet Gynecol 1976; 126:110–116.

(19) Estadísticas de Salud Serie A 1974; 1975; 1976; 1977; 1978. Dirección General de Salud, Departamento de Estadísticas y Computos Electrónicos, Panamá.

(20) Clarke AE, Anderson TW. Does screening by "Pap" help prevent cervical cancer? Lancet 1979; 2:1–4.

(21) Kessler II, Aurelian L. Uterine cervix. In: Schottenfeld D, ed. Cancer epidemiology and prevention, current concepts. Springfield, Ill.: Thomas, 1975: 262–317.

(22) Alexander ER. Possible etiologies of cancer of the cervix other than herpesvirus. Cancer Res 1973; 33:1485–1496.

(23) World Health Organization. WHO handbook for standardized cancer registries. Geneva: WHO, 1975.

blank page

Phase I–Phase II Trial of *N*-Phosphonacetyl-L-Aspartic Acid Given by Intravenous Infusion and 5-Fluorouracil Given by Bolus Injection[1,2]

Charles Erlichman,[3,4] Ross C. Donehower,[5] James L. Speyer,[6] Ray Klecker,[7] *and* Bruce A. Chabner[7]

ABSTRACT—A phase I clinical trial of *N*-phosphonacetyl-L-aspartic acid (PALA) and 5-fluorouracil (FUra) was performed on 30 patients. PALA was given as a 15-minute iv infusion once daily for 5 days, and FUra was given as a bolus injection on days 2, 3, 4, and 5. Cycles of treatment were repeated every 3 weeks. Dose-limiting toxicity was manifested by stomatitis and diarrhea. Skin rash was observed also but was not dose limiting. No consistent hematopoietic or renal toxicity was observed. Seventeen patients with disseminated metastatic melanoma and measurable disease were evaluated for response. One partial response was seen; however, the response was associated with significant toxicity, and the treatment could not be repeated. Stable disease was observed in 3 patients with melanoma, 1 patient with colon carcinoma, and 1 patient with ovarian carcinoma. Our findings suggest that the clinical activity of PALA and FUra given according to the above schedule for melanoma is less than 25% ($P<0.05$). Pharmacokinetic studies of FUra revealed no consistent effect of PALA pretreatment on FUra disappearance in plasma. The mean FUra elimination half-life in plasma was 7.11±0.84 minutes (SEM), which is no different from that reported for FUra alone. The recommended doses on this schedule for phase II studies are 1,000 mg PALA/m^2/day iv daily for 5 days and 200 mg FUra/m^2/day iv on days 2, 3, 4, and 5—JNCI 1982; 68:227–231.

The use of combination chemotherapy has become commonplace in the treatment of many neoplastic diseases. In general, drugs have been combined on the basis of their single-agent activity and their lack of overlapping toxicity for normal tissues. Some consideration also has been given to the ability of drugs to act at different phases of the cell cycle. Increasing interest is now being directed to drug combinations designed to take advantage of biochemical interactions at the cellular level. We report here a phase I trial of a combination of PALA and FUra, which was designed with the biochemical mechanisms of these agents in mind.

PALA, a potent inhibitor of aspartate transcarbamylase, acts to inhibit de novo pyrimidine biosynthesis, as demonstrated in several murine solid tumors (*1, 2*). PALA has undergone extensive phase I (*3, 4*) and phase II trials (*5–7*) in humans over the last few years, but this agent has shown little clinical activity. FUra, a synthetic pyrimidine base analog, has been widely used in clinical chemotherapy for more than 20 years. In the cell, FUra is converted enzymatically to nucleotides. 5-Fluorouridine triphosphate is incorporated into RNA, and 5-fluorodeoxyuridine monophosphate potently inhibits cellular thymidylate synthetase. Pretreatment with PALA before FUra administration could result in increased FUra nucleotide formation, inasmuch as PALA has been shown to decrease intracellular pyrimidine nucleotide pool size in some cell lines (*8*), and could result in less competing substrate for FUra conversion to nucleotides, incorporation into RNA, and inhibition of thymidylate synthetase. Additionally, inhibition of the de novo pathway for pyrimidine biosynthesis by PALA might result in increased cellular levels of PRPP because of decreased use by this pathway. Drugs that increase PRPP levels, such as methotrexate, have been shown in vitro to result in enhanced FUra nucleotide formation (*9*).

In support of this hypothesis that pretreatment with PALA would enhance FUra activity, animal studies have shown that PALA and FUra together have greater antitumor activity in CD8F1 mammary carcinoma (*10*), colon 38 and 26 carcinomas, Lewis lung carcinoma, and M5076 carcinoma than do single agents (*11*). On the basis of this hypothesis, a study of PALA and FUra was performed on patients with extensive malignant disease. A dose schedule was chosen that included pretreatment with PALA, to decrease intracellular pyrimidine nucleotide levels before administration of FUra.

MATERIALS AND METHODS

This phase I–phase II trial was conducted cooperatively by the Medicine Branch and the Clinical Pharmacology Branch of the National Cancer Institute. Entered in the study were 30 patients, 26–68 years old. The male:female

---

ABBREVIATIONS USED: AUC=area under the curve; FUra=5-fluorouracil; PALA=*N*-phosphonacetyl-L-aspartic acid; PRPP=5-phosphoribosyl-1-pyrophosphate; $t_{\frac{1}{2}}$=half-life; WBC=white blood cell(s).

---

[1] Received May 4, 1981; accepted September 18, 1981.

[2] Research procedures were in accord with the ethical standards of the Clinical Research Committee, National Cancer Institute.

[3] Fellow of the Medical Research Council of Canada.

[4] Department of Medicine, Princess Margaret Hospital, 500 Sherbourne St., Toronto, Ontario, Canada M4X 1K9.

[5] The Johns Hopkins Oncology Center, 600 North Wolfe St., Baltimore, Md. 21205.

[6] Division of Oncology, New York University Medical Center, 550 First Ave., New York, N.Y. 10016.

[7] Clinical Pharmacology Branch, Division of Cancer Treatment, National Cancer Institute, National Institutes of Health, Public Health Service, U.S. Department of Health and Human Services, Bethesda, Md. 20205.

ratio was 1.6:1. The presence of cancer in all 30 patients was pathologically confirmed: 18 had melanomas, 8 had carcinomas of the colon, 2 had carcinomas of the ovary, 1 had a sarcoma, and 1 had carcinoma of the pancreas. Prior therapy with other chemotherapeutic agents (mean, two drugs) had been administered to 24 patients; 3 patients with carcinoma of the colon and 1 patient with carcinoma of the ovary had had prior FUra chemotherapy. The patient performance status was 30-90 on the Karnofsky scale; 24 of 30 had a performance status greater than or equal to 50.

Every 3 weeks patients received a daily 15-minute iv infusion of PALA for 5 consecutive days. FUra was given as a bolus injection shortly after completion of the PALA infusion on days 2, 3, 4, and 5. This dose schedule was chosen on the assumption that 1-day pretreatment with PALA would significantly decrease the levels of intracellular pyrimidine nucleotides prior to administration of FUra. Dose escalation for new patients was permitted after a minimum of 3 patients had completed 2 therapy cycles. In the absence of known cumulative toxicity for either drug, dose escalation was allowed for patients who had successfully completed a therapy cycle with no toxicity. Two drug escalation programs were used. Initially, the PALA dose was 1,500 mg/m^2/day for 5 days, and FUra was increased from 100 to 150 to 250 mg/m^2/day. The PALA dose was then decreased to 1,000 mg/m^2/day, and FUra was escalated from 150 to 200 to 250 mg/m^2/day. The 6 patients who received 700 mg PALA/m^2/day and 150 mg FUra/m^2/day had developed significant toxicity at a higher dose level in this trial. Patients were considered to be assessable for acute toxicity if they completed one course of therapy.

Skin and gastrointestinal toxicities were graded 1+ to 3+ according to the following criteria: Patchy areas of skin involvement were considered 1+, generalized skin involvement was graded 2+, and patients experiencing generalized exfoliation were assigned 3+. Patients who had loose bowel movements (<4 movements/day and none at night) or minimal stomatitis were considered to have 1+ gastrointestinal toxicity. Frank diarrhea (>4 movements/day) and/or stomatitis, which was uncomfortable but still permitted oral intake of food, was graded 2+. A 3+ gastrointestinal toxicity was assigned to patients having diarrhea with guaiac-positive stool and/or severe stomatitis associated with an inability to ingest any liquids or solids.

Pharmacologic studies were performed on selected patients at dose levels of 100, 200, and 250 mg FUra/m^2. By means of a high-pressure liquid chromatography technique (*12*), drug levels in plasma were monitored for 2 hours after the FUra iv bolus injection (*12*).

RESULTS

Renal function before therapy, as indicated by 24-hour creatinine clearance, was assessed in 22 patients: 14 had normal renal function (clearance ≥70 ml/min), 7 had moderate impairment of renal function (clearance <70 but ≥40 ml/min), and 1 had marked renal impairment (clearance <40 ml/min). In 8 patients for whom information on creatinine clearance was not available, the blood urea nitrogen was normal in all, and serum creatinine was less than 1 mg/100 ml in 6. Serum creatinine values of 1.3 mg/100 ml were recorded for 2 patients. The total bilirubin level in all 30 patients was normal. All patients except 2 had WBC counts of 3,500 or more/mm^3. The WBC counts for these 2 were 3,200 and 3,100/mm^3. All patients had platelet counts greater than 100,000/mm^3.

TABLE 1.—*PALA and FUra dose levels*

Dose level, mg/m^2/day		No. of patients[a]	No. of therapy courses
PALA	FUra		
700	150	6	15
1,000	150	1	3
1,000	200	21	59
1,000	250	2	8
1,500	100	2	4
1,500	150	4	6
1,500	250	3	3

[a] Due to dose escalation in some patients, the total number is >30.

One patient died before completion of 1 cycle of therapy due to progression of the disease and was not included in toxicity evaluations. For the remaining 29 patients, the dose levels evaluated and the number of patients and therapy courses administered at each level are summarized in table 1. Six patients received 1 cycle of therapy only, 17 patients received between 2 and 5 cycles, and 5 patients received between 6 and 10 cycles. One patient received more than 14 therapy cycles.

The major clinical toxicities affected the skin and gastrointestinal tract and are summarized in tables 2 and 3. Skin toxicity was manifested most commonly by a macular, erythematous eruption that occasionally was pruritic. It usually began on days 5-8 of a cycle and was resolved in approximately 10-14 days. Skin toxicity did not occur consistently with each cycle. Prior chemotherapy or radiotherapy did not appear to predispose patients to skin toxicity. Although skin toxicity was a common occurrence, at none of the dose levels evaluated was it dose limiting.

Gastrointestinal toxicity was the dose-limiting toxicity for the PALA-FUra combination used in this study. The major symptoms were mucositis and severe diarrhea. All 3 patients treated at a dose level of 1,500 mg PALA/m^2/day and 250 mg FUra/m^2/day developed severe mucositis and diarrhea with guaiac-positive stool. One patient treated at 1,500 mg PALA/m^2/day and 250 mg FUra/m^2/day became hypovolemic, secondary to fluid loss from diarrhea, and developed renal failure. Careful management of these complications reversed the renal failure and the patient recovered.

TABLE 2.—*Skin toxicity*

Dose level, mg/m^2/day		Toxicity grade			No. of toxic therapy courses/total No. of courses
PALA	FUra	1+	2+	3+	
700	150	1	1	0	2/15
1,000	150	3	0	0	3/3
1,000	200	21	2	0	23/59
1,000	250	3	0	0	3/8
1,500	100	0	0	0	0/4
1,500	150	3	1	0	4/6
1,500	250	3	0	0	3/3

TABLE 3.—*Gastrointestinal toxicity*

Dose level, mg/m²/day		Toxicity grade			No. of toxic therapy courses/total No. of courses
PALA	FUra	1+	2+	3+	
700	150	3	0	0	3/15
1,000	150	0	1	0	1/3
1,000	200	26	7	2	35/59
1,000	250	4	0	1	5/8
1,500	100	3	0	0	3/4
1,500	150	0	1	2	3/6
1,500	250	0	0	3	3/3

At 1,500 mg PALA/m²/day and 150 mg FUra/m²/day, 2 patients developed significant gastrointestinal toxicity manifested by prolonged oral mucositis. At 1,000 mg PALA/m²/day and 200 mg FUra/m²/day, most episodes of toxicity were relatively mild and tolerable. However, 2 of 59 therapy courses were associated with significant mucositis, which varied from angular stomatitis to complete oral mucosal ulceration. The mucositis began most commonly on day 4 and lasted 2–14 days. Diarrhea usually began during the second week of a cycle and was associated with occasional cramping. Gastrointestinal toxicity appeared to depend on the dose of FUra given with 1,500 mg PALA/m², but this relationship was not demonstrated when the PALA dose was 1,000 mg/m². Three patients complained of a gritty sensation in the eyes and photophobia. Two of these had obvious conjunctivitis. None of the three had any visual acuity disturbance, and ophthalmoscopic examination did not reveal any retinal abnormalities.

Hematologic toxicity was assessed by measurement of WBC and platelet counts during the course of therapy (table 4). For 52 of 98 therapy courses, nadir blood counts were available for assessment of hematologic toxicity. No patient developed a platelet count of less than 50,000/mm³. Five courses of therapy were associated with a fall in platelet counts to less than 100,000 but greater than 50,000/mm³. After receiving 1,500 mg PALA/m²/day and 100 mg FUra/m²/day, 1 patient developed a platelet count of 73,000/mm³. A second patient on 2 cycles of 1,000 mg PALA/m²/day and 250 mg FUra/m²/day developed platelet counts of 95,000 and 59,000/mm³. This patient had platelet counts of 74,000 and 59,000 when treated with 2 cycles at 1,000 mg PALA/m² and 200 mg FUra/m²/day. The WBC nadir was less than 2,000 in 2 patients both treated with 1,000 mg PALA/m²/day and 200 mg FUra/m²/day. One of these individuals had been treated previously with cisplatin, chlorozotocin, and BCG. The other patient had received no previous therapy.

While receiving PALA–FUra therapy, 5 patients developed neurologic abnormalities. The 2 patients who had generalized seizures on 1,000 mg PALA/m²/day and 200 mg FUra/m²/day were simultaneously documented to have central nervous system metastases. One patient treated with 1,500 mg PALA/m²/day and 250 mg FUra/m²/day had focal seizures during a period when he was uremic and had a serum creatinine of 12.2 mg/100 ml. In 2 patients in whom bizarre affects and thought disorders were observed, no underlying central nervous system lesions were found. In 1 of these patients treated with 1,000 mg PALA/m²/day and 150 mg FUra/m²/day, the abnormal behavior was resolved when chemotherapy was suspended. However, in the other who received 1,500 mg PALA/m²/day and 150 mg FUra/m²/day, no improvement occurred after therapy was stopped.

Due to disease progression, 24 patients were removed from the study, and 2 patients died from the disease during the study. Two were removed from the study after they refused further therapy. Two at this writing have stable disease and continue in the study. The 17 patients with pathologic diagnosis of melanoma were treated at adequate doses that produced mild but significant toxicity, and all had measurable disease. No patient had a complete response. One developed a partial response with greater than 50% decrease in a skin nodule and lung metastases. Another patient had a mixed response: a greater than 50% decrease in the size of skin lesions but developed liver metastases on therapy. Three patients with melanoma were considered to have stable disease for 2 and 3 months. None of these patients had had previous FUra therapy. One patient with ovarian carcinoma, who had previously received FUra, was stable for 10 months, and another with colon carcinoma was stable for 4 months.

Pharmacologic studies were performed on 9 patients. Maximum plasma FUra levels were 3.27 m*M* at a dose of 250 mg/m². Plasma FUra levels dropped below the level of assay sensitivity (5×10^{-8} *M*) within 60 minutes. In some patients, a distinct bi-exponential decline could not be

TABLE 4.—*Hematologic toxicity*

Myelosuppression indicator	Dose level, mg/m²/day		No. of therapy courses[a]
	PALA	FUra	
Platelets, <100,000 but >50,000/mm³	1,500	100	1
	1,500	250	2
	1,000	200	2
WBC, <2,000/mm³	1,000	200	2

[a] Hematologic toxicity data were available for 52 of 98 administered courses.

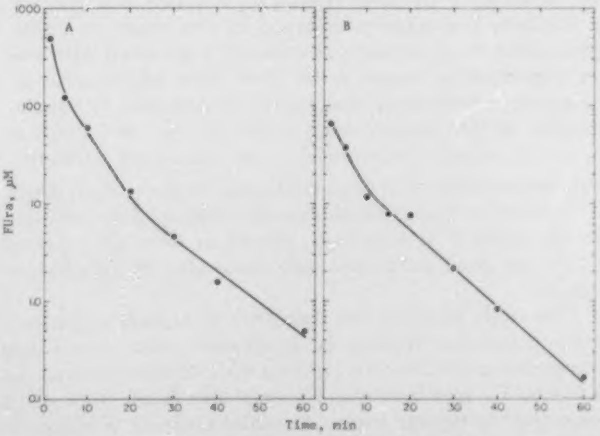

TEXT-FIGURE 1.—Plot of plasma FUra vs. time. A) Patient was treated with 250 mg FUra/m². B) Patient was treated with 200 mg FUra/m².

TABLE 5.—*FUra pharmacokinetics*

Patient	Dose level, mg/m²/day		k, min^{-1}[a]	$t_{1/2}$, min[b]	AUC, mmol·min/liter	r[c]
	PALA	FUra				
#1	1,500	100	0.0801	8.65	0.545	−0.893
#2	1,500	100	0.124	5.57	0.047	−0.999
#3	1,500	100	0.0633	10.94	0.029	−0.944
#4	1,500	200	0.0875	7.88	0.360	−0.995
#5	1,000	200	0.0668	10.38	1.800	−0.975
#6	1,000	200	0.1011	6.85	0.550	−0.994
#7	1,000	200	0.1559	4.44	0.319	−0.936
#8	1,500	250	0.138	5.02	1.86	−0.995
#9	1,500	250	0.164	4.24	1.64	−0.963

[a] Plasma FUra elimination rate constant.

[b] Plasma FUra elimination $t_{1/2}$.

[c] Correlation coefficient (r) from linear regression of 10–60 min Log FUra levels vs. time.

clearly defined because of difficulties in obtaining adequate numbers of early samples during this distribution phase (text-fig. 1). Therefore, individual FUra profiles were analyzed in terms of a pharmacokinetic, one-compartment, open model similar to that of MacMillan et al. (*13*). The dose levels, plasma FUra elimination rate constant k, plasma FUra elimination $t_{1/2}$, and the AUC are summarized in table 5. The mean $t_{1/2}$ was 7.11±0.84 minutes (SEM). The mean AUC values obtained in this analysis did not increase linearly with dose, but a rapid nonlinear increase in the mean AUC level was observed for those patients treated with 250 mg FUra/m²/day (text-fig. 2).

DISCUSSION

An initial trial of PALA given as a 15-minute daily iv infusion for 5 days and FUra on days 2, 3, 4, and 5 as a bolus injection, repeated every 3 weeks, demonstrated dose-limiting toxicity to gastrointestinal mucosa. The major toxicity of PALA as a single agent is manifested in the skin and gastrointestinal organs, whereas FUra when given by bolus injection most commonly results in myelosuppression. However, gastrointestinal and skin toxicity can occur with FUra even when given by bolus injection. Therefore, it is difficult to attribute the toxicity observed in this study to either agent alone. In 2 patients, neurotoxicity occurred that was not explained by causes other than drug administration. Inasmuch as neurologic abnormalities secondary to administration of PALA have been reported (*14*), and because FUra is known to occasionally cause neurologic problems, the neurotoxicity of the 2 patients may be due to both drugs. Conjunctivitis and photophobia after PALA administration, which occurred in 3 patients, previously were not reported (*3, 4*), but these conditions may occur after FUra administration.

This study involved the treatment of numerous patients with melanoma because other clinical trials were being conducted at the time for patients with this diagnosis at the National Cancer Institute. Patients who failed those trials were eligible for our study. A partial response was experienced by 1 of 17 patients with melanoma. However, this patient, treated with 1,500 mg PALA/m²/day and 250 mg FUra/m²/day, developed severe diarrhea with associated hypovolemia and subsequent acute tubular necrosis. Careful management reversed the renal failure and the patient recovered, but subsequent courses of treatment with PALA and FUra could not be administered to him. Our findings suggest that this particular dose schedule for PALA and FUra would result in less than a 25% response rate (P<0.05) for patients with melanoma and, therefore, would not be a useful combination for clinical therapy of melanoma.

The FUra pharmacokinetic studies on patients treated with PALA and FUra suggest two points: *a*) The plasma elimination $t_{1/2}$ of 7.11 minutes that we observed is not different from that reported by others in single-agent studies (*13*). This implies that any enhanced toxicity observed for the PALA-FUra combination was not due to a change in plasma clearance of FUra by PALA. Because PALA is excreted primarily by a renal mechanism and is not highly protein-bound and FUra is primarily metabolized, pharmacokinetic interaction between these agents in plasma would not be expected. Such a conclusion is supported by our studies. Therefore, it is more likely that any enhanced toxicity is the result of an interaction at the cellular level. *b*) A saturable mechanism in the elimination of FUra is suggested by the nonlinear relationship between the AUC and the administered FUra dose. This interpretation must be made cautiously because of the small numbers of patients treated at each dose level and the wide variation in the calculated AUC; however, this interpretation agrees with suggestions made in other reports (*15, 16*).

The dose schedule in this study was chosen to take advan-

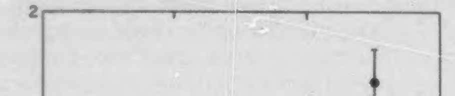

TEXT-FIGURE 2.—Plot of mean AUC vs. FUra dose level. *Error bars* represent SEM.

tage of the mechanism proposed for PALA and FUra interaction at the cellular level. We had previously noted that on the PALA schedule of a 15-minute infusion daily for 5 days, aspartate transcarbamylase levels in leukocytes were significantly depressed within 24 hours of the first dose (*17*). If similar changes occur in other tissues, pyrimidine nucleotide levels would probably decrease in parallel by 24 hours after the first dose of PALA. Addition of FUra at that time could result in metabolism of this pyrimidine analog to active metabolites at a rate greater than that normally observed. However, a therapeutic benefit of this PALA-FUra dose schedule was seen in only 1 patient with melanoma. Other investigators using other schedules have reported responses in colon carcinoma, large cell carcinoma of the lung, fibrous histiocytoma, and sarcoma (*18, 19*). Although we found very limited activity of this drug combination in patients who had received prior chemotherapy for metastatic melanoma, phase II studies with other dose schedules may be warranted on patients with other malignant diseases responsive to FUra. A schedule that involves PALA and FUra administration by continuous infusion may be more efficacious than the one used in this study. Such a schedule may allow more incorporation of FUra into RNA throughout the cell cycle. For future phase II studies, we recommend 1,000 mg PALA/m^2/day given iv over a period of 15 minutes for 5 days and 200 mg FUra/m^2/day given by bolus injection on days 2, 3, 4, and 5.

REFERENCES

(*1*) Johnson RK, Inouye T, Goldin A, Stark GR. Antitumor activity of *N*-(phosphonacetyl)-L-aspartic acid, a transition-state inhibitor of aspartate transcarbamylase. Cancer Res 1976; 36:2720–2725.

(*2*) Johnson RK, Swyryd EA, Stark GR. Effects of *N*-(phosphonacetyl)-L-aspartate on murine tumors and normal tissues in vivo and in vitro and the relationship of sensitivity to rate of proliferation and level of aspartate transcarbamylase. Cancer Res 1978; 38:371–378.

(*3*) Erlichman C, Strong JM, Wiernik PH, et al. Phase I trial of *N*-(phosphonacetyl)-L-aspartate. Cancer Res 1979; 39:3992–3995.

(*4*) Valdivieso M, Moore EC, Burgess AM, et al. Phase I clinical study of *N*-(phosphonacetyl)-L-aspartic acid (PALA). Cancer Treat Rep 1980; 64:285–292.

(*5*) Carroll DS, Gralla RJ, Kemeny NE. Phase II evaluation of *N*-(phosphonacetyl)-L-aspartic acid (PALA) in patients with advanced colorectal carcinoma. Cancer Treat Rep 1980; 64:349–351.

(*6*) Creagan ET, Ahmann DL, Ingle JN, Purvis JD III. Phase II study of *N*-(phosphonacetyl)-L-aspartate (PALA) in disseminated malignant melanoma. Proc Am Soc Clin Oncol 1980; 21:344.

(*7*) Yagoda A, Watson RC, Blumenreich R, Young CW. Phase II trials in urothelial tumors with Amsa and PALA. Proc Am Soc Clin Oncol 1980; 21:427.

(*8*) Moyer JD, Handschumacher RE. Selective inhibition of pyrimidine synthesis and depletion of nucleotide pools by *N*-(phosphonacetyl)-L-aspartate. Cancer Res 1979; 39:3089–3094.

(*9*) Cadman E, Heimer R, Davis L. Enhanced 5-fluorouracil nucleotide formation after methotrexate: Explanation for drug synergism. Science 1979; 205:1135–1137.

(*10*) Spiegelman S, Sawyer R, Nayak R, Ritzi E, Stolfi R, Martin D. Improving the antitumor activity of 5-fluorouracil by increasing its incorporation into RNA via metabolic modulation. Proc Natl Acad Sci USA 1980; 77:4966–4970.

(*11*) Johnson RK, Clement JJ, Howard WS. Treatment of murine tumors with 5-fluorouracil in combination with de novo pyrimidine inhibitors PALA or pyrazofurin. Proc Am Assoc Cancer Res 1980; 21: 292.

(*12*) Buckpitt AR, Boyd MR. A sensitive method for determination of 5-fluorouracil and 5-fluorodeoxyuridine in human plasma by high pressure liquid chromatography. Anal Biochem 1980; 106:432–437.

(*13*) MacMillan WE, Wolberg WH, Welling PG. Pharmacokinetics of fluorouracil in humans. Cancer Res 1978; 38:3479–3482.

(*14*) Gralla RJ, Kemeny N, Young CW, Sykes MP. Central nervous system toxicity of PALA (*N*-phosphonacetyl-L-aspartate). Proc Am Soc Clin Oncol 1980; 21:350.

(*15*) Collins JM, Dedrick RL, King FG, Speyer JL, Myers CE. Nonlinear pharmacokinetic models for 5-fluorouracil in man: Intravenous and intraperitoneal routes. Clin Pharmacol Ther 1980; 28:235–246.

(*16*) Speyer JL, Collins JM, Dedrick RL, et al. Phase I and pharmacological studies of intraperitoneal 5-fluorouracil. Cancer Res 1980; 40:567–572.

(*17*) Kensler TW, Erlichman C, Jayaram HN, Tyagi AK, Ardalan B, Cooney DA. Peripheral leukocytes as indicators of the enzymic effect of *N*-(phosphonacetyl)-L-aspartic acid on human L-aspartate transcarbamylase activity. Cancer Treat Rep 1980; 64:967–973.

(*18*) Bedikian AY, Valdivieso M, Stroehlein JR, Karlin DA, Bennet RW, Bodey GP. Phase I–II evaluation of PALA-5-fluorouracil combination in patients with colorectal carcinoma. Proc Am Soc Clin Oncol 1980; 21:415.

(*19*) Meshad MW, Ervin TJ, Johnson RK. A phase I trial of combined therapy with *N*-(phosphonacetyl)-L-aspartate and 5-fluorouracil. Proc Am Soc Clin Oncol 1980; 21:341.

blank page

Phytohemagglutinin or Pokeweed Mitogen Induction of In Vitro Colony Formation by T-Cells From Patients With Chronic Lymphocytic Leukemia [1,2,3]

Vito Pistoia,[4] Arcangelo Nocera,[4] Riccardo Ghio,[5] Paola Minale,[4] *and* Manlio Ferrarini[4,6]

ABSTRACT—The colony-forming capacity of peripheral blood T-cells isolated from B-cell chronic lymphocytic leukemia patients was studied and compared with that of peripheral blood T-cells isolated from 2 groups of normal controls (young and aged healthy donors). Upon stimulation with phytohemagglutinin or pokeweed mitogen, T-cells from both the patients and the controls developed into colonies but only in the presence of the appropriate conditioned media. When the responses of the 3 groups were compared, no statistically significant differences were detected. However, the number of patients who failed to respond to phytohemagglutinin was larger than that of normal controls. Studies on a selected group of patients demonstrated that such unresponsiveness was unrelated to the presence of suppressor cells or to inadequate conditions used for stimulation in culture. Rather, this unresponsiveness may be connected with an intrinsic T-cell defect present in certain B-cell chronic lymphocytic leukemia patients.—JNCI 1982, 68:233–237.

B-cell CLL is a lymphoid cancer derived from the proliferation of a single clone of B-lymphocytes arrested at early stages of maturation and incapable of differentiating further into more mature cells (*1*).

In recent years the question has been raised whether or not T-cells from B-cell CLL patients may be responsible, at least in part, for the poor B-cell maturation; this problem has been investigated in several in vitro experimental systems (*2-8*).

Colony formation in semisolid media represents a most valuable tool for the study of both the proliferative and clonogenic capacities of T-cells (*9-11*). Furthermore, this in vitro technique has been progressively modified so that it is now possible to investigate the function of T-cells independently of the influence of any other accessory cell from the same subject. The present study deals with the colony-forming capacity of T-cells from B-cell CLL patients and shows that these cells do not behave differently from those of normal subjects.

MATERIALS AND METHODS

Patients.—Twenty-one patients aged 45–79 years (mean, 65 yr old) were studied. All had diagnoses of CLL confirmed by both clinical and histologic criteria. The white blood cell count ranged from 20,000 to 400,000 cells/mm^3 with a minimum of 70% lymphocytes.

According to the Rai classification (*12*), 6 of the patients had CLL in stage 0; 4, in stage 1; 3, in stage 2; 3, in stage 3; and 5, in stage 4. Most peripheral blood cells ($\geq$80%) had monoclonal membrane immunoglobulins in 20 of 21 patients, as assessed by immunofluorescence (*13*). In the remaining patient, the B-cell nature of the malignant cells was documented by their capacity to form rosettes with mouse red blood cells (*14*) and with antibody- and complement-coated erythrocytes (*15*).

None of the patients had serum monoclonal components or a positive Coombs' test. All but 5 patients had received treatment with chlorambucil before testing. For controls 28 normal healthy volunteers were used. They were subdivided into 2 groups: Control group I consisted of 13 individuals aged 21–35 years (mean, 28 yr old), whereas control group II was comprised of 15 individuals aged 45–72 years (mean, 62 yr old).

Cell separation.—MNC were separated from heparinized peripheral blood on F–H gradients. AC were removed from normal cell suspensions by adherence to plastic flasks. T-cells were isolated from MNC by rosetting with E_N, followed by F–H density gradient centrifugation (*16*). The rosettes in the pellets were passed on F–H gradients up to five times in the case of CLL or three times in the normal controls. E_N were lysed with ammonium chloride. The proportions of E_N rosettes in the purified suspensions were 96–98% and 85–90% for the normal subjects and the CLL patients, respec-

---

ABBREVIATIONS USED: AC=adherent cell(s); BFU-E=erythroid burst-forming unit(s); CFU-C=granulocyte colony-forming unit(s); CFU-E=erythroid colony-forming unit(s); CLL=chronic lymphocytic leukemia; CM=conditioned medium (media); E_N=neuraminidase-treated sheep erythrocyte(s); F–H=Ficoll–Hypaque; GM-CSA=granulocyte–monocyte colony-stimulating activity; MNC=mononuclear cell(s); PHA=phytohemagglutinin; PWM=pokeweed mitogen; T_G=T-cells bearing receptors for the Fc portion of IgG.

---

[1] Received May 13, 1981; accepted September 10, 1981.

[2] Supported by grants from Consiglio Nazionale delle Ricerche (Progetto Finalizzato Controllo Crescita Neoplastica) and from the North Atlantic Treaty Organization.

[3] Research procedures were in accord with the ethical standards of the Committee on Human Experimentation, University of Genoa.

[4] Department of Immunology, University of Genoa, Viale Benedetto XV, 10, 16132 Genoa, Italy.

[5] Department of Internal Medicine, University of Genoa.

[6] We thank Dr. A. Marmont (Division of Hematology, Ospedale S. Martino, Genoa); Dr. P. Boccaccio, Dr. I. Pannacciulli, Dr. C. Sacchetti, Dr. E. Salvidio (Department of Internal Medicine, University of Genoa); the members of their staff for permission to study their patients; and Dr. S. Rovida (Department of Medical Statistics, University of Genoa) for help in statistical analysis.

tively. T_G were removed from unfractionated T-lymphocytes by rosetting with ox red blood cells coated with rabbit IgG anti-ox antibodies. The rosettes were separated from the nonrosetting cells on F–H density gradients (*16*).

Preparation of CM—Two different CM were used. The first one was used for the PHA-stimulated cultures, whereas the other was employed in the PWM-stimulated cultures. The reasons for the use of different CM will be apparent below and have already been discussed in part previously (*17–19*).

1) AC CM: MNC, 1×10^6, were incubated in RPMI-1640 medium supplemented wtih 10% fetal calf serum in plastic flasks at 37°C for 1 hour. Non-AC were removed and AC were washed three times and cultured in the same medium at 37°C for 48 hours. CM were dyalized against phosphate-buffered saline (4 hr) and distilled water (24 hr), filtered, and stored at −20°C (*17*).

2) PWM-stimulated MNC CM: Tonsillar MNC were cultured for 48 hours at a concentration of 7×10^6/ml in RPMI-1640 medium supplemented with 10% AB serum and PWM at a final concentration of 1:50. CM was recovered, filtered, and stored at −20°C. AC CM and MNC CM were titrated according to the ability to support colony formation by purified T-cells and used at the optimal concentration.

Cell cultures.—Isolated T-cells were plated in semisolid medium with the use of a two-layer agar system, according to a modification of the method of Sachs (*20*). In 35-mm petri dishes cells were seeded in 1 ml of 0.4% agar, RPMI-1640, and 20% heat-inactivated AB serum over a 1-ml underlayer containing 0.5% agar, RPMI-1640, 20% AB serum, 6×10^6 human red blood cells, 5×10^{-5} *M* 2-mercaptoethanol, and 0.03 ml mitogen (PHA-M or PWM). CM were usually included in the underlayers. Their concentration (determined by preliminary titration experiments) ranged from 10 to 25% of the total volume of the agar. CFU-C, BFU-E, and CFU-E assays were performed according to published methods (*21, 22*). Cultures were incubated in a fully humidified atmosphere with 5% CO_2.

Statistical analysis.—The results were statistically analyzed by Student's *t*-test on logarithmically transformed data, the chi-square test with Yates' continuity correction, Fisher's exact probability test, and the nonparametric Mann-Whitney U test.

RESULTS

PHA Induction of Colony Formation by CLL T-Cells

T-cells from peripheral blood of CLL patients and the 2 control groups were tested for colony formation with the use of PHA as a mitogen. Preliminary experiments demonstrated that normal T-cells when cultured alone formed very few or no colonies. However, their colony-forming ability was raised to the values obtained with unseparated MNC by the addition of AC CM. Consequently, all of the T-cell cultures were supplemented with AC CM. With this technique colonies appeared after 72 hours and reached their maximum number after 6–7 days. Most of the colonies grew on top of the agar, whereas only a few (≈10%) developed inside the agar.

Since control studies demonstrated a strong GM-CSA in the AC CM, one could argue that the colonies detected in the purified T-cell fractions were not of lymphoid origin and could likely represent myeloid cells. However, to develop they had an absolute requirement for the presence of PHA. This requirement is different from that observed for the colonies of other lineages that grow in the presence of the GM-CSA (or erythropoietin) only. Moreover, specific tests for CFU-E, BFU-E, and CFU-C on purified normal T-cells failed to detect any colony formation. The same tests performed on CLL patients' purified T- or B-cells gave identical results (data not shown). Finally, separation studies on normal peripheral blood cells showed that CFU-E, BFU-E, and myeloid CFU-C precursors fractionated within the non-T–non-B cells (Ghio R, Pistoia V, Nocera A, and Ferrarini M: Manuscript in preparation).

Text-figure 1 shows the responses of T-cells from patients and those from normal controls. Statistical analysis of the data with the Mann-Whitney U test did not demonstrate a significant difference in the colony-forming capacity of the 3 groups. In addition, no correlation was found between the number of colonies and the clinical stage within the patient group. T-cells from 8 of 21 patients and from only 1 of the healthy donors of control group II failed to respond. However, the frequency of nonresponder individuals in the 3 groups was not significantly different, as demonstrated by the analysis of the data by the chi-square test and Fisher's exact probability test.

The abundance of nonresponders in the CLL group

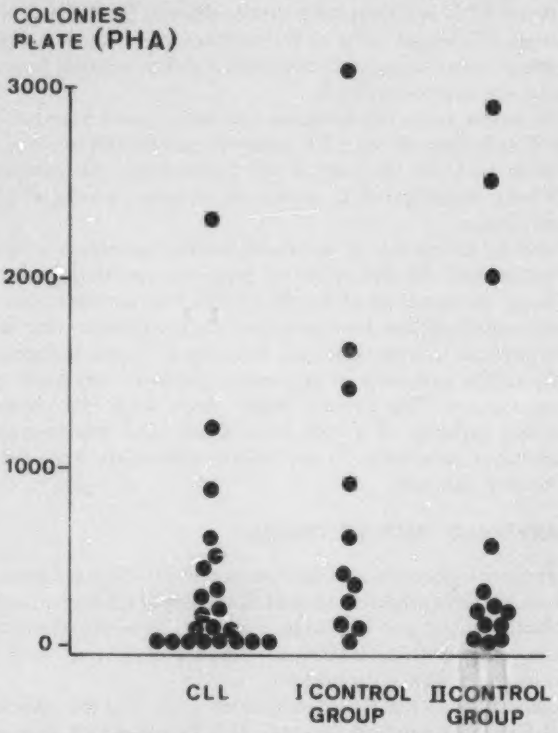

TEXT-FIGURE 1.—Colony formation by T-cells from B-cell CLL patients and control groups stimulated with PHA. Cells were plated at a concentration of 3×10^5/dish. Colonies were counted on day 6. Results are expressed as numbers of colonies/plate.

prompted further studies on the possible mechanisms of the unresponsiveness. T-cells from the 8 nonresponder patients failed to form colonies also when cultured with a wide range of mitogen concentrations or with media containing different proportions of AC CM. Furthermore, we observed no colonies even by culturing the cells for long periods (up to 12 days).

Colony formation was not detected in 3 CLL patients also when T_G, which are generally increased in CLL (*3*) and exert a suppressive effect on certain in vitro responses (*23, 24*), were removed from the T-cell suspensions. Moreover, we studied the presence or absence of suppressor cells by mixing the patients' T-cells with normal T-cells and by testing the mixture for colony formation. In three experiments with 3 different patients, the normal T-cells formed the expected number of colonies in the presence of CLL T-cells. The problem of whether or not the low proportion of the malignant B-cells contaminating the T-cells could exert a suppressive effect was also investigated. Peripheral blood cells from the patients were depleted of T-cells by rosetting with E_N, mixed with normal T-cells, and cultured.

Table 1 shows one representative experiment of three. Suppression of colony growth was not observed. Rather a threefold to fourfold enhancement of numbers of colonies was detected. This result is in agreement with that observed in different experimental systems (*25*).

Two of the nonresponder patients had CLL in stage 0; 1, in stage 1; 1, in stage 2; 1, in stage 3; 3, in stage 4; and 2, untreated. This finding seems to exclude a correlation between lack of response and clinical stage or treatment.

PWM Induction of Colony Formation by CLL T-Cells

Purified T-cells from 15 CLL patients and normal controls were cultured in agar in the presence of both PWM and MNC CM. Preliminary experiments showed that this CM was necessary for the induction of colony formation, whereas AC CM failed to support colony growth (*19*). Under these conditions PWM-stimulated T-lymphocytes formed colonies that displayed the same morphology and kinetics of appearance as those of PHA-stimulated T-lymphocytes described above. Since MNC CM contained a strong GM-CSA, the same specific tests already described for the PHA system had to be performed to rule out the possibility that the colonies detected were of myeloid origin.

The results of the experiments are reported in text-figure 2. Some nonresponders were detected in all of the groups, and no significant difference between the responses of the patients and the controls was found. Only 3 of 7 patients who responded to PWM also responded to PHA. Again, no correlation was found between the cloning efficiency of T-cells and the clinical stage of the disease in each patient.

DISCUSSION

The present study demonstrates that T-cells from CLL patients display normal colony-forming capacity in agar. These results were obtained with an experimental system in which: 1) The responsiveness of highly purified T-cells from both patients and controls could be compared under identical conditions and 2) the influence of factors other than the "intrinsic" responsiveness of T-cells could be minimized or abolished.

TABLE 1.—*Influence of CLL B-cells on normal T-lymphocyte colony formation*[a]

Cell population	No. of colonies
Normal T-cells	400
Normal T-cells+CLL B-cells (3×10^4/plate)	650
Normal T-cells+CLL B-cells (6×10^4/plate)	850
Normal T-cells+CLL B-cells (9×10^4/plate)	1,100
CLL B-cells	0

[a] T-cells from a normal donor (3×10^5/plate) were cocultured with increasing amounts of B-cells from a CLL-patient (3×10^4, 6×10^4, and 9×10^4/plate) in the presence of PHA. CLL B-cells were cultured alone as a control. Colonies were counted on day 6. Results are expressed as numbers of colonies/plate.

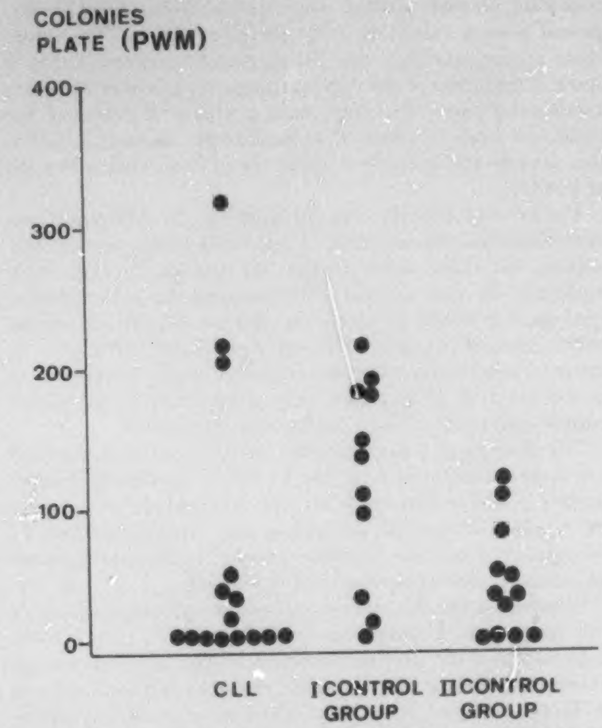

TEXT-FIGURE 2.—Colony formation by T-cells from B-cell CLL patients and control groups stimulated with PWM. Cells were plated at a concentration of 3×10^5/dish. Colonies were counted on day 6. Results are expressed as numbers of colonies/plate.

The use of purified T-cells instead of unfractionated MNC overcame the difficulties represented by the presence of many malignant cells diluting out the T-cells in the CLL cell suspensions. Furthermore, the accessory cells needed for the induction of colonies could be substituted by the appropriate CM. Control experiments excluded the possibility that the observed colonies were formed by myeloid or erythroid precursors contaminating the T-cells. T-cells were induced to form colonies by PWM only in the presence of PWM-stimulated MNC CM. This special requirement is explained by the results of recent experiments demonstrating that, in addition to monocyte-derived factors, factors released by another nonadherent non-T accessory cell are needed for PWM-induced colony formation (*19*). PWM, together with these factors, activates a cell population, which, although overlapping, is not identical with that stimulated by PHA. This observation might also account for the differences in the response to PHA and PWM in each individual.

The statistical analysis of the data did not demonstrate any difference between the responses of the patients and those of the controls. These data and the results of previous experiments with liquid culture systems (*4, 7, 26–29*) would indicate normal proliferative and clonogenic capacities of T-cells from most CLL patients. In all of these studies the responses of each patient and control were generally dispersed over a relatively wide range of values. Therefore, these techniques may not be adequate to reveal either a small diminution of the response in each patient or to detect small subgroups of unresponsive patients. Because of the relatively high number of nonresponder normal subjects, this may be particularly true for the systems that make use of PWM.

Unlike that reported by others (*30*), no difference was noted between the responses of aged and young people. The reasons for these discrepancies are not easily explained, especially in view of the differences in the experimental systems, but could be traced to the use of unfractionated MNC, instead of purified T-cells. Age-related differences in the in vitro mitogen responses, therefore, might be connected to the function of accessory cells rather than to the proliferative capacities of the lymphocytes themselves.

The finding of a high number of CLL patients who did not form colonies in response to PHA warranted further studies. These studies ruled out the involvement of suppressor T-cells (*31*) and the possibility that insufficient doses of mitogen or of medium supplements were used and suggested an intrinsic unresponsiveness of the T-cells.

Whether or not this unresponsiveness represents a distinctive feature of a subgroup of CLL patients is presently unknown and the problem is being investigated further on a larger number of CLL patients. However, intrinsic defects of T-cell functions have been detected in certain lymphoproliferative disorders with the use of various experimental systems (*2, 3, 6*). In some cases the explanation for such defects could reside in the circulating T-cells' being part of the same malignant clone as that of the B-cells (*32, 33*).

REFERENCES

(*1*) Preud'homme JL, Brouet JC, Seligmann M. Lymphocyte membrane markers in human lymphoproliferative diseases. In: Seligmann M, Preud'homme JL, Kourilsky FM, eds. Membrane receptor on lymphocytes. Amsterdam: Elsevier/North-Holland, 1975:417–429.

(*2*) Fu SM, Chiorazzi N, Kunkel HG. Differentiation capacity and other properties of the leukemic cells of chronic lymphocytic leukemia. Immunol Rev 1979; 48:23–44.

(*3*) Chiorazzi N, Fu SM, Montazeri G, Kunkel HG, Rai KR, Gee T. T cell helper defect in patients with chronic lymphocytic leukemia. J Immunol 1979; 122:1087–1090.

(*4*) Fauci AS, Pratt KR, Whalen G. Intrinsic B cell defect in the immunoglobulin deficiency of CLL. Clin Res 1977; 25 (2A):48.

(*5*) Callery RT, Strelkauskas AJ, Yanovich P, Marks S, Rosenthal D, Schlossman SF. Functional abnormalities associated with T lymphocytes from patients with CLL. Clin Immunol Immunopathol 1980; 17:451–458.

(*6*) Foa R, Catovsky D. T lymphocyte colonies in normal blood, bone marrow and lymphoproliferative disorders. Clin Exp Immunol 1979; 36:488–495.

(*7*) Wybran J, Chantler S, Fudenberg HH. Isolation of normal T cells in chronic lymphatic leukemia. Lancet 1973; 1:126–129.

(*8*) Douer D, Sachs L. Differences in the formation of normal T lymphocyte colonies by peripheral blood cells from patients with chronic lymphocytic leukemia and Hodgkin's disease. Clin Exp Immunol 1979; 38:514–522.

(*9*) Fibach E, Gerassi E, Sachs L. Induction of colony formation in vitro by human lymphocytes. Nature 1976; 259:127–129.

(*10*) Rozenszajn LA, Goldman I, Kalechman Y, et al. T-lymphocyte colony growth in vitro: Factors modulating clonal expansion. Immunol Rev 1981; 54:157–186.

(*11*) Claesson MH, Rodger MB, Johnson GR, Whittingham S, Metcalf D. Colony formation by human T lymphocytes in agar medium. Clin Exp Immunol 1977; 28:526–534.

(*12*) Rai KW, Sawitsky A, Cronkite EP, Chanana A, Levy RN, Pasternak BS. Clinical staging of chronic lymphocytic leukemia. Blood 1975; 46:219–234.

(*13*) Ferrarini M, Bargellesi A, Corte G, Viale G, Pernis B. Comparative study of membrane and intracytoplasmic Ig classes in human lymphoid cells. Ann NY Acad Sci 1975; 254:243–249.

(*14*) Gupta S, Good RA, Siegal FP. Rosette formation with mouse erythrocytes. II. A marker of human B and non-T lymphocytes. Clin Exp Immunol 1976; 25:319–327.

(*15*) Ross GD, Winchester RJ, Rabellino RM, Hoffman T. Surface markers of complement receptor lymphocytes. J Clin Invest 1978; 62:1086–1092.

(*16*) Moretta L, Ferrarini M, Cooper MD. Characterization of human T-cell subpopulations as defined by specific receptors for immunoglobulins. Contemp Top Immunobiol 1978; 8:19–53.

(*17*) Claesson MH, Whittingham S, Rodger MB, Burgess AW. Colony growth of human T lymphocytes in agar: Effect of a soluble factor from adherent cells. Eur J Immunol 1977; 7:608–612.

(*18*) Pistoia V, Ghio R, Canonica GW, Colombatti M, Moretta L. Comparison of the colony forming capacities of human T lymphocyte subpopulations. Clin Immunol Immunopathol. In press.

(*19*) Pistoia V, Nocera A, Ferrarini M, Ghio R. Cellular interactions in the colony formation by human T lymphocytes induced by pokeweed mitogen (PWM). Exp Hematol 1981; 9 (suppl 9):131.

(*20*) Sachs L. Control of cloning of normal human T lymphocytes by transferrin, albumin and different lectins. Clin Exp Immunol 1978; 33:495–498.

(*21*) Iscove NN, Seiber F, Winterhalter KH. Erythroid colony formation in cultures of mouse and human bone marrow. Analysis of the requirement for erythropoietin by gel filtration and affinity chromatography on agarose concanavalin A. J Cell Physiol 1974; 83:309–318.

(*22*) Pike BL, Robinson WA. Human bone marrow colony growth in agar gel. J Cell Physiol 1970; 76:77–84.

(*23*) Moretta L, Webb SR, Grossi CE, Lydyard PM, Cooper MD. Functional analysis of two human T cell subpopulations: Help and suppression of B cell responses by T cells bearing receptors for IgM (T_M) or IgG (T_G). J Exp Med 1977; 146:184–200.

(*24*) Canonica GW, Pistoia V, Ghio R, Mingari MC, Moretta L. Suppressor activity of T cells bearing Fc receptors for IgG on lymphoid colony formation. Scand J Immunol 1980; 12:507–511.

(*25*) Douer D, Sachs L. Production of human T cell colony inducing activity (TCI) by malignant cells from patients with lymphocytic and myeloid leukemia. J Immunol 1979; 122:2473–2477.

(*26*) Han T, Dadey B. In vitro functional studies of mononuclear cells in patients with CLL. Cancer 1979; 43:109–117.

(*27*) Fernandez LA, MacSween JM, Langley GR. T cell function in untreated B cell chronic lymphocytic leukemia. Cancer 1977; 39:1168–1174.

(*28*) Semenzato G, Pezzutto A, Agostini C, Albertin M, Gasparotto G. T lymphocyte subpopulations in chronic lymphocytic leukemia: A quantitative and functional study. Cancer. In press.

(*29*) Guglielmi P, Preud'homme JL. Stimulation of T lymphocytes by protein A from *Staphylococcus aureus* in B-derived chronic lymphocytic leukemia. Clin Exp Immunol 1980; 41:136–140.

(30) Weksler ME, Hütteroth T. Impaired lymphocyte function in aged humans. J Clin Invest 1974; 53:99–104.

(31) Faguet GB. Mechanisms of lymphocyte activation: The role of suppressor cells in the proliferative responses of chronic lymphatic leukemia lymphocytes. J Clin Invest 1979; 63:67–74.

(32) Lea T, Førre ØT, Michaelsen TE, Natvig JB. Shared idiotypes on human peripheral blood B and T lymphocytes. J Immunol 1979; 122:2413–2417.

(33) Preud'homme JL, Klein M, Labaume S, Seligmann M. Idiotype-bearing and antigen binding receptors produced by blood T lymphocytes in a case of human myeloma. Eur J Immunol 1977; 7: 840–846.

blank page

Causes of Death and Sex Differences in Survival Times of Pigs With Untreated Hereditary Lymphosarcoma (Leukemia)[1,2,3]

H. S. McTaggart,[4] **P. Imlah,**[4] *and* **K. W. Head**[4,5]

ABSTRACT—The survival times from birth of 39 entire male Large White pigs with hereditary lymphosarcoma (L/S) were significantly shorter than those of 76 affected females. The survival times of 19 male castrates were for the most part intermediate between those for entire males and females. Analysis of the cause of death revealed that pigs with L/S (L/S-P) were more likely than pigs without L/S to die from colibacillosis, but this disease showed no sex predisposition. In uncomplicated deaths from L/S, weights of splanchnic lymph nodes, spleen, and thymus were greatest in females. The cell-mediated and humoral antibody responses of L/S-P were significantly poorer against 2,4-dinitrofluorobenzene (DNFB) and sheep red blood cells, poorer against skin homografts, but better against bovine serum albumin than those of healthy littermates. Healthy females had stronger DNFB reactions than did healthy males or castrates. Castrated L/S-P responded to DNFB better than did females and significantly better than did entire males.—JNCI 1982; 68:239–246.

Hereditary L/S of pigs is an autosomal recessive condition (*1*) that manifests itself during the first few weeks or months of the animal's life by the development of solid lymphoid tumors, especially in the splanchnic lymph nodes, and is accompanied by a lymphoblastic leukemia (*2*). In no observed case of L/S have these leukemia cells shown surface markers characteristic of either T-cells or B-cells.

In terms of morbid anatomy and histopathology, affected animals constitute a homogeneous group (apart from the increasing involvement of various organs with age) distinct from the various sporadic forms of L/S. The epididymis and testes of affected males, though usually macroscopically normal, are frequently found by histologic examination to have been invaded by the tumor as early as 100 days after the animal's birth. Conversely, the ovary and uterus have never been found to be affected, even in the oldest female examined (437 days).

In the ALL of childhood, the prognosis for boys is poorer than for girls (*3*). Testicular relapse is a special hazard in boys, although its role as either a cause of poorer prognosis or as an indicator of multiple organ involvement is still debatable (*4*, *5*). Because of the testicular invasion we observed in our pigs, we instituted a retrospective study of untreated cases of L/S to ascertain whether there was any difference in survival times of males and females and what effects, if any, resulted from early castration of males.

MATERIALS AND METHODS

Pigs.—L/S cases in this survey consisted of 134 animals (76 F, 39 M, 19 C) from 74 litters sired by 12 boars and out of 36 sows in the herd of Large White pigs described by Head et al. (*2*). All pigs were bred, reared, and kept under the same "minimal disease" conditions, though accidental breakdowns occasionally occurred. There was no intentional segregation of the sexes.

Of these animals, 100 (53 F, 28 M, and all 19 C) were allowed to live out their lives without antineoplastic treatment and either died of natural causes or were killed for humane reasons in the terminal stage of disease. The remaining 34 pigs were randomly selected for antineoplastic treatment or were killed to provide experimental material. At the commencement of such treatment or on being killed, they were classified as "withdrawn" in accordance with the requirements of the log rank test (*see* below). As each animal was withdrawn, the number of animals at risk in the overall survival analysis (text-fig. 1) was reduced by one, but the removal was not counted as an event within the meaning of the test. The cause of death of the withdrawn animals was classified as "miscellaneous." Confirmation of L/S in all the animals was made by necropsy and subsequent histopathology.

In earlier years, castration was performed routinely on males before 3 weeks of age, i.e. at an earlier age than that of any pig in which hereditary L/S has ever been detected. Castration had no demonstrable effect on the death rate. Males were left entire only if a working boar would be needed in about 12 months, in which case no male of the selected litter was castrated. In later years all males were left entire.

Survival curves based on age at death were constructed

ABBREVIATIONS USED: ALL=acute lymphoblastic leukemia; BSA=bovine serum albumin; C=castrated male(s); df=degrees of freedom; DNFB=2,4-dinitrofluorobenzene; F=female(s); LH=luteinizing hormone; L/S=lymphosarcoma; L/S-P=pig(s) with L/S; non-L/S-P=pig(s) without L/S; M=entire male(s); PBS=phosphate-buffered saline; PCV=postcapillary venule; PIA=porcine intestinal adenomatosis; SRBC=sheep red blood cells.

---

[1] Received March 3, 1980; revised May 14, 1981; accepted July 22, 1981.

[2] Supported by grants from the Agricultural Research Council and the Cancer Research Campaign of Great Britain.

[3] Animals were maintained under the guidelines of the Home Office of Great Britain.

[4] Royal (Dick) School of Veterinary Studies, University of Edinburgh, Edinburgh, Scotland.

[5] We are indebted to Dr. R. J. Prescott, Medical Computing and Statistics Unit, University of Edinburgh, for statistical advice and to Dr. G. H. K. Lawson, Department of Veterinary Pathology, University of Edinburgh, for bacteriologic examinations.

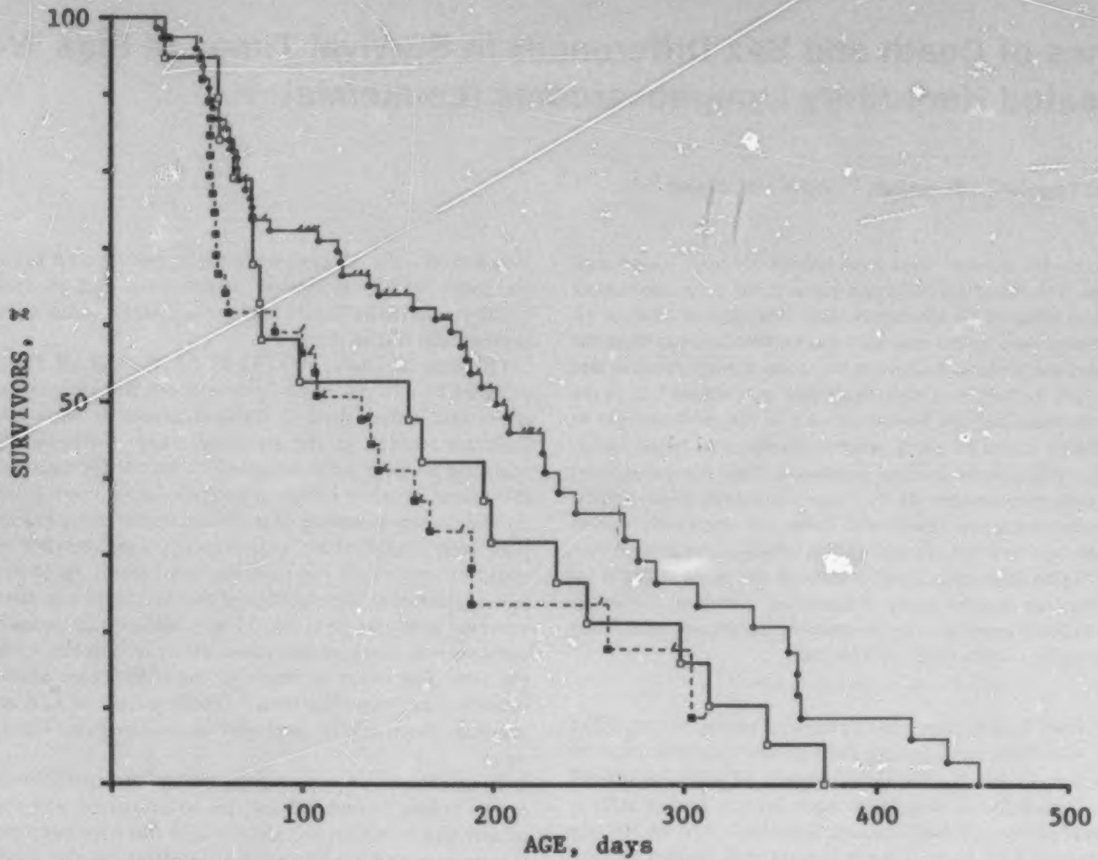

TEXT-FIGURE 1.—Survival curves based on age at death of pigs with untreated L/S. Females, ●—●; entire males, ■- - -■; castrated males, □—□; animals withdrawn from survival analysis (antineoplastic treatment had commenced or they were slaughtered for experimental reasons), /.

for the three sex categories and analyzed by the log rank (Mantel-Haenzel) test (*6*). All pigs that died in the piggery were examined by appropriate methods to establish the cause of death.

Diagnosis of death from colibacillosis was based on the postmortem condition of the gastrointestinal tract and confirmed if heavy growths of hemolytic *Escherichia coli* of known pathogenic serotypes could be cultured from the intestinal contents. Some cases of suspected colibacillosis were not serotyped because the pig had been dead too long before necropsy, it had been treated chemotherapeutically, or littermates dying from the same outbreak of the disease already had been serotyped. A litter was regarded as being at risk of death from colibacillosis if the death of any pig in that litter was attributable to a pathogenic strain.

The cell-mediated and humoral antibody responses of L/S-P were compared with those of their healthy littermates. All tests were performed in pigs at 3–4 months of age.

Immune response tests.—Cell-mediated response: *a*) Skin sensitivity reaction to DNFB. Skin sensitivity reaction to 10% DNFB was tested and scored as described in (*7*). The responses in 18 L/S-P (10 F, 5 M, 3 C) were compared with those in 38 healthy pigs (18 F, 14 M, 6 C). Up to 4 L/S-P came from each of 9 litters of L/S carrier × L/S carrier parentage. Of the healthy pigs, 8 were from 2 of those litters. The remaining 30 healthy pigs were from 4 litters of noncarrier × noncarrier parentage. *b*) Skin graft rejection. An exchange of full-thickness skin grafts of 6.26-cm^2 area was made between 6 L/S-P (2 F, 4 C) and 6 healthy littermates (2 F, 1 M, 3 C). Grafts were exchanged at a site approximately 5 cm below the dorsum behind the shoulder blade. Rejection time was assessed on total separation of the graft.

Humoral antibody response: *a*) Primary and secondary antibody response to SRBC. Two complete litters, one containing 2 L/S-P and 5 healthy pigs and the other containing 4 L/S-P and 4 healthy pigs, were given two 10-ml sc injections, 4 weeks apart, of a 30% suspension of washed SRBC in PBS, (pH 7.2) from a type O sheep. Serum samples were taken before immunization and on the 10th day after each injection. Type O SRBC were used as the source of antigen and as the test cell to avoid the possibility of reaction with the natural blood group antiserum anti-A, in the serum of blood group O, and "−" (i.e., A − ve, O − ve) pigs. All sera were subjected to a hemolytic test after heat inactivation at 56°C for 0.5 hour, with neat rabbit sera absorbed with type R SRBC as the source of complement. The test was set up in 7-mm disposable tubes with sera titered in doubling dilutions. Test serum (5 μl) was mixed with 5 μl of a 1.5% suspension of washed (four times) SRBC in PBS. After 10 minutes, 5 μl of absorbed neat rabbit complement was added to each tube. The tubes were incubated at 20°C and shaken for 1 minute at the end of each hour, for a total period of 6 hours. At the end of that time, a hemolytic reaction score ranging from 0 to 5 was made at each dilution. Due to antispecies reaction, an additive score was calculated for the preimmune sera, and this score was deducted from the additive score calculated for the primary and secondary test sera reactions. The remaining score was taken as the measure of the humoral antibody response.

b) Primary and secondary antibody response to BSA: Two complete litters, one containing 1 L/S-P and 11 healthy pigs and the other containing 1 L/S-P and 6 healthy pigs, were given two 5-ml sc injections, 4 weeks apart, of a 5% mixture of BSA in PBS (pH 7.2). Preimmune, primary, and secondary response serum samples were taken 10 days after each injection. The tanned red cell (*8*) was used as a test system. Type O SRBC were formalized by the suspension of 25 ml of packed, washed (five times) cells in 200 ml of PBS, to which 50 ml of 40% Formalin in a dialysis tube was added. The tube was agitated for 3 hours and then punctured and removed. The mixture was left overnight at room temperature. Cells were then filtered through muslin, washed five times in PBS, and kept at 4°C in 100 ml PBS. For tanning, 10 ml of formalized cells (≈25% concentration) was suspended in 90 ml of 0.01% tannic acid and incubated for 15 minutes at 37°C in a water bath. Cells were then washed three times with PBS and made into a final 1% suspension with PBS. The cells were coated with BSA. (An equal volume of 1% tanned cells was mixed with an equal volume of 1% BSA in PBS and incubated for 1 hour at 37°C.) The cells were then washed five times in PBS and made into a 1.5% suspension in PBS containing 1% normal rabbit serum that had previously been heat inactivated at 56°C for 0.5 hour and absorbed with uncoated tanned SRBC to remove nonspecific agglutinins before being tested against coated cells. Tests were set up in microtiter plates with V-shaped wells. In each well, 5 µl of doubling dilutions of test sera was mixed with 5 µl of a 1.5% suspension of coated cells. Agglutination was read after the mixture had remained overnight at room temperature. An agglutination reaction ranging from 0 to 5 was scored for each well for preimmune, primary, and secondary test sera. No preimmunization reaction was observed.

RESULTS

Survival Curves

Text-figure 1 presents the overall survival curves, based on age at death, for three sex categories. The relative death rate (the ratio of observed to expected deaths) for females was 0.82; for entire males, 1.43; and for castrates, 1.20. The median survival time was 201 days for females and 131 days for entire males. The median survival time of castrates again was intermediate at 156 days. Although the log rank test indicates that the overall differences among the three survival curves were significant (X^2, 6.4; df, 2; $P<0.05$), the difference between entire males and castrates was not (X^2, 0.4; df, 1; $P>0.5$). When the data for males were combined, the difference in survival times of females and males (including C) was significant (X^2, 5.9; df, 1; $P<0.02$).

Sex Distribution of L/S Cases

In earlier publications (*1, 2*) we stated that we had observed no significant sex bias in the distribution of L/S cases. In the present survey, the observed number of females with L/S was only one less than the expected 25% for those of L/S carrier × L/S carrier parentage and old enough to be diagnosed (table 1). However, males (including C) were underrepresented, though the shortfall from expectation was not statistically significant (χ^2, 1.5; df, 1; $P>0.2$).

Usually, the number of male pigs born exceeds that of females by a few units of percentage, and the mortality of males is higher than that of females (*9–11*). These male-to-female ratios were reflected in the 75 litters of non-L/S carrier × non-L/S carrier parentage (non-L/S litters) in our piggery that were contemporaneous with the 74 litters of L/S carrier × L/S carrier parentage (L/S litters) from which the L/S cases were derived (table 1). Males accounted for 52.30% of the total number of pigs born in non-L/S litters but for only 50.37% in L/S litters. During the first 3 weeks of life, the death rate in non-L/S litters was 11.9% for females and 25.2% for males. In L/S litters the death rate was much higher for both sexes (F, 22.75%, M, 34.5%). At 3 weeks of age, males were fewer than females: 48.2% in non-L/S litters, 46.3% in L/S litters.

Causes of Death

All 134 pigs in this survey (table 2) showed L/S lesions at necropsy, which were confirmed by histopathology. The postmortem data for the 100 untreated pigs were similar to those recorded in more detail for the series of 53 in our previous paper (*2*). As noted in that paper, some pigs also exhibited lesions of intercurrent disease. Where the lesions were similar to those found in non-L/S-P that had died, we assumed that the L/S-P had died or were dying from intercurrent disease. When no lesions of lethal intercurrent disease were present, we classified the cause of death as L/S.

Colibacillosis.—L/S-P that died from colibacillosis were between 25 and 108 days old. By that time non-L/S littermates also had died from similar symptoms and had the current pathogenic *E. coli* serotype. The colonization and adhesion of enterotoxigenic *E. coli* in the intestine, and the animal's subsequent development of disease with eventual death or recovery, have a complex etiology (*12, 13*). Because of the complicated interaction of managemental factors, microbiologic considerations, and the inherent reactivity of the host pig, we could not be certain, even in a single litter, that all pigs were equally at risk. Nevertheless, we considered the possibility that L/S pigs were more susceptible to coli-

TABLE 1.—*Sex distribution in litters of L/S-P and non-L/S-P*

Parentage	No. of litters	Sex	Total born	Stillborn or dead at 3 wk	Alive at 3 wk	L/S diagnosis
L/S carrier × L/S carrier	74	♀	400	91	309	76
		♂	406	140	266	58
Non-L/S carrier × non-L/S carrier	75	♀	394	47	347	0
		♂	432	109	323	0

TABLE 2.—*Causes of death of L/S-P*

Age, days	Intercurrent disease																												
	Colibacillosis			PIA			Perforated ulcer[a]			*Haemophilus* or *Salmonella* infection			β-HS[b]			Pneumonia			Trauma			Tumor			Miscellaneous[c]			Total		
	F	C	M	F	C	M	F	C	M	F	C	M	F	C	M	F	C	M	F	C	M	F	C	M	F	C	M	F	C	M
25–74	17	6	13	1	0	1	1	0	1										1	0	0				1	0	0	21	6	15
75–124	0	1	2	2	0	0				0[d]	2[d]	0				1	0	1				2	0	1	3	0	3	8	3	7
125–174				0	0	1																4	2	4	8	0	4	12	2	9
175–224							1	0	0													7	2	2	8	0	1	16	2	3
225–274										1[e]	1[e]	0	1	0	0							3	1	1	3	0	1	8	2	2
275–324										0	0	1[d]										3	2	0	0	0	2	3	2	3
325–374													1	0	0				1	0	0	3	2	0				5	2	0
375–424																						1	0	0				1	0	0
425–474							1	0	0													1	0	0				2	0	0
Total	17	7	15	3	0	2	3	0	1	1	3	1	2	0	0	1	0	1	2	0	0	24	9	8	23	0	11	76	19	39

[a] Peritonitis due to perforation of an ulcer of the gastrointestinal tract.

[b] β-Hemolytic group L streptococcal infection.

[c] L/S-P that died after antineoplastic treatment or were killed to provide experimental material. Data for these animals were removed from survival analyses, and the animals were classified as "withdrawn." The ages indicated are ages at withdrawal and not at death.

[d] *H. parainfluenzae suis* infection.

[e] *S. dublin* infection.

bacillosis than non-L/S pigs worthy of examination (*see* later).

PIA.—The outbreak of a hemorrhagic bowel syndrome associated with intestinal adenomatosis, described by Rowland and Rowntree (*14*), occurred in the same minimal-disease, hysterectomy-derived herd in which the L/S cases occurred. In the period covered in this paper, only a few deaths occurred in L/S-P and non-L/S-P in which PIA lesions were found and the presence of *Campylobacter sputorum mucosalis* was demonstrated by the method of Lawson and Rowland (*15*). The etiology of PIA seems to be even more complex than that of colibacillosis, and any relationship to coexisting L/S is even more debatable.

Perforated ulcer.—A perforating ulcer of the gastrointestinal tract, with subsequent peritonitis and death, was found in the colon of a 60-day-old male, the duodenum of a 67-day-old female, the jejunum of a 205-day-old female, and the fundus of the stomach of a 437-day-old female. Similar deaths were recorded in non-L/S-P but with much less frequency. Although the gut might be diffusely involved with the tumor, ulceration was not in an area of gut particularly severely affected; i.e., ulceration did not occur in a localized L/S. Many factors may interact to devitalize the gut and allow ulceration to occur. Among these are the diffuse involvement of the lymphoid tissue of the gastrointestinal tract, which displaces normal tissues; the possible interference with immune defense; the weight of the gastric-mesenteric lymph node mass hanging on the mesentery; and the erratic feeding associated with the animal's depression in the late anemic and emaciation stages of the disease.

Haemophilus *serositis.*—New pathogens introduced into a minimal disease herd tend to cause an explosive disease outbreak, as happened with *Haemophilus*. In 1 month before the outbreak was controlled by therapy and management, of 12 sows and gilts, 3 non-L/S-P (455, 897, and 1,152 days old) and 1 L/S-P (304 days old) died of pneumonia, pleurisy, and pericarditis. *H. parainfluenza suis* was recovered in all cases. Of the other sows, 4 became ill but recovered. The disease affected the whole piggery and despite treatment, 2 piglets (13 days old), a male and a castrated non-L/S-P (120 and 102 days old), and 2 castrated L/S-P pigs (79 and 99 days old) died. That a pig had L/S did not apparently influence the morbidity or mortality.

Salmonellosis.—A similar accidental break in the minimal disease status of the piggery was caused by a *Salmonella* infection. At the time of the occurrence the cattle in a nearby barn were affected with salmonellosis (*16*). The drainage from a part of the piggery is to a common drain with that of the cow barn. This drain became blocked, the piggery was flooded and 2 L/S-P died of salmonellosis during the resultant outbreak. One was a 243-day-old female that had an extensive necrotizing bronchopneumonia from which *S. dublin* and *Corynebacterium pyogenes* were recovered. The other, a 249-day-old castrate, died as a result of a fibrino-necrotic enteritis from which *S. dublin* was recovered. A 2-cm spherical nodule present at the castration site on one side proved to be a remnant of epididymis infiltrated by L/S tissue.

Streptococcal infections.—Within 6 days, 2 gilts with L/S died, and β-hemolytic group L streptococci were recovered. In a 227-day-old animal, the recovery was made from aortic valve endocarditis lesions, kidney abscesses, and polyarthritis of all major limb joints. Identification of infection also was made from the culture of joint tissue from a 359-day-old sow that exhibited such severe polyarthritis that she was destroyed for humane reasons. Much of the last week of her life was spent lying on her left side, and at necropsy the left cardiac lobe of the lung showed a purulent pneumonia from which *C. pyogenes* was recovered.

Pneumonia.—Despite the occasional accidental breakdown of minimal disease conditions in the piggery, enzootic pneumonia never was present. A very small, ill-thriven male L/

S-P (86 days old) died after being moribund for several days, and at necropsy he showed an extensive necrotizing pneumonia from which *C. pyogenes* was recovered. Another very small, ill-thriven female L/S-P (83 days old) died, despite antibiotic therapy, after 3 days of dyspnea. Necropsy revealed marked pleural effusion and an interstitial pneumonia, but only *E. coli* could be recovered on examination of the cultured tissues.

Trauma.—A 70-day-old female L/S-P was savaged by her littermates and died as a result of a fractured rib that lacerated the lung and caused hemothorax. This type of lesion had not been seen in non-L/S-P of that age, though fighting in the piggery sometimes breaks out. The lesion may have occurred because the L/S-P was so much smaller than her penmates. A 361-day-old female L/S-P was destroyed because she could not rise after she slipped and fell. Necropsy revealed severe tearing of the muscles of the hindlimb. Heavy sows that did not have L/S have damaged themselves in falls, but this gilt with L/S, though not emaciated, could not be classed as overweight. The fall may have occurred because of the weakness sometimes observed in advanced cases of L/S.

Tumor.—In addition to involvement of the lymphoid tissues of lymph nodes and spleen, we found tumor replacement of bone marrow with resultant anemia and thrombocytopenia. The lymphoid tissue of the gastrointestinal tract was always involved in a diffuse manner, and the liver became progressively infiltrated; interference with digestion, absorption, and metabolism could therefore be expected. In a disease in which so many organ systems are involved, difficulty is often encountered in deciding which site of maximum dysfunction is responsible for the death of the pig.

Effect of Sex on Risk of Death from Various Causes in L/S-P

When the data for all 134 pigs were examined together, the survival time of males was significantly shorter than that of the females. Table 2 shows that the two untreated categories with the largest number of deaths were colibacillosis and tumor. We decided to analyze these groups to determine whether sex differences in survival were associated with a particular category.

Death from colibacillosis.—As seen in table 2, all of the animals with colibacillosis had died by age 124 days. In the present survey, 65 L/S pigs were at risk of death from colibacillosis. Table 3 indicates no significant difference among the three sex categories (χ^2, 2.7; df, 2; $P>0.2$) in the number of deaths from the disease. Thus, although text-figure 1 shows a more precipitous fall in male and castrate than in female survival curves before 100 days, the fall was not due to increased susceptibility to colibacillosis, which is the most common cause of death in this age group (*see* table 2). The difference in survival curves is due to the fact that male deaths from colibacillosis were spread over a narrower age range (30–61 days) than that of castrates (28–78 days) or that of females (25–74 days). Moreover, no obvious differences were present in the histopathologic findings for the sexes in this group of L/S-P—only minor differences in organ weights.

TABLE 3.—*Causes of death of L/S-P in litters at risk of colibacillosis: Present survey*

Cause of death	F	C	M	Total no.
Colibacillosis	17	7	15	39
Other causes	15	6	5	26
Total No. at risk	32	13	20	65

Before the present survey was undertaken, an earlier study (McTaggart HS, Imlah P, Head KW: Unpublished data) had been made of the effects of colibacillosis. It involved 207 pigs in 27 litters of L/S carrier × L/S carrier parentage, in which L/S occurred or was expected and in which L/S-P were also at risk of death from colibacillosis. Table 4 shows that of these pigs, 61.5% (but only 16.7% of non-L/S-P) died of colibacillosis. The difference is very highly significant (χ^2, 33.9; df, 1; $P\ll0.001$). Use of the chi-square test was not fully justified because there could conceivably be a litter effect on mortality from colibacillosis (although such an effect was not obvious from the data), and the independence assumption of the test would not be satisfied. Nevertheless, the magnitude of such an effect could not be large enough to affect the conclusion of an association between L/S and death from colibacillosis. However, no significant difference in susceptibility to death from colibacillosis was apparent among the three sex categories in either L/S-P (χ^2, 2.0; df, 2; $P>0.1$) or non-L/S-P (χ^2, 1.7; df, 2; $P>0.1$).

Death from tumors.—As seen in table 2, only 3 (2 F, 1 M) of the 41 animals in this category died before they were 125 days old. Although the figures suggest that females survive longer than castrates and that both survive longer than entire males, when the data were subdivided into sex and age subsets the numbers were too small in some groups for meaningful statistical analysis.

We concluded that although there is a significant difference between the overall survival of males and females, our data do not warrant our attributing the difference to any particular cause or causes of death.

Lymph Node and Organ Weights of L/S-P That Died from Colibacillosis

Because L/S cases progress clinically at different speeds, we decided to test the hypothesis that there might be a critical lymph node weight at which pigs die and that males reach this weight before females. Analyses were made of absolute weights and relative weights (g/kg body wt). Inasmuch as the conclusions from both sets of data were the same, only absolute weights were considered.

TABLE 4.—*Causes of death in L/S carrier × L/S carrier litters at risk of colibacillosis: Study prior to present survey*

Group	Cause of death	F	C	M	Total
L/S-P	Colibacillosis	11	4	9	24
	Other causes	7	5	3	15
Non-L/S-P	Colibacillosis	10	13	5	28
	Other causes[a]	65	47	28	140
Total No. at risk		93	69	45	207

[a] Including pigs commercially slaughtered.

Increases in L/S lymph node weights occur with age (row 1, tables 5, 6). Thus in comparisons of lymph node weights of pigs of similar ages that died from similar causes, the variable was their sex. When the data for the three sex categories were compared, Duncan's new multiple-range test was used to determine significant differences. When the data for males and castrates were combined because of small numbers, Student's *t*-test was used.

Rows 1–3, table 5, present the data for 30 L/S-P, of a narrow age range, that died from colibacillosis. Data for lymph nodes are given in order of decreasing weight, and the order is the same for each sex. The mesenteric lymph node, gastric lymph node, spleen, and thymus weights of females were greater than those of males and castrates, but none of the differences among the groups were significant.

In rows 4–9, table 5, the data were separated into three categories according to body weight. Because the lymph node and organ weights for males and castrates were similar in rows 1 and 2, the data were grouped together. The order of lymph node weights remained the same as in rows 1–3, but as the body weight increased so did the lymph node and organ weights. The greater thymus and spleen weights in row 3 mainly reflect the weights in the heaviest female category (row 9). The mesenteric and gastric lymph node weights were greater for females than for males (including C) in each body weight category, but the differences among the sex groups were not significant. In the heaviest body weight category, the female thymus was significantly heavier than that of the males plus castrates (*t*-test, 4.2; df, 4; $P<0.02$).

Because healthy pigs were not killed at age 44–79 days, data for non-L/S-P that died of colibacillosis (rows 10–15, table 5) were used for comparison with data for the L/S-P. Weight categories were the same as for the L/S-P. Comparison of the data in row 10 with those in row 11, 12 with 13, and 14 with 15, shows no obvious sex differences in non-L/S-P. In non-L/S-P, the smaller the body weight the smaller the thymus was, indicating that thymus involution is greatest in poorly nourished pigs even when no L/S was present. All lymph nodes were enlarged in the L/S pigs, as compared

TABLE 5.—*Body weights, ages, and organ weights of L/S-P and non-L/S-P that died from colibacillosis at ages 44–74 days*[a]

Row No.	Sex	No. of pigs	Body wt, (kg)	Age, days	Lymph node wt, g[b]									Organ wt, g		
					Mesenteric-colonic	Gastric-splenic	Head group	Bronchial	Inguinal	Iliac group	Precrural[c]	Prescapular	Popliteal	Liver	Spleen	Thymus
					L/S-P: body wt, 4–21.9 kg[d]											
1	C	5	11.7	64.8	247	41	34	20	9	5	5	3	1	508	49	6
2	M	11	9.6	52.5	239	47	26	8	7	5	3	2	1	387	44	12
3	F	14	10.2	56.9	312	75	31	13	7	6	3	3	1	394	61	24
					L/S-P: body wt, 4–7.9 kg											
4	C M	1 4	5.8	54	94	19	15	4	4	3	1.5	1	0.3	235	30	3
5	F	4	5.8	56	136	27	20	3.5	3	3	1.5	2	0.6	219	30	5
					L/S-P: body wt, 8–14.9 kg											
6	C M	2 6	11.0	54	247	49	30	8	8	5	3	2	1.6	449	48	13
7	F	7	10.5	55	264	65	29	12	6	4	3	2	0.8	366	59	14
					L/S-P: body wt, 15–21.9 kg											
8	C M	2 1	15.6	67	471	80	52	36	14	8	4	3	1.2	697	61	13±12
9	F	3	15.3	64	660	163	50	29	18	14	4	6	1.4	693	128	71±21
					Non-L/S-P: body wt, 4–7.9 kg											
10	C M	0 4	5.3	49	22	2	4	1	2	2	1	1	0.6	178	11	6
11	F	3	4.5	51	20	2.5	5	1	2	2	0.6	1	0.2	168	9	3.5
					Non-L/S-P: body wt, 8–14.9 kg											
12	C M	1 6	10.4	52	37	3	7	1.5	2	1.5	1	1.5	0.5	354	18	18
13	F	14	10.8	58	43	4	7	2	2.5	2	1	1	0.2	354	25	18
					Non-L/S-P: body wt, 15–21.9 kg											
14	C M	4 2	18.6	62	80	9	12	6	4	3	2	2	0.4	549	35	44
15	F	2	16.9	62	63	6	12	3	3	2.5	1	3	0.2	578	34	36

[a] Values are means. SD are included only where significant differences among the sex categories were detected (last column).

[b] Weights of bilateral nodes are totals of both sides.

[c] Prefemoral.

[d] Data for these L/S-P are subdivided under the next three weight categories.

TABLE 6.—*Body weights, ages, and organ weights of older pigs that died or were killed*[a]

<table>
<tr><th rowspan="2">Row No.</th><th rowspan="2">Sex</th><th rowspan="2">No. of pigs</th><th rowspan="2">Body wt, kg</th><th rowspan="2">Age, days</th><th colspan="9">Lymph nodes wt, g[b]</th><th colspan="3">Organ wt, g</th></tr>
<tr><th>Mesenteric-colonic</th><th>Gastric-splenic</th><th>Head group</th><th>Bronchial</th><th>Inguinal</th><th>Iliac group</th><th>Precrural[c]</th><th>Prescapular</th><th>Popliteal</th><th>Liver</th><th>Spleen</th><th>Thymus</th></tr>
<tr><td colspan="17">L/S-P: body wt, 110–209 kg</td></tr>
<tr><td>1</td><td>C</td><td>4</td><td>28</td><td>178</td><td>1,359</td><td>432</td><td>106</td><td>26</td><td>27</td><td>17</td><td>14</td><td>3.5</td><td>5</td><td>1,471</td><td>557</td><td>1.5</td></tr>
<tr><td>2</td><td>M</td><td>6</td><td>31</td><td>159</td><td>943</td><td>367</td><td>87</td><td>29</td><td>30</td><td>23</td><td>7</td><td>8</td><td>6</td><td>2,104</td><td>560</td><td>5.1</td></tr>
<tr><td>3</td><td>F</td><td>13</td><td>25</td><td>168</td><td>1,096</td><td>346</td><td>82</td><td>26</td><td>19</td><td>15</td><td>5</td><td>5</td><td>4</td><td>1,676</td><td>331</td><td>3.4</td></tr>
<tr><td colspan="17">Healthy pigs (abattoir or experimental controls): body wt, 110–209 kg</td></tr>
<tr><td>4</td><td>C
M
M-CR[d]</td><td>16
1
2</td><td>58</td><td>170</td><td>136</td><td>17</td><td>26</td><td>6</td><td>9</td><td>6.5</td><td>4</td><td>3.5</td><td>1.5</td><td>1,404</td><td>139</td><td>81.5</td></tr>
<tr><td>5</td><td>F</td><td>8</td><td>57</td><td>169</td><td>135</td><td>17</td><td>31</td><td>4</td><td>11</td><td>8</td><td>4</td><td>6</td><td>1.5</td><td>1,346</td><td>117</td><td>64.5</td></tr>
<tr><td colspan="17">L/S-P: body wt, 290–360 kg</td></tr>
<tr><td>6</td><td>C</td><td>2</td><td>74.5</td><td>305.5</td><td>795</td><td>1,338</td><td>256</td><td>127</td><td>100</td><td>42</td><td>45</td><td>12</td><td>19</td><td>3,008</td><td>2,338</td><td>10</td></tr>
<tr><td>7</td><td>F</td><td>5</td><td>60</td><td>332</td><td>2,282</td><td>1,558</td><td>153</td><td>57</td><td>57</td><td>27</td><td>21.5</td><td>10.5</td><td>8.5</td><td>3,593</td><td>2,397</td><td>18.5</td></tr>
</table>

[a] Values are means. SD were excluded because no significant differences among the sex categories were detected.

[b] Weights of bilateral nodes are totals of both sides.

[c] Prefemoral.

[d] Males with unilateral cryptorchidism.

to those in non-L/S-P, with enlargement greatest for the gastric nodes, then the mesenteric nodes, and least for the prescapular nodes.

Lymph Node and Organ Weights of Older Pigs

Rows 1–3 (table 6) present data by sex on causes of death in L/S-P at ages 110–209 days. The order of the lymph node weights remained essentially the same as those for the younger L/S-P (table 5), but no significant sex differences in lymph node or organ weights were apparent. Rows 4 and 5 show weights for healthy pigs slaughtered at the abattoir for meat or killed to supply experimental material. In a comparison of rows 4 and 5 with rows 1–3, the most noticeable feature was the marked involution of the thymus in the L/S-P and the marked increase in their spleen weights. The order of lymph node enlargement in L/S-P was similar to that seen in the younger pigs (table 5).

Rows 6 and 7 (table 6) give the data for L/S-P that were more than 290 days old, at which time the entire males had died. (There was no control group for this weight category.) Three interesting developments were noted: The older L/S-P had more thymus than did the younger L/S-P (rows 1–3); the spleen enlargement was massive due to a mixture of tumor and extramedullary hemopoiesis; and although the lymph node weights had become massive, the order of lymph node enlargement was maintained.

We concluded that no simple difference in lymph node involvement from L/S accounted for the difference in survival between the sexes.

Immunologic Responsiveness

The cell-mediated responses of L/S-P and healthy pigs, as measured by skin reaction to 10% DNFB and skin graft rejection time, are shown in table 7. The mean DNFB skin reaction score for healthy pigs was very significantly greater than that for L/S-P (*t*-test, 6.6; df, 54; $P<0.001$). For healthy females the mean reaction to DNFB was significantly greater than that for males (*t*-test, 2.6; df, 30; $P<0.02$). The mean reaction scores for castrates were intermediate and were not significantly different from those for females or those for males ($P>0.3$ in both cases).

The mean response for healthy pigs of L/S carrier × L/S carrier parentage was almost identical to the response for pigs of non-L/S carrier × non-L/S carrier parentage. We cannot conceive that the difference between L/S-P and healthy pigs could be due to litter effects, and we have been unable to demonstrate any strong litter effects in the sex differences.

In L/S-P the mean DNFB reactions for females and males were not significantly different (*t*-test, 1.3; df, 13; $P>0.2$). The mean reaction for castrates was greater than that of either but was significantly different only from the mean reaction for males (*t*-test, 4.9; df, 6; $P<0.01$). The mean skin graft rejection time for L/S-P was 4 days longer than that for healthy littermates; the difference was very highly significant (*t*-test, 6.9; df, 5; $P<0.001$). Insufficiency of numbers of animals prevented any comparison by sex.

The humoral antibody response scores for reaction to SRBC and BSA are shown in table 8. For healthy pigs the mean accumulated scores for reaction to SRBC were the same for the primary and secondary responses. For L/S-P the mean primary and secondary responses to SRBC were not significantly different. The mean primary response for L/S-P was significantly weaker than that for healthy pigs (*t*-test, 3.7; df, 13; $P<0.01$). The mean secondary response was very significantly weaker for L/S-P than for healthy pigs (*t*-test, 6.5; df, 13; $P<0.001$).

The mean primary and secondary responses to BSA for healthy pigs were not significantly different (*t*-test, 0.9; df, 16; $P>0.3$). In L/S-P the mean secondary response was significantly stronger than the mean primary response (*t*-test, 14.0; df, 1; $P<0.05$), and both responses were very significantly greater than the corresponding responses for

TABLE 7.—*Cell-mediated reactions of L/S-P and healthy littermates as measured by DNFB skin sensitivity reaction scores[a] and skin graft rejection times*

Sex	10% DNFB reaction score, mean ± SD				Skin graft rejection time, mean ± SD[b]			
	Healthy pigs		L/S-P		Healthy pigs		L/S-P	
	No. tested	Score	No. tested	Score	No. tested	Days	No. tested	Days
M, C, F	38	3.4±1.08	18	1.2±1.35	6	8.67±2.07	6	12.67±2.58
M	14	2.9±1.07	5	0.4±0.55	—		—	
C	6	3.3±1.41	3	2.0±0	—		—	
F	18	3.8±0.92	10	1.4±1.65	—		—	

[a] For interpretation of DNFB reaction scores, *see* text.

[b] — indicates insufficient number of animals for comparison of data.

TABLE 8.—*Humoral antibody accumulated scores for reactions of L/S-P and healthy littermates to SRBC and BSA as sources of antigen*

Antigen source	Pigs			Accumulated reaction scores, mean ± SD	
	Litter No.	Condition	No. tested	Primary response	Secondary response
SRBC	1	Healthy	5	19.6±6.6	20.0±3.7
		L/S	2	10.0±2.8	7.5±2.1
	2	Healthy	4	15.8±3.4	15.3±2.5
		L/S	4	7.5±4.1	6.0±2.2
	1 and 2	Healthy	9	17.9±5.5	17.9±3.9
		L/S	6	8.3±3.6	6.5±2.1
BSA	3	Healthy	6	0.8±2.0	2.3±2.7
		L/S	1	6.0	19.0
	4	Healthy	11	0.8±1.6	0.3±0.7
		L/S	1	9.0	24.0
	3 and 4	Healthy	17	0.8±1.7	1.0±1.9
		L/S	2	7.5±2.1	21.5±3.5

healthy pigs (primary: *t*-test, 5.2; df, 17; $P<0.001$; secondary: *t*-test, 13.5; df, 17; $P \ll 0.001$).

DISCUSSION

Although we demonstrated that male L/S-P have a significantly shorter survival time than do females and that testicular involvement is common in entire males, any analogy with childhood ALL is only superficial. In the pig, the sex differences in survival are apparent in untreated animals, whereas in children they have become apparent only in recent years with the long follow-up of aggressively treated individuals [(*3*); Innes EM: Personal communication].

ALL can be classified according to at least four main cell types (*17*). Of these, the T-cell type (15% of ALL cases) has a poor prognosis with present conventional chemotherapy and is four times more common in boys than in girls (*17, 18*). Hereditary L/S of pigs is probably a homogeneous, non-B- non-T-cell entity but to which of the human ALL types it corresponds, if to any, is not clear. Even morphologically, the abnormal mononuclear cells seen in the blood of L/S-P are not quite like those in any human ALL (Innes EM: Personal communication); for one thing, the cells have more cytoplasm. Furthermore, whereas ALL is about one and one-half times more common in boys than in girls (*3*), we found that hereditary L/S occurred less frequently than the 25% expected in male pigs of L/S carrier × L/S carrier parentage.

The higher death rate for males in L/S litters during the first 3 weeks of life possibly may be associated with a proportion of L/S cases not diagnosed at necropsy and subsequent histopathology. Similarly, the unexpectedly low proportion of males born may have been associated with prenatal deaths due to L/S, but as yet we do not have the techniques to establish the validity of this hypothesis.

Comparison of liver, spleen, and some lymph node weights for L/S-P and non-L/S-P that died from colibacillosis shows that the weights are heavier for LS-P, but that the thymus weights of the 2 groups were not markedly different (table 5). The increased likelihood that L/S-P will die of colibacillosis, therefore, does not seem to be thymus-dependent. Indeed, the involution of the thymus seems to correlate with the body weight of the pig rather than with the cause of death. If the decrease in thymus weight was inversely proportional to the increase in lymph node weight, one would expect a smaller thymus than that actually observed in the older L/S-P. The longest surviving females and castrates with L/S, although six times as old as the pigs that died of colibacillosis, had thymuses of comparable weight (tables 5 and 6), which might be interpreted as indicating that the ability of an L/S-P to survive depends on the retention of a moderate amount of thymus. Certainly, these organ weight figures show that the longer a pig survives the greater the weight of tumor tissue it carries, and apparently death does not automatically intervene at any fixed tumor weight.

Male and castrate L/S pigs that died from colibacillosis between the ages of 44 and 74 days had lighter gastric lymph node, mesenteric lymph node, spleen, and thymus weights than did females of the same age that died of the same disease. The critical regulators of sexual maturation in healthy male pigs are the LH and testosterone plasma levels, which do not start to rise until approximately 80 days of age; these levels peak at about 110 and 138 days, respectively, and then return to a low level [Florcruz SV, Lapwood KR (*19*)]. In addition, those authors believe that body weight is important in the regulation of spermatogenesis, which they found occurred between 90 and 127 days. Separation of the data into three ascending weight categories for the 44- to 74-day-old pigs that died of colibacillosis revealed that the heavier weights of gastric and mesenteric lymph nodes occurred in the females in each category. However, spleen and thymus weights were greatest only in the heaviest females (table 5).

Sex differences in organ and lymph node weights are difficult to explain simply as an increase in tumor or as an increase in host defense cells. The differences occur before male puberty sex hormones arise in males—not when male puberty sex hormones peak and establish the adult pattern (at 110–209 days old; table 6)—and before estrus cycles are apparent in females. In the oldest age group (290–360 days old), in which no entire male L/S-P still were alive, the females had heavier gastric lymph nodes, mesenteric lymph nodes, and thymuses, but not spleens, than did castrates. Therefore, we believe that sex hormones at levels governing normal, functional sexual maturity are not responsible for the differences in survival and tumor progress, because even in older pigs normal spermatogenesis and normal ovarian cycling were not observed. The observation that cellular immune responses were reduced in L/S-P is compatible with the marked regression of the thymus in all cases. The significantly better sensitivity reactions to DNFB of castrates as opposed to those of male L/S-P (table 7) suggest a possible reason for the better survival rates for castrates. Unfortunately, only for the DNFB immune response test system were sufficient animals involved to permit a comparison between the sexes, and generalizations should not be made on the basis of one system.

The significantly better humoral antibody responses to SRBC of healthy pigs as compared to those of littermates with L/S could possibly give some indication as to why the L/S-P are more susceptible to *E. coli* infections (table 4). The immune systems probably are quite different. The SRBC reaction depends mainly on an IgM and IgG response, whereas in *E. coli* infections an IgA response is favored along with the adhesive "stick" gene for K88 antigen (*13*). This difference in the immune response of L/S-P has not been investigated.

The enhanced responses of the 2 L/S-P to BSA (table 8) are evidence that all immune mechanisms are not depressed by the disease. In these pigs, the immune mechanisms were improved. As reported previously (*20*), an increase occurs in the levels of IgM and IgG in the sera of L/S-P. The direct agglutination reaction against BSA-coated tanned cells may involve IgM in the primary and, to a certain extent, in the secondary response. To judge the entire immune responsiveness of L/S-P as being inferior to that of their healthy littermates, on the basis of observations made with the use of certain immune test systems, would be unwise. With regard to thymus-dependent systems, the responses of L/S-P are obviously inferior to those of their healthy littermates. The responses of L/S-P to certain other humoral antibody systems, involving complement fixation and reaction to particulate antigens, are also inferior but to other systems, involving soluble antigens, they are superior.

The observation that healthy female pigs had a better immune response to DNFB than did healthy male pigs is in general agreement with immune response studies in humans (*21*) and mice (*22*). Studies of thymus-dependent and thymus-independent responses of entire male, female, and castrated mice (*23*), demonstrated that the responses of female and castrated mice were superior to those of the entire males, but that the thymus-independent responses of castrated mice were superior to those of the females. In our study, the 3 castrated L/S-P pigs showed a better reaction to DNFB than did the male or female L/S-P. However, McFarlin and Balfour (*24*) demonstrated that skin contact sensitivity induced by DNFB is inhibited in thymectomized newborn pigs, which implies that the DNFB reaction is mainly thymus-dependent in the pig. In this respect castrated L/S-P appear to have some superiority in their degree of reaction. The superior immune response of castrated mice (*23*) was related to hyperplasia of the thymus and spleen, with an increase in the number of cortisone-sensitive cells in the thymus and an increase in the number of peripheral lymphocytes. Such differences have not been investigated in detail in pigs; however, as can be seen in table 6, healthy male pigs (16 of 19 were C) had heavier spleen and thymus weights than did comparable females. We have therefore demonstrated a reduction in the ability of male pigs to survive with L/S and that this reduction is not related to an increased susceptibility to some infections (e.g., colibacillosis) or to a more rapid growth of tumor mass in males than in females. In part, the difference in biologic behavior of untreated L/S-P of different sexes may be due to differences in their immune responsiveness. There are, however, fragments of evidence to suggest that the difference is mediated through the testes and epididymis. Batchelor and Chapman (*25*) concluded that a higher rate of antibody synthesis in female mice was not because of the presence of ovarian tissues, but rather that males were immunologically inferior due, in part, to the presence of the testes, although the immune system deficiency was not attributable to testosterone. Any effect of sex hormones in male L/S-P presumably must be at a time when those hormones are at a low level in the plasma, because tumor growth is not exacerbated with the normal occurrence of puberty. Moreover, the involvement of the epididymis remnant in an incompletely castrated pig that died from salmonellosis 228 days after castration showed that only traces of testes may reduce immunity. A castrated male fetus has a neutral or female sex pattern because the testes of the male superimposes "maleness" by stimulating wolffian duct growth by an androgen and by suppressing the müllerian duct by an unknown hormone (*26*). This phenotypic sex determination occurs in the womb when LH and testosterone levels are very low and may, in part, be mediated through the H-Y antigen, a product of the testes-determining Y-chromosome gene (*27*).

Castration of male mice results in the lymph node PCV endothelial cells becoming nearer in character to those of the female, presumably, because of their release from a direct depressive effect of androgens [Kittas L, Henry C (*28*)]. Those authors discuss the ways in which gonadectomy and estrogen administration may influence both thymus activity and PCV control of lymphocyte recirculation. The gonad would seem to be more important than the Y-chromosome in influencing immunologic responsiveness. Gonadectomy and administration of estrogen could have the type of moderating effect on the biologic behavior of L/S that we have outlined.

In summary, the expected life-span of a pig may be shortened by many factors. L/S invariably leads to the death of the pig at an early age. Moreover, an L/S-P may die from intercurrent disease sooner than from the tumor alone. Conversely, some factors appear to be present in the L/S-P that may slightly extend its life-span. We believe that there is a hierarchy of factors that influence the life-span: *a*) Intercurrent diseases acting alone that cause death at any age and are unrelated to the progress of the L/S (e.g., *Haemophilus* and *Salmonella* infections). The number of deaths in a group of L/S pigs due to such diseases will be governed by the number of pigs exposed to the causal agent. In a conventional piggery, more deaths would be expected in this category than occurred in our minimal disease herd. *b*) Intercurrent diseases that have a characteristic morbidity age distribution (e.g., colibacillosis). Mortality from such diseases is increased in pigs already affected with L/S. The number of deaths in a group of L/S-P due to intercurrent diseases will be governed by such factors as a new pathogenic strain of the disease organism, the herd immune status in respect to the current organism's serotype, and changes in feeding and management. *c*) The intrinsic growth rate of the L/S in a particular pig, with eventual death due to multiple organ system failure. *d*) Host pig factors that modify the rate of L/S growth to a limited extent (e.g., sex).

REFERENCES

(*1*) McTaggart HS, Laing AH, Imlah P, Head KW, Brownlie SE. The genetics of hereditary lymphosarcoma of pigs. Vet Rec 1979; 105:36.

(*2*) Head KW, Campbell JG, Imlah P, Laing AH, Linklater KA, McTaggart HS. Hereditary lymphosarcoma in a herd of pigs. Vet Rec 1974; 95:523–527.

(*3*) Baumer JH, Mott MG. Sex and prognosis in childhood acute lymphoblastic leukaemia. Lancet 1978; 2:128–129.

(*4*) Editorial: Testicular infiltrates in childhood leukaemia: Harbour or harbinger? Lancet 1978; 2:136–137.

(*5*) Baumer JH, Mott MG, Gentle TA. Letter: Sex and prognosis in childhood acute lymphoblastic leukaemia. Lancet 1978; 2:673.

(*6*) Peto R, Pike MC, Armitage P, et al. Design and analysis of randomised clinical trials requiring prolonged observation of each patient. II. Analysis and examples. Br J Cancer 1977; 35:1–35.

(*7*) Brownlie SE, Campbell JG, Head KW, Imlah P, McTaggart HS, McVie JG. The effects of prednisolone on normal pigs. Eur J Cancer 1978; 14:567–578.

(*8*) Boyden SV. The adsorption of proteins on erythrocytes treated with tannic acid and subsequent haemagglutination by anti-protein sera. J Exp Med 1951; 93:107–120.

(*9*) Mathai E, Ramachandran P. A study on litter size and sex ratio in pigs. Kerala J Vet Sci 1972; 3:1–5.

(*10*) Bereskin B, Shelby CE, Cox DF. Some factors affecting pig survival. J Anim Sci 1973; 36:821–827.

(*11*) Vangen O. Studies on a two trait selection experiment in pigs. Acta Agric Scand 1980; 30:309–319.

(*12*) Kenworthy R. Digestibility and balance studies of gnotobiotic pigs undergoing acute intestinal infection with *E. coli*. Res Vet Sci 1974; 16:208–215.

(*13*) Rutter JM. *E. coli* infection in piglets: Pathogenesis, virulence and vaccination. Vet Rec 1975; 96:171–175.

(*14*) Rowland AC, Rowntree PG. A haemorrhagic bowel syndrome associated with intestinal adenomatosis in the pig. Vet Rec 1972; 91:235–241.

(*15*) Lawson GH, Rowland AC. Intestinal adenomatosis in the pig: A bacteriological study. Res Vet Sci 1974; 17:331–336.

(*16*) Lawson GH, McPherson EA, Laing AH, Wooding P. The epidemiology of *Salmonella dublin* infection in a dairy herd. I. Excretion and persistence of the organism. J Hyg Camb 1974; 72:311–328.

(*17*) Greaves MF. Molecular phenotypes: A new perspective in diagnosis and classification of leukemias. In: Morris-Jones PH, ed. Topics in paediatrics. I. Haematology and oncology. London: Pitman Med, 1979:36–50.

(*18*) Chessels J. Presentation and prognosis in childhood leukaemia. In: Morris-Jones PH, ed. Topics in paediatrics. I. Haematology and oncology. London: Pitman Med, 1979:27–35.

(*19*) Florcruz SV, Lapwood KR. A longitudinal study of pubertal development in boars. Int J Androl 1978; 1:317–330.

(*20*) Imlah P, Brownlie SE, Head KW, McTaggart HS, McVie JG. Serum gamma globulin levels and the detection of heavy chain and light chain in the serum and urine of cases of pig hereditary lymphosarcoma. Eur J Cancer 1979; 15:1337–1349.

(*21*) Rowley MJ, Mackay IR. Measurement of antibody-producing capacity in man. Clin Exp Immunol 1969; 5:407–418.

(*22*) Terres G, Morrison SL, Habicht GS. A quantitative difference in the immune response between male and female mice. Proc Soc Exp Biol Med 1968; 127:664–667.

(*23*) Eidinger D, Garrett TJ. Studies of the regulatory effects of the sex hormones on antibody formation and stem cell differentiation. J Exp Med 1972; 136:1098–1116.

(*24*) McFarlin DE, Balfour B. Contact sensitivity in the pig. In: Jankovic BD, Isakovic K, eds. Microenvironmental aspects of immunity. New York: Plenum, 1973:539–544.

(*25*) Batchelor JR, Chapman BA. The influence of sex upon the antibody response to an incompatible tumour. Immunology 1965; 9:553–563.

(*26*) Short RV. An introduction to some of the problems of intersexuality. J Reprod Fertil [Suppl] 1969; 7:1–8.

(*27*) Ohno S, Christian LC, Wachtel SS, Koo GC. Hormone-like role of H-Y antigen in bovine freemartin gonad. Nature 1976; 261:597–598.

(*28*) Kittas C, Henry L. Ultrastructural effects of sex hormones and infection on lymph node post-capillary venules. J Pathol 1980; 132:121–132.

Calorie Restriction: Effect on Growth of Human Tumors Heterotransplanted in Nude Mice[1,2,3]

Beppino C. Giovanella,[4,5] **Randall C. Shepard,**[4] **John S. Stehlin,**[4] **John M. Venditti,**[6] *and* **Betty J. Abbott**[6,7]

ABSTRACT—The presence of 4 human malignant tumors (1 breast, 1 lung, and 2 colon carcinomas) growing subcutaneously as heterotransplants in nude mice did not significantly affect the body weights of adult animals until the tumors reached very large dimensions (tumor wt >15% of the body wt). However, a colon carcinoma (HT 29) induced a cessation of the natural rate of body weight increase when it grew in young adults (animals weighing ≈25 g which will gain 6 g or ≈25% body wt in 1 mo). Calorie restriction at all the levels tested (8, 6, 4, and 2 g/day/mouse) with standard pelletized mouse food produced both weight loss in the animals (with and without tumor) and a lowering of the growth rate of all the 4 tumors tested growing at a subcutaneous site and/or under the kidney capsule. Each tumor responded differently to the calorie restriction. The 4 tumors tested grew equally in both male and female nude mice. Young animals weighing 20 g inoculated with a fifth tumor (MeWo melanoma) exhibited tumor growth inhibition proportional to restriction of calorie intake. Their survival, however, did not improve.—JNCI 1982; 68:249–257.

The effect of calorie restriction on the incidence and growth rate of malignant tumors in animals has been the subject of many papers (*1–18*). However, much less is known about the effect of calorie restriction on the incidence and growth rate of malignant tumors in humans (*19*) because it is not possible to starve human cancer patients for evident ethical and practical reasons. Since the nude mouse (*20, 21*) is capable of accepting human tumor heterotransplants because of its immunologic deficiency (*22, 23, 24*), it is now possible to submit human tumors in the nude mouse host to calorie restriction under the same rigorous experimental conditions used for the study of animal tumors. We have studied the effects of different degrees of calorie restriction on the growth rate of 5 human malignant tumors (2 colon carcinomas, 1 breast carcinoma, 1 lung carcinoma, and 1 melanoma) serially transplanted into nude mice.

MATERIALS AND METHODS

Mice—Noninbred nude Swiss mice were bred and experimented on within the Cancer Research Laboratory, St. Joseph Hospital, under strictly pathogen-free conditions according to the procedures described by Giovanella and Stehlin (*25*). For the calorie restriction experiments, the mice were isolated singly in polycarbonate cages. The desired daily amount (2, 4, 6, 8 g) of sterile pelletized autoclavable mouse food (Wayne Lab Blox Sterilizable; Allied Mills, Inc., Chicago, Ill.) was introduced under sterile conditions into each cage. Such pelletized food contains 24% proteins, 4% fats, and 4.5% crude fiber. It is composed of corn and wheat flakes, soybean meal, wheat red dog, wheat middlings, fish meal, brewer's dried yeast, soybean oil, animal liver meal, vitamins, and minerals. One gram is equivalent to 3.7 calories. The controls fed ad libitum always had an excess of the same food present in the cages. We determined ad libitum food intake by feeding animals weighed amounts of powdered food placed at the bottom of a narrow-necked container. Under such conditions, the animal could eat as much as it wished, but spillage was minimized because to obtain food the mouse was forced to introduce its head and neck only and not its front paws into the opening. Every 24 hours, the container was withdrawn, the contents were weighed, and the amount eaten was established by the subtraction of the amount of food still present from the original amount introduced in the container. As an additional precaution, the small container was fixed at the center of a petri dish 10 cm in diameter. When eating, the mouse had to perch itself on the rim of the petri dish so that urine and feces fell outside the petri dish. This arrangement allowed us to collect (with a brush) and weigh even the smallest amounts of powdered food spilled by the mouse. All the animals received water ad libitum. To the water, sterilized by passage through a Millipore filter, was added 1 ml multivitamin infusion/liter (U.S. Vitamin and Pharmaceutical Corp., Tuckahoe, N.Y.) [*See* (*25*) for complete composition of the multivitamin infusion.] This diet was fully balanced, and the only restriction practiced was on the calorie intake.

Tumors.—Human breast carcinoma Clouser (CL #1; also

ABBREVIATIONS USED: EMEM=Eagle's minimum essential medium; NCI=National Cancer Institute; OMU=optical micrometer unit(s).

---

[1] Received April 14, 1980; revised September 10, 1981; accepted September 25, 1981.

[2] Supported by Public Health Service contract N01CM-67073-TQ from the National Cancer Institute.

[3] Animals were maintained under the guidelines set forth by The Stehlin Foundation for Cancer Research.

[4] Cancer Research Laboratory, St. Joseph Hospital, Houston, Tex. 77002.

[5] *Address reprint requests to* Dr. Giovanella at The Stehlin Foundation for Cancer Research, 777 St. Joseph Professional Bldg., Houston, Tex. 77002.

[6] Division of Cancer Treatment, National Cancer Institute, National Institutes of Health, Public Health Service, U.S. Department of Health and Human Services, Bethesda, Md. 20205.

[7] We thank Mr. Peter DeMarsh, Mr. John Mendoza, Mr. Dana Vardeman, Mr. Michael Harlow, Mr. Douglas Coil, and Mr. Gregory Bartel for their skillful technical assistance; Miss Betty Mendoza for the preparation of the manuscript; and Dr. Shih-shun Lee, Cancer Research Laboratory, for his invaluable help with the statistical calculations.

BX #1 in the screening panel, Division of Cancer Treatment, NCI) is an invasive ductal cell carcinoma of the breast heterotransplanted in our laboratory from a primary tumor of a 29-year-old woman and serially carried for 48 passages in nude mice. This tumor has been extensively studied, especially for its response to experimental chemotherapy (*26–29*). Human lung carcinoma Doyle (DO #1; also LX #1 in the screening panel, Division of Cancer Treatment, NCI) is an undifferentiated epidermoid carcinoma of the lung heterotransplanted in our laboratory from a subcutaneous metastasis of a 48-year-old man and serially carried for 39 passages in nude mice; it has been extensively studied (*27, 28, 30*). Human colon carcinoma Squires (SQ #1), also extensively studied in our laboratory and other laboratories (*27*), is a moderately differentiated adenocarcinoma of the colon; it was heterotransplanted in our laboratory from an iliac lymph node metastasis of a 50-year-old man and serially carried for 16 passages in nude mice. Human colon carcinoma HT 29 (CX #1 in the screening panel, Division of Cancer Treatment, NCI) was received from the Mason Research Institute, Worcester, Mass., as a nude mouse tumor serially transplantable. It was obtained by the injection in nude mice of cells of the tissue-cultured line HT 29 (passage 100) received from Dr. Jørgen Fogh, Sloan-Kettering Institute, Rye, N.Y., who established it in culture from a primary mucinous adenocarcinoma of the colon in a 44-year-old woman (*31*). This tumor has been carried for 26 passages in nude mice and is also well studied (*29, 32*). The MeWo cell line was originated by Kodera and Bean from a malignant melanoma metastatic to a lymph node of a 74-year-old male in 1974. It has been well studied and characterized both in vitro and in vivo in nude mice (*33*). All of these tumors were transplanted in our laboratory either by the sc injection of 0.5 ml of the finely minced tumor suspended in EMEM (GIBCO, Grand Island, N.Y.) (10% wt/vol, equivalent to ≈50 mg wet wt tumor) or by the surgical insertion of a small fragment of the tumor under the kidney capsule according to the method of Bogden et al. (*29*).

TABLE 1.—*Food intake of nude and heterozygous Swiss mice, groups of 4 mice*

Mice	Age, mo[a]	Food intake[b]	
		g/mouse/day	mg/g/day
Nude	1	6.5±0.4	399
	3	8.1±0.7	245
Heterozygous	1	5.9±0.6	272
	3	5.5±0.2	166

[a] Average body weights at 1 mo of age were 16.3 g for the nude mice and 21.7 g for the heterozygous mice. Average weights at 3 mo of age were 33.1 g for the nude mice and 40.5 g for the heterozygous mice.

[b] Values are means ± SD.

Food intake and experimental procedures.—Groups of 50 nude mice fed ad libitum were inoculated with the same tumor. When the tumors reached the desired size, the animals were divided into groups of 10 (5 males and 5 females). From then on, each group received one of five food quantities: ad libitum, 8 g/mouse/day, 6 g/mouse/day, 4 g/mouse/day, and 2 g/mouse/day. The animals with subcutaneous tumors were individually weighed, and the tumor was measured every 2d day for at least 30 days after the start of treatment. The tumor weight in milligrams was calculated according to the formula $(ab^2)/2$, where a and b were expressed in millimeters. The subrenal capsule transplants were measured in situ at the moment of implantation by means of a micrometric ocular applied to a stereomicroscope and then by the same instrument when the mice were killed 11 days later.

The size of the tumor is given as average diameter, $(a + b)/2$, expressed in OMU (1 OMU = 0.1 mm). In most experiments, adult nude mice were used (i.e., animals whose weights do not increase any further or increase very slowly even if fed ad libitum). In some experiments, however, the effects of calorie restriction were compared in adult nude and young adult nude mice (i.e., animals that are in the last part of their normal weight gain period). Young adult mice will gain 25% body weight before they reach the adulthood plateau. The MeWo survival experiment was conducted with the use of groups of 8 animals that were inoculated sc with the tumor and fed ad libitum (6 g/day, 4 g/day, and 3 g/day) starting when the mice weighed 20 g. The animals were then followed until all the mice in a group died.

RESULTS

The results are summarized in tables 1–16 and in text-figures 1 and 2. No sex differences were observed. Accordingly, all the results are given as averages of groups composed of 50% males and 50% females. Table 1 shows the amounts of food consumed by young and adult mice when

TABLE 2.—*Body weights of tumor-free adult mice*

Food intake	Body weight, g, after diet was instated on day:[a]			
	0	8	18	28
Ad libitum	34.2±3.0 (16)	34.3±2.7 (16)	34.9±3.7 (16)	35.4±2.8 (16)
Weight loss [g], %		[+0.1], 0	[+0.7], +2	[+1.2], +4
8 g	34.2±4.0 (12)	28.8±3.7 (12)	32.2±5.2 (12)	33.2±4.7 (12)
Weight loss [g], %		[5.4], 16	[2.0], 6	[1.0], 3
6 g	34.3±3.4 (12)	28.3±2.6 (12)	28.0±2.5 (12)	27.7±3.4 (12)
Weight loss [g], %		[6.0], 17	[6.3], 18	[6.6], 19
4 g	33.8±3.2 (16)	21.9±2.0[b] (14)	19.6±1.2 (12)	20.2±1.4 (11)
Weight loss [g], %		[11.9], 35	[14.2], 42	[13.6], 40
2 g	33.8±3.3 (16)	20.6±2.0[b] (11)	20.2±1.5 (5)	20.2±1.3 (4)
Weight loss [g], %		[13.2], 39	[13.6], 40	[13.6], 40

[a] Values are means ± SD. *Numbers in parentheses* are numbers of animals. *Numbers with plus signs in brackets*=weight gain, g.

[b] $P<0.01$ vs. day 0 data.

fed ad libitum. Nude mice consumed more food than did their heterozygous furry littermates. Also, for adult nude mice, feeding 8 g/day/mouse is almost equivalent to ad libitum feeding. Table 2 shows that tumor-free adult nude mice (≈90 days old) if fed ad libitum very slowly increased their body weights. Such increase, although slow, was significant so that a male 1-year-old Swiss nude mouse in our colony not infrequently reached a body weight of 45–50 g. If calorie restriction was instituted, the body weight dropped initially and then rebounded if the calorie restriction was minimal (8 g/mouse/day) or leveled off at different levels if the calorie restriction was more severe. This phenomenon is explained in table 3, which shows the level of food intake (in mg/g body wt) with different diets and the leveling off of food intake after 3 days when the body weight stabilized. Table 2 shows that animals fed at 2 and 4 g/mouse/day, after initially losing some weight, leveled off at the same body weight, although the 2-g animals had a food intake that was one-half that of the 4-g mice (table 3). However, a profound difference existed between these two levels of calorie intake. Mice fed 4 g/mouse/day can live indefinitely, whereas mice fed 2 g/mouse/day will all die within 30–40 days. Thus for nude Swiss mice, the minimum food intake is about 200 mg/g/day, which will maintain them indefinitely at a lean 20- to 21-g body weight. If the diet was instated at a younger age when the animal was still growing and not just slowly fattening, the same basic observations were made (tables 4, 5). If the animals were provided with more than 200 mg food/g/day, they kept growing. Comparisons at the level of 2 g/mouse/day were not possible because the adults under these conditions had available only 100 mg food/g/day versus 150 mg for the young animals.

With ad libitum feeding, the growth of all 4 tumors depressed the body weights of nude mice. The depression was greatest with DO #1 lung carcinoma, a very invasive tumor. HT 29 colon carcinoma mildly depressed the weights of adult animals, but it totally suppressed the growth of young animals (table 6).

Calorie restriction reduced the growth of all 4 subcuta-

TABLE 3.—*Food intake of tumor-free adult mice*

Food intake[a]	Food intake, mg/g body wt, after diet was instated on day:[b]			
	0	8	18	28
8 g	234 (12)	278 (12)	248 (12)	241 (12)
Weight loss, %		16	+10[c]	+3[c]
6 g	175 (12)	212 (12)	214 (12)	217 (12)
Weight loss, %		17	1	1
4 g	118 (16)	183 (14)	210 (12)	198 (11)
Weight loss, %		35	7	+2[c]
2 g	59 (16)	97 (11)	99 (5)	95 (4)
Weight loss, %		39	1	0

[a] Weight loss is relative to previous measurement.
[b] *Numbers in parentheses* are numbers of animals.
[c] Weight gain, %.

TABLE 5.—*Food intake of tumor-free young mice weighing 24 g*

Food intake[a]	Food intake, mg/g body wt, after diet was instated on day:[b]			
	0	8	18	28
8 g	327 (4)	311 (4)	265 (4)	249 (4)
Weight loss, %		+5[c]	+18[c]	+8[c]
6 g	246 (4)	284 (4)	240 (4)	223 (4)
Weight loss, %		13	+16[c]	+7[c]
4 g	167 (4)	250 (4)	227 (4)	209 (4)
Weight loss, %		33	+7[c]	+9[c]
2 g	83 (4)	150 (4)	143 (4)	133 (4)
Weight loss, %		45	+3[c]	+5[c]

[a] Weight loss is relative to previous measurement.
[b] *Numbers in parentheses* are numbers of animals.
[c] Weight gain, %.

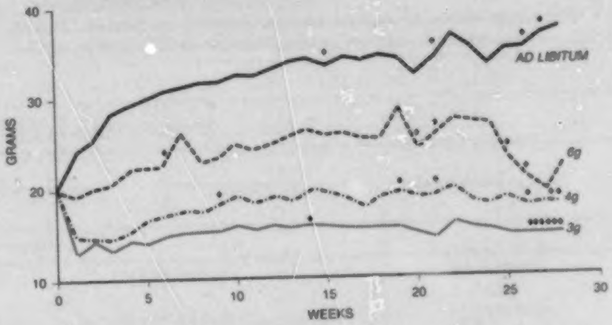

TEXT-FIGURE 1.—Changes in body weight as a function of time at various levels of food intake. Mice inoculated sc with MeWo melanoma at day 0 when diet was also instated. Groups of 8 animals were used for each level of food intake. ◆, death of 1 mouse.

TABLE 4.—*Body weights of tumor-free young mice weighing 24 g*

Food intake	Body weight, g, after diet was instated on day:[a]			
	0	8	18	28
Ad libitum	23.9±2.5 (4)	26.8±4.6 (4)	31.3±4.0 (4)	33.4±3.4 (4)
Weight loss [g], %		[+2.7], +11	[+7.4], +31	[+9.5], +40
8 g	24.5±2.7 (4)	25.7±4.4 (4)	30.2±4.5 (4)	32.2±5.1 (4)
Weight loss [g], %		[+1.2], +5	[+5.7], +23	[+7.7], +31
6 g	24.4±2.3 (4)	21.1±3.1 (4)	25.0±3.4 (4)	26.9±3.6 (4)
Weight loss [g], %		[3.3], 13	[+0.6], +3	[+2.5], +10
4 g	23.9±2.0 (4)	16.0±1.5[b] (4)	17.6±1.1 (4)	19.9±1.0 (4)
Weight loss [g], %		[7.9], 33	[6.3], 26	[4.0], 17
2 g	24.0±3.1 (4)	13.3±1.9[b] (4)	14.0±2.9 (4)	15.0±2.6 (4)
Weight loss [g], %		[10.7], 45	[10.0], 42	[9.0], 37

[a] Values are means ± SD. *Numbers in parentheses* are numbers of animals. *Numbers with plus signs in brackets*=weight gain, g.
[b] $P<0.01$ vs. day 0 data.

TABLE 6.—*Body weights of animals fed ad libitum*

Parameter[a]	Body weight, g[b]	
	HT 29 colon cancer, adults	
	Day 12	Day 40
No tumor	37.7	35.9 (+0.2) [+0.6]
Tumor	34.6	31.3 (−3.3) [−9.5] {−10.1}
	HT 29 colon cancer, young animals	
	Day 3	Day 38
No tumor	23.9	33.4 (+9.5) [+39.7]
Tumor	24.2	24.3 (−0.1) [−0.4] {−40.1}
	CL #1 breast cancer, adults	
	Day 10	Day 38
No tumor	34.1	36.5 (+2.4) [+7.0]
Tumor	33.8	31.6 (−2.2) [−6.5] {−13.5}
	SQ #1 colon cancer, adults	
	Day 13	Day 41
No tumor	33.6	35.3 (+1.7) [+5.0]
Tumor	33.7	33.3 (−0.4) [−1.2] {−6.2}
	DO #1 lung cancer, adults	
	Day 5	Day 33
No tumor	33.3	33.9 (+0.6) [+2.0]
Tumor	35.4	29.2 (−6.2) [−17.4] {−19.4}

[a] No tumor refers to control animals bearing no tumors. Tumor refers to experimental animals bearing tumors. In this and in all the following tables, the host weight of a tumor-bearing animal is obtained by subtraction of the tumor weight from the total weight.

[b] Days listed are days after tumor inoculation. *Numbers in parentheses* are body weight gains (+) or losses (−), in grams, after 28 days. *Numbers in brackets* are percent body weight gains (+) or losses (−) after 28 days. *Numbers in braces* are percent body weight losses (−) after 28 days of tumor-bearing animals relative to the weights of their non-tumor-bearing controls.

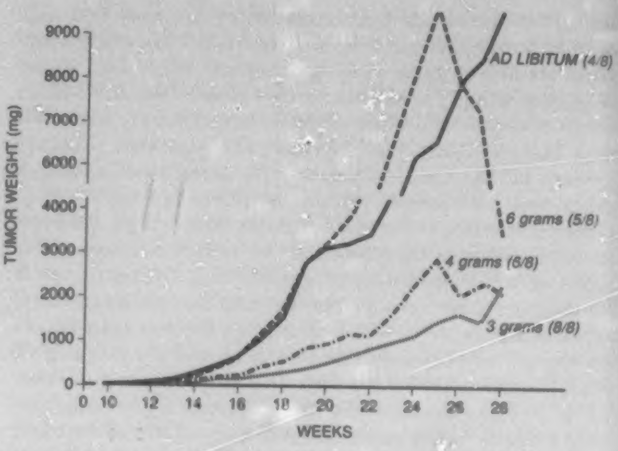

TEXT-FIGURE 2.—Tumor growth in same animals as in text-fig. 1. *Numbers in parentheses* at the end of each curve indicate No. of survivors at the end of the experiment/total No. of mice in the experiment.

TABLE 7.—*Breast carcinoma CL #1 growing subcutaneously in adult mice*

Food intake[a]	Days after tumor inoculation[b]			
	10	18	28	38
	Tumor weight, g			
Ad libitum	0.16±0.07 (10)	0.87±0.44 (10)	3.24±1.16 (10)	6.75±3.35 (10)
WT/W0		5	20	42
8 g	0.15±0.01 (10)	0.86±0.34 (10)	3.09±0.59 (9)	4.90±1.69 (8)
WT/W0		6	19	31
Inhibition, %		+20	5	26
6 g	0.16±0.08 (10)	0.64±0.43 (10)	1.80±1.10 (10)	2.86±1.12 (10)
WT/W0		4	11	18
Inhibition, %		20	45	57
4 g	0.15±0.07 (10)	0.36±0.20 (8)	0.84±0.46 (8)	1.31±0.69[c] (8)
WT/W0		2	6	9
Inhibition, %		60	70	79
	Body weight, g			
Ad libitum	33.9±3.1 (10)	34.7±2.7 (10)	33.6±2.6 (10)	31.6±3.5 (10)
Weight loss [g], %		[+0.8],[d] +2	[0.3], 1	[2.3], 7
8 g	33.8±2.7 (10)	30.0±2.3 (10)	31.3±2.9 (9)	26.6±4.1 (8)
Weight loss [g], %		[3.8], 11	[2.5], 7	[7.2], 21
6 g	33.7±3.8 (10)	24.4±5.7 (10)	25.4±2.6 (10)	26.4±2.8 (10)
Weight loss [g], %		[9.3], 28	[8.3], 25	[7.3], 22
4 g	33.9±3.6 (10)	23.2±1.7[e] (8)	21.7±1.9 (8)	22.9±2.3 (8)
Weight loss [g], %		[10.7], 32	[12.2], 36	[11.0], 32

[a] WT/W0=weight at time *t*/weight at time 0.

[b] Values are means ± SD. *Numbers in parentheses* are numbers of animals.

[c] $P<0.05$ vs. ad libitum data.

[d] Weight gain, g.

[e] $P<0.01$ vs. day 10 data.

neously transplanted tumors and reduced the body weights of their hosts. These results also held true with subcapsular renal transplantation. [*See* subcutaneous data 8 days after instatement of diet (tables 7-11) compared with subcapsular data 11 days after instatement (tables 13-16).] Calorie restriction at these levels minimally affected the body weights of tumor-free animals over 11 days (table 12).

A survival experiment was performed with MeWo mela-

TABLE 8.—*Lung carcinoma DO #1 growing subcutaneously in adult mice*

Food intake[a]	Days after tumor inoculation[b]			
	5	13	23	33
	Tumor weight, g			
Ad libitum	0.37±0.12 (8)	1.52±0.59 (8)	5.11±1.85 (7)	6.01±2.3 (6)
WT/W0		4	14	16
4 g	0.45±0.24 (8)	0.31±0.22 (5)	0.85 (1)	1.30 (1)
WT/W0		0.7	2	3
Inhibition, %		82	86	81
2 g	0.41±0.25 (9)	0.49±0.41 (5)		
WT/W0		1		
Inhibition, %		75		
	Body weight, g			
Ad libitum	35.4±5.4 (8)	30.2±4.3 (8)	27.4±5.0 (7)	29.2±4.4 (6)
Weight loss [g], %		[5.2], 15	[8.0], 23	[6.2], 17
4 g	35.7±4.0 (8)	23.0±3.5[c] (5)	20.1 (1)	18.1 (1)
Weight loss [g], %		[12.7], 36	[15.6], 44	[17.6], 49
2 g	35.[illegible]±3.6 (9)	22.6±2.2[c] (5)		
Weight loss [g], %		[12.4], 35		

[a] WT/W0=weight at time *t*/weight at time 0.
[b] Values are means ± SD. *Numbers in parentheses* are numbers of animals.
[c] *P*<0.01 vs. day 5 data.

TABLE 9.—*Colon carcinoma SQ #1 growing subcutaneously in adult mice*

Food intake[a]	Days after tumor inoculation[b]			
	13	21	31	41
	Tumor weight, g			
Ad libitum	0.19±0.8 (10)	0.70±0.25 (10)	2.66±1.24 (10)	6.12±2.56 (10)
WT/W0		4	14	32
8 g	0.19±0.14 (10)	0.77±0.73 (10)	2.39±2.16 (10)	4.07±1.64 (10)
WT/W0		4	13	32
Inhibition, %		0	7	0
6 g	0.19±0.10 (10)	0.55±0.21 (9)	1.76±0.98 (9)	3.39±1.83 (9)
WT/W0		3	9	18
Inhibition, %		25	36	44
4 g	0.18±0.10 (10)	0.33±0.15 (9)	0.86±0.52 (8)	1.72±0.74 (6)
WT/W0		2	5	10
Inhibition, %		50	64	69
2 g	0.21±0.10 (10)	0.31±0.10 (6)	0.39±0.15 (3)	
WT/W0		2	2	
Inhibition, %		50	86	
	Body weight, g			
Ad libitum	33.7±4.0 (10)	33.8±3.4 (10)	32.9±3.9 (10)	33.3±3.9 (10)
Weight loss [g], %		[+0.1],[c] +1	[0.8], 2	[0.4], 1
8 g	33.7±3.4 (10)	29.5±4.3 (10)	29.4±4.9 (10)	29.3±3.3 (10)
Weight loss [g], %		[4.2], 12	[4.3], 13	[4.4], 13
6 g	34.0±3.6 (10)	26.5±2.0[d] (9)	26.7±1.9 (9)	24.2±3.2 (9)
Weight loss [g], %		[7.5], 22	[7.3], 21	[9.8], 29
4 g	34.3±3.1 (10)	21.7±2.1[e] (9)	21.7±2.6 (8)	21.0±1.6 (6)
Weight loss [g], %		[12.7], 37	[12.7], 37	[13.4], 39
2 g	33.7±3.2 (10)	19.6±1.4[e] (6)	18.0±1.8 (3)	
Weight loss, [g], %		[14.1], 42	[15.7], 47	

[a] WT/W0=weight at time *t*/weight at time 0.
[b] Values are means ± SD. *Numbers in parentheses* are numbers of animals.
[c] Weight gain, g.
[d] *P*<0.05 vs. day 13 data.
[e] *P*<0.01 vs. day 13 data.

TABLE 10.—*Colon carcinoma HT 29 growing subcutaneously in adult mice*

Food intake[a]	Days after tumor inoculation[b]			
	12	20	30	40
		Tumor weight, g		
Ad libitum	0.49±0.21 (10)	1.4±0.5 (10)	2.9±1.4 (10)	6.7±2.9 (9)
WT/W0		3	6	14
8 g	0.49±0.24 (10)	1.3±0.5 (10)	2.9±1.1 (10)	3.9±1.8 (10)
WT/W0		3	6	8
Inhibition, %		0	0	43
6 g	0.50±0.28 (10)	1.3±0.6 (10)	2.0±0.8 (10)	3.6±1.5 (10)
WT/W0		3	4	6
Inhibition, %		0	33	57
4 g	0.49±0.16 (10)	0.9±0.5 (10)	1.5±0.8 (9)	1.1±0.6[c] (8)
WT/W0		2	3	2
Inhibition, %		33	50	86
2 g	0.50±0.24 (10)	0.7±0.3 (10)	0.8±0.3 (7)	0.6±0.5[c] (5)
WT/W0		1	2	1
Inhibition, %		67	67	93
		Body weight, g, tumor-bearing mice		
Ad libitum	34.6±3.5 (10)	33.8±3.4 (10)	32.7±3.3 (10)	31.3±4.1 (9)
Weight loss [g], %		[0.8], 2	[1.9], 5	[3.3], 9
8 g	34.0±4.2 (10)	29.2±3.7 (10)	26.5±3.8 (10)	26.6±4.1 (10)
Weight loss [g], %		[4.8], 14	[7.5], 22	[7.4], 22
6 g	35.0±2.7 (10)	26.3±2.0[d] (10)	25.0±2.8 (10)	26.0±2.6 (10)
Weight loss [g], %		[8.7], 25	[10.0], 29	[9.0], 26
4 g	33.7±3.9 (10)	21.8±2.6[d] (10)	20.4±2.3 (9)	20.9±2.6 (8)
Weight loss [g], %		[11.9], 35	[13.3], 39	[12.8], 38
2 g	33.2±2.8 (10)	21.4±1.9[d] (10)	19.8±2.3 (7)	18.8±2.7 (5)
Weight loss [g], %		[11.8], 35	[13.4], 40	[14.4], 43

[a] WT/W0=weight at time *t*/weight at time 0.
[b] Values are means ± SD. *Numbers in parentheses* are numbers of animals.
[c] $P<0.05$ vs. ad libitum data.
[d] $P<0.01$ vs. day 12 data.

TABLE 11.—*Colon carcinoma HT 29 growing subcutaneously in young mice*

Food intake[a]	Days after tumor inoculation[b]			
	8	16	26	36
		Tumor weight, g		
Ad libitum	0.20±0.03 (9)	0.66±0.17 (9)	3.68±0.62 (9)	7.01±2.03 (9)
WT/W0		3	18	35
8 g	0.20±0.05 (10)	0.66±0.25 (10)	2.62±0.71 (10)	4.95±0.97 (10)
WT/W0		3	13	25
Inhibition, %		0	28	29
6 g	0.20±0.06 (10)	0.46±0.19 (10)	2.22±0.81 (10)	4.45±2.04 (10)
WT/W0		2	11	22
Inhibition, %		33	39	37
4 g	0.20±0.04 (10)	0.35±0.10 (10)	1.49±0.44 (9)	3.05±0.82[c] (9)
WT/W0		2	8	15
Inhibition, %		33	66	57
2 g	0.20±0.06 (10)	0.25±0.15 (9)	0.72±0.50 (9)	0.95±0.51[d] (7)
WT/W0		1	4	5
Inhibition, %		66	78	86
		Body weight, g		
Ad libitum	24.4±2.5 (9)	25.1±2.3 (9)	26.0±2.6 (9)	24.2±2.5 (9)
Weight loss [g], %		[+0.7],[e] +3	[+1.6],[e] +7	[0.2], 1
8 g	24.0±1.9 (10)	22.5±2.3 (10)	23.7±3.3 (10)	20.7±2.0 (10)
Weight loss [g], %		[1.5], 6	[0.3], 1	[3.3], 14
6 g	24.5±2.1 (10)	18.8±1.9[f] (10)	20.7±2.9 (10)	20.8±3.2 (10)
Weight loss [g], %		[5.7], 23	[3.8], 15	[3.7], 15
4 g	24.6±2.3 (10)	15.7±1.4[g] (10)	17.2±1.8 (9)	17.7±2.3 (9)
Weight loss [g], %		[8.9], 36	[7.4], 30	[6.9], 28
2 g	24.5±2.4 (10)	13.5±1.0[g] (9)	13.5±1.2 (9)	14.0±1.0 (7)
Weight loss [g], %		[11], 45	[10.9], 44	[10.5], 43

[a] WT/W0=weight at time *t*/weight at time 0.
[b] Values are means ± SD. *Numbers in parentheses* are numbers of animals.
[c] $P<0.05$ vs. ad libitum data.
[d] $P<0.01$ vs. ad libitum data.
[e] Weight gain, g.
[f] $P<0.05$ vs. day 8 data.
[g] $P<0.01$ vs. day 8 data.

TABLE 12.—*Animal weights of tumor-free mice*

Food intake	Animal weight, g, after diet instated on day:[a]	
	0	11
Ad libitum	33.9±2.8 (16)	33.6±2.8 (16)
Weight loss [g], %		[0.3], 1
8 g	33.9±3.1 (16)	[illegible] (16)
Weight loss [g], %		[illegible], 4
6 g	33.9±3.4 (16)	26.4±2.7^{b} (16)
Weight loss [g], %		[1.5], 4
4 g	33.7±2.7 (16)	21.8±2.2^{c} (14)
Weight loss [g], %		[11.9], 35
2 g	34.1±3.4 (16)	19.8±2.1^{c} (11)
Weight loss [g], %		[14.3], 42

[a] Values are means ± SD. *Numbers in parentheses* are numbers of animals.

[b] $P<0.05$ vs. day 0 data.

[c] $P<0.01$ vs. day 0 data.

TABLE 13.—*Breast carcinoma CL #1 growing under the kidney capsule*

Food intake[a]	Days after tumor inoculation[b]	
	0	11
Average tumor diameter, OMU		
Ad libitum	21.9±3.2 (10)	47.0±9.0 (10)
DT/D0		2.2
8 g	21.7±4.1 (10)	39.5±6.9 (10)
DT/D0		1.8
Inhibition, %		15
6 g	21.8±6.8 (10)	40.4±11.3 (10)
DT/D0		1.9
Inhibition, %		14
4 g	22.0±5.9 (10)	30.4±6.6^{c} (10)
DT/D0		1.4
Inhibition, %		36
2 g	21.7±4.2 (10)	25.5±4.7^{d} (9)
DT/D0		1.2
Inhibition, %		45
Body weight, g		
Ad libitum	33.7±2.5 (10)	32.8±3.3 (10)
Weight loss [g], %		[0.9], 3
8 g	33.9±2.3 (10)	31.8±3.0 (10)
Weight loss [g], %		[2.1], 6
6 g	34.3±2.8 (10)	26.2±1.3^{e} (10)
Weight loss [g], %		[8.1], 23
4 g	33.6±3.2 (10)	22.1±1.9^{e} (10)
Weight loss [g], %		[11.5], 38
2 g	34.2±2.8 (10)	19.7±2.1^{e} (9)
Weight loss [g], %		[14.5], 41

[a] DT/D0=average diameter after 11 days/average diameter at day 0.

[b] Values are means ± SD. *Numbers in parentheses* are numbers of animals.

[c] $P<0.05$ vs. ad libitum data.

[d] $P<0.01$ vs. ad libitum data.

[e] $P<0.01$ vs. day 0 data.

TABLE 14.—*Lung carcinoma DO #1 growing under the kidney capsule*

Food intake[a]	Days after tumor inoculation[b]	
	0	11
Average tumor diameter, OMU		
Ad libitum	25.3±4.8 (10)	53.2±10.8 (9)
DT/D0		2.1
8 g	25.0±4.0 (10)	48.6±9.2 (9)
DT/D0		1.9
Inhibition, %		9
6 g	25.3±3.9 (10)	53.4±7.7 (10)
DT/D0		2.1
Inhibition, %		0
4 g	25.1±3.0 (10)	38.7±8.5 (10)
DT/D0		1.5
Inhibition, %		27
2 g	25.1±4.7 (10)	26.3±4.6^{c} (3)
DT/D0		1.1
Inhibition, %		51
Body weight, g		
Ad libitum	35.0±2.9 (10)	33.8±2.5 (9)
Weight loss [g], %		[1.2], 3
3 g	35.9±2.6 (10)	30.0±1.7^{d} (9)
Weight loss [g], %		[5.9], 16
6 g	36.0±3.5 (10)	26.1±2.5^{e} (10)
Weight loss [g], %		[9.9], 27
4 g	36.9±4.2 (10)	21.9±2.7^{e} (10)
Weight loss [g], %		[15], 41
2 g	35.2±2.0 (10)	19.2±0.9^{e} (3)
Weight loss [g], %		[16], 45

[a] DT/D0=average diameter after 11 days/average diameter at day 0.

[b] Values are means ± SD. *Numbers in parentheses* are numbers of animals.

[c] $P<0.05$ vs. ad libitum data.

[d] $P<0.05$ vs. day 0 data.

[e] $P<0.01$ vs. day 0 data.

noma inoculated sc into young nude mice weighing 20 g. Immediately after tumor inoculation, the mice were divided into 4 groups of 8 animals each and fed various levels of food (ad libitum or 6, 4, and 3 g/mouse/day). The body weights of the animals and the tumor growth curves are shown in text-figures 1 and 2. The number of deaths among the tumor-bearing animals are also indicated. The experiment was terminated after 28 weeks when all the mice in the 3-g group were dead. At that time, there were still 2, 3, and 4 survivors, respectively, in the 4-g, 6-g, and ad libitum groups.

DISCUSSION

The data obtained show that calorie restriction inhibited the growth of human tumors heterotransplanted at subcutaneous sites or under the kidney capsule in nude mice. Such inhibition of growth was both dose-dependent and tumor-dependent. For a given tumor, the more severe the calorie restriction, the larger the tumor growth inhibition. However, the same calorie restriction applied to different tumors caused different degrees of inhibitions of growth. These results parallel quite closely the results obtained by Tannenbaum and Silverstone (*17*) using animal tumors. Our data and those of Tannenbaum and Silverstone showed that tumor growth inhibition and host weight loss were closely correlated. The 4 tumors studied did not significantly affect the weights of the adult hosts until these tumors had reached very large dimensions. When 1 of these tumors was transplanted into young mice still increasing their body mass, the body weight gain was completely stifled. This inhibition of

TABLE 15.—*Colon carcinoma SQ #1 growing under the kidney capsule*

Food intake[a]	Days after tumor inoculation[b]	
	0	11
	Average tumor diameter, OMU	
Ad libitum	25.1±3.7 (10)	34.9±6.1 (10)
DT/D0		1.4
8 g	25.2±4.1 (10)	36.4±6.3 (9)
DT/D0		1.4
Inhibition, %		0
6 g	25.3±3.7 (10)	29.8±6.8 (10)
DT/D0		1.2
Inhibition, %		14
4 g	25.1±2.8 (10)	30.2±11.4 (8)
DT/D0		1.2
Inhibition, %		14
2 g	25.4±4.1 (10)	25.2±7.1 (7)
DT/D0		1.0
Inhibition, %		29
	Body weight, g	
Ad libitum	35.3±3.5 (10)	33.5±2.6 (1)
Weight loss [g], %		[1.8], 5
8 g	34.1±2.2 (10)	30.6±3.2 (9)
Weight loss [g], %		[3.5], 10
6 g	35.6±3.3 (10)	26.7±4.4[c] (10)
Weight loss [g], %		[8.9], 25
4 g	34.4±3.1 (10)	21.7±1.6[d] (8)
Weight loss [g], %		[12.7], 37
2 g	33.8±2.3 (10)	18.7±1.3[d] (7)
Weight loss [g], %		[15.1], 45

[a] DT/D0=average diameter after 11 days/average diameter at day 0.

[b] Values are means ± SD. *Numbers in parentheses* are numbers of animals.

[c] $P<0.05$ vs. day 0 data.

[d] $P<0.01$ vs. day 0 data.

body weight gain occurred even with a small tumor mass. Clearly, different tumors interfere in different ways with the host's metabolism. Substances secreted by the tumor probably play a major role in effects not directly attributable to the mechanical action of the tumor mass (such as increase in body weight and compression of vital organs). That human tumors can secrete toxic substances is well known (*34*). We also know that human tumors heterotransplanted into nude mice can and do secrete various products (such as hormones and unidentified proteins) (*35*). Some such products have already been identified as being toxic for the host mice (*36, 37*), and some have already been held responsible for weight loss among nude mice after heterotransplantation of certain human tumors (*38*).

Our findings should caution everybody engaged in experimental therapy studies involving human tumors heterotransplanted into nude mice about the need to keep a close watch on the weights of the treated animals throughout the experiment. Even short-term experiments are not exempt from such a caveat, as clearly shown by the kidney capsule experiments. Simple calorie restriction induced up to 62% tumor growth inhibition in the kidney experiments and 93% in the subcutaneous experiments. Fortunately, such inhibitions correlate closely with body weight loss, which can be easily monitored. Such losses must be minimized if reliable results are desired. For the achievement of such a goal, the first necessary precaution is the use of nude mice in good health. Nude mice affected by murine viral hepatitis and other infectious diseases lose weight rapidly (*39, 40*) due to both their reduced food intake and the extensive destruction of the liver, in the case of hepatitis. Such animals have no place in experimental therapy experiments, as we have already stated (*30*). Second, but no less important, is the monitoring of the debilitating effect of the antitumor treatment itself on the mice, as measured by weight loss. Our data indicate that any weight loss above 20% renders unreliable the results obtained. Also, our results clearly show the need for further studies on the role of calorie intake in cancer growth. It has already been demonstrated in animals that hyperalimentation stimulates considerably the growth of transplantable tumors (*41*). Nobody would deny the need to nutritionally support an emaciated cancer patient undergoing strenuous chemotherapy. Also, our own preliminary survival experiment shows that calorie restriction, although capable of limiting tumor growth, does not prolong and, if anything, shortens the life-span of the host. However, in view of our findings and those of others, it would not seem unreasonable to suggest a low calorie intake to cancer-free patients at high risk of tumor recurrence. Further studies are in process, with the use of the nude mouse model, on the incidence of takes of human tumors inoculated at minimum effective inoculum doses in animals fed at various calorie

TABLE 16.—*Colon carcinoma HT 29 growing under the kidney capsule*

Food intake[a]	Days after tumor inoculation[b]	
	0	11
	Average tumor diameter, OMU	
Ad libitum	22.9±6.2 (10)	32.8±7.1 (10)
DT/D0		1.4
8 g	22.8±5.9 (10)	25.6±8.3 (9)
DT/D0		1.1
Inhibition, %		21
6 g	22.9±5.4 (10)	25.1±5.9 (9)
DT/D0		1.1
Inhibition, %		21
4 g	23.2±4.8 (10)	22.9±6.2 (9)
DT/D0		1.0
Inhibition, %		29
2 g	22.8±4.9 (10)	23.4±4.5 (8)
DT/D0		1.0
Inhibition, %		29
	Body weight, g	
Ad libitum	35.0±6.1 (10)	31.1±3.0 (10)
Weight loss [g], %		[3.9], 11
8 g	33.9±3.6 (10)	26.9±3.4 (9)
Weight loss [g], %		[7.0], 21
6 g	33.1±3.4 (10)	23.7±2.8[c] (9)
Weight loss [g], %		[9.4], 28
4 g	33.6±3.4 (10)	20.3±2.7[c] (9)
Weight loss [g], %		[13.3], 40
2 g	33.8±2.9 (10)	19.6±2.1[c] (8)
Weight loss [g], %		[14.2], 42

[a] DT/D0=average diameter after 11 days/average diameter at day 0.

[b] Values are means ± SD. *Numbers in parentheses* are numbers of animals.

[c] $P<0.01$ vs. day 0 data.

levels. Such a model best approximates the case of a human patient whose primary tumor has been surgically removed but who has most probably disseminated micrometastases.

REFERENCES

(*1*) Moreschi C. Beziehungen zwischen Ernagrung und Tumorwachstein. Z Immunitatsforsch 1909; 2:651–685.

(*2*) Rous P. Sarcoma of fowl transmissible by an agent separable from the tumour cells. J Exp Med 1911; 13:397–411.

(*3*) ———. The influence of diet on transplanted and spontaneous mouse tumors. J Exp Med 1914; 20:433–451.

(*4*) Flory CM, Furth J, Saxton JA Jr, Reiner L. Chemotherapeutic studies on mouse leukemia. Cancer Res 1943; 3:729–743.

(*5*) Bischoff F, Long ML, Maxwell LC. Influence of caloric intake upon the growth of sarcoma 180. Am J Cancer 1935; 24:549–553.

(*6*) Bischoff F, Long ML. The influence of calories per se upon the growth of sarcoma 180. Am J Cancer 1938; 32:418–421.

(*7*) Sugiura K, Benedict SR. The influence of insufficient diets upon tumor recurrence and growth in rats and mice. J Cancer Res 1926; 10:309–318.

(*8*) Tannenbaum A. The initiation and growth of tumors. Introduction. I. Effects of underfeeding. Am J Cancer 1941; 38:335–350.

(*9*) ———. Relationship of body weight to cancer incidence. Arch Pathol 1940; 30:509.

(*10*) ———. The genesis and growth of tumors. II. Effects of caloric restriction per se. Cancer Res 1942; 2:460–467.

(*11*) Ross MH, Bras G. Tumour incidence patterns and nutrition in the rat. J Nutr 1965; 87:245–260.

(*12*) ———. Lasting influence of early caloric restriction on prevalence of neoplasms in the rat. J Natl Cancer Inst 1971; 47:1095–1113.

(*13*) Saxton JA, Sperling GA, Barnes LL, McKay CM. The influence of nutrition upon the incidence of spontaneous tumours of the albino rat. Acta Un Int Cancr 1948: 6:423.

(*14*) Tannenbaum A. The dependence of tumor formation on the degree of caloric restriction. Cancer Res 1945; 5:609–615.

(*15*) ———. The dependence of the genesis of induced skin tumours on the caloric intake during different stages of carcinogenesis. Cancer Res 1944; 4:673–677.

(*16*) ———. Effects of varying caloric intake upon tumour incidence and tumour growth. Ann NY Acad Sci 1947; 49:5–18.

(*17*) Tannenbaum A, Silverstone H. The influence of the degree of caloric restriction on the formation of skin tumours and hepatomas in mice. Cancer Res 1949; 9:724–727.

(*18*) Jose DG. Dietary deficiency of protein, amino acids and total calories on development and growth of cancer. Nutr Cancer 1979; 1:58–63.

(*19*) Wynder EL. Nutrition and cancer. Fed Proc 1976; 35:1309–1315.

(*20*) Flanagan SP. "Nude," a new hairless gene with pleiotropic effects in the mouse. Genet Res 1966; 8:295–309.

(*21*) Pantelouris EM. Absence of thymus in a mouse mutant. Nature 1968; 217:370–371.

(*22*) Rygaard J, Povlsen CO. Heterotransplantation of a human malignant tumour to "nude" mice. Acta Pathol Microbiol Scand 1969; 77:758–760.

(*23*) Giovanella BC, Yim SO, Stehlin JS, Williams LJ Jr. *Brief communication:* Development of invasive tumors in the "nude" mouse after injection of cultured human melanoma cells. J Natl Cancer Inst 1972; 48:1531–1533.

(*24*) Giovanella BC, Fogh J. Present and future trends in investigations with the nude mouse as a recipient of human tumor transplants. In: Fogh J, Giovanella BC, eds. The nude mouse in experimental and clinical research. New York: Academic Press, 1978:282–312.

(*25*) Giovanella BC, Stehlin JS. Heterotransplantation of human malignant tumors in "nude" thymusless mice. I. Breeding and maintenance of "nude" mice. J Natl Cancer Inst 1973; 51:615–619.

(*26*) Giovanella BC, Stehlin JS, Shepard RC. Experimental chemotherapy on human breast carcinomas heterotransplanted in nude mice. In: Nomura T, Ohsawa N, Tamaoki N, Fujiwara K, eds. Proceedings of the second international workshop on nude mice. Tokyo: Univ Tokyo Press, 1977:475–481.

(*27*) Giovanella BC, Stehlin JS, Fogh J, Sharkey FE. Serial transplantation of human malignant tumors in nude mice and their use in experimental chemotherapy. In: Houchens DP, Ovejera AO, eds. The use of athymic (nude) mice in cancer research. New York: Fischer, 1978:163–179.

(*28*) Houchens DP, Ovejera AO, Barker AD. The therapy of human tumors in athymic (nude) mice. In: Houchens DP, Ovejera AO, eds. The use of athymic (nude) mice in cancer research. New York: Fischer, 1978:267–280.

(*29*) Bogden AE, Kelton DE, Cobb WR, Esber HJ. A rapid screening method for testing chemotherapeutic agents against human tumor xenografts. In: Houchens DP, Ovejera AO, eds. The use of athymic (nude) mice in cancer research. New York: Fischer, 1978:231–250.

(*30*) Giovanella BC, Stehlin JS, Williams LJ, Lee SS, Shepard RC. Heterotransplantation of human cancers into nude mice—a model for human cancer chemotherapy. Cancer 1978; 42:2269–2281.

(*31*) Fogh J, Trempe G. New human tumor cell lines in human tumor cells in vitro. In: Fogh J, ed. Human tumor cells in vitro. New York: Plenum Press, 1975:115–159.

(*32*) Osieka R, Johnson RK. Evaluation of chemical agents in phase I clinical trials and earlier stages of development against xenografts of human colon carcinoma. In: Houchens DP, Ovejera AO, eds. The use of athymic (nude) mice in cancer research. New York: Fischer, 1978:217–223.

(*33*) Fogh J, Bean MA, Bruggen J, et al. Comparison of human tumor cell line before and after growth in the nude mouse. In: Fogh J, Giovanella BC, eds. The nude mouse in experimental and clinical research. New York: Academic Press, 1978:215–234.

(*34*) Nakahara W, Fukuoka F. Chemistry of cancer toxin toxohormone. Springfield, Ill.: Thomas, 1961.

(*35*) Shimosato Y, Kameya T, Kubota T, et al. Experimental chemoradio and endocrine therapy for human cancers transplanted in nude mice. In: Nomura T, Ohsawa N, Tamaoki N, Fujiwara K, eds. Proceedings of the second international workshop on nude mice. Tokyo: Univ Tokyo Press, 1977:499–508.

(*36*) Tamaoki N, Hata J, Izumi S, Ueyama Y, Toyama K. Systemic effect of human renal cell carcinoma on nude mice, polycythemia, anemia, hypervolemia and hepatomegaly. In: Nomura T, Ohsawa N, Tamaoki N, Fujiwara K, eds. Proceedings of the second international workshop on nude mice. Tokyo: Univ Tokyo Press, 1977: 499–508.

(*37*) Shin S, Kadish AS, Bancroft FC. Host response to heterologous endocrine tumor transplants in nude mice. In: Houchens DP, Ovejera AO, eds. The use of athymic (nude) mice in cancer research. New York: Fischer, 1978:133–143.

(*38*) Kondo Y, Ueyama Y, Ohsawa N. Cachexia in nude mice bearing a human malignant melanoma. In: Nomura T, Ohsawa N, Tamaoki N, Fujiwara K, eds. Proceedings of the second international workshop on nude mice. Tokyo: Univ Tokyo Press, 1977:441–448.

(*39*) Sebesteny A. Hepatitis and brain lesions due to mouse hepatitis virus associated by wasting in nude mice. Lab Anim 1974; 8:317–323.

(*40*) Ueda K, Tamura T, Machii K, Fujiwara K. An outbreak of Sendai virus infection in a nude mouse colony. In: Nomura T, Ohsawa N, Tamaoki N, Fujiwara K, eds. Proceedings of the second international workshop on nude mice. Tokyo: Univ Tokyo Press, 1977:61–69.

(*41*) Cameron IL, Pavlat WA. Stimulation of growth of a transplantable hepatoma in rats by parenteral nutriton. J Natl Cancer Inst 1976; 56:597–602.

Resting State Depth and Saturation Density as Modulated by Tumor Promoters and Culture Conditions: Relationship to Chemical Transformation in C3H/10T½ Cells [1,2]

David Miska [3] *and* **H. Bruce Bosmann** [4,5]

ABSTRACT—With the use of cultures of C3H/10T½ fibroblasts, the relationships of saturation density and cell resting state (G_0) depth to oncogenic transformation by 3-methylcholanthrene (MCA) were investigated. The tumor promoter 12-*O*-tetradecanoylphorbol 13-acetate (TPA), caused a small increase in the saturation density, but saccharin (SAC), a suspected promoter, did not. Correspondingly, TPA tested positively as a promoter of transformation in a typical two-stage transformation assay with these cells while SAC did not. By altering the confluent-phase serum concentration and/or the medium renewal frequency of MCA-treated cultures, it was found that the magnitude of transformation for a given concentration of MCA was independent of the saturation density. Oscillations in this density were observed even when the medium was renewed as frequently as every 3 days, indicating that cell death and replacement occur during what is generally regarded to be a period of cellular stability. Neither TPA nor SAC blocked the cells from progressing into deeper resting states over time, as indicated by the prereplicative lag time after a medium change at 42 days. However, the serum concentration and medium renewal frequency did affect the resting state depth. Daily renewals with medium containing 10% serum blocked the resting state from deepening and kept the cells from achieving a saturation density. Under these circumstances, transformation was completely inhibited in MCA-treated cultures.—JNCI 1982; 68:259–266.

Whereas sustained hyperplasia by itself may be sufficient to promote tumors (*1*, *2*), the mechanism of the distinctly powerful tumor promoting action of certain hyperplastic agents such as the phorbol ester TPA (*3*) has not yet been established. One research area attracting considerable attention is the ability of phorbol esters to block cellular differentiation (*4*). The main contribution of TPA-type compounds to the promotion process might therefore involve keeping initiated cells from differentiating into nondividing cells (*5*, *6*) as opposed to their merely stimulating cell division.

Using the C3H/10T½ mouse embryo cell line for which a two-stage transformation assay has been developed (*7*), Mondal and Heidelberger (*8*, *9*) have shown that the ability of promoting compounds from different chemical classes to block the differentiation of these cells into either fat or muscle cells is inconsistent. However, for TPA-type compounds, there is a good correlation between promoting activity and ability to block both types of differentiation.

Another expression of differentiation in C3H/10T½ cells may be their ability to enter deeper resting states as the time spent in a confluent state increases, as indicated by lengthened prereplicative lag times after a stimulus to divide (*10*). This behavior is similar to that seen in other culture systems (*11–13*) and analogous to what occurs in a variety of aging organs (*14–16*). The elongation of the prereplicative period may be the consequence of the cells entering into deeper levels of the hypothetical resting state G_0 (*11*). Evidence from the literature suggests that this resting state is important to the process of promotion: 1) Croton oil shortens the total cell cycle time eightfold in mouse epidermis, with most of this shortening occuring in the G_1 portion of the cycle (*17*). Even though these authors do not refer to a G_0 compartment, it can be argued that the cells' G_1 residence time includes time spent in a G_0 state. 2) Retinoic acid, which can inhibit TPA's tumor promoting properties (*18*), increases the prereplicative lag time of HeLa cells relative to untreated cells (*19*). 3) TPA can substitute for PDGF, a serum polypeptide that confers upon resting phase 3T3 cells the competency to enter the cell cycle (*20*). Correspondingly, PDGF can block cycling cells from entering G_0 (*21*), an action for which TPA has not been tested. 4) In the initiation/promotion assay with C3H/10T½ cells, the promotion phase must begin before confluency is achieved (*7*, *22*), a time when the cells are beginning to acquire lengthened prereplicative lag times (*10*).

The above points led us to test TPA and SAC (a nonphorbol compound), which have been shown to promote transformation in C3H/10T½ cells (*7*, *23*), for their ability to interfere with cellular progression into G_0. We varied the serum concentration and medium renewal frequency in other experiments as an alternative method of manipulating

---

Abbreviations used: FGRF=fibroblast growth regulatory factor; MCA=3-methylcholanthrene; PDGF=platelet-derived growth factor; SAC=saccharin; TPA=12-*O*-tetradecanoylphorbol 13-acetate.

---

[1] Received October 20, 1980; revised September 14, 1981; accepted September 16, 1981.

[2] Supported in part by Public Health Service (PHS) grant 5-T32ES-07026 from the National Institute of Environmental Health Sciences (D. M.) and by PHS grant 5-R01CA-19767 from the National Cancer Institute. (H. B. B.).

[3] Department of Pharmacology and Toxicology, University of Rochester School of Medicine and Dentistry, Rochester, N.Y. 14642.

[4] Department of Pharmacology and Toxicology and University of Rochester Cancer Center, University of Rochester School of Medicine and Dentistry.

[5] Geriatric Academic Medicine Awardee of the National Institute on Aging.

the resting state depth. We also measured the effects of these compounds and the medium renewal protocols on the saturation density. Conflicting data exist on TPA's effect on the saturation density of C3H/10T½ cells (*22, 24*); the effect of saccharin has not been studied. The measurements of resting state depth and cell density were compared to the transformation incidence in experiments where cells were given similar treatments after exposure to the carcinogen MCA.

MATERIALS AND METHODS

Cells.—C3H/10T½ CL8 mouse embryo fibroblasts were provided by Dr. Charles Heidelberger and Dr. Sukdeb Mondal. Our original stock was expanded and frozen according to Reznikoff et al (*25*), with the use of DMSO as the cryopreservative. Frozen cell stocks from passage 6 were thawed when needed and seeded into 150-cm^2 Costar or 75-cm^2 Falcon tissue culture flasks containing Eagle's basal medium with Earle's salts (GIBCO, Grand Island, N.Y.) supplemented with 10% heat-inactivated fetal calf serum (GIBCO). When the cultures were in their late growth phase they were rinsed with Ca^{2+}- and Mg^{2+}-free Hank's balanced salt solution. We then added 0.1% trypsin solution prepared from 2.5% stock trypsin (GIBCO) and the same salt solution, whose activity was quenched with serum approximately 6 minutes later. Samples were enumerated with a Coulter Counter (Coulter Electronics Inc., Hialeah, Fla.) and the cells were then suspended in medium with 10% serum to give the desired cell concentration. All of the experiments were performed in Costar 24-well (16-mm diameter) cluster dishes. The suspensions were stirred with an umbrella stirrer (Fisher Scientific Co., Rochester, N.Y.) at 1 rpm, and aliquots were dispensed into the wells using a repeatable pipetter (Manostat Corp., New York, N.Y.) fed from a sideport on the reservoir bottle. These procedures allowed an equal number of cells to be seeded into a large number of wells within a short time, ensuring uniform viability between the first and the last wells plated. The cultures were maintained at 37°C in a humidified incubator with 5% CO_2 atmosphere. Stock cultures were not exposed to antibiotics. In one experiment, as noted, cells were treated with gentamicin (Schering-Plough Corp., Kenilworth, N.J.) at 20 μg/ml after confluency, a concentration shown not to affect transformation in these cells (*26*). Serum from a single lot was used in all of the experiments and was added to the medium shortly before use. No serum was frozen and thawed more than twice. All solutions added to the cultures were prewarmed to 37°C. The cells tested negatively for mycoplasma contamination by means of Hoechst 33258 stain (American Hoechst Corp., North Sommerville, N.Y.) (*27*).

Cell counting.—The normal cell harvesting procedure with 0.1% trypsin in buffer solution (*25*) does not produce a complete yield when the cells have been confluent for extended periods. We found that a combined treatment with Na-EDTA and trypsin gave substantially improved harvests: the medium is poured off and the wells are preexposed to a 0.02% solution of Na-EDTA in Puck's salt solution (8.0 g NaCl, 0.4 g KCl, 1.0 g glucose, 0.35 g $NaHCO_3$, 1,000 ml H_2O) for approximately 1 minute (less for cells that are preconfluent or freshly confluent). This is replaced by Puck's saline containing both 0.02% Na-EDTA and 0.1% trypsin. Treatment continued until the majority of the cells were dislodged, at which time medium containing serum was added to quench the process, and the entire solution was then pipetted up and down against the bottom of the well several times to obtain a monodispersion. The entire suspension was diluted for counting in balanced electrolyte solution (Coulter Electronics, Inc.). A model ZB Coulter Counter with an attached Channelyzer was used to count the cells and to determine the median cell volume.

Transformation assays.—Cells were plated 100 per well in 0.5 ml medium containing 10% serum. After 24 hours this was replaced by 0.5 ml of fresh 10%-serum-containing medium that included the carcinogen MCA (Sigma Chemical Co., St. Louis, Mo.). The MCA was dissolved in acetone earlier to give a final concentration of 0.5% acetone in the medium. The treated wells and their acetone controls were rinsed with fresh medium 24 hours later and refilled with 0.5 ml of fresh medium. The medium was replaced again 4 days later, this time with 1 ml fresh medium per well. When the cultures became confluent, a medium change was made, and at this time the serum concentration of the medium in some wells was changed from 10 to 3%. Medium changes were then made at half-, 1-, or 4-day intervals for the remainder of the experiment.

In the initiation-promotion experiment, TPA (Consolidated Midland Corp., Brewster, N.Y.) or purified type C SAC (provided by Dr. D. R. Stoltz, Department of Health and Welfare, Canada) were incorporated into the medium changes. TPA or SAC addition started 4 days after treatment with subtransforming concentration of MCA. TPA was dissolved in acetone and added to the medium to yield 0.5% acetone concentration, whereas SAC was added in a freshly prepared, filter-sterilized, aqueous solution. The medium contained 10% serum throughout the experiment and was changed at 4-day intervals.

The concentrations of MCA, TPA and SAC were nontoxic as determined by plating efficiency studies. The wells were scored for type III foci (*28*) 6 weeks after plating, after fixing the cells with methanol and staining with Giemsa. In one experiment, the wells were checked for foci every 2 to 3 days after confluency using a phase-contrast inverted microscope.

Autoradiography.—To determine if TPA, SAC, or altered serum concentration or medium renewal frequencies could interfere with the deepening of the resting state over time, wells treated identically to those in transformation experiments but not exposed to MCA were stimulated to divide at 42 days by a medium change incorporating 15% of serum. At 3-hour intervals, stimulated and unstimulated wells were pulse-labeled for 30 minutes with medium containing 5 μCi [^{3}H]thymidine/ml, (1 mCi/ml, 43-45 μCi/mmol; Amersham Corp., Arlington Heights, Ill.), followed by a 10-minute chase with medium containing 20 μg/ml unlabeled thymidine. The cells were then rinsed with a 0.9% NaCl solution and subsequently fixed in methanol-0.9% NaCl (1:1) solution followed by 100% methanol. After drying, the well bottoms were punched out and mounted on glass microscope slides with Permount (Fisher Scientific Co., Rochester, N.Y.), allowed to set, and coated with Kodak nuclear emulsion NTB 3 diluted 50% with water. The preparations were air-dried and exposed for 2 days in the dark, at which time they were developed and counterstained with Giemsa. At least 500 nuclei were scored per well.

RESULTS

Daily cell counts of wells that were treated with SAC or TPA, at concentrations shown to promote transformation in these cells (*7, 23*), are displayed in text-figure 1 relative to cell counts of untreated wells. The medium was renewed every 3 days. TPA treatment caused an initial lag in cell growth, as seen previously in this (*24*) and other systems (*29*), but the cells eventually grew to a higher saturation density than either the untreated or SAC-treated cells. This latter group may have had a slightly depressed cell density late after reaching confluency. TPA also produced a decrease in cell volume, as has been documented with many cell types (*29, 30*), but this effect diminished with time. We observed the ability of confluent-phase medium renewals to produce oscillations in the saturation density and cell volume not previously described in the literature. In general, volume increases followed the medium changes by 1 day, followed a day later by a coincident decline in the volume and an increase in the cell number. This is especially noticeable in the case of TPA-treated wells, whereas the effect on untreated and SAC treated wells appears to taper off after a few medium changes. The experimental results in text-figure 4 show a similar pattern for the groups receiving medium renewals every 4 days.

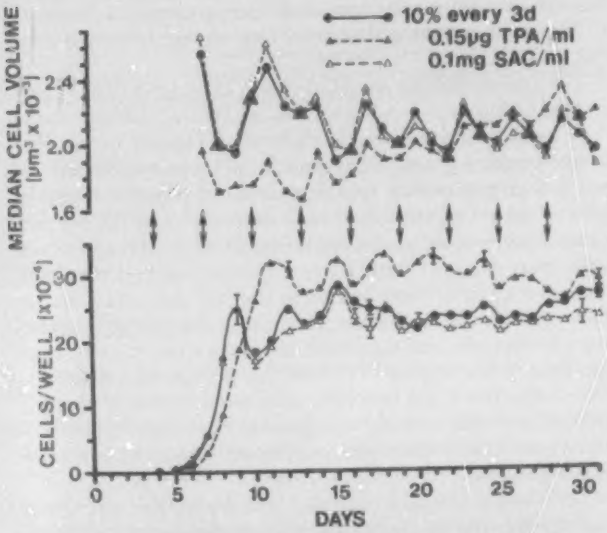

Text-figure 1.—Cells were seeded at 400/well in 1 ml of medium containing 10% serum. Indicated treatments were included in the medium starting with the first medium change (day 4) and continued for the duration of the experiment. Medium changes, *indicated by the arrows*, were at 1 ml/well and included 10% serum. Control wells contained 0.5% acetone starting with the first medium change. *Each point* on the cell growth curve represents the average of 3 wells. The SE for these points is shown where >10,000. Median cell volume was determined from the cumulative cell size distribution of the 3 wells.

Cell counts of wells not exposed to MCA (text-fig. 2), but otherwise treated identically to wells from accompanying transformation experiments, shows a similar increase in the saturation density for TPA-treated cells compared to untreated cells. In this experiment, the effects of confluent-phase serum concentration and medium renewal frequency were also measured. The saturation density is usually considered to be determined by the concentration of serum in the medium (*31, 32*). However, this text-figure shows that the frequency of the medium renewals can also have a substantial effect upon the saturation density. Cells given twice daily changes of medium containing 3% serum starting at confluency reached a 4.5-times greater saturation density than that achieved by the group given 3% serum-containing medium every 4 days. The 3% serum per half-day group also outgrew twofold the wells receiving 10% serum with medium changes every 4 days.

Results from transformation experiments corresponding to the groups in text-figure 2 are shown in tables 1 and 2. The first table shows that there were no statistically significant differences in transformation between groups on different medium renewal protocols in spite of their widely different saturation densities, although the highest density group (3% serum per half-day) showed a tendency toward enhanced transformation. The effect of administering TPA or SAC to initiated cultures is shown in table 2. The magnitude of TPA's ability to enhance transformation contrasts with its modest ability to stimulate cell growth. The inability of SAC to increase the saturation density was parallelled by its ineffectiveness as a promoter in our experiments. This was a surprising finding, since we used the same concentration that had previously been shown to produce a substantial increase in transformation (*23*). We obtained our SAC supply from the same source as those researchers.

At 42 days, corresponding to the termination of the

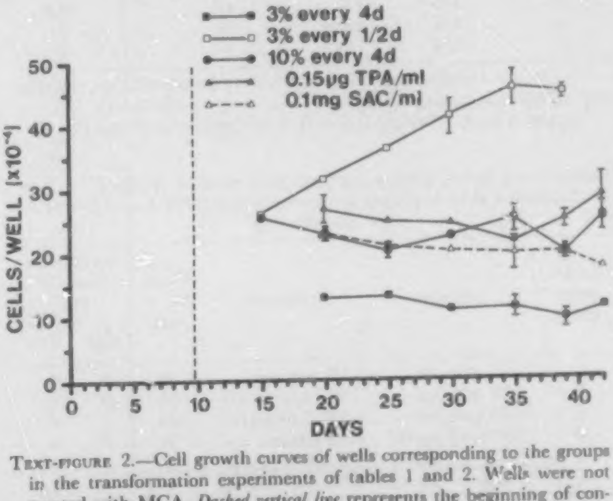

Text-figure 2.—Cell growth curves of wells corresponding to the groups in the transformation experiments of tables 1 and 2. Wells were not treated with MCA. *Dashed vertical line* represents the beginning of confluency. MCA-treated wells became confluent at about the same time. *Each point* is the average of 2 wells and the SE is given where >10,000. Wells were continuously treated with 20 µg/ml gentamicin starting with the medium changes at day 14.

transformation assays, representative wells from all of the groups were evaluated for their resting state depth (text-fig. 3). Countering our hypothesis, neither TPA nor SAC had an effect upon the movement of cells into deeper resting states with time. However, it appeared that the confluent-phase serum concentration and medium renewal frequency could influence this progression.

A second group of experiments investigated further the relationships between resting state depth, cell growth and transformation by manipulating these two culture conditions. As with the first set of experiments, a 10% serum per 4-days group and a 3% serum per 4-days group were included. The previous 3% per half-day group was replaced by a 3% per day group, and a 10% per day group was added. Cell counts of wells maintained under these culture conditions are shown in text-figure 4. By changing the medium every day starting at confluency, wells receiving 10% serum failed to stop growing over the course of the experiment, ultimately achieving a density of 7.2×10^5 cells/well at day 42, or 3.2-times the saturation density for cells receiving the same serum concentration but with medium changes every 4 days. This latter group, as well as both 3% serum groups, had cell densities at 42 days that were similar to their respective saturation densities achieved during the daily counting period. The 3% per day group reached a saturation density almost the same as that for the 10% per 4-days group. The 3% and 10% per 4-days groups showed the same oscillatory pattern for cell number and volume relative to medium changes as did the groups in text-figure 1. The wells receiving daily medium changes did not show this periodicity.

TABLE 1.—*Effect of altering the confluent-phase serum concentration and medium renewal frequency on the appearance of type III foci in wells treated with MCA and scored 6 wk after plating*[a]

Treatment group	Serum concentration/renewal frequency, %/day	MCA, µg/ml	Total No. of wells	Wells with type III foci	
				No.	%[b]
a	3/4	none	37	0	0
b	3/4	1.0	47	4	8.5
c	3/½	none	34	0	0
d	3/½	1.0	47	7	14.9
e	10/1	none	36	0	0
f	10/4	1.0	48	3	6.2

[a] Wells were continuously treated with 20 µg gentamicin/ml, starting with the medium change at day 14.

[b] G-test: b vs. d, 0.5>*P*>0.1; b vs. f, 0.9>*P*>0.5; d vs. f, 0.5>*P*>0.1.

TABLE 2.—*Effect of TPA or SAC on the formation of type III foci in wells given a subtransforming concentration of MCA and scored 6 wk after plating*[a]

Treatment group	Initiator	Promoter	Total No. of wells	Wells with type III foci	
				No.	%[b]
a	0.5% acetone	0.5% acetone	36	0	0
b	0.5% acetone	TPA, 0.15 µg/ml	36	0	0
c	0.5% acetone	SAC, 0.10 mg/ml	36	0	0
d	MCA, 0.1 µg/ml	0.5% acetone	48	0	0
e	MCA, 0.1 µg/ml	TPA, 0.15 µg/ml	48	5	10.4
f	MCA, 0.1 µg/ml	SAC, 0.10 mg/ml	48	1	2.1

[a] Wells were treated continuously with gentamicin, 20 µg/ml, starting with the medium change at day 14.

[b] G-test; d vs. e, 0.01>*P*>0.005; d vs. f, 0.5>*P*>0.1; b vs e, 0.025>*P*>0.01.

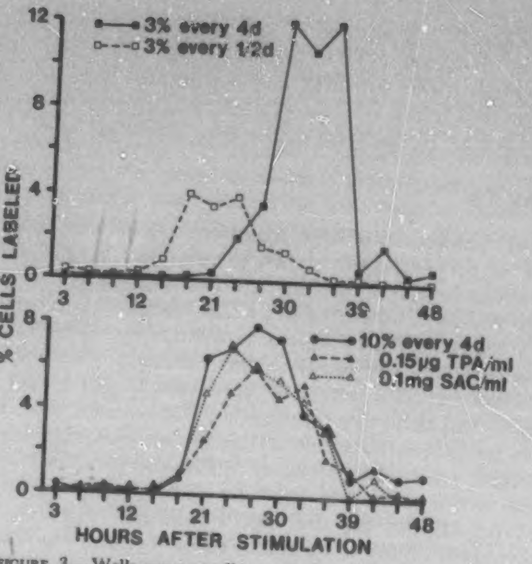

TEXT-FIGURE 3.—Wells corresponding to the groups in the transformation experiments of tables 1 and 2 were tested at day 42 for their resting state depth as reflected by the prereplicative lag time after a medium change incorporating 15% serum. *Each point* represents a 30-min uptake of [^{3}H]thymidine. Wells were not treated with MCA. The curves are presented on separate graphs for clarity. Unstimulated wells had the following average nuclear labeling indices: 3%/4 days, 0.0%; 3%/half-day, 1.2%; 10%/4 days, 0.2%; TPA, 0.1%, SAC, 0.1%.

The corresponding transformation experiments were performed using two concentrations of MCA. Table 3 shows that focus formation was completely inhibited in the 10% serum per day group, whereas the 10% per 4-days and 3% per 4-days groups had similar degrees of transformation in spite of their different saturation densities. The 3% per day group had a significantly higher percentage of transformed wells than either of these latter 2 groups, yet had about the same overall saturation density as the 10% per 4-days group. These results confirmed the previous findings that transformation does not correlate with the saturation density. Also apparent from a comparison of the groups which showed transformation is the lack of a correlation between transformation and the cumulative growth that each group has undergone before settling at its respective saturation density (text-fig. 4).

Text-figure 5 shows that the 10% serum per day group had the shortest lag time prior to replication for any group in this text-figure or in text-figure 3. This lag is virtually identical to what we have seen previously for cultures which have just become confluent (approximately 16 hr median lag time) (*10*). This indicates that the culture conditions were such that cells had not progressed into deeper resting states even after 4½ weeks in a confluent state. The 3% serum per half-day group of text-figure 3 had the shortest

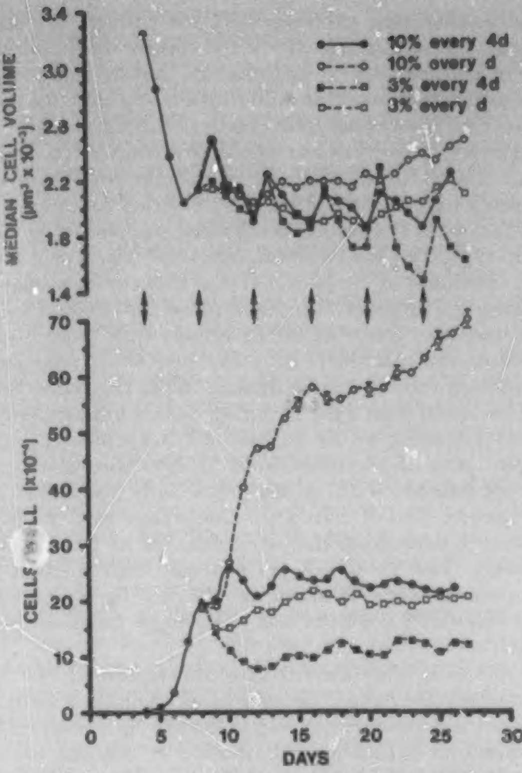

TEXT-FIGURE 4.—Cells were seeded at 400/well in 1 ml of medium containing 10% serum. Starting at confluency (day 8), the medium changes were made with the indicated serum concentration and frequency. Medium change preceding confluency (day 4) included 10% serum and was performed on each group. All medium changes were made at 1 ml/well and are indicated for groups receiving changes every 4 days (*arrows*). *Each point* on the cell growth curve represents the average of 3 wells. The SE is shown where >10,000. Median cell volume was determined from the cumulative cell size distribution of the 3 wells.

prereplicative lag time of any of the groups that showed transformation in either experiment. However, this lag was still 3–6 hours longer than that indicated above for freshly confluent cells or for the 10% serum per day group in text-figure 5.

DISCUSSION

Even though neither TPA nor SAC prevented the cultures from acquiring longer prereplicative lag times, it is still possible that promoters selectively block initiated cells from going into deeper resting states. This is an effect that studies such as these, which measure population response, would be unable to discern. Sivak's study (*33*) on the ability of phorbol ester-containing croton resin to cause selective outgrowth of virally transformed 3T3 cells when mixed with normal cells lends support to this possibility. Additionally, Schulte-Hermann et al. (*34*) have recently shown that cells in areas of liver that were rendered preneoplastic by carcinogen treatments are preferentially stimulated to proliferate by liver tumor promotors.

The various combinations of confluent-phase serum concentrations and renewal frequencies produced a range of saturation densities and cumulative cell division that did not relate in any consistent manner to the transformation incidence. By analogy, the small enhancement of the saturation density and cumulative cell division by TPA is not likely to explain its ability to stimulate transformation in these cells. In spite of this, the ability of a compound to stimulate cell growth in vitro, even if such action is only epiphenomenally linked to the promotion process, may be a prerequisite for promoting potency in vitro: SAC, which did not stimulate cell growth, did not promote transforma-

TABLE 3.—*Effect of altering the confluent-phase serum concentration and medium renewal frequency on the appearance of type III foci in wells treated with MCA and scored 6 wk after plating*

Treatment group	Serum concentration/ renewal frequency, %/ day	MCA, µg/ml	Total No. of wells	Wells with type III foci	
				No.	%[a]
a	3/4	None	24	0	0
b	3/4	1.0	24	3	12.5
c	3/4	5.0	23	9	39.1
d	3/1	None	24	0	0
e	3/1	1.0	24	9	37.5
f	3/1	5.0	24	18	75.0
g	10/4	None	24	0	0
h	10/4	1.0	24	4	16.7
i	10/4	5.0	24	11	45.8
j	10/1	None	24	0	0
k	10/1	1.0	24	0	0
l	10/1	5.0	24	0	0

[a] G-test; b+c vs. e+f, $P<0.005$; b+c vs. h+i, $0.9>P>0.5$; e+f vs. h+i, $0.025>P>0.01$.

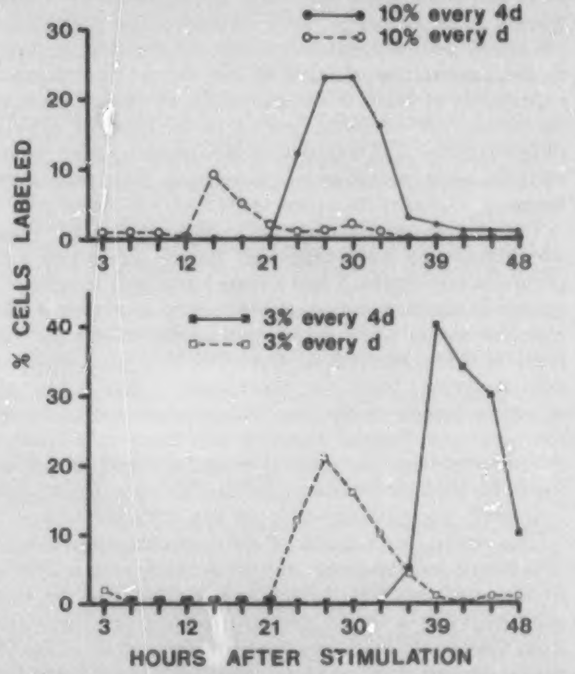

TEXT-FIGURE 5.—Same as text-fig. 3 except that the groups correspond to those in table 3.

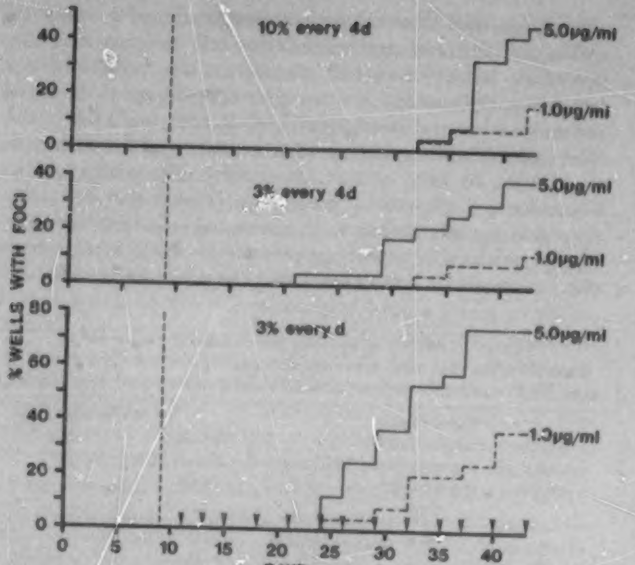

TEXT-FIGURE 6.—Appearance of type III foci in the transformation experiment of table 3. *Arrows* indicate when the wells were scored. *Dashed vertical line* indicates when confluency was achieved.

tion. While our work was in progress, Kennedy et al (*22*) reported similar results that the ability of TPA to increase radiation-induced transformation in these cells is not explained solely by the fact that it stimulates cellular proliferation.

An unexpected finding was the apparent requirement for a cellular progression into deep resting states for transformation to be expressed. Such a requirement may relate to the latent period in carcinogenesis. As shown in text-figure 6, the appearance of type III foci in the transformation experiment of table 3 was scored for every 2-3 days after confluency. A confluent period of at least 12 days was required before foci began to appear, during which time the cultures were presumably progressing into deep resting states.

We cannot readily offer an explanation of the reasons why the resting state depths of the 3% serum per 4 days groups in text-figures 3 and 5 varied so widely in spite of the groups being maintained as identically as practical. However, we do not think that it necessarily reflects the variability of this parameter for the other treatment groups nor does it detract from our conclusions. There was a good correspondence between the 10% serum per 4 days curves in the same text-figures. Furthermore, there is a consistent relationship between renewal frequency and resting state depth for each serum concentration (10% per day <10% per 4 days; 3% per half-day <3% per day <3% per 4 days).

The resting state depth of the transformation-inhibited 10% serum per day group, as well as being similar to that of freshly confluent cells (*10*), was also similar to the resting state depth of a chemically transformed cell line derived from C3H/10T½ cells reported by Moses et al. (*35*). Their results suggest that, unlike normal cells, transformed cells are unable to submerge into deeper resting states with time.

It is possible that carcinogen-treated cultures are able to express transformation only if the culture conditions allow the unaffected cells to progress into resting states beyond this apparent limit. This would then give a selective growth advantage to any transformed cells in the culture since these cells would be the first to respond to a stimulus to divide. A series of such stimuli might occur with the periodic medium renewals that maintain the cultures during confluency. The oscillations in the saturation density, seen for those groups with confluent-phase medium renewals every 3 or 4 days, is one indication of the potential that these renewals have for causing cell turnover. Confluent-phase cell division and cell loss were also probable in the groups with more frequent medium changes (half- or 1-day intervals), even though text-figure 4 shows that oscillations in the saturation density did not occur with daily renewals. This is indicated in text-figure 3 (legend) by the amount of DNA synthesis that was occurring in unstimulated wells 42 days after plating. The 3% per half-day wells, which presumably also lacked these oscillations, had at least a 6-times greater rate of [^{3}H]thymidine-incorporation than either the 3% or 10% per 4 day cultures. The 3% serum per half-day cells reached their saturation density by about day 39 (text-fig. 2), indicating that this DNA synthesis was likely to be balanced by cell loss.

Since daily renewals with medium containing 10% serum apparently prevented the cells from reaching a saturation density, it is possible that type III focus formation requires a minimum period in such a state in contrast to, or in concert with, a minimum resting state depth. Again, periodic medium changes while the cells are at their saturation density may provide a stimulus for the selective outgrowth of carcinogen-altered cells. In a careful study of cell density kinetics, Van Der Bosch (*36*) demonstrated that graduated cell death is a normal means by which cultures adjust to reduced serum levels. The cell turnover we have described is possibly then a consequence of a differential in the potency of fresh medium versus medium that has become partially depleted of serum components after a time in culture, in terms of its ability to sustain all of the cells in a viable state. It is known that transformed cells have a lower serum requirement for growth than their normal counterparts (*35*), thus normal cells may be preferentially lost during these die-off periods. Another possibility is that the confluent cells release a growth-inhibiting factor such as FGRF (*37*) that counteracts the ability of serum to maintain cells at a particular density. FGRF does not restrict virally transformed cells, making this another means by which nontransformed cells could be discriminated against. Both of these proposed mechanisms can also be used to explain the effect that frequent medium renewals have upon the overall cell density. Increased renewal frequencies could prevent either nutrient deprivation or accumulation of growth inhibitory factors, or both. Furthermore, FGRF has been shown to delay the onset of DNA synthesis in resting cultures, with higher concentrations causing greater delays (*37*). This may explain our observation that frequent medium renewals slow the progression of cultures into deeper G_0 states, possibly by keeping such factors from accumulating. It may also be that resting state deepening occurs only after the cells have reached their saturation density—something that is delayed by frequent medium renewals.

The inhibition of transformation seen in the 10% serum per day group is unlikely to be a consequence of the high cell density it achieved: There was no indication from the other groups of either experiment of an inverse correlation between the saturation density and transformation incidence. This would initially appear to be in conflict with the results by Bertram (*32*), where lowered serum levels reduced the saturation density and enhanced transformation in C3H/10T½ cells, while high serum levels increased the saturation density and inhibited transformation. However, there are circumstances that may account for this discrepancy: 1) We do not know how the growth-promoting properties of our serum compare with the serum used by Betram, who also showed that different serum lots produce widely different saturation densities, especially at low concentrations; 2) The medium renewal interval in his experiments was 7 days in comparison with our maximum of 4 days. We have noticed that the cell die-off becomes greater as this interval increases. The relationship between saturation density and transformation incidence may increasingly become obscured as the renewal interval is lengthened.

Type II foci were discernible in a small number of the 10% per day wells. Their occurence was inhibited nonetheless compared to the other MCA-treated groups from the same experiment. However, their detection makes it unlikely that the high cell density achieved in the 10% per day group obscured the identification of foci. It also suggests that this lower grade of transformation is not as sensitive to the conditions that blocked the appearance of type III foci.

From replating experiments with C3H/10T½ cells, Haber et al. (*38*) conclude that transformation is independent of the absolute time or number of cell divisions occurring between carcinogen treatment and expression. Our experiments indicate that cell division occurs in confluent cultures that receive periodic medium renewals even after they have reached their saturation density. Cultures reaching this growth plateau are usually considered to be dormant but are actually more likely to be in a state in which cell division and loss are balanced. Cell turnover during this period may be required for the expression of transformation, thus providing a selective growth stimulus for initiated or transformed cells that does not exist when the cells are in a preconfluent growth phase.

REFERENCES

(*1*) Frei JV. Comment on epidermal hyperplasia and tumor promotion. J Natl Cancer Inst 1977; 59:299.

(*2*) Argyris TS. The regulation of epidermal hyperplastic growth. Crit Rev Toxicol 1981; 9:151–200.

(*3*) Boutwell RK. The function and mechanism of promoters of carcinogenesis. Crit Rev Toxicol 1974; 2: 419–443.

(*4*) Diamond L, O'Brien TG, Baird WM. Tumor promoters and the mechanism of tumor promotion. Adv Cancer Res 1980; 32:1–74.

(*5*) Rovera G. O'Brien TG, Diamond L. Tumor promoters inhibit spontaneous differentiation of Friend erythroleukemia cells in culture. Proc Natl Acad Sci USA 1977; 74:2894–2898.

(*6*) Weinstein IB, Yamasaki H, Wigler M, et al. Molecular and cellular events associated with the action in initiating carcinogens and tumor promoters. In. Griffin AC, Shaw CR, eds. Carcinogens: Identification and mechanisms of action. New York: Raven, 1979: 399–418.

(*7*) Mondal S, Brankow DW, Heidelberger C. Two-stage chemical oncogenesis in cultures of C3H/10T½ cells. Cancer Res 1976; 36: 2254–2260.

(*8*) Mondal S, Heidelberger C. Cell differentiation and tumor promotion. Proc Am Assoc Cancer Res 1980; 21:96.

(*9*) ———. Inhibition of induced differentiation of C3H/10T½ clone 8 mouse embryo cells by tumor promoters. Cancer Res 1980; 40: 334–338.

(*10*) Miska D, Bosmann HB. Existence of an upper-limit to elongation of the prereplicative period in confluent cultures of C3H/10T½ cells. Biochem Biophys Res Commun 1980; 93:1140–1145.

(*11*) Augenlicht LH, Baserga R. Changes in the G_0 state of WI-38 fibroblasts at different times after confluence. Exp Cell Res 1974; 89: 255–262.

(*12*) Crane MS, Thomas DB. Cell-cycle, cell-shape mutant with features of the G_0 state. Nature 1976; 261:205–208.

(*13*) Terskikh VV, Zosimovaskaya AI, Gasparian GH, Zakarian GG. Deepening of cells into the resting state (abstract). Cell Tissue Kinet 1980; 13:215–216.

(*14*) Bucher NL. Regeneration of mammalian liver. Int Rev Cytol 1963; 15:245–309.

(*15*) Adleman RC, Stein G, Roth GS, Englander D. Age-dependent regulation of mammalian DNA synthesis and cell proliferation in vivo. Mech Aging Dev 1972; 1:49–59.

(*16*) Russo J, Russo I. Influence of differentiation and cell kinetics on the susceptibility of the rat mammary gland to carcinogenesis. Cancer Res 1980; 40:2677–2687.

(*17*) Frankfurt OS, Raitcheva E. Effect of tumor promoters on cell kinetics in mouse epidermis. J Natl Cancer Inst 1972; 49:131–137.

(*18*) Mueller GC, Kensler TW, Kajiwara K. Mechanisms of DNA and chromatin replication: Possible targets of cocarcinogenesis. In: Slaga TJ, Sivak A, Boutwell RK, eds. Carcinogenesis. Vol II. Mechanisms of tumor promotion and cocarcinogenesis. New York: Raven, 1978:79–90.

(*19*) Dion LD, Gifford GE. Retinoic acid induces a G_1 cell cycle block in HeLa cells. Proc Soc Exp Biol Med 1980; 163:510–514.

(*20*) Frantz CN, Stiles CD, Scher CD. The tumor promoter 12-*O*-tetradecanoyl-phorbol-13-acetate enhances the proliferative response of Balb/c-3T3 cells to hormonal growth factors. J Cell Physiol 1979; 100:413–424.

(*21*) Scher CD, Stone ME, Stiles CD. Platelet-derived growth factor prevents G_0 growth arrest. Nature 1979; 281:390–392.

(*22*) Kennedy AR, Murphy G, Little JB. Effect of time and duration of exposure to 12-*O*-tetradecanoylphorbol-13-acetate on X-ray transformation of C3H/10T½ cells. Cancer Res 1980; 40:1915–1920.

(*23*) Mondal S, Brankow DW, Heidelberger C. Enhancement of oncogenesis in C3H/10T½ mouse embryo cell cultures by saccharin. Science 1978; 201:1141–1142.

(*24*) Peterson R, Mondal S, Brankow DW, Thon W, Heidelberger C. Effects of promoters on DNA synthesis in C3H/10T½ mouse fibroblasts. Cancer Res 1977; 37:3223–3227.

(*25*) Reznikoff CA, Brankow DW, Heidelberger C. Establishment and characterization of a cloned line of C3H mouse embryo cells sensitive to postconfluence inhibition of division. Cancer Res 1973; 33:3231–3238.

(*26*) Bertram JS. Reduction in the formation of carcinogen-induced transformed foci by penicillin G sodium in the C3H/10T½ C1.8 cell line. Cancer Lett 1979; 7:289–298.

(*27*) Chen TR. In situ detection of mycoplasma contamination in cell cultures by fluorescent Hoechst 33258 stain. Exp Cell Res 1977; 104:255–262.

(*28*) Reznikoff CA, Bertram JS, Brankow DW, Heidelberger C. Quantitative and qualitative studies of chemical transformation of cloned C3H mouse embryo cells sensitive to postconfluence inhibition of cell division. Cancer Res 1973; 33:3239–3249.

(*29*) Diamond L, O'Brien S, Donaldson C, Shimizu Y. Growth stimulation of human diploid fibroblasts by the tumor promoter 12-*O*-tetradecanoylphorbol-13-acetate. Int J Cancer 1974; 13:721–730.

(*30*) Driedger PE, Blumberg PM. The effect of phorbol diesters on chicken embryo fibroblasts. Cancer Res 1977; 37:3257–3265.

(31) HOLLEY RW, KIERNAN JA. Studies of serum factors required by 3T3 and SV3T3 cells. In: Wolstenholme GE, Knight J, eds. Growth control in cell cultures. Edinburgh: Churchille-Livingstone, 1971: 3–10.

(32) BERTRAM JS. Effects of serum concentration on the expression of carcinogen-induced transformation in the C3H/10T½ CL8 cell line. Cancer Res 1977; 37:514–523.

(33) SIVAK A, VAN DUUREN BL. Phenotypic expression of transformation; induction in cell culture by a phorbol ester. Science 1967; 157: 1443–1444.

(34) SCHULTE-HERMANN R, OHDE G, SCHUPPLER J, TIMMERMANN-TROSIENER I. Enhanced proliferation of putative preneoplastic cells in rat liver following treatment with the tumor promotors phenobarbital, hexachlorocyclohexane, steroid compounds, and nafenopin. Cancer Res 1981; 41:2556–2562.

(35) MOSES HL, PROPER JA, VOLKENANT ME, WELLS DJ, GETZ MJ. Mechanism of growth arrest of chemically transformed cells in culture. Cancer Res 1978; 38:2807–2812.

(36) VAN DER BOSCH J. Complex population kinetics in 3T3 and SV40-3T3 cell cultures. Exp Cell Res 1978; 117:111–119.

(37) DATTA P, NATRAJ CV. Fibroblast growth regulatory factor inhibits DNA synthesis in BALB/c 3T3 cells by arresting in G_1. Exp Cell Res 1980; 125:431–439.

(38) HABER DA, FOX DA, DYNAN WS, THILLY WG. Cell density dependence of focus formation in the C3H/10T½ transformation assay. Cancer Res 1977; 37:1644–1648.

Vasopressin: Action on WRK-1 Rat Mammary Tumor Cells[1]

M. E. Monaco,[2,3] **P. H. Kohn,**[4] **W. R. Kidwell,**[5] **J. S. Strobl,**[6] *and* **M. E. Lippman**[7]

ABSTRACT—WRK-1, a cell line in long-term culture derived from a 7,12-dimethylbenz[a]anthracene-induced rat mammary tumor, responds to physiologic concentrations of vasopressin with increased precursor incorporation into phospholipids and with increased protein accumulation. Because vasopressin has been reported to be a potent mitogen for Hela cells and 3T3 cells, a study was conducted to determine whether it could act as a mitogen for WRK-1 cells. Under no conditions was a clear-cut mitogen response to vasopressin demonstrated.—JNCI 1982; 68:267–270.

In recent years vasopressin has been reported to have activities other than antidiuresis and pressor that may have physiologic relevance. Its ability to stimulate smooth muscle contraction in the breast and uterus under certain conditions has been well documented (*1, 2*). A role for vasopressin as a neurotransmitter has been suggested by the findings of Walter and his colleagues (*3*); Hems and Whitton (*4*) and Kirk et al. (*5*) have reported effects of vasopressin on liver metabolism. Lastly, vasopressin can act as a potent mitogen for Hela cells (*6*) and 3T3 cells (*7*). The mitogenic activity has led to speculation concerning a role for vasopressin in cancer growth (*8*).

We have recently reported the establishment and characterization of WRK-1, a cell line derived from a DMBA-induced rat mammary tumor (*9–11*). Morphology and response to neurohypophyseal hormones suggest these cells may be of myoepithelial origin. Physiologic concentrations of vasopressin (10^{-10} *M*) and pharmacologic concentrations of oxytocin (10^{-8} *M*) stimulate a variety of metabolic alterations in WRK-1 cells: 1) increased incorporation of [^{14}C]-acetate into fatty acids (*11*), 2) increased rate of turnover of phosphatidylinositol (Monaco ME, Lippman ME: Manuscript in preparation), and 3) increased protein accumulation (*11*). The fact that the protein concentration is increased as well as the observation that the radiolabeled fatty acids are present predominantly as phospholipids suggested that vasopressin acts as a mitogen for these cells.

MATERIALS AND METHODS

Carrier-free [^{32}P]orthophosphate was obtained from ICN Pharmaceuticals Inc. [^{33}P]orthophosphate was from New England Nuclear Corp. [^{3}H]thymidine (45 Ci/mmol) and [^{14}C]acetate (59 mCi/mmol) were supplied by Amersham/Searle Corp. Normal rat serum and fetal calf serum were from Grand Island Biological Co. Tissue culture media, trypsin solutions, and Dulbecco's PBS were prepared by the National Institutes of Health Media Unit. BrdUrd and colchicine were purchased from Sigma Chemical Co. Vasopressin was obtained from Calbiochem-Behring Corp. Aquasol came from New England Nuclear Corp.

Cell culture.—WRK-1 cells were derived from a DMBA-induced rat mammary tumor as previously described (*9*). The morphology, growth characteristics, and response of these cells to neurohypophyseal hormones have also been described (*10*). Cells were routinely grown in MEM supplemented with glutamine (1.168 mg/ml), penicillin (100 U/ml), streptomycin (100 µg/ml), fetal calf serum (10%), and rat serum (2%). This growth medium will be referred to as complete medium. For experiments, cells were harvested with trypsin (0.05%) and EDTA (0.02%) solution in PBS without Ca^{2+} or Mg^{2+} and replicately plated into six-well (35 mm/well) plastic dishes or 100-mm plastic petri dishes in 2 ml or 10 ml complete medium, respectively. When the cells had attached to the surface of the dish, the complete medium was exchanged for the experimental media, as described in the text-figure legends.

Measurement of [^{33}P]orthophosphate incorporation.—Cells were replicately plated in complete medium containing 10 µCi [^{32}P]orthophosphate/ml. After 48 hours, half of the cultures was treated with vasopressin (5×10^{-9} *M*), and [^{33}P]orthophosphate (10 µCi) was added to all the cultures. Cells were harvested 2 hours later with 0.02% EDTA in PBS and collected by centrifugation in a Clay-Adams serofuge II. Phospholipids were extracted from the cell pellets with chloroform:methanol:HOH (2:1:0.75, vol/vol/vol) as previously described (*11*). A fraction of the chloroform layer was transferred to a glass scintillation vial and allowed to evaporate to dryness in air. Aquasol, 5 ml, was then added to each sample, and the radioactivity was determined with a Packard liquid scintillation spectrometer (model #3044). Results are expressed as the ratio of ^{33}P/^{32}P.

Growth curves.— For growth experiments, cells were repli-

ABBREVIATIONS USED: BrdUrd=5-bromo-2′-deoxyuridine; DMBA=7,12-dimethylbenz[a]anthracene; MEM=minimum essential medium; PBS=phosphate-buffered saline.

---

[1] Received February 13, 1981; revised August 28, 1981; accepted September 25, 1981.

[2] Department of Physiology and Biophysics, School of Medicine, New York University Medical Center, New York, N.Y. 10016.

[3] Veterans Administration Hospital, 16 West, 408 First Ave., New York, N.Y. 10010. *Address reprint requests to* Dr. Monaco *at this address.*

[4] Division of Genetics, Department of Pediatrics, University of Florida, Gainsville, Fla. 32611.

[5] Laboratory of Pathophysiology, Division of Cancer Biology and Diagnosis (DCBD), National Cancer Institute (NCI), National Institutes of Health, Public Health Service, U.S. Department of Health and Human Services, Bethesda, Md. 20205.

[6] Laboratory of Biochemistry, DCBD, NCI.

[7] Medicine Branch, Division of Cancer Treatment, NCI.

cately plated in 35-mm plastic wells. If complete medium was used for the duration of the experiment, vasopressin (5×10^{-9} *M*) was added to half the cultures at the time of plating. If a depleted medium was used, the complete medium was removed after the cells had attached to the surface of the dish and replaced with the depleted variant, plus or minus vasopressin. Cell numbers were determined with the use of a hematocytometer.

Measurement of thymidine incorporation.—After attachment of the cells to the dish, the complete medium was exchanged for serum-free medium supplemented with insulin (10^{-6} *M*). The medium was replaced 12 hours later with fresh medium with insulin, and vasopressin (5×10^{-10} *M*) was added to half the cultures. At various times following the addition of the hormone, cells were incubated for 2 hours with [^{3}H]thymidine (1 μCi/ml). Incorporation of [^{3}H]thymidine into acid-precipitable material was measured as previously described (*12*).

Measurement of mitotic index and BrdUrd incorporation.—Cells were replicately plated in 100-mm petri dishes in complete medium. When the cultures were approximately 50% confluent, the medium was exchanged for serum-free medium with insulin, and vasopressin (5×10^{-9} *M*) was added to half the cultures. BrdUrd (10^{-6} *M*) was added to all the cultures. At designated times, cells were treated for 4 hours with colchicine (200 ng/ml) and then harvested with 0.02% EDTA in PBS. Cells were collected by centrifugation and the pellets were treated at 37°C with 0.075 *M* KCl for 10 minutes. They were then fixed two times in cold methanol: acetic acid (3:1, vol/vol). Slides were prepared in a standard manner, air dried, and stained for sister chromatid differentiation as described by Goto et al. (*13*).

Protein determinations.—Protein concentrations were measured by the methods of Lowry et al. (*14*).

RESULTS

Effect of vasopressin on phospholipid metabolism in complete medium.—WRK-1 cells do not increase in number under the serum-free conditions generally employed when the effects of vasopressin are measured; therefore, to assess the mitogenic potential of the hormone, we first determined its ability to alter metabolism in cells under growth conditions. Stimulation by vasopressin of [^{32}P]orthophosphate incorporation into phospholipids was used as the end point of hormonal activity. Results are seen in table 1. Vasopressin treatment resulted in an 87% increase in ^{32}P incorporation above control values. In a second experiment (results not shown) stimulation was 50%. These values are approximately half those seen under serum-free conditions. A general increase in overall basal metabolic rates produced by serum probably explains the lesser folds of stimulation observed under these conditions.

TABLE 1.—*Effect of vasopressin on ^{32}P incorporation into phospholipids in the presence of serum*

Cells with complete medium	^{32}P, cpm	^{33}P, cpm	^{32}P/^{33}P, × 10^3
Control	287	5,872	48.8
Vasopressin added	459	5,015	91.5

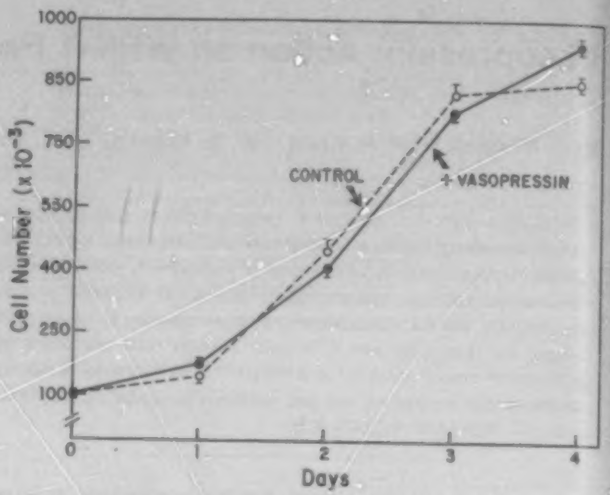

TEXT-FIGURE 1.—Effect of vasopressin on the growth of WRK-1 cells in complete medium. Cells were plated in MEM plus 10% fetal calf serum and 2% rat serum, plus or minus vasopressin. On days 1-4, cells were harvested and counted as described in "Materials and Methods." Controls, ○- - -○; cultures treated with 5×10^{-9} vasopressin, ●—●. Values are the means of three determinations ± 1 SD.

Effects of vasopressin on growth in complete medium.—Having ascertained that vasopressin is effective in the presence of complete medium, we studied growth under these conditions. Text-figure 1 illustrates the results. The cell number increased from 100,000 per dish at the start of the experiment to 850,000 per dish by day 4. No significant difference was seen between control and vasopressin-treated cells during this time.

Effect of vasopressin on growth in depleted medium.—Mitogenic actions of a growth agent are sometimes abolished in the presence of other mitogens. We, therefore, carried out growth experiments in depleted medium in which WRK-1 cells grew more slowly (doubling time=72 hr) than in complete medium. Two variations were made: 1) Serum concentrations were lowered to 0.5% rat serum and 0% fetal calf serum (text-fig. 2A) and 2) rat serum obtained from animals with hereditary diabetes insipidus (vasopressin deficiency) was substituted for normal rat serum (text-fig. 2B). In neither case did vasopressin increase the growth rate of the cells. The difference on day 5 seen in text-figure 2B was not statistically significant. When the ability of insulin to increase the growth rate of the cells was tested under identical conditions, the results shown in table 2 were obtained. Thus insulin increased the numbers of WRK-1 cells under conditions in which vasopressin did not.

Effect of vasopressin on growth parameters in serum-free medium.—Because maximal metabolic and morphologic effects of vasopressin are generally observed under serum-free conditions, mitogenicity was also assessed in serum-free medium containing insulin. Since cells do not divide under these conditions, three parameters other than cell number were used to assay the mitogenic capacity of vasopressin: *a*) [^{3}H]thymidine incorporation into acid-precipitable material, *b*) mitotic index, and *c*) BrdUrd incorporation into DNA. That the DNA was replicating under these conditions

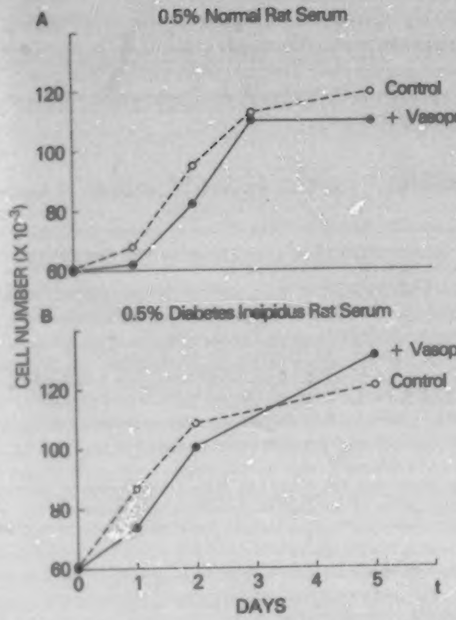

TEXT-FIGURE 2.—Effect of vasopressin on the growth of WRK-1 cells in depleted medium. Cells were plated in complete medium. When the cells had attached, the complete medium was exchanged for MEM + 0.5% rat serum (A) or MEM + 0.5% diabetes insipidus rat serum (B). Cells were harvested and counted as described in "Materials and Methods." Controls, O---O; cultures treated with vasopressin, ●—●. Values given are means of triplicate determinations. SD averaged ≈10%.

TABLE 2.—*Effect of insulin on growth of WRK-1 cells in 0.5% rat serum*

Day	Cell No., $\times 10^{-3\,a}$		
	Control cells with depleted medium	Cells with depleted medium and vasopressin, 5×10^{-9} *M*	Cells with depleted medium and insulin, 10^{-6} *M*
0	241±24		
1	454±54	382±73	549±46
2	610±117	609±101	838±12

[a] Values are means of triplicate determinations ± 1 SD.

can be demonstrated by the appearance of BrdUrd-labeled chromosomes as described below.

a) [^{3}H]thymidine incorporation: The results of this experiment are misleading. Incorporation of [^{3}H]thymidine into acid-precipitable material was greater in the presence of vasopressin at a given time point; however, if one follows a time course of incorporation (text-fig. 3), one observes that vasopressin acted to decrease the rate at which cells slowed down metabolically following the removal of serum from the medium. Measurements of thymidine kinase activity paralleled those of thymidine incorporation (data not shown). Thus, rather than inducing mitosis, vasopressin probably increases the survival of the cells under adverse conditions. The appearance of the cells supports this notion.

b) Mitotic index: When the number of mitotic figures per 1,000 cells was compared for control and vasopressin-treated cells in serum-free medium, the results shown in table 3 were obtained. Whereas the mitotic index increased with time in culture, there was no stimulatory effect of vasopressin. The increase in the number of mitotic figures with time suggests that, in the absence of serum, cells are able to replicate their DNA but not divide. Possibly however, the rate of cell death is equal to the rate of cell division.

c) BrdUrd incorporation: Adding BrdUrd to thymidine-deficient medium leads to the incorporation of BrdUrd in place of thymidine into newly synthesized strands of DNA. Through a process of photolysis, heating, and subsequent staining with Giemsa, cells having DNA that has replicated once after BrdUrd addition (M1), twice after BrdUrd addition (M2), and three more times after BrdUrd addition (M3) can be distinguished by arresting the cultures in metaphase and observing the differential staining patterns of each type in a metaphase spread. M1 figures have two of four strands from each chromosome labeled with BrdUrd; M2 figures have three of four strands from each chromosome labeled; M3 figures have some chromosomes with three and others with all four labeled. When mitotic figures from control cells and vasopressin-treated cells were scored, the results shown in table 4 were obtained. Vasopressin had no effect on the distribution, indicating no difference in rates of DNA replication.

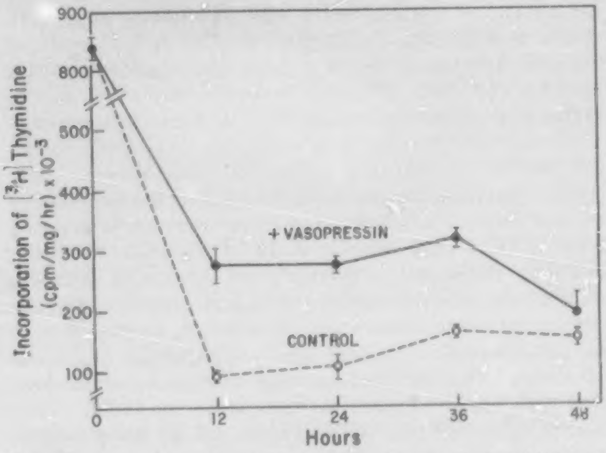

TEXT-FIGURE 3.—Effect of vasopressin on the incorporation of [^{3}H]thymidine into acid-precipitable material in WRK-1 cells. Cells were plated and allowed to attach to the surface of the dish in complete medium. The complete medium was exchanged for fresh serum-free medium with 10^{-6} *M* insulin, plus or minus vasopressin (5×10^{-9} *M*). At the time indicated, cells were incubated with 1 μCi/ml [^{3}H]thymidine for 2 hr and harvested as described in "Materials and Methods." Control cells, O---O; vasopressin-treated cultures, ●—●. Values are means of triplicate determinations ±1 SD.

TABLE 3.—*Effect of vasopressin on mitotic index in WRK-1 cells*

Cells in serum-free medium	Time of treatment, hr	Mitotic index, per 1,000 cells[a]
Control	24	3.22
Vasopressin added	24	3.00
Control	54	13.70
Vasopressin added	54	10.00

[a] Each value is the average of two determinations.

TABLE 4.—*Effect of vasopressin on BrdUrd labeling of DNA in WRK-1 cells*

Cells with thymidine-deficient medium	Time of treatment, hr	Percent of mitotic figures[a]		
		M1	M2	M3
Control	24	97	3	
Vasopressin added	24	94	6	
Control	54	53	42	5
Vasopressin added	54	48	50	2

[a] Each value is the average of two determinations.

DISCUSSION

Vasopressin has been reported to act as a mitogen for both Hela cells (*6*) and 3T3 cells (*7*) in culture. We (*10, 11*) have previously reported that WRK-1 rat mammary tumor cells respond to vasopressin with a variety of biochemical alterations. To determine whether or not vasopressin was a mitogen for WRK-1 cells, we performed the preceding series of experiments. Under no conditions were we able to detect a clear-cut mitogenic effect of the hormone. No consistent differences were seen in cell number, mitotic index, or rate of DNA replication. Thymidine incorporation was higher in vasopressin-treated cells; however, the time course suggested that under serum-free conditions vasopressin was increasing the survival of the cells rather than stimulating growth. In similar experiments, insulin (10^{-6} *M*) clearly increased cell number. The possibility of endogenous serum vasopressin masking the effect of added hormone was ruled out by experiments in serum-free medium, by experiments in medium containing serum from animals with diabetes insipidus, and by the fact that vasopressin could stimulate precursor incorporation into phospholipid in the presence of normal serum. The exact nature of vasopressin's interaction with WRK-1 cells remains to be determined. However, although vasopressin is probably not a mitogen for these cells, a role for this hormone in cancer growth cannot be eliminated. Vasopressin may, for example, predispose cells for mitogenization by other agents or influence metastatic potential. Other morphologic and biochemical data show that vasopressin increases the survival of the WRK-1 cells and as such may play an important role in the growth of cancers. Factors that influence cancer growth in vivo need not be directly mitogenic. Certainly, the relationship between vasopressin and mammary cancer cells is worthy of further investigation. We are currently attempting to dissect the mechanism by which vasopressin stimulates overall metabolism in WRK-1 cells.

REFERENCES

(*1*) VanDongen CG, Marshall JM. Effect of various hormones on the milk ejection response of tissue isolated from the rat mammary gland. Nature 1967; 213:632–683.

(*2*) Coutinho EM, Lopes AV. Responses of the nonpregnant uterus to vasopressin as an index of ovarian function. Am J Obstet Gynecol 1968; 102:479–489.

(*3*) Walter R, VanRee JM, DeWied D. Modifications of conditioned behavior of rats by neurohypophysial hormones and analogs. Proc Natl Acad Sci USA 1978; 75:2493–2496.

(*4*) Hems DR, Whitton PO. Stimulation by vasopressin of glycogen breakdown and gluconeogenesis in the perfused rat liver. Biochem J 1973; 136:705–709.

(*5*) Kirk CJ, Verrinder TR, Hems DA. Rapid stimulation by vasopressin and adrenaline, of ionorganic phosphate incorporation into phosphatidyl inositol in isolated hepatocytes. FEBS Lett 1977; 83:267–271.

(*6*) Bernard-Weil E, Da Lage C. Inhibition by control of the favourable action of lysine-vasopressin on the growth of Hela cell cultures. Experientia 1968; 24:1001.

(*7*) Rozengurt E, Legg A, Pettican P. Vasopressin stimulation of mouse 3T3 cell growth. Proc Natl Acad USA 1979; 76:1284–1287.

(*8*) Bernard-Weil E, Patterson JP. Association between vasopressin and corticosteroids in the palliative treatment of advanced breast cancer. Oncology 1973; 28:497–508.

(*9*) Kidwell WR, Monaco ME, Wiche M, Smith G. Unsaturated fatty acid requirements for growth and survival of a rat mammary tumor cell line. Cancer Res 1978; 38:4091–4100.

(*10*) Monaco ME, Lippman ME, Knazek RA, Kidwell WR. Vasopressin stimulates acetate incorporation into lipids in a dimethylbenz[*a*]-anthracene-induced rat mammary tumor cell line. Cancer Res 1978; 38:4101–4103.

(*11*) Monaco ME, Kidwell WR, Lippman ME. Neurohypophyseal-hormone-responsive cell line derived from a dimethylbenzanthracene-induced rat mammary tumour. Biochem J 1980; 188:437–442.

(*12*) Osborne CK, Bolan G, Monaco ME, Lippman ME. Hormone-responsive human breast cancer in long-term culture: Effect of insulin. Proc Natl Acad Sci USA 1976; 73:4536–4540.

(*13*) Goto K, Maeda S, Kano Y, Sugiyama T. Factors involved in differential Giemsa-staining of sister chromatids. Chromosoma 1978; 66:351–359.

(*14*) Lowry OH, Rosebrough NJ, Farr AL, Randall RJ. Protein measurement with the Folin phenol reagent. J Biol Chem 1951; 193:265–275.

Cholangiocellular Carcinomas Induced in Syrian Golden Hamsters Administered Aflatoxin B_1 in Large Doses[1,2,3]

Michael R. Moore,[4,5] Henry C. Pitot,[4] Elizabeth C. Miller,[4,6] *and* James A. Miller[4,7]

ABSTRACT—The hepatocarcinogenicity of aflatoxin B_1 (AFB_1) was compared in male Syrian golden hamsters and inbred F344 rats. AFB_1 was administered by gavage 5 days/week for 6 weeks at doses of 1 and 2 mg/kg body weight/day to rats and hamsters, respectively; rats did not survive beyond 3 weeks with doses of 2 mg/kg/day. After 6 weeks the animals either received no further treatment or were given 0.1% phenobarbital sodium in the drinking water. ATPase-deficient foci of hepatic parenchymal cells, neoplastic nodules, and hepatocellular carcinomas were observed in liver sections from AFB_1-treated rats killed at 6, 14, or 23 weeks; they were not seen in sections from AFB_1-treated hamsters killed at 6, 14, or 46 weeks. Each of the 50 AFB_1-treated rats developed hepatocellular carcinomas by 46 weeks; many also had cholangiocarcinomas and mixed hepatocellular–cholangiocellular carcinomas. Hepatocellular carcinomas were found in only 2 of 49 AFB_1-treated hamsters by 78 weeks. At this time cholangiocarcinomas were found in 15 hamsters, and microscopic cholangiomas were seen in all of the livers. Compared to the rat, the hamster was resistant to the hepatotoxic and hepatocellular carcinogenic effects of AFB_1.—JNCI 1982; 68:271–278.

Considerable evidence indicates that in the rat AFB_1-2,3-oxide is an ultimate electrophilic, mutagenic, and carcinogenic metabolite of the hepatocarcinogenic mycotoxin AFB_1 (*1–5*). The capacity of fortified liver microsomes from adult male Syrian golden hamsters to metabolize AFB_1 to AFB_1-2,3-oxide in vitro, as measured by the yields of 2,3-dihydro-2,3-dihydroxy-AFB_1 or of aflatoxin–nucleic acid adducts, is equivalent to that of hepatic microsomes from phenobarbital-treated male F344 rats and about four times that of hepatic microsomes from untreated rats (*5–7*). However, in spite of this high enzymatic activity in vitro, hamsters given AFB_1 form lower levels of hepatic nucleic acid-bound aflatoxin adducts in vivo than do rats given AFB_1 [(*8*); Moore MR, Miller EC, Miller JA: Unpublished data].

The acute hepatotoxicity of AFB_1 is also somewhat lower for the hamster than for the rat; a median lethal dose of 10 mg/kg body weight was reported for 30-day-old hamsters as compared to that of 5 mg/kg body weight for 21-day-old male rats (*9*). Furthermore, in contrast to the high susceptibility of rat liver to the carcinogenicity of AFB_1 (*10*), in early studies no hepatic tumors, regenerative nodules, or cirrhosis was observed in Syrian hamsters given a mixture of aflatoxins (total doses of 5–10 mg; ≈40% AFB_1) over 6–11 months and maintained for their life-span (≤30 mo) (*11*). Some histopathologic changes were noted in the hamster tissues, but more recent studies have shown that dimethylformamide, the solvent used in the previous study (*11*) for the ip administration of the aflatoxins, is also hepatotoxic (*12, 13*). To examine this problem further, we have given high doses of AFB_1 orally for 6 weeks to weanling male Syrian hamsters and F344 rats; the histopathologic changes in the livers and tumor induction were studied as a function of time. Although considerably more resistant than rats to the hepatotoxic and hepatocarcinogenic effects of AFB_1, the treated hamsters developed cholangiomas and cholangiocarcinomas, in addition to cholangiofibrosis and cystic changes, by 32–78 weeks.

MATERIALS AND METHODS

Male Syrian golden hamsters and F344 rats, both 4 weeks old (Charles River Breeding Laboratories, Wilmington, Mass.), with average initial weights of 54±6 and 66±8 g, respectively, were housed in pairs in screen-bottom cages and fed Wayne Breeder Blox pellets (Allied Mills, Inc., Chicago, Ill.) and tap water ad libitum.

AFB_1 (Calbiochem, La Jolla, Calif.), dissolved in DMSO and diluted with an equal volume of sterile trioctanoin (Sigma Chemical Co., St. Louis, Mo.), was given by gavage without anesthesia 5 days/week for 6 consecutive weeks. The daily dose for the hamsters was 2 mg/kg body weight, and that for the rats was either 1 or 2 mg/kg body weight. Control animals of both species received only the vehicle, 50% DMSO–trioctanoin, on the same schedule. All animals received 2 ml of DMSO–trioctanoin/kg/day. Uniform suspensions were maintained by use of a magnetic stirrer. Starting 24 hours after the last dose of AFB_1 or solvent, we

---

ABBREVIATIONS USED: AFB_1=aflatoxin B_1; DMSO=dimethyl sulfoxide; GGT=γ-glutamyltranspeptidase; Glc-6-Pase=glucose-6-phosphatase; H & E=hematoxylin and eosin; IARC=International Agency for Research on Cancer.

---

[1] Received February 20, 1981; revised September 11, 1981; accepted September 23, 1981.

[2] Supported by Public Health Service grants CA-07175 and CA-22484 from the National Cancer Institute.

[3] Animals were maintained under the guidelines set forth in the "Guide for the Care and Use of Laboratory Animals" by the Institute of Laboratory Animal Resources, National Research Council.

[4] McArdle Laboratory for Cancer Research, University of Wisconsin Medical School, 450 North Randall Ave., Madison, Wis. 53706.

[5] *Present address:* Department of Chemistry and Metabolism, Litton Bionetics, Inc., 5516 Nicholson Lane, Kensington, Md. 20795.

[6] *Address reprint requests to* Dr. E. C. Miller.

[7] We thank Mr. Randy Knibbs, Ms. Priscilla Kimberly, and Mr. Jon Springer for excellent technical assistance. We are grateful to Ms. Jane Weeks and Ms. Mary Folz for preparation of the histologic slides.

gave some of the animals 0.1% phenobarbital sodium in the drinking water (*14*) until the experiments were terminated.

At least 6 rats/group were killed at 6, 14, and 23 weeks after the beginning of treatment, and at least 6 hamsters/group were killed at 6, 14, and 46 weeks. For the 6-week time point the animals were all killed 24 hours after receiving the last of the 30 doses of AFB_1 or solvent. In addition, groups of 30 rats or hamsters were observed for tumor development; the surviving rats and hamsters were killed at 46 and 78 weeks, respectively. At each time both AFB_1-treated and control animals were autopsied. The hamsters and rats killed at or after 23 weeks included groups given phenobarbital in the drinking water, starting at the 7th week, and groups given only tap water.

All animals found dead and those killed at the times indicated above were subjected to gross routine autopsies, which included examination of the skin and subcutaneous tissue and the organs of the abdominal and peritoneal cavities. Sections of the livers from all animals, of the harderian glands and kidneys from the animals killed at the specified intervals, and of the harderian glands from the hamsters that survived to the end of the experiment were fixed in buffered 10% Formalin and stained with H & E for histologic examination. The histopathologic criteria for the diagnosis of hepatic lesions, including the cholangiocellular neoplasms, were those of the IARC (*15*) and of the National Research Council (*16*).

For the animals killed at one of the designated times, each liver lobe was bisected and one of the two sections from each lobe was fixed in buffered 10% Formalin. The remaining sections from each of the liver lobes were juxtapositioned on a filter paper square to form a single tissue block, which was immediately frozen on Dry Ice. Consecutive 6-μm sections with areas approximately 3 cm^2 from the frozen tissues were stained for ATPase (*17*) or with H & E. In addition, four consecutive sections cut from frozen tissue blocks from the livers of a few of the tumor-bearing animals were stained for ATPase, Glc-6-Pase (*18*), or GGT (*19*) or with H & E. The size and total number of ATPase-deficient foci per liver were estimated as described previously (*20, 21*).

RESULTS

The rats were much more susceptible to the hepatotoxic and hepatocarcinogenic effects of AFB_1 than were the hamsters. Thus none of the rats given 5 doses of AFB_1/week at the rate of 2 mg/kg/dose survived past the 3d week; the livers of these rats all showed moderate bile duct proliferation and portal fibrosis, as well as focal areas of atypical hepatocyte proliferation. The 6-week survival rates of the rats given doses of 1 mg/kg and of hamsters given doses of 2 mg/kg, five times per week for 6 weeks, were 95 and 85%, respectively; 100 and 88% of the control rats and hamsters, respectively, given only the vehicle survived for this period. The weight gains of the AFB_1-treated (1 mg/kg/dose) and control rats during the 6-week treatment period were 83 and 141 g, respectively. During the same period the AFB_1-treated hamsters gained 30 g, while the control hamsters gained 83 g. These weight differentials were essentially eliminated during the next 8 weeks because the AFB_1-treated animals, with or without phenobarbital administration, had weight gains of 1.5–2 times those of controls. These large doses were administered in view of the reported refractoriness of hamsters to the induction of hepatic tumors by AFB_1 (*11*).

The results of the gross and histologic studies of the livers, kidneys, and harderian glands indicated that, as in previous studies with rats (*10*), the pathologic changes induced by AFB_1 occurred primarily in the liver. The hepatic damage occurred earlier and was more severe in rat liver than in hamster liver. Further, the hepatic toxicity resulted in cholangiofibrosis, cholangiomas, and cholangiocellular carcinomas in the hamsters, whereas the hepatic parenchymal cells were the major target in rat liver.

Liver Pathology at 6 Weeks

At 24 hours after the last of 30 doses (1 mg/kg) of AFB_1, rat liver sections stained with H & E showed numerous transections of both eosinophilic and basophilic foci (*16*) of hepatic parenchymal cells (table 1; figs, 1, 2). Several transections of neoplastic nodules (*22*) were noted in sections from four of six livers examined. The livers were also calculated (*20, 21*) to contain an average of 2,110±1,050 ATPase-deficient foci of parenchymal cells; the foci had an average diameter of 0.34±0.19 mm. Since a deficiency in ATPase was evident throughout the tissue sections, only those focal areas devoid of any ATPase staining were counted. Moderate ductular proliferation and focal hepatocyte degeneration, predominantly around the portal areas, were noted in all the sections. Occasional areas of moderate to marked oval cell proliferation and focal megalocytosis were detected. Liver sections from rats given only the vehicle were free of any notable abnormalities.

In contrast, neither neoplastic nodules nor any transections of eosinophilic or basophilic foci of parenchymal cells were seen in H & E-stained liver sections from hamsters given AFB_1 at 2 mg/kg/dose—twice the level tolerated by the rats (table 1). Furthermore, at 6 weeks no ATPase-deficient foci of hepatic parenchymal cells were seen in liver sections from AFB_1-treated hamsters or in the vehicle controls. Pathologic changes common to the livers from AFB_1-treated hamsters killed at 6 weeks (24 hr after the last dose) included focal hepatocyte degeneration and a marked accentuation of acinar zone 1 (*23*) with occasional megalocytosis (fig. 3). These changes were not seen in liver sections from control hamsters given only the vehicle (50% DMSO–trioctanoin) (fig. 4).

Liver Pathology at 14 Weeks

At 14 weeks after the first dose of AFB_1, multiple gray-white nodules about 1 mm in diameter were detected on the surface and in the interior of the liver lobes of all carcinogen-treated rats; transections of eosinophilic foci of hepatic parenchymal cells and of neoplastic nodules (fig. 5) were prevalent in virtually all of the sections examined microscopically (table 1). Microscopic hepatocellular carcinomas were observed in liver sections from 3 of the 9 rats. The livers contained an average of 3,440±535 ATPase-deficient foci with an average diameter of 0.76±0.48 mm.

No foci of ATPase-deficient parenchymal cells and no eosinophilic or basophilic foci were detected in the liver sections from AFB₁-treated hamsters or from vehicle-treated controls killed at 14 weeks. Focal megalocytosis and cellular vacuolization were the only notable abnormalities seen at 14 weeks (8 wk after the last dose) in liver sections from hamsters given AFB₁ (fig. 6).

Liver Pathology at 23 Weeks

As table 2 shows, 23 weeks after the first dose of AFB₁, all of the livers from the AFB₁-treated rats contained one or more gray-white nodules that were at least 0.5 cm in diameter and that were diagnosed microscopically as hepatocellular carcinomas. These carcinomas exhibited a histologic pattern similar to that of the Morris hepatoma 7316 (*24*). In addition, the livers also frequently contained multiple hyperplastic and neoplastic nodules (*22*). Administration of 0.1% of phenobarbital sodium in the drinking water did not increase the tumor incidence. No cholangiocarcinomas were detected in the livers from AFB₁-treated rats, and no significant abnormalities were observed in liver sections from control rats given only 50% DMSO–trioctanoin with or without subsequent phenobarbital administration.

TABLE 1.—*Liver histopathology at 6 and 14 weeks in F344 rats and Syrian golden hamsters given AFB₁*[a]

Parameter	6 wk				14 wk			
	Rats given:		Hamsters given:		Rats given:		Hamsters given:	
	Vehicle only	AFB₁	Vehicle only	AFB₁	Vehicle only	AFB₁	Vehicle only	AFB₁
No. of animals examined	6	6	6	6	9	9	7	7
No. of animals with:								
No remarkable hepatic changes	6	0	6	0	9	0	7	0
Hepatocellular degeneration	0	6	0	6	0	0	0	0
Portal necrosis	0	6	0	0	0	0	0	0
Focal cellular vacuolization	0	0	0	0	0	0	0	7
Focal hepatic megalocytosis	0	0	0	5	0	0	0	5
Focal bile duct proliferation	0	6	0	0	0	0	0	0
Eosinophilic foci of hepatocytes	0	6	0	0	0	9	0	0
Neoplastic hepatic nodules	0	4	0	0	0	8	0	0
Early hepatocellular carcinoma (microscopic)	0	0	0	0	0	3	0	0

[a] AFB₁ dissolved in 50% DMSO-trioctanoin (2 ml/kg/dose) was given daily by gavage, 5 days/wk, for 6 wk. Rats and hamsters received 1 mg/kg/day and 2 mg/kg/day, respectively. Controls for both species were given only the vehicle. Animals were killed at 6 wk (24 hr after the last dose) and at 14 wk (8 wk after the last dose), and sections of the livers were fixed in buffered Formalin and stained with H & E.

TABLE 2.—*Hepatic tumor incidences in AFB₁-treated male rats and hamsters*[a]

Parameter	Rats								Hamsters							
	Killed at 23 wk				Killed at 46 wk[b]				Killed at 46 wk				Died at 24–78 wk or killed at 78 wk[c]			
	Vehicle only		AFB₁		Vehicle only		AFB₁		Vehicle only		AFB₁		Vehicle only		AFB₁	
Phenobarbital[d]	–	+	–	+	–	+	–	+	–	+	–	+	–	+	–	+
No. of animals autopsied	12	12	7	10	30	30	25	25	7	6	8	6	26	27	25	24
No. of animals with gross hepatic tumors	0	0	7	10	0	0	25	25	0	0	0	1	0	0	6	7
No. of gross tumors/liver[e]	0	0	7.0±5.7	6.8±3.7	0	0	7.2±3.5	7.4±1.9	0	0	0	0	0	0	0.2±0.4	0.4±0.6
No. of animals with:																
Hepatocellular carcinomas	0	0	7	10	0	0	25	25	0	0	0	0	0	0	1	1
Mixed hepatocellular–cholangiocellular carcinoma	0	0	1	5	0	0	5	18	0	0	0	0	0	0	0	0
Cholangiocarcinoma	0	0	0	0	0	0	2	5	0	0	1	1	0	0	8	7
Cholangiomas only (microscopic)	0	0	0	0	0	0	0	0	0	0	4	2	0	0	17	17

[a] AFB₁ was given daily, 5 days/wk, for 6 wk to rats at a level of 1 mg/kg/day and to hamsters at 2 mg/kg/day. Controls for both species were given only the vehicle. Beginning 24 hr after the last dose, 1 group of rats and 1 group of hamsters were given 0.1% phenobarbital sodium in the drinking water until the experiment was terminated. Formalin-fixed liver sections stained with H & E were examined from all rats killed at 23 or 46 wk, hamsters killed at 46 or 78 wk, and animals of either species that were found moribund or dead.

[b] Data for groups of 30 rats designated in the protocol for analysis of tumor incidence. None of the rats killed at 6, 14, or 23 wk are included in these tabulations.

[c] Data for groups of 30 hamsters designated in the protocol for analysis of tumor development. None of the hamsters killed at 6, 14, or 46 wk are included in these tabulations.

[d] + = phenobarbital was administered as 0.1% of the drinking water starting at 7 wk. – = phenobarbital was not administered.

[e] Tumors ≥0.5 cm in diameter were tabulated.

Liver Pathology at 46 Weeks

Twenty-five of the 30 AFB_1-treated rats in each group, whether or not they were given phenobarbital in the drinking water, survived until they were killed at 46 weeks (table 2). Gray-white nodules that were at least 0.5 cm in diameter and were diagnosed microscopically as hepatocellular carcinomas were found in the liver of each of the treated rats; the average number per liver was 7. However, the number of rats that also had mixed hepatocellular–cholangiocellular carcinomas (18/25 or 72%) or cholangiocellular carcinomas (5/25 or 20%) (*15*) was greater for the AFB_1-treated rats given phenobarbital than for those not given the drug. The incidences of these tumors in the rats not given phenobarbital were 5 of 25 (20%) and 2 of 25 (8%), respectively. Liver sections from controls treated only with the DMSO–trioctanoin emulsion, whether or not they received phenobarbital, showed no remarkable abnormalities.

In contrast, hepatocellular carcinoma was not detected in any of the AFB_1-treated hamsters killed at 46 weeks. However, 2 hamsters each had a cholangiocellular carcinoma 1 cm in diameter, and microscopic cholangiomas were seen in sections from 6 of the 14 hamster livers. In addition, from the groups of AFB_1-treated hamsters reserved for determination of tumor incidence, 3 that received phenobarbital in the drinking water and 4 that received only tap water died with gross cholangiocellular carcinomas between 28 and 38 weeks. Focal areas of hepatocyte hyperplasia and bile duct proliferation were also observed microscopically in liver sections from AFB_1-treated hamsters, whereas no notable changes were seen in the control livers.

Liver Pathology at 78 Weeks

The 15 surviving hamsters given AFB_1 and the 23 surviving solvent-treated controls were killed at 78 weeks. No gross hepatocellular carcinomas were detected, but microscopic hepatocellular carcinomas were seen in liver sections from 2 AFB_1-treated hamsters, 1 of which was given phenobarbital in the drinking water (fig. 7). The livers from all of the AFB_1-treated hamsters, whether or not they received phenobarbital, exhibited multiple cystic cholangiomas and cholangiofibrosis (fig. 8); 30% of the livers contained hard, white masses that were diagnosed as cholangiocellular carcinomas (figs. 9, 10). Another 3 AFB_1-treated hamsters from these groups died with gross cholangiocellular carcinomas and microscopic cholangiomas between 46 and 52 weeks

Thus the tumor incidence (table 2) for the hamsters includes those that died before 78 weeks and those killed at the termination of the experiment. The mean survival times for the AFB_1-treated hamsters that survived at least 24 weeks were 64 weeks for hamsters given subsequent treatment with phenobarbital and 66 weeks for hamsters not given subsequent phenobarbital treatment. Hamsters given only the vehicle, with or without subsequent phenobarbital treatment, did not develop grossly or microscopically notable hepatic abnormalities. For the control hamsters that survived at least 24 weeks, the mean survival times were 67 or 70 weeks, respectively, for those that did or did not receive phenobarbital.

Three cholangiocarcinomas from the AFB_1-treated hamsters (2 from animals given phenobarbital and 1 from a nonphenobarbital-treated hamster) were each examined with histochemical stains. Each of these carcinomas was ATPase-deficient, Glc-6-Pase-deficient, and GGT-positive. Sections of nontumor hepatic tissue from each of these 3 hamsters and from 1 other AFB_1-treated hamster, without phenobarbital treatment, contained five to ten ATPase-deficient focus transections of hepatic cells per 2- to 3-cm^2 tissue section (fig. 11). These focus transections in the nonneoplastic tissue were not detectable in consecutive sections stained for Glc-6-Pase or GGT or with H & E (fig. 12). The number of ATPase-deficient foci per liver could not be estimated (*20, 21*), since the contribution to the liver weight of numerous hepatic cysts was unknown. Liver sections taken at 78 weeks from 8 hamsters that received only the vehicle (DMSO-trioctanoin), with or without subsequent phenobarbital administration, did not contain any focus transections of hepatic cells that were detectable with the histochemical stains used.

Other Pathology

Only limited study of other tissues was made, since the major focus of this study was a comparison of hepatic tumor development. However, the harderian glands were examined in view of the earlier report of the occurrence of adenomas in these glands in AFB_1-treated hamsters (*11*). Focal glandular atrophy and focal pigmentation of the glands were observed in 2 of 6 rats killed at the termination of the AFB_1 treatments at 6 weeks. No histologic changes were observed in the harderian glands from hamsters at 6 weeks or in any of the rats or hamsters examined at later times up to 78 weeks. However, at 78 weeks 5 of 6 or 6 of 9, respectively, of the AFB_1-treated hamsters that were or were not given phenobarbital had microscopic adenomas of the harderian gland. Similarly, for the vehicle-treated controls the incidences were 3 of 9 or 6 of 14, respectively, for the hamsters that did or did not receive phenobarbital. Harderian gland adenomas were not observed in any of the rats.

The kidneys of the hamsters that received AFB_1 and of the controls showed varying degrees of nephritis with interstitial fibrosis and chronic inflammation, tubular dilatation, cast formation, and occasional hyperplasia. A renal cell carcinoma was found in 1 AFB_1-treated hamster at 78 weeks.

DISCUSSION

These data confirm previous impressions (*9, 11*) that livers of Syrian golden hamsters are much less susceptible than those of rats to the toxic and carcinogenic effects of AFB_1. This finding is consistent with the lower levels of macromolecule-bound AFB_1 residues in the livers of AFB_1-treated hamsters as compared to those of AFB_1-treated rats [(8); Moore MM, Miller EC, Miller JA: Unpublished data]. Both findings are in marked contrast to the severalfold greater capacity of NADPH-fortified hamster liver microsomes, as compared to those of rat liver, to metabolize AFB_1 to the apparent ultimate carcinogen AFB_1-2,3-oxide in vitro (*5–7*). The livers of both species contain glutathione *S*-

transferase activity that forms a conjugate from an AFB$_1$ metabolite, presumably the 2,3-oxide (*25, 26*). Differences in the level of this enzyme or of other metabolizing systems may be one of the factors responsible for the very different susceptibilities of rat and hamster livers to AFB$_1$.

The hepatotoxic and carcinogenic effects of AFB$_1$ in the rat were directed primarily toward the parenchymal cells, as evidenced by the formation of foci of parenchymal cells with altered histochemical staining properties and the development of neoplastic nodules and hepatocellular carcinomas. Although cholangiocellular carcinomas were rare, many hepatocellular carcinomas contained cholangiocellular components, especially at the termination of the experiment for those rats that also received phenobarbital. By contrast, the bile duct cells appeared to be the primary target in hamster livers, since essentially the only neoplasms observed were cholangiomas and cholangiocellular carcinomas that arose late in the experiment. Thus the differences in the susceptibilities of rat and hamster bile duct cells to AFB$_1$ appear to be relatively small as compared to those of their hepatic parenchymal cells.

Since phenobarbital promotes the formation of hepatocellular carcinomas in rats when it is given subsequent to minimal doses of a variety of carcinogens, including 2-acetylaminofluorene, diethylnitrosamine, and certain aminoazo dyes (*14, 27–29*), it was anticipated that phenobarbital might facilitate hepatic tumor induction in the hamster. Whether the negative result that was observed reflects only the strong refractoriness of the hamster hepatic parenchymal cells to the initiation of carcinogenesis by AFB$_1$ or also a lack of promoting activity of phenobarbital in hamsters requires further investigation. Phenobarbital administration to rats appeared to promote the formation of carcinomas that contained cholangiocellular elements. The lack of effect of phenobarbital on the incidence of carcinomas of parenchymal cell origin in rats is readily explicable by the massive dose of AFB$_1$ administered to these animals.

As noted in Herrold's experiment (*11*), a number of the AFB$_1$-treated hamsters developed adenomas of the harderian gland. Although Herrold did not find these adenomas in any of her control animals, these tumors did occur in some of our control hamsters and thus cannot be ascribed to the action of AFB$_1$. Adenomas of the harderian gland have been found in untreated hamsters studied in other laboratories (*30–32*), but the incidences were much lower (≈2%) than those observed in this experiment.

REFERENCES

(*1*) Campbell TC, Hayes JR. The role of aflatoxin metabolism in its toxic lesion. Toxicol Appl Pharmacol 1976; 35:199–222.

(*2*) Lin JK, Miller JA, Miller EC. 2,3-Dihydro-2-(guan-7-yl)-3-hydroxy-aflatoxin B$_1$, a major acid hydrolysis product of aflatoxin B$_1$-DNA or -ribosomal RNA adducts formed in hepatic microsome-mediated reactions and in rat liver in vivo. Cancer Res 1977; 37: 4430–4438.

(*3*) Essigmann JM, Croy RG, Nadzan AM, et al. Structural identification of the major DNA adduct formed by aflatoxin B$_1$ in vitro. Proc Natl Acad Sci USA 1977; 74:1870–1874.

(*4*) Martin CN, Garner RC. Aflatoxin B$_1$-oxide generated by chemical or enzymic oxidation of aflatoxin B$_1$ causes guanine substitution in nucleic acids. Nature 1977; 267:863–865.

(*5*) Swenson DH, Miller JA, Miller EC. 2,3-Dihydro-2,3-dihydroxy-aflatoxin B$_1$: An acid hydrolysis product of an RNA-aflatoxin B$_1$ adduct formed by hamster and rat liver microsomes in vitro. Biochem Biophys Res Commun 1973; 53:1260–1267.

(*6*) Lin JK, Kennan, KA, Miller EC, Miller JA. Reduced nicotinamide adenine dinucleotide phosphate-dependent formation of 2,3-dihydro-2,3-dihydroxyaflatoxin B$_1$ from aflatoxin B$_1$ by hepatic microsomes. Cancer Res 1978; 38:2424–2428.

(*7*) Garner RC, Miller, EC, Miller, JA. Liver microsomal metabolism of aflatoxin B$_1$ to a reactive derivative toxic to *Salmonella typhimurium* TA 1530. Cancer Res 1972; 32:2058–2066.

(*8*) Garner RC, Wright CM. Binding of [^{14}C]aflatoxin B$_1$ to cellular macromolecules in the rat and hamster. Chem Biol Interact 1975; 11:123–131.

(*9*) Wogan GN. Chemical nature and biological effects of the aflatoxins. Bacteriol Rev 1966; 30:460–470.

(*10*) Wogan GN, Newberne PM. Dose-response characteristics of aflatoxin B$_1$ carcinogenesis in the rat. Cancer Res 1967; 27:2370–2376.

(*11*) Herrold KM. Aflatoxin induced lesions in Syrian hamsters. Br J Cancer 1969; 23:655–660.

(*12*) Ungar H, Sullman SF, Zuckerman AJ. Acute and protracted changes in the liver of Syrian hamsters induced by a single dose of aflatoxin B$_1$: Observations on pathological effects of the solvent (dimethylformamide). Br J Exp Pathol 1976; 57:157–164.

(*13*) Mathew T, Karunanithy R, Yee MH, Natarajan PN. Hepatoxicity of dimethylformamide and dimethylsulfoxide at and above the levels used in some aflatoxin studies. Lab Invest 1980; 42:257–262.

(*14*) Peraino C, Fry RJ, Staffeldt E. Reduction and enhancement by phenobarbital of hepatocarcinogenesis induced in the rat by 2-acetylaminofluorene. Cancer Res 1971; 31:1506–1512.

(*15*) Schauer A, Kunze E. Tumours of the liver. In: Turusov VS, ed. Pathology of tumours in laboratory animals. Vol 1. Lyon: IARC, 1976:41–72.

(*16*) Institute of Laboratory Animal Resources, National Research Council, National Academy of Sciences. Histologic typing of liver tumors of the rat. JNCI 1980; 64:177–206.

(*17*) Wachstein M, Meisel E. Histochemistry of hepatic phosphatases at a physiologic pH. Am J Clin Pathol 1957; 27:13–23.

(*18*) ———. On the histochemical demonstration of glucose-6-phosphatase. J Histochem Cytochem 1956; 4:592.

(*19*) Rutenberg AM, Kim H, Fischbein JW, Hankers JS, Wasserkrug HL, Seligman AM. Histochemical and ultrastructural demonstration of γ-glutamyltranspeptidase activity. J Histochem Cytochem 1969; 17:517–526.

(*20*) Moore MM, Drinkwater NR, Miller EC, Miller JA, Pitot HC. Quantitative analysis of the time-dependent development of glucose-6-phosphatase-deficient foci in the livers of mice treated neonatally with diethylnitrosamine. Cancer Res 1981; 41:1585–1593.

(*21*) Drinkwater NR. Physical and chemical effects of carcinogen binding to DNA in relation to biological activity and statistical problems in chemical carcinogenesis. Ph.D. dissertation. Madison: University of Wisconsin, 1980.

(*22*) Squire RA, Levitt MM. Report of a workshop on classification of hepatocellular lesions in rats. Cancer Res 1975; 35:3214–3223.

(*23*) Rappaport AM. The structural and functional unit in the human liver (liver acinus). Anat Rec 1958; 130:673–689.

(*24*) Miyaji H, Morris HP, Wagner BP. Histological study of some primary and transplantable hepatic tumors in rats. Methods Cancer Res 1968; 4:153–178.

(*25*) Lotlikar PD, Insetta SM, Lyons PR, Jhee E-C. Inhibition of microsome-mediated binding of aflatoxin B$_1$ by glutathione *S*-transferase. Cancer Lett 1980; 9:143–149.

(*26*) Degen GH, Neumann HG. The major metabolite of aflatoxin B$_1$ in the rat is a glutathione conjugate. Chem Biol Interact 1978; 22: 239–255.

(*27*) Kitagawa T, Pitot HC, Miller EC, Miller JA. Promotion by dietary phenobarbital of hepatocarcinogenesis by 2-methyl-*N,N*-dimethyl-4-aminoazobenzene in the rat. Cancer Res 1979; 39:112–115.

(*28*) Pitot HC. Drugs as promoters of carcinogenesis. In: Estabrook RW, Lindenlaub E, eds. The induction of drug metabolism. Stuttgart and New York: Schattauer-Verlag, 1979:471–483.

(*29*) Miller EC, Kadlubar FF, Miller JA, Pitot HC, Drinkwater NR. The N-hydroxy metabolites of *N*-methyl-4-aminoazobenzene and related dyes as proximate carcinogens in the rat and mouse. Cancer Res 1979; 39:3411–3418.

(30) Pour P, Mohr U, Althoff, J, Cardesa A, Kmoch N. Spontaneous tumors and common diseases in two colonies of Syrian hamsters. IV. Vascular and lymphatic systems and lesions of other sites. J Natl Cancer Inst 1976; 56:963-974.

(31) Dontenwill W, Chevalier, HJ, Harke HP, LaFrenz U, Reckzeh G, Schneider B. Spontantumoren des Syrischen Goldhamster. Z Krebsforsch 1973; 80:127–158.

(32) Fortner JC. Spontaneous tumors, including gastrointestinal neoplasms and malignant melanomas, in the Syrian hamster. Cancer 1957; 10:1153–1156.

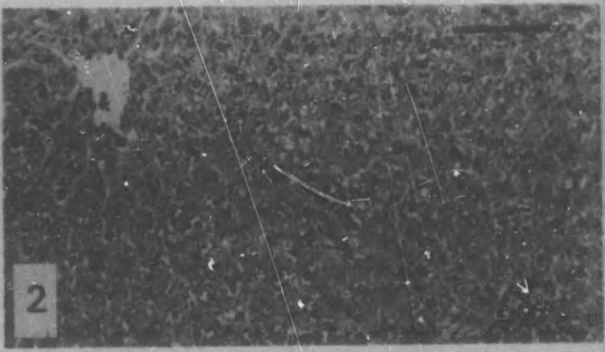

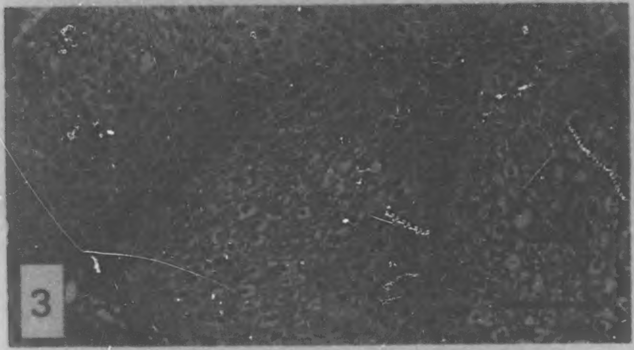

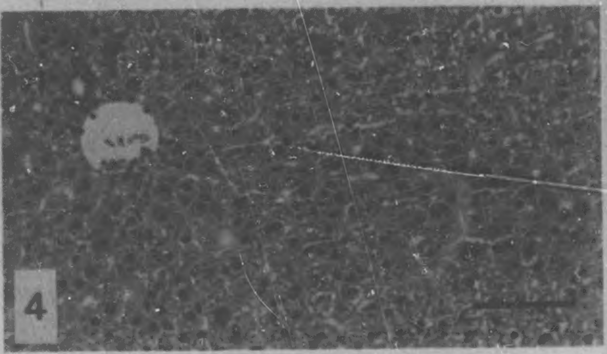

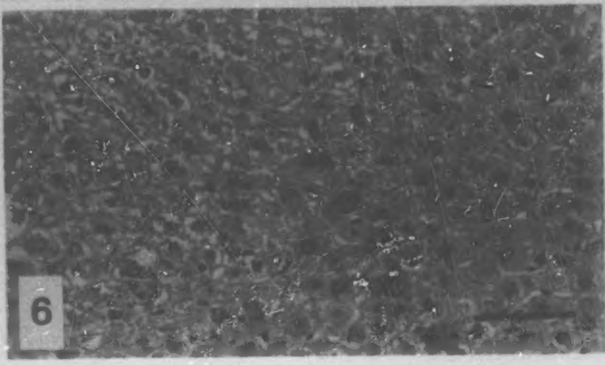

Figure 1.—Transection of hepatic basophilic focus with surrounding normal rat liver. The rat was killed 24 hr after the last dose of AFB$_1$, 1 mg/kg/day, five times/wk for 6 wk. *Bar*=150 μm. H & E. × 96

Figure 2.—Liver section from a control rat killed 24 hr after the last dose of 50% DMSO-trioctanoin at 2 ml/kg/day, five times/week for 6 wk. H & E. *Bar*=75 μm. × 190

Figure 3.—Hepatic megalocytosis, ductular proliferation, and cellular vacuolation in acinar zone 1 (*23*) of the liver section from a hamster killed 24 hr after the last dose of AFB$_1$, 2 mg/kg/day, five times/wk for 6 wk. H & E. *Bar*=150 μm. × 93

Figure 4.—Hepatocytes of acinar zone 1 in a liver section from a control hamster killed 24 hr after the last dose of 50% DMSO-trioctanoin at 2 ml/kg/day, five times/wk for 6 wk. H & E. *Bar*=75 μm. × 190

Figure 5.—Edge of neoplastic nodule (*upper left*) exhibiting a border with normal hepatic tissue (*lower right*). This lesion was taken from the liver of an AFB$_1$-treated rat killed at 14 wk. H & E. *Bar*=75 μm. × 195

Figure 6.—Focal megalocytosis and cellular vacuolization in the liver of an AFB$_1$-treated hamster killed at 14 wk. H & E. *Bar*=75 μm. × 195

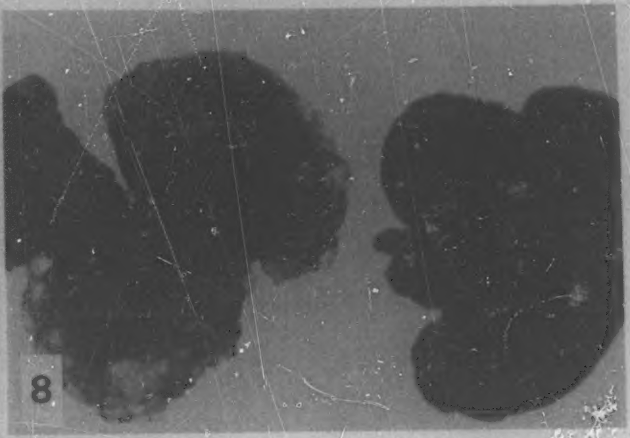

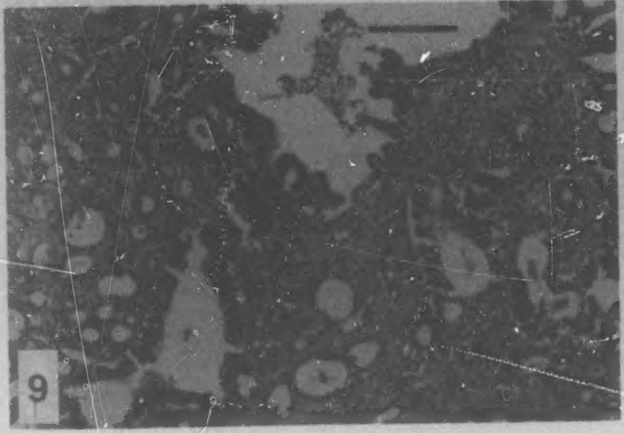

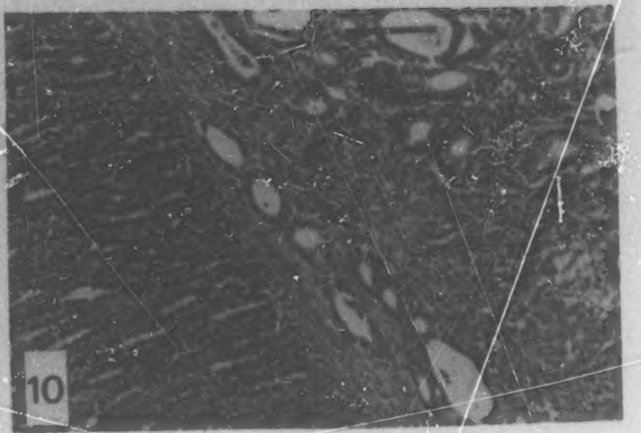

FIGURE 7.—Well-differentiated hepatocellular carcinoma (*upper left*) invading adjacent normal liver (*lower right*). Lesion was obtained from the liver of a hamster administered AFB$_1$ and killed at 78 wk. *Note* the darker staining of both nuclei and cytoplasm of the neoplastic cells as well as moderate cytologic anaplasia and several cell-thick plates in the neoplasm. H & E. *Bar*=150 µm. × 98

FIGURE 8.—Livers from AFB$_1$-treated (*left*) and control (*right*) hamsters killed at 78 wk.

FIGURE 9.—Cholangiocellular carcinoma from the liver of a hamster administered AFB$_1$ for 6 wk and killed at 78 wk. *Note* variable sizes of the neoplastic glands as well as some papillary projections in the upper large duct. H & E. *Bar*=150 µm. × 85

FIGURE 10.—Metastasis of cholangiocellular carcinoma to the submucosa of the stomach of a hamster administered AFB$_1$ for 6 wk and killed at 78 wk. *Note* the somewhat more uniform size of the glands in the metastatic as compared to the primary lesion (fig. 9). H & E. *Bar*=150 µm. × 85

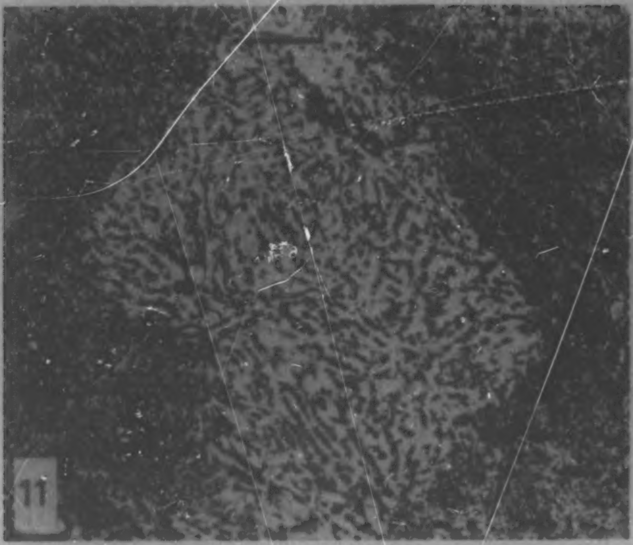

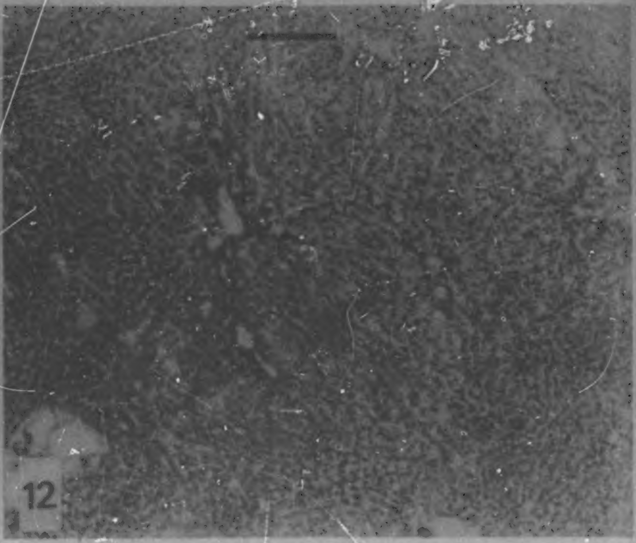

FIGURE 11.—ATPase-deficient focus in the liver from a hamster administered AFB$_1$ for 6 wk and killed at 78 wk. H & E. *Bar*=150 µm. × 82

FIGURE 12.—Serial section to the liver section shown in fig. 11 stained with H & E. *Note* that the focus seen in fig. 11 is not evident with H & E staining. *Bar*=150 µm. × 82

L-Histidinol Protection Against Cytotoxic Action of Cytosine Arabinoside and 5-Fluorouracil in Cultured Mouse Spleen Cells[1,2]

Robert C. Warrington[3,4] *and* **Wei D. Fang**[3,5]

ABSTRACT—The effects of L-histidinol, a structural analog of the essential amino acid L-histidine, on the proliferative responses and anticancer drug vulnerability of cultured spleen cells from male C57BL/6J mice exposed to optimal mitogenic doses of concanavalin A (Con A) or *E. coli* lipopolysaccharide (LPS) were investigated. By means of tritiated thymidine ([^{3}H]dThd) incorporation into acid-insoluble material as the criterion for proliferation, L-histidinol was shown to provide a dose-dependent inhibition of mitogenic responses elicited by Con A and LPS. Total (apparent) inhibition was provided by 1-m*M* concentrations of the analog and, at this concentration, [^{3}H]dThd incorporation was totally reversible even after 72 hours of sustained exposure. Simultaneous addition of L-histidinol and either of the mitogens provide a G_0-like arrest for 24 hours. Thereafter, the cells appeared to begin slow cell cycle transit but did not traverse the G_1/S boundary within 96 hours of incubation. These responses of cultured murine lymphocytes to L-histidinol provided dramatic and extended protection from the cell cycle phase-specific drug cytosine arabinoside and dramatic but transient protection from the cell cycle-specific drug 5-fluorouracil. In principle, these findings extend the L-histidinol anticancer drug approach for improving the therapeutic index of antineoplastic agents, not only to both *cycle-* and *phase-specific* drugs, but also to primary cells of myeloid origin.—JNCI 1982; 68:279–286.

The failure of anticancer drugs to act specifically against malignant cells in vivo represents a major weakness in the armamentarium of cancer treatment (*1*). Many anticancer drugs act against actively proliferating cells, regardless of their status, with resultant toxicities for non-malignant cells of the myelopoietic, gastrointestinal and epidermal tissues. One means of improving significantly the therapeutic index of several classes of currently used anticancer agents would be to reduce, selectively, the number of normal cells in cycle, while not altering the proliferative status of the malignant cell population. A priori, such an approach would increase the specificity of cytotoxic drugs, allow more aggressive treatment regimens, and reduce the deleterious side-effects of chemotherapeutic agents. One means of approaching this goal is to exploit the different growth properties of normal and neoplastic cells. This idea, first proposed in 1974 (*2*) and demonstrated in principle independently by Pardee and James (*3*) and O'Neill (*4*) in 1975, has been endorsed by others subsequently (*5–9*). The assumption inherent in these studies is that appropriate manipulation of the differences in growth responses of normal and neoplastic cells may be a means of conferring specificity upon cell cycle phase-specific drugs in vivo. Unfortunately, many of the reagents employed to date possess too high an inherent toxicity for in vivo applicability (*4, 10, 11*). Nevertheless, if an effective and nontoxic means of evoking differential proliferative responses from normal and neoplastic cell populations in the in vivo situation can be devised, such an approach could offer an improvement for cancer chemotherapy.

Studies from this laboratory (*12–14*) suggest that L-histidinol, a structural analog of the essential amino acid L-histidine, possesses a number of the properties required of an agent capable of enchancing the therapeutic index of anticancer drugs in vivo. L-Histidinol arrests reversibly the growth of a number of cells with normal phenotype and confers total protection from otherwise lethal doses of S-phase drugs. In contrast, the analog does not similarly arrest cell cycle transit of some tumorigenic cell lines and, consequently, does not diminish the susceptibility of these cells to S-phase drugs. In an on-going study, for example, the differential growth response elicited by L-histidinol from the normal/transformed CHO cell pair LR73/TR3 can provide an increase in the therapeutic index of Ara C in excess of 3×10^5 (Warrington RC, Fang WD: In preparation). Among the normal cells shown to be protected from S-phase drugs by histidinol are Balb/3T3 (*12*), LR73, low passage human foreskin fibroblasts (*14*), and 3T3 (*15*). Transformed lines tested to date include mouse L-cells, Balb/3T12, SV101, SVA31 (*15*), TR3, and a rat mammary adenocarcinoma, R13762 (Warrington RC: Unpublished observations).

In this study we extend our investigations of the effects of L-histidinol on proliferative responses and on cytotoxic drug vulnerability to primary cultures of mouse spleen cells. We demonstrate that histidinol not only inhibits the proliferative responses elicited by the mitogens Con A and LPS but also provides significant protection upon these cells from the cytotoxic action of the cell cycle phase-specific drug Ara C as well as the cell cycle-specific drug FUra.

ABBREVIATIONS USED: Ara C=cytosine arabinoside; Con A=concanavalin A; FBS=fetal bovine serum; FUra=5-fluorouracil; [^{3}H]dThd=tritiated thymidine; LPS=lipopolysaccharide.

---

[1] Received March 10, 1981; accepted September 1, 1981.

[2] Supported by Public Health Service research grant CA23823 from the National Cancer Institute.

[3] Department of Biochemistry, University of Saskatchewan, Saskatoon, Saskatchewan, S7N 0W0 Canada.

[4] Medical Research Council of Canada Scholar.

[5] We thank Dr. I. A. Ramshaw, Department of Microbiology, University of Saskatchewan, for advice and interest during the initial phase of this study. We also thank Mr. Kevin Atchison for his expert assistance in the early investigations.

MATERIALS AND METHODS

L-Histidinol was purchased from Aldrich Chemical Company, Milwaukee, Wis., Con A from Pharmacia, Piscataway, N. J., LPS W (*E. coli*) from Difco Laboratories, Detroit, Mich., and [*methyl*-^{3}H]dThd (6.7 Ci/mmol) from New England Nuclear Corp., Boston, Mass. Mice (20–25 grams body weight) were C57BL/6J males, bred and maintained in the Department of Microbiology, University of Saskatchewan animal facility. FUra was a product of Hoffmann-La Roche Inc., Nutley, N. J., and Ara C was a product of the Upjohn Co., Kalamazoo, Mich.

An appropriate number of C57BL/6J male mice were killed by ether anesthesia and subsequent cervical dislocation. Spleens were removed aseptically and forced gently through a sterile 64-mesh stainless steel screen. The resultant cell suspensions were swirled and pelleted (1,000 rpm, 15 minutes) three times from RMPI 1640 medium supplemented with 5% (vol/vol) FBS. Cell suspensions (0.1 ml, 3 × 10^6/ml) were made up in RPMI 1640+5% FBS, placed in Linbro tissue culture plates, and incubated in a humidified CO_2 incubator (5% CO_2, 37°C). "Nil" samples received no mitogens, whereas the mitogens Con A, 1 µg/ml, LPS, 100 µg/ml, were used at concentrations providing maximal incorporation of [^{3}H]dThd into acid-insoluble material after 48 hours of incubation. Each well was brought to a final volume of 0.2 ml by appropriate additions then 1 µCi [*methyl*-^{3}H]dThd was added. After 6 more hours of incubation (incorporation was shown to be linear over 8 hours), the cells were collected and washed onto filter paper by a semiautomated cell harvester. The filters were dried, placed in vials containing 6 ml scintillation fluid, and the radioactivity (incorporated into acid-insoluble material) was determined. For protein synthesis, [^{3}H]leucine was used in place of [^{3}H]dThd. Each data point represents the average incorporation of four replica wells. Where indicated, bulk (1.0 ml) cultures that had been exposed to various reagents were transferred to sterile siliconized tubes and centrifuged. The cells were washed by three successive resuspension–pelleting cycles. The washed cells were then resuspended in an appropriately reconstituted medium, incubated in Linbro wells and exposed to [^{3}H]dThd as above.

RESULTS

General Assessment of the Effects of L-Histidinol on DNA and Protein Biosynthesis in Cultured Spleen Cells

Initial characterizations of the C57 spleen culture system employed in this study included an evaluation of the concentrations of the mitogens Con A and LPS providing maximal incorporation of [^{3}H]dThd into acid-insoluble material, and an assessment of the duration of the linearity of isotope incorporation under optimized conditions. The dose responses of the cells to Con A and LPS, scored by a 6-hour exposure to [^{3}H]dThd after 48 hours of incubation in mitogens, are shown in the insets of text-figure 1. Incorporation after 24 hours of incubation with these mitogens gave qualitatively identical dose responses, although the total incorporation at 24 hours was typically 80–90% of that observed after the 48-hour exposure. Pulse experiments verified that label incorporation was linear for up to 8 hours (not shown) under optimized conditions. This argues that isotope availability is not a rate-limiting factor for the 6-hour pulse period used in all subsequent studies.

The effects of L-histidinol on proliferative responses were assessed initially by examining incorporation in cultures incubated for 24 hours with either no additions (nil) or optimal concentrations of Con A and LPS. In this instance, cultures received simultaneously various concentrations of the analog. Text-figure 1 shows that L-histidinol, added at the time of mitogen addition, provides a dose-dependent inhibition of [^{3}H]dThd incorporation which is qualitatively identical in Con A- and LPS-supplemented cultures, as well as nil cultures. Total inhibition of incorporation, in all cases, was obtained by 1 m*M* L-histidinol.

The time dependency of histidinol inhibition of proliferative responses is documented in text-figure 2. As is the case in most cells exiting quiescence or G_0 (*16*), cultured lymphocytes show a quasi-synchronous proliferative response on exposure to mitogens (*16, 17*). Murine lymphocytes in culture traverse the G_0/G_1 boundary between 3 and 6 hours after mitogen exposure (*18*) and cross the G_1/S boundary approximately 20 hours after stimulation (*18*). Text-figure 2 indicates that L-histidinol inhibits the proliferative re-

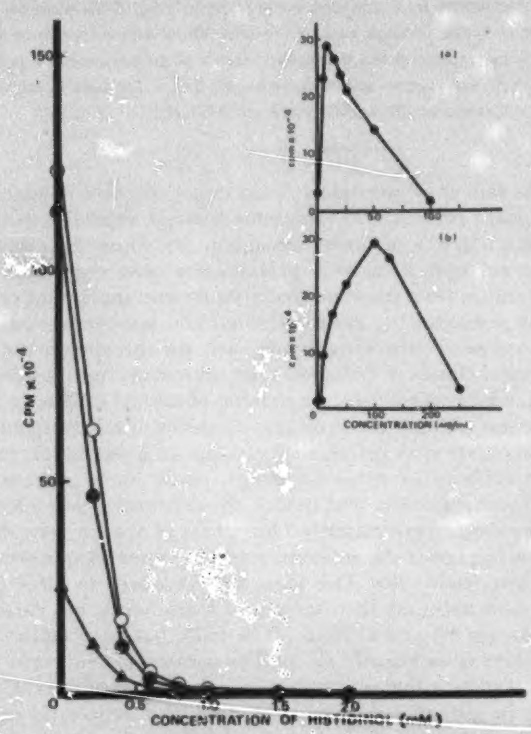

TEXT-FIGURE 1.—*Inset*: Dose dependence of Con A (a) and LPS (b) on [^{3}H]dThd incorporation into acid-insoluble material (hereafter, this will be referred to as the less qualified term DNA synthesis). Text-fig.: Inhibition of DNA synthesis by L-histidinol. Cultures were treated with 1 µg Con A/ml (●), 100 µg LPS/ml (○), or no additions (▲) and, at the same time, with the noted concentrations (final) of L-histidinol. After 24 hr of incubation, DNA synthesis was determined as for the inset.

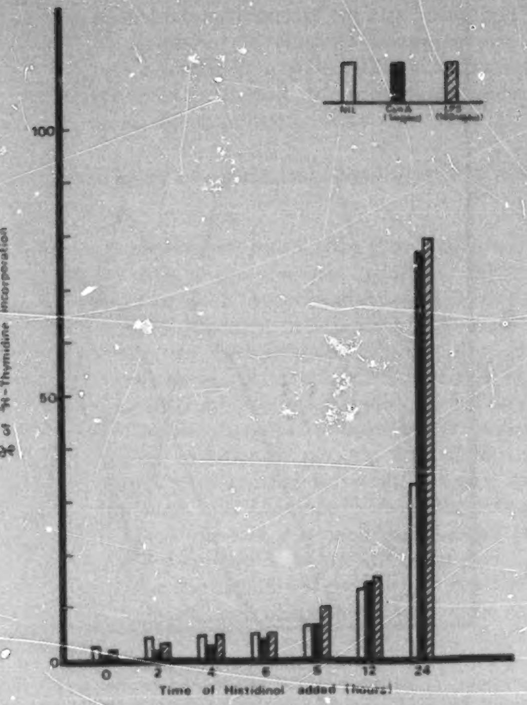

TEXT-FIGURE 2.—Time dependence of the inhibition of DNA synthesis by L-histidinol. Taking the zero time as the time of mitogen addition, at zero time and various intervals thereafter, L-histidinol (1 m*M*) was added to nil-, Con A-, or LPS-treated cells. At 24 hr, DNA synthesis was determined and scored relative to the incorporation observed in cultures not receiving L-histidinol (100%).

sponses of murine spleen cells maximally if added to G_0 cells, that inhibition diminishes as the drug is added to G_0/G_1 transitting and G_1-committed cells, and that minimal inhibition ensues in S-phase committed cells.

The major and initial effect of L-histidinol on eukaryotic cells is a competitive inhibition of histidyl-tRNA synthetase (*19*). This results in a dramatic elevation of the deacylated form of $\mathrm{tRNA^{His}}$ which, in turn, causes not only an abrupt inhibition of protein biosynthesis (*19, 20*) but also a number of alterations of cellular physiology. These include a profound and specific reduction in rRNA production (*20*) and diminished uptake of various nutrients (*21*), effects collectively termed as negative pleiotypic response (*22*). To establish that L-histidinol was inhibiting protein biosynthesis in spleen cells, the effects of the analog on [^{3}H]leucine incorporation into acid-insoluble material were examined at both early (0–5 hours) and late (17–22 hours) times relative to the time of mitogen addition. Text-figure 3 demonstrates that L-histidinol provided a dose-dependent inhibition of leucine into acid-insoluble material. However, cells treated with L-histidinol early appeared somewhat less inhibited than cells which are assumed to be at or beyond the G_1/S boundary (17–22 hours). Although the significance of this observation is not clear, it does argue that the apparent inability of the analog to inhibit [^{3}H]dThd incorporation in G_1 and S-phase cells is not simply a result of an inability of histidinol to inhibit protein biosynthesis in committed spleen cells.

Histidine Reversal of the Histidinol-Mediated Inhibition of Proliferative Responses of Con A- and LPS-Treated Spleen Cells

Having verified that L-histidinol provided total inhibition of mitogenic responses for 24 hours (text-fig. 1), it was of interest to examine further aspects of its antiproliferative effects. These aspects included an evaluation of the duration of the inhibition, an assessment of whether the inhibition was reversible and, if so, an investigation of alterations in the kinetics of reversal as a function of the duration of incubation. These objectives were examined by preparing cultures treated with either Con A or LPS as well as 1 m*M* L-histidinol. At daily intervals, such cultures were released from the histidinol-mediated proliferative arrest by the addition of excess L-histidine and pulsed with [^{3}H]dThd immediately after reversal and at 24-hour intervals thereafter. One distinct advantage of L-histidinol as an antiproliferative agent is that its effects can be reversed simply by supplementing the treated cultures with excess L-histidine. Since histidinol exerts its effects by a competitive inhibitory mode, the inhibitor itself may be competed against effectively by providing excess histidine (*19, 20*). Therefore, the release of cultures from the histidinol block was achieved by adding L-histidine to the appropriate cultures. The results of these experiments are presented in text-figures 4 and 5.

Neither Con A- nor LPS-treated cultures reveal any spontaneous recovery from the block to dThd incorporation mediated by 1 m*M* L-histidinol for up to 96 hours of incubation. That such cultures were incubated continuously

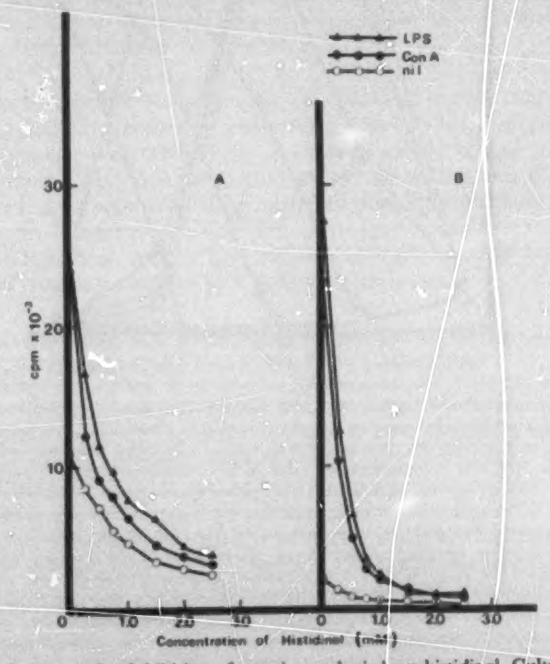

TEXT-FIGURE 3.—Inhibition of protein synthesis by L-histidinol. Cultures supplemented with Con A (●), LPS (▲), or no mitogen (○) were treated with 1 m*M* L-histidinol and 1 μCi [^{3}H]leucine/ml at 0 (A) or 17 hr (B). After 5 hr of incubation, the incorporation of [^{3}H]leucine into acid-insoluble material was determined.

best copy available

in optimal concentrations of the mitogens Con A and LPS, attests to the substantial and long-term effectiveness of histidinol as an antiproliferative agent. Mitogen-treated cultures not receiving L-histidinol showed substantial DNA synthesis for 48 hours with a drastic reduction by 72 hours. Significant restoration of the capacity for [^{3}H]dThd incorporation was observed in L-histidinol-treated cultures supplemented with histidine, even after 3 days of continuous treatment. This observation demonstrates that the L-histidinol-mediated inhibition of proliferative responses is one that is characterized by reversibility. Although the overall apparent rates and maximum levels of incorporation in released cultures are comparable to those observed in the mitogen-treated controls, it is clear that as the incubation continues prior to reversal, the kinetics of incorporation of [^{3}H]dThd change in a consistent manner. In both Con A- and LPS-treated cultures, the level of incorporation observed in the pulse period given immediately after reversal with histidine increases with incubation time. Another trend, which appears to be correlated with the former pattern, is a tendency for cultures held longer in histidinol prior to reversal, to reach maximal apparent rates of incorporation in shorter and shorter reversal periods. Both of these observations suggest, but by no means prove, that histidinol provides a transient G_0 arrest. The transience of the block is presumably a result of chronic mitogenic stimulus that allows the cells to exit slowly from G_0 and to approach but not traverse the G_1/S boundary. The latter point is suggested by the lack of incorporation in histidinol-treated cells not subjected to reversal. These interpretations are further substantiated by the anticancer drug experiments described below.

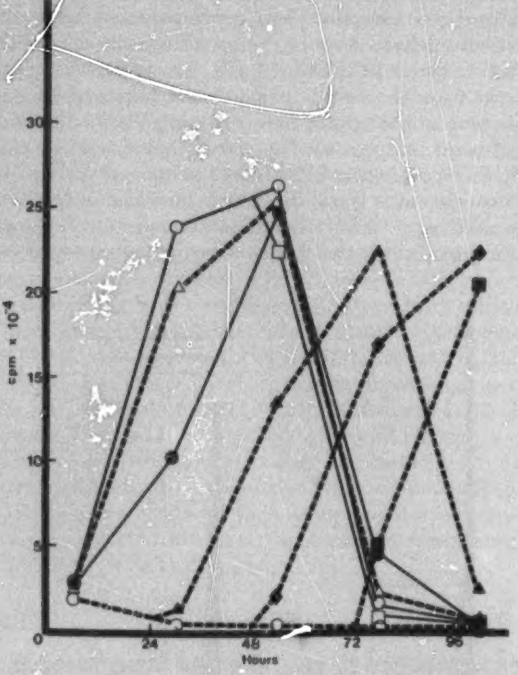

TEXT-FIGURE 4.—Recovery of DNA synthesis by the addition of L-histidine to L-histidinol–Con A-treated cells. Release from the L-histidinol-mediated proliferative arrest in Con A–L-histidinol-treated cells, 1 µg/ml and 1 m*M*, respectively, was achieved by adding L-histidine dihydrochloride (2 m*M*). For cultures released after 24 hr of exposure to Con A and L-histidinol, ▲- - -▲, replica wells were pulsed from 0–6, 24–30, 48–54, and 72–78 hr relative to the time of addition of L-histidine. Similarly, cultures released after 48 hr, ◆- - -◆, were pulsed from 0–6, 24–30, and 48–54 hr relative to the time of addition of L-histidine. Likewise, cultures incubated for 72 hr in Con A (L-histidinol) prior to release, ■- - -■, were pulsed from 0–6 and 24–30 hr relative to the time of L-histidine addition. Subsequent experiments (not shown) employing L-histidine, rather than L-histidine dihydrochloride, showed an absence of the minor perturbation of DNA synthesis observed here for cultures receiving Con A, L-histidinol, and L-histidine △- - -△. Hence, all subsequent reversal experiments employed L-histidine. ○——○=Con A; ●——●=Con A+L-histidinol+L-histidine; □——□=L-histidine added at 48 hr; ○- - -○=Con A+L-histidinol.

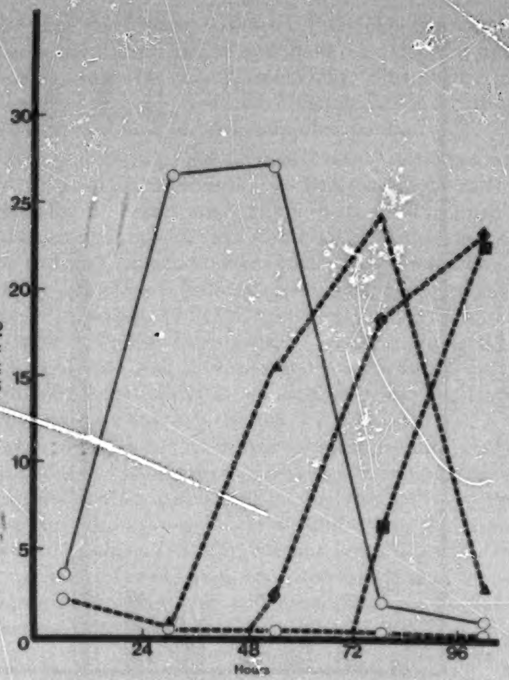

TEXT-FIGURE 5.—Recovery of DNA synthesis by the addition of L-histidine to L-histidinol–LPS-treated cells. Release from the L-histidinol-mediated inhibition of DNA synthesis in LPS–L-histidinol-treated cells, 100 µg/ml and 1 m*M*, respectively, was achieved by adding 2 m*M* L-histidine at 24 (▲), 48 (◆), or 72 (■) hr. The recovery of DNA-synthetic capacity was determined as in text-fig. 4. ○——○=LPS; ○- - -○=LPS+L-histidinol.

Toxicity of Ara C and FUra to Spleen Cells

To assess the possibility that the L-histidinol-mediated proliferative arrest of spleen cells would confer protection from cytotoxic action of the cell cycle phase-specific drug Ara C and the cell cycle-specific drug FUra (*23*), it was necessary to evaluate the inherent toxicity of these drugs. Text-figure 6 demonstrates the dose dependency of inhibition of [^{3}H]dThd incorporation by these drugs in Con A- and LPS-treated cultures. The cells were exposed to various concentrations of the drugs for 24 hours and residual DNA-synthetic capacity was scored without removal of the cytotoxic drug. As will be shown below, assessment of residual DNA-synthetic capacity without removal of the drugs provides a substantial overestimate of toxicity. Although low levels of FUra appeared to enhance incorporation, this response may be interpreted as reflecting a perturbation in the specific activity of the thymidine triphosphate precursors rather than an actual stimulatory effect.

Dose Dependency of L-Histidinol-Mediated Protection From Ara C

The previous experiment established that 5 μg Ara C/ml was sufficiently toxic to provide total (apparent) inhibition of [^{3}H]dThd incorporation. Accordingly, Con A-treated cells were given varying doses of L-histidinol and 5 μg Ara C/ml for 24 hours. To score for putative protection, it was necessary to wash these cultures to eliminate Ara C. To facilitate this essential manipulation, bulk (1.0 ml) cultures were prepared and incubated after appropriate additions. At the end of the incubation period, the cultures were transferred to sterile, siliconized tubes and washed as described in "Materials and Methods." The cells were then resuspended in medium and dispersed into Linbro plates (0.2 ml/well) and processed as before. In text-figure 7, the residual DNA-synthetic capacity of the cultures as a function of L-histidinol concentration is shown scored relative to Con A-treated control cultures similarly manipulated. In contrast to the former experiment, wherein the Ara C was not removed prior to assessment, this protocol reveals that Ara C and Con A-treated cells retain, after 24-hour exposure, approximately 15% of the capacity of control cells to incorporate [^{3}H]dThd. The addition of L-histidinol provides a dramatic protective effect, which is dose-dependent up to 1 m*M*. The latter concentration provided total apparent protection from Ara C. The addition of higher concentrations of the analog results in a decline of protection.

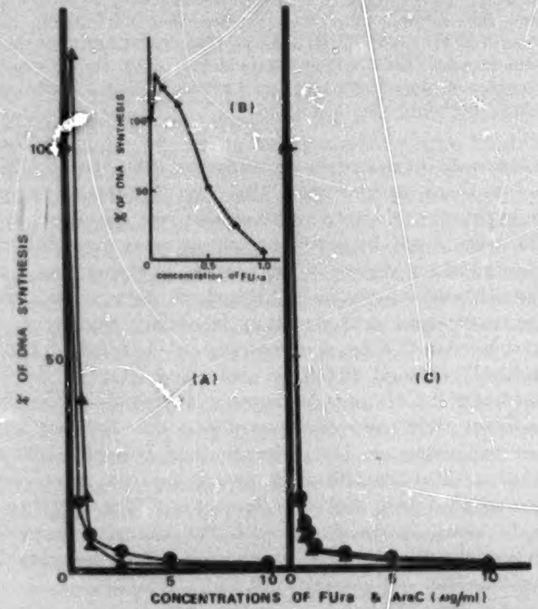

TEXT-FIGURE 6.—Inhibition of DNA synthesis in Con A- and LPS-treated lymphocytes by Ara C and FUra. A) Spleen cells received 1 μg Con A/ml and the noted concentrations of Ara C (●) or FUra (▲). After 24 hr, DNA-synthetic capacity was determined without prior removal of drugs and expressed as a percentage of DNA synthesis in cells receiving only Con A (100%) (concentration terms 1, 5, and 10 μg/ml for Ara C and FUra correspond to 4.1, 20.56, and 41.1 μmol and to 7.69, 38.4, and 76.9 μmol, respectively). B) The experiment was as for A except a larger number of low concentrations of FUra were used. C) Spleen cells received 100 μg LPS/ml and the indicated concentrations of Ara C (●) or FUra (▲). DNA synthesis was scored as in A.

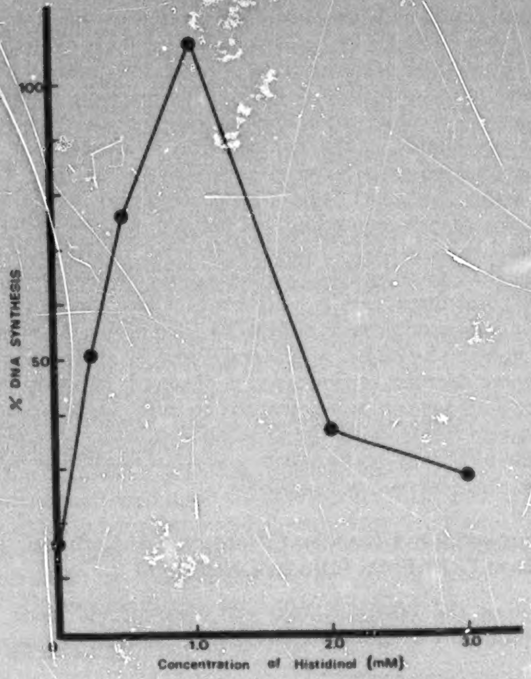

TEXT-FIGURE 7.—Dose dependency of L-histidinol-mediated protection from Ara C. Bulk, 1.0 ml, cultures of spleen cells received 1 μg Con A/ml, 5 μg Ara C/ml, and the noted concentrations of L-histidinol. After 24 hr of incubation, the bulk cultures were washed three consecutive times to remove drugs. The cells were then reincubated with Con A alone for 24 hr and then pulsed for 6 hr with [^{3}H]dThd. The incorporation is plotted as a percentage of a control culture, Con A-treated for 24 hr, followed by [^{3}H]dThd pulse.

Substantial and Prolonged Protection of Cultured C57 Spleen Cells From Ara C by L-Histidinol

The previous experiment verified that 1 m*M* L-histidinol provided total protection to spleen cells treated with an optimum mitogenic dose of Con A and a decidedly toxic level of Ara C. It was of interest to attempt to define the duration of the protective influence over a range of Ara C concentrations. The results of such a study are represented in text-figure 8, wherein residual DNA synthesis is equated operationally with cell survival.[6] For cultures receiving Con

---

[6] Since there is a principled, but not verified, justification of equating residual DNA-synthetic capacity with the more meaningful relative cell survival assay, the data in text-figs. 8 and 9 are presented as *pseudo*-relative cell survival.

A and Ara C without L-histidinol, it appears that a dose of 1 μg Ara C/ml for 24 hours confers near maximal toxicity. Increased drug concentrations or increased duration of exposure to the drug provide but a rather marginal additional toxicity. This observation may indicate that the majority of cells responding to the mitogen Con A are brought into cycle (and hence rendered vulnerable to this low dose of Ara C) within the initial 24-hour exposure period, with a lesser fraction of cells responding in a delayed manner. However, other modes of Ara C toxicity may be involved (*24*). A different type of response is observed in cultures receiving 1 m*M* L-histidinol, Con A, and Ara C. L-Histidinol provides essentially total protection from all doses of Ara C tested for 24 hours. Thereafter, a moderate dose- and duration-dependent decrease of protection is observed. However, even after 3 days of continuous incubation in the highest concentration of Ara C tested, the histidinol-supplemented cultures retain a DNA-synthetic capacity which is fourfold or higher than that observed in its absence.

Substantial but Transient Protection of Cultured Spleen Cells From FUra by L-Histidinol

Given the generality that cell cycle-specific drugs are useful agents in the chemotherapeutic management of cancer, we were interested in assessing the influence of L-histidinol on FUra, a prototype of this class of anticancer agents. The experimental protocol employed was the same as described for Ara C experiments above, and the results are presented in text-figure 9. For cultures receiving Con A and FUra without L-histidinol, the toxicity patterns are somewhat more dose- and duration-dependent than were observed for Ara C–Con A combinations. Although 1 m*M* L-histidinol provided dramatic protection from all doses of FUra tested for 24 hours of exposure, thereafter we observed significant dose- and duration-dependent decrease in its protective influence. The rather marked difference between the influence of L-histidinol on protection from Ara C, an S-phase specific drug and its influence on FUra, a cell cycle-specific drug, is consistent with the duration-dependent effects of the analog. This observation will be elucidated in the discussion.

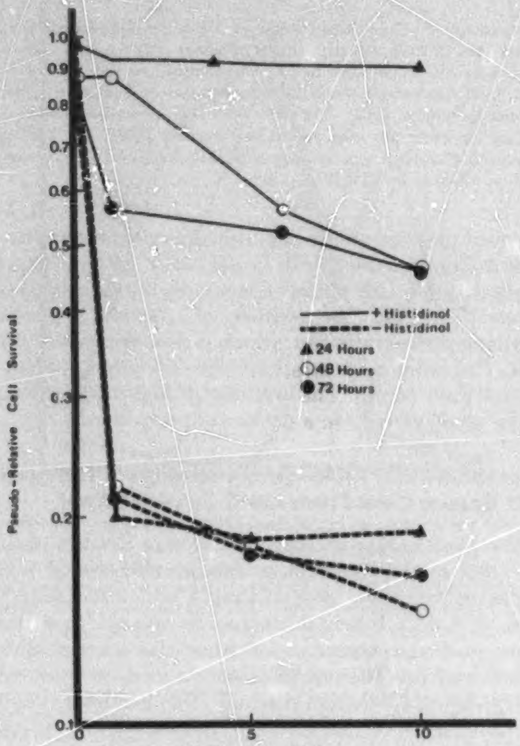

TEXT-FIGURE 8.—Protection of Con A-treated cells from Ara C by L-histidinol. Bulk cultures, 1.0 ml, were supplemented with 1 μg Con A/ml, L-histidinol (1 m*M*), or 1, 5, or 10 μg Ara C/ml or 4.1, 20.56, or 41.1 μmol, respectively, as noted. After 1, 2, or 3 days of incubation, the cultures were washed and reincubated with 2 μg Con A/ml for 24 hr and finally pulsed with [^{3}H]dThd for 6 hr.

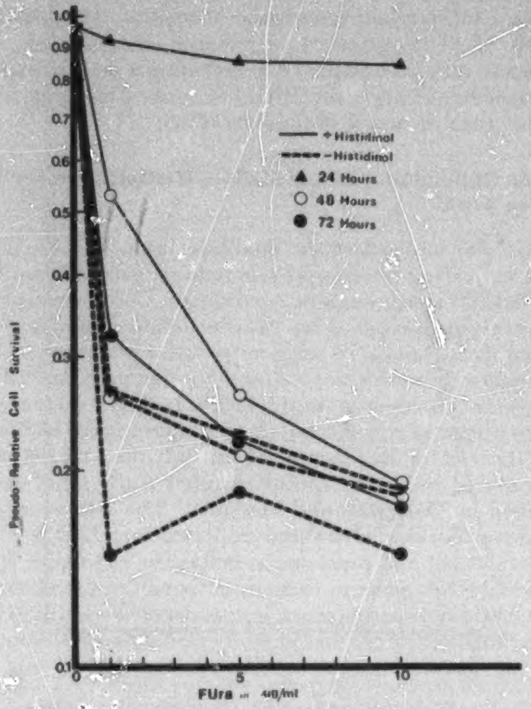

TEXT-FIGURE 9.—Protection of Con A-treated cells from FUra by L-histidinol. Bulk cultures, 1.0 ml, were supplemented with 1 μg Con A/ml, L-histidinol (1 m*M*), or 1, 5, or 10 μg FUra/ml or 7.69, 38.4, or 76.9 μmol, as noted. After 1, 2, or 3 days of incubation, the cultures were washed, reincubated with 1 μg Con A/ml for 24 hr and finally pulsed with [^{3}H]dThd for 6 hr.

DISCUSSION

The studies presented here establish that murine splenic lymphocytes of both T- and B-cell designation (scored as Con A- and LPS-responsive cells, respectively) are influenced by the histidine analog L-histidinol in a manner reminiscent of that of nonmyeloid normal cells in culture. The histidine analog inhibits B- and T-lymphocyte mitogenic responses, evaluated by the criterion of [^{3}H]dThd incorporation into an acid-soluble form. This inhibition, as seen in nonmyeloid lines, is dependent both upon the dose of the analog as well as upon the time of addition relative to the mitogenic stimulus. A maximal and prolonged inhibition is observed if the analog is added at the time of mitogen addition, whereas delaying the addition of L-histidinol with regard to mitogen addition results in a diminishing suppression of the proliferative response. Cultures receiving both mitogen and L-histidinol simultaneously show total apparent reversibility after 3 days of inhibition, even though these cultures show no spontaneous G_1/S transit for up to 4 days in culture. It is essential that any agent that is contemplated as a means of improving the therapeutic index of anticancer drugs in vivo, should not only provide selective and long-term inhibition of proliferative responses for cells of normal phenotype, but also, it should allow complete reversal following the phase of inhibition. Similar long-term but completely reversible states of proliferative arrest mediated by L-histidinol are observed in other types of cells possessing normal phenotype (*12-15*).

A more critical evaluation of the data presented herein reveals, however, that these myeloid cells are not maintained in a persistent G_0-like state on histidinol treatment, as is the case for their normal but nonmyeloid counterparts (*12-15*). Con A- and LPS-treated murine spleen lymphocytes supplemented with L-histidinol appear to be maintained in a G_0-like state for approximately 24 hours. Thereafter, a cell-cycle progression toward, but not traversing, the G_1/S boundary appears to ensue. The strongest evidence for this interpretation derives from the decay of FUra protection observed in text-figure 9. G_0-exiting cells become vulnerable to FUra, initially, as a result of the marked elevations in RNA synthesis (*23*), which delineates the G_0/G_1 boundary transition (*17*). This macromolecular event begins between 3-6 hours after mitogen treatment of murine lymphocytes (*18*) in the absence of an agent such as L-histidinol. Hence, the vulnerability of analog-treated cells subjected to FUra for periods in excess of 24 hours, combined with the changing kinetics of DNA synthesis following reversal of histidinol treatment (text-figs. 4, 5), suggest that the analog establishes a G_0-sojourn of approximately 24 hours followed thereafter by progression into G_1. We note that essentially identical interpretations were made by Taudou et al. (*26*) in their analysis of the effects of L-histidinol on DNA synthesis in Con A-treated guinea pig lymphocytes. Although these descriptions are consistent with the [^{3}H]dThd incorporation studies and with the duration-toxicity studies using Ara C and FUra, they remain suggestive, nevertheless, pending an investigation by a more definitive approach like the flow cytometric analysis of lymphocyte responses with the use of acridine orange (*17, 25*). Such uncertainties notwithstanding, the inhibition of proliferative responses mediated by L-histidinol is sufficient to provide a dramatic and prolonged protection from the cell-phase specific drug Ara C, as well as a dramatic but transient protection from the cycle-specific drug FUra.

The data presented in this study represent, to our knowledge, the first report that *primary* cells in culture can be protected from anticancer drugs by manipulating their proliferative status using an agent like L-histidinol. Furthermore, we believe that this is also the first documentation that this type of approach can be extended to *cell cycle-specific* anticancer drugs. In principle these observations suggest that a combined histidinol-anticancer drug approach for improving the therapeutic index of anticancer agents may be applicable to a much broader spectrum of drugs than was envisaged originally (*14*). Should the spleen lymphocytes prove to be reminiscent of their more immediate or pluripotent myeloid precursors in terms of their response to L-histidinol, then these results also suggest that the crucial marrow population cells may likewise be provided protection from anticancer drugs by means of the histidinol-anticancer drug approach. This possibility is under investigation currently. We have demonstrated that L-histidinol, given at appropriate schedules in conjunction with a large, single challenge of Ara C, confers substantial protection upon the bone-marrow cell population of intact mice (Warrington RC, Fang WD: Unpublished observation). These observations, based upon the resumption of de novo erythropoiesis and lymphopoiesis following drug treatments, have been confirmed (Warrington RC, Fang WD: Unpublished observation) by experiments relying on the quantitative CFU-C assay for murine bone marrow cells (*27*).

REFERENCES

(*1*) Tannock I. Cell kinetics and chemotherapy: A critical review. Cancer Treat Rep 1978; 62:1117-1133.

(*2*) Halpern BC, Clark BR, Hardy DH, Halpern RM, Smith RA. The effect of replacement of methionine by homocysteine on survival of malignant and normal adult mammalian cells in culture. Proc Natl Acad Sci USA 1974; 71:1133-1136.

(*3*) Pardee AB, James LT. Selective killing of transformed baby hamster kidney cells. Proc Natl Acad Sci USA 1975; 72:4994-4998.

(*4*) O'Neill FJ. Selective destruction of cultured tumor cells with uncontrolled nuclear division by cytochalasin B and cytosine arabinoside. Cancer Res 1975; 35:3111-3115.

(*5*) Rozengurt E, Po CC. Selective cytotoxicity for transformed 3T3 cells. Nature 1976; 261:701-702.

(*6*) Bradley MO, Kohn KW, Sharkey NA, Ewig RA. Differential cytotoxicity between transformed and normal human cells with combinations of aminonucleoside and hydroxyurea. Cancer Res 1977; 37:2126-2131.

(*7*) Schiaffonati L, Baserga R. Different survival of normal and transformed cells exposed to nutritional conditions nonpermissive for growth. Cancer Res 1977; 37:541-545.

(*8*) Fernandez-Pol JA, Bono VH, Johnson GS. Control of growth by picolinic acid: Differential responses from normal and transformed cells. Proc Natl Acad Sci USA 1977; 74:2889-2893.

(*9*) Rupniak HT, Paul D. Selective killing of transformed cells by exploitation of their defective cell cycle controls by polyamines. Cancer Res 1980; 40:293-297.

(*10*) Lin H, Bruce WR, Walcroft MJ. Concanavalin A (NSC-143504): Its action on experimental tumor cells and possible use in cancer chemotherapy. Cancer Chemother Rep 1975; 59 (pt. 1):319-326.

(*11*) Ben-Ishay Z, Farber E. Protective effects of an inhibitor of protein synthesis cycloheximide, on bone marrow damage by cytosine arabinoside or nitrogen-mustard. Lab Invest 1977; 33:478-490.

(*12*) Warrington RC, Hechtman R. The histidine analogue L-histidinol arrests the growth of Balb/3T3 cells in G_0. Cell Biol Int Rep 1977; 1:571-579.

(*13*) Yen A, Warrington RC, Pardee AB. Serum-stimulated 3T3 cells undertake a histidinol-sensitive process which G1 cells do not. Exp Cell Res 1978; 114:458-462.

(*14*) Warrington RC. Selective killing of oncogenic human cells cocultivated with normal human fibroblasts. JNCI 1978; 61:69-73.

(*15*) ———. Differential responses of normal and transformed mouse cell lines to L-histidinol. Am Soc Microbiol 1977; 1:120.

(*16*) Baserga R. Multiplication and division in mammalian cells. New York: Marcel Dekker, Inc. 1976;53-72.

(*17*) Darzynkiewicz F, Traganos T, Sharpless T, Melamed MR. Lymphocyte stimulation: A rapid multiparameter analysis. Proc Natl Acad Sci USA 1976; 73:2881-2884.

(*18*) Chambers DA, Martin DW, Weinstein Y. The effect of cyclic nucleotides on purine biosynthesis and the induction of PRPP synthetase during lymphocyte activation. Cell 1974; 3:375-380.

(*19*) Hansen BS, Vaughan MH, Wang L. Reversible inhibition by histidinol of protein synthesis in human cells at the activation of histidine. J Biol Chem 1972; 247:3854-3857.

(*20*) Warrington RC, Wratten N, Hechtman R. L-Histidinol inhibits specifically and reversibly protein and ribosomal RNA synthesis in mouse L-cells. J Biol Chem 1977; 252:5251-5257.

(*21*) Grummt F, Grummt I. Studies on the role of unchanged tRNA in pleiotypic responses of animal cells. Eur J Biochem 1976; 64:307-312.

(*22*) Hershko A, Mamont P, Shields R, Tomkins GM. Pleiotypic response. Nature [New Biol] 1971; 232:206-211.

(*23*) Evans RM, Laskin JD, Hakala MT. Assessment of growth-limiting events caused by 5-fluorouracil in mouse cells and human cells. Cancer Res 1980; 40:4113-4122.

(*24*) Hawtrey AO, Scott-Burden T, Robertson G. Inhibition of glycoprotein and glycolipid synthesis in hamster embryo cells by cytosine arabinoside and hydroxyurea. Nature 1974; 252:58-60.

(*25*) Darzynkiewicz Z. Acridine orange as a molecular probe in studies of nucleic acids in situ. In: Melamed MR, Mullaney PF, Mendelsohn ML, eds. Flow cytometry and sorting. New York: Wiley. 1979:285-316.

(*26*) Taudou G, Wiart J, Panijel J. An inhibitor of tRNA aminoacylation reversibly inhibits DNA synthesis in concanavalin A-treated lymphocytes. Mol Immunol 1979; 16:137-139.

(*27*) Stohlman F, Quesenberry PJ, Tyler WS. The regulation of myelopoiesis as approached with in vivo and in vitro techniques. In: Brown EB, ed. Progress in hematology. New York: Grune. 1972: 259-297.

Murine Lymphoma L5178Y Cells Resistant to Purine Antagonists: Differences in Cross-Resistance to Thioguanine-Platinum(II) and Selenoguanine-Platinum(II)[1, 2]

Fumihiko Kanzawa,[3] Mitsuaki Maeda,[4] Takuma Sasaki,[4] Akio Hoshi,[3] *and* Kazuo Kuretani[3]

ABSTRACT—To determine whether the antitumor activities of thioguanine-platinum(II) [TG-Pt(II)] and selenoguanine-platinum(II) [SeG-Pt(II)] are due to direct actions of these compounds or to the actions of their hydrolysis products, studies were made on a purine antagonist-resistant, murine lymphoma L5178Y/MP subline that lacked the anabolic enzyme hypoxanthine-guanine phosphoribosyltransferase necessary for tumor inhibition. The L5178Y/MP subline proved to be highly resistant to both TG-Pt(II) and thioguanine; the resistance ratios to the two compounds were almost identical. The subline showed high resistance to selenoguanine, but the cross-resistance to SeG-Pt(II) was negligible. Whether the compounds exhibit the delayed cytotoxicity characteristic of purine antagonists was also investigated. Delayed cytotoxicity was demonstrated for TG-Pt(II) as well as for thioguanine and other purine antagonists but not for SeG-Pt(II) or *cis*-dichlorodiammineplatinum(II). Experiments on cross-resistance and delayed cytotoxicity showed differences in the cytotoxicities of TG-Pt(II) and SeG-Pt(II): TG-Pt(II) exerted its activity through its hydrolysis product thioguanine, whereas SeG-Pt(II) compound was cytotoxic itself.—JNCI 1982; 68:287–291.

Since the antitumor activity of cisplatin [*cis*-dichlorodiammine-platinum(II)] has proved to be effective as an inhibitor to the growth of several experimental tumors (*1, 2*), considerable efforts have been made towards finding platinum derivatives with better antitumor activity and less toxicity (*3–9*). Previously, several complexes of TG and SeG with platinum, such as TG-Pt(II) and SeG-Pt(II), have been reported to be effective antitumor agents in experimental animals (*10*). They had at least as much cytotoxic activity as the parent compounds but were less toxic to the host. The mechanism of action of these compounds is not fully understood. Their cytotoxicity is thought to be produced by their direct antitumor effects, or through splitting to their respective nucleo-bases (TG or SeG) with subsequent metabolic conversion to their respective nucleotides by HGPRT, a process necessary for tumor inhibition (*11*). Our purpose in this study was to determine which of these two possibilities is correct. To this end, we tested against these compounds the cross-resistance of a cell line lacking HGPRT activity, and, hence, resistant to purine antagonists. We also tested TG-Pt(II) and SeG-Pt(II) for delayed cytotoxicity, which is a characteristic property found in purine antagonists such as MP and TG (*12–14*).

MATERIALS AND METHODS

Chemicals.—TG-Pt(II) and SeG-Pt(II) were prepared as described previously (*10*). Their chemical structures are shown in text-figure 1. SeG was synthesized by the method of Mautner et al. (*11*). Cisplatin and TG, used as reference compounds, were purchased from Strem Co. Ltd., Newburyport, Mass., and Sigma Chemical Co., St. Louis, Mo., respectively. ^{14}C-labeled hypoxanthine (sp act, 55 mCi/mmol) was purchased from the Radiochemical Centre, Amersham, England.

Cell culture.—A clone of murine lymphoma L5178Y cells designated L5178Y/O, sensitive to purine antagonists, was used in the experiments and was also used as the parental line for isolating the MP-resistant cell line. Stock cultures of L5178Y cells were maintained as suspension cultures in exponential growth by three subcultures a week in Fischer's medium (GIBCO, Grand Island, N.Y.) supplemented with 10% horse serum, 100 μg streptomycin/ml and 100 U penicillin/ml in a CO_2 incubator with a humid atmosphere of 5% CO_2 and 95% air as described previously (*15*). Cultures were restarted from frozen stock every 6 weeks.

Evaluation of antitumor action.—We tested the effects of drugs on the proliferation of L5178Y cells in vitro (*16*) by two different methods. First, we evaluated the cytotoxic effect of continuous exposure to drugs on cell proliferation. Duplicate 10-ml cultures, initially containing 2.5×10^4 cells/ml, were incubated in medium with test compounds at various concentrations in capped 50-ml bottles for 48 hours at 37°C. After incubation, cells were counted in either a TOA Microcellcounter CC-108 (TOA Medical Electronics Co., Kobe, Japan) or under a microscope, and the cell proliferation ratio of treated versus control cultures was calculated. Antiproliferating activities were determined as IC_{50} values—the concentrations required for 50% inhibition of cell proliferation of control cultures during incubation for 2 days. The second method was designed to determine delayed cytotoxicity, i.e., the effect of brief exposure to drugs on subsequent cell growth in drug-free medium. Duplicate 20-ml cultures

---

ABBREVIATIONS USED: HGPRT=hypoxanthine-guanine phosphoribosyltransferase; MNNG=*N*-methyl-*N'*-nitro-*N*-nitrosoguanidine; MP=6-mercaptopurine; SeG=6-selenoguanine; SeG-Pt(II)=selenoguanine-platinum(II); TG=6-thioguanine; TG-Pt(II)=thioguanine-platinum(II).

---

[1] Received May 20, 1981; accepted September 18, 1981.

[2] Supported by a grant-in-aid for cancer research from the Ministry of Health and Welfare of Japan.

[3] Pharmacology Division, National Cancer Center Research Institute, 1-1 Tsukiji 5-chome, Chuo-ku, Tokyo 104, Japan.

[4] Chemotherapy Division, National Cancer Center Research Institute.

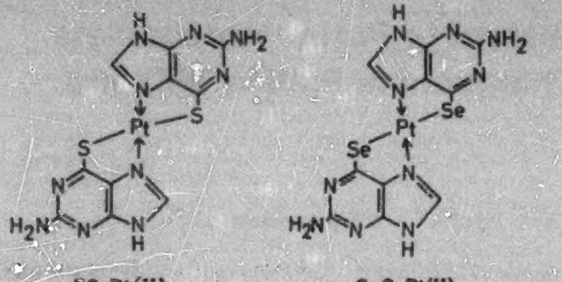

TG-Pt(II) SeG-Pt(II)

TEXT-FIGURE 1.—Chemical structures of TG-Pt(II) and SeG-Pt(II).

containing 2×10^4 cells/ml were exposed to drugs at various concentrations for 24 hours. The cells were then collected by centrifugation (500×*g*, for 3 min), washed once with warm drug-free medium, resuspended in fresh medium, and incubated for 4 days at 37°C. Samples were taken at regular intervals to determine cell density. After culture for 4 days, the cumulative cell number was calculated by multiplying the cell densities by the dilution factors for each subculture. The cytotoxicity of the drug was expressed as the IC_{99} value—the concentration required for 99% inhibition of cell proliferation in the 4-day period.

Isolation of the resistant cell line.—A cell line resistant to purine antagonists was established by the technique described previously for the selection of the L5178Y/FU subline (*17*). L5178Y cells were submitted to the mutagenic action of 3.0 µ*M* MNNG for 24 hours, then exposed to MP for 24 hours, washed once, and cultured in drug-free medium until cell proliferation resumed. The resulting cells were then exposed to about three times the previous drug concentration. This procedure, termed the drug-treatment episode, was repeated when the cells showed the same proliferation ratio as untreated cultures. After the last episode, the cells were cloned by the soft agar technique using 0.15% Nobel's agar in medium consisting of 9 volumes of Fischer's medium supplemented with 10% horse serum and antibiotics plus 1 volume of conditioned medium.

Assay of HGPRT activity.—The ability of sonic extracts of L5178Y cells to convert [8-^{14}C]hypoxanthine to inosinate was assayed by the method of Henderson et al. (*18*). Sonic extracts were prepared by subjecting L5178Y cell suspensions (3×10^7 cells/ml in 50 m*M* Tris-HCl buffer, pH 7.4) to three successive (10 sec) 20-kc bursts of ultrasound with 60-second intervals of cooling at 4°C between bursts. The sonicates were then centrifuged (15,000×*g*, 45 min) and the supernatants were used to assay HGPRT activity. Assay mixtures contained 1 m*M* 5-phosphorylribose-1-pyrophosphate, 1 m*M* magnesium sulfate, 25 m*M* Tris-HCl buffer (pH 7.4), 0.1 m*M* [8-^{14}C]hypoxanthine and sonic extracts of 2×10^5 cells in a final volume of 0.1 ml. After incubation at 37°C, 4 *M* formic acid was added, the mixtures were centrifuged, and an aliquot of the supernatant was chromatographed on cellulose thin-layer chromatography plastic sheets in 5% disodium hydrogen phosphate with appropriate carriers to isolate the reaction product, inosinate. We determined the radioactivities associated with the spots of base, nucleoside and nucleotide on the chromatogram by sectioning the chromatogram and measuring the radioactivity directly in the scintillation fluid.

RESULTS AND DISCUSSION

Isolation and Characterization of MP-Resistant L5178Y Cells

After mutation the L5178Y cells were exposed to 10 µ*M* MP for 24 hours, then passaged for 11 days in drug-free medium. After that, they were cultured for three successive 24-hour episodes in media containing MP at increasing concentrations such as 300, 1,000 and 3,000 µ*M*. Each MP treatment was followed by recovery periods consisting of passage for 5, 8, and 2 days, respectively, in drug-free medium. After the last episode, cells were cloned and 54 clones were picked up at random from individual colonies. Twenty-one of the colonies were discarded because they grew slowly on large-scale culture in normal medium. The other colonies were tested for their ability to grow in medium containing 1,000 µ*M* MP. A clone designated as L5178Y/MP was selected for further studies because of its high resistance to MP. Text-figure 2 shows the proliferation curves of the L5178Y/O parent line and MP-resistant L5178Y/MP subline in drug-free medium 4 days after the treatment with MP at various concentrations for 24 hours. The L5178Y/MP subline was clearly more resistant to MP than the parent line. For example, the L5178Y/O line scarcely grew with 0.3 µ*M* MP (*see* left side of text-fig. 2), whereas with as much as 3,000 µ*M* MP the L5178Y/MP subline grew well (*see* right panel of text-fig. 2). Moreover, the L5178Y/MP subline was at least 1,000-fold more resistant than the L5178Y/O line to continuous exposure to MP (data not shown). This subline also showed cross-resistance to TG and SeG, with ratios of 3,750 and 438, respectively, as shown in table 1. It retained this resistance for at least 6 months during passage in the absence of drugs.

The mechanism of resistance to purine antagonists has

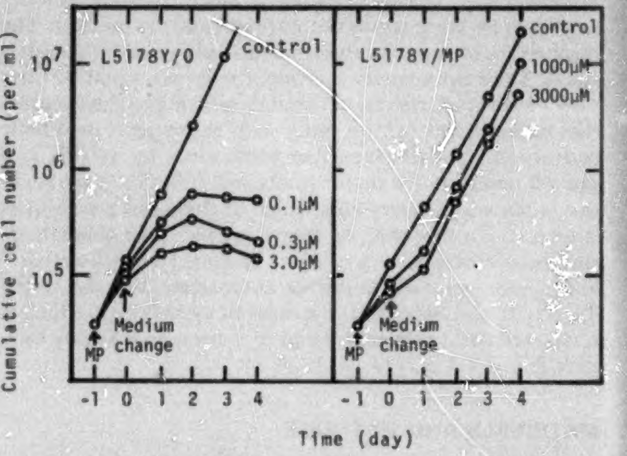

TEXT-FIGURE 2.—Effects of exposure to MP for 24 hr on proliferation of L5178Y/O and L5178Y/MP cells in drug-free medium. Cultures were treated with MP at the indicated concentration for 24 hr. On day 0, cells were transferred to drug-free medium and incubated at 37°C.

TABLE 1.—*Cross-resistance of L5178Y/MP cells to cytotoxicity of test compounds*

Compound	Sensitivity, IC_{50}, μM[a]		Resistance	
	L5178Y/O	L5178Y/MP	Ratio[b]	Degree[c]
Cisplatin	2.9	2.4	0.83	–
TG	0.080	300	3,750	+++
TG-Pt(II)	0.19	740	3,890	+++
SeG	0.40	175	438	++
Seg-Pt(II)	1.40	4.5	3.2	–

[a] Cells were cultured in medium containing test compounds at various concentrations. After 2 days the proliferation ratio was calculated by dividing the No. of cells in the test cultures by those in control cultures. Sensitivity is expressed as the concentration causing 50% inhibition of growth (IC_{50}) determined from the dose-response curve.

[b] Resistance ratio, the ratio of the IC_{50} value of L5178Y/MP cells to that of the L5178Y/O subline, was used as a parameter for the evaluation of cell resistance.

[c] Resistance degree is the resistance ratio expressed on an arbitrary scale: – = ratio of ≤9; + = ratio of 10–99; ++ = ratio of 100–999; +++ = ratio of ≥1,000.

been studied for over a decade. Human tumors become unresponsive to purine antagonists in various ways, including by significant elevation of membrane-bound alkaline phosphatase activity (*19–22*), whereas, in nonhuman systems (*23*, *24*), the most frequent cause of resistance is the absence of the anabolic enzyme, HGPRT, required to convert these antimetabolites to nucleotides, a process necessary for tumor inhibition. Text-figure 3 shows the HGPRT activity of sonic extracts of cultures of L5178Y/O and L5178Y/MP cells. Enzymatic phosphoribosylation of hypoxanthine to inosinate started at the beginning incubation of the sonic extract of L5178Y/O cells, whereas no inosinate was produced by the sonic extract of L5178Y/MP cells under the same conditions. These facts suggested that loss, or marked decrease, of the activity of the anabolic enzyme HGPRT in L5178Y/MP cells contributes to the resistance of these cells to purine antagonists such as MP, TG, and SeG.

Cross-Resistance of L5178Y/MP to Platinum Complexes

The cytotoxic effects of drugs on the proliferation of the L5178Y/O and L5178Y/MP cells were examined. From the linear log dose-probit plots observed, the IC_{50} values were determined and are shown in table 1. First, as a reference, cisplatin was tested. Cisplatin exhibited almost full activity against the L5178Y/MP subline as well as L5178Y/O parent line indicating that the subline has no cross-resistance to cisplatin. The IC_{50} value of the L5178Y/O line for TG was 0.08 μM and that of the L5178Y/MP subline was 300 μM; that is, the L5178Y/MP subline was about 3,750-fold more resistant to TG than the L5178Y/O line. Further, the IC_{50} value of the L5178Y/MP line for TG-Pt(II) was 740 μM, or 3,890 times greater than that of the sensitive line. Thus the resistance ratio of TG-Pt(II) was almost identical with that for TG. The cross-resistances of the L5178Y/MP subline to SeG and SeG-Pt(II) were also tested under similar conditions. The L5178Y/MP subline exhibited a high resistance ratio, 458, to SeG, but its cross-resistance to SeG-Pt(II) was negligible as shown in table 1.

The modes of action of the two platinum complexes can be explained on the basis of the resistance ratios. TG-Pt(II) is not directly active but is hydrolyzed to cytotoxic TG in the cell or medium. This explains the similiarity between the resistance ratios of TG-Pt(II) and TG. Conversely, SeG-Pt(II) itself is cytotoxic and its effect is not the result of hydrolysis to SeG.

Delayed Cytotoxicity

Text-figure 4 shows the proliferation curves of the subsequent growth of the L5178Y/O parent cells when cultured in drug-free medium for 10 days, after treatment with drugs at various concentrations for 24 hours. After brief exposure to MP, the cumulative cell number gradually increased and showed downward concavity at about the time that the cell numbers began to decrease. This behavior pattern, defined as "delayed cytotoxicity" by Tidd et al. (*12*) and Tidd and Paterson (*13*), is a characteristic of the antitumor action of purine antagonists. The delayed cytotoxicity is believed to be caused by a time-lag between the exposure of the tumor cells to drugs and the physical manifestation of drug toxicity (*13*). The phenomenon indicates that cell division continued in the presence of drugs, and that after removal of the drugs one to two doublings still occurred before the anabolism of MP to TG nucleotides, and the incorporation of TG nucleotides into DNA (*25*). In this study, TG and SeG also showed delayed cytotoxicity (text-figs. 4B, 4C). The delayed response of the cells to TG-Pt(II) became apparent when the cells were exposed to the drug at concentrations of 0.3 and

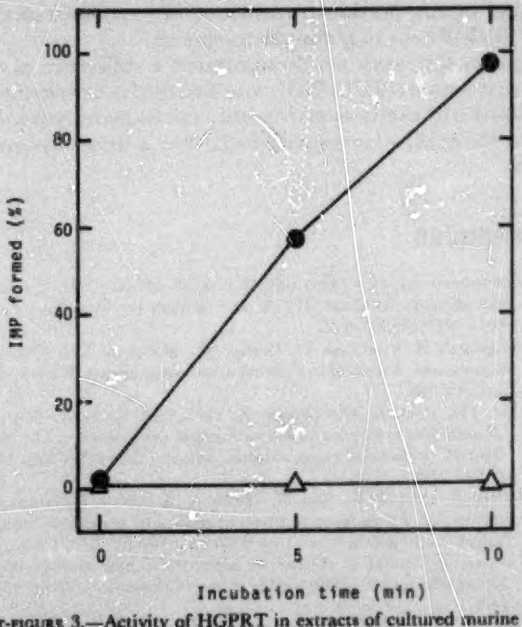

TEXT-FIGURE 3.—Activity of HGPRT in extracts of cultured murine lymphoma L5178Y cells sensitive or resistant to MP. The procedure for enzyme assay is described in the text. (●—●) L5178Y/O; (△—△) L5178Y/MP.

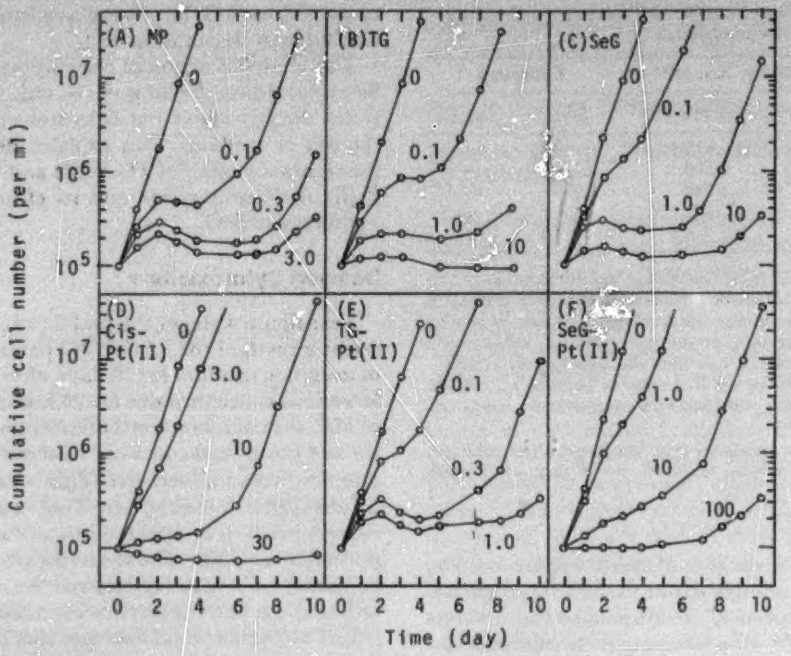

TEXT-FIGURE 4.—Proliferation curves of murine lymphoma L5178Y cells treated with MP (A), TG (B), SeG (C), cisplatin (D), TG-Pt(II) (E), and SeG-Pt(II) (F). Cultures were treated with drugs at the concentrations (*μM*) indicated for 24 hr. On day 1, the culture fluid was replaced by drug-free medium.

1.0 *μM*. Conversely, the response of the cells to identical treatment with SeG-Pt(II) (text-fig. 4F) showed no delayed cytotoxicity, an effect similar to that of cisplatin (text-fig. 4D). The demonstration of delayed cytotoxicity of antitumor activity of TG-Pt(II) but not SeG-Pt(II) confirms the findings of the previous experiment of cross-resistance of L5178Y/MP cells to platinum complexes.

Thus in this work we demonstrated a difference in the cytotoxic actions of TG-Pt(II) and SeG-Pt(II) by two methods. TG-Pt(II) exerts its activity through its hydrolysis product in the cells, whereas SeG-Pt(II) has a direct cytotoxic action.

REFERENCES

(*1*) ROZENCWEIG M, VON HOFF DD, SLAVIK M, MUGGIA FM. Cis-diamminedichloroplatinum (II). A new anticancer drug. Ann Intern Med 1977; 86:803-812.

(*2*) ROSENBERG B, VANCAMP L, TROSCK JE, MANSOUR VH. Platinum compounds: A new class of potent antitumour agents. Nature 1969; 222:385-386.

(*3*) HILL JM, LOEB E, MACLELLAN A, HILL NO, KHAN A, KING JJ. Clinical studies of platinum coordination compounds in the treatment of various malignant diseases. Cancer Chemother Rep 1975; 59:647-659.

(*4*) KIDANI Y, INAGAKI K, IIGO M, HOSHI A, KURETANI K. Antitumor activity of 1,2-diaminocyclohexane-platinum complexes against Sarcoma 180 ascites form. J Med Chem 1978; 21:1315-1318.

(*5*) TASHIRO T, KIDANI Y. Antitumor activities of new analogs of cis-dichlorodiammine-platinum(II). Curr Chemother 1978; 1313-1315.

(*6*) LEH FK, WOLF W. Platinum complexes: A new class of antineoplastic agents. J Pharm Sci 1976; 65:315-328.

(*7*) CLEARE MJ, HOESCHELE JD. Studies on the antitumor activity of group VIII transition metal complexes. Part I. Platinum (II) complexes. Bioinorganic Chem 1973; 2:187-210.

(*8*) LIPPARD SJ. Platinum complexes: Probes of polynucleotide structure and antitumor drugs. Accounts Chem Res 1978; 11:211-217.

(*9*) DAVIDSON JP, FABER PJ, FISCHER RG JR, et al. "Platinum-pyrimidine blues" and related complexes: A new class of potent antitumor agents. Cancer Chemother Rep 1975; 59:287-300.

(*10*) MAEDA M, ABIKO N, SASAKI T. Synthesis of seleno- and thioguanine-platinum(II) complexes and their antitumor activity in mice. J Med Chem 1981; 24:167-169.

(*11*) MAUTNER HG, CHU SH, JAFFE, JJ, SARTORELLI AC. The synthesis and antineoplastic properties of selenoguanine, selenocytosine and related compounds. J Med Chem 1963; 6:36-39.

(*12*) TIDD DM, KIM SC, HORAKOVA K, MORIWAKI A, PATERSON AR. A delayed cytotoxic reaction for 6-mercaptopurine. Cancer Res 1972; 32:317-322.

(*13*) TIDD DM, PATERSON AR. A biochemical mechanism for the delayed cytotoxic reaction of 6-mercaptopurine. Cancer Res 1974; 34:738-746.

(*14*) TOMIZAWA S, ARONOW L. Studies on drug resistance in mammalian cells. II. 6-Mercaptopurine resistance in mouse fibroblasts. J Pharmacol Exp Ther 1960; 128:107-114.

(*15*) KANZAWA F, HOSHI A, KURETANI K. Differences between 5-fluoro-2′-deoxyuridine and 5-fluorouridine in their cytotoxic effect on growth of murine lymphoma L5178Y cells in in vivo and in vitro systems. Eur J Cancer 1980; 16:1087-1092.

(*16*) ———. Antitumor activity of alkyl esters of 1-*β*-D-ribofuranosyl-5-fluorouracil-5′-phosphate against murine lymphoma L5178Y resistant to 1-*β*-D-ribofuranosyl-5-fluorouracil. Bull Cancer (Paris) 1979; 66:497-501.

(*17*) ———. Isolation and characterization of the murine lymphoma L5178Y cell line highly resistant to 5-fluorouracil. J Pharmacobiodyn 1980; 3:390-394.

(*18*) HENDERSON JF, BROX LW, KELLY WN, ROSENBLOOM FM, SEEGMILLER JE. Kinetic studies of hypoxanthine-guanine phosphoribosyltransferase. J Biol Chem 1968; 243:2514-2522.

(*19*) ROSMAN M, LEE MH, CREASEY WA, SARTORELLI AC. Mechanism of resistance to 6-thiopurines in human leukemia. Cancer Res 1974; 34:1952-1956.

(*20*) DAVIDSON JD, WINTER TS. Purine nucleotide pyrophosphorylases in

6-mercaptopurine-sensitive and -resistant human leukemias. Cancer Res 1964; 24:261–267.

(21) Wolpert MK, Damle SP, Brown JE, Sznycer E, Agrawal KC, Sartorelli AC. The role of phosphohydrolases in the mechanism of resistance of neoplastic cells to 6-thiopurines. Cancer Res 1971; 31:1620–1626.

(22) Kessel D, Hall TC. Retention of 6-mercaptopurine derivatives by intact cells as an index of drug response in human and murine leukemias. Cancer Res 1969; 29:2116–2119.

(23) Brockman RW, Anderson EP. Biochemistry of cancer (metabolic aspects). Ann Rev Biochem 1963; 32:463–512.

(24) Brockman RW. Mechanism of resistance to anticancer agents. Adv Cancer Res 1963; 7:129–234.

(25) Hirshaut Y, Weiss GH, Petry S. The use of long-term human leukocyte cell cultures as models for the study of antileukemic agents. Cancer Res 1969; 29:1732–1740.

blank page

Production of Kidney Tumors in Rats With Low Dose of Dimethylnitrosamine After Partial Hepatectomy[1]

Ritva P. Evarts,[2] Carolyn A. Brown,[2] *and* Mostafa Hassan Mostafa[3,4,5]

ABSTRACT—The occurrence of kidney tumors in inbred Wistar rats as a result of dimethylnitrosamine (DMN) administration at different intervals after partial hepatectomy was studied. The schedule for DMN administration was determined on the basis of the levels of liver dimethylnitrosamine demethylase (DMN-*d*) at different intervals after the operation. DMN-*d* was 62% of the control values at 24 hours, 72% at 72 hours, and 96% at 92 hours after the operation. At these intervals a single dose of DMN (10 mg/kg body wt) was given to partially hepatectomized animals and to untreated controls. At termination, when the animals were 94 weeks old, no kidney tumors were found in the control animals, whereas 23 of 54 animals (43%) that had been given injections of DMN 24 hours after partial hepatectomy developed kidney tumors. Kidney tumor incidence was 28 or 12%, respectively, when the carcinogen was administered 72 or 92 hours after the operation. The kidney tumor incidence and the activity of liver DMN-*d* were inversely related.—JNCI 1982; 68:223–298.

When administered to animals in small doses during extended time periods, DMN produces liver tumors, whereas one large dose of this carcinogen produces kidney tumors in the surviving animals (*1*). The activity of the microsomal enzyme system that metabolizes DMN, DMN-*d*, is low in the newborn liver, reaches its maximum at puberty, and is again low in adult liver (*2*). This enzyme produces from DMN the ultimate reactive carcinogenic species that form covalent bonds with body macromolecules. Despite the high labeling of liver DNA by DMN after one injection of carcinogen (*3–5*), only kidney tumors are produced (*6*). Thus liver seems to be resistant to tumor production by a single large dose of DMN. When the activity of the microsomal enzyme system is low naturally as in newborn animals (*2, 7*) or when it is lowered by dietary (*8–11*) or chemical means (*12–15*), peripheral tissues, especially kidney, become more sensitive to the carcinogenic action of DMN (*8–14*). Besides removing a large portion of the liver, partial hepatectomy lowers the activity of DMN-*d*, which returns to a normal level after a few days (*16, 17*). In the present experiment we took advantage of this effect of partial hepatectomy on DMN-*d* to investigate the occurrence of kidney tumors in rats as a result of DMN administration at different intervals after partial hepatectomy.

MATERIALS AND METHODS

In the first part of the experiment 64 Wistar inbred female rats (average wt±SD, 135±8.21 g) from Charles River Breeding Laboratories, Wilmington, Mass., were used. Half of these rats were partially hepatectomized according to the procedure of Higgins and Anderson (*18*), with removal of the left lateral and median lobes. The operation was timed such that the subsequent termination of the animals could be performed between 9 and 12 a.m. Four control rats without operation and 4 partially hepatectomized animals were killed at the following intervals after the operation: 6, 13, 24, 32, 48, 72, 92, and 168 hours. Livers were removed, homogenized in 4 volumes of 0.1 *M* potassium phosphate buffer (pH 7.4), and centrifuged for 20 minutes at 9,000×*g*. The supernatant was centrifuged at 105,000×*g* for 1 hour. The microsomal pellet was suspended in 0.1 *M* phosphate buffer and the centrifugation at 105,000×*g* was repeated. DMN-*d* activity was determined as described earlier (*19*). The substrate concentration used was 4 m*M*. Protein was measured by the method of Lowry et al. (*20*). Cytochrome P_{450} was measured by the method of Omura and Sato (*21*) with 91 $mM^{-1}\times cm^{-1}$ as the molecular extinction coefficient for the reduced cytochrome P_{450}–CO complex.

In the second part of the experiment 167 Wistar inbred female rats (average wt±SD, 138±4.66 g) also from Charles River Breeding Laboratories were used. Partial hepatectomy was performed on 116 animals that were divided into 3 groups. DMN (10 mg/kg body wt) was given by ip injection to the first group at 24 hours (61 rats), to the second group at 72 hours (37 rats), and to the third group at 92 hours (18 rats) after the operation. The timing of the operation was such that the animals were given injections between 9 and 12 a.m. Control rats (51) received the same amount of DMN, also by ip injection. The animals were fed Wayne Lab Blox and water ad libitum and their weights were recorded monthly. Animals were killed if moribund; the entire experiment was terminated when the animals were 94 weeks old, and all the animals were necropsied. Kidneys, liver, lungs, stomach, and bladder were examined for evidence of neoplasms. Tissues were fixed in Bouin's solution

ABBREVIATIONS USED: DMN=dimethylnitrosamine; DMN-*d*=dimethylnitrosamine demethylase; H & E=hematoxylin and eosin.

---

[1] Received May 26, 1981; accepted September 23, 1981.

[2] Laboratory of Carcinogen Metabolism, Division of Cancer Cause and Prevention, National Cancer Institute, National Institutes of Health, Public Health Service, U.S. Department of Health and Human Services, Bethesda, Md. 20205.

[3] Visiting Scientist, Laboratory of Carcinogen Metabolism, National Cancer Institute.

[4] *Present address*: Medical Research Institute, Alexandria University, Alexandria, Egypt.

[5] We thank Dr. E. K. Weisburger, Chief of the Laboratory of Carcinogen Metabolism, and Ms. Frances Williams.

and the histologic preparations were stained with hematoxylin and eosin. For microscopic examination each kidney was sectioned sagittally in three or four planes. For statistical analyses the chi-square test was used.

RESULTS

The activity of DMN-*d* was lowest 24 hours after partial hepatectomy and gradually returned to the normal levels in 4–7 days (text-fig. 1). The total amount of cytochrome P_{450} was also lowest 24 hours after the operation, but it remained low several days after the operation. However, in 1 week it had returned to the normal level.

To study the relationship between liver DMN-*d* activity and the incidence of kidney tumors, we selected the 24-, 72-, and 94-hour intervals after partial hepatectomy for administration of DMN. At these intervals the activity of liver DMN-*d* was, respectively, 58, 67, and 89 nmol/hour/mg microsomal protein. The pooled value for control animals was 93 nmol/hour/mg microsomal protein. Table 1 shows the incidence of kidney tumors in the different groups. No kidney tumors were produced among the controls when the same dose of DMN per kilogram body weight was administered, whereas nearly half of the animals that received DMN 24 hours after the partial hepatectomy developed kidney tumors. The tumor incidence was 28% when DMN was administered 72 hours after the partial hepatectomy, whereas in the 92-hour group only 2 of the 17 animals developed renal rumors.

According to Higgins and Anderson (*18*), percentages of restored weights of liver at 24-, 72-, and 92-hour intervals during restoration were 45.3, 70.6, and 74.3% of the controls, respectively, when median and left lateral lobes of the liver were removed at operation. Table 2 shows the restored liver weights calculated from the average liver weights of the control rats killed at the same intervals and the specific and total liver microsomal DMN-*d* activities of the operated rats. When the specific activity of liver DMN-*d* was plotted against the incidence of kidney tumors, an inverse relationship was obtained. When the total DMN-*d* activities of the restored livers 24, 72, and 92 hours after the operation were plotted against the incidence of kidney tumors (text-fig. 2), a similar inverse relationship was obtained.

Macroscopically, most of the kidney tumors were visible beneath the renal capsule. Either they were well demarcated from the adjacent renal parenchyma with a pale cut surface

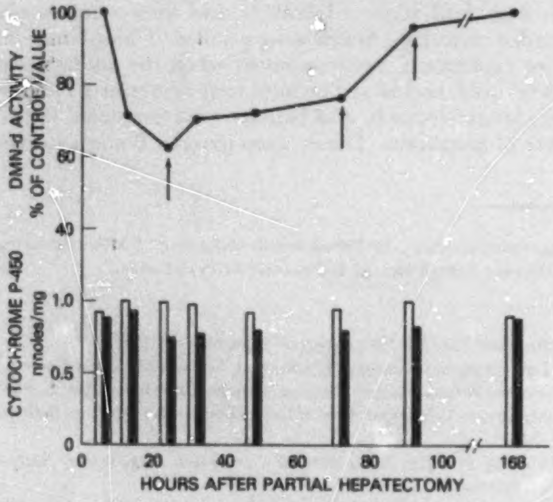

TEXT-FIGURE 1.—Four control and 4 partially hepatectomized rats were killed 6, 13, 24, 32, 48, 72, 92, and 168 hr after the operation. Liver microsomal DMN-*d* activity is expressed as percentage of the corresponding control values. Cytochrome P_{450} is expressed as nmol/mg microsomal protein. *Open bars* = control rats; *solid bars* = partially hepatectomized rats.

TABLE 1.—*Distribution of kidney tumors among animals*

Time of administration of DMN after partial hepatectomy	Initial No. of animals	Effective No. of animals[a]	Total No. of animals with kidney tumors[b]
Control	51	46	0
24 hr	61	54	23[c] (43)
72 hr	37	32	9[c] (28)
92 hr	18	17	2[d] (12)

[a] No. of animals that survived ≥14 mo.

[b] *Numbers in parentheses* are the percentages of the effective No. of animals.

[c] Significant at 0.1% level.

[d] Significant at 5% level.

TABLE 2.—*Restored liver weights and specific and total liver microsomal DMN-*d *activities of partially hepatectomized rats*

Interval after the operation, hr	Restored liver weights, g[a]	Liver microsomal protein, mg/g	DMN-*d*, nmol/hr/mg microsomal protein	Totel liver microsomal DMN-*d* activity, μmol/hr
24	2.67	20	58	3.1
72	4.52	21	67	6.4
92	4.76	23	89	9.7

[a] Calculated from the liver weights of the control rats killed at the same intervals.

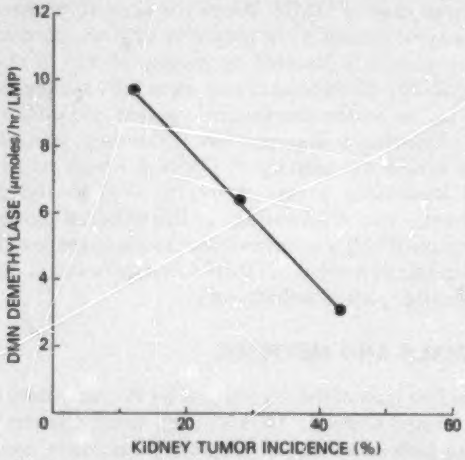

TEXT-FIGURE 2.—Kidney tumor incidence of animals administered DMN (10 mg/kg body wt) 24, 72, and 92 hr after partial hepatectomy vs. DMN-*d* activity in liver microsomal proteins (LMP) at the same intervals after the operation.

or the whole kidneys seemed to be transformed into large cystic tumors that were partly necrotic and partly filled with brownish fluid. The weight of the necrotic tumors including the kidney varied from 4 to 20 g.

Table 3 shows the distribution of the histologically different renal tumors. The difference between adenomas and adenocarcinomas was difficult to assess. Both tumors were usually well demarcated against the normal kidney parenchyma and both showed an expansive mode of growth. However, adenocarcinomas frequently seemed to be multifocal or bilateral. Cellular pleomorphism, mitotic activity, and focal necrosis were the criteria on which the difference between the adenomas and adenocarcinomas was based. Adenomas were mostly solid with acidophilic or pale-staining cytoplasm (fig. 1). The nuclei were small, round, or oval or vesicular with prominent nucleoli (fig. 2). Mesenchymal tumors were rare. They seemed to infiltrate the kidney parenchyma and extended more deeply into the subcortical area. The tumor cells were small, dark-staining spindle cells (fig. 3).

In addition, cystic lesions lined by eosinophilic or basophilic epithelium were encountered in partially hepatectomized animals but not in the controls (fig. 4). The tissue around the cyst showed distinct morphologic changes.

In the present experiment only a few neoplastic or preneoplastic liver changes were encountered. Fibromas seemed to originate from the incision site in the liver. Only one liver cell tumor was present. However, acidophilic liver cell nodules and basophilic and clear cell areas were present among the operated animals (table 4). No tumor or histologic changes were found in the other tissues examined.

DISCUSSION

The purpose of the present experiment was to assess the importance of active liver DMN metabolism for tumor production in extrahepatic tissue, especially in the kidney. In the past, kidney tumors have been produced by high doses of DMN (up to 40 mg/kg body wt). This dose usually gives about 50% tumor incidence (*10*). To produce kidney tumors with lower doses of DMN, previous workers have used treatments that decrease the activity of DMN-metabolizing enzymes in liver. Either administration of CCl_4, which decreases the amount of cytochrome P_{450} and the activity of DMN-*d* (*13-15*), or administration of high-carbohydrate, low-protein diets, which have similar effects (*22*), has been used to produce kidney tumors with a relatively low dose of DMN. Craddock (*23*) produced a 43% liver tumor incidence and a 71% kidney tumor incidence with a single dose of DMN after partial hepatectomy. In another study dimethylformamide, which lowers the metabolism of DMN, had no effect on liver tumor production of DMN; however, the incidence of kidney tumors was not reported (*24*). In the same study a 33% kidney tumor incidence was produced when 9 mg DMN/kg was given 31 hours after partial hepatectomy. However, one question remains to be answered. Do these treatments affect the kidney as well and thereby increase the susceptibility of the kidney to tumorigenesis by DMN? We tried to approach the question of the importance of active liver metabolism for the peripheral tissue by administering relatively low doses of DMN to the partially hepatectomized rats at appropriate intervals after partial hepatectomy. The timing of the administration was based on determinations of the activity of DMN-*d* at the different intervals after the operation. A similar approach has been used by other workers, but the number of animals used in previous work limited the conclusion that could be drawn (*16*). In our experiment the enzyme activity was lowest 24 hours after the operation and then gradually increased until in 1 week it was back to normal. However, the amount of cytochrome P_{450} remained low for a long time. In our study only 1 of the partially hepatectomized rats developed a hepatocellular neoplasm. There were 2 fibromas and 3 nodules present among these animals.

TABLE 3.—*Distribution of kidney tumors in rats*

Group	Total No. of animals with tumors	No. of adenocarcinomas	No. of adenomas	No. of mesenchymal tumors	No. of cysts
Control	0	0	0	0	0
24 hr	23	7	14	2	2
72 hr	9	2	5	2	1
92 hr	2	0	2	0	1

TABLE 4.—*Distribution of liver cell alterations and tumors in rats*

Group	Hepatoma	Fibroma	Liver cell nodule	Clear cell areas	Basophilic areas
Control	0	0	0	0	0
24 hr	1	1	2	1	3
72 hr	0	1	1	3	5
92 hr	0	0	0	1	0

When the pooled kidneys from control rats and partially hepatectomized rats were analyzed for DMN-*d* activity, no difference in the kidney DMN-*d* activity was found. The value for the control kidneys was 37 nmol/hour/mg microsomal protein and for the operated animals 31 nmol/hour/mg microsomal protein. Thus the change in the kidney DMN-*d* does not seem to play an important part in the production of kidney tumors after partial hepatectomy. However, the determination of DMN-*d* activity when whole kidney is used can be inaccurate because the kidney is composed of anatomically and functionally different parts. The kidney cortex is known to have a drug-metabolizing enzyme system (*25, 26*). This enzyme system can be confined to a relatively small population of renal cells and still exist in concentrations similar to those in hepatocytes (*27*). All the tumors encountered in the kidney were in the cortical area. Large cysts lined with transformed epithelium that formed fold and papillary projections to the lumen of the cysts seemed to be the first step toward tumor production.

Our experiments showed an inverse relationship between the activity of liver DMN-*d* and kidney tumor production. There was also an inverse relationship between the total liver DMN-*d* activity and kidney tumor production (text-fig. 2). Most likely, both the removal of a large portion of the liver and the decrease of the specific activity of the enzyme that metabolizes DMN play an important role in the production of the kidney tumors by DMN. However, many other studies have shown that only a decrease in the specific activity of the liver is enough for tumor production in the kidney (*3, 10, 16*). In addition, alkylation of kidney DNA increased when liver enzyme activity decreased as shown by Swann et al. (*5*) when a protein-free diet was fed to the animals. The kidneys become the target whenever higher doses of DMN reach them due to impairments in the liver mixed-function oxidase system.

REFERENCES

(*1*) Swann PF, Magee PN. Nitrosamine-induced carcinogenesis. Adv Cancer Res 1968; 110:39-47.

(*2*) Davies DL, Bryant GM, Arcos JC, Argus MF. *Brief Communication*: Age-dependence of hepatic dimethylnitrosamine-demethylase activity in the rat. J Natl Cancer Inst 1976; 56:1057-1058.

(*3*) Swann PF, McLean AE. Cellular injury and carcinogenesis. The effect of a protein-free high-carbohydrate diet on the metabolism of dimethylnitrosamine in the rat. Biochem J 1971; 124:283-288.

(*4*) Nicoll JW, Swann PF, Pegg AE. Effect of dimethylnitrosamine on persistence of methylated guanines in rat liver and kidney DNA. Nature 1975; 254:261-262.

(*5*) Swann PF, Kaufman DG, Magee PN, Mace R. Induction of kidney tumours by a single dose of dimethylnitrosamine: Dose response and influence of diet and benzo(*a*)pyrene pretreatment. Br J Cancer 1980; 41:285-294.

(*6*) Magee PN, Barnes JM. Induction of kidney tumors in the rat with dimethylnitrosamine (*N*-nitrosodimethylamine). J Pathol Bacteriol 1962; 84:19-31.

(*7*) Della Porta G, Terracini B. Chemical carcinogenesis in infant animals. Prog Exp Tumor Res 1969; 11:334-363.

(*8*) Swann PF, McLean AE. The effect of diet on the toxic and carcinogenic action of dimethylnitrosamine. Biochem J 1968; 107:14.

(*9*) Hard GC, Butler WH. Cellular analysis of renal neoplasia: Induction of renal tumors in dietary-conditioned rats by dimethylnitrosamine with a reappraisal of morphological characteristics. Cancer Res 1970; 30:2796-2805.

(*10*) McLean AE, Magee PN. Increased renal carcinogenesis by dimethylnitrosamine in protein deficient rats. Br J Exp Pathol 1970; 51:587-590.

(*11*) McLean AE, Day PA. The use of new methods to measure the effect of diet and the inducers of microsomal enzyme synthesis on cytochrome P-450 in liver homogenates and on metabolism of dimethylnitrosamine. Biochem Pharmacol 1974; 23:1173-1180.

(*12*) Pound AW, Lawson TA, Horn L. Increased carcinogenic action of dimethylnitrosamine after prior administration of carbon tetrachloride. Br J Cancer 1973; 27:451-459.

(*13*) Smuckler EA, Arrhenius E, Hultin T. Alterations in microsomal elution transport, oxidative N-demethylation and azo-dye cleavage in carbon tetrachloride and dimethylnitrosamine-induced liver injury. Biochem J 1967; 103:55-64.

(*14*) Pound AW, Horn L, Lawson TA. Decreased toxicity of dimethylnitrosamine in rats after treatment with carbon tetrachloride. Pathology 1973; 5:233-242.

(*15*) Pound AW, Lawson TA. Protection by a small dose of carbon tetrachloride against the toxic effect of dimethylnitrosamine in rats. Br J Exp Pathol 1974; 55:203-212.

(*16*) ———. Partial hepatectomy and toxicity of dimethylnitrosamine and carbon tetrachloride, in relation to the carcinogenic action of dimethylnitrosamine. Br J Cancer 1975; 32:596-603.

(*17*) Evarts RP, Mostafa MH. Dimethylnitrosamine demethylase activity of rat liver microsomes after partial hepatectomy. Biochem Pharmacol 1978; 27:2751-2753.

(*18*) Higgins GM, Anderson RM. Experimental pathology of the liver. I. Restoration of the liver of the white rat following partial surgical removal. Arch Pathol 1931; 12:186-202.

(*19*) Evarts RP, Mostafa MH. The effect of L-tryptophan and certain other amino acids on liver nitrosodimethylamine demethylase activity. Food Cosmet Toxicol 1978; 16:588-589.

(*20*) Lowry OH, Rosebrough NJ, Farr AL, Randall RJ. Protein measurement with Folin phenol reagent. J Biol Chem 1951; 193:265-275.

(*21*) Omura T, Sato R. The carbon monoxide-binding pigment of liver microsomes. Evidence for its hemoprotein nature. J Biol Chem 1964; 239:2370-2378.

(*22*) Venkatesan N, Arcos JC, Argus MF. Amino acid induction and carbohydrate repression of dimethylnitrosamine demethylase in rat liver. Cancer Res 1970; 30:2563-2567.

(*23*) Craddock VM. Effect of a single treatment with the alkylating carcinogen dimethylnitrosamine, diethylnitrosamine and methyl methane sulfonate, on liver regenerating after partial hepatectomy. Chem Biol Interact 1975; 10:313-321.

(*24*) Craddock VM. Liver carcinomas induced in rats by single administration of dimethylnitrosamine after partial hepatectomy. J Natl Cancer Inst 1971; 47:899-907.

(*25*) Zenser TV, Mattammal MB, Davis BB. Differential distribution of the mixed-function oxidase activities in rabbit kidney. J Pharmacol Exp Ther 1978; 207:719-725.

(*26*) Zenser TV, Armbrecht HJ, Birnbaum LS, Mattammal MB, Davis BB. Characterization of renal cytochrome P-450 systems. Fed Proc 1979; 22:658.

(*27*) Hook JB. Modulation of nephrotoxicity by environmental chemicals. In: Eighth International Congress of Pharmacology, Tokyo: 1981: 86.

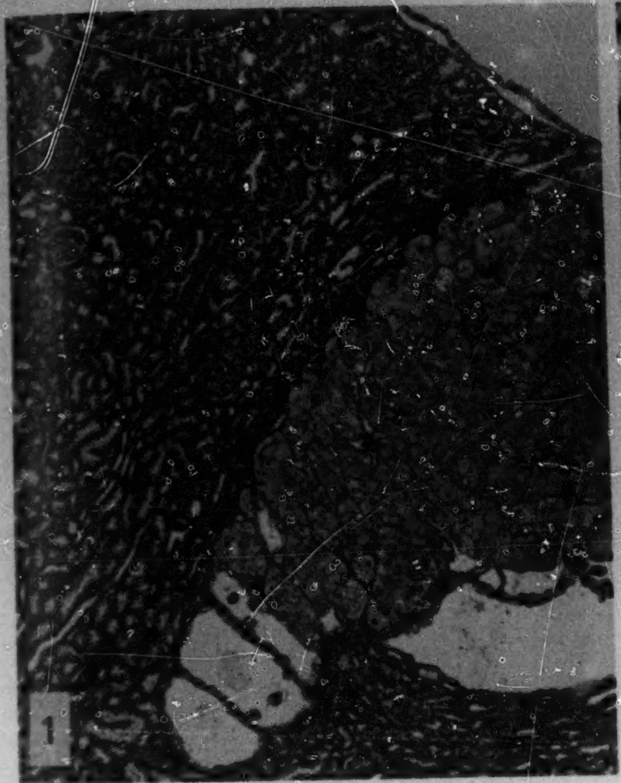

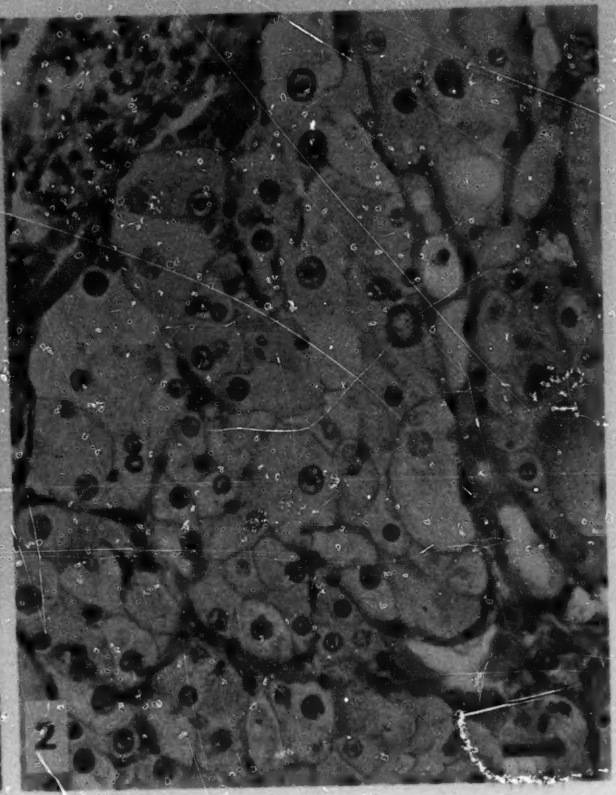

FIGURE 1.—Adenoma of outer layer of renal cortex. *Note* clear demarcation of the tumor and compression of the renal parenchyma. Cystic spaces lined with transformed epithelium give the impression that the cyst formation is the first step toward the neoplastic growth. H & E. *Bar* = 230 µm. × 54

FIGURE 2.—Higher magnification of the adenoma in fig. 1. Tumor cells are pleomorphic with pale eosinophilic cytoplasm. Nuclei are round with prominent nucleoli. H & E. *Bar* = 38 µm. × 330

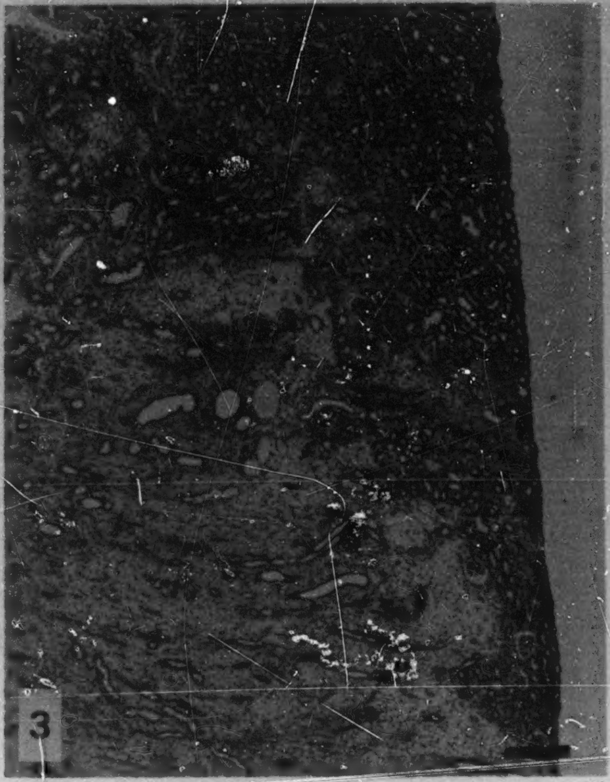

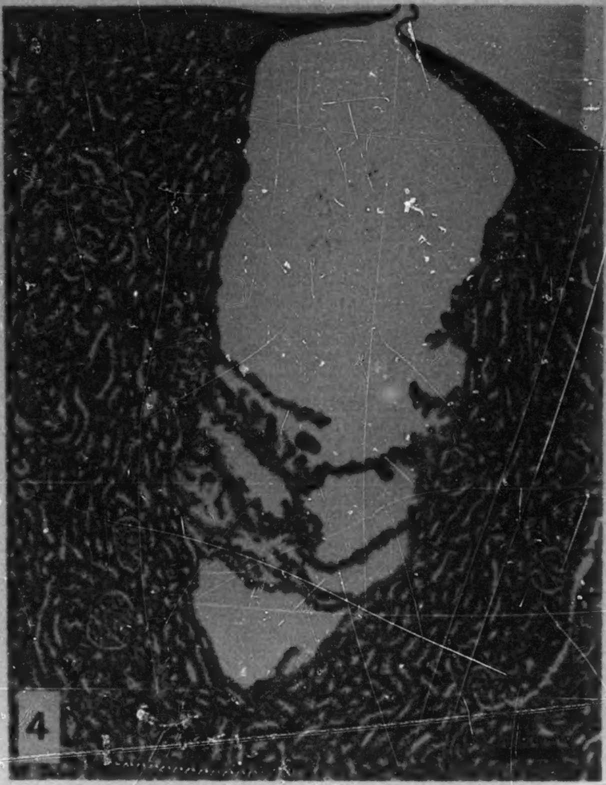

FIGURE 3.—Mesenchymal tumor extending throughout the kidney cortex. At the edge of the tumor, spindle cells surround the kidney tubules. At higher magnification many mitotic figures can be seen at that area. H & E. *Bar* = 330 μm. × 38

FIGURE 4.—Cortical cyst lined with transformed epithelium that form folds and bridges across the luminal space. First step in the formation of tumor. H & E. *Bar* = 230 μm. × 54

Inhibition of Iodinated Nerve Growth Factor Binding by the Suspected Tumor Promoters Saccharin and Cyclamate[1,2]

Douglas N. Ishii, *Ph.D.*[3,4]

ABSTRACT—The strong correlation between tumor-promoting activity and the capacity to inhibit nerve growth factor-induced neurite outgrowth for a number of compounds prompted studies on the suspected bladder tumor promoters saccharin and cyclamate. These artificial sweeteners reversibly inhibited neurite outgrowth and binding of $[^{125}I]$nerve growth factor in embryonic chick sensory ganglia cells. Curves showing the dose-dependent inhibition of response and the dose-dependent inhibition of binding to high affinity sites were closely parallel. The inhibition appeared to be due to a reduction in the affinity rather than to a change in the number of binding sites, as indicated by the extent of reduction in the association rate. These results suggest that alteration of cellular differentiation by tumor promoters may result from interactions with receptor systems that regulate specialized cell functions.—JNCI 1982; 68:299–303.

Certain plant diterpene esters, such as TPA, that are potent tumor promoters in the two-stage mouse skin carcinogenesis system (*1–3*) are reversible inhibitors of neurite outgrowth, while their nonpromoting structural congeners are not (*4, 5*). The suspected bladder tumor promoters saccharin (*6–10*) and cyclamate (*8, 9*) have recently been shown to share this property with the tumor-promoting plant diterpenes (*11*). This inhibitory action is significant, since different chemical classes of promoters often do not show similar effects in a given tissue (*12, 13*). Non-phorbol ester promoters have received scanty attention, but any general mechanism of promoter action must, of course, satisfactorily explain how these other chemical classes of promoters act. This study was conducted to determine whether antagonism of NGF-induced morphologic differentiation in cultured embryonic chick DRG by these artificial sweeteners could be accounted for by inhibition of NGF binding. Little is known of the mechanism of how neurite outgrowth and how the specialized topography of neurons are regulated, although cell shape is of obvious importance to neuronal function. Studies on the mechanism of NGF action may be aided by the availability of antagonists. Reviews on the chemistry of NGF and its effects on the growth and development of the vertebrate nervous system are available (*14–18*). The data are discussed in light of the known effects of tumor promoters on differentiation in other cell systems.

MATERIALS AND METHODS

Chemicals.—Sodium saccharin (S-1002 lot 117C-0154) and sodium cyclamate (C-9131, lot 57C-0157) were purchased from Sigma Chemical Co., St. Louis, Mo. According to the manufacturer, sodium saccharin was synthesized by the Maumee procedure. Sodium cyclamate was more than 99% pure and the content of cyclohexylamine was unknown. Other chemicals were of the best commercially available grades.

Ganglia culture and bioassay.—The detailed procedures for ganglia culture and bioassay are described elsewhere (*4*). DRG from embryonic 7- to 10-day-old white leghorn chick embryos were cultured in RPMI-1640 containing 1 mg BSA/ml and 2 ng NGF/ml on a rattail collagen-coated Microwell plate. The Na^+ concentration and osmolarity of the medium was kept constant by regulation of the NaCl content of the RPMI-1640 medium. The extent of nerve fiber outgrowth was monitored as described in the text-figure legends.

Preparation and iodination of NGF.—NGF was prepared from male mouse saliva (*19, 20*) and purity was confirmed by the presence of a single band on isoelectric focusing (pH 3.5–10) in 7.5% polyacrylamide gels. Purified NGF was iodinated with lactoperoxidase (*21*) and a single band was detected on isoelectric focusing and on sodium dodecyl sulfate gel electrophoresis.

Binding of $[^{125}I]$NGF.—Assay of binding to intact cells obtained from dissociated DRG closely followed procedures described by others (*22*), except that cells ($1\text{–}2\times10^6$/ml) were incubated at 37°C in RPMI-1640 containing 5 mg BSA/ml and $[^{125}I]$NGF. Since Na^+ ions slightly inhibit binding, it is important that Na^+ concentration and total osmolarity be controlled as described above. Incubates were subjected to equilibrium sedimentation for 30 seconds in a Beckman Model 152 Microfuge (Beckman Instruments, Inc., Palo Alto, Calif.), and the cell pellet fraction, and sometimes the supernatant fraction, were assayed for total radioactivity content. Binding to two classes of high affinity sites (*22*) can be distinguished. After incubation for 10 minutes on ice with excess (10 μg/ml) nonradioactive NGF,

---

ABBREVIATIONS USED: BSA=bovine serum albumin; DRG=dorsal root ganglia; NGF=nerve growth factor (the β-subunit); TPA=12-*O*-tetradecanoylphorbol 13-acetate.

---

[1] Received June 4, 1981; accepted September 8, 1981.

[2] Supported in part by Public Health Service (PHS) grant R01NS-14218 from the National Institute of Neurological and Communicative Disorders and Stroke and by PHS Research Career Development Award 1-K04NS-00375.

[3] Department of Pharmacology and Cancer Research Center, College of Physicians and Surgeons, Columbia University, 630 West 168th St., New York, N.Y. 10032.

[4] I thank Ms. Vicki M. Stovall for the fine technical assistance.

binding to the high affinity component (site I) was quantitatively retained. Binding to the lower affinity component (site II) was defined as the difference between total binding and site I binding and was rapidly and quantitatively lost. Nonspecific binding was determined from other incubates containing an excess of 10 μg NGF/ml at the onset and was subtracted from reported values.

RESULTS

Reversible Effect of Promoters on [^{125}I]NGF-Binding and DRG Response.

The total amount of radioactivity specifically bound to DRG cells incubated with [^{125}I]NGF was inhibited at about the rate of 50% with 50 m*M* sodium saccharin and about 64% with 56 m*M* cyclamate (text-fig. 1). Binding recovered rapidly and completely after the artificial sweeteners were washed out. With cyclamate, however, recovery of binding after washout reached a transient maximum followed by a decline to a plateau level of about 62% of the total binding. These unusual kinetics invite further study. Concentrations of about 50 m*M* of artificial sweeteners cause substantial inhibition of neurite outgrowth in cultured DRG, which is rapidly and completely reversible by washout of the compounds, whereas 50 m*M* glucose or sucrose cause no detectable effect on neurite outgrowth (*11*).

Relationship Between Promoter Concentration, DRG Response, and [^{125}I]NGF Binding.

The effect of various concentrations of saccharin and cyclamate on neurite outgrowth was studied (text-fig. 2). Previously, DRG response was scored (*11*) by the classical semiquantitative bioassay method (*23*). We have chosen an alternative method to detect DRG response, and measured the neurite length. Ganglia were exposed to NGF for 1 day to permit neurites to penetrate the ganglia capsule. Neurite length was measured before and after exposure to artificial sweetener compounds for an additional day. The rate of neurite outgrowth in control cultures appeared linear over 2 days. Neurite length increase was inhibited by saccharin or cyclamate concentrations above 5–10 m*M* (approximately 1–2 mg/ml), and half-maximally by about 25 m*M*. Established neurites were not caused to retract by any drug concentration; other experiments showed that artificial sweeteners decrease the rate of neurite elongation. Half-maximal inhibition of the classical bioassay score was at about 33 m*M* for cyclamate and 50 m*M* for saccharin (*11*). These data correlate reasonably well with effects on inhibition of radioactive NGF binding (text-fig. 3).

Instead of studying the effect of cyclamate and saccharin concentrations on total binding, I studied the effect on binding to the two high affinity components termed site I ($K_d \cong 2.3 \times 10^{-11}$ *M*) and site II ($K_d \cong 1.7 \times 10^{-9}$ *M*) by Sutter et al. (*22*). NGF binding to site I was inhibited by artificial sweetener concentrations above 5–10 m*M*, and the curves for the dose-dependent inhibition following closely those of the inhibition of neurite outgrowth. Saccharin inhibited NGF binding to site II as well, but in this experiment, cyclamate did not. However, in other experiments, cyclamate could clearly inhibit site II binding. In contrast to artificial sweeteners, high concentrations of glucose and sucrose had little, if any, effect on binding. Since regulation of neurite outgrowth correlates best with NGF binding to site I (*22*), I shall not discuss further the effects on binding to site II here. Significant differences between effects on site I and site II will be presented elsewhere.

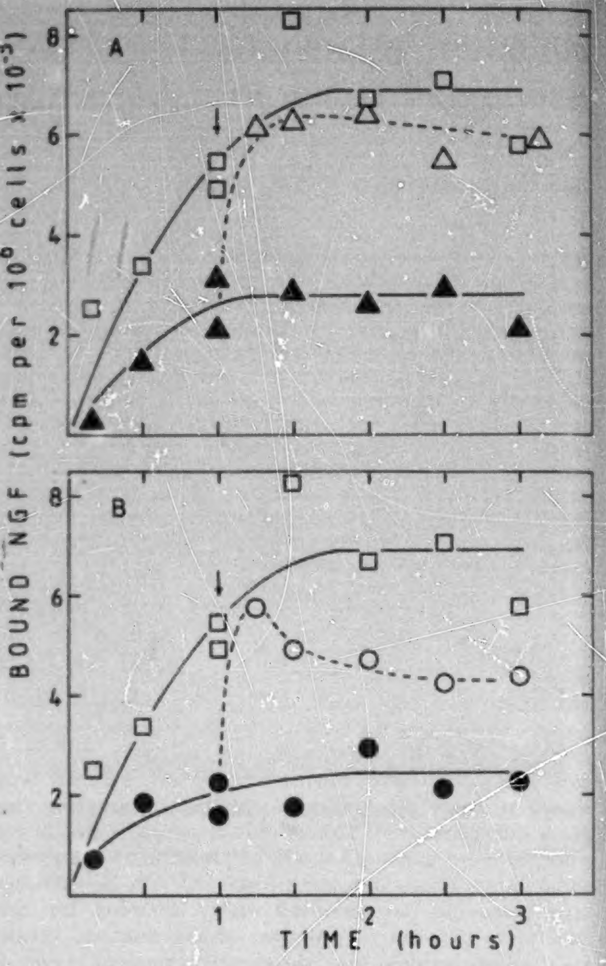

TEXT-FIGURE 1.—Time course of saccharin and cyclamate inhibition of total specific [^{125}I]NGF binding to DRG cells, and recovery following washout of sweeteners. Intact cells from dissociated 8-day-old embryonic chick DRG were incubated at 37°C with 5 ng [^{125}I]NGF/ml (sp act, 58 cpm/pg; 2×10^{-10} *M*) alone and with saccharin or cyclamate. At the time shown (*arrow*) incubates were centrifuged and the cells were resuspended in the same initial incubation solutions. Some treated incubates were resuspended in the absence of sweeteners. At various times, aliquots were removed and assayed for total bound radioactivity. Nonspecific binding was estimated from parallel incubates containing excess nonradioactive NGF (10 μg/ml), and values were subtracted from total binding. Panel A: □, control; ▲, plus 50 m*M* sodium saccharin; and △, incubates initially with saccharin followed by washout. Panel B: □, control; ●, 56 m*M* sodium cyclamate added; and ○, incubates initially with cyclamate followed by washout.

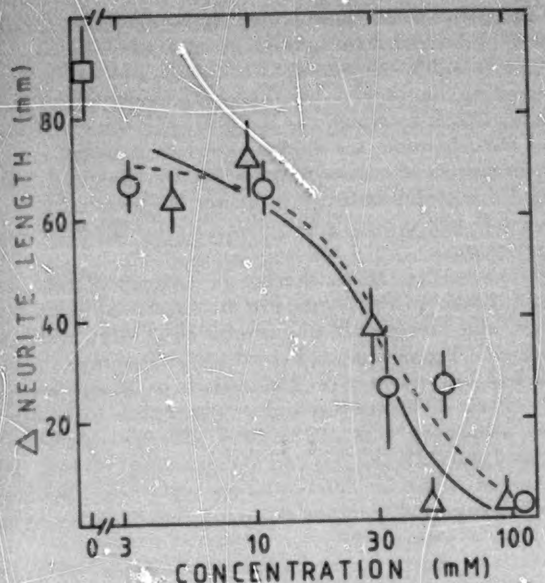

TEXT-FIGURE 2.—Relationship between saccharin and cyclamate concentration and neurite outgrowth in cultured DRG. To establish neurite outgrowth, DRG were incubated on rattail collagen-coated Microwell plates for 1 day with 2 ng NGF/ml (8×10^{-11} *M*) and the neurite length from the edge of the explant to the fiber tip was measured. Then various concentrations of artificial sweeteners were added, the incubations were continued for another day, and neurite length was measured again. The text-figure shows the *change* in neurite length between days 1 and 2: □, no additions; Δ, saccharin added; ○, cyclamate added.

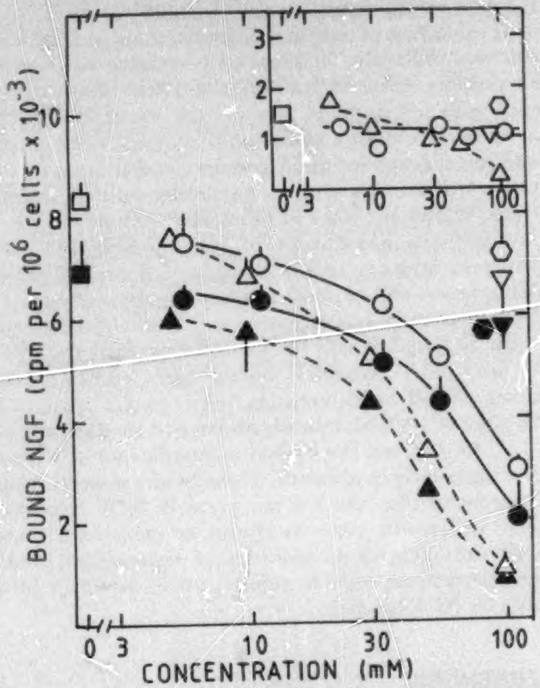

TEXT-FIGURE 3.—Effect of saccharin and cyclamate concentration on [^{125}I]NGF binding to DRG cells. Cells from 9-day-old embryonic chick DRG were incubated for 1 hr with [^{125}I]NGF (2×10^{-10} *M*) and the indicated concentrations of sweeteners. Specific total (*open symbols*) and site I (*solid symbols*) bound radioactivity were assayed: □, no additions; Δ, saccharin added; ○, cyclamate added; ⬡, sucrose added; and ▽, glucose added. Values are means ± SE, *n*=3. *Inset* shows radioactivity bound to site II, defined as the difference between specific total and site I-bound radioactivity. Corresponding symbols are used.

Effect of Promoters on [^{125}I]NGF Affinity and Association Rate.

To study the mechanism by which binding to site I is inhibited, DRG cells were incubated with various concentrations of [^{125}I]NGF for 1 hour, a time sufficiently long to reach a steady state in binding, and enough saccharin or cyclamate was added to inhibit [^{125}I]NGF binding by more than 50% (text-fig. 4). The data, excluding binding to site II, were plotted according to Scatchard (*24*). There was no effect on the number of available high affinity sites, but the binding affinity (equilibrium constant of association) was reduced to about 20% and 25% of the control value by 50 m*M* saccharin and 80 m*M* cyclamate, respectively. Binding to a low affinity nonsaturable component was unaltered. Consistent with this finding, the binding isotherms shifted

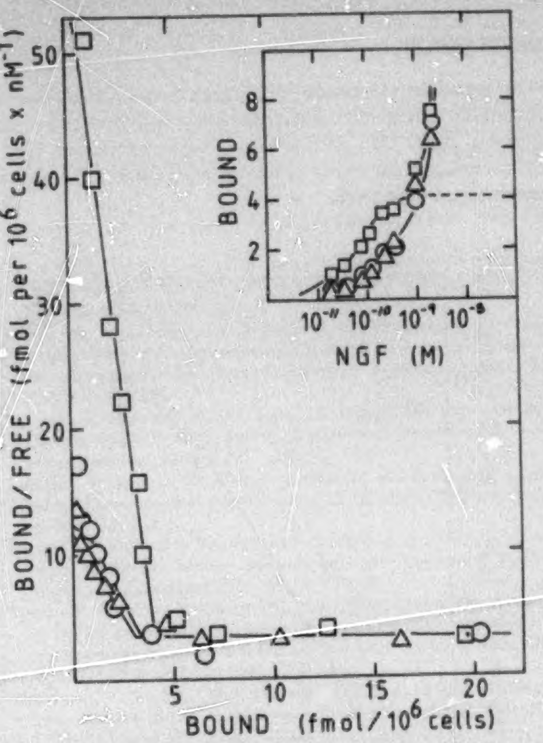

TEXT-FIGURE 4.—Effect of cyclamate and saccharin on the Scatchard analysis of [^{125}I]NGF binding to embryonic chick DRG cells. Cells obtained from 8-day-old embryonic DRG were incubated for 1 hr with various concentrations of [^{125}I]NGF alone (□) and with 50 m*M* saccharin (Δ), or 80 m*M* cyclamate (○). Binding to site I was assayed and values plotted according to Scatchard (*24*). *Inset* shows the relationship between bound radioactivity and low concentrations of [^{125}I]NGF. *Dashed line* indicates the saturation of site I as determined from the Scatchard plot. Units for bound NGF are in fmol/10^6 cells. The calculation of molarity is based on the dimer mol wt of 26,500 for NGF.

in parallel to the right when these agents were present (text fig. 4, inset).

The decreased affinity of [^{125}I]NGF binding could be due to a decrease in the association rate constant or to an increase in the dissociation rate constant. At the appropriately low concentration of 1.6×10^{-11} *M* [^{125}I]NGF, more than 95% of the radioactivity is estimated to bind exclusively to site I (*22*), permitting study of the association rate (text-fig. 5). Saccharin (50 m*M*) inhibited the initial velocity of binding to site I by 85% and 50 m*M* cyclamate by about 78%, inhibition values which could quantitatively account for the observed decrease in the affinity constant. Saccharin or cyclamate had no detectable effect on the rate of loss of bound radioactivity (data not shown). While these results suggest that inhibition is due to a decrease in the association rate, the data do not reveal whether the effect is direct or due to perturbation of other membrane components.

DISCUSSION

A number of tumor promoters are now known to be reversible inhibitors of morphologic differentiation in cells derived from the neural crest, and promoters can alter differentiation in many cell systems, possibly by a common mechanism of action.

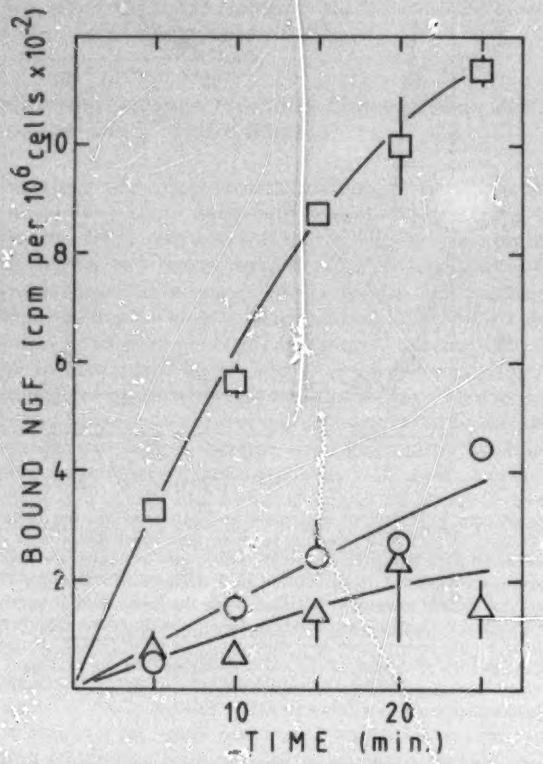

TEXT-FIGURE 5.—Effect of saccharin or cyclamate on the initial rate of [^{125}I]NGF binding to site I on DRG cells. Cells from 9-day-old embryonic DRG were incubated with 0.40 ng [^{125}I]NGF/ml (1.6×10^{-11} *M*) alone (□), and with 50 m*M* saccharin (Δ), or 50 m*M* cyclamate (○). At various times aliquots were removed for assay of radioactivity bound to site I. Values are means ±SE, $n=3$.

The potent tumor-promoting macrocyclic plant diterpene esters inhibit neurite outgrowth in cultured DRG (*4*) and in mouse neuroblastoma cells (*5*), but structurally related nonpromoting congeners do not. The weak mouse skin promoter phenol (*25*) is an antagonist in DRG (*11*), whereas benzene and fluorobenzene are neither skin tumor promoters (*25*) nor inhibitors of neurite outgrowth (*11*). Moreover, I have found that deoxycholate, a promoter in colon (*26, 27*), also reversibly blocks neurite outgrowth (Ishii DN:Unpublished observation).

Promoters may act by altering the program of differentiation in a variety of cell types. Phorbol ester promoters inhibit fusion and myogenesis of cultured chick myoblasts (*28*), terminal differentiation of Friend erythroleukemia cells (*29, 30*), and conversion of 3T3 fibroblasts to adipose-like cells (*31*). These compounds can also induce phenotypic expressions associated with the normal differentiated state in myeloid leukemia (*32, 33*) and in melanoma (*34*) cells. Thus alteration of cellular differentiation, particularly because it was also reported in mouse skin (*35*), may be an important property of promoters.

While saccharin and cyclamate clearly inhibit NGF binding, TPA (*4, 36*) and phenol (*11*) do not, suggesting that tumor promoters may antagonize morphologic differentiation of neuronal cells by more than one mechanism. Interestingly, binding of epidermal growth factor to cultured mammalian cells is inhibited by the tumor-promoting phorbol esters (*36–38*). Binding of other ligands to the cell surface was not affected (*36*), suggesting specificity. This report shows that binding of other physiologically important polypeptides can be inhibited. The induction of globin mRNA in erythroleukemia cells is inhibited by TPA (*39*) during inhibition of terminal differentiation, indicating that promoters probably act prior to processing of transcripts and, possibly, prior to transcription itself. These data, together with my findings, support the tentative hypothesis that tumor-promoting compounds may alter the program of cellular differentiation in a variety of cell types by interacting with receptor systems regulating cellular functions. Various chemical classes of promoters may interact at different steps in a sequence of receptor-activated events; whether interaction results in induction or inhibition of differentiation will depend on the program of the involved receptor system in a particular tissue. This tentative hypothesis can be tested. It will be of interest to study the effect of TPA and other promoters on the early events following binding of NGF to its receptors.

Binding of [^{125}I]NGF has been studied by several groups (*21, 22, 40, 41*), but the biological significance of identified sites is not clearly established. These results strongly support the argument that site I is the putative NGF receptor for neurite outgrowth since saccharin or cyclamate cause a parallel dose-dependent inhibition of response and binding. These compounds will, hopefully, prove useful in further studies on NGF binding.

REFERENCES

(*1*) BERENBLUM I. The co-carcinogenic action of croton resin. Cancer Res 1941; 1:44–48.

(2) Hecker E. Isolation and characterization of the co-carcinogenic principles from croton oil. Methods Cancer Res 1971; 6:439–484.

(3) Van Duuren BL. Tumor promoting agents in two-stage carcinogenesis. Prog Exp Tumor Res 1969; 11:31–68.

(4) Ishii DN. Effect of tumor promoters on the response of cultured embryonic chick ganglia to nerve growth factor. Cancer Res 1978; 38:3886–3893.

(5) Ishii DN, Fibach E, Yamasaki H, Weinstein IB. Tumor promoters inhibit morphological differentiation in cultured mouse neuroblastoma cells. Science 1978; 200:556–559.

(6) Fitzhugh OG, Nelson AA, Frawley JP. A comparison of the chronic toxicities of synthetic sweetening agents. J Am Pharmaceut Assoc 1951; 40:583–586.

(7) Bryan GT, Ertürk E, Yoshida O. Production of urinary bladder carcinomas in mice by sodium saccharin. Science 1970; 168:1238–1240.

(8) Price JM, Biava CG, Oser BL, Vogin EE, Steinfeld J, Ley HL. Bladder tumors in rats fed cyclohexylamine or high doses of a mixture of cyclamate and saccharin. Science 1970; 167:1131–1132.

(9) Hicks RM, Wakefield J, Chowaniec J. Evaluation of a new model to detect bladder carcinogens or co-carcinogens; results obtained with saccharin, cyclamate and cyclophosphamide. Chem Biol Interact 1975; 11:225–233.

(10) Cohen SM, Arai M, Jacobs JB, Friedell GH. Promoting effect of saccharin and DL-tryptophan in urinary bladder carcinogenesis. Cancer Res 1979; 29:1207–1217.

(11) Ishii DN. Effect of the suspected tumor promoters saccharin, cyclamate and phenol on nerve growth factor binding and response in cultured embryonic chick ganglia. Cancer Res. (In press).

(12) Wigler M, Defeo D, Weinstein IB. Induction of plasminogen activator in cultured cells by macrocyclic plant diterpene esters and other agents related to tumor promotion. Cancer Res 1978; 38: 1434–1437.

(13) Driedger PE, Blumberg PM. Non-phorbol mouse skin tumor promoters do not mimic phorbol myristate acetate in its effects on chick embryo fibroblasts. Int J Cancer 1978; 22:63–69.

(14) Varon S. Nerve growth factor and its mode of action. Exp Neurol 1975; 48:75–92.

(15) Hendry IA. Control in the development of the vertebrate sympathetic nervous system. Rev Neuroscience 1976; 2:149–194.

(16) Mobley WC, Server AC, Ishii DN, Riopelle RJ, Shooter EM. Nerve growth factor (first of three parts). N Engl J Med 1977; 297: 1096–1104.

(17) ———. Nerve growth factor (second of three parts). N Engl J Med 1977; 297:1149–1158.

(18) ———. Nerve growth factor (third of three parts). N Engl J Med 1977; 297:1211–1218.

(19) Burton LE, Wilson WH, Shooter EM. Nerve growth factor in mouse saliva: Rapid isolation procedures for and characterization of 7 S nerve growth factor. J Biol Chem 1978; 253:7807–7812.

(20) Varon S, Nomura J, Shooter EM. Reversible dissociation of mouse nerve growth factor protein into subunits. Biochemistry 1968; 7: 1296–1303.

(21) Herrup K, Shooter EM. Properties of the β-nerve growth factor receptor of avian dorsal root ganglia. Proc Natl Acad Sci USA 1973; 70:3884–3888.

(22) Sutter A, Riopelle RJ, Harris-Warrick RM, Shooter EM. Nerve growth factor receptors: Characterization of two distinct classes of binding sites on chick embryo sensory ganglia cells. J Biol Chem 1979; 254:5972–5982.

(23) Levi-Montalcini R, Hamburger V. Selective growth-stimulating effects of mouse sarcoma on the sensory and sympathetic nervous system of the chick embryo. J Exp Zool 1951; 116:321–362.

(24) Scatchard G. The attraction of proteins for small molecules and ions. Ann NY Acad Sci 1949; 51:660–675.

(25) Boutwell RK, Bosch DK. The tumor-promoting action of phenol and related compounds for mouse skin. Cancer Res 1959; 19:413–424.

(26) Cook JW, Kennaway EL, Kennaway NM. Production of tumors in mice by deoxycholic acid. Nature 1940; 145:627.

(27) Reddy BS, Narasawa T, Weisburger JH, Wynder EL. Promoting effect of sodium deoxycholate on colon adenocarcinoma in germfree rats. J Natl Cancer Inst 1976; 56:441–442.

(28) Cohen R, Pacifici M, Rubinstein N, Biehl J, Holtzer H. Effect of a tumor promoter on myogenesis. Nature 1977; 266:538–540.

(29) Rovera G, O'Brien T, Diamond L. Tumor promoters inhibit spontaneous differentiation of Friend erythroleukemia cells in culture. Proc Natl Acad Sci USA 1977; 74:2894–2898.

(30) Yamasaki H, Fibach E, Nudel U, Weinstein IB, Rifkind RA, Marks PA. Tumor promoters inhibit spontaneous and induced differentiation of murine erythroleukemia cells in culture. Proc Natl Acad Sci USA 1977; 74:3451–3455.

(31) Diamond L, O'Brien TG, Rovera G. Inhibition of adipose conversion of 3T3 fibroblasts by tumor promoters. Nature 1977; 269:247–249.

(32) Huberman E, Callaham MF. Induction of terminal differentiation in human promyelocytic leukemia cells by tumor-promoting agents. Proc Natl Acad Sci USA 1979; 76:1293–1297.

(33) Sachs L. Control of normal cell differentiation and the phenotypic reversion of malignancy in myeloid leukaemia. Nature 1978; 274: 535–539.

(34) Tveit KM, Fodstad O, Johannessen JV, Olsnes S. A human melanoma cell line established from xenograft in athymic mice. Br J Cancer 1980; 41:724–733.

(35) Raick AN. Ultrastructural, histological and biochemical alterations produced by 12-*O*-tetradecanoyl-phorbol-13-acetate on mouse epidermis and their relevance to skin tumor promotion. Cancer Res 1973; 33:269–286.

(36) Shoyab M, Delarco JE, Todaro GE. Biologically active phorbol esters specifically alter affinity of epidermal growth factor membrane receptors. Nature 1979; 279:387–391.

(37) Lee LS, Weinstein IB. Tumor-promoting phorbol esters inhibit binding of epidermal growth factor to cellular receptors. Science 1978; 202:313–315.

(38) Brown KD, Dicker P, Rozengurt E. Inhibition of epidermal growth factor binding to surface receptors by tumor promoters. Biochim Biophys Res Commun 1979; 86:1037–1043.

(39) Fibach E, Gambari R, Shaw PA, et al. Tumor promoter-mediated inhibition of cell differentiation: Suppression of the expression of erythroid functions in murine erythroleukemia cells. Proc Natl Acad Sci USA 1979; 76:1906–1910.

(40) Banerjee SP, Snyder SH, Cuatrecasas P, Greene LA. Binding of nerve growth factor receptor in sympathetic ganglia. Proc Natl Acad Sci USA 1973; 70:2519–2523.

(41) Frazier WA, Boyd LF, Bradshaw RA. Properties of the specific binding of ^{125}I-nerve growth factor to responsive peripheral neurons. J Biol Chem 1974; 249:5513–5519.

blank page

Granulopoiesis Longevity in Continuous Bone Marrow Cultures and Factor-Dependent Cell Line Generation: Significant Variation Among 28 Inbred Mouse Strains and Outbred Stocks [1, 2, 3]

Mary Ann Sakakeeny [4] *and* **Joel S. Greenberger** [4, 5, 6]

ABSTRACT—Longevity of granulopoiesis in corticosteroid-supplemented continuous bone marrow cultures and generation of permanent WEHI-3 dialyzed conditioned medium (DCM)-dependent hematopoietic progenitor cell lines were evaluated for 28 inbred mouse strains and outbred stocks. Cultures from AKR/J, NZW, C58/J, DBA/2J, and C57BL/KsJ mice generated granulocytes for 45–58 weeks and released more than 10^5 murine sarcoma virus (MuSV) rescue units of endogenous retrovirus; nonadherent (NA) cells from 50% or more cultures produced permanent WEHI-3 DCM-dependent cell lines. Cultures from 129/J, BALB/cJ, SJL/J, RF/J, CD-1 Swiss, C57BR/cdJ, C57BL/Ka, CBA/J, RFM/Sn, NZB, C3H/HeJ, NIH Swiss [N:NIH(S)], C57BL/10J, C57L/J, SWR/J, HRS/J, and C57BL/6J mice generated granulocytes for 12–38 weeks; some released 10^1–10^2 MuSV rescue units of retrovirus, and NA cells from less than 50% of cultures from all but SWR/J and C57L/J mice produced WEHI-3 DCM-dependent cell lines. Thus longevity of granulopoiesis in mouse continuous bone marrow cultures varies significantly among strains.—JNCI 1982; 68: 305–317.

The development of a method for maintenance and proliferation of pluripotential hematopoietic stem cells in vitro from a single bone marrow inoculum (*1–3*) has led to a number of studies of the biology of normal and abnormal hematopoiesis in vitro (*3–15*). The initial difficulty with reproduction of the system of Dexter and Testa (*1*) has been overcome by addition of 17-hydroxycorticosteroid at a concentration of 10^{-7} to 10^{-5} *M* to horse serum or FCS and sustains hematopoiesis in vitro for several months (*2*). The addition of hydrocortisone to long-term bone marrow cultures also eliminates the need for addition of a second marrow inoculum at 3–4 weeks (recharge) as initially described by Dexter and Testa (*1*). While longevity of hematopoiesis in murine continuous bone marrow cultures is improved by corticosteroid, differences in culture longevity between laboratories (*1, 2, 7, 13, 16–18*) suggested that mouse strain genotype might independently influence the duration of hematopoiesis in vitro. Furthermore, cells removed from continuous bone marrow cultures of some (*6, 14*), but not all (*6, 9*), mouse strains form permanent lines of self-renewing hematopoietic progenitor cells if transferred to suspension culture in DCM from the WEHI-3 cell line (*9, 19*) or pokeweed mitogen spleen cell-conditioned medium (*8*). The observation that infection of cultures from N:NIH(S) mice with specific murine leukemia viruses prolonged the duration of granulopoiesis in primary cultures and induced formation of WEHI-3-dependent cell lines (*9, 10*) indicated that regulation of self-renewal of hematopoietic cells in vitro was altered by retrovirus replication. The site(s) and mechanism of action of retrovirus replication on hematopoietic and/or adherent stromal cells in the cultures are unknown.

In the present studies, we evaluated the role of genetic variables, including endogenous retrovirus replication, in regulation of hematopoiesis in long-term bone marrow cultures from 20 inbred mouse strains, four F_1 hybrid strains, and several F_2, backcross, and outbred mouse stocks. We specifically sought to determine *a*) whether longevity of hematopoiesis was associated with spontaneous induction of replication of endogenous ecotropic retrovirus, as suggested by previous studies (*7*); *b*) whether stromal and/or hematopoietic stem cell genotype regulated longevity; and *c*) whether longevity could be correlated with differences in the morphology of NA cells, including maintenance of adipocytes in the adherent cell layer.

MATERIALS AND METHODS

Mice.—Mice were obtained from The Jackson Laboratory, Bar Harbor, Maine, and included the following: AKR/J, BALB/cJ, CBA/J, C57BL/6J, C57BL/10J, C57BL/KsJ, C57BR/cdJ, C3H/HeJ, C58/J, C57L/J, DBA/2J, RF/J, SJL/J, SWR/J, 129/J, HRS/J,

---

ABBREVIATIONS USED: CFU$_c$=colony-forming unit(s) of progenitor cells; CSF=colony-stimulating factor(s); DCM=dialyzed conditioned medium; FCS=fetal calf serum; GM=granulocyte-macrophage; GM-CFU$_c$=CFU$_c$ of GM progenitor cells; MuSV=murine sarcoma virus; K-MuSV=Kirsten MuSV; NA=nonadherent.

---

[1] Received June 9, 1981; accepted September 9, 1981.

[2] Supported by Public Health Service grants CA-25412-02 and CA-26785-01 from the National Cancer Institute and by American Cancer Society research grant ACS-CH-171.

[3] Animals were maintained under the guidelines set forth by the Sidney Farber Cancer Institute.

[4] Joint Center for Radiation Therapy, Department of Radiation Therapy, Harvard Medical School and Sidney Farber Cancer Institute, 44 Binney St., Boston, Mass. 02115.

[5] *Address reprint requests to* Dr. Greenberger.

[6] We thank Dr. Stuart A. Aaronson, National Cancer Institute, Bethesda, Md., and Dr. Samuel Hellman, Joint Center for Radiation Therapy, Boston, Mass., for helpful discussions; Dr. William C. Moloney, Peter Bent Brigham–Women's Hospital, Boston, Mass., for review of microscopic slides; and Mr. Thomas Novak, Ms. Nancy Hoffman, and Ms. Karen Berndtson for technical assistance.

(C57BL/6J × DBA/2)F_1 [(B6D2)F_1/J] and (C3H/HeJ × DBA/2J)F_1 [(C3D2)F_1/J]. C57BL/Ka mice were provided by Dr. Alain DeCleve and Dr. Henry Kaplan, Stanford University, Palo Alto, Calif. CD-1 Swiss mice were obtained from the Charles River Breeding Laboratories, Boston, Mass. NIH Swiss [N:NIH(S)], NZB, and NZW mice were obtained from the Small Animal Section, Veterinary Resources Branch, Division of Research Services, National Institutes of Health, Bethesda, Md. RFM/Sn mice were provided by Dr. Harvey Preissler, Roswell Park Memorial Institute, Buffalo, N.Y. (CBA/J × C57BL/6J)F_1, [N:NIH(S) × C57BL/KsJ]F_1, [NIH:NIH(S) × C57BL/KsJ]F_1 × N:NIH(S) backcross, and [(N:NIH(S) × C57BL/KsJ]F_2 mice were bred in our laboratory. All mice were standardized to 30–33 g, and only female mice were used unless otherwise designated.

Cell lines.—Cells were grown in Dulbecco's modified Eagle's minimum essential medium with 10% FCS and included embryo fibroblast lines NIH/3T3 (*20*) and BALB/3T3 (*21*) and a normal rat kidney line, NRK (*22*). A K-MuSV-transformed nonproducer cell line of each has been described; they are termed KNIH, KBALB, and KNRK, respectively (*23*).

The cell lines L929 and WEHI-3 clone 5 (*15*) have been reported. Conditioned medium was harvested from each line after growth at 37°C for 72 hours. For WEHI-3 conditioned medium was then dialyzed against a hundredfold excess of distilled water for 72 hours. The dialysate was then concentrated fivefold by Amicon PM10 filtration (Amicon Corp., Lexington, Mass.) according to published procedures. The resulting DCM was added in a 10% volume to McCoy's 5-A supplemented medium (*11*) with 15% FCS (Flow Laboratories, Inc., Rockville, Md.).

Virus assays.—A method for detection of retrovirus virion-associated reverse transcriptase in the culture fluid of normal long-term bone marrow cultures has been reported previously (*9*). A focus assay has been described for detection of low levels of infectious retrovirus by 7 days' cocultivation of marrow culture cells with exponential phase cultures of KNIH, KBALB, or KNRK cells followed by transfer of this culture medium in serial tenfold dilutions to exponential phase cultures of Balb/3T3, NIH/3T3, and NRK cells for focus assay of rescued K-MuSV (*7*). Virus detected by rescue of K-MuSV from KNIH cells with focus formation on NIH/3T3 cells was designated N-tropic according to published criteria of host range for infectivity (*24*). The level of virus production was designated as the end-point dilution at which K-MuSV was rescued (MuSV rescue units) (*7*).

Long-term bone marrow cultures.—The contents of a tibia and femur were flushed via a 22-gauge needle into Corning plastic flasks (40 cm^2) in 10.0 ml Fisher's medium supplemented with 10^{-5} *M* hydrocortisone sodium hemisuccinate (Solu-Cortef; The Upjohn Co., Kalamazoo, Mich.) and 25% horse serum (Flow Laboratories, Inc., Rockville, Md.). Cultures were maintained at 33°C in a high-humidity incubator (Wedco, Rockville, Md.) with 7% CO_2 and were fed by weekly removal of all NA cells and medium with replacement by a 10.0-ml volume of fresh medium. Cultures were not recharged with any additional marrow. By week 4, all cultures were switched to weekly refeeding with 8.0 ml of medium containing 25% FCS with 10^{-5} *M* hydrocortisone (*3*).

Hematopoietic colony-forming cell assays.—The assay for GM-CFU$_c$ (*25*) has been described. The method for quantitation of adipocyte colonies (≥50 cells) and clusters (10–49 cells) in primary marrow cultures was reported previously (*2, 3*).

Establishment of permanent WEHI-3 DCM-dependent hematopoietic progenitor cell lines.—NA cells from individual marrow cultures were centrifuged to a pellet (1,000×*g* for 10 min) and transferred at 5×10^5 cells to 4.0-ml petri dishes containing McCoy's 5-A supplemented medium (*9, 10*) and 10% WEHI-3 DCM (*11*). The methods for establishing cloned cell lines and for preparing dialyzed, Amicon filtration-concentrated WEHI-3 conditioned medium have been reported previously (*11*).

Histochemical and hematologic staining.—The methods for detection of intracellular myeloperoxidase, lysozyme, esterase-M (ASD-chloroacetate substrate-specific), and metachromasia by toluidine blue dye (*26–30*) have been described. Metachromasia has been shown to be a reliable indicator of mast cell–basophil differentiation of GM-CFU$_c$, derived from long-term marrow cultures and correlates with intracellular synthesis of histamine and the presence of surface IgE receptors (*28*). The Wright's–Giemsa staining technique was used as reported previously (*30*).

Assay for in vivo leukemogenicity.—Cell lines grown in WEHI-3 DCM were inoculated ip into newborn mice on the 1st day of life or iv into adult 30- to 33-g mice of each indicated strain. Mice were observed weekly for lymph node or spleen enlargement and peripheral blood leukocyte counts. According to published methods (*9*), dead or dying mice were subjected to complete postmortem evaluation of liver, spleen, lymph nodes, bone marrow, and central nervous system.

RESULTS

Continuous bone marrow cultures were established from the contents of a femur and tibia of each of the mouse strains shown in table 1. Each experiment for each strain contained at least eight cultures (femurs and tibias from four mice); cultures were initiated in 25% horse serum supplemented with 10^{-5} *M* hydrocortisone and switched by day 28 (the fourth weekly feeding) to 25% FCS with the same hydrocortisone concentration. At least two separate experiments containing at least eight flasks each were performed with each mouse strain or stock. To minimize variation due to differences in lots of horse serum or FCS, we reserved specific lots of serum for use exclusively in these experiments. Cultures were maintained at 33°C, and assays for GM-CFU$_c$ were performed with the use of a single preparation of L929 cell-conditioned medium as a source of CSF. Cultures were incubated at 37°C and scored by one observer (M. A. S.) on day 7. Thus differences in the biologic properties between the strains could not be attributed to differences in culture conditions.

Each culture had the medium changed every 7th day, according to published procedures (*3*), by removal of all NA cells and medium and replacement by a fresh volume of medium. Cells from each group of cultures were spun to a pellet at 1,000×g for 10 minutes, resuspended in 4.0 ml of McCoy's 5-A medium supplemented with 10% WEHI-3 DEM, and maintained at 31°C with passage every 3d day as described in "Materials and Methods." The number of cultures generating a suspension cell line from 5×10^5 NA cells, which could be maintained continually with passage twice a week and could be cloned in 0.3% agar, was determined for each strain in each experiment. Extra NA cells from all the cultures of each strain were then pooled and prepared for differential cell count and GM-CFU$_c$ assay.

Longevity of Granulopoiesis and Generation of WEHI-3 DCM-Dependent Cell Lines: Significant Variation Among Mouse Strains

As shown in table 1, the duration of generation of mature granulocytes and cells that formed GM-CFU$_c$ (>50 cell colonies in 0.3% agar supplemented with L929 cell CSF) varied significantly among strains. Cultures from AKR/J, NZW, DBA/2J, and C58/J marrow produced granulocytes for over 50 weeks and generated GM-CFU$_c$ for at least 40 weeks. Within each of these strains, individual cultures varied, but the range of fluctuation was less than 20% of the mean (table 1). NA cells from at least 50% of cultures from each of these strains generated permanent cell lines in WEHI-3 DCM. Marrow cultures from C57BL/KsJ mice generated granulocytes and GM-CFU$_c$ for at least 40 weeks, and a very high fraction of cultures (10/16) generated WEHI-3 DCM-dependent cell lines. The earliest culture harvest generating a permanent line was detected at week 4 with AKR/J and NZW marrow, but the cultures produced NA cells that were capable of forming cell lines for very long periods (with AKR/J up to 40 wk). Continuous bone marrow cultures established from 129/J, BALB/cJ, SJL/J, RF/J, CD-1 Swiss, C57BR/cdJ, C57BL/Ka, CBA/J, RFM/Sn, NZB, C3H/HeJ, and N:NIH(S) mice generated mature granulocytes and GM-CFU$_c$ for periods ranging between 25 and 38 weeks. In each case, the decline of hematopoiesis was associated with a relative increase in the percentage of macrophages detected in NA cell harvests and decreased numbers of hematopoietic cell islands in the adherent compartment of the culture. These adherent islands have previously been shown by use of the inverted microscope to consist of flat cells with rounded, rather than polygonal or elongate, shape and a nonrefractile appearance (*15*). The morphologic appearance of such tightly interlocking round cells has been termed "cobblestone areas." Round, refractile hematopoietic cells were observed to evolve in sheets from these cobblestone areas, and cessation of hematopoiesis was associated with decreased numbers of such cobblestone areas (*15*).

The density of cobblestone areas in cultures at weeks 4 and 8 was compared for AKR/J, NZW, C57BL/KsJ, 129/J, N:NIH(S), and C3H/HeJ mice. The morphology of cultures at weeks 4 and 8 was indistinguishable among representatives of each group when scored for the percentage

TABLE 1.—*Longevity of granulopoiesis and generation of WEHI-3 DCM-dependent hematopoietic progenitor cell lines in continuous bone marrow cultures from various inbred and outbred mice*[a]

Mouse strain or stock	Duration of generation of mature granulocytes $>10^4$/culture, mean (range), wk[b]	Duration of generation of GM-CFU$_c$, mean (range), wk[c]	No. of cultures[d] generating WEHI-3 DCM-dependent cell line/No. tested
Mouse strain, inbred			
AKR/J	58 (52–65)	56 (52–58)	10/16
BALB/cJ	35 (30–41)	33 (23–41)	2/16
CBA/J	28 (27–30)	19 (13–29)	1/16
C57BL/6J	20 (18–27)	19 (18–25)	2/16
C57BL/10J	24 (18–25)	24 (20–26)	3/16
C57BL/KsJ	45 (40–52)	40 (38–50)	10/16
C57BL/Ka	28 (20–30)	28 (20–29)	2/16
C57BR/cdJ	27 (20–31)	28 (26–32)	5/16
C3H/HeJ	26 (18–28)	20 (18–22)	1/16
C58/J	50 (48–52)	42 (40–47)	9/16
C57L/J	24 (21–26)	22 (19–23)	8/16
DBA/2J	48 (41–50)	48 (42–49)	8/16
RF/J	32 (21–35)	24 (21–26)	0/16
RFM/Sn	27 (25–29)	26 (21–28)	0/16
SJL/J	32 (30–33)	30 (28–31)	2/16
SWR/J	24 (21–27)	18 (15–21)	9/16
129/J	38 (34–40)	38 (35–41)	0/16
NZB	26 (21–27)	24 (21–26)	0/16
NZW	53 (51–65)	51 (47–62)	11/16
HRS/J	12 (10–17)	10 (9–12)	0/16
F_1 hybrid strain			
(B6D2)F_1/J (C57BL/6J♀ × DBA/2J♂)	51 (45–53)	50 (47–53)	10/16
(C3D2)F_1/J (C3H/HeJ♀ × DBA/2J♂)	41 (38–46)	40 (31–41)	3/16
CBA/J♀ × C57BL/6J♂	23 (20–30)	23 (21–27)	2/16
N:NIH(S)♀ × C57BL/KsJ♂	43 (28–52)	40 (29–47)	4/24
F_2 hybrid strain			
[N:NIH(S)♀ × C57BL/KsJ♂]F_2	42 (21–51)	43 (22–51)	0/24
Backcross strain			
[N:NIH(S)♀ × C57BL/KsJ♂]F_1♀ × N:NIH(S)♂	43 (22–51)	42 (23–50)	1/24
Mouse stock, outbred			
CD-1 Swiss	31 (21–41)	29 (18–40)	4/16
N:NIH(S)	25 (20–29)	21 (18–25)	0/240

[a] Groups of at least 16 cultures were established from the contents of femur and tibia marrow from mice of each indicated strain or stock. All cultures were initiated in 25% horse serum and switched at day 28 (the fourth weekly feeding) to 25% FCS. Fresh hydrocortisone (10^{-6} *M*) was added weekly. F_1 and F_2 hybrid mice and backcross mice were bred or obtained as described in "Materials and Methods."

[b] Total removed cells were counted, and the mean cell No. produced per week per culture was recorded. Results are presented as the mean longest duration of production of at least 10^4 granulocytes/wk for each culture. The range of production of 10^4 cells/culture is also shown for each group.

[c] Results represent the mean and range of duration of production of at least one ≥50-cell GM-CFU$_c$ colony/5×10^4 cells in 10% L929-conditioned medium as a source of CSF. The mean and range of GM cluster production (10–49 cells/colony) are not shown but averaged 1–2 wk longer than those for GM-CFU$_c$.

[d] The NA cells from each group of cultures after cells were removed for GM-CFU$_c$ assay and hematologic staining were centrifuged to a pellet and transferred to suspension cultures in McCoy's 5-A supplemented medium containing 10% concentrated (five times) WEHI-3 DCM (11). The No. of cultures in each group establishing a permanent cell line that sustained exponential phase growth in suspension culture for >10 mo is shown over the total No. of cultures tested.

of surface area covered by cobblestone areas and percentage of culture surface area covered by adherent fibroblast-like cells or adipocytes. Thus the appearance of long-term marrow cultures at early time points (before wk 8) did not predict the ultimate longevity of the cultures.

Continuous marrow cultures from C57BL/10J, C57L/J, SWR/J, C57BL/6J, and HRS/J mice showed longevity ranging from 12 to 24 weeks. The decreased longevity of cultures from HRS/J mice compared to that of AKR/J mice was highly significant (P<0.001) as was the difference between cultures from either AKR/J or C57BL/Ks/J and C3H/HeJ or C57BL/6J mice (P<0.02). There were no visible differences as judged by inverted microscopic examination of culture groups, except that HRS/J cultures began to demonstrate decreased cobblestone islands and decreased density of NA cells at week 6.

Generation of GM-CFU$_c$ by cultures from each of the inbred strains fluctuated from week to week. This phenomenon could not be correlated with differences in the total number of cells produced during a particular week or to the percentage of immature cells detected that week. As shown in text-figure 1, AKR/J long-term marrow cultures generated GM-CFU$_c$ for over 56 weeks. The peaks of production of GM-CFU$_c$ seen at weeks 31, 42, and 50, when cells were plated at 2×10^5/dish, were not associated with increases in the percentage of immature granulocytes at those time points. Immature granulocytes ranged between 20 and 30% of cells in the culture. The peaks of GM-CFU$_c$ also did not correlate with increases in the total number of NA cells removed at that time point. Total cell numbers varied between 10^5 and 5×10^6 cells/culture.

Fluctuation in production of GM-CFU$_c$ also occurred in marrow cultures from NZW, DBA/2J, and C58/J marrow cultures (text-figs. 2-4), although in NZW cultures an increased number of GM-CFU$_c$ was detected between week 36 and week 44 compared to that for weeks 4-12. An increased relative number of GM-CFU$_c$ was also seen between week 30 and week 44 compared to that for earlier weeks in DBA/2J and C58/J marrow cultures. A similar fluctuation in production of GM-CFU$_c$ was seen in marrow cultures from strains with decreased in vitro longevity. As shown in text-figure 5, cultures from 129/J mice produced GM-CFU$_c$ that cycled rapidly between week 1 and week 24, with the greater numbers of colonies detected at the higher plating density (2×10^5) compared to those at the lower (5×10^4) one. A fluctuation was also seen in cultures from SJL/J, C57BR/cdJ, and C57BL/10J mice (text-fig. 6; data not shown). The percentage of immature granulocytes scored in cultures from 129/J and SJL/J mice was significantly lower than that in cultures from AKR/J, NZW, DBA/2J, or C58/J mice. Cultures from those strains with decreased longevity were also observed to have a persistently lower percentage of immature granulocytes in the removed cell number; however, there was no detectable difference in the absolute number of cells removed among strains with long and short durations of hematopoiesis. Cultures from C57BR/cdJ, C57BL/10J, RF/J, NZB, C57L/J, CBA/J, C57BL/6J, and SWR/J mice persistently demonstrated less than 25% immature granulocytes in the harvests between week 1 and week 20 (text-fig. 7; data not shown). Included in the designation of immature granulocytes are cells with blast, promyelocyte, or myelocyte morphology. Excluded are cells with toluidine blue-positive mast cell–basophil granules, megakaryocytes, and multinucleated cells including detached macrophages.

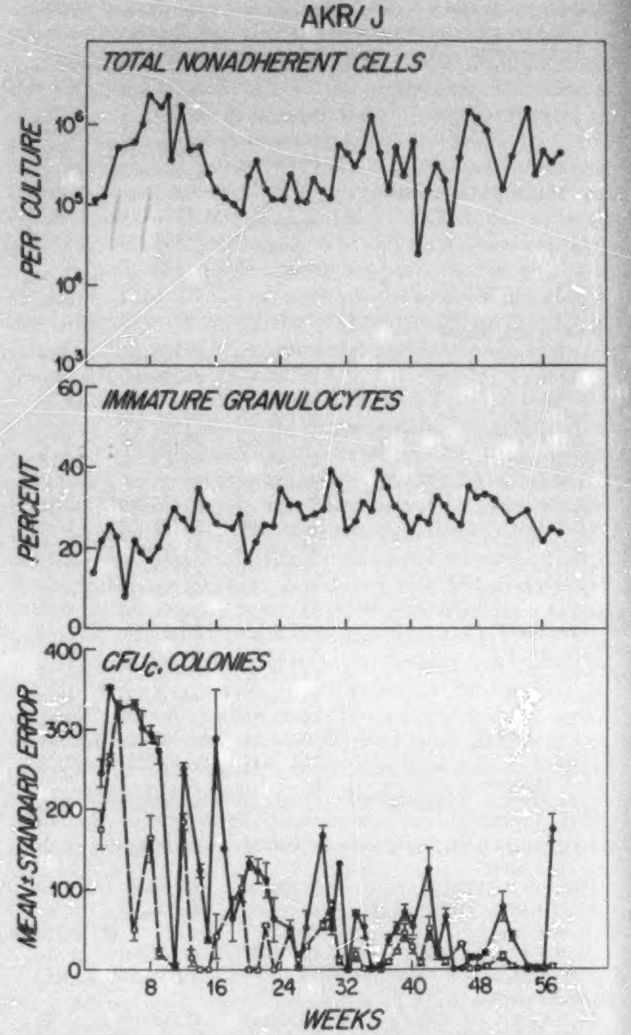

TEXT-FIGURE 1.—Granulopoiesis in continuous marrow cultures from AKR/J mice. Results represent the mean total NA cells counted per culture each week in the total volume of medium removed that week. Loosely adherent cells were not washed off. At least six cultures in each of 2 expts were counted at each time point. The percent immature granulocytes is based on a differential cell count of a Wright's–Giemsa-stained preparation of NA cells removed each week and is the mean of at least three counts at each point scoring 1,000 cells/slide. The No. includes blasts, promyelocytes, and myelocytes excluding detached macrophages, megakaryocytes, and subtraction of the percent mast cell–basophils scored on parallel toluidine blue-stained slides. The standard error was <10% of the mean for these determinations. The CFU$_c$ are the mean ± standard error of the mean for GM colonies of ≥50 cells/colony scored at day 7 following incubation at 37°C of 2×10^5 (●) or 5×10^4 (○) NA cells/1.0 ml culture containing 0.3% agar. (Text-figs. 2–8 are prepared in an identical fashion.)

The number of NA cells recovered weekly from cultures of each strain clearly fluctuated. This fluctuation was often precipitous, as seen in the variation of cells removed weekly from NZB cultures (text-fig. 8). In contrast, AKR/J cultures produced a consistently higher number of cells that fluctuated over a shorter tenfold range (10^5–10^6) per week, compared to the fluctuations in NZB cultures over a hundredfold range (10^4–10^6). An overall trend toward decreased production of cells per week was observed with each strain tested; however, the plateau of production lasted over 56 weeks for AKR/J cultures (text-fig. 1), over 52 weeks for NZW cultures (text-fig. 2), and for a much shorter duration with strains such as NZB (text-fig. 8). In cultures that produced GM-CFU$_c$ and/or granulocytes at more than 10^4/culture/week for over 40 weeks, a gradual decline in the total cell number produced per week correlated with an increase in the relative percentage of macrophage-like cells in the NA cell harvest. The decrease in cell number is shown for C58/J cultures in text-figure 4 and for 129/J cultures in text-figure 5 and is compared to that for the shorter duration cultures of NZB marrow in text-figure 8 and of SWR/J marrow in text-figure 7. In DBA/2J cultures, a downward trend in cell numbers was observed from weeks 8 to 32 followed by a gradual increase in the production of GM-CFU$_c$ and total cell numbers between week 36 and week 48. A second increase in cell number was associated with a gradual increase in the percentage of immature granulocytes also seen at that time (text-fig. 3). In each of the strains tested, the number of GM-CFU$_c$ was greater at the high cell density (2×10^5/ml) compared to that at the lower cell density (5×10^4/ml) (text-figs. 1–8), arguing against production of NA inhibitory cells for the GM-CFU$_c$.

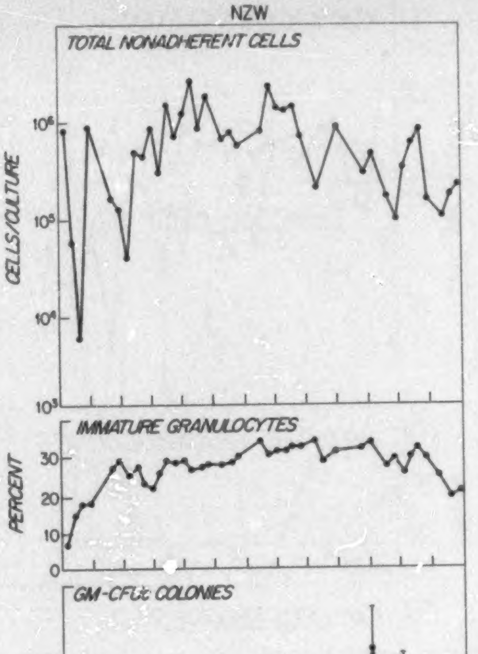

TEXT-FIGURE 2.—Granulopoiesis in continuous marrow cultures from NZW mice.

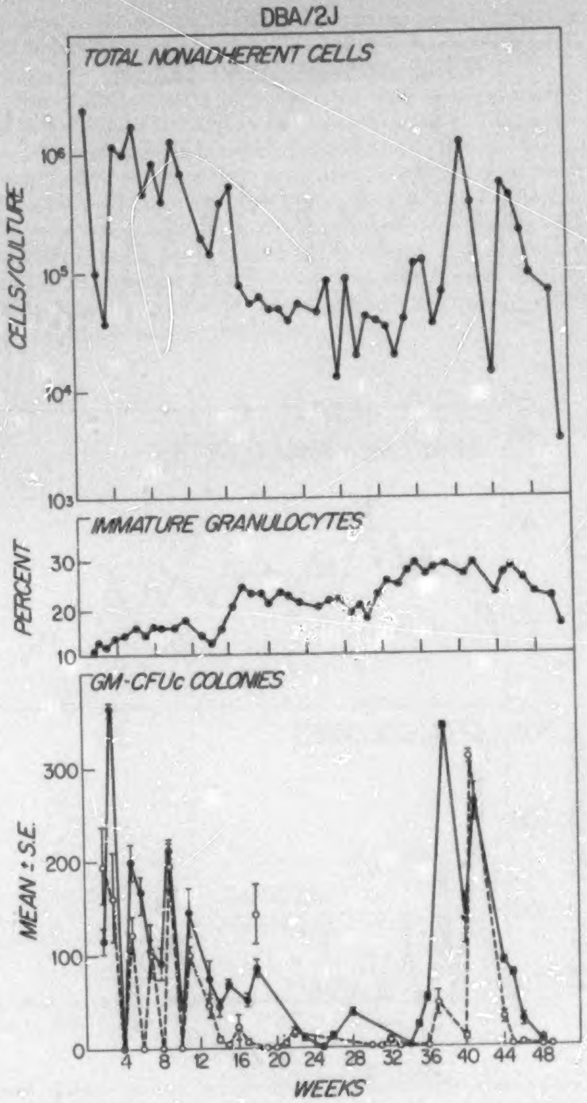

TEXT-FIGURE 3.—Granulopoiesis in continuous marrow cultures from DBA/2J mice.

The morphology of GM-CFU$_c$ produced in cultures from representative strains at extremes of the spectrum was tested next. GM-CFU$_c$ produced at week 50 by C57BL/KsJ and

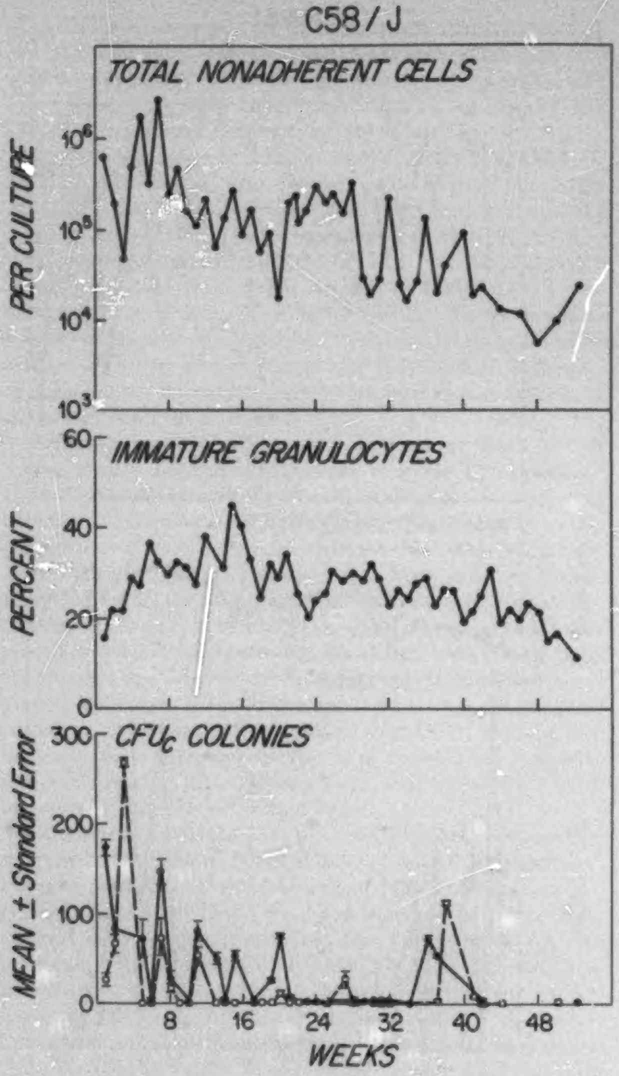

Text-figure 4.—Granulopoiesis in continuous marrow cultures from C58/J mice.

AKR/J were 82–85% macrophage and 15–18% mixed GM (range for 6 separate expts). GM-CFU$_c$ produced by these same cultures at earlier time points were not detectably different and did not differ from GM-CFU$_c$ produced at week 10 by HRS/J cultures (83–86% macrophage and 16–17% GM).

Duration of Hematopoiesis Influenced by a Mendelian Genetic Mechanism

Several F$_1$ hybrid strains were next tested to determine whether longevity of hematopoiesis in long-term marrow cultures was a dominant or recessive trait or whether it was regulated by a more complex genetic mechanism. Results with several of these hybrids are shown in table 1. For these studies at least four separate experiments with eight cultures per strain were performed. (B6D2)F$_1$ marrow cultures derived from a DBA/2 parent, with a mean longevity of 48 weeks, and a C57BL/6J parent, with a duration of hematopoiesis of 20 weeks, demonstrated longevity similar to that of the DBA/2 parent with generation of granulocytes for 51 weeks and GM-CFU$_c$ for 50 weeks. Similarly, (C3D2)F$_1$ mice demonstrated characteristics similar to those of the DBA/2 parent with generation of granulocytes for 41 weeks and GM-CFU$_c$ for 40 weeks. The F$_1$ hybrid between CBA/J and C57BL6/J mice demonstrated an intermediate longevity of 23 weeks for production of granulocytes and of 23 weeks for production of GM-CFU$_c$. Data with three F$_1$ strains indicated that longevity was dominant if measured by mean duration of hematopoiesis. The range of individual cultures within each F$_1$ group indicated that the longevity of most cultures in the group was increased above that of the short-duration parent strain. NA cells from each F$_1$

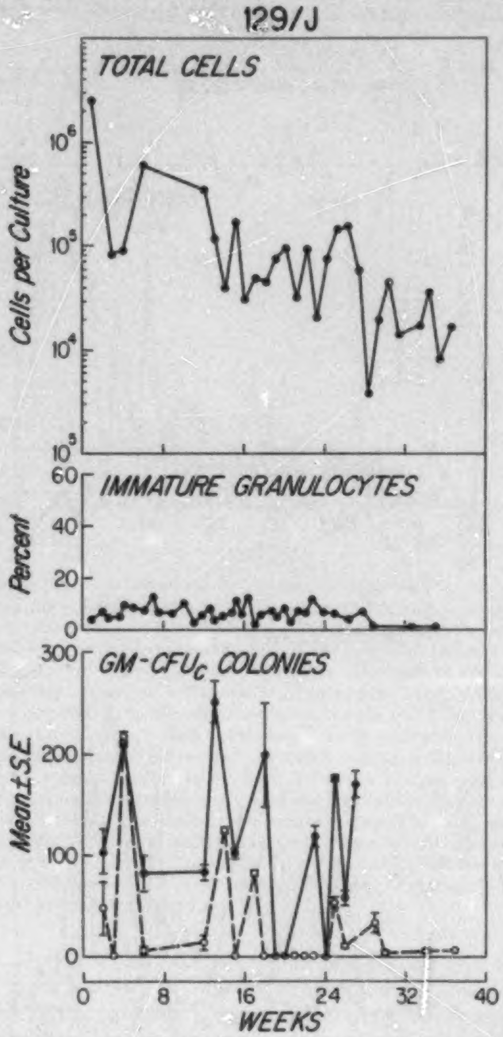

Text-figure 5.—Granulopoiesis in continuous marrow cultures from 129/J mice.

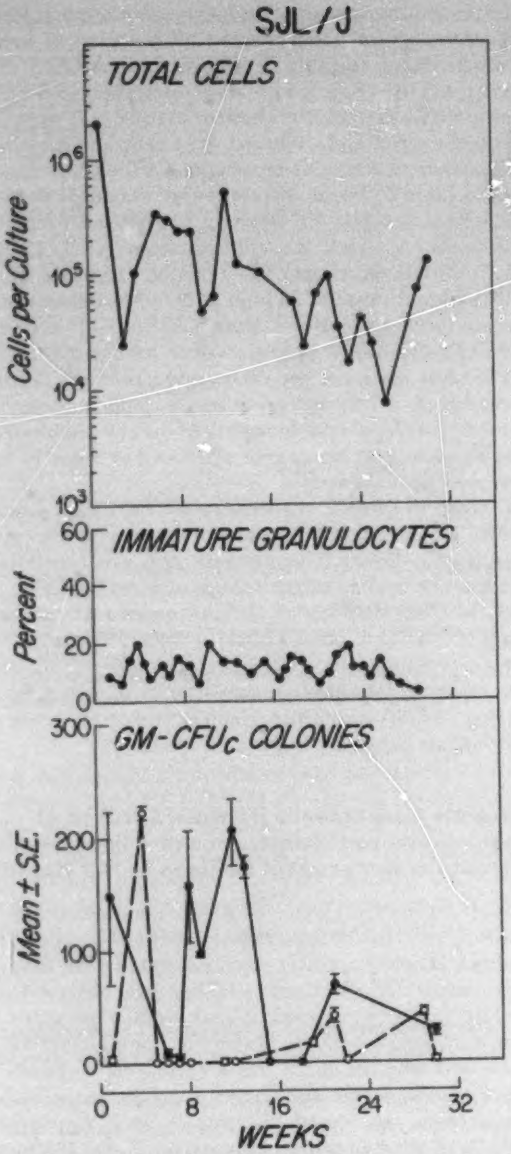

TEXT-FIGURE 6.—Granulopoiesis in continuous marrow cultures from SJL/J mice.

hybrid tested generated permanent WEHI-3 DCM-dependent cell lines (table 1).

Examination of cultures from [N:NIH(S) × C57BL/-KsJ]F$_1$ mice was next done and revealed an intermediate longevity, which was, however, closer to that of the long-duration parent C57BL/KsJ. These F$_1$ cultures generated GM-CFU$_c$ for 40 weeks and granulocytes for 43 weeks. To determine if longevity segregated in genetic crosses, we derived F$_2$ hybrid mice from N:NIH(S) and C57BL/KsJ mice and backcross mice of the F$_1$ generation on the shorter duration N:NIH(S) parent. Results with these cultures are shown in table 1 and indicate that longevity was consistently higher than that for the short-duration parent; however, the range of individual cultures widened as the genetic influence of the N:NIH(S) parent was increased in backcross and F$_2$ strains.

Two outbred stocks of Swiss mice were next compared: CD-1 Swiss and N:NIH(S). As shown in table 1, the longevity of hematopoiesis between the two stocks was not significantly different; however, generation of WEHI-3 cell-conditioned medium-dependent lines was markedly different. Combined results from experiments done over 3 years with N:NIH(S) mice are included for reference. No permanent lines were obtained from NA cells removed from N:NIH(S) cultures; however, 4 of 16 cultures from CD-1 Swiss marrow generated permanent cell lines.

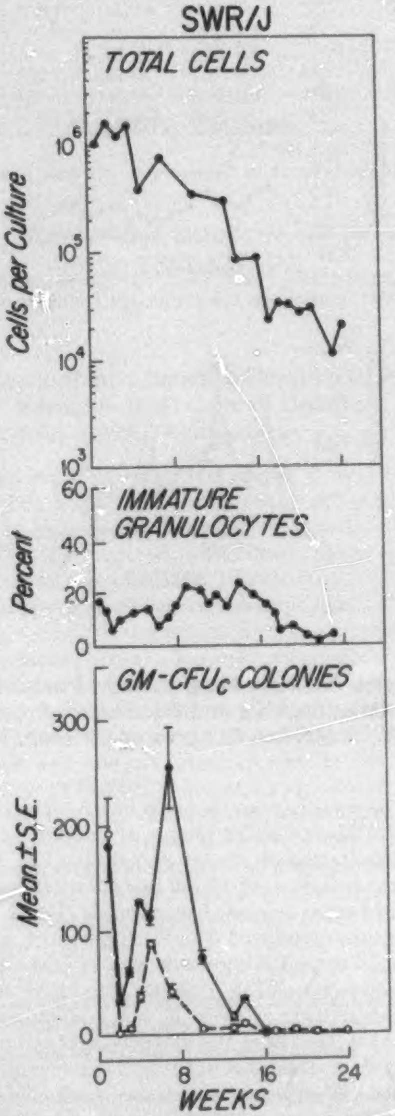

TEXT-FIGURE 7.—Granulopoiesis in continuous marrow cultures from SWR/J mice.

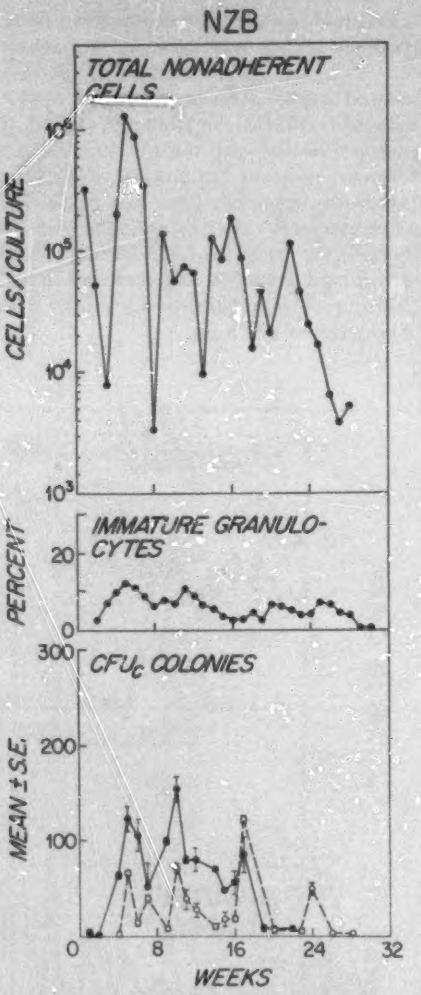

TEXT-FIGURE 8.—Granulopoiesis in continuous marrow cultures from NZB mice.

Concordance Between Magnitude of Production of Immature Granulocytes and Duration of Production of GM-CFU$_c$ in Marrow Cultures of Different Mouse Strains

Table 2 shows the mean numbers of NA cells produced at weeks 10, 20, 30, and 40 for groups of cultures from each of 17 representative mouse strains and stocks. The magnitude of cell production at week 10 did not reflect the subsequent longevity of hematopoiesis. For example, RF/J long-term marrow cultures produced 3×10^6 cells/culture at week 10 and continued to produce granulocytes or GM-CFU$_c$ for 24 weeks. In contrast, NZW cultures produced fewer cells (5.0×10^5) per culture at week 10 but maintained hematopoiesis for 51 weeks. Thus the magnitude of cell production at the early time point did not reflect the overall longevity of the cultures. These experiments also confirmed our observation that density of cobblestone and round cell areas in the cultures at the early time of 10 weeks could not predict long-duration cultures.

The percent immature granulocytes generated at week 10 more accurately reflected the overall duration of hematopoiesis. As shown in table 2, cultures from AKR/J, NZW, DBA/2J, C57BL/KsJ, and C58/J mice produced 16–38% immature cells at week 10. These immature cells were of the granulocyte series and excluded mast cells and multinucleated megakaryocytes or macrophages. Of the 12 other strains shown in table 2, 5 demonstrated more than 16% immature granulocytes at week 10, whereas 7 produced consistently lower levels. At week 20, cultures from AKR/J, NZW, DBA/J, C57BL/KsJ, and C58/J mice produced at least 15% NA immature cells; as high as 36% NA immature cells were produced by cultures from C57BL/KsJ. Of the 12 other strains shown, 3 produced over 15% immature cells. Thus in most instances the early production and increased percentage of immature granulocytes appeared to more accurately predict overall longevity of the cultures compared to the absolute number of cells produced at week 10 for 17 strains and stocks tested.

As shown in table 2, the density of GM-CFU$_c$ produced at week 10, 20, or 30 did not correlate with the overall longevity of cultures. This phenomenon was attributed to fluctuation or cycling of the release of NA GM-CFU$_c$ (text figs. 1–8). Thus analysis of differences between strains by looking at one time point either at week 10 or at week 20 did not accurately predict the overall longevity of the cultures; however, persistent production of a relatively high percentage of NA immature granulocytes (>10%) best predicted culture longevity beyond 30 weeks.

Incomplete Concordance Between Duration of Hematopoiesis and Maintenance of Adipocytes in Adherent Compartment of Cultures or *H-2* Haplotype

Initial studies by Dexter et al. (*31*) indicated that fat-containing cells in the adherent microenvironment of long-term bone marrow cultures were associated with long-term hematopoiesis. To determine whether cells observed to accumulate fat between week 1 and week 4 persisted over longer duration in cultures producing granulocytes for long periods and whether there was a correlation between persistence of adipocytes and longevity of hematopoiesis between strains, we scored cultures of each mouse strain weekly, according to published criteria (*2*), for the number of adipocyte colonies and clusters seen in the adherent microenvironment. As shown in table 3, there was no concordance between the duration of granulopoiesis as reflected in the production of GM-CFU$_c$ and the duration of detectable adipocytes in the adherent layer of the cultures. Adipocytes were seen for 17 weeks in AKR/J cultures that generated GM-CFU$_c$ for 56 weeks. In contrast, adipocytes were seen for 37 weeks in cultures from N:NIH(S) mice, while hematopoiesis persisted for 21 weeks. Adipocytes were detected for 21 weeks in cultures from SWR/J, DBA/2J, C58/J, and CD-1 Swiss mice. The difference in longevity of hematopoiesis between SWR/J (18 wk) and DBA/2J (48 wk) was significant ($P<0.001$), whereas adipocyte maintenance was not detectably different ($P>0.5$).

There was no detectable correlation between a specific *H-2* haplotype and duration of hematopoiesis. C57BL/KsJ

TABLE 2.—*Concordance between magnitude of production of immature granulocytic cells and GM-CFU$_c$ in long-term bone marrow cultures from different mouse strains*[a]

Mouse strain or stock[b] (longevity of GM-CFU$_c$ production, wk)	Mean No. of NA cells/culture, $\times 10^5$, at wk:[c]				Percent immature cells at wk:[d]				Mean No. of GM-CFU$_c$/2×10^5 cells/5×10^4 cells at wk:[e]			
	10	20	30	40	10	20	30	40	10	20	30	40
AKR/J (56)	40.0	2.7	1.7	6.5	20	15	38	22	273/21	133/5	52/80	54/29
NZW (51)	5.0	18.0	14.0	4.7	28	26	30	32	216/33	39/17	101/13	415/114
DBA/2J (48)	13.0	0.5	0.4	12.0	16	22	20	28	52/1.8	NT/0	NT/25	136/10
C57BL/KsJ (45)	5.0	3.8	4.6	0.66	38	36	14	26	252/0	2.5/1.0	NT	NT
C58/J (42)	4.4	0.59	1.0	0.29	30	28	28	20	0/0	75/11	0/0	NT
129/J (38)	8.5	0.96	0.46	NT	10	8	1	NT	50/3	0/0	NT/4.5	NT
BALB/cJ (33)	13.0	1.2	0.1	NT	4	9	1	NT	120/19	88/NT	NT	NT
SJL/J (30)	0.47	0.67	1.3	NT	20	13	6	NT	18/8	31/3	0/0	NT
C57BR/cdJ (28)	8.1	0.73	0.062	NT	22	20	18	NT	0/0	34/20	NT	NT
C57BL/10J (24)	3.5	0.50	NT	NT	16	15	NT	NT	35/8.5	0/3	NT	NT
RF/J (24)	30.0	0.83	0.066	NT	10	5	NT	NT	91/6	69/0	NT	NT
NZB (24)	0.55	0.19	NT	NT	8	8	1	NT	154/70	NT/5	NT	NT
C57L/J (22)	10.0	0.41	NT	NT	8	6	NT	NT	26/5	NT/2.5	NT	NT
N:NIH(S) (20)	10.0	1.2	2.3	0.15	8	6	3	4	96/53	113/10	0/0	NT
CBA/J (19)	8.7	0.52	0.028	NT	18	16	16	NT	26/0	0/0	NT	NT
C57BL/6J (19)	1.1	0.75	NT	NT	12	8	NT	NT	140/30	0/NT	NT	NT
SWR/J (18)	3.4	0.27	NT	NT	20	3	NT	NT	74/6.5	NT	NT	NT

[a] NT=not tested.

[b] Results for 17 representative strains and stocks are presented in decreasing order of longevity as measured in duration of production of detectable L929 CSF-responsive GM-CFU$_c$.

[c] Results are the means of at least eight cultures counted at that week.

[d] Results are presented as the mean percents of NA cells classified as blasts, promyelocytes, or myelocytes. Excluded are mast cells, macrophages, and megakaryocytes.

[e] Results are presented as the means of four GM-CFU$_c$ cultures scored at each cell plating density (2×10^5/5×10^4 NA cells/culture) and are for ≥50 cell colonies scored at day 7 after incubation at 37°C in 7% CO_2 and 0.3% agar containing 10% L929-conditioned medium and 15% FCS.

marrow cultures (*H-2^d*) produced granulocytes for 45 weeks, and cultures from DBA/2J (*H-2^d*) marrow produced granulocytes for 48 weeks. However, cultures from BALB/cJ (*H2^d*) marrow produced granulocytes for 33 weeks, a significantly shorter time (P<0.02). Both AKR/J and CBA/J mice have the *H-2^k* haplotype, and hematopoiesis varied significantly from 56 weeks with AKR/J to 19 weeks with CBA/J (P<0.02).

Concordance of Longevity of Granulopoiesis with High-Level Replication of Endogenous Retrovirus

Detectable spontaneous induction of endogenous retrovirus replication was next correlated with the longevity of hematopoiesis. As shown in table 4, AKR/J, NZW, DBA/2J, C57BL/KsJ, and C58/J long-term marrow cultures generated granulocytes for over 40 weeks and spontaneously released N-tropic endogenous virus. The level of virus released was more than 10^5 MuSV rescue units for each of these strains (table 4). In contrast, CBA/J, C57BL/6J, and BALB/cJ marrow cultures also released N-tropic virus but at a significantly lower level (10^1-10^2 MuSV rescue units) and generated granulocytes for 19 weeks (33 wk for BALB/cJ). While 129/J long-term marrow cultures produced granulocytes for 38 weeks, these cultures did not release detectable N-tropic virus. Thus spontaneous induction of detectable endogenous virus replication did not absolutely correlate with longevity of hematopoiesis. There was a positive correlation between high-level replication of retrovirus and longevity of hematopoiesis beyond 40 weeks (P<0.05).

Lack of Concordance Between Duration of Production of Basophil–Mast Cells or Lymphocytes and Neutrophilic Granulocytes

To determine whether production of a morphologically detectable NA helper cell or inhibitory cell accounted for variations in duration of hematopoiesis, we tested weekly NA cells from five representative strains for production of morphologically recognizable megakaryocytes, erythroid cells, lymphocytes, monocytes, plasma cells, or toluidine blue-positive mast cell–basophils. As shown in table 5, there was no correlation between longevity of production of granulocytes and the number of weeks during which basophil-mast cells were detected in the NA cell compartment. C57BL/KsJ marrow cultures produced detectable mast cells for 7 weeks and mature granulocytes for 45 weeks. In contrast, while N:NIH(S) cultures also produced basophil-mast cells for 7 weeks, granulocytes were generated for 25 weeks, a significantly shorter duration (P<0.01). No correlation was observed if duration of granulopoiesis was compared to numbers of NA megakaryocytes, monocytoid or lymphoid cells, or plasma cells detected in the NA compartment (data not shown).

Effect of Genotype of Adherent Stromal Cells and NA Hematopoietic Stem Cells on Longevity of Hematopoiesis in Mixed Marrow Cultures

To determine whether the longevity of AKR/J and C57BL/KsJ marrow cultures was a property of the adherent and/or NA cell population, we established, according to published methods (15), purified stromal cell cultures from

TABLE 3.—*Lack of concordance between duration of hematopoiesis and maintenance of adipocytes in mouse long-term bone marrow cultures*

Mouse strain or stock	Duration of granulopoiesis, mean,[a] GM-CFU_c	Duration of detectable adipocytes in adherent layer, >1 colony or >10 clusters, wk[b]
AKR/J	56	17
BALB/cJ	33	20
CBA/J	19	15
C57BL/6J	19	17
C57BL/10J	24	16
C57BL/KsJ	45	19
C57BL/Ka	28	17
C57BR/cdJ	28	16
C3H/HeJ	20	19
C58/J	42	21
C57L/J	22	17
DBA/2J	48	21
RF/J	24	14
RFM/Sn	26	12
SJL/J	30	16
SWR/J	18	21
129/J	38	10
NZB	24	10
NZW	51	17
HRS/J	10	10
$(B6D2)F_1$	50	17
$(C3D2)F_1$	40	21
CBA/J × C57BL/6J	23	17
N:NIH(S) × C57BL/KsJ	40	19
$[\text{N:NIH(S)} \times \text{C57BL/KsJ}]F_2$	43	16
$[\text{N:NIH(S)} \times \text{C57BL/KsJ}]F_1 \times \text{N:NIH(S)}$	42	15
CD-1 Swiss	29	21
N:NIH(S)	21	37

[a] Results are presented as the mean longest duration of production in weeks of ≥1 GM-CFU_c in L929 cell CSF from each group of cultures.

[b] Each culture was scored weekly by examination, according to published methods (*2*), with the use of a Zeiss inverted microscope for the total No. of adherent fat-containing cell islands. The results are presented as the mean longest No. of weeks during which at least 1 adipocyte colony (≥50 cells/area) or 10 adipocyte clusters (10–49 cells/area) were visualized.

TABLE 4.—*Incomplete concordance between either spontaneous induction of detectable endogenous retrovirus replication or H-2 haplotype and longevity of granulopoiesis in continuous bone marrow cultures*

Mouse strain or stock	Longevity of production of GM-CFU_c, wk	*H-2* haplotype	Virus release detectable by reverse[a] transcriptase assay of culture fluid or cocultivation of NA cells with K-MuSV nonproducer cells (host range of virus) (titer)
AKR/J	56	*K*	+ (N-tropic) $>10^5$
NZW	51	*Z*	+ (N-tropic) $>10^5$
DBA/2J	48	*d*	+ (N-tropic) $>10^5$
C57BL/KsJ	45	*d*	+ (N-tropic) $>10^5$
C58/J	42	*K*	+ (N-tropic) $>10^5$
129/J	38	*bc*	−
BALB/cJ	33	*d*	+ (N-tropic) $(10^1–10^2)$
SJL/J	30	*s*	−
C57BR/cdJ	28	*K*	−
C57BL/10J	24	*b*	−
RF/J	24	*K*	−
NZB	24	*b*	−
C57L/J	22	*b*	−
N:NIH(S)	21	*s*	−
CBA/J	19	*K*	+ (N-tropic) $(10^1–10^2)$
C57BL/6J	19	*b*	+ (N-tropic) $(10^1–10^2)$
SWR/J	18	*q*	−

[a] Pooled culture supernatants from weekly harvests were concentrated by ultracentrifugation and tested for virion-associated reverse transcriptase according to "Materials and Methods." Negative groups of cultures were next tested by cocultivation of 10^6 NA cells with polybrene-treated (*32*) exponential phase cultures of KNIH, KBALB, or KNRK cells, and 7-day supernatants were tested for rescue of focus-forming virus as described (*23*). Host range for infectivity is as previously described (*24*). Titer is expressed in MuSV rescue units as described in "Materials and Methods." − = <1.0.

TABLE 5.—*Lack of concordance between duration of production of basophil-mast cells and neutrophilic granulocytes in long-term bone marrow cultures from different mouse strains*

Mouse strain or stock	Basophil-mast cells[a] $>1/10^4$ cells/culture at wk	Neutrophilic granulocytes[a] $>10^4$/culture at wk
C57BL/KsJ	7	45
C57BL/6J	4	20
C3H/HeJ	6	26
N:NIH(S)	7	25
CD-1 Swiss	8	31

[a] NA cells harvested weekly were assayed, according to published procedures (*28*), for the No. of metachromasia-positive cell lines by toluidine blue staining. Results are presented as the mean No. of weeks during which at least one mast cell–basophil was detected/10^4 NA cells harvested compared to the mean duration of production of neutrophils/culture.

each strain by corticosteroid deprivation. NA cells from other corticosteroid-rich cultures were harvested at week 8 and engrafted to each syngeneic or allogeneic population at 5×10^6 NA cells/culture (*15*).

As shown in table 6, AKR/J or C57BL/KsJ NA cells proliferated in vitro for a significantly longer period on syngeneic or allogenic stromal cell cultures, including those from strains with a shorter duration of hematopoiesis following addition of their own syngeneic hematopoietic cells. For example, AKR/J NA cells engrafted to C3H/HeJ stromal cultures produced granulocytes for more than 20 weeks, whereas C3H/HeJ stromal cultures receiving syngeneic C3H/HeJ NA cells produced granulocytes for 8 weeks ($P<0.001$). In the reciprocal mix C3H/HeJ NA cells engrafted to AKR/J cultures produced granulocytes for 6 weeks, a shorter duration ($P<0.01$). The data indicate that the longevity of AKR/J marrow cultures compared to that of C3H/HeJ cultures was attributable to cells in the AKR/J NA cell compartment. When transferred to empty plastic flasks, AKR/J 8-week NA cells produced granulocytes for 2 weeks. These results confirm previous studies showing that stromal adherent cells are required for in vitro proliferation of 8-week NA cells harvested from murine continuous marrow cultures (*15*).

DISCUSSION

The present studies with 28 inbred mouse strains and outbred mouse stocks demonstrate significant differences in

TABLE 6.—*Effect of source of purified hematopoietic stem cells or stromal cells on longevity of reconstituted mouse bone marrow cultures*

Source of purified stromal culture[a]	Source of purified hematopoietic stem cells[b]					
	Long duration, wk		Intermediate duration, wk			
	AKR/J[c]	C57BL/KsJ[c]	N:NIH(S)	C3H/HeJ	C57BL/10J	C57BL/6J
Long duration						
AKR/J	>20	NT	NT	6	NT	7
Intermediate duration						
N:NIH(S)	>20	>20	9	NT	6	7
C3H/HeJ	>20	>20	NT	8	NT	6
C57BL/10J	NT	NT	6	NT	7	NT
C57BL/6J	>20	NT	8	19	NT	17
CD-1 Swiss	>20	NT	NT	NT	NT	NT

[a] Groups of 20 marrow cultures were established as described in "Materials and Methods"; however, with the use of 25% FCS and no added corticosteroid as in (*15*), cultures were medium changed as described in "Materials and Methods," and at day 28 representative cultures were scraped to remove NA cells and adherent cells and tested for GM-CFU$_c$ formation. Under these conditions, <1 GM-CFU$_c$/10^5 cells was detected. These groups were then used as recipient purified stromal cultures.

[b] Longest duration generation of 10^4 granulocytes/culture/wk. NA cells from corticosteroid-rich cultures of each strain were removed at wk 8 and transferred at 5×10^6 cells to each culture of purified stroma. Reconstituted cultures were then weekly medium changed, and NA cells were tested for granulocyte morphology and GM-CFU$_c$ as described in "Materials and Methods." NT = not tested.

[c] AKR or C57BL/KsJ cell groups engrafted to each recipient stroma produced a significantly greater No. of granulocytes than N:NIH(S), C3H/HeJ, C57BL/6J, or C57BL/10J stem cells engrafted to the same groups of stroma ($P < 0.05$).

the longevity of hematopoiesis in a continuous marrow culture system that involves use of a single inoculum of bone marrow in 10^{-5} *M* hydrocortisone. Longevity of production of GM-CFU$_c$ and neutrophilic granulocytes did not correlate with *H-2* haplotype, production of basophil–mast cells, persistence of adherent adipocytes, or cumulative number of NA cells produced during the initial 8 weeks. The present studies did not attempt to correlate longevity of granulopoiesis with production of pluripotential, erythroid, megakaryocytic, or lymphoid CFU$_c$. Significant differences among strains may also be detected when these data are collected. Cultures from each strain were tested for replication of endogenous retrovirus. Cultures from those strains releasing high levels of N-tropic virus, including AKR/J, NZW, DBA/2J, C7BL/KsJ, and C58/J, were those with the greatest longevity; however, lower levels of N-tropic virus were also detectably released by cultures from the following strains that showed a significantly shorter duration of granulopoiesis: BALB/cJ, CBA/J, and C57BL/6J. Still other strains known to contain an endogenous N-tropic virus (e.g., RF/J, C57BR/cdJ, and SWR/J) (*7*) did not release detectable levels of virus despite identical culture methods.

An explanation for the significant differences in longevity of AKR/J long-term marrow cultures (that generated granulocytes in excess of 58 wk) and HRS/J marrow cultures (that produced granulocytes for 12 wk) was approached through several genetic and mixing experiments. The differences were not attributable to our use of FCS and hydrocortisone, since similar differences were detected if cultures were established in a "special" lot of horse serum that supports hematopoiesis with no added corticosteroid (*33*).

To determine whether genetic factors in the adherent stromal cell and/or NA hematopoietic stem cell compartment determined longevity of granulopoiesis, we transferred NA cells from 8-week-old AKR/J or C57BL/KsJ cultures to purified stromal cell cultures of the same or other strains with a shorter duration of granulopoiesis. These experiments indicated that the genotype of the NA AKR/J or C57BL/KsJ hematopoietic cells stimulated a significantly longer duration of granulopoiesis following engraftment of these cells to stromal cultures of short-duration strains (C3H/HeJ or C57BL/6J) compared to that observed following engraftment of hematopoietic stem cells from C3H/HeJ or C57BL/6J cultures to their syngeneic stromas. Furthermore, AKR/J stromal cultures did not confer greater longevity to engrafted C3H/HeJ or C57BL/6J hematopoietic stem cells. These data indicate that a factor in the hematopoietic stem cell compartment of AKR/J or C57BL/KsJ cultures determined longevity. Whether this factor is replication of the N-tropic endogenous virus is not yet known.

There are a number of possible interpretations of the data showing correlation of retrovirus replication with increased longevity of hematopoiesis in vitro. Limited hematopoiesis in marrow cultures of some strains may be due to an inhibitory effect of their adherent stromal cells, and retrovirus replication may block the synthesis of an inhibitor. The failure of virus-positive AKR/J stromal cultures to increase the longevity of hematopoiesis by added C3H/HeJ or C57BL/6J stem cells argues against this mechanism. Alternatively, retrovirus replication may stimulate adherent stromal cells to produce a growth factor for early hematopoietic progenitor cells. Evidence in support of such stimulation comes from data showing that retrovirus infection of bone marrow stromal cells results in elevated production of a CSF that is active for macrophage progenitor cells (*12*). Other such molecules might be induced by virus replication, and genetic factors might determine stem cell response to this factor.

WEHI-3 DCM-dependent cell lines derived from NA cells removed from marrow cultures showed a range of morphological, biological, and biochemical properties with differences persisting after cloning in some of the lines and in others in the separation of multiple subclones (*6*). While most clonal lines from most strains demonstrated predominantly neutrophilic granulocyte or macrophage differentiation capacity, several cloned lines persistently produced 1–

20% toluidine blue-positive mast cells, and others were purely mast cell–basophil. WEHI-3 DCM-dependent cultures obtained from one experiment with C57BL/6JUt and B6.S marrow cultures contained multipotential stem cell populations including those capable of forming erythroid, GM, and mast cell colonies (Humphries K, Eaves CG, Greenberger JS: Manuscript in preparation). Whether a single protein or multiple factors produced by the WEHI-3 cell line or found in concanavalin A spleen conditioned medium stimulate each of the cell phenotypes found in these cell lines (mast cell, granulocyte progenitor, and multipotential progenitor) is not yet known.

Some clonal cell lines derived from virus-positive marrow cultures maintained in WEHI-3 DCM continued to release ecotropic virus, whereas other cell lines from virus-positive primary cultures were observed to be virus-negative (*6, 8*). Thus induction of endogenous virus and persistent replication of either that induced virus or an infecting exogenous virus may occur through different mechanisms in bone marrow cultures. Divergence of mechanisms for induction and persistence of mouse retrovirus replication has been demonstrated with embryo fibroblast lines treated with 5-iodo-2′-deoxyuridine (*34*) and with lipopolysaccharide induction of virus from B-lymphocytes (*35*). None of the spontaneously generated cell lines tested produces detectable leukemia in vivo; however, further studies are required to explain elevated peripheral blood counts that were seen in mice given C57BL/KsJ cell lines, and cell lines from other strains remain to be tested.

The present studies indicate that necessary interactions between adherent and NA cell populations in the hematopoietic microenvironment of long-term bone marrow cultures vary significantly among mouse strains. These variations occur over a much broader spectrum than that initially ascribed to mutational defects in specific strains (*36, 37*) and may be attributed in part to the effect of retrovirus replication or other forms of chronic in vitro stimulation of the adherent cell compartment of the cultures (*38*). While the system appears to be complicated, understanding the mechanism by which bone marrow cultures regulate the longevity of hematopoietic stem cells should provide insight into our understanding of genetic and environmentally altered diseases of the bone marrow.

REFERENCES

(*1*) Dexter TM, Testa NG. Differentiation and proliferation of hemopoietic cells in culture. In: Prescott D, ed. Methods in cell biology. Vol 14. New York: Academic Press, 1976:387–405.

(*2*) Greenberger JS. Sensitivity of corticosteroid-dependent, insulin-resistant, lipogenesis in marrow preadipocytes of obese-diabetic (db/db) mice. Nature 1978; 275:752–754.

(*3*) Greenberger JS, Gans PJ, Davisson PB. Murine sarcoma viruses block corticosteroid inducible differentiation of bone marrow preadipocytes associated with long-term in vitro hemopoiesis. Virology 1979; 45:217–233.

(*4*) Dexter TM, Scott D, Teich NM. Infection of bone marrow cells in vitro with FLV: Effects on stem cell proliferation, differentiation and leukemogenic capacity. Cell 1977; 12:355–364.

(*5*) Greenberger JS. Phenotypically distinct target cells for murine sarcoma virus and murine leukemia virus marrow transformation in vitro. JNCI 1979; 62:337–348.

(*6*) ———. Self-renewel of factor-dependent hemopoietic progenitor cell lines derived from long-term marrow cultures demonstrates significant mouse strain genotypic variation. J Supramol Struct 1980; 13:501–511.

(*7*) Greenberger JS, Donohue D, Sakakeeny MA. Induction of ecotropic endogenous retroviruses in long-term bone marrow cultures from mouse strains of varying natural leukemia incidence. J Reticuloendothel Soc 1979; 26:839–853.

(*8*) Greenberger JS, Eckner RJ, Ostertag W, et al. Release of spleen focus-forming virus (SFFV) in differentiation inducible granulocytic leukemia cell lines transformed in vitro by Friend leukemia virus. Virology 1980; 105:425–435.

(*9*) Greenberger JS, Gans PJ, Davisson PB, Moloney WC. In vitro induction of continuous acute promyelocyte leukemia cell lines by Friend or Abelson murine leukemia viruses. Blood 1979; 53:987–1001.

(*10*) Greenberger JS, Newburger PE, Lipton JM, Moloney WC, Sakakeeny MA, Jackson PL. Virus and cell requirements for Friend virus granulocytic leukemogenesis in long-term bone marrow cultures of NIH Swiss [N:NIH(S)] mice. 1980; 64:867–878.

(*11*) Greenberger JS, Newburger PE, Sakakeeny MA. Phorbol myristate acetate stimulates macrophage proliferation and differentiation and alters granulopoiesis and leukemogenesis in long-term bone marrow cultures. Blood 1980; 56:368–379.

(*12*) Greenberger JS, Wroble LM, Sakakeeny MA. Murine leukemia viruses: Induction of macrophage production of granulocyte–macrophage colony stimulating factor in vitro. JNCI 1980; 65:841–851.

(*13*) Jones-Villeneuve EV, Rusthoven JJ, Miller RG, Phillips RA. Differentiation of THY1-bearing cells from progenitors in long-term marrow cultures. J Immunol 1980; 124:567–701.

(*14*) Dexter TM, Garland J, Scott D, Scolnick E, Metcalf D. Growth of factor-dependent hematopoietic precursor cell lines. J Exp Med 1980; 152:1036–1047.

(*15*) Cohen GI, Canellos GP, Greenberger JS. In vitro quantitation of engraftment between purified populations of bone marrow hemopoietic stem cells and stromal cells. In: Gale P, Golde D, eds. Proceedings of the Keystone ICN–UCLA symposium on autologous bone marrow transplantation, Keystone, Colo., Feb 18–21, 1980. New York: Academic Press. 1980:491–505.

(*16*) Hays EF, Warren J, Hale L, Rodensky D. AKR murine leukemia viruses and long-term bone marrow cultures from AKR and SJL mice. Exp Hematol 1980; 8:134–146.

(*17*) Williams N, Jackson H, Sheridan AP, Murphy MJ, Elste A, Moore MA. Regulation of megakaryopoiesis in long-term bone marrow cultures. Blood 1978; 51:245.

(*18*) Humphries RK, Eaves AC, Eaves CJ. Characterization of a primitive erythropoietic progenitor found in mouse marrow before and after several weeks in culture. Blood 1979; 53:746–762.

(*19*) Greenberger JS, Newburger P, Karpas A, Moloney W. Constitutive and inducible granulocyte-macrophage functions in mouse, rat, and human myeloid leukemia-derived continuous tissue culture lines. Cancer Res 1978; 38:3340–3348.

(*20*) Jainchill JC, Aaronson SA, Todaro GJ. Murine sarcoma and leukemia viruses: Assay using clonal lines of contact-inhibited mouse cells. J Virol 1969; 4:549–553.

(*21*) Aaronson SA, Todaro GJ. Basis for the acquisition of malignant potential by mouse cells cultivated in vitro. Science 1968; 162:1024–1026.

(*22*) Duc-Nguyen H, Rosenbaum EN, Ziegel RF. Persistent infection of a rat kidney cell line with Rauscher leukemia virus. J Bacteriol 1966; 92:1133–1140.

(*23*) Aaronson SA, Weaver CA. Characterization of murine sarcoma virus (Kirsten) transformation of mouse and human cells. J Gen Virol 1971; 13:245–252.

(*24*) Hartley JW, Rowe WP, Huebner RJ. Host range restrictions of murine leukemia viruses in mouse embryo cell cultures. J Virol 1970; 5:221–225.

(*25*) Bradley TR, Metcalf D. The growth of mouse bone marrow cells in vitro. Aust J Exp Biol Med Sci 1966; 44:285–300.

(*26*) Greenberger JS, Aaronson SA, Rosenthal DS, Moloney WC. Continuous production of peroxidase, esterase, alkaline phosphotase, and lysozyme by clones of promyelocytes. Nature 1975; 257:143–144.

(*27*) Kincaide PW, Paige CJ, Parkhouse ME, Lee G. Characterization of murine colony-forming B cells. I. Distribution, resistence to anti-immunoglobulin antibodies and expression of Ia antigens. J Immunol 1978; 120:1289–1296.

(28) Nagao K, Tokoro K, Aaronson SA. Continuous lines of mast cells derived from normal bone marrow. Science 1981; 212:333–335.

(29) Till JE, McCulloch EA. A direct measurement of the radiation sensitivity of normal mouse bone marrow. Radiat Res 1961; 14: 213–220.

(30) Greenberger JS, Karpas A, Gans PJ, Newman H, Moloney WC. Increased myeloid-associated enzymes in Epstein-Barr virus nuclear antigen positive human cell lines exposed to butyric acid in vitro. Blood 1978; 51:1073–1085.

(31) Dexter TM, Allen TD, Lajtha LG. Conditions controlling the proliferation of hemopoietic stem cells in vitro. J Cell Physiol 1977; 91:335–344.

(32) Toyoshima K, Vogt PK. Temperature sensitive mutants of an avian sarcoma virus. Virology 1969; 38:930–931.

(33) Dexter TM, Moore MA, Sherridan AP. Maintenance of hematopoietic stem cells and production of differentiated progeny in allogeneic and semi-allogeneic bone marrow chimeras in vitro. J Exp Med 1977; 145:1612–1616.

(34) Aaronson SA, Stephenson JR, Greenberger JS. Cellular replication and the persistence of inducible RNA type-C viruses. J Virol 1974; 13:1403–1407.

(35) Greenberger JS, Phillips SM, Stephenson JR, Aaronson SA. Induction of mouse type-C RNA virus by lipopolysaccharide. J Immunol 1975; 115:317–320.

(36) Dexter TM, Moore MA In vitro duplication of "cure" of hematopoietic defects in genetically anemic mice. Nature 1977; 269:412–414.

(37) Blackburn MJ, Patt HM. Increased survival of CBA pluripotent hematopoietic stem cells in vitro induced by marrow stromal factor in SL/SL2 mice. Exp Hematol 1979; 7:324–328.

(38) Greenberger JS, Shadduck RK, Jaenisch R, Waheed A, Sakakeeny MA. Effects on murine leukemia virus infection on long-term hematopoiesis in vitro emphasized by increased survival of bone marrow cultures derived from BALB/Mo mice. Cancer Res 1981; 41:3556–3565.

blank page

Effects of Dietary Lipids on Lactogenic Hormone Receptor Binding in Rat Mammary Tumors[1, 2, 3, 4]

William T. Cave, Jr.,[5] *and* **Marsha J. Erickson-Lucas**[5, 6]

ABSTRACT—Both epidemiologic studies in humans and experiments in laboratory animals have indicated that high-fat (HF) diets promote mammary tumor growth; however, the biochemical mechanisms responsible for this accelerated tumor growth are poorly understood; thus this study was designed to determine whether diet-induced alterations in the lipid composition of mammary tumor cell membranes were associated with differences in lactogenic hormone binding capacity. Mammary tumors were induced with *N*-methyl-*N*-nitrosourea in 50-day-old female inbred Buffalo rats that were maintained on either HF or low-fat (LF) diets composed of either 20% corn oil or 0.5% corn oil, respectively. The microsome-membrane fractions of these tumors were then analyzed for specific lactogenic hormone binding with the use of ^{125}I-labeled human growth hormone. Methylated extracts of these same membrane fractions were also subjected to gas–liquid chromatography. Our results demonstrated that the mammary tumor membranes of the HF group did have a significantly greater lactogenic binding capacity than those of the LF group and that these differences in hormone binding were accompanied by significant alterations in the membrane qualitative fatty acid profiles of each group. Therefore, one way in which dietary lipids may be able to influence mammary tumor growth is by modification of the lactogenic hormone binding capacity of tumor cell membranes.—JNCI 1982; 68:319–324.

In recent years, much evidence has accumulated that indicates that dietary lipids can influence the development of breast cancer. Data from epidemiologic surveys, for example, have revealed that human populations maintained on HF diets have a selectively increased mortality from breast cancer (*2*); prospective studies with laboratory animals have repeatedly documented that HF diets accelerate the growth rates of both spontaneous and carcinogen-induced tumors (*3–7*).

Very little is known, however, about the specific biologic mechanisms responsible for this lipid-dependent enhancement of mammary tumor growth. All that can be stated at present is that these dietary lipid effects are closely linked temporally to events occurring after tumor initiation (*8*) and that they require the presence of certain hormones such as prolactin and estrogen for their maximal expression (*4, 9*). Some investigators have postulated that these facts indicate that dietary fats can promote mammary tumor growth by modifying the normal relationship that usually exists between the initiated tumor cells and their hormonal environment (*2*); but to date how these hormone–tumor cell alterations occur has not been precisely defined.

One recently proposed hypothesis on this subject is that lipids, particularly polyunsaturated lipids, may be able to alter the physiologic activities of certain membrane-associated hormone receptors by changing the structural composition of the tumor cell membranes (*10*). This study was designed to experimentally evaluate this possibility. Its specific objectives were to establish whether quantitative changes in dietary fat could alter the lactogenic binding capacity of mammary tumor cells and, if so, to determine whether there were any particular qualitative differences in membrane lipid composition associated with these hormone receptor alterations.

METHODS AND MATERIALS

Treatment groups.—Female inbred Buffalo rats (Simonsen Laboratories, Gilroy, Calif.), 44 days old, were randomly divided into 2 groups. Group 1 was fed an LF diet containing 0.5% corn oil, while group 2 was fed an HF diet containing 20% corn oil. The specific composition of these diets (table 1) was closely patterned after previously established experimental models (*7, 8, 11*). Both diets had an equivalent ratio of protein calories to total calories.

Tumor induction.—When the rats were 51 days of age, mammary tumors were induced following the methods of Gullino et al. (*12*). MNU (K & K Laboratories, Plainview, N.Y.) was dissolved in water (10 mg/ml) and administered iv to the rats (5 mg/100 g body wt) with subsequent injections 4 and 8 weeks later. All animals were maintained under identical laboratory conditions and the developing tumors were measured weekly. When each animal's tumor reached a size of approximately 1–2 cm in diameter, the

---

Abbreviations used: BSA=bovine serum albumin; HF=high fat (high-fat); hGH=high-growth hormone; LF=low fat (low-fat); MNU=*N*-methyl-*N*-nitrosourea; oPRL=ovine prolactin; TM=0.025 *M* Tris HCl–0.1 *M* $MgCl_2$.

---

[1] Received July 2, 1981; accepted September 25, 1981.

[2] Supported by grant 1N-18T from the American Cancer Society, by a grant from the United Cancer Council, and by Public Health Service grant CA-30629 from the National Cancer Institute.

[3] A preliminary report of this material was presented at the 72nd Annual Meeting of the American Association of Cancer Research, April 1981, in Washington, D.C. (*1*).

[4] Guidelines for the care and use of laboratory animals were followed as set forth by the National Research Council and the National Institutes of Health.

[5] Endocrine Unit, Department of Internal Medicine, University of Rochester School of Medicine, St. Mary's Hospital, 89 Genesee St., Rochester, N.Y. 14611.

[6] We acknowledge the technical assistance of Ms. Corrine Schutrum, Mr. Robert Amberger, and Mr. Michael Lynch, as well as the secretarial assistance of Ms. Bonnie DeConinck.

TABLE 1.—*Diet composition*

Component	LF diet	HF diet
Corn oil (100% pure; vitamin free)	5 g/kg	200 g/kg
Casein (vitamin free)	180 g/kg	230 g/kg
Sucrose	220 g/kg	145 g/kg
Dextrose	260 g/kg	175 g/kg
Dextrin	260 g/kg	175 g/kg
Rogers Harper vitamin mix	5 g/kg	5 g/kg
Rogers Harper salt mix	50 g/kg	50 g/kg
Vitamin B_{12} (10 μg/ml water)	5 ml/kg	5 ml/kg
Choline (0.20 g/ml water)	15 ml/kg	15 ml/kg

animal was killed unanesthetized by cervical transection early in the day during diestrus. Immediately afterward, an autopsy was performed and samples of tumor and liver tissue were snap frozen in liquid nitrogen and stored at −80°C.

Subcellular fractionation.—The frozen samples were initially powdered in a pulverizer (Thermovac Industries Corp., St. Copiague, N.Y.) and then homogenized in a tissumizer (Tekmar Co., Cincinnati, Ohio) with 6 volumes (wt/vol) of TM buffer (pH 7.55). After homogenization, the samples were separated into subfractions by an initial centrifugation at 15,000×*g* for 20 minutes and then a subsequent spin of the supernatant at 190,000×*g* for 60 minutes. This 190,000×*g* pellet (microsome-membrane fraction) was then divided into two portions. One portion was saved for lipid analysis by storage at −80°C in a gaseous nitrogen atmosphere, while the remainder was resuspended in TM buffer and used for receptor analysis.

Hormone iodination.—Carrier-free ^{125}I was obtained from Amersham Corp., Arlington Heights, Ill., and hGH-I-1 and oPRL-I-1 were obtained from the National Institute of Arthritis, Diabetes, and Digestive and Kidney Diseases, Bethesda, Md. Both of these hormones were iodinated with lactoperoxidase according to the general methodology of Thorell and Johansson (*13*), but with the use of an immobilized preparation of lactoperoxidase and glucose oxidase (Enzymobead; BioRad Laboratories, Richmond, Calif.). The iodinated hormone was separated from the free ^{125}I on a Sephadex G-25 column with a 0.01-*M* borate buffer (pH 8.0) for elution. The specific activity of the iodinated hormones ranged from 90 to 130 μCi/μg.

Hormone binding assays.—We measured the hormone binding in these studies by using the previously established methodology of Posner et al. (*14*), Posner (*15*), and Shiu and Friesen (*16*). ^{125}I-labeled hormone was incubated with 140 μg of the microsome-membrane protein in a final volume of 0.5 ml containing 0.2% BSA–TM buffer (pH 7.55) for 22 hours at 24°C. Parallel incubations were performed in the presence of excess unlabeled hormone (hGH, 2.5 μg; or oPRL, 2.5 μg) to determine nonspecific binding. The assay was terminated by the addition of 3 ml of 0.1% BSA–TM buffer, and the bound and the free-labeled hormones were separated by centrifugation as described by Posner (*15*). Specific hormone binding was calculated by subtraction of the nonspecific counts from the total radioactivity bound. Measurements of lactogenic binding capacity (^{125}I-labeled hGH) were made on the microsome-membrane fractions of both mammary tumors and liver tissues; however, due to a limited amount of tumor tissue, measurements of ^{125}I-labeled oPRL binding were made only on the hepatic tissue.

Fatty acid extraction, hydrolysis, and methylation.—Lipid extraction was performed according to the methods of Folch et al. (*17*). Approximately 10–30 mg of microsomal membrane fraction was suspended in 2.0 ml of methanol containing 1 mg/100 ml (wt/vol) butylated hydroxytoluene and mixed with 2.0 ml of chloroform. After sitting in this mixture overnight at 4°C in a nitrogen atmosphere, the samples were centrifuged at 1,100×*g* for 5 minutes. The supernatant was removed and then mixed with 2.0 ml of chloroform and 1.5 ml of 0.74% aqueous KCl. After centrifugation the bottom layer was dried down under nitrogen. The residue was then resolubilized in 2 ml of 3 *N* HCl in methanol and incubated in a water bath at 75°C for 2 hours. After incubation, the methylated lipids were washed with 2 ml of water and 4 ml of *n*-hexane. The resultant supernatant was then mixed with 0.1% Na_2CO_3; after a further centrifugation step, the upper layer was removed and stored under gaseous nitrogen at 4°C until ready to be analyzed by gas-liquid chromatography.

Qualitative fatty acid analysis—At the time of final analysis, the stored methylated lipids were dried down under gaseous nitrogen and redissolved in 50 μl of *n*-hexane. Two microliters of this solution was then analyzed in a gas chromatograph (Hewlett-Packard 5830A) with the use of a 6-foot glass column packed with 10% SP-2330 on a 100/120 chromosorb W acid-washed support (Supelco, Inc., Bellefonte, Pa.). The retention times of the individual fatty acids and the integrated areas under each peak were obtained directly from the computer associated with the instrument. We determined the identity of the specific peaks by comparing them to known standards (Supelco, Inc. and Sigma Chemical Co., St. Louis, Mo.) run at the time of the assay.

Data analysis.—All results are presented as the mean plus or minus the standard error of the mean. The data were evaluated statistically by analysis of variance with a Hewlett-Packard Model 9830A desk top computer and its program.

RESULTS

Autopsy data.—The autopsy findings on the animals from this study are presented in table 2. Although we observed a slight but significant difference in the body weights of the 2 groups, we saw no clinical or autopsy evidence (e.g., scaly skin, roughened hair coat, or necrosis of the tail) to suggest that this was due to any dietary deficiency in the LF group. There were no statistical differences between the liver weights of the 2 groups.

All animals in both groups developed mammary tumors; however, the animals given HF diets had more tumors per animal than did the animals given LF diets. Furthermore, the animals given HF diets, despite a significantly earlier mean age at death, had a tumor burden that was equivalent, if not slightly greater, than that of the animals given LF diets. This observation indicated that the animals given HF diets had required significantly less time than did the animals given LF diets to develop a similar tumor burden. A graphic illustration of these relationships is presented in text-figure 1.

TABLE 2.—*Mammary carcinogenesis MNU-treated rats on HF and LF diets*

Diet	No. of rats	Age at death, days[a]	Body weight, g[a]	Liver weight, g[a]	Tumor No.[a]	Tumor burden, g[a]
LF	19	150.5±2.9[b]	209.3±3.4[c]	8.54±0.23	3.0±0.3[b]	14.3±2.2
HF	19	129.5±3.2	226.6±2.9	8.69±0.28	3.9±0.3	17.23±2.0

[a] Values are means ± SE.

[b] Difference from HF group significant at $P<0.05$ by analysis of variance.

[c] Difference from HF group significant at $P<0.01$ by analysis of variance.

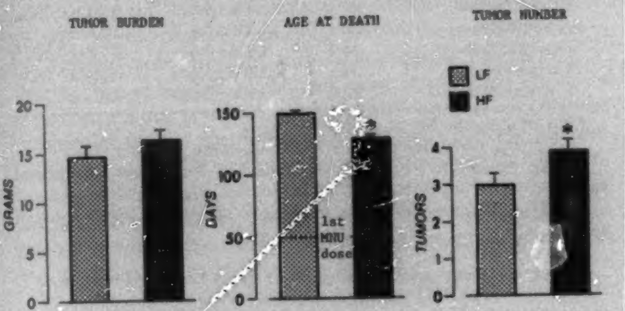

TEXT-FIGURE 1.—Autopsy findings on the animals used in this study. Each group consists of data from 19 animals. *Bar graphs* depict the means±SE for each group. *Single asterisks* indicate that the differences between the 2 groups was significant at $P<0.05$ by analysis of variance.

Mammary tumor membrane hormone binding data.—The results of the studies on the binding of ^{125}I-labeled hGH to the mammary tumor microsome-membrane fractions of the 2 treatment groups are presented in text-figure 2. This text-figure clearly shows that the binding capacity of the HF samples (54.8±4.0 fmol/mg protein) was significantly greater ($P<0.01$) than that of the LF samples (32.8±3.2 fmol/mg protein).

Liver membrane hormone binding data.—The results of comparable studies measuring the binding of ^{125}I-labeled hGH to the microsome-membrane fractions of hepatic tissue are presented in text-figure 3A. As this text-figure indicates, the lactogenic hormone binding capacities of the hepatic membranes of the HF group (92.9±9.4 fmol/mg protein) were also greater than those of the LF group (75.4±6.2 fmol/mg protein). These differences in hepatic binding, however, were not quite great enough to be statistically significant.

An almost identical pattern of binding was observed when these same hepatic microsome-membrane fractions were incubated with ^{125}I-labeled oPRL (text-fig. 3B). Although the differences between the 2 groups again failed to reach statistical significance, the HF samples persistently demonstrated a greater binding capacity for the ^{125}I-labeled oPRL (38.8±6.7 fmol/mg protein) than the LF samples (26.7±5.0 fmol/mg protein). In addition, despite the fact that the absolute amount of the ^{125}I-labeled oPRL bound to the hepatic membrane fraction was somewhat less than that observed for the ^{125}I-labeled hGH, the actual measured differences in hormone binding capacity between the HF and LF samples were almost the same, regardless of which hormone binding assay results were used. This observation would appear to indicate that the differences observed in hepatic ^{125}I-labeled hGH binding can be attributed almost completely to changes in prolactin receptor binding as measured by ^{125}I-labeled oPRL.

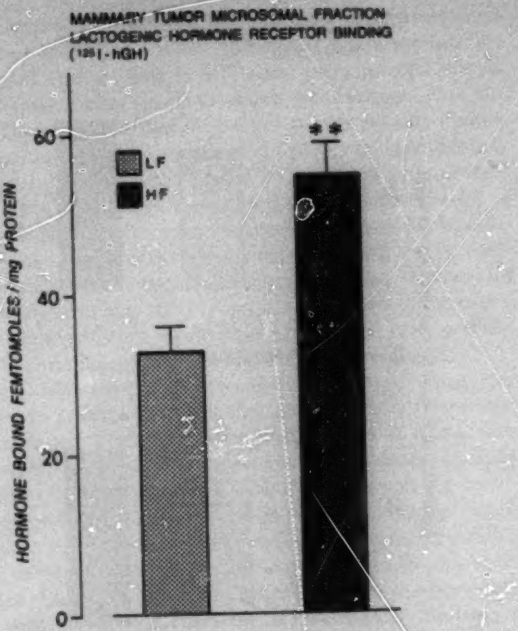

TEXT-FIGURE 2.—Lactogenic hormone binding capacity of mammary tumor microsomes as measured with ^{125}I-labeled hGH. Data from the LF diet group represent the results of determinations made on tumors from 12 individual animals, whereas data from the HF diet group represent the results of determinations made on tumors from 11 individual animals. *Bar graphs* depict the means±SE values for each diet group. *Double asterisk* indicates that the difference between the 2 groups is statistically significant at $P<0.01$ by analysis of variance.

Mammary tumor fatty acid profile.—The distribution profiles of the fatty acids extracted from the tumor microsome-membrane fractions are represented in table 3. Several significant differences were readily detectable between the 2 groups. In general, the HF samples had significantly greater percentages of their total lipids in the form of the polyunsaturated fatty acids linoleic acid (18:2) and ecosatrienoic acid (20:3) than the LF group and significantly lower percentages of the saturated fatty acids *n*-pentadecanoic acid (15:0), palmitic acid (16:0), palmitoleic acid (16:1), stearic acid (18:0), and oleic acid (18:1). The only exception to this trend was the slight but significant decrease in the percentage of arachidonic acid (20:4) observed in the HF samples.

Hepatic fatty acid profile.—Comparable data outlining the distribution profile of the fatty acids in the hepatic microsome-membrane fraction are presented in table 4. Very similar to the results obtained from the analysis of the tumor lipid samples, the hepatic HF samples also had significantly less of their total lipid in the form of the more saturated fatty acids—palmitic acid (16:0), palmitoleic acid (16:1), and oleic acid (18:1)—than the LF samples. There were some additional differences that were not noted in the tumor samples, such as significantly greater percentages of stearic

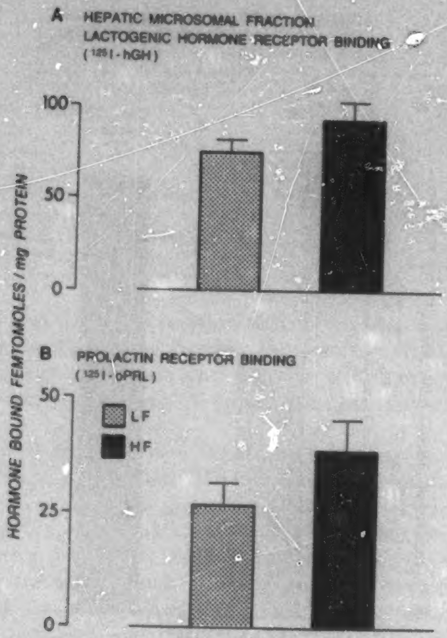

TEXT-FIGURE 3.—A) *Bar graphs* depict the mean plus or minus standard error of the lactogenic binding capacities of hepatic microsomes as measured with ^{125}I-labeled hGH. Data from the LF diet group represent determinations made on livers from 18 animals, whereas data from the HF diet group represent determinations made on 17 animals. B) *Bar graphs* depict the means±SE of the binding capacities of hepatic microsomes for ^{125}I-labeled oPRL. The number of livers sampled in each group are the same as noted in 3A.

acid (18:0), arachidonic acid (20:4), docosatetranoic acid (22:4), and docosahexanoic acid (22:6) in the HF samples and a significantly lower percentage of myristic acid (14:0).

DISCUSSION

The ability of dietary fat to enhance mammary tumor growth in laboratory animals was initially documented by Tannenbaum (*3*) in 1942 when he reported that DBA mice fed an HF diet had an increased incidence of spontaneous mammary tumors. Since then many others have confirmed this relationship in rodents, not only for spontaneous mammary tumors but also for carcinogen-induced and transplanted mammary tumors (*4–7, 18*). In the present experiments, this effect of dietary lipids on mammary tumor growth was reflected in the finding that the animals given HF diets had more tumors per animal and a faster tumor growth rate than the animals given LF diets.

The scientific importance of this relationship rests in the fact that it is uniquely restricted to dietary lipids and is independent of caloric intake. Animals on HF diets have been consistently shown to have greater mammary tumor growth rates than pair-fed animals on equal caloric LF diets (*19, 20*). Such effects have not been observed to occur as a result of comparable variations in any of the other dietary components such as protein, vitamins, or minerals above those required for normal maintenance (*21*).

TABLE 3.—*Fatty acid composition of lipids extracted from mammary tumor microsomes*

Fatty acid	Proportion[a]	Percent of total lipid[b]	
		LF group	HF group
Myristic	14:0	0.899±0.115	0.578±0.047
Pentadecanoic	15:0	1.593±0.068[c]	1.281±0.053
Palmitic	16:0	20.386±0.765[c]	17.838±0.241
Palmitoleic	16:1	3.320±0.414[c]	1.246±0.037
Stearic	18:0	11.882±0.439[c]	9.996±0.298
Oleic	18:1	30.140±1.235[c]	23.522±0.532
Linoleic	18:2	2.592±0.213[c]	22.932±1.249
Linolenic	18:3	0.043±0.021	0.072±0.025
Eicosenoic	20:1	0.649±0.150	0.596±0.214
Eicosatrienoic	20:3	0.338±0.113[d]	0.603±0.185
Arachidonic	20:4	13.123±0.817[d]	10.710±0.727
Docosatetranoic	22:4	4.854±0.699	3.759±0.264
Tetracosenoic	24:1	0.904±0.433	0.727±0.280
Docosahexanoic	22:6	0.689±0.089	0.821±0.106

[a] No. of C-atoms:No. of double bonds.

[b] LF group, $n=12$; HF group, $n=11$. Values are means ± SE.

[c] Difference from HF group significant at $P<0.01$ by analysis of variance.

[d] Difference from HF group significant at $P<0.05$ by analysis of variance.

TABLE 4.—*Fatty acid composition of lipids extracted from liver microsomes*

Fatty acid	Proportion[a]	Percent of total lipid[b]	
		LF group	HF group
Myristic	14:0	0.387±0.080[c]	0.050±0.026
Pentadecanoic	15:0	0.132±0.029	0.156±0.008
Palmitic	16:0	19.923±0.816[c]	15.226±0.448
Palmitoleic	16:1	5.738±0.572[c]	0.703±0.087
Stearic	18:0	14.299±0.686[d]	16.750±0.931
Oleic	18:1	29.152±1.039[c]	12.303±0.384
Linoleic	18:2	3.553±0.397[c]	22.448±0.764
Linolenic	18:3	0.101±0.022[c]	0.434±0.044
Eicosenoic	20:1	0.183±0.069	0.067±0.016
Eicosatrienoic	20:3	0.740±0.121	0.494±0.060
Arachidonic	20:4	13.194±0.359[c]	15.944±0.855
Docosatetranoic	22:4	1.050±0.303[d]	1.977±0.180
Tetracosenoic	24:1	2.923±0.319	3.441±0.238
Docosahexanoic	22:6	2.816±0.358[c]	5.297±0.377

[a] No. of C-atoms:No. of double bonds.

[b] LF group, $n=9$; HF group $n=9$. Values are means ± SE.

[c] Difference from HF group significant at $P<0.01$ by analysis of variance.

[d] Difference from HF group significant at $P<0.05$ by analysis of variance.

Precisely how dietary lipids specifically enhance mammary tumor growth is poorly understood. It has been documented that qualitative and quantitative differences in dietary lipids can significantly modify the biochemical composition of mammary tumor cells (*18*), but to what extent these changes in tumor lipid composition can be directly correlated with the enhanced tumor growth observed is still unclear. For example, even though it has been shown that some tumor cell lines do increase their growth rates in response to dietary increases in linoleic acid, it has not been possible to define any universal correlation between the precise amount of linoleic acid in a tumor and its specific growth rate (*22*). Therefore, most investigators have concluded that if differences in the lipid composition of mammary tumor cells do affect tumor growth, they must do so in a relatively complex fashion. Certainly, the evidence would indicate that other factors such as the genetic character of the cell line and the physiologic characteristics of the host can also significantly influence the final rate of lipid-dependent mammary tumor growth.

Our knowledge of the physiologic parameters of the host, which are most important in facilitating lipid-dependent mammary tumor growth, is still rather limited. The data that have been accumulated, however, strongly suggest that the hormonal environment is especially important. Wicha et al. (*10*), for example, have shown quite clearly that the growth rates of primary cultures of 7,12-dimethylbenz[*a*]-anthracene-induced rat mammary tumor cells are much greater when specific hormones (i.e., 17β-estradiol, prolactin, progesterone, insulin, and hydrocortisone) are added to the media with oleic or linoleic acid than when either of these fatty acids is added alone. Which hormones are most influential in this lipid-dependent growth process has not been unequivocally resolved, but data showing that prolactin-inhibiting drugs, estrogen antagonists, and ovariectomy can greatly reduce or totally abolish this lipid-dependent growth process have made it clear that prolactin and estrogen must be critically involved (*4, 9*).

In the past, our concepts of how prolactin might facilitate lipid-dependent mammary tumor growth have been very speculative. It was proposed initially that dietary lipids might be able to directly stimulate pituitary gland production (*23*), but subsequent experimental studies revealed that animals on HF diets and with accelerated mammary tumor growth do not have elevated basal serum prolactin levels and their pituitary glands do not synthesize increased quantities of prolactin in vitro (*4*). Moreover, other studies (*24*) have shown that even when the serum prolactin levels of animals on LF and HF diets are increased to equally high levels by hypothalamic lesions, a difference in mammary tumor growth rates persists. Therefore, it has remained necessary to continue to search for alternate possible mechanisms of prolactin–lipid interaction in mammary tumorigenesis.

We believe that our results have now resolved some of this previous uncertainty by providing substantial evidence in favor of the hypothesis that dietary fats can alter the sensitivity of mammary tumor cells to prolactin. Our data show very clearly that the tumor membranes of the animals given HF diets have significantly greater lactogenic hormone binding capacities than those of the animals given LF diets; and since it is well recognized that prolactin initiates its hormonal action via such membrane receptors (*25*), it is highly probable that, at any comparable physiologic prolactin level, there would be a greater mammotrophic stimulation of the tumor cells from animals given HF diets than from animals given LF diets. We cannot state conclusively, at this time, whether these differences in hormone binding are due to generalized alterations in the total mammary tumor cell population or selective changes in a specific subpopulation of tumor cells; but the observation that dietary lipids can induce similar, though less significant, changes in the hormone binding capacities of liver cells suggests that modifications in prolactin responsiveness very likely occur in a variety of target cells as well.

Our perception of the biochemical mechanisms responsible for these alterations in the lactogenic hormone binding capacities of tumor cells is still very incomplete. Several recent investigations, however, have pointed out that the structural changes induced in the cell membranes by dietary lipids, particularly polyunsaturated lipids, can significantly increase membrane fluidity (*26, 27*). Such changes in membrane fluidity have been postulated to be great enough to regulate the accessibility of membrane receptors to circulating hormones. Our results would certainly seem very compatible with this concept. They show that the tumor and liver membranes from the HF group had both the greatest degree of unsaturation evident in their fatty acid profiles and the highest lactogenic hormone binding capacities.

We conclude, therefore, that our experimental results not only confirm previous reports that dietary lipid alterations can significantly affect the fatty acid profiles of mammary tumor membranes but also show that such changes in lipid composition can be associated with differences in the lactogenic hormone binding capacities of these tumor membranes. Certainly, further studies will be needed to establish whether these changes in binding capacity are functionally significant; but if this can be accomplished, it would strongly suggest that one way dietary lipids can modify mammary tumor growth is by inducing changes in the lactogenic hormone binding capacities of tumor cell membranes.

REFERENCES

(*1*) Cave WT Jr, Erickson-Lucas MJ. Effects of dietary lipids on lactogenic hormone receptor binding in rat mammary tumors. Proc Am Assoc Cancer Res 1981; 22:7.

(*2*) Carroll KK, Khor HT. Dietary fat in relation to tumorigenesis. Prog Biochem Pharmacol 1975; 10:308–353.

(*3*) Tannenbaum A. The genesis and growth of tumors. III. Effects of a high fat diet. Cancer Res 1942; 2:468–475.

(*4*) Cave WT Jr, Dunn JT, MacLeod RM. Effects of iodine deficiency and high-fat diet on *N*-nitrosomethylurea-induced mammary cancers in rats. Cancer Res 1979; 39:729–734.

(*5*) Davis RK, Stevenson GT, Busch KA. Tumor incidence in normal Sprague-Dawley female rats. Cancer Res 1956; 16:194–197.

(*6*) Engel RW, Copeland DH. Influence of diet on the relative incidence of eye, mammary, ear duct, and liver tumors in rats fed 2-acetylaminofluorene. Cancer Res 1951; 11:180–183.

(*7*) Gammal EB, Carroll KK, Plunkett ER. Effects of dietary fat on mammary carcinogenesis by 7,12-dimethylbenz[*a*]anthracene in rats. Cancer Res 1967; 27:1737–1742.

(*8*) Carroll KK, Khor HT. Effects of dietary fat and dose level on 7,12-dimethylbenz[*a*]anthracene on mammary tumor incidence in rats. Cancer Res 1970; 30:2260–2264.

(*9*) Chan P-C, Cohen LA. Effect of dietary fat, antiestrogen, and antiprolactin on the development of mammary tumors in rats. J Natl Cancer Inst 1974; 52:25–30.

(*10*) Wicha MS, Liotta LA, Kidwell WR. Effects of free fatty acids on the growth of normal and neoplastic rat mammary epithelial cells. Cancer Res 1979; 39:426–435.

(*11*) Carroll KK, Khor HT. Effects of the level and type of dietary fat on incidence of mammary tumors induced in female Sprague-Dawley rats by 7,12-dimethylbenz[*a*]anthracene. Lipids 1971; 6:415–420.

(*12*) Gullino PM, Pettigrew HM, Grantham FH. *N*-Nitrosomethylurea as mammary gland carcinogen in rats. J Natl Cancer Inst 1975; 54:401–414.

(*13*) Thorell JI, Johansson BG. Enzymatic iodination of polypeptides with ^{125}I to high-specific activity. Biochim Biophys Acta 1971; 251:363–369.

(*14*) Posner BI, Kelly PA, Shiu RP, Friesen HG. Studies on insulin, growth hormone, and prolactin binding: Tissue distribution, species variation, and characterization. Endocrinology 1974; 95:521–531.

(*15*) Posner BI. Regulation of lactogen-specific binding sites in rat liver: Studies on the role of lactogens and estrogen. Endocrinology 1976; 99:1168–1177.

(*16*) Shiu RP, Friesen HG. Properties of a prolactin receptor from the rabbit mammary gland. Biochem J 1974; 140:301–311.

(*17*) Folch J, Lees M, Sloane Stanley GH. A simple method for the isolation and purification of total lipids from animal tissues. J Biol Chem 1957; 226:497–509.

(*18*) Rao GA, Abraham S. *Brief communication:* Enhanced growth rate of transplanted mammary adenocarcinoma induced in C3H mice by dietary linoleate. J Natl Cancer Inst 1976; 56:431–432.

(*19*) Tannenbaum A. The dependence of tumor formation on the composition of the calorie-restricted diet as well as on the degree of restriction. Cancer Res 1945; 5:616–625.

(*20*) Dunning WF, Curtis MR, Maun ME. The effects of dietary fat and carbohydrate on diethylstilbestrol-induced mammary cancer in rats. Cancer Res 1949; 9:354–361.

(*21*) Carroll KK. Experimental evidence of dietary factors and hormone-dependent cancers. Cancer Res 1975; 35:3374–3383.

(*22*) Hillyard L, Rao GA, Abraham S. Effect of dietary fat on fatty acid composition of mouse and rat mammary adenocarcinomas. Proc Soc Expt Biol Med 1980; 163:376–383.

(*23*) Chan PC, Cohen LA. Dietary fat and growth promotion of rat mammary tumors. Cancer Res 1975; 35:3384–3386.

(*24*) Ip C, Yip P, Bernardis LL. Role of prolactin in the production of dimethylbenz[*a*]anthracene-induced mammary tumors by dietary fat. Cancer Res 1980; 40:374–378.

(*25*) Kelly PA, Labrie F, Asselin J. The role of prolactin in tumor development. In: Keller JA, Hilf R, eds. Influence of hormones in tumor development. Vol II. Boca Raton, Fla.: CRC Press, 1979: 157–194.

(*26*) Knazek RA, Liu SC. Dietary essential fatty acids are required for maintenance and induction of prolactin receptors. Proc Soc Expt Biol Med 1979; 162:346–350.

(*27*) Dave JR, Knazek RA, Sears ME. Bradykinin modifies both prolactin binding capacity and fluidity of mouse liver membranes. Proc Am Assoc Cancer Res 1981; 22:10.

Lipopolysaccharide and Pristane-Induced Peritoneal Exudate Requirements for Plasma Tumor Cell Colony Formation[1,2,3]

Micsunica Platica,[4] Catherine Bojko,[4] Radu Clincea,[4] *and* Vincent Hollander[4,5,6]

ABSTRACT—The role for lipopolysaccharide (LPS) and a pristane-induced peritoneal exudate (PIPE) on the in vitro development of murine plasmacytoma was studied. MOPC-315 cell suspensions showed little tendency for colony formation in a soft agar culture medium. Additions of LPS and PIPE were required for maximal colony formation. The LPS effect was dose-dependent down to nanogram quantities. PIPE prepared from inbred strains of mice not susceptible to pristane-induced plasmacytoma (DBA/2) or from normal peritoneal washings was ineffective. PIPE activity was radioresistant and not transferable by cell-free conditioned medium. Three strains of transplantable plasmacytomas showed colony formation stimulation by LPS plus PIPE, but LPS and PIPE were ineffective with lymphosarcoma P1798.—JNCI 1982; 68:325-328.

Soft agar techniques are widely used for cloning of normal hematopoietic and myeloid leukemia cells in mice and humans (*1–9*). Colony formation can be potentiated by various factors (*1, 5, 10–17*). When cultured in semisolid agar, some myeloma cell lines also have the ability to form colonies (*18–23*). For these reasons, the soft agar technique was selected to assess the role of LPS and PIPE in vitro.

Administration ip of mineral oil and/or related compounds induces plasmacytomas in inbred BALB/c mice. Work done in our laboratory suggested that LPS and PIPE play a role in the pathogenesis of such plasmacytomas (*24–26*). Now we report that PIPE along with LPS induces colony formation by transplantable plasma tumor cell lines in soft agar.

MATERIALS AND METHODS

Mice.—Female inbred BALB/c and DBA/2 mice 6–8 weeks old (Simonsen Laboratories, Gilroy, Calif.) were used.

Tumors.—MOPC-315, a transplantable plasma tumor cell line, was transplanted and carried as previously described (*27*). MPC-11 (supplied by Dr. Susan Zolla, Veterans Administration Hospital, New York, N.Y.) and MOPC-104 (obtained from The Salk Institute, San Diego, Calif.) were transplanted and prepared as described for MOPC-315. P1798, a murine lymphosarcoma induced in BALB/c mice by diethylstilboestrol–cortisol, was obtained from Dr. John Stevens (American Cancer Society, New York, N.Y.). It was prepared and transplanted by the method described by Stevens et al. (*28*) with slight modifications.

Preparation of PIPE and NPW.—PIPE and NPW were prepared as described previously (*26*). In some experiments the cellular component of PIPE or NPW was destroyed by repetitive freezing and thawing. The procedure was repeated until 100% dead cells were found by the trypan blue exclusion test. In other experiments the PIPE was irradiated (2,500 rad/1×10^7 PIPE cells). In some experiments the PIPE-conditioned medium was used; 1.5×10^7 cells were cultured in 2 ml of McCoy's 5-A medium with and without LPS. The cultures were collected at 4, 7, and 10 days after plating and centrifuged at $504\times g$ for 10 minutes, and the supernatant representing PIPE-conditioned medium was used in colony assay.

LPS preparation.—LPS *Escherichia coli* 055:B5 was obtained from Difco Laboratories, Detroit, Mich. Dilutions of LPS were made in LPS-free 0.85% NaCl.

Karyotypic analysis.—The method of Worton and Duff (*29*) was used for karyotypic analysis of cells in colonies.

Assay for colony-stimulating activity.—A slightly modified method from that described by Kincade et al. (*30*) for B-cell cloning was used. All cultures were done in plastic petri dishes 35×10 mm (Corning Glass Works, Corning, N.Y.). The culture medium was a 9:1 mixture of enriched McCoy's 5-A medium (M.A. Bioproducts, Walkersville, Md.) supplemented with 10% heat-inactivated fetal calf serum and 0.3% agar (Difco Laboratories). Triplicate cultures were prepared; each contained 1×10^5 plasma tumor cells (MOPC-315, MPC-11, or MOPC-104) or 1×10^4 P1798 cells in 1 ml agar medium. Various amounts of PIPE, NPW (collected from BALB/c or DBA/2 mice), PIPE-conditioned medium, or LPS were added to each culture from the beginning unless otherwise indicated. The PIPE, NPW, or PIPE-conditioned medium was added to the agar medium containing the tumor cells; then 1 ml of this mixture was pipetted into culture dishes with or without LPS. After testing a wide range of PIPE cell numbers (5×10^4–5×10^6 cells/plate) and LPS doses ranging from 5 ng to 125 µg/plate, we found that 1–2×10^5 PIPE cells in the presence of 50 µg *E. coli* LPS were

---

ABBREVIATIONS USED: LPS=lipopolysaccharide; NPW=normal peritoneal washings; PCT=plasma cell tumor; PIPE=pristane-induced peritoneal exudate.

---

[1] Received July 9, 1981; accepted October 7, 1981.

[2] Supported by Public Health Service grants CA-26041 and CA-14194 from the National Cancer Institute.

[3] Animals were maintained under the guidelines set forth by the National Institutes of Health.

[4] Research Institute of the Hospital for Joint Disease, Mount Sinai School of Medicine, 1919 Madison Ave., New York, N.Y. 10035.

[5] *Address reprint requests to* Dr. Hollander.

[6] We thank Dr. Paul W. Kincade and Dr. Hal E. Broxmeyer (Sloan-Kettering Institute for Cancer Research, New York, N.Y.) for their helpful suggestions in setting up the assay and Dr. Alexander Pearlman (Joint Diseases North General Hospital, New York, N.Y.) for irradiation of the cells.

optimal for PCT colony formation. The plates were incubated at 37°C in a fully humidified atmosphere of 7% CO_2 in air. Colonies were counted 6–7 days after plating by use of an inverted microscope. Only aggregates of more than 20 cells were scored as colonies. Plating efficiency was defined as (number of colonies/number of cells per plate)×100. The cells that grew in colonies were identified as typical plasma tumor cells by morphology, karyotype analysis (only for MOPC-315), and their ability to induce typical plasmacytomas when transplanted sc into BALB/c mice. MOPC-315 cells are polyploid (modal number, 66) with a submetacentric marker; metaphase preparations from cells that develop colonies were also polyploid (modal number, 66; range, 62–70) with one submetacentric marker.

RESULTS

Table 1 shows that MOPC-315 cells, regardless of the number used per culture, produced no colonies when these cells were cultured alone in soft agar under conditions described above. When given independently, neither LPS (doses ranging from 5 ng to 125 μg/plate) nor PIPE collected from BALB/c mice 2 months after pristane administration (5×10^4–5×10^6 cells/plate) stimulated MOPC-315 colony formation. In contrast, PIPE plus LPS consistently produced a number of colonies of typical plasmacytomas. Within each experiment we ran a control containing PIPE alone, cultured under the same conditions as those described in "Materials and Methods" but without PCT. Only a very few isolated cells could be seen after the PIPE was kept in agar–McCoy's 5-A medium for 6 days. No colonies were observed. Similar results were obtained with PIPE collected 3 days after pristane inoculation into BALB/c mice (data not shown).

Either alone or combined with different amounts of LPS, PIPE collected from DBA/2 mice, a strain resistant to plasmacytoma induction, was unable to induce colonies. When tested alone or with LPS, NPW prepared from strains of mice resistant (DBA/2) or susceptible (BALB/c) to plasmacytomas, containing amounts of cells similar to those found to be active in PIPE, were also ineffective on MOPC-315 colony formation. The effect of delayed addition of LPS or PIPE on colony formation by PCT was also evaluated. When PCT cells were incubated in semisolid medium in the presence of LPS and PIPE was added 24 hours later, almost no colonies were obtained. Similar results were obtained when LPS was added 24 hours after the beginning of the experiment.

From our present results it seems that PIPE and LPS activities show at least some specificity. PIPE alone or combined with LPS did not stimulate the colony formation by P1798, a murine lymphosarcoma. In contrast, PIPE and LPS potentiated the colony formation by MOPC-315, MPC-11, and MOPC-104, three transplantable plasma tumor cell lines. No colonies were found in the presence of either LPS or PIPE alone (table 2) except for MOPC-104, which has the ability to form colonies even in the absence of PIPE or LPS, but the number of colonies formed was greatly increased by the presence of PIPE plus LPS.

When PIPE was fractionated by centrifugation at 1,080×*g* for 10 minutes into a supernatant and pellet, a highly stimulatory effect on MOPC-315 colony production was seen with the pellet fraction. Almost no effect was obtained with the supernatant. Repetitive freezing and thawing of PIPE completely abolished the ability to induce colonies in soft agar, whereas irradiation (2,500 rad/1×10^7 PIPE cells) had no diminishing effect on the capacity of PIPE to stimulate the colony formation. PIPE-conditioned medium (over a wide concentration range) was unable to induce MOPC-315 colony formation whether or not it was obtained from PIPE cultured in the presence of LPS and plated with or without LPS (table 3).

Text-figure 1 shows that the MOPC-315 colony formation in the presence of LPS and PIPE was LPS dose-dependent. A linear relationship between the log of LPS concentration and the number of colonies formed was observed. The correlation coefficient (0.93) and 95% confidence limits are

TABLE 1.—*Effect of PIPE plus LPS on MOPC-315 colony formation*

Group No.	Tumor used[a]	Material added[b]	Mean No. of colonies[c]	Plating efficiency
1	MOPC-315	None	3±2	0.003
2	MOPC-315	LPS	5±4	0.005
3	MOPC-315	PIPE[d]	25±4	0.025
4	MOPC-315	PIPE + LPS	1,065±250	1.06
5	MOPC-315	PIPE + saline	35±10	0.035
6	None	PIPE[e]	0	—

[a] MOPC-315 cells were plated at 1×10^5 cells/culture, except in group 1 where a range of cell numbers of 1×10^4–5×10^6 cells/plate was used. Colonies were scored after 6 days of culture.

[b] PIPE was collected 2 mo after ip administration of pristane to BALB/c mice.

[c] Mean of triplicate cultures ± SD. Four experiments with similar results were done.

[d] In 2 of 20 experiments PIPE alone gave similar colony counts to PIPE plus LPS.

[e] PIPE was cultured as described in "Materials and Methods" but without plasma tumor cells added.

TABLE 2.—*Effect of PIPE and LPS on MPC-11, MOPC-104, and P1798 colony formation*

Group No.	Tumor used[a]	Material added[b]	Mean No. of colonies[c]
1	MPC-11	None	15±10
2	MPC-11	LPS	25±5
3	MPC-11	PIPE	32±16
4	MPC-11	LPS + PIPE	890±110
5	MOPC-104	None	83±12
6	MOPC-104	LPS	125±15
7	MOPC-104	PIPE	206±52
8	MOPC-104	LPS + PIPE	1,100±180
9	P1798	None	2±3
10	P1798	LPS[d]	5±2
11	P1798	PIPE	4±3
12	P1798	LPS[d] + PIPE	6±5

[a] MPC-11 and MOPC-104 were plated at 1×10^5 cells/culture. P1798 was plated at 1×10^4 cells/culture.

[b] PIPE was collected 2 mo after ip administration of pristane to BALB/c mice.

[c] Mean of triplicate cultures ± SD. Three experiments with similar results were done.

[d] LPS dose range: 5 ng–50 μg/plate.

shown. The text-figure also shows that nanogram doses of LPS have potentiating effects on MOPC-315 colony formation.

TABLE 3.—*Effect of LPS, PIPE fractions, irradiated and freeze-thaw-treated PIPE, or PIPE-conditioned medium on MOPC-315 colony formation*[a]

Group No.	Material added[b]	Mean No. of colonies[c]
1	None	6±3
2	Supernatant[d] + LPS	18±7
3	Pellet[d] + LPS	830±53
4	Irradiated PIPE + LPS	740±61
5	Freeze-thaw-treated PIPE + LPS	28±5
6	PIPE-conditioned medium[e] + LPS	13±4
7	PIPE-conditioned medium[f] + LPS	20±5
8	PIPE + LPS[g]	35±10
9	PIPE[g] + LPS	20±5

[a] All cultures contained 1×10^5 MOPC-315 cells.

[b] PIPE was collected 2 mo after ip administration of pristane to BALB/c mice. No colonies were obtained in the absence of LPS in the experimental groups. For brevity these negative results were not presented.

[c] Mean of triplicate cultures ± SD. Three experiments with similar results were done.

[d] These fractions were obtained by centrifugation at 1,080×*g* for 10 min.

[e] PIPE was cultured in medium without LPS and processed as described in "Materials and Methods."

[f] PIPE was cultured in medium with LPS and processed as described in "Materials and Methods."

[g] This material was added 24 hr after plating.

DISCUSSION

Administration ip of mineral oil and related substances into susceptible strains of mice induced plasmacytomas after a latent period (*31, 32*).

We have presented evidence that chronic administration of LPS enhances pristane-induced tumorigenesis (*24*). Small inocula of primary plasma tumor cells are not able to transplant into new recipients unless the animals are conditioned by ip administration of pristane at least 3 days before tumor inoculation (*33, 34*). Recently, we showed that such small inocula could also be transplanted into mice pretreated with a peritoneal exudate induced by pristane in BALB/c mice (*26*).

The present work extends these earlier observations concerning the role of LPS and PIPE on the pathogenesis of PCT. With the soft agar technique, we were able to show that PIPE along with LPS consistently induced colony formation by MOPC-315, a plasma tumor cell line. Neither LPS nor PIPE alone was able to induce MOPC-315 colony production except in 2 of 20 experiments in which PIPE alone potentiated the PCT colony formation. Possibly, these two positive results were due to contamination of PIPE with LPS (*35*). The number of colonies obtained was LPS dose-dependent. LPS was effective even in nanogram dose ranges. A temporal relationship was observed. A 24-hour delay in the addition of either one of these two fractions to MOPC-315 cultures resulted in far less colony formation. These data are consistent with a synergistic role of peritoneal cells and LPS in the growth and development of PCT. PIPE and

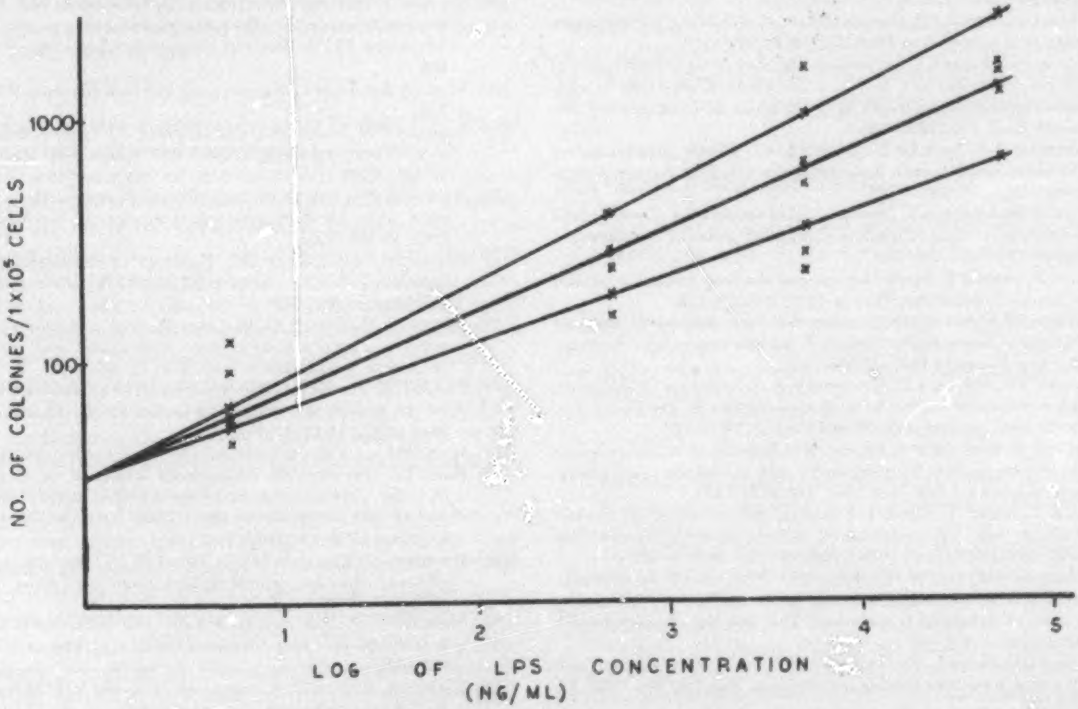

TEXT-FIGURE 1.—LPS dose response.

LPS activities seem to be specific for plasmacytomas. The three transplantable plasma tumor cell lines studied presented colonies under the experimental conditions described, whereas no colonies were formed by the murine lymphosarcoma P1798.

The novelty of our work consists of stressing the role of nanogram amounts of LPS in the pathogenesis of PCT. Only a few reports have shown the effect of small amounts of LPS (*36–39*), and to our knowledge none have dealt with the effect of nanogram doses of LPS on plasma tumor cells. Possibly, LPS interacted with particular cells from PIPE causing them to produce or release factors stimulating PCT colony formation. However, since PIPE-conditioned medium does not stimulate colony formation, it is unlikely that the effect results from a soluble mediator produced by PIPE.

Different factors were reported as promoting PCT colony formation (*18–21*). The relationship between the colony-stimulating factor and PIPE cells stimulated by LPS and other PCT-stimulating factors described is not clear. Studies concerned with further identification of the active part of PIPE and its effect on other T- and B-cell lymphomas as well as other plasmacytomas are in progress.

REFERENCES

(*1*) Bradley TR, Metcalf D. The growth of mouse bone marrow cells in vitro. Aust J Exp Biol Med Sci 1966; 44:287–299.
(*2*) Ichikawa YD, Pluznik H, Sachs L. In vitro control of the development of macrophage and granulocyte colonies. Proc Natl Acad Sci USA 1966; 56:488–495.
(*3*) Fibach E, Hayashi M, Sachs L. Control of normal differentiation of myeloid leukemic cells to macrophages and granulocytes. Proc Natl Acad Sci USA 1973; 70:343–345.
(*4*) Metcalf D, Nossal GJ, Warner NL, et al. Growth of B-lymphocyte colonies in vitro. J Exp Med 1975; 142:1534–1549.
(*5*) Kincade PW, Paige CJ, Parkhouse RM, Lee G. Characterization of murine colony-forming B cells. I. Distribution, resistance to anti-immunoglobulin antibodies, and expression of Ia antigens. J Immunol 1978; 120:1289–1296.
(*6*) Rozenszajn LA, Shoham D, Kalechman I. Clonal proliferation of PHA-stimulated human lymphocytes in soft agar culture. Immunology 1975; 29:1041–1055.
(*7*) Sredni B, Kalechman Y, Nichlin H, Rozenszajn LA. Development of colonies in vitro of mitogen-stimulated mouse T lymphocytes. Nature 1976; 259:131–132.
(*8*) Fibach E, Gerassi E, Sachs L. Induction of colony formation in vitro by human lymphocytes. Nature 1976; 259:126–128.
(*9*) Claësson MH, Roder MB, Johnson GR, Whittingham S, Metcalf D. Colony formation by human T-lymphocytes in agar medium. Clin Exp Immunol 1977; 28:526–534.
(*10*) Bradley TR, Metcalf D, Robinson WA. Stimulation by leukaemic sera of colony formation in solid agar cultures by proliferation of mouse bone marrow cells. Nature 1967; 213:926–927.
(*11*) Kurland JI, Kincade PW, Moore MA. Regulation of B lymphocyte clonal proliferation by stimulatory and inhibitory macrophage-derived factors. J Exp Med 1977; 146:1420–1435.
(*12*) Fibach E, Sachs L. Control of normal differentiation of myeloid leukemic cells. IV. Induction of differentiation by serum from endotoxin treated mice. J Cell Physiol 1973; 83:177–185.
(*13*) Abdelnoor AM, Chang HL, Pham PH, Nowotny A. Lack of relationship between toxicity and bone marrow cell colony stimulating activity of endotoxin preparations. Proc Soc Exp Biol Med 1980; 163:15–18.
(*14*) Pluznik DH, Sachs L. The induction of clones of normal "mast" cells by a substance from conditioned medium. Exp Cell Res 1966; 43:553–563.
(*15*) Stanley ER, Metcalf D. Partial purification and some properties of the factor in normal and leukemic human urine stimulating mouse bone marrow colony growth in vitro. Aust J Exp Biol Med 1969; 43:553–563.
(*16*) Apte RN, Hertogs CF, Pluznik DH. Generation of colony stimulating factor by purified macrophages and lymphocytes. J Reticuloendothel Soc 1979; 26:491–500.
(*17*) Joshi JH, Entringer MA, Robinson WA. Bacterial stimulation of serum colony-stimulating activity and neutrophyl production in germ-free mice. Proc Soc Exp Biol Med 1979; 162:44–47.
(*18*) Coffino P, Laskov R, Scharff MD. Immunoglobulin production: Method for quantitatively detecting variant myeloma cells. Science 1970; 167:186–188.
(*19*) Park CH, Bergsagel DE, McCulloch EA. Mouse myeloma tumor stem cells: A primary cell culture assay. J Natl Cancer Inst 1971; 46:411–422.
(*20*) Metcalf D. Colony formation in agar by murine plasmacytoma cells: Potentiation by hemopoietic cells and serum. J Cell Physiol 1973; 81:397–410.
(*21*) ———. The serum factor stimulating colony formation in vitro by murine plasmacytoma cells: Response to antigen and mineral oil. J Immunol 1974; 113:235–243.
(*22*) Baumal R, Birshtein BK, Coffino PR, Scharff MD. Mutations in immunoglobulin-producing mouse myeloma cells. Science 1973; 182:164–166.
(*23*) Hamburger A, Salmon SE. Primary bioassay of human myeloma stem cells. J Clin Invest 1977; 60:846–854.
(*24*) Bober LA, Kranepool MJ, Bojko C, Steiner G, Hollander VP. Endotoxin enhancement of plasma cell tumor development in mice given injections of mineral oil. Cancer Res 1976; 36:1947–1949.
(*25*) Platica M, Hollander VP. Role of lipopolysaccharides in the production of plasma cell tumors in mice given mineral oil injections. Cancer Res 1978; 38:703–705.
(*26*) Platica M, Bojko C, Hollander VP. Transplantation of primary plasma cell tumor without 2,6,10,14-tetramethylpentadecane (pristane) treatment of the hosts. Cancer Res 1980; 40:579–581.
(*27*) Bober LA, Kranepool MJ, Hollander VP. Inhibitory effect of endotoxin on the growth of plasma cell tumor. Cancer Res 1976; 36:927–929.
(*28*) Stevens J, Stevens YW, Behrens U, Hollander VP. Role of nucleoside transport in glucocorticoid-induced regression of mouse lymphoma P1798. Biochem Biophys Res Commun 1973; 50:799–806.
(*29*) Worton RG, Duff C. Karyotyping. Methods Enzymol 1979; 58:322–344.
(*30*) Kincade PW, Moore AS, Lee G, Paige CJ. Colony-forming B cells in F_1 hybrid and transplanted CBA/N mice. Cell Immunol 1978; 40:294–302.
(*31*) Anderson PN, Potter M. Induction of plasma tumours in BALB/c mice with 2,6,10,14-tetramethylpentadecane (pristane). Nature 1969; 22:994–995.
(*32*) Potter M, MacCardle RC. Histology of developing plasma cell neoplasia induced by mineral oil in BALB/c mice. J Natl Cancer Inst 1964; 33:497–515.
(*33*) Potter M, Pumphrey JG, Walters JL. *Brief communication:* Growth of primary plasmacytomas in mineral oil-conditioned peritoneal environment. J Natl Cancer Inst 1972; 49:305–308.
(*34*) Cancro M, Potter M. The requirement of an adherent substratum for the growth of developing plasmacytoma cells in vitro. J Exp Med 1976; 144:1554–1567.
(*35*) Weir DM, ed. Cellular immunology. Vol 2. Oxford: Blackwell, 1973.
(*36*) Ruco LP, Meltzer MS. Macrophage activation for tumor cytotoxicity: Development of macrophage cytotoxic activity requires completion of a sequence of short lived intermediary reactions. J Immunol 1978; 121:2035–2042.
(*37*) Weinberg JB, Chapman HA Jr, Hibbs JB Jr. Characterization of the effects of endotoxin on macrophage tumor cell killing. J Immunol 1978; 121:72–80.
(*38*) Metcalf D. Role of mercaptoethanol and endotoxin in stimulating B lymphocyte colony formation in vitro. J Immunol 1976; 116:635–638.
(*39*) Vaheri A, Ruoslahti E, Sarvas M, Nurmine NM. Mitogenic effect by lipopolysaccharides and pokeweed lectin on density-inhibited chick embryo fibroblasts. J Exp Med 1973; 138:1356–1364.

Plasminogen Activator, Fibronectin, Lymphotoxin Sensitivity, and Natural Skin Reactivity Relationships to Guinea Pig Cell Tumorigenicity[1, 2]

Richard P. McCabe[3] *and* **Charles H. Evans**[3, 4]

ABSTRACT—The quantitative expression of five properties of chemical carcinogen-induced, neoplastically transformed NIH strain 2 guinea pig fibroblasts was compared in cells possessing thousandfold differences in tumorigenicity. Plasminogen activator synthesis, sensitivity to lymphotoxin inhibition of cell proliferation, and the ability to induce a natural delayed tuberculin-type skin reaction in nonimmune syngeneic guinea pigs correlated directly with the number of cells required to produce a tumor. The most tumorigenic cells (10^2-cell threshold dose) produced the most plasminogen activator, were most sensitive to lymphotoxin, and produced the greatest skin reactivity. Cells with a threshold tumor dose of 10^6–10^7 cells exhibited the lowest expression of these properties. Fibronectin incorporation into an extracellular matrix was diminished in tumorigenic cells, as was anchorage-dependent growth; but neither diminished fibronectin incorporation nor the decreased anchorage requirement correlated quantitatively with the number of cells required to produce a tumor. The present investigation indicates that plasminogen activator synthesis, sensitivity to lymphotoxin, and the capacity of tumorigenic cells to induce natural delayed-type skin reactivity are among the factors that influence initial tumor growth. Plasminogen activator, an extracellular protease, may aid in the growth and spread of tumor cells in vivo by interfering with host fibrin deposition and by inactivating other host proteins such as lymphotoxin.—JNCI 1982; 68:329–336.

One of the central objectives of tumor biology is to define the interactions between tumorigenic cells and the host during the early stages of carcinogenesis that culminate in a progressively growing tumor. Cells most efficient in tumor formation are likely to express altered characteristics that function to the advantage of these efficient cells in these interactions and distinguish them from less efficient cells. Properties that may be altered in tumorigenic cells as compared to nontumorigenic cells include protease production (*1–3*), expression of cell surface antigens (*4–6*), production of extracellular matrix components such as fibronectin (*7, 8*), and sensitivity to a variety of natural cytotoxic host effector mechanisms (*9, 10*). The question remains as to the role of the altered properties in the formation of a primary autochthonous tumor.

In vitro models of carcinogenesis, especially those that are syngeneic and adequately studied with respect to their tumor immunology and natural immune capacity, provide the opportunity for elucidation of the initial cell–host interactions which facilitate or prevent tumor growth. Previous work with a series of NIH strain 2 (2/N) guinea pig cells transformed in culture by chemical carcinogens described the development of tumorigenicity (*11*), karyologic alterations (*12*), immunogenicity (*13, 14*), sensitivity to the growth inhibitory effects of homologous lymphotoxin (*9, 15*), and ability to induce an id delayed tuberculin-like skin response in nonimmune syngeneic animals (*9*). These cells do not express detectable cell line-specific tumor rejection antigens or have the ability to induce serologic or cellular tumor-specific immunity (*13*), yet they have acquired individually distinctive susceptibilities to cytotoxicity mediated by lymphotoxin and by normal (naturally immune) syngeneic leukocytes (*10, 15*). Guinea pig cells produce plasminogen activator, and the expression of this property occurs during the process of carcinogenesis as the cells become tumorigenic (*16*). These previous investigations established the characteristic properties of this model and the reactivity of the tumorigenic cells with various immunologic effectors but did not address the interrelationship of any of the cellular properties to the ability of the cells to produce a tumor. The present study investigates the quantitative relationship of these properties to the specific tumorigenic ability of the cells. Accordingly, the quantitative expression of plasminogen activator, anchorage-independent growth, fibronectin production and incorporation, lymphotoxin sensitivity, and natural skin reactivity were assessed in five lines of tumorigenic syngeneic 2/N guinea pig cells. The expression of each of the properties was related to the distinctive tumorigenicity of each cell line as measured by its minimum tumorigenic dose.

MATERIALS AND METHODS

Cell cultures.—Table 1 lists some properties of the guinea pig fibroblasts used. Tumorigenic cell lines were selected to

---

ABBREVIATIONS USED: FBS=fetal bovine serum; [^{3}H]dThd=tritiated thymidine; id=intradermal(ly); NGPS=normal guinea pig serum; OA=ovalbumin; PBS=phosphate-buffered saline; SpA=staphylococcal protein A; SRBC=sheep red blood cells.

---

[1] Received July 15, 1981; accepted October 7, 1981.

[2] Animals were maintained under the guidelines of the National Institutes of Health.

[3] Tumor Biology Section, Laboratory of Biology, Division of Cancer Cause and Prevention, National Cancer Institute, National Institutes of Health, Public Health Service, U.S. Department of Health and Human Services, Bethesda, Md. 20205.

[4] We thank Dr. Joseph DiPaolo and Dr. Tibor Borsos, both of the National Cancer Institute, for advice and critical review of the manuscript. We also acknowledge the technical assistance of Mr. James Pomponio and Ms. Nancee Cahill and the secretarial assistance of Mrs. Diana Shaw.

TABLE 1.—*Strain 2/N guinea pig cells*

Culture designation[a]	Passages	Previous chemical treatment	Tumorigenicity[b]
2°	2–5	None	–
103	40–50	Acetone	–
106[c]	117–127	7,12-Dimethylbenz[*a*]anthracene	–
104C1	43–45	Benzo[*a*]pyrene	+
107C3	77–87	*N*-Methyl-*N*′-nitro-*N*-nitrosoguanidine	+
HM4C1	98–108	*N*-Methyl-*N*′-nitro-*N*-nitrosoguanidine	+
74C3	69–79	3-Methylcholanthrene	+
HM2C1	95–105	Diethylnitrosamine	+
L1C1[d]	24–34	Diethylnitrosamine	+

[a] Designation suffixes C1 and C3 refer to clones derived from single cells obtained from colonies growing in 0.35% agar.

[b] Tumorigenicity (+ or –) was determined by the ability of as many as 10^6 cells to produce a progressively growing tumor after sc injection into nonirradiated or gamma-irradiated 1-day-old or 4- to 6-month-old male 2/N guinea pigs (*11*), respectively. All tumorigenic cells gave rise to fibrosarcomas except L1C1, which produced a carcinoma.

[c] Cells designated 106 were derived from the same fetus as 103, 104, and 107 cells. The 106 cells exhibit the transformed colony morphology typical of tumorigenic cells but at 125 passages after carcinogen treatment remain nontumorigenic at an sc dose of 10^6 cells/animal.

[d] L1C1 is a cloned line obtained from an ascites variant of an in vivo induced guinea pig hepatocellular carcinoma (*17, 23*). L1C1 was included as a tumor cell control in some experiments. All other cell lines were derived from guinea pig fetuses and exhibit a fibroblast-like appearance (*11*).

represent a range of tumorigenic thresholds. When injected sc or id into syngeneic animals (*13, 14*) under the conditions used in this study, none of these cells induces tumor-specific immunity. Nontumorigenic control cells were selected to include short-term (culture 2°), intermediate-term (culture 103), and long-term (culture 106) passaged cells, including the carcinogen-induced, morphologically transformed but nontumorigenic (culture 106) cells. All cells were obtained from stocks preserved in liquid nitrogen, were studied within 10 passages after reintroduction into culture, and were grown in RPMI-1640 medium with 10% FBS (complete medium) at 37°C in a water-saturated atmosphere containing 5% CO_2 (*9*).

Analysis of plasminogen activator.—Plasminogen activator was assayed essentially as described by Strickland and Beers (*18*). Fibrinogen (bovine, 98% clottable protein; Calbiochem-Behring Corp., Los Angeles, Calif.) was radiolabeled by the chloramine-T method (*19*) to a specific activity of 3–6×10^5 cpm/µg. Radiolabeled fibrinogen and unlabeled fibrinogen were mixed in phosphate-saline buffer (0.68 m*M* Na_2HPO_4, 0.12 m*M* KH_2PO_4, 0.22 m*M* KCl, and 11.42 m*M* NaCl) and applied to 6-well (10^5 cpm, 100 µg, 0.2 ml) tissue culture plates. Coated plates were dried under vacuum at room temperature for 3 days and used for the assay of plasminogen activator within 10 days.

The 6-well tissue culture dishes coated with ^{125}I-labeled fibrinogen were washed with Dulbecco's PBS to remove nonadherent material. At this stage each well contained 50,000–70,000 cpm, as determined by pronase digestion. Then, 5×10^4 tumorigenic or nontumorigenic cells were plated in 3 ml complete medium previously depleted of plasminogen by passage over lysine-Sepharose 4B (*20*). Soybean trypsin inhibitor (300 µg/ml) was added to inhibit any residual plasmin activity. Cells were incubated (37°C, 5% CO_2) overnight, the medium was removed, the cell layer was washed, and 1.5 ml RPMI-1640 medium containing 10% acid-treated NGPS was added. After a further 5-hour incubation, which permitted fibrin digestion, the medium was removed and counted for ^{125}I (cpm). Controls for spontaneous release due to cells alone (no NGPS), spontaneous release with no cells (medium plus NGPS), and total release (pronase, 80 µg) were included for each 6-well plate. The percentage of the total cpm released in each test well was calculated after correction for the activity in the two spontaneous release controls. The cell lines were assayed twice in triplicate, and the results were expressed as the mean of six determinations. NGPS was acid treated by titration to pH 3.0 with 1 *N* HCl, which inactivated acid-labile protease inhibitors, and was neutralized after 30 minutes with NaOH (*21*).

Assessment of anchorage-independent growth.—Cloning efficiency of tumorigenic cells in 0.35% agar in complete medium was assessed as described (*11*). Suspensions of 10^2 or 10^3 trypsinized cells in 5 ml complete medium containing 0.35% liquid agar at 40°C were prepared and immediately poured onto a 4-ml basal layer of 0.7% agar in complete medium in a 60-mm petri dish. The dishes were incubated (37°C, 5% CO_2) and examined by phase-contrast microscopy at 7, 14, and 21 days for the presence of colonies growing in the 0.35% agar. After 21 days the colonies were stained by the addition of 1 ml of a 1:100 dilution in medium of a 1:300 solution of neutral red/dish. Only colonies containing more than 100 cells were counted.

Fibronectin localization and quantitation.—Fibronectin was purified from normal guinea pig plasma by gelatin-Sepharose 4B affinity chromatography as described by Engvall and Ruoslahti (*22*). Xenoantisera were produced in New Zealand White rabbits, heat inactivated (56°C, 30 min), and absorbed with three volumes of SRBC and two volumes of guinea pig erythrocytes. Control sera obtained from the same rabbits before immunization were similarly absorbed. Analysis of the xenoantisera by double diffusion and immunoelectrophoresis against normal guinea pig plasma indicated specificity for fibronectin.

Immunofluorescence was evaluated in tumorigenic and nontumorigenic cells on Lab-Tek 8-chamber culture slides seeded with 2.5×10^4 cells in complete medium and incubated (37°C, 5% CO_2) until confluent. The slides were washed in PBS, fixed with 3.5% phosphate-buffered Formalin (60 min, 25°C), and rinsed with PBS. Xenoantisera or control sera (50 µl/chamber, 1:80 dilution) were added for 60 minutes, and the slides were rinsed and incubated with fluorescein isothiocyanate-conjugated goat anti-rabbit IgG (50 µl/chamber, 1:20 dilution) for another 60 minutes. The slides were washed, and fluorescence was determined with a Leitz Ortholux II equipped for fluorescence microscopy with Ploem illumination for fluorescein, as previously described (*23*). Photomicrographs were taken with Kodak Tri X-film (ASA 400). No fluorescence was seen with the control sera on any of the cells tested, and none of the absorbed sera when reacted with SRBC showed fluorescence.

Relative quantitation of the amount of fibronectin bound to the cells and incorporated into the extracellular matrix was obtained in a radiobinding assay in which the erythrocyte-absorbed xenoantisera and ^{125}I-labeled SpA were used. The procedure has been described in detail (*24*). Protein A was radiolabeled to a specific activity of 4×10[illegible] cpm/μg with Bolton-Hunter reagent (*25, 26*). Tumorigenic and nontumorigenic cells (5×10^4, 0.1 ml) in complete medium were seeded in 96-well flat-bottom tissue culture plates and incubated (37°C, 5% CO_2). The next day, the medium was removed by a quick shake of the inverted plate, the adherent cells were washed with 0.1% OA in PBS, and 50 μl of diluted xenoantisera (1:10–1:80 in OA–PBS) was added. After 60 minutes' incubation at room temperature, unbound antisera were removed by three washes with OA–PBS, 50 μl of ^{125}I-labeled SpA (20 ng) was added to the cells, and incubation was continued for 30 minutes at room temperature. Excess ^{125}I-labeled SpA was removed by washing the wells with OA–PBS, the cells were then digested with 1 *N* NaOH, and the digest was counted for ^{125}I (cpm). The results were expressed as the percentage of total cpm of ^{125}I (^{125}I-cpm) bound to the digested cells.

Lymphotoxin inhibition of cell growth.—Production of 2/N guinea pig lymphotoxin by peritoneal leukocytes and analysis of the activity were described in detail (*9*). Mineral oil-induced leukocytes were harvested, washed, and suspended in serum-free RPMI-1640 medium at 5×10^5 cells/ml (20 ml/100-mm dish). Phytohemagglutinin (100 μg/ml) was added immediately, and the guinea pig lymphotoxin-containing culture medium was collected after 24 hours and frozen at −40°C. Guinea pig lymphotoxin was assayed in a [^{3}H]dThd release assay with murine αL929 target cells. One U of lymphotoxin induced 50% release of [^{3}H]dThd from 10^4 target cells in 72 hours (*27*).

Measurement of target cell susceptibility to the colony inhibitory activity of guinea pig lymphotoxin has been previously described in detail (*15*). Single cell suspensions of target cells were obtained by mild trypsinization (0.1% trypsin) of exponentially growing cultures of tumorigenic and nontumorigenic cells. The cell suspensions were diluted with complete medium to contain 100–1,000 cells/4 ml to produce 30–60 colonies and were plated in 60-mm petri dishes. Guinea pig lymphotoxin was included in the complete medium at 6, 60, or 600 U/ml. Each assay was performed in sextuplicate. After 7 days of incubation (37°C, 5% CO_2), the medium was removed and the colonies were washed with PBS, fixed in methanol, and stained with 10% aqueous Giemsa. Colonies greater than 0.2 mm in diameter were counted. Target cell response to guinea pig lymphotoxin was expressed as a percentage of the number of colonies in the untreated control group. Less than 10% inhibition of colony formation was not considered significant. The reproducibility of this assay is ±5%.

Intradermal skin tests.—Exponentially growing tumorigenic and nontumorigenic cells were harvested from 100-mm culture dishes with 5 ml 1:5,000 EDTA and were washed twice with RPMI-1640 medium. The cells, resuspended at 2.5 or 5.0×10^7 cells/ml RPMI-1640 medium, were injected (0.1 ml) id into the shaved abdomen of healthy nonimmunized 14- to 16-week-old male 2/N guinea pigs. Each cell line was tested in 6 animals; each animal received four injections of different cell lines at separate sites 4 cm apart. Reactivity was determined by the calculation of the average diameter of induration of two perpendicular measurements 1, 2, 3, and 4 days after inoculation. Results were expressed as an index of reactivity, which was the ratio of the mean induration on day 4 to the mean induration on day 1 calculated by linear regression analysis of the indurations on days 1, 2, 3, and 4. Portions of these data were included as part of another report (*9*).

Determination of tumorigenic threshold dose.—Chemical carcinogen-treated neoplastic cells were assessed for their tumorigenic ability in adult guinea pigs. Exponentially growing cultures of cells were harvested by mild (0.1%) trypsinization, washed twice with RPMI-1640 medium, and resuspended in this medium at tenfold increments from 10^2 to 10^6 cells/ml. Groups of six 12- to 20-week-old 2/N guinea pigs received sc injections in the flank of 1.0 ml of each cell suspension. Each guinea pig received only cells of one cell line. Tumor growth was monitored for 6 months. The lowest number of cells producing a progressively growing tumor in at least half the group during this period was the minimum tumorigenic dose. Line 74C3 failed to produce a tumor in any guinea pig inoculated with 10^2–10^6 cells. However, within 2 months after injection of 10^7 cells, tumors appeared in 2 of 2 animals tested.

RESULTS

Five lines of in vitro transformed tumorigenic syngeneic 2/N guinea pig cells and four controls were studied for expression of selected phenotypic properties. Three of the four controls were nontumorigenic guinea pig cells representing *a*) long-term-cultured (culture 106) carcinogen-induced morphologically transformed nontumorigenic cells, *b*) intermediate-term-cultured (culture 103) cells treated with acetone (a noncarcinogen) and possessing a nontransformed morphology, and *c*) low-passage secondary culture (2°) untreated cells.

Tumorigenic cells were distinguishable from nontumorigenic cells by production of plasminogen activator. Plasminogen activator was produced by all tumorigenic cells in amounts that correlated with their tumorigenicity (table 2). Nontumorigenic cells were not active, as evidenced by their failure to release ^{125}I-cpm after plasminogen was added, even when the incubation time with plasminogen was extended to 24 hours and the cell number in each well was increased to 1×10^5. In a 48-hour assay with 2×10^5 cells, culture 103 had sufficient activity to digest 34% of the ^{125}I-labeled fibrin; culture 106 and the 2° culture cells produced no activity under these conditions (data not shown).

Activation of plasminogen by tumorigenic cells may be a factor in the expression of anchorage-independent growth and in the determination of the amount of fibronectin deposition in intercellular areas. To see whether a relationship exists among plasminogen activator production, anchorage-independent growth, fibronectin deposition, and tumorigenicity, we determined the cloning efficiency of guinea pig cells in medium containing 0.35% agar and the

TABLE 2.—*Properties of tumorigenic guinea pig fibroblast-like cells*

Culture designation	Tumor threshold, No. of cells sc	Plasminogen activator production, % fibrin digested ± SE[a]	Percent cloning efficiency in 0.35% agar ± SE	Fibronectin production, % antibody binding at 1:10 antiserum dilution	Lymphotoxin susceptibility, U[b]	Index of skin reactivity, mean ± SE (range)[c]
HM2C1	10^2	22.0±1.5	4.6±0.7	31	28	1.16±0.07
104C1	10^2	16.9±0.6	2.4±0.7	35	90	1.11±0.16
HM4C1	10^3	14.3±0.4	24.8±1.6	27	200	0.98±0.09
107C3	10^5	6.3±0.6	12.9±0.9	24	450	0.78±0.14
74C3	10^7	6.2±1.1	27.1±1.3	29	3,500	0.51±0.08
103, 106, 2°	—[d]	0	0	33–48	—[e]	(0.14–0.45)

[a] Range of plasminogen-independent digestion of fibrin was 1.0–1.5%.

[b] Number of lymphotoxin units required to reduce tumorigenic cell colony formation by 50%.

[c] Determined as the ratio of the mean induration on day 4 to the mean induration on day 1, calculated by linear regression analysis of the indurations on days 1, 2, 3, and 4.

[d] No tumors were observed after injection of 10^8 cells.

[e] Nontumorigenic cells were not sensitive to lymphotoxin-inhibited colony formation.

pattern and quantity of fibronectin incorporation into an extracellular matrix.

Only tumorigenic guinea pig cells formed colonies in soft agar. Efficiency of colony formation by tumorigenic cells ranged from 2.4 to 27.1%, but the ranking showed correlation neither with the amount of plasminogen activator produced by the cells nor with the minimum required tumorigenic dose (table 2). Lowest cloning efficiencies were seen with highly tumorigenic cells producing the most plasminogen activator (HM2C1 and 104C1), and highest efficiency was obtained with the weakly tumorigenic cells producing the least amount of plasminogen activator (line 74C3). The relationship was not strictly reversed since cells of line HM4C1 showed a higher cloning efficiency, higher plasminogen activator activity, and greater tumorigenicity than cells of line 107C3.

Fibronectin production and extracellular deposition by the guinea pig cells were studied by indirect immunofluorescence in which rabbit antisera to guinea pig plasma fibronectin were used. A distinctly different pattern of immunofluorescence was seen with the nontumorigenic cells as compared to the tumorigenic cells. Nontumorigenic 2° culture cells (fig. 1A) and culture 103 cells showed a pattern of extracellular matrix-associated fluorescence that outlined the cells and revealed their ordered arrangement. Carcinogen-treated morphologically transformed nontumorigenic culture 106 cells exhibited a fluorescence pattern similar to that seen with nontumorigenic culture 103 and 2° cells, revealing an extracellular matrix of fibronectin that outlined the cells, illuminating their random pattern of growth (fig. 1B). In contrast, tumorigenic cells showed a surface rather than an extracellular matrix-associated fluorescence of weak intensity and patchy appearance (fig. 1C). Tumorigenic cells could not be distinguished from each other by their pattern of immunofluorescence. A rabbit antiserum to human plasma fibronectin was used with similar results.

We determined the relative amount of cell-bound and extracellular fibronectin produced by each cell line in a radiobinding assay with rabbit anti-guinea pig fibronectin antisera and ^{125}I-labeled SpA to learn whether differences between tumorigenic and nontumorigenic cells could be quantitated. Nontumorigenic cells, after incubation with antisera to fibronectin, bound more ^{125}I-labeled SpA and thus produced more fibronectin than did tumorigenic cells, but in all assays no clear distinction between tumorigenic and nontumorigenic cells was possible on the basis of the quantity of fibronectin produced (text-fig. 1; table 2). The binding data were confirmed in three similar experiments, with the only differences attributed to decay of the radiolabel.

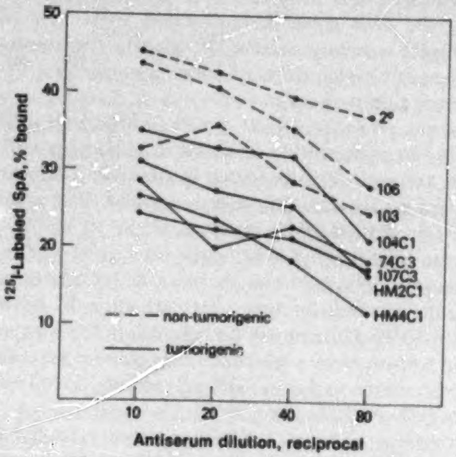

TEXT-FIGURE 1.—^{125}I-labeled SpA quantitation of anti-guinea pig fibronectin xenoantisera bound to tumorigenic and nontumorigenic guinea pig cells. Diluted xenoantisera (50 µl) were reacted with 5×10^4 cells per line per 96-well tissue culture plate. After removal of unbound xenoantibody, bound antibody was reacted with 20 ng (10^5 cpm) ^{125}I-labeled SpA. *Each point* is the mean of duplicate determinations. In the absence of antisera, the amount of bound ^{125}I-labeled SpA ranged from 1.1 to 1.4%.

Tumorigenicity, plasminogen activator synthesis, soft agar cloning efficiency, and fibronectin production by tumorigenic guinea pig cell lines were also compared. No correlation of fibronectin production with any of the other properties of the cells was revealed (table 2).

Since tumorigenic cells are sensitive to the colony-inhibitory activity of homologous lymphotoxin and nontumorigenic cells are not sensitive, we were interested in determining whether this sensitivity correlates with any of the other phenotypic properties. Lymphotoxin inhibited colony formation by tumorigenic cells but had no inhibitory effect on nontumorigenic cells. In the colony formation assay the tumorigenic but not the nontumorigenic cells were inhibited as much as 85% by 600 U lymphotoxin. Lymphotoxin sensitivity showed a direct correlation both with the amount of plasminogen activator produced and with the tumorigenicity of the cells (table 2): The most highly tumorigenic cells produced the most plasminogen activator and were most sensitive to lymphotoxin (line HM2C1), the least tumorigenic cells produced the least amount of plasminogen activator and were least sensitive to lymphotoxin (lines 743C3 and 107C3), and the other two cell lines were intermediate in tumorigenicity and ranked in the same order of plasminogen activator production and lymphotoxin sensitivity. Lymphotoxin sensitivity did not correlate with soft agar cloning efficiency or fibronectin production.

Within 24 hours after id injection of 2–5$\times 10^6$ cells into syngeneic nonimmune guinea pigs, an area of induration up to 5-mm diameter appears (*9*). When nontumorigenic cells are injected, the response rapidly subsides, but with tumorigenic cells the response increases, persists, or subsides slowly over 4 days at a rate characteristic of the cell line (*9*). Expression of this natural delayed-type skin reactivity by tumorigenic guinea pig cells correlated with the tumorigenic ability of the cells, the production of plasminogen activator, and sensitivity to lymphotoxin. No correlation was seen with soft agar cloning efficiency or fibronectin production (table 2).

DISCUSSION

Three properties of tumorigenic guinea pig cells—plasminogen activator production, lymphotoxin sensitivity, and the capacity to elicit a tuberculin-like delayed id skin response in nonimmune syngeneic guinea pigs—correlated quantitatively with the capacity of the cells to produce a progressively growing tumor in syngeneic animals. Two properties—cloning efficiency in 0.35% agar and the pattern of extracellular fibronectin deposition—distinguished the tumorigenic and nontumorigenic cells, but the quantitative expression of these properties did not correlate with the degree of tumorigenicity. This finding is in accord with results from other laboratories indicating a frequent but not a necessary correlation among the properties of anchorage-independent growth, decreased fibronectin incorporation, and tumorigenic ability (*28–30*). Our findings with regard to fibronectin may have been influenced by the period of in vitro culture. Yamada et al. (*31*) and Chen et al. (*32*) reported decreased fibronectin production by cells after, respectively, establishment of a permanent cell line and extensive passage in culture. The possibility that the amount of fibronectin detected in our experiments was related to those factors was not excluded, and among fresh cell isolates, a clear quantitative distinction among cells of differing tumorigenic abilities may be observed. It is also possible that further experiments will show, as suggested by current data, that the change in fibronectin production with transformation covers a continuous spectrum, with no clear distinction among tumorigenic cells or between groups of nontumorigenic and tumorigenic cells.

That tumorigenic cells produced plasminogen activator in amounts which correlated directly with their tumorigenic ability and that nontumorigenic cells produced no activator in the same assay suggest a functional relationship between in vivo growth of tumor cells and plasminogen activator. In vivo evidence implicating plasminogen activator and tumor development also includes the identification of plasminogen activator in extracts of established tumors (*33–35*) and in histologic tumor tissue sections (*2*) and the demonstration of relatively greater plasminogen activator concentrations in metastatic as compared to primary tumor tissue (*36*). Dvorak et al. (*37, 38*) suggested a mechanism whereby plasminogen activator may promote tumor formation. They reported that a principal difference between spontaneously regressing (line 1) and highly malignant (line 10) guinea pig tumors was the amount of fibrin gel surrounding the growing tumors. Line 1 tumors were encapsulated by fibrin to a greater extent than line 10 tumors; Dvorak et al. postulated that plasminogen activator promoted fibrin digestion which permitted tumor growth and possibly stimulated growth of blood vessels into the developing tumor mass. Extensive fibrin deposition during tumor growth has also been observed by other workers (*39, 40*), and our studies of the histology of the induration produced by id injected tumorigenic guinea pig cells indicate that within 4 days a well-ordered fibroblast-rich matrix begins to develop around the nascent tumor cells (McCabe RP, Oneson R, Evans CH: Unpublished data). In the light of these observations, we may reasonably suggest that in some instances plasminogen activator can influence tumor development by limiting the isolation of the tumor within a fibrin matrix and by promoting angiogenesis.

Our laboratory (*9*) described the sensitivity of tumorigenic guinea pig fibroblasts to the colony inhibitory activity of homologous lymphotoxin and the capacity of these fibroblasts to induce natural delayed tuberculin-like skin reactivity in nonimmune animals. These properties of tumorigenic fibroblasts were shown to develop during the course of carcinogenesis at approximately the same time as the cells became tumorigenic. In the present work we show that these two properties correlate quantitatively with tumorigenicity, as measured by the minimum tumorigenic dose, and that their expression is related to a third factor, plasminogen activator. Zwilling et al. (*10*) demonstrated that the susceptibility of these guinea pig fibroblasts to lymphoid cell natural cytotoxic activity also correlated with tumorigenicity. That study showed a continuum in natural leukocyte cytotoxicity, as observed for natural delayed skin reactivity in the present investigation. Together, these responses indicate the differential capacity on the part of the recipient or host animal to recognize and respond to nascent tumorigenic cells and the differential susceptibility of these cells to possible defense mechanisms. The correlation with plasminogen activator activity does not provide a clear picture; yet these findings, together with the known importance of protease activities in cell functions (*41–44*), the inhibitory effect of protease inhibitors on lymphotoxin activity (*45*), and the mitogenic activity of some proteases for lymphocytes (*46*), indicate the need for further investigation into the relationships of these activities to each other. Since cells most sensitive to effectors of natural immunity also produce the greatest amount of plasminogen activator, a mechanism may exist whereby immunologic effector cells or soluble factors mediate their activity through the action of target cell proteases.

REFERENCES

(*1*) Barrett JC, Crawford BD, Mixter LO, Schechtman LM, Ts'o PO, Pollack R. Correlation of in vitro growth properties and tumorigenicity of Syrian hamster cell lines. Cancer Res 1979; 39: 1504–1510.

(*2*) Cliffton EE, Grossi CE. Fibrinolytic activity of human tumors as measured by the fibrin plate method. Cancer 1955; 8:1146–1154.

(*3*) Unkeless JC, Tobia A, Ossowski L, Quigley JP, Rifkin DB, Reich E. An enzymatic function associated with transformation of fibroblasts by oncogenic viruses. I. Chick embryo fibroblast cultures transformed by avian RNA tumor viruses. J Exp Med 1973; 137: 85–111.

(*4*) Alexander P. Foetal "antigens" in cancer. Nature 1972; 235:137–140.

(*5*) Klein G. Tumor antigens. Ann Rev Microbiol 1966; 20:223–252.

(*6*) Prehn RT, Main JM. Immunity to methylcholanthrene-induced sarcomas. J Natl Cancer Inst 1957; 18:769–778.

(*7*) Furcht LT, Mosher DF, Wendelschafer-Crabb G. Effects of cell density and transformation on the formation of a fibronectin extracellular filamentous matrix on human fibroblasts. Cancer Res 1978; 38:4618–4623.

(*8*) Hynes RO. Alterations of cell surface proteins by viral transformation and by proteolysis. Proc Natl Acad Sci USA 1973; 70:3170–3174.

(*9*) Evans CH, Cooney AM, DiPaolo JA. Colony inhibition mediated by nonimmune leukocytes in vitro and skin reactivity in vivo as indices of tumorigenicity of guinea pig cultures transformed by chemical carcinogens. Cancer Res 1975; 35:1045–1052.

(*10*) Zwilling BS, Meltzer MS, Evans CH. Differential cytotoxicity of tumorigenic and nontumorigenic strain-2 guinea pig cells as mediated by syngeneic phytohemagglutinin-stimulated peritoneal exudate cells. J Natl Cancer Inst 1975; 54:743–747.

(*11*) Evans CH, DiPaolo JA. Neoplastic transformation of guinea pig fetal cells in culture induced by chemical carcinogens. Cancer Res 1975; 35:1035–1044.

(*12*) Popescu NC, Evans CH, DiPaolo JA. Chromosome patterns (G and C bands) of in vitro chemical carcinogen-transformed guinea pig cells. Cancer Res 1976; 36:1404–1413.

(*13*) Ohanian SH, McCabe RP, Evans CH. Immunogenicity of guinea pig cells transformed in culture by chemical carcinogens. JNCI 1981; 67:1363–1368.

(*14*) Zbar B, Ribi E, Kelly M, Granger D, Evans CH, Rapp HJ. Immunological approaches to the treatment of human cancer based on a guinea pig model. Cancer Immunol Immunother 1976; 1:127–138.

(*15*) Evans CH, Rabin ES, DiPaolo JA. The susceptibility of guinea pig cells to the colony-inhibitory activity of lymphotoxin during carcinogenesis. Cancer Res 1977; 37:898–903.

(*16*) Sisskin EE, Weinstein IB, Evans CH, DiPaolo JA. Plasminogen activator synthesis accompanying chemical carcinogen-induced in vitro transformation of Syrian hamster and guinea pig fetal cells. Int J Cancer 1980; 26:331–335.

(*17*) Rapp HJ, Churchill WH Jr, Kronman BS, Rolley RT, Hammond WG, Borsos T. Antigenicity of a new diethylnitrosamine-induced transplantable guinea pig hepatoma: Pathology and formation of ascites variant. J Natl Cancer Inst 1968; 41:1–11.

(*18*) Strickland S, Beers WH. Studies on the role of plasminogen activator in ovulation. J Biol Chem 1976; 251:5694–5702.

(*19*) Hunter WM. The preparation of radioiodinated proteins of high activity, their reaction with antibody in vitro: The radioimmunoassay. In: Weir DM, ed. Handbook of experimental immunology. Philadelphia: Davis, 1967:647–651.

(*20*) Deutsch DG, Mertz ET. Plasminogen purification from human plasma by affinity chromatography. Science 1970; 170:1095–1096.

(*21*) Loskutoff DJ, Edgington T. Synthesis of fibrinolytic activator and inhibitor by endothelial cells. Proc Natl Acad Sci USA 1977; 74: 3903–3907.

(*22*) Engvall E, Ruoslahti E. Binding of soluble form of fibroblast surface protein, fibronectin, to collagen. Int J Cancer 1977; 20:1–5.

(*23*) Evans CH, Ohanian SH, Cooney AM. Tumor specific and Forssman antigens of guinea pig hepatoma cells. Comparison of tumor cells grown in vivo and in vitro. Int J Cancer 1975; 15:512–521.

(*24*) McCabe RP, Quaranta V, Frugis L, Ferrone S, Reisfeld RA. A radioimmunometric antibody-binding assay for evaluation of xenoantisera to melanoma-associated antigens. JNCI 1979; 62:455–463.

(*25*) Bolton AE, Hunter WM. The labelling of proteins to high specific radioactivities by conjugation to a ^{125}I-containing acylating agent. Biochem J 1973; 133:529–539.

(*26*) Langone JJ, Boyle MD, Borsos T. ^{125}I protein A: Applications to the quantitative determination of fluid phase and cell bound IgG. J Immunol Methods 1977; 18:281–293.

(*27*) Rundell JO, Evans CH. Species specificity of guinea pig and human lymphotoxin colony inhibitory activity. Immunopharmacology 1981; 3:9–18.

(*28*) Gallimore PH, McDougall JK, Chen LB. Malignant behaviour of three adenovirus-2-transformed brain cell lines and their methyl cellulose-selected sub-clones. Int J Cancer 1979; 24:477–484.

(*29*) Kahn P. Cellular tumorigenicity in nude mice: Test of associations among loss of cell surface fibronectin, anchorage independence, and tumor-forming ability. J Cell Biol 1979; 82:1–16.

(*30*) Der CJ, Stanbridge EJ. Lack of correlation between decreased expression of cell surface LETS protein and tumorigenicity in human cell hybrids. Cell 1978; 15:1241–1251.

(*31*) Yamada KM, Yamada SS, Pastan I. Quantitation of a transformation sensitive, adhesive cell surface glycoprotein: Decrease on several untransformed permanent cell lines. J Cell Biol 1976; 74:649–654.

(*32*) Chen LB, Maitland N, Gallimore PH, McDougall JK. Detection of the large external transformation-sensitive protein on some epithelial cells. Exp Cell Res 1977; 106:39–46.

(*33*) Corasanti JG, Celik C, Camiolo SM, et al. Plasminogen activator content of human colon tumors and normal mucosae: Separation of enzymes and partial purification. JNCI 1980; 65:345–351.

(*34*) Markus G, Takita H, Camiolo SM, Corasanti JG, Evers JL, Hobika GH. Content and characterization of plasminogen activators in human lung tumors and normal lung tissues. Cancer Res 1980; 40:841–848.

(*35*) Nagy B, Ban J, Brdar B. Fibrinolysis associated with human neoplasia: Production of plasminogen activator by human tumors. Int J Cancer 1977; 19:614–620.

(*36*) Wang BS, McLoughlin GA, Richie JP, Mannick JA. Correlation of the production of plasminogen activator with tumor metastases in B16 mouse melanoma cell lines. Cancer Res 1980; 40:288–292.

(*37*) Dvorak HF, Dvorak AM, Manseau EJ, Wiberg L, Churchill WH. Fibrin gel investment associated with line 1 and line 10 solid tumor growth, angiogenesis, and fibroplasia in guinea pigs. Role of cellular immunity, myofibroblasts, microvascular damage, and infarction in line 1 tumor regression. JNCI 1979; 62:1459–1472.

(*38*) Dvorak HF, Orenstein NS, Carvalho AC, et al. Induction of a fibrin gel investment. An early event in line 10 hepatocarcinoma growth mediated by tumor secreted products. J Immunol 1979; 122:166–174.

(*39*) Kodama Y, Tanaka K. Thromboplastic and fibrinolytic activities of V2 and V7 carcinomas of rabbits, with special reference to fibrin deposition and thrombus formation in the tumors. Acta Pathol Jpn 1978; 28:279–286.

(*40*) O'Meara RA. Fibrin formation and tumor growth. Thromb Diathes Haemorrh 1968; suppl 28:137–142.

(*41*) Astrup T. Tissue activators of plasminogen. Fed Proc 1964; 25:42–51.

(*42*) Ossowski L, Biegel D, Reich E. Mammary plasminogen activator: Correlation with involution, hormonal modulation and comparison between normal and neoplastic tissues. Cell 1979; 16:929–940.

(*43*) Reich E. Activation of plasminogen: A widespread mechanism for generating localized extracellular proteolysis. In: Ruddon R, ed. Biological markers of neoplasia: Basic and applied aspects. New

York: Elsevier, 1978:491–498.
(44) Unkeless JC, Gordon S, Reich E. Secretion of plasminogen activator by stimulated macrophages. J Exp Med 1974; 139:834–850.
(45) Weitzen M, Granger GA. The human LT system. VIII. A target cell-dependent enzymatic activation step required for the expression of the cytotoxic activity of human lymphotoxin. J Immunol 1980; 125:719–724.
(46) Carney DH, Glenn KC, Cunningham DD. Conditions which affect initiation of animal cell division by trypsin and thrombin. J Cell Physiol 1978; 95:13–22.

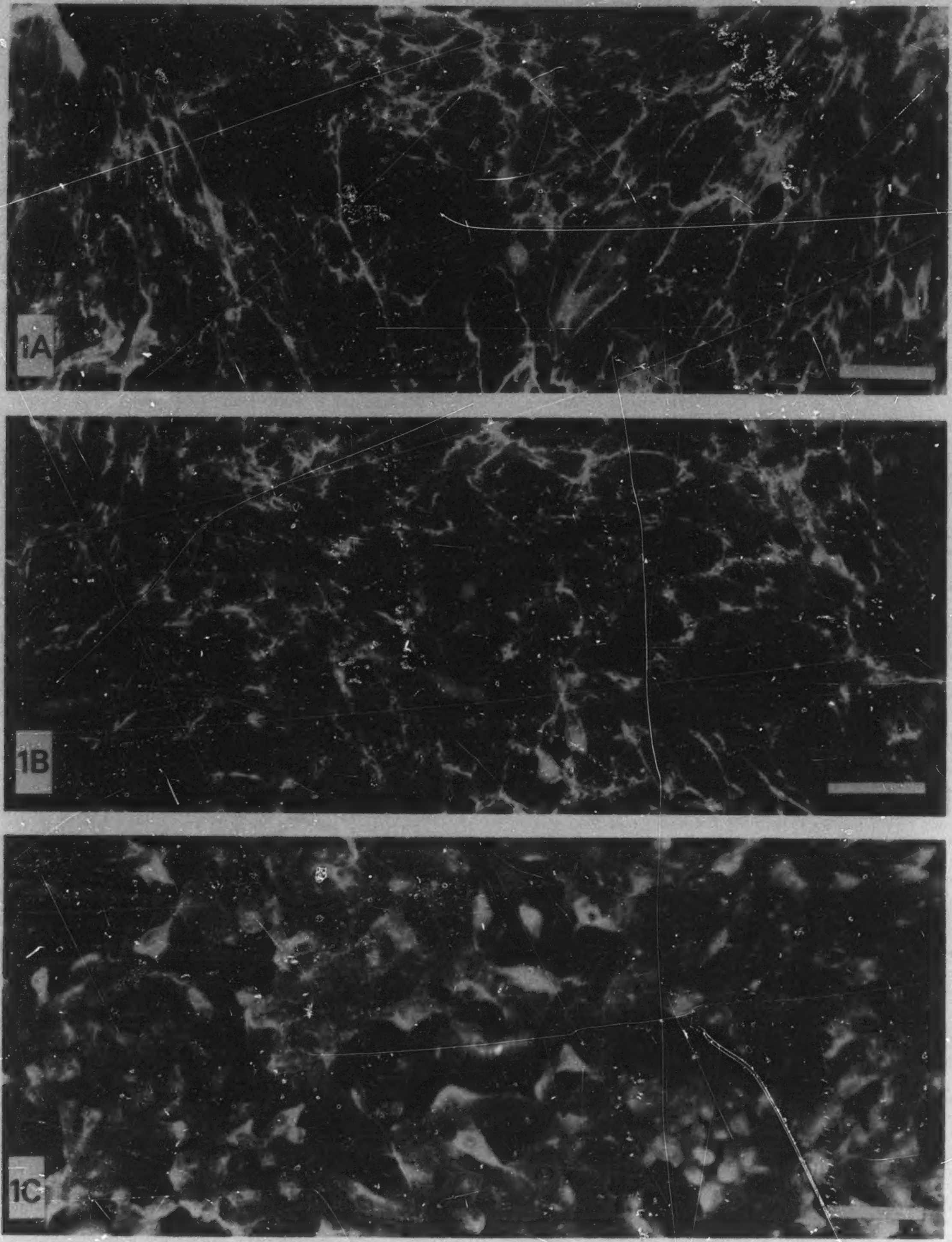

FIGURE 1.—Immunofluorescence with anti-guinea pig fibronectin xenoantisera on A) nontumorigenic 2° culture cells, B) morphologically transformed nontumorigenic line 106 cells, and C) tumorigenic line 104Cl cells. *Bar* = 100 µm. × 170

Meeting Highlights

Kaposi's Sarcoma in Homosexual Men

On September 15, 1981, a meeting was convened at the National Cancer Institute (NCI), Bethesda, Maryland, to discuss an apparent epidemic of Kaposi's sarcoma in homosexual men living in New York and California over the past 2 years. This conference was sponsored jointly by the Division of Cancer Treatment, NCI, and the Communicable Disease Centers (CDC), Atlanta, Georgia.

Kaposi's sarcoma was first described in 1872 as a rare, multicentric, pigmented sarcoma of uncertain histogenesis, commonly found among older men of Jewish, Italian, or Eastern European origin. It was later discovered to be endemic in parts of tropical Africa. More recently, a large excess of Kaposi's sarcoma was noted among renal allograft recipients and other immunosuppressed patients. Since 1979, the CDC reported over 70 cases of Kaposi's sarcoma among homosexual males, many of whom are profoundly immunodeficient and are afflicted with opportunistic infections such as *Pneumocystis carinii* pneumonia. The NCI–CDC meeting focused on the "state of the art" of clinical features, epidemiology, etiology, and treatment of Kaposi's sarcoma.

Histologically, the tumor consists of spindle cells, some containing vascular "slits," with an admixture of lymphocytes. Monomorphic or anaplastic patterns are also described; the anaplastic pattern correlates with more aggressive clinical lesions. Kaposi's sarcoma in endemic areas of Africa follows several clinical patterns: a lymphadenopathic type, common in childhood; a nodular type, characteristically subcutaneous and indolent; a "florid" or sarcomatous type, showing aggressive local behavior; and an infiltrative, deeply invasive type. In nonendemic areas, Kaposi's sarcoma first appears as bluish cutaneous nodules, patches, or plaques.

The varied clinical appearance and course of Kaposi's sarcoma do not adapt well to classical staging systems. At the NCI meeting, a staging scheme was adopted that encompasses all cases, whether endemic, nonendemic, or epidemic. Anatomic distribution defines two categories: local–regional or generalized. Clinical behavior in each category may be "indolent" or "aggressive," features that reflect disease tempo and progression.

The consensus as to treatment was that local–regional cases should be treated with radiotherapy, while patients with generalized disease require chemotherapy with the use of single agents (e.g., Velban or a trial of VP-16 vs. ICRF-187) for indolent tumors or combination chemotherapy for aggressive tumors. Because of the favorable chemosensitivity of this tumor, two non-cross-resistant regimens were selected: dactinomycin, dacarbazine, and vincristine, alternating every 3 weeks with doxorubicin, Velban, and bleomycin.

Data associating Kaposi's sarcoma with cytomegalovirus (CMV) were reviewed. Five of 8 tissue cultures of African biopsy specimens disclosed a CMV-like virus on electron microscopy. Compared to controls, African patients do not show elevation of CMV antibody titers, but control levels are high anyway, possibly obscuring a difference. Seroepidemiology in European patients, however, revealed a strong association with CMV antibody elevation. Studies of allograft recipients receiving immunosuppressive therapy and of homosexual males with Kaposi's sarcoma also reveal high antibody titers to CMV. The most compelling link was the detection of the CMV-related antigen in 7 of 31 African tumor biopsy specimens and in 4 of 12 tumor cell lines and CMV–DNA homology in 3 of 8 tumor biopsy specimens. Since CMV has oncogenic potential in vitro, its association with human neoplasia, both in endemic and epidemic cases, needs more study.

Epidemiologic data disclose two recent patterns associated with the risk of Kaposi's sarcoma. One is an acquired immunodeficiency syndrome, characterized by multiple opportunistic infections, anergy, and in extreme cases, a "wasting" syndrome. *Pneumocystis carinii* is a particularly prominent pathogen, reported in 54 homosexual men over a 4-year period. Fourteen additional patients with *Pneumocystis carinii* pneumonia also had Kaposi's sarcoma. The pathogenesis of this apparently sex-linked immunodeficiency syndrome is not known. Postulated mechanisms include CMV infection (perhaps a strain that is tropic for T-lymphocytes) or adverse effects of inhaled or ingested drugs on the immune system.

The second risk feature is the use of nitrite inhalants among homosexual men. Up to 88% of Kaposi's sarcoma patients report regular use of isobutyl or amyl nitrite inhalants; the frequency of use parallels the number of sex partners. Possibly, the excessive use of nitrites in recent years accounts for the epidemic of Kaposi's sarcoma: Inhaled nitrites could combine with secondary amines to form highly carcinogenic nitrosamines that act on capillary endothelium to produce mutations and neoplastic transformation. In the setting of profound immunodeficiency, neoplasia would proceed unchecked by normal immunosurveillance mechanisms. It is further possible that the inhaled nitrites are in some way directly toxic to pulmonary macrophages, increasing local susceptibility to opportunistic pulmonary infection.

The workshop concluded with a number of recommendations. First, the coordination of investigations was essential and should be centralized by NCI. Representatives from the major epidemic areas, New York and California, agreed to collaborate on the epidemiology (through the CDC) and treatment programs (through the cooperative groups). Communications and procedures were established to study virologic and serologic aspects of Kaposi's sarcoma patients and controls. Various clinical and laboratory immunologic studies were proposed. Dr. William DeWys, Chief, Clinical Investigations Branch, Cancer Therapy Evaluation Program, Division of Cancer Treatment, NCI, agreed to coordinate the NCI activities, and Dr. James Curran, CDC, will manage the epidemiologic aspects. The epidemic of Kaposi's sarcoma in homosexual men is an "accident of nature" that requires prompt clinical attention to the victims and affords a unique opportunity to study a rare tumor.

JOHN L. ZIEGLER, *M.D.*
Associate Chief of Staff for Education
Veterans Administration Medical Center
San Francisco, California 94121

Monoclonal Antibodies and Breast Cancer

The Diagnosis Working Group of the Breast Cancer Task Force, National Cancer Institute (NCI), sponsored a workshop on the use of monoclonal antibodies in breast cancer on June 29, 1981, in Bethesda, Maryland. The purpose of the workshop was to determine whether monoclonal antibodies are available that can assist physicians in establishing a diagnosis of breast cancer or in estimating prognosis. We were also interested in learning about the major advances and in determining which areas needed further stimulation. The workshop proved especially informative since most of the work presented had not been published. In addition, the workshop helped to foster communication between investigators making monoclonal antibodies and pathologists who would ultimately use them.

Investigators have used a variety of approaches for producing monoclonal antibodies that react with malignant or normal breast tissue. One approach was to use antigens known to be present on breast cancer cells, such as estrogen receptor(s) (ER) (G. Greene, University of Chicago, Chicago, Ill.) or histocompatibility antigens (S. Ferrone, Scripps Clinic and Research Foundation, La Jolla, Calif.). Another approach has been to use whole cells or the membrane fractions as antigens. One group used membrane fractions from liver metastases (J. Schlom, NCI), while others (Z. Steplewski, The Wistar Institute, Philadelphia, Pa.; D. Yuan and F. Hendler, University of Texas Southwestern Medical School, Dallas, Tex.; K. Grzyb, University of Texas Health Science Center at San Antonio, San Antonio, Tex.) preferred cell lines because of their accessibility and reproducibility. One problem, however, associated with the use of cell lines is the loss of some antigens during prolonged passage (Schlom; R. Ceriani, Children's Hospital Medical Center, Oakland, Calif.). For example, one of Schlom's monoclonal antibodies reacts with MCF-7 cells, but only up to passage 319, while another monoclonal antibody no longer reacts with MCF-7 after passage 317. A third approach taken by J. Hilgers (The Netherlands Cancer Institute, Amsterdam, The Netherlands) and Ceriani was to use milk fat globules as the immunogen. These milk fat globule antigens are produced by cells that have reached the most highly differentiated state and therefore may be useful markers for differentiation.

The importance of using multiple assays to screen and characterize monoclonal antibodies was emphasized by J. D. Minna (NCI–Veterans Administration Medical Oncology Branch, Washington, D.C.). Since several thousand hybridoma supernatants must be screened to obtain only a few interesting monoclonal antibodies, the initial screening assay should test several hundred supernatants rapidly and reproducibly. Most investigators preferred a solid-phase assay in which the binding of monoclonal antibody to antigen was detected by either an enzyme-linked second antibody or iodinated protein A.

In addition to screening monoclonal antibodies for binding to cells, several investigators tested monoclonal antibodies for other properties. For instance, some monoclonal antibodies were screened by Schlom for antibody-dependent cellular cytotoxicity to determine which antibodies may be useful for immunotherapy. Ferrone uses only monoclonal antibodies that identify antigens by immunoprecipitation so that there is no question about the antigen under study. Minna is measuring antibody against tumor-associated antigens in human sera by inhibition of the binding of monoclonal antibody. The assay can detect as little as 7–10 ng of antibody.

Of greatest interest to pathologists were the patterns of reactivity on tissue sections. These were revealed by several common immunohistochemical methods—fluorescence, peroxidase, or avidin–biotin-coupled systems. Yuan and Hendler have developed an assay utilizing iodinated monoclonal antibodies to measure their binding to tissue sections. By this method over a hundred tissue sections can be assayed overnight, and several observers can assess the results simultaneously.

As one would expect, the method of fixation is very important for the binding of monoclonal antibodies to tissue sections. Only some antigens recognized by monoclonal antibodies survive Formalin fixation, which is unfortunate since it will limit retrospective studies with stored Formalin-fixed tissues. B-5, a mercuric chloride Formalin fixative (R. Cardiff, University of California at Davis, Davis, Calif.), ethanol on frozen sections (L. Pertschuk, Downstate Medical Center, Brooklyn, N.Y.), and B-5 plus Bouin's fixative (M. Nadji, University of Miami, Miami, Fla.) were all superior to Formalin. Zenker's and Bouin's fixatives tended to displace the antigens into the cytoplasm, even those that were located along the cell surface in frozen sections. Because of the vagaries of fixation, it may be advisable to use frozen tissue for immunocytochemical staining.

None of the investigators were able to produce a monoclonal antibody that reacted exclusively with breast cancer. The patterns of cross-reactivity with normal tissues and other tumors varied with each monoclonal antibody and were unpredictable. Some monoclonal antibodies obtained by Schlom reacted with a majority of malignant breast tumors, whereas others reacted with only certain cells of some cancers other than breast cancers. None of the monoclonal antibodies tested reacted with the cell surface of melanomas or sarcomas, which is not unexpected in view of the epithelial origin of breast carcinomas. Many monoclonal antibodies, however, reacted with various carcinoma cell lines, especially those derived from the colon. Whether this indicates broad antigenic overlap between colon and breast carcinomas remains to be determined. Some monoclonal antibodies reacted with the cytoplasm or secreted proteins of certain breast biopsy specimens as detected by immunoperoxidase staining.

One monoclonal antibody also stained sweat glands, which is not surprising in view of the embryologic origin of the mammary glands. Perhaps this monoclonal antibody will be useful in the diagnosis of sweat gland tumors. Some monoclonal antibodies that reacted against breast cancer tissue also reacted with the normal epithelium adjacent to the tumor. Schlom suggested that this could be the result of adsorption of shed tumor antigens, preneoplastic changes in adjacent epithelium, or production of some factor by the tumor that stimulated the normal tissue to express this antigen. Cardiff mentioned that because of the sensitivity of tissue sections, one positive cell in 10^6 could be detected. Thus a monoclonal antibody that appeared to be very specific by routine binding assays could show a much wider reactivity on tissue sections. Hilgers reminded the audience that one of the first differentiation antigens to be discovered, i.e., theta for thymocytes, is also present in brain tissue. Furthermore, this antigen can be detected in the stroma of mammary and colon tissues.

It will be very surprising if antigens are discovered that are present on only cancerous breast tissue. More likely, what will be found are antigens present on several tissues, but there will be quantitative differences in the expression of these antigens. The monoclonal antibodies will appear to be more specific the less sensitive the assay system. It is also possible that some monoclonal antibodies that bind to both benign and malignant breast tumors may indicate a better prognosis, since this overlap may mean that a high proportion of differentiated cells is present in the malignant tumors (Yuan and Hendler).

It was suggested that some of the cross-reactions seen with other tumor tissues may indicate a common cell within the tumors. For instance, Minna reported a monoclonal antibody that reacted with small cell carcinoma of the lung in addition to breast carcinoma, and Schlom found that many of his monoclonal antibodies against breast cancer also reacted with colon cancer. This phenomenon is possible if a common cell, such as an uncommitted stem cell, is present in many tumors.

Heterogeneous reactivity of tumor cells has been previously observed with xenogeneic antisera, but there was always some doubt that this represented true heterogeneity, because of the possible polyspecificity of the xenoantibodies. This heterogeneity has now been firmly established by monoclonal antibodies. In fact, this may be an important contribution of monoclonal antibodies to our understanding the nature of neoplasia. This heterogeneity was observed in different ways. For example, monoclonal antibodies may react with only some cells in the primary tumor or not with all metastatic foci in lymph nodes (Cardiff and Ceriani). There is heterogeneity in cell lines as well, even after cloning (Ceriani). Some variations in staining may not be the result of true heterogeneity, but rather the differential expression of antigens during the cell cycle or loss of antigens after many mitoses. Tumor cell lines are heterogeneous with respect to both stain intensity and size after analysis in the fluorescence-activated cell sorter (Schlom and collaborators; Yuan and Hendler).

Some of the antigens reacting with monoclonal antibodies have been characterized by immune precipitation and sodium dodecyl sulfate polyacrylamide gel electrophoresis (Schlom, Ferrone, and Hilgers). These antigens range from 30,000 to over 200,000 daltons. Yuan and Hendler identified an antigen on two-dimensional gel electrophoresis that was composed of two chains of 30,000 daltons, each chain with a different pI. Clearly, monoclonal antibodies will be valuable tools for the purification and characterization of tumor-associated antigens.

Ferrone studied the expression of the human histocompatibility antigens (HLA-A, HLA-B, HLA-C, and HLA-DR) on breast tumor cells. It has been shown in other systems that cells undergoing malignant transformation exhibit quantitative and sometimes qualitative changes in the expression of these antigens. In addition, evidence indicates that there may be an association of histocompatibility antigens with some tumor antigens.

The following patterns were seen with breast cancer cell lines. The monoclonal antibody against HLA-A, HLA-B, and HLA-C heavy chain was positive with all cell lines tested, but there were quantitative differences among the cell lines. There was an excess of β_2-microglobulin compared to the HLA heavy chain on some breast tumors, especially on infiltrating ductal carcinomas, lobular carcinomas, and tubular carcinomas, but not on medullary carcinomas. The Ia-like monoclonal antibody that reacts with melanoma cells was negative on three breast cell lines and weakly positive on two cell lines. The monoclonal antibody directed against the 85,000-dalton component that is present on melanomas and lymphocytes was present on all breast cell lines, but the degree of reactivity varied widely. The 94,000 component that is present on melanomas and absent on lymphocytes was present on only some breast cell lines, and the amount of antigen present varied with each cell line. The high-molecular-weight antigen that is found on melanomas was absent on lymphocytes and all breast cell lines tested.

M. Unger (The Salk Institute, La Jolla, Calif.) has obtained several monoclonal antibodies against rat mammary differentiation antigens. Two of these also reacted with normal rat ovary. These monoclonal antibodies may be useful for the study of normal differentiation antigens in other tissues in addition to the mammary gland.

Monoclonal antibodies prepared against ER can provide a more sensitive and reproducible assay for evaluating the ER status of breast cancer (Greene). The assay consists of a monoclonal antibody directed against one epitope on the receptor as a bridge between a plastic surface and the receptor and a second, radiolabeled monoclonal antibody against a different epitope to measure the amount of ER bound and thus the amount of receptor present in the cytosol. The assay, which is as sensitive as current biochemical methods, is simpler to perform and does not require labeled estrogen.

Pertschuk and Nadji are using these monoclonal antibodies to localize ER with either fluorescence or peroxidase staining. The method of tissue fixation is very important for preservation of the reaction of the monoclonal antibody with the hormone receptors. Slow dehydration in ethanol appears to be optimal in Pertschuk's laboratory. Heterogeneity of staining is commonly observed, as mentioned by previous speakers. In fact, fixation adds another variable over and above the heterogeneity. In a retrospective study, 23 tumors were ER-positive by immunohistochemical and biochemical measurements, 20 were negative by both methods, 6 were negative by fluorescence but positive by biochemical methods, and 4 were the reverse. In a prospective study, 28 were positive by both methods, 2 negative by both methods, 5 negative by fluorescence and positive by biochemical methods, and none the reverse.

Our ability to assess the ER status directly on tissues will become more important as smaller tumors are detected and sample size is limited. We should also be able to assess the ER status of needle aspirates, bone biopsy specimens, and pleural effusions. The proportion of normal or necrotic tissue to the tumor mass can be visualized directly in histological sections, which is an advantage, especially when ER concentration is measured on a unit per weight basis in cytosols. Yuan and Hendler have an interesting monoclonal antibody that binds only to cells that have a cytoplasmic ER, but the monoclonal antibody is directed against a cell surface component.

S. Halter (Vanderbilt University, Nashville, Tenn.) described a retrospective study of stage II mammary carcinomas evaluated for the association of either carcinoembryonic antigen or pregnancy-specific β_1-glycoprotein with survival. Since there was no correlation with survival, she concluded that monoclonal antibodies directed against other oncofetal antigens may be more useful for assessing prognosis.

W. L. McGuire (University of Texas Health Science Center at San Antonio) led the general discussion on the usefulness of monoclonal antibodies for detection and treatment of breast cancer. One concern expressed by all discussants was the heterogeneity of breast cancer cells, which seems to preempt the use of a single monoclonal antibody for diagnostic or therapeutic purposes. There was agreement that a mixture, or a cocktail, of monoclonal antibodies directed against many antigens will be necessary for treatment. It was also noted that some cytotoxic monoclonal antibodies will kill tumors if these antibodies are injected as late as 6 days after tumor implantation in mice.

However, in vivo killing has not been observed with ricin-conjugated antibody, presumably because of dissociation, although cells are killed in vitro by the complex. Chemical modification of the ricin A- and B-chains is being tried as a means to stabilize the conjugate in vivo. It was also suggested that a monoclonal antibody be used to isolate the antigen of interest and that the isolated antigen be used to produce xenoantisera against all epitopes on the antigen.

Results with the use of the monoclonal antibodies for imaging have been disappointing, but several groups are working to improve the technology, especially in the search for an isotope that is better than iodine-131.

P. E. Fast (The Upjohn Co., Kalamazoo, Mich.) and H. Battifora (City of Hope National Medical Center, Duarte, Calif.) summarized the workshop. Both believed that the available monoclonal antibodies will improve our understanding of the biology of breast cancer. Some will even prove useful for identifying breast cancer cells and for estimating prognosis. More research is needed to determine whether any of the monoclonal antibodies can detect an antigen present in serum that would be diagnostically useful. Frozen tissue banks may be necessary for retrospective studies, since many monoclonal antibodies do not react on Formalin-fixed tissues.

The general status of the field was best summarized by Hilgers who stated that we are now in an optimistic period. However, there are many details that must be worked out. It will take some time to sort out the data before we reach a more realistic period, when monoclonal antibodies can be applied to practical problems.

A feeling of optimism pervaded the workshop. All seemed to recognize that monoclonal antibodies have given us a new Kismet but that heterogeneity was swift to inflict retribution.

Marianne L. Egan, *Ph.D.*
Chairperson, Diagnosis Working Group
Breast Cancer Task Force
Department of Microbiology
University of Alabama in Birmingham
Birmingham, Alabama 35294

Donald E. Henson, *M.D.*
Chief, Diagnostic Projects Section
Breast Cancer Task Force
Division of Cancer Biology and Diagnosis
National Cancer Institute
National Institutes of Health
Public Health Service
U. S. Department of Health and Human Services
Bethesda, Maryland 20205

Announcements

The Journal *will publish notices of major meetings dealing with cancer. Submission of notices 6 months in advance is requested to permit timely publication.*

National Toxicology Program Conference

The National Toxicology Program of the U.S. Department of Health and Human Services will sponsor this conference entitled "Photobiologic, Toxicologic, Pharmacologic, and Therapeutic Aspects of Psoralens" to be held at the National Institutes of Environmental Health Science, Research Triangle Park, North Carolina, on March 1–3, 1982. The meeting will cover the basic and clinical aspects of psoralen photochemotherapy with special emphasis on psoralen photochemistry, interactions of psoralens with DNA, RNA, and proteins, acute and chronic toxicity, mutagenicity, carcinogenicity, structure and photosensitivity activity relationship, and clinical responses of various psoralens in relationship to photochemotherapy of psoriasis and vitiligo.

For additional information please contact Dr. Madhu A. Pathak at the Department of Dermatology, Harvard Medical School, Massachusetts General Hospital, Boston, Massachusetts 02114 (telephone: 617-726-3996) or Dr. June K. Dunnick at the National Toxicology Program, NIEHS, Research Triangle Park, North Carolina 27709 (telephone: 919-541-4811).

Latest NCI Monographs Published

Monograph No. 56: *Sarcomas of Soft Tissue and Bone in Childhood*: Topics presented and discussed during this Symposium included recent developments in diagnosis and treatment of rhabdomyosarcomas and Ewing's sarcoma, based on Intergroup studies and those at other medical centers here and abroad. Various aspects were covered: evaluation, epidemiology, pathology, psychological support of patients, surgical treatment, immunotherapy, and multimodal therapy. GPO Stock No.: 017-042-00150-1. Price: $14.00 in the United States, Canada, and Mexico; $17.50 elsewhere (includes mailing charges).

Monograph No. 57: *Surveillance, Epidemiology, and End Results Program: Incidence and Mortality Data: 1973–1977.* This volume provides detailed tabular information on the incidence of and mortality from cancer in 11 representative areas of the United States during the initial 5 years of the SEER Program. Data are classified according to the sex, race, age, and residence of the patient; anatomic site; and histologic type of cancer. An introduction explains the goals and operation of the SEER Program as well as the organization and presentation of the data. Tables for each SEER area are also introduced by the persons responsible for reporting the data. GPO Stock No.: 017-042-00156-1. Price: $23.00 in the United States, Canada, or Mexico; $28.75 elsewhere (includes mailing charges).

NOTE: Errata on pages 982–983, Appendix Table I, have been brought to our attention: Numbers of deaths are double the correct numbers. The rates are correct as given.

Other Monographs Available

No. 41: A limited number of the Third National Cancer Survey: Incidence Data were located and can now be ordered from the Government Printing Office. GPO Stock No.: 017-042-00180-1; price $11.50 ($14.40)*

No. 49: Workshop on Genitourinary Cancer Immunology; GPO Stock No. 017-042-00133-1; price $11.85 ($15.80)

No. 50: International Conference on Ultraviolet Carcinogenesis (soft cover only); GPO Stock No. 017-042-00149-8; price $7.70 ($9.60)

No. 51: Perinatal Carcinogenesis (soft cover only); GPO Stock No. 017-042-00146-3; price $7.70 ($9.60)

No. 52: Aspects of Cancer Research 1971–1978: Editorials from the Journal of the National Cancer Institute; GPO Stock No. 017-042-00140-4; price $14.30 ($17.90)

No. 53: Second Symposium on Epidemiology and Cancer Registries in the Pacific Basin; GPO Stock No. 017-042-00142-1; price $8.25 ($10.30)

No. 54: The Occurrence of Tumors in Domestic Animals; GPO Stock No. 017-042-00145-5; price $9.35 ($11.70)

No. 55: Experimental Evaluation of Antitumor Drugs in the USA and USSR and Clinical Correlations; GPO Stock No. 017-042-00144-7; price $12.10 ($15.10)

Send orders to Superintendent of Documents, U.S. Government Printing Office, Washington, D.C. 20402. Be sure to include title and stock number of volume desired. Payment is required in advance; make check or money order (foreign or domestic) payable to Superintendent of Documents. Please **DO NOT SEND** orders to the Editorial Office or the National Cancer Institute.

*Prices *in parentheses* are for countries other than the United States, Canada, or Mexico.

☆U.S. GOVERNMENT PRINTING OFFICE: 1982-361-145/51

blank page

JNCI (NIH Publication No. 82-13)

68/3

NEWARK PUBLIC LIBRARY

APR 20 1982

U. S. GOV'T DEPOSITORY

JNCI Journal of the National Cancer Institute

March 1982
Volume 68
Number 3

U.S. DEPARTMENT OF HEALTH AND HUMAN SERVICES   Public Health Service   National Institutes of Health

Number 3   PP. 343-[illegible]   March 1982

HE 20. 3161:

The photomicrograph on the cover shows immunofluorescence of cytoskeletal filaments in a human cell line from a poorly differentiating cutaneous squamous cell carcinoma. In the indirect immunofluorescence test, antibodies against bovine keratin decorated a three-dimensional network of fiber (*see* paper by Boukamp et al. on pages 415–427).

JNCI

Journal of the National Cancer Institute

March 1982
Volume 68
Number 3

THE JOURNAL of the National Cancer Institute solicits manuscripts on original observations in laboratory and clinical research from all scientists. A manuscript is considered for publication with the understanding that it has not been published previously and is submitted exclusively to the Journal. Opinions expressed by the authors are not necessarily those of the publisher or its editors.

THE JOURNAL is published monthly (two volumes a year). The Secretary of Health and Human Services has determined that the publication of this periodical is necessary in the transaction of the public business required by law of this Department.

A MONOGRAPH SERIES covering proceedings of scientific meetings pertaining to cancer is also published. These books may be purchased from the Superintendent of Documents. Series subscriptions are not available and monographs are not included in a subscription to the Journal.

THE JOURNAL is for sale by the Superintendent of Documents, U.S. Government Printing Office, Washington, D.C. 20402. Price per copy, $6.00. Subscription price for two volumes per year in the United States, $65.00; foreign, $81.25. Payment is required in advance, and check or money order should be made payable to the Superintendent of Documents.

All inquiries regarding purchase of subscriptions or depository library distribution, including inquiries about missing issues and change of address, should be addressed to the Government Printing Office. The Government Printing Office requires payment in advance on all orders. Inquiries regarding missing issues or change of address for official subscriptions should be addressed to the Editorial Office, Room 850, Westwood Building, 5333 Westbard Avenue, Bethesda, Md. 20016.

VINCENT T. DEVITA, JR., *Director, National Cancer Institute*

BOARD OF EDITORS

PETER GREENWALD, *Editor in Chief*

ELIZABETH K. WEISBURGER, *Assistant Editor in Chief*

STUART A. AARONSON, *Associate Editor*

CHARLES H. EVANS, *Associate Editor*

MARY A. FINK, *Associate Editor*

JANET W. HARTLEY, *Associate Editor*

DONALD HENSON, *Associate Editor*

RONALD B. HERBERMAN, *Associate Editor*

GEORGE S. JOHNSON, *Associate Editor*

KURT W. KOHN, *Associate Editor*

ARTHUR S. LEVINE, *Associate Editor*

JOHN J. MULVIHILL, *Associate Editor*

ALAN S. RABSON, *Associate Editor*

RICHARD M. SIMON, *Associate Editor*

EDITORIAL STAFF

EDWIN A. HAUGH, *Managing Editor*

PAMELA T. ALLEN, *Assistant Managing Editor*

FLORENCE I. GREGORIC, *Monograph Editor*

Editors: DOROTHY D. KATZ, MERCEDES B. LA CHARITY, I. AGNES REVESZ, JOAN O'BRIEN RODRIGUEZ, CONSTANCE R. STONESTREET, and ANNA B. WITTIG

JNCI (NIH Publication No. 82-13)

U.S. DEPARTMENT OF HEALTH AND HUMAN SERVICES   Public Health Service   National Institutes of Health

Instructions to Authors

Text: Send one original and two copies. **Text-figures** (graphs, charts, and line drawings): Send one original and two copies. **Figures** (photomicrographs and photographs): Send three original glossy prints, unmounted. **Tables:** Send tabular material in typewritten form; do not submit tables as glossy prints to be photographed. The entire manuscript including footnotes, legends, and references must be typed double spaced. Single-spaced portions of a manuscript will be returned to the author for retyping. The mailing address is: Journal of the National Cancer Institute, Westwood Building, Room 850, 5333 Westbard Avenue, Bethesda, Maryland 20016.

Manuscripts should be accompanied by a covering letter from the author responsible for correspondence about the manuscript. The covering letter should contain a statement that the manuscript has been seen and approved by all authors and that all persons listed as authors have made significant (not merely administrative, technical, or supervisory) contributions to the content of the paper. The letter should also state that the manuscript or substantial portions thereof have not been previously published nor are they under consideration for publication in another journal.

Data too extensive for inclusion in a manuscript, but which may be of interest to other investigators, may be deposited with the National Auxiliary Publications Service (NAPS), c/o Microfiche Publications, P.O. Box 3513, Grand Central Station, New York, New York 10017. Authors using the NAFS facilities should indicate in a footnote how their additional data may be obtained.

TITLE: Be brief (no more than 14 words, if possible), but for indexing purposes include all key words. The annual subject index is prepared directly from the titles. Titles that form complete sentences are not acceptable. Do not use abbreviations or chemical formulas in titles.

BYLINE: Supply the complete first name, middle initial, and last name of each author. Avoid use of nicknames. Academic degree is optional; however, if a degree is provided for one author, it should be provided for all authors on a manuscript. Include the name of the institution, address, and zip code for each author. Indicate address for reprint requests in a footnote on the byline.

ACKNOWLEDGMENTS: Financial aid in support of research should be recognized in a footnote. Aid in technical fields, animal care, photography, stenography, and other areas may be mentioned in a separate footnote. Indicate the title (Dr., Mr., Mrs., Miss, Ms.) and affiliation of each person acknowledged.

ABSTRACT: Provide an abstract, 150 words or less, on a separate page. The abstract should describe only *results* of the work being reported. Speculation, historical background, or reference to published works will be deleted from abstracts. Any inbred strains, noninbred stocks, cell lines, or other living materials used in the work should be noted in the abstract.

TEXT: Avoid the use of laboratory jargon and abbreviations not in common usage. When possible, refrain from the use of abbreviations that form words (exceptions are PAGE, ALL). Whenever possible, write mathematical equations and chemical formulas on a single line; submit complicated chemical structures as artwork. Avoid repetition of data in the text when it is presented in tables or text-figures.

Use the following style sources: Webster's *Third New International Dictionary* and Dorland's *Illustrated Medical Dictionary* (25th ed) for spelling; *Council of Biology Editors Style Manual* (4th ed) for scientific abbreviations and symbols: *Government Printing Office Style Manual* for other abbreviations and symbols, punctuation, and hyphenation; *Biochemical Nomenclature and Related Documents* (IUB, 1978) for abbreviations of chemical substances; *Enzyme Nomenclature*, recommendations (1978) of the IUB for recommended names of enzymes and information on nomenclature of isozymes; *The Merck Index* (9th ed) for chemical compounds; "Standard Nomenclature for Inbred Strains of Mice: Seventh Listing" by Joan Staats (Cancer Res 1980;40: 2083-2128) for inbred mouse strains; "Standardized Nomenclature for Inbred Strains of Rats: Fourth Listing" by Joan Staats and Michael Festing (Transplantation 1973;16:221-245) for designations of inbred rat strains; *Animals for Research* (9th ed) prepared by the Institute of Laboratory Animal Resources, National Academy of Sciences, for designations of laboratory animal stocks and strains.

TABLES: Submit tabular material typed double spaced on a separate page. Computer print-outs of tables are acceptable only if they are double spaced and with satisfactory title, column headings, legends and other textual material. Provide headings for all columns of a table and indicate units of measurement where applicable.

TEXT-FIGURES: Refer to graphs, charts, and line drawings as text-figures. Make the abbreviations on text-figures identical to the abbreviations used in the text and legends. Symbols and lettering should be large enough to be legible if reduced. Glossy prints or original drawings in black ink are acceptable; orient vertically instead of horizontally.

FIGURES: Refer to photomicrographs and photographs as figures. Figures and their legends should fit a 7.5- by 9-inch dimension. Calculate that nine typewritten lines of legend will require 1 inch of vertical space. Type figure legends on a separate sheet and identify in the legend any lettering used on the figure. Trim photographs to show only important areas. Do not number face of photographs; use the back or overlay to indicate the top and number of each. Printed indicators may be included on photographs; do not use hand-drawn indicators. *Insert internal scale markers on all photomicrographs.* Color photographs must be grouped as a single plate. For color reproduction, submit both color transparencies and high-quality black and white reproductions. The need for color must be documented before it will be considered.

REFERENCES: Use any recent issue of the Journal as a style guide for reference lists. Number references in order of citation in both text and reference list. For periodicals, provide author(s), title of paper, journal, year, volume, and first and last page numbers. For books, give the author(s), title, name(s) of editor(s), location and name of publisher, year, pertinent chapter or section title, and page numbers. Follow *Index Merdicus* for punctuation and abbreviations. Citations of papers in preparation or submitted for publication, unpublished observations, and personal communications should be noted parenthetically in the text. Do *not* include them in the reference list. The accuracy of all references is the responsibility of the authors and not of the editorial staff.

LETTERS TO THE EDITOR should pertain to recent articles in the Journal and should not contain new data unless relevant to the discussion of a particular paper. The authors addressed will be invited to reply to comments before correspondence is published. Letters will be edited by the Staff, subject to contributor approval.

FURTHER DETAILS on the preparation of manuscripts are set forth in the document "Uniform Requirements for Manuscripts Submitted to Biomedical Journals" prepared by the International Steering Committee of medical editors (*see* Am Rev Respir Dis 1979;119:3-10/Ann Intern Med 1979;90:95-99/Br Med J 1979;1:532-535/ or Lancet 1979;1:428-430).

UNITED STATES GOVERNMENT PRINTING OFFICE, WASHINGTON, D.C.: 1982

Table of Contents

Vol. 68, No. 3——March 1982

Guest Editorial

343	What are isozymes telling us about gene regulation in cancer?	*Sidney Weinhouse*

Investigations on Man

351	Single oblique-view mammography for periodic screening for breast cancer in women	*Bengt Lundgren, Anders Helleberg*
357	Observer variation in the interpretation of xeromammograms	*Norman F. Boyd, Christina Wolfson, Myron Moskowitz, Thomas Carlile, Michel Petitclerc, Helen A. Ferri, Eve Fishell, Andre Gregoire, Matthew Kiernan, J. Donald Longley, Imre S. Simor, Anthony B. Miller*
365	Multiple cell lines from patients with malignant melanoma: Morphology, karyology, and biochemical analysis	*Toni U. Semple, George E. Moore, Robert T. Morgan, Linda K. Woods, Laurie A. Quinn*
381	Prolactin receptors in human breast tumors	*Lucile Turcot-Lemay, Paul A. Kelly*
385	Tumor promoter 12-O-tetradecanoylphorbol 13-acetate: Effect on complement and Epstein-Barr virus receptors in human lymphoblastoid cell lines	*Naoki Yamamoto, Takashi Mitsuma, Arnold Vogt*
391	Cerebrospinal fluid levels of 2′-deoxycoformycin after systemic administration in monkeys	*Julie Blatt, Peter M. Venner, Riccardo Riccardi, Lawrence F. Cohen, Daimon Gangji, Robert I. Glazer, David G. Poplack*
395	Smoking history and lung cancer survival in women	*M. Ward Hinds, Hong-Yi Yang, Grant Stemmermann, James Lee, Laurence N. Kolonel*
401	Intestinal metaplasia in Japan: Association with diet	*Abraham Nomura, Hiroshi Yamakawa, Takuzo Ishidate, Sigetosi Kamiyama, Hisayuki Masuda, Grant N. Stemmermann, Lance K. Heilbrun, Jean H. Hankin*
407	Basis for the differential action of aminonucleoside on normal and transformed human fibroblasts	*Ernest A. Albanese, George P. Studzinski*
415	Phenotypic and genotypic characteristics of a cell line from a squamous cell carcinoma of human skin	*Petra Boukamp, Wolfgang Tilgen, Rule T. Dzarlieva, Dirk Breitkreutz, Dietrich Haag, Rüdiger K. Riehl, Axel Bohnert, Norbert E. Fusenig*
429	Epidemiological features of Wilms' tumor: Results of the National Wilms' Tumor Study	*Norman E. Breslow, J. Bruce Beckwith*
437	Growth and characterization of childhood rhabdomyosarcomas as xenografts	*J. A. Houghton, P. J. Houghton, B. L. Webber*

445 Intrastage prognostic heterogeneity: Implications for adjuvant chemotherapy of breast cancer — *Maurice M. Black, Benjamin F. Hankey, Thomas H. C. Barclay*

Investigations on Nonhuman Systems

449 Morphology and function of ganglio-*N*-tetraosylceramide-positive lymphocyte mediators of natural killer activity — *Kazuo Shimamura, Sonoko Habu, Hiroyasu Fukui, Akira Akatsuka, Ko Okumura, Norikazu Tamaoki*

457 Friend erythroleukemia virus complex: Role of viral components in modifying erythroid differentiation in mice — *Barbara Fagg, Wolfram Ostertag*

461 Growth and spontaneous regression of swine melanoma: Relationship of in vitro leukocyte reactivity — *Jane Berkelhammer, Bonnie M. Ensign, Reuel R. Hook, Jr., Cynthia J. Hecker, Gerald D. Smith, Ronald W. Oxenhandler*

469 Ganglioside changes induced by tumor promoters in promotable JB6 mouse epidermal cells: Antagonism by an antipromoter — *Leela Srinivas, Nancy H. Colburn*

475 Microcirculatory blood flow, capillary morphology, and local oxygen pressure of the hamster amelanotic melanoma A-Mel-3 — *Bernhard Endrich, Frithjof Hammersen, Alwin Götz, Konrad Messmer*

487 Effect of rate of heating on lethality due to hyperthermia and selected chemotherapeutic drugs — *Terence S. Herman, Cynthia C. Sweets, David M. White, Eugene W. Gerner*

493 Glutathione *S*-transferase activity: Enhancement by compounds inhibiting chemical carcinogenesis and by dietary constituents — *Velta L. Sparnins, Placida L. Venegas, Lee W. Wattenberg*

497 Organ-specific promoting effects of phenobarbital sodium and sodium saccharin in the induction of liver and urinary bladder tumors in male F344 rats — *Keisuke Nakanishi, Shoji Fukushima, Akihiro Hagiwara, Seiko Tamano, Nobuyuki Ito*

501 Serologic analysis of nitrosourea-induced rat gliomas — *Michael Pfreundschuh, Humberto Cravioto, Gerald Hochwald, Joseph Ransohoff*

507 Development and biologic properties of malignant cell sublines and clones of a spontaneously metastasizing rat mammary adenocarcinoma — *Anthony Neri, Dan Welch, Takanori Kawaguchi, Garth L. Nicolson*

519 Temperature gradients and local perfusion in a mammary carcinoma — *Pietro M. Gullino, Rakesh K. Jain, Flora H. Grantham*

Correction

535 November 1981, Vol. 67, No. 5, page 991: Letters to the Editor, "BCG and Cancer" (reply) — *George W. Comstock*

Announcements

535 Harvard Medical School Continuing Education Program

535 Aspirin Foundation of America

535 Cancer Management 1982

535 World Symposium on Asbestos

535 First International Symposium on the Endocrine Lung in Health and Disease

535 World Congress of Gastroenterology, Digestive Endoscopy, and Colo-Proctology

536 Annual Course in Advanced Immunology

536 First Conference on Radioprotectors and Anticarcinogens

536 Design and Analysis of Scientific Experiments

536 Veterinary Cancer Society

blank page

Guest Editorial

Sidney Weinhouse[1,2]

What are Isozymes Telling Us About Gene Regulation in Cancer?[3,4]

There is an increasing recognition that cancer is associated with abnormalities of gene regulation, manifested by misprogramming of protein synthesis. Whether or not this phenomenon is causal, consequential, or incidental to the neoplastic transformation, it is interwoven throughout the whole fabric of cancer biology and may therefore be a key to the long-sought molecular basis of neoplasia. It encompasses virtually every means we have of identifying gene products, including antigens, polypeptide hormones, membrane glycoproteins, growth factors, and of course enzymes, the subject of this essay.

Because enzymes constitute the machinery of the cell, they are obvious sites of functional importance in tumor growth and metabolism. For this reason they have been the focus of several generations of biochemical effort which, unfortunately, has resulted in an unwieldy mass of data that have confused rather than illuminated our conceptions of the enzymatic basis of the neoplastic process. Early attempts to relate neoplasia to changes in enzyme activity are highlighted in the enzyme convergence hypothesis of Greenstein (*1*). Potter has spent a lifetime career in a study of the significance of enzyme composition in tumors and recently summarized his ideas as they evolved from the original enzyme deletion hypothesis to his current views on cancer as an aberration of embryonic development (*2*). More recently, Weber (*3*) has brought a degree of order into the relationships between tumor growth rates and enzyme activity. He classified a large number of enzymes, primarily of carbohydrate and nucleotide metabolism, into anabolic and catabolic species and demonstrated a good correlation in liver and kidney neoplasms between ratios of the activities of the so-called anabolic and catabolic enzymes and their growth rates.

ROLES OF ISOZYMES[5]

The development of highly sensitive methods of protein separation and identification led to the realization that many enzymes exist in multiple forms that catalyze the same reaction but differ in chemical and kinetic properties (*4*). The existence of enzymes structured specifically for individual organ function has added a new dimension to our conception of metabolic regulation. Since it is presumed (though not always proved) that isozymes are products of different genes, they provide additionally, elegant opportunities for understanding the genetic basis of metabolic dysfunction. As a result, a renewed interest is being kindled in studies on the enzymatic machinery of the cancer cell, bringing with it the discovery of a host of isozyme alterations in tumors (*5–8*). These studies have had a dual impact—not only have they broadened our insights on the molecular basis of tumor metabolism, but also they have brought isozyme alterations within an already impressive conceptual framework built from a variety of other abnormalities of genetic regulation in cancer.[6]

TWO EXAMPLES OF ISOZYME ALTERATION IN HEPATOMAS

Because of the rich diversity of enzymes catalyzing the many specialized functions of the liver, this organ and its neoplastic counterpart, the hepatoma, are especially advantageous model systems for comparative studies of isozyme composition. Happily also, there are available the Morris hepatomas (*9*), a spectrum of chemically induced, transplantable rat tumors ranging widely in growth rate, degree of differentiation, and in their retention and loss of hepatic functions. Although much of our knowledge of isozyme alterations is thus somewhat narrowly based on the rat liver-hepatoma model, several clearcut isozyme alterations in nonhepatic organ–tumor systems, attest to the generality of this phenomenon.

Aldolase

Aldolase is especially noteworthy because it was the first

---

[1] Fels Research Institute, Temple University School of Medicine, Health Sciences Center, Philadelphia, Pa. 19140.

[2] Thanks are due to Jennie B. Shatton, Albert Williams, and Harold P. Morris for their contribution to this work.

[3] Received September 3, 1981.

[4] The experimental work of the author is supported by Public Health Service grants CA-12227 and CA-10916 from the National Cancer Institute and by grant 74-BC from the American Cancer Society.

[5] A detailed discussion of the definition and properties of isozymes is beyond the scope of this brief essay. The reader is referred to the commission on biochemical nomenclature of the International Union of Biochemistry (Enzyme nomenclature. Amsterdam: Elsevier Sci Publ, 1972:24). The term isozymes is restricted to enzymes that are products of different genes and to heteropolymers thereof, where applicable. The term excludes those enzymes derived by chemical modification or by allosteric modification through interaction with substrates or effectors.

To save space, the reference list is largely confined to review articles, from which references to the primary literature can be obtained.

[6] Isozymes of glucose-6-phosphate dehydrogenase have played an important part in establishing a clonal origin for human tumors (Fialkow PJ. Clonal origin of human tumors. Biochim Biophys Acta 1976; 458:283-321). However, this topic is not covered in this paper.

Editor's note: Periodically, the Journal publishes solicited guest editorials as a means of transmitting to investigators in cancer research the essence of current work in a special field of study. The Board of Editors welcomes suggestions for future editorials that succinctly summarize current work toward a clearly defined hypothesis regarding the causes or cure of cancer.

to have its isozyme composition studied in tumors; and it exemplifies the many other subsequently revealed isozyme alterations in neoplastic tissues. It occurs in cells as a tetramer, the composition of which depends on the relative abundance of the subunit isozymes (*5*). These subunits are denoted as A, B, and C. Isozyme C appears very early in embryonic development and is accompanied, and ultimately replaced to a large extent, by isozyme A in the fetus. Isozyme A persists into adulthood in most organs and is accompanied by isozyme C in adult brain. In contrast, isozyme A, the major form in fetal liver, is essentially replaced completely by isozyme B in the adult liver. The B-isozyme is kinetically geared for two highly specific liver functions: the utilization of fructose and the conversion of triose phosphates to hexose phosphate in the synthesis of glucose.

The first clear-cut demonstration of enzyme alteration in cancer can be credited to Schapira (*5*), who observed a striking change in the properties of serum aldolase in several human diseases. The serum enzyme resembled that of muscle aldolase in some muscular diseases and resembled that of liver aldolase in hepatitis or liver glycogen storage disease. Thus the serum isozyme reflected its probable derivation from the diseased tissue. However, in liver tumor patients the serum had the muscle isozyme. Subsequent studies by Schapira and other investigators revealed that liver neoplasms, in contrast with adult liver, consistently exhibit an aldolase isozyme pattern resembling that of fetal liver or nonhepatic adult tissues with preponderance of isozymes A or A and C (*5*). My colleagues and I found (*10*) for example, that aldolase B is lost to a varying degree from the "spectrum" of Morris hepatomas, depending on their growth rate and degree of dedifferentiation; in rapidly growing, poorly differentiated liver tumors we found aldolase B to be completely replaced by aldolase A.

Hexokinases

Three hexokinase isozymes termed I, II, and III are present in varying proportions in fetal and adult tissues. Shortly after birth, a fourth form, IV, appears in liver (*11*). Because of its specificity toward glucose, it has been termed glucokinase. It is endowed with several special properties, two of which are extremely important to hepatic glucose metabolism; a low affinity for glucose, which ensures the physiologically appropriate hepatic glucose uptake only during hyperglycemia, and a marked responsiveness in activity toward glucose and dependence on various hormones, particularly insulin (*11*). As with aldolase B, glucokinase is lost to varying degrees in hepatomas, depending on the growth rate and and degree of dedifferentiation, and is replaced completely in fast-growing, poorly differentiated hepatomas by one or more of the other three hexokinase isozymes that are present in fetal liver (*12*).

FETAL ISOZYME EXPRESSION IN HEPATOMAS

These examples illustrate two noteworthy features of isozyme alterations in cancer. In each instance, an isozyme geared kinetically for specific adult liver functions is lost and is replaced by isozymes with different kinetic properties, presumably only geared for efficient substrate utilization. This type of change can be perceived as a molecular foundation for the loss of host control over tumor growth that characterizes cancer. The second notable feature is that isozyme alterations cut both ways. While fetal isozymes appear, there is also a loss of adult forms. Thus not only is there an apparent reactivation of genes that were active during fetal stages but were inactivated during normal embryonic development; there is also a suppression of genes coding for adult liver enzymes.

As isozyme alterations in tumors unfold, it is becoming increasingly evident that fetal isozyme expression in hepatomas is a wide-ranging general phenomenon. In a recent review, Ibsen and Fishman (*13*) collected 22 instances of fetal isozyme expression in tumors of various types. These are listed in table 1. It is obvious that in liver tumors there is a massive switch in enzyme protein expression; it is likely that many more remain to be discovered. For those proteins that appear in cancer and are also found in the fetus and various embryonal-derived tissues such as the trophoblast and the placenta, Fishman (*14*) has proposed the term oncodevelopmental proteins. The widespread interest in such tumor-associated proteins, which reflects their biologic and potential diagnostic importance, has given birth to an International Society of Oncodevelopmental Biology.

Although most of our information has been gained thus far from studies on hepatomas, the shift to fetal isozyme expression does occur also in nonhepatic tumors. Schapira (*5*) observed fetal aldolase C in human rhabdomyosarcoma; Failly-Crepin and Uriel (*15*) reported the presence of a fetal brain carboxyl esterase in murine teratocarcinoma; and Omenn and Hermodson (*16*) found that whereas both fetal and adult normal human brain have the same phosphoglycerate mutase isozyme as do relatively benign brain tumors, highly malignant astrocytomas have the muscle- or hybrid-type isozymes. Farron et al. (*17*) observed fetal muscle pyruvate kinase III in a rat rhabdomyosarcoma, and my colleagues and I (*18*) found fetal muscle creatine kinase B in rat rhabdomyosarcomas. Herzfeld and Greengard (*19*) have reported fetal patterns of enzyme composition in colon and lung neoplasms. Further studies will surely yield more examples of fetal isozyme expression in other experimental tumor models.

Among the enzymes listed in table 1, several are especially worthy of mention.

Alkaline Phosphatase

This enzyme has clinical importance because the genotypic forms and their several variants in human cancer are being explored as diagnostic aids (*14*). There are at least three distinct genotypic forms in human tumors and in plasmas of cancer patients. One of these is present in hepatomas and, though not found in fetal liver, is present in fetal and adult intestine. Another isozyme is present at all phases of embryonic development. A third, the so-called Regan isozyme seen commonly in ovarian, testicular, and pancreatic tumors, is most prominent in term placenta but not in the fetus.

γ-Glutamyl Peptidotransferase

A striking example of the resurgence of a fetal isozyme in

TABLE 1.—*Isozymes expressed in hepatomas and various other tumors and in embryonal, fetal, or placental tissue*[a]

Isozyme	Developmental stage of expression	Neoplasms expressed in:
Aldolase A	Fetal liver and gut	Hepatoma, duodenal, adenocarcinoma
Aldolase C	Embryonic liver, fetal muscle	Hepatoma, rhabdomyosarcoma
Pyruvate kinase K	Fetal liver, muscle, brain	Hepatoma, rhabdomyosarcoma, brain tumors
Glycogen phosphorylase (low Pi)	Fetal liver, placenta	Hepatoma
Hexokinase II	Fetal liver, placenta	Hepatoma
Hexokinase III	Neonatal liver, placenta	Kidney tumors, mammary tumors, rhabdomyosarcoma
L-Glycerol 3-phosphate dehydrogenase (anodal form)	Embryo, early fetus	Ascites tumors
Alcohol dehydrogenase (anodal form)	Fetal liver	Hepatoma
Branched chain amino acid amino-transferase III	Placenta	Hepatomas
Glutaminase K	Fetal liver	Hepatoma, mammary tumors
Histaminase	Fetal liver	Various tumors
Carbamyl phosphate synthetase II	Fetal	Hepatoma, mammary tumors
Ornithine decarboxylase (low Km)	Fetal	Various tumors
tRNA methylases	Fetal liver	Hepatoma, other tumors
CDP-reductase	Fetal liver	Hepatoma
Thymidine kinase, cytoplasmic	Fetal liver, gut	Hepatoma, gastrointestinal neoplasms
Uridine kinase II	Fetal liver	Hepatoma, leukemia
DNA polymerase γ	Fetal liver	Hepatoma
dCMP deaminase	Fetal liver	Hepatoma
Glucosamine 6-P synthetase (low Pi)	Fetal liver	Hepatoma
Hexosaminidase (fast)	Fetal liver	Hepatoma
Alkaline phosphatase (Regan)	Placenta	Many tumors
Alkaline phosphatase (hepatoma form)	FL amnion cells, fetal intestine	Hepatoma
Alkaline phosphatase (non-Regan)	Chorion, fetal	Many tumors
γ-Glutamyl transpeptidase (fetal)	Fetal liver	Hepatoma
Arylamidase	Placenta	Hepatoma

[a] Data from Ibsen and Fishman (*13*). Reprinted courtesy of Elsevier/North Holland Biomedical Press.

tumors is γ-glutamyl transpeptidase. This enzyme is bound to the plasma membrane, and it is normally low in adult rat liver but very high in fetal liver and chemically induced hepatomas. According to Fiala (*20*), who originally noted the dramatic increase of this enzyme in tumors, it appears very early in the liver (within 10–20 hours) after carcinogen administration. Its functional role in amino acid transport, particularly in the kidney, and in the formation and breakdown of glutathione has been pointed out recently by Allison and Meister (*21*).

Pyruvate Kinase

This enzyme is located at a strategic site in the pathways of carbohydrate metabolism and, because it utilizes ADP as a substrate and yields ATP as a product, plays a particularly important role in the energy transduction associated with glucose metabolism. Sixty years ago Otto Warburg discovered that certain tumors avidly utilize glucose aerobically and in common with normal tissues utilize less glucose in the presence of oxygen than in its absence; a phenomenon he termed the Pasteur effect. This name was based on an observation made by Pasteur some 100 years earlier that when yeast is exposed to oxygen it ceases to ferment glucose. The significance of the high aerobic glycolysis of tumors and the Pasteur effect have been perennial and still unresolved subjects of much experiment, discussion, and controversy (*22*). These complex interrelationships between oxygen and glucose utilization in tumors may be mediated in part at least by changes in the activities and isozyme composition of pyruvate kinase. Since this enzyme competes for ADP with the phosphorylation of ADP to ATP that is also coupled with respiration, the reciprocal relationship between respiration and glucose utilization implied in the Pasteur effect is understandable. For the same reason, a high pyruvate kinase activity, which typifies many tumors, can be perceived as a major factor in their high glycolytic activity. Evidence for such a role of pyruvate kinase has been obtained by us in collaboration with Gosalvez et al. (*23, 24*). By manipulating the relative activities of pyruvate kinase and mitochondrial respiration, competition for ADP between those systems was demonstrated (*23*); and further studies in which pyruvate kinase was specifically inhibited in Ehrlich ascites cells (*24*) provided further suggestive evidence that the replacement of a tightly controlled hepatic pyruvate kinase by a high activity of the fetal form may be responsible for the high glycolytic activity of the rapidly growing, poorly differentiated hepatomas.

OTHER TUMOR-ASSOCIATED PROTEINS

If isozyme alterations were the only manifestation of altered gene regulation, they would represent merely one more peculiarity to be added to an already large array of perplexities that contribute to the mystery of cancer. However, it is clear now that isozyme alterations are merely one manifestation of what is evidently a wide-ranging phenomenon, encompassing virtually every means we have of identifying proteins. Immunologic methods applied over nearly a century have identified a host of tumor-associated antigens, many of which are found in normal fetal tissues. Some of these, for example carcinoembryonic antigen and α-fetoprotein, figure prominently in diagnosis of cancer and monitoring of treatment (*25–27*). Another striking example of transformation-associated gene activation is the many changes in enzyme activities, cell composition, and metabolism of somatic cell hybrids resulting from transformation by simian virus (*28*).

Plasminogen activators are proteolytic enzymes that convert plasminogen to plasmin and may be responsible for tumor invasiveness. They occur in the early embryo and are produced and secreted from transformed cells in culture (*29*). The synthesis and secretion of angiogenesis factor(s), upon which the developing embryo depends for the ingrowth of capillaries from nearby blood vessels are also required for growth of solid tumors (*30*). Tumors are generally less fastidious in their requirements for growth in culture than normal cells, a property due, according to Todaro and Delarco (*31*), to acquisition of the ability of these cells to synthesize their own growth factors.

A bizarre phenomenon, increasingly recognized to occur commonly in human nonendocrine tumors is the ectopic production of polypeptide hormones. Virtually every known polypeptide hormone has been identified as a tumor product. Recently Imura (*32*), and earlier Levine and Metz (*33*), pointed out an underlying pattern according to which the hormones produced can be classified consistent with the embryologic background of the tissue of origin. As seen in table 2, a wide variety of tumors in Group I arise from so-called APUD (amino acid precursor uptake and decarboxylating) cells, considered to be of ectodermal origin, whereas tumors of Group II arise from tissues derived from endoderm and mesoderm. In addition, some tumors, classified in Group III, produced polypeptides, which may not be ectopic in the strict sense because the normal tissues of origin are unknown.

Thus the ectopic production of polypeptide hormones by tumors reflects some limitations already imposed upon gene expression of cells at an early stage in embryogenesis. Once considered rare, the development of ultrasensitive methods of radioimmunoassay has rendered ectopic hormone production so common as to suggest that it may occur with all tumors (*34*). It is likely that these ectopic hormones, as well as other hormones waiting to be discovered, may well be responsible for the many otherwise inexplicable effects of tumors on host metabolism and behavior (*35*).

TABLE 2.—*A classification of hormone-producing tumors*[a]

Group	Hormones produced	Common tumors
I	ACTH, LPH, α-MSH, CLIP	Oat-cell cancer (lung)
	β-endorphin, γ-MSH	Carcinoid
	Vasopressin, oxytocin, neurophysin	Thymic cancer
	Calcitonin	Islet-cell cancer
	Other APUD hormones (CRF, GRF, VIP, somatostatin, gastrin, etc.)	Medullary thyroid cancer
		Pheochromocytoma
II-A	PTH	Renal cancer, hepatoma
		Epidermoid cancer (lung)
II-B	GH	Lung cancer
	PRL	Gastric cancer
II-C	hCG	Large-cell cancer (lung)
	hCS	Hepatoma
III[b]	Erythropoietin	Hepatoma, cerebellar hemangioblastoma
	Colony-stimulating factor	Epidermoid cancer etc.
	NSILA (insulin-like growth factor)	Mesodermal tumor, hepatoma, etc.

[a] Data are from Imura (*32*). Reprinted courtesy of Academic Press.

[b] Group III tumors may not be "ectopic" hormone-producing tumors in a strict sense.

SOME ECTOPIC ISOZYMES

Ectopic protein expression is not entirely confined to polypeptide hormones. We recently observed that neoplasms of rat liver, kidney, and brain contain the M-form of creatine kinase characteristic of adult muscle, as well as the B-form, which is the only detectable isozyme in the tissue of origin (*18*). Phosphoglycerate mutase is another enzyme in which the sole form in human brain is the B-isozyme, whereas highly malignant brain tumors also carry the adult muscle, M-form (*16*). Tanaka et al. (*36*) observed the ectopic occurrence of the adult liver form of phosphofructokinase in several nonhepatic neoplasms. No doubt other examples are awaiting discovery.

LOSS OF ADULT LIVER ENZYMES

Another facet of enzyme alteration in tumors can be considered to be within the realm of fetal expression—namely, the loss in hepatomas of many adult liver enzymes that are also normally low or absent in fetal liver. This category includes for the most part enzymes participating in specialized adult liver functions such as gluconeogenesis, fructose metabolism, and fatty acid oxidation. In a study of 82 enzymes occurring in normal adult rat liver, Knox (*37*) found that 32 of these had low or negligible activity in fast growing hepatomas. Of this number, 24 also had low or negligible activity in fetal liver. Of the 50 enzymes that retained high activity in fast growing hepatomas, 42 of these also had high activity in fetal liver.

In a comprehensive study of human intestinal and pulmonary tissue and their neoplastic counterparts, Herzfeld and Greengard (*19*) found a close resemblance in enzyme pattern between fetal and neoplastic tissues but a lesser correlation with the normal tissues. Though these observations are not as striking as the resurgence of fetal liver-associated isozymes in hepatomas, they emphasize further the similarities of enzyme expression shared by fetal liver and rapid-growing tumors.

SOME CONCERNS ABOUT SIGNIFICANCE OF ISOZYME ALTERATIONS

The cancer problem is characteristically plagued by uncertainties, and the alterations of isozyme expression in hepatomas are not without their ambiguities. First is the question of definition. It is implicit in considering isozyme alterations as abnormalities of gene expression that isozymes are products of different genes. This is not generally easy to establish and in many instances is an article of faith rather than fact. The growing recognition of enzyme variants and the existence of post-translation modifications of proteins necessitate caution in assuming the existence of true isozymes without definitive evidence. Second, alterations in enzyme activities in hepatomas occur against a background of normal physiological variation. Many isozymes of adult liver undergo substantial changes in activity in response to normal dietary and hormonal alterations. It is important to establish, therefore, that the observed alterations in tumors are not merely consequences of metabolic changes that may occur in tumor-bearing animals. Third, isozyme alterations are almost never all or none. Fetal isozymes generally do not disappear completely from adult liver, and adult liver isozymes generally do not disappear completely, even from the least differentiated hepatomas. Moreover, enzymatic differentiation follows separate temporal sequences in different tissues; what may be a fetal liver isozyme also may be an adult isozyme of other tissues. Another question that needs resolution concerns tumor heterogeneity. In many instances we are not sure whether isozyme alterations are due to true changes in isozyme composition of a homogeneous cell population or to differences in the cell populations comprising the tumor. Granting that isozymes are truly products of different genes, another question concerns the extent to which the activity levels observed are due to variations in rates of synthesis and degradation, or to factors concerned with the activation or inactivation of preexisting protein structures. These questions are coming to the fore increasingly with the development of highly sensitive enzyme radioimmunoassays.

In comparing adult liver or hepatomas with fetal liver, one should also note that prior to birth there is a change in cell population. Early in fetal development the liver contains a substantial portion of hematopoietic cells. However, at 1–3 days before birth, when fetal liver is usually taken for enzyme assays, the large majority of cells are hepatocytes (*37*).

Finally, a thoughtful assessment of abnormal gene regulation in cancer must also consider that the expression of fetal or ectopic proteins may occur fleetingly during cell proliferation induced either by partial hepatectomy or by growth of liver cells in culture (*38*). The crucial difference is of course that in hepatomas the change persists. Nonetheless, any conclusion as to the significance of isozyme alterations must be tempered by the possibility that those changes may be the result rather than the cause of cell proliferation.

Despite the many above-mentioned uncertainties, there is no doubt that cancer is associated with a massive switch in protein composition. The expression of fetal and ectopic proteins by tumors provides a plausible explanation for the many metabolic peculiarities of cancer cells and their effects on the host, and their functional significance should be a promising direction for future progress in the diagnosis and management of human cancer. More important, perhaps, is what these phenomena are trying to tell about the molecular nature of the neoplastic transformation. In the following concluding paragraphs a few personal reflections are presented, without attempting the virtually impossible task of reviewing the voluminous speculations on the role of gene regulation in cancer.

Genetic Versus Epigenetic Mechanisms

One of the long-standing unresolved problems is the significance of somatic mutation in cancer causation. The association between increased cancer incidence in a variety of genetic disorders and chromosomal abnormalities (*39*), the increasing recognition of DNA as a target of oncogenic viruses, radiation, and chemicals, the role of deficiency or infidelity of DNA repair in cancer causation (*40*), and the close correlations between carcinogenesis and microbial mutagenesis (*41*) provide a body of such compelling evidence as to place the somatic mutation hypothesis in the status of dogma.

It is ironic, therefore, that equally compelling evidence exists for an epigenetic process of cancer induction to which the misprogramming of isozyme and other protein expression adds strong support. Whether these proteins are identified as isozymes or antigens or polypeptide hormones, it is very important to recognize that these are not new proteins. They are mislocated either temporally or geographically and are therefore assumed to be products of genes that are not new. However, these proteins are newly activated by some mechanism that overcomes the normally rigid process by which genes are selected for expression or repression in each tissue during normal embryonic development. Discussions and speculations on epigenetic mechanisms in neoplastic development may be found in several recent papers (*42–45*).

A substantial proportion of the DNA in the genome probably serves a regulatory function, and we might assume that mutations leading to cancer occur in regulatory genes. This otherwise plausible assumption is not compatible, however, with a body of convincing evidence that the genome of at least some cancer cells can survive the neoplastic transformation with an intact, totipotential genome.

The genomes of many-times-transplanted frog or mouse cancer cells retain all of the encoded information and the capability, under appropriate circumstances, for normal embryonic development and to yield normal viable progeny with the genetic properties of the original tumor host intact (*42–46*). Plant tumors grown in culture for many generations, can in the proper environment, also undergo redifferentiation to yield plants that can flower and produce seed and ultimately new plants that are genetically indistinguishable from the original plant tumor host (*47*). This degree of genetic fidelity toward one of life's most highly orchestrated processes hardly seems compatible with a somatic mutation, whether in genes that code for structural, functional, or regulatory proteins.

Additionally, there is an increasing awareness that the neoplastic transformation may not be as immutable as was generally believed. Partial temporary redifferentiation of cultured transformed cells by addition of chemicals (*48*) or in some instances merely by change in temperature are common phenomena (*49*); there are rare but well-documented instances of "spontaneous" reversion of human cancers (*50*).

A pervasive question is why is there a preferential if not obligatory activation of embryonal or fetal genes in cancer? A plausible hypothesis in the light of current knowledge is that of Uriel (*51*). He has proposed that cells attacked by carcinogens have to undergo retrodifferentiation to a partially differentiated state as a normal physiological response to damage, thereby enabling cells to assume their fully differentiated state by way of normal regenerative mechanisms.

As Uriel points out, the regeneration of limbs, tails, and other organs, a process that occurs commonly in amphibia following resection, is preceded by a retrodifferentiation of those cells destined for redifferentiation to the new organ. Apparently, a reversion to what appears to be an embryonic stage of development is a general requirement for a normal reordering of gene regulation following tissue injury. This retrodifferentiated state probably accounts for the transitory appearance of fetal gene products during liver regeneration (*38*). When, however, a cell becomes transformed, differentiation is not completed, and the regulatory restraints that normally operate would not be fully functional. Under these circumstances, control of cellular proliferation would be impaired. Failure to reach the fully differentiated state would probably result in an unstable genome. It is conceivable that such an unstable genome, lacking host control of cell division, would lead to variability of progeny, thus accounting for the diversity of tumor phenotypes. Selection of such variable progeny for rapid growth could then account for tumor progression (*52*), an intractable common feature of human cancer, trending inexorably toward increased growth rate, autonomy, anaplasia, and resistance to treatment. Potter (*2, 53*) has over many years also envisioned the neoplastic condition in terms of an inability of cells to complete the full program of differentiation that is required for harmonious integration of tissues into the totality of functions in the whole organism. His view, expressed in the aphorism, "Oncogeny is blocked ontogeny," exemplifies the growing recognition that cancer is associated with abnormalities in the maintenance of the fully differentiated state.

With such strong evidence for and against the somatic mutation hypothesis, the question is, How can this situation be reconciled? What kind of change in DNA can be induced that will not involve a change in its primary structure, yet will lead to a quasi-permanent disruption of the normally rigid selective mechanisms for gene expression. Without mutation in the strict sense, how can the relationships of regulatory to structural genes be so altered as to yield new stable conformations that lead to an abnormally differentiated state with the acquisition of proliferative potential? These questions are of course central to our understanding of developmental biology, and they place the cancer problem directly within this as-yet-underdeveloped field. It would appear that somewhere within the temporally programmed modulation of gene readouts involved in normal embryonic development leading to the fully differentiated state there probably lies the key to the understanding of the neoplastic transformation.

Although little is yet known of the molecular processes involved, a great deal of effort is currently directed to mechanisms of gene transcription and translation. Some particularly promising clues to regulation of genomic expression follow from recent findings on a possible role of macromolecular methylation. Forrester and Hancock (*54*) have proposed that methylation of a repressor protein is required for activity in normal differentiation. Methylated bases, e.g., 5-methylcytosine in DNA, have been suggested for a regulatory role in eukaryotic as well as prokaryotic cells (*42, 55, 56*), and tRNA methylation also has been implicated in differentiation and neoplasia (*57*). The pace of activity in these and other studies of molecular mechanisms of gene regulation bode well for early answers to the enigma of cancer.

REFERENCES

(*1*) Greenstein JP. Biochemistry of cancer. 2d ed. New York: Academic Press, 1954.

(*2*) Potter VR. Initiation and promotion in cancer formation: The importance of studies on intercellular communication. Yale J Biol Med 1980; 53:367–388.

(*3*) Weber G. Enzymology of cancer cells. Parts 1 and 2. N Engl J Med 1977; 296:541–555.

(*4*) Markert CL. Biology of isozymes. In: Markert CL, ed. Isozymes. Vol 1. New York: Academic Press, 1975:1–9.

(*5*) Schapira F. Isozymes and cancer. Adv Cancer Res 1973; 18:77–153.

(*6*) Weinhouse S. New dimensions in the biology of cancer. Cancer 1980; 45:2975–2980.

(*7*) Criss WE. A review of isozymes and cancer. Cancer Res 1971; 31: 1523.

(*8*) Weinhouse S. Glycolysis, respiration and anomalous gene expression in experimental hepatomas. G. H. A. Clowes memorial lecture. Cancer Res 1972; 32:2007–2016.

(*9*) Morris HP. Induction and characteristics of "minimal" deviation and other transplantable hepatomas. Recent Results Cancer Res 1974; 44:103–114.

(*10*) Adelman RC, Morris HP, Weinhouse S. Fructokinase, triokinase, and aldolases in liver tumors of the rat. Cancer Res 1967; 27:2408–2413.

(*11*) Weinhouse S. Regulation of glucokinase in liver. Curr Top Cell Regul 1976; 11:1–50.

(*12*) Shatton JB, Morris HP, Weinhouse S. Kinetic, electrophoretic, and chromatographic studies on glucose-ATP phosphotransferases in rat hepatomas. Cancer Res 1969; 29:1161–1172.

(*13*) Ibsen KH, Fishman WH. Developmental gene expression in cancer. Biochim Biophys Acta 1979; 560:243–280.

(*14*) Fishman WH. Perspectives on alkaline phosphatase isoenzymes. Am J Med 1974; 56:617–650.

(*15*) Failly-Crepin C, Uriel J. A fetal carboxylesterase of mouse origin common to normal embryonic brain and murine experimental teratocarcinoma. FEBS Lett 1973; 33:351–354.

(*16*) Omenn GS, Hermodson MA. Human phosphoglycerate mutase: Isozyme marker for muscle differentiation and for neoplasia. In: Markert CL, ed. Isozymes. Vol III. New York: Academic Press, 1975: 1005–1018.

(*17*) Farron F, Hsu HH, Knox WE. Fetal-type isozymes in hepatic and nonhepatic rat tumors. Cancer Res 1972; 32:302–308.

(*18*) Shatton JB, Morris HP, Weinhouse S. Creatine kinase isozymes in normal tissues and neoplasms of rats and mice. Cancer Res 1979; 39:492–502.

(*19*) Herzfeld A, Greengard O. Enzyme activities in human fetal and neoplastic tissues. Cancer 1980; 46:2047–2054.

(*20*) Fiala S, Mohindru A, Kettering WG, Fiala AE, Morris HP. Glutathione and γ-glutamyl transpeptidase in rat liver during chemical carcinogenesis. J Natl Cancer Inst 1976; 57:591–598.

(*21*) Allison RD, Meister A. Evidence that transpeptidation is a significant function of γ-glutamyl transpeptidase. J Biol Chem 1981; 256:2988–2992.

(*22*) Weinhouse S. The Warburg hypothesis fifty years later. Guest editorial. Z Krebsforschung 1976; 87:115–120.

(*23*) Gosalvez M, Perez-Garcia J, Weinhouse S. Competition for ADP between pyruvate kinase and mitochondrial oxidative phosphorylation. Eur J Biochem 1974; 46:133–140.

(*24*) Gosalvez M, Lopez-Alarcon L, Garcia-Suarez S, Montalvo A, Weinhouse S. Stimulation of tumor-cell respiration by inhibitors of pyruvate kinase. Eur J Biochem 1975; 55:315–321.

(*25*) Gold P. Embryonic origin of human tumor-specific antigens. Prog Exp Tumor Res 1971; 14:43–58.

(*26*) Goldenberg DM. Oncofetal and other tumor-associated antigens of the human digestive system. In: Current topics in pathology. Berlin and Heidelberg: Springer-Verlag, 1979:290–342.

(*27*) Coggin JH Jr, Anderson NG. Embryonic and fetal antigens in cancer. In: King TJ, ed. Developmental aspects of carcinogenesis and immunity. New York: Academic Press, 1974:173–185.

(28) Martin RG. The transformation of cell growth and transmogrification of DNA synthesis by simian virus 40. Adv Cancer Res 1981; 34:1–68.

(29) Strickland S, Reich E, Sherman MI. Plasminogen activator in early embryogenesis: Enzyme production of trophoblast and parietal endoderm. Cell 1976; 9:231–240.

(30) Folkman J. Tumor angiogenesis. Adv Cancer Res 1974; 19:331–364.

(31) Todaro GJ, Delarco JE. Transformation by murine and feline sarcoma viruses specifically blocks binding of epidermal growth factor to cells. Nature 1976; 264:26–31.

(32) Imura H. Ectopic hormone production viewed as an abnormality in regulation of gene expression. Adv Cancer Res 1980; 33:39–75.

(33) Levine RJ, Metz SA. A classification of ectopic hormone-producing tumors. Ann N Y Acad Sci 1974; 230:533–546.

(34) Odell W, Wolfsen A, Yoshimoh Y, Weitzman R, Fisher D, Hirose F. Ectopic peptide synthesis: A universal concomitant of neoplasia. Trans Assoc Am Physicians 1977; 90:204–207.

(35) Hall TC. Paraneoplastic syndromes. Ann NY Acad Sci 1974; 230:1–577.

(36) Tanaka T, Imamura K, Ann T, Taniuchi K. Biochemical studies of the neoplastic state. Gan Monogr 1972; 13:219–234.

(37) Knox WE. Enzyme patterns in fetal, adult and neoplastic rat tissues. 2d ed. Basel: Karger, 1976.

(38) Leffert H, Moran T, Sell S, et al. Growth-state dependent phenotypes of adult hepatocytes in primary monolayer culture. Proc Nat Acad Sci USA 1978; 75:1834–1838.

(39) Knudson AG Jr. Mutation and human cancer. Adv Cancer Res 1973; 17:317–352.

(40) Cleaver JE. DNA repair and its coupling to DNA replication in eukaryotic cells. Biochim Biophys Acta 1978; 516:489–518.

(41) Ames BN, McCann J, Yamasaki E. Methods for testing carcinogens and mutagens with the Salmonella/mammalian microsome mutagenicity test. Mutat Res 1975; 31:347–364.

(42) Holliday R. A new theory of carcinogenesis. Br J Cancer 1979; 40: 513–522.

(43) Sherbet GV. Epigenetic processes and their relevance to the study of neoplasia. Adv Cancer Res 1970; 13:97–167.

(44) Rubin H. Is somatic mutation the major mechanism of malignant transformation? JNCI 1980; 64:995–1000.

(45) Mintz B, Fleischmann RA. Teratocarcinomas and other neoplasms as developmental defects in gene expression. Adv Cancer Res 1981; 34:211–278.

(46) McKinnell RG, Deggins BA, Labat DD. Transplantation of pluripotential nuclei from triploid frog tumors. Science 1969; 165:394–396.

(47) Braun AC. Plant tumors. In: Beck FF, ed. A comprehensive treatise. Vol 4. New York and London: Plenum Press, 1975:411–428.

(48) Marks PA, Rifkind RA. Erythroleukemia differentiation. Ann Rev Biochem 1978; 47:419–448.

(49) Basilico C. Temperature-sensitive mutations in cancer cells. Adv Cancer Res 1977; 24:223–266.

(50) Everson TC, Cole WH. Spontaneous regression of cancer. Philadelphia: Saunders, 1966.

(51) Uriel J. Retrodifferentiation and the fetal patterns of gene expression in cancer. Adv Cancer Res 1979; 29:127–174.

(52) Foulds L. Neoplastic development. New York: Academic Press, 1960.

(53) Potter VR. Phenotypic diversity in experimental hepatomas: The concept of partially blocked ontogeny. Br J Cancer 1978; 38:1–23.

(54) Forrester PI, Hancock RL. Theoretical mechanisms for synthesis of carcinogen-induced embryonic proteins. Med Hypotheses 1978; 4: 31–36.

(55) Ehrlich M, Wang RY-H. S-Methylcytosine in eukaryotic DNA. Science 1981; 212:1350–1357.

(56) Razin A, Riggs AD. DNA methylation and gene function. Science 1980; 210:604–610.

(57) Kerr SJ, Borek E. Regulation of the tRNA methyltransferases in normal and neoplastic tissues. Adv Enzyme Reg 1973; 11:63–77.

blank page

Single Oblique-View Mammography for Periodic Screening for Breast Cancer in Women[1,2]

Bengt Lundgren, *M.D.*,[3] *and* **Anders Helleberg**, *M.D.*[4]

ABSTRACT—A population, originally 6,845 women, 40 years of age and over, was screened for breast cancer by single oblique-view mammography in 1974, 1977, and 1980. Of the 5,789 women remaining in their parish in 1980, 94% had attended the screening at least once. Of 111 breast cancers diagnosed in the 6.25-year study period, 78% were detected at screening, 15% as interval cancers, and 7% among nonresponders. Sixty-three percent of the women had tumors in clinical stage I, and 59% had tumors less than or equal to 10 mm. The predictive value for biopsy recommendations by mammography was 78%. This method was considered very suitable for screening. In the older age groups there was probably some overdiagnosis of cancers that would never have become symptomatic.—JNCI 1982; 68: 351–355.

The most important question still to be definitely answered regarding screening for breast cancer is that of screening's impact on breast cancer mortality. Breast cancers vary widely in growth rates, and growth rate may strongly influence the outcome of treatment. The fast-growing cancers probably metastasizing early may be beyond any type of treatment, whereas the very slow ones perhaps need not be treated at all. Probably, an intermediate tumor group exists that is influenced positively by early treatment, and screening would be beneficial for this group. However, if screening and early treatment were proved to have no effect on mortality, the concept of biologic predeterminism would be true. But important evidence contrary to this concept exists, of which the most convincing is the Health Insurance Plan of Greater New York (HIP) study showing long-term reduction of mortality as a result of screening. (*1*)

Another important point in the evaluation of screening programs is whether high attendance rates can be maintained through several repeat screenings. The falling off of participation to unprofitably low levels could be one reason to abandon this procedure (even if the screening were well performed in other respects) because then the impact of screening on the disease in the population would be too small to merit its use.

Also, overdiagnosis of cancer is conceivable in elderly patients and/or in those with very slow-growing tumors.

Beginning in 1974, population screening by single oblique-view mammography has been performed in an increasing number of regions in Sweden. The technique was developed in Gävleborg County, starting with a pilot study (*2*) in the town of Sandviken on a population since then closely followed. This population was screened a second time in 1977 (*3*) and a third time in 1980. Actually, all the females of the county 40 years and older were screened at least once. This report deals with the pilot study population; it emphasizes the third screening and refers back through the period of 6.25 years from the start of the program. Our aims were to study participation and detection rates, incidence of breast cancer in the population, tumor stages, and the likelihood of overdiagnosis and, if possible, to reach a conclusion regarding the optimum interval time for effective screening by single oblique-view mammography.

The present study was not randomized, since it was extended from a methodic development project. However, randomized and controlled screenings to study effects on breast cancer mortality have been used by this method in Kopparberg County since 1977, in Östergötland County since 1978 (*4*, *5*), and in the city of Stockholm since 1981.

MATERIALS AND METHODS

The original population defined in March 1974 was comprised of 6,845 women 35 years or older living in the urban parish of Sandviken, a small industrial town in middle Sweden. In August 1977, when the second screening was begun, 6,231 remained alive and in the study area, 315 women had died, and 299 had moved out of the parish. The average time between screenings was 3.4 years, and the average yearly decline in number of women was 2.6% (*6*).

In January 1980 a new census was done (table 1); 5,789 women, then aged 40 years old and above, remained in the parish. The average yearly decrease in number of women since 1974 was 2.7%. The greatest change was, naturally, in the oldest age group (>69 yr old), where deaths accounted for most of the population decrease, and the next greatest change was in the youngest age group, where relocation accounted for most of the 15% decrease.

The screening method in 1980 was that of the previous screening, i.e., single oblique-view mammography (*2*, *7*) (one X-ray film of each breast available to the reader). Physical examination was not done at screening. The participants were asked if they had felt any lumps; if they had, clinical examination was prescribed, irrespective of mammography results. Also, in instances of suspicious mammography findings, patients were clinically examined.

The screening was done by two radiographers in a mobile unit. Each full working day about 125 women were invited to participate, and normally 95–105 of them attended. They were invited by computer-printed letters with appointment

---

ABBREVIATIONS USED: PV=predictive value(s); TIS=tumor in situ; TNM=International Union Against Cancer classification system based on extent of primary tumor (T), condition of lymph nodes (N), and absence or presence of metastases (M).

---

[1] Received October 21, 1980; revised September 21, 1981; accepted October 14, 1981.

[2] Research procedures were in accord with the ethical standards of the Helsinki Declaration of 1975.

[3] Mammography Department, Gävle Hospital, S-801 17 Gävle, Sweden.

[4] Department of Surgery, Gävle Hospital.

TABLE 1.—*Study population as registered at beginnings of three screenings*[a]

Age, yr, of subjects in 1974	No. of subjects in 1974	No. of subjects in 1977	Population decrease, %, 1974–77	No. of subjects in 1980	Population decrease, %, 1974–80	Mean yearly decrease, %
35–39	756	668	11	634	16	3.2
40–49	1,439	1,342	7	1,282	11	2.2
50–59	1,679	1,609	4	1,539	9	1.8
60–69	1,721	1,601	7	1,507	12	2.4
≥70	1,250	1,021	18	827	34	6.8
≥35	6,845	6,241	9	5,789	155	3.0
35–69	5,595	5,220	7	4,962	11	2.2

[a] Decrease in numbers in 1974–77 and 1974–80 caused by deaths and relocation out of the study parish.

times. The exposed X-ray films were sent to the central screening unit at Gävle Hospital, where they were processed and read the day after the examination. Letters reporting good health were normally received by the participants on day 2 after examination. If findings at mammography screening were doubtful, a complete three-view examination was done; if suspicions still remained, the patients were referred to the Gävle Hospital breast unit for clinical examination, upon which a few patients were found to have benign conditions, usually cysts, and were then given reports of good health. The remaining patients usually underwent surgical biopsy. Nonpalpable lesions were first localized by needle and hook and then received injections of methylene blue dye. Specimen radiography was always performed. If the suspicious lesion consisted of microcalcifications, the paraffin-embedded specimens were X-rayed to substantiate the microscopic findings.

Information on growth rates of the cancers in the present study is incomplete. A prerequisite for such knowledge is that previously recorded mammographies are available for all cancer cases. However, such mammographies were not available at the first screening occasion and for nonresponders. The rate of growth can be estimated for cancers that generate at least a moderately well-defined tumor shadow. For cancers that are visible as microcalcifications only, the size of the tumors cannot be determined. In several cases growth rates could be calculated, however.

The curative treatment varied. Some of the oldest patients were given Tamoxifen orally as the only therapy, without excision of the tumors. In these cases there were positive cytologic cancer diagnoses. On some patients tylectomy and exploration of the axilla were done, without subsequent radiotherapy. The most "radical" treatment was total mastectomy with exploration of the axilla.

The X-ray equipment was a Philips Mammodiagnost. Kodak-Pathé NMB film was used with Kodak min-R screens. The average absorbed radiation dose was 0.7 mGy (70 mrad).

RESULTS

Participation.—Of the 5,789 women remaining in 1980, aged 40 years and over, 82% participated at the third screening. Table 2 shows the participation of these women at all three screenings. The attendance rate of women at the ages below 70 years old was over 90% on all three occasions and much lower in those at ages over 69 years old.

Table 3 demonstrates numbers and rates of women participating in the screening once only, twice, or three times. Of the total population, the percentage of participants with at least one attendance was 94% for those 40 years old or more and 96% for those 40–69 years old.

Of the 1,057 nonparticipants at the third screening, 90 entered the Gävle Hospital breast unit in 1979 or the first half of 1980.

Referrals and detections at third screening.—Table 4 shows numbers and rates of referred patients and cancer cases. The cancer detection rate among participants over 40 years old was 4.4 per 1,000 and among those 40–69 years old, 3.2 per 1,000; the predictive value for patients referred from screening to clinical examination was 55% and 44%, respectively. In all, 38 patients were referred (0.8%), of whom 9 were found to have clinically benign lesions, mostly cysts. Of the remaining 29 patients, 21 had histopathologically

TABLE 2.—*Persons still alive and in the parish in 1980 and their participation in 1974, 1977, and 1980 screenings*

Age, yr, in 1980	Invited No.	No. of participants (%)		
		1974	1977	1980
40–49	1,262	1,188 (94)	1,161 (92)	1,159 (92)
50–59	1,436	1,345 (94)	1,308 (91)	1,296 (90)
60–69	1,547	1,433 (93)	1,366 (88)	1,350 (87)
≥70	1,544	1,303 (84)	1,029 (67)	927 (60)
≥40	5,789	5,269 (91)	4,864 (84)	4,732 (82)
40–69	4,245	3,966 (93)	3,835 (90)	3,805 (90)

TABLE 3.—*Participation in the three screenings; remaining population in 1980*

Age, yr, in 1980	Invited population No.	No. of participants (%)			
		One time	Two times	Three times	Sometimes
≥40	5,789	399 (7)	624 (11)	4,406 (76)	5,429 (94)
40–69	4,245	146 (3)	354 (8)	3,584 (84)	4,084 (96)

TABLE 4.—*Number and rates of patients referred from the 1980 screening; number and rates of cancer cases*

Age, yr	Invited population No.	No. of participants	Referred patients		Cancer cases		
						Rate/1,000	
			No.	Rate/1,000	No.	Invited women	Participating women
40–49	1,262	1,159	8	7	3	2.4	2.6
50–59	1,436	1,296	8	6	3	2.1	2.3
60–69	1,547	1,350	12	9	6	3.9	4.4
≥70	1,544	927	10	11	9	5.8	9.7
≥40	5,789	4,732	38	8	21	3.6	4.4
40–69	4,245	3,805	28	7	12	2.8	3.2

verified breast cancers and 8 had benign lesions at surgical biopsy (PV, 72%).

Thirty-one patients were referred by mammography only, of whom 21 had cancer (PV, 68%). One of the cancer patients had felt a lump; the other patients were nonsymptomatic. A further 7 patients had reported lumps but had normal mammography and physical examination results. Of the 31 patients referred by mammography, 4 had benign lesions diagnosed at clinical examination, and biopsy was recommended in 27 patients (PV, 78%), 21 of whom had cancer. There were 4 noninvasive ductal cancers (TIS); 11 were stage I, 4 were stage II, and 2 were stage III invasive cancers. The stage III cancers (T2aN2M0 and T4bN2M0) were considered inoperable. Of the remaining 19, only 1 had axillary metastases diagnosed after biopsy.

Breast cancer detections.—The stages (according to the TNM system) of all 111 cancers detected during the study period, i.e., at screening, at follow-up of suspicious cases, during intervals between screenings, and among the nonresponders, are shown in table 5. At screening, 7 of 86 (8%) of the cases detected were in stages III and IV, compared to 6 of 16 (38%) of the interval cases.

Sizes of the tumors detected at screening, measured as the largest diameter in the biopsy specimens or in some cases in the radiographies, are shown in table 6. The total rate of noninvasive and invasive cancers 10 mm or less was 59%.

Table 7 shows the ages of all breast cancer patients diagnosed in the population since the start of the first screening and includes screening detections, interval cases, and cases among nonresponders.

Overdiagnoses.—There is an obvious possibility that some cases of cancer detected in a screening would never have developed into clinically detectable tumors during the patient's normal life expectancy; some may not be lethal, given even several decades of growth. Our hypothesis is that this could occur only at an initial screening, when no evidence exists about the biologic behavior of the individual tumors. At subsequent screenings, there will always be available "base-line" mammographies, and only tumors with radiologically verifiable growth will be diagnosed. A way to gain more solid evidence on this point was tested in the present study, although the number of cancer cases was small.

Table 5.—*Stages according to the TNM system of all tumors detected at three screenings, during intervals, and among nonresponders*

Stage	No. of cancer cases detected						
	At screening and follow-up			During intervals	Among nonresponders	Total No.	Percent
	1974	1977	1980				
TIS			4	2		6	5
I	31	17	11	2	3	64	58
II	9	3	4	6	3	25	23
III		1	2	4	3	10	9
IV	4			2		6	5
Total	44	21	21	16	9	111	100

Table 6.—*Tumor sizes measured as largest diameter in biopsy specimen or radiograph; all three screenings and follow-up*

Tumor size, mm	No. in 1974	No. in 1977	No. in 1980	Total No.	Percent
TIS	—	—	4	4	5
≤10	24	12	10	46	54
11–20	12	6	4	22	26
21–50	7	3	2	12	14
>50	1	—	1	2	1
Total	44	21	21	86	100

Table 7.—*All cancer cases diagnosed in target populations from start of first screening in 1974 to end of third screening in 1980*

Age, yr	Cancer cases diagnosed			
	At screening and follow-up (%)	Intervals (%)	Nonresponders (%)	Total No.
35–39	1 (50)	1 (50)		2
40–49	5 (56)	3 (33)	1 (11)	9
50–59	13 (76)	4 (24)		17
60–69	36 (86)	4 (10)	2 (4)	42
≥70	31 (76)	4 (10)	6 (14)	41
≥35	86 (78)	16 (15)	9 (7)	111
40–69	55 (79)	12 (17)	3 (4)	70

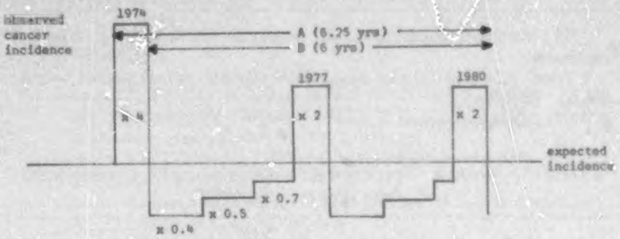

Text-figure 1.—Cancer incidence variations caused by three screenings.

Text-figure 1 demonstrates schematically the incidence of breast cancer in the study population during the study period. On the first screening a rather high rate of prevalent cases was detected, giving 4.3 times the expected incidence in 1974 (*2*), which lowered at the two following screenings. In the interval years the incidence rates were well below the average expected (*6*). Average yearly observed standardized incidence rates were calculated for the whole period (A) and for the period after the first screening (B), and these were compared to the expected standardized national incidence.

Table 8 shows the total average rate of observed incidence (detections at screening, interval cases, and cases among nonresponders) against expected incidence for period A, estimated on a standard population with the use of the census from the midpoint screening in 1977. Only those of ages up to 69 years old were tested, and the age group 35–39 years old was too small both in number of persons and cancer cases to be useful. It would seem that over this period 1.5 times as many cases were detected as expected; in the age group 60–69 years old, twice as many as those expected were detected.

Table 9 demonstrates period B studied in the same manner. When the first screening occasion was excluded, the rate of observed to expected incidence was 1.0; i.e., no excess cancers were diagnosed.

Growth rates.—Growth rates could be calculated for 16 of

TABLE 8.—*Mean incidence test for overdiagnosis for the 6.25-year period A, March 1974 to June 1980; expected age-adjusted standardized incidence for Sweden 1974; mean study population defined in 1977; Swedish ST*[a]

Age, yr	Mean population No.	Cancer cases		Incidence per 100,000[b]		OI/EI	ST, %	OI × ST
		Total No.	Average No./yr	OI	EI			
35–39	271	2	0.32	118	39	3.0[c]	5.5	649
40–49	1,338	9	1.44	108	113	1.0	12.3	1,328
50–59	1,508	17	2.72	180	154	1.2	12.8	2,304
60–69	1,671	42	6.72	402	204	2.0	10.9	4,382
35–69	4,788	70	11.2		140	1.5	41.5	8,662

[a] ST, standard population; OI, observed incidence; EI, expected incidence.

[b] Total EI=140/100,000; total OI=(OI×ST)/ST=8,662/41.5=209/100,000; OI/EI=1.5.

[c] Of little significance.

TABLE 9.—*Mean incidence test for overdiagnosis for 6-year period B, June 1974 to June 1980*[a]

Age, yr	Mean population No.	Cancer cases		Incidence per 100,000[b]		OI/EI	ST, %	OI × ST
		Total No.	Average/yr	OI	EI			
35–39	271	1	0.2	74	39	(1.9)	5.5	407
40–49	1,338	9	1.5	112	113	1.0	12.3	1,378
50–59	1,508	12	2.0	133	154	0.9	12.8	1,702
60–69	1,671	23	3.8	227	204	1.1	10.9	2,474
35–69	4,788	45	7.5		140	1.0	41.5	5,961

[a] First screening excluded. OI, observed incidence; EI, expected incidence; ST, standard population.

[b] Total OI=5,961/41.5=144/100,000. Total EI=140/100,000.

21 carcinomas at the second screening, for 18 of 21 carcinomas at the third screening, and for 12 of 16 interval cases. The rates varied from a volume doubling time of less than 1 month to 13 months. Arbitrarily, the tumors were divided into 3 groups: "fast," "medium," and "slow" in regard to growth rate (table 10). Of the cancers detected at screening, 71% were medium types and 9% were fast, whereas of the interval cases 41% were fast and 34% were slow.

DISCUSSION

Here, as in other reports (*2–4, 6, 7*), the single oblique view was used. This method is employed at four of (at the present) five Swedish breast screening centers. At the fifth center the oblique view is combined with a craniocaudad view for screening (*8*). No differences in pick-up rates or interval cancer rates have been observed between these two variants of single modality screening (*5*). The costs, however, increase by a total of at least 60% by the apparently unimportant addition of the second view (*9*). The sensitivity of single oblique-view mammography expressed as the efficiency index, which takes into account interval cancers found during year 1 after screening, is 93% (*10*). The sensitivity of three-view mammography at our hospital is 95%. It is improbable that two views would surpass that. Given the very substantial cost increase incurred by addition of the second view, the price for the doubtful marginal gain seems exorbitant.

Though the rate of cases referred from screening by single-view mammography in our project was never high—1.4% in the pilot study (*2*)—it was lower at the third screening, only 0.8%. The specificity at the first screening was 99.2% and at the third, 99.8%. The decreasing referral rate had several causes: mounting experience, decreasing cancer detection rates, and the facts that a number of benign lesions with doubtful mammographic appearance had been excised at the first screening and that base-line X-rays were available for comparison.

The PV for biopsy recommendations by mammography was very high (78%), meaning that very few "unnecessary" biopsies were performed. The low negative biopsy rate could theoretically mean that some cancers were missed. Such tumors always turn up as interval cancers, and we do not believe that our rate of such cancers is unduly high; on the contrary, we consider it satisfactorily low. PV rates from other sources tend to be much lower; for instance, Moskowitz and Fox (*11*) reported 12% and Rombach (*12*), 31%. The four Swedish screening centers, of which ours is one, were found to have very similar PV (61–66%) at initial screening (*5*). In the report on the Breast Cancer Detection Demonstration Projects, this important aspect of screening was not mentioned. Those PV rates were probably lower than ours. The interval cancer rates were higher (*13*). The wide span in reported PV rates may reflect either differences of quality (examination and interpretation) or attitude or a combination of the two. The quality aspect is obvious and should need no further analysis: Bad examinations by inexperienced or badly motivated people lead to higher rates of both false positives and false negatives. The attitude current in Sweden includes concern both about the integrity and well-being of the individual participants and the buildup of public good will for the future benefit of the screening. We believe that it is extremely important to make every effort to keep the number of false-positive cases at an absolute minimum, since the fear and anxiety the women concerned have to live with until a definite diagnosis is reached may be devastating. From a practical viewpoint it is also important to reduce the number of false positives, because high rates may adversely affect future participation.

The participation rates were good throughout the period

TABLE 10.—*Growth rates of carcinomas detected at screening or in intervals between screenings*

Growth type	Doubling time, mo	Detections		
		At screening (%)	In intervals (%)	Total (%)
Fast	0–2	3 (9)	5 (41)	8 (17)
Medium	2.1–5	24 (71)	3 (25)	27 (59)
Slow	5.1–13	7 (20)	4 (34)	11 (24)
Total		34 (100)	12 (100)	46 (100)

reported. In fact, to our knowledge none better have ever been reported from any screening program. No less than 96% of women 40–69 years old participated in at least one screening, showing that the concept of breast screening and the way it was done were acceptable, despite mammography and breast screening being given a less-than-benevolent coverage by the mass media during the first 2 or 3 years of the period.

The rate of noninvasive and invasive cancers, 10 mm and less, was 55% at the first screening and 67% at the third screening and totaled 59%. Detecting "early" cancers, one aim of breast screening, was achieved. Though the actual number of cancer cases is quite small for each age group, there is no doubt that the efficiency of the screening was lower in younger women, partly because of the inherent lower diagnostic accuracy of mammography in the denser breasts of younger women and also because of too-long screening intervals. These intervals were longer than intended, 3.4 and 2.7 years, whereas we would have preferred 2.5 years at the most. However, it is possible that different intervals should be chosen, e.g., 1.5 years for women below 55 years of age and 3 years for those over that age. We still do not believe that there is enough evidence for a final decision on the optimum interval time, which also must include cost-benefit calculations. In the end a decision will probably be based as much on political and economical arguments as on strictly medical ones.

The model for observing possible overdiagnosis is certainly based on limited material, and nothing definite may be concluded from it. It could, however, be useful in ultimately proving or disproving our hypothesis that overdiagnosis could occur at a first screening only. Logically, it is probable that the tendency seen in the model will persist as the observation time increases. If that tendency turns out to represent a truth, we believe that this type of overdiagnosis may be an acceptable "cost," especially in view of the increasing use of very conservative treatment methods. The interpretation of the results is, however, complicated by earlier diagnosis (lead time) which will cause an age group shift. A cancer that should normally become clinically obvious for instance at age 72 years may well have its detection advanced to age 67 years because of screening. Thus some cases in lower age groups actually "belong" to the next older group.

The material on growth rates is small, at least concerning interval cancers. The rate of fast-growing cancers was higher among the interval cases, which could be expected, if one bears in mind length bias. There were also several slow-growing carcinomas, which represent observer interpretation errors at the screening examination.

Our opinion is that single oblique-view mammography, strictly monitored for high quality, has been proved to be very suitable for mass screening for breast cancer. It has a high sensitivity and specificity, is acceptable and reproducible, has a very high capacity, can be used in out-reaching mobile units, and is relatively cheap to implement. The most important issue, the impact of efficient breast screening by this method on breast cancer mortality, is at present under study in controlled, randomized trials in Sweden, with results forthcoming in 1 or 2 years.

REFERENCES

(*1*) Shapiro S. Efficacy of breast cancer screening. In: Miller AB, ed. Screening in cancer. Geneva: UICC, 1978:133–157 (UICC technical report series, vol 40).

(*2*) Lundgren B, Jakobsson S. Single view mammography. Cancer 1976; 38:1124–1129.

(*3*) ———. Repeat screening by single oblique view mammography. Breast Cancer Res Treat. In press.

(*4*) Tabar L, Gad A, Fagerberg G, et al. Screening for breast cancer in Sweden. A randomized controlled trial. In: Logan WW, Muntz EP, eds. Reduced dose mammography. New York: Masson, 1979: 407–414.

(*5*) Andersson I, Fagerberg G, Lundgren B, Tabar L. Breast cancer screening in Sweden. Radiologe 1980; 20:608–611.

(*6*) Lundgren B, Jakobsson S. Single view mammography screening. Radiology 1979; 130:109–112.

(*7*) Lundgren B. Single oblique view mammography. An efficient method for breast cancer screening. Academic thesis. Gävle/Stockholm: Karolinska Institute, 1980:95.

(*8*) Andersson I. Mammographic screening for breast carcinoma. An academic thesis. Malmö/Lund: University of Lund, 1981:146.

(*9*) Lundgren B, Medin B. One or two mammography views at breast cancer screening? A cost-effectiveness analysis. Lakartidningen 1981; 78:2455–2457.

(*10*) Lundgren B. Efficiency of single-view mammography: Rate of interval cancer cases. JNCI 1979; 62:799–803.

(*11*) Moskowitz M, Fox SH. Cost analysis of aggressive breast cancer screening. Radiology 1979; 130:253–256.

(*12*) Rombach JJ. Breast cancer screening. Alphen aan den Rijn and Brussels: Stafleu's 1980:132.

(*13*) Beahrs OH, Shapiro S, Smart C. Report of the working group to review the National Cancer Institute–American Cancer Society Breast Cancer Detection Demonstration Projects. JNCI 1979; 62: 639–709.

blank page

Observer Variation in the Interpretation of Xeromammograms[1,2]

Norman F. Boyd,[3,4] Christina Wolfson,[5] Myron Moskowitz,[6] Thomas Carlile,[7] Michel Petitclerc,[8] Helen A. Ferri,[9] Eve Fishell,[10] Andre Gregoire,[11] Matthew Kiernan,[12] J. Donald Longley,[13] Imre S. Simor,[10] *and* **Anthony B. Miller[3]**

ABSTRACT—We have examined variation in the interpretation of xeromammograms among radiologists designated to take part in a Canadian multicenter randomized controlled trial of screening for breast cancer. Radiologists read 100 xeromammograms comprising 10 histologically proved cancers, 40 benign abnormalities, and 50 normal films. Radiologists' opinions differed widely on the frequency of suspected or identified cancer. The diagnostic category "suspicion of cancer" or "cancer" was selected by radiologists for 10–55% of the films, and biopsy or aspiration was recommended for 21 to 53% of patients whose films were examined. Agreement on specific diagnostic categories was greatest for the diagnosis of cancer; agreement was least for the diagnosis of benign abnormalities and intermediate for the diagnosis of normality. Known cancers were in general correctly identified. These results indicate a need for development of methods to reduce observer variation in the interpretation of xeromammograms while preserving diagnostic sensitivity and validity. Results also emphasize the importance of developing strategies to ensure quality control in multicenter trials.—JNCI 1982; 68:357–363.

Experienced radiologists may differ in their interpretation of radiographs, and the subject of observer variation in clinical radiology has received particular attention in connection with screening for pulmonary tuberculosis. Radiologists may fail to identify a substantial proportion of cases with roentgenographic evidence of tuberculosis and frequently change their readings on positive cases upon later rereading of the same films (*1–4*). These findings indicate the possibility that the detection of breast cancer by mammography might also be influenced by the observer who interprets the film.

While planning a multicenter randomized controlled trial of screening for breast cancer with mammography, we recognized that differences in mammogram interpretation between radiologists in the various centers could influence the number and stage of evolution of detected cancers and thus influence any effect of screening with mammography on breast cancer mortality. To determine the extent of differences between the diagnostic interpretations of mammograms and in the radiologists' recommendations for subsequent action, we conducted a study of observer variation in which all participating radiologists read the same set of mammograms.

MATERIALS AND METHODS

Xeromammograms and readers.—The xeromammograms were selected by two of us (M. M. and T. C.) from the files of two Breast Cancer Detection Demonstration Project screening centers. Fifty xeromammograms were selected from each center, and each set of 50 comprised 5 histologically proved cancers, 10 benign abnormalities confirmed by biopsy, 10 benign abnormalities not proved by biopsy, and 25 films that were regarded as normal. All "normal" films were of subjects who had been followed for at least 4 years after the film was taken and in whom breast cancer did not develop. No other criteria were established for the selection of films. One radiologist selected films thought to be representative of the three principal diagnostic classes; the other radiologist selected films from the Department's teaching file that for cancers showed only subtle radiologic features of the disease and for the benign abnormalities showed shared radiologic signs with the minimal breast cancers. The films from each subject comprised a mediolateral and craniocaudal view of each breast. All were regarded as technically satisfactory by the radiologist who selected them.

The set of 100 selected mammograms was copied by an industrial photographic process and arranged in random sequence. A complete set was sent to the two radiologists who had submitted films and to the other seven radiologists who had agreed to participate in a Canadian multicenter randomized controlled trial of breast cancer screening. All radiologists were members of university departments and had a special interest in mammography. The composition of the set of xeromammograms was known only to the two radiologists who provided the films. The technical quality of the reproduced films was assessed, in the absence of established physical methods of comparison, by the radiologists who submitted the original films. Some degradation of the image was thought to have occurred in the process of copying, but the copied images were considered adequate for diagnostic purposes. In the copying process the color of the background was changed from blue in the original to black in the copy. Each radiologist described each film, recorded a diagnosis, and made a recommendation for further action on a standardized precoded recording form.

---

[1] Received December 24, 1980; revised August 25, 1981; accepted September 14, 1981.

[2] Supported by a grant from the National Cancer Institute of Canada.

[3] Epidemiology Unit, National Cancer Institute of Canada, Toronto, Canada.

[4] *Address reprint requests to* Dr. Boyd at The Princess Margaret Hospital, 500 Sherbourne St., Toronto, Ontario, Canada M4X 1K9.

[5] Department of Epidemiology and Health, McGill University, Montreal, Canada.

[6] Department of Radiology, University of Cincinnati, Cincinnati, Ohio.

[7] Department of Radiology, Virginia Mason Medical Centre, Seattle, Wash.

[8] Department of Radiology, Laval University, Quebec, Canada.

[9] Department of Radiology, University of Alberta, Canada.

[10] Department of Radiology, University of Toronto, Canada.

[11] Department of Radiology, University of Montreal, Canada.

[12] Department of Radiology, University of Manitoba, Canada.

[13] Department of Radiology, University of British Columbia, Vancouver, Canada.

No time limits were imposed for the completion of this process.

Assessment of agreement.—The recording form listed 11 diagnostic categories that were condensed to 5 categories for the purposes of the analysis of agreement. These categories were: *a*) technically unsatisfactory film, *b*) normal breast, *c*) benign abnormality, *d*) suspicion of cancer, *e*) cancer present. As discussed below, films that were read as technically unsatisfactory were subsequently excluded for the purpose of analysis of agreement.

The readers recommended further therapeutic action for each patient by indicating if aspiration or biopsy should be performed, and if no immediate action was needed, when the next examination should be done. The recommendations made were then grouped into the following categories to assess agreement: *a*) aspiration and/or biopsy, *b*) reexamination in less than 6 months, *c*) reexamination in 6–12 months, *d*) reexamination in 12 months or more.

Statistical procedures.—Agreement on the use of the categories of diagnosis and recommendation was determined, after correction for expected chance agreement, with the use of the weighted kappa statistic (κ_w) (*5*) for each of the possible pairs of readers that could be formed from the participating radiologists. Weighted kappa was used because not all disagreements were considered to be of the same importance. For example, a disagreement in which a film was classified as normal by one radiologist and as benign by another was thought less serious than one in which a film was classified as normal by one reader and as cancerous by another. The weighted kappa statistic allows that not all disagreements are of equal importance and that some classes of disagreement, after adjustment with appropriate weights, can contribute to the overall level of agreement.

The weights used in calculating weighted kappa were those proposed for dichotomous ordinal scales by Cicchetti (*6*). (A dichotomous ordinal scale is one that is used to rate conditions that may be present or absent, and if present, that may exist in a number of states which can be ordinally ranked according to increasing levels of severity or seriousness.) With the weighted kappa statistic, a score of 1.0 indicates perfect agreement, and a score of zero indicates agreement that is not better than expected by chance. An example of the application of weighted kappa to the data presented here is given in the "Appendix."

For the analysis of agreement on diagnosis, with the weighted kappa, the scale comprised the diagnostic categories listed above after exclusion of the category of technically unsatisfactory. This exclusion was made because judgments about the technical merit of a film were thought to differ qualitatively from judgments about the diagnostic information that the film contained, and opinions about the technical merit of the film could not be ordinally ranked with diagnostic interpretations. One reader (radiologist G), who regarded 18 films as technically unsatisfactory, was excluded from the analysis of agreement on diagnosis, and any film regarded as technically unsatisfactory by any of the remaining readers was also excluded. The composition of the set of 85 films remaining after these exclusions is described in table 1.

TABLE 1.—*Composition of sets of films used for the analysis of agreement*[a]

Diagnostic category	Original set No.	Analysis of diagnosis No.	Analysis of recommendation No.
Cancer	10	10	9
Benign disease	40	33	27
Normal	50	42	25
Total	100	85	61

[a] *See test for reasons for exclusion.*

TABLE 2.—*Diagnostic classification of 100 films according to radiologist*

Diagnostic category	Diagnostic film classification according to radiologist								
	A	B	C	D	E	F	G	H	I
Technically unsatisfactory film	0	0	1	0	2	8	18	5	2
Normal	37	32	24	59	27	9	4	9	14
Benign disease	29	49	41	16	61	36	54	31	58
Suspicion of cancer	33	16	32	23	10	42	23	45	24
Cancer	1	3	2	2	0	5	1	10	2
Total	100	100	100	100	100	100	100	100	100

For the analysis of agreement on recommendations, with the weighted kappa statistic, the scale comprised the four categories listed above, and an additional category of films on which the radiologist had been unable to make a recommendation. The usual reason cited for not making a recommendation was that additional information, such as the patient's age or the findings of physical examination, was required. One reader (radiologist E), who was unable to make a recommendation on 32 films, was excluded from the analysis of agreement on recommendation, and any film on which any of the remaining readers could not make a recommendation was also excluded. The composition of the set of 61 films remaining after these exclusions is described in table 1.

In addition to overall agreement on the use of the four categories of diagnosis and recommendation, agreement on the use of each individual category was calculated (specific category agreement) to determine if there were particular categories that could not be reliably distinguished. Specific category agreement was calculated for each of the pairs of radiologists, and an example of the calculation is given in the "Appendix."

RESULTS

Diagnosis

Table 2 shows the frequency with which each radiologist used the four diagnostic categories and identified films as technically unsatisfactory. Use of the category "normal breast" varied from 4 to 59% according to reader, and between 16 and 61% of the films were read as showing a benign abnormality. The number of films suspected of containing cancer varied from 10 to 45%, and the number of films in which cancer was thought definitely to be present varied from 0 to 10%. Between 0 and 18% of the films were regarded as technically unsatisfactory according to the radiologists. Reader G, who classified 18 of the films as technically unsatisfactory, was excluded from the analysis of agreement on diagnosis shown in table 3. The radiologists who selected the films for this study are identified as readers A and B in the results that follow.

Table 3 shows the weighted kappa scores for agreement between all 28 possible pairings of these radiologists (excluding radiologist G) on the classification of the films. This analysis is confined to the 85 films that all of the remaining 8 readers agreed were technically satisfactory. All values of kappa indicated that agreement was significantly greater than expected chance agreement. The lowest value for κ_w was 0.23 between readers D and H, and the highest value was 0.59 between readers A and B. Five of the 28 values of kappa were less than 0.30, and only 4 were greater than 0.50.

Table 4 shows the mean kappa scores for agreement between radiologists (again excluding reader G) on the use of each individual diagnostic category. The scores cited for each radiologist are mean values for agreement between that reader and all other readers in the study on the use of each diagnostic group. (An example is worked out in the "Appendix" to illustrate how specific category agreement was determined.) Agreement was greatest on the category "cancer" with mean kappa values of 0.50 or more for all readers but one. Agreement was least on the category "benign abnormality" for all radiologists. Agreement on the categories "normal breast" and "suspicion of cancer" was intermediate.

To assess the possible influence on the results of excluding radiologist G, we repeated the analyses shown in tables 3 and 4 but limited them to the 71 films that all nine radiologists agreed were technically satisfactory. The results obtained were very similar to those shown in tables 3 and 4 and did not alter the conclusions drawn from those tables.

All 10 films known to contain histologically verified carcinoma of the breast were included in the set of films used for the analysis of agreement, and four were identified by all eight radiologists as cancerous or suspicion of cancer. Four of the eight readers identified all 10 films as cancerous or suspicion of cancer.

TABLE 3.—*Kappa scores for agreement on diagnosis*

Radiologist	Kappa scores according to radiologist							
	A	B	C	D	E	F	H	I
A		0.59	0.47	0.53	0.43	0.34	0.32	0.45
B			0.41	0.47	0.43	0.34	0.28	0.53
C				0.42	0.46	0.43	0.51	0.42
D					0.37	0.25	0.23	0.30
E						0.24	0.28	0.30
F							0.46	0.44
H								0.36

TABLE 4.—*Mean kappa scores for agreement on the use of specific diagnostic categories*

Diagnostic category	Mean kappa scores according to radiologist							
	A	B	C	D	E	F	H	I
Normal	0.48	0.46	0.50	0.40	0.45	0.35	0.40	0.42
Benign disease	0.18	0.24	0.20	0.08	0.15	0.25	0.17	0.21
Suspicion of cancer	0.55	0.54	0.53	0.52	0.47	0.39	0.34	0.56
Cancer	0.77	0.66	0.68	0.53	0.46	0.63	0.59	0.57

TABLE 5.—*Frequency of recommendations made by radiologists*

Recommendation	Recommendation frequency for radiologist								
	A	B	C	D	E	F	G	H	I
No recommendation	0	1	15	0	32	15	17	3	0
Follow-up in ≥12 mo	45	60	44	58	33	30	30	33	54
Follow-up in 6–12 mo	5	10	8	13	12	19	1	3	15
Follow-up in <6 mo	6	0	1	0	2	5	20	8	2
Aspiration and/or biopsy	44	29	32	29	21	31	32	53	29
Total	100	100	100	100	100	100	100	100	100

TABLE 6.—*Mean kappa scores for agreement on recommendation*

Radiologist	Mean kappa scores according to radiologist							
	A	B	C	D	F	G	H	I
A		0.53	0.39	0.48	0.51	0.52	0.48	0.43
B			0.36	0.53	0.60	0.45	0.42	0.52
C				0.49	0.37	0.38	0.15[a]	0.41
D					0.53	0.46	0.33	0.40
F						0.56	0.45	0.51
G							0.47	0.43
H								0.28

[a] Agreement not significantly greater than expected by chance.

Recommendations for Therapy

Table 5 shows the frequency with which each radiologist used the four categories of recommendation or did not make a recommendation. Aspiration and/or biopsy was recommended for 21–53% of these cases according to the reader, and re-examination in 12 months or more was recommended in 30–60% of instances. The recommendation for reexamination in less than 6 months was not used at all by some radiologists and in as many as 20% of instances by others. The recommendation for reexamination in 6–12 months was also used quite variably. Radiologist E did not make a recommendation regarding 32% of the films and was excluded from the analyses of agreement that are shown in tables 6 and 7.

Table 6 shows the weighted kappa scores for agreement between radiologists on the use of these categories of therapy recommendation for the 61 films on which all remaining readers made a recommendation. All but one of the values for kappa differed significantly from expected chance agreement, and the highest value was 0.63. Of the 10 kappa values, eight were 0.50 or more, and two values were less than 0.30.

Table 7 shows the mean kappa scores for agreement between radiologists on the use of each category of recommendation. Agreement was greatest on the recommendation for aspiration and/or biopsy or for follow-up in a year or more. Substantially lower levels of agreement were seen for

TABLE 7.—*Mean kappa scores for agreement on the use of specific categories of recommendation*

Recommendation	Mean kappa scores according to radiologist							
	A	B	C	D	F	G	H	I
Follow-up in ≥12 mo	0.51	0.54	0.38	0.50	0.54	0.51	0.39	0.48
Follow-up in 6–12 mo	0.07	0.08	0.14	0.12	0.20	0.04	0.12	0.01
Follow-up in <6 mo	−0.01	−0.18	−0.19	−0.12	−0.19	0.02	−0.07	−0.15
Aspiration and/or biopsy	0.58	0.58	0.44	0.54	0.51	0.63	0.48	0.54

all readers on both categories of recommendation for reexamination in less than a year.

We performed two additional analyses to assess the influence of exclusion on the results shown in tables 6 and 7. In the first, radiologist E was included, but the analysis was confined to the 47 films on which all radiologists made a recommendation. In the second, radiologists E, C, F, and G, all of whom did not make a recommendation for several films, were omitted, and the analysis was performed on the 97 films on which the remaining 5 radiologists did make a recommendation. Both analyses gave results that were very similar to those shown in tables 6 and 7.

Table 8 shows the number of radiologists who recommended biopsy according to the original diagnostic classification of the films. Three of the 10 films known to contain histologically verified breast cancer were recommended for aspiration or biopsy by all nine readers, eight of the 10 were recommended for biopsy by seven readers, and all 10 cases were recommended for biopsy or aspiration by at least five readers. Two of the films from breast cancer patients that were not recommended for biopsy by all readers appeared to give rise to particular difficulty. Both had been submitted by the radiologist who selected films showing only subtle radiologic signs of cancer. For one case of the five so selected, four radiologists did not recommend biopsy, and one radiologist did not make a recommendation. For another patient's film, three radiologists did not recommend biopsy. In 2 other patient's films submitted by this radiologist, one reader did not recommend biopsy. There were three films of cases submitted by the other radiologist for which one reader did not recommend biopsy and one for which no recommendation was made.

Of the 50 films from normal subjects, 14 were recommended for biopsy or aspiration by at least one reader, but there was little agreement on the recommendation for biopsy. In only three instances did three or more readers agree on the recommendation for biopsy or aspiration. Agreement on the need for aspiration and/or biopsy on films from patients thought to have benign breast disease was less than that for the known cancers, but it was greater than that for the known normal subjects.

DISCUSSION

As with other studies of observer variation, it should not be assumed without further evidence that these results apply to other radiologists or to other sets of xeromammograms. However, these results show that the radiologists who took part in this study varied greatly both in their diagnostic interpretation of xeromammograms and in their recommendations for further action. Although observer variation has been encountered in many radiologic prrocedures, it is likely to be particularly important in mammography. The concept of screening for breast cancer with mammography is based on the premise that radiologic signs suggesting the presence of cancer may be detected before other abnormalities, such as a palpable mass, are present. The performance of biopsy in response to the detection of such radiologic signs is expected to advance the time at which the diagnosis of breast cancer is made in an affected individual and so to increase the proportion of cancers found at a curable stage of their evolution (*7*). It can be expected, therefore, that in the context of screening for breast cancer with mammography, advice that a biopsy should be performed will often be based on the appearance of the mammogram alone and given in the absence of other evidence of breast disease that might help in making a clinical decision. Our results show that the advice to perform a biopsy based on the reading of a particular film may vary greatly from one radiologist to another. The known cancers included in the set of mammograms used in this study were, however, generally recommended for biopsy, and the analysis of specific category agreement showed that agreement on the presence of cancer was consistently higher than that for any of the other diagnostic categories. However, since the number of known cancers included in this set of films was small, it is unlikely that they included the full spectrum of radiologic signs of cancer. Therefore, no general conclusion regarding the diagnostic accuracy of mammography with respect to breast cancer should be drawn.

The principal sources of observer variation in this study were the diagnostic readings and therapy recommendations made about films from patients who did not have breast cancer. Whereas the actual prevalence of cancer in this set of mammograms was 10 of 85 (12%), the reported prevalence

TABLE 8.—*Agreement on the recommendation for biopsy according to diagnosis*[a]

Diagnostic category	No. of films	Agreement among following No. of radiologists recommending biopsy								
		9	8	7	6	5	4	3	2	1
Cancer	10	3	7	8	9	10	10	10	10	10
Benign disease, biopsy	20	1	7	10	13	14	17	18	19	19
Benign disease, no biopsy	20	2	2	5	6	7	9	9	12	18
Normal	50	0	0	0	1	1	2	3	6	14

[a] The rows of this table show, for each diagnostic category, the number of films recommended for biopsy and the number of radiologists recommending biopsy. Thus in the first row, of the 10 films from patients with cancer, 3 were recommended for biopsy by 9 readers, 7 by 8 readers, 8 by 7 readers, and so on.

of mammograms suspected of containing cancer varied from 10 to 55% according to the reader; there was also great variation in the frequency with which aspiration or biopsy was recommended. This problem is magnified by the composition of the set of films that we assembled and in particular by the inclusion of a relatively large number of films from patients with benign breast disease who had previously been judged to require biopsy. While such patients can be expected to have radiologic signs that cannot be reliably distinguished from cancer, it is clear from our results that radiologists may differ widely in their interpretation of these signs. As a result, as many as six of the 50 films from normal subjects were recommended for biopsy by at least one radiologist. This finding may arise in part from diagnostic habits formed in clinical practice, where there is a high prevalence of cancer in the films examined, and particular importance is placed on the need to avoid missing patients with breast cancer. Another contributing factor to this finding may be that radiologists were influenced by the circumstances of studying observer variation. Variability in the classification of patients who do not have breast cancer, however, is likely to have particularly important consequences in screening, where the prevalence of breast cancer is likely to be low, and the great majority of the women examined are free of breast cancer.

The results presented suggest some methods by which observer variation might be reduced. The analysis of specific category agreement on diagnosis showed that agreement on the category "benign abnormality" was so poor for all readers that it might be advantageous to eliminate this category. At least in context of screening for breast cancer, a diagnostic classification that seeks only to distinguish from all others those patients in whom cancer is present or suspected might be simpler to use and less subject to variability. Similarly, agreement on the recommendation to reexamine in less than 12 months was so poor that future studies might limit recommendations to the two categories of immediate aspiration and/or biopsy and follow-up in 12 months or more.

In addition to simplifying the classification of diagnosis and recommendation, explicit criteria for the recognition of those mammographic appearances that are most likely to be associated with invasive breast cancer, minimal breast cancer, and benign proliferative disorders need to be developed and tested. These criteria should, however, be based on mammographic signs that can themselves be reliably identified. Analysis of agreement on the mammographic signs recorded in this study showed that agreement on the presence or absence of architectural distortion, radiologic evidence of a breast mass, or of calcification, was less than that achieved for diagnosis. Thus for these readers none of the mammographic features recorded in this study offered a suitable basis for the formulation of criteria. Other methods of describing the observed information in a more reliable way need to be sought.

A further procedure whose feasibility and effects on observer variation merit study is that of dual reading of mammograms by two radiologists. When the dual reading of chest radiographs was introduced to screening for pulmonary tuberculosis, fewer films with radiologic evidence of active disease were missed (*8, 9*). In the present study the number of films available for the analysis for agreement on recommendation according to each of the four major diagnostic categories is small and any conclusions must be tentative. However, it appears that most readers were in agreement on the need for biopsy in those films that were subsequently shown to contain breast cancer, while there was less agreement about the need for biopsy when films in the other diagnostic categories were read. It is possible, therefore, that dual reading may reduce the effects of observer variation in the interpretation of xeromammograms and help to ensure that the greatest possible number of breast cancers are detected while minimizing the number of breast biopsies performed on women who do not have breast cancer.

APPENDIX

The example given here is intended to illustrate the way in which the results were calculated. More mathematical discussions of these indices of agreement may be found elsewhere (*5, 6, 10*) as may more detailed discussions written for clinicians (*11*).

Appendix table 1 shows the way in which radiologists A and B classified the 85 mammograms regarded as technically satisfactory according to diagnosis. Perfect agreement occurs in the cells of the table where both readers assigned the same diagnosis and the cells in which there is perfect agreement lie along the diagonal from the top left cell to the bottom right cell.

Calculation of Agreement and Weighted Agreement (PO_w)

The simplest method of calculating agreement is to add the number of films classified in each of the four cells in appendix table 1 that lie on the diagonal indicating perfect agreement and to divide this number by the total number of films classified. Thus the proportion of perfect agreement was: (21+17+15+1)/85=54/85=0.64.

This method of calculation regards all disagreements as being of equal importance. However, we may regard disagreements between suspicion of cancer and cancer or between normal and benign as being of little importance; we

APPENDIX TABLE 1.—*Diagnostic classification of films according to radiologists A and B*

	Diagnostic film classification according to:[a]				
	Radiologist B				
Radiologist A	Normal	Benign disease	Suspicion of cancer	Cancer	Total
Normal	21(1.00)	12(0.60)	0(0.20)	0(0.00)	33
Benign disease	4(0.60)	17(1.00)	1(0.80)	0(0.40)	22
Suspicion of cancer	3(0.20)	9(0.80)	15(1.00)	2(0.80)	29
Cancer	0(0.00)	0(0.40)	0(0.80)	1(1.00)	1
Total	28	38	16	3	85

[a] No. of films (cell weights in parentheses throughout).

may regard disagreements between normal and cancer as being of greater importance. To allow for differences in the importance of some categories of disagreement, we may "weight" disagreements differently. The weights used in this process are shown *in parentheses* in appendix table 1 and are proposed by Cicchetti (*6*).

Weighted agreement is calculated by multiplying the number in each cell by its associated weight and adding the products for the entire table. This sum is then divided by the total number of films classified. Thus weighted agreement in appendix table 1 becomes: $[(21\times1)+(12\times0.60)+(0\times0.20)+(4\times0.60)+(17\times1.0)+(1\times0.80)+(0\times0.40)+(3\times0.20)+(9\times0.80)+(15\times1.0)+(2\times0.80)+(0\times0.40)+(0\times0.80)+(1\times1.0)]/85=0.8682$.

Calculation of Weighted Agreement Expected by Chance (PC_w)

The calculation of agreement that was performed in the previous section did not take into account the amount of agreement expected by chance. To do this, an expected value is calculated for each cell. This is done by multiplying the row totals (that is, the cassifications of radiologist A) by the column totals (the classifications of radiologist B) and dividing by the grand total. Thus, for the top left cell of appendix table 1 the expected number is derived by: $(28\times33)/85=10.87$.

After an expected number has been calculated for each of the 16 cells of appendix table 1, expected agreement is determined by multiplying the expected number in each cell by the cell weight, in an identical manner to that used when weighted observed agreement was calculated, and then adding up the products. For appendix table 1: $PC_w=\{(10.87\times1.0)+(14.75\times0.60)+(6.21\times0.20)+(7.25\times0.60)+(9.84\times1.0)+(4.14\times0.80)+(0.78\times0.40)+(9.55\times0.20)+(12.96\times0.80)+(5.46\times1.0)+(1.02\times0.80)+(0.45\times0.40)+(0.19\times0.80)+(0.04\times1.0)\}/85=0.6788$.

Calculation of Weighted Kappa (κ_w)

As shown above, some agreement on the diagnostic classification of films can be expected by chance alone. The kappa statistic corrects the amount of agreement observed for the agreement that is expected by chance. It is preferred to other indices of association, such as the correlation coefficient, because it expresses the extent to which two sets of observations agree, and not merely the extent to which they are related (*11*). Weighted kappa is calculated by the formula: $PO_w-PC_w/1-PC_w$, where PO_w is the proportion of weighted agreement, calculated as in the first section above, and PC_w is the proportion of weighted agreement expected by chance, calculated as in the second section above. For the example shown in appendix table 1, $\kappa_w=(0.8682-0.6788)/(1-0.6788)=0.5898$.

Kappa will have the value 0 if agreement observed is equal to agreement expected by chance ($PO_w=PC_w$); kappa will be +1 if observed agreement is perfect ($PO_w=1.0$). Kappa will be less than 0 if observed agreement is less than agreement expected by chance.

Calculation of Specific Category Agreement

Calculation of kappa values for agreement in specific categories also required calculation of the amount of agreement observed for a specific category (*SO*), the amount of agreement expected by chance for that category (*SC*), and correction of the agreement observed for the agreement expected by chance (kappa).

The amount of specific category agreement observed (*SO*) is calculated from the number of agreed upon cases in a particular diagnostic category, divided by the average number of cases to which that diagnostic category is applied. For example, in appendix table 1 radiologists A and B agreed that 21 films were normal. The category ""normal" was applied to 33 films by reader A and to 28 films by reader B. The average frequency to which the category was applied is then $33+28/2=30.5$. Observed specific category agreement is thus $21/30.5=0.69$.

With the use of cell weights, calculation of specific category agreement was expanded to take into account partial disagreements in an analogous manner to that described in the first section of this appendix.

The amount of specific category agreement expected by chance (*SC*) was calculated for each cell and each pair of readers by first determining the expected number for the cell. This was done by multiplying the number of films placed in that category by one reader by the number placed in the category by the other reader and then dividing the product by the total number of films. The amount of specific category agreement expected by chance is then obtained by dividing the expected cell number by the average frequency with which the two readers used the category. Thus for the category "normal" in appendix table 1, the expected number of films in the cell is $(33\times28)/85=10.87$. Expected specific category agreement on the category "normal" is then $10.87/30.5=0.36$.

Finally, the chance corrected specific category agreement (Kappa) for any given nominal category is given by: kappa$=(SO-SC)/(1-SC)$. In the example considered above for the category "normal", and not taking into account weights for partial agreement, kappa$=(0.69-0.36)/(1-0.36)=0.52$.

The assessment of specific category agreement is fully discussed by Cicchetti et al. (*10*).

REFERENCES

(*1*) Birkelo CC, Chamberlain WE, Phelps PS, Schools PE, Zacks D, Yerushalmy J. Tuberculosis case finding: Comparison of effectiveness of various roentgenogram and photofluorographic methods. JAMA 1947; 133:359–366.

(*2*) Cochrane AL, Garland LH. Observer error in interpretation of chest films: International investigation. Lancet 1952; 2:505–509.

(*3*) Garland LH, Miller ER, Zwerling HB, et al. Studies on the value of serial films in estimating progress of pulmonary disease. Radiology 1952; 58:161–177.

(*4*) Groth-Petersen E, Lovgreen A, Thillemann J. On the reliability of photofluorograms and value of dual reading. Acta Tuberc Scand 1952; 26:13–37.

(*5*) Cohen J. Weighted kappa: Nominal scale agreement with provision for scaled disagreement or partial credit. Psychol Bull 1968; 70: 213–220.

(6) Cicchetti DV. Assessing inter-rater reliability for rating scales: Resolving some basic issues. Br J Psychiat 1976; 129:452–456.

(7) Shapiro S. Evidence on screening for breast cancer from a randomized trial. Cancer 1977; 39:2772–2782.

(8) Stradling P, Johnston RN. Reducing observer error in a 70-mm chest-radiography service for general practitioners. Lancet 1955; 1: 1247–1250.

(9) Yerushalmy J, Harkness JT, Cope JH, Kennedy BR. Role of dual reading in mass radiography. Am Rev Tuberc 1950; 61:443–464.

(10) Cicchetti DV, Lee C, Fontanna AF, Dowds BN. Computer program for assessing specific category rater agreement for qualitative data. Educ Psychol Measur 1978; 38:805–813.

(11) Kramer MS, Feinstein AR. Clinical biostatistics. LIV. The biostatistics of concordance. Clin Pharmacol Ther 1981; 29:111–123.

Multiple Cell Lines From Patients With Malignant Melanoma: Morphology, Karyology, and Biochemical Analysis[1,2,3]

Toni U. Semple,[4] George E. Moore,[4] Robert T. Morgan,[4] Linda K. Woods,[4] *and* Laurie A. Quinn[4,5]

ABSTRACT—Of 23 cell lines representing 8 patients with malignant melanoma, one cell line from each patient has been extensively characterized by means of phase morphology, ultrastructural morphology, biochemical markers, steroid receptor protein analysis, and steroid hormone production. Extensive cytogenetic characterization was compiled from seven of the eight cell lines. The melanocytic derivation of the tumor cell lines was supported by the detection of the catecholamines epinephrine, norepinephrine, and dopamine. In addition, well-defined melanosomes were present in six of the seven lines whose ultrastructures were examined morphologically. None of the lines produced α-fetoprotein, β-human chorionic gonadotropin, or carcinoembryonic antigen in detectable amounts. The individuality of the cell lines was confirmed by phenotypic patterns of isozymes and by karyology.—JNCI 1982; 68:365–380.

Mammalian cells established as permanent lines in vitro are increasingly useful in many areas of scientific pursuit not previously associated with tissue culture. Normal and abnormal substances produced eutopically or ectopically by cells in culture are a valuable resource. The effects of various hormones, nutrients, and growth factors on the metabolism and survival of mammalian cells can be assayed in vitro. Cell lines established from different types of cancers can be used by the oncologist to identify and categorize clinically significant patterns of biological aberrations in neoplastic disease.

It is imperative that every cell line used for in vitro studies be characterized as fully as possible. The array of attributes so delineated allows investigators interested in a particular attribute to select a cell line for use without preliminary screening of many cell lines. More importantly, the characteristics described provide for periodic reidentification of each cell line.

We have almost 40% success in establishing continuous cell lines from patients with malignant melanoma. Malignant melanoma cell lines are common; multiple cell lines from a [illegible] are less common. Very few malignant [illegible] [illegible] literature have been thoroughly [illegible]. We [illegible] of 23 cell lines from 8 patients [illegible] malignant melanoma.

MATERIALS AND METHODS

Case histories.—Patient A (COLO 297 cell line): On September 2, 1976, a [illegible] removed from a 76-year-old white [illegible] and cultured. The pathologic diagnosis was malignant melanoma with sheets of heavily pigmented pleomorphic cells.

Patient B (COLO 296, COLO 298, COLO 300, and COLO 302 cell lines): On October 5, 1976, a 47-year-old white woman was seen with a 6-cm mass in the inguinal area, subsequent to the excision of a malignant melanoma from the leg that was done elsewhere. The tissue excised by groin dissection was confirmed as a pigmented malignant melanoma. The metastatic tumor tissue was cultured by our laboratories. The patient is alive and well.

Patient C (COLO 322 and COLO 324 cell lines): A 42-year-old white male had a black spot removed from his cheek by dermabrasion, but local regrowth and probable metastases were noted. Following chemotherapy, a neck dissection and subsequently an axillary dissection were performed in October 1975. Tissue culture from the regional lymph nodes contained malignant melanoma cells with pleomorphic forms, prominent nucleoli, and some bizarre mitoses. This metastatic tumor tissue was cultured.

Patient D (COLO 342, COLO 343, and COLO 349 cell lines): This 69-year-old white male had undergone excision of a malignant melanoma from the arm and the axillary nodes some years ago. A melanotic metastasis in a groin lymph node was excised in January 1978 and cultured.

Patient E (COLO 358, COLA 361, COLO 362, and COLO 363 cell lines): On September 7, 1971, a 63-year-old white male patient was admitted with axillary and cervical metastases 7 years after excision of a malignant melanoma of the skin over the left scapula. The diagnosis was confirmed and the tumor tissue was cultured. The patient was given chemotherapy and is well.

Patient F (COLO 368 and COLO 381 cell lines): A right axillary mass was excised in July 1977, 6 months after a bleeding mole had been removed by cautery from the back of this 35-year-old white male; local recurrence was also present. A third metastasis in the right flank was excised, confirmed as a pigmented malignant melanoma, and cultured. Despite chemotherapy, the patient died in a few months.

Patient G (COLO 383 and COLO 415 cell lines): On November 15, 1978, a large neck mass was excised from a 21-year-old white woman 2 years after a lightly pigmented malignant melanoma was removed from her back. A pathologic diagnosis of amelanotic melanoma was made and

---

ABBREVIATIONS USED: AFP=α-fetoprotein; CEA=carcinoembryonic antigen; DAPI=4',6-diamidino-2-phenylindol dihydrochloride; DM=double minute(s); FBS=fetal bovine serum; β-HCG=β-human chorionic gonadotropin.

---

[1] Received February 20, 1981; revised October 5, 1981; accepted October 22, 1981.

[2] Supported by Public Health Service grant 1-R01CA-15018 from the National Cancer Institute and by the Mary B. and L. H. Marshall Fund.

[3] Research procedures were in accord with the Human Subjects Committee, Denver General Hospital.

[4] Division of Surgical Oncology, Denver General Hospital, 750 Cherokee St., Denver, Colo. 80204.

[5] We are indebted to Ms. Loris McGavran for excellent cytogenetic analyses.

tissue sent to our cell culture laboratory. Both this patient and her father died of malignant melanoma.

Patient H (COLO 417, COLO 419, COLO 437, COLO 441v, and COLO 442v cell lines): In July 1979 a 30-year-old white male with schizophrenia was noted to have developed a huge axillary mass that an examination proved to be a pigmented malignant melanoma. This tissue was cultured. The patient died 1 year later from extensive disease.

Cell culture.—Our methods for tumor cell cultures have been described (*1*). Tumor specimens were finely minced in RPMI-1640 medium (Irvine Scientific, Irvine, Calif.) with 20% FBS (heat inactivated at 56°C for 30 min), and 0.25 ml of the resultant cell suspension was pipetted in 4-ounce flint-glass bottles. No more than 1 ml of a selected medium was added to each flask. The flasks were loosely capped and placed in a humidified 37°C incubator containing 10% CO_2 in air for 24–48 hours. Each week, or as needed, 1–5 ml of appropriate medium was added to the culture until growth stabilized. We made subcultures either by sharply rapping the flask on the palm of the hand to loosen cells or by using a rubber scraper and then pouring suspended cells into another flask.

The lymphoid cell lines were established by methods previously described (*2*).

Representative cell lines were selected for extensive characterization.

Morphology.—Morphologic studies were accomplished by the examination with phase optics of Leighton tube subcultures of the cell lines. Duplicate cover slips were fixed for 3 minutes in absolute ethanol, stained with May-Grünwald-Giemsa, and mounted for permanent records.

For the study of the ultrastructural morphology, cells were harvested, pelleted, and fixed in 4% glutaraldehyde in 0.1 *M* phosphate buffer (pH 7.3). The methodology for embedding and staining has been reported elsewhere (*3*).

Chromosome analyses.—Chromosome preparations for each line analyzed were made according to techniques described previously (*4*). Slides were also stained conventionally with Giemsa to determine the presence of DM chromosomes (small, acentric chromosomes). Chromosome mode was determined by direct microscopic observation of 50 cells at metaphase. We selected 8–14 metaphase plates to be photographed and karyotyped.

Pigment formation.—For enhancement of pigment formation, cells were grown for 2 weeks in GEM 1717 media (Irvine Scientific) with 10% FBS containing 0.44 m*M* L-tyrosine and pelleted into round-bottomed test tubes. The resultant pellet was allowed to stand in the light for 2 weeks. The color of the pellet was then compared visually to that of control pellets treated in the identical manner except for the additional tyrosine.

CEA.—CEA levels were determined with a radioimmunoassay technique available in kit form by Roche Diagnostics, Nutley, N.J. Preparation of cultures for this assay has been described previously (*5*).

Isozyme phenotypic patterns.—Phenotypic isozyme analyses were performed in accord with the starch-gel electrophoretic methods of Harris and Hopkinson (*6*). Glucose-6-phosphate dehydrogenase mobility was determined with the use of the standard clinical procedure of Helena Laboratories, Beaumont, Tex. For sample preparation, 10^6 cells were freeze-thawed three times in 0.1 ml deionized water.

Plating efficiency.—For each cell line, 3×10^2 or 6×10^2 cells were plated in each of three 35-mm tissue culture dishes; 1.2 ml of RPMI-1640 plus 20% FBS was the final volume in the plates. The plates were placed undisturbed for 7 days in a humidified 37°C incubator containing 10% CO_2. After the incubation period, the medium was aspirated from the plates, and cell colonies were fixed with methanol–acetic acid (3:1) and stained with Gram's crystal violet. The plating efficiency was calculated by: (Average number of colonies/number of cells originally seeded)×100=plating efficiency.

Ectopic elaboration of cell products.—β-HCG and AFP determinations were performed by Immunological Associates of Denver, Denver, Colo. Calcitonin, serotonin, and the fractionated catecholamines were determined by UpJohn Laboratories, Woodland Hills, Calif., and Kalamazoo, Mich. In all cases, aliquots from 15 ml of spent medium from cultures not fed for the preceding 48 hours and containing 1.5×10^6 cells were used for the determinations. These determinations were all performed in 1980 on cultures in continuous culture since their establishment.

Production of steroid hormones.—Estrogen and progesterone production was determined by use of an Estrogen Pak (^{3}H-labeled estrogens, estradiol, and estrone; New England Nuclear Corp., Boston, Mass.) and a Progesterone Pak (^{3}H-labeled progesterone; New England Nuclear Corp.), respectively. Preparation of cultures for steroid hormone production assays has been described elsewhere (*7*).

Steroid receptor assays.—Assays of 4S and 8S receptor proteins were determined as previously described (*7*).

Mycoplasma.—We monitored mycoplasma contamination by staining cytocentrifuge preparations of the cells with Hoechst dye 33258 (bisbenzamide) according to the methods of Chen (*8*) or with DAPI by the method of T. E. Swanson (personal communication). Cell preparations were fixed in methanol–acetic acid (3:1) for 10 minutes, stained in 0.1 μl DAPI/ml for 5 minutes, leached in distilled water for 10 seconds, mounted in phosphate-buffered saline, and viewed with UV epi-illumination.

Storage in cell banks.—Cell lines were preserved in ampuls by the suspension of 10^6 cells/ml in RPMI-1640 medium plus 20% FBS, 12.5% dimethyl sulfoxide, and antibiotics and then slowly cooled to −80°C.

RESULTS

Cell culture.—The history of each cell line is presented in table 1. All cell lines were established from metastases.

Phase morphology.—All cell lines (with the exception of COLO 417) grew as spindle-shaped to triangular–dendritic and cuboidal cells. The percentage of each cell type varied among the different lines. Bizarre cells with extensive dendritic processes were observed in all the lines. When confluent, all lines formed clumps of viable cells that either loosely attached to the monolayer or floated free in the supernatant. COLO 417 was comprised primarily of round to oval cells that were loosely attached or grew in the supernatant. Spindle cells were occasionally observed, be-

TABLE 1.—*Histories of 23 cell lines from patients with malignant melanoma*

Patient	Cell line[a]	Tissue of origin	Date of initiation	Date of establishment	Therapy prior to culture[b]	Cell type
A	COLO 297*	Biopsy	9/2/76	12/28/76	None	Monolayer
B	COLO 296	Node	9/20/76	12/27/76	None	Monolayer
	COLO 298*	Node	10/20/76	1/17/77	None	Monolayer
	COLO 300	Node	10/20/76	2/8/77	None	Monolayer
	COLO 302	Node	10/20/76	3/9/77	None	Monolayer
C	COLO 322	Biopsy	4/19/77	6/21/77	DTIC	Monolayer
	COLO 324*	Biopsy	4/19/77	7/19/77	DTIC	Monolayer
D	COLO 342	Biopsy	12/9/77	12/23/77	Adriamycin	Monolayer
	COLO 343	Biopsy	12/9/77	12/23/77	Adriamycin	Monolayer
	COLO 349*	Biopsy	1/27/78	3/21/78	Adriamycin	Monolayer
E	COLO 358	Blood	3/21/78	5/16/78	None	Lymphoid
	COLO 361*	Node	3/22/78	6/22/78	None	Monolayer
	COLO 362	Node	3/22/78	6/22/78	None	Monolayer
	COLO 363	Node	3/22/78	6/22/78	None	Monolayer
F	COLO 368	Biopsy	4/27/78	7/25/78	DTIC	Monolayer
	COLO 381*	Biopsy	4/27/78	12/15/78	DTIC	Monolayer
G	COLO 383	Biopsy	11/16/78	1/24/79	None	Monolayer
	COLO 415*	Biopsy	11/16/78	5/25/79	None	Monolayer
H	COLO 417*	Biopsy	7/3/79	7/17/79	None	Monolayer
	COLO 419	Biopsy	7/3/79	7/25/79	None	Monolayer
	COLO 437	Biopsy	7/3/79	7/20/79	None	Monolayer
	COLO 441v	Blood	7/24/79	9/7/79	None	Lymphoid
	COLO 442v	Blood	7/24/79	9/7/79	None	Lymphoid

[a] Cell lines marked with an *asterisk* were selected for extensive characterization.
[b] DTIC=imidazole carboximide.

coming more common with confluence. Giant cells with multiple nuclei were frequent in COLO 417.

Pigment granules were observed in all cell lines. The heaviest pigmentation was observed in COLO 297. Nuclei of the cells were round to ovoid with prominent nucleoli. Intracellular bridges were seen in COLO 361 and COLO 415. All the lines with the exception of COLO 361 grew rapidly and formed confluent monolayers in 4–5 days; COLO 361 formed a confluent monolayer in 2–3 weeks.

Section A of figures 1–8 show phase morphology for all lines described.

Ultrastructural morphology.—Electron photomicrographs revealed melanosomes that ranged from abundant and heavily pigmented in COLO 297 to rare and lightly pigmented or nonpigmented in COLO 417. COLO 415 did not have any ultrastructure clearly identifiable as that of a melanosome or premelanosome. All cells displayed endoplasmic reticulum in varying amounts, but the endoplasmic reticulum appeared abnormal in all cells. Unusual endoplasmic reticulum incorporated into circular patterns was observed in COLO 415. Polysomes were abundant in COLO 297, COLO 324, and COLO 417. Numerous, but aberrant mitochondria were observed in all lines. Well-formed Golgi structures were abundant. Lipid vacuoles and glycogen deposits were observed in all lines. Fenestrated nucleoli were apparent in all lines. Microvillar projections were seen only in COLO 349 and COLO 417, being most plentiful in COLO 417. Tight junctions are not expected in melanoma cell lines but were plentiful in COLO 417.

Sections B of figures 1–8 exemplifies the ultrastructural morphology of these lines. The ultrastructural morphology of COLO 361 is not available.

Chromosome analyses.—Due to a laboratory accident, one cell line (COLO 361) has been lost. Therefore, chromosome analysis of this line is not available. Early harvests of this line had structural and numerical chromosome abnormalities. Karyotypes for the other cell lines appear in figures 9–15. Major chromosome markers were defined as those appearing in 50% of the cells analyzed and were designated by "M." No marker chromosomes common to all cell lines were observed. Chromosomes 1, 3, 5, 6, and 7 were the most frequently involved, whereas chromosomes 2, 4, 9, 11, 15, 20, 21, 22, X, and Y were infrequently involved (table 2). The chromosome mode and range near the mode for the seven cell lines examined are listed in table 3. All lines exhibited chromosome numbers within the triploid or tetra-

TABLE 2.—*Chromosome involvement in markers of malignant melanoma cell lines*

Parameter	Chromosome																							
	1	2	3	4	5	6	7	8	9	10	11	12	13	14	15	16	17	18	19	20	21	22	X	Y
No. of markers with involvement of specific chromosomes	13	4	9	3	7	9	9	6	2	3	3	4	5	5	1	5	4	4	3	1	2	1	1	0
No. of cell lines with marker involvement of specific chromosomes	7	3	5	3	2	6	4	5	2	2	2	4	4	4	1	5	4	4	2	1	2	1	1	0

TABLE 3.—*Chromosome modes in malignant melanoma cell lines*

Cell line	No. of months post establishment	Chromosome mode (range)	Percent of cells within range
COLO 297	23	87 (78–94)	64
	26	(82–86)[a]	60
	39	(79–82)[a]	43
COLO 298	18	40 (39–43)	70
		80 (70–80)[b]	25
	35	69 (62–74)	93
COLO 324	30	(71–78)[a]	32
		(130–151)[a,b]	48
COLO 349	5	80 (79–92)	45
	22	(84–96)[a]	70
COLO 381	13	77 (73–80)	68
	25	77 (72–83)	85
COLO 415	21	86 (82–91)	37
COLO 437	4	66 (63–71)	70

[a] No definitive mode.
[b] Bimodal.

ploid range. Four of the seven lines have sequential analysis data. Those lines showed no particular pattern of chromosome gain or loss. The percentage of cells with chromosome counts near the mode increased in three of four cases. No correlation was observed among patients' stage of disease, number of months until death, length of time of cell lines in culture, number of chromosome abnormalities, or cell line stability. Table 4 lists the marker and DM chromosome occurrence in the cell lines examined. The frequency of cells with DM varied from 4 to 50%.

Isozyme analyses.—Results of isozyme analyses are presented in table 5.

Pigment production and ectopic elaboration of cell products.—The results of enhanced pigment production and elaboration of cell products are presented in table 6.

Steroid receptors.—Steroid receptor analyses are presented in table 7. Of three biopsy specimens that expressed positive estrogen receptor proteins, only COLO 342 retained this characteristic in culture.

Steroid hormone production.—COLO 296, COLO 297, COLO 342, COLO 368, and COLO 381 were examined for hormone production; none were positive.

Plating efficiencies.—Plating efficiencies were as follows: COLO 297=12%, COLO 298=27%, COLO 349=26%, COLO 324 and COLO 417=19%, and COLO 381 and COLO 415=17%. These figures were obtained from plates containing 300 cells/dish. There was no statistically significant difference ($P>0.1$) in the plating efficiency in plates containing 600 cells/dish.

TABLE 4.—*Marker and DM chromosome occurrence in malignant melanoma cell lines*

Cell line	Mean No. of chromosomes per cell	Percent of marker contribution to chromosome No.	Percent of cells with DM
COLO 297	74	25	50.0
COLO 298	73	23	9.3
COLO 324	120	10	41.1
COLO 349	79	20	4.0
COLO 381	75	14	5.7
COLO 415	86	19	40.2
COLO 437	59	14	10.0

Mycoplasma.—Although rare, sparse mycoplasma contamination was seen in some lines; at no time were all cultures of these lines positive. Positive cultures were treated with Tylocine or tetracycline until all evidence of mycoplasma had been eliminated and the cultures remained free of contamination, or the positive cultures were discarded. All characterizations were performed on cultures free from mycoplasma.

DISCUSSION

To derive maximum benefit from cultured mammalian cells, investigators must be informed of cellular characteristics that satisfy their particular area of investigation. Additionally, for those investigators interested in the histogenesis of a particular type of cancer, evidence of the ascribed origin of the cells is important. Finally, characteristics fingerprinting a particular cell line are mandatory for the subsequent reidentification of that cell line. Cross-contamination is an increasingly common occurrence and is recognizable only when cell lines have had marker properties identified previously. The variety of markers presented in our report may be utilized to assess the potential value of these lines to investigators and to provide a means to identify the cell lines described.

We have characterized eight cell lines representative of 23 tumor cell lines established from 8 patients with malignant melanoma. Cell lines from 6 of our 8 patients are similar to each other with respect to morphology by phase optics, ultrastructural morphology, and growth characteristics. They also resemble melanoma cell lines previously described by us (*9*). Two cell lines, COLO 361 from patient E and COLO 415 from patient G, differ from most malignant melanoma cell lines established in our laboratory. For example, melanosomes were not observed in COLO 415, and addition of extra tyrosine failed to increase pigment production in either line. Although the morphology of the two lines was similar, their isozyme phenotypes were differ-

TABLE 5.—*Isozyme phenotypes of malignant melanoma cell lines*

Cell line	Phenotype of					Frequency of occurrence
	Glc-6-*PD*[a]	PGM1[b]	PGM3[c]	ESD[d]	GOT2[e]	
COLO 297	B	1	1	2–1	1	0.052
COLO 298	B	1	1	1	1	0.249
COLO 324	B	2	1	1	1	0.026
COLO 349	B	2–1	1	1	1	0.162
COLO 361	B	2–1	2–1	1	1	0.112
COLO 381	B	2–1	1	1	1	0.162
COLO 415	B	2–1	1	1	1	0.162
COLO 417	B	1	1	1	1	0.249

[a] Glucose-6-phosphate dehydrogenase.
[b] First locus of phosphoglucomutase.
[c] Third locus of phosphoglucomutase.
[d] Esterase D.
[e] "Mitochondrial" glutamate–oxaloacetate transaminase.

TABLE 6.—*Stimulation of pigment production and ectopic secretion of cell products from melanoma cell lines*

Parameter	Media blank	COLO 297	COLO 298	COLO 324	COLO 349	COLO 361[a]	COLO 381	COLO 415	COLO 417
CEA, ng/ml	2	0	0	0	0	0	0	0	0
β-HCG, nIU/ml	0	0	0	0	0	ND	0	0	0
AFP, ng/ml	6	5	5	4	6	ND	1	4	7
Calcitonin, pg/ml	<30	36	123	65	35	<30	61	34	37
Serotonin, ng/ml	<22	<22	<22	<22	<22	<22	<22	<22	<22
Catecholamines, pg/ml:									
Dopamine	2	54	<1	19	<1	25	43	45	7
Epinephrine	<1	9	5	3	4	9	14	8	9
Norepinephrine	12	<1	11	<1	13	16	39	3	12
Tyrosine (four times medium concentration)[b]	–	++++	++++	++++	+++	+	+++	–	++++

[a] ND=not determined.

[b] Relative visual assessments.

ent, indicating that they were distinct cell lines. The histopathology studies on both of these metastatic lesions did not reveal pigment in the cells. Both patients had "malignant melanoma" lesions removed previously from different sites. The possibility of the derivation of these cell lines from secondary primary lesions should be considered; however, there was no clinical evidence of other primary cancers in these patients. It is also possible that these two cell lines represent a population of melanoma cells that does not usually survive culture, is primitive and/or undifferentiated, and does not generate melanosomes.

Occurrence of aberrant karyotypes was expected in the malignant cell lines. All human tumor cell lines established in this laboratory (>165 different lines) exhibit abnormal chromosome constitutions. All of the lines derived from different individuals can be distinguished on the basis of karyotype. The extensive analyses that were possible through the use of cultured cells did not reveal specific chromosome breakpoints in common markers. Such breakpoints would indicate that the observed chromosome abnormalities were related to the malignant melanoma disease process, as has been observed for some other types of cancers (*10–13*). In this case, however, the significance of chromosome aberrations remains speculative. The presence of DM is also expected. DM have been detected in all but one tumor cell line scanned for their presence by us. Theoretically, malignant melanomas are derived from neural-ectodermal tissue and might be expected to produce some of the products associated with amine precursor uptake and decarboxylase cells. The selection of biochemical markers was

TABLE 7.—*Analysis of steroid and glucocorticoid receptor proteins*[a]

Patient	Fresh tumor estrogen receptor protein[b]	Cell line analyzed	Receptor protein			
			Estrogen	R5020 (promogestone)	Dexamethasone	5α-Dihydroxytestosterone
A	222—4S 136—8S 358—total	COLO 297	0	0	108—4S 0—8S 108—total	0
B	Not determined	COLO 296	0	0	0	0
C	Not determined	COLO 322	0	0	0	0
D	1) 87—4S 0—8S 87—total 2) 273—4S 359—8S 632—total	COLO 342	60—4S 91—8S 151—total	0	0	0
E	0	COLO 363	0	0	718—4S 321—8S 1,039—total	0
F	1) 345—4S 129—8S 474—total 2) 0	COLO 368	0	0	0	0
G	Not determined	COLO 415	0	0	90—4S 0—8S 90—total	304—4S 0—8S 304—total
H	0	COLO 417	0	0	0	0

[a] Values are expressed in femtamoles per gram of packed cells.

[b] Where numbered, values represent two different tumor specimens.

made in part on this basis. The cell lines were assayed for the production of serotonin, calcitonin, and the catecholamines epinephrine, norepinephrine, and dopamine. The synthesis of the catecholamines from 3,4-dihydroxy-L-phenylalanine, a precursor to 5,6-indolequinone (the monomer of melanin pigments), might be expected of a melanocyte whose metabolic controls are abnormal. In addition, AFP and CEA assays were selected to demonstrate the possible dedifferentiation of the cells to a more embryonic stage of ontogeny. β-HCG was assayed and has been previously associated with melanoma cell lines (*14*).

All the cell lines tested produced significant levels of one or more of the catecholamines. Although there has recently been a report of melanoma producing serotonin in vivo (*15*), the failure of these cell lines to produce either serotonin or β-HCG may reflect the variable gene derepression which is perhaps associated with chromosome aberrations. Alternatively, the culture environment may have selected against those cells producing these substances. The lack of detectable CEA or AFP may simply indicate that there is still sufficient genetic control in these cell lines to prevent expression of the embryonic antigens.

The detection of estrogen receptors in three of six fresh tumor specimens is compatible with other reports (*16*). Only one cell line retained detectable levels of estrogen receptors. Three of eight had glucocorticoid receptors, and one of eight had androgen receptors. Such cell lines should be valuable for studies of receptor activity. Selective pressures of the culture media with sera containing variable amounts of hormones probably influence survival of cells from the heterologous mosaic of mutant cells in the original tumor with or without hormone receptors.

This spectrum of melanoma cell lines is also valuable to investigators seeking a common specific melanoma antigen.

In summary, the individuality of eight human malignant melanoma cell lines has been established through phenotypic isozyme fingerprinting, karyotypes, and biochemical markers. The original histologic diagnosis of melanoma has been conclusively confirmed in six of these lines, but the characteristics of two cell lines are atypical and cause one to reconsider the nature of the tumor from which the lines were established. However, the biochemical data indicated that these lines are probably of malignant melanotic origin, despite the absence of melanin in subsequent metastases. In our opinion, there will always be primitive cancers derived from precursors of entities such as melanoma that may not contain type-specific structures, functions, cell products, biologic behavior, or antigens. These cancers will give question to the histogenesis, diagnosis, and therapy of the lesion.

REFERENCES

(*1*) Morgan RT, Quinn LA, Woods LK, Moore GE. Marker properties of tumor and lymphoid cell lines derived from a patient with squamous cell carcinoma. Cancer Res 1977; 37:2030–2035.

(*2*) Moss DJ, Pope JH. Assay of infectivity of Epstein-Barr virus by transformation of human leukocytes in vitro. J Gen Virol 1972; 17:233–236.

(*3*) Mitchen JR, Moore GE, Gerner RE, Woods LK. Interaction of human melanoma cell lines with autochthonous lymphoid cells. Yale J Biol Med 1973; 46:669–680.

(*4*) Semple TU, Quinn LA, Woods LK, Moore GE. Tumor and lymphoid cell lines from a patient with carcinoma of the colon for a cytotoxicity model. Cancer Res 1978; 38:1345–1355.

(*5*) Moore GE, Morgan RT, Quinn LA, Woods LK. A transitional cell carcinoma cell line. In Vitro 1978; 14:301–306.

(*6*) Harris H, Hopkinson DA. Handbook of enzyme electrophoresis in human genetics. New York: Elsevier, 1976.

(*7*) Woods LK, Morgan RT, Quinn LA, Moore GE, Semple TU, Stedman KE. Comparison of four new cell lines from patients with adenocarcinoma of the ovary. Cancer Res 1979; 39:4449–4459.

(*8*) Chen TR. Microscopic determination of *Mycoplasma* contamination in cell cultures and cell culture media. Tissue Culture Assoc Manual 1975; 1:229–232.

(*9*) Quinn LA, Woods LK, Merrick SB, Arabasz NM, Moore GE. Cytogenetic analysis of twelve human malignant melanoma cell lines. J Natl Cancer Inst 1977; 59:301–307.

(*10*) Cruciger QV, Pathak S, Cailleau R. Human breast carcinoma: Marker chromosomes involving 1q in seven cases. Cytogenet Cell Genet 1976; 17:231–235.

(*11*) Kakati S, Hayata I, Oshimura M, Sandberg AA. Chromosomes and causation of human cancer and leukemia. X. Banding patterns in cancerous effusions. Cancer 1975; 36:1729–1738.

(*12*) Rowley JD. Duplication of part of chromosome No. 1 in myeloproliferative diseases. Lancet 1978; 1:96–97.

(*13*) Manolov G, Manolova Y. Marker band in one chromosome 14 from Burkitt's lymphoma. Nature 1972; 237:33–34.

(*14*) Neuwald PD, Anderson C, Salivar WO, et al. Expression of oncodevelopmental gene products by human tumor cells in culture. JNCI 1980; 64:447–459.

(*15*) Harai T, Nishihara H, Hattori S, Tateishi T. Malignant melanoma producing serotonin. Cancer 1979; 43:294–298.

(*16*) Stedman KE, Moore GE, Morgan RT. Estrogen receptor proteins in diverse human tumors. Arch Surg 1980; 115:244–248.

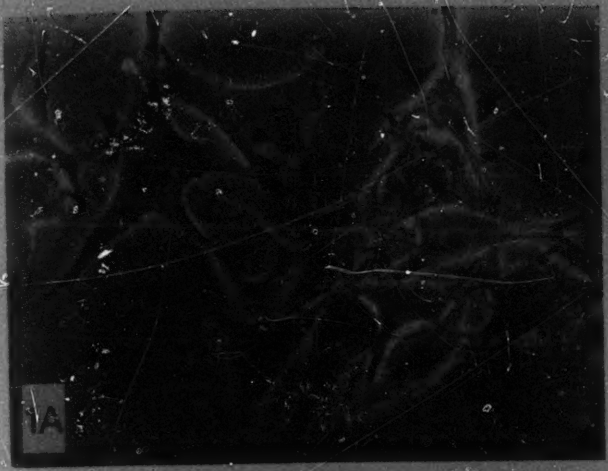

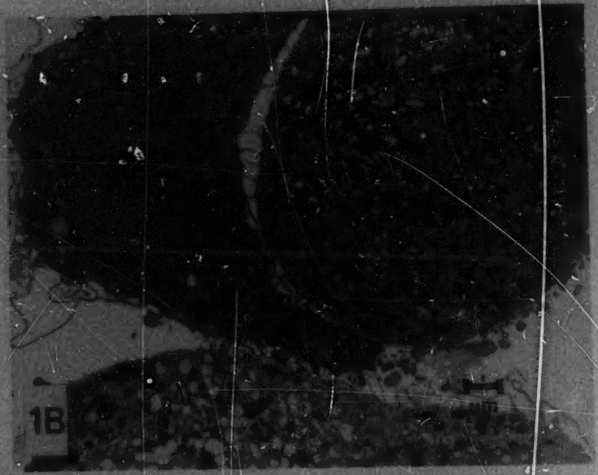

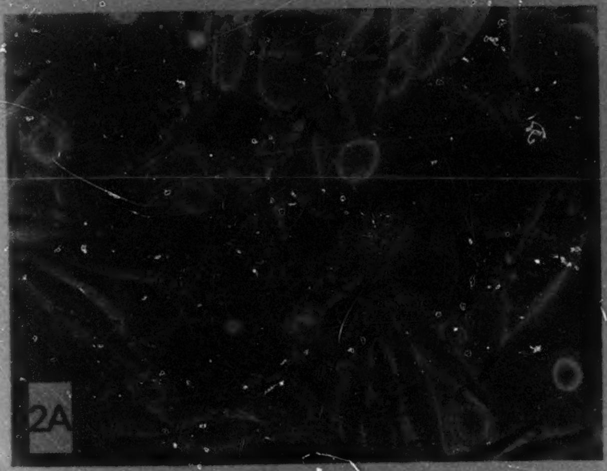

FIGURES 1A, 2A, AND 3A.—Representative phase morphology of COLO 297, COLO 298, and COLO 324, respectively. All cells show spindle to dendritic shapes with occasional dendritic processes and large nuclei with predominantly single or double nucleoli. Dark inclusion granules are prevalent. × 325. FIGURES 1B, 2B, AND 3B.—Ultrastructural morphology of COLO 297, COLO 298, and COLO 324, respectively. Melanosomes are abundant in all lines, especially COLO 297. All lines demonstrated aberrant mitochondria and numerous Golgi, ribosomes, and lipid deposits. *Bars*=1 μm.

best copy available

4A

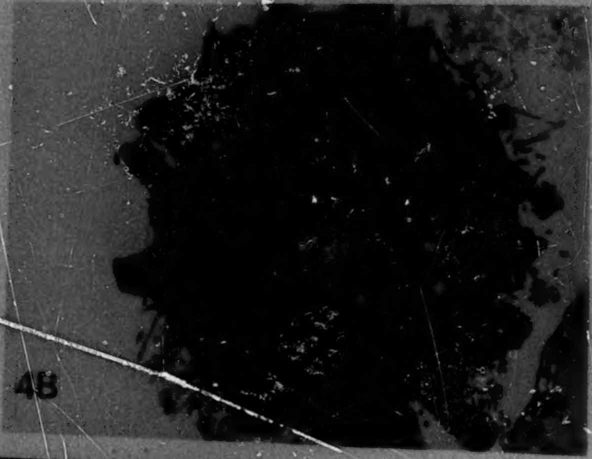
4B

5

6A

6B

FIGURES 4A, 5, AND 6A.—Phase morphology of COLO 349, COLO 361, and COLO 381, respectively. Typical melanoma morphology is exhibited by COLO 349 and COLO 381. Two types of morphology are shown in COLO 361. × 230. FIGURES 4B AND 6B.—Ultrastructural morphology of COLO 349 and COLO 381, including melanosomes, polysomes, and abnormal mitochondria. *Bars*=1 μm.

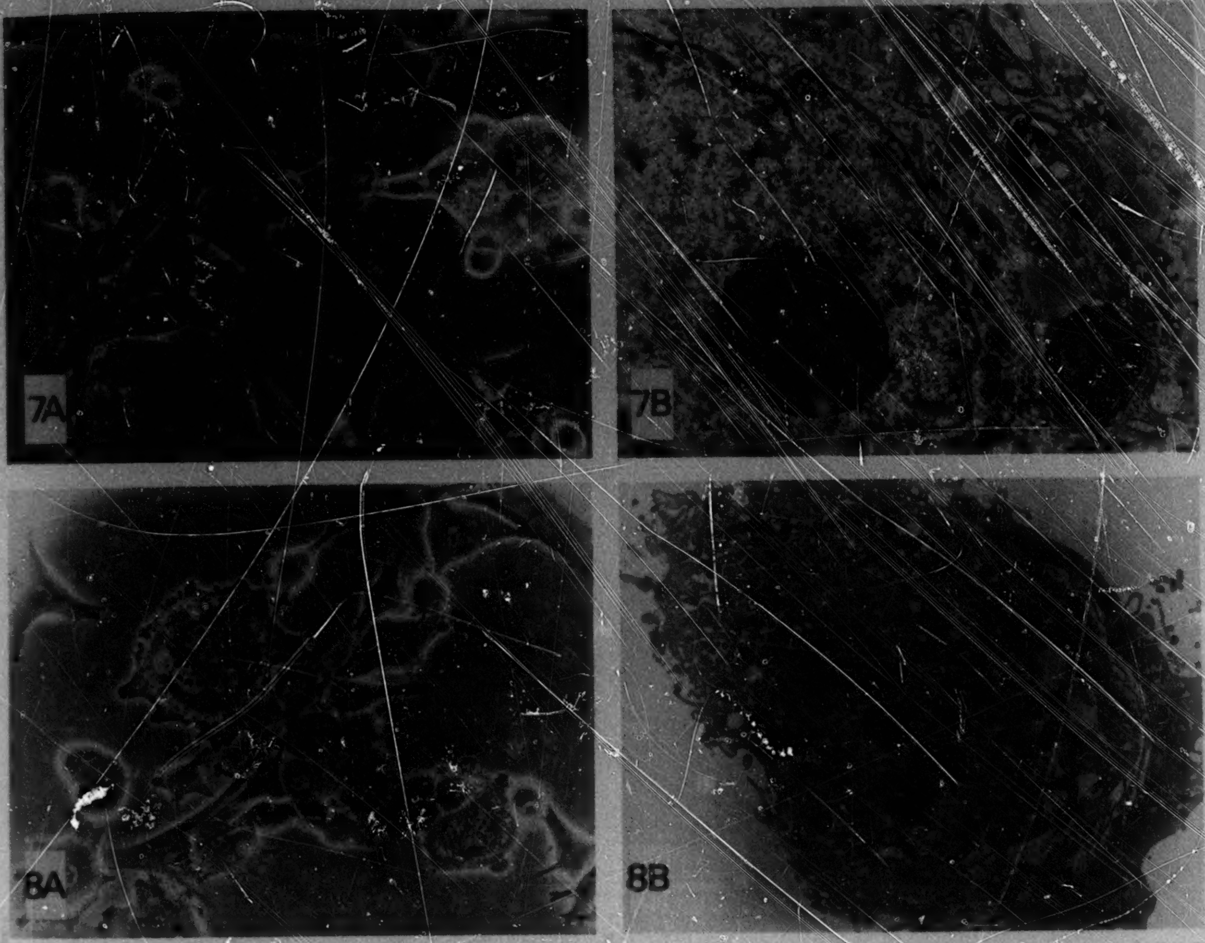

FIGURES 7A AND 8A.—Phase morphology of COLO 415 and COLO 417, respectively. These cell lines possess characteristics similar to those of other lines described. × 280. FIGURE 7B.—Highly irregular circular patterns of endoplasmic reticulum exhibited by COLO 415. FIGURE 8B.—Typical melanoma characteristics with the exception of tight junctions visible around periphery of central cell. *Bars*=1 µm.

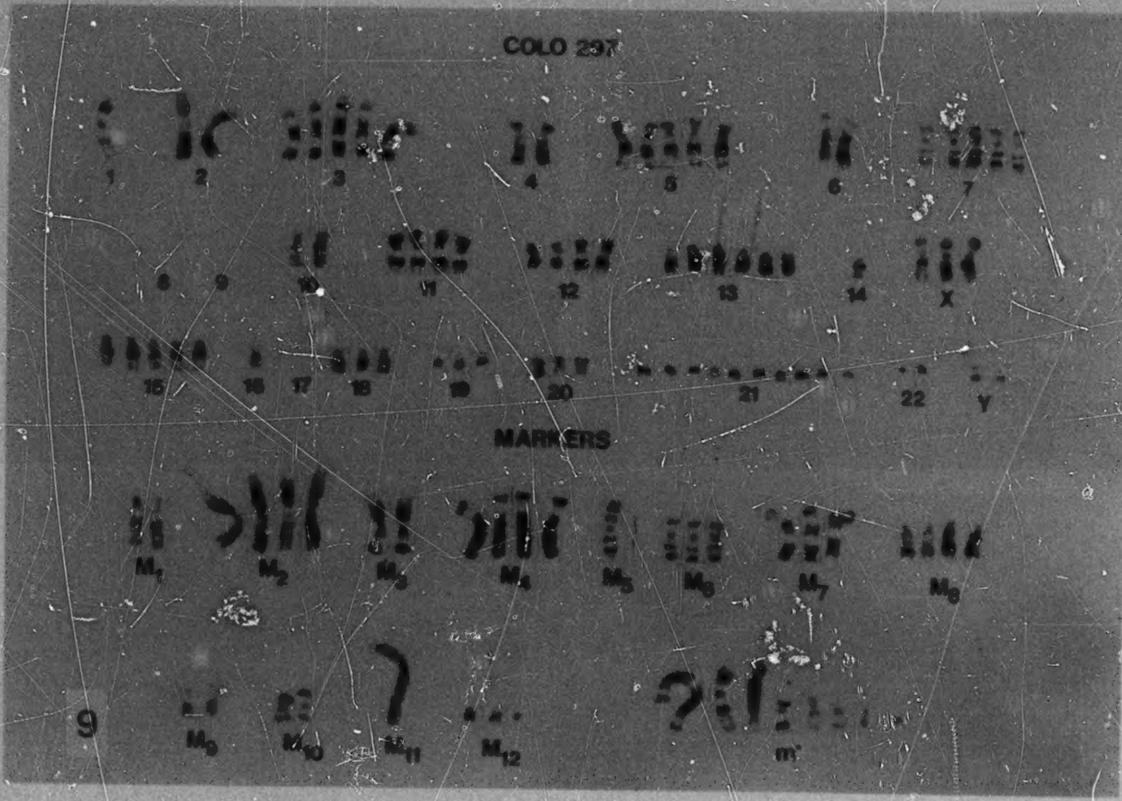
COLO 297
1
2
3
4
5
6
7
8
9
10
11
12
13
14
X
15
16
17
18
19
20
21
22
Y
MARKERS
M1
M2
M3
M4
M5
M6
M7
M8
9
M9
M10
M11
M12
m'

FIGURE 9.—Karyotype of COLO 297

Major marker chromosome	Karyotype
M1	del(1) (qter→p13:)
M2	t(1;2) (lpter→1p34::2p23→2qter)
M3	t(1;3) (lpter→1q11::3p13→3pter)
M4	t(4;6;?) (4qter→4q12::6q11→6p21::?)
M5	i(7) (qter→cen→qter)
M6	del,t(7;17) (7q32→7q11::17p13→17qter)
M7	t(9;?;8) (9pter→9q34::?::8q12?→8qter)
M8	del,t(10;12) (10p13→10q24::12q14→12qter)
M9	t(16;?) (16qter→16p13::?)
M10	i(17) (qter→cen→qter)
M11	Submetacentric larger than chromosome 1 with lightly stained short arm; dark band near centromere; remainder of long arm had intermediate staining intensity with no distinct bands (homogenous staining region?)
M12	Small centric fragment

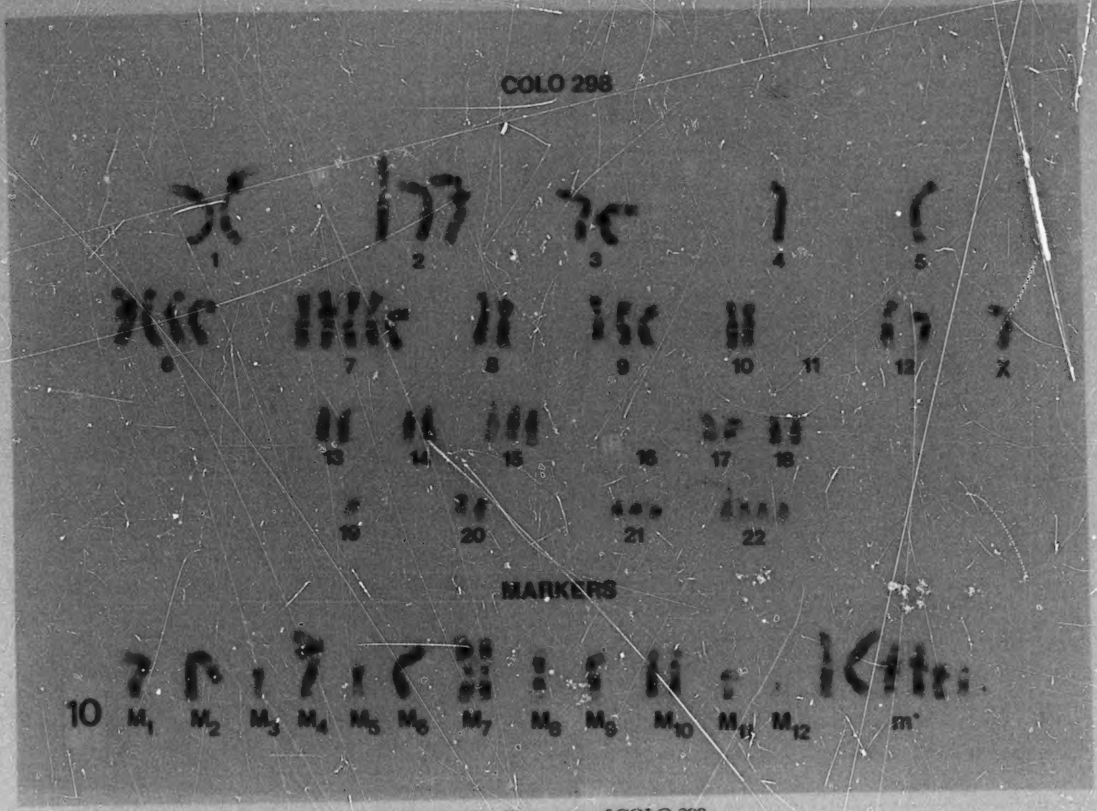
COLO 298
1
2
3
4
5
6
7
8
9
10
11
12
X
13
14
15
16
17
18
19
20
21
22
MARKERS
10
M_1
M_2
M_3
M_4
M_5
M_6
M_7
M_8
M_9
M_{10}
M_{11}
M_{12}
m*

FIGURE 10.—Karyotype of COLO 298

Major marker chromosome	Karyotype
M1	del(3) (qter→p23:)
M2	t(4;7) (4qter→4p16::7p11→7qter)
M3	del(5) (pter→q22:)
M4	t(5;17) (5qter→5q13::17p11→17qter)
M5	t(5;19) (5pter→5p13::19p131→19qter)
M6	i(8) (qter→cen→qter)
M7	i(11) (qter→cen→qter)
M8	The q-arm was derived from 11 or 12q; p-arm has sharp, dark band near centromere; nonbanded pter
M9	t(12; ?) (12qter→12p13::?)
M10	t(13;16) (13qter→13q12::16q13→16pter)
M11	t(19; ?) (19?::?)
M12	Centric fragment

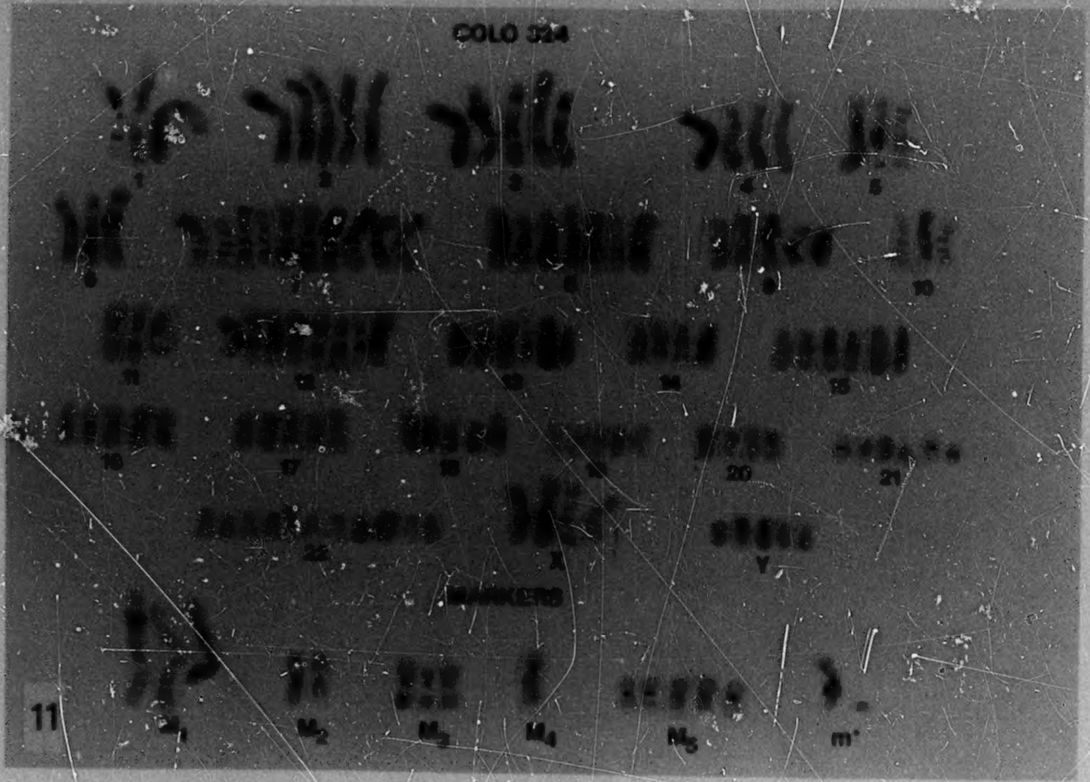
COLO 324
1
2
3
4
5
6
7
8
9
10
11
12
13
14
15
16
17
18
19
20
21
22
X
Y
MARKERS
11
M1
M2
M3
M4
M5
m'

FIGURE 11.—Karyotype of COLO 324

Major marker chromosome	Karyotype
M1	t(1; ?) (1pter→1p35::?)
M2	del(6) (pter→q21:)
M3	del(11) (pter→q23:)
M4	t(14; 21) (14qter→cen→21qter)
M5	del(16) (pter→q22:)

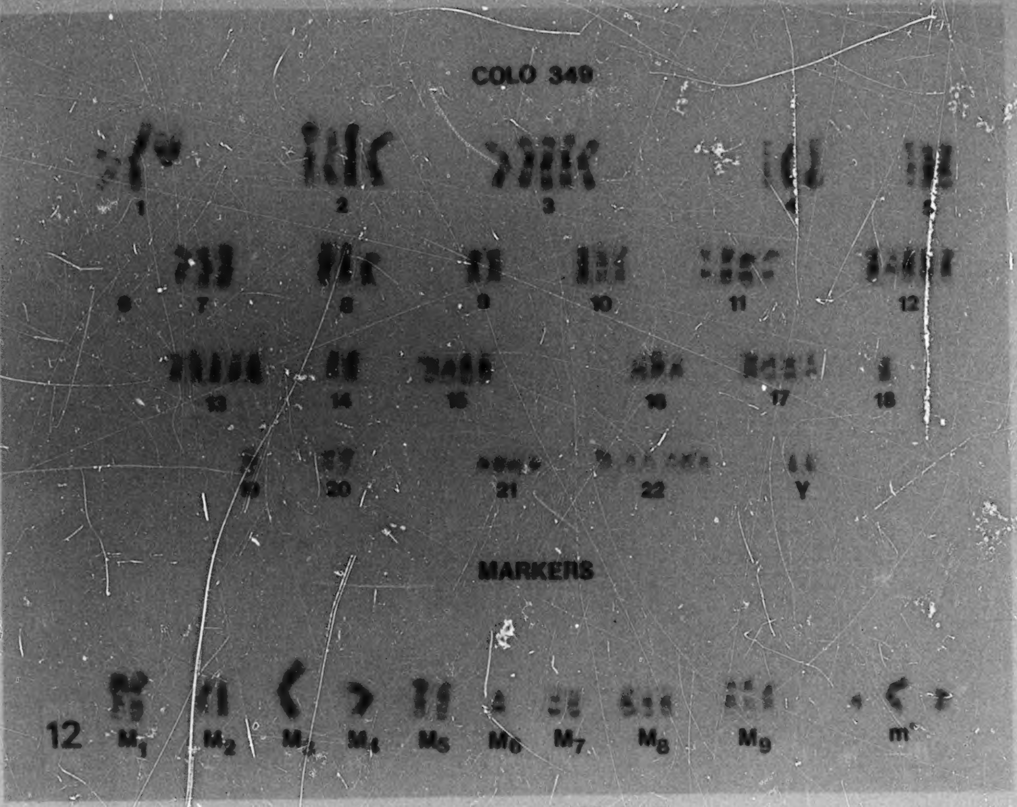
COLO 349
1
2
3
4
5
6
7
8
9
10
11
12
13
14
15
16
17
18
19
20
21
22
Y
MARKERS
12
M_1
M_2
M_3
M_4
M_5
M_6
M_7
M_8
M_9
m

FIGURE 12.—Karyotype of COLO 349

Major marker chromosome	Karyotype
M1	t(1; ?) (lqter→lp12::?)
M2	t(6; ?) (6qter→cen→?)
M3	t(7; ?) (7qter→7pl?::?)
M4	t(8; ?) (8qter→8p21::?)
M5	t(15; ?) (15pter→15q26?::?)
M6	del(17) (qter→pi1)
M7	t(19; ?) (19pter→19q12::?)
M8	Submetacentric E-sized marker; medium-intensity band near centromere; small terminal band in q-arm, light staining of p-arm
M9	Submetacentric E-sized marker; pericentric C-band, 2 equal bands of medium intensity on q-arm, light staining of terminus

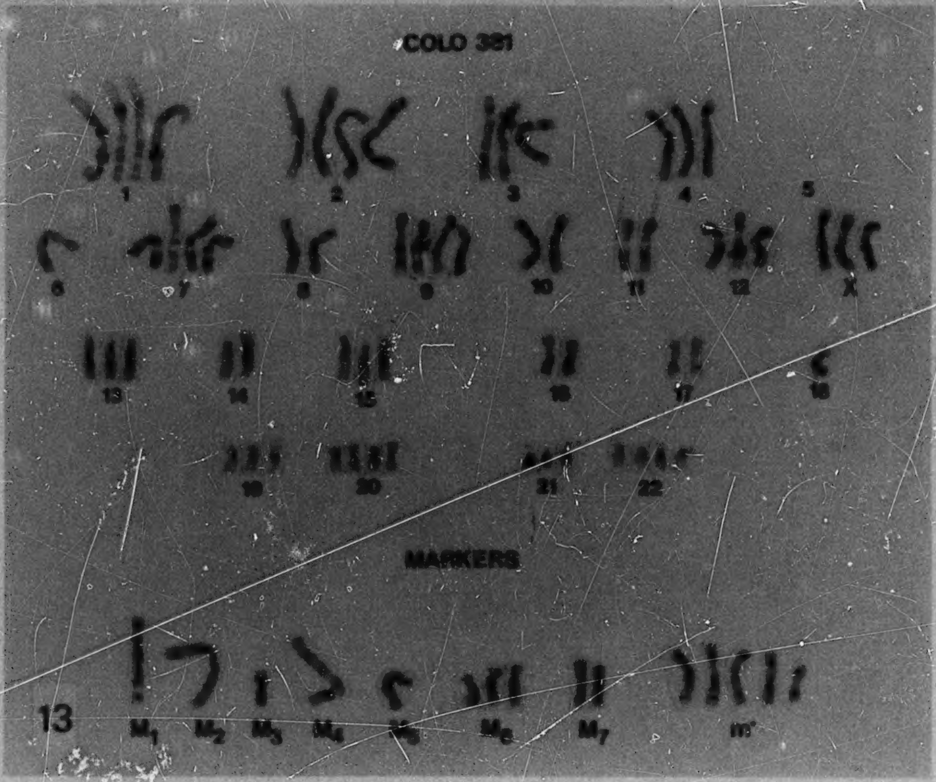
COLO 381
1
2
3
4
5
6
7
8
9
10
11
12
X
13
14
15
16
17
18
19
20
21
22
MARKERS
13
M1
M2
M3
M4
M5
M6
M7
m'

FIGURE 13.—Karyotype of COLO 381

Major marker chromosome	Karyotype
M1	t(3;6) (3p25→3p21::6q27→6pter)
M2	i(5) (qter→cen→qter)
M3	del(5) (pter→q14:)
M4	t(12;?;?) (12qter→12p13::?::?)
M5	Acrocentric marker derived from M4
M6	t(18;?) (18pter→18q23::?)
M7	Unidentifiable marker; q-arm has 3 prominent bands; p-arm has 2–3 less distinctive bands of short arm and no identifiable bands in long arm

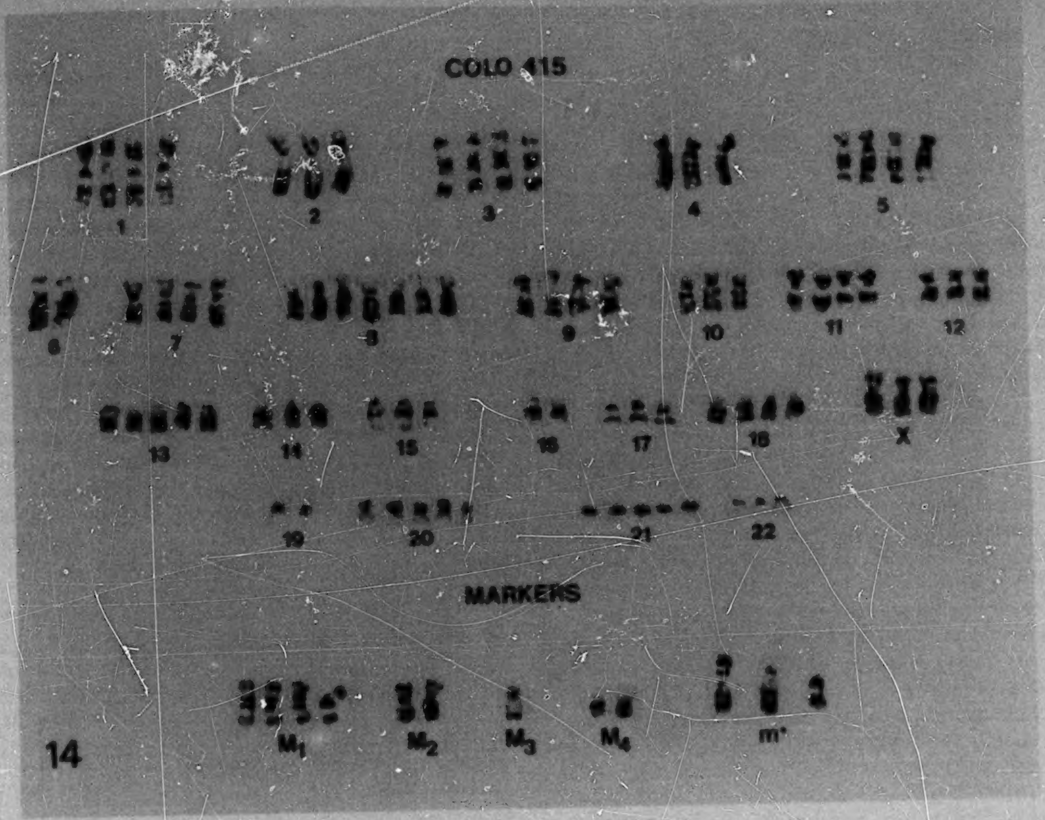
COLO 415
1
2
3
4
5
6
7
8
9
10
11
12
13
14
15
16
17
18
X
19
20
21
22
MARKERS
M_1
M_2
M_3
M_4
m*
14

Figure 14.—Karyotype of COLO 415

Major marker chromosome	Karyotype
M1	i(6) (pter→cen→pter)
M2	del(7) (pter→q32:)
M3	t(7;17) (7pter→7p13::17q21→17pter)
M4	del(16) (pter→q22:)
M5	Centric fragment

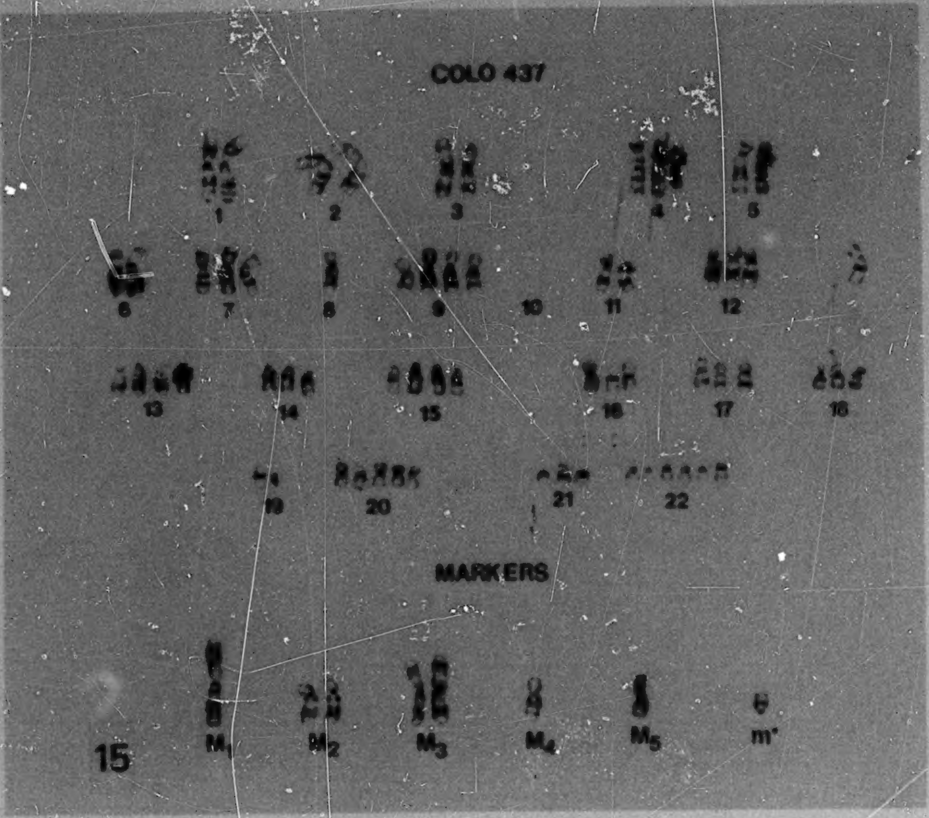
COLO 437
1
2
3
4
5
6
7
8
9
10
11
12
13
14
15
16
17
18
19
20
21
22
MARKERS
15
M1
M2
M3
M4
M5
m'

FIGURE 15.—Karyotype of COLO 437

Major marker chromosome	Karyotype
M1	t(1;2) (1qter→cen→2qter)
M2	t(3;10) (3qter→3q21::10q22→10pter)
M3	t(3;13) (3qter→3p13::13q11→13qter)
M4	t(8;14) (8pter→8q21::14q23→14qter)
M5	t(X;?) (Xq25→Xp22::?)
M6	del(16) (pter→q23:)

Prolactin Receptors in Human Breast Tumors[1,2]

Lucile Turcot-Lemay[3,4,5] *and* **Paul A. Kelly**[3,6]

ABSTRACT—Prolactin-binding sites were determined in 759 human breast tumor biopsy specimens. Ovine prolactin (oPRL) was used in the binding assay of 569 tumors with 13% of the tumors showing a positive content with more than 1% specific binding. Human prolactin (hPRL) was utilized for 343 tumors with 38% of the tumors binding 1% or greater of the added radioactivity. When human growth hormone (hGH) was used as the labeled ligand in 95 tumors, only 2% of the tumors specifically bound more than 1% of the hGH. A total of 153 tumors were assayed simultaneously with the use of labeled hPRL and oPRL. Whereas 10.4% of the tumors showed the presence of prolactin-binding sites (>1% specific binding) when oPRL was used, an approximately threefold increase (29.4%) in tumors possessing prolactin receptors was revealed when hPRL was used as the labeled ligand. Therefore, hPRL is the preferred ligand for the assessment of prolactin receptor levels in human breast cancer biopsy specimens.—JNCI 1982; 68:381–383.

The measurement of hormone receptor levels for estrogen and progesterone in breast cancer biopsy specimens has become a routine procedure to establish the hormonal dependency of these tumors and to direct the type of therapy to be given to these patients (*1–3*). It has been demonstrated, however, that only 55–60% of the receptor-positive tumors respond to various forms of endocrine treatment, whereas less than 10% of the patients with receptor-negative tumors respond to such treatment (*1*, *4*, *5*). Therefore, something not predicted by assessment of steroid receptor levels might be involved in the growth and development of these tumors. Prolactin has a well-established role in the development and growth of experimental rat and mouse mammary tumors (*6–9*), and prolactin receptors have been identified in these tumors as well as more recently in human breast tumors (*10–14*).

During the last 2 years, we have assayed prolactin receptors in 759 human breast tumors sent to our laboratory by the surrounding medical centers for steroid receptor determination. A comparison of the optimum type of labeled ligand to use in the assay of prolactin receptors in breast tumor biopsies was done.

MATERIALS AND METHODS

Membrane preparation.—Human breast tumor specimens or biopsy specimens were received for 17β-estradiol and progesterone receptor assays from several regional hospitals and were frozen on Dry Ice or in liquid nitrogen. Tumors were first pulverized, then homogenized with 2- to 10-second bursts of a Polytron PT-10 homogenizer in 25 m*M* Tris–HCl (pH 7.4), 1.5 m*M* EDTA, 10 m*M* thioglycerol, and 10% glycerol, and finally centrifuged at 13,000×*g* for 15 minutes. The supernatant was centrifuged at 105,000×*g* for 90 minutes. The resulting cytosol was used for the steroid receptor-binding assays. The crude microsomal pellet was resuspended in 25 m*M* Tris–HCl and 10 m*M* $MgCl_2$ (pH 7.4) with a Teflon–glass homogenizer, and the protein concentration was measured (*15*) with bovine serum albumin as standard.

Hormones.—oPRL (NIH-P-S12; 35 IU/mg) and hGH (HS-2160E; 1.7 IU/mg) were gifts of the National Pituitary Agency, University of Maryland School of Medicine, Baltimore, Md. and by the National Institute of Arthritis, Metabolism, and Digestive Disease, National Institute of Health. The hPRL for iodination was provided by Dr. Henry Friesen, University of Manitoba, Winnipeg, Manitoba.

[^{125}I]oPRL-, [^{125}I]hPRL-, and [^{125}I]hGH-binding assays.—The oPRL, hPRL, and hGH (5 μg each) were iodinated with low concentrations of chloramine-T (500 ng). The specific activities varied from 35 to 65 μCi/μg for oPRL and from 72 to 75 μCi/μg for hPRL and was 36.4 μCi/μg for hGH, as calculated by isotope recovery.

Approximately 100,000 cpm of [^{125}I]oPRL, [^{125}I]hPRL, or [^{125}I]hGH was incubated with 300 μg of tumor membrane protein in a final volume of 0.5 ml in 25 m*M* Tris–HCl and 10 m*M* $MgCl_2$ (pH 7.4) containing 0.1% bovine serum albumin. The incubation was performed at 23°C in the presence or absence of an excess of unlabeled oPRL for 16–20 hours. The incubation was stopped by addition of 3 ml of the incubation buffer. Bound and free hormones were separated by low-speed centrifugation (2,000×*g*) at 4°C for 15 minutes. After decantation, the pellets were counted in an LKB gamma spectrometer. Specific binding was obtained by subtraction of nonspecific from total bound radioactivity. This value was expressed as percentage of the total radioactivity added to the tube (*7*). Nonspecific binding ranged from 2 to 4% of the added radioactivity. We established a limit of sensitivity of 0.5% by obtaining a difference of at least 500 cpm between total counts and nonspecific counts for the biopsy samples. Differences of less than 500 cpm (corresponding to 0.5% of the 100,000 cpm of added radioactivity) were considered below the limit of sensitivity for the technique, on the basis of a combination of a number of factors routinely examined including counter background, homogeneity of labeled hormones from one iodi-

---

ABBREVIATIONS USED: hGH=human growth hormone; hPRL= human prolactin; oPRL=ovine prolactin.

---

[1] Received March 11, 1981; revised October 27, 1981; accepted November 2, 1981.

[2] Supported by a grant from the Medical Research Council of Canada.

[3] Department of Molecular Endocrinology, Le Centre Hospitalier de l'Université Laval, Quebec GIV 4G2, Canada.

[4] Recipient of a Fellowship from the Conseil de la Recherche en Santé du Québec.

[5] *Present address*: Molecular Oncology Laboratory, Hôtel-Dieu de Québec, 11, Côte du Palais, Quebec GIR 2J6, Canada.

[6] We thank Mr. Réjean Mélançon for homogenizing and preparing the cytosol and membrane fractions of human breast cancer biopsy specimens.

TABLE 1.—*Comparison of specific binding to 153 human breast cancer biopsy specimens with oPRL and hPRL as the labeled ligand*[a]

Ligand	Specific binding at binding values of:				
	0%	0.1–0.4%	0.5–0.9%	1.0–1.9%	>2.0%
[^{125}I]hPRL	25.5% (39)	18.3% (28)	26.8% (41)	20.3% (31)	9.1% (14)
				29.4%	
[^{125}I]oPRL	50.4% (77)	25.5% (39)	13.7% (21)	7.8% (12)	2.6% (4)
				10.4%	

[a] *Numbers in parentheses* indicate the numbers of tumors.

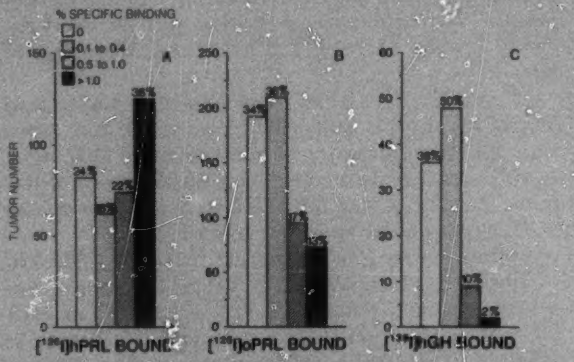

TEXT-FIGURE 1.—Comparison of specific binding of prolactin with [^{125}I]hPRL (A, 343 tumors), [^{125}I]oPRL (B, 569 tumors), and [^{125}I]hGH (C, 95 tumors). Binding values are arbitrarily divided into four categories (0, 0.1–0.4, 0.5–0.9, and 1.0% of the added radioactivity specifically bound).

nation to the next, nonspecific binding values, and degree of binding, which can be competed by an excess of unlabeled prolactin.

RESULTS

Text-figure 1 shows a comparison of prolactin-binding sites. Three different labeled ligands in human breast cancer biopsy samples were used. On the basis of the background sensitivity of the technique in our laboratory, values greater than 0.5% of the added radioactivity represented significant specific binding of prolactin. With [^{125}I]hPRL (text-fig. 1A), 58% of the biopsy specimens fell into this category compared to 30% with [^{125}I]oPRL (text-fig. 1B) and only 12% with [^{125}I]hGH (text-fig. 1C). When 1% or greater of the added radioactivity was used as the criterion for selecting tumors that showed positive prolactin binding, the values were 36, 17, and 2%, respectively, for hPRL, oPRL, and hGH. There were equally less tumors showing no measurable prolactin binding (0%) or borderline values (0.1–0.4%) when hPRL was used as the tracer.

Table 1 compares ^{125}I-labeled oPRL and hPRL binding to 153 human breast cancer biopsy specimens. Binding studies were done in parallel with both freshly iodinated hormones. Compared to the use of oPRL as tracer, the use of [^{125}I]hPRL as tracer allowed the detection of almost three times as many tumors possessing prolactin receptors (29.4 vs. 10.4%) and also resulted in a twofold increase in the tumors showing moderate binding values (0.5–0.9%). There was no correlation between the level of prolactin receptors and the concentration of receptors for either 17β-estradiol or progesterone in these tumors (data not shown).

DISCUSSION

Human breast tumors possess membrane prolactin-binding proteins in sufficient amounts to be detected when the appropriate procedure is used. Specific binding of 1% or greater of the added radioactivity has been considered positive (*10*). Di Carlo and Muccioli (*14*), using an assay similar to ours, found positive values for prolactin receptors in 32.5% of their tumors, which is very close to our value of 36%. The present studies indicate the importance of the use of hPRL rather than oPRL for the determination of prolactin receptors to human breast cancer biopsy specimens. A rather puzzling result was the low binding values found when hGH was used as a labeled ligand. We and others have reported that hGH effectively competes with [^{125}I]-oPRL or [^{125}I]hPRL in breast tumor samples (*9*, *14*). The restrictions involved in performing a study such as this limit the type of basic information that can be obtained therefrom. We were limited to using the homogenization buffers and techniques that are optimum for the determination of steroid receptor levels. Studies are in progress to investigate methods to increase prolactin binding by differential gradient centrifugation. Also, the use of [^{125}I]hGH will be compared more extensively with that of hPRL in the same tumor specimens, especially in view of the increased efficacy of labeled hGH binding to human mammary epithelial cells (Turcot-Lemay L, Kelly PA: Unpublished observations).

These studies confirm the existence of prolactin receptors in human breast cancer biopsy specimens. It will be important to investigate the possible therapeutic implications of the determination of prolactin receptor levels in the prediction of the response of breast cancer patients to endocrine therapy.

REFERENCES

(*1*) JENSEN EV, BLOCK GE, SMITH S, KYSER K, DESOMBRE E. Estrogen receptors and breast cancer response to adrenalectomy. Natl Cancer Inst Monogr 1971; 34:55–70.

(*2*) MCGUIRE WL. Estrogen receptors in human breast cancer. J Clin Invest 1973; 52:73–77.

(*3*) HORWITZ KB, MCGUIRE, NL, PEARSON OH, SEGALOFF A. Predicting response to endocrine therapy in human breast cancer: A hypothesis. Science 1975; 189:726–727.

(4) McGuire WL, Carbone PP, Sears ME, Escher GL. Estrogen receptors in human breast cancer: An overview. In: McGuire WL, Carbone PP, Vollmer EP, eds. Estrogen receptors in human breast cancer. New York: Raven Press, 1975:1–7.

(5) McGuire WL, Horwitz KB, Pearson DH, Segaloff A. Current status of estrogen and progesterone receptors in breast cancer. Cancer 1975; 39:2934–2947.

(6) Costlow ME, Buschow RA, Richert NO, McGuire WL. Prolactin and estrogen binding in transplantable hormone-dependent and autonomous rat mammary carcinoma. Cancer Res 1975; 35:970–974.

(7) Kelly PA, Bradley, C, Shiu RP, Meites J, Friesen HG. Prolactin binding to rat mammary tissues. Proc Soc Exp Biol Med 1974; 146:816-819.

(8) Turkington RW. Prolactin receptors in mammary carcinoma cells. Cancer Res. 1974; 34:758–763.

(9) Kelly PA, Labrie F, Asselin J. The role of prolactin in tumor development. In: Kellen JA, Hilf R, eds. Influences of hormones in tumor development. Vol 2. Boca Raton, Fla.: CRC Press, 1978: 157–194.

(10) Holdaway IM, Friesen HG. Hormone binding by human mammary carcinoma. Cancer Res 1977; 37:1946–1952.

(11) Pearson OH, Manni A, Chambers M, Brudkey J, Marshall JS. Role of pituitary hormones in the growth of human breast cancer. Cancer Res 1978; 38:4323–4326.

(12) Partridge RK, Hähnel R. Prolactin receptors in human breast carcinoma. Cancer 1979; 43:643–646.

(13) Di Carlo R, Muccioli G, Conti G, Reboani C, Di Carlo F. Estrogen and prolactin receptor concentrations in human breast tumors. In: Genazzani E, Di Carlo F, Mainwaring W, eds. Pharmacological modulation of steroid action. New York: Raven Press, 1980:261–266.

(14) Di Carlo R, Muccioli G. Prolactin receptor in human mammary carcinoma. Tumori 1979; 65:695–702.

(15) Lowry OH, Rosebrough NJ, Farr AL, Randall RJ. Protein measurement with the Folin phenol reagent. J Biol Chem 1951; 193:265–275.

blank page

Tumor Promoter 12-*O*-Tetradecanoylphorbol 13-Acetate: Effect on Complement and Epstein-Barr Virus Receptors in Human Lymphoblastoid Cell Lines[1,2]

Naoki Yamamoto,[3] Takashi Mitsuma,[4,5] *and* Arnold Vogt[4,6,7]

ABSTRACT—The effect of the tumor promoter 12-*O*-tetradecanoylphorbol 13-acetate (TPA) on the C3 and Epstein-Barr virus (EBV) receptors in various human lymphoblastoid cells was investigated with the use of the erythrocyte-antibody-complement (EAC) rosette formation method and a quantitative bioassay for EBV receptors. TPA caused a significant decrease of C3 receptors in the cultures of both Raji and SB4 cells (by ≈50% of the C3 receptors in untreated cultures at 10 ng/ml). Kinetic studies revealed that the rate of reduction was rather moderate but progressive, reaching a maximum 5 days after treatment with TPA. Kinetic studies showed that EBV receptors also decreased, similar to the reduction seen with C3 receptors after TPA treatment. The effect of TPA on the reduction of C3 receptors was observed not only in these cells but also in other EBV-positive B-cells, subclones of SB4 cells, and MOLT-4 cells. However, in an EBV-negative B-cell line, BJAB, EAC rosette formation was significantly enhanced.—JNCI 1982; 68:385–390

It has been well established that initiators and promoters regulate the two-stage mouse skin carcinogenesis model (*1*). Most initiators generate elecrophilic metabolites that covalently bind to DNA. However, the promoters are thought to interact directly with the cells without requiring such metabolic activation and do not bind covalently to DNA (*2*). When a tumor promoter is painted periodically on mouse skin, following application of an initiator, papillomas develop. If treatment with the promoter is discontinued too soon, the papilloma regresses. However, when applied alone, the promoter may induce skin hyperplasia but does not generally induce papilloma (*3*). These data suggest that tumor promoters act "epigenetically" on the cells and their effects are reversible, whereas initiators genetically and irreversibly alter the cells.

At concentrations as low as 5×10^{-10} *M*, the phorbol diester tumor promoters, the most potent of which is TPA, induce a number of biologic and biochemical effects on cells in vitro. These effects include alterations in surface receptor, cell morphology, cell growth pattern, saturation density, cell-to-cell communication, anchorage dependence, membrane transport, and cyclic nucleotide synthesis, stimulation of mitoses and cell glycoproteins, induction of plasminogen activator and ornithine decarboxylase, modulation of cell differentiation, induction of oncogenic viruses, and enhancement of virus-induced cell transformation (*4–15*).

Among the pleiotropic effects of TPA, some changes (e.g., in morphology, cell adhesion, or inhibition of epidermal growth factor binding to membrane receptors) occur immediately or within a few hours after TPA treatment and do not require macromolecular synthesis (*16, 17*). This observation suggests that these changes are caused by the direct interaction of TPA with the cell membrane.

These facts prompted us to investigate the influence of TPA on C3 receptors and EBV receptors on the surface of a number of cell types including cell lines originating from a healthy adult, from Burkitt's lymphoma, and from T-cell leukemia. The results show that treatment with TPA decreases the number of C3 and EBV receptors at the same time in the several lymphoblastoid cell lines. However, in one cell line, significant stimulation of rosette formation was observed.

MATERIALS AND METHODS

Cells and viruses.—All cell lines were maintained in RPMI-1640 medium (Flow Laboratories, Inc., Irvine, Scotland) supplemented with 10% fetal calf serum, 100 IU penicillin/ml, and 100 µg streptomycin/ml. They were passaged routinely once weekly. The origin of each cell line is described in table 2. Infectious EBV was obtained from supernatants of P3HR-1 cells by differential centrifugation and concentrated about a hundredfold as described (*18*). SB4 cells were subcloned by the use of soft agarose (*18*). Cells were suspended at appropriate dilutions in 2 ml of RPMI-1640 medium containing 20% fetal calf serum and 0.35% sea plaque agarose (Marine Colloids, Inc., Rockland, Maine) and seeded in a 60-mm plastic petri dish containing a 5-ml base layer of 0.5% agarose in the same medium. The plates were then placed in a 5% CO_2 atmosphere at 37°C in a humidified incubator. Individual colonies were isolated by aspiration through the soft agar after 3 weeks from plates containing no more than 10–20 colonies.

Chemicals.—TPA, AMD, CH, Ara-C, IdUrd, and PM were purchased from Sigma Chemical Co., St. Louis, Mo.

ABBREVIATIONS USED: AMD=actinomycin D; Ara-C=β-cytosine arabinoside hydrochloride; CH=cycloheximide; DMSO=dimethyl sulfoxide; EA=early antigen(s); EAC=erythrocyte-antibody-complement; EBV=Epstein-Barr virus; IdUrd=5-iodo-2′-deoxyuridine; PM=puromycin; RA=13-*cis*-retinoic acid; SRBC=sheep red blood cells; TPA=12-*O*-tetradecanoylphorbol 13-acetate.

---

[1] Received April 2, 1981; revised September 21, 1981, accepted October 7, 1981.

[2] Supported by the Deutsche Forschungsgemeinschaft (SFB 31, Medizinische Virologie–Tumorentstehung und Entwicklung).

[3] Institut für Virologie, Zentrum für Hygiene, Universität Freiburg, Hermann-Herder-Str. 11, 7800 Freiburg, Federal Republic of Germany.

[4] Institut für Immunologie, Zentrum für Hygiene, Universität Freiburg.

[5] *Present address*: College of Biomedical Technology, University of Niigata, 1 Asahimachi, Niigata, Japan 751.

[6] *Address reprint requests to* Dr. Vogt.

[7] We are indebted to Professor H. zur Hausen and Dr. S. Batsford for the critical reading of this manuscript and to M. Dieterle for excellent technical assistance.

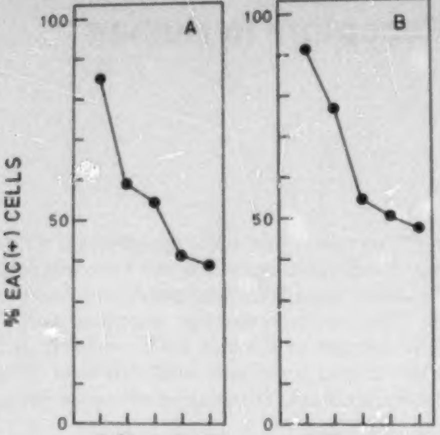

TEXT-FIGURE 1.—Effect of various concentrations of TPA on EAC rosette formation in Raji and SB4 cells. Raji (A) and SB4 (B) cells were incubated at a density of 4×10^5 cells/ml. Five days after addition of various concentrations of TPA, the percentage of EAC rosette-forming cells was determined as described in "Materials and Methods."

4α-phorbol-12,13-didecanoate and Ingenol prepared as previously described (*19*) were supplied by Dr. E. Hecker, Deutsches Krebsforschungszentrum, Heidelberg, Federal Republic of Germany. RA was obtained from Nordmark Co., Hamburg, Federal Republic of Germany. TPA and all other chemicals were dissolved in DMSO and phosphate-buffered saline, respectively.

Preparation of EAC.—A 1.5% suspension of washed SRBC was mixed with an equal volume of anti-SRBC antibody, diluted to one step lower than the agglutinating titer, and incubated at 37°C for 30 minutes. To this mixture an equal volume of fresh mouse serum diluted 1:20 was added and incubated at 37°C for 15 minutes. The preparation was placed on ice and used within 1 day.

EAC rosette assays.—Target cells, 2×10^5, were incubated with 2×10^7 EAC in a total volume of 300 μl medium for 5 minutes at room temperature, then centrifuged at 200×*g* for 5 minutes, and incubated again at room temperature for 20 minutes. Afterward, the cells were gently resuspended and kept on ice until they were counted. We determined the portion of rosette-forming cells (≥3 bound indicator cells/target cell) by viewing about 200 viable target cells on a glass slide.

EBV receptors.—The concentration of EBV receptors was quantitated by the bioassay of Sairenji and Hinuma (*20*). An EBV concentrate from P3HR-1 supernatants was used as the virus source at a dilution of 1:8. In 10^6 Raji cells, 1 ml of this virus induced about 15% EBV-related EA-positive cells after 2 days. At intervals, TPA-treated and untreated cells were washed three times with complete medium and then suspended in 550 μl EBV. Incubation was continued at 37°C with gentle shaking. Thirty minutes after incubation, supernatants of the cultures were collected after centrifugation and processed for EA induction experiments, as described before (*20*). The adsorption index was calculated as described by Klein et al. (*21*) according to the formula: adsorption index = [maximal (control) % EA induction − test % EA induction]/maximal (control) % EA induction.

Treatment of the cells with TPA.—TPA was added to the tissue culture medium at the indicated concentration. Control cultures received DMSO alone.

RESULTS

First we investigated the effect of different concentrations of TPA on C3 receptors of Raji and SB4 cells. As shown in text-figure 1, EAC rosette-forming cells were significantly reduced 5 days after treatment with TPA in both cell lines. At 10 ng/ml the rate of rosette-forming cells was reduced by about 50%. There seemed to be no significant differences in the rate of reduction above 10 ng TPA/ml in both cell lines. Therefore, we used 10 ng TPA/ml for further investigations, unless otherwise indicated.

Then we studied kinetically the effect of TPA on the number of C3 receptors by correlating the C3 receptors to cell growth. In both cell lines, TPA caused a gradual decrease in the proportion of C3 receptor-positive cells, reaching a minimum 5 and 6 days after TPA treatment in Raji and SB4 cells, respectively (text-fig. 2). Under these conditions cell growth was significantly inhibited by TPA treatment, resulting in only about 50% of the control growth in

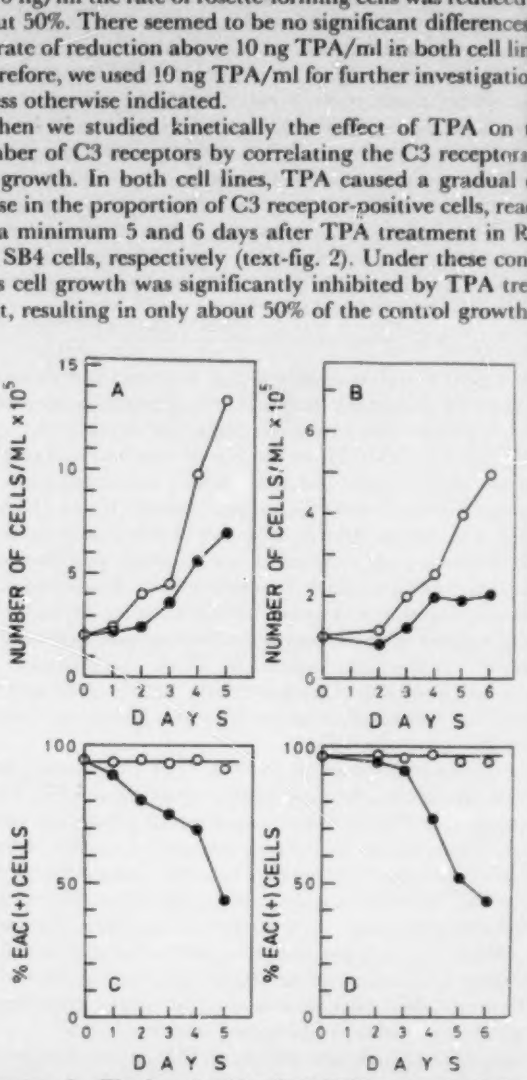

TEXT-FIGURE 2.—Kinetic study of the effect of TPA on growth of cells and on EAC rosette formation in Raji and SB4 cells. Raji and SB4 cells were incubated in the presence (●—●) or absence (○—○) of 10 ng TPA/ml at a density of 2×10^5 cells/ml and 1×10^5 cells/ml, respectively. At the indicated times the number of viable (trypan blue excluded) cells/ml was determined in a hemacytometer (Raji, A; SB4, B). At the same time the percentage of EAC rosette-forming cells was determined (Raji, C; SB4, D).

both lines. Viability of these cells, however, was not significantly affected by the presence of TPA. In a representative experiment with the use of Raji cells, viability was 83% 5 days after TPA treatment compared to 84% in control cultures. Raji and SB4 cells did not show significant differences after TPA treatment, as far as the viability of the cells was concerned. In contrast to TPA, no reduction in C3 receptors on Raji or SB4 cells was seen with two nonpromoting diterpenes, 4α-phorbol-12,13-didecanoate and Ingenol, used at concentrations of 1–100 ng/ml.

We then studied whether the reduction of C3 receptors caused by TPA was linked to that of EBV receptors. For this purpose we used the quantitative bioassay described by Sairenji and Hinuma (*20*). To avoid the complication arising from cell proliferation, we treated Raji cells with 5 μg of the DNA inhibitor Ara-C/ml. Under this condition cell growth was completely inhibited without affecting the rate of the C3 receptors (table 1). Text-figure 3 shows that the adsorption index decreased at the same time as the number of receptor-positive cells.

Further experiments were done to determine whether the TPA-induced reduction of C3 receptors was seen in other human lymphoblastoid cell lines and in subclones of SB4 cells. We tested 9 C3 receptor-positive cell lines that have some differences in their origins and in the EBV genome status. Table 2 shows that all tested cell lines, except BJAB cells, responded to TPA treatment. The extent of reduction of C3 receptors after TPA treatment seemed to vary greatly depending on the cells and lay between 15 and 75% of that seen in the control cultures. In BJAB cells, an EBV-negative Burkitt's lymphoma-derived line, rosette formation was significantly stimulated after TPA treatment. As compared to the reduction of rosette formation, a rather rapid response was seen, reaching a maximum 3 days after TPA addition (table 2). This effect was reproducible in two further experiments, although the enhancement of EAC rosette formation was not large.

TABLE 1.—*Effect of various inhibitors of macromolecular synthesis on the TPA-induced reduction of C3 receptors in Raji cells*

Treatment[a]	Percent EAC at:[b]	
	3 days	5 days
AMD (100 ng/ml) + TPA	71±6	45±5
CH (5 μg/ml) + TPA	56±7	40±3
PM (5 μg/ml) + TPA	50±6	41±3
Ara-C (10 μg/ml) + TPA	61±8	57±5
IdUrd (10 μg/ml) + TPA	61±6	59±8
RA (10 *μM*) + TPA	67±10	56±12
TPA	65±11	54±11
AMD (100 ng/ml)	87±8	81±9
CH (5 μg/ml)	92±4	87±1
PM (5 μg/ml)	78±8	71±6
Ara-C (10 μg/ml)	91±4	90±5
IdUrd (10 μg/ml)	90±8	91±5
RA (10 *μM*)	93±3	88±8
No treatment (control)	93±10	89±9

[a] In the presence of inhibitors the appropriate macromolecular syntheses were inhibited completely within 24 hr without affecting the cell viability. In all instances, TPA was administered at 10 ng/ml.

[b] Percent of EAC rosette-forming cells. Values are means ± SD of triplicate assays.

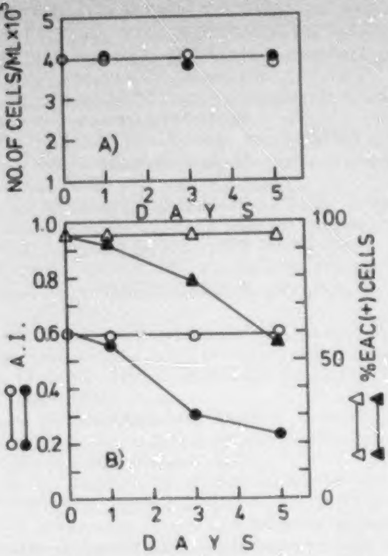

TEXT-FIGURE 3.—Comparative study of the effect of TPA on C3 and EBV receptors in Raji cells. Cells were incubated with Ara-C (5 μg/ml) at a density of 4×10⁵ cells/ml in the presence or absence of TPA. At intervals, the number of viable cells was determined (A). At the same time, the adsorption index (A.I.) [●——● (+TPA); ○——○ (−TPA)] and EAC rosette-forming cells [▲——▲ (+TPA); △——△ (−TPA)] were determined as described in "Materials and Methods" (B).

Finally, we investigated the effect of various inhibitors of macromolecular synthesis on the TPA-induced reduction of C3 receptors of Raji cells. Table 1 shows that in the presence of an inhibitor of RNA synthesis (AMD) and of inhibitors of protein synthesis (CH and PM) together with TPA, some enhancement was seen in the reduction of C3 receptors even though these chemicals when used alone did not affect EAC rosette formation. Inhibitors of DNA synthesis (Ara-C and IdUrd) did not significantly affect the results. RA has been reported to inhibit various alterations induced by TPA (*22–24*). However, the results showed that RA did not inhibit the TPA-mediated reduction of C3 receptors.

DISCUSSION

Evidence is increasing that an early site of action of TPA is the cell membrane (*25–27*). For example, inhibition of the epidermal growth factor binding to receptors in HeLa cells occurs within a few minutes after exposure to TPA, and adhesion of murine erythroleukemia cells to the surface occurs within 20 minutes of addition of compound. The fact that these changes do not require de novo syntheses of RNA and protein also supports the assumption that tumor promoters have a direct effect on cell membranes and their functions (*16, 17*). The current studies show that the reduction of C3 and EBV receptors takes place much more slowly than do the above-mentioned alterations induced by TPA. This finding suggests that the decrease of C3 and EBV receptors is not caused by the direct action of TPA but rather by the indirect action. As far as the kinetic studies are concerned, our results resemble the decrease of large, external transformation-sensitive protein or induction of

TABLE 2.—*Effect of TPA on the concentration of C3 receptors in several lymphoblastoid cell lines*

Cell line	Origin	EBV genome	TPA[a]	Percent EAC at:[b]		
				1 day	3 days	5 days
Raji	Burkitt's lymphoma	+	−	94±6	93±3	89±3
			+	93±7	65±11	54±11
NC37	Burkitt's lymphoma	+	−	95±5	92±6	90±3
			+	95±1	75±8	41±12
Daudi	Burkitt's lymphoma	+	−	61±8	59±12	66±8
			+	60±9	50±8	50±5
SB4	PBL[c]	+	−	97±3	98±1	98±5
			+	94±4	93±2	53±8
SB4-4	Subclone of SB4	+	−	97±1	99±1	93±7
			+	98±1	76±4	43±5
SB4-8	Subclone of SB4	+	−	95±1	97±2	90±5
			+	95±3	64±5	49±3
SB4-9	Subclone of SB4	+	−	95±3	95±3	92±6
			+	89±8	58±5	51±6
BJAB	Burkitt's lymphoma	−	−	3±2	2±1	2±1
			+	7±2	14±1	8±4
MOLT-4	T-cell leukemia	−	−	ND	ND	34±9
			+	ND	ND	5±1

[a] Administered at 10 ng/ml.

[b] Percent of EAC rosette-forming cells. Values are means ± SD of triplicate assays. ND=not determined.

[c] PBL=peripheral blood lines. Establishment and characteristics of this cell line are described elsewhere (Mitsuma T, Vogt A, Takamiya H, Galli C, Yamamoto N: Manuscript in preparation).

EBV antigens after treatment with TPA, which also requires a few days for maximal expression (*5*). Some additional steps are apparently required after the initial interaction of TPA with the cell membrane, leading to the modification of the gene expression and to an increase or decrease in the various metabolites, proteins, and enzymes plus modifications of the differentiation of the cells.

Several lines of evidence suggested that phorbol esters have effects on cell differentiation. These effects include the inhibition of differentiation and, conversely, promotion of it. In the inhibition of differentiation, the phenotypes and cell types that are affected by phorbol esters vary greatly, e.g., hemoglobin synthesis in mouse Friend erythroleukemia cells, myotubule formation in chick myoblast, sulfated proteoglycan synthesis in chick chondroblast, lipid accumulation in mouse Balb/3T3 fibroblasts, neurite formation in mouse neuroblastoma cells, melanin synthesis in mouse melanoma cells, and changes in morphology and phagocytic activity in mouse myeloid leukemia cells (*6, 12, 28-32*). Among these cell types, mouse Friend erythroleukemia cells are used most frequently. These cells are induced to differentiate to produce benzidine by treatment with various chemicals (e.g., DMSO), and finally cell growth ceases after expression of such a phenotype. TPA inhibits reversibly this induction of cell differentiation. These data would support the idea that cancer cells arise from aberrant differentiation and that disturbance of differentiation may be involved in the promotion step of chemical carcinogenesis (*33*). However, several groups have found that tumor promoters also may stimulate several types of cell differentiation (*34-37*). These conflicting observations on cell differentiation were even seen in the experiments in which the same cell line was used. A murine myeloid leukemia cell line (M1 cells) has indeed shown both stimulation and inhibition of differentiation by phorbol esters (*34, 37*).

In the present studies C3 and EBV receptors in several lines were specifically reduced by TPA. In the EBV-negative cell line BJAB, the same treatment stimulated EAC rosette formation. Moreover, previous experiments have shown that after TPA treatment SB4 cells could be stimulated to produce IgG and to phagocytize *Candida* cells, while the concentration of Fc receptors was not affected (Mitsuma T, Vogt A, Takamiya H, Galli C, Yamamoto N: Manuscript in preparation). Conceivably, these alterations were also related to cell differentiation.

Table 1 shows that the inhibitors of RNA and protein syntheses enhanced the reduction of EAC rosette formation by TPA even though the chemicals per se had very little effect. It is likely that production of C3 receptor protein is inhibited and old receptor proteins decay gradually on the cell surface without being replaced by newly synthesized receptor proteins in the presence of these agents. At the moment, however, it is difficult to explain how these chemicals exert their effects on the TPA-induced reduction of EAC rosette formation. Inhibitors of DNA synthesis did not affect the EAC rosette formation when they were used alone or together with TPA. Similarly, RA had no effect on EAC rosette formation.

Under our experimental conditions TPA inhibited cell growth considerably, although both TPA-treated and untreated cultures did not show significant differences in cell viability at the termination of the experiments. The decrease of C3 and EBV receptors by TPA, however, is not attributable to this cell growth inhibition, since inhibitors of DNA synthesis do not decrease the number of C3 receptors even though they have stronger effects as far as growth inhibition is concerned.

A number of experiments have suggested that the receptor for EBV on B-cells is identical to or closely associated with the receptor for the C3 component of complement (*38*). It was therefore of interest to determine whether the decrease of C3 receptors is associated with that of EBV receptors after the treatment with TPA. Text-figure 3 shows that it is. This observation does not, of course, exclude the possibilities that the EBV receptor either includes components in addition to the complement receptor or is closely linked to but separate from the complement receptor. Nevertheless, the fact that these independent methods revealed the reduction of C3 and EBV receptors, respectively, suggests that the cell membrane containing these receptors was indeed modified by TPA.

TPA efficiently induces EBV-specific antigens in genome-carrying cells. In producer cell lines, not only viral antigens but also viral particles are induced, while induction is restricted only to the functional viral proteins, EA in nonproducer lines (*13*, *38*). Most of the cells that we used in the present study were EBV nonproducers or even EBV-negative cell lines. Therefore, the possibility that the decrease of C3 and EBV receptors was due to readsorption of induced virus particles onto these receptors, blocking them in the process, is clearly excluded. However, whether the effect is due to interaction of receptor protein with viral proteins remains to be determined.

The aim of the present study was to investigate the influence of TPA on C3 receptors and EBV receptors on the surface of various cell lines, including those originating from a healthy subject and from patients with tumors. The inhibitory effect of the tumor promoter TPA on EAC rosette formation was considered to be due to TPA itself, not to DMSO used as a solvent since the DMSO had no effect at any concentration used (≤0.1%). In addition, two nonpromoting diterpenes exerted no influence on C3 receptors. The present study adds one more effect to the panel of pleiotropic effects of TPA in vitro. Several authors have tried to correlate the level of such effects [e.g., (*16*, *19*)] caused by various tumor promoters with that of tumor-promoting activity in vivo. Further study will clarify whether other tumor promoters have similar effects and if their effects then parallel the degree of tumor-promoting activity.

REFERENCES

(*1*) Berenblum I, Shubik P. A new quantitative approach to the study of the stages of chemical carcinogenesis in the mouse's skin. Br J Cancer 1947; 1:383–391.

(*2*) Weinstein IB, Troll W. National Cancer Institute workshop on tumor promotion and cofactors in carcinogenesis. Cancer Res 1977; 37:3461–3463.

(*3*) Berenblum I. Sequential aspects of chemical carcinogenesis: Skin. In: Becker FF, ed. Cancer: A comprehensive treatise. Vol 1. New York: Plenum, 1975:323–344.

(*4*) Lee LS, Weinstein IB. Tumor-promoting phorbol esters inhibit binding of epidermal growth factor to cellular receptors. Science 1978; 202:313–315.

(*5*) Blumberg PM, Driedger PE, Rossow PW. Effect of a phorbol ester on a transformation sensitive surface protein of chick fibroblasts. Nature 1976; 264:446–447.

(*6*) Yamasaki H, Fibach E, Nudel U, Weinstein IB, Rifkind RA, Marks PA. Tumor promoters inhibit spontaneous and induced differentiation of murine erythroleukemia cells in culture. Proc Natl Acad Sci USA 1977; 74:3451–3455.

(*7*) Sivak A, Van Duuren BL. Phenotypic expression of transformation: Induction in cell culture by a phorbol ester. Science 1967, 157: 1443–1444.

(*8*) Diamond L, O'Brien TG, Donaldson C, Shimizu Y. Growth stimulation of human diploid fibroblasts by the tumor promoter, 12-*O*-tetradecanoylphorbol-13-acetate. Int J Cancer 1974; 13:721–730.

(*9*) Moroney J, Smith A, Tomel LD, Wenner CE. Stimulation of ^{86}Rb + and ^{32}Pi movements in 3T3 cells by prostaglandins and phorbol esters. J Cell Physiol 1978; 95:287–294.

(*10*) Wigler M, Weinstein IB. Tumour promoter induces plasminogen activator. Nature 1976; 259:232–233.

(*11*) Yuspa SH, Lichti U, Ben T, et al. Phorbol esters stimulate DNA synthesis and ornithine decarboxylase activity in mouse epidermal cell culture. Nature 1976; 262:402–404.

(*12*) Rovera G, O'Brien TG, Diamond L. Tumor promoters inhibit spontaneous differentiation of Friend erythroleukemia cells in culture. Proc Natl Acad Sci USA 1977; 74:2894–2898.

(*13*) zur Hausen H, O'Neill FJ, Freese UK, Hecker E. Persisting oncogenic herpesvirus induced by tumour promoter TPA. Nature 1978; 272:373–375.

(*14*) Fisher PB, Weinstein IB, Eisenberg D, Ginsberg HS. Interaction between adenovirus, a tumor promoter, and chemical carcinogens in transformation of rat embryo cell cultures. Proc Natl Acad Sci USA 1978; 75:2311–2314.

(*15*) Yamamoto N, zur Hausen H. Tumour promoter TPA enhances transformation of human leukocytes by Epstein-Barr virus. Nature 1979; 280:244–245.

(*16*) Yamasaki H, Weinstein IB, Fibach E, Rifkind RA, Marks PA. Tumor promoter-induced adhesion of the DS19 clone of murine erythroleukemia cells. Cancer Res 1979; 39:1989–1994.

(*17*) Lee LS, Weinstein IB. Studies on the mechanism by which a tumor promoter inhibits binding of epidermal growth factor to cell receptors. Carcinogenesis 1980; 1:669–679.

(*18*) Bister K, Yamamoto N, zur Hausen H. Differential inducibility of Epstein-Barr virus in cloned Raji cells. Int J Cancer 1979; 23:818–825.

(*19*) zur Hausen H, Bornkamm GW, Schmidt R, Hecker E. Tumor initiators and promoters in the induction of Epstein-Barr virus. Proc Natl Acad Sci USA 1979; 76:782–785.

(*20*) Sairenji T, Hinuma Y. Modes of Epstein-Barr virus infection in human floating cell lines. Gan 1973; 64:582–590.

(*21*) Klein G, Manneborg A, Steinitz M. Differences in EBV receptor concentration between in vitro EBV-converted lymphoma sublines reflect biological differences between the converting viral strains. Int J Cancer 1979; 23:197–200.

(*22*) Verma AK, Boutwell RK. Vitamin A acid (retinoic acid), a potent inhibitor of 12-*O*-tetradecanoylphorbol-13-acetate induced ornithine decarboxylase activity in mouse epidermis. Cancer Res 1977; 37:2196–2201.

(*23*) Sporn M. Pharmological prevention of carcinogenesis by retinoids. In: Slaga TJ, Sivak A, Boutwell RK, eds. Carcinogenesis. Vol 2. Mechanisms of tumor promotion and cocarcinogenesis. New York: Raven Press, 1978:545–551.

(*24*) Yamamoto N, Bister K, zur Hausen H. Retinoic acid inhibition of Epstein-Barr virus induction. Nature 1979; 278:553–554.

(*25*) Weinstein IB, Yamasaki H, Wigler M, et al. Molecular and cellular events associated with the action of initiating carcinogens and tumor promotion. In: Griffin AC, Shaw CR, eds. Carcinogens: Identification and mechanisms of action (M. D. Anderson, Symposium). New York: Raven Press, 1979:399–418.

(*26*) Castagna M, Rochette-Egly C, Rosenfeld C. Tumor promoting phorbol diester induces substrate adhesion and growth inhibition in lymphoblastoid cells. Cancer Lett 1979; 6:227–234.

(*27*) Lee LS, Weinstein IB. Membrane effects of tumor promoters: Stimulation of sugar transport in mammalian cell cultures. J Cell Physiol 1979; 99:451–460.

(*28*) Cohen R, Pacifici M, Rubenstein N, Biehl J, Holtzer H. Effect of a tumour promoter on myogenesis. Nature 1977; 266:538–540.

(*29*) Pacifici M, Holtzer H. Effects of tumor-promoting agents on chondrogenesis. Am J Anat 1977; 150:207–212.

(*30*) Diamond L, O'Brien TG, Rovera G. Inhibition of adipose conversion of 3T3 fibroblasts by tumour promoters. Nature 1977; 269:247–248.

(*31*) Mufson RA, Fisher PB, Weinstein IB. Phorbol esters produce a delay in the expression of melanogenesis by B-16 melanoma cells. Proc Am Assoc Cancer Res 1978; 19:183.

(*32*) Ishii DN, Fibach E, Yamasaki H, Weinstein IB. Tumor promoters inhibit morphological differentiation in cultured mouse neuroblastoma cells. Science 1978; 200:556–559.

(33) Gurchot C. The trophoblast theory of cancer (John Beard, 1857–1924) revisited. Oncology 1975; 31:310–333.

(34) Sugimura T, Kawachi T, Nakayasu N, Matsukura N, Takayama S. Enhancement of differentiation of mouse leukemia cells by TPA and promotion of stomach carcinogenesis of rats by orally given croton oil. Abstracts of papers presented at the meeting on phorbol esters. Cold Spring Harbor, N.Y.: Cold Spring Harbor Laboratory, 1978:30.

(35) Miao RM, Fieldsteel AH, Fodge DW. Opposing effects of tumour promoters on erythroid differentiation. Nature 1978; 274:271–272.

(36) Nagasawa K, Mak TW. Phorbol esters induce differentiation in human malignant T lymphoblasts. Proc Natl Acad Sci USA 1980; 77:2964–2968.

(37) Kasukabe T, Honma Y, Hozumi M. Inhibition of functional and morphological differentiation of cultured mouse myeloid leukemia cells by tumor promoters. Gan 1979; 70:119–123.

(38) Jondal M, Klein G, Oldstone MB, Bokisch V, Yefenof E. An association between complement and Epstein-Barr virus receptors on human lymphoid cells. Scand J Immunol 1976; 5:401–410.

Cerebrospinal Fluid Levels of 2′-Deoxycoformycin After Systemic Administration in Monkeys[1,2]

Julie Blatt,[3] Peter M. Venner,[4,5,6] Riccardo Riccardi,[3,7] Lawrence F. Cohen,[3] Diamon Gangji,[3,8] Robert I. Glazer,[4] *and* David G. Poplack[3,9]

ABSTRACT—2′-Deoxycoformycin (DCF) is an inhibitor of the enzyme adenosine deaminase (ADA) and has shown promise as an antileukemia agent. For the assessment of the extent to which systemically administered DCF crosses into the central nervous system (CNS), rhesus monkeys were given iv boluses of DCF. Simultaneous blood and cerebrospinal fluid (CSF) samples were assayed for DCF levels at times ranging from 10 minutes to 6 hours after the drug was given. Average peak CSF drug levels of 5.5×10^{-8} *M* and 3×10^{-7} *M* were reached 1½–2 hours following injections of 0.25 and 1.0 mg DCF/kg, respectively. The ratio of peak CSF to simultaneous plasma levels was 1 to 10. Data obtained from a patient who had acute lymphocytic leukemia and who was given iv DCF were comparable. Drug levels achieved within the CSF following iv administration of 0.25 mg DCF/kg are similar to those previously demonstrated to inhibit ADA. These results may be important both for understanding DCF-related CNS toxicity and for designing combination chemotherapy with DCF.—JNCI 1982; 68: 391–393.

DCF is a tight-binding inhibitor of the enzyme ADA and has shown promise as an antileukemia agent (*1–5*). In particular, the demonstration that lymphoblasts with T-cell characteristics have elevated ADA activity has raised the possibility that DCF might provide a means of selective chemotherapy for patients with T-cell ALL, a group known to have a poor prognosis with currently available chemotherapy (*6*). The systemic administration of DCF has been associated with dose-limiting toxicity to the CNS. Severe encephalopathy, seizures, confusion, and emotional lability have been noted (*1–3*). However, little information is available on the ability of DCF to cross the blood-brain barrier in primates, and the relationship of DCF levels in the CNS to toxicity is not known.

The concentration of DCF in the CNS may also be important because of the anticipated use of this agent in combination with Vira-A in anticancer clinical trials. The presence of DCF in the CNS in amounts sufficient to inhibit ADA might enhance the therapeutic efficacy or increase the toxicity of Vira-A within the CNS.

To better define the extent to which DCF crosses the blood-brain barrier, we administered DCF iv to rhesus monkeys and measured serial plasma and CSF drug levels. In addition, DCF levels were determined in plasma and CSF samples from 1 CNS leukemia patient who had participated in a phase I trial of DCF (*3*).

MATERIALS AND METHODS

Animals.—Four adult male rhesus monkeys (*Macaca mulatta*) weighing between 6.0 and 7.6 kg were obtained from the National Institutes of Health Primate Center. A subcutaneous Ommaya reservoir was placed in each animal as previously described (*7*) such that sterile ventricular CSF sampling could be accomplished over an extended period of time. All injections and sampling were performed on conscious animals sitting in primate chairs. Venous blood samples were obtained from a heparinized indwelling femoral vein catheter. Monkeys were monitored daily for 1 week after DCF administration for signs of toxicity with neurologic and ophthalmologic examinations, complete blood counts with platelet and differential counts, liver enzymes, blood urea nitrogen, and creatinine.

Humans.—One 6-year-old male with ALL participating in a phase I trial of DCF received iv 0.25 mg DCF/kg/day for 3 successive days. During and after a course of DCF therapy he underwent two lumbar punctures for evaluation of concurrent CNS disease. Aliquots of CSF as well as simultaneous plasma samples were assayed for DCF levels.

DCF preparation and administration.—DCF (NSC-218321) was obtained as Pentostatin from the Investigational Drug Branch, Division of Cancer Treatment, National Cancer Institute. A 2 mg/ml solution was prepared with the use of injectable sodium chloride. This solution was administered as an iv bolus via the femoral vein to each of 2 monkeys at a dose of 0.25 mg/kg and to another 2 monkeys at 1.0 mg/kg.

Sample collection and processing.—Samples of CSF, 0.25–1.0 ml, were obtained from the Ommaya reservoir before and periodically following iv injection of DCF (10, 30, 60, and 90 min and 2, 4, and 6 hr). Simultaneous venous blood samples were obtained and centrifuged, and the resultant plasma was removed. All specimens were frozen at −20°C until immediately before use in DCF assays.

DCF assay.—DCF activity in plasma and CSF was deter-

ABBREVIATIONS USED: ADA=adenosine deaminase; ALL=acute lymphocytic leukemia; CNS=central nervous system; CSF=cerebrospinal fluid; DCF=2′-deoxycoformycin; $t_{1/2}$=half-life; Vira-A=vidarabine.

---

[1] Received April 22, 1981; accepted October 22, 1981.

[2] Animals were maintained under the guidelines set forth by the National Institutes of Health (NIH). For human studies, the research procedures were in accord with the ethical standards of the Clinical Research Committee, NIH.

[3] Pediatric Oncology Branch, Division of Cancer Treatment, National Cancer Institute, NIH, Public Health Service, U.S. Department of Health and Human Services, Bethesda, Md. 20205.

[4] Applied Pharmacology Section, Laboratory of Medicinal Chemistry and Biology, Division of Cancer Treatment, National Cancer Institute.

[5] Recipient of a McEachern Fellowship awarded by the Canadian Cancer Society.

[6] *Present address*: MacEachern Laboratory, Cancer Research Unit, University of Alberta, Edmonton, Alberta, Canada T6G 2H7.

[7] *Present address*: Department of Pediatrics, Catholic University of Rome, Largo A. Gemelli N. 8, Rome, Italy.

[8] *Present address*: Jules Bordet Institute, Brussels, Belgium.

[9] We thank Mrs. Dondra O'Neill and Ms. Ann Piety for superb technical assistance, Dr. Daniel Glaubiger and Dr. Marvin Chassin for their interest and advice, and Ms. Betty Foy for typing the manuscript.

mined by inhibition of the ADA-catalyzed conversion of adenosine to inosine according to a previously described method (*8*). Samples were not boiled or filtered before DCF assay. Standard curves were determined by incubation of calf intestinal ADA (Sigma Chemical Co.), 0.0067 U, with known amounts of DCF (0.2–06 n*M*) in 0.05 *M* potassium phosphate buffer (pH 7.4) at 37°C for 10 minutes. Adenosine (final concentration, 0.1 m*M*) was then added for a total volume of 1.0 ml, and the reaction was followed at 265 nm with the use of a Gilford 250 spectrophotometer. A plot of DCF concentration versus percentage of control rate of adenosine deamination was used to calculate all plasma and CSF DCF levels. These levels were determined by the dilution of samples to cuvette concentrations so as to obtain a rate of 40–75% of the uninhibited control with the use of a reaction mixture as described above. The assay was validated by the addition of known concentrations of DCF to plasma and CSF.

Pharmacokinetics.—DCF serum levels were analyzed for pharmacokinetic parameters. Data were tested for statistical fit to one, two, or three compartment models according to general formulae (*9*). The best fit for serum data was a two-compartment open model described by $C = Ae^{-\alpha t} + Be^{-\beta t}$, where A, α refer to the fast, initial component and B, β to the terminal, slow component. A and B are the zero time concentrations of the respective components, and C is the total concentration at time t. The α and β are the elimination rate constants for the respective components. Calculations were made sequentially with A initially zero, and the respective components were tested for fit with the use of linear regression and the Pearson moment product of correlation. Calculations for the fast component were made with serum levels adjusted for the slow component elimination results. The curves for the serum data in text-figure 1 were generated from the equation above and the derived parameters. The curves for the CSF data were optically fit.

RESULTS

Plasma and CSF levels following iv bolus injection of 0.25 mg DCF/kg or 1.0 mg DCF/kg in the rhesus monkey are shown in text-figure 1. The α $t_{1/2}$ for plasma was 10–15 minutes and the β $t_{1/2}$ was 2 hours. Average peak CSF levels were 5.5×10^{-8} *M* and 3×10^{-7} *M* for the two dosages. These were reached 1½–2 hours after the drug was given. Peak CSF levels of DCF were one-tenth of simultaneous plasma levels.

Comparable data on CSF to plasma ratios were obtained from the samples available on 1 patient. Four hours after the first 0.25 mg/kg iv bolus, the DCF concentrations in the CSF and plasma were 7×10^{-8} *M* and 5.5×10^{-7} *M*, respectively. One hour after the third daily dose of DCF, the CSF level was 1.3×10^{-7} *M* with a concurrent plasma level of 9×10^{-7} *M*. Neither the monkeys nor the 1 patient developed any neurologic toxicity.

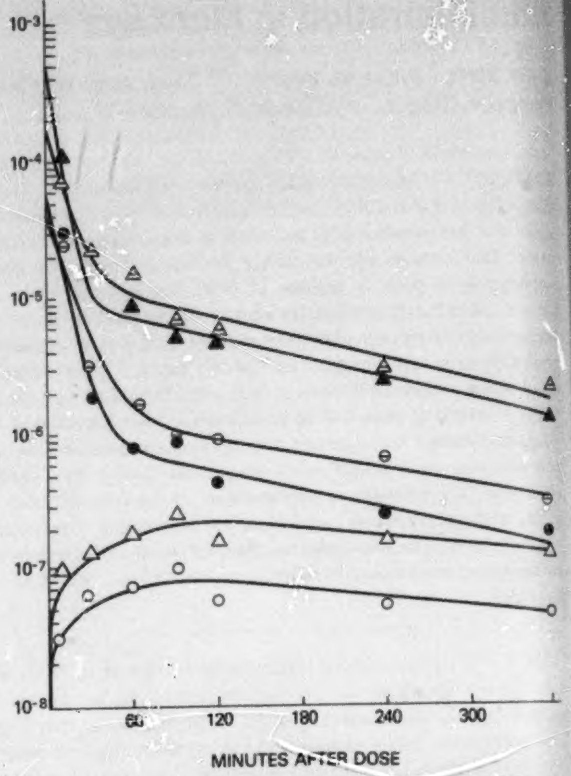

Text-figure 1.—Plasma and CSF levels of DCF. △, ▲: plasma DCF levels in each of 2 monkeys following 1.0 mg/kg iv bolus. ⊖, ●: plasma DCF levels in each of 2 monkeys following 0.25 mg/kg iv bolus. ○, △: CSF levels following 0.25 mg/kg iv bolus and 1.0 mg/kg, respectively.

DISCUSSION

DCF has been demonstrated to have activity against systemic ALL and is presumed to act by inhibiting ADA. In vitro studies have shown that levels of DCF of 4×10^{-8} *M* result in 50% inhibition of ADA in L1210 cells and that DCF levels of 5×10^{-7} *M* result in 100% ADA inhibition (*10*). Phase I studies in humans have suggested that doses greater than or equal to 0.25 mg DCF/kg iv can temporarily inhibit ADA in leukemia and normal white blood cells in bone marrow and peripheral blood (*1–5*).

In dogs, a single 0.25 mg/kg iv bolus of DCF has been found to reduce ADA activity of normal intracerebral tissue to 20% of base-line levels for at least 24 hours following peak CSF levels of only 1.5×10^{-8} *M* (*8*). Whether sufficient levels of DCF can be achieved in the CNS to inhibit ADA in resident leukemia cells following systemic drug administration is uncertain. The results of the present study are consistent with pharmacokinetics demonstrated in dogs and show that when DCF is given as a single iv bolus to rhesus monkeys, peak CSF levels of DCF are about one-tenth of simultaneous plasma levels. In addition, a recent study has shown similar ratios of peak CSF to simultaneous plasma levels in an ALL patient who was treated with multiple daily doses of DCF (*11*). Increases in drug dosage result in approximately linear increases in both plasma and CSF drug levels. Extrapolation from these results, for example, might suggest that a systemic dose of 0.5 mg/kg would produce peak CSF levels of approximately 10^{-7} *M*. On the basis of the above-mentioned human, L1210, and dog studies, these levels might be expected to inhibit ADA in normal monkey brain cells as well as ALL cells sequestered in the CNS. The applicability to humans of studies in monkeys on drug transport across the blood-brain barrier has already been established (*12*).

In a recent phase I trial, 0.5 mg DCF/kg/day for each of 3 successive days resulted in no significant neurotoxicity (*3*). None of the monkeys studied here given either 0.25 mg DCF/kg or 1.0 mg DCF/kg demonstrated neurotoxicity. Thus results of the present study do not permit a definitive statement regarding the relationship of either DCF levels or ADA inhibition within the CNS and the production of neurotoxicity. Measurement of ADA activity in ALL cells in the CSF before and after systemic DCF administration and correlation with neurotoxicity will be of interest.

REFERENCES

(*1*) Benjamin RS, Plunkett W, Keating MJ, et al. Phase I and biochemical pharmacological studies of deoxycoformycin. Proc Am Soc Clin Oncol 1980; 21:337.

(*2*) Kufe D, Major P, Agarwal R, Reinherz E, Frei E III. Phase I–II trial of deoxycoformycin (DCF) in T cell malignancies. Proc Am Soc Clin Oncol 1980; 21:328.

(*3*) Poplack DG, Sallan SE, Rivera G, et al. Phase I study of 2′-deoxycoformycin in acute lymphoblastic leukemia. Cancer Res 1981; 41:3343–3346.

(*4*) Schneider R, Korngold G, Vale K, Woodcock T, Tan C, Young C. Clinical and pharmacologic investigation of deoxycoformycin. Proc Am Assoc Cancer Res 1980; 21:185.

(*5*) Smyth JF, Chassin MM, Payne RM, Jackman AL, Harrap KR, Johns DG. The clinical pharmacology of the adenosine deaminase inhibitor 2′-deoxycoformycin. Cancer Chemother Pharmacol 1980; 5:93–101.

(*6*) Smyth JF, Poplack DG, Holiman BJ, Leventhal BG, Yarbro G. Correlation of adenosine deaminase activity with cell surface markers in acute lymphoblastic leukemia. J Clin Invest 1978; 62: 710–712.

(*7*) Wood JH, Poplack DG, Flor WF, Gunby FN, Ommaya AK. Chronic ventricular cerebrospinal fluid sampling, drug injections and pressure monitoring using subcutaneous reservoirs in monkeys. Neurosurgery 1977; 1:132–135.

(*8*) Chassin NM, Adamson RH, Zaharevitz DW, Johns DG. Enzyme inhibition titration assay for 2′-deoxycoformycin and its application to the study of the relationship between drug concentration and tissue adenosine deaminase in dogs and rats. Biochem Pharmacol 1979; 28:1849–1855.

(*9*) Gibaldi M, Perrier D. Pharmacokinetics. New York: Marcel-Dekker, 1975; 2, 53, 91.

(*10*) Glazer RI, Lott TJ, Peale AL. Potentiation by 2′-deoxycoformycin of the inhibitory effect by 3′-deoxyadenosine (cordycepin) on nuclear RNA synthesis in L1210 cells in vitro. Cancer Res 1978; 38: 2233–2238.

(*11*) Major PP, Agarwal RP, Kufe DW. Deoxycoformycin: Neurological toxicity. Cancer Chemother Pharmacol 1981; 5:193–196.

(*12*) Wood JH, Poplack DG, Bleyer WA, Ommaya AK. Primate model for long term study of intraventricularly or intrathecally administered drugs and intracranial pressure. Science 1977; 195:499–501.

blank page

Smoking History and Lung Cancer Survival in Women[1,2]

M. Ward Hinds, *M.D., M.P.H.,*[3] **Hong-Yi Yang,** *M.D.,*[4] **Grant Stemmermann,** *M.D.,*[5] **James Lee,** *Ph.D.,*[3] *and* **Laurence N. Kolonel,** *M.D., Ph.D.*[3,6]

ABSTRACT—The 12-month survival of 223 women with primary lung cancer was examined according to their smoking status given in the hospital record. A multivariate regression model was used to adjust simultaneously for age, tumor stage at diagnosis, tumor histology, and treatment. With adjustment for all these covariates, the 136 ever-smokers demonstrated a significantly greater probability of dying during the 12 months after diagnosis than the 87 never-smokers (odds ratio=1.74; *P*=0.023).—JNCI 1982; 68:395–399.

Many nontherapeutic factors have been associated with survival of patients with lung cancer. These factors include age (*1–3*), sex (*1, 2*), race (*2, 4*), socioeconomic status (*2, 5*), tumor histology (*1, 6, 7*), pretreatment performance status (*3, 7*), disease stage (*2, 3, 6, 7*), weight loss history (*3*), and pattern of metastases (*3*). Still another factor, smoking status, was recently suggested to have prognostic value for patients with small cell lung cancer (*8*); patients who had never smoked or quit smoking before diagnosis had the best survival, patients who quit at the time of diagnosis had intermediate survival, and patients who continued smoking had the worst survival. An earlier study (*9*), however, found no association between smoking history and lung cancer survival. Experimental studies of murine tumor cell transplants lend some support to the hypothesis that exposure to cigarette smoke may promote tumor growth and decrease survival (*10*).

We recently investigated the relationship of smoking to lung cancer risk among Japanese, Chinese, and Hawaiian women in Hawaii (*11*) and found that a substantial proportion of lung cancer patients in these groups had never smoked. When we further examined the survival of these women with respect to their smoking status, we found that those who had never smoked demonstrated superior survival. The details of this finding are reported herein.

METHODS

The method of identification of the lung cancer patients through the HTR has been described in detail elsewhere (*11*). All patients were Japanese, Chinese, or Hawaiian–part-Hawaiian women diagnosed with primary lung cancer from 1968 to 1978. Smoking histories were obtained by a review of the medical records, and a patient was not considered a never-smoker unless specifically so called in her record. Patients with any history of smoking were classified as smokers. Lack of record detail precluded quantification of smoking history. Pathology slides were independently reviewed by two of us (H. Y. Y. and G. S.). When independent slide reviews were not in agreement (16%), mutual agreement was reached in a joint review. The pathologists reviewing the slides were kept blind to all information about the patient.

We included in our survival analysis only those patients for whom we knew age and stage at diagnosis, smoking history, initial treatment, and follow-up status for at least 12 months post diagnosis and for whom the pathologic slide review indicated an epidermoid, adenocarcinoma, small cell, or large cell histologic pattern. We were thus able to include in the survival analysis 223 of the original 397 patients identified by the HTR. The remaining 174 patients could not be included because their records were not found (No.=22), readable tissue slides were not available (No.=84), smoking histories were not present in the records (No.=55), an unusual histologic pattern was found (No.=7), or the stage at diagnosis was unknown (No.=6).

Staging categories used were as follows: *a*) *localized*—restricted to the lung, *b*) *regional*—spread by direct extension to immediately adjacent tissues or organs and/or spread into regional lymph nodes, and *c*) *distant*—spread beyond immediately adjacent tissues or organs or regional lymph nodes. Staging was standardized by a review of all 223 HTR abstracts.

The first course of cancer-directed therapy was coded by the HTR. We categorized treatment as surgery alone, radiation alone, or other modalities (primarily chemotherapy) alone or in combination. Further subcategorization was possible but not practical due to the small number of patients in each subcategory.

Using the proportional hazards regression model described by Prentice and Gloeckler (*12*), we compared the survival experience of smokers versus never-smokers. This multivariate method allows examination of the influence of any single factor on survival while simultaneous adjustment can be made for other factors (covariates) in the model. We included the following covariates in various stages in our model: age, ethnic group, disease stage at diagnosis, treatment, and tumor histology. We computed the covariate-adjusted relative risk of dying in smokers compared to never-smokers. Using a rationale and method similar to those described by Lee (*13*) for the logistic regression model, we further computed interval-specific covariate-adjusted sur-

---

Abbreviation used: HTR=Hawaii Tumor Registry.

---

[1] Received April 24, 1981; revised October 28, 1981; accepted November 6, 1981.

[2] Research was funded in part by the Leahi Foundation, Honolulu, and by Public Health Service contract N01CP-53511 from the Division of Cancer Cause and Prevention, National Cancer Institute.

[3] Epidemiology Program, Cancer Center of Hawaii, University of Hawaii at Manoa, 1236 Lauhala St., Room 407, Honolulu, Hawaii 96813.

[4] Department of Pathology, University of Hawaii, School of Medicine, Honolulu.

[5] Kuakini Medical Center, Honolulu.

[6] We thank Ms. Virginia Sieburg of the Hawaii Tumor Registry for the review and stage standardization of the medical record abstracts.

vival rates. Survival analysis was restricted to 12 months after diagnosis because 56% of the patients were deceased by that time, and the small number of patients remaining after 12 months would not allow convergence of the iterative procedure of the computer program while all covariates were included in the model.

RESULTS

As can be seen in table 1, smokers and never-smokers differed in their distribution of all of the covariates, although the differences were statistically significant ($P<0.05$) only for age, ethnic group, and tumor histology. As would be expected, smokers tended to be younger than never-smokers, epidermoid and small cell cancers were more common among smokers, and adenocarcinomas were more common among never-smokers. Smokers were also more likely to be Hawaiian. However, since our survival analyses consistently showed that ethnicity of these lung cancer patients was not significantly related to their risk of dying, ethnicity was omitted as a covariate in the final analyses. Although neither disease stage at diagnosis nor treatment was significantly related to smoking status, the distribution of both would tend to favor better survival of never-smokers because more never-smokers were diagnosed while their disease was still in a localized stage and more were treated with surgery only. Stage of disease at diagnosis has been consistently shown to be a strong predictor of survival (*2, 3, 6, 7*), and our analysis likewise showed this tendency so that this covariate was included in the model to preclude any stage bias in favor of the survival of never-smokers. Our analysis suggested that treatment was only a weak predictor of survival after adjustment was made for other covariates, however, so that analyses both with and without adjustment for treatment are reported.

When adjustments were made for age, stage, and histology, the multivariate model gave a relative risk of 1.86 ($P=0.011$) for dying within 12 months of diagnosis among smokers compared to never-smokers. As would be expected, age, stage, and histology were also significantly ($P<0.05$) related to risk of dying in this model. When treatment was added to the model, the relative risk of dying among smokers compared to never-smokers was slightly reduced to 1.74 ($P=0.023$). However, as noted above, treatment itself was not quite significantly related ($P=0.075$) to risk of dying in this model. Age, stage, and histology remained significantly related to risk of dying in the model including treatment.

We present a model-independent description of the survival of never-smokers versus smokers within several age, stage, and histology strata in table 2. Because the degree of stratification used in the regression model (and shown in table 1) resulted in very small numbers in some cells, several strata were collapsed in table 2. The superior survival of never-smokers versus smokers is evident in six of the eight strata, with the only exceptions being patients less than age 65 with distant disease stage and nonadenocarcinoma histology and patients over age 64 with localized or regional disease stage and adenocarcinoma histology.

Because histology appeared to have the greatest potential for confounding the smoking status–survival association, we performed a separate multivariate regression analysis of adenocarcinoma cases only, again comparing the survival of smokers and never-smokers while simultaneously adjust-

TABLE 1.—*Distribution of lung cancer cases by smoking status and age, ethnic group, disease stage, treatment, and tumor histology*

Covariate	Smokers		Never-smokers		χ^2	P
	No.	Percent	No.	Percent		
Age, yr						
0–49	33	24.3	9	10.3	17.8	<0.001
50–64	65	47.8	30	34.5		
≥65	38	27.9	48	55.2		
Total	136	100	87	100		
Ethnic group						
Japanese	47	34.6	44	50.6	51.5	<0.001
Hawaiian-part-Hawaiian	80	58.8	13	14.9		
Chinese	9	6.6	30	34.5		
Total	136	100	87	100		
Disease stage at diagnosis						
Localized	32	23.5	26	29.9	1.32	$0.5<P<0.75$
Regional	39	28.7	25	28.7		
Distant	65	47.8	36	41.4		
Total	136	100	87	100		
Treatment						
Surgery only	42	30.9	36	41.4	3.03	$0.1<P<0.25$
Radiation only	33	24.3	15	17.2		
Other	61	44.8	36	41.4		
Total	136	100	87	100		
Tumor histology						
Epidermoid	31	22.8	6	6.9	24.9	<0.001
Small cell	30	22.1	6	6.9		
Adenocarcinoma	54	39.7	61	70.1		
Large cell	21	15.4	14	16.1		
Total	136	100	87	100		

TABLE 2.—*Survival comparison of lung cancer patients by smoking status, age, disease stage, and tumor histology*

Age, yr	Disease stage at diagnosis	Tumor histology	Never-smokers		Smokers	
			No.	Survival, %[a]	No.	Survival, %[a]
≤64	Localized + regional	Adenocarcinomas	19	95.2	26	82.1
≤64	"	Other	4	100.0	28	53.3
≤64	Distant	Adenocarcinomas	9	66.7	15	35.3
≤64	"	Other	7	10.0	29	19.4
≥65	Localized + regional	Adenocarcinomas	23	81.8	6	83.3
≥65	"	Other	5	60.0	11	54.5
≥65	Distant	Adenocarcinomas	10	30.0	7	20.0
≥65	"	Other	10	14.3	14	8.3

[a] Survival of >12 mo from diagnosis date.

TABLE 3.—*Distribution of lung cancer cases by smoking status and time period of diagnosis*[a]

Diagnosis, yr	Smokers		Never-smokers	
	No.	Percent	No.	Percent
1968–71	24	17.6	21	24.1
1972–75	51	37.5	29	33.4
1976–78	61	44.9	37	42.5
Total	136	100	87	100

[a] χ^2=1.39; degrees of freedom=2; P=0.50.

ing for age, tumor stage, and treatment. We found a relative risk of 2.1 (P=0.057) for dying within 12 months of diagnosis among smokers compared to never-smokers. Thus although statistical significance was borderline, the superior survival of never-smokers found in the analysis of all cases was supported in the analysis of adenocarcinoma cases alone.

Because treatment of lung cancer has been changing substantially and because there is evidence that survival of lung cancer patients is improving (*4*), we considered the possibility that our comparison of survival among smokers versus never-smokers might be biased by more never-smokers having been diagnosed and treated in the latter part of the study period. However, as shown in table 3, there was no statistically significant difference in the distribution of smokers and never-smokers with respect to time period of diagnosis. Such differences as did exist would favor a better survival of smokers because more were diagnosed in the latter part of the study period.

In text-figure 1 we show the model-predicted survival curves for smokers and never-smokers after adjustment for age, disease stage at diagnosis, and tumor histology. This model predicts that 68.1% of never-smokers but only 49.1% of smokers with lung cancer would be living at 12 months after diagnosis.

DISCUSSION

The findings of this investigation and those of Johnston-Early et al. (*8*) suggest that smoking status of lung cancer patients may be an independent predictor of survival. Such a conclusion is, however, in contradiction to the findings of Linden et al. (*9*) in an earlier study. Although these disparate results cannot be easily reconciled, it is worth noting several characteristics of the study of Linden et al. that make its results difficult to interpret. Although 5% of the cases were not histologically confirmed, they were nevertheless included as lung cancers. Perhaps more importantly, 43% of the cases had no specific histologic classification other than "carcinoma." Thus any adjustment for histology in the survival analysis (none was attempted) was precluded. However, the available histologic data of Linden et al. indicated that the survival for squamous carcinoma patients was superior to that for adenocarcinoma patients up to 27 months after diagnosis and that squamous carcinoma patients were more likely to be smokers. Therefore, a bias favoring survival of smokers is suggested. Similarly, there was no attempt to adjust for age in the survival comparisons, although it was stated that a higher proportion of nonsmokers were age 65 or older. Because older age is associated with decreased survival, this again suggests a bias favoring better survival of smokers. The number of never-smokers was very small (No.=15), and there was no attempt to identify those who may have stopped smoking before their lung cancer diagnosis. Finally, the cases in the study of Linden et al. were diagnosed over a broad time period (1953–68), and there was no attempt to examine the data to see if the smoking categories of cases were distributed by time of diagnosis in

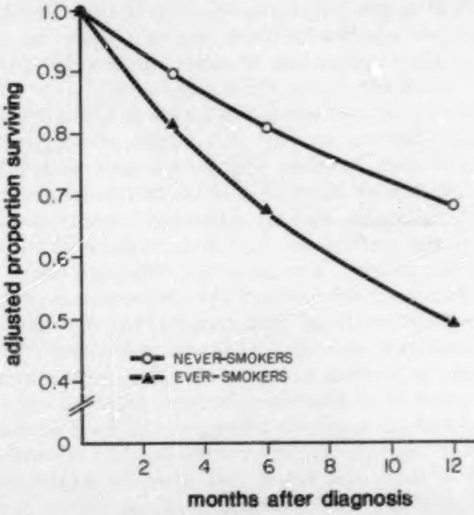

TEXT-FIGURE 1.—Model-predicted survival curves for ever-smokers and never-smokers with lung cancer after simultaneous adjustment for age, disease stage at diagnosis, and histologic classification of tumor. The curves are significantly different (P=0.01).

a manner that might favor survival of smokers. Considering all these shortcomings, it is not difficult to see how Linden et al. (*9*) might have failed to detect a survival advantage among nonsmokers of the small magnitude suggested by our findings and those of Johnston-Early et al. (*8*).

One shortcoming of our own study is the lack of information on pretreatment performance status of the lung cancer patients. Performance status is a very strong predictor of lung cancer survival (*7*) and is now routinely controlled for by stratified randomization in lung cancer treatment studies (*14*). Unfortunately, performance status of our patients was not available from the HTR records. The study of Johnston-Early et al. (*8*), however, did contain information on performance status, and they found no statistically significant association between this variable and smoking status. Nevertheless, they adjusted for performance status in one analysis comparing survival of patients according to smoking categories and found that survival differences remained significant ($P<0.04$). Therefore, although we could not examine the effect of adjusting for performance status in the current study, the findings of Johnston-Early et al. (*8*) suggest that such adjustment would be unlikely to alter our results.

Our adjustment for treatment had only a small effect on the association between smoking status and lung cancer survival. When Johnston-Early et al. (*8*) adjusted for treatment protocol in a similar fashion, they also found that the association between smoking status and survival remained significant ($P<0.04$). We could find no significant difference in the treatment given to smokers compared to never-smokers, and such difference as existed was primarily related to the earlier disease stage at diagnosis among never-smokers and their different histologic pattern of lung cancer (more adenocarcinomas). Adjusting for stage and histology thus largely adjusted for treatment also, which possibly explains the lack of statistical significance for the association of treatment and survival in the multivariate model. Attempting to subcategorize treatment more finely than in table 1 did not suggest any bias favoring survival of never-smokers. In fact, a larger percentage of never-smokers (10.3%) received no treatment than did smokers (7.4%).

Two survival-related covariates (age and histology) were significantly different in their distribution among smokers and never-smokers. Smokers with lung cancer tended to be younger and to have more often either epidermoid or small cell tumor histologies. The age difference is understandable in view of the well-known higher prevalence of smokers among young women. The histologic difference is also understandable in consideration of the higher relative risk for epidermoid and small cell lung cancers than for adenocarcinoma associated with smoking in this population (*11*).

The findings of some animal studies may have relevance to the question of an association between smoking and lung cancer survival. Holt and his colleagues (*15*) have examined the effects of cigarette smoke exposure on the cell-mediated immunity of mice and found that exposure to the body-weight equivalent of 20–30 cigarettes a day results in substantial changes in immunologic function, both systemically and locally in the respiratory tract. Most interesting are the effects of cigarette smoke exposure on the growth rates of murine tumor cells inoculated sc and intratracheally (*10*). Mice exposed to cigarette smoke for 26 weeks and then inoculated sc with tumor cells showed significantly greater mean tumor volumes after day 14 post inoculation than did mice not smoke exposed. In addition, smoke-exposed mice developed significantly more lung metastases. In mice inoculated intratracheally with tumor cells, 70% of smoke-exposed animals died within 60 days compared to only 25% of controls (*10*).

If an independent relationship does exist between smoking status and cancer survival, it may not be limited to lung cancer. A study of patients with malignant melanoma suggests that nonsmokers remain disease-free significantly longer than do smokers (*16*). A general effect of smoking on cancer survival might be expected if the effect were mediated through alteration in immunologic functions (*15*).

The current study and other studies (*8*, *10*) suggest that lung cancer survival may be independently related to smoking status. The question of such an association is an important one with implications for the design and analysis of lung cancer treatment protocols. Furthermore, at least one study (*8*) suggests that some survival benefit may be derived by cessation of smoking at the time of lung cancer diagnosis. Although the current study cannot directly address this issue, the results do suggest the need for future research designed to do so. Such research with larger data sets that allow control for pretreatment performance status as well as other potentially confounding variables is needed before any conclusions can be reached about the true nature of the relationship between smoking status and lung cancer survival.

REFERENCES

(*1*) CONNELLY RR, CUTLER SJ, BAYLIS P. End results in cancer of the lung: Comparison of male and female patients. J Natl Cancer Inst 1966; 36:277–287.

(*2*) NOMURA A, KOLONEL L, RELLAHAN W, LEE J, WEGNER E. Racial survival patterns for lung cancer in Hawaii. Cancer 1981; 48:1265-1271.

(*3*) LANZOTTI VJ, THOMAS DR, BOYLE LE, SMITH TL, GEHAN EA, SAMUELS ML. Survival with inoperable lung cancer. Cancer 1977; 39: 303–313.

(*4*) MYERS MH, HANKEY BF. Cancer patient survival experience. Washington, D.C.: U.S. Dept of Health and Human Services, 1980 (Publication No. 80-2148).

(*5*) BERG JW, ROSS R, LATOURETTE HB. Economic status and survival of cancer patients. Cancer 1977; 39:467–477.

(*6*) CAMPOBASSO O, INVERNIZZI B, MUSSO M, BERRINO F. Survival rates of lung cancer according to histological type. Br J Cancer 1974; 29: 240–246

(*7*) ZELEN M. Keynote address on biostatistics and data retrieval. Cancer Chemother Rep Part 3 1973; 4:31–42.

(*8*) JOHNSTON-EARLY A, COHEN MH, MINNA JD, et al. Smoking abstinence and small cell lung cancer survival. JAMA 1980; 244:2175–2179.

(*9*) LINDEN G, DUNN JE, HOM PH, MANN M. Effect of smoking on the survival of patients with lung cancer. Cancer 1972; 30:325–328.

(*10*) CHALMER, J, HOLT PG, KEAST D. Cell-mediated immune responses to transplanted tumors in mice chronically exposed to cigarette smoke. J Natl Cancer Inst 1975; 55:1129–1134.

(*11*) HINDS MW, STEMMERMANN GN, YANG H-Y, KOLONEL L, LEE J, WEGNER E. Differences in lung cancer risk from smoking among Japanese, Chinese and Hawaiian women in Hawaii. Int J Cancer 1981; 27:297–302.

(*12*) PRENTICE RL, GLOECKLER LA. Regression analysis of grouped survival data with application to breast cancer data. Biometrics 1978; 34:

57–67.

(*13*) Lee J. Covariance adjustment of rates based on the multiple logistic regression model. J Chronic Dis 1981; 34:415–426.

(*14*) Livingston RB, Moore TN, Heilbrun L, et al. Small-cell carcinoma of the lung: Combined chemotherapy and radiation. Ann Intern Med 1978; 88:194–199.

(*15*) Holt PG, Keast D, MacKenzie JS. Immunosuppression in the mouse induced by long-term exposure to cigarette smoke. Am J Pathol 1978; 90:281–284.

(*16*) Shaw HM, Milton GW, McCarthy WH, Farago GA, Dilworth P. Effect of smoking on the recurrence of malignant melanoma. Med J Aust 1979; 1:208–209.

blank page

Intestinal Metaplasia in Japan: Association With Diet[1,2]

Abraham Nomura,[3] Hiroshi Yamakawa,[4] Takuzo Ishidate,[5] Sigetosi Kamiyama,[5] Hisayuki Masuda,[5] Grant N. Stemmermann,[3] Lance K. Heilbrun,[3] *and* Jean H. Hankin[6,7]

ABSTRACT—Of 1,749 volunteers in a screening program for gastric cancer in Japan, 206 men and 181 women received a systematic gastroscopic examination and responded to a dietary questionnaire estimating their quantitative intake of 33 food items during the past week. When diet was correlated with intestinal metaplasia (a precursor lesion of gastric carcinoma) found in gastroscopic biopsies, it was observed that more dried fish consumption and less vitamin A intake increased the extent of intestinal metaplasia in men. For women, there was a significant negative association of ume (pickled plum) intake with intestinal metaplasia. The implications of these findings were discussed in relation to gastric cancer.—JNCI 1982; 68:401–405.

Intestinal metaplasia of the stomach is considered to be a precursor lesion of intestinal gastric carcinoma as defined by histologic criteria (*1*). Many studies have consistently supported this view (*2–13*). For this reason, we decided to study the relationship of intestinal metaplasia with diet among the Japanese in Japan who are at high risk for gastric carcinoma.

Although many case–control studies of diet and gastric cancer have been done in the past (*14–21*), the interpretation of their findings has been cautious, partly because of the acknowledged long interval from gastric cancer induction to clinical manifestation (*22, 23*). Much reliance must be placed on the assumption that dietary information obtained after diagnosis reflects a person's usual diet over a long time. By the study of intestinal metaplasia, a precursor lesion, the time between exposure and the presence of disease is shortened considerably.

MATERIALS AND METHODS

Chokai Village is a rural community in Akita prefecture, Japan, with a population of 9,082 according to the 1975 National Census. From 1973 to 1978, 1,749 adult volunteer residents of Chokai Village received a fluoroscopic examination for the early detection of gastric cancer. On the basis of fluoroscopic findings or other clinical indications, 419 (24% of 1,749) subsequently received a gastroscopic examination along with a diet questionnaire. This report is limited to the 387 (92.4% of 419) subjects who systematically had a gastric biopsy taken from each of five sites in the stomach, as numbered and illustrated in text-figure 1.

Each biopsy specimen was assessed for the presence of intestinal metaplasia and was graded as follows: grade 0 = none; grade 1 = the presence of a single metaplastic gland; grade 2 = intestinal metaplasia involving two or more glands; grade 3 = intestinal metaplasia of the entire specimen. As a consequence, the intestinal grade scored for each subject ranged from 0 to 15 (five sites with a maximum grade of 3 each).

The participants were asked questions relating to education, occupation, cigarette smoking, alcohol intake, and recent dietary intake. Details of the dietary method used in this study have been previously published (*24*). We designed the study to quantitate the recent intakes of 33 specific food items by asking the participants to choose appropriate photographs of weighed small, medium, and large portions of each item. The 33 items were selected because of their suspected association with gastrointestinal neoplasms. The method consisted of an item-by-item recall to learn which items were eaten during the past week. When the respondent recalled eating a particular item, the interviewer asked him or her to choose the serving size from the picture. The dish in the photograph was present at the time of interview to provide the respondent with a sense of scale. The frequency of consumption and the estimated amount consumed during the past week were then recorded. For example, if a person ate three large servings of eggs (two eggs or 100 g) during the past week, his or her egg consumption was coded "3" for frequency and "3" (which designated large serving) for amount. The quantitative weekly amount would then be equivalent to 300 g (3×100 g).

Vitamin A and vitamin C intake was estimated mainly from food composition tables (*25, 26*) applied to the 33 food items. There were 16 food items containing varying amounts of vitamin A, and 11 containing varying amounts of vitamin C.

Age- and sex-adjusted mean metaplasia scores by cigarette use, alcohol use, and demographic variables were computed by the direct method of adjustment (*27*). The entire set of 387 subjects was the reference population. Comparisons of these mean metaplasia scores involved *t*-tests for independent samples.

The percent of subjects who consumed a given food item at least once during the week ranged from 1 to 98. As a result, 3 consumption-level groups (g/wk) in the analysis of the 33 food items were defined: none or low, intermediate, and high. To permit good estimates of age-adjusted mean metaplasia scores, we arbitrarily required at least 10 subjects in each of the 3 groups. Cutoff points were chosen accordingly for each food item. For vitamins A and C, 3 consump-

ABBREVIATION USED: *r*=coefficient of correlation.

---

[1] Received April 29, 1981; accepted October 28, 1981.

[2] Supported by Public Health Service contracts N01CP-61060 and N01CP-23213 from the Division of Cancer Cause and Prevention, National Cancer Institute.

[3] Japan–Hawaii Cancer Study, Kuakini Medical Center, 347 North Kuakini St., Honolulu, Hawaii 96817.

[4] Kawauchi Clinic, Chokai Village, Akita Prefecture, Japan.

[5] Akita University School of Medicine, Akita, Japan.

[6] University of Hawaii School of Public Health, Honolulu, Hawaii 96822.

[7] We thank Mrs. Carol Miyahira for her technical assistance.

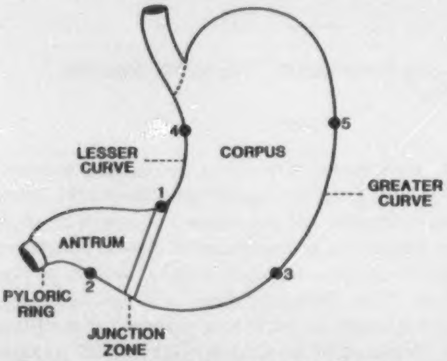

TEXT-FIGURE 1.—1=the lesser curvature at the junction of the antrum with the corpus and roughly corresponding with the incisura—the area most likely to show intestinal metaplasia; 2 = the greater curvature of the pyloric antrum 2–4 cm proximal to the pyloric ring—an area at intermediate risk for intestinal metaplasia; 3=the greater curvature of the stomach opposite the incisura; 4=the lesser curvature midway between the incisura and cardia; 5=the greater curvature opposite site #4. The last three sites are areas of low risk for intestinal metaplasia.

tion level groups (low, intermediate, high) were defined with approximately equal numbers of subjects. For both men and women, the same nine foods did not meet the sample size criterion: beef, Spam–lunchmeat, bacon, dried cuttlefish, corn on the cob, cut corn, tomato juice, celery, and black tea. For the remaining 24 foods and for vitamins A and C, age-adjusted mean metaplasia scores by consumption level were computed by the direct method of adjustment (*27*).

Preliminary data analysis indicated major differences in the foods that were most related to extent of metaplasia in males compared with females. Therefore, the described food consumption categories, age adjustments, and all subsequent analyses were done separately by sex. As an initial variable-screening step, a test for (linear) trend in the metaplasia scores with increasing consumption of each food item and vitamin was done by means of bivariate regression (*28*), which accounted for age. Dietary items were retained for subsequent multivariate analysis if they showed notable linear trends ($P<0.15$) in metaplasia scores. Multivariate analysis of the relationship of metaplasia score to age and the selected dietary items was done (separately by sex) with ordinary multiple linear regression (*28*).

RESULTS

A total of 206 men and 181 women had the diet questionnaire and gastric biopsies from the five specified sites. The age range of the study subjects at time of examination was 22–78 years. The distribution of metaplasia score by sex and age is presented in table 1. The presence of extensive intestinal metaplasia peaked at ages 50–59 in men. In women, extensive metaplasia continued to increase with age.

Table 2 shows comparisons of metaplasia scores by social or personal characteristics. Although consumers of hard liquor had a lower average metaplasia score than nonconsumers, there was a lack of consistency in metaplasia scores between consumers and nonconsumers of different types of alcoholic beverages. Farmers had a higher mean metaplasia score than subjects with other occupations, but the difference was not significant ($P=0.06$).

The notable trends in mean metaplasia scores with increasing consumption of different foods and vitamins are shown separately for men and women in table 3. For men, the dietary items most related to metaplasia score were dried fish, saimin or udon (noodles), vitamin A, sashimi (raw fish), tsukudani (seaweed paste), fruit drinks–ades, and shrimp. Dietary items with $P>0.15$ for linear trend for men were chicken, wieners, Vienna–pork sausage, eggs, char siu (sweetened roast pork), kamaboko (fish cake), tofu (soybean curd), rice, Japanese soup, sliced tomatoes, lettuce, hakusaizuke (pickled Chinese cabbage), takuwan (pickled turnip), ume (pickled plum), green tea, genmai cha (tea), coffee, milk, and vitamin C. For women, foods most related to metaplasia score were only ume, chicken, and shrimp.

TABLE 1.—*Distribution of metaplasia scores by sex and age*

Sex	Age, yr	No. of subjects by metaplasia scores (%)			
		0	1–5	6–15	Total
Men	<40	23 (61)	15 (39)	0 (0)	38 (100)
	40–49	14 (27)	23 (45)	14 (27)	51 (99)
	50–59	8 (14)	17 (30)	31 (55)	56 (99)
	≥60	11 (18)	20 (33)	30 (49)	61 (100)
Total		56 (27)	75 (36)	75 (36)	206 (99)
Women	<40	19 (68)	9 (32)	0 (0)	28 (100)
	40–49	17 (43)	19 (48)	4 (10)	40 (101)
	50–59	26 (43)	21 (35)	13 (22)	60 (100)
	≥60	18 (34)	19 (36)	16 (30)	53 (100)
Total		80 (44)	68 (38)	33 (18)	181 (100)

TABLE 2.—*Sex- and age-adjusted mean metaplasia scores by social or personal characteristics*

Characteristics (*n*)	Metaplasia score	*P*-value[a]
Education		
Senior primary or more (198)	3.2	0.90
Primary or less (189)	3.2	
Occupation		
Farmer (253)	3.7	0.06
Other (134)	3.0	
Cigarettes		
Smoker (150)	2.6	0.10
Nonsmoker (237)	3.4	
Wine		
Drinker (139)	4.0	0.09
Nondrinker (248)	3.3	
Fermented sake		
Drinker (333)	3.5	0.61
Nondrinker (54)	3.3	
Beer		
Drinker (261)	3.4	0.10
Nondrinker (126)	4.0	
Hard liquor		
Drinker (98)	2.6	0.01
Nondrinker (289)	3.7	
Home brew		
Drinker (218)	3.6	0.29
Nondrinker (169)	3.2	
Nonfermented sake		
Drinker (157)	3.6	0.64
Nondrinker (230)	3.4	

[a] Two-tailed *t*-test.

TABLE 3.—*Age-adjusted mean metaplasia scores by consumption level of selected[a] dietary items and by sex*

Sex	Dietary item	Consumption level, g/wk			*P*-value[b]
		None or low	Intermediate	High	
Men	Dried fish	3.6	4.3	5.7	0.006
	Saimin or udon (noodles)	5.3	2.7	4.1	0.011
	Vitamin A	5.3	4.6	3.6	0.017
	Sashimi (raw fish)	5.0	2.9	4.0	0.034
	Tsukudani (seaweed paste)	4.1	4.5	5.8	0.043
	Fruit drinks–ades	4.8	4.3	3.7	0.107
	Shrimp	4.5	3.8	3.1	0.123
Women	Ume (pickled plum)	2.8	2.7	0.7	0.017
	Chicken	1.7	2.5	2.9	0.070
	Shrimp	2.6	1.8	1.2	0.111

[a] Those selected had linear trend with $P<0.15$ (for screening purposes). Dietary items listed by *P*-value for trend.

[b] From two-tailed *t*-test for linear trend in the mean metaplasia scores.

TABLE 4.—*Results[a] of multiple linear regression of metaplasia scores on age and selected dietary items by sex*

Variable[b]	$\hat{b}$[c]	SE, $\hat{b}$[d]	$\hat{\beta}$[e]	*P*-value[f]
Men: $n=164$; $R^2=0.221$				
Age	0.088	0.024	0.271	<0.001
Dried fish	0.001	0.0004	0.242	0.002
Vitamin A	−0.0001	0.00004	−0.170	0.025
Tsukudani (seaweed paste)	0.057	0.036	0.116	0.110
Sashimi (raw fish)	−0.005	0.006	−0.054	0.399
Shrimp	−0.013	0.018	−0.053	0.459
Saimin–udon (noodles)	0.0003	0.0006	0.031	0.681
(Constant term)	0.288	1.474	NA	0.845
Women: $n=176$; $R^2=0.163$				
Age	0.094	0.020	0.323	<0.001
Ume (pickled plum)	−0.029	0.014	−0.142	0.045
Shrimp	−0.018	0.010	−0.121	0.087
Chicken	0.004	0.003	0.111	0.117
(Constant term)	−2.471	1.149	NA	0.033

[a] Results are listed in descending order of statistical significance, except for the constant term of the multiple regression model.

[b] n=No. of subjects; R^2=proportion of total variation in metaplasia scores explained by the particular set of variables in the regression model.

[c] $\hat{b}$=estimated (unstandardized) regression coefficient.

[d] SE, $\hat{b}$=estimated standard error of $\hat{b}$.

[e] $\hat{\beta}$=estimated standardized regression coefficient. NA=not applicable.

[f] For testing (via *F*-statistics) whether the regression coefficient is significantly different from zero.

Table 3 suggests that seven dietary items should enter into the multiple regression analysis for men. However, vitamin A and fruit drinks–ades were too highly intercorrelated ($r=0.64$) to permit both of them in the model. Since vitamin A initially had the more significant association ($P=0.017$) and since it represents a summary measure of 16 foods, it was selected in preference to fruit drinks–ades.

The results of the multiple regression analyses, in which the simultaneous effects of age and the various dietary items can be assessed, are shown in table 4. For men, increasing metaplasia scores were significantly associated ($P<0.05$) with increasing age, increasing consumption of dried fish, and decreasing consumption of vitamin A. For women, however, increasing metaplasia scores were significantly associated with increasing age and decreasing consumption of ume.

DISCUSSION

The presence of intestinal metaplasia is common in this study population. Its greater prevalence in men than women and its increase with age have been previously reported (*29*). The systematic biopsies of the gastric mucosa represented only a very small portion of the gastric mucosal surface area. For this reason, subjects with focal metaplasia may have false-negative biopsies. The metaplasia score, therefore, probably underestimates the extent of metaplasia in the stomachs examined.

Alcohol intake in general and cigarette smoking in particular did not appear to be clearly associated with the degree of intestinal metaplasia. A separate investigation found that alcohol drinkers or current smokers had a slightly lower prevalence of precursor lesions such as intestinal metaplasia or chronic atrophic gastritis than was found for nondrinkers or nonsmokers, respectively (*11*). The authors attributed this pattern to a tendency to discontinue use of items that exacerbated gastric symptoms. With respect to stomach cancer, the findings from earlier studies on the use of alcohol have been equivocal (*15, 18, 30*). A positive association between cigarette smokers and stomach cancer has been observed mainly in prospective studies (*31, 32*), but the lack of a dose-response relationship has suggested that the association was not a causal one.

Haenszel and co-workers (*11*) found a negative association of precursor lesions of stomach cancer with social class status, which is consistent with the view of many past studies (*15, 18, 33, 34*) that stomach cancer is a disease of the low social class. We observed that farmers (low social class) had a notably ($P=0.06$) higher mean metaplasia score than persons engaged in other occupations.

Regression analysis revealed that more dried fish consumption and less vitamin A intake in men and less ume intake in women increased the extent of intestinal metaplasia. Dried fish is a common protein source in Chokai Village with an average weekly consumption of 626 g for men and 604 g for women. It consists mainly of dried sardine, cod, mackerel, or herring, with salt often included. The positive relationship of dried fish with its high salt content to intestinal metaplasia corresponds with findings in a previous study that showed a strong association between salt use and intestinal metaplasia (*35*). Workers have shown that dried fish is rich in nitrites or secondary amines (*36*), which are needed in the formation of N-nitroso compounds. N-nitroso compounds are known carcinogens (*37*), and some workers suspect that they may be associated with the development of gastric cancer (*1*).

Recent studies have suggested that low vitamin A intake may increase susceptibility to cancer (*38, 39*). Our findings among the men indirectly support this impression. Because vitamin C blocks the formation of N-nitroso compounds in vitro or in vivo (*40, 41*), it may be protective against gastric neoplasms. However, our data showed no association between vitamin C intake and the degree of intestinal metaplasia. On the basis of the 1975 National Nutrition Survey in Japan, the average daily intake for all persons of vitamins A and C was 1,602 IU and 117 mg, respectively (*42*). The average daily intakes for the adults in our study were 2,006 IU of vitamin A and 39 mg of vitamin C. The low level of vitamin C intake, as measured by our dietary questionnaire, may have contributed to its lack of association with intestinal metaplasia.

The reasons for the sex difference in the association of intestinal metaplasia with dried fish intake and vitamin A intake are not readily apparent. Several possibilities need to be explored, such as subtle differences in food use between the sexes. It is a common household custom in rural Japan for the husband to be served from the anterior portion of the fish. This would expose him to a higher salt intake if the body cavity of the fish has been packed with salt as part of the preservation process. It is also possible that women in this population might have a higher intake of substances that block the nitrosation of dietary amines.

Even though the mean weekly intake of ume was only 9 g, it had a significant negative association with metaplasia score in women. This was an unexpected finding because the process of pickling has been shown to increase the nitrite content of food items (*36*). Ume and other pickled items were found to be positively associated with stomach cancer among the Japanese in Hawaii (*15*) but not in Japan (*16*). When we correlated the intake of ume with the other 32 food items for the women, we found that it was strongly associated with only tomatoes (r=0.17) and celery (r=0.18), vegetables that have been negatively associated with stomach cancer in past studies (*14-16, 18*). The women had a higher mean weekly intake than did the men for tomatoes (136 vs. 85 g) and celery (11.8 vs. 9.4 g). Although this negative association of ume with metaplasia score possibly is a chance finding, further clarification is needed with regard to this observation.

Overall, only dried fish of the 33 food items in the questionnaire had a significantly positive association with intestinal metaplasia of the stomach. Several past studies have also shown that dried or salted fish increased the risk for gastric cancer (*14, 15, 18*). Because dried fish is so commonly consumed in Chokai Village and elsewhere in Japan, it is important to study further its relationship to intestinal metaplasia and stomach cancer.

REFERENCES

(*1*) Correa P, Haenszel W, Cuello C, Tannenbaum S, Archer M. A model for gastric cancer epidemiology. Lancet 1975; 2:58-59.

(*2*) Morson BC. Carcinoma arising from area of intestinal metaplasia in the gastric mucosa. Br J Cancer 1955; 9:365-376.

(*3*) Correa P, Cuello C, Duque E. Carcinoma and intestinal metaplasia of the stomach in Columbian migrants. J Natl Cancer Inst 1970; 44:297-306.

(*4*) Ming SC, Goldman H, Freiman DG. Intestinal metaplasia and histogenesis of carcinoma of human stomach. Cancer 1967; 20: 1418-1429.

(*5*) Lauren P. Two histological main types of gastric carcinoma. Acta Pathol Microbiol Scand 1965; 64:31-49.

(*6*) Jarvi O, Lauren P. On the role of heteropias of the intestinal epithelium in the pathogenesis of gastric cancer. Acta Pathol Microbiol Scand 1951; 29:26-44.

(*7*) Munoz N, Asvall J. Time trends of intestinal and diffuse types of gastric cancer in Norway. Int J Cancer 1971; 8:144-157.

(*8*) Munoz N, Correa P, Cuello C, Duque E. Histologic types of gastric carcinoma in high and low risk areas. Int J Cancer 1968; 3:809-818.

(*9*) Munoz N, Connelly R. Time trends of intestinal and diffuse types of gastric cancer in the United States. Int J Cancer 1971; 8:158-164.

(*10*) Correa P, Sasano N, Stemmermann GN, Haenszel W. Pathology of gastric carcinoma in Japanese populations: Comparisons between Miyagi prefecture, Japan, and Hawaii. J Natl Cancer Inst 1973; 51:1449-1459.

(*11*) Haenszel W, Correa P, Cuello C, et al. Gastric cancer in Colombia. II. Case-control epidemiologic study of precursor lesions. J Natl Cancer Inst 1976; 57:1021-1026.

(*12*) Matsukura N, Kawachi T, Sasajima K, Sano M, Sugimura T, Hirota T. Induction of intestinal metaplasia in the stomachs of rats by *N*-methyl-*N'*-nitro-*N*-nitrosoguanidine. JNCI 1978; 61:141-144.

(*13*) Watanabe H. Experimentally induced intestinal metaplasia in Wistar rats by X-ray irradiation. Gastroenterology 1978; 75:796-799.

(*14*) Bjelke E. Epidemiologic studies of cancer of the stomach, colon, and rectum. Scand J Gastroenterol 1974; 9 (suppl 31):42-53.

(*15*) Haenszel W, Kurihara M, Segi M, Lee RK. Stomach cancer among Japanese in Hawaii. J Natl Cancer Inst 1972; 49:969-988.

(*16*) Haenszel W, Kurihara M, Locke FB, Shimuzu K, Segi M. Stomach cancer in Japan. J Natl Cancer Inst 1976; 56:265-278.

(*17*) Graham S, Lilienfeld AM, Tidings JE. Dietary and purgation factors in the epidemiology of gastric cancer. Cancer 1967; 20: 2224-2234.

(*18*) Hirayama T. Epidemiology of stomach cancer. Gan 1971; 11:3-19.

(*19*) Higginson J. Etiological factors in gastrointestinal cancer in man. J Natl Cancer Inst 1966; 37:527-545.

(*20*) Modan B, Lubin F, Barell V, Greenberg RA, Modan M, Graham S. The role of starches in the etiology of gastric cancer. Cancer 1974; 34:2087-2092.

(*21*) Acheson ED, Doll R. Dietary factors in carcinoma of the stomach: A study of 100 cases and 200 controls. Gut 1964; 5:126-131.

(*22*) Haenszel W. Cancer mortality among the foreign-born in the United States. J Natl Cancer Inst 1961; 26:37-132.

(*23*) Haenszel W, Kurihara M. Studies of Japanese migrants. I. Mortality from cancer and other diseases among Japanese in the United States. J Natl Cancer Inst 1968; 40:43-68.

(*24*) Hankin JH, Rhoads GG, Glober GA. A dietary method for an epidemiologic study of gastrointestinal cancer. Am J Clin Nutr 1975; 28:1055-1061.

(*25*) Watt BK, Merrill AL. Composition of foods—raw, processed, prepared. Washington, D.C.: U.S. Govt Print Off, 1963 [Agr Res Serv Handbook No. 8, U.S. Dept Agr].

(*26*) Japan Dietetic Association. Standard tables of food composition. Suppl 3d revision. Tokyo: Ishiyaku Shuppan Co., 1980.

(*27*) Lilienfeld AM, Pederson E, Dowd JE. Cancer epidemiology: Methods of study. Baltimore: Johns Hopkins Press, 1967:102-103.

(*28*) Draper NR, Smith H. Applied regression analysis. New York: Wiley, 1966:44-85.

(*29*) Stemmermann GN, Ishidate T, Samloff IM, et al. Intestinal metaplasia of the stomach in Hawaii and Japan. Am J Dig Dis 1978; 23:815-820.

(*30*) Wynder EL, Kmet J, Dungal N. An epidemiological investigation of gastric cancer. Cancer 1963; 16:1461-1496.

(*31*) Kahn HA. The Dorn study of smoking and mortality among U.S. veterans: Report on eight and one-half years of observation. Natl Cancer Inst Monogr 1966; 19:1-125.

(*32*) Hammond EC. Smoking in relation to the death rates of 1 million men and women. Natl Cancer Inst Monogr 1966; 19:127-204.

(*33*) Sigurjonsson J. Occupational variations in mortality from gastric cancer in relation to dietary differences. Cancer 1967; 21:651-656.

(*34*) Cohart EM. Socioeconomic distribution of stomach cancer in New Haven. Cancer 1954; 7:455-461.

(*35*) Stemmermann G, Haenszel W, Locke F. Epidemiologic pathology of gastric ulcer and gastric carcinoma among Japanese in Hawaii. J Natl Cancer Inst 1977; 58:13–20.

(36) Ishidate M, Tanimura A, Ito Y, et al. Secondary amines, nitrites and nitrosamines in Japanese foods. In: Nakahara W, et al., eds. Topics in chemical carcinogenesis. Proceedings of the second international symposium of the Princess Takamatsu Cancer Research Fund. Baltimore: University Park Press, 1972:313–322.

(37) Lijinsky W, Epstein SS. Nitrosamines as environmental carcinogens. Nature 1970; 225:21–23.

(38) Wald N, Idle M, Boneham J, Bailey A. Low serum vitamin A and subsequent risk of cancer. Lancet 1980; 2:813–815.

(39) Kark JD, Smith AH, Switzer BR, Hames CG. Serum vitamin A (retinol) and cancer incidence in Evans County, Georgia. JNCI 1981; 66:7–16.

(40) Mirvish S, Wallcave L, Eagen M, Shubik P. Ascorbate-nitrite reaction: Possible means of blocking the formation of carcinogenic N-nitroso compounds. Science 1972; 177:65–68.

(41) Raineri R, Weisburger JH. Reduction of gastric carcinogens with ascorbic acid. Ann NY Acad Sci 1975; 258:181–189.

(42) Kagawa Y. Impact of westernization on the nutrition of Japanese: Change in physique, cancer, longevity and centenarians. Prev Med 1978; 7:205–217.

blank page

Basis for the Differential Action of Aminonucleoside on Normal and Transformed Human Fibroblasts[1, 2]

Ernest A. Albanese[3] *and* **George P. Studzinski**[3, 4, 5]

ABSTRACT—Acid-soluble extracts of normal human fibroblasts (IMR 90 cells) exposed to [^{3}H]aminonucleoside of puromycin ([^{3}H]AMS) contained larger amounts of unchanged AMS than did similar extracts of their transformed counterparts (AG 2804 cells). The radioactive compounds present in IMR 90 cells were further analyzed by sequential high-voltage paper electrophoresis, enzyme digestion, and paper chromatography. In addition to unchanged [^{3}H]AMS, only [^{3}H]adenosine, [^{3}H]inosine, and [^{3}H]adenosine monophosphate could be detected, apparently derived from [^{3}H]adenosine present in the [^{3}H]AMS samples added to the cultures. Consistent with the absence of metabolism of AMS in IMR 90 cells was the failure to find AMS derivatives in the RNA or DNA of these cells. The content of ribonucleoside triphosphates (rNTPs) in acid-soluble extracts of IMR 90 cells was significantly reduced by AMS treatment, and nuclei or broken cell preparations obtained from AMS-treated IMR 90 cells incorporated [^{3}H]UTP into macromolecules at approximately control rates, when supplemented with rNTPs. These findings indicated that the reduced level of rNTPs may be responsible for the AMS-induced inhibition of RNA synthesis in normal cells.—JNCI 1982; 68:407–413.

The adenosine analog AMS has been shown to have markedly different effects on the nucleic acid metabolism and growth of various cultured normal and transformed mammalian cells (*1–7*). In normal cells AMS inhibits nonselectively the synthesis of all species of RNA and arrests the cell cycle traverse, principally in the G_1 phase. However, in fibroblasts transformed by an oncogenic virus, simian virus 40, AMS has a particularly marked inhibitory effect on ribosomal RNA synthesis but permits continued, though increasingly retarded, traverse of the cell cycle by the treated fibroblasts.

Our recent work has provided an explanation for the selective inhibition of ribosomal RNA synthesis in transformed cells (*8–10*). It appears that in these cells AMS is slowly demethylated, then sequentially phosphorylated to a triphosphate derivative, which can be incorporated by RNA polymerases into growing RNA chains, thereby causing premature termination of these chains. The severity of the effect on ribosomal RNA can be explained by structural changes in the nucleolus, which result from incorporation of demethylated AMS into preribosomal RNA and which greatly potentiate the biochemical effect (*10*). The explanation for the absence of such an effect on ribosomal RNA synthesis in normal cells was not available.

In this communication we present data indicating that AMS is not metabolized by the normal fibroblast and therefore cannot be incorporated into the RNA of the nucleolus. The inhibitory effects of this drug can be attributed to the reduction in the intracellular concentration of rNTPs for RNA synthesis.

MATERIALS AND METHODS

Materials.—The purine derivatives AMS, AMP, adenosine, adenine, N^6-monomethylaminopurine-9-riboside, and the enzymes nucleotide pyrophosphatase (EC 3.6.1.9), alkaline phosphatase from *Escherichia coli* (EC 3.1.3.1), deoxyribonuclease I (EC 3.1.4.5), and snake venom phosphodiesterase I (EC 3.1.4.1) were purchased from Sigma Chemical Co., St. Louis, Mo. N^6,N^6-Dimethylaminopurine-9-riboside was purchased from Vega Biochemicals, Tucson, Ariz. Nucleoside triphosphates were obtained from ICN Chemical and Radioisotope Division, Irvine, Calif. The [^{3}H]AMS was purchased from Amersham Corp., Arlington Heights, Ill. (10.6 Ci/mmol; general label). It was found to contain a small percentage of contaminating adenosine (*see* text-fig. 2), but attempts at further purification by electrophoresis resulted in the appearance of unidentified breakdown products. New England Nuclear Corp., Boston, Mass. supplied [5,6-^{3}H]uridine (38.8 Ci/mmol), [^{32}P]orthophosphate (carrier-free), and [5,6-^{3}H]UTP (46.3 Ci/mmol).

Cell culture.—Human lung fibroblasts (IMR 90 cells) and their simian virus 40-transformed derivatives (AG 2804 cells) were obtained from the Institute for Medical Research, Camden, N.J. The IMR 90 cells were grown as monolayers in 75-cm^2 plastic flasks (Corning Glass Works, Corning, N.Y.,) with the use of McCoy's 5-A medium supplemented with 20% fetal bovine serum (heat inactivated at 55°C for 30 min) and 1% glutamine. AG 2804 cells were grown in Corning flasks, and Eagle's minimum essential medium supplemented with 10% newborn calf serum (also heat inactivated) and 1% glutamine was used. Antibiotic supplements were not used for either cell line.

Preparation of PCA extracts for electrophoretic analysis.—Ten flasks of IMR 90 cells or four flasks of AG 2804 cells were exposed to 12.5 µCi of [^{3}H]AMS and 100 µg of unlabeled AMS/ml of McCoy's 5-A medium. Each flask was given 10 ml of the labeling medium. Following 18 hours of incubation at 37°C, the medium was removed and the cell sheets were rinsed four times with ice-cold 0.1 *M* sodium PBS (0.85% NaCl; pH 7.0). The cells were gently suspended in PBS with a rubber spatula and centrifuged at 800×*g* at 4°C for 10

ABBREVIATIONS USED: AMS=aminonucleoside of puromycin; DDT=1,4-dithiothreitol; PBS=phosphate-buffered saline; PCA=perchloric acid; PEI=polyethyleneimine; rNTPs=ribonucleoside triphosphates; TCA=trichloroacetic acid.

---

[1] Received May 14, 1981; accepted October 22, 1981.

[2] Supported by Public Health Service grant CA-19750 from the National Cancer Institute.

[3] Department of Pathology, College of Medicine and Dentistry of New Jersey, New Jersey Medical School, Newark, N.J. 07103.

[4] *Address reprint requests to* Dr. Studzinski.

[5] We thank Ms. Marsha Trocola-Simchera for tissue culture preparations.

minutes. The cells were washed once by resuspension in PBS and centrifugation. The pellets were suspended in 2 ml of ice-cold distilled water and disrupted by 25 strokes in an 8-ml Potter-Elvehjem homogenizer (Kontes #22). Then 70% PCA was added to a final concentration of 5%. The homogenate was mixed in a vortex and kept on ice for 15 minutes before being centrifuged for 10 minutes at 800×*g*. The supernatant was saved, and the pellet washed two times with 2.5% ice-cold PCA and kept for further analysis. The supernatant and washes were combined, neutralized with KOH, and centrifuged at 2,900×*g* for 10 minutes. The final extract was lyophilized and stored for further analysis.

Determination of the incorporation of [^{3}H]AMS into nucleic acid.—Thirty flasks of IMR 90 cells were exposed to 333 μCi of [^{3}H]AMS with unlabeled 340 μ*M* AMS (100 μg/ml) in 10 ml of McCoy's 5-A medium per flask and incubated for 18 hours. PCA pellets obtained as described above were washed twice with 10 ml of 2.5% PCA and precipitated three times out of ice-cold 0.1 *N* NaOH with 10% PCA as previously described (*9*). The final pellet was hydrolyzed in 3 ml of 0.3 *N* KOH at 37°C for 24 hours. The hydrolysate was neutralized with PCA, centrifuged at 2,900×*g* for 10 minutes, and lyophilized. The remaining pellet, containing the DNA, was subjected to successive digestion with DNase I and snake venom phosphodiesterase I (*9*).

High-voltage electrophoresis.—The lyophilized samples were resuspended in 700 μl of distilled water and spotted across 5-cm-wide Whatman 3MM electrophoresis paper. The buffer contained pyridine, acetic acid, and water (1:10:89; pH 3.5). Electrophoresis was done on a Gilson model D high-voltage electrophorator for 1.5–3 hours at 2,000 V.

Elution of compounds from electrophoretic strips.—Sections of the paper strip (1 cm) were suspended over beakers of distilled water, and the compounds in the paper were allowed to concentrate at the tip of the paper by capillary action. The sections were then attached to the lip of a conical centrifuge tube with the tip of the paper pointing into the tube. The tubes were centrifuged at 300×*g*, and the water drawn out of the paper carried the compound into the tube. The eluted samples were lyophilized for further analysis.

Enzymatic digestion of compounds eluted from electrophoretic strips.—In the case of alkaline phosphatase, the lyophilized material was dissolved in 0.2 ml of 0.1 *M* Tris buffer (pH 8.0) and incubated at 37°C, with a total of 150 μg of enzyme added in 50-μg aliquots at 15-minute intervals. For nucleotide pyrophosphatase digestion the sample was dissolved in 0.2 ml of 0.02 *M* Tris buffer (pH 7.4) containing 1 m*M* $MgCl_2$. Then 0.01 U of the enzyme was added to the sample and incubated at 37°C for 15 minutes, after which all samples were stored at −20°C until electrophoresis could be performed.

Acid hydrolysis of compounds eluted from electrophoretic strips.—The lyophilized material was dissolved in 50 μl of 1 *N* HCl and heated at 100°C for 1 hour. The samples were chromatographed along with adenine and hydrolysates of N^6-methyladenosine and N^6,N^6-dimethyladenosine. The paper used was Whatman 3MM, and the solvent system contained isopropanol, NH_4OH, and H_2O (7:1:2; pH 11) (*9*).

Radioactivity measurements of electrophoretic strips and chromatograms.—Sections of paper (1 cm) were minced with scissors and placed in scintillation vials. Then 1 ml of water was added and the vials were heated at 60°C for 2 hours. The vials were mixed in a vortex for 30 seconds, Biofluor was added, and the vials were mixed in a vortex for another 30 seconds. The radioactivity was measured in an Intertechnique scintillation counter (model 4000).

Preparation of nuclei and cell homogenates.—Flasks of cells treated with 340 μ*M* AMS for varying periods of time were rinsed with PBS and harvested as described above. The washed pellet was suspended in buffer A [0.12 *M* Tris (pH 7.8), 0.02 *M* KCl, 0.01 *M* $MgCl_2$, and 0.3 *M* sucrose] and centrifuged at 800×*g* for 10 minutes. The cells were resuspended in buffer A and disrupted by 12 strokes in an 8-ml Potter-Elvehjem homogenizer. The homogenate was centrifuged at 800×*g* for 10 minutes and washed once in buffer A. The pellet was then suspended in buffer B [0.25 *M* sucrose, Tris (pH 7.5), 25 m*M* KCl, and 5 m*M* $MgCl_2$] and rehomogenized with 12 strokes. The crude nuclear suspension was placed over buffer C [1.1 *M* sucrose, 50 m*M* Tris (pH 7.5), 25 m*M* KCl, and 5 m*M* $MgCl_2$) and centrifuged at 2,900×*g* for 30 minutes. The final nuclear pellet was resuspended in buffer A containing 1 m*M* DTT.

In the case of cell homogenates, cell pellets, after being washed in PBS, were directly homogenized in buffer A with 1 m*M* DTT (12 strokes) and used in RNA polymerase assays.

Assays of RNA synthesis by isolated nuclei or cell homogenates.—The incubation mixture contained 50 μl of nuclei or cell homogenate (8–12 μg DNA), ATP, GTP, and CTP (all 0.6 m*M*), and 5 μCi [5,6-^{3}H]UTP. (Specific activity after addition of unlabeled UTP was 304 mCi/mmol.) The final volume was adjusted to 100 μl with distilled water. In some experiments cell homogenates were not exposed to exogenous unlabeled rNTPs, but only to 5 μCi of high specific activity [5,6-^{3}H]UTP (sp act, 46.3 Ci/mmol). The preparations were incubated at 37°C for indicated periods of time, the reaction was stopped by the addition of 1 ml ice-cold 10% TCA, and the precipitate was collected by centrifugation, dissolved in 0.1 *N* NaOH, and reprecipitated with 10% TCA. This procedure was repeated, and the final pellet was dissolved in 250 μl of 0.1 *N* NaOH mixed with 10 ml of Biofluor. Radioactivity was determined in the liquid scintillation counter.

Incorporation of [5,6-^{3}H]uridine into intact cells.—Cells were seeded in Costar six-well cluster dishes and exposed to 340 μ*M* AMS for varying periods of time. After incubation with the drug, the medium was removed and replaced with 1 ml of fresh medium without serum or AMS, containing [5,6-^{3}H]uridine (5 μCi/ml). One hour later the labeling medium was removed, the cells were rinsed three times with 1 ml of PBS, 500 μl of 5% TCA was added to the wells, and the dishes were kept at 4°C for 30 minutes. The TCA was then removed and the cell sheet washed two times with 1 ml of fresh 5% TCA. The final sample containing acid-precipitable material was dissolved in 500 μl of 0.1 *N* NaOH. A 250-μl aliquot of this solution was added to 10 ml of Biofluor, and the radioactivity was counted by liquid scintillation.

Measurement of relative concentrations of rNTPs.—IMR 90 cells, grown in 75-cm^2 plastic flasks, were incubated with 5 µCi [^{32}P]orthophosphate/ml in 9 ml of Dulbecco's medium supplemented with 20% fetal bovine serum and 1% glutamine. After 24 hours at 37°C, AMS was added in 1 ml of sterile water to a final concentration of 340 µ*M*. Control flasks received 1 ml of sterile water. The cells were incubated with AMS for 18 hours, the medium was removed, and the cells were rinsed and harvested with PBS as described above. The cell pellet was extracted with 500 µl of ice-cold 1 *M* formic acid. The mixture was mixed in a vortex at 15-minute intervals for 1 hour, then centrifuged at 2,900×*g* for 30 minutes. The supernatant was mixed with unlabeled standard triphosphates, and 5-µl aliquots were spotted on PEI cellulose thin-layer sheets. Chromatograms were developed with 0.85 *M* KH$_2$PO$_4$ (pH 3.4) (*11*). The spots were visualized by UV light, cut out, and added to vials with 3 ml of Biofluor, and the radioactivity was counted by liquid scintillation.

DNA measurement.—DNA content was measured by Fleck and Munro's (*12*) modification of the Schmidt-Thannhauser procedure (*13*).

RESULTS

Analysis of Radioactive Compounds in the Acid-Soluble Extracts of Fibroblasts Treated With [^{3}H]-AMS

The IMR 90 fibroblasts were incubated with [^{3}H]AMS for 18 hours, and the PCA extract was analyzed by high-voltage electrophoresis (text-fig. 1A). The pattern of radioactive compounds thus obtained was compared with the pattern obtained for identically treated transformed fibroblasts (text-fig. 1B). In both cell lines, unchanged AMS was the principal radioactive compound, but the drug accumulated to a much greater extent in normal than in transformed cells. Conversely, smaller amounts of radioactive compounds other than AMS were present in extracts of normal cells.

We have previously established that in transformed cells AMS must be demethylated in the N^6 position before it can be further metabolized and incorporated into cellular RNA (*9*). Demethylated derivatives of AMS cannot be separated from the parent compounds by electrophoresis, but the separation can be easily accomplished by paper chromatography in appropriate solvents. Therefore, for the determination of whether area 1 of the electrophoretogram shown in text-figure 1A contained demethylated AMS (3′-amino-3′-deoxyadenosine) as well as unchanged AMS, this area was eluted, hydrolyzed with HCl to liberate the purine bases, and subjected to paper chromatography in a system that separates adenine from its methylated derivatives. As shown in the inset to text-figure 1A, area 1 contained only N^6,N^6-dimethyladenine, indicating that no detectable demethylation took place in the normal cells incubated with the drug for 18 hours.

Radioactive compounds found in the cells exposed to [^{3}H]AMS can be derived from this component and also from [^{3}H]adenosine, which contaminates the available [^{3}H]AMS preparations as shown in text-figure 2 (*9, 10*). The minor peaks in text-figure 1A, areas 2–4, were therefore eluted from the electrophoretograms and subjected to an analysis summarized in table 1. It is clear that these peaks represented contaminant [^{3}H]adenosine and its metabolites inosine and AMP. No metabolites of AMS could be detected in the intracellular pools of IMR 90 cells.

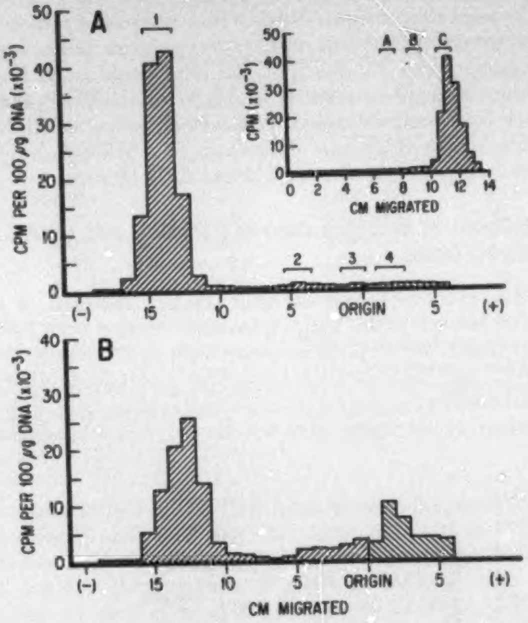

TEXT-FIGURE 1.—Electrophoretograms of the radioactive compounds in the PCA extracts of IMR 90 and AG 2804 cells after exposure to 12.5 µCi [^{3}H]AMS/ml and unlabeled AMS (340 µ*M*) for 18 hr. A) Acid-soluble extract of IMR 90 cells. Areas 1 through 4 were eluted for further analysis. *Inset* represents a chromatogram of the HCl hydrolysate of the material eluted from area 1. Adenine and acid hydrolysates of N^6-mono and N^6,N^6-dimethyl derivatives of adenosine were cochromatographed as standards and visualized by UV light. These standards are designated A, B, and C, respectively, in the *inset*. B) Acid-soluble extract of AG 2804 cells.

Absence of Incorporation of [^{3}H]AMS Into RNA in IMR 90 Cells

Preliminary experiments, performed according to protocols that demonstrated the incorporation of [^{3}H]3′-amino-3′-deoxyadenosine derived from [^{3}H]AMS into the RNA of transformed cells (*9, 10*), failed to show such incorporation into the RNA of IMR 90 cells. This observation is in keeping with the lack of conversion of AMS in these cells into phosphorylated metabolites that could form the substrates for RNA polymerases and was confirmed by the use of a larger number of cells (fourfold increase) exposed to a higher concentration of [^{3}H]AMS (fivefold increase).

Text-figure 3 shows that the alkaline hydrolysate of the residual pellet obtained after PCA precipitation and washes of IMR 90 cells exposed to [^{3}H]AMS contained only the radioactivity migrating with AMS. This radioactivity could be attributed to [^{3}H]AMS adsorbed to pellet contents by noncovalent bonds. Radioactivity derived from the [^{3}H]3′-amino-3′-deoxyadenosine intermediate, covalently incorporated into RNA, would migrate with AMS due to its ribose amino group, but acid hydrolysis would liberate adenine.

The inset to text-figure 3 shows that no peak of radioactivity was present in the area of the chromatogram migrating with adenine (area A) and that the only peak noted had the chromatographic mobility of N^6,N^6-dimethyladenine and, therefore, was presumably derived from adsorbed [^{3}H]AMS. Thus we conclude that demethylated AMS derivatives are not incorporated into the RNA of IMR 90 cells.

Absence of Incorporation of [^{3}H]AMS Into DNA of IMR 90 Cells

The material remaining after alkaline hydrolysis of PCA-extracted cell pellet was sequentially treated with DNase I and snake venom phosphodiesterase I as described in "Materials and Methods." Radioactive compounds migrating with AMS were not detected on high-voltage paper electrophoresis of the digest (data not shown), which indicates that AMS or a derivative is not incorporated into the DNA of IMR 90 cells treated for 18 hours with the drug.

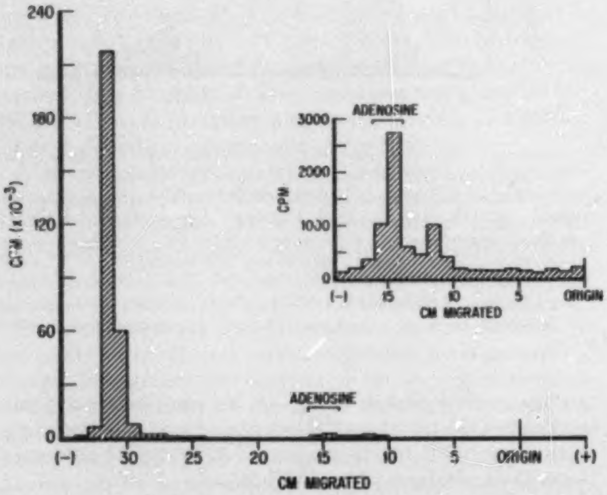

TEXT-FIGURE 2.—Electrophoretogram of [^{3}H]AMS as received from the supplier. The sample contained 0.5 μCi [^{3}H]AMS and 100 μg of unlabeled AMS. *Inset* is an enlargement of area showing the minor peak that migrated with standard adenosine.

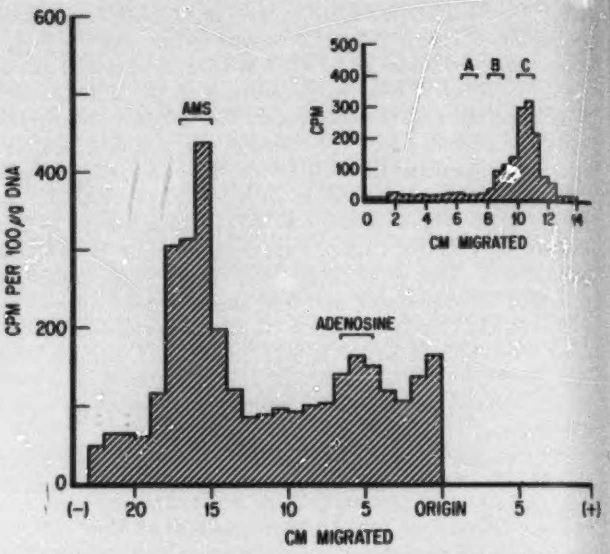

TEXT-FIGURE 3.—Electrophoretogram of the KOH hydrolysate of the PCA pellet obtained from 30 flasks of IMR 90 cells exposed for 18 hr to 33.3 μCi [^{3}H]AMS/ml; unlabeled AMS was added to 340 μM. Unlabeled AMS and adenosine were coelectrophoresed as markers and visualized by UV light *Inset* represents a chromatogram of the HCl hydrolysate of the material eluted from the area migrating with the marker AMS. Adenine and acid hydrolysates of N^6-mono and N^6,N^6-dimethyl derivatives of adenosine were cochromatographed as standards and visualized by UV light. These standards are designated A, B, and C, respectively, in the *inset*.

Comparison of the Inhibitory Effect of AMS on RNA Synthesis in Nuclei Isolated From IMR 90 Cells, in Cell Homogenates, and in Intact Cells

The absence of any evidence of metabolism of AMS or its incorporation into RNA of IMR 90 cells raised the question as to the mechanism of the inhibition of growth and nucleic acid synthesis that this drug induces in normal fibroblasts

TABLE 1.—*Summary of the analyses performed on PCA extract of IMR 90 cells incubated for 18 hours with [^{3}H]AMS*

Area of electrophoretic strip	Electrophoresis[a]	Paper chromatography[b]	Paper chromatography after HCl digest	Electrophoresis after alkaline phosphatase treatment	Electrophoresis after pyrophosphatase treatment	Compound identified as:
1	Migrated with standard AMS	Cochromatographed with standard AMS	Cochromatographed with N^6,N^6-dimethyladenine	Not applicable	Not applicable	AMS
2	Migrated with standard adenosine	Cochromatographed with standard adenosine	Cochromatographed with standard adenine	Not applicable	Not applicable	Adenosine
3	Migrated with standard inosine	Cochromatographed with standard inosine	Cochromatographed with standard hypoxanthine	Not applicable	Not applicable	Inosine
4	Migrated with standard AMP	Not applicable	Cochromatographed with standard adenine	Migrated with standard adenosine	Migrated with AMP+	AMP

[a] As described in "Materials and Methods."

[b] A small amount of conversion to adenosine was noted, which was due to a slight phosphomonoesterase activity in the nucleotide pyrophosphatase preparation reported by the supplier.

(3–5). A clue to the basis of the inhibitory effect of AMS on RNA synthesis was obtained by a comparison of the results obtained when AMS inhibition of RNA synthesis was measured by different methods (text-fig. 4). The inhibition of RNA synthesis became apparent after 4 hours of AMS treatment when determined by incorporation of uridine into acid-insoluble material of intact cells. That this was not due to a cell membrane effect on cellular uptake of uridine is shown by the almost identical results obtained when UTP was incorporated into the RNA of mechanically disrupted cells.

In contrast, measurement of UTP incorporation into the RNA of nuclei isolated from AMS-treated IMR 90 cells showed no effect of AMS during the first 18 hours of AMS treatment and only a minor depression of RNA synthesis thereafter. A possible explanation for the lack of the inhibitory effect of AMS as determined in isolated nuclei could be that RNA synthesis in isolated nuclei is measured in the presence of exogenously supplied rNTPs, whereas the incorporation of an RNA precursor in intact cells or homogenates depends on the presence of endogenous substrates. The possibility that the level of ATP or other rNTPs limited the rate of RNA synthesis in AMS-treated IMR 90 cells and homogenates was tested by supplementation of cell homogenates with such exogenous substrates. The data in table 2 show that addition of rNTPs to homogenates prepared from AMS-treated cells abolishes the effect of AMS on RNA synthesis in these homogenates. These results suggest that AMS inhibits the synthesis of RNA in IMR 90 cells by reducing the pool of available substrates for RNA polymerase action.

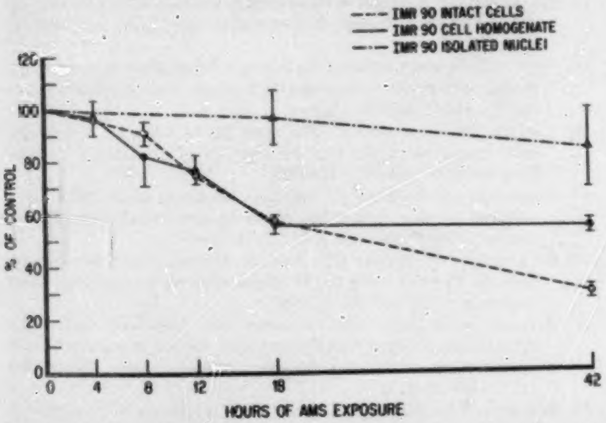

TEXT-FIGURE 4.—Time course of the effect of AMS (340 *μM*) on the RNA synthesis in IMR 90 cells as measured by incorporation of [5,6-^{3}H]uridine in intact cells (○- - -○), incorporation of [5,6-^{3}H]UTP in cell homogenates (●—●), and incorporation of [5,6-^{3}H]UTP in isolated nuclei supplemented with exogenous rNTPs (△-·-·-△). Incubation time with the radiolabel for cell homogenates and isolated nuclei was 2 min; for intact cells, it was 60 min. Other incubation conditions are described in "Materials and Methods."

TABLE 3—*Effect of AMS (340 μM for 18 hr) on the rNTPs pools of IMR 90 cells*[a]

Expt No.	rNTPs	[^{32}P]orthophosphate/10 μg DNA		Control, %
		Control, mean ± SD	AMS-treated, mean ± SD	
1[b]	GTP	2,480±490	1,879±218	75.8
	ATP	6,513±972	4,089±482	62.8
	CTP	1,442±234	1,030±297	71.4
	UTP	5,283±883	4,424±325	83.7
2[c]	GTP	4,073±531	2,736±365	67.2
	ATP	6,645±626	5,045±315	75.9
	CTP	1,448±228	1,114±94	76.9
	UTP	8,429±1,203	7,092±1,002	84.2

[a] IMR 90 cells were exposed to 5 μCi [^{32}P]orthophosphate/ml for 24 hr and then to 340 *μM* AMS and 5 μCi [^{32}P]orthophosphate/ml for 18 hr. Formic acid extract was analyzed for rNTPs by PEI anion-exchange chromatography as described in "Materials and Methods."

[b] *n*=12.

[c] *n*=6.

Effect of AMS on the Intracellular Content of rNTPs

Levels of rNTPs were measured in IMR 90 cells allowed to equilibrate with [^{32}P]orthophosphate for 24 hours and then treated with AMS for 18 hours in the presence of [^{32}P]orthophosphate. The results shown in table 3 indicate that the levels of rNTPs were reduced by AMS to a moderate degree. Unexpectedly, pyrimidine rNTPs as well as the purine rNTPs were lowered by the treatment, though the reduction in UTP concentration was less marked than the reduction in the concentration of other rNTPs. These data strengthen the view that the inhibition of RNA synthesis seen in IMR 90 cells after prolonged treatment with AMS is mediated by a reduction in the cellular content of rNTPs.

Similar measurements of rNTP levels in AG 2804 cells showed that treatment with AMS for 18 hours also caused a drop in the pools of rNTPs (table 4), which may contribute to the more delayed effects of AMS on these cells.

DISCUSSION

The essential difference between the normal and transformed cell response to AMS seems to be the low ability of

TABLE 2.—*Effect on the incorporation of [^{3}H]UTP into RNA of the addition of rNTPs to homogenates of IMR 90 cells treated with AMS*[a]

Time of incubation with [^{3}H]UTP, min	Experimental group	Incubation with [^{3}H]UTP only		Incubation with [^{3}H]UTP + rNTPs	
		cpm/10 μg DNA	Control, %	cpm/10 μg DNA	Control, %
2	Control	3,148±33	100±1.1	727±74	100±10.3
	AMS-treated	1,764±84	56±4.8	647±25	89± 3.8
10	Control	12,271±802	100±6.6	18,202±848	100± 4.7
	AMS-treated	8,402±745	68±8.9	20,919±3,020	115±14.5

[a] Intact IMR 90 cells were treated with 340 *μM* AMS and mechanically disrupted, and aliquots were incubated with 5 μCi of [^{3}H]UTP in the presence or absence of 600 *μM* ATP, GTP, and CTP, and 16.4 *μM* unlabeled UTP. Mean values for four determinations ± SD are shown.

TABLE 4.—*Effect of AMS (340 μM for 18 hr) on the pools of rNTPs of AG 2804 cells*[a]

rNTPs	CPM [^{32}P]orthophosphate/10 μg DNA		Control, %
	Control, mean ± SD	AMS-treated, mean ± SD	
GTP	3,399±147	2,440±195	71.7
ATP	12,422±750	7,951±965	64.0
CTP	2,319±331	1,946±216	83.9
UTP	4,801±509	3,826±238	79.7

[a] AG 2804 cells were exposed to 5 μCi [^{32}P]orthophosphate/ml for 24 hr and then to 340 μ*M* AMS and 5 μCi [^{32}P]orthophosphate/ml for 18 hr (total of 42 hr of incubation with [^{32}P]orthophosphate). Formic acid extract was analyzed for rNTPs by PEI anion-exchange chromatography as described in "Materials and Methods." The means and SD are for six determinations.

the normal cells to metabolize AMS. This low ability may explain the observed greater accumulation of nonmetabolized AMS in the acid-soluble pools of normal fibroblasts when compared to its accumulation in transformed fibroblasts, though the greater rate of uptake of this compound by normal fibroblasts may have contributed to this effect (*14*). Evidence that the accumulated AMS is not appreciably metabolized by normal cells was difficult to gather because it was not possible in these studies to obtain (or completely purify) [^{3}H]AMS samples totally free of the small amounts of [^{3}H]adenosine. However, it was possible to obtain such evidence mainly because the 3′-amino group in AMS is highly charged and thus confers high electrophoretic mobility to AMS and all its metabolites, and there is no known mechanism for removing this amino group from the sugar molecule.

Special efforts were also made to ensure detection of small amounts of AMS metabolites that could perhaps be incorporated into cellular RNA. Nonetheless, in spite of increasing the amounts of [^{3}H]AMS and of cell cultures used for these studies, to the point that less than 1% of the transformed cell rate of AMS incorporation into RNA would have been detected if it also occurred in the normal fibroblasts, we were unable to find any incorporation. We conclude, therefore, that if incorporation of AMS into RNA occurs in normal fibroblasts, it is insignificant when compared to the amount incorporated by transformed fibroblasts.

Data presented here also indicate that treatment with AMS reduces the levels of ribonucleoside triphosphate precursors in normal and transformed fibroblasts, and this reduction may be responsible for the gradual onset of inhibition of RNA synthesis brought about in normal cells by this treatment. This effect may also be a secondary cause of the inhibition by AMS of the growth of the transformed fibroblasts. A similar sequence of events has been reported for histidine-starved Ehrlich ascites cells, in which purine nucleoside triphosphate pools shrank to about 70% and nucleolar RNA synthesis was reduced to about 40% of the control value (*15*). The importance of changes in purine precursor pool levels to the mechanism of AMS action in these cells is also suggested by the observations that the inhibitory or differentiation-inducing effects of AMS can be blocked by simultaneous addition of equimolar inosine (*3*, *16*) and that cordycepin, a compound with great structural similarity to AMS (*17*), may exert its inhibitory effect by interfering with the de novo biosynthesis of purines, thus causing a depletion of the cellular adenine nucleotide pools (*18–20*), though this compound can also cause premature termination of RNA chains (*21*, *22*). However, purine analogs which have a 3′-hydroxyl group and are incorporated into RNA have been shown to interfere with its maturation (*23*).

In view of these results, we conclude that the altered cellular responses to AMS that are seen after simian virus 40 transformation stem from the greatly enhanced ability of the transformed cells to remove the methyl groups from the N^6 position of AMS, probably due to the increased activity of demethylating or transmethylating enzymes. This ability leads to the phosphorylation and incorporation of AMS metabolites into RNA of transformed cells, where additional effects occur in the nucleolus (*10*). The mechanism through which AMS causes a reduction in the levels of pools of rNTPs, presumably by the unchanged drug, remains to be elucidated.

REFERENCES

(*1*) FARNHAM AE, DUBIN DT. Effect of puromycin aminonucleoside on RNA synthesis in L cells. J Mol Biol 1965; 14:55–62.

(*2*) STUDZINSKI GP, ELLEM KA. Relationship between RNA synthesis, cell division and morphology of mammalian cells. J Cell Biol 1966; 29: 411–421.

(*3*) ———. Differences between diploid and heteroploid cultured mammalian cells in their response to puromycin aminonucleoside. Cancer Res 1968; 28:1773–1782.

(*4*) TAYLOR JM, STANNERS CP. The synthesis of RNA by mammalian cells treated with the aminonucleoside of puromycin. Biochim Biophys Acta 1968; 155:424–432.

(*5*) STUDZINSKI GP, GIERTHY JF. Selective inhibition of the cell cycle of cultured human diploid fibroblasts by aminonucleoside of puromycin. J Cell Physiol 1973; 81:71–84.

(*6*) GIERTHY JF, STUDZINSKI GP. Absence of aminonucleoside-sensitive steps in the cell cycle of SV40-transformed human fibroblasts. Cancer Res 1973; 33:2673–2676.

(*7*) BRADLEY MO, KOHN KW, SHARKEY NA, EWIG RA. Differential cytotoxicity between transformed and normal human cells with combinations of aminonucleoside and hydroxyurea. Cancer Res 1977; 37:2126–2131.

(*8*) ALBANESE EA, STUDZINSKI GP. Selective inhibition of preribosomal RNA synthesis by puromycin aminonucleoside in transformed human fibroblasts: Studies of the nature of the inhibition in isolated nuclei and nucleoli. J Cell Physiol 1979; 99:55–66.

(*9*) ———. Metabolism of puromycin aminonucleoside in transformed human lung fibroblasts and the mechanism of its inhibition of RNA synthesis. Mol Pharmacol 1980; 17:262–267.

(*10*) STUDZINSKI GP, ALBANESE EA. Nascent RNA chain termination and ultrastructural changes in nucleoli isolated from SV40-transformed fibroblasts treated with aminonucleoside of puromycin. Lab Invest 1980; 43:427–433.

(*11*) CASHEL M, LAZZARINI RA, KALBACHER B. An improved method for thin-layer chromatography of nucleotide mixtures containing ^{32}P-labeled orthophosphate. J Chromatogr 1969; 40:103–109.

(*12*) FLECK A, MUNRO HN. The precision of ultraviolet absorption measurements in the Schmidt-Thannhauser procedure for nucleic acid estimation. Biochim Biophys Acta 1962; 55:571–583.

(*13*) SCHMIDT G, THANNHAUSER SJ. A method for the determination of deoxyribonucleic acid, ribonucleic acid and phosphoproteins in animal tissue. J Biol Chem 1945; 161:83–89.

(*14*) STUDZINSKI GP, ALBANESE EA, SCATENA J, TROCOLA-SIMCHERA M. Fibroblasts transformed by an oncogenic virus show decreased uptake of puromycin aminonucleoside. Biochem Biophys Res Commun 1980; 95:1446-1451.

(*15*) Grummt I, Grummt F. Control of nucleolar RNA synthesis by the intracellular pool sizes of ATP and GTP. Cell 1976; 7:447-453.

(*16*) Lacour F, Harel L, Friend C, Huynh T, Holland JG. Induction of differentiation of murine erythroleukemia cells by aminonucleoside of puromycin and inhibition of this induction by purines and purine derivatives. Proc Natl Acad Sci USA 1980; 77:2740-2742.

(*17*) Suhadolnick RJ. Naturally occurring nucleoside and nucleotide antibiotics. Progr Nucleic Acid Res Mol Biol 1979; 22:193-291.

(*18*) Klenow H. Inhibition by cordycepin and 2-deoxyglucose of the incorporation of [^{32}P]orthophosphate into the nucleic acids of Ehrlich ascites-tumor cells in vitro. Biochim Biophys Acta 1963; 76: 354-365.

(*19*) Rottman F, Guarino AJ. The inhibition of phosphoribosyl-pyrophosphate amidotransferase activity by cordycepin monophosphate. Biochim Biopys Acta 1964; 89:465-472.

(*20*) Overgaard-Hansen K. The inhibition of 5-phosphoribosyl-1-pyrophosphate formation by cordycepin triphosphate in extracts of Ehrlich ascites tumor cells. Biochim Biophys Acta 1964; 80:504-507.

(*21*) Shigeura H, Boxer GE. Incorporation of 3′-deoxyadenosine-5′-triphosphate into RNA by RNA polymerase from *Micrococcus lysodeikticus*. Biochem Biophys Res Commun 1964; 17:758-763.

(*22*) Cory J, Suhadolnik RJ, Resnick B, Rich MA. Incorporation of cordycepin (3′-deoxyadenosine) into ribonucleic acid and deoxyribonucleic acid of human tumor cells. Biochim Biophys Acta 1965; 103:646-653.

(*23*) Weiss JW, Pitot HC. Inhibition of ribosomal RNA maturation in Novikoff hepatoma cells by toyocamycin, tubercidin, and 6-thioguanosine. Cancer Res 1974; 34:581-587.

blank page

Phenotypic and Genotypic Characteristics of a Cell Line From a Squamous Cell Carcinoma of Human Skin[1,2]

Petra Boukamp,[3] Wolfgang Tilgen,[4] Rule T. Dzarlieva,[3] Dirk Breitkreutz,[3] Dietrich Haag,[5] Rüdiger K. Riehl,[4] Axel Bohnert,[3] *and* Norbert E. Fusenig[3,6,7]

ABSTRACT—A human cell line (SCL-1) from a poorly differentiating cutaneous squamous cell carcinoma (SCC) was studied through 20 passages during 2 years. Cells maintained their original morphology with low degree of keratinization, as indicated by light and electron microscopy. The keratin peptide pattern resembled the type in SCC tumors, and the corresponding filaments were detected by immunofluorescence at all passage levels. Cells did not grow in soft agar but formed tumor-like nodules in an "organotypic" culture assay (on lifted collagen gels) and grew invasively after transplantation to immunosuppressed inbred C3H mice. After injection into BALB/c *nu/nu* mice, tumors of SCC morphology were formed. The hypodiploid tumor stemline was maintained for about 10 passages, when a shift to hyperploidy started, as determined by chromosome and DNA flow microfluorometric analyses. Two stable marker chromosomes (in 100 and 70% of the metaphases, respectively), involving chromosomes 7 and 9, strongly indicated a monoclonal origin of this cell line.—JNCI 1982; 68:415–427.

The availability of cell lines from various carcinomas with well-defined morphology, cytogenetics, and biologic behavior will greatly facilitate in vitro studies of the properties of malignant human epithelial cells, as well as studies of their sensitivity or resistance to radiation and chemotherapy. Investigations with several cell lines derived from individual tumors of the same type and tissue may clarify problems concerning the similarities and heterogeneity of tumor cells from the same tissue.

Although tissue culture models offer considerable advantages in the study of normal and tumor cells, the likeness of long-term-cultured cells to cells of the original normal or tumor tissue has rarely been substantiated. Due to selection for the most efficiently attaching and proliferating cells in primary culture and at each passage level, the original tumor cell population may have been considerably changed. Further alterations may occur within the cultivated cell population due to growth conditions in vitro. Thus preparations from tumor biopsies have to be compared with primary, early- and late-passage cultures to discriminate characteristics associated with the predominant tumor cell population in vivo from those that are merely consequences of culture conditions.

Since the first human epithelial cell line HeLa was established by Gey in 1951 (*1*), many carcinoma cell lines from different human organs have been characterized with respect to their tissue specificity and malignancy (*2–7*). It is still rather difficult to establish defined human epithelial tumor lines, as evidenced by the low success rate of 1–38%, probably due mainly to the low tendency of epithelial cells to grow in vitro. Most of the successful attempts started with cells from metastases, effusions, or ascitic fluids, and those cells might have acquired growth abilities different from those of cells of the primary tumor (*5, 8–13*). To our knowledge, no report has characterized in detail a cell line derived from a primary SCC of the skin.

In this paper, we report the development of a human epithelial cell line (SCL-1) derived from biopsy material of a cutaneous SCC. The studies include the analysis of cell growth and morphology, neoplastic behavior in vivo and in vitro, the determination of differentiation functions such as keratin polypeptides and cytoskeleton pattern, and the cytogenetic and cytometric analyses of the cell populations. The SCC cells were studied in explant cultures and through the first 20 passages over a period of 2 years.

MATERIALS AND METHODS

Culture medium.—A modified Eagle's minimum essential medium (four times the concentrated ingredients) (*14*) with 17% fetal calf serum was used throughout. All medium components were obtained from Seromed (Munich, FRG). Penicillin (100 U/ml), streptomycin (50 µg/ml), and ampicillin (50 µg/ml) were added. Dulbecco's PBS and EDTA were obtained from Serva (Heidelberg, FRG), and trypsin (1:250) came from Boehringer (Mannheim, FRG).

Culture conditions.—A poorly differentiated solid SCC of the face from a 74-year-old woman was removed surgically and immediately prepared for tissue culture, electron microscopy, and cytometry. At surgery no metastases were observed. The biopsy material was rinsed several times in complete growth medium with antibiotics, freed of necrotic or surrounding connective tissue, and cut with scalpels into cubes of about 2-mm diameter. Then 6–8 of these specimens were placed individually in 35-mm plastic petri dishes (Fal-

---

ABBREVIATIONS USED: FMF=flow microfluorometry (microfluorometric); FRG=Federal Republic of Germany; H & E=hematoxylin and eosin; PBS=phosphate-buffered saline; SCC=squamous cell carcinoma(s); SDS=sodium dodecyl sulfate.

---

[1] Received May 26, 1981; accepted Sepember 23, 1981.

[2] Supported in part by the Deutsche Forschungsgemeinschaft (SFB 136).

[3] Deutsches Krebsforschungszentrum (DKFZ), 6900 Heidelberg, Federal Republic of Germany.

[4] Department for Dermatology, University of Heidelberg, 6900 Heidelberg.

[5] Department for Pathology, University of Heidelberg.

[6] *Address reprint requests to* Dr. Fusenig.

[7] We thank Dr. W. W. Franke (Division of Membrane Biology and Biochemistry, DKFZ) for kindly providing the anti-keratin antiserum and Dr. W. Nicklas (Zentrales Tierlabor, DKFZ) for testing cells for contamination. The excellent technical assistance of Mrs. Birgit Kahl, Miss Jutta Pöhlmann, and Mrs. Sabine Stuhlert and the assistance of Miss Monika Matejka in the preparation of the manuscript are gratefully acknowledged.

con Plastics, Oxnard, Calif.), covered by a plasma clot (Difco Laboratories, Detroit, Mich.), and left for 30 minutes at room temperature, after which 2 ml of complete culture medium was added. The dishes were then incubated at 37°C in a humidified atmosphere of 5% CO_2 in air. Medium was changed once a week. Cultures were examined and photographed under an inverted microscope with the use of phase-contrast optics (Wild Heerbrugg Instruments Inc., Heerbrugg, Switzerland). Fibroblasts that usually would grow at the periphery of the outgrowing epithelial sheet were eliminated with brief trypsin treatment (0.25% at 37°C for 1–2 min).

For generation of subcultures, the cells were rinsed in EDTA (0.2% for 2 min), incubated in EDTA–trypsin (5–7 min; final concentration), and flushed by pipette. Cells were enumerated in an electronic counter (Coulter Electronics Inc., Boulder, Colo.) and replated at high densities (5×10^5/cm^2). At different cell passage levels, growth curves were established by daily cell counts of duplicate dishes. Cloning efficiency was determined by plating 10^3 cells per 60-mm dish with or without conditioned medium (from confluent SCL-1 culture).

Three-dimensional growth behavior was tested of cells from different passages by plating 2×10^5 cells on collagen gels prepared in silicon chambers ("organotypic" culture assay) (*15, 16*). After cell attachment, the collagen layer was lifted to the medium–air interphase [with the use of "Stanzen" dishes (*15*)] while the medium covering the cells was drained. Thus cultures were nourished only from below by diffusion through the collagen, and the upper cell surface was exposed to air. For histologic examination, these organotypic cultures were fixed at weekly intervals in buffered Formalin and cross sections of paraffin-embedded specimens were stained with H & E or Masson-Goldner.

Anchorage-independent growth was examined in 0.3% soft agar on top of a 0.5% agar base (*17*). The agar (Bacto; Difco Laboratories) was prepared in complete culture medium with 17% fetal calf serum (final concentration); 10^4, 10^5, and 10^6 cells were plated in 60-mm dishes. Dishes were examined weekly, finally stained with 2-(*p*-iodophenyl)-3-*p*-nitrophenyl-5-phenyltetrazolium chloride (*18*) to detect viable colonies, and inspected under low-magnification optics.

Cultures from passage 17 were monitored for mycoplasma by inoculation in agar and broth and were found free of contamination.

Electron microscopy.—Electron microscopy was performed on the original tumor biopsy specimen and on intact cultures growing on plastic or collagen, as well as on the tumors induced in nude mice. Specimens from tumor material were prepared according to the technique of Peracchia and Mittler (*19*). Cells grown on plastic petri dishes were processed as described in (*20*). Ultrathin sections of an Epon-embedded specimen were stained with uranyl acetate and examined with a Zeiss electron microscope EM 109 or a Philips electron microscope, EM 400.

Extraction of cytoskeletal (keratin) proteins.—Confluent cell cultures were sequentially treated with isotonic buffer containing 0.5–1% Triton X-100 followed by high-salt buffer (1.5 *M* KCl) as described earlier (*16, 21, 22*). The remaining cytoskeletons were rinsed with isotonic buffer and extracted with 5% SDS, 10% mercaptoethanol, and 2 m*M* EDTA in 20 m*M* phosphate buffer (pH 7.2). The suspensions were heated at 100°C for 5 minutes, homogenized, and (after 30-60 min) centrifuged at $20{,}000\times g$ for 20 minutes to remove the insoluble material. For the preparation of total cellular proteins, culture dishes were rinsed extensively with PBS and extracted with SDS and mercaptoethanol as above. Corresponding preparations from frozen tumor tissue (stored in liquid nitrogen) were obtained by homogenization either in Triton X-100-containing buffers (isotonic and high salt) at 4°C followed by extraction ("cytoskeletal proteins") or directly in extraction buffers ("total proteins") as outlined above. To all buffers, fresh 0.1–1 m*M* phenylmethylsulfonyl fluoride was added before use.

Gel electrophoresis.—Proteins were analyzed by electrophoresis on slab gels in the presence of SDS according to the methods of Weber and Osborn (*23*) and Laemmli (*24*). Samples were heated at 100°C for 1 minute and applied to 10% acrylamide gels. Bromphenol blue was used as a tracking dye. Gels were stained with 0.05% Coomassie blue in 25% isopropanol and 7.5% acetic acid and destained with 7.5% acetic acid.

Indirect immunofluorescence test.—The intracellular distribution of the cytoskeletal network was visualized by the use of specific antibodies. Cells were grown on glass cover slips, washed in PBS, air dried, and fixed in acetone for 15 minutes at room temperature. The hydrated cover slips were first incubated for 45 minutes at 30°C with a guinea pig anti-bovine keratin antiserum (*20*) and thereafter with fluorescein-labeled goat anti-guinea pig IgG (Miles-Yeda, Rehovot, Israel). The cover slips were rinsed in PBS and Tris-HCl buffer (pH 8.5), mounted in Aqua-Mount (Lerner Laboratories, Stamford, Conn.), and examined with an inverted microscope with fluorescence optics (IM 35; Carl Zeiss, Inc., Oberkochen, FRG).

Tumorigenicity test.—We tested tumorigenicity in vivo by injecting 1×10^6 and 4×10^6 cells, respectively, im or sc into 7-week-old *nu/nu* mice (BALB/c and NMRI back-crosses). The animals were killed after about 3 months and the tumor material was taken for histology and biochemical analysis.

Invasive growth was tested in a transplantation assay with 2×10^5 cells implanted in 200 μl medium onto an induced subcutaneous graft bed (*15, 25*) in thymectomized and irradiated (400 rad) adult inbred C3H mice. Animals were killed after 7, 14, and 21 days, and the transplants were processed for routine histology. Serial sections were cut and stained with H & E, Masson-Goldner, and periodic acid–Schiff.

Cytogenetic studies.—Chromosome analysis was performed on cultures as soon as adequate growth was achieved (passage 2) and at regular intervals at subsequent passages. The cells arrested at metaphase with Colcemid (10^{-7} *M* for 2 hr) were harvested by EDTA–trypsin treatment (5 min) and processed according to the technique of Moorehead et al. (*26*).

For chromosome identification, G-banded preparations were made according to the method of Seabright (*27*). Slides, bearing good metaphase spreads, were allowed to age in the dark 2–3 weeks and then treated with 0.025% trypsin for 20–45 seconds and stained with 3% Giemsa in Sörensen's buffer (pH 6.8) for 12 minutes. Staining of centromeric heterochromatin (C-bands) was achieved according to methods reported by Sumner (*28*). Slides were examined on an Ortholux microscope (E. Leitz, Inc., Wetzlar, FRG). At least 50 G-banded metaphases were analyzed per passage.

Cytometric DNA determination.—DNA distribution patterns were determined in biopsy material and cultured cells by FMF and single cell analyses. Tumor tissues were prepared and stained according to the procedure of Zante et al. (*29*). The FMF–DNA histograms were evaluated as described (*30*). Cell cultures were trypsinized, filtered through 70-µm mesh, and centrifuged at 100×*g*; cells were stained in a solution of homidium bromide and 4′-6-diamidino-2-phenylindole or aureolic acid in 0.1 *M* Tris buffer (pH 7.6). DNA measurement was performed with an ICP 22 pulse cytophotometer (Phywe AG, Göttingen, FRG). Pulse height analysis was displayed with a multichannel analyzer (MCA 8100; Canberra Industries, Meriden, Conn.). Cell compartments were calculated according to their DNA content from up to 100,000 counts.

Single cell DNA measurements were performed on smears of cell suspensions from biopsies or on intact cultures after fixation in 95% ethanol and staining by the acriflavine–Feulgen procedure according to Prenna and Bianchi (*31*). Preparations were measured by light absorbance and fluorescence with the use of a scanning microspectrophotometer and a microscope fluorescence photometer (UMSP I and MPM; Carl Zeiss, Inc.). We determined ploidy stages by measuring at least 100 individual cell nuclei.

RESULTS

Development of the Cell Line

In SCC explant cultures epithelial outgrowth was first visible within 3–5 days. The cell sheets, composed of cuboidal, densely packed epithelial cells, continuously enlarged (fig. 1A), but a nearly complete monolayer was observed only after about 4 months. Then cells could be subcultured, but proliferation was low in early and later subcultures and was dependent on high cell density. During the first four passages, cultures reached confluence after about 2 months, whereas later (starting from passage 13) cells could be subcultured every 3 weeks. The mean population doubling time decreased from 6 days to about 60 hours (table 1), whereas the attachment rate stayed constant at 60% when determined 24 hours after plating. Growth at clonal or low cell density was not achieved until passage 18 and even then strictly depended on the addition of conditioned medium from SCL-1 cultures. Cloning efficiency was 6–10% in conditioned medium as compared to less than 1% in unconditioned medium.

Morphologic Characteristics of Cultured Cells

Explant cultures were composed of rather uniform, small polygonal cells with large nuclei and prominent nucleoli. Mitotic figures, sometimes with abnormal configurations were frequent (fig. 1B).

Subcultures were more heterogeneous, revealing two types of cell colonies with clearly different morphologies. Colonies of tightly packed, uniform polygonal cells (fig. 2A) alternated with defined areas of smaller cells exhibiting wider intercellular spaces (fig. 2B). This type of smaller cells eventually started to pile up and formed large nodules of proliferating cells (figs. 2C, D). Occasionally, some regions revealed the striated appearance typical for the differentiating upper layers of normal (mouse) keratinocytes (fig. 2C) (*14, 32*). Large and often multinucleated cells between the compact cell islands were frequent in all cultures (fig. 2B).

Ultrastructurally, SCL-1 cells could be identified as epidermal by their desmosomes and tonofilament bundles. Tonofilament bundles appeared less dense and more evenly distributed in later passage cultures (fig. 3) as compared to explant cultures. Cell and nuclear polymorphism with large, often indented nuclei was similar to that observed in the original tumor (fig. 4A), which was diagnosed as poorly differentiated with numerous atypical mitoses and few individual keratinized (dyskeratotic) cells (fig. 4B). The cytoplasmic organelles were well developed and microvilli were prominent at the cell borders.

Differentiation in Culture

Typical keratinization, including stratification and formation of continuous horny layers, was not observed in cultures of SCL-1 cells but keratinized cells with keratohyalin granules could be identified in explant cultures and subcultures. Occasionally, flat translucent cells with thickened membranes and pyknotic nuclei—resembling parakeratotic cells—were seen on top of the monolayers. These cells eventually detached and their "cornified envelopes" (*33*) could be identified by the insolubility in SDS. When grown on lifted collagen layers (organotypic culture assay), SCL-1 cells formed three-dimensional nodules, sometimes with central necroses or horn pearl-like structures (fig. 5A) but with no features of normal epidermal differentiation as observed with normal mouse keratinocytes (*34*). Unlike confluent cultures on plastic, cells could be grown on collagen for up to 3 months without detaching from the substrate. The ultrastructure of these nodules revealed only few dyskeratotic cells but wide intercellular spaces, often filled with long villous projections interdigitating with adjacent cells, and numerous mitoses were conspicuous (fig. 5B).

The cytoskeletal filaments of the cultured cells were com-

TABLE 1.—*Growth behavior of SCL-1 cells in vitro and in vivo, depending on passage number*[a]

Passage No.	Mean doubling time, hr	Single cell cloning	Abnormal growth in organotypic cultures	Colony formation in soft agar	Invasive growth in vivo	Tumor growth in nude mice
5	NT	–	+	NT	+	NT
8	144	–	+	–	+	NT
10	144	–	+	–	+	NT
18	60	+[b]	NT	–	NT	+
20	60	+[b]	NT	–[b]	NT	+

[a] Not tested, NT; no growth, –; growth, +.

[b] In medium conditioned on SCL-1 cultures.

posed of keratin proteins (tonofilaments), as also demonstrated earlier by immunologic and biochemical methods with keratinocytes from other species including humans (*20, 22, 35, 36*). In the indirect immunofluorescence test, antibodies against bovine keratin decorated a three-dimensional meshwork of fibers in SCL-1 cells (fig. 6). In early passages heavily labeled filaments were located especially around the nucleus, and numerous correspondences in adjacent cells indicated an extended filamentous system linked by desmosomal junctions. In later culture passages, fluorescence labeling of cytoskeletal filaments appeared weaker, corresponding to the ultrastructural observations. However, this finding might be due to an altered distribution of keratin fibrils rather than to a decrease in keratin content, as indicated by biochemical analysis.

The cystoskeletal proteins of SCL-1 cells were composed mainly of two strong and four somewhat less prominent peptide bands (size range, 45,000–59,000 daltons) in addition to some residual actin (fig. 7). The larger peptides (≥60,000 daltons) present in whole normal epidermis were virtually absent in both tumor tissue and SCL-1 cell cultures, a feature that might be common to most neoplastic lesions of the skin (*37, 38*). Qualitatively, the typical keratin pattern of SCC cells remained unchanged in culture when cells from passages 8 and 19 were compared. There was a striking similarity between the keratins in SCL-1 cultures and keratins in the original SCC tumor. The keratin protein pattern of the tumors formed after injection of SCL-1 cells in the nude mouse (fig. 7) resembled even more closely that of the primary tumor biopsy specimen than the pattern from cultured cells (data not shown).

Cytogenetic Characteristics

Chromosome analysis of SCL-1 cells, first done on second passage cultures 6 months after plating, revealed a heterogeneous (female) karyotype with a main hypodiploid stemline of 45 chromosomes. The G-banded karyotype showed monosomy for chromosomes 7, 9, and 15 and two metacentric marker chromosomes (fig. 8). The larger marker chromosome (M1) was derived from the long arms of chromosomes 7 and 9 (7q9q), and the smaller one (M2) was derived from the short arms of the same chromosomes (7p9p). These marker chromosomes were present at each passage level in 100% and 60–70%, respectively (table 2). No marker chromosome characteristic for HeLa cells or other similarities to the HeLa karyotype were found. Starting with passage 11, a side stemline with additional monosomy for chromosome 4 and trisomy for chromosome 20 appeared. Structural chromosome aberrations, including chromatid and chromosome breaks, fragments, minutes, and exchange figures, drastically increased with culture time, and additional marker chromosomes appeared mainly involving chromosomes 1 and 4.

The hypodiploid stemline as well as the hypotetraploid fraction stayed relatively stable up to passage 11, whereas the hypertetraploid fraction increased constantly and the level of endoreduplication diminished (table 3). With higher passages, however, the modal chromosome number increased to hypotetraploidy (73–90) and near-diploid cells had disappeared. Giant metaphases were observed only at later passages (20–30).

TABLE 2.—*Structural chromosome aberrations in the SCL-1 cell line*

Type of chromosome aberration	Percent of chromosome aberration in cell line at passage No.:			
	2	6	11	20
Chromatid and isochromatid breaks	0	2	5	6
Chromosome fragments	0	0	2	6
Minutes	0	0	4	10
Double minutes	0	0	4	16
Exchange figures[a]	0	0	0	10
Premature chromosome condensation	0	2	2	2
Marker chromosome M1 (7q9q)	100	100	100	100
Marker chromosome M2 (7p9p)	70	60	90	70
Other markers	0	0	5	12

[a] Triradials, quadriradials, rings.

TABLE 3.—*Numerical chromosome changes during culture time*

No. of chromosomes per metaphase	Percent of chromosomes per metaphase changed during cell line passage No.:			
	2	6	11	20
40–43	8	4	4	0
44	18	16	16	0
45	36	44	32	0
46	8	10	16	0
Hypotriploidy and triploidy, 50–69	6	0	0	4
Hypotetraploidy, 73–90	12	12	14	66
Pseudotetraploidy, 92	2	2	4	8
Hypertetraploidy	0	6	10	18
Endoreduplication	10	6	4	0
Giant metaphases	0	0	0	4

Cytometric DNA Analysis

In addition to chromosome analysis, quantitative DNA determinations such as those provided by pulse cytometry (FMF) or single-cell DNA measurement represent further means to follow-up changes in cell populations as far as stemlines and ploidy degrees are concerned. Moreover, data obtained by these methods provide information about the proliferative activity of cell populations (S-phase fractions).

The data show that the main tumor cell population in vivo was approximately diploid (2c) in its DNA content. Only a minor proportion of cells had a DNA content higher than 4c (text—fig. 1; table 4). Cells from 8-day-old explant cultures as well as from early passages (up to passage 10) revealed a similar DNA distribution pattern. However, in culture, the percentage of cells with an 8c DNA content had increased. Starting with passage 13, the population shifted toward a 4c DNA content, paralleled by a decrease in near-diploid (2c) cells. By passage 23, virtually all cells with a 2c DNA content had disappeared.

Thus both cytometric and cytogenetic analyses demonstrated that the original near-diploid tumor stemline was stable for up to 1.5 years or about 12 passages in culture and then shifted to a near-tetraploid level. The proportion of cells with higher ploidy levels stayed relatively un-

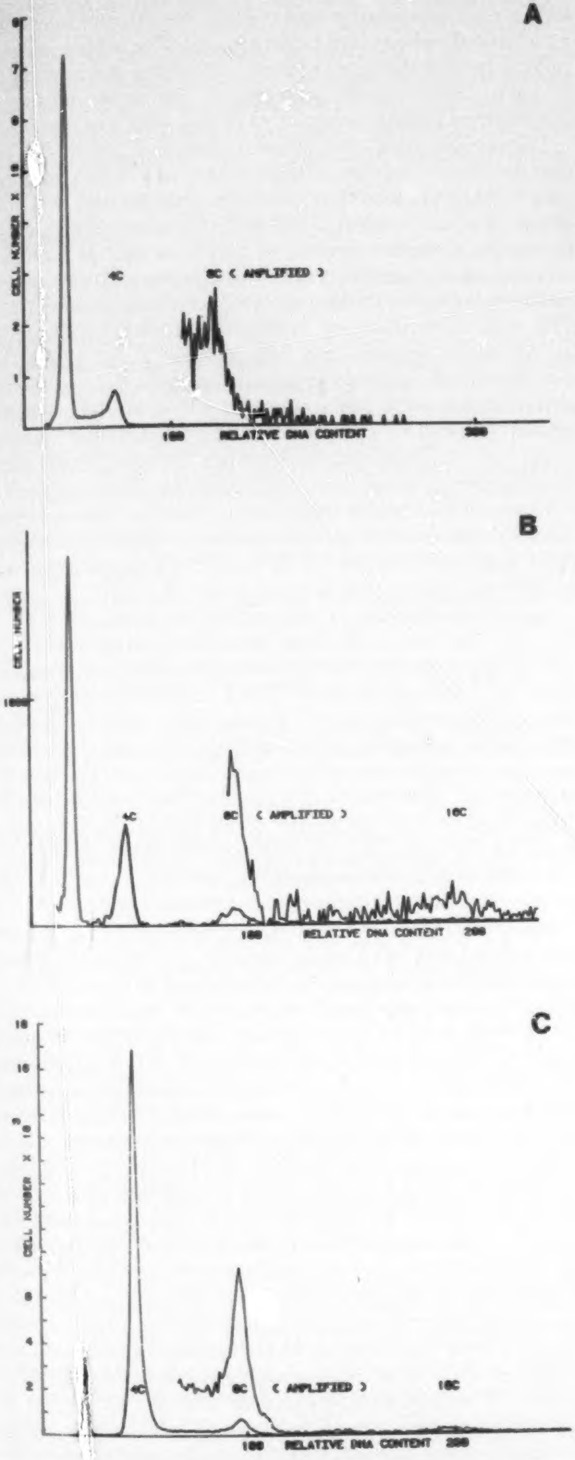

TEXT-FIGURE 1.—DNA distribution pattern determined by flow microfluorometric analysis. A) Primary tumor biopsy material with predominantly 2c DNA content (tumor stemline). B) Early passage (9) of SCL-1 with a similar DNA distribution. C) Later passage (16) of SCL-1 showing a predominant stemline with 4c DNA content.

TABLE 4.—*DNA histograms of human cutaneous SCC cells in primary and long-term cultures*

Source of cells	Percent of cells with relative DNA content:				
	2c[a]	4c	8c	16c	S-phase[b]
Tumor biopsy	76.5	13.0	1.0	0.0	9.5
Explant culture	38.0	38.0	11.5	0.5	12.0
Passage 7	55.0	27.0	7.5	2.5	8.0
Passage 13	30.0	53.0	5.0	0.0	12.0
Passage 16	6.0	81.0	4.0	1.0	8.0
Passage 23	0.0	83.0	8.0	0.0	9.0

[a] Human lymphocytes were used as standards and were located in the 2c region.

[b] Represents the sum of all fractions, positioned between the peaks of 2c, 4c, 8c, and 16c, i.e., both the cells in true S-phase and the heteroploid cells.

changed. Single cell measurements of Feulgen-stained cultures revealed a comparable DNA distribution pattern.

Malignant Growth Characteristics

Heterogeneous cell morphology, atypical mitoses, and the variations in DNA histogram and karyotype were strong indications of the transformed state of the SCL-1 cells. The low growth rate and the nearly normal (diploid) DNA content of cells in explant and early subcultures, however, were not typical for malignant cells. Moreover, SCL-1 cells up to passage 20 did not easily grow at clonal densities nor did they form colonies in soft agar (table 1). The addition of conditioned medium to the agar overlay did not stimulate colony growth, although it improved single cell cloning on solid substrate.

While the agar test failed to identify the transformed state of SCL-1 cells (i.e., anchorage independency), the growth behavior in the organotypic culture assay (described in "Materials and Methods") was abnormal and comparable to that of transformed mouse epidermal cells (*15, 16*). Cross sections from 1- to 3-week-old cultures showed actively proliferating nodules (fig.. 5) resembling ultrastructurally the primary tumor biopsy specimen.

Malignancy of SCL-1 cells could clearly be demonstrated at later passages in nude mice. Tumors developed after a long latency period of about 2 months when cells were injected (sc or im) into 7-week-old (BALB/c) *nu/nu* mice (table 1). We reduced the latency period, however, by using newborn animals (NMRI *nu/nu*). Histologically, the solid encapsulated tumors were SCC with a low degree of differentiation quite similar to that of the original SCC (fig. 9 cf. to fig. 4B).

Invasive growth behavior could already be demonstrated with SCL-1 cells from passage 5 when the available cell number was still insufficient for the nude mouse test (*15, 16, 39, 40*). When transplanted onto induced granulation tissue in immunosuppressed adult C3H mice, multilayered and invasively growing cell masses developed in 100% of the animals. Histologically, these tumor masses revealed features of the original tumor such as atypical mitoses, dyskeratotic cells, and giant cells (fig. 10). Invasiveness was clearly visible 1-3 weeks after transplantation of 2×10^5 cells. However, at the start of week 3, rejection of the transplants commenced.

Preliminary experiments demonstrated that the transplantation assay is also feasible with nude mice and may thus provide a more sensitive in vivo test for the study of invasion and metastasis of human tumor cells.

DISCUSSION

We have previously demonstrated by morphologic and biochemical criteria and by cell kinetics that the predominant cell population from cutaneous epithelial tumors can be propagated in explant cultures (*41, 42*). Here we describe the long-term cultivation of cells from an SCC from human skin obtained by a routine explant culture technique. Serial subcultures were achieved only by high seeding density, and cell growth could be improved by conditioned medium (from SCC cultures). A second cell line (SCL-2) was more rapidly adapted by use of these conditions (Tilgen W, Boukamp P, Breitkreutz D, et al: In preparation). Growth at lower temperature (30°C) or cocultivation with irradiated 3T3 feeder cells was not advantageous. Rheinwald and Beckett (*43*) reported, however, that successful cultivation of SCC from tongue and facial epidermis depended on the presence of mesenchymal (3T3) cells.

Morphologically, SCC cells in explant and subcultures revealed characteristics similar to those of the tumor biopsy specimen, as far as polymorphism, mitotic activity, abnormalities, and the low degree of keratinization were concerned. The low degree of keratinization was strongly indicated by the rare formation of cornified envelopes. Moreover, the keratin peptide patterns of the epithelial outgrowth in explant cultures of this and other SCC tumors compared well with those of the respective tumor biopsy specimens. In addition, quantitative keratin protein analysis revealed the poor degree of differentiation of the tumor cells, correlating well with the morphologic findings (data not shown). Larger peptide bands (62,000–68,000 daltons), which are major components of epidermis, were detected neither in tumor tissue nor in culture. In regard to the DNA distribution, the cultured cells were also nearly identical to the preparations made from the primary tumor. All these observations strongly indicated that the major tumor cell population of the SCC has been grown in short-term culture.

When early and later passages were compared, the SCL-1 cells demonstrated high phenotypic stability, since the peptides ranging from 45,000 to 59,000 daltons were quite consistent. Tonofilaments, however, seemed to be reduced in later passages, although the cytoskeletal network of keratin fibers remained clearly visible after decoration with specific antibodies.

Abnormal or malignant growth behavior could be tested only after at least 1 year in culture and was clearly positive in the organotypic culture and transplantation assay. At later passages, tumorigenicity of SCL-1 cells was also demonstrated in nude mice, but higher cell numbers and longer latency periods were required as compared to those in the transplantation assay. Although single cell cloning was possible in late passages with the use of conditioned medium, cells did not express anchorage-independent growth (even in conditioned medium). Anchorage-independent growth is not always correlated with tumorigenicity in vivo, particularly with human carcinoma cells (*6, 44–46*), and may often be acquired only at late culture stages. The ability possibly reflects further changes in growth behavior, due to selection in vitro. Up to 20–30 passages, no significant change in transformed growth behavior of SCL-1 cells was noted.

Despite the good phenotypic stability of the SCL-1 cell population in culture, chromosome and DNA analyses clearly demonstrated that genotypic changes occurred after about 1½ years in culture. The shift of tumor cell karyotypes in culture to higher degrees of ploidy as well as increased chromosomal aberrations in relation to the culture time has also been reported for human lymphatic cells lines (*47, 48*). The shift to hyperploidy in SCL-1 cultures, paralleled by an increased growth rate, was evidently not caused by overgrowth of a minor subpopulation since the two marker chromosomes were maintained in 100 and 70% of metaphases from culture passages 2–20. Although biopsy material could not be examined cytogenetically, nevertheless these marker chromosomes were very likely also characteristic for the hypodiploid tumor stemline in vivo. The almost identical DNA distribution in tumor and early cultured cells gives good evidence that the SCC tumor cell population was transferred into culture without major changes.

The predominance of hypodiploid stemlines in SCC of the skin has previously been determined with the use of DNA cytophotometry (*49*). The methodologic advantage of automated cytophotometric DNA analyses over conventional cytogenetic studies is obvious, since large numbers of cells can be rapidly analyzed. Although the technique is not sensitive enough to detect very small changes in chromosome number and structure, variations in DNA content can be determined with a fair degree of confidence. By cytometry alone, however, the slight hypodiploid deviation of the SCL-1 stemline could not be detected, whereas the shift of the karyotype to hyperploid levels was clearly visible.

Marker chromosomes have been studied in human tumors and derived cell cultures to correlate chromosomal alterations with tumorigenicity or specific tumor types (*50–53*). These studies are complicated by the rapid karyotypic changes observed in many tumors and further aberrations occurring during prolonged cultivation. Nevertheless, evidence exists for nonrandom changes of marker chromosomes in human tumor cells. With carcinomas, a frequent occurrence of maker chromosomes involving chromosomes 1, 3, 5, 7, and 8 was observed (*54–56*). In the SCL-1 cell line, described here and in short-term subcultures of a second skin SCC (Tilgen W, et al: In preparation), the most frequent markers involved chromosomes 7 and 1 and possibly chromosome 8. Similar observations were made earlier with an SCC line by Moore et al. (*9*). Further studies with more tumors and derived cell lines are needed to prove whether translocations involving these particular chromosomes are indicative of SCC or have general relevance for transformation. It should also be clarified whether the degree of differentiation and growth behavior of cells in vivo and in vitro are related and are reflected by the respective karyotypes.

The remarkable stability of the genotypic and phenotypic characteristics clearly indicated that the relevant tumor cell population could be maintained for about 10 passages during a period of more than 1½ years. While in further passages the phenotypic expression seemed to be largely conserved, continued genetic changes were observed. Thus our data demonstrate that cell culture models can be used for limited intervals to study the biologic characteristics of carcinoma cells and their sensitivity to therapeutic manipulations, provided the integrity of the cultured cells is carefully determined.

REFERENCES

(*1*) Gey GO, Coffman WD, Kubicek MT. Tissue culture studies on the proliferative capacity of cervical carcinoma and normal epithelium. Cancer Res 1952; 12:264–265.

(*2*) Giard DJ, Aaronson SA, Todaro GJ, et al. In vitro cultivation of human tumors: Establishment of cell lines derived from a series of solid tumors. J Natl Cancer Inst 1973; 51:1417–1423.

(*3*) Owens RB, Smith HS, Nelson-Rees WA, Springer EL. *Brief communciation*: Epithelial cell cultures from normal and cancerous human tissues. J Natl Cancer Inst 1976; 56:843–849.

(*4*) Fogh J, Wright WC, Loveless JD. Absence of HeLa cell contamination in 169 cell lines derived from human tumors. J Natl Cancer Inst 1977; 58:209–214.

(*5*) Fischer P, Vetterlein M. Establishment and cytogenetic analysis of a cell line derived from a human epithelioma of the lung. Oncology 1977; 34:205–208.

(*6*) Cailleau R, Olive M, Cruciger QV. Long-term human breast carcinoma cell lines of metastatic origin: Preliminary characterization. In Vitro 1978; 14:911–915.

(*7*) Smith HS. In vitro properties of epithelial cell lines established from human carcinomas and nonmalignant tissue. JNCI 1979; 62:225–230.

(*8*) Fogh J, Trempe G. New human tumor cell lines. In: Fogh J, ed. Human tumor cells in vitro. New York and London: Plenum, 1975: 115–159

(*9*) Moore GE, Merrick SB, Woods LK, Arabasz NM. A human squamous cell carcinoma cell line. Cancer Res 1975; 35:2684–2688.

(*10*) Morgan RT, Quinn LA, Woods LK, Moore GE. Marker properties of tumor and lymphoid cell lines derived from a patient with squamous cell carcinoma. Cancer Res 1977; 37:2030–2035.

(*11*) Okabe T, Sato N, Kondo Y, et al. Establishment and characterization of a human cancer cell line that produces human colony-stimulating factor. Cancer Res 1978; 38:3910–3917.

(*12*) Dodson MG, Klegerman ME, Menon M, Kerman RH, Lange CF, O'Leary JA. Establishment and characterization of a squamous cell carcinoma of the vulva in tissue culture and immunologic evaluation of the host. Am J Obstet Gynecol 1978; 131:606–619.

(*13*) Lasfargues EY, Coutinho WG, Redfield ES. Isolation of two human tumor epithelial cell lines from solid breast carcinomas. JCNI 1978; 61:967–978.

(*14*) Fusenig NE, Worst PK. Mouse epidermal cell cultures. II. Isolation, characterization, and cultivation of epidermal cells from perinatal mouse skin. Exp Cell Res 1975; 3:443–457.

(*15*) Fusenig NE, Amer SM, Boukamp P, Worst PK. Characteristics of chemically transformed mouse epidermal cells in vitro and in vivo. Bull Cancer (Paris) 1978; 65:271–280.

(*16*) Fusenig NE, Breitkreutz D, Boukamp P, Lüder M, Irmscher G, Worst PK. Chemical carcinogenesis in mouse epidermal cell cultures: Altered expression of tissue specific functions accompanying cell transformation. In: Franks LM, Wigley CB, eds. Neoplastic transformation in differentiated epithelial cell systems in vitro. New York: Academic Press, 1979:37–98.

(*17*) MacPherson J. Soft agar techniques. In: Kruse PF, Patterson MK, eds. Tissue culture, methods and applications. New York: Academic Press, 1973:276–280.

(*18*) Schaeffer WL, Friend K. Efficient detection of soft agar grown colonies using a tetrazolium salt. Cancer Lett 1976; 1:259–262.

(*19*) Peracchia C, Mittler BS. Fixation by means of glutaraldehyde-hydrogen peroxide reaction products. J Cell Biol 1972; 53:234–238.

(*20*) Franke WW, Schmid E, Breitkreutz D, et al. Simultaneous expression of two different types of intermediate size filaments in mouse keratinocytes proliferating in vitro. Differentiation 1979; 14:35–50.

(*21*) Franke WW, Weber K, Osborn M, Schmid E, Freudenstein C. Antibody to prekeratin. Decoration of tonofilament-like arrays in various cells of epithelial character. Exp Cell Res 1978; 116:429–445.

(*22*) Breitkreutz D, Boukamp P, Lüder M, Fusenig NE. Morphological and biochemical criteria for keratinization in primary and permanent mouse epidermal cell cultures. Front Matrix Biol 1981; 9:57–82.

(*23*) Weber K, Osborn M. The reliability of molecular weight determinations by dodecyl sulfate-polyacrylamide gel electrophoresis. J Biol Chem 1969; 244:4406–4412.

(*24*) Laemmli UK. Cleavage of structural proteins during the assembly of the head of bacteriophage T4. Nature 1970; 227:680–685.

(*25*) Worst PK, Valentine EA, Fusenig NE. Formation of epidermis after reimplantation of pure primary epidermal cell cultures from perinatal mouse skin. J Natl Cancer Inst 1974; 53:1061–1064.

(*26*) Moorehead PS, Nowell PC, Mellman WJ, Battips DM, Hungerford DA. Chromsome preparations of leukocytes cultured from human peripheral blood. Exp Cell Res 1960; 20:613–616.

(*27*) Seabright M. A rapid banding technique for human chromosomes. Lancet 1971; 2:971–972.

(*28*) Sumner AT. A simple technique for demonstrating centromeric heterochromatin Exp Cell Res 1972; 75:304–305.

(*29*) Zante J, Schumann J, Barlogie W, Göhde W, Büchner TH. New preparation and staining procedures for specific and rapid analysis of DNA distributions. In: Göhde W, Schumann J, Büchner T, eds. Pulse cytophotometry. Ghent, Belgium: European Press, 1976:97.

(*30*) Haag D. Flow microfluorometric de(s)oxyribonucleic acid (DNA) analysis supplementing routine histopathologic diagnosis of biopsy specimens. Lab Invest 1980; 42:85–90.

(*31*) Prenna G, Bianchi UA. Reazioni di Feulgen fluorescenti e loro possibilitia citofluorometriche quantitative. 5. Citofotometria quantitativa in fluorescenza ed assorbimento della reazione di Feulgen eseguita con Acrivlavina-SO_2. Riv Istoch Norm Pathol 1964; 10: 667.

(*32*) Voigt W-H, Fusenig NE. Organotypic differentiation of mouse keratinocytes in cell culture: A light- and electron-microscopic study. Biol Cellulaire 1979; 34:111–118.

(*33*) Rice RH, Green H. The cornified envelope of terminally differentiated human epidermal keratinocytes consists of cross-linked protein. Cell 1977; 11:417–422.

(*34*) Fusenig NE, Breitkreutz D, Lueder M, Boukamp P, Worst PK. Keratinization and structural organization in epidermal cell cultures. In: Schweiger HG, ed. International cell biology 1980–1981. Heidelberg: Springer-Verlag. 1981:1004–1014.

(*35*) Steinert P, Yuspa SH. Biochemical evidence for keratinization by mouse epidermal cells in culture. Science 1978; 200:1491–1493.

(*36*) Sun T-T, Green H. Keratin filaments of cultured human epidermal cells. J Biol Chem 1978; 253:2053–2060.

(*37*) Breitkreutz D, Tilgen W, Boukamp P, Fusenig NE. Alterations of keratin peptides in malignant lesions of human skin. J Cancer Res Clin Oncol 1981; 99:6A.

(*38*) Winter H, Schweizer J, Goerttler K. Keratins as markers of malignancy in mouse epidermal tumors. Carcinogenesis 1980; 1: 391–398.

(*39*) Worst PK, Fusenig NE. Histocompatibility antigens on the surface of cultivated epidermal cells from mouse embryo skin. Transplantation 1973; 15:375–382.

(*40*) ——Rücktransplantation epidermaler Mäusezellkulturen mit Ausbildung einer neuen Epidermis in syngenen und allogenen Empfängern. Z Immunitaetsforsch 1976; 152:323–326.

(*41*) Tilgen W, Haag D, Boukamp P, Riehl R, Breitkreutz D, Fusenig NE. Morphological and cell kinetic aspects of human malignant skin tumors in vitro. Eur J Cell Biol 1980; 22:389A.

(*42*) Tilgen W, Riehl R, Haag D, Breitkreutz D, Boukamp P, Fusenig NE. Human malignant skin tumors in vivo and in vitro. J Cancer Res Clin Oncol 1981; 99:58A

(*43*) Rheinwald JG, Beckett MA. Defective terminal differentiation in culture as a consistent and selectable character of malignant human keratinocytes. Cell 1980; 22:629–632.

(*44*) Katsuta H, Takaoka T. Parameters for malignant transformation of mammalian cells treated with chemical carcinogens in tissue culture. In: Nakahara W, Takayama S, Sugemura T, et al., eds. Topics in chemical carcinogenesis. Tokyo: Univ Tokyo Press, 1972: 389-400.

(45) Hackett AJ, Smith HS, Springer EL, et al. Two syngeneic cell lines from human breast tissue: The aneuploid mammary epithelial (Hs578T) and the diploid myoepithelial (Hs578Bst) cell lines. J Natl Cancer Inst 1977; 58:1795-1806.

(46) Marshall CJ, Franks LM, Carbonell AW. Markers of neoplastic transformation in epithelial cell lines derived from human carcinomas. J Natl Cancer Inst 1977; 58:1743-1751.

(47) Steel CM, Shade M, Woodward MA. Chromosome aberrations acquired in vitro by human B-cell lines. I. Gains and losses of material. JNCI 1980; 65:95-99.

(48) Shade M, Woodward MA, Steel CM. Chromosome aberrations acquired in vitro by human B-cell lines. II. Distribution of break points. JNCI 1980; 65:101-109.

(49) Manocha SL, Steele HD, Stich HF. The mosaic composition of the DNA content of the epidermal carcinomas of man. Z Krebsforsch 1969; 72:144-154.

(50) Lin CC, Goldstein S. Analysis of Q-banding patterns in human cell lines. J Natl Cancer Inst 1974; 53:298-304.

(51) Nelson-Rees WA, Flandermeyer RR, Hawthorne PK. Distinctive banded marker chromosomes of human tumor cell lines. Int J Cancer 1975; 16:74-82.

(52) Engel LW, Young NA, Tralka TS, Lippman ME, O'Brien SJ, Joyce J. Establishment and characterization of three new continuous cell lines derived from human breast carcinomas. Cancer Res 1978; 38: 3352-3364.

(53) Slater RM, Philip P, Badsberg E, Behrendt H, Hansen NE, van Heerde P. A 14q+ chromosome in a B-cell acute lymphocytic leukemia and in a leukemic non-endemic Burkitt lymphoma. Int J Cancer 1979; 23:639-647.

(54) Cruciger QV, Pathak S, Cailleau R. Human breast carcinomas: Marker chromosomes involving 1q in seven cases. Cytogenet Cell Genet 1976; 17:231-235.

(55) Mitelman F, Levan G. Chromosomes in neoplasia: An appeal for unpublished data. Cancer Genet Cytogenet 1979; 1:29-32.

(56) Kakati S, Hayata I, Oshimura M, Sandberg AA. Chromosomes and causation of human cancer and leukemia. Cancer 1975; 36:1729-1738.

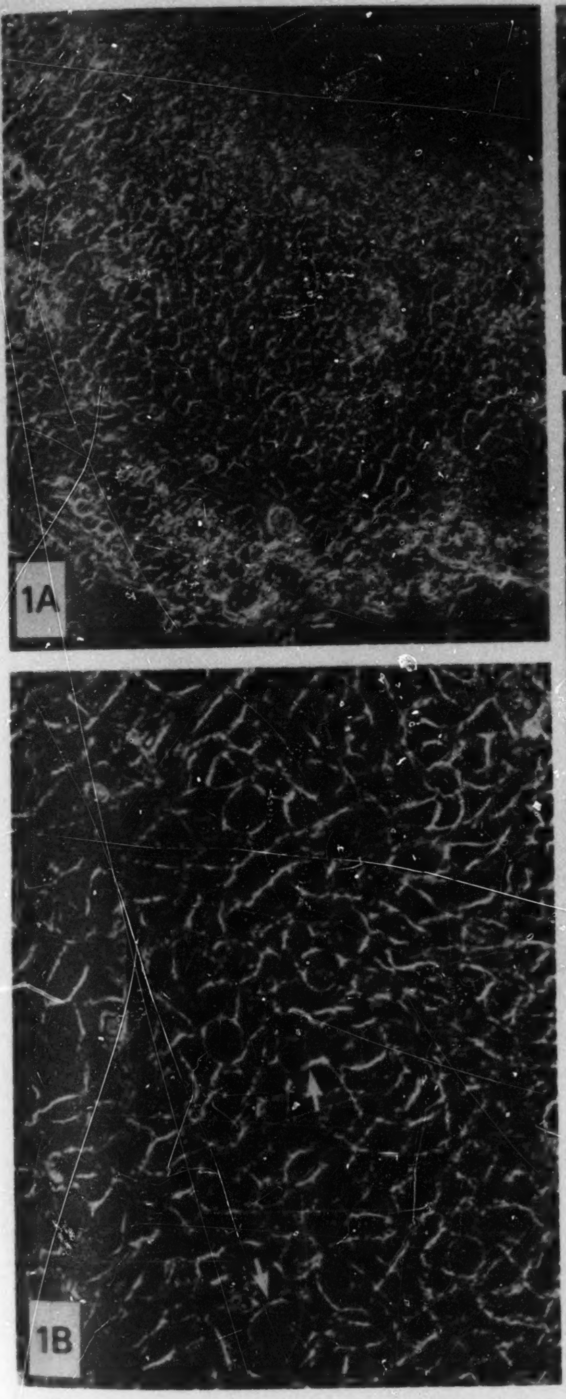

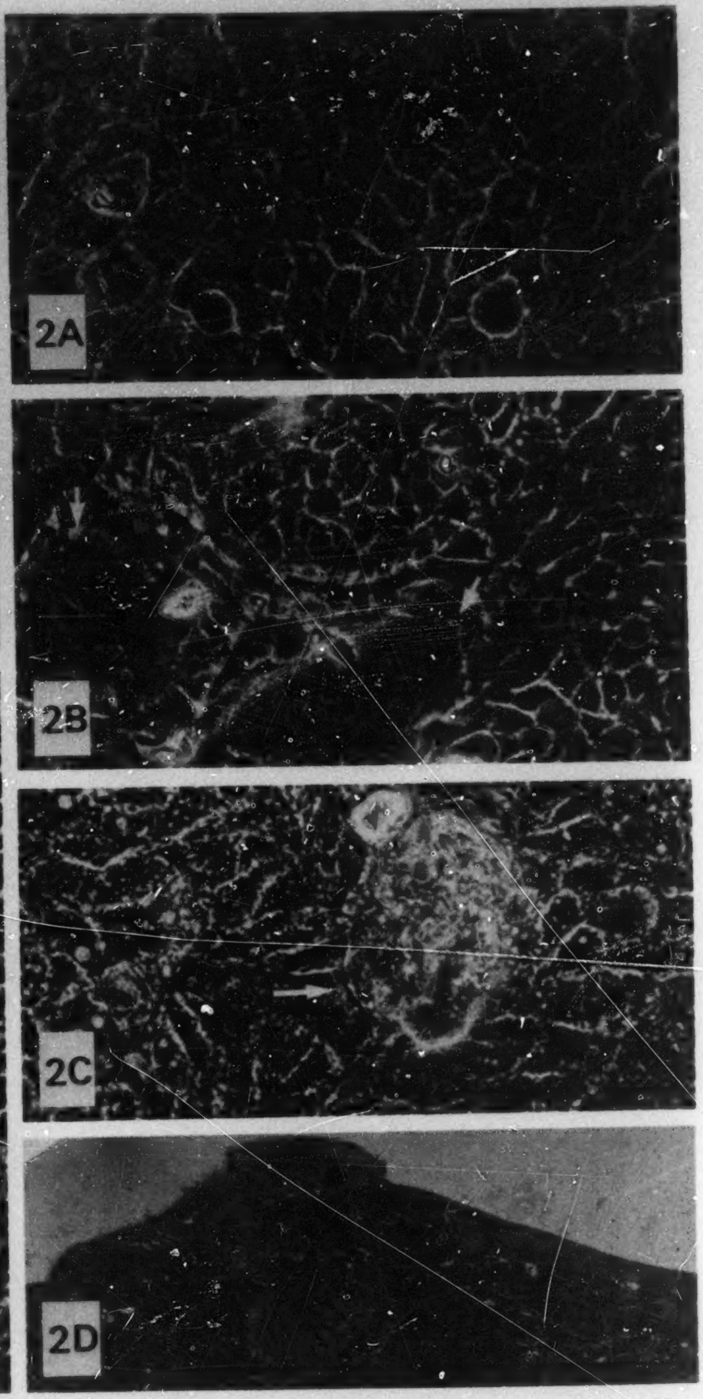

FIGURE 1.—Explant culture of SCC 8 days after plating. A) Explanted specimen (*upper right corner*) surrounded by the expanding epithelial sheet. Phase contrast. *Bar*=100 µm. × 100. B) Magnification of a section in 1A: The heterogeneous, densely packed, and actively proliferating epithelial cells are seen with atypic mitoses (*arrows*). *Bar*=50 µm. × 260. FIGURE 2.—Confluent SCL-1 culture (passage 10). A) Homogeneous area. H & E. *Bar*=50 µm. B) Area of small cells with enlarged intercellular spaces and giant cells (*arrows*). H & E. *Bar*=50 µm. C) Dense area with striated, presumably multilayered cells and a nodule with piled-up cells. Phase contrast. *Bar*=50 µm. × 260. D) Ultrastructure of cross section through a cell nodule of piled-up cells. *Bar*=20 µm. × 925

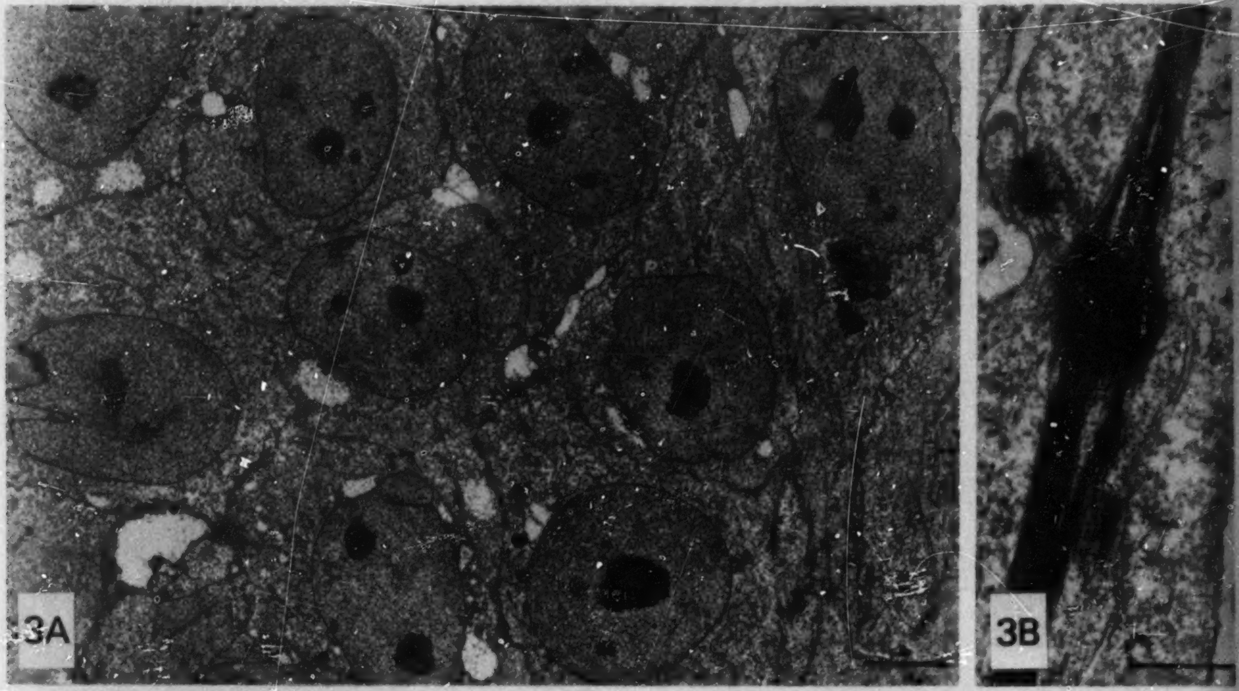

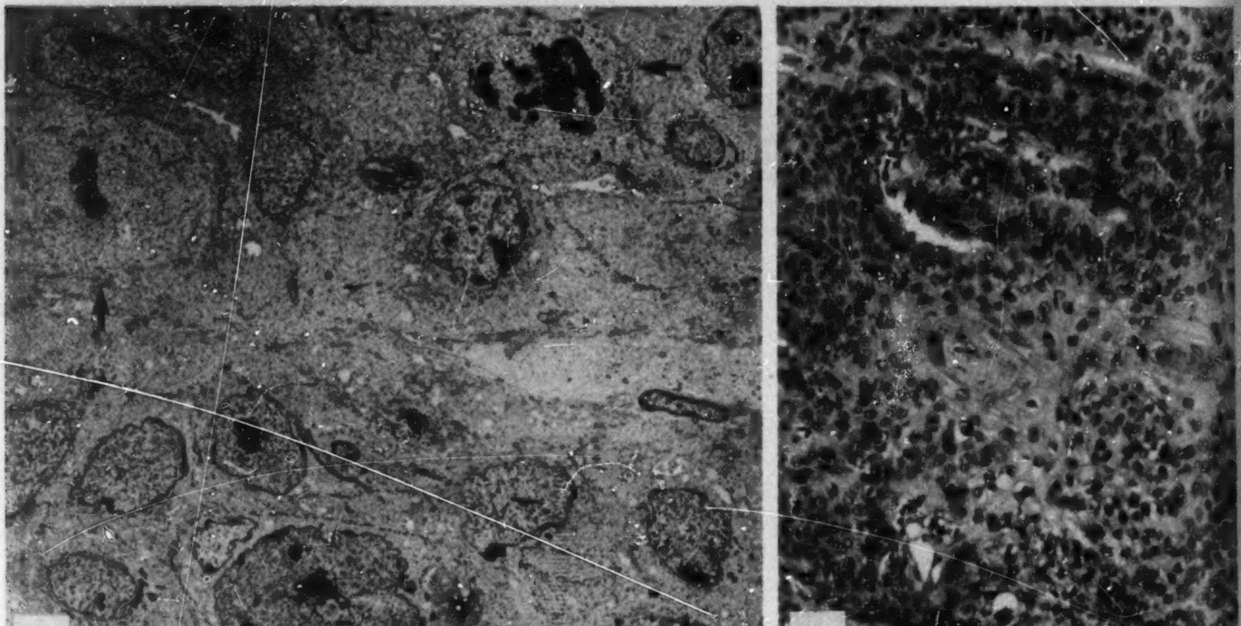

FIGURE 3.—Ultrastructure of an SCL-1 culture (passage 9) sectioned parallel to the petri dish. A) Tightly packed cuboidal cells with large nuclei and distinct nucleoli. Uranyl acetate. *Bar*= 5 µm. × 2,500. B) Magnification of a section in 1A: Desmosomes with connected tonofilament bundles. *Bar*=5 µm. × 3,400. FIGURE 4.—SCC biopsy. A) Ultrastructure of heterogeneous, tightly packed and actively proliferating cell population (*arrows*) with low degree of keratinization. Uranyl acetate. *Bar*=5 µm. × 2,500. B) Histologic aspect with keratinizing area of the otherwise poorly differentiated tumor. H & E. *Bar*=100 µm. × 180

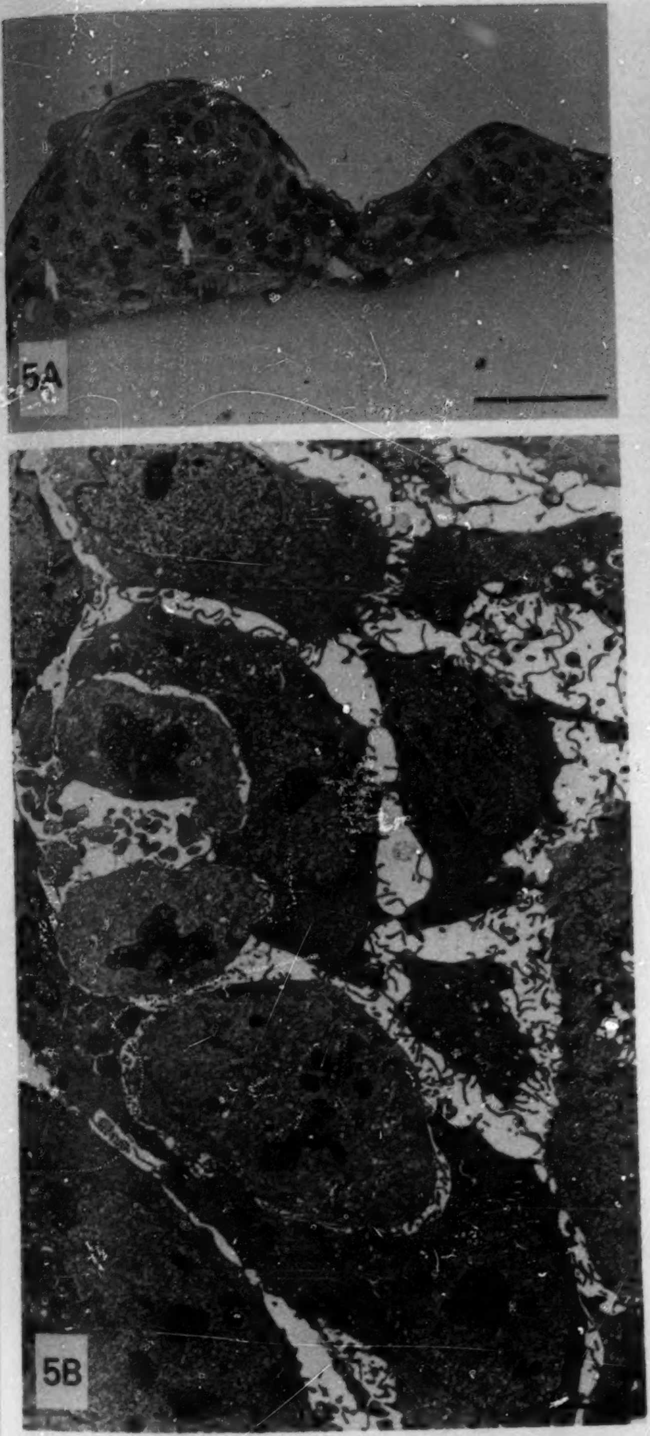

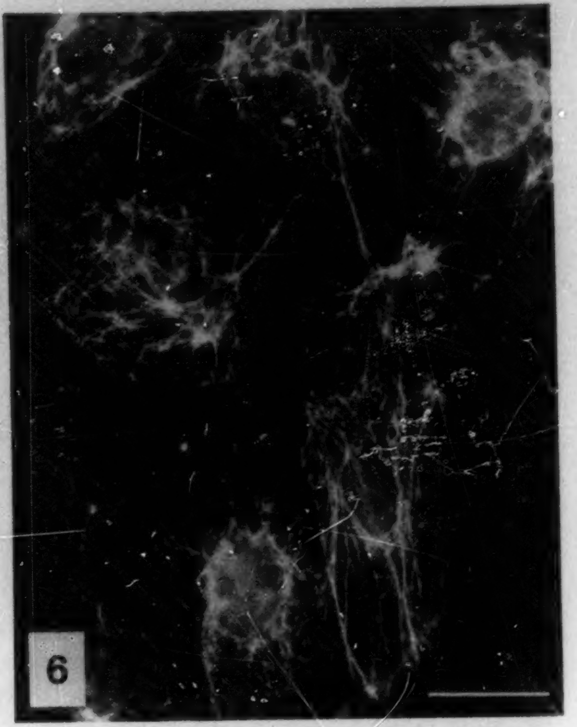

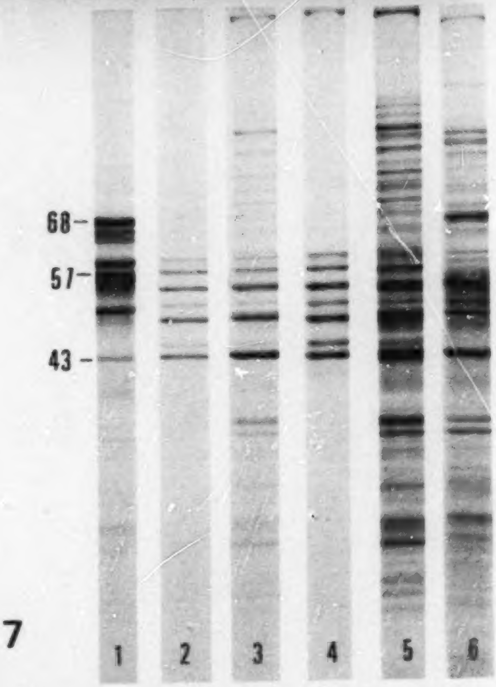

FIGURE 5.—Tumor-like nodules grown on lifted collagen gels (organotypic culture assay). A) Histology of a cross section with irregularly distributed mitoses (*arrows*). *Bar*=100 µm. H & E. × 195. B) Ultrastructure of a horizontal section showing large intercellular spaces, numerous microvilli, and high mitotic activity. *Bar*=5 µm. × 2,500

FIGURE 6.—Immunofluorescence of cytoskeletal filaments in SCL-1 cells decorated by an antikeratin antiserum. *Bar*=50 µm. × 360

FIGURE 7.—Electrophoresis of cytoskeletal proteins of normal epidermis, SCL-1 cells, and SCC on SDS slab gels. 1) Normal human epidermis—total protein; 2) SCL-1 cells, passage 8—cytoskeleton; 3) SCL-1 cells passage 8—total protein; 4) SCL-1 cells, passage 19—cytoskeleton; 5) SCL-1 cells, passage 19—total protein; 6) SCC tumor biopsy—total protein.

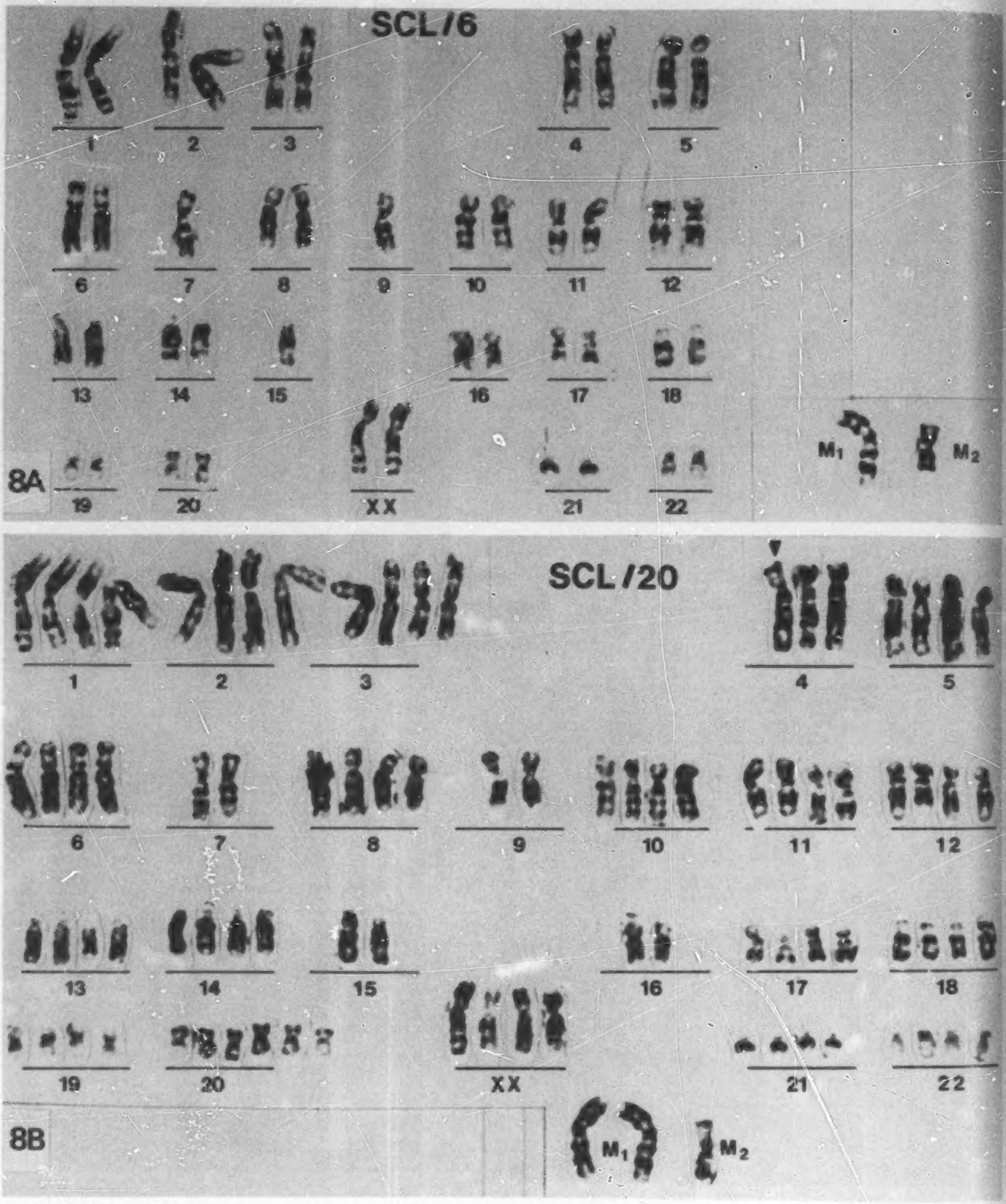
SCL/6
1
2
3
4
5
6
7
8
9
10
11
12
13
14
15
16
17
18
8A
19
20
XX
21
22
M1
M2
SCL/20
1
2
3
4
5
6
7
8
9
10
11
12
13
14
15
16
17
18
19
20
XX
21
22
8B
M1
M2

FIGURE 8.—Karyotypes of G-banded metaphases from SCL-1 cultures. A) Metaphase from passage 6 with 45 chromosomes, monosomy for chromosome 7, 9, and 15 and two marker chromosomes (M1: 7q9q; M2: 7p9p). B) Metaphase from passage 20 with a hypotetraploid chromosome mode with two M1 and one M2 marker chromosomes.

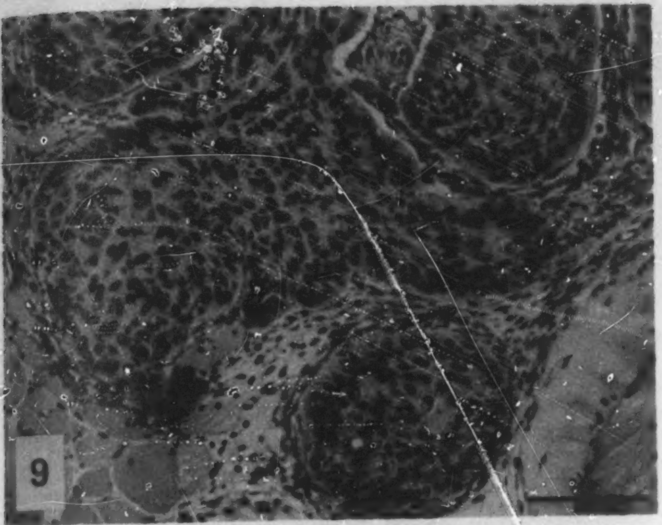

Figure 9.—Cross section of a tumor formed 3 mon after im injection of 1×10^6 cells (passage 17) into BALB/c *nu/nu* mice. H & E. *Bar*=100 μm. × 180

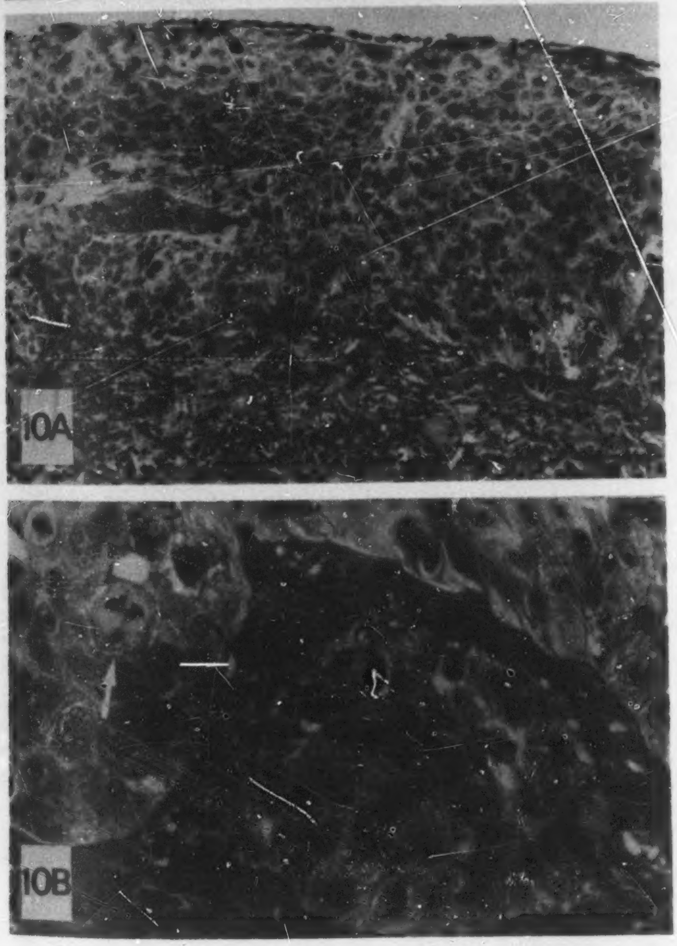

Figure 10.—SCL-1 transplant on a granulation tissue in adult thymectomized and irradiated (400 rad) C3H mice (passage 9). A) Cells grow on the surface and invade deeply into the granulation tissue. H & E. *Bar*=50 μm. × 225. B) Atypic mitosis (*arrow*) and dyskeratosis near the advancing front of invading tumor masses. H & E. *Bar*=50 μm. × 385.

Epidemiological Features of Wilms' Tumor: Results of the National Wilms' Tumor Study[1, 2]

Norman E. Breslow[3, 4] and J. Bruce Beckwith[5, 6]

ABSTRACT—Nearly 2,000 children with Wilms' tumor registered in a national clinical trial during 1969–81 showed high rates of aniridia, hemihypertrophy, cryptorchidism, hypospadias, and other genitourinary anomalies. Patients with bilateral disease, who constituted 5% of the total, had younger ages at diagnosis and an increased incidence of congenital anomalies and renal blastemal rests. Those with multicentric unilateral lesions had more blastemal rests but were otherwise indistinguishable from the unicentric cases. The 20 familial cases had none of the features usually associated with genetic tumors: neither younger ages nor an increase in bilaterality nor associated congenital anomalies. These observations suggest that the fraction of Wilms' tumors that is due to an inherited mutation may be substantially smaller than previously supposed and support the concept that the disease arises from a variety of pathogenetic pathways.—JNCI 1982; 68:429–436.

Several features of the epidemiology of Wilms' tumor suggest that genetic factors may play a major role in its etiology. The occurrence of the disease is remarkably constant among peoples in scattered parts of the world who have different environments, life-styles, and highly variable incidence rates for most cancers (*1*) Regardless of race, country, or epoch of birth, about one child in every 10,000 may be expected to develop by age 15 a malignant tumor of the kidney (*2*), of which the vast majority have the histologic characteristics of nephroblastoma.

Wilms' tumors are well known to be associated with certain congenital defects including aniridia, hemihypertrophy, and various anomalies of the GU tract (*3*). Cytogenetic studies have established that the aniridia–Wilms' tumor syndrome invariably occurs in persons with a specific chromosomal deletion (*4*). Although these cases tend to be sporadic rather than familial (*5*), aniridia has been diagnosed in both members of a pair of identical twins of whom one had Wilms' tumor (*6*). Reports of familial Wilms' tumor are fairly common (*7*). According to a two-stage mutational model for embryonal tumors, the disease may occur in both hereditary and sporadic forms depending upon whether or not the first mutation is germinal or somatic (*8*). Nodular renal blastema, which is found in approximately one-third of patients with Wilms' tumor (*9*), has been suggested as a precursor lesion in individuals who carry the "Wilms' gene" (*10*).

Most of the published information about genetic factors and Wilms' tumor has come from the aggregation of small series or case reports gathered from widely scattered sources. A unique opportunity for systematic study of the subject in a large and relatively unselected population was created by the NWTS. Some relevant data on congenital anomalies among 547 NWTS patients registered between 1969 and 1973 have already appeared (*11*). The purpose of the present report is to extend these observations to the roughly 2,000 patients registered with the study during the past decade, emphasizing particularly the quantitative differences between bilateral-familial versus unilateral-sporadic cases vis-à-vis age at onset, the occurrence of congenital anomalies, and certain histologic findings.

MATERIALS AND METHODS

Study population.—Between October 1969 and March 1981, a completed registration form was submitted to the NWTS Statistical Center for 2,073 patients. Excluded from consideration here were those whose final diagnosis was other than Wilms' tumor: 59 cases of congenital mesoblastic nephroma, 16 neuroblastomas, 7 polycystic kidneys, 6 renal cell carcinomas, and 13 cases with various benign and malignant conditions. Also excluded were 60 patients identified by the NWTS Pathology Center as having monophasic, clear cell, or rhabdoid sarcoma of the kidney (*12*) and 7 patients who were over 15 years of age at the time of diagnosis. This left 1,905 cases for analysis.

There were three different therapeutic trials in force since the beginning of the study (*13, 14*). Most patients were duly randomized on one of these trials and had base-line and follow-up data submitted at regular intervals. Others, including those registered during interim periods following closure of randomization rolls and the start of a new study, followed one of the NWTS protocol therapies without benefit of randomization. A few, whose treatment did not correspond to any of the defined NWTS regimens, were simply registered with the data center according to an agreement with the nearly 100 participating institutions that all Wilms' tumor patients would be reported. Details of their treatment and follow-up were not routinely requested and are substan-

---

ABBREVIATIONS USED: GU=genitourinary; ICD=International Classification of Diseases; NWTS=National Wilms' Tumor Study.

---

[1] Received June 25, 1981; accepted October 9, 1981.

[2] Supported in part by Public Health Service grants 2-R10CA-11722 and 1-K07CA-00723 from the National Cancer Institute.

[3] Department of Biostatistics SC-32, University of Washington, Seattle, Wash. 98195; and Fred Hutchinson Cancer Research Center, Seattle, Wash. 98104.

[4] *Address reprint requests to* Dr. Breslow, Department of Biostatistics SC-32, University of Washington, Seattle, Wash. 98195.

[5] Pathology Laboratory, Children's Orthopedic Hospital, Seattle, Wash. 98195.

[6] We gratefully acknowledge the contributions made by the many surgeons, pediatricians, and radiation therapists who treated these children and without whom the study would have been impossible. We also extend grateful thanks to Mrs. S. Jacobson, Dr. D. A. Sim, and Dr. P. Raju for technical assistance, and to Dr. N. F. Palmer and Dr. R. W. Miller for their assistance with the design of the study.

TABLE 1.—*Source of study patients*

Case category	No. of cases included in study			
	NWTS1, 10/69–12/74	NWTS2, 1/75–4/79	NWTS3, 5/79–3/81	Totals
Randomized	[illegible]	517	350	1,200
Followed	191	226	59	476
Registration only	121	80	28	229
Total	645	823	437	1,905

tially less complete than those for randomized or followed patients. Table 1 shows the number of cases of each type.

Sources of data.—The two main sources of data on demographic characteristics and congenital defects were the NWTS registration form, available for all study patients, and a family questionnaire which was filled out and returned by the parent or guardian for 1,370 cases. The questionnaire was available for 78% of randomized, 68% of followed, and 47% of registered patients. The registration form specifically requested information from the referring physician on GU anomalies, aniridia or other eye defects, hemihypertrophy, nevi, hemangiomas, neoplasms, and other congenital defects. The questionnaire asked for a history of pregnancies and family illnesses. Neither form was completely reliable; conditions shown on one were sometimes missing from the other (*11*). The occurrence of a few anomalies was ascertained only after careful reading of the pathology-surgery narratives and flow sheets submitted for most randomized and followed cases. Some relevant conditions have undoubtedly gone unreported or unnoticed.

Slides of the tumor specimen from the initial nephrectomy were submitted and reviewed by the NWTS Pathology Center for 74% of randomized, 63% of followed, and 33% of registered patients in this study. Four or more slides were available for 75% of such patients on the first study. Current guidelines for minimal histologic sampling call for one section to be taken for each centimeter of the largest tumor diameter, plus one section for each nodule of a multicentric tumor. Tumors were classified in one of 30 pattern recognition categories, given a percentage breakdown into stromal, blastemal, and epithelial elements, and scored for the presence of focal or diffuse cellular atypism (anaplasia) (*12*). More recently, the presence or absence of renal dysplasia, Beckwith's medullary dysplasia (*15*), blastemal rests, and immature glomeruli has been noted when the histologic sampling was sufficiently complete.

Bilateral and multicentric tumors.—Of the 1,905 cases analyzed, 84 were bilateral at onset, and an additional 19 developed disease in the contralateral kidney during the course of follow-up. Patients in this latter group were too few for separate evaluation and seemed comparable to the 84 vis-à-vis age and other relevant characteristics. Therefore a single category of 103 bilateral cases was utilized in the data analyses. A second category consists of 133 patients with unilateral multicentric lesions. Some of these were identified from the gross description provided by the pathologist making the initial diagnosis. Others were found during the central pathology review with the use of a criterion of separate tumor nodules of distinct histology. Specimens having a contiguous mass of tumor of uniform histology, but with isolated rests of blastema appearing elsewhere in the kidney, were not scored as multicentric. In view of the absence of central review for many cases, and the variability in the histologic sampling for others, the 133 cases cannot be regarded as a complete enumeration of those with multicentric disease. The third category consists of the remaining 1,669 unilateral cases without evidence of multicentricity.

Statistical methods.—Standard statistical methods (*16*) including *t*-tests, chi-square tests and rank sum tests were used to compare the three categories of patients. Since the family questionnaire was available for only 66% of the bilateral versus 72% of the unilateral cases, some of the analyses were adjusted for presence or absence of this source of information with the use of the odds ratio estimator and chi-square test of Mantel and Haenszel (*17*). The shape of the three age distributions was studied by hierarchical fitting of exponential, Weibull, and log gamma models with the use of the maximum likelihood method (*18*).

RESULTS

Age, Sex, and Race

Table 2 summarizes the demographic characteristics of patients in each of the 3 categories. The differences by sex and race are well within the bounds of change ($\chi^2_2=1.9$, $P=0.39$ for sex and $\chi^2_2=4.2$, $P=0.13$ for race), and the averages of the mother's age at birth are nearly identical. Comparison of the age distributions using the rank sum test shows no difference between the multicentrics and unicentrics ($P=0.72$) but shows a highly significant difference between the bilaterals and the combined unilateral group ($P<0.0001$).

Text-figure 1 presents semilog plots of the cumulative age distribution for each category. The shape parameters of the fitted Weibull distributions (table 3) confirm the visual impression of a similar degree of curvature: All three estimates of σ are significantly less than unity ($P<0.0001$), indicating that none of the age distributions are exponential. However, the Weibull model fits quite adequately in comparison with the log normal and other members of the log gamma class.

TABLE 2.—*Demographic characteristics of patients with bilateral, multicentric and unicentric Wilms' tumor*

Demographic characteristic	Wilms' tumor category		
	Bilateral	Multicentric	Unicentric
No. of patients	103	133	1,669
Sex, % male	44.7	42.1	47.8
Age at diagnosis, mo:			
Median	25.5	43.3	36.1
Mean	30.5	44.6	45.1
SD	21.6	29.3	33.9
Race, % nonwhite	13.6	16.0	20.5
Mother's age at birth, yr:			
Mean	25.2	25.0	25.4
SD	5.9	5.4	5.5
(*n*)[a]	(67)	(103)	(1,173)

[a] No. of cases for which mother's age was known.

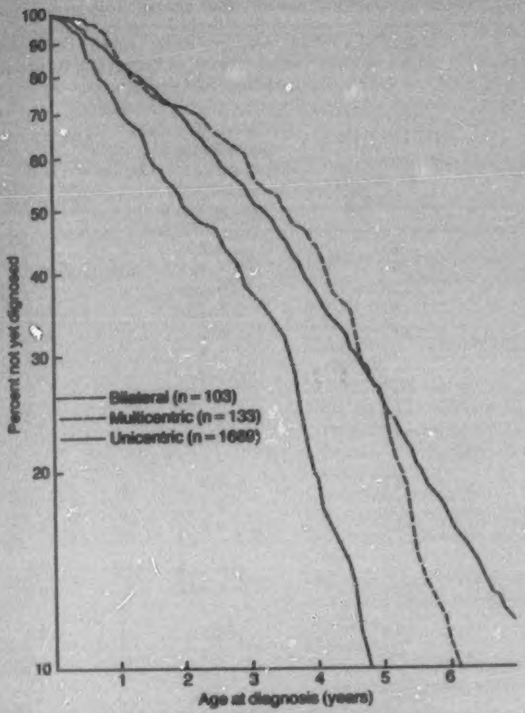

TEXT-FIGURE 1. —Cumulative distributions of age at diagnosis for three categories of patients with Wilms' tumor.

TABLE 3.—*Parameters of Weibull age distributions fitted to each category of tumor*

Tumor category	Estimated parameters of Weibull distribution[a] ±SE	
	$\alpha = -\log \lambda$	$\sigma = 1/\rho$
Bilateral, *n*=103	3.12±0.09	0.71±0.08
Multicentric, *n*=133	3.56±0.07	0.62±0.05
Unicentric, *n*=1,669	3.49±0.02	0.73±0.02

[a] Parameters were chosen according to Farewell and Prentice (*18*).

An unexpected finding was that the age distribution depended on sex. Male cases tended to be diagnosed a few months earlier, having a mean (±SD) age of 42.1±32.7 versus 46.1±33.7 months for females. The frequency distributions (text-fig. 2) show that male incidence peaks in the 2d or 3d year of life, whereas for females it remains high into the 4th year. The large number of cases ensures that the observed differences are statistically significant (P=0.003 by the rank sum test).

Incidence of Congenital Anomalies

Rates of congenital anomalies among NWTS patients, classified according to the ninth revision of the ICD (*19*), were compared with those from two other large series (table 4). The Collaborative Perinatal Project appears to have the highest incidence yet reported for a general population (*20*). Rates shown in table 4 for this series resulted from aggregation of data for specific conditions coded in the range ICD 741–759 and involved direct adjustment to the race distribution of the NWTS population. A second control series was provided by the surveillance program of the Center for Disease Control in Atlanta, Ga. (Erickson D: Personal communication). Several features complicate the comparability of these data. For example, NWTS patients are examined intensively at diagnosis and have surgical exploration of the kidney and other abdominal organs which would tend to elevate their rates for some conditions. Also, the population series include conditions found at autopsy in stillborn babies and count multiple anomalies within each of the ICD categories, whereas NWTS cases are counted only once. Thus the control rates are shown simply with a view toward providing "order of magnitude" figures for the general population; statistical tests were not considered relevant.

One NWTS patient was reported with spina bifida. Of 8 others with central nervous system anomalies, 5 had hydrocephalus, 2 had microcephaly, and 1 had a meningiomyelocele.

Table 5 lists the characteristics of 16 NWTS patients with aniridia–Wilms' tumor syndrome. Their high frequencies of associated eye anomalies and GU disorders confirm earlier work (*5*). The average age at diagnosis, 24.4±11.2 months, is significantly lower than that for the other cases (P=0.02). There was an assortment of other, mostly minor eye disorders in 7 more children including ptosis, heterochromia, blocked tear ducts, anisocoria, and cataracts. Ear and face deformities in 4 patients included 1 possible case of Noonan's syndrome (i.e., low set ears, slant eyes, and valvar pulmonic stenosis) and 1 with a cleft palate. Cleft palate was the sole anomaly in 1 other patient.

There were 29 patients reported with anomalies of the cardiovascular or respiratory systems of which 3 were associated with the aniridia syndrome (table 5). The remainder of the cases included 9 septal defects, 7 accessory or anomalous renal vessels, 2 coarctations of the aorta, and miscellaneous other conditions. The 13 anomalies of the upper alimentary tract–digestive systems included 3 Meckel's diverticula, 2 high-arched palates, 2 intestinal malrotations,

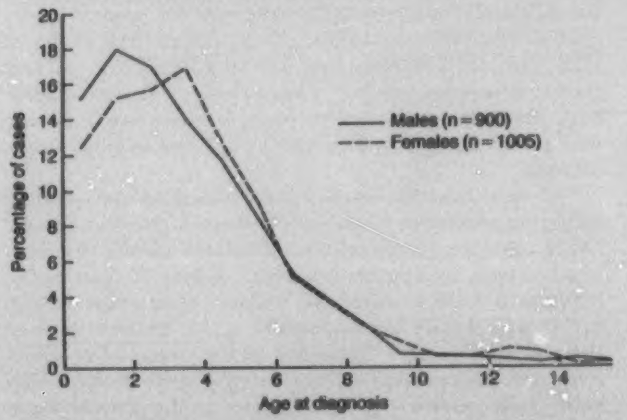

TEXT-FIGURE 2.—Histograms of age at diagnosis for male and female patients with Wilms' tumor.

TABLE 4.—*Rates of congenital anomalies noted in NWTS patients versus those in two other series*

ICD classification, 9th rev.	Anomaly–organ system(s)	Congenital anomaly rates per 1,000 cases in study series: Years of observation, ages of patients at observation, and No. of M and F[a]		
		NWTS: 1969–81, ages 0–15 yr, 900 M+1,005 F	Collaborative Perinatal Project:[b] 1959–66, ages 0–11 mo, 27,087 M+26,170 F	Atlanta:[c] 1968–78, ages 0–11 mo, 144,025 M+136,689 F
741–2	Central nervous system	4.7	4.2	1.9
743.45	Aniridia	8.4	0.01	0.02
743	Eye, excluding aniridia cases	3.7	2.5–4.0	0.9
744	Ear, face, and neck	2.1	0.5–13.3	3.9
745–8	Cardiopulmonary system	15.2	10.2	10.3
749	Cleft palate–lip	1.0	2.5	2.4
750–1	Upper alimentary tract–digestive system	6.8	5.7–7.4	3.5
752.5[d]	Cryptorchidism	27.8	11.9	1.5
752.6[d]	Hypospadias	17.8	8.7	4.9
752, excluding 752.5 and 752.6	Genital	2.1	0.9–3.5	1.4
753.3	Fused kidney	3.7	0.2	—
753.3	Double-collecting system	15.2	0.1	—
753	Urinary system excluding fused kidney, double-collecting system	7.3	3.3	1.7
754.5–754.7	Clubfoot	3.7	6.6–23.6	3.9
754–6, excluding 754.5–754.7	Musculoskeletal system	22.6	16.9–28.0	10.9
757	Hair, skin, and nails	17.8	37.4	2.3
758	Chromosome defects, Down's syndrome	0.5	1.1	—
759.0	Accessory spleen	6.3	0.2	—
759.8	Hemihypertrophy	24.7	0.03	—

[a] M=males; F=females.

[b] Data from Myrianthopoulos and Chung (20). When 2 values are given, the lower is the "major" anomalies only; upper and single values include "minor" conditions.

[c] Data from Erickson D.: Personal communication.

[d] Rates for males only.

and 1 each tongue tied at birth, macroglossia, imperforate anus, congenital megacolon (Hirschsprung's disease), hyperplasia of the small bowel, and persistent cloacus.

The predominant genital anomalies in males were 25 cases of cryptorchidism and 16 cases of hypospadias; 4 patients had both. Mean ages at diagnosis were 32.9±26.2 and 23.9±20.5 months for the 2 groups. These were less than the mean age of 42.1±32.7 months for all males, and the difference for hypospadias ($P<0.0001$) but not cryptorchidism ($P=0.08$) was statistically significant. Five of the 10 male cases with aniridia had one or the other of the two genital anomalies (table 5). Other kinds of abnormal genitalia were seen in 4 more patients: 2 males and 1 female were pseudohermaphrodites and 1 male had an extra testicular sac.

The most common urinary tract anomalies were double collecting systems in 29 patients or fused kidneys in 7 cases. Other cases were reported with lobulated kidney (4 cases), renal ectopia, hydronephrosis, cystic kidney (2 cases each), malformed kidney, dysplastic kidney, obstruction of the ureter, and female hypospadias (1 each). Because most of these anomalies were discovered in the course of nephrectomy and because results from autopsy series indicate that many such conditions go undiagnosed in the general population (*21*), the control comparisons have little relevance. Similar remarks apply to the 12 cases of accessory spleen coded under ICD 759.

The 51 musculoskeletal anomalies included clubfoot (7 cases), conditions involving the hip (8 cases), face or skull (11 cases), leg or ankle (2 cases), ribs or sternum (6 cases), spine (scoliosis, 5 cases), and the hand (6 cases). There were also single occurrences of spina bifida occulta, phocomelia, Klippel–Feil syndrome, prune belly syndrome, a missing toe, and the combination of claw hand with claw feet. Strawberry nevi, birthmarks, accessory skin tags, or other integumentary disorders coded under ICD 757 were seen in 34 patients.

The average age of 20 male and 27 female patients diagnosed with hemihypertrophy was 39.5 months, almost identical to that for the sample as a whole. One had aniridia and 4 had various anomalies of the GU tract. For 35 of these 47 patients, the laterality of both tumor and hemihypertrophy was known; however, there was no indication that the two were related.

Data were collected on a number of congenital conditions besides those that could be coded to ICD categories 741–759. For example, 21 male cases were reported with inguinal hernia, varicocele or hydrocele, and 2 females had inguinal hernia. Umbilical hernias occurred in 6 males and 8 females, 3 of them in 4 children reported by their institutions as having the Beckwith–Wiedemann syndrome. Hereditary disorders included 3 cases of sickle cell anemia, 2 Hashimoto's diseases, 2 von Willebrand's diseases, and 1 each of hemoglobinopathy and Mediterranean anemia. There were 10 mentally retarded patients without seizures, and 5, all of whom also had other anomalies, with seizures. An additional 5 cases were reported as having seizures but no retardation.

TABLE 5.—*Characteristics of NWTS cases with the aniridia-Wilms' tumor syndrome*

Case identification No.	Sex	Race[a]	Age at diagnosis, mo	Laterality-centricity[b]	Associated anomalies and diseases
14	♂	W	15	Uc	Glaucoma, cryptorchidism, hydrocele
31	♀	B	44	Uc	Mitral insufficiency
95	♂	B	24	Uc	Crossed renal ectopia, septal defect, myelomonocytic leukemia, rhabdomyosarcoma, neuroblastoma
195	♂	W	27	Uc	Glaucoma, hydrocele
384	♂	W	33	Uc	Cryptorchidism, fused kidney
451	♀	W	13	LB	Cataracts, glaucoma, microlentis
489	♂	W	27	Uc	Glaucoma, cryporchidism, ventricular septal defects, high palate
505	♀	B	18	Uc	Cataracts
2,006	♀	W	20	Uc	Cataracts, retinal detachment, double collecting system
2,092	♂	W	23	Uc	None
2,102	♂	W	12	B	Hypospadias, dysplastic kidney, skull deformity
2,626	♂	W	15	M	None
2,663	♂	W	12	Uc	Cataracts, cryptorchidism, hypospadias, inguinal hernia
3,240	♀	W	30	Uc	Bowel malrotation
3,272	♂	W	51	Uc	Male pseudohermaphrodite, partial blindness, mild mental retardation, fetal lobulation of the unaffected kidney
3,279	♀	W	25	Uc	Hemihypertrophy

[a] B=black; W=white.

[b] Uc=unicentric; M=multicentic; LB=late bilateral; B=bilateral at onset.

Association of Congenital Anomalies With Bilaterality and Multicentricity

Table 6 compares the incidence of common anomalies among the three patient categories. More than twice as many bilateral than unilateral cases were reported with at least one anomaly ($P<0.0001$). The association was particularly strong with hemihypertrophy and with hypospadias and other abnormalities of the male genitalia. There was no evidence, however, for an excess of congenital anomalies of any kind among the (unilateral) multicentric cases as compared to unicentric cases.

Histopathology

Most tumors, regardless of laterality or centricity, exhibited the typical mixed pattern of stromal, epithelial, and blastemal elements. For one particular subtype, anaplastic blastema, 3 of the 10 cases were found among the bilaterals ($P<0.001$). However, the significance of the finding is obscured by the fact that 30 or more distinct subtypes have been defined (*12*).

More interesting differences between categories were found in the presence of certain embryonic or premalignant structures (table 7). The bilateral and multicentric cases all tended to have a higher frequency of renal dysplasia, Beckwith's medullary dysplasia, blastemal rests, and immature glomeruli. Particularly striking was the occurrence of blastemal rests in more than one-half of the bilateral and multicentric lesions versus 14% of unicentric lesions. However, there was no indication that 175 NWTS patients observed with blastemal rests were diagnosed any earlier than 705 scored negative or uncertain; mean ages (±SD) were 42.3±26.8 and 43.2±32.7 months, respectively.

Familial Wilms' Tumor

There were 20 patients (1.0%) reported who had one or more relatives with Wilms' tumor, a sibling being involved in 7 cases and a parent in 1. These cases generally seem quite comparable to their nonfamilial counterparts (table

TABLE 6.—*Association of selected congenital anomalies with bilaterality and multicentricity*

Anomaly-organ system(s)	No. of cases in each category			Degree of association			
				Bilateral vs. unilateral		Multicentric vs. unicentric	
	Bilateral, $n=103$	Multicentric, $n=133$	Unicentric, $n=1,669$	ψ[a]	P[b]	ψ	P
Aniridia	2	1	13	2.6	0.47	1.0	0.63
Cardiopulmonary	2	2	25	1.3	0.95	1.0	0.72
Cryptorchidism[c]	4	0	21	3.7	0.04	0.0	0.42
Hypospadias[c]	5	0	11	9.2	<0.0001	0.0	0.77
All genital[d]	9	0	30	5.8	<0.0001	0.0	0.22
All urinary tract	5	1	44	2.0	0.25	0.3	0.29
Musculoskeletal	2	2	47	0.7	0.90	0.5	0.51
Integumentary	1	3	30	0.6	0.86	1.2	0.95
Hemihypertrophy	8	4	35	4.0	0.001	1.4	0.76
All anomalies[e]	26	19	217	2.3	0.001	1.1	0.49

[a] ψ=odds ratio measure of association (adjusted).

[b] P=significance level (adjusted).

[c] Only males considered.

[d] Both sexes; includes cryptorchidism and hypospadias.

[e] ICD 741-759.

TABLE 7.—*Histologic features of bilateral, multicentric, and unicentric Wilms' tumor*

Feature	Wilms' tumor category: No. of cases positive/No. examined (%)			P^a
	Bilateral	Multicentric	Unicentric	
Renal dysplasia	5/28 (18)	6/76 (8)	16/732 (2)	<0.0001
Beckwith medulla	3/20 (15)	11/63 (17)	35/523 (7)	0.01
Blastemal rests	18/33 (55)	52/87 (60)	104/760 (14)	<0.0001
Immature glomeruli	8/28 (29)	14/75 (19)	86/735 (12)	0.01

[a] Significance level based on χ^2_3 statistic for homogeneity.

8). Mean ages for the patient at diagnosis and the mother at birth are 44.4±22.1 months and 26.3±4.8 years, respectively, both figures being close to those for the series as a whole (table 2). Three patients had congenital anomalies, none of them typically associated with Wilms' tumor. Only 1 familial case had bilateral disease and 2 were multicentric; however, several bilateral tumors were reported among the affected family members. The range of cell types and other histopathologic features was fairly characteristic.

DISCUSSION

Certain of the NWTS findings confirm the observations made by Knudson and Strong (*8*) and others (*6, 22*) in support of a two-stage mutational model for the etiology of Wilms' tumor. Other findings conflict with this notion. In agreement are the earlier ages at diagnosis and the higher incidence of associated congenital anomalies for the bilateral cases, although the differences are not nearly so great as in the small study of Bond (*22*), and the younger ages for those with aniridia but not with hemihypertrophy. Similarly, the NWTS data (table 7) confirm an association of blastemal rests with bilaterality which was previously noted in a much smaller series and was used to suggest that nodular blastema is a precursor lesion occurring in patients with the putative mutation (*23*).

An essential feature of the etiologic model is the young median age of the hereditary cases, which are assumed to encompass all bilateral and familial tumors and a fraction of the remainder. Indeed, it is largely on the basis of an age distribution typical of unilateral cases that those accompanied by hemihypertrophy have been identified as sporadic. According to the theory, the hereditary cases occur earlier since only the second mutational event need take place. The original model for both retinoblastoma (*24*) and Wilms' tumor (*8*) asserted further that the ages of such cases followed the "one-hit" or exponential distribution expected from a constant rate of occurrence for this event. However, this was subsequently modified to accommodate a changing population of susceptible embryonic cells (*25–27*). Moreover, the percentage of Wilms' tumors estimated to be of hereditary origin has recently been revised downward from 38 to 15–20% (*28*).

The age distributions of the unilateral and bilateral NWTS cases display rather similar degrees of curvature on the semilog plot and as measured by the shape parameters of the fitted Weibull distributions (table 3): $\rho = \sigma^{-1} = 1.41$ for the bilateral cases and $\rho = 1.37$ for unilateral, unicentric cases. The density of the age distribution for the unilateral–sporadic cases is proportional to the age incidence function which, since these cases predominate numerically, has roughly the shape shown in text-figure 2. The peak in incidence at ages 2–4 is consistent with a rise and subsequent decline in the number of susceptible embryonic cells (*29*). Alternatively, the density of the age distribution for the bilateral–hereditary cases should reflect the attenuation of a population of susceptibles, most of whom acquire the disease. We have not yet attempted to verify the complicated relationship between the two curves which is predicted by the most recent model (*27*).

One aspect of the theory that needs some modification or clarification in light of the NWTS data is the classification of patients with (unilateral) multicentric tumors in the hereditary class. The characteristics of 133 multicentric cases in this series are closer to those of patients with unicentric tumors than to those with bilateral tumors with regard to age at diagnosis and the association with congenital anomalies. The single feature that they share with the bilaterals is a high frequency of association with nodular blastema and other embryonic remnants. While this perhaps fits in with the idea of a common mutational etiology, the observation of identical age distributions for cases with and without blastemal rests does not.

Another group for whom NWTS data fail to confirm earlier observations made in support of the mutational theory is the group of the familial cases shown in table 8, of which tumors 69 and 2,230 have been reported previously (*30, 31*). Although these are admittedly few in number and include 1 or 2 questionable patients, it is instructive that they display none of the features usually associated with genetic tumors: neither younger ages at onset, nor a high degree of bilaterality, nor a heightened association with congenital anomalies, nor a clear pattern of autosomal dominance. However, a greater incidence of bilaterality was apparent among family members with the disease. The concepts of delayed mutation and host resistance have been advanced to explain the occurrence of pedigrees, such as observed here, where affected distant cousins are related via unaffected family members (*32*). Also, the small number of cases means that the story could change dramatically after another decade of case collection and observation. By that time a number of the survivors of bilateral Wilms' tumor (*33*) will themselves be parents, and the answer should be clearer. Nevertheless, the recent report of no tumors being found in 54 children of a series of patients who survived the unilateral disease reinforces our belief that the hereditary fraction may be rather small (*34*).

If bilateral Wilms' tumors are not usually the result of an inherited mutation, one must search elsewhere to explain their earlier age at diagnosis and the clear link to hypo-

TABLE 8.—*Characteristics of NWTS patients with familial Wilms' tumor*

Case identification No.	Sex	Age at diagnosis, mo	Mother's age at birth, yr	Associated anomalies	Laterality–centricity[a]	Family member(s) with Wilms' tumor: Relation	Sex	Age at diagnosis, yr	Laterality[b]
13[c]	♂	34	27	Congenital ptosis, aortic stenosis, arrested hydrocephalus	Uc	Sibling	♂	5	Ul
69	♂	61	29	None	M	Sibling	♂	6	B
						Sibling	♀	2	Ul
156	♀	29	19	None	Uc	First cousin	♂		B
						Mother's first cousin	♂		Ul
						Aunt	♀	3	
267	♂	40	22	None	B	Father's first cousin	♂	6	
277[d]	♂	6		None	Uc	Parent's second cousin	♂	1	Ul
310	♀	69	25	None	Uc	Sibling	♂	3	
469[c]	♂	66	25	None	Uc	Sibling	♂	1	Ul
636	♂	51	24	None	M	Sibling	♀	0	
647	♀	67	23	None	Uc	Second cousin	♂	4	
						Uncle (maternal)	♂	0	
2,144[e]	♂	64	30	Accessory spleen	Uc	Sibling	♂	2	Ul
2,159	♂	69	31	None	Uc	Mother	♀		
2,181	♂	63		None	Uc	Second cousin, once removed	♂		
2,230	♂	39		None	Uc	Father's first cousin	♀	9	Ul
						Father's first cousin	♂	2	LB
						Father's first cousin	♂	3	B
						Father's first cousin	♂	3	Ul
2,298[d]	♂	18	26	Clubfoot	Uc	Mother's second cousin	♂	0	Ul
2,391[e]	♂	21	32	None	Uc	Sibling	♂	5	Ul
2,417	♂	64		None	Uc	Mother's first cousin			Ul
2,550	♂	0	24	None	Uc	Mother's first cousin	♂	5	
2,556	♂	27	37	None	Uc	First cousin, once removed	♀	1	
2,699	♀	39	20	None	Uc	Maternal uncle	♂	5	
2,937	♂	60		None	Uc	Paternal uncle	♂	5	

[a] Uc=unicentric; M=multicentric; B=bilateral.

[b] Ul=unilateral; B=bilateral; LB=late bilateral.

[c] Related cases.

[d] Related cases.

[e] Related cases.

spadias and other anomalies. These features could indeed be due to a two-stage process, but one in which the first event occurs postzygotically rather that prezygotically, and early enough in embryogenesis to affect developing renal and genital tissue on both sides of the midline. The age at diagnosis would then be determined by the time it takes for the second event to occur in either of two kidneys. Consequently, the age at diagnosis would be less on the average than if only one kidney were at risk.

The observations made here support the concept that Wilms' tumors may arise by a variety of pathogenetic pathways. One subgroup comprises the aniridia cases, with their young ages, high incidence of associated GU anomalies, and specific chromosome abnormalities. Another group consists of patients with Wilms' tumor and gonadal dysgenesis, for which a common defect in the embryonic urogenital ridge has been suggested as a possible cause (*35*). The cases arising in association with hemihypertrophy seem to form a rather different group; the familial cases, however, may turn out to be a heterogeneous collection, some of which are indeed carriers of a particular mutation and others of which are not.

Another interesting finding from this large and systematic study of patients registered in a national clinical trial is male-to-female sex ratio of 900:1,005=0.896, which is significantly different from unity (P=0.05). This agrees with the ratio of 0.9 found in a French series of 248 cases diagnosed during 1957–67 (*36*) but conflicts with the ratio of 184:151=1.2 observed in 1962–66 in a population-based series (*37*) in Great Britain and with the ratio of 81:66=1.2 observed for kidney tumors under 15 years of age in the Third National Cancer Survey (*38*). Because all these ratios are sufficiently close to 1, further data from incidence registers will be required to resolve the issue of a possible sex difference. Of greater potential significance are the distinct age distributions noted for the two sexes (text-fig. 2). The difference of 4 months in mean ages is rather small; therefore, it could easily have gone undetected in earlier studies with fewer cases. Nevertheless, a similar pattern, which could reflect a slight sex difference in the rate of growth or maturation of susceptible embryonic tissue, was observed in Great Britain (*37*).

REFERENCES

(1) Innis MD. Nephroblastoma: Possible index cancer of childhood. Med J Aust 1972; 1:18–20.

(2) Stukonis MK. Cancer incidence cumulative rates. IARC internal technical report No. 78/002. Lyon: IARC, 1978.

(3) Miller RW, Fraumeni JF Jr, Manning MD. Association of Wilms' tumor with aniridia, hemihypertrophy and other congenital malformations. N Engl J Med 1964; 270:922–927.

(4) Francke U, Holmes LB, Atkins L, Riccardi VM. Aniridia–Wilms' tumor association: Evidence for specific deletion of 11p13. Cytogenet Cell Genet 1979; 24:185–192.

(5) Fraumeni JF, Glass AG. Wilms' tumor and congenital aniridia. J Am Med Assoc 1968; 206:825–828.

(6) Maurer HS, Pendergrass TW, Borges W, Hornig GR. The role of genetic factors in the etiology of Wilms' tumor. Cancer 1979; 43: 205–208.

(7) Juberg RC, St. Martin EC, Hundley JR. Familial occurrence of Wilms' tumor: Nephroblastoma in one of monozygous twins and in another sibling. Am J Hum Genet 1975; 27:155–164.

(8) Knudson AG, Strong LC. Mutation and cancer: A model for Wilms' tumor of the kidney. J Natl Cancer Inst 1972; 48:313–324.

(9) Machin GA. Persistent renal blastema (nephroblastomatosis) as a frequent precursor of Wilms' tumor: A pathological and clinical review. Am J Pediatr Hematol Oncol 1980; 2:165–172, 253–261, 353–362.

(10) Bove KE, McAdams AJ. The nephroblastomatosis complex and its relationship to Wilms' tumor: A clinicopathologic treatise. Perspect Pediatr Pathol 1976; 3:185–223.

(11) Pendergrass TW. Congenital anomalies in children with Wilms' tumor. A new survey. Cancer 1976; 37:403–409.

(12) Beckwith JB, Palmer NF. Histopathology and prognosis of Wilms' tumor. Results from the first National Wilms' Tumor Study. Cancer 1978; 41:1937–1948.

(13) D'Angio GJ, Evans AE, Breslow N, et al. The treatment of Wilms' tumor. Results of the National Wilms' Tumor Study. Cancer 1976; 38:633–646.

(14) D'Angio GJ, Evans AE, Breslow N, et al. The treatment of Wilms' tumor: Results of the second National Wilms' Tumor Study. Cancer 1981; 47:2302–2311.

(15) Beckwith JB. Macroglossia, omphalocele, adrenal cytomegaly, gigantism and hyperplastic visceromegaly. In: Bergsma D, McKusick VA, Hall JG, Scott CI, eds. Birth defects: Original article series. New York: Stratton Intercon, Vol 5. 1969:188–196.

(16) Armitage P. Statistical methods in medical research. Oxford: Blackwell, 1971.

(17) Mantel N, Haenszel W. Statistical aspects of the analysis of data from retrospective studies of disease. J Natl Cancer Inst 1959; 22: 719–748.

(18) Farewell VT, Prentice RL. A study of distributional shape in life testing. Technometrics 1977; 19:69–75.

(19) World Health Organization: International classification of diseases. 9th rev. Geneva: WHO, 1978.

(20) Myrianthopoulos NC, Chung CS. Congenital malformations in singletons: Epidemiologic survey. In: Bergsma D, Paul NW, eds. Birth defects: Original article series, Vol 10, No. 11. New York: Stratton Intercon, 1974:1–58.

(21) Felton L. Should intravenous pyelography be a routine procedure for children with cryptorchidism or hypospadias? J Urol 1959; 81: 335–338.

(22) Bond JV. Bilateral Wilms' tumor. Age at diagnosis, associated congenital anomalies and possible pattern of inheritance. Lancet 1975; 2:482–484.

(23) Bove KE, Koffler H, McAdams AJ. Nodular renal blastema. Definition and possible significance. Cancer 1969; 24:323–332.

(24) Knudson AG. Mutation and cancer. Statistical study of retinoblastoma. Proc Natl Acad Sci USA 1971; 68:820–823.

(25) Bonaiti-Pellie ML, Briard-Guillemot J, Feingold J, Frezal J. Mutation theory of carcinogenesis in retinoblastoma. J Natl Cancer Inst 1976; 57:269–276.

(26) Knudson AG, Hethcote HW, Brown BW. Mutation and childhood cancer: A probabilistic model for the incidence of retinoblastoma. Proc Natl Acad Sci USA 1975; 72:5116–5220.

(27) Hethcote HW, Knudson AG. Model for the incidence of embryonal cancer: Application to retinoblastoma. Proc Natl Acad Sci USA 1978; 75:2543–2547.

(28) Knudson AG. Genetics and the child cured of cancer. In: Van Eys J, Sullivan MP, eds. Status of the curability of childhood cancers. New York: Raven Press, 1980:295–305.

(29) Moolgavkar SH, Knudson AG. Mutation and cancer: A model for human carcinogenesis. JNCI 1980; 66:1037–1052.

(30) Meadows AT, Lichtenfeld JL, Koop CE. Wilms' tumor in three children of a woman with congenital hemihypertrophy. N Engl J Med 1974; 293:23–24.

(31) Cordero JF, Li FP, Holmes LB, Gerald PS. Wilms' tumor in five cousins. Pediatrics 1980; 66:716–719.

(32) Matsunaga E. Hereditary retinoblastoma: Delayed mutation or host resistance? Am J Hum Genet 1978; 30:406–424.

(33) Bishop HC, Tefft M, Evans AE, D'Angio GJ. Survival in bilateral Wilms' tumor—review of 30 National Wilms' Tumor Study cases. J Pediatr Surg 1977; 12:631–638.

(34) Green DM, Fine WE, Li FP. The offspring of patients treated for unilateral Wilms' tumor in childhood. Cancer. In press.

(35) Rajfer J. Association between Wilms' tumor and gonadal dysgenesis. J Urol 1981; 125:388–390.

(36) Lemerle J, Tournade M, Gerard-Marchant R, et al. Wilms' tumor: Natural history and prognostic factors. A retrospective study of 248 cases treated at the Institut Gustave-Roussy 1952–1957. Cancer 1976; 37:2557–2566.

(37) Ledlie EM, Mynors LS, Draper GJ, Gorbach PD. Natural history and treatment of Wilms' tumour: An analysis of 335 cases occurring in England and Wales 1962–6. Br Med J 1970; 4:195–200.

(38) Cutler SJ, Young JL Jr, eds. Third National Cancer Survey: Incidence data. Natl Cancer Inst Monogr 1975; 41:1–454.

Growth and Characterization of Childhood Rhabdomyosarcomas as Xenografts[1,2,3]

J. A. Houghton,[4] P. J. Houghton,[4,5] *and* B. L. Webber[6]

ABSTRACT—Eleven surgical specimens of childhood rhabdomyosarcoma (RMS), two bone marrow samples, and cells from ascitic fluid from 1 patient were implanted sc into immune-deprived inbred CBA/CaJ mice. From these, seven lines of RMS were obtained as xenografts, each retaining the histologic characteristics of the tumor of origin and human lactate dehydrogenase isozymes; these represented 6 of the 11 surgical specimens, whereas one line originated from the transplanted cells from ascitic fluid. It was concluded that childhood RMS has a fairly high frequency of heterotransplantability in this system and that such a laboratory model may prove useful in the development of new therapeutic regimens in this disease.—JNCI 1982; 68:437–443.

RMS represents 5–15% of all malignant solid tumors and 4–8% of all malignant diseases in children under 15 years of age (*1–3*). It is the most common soft tissue sarcoma in children (*4–6*) and represents approximately 10% of the solid neoplasms at this institution (*7*).

In children, RMS is a relatively sensitive tumor to treatment with radiation and several chemotherapeutic agents, particularly cyclophosphamide (*8, 9*) dactinomycin (*10, 11*), and vincristine (*12, 13*), although relatively few agents have been evaluated against previously untreated disease (*14*). The prognosis for patients with advanced disease is poor; thus in one study (*15*) only 56% of patients with incomplete resection or with gross residual but nondisseminated disease and only 29% of those with disseminated disease at diagnosis remained in continuous remission. RMS of the peritoneum and extremities have a poor prognosis (*2, 16*). Because of variations in therapeutic protocols according to the stage or site of primary disease, new therapeutic approaches are difficult to evaluate. Accordingly, an appropriate laboratory model of childhood RMS would afford the opportunity to evaluate, under carefully controlled experimental conditions, new therapeutic regimens in both untreated and drug-resistant forms of RMS. Xenografts of various human cancer types retain many characteristics of the tumor of origin (*17–19*), including chemosensitivity associated with the human disease (*20–23*), and in specific instances show similar responses to those determined in the particular tumor of origin (*24, 25*). The current study demonstrates the growth and characteristics of a series of childhood RMS xenografts, established directly from patient specimens, in mice immune deprived by infant thymectomy and irradiation.

MATERIALS AND METHODS

CBA/CaJ inbred female mice were immune deprived by the technique of infant thymectomy (in 4-wk-old mice), followed 3 weeks later by whole-body irradiation (850 rad; Varian 4 MeV linear accelerator). Within 4 hours of irradiation, each mouse received iv injections of 2.5×10^6 bone marrow cells derived from thymectomized syngeneic mice (*17*). Mice were used for the implantation of neoplastic tissue 2 weeks after the transplantation of murine bone marrow.

Specimens of human RMS were obtained from surgery, needle biopsy, bone marrow aspirate, or peritoneal washout; these specimens were implanted sc into the dorsal flanks of mice, the number of mice used being dependent on the size of the specimen. In general, 2- to 4-mm^3 pieces of tumor were implanted. The incision wound was irrigated with a solution containing penicillin (20,000 U/ml) and streptomycin (20 mg/ml). All procedures were done in a type B laminar flow hood. Mice were caged in an air-conditioned room (26–28°C) lighted for 12 hours each day. Cages, litter, and food (Purina #5010, autoclavable) were sterilized, and mice were placed in fresh cages twice weekly.

We assessed the growth of tumors by measuring two perpendicular diameters at 7-day intervals. As tumor shape approximated that of a sphere, tumor volumes were calculated with the use of the formula $(\pi/6)\times d^3$, where d is the mean diameter (*26*). Tumors were serially passaged when they had grown to 2–3 cm in diameter. Glycogen and collagen contents were estimated histochemically by standard procedures.

Isozymes of LDH were separated by electrophoresis as previously described (*17*). Tumors were rapidly excised and pieces (>100 mg) were stored in liquid nitrogen until analysis. Mouse and human isozymes were separated by flat bed electrophoresis (200 V, 95 min, 2°C) on cellogel analytical strips (Kalex Scientific Co., Manhasset, N.Y.).

Data presented are from tumors between passage #2 and 7 in mice.

RESULTS

Eleven surgical specimens of RMS, two bone marrow samples, and cells from ascitic fluid of 1 patient were

---

Abbreviations used: H & E=hematoxylin and eosin; LDH=lactate dehydrogenase; RMS=rhabdomyosarcoma(s); T^-B^+=depleted for T-cells and positive for B-cells; TD_2=volume doubling time(s).

---

[1] Received July 13, 1981; accepted October 9, 1981.

[2] Supported by a Willie Mae Darwin Memorial grant, CH-156, from the American Cancer Society and by Algerian Lebanese Syrian Associated Charities.

[3] Research procedures on human experimentation were in accord with the ethical standards of the Clinical Trials of St. Jude Children's Research Hospital. Guidelines for the care and use of laboratory animals were followed as set forth by St. Jude Children's Research Hospital.

[4] Division of Biochemical and Clinical Pharmacology, St. Jude Children's Research Hospital, 332 North Lauderdale, Memphis, Tenn. 38101.

[5] *Address reprint requests to* Dr. P. J. Houghton.

[6] Division of Pathology, St. Jude Children's Research Hospital.

implanted into immune-deprived (T⁻B⁺) mice. Generally, only a few mice received implants due to the small size of the specimen. Six lines of RMS have been established as xenografts from specimens of solid tumor, and one line from ascites cells. No tumors grew from the two bone marrow samples (table 1).

Histology

We have attempted to compare human tumors with their corresponding xenografts with respect to growth pattern (embryonal or alveolar), cell differentiation, cross-striations, and glycogen. Results are summarized in table 2. In no case were major differences noted histologically between the human tumor and the xenograft. The human tumor and xenograft in cases HxRh7 and HxRh10 were essentially identical. Human tumor MS showed more tumor necrosis and slightly better differentiation (lower nucleus-cytoplasmic ratio) than in the xenograft (HxRh8). Focal areas in the human tumor showed an alveolar pattern with loss of cohesion of individual cells. The xenograft showed similar nesting of the cells but no loss of cohesion. The HxRh18 tumors were very similar. A relatively small amount of xenograft material was available for study, and the human tumor did show slightly more collagen than did the xenograft in degenerate areas. A few foci showed an alveolar pattern in the human tumor; this pattern was not seen in the xenograft. Both human tumor RK and xenograft HxRh12 showed good muscle differentiation (fig. 1), cross-striations being demonstrated in both the human and xenograft material. The only minor differences noted were apparently slightly better muscle differentiation in the human tumor, whereas the xenograft showed more spindle-shaped cells than did the human tumor. The sample from 1 patient (tumor RJ) had a more nested pattern than did that of the xenograft, and the xenograft had a looser, more myxoid appearance than did the human tumor; both contained demonstrable cross-striations (fig. 1). HxRh6 was difficult to compare because of the scanty material available in the human biopsy specimen. The xenograft showed necrosis, calcification, and deposition of DNA in vessel walls (as determined by Feulgen stain), none of which was noted in the human biopsy specimen. In essentially all cases, the human biopsy specimens and xenografts were remarkably similar histologically and the differences described were very minor. Each tumor line growing in mice produced human-specific LDH isozymes, indicating the presence of the human genome (fig. 2).

Growth Characteristics

The growth rate of tumors growing as xenografts was determined usually on passage #2, when sufficient numbers of tumors were available. TD_2 ranged from 7 to 20 days for individual lines (table 3), although some variation was noted

TABLE 1.—*Surgical specimens of RMS and growth as xenografts*

Sample	Tumor site	No. of mice	No. of pieces implanted[a]	No. of tumors
HxRh1	Orbit	1	2	0
HxRh3	Lung	2	4	0
HxRh4	Breast	1	1	0
HxRh6	Ascites	13	—	1
HxRh7	Bladder	14	28	5
HxRh8	Groin	1	1	1
HxRh9	Nose	6	12	0
HxRh10	Perineum	7	14	4
HxRh12	Buttock	4	8	3
HxRh13	Abdominal wall	1	1	0
HxRh14	Inguinal region	5	10	3
HxRh15	Marrow	1	—	0
HxRh16	Marrow	3	—	0
HxRh18	Perineum	3	6	3

[a] Implanted as cell suspension: —.

TABLE 2.—*Histologic comparison of human tumors and their corresponding xenografts*[a]

Human tumor compared to corresponding xenograft	Tumor pattern	Tumor differentiation	Collagen	Glycogen	Necrosis
Human RRJ	Embryonal with solid nesting	Poor	ND	+++	++
Xenograft HxRh6	Embryonal with solid nesting	Poor	++	+++	++
Human ED	Embryonal	Poor	+++	+++	+
Xenograft HxRh7	Embryonal	Poor	+++	+++	+
Human MS	Alveolar plus embryonal	Fair	+	+++	++
Xenograft HxRh8	Alveolar but without loss of cohesion	Poor	±	+++	–
Human EK	Embryonal	Poor	+	+++	+
Xenograft HxRh10	Embryonal	Poor	+	+++	+
Human RK	Embryonal	Quite good; cross-striations	±	+++	+++
Xenograft HxRh12	Embryonal, more spindled	Quite good; cross-striations	±	+++	+++
Human RJ	Embryonal plus alveolar	Good; cross-striations	++	+++	–
Xenograft HxRh14	Embryonal plus less alveolar	Good; cross-striations	++	+++	–
Human AP	Embryonal plus small amount of alveolar	Moderate	++	+++	++
Xenograft HxRh18	Embryonal	Moderate	+	+++	++

[a] ND = not determined due to poor specimen; +++ = abundant, ++ = moderate, + = slight, ± = occasional, – = absent.

in the rate of growth between xenografts of the same line growing in different host mice. Growth rates of these tumors in mice did not correlate with the degree of tumor cell differentiation; for example, HxRh6, derived from ascites cells, grew most slowly but was poorly differentiated, whereas the moderately differentiated HxRh18 line grew most rapidly. Growth curves for individual tumors are shown in text-figure 1. The growth pattern approximated to logarithmic rather than to Gompertz' growth (i.e., increasing TD_2 with time), as has been observed in xenografts established from human colorectal adenocarcinomas (*26*).

DISCUSSION

The growth of a human RMS cell line in heterologous hosts, with the use of transplantation into fetal and newborn kittens (intracerebrally) (*27*), into cogenitally athymic mice (*28*), or into mice and hamsters treated with antithymocyte serum (*29*, *30*) has been reported. Our present study demonstrated that RMS tissue obtained at surgery may be transplanted directly into mice T^-B^+ with a high frequency of subsequent tumor development. Considering the limited material available (5–100 mg), rates of takes were high. Six xenograft lines were established, with the use of material derived from 11 human tumors (solid). In 1 case, HxRh8, the line was established from a single implant. Each tumor line established directly from patient samples has proved transplantable into subsequent hosts for periods from 14 to 20 months. During this time no significant changes in growth rate, histology, or transplantability have been observed. Successful grafts were not obtained from bone marrow samples, which is not surprising, since this material may have contained only a few tumor cells, whereas normal cells in the marrow may have induced a T-cell-independent rejection in the host T^-B^+ (*31*). Alternatively, the failure to grow tumor from bone marrow samples may be a result of transplantation into only 4 mice. The 1 sample from ascitic fluid, HxRh6, proved transplantable; however, sc inoculation may not have been the optimal route and injection of such a sample into the leg muscle may prove to be desirable, wherein the ascites cells might be more localized.

Each of the xenografts produced human-specific LDH, indicating retention of the human genome, and each line retained the histologic integrity of its tumor of origin during the period studied. Only HxRh12 and HxRh14 demonstrated cross-striations under the light microscope, as did the original tumors. Subtle differences between xenografts and their human tumors were observed, although the significance of these differences is not known; for instance, the xenograft HxRh8 was less differentiated than its tumor of origin, although it still possessed a similar alveolar pattern. In HxRh6 xenografts established from ascites cells, necrosis, calcification, and deposition of DNA in vessel walls were observed, but these were not present in the specimen of the human primary tumor which, however, was regarded as being of poor quality. Consequently, these observed differences may reflect sampling variation.

TABLE 3.—*TD_2 for xenografts growing at the subcutaneous site*[a]

Tumor line	Passage No.	TD_2, days ± 1 SD
HxRh6	2	19.8±2.3
HxRh7	3	15.9±5.9
HxRh8	3	10.8±3.1
HxRh10	2	12.0±4.3
HxRh12	2	12.5±4.6
HxRh14	2	10.2±2.5
HxRh18	2	7.2±1.5

[a] Tumor fragments were implanted sc, and diameters were measured at 7-day intervals as soon as the tumors became palpable. TD_2 values were calculated during the initial two volume doublings.

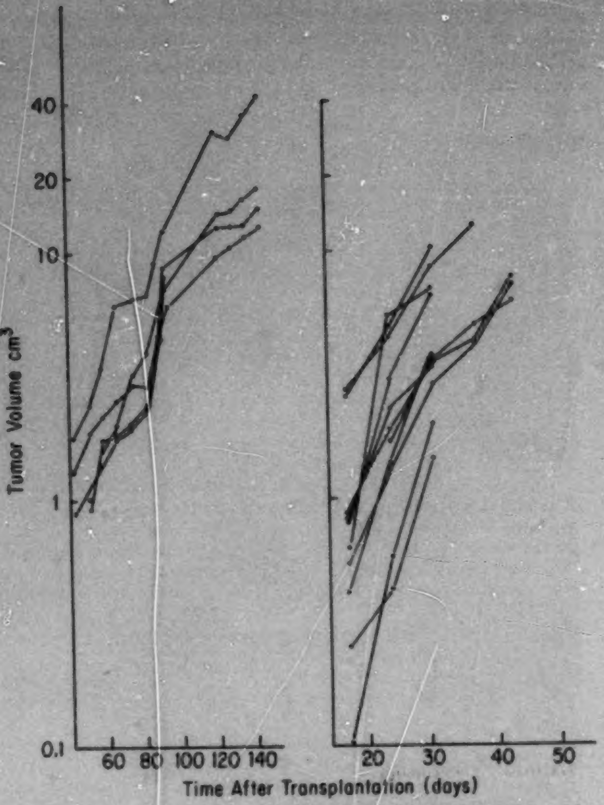

TEXT-FIGURE 1.—Growth curves for HxRh6 (*left*) and HxRh18 (*right*) growing subcutaneously in immune-deprived mice.

Whether these xenografts retain the chemosensitivity associated with RMS as a disease or more specifically correlate with the drug responsiveness of the tumor of origin remains to be elucidated. Initial results do indicate that RMS xenografts retain the chemosensitivity associated with the clinical disease. The clinically effective agents, vincristine, cyclophosphamide, dactinomycin and doxorubicin, have each shown significant activity in 1 or more xenograft lines (*32*, *33*). Detailed chemosensitivity of RMS xenografts will be seen in (*33*). The present study has shown that the growth of RMS xenografts is progressive, often with relatively slow TD_2, in the order of 12 days. Each tumor line remains serially transplantable 14–20 months after initial implantation of the human material and retains histologic characteristics of the human tumor. This laboratory model of childhood RMS could prove to be of value, because new classes of agents and many known anticancer drugs, in addition to compounds that have not received evaluation against previously untreated RMS in children, may be examined relatively rapidly in xenografted mice.

REFERENCES

(*1*) Maurer HM, Moon T, Donaldson M, et al. The intergroup rhabdomyosarcoma study. A preliminary report. Cancer 1977; 40:2015-2026.

(*2*) Sutow WW, Sullivan MP, Reid HL, Taylor HG, Griffith KM. Prognosis in childhood rhabdomyosarcoma. Cancer 1970; 25:1385-1390.

(*3*) Young JL, Miller RW. Incidence of malignant tumors in U.S. children. J Pediatr 1975; 86:254-258.

(*4*) Enzinger FM, Shiraki M. Alveolar rhabdomyosarcoma. An analysis of 110 cases. Cancer 1969; 24:18-31.

(*5*) Pinkel D, Pickren J. Rhabdomyosarcoma in children. JAMA 1961; 175:293-298.

(*6*) Heyn RM. The role of chemotherapy in the management of soft tissue sarcomas. Cancer 1975; 35:921-924.

(*7*) Ransom JL, Pratt CB, Shanks E. Childhood rhabdomyosarcoma of the extremity: Results of combined modality therapy. Cancer 1977; 40:2810-2816.

(*8*) Haddy TB, Nora AH, Sutow WW, Vietti TJ. Cyclophosphamide treatment for metastatic soft tissue sarcoma (intermittent large doses in the treatment of children). Am J Dis Child 1967; 114:301-308.

(*9*) Pinkel D. Cyclophosphamide in children with cancer. Preliminary report. Pediatrics 1959; 23:342-347.

(*10*) Farber S, D'Angio G, Evans A, Mitus A. Clinical studies of actinomycin D with special reference to Wilms' tumor in children. Ann NY Acad Sci 1960; 89:421-424.

(*11*) Tan CT, Dargeon HW, Burchenal JH. Effect of actinomycin D in childhood cancer. Pediatrics 1969; 24:544-561.

(*12*) James DH, George P. Vincristine in children with malignant solid tumors. J Pediatr 1964; 64:534-541.

(*13*) Selawry OS, Hananian J. Vincristine treatment of cancer in children. JAMA 1963; 183:741-746.

(*14*) Green DM, Jaffe N. Progress and controversy in the treatment of childhood rhabdomyosarcoma. Cancer Treat Rev 1978; 5:7-27.

(*15*) Maurer HM. Rhabdomyosarcoma. Pediatr Ann 1979; 8:35-48.

(*16*) Ransom JL, Pratt CB, Hustu HO, Kumar AP, Howarth CB, Bowles D. Retroperitoneal rhabdomyosarcoma in children. Results of multimodality therapy. Cancer 1980; 45:845-850.

(*17*) Houghton JA, Taylor DM. Maintenance of biological and biochemical characteristics of human colorectal tumours during serial passage in immune-deprived mice. Br J Cancer 1978; 37:199-212.

(*18*) Bailey MJ, Ormerod MG, Imrie SF, et al. Comparative functional histopathology of human breast carcinoma xenografts. Br J Cancer 1981; 43:125-134.

(*19*) Povlsen CO, Rygaard J. Heterotransplantation of human epidermoid carcinomas to the mouse mutant "nude." Acta Pathol Microbiol Scand [A] 1972; 80:713-717.

(*20*) Bailey MJ, Gazet J-C, Smith IE, Steel GG. Chemotherapy of human breast-carcinoma xenografts. Br J Cancer 1980; 42:530-536.

(*21*) Giulani FC, Zirvi KA, Kaplan NO, Goldin A. Chemotherapy of human colorectal xenografts in athymic mice with clinically active agents: 5-Fluorouracil and 1-3-bis-(-2-chloroethyl)-1-nitrosurea (BCNU). Comparison with doxorubicin derivatives: 4'-Deoxydoxorubicin and 4'-*O*-methyldoxorubicin. Int J Cancer 1981; 27:5-13.

(*22*) Goldin A, Venditti JM, Macdonald JS, Muggia FM, Henney JE, De Vita VT. Current results of the screening program of the Division of Cancer Treatment, National Cancer Institute. Eur J Cancer 1981; 17:129-142.

(*23*) Houghton PJ, Houghton JA. Evaluation of single-agent therapy in human colorectal tumour xenografts. Br J Cancer 1978; 37:833-840.

(*24*) Shorthouse AJ, Peckham MJ, Smyth JF, Steel GG. The therapeutic response of bronchial carcinoma xenografts: A direct patient-xenograft comparison. Br J Cancer 1980; 41 (suppl IV):142-145.

(*25*) Fujita M, Taguchi T. Comparison between the chemotherapy on human cancer xenografts in nude mice and the clinical response observed in their donor patients. In: Proceedings of the Third International Workshop on Nude Mice. New York: Gustav Fischer. In press.

(*26*) Houghton JA, Taylor DM. Growth characteristics of human colorectal tumours during serial passage in immune-deprived mice. Br J Cancer 1978; 37:213-223.

(*27*) Gardner MB, Johnson EY, Rasheed S, McAllister RM. Intracerebral transplantation of human rhabdomyosarcoma cells into fetal and newborn kittens. Int J Cancer 1973; 12:563-567.

(*28*) Gershwin ME, Ikeda RM, Kawakami TG, Owens RB. Immunobiology of heterotransplanted human tumors in nude mice. J Natl Cancer Inst 1977; 58:1455-1460.

(*29*) Todaro GJ, Arstein P, Parks WP, Lenette EH, Huebner RJ. A type C virus in human rhabdomyosarcoma cells after inoculation into NIH Swiss mice treated with antithymocyte serum. Proc Natl Acad Sci USA 1973; 70:859-862.

(*30*) McAllister RM, Isaacs H, Gardner MB, Klement V. Transplantation of human rhabdomyosarcoma cells in heterogous hosts' tumors formed and viruses recovered. Bibl Haematol 1975; 40:659-662.

(*31*) Cudkowicz G. Rejection of bone marrow allografts by irradiated athymic nude mice. Proc Am Assoc Cancer Res 1975; 16:170.

(*32*) Houghton PJ, Houghton JA, Brodeur GM, Green AA. Characterization, chemosensitivity and drug resistance in xenografts of human childhood rhabdomyosarcoma (RMS). Proc Am Assoc Cancer Res 1981; 22:245.

(*33*) Houghton JA, Houghton PJ, Green AA. Chemotherapy of childhood rhabdomyosarcoma growing as xenografts in immune-deprived mice. Cancer Res. In press.

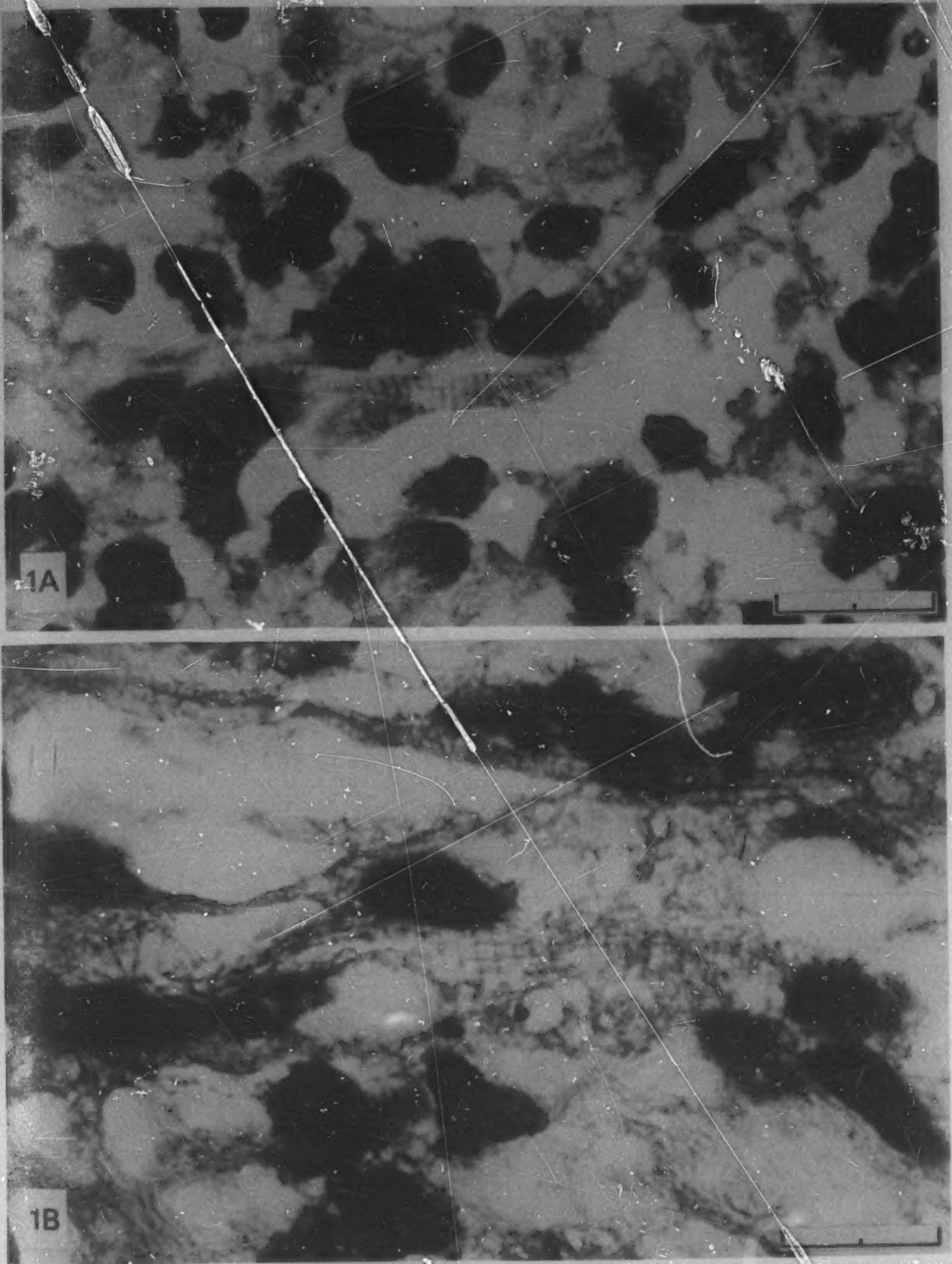

FIGURE 1.—A) Human tumor RK. B) Corresponding xenograft HxRh12. Both demonstrate cross-striations. H & E. *Bar*= 20 μm. × 1,380

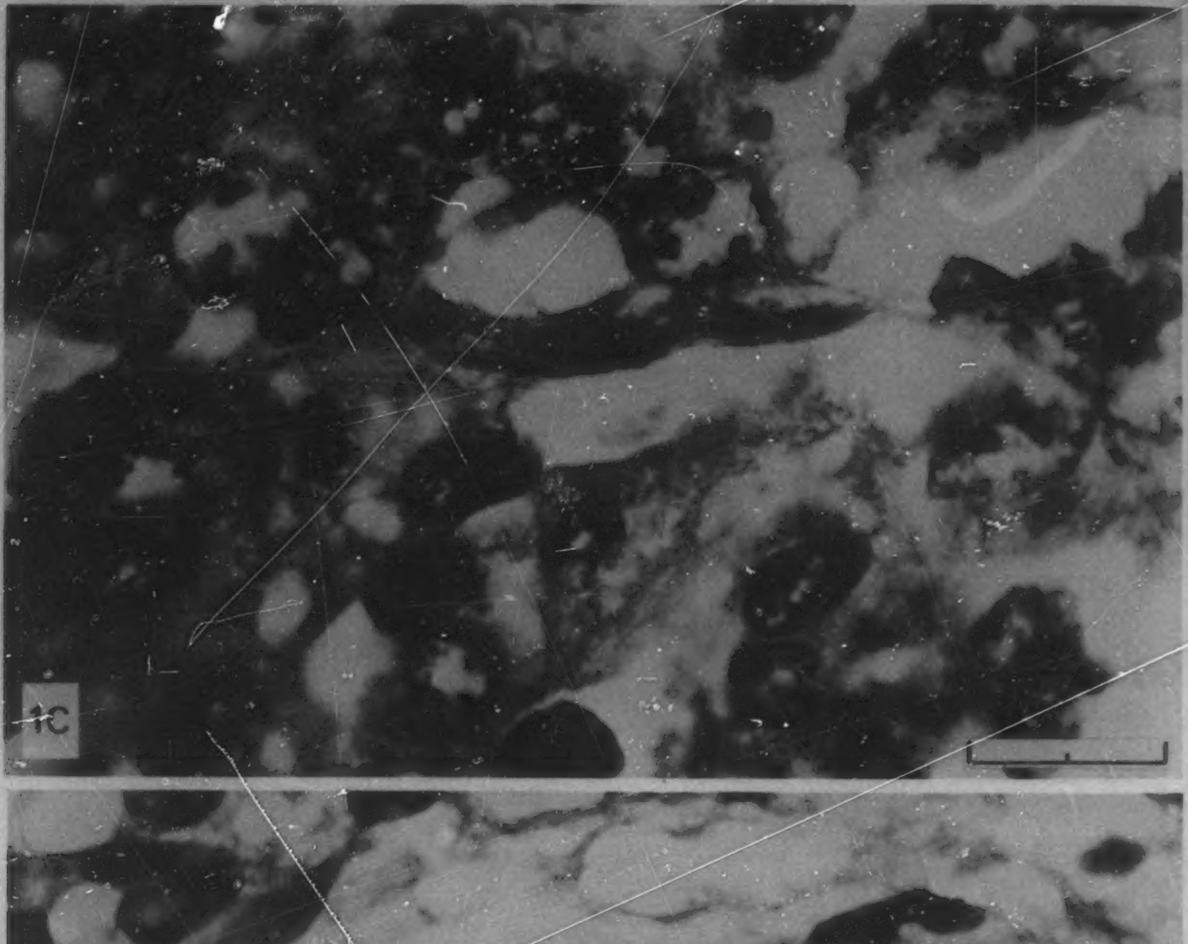

FIGURE 1.—C) Human tumor RJ with cross-striations. D) Corresponding xenograft HxRh14 with a giant cell. Both exhibit cross-striations. H & E. Bar=20 µm. × 1,380

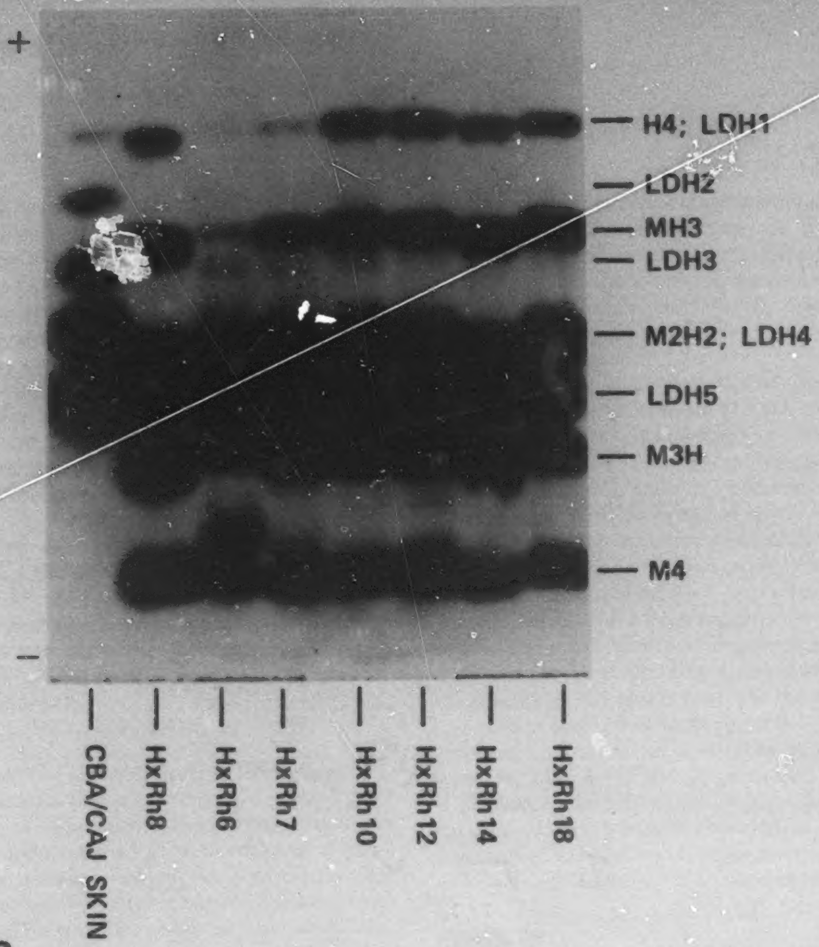
+
−
H4; LDH1
LDH2
MH3
LDH3
M2H2; LDH4
LDH5
M3H
M4
CBA/CAJ SKIN
HxRh8
HxRh6
HxRh7
HxRh10
HxRh12
HxRh14
HxRh18

2

FIGURE 2.—Separation of mouse-specific and human-specific isozymes of LDH by electrophoresis. Mouse isozymes are designated LDH 1–5 and human isozymes, H4–M4. Each line of xenograft demonstrated human-specific LDH isozymes. CBA/CaJ mouse skin (*lane 1*) was used to represent the murine pattern.

blank page

Intrastage Prognostic Heterogeneity: Implications for Adjuvant Chemotherapy of Breast Cancer[1,2]

Maurice M. Black, *M.D.*,[3] **Benjamin F. Hankey**, *Sc.D.*,[4] *and* **Thomas H. C. Barclay**, *M.D.*[5]

ABSTRACT—The precise role of the use of adjuvant chemotherapy in the treatment of primary breast cancer has been questioned by some clinicians. One of the most important questions regarding the use of adjuvant chemotherapy is the identification of appropriate patients to receive it. The presence of positive axillary nodes has been the determining factor for the evaluation of chemotherapy in clinical trials. The possibility that other factors should be considered in deciding on the routine use of chemotherapy is discussed here on the basis of data from breast cancer patients diagnosed in the Province of Saskatchewan, Canada, none of whom received chemotherapy as part of their primary treatment. The data illustrate the prognostic heterogeneity that exists among patients with negative axillary nodes and among patients with positive axillary nodes. The implications of such heterogeneity include the possibilities that some patients may not benefit from adjunctive chemotherapy and that some may actually be harmed by it. Specific procedures are described for the analysis of existing clinical trial data to determine whether there is any evidence that some patients may not have benefited from adjunctive chemotherapy. Additional clinical trials would have to be done to substantiate such observations.—JNCI 1982; 68:445–447.

A recent editorial in The Lancet (April 4, 1981) regarding adjuvant chemotherapy for breast cancer patients concluded that "the precise role of adjuvant chemotherapy remains in doubt; adjuvant chemotherapy is still an experimental treatment, and should be confined largely to controlled trials designed to show what sort of patients benefit, for how long, and at what price." The need for more precise prognostic characterization of breast cancer patients selected for adjuvant chemotherapy was also addressed by Packard, et al. (*1*) in 1977 and before that by Black and coworkers (*2–4*). These studies suggested that prognostic heterogeneity was still present among patients grouped according to node involvement. Axillary node involvement is currently the primary determinant of whether or not adjunctive chemotherapy is part of a patient's treatment regimen. This report presents a reanalysis of data previously reported (*4*) in an attempt to further illustrate the prognostic heterogeneity within breast cancer patients grouped by node status. Also, statistical procedures are discussed which, if applied to existing clinical trial data, could lead to further refinement of the identification of breast cancer patients who should receive adjuvant chemotherapy.

MATERIALS AND METHODS

The data analyzed here have been described previously (*4*). The data were obtained from 333 patients with operable invasive breast cancer for whom tumor and lymph node slides were available and who were diagnosed in 1946, 1951, 1960, or 1968 in one of two breast cancer clinics serving the Province of Saskatchewan, Canada. The previous report (*4*) referred to 348 patients; however, those patients who did not undergo radical mastectomy were excluded. None of the patients received chemotherapy as part of their primary treatment. Follow-up on these patients extended into 1972. Various clinical data were obtained for all patients and the slides for each tumor were read by one of us (M. M. B.) for purposes of rediagnosis and determination of various histologic characteristics.

The histologic characteristics of the tumor included NG and the presence or absence of LRE response to the tumor. A LRE response was defined as the presence of either specified amounts of periductal lymphoid infiltrate, or perivenous lymphoid cellular infiltrate associated with the ducts, or specified amounts of lymphoid infiltrate, or perivenous lymphoid infiltrate associated with the invasive tumor. The presence of one or more of these four factors was taken as evidence of an LRE response. Detailed descriptions of these factors have been reported previously (*2–5*).

The statistical methods employed in the analysis of the data included the life table method of computing observed survival rates (*6*) and a multiple regression model referred to as the proportional hazards model (7) for simultaneously assessing the effects of a number of prognostic factors on survival. The use of the proportional hazards model made it possible to attach statistical significance to the effect on survival of each variable included in the model, by testing whether or not the value of its associated regression coefficient was consistent with a value of zero.

RESULTS

Since the patients included in this analysis were diagnosed and treated prior to the use of chemotherapy in the treatment of patients with regional lymph node involvement, they are of particular value in illustrating prognostic heterogeneity with respect to lymph node status in the absence of any effect of chemotherapy. Prognostic heterogeneity by lymph node status is illustrated in table 1. The patients were classified by number of positive nodes, (0, 1–3, ≥4), NG (I, II, or III) of their primary tumor, and whether there was an

---

ABBREVIATIONS USED: LRE=lymphoreticuloendothelial; NG=nuclear grade.

---

[1] Received August 13, 1981; accepted November 2, 1981.

[2] Supported by Public Health Service contract N01-CP-33321 from the Field Studies and Statistics Program, National Cancer Institute.

[3] Institute of Breast Diseases, Macy Pavilion, Suite 1039, Westchester County Medical Center, Valhalla, N.Y. 10595.

[4] Biometry Branch, Field Studies and Statistics Program, National Cancer Institute, National Institutes of Health, Public Health Service, U.S. Department of Health and Human Services, Bethesda, MD. 20205.

[5] University Hospital, Saskatoon, Saskatchewan, Canada.

LRE response to the tumor. For negative-node patients, the best survival was associated with NG=III, LRE-positive tumors, and the worst survival was associated with NG=I, LRE-negative tumors. For patients with positive nodes a similar relationship to survival was seen for NG and LRE response and the number of nodes positive was also of prognostic significance. Had data on tumor size been available, such data could have provided further evidence of prognostic heterogeneity by node status.

To determine the statistical significance of these observations, the effects on survival of number of nodes positive, NG, and LRE response were simultaneously assessed with the use of the proportional hazards regression model. The estimated coefficients, their standard errors, and the ratio of the estimated coefficients to their standard errors are given in table 2. Variables for age were also included. The variables were introduced into the model as: $X_1=0$ (NG=I), $X_1=1$ (NG=II), $X_1=2$ (NG=III); $X_2=0$ (LRE-negative), $X_2=1$ (LRE-positive); $X_3=0$ (1–3 nodes positive), $X_3=1$ (≥4 nodes positive); $X_4=1$ (age 45–54 yr), $X_4=0$ (otherwise); $X_5=1$ (age≥55 yr), $X_5=0$ (otherwise).

A review of table 2 indicates that none of the variables included for negative-node patients has regression coefficients significantly different from zero at the 0.05 level of significance. For those patients with positive nodes the coefficients for NG and LRE response are significantly different from zero as is the coefficient for number of nodes positive. The absolute value of the estimated coefficients for NG and LRE response are also larger than those for patients with negative nodes indicating that statistical significance is not due to the slightly larger number of patients with positive nodes.

DISCUSSION

These observations provide some evidence that the variation in survival observed for the positive-node patients is not due to chance variation and would suggest the need to question the propriety of treating patients with an already good prognosis with chemotherapy. Even though NG and LRE response were not statistically significant for negative-node patients, the pattern of the survival rates in table 1 is consistent with some effect of NG and LRE response. If the effects of these variables are really smaller in negative-node patients, as is suggested in table 2, then it would have required a larger number of patients to detect such effects as being significant. If the survival rates for negative-node patients in table 1 are taken as representative of the variation in that patient group, it would appear that negative-node patients with NG=I tumors could possibly benefit from chemotherapy, particularly those with no LRE response.

With the use of data on number of nodes positive, tumor size, NG, and LRE response for patients entered into randomized clinical trials, it might be possible to make some further determination of the types of tumors that respond to chemotherapy. An asssessment of deleterious effects of chemotherapy on certain subgroups of patients might also be possible. Detailed procedures for making such determi-

TABLE 1.—*Observed survival rates by node status, NG, and LRE response*[a]

NG/LRE response	Negative nodes			1–3 positive nodes			≥4 positive nodes		
	No. of patients	3-yr rate	5-yr rate	No. of patients	3-yr rate	5-yr rate	No. of patients	3-yr rate	5-yr rate
I Negative	12	0.50(8)	0.50(6)	15	0.60(10)	0.28(6)	13	0.15(5)	0.15(2)
Positive	33	0.88(30)	0.70(23)	19	0.61(11)	0.61(9)	17	0.52(10)	0.26(3)
II Negative	44	0.93(43)	0.77(30)	40	0.60(28)	0.42(19)	33	0.39(22)	0.25(12)
Positive	25	0.92(24)	0.81(14)	17	0.88(16)	0.88(13)	6	0.50(6)	0.50(3)
III Negative	26	0.85(23)	0.81(20)	8	0.87(8)	0.87(5)	8	0.75(7)	0.61(6)
Positive	12	0.92(11)	0.92(7)	3	1.00(3)	1.00(3)	2	1.00(2)	1.00(1)

[a] No. of patients at risk of dying at beginning of the 3d yr and 5th yr for each rate is in parentheses.

TABLE 2.—*Fits of proportional hazards model for patients with negative nodes and for patients with positive nodes*

Variable	Patients with negative nodes[a]			Patients with positive nodes[b]		
	Estimated regression coefficient	SE	Ratio[c]	Estimated regression coefficient	SE	Ratio[c]
NG	−0.240	0.178	−1.35	−0.564	0.146	−3.87[d]
LRE response	−0.452	0.272	−1.66	−0.632	0.207	−3.05[e]
No. nodes positive	—	—	—	0.608	0.181	3.37[e]
Age 45–54 yr	0.160	0.392	0.41	0.011	0.259	−0.04
Age ≥55 yr	0.379	0.355	1.06	0.189	0.224	0.85

[a] No. of patients=152.

[b] No. of patients=181.

[c] Ratio of the estimated regression coefficient and its SE. This ratio is asymptotically normally distributed with a mean of 0 and a variance of 1 and can be used to test the hypothesis that the associated sample estimate of the regression coefficient is consistent with a population value of 0.

[d] $P<0.001$.

[e] $P<0.005$.

nations from clinical trial data have been described by Byar and Green (*8*). They present statistical methodology including multivariate methods that can be used to identify interactions between the effects of treatment and important prognostic factors. Statistically significant interactions of this type suggest the possibility that the treatment being tested was not the "best" treatment for all patients who received it. They illustrate the use of the methodology by analyzing the data from a clinical trial for patients with stage III or stage IV cancer of the prostate where the treatment being tested was diethylstilbestrol. Their analysis suggested "that young patients with high-grade tumors should have been treated with estrogens, but that older patients with low-grade tumors were harmed by estrogen treatment." They emphasize that such an observation is not definitive, but suggests a hypothesis to be further tested in a clinical trial.

It is important to emphasize that the use of cytotoxic chemotherapeutic agents as adjuvant therapy for breast cancer patients is done under the assumption that acute and chronic morbidity from treatment is justified because of improved recurrence and survival rates. If there is evidence that those patients identified to receive such adjuvant therapy are a prognostically heterogeneous group (as is the case here), then possibly some patients may be unnecessarily treated or even harmed by the treatment even though clinical trials have shown that adjuvant chemotherapy is beneficial for breast cancer patients with positive axillary lymph nodes.

Our primary concern is that the routine use of adjuvant chemotherapy for breast cancer patients with positive nodes may be no more consistent with the biology of the disease than was the routine use of radical mastectomy as the primary treatment for breast cancer. We would hope that an effort will be made to further analyze existing clinical trial data utilizing the previously mentioned procedures (*8*) in an attempt to develop hypotheses that could be tested in future trials. Such studies could further refine the identification of patients who might benefit from adjunctive chemotherapy.

REFERENCES

(*1*) Packard RA, Prosnitz LR, Bobrow SN. Selection of breast cancer patients for adjuvant chemotherapy. JAMA 1977; 233:1034–1038.

(*2*) Black MM. Immunology of cancer. Surg Gynecol Obstet 1959; 109: 105–116.

(*3*) Cutler SJ, Black MM, Goldenberg IS. Prognostic factors in cancer of the female breast. Cancer 1963; 16:1589–1597.

(*4*) Black MM, Barclay TH, Hankey BF. Prognosis in breast cancer utilizing histologic characteristics of the primary tumor. Cancer 1975; 36:2048–2055.

(*5*) Black MM. Immunology of breast cancer: Clinical implications. In: Progress in Clinical Cancer, Vol VI. Ariel IM, ed. New York: Grune, 1975;115–137.

(*6*) Cutler SJ, Ederer F. Maximum utilization of the life table method in analyzing survival. J Chronic Dis 1958; 8:699–712.

(*7*) Cox DR. Regression models and life tables (with discussion). J R Stat Soc (B) 1972; 34:187–220.

(*8*) Byar DP, Green SB. The choice of treatment for cancer patients based on covariate information. Bull Cancer (Paris) 1980; 67:477–490.

blank page

Morphology and Function of Ganglio-*N*-tetraosylceramide-Positive Lymphocyte Mediators of Natural Killer Activity[1,2,3]

Kazuo Shimamura,[4] Sonoko Habu,[4] Hiroyasu Fukui,[4] Akira Akatsuka,[5] Ko Okumura,[6] *and* Norikazu Tamaoki[4,7]

ABSTRACT—More than 90% of nylon wool-passed spleen cells from nude mice reacted with ganglio-*N*-tetraosylceramide (asialo G_{M1}) which eliminated mouse natural killer (NK) cell activity in the presence of complement. The successful enrichment of asialo G_{M1}-positive (asialo G_{M1}^+) cells made possible the demonstration that the number of asialo G_{M1}^+ cells was correlated with NK cell activity as well as with binding frequency to YAC-1 target cells. Morphologically, by light and immunoelectron microscopic examinations, the enriched asialo G_{M1}^+ cells were composed of 90% lymphocytes and 10% large cells with the characteristics of monocytes. However, the asialo G_{M1}^+ lymphocytes (but not the monocytes) bound to the target cells and gave rise to the sequential cytolysis. Although asialo G_{M1}-negative lymphocytes and asialo G_{M1}^+ monocytes were sometimes observed to bind to target cells, cytolytic features of the target cells were not demonstrated. These results strongly suggest that asialo G_{M1}^+ lymphocytes are essential for NK cytolysis by directly binding to target cells.—JNCI 1982; 68:449–455.

We previously reported that cytotoxic treatment with anti-asialo G_{M1} eliminates the NK activity of mouse spleen cells (*1*) and decreases the number of cells reactive with anti-asialo G_{M1} by the indirect immunofluorescence method in vitro as well as in vivo (*2*). Since it was also proved that anti-asialo G_{M1} did not affect T-cell or B-cell function, positive selection of asialo G_{M1}^+ cells allowed us to determine morphologic and functional characteristics of the cell types required for NK cytolysis. Evidence is increasing that NK cells are lymphocytes (*3–5*), whereas the reports are few that monocytes or macrophages are involved in NK cytolysis (*6*). Light and electron microscopic examinations by Roder et al. (*7*) demonstrated that spleen cells that bind to NK-sensitive target cells were lymphocytes.

However, it has not been proved that such lymphocytes express surface antigens such as NK-1 (*8*), Ly-5 (*9*), low Thy-1 (*10, 11*), and Qa-4 and Qa-5 (*12*) for NK cells. In addition, it also remains unclear whether the cells possessing these antigens eventually bind to and directly lyse target cells. Although Tam et al. (*13*) recently reported that NK-1^+ cell populations sorted by a fluorescence-activated cell sorter had increased NK activity as well as increased binding frequency, the detailed features of the binding and lytic process by NK-1^+ cells are still unclear. In this paper, asialo G_{M1}^+ cells from nude mice were enriched by the use of a nylon wool column and then were examined by immunoelectron microscopy to determine whether asialo G_{M1}^+ cells that directly bind to target cells are lymphocytes or some other type of cells. The study reported here, which includes a functional analysis of asialo G_{M1}^+ cells, demonstrated that asialo G_{M1}^+ lymphocytes bind to target cells and thus achieve NK cytolysis.

MATERIALS AND METHODS

Mice.—Nude mice of the BALB/cA background and 8–12 weeks old were obtained from the Central Institute for Experimental Animals, Kawasaki, Japan.

Tumor cells.—YAC-1, a Moloney virus-induced lymphoma in A/Sn mice, was maintained in our laboratory in 10% RPMI-1640.

Enrichment of NK cells.—We prepared the spleen cell suspension by pressing spleens from nude mice between two glass slides in 10% RPMI-1640. Two grams of nylon wool were packed into a 10-ml plastic syringe and moistened with prewarmed (37°C) 10% RPMI-1640. A suspension of 10^9 spleen cells in 10% RPMI-1640 was applied to the column and incubated (37°C, 5% CO_2). After 45 minutes of incubation, the cells were washed from the nylon wool column with 30 ml warm 10% RPMI-1640. The eluate constituted fraction 1. Recovery of the washed-out cells was 2–3% of the applied cells. A subsequent 45-minute incubation of the column was performed, and the second fraction was obtained by washing the column with the same medium (fraction 2).

Fluorescence study on asialo G_{M1}^+ cells.—Indirect staining of the cells with anti-asialo G_{M1} was performed. Rabbit antiserum against asialo G_{M1} was prepared by the method described in the previous paper (*1*). After incubation of 2×10^6 cells with 0.1 ml anti-asialo G_{M1} diluted 1:20 (4°C, 30 min), the cells were washed three times and were stained (4°C, 30 min) with FITC-conjugated goat anti-RIg diluted 1:10. Stained cells were determined under a fluorescence

---

ABBREVIATIONS USED: C=complement; CTL=cytotoxic T-lymphocyte; ER=endoplasmic reticulum (reticula); FITC=fluorescein isothiocyanate; asialo G_{M1}=ganglio-*N*-tetraosylceramide; asialo G_{M1}^+=asialo G_{M1}-positive; asialo G_{M1}^-=asialo G_{M1}-negative; HRPO=horseradish peroxidase; Ia^+=Ia-positive; NK=natural killer; NK-1^+=NK-1-positive; PBS=phosphate-buffered saline; RIg=rabbit immunoglobulin; 10% RPMI-1640=RPMI-1640 medium containing 10% heat-inactivated fetal calf serum and 100 U penicillin–streptomycin/ml.

---

[1] Received March 4, 1981; revised September 1, 1981; accepted October 14, 1981.

[2] Supported in part by a Grant-in-Aid from the Ministry of Education, Science and Culture, the Ministry of Health and Welfare, and by a research contract for the discovery of the factors regulating aging from the Institute of Physical and Chemical Research, Japan.

[3] Animals were maintained under the guidelines of the Central Institute for Experimental Animals as followed by the Department of Pathology, Tokai University School of Medicine.

[4] Department of Pathology, Tokai University School of Medicine, Isehara, Kanagawa, Japan.

[5] Division of Electromicroscopy, Tokai University School of Medicine.

[6] Department of Immunology, Faculty of Medicine, University of Tokyo, Tokyo, Japan.

[7] We are grateful to Mr. M. Tokunaga and Mr. T. Itoh for excellent technical assistance and to Mrs. M. Ohshiba for excellent secretarial assistance.

microscope (Standard IV; Carl Zeiss, Inc., Oberkochen, Federal Republic of Germany).

Immunoelectron microscopic study.—The cells incubated (4°C, 30 min) with pepsin-digested $F(ab')_2$ fragments of anti-asialo G_{M1} were stained (4°C, another 30 min) with $F(ab')_2$ fragments of goat anti-RIg labeled with HRPO by Nakane's method (*14*). After being washed, the cells were fixed for 20 minutes in 2% glutaraldehyde on ice and washed in PBS (pH 7.2) three times. They were incubated (5 min) in Karnovsky's solution (3,3'-diaminobenzidine:4 $HCl-H_2O_2$ solution) at room temperature. After osmium fixation and graded alcohol dehydration, thin sections cut with an LKB-8800 microtome were examined under an electron microscope JEM-100C (JEOL, Tokyo, Japan). We omitted staining some sections with a metal salt to distinguish reaction products from nonspecific density. A control study on the samples treated with normal rabbit serum instead of $F(ab')_2$ fragments of anti-asialo G_{M1} showed no reaction products on the surface of any of the spleen cells.

Determination of asialo G_{M1}^+ large cells.—When stained for anti-asialo G_{M1} by indirect immunofluorescence or enzyme-labeled antibody, the large cells of nylon-passed spleen cells were determined as having diameters of more than 8 μm under a light microscope. Endogenous peroxidase-positive granules were visualized as brown dots and dense granules under light and electron microscopes, respectively, by incubation in Karnovsky's solution after fixation described previously in "Immunoelectron microscopic study."

Target binding assay.—For investigation of the binding of NK cells to target cells, 10^6 spleen cells and 10^5 YAC-1 cells were mixed in 0.2 ml 10% RPMI-1640 and centrifuged at 800 rpm in round-bottomed microtiter plates. After incubation in 5% CO_2 (37°C, 10 min to 4 hr), the cells were pipetted with a micropipette into the microplates and were indirectly stained for anti-asialo G_{M1} by the methods described previously in "Fluorescence study on asialo G_{M1}^+ cells" and "Immunoelectron microscopic study," respectively. When washed by pipetting three times with PBS in the wells, FITC-conjugated cells binding to target cells were counted under a fluorescence microscope. For electron microscopic examination of target-binding cells, the cells stained with peroxidase-labeled $F(ab')_2$ fragments of goat anti-RIg antisera were dropped onto the albumin-coated glass slides and were fixed in 2% glutaraldehyde. The same procedure was performed in the presence of 25 m*M* EDTA, which blocked binding of NK and target cells.

Cytotoxic treatment of spleen cells with anti-asialo G_{M1}.—After 10^7 spleen cells were incubated (37°C, 30 min) with 1:100 diluted anti-asialo G_{M1}/ml, they were washed three times before being incubated (37°C, 30 min) with guinea pig C diluted 1:15. In washed spleen cells, no asialo G_{M1}^+ cells were observed.

Chromium release assay for NK activity.—The procedure used for mixing 10×10^3 target cells, labeled with ^{51}Cr-sodium chromate, with various numbers of spleen cells was the same as that used for the target binding assay, but all incubations were for 4 hours at 37°C in 0.2 ml Microwell plates. At the completion of incubation, radioactivity released from triplicate cultures was measured by a gamma counter. We determined spontaneous release by culturing ^{51}Cr-labeled target cells alone. We determined maximum release by counting 1 ml of the supernatant after ^{51}Cr-labeled target cells were incubated in 2 ml of water. Percent lysis was computed by the following formula (with standard deviation in triplicates being <2% of the mean value): Percent lysis = [(experimental release − spontaneous release)/(maximum release − spontaneous release)]×100.

RESULTS

Since anti-asialo G_{M1} serum was proved to eliminate mouse NK activity in the presence of C (*1, 15*) and there were two types of asialo G_{M1}^+ cells (small and large) in nude mouse spleens observed under the fluorescent microscope, further morphologic studies were performed with immunoelectron microscopy. The asialo G_{M1}^+ cells were clearly identified by the linear localization of reaction products with anti-asialo G_{M1} antibody on the cell surface at both light and electron microscopic levels. By an indirect staining method, in which a peroxidase-labeled second-step antiserum was used, the asialo G_{M1}^+ small cells were identified to be typical mature lymphocytes possessing heterochromatic nuclei and numerous free ribosomes as well as a few rough ER in the cytoplasm (fig. 1). In contrast, asialo G_{M1}^+ large cells showed characteristics of endogenous peroxidase-positive granules in the abundant cytoplasm, well-developed ER, and less prominent nuclear heterochromatin (fig. 2). From these electron microscopic features, asialo G_{M1}^+ small and large cells were proved to be lymphocytes and monocytes, respectively.

To determine which type of cell was really involved in NK activity, we enriched NK cells from nude mouse spleen cells by using a nylon wool column, which is known to enrich NK activity in spleen cells of euthymic mice (*3, 6*). Spleen cells from non-immunized nude mice were incubated in a tightly packed nylon wool column and then eluted by the two-step method described in "Materials and Methods." Of the spleen cells obtained from fraction 1 (the first wash of the nylon wool column and accounting for 2–3% of the total applied cells), almost 90% were stained for anti-asialo G_{M1} (text-fig. 1). As shown, asialo G_{M1}^+ cells of fraction 1 consisted of 90% small cells and 10% large (>8 μm diameter) cells. By immunoelectron microscopic study, these enriched asialo G_{M1}^+ small and large cells were confirmed to be the same morphologically as the cells referred to as lymphocytes and monocytes in untreated spleen cells. Endogenous peroxidase-positive granules were detectable by incubation in Karnovsky's solution, by which antibody labeled with HRPO was visualized (*see* "Materials and Methods"), and the resulting granules were observed in 70% of the large but in less than 5% of the small asialo G_{M1}^+ cells.

Cells eluted as fraction 2 by the second wash performed after a further forty-five-minute incubation contained the same percentage of asialo G_{M1}^+ cells, but the proportion of large cells was increased to 40%. The results of functional studies of NK cells in which these fractions were used are depicted in text-figure 2. Corresponding to the percentage of asialo G_{M1}^+ cells and especially coincident with the proportion of asialo G_{M1}^+ small cells, NK activity was prominently increased in fraction 1. To know further

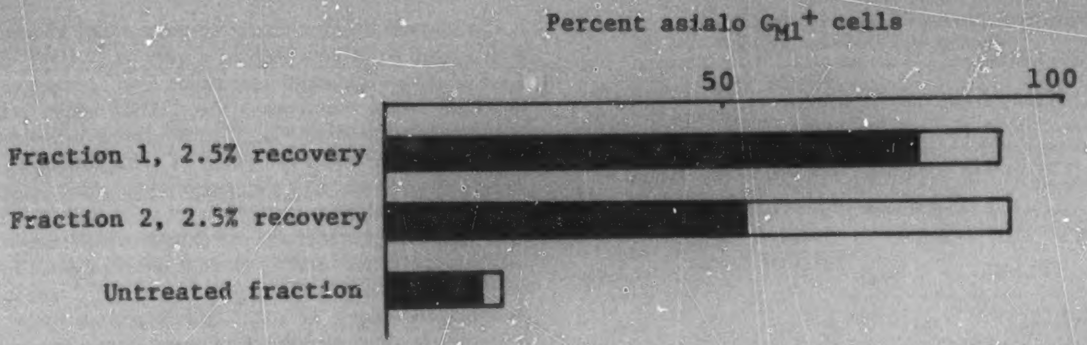

TEXT-FIGURE 1.—Morphologic analysis of asialo G_{M1}^+ cells enriched by use of nylon wool column. The untreated fraction was obtained from spleen cells incubated in medium for 45 min at 37°C and was not applied to a nylon wool column. Fraction 1 was obtained from nude mouse spleen cells as the eluate of the first wash and fraction 2 was obtained by the second wash of the nylon wool column (*see* "Materials and Methods"). The recovery percentage was calculated from the fact that 2.5×10^6 cells were obtained by first and second washings of the column after 10^8 spleen cells were applied. Small (▬) and large (▭) cells were determined as having diameters of less than and more than 8 µm, respectively.

whether the asialo G_{M1}^- cells had a role in NK cytolysis, we performed a quantitative add-back experiment in which cells were passed through nylon wool (fraction 1), and asialo G_{M1}^- cells were obtained by cytotoxic treatment with anti-asialo G_{M1}. As shown in table 1, consistent with our previous observation presented in text-figure 2, the number of asialo G_{M1}^+ small cells was correlated with the NK activity, but adding back asialo G_{M1}^- cells did not have any effect on NK activity.

Since the binding of effector and target cells is required for cytolysis by NK cells (*6, 12*), experiments were performed to determine if asialo G_{M1}^+ lymphocytes bind directly to target cells, with the eventual result of target cell lysis, or if other additional phenotypically distinct cells bind to target cells. As shown in table 2, enriched asialo G_{M1}^+ lymphocytes (fraction 1) were shown to bind to target cells more frequently than to lymphocytes from the untreated cell population, which contained a larger percentage of asialo G_{M1}^- cells. In addition, an immunofluorescence study revealed that the percentage of asialo G_{M1}^+ cells in lymphocytes binding to target cells was also higher in fraction 1. Both the binding frequency and percentage of asialo G_{M1}^+ cells in these binding lymphocytes were correlated with NK activity and were confirmed to be abolished by cytotoxic treatment with anti-asialo G_{M1}. Furthermore, a binding inhibition experiment in which cells were treated with EDTA strongly supported the importance of binding for asialo G_{M1}^+ cells to function as NK cells.

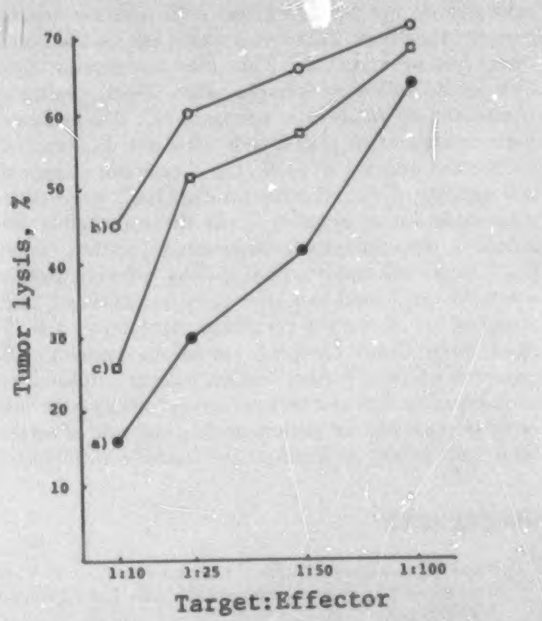

TEXT-FIGURE 2.—NK activity of effector cells from a) untreated cells, b) fraction 1, and c) fraction 2 of nude mice. Effector cells are defined in text-fig. 1.

An immunoelectron microscopic examination, in which $F(ab')_2$ was used for staining anti-asialo G_{M1}, was performed to determine if asialo G_{M1}^+ lymphocytes really bind to target cells. In the first 20-minute incubation of target and nylon

TABLE 1.—*Dependence of NK activity on the number of asialo G_{M1}^+ small cells from nude mouse spleens*

Effector cells, $\times 10^{-4}$			Tumor lysis, %
Total cells[a]	Asialo G_{M1}^+ small cells[b]	Asialo G_{M1}^- cells[c]	
25	25	0	54
25	12.5	12.5	46
25	6	19	37
25	3	22	22
25	0	25	−1
25	25	0	55
35	25	10	57
47	25	22	59
85	25	60	58
100	25	75	59

[a] Total is sum of asialo G_{M1}^+ cells (column 2) and G_{M1}^- cells (column 3).

[b] Asialo G_{M1}^+ small cells referred to in text-fig. 1 were determined for fraction 1, which consisted of 88% asialo G_{M1}^+ cells. *See* "Materials and Methods" for description of fraction 1.

[c] Asialo G_{M1}^- cells were obtained by treatment of nude mouse spleen cells with 1:100 diluted anti-asialo G_{M1} and guinea pig C (1:15). After cytotoxic treatment, no asialo G_{M1}^+ cell was observed.

TABLE 2.—*Relationship between binding of asialo G_{M1}^+ lymphocytes to target cells and NK cytolysis*

Treatment	Percent asialo G_{M1}^+ cells in lymphocytes	Percent tumor lysis at effector:target of:		Percent of cells binding to target cells at effector:target of 10:1	
		10:1	100:1	Lymphocytes[a]	Asialo G_{M1}^+ lymphocytes[b]
Nylon wool column, fraction 1[c]	81	31	68	87	88
Untreated	11	10	38	8	28
Anti-asialo G_{M1} plus C[d]	1	0	0	4	2
EDTA[e]	11	0	0	3	ND

[a] The number of cells in all lymphocytes binding to target cells was counted under a light microscope, and the percentage was calculated.

[b] The number of asialo G_{M1}^+ cells in lymphocytes binding to target cells was counted, and the percentage was calculated.

[c] Fraction 1 was obtained as described in "Materials and Methods."

[d] Asialo G_{M1}^- cells were obtained as mentioned in table 1 and in "Materials and Methods."

[e] Spleen cells were incubated with target cells in 10% RPMI-1640 containing 25 m*M* EDTA at 37°C for 30 min.

wool-passed cells, the asialo G_{M1}^+ cells were found to contact target cells with a broad and penetrating projection of their lymphocyte cytoplasm (fig. 3). After 1–2 hours of incubation with asialo G_{M1}^+ lymphocytes (fig. 4), degeneration of fused target cells was observed in the first hour, and the number of degenerated fused cells increased with time. However, target cells bound to asialo G_{M1}^- lymphocytes, which were occasionally found, remained nondegenerated even after 4 hours of incubation (fig. 5). Although large cells, including both asialo G_{M1}^+ and G_{M1}^- cells, were rarely found tightly bound to target cells, they were found gathered around degenerated dying cells and cell debris. All of the above data suggest that asialo G_{M1}^+ but not asialo G_{M1}^- lymphocytes function as NK cells by directly binding to target cells.

DISCUSSION

Successful isolation of asialo G_{M1}^+ cells from spleens of nude mice enabled us to study the detailed morphologic and functional aspects of target cell cytolysis by NK cells. It was concluded that the number of asialo G_{M1}^+ cells correlates positively with NK activity as well as with the frequency of target cell–effector cell contact. Very recently, other investigators (Beaumont TJ, et al: Personal communication) have indicated that more than 60% of effector cells in contact with target cells were asialo G_{M1}^+. These asialo G_{M1}^+ cells seem to be consistent with the target-binding cells of Roder et al. (*7*) or NK-1$^+$ cells with NK activity isolated by a fluorescence-activated cell sorter (*13*). The essentiality of the binding between NK cells and target cells for NK cell activity was also demonstrated in this study in that cytotoxic treatment of the spleen cell population with anti-asialo G_{M1} drastically reduced the cell–cell binding as well as the NK activity.

Immunoelectron microscopic observation revealed that cells bound to targets both at a very early stage and at a later degenerating stage were asialo G_{M1}^+ lymphocytes but not G_{M1}^- ones. Although a few YAC-1 target cells were found to bind to asialo G_{M1}^- lymphocytes, no degenerating or dying target cells were detected. This functional observation considered with the morphologic observation that the nature of the contact of target cells with asialo G_{M1}^+ and G_{M1}^- lymphocytes did not differ strongly suggests that target and effector binding alone is not always sufficient for target cell lysis in the NK system, although it was sufficient in the CTL system (*16, 17*). While a number of studies regarding binding and the subsequent lytic process of target cells in CTL and NK systems have been reported, the lytic mechanism has not been satisfactorily defined, particularly at the molecular level (*16–19*). Recently, it has been reported that T-cell-mediated and NK-cell-mediated cytolysis were blocked by the addition of anti-Lyt-2 (*20, 21*) and anti-Ly-5 (*9*), respectively. It is likely that the surface antigens function in the two types of cytolysis. We used anti-asialo G_{M1} alone in a blocking experiment, but target cell lysis was not affected (unpublished data). The same result was also reported for anti-NK-1 antiserum (*13*). Asialo G_{M1} expressed on NK cells, therefore, seems unrelated to "recognition" receptors and/or structures for NK lysis.

Anti-asialo G_{M1} was shown to react not only to a subpopulation of lymphocytes but also to less than 10% of nylon wool-passed cells, which we refer to as monocytes because of their morphologic characteristics. The involvement of these asialo G_{M1}^+ monocytes in NK activity could not be ruled out because both asialo G_{M1}^+ lymphocytes and monocytes are simultaneously eliminated by cytotoxic treatment, resulting in abolished NK activity. However, the morphologic observation that asialo G_{M1}^+ monocytes rarely bind to target cells and do not bind to target cells that are degenerating suggests that these monocytes might not be associated with direct lysis of target cells. They may function as "accessory" cells as do Ia$^+$ macrophages when T-cell proliferation is stimulated by antigens or mitogens (*22, 23*); however, cytotoxic treatment of spleen cells with anti-Ia serum did not reduce the number of asialo G_{M1}^+ cells nor reduce the NK cell activity (*24*). Whether asialo G_{M1}^+ large cells are a subpopulation of accessory cells distinguishable from Ia$^+$ accessory cells presents an interesting question. Since asialo G_{M1}^+ large cells are morphologically different from typical macrophages found as a peritoneal exudate cell and characterized by abundant cytoplasm containing a well-developed large Golgi complex, numerous vesicles, ER, and eccentric nucleus, further studies such as combination of or recovery of surface markers and single cell agarose assay will be of importance for understanding the role of asialo G_{M1}^+ large cells as well as macrophage function in NK activity.

REFERENCES

(*1*) KASAI M, IWAMORI M, NAGAI Y, OKUMURA K, TADA T. A glycolipid on the surface of mouse natural killer cells. Eur J Immunol 1980; 10:175–180.

(*2*) KIESSLING R, KLEIN E, PROSS H, WIGZELL H. "Natural" killer cells in the mouse. II. Cytotoxic cells with specificity for mouse Moloney leukemia cells. Characteristics of the killer cell. Eur J Immunol

1975; 5:117–121.

(3) Herberman RB, Nunn ME, Holden HT, Lavrin DH. Natural cytotoxic reactivity of mouse lymphoid cells against syngeneic and allogeneic tumors. II. Characterization of effector cells. Int J Cancer 1975; 16:230–239.

(4) Cantor H, Kasai M, Shen FW, Leclerc JC, Glimcher L. Immunogenetic analysis of "natural killer" activity in the mouse. Immunol Rev 1979; 44:3–12.

(5) Lohmann-Matthes ML, Domzig W, Roder J. Promonocytes have the functional characteristics of natural killer cells. J Immunol 1979; 123:1883–1886

(6) Habu S, Fukui H, Shimamura K, et al. In vivo effects of anti-asialo G_{M1}. 1. Reduction of NK activity and enhancement of transplanted tumor growth in nude mice. J Immunol 1981; 127:34–38.

(7) Roder JC, Kiessling R, Biberfeld P, Andersson B. Target–effector interaction in the natural killer (NK) cell system. II. The isolation of NK cells and studies on the mechanism of killing. J Immunol 1978; 121:2509–2517.

(8) Pollack SB, Tam MR, Nowinski RC, Emmons SL. Presence of T cell-associated surface antigens on murine NK cells. J Immunol 1979; 123:1818–1821.

(9) Kasai M, Leclerc JC, Shen FW, Cantor H. Identification of Ly-5 on the surface of "natural killer" cells in normal and athymic inbred mouse strains. Immunogenetics 1979; 8:153–159.

(10) Herberman RB, Nunn ME, Holden HT. Low density of Thy-1 antigen on mouse effector cells mediating natural cytotoxicity against tumor cells. J Immunol 1978; 121:304–309.

(11) Mattes MJ, Sharrow SO, Herberman RB, Holden HT. Identification and separation of Thy-1 positive mouse spleen cells active in natural cytotoxicity and antibody-dependent cell-mediated cytotoxicity. J Immunol 1979; 123:2851–2860.

(12) Koo GC, Jacobson JB, Hammerling GJ, Hammerling U. Antigenic profile of murine natural killer cells. J Immunol 1980; 125:1003–1006.

(13) Tam MR, Emmons SL, Pollack SB. Analysis and enrichment of murine natural killer cells with the fluorescence-activated cell sorter. J Immunol 1980;124:650–655.

(14) Nakane PK. Recent progress in the peroxidase-labeled antibody method. Ann NY Acad Sci 1975; 254:203–211.

(15) Young WW Jr, Hakomori SI, Durdik JM, Henney CS. Identification of ganglio-*N*-tetraosylceramide as a new cell surface marker for murine natural killer (NK) cells. J Immunol 1980; 124:199–201.

(16) Roder JC, Argov S, Klein M, et al. Target–effector cell interaction in the natural killer cell system. V. Energy requirements, membrane integrity, and the possible involvement of lysosomal enzymes. Immunology 1980; 40:107–116.

(17) Wagner H, Röllinghoff M. T cell-mediated cytotoxicity: Discrimination between antigen recognition, lethal hit and cytolysis phase. Eur J Immunol 1974; 4:745–750.

(18) Zagury D, Bernard J, Jeannersson P, Thiernesse N, Cerottini JC. Studies on the mechanism of T cell-mediated lysis at the single effector cell level. I. Kinetic analysis of lethal hits and target cell lysis in multicellular conjugates. J Immunol 1979; 123:1604–1609.

(19) Grimm E, Bonavida B. Mechanism of cell-mediated cytotoxicity at the single cell level. I. Estimation of cytotoxic T lymphocyte frequency and relative lytic efficiency. J Immunol 1979; 123:2861–2869.

(20) Shinohara N, Sachs DH. Mouse alloantibodies capable of blocking cytotoxic T-cell function. I. Relationship between the antigen reactive with blocking antibodies and the *Lyt-2* locus. J Exp Med 1979; 150:432–444.

(21) Shevach EM. The function of macrophage in antigen recognition by guinea pig T lymphocytes. III. Genetic analysis of the antigens mediating macrophage–T lymphocyte interaction. J Immunol 1976; 116:1482–1489.

(22) Schwartz RH, David CS, Sachs DH, Paul WE. T lymphocyte-enriched murine peritoneal exudate cells. III. Inhibition of antigen-induced T lymphocyte proliferation with anti-Ia antisera. J Immunol 1976; 117:531–540.

(23) Habu S, Raff ME. Accessory cell dependence of lectin-induced proliferation of mouse T lymphocytes. Eur J Immunol 1977; 7:451–457.

(24) Habu S, Hayakawa K, Okumura K, Tada T. Surface markers on natural killer cells of the mouse. Eur J Immunol 1979; 9:938–942.

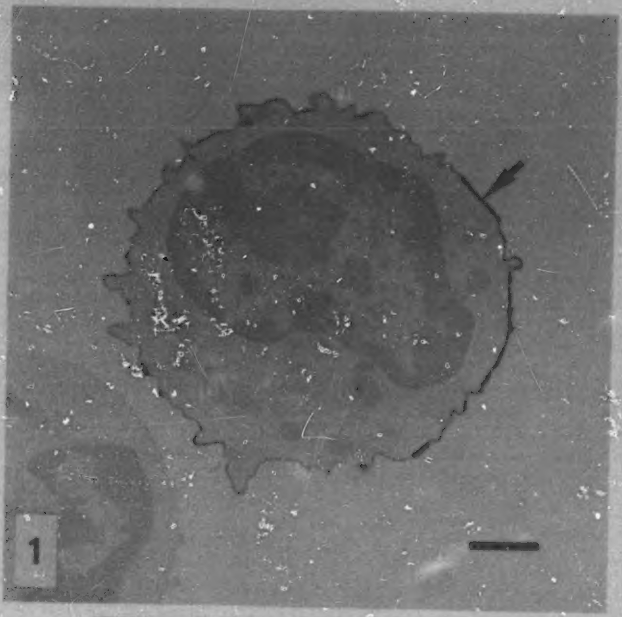

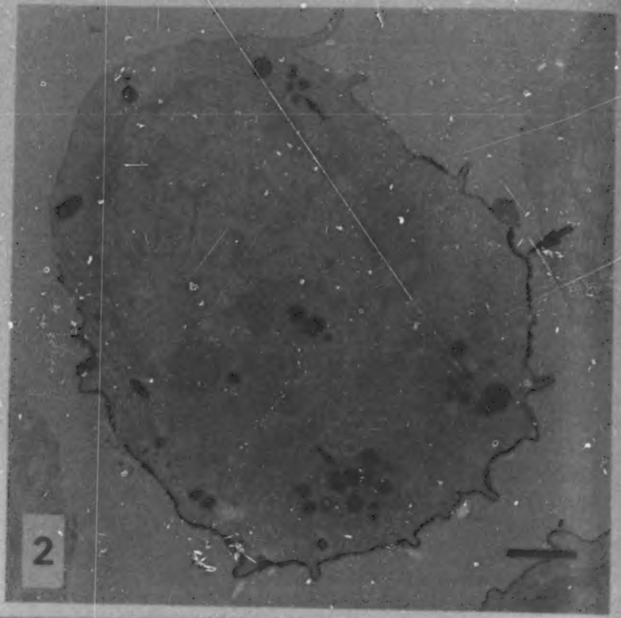

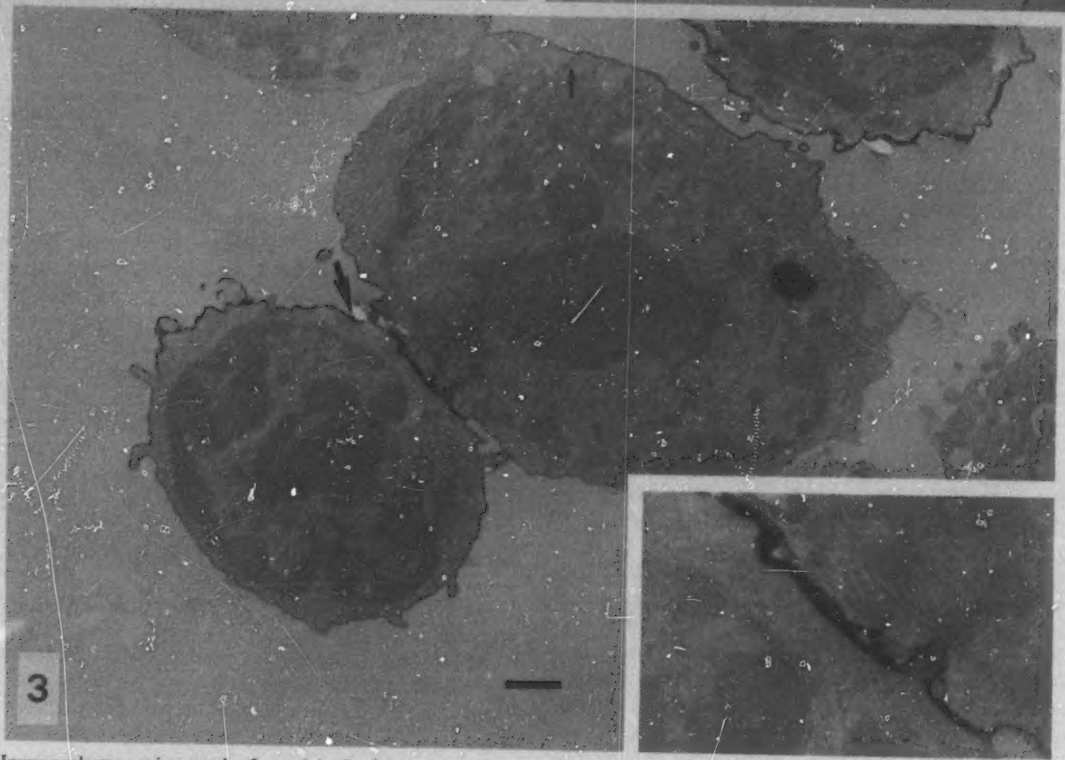

FIGURE 1.—Immunoelectron micrograph of an asialo G_{M1}^{+} lymphocyte. Reaction products with anti-asialo G_{M1} antibody are noted on the surface of the small lymphocyte as dark fine deposits (*single arrow*). Counterstain is omitted. *Bar*=1 µm. × 10,000. FIGURE 2.—Immunoelectron micrograph of an asialo G_{M1}^{+} monocyte. In addition to the specific reaction products with anti-asialo G_{M1} antibody on the cell surface (*large arrow*), cytoplasmic granules are stained for the presence of endogenous peroxidase (*small arrow*). *Bar*=1 µm. × 10,000. FIGURE 3.—Immunoelectron micrograph of a lymphocyte-target cell interaction after 20 min of incubation. The YAC-1 tumor cell (*right*) is distinguishable by the presence of nuclear atypism, fat droplets, and virus particles (*small arrow*) from the effector lymphocyte (*left*) that shows reaction products with anti-asialo G_{M1} antibody on its cell surface (*large arrow*). *Bar*=1 µm. × 9,900. *Inset* shows effector-target cell contact with protrusion of lymphocyte cytoplasm into tumor. × 30,000

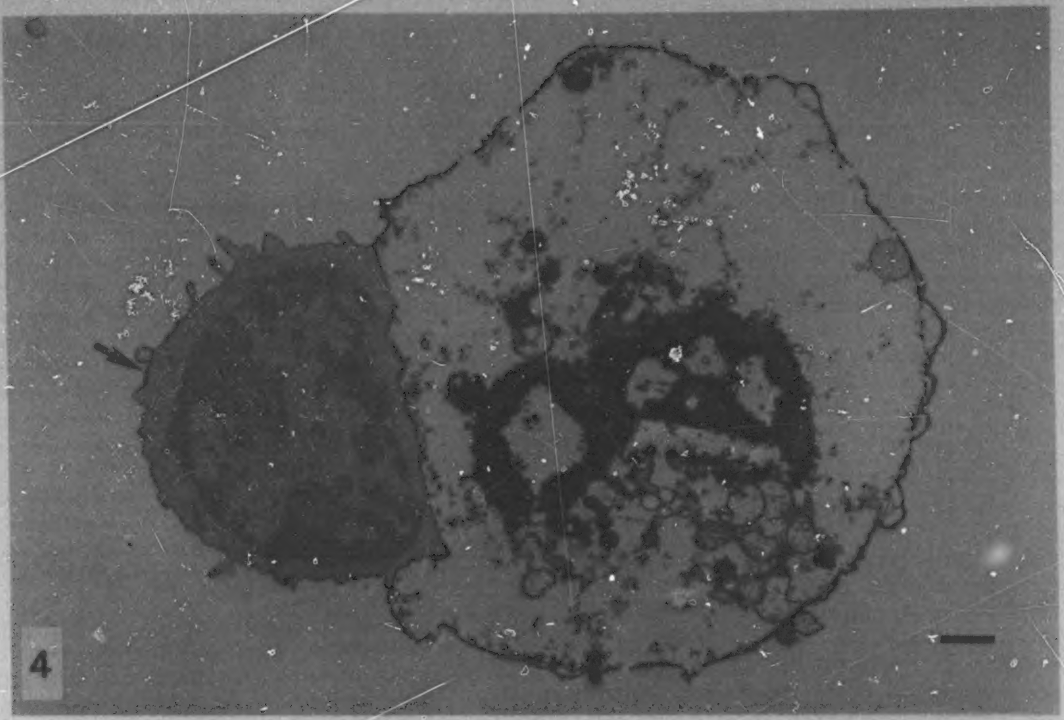

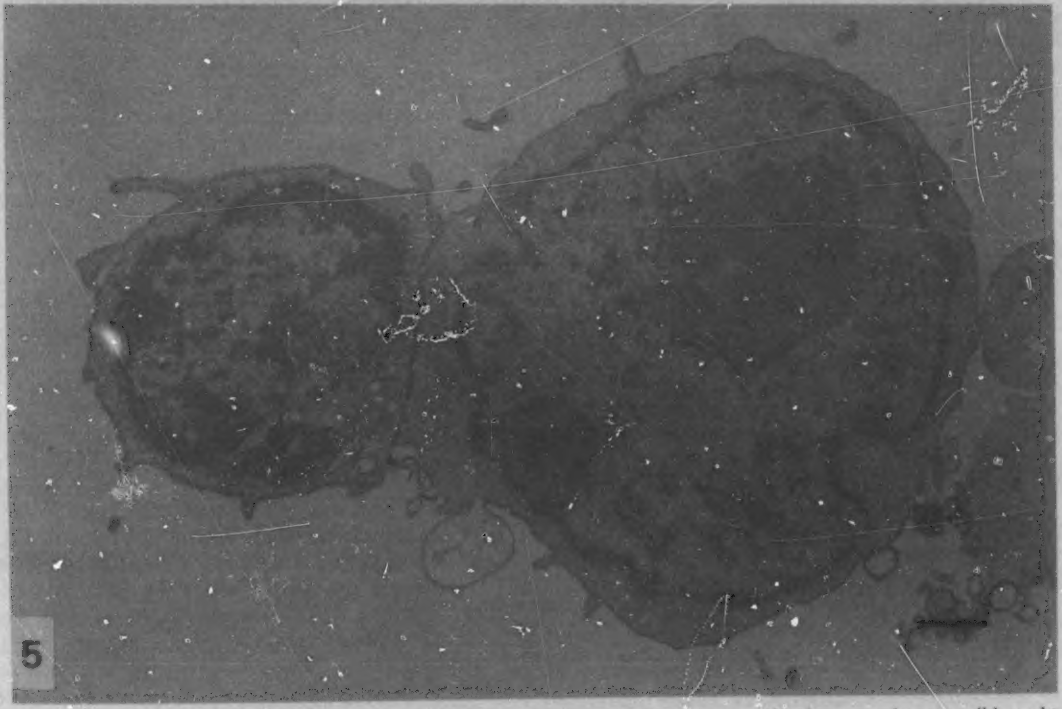

FIGURE 4.—Immunoelectron micrograph of lymphocyte–target cell interaction after 2 hr of incubation. *Note* degenerated tumor cell bound to the asialo G_{M1}^{+} lymphocyte (*arrow*) with fused cell membrane. *Bar*=1 µm. × 7,300

FIGURE 5.—Immunoelectron micrograph of lymphocyte–target cell interaction after 4 hr of incubation. No sign of degeneration is noted in the tumor cell bound to the asialo G_{M1}^{-} lymphocyte. *Bar*=1 µm. × 8,000

Friend Erythroleukemia Virus Complex: Role of Viral Components in Modifying Erythroid Differentiation in Mice[1,2,3]

Barbara Fagg[4,5,6] *and* Wolfram Ostertag[4,7]

ABSTRACT—The present study was carried out to determine which component of the polycythemic strain of Friend erythroleukemia virus (FV-P)—Friend helper virus [Friend murine leukemia virus (F-MuLV)] or the replication-defective spleen focus-forming virus (SFFV)—is responsible for inducing erythropoietin-independent erythropoiesis and expansion of the erythroid compartment in infected mice. F-MuLV and SFFV were cloned in SC1 cells to give a cell line 643/22N, which released only F-MuLV and SC204, a nonproducer cell line carrying SFFV. On superinfection with specific helper viruses, SC204 yielded further cell lines, which released SFFV in conjunction with 1) Friend, 2) Moloney, or 3) Gross helper viruses. With the use of an in vitro colony formation assay to monitor erythropoiesis in the bone marrow of inbred DBA/2J mice infected with any of the virus preparations containing SFFV plus helper virus, the erythroid precursor cell population was found to become erythropoietin-independent and amplified; adult mice infected with any of the helper viruses alone did not develop any symptoms of Friend disease. Thus the biologic activity of the FV-P complex was unaffected by replacement of the F-MuLV with an unrelated helper virus (Moloney or Gross). These results indicated that the SFFV component of FV-P is responsible for modifying erythroid differentiation in adult mice.—JNCI 1982; 68:457–460.

Friend virus causes an erythroleukemia in adult susceptible mice. Two strains of the virus have been distinguished in infected mice: FV-A and FV-P. Mirand (*1*) obtained FV-P from animals infected with the original virus FV-A, which had been isolated by Friend (*2*). Committed erythroid precursor cells appear to be the major target cells for both strains of Friend virus (*3, 4*), and in vivo studies have shown that, after infection by FV-P, erythropoiesis rapidly becomes independent of the normal regulator, Epo (*5*).

With the development of in vitro colony formation assays for erythroid precursors (*6, 7*), it was possible to examine the differentiation of erythroid precursors from virus-infected animals in vitro. In cultures of normal mouse bone marrow, the formation of early (2-day) erythroid colonies derived from the CFU-E (a committed erythroid precursor cell near the end of the erythroid pathway) is strictly dependent on the presence of Epo in the culture medium. Growth of Epo-independent colonies from the bone marrow of FV-P-infected mice was first described by Liao and Axelrad (*8*) and Horoszewicz et al. (*9*) and was shown to be a direct consequence of virus infection.

FV-P is not a single entity but comprises an SFFV that is defective and a helper virus F-MuLV that is required for replication. It was therefore of considerable interest to determine which of these FV-P components causes erythropoiesis to become Epo-independent and produces overt disease in the mouse—properties of SFFV, evidenced in (*5, 10, 11*), although such evidence is necessarily of an indirect nature since SFFV is replication-defective and cannot be studied independently of a helper virus. Our approach was to exchange the Friend helper virus with other unrelated helper viruses, which do not themselves alter erythroid differentiation, and to examine erythroid colony formation in cultures of bone marrow taken from mice infected with these new virus complexes. A similar rationale has been used to examine the role of the helper virus in the transformation of lymphoid cells by the Abelson virus complex (*12, 13*) and of hematopoietic cells by Kirsten virus (*13*).

MATERIALS AND METHODS

Cell lines and virus isolates.—Cell lines were grown in a modification of Eagle's minimum essential medium containing 10% FCS, as described previously (*14*). F4–6 is a subclone of the cell line F4N, which consistently releases high levels of FV-P (*15*). The SFFV and F-MuLV components of FV-P were cloned by successive end-point dilutions (*16, 17*) to give SC204, which is an SFFV-positive, F-MuLV-negative cell line, and 643/22N, which is SFFV-negative and F-MuLV-positive. The SFFV was rescued from SC204 cells by superinfection with the following cloned viruses: F-MuLV from 643/22N cells, which is free of detectable xenotropic sequences (Ostertag W: Unpublished work); M-MuLV from cell line 1.1A (provided by Dr. R. Weinberg, MIT, Cambridge, Mass.); and Gross helper virus (Gross-MuLV) from NIH Swiss mouse fibroblasts (provided by Dr. D. Baltimore, MIT) to give cell lines that released SFFV plus F-MuLV, SFFV plus M-MuLV, and SFFV plus Gross MuLV, respectively.

Virus infection.—Supernatants from the cell lines were routinely assayed for reverse transcriptase activity (*15*) and for SFFV titer determined by the spleen focus-formation assay

---

ABBREVIATIONS USED: CFU-E=colony-forming unit(s)—erythroid; Epo=erythropoietin; FCS=fetal calf serum; F-MuLV=Friend MuLV; FV-A=anemia-producing strain of Friend virus; FV-P=polycythemia-producing strain of Friend virus; MIT=Massachusetts Institute of Technology; MuLV=murine leukemia (helper) virus; M-MuLV=Moloney MuLV; SFFU=spleen focus-forming unit(s); SFFV=spleen focus-forming virus.

---

[1] Received July 28, 1980; accepted July 30, 1981.

[2] Supported by the Max-Planck Gesellschaft and the Deutche Forschungsgemeinschaft

[3] A preliminary report of this work was presented at a conference of the International Union Against Cancer in Geneva, Switzerland; Experientia 1979; 35:362.

[4] Max-Planck-Institut für experimentelle Medizin, D-3400 Göttingen, Federal Republic of Germany.

[5] *Address reprint requests to* Dr. Fagg at her *present address:* Department of Microbiology, University of California, Irvine, Calif. 92717.

[6] Recipient of a European Fellowship from the Royal Society (London).

[7] *Present address:* Beatson Institute for Cancer Research, Garscube Estate, Switchback Rd., Glasgow, Scotland.

(*18*) and expressed as SFFU per milliliter of supernatant. When the reverse transcriptase activity was approximately 10 pmol thymidine 5′-triphosphate incorporated into trichloroacetic acid-precipitable material per 10 μl supernatant, the supernatants were concentrated 10–100 times with the use of an Amicon DC2 hollow-fiber unit fitted with a 100,000-molecular weight cut-off membrane followed by use of an Amicon 402 unit fitted with an XM300 membrane. These preparations were filtered (0.2 μm, Acrodisc, Gelman Instrument Co., Ann Arbor, Mich.) and stored in liquid nitrogen until use. Preparations were thawed, diluted as appropriate, and administered iv to 3- to 4-month-old male DBA/2J mice.

Methyl cellulose cultures.—Virus-infected mice were used for experiments at a time when the spleen was easily palpated. Uninfected animals of a similar age were used as controls. Mice were killed by cervical dislocation, the spleen and both femurs were removed under sterile conditions, and the wet weight of the spleen was recorded. The marrow was flushed from both femurs into α-medium (Flow Laboratories Inc., Bonn, Federal Republic of Germany) containing 2% FCS and was dispersed by repeated passage through syringe with a 22-gauge needle. The resultant single cell suspension was plated in α-medium containing 25% FCS, 0.1 m*M* α-thioglycerol, and 1% methyl cellulose (Fluka, Buchs, Switzerland), essentially as described by Iscove et al. (*7*). For each bone marrow sample, duplicate cultures were prepared containing 0.5, 1.0, and, in some experiments, 0.25 and 2.0×10^5 cells/ml with or without 0.15 U of human Epo/ml (this dose of Epo was shown to give maximum numbers of CFU-E colonies in normal bone marrow cells). Human Epo was either provided by Dr N. Iscove (Basel Institute for Immunology, Switzerland) or was prepared by means of the same procedure in (*7*) and calibrated in vitro against Step III Epo (Connaught Medical Research Laboratories, Ontario, Canada). After 2 days' incubation at 37°C in 5% CO_2-air, the number of colonies arising from CFU-E cells (CFU-E colonies) was counted with an inverted microscope (× 100). We confirmed the identification of colonies as erythroid by staining with benzidine either in the culture dish or after smearing colonies on a glass slide. In all cases examined a linear relationship existed between the number of cells plated and the number of colonies formed both in the presence and absence of Epo.

RESULTS

Effects of FVP on the CFU-E Population

The number of CFU-E colonies formed in the presence and absence of Epo was determined from 1.5 to 12 days after infection of DBA/2J mice with FVP derived from F4–6 cells. Over the period of 5–12 days after infection, a steady increase in both spleen weight (text-fig. 1A) and the numbers of Epo-dependent and Epo-independent colonies (text-fig. 1B) was observed. These results are in close agreement with those of other authors (*8, 19*), who used FV-P that had been continually passaged in mice, except that the virus from F4–6 cells resulted in a larger expansion of the CFU-E compartment.

The relationship between the number of SFFU administered and the induction of splenomegaly, Epo independence, and amplification of the CFU-E population was examined in more detail with the F4-6-derived virus. For spleen weight, a plot of logarithm dose versus response was sigmoid (text-fig. 2A) and, at all doses suprathreshold for this response, the CFU-E population was Epo-independent (text-fig. 2B). Expansion of the CFU-E population was also related to the amount of SFFV injected (text-fig. 2B), although the threshold for this response was higher than that for induction of Epo independence or splenomegaly. For this reason, mice were used in subsequent experiments only when they exhibited pronounced splenomegaly (≈2 g wet wt).

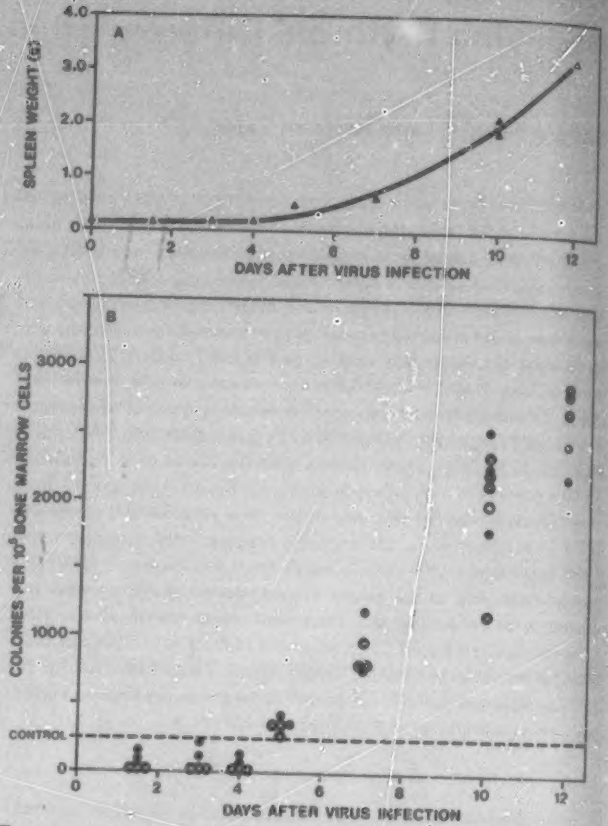

TEXT-FIGURE 1.—Effects of FV-P infection (2×10^3 SFFU/mouse, derived from F4–6 cells) on: A) spleen wt (▲) and B) numbers of CFU-E colonies developing in bone marrow cells grown for 2 days in the presence (●) or absence (○) of 0.15 U Epo/ml. The control value (- - - -) represents the number of CFU-E colonies found in normal bone marrow cells cultured in the presence of Epo

Cause of Epo-independent Erythropoiesis: SFFV or F-MuLV?

The SFFV-positive, F-MuLV-negative nonproducer cell clone SC204 was superinfected with F-MuLV, M-MuLV, or Gross MuLV. Reverse transcriptase assays indicated that the 3 resultant cell lines released similar levels of virus (table 1), although the Gross MuLV infected cell line required longer to attain this level. However, the SFFV titer differed

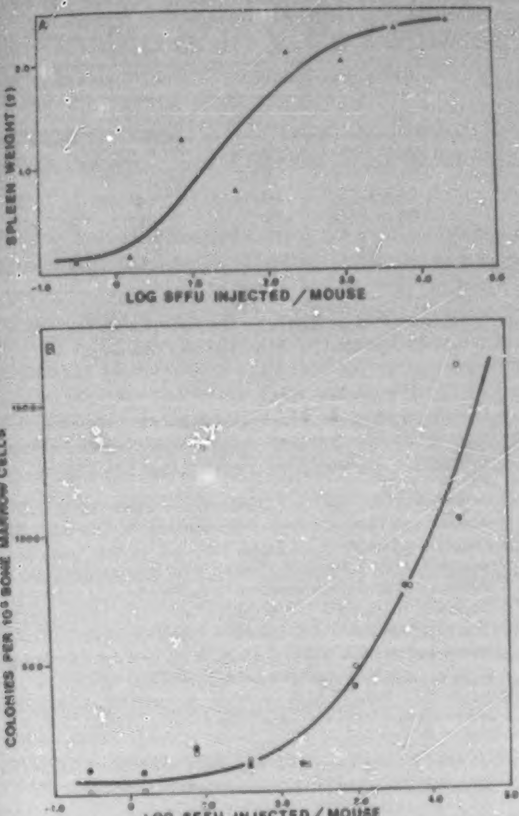

TEXT-FIGURE 2.—Relationship between the number of SFFU (from F4–6 virus) injected/mouse and A) spleen wt (▲) and B) numbers of CFU-E colonies developing in bone marrow cells grown for 2 days in the presence (●) or absence (○) of 0.15 U Epo/ml, when the animals were killed 20 days after virus infection.

markedly between the 3 cell lines (table 1). The ratio of SFFV to reverse transcriptase activities was at least fiftyfold higher in SC204 cells infected with F-MuLV than in those exposed to M-MuLV or Gross MuLV. Experiments involving M-MuLV or Gross MuLV were therefore conducted with both the cell supernatants and the virus concentrates. All virus complexes examined induced splenomegaly in all mice when doses greater than 50 SFFU/animal were injected.

Erythroid colonies developed in the absence of Epo when bone marrow cells from animals infected with any of the SFFV plus helper virus preparations were grown in vitro (table 2). This is in contrast to normal bone marrow cells requiring Epo to complete their differentiation in vitro (table 2). In all cases, similar numbers of erythroid colonies were formed in the presence or absence of Epo, indicating that almost the entire CFU-E population had become Epo-independent as a result of virus infection. Induction of Epo independence was not dependent on the helper virus present with SFFV. Adult mice were unaffected by inoculation with comparable doses of F-MuLV, M-MuLV, or Gross MuLV alone; they showed no evidence of splenomegaly or symptoms of Friend disease.

In addition to becoming Epo-independent, the CFU-E population was amplified in animals infected with F4–6-derived FV-P, SFFV plus F-MuLV, and concentrated preparations of SFFV plus M-MuLV or SFFV plus Gross MuLV (table 2). The absence of erythroid expansion in mice inoculated with untreated cell supernatants containing SFFV plus M-MuLV or SFFV plus Gross MuLV can be attributed to the low amount of SFFU in these virus preparations since text-figure 2 demonstrates that FVP administered at an equivalent SFFU dose also caused the CFU-E population to become Epo-independent without altering its size.

DISCUSSION

Epo-independent erythropoiesis is a prominent feature of FV-P infection in vivo (*5*). The results presented here provide a direct demonstration that this change is caused by the SFFV component of the virus and not the F-MuLV component. Previously, some uncertainty existed concerning the role of SFFV and F-MuLV in the induction of Friend disease. Some evidence indicating the importance of SFFV has been obtained in studies showing *a*) that no Epo-independent erythropoiesis is found in the absence of SFFV in vivo (*5*) or in vitro (*11*) and *b*) that bone marrow cells infected with FV-P in vitro develop erythroid colonies independently of Epo in proportion to the number of SFFU used for infection (*10, 11*). However, recent data indicate that the helper viruses isolated from both FV-A and FV-P are capable of inducing an erythroleukemia (splenomegaly and erythroid expansion but not Epo independence) in newborn but not adult mice (*20, 21*). Furthermore, studies of the Abelson virus complex, which also comprises a helper virus and a replication-defective component, suggest that the helper virus is required for lymphocyte transformation (*12, 13*).

This question has been difficult to answer directly because SFFV is replication-defective and therefore cannot function without a helper virus. In the present study, this problem was circumvented by construction of virus pseudotypes that contained helper viruses unrelated to F-MuLV. Regardless of the helper virus present with SFFV, all complexes prepared were capable of inducing both Epo independence and

TABLE 1.—*Spleen focus-forming titers and reverse transcriptase levels in the supernatants of cell lines producing different FVP complexes*[a]

Cell line	Reverse transcriptase activity, pmol TTP/10 µl cell supernatant	SFFU/ml	SFFU/pmol TTP
F4-6	16	1.2×10^3	0.75
SC204 plus F-MuLV	13	1.5×10^3	1.15
SC204 plus M-MuLV I	9	20	0.022
SC204 plus M-MuLV II	12,500	2.0×10^4	0.016
SC204 plus Gross MuLV I	8	6	0.008
SC204 plus Gross MuLV II	240	1.5×10^2	0.006

[a] Details of the virus preparations, reverse transcriptase, and SFFV assays are given in "Materials and Methods." I=untreated cell supernatant, II=supernatant concentrated as described in "Materials and Methods."

TABLE 2.—*Effects of infection with different virus preparations on spleen weight and erythroid colony formation in bone marrow cells cultured for 2 days in the presence or absence of Epo*[a]

Parameters	No virus	FV-P from F4-6 cells	SFFV plus F-MuLV	SFFV plus M-MuLV		SFFV plus Gross MuLV	
				I	II	I	II
No. of SFFU injected/mouse	0	600	750	250	5,000	5	90
Spleen wet wt, g[b]	0.12	2.73	2.78	1.13	2.44	2.39	2.28
Days after infection	0	10–12	19–25	25–40	18–46	25–40	38–46
Mean No. of CFU-E colonies/10^5 cells without Epo[b]	1	2,606	1,053	105	469	151	600
Mean No. of CFU-E colonies/10^5 cells with Epo[b]	178	2,183	863	91	598	189	833

[a] 0.15 U EPO/ml. Virus preparations and assays are described in "Materials and Methods." Two preparations of SFFV plus M-MuLV and SFFV plus Gross MuLV were used: I=untreated cell supernatant, II=supernatant concentrated as described in "Materials and Methods."

[b] Values are means of data from 3 to 6 separate mice.

some degree of erythroid expansion, demonstrating that it is the SFFV that is primarily responsible for modifying erythropoiesis in FV-P-infected mice. These data are reinforced by recent studies (*21, 22*) (in which the helper viruses from FV-A and FV-P complexes were reciprocally exchanged) indicating that SFFV determines the nature (anemia or polycythemia) of the disease in vivo.

It is interesting that erythroid expansion was only observed when concentrated preparations of SFFV plus M-MuLV or SFFV plus Gross MuLV were used. The possibility that the helper viruses may carry a common function that affects the size of the erythroid population cannot be entirely excluded. However, the untreated virus preparations contained very low levels of SFFV: An equivalent dose (SFFU) of FV-P (F4-6) similarly produced Epo independence but no erythroid expansion, whereas higher doses induced both changes (text-fig. 2). Therefore, SFFV appears to control the size of the erythroid population in addition to its responsiveness to Epo, although the threshold for expression of these functions may differ.

The present study provides strong evidence that it is the SFFV component of Friend virus that induces the symptoms of Friend disease in mice and indicates that F-MuLV principally serves a replicative function.

REFERENCES

(*1*) MIRAND EA. Virus-induced erythropoiesis in hypertransfused-polycythemic mice. Science 1967; 156:832–833.

(*2*) FRIEND C. Cell-free transmission in adult Swiss mice of a disease having the character of a leukemia. J Exp Med 1957; 105:307–318.

(*3*) FRIEND C, SCHER W, HOLLAND JG, SATO T. Hemoglobin synthesis in murine virus-induced leukemic cells in vitro: Stimulation of erythroid differentiation by dimethyl sulfoxide. Proc Natl Acad Sci USA 1971; 68:378–382.

(*4*) TAMBOURIN PE, WENDLING F. Target cell for oncogenic action of polycythaemia-inducing Friend virus. Nature 1975; 256:320–322.

(*5*) MIRAND EA, STEEVES RA, LANGE RD, GRACE JT. Virus-induced polycythemia in mice: Erythropoiesis without erythropoietin. Proc Soc Exp Biol Med 1968; 128:844–849.

(*6*) STEPHENSON JR, AXELRAD AA, MCLEOD DL, SHREEVE MM. Induction of colonies of hemoglobin-synthesizing cells by erythropoietin in vitro. Proc Natl Acad Sci USA 1971; 68:1542–1546.

(*7*) ISCOVE NN, SIEBER F, WINTERHALTER KH. Erythroid colony formation in cultures of mouse and human bone marrow: Analysis of the requirement for erythropoietin by gel filtration and affinity chromatography on agarose-concanavalin A. J Cell Physiol 1974; 83:309–320.

(*8*) LIAO S-K, AXELRAD AA. Erythropoietin-independent erythroid colony formation in vitro by hemopoietic cells of mice infected with Friend virus. Int J Cancer 1975; 15:467–482.

(*9*) HOROSZEWICZ JS, LEONG SS, CARTER WA. *Brief communication:* Friend leukemia: Rapid development of erythropoietin-independent hematopoietic precursors. J Natl Cancer Inst 1975; 54:265–267.

(*10*) CLARKE BJ, AXELRAD AA, SHREEVE MM, MCLEOD DL. Erythroid colony induction without erythropoietin by Friend leukemia virus in vitro. Proc Natl Acad Sci USA 1975; 72:3556–3560.

(*11*) HANKINS WD, KOST TA, KOURY MJ, KRANTZ SB. Erythroid bursts produced by Friend leukemia virus in vitro. Nature 1978; 276:506–508.

(*12*) ROSENBERG N, BALTIMORE D. The effect of helper virus on Abelson virus-induced transformation of lymphoid cells. J Exp Med 1978; 147:1126–1141.

(*13*) SCHER CD. Effect of pseudotype on Abelson virus and Kirsten sarcoma virus-induced leukemia. J Exp Med 1978; 147:1044–1053.

(*14*) OSTERTAG W, MELDRIS H, STEINHEIDER G, KLUGE N, DUBE S. Synthesis of mouse haemoglobin and globin mRNA in leukaemic cell cultures. Nature [New Biol] 1972; 239:231–234.

(*15*) PRAGNELL IB, OSTERTAG W, PAUL J. The expression of viral and globin genes during differentiation of the Friend cell. Exp Cell Res 1977; 108:269–278.

(*16*) PRAGNELL IB, MCNAB A, HARRISON PR, OSTERTAG W. Are spleen focus-forming virus sequences related to xenotropic viruses and expressed specifically in normal erythroid cells? Nature 1978; 272:456–458.

(*17*) OSTERTAG W, PRAGNELL IB. Changes in genome composition of the Friend virus complex in erythroleukemia cells during the course of differentiation induced by dimethyl sulfoxide. Proc Natl Acad Sci USA 1978; 75:3278–3282.

(*18*) AXELRAD AA, STEEVES RA. Assay for Friend leukemia virus: Rapid quantitative method based on enumeration of macroscopic spleen foci in mice. Virology 1964; 24:513–518.

(*19*) OPITZ U, SEIDEL HJ, BERTONCELLO I. Erythroid stem cells in Friend-virus infected mice. J Cell Physiol 1978; 96:95–104.

(*20*) TROXLER DH, SCOLNICK EM. Rapid leukemia induced by cloned Friend strain of replicating murine type-C virus. Virology 1978; 85:17–27.

(*21*) MACDONALD ME, MAK TW, BERNSTEIN A. Erythroleukemia induction by replication-competent type-C viruses cloned from the anemia- and polycythemia-inducing isolates of Friend leukemia virus. J Exp Med 1980; 151:1493–1503.

(*22*) TROXLER DH, RUSCETTI SK, LINEMEYER DL, SCOLNICK EM. Helper-independent and replication-defective erythroblastosis-inducing viruses contained within anemia-inducing Friend virus complex (FV-A). Virology 1980; 102:28–45.

Growth and Spontaneous Regression of Swine Melanoma: Relationship of In Vitro Leukocyte Reactivity[1,2,3]

Jane Berkelhammer,[4,5,6,7] Bonnie M. Ensign,[4,5,8] Reuel R. Hook, Jr.,[4,9] Cynthia J. Hecker,[4,5] Gerald D. Smith,[4,10] *and* Ronald W. Oxenhandler[6,11,12,13]

ABSTRACT—A visual microcytotoxicity technique was used to evaluate the leukocyte reactivity of melanoma swine against allogeneic swine melanoma target cells. Peripheral blood leukocytes, which had been collected and cryopreserved in liquid nitrogen at various times during in vivo tumor growth and regression, were thawed and tested on the same day. Comparison of longitudinal leukocyte reactivity with in vivo tumor volume indicated that swine with regressing melanomas exhibited increased leukocyte reactivity during tumor regression. Swine with maximum tumor volumes less than 30,000 mm³ exhibited patterns of leukocyte reactivity that paralleled the patterns of in vivo tumor growth and regression. However, swine with maximum tumor volumes greater than 30,000 mm³ demonstrated increased in vitro leukocyte reactivity at the time of maximum in vivo tumor volume. Histopathologic analyses revealed that increases in tumor volume were frequently a result of host inflammatory cells, particularly pigment-laden macrophages, infiltrating the tumors. Thus at the time of maximum tumor volume, malignant melanocytes were proportionately decreasing in number while pigment-laden macrophages were proportionately increasing. These studies provide additional evidence that the spontaneous tumor cell regression of swine melanoma is associated with immunologic events and that assays of leukocyte reactivity are useful in vitro correlates of host antitumor immunity.—JNCI 1982; 68: 461–468.

Results of in vitro leukocyte cytotoxicity assays in cancer patients have been difficult to interpret because of the frequent toxicity observed with leukocytes from tumor-free individuals and because of the wide technical variation in assays performed on different days (*1*). The demonstration by several investigators (*2–5*) that cryopreserved leukocytes retain their reactivity in in vitro immunologic assays has permitted the simultaneous testing of several samples collected at various times, thus minimizing the day-to-day variation in assays.

Using cryopreserved leukocytes from melanoma patients and tumor-free donors, Berkelhammer et al. found that melanoma patients receiving either autologous (*2*) or allogeneic (*6*) irradiated melanoma cells plus BCG exhibited increased leukocyte reactivity against allogeneic melanoma cells. However, the increase in reactivity did not correlate with the clinical response to the immunotherapy. It was not clear whether the lack of correlation between in vitro leukocyte reactivity and the clinical course of human melanoma represented a lack in the assay system or was instead a result of the fact that most of the melanoma patients had tumor burdens too great to be destroyed by immunocompetent leukocytes in vivo.

The Sinclair swine melanoma system provides a unique opportunity to resolve some of the controversy surrounding in vitro leukocyte reactivity assays. Swine melanoma, while very similar histopathologically to human malignant melanoma, exhibits an extremely high rate (90%) of spontaneous regression. Evidence exists both in vivo and in vitro (*7–11*) that a host immune response plays a role in the spontaneous regression of this neoplasm. The objective of this investigation was to determine if in vitro leukocyte reactivity to swine melanoma cells could be correlated with in vivo tumor volume.

MATERIALS AND METHODS

Swine.—The Sinclair melanoma swine used in this study were derived from miniature swine originally developed at the Hormel Institute, Austin, Minn. These swine were derived from matings of melanoma females × melanoma males. All animals were housed indoors and given free access to water and a commercial swine diet that contained 18% protein. The swine were examined individually for the presence of melanocytic lesions within 72 hours after birth and at 2-week intervals thereafter. Total tumor volume was determined as the sum of all raised cutaneous lesions; individual tumor volumes were calculated as cylinders. Serial

---

ABBREVIATIONS USED: EMEM—C=Eagle's minimum essential medium—complete medium for culture of cells; EMEM—F=EMEM—freeze medium for cryopreservation of cells; FCS=fetal calf serum; NK=natural killer; PBL=peripheral blood leukocytes; PBS=phosphate-buffered saline; PLM=pigment-laden macrophage(s).

---

[1] Received November 26, 1980; revised October 21, 1981; accepted November 6, 1981.

[2] Supported by Public Health Service grants CA-08023, CA-25718, and CA-28230 from the National Cancer Institute.

[3] Animals were maintained under the guidelines of the National Research Council.

[4] Sinclair Comparative Medicine Research Farm, University of Missouri, Route 3, Columbia, Mo. 65201.

[5] Department of Medicine, University of Missouri School of Medicine, Columbia, Mo. 65212.

[6] Cancer Research Center, Columbia, Mo. 65201.

[7] *Address reprint requests to* Dr. Berkelhammer at the Sinclair Comparative Medicine Research Farm.

[8] Recipient of a scholarship for research in medicine from the Department of Medicine, University of Missouri—Columbia.

[9] Department of Microbiology, University of Missouri School of Medicine.

[10] *Present address*: Veterinary Clinical Sciences, School of Veterinary Medicine, Louisiana State University, Baton Rouge, La. 70803.

[11] Department of Pathology, University of Missouri School of Medicine.

[12] Ellis Fischel State Cancer Hospital, Columbia, Mo. 65201.

[13] We thank Ms. Marcia Tidwell and Mrs. Sandra Cottrell for excellent technical assistance and Mrs. Dorothy Tumulty for typing the manuscript. We gratefully acknowledge the enthusiastic support of Dr. C. E. Mengel, Dr. C. C. Middleton, and Dr. J. W. Yarbro on behalf of this project.

laparotomies and thoracotomies on 13 swine indicated that internal tumors did not represent a significant portion of the total tumor volume.

To limit the variables affecting in vitro leukocyte reactivity, we did not perform sequential biopsies on most animals studied prospectively in this report. On 2 pigs (#5319 and 5434) sequential biopsies were done with aseptic technique. Tissues for light microscopy were processed as previously described (*7*).

Previous gross classification schemes in which the swine were classified as progressors or regressors according to changes in measured tumor volume were not used in this study. This practice has resulted in the frequently fallacious assumption that neoplastic cells were responsible for the change in the size of the *tumor*. Tumor is used here in the classical gross sense to mean swelling.

Media.—EMEM—C used for all cell culture procedures consisted of Eagle's minimum essential medium (Auto-Pow MEM; Flow Laboratories, Inc., McLean, Va.) supplemented with sodium bicarbonate, 4 m*M* L-glutamine, 1% vitamins, 1% sodium pyruvate, 1% nonessential amino acids, 100 IU penicillin and 100 μg streptomycin/ml, 25 μg Fungizone/ml, 30 m*M* HEPES[14] buffer (Flow Laboratories, Inc.), 50 μg gentamicin/ml (M.A. Bioproducts, Walkersville, Md.), and 8% FCS (KC Biologicals, Lenexa, Kans.). EMEM—F contained the same ingredients as EMEM—C, except that 12% dimethyl sulfoxide was added and 30%, rather than 8%, FCS was added.

Target cells and leukocytes.—An allogeneic swine melanoma cell line, #4187, which was established in culture as described previously (*10*), served as the target cell population for all leukocyte microcytotoxicity assays. PBL were separated from whole blood on a Ficoll-Hypaque gradient (Histopaque-1077; Sigma Chemical Co., St. Louis, Mo.). Heparinized blood was diluted with an equal volume of PBS, and four volumes of diluted blood were layered onto one volume of Ficoll-Hypaque. The gradient was centrifuged at 750×*g* at room temperature for 30 minutes, and the middle leukocyte-rich layer was removed and washed with PBS. The washed PBL were then suspended in EMEM—F and frozen in liquid nitrogen as described below. It should be noted that 750×*g* is considerably greater than the speed usually described for separation of human leukocytes. However, this was found to be the optimum rate for the separation of swine leukocytes.

For cryopreservation of leukocytes and tumor cells, cells were suspended in EMEM—F and placed in plastic serum test tubes (A/S Nunc, Roskilde, Denmark). The vials were then placed in a −70°C freezer for at least 24 hours and then stored in liquid nitrogen until used. Before use, frozen samples were thawed rapidly in warm water, diluted with EMEM—C, and washed by centrifugation. Cell viability was assessed by trypan blue exclusion.

Leukocyte microcytotoxicity.—A modification (*2*) of the microcytotoxicity technique of Takasugi and Klein (*12*) was used. Melanoma cell monolayers were harvested by trypsinization, and the number of cells was adjusted to a concentration known to yield 100–400 cells/well after plating. The tumor cell suspension was dispensed in MicroTest plates (#3034; Falcon Plastics, Oxnard, Calif.) in volumes of 0.01 ml/well. The plates were then wrapped in moist gauze and placed in a plastic box with the lid slightly open, and the box was incubated at 37°C in a CO_2 incubator for 12–24 hours. Leukocytes were then thawed, washed in EMEM—C, counted, and added to the tumor cells at concentrations of 1×10^5/0.01 ml. Control groups consisted of tumor cells without leukocytes. Each leukocyte and control group consisting of eight replicates was distributed over the entire plate rather than in horizontal rows to randomize variability in cell plating caused by position on the plate. The leukocyte-tumor cell mixture was then incubated for an additional 40–48 hours.

The leukocytes were then removed, and the surviving tumor cells were visually counted (*2*). Visual counts were assessed after the remaining cells were fixed with acetone-alcohol and stained with Giemsa. Survival fractions were determined by dividing the mean number of tumor cells remaining in wells containing leukocytes by the number remaining in wells without leukocytes (medium control).

RESULTS

Comparison of Fresh Versus Frozen Swine PBL

Swine PBL from 2 donors were tested immediately after preparation and after storage in liquid nitrogen for 1 week. The results shown in table 1 indicate that there was no decrease in leukocyte reactivity (i.e., increase in tumor cell survival) after cryopreservation of the leukocytes.

Relationship Between Leukocyte Reactivity and In Vivo Tumor Volume

For the investigation of the relationship between leukocyte reactivity and in vivo melanoma growth and regression, the leukocyte reactivity of a swine (#5319) with many small tumors which ultimately regressed was compared to that of a swine (#5338) with a large rapidly growing tumor. Text-figure 1A shows that both the rate of tumor growth and the maximum tumor volume (150,000 mm^3) were much greater in swine #5338 than in #5319. Cryopreserved leukocytes from both animals were then tested simultaneously against

TABLE 1.—*In vitro reactivity of swine leukocytes*[a]

Lymphocyte source	Mean No. of tumor cells ± SD (% survival)[b]	
	Before freezing	After freezing
Swine #5767	184±52 (79)[c]	125±34 (83)[c]
Swine #5771	160±38 (68)[d]	102±26 (68)[d]
Medium control	234±63	150±35

[a] Lymphocytes were tested in a 48-hr visual microcytotoxicity assay before freezing or after freezing with subsequent storage in liquid nitrogen for 1 wk.

[b] Mean is of 8 wells/group. Percent survival was calculated as (mean cell number in experimental wells/mean cell number in medium control wells) × 100. Differences between experimental and control groups were tested by two-tailed Mann-Whitney *U* test.

[c] Not significant.

[d] $P<0.05$.

---

[14] 4-(2-Hydroxyethyl)-1-piperazine ethanesulfonic acid.

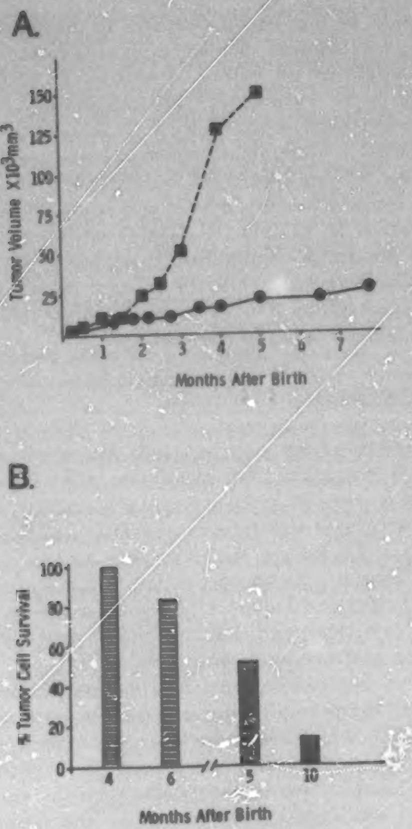

TEXT-FIGURE 1.—A) Comparison of tumor growth in progressor swine #5338 (- -■- -) and regressor swine #5319 (—●—). B) Comparison of leukocyte reactivity in progressor swine #5338 (▥) and regressor swine #5319 (▨). Cryopreserved leukocytes were tested simultaneously in a visual microcytotoxicity assay.

allogeneic swine melanoma cells. The results shown in text-figure 1B indicate that the samples collected from swine #5319 were substantially more reactive (52 and 14% survival or 48 and 86% reactivity) than were the samples collected from swine #5338 (99 and 84% survival or 1 and 16% reactivity).

Sequential histologic sampling was performed on pig #5319, tumor #1. Text-figure 2 compares measured tumor volume to the content of PLM and tumor cells. We have arbitrarily assigned the sum of tumor cells and macrophages to be 100%, although we are well aware that other cellular and noncellular elements contribute to tumor volume. At the time of maximum tumor volume, approximately 90% of the pigmented cells were macrophages and only 10% were malignant cells, which corresponds to an in vitro tumor cell survival of 52%.

Figures 1 and 2 illustrate the two extremes in the growth and regression of the cutaneous melanoma. Figure 1 is a histologic example of early tumor growth (day 10) when more than 90% of the pigmented cells were tumor cells. At a much later time (276 days), the regressed tumor was characterized by complete epidermal depigmentation (fig. 2) with isolated large nests of PLM in the dermis.

To determine if longitudinal leukocyte reactivity could be correlated with in vivo measured tumor volumes of swine melanoma, we tested the sequential reactivities of 7 swine in the visual microcytotoxicity assay. Leukocytes were collected and cryopreserved at 2- to 4-week intervals during the first 3–6 months after birth. All leukocyte samples from individual swine were thawed and tested on the same day. Text-figure 3 indicates that cryopreserved leukocytes that were from a single swine and that were tested on four different dates exhibited essentially the same pattern of sequential reactivity on all four dates.

The sequential reactivities of the 7 swine were compared to their in vivo tumor growth. All 7 swine exhibited easily

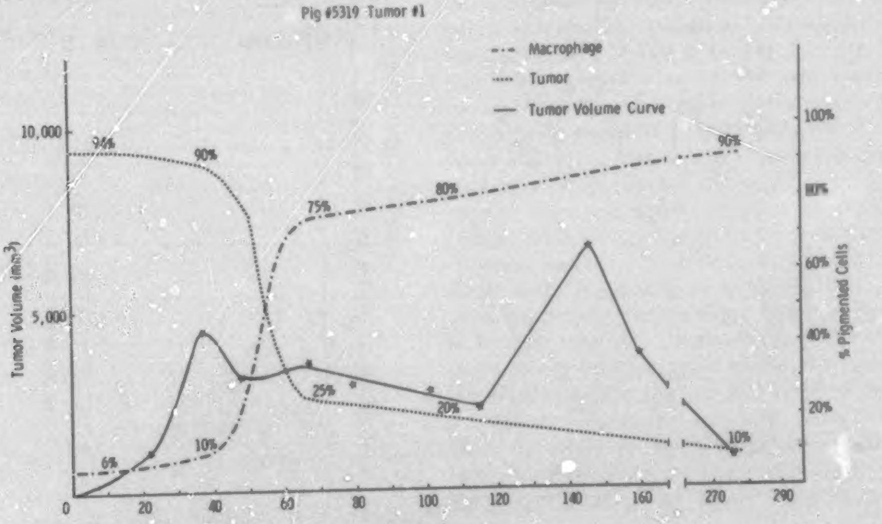

TEXT-FIGURE 2.—Sequential tumor volume measurements (—★—) compared to relative changes in numbers of malignant cells (····) and PLM (—·—).

detectable decreases in tumor volume during the period of observation. Four of the swine had maximum tumor volumes less than 30,000 mm^3 (text-fig. 4), and 3 swine had maximum tumor volumes greater than 30,000 mm^3 (text-fig. 5). The pattern of leukocyte reactivity in the 4 swine with relatively small tumor burdens (text-fig. 4) followed quite closely the pattern of tumor growth. In general, for tumor volumes less than 30,000 mm^3, tumor cell survival in vitro increased when in vivo tumor volume increased and decreased when in vivo tumor volume decreased. Swine #6003, which had the smallest tumor burden (maximum, 6,000 mm^3), exhibited the least variation in leukocyte reactivity throughout the period of tumor growth and regression.

In the 3 swine with maximum tumor volumes greater than 30,000 mm^3 (text-fig. 5), a consistent trend in reactivity was also observed, but this trend was different from that of swine with smaller tumor burdens. In the swine with large tumors, a substantial increase in in vivo tumor volume was accompanied by an *increase* in leukocyte reactivity (i.e., a decrease in in vitro tumor cell survival). This dramatic increase in leukocyte reactivity was followed by a refractory period with a subsequent return to increased reactivity as the tumor volume continued to decrease.

One tumor from pig #5434 was sampled for histologic examination at 42 and 71 days. Text-figure 6 illustrates that, as the tumor volume decreased, the number of malignant cells decreased, while the relative percentage of macrophages increased. This decrease in tumor cells was paralleled by a decrease in in vitro survival.

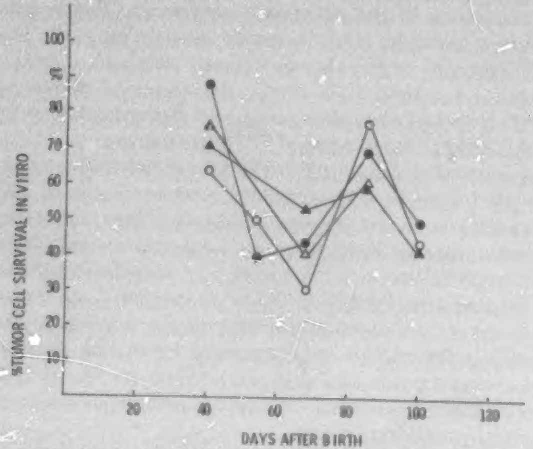

TEXT-FIGURE 3.—Sequential leukocyte reactivity of cryopreserved leukocytes from swine #5895 tested on 4 different days: ●=tested Jan. 30, 1981; ○=tested Feb. 16, 1981; ▲=tested March 10, 1981; △=tested May 19, 1981.

DISCUSSION

The results of the present study demonstrate that cryopreserved leukocytes from melanoma swine can be used to evaluate sequential leukocyte reactivity throughout the in vivo growth and spontaneous regression of Sinclair swine melanoma. Leukocyte reactivity was assayed by a visual microcytotoxicity technique, which utilized small numbers of tumor cells and leukocytes. Plating leukocytes in mixed patterns over the entire plate minimized position effects and prevented subjectivity during visual counting.

Initial comparisons of leukocyte reactivity in swine #5319, which had many small regressing tumors, with reactivity in swine #5338, which had a single large progressively growing tumor, suggested an association between in vitro leukocyte reactivity and in vivo tumor volume (text-fig. 1). Leukocyte reactivity was significantly greater in the swine with the slower rate of tumor growth and lower tumor volume (#5319).

Longitudinal studies of leukocyte reactivity in an additional 7 melanoma swine (all of which ultimately had complete tumor regression) indicated two patterns of leukocyte responses, both of which could be associated with

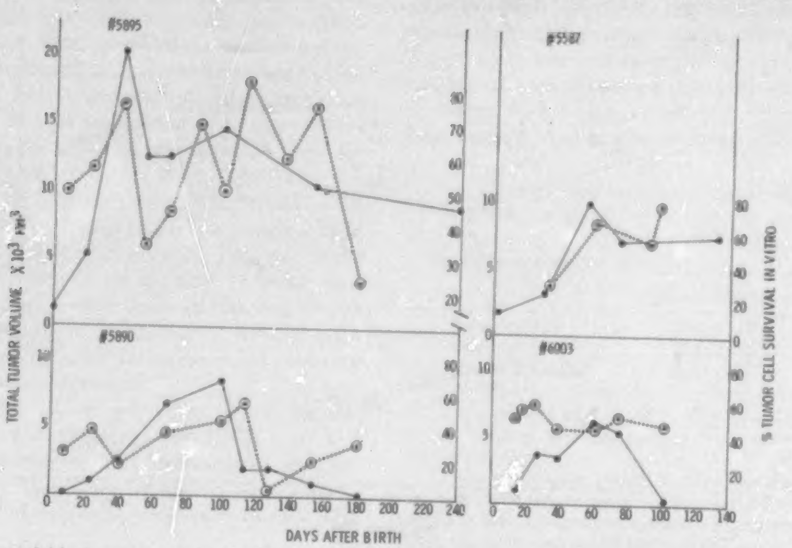

TEXT-FIGURE 4.—In vitro sequential leukocyte reactivity (- -⊙- -) compared with in vivo tumor growth (—●—) in 4 swine with tumor volumes <30,000 mm^3. *Left vertical axes* represent in vivo tumor volume; *right vertical axes* represent in vitro percent tumor cell survival.

changes in cutaneous tumor volume. In swine with cumulative tumor volumes less than 30,000 mm^3, substantial increases and decreases in tumor volume were paralleled by increases and decreases in in vitro tumor cell survival (text-fig. 4). In 1 swine (#6003), which had an extremely small tumor burden, little variation in leukocyte reactivity was observed throughout the 3 months of observation. This lack of variation may have resulted from a low level of sensitizing tumor antigen in the circulation, possibly due to the fact that tumor cells were confined to the epidermis, which lacks a vascular supply.

In 3 swine with tumor volumes greater than 30,000 mm^3, a peak in in vivo tumor volume was accompanied by low in vitro tumor cell survival (i.e., high leukocyte reactivity) (text-fig. 5). Histopathologic analysis of tumor biopsy specimens indicated that the period of maximum increase in tumor volume could be attributed, in part, to infiltration by host inflammatory cells, especially by PLM (*13*). Therefore, the increase in tumor volume, rather than representing neoplastic cell growth, actually may have been a sign of in vivo tumor regression.

The cutoff point of 30,000 mm^3 was chosen empirically because the leukocyte reactivity divided naturally into these 2 groups. Although most lesions in this study were not examined by biopsy procedures, biopsy data from other melanoma swine suggest that the individual tumors that comprised the cumulative tumor volumes probably exhibited a histologic spectrum ranging from noninvasive to frankly invasive melanomas.

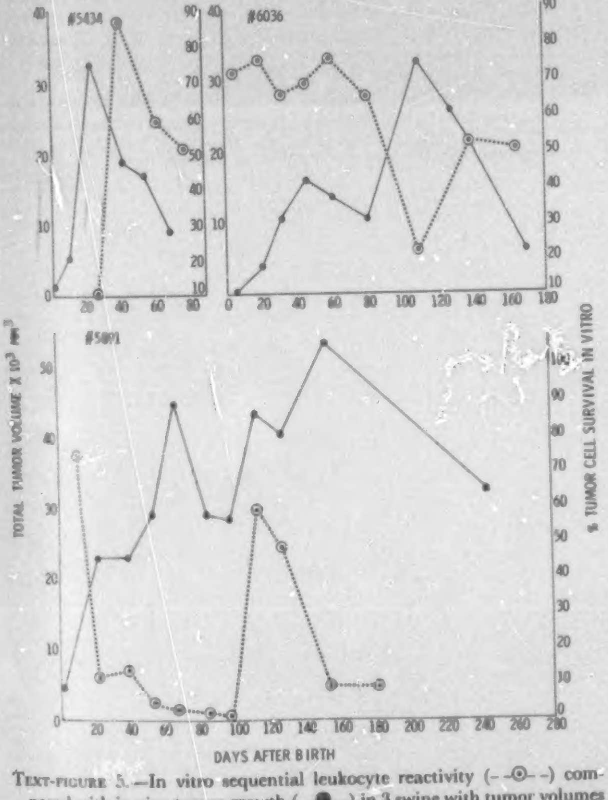

TEXT-FIGURE 5.—In vitro sequential leukocyte reactivity (- -⊙- -) compared with in vivo tumor growth (—●—) in 3 swine with tumor volumes >30,000 mm^3. *Left vertical axes* represent in vivo tumor volume; *right vertical axes* represent in vitro percent tumor cell survival.

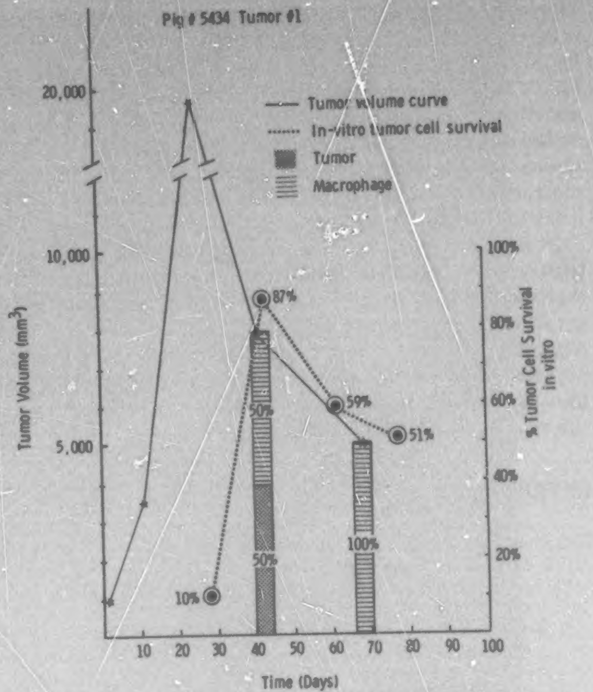

TEXT-FIGURE 6.—Sequential changes in tumor volume (—★—) of a *single* cutaneous malignant melanoma in relation to in vitro leukocyte reactivity (- -⊙- -). Total height of the two bars at 42 and 69 days represents 100% of the pigmented cells comprising the tumor volume on those days. The relative percentage of malignant cells is indicated by ▩ and of PLM by ▤.

In this study, the swine with larger cumulative tumor volumes tended to have larger individual melanomas, while swine with smaller cumulative volumes usually had multiple smaller tumors. Previous biopsy data have indicated that palpable tumors having low volumes may consist of purely intraepidermal proliferation of neoplastic melanocytes with the palpable components contributed by PLM in the dermis. More definitive conclusions concerning the relationship of leukocyte reactivity to melanoma growth and regression require that sequential biopsies be performed on every tumor. Such studies are currently under way.

Initial increases in leukocyte reactivity, particularly in swine with larger tumors, were followed consistently by a transient decrease in reactivity. The reasons for this "eclipse" in in vitro reactivity are not known. However, the decrease in reactivity could have resulted from either a decrease in stimulating tumor antigen as a result of regression or from the release of antigen–antibody complexes which might block the leukocyte response. Several investigators (*14–16*) have reported transient losses in leukocyte reactivity after surgical removal of tumor or radiotherapy in cancer patients.

The effector cell population has not been purified and is composed of the entire PBL layer recovered from a Ficoll–

Hypaque gradient. Thus we cannot at this time identify the cell(s) responsible for the reactivity. In light of recent reports by other investigators on NK activity in melanoma patients (*17*, *18*), we will be interested in determining if the NK activity in Sinclair melanoma swine is increased during melanoma regression. In addition, since PLM are the most numerous cells found in biopsy specimens of regressing swine melanomas, we would like to determine if monocytes participate in the in vitro leukocyte response.

In conclusion, these results indicate a strong relationship between the spontaneous regression of swine melanoma and increased in vitro leukocyte reactivity. These studies do not prove that host immunologic responses cause the in vivo regression. However, they do indicate that the regression process is associated with a host immunologic response and that in vitro assays of leukocyte reactivity are useful indicators of in vivo antitumor immunity.

REFERENCES

(*1*) Cummings FJ, Heppner GH. Cellular and humoral immunity in patients with solid tumors. In: Waters H, ed. The handbook of cancer immunology. Vol 4. New York: Garland Publishing, 1978: 219–233.

(*2*) Berkelhammer J, Mastrangelo MJ, Laucius JF, Bodurtha AJ, Prehn RT. Sequential in vitro reactivity of lymphocytes from melanoma patients receiving immunotherapy compared with the reactivity of lymphocytes from healthy donors. Int J Cancer 1975; 16:571–578.

(*3*) Oldham RK, Dean JH, Cannon GB, et al. Cryopreservation of human lymphocyte function as measured by in vitro assays. Int J Cancer 1976; 18:145–155.

(*4*) Thierry C, Turc JM, Valles H, Serrou B. Routine technique of lymphocyte cryopreservation evaluated by in vitro tests of immune response. Eur J Cancer 1977; 13:367–371.

(*5*) Birkeland SA. Cryopreservation of human lymphocytes for sequential testing of immune competence. Eur J Cancer 1980; 35:57–67.

(*6*) Berkelhammer J, Mastrangelo MJ, Bellet RE, Berd D, Prehn RT. Chemoimmunotherapy increases the lymphocyte reactivity of melanoma patients. Eur J Cancer 1979; 15:197–204.

(*7*) Oxenhandler RW, Adelstein EH, Haigh J, Hook RR Jr, Clark WH Jr. Malignant melanoma in the Sinclair miniature swine: An autopsy study of 60 cases. Am J Pathol 1979; 96:707–720.

(*8*) Hook RR Jr, Aultman MD, Adelstein EH, Oxenhandler RW, Millikan LE, Middleton CC. Influence of selective breeding on the incidence of melanomas in Sinclair miniature swine. Int J Cancer 1979; 24:668–672.

(*9*) Aultman MD, Hook RR Jr. In vitro lymphocyte reactivity to soluble tumor extracts in Sinclair melanoma swine. Int J Cancer 1979; 24: 673–678.

(*10*) Berkelhammer J, Caines SM, Dexter DL, Adelstein EH, Oxenhandler RW, Hook RR Jr. Adaptation of Sinclair swine melanoma cells to long-term growth in vitro. Cancer Res 1979; 39:4960-4964.

(*11*) Berkelhammer J, Hook RR Jr. Growth of Sinclair swine melanoma in the hamster cheek pouch. Transplantation 1980; 29:193–195.

(*12*) Takasugi M, Klein E. A microassay for cell mediated immunity. Transplantation 1970; 9:219–227.

(*13*) Kovacs SA, Geekie KM, Oxenhandler RW, Agris PF. Tyrosinase activity and isoenzyme distribution corresponding to growth and regression of melanoma in Sinclair miniature swine. JNCI 1981; 67:645–651.

(*14*) Byrne M, Heppner G, Stolbach L, Cummings F, McDonnough E, Calabresi P. Tumor immunity in melanoma patients as assessed by colony inhibition and microcytotoxicity methods: A preliminary report. Natl Cancer Inst Monogr 1973; 37:3–8.

(*15*) Cochran AJ, Spilg WG, Mackie RM, Thomas CE. Post-operative depression of tumour-directed cell-mediated immunity in patients with malignant disease. Br Med J 1972; 4:67–70.

(*16*) Perlmann P, O'Toole C, Unsgaard B. Lymphocyte-mediated tumor cell destruction in vitro. Some general principles and reactivities in bladder carcinoma. Natl Cancer Inst Monogr 1972; 35:223–229.

(*17*) Hersey P, Edwards A, Honeyman M, McCarthy WH. Low natural-killer-cell activity in familial melanoma patients and their relatives. Br J Cancer 1979; 40:113–122.

(*18*) Hersey P, Edwards A, McCarthy WH. Tumour-related changes in natural killer cell activity in melanoma patients. Influence of stage of disease, tumour thickness and age of patients. Int J Cancer 1980; 25:187–194.

FIGURE 1.—Tumor #1 from pig #5319 at 10 days of age. More than 90% of the pigmented cellular elements were tumor cells (⇧) and less than 10% were PLM (⬆). *White shaded arrow* indicates a tumor cell undergoing mitosis. Melanin bleach stain. *Bar*=20 µm. × 250

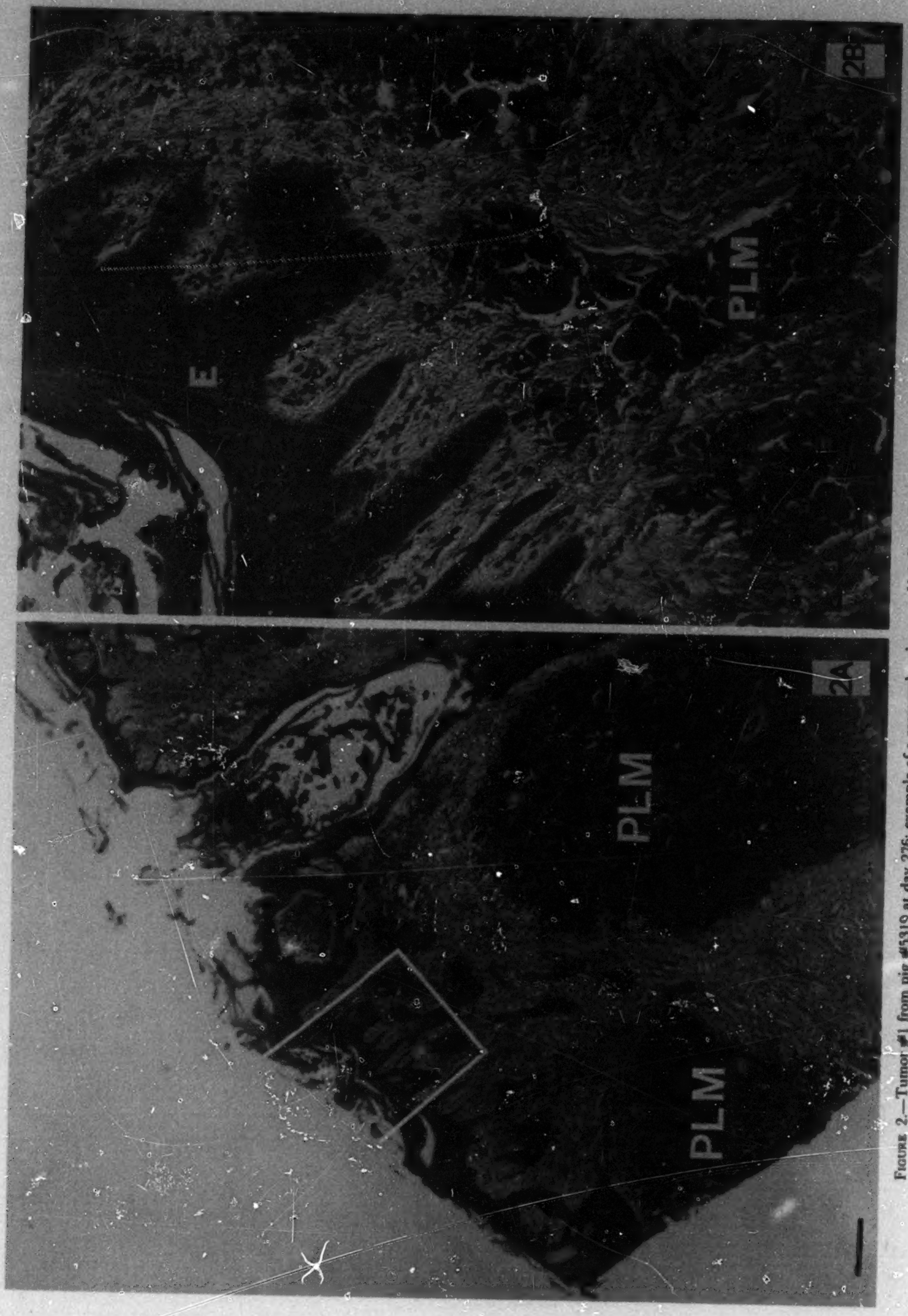

FIGURE 2.—Tumor #1 from pig #5319 at day 276: example of a regressed melanoma. H & E. A) Only islands of PLM are seen in the dermis. *Bar*=360 μm. × 16. B) Detail from *inset* in 2A. Epidermis (E) lacks any neoplastic cells. Approximately 90% of the pigmented cellular elements were PLM, and 10% were residual malignant cells (not shown here). *Bar*=55 μm. × 100

Ganglioside Changes Induced by Tumor Promoters in Promotable JB6 Mouse Epidermal Cells: Antagonism by an Antipromoter[1]

Leela Srinivas[2] *and* Nancy H. Colburn[2, 3, 4]

ABSTRACT—Since cell surface gangliosides have been implicated in the regulation of cell growth and differentiation and since tumor-promoting phorbol esters produce a number of membrane changes, the possibility was investigated that ganglioside changes may play a role in promotion of transformation in JB6 mouse epidermal cells. The studies showed that tumor-promoting but not non-promoting phorbol esters produced decreased precursor incorporation into trisialoganglioside G_T and increased incorporation into disialoganglioside GD_1b and an unknown ganglioside, G_X. These ganglioside responses to promoters were antagonized by the antipromoter retinoic acid, thus suggesting that alterations in ganglioside levels may be involved in promotion of transformation.—JNCI 1982; 68:469–473.

TPA is a highly active tumor promoter, having a wide range of effects on cultured cells (*1–9*). TPA and other tumor promoters promote anchorage independence and tumorigenicity in JB6 mouse epidermal cells (*2–4*). These cells are useful as a model for studying late-stage tumor promotion because they respond to promoters with an irreversible shift to tumor cell phenotype as measured by anchorage independence. Promoter-induced anchorage-independent JB6-derived cell lines are also tumorigenic as determined by injection into nude mice (*3*). TPA also elicits a number of plasma membrane and other glycoprotein changes, such as fibronectin and collagen loss, stimulated hexose uptake, inhibited binding of epidermal growth factor, and stimulated phospholipid synthesis (*1, 10–13*). One hypothesis of tumor promotion proposes that the promoting activity is mediated by specific plasma membrane changes. A candidate for membrane-mediated changes could be glycolipids, which are postulated to function in the regulation of cell growth and morphology (*14–16*). Among the glycolipids, gangliosides are of interest to study because they function specifically in the binding of fibronectin (*17*), cholera toxin (*18*), tetanus toxin (*19*), thyroid-stimulating hormone (*20*), and serotonin (*21*). Glycolipids have been implicated in the induction and maintenance of malignant transformation (*14*). Gangliosides in particular are sensitive to viral and chemical transformation (*22–26*). Specific ganglioside changes are brought about by TPA-induced differentiation in human melanoma cells (*7*).

Retinoids have been shown to be antipromoters both in vivo and in cell culture (*9, 27, 28*). Promotion of anchorage independence and tumorigenicity by TPA in JB6 cells is blocked by retinoids (*4, 28*). It was therefore of interest to investigate whether ganglioside synthesis might be a target for the tumor-promoting action of phorbol esters and for the anti-tumor-promoting action of retinoids. We report here that promoting but not nonpromoting phorbol esters induce specific ganglioside changes in promotable JB6 cells and that these changes are prevented by the antipromoter RA.

MATERIALS AND METHODS

Chemicals.—TPA and its ester analogs were purchased from Dr. Peter Borchert, Chemical Carcinogenesis (Eden Prairie, Minn.), and were stored at −20°C in a desiccated container at 1 mg/ml concentration in spectral grade DMSO. At the time of use they were diluted appropriately in the medium in which the concentration of DMSO was always 0.1% or less. RA was a gift from Hoffmann-La Roche Inc. (Nutley, N.J.) and was used at 10^{-6} *M* final concentration under yellow light. Bovine brain gangliosides and standard individual gangliosides G_{M1}, G_{D1a}, and G_T were purchased from Supelco, Inc. (Bellefonte, Pa.). D-[1-^{14}C]glucosamine hydrochloride (55 mCi/mmol) was procured from Amersham/Searle Corp. (Arlington Heights, Ill.). Solvents used were of analytic grade from Fisher Scientific Co. (Fair Lawn, N.J.). Silica Gel-G plates were purchased from Analtech, Inc. (Newark, Del.). *Clostridium perfringens* neuraminidase was purchased from Boehringer Mannheim Biochemicals (Indianapolis, Ind.), and *N*-acetylneuraminic acid was purchased from Sigma Chemical Co. (St. Louis, Mo.).

Cell culture.—The JB6 cell line was derived from mouse primary epidermal cell cultures as described by Colburn et al. (*2, 29*). These cells were passed by trypsinization (0.06% trypsin), and cultures were always maintained in logarithmic growth. Cells were grown in 15-cm petri dishes in minimum essential medium with Earle's salts (GIBCO, Grand Island, N.Y.) and were supplemented with 8% fetal calf serum (Flow Laboratories, Inc., Rockville, Md.) and antibiotics.

TPA exposure and labeling.—TPA was added to the cells at 10 ng/ml (1.6×10^{-8} *M*) concentration (unless otherwise stated in 5% fetal bovine serum medium), and time of exposure was 24 hours. The cells were terminally labeled with D-[1-^{14}C]glucosamine hydrochloride for 4 hours at a final concentration of 4 μCi/ml. DMSO controls were always included, and all experiments were conducted in duplicate or triplicate.

Ganglioside isolation.—The medium was removed, and cells were washed thoroughly with phosphate-buffered saline and scraped in 4 ml methanol to which 8 ml chloroform was

ABBREVIATIONS USED: DMSO=dimethyl sulfoxide; RA=retinoic acid; R_f=retardation factor(s); TLC=thin-layer chromatography; TPA=12-*O*-tetradecanoylphorbol 13-acetate.

---

[1] Received May 18, 1981; accepted November 6, 1981.

[2] Laboratory of Viral Carcinogenesis, NCI-Frederick Cancer Research Facility, Frederick, Md. 21701.

[3] *Address reprint requests to* Dr. Colburn.

[4] We thank Dr. Roscoe Brady, Dr. Peter Fishman, and Dr. Hynda Kleinman, National Institutes of Health, for their comments on the manuscript.

best copy available

then added. The gangliosides were isolated according to the procedure of Suzuki (*30*) as modified by Langenbach (*31*). This method involved sonication of cells in chloroform:methanol (2:1; vol/vol) in the presence of 100 µg bovine brain gangliosides followed by removal of cell debris. Water was added to one-fifth of the total volume and mixed thoroughly. The upper phase containing gangliosides was removed and saved. The lower phase was carefully washed with the theoretical upper phase (48:47:1) (CH_3OH:H_2O:$CHCl_3$; vol/vol/vol), and the washes were combined with the upper phase. The upper phase was dialyzed in boiled and washed dialysis bags against distilled water for 24 hours at 4°C. The contents of the dialysis bag were lyophilized and dissolved in chloroform:methanol (2:1; vol/vol). Gangliosides were separated by thin-layer chromatography on Silica Gel-G-coated plates with a solvent system of chloroform:methanol:ammonium hydroxide:water (60:35:0.5:7.5; vol/vol/vol/vol). This solvent system separates gangliosides clearly from the origin due to the low concentration of ammonium hydroxide used. The gangliosides were identified by cochromatography with authentic standards. The gangliosides' R_f were G_X (an unidentified ganglioside): 0.08; G_T: 0.18; G_{D1b}: 0.3; G_{D1a}: 0.38; G_{M1}: 0.48; G_{M2}: 0.8; and G_{M3}: 0.95. The mode of ganglioside detection was by exposure to iodine vapor with the lid of the chamber open to a slit. The stained bands were marked, and iodine was allowed to sublime. We determined the incorporation of [^{14}C]glucosamine by scraping the band, extracting the ganglioside into 1.0 ml of chloroform:methanol:water (10:10:1; vol/vol/vol), and counting in a Beckman liquid scintillation counter with the use of Hydroflour as scintillant. The efficiency of ganglioside extraction from the TLC plate was 80–90% for all gangliosides. Scintillation counting efficiency in 1.0 ml solvent was 50%. The nomenclature of the gangliosides is that of Svennerholm (*32*).

Neuraminidase assay.—JB6 mouse epidermal gangliosides G_X, G_T, and G_{D1b} were scraped off the plate and used as substrates. The incubation medium contained purified ganglioside (±5 µg sialic acid), 100 µl of 200 m*M* acetate buffer (pH 5.2) containing 2 m*M* calcium chloride plus or minus 0.1 U enzyme (50 µl), and water to a final volume of 200 µl. The reaction mixture was incubated for 4 hours at 37°C, and the reaction was stopped by addition of 10 volumes of $CHCl_3$:CH_3OH (2:1 vol/vol). The mixture was evaporated under a stream of nitrogen and dissolved in chloroform:methanol (1:1; vol/vol). An aliquot was applied to a Silica Gel-G plate that was prerun with a solvent system of petroleum ether:diethyl ether:acetic acid (80:20:1; vol/vol/vol) and dried overnight. This system obviates the need to desalt the reaction mixture and does not interfere with separation of gangliosides with the use of the previously mentioned solvent system (*33*) but yields different R_f.

RESULTS

TPA exposure for 24 hours produced about a 50% decrease in de novo synthesis of total gangliosides as measured by a terminal 4-hour incorporation of D-[1-^{14}C]glucosamine. Separation of gangliosides by TLC gave the following R_f, as illustrated in text-figure 1: G_X (an unidentified ganglioside): 0.08; G_T: 0.18; G_{D1b}: 0.30; G_{D1a}: 0.38; G_{M1}: 0.48; G_{M2}: 0.8; and G_{M3}: 0.95. Determination of the distribution of precursor incorporation into individual gangliosides revealed that TPA produces three specific changes in ganglioside synthesis (text-fig. 1). The precursor incorporation into a trisialoganglioside G_T decreased eightfold to tenfold, while incorporation into an unidentified ganglioside G_X and a disialoganglioside G_{D1b} increased twofold. That the unknown band G_X is a ganglioside is indicated by three observations: *a*) It shows incorporation of palmitic acid and is therefore a lipid and not a glycopeptide. *b*) It gives a positive reaction with resorcinol, thereby indicating the presence of sialic acid moieties. *c*) When treated with *C. perfringens* neuraminidase (fig. 1), G_X from JB6 cells is completely converted to monosialoganglioside G_{M1}. This result is expected for complex gangliosides and in fact occurs for the other complex JB6 gangliosides G_T and G_{D1b} as shown in figure 1, lanes 3 and 4.

The TPA-sensitive gangliosides have been identified on the basis of the solvent system shown in text-figure 1 as well as on the basis of two others. These included *N*-propanol:water (7:3; vol/vol) and chloroform:methanol:0.25% $CaCl_2$ (60:35:8; vol/vol/vol). However, the identities of these gangliosides are exclusively based on TLC. More exact methods of identification, such as gas-liquid chromatography and mass spectrometry, are being developed in our laboratory to determine the structure (Muschik G, Srinivas L, Colburn NH: Unpublished data).

The TPA-induced changes in ganglioside synthesis were observed as early as 0–4 hours after TPA exposure and persisted for at least 48 hours (text-fig. 2). Maximal effects were observed by 24 hours of exposure to TPA. The time course suggests coordinate regulation by TPA of shifts in the synthesis of all three gangliosides (G_T, G_X, and G_{D1b}).

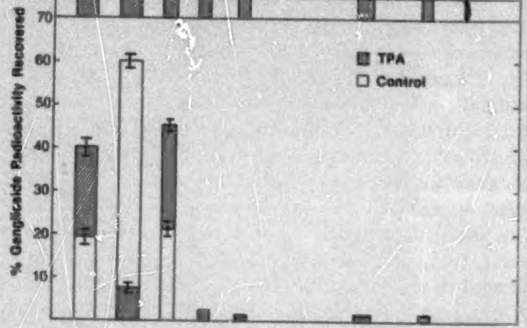

TEXT-FIGURE 1.—TPA treatment of JB6 cells produces a specific decrease in D-[1-^{14}C]glucosamine incorporation into trisialoganglioside G_T and an increase in incorporation into G_{D1b} and G_X. Gangliosides were separated on precoated Silica Gel-G plates (250 µm) with $CHCl_3$:CH_3OH:NH_3OH:H_2O (60:35:0.5:7.5; vol/vol/vol/vol). Plates were exposed to iodine vapors, and ganglioside bands were marked. After the iodine sublimed, the gangliosides were scraped, dissolved in $CHCl_3$:CH_3OH:H_2O 10:10:1; vol/vol/vol), and counted in a scintillation counter with Hydroflour at an efficiency of 50% for 1-ml samples. The radioactivity incorporated into each ganglioside was expressed as percent of total ganglioside-associated radioactivity with I indicating the range of duplicates. The radioactivity recovered from the plate was 80–90% of the total activity applied. Ganglioside-associated radioactivity recovered from control plates was ≈2,000 cpm, and from TPA-treated plates it was ≈1,100 cpm from a typical experiment. OR=origin; SF=solvent front.

The variation of ganglioside response with TPA concentration (text-fig. 3) indicates a correlation with the promotion of tumor cell phenotype by JB6 cells. As reported previously (*2*), 1-100 ng TPA/ml is active in promotion of anchorage independence with 10 ng/ml showing near-saturating activity. The 10-ng (1.6×10^{-8} *M*) TPA/ml concentration also appeared to be near saturating for the G_T decrease. To ascertain whether the changes are promoter-specific, we tested several analogs of TPA. The order of promoting activity in vivo and in JB6 cells in culture (*2*) for phorbol esters tested at 100 ng/ml was TPA>phorbol 12,13-dibenzoate>phorbol 12,13-dibutyrate>phorbol 12,13-diacetate=phorbol. As shown in text-figure 4, the non-tumor promoters phorbol 12,13-diacetate and phorbol showed no activity; the weak promoter phorbol 12,13-dibutyrate showed little or no activity; and phorbol 12,13-dibenzoate, which is less active as a promoter than TPA, showed intermediate activity in producing ganglioside shifts.

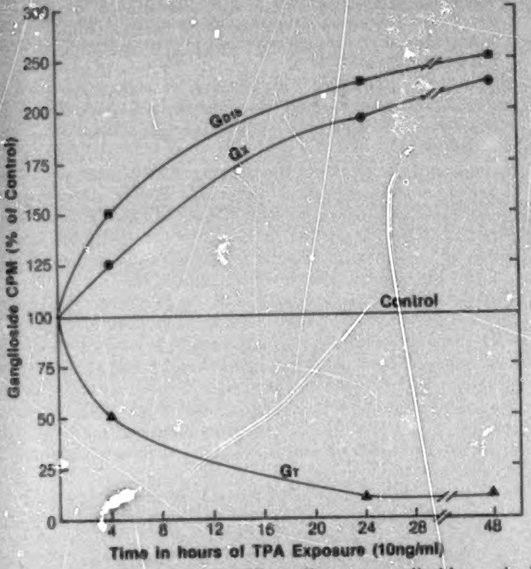

TEXT-FIGURE 2.—Time course of TPA effect on ganglioside synthesis in JB6 cells. D-[1-^{14}C]glucosamine incorporation was done for the terminal 4 hr of TPA exposure. Control values (100%) represent the incorporation of [1-^{14}C]glucosamine obtained without TPA at each time point as a percent of total ganglioside-associated radioactivity. The graph shows the [1-^{14}C]glucosamine incorporation into each ganglioside compared to that of control at each time point. *Each point* is the mean value for duplicate dishes.

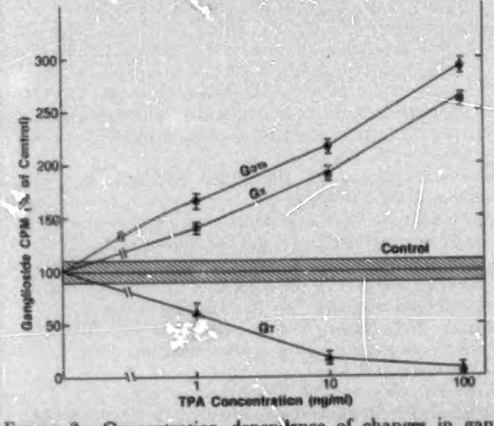

TEXT-FIGURE 3.—Concentration dependence of changes in ganglioside synthesis in response to TPA. TPA-induced changes in ganglioside synthesis (cpm [1-^{14}C]glucosamine incorporated as % of control) were determined as described in the legend to text-fig. 2. ▨=mean plus or minus the standard error of control values. ⟍=the range for duplicate TPA-treated samples.

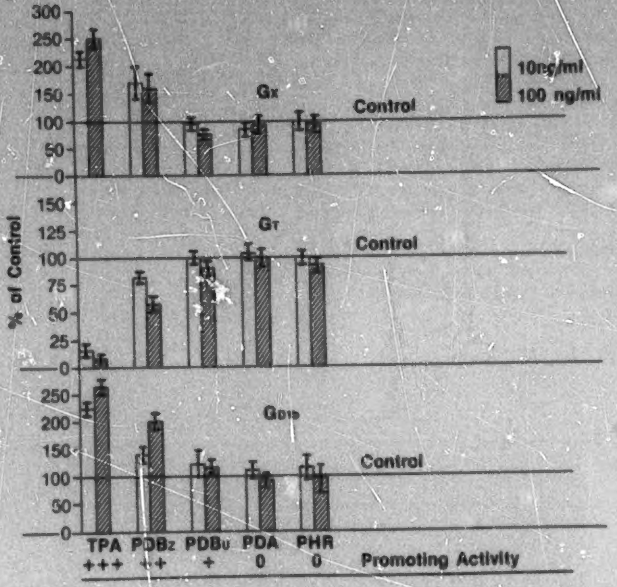

TEXT-FIGURE 4.—Ganglioside changes correlate with promoting activity of phorbol esters. [1-^{14}C]glucosamine incorporation into gangliosides was determined 20-24 hr after exposure to phorbol (PHR) or phorbol ester, and the results are expressed as described for text-fig. 2. I, the range of duplicate values. PDB_Z=phorbol 12,13-dibenzoate; PDB_U=phorbol 12,13-dibutyrate; PDA=phorbol 12,13-diacetate.

RA, an antipromoter both in vivo and in vitro (*9*), was investigated as a possible antagonist of TPA-induced ganglioside changes. Text-figure 5 shows the effects on ganglioside synthesis of an antipromoting concentration of RA alone or in combination with TPA. The 4-hour terminal incorporation of [1-^{14}C]glucosamine into gangliosides was unaffected by a 24-hour exposure to RA alone. In combination with TPA, RA completely prevented the TPA-induced changes in G_X, G_T, and G_{D1b}.

DISCUSSION

These studies have shown that tumor-promoting but not nonpromoting phorbol esters produce substantially decreased synthesis of G_T and increased synthesis of G_{D1b} and an unidentified ganglioside G_X in promotable JB6 cells. This observation, together with the demonstration that an antipromoting (*4, 27*) concentration of RA antagonizes the changes, suggests that the ganglioside response to TPA could be involved in promotion of transformation in JB6 cells.

The gangliosides affected by TPA in mouse JB6 cells differ from those involved in the TPA response in human melanoma cells (*7*). Undoubtedly, tissue and species specific-

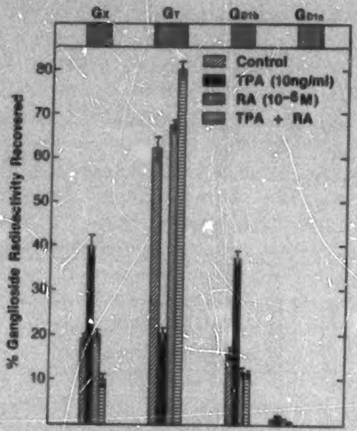

TEXT-FIGURE 5.—Anti-tumor-promoting concentration of RA antagonizes TPA effects on G_X, G_T, and G_{D1b} synthesis. JB6 cells were treated with 10 ng (1.6×10^{-8} *M*) TPA/ml for 24 hr. RA (10^{-6} *M*) exposure was done alone or simultaneously with TPA. The cells were labeled with [1-^{14}C]glucosamine for the last 4 hr. Gangliosides were isolated, separated, detected, and counted as described in text-fig. 1.

ity can be expected to give rise to characteristic ganglioside profiles and responses to external stimuli as is found for a variety of other cell surface molecules.

The similar time courses of G_T, G_{D1b}, and G_X changes suggest that TPA triggers some coordinate control mechanism that affects all three gangliosides. Decreased activity of anabolic enzymes, such as a glycosyltransferase, or increased activity of a catabolic enzyme, such as a neuraminidase, might be involved in producing such coordinate regulation with G_T as a primary target. We have recently found that JB6 cells produce a neuraminidase that utilizes G_T as a substrate (Srinivas L, Colburn NH: Unpublished data). Such an activity could be a candidate for a mediator of the G_T response to TPA.

The observation that the promoter-induced changes in ganglioside synthesis are completely blocked by the antipromoter suggests that: *a*) These gangliosides are involved in promotion of transformation, and *b*) they may be the target of the antipromoting action of RA. We have recently reported that RA also antagonizes the TPA-induced collagen decrease (*13*) in JB6 cells. Since the time courses of the collagen and ganglioside responses to TPA are similar, coordinate regulation of the two events by RA might be possible. However, the data suggest that the pathways may be different for the antagonism of TPA-induced collagen and ganglioside changes since RA alone increases collagen levels (*13*) but is without effect on ganglioside levels (text-fig. 5).

Further evidence for a role of the G_T switch in promotion of transformation by TPA in JB6 cells comes from our recent observation that promotion-sensitive but not promotion-resistant variants consistently undergo this G_T decrease (*34*).

REFERENCES

(*1*) Colburn NH. Tumor promotion and preneoplastic progression. In: Slaga TJ, ed. Carcinogenesis. Vol 5. Modifiers of carcinogenesis. New York: Raven Press, 1980:35–56.

(*2*) Colburn NH, Former BF, Nelson KA, Yuspa SH. Tumour promoter induces anchorage independence irreversibly. Nature 1979; 282: 589–591.

(*3*) Colburn NH. Tumor promoter produces anchorage independence in mouse epidermal cells by an induction mechanism. Carcinogenesis 1980; 1:951–954.

(*4*) Colburn NH, Koehler BA, Nelson KJ. A cell culture assay for tumor promoter dependent progression toward neoplastic phenotype: Detection of tumor promoters and promotion inhibitors. Teratogen Carcinogen Mutagen J 1980; 1:87–96.

(*5*) Yamasaki H, Fibach E, Nudel V, Weinstein IB, Rifkind RA, Marks PA. Tumor promoters inhibit spontaneous and induced differentiation of murine erythroleukemia cells in culture. Proc Natl Acad Sci USA 1977; 74:3451–3453.

(*6*) Delclos KB, Blumberg PM. Decrease in collagen production in normal and Rous sarcoma virus transformed chick embryo fibroblasts induced by phorbol myristate acetate. Cancer Res 1979; 39: 1667–1672.

(*7*) Huberman E, Heckman C, Langenbach R. Stimulation of differentiated functions in human melanoma cells by tumor promoting agents and dimethyl sulfoxide. Cancer Res 1979; 39:2618–2624.

(*8*) Huberman E, Callahan MF. Induction of terminal differentiation in human premyelocytic leukemia cells by tumor promoting agents. Proc Natl Acad Sci USA 1979; 76:1293–1297.

(*9*) Colburn NH, VorderBruegge WF, Bates JR, Yuspa SH. Epidermal cell transformation in vitro. In: Slaga TJ, Sivak A, Boutwell RK, eds. Carcinogenesis. Vol 2. Mechanisms of tumor promotion and cocarcinogenesis. New York: Raven Press, 1978; 37:3257–3265.

(*10*) Driedger PE, Blumberg PM. The effect of phorbol diesters on chicken embryo fibroblasts. Cancer Res 1977; 37:3257–3265.

(*11*) Lee LS, Weinstein IB. Tumor promoting phorbol esters inhibit binding of epidermal growth factor to cellular receptors. Science 1978; 202:313–315.

(*12*) Shoyab M, DeLarco JE, Todaro GJ. Biologically active phorbol esters specifically alter affinity of epidermal growth factors membrane receptor. Nature 1979; 279:387–391.

(*13*) Dion DL, De Luca LM, Colburn NH. Phorbol ester induced anchorage independence and antagonism by retinoic acid correlates with altered expression of specific glycoproteins. Carcinogenesis. In press.

(*14*) Hakomori S. Structures and organization of cell surface glycolipids. Dependence on cell growth and malignant transformation. Biochim Biophys Acta 1975; 417:56–89.

(*15*) Richardson CL, Baker SR, Moore DJ, Keenan TW. Glycosphingolipid synthesis and tumorigenesis. A role for the Golgi apparatus in the origin of specific receptor molecules of mammalian cell surface. Biochim Biophys Acta 1975; 417:175–186.

(*16*) Fishman PH, Henneberry RC. Induction of ganglioside biosynthesis in cultured cells by butyric acid. In: Sweeley CC, ed. Cell surface glycolipids. American Chemical Society symposium series. Vol 128. Washington, D. C.: American Chemical Society, 1980:223–239.

(*17*) Kleinman HK, Martin GR, Fishman PH. Ganglioside inhibition of fibronectin mediated cell adhesion to collagen. Proc Natl Acad Sci USA 1979; 76:3367–3371.

(*18*) Fishman PH, Brady RO. Biosynthesis and function of gangliosides. Science 1976; 194:906–915.

(*19*) Van Heyningen WE. Gangliosides as membrane receptors for tetanus toxin, cholera toxin and serotonin. Nature 1974; 139:415–417.

(*20*) Mullin BR, Fishman PH, Lee G, et al. Thyrotropin–ganglioside interactions and their relationship to the structure and function of thyrotropin receptors. Proc Natl Acad Sci USA 1976; 73:842–846.

(*21*) Wooley DW, Gommi BW. Serotonin receptor. VII. Activities of various pure gangliosides as their receptors. Proc Natl Acad Sci USA 1965; 53:959.

(*22*) Brady RO, Fishman PH. Biosyntheses of glycolipids in virus-transformed cells. Biochim Biophys Acta 1974; 355:121–148.

(*23*) Sekeyama H, Robbins PW. Glycolipid synthesis and tumorigenicity of clones isolated from the HIL2 line of hamster embryo fibroblasts. Fed Proc 1973; 32:86–90.

(*24*) Coleman PL, Fishman PH, Brady RO, Todaro GT. Altered ganglioside biosynthesis in mouse cell cultures following transformation with chemical carcinogens and X-irradiation. J Biol Chem 1975; 250:55–60.

(25) Critchley DR, Vicker MG. Glycolipids as membrane receptors are important in growth regulation and cell interaction. In: Poste G, Nicolson GL, eds. Dynamic aspects of cell surface organization. Amsterdam: Elsevier/North-Holland, 1977:307–370.

(26) Kloppel TM, Morré DJ. Characteristics of transplantable tumors induced in the rat by *N*-2-fluorenylacetamide: Elevation in tissue and serum sialic acid. JNCI 1980; 64:1401–1411.

(27) Sporn MM, Dunlop NM, Newton DL, Smith JM. Prevention of chemical carcinogenesis by vitamin A and its synthetic analogs (retinoids). Fed Proc 1976; 35:1332–1338.

(28) Colburn NH, Ozanne S, Litchi U, et al. Retinoids inhibit promoter dependent preneoplastic progression in mouse epidermal cell lines. Proc Natl Acad Sci USA 1981; 359:251–259.

(29) Colburn NH, VorderBruegge WE, Bates JR, et al. Correlation of anchorage-independent growth with tumorigenicity of chemically transformed mouse epidermal cells. Cancer Res 1978; 38:624–634.

(30) Suzuki KJ. The patterns of mammalian brain gangliosides. II. Evaluation of the extraction procedures, postmortem changes and the effect of formalin preservation. J Neurochem 1965; 12:629–638.

(31) Langenbach R. Gangliosides of chemically and virally transformed rat embryo cells. Biochim Biophys Acta 1975; 388:231–242.

(32) Svennerholm L. The gangliosides. J Lipid Res 1964; 5:145–155.

(33) Rey G, Gosselin L, Bacqu C, et al. The ganglioside content of the milk fat globule membrane and the mouse mammary tumor virus isolated from the milk of infected mice. Eur J Biochem 1980; 107:25–30.

(34) Colburn NH, Wendel EJ, Srinivas L. Responses of preneoplastic epidermal cells to tumor promoters and growth factors: Use of promoter-resistant variants for mechanism studies. J Supramol Struct Cell Biochem. In press.

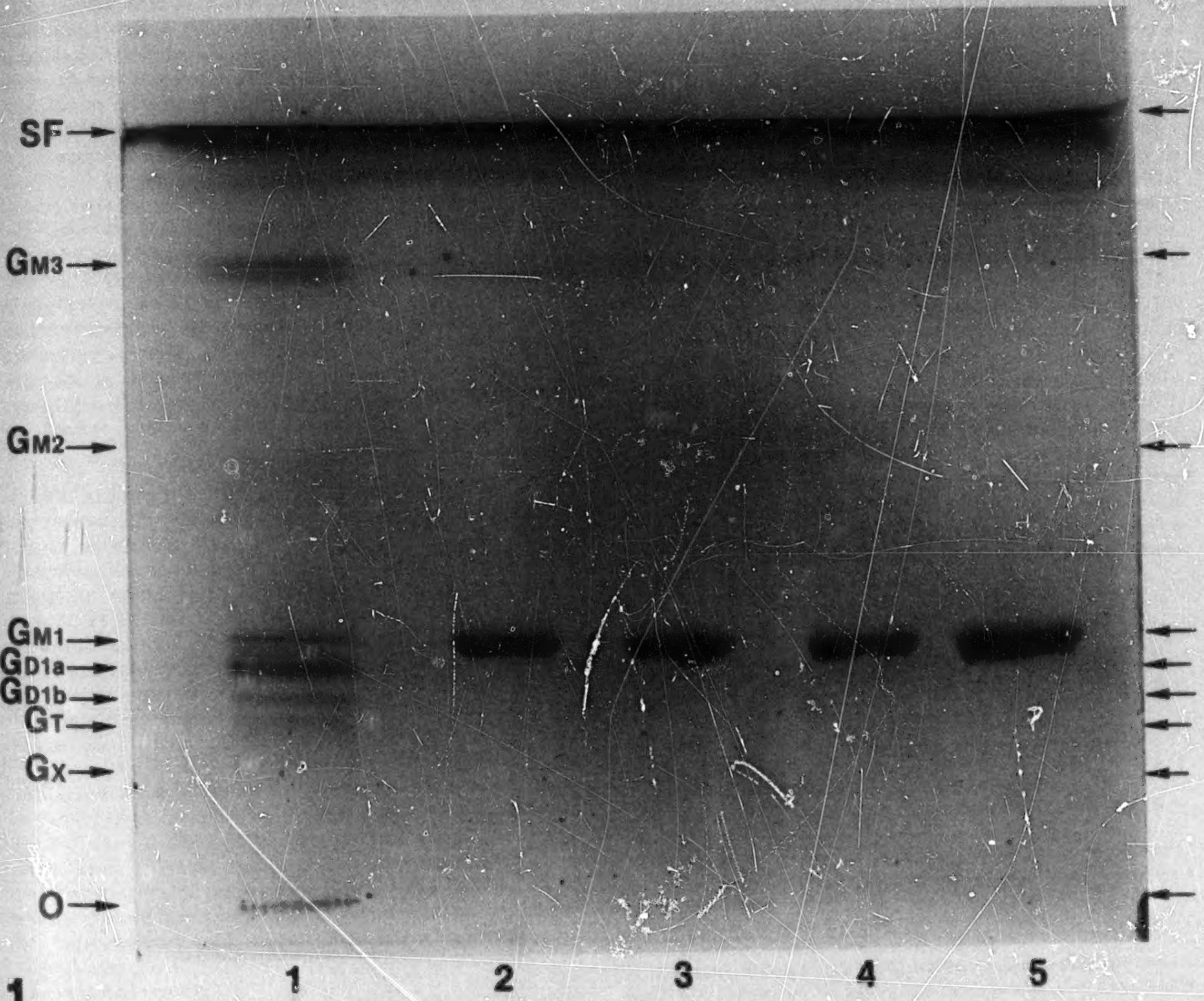

1

Figure 1.—Evidence that G_X is a complex ganglioside: Conversion to G_{M1} by *C. perfringens* neuraminidase. Neuraminidase treatment was done in the presence of 2 m*M* $CaCl_2$ in acetate buffer at pH 5.2. The reaction was stopped by addition of 10 vol of $CHCl_3$:CH_3OH (2:1). The reaction products were separated with the solvent system used in text-fig. 1, but the plate was prerun with petroleum ether:diethyl ether:acetic acid (80:20:1; vol/vol/vol) and was dried overnight, which obviated the need for desalting. Gangliosides were detected and counted as shown in the legend to text-fig. 1. Lane 1: standard bovine brain gangliosides untreated. Lane 2: JB6 G_X + neuraminidase. Lane 3: JB6 G_T + neuraminidase. Lane 4: JB6 G_{D1b} + neuraminidase. Lane 5: Standard bovine brain G_{M1}.

blank page

Microcirculatory Blood Flow, Capillary Morphology, and Local Oxygen Pressure of the Hamster Amelanotic Melanoma A-Mel-3 [1,2,3]

Bernhard Endrich, *M.D.*,[4,5] **Frithjof Hammersen**, *M.D.*,[6] **Alwin Götz**,[4,7] *and* **Konrad Messmer**, *M.D.*[4,8]

ABSTRACT—Transparent chambers and permanent indwelling catheters were implanted in the dorsal skin flaps of 24 inbred golden Syrian hamsters. After 48 hours, 4×10⁴ amelanotic melanoma cells (A-Mel-3) were transplanted sc (12 hamsters) in areas exposed for intravital microscopy. A platinum multiwire electrode and techniques for a quantitative analysis of television images were used for measurements of local oxygen pressure (P_{O_2}), capillary blood cell velocity, capillary density, and capillary diameter and length, whereas capillary morphology was evaluated by electron microscopy. Compared to the mean local P_{O_2} of the skin flaps of controls (12 hamsters), the mean local P_{O_2} on the tumor surface of melanoma-bearing hamsters decreased with tumor size. Although capillary density of the melanoma was elevated 4 days after tumor transplantation, it decreased significantly until day 12. Of hemodynamic significance were huge platelet conglomerates in short, dilated capillaries. Electron microscopy revealed endothelial hyperplasia, open endothelial junctions, and disintegration of the capillary endothelium. These findings strongly suggest that elevated microvascular resistance, intratumor tissue pressure, and widening of intercapillary distances in the melanoma might significantly diminish the impact of chemotherapeutic treatment.—JNCI 1982; 68:475–485.

One important feature of malignant melanomas is the unpredictability of growth and metastatic spread. A primary tumor as small as 5 mm³ can be accompanied by distant dissemination and metastases. In general, such small lesions reveal an established, characteristic microcirculatory pattern (*1-4*) on which cancer cells depend for maintenance and proliferation. The distribution of oxygen and nutrients at the capillary barrier is achieved after a distinct endothelial proliferation of postcapillaries and collecting venules into the tumor mass. By contrast, arterial blood is supplied to the tumor by morphologically normal arterioles (*5, 6*).

The total volume of blood supplying the malignant mass will, however, depend on both morphology and reactivity of arterioles and precapillaries located *in the tumor* as well as on the reactivity of the microcirculation in tissue *surrounding the tumor*. Only in vivo studies on single microvessels allow characterization of the structural and functional elements within the microvascular system. When transparent chamber techniques are used, the growth progression of malignant tumors and the alterations of their neovascular systems can be evaluated readily.

If these techniques are combined with a quantitative analysis of TV images, microhemodynamic parameters can be quantitated in individual vessels of both the melanoma and the surrounding subcutaneous structures. The present study reports on morphologic and microhemodynamic features of the hamster amelanotic melanoma A-Mel-3 with information gathered from in vivo and in situ observations.

MATERIALS AND METHODS

Quantitative analysis of the microcirculation.—Techniques of intravital microscopy and hemodynamic analysis in the terminal vascular bed have been described by Intaglietta and Zweifach (*7*) and by Zweifach and Lipowsky (*8*) (text-fig. 1) and were followed up with minor modifications of the optical system as reported previously (*9*). For microscopic observations and measurements, the original transparent double-frame-type chamber of Algire (*10*) was modified and aluminum chambers were implanted in the dorsal skin flaps of 24 hamsters, with the tissue thickness fixed at 450±5 µm. Because hamster skin is extremely translucent, such a large tissue thickness could be used, allowing for prolonged observation of a rapidly growing tumor. Two permanent indwelling catheters were inserted through the right jugular vein and the carotid artery and were directed toward the right and left ventricles, respectively (*9*).

After a 48-hour recovery from anesthesia and microsurgery, the hamsters' systemic pressures were monitored at 2-day intervals by Statham pressure transducers via both catheters. Concurrently, intravascular velocity of red blood cells was measured on-line from the photometric signal provided by two optical windows (Video Photometric Analyzer, model 204; IPM Inc., San Diego, Calif.) that were placed along the centerline of a given blood vessel within the televised site (*11*).

ABBREVIATIONS USED: FITC–Dextran 150=fluorescein isothiocyanate covalently bound to dextran, mol wt 150,000 (Pharmacia AB, Uppsala, Sweden); P_{O_2}=pressure of oxygen; TV=television.

---

[1] Received June 4, 1981; accepted October 19, 1981.

[2] Supported by a grant from the Abbott Foundation, Abbott Laboratories, North Chicago, Ill.

[3] Guidelines for the care and use of laboratory animals were followed as set forth by Good Laboratory Practice Regulations of the U.S. Food and Drug Administration.

[4] Institute for Surgical Research, Klinikum Grosshadern, University of Munich, Munich, Federal Republic of Germany.

[5] *Address reprint requests to* Dr. Endrich at the Department of Experimental Surgery, University of Heidelberg, Im Neuenheimer Feld 347, D-6900 Heidelberg 1, Federal Republic of Germany.

[6] Department of Anatomy, Technical University of Munich, Munich, Federal Republic of Germany.

[7] Candidate for the medical degree.

[8] We thank Ms. A. Hetzer, Ms. B. Lenze, Ms. A. Kreisle, and Ms. A. Bieber for their skillful technical assistance and Ms. I. Moll for typing the manuscript.

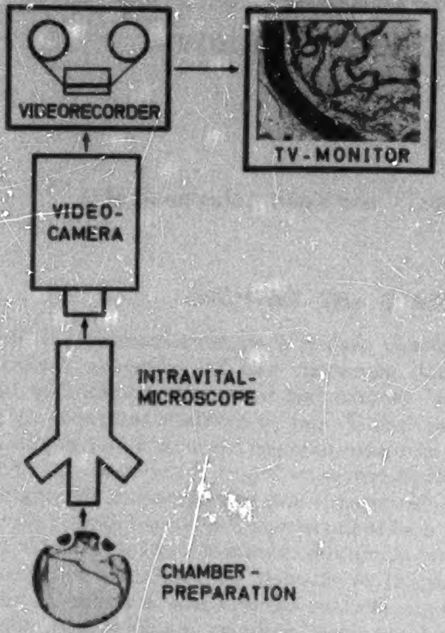

TEXT-FIGURE 1.—Scheme of the optical and electronic system for in vivo studies of the microcirculation.

In vitro calibration of the velocity system was performed before the experiment by measurement of the velocity of a disk rotating in a plane tangential to the optical axis. The windows were aligned manually along lines previously scratched into the translucent disk at a known radius and were filled with (8–10 µm) silicon carbon particles. These particles modulated the light reflected from the translucent disk and provided a signal size of 0.2–0.3 V. Even though a rotating disk containing a freshly prepared blood smear yielded the same signal size, in vitro measurements provided by constant size particulate matter were found to be more reproducible over an extended time (due to the shrinkage and discoloration of blood cells).

By this modified technique, the velocity system demonstrated a linearity of within 5% for all velocities from 0 to 10 mm/second. Due to framing rate limitations of European TV standards, however, large window spacings between 50 and 200 µm were necessary to measure velocities above 2.5 mm/second in vitro. Velocities above 10 mm/second could not be measured because the distance between the two sensors exceeded the vertical axis of the TV monitor at the given magnification (900×).

In vivo, however, the maximum blood cell velocity that can be reliably measured with the photometric analyzer and European TV standards is limited to approximately 2.5 mm/second. As a result of larger window spacings required to measure higher velocities, the computation of other events, i.e., autocorrelation, diminished the sharpness of the peak cross-correlation due to the light scintillation of the bloodstream, hence decreasing its detectability (*11, 12*). This problem, however, could be neglected in our study because the velocity data obtained only occasionally exceeded 2.5 mm/second. Each value above 2.5 mm/second was double checked with both the photometric analyzer and the photodiode as described below.

Intravital microscopy and video recordings were obtained from selected areas in subcutaneous tissues of chamber-bearing animals that were not tumor bearing (n=12) and that were tumor bearing (n=12). The region selected covered at least 1,800×1,000 µm. To minimize bias, we selected the region on day 0 (48 hr after implantation of the chamber and before inoculation of the melanoma) entirely on the basis of tissue transparency and visibility of large blood vessels (20–40 µm). When transillumination is used, capillaries are barely visible in this chamber model; consequently, any measurement at the capillary level refers to a single blind selection of this type of microvessel. After being committed to one region, we could better visualize the microvascular beds with the use of fluorescent microscopy after the hamsters received iv injections of 0.2 ml of 5% FITC-Dextran 150. This technique improved the poor contrast in vivo between the vessel wall of larger vessels and capillaries, the adjoining tissue, and the vascular contents to such an extent that blood cells were delineated as dark structures versus a bright background of plasma. Since microvascular entities were analyzed in a "dynamic" system, a given region could be as large as 5,000×3,500 µm, a size that then required several separate photomontages for microvascular analysis (*12*). In each animal, the identical area was observed throughout the experiment.

Videotape recordings needed for measurements of blood cell velocities and vascular diameters were performed in restrained, unanesthetized animals. At the conclusion of the experiments, the videotapes were played back, and the raster-line signals produced by the movement of blood cells were passed through the Video Photometric Analyzer. The comparison of velocity data from the videotape with data obtained during the recording procedure did not show any differences and the velocity data were not related to the use of either the Video Photometric Analyzer or a photodiode (fiber optic pickup system; IPM Inc.) which should be used for European TV standards if the velocity exceeds 2.5 mm/second (*11*). However, data from videotape recordings were included in this study primarily for the following reasons: 1) to shorten the time needed to restrain the unanesthetized animal for observation and videotape recordings, 2) to allow sufficient time for analysis because a dense capillary network (mean intercapillary spacing, ≈10 µm) was consistently seen providing a redundancy of information, and 3) to allow a double check of measurements by the principal investigator.

By measuring blood cell velocity and diameter in each vessel supplying the tumor with blood, we could calculate volume flow through any "inflow" vessel and thus, by addition of volumetric blood flows of all feeding vessels, could obtain total volume flow to the tumor. The conversion of these values into the usual dimension of blood flow (ml/min/100 g) was done by the calculation of the tumor weight. To calculate the tumor weight, we measured the tumor radius from the opaque area associated with the presence of the tumor, and we determined the equivalent radius of a circle covering the same surface. Since the tissue thickness was known (450 µm), the tumor volume and weight (specific density assumed to be 1) were readily calculated by the multiplication of the tumor surface by the tissue thickness. The blood inflow (ml/min/100 g) was determined by division of the total volumetric flow through the calculated tumor weight and by multiplication of this value by 100 (g).

On various days, we used a platinum multiwire electrode to measure local Po_2 on the surface of subcutaneous tissue (*13, 14*). The design of this Po_2 electrode consists of eight 15-μm-diameter platinum wires sealed in glass and covered with a Teflon membrane. The electrode registers O_2 tension on the tissue's surface simultaneously at eight different positions in a hemispherical catchment area of 30–50 μm. A micromanipulator was used to place the electrode on the tissue preparation after the cover glass was lifted from the chamber. By controlled movement of the electrode on the tissue's surface, a statistical distribution of Po_2 values could be obtained. The data are shown as Po_2 histograms.

During the Po_2 measurements, the local temperature was measured in the subcutis (small animal temperature probe; Ellab Instruments, Copenhagen, Denmark) and on the tumor's surface. This parameter remained constant in all animals (mean value ± SEM: 30.1±0.1°C).

Morphologic studies of the vascularization patterns were performed by construction of photomontages from black-and-white prints taken from the TV monitor at 500× (final magnification of printed montage=150×). The size of the areas selected in the preparation was measured from montages by a planimeter with an accuracy of ±5%. Lengths of vessels within a given area were also measured from the montage by the use of a map measure (*15*). In addition, an electronic video-image shearing technique was used to determine the internal vessel diameter for all vessels in which velocity measurements were made. This was performed at an effective magnification of 600×, as observed on a TV monitor (*16*). For morphometric measurements of capillary density, i.e., the density of FITC–Dextran 150-stained visible capillaries, the total length of vessels per unit area was calculated by stereologic techniques (*15*).

A rectangular grid was superimposed on the vessel's overlay. The total number of intersections between vessels and grid within a designated area were counted. If one assumes a random orientation of individual vessels, capillary density (L_A) was calculated from the probability of these intersections according to the equation $L_A = \pi \cdot N \cdot X / 2L_G$ (cm^{-1}), where N equals the number of intersections between vessels and grid, X equals the total magnification, and L_G equals the total length of grid lines enclosed in the designated area.

For routine L_A counts at 150×, a grid spacing of 10 mm was chosen. Despite a spacing of 450 μm between the two chamber frames, the depth of focus, as obtained by epi-illumination and fluorescent microscopy, was approximately 70 μm. This value is within the limits for the analysis of a three dimensional structure (*15*); consequently, the capillary density was analyzed precisely as described by Schmid-Schoenbein et al. (*15*). Routine histologic sections from tumor and controls confirmed that the vasculature studied in vivo very much resembled the typical microvascular pattern of the melanoma and subcutaneous tissue, respectively. Furthermore, all feeding vessels were found within this depth of focus.

Preparation and inoculation of tumor cells.—Tumor cells were received from a solid, virus-induced amelanotic melanoma A-Mel-3 established by Fortner et al. (*17*) from hamster cells. After sc injection of 1×10^6 cells in the hamster's back, a solid tumor 2 cm in diameter grew within 14 days. The tumor became necrotic by that time and killed the animal within 3 weeks. Before becoming necrotic, the tumor was maintained by being passed once every other week in inbred Syrian hamsters and was harvested by being sterilely excised. Cell suspensions of sterile hamster melanoma cells were stored in RPMI-1640 medium containing 10% fetal calf serum plus 10% dimethyl sulfoxide and kept frozen in liquid nitrogen. After a rapid thaw to 37°C, the cells were washed three times in RPMI-1640 medium plus 1% penicillin–streptomycin and checked for viability by trypan blue exclusion. Usually, 70–80% of the tumor cells were alive.

For tumor cell transplantation in the chamber preparation, 1 μl (microliter syringe; Hamilton, Bonaduz, Switzerland) of a concentrated tumor cell suspension was inoculated 48 hours after the chamber was implanted. This measure served to distinguish trauma-induced neovascularization from the development of capillary buds due to tumor growth. We evaluated the precise number of living cells by counting several samples with identical volumes and then adjusting the number of cells to 35,000–40,000 living tumor cells. All animals were housed in single cages in an environment that was controlled at 28°C. After tumor cells were inoculated, animals bearing the melanoma as well as control animals were kept for 4 days at 35°C and 50% humidity (Intensive Care Incubator 7510; Dräger, Lübeck, Federal Republic of Germany). This measure increased the tumor take to more than 90%. As the tumor became vascularized after 4 days, the environmental temperature was decreased to 28°C. All videotape recordings and measurements were done in animals taken from the 28°C environment and placed under the microscope. As mentioned earlier, the local subcutaneous temperature was constant at 30.1°C in the unanesthetized animal.

RESULTS

Microvascular Pattern of Amelanotic Melanoma A-Mel-3

The tumor portion in the tissue chambers was usually ovoid (fig. 1) with 1–4 vessels of arteriolar dimension and a moderate number of precapillaries feeding the melanoma. A narrow zone of edematous connective tissue separated the periphery of the tumor from a leash of dilated capillaries and collecting venules that surrounded the tumor (fig. 2). All of these vessels appeared to have thin walls lined by a single endothelial layer. There were also a few residual vessels remaining from those long, parallel capillaries at the inoculation site, which were typical of skeletal muscle tissue.

Direct attachment of tumor cells to capillaries was seen (fig. 3) and was frequently associated with formation of thrombi. Electron microscopy further revealed occasional diapedesis of erythrocytes (fig. 4). After approximately 4 days, a typical vascular configuration of short, thin-walled, sometimes dilated capillaries was seen primarily at the edge of the tumor (fig. 5). The appearance of these new blood vessels was associated with rapid growth of the malignant tissue. By 12 days after transplantation, the radius of the tumor portion became 2,718±664 μm. Due to continuous growth, the tumor obscured the preparation after 18 days, and observations in the microvasculature of the tumor were no longer possible.

The length of capillaries revealed a statistically significant difference ($P<0.02$–<0.005, Student's paired *t*-test) between tumor-bearing and control animals. The average capillary length in amelanotic melanoma was 198.2±8.9 µm on day 4 and 230.5±10.3 µm 8 days later (text-fig. 2). Capillary length in subcutaneous tissue of control tumor-free animals was 414.4±30.9 µm on day 4 and 418.5±21.8 µm on day 12, i.e., 14 days after implantation of the aluminum chamber.

Large necrotic, avascular areas appeared in the center part of the tumor approximately 5 days after its transplantation. At that time, platelet conglomerates were consistently noted in capillaries of the amelanotic melanoma, temporarily blocking the blood flow. As the melanoma grew further, the vasculature continually pushed the existing microvascular channels toward the tumor's growing edges, while more centric blood vessels were obliterated.

On the basis of 71 determinations from 8 animals (control, $n=4$; A-Mel-3-bearing, $n=4$), a rise in capillary density was found in tumor-free control preparations, whereas in the tumor-containing chambers, the slight increase in the density of erythrocyte-perfused capillaries at 4 days after tumor transplantation was followed by a consecutive decrease as tumor growth continued (text-fig. 3).

Hemodynamic Characteristics of Amelanotic Melanoma A-Mel-3

Table 1 demonstrates that, with the exception of a slight hypovolemia on day 0 in our control group, significant changes of mean arterial pressure, central venous pressure, and heart rate did not occur. The microcirculation of the amelanotic melanoma A-Mel-3, however, revealed typical alterations.

In most microvessels, the direction of blood flow *encircled* the center of the tumor, with intermittent or regurgitant blood flow in capillary channels. This phenomenon was strongly related to the presence of platelet conglomerates in tumor blood vessels. Tables 1 and 2 summarize measurements of blood cell velocity and vessel diameter at various days after tumor transplantation in amelanotic melanoma and in tumor-free control preparations. Mean blood cell velocity in capillaries was significantly different, and blood flow in single capillaries of the amelanotic melanoma A-Mel-3 revealed localized irregularities in those segments where microaneurysms or platelet conglomerates were observed. Despite the progressive dilation of arterioles and precapillaries, blood cell velocity in precapillaries of the tumor was significantly lower when compared to blood cell velocity in tumor-free preparations.

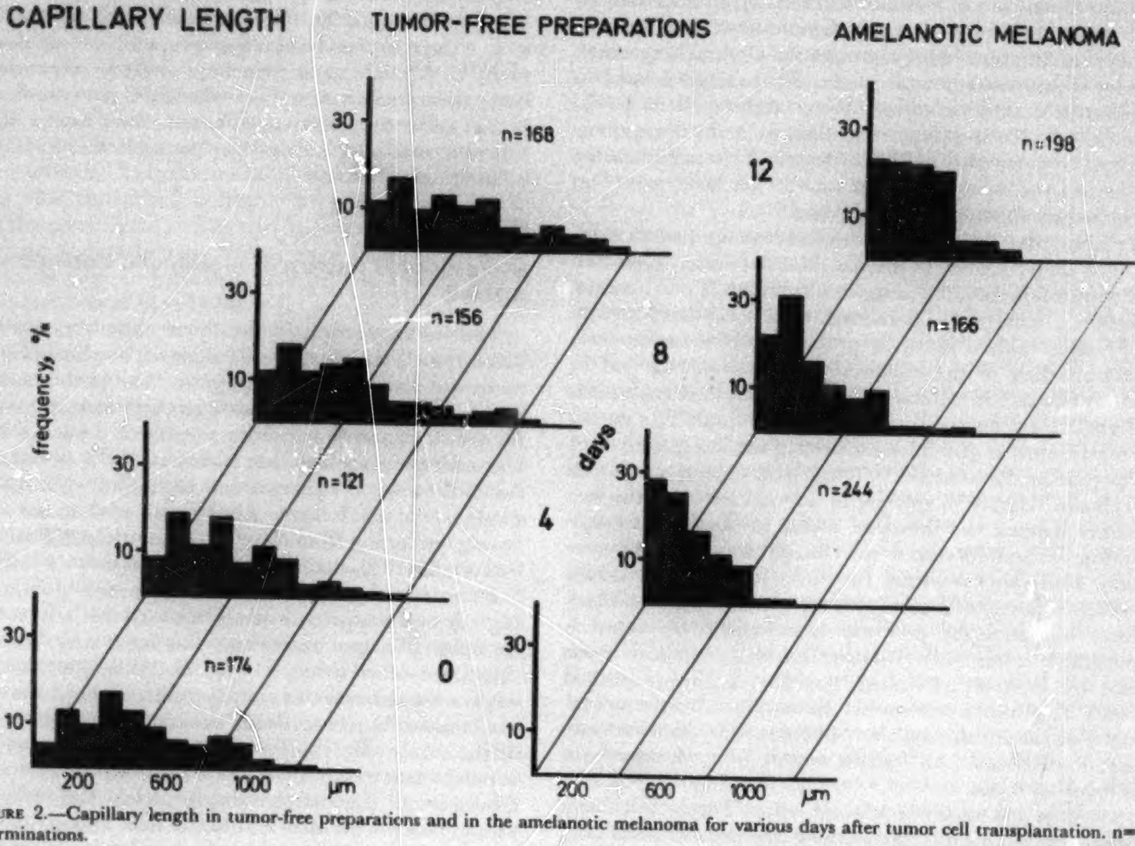

TEXT-FIGURE 2.—Capillary length in tumor-free preparations and in the amelanotic melanoma for various days after tumor cell transplantation. n=No. of determinations.

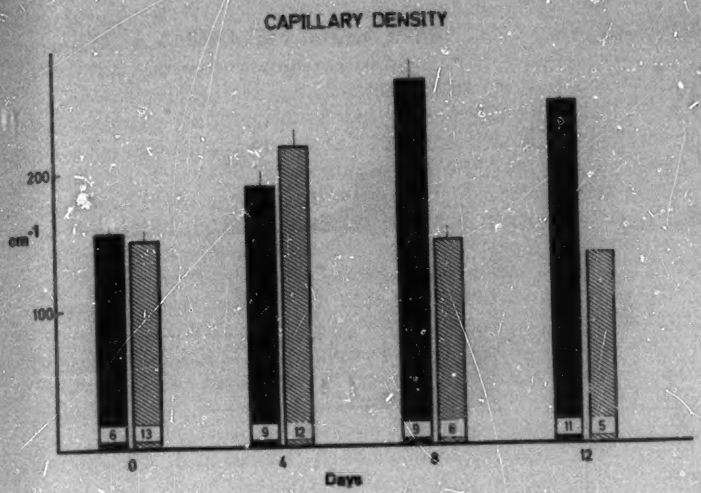

TEXT-FIGURE 3.—Capillary density in tumor-free preparations and in the amelanotic melanoma A-Mel-3. *Black columns*=tumor-free preparations; *hatched columns*=amelanotic melanoma A-Mel-3. *Hatched column* on day 0 reflects capillary density in the area subsequently transplanted with tumor cells. *Numbers within each column* are No. of determinations for a given day.

TABLE 1.—*Melanoma microcirculation: Parameters along different microvascular segments*[a]

Parameter	Day[a]			
	0	4	8	12
Mean arterial pressure, mm Hg	111.1±6.1	96.3±3.6	114.6±4.4	111.0±13.0
Central venous pressure, mm Hg	−0.4±0.7	−0.4±1.4	2.6±2.2	3.0±2.1
Heart rate/min	374±13	348±12	351±37	415±35
Blood cell velocity, mm/sec				
Arterioles	—	1.30±0.12 (13.5–35.0) [14]	1.18±0.27 (17.0–41.4) [12]	1.56±0.31 (19.5–44.4) [12]
Precapillaries	—	1.17±0.09 (6.3–21.9) [42]	1.08±0.15 (9.4–28.0) [19]	0.89±0.11 (9.9–35.6) [10]
Capillaries	—	0.46±0.03 (4.3–22.7) [138]	0.50±0.03 (5.1–27.0) [146]	0.51±0.05 (4.8–34.8) [70]
Postcapillaries	—	0.44±0.03 (8.1–26.1) [89]	0.56±0.06 (8.9–20.7) [54]	0.47±0.04 (7.2–36.7) [46]
Collecting venules	—	0.51±0.04 (13.8–53.2) [53]	0.92±0.10 (14.4–53.4) [42]	0.90±0.07 (15.0–51.3) [17]

[a] Determinations were made at a local subcutaneous temperature of 30.1°C. Values are means ± SEM. *Numbers in parentheses* are ranges of diameters in micrometers. *Numbers in brackets* are No. of determinations. — = not applicable.

TABLE 2.—*Subcutaneous tumor-free control circulation: Parameters along different microvascular segments*[a]

Parameter	Day[a]			
	0	4	8	12
Mean arterial pressure, mm Hg	93.2±5.2	107.6±7.2	117.2±5.4	115.3±6.7
Central venous pressure, mm Hg	−1.7±1.1	0±1.5	−0.4±1.2	−0.6±0.8
Heart rate/min	380±10	350±46	392±15	382±7
Blood cell velocity, mm/sec				
Arterioles	1.20±0.34 (15.6–30.0) [6]	0.94±0.13 (15.0–51.6) [5]	1.38±0.22 (18.7–50.6) [7]	1.61±0.46 (16.1–39.9) [6]
Precapillaries	1.21±0.20 (8.1–11.9) [12]	1.70±0.16 (7.3–11.3) [29]	1.88±0.12 (6.4–16.0) [48]	1.94±0.17 (6.5–13.8) [31]
Capillaries	0.48±0.04 (4.4–13.1) [82]	0.79±0.05 (4.1–7.9) [139]	0.70±0.03 (4.5–11.0) [181]	0.73±0.06 (3.5–7.9) [78]
Postcapillaries	0.34±0.05 (11.3–21.3) [23]	0.70± 0.06 (7.4–13.0) [71]	0.64±0.04 (7.0–19.4) [81]	0.53±0.05 (8.1–14.6) [52]
Collecting venules	0.47±0.04 (14.1–36.3) [22]	0.75±0.04 (14.6–38.5) [92]	0.90±0.05 (14.3–43.5) [102]	0.65±0.05 (14.2–34.2) [67]

[a] Determinations were made at a local subcutaneous temperature of 30.1°C. Values are means ± SEM. *Numbers in parentheses* are ranges of diameters in micrometers. *Numbers in brackets* are No. of determinations.

After measuring blood cell velocity and diameter in each vessel supplying the tumor with blood, we calculated the volume flow through any inflow vessel and determined the total tumor blood flow. The mean blood flow of the amelanotic melanoma was 40.4 ml/minute/100 g on day 4 and 21.1 ml/minute/100 g on day 12, respectively. Further growth of the tumor resulted in large, unperfused areas in the amelanotic melanoma. Petechial hemorrhage developed in those segments where blood flow was re-established after a period of very slow (<0.10 mm/sec) or zero flow.

As a result of nonhomogeneous capillary perfusion, decreased capillary density, and central necrosis, the local tissue Po_2 decreased as the tumor grew. While the Po_2 histograms in subcutaneous tissue of tumor-free animals were homogeneous with a mean value between 20 and 35 mm Hg, the Po_2 histograms shifted to the left in all animals

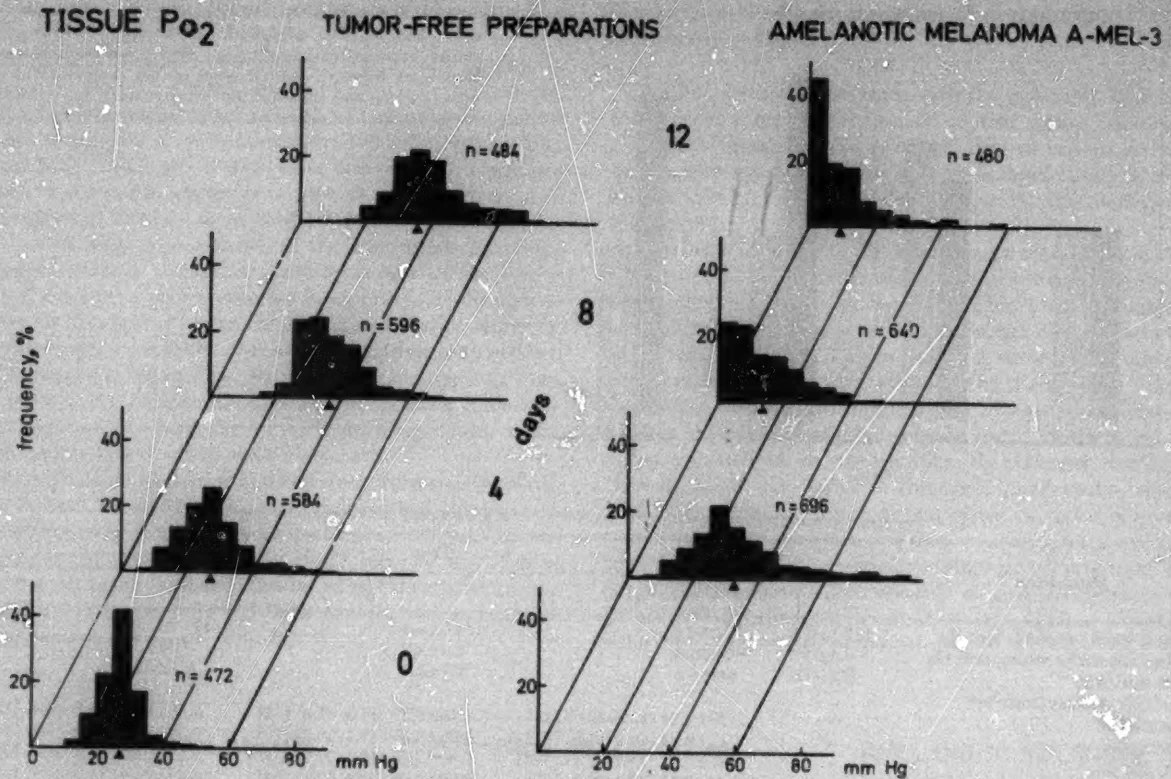

Text-figure 4.—Frequency distribution of local P_{O_2} for tumor-free preparations and for the amelanotic melanoma A-Mel-3 at days 0, 4, 8, and 12. n=No. of determinations as obtained by movement of the platinum multiwire electrode. Measurements were done in 12–15 different positions on the given tissue surface.

studied from earliest tumor growth throughout day 12. The P_{O_2} distribution in the sum histograms (text-fig. 4), with a mean value of 9.7±2.4 mm Hg on day 12, and the distinct change in skewness obtained in each animal reflect a progressive tissue hypoxia in the amelanotic melanoma A-Mel-3. This finding was not related to a difference in the number of single determinations.

DISCUSSION

For the prediction of antimalignant action of chemotherapy and radiation therapy in humans, preclinical screening systems are important because individual tumors, even those appearing identical by histologic grading, differ considerably in their response to treatment (*18*, *19*).

If human tumors were used in nude mice or hamsters, an experimental model could be designed to resemble human cancers biologically, immunologically, and genetically. However, host versus graft effects, particularly on the microvasculature, restrict this approach. From implanting pieces of different human tumors and small fragments of the amelanotic melanoma A-Mel-3, Witte and Goldenberg (*4*) concluded that homologous tumors are better adapted to the host's vascular system. When they used human tumor specimens, they noted, even in the immunologically privileged hamster cheek pouch, a pronounced reactive hyperemia in capillaries and larger blood vessels, a finding that is contrary to the established pathomechanism of capillary vascularization of a tumor mass (*1*, *2*, *4*, *20–22*). Consequently, human tumors cannot be used in animals for quantitative studies of the microcirculation within and around the transplant because "tumor-typical reactions" of the terminal vascular bed are most likely superimposed by the host versus graft reaction.

With a homologous tumor in the hamster's skin flap, distinct discrepancies of our blood cell velocity data, particularly at the arteriolar site, became apparent when these results were compared to data reported in the literature (*8*, *23*, *24*). However, recent studies on effects of anesthesia strongly suggest that anesthesia per se as well as the exposure of tissues affects most microvascular preparations and causes varying degrees of inflammation and vasodilation (*25*). Consequently, intravital microscopic exposure of tissues in the anesthetized animal very likely eliminates control mechanisms, namely, vasomotor activity (*26*). Contrary to current microcirculatory preparations, this phenomenon in our control animals was observed in about 60% of all arteriolar vessels studied (periodicity of this effect=2–3 cycles/min). Since data on blood cell velocity are usually reported as mean values for a certain period of time (20 sec in our study), the presence of vasomotor activity will yield lower blood cell velocities in arterioles. Furthermore, in contrast to our study, a great number of microcirculatory studies have been conducted with the local temperature adjusted to approximately 37°C (*8, 23, 24*). This temperature difference of approximately 7°C may provide another likely explanation for this apparent discrepancy in blood cell velocities.

It is a well-established fact that histograms of local Po_2 reflect perfectly the integrity of the microvascular network and the O_2 supply of the tissue (*27, 28*). The measurements of local Po_2 in control preparations and bell-shaped, homogeneous Po_2 histograms over a period of 12 days provide clear evidence of a normal, physiologic microcirculatory bed (*27, 28*) in our chamber model. The pattern of the capillary network and its flow characteristics, both quantitatively analyzable by the combination of local Po_2 measurements with the quantitative analysis of TV images, will directly affect the local Po_2. This combination is essential for the elucidation of the mechanism of tissue hypoxia in a malignant tumor.

Significant discrepancies between tumor-free and melanoma-bearing animals are 1) short, tortuous capillaries aligned only along the edge of the tumor; 2) capillary density/unit of tissue decreased as tumor grew while capillary density rose slightly in tumor-free preparations; 3) blood cell velocity at precapillary and capillary sites less in tumors than in subcutaneous tissues of tumor-free animals; and 4) lack of arteriolar vasomotion in the amelanotic melanoma. Moreover, any extravascular pressure on arteriolar tumor vessels results in both a complete stop of blood flow to the tumor center and a decrease of blood flow rate to large tumor areas, finally followed by necrosis. Low blood flow to large, central parts of the melanoma and higher blood flow to a very small volume of cells at the tumor's margin resulted in an overall decreased blood flow in the amelanotic melanoma A-Mel-3. Moreover, local variations in capillary morphology and alignment provide evidence that the tumor per se affects its blood supply (*20, 29–33*), a finding that could be quantitatively assessed by the measurement of capillary density.

The elevated capillary density 4 days after tumor transplantation and the subsequent, statistically significant decrease of this parameter indicate 1) tumor cell transplantation as a strong, angiogenic stimulus evoking an initial increase of capillary density (as a consequence, blood flow in the amelanotic melanoma A-Mel-3 was higher than that in subcutaneous tissue of tumor-free animals at the time of tumor development) and 2) significant effects of extravascular but intratumoral mechanical forces leading to a collapse of a great number of exchange vessels, hence reducing the overall rate of blood flow. One might argue that the decrease of capillary density in the tumor resulted from the given experimental conditions where the frame-to-frame distance of only 450 μm might apply external compression to the tumor. In fact, Eddy and Casarett (*22*) and Peters et al. (*29*) reported self-compression of "sandwich" tumors. Blood flow in their preparations could quickly be restored by an increase in the distance between the chamber frames. Peters et al. (*29*) reported that microcirculatory channels could not tolerate the sudden impact of resumed blood flow after ischemia; consequently, the area exposed was later covered with blood. Identical observations were made in our study, however, only after day 16 when the cover glass was removed. By contrast, during earliest tumor growth (days 0–12), when repeated opening and reinsertion of the cover glass were performed for measurements of local Po_2, microscopic inspection and quantitative analysis of blood cell velocity and capillary density before and after Po_2 measurements did not reveal any significant morphologic or microhemodynamic changes, thus indicating that our tumor was apparently not subjected to external compression until day 16 after tumor cell transplantation.

In particular, we never observed during the first 12 days of tumor development that blood flow or tumor volume (congestion of blood within the melanoma) increased when we lifted the cover glass. Consequently, any obstruction of capillary blood flow cannot result from external compression by cover glass or chamber frame but from "mechanical forces" within the proliferative system ("self-compression") of a malignant tumor because its microcirculation is characterized by a lack of organization, differentiation, and strictly correlated development of capillaries (*1–4, 22, 33*). Moreover, rarefaction and uneven distribution of capillaries within malignant tumors will inevitably cause local tissue hypoxia (*34, 35*).

A low capillary density, however, does not necessarily imply that the capillaries were not present. In fact, compression of larger microvascular entities associated with tissue hypoxia was frequently observed during tumor growth and was probably caused by an "internal tumor tissue pressure." This hypothesis can further be supported by 1) the fact that values of interstitial tissue pressure up to 23 mm Hg have been reported for the 7,12-dimethylbenz[*a*]-anthracene-induced adenocarcinoma of the rat (*36*); 2) the fact that, in the same tumor, the postcapillary and venular pressure was found to be significantly lower than that in subcutaneous tissue [a lower microvascular pressure might favor compression and obstruction of microscopic vessels in malignant tumors (*29, 36*)]; and 3) the finding of disintegration of the capillary endothelium and wide-open endothelial junctions in the amelanotic melanoma A-Mel-3 facilitating the filtration of fluid into the extravascular space (fig. 4).

These findings suggest that interstitial edema and proliferative activity in malignant tumors might compress a great number of nutritional capillaries. This "self-destroying capacity" may finally result in hypoxia or low-flow anoxia of large parts of the melanoma, whereas only a small tumor margin is still sufficiently supplied with blood.

REFERENCES

(*1*) Warren BA, Shubik P. The growth of the blood supply to melanoma transplants in the hamster cheek pouch. Lab Invest 1966; 15:464–478.

(*2*) Warren BA. The microcirculation in two transplantable melanomas of the hamsters. II. Scanning electron microscopy. Cancer Lett 1978; 4:117–124.

(*3*) ———. Metastasis via the blood stream: The method of intravasation of tumor cells in a transplantable melanoma of the hamster. Cancer Lett 1978; 4:245–251.

(*4*) Witte S, Goldenberg DM. Microcirculation in tumours and reaction to transplantation. Bibl Anat 1967; 9:396–402.

(*5*) Yamaura H, Sato H. Quantitative studies on the developing vascular system of rat hepatoma. J Natl Cancer Inst 1974; 53:1229–1240.

(*6*) Intaglietta M, Myers RR, Gross JF, Reinhold HS. Dynamics of microvascular flow in implanted mouse mammary tumours. Bibl

Anat 1977; 15:273–275.

(7) Intaglietta M, Zweifach BW. Microcirculatory basis of fluid exchange. Adv Biol Med Phys 1974; 15:111–159.

(8) Zweifach BW, Lipowsky HH. Quantitative studies of the microcirculatory structure and function. III. Microvascular hemodynamics of cat mesentery and rabbit omentum. Circ Res 1977; 41:380–390.

(9) Endrich B, Asaishi K, Goetz A, Messmer K. Technical report. A new chamber technique for microvascular studies in unanesthetized hamsters. Res Exp Med (Berl) 1980; 177:125–134.

(10) Algire GH. An adaption of the transparent-chamber technique to the mouse. J Natl Cancer Inst 1943; 4:1–11.

(11) Intaglietta M, Silverman NR, Tompkins WR. Capillary flow velocity measurements in vivo and in situ by television methods. Microvasc Res 1975; 10:165–179.

(12) Zweifach BW. Quantitative studies of microcirculatory structure and function. I. Analysis of pressure distribution in the terminal vascular bed in cat mesentery. Circ Res 1974; 34:843–857.

(13) Kessler M, Grunewald WA. Possibilities of measuring oxygen pressure fields in tissue by multiwire platinum electrodes. Prog Respir Res 1969; 3:147–152.

(14) Luebbers DW. Principle of construction and application of various platinum electrodes. Prog Respir Res 1969; 3:136–146.

(15) Schmid-Schoenbein GW, Zweifach BW, Kovalcheck S. The application of stereological principles to morphometry of the microcirculation in different tissues. Microvasc Res 1977; 14:303–317.

(16) Intaglietta M, Tompkins WR. Microvascular measurements by video image shearing and splitting. Microvasc Res 1973; 5:309–312.

(17) Fortner JG, Mahy AG, Schrodt GR. Transplantable tumors of the Syrian (golden) hamster. Part I: Tumors of the alimentary tract, endocrine glands and melanomas. Cancer Res 1961; 21(6)pt 2:161–198.

(18) Smith GM. The effect of cytotoxic agents on human tumours transplanted to the hamster cheek pouch. Br J Cancer 1969; 23:78–87.

(19) Lee YT. Diagnosis, treatment and prognosis of early melanoma. Ann Surg 1980; 191:87–97.

(20) Gullino PM, Grantham FH. Studies on the exchange of fluids between host and tumor. II. The blood flow of hepatomas and other tumors in rats and mice. J Natl Cancer Inst 1961; 27:1465–1491.

(21) Reinhold HS, Blachiwiecz B, Blok A. Oxygenation and reoxygenation in "sandwich" tumours. Bibl Anat 1977; 15:270–272.

(22) Eddy HA, Casarett GW. Development of the vascular system in the hamster malignant neurilemmoma. Microvasc Res 1973; 6:63–82.

(23) Fronek K, Zweifach BW. Microvascular blood flow in cat tenuissimus muscle. Microvasc Res 1977; 14:181–189.

(24) Lipowsky HH, Zweifach BW. Methods for the simultaneous measurement of pressure differentials and flow in single unbranched vessels of the microcirculation for rheological studies. Microvasc Res 1977; 14:345–361.

(25) Longnecker DE, Harris PD. Anesthesia. In: Kaley G, Altura BM, eds. Microcirculation. Vol. III. Baltimore: Univ Park Press, 1980: 333–369.

(26) Intaglietta M. Vasomotor activity, time-dependent fluid exchange and tissue pressure. Microvasc Res 1981; 21:153–164.

(27) Luebbers DW. Local tissue Po_2: Its measurement and meaning. In: Kessler M, Bruley DF, Clark LC, Luebbers DW, Silver IA, Strauss J, eds. Oxygen supply. Munich, Berlin, and Vienna: Urban Schwarzenberg, 1973:151–155.

(28) Kessler M, Görnandt L, Lang H. Correlation between oxygen tension in tissue and hemoglobin dissociation curve. In: Kessler M, Bruley DF, Clark LC, Luebbers DW, Silver IA, Strauss J, eds. Oxygen supply. Munich, Berlin, and Vienna: Urban Schwarzenberg, 1973:156–159.

(29) Peters W, Teixeira M, Intaglietta M, Gross JF. Microcirculatory studies in rat mammary carcinoma. I. Transparent chamber method, development of microvasculature, and pressures in tumor vessels. JNCI 1980; 65:631–642.

(30) Endrich B, Intaglietta M, Reinhold HS, Gross JF. Hemodynamic characteristics in microcirculatory blood channels during early tumor growth. Cancer Res 1979; 39:17–23.

(31) Endrich B, Reinhold HS, Gross JF, Intaglietta M. Tissue perfusion inhomogeneity during early tumor growth in rats. JNCI 1979; 62: 387–395.

(32) Endrich B, Zweifach BW, Reinhold HS, Intaglietta M. Quantitative studies on microcirculatory function in malignant tissue: Influence of temperature on microvascular hemodynamics during the early growth of the BA 1112 rat sarcoma. Int J Radiat Oncol Biol Phys 1979; 5:2021–2030.

(33) Asaishi K, Endrich B, Götz A, Messmer K. Quantitative analysis of microvascular structure and function in the amelanotic melanoma A-Mel-3. Cancer Res 1981; 41:1898–1904.

(34) Urbach F, Noell WK. Effects of oxygen breathing on tumor oxygen measured polarographically. J Appl Physiol 1958; 13:61–65.

(35) Vaupel P. Hypoxia in neoplastic tissue. Microvasc Res 1977; 13:399–408.

(36) Wiig H, Tveit E, Hultborn R, Weiss L. Interstitial and vascular pressures in rat mammary tumours. Bibl Anat 1981; 20:620–623.

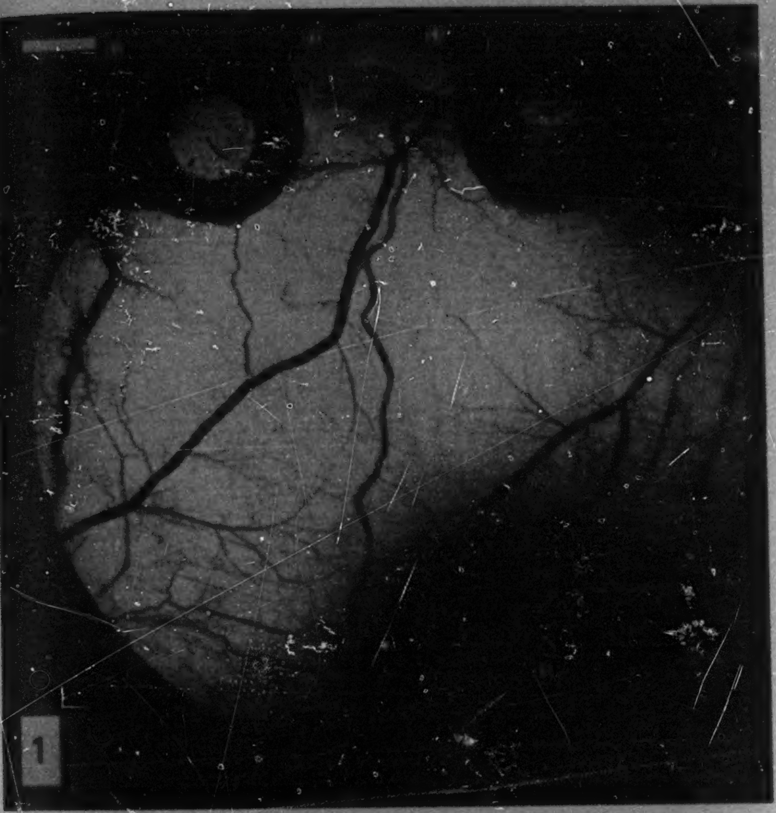

FIGURE 1.—Typical overview of a tumor preparation. Tumor is located in the *right lower part* of the chamber 6 days after transplantation. Unstained. *Bar*=1 mm. ×10

FIGURE 2.—Chaotic microcirculatory alignment at tumor's edge. Capillaries were visualized after iv injection of 0.2 ml 5% FITC-Dextran 150 solution. *Bar*=50 μm. Photographed from TV monitor. ≈×220

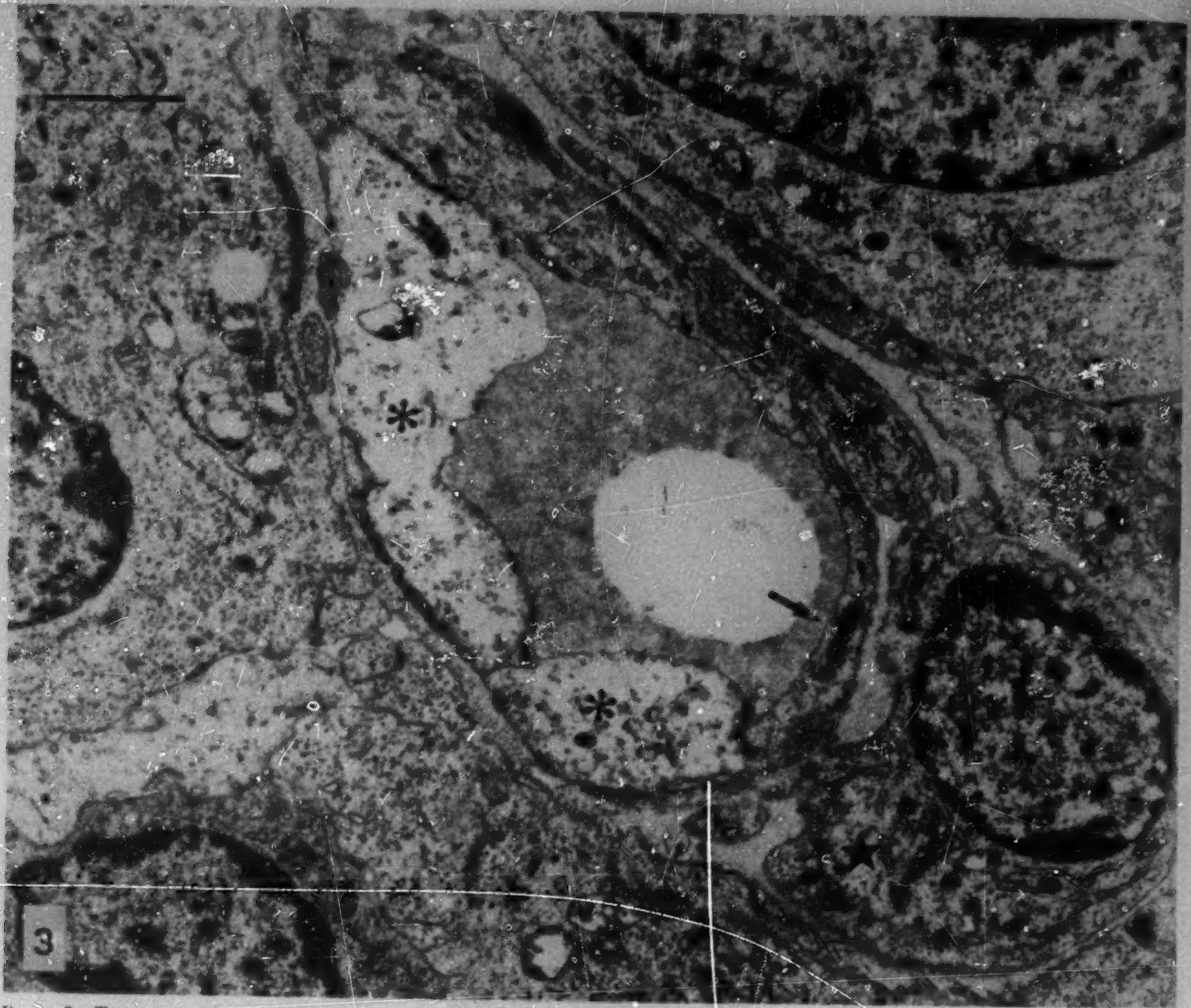

3

FIGURE 3.—Transverse section through a capillary of tumor grown for 8 days in tissue chamber. Two endothelial cells display prominent edema (*), whereas another "endothelial" cell (→) represents obvious cytoplasmic extension of the nucleated cell body (★) located beyond capillary wall proper. *Note* structural similarities between this cell and adjoining tumor cells. *Bar*=2 µm. × 11,500

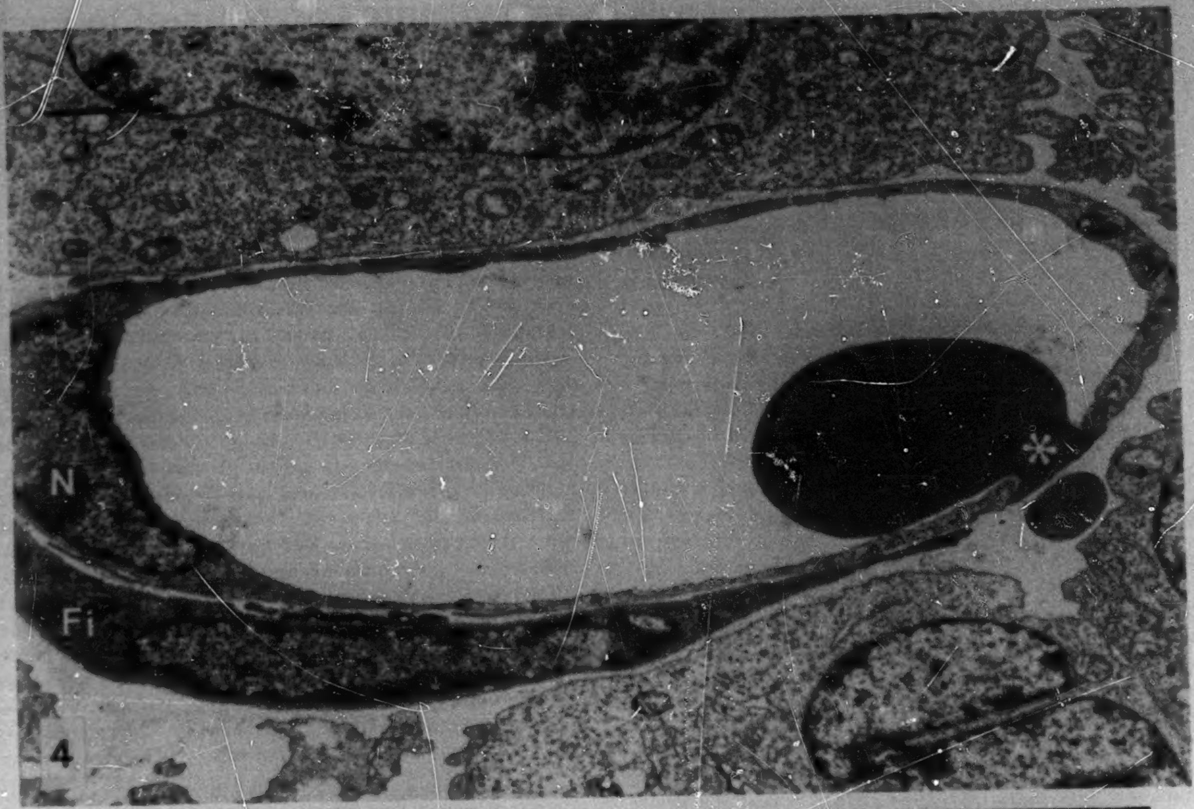

4

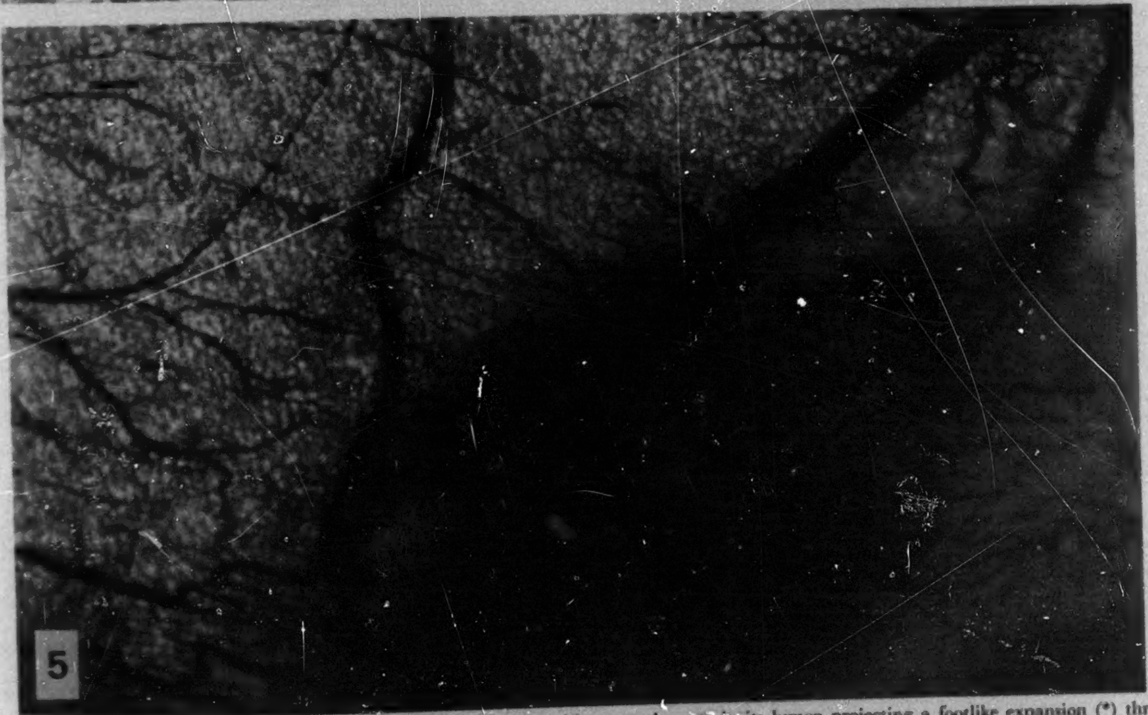

5

FIGURE 4.—Oblique section of thin-walled venous capillary segment with an erythrocyte in its lumen projecting a footlike expansion (*) through an interendothelial gap (from 8-day-old tumor). N=endothelial nucleus; Fi=fibroblast. *Bar*=2 µm. × 9,000

FIGURE 5.—Close-up of tumor preparation. Narrow zone of edema separated the periphery of the tumor from capillaries and collecting venules surrounding the tumor. These vessels were slightly dilated. A few vessels also remained from those long, parallel capillaries at the inoculation site which were typical for skeletal muscle structures and from which occasional extravasation of erythrocytes occurred. Unstained. *Bar*=100 µm. × 70

blank page

Effect of Heating on Lethality Due to Hyperthermia and Selected Chemotherapeutic Drugs [1, 2]

Terence S. Herman,[3, 4] Cynthia C. Sweets,[3] David M. White,[3] *and* Eugene W. Gerner[5]

ABSTRACT—Because the rate of heating alters various cellular events associated with exposure to hyperthermia (including the rate of cell death), effect of this parameter on the cytotoxic interaction between selected anticancer drugs and hyperthermia was studied. The drugs cisplatin, 1,3-bis(2-chloroethyl)-1-nitrosourea, and adriamycin at 42.4°C and bleomycin and methotrexate at 43°C were tested in Chinese hamster ovary (CHO) cells in vitro. Heating times ranged from less than 3 minutes (immediate exposure) to 3 hours. For all drugs tested, synergistic cytotoxicity was not significantly altered by heating to peak temperature over 30 minutes as compared with immediate exposure. When heating to peak temperatures was prolonged to 3 hours, however, cell killing was markedly reduced, although significant sensitization to the drug remained. This was true despite the fact that, in CHO cells, heating to 42.4°C over 3 hours produced no cell killing for up to 6 hours at that temperature. These results suggested that the mechanism(s) responsible for induced thermotolerance are probably different from those that cause cellular resistance to the cytotoxic effects of the drugs tested. These results may also partially explain the relative lack of clinical success with whole-body hyperthermia and chemotherapeutic drugs as anticancer treatment, because heating to therapeutic temperatures often requires 2–3 hours.—JNCI 1982; 68: 487–491.

The treatment of cancer with chemotherapeutic drugs and hyperthermia has been stimulated by in vitro studies that have demonstrated markedly increased activity of several anticancer agents when used at clinically achievable hyperthermia temperatures (*1*). Our own pilot experiment utilizing whole-body hyperthermia in conjunction with anticancer drugs (*2*) was prompted by these observations. Our clinical work, however, revealed that whole-body heating to a peak temperature of 42.4°C required an average of about 170 minutes. Previously reported in vitro studies (*1, 3*) had employed heating techniques that were able to reach temperatures of 42–43°C within 3–5 minutes. Since this discrepancy seemed potentially important, we examined the rate of heating as a determinant of hyperthermic cytotoxicity. We found that cell survival over time at 42.4°C was dependent on the rapidity of heating to that temperature (*4*). We were also interested in determining whether the positive cytotoxic interaction between selected anticancer agents and hyperthermia would be altered by differing rates of heating. We can now report that this seems to be true for several chemotherapeutic drugs that we have tested with hyperthermia in CHO cells in vitro.

MATERIALS AND METHODS

Cell culture.—CHO cells, originally obtained in 1974 from Dr. Ronald M. Humphrey, University of Texas Cancer Center, M. D. Anderson Hospital, Houston, Tex., were grown in McCoy's 5-A medium supplemented with 20% (vol/vol) fetal calf serum, penicillin (11 U/ml), and streptomycin (100 μg/ml) (all from Grand Island Biological Co., Grand Island, N.Y.). Cells were maintained in logarithmic growth phase at 37°C in a 5% CO_2–95% air atmosphere. Doubling time was 13–14 hours for the CHO cells. Cell numbers were determined with an electronic particle counter (model ZBI; Coulter Electronics Inc., Hialeah, Fla.).

Cell viability measurements.—Cell viability was measured by the ability of single cells to form colonies in vitro, as described previously (*5, 6*). The colony-forming efficiencies of control cultures are between 85 and 95% for CHO cells. The results from colony-forming experiments, described in the text-figures, represent at least three replicate experiments per text-figure.

Heat treatments.—Exponentially growing cells were exposed to a peak temperature of 42.4°C or 43°C for 1 hour. In selected studies, the cells were taken from 37°C to peak temperature over times that varied from 30 minutes to 3 hours (rates of heating between 1.8°C and 12.0°C/hr). Other cells were exposed to 42.4°C or 43°C immediately (i.e., heated to peak temperature within 3 min). Heating was accomplished in a Plexiglas water tank with a continuous in-flow and out-flow system connected to a Haake model FK water heater. With this apparatus, the rate of heating could be adjusted so that continuous monitoring of bath temperature allowed different rates of heating, between 37°C and 42.4° or 43°C, to be achieved. Cells underwent heating in either T-25 or T-75 flasks (Falcon Plastics, Oxnard, Calif.) containing 5 or 15 ml, respectively, of fresh medium. Temperatures quoted are those of the cell monolayer position and were recorded with thermistor probes.

Drug treatments.—Exponentially growing cells were exposed to varying concentrations of BCNU (Bristol Laboratories Inc., Syracuse, N.Y.), *cis*-diamminedichloroplatinum(II) (cisplatin; Bristol Laboratories Inc., Syracuse, N.Y.), bleomycin (Bristol Laboratories Inc.), adriamycin (Farmitalia Co., Milan, Italy), or methotrexate (Lederle Laboratories, Pearl River, N.Y.) in 60-mm petri dishes for

---

ABBREVIATIONS USED: BCNU=1,3-bis(2-chloroethyl)-1-nitrosourea; CHO=Chinese hamster ovary.

---

[1] Received June 4, 1981; accepted September 18, 1981.

[2] Supported in part by Public Health Service grants CA-26220 and CA-17343 from the National Cancer Institute and by Veterans Administration Research Support.

[3] Section of Hematology/Oncology, Department of Medicine, University of Arizona College of Medicine, and Veterans Administration Medical Center, Tucson, Ariz. 85723.

[4] *Address reprint requests to* Dr. Herman at Section of Hematology–Oncology, University of Arkansas for Medical Science, Little Rock, Ark. 72205.

[5] Division of Radiation Oncology, Department of Radiology, Health Sciences Center, University of Arizona College of Medicine, Tucson, Ariz. 85724.

1 hour at 37°C or at 42.4° or 43°C in T-25 or T-75 flasks once cells had reached peak temperature. Small numbers of flasks were used so that all could be removed from the heating chamber, media poured off, and fresh media and drug added in less than 5 minutes by a team of investigators. Non-drug-treated controls were handled identically. We always prepared drug solutions immediately before use by dissolving the drug in sterile water (except for BCNU, which was dissolved primarily in 100% ethanol). Appropriate dilutions of drugs were added to fresh medium, with the volume of drug solution never exceeding 20% (1 ml) of the total volume of 5 ml. After treatment, the medium was removed and the cultures were washed twice with warmed Puck's Saline A (Grand Island Biological Co.) and trypsinized (0.05% for 2-3 min). Following this procedure, known numbers of cells were plated into plastic petri dishes for colony growth as described above.

RESULTS

Text-figure 1 depicts the effect of differing rates of heating on the cytotoxic interaction between cisplatin and exposure to 42.4°C for 1 hour. As compared with cell killing due to cisplatin at 37°C, cytotoxicity was strikingly enhanced when the 1-hour exposure to the drug occurred at 42.4°C if cells were rapidly heated to this temperature. At a drug concentration of 1 μg/ml, for instance, a 1-hour exposure at 37°C produced only about a 28% cell kill, whereas the same drug treatment at 42.4°C in cells heated over less than 3 minutes resulted in about a 96% cell kill. This is evidence of significant synergy, since immediate exposure to 42.4°C alone caused about a 25% cell kill, and simple additive lethality would have resulted in only about a 46% cell kill. Similarly, at other drug concentrations the resulting cell survivals indicated cytotoxic synergy between cisplatin and exposure to 42.4°C for 1 hour when heating from 37°C to 42.4°C occurred in 30 minutes or less. When heating of cells occurred over 3 hours, however, the cytotoxicity achieved by cisplatin and exposure to 42.4°C decreased. In this circumstance, after exposure to 1.0 μg/ml for 1 hour at 42.4°C, cell kill was only about 60% as opposed to about 96% when heating to 42.4°C was immediate. However, despite the fact that a 1-hour treatment at 42.4°C caused no cell kill if heating was accomplished over 3 hours, cells were still altered in a manner that increased significantly the cytotoxicity of cisplatin.

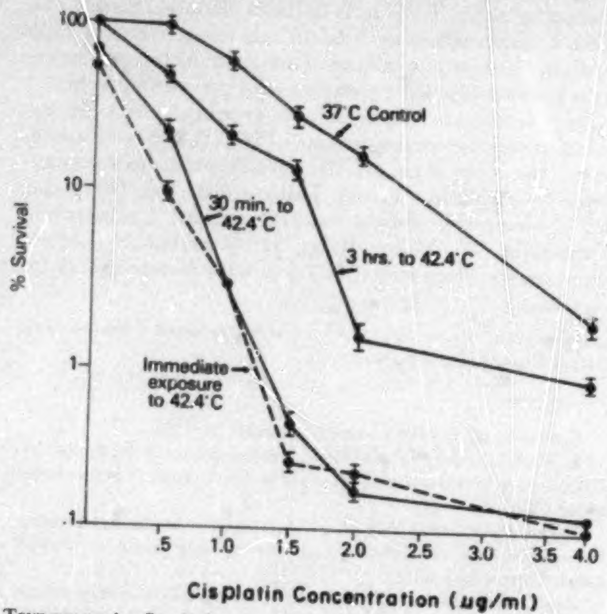

TEXT-FIGURE 1.—Survival curve of exponentially growing CHO cells exposed to the concentrations of cisplatin indicated at 37°C or 42.4°C for 1 hr after heating times from 37°C to 42.4°C as indicated. *Bars* represent standard errors.

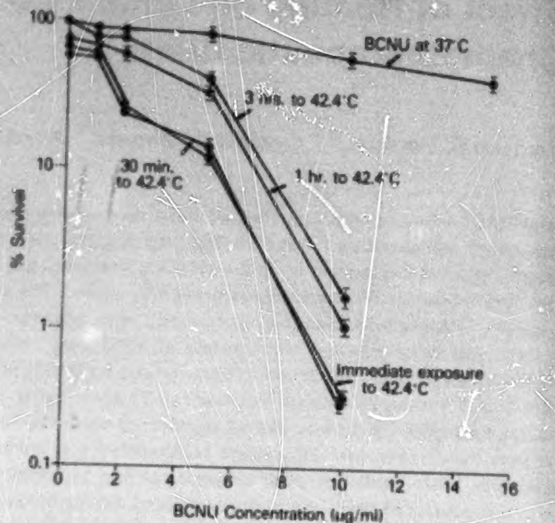

TEXT-FIGURE 2.—Survival curve of exponentially growing CHO cells exposed to the concentrations of BCNU indicated at 37°C or 42.4°C for 1 hr after heating times from 37°C to 42.4°C as indicated. *Bars* represent standard errors.

Text-figure 2 shows the effect on cytotoxicity due to hyperthermia and BCNU when differing rates of heating to 42.4°C were used. As was true for cisplatin, significant cytotoxic synergism was observed between exposure to BCNU and 42.4°C for 1 hour. Heating times of 30 minutes or less produced the greatest synergy. At a concentration of 5 μg BCNU/ml, for instance, about an 85% cell kill occurred after a 1-hour exposure at 42.4°C if heating occurred over 30 minutes or less than 3 minutes, but only about a 60% cell kill was observed if heating occurred over 1 hour or 3 hours. Again, heating over 3 hours to 42.4°C, which resulted in no measurable cell kill in itself, did sensitize cells to BCNU.

When this same experiment was conducted with adriamycin, the effect of the rate of heating was more difficult to appreciate (text-fig. 3). Our CHO cells are extremely sensitive to relatively low concentrations of adriamycin at 37°C as we have previously reported (*7*). Exposure to adriamycin at 42.4°C, however, did result in significantly increased cytotoxicity above that attributable to a simple additive effect. For instance, cell kill following exposure to 0.2 μg adriamycin/ml for 1 hour at 37°C was 90%. A 92.5% cell kill would have been expected to have resulted from an additive interaction between immediate heating to 42.4°C

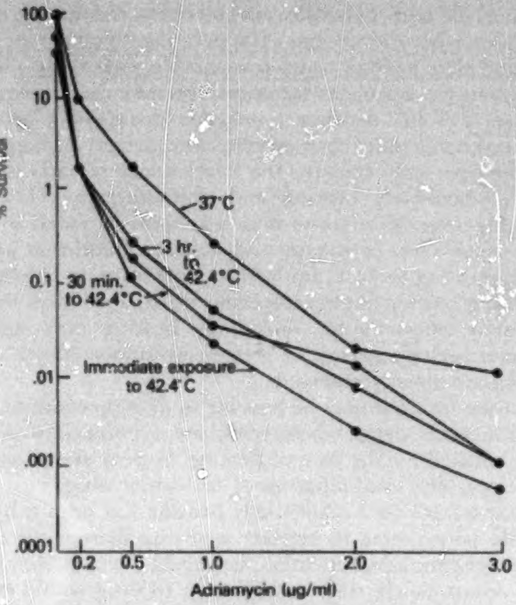

TEXT-FIGURE 3.—Survival curve of exponentially growing CHO cells exposed to the concentrations of adriamycin indicated at 37°C or 42.4°C for 1 hr after heating times from 37°C to 42.4°C as indicated. Largest standard error=±0.8%. Cell survivals after exposure to 42.4°C and these doses of adriamycin are significantly different for heating times of 3 hr as compared with immediate exposure [$P<0.01$ by the nonparametric Wilcoxon test (*7*)].

for 1 hour and this concentration of adriamycin. Instead, however, about a 98% cell kill was observed. When heating to 42.4°C occurred over 3 hours or 30 minutes, somewhat less cell kill occurred throughout the dose range of adriamycin used. Clear differences between the cytotoxicity caused by adriamycin and 1-hour exposure to 42.4°C when heating occurred over 3 hours or 30 minutes were not observed (error bars have been omitted for ease of presentation). A significant decrease, however, was seen between the cell kill caused by 1-hour exposures to these concentrations of adriamycin at 42.4°C if heating to this temperature required 3 hours as opposed to less than 3 minutes [$P<0.01$ by the nonparametric Wilcoxon test (*8*)].

We also examined cell killing due to bleomycin and methotrexate at 43°C in relationship to the rate of heating (text-figs. 4, 5). In text-figure 4 cell survivals graphed on the *y* axis show the effect of hyperthermia alone and demonstrated that the rate of heating altered cell killing due to a 1-hour exposure to 43°C as well as 42.4°C. Instead of about an 80% cell kill due to exposure to 43.0°C for 1 hour when heating was immediate, heating over 3 hours resulted in only about a 50% cell kill. No significant reduction in the synergistic cytotoxicity due to the dose range of bleomycin employed and exposure to 43°C for 1 hour was appreciated when heating occurred over 30 minutes as compared with immediate heating. When heating time was 3 hours, however, the cell kill achieved was markedly reduced. For instance, only about an 80% cell kill occurred after exposure to 1 µg bleomycin/ml for 1 hour at 43°C when heating was conducted over 3 hours as opposed to a 95% cell kill when heating time was 30 minutes or less than 3 minutes. At other concentrations of bleomycin, a similar pattern was observed. As with the other drugs, however, except for cell survival after 1 µg/ml in cells heated over 3 hours to 43.0°C where lethality was roughly additive, cell killing due to higher concentrations of bleomycin at 43.0°C for 1 hour remained greater than additive even when heating occurred over 3 hours.

Text-figure 5 shows the effect of rate of heating on cytotoxicity due to methotrexate and 1-hour exposure to 43°C. As we have previously reported (*7*), our CHO cells are extremely resistant to methotrexate and no cell kill was observed after a 1-hour exposure to 200 µg/ml at 37°C. If, however, cells were exposed immediately to 43°C, treatment with a range of methotrexate concentrations above 5 µg/ml for 1 hour reduced survival about 50% beyond that due to a 1-hour immediate exposure to 43°C (from ≈20% to ≈10%). This was the expected maximum cell kill from methotrexate, since only about 50% of CHO cells were in S-phase during exponential growth. When heating to 43°C was conducted over 3 hours, however, no increase in cell kill over that due to hyperthermia (≈50%) was caused by methotrexate over the dose range tested. When heating time was 30 minutes, an interesting survival pattern was observed. Cells surviving hyperthermia seemed partially sensitized to methotrexate so that only at 50 and 200 µg/ml concentrations did a 1-hour exposure to methotrexate result in a full 50% additional cell kill.

DISCUSSION

We have demonstrated in our in vitro system that the magnitude of cell killing due to hyperthermia and selected anticancer drugs is partially dependent on the rate of heating from 37°C to peak temperature. We have previously reported (*4*) that the killing in CHO cells due to exposure

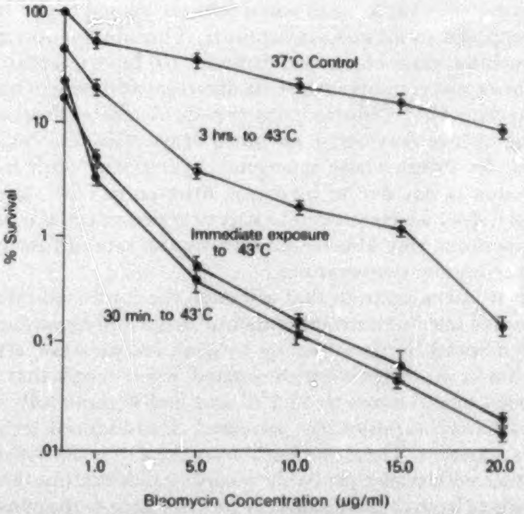

TEXT-FIGURE 4.—Survival curve of exponentially growing CHO cells exposed to the concentrations of bleomycin indicated at 37°C or 43.0°C for 1 hr after heating times from 37°C to 43.0°C as indicated. *Bars* represent standard errors.

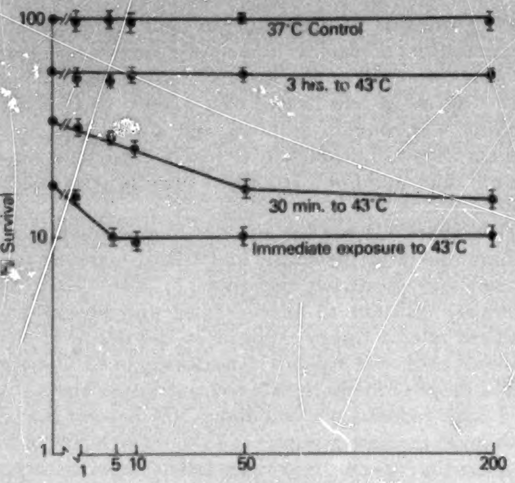

TEXT-FIGURE 5.—Survival curve of exponentially growing CHO cells exposed to the concentrations of methotrexate indicated at 37°C and 43.0°C for 1 hr after heating times from 37°C to 43.0°C as indicated. *Bars* represent standard errors.

to 42.4°C over time is dependent on the rate of heating from 37°C. We were able to correlate these survival differences with an increase in total cellular protein within the particulate fraction of cells heated to temperatures over 3 hours, whereas rapidly heated cells showed a significant reduction in protein. In addition, slowly heated cells showed no significant change in size or cholesterol content, while rapidly heated cells showed marked fluctuations over time at peak temperature in these indirect measures of plasma membrane integrity (*9*).

We have not reported studies here of drug uptake in slowly heated cells as compared with rapidly heated cells, but preliminary investigations indicate that uptake is decreased with adriamycin when cells are heated over 3 hours as opposed to immediate exposure. This observation is not surprising, since Hahn and Strande (*10*) have reported that prior exposure to hyperthermia decreases adriamycin uptake into their HA1 Chinese hamster cells. A similar decrease in drug uptake may occur for other drugs after slow heating, even for drugs whose synergistic cytotoxicity with hyperthermia is not due to increased drug entry (*10*). Alternatively, drug access to cellular sites of action or cellular repair capabilities may also be affected by the rate of heating to hyperthermic temperatures.

It is intersting to us that although the combined cytotoxicities of selected chemotherapeutic drugs and hyperthermia are reduced by slow heating to peak temperature, sensitization to the drugs is not eliminated. Even in cells that were heated over 3 hours to 42.4°C and had become fully thermotolerant, significantly increased drug-induced lethality was apparent. These observations suggest that the induction of thermotolerance probably occurs by mechanisms that are separate from those responsible for resistance to the cytotoxic actions of these drugs.

While it is difficult to extrapolate from in vitro data to clinical results, reported response rates in patients treated with whole-body hyperthermia and chemotherapeutic drugs (*12*) have been somewhat disappointing. We have demonstrated that heating times comparable with those usually necessary to raise core temperature into the therapeutic range (2–3 hr) decrease synergistic cytotoxicity between hyperthermia and chemotherapeutic drugs. Perhaps this finding partially explains the relative lack of early success with whole-body heating and chemotherapy. However, heating over 30 minutes does not seem to result in any appreciable loss of synergy and we have found that whole-body heating to 42°C from 37°C in 30 minutes is possible utilizing heating of extracorporally circulated blood. Unfortunately, more rapid whole-body heating may lead to greater toxicity as well as greater antitumor effects as we may have already observed.

In the future it may be possible to develop combinations of anticancer drugs whose combined cytotoxicities will be less affected by the rate of heating to peak temperatures. Alternatively, local infusions of anticancer drugs into large tumor masses once whole-body heating has been achieved would be expected to produce a greater therapeutic index than systemic administration, especially if whole-body heating occurs slowly since sensitization to drug would be expected to be preserved while toxicity from hyperthermia in normal tissues should be minimized. It may also be possible that slow heating to lower hyperthermic temperatures in the range of 41–41.5°C for sustained times may result in a greater therapeutic index. In this regard the work of Read et al. (*13*) may be pertinent. These investigators have demonstrated that CHO cells heated at 41–42°C for prolonged periods show the loss of thermotolerance after about 18–20 hours. Cell killing then proceeds exponentially. Delayed administration of drugs until this time may also provide greater therapeutic benefit and needs to be studied preclinically. Finally, the data we have reported would suggest that the use of selected chemotherapeutic drugs with regional-local hyperthermia should be very effective since rapid heating times are possible.

REFERENCES

(*1*) HAHN GM. Potential for therapy of drugs and hyperthermia. Cancer Res 1979; 39:2264–2268.

(*2*) HERMAN TS, ZUKOSKI CF, ANDERSON RM, ET AL. Whole body hyperthermia in patients with advanced refractory malignancy. Cancer Treat Rep. In press.

(*3*) KOWAL CD, BERTINO JR. Possible benefits of hyperthermia to chemotherapy. Cancer Res 1979; 39:2285–2289.

(*4*) HERMAN TS, SICKNEY DG, GERNER EW. Differential rates of heating influence hyperthermia induced cytotoxicity in normal and transformed cells in vitro. Proc Am Assoc Cancer Res 1979; 20:165.

(*5*) GERNER EW, BOONE R, CONNOR WG, HICKS JA, BOONE ML. Transient thermotolerant survival response produced by single thermal doses in HeLa cells. Cancer Res 1976; 36:1035–1040.

(*6*) GERNER EW, SCHNEIDER MS. Induced thermal resistance in HeLa cells. Nature 1975; 256:500–502.

(*7*) HERMAN TS, CRESS AE, GERNER EW. Collateral sensitivity to methotrexate in cells resistant to adriamycin. Cancer Res 1979; 39:1937–1942.

(*8*) ARMITAGE P. Wilcoxon's rank sum test in statistical methods in medical research. New York: Wiley, 1977:398.

(*9*) HERMAN TS, GERNER EW, MAGUN BE, STICKNEY D, SWEETS CC, WHITE DM. Rate of heating as a determinant of hyperthermic cytotoxicity. Cancer Res. In press.

(*10*) HAHN GM, STRANDE DP. Cytotoxic effect of hyperthermia and adriamycin on Chinese hamster cells. J Natl Cancer Inst 1976; 57:1063–1067.

(*11*) Hahn GM, Braun J, Har-Kedar I. Thermochemotherapy: Synergism between hyperthermia (42–43°C) and adriamycin (or bleomycin) in mammalian cell inactivation. Proc Natl Acad Sci USA 1975; 79: 937–940.

(*12*) Larkin JM. A clinical investigation of total body hyperthermia as cancer therapy. Cancer Res 1979; 39:2252–2254.

(*13*) Read RA, Fox MH, Bedford JS. Thermotolerance and chronic hyperthermia. In: Proceedings of third international symposium on cancer therapy by hyperthermia, drugs, and radiation. Natl Cancer Inst Monogr. In press.

blank page

Glutathione *S*-Transferase Activity: Enhancement by Compounds Inhibiting Chemical Carcinogenesis and by Dietary Constituents[1,2,3]

Velta L. Sparnins,[4] Placida L. Venegas,[4] *and* Lee W. Wattenberg[4]

ABSTRACT—Benzyl isothiocyanate, β-naphthoflavone, coumarin, α-angelicalactone, disulfiram, indole-3-carbinol and indole-3-acetonitrile induced increased glutathione (GSH) *S*-transferase activity in the liver and small intestine in female ICR/Ha mice. All seven compounds are inhibitors of chemical carcinogenesis. In additional work, several dietary constituents increased GSH *S*-transferase activity. Consumption of diets containing dried powdered preparations of brussels sprouts, cabbage, coffee beans, or tea leaves resulted in increased GSH *S*-transferase activity. Mice fed an unrefined diet (Purina Rat Chow) had a higher GSH *S*-transferase activity than those fed a semipurified diet. The results of the present study indicated that the composition of the diet can alter the activity of an important enzyme system having the capacity to detoxify chemical carcinogens.—JNCI 1982; 68:493–496.

An increasing number of compounds have been found to inhibit the neoplastic effects of chemical carcinogens when these compounds are administered before and/or simultaneously with exposure to the carcinogen (*1–3*). One of the most effective compounds of this type is 2(3)-BHA, which inhibits a wide range of chemical carcinogens (*2*). Studies by Benson et al. (*4, 5*) have shown that 2(3)-BHA administered in the diet markedly increased GSH *S*-transferase activity. The greatest effect was on the GSH *S*-transferase activity of the liver, which was enhanced eightfold. Smaller increases were found in other tissues. Ethoxyquin, which suppresses BP-induced neoplasia, also was found to enhance GSH *S*-transferase activity (*4*).

GSH *S*-transferase has been studied extensively as a major detoxification system that catalyzes the binding of various electrophiles to GSH (*6, 7*). Since the reactive ultimate carcinogenic forms of chemical carcinogens are electrophiles, GSH *S*-transferase takes on considerable importance as a mechanism for carcinogen detoxification. Enhancement of the activity of this system potentially could increase the capacity of the organism to withstand the neoplastic effects of chemical carcinogens. Experiments have been performed to determine if there is a relationship between increased GSH *S*-transferase activity in a target organ of chemical carcinogenesis and response to the carcinogen. For this purpose, the forestomach of the mouse was used. Members of several classes of inhibitors of BP-induced neoplasia of the mouse forestomach were studied for their effects on the GSH *S*-transferase activity in that structure. Five of the compounds increased the GSH *S*-transferase activity of the forestomach between 78 and 182%. The five compounds were *p*-methoxyphenol, 2-BHA, coumarin, α-angelicalactone, and benzyl isothiocyanate. All five inhibited BP-induced neoplasia of the forestomach. These data indicate that enhancement of the GSH *S*-transferase activity by an amount of about 75% or greater is associated with a reduced carcinogenic response of the forestomach to BP (*8*). The data also suggest that the capacity to enhance GSH *S*-transferase activity might be used as a method of identifying compounds or natural products likely to inhibit BP or other carcinogens detoxified in a similar manner.

In many instances carcinogens are consumed in the diet and have target sites of action in organs such as lung or breast, which are distant from the gastrointestinal tract. Under these conditions, the carcinogen could be detoxified in the small intestine and liver. The reaction of the liver and small bowel to a particular inducer of increased GSH *S*-transferase activity and that of the forestomach may be very different. Thus 3-BHA is a potent inhibitor of GSH *S*-transferase activity of the liver and small bowel but is weak for forestomach (*4, 5, 8*). The liver and the small intestine have high levels of GSH *S*-transferase activity and also show very marked increases in GSH *S*-transferase activity in response to appropriate inducers. Thus the levels of GSH *S*-transferase activity in liver and small bowel could be exceedingly important for the response of many tissues to exposures to chemical carcinogens. In the present work the effects of several inhibitors of carcinogen-induced neoplasia of tissues distant from the alimentary tract have been studied on the GSH *S*-transferase activity of small bowel mucosa and liver. These inhibitors included benzyl isothiocyanate, β-naphthoflavone, coumarin, α-angelicalactone, disulfiram, indole-3-carbinol, and indole-3-acetonitrile (*3, 9–15*). In addition, the effects of some natural products on GSH *S*-transferase activity have been ascertained.

MATERIALS AND METHODS

Animal experiments.—Female ICR/Ha mice from the Madison, Wis., facility of the Harlan-Sprague-Dawley Co., Indianapolis, Ind., were used in all experiments. Mice were randomized by weight at 7 weeks of age. At that time they were divided into groups of 5 to 10 animals each and placed on experimental diets. A semipurified diet was given consisting of 27% vitamin-free casein, 59% starch, 10% corn oil, 4% salt mix (U.S. Pharmacopeia XIV) and a complete

---

ABBREVIATIONS USED: AHH=aryl hydrocarbon hydroxylase; 2-BHA=2-*tert*-butyl-4-hydroxyanisole (the minor isomer occurring in the commercial mixture); 2(3)-BHA=2(3)-*tert*-butyl-4-hydroxyanisole (mixture of isomers found in commercial preparations); 3-BHA=3-*tert*-butyl-4-hydroxyanisole (the major isomer occurring in the commercial mixture); BP = benzo[*a*]pyrene; GSH=glutathione.

---

[1] Received June 4, 1981; accepted October 6, 1981.

[2] Supported by Public Health Service grants CA-14146 and CA-09599 from the National Cancer Institute.

[3] Animals were maintained under guidelines set forth by the University of Minnesota.

[4] Department of Laboratory Medicine and Pathology, University of Minnesota, Minneapolis, Minn. 55455.

mixture of vitamins (Teklad, Inc., Madison, Wis.). To this semipurified diet were added the test compounds. In experiments comparing the semipurified diet with an unrefined diet, pulverized Purina Rat Chow (Ralston Purina Co., St. Louis, Mo.) was used. Inhibitors were employed in concentrations shown to inhibit carcinogen-induced neoplasia. Inactive compounds were used in concentrations for which they were shown to lack carcinogen-inhibitory capacities. The diets were fed for 2 weeks, at which time the mice were killed. The liver and proximal half of the small bowel were removed. The small bowel was opened and washed, and the musosa was scraped off gently.

Preparation of homogenates and cytosol.—All steps were done at 0-4°C. The tissues to be studied were homogenized in 0.1 *M* phosphate buffer (pH 7.5). The homogenate was centrifuged at 9,000×*g* for 20 minutes and then at 100,000×*g* for 1 hour. The supernatant was used for the assay of GSH *S*-transferase activity.

Determinations of GSH S-*transferase activity.*—The activity of cytosol GSH *S*-transferase was determined spectrophotometrically at 30°C with 1-chloro-2,4-dinitrobenzene as substrate according to the procedure of Habig et al. (*16*). The reaction mixture (1 ml) contained 100 μmol phosphate buffer (pH 6.5), 5 μmol GSH, and 1 μmol 1-chloro-2,4-dinitrobenzene. The reaction was started by addition of cytosol.

Chemicals.—Benzyl isothiocyanate was obtained from Eastman Organic Chemicals (Rochester, N.Y.); β-naphthoflavone, disulfiram, coumarin, α-angelicalactone, umbelliferone, γ-valerolactone, indole-3-carbinol, indole-3-acetonitrile, and 1-chloro-2,4-dinitrobenzene were from Aldrich Chemical Co. (Milwaukee, Wis.); 2(3)-BHA was purchased from Sigma Chemical Co. (St. Louis, Mo.). 3-BHA was prepared from the commercially obtained 2(3)-BHA by recrystallization from acetone as described previously (*17*).

Natural products.—Green coffee beans from Guatemala were purchased from the McGarvey Coffee Company (Minneapolis, Minn.). Chieftain Savoy variety cabbage and Jade Cross variety brussels sprouts were grown on the St. Paul campus of the University of Minnesota without use of chemical pesticides. Bulk black tea leaves from Ceylon were obtained from Coffee & Tea, Ltd. (St. Paul, Minn.). A commercial brand of instant tea, Lipton Co., Englewood Cliffs, N.J. was used. For addition to the diet, the green coffee beans, vegetables (after chopping and air drying), and tea leaves were converted to a powder form in a Waring Blendor.

RESULTS

All of the compounds that have been shown to protect against chemical carcinogenesis induced an increase in GSH *S*-transferase activity. These included 3-BHA, β-naphthoflavone, disulfiram, α-angelicalactone, coumarin, indole-3-carbinol, and indole-3-acetonitrile (table 1). In contrast, three compounds ineffective as inhibitors of carcinogen-induced neoplasia, i.e., tetrafluorophenol, γ-valerolactone, and umbelliferone, did not induce increased GSH *S*-transferase activity. Compounds inducing increased activity invariably did so in both tissues. The two lactones α-angelicalactone and coumarin and indole-3-acetonitrile have a more potent effect on liver than on the small bowel.

The results of studies of effects of natural materials and dietary constituents on GSH *S*-transferase activity are recorded in experiments 5-8 in table 1. Substituting an unrefined commercial diet (Purina Rat Chow) for the semipurified diet resulted in enhancement of GSH *S*-transferase activity. Cabbage produced a similar magnitude of enhancement and brussels sprouts and tea leaves caused a greater induction. Of the natural products tested, the largest effect occurred with green coffee beans. The increase in GSH *S*-transferase was particularly prominent in the mucosa of the small bowel. The green coffee beans caused the greatest enhancement of GSH *S*-transferase activity in the mucosa of the small bowel of any of the test substances studied.

DISCUSSION

The results of the present study show that diverse groups of compounds having the capacity to inhibit carcinogen-induced neoplasia all induce an increase in GSH *S*-transferase activity in liver and the mucosa of the small bowel (*3, 9-15*). Compounds inducing increased GSH *S*-transferase activity have been found to have other biological effects as well. The best studied of these compounds is 3-BHA, which has been shown to increase the activity of UDP-glucuronosyl transferase, epoxide hydrolase, and NADPH:quinone reductase and also to alter the microsomal metabolism of BP (*2, 18-24*). The data obtained in the present investigation show an association between inhibition of carcinogen-induced neoplasia and induction of increased GSH *S*-transferase activity. However, it is not clear whether induction of GSH *S*-transferase is directly or partially responsible for inhibition of neoplasia, or represents a marker parameter.

In previous studies, consumption of crude diets was found to increase AHH activity. This induction was shown to be due to xenobiotic compounds of vegetable origin (*25, 26*). Since both AHH and GSH *S*-transferase are involved in the metabolism of foreign compounds, the question arose as to whether crude diets would also enhance GSH *S*-transferase activity. In the present investigation, mice fed Purina Rat Chow had a higher GSH *S*-transferase activity than those fed a purified diet. The inducing compound or compounds in the Purina Rat Chow have not been identified. In addition to the crude diet, brussels sprouts and cabbage were investigated. These two vegetables contain indoles and aromatic isothiocyanates, compounds that induce increased GSH *S*-transferase activity (*26-28*). Both of these vegetables were found to enhance GSH *S*-transferase activity. Coffee beans also were investigated in the present study. Consumption of green coffee beans resulted in exceedingly high levels of GSH *S*-transferase activity. Subsequently, tea was studied. It also had inducing capacity but was less potent than coffee. Work is in progress aimed at the identification of the active constituent in these two materials. The enhancement of GSH *S*-transferase activity by natural products is of interest because it suggests that one way in which the composition of the diet may alter responses to chemical carcinogens is by enhancing GSH *S*-transferase activity and/or associated detoxification systems.

TABLE 1.—*Effects of β-naphthoflavone, disulfiram, benzyl isothiocyanate, phenols, lactones, coumarins, indoles, green coffee beans, vegetables, instant tea, and tea leaves on the GSH S-transferase activity in the cytosols of mouse liver and mucosa of the small intestine*

Expt No.	Additions to diets	Amounts, g diet^{a}	Mucosa of small intestine: GSH S-transferase activity^{b}		Liver: GSH S-transferase activity^{b}	
			nmol/min/mg	Ratio^{c}	nmol/min/mg	Ratio^{c}
1	None	—	685±37	—	2,170±60	—
	Disulfiram	0.02	1,960±110	2.86±0.22^{d}	3,630±80	1.67±0.06^{d}
	Benzyl isothiocyanate	0.03	3,000±370	4.38±0.[illegible]^{d}	6,950±230	3.20±0.14^{d}
2	None	—	704±69	—	2,490±180	—
	3-BHA	0.03	3,650±180	5.18±0.57^{d}	16,700±960	6.71±0.61^{d}
	Tetrafluorophenol	0.03	664±88	0.94±0.16	2,840±110	1.14±0.09^{e}
3	None	—	509±69	—	1,780±100	—
	α-Angelicalactone	0.03	1,250±57	2.46±0.35^{d}	7,510±30	4.22±0.25^{d}
	γ-Valerolactone	0.03	474±30	0.93±0.14	1,710±200	0.96±0.13
	Coumarin	0.03	868±27	1.71±0.18^{f}	9,430±470	5.29±0.41^{d}
	Umbelliferone	0.05	424±29	0.83±0.13	1,820±70	1.02±0.07
4	None	—	406±49	—	1,600±60	—
	Indole-3-carbinol	0.04	1,430±10	3.52±0.43^{d}	4,410±400	2.76±0.27
	Indole-3-acetonitrile	0.04	740±9	1.82±0.22^{d}	5,830±360	3.64±0.26^{d}
5	None	—	468±29	—	1,610±40	—
	β-Naphthoflavone	0.02	1,840±160	3.93±0.43^{d}	3,180±200	1.98±0.13^{d}
	Green coffee beans	5%	2,650±270	5.66±0.67^{d}	4,170±250	2.59±0.17^{d}
6	None	—	391±26	—	1,740±210	—
	Purina Rat Chow	100%	621±21	1.59±0.12^{d}	2,110±130	1.21±0.16^{e}
	Green coffee beans	20%	4,280±540	10.95±1.56^{d}	8,600±520	4.94±0.67^{d}
7	None	—	359±23	—	2,170±360	—
	Purina Rat Chow	100%	615±77	1.71±0.24^{e}	2,800±80	1.29±0.22
	Cabbage	20%	751±80	2.09±0.23^{e}	1,690±20	0.78±0.13
	Brussels sprouts	20%	1,110±90	3.09±0.31^{d}	3,910±300	1.80±0.33^{e}
8	None	—	501±40	—	2,280±200	—
	Instant tea	10%	1,070±115	2.14±0.29^{d}	5,670±380	2.49±0.28^{d}
	Tea leaves	10%	927±48	1.85±0.18^{d}	5,420±300	2.38±0.25^{e}
	Tea leaves	20%	948±93	1.89±0.24^{d}	5,660±170	2.48±0.23^{d}

[a] Amounts of test substances added to the diets are expressed as mmol/g diet for chemicals and as the percent of diet for natural products.

[b] GSH S-transferase activity was determined with use of 1-chloro-2,4-dinitrobenzene as the substrate. Values given are mean values of two to five determinations ± SD.

[c] Ratio of GSH S-transferase activity from mice receiving the test substance to that of the activity in control mice.

[d] $P < 0.005$.

[e] $P < 0.025$.

[f] $P < 0.010$.

REFERENCES

(*1*) WATTENBERG LW. Inhibitors of chemical carcinogenesis. Adv Cancer Res 1978; 26:197–226.

(*2*) ———. Inhibitors of chemical carcinogens. In: Burchenal JH, ed. Cancer: Achievements, challenges and prospects for the 1980's. New York: Grune, 1980:517–539.

(*3*) ———. Naturally-occurring inhibitors of chemical carcinogens. In: Miller EC, Miller JA, Hiromo I, Sugimura T, Takayama S, eds. Naturally-occurring carcinogens-mutagens and modulators of carcinogenesis. New York: University Park Press, 1980:315–329.

(*4*) BENSON AM, BATZINGER RP, OU SL, BUEDING E, CHA YN, TALALAY P. Elevation of hepatic glutathione S-transferase activities and protection against mutagenic metabolites of benzo(a)pyrene by dietary antioxidants. Cancer Res 1978; 38:4486–4495.

(*5*) BENSON AM, CHA YN, BUEDING E, HEINE, HS, TALALAY P. Elevation of extrahepatic glutathione S-transferase and epoxide hydratase activities by 2(3)-*tert*-butyl-4-hydroxyanisole. Cancer Res 1979; 39: 2971–2977.

(*6*) JAKOBY WB. The glutathione S-transferases: A group of multifunctional detoxification proteins. Adv Enzymol 1978; 46:383–414.

(*7*) CHASSEAUD LF. The role of glutathione and glutathione S-transferases in the metabolism of chemical carcinogens and other electrophilic agents. Adv Cancer Res 1979; 29:175–274.

(*8*) SPARNINS VL, WATTENBERG LW. Enhancement of glutathione S-transferase activity of the mouse forestomach by inhibitors of benzo[*a*] pyrene-induced neoplasia of the forestomach. JNCI 1981; 66:769–771.

(*9*) WATTENBERG LW. Inhibition of carcinogenic and toxic effects of polycyclic hydrocarbons by several sulfur-containing compounds. J Natl Cancer Inst 1974; 52:1583–1587.

(*10*) ———. *Brief communication:* Inhibition of dimethylhydrazine-induced neoplasia of the large intestine by disulfiram. J Natl Cancer Inst 1975; 54:1005–1006.

(*11*) WATTENBERG LW, LAM LK, FLADMOE A, BORCHERT P. Inhibitors of colon carcinogenesis. Cancer 1977; 40:2432–2435.

(*12*) WATTENBERG LW, LEONG JL. Inhibition of the carcinogenic action of 7,12-dimethylbenz(*a*)anthracene by β-naphthoflavone. Proc Soc Exp Biol Med 1968; 128:940–943.

(*13*) ———. Inhibition of the carcinogenic action of benzo(*a*)pyrene by flavones. Cancer Res 1970; 30:1922–1925.

(*14*) WATTENBERG LW, LOUB WD. Inhibition of polycyclic hydrocarbon-induced neoplasia by naturally-occurring indoles. Cancer Res 1978; 38:1410–1413.

(*15*) WATTENBERG LW, LAM LK, FLADMOE A. Inhibition of chemical carcinogen-induced neoplasia by coumarins and α-angelicalactone. Cancer Res 1979; 39:1651–1654.

(*16*) HABIG WH, PABST MJ, JAKOBY WB. Glutathione S-transferases. J Biol Chem 1974; 249:7130–7139.

(*17*) LAM LK, PAI RP, WATTENBERG LW. Synthesis and chemical carcinogen inhibitory activity of 2-*tert*-butyl-4-hydroxyanisole. J Med Chem 1979; 22:569–571.

(*18*) CHA YN, BUEDING E. Effects of 2(3)-*tert*-butyl-4-hydroxyanisole administration on the activities of several hepatic microsomal and cytoplasmic enzymes in mice. Biochem Pharmacol 1979; 28:1917–1921.

(*19*) Cha YN, Martz F, Bueding E. Enhancement of liver microsome epoxide hydratase activity in rodents by treatment with 2(3)-*tert*-butyl-4-hydroxyanisole. Cancer Res 1978; 38:4496–4498.

(*20*) Benson AM, Hunkeler MJ, Talalay P. Increase of NAD(P)H: quinone reductase by dietary antioxidants: Possible role in protection against carcinogenesis and toxicity. Proc Natl Acad Sci USA 1980; 77:5216–5220.

(*21*) Lam LK, Fladmoe AV, Hochalter JB, Wattenberg LW. Short time interval effects of butylated hydroxyanisole on the metabolism of benzo(*a*)pyrene. Cancer Res 1980; 40:2824–2828.

(*22*) Lam LK, Wattenberg LW. Effects of butylated hydroxyanisole on the metabolism of benzo[*a*]pyrene by mouse liver microsomes. J Natl Cancer Inst 1977; 58:413–417.

(*23*) Speier JL, Lam LK, Wattenberg LW. Effects of administration to mice of butylated hydroxyanisole by oral intubation on benzo[*a*]pyrene-induced pulmonary adenoma formation and metabolism of benzo[*a*]pyrene. J Natl Cancer Inst 1978; 60:605–609.

(*24*) Speier JL, Wattenberg LW. Alterations in microsomal metabolism of benzo[*a*]pyrene in mice fed butylated hydroxyanisole. J Natl Cancer Inst 1975; 55:469–472.

(*25*) Wattenberg LW. Enzyme reactions and carcinogenesis. In: Environment and cancer. Twenty-fourth annual symposium on fundamental cancer research at the University of Texas M. D. Anderson Hospital and Tumor Institute. Baltimore: Williams & Wilkins, 1972:241–255.

(*26*) Loub WD, Wattenberg LW, Davis DW. Aryl hydrocarbon hydroxylase induction in rat tissues by naturally occurring indoles of cruciferous plants. J Natl Cancer Inst 1975; 54:985–988.

(*27*) Virtanen AI. Some organic sulfur compounds in vegetables and fodder plants and their significance in human nutrition. Angew Chem [Engl] 1962; 1:299–306.

(*28*) Kjaer A. Naturally occurring isothiocyanates and their parent glycosides. In: Kharasch N, ed. Vol 1. Chemistry of organic sulfur compounds. New York: Pergamon Press, 1961:409–420.

Organ-Specific Promoting Effects of Phenobarbital Sodium and Sodium Saccharin in the Induction of Liver and Urinary Bladder Tumors in Male F344 Rats [1, 2, 3]

Keisuke Nakanishi,[4] Shoji Fukushima,[4] Akihiro Hagiwara,[4] Seiko Tamano,[4] *and* Nobuyuki Ito[4, 5]

ABSTRACT—Studies were conducted to determine whether initial treatment with *N*-2-fluorenylacetamide (2-FAA) or *N*-butyl-*N*-(4-hydroxybutyl)nitrosamine (BBN) followed by treatment with either phenobarbital sodium (PB) or sodium saccharin (SS) induced or enhanced liver and/or bladder tumorigenesis. Male inbred F344 rats were given 0.05% PB and 5.0% SS in the diet for 32 weeks after 4-week administration of 0.02% 2-FAA or 0.01% BBN. PB significantly enhanced hepatocarcinogenesis after 2-FAA treatment and induced hyperplastic liver nodules after BBN treatment. The SS significantly enhanced induction of bladder hyperplasias, but not papilloma after BBN treatment, and induced bladder hyperplasias after 2-FAA treatment. However, PB had no effect on the bladder and SS had no effect on the liver after either 2-FAA or BBN treatment. The data indicate that although 2-FAA and BBN have tumor-initiating effects in the liver and urinary bladder, the tumor-promoting effects of PB and SS are organ-specific. The tumor-promoting effect of PB for the liver is relatively greater than that of SS for the urinary bladder.—JNCI 1982; 68:497–500.

The two-stage process of carcinogenesis involving initiation and promotion has been demonstrated in the skin (*1, 2*) and in various organs, such as the liver (*3–7*), urinary bladder (*8–10*), breast (*11, 12*), colon (*13*), lung (*7, 14*), and stomach (*15, 16*), with a variety of chemicals used as initiating and promoting agents. Whether the initiating and/or the promoting agent is responsible for organ specificity is presently unclear (*17*). It has been established that cancer in humans and other animals can be induced by a multistage process and that cofactors play a role in cancer induction (*18*).

It has been shown that 2-FAA has carcinogenic activity toward various organs in rats including the liver and urinary bladder (*19*). BBN induced tumors only in the urinary tract, especially the urinary bladder, in rats (*10, 20*). However, several carcinogens not specific for the liver combined with partial hepatectomy have been shown to act as initiators in the liver and induce liver neoplasia in rats when promoting agents are subsequently administered (*4, 5*). We concluded, therefore, that BBN may also have initiating activity in the liver.

It has been shown that PB (*3, 6*) and SS (*8–10*) act as promoters for the liver and urinary bladder, respectively, if administered after initiation. However, the promoting effect of PB or SS on the induction of both liver and bladder tumors and the direct comparison of the promoting effect of PB for the liver and of SS for the bladder have not been evaluated. In the present experiment, the promoting effect of PB or SS for the liver and bladder was evaluated following initiation with either 2-FAA or BBN.

MATERIALS AND METHODS

Chemicals—2-FAA was purchased from Nakarai Chemical, Kyoto; BBN from Izumi Chemical Co., Yokohama; SS, containing 7 ppm orthotoluenesulfonamide, from Okuno Chemical Co., Osaka; PB from Iwaki Pharmaceutical Co., Tokyo; and Tween 80 from Katayama Chemical Co., Osaka.

Animals and experimental design.—A total of 272 male inbred F344 rats (Charles River Japan Co., Kanagawa) weighing 100–120g were divided into 3 groups. These groups were further separated into 3 subgroups (A–C) for testing on PB, SS, or control diet.

Group 1: Rats were fed basal diet (Oriental M; Oriental Yeast Co., Tokyo) containing 0.02% 2-FAA for 4 weeks and then given 0.05% PB (A), or 5.0% SS (B) in the diet, or basal diet (C).

Group 2: Rats were given 0.01% BBN in the drinking water containing 0.01% Tween 80 for 4 weeks followed by the treatments for subgroups A, B, and C as described for group 1.

Group 3: Rats were fed untreated diet and water for 4 weeks followed by the treatments for the 3 subgroups as described for group 1. All subgroups consisted of 30 rats except subgroups 1B and 2B, which consisted of 31 rats at the start of the experiment.

Rats were housed 5/cage in plastic cages in an airconditioned room at 24°C with 50% humidity and were weighed weekly. Food and water consumption were determined periodically during the experiment. Animals that died during the experimental period were autopsied and examined, but they were not included in the final count.

Histologic observation.—All rats were killed with ether at the end of week 36. Their urinary bladders were inflated with 10% phosphate-buffered Formalin solution via the urethra

---

ABBREVIATIONS USED: BBN=*N*-butyl-*N*-(4-hydroxybutyl)nitrosamine; 2-FAA=*N*-2-fluorenylacetamide; PB=phenobarbital sodium; SS=sodium saccharin.

---

[1] Received June 17, 1981; accepted September 23, 1981.

[2] Supported in part by Grants-in-Aid for Cancer Research 501061, 501069, and 501077, 1980 from the Ministry of Education, Science and Culture, Japan; by the Experimental Pathological Research Association; and by the Society for Promotion of Pathological Research of Nagoya.

[3] Animals were maintained under the guidelines set forth by the Nagoya City University Medical School.

[4] First Department of Pathology, Nagoya City University Medical School, 1 Kawasumi, Mizuho-cho, Mizuho-ku, Nagoya 467, Japan.

[5] We gratefully acknowledge the assistance of Dr. Samuel M. Cohen, University of Nebraska Medical Center, in the preparation of this manuscript.

and removed. The liver, both kidneys, and the spleen were also removed and weighed and fixed in the same fixative solution. The liver lobes were cut off and cut into serial sections 2–3 mm thick. Several of these sections were prepared for histologic examination. When gross nodular lesions were observed in a few serial sections, the section in which the nodule was largest was examined. The urinary bladder was cut into left and right halves, and six to eight serial sections were cut from each half. All tissue sections were stained with hematoxylin and eosin. Other tissues with abnormalities by gross examination were also examined histologically.

Cross sections of each liver lobe were prepared for histologic examination. Proliferative lesions of parenchymal cells greater than 0.2 mm in diameter were classified as hyperplastic nodules. Relatively large nodular areas with a trabecular or papillary structure and cytological atypia were classified as hepatocellular carcinomas. For quantitative analysis of these lesions (number and total area per 1 cm^2 of liver specimen), a general purpose color image processor (model VIP-21C; Olympus-Ikegami Co., Tokyo) was used as described previously (*21*).

Serial sections of the urinary bladder were prepared for histologic examination. Histologic changes of the urinary bladder were classified into four types: simple hyperplasia, papillary or nodular hyperplasia, papilloma, and cancer. The average numbers of all these lesions except simple hyperplasia per 10-cm length of basement membrane was calculated for each group with a divider or the color image processor as described previously (*10*).

The data were subjected to analysis of variance, and differences between means were tested by Student's *t*-test. Comparison between groups was made by the χ^2-test.

RESULTS

All rats except those given 2-FAA or SS gained weight at rates similar to those of the control group (group 3C). Some rats died of pneumonia or other causes during the experiment. Liver or bladder lesions were seen in few of these rats and no other neoplastic lesions were found. The intake of chemicals did not differ for the different groups, and the average consumptions of 2-FAA, BBN, PB and SS were approximately 7–11, 10–15, 23–33, and 2,000–3,000 mg/kg/day, respectively. However, water intake was about 50% greater per kilogram body weight in groups of rats given SS compared to water intake in other groups.

Liver Changes

Gross white spots or masses were frequently seen on the liver surface in the group treated with 2-FAA (group 1), especially subgroup B, and the liver was enlarged in rats given PB (all subgroups A). Findings in the liver for each group are shown in table 1.

In the groups pretreated with 2-FAA (group 1), almost all rats (93–100%) had hyperplastic nodules. In group 1A, treated with PB after 2-FAA, hepatocellular carcinomas were seen in 5 of 24 rats (21%), but no metastases were observed. The average numbers and areas of hyperplastic nodules per 1 cm^2 of liver in group 1 A were significantly higher ($P<0.05$) than those in the group treated with 2-FAA alone (group 1C). However, no significant differences in the liver were seen between groups 1B and 1C. The incidence, average number, and area of hepatocellular carcinomas per 1 cm^2 of liver specimen in the group treated with 2-FAA and then PB (group 1A) were significantly higher ($P<0.05$, $P<0.01$, and $P<0.05$, respectively) than those in the group treated with 2-FAA alone (group 1C). Although treatment with BBN alone (group 2C) or PB alone (group 3A) induced no liver lesions, sequential administration of these two chemicals (group 2A) resulted in a significant ($P<0.01$) incidence of hyperplastic nodules. However, the number and the area of the nodules per liver were negligible. Cholangiofibrosis was seen in group 1 (table 1). Other liver lesions seen were oval cell proliferation and cystic change of the bile ducts in group 1, and bile duct proliferation and fatty change in all subgroups A. No specific changes were observed in other groups treated with BBN and/or SS or in control rats.

Urinary Bladder Changes

In group 2, initially treated with BBN, we observed gross papillary lesions extending into the bladder lumen. The average length of the basement membrane was 11–14 cm in each subgroup. Findings in the urinary bladder are summarized in table 2.

Although treatment with 2-FAA (group 1C) or SS (group

TABLE 1.—*Histopathologic changes of the liver in rats treated with 2-FAA or BBN followed by PB and SS*

Group	Treatment	No. of rats	Hyperplastic nodules: Incidence (%)	Hyperplastic nodules: No./cm^{2a}	Hyperplastic nodules: Area, mm^2/cm^{2a}	Hepatocellular carcinoma: Incidence (%)	Hepatocellular carcinoma: No./cm^{2a}	Hepatocellular carcinoma: Area, mm^2/cm^{2a}	Cholangiofibrosis (%)
1A	2-FAA→PB	24	24 (100)	5.5±3.2[b]	3.5±2.1[b]	5 (21)[b]	0.1±0.1[c]	1.3±3.0[b]	7 (29)
1B	2-FAA→SS	29	27 (93)	3.0±3.6	1.9±2.4	0	0	0	3 (10)
1C	2-FAA	28	27 (96)	3.6±2.6	1.9±1.8	0	0	0	2 (7)
2A	BBN→PB	30	8 (27)[c]	0±0	0±0	0	0	0	0
2B	BBN→SS	29	0	0	0	0	0	0	0
2C	BBN	28	0	0	0	0	0	0	0
3A	PB	29	0	0	0	0	0	0	0
3B	SS	28	0	0	0	0	0	0	0
3C	None	29	0	0	0	0	0	0	0

[a] Values are means ± SD.

[b] $P<0.05$, compared with subgroup C (basal diet).

[c] $P<0.01$, compared with subgroup C (basal diet).

TABLE 2.—*Histopathologic changes of the urinary bladder in rats treated with 2-FAA or BBN followed by PB or SS*

Group	Treatment	No. of rats	Simple hyperplasia/incidence (%)	Papillary or nodular hyperplasia		Papilloma	
				Incidence (%)	No./10-cm basement membrane[a]	Incidence (%)	No./10-cm basement membrane[a]
1A	2-FAA→PB	24	0	0	0	0	0
1B	2-FAA→SS	29	6 (21)[b]	4 (14)[b]	0.3±1.1	0	0
1C	2-FAA	28	0	0	0	0	0
2A	BBN→PB	30	19 (63)	14 (47)	0.6±0.7	9 (30)	0.4±0.8
2B	BBN→SS	29	27 (93)[b]	24 (83)[b]	2.6±2.2[c]	6 (21)	0.2±0.4
2C	BBN	28	19 (68)	11 (39)	0.7±1.0	8 (29)	0.4±0.7
3A	PB	29	0	0	0	0	0
3B	SS	28	0	0	0	0	0
3C	None	29	0	0	0	0	0

[a] Values are means ± SD.
[b] $P<0.05$, compared with subgroup C (basal diet).
[c] $P<0.01$, compared with subgroup C (basal diet).

3B) alone induced no lesions in the urinary bladder epithelium, sequential administration of these two chemicals (group 1B) resulted in a significant ($P<0.05$) incidence of simple hyperplasia and papillary or nodular hyperplasia. However, the average number of papillary or nodular hyperplastic lesions was not significantly increased. Treatment with PB after initiation with 2-FAA (group 1A) had no significant effect on the urinary bladder epithelium.

In group 2, pretreated with BBN, three types of epithelial changes—simple hyperplasia, papillary or nodular hyperplasia, and papilloma—were seen in the urinary bladder epithelium. However, carcinoma was not observed in any of the groups in this experiment. Treatment with SS after BBN (group 2B) resulted in significantly higher ($P<0.05$) incidences of simple hyperplasia and papillary or nodular hyperplasia than those in group 2C and a significant increase ($P<0.01$) in the average number of papillary or nodular hyperplastic lesions per 10-cm length of basement membrane. No significant difference was observed in the values between groups 2A and 2C. Groups of rats given PB alone (group 3A) or basal diet (group 3C) had normal bladder epithelium.

In this experiment, 6 rats in group 1B and 7 rats in group 2A had both liver and bladder neoplastic lesions. In the urinary bladder, neither calculi nor parasites were observed in any rat, and neoplasms other than in the liver or bladder were not observed.

DISCUSSION

In the present 36-week experiment, the total doses of 2-FAA (group 1C) or BBN alone (group 2C) were subcarcinogenic for liver and bladder. Following 2-FAA treatment, PB enhanced the induction of hyperplastic liver nodules and induced hepatocellular carcinomas, but did not affect the bladder mucosa. PB also induced hyperplastic liver nodules after BBN treatment, but it did not enhance bladder neoplasia induction. Conversely, after BBN treatment, SS enhanced the induction of bladder hyperplastic lesions but did not affect the liver. SS also induced bladder hyperplasia after 2-FAA treatment but did not enhance liver neoplasia induction. These data indicate that 2-FAA and BBN act as initiators for the liver and bladder—2-FAA with greater activity for the liver and BBN with greater activity for the bladder. BBN, in contrast to 2-FAA, appears to have only initiating activity for the liver similar to that of other nonhepatocarcinogens (*4, 5*), but it is not a complete carcinogen for the liver.

SS promoted the induction of bladder neoplastic lesions in rats after initiation with 2-FAA (group 1B) and BBN (group 2B), with similar results to those after administration of other bladder carcinogens (*8, 9*). However, the described effects of PB on the liver after 2-FAA treatment (group 1A, table 1) and of SS on the bladder after BBN treatment (group 2B, table 2) have already been reported previously (*3, 10*). Since hyperplastic nodules and papillary or nodular hyperplasias are thought to be preneoplastic lesions of the hepatocellular and bladder carcinomas, respectively, if the experimental period is extended over 36 weeks, similar results might be obtained to those of Tatematsu et al. (*21*) and Ito et al. (*22*).

The results of the present experiment indicate that PB and SS act as promoters specific for liver and bladder, respectively. These results are consistent with other results showing that PB did not enhance the appearance of 7,12-dimethylbenz[*a*]anthracene-induced skin tumors (*23*) or dimethylnitrosamine-induced lung tumors (*6*), and that PB increased the incidence of spontaneous liver tumors but had no effect on the incidences of other spontaneous tumors (*24*). Also, SS did not enhance the appearance of benzo[*a*]pyrene-induced forestomach tumors (*25*). In contrast, promoters of skin carcinogenesis in mice, including croton oil (*1*), phorbol (*2*), and 12-*O*-tetradecanoylphorbol 13-acetate (*2*), have been reported to have promoting effects on carcinogenesis of various organs, such as breast (*11*), liver and lung (*7*), forestomach (*15*), and glandular stomach (*16*). Additional studies are needed to determine the mechanisms involved for the organ specificity of tumor promoters.

REFERENCES

(*1*) BERENBLUM I, SHUBIK PA. A new quantitative approach to the study of stages of chemical carcinogenesis in the mouse's skin. Br J Cancer 1947; 1:383–391.

(*2*) Baird WM, Boutwell RK. Tumor-promoting activity of phorbol and four diesters of phorbol in mouse skin. Cancer Res 1971; 31: 1074–1079.

(*3*) Peraino C, Fry RJ, Staffeldt E. Reduction and enhancement by phenobarbital of hepatocarcinogenesis induced in the rat by 2-acetylaminofluorene. Cancer Res 1971; 31:1506–1512.

(*4*) Kitagawa T, Hirakawa T, Ishikawa T, Nemoto N, Takayama S. Induction of hepatocellular carcinoma in rat liver by initial treatment with benzo(*a*)pyrene after partial hepatectomy and promotion by phenobarbital. Toxicol Lett 1980; 6:167–171.

(*5*) Tsuda H, Lee G, Farber E. Induction of resistant hepatocytes as a new principle for a possible short-term in vivo test for carcinogens. Cancer Res 1980; 40:1157–1164.

(*6*) Uchida E, Hirono I. Effect of phenobarbital on induction of liver and lung tumors by dimethylnitrosamine in newborn mice. Gan 1979; 70:639–644.

(*7*) Armuth V, Berenblum I. Systemic promoting action of phorbol in liver and lung carcinogenesis in AKR mice. Cancer Res 1972; 32: 2259–2262.

(*8*) Hicks RM, Wakefield JS, Chowaniec J. Evaluation of a new model to detect bladder carcinogens or co-carcinogens; results obtained with saccharin, cyclamate and cyclophosphamide. Chem Biol Interact 1975; 11:225–233.

(*9*) Cohen SM, Arai M, Jacobs JB, Friedell GH. Promoting effect of saccharin and DL-tryptophan in urinary bladder carcinogenesis. Cancer Res 1979; 39:1207–1217.

(*10*) Nakanishi K, Hirose M, Ogiso T, Hasegawa R, Arai M, Ito N. Effects of sodium saccharin and caffeine on the urinary bladder of rats treated with *N*-butyl-*N*-(4-hydroxybutyl)nitrosamine. Gan 1980; 71:490–500.

(*11*) Armuth V, Berenblum I. Promotion of mammary carcinogenesis and leukemogenic action by phorbol in virgin female Wistar rats. Cancer Res 1974; 34:2704–2707.

(*12*) Huggins C, Moon RE, Morii S. Extinction of experimental mammary cancer. I. Estradiol—17β and progesterone. Proc Natl Acad Sci USA 1962; 48:379–386.

(*13*) Reddy BS, Watanabe K, Weisburger JH, Wynder EL. Promoting effect of bile acids in colon carcinogenesis in germ-free and conventional F344 rats. Cancer Res 1977; 37:3238–3242.

(*14*) Witschi H, Williamson D, Lock S. Enhancement of urethane tumorigenesis in mouse lung by butylated hydroxytoluene. J Natl Cancer Inst 1977; 58:301–305.

(*15*) Goerttler K, Loehrke H, Schweizer J, Hesse B. Systemic two-stage carcinogenesis in the epithelium of the forestomach of mice using 7,12-dimethylbenz[a]anthracene as initiator and the phorbol ester 12-*O*-tetradecanoylphorbol-13-acetate as promoter. Cancer Res 1979; 39:1293–1297.

(*16*) Matsukura N, Kawachi T, Sano T, Sasajima K, Sugimura T. Promoting action of croton oil on gastrocarcinogenesis by *N*-methyl-*N'*-nitro-*N*-nitrosoguanidine in rats. J Cancer Res Clin Oncol 1979; 93:323–327.

(*17*) Ito N, Tatematsu M, Imaida K, Hasegawa R, Murasaki G. Effects of various promoters on the induction of hyperplastic nodules in rat liver. Gan 1980; 71:415–416.

(*18*) Weinstein IB, Troll W. National Cancer Institute workshop on tumor promotion and cofactors in carcinogenesis. Cancer Res 1977; 37:3461–3463.

(*19*) Oyasu R, Miller DA, McDonald JH, Hass GM. Neoplasms of rat urinary bladder and liver. Arch Pathol 1963; 75:184–190.

(*20*) Ito N, Arai M, Sugihara S, et al. Experimental urinary bladder tumors induced by *N*-butyl-*N*-(4-hydroxybutyl)nitrosamine. Gan Monogr Cancer Res 1975; 17:367–381.

(*21*) Tatematsu M, Takano T, Hasegawa R, Imaida K, Nakanowatari J, Ito N. A sequential quantitative study of the reversibility or irreversibility of liver hyperplastic nodules in rats exposed to hepatocarcinogens. Gan 1980; 71:843–855.

(*22*) Ito N, Hiasa Y, Tamai A, Okajima E, Kitamura H. Histogenesis of urinary bladder tumors induced by *N*-butyl-*N*-(4-hydroxybutyl)nitrosamine in rats. Gan 1969; 60:401–410.

(*23*) Grube MS, Peraino C, Fry RJ. The effect of dietary phenobarbital on the induction of skin tumor in hairless mice with 7,12-dimethylbenz[*a*]anthracene. Invest Dermatol 1975; 64:258–262.

(*24*) Ponomarkov V, Tomatis L, Turasov V. The effect of long-term administration of phenobarbitone in CF-1 mice. Cancer Lett 1976; 1:165–172.

(*25*) Roe JF, Levy LS, Carter RL. Feeding studies on sodium cyclamate, saccharin and sucrose for carcinogenic and tumor-promoting activity. Food Cosmet Toxicol 1970; 8:135–145.

Serologic Analysis of Nitrosourea-Induced Rat Gliomas[1,2,3,4]

Michael Pfreundschuh,[5] Humberto Cravioto,[6,7] Gerald Hochwald,[8] *and* Joseph Ransohoff[9,10]

ABSTRACT—Inbred CDF rats (cesarean-delivered F344 rats) were immunized with either a nitrosourea-induced glioma EA-285 or its subline EA-285A and both with and without *Corynebacterium parvum*. A humoral immune response in syngeneic rats to the immunizing tumor was demonstrated with micromodifications of different rosette assays (immune adherence assay, protein-A assay, and anti-C3-mixed hemadsorption assay). Extensive absorption studies of two immune sera with the highest reactivity revealed two glioma-specific antigens (or two components of one antigen) on the cell surface of the cloned tumor subline. One antigen was present only on the cell surface of the subline of the glioma used for both immunization and absorption analyses. The other antigen appeared on the cell surface of both the cloned subline EA-285A and the parental cell line EA-285. These preliminary studies showed that CDF rats immunized against a syngeneic glioma mounted a humoral immune response that appeared to be individually tumor-specific.—JNCI 1982; 68:501–505.

Nitrosourea compounds are highly selective carcinogens for the nervous systems of rats (*1–4*). Nitrosourea-induced neurogenic tumors grow well in tissue culture, and the cultured tumor cells grow intracerebrally or sc when transplanted to syngeneic hosts (*5–11*). The immunogenicity of these tumors has been observed in vivo (*12, 13*) and by in vitro procedures (*14–17*). In all of these studies, however, the specificity of the immune response was not extensively or sufficiently tested by absorption studies with normal or neoplastic allogeneic and syngeneic cell lines (*17*). The aim of this work was a study of the specific humoral immune responses of syngeneic rats to an *N*-methyl-*N*-nitrosourea-induced glioma from the inbred, cesarean-delivered F344 rat (CDF rat). All CDF glioma cell lines studied here were induced by nitrosourea compounds and were kept in our laboratory. The sensitive C3MHA assay was used, because it allows serum-saving dilutions for extensive absorption analysis (*18*). For comparison, the IA assay and the PA assay were also used (*18*).

MATERIALS AND METHODS

Tumor cell line.—The glioma cell line EA-285 was a cerebral astrocytoma induced after eight monthly iv injections of 20 mg *N*-methyl-*N*-nitrosourea/kg body weight (total dose, 45 mg) into a CDF male rat from the Charles River Breeding Laboratories, Wilmington, Mass. The in vivo and in vitro morphology and some of the biologic characteristics of this tumor have been described in detail (*4, 9, 13*). EA-285A is a subline derived from this tumor that, in contrast to the uncloned parent tumor, kept its astrocytoma-like morphology even after long-term tissue culture (*13*). The cell lines were examined regularly for bacterial, fungal, and mycoplasma infections. If contaminated, the cultures were discarded. The cell lines used for absorption studies (*see* table 2) have been previously described (*17–20*). The allogeneic rat sarcomas SP 72, SP 73, and SP 76 were from Dr. S. Matzku, the German Cancer Research Center, Heidelberg.

Immunization.—Syngeneic CDF rats were immunized by injections of either irradiated (10^4 rad) trocar tumor pieces or 10^6 irradiated (5×10^3 rad) cultured cells (Gammator M. Radiation Machinery Corp., Parsippany, N.J.). In some rats the tumor cells were mixed with *Corynebacterium parvum* (Formalin-killed organisms, active strain 6434; Burroughs-Wellcome Co., Research Triangle Park, N.C.). The two immune sera with the highest tumor antibody titer were 230 and 352. Serum 230 was obtained from a male CDF rat given an sc injection in the right and left limbs of 1×10^5 EA-285A cultured cells together with 0.007 mg of *C. parvum*. Serum 352 was obtained from a male CDF rat immunized with irradiated trocar pieces of EA-285 tumor. The trocar used for sc transplant was an 18-gauge, 3.5-cm-long needle fitted with a plunger and filled with irradiated tumor. Three sc injections and one ip injection of trocar tumor pieces at weekly intervals were followed 2 weeks later by an sc challenge of 10^5 cultured EA-285 cells. Allogeneic serum 266 was obtained after two sc injections of a WF rat with 10^7 CDF glioma EA-285A cultured cells. Serum 255 was taken from a normal male nonimmunized CDF rat.

IA assay.—Indicator cells were huRBC stored in Alsever's solution up to 4 weeks. The huRBC were washed three times in VBM at 4°C and resuspended to a 0.2% (vol/vol) solution

---

ABBREVIATIONS USED: C3MHA=anti-C3-mixed hemadsorption; EA=erythrocyte-antibody; EAC=erythrocyte-antibody-complement; huRBC=human O-positive red blood cell(s); IA=immune adherence; PA=protein A; PBS=phosphate-buffered saline; SRBC=sheep red blood cells; VBM=Veronal buffer medium.

---

[1] Received June 18, 1981; accepted October 14, 1981.

[2] Supported in part by the Sonderforschungsbereich 136 and by the Ludwig W. Froelich Brain Tumor Research Fund.

[3] Presented in part (*19*) at the 1981 annual meeting of the American Association for Cancer Research, Washington, D.C.

[4] Animals were maintained under the guidelines set forth in the "Guide for the Care and Use of Laboratory Animals" by the Institute of Laboratory Animal Resources, National Research Council, and by New York University Medical Center.

[5] Medizinische Universitats—Poliklinik, Heidelberg, Federal Republic of Germany.

[6] Laboratory of Neuropathology, Department of Pathology, School of Medicine, New York University Medical Center, 550 First Ave., New York, N.Y. 10016.

[7] *Address reprint requests to* Dr. Cravioto.

[8] Department of Neurology, School of Medicine, New York University Medical Center.

[9] Department of Neurosurgery, School of Medicine, New York University Medical Center.

[10] We gratefully acknowledge the technical help of Mrs. Brigitte Geisler, Mrs. Ingrid Prechtel, Dr. Erica De Bernardo, and Mr. Frank Drnovsky and the secretarial assistance of Mrs. Mary Pino.

in VBM. The complement source, 7.5-µl aliquots of 1:50 dilutions of guinea pig serum in a 0.2% (vol/vol) suspension of huRBC in VBM, was added to each well and incubated at 37°C for 30 minutes. The guinea pig serum was screened for high complement activity and low heteroantibody reactivity for rat cells as previously described (*18*). The plates were then washed once in VBM and scored.

C3HMA assay.—For preparation of the C3MHA assay indicator cells, SRBC, which were stored in Alsever's solution up to 2 weeks, were washed three times in PBS and resuspended in a 20% (vol/vol) concentration. Equal volumes of this SRBC solution and heat-inactivated rabbit anti-SRBC serum (Cappel Laboratories, Cochranville, Pa.) at a subagglutinating concentration of 1:200 were incubated for 30 minutes at room temperature. The antibody-coated SRBC (EA) were washed once in PBS and once in VBM and resuspended at 10% (vol/vol) in VBM. To obtain EAC14 cells, we incubated this EA solution on ice with prescreened guinea pig serum at a final concentration of 1:40 for 7.5 minutes, after which we washed the solution twice and resuspended it at 2% (vol/vol) in VBM. Equal volumes of this EAC14 solution and guinea pig complement components C2 and C3 (Cordis Laboratories, Miami, Fla.) at 200 U/ml in VBM were mixed and incubated for 30 minutes at 30°C to produce EAC423. The cells were washed twice in VBM, resuspended at 0.5% in VBM, and incubated with an equal volume of a subagglutinating concentration (1:80) of goat anti-guinea pig C3 (Cappel Laboratories) at room temperature for 1 hour. The EAC423 anti-C3 cells were washed twice and resuspended at 0.5% (vol/vol) in VBM. Preparation of target cells and serum incubation were performed as described for the other assays. After serum incubation, the plates were washed three times in VBM. Then 10 µl of prescreened guinea pig serum was added as a source of complement at a concentration of 1:50 in VBM and incubated for 10 minutes at 37°C. The wells were washed three times in VBM, and 7.5 µl of the 0.5% (vol/vol) EAC423 anti-C3 indicator cell solution in VBM was added to each well. After 30 minutes at room temperature, the wells were washed once in VBM and scored.

PA assay.—The huRBC were washed twice in VBM and once in saline. To 1 volume of a 10% (vol/vol) huRBC solution in saline, a 1/10 volume of PA (1 mg/ml; Pharmacia Fine Chemicals, Freiburg, Federal Republic of Germany) was added slowly and mixed. One volume of chromium chloride ($CrCl_3$–$6H_2O$; E. Merck A.G., Darmstadt, Federal Republic of Germany), 0.02% (wt/vol) in saline, was added dropwise while the mixture was being shaken. The mixture was incubated for 5 minutes at room temperature. The reaction was stopped by addition of excess VBM, and the PA-coated huRBC were washed twice and resuspended at 10% (vol/vol) in VBM. After serum incubation, plates were washed three times with VBM, and 7.5 µl of 0.2% (vol/vol) PA indicator cell suspension in VBM was added to each well. The plates were incubated for 45 minutes at room temperature, washed once with VBM, and scored.

Evaluation.—All tests were scored with the aid of an inverted microscope. Individual cells were scored positive when 50% or more of the cell perimeter was covered by indicator cells. In each case, at least three red blood cells were attached to a positive cell. Target cells showed a clear-cut positive or negative phenomenon. On the rare occasion when only one or two indicator cells were attached to a target cell, the test was scored as negative. The serum titer was read as the highest serum dilution to give at least 10% positive target cells in the respective well. For a test to be valid, control wells that had been incubated with VBM alone had to have less than 1% positive cells ("no background").

Background reactivity.—When seen, background reactivity is probably due to heteroantibody. As shown previously (*18*), background reactivity can be abolished by shortening the complementation time, probably because attachment of heteroantibody in the guinea pig serum to the surface of the target cells takes more time than complementation. This modification proved to be more consistent than preabsorption of guinea pig serum with rat target cells, which often led to variable reduction of complement activity. When the assay protocol was strictly adhered to, the modification of the serologic assays for microtiter plates #3034 (instead of #3040) did not affect sensitivity and reproducibility. Plates must not stand too long; otherwise, the wells may dry out. Plates must also be thoroughly washed.

RESULTS

The IA assay reactivity of different sera against EA-285A is shown in text-figure 1. The allogeneic serum had the highest reactivity at a titer of 1:32. The immune serum 352 had an IA assay titer of 1:8. In this experiment serum 355, a control serum from a non-tumor-bearing CDF rat, had no detectable reactivity against EA-285A. Text-figure 2 shows that the reactivity of serum 230 was highest in the C3MHA assay with a titer of 1:32. Reactivity of serum 230 as detected by PA and IA assays was lower, 1:8 and 1:16, respectively. Serum 352 showed a pattern similar to that of serum 230. The maximal serum reactivity obtained by the three assays is shown in table 1. The highest reactivity was obtained with allogeneic immune serum 266. In the C3MHA assay, sera 230 and 352 showed the highest reactivity (1:128) and were used in absorption studies (*see* below). Serum 355 from

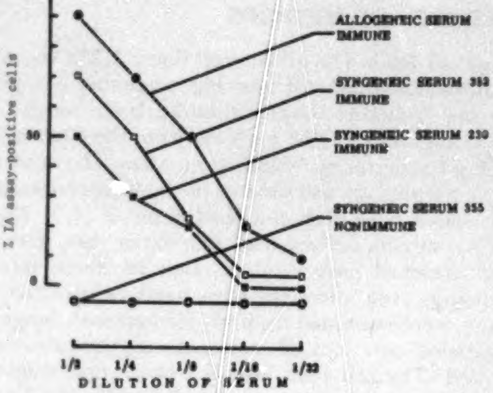

TEXT-FIGURE 1.—IA assay reactivity of various rat sera against EA-285A.

a normal male rat, similar to sera 451 and 455 (obtained from rats immunized with *C. parvum* only), showed no reactivity in the PA assay, a weak reactivity of 1:2 to 1:4 in the IA assay, and a reactivity of 1:4 to 1:8 in the C3MHA assay. However, this reactivity did not appear tumor-specific since it was absorbed by normal cultured CDF skin. The assay that gave the highest titer was the C3MHA assay. This assay was chosen to analyze the specificity of the anti-EA-285A reactivity because it allowed extensive absorptions with the use of diluted sera. These antisera were absorbed with a wide spectrum of syngeneic, allogeneic, and heterologous benign and malignant cells. Text-figure 3 illustrates individual absorption tests of serum 230 and serum 352. Table 2 summarizes the results of absorption studies performed with these sera. The antigen detected by serum 230 was restricted to syngeneic EA-285A glioma cells. Other cell types, including other syngeneic nitrosourea-induced CDF tumors of the nervous system and a panel of normal CDF tissue and fetal rat cells, did not absorb reactivity of serum 230. Serum 352 showed a similar absorption pattern as did serum 230. However, the C3MHA assay reactivity of serum 352 to EA-285A cells was also absorbed by the parental cell line EA-285.

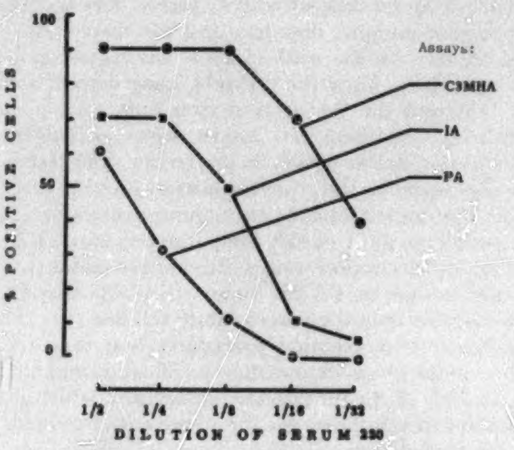

TEXT-FIGURE 2.—Reactivity of serum 230 against syngeneic glioma EA-285A as detected by C3MHA, IA, and PA assays.

TABLE 1.—*Maximal rat serum reactivity in three rosette assays*

Serum No.	Rat strain	Rat immunized with:	Titers obtained in		
			IA assay	PA assay	C3MHA assay
230	CDF	Irradiated EA-285A cells mixed with *C. parvum*	1:16	1:8	1:128
266	WF	Irradiated EA-285A cells	1:64	1:16	1:256
352	CDF	Irradiated EA-285 trocar pieces	1:16	1:8	1:128
300	CDF	Irradiated EA-285A cells	1:8	1:4	1:32
355	CDF	Not immunized	1:4	0	1:8
451	CDF	*C. parvum*	1:2[a]	0	1:4[a]
455	CDF	*C. parvum*	1:2[a]	0	1:4[a]

[a] Titers seen in these sera were nonspecific and were absorbed with EA-285A tumor cells as well as with CDF skin fibroblasts.

Quantitative absorption analysis of the antigen detected by serum 352.—Quantitative absorption tests were performed with the two cell lines expressing the antigen detected by serum 352. As measured by absorption capacity per cell, the original cell line EA-285 as compared to the cloned cell line EA-285A expressed one-third of this antigen on the cell surface (text-fig. 4).

Stability of antigen expression by cultured rat glioma cells.—Late in vitro passages of tumor cell lines EA-285 and EA-285A (147–215) were tested for the presence of the antigen detected by serum 230 or 352. In general, only minimal fluctuations (5–10% of early passages) in the strength of this syngeneic reaction and antibody titer could be detected. The specificity of the reactions, as determined by absorption analysis, remained constant, despite the late in vitro passage number.

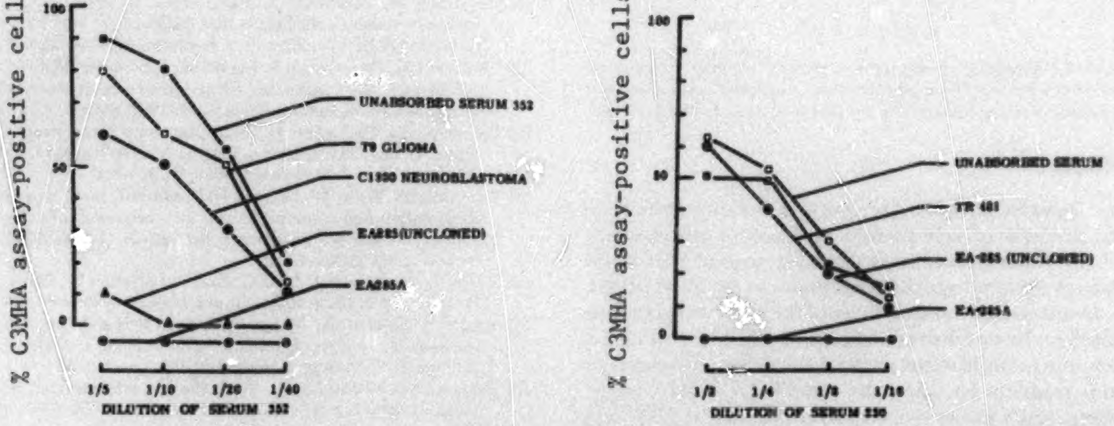

TEXT-FIGURE 3.—Individual absorption tests of serum 352 (*left*) and serum 230 (*right*) C3MHA assay reactivity. Serum 230 was absorbed with the immunizing cell line EA-285A only, whereas serum 352 was also absorbed with the parental cell line EA-285. TR 481 is a malignant neuroma cell line (*13*).

TABLE 2.—*Absorption studies of syngeneic immune serum 352 to rat glioma EA-285 and serum 230 to rat glioma EA-285A*

Absorption	Serum 230[a]	Serum 352[a]
EA-285A (cloned)	+	+
EA-285 (uncloned)	−	+
YE2/2 CDF glioma	−	−
T9 CDF glioma	−	−
TR 481 CDF neuroblastoma	−	−
SP 6 rat sarcoma	−	−
SP 11 rat sarcoma	−	−
SP 50 rat sarcoma	−	−
SP 73 rat sarcoma	−	−
CDF brain	−	−
CDF lung	−	−
CDF fibroblasts	−	−
CDF liver	−	−
CDF spleen lymphocytes	−	−
CDF red blood cells	−	−
Fetal rat brain	−	−
Fetal rat lung	−	−
Fetal rat liver	−	−
Fetal rat kidney	−	−
C1300 mouse neuroblastoma	−	−
Guinea pig kidney	−	−
SRBC	−	−
Fetal calf serum	−	−
AJ human glioma	−	−
BK human glioma	−	−
ME 180 human cervical cancer	−	
SK-LC-LL human lung cancer	−	−
SK-RC-VO human renal cancer	−	
O⁺ huRBC	−	−

[a] + = absorbed; − = not absorbed.

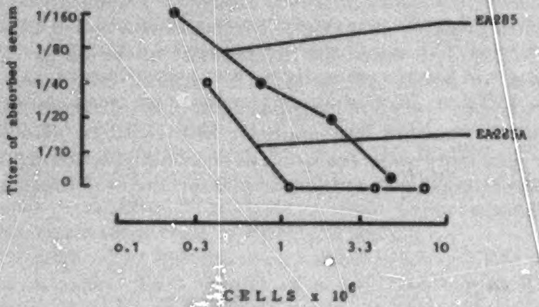

TEXT-FIGURE 4.—Quantitative absorption analysis of serum 352 reactivity. The cloned cell line EA-285A expresses three times more tumor antigen on the surface of one cell than does the parent tumor cell line EA-285.

DISCUSSION

To our knowledge this study contains the most extensive serologic analysis of cell surface antigens of nitrosourea-induced rat gliomas. Although there are several reports on the existence of tumor-specific antibodies to rat gliomas (*14, 15, 17*), an analysis of the specificity of the observed reactions was limited in the number of antigens tested. This limitation was often due to insufficient amounts of serum. We can now avoid this problem by using the modified C3MHA assay. The present study shows two important results: 1) CDF rats immunized against a syngeneic nitrosourea-induced glioma are able to mount a humoral immune response against this tumor, which seems to be individually tumor-specific [class I antigen (*20*)]. 2) Immunization with the in vitro cultured cells of the subline EA-285A gives rise to an antibody that detects an antigen present only in the subline; in contrast, immunization with the in vivo transplanted subline of the glioma induces in the syngeneic rat the production of an antibody that reacts with an antigen present in both the EA-285 tumor cell line and in the EA-285A cloned subline. The quantitative absorption analysis shows that this antigen is present in the subline at a concentration threefold greater than that found in the parental line EA-285. It is not clear whether the antigens detected by sera 230 and 352 are different antigens or different components of the same antigen. It is also uncertain whether or not the antigen present only in the cloned cell line and detected by serum 230 represents a new antigen that developed in vitro after cloning.

The addition of *C. parvum* to enhance the response to the tumor may result in the formation of antibodies to minor components and contribute to the production of the tumor-specific antibody in serum 230. The injection of the same number of tumor cells without *C. parvum* does not result in a consistent immune response, and the reactivities of the resulting sera are too weak to allow absorption analysis of their specificity. Since the C3MHA assay detects both IgG and IgM and the PA assay detects only IgG, it can be speculated that these two assays detect antibodies with different specificities present in one serum. A similar conclusion was made in the study of human astrocytomas (*20*). Again, the limited amount of immune serum available did not permit analysis of the comparatively weak PA assay reaction by absorption studies. Studies are under way with another subline of EA-285 tumor (EA-528) that is more immunogenic than the parent tumor cell line (*21*). The use of different immunization procedures that may result in higher titered serum should allow purification and biochemical analysis of the glioma-specific antigen, which may be important in the future for the treatment of animals with transplanted tumors.

REFERENCES

(*1*) DRUCKREY H, IVANKOVIC S, PREUSSMANN R. Selektive Erzeugung maligner Tumoren im Gehirn und Rückenmark von Ratten durch *N*-Methyl-*N*-Nitrosoharnstoff. Z Krebsforsch 1965; 66:389–408.

(*2*) DRUCKREY H, PREUSSMANN R, IVANKOVIC S, SCHMÄHL D. Organotrope carcinogene Wirkungen bei 65 verschiedenen N-Nitroso-Verbindungen an BD-Ratten. Z Krebsforsch 1967; 69:103–201.

(*3*) IVANKOVIC S, DRUCKREY H. Transplacentare Erzeugung maligner Tumoren des Nervensystems. I. Äthyl-Nitroso-Harnstoff (ANH) an BD IX Ratten. Z Krebsforsch 1968; 71:320–360.

(*4*) CRAVIOTO H, WEISS JF, GOEBEL HH., WEISS E DE C, RANSOHOFF J. Preferential induction of central or peripheral nervous system tumors in rats by nitrosourea derivatives. J Neuropathol Exp Neurol 1974; 33:595–615.

(*5*) BENDA P, LIGHTBODY J, SATO G, LEVINE L, SWEET W. Differentiated rat glial cell strain in tissue culture. Science 1968; 161:370–371.

(*6*) BENDA P, SOMEDA K, MESSER J, SWEET WH. Morphological and immunochemical studies of rat glial tumors and clonal strains propagated in culture. J Neurosurg 1971; 34:310–323.

(*7*) PFEIFFER SE, WECHSLER W. Biochemically differentiated neoplastic clone of Schwann cells. Proc Natl Acad Sci USA 1972; 69:2885–2889.

(*8*) CRAVIOTO H, WEISS JF, WEISS E DE C, GOEBEL HH, RANSOHOFF J. Biological characteristics of peripheral nerve tumors induced with ethylnitrosourea. Acta Neuropathol (Berl) 1973; 23:265–280.

(9) Cravioto H, Hirt P, Chabora J. Studies on transplantation of nitrosourea-induced brain tumors. In: Kornyey ST, Tariska ST, Gosztonyi G, eds. Proceedings of the seventh international congress of neuropathology. Vol I. Amsterdam: Excerpta Medica, 1975:483–490.

(10) Lantos PL, Roscoe JP, Shickmore CJ. Studies of the morphology and tumourigenicity of experimental brain tumours in tissue culture. Br J Exp Pathol 1976; 57:95–104.

(11) Cravioto H. Immunology of experimental brain tumors, chapt 7. In: Water H, ed. The handbook of cancer immunology. Vol 3. Immune status in cancer treatment and prognosis. New York and London: Garland STPM Press, 1978:329–363.

(12) Denlinger RH, Swenberg A, Koestner A, Liss L. Tumor-specific transplantation immunity to intracerebral challenge with cells from a methylnitrosourea-induced brain tumor. J Med 1975; 6:249–259.

(13) Yoshida J, Cravioto H. Nitrosourea-induced brain tumors: An in vivo and in vitro tumor model system. JNCI 1978; 61:365–374.

(14) Toh BH, Guli PG. In vitro immunoreactivity against ethylnitrosourea-induced tumors of the nervous system in the rat. Experientia 1974; 30:1472–1473.

(15) Stavrou D, Anzil AP, Elling H. Tumor specific fluorescent and complement-dependent cytotoxic antibodies in the serum of rats with chemically induced brain gliomas. Acta Neuropathol (Berl) 1978; 43:111–117.

(16) Spence AM, Hellström KE, Hellström I, Van Belle G, Sullivan K, Wallström T. Immunization against ethylnitrosourea-induced autochthonous neurogenic rat tumours. Br J Cancer 1979; 40:164–167.

(17) Yoshida J, Cravioto H, Ransohoff J. In vitro transformation of fetal brain cells from CDF rats exposed in utero to *N*-ethyl-*N*-nitrosourea: Morphologic and immunologic studies. JNCI 1980; 64:1231–1239.

(18) Pfreundschuh M, Ueda R, Rauterberg EW, Dorken BH, Shiku H. Comparison of multiple rosetting assay for detecting reactivity of different immunoglobulin classes against surface antigens of benign and malignant tissue culture cells. J Immunol Methods 1980; 37:71–81.

(19) Pfreundschuh M, Cravioto H. Serological analysis of nitrosourea-induced rat gliomas. Proc Am Assoc Cancer Res 1981; 22:294.

(20) Pfreundschuh M, Shiku H, Takahashi T, et al. Serological analysis of cell surface antigens of malignant human brain tumors. Proc Natl Acad Sci USA 1978; 75:5122–5126.

(21) Morantz RA, Wood GW, Foster M, Clark M, Gollahon K. Macrophages in experimental and human brain tumors. Part I. Studies of the macrophage content of experimental rat brain tumors of varying immunogenicity. J Neurosurg 1979; 50:298–304.

Development and Biologic Properties of Malignant Cell Sublines and Clones of a Spontaneously Metastasizing Rat Mammary Adenocarcinoma[1,2,3]

Anthony Neri,[4,5] Dan Welch,[6] Takanori Kawaguchi,[6,7] *and* Garth L. Nicolson[6,8]

ABSTRACT—With the use of the rat 13762 mammary adenocarcinoma tumor, an animal model for spontaneous mammary tumor metastasis was developed. The parental tumor implanted sc into the mammary fat pads of female Fischer 344 rats metastasized at low frequency to lymph nodes and lung and did not metastasize to other organs. Oophorectomy did not modify the metastatic properties of the parental 13762 tumor. Cell lines were adapted to tissue culture from lymph node or lung metastases, and these were compared to parental tumor transplants in spontaneous metastasis assays. Only the cell lines established from metastases were spontaneously metastatic within 23 days after sc implantation, indicating that tumor cell populations from metastases are more metastatic than are cells from the parental tumor. Several individual parental tumor-derived and lung metastasis-derived clones were compared for spontaneous metastatic potentials, cell culture morphologies, histologic structures at primary implant and secondary metastatic sites, and growth characteristics in vivo and in vitro. There was no correlation between any of these tumor and cellular properties and metastatic potential. The parental mammary tumor-derived, lymph node metastasis-derived, and lung metastasis-derived cell lines and clones with differing spontaneous metastatic properties should prove useful in studies on the roles of tumor cell and host properties in lymphatic and blood-borne metastasis.—JNCI 1982; 68: 507–517.

Tumor metastasis is probably the most urgent problem in the management of cancer, because primary tumors can in most cases be treated effectively by a combination of treatments usually involving surgery, chemotherapy, and radiotherapy. However, metastatic tumor cells have often spread to other sites before they are detected and treated (*1*, *2*). Therefore, efforts to elucidate and better understand the events and processes involved in metastasis should lead to improved and more effective means of cancer control.

For malignant cells to spread from the primary sites to near and distant secondary sites, the tumor cells must invade surrounding normal tissues, penetrate blood and/or lymphatic vessels, dislodge from the primary tumor mass, disseminate to distant sites, arrest in the lymph nodes or microvasculature of distant organs, and finally invade the parenchyma and stroma at these sites to survive and grow into gross metastatic colonies (*3–5*). Metastasis is a complex biologic process, and its final outcome is influenced by both host factors and tumor cell properties (*5–7*). That this process is the end result of several highly selective sequential steps during which only a few cells eventually survive suggests that only a small fraction of cells in the primary tumor is capable of completing the entire sequence (*4–6*). Heterogeneity in metastatic potential within malignant cell populations has been found in several animal tumor model systems (*8*, *9*, *10–14*). In addition to heterogeneity in metastasis, evidence is increasing that single neoplasms can be comprised of subpopulations that vary in other characteristics such as in vivo and in vitro growth potential (*15*, *16*), drug sensitivity (*15*, *17–20*), immunogenicity (*21–23*), and radiosensitivity (*24*, *25*). Therefore, it is not surprising that therapeutic measures taken against metastatic disease are often ineffective.

To better define tumor cell and host properties related to the metastatic process, one must have suitable animal tumor models that resemble human metastatic disease (*5*, *26*). In addition, the experimental models should allow for the selection of malignant subpopulations with low and high metastatic potentials. Such animal metastatic models have been developed for certain histologic types of tumors, such as melanoma (*27–30*), fibrosarcoma (*10*, *11*), carcinoma (*12*, *31*, *32*), lymphosarcoma (*33*), and sarcoma (*9*, *34*). Although breast cancer metastasis is the leading cause of death in women 35–54 years old (*35*), suitable animal models for studying mammary tumor metastasis with the use of high and low metastatic cell sublines from the same parental tumor have not been available. We now report on the establishment of an animal tumor model for the experimental study of spontaneous metastasis of a rat mammary adenocarcinoma from mammary sites to distant secondary sites as well as biologic characterization in vivo and in vitro of cell lines and clones isolated from the parent tumor and metastases that exhibit different metastatic potentials.

ABBREVIATIONS USED: AMEM=alpha modification of minimum essential medium; CM=complete medium; DPBS=Dulbecco's phosphate-buffered saline; DPBS-CMF=Ca^{2+}- and Mg^{2+}-free DPBS; H & E=hematoxylin and eosin.

---

[1] Received July 16, 1981; accepted November 2, 1981.

[2] Supported by Public Health Service grant R01CA 28844 from the National Cancer Institute (to G. L. N.).

[3] Animals were maintained under the guidelines set forth by The University of Texas System Cancer Center and in the "Guide for the Care and Use of Laboratory Animals" by the Institute of Laboratory Animal Resources, National Research Council.

[4] Department of Developmental and Cell Biology, University of California, Irvine, Calif. 92717.

[5] *Present address:* Department of Biochemistry, University of Southern California Comprehensive Cancer Center, Los Angeles, Calif. 90033.

[6] Department of Tumor Biology, The University of Texas System Cancer Center, M. D. Anderson Hospital and Tumor Institute, Houston, Tex. 77030.

[7] *Permanent address:* Second Department of Pathology, Fukushima Medical College, Fukushima 960, Japan.

[8] *Address reprint requests to* Dr. Nicolson at Department of Tumor Biology-108, The University of Texas System Cancer Center, M. D. Anderson Hospital and Tumor Institute, 6723 Bertner Ave., Houston, Tex. 77030.

MATERIALS AND METHODS

Animals.—Female Fischer 344/CRBL rats 6–9 weeks of age were used. They were fed a diet of Wayne Lab-Blox (Allied Mills, Inc., Chicago, Ill.) and tap water with a chlorine content of 0.35–0.80 ppm. All animals used for experimentation were healthy as determined by visual observations and by diagnostic laboratory tests performed by the Veterinary Laboratory Services (Irvine, Calif.) for viral, bacterial, fungal, and parasitic infections.

Mammary adenocarcinoma tumor line.—The mammary adenocarcinoma line 13762 was originally developed by Segaloff (*36*) by dietary administration of 7,12-dimethylbenz[*a*]anthracene. The tumor has since been maintained by in vivo sc serial passages in syngeneic female Fischer 344 rats and as frozen stocks in liquid nitrogen. The frozen form of the 13762NF solid tumor was obtained in 1977 from the Mason Research Institute, Worcester, Mass. Upon arrival, the frozen tumor specimen was thawed quickly in a 37°C water bath, washed three times with 10 ml AMEM (*37*) without antibiotics or serum. The tumor tissue was then transferred to a 35-mm plastic petri dish (Corning Glass Works, Corning, N.Y.) and cut into 2×3-mm pieces with the use of iridectomy scissors. Eight rats were lightly anesthetized with Metofane (methoxyflurane; Pitman-Moore, Inc., Washington Crossing, N.J.), and tumor pieces measuring 2–3 mm were individually implanted sc by surgical incision in the mammary fat pad. The incision was closed with wound clips. Tumor-bearing animals were observed and palpated twice weekly for primary tumor growth and possible metastases to inguinal and axillary lymph nodes. Animals suspected of having metastases were killed, the primary tumors were measured, and the pleural and visceral organs were examined with the aid of a dissecting microscope for the presence of tumor lesions. In all cases, secondary tumors were verified by histologic examination of paraffin-embedded samples prepared from tumor-involved tissues.

Oophorectomy.—Animals were oophorectomized to determine whether the growth and metastasis of the parental 13762 adenocarcinoma tumor were affected by ovarian hormones. The ovaries of 10 rats were surgically excised, and the animals were allowed to recover for 14 days. Following the recovery period each oophorectomized rat received an sc implant of 2×3-mm tissue from the parental tumor in the mammary fat pad. The source of tumor tissue fragments used for transplantation was a subcutaneous growth of the parental tumor. The fragments were derived from fleshy, peripheral areas of the tumor distant from any necrotic regions. Rats that did not have their ovaries removed but had received equivalent fragments of parental tumor tissue served as controls. After 40 days the animals were killed by anesthesia (Metofane), their primary tumors measured, and their organs examined with the aid of a dissecting microscope for the presence of surface tumor nodules.

In vivo growth and spontaneous metastasis of the parent tumor 13762 line.—Tumor tissue obtained from peripheral, nonnecrotic regions of the parental tumor was cut into 2×3-mm fragments and implanted sc into the mammary fat pads of recipient rats. The animals were killed by anesthesia (Metofane) at 23 and 40 days post tumor implantation. The implanted (subcutaneous primary) tumors were then measured, and the organs of all animals were examined with the aid of a dissecting microscope for surface tumor lesions.

Establishment of tissue culture cell lines and clones from the parental 13762 adenocarcinoma and its metastases.—Parental tumor tissue fragments were removed with the use of sterile forceps and a scalpel from peripheral, nonnecrotic regions of a single tumor measuring 4 cm in diameter after 40 days of subcutaneous growth. Four tissue fragments having a total wet weight of approximately 1.5 g were transferred to a sterile 35-mm plastic petri dish containing 5 ml of cold AMEM without antibiotics plus 10–20% heat-inactivated fetal bovine serum (Flow Laboratories, Inc., Inglewood, Calif.) (CM). The fragments were subjected to ten rinses (5 ml each) with cold CM. After the final rinse the medium was aspirated and the fragments were finely minced with sterile iridectomy scissors. After 5 ml CM was added to the minced tissue, the tissue was transferred with the use a wide-bore sterile pipette to a 15-ml sterile plastic conical centrifuge tube. The tube was placed in an ice bath, and the minced tissue was allowed to settle. The supernatant was decanted, and the settled tissue mince was washed three times with 10 ml each of cold CM. Finally, the minced tissue was resuspended in 10 ml of CM containing 1 mg crude collagenase/ml (100 U/mg, CLS III; Worthington Biochemical Corp., Freehold, N.J.). The tissue was distributed into ten 75-cm^2 tissue culture flasks (Corning Glass Works) containing 9 ml of CM with 1 mg collagenase/ml each and incubated at 37°C in a humid atmosphere of 95% air–5% CO_2. After 72 hours of incubation in the presence of collagenase, very few cells were found to be attached to the substratum; instead, most cells were found to be floating in the medium as single cells or loosely adhering cell aggregates. The medium containing the single cells and aggregates was collected from each culture and centrifuged at $180\times g$ for 5 minutes. The cell pellets were resuspended in 10 ml of fresh CM and distributed into five 75-cm^2 culture flasks containing 9 ml of CM each. To facilitate attachment to the substratum, we left the cultures undisturbed for 5 days at 37°C. The cultures were then examined for cellular attachment and growth. When the cultures had reached approximately 50–60% confluence, they were detached with the use of 3 ml of prewarmed 0.25% trypsin (Difco Laboratories, Detroit, Mich.; 1:250) in DPBS-CMF (*38*). CM (10 ml) was then added to each flask to inhibit trypsin activity. Viable cell counts were determined with the use of 0.1% trypan blue in DPBS-CMF with a hemacytometer.

Metastatic tumor lesions from lungs and axillary lymph nodes were established in tissue culture. The source of metastases was the same animal whose primary parental tumor was established in tissue culture. An enlarged axillary lymph node measuring 8 mm in diameter was excised surgically and aseptically and placed in a 35-mm petri dish containing 5 ml of cold CM. The lungs of an animal possessing over 15 surface tumor nodules were removed and placed in a separate petri dish containing 5 ml of CM. Five surface tumor nodules were selected, dissected away from normal lung tissue, and transferred to another petri dish containing 5 ml of CM. Tissue cultures of the parent tumor and its lung metastases were subjected twice to single cell cloning procedures according to Neri and Nicolson (*39*).

In vitro analysis of growth rates and saturation densities.—Tumor cell clones derived from tissue culture of parental tumor and metastatic lung lesions were analyzed for differences in growth rates and saturation densities. For growth rate studies, established cultures of individual clones were detached with the use of 0.25% trypsin in DPBS-CMF, reseeded into 25-cm² flasks at an initial density of 4×10³ viable cells/cm² in 5 ml of CM, and incubated for 6 days without medium change. Cell counts were obtained every 24 hours on triplicate cultures with the use of a hemacytometer. The conditions used for the determination of saturation densities were identical to those used for the growth rate analysis except for the addition of fresh CM at 96 hours during log phase growth and thereafter every 24 hours until each clonal culture reached stationary growth phase.

In vivo biologic assays.—Individual clones derived from the parental tumor and from lung metastases were analyzed for their extent of growth and capacity to metastasize spontaneously from subcutaneous sites. Tissue cultures of tumor cell clones that were 80–90% confluent were detached with the use of 0.25% trypsin in DPBS-CMF and washed twice with 15 ml of cold AMEM, and cell numbers and viabilities were determined. Cell suspensions over 90% viable were used for all injections. Animals were anesthetized lightly with Metofane and given injections sc with the use of a 25-gauge needle on a 1-ml syringe in the mammary fat pad with 1×10⁶ viable cells in 0.5 ml of AMEM. All animals were killed with Metofane 23 days post tumor cell injection. Tumors growing at the site of injection were measured, organs were removed and rinsed in DPBS, and each organ was examined with the aid of a dissecting microscope for tumor involvement. Tissue samples from primary tumor sites and metastatic sites were prepared for histology.

Histology.—Tissues were prepared for histology by fixation in Bouin's solution (24 hr) followed by dehydration, paraffin embedding, and sectioning. Sections 4–6 μm thick were stained with H & E.

Mycoplasma testing—Tissue cultures of all cell lines and clones were routinely screened with the use of Hoechst 33258 stain (Calbiochem-Behring Corp., Los Angeles, Calif.) for the presence of mycoplasma contamination prior to animal injections by the procedures of Chen (*40*).

RESULTS

Growth and Spontaneous Metastasis of the Parental Tumor in Oophorectomized Rats

No significant differences in the extent of growth or spontaneous metastases of the parental mammary adenocarcinoma tumors were observed between oophorectomized and control animals. Forty days after tumor implantation the oophorectomized group (10 rats) and the control animals (15 rats) had subcutaneous tumors measuring 44.6±8.4 and 45.6±7.2 mm (average diameters ± SD), respectively. Gross observations of pleural and visceral organs for metastases also revealed no apparent differences. Of the oophorectomized animals, 20% (2/10) had surface pulmonary tumor nodules (median=11; range=1, 112). In the control group that had not undergone oophorectomy, 5 of 15 animals had visible surface pulmonary tumor nodules (median=5; range=1, 72). Lymph node metastases were found in 60% (6/10) and 53% (8/15) of the oophorectomized and control animals, respectively; other organs in both groups were negative.

In Vivo Biologic Characteristics of the Parental Tumor

The growth and metastatic profiles of the parental mammary adenocarcinomas in syngeneic female Fischer 344 rats were examined (table 1). Animals receiving parental tumor tissue fragments (2×3 mm) sc were killed 23 days later and examined. Metastases were not detectable, including metastases in lymph nodes or pleural and visceral organs. The subcutaneous tumors at this time had mean diameters of 29±4.8 mm, grew as scirrous-like masses that did not erupt through the skin, and exhibited only slight central necrosis with very little fluid accumulation. In contrast, among the 56 animals that were killed 40 days after sc tumor implantation, 31 rats had metastases to the lymph node (inguinal, axillary, lumbar, and/or mesenteric nodes) and 23 had lung metastases (median number of lung surface tumor foci=5; range=1, 65). All other organs examined, such as liver, spleen, kidneys, and ovaries, were negative for visible tumor metastases. The subcutaneous tumors had mean diameters of 45.90±9.3 mm. At that stage, the tumors had erupted through the overlying skin and exhibited centers of necrosis.

To minimize the possibility that subclinical micrometastases were present deep within the organs and therefore not detected by visual observations, we excised and minced the organs from randomly selected animals with no visual indication of tumor involvement. Portions of the tissue minces representing each organ (i.e., lungs, liver, spleen, kidneys, ovaries, and regional and distant lymph nodes) were implanted sc in mammary fat pads of groups of rats. The animals were observed for tumor growth over 3 months, but no tumors developed in these animals within that period.

Established Cell Lines and Clones of 13762 Adenocarcinoma

Primary cultures established from the parental tumor were comprised of cells with different morphologies. Morphologic heterogeneity ranged from fibroblastic to epithe-

TABLE 1.—*In vivo biologic characteristics of the 13762 mammary adenocarcinoma parental tumor*

Days after implantation	Primary tumor average diameter, mm ± SD[a]	Animals with lung metastases[b] (%)	Median No. of visible lung metastases (range)	Animals with regional lymph node metastases[b] (%)
23	29.0±4.8	0/24 (0)	0	0/24 (0)
40	45.9±9.3	23/56 (42)	5 (1, 65)	31/56 (55)

[a] We calculated average tumor diameters by performing two measurements 90° to each other, dividing the sum by 2, averaging all values for each experimental animal group, and computing the standard deviations.

[b] No. of animals with metastases/total No. of animals given tumor implants.

lial, and these morphologic types were often separated by distinct boundaries. Parallel primary cultures not subjected to cloning were allowed to reach confluence and were subcultured continuously for 6–7 weeks, which resulted in cell lines that were morphologically uniform and exhibited only fibroblastic morphologies. That these cultures represented overgrowth by normal host fibroblasts was suggested by their inability to produce subcutaneous tumors over 4 months in syngeneic rats (5 rats/group; injection, up to 10×10^6 viable cells/rat). We concluded that the cloning of parental tumor lines must be initiated as early as possible to prevent subsequent overgrowth of tumor cells by normal fibroblasts.

Primary cultures of parental tumor exhibiting a large degree of morphologic heterogeneity were subcultured and immediately subjected to cloning procedures. Selected clonal variants possessed mainly fibroblastic or epithelial-like morphologies (fig. 1). Cell clones derived from cultures of lung metastases were not as morphologically heterogeneous as were clones obtained from the parental primary tumor (fig. 2).

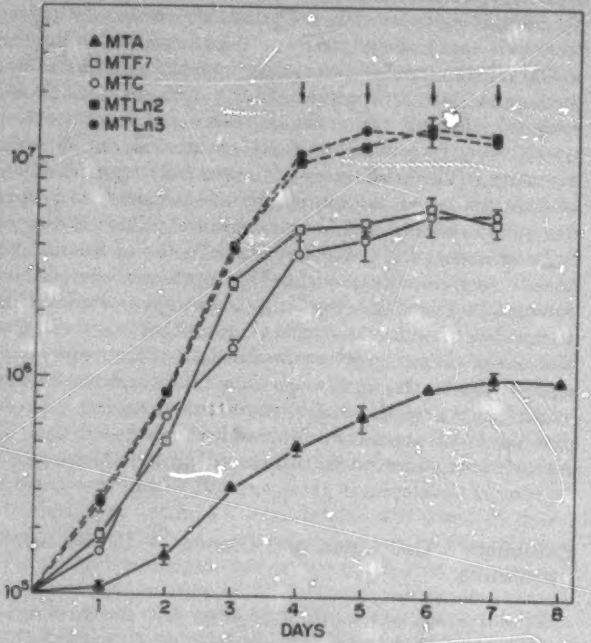

TEXT-FIGURE 1.—*In vitro* growth rates of mammary tumor clones. Cultures were seeded initially at 10^5 cells/25-cm² flask and refed at the indicated (*arrows*) times.

In Vitro Growth Rates and Saturation Densities of Adenocarcinoma Clones

In vitro growth studies of the selected clones revealed differences in growth rates and saturation densities (text-fig. 1). Clones derived from metastatic lung lesions (MTLn2 and MTLn3) had generation times of 13.5 hours and final saturation densities of 6×10^5 cell/cm², while clones obtained from the parental tumor (MTC and MTF7) possessed mean generation times of approximately 16.5 hours and saturation densities of $2.2–2.4 \times 10^5$ cells/cm². Clone MTA differed dramatically from the other clones; it exhibited a generation time of approximately 28.6 hours and a final saturation density of 4×10^4 cells/cm² (text-fig. 1).

In Vivo Biologic Characteristics of Adenocarcinoma Cell Lines and Clones

To determine whether the tumor cells from secondary metastatic lesions represented cells with enhanced metastatic potentials, we injected sc the uncloned tumor cell cultures established from axillary lymph nodes and lung metastases (1×10^6 viable cells in the mammary fat pad). The animals were killed 23 days later and examined for gross metastases. A striking difference in the extent of subcutaneous growth and potential to metastasize was found between lung metastasis or lymph node-derived tumor cell lines and cells from the parental tumor (table 2). All animals receiving injections sc in the mammary fat pads of metastasis-derived tumor cells developed both lymph node (inguinal, axillary, and lumbar) and lung metastases, whereas animals implanted with parental tumor tissue (2×3 mm, sc in the mammary fat pads) showed no detectable metastases in organs or lymph nodes. The difference in the metastatic potentials of metastasis-derived tumor cells compared to the parental tumor-derived cells was not simply due to in vitro cultivation, because direct sc transfer of lymph node and lung metastatic lesions (5 rats with lung and 5 rats with axillary lymph node metastases) resulted in patterns of metastasis similar to those found with tissue culture-adapted cells (data not shown). These results indicated that in this system tumor cell populations from secondary lesions pos-

TABLE 2.—*In vivo comparison of the parental 13762 mammary adenocarcinoma with its metastatic variant cell lines selected from tumor-involved lymph nodes and lungs*

Origin of tumor tissue	Primary tumor average diameter, mm ± SD[a]	Time of animal examination, days	Animals with lung metastases[b]	No. of surfece lesions per lung, median (range)	Animals with lymph node metastases[b]
Lung metastasis (1×10^6 tumor cells injected)	18.8±3.7	23	5/5	53 (15, >250)	5/5
Lymph node metastasis (1×10^6 tumor cells injected)	15.5±3.2	23	5/5	37 (1, >250)	5/5
Parental 13762 tumor (2×3-mm tumor pieces transplanted)	27.7±4.3	23	0/10	0	0/10

[a] *See* table 1 for calculations.

[b] No. of animals with metastases/total No. of animals given tumor implants.

sessed enhanced metastatic potentials when compared to those found in cells from the parental tumor.

Evidence that the parental tumor was comprised of subpopulations of tumor cells that varied in their capacity to metastasize was revealed by in vitro cloning followed by the analysis of the clones for their in vivo biologic behaviors. Tumor cell clones from primary cultures of the parental tumor varied widely in their ability to grow at the site of inoculation and produce distant metastases after 23 days of subcutaneous growth (table 3). This end point was chosen because some of the clones killed their host before 40 days. Tumor clone MTA displayed the highest metastatic potential with approximately 94% of the animals exhibiting pulmonary metastases, although the sizes of the primary tumors at the subcutaneous sites of injection were comparatively small. In contrast, tumor clone MTF7 produced significantly larger tumors at the injection site; but it was intermediate in metastatic potential, producing pulmonary metastases in 52% of the animals. Clone MTC gave rise to primary implanted tumors of intermediate size and demonstrated the lowest metastatic potential of the clones examined with only 10% of the animals given injections developing pulmonary metastases (median No.=2; range=1, 6). Clones obtained from the parental tumor (MTA, MTF7, and MTC) did not form detectable extrapulmonary metastases in any of the experiments, as confirmed by gross observations and direct subcutaneous transfer of randomly selected organ and lymph node tissues.

The lung metastasis-derived clones MTLn2 and MTLn3 were also examined for their ability to produce spontaneous metastases after 23 days of in vivo subcutaneous growth (table 3). Clone MTLn3 produced lung metastases in 76% of the animals examined and lymph node metastases (axillary, inguinal, and lumbar) in 21% of the animals examined. Although clone MTLn2 originated from metastatic lung lesions, it had a low metastatic potential, producing pulmonary metastases in only 11% of the animals and no apparent lymph node involvement. These results indicate that both the parental tumor and its metastases are composed of subpopulations of tumor cells that vary not only in their growth properties but also in their metastatic potentials.

Histology

The tumors formed from subcutaneous mammary pad implants of parental tumor and cloned cell lines are shown histologically in figure 3. The parental 13762NF tumor grew in small, dense cell clusters or strands of varying morphologic types, sizes, and staining characteristics, but common to most cells were a slightly basophilic cytoplasm and high mitotic index. Within the tumor mass only small amounts of fibrous tissue could be found, and very little overall cellular organization was seen except for some luminal formation. The parental tumor was classified histologically as an undifferentiated adenocarcinoma. Clones derived from the parental tumor or lung metastases varied histologically from poorly differentiated adenocarcinoma with definite luminal formation (i.e., MTLn2) to scirrous-like, well-vascularized undifferentiated carcinoma (i.e., clones MTC and MTF7). Clone MTA was quite different from the other clones and was similar in structure to a giant cell sarcoma of unknown origin (fig. 3). Metastases formed by the sc implantation of the tumor cell clones also reflected the structural heterogeneity of the parental tumor (fig. 4). Lung metastases were more uniform in histologic structure, often representing the morphologies of minor subpopulations present in the subcutaneous tumors (i.e., clone MTA) (fig. 4). In many cases host lymphocytes, granulocytes, or polymorphonuclear cells were present in the metastatic lesions (fig. 4).

DISCUSSION

The results of these studies and those of others show that parental tumors and their metastases are composed of subpopulations of tumor cells that differ in certain in vitro and in vivo biologic characteristics. We have shown that variant cell subpopulations (clones) can be obtained from cultures of both the parental tumor and its lung metastases, and this heterogeneity was confirmed when these clones were assayed

TABLE 3.—*Biologic analysis of cloned 13762 adenocarcinoma tumor cell clones and in vivo-selected metastatic variants*

13762 adenocarcinoma clone	Culture passage No.	Primary tumor average diameter, mm ± SD[a]	Animals with lung metastases[b]	No. of lesions per lung, median (range)	Animals with lymph node metastases[b]	Metastatic potential
MTA	10	5.2±1.21	10/10	120 (7, >250)	0/10	High
	17	2.65±1.24	8/10	27 (2, >250)	0/10	
	18	2.48±0.95	19/19	65 (1, >250)	0/19	
MTF7	10	15.94±2.16	7/20	54 (4, 127)	0/20	Intermediate
	12	18.69±2.25	13/21	41 (1, >250)	0/21	
	12	14.03±2.84	12/20	87 (1, >250)	0/20	
MTC	9	6.1±0.90	0/10	0	0/10	Low
	11	5.67±1.06	0/10	0	0/10	
	14	8.56±0.97	4/20	2 (1, 6)	0/20	
MTLn2	35	13.94±4.05	1/20	15 (—)	0/20	Low
	38	15.38±1.94	5/20	8 (1, 39)	0/20	
	41	17.00±3.30	1/20	1 (—)	0/20	
MTLn3	13	9.51±1.84	14/20	64 (15, >250)	0/20	High
	14	10.93±2.20	16/20	95 (2, >250)	7/20	
	15	10.18±3.05	16/20	42 (1, >250)	6/20	

[a] See table 1 for calculations.

[b] No. of animals with metastases/total No. of animals given tumor implants.

for in vivo and in vitro growth properties, in vitro saturation densities, in vitro morphologies, and in vivo histologic appearance. Although the several clones that were tested varied in their in vitro growth rates and saturation densities, these parameters did not correlate with their metastatic potentials. Two parental tumor clones, MTC and MTF7, had similar growth rates and saturation densities in vitro but differed significantly in their abilities to metastasize. The same was true for clones MTLn2 and MTLn3 that were selected from lung metastases. Both of these clones exhibited similar growth rates and saturation densities in vitro, but they differed in their ability to form distant metastases. Parental clone MTA, which had the lowest growth rate and saturation density of all clones in vitro, displayed the highest metastatic potential. In contrast, lung metastasis-derived clone MTLn2, which demonstrated a high growth rate and saturation density in vitro, had a relatively low metastatic potential.

The extent of subcutaneous tumor growth at the site of inoculation was unique for each clone and did not correlate with their metastatic potentials. That the subcutaneous tumor size and growth rate of a tumor are poor indicators of the capacity of the tumor to metastasize successfully has also been reported in other animal tumor systems (*8–16, 41, 42*) and in human breast cancer (*1, 2*). In light of the findings presented here and elsewhere (*9–15*), that single neoplasms contain heterogeneous subpopulations of tumor cells with differing metastatic potentials, it is not surprising that the overall size or growth rate of a tumor may not reflect its metastatic potential. More likely, the metastatic potential of a tumor is determined by the relative frequency and/or emergence of highly malignant subpopulations (*43*) that possess characteristics allowing them to metastasize successfully. The direct in vitro isolation of metastatic clones from the parent tumor indicates that these metastatic subpopulations preexisted and were not formed by adaptive processes (*44, 45*). Furthermore, that the lung metastasis-derived clones reflect an organ adaptive process is unlikely, since the two clones examined here differed significantly in their capacity to form pulmonary metastases and the derivation of clones from lung metastases did not involve repeated in vivo cycling of metastatic variants with the use of the lungs as a selective environment. The presence of a poorly metastatic subpopulation of tumor cells within lung metastatic lesions suggests that metastases are comprised of tumor cell subpopulations that vary in their ability to form subsequent metastases. A similar conclusion was reported for metastatic subpopulations and clones obtained from a fibrosarcoma (*44*).

Of the animal models that exist for studying mammary tumor metastasis, most are mouse tumor models that exhibit few similarities to human breast cancer (*46*). Carcinomas from mice generally grow rapidly, and most express high levels of mammary tumor virus and rarely metastasize; when metastasis occurs, it is usually hematogenous (*46*). In contrast, rat mammary carcinomas show many similarities to human breast cancer, such as tumor histologic structure, mode of metastasis (*47*), immunogenicities and sensitivies to immunotherapy (*48*), and responsiveness to hormone (*36, 49, 50*) or steroid manipulations (*51, 52*).

The rat mammary adenocarcinoma used in these studies was induced chemically in female Fischer 344 rats. The clones obtained from this tumor exhibit significant differences in their histologic appearances, ranging from sarcoma-like to poorly differentiated ductal structures. The apparent histologic variations that we found are consistent with those reported by others who observed that chemically induced rat mammary tumors can display histologic heterogeneity between tumors and within the same tumor (*53, 54*). Although one can argue that the heterogeneous nature of the 13762 adenocarcinoma is due to its long-term existence as a transplanted tumor, such phenotypic diversity has also been noted in tumors of recent origin (*55*). We attempted to obtain not only variant cell subpopulations that differed in their metastatic capacities but also subpopulations that were histologically similar to human mammary carcinomas. We do not imply here that we have obtained even a fraction of the subpopulations that may exist within a mammary tumor; however, the tumor clones described here serve to illustrate the heterogeneous nature of this neoplasm in respect to growth, histology, and metastasis. In addition, the tumors formed by these cell clones display varying degrees of host lymphoid cell infiltration both at the subcutaneous sites and their metastases. The relationship between host cell infiltration and biologic or metastatic behavior of these tumors is at present unclear and will require further studies.

Among the clones tested, only MTLn3 exhibited extensive and reproducible lymph node metastasis. This clone is of special interest since human mammary adenocarcinomas frequently metastasize to regional lymph nodes (*2*). The possibility that a difference in the mode of metastasis was imposed at the injection site can be ruled out since all clones were introduced at the same subcutaneous site in the mammary fat pad. Although lymph nodes were examined histologically for the presence of occult metastases, we cannot rule out the possibility that tumor cells from the other clones did in fact reach lymph nodes, but in such small numbers that they were either destroyed by host immunocytes or were unable to grow.

The process of tumor metastasis is biologically complex, and its study requires appropriate experimental models (*3, 5, 26, 32*). The model that we have established for mammary tumor metastasis has already shown its usefulness in studies on the differences in cell surface glycoproteins between cells of diverse metastatic potential (*39, 56*) and heterogeneity in therapeutic response to ionizing radiation (Welch D, Milas L, Nicolson GL: In preparation) and hyperthermia (*57*). By the examination and comparison of cell clones of low and high metastatic potentials for their biologic, biochemical, and other properties, it is hoped that unique characteristics possessed by metastatic populations will be better defined.

REFERENCES

(*1*) Sugarbaker EV. Cancer metastasis: A product of tumor-host interactions. Curr Probl Cancer 1979; 7:3–59.
(*2*) Fisher B, Slack NH, Bross ID. Cancer of the breast: Size of neoplasm and prognosis. Cancer 1969; 24:1071–1080.
(*3*) Fidler IJ, Gersten DM, Hart IR. The biology of cancer invasion and metastasis. Adv Cancer Res 1978; 28:149–250.
(*4*) Poste G, Fidler IJ. The pathogenesis of cancer metastasis. Nature 1980; 283:139–146.
(*5*) Fidler IJ, Nicolson GL. The immunobiology of experimental met-

astatic melanoma. Cancer Biol Rev 1981; 2:171–234.

(6) Fidler IJ. Tumor heterogeneity and the biology of cancer invasion and metastasis. Cancer Res 1978; 38:2651–2660.

(7) Carter RL. General pathology of the metastatic process. In: Baldwin RW, ed. Secondary spread of cancer. New York: Academic Press, 1978:1–52.

(8) Fidler IJ, Kripke ML. Metastasis results from pre-existing variant cells within a malignant tumor. Science 1977; 197:893–895

(9) Nicolson GL, Brunson KW, Fidler IJ. Specificity of arrest, survival and growth of selected metastatic variant cell lines. Cancer Res 1978; 38:4105–4111.

(10) Suzuki N, Withers HR, Koehler MW. Heterogeneity and variability of artificial lung colony-forming ability among clones from a mouse fibrosarcoma. Cancer Res 1978; 38:3349–3351.

(11) Kripke ML, Gruys E, Fidler IJ. Metastatic heterogeneity of cells from an ultraviolet light-induced murine fibrosarcoma of recent origin. Cancer Res 1978; 38:2962–2967.

(12) Talmadge JE, Starkey JR, Davis WC, Cohen AL. Introduction of metastatic heterogeneity by short-term in vivo passage of a cloned transformed cell line. J Supramol Struct 1979; 12:227–243.

(13) Reading CL, Brunson KW, Torrianni M, Nicolson GL. Malignancies of metastatic murine lymphosarcoma cell lines and clones correlate with decreased cell surface display of RNA tumor virus envelope glycoprotein gp70. Proc Natl Acad Sci USA 1980; 77:5943–5947.

(14) Chambers AF, Hill RP, Ling V. Tumor heterogeneity and stability of the metastatic phenotype of mouse KHT sarcoma cells. Cancer Res 1981; 41:1368–1372.

(15) Dexter DL, Kowalski HM, Blazar BA, Fligiel Z, Vogel R, Heppner GH. *Heterogeneity of tumor cells from a single mouse mammary tumor. Cancer Res 1978; 38:3174–3181.*

(16) Cifone MA, Kripke ML, Fidler IJ. Growth rate and chromosome number of tumor cell lines with different metastatic potential. J Supramol Struct 1979; 11:467–476.

(17) Fuji H, Mihich E. Selection for high immunogenicity in drug-resistant sublines of murine lymphomas demonstrated by plaque assay. Cancer Res 1975; 35:946–952.

(18) Heppner GH, Dexter DL, Denucci T, Miller FR, Calabresi P. Heterogeneity in drug sensitivity among tumor cell subpopulation of a single mammary tumor. Cancer Res 1978; 38:3758–3763.

(19) Biorklund A, Hakansson L, Stenstam B, Tropes C, Akerman M. On heterogeneity of non-Hodgkin's lymphomas as regards sensitivity to cytostatic drugs. Br J Cancer 1980; 16:647–654.

(20) Lotan R, Nicolson GL. Heterogeneity in growth inhibition by β-*trans*-retinoic acid of metastatic B16 melanoma clones and in vivo-selected cell variant lines. Cancer Res 1979; 39:4767–4771.

(21) Byers VS, Johnston JO. Antigenic differences among osteogenic sarcoma tumor cells taken from locations in human tumors. Cancer Res 1977; 37:3173–3183.

(22) Pimm MV, Baldwin RW. Antigenic differences between primary methylcholanthrene-induced rat sarcomas and post-surgical recurrences. Int J Cancer 1977; 20:37–43.

(23) Fogel M, Gorelik E, Segal S, Feldman M. Differences in cell surface antigens of tumor metastases and those of the local tumor. JNCI 1979; 62:585–588.

(24) Révész L, Norman U. Relationship between chromosome ploidy and radiosensitivity in selected tumor sublines of common origin. J Natl Cancer Inst 1960; 25:1041–1063.

(25) Hill HZ, Hill GJ, Miller CF, Kwong F, Purdy J. Radiation and melanoma: Response of B16 mouse tumor cells and clonal lines to in vitro irradiation. Radiat Res 1979; 80:259–276.

(26) Nicolson GL. Properties of metastatic tumor cells. In: Burchenal JH, Oettegen HF, eds. Cancer achievements, challenges, prospects for the 1980s. New York: Grune, 1981:477–490.

(27) Fidler IJ. Selection of successive tumor lines for metastasis. Nature [New Biol] 1973; 242:148–149.

(28) Brunson KW, Beattie C, Nicolson GL. Selection and altered tumour cell properties of brain-colonising metastatic melanoma. Nature 1978; 272:543–545.

(29) Brunson KW, Nicolson GL. Selection of malignant melanoma variant cell lines for ovary colonization. J Supramol Struct 1979; 11:517–528.

(30) Raz A, Hart IR. Murine melanoma. A model for intracranial metastasis. Br J Cancer 1980; 42:331–341.

(31) Klein E. Gradual transformation of solid into ascites tumors. Evidence favoring the mutation-selection theory. Exp Cell Res 1955; 8:188–212.

(32) Fidler IJ. General consideration for studies of experimental cancer metastasis. Methods Cancer Res 1978; 15:399–439.

(33) Brunson KW, Nicolson GL. Selection and biologic properties of malignant variants of a murine lymphosarcoma. JNCI 1978; 61:1499–1503.

(34) Hart IR, Talmadge JE, Fidler IJ. Metastatic behavior of a murine reticulum cell sarcoma exhibiting organ-specific growth. Cancer Res 1981; 41:1281–1287.

(35) Silverberg E. Cancer statistics, 1981. CA—Cancer J Clinicians 1981; 31:13–28.

(36) Segaloff A. Hormones and breast cancer. Recent Prog Horm Res 1966; 22:351–379.

(37) Stanners CP, Eliceiri GL, Green H. Two types of ribosomes in mouse-hamster hybrid cells. Nature [New Biol] 1971; 230:52–54.

(38) Dulbecco R. Topoinhibition and serum requirement of transformed and untransformed cells. Nature 1970; 227:802–806.

(39) Neri A, Nicolson GL. Phenotypic drift of metastatic and cell surface properties of mammary adenocarcinoma cell clones during growth in vitro. Int J Cancer. In press.

(40) Chen TR. In situ detection of mycoplasma contamination in cell cultures by fluorescent Hoechst 33258 stain. Exp Cell Res 1977; 104:255–262.

(41) Hart IR. The selection and characterization of an invasive variant of B16 melanoma. Am J Pathol 1979; 97:587–600.

(42) Vaage J. A survey of the growth characteristics of and the host reactions to one hundred C3H/He mammary carcinomas. Cancer Res 1978; 38:331–338.

(43) Nowell PC. The clonal evolution of tumor cell populations. Science 1976; 194:23–28.

(44) Raz A, Hanna N, Fidler IJ. In vivo isolation of a metastatic tumor cell variant involving selective and nonadaptive processes. JNCI 1981; 66:183–189.

(45) Nicolson GL, Custead SE. Tumor metastasis is not due to adaptation to an organ environment. Science 1982; 215:176–178.

(46) Kim U. Factors influencing metastasis of breast cancer. In: McGuire WL, ed. Breast cancer. Vol 3. New York: Plenum, 1979:1–49.

(47) Young S, Hallowes RC. Tumors of the mammary gland. In: Turusov US, ed. Pathology of tumors in laboratory animals. Vol I. Tumors of the rat. Lyon: IARC, 1973:31–74.

(48) Kreider JW, Bartlett GL, Purnell DM. Suitability of rat mammary adenocarcinoma 13762 as a model for BCG immunotherapy. J Natl Cancer Inst 1976; 56:797–802.

(49) Huggins C, Brigiarelli G, Sutton H. Rapid induction of mammary carcinoma in the rat and the influence of hormones on the tumors. J Exp Med 1959; 109:25–52.

(50) Dao TL. Carcinogenesis of mammary gland in rat. Prog Exp Tumor Res 1964; 5:157–217.

(51) Huggins C, Yang NC. Induction and extinction of mammary cancer. A striking effect of hydrocarbons permits analysis of mechanisms of causes and cure of breast cancer. Science 1962; 137:257–262.

(52) Daniel PM, Prichard MM. The response of experimentally induced mammary tumours in rats to ovariectomy. Br J Cancer 1964; 17:687.

(53) Stevens L, Stevens E, Currie AR. Histological studies and measurement of nucleic acid synthesis in rat mammary tumours induced by 9,10-dimethyl-1,2-benzanthracene (DMBA). J Pathol Bacteriol 1965; 89:581–589.

(54) Archer FL, Orlando RA. Morphology, natural history and enzyme patterns in mammary tumors of the rat induced by 7,12-dimethylbenz(*a*)anthracene. Cancer Res 1968; 28:217–224.

(55) Fidler IJ, Gruys E, Cifone MA, Barnes Z, Bucana C. Demonstration of multiple phenotypic diversity in a murine melanoma of recent origin. JNCI 1981; 67:947–956.

(56) Neri A, Ruoslahti E, Nicolson GL. The distribution of fibronectin on clonal cell lines of a rat mammary adenocarcinoma growing in vitro and in vivo at primary and metastatic sites. Cancer Res 1981; 41:5082–5095.

(57) Tomasovic SP, Thames HD Jr, Nicolson GL. Heterogeneity in hyperthermic sensitivity of rat 13762NF mammary adenocarcinoma cell clones of differing metastatic potential. Radiat Res. In press.

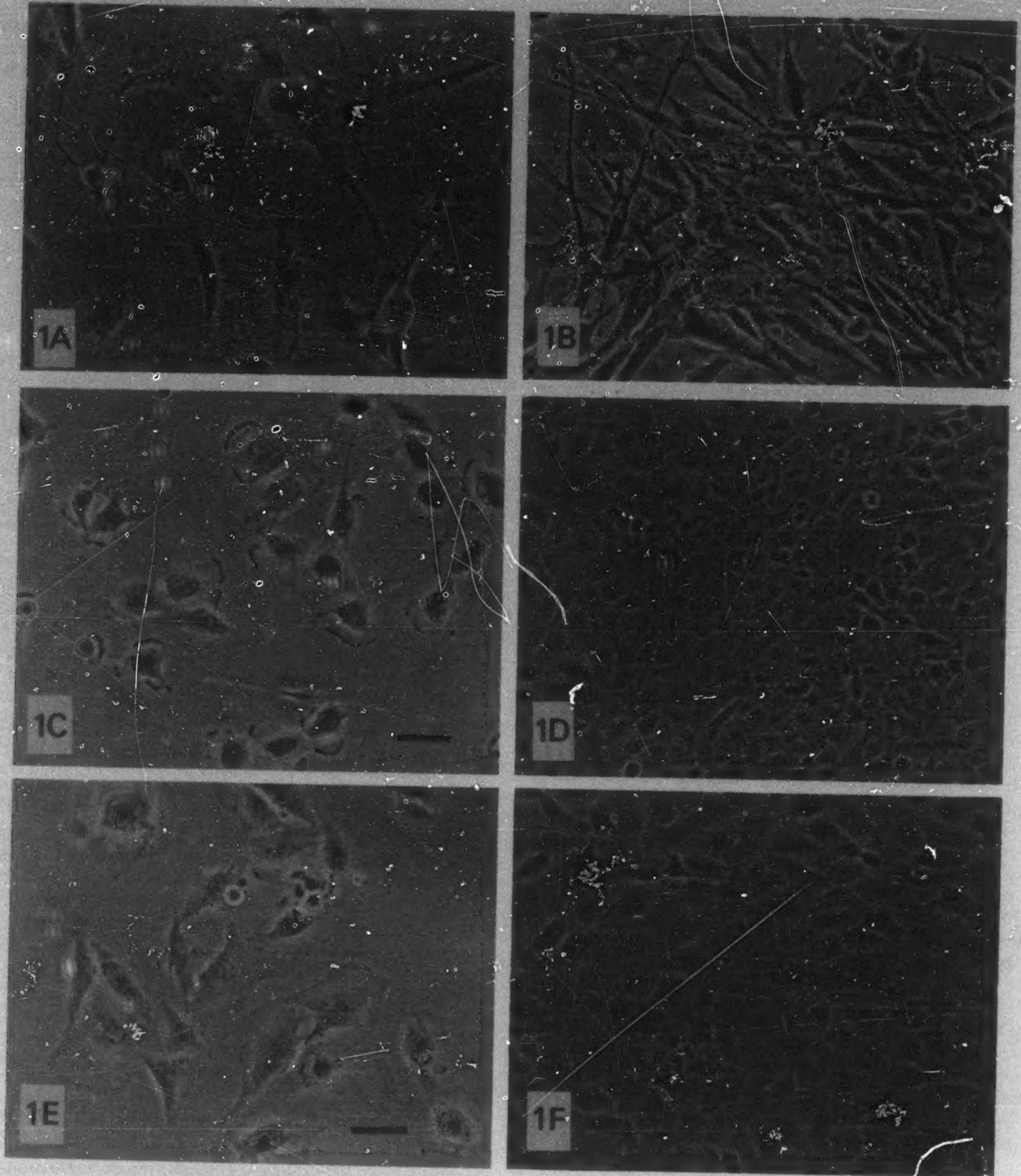

FIGURE 1.—In vitro tissue culture morphologies of parental mammary tumor clones growing on plastic substrate at low (48 hr of growth) or high (120 hr of growth) densities. A) Clone MTA at low density. *Note* fibroblastic-like appearance. B) Clone MTA at high density. Cells are often polynucleated with a high cytoplasm-to-nuclear ratio and exhibit extensive nuclear overlapping. C) Clone MTC at low density. *Note* epithelial-like cellular morphologies. D) Clone MTC at high density. Polynucleation and nuclear overlapping are not apparent. E) Clone MTF7 at low density. *Note* epithelial-like cellular morphologies. F) Clone MTF7 at high density. Cells rarely show polynucleation, have a low cytoplasm-to-nuclear ratio, and do not exhibit nuclear overlapping. Phase contrast. *Bars*=50 µm. × 180

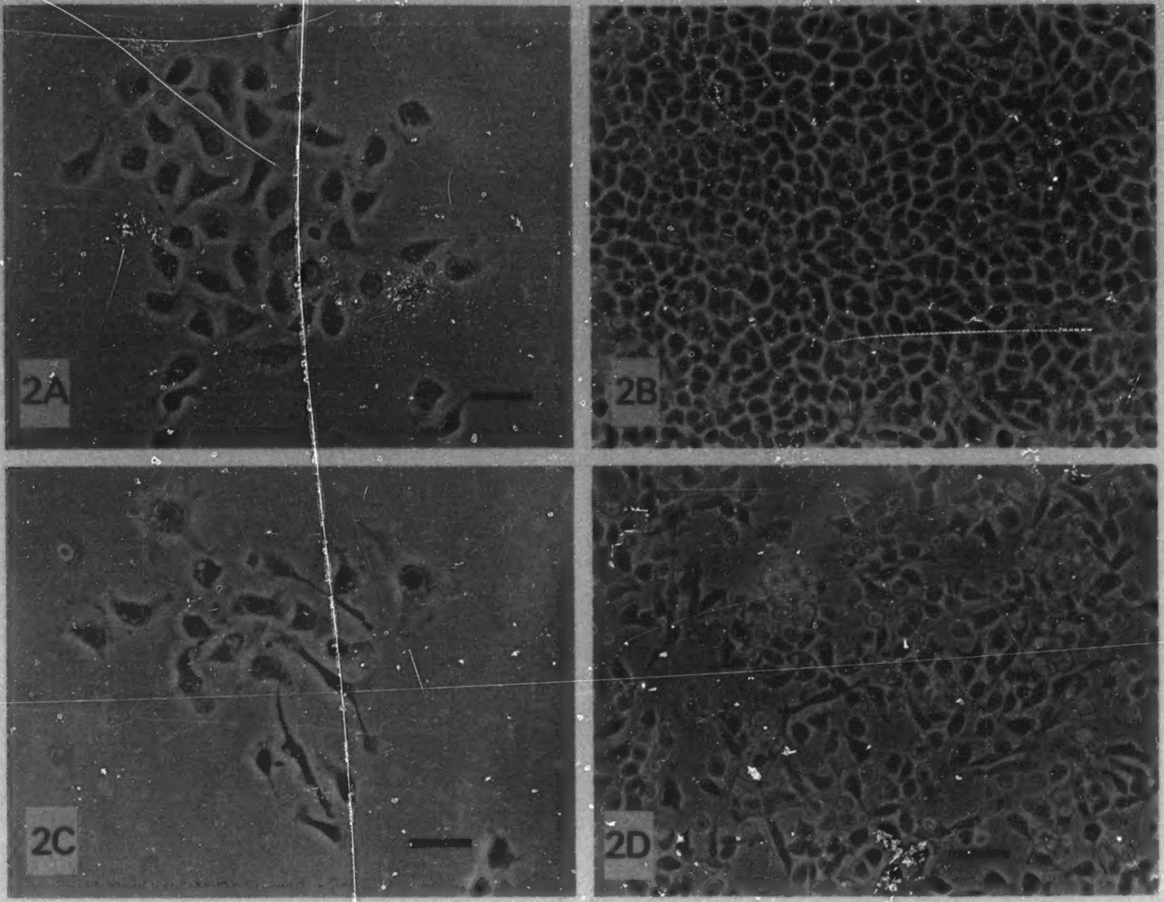

FIGURE 2.—In vitro tissue culture morphologies of lung metastases-derived mammary tumor clones growing on a plastic substrate at low (48 hr of growth) or high (120 hr of growth) densities. A) Clone MTLn3 at low density. *Note* epithelial-like morphologies. B) Clone MTLn3 at high density. Cells do not show nuclear overlapping or tendency to grow in multilayers. C) Clone MTLn2 at low density. *Note* loosely adherent, more spindle-shaped cells with cytoplasmic projections. D) Clone MTLn2 at high density. Cells are prone to undergo nuclear overlapping and formation of multilayers. Phase contrast. *Bars*=50 µm. × 180

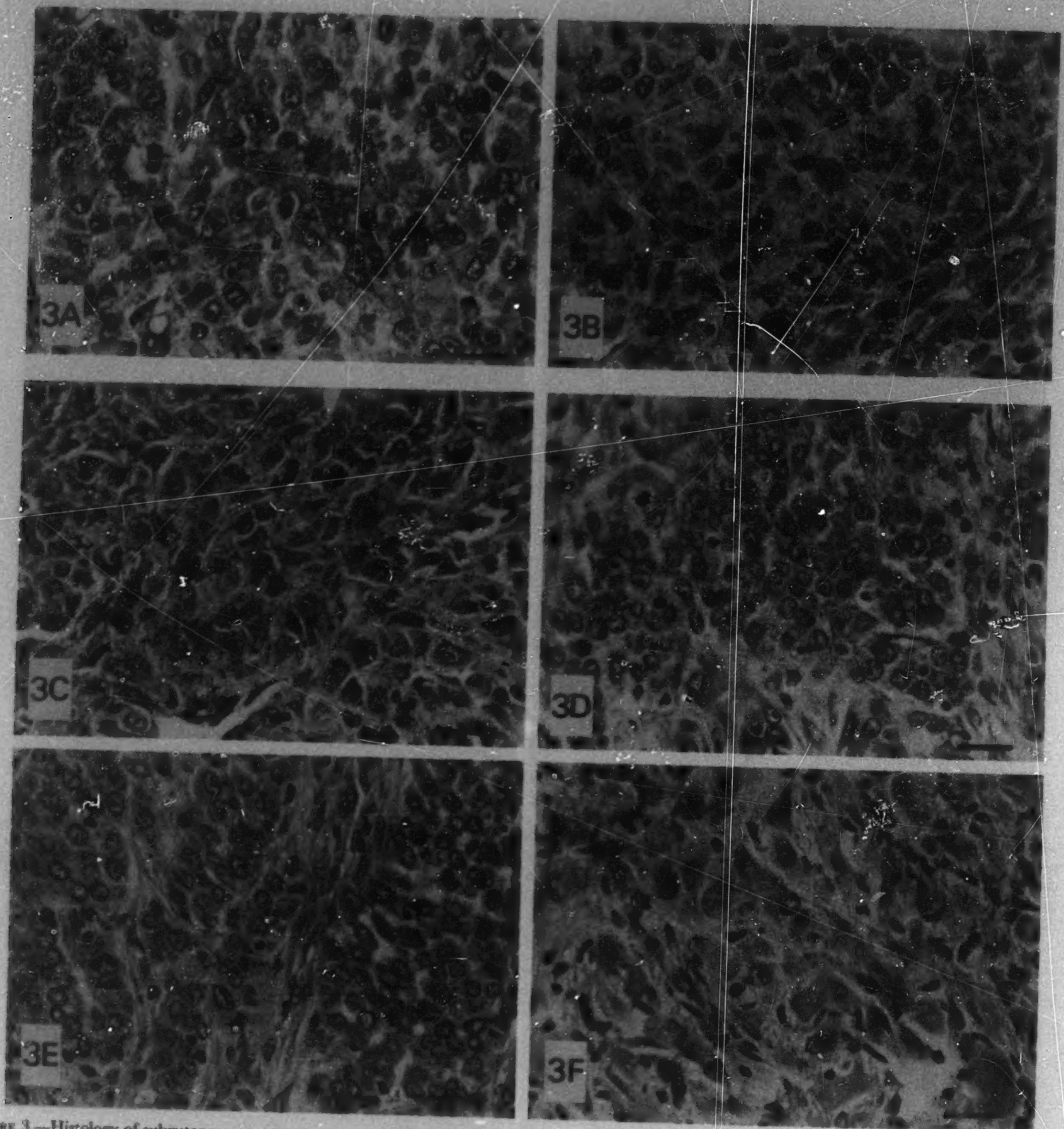

FIGURE 3.—Histology of subcutaneous mammary tumors 23 days after injection of parental tumor or cell clones into the mammary fat pad. A) Parental tumor. *Note* cells of varying sizes, histologic types, and staining characteristics. Some luminal formation and only small amounts of fibrous material can be found. B) Clone MTC tumor. Tumors possessed generally large cells (two distinct cell populations) with large nuclei and nucleoli. C) Clone MTF7 tumor. *Note* large tumor cells with abundant cytoplasm and peripheral nuclei. This tumor possesses large amounts of fibrous, filamentous tissue with less host lymphoid cell infiltration compared to that in other clones. D) Clone MTLn3 tumor. *Note* mixed cell population having no definitive arrangement except for some nodule-like structures. Cells in these tumors are large and often have 1–2 large, irregularly shaped nucleoli. Host reaction against this tumor is evident only along invading edges; otherwise, tumors are generally devoid of infiltrating host lymphoid cells. E) Clone MTLn2 tumor. This clone produced tumors with large amounts of fluid and necrosis. There are connective tissues and host-infiltrating cells in the tumors. F) Clone MTA tumor. The tumors appear to be similar to giant cell sarcomas of unknown origin and are composed of giant, polynucleated cells possessing 1–2 nucleoli and abundant acidophilic cytoplasm. A minor population of smaller cells is also evident. *Note* very large amounts of connective tissue and limited host lymphoid cell infiltration. H & E. *Bars*=50 µm. × 160

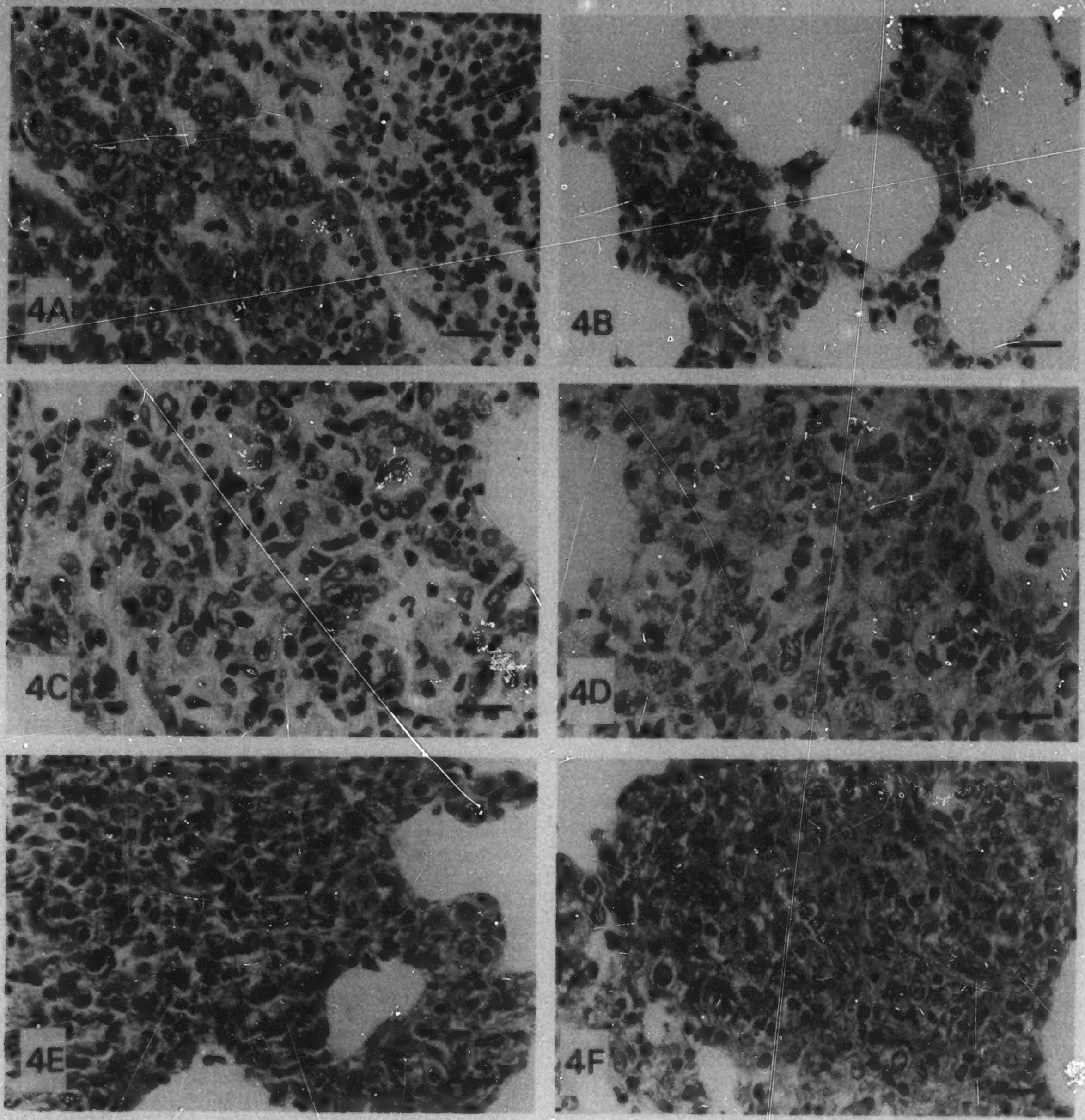

FIGURE 4.—Histology of lymph node and lung metastases 23 days after injection sc of mammary tumor clones. A) Clone MTLn3 metastasis to lumbar lymph node. *Note* the involved node at the tumor–normal cell interface with MTLn3 cells of similar structure to MTLn3 cells found at the subcutaneous site. B) Clone MTLn3 lung metastasis. *Note* tumor cells in the alveolar septum without substantial host lymphoid cell infiltration. C) Clone MTC lung metastasis. A rare MTC lesion in the alveolar septum. This metastasis is characterized by host lymphoid and granulocytic cell infiltration. D) Clone MTA lung metastasis. *Note* that the MTA metastasis tumor structure does not resemble the predominant large cell population present in the subcutaneous tumor but appears to be made up of the small cell population infrequently found in the subcutaneous tumor. E) Clone MTF7 lung metastasis. Some cells in alveolar lumen resemble cells found in the subcutaneous tumor. These lesions are characterized by extensive infiltration by lymphocytes, monocytes, and granulocytes. F) Clone MTLn2 lung metastasis. Tumor cells in the alveolar septum have retained much of the nodular organization seen in subcutaneous tumors. Tumors were also characterized by large numbers of lymphocytes and granulocytes and a few polymorphonuclear cells. H & E. *Bars*=50 µm. × 160

Temperature Gradients and Local Perfusion in a Mammary Carcinoma[1,2]

Pietro M. Gullino,[3,4] **Rakesh K. Jain,**[5] *and* **Flora H. Grantham**[3]

ABSTRACT—Temperature gradients of mammary tumors in randombred Sprague-Dawley rats under normothermia, hypothermia, and hyperthermia were determined, and their experimental modifications were utilized to assess differences in perfusion rates within the neoplastic tissue. Normothermic tumors showed a circadian rhythm with zenith at midnight and nadir at midday. Differences between highest and lowest temperatures recorded during the 24-hour period reached up to 3°C. Similar oscillations were observed in subcutaneous tissue without tumor. An average temperature increment of 0.5–1.0°C was observed when a tumor was transferred from the subcutaneous to the abdominal location. Gradients larger than 1°C were observed within the same tumor in locations only a few millimeters distance from each other. The nonuniformity in temperature within normothermic tumors was exaggerated during hyperthermia. No appreciable change in temperature gradients was seen within a normothermic tumor when tumor blood flow was doubled or reduced to one-third of the basal level. Hyperthermia increased both volume and temperature of tumor efferent blood. As expected, decrease or increase in blood flow during hyperthermia increased or decreased tumor temperature, respectively, but substantial temperature gradients up to 2°C still persisted within adjacent regions. The extent of temperature changes in the tumor could not be correlated with a known change in blood supply. A pulse of cold serum into the tumor afferent artery produced a substantial reduction of tumor blood flow, but only a small depression in tumor temperatures, and a very small change in tumor temperature gradients. No appreciable modification could be brought about in tumor temperature levels and temperature gradients within the tumor by pulses of cold serum in the afferent artery during hyperthermia. After external cooling of the tumor, the time necessary to compensate for temperature depression did not correlate with either the reduction of temperature or with the thickness of the tumor tissue separating the thermistor from the cold source. The results indicate extensive anisotropy of temperature and blood distribution within growing neoplastic tissue and suggest that heat transfer by convection within the tumor is much less effective than it is commonly assumed.—JNCI 1982; 68:519–533.

In human and rodent tumors survival of cancer cells is sharply reduced at 42°C while normal tissues do not suffer irreparable damage. At temperature above 42°C, although neoplastic cells are more rapidly damaged, normal tissues are also severely affected. Temperatures below 42°C but above physiologic levels may accelerate growth and dissemination of neoplastic cells (*1–5*). These observations indicate the need for accurate knowledge of temperature distribution within tumors in view of the importance that thermography and hyperthermia have acquired in cancer detection and treatment.

In the experiments reported here, we evaluated the temperature gradients of the virgin mammary gland and of mammary tumors under normothermia, hypothermia, and hyperthermia in rats. We also evaluated the effects of changes in local blood perfusion rates on temperature gradients within the tumor and assessed the implications of the results on thermography and hyperthermia.

MATERIALS AND METHODS

Experimental approach.—The temperature gradients within normothermic tumors were measured continuously by three thermistors from the 1st day of tumor transplantation until the host died 15–18 days later. The thermistors were incorporated by the growing tumor tissue; therefore, damages due to the insertion of measuring probes were avoided. The animal was kept in an appropriate cage and was free to move during the experimental period (*6*).

Temperature gradients during hyperthermia were measured in anesthetized rats. Heat was produced by an electric bulb with appropriate shielding and controlled energy input. The distance between heat source and skin was 20 cm. The animal was shielded by styrofoam, and only the skin covering the tumors was directly exposed to heat. Tumors grown at the extremity of a vascular pedicle (*7*) were utilized to measure volume and temperature of blood leaving the tumor. Changes in temperature gradients within tumors were obtained by rapid cooling of the tumor. In the first approach, a pulse of cold serum was injected in the artery feeding the tumor. In the second approach, 300 µl ethanol was applied to the skin covering the tumor and was then rapidly evaporated during 2 minutes by a stream of air.

Animals and tumors.—Randombred Sprague-Dawley female rats 3–4 months old, 200–250 g body weight were utilized (Small Animal Section, Veterinary Resources Branch, Division of Research Services, NIH, Bethesda, Md.). W256 was used as a model in all experiments. The tumor was transplanted from the NIH line, carried in Sprague-Dawley females for almost 5 decades (*8*) in subcutaneous implants alternated with intraperitoneal passages at a ratio of 5:1. The rats were anesthetized with ether for

---

ABBREVIATIONS USED: ia=intra-arterial; NIH=National Institutes of Health; W256=Walker 256 carcinoma.

---

[1] Received July 31, 1981; accepted October 22, 1981.

[2] Animals were maintained under the guidelines set forth by the National Institutes of Health Policy on Humane Care and Use of Animals and by the Animal Welfare Act in facilities accredited by the American Association for Accreditation of Laboratory Animal Care.

[3] Laboratory of Pathophysiology, Division of Cancer Biology and Diagnosis, National Cancer Institute (NCI), National Institutes of Health, Public Health Service, U.S. Department of Health and Human Services, Bethesda, Md. 20205.

[4] *Address reprint requests to* Dr. Gullino, Building 10, Room 5B-36, NCI, National Institutes of Health, Bethesda, Md. 20205.

[5] Department of Chemical Engineering, Carnegie-Mellon University, Pittsburgh, Pa. 15213.

minor surgery, such as preparation of the subcutaneous pouch or positioning of thermistors; otherwise, 50 mg pentobarbital/kg body weight, or 1 mg urethan/kg body weight was used for anesthesia. The animals were kept in a room with a 12-hour light cycle, from 6 a.m. to 6 p.m. light and from 6 p.m. to 6 a.m. dark. Room temperature was controlled at 24±1°C. The temperature of the operating table was 30±1°C. No precaution was taken to prevent heat loss from anesthetized animals. In long-term experiments tumor temperature was recorded every 30 minutes; in short-term experiments, every 10–30 seconds.

Tumor preparations.—Measurements of temperature gradients were conducted on subcutaneous transplants during the life-span of the tumor. A pouch was prepared in the subcutaneous tissue of the lumbar region, and three thermistors bound together at a distance of approximately 0.5 cm from each other were placed in it with a few fragments of W256. The wires of the thermistors were driven through a subcutaneous tunnel to the nuchal region and then out of the animal into a stainless steel spring for protection. One end of the spring was fixed to the skin of the nuchal region, and the opposite end was attached to the top of the cage that rested on a 30×30-cm plastic base. The length of the spring was adjusted to permit the animal to move at will around the cage. An appropriate device previously described (*6*) compensated for the torsion produced by the movements.

The temperature of the host was also continuously monitored by a thermistor placed in the abdominal cavity. The wire of this thermistor exited from the lumbar region opposite to the tumor implant and joined the wires of the tumor thermistors in the subcutaneous tunnel and the protective stainless spring. This preparation permitted continuous temperature monitoring during the life-span of the tumor.

In experiments where measurements started only after the tumor had grown to incorporate the thermistors, the wires of the thermistors were kept in a pouch of the nuchal region until the time of measurement.

Experiments that involved a pulse of cold serum were performed on a tumor preparation where *a*) three thermistors were incorporated by the tumor, *b*) the tumor was connected to the host by one artery and one vein only so that all the blood flowing through the tumor could be collected when the vein was cannulated, *c*) the tumor was grown subcutaneously in a paraffin sack to prevent infiltration of the surrounding tissues so that the measured blood supply pertained exclusively to the tumor, and *d*) the experiment was performed in an anesthetized animal.

A preparation with these characteristics was in the past obtained by transplanting the tumor at the distal end of the ovarian pedicle (*7*). In the experiments with a pulse of cold serum, however, the rat ovarian artery was too small to accept any available catheter without being occluded. We therefore developed a second system that utilizes the artery and vein of the left inguinal mammary gland as blood supplier to the transplanted tumor.

As previously described (*9*), in this system an arterial and venous branch of the superficial epigastric vessels reach the second inguinal mammary gland as a pair of vessels that run isolated in the adipose tissue and penetrate the gland through a circumscribed area. As a first step, this vascular pedicle was isolated with a fragment of gland about 0.5 cm^3 at the distal extremity. Then about 0.1 ml of tumor slurry was injected into the isolated gland fragment, and three thermistors were anchored around it. The implant was then enveloped by a sheet of paraffin (American Can Company, Marathon Products, Neenah, Wisc.) and placed into a pouch of the subcutaneous tissue. The purpose of the paraffin envelope was to avoid invasion of and vascular input from the surrounding tissues.

After 4–5 days, the subcutaneous pouch was opened and the paraffin sack was discarded. At this time, the tumor appeared like a ball about 1 cm in diameter. Inspection permitted an assessment of its growth and allowed us to correct the thermistor's position when necessary. The preparation was again placed in a paraffin sack and returned to the subcutaneous pouch. During the following 4–5 days, the tumor volume doubled, the thermistors were completely incorporated by the growing tissue, and the preparation was ready for measurements.

The abdominal cavity of the anesthetized rat was opened and the iliac vessels exposed. The femoral artery and the collateral branches leaving the third distal of the left iliac artery were tied off, except for the superficial epigastric and rectal branches. The right iliac artery was then tied off at the caudal extremity. A catheter (PE10; Clay-Adams Inc., New York, N.Y.) was inserted and the tip positioned a few millimeters from the origin of the epigastric artery feeding the tumor. The catheter was heat pulled to reach an outside diameter about one-fifth of the original. This kind of catheter is sufficient to permit the injection of 2 ml serum within 2 minutes and does not obstruct the blood supply to the tumor, as proved by the unaltered volume of tumor efferent blood after catheter insertion.

Figure 1 summarizes the conditions necessary for the cold pulse experiment. In the preliminary experiments the catheter delivering the cold pulse was positioned into the iliac artery via the left external carotid and the aorta. This procedure was simpler and less traumatic than the modified procedure, but the results were unsatisfactory. Only minimal changes in temperature gradients were recorded within the tumor, presumably because the cold serum flowing through a thin catheter immersed in warm blood through several centimeters became too warm by the time it reached the tumor capillary system. With the modified procedure, however, a pulse of cold serum could be rapidly delivered to the vascular system of the tumor in a reliable and consistent way.

The reduction in tumor temperature by an external coolant was obtained with 300 µl of ethanol dispersed in 30 seconds over the skin overlaying the tumor and immediately evaporated by a constant stream of room air directed on the wet surface for 2 minutes. The procedure induced sharp temperature reduction in the tissues covered by the skin.

At the end of the experiment, we measured accurately with a caliper the thickness of the tumor tissue that separated each thermistor from the tumor surface facing the skin, or from the abdominal wall, or from each other (fig. 2).

Changes in tumor blood supply.—The vein draining the tumor grown at the extremity of a vascular pedicle was cannulated and the volume of efferent blood was measured continusouly throughout the experiment. Arterial pressure was kept constant by reintroducing blood via the external jugular vein in about the same amount as that lost by the tumor vein (fig. 1A). The blood temperature was stabilized at 35.5°C and was returned to the animal. When the volume of blood pumped into the jugular vein was reduced, hypovolemia occurred, the aortic pressure decreased, and the flow of tumor efferent blood diminished. When the aortic pressure was kept at 50 mm Hg, the efferent tumor blood was usually reduced to one half of the volume measured at the physiologic aortic pressure of about 100 mm Hg. When the volume of blood return to the jugular vein was increased, hypervolemia occurred and tumor efferent blood volume rose. An aortic pressure of 140 mm Hg usually doubled the outflow of tumor blood measured at physiologic pressure.

Measuring devices.—Tumor temperature was measured with epoxy-coated linear thermistors (#44201; Yellow Spring Instrument Co., Yellow Spring, Ohio). The response time of the thermistor is 1 second in unstirred oil and 10 seconds in still air. A bridge circuit containing the thermistor in one arm was built according to the suggestions of the manufacturers of the thermistor. The bridge circuit, balanced at a low reference temperature, gave an output proportional to the temperature change. When the bridge circuit was calibrated correctly, deviation from the true temperature was less than 0.1°C within the temperature ranges of the experiment. The unbalanced output of the circuit was connected to a recorder (Autodata Nine; Acurex, Mountain View, Calif.). A mercury-in-glass thermometer corrected by the Institute for Basic Standards (National Bureau of Standards, U.S. Department of Commerce, Washington, D.C.) was used to calibrate the thermistors. Temperature changes due to self-heating of the thermistors were negligible. The thermistors were calibrated in water before implantation and again at the end of each experiment.

The thermistor wires were carefully isolated and contained within a polyethylene catheter (PE10). The area of tissue in contact with the sensitive surface of the thermistor was estimated to be about 0.5 mm in diameter.

RESULTS

Temperature Gradients in the Virgin Mammary Gland

For the purpose of background information, the temperature of the rat's second inguinal mammary gland was measured with two thermistors—one located between the gland and the abdominal muscle and the other located between the gland and the skin. This was considered the most effective way of obtaining data with minimum damage to the gland that is spread out as a sheet in the subcutaneous tissue. Each experiment lasted for 5 days while the animals were free to move in an appropriate cage. Text-figure 1 shows 3 days of recording of one of four experiments.

A circadian rhythm was evident in all the mammary glands with the highest temperatures toward midnight and the lowest at noon. The skin side of the gland was consistently colder, as one would expect, but the differences between skin and abdominal sides did not follow any obvious pattern. The amplitude of these differences was largest in the experiment of text-figure 1, where differentials of 2°C were occasionally observed. In three other experiments, however, the largest differences remained within 0.7°C.

Comparisons between temperatures of the second inguinal and third thoracic glands were also made with two thermistors, both placed either on the skin side or on the abdominal side of the glands. In four out of six experiments, the temperature tracings overlapped or intersected each other indicating that the temperature gradients were not substantially different for the two glands. In one animal, the thoracic gland was consistently up to 1°C warmer than the inguinal gland over the 5-day measurement period, and in another animal the reverse condition was observed (data not shown).

From the experiments aimed at assessing the temperature gradients of the normal mammary gland of rats kept at room temperature, we concluded that differences of about 0.7°C between the skin side and abdominal wall side of the gland were common and differences up to 2°C were possible.

Temperature Gradients Within Normothermic Tumors

Temperature Gradients at the Site of Tumor Implant

As a preliminary experiment, the temperature gradients of the subcutaneous tissue were recorded by three thermistors in the lumbar region where the tumors were transplanted. A fourth thermistor was placed in the abdominal cavity. In three separate experiments temperatures were recorded for 15 consecutive days, the time required by W256 to kill or make the animal moribund.

The circadian rhythm was not evident until 48 hours after the implant of the three thermistors. The abdomen was consistently warmer than the subcutaneous region, and the largest difference observed in the three experiments was 2.2°C. The tracings of the the three subcutaneous thermistors were often overlapping or intersecting each other. Oc-

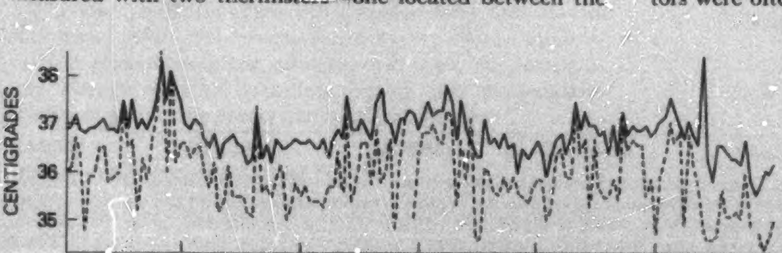

TEXT-FIGURE 1.—Temperature gradients in the left second inguinal mammary gland of a virgin, female 170-g rat. Measurements started 2 days after thermistors were implanted. ——=temperature recording between the skin and the gland. — — —=temperatures between abdominal wall and gland surface. *Note* the circadian rhythm of temperature changes with zenith at midnight and nadir at midday. Room temperatures varied between 25.5 and 27.5°C with the coldest peaks at midnight.

casionally, there were differences up to 2.0°C persisting for two to three recordings at 30-minute intervals, suggesting that these gradients were indeed real and possibly of physiologic significance.

Temperature Gradients Within the Tumor

The W256 was implanted in the lumbar region, and as it grew it incorporated the three thermistors. The temperature was recorded from the day of the implant until the tumor killed the animal. At the time of tumor implant, a thermistor was also placed in the abdominal cavity to monitor host temperature. The objective was to measure the range of temperature changes during tumor growth and to assess the possible influence of necrosis on these changes. Indeed, as the tumors grew, areas of necrotic tissue around the thermistor were increasing in number to the point where the thermistors were embedded almost completely in necrotic material during the last days of the host's life.

Text-figure 2 shows a recording, from day 6 to day 9 after transplantation, obtained in one of four experiments. All tumors consistently showed circadian rhythm in synchrony with that of the host, i.e., the highest temperatures occurred at midnight and the lowest temperatures occurred at midday. Differences between the highest and lowest temperatures recorded during the circadian changes are reported (table 1) from the time of tumor implant until the death of the animal. They are comparable with the changes observed in the subcutaneous tissue of the lumbar region where the tumor was transplanted. Surprisingly, no substantial modification of these gradients was apparent during the increase in tumor size with prevalence of necrosis around the thermistors. As the host became moribund, the absolute value of body temperature decreased. However, substantial temperature gradients within the tumor persisted until the last day of host survival (table 1).

At any given time, temperature gradients were also consistently present among different areas of the same tumor (text-figure 2), with ranges comparable to those observed in the subcutaneous tissue. As expected, thermistors closer to the skin surface of the tumor usually measured the lowest temperatures. Only exceptionally, and for a brief period of time, was the temperature of the subcutaneous tumor equal to or higher than that of the abdomen. When the animal became moribund, the amplitude of temperature changes was reduced both during the circadian rhythm and within the tumor at any given time. Occasionally, the tumor was warmer than the abdomen during the last 48–72 hours of host survival.

Temperature Gradients in the Same Tumor Grown Consecutively in Two Locations

Each tumor was grown at the extremity of a vascular pedicle and incorporated three thermistors. Initially, the tumor was located in a pouch of the subcutaneous tissue and was enveloped in a paraffin bag. When the tumor size was sufficiently large to ensure incorporation of the three thermistors, the temperature gradients were recorded for 2 days. Then the tumor was transferred from the subcutaneous pouch into the abdominal cavity and the temperature gradients were recorded for 2 additional days. The transfer of the tumor from the subcutaneous to the abdominal location was possible because the paraffin bag, in which the tumor grew, kept it isolated from the surrounding tissues. Moreover, the location of the tumor at the extremity of the long

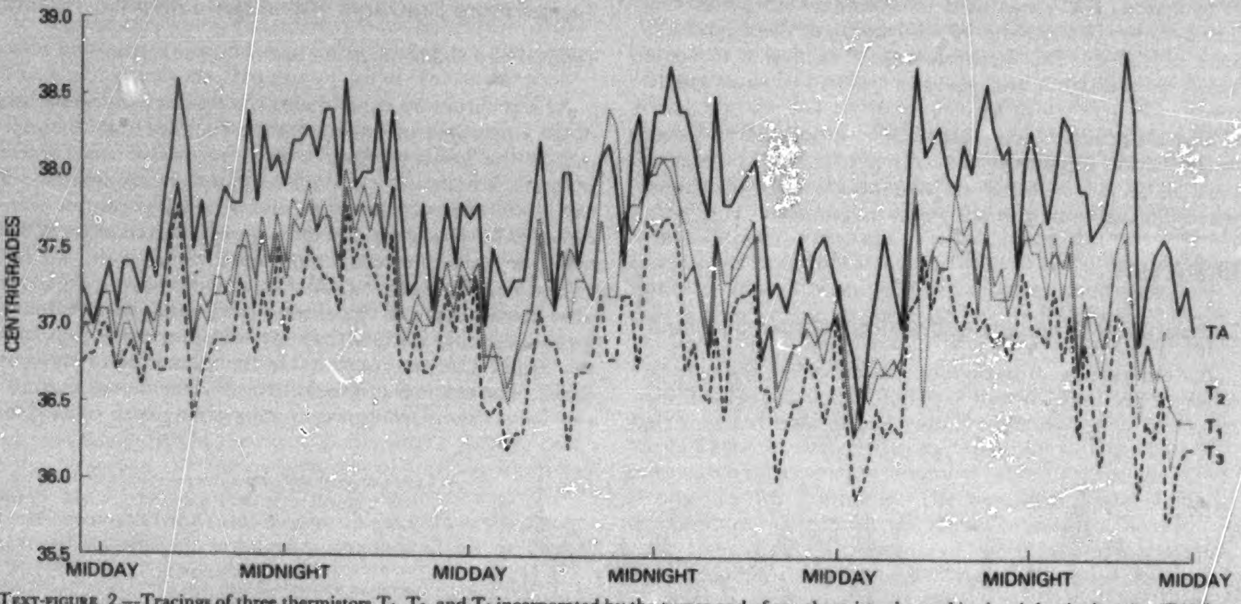

TEXT-FIGURE 2.—Tracings of three thermistors T_1, T_2, and T_3 incorporated by the tumor and of one thermistor located in the abdominal cavity (TA) from day 6 to day 9 for a subcutaneous W256 growing in the left lumbar region of the rat. *Note* the circadian rhythm, with zenith and nadir at midnight and midday, respectively, synchronous with that of the abdominal cavity which is consistently warmer than the subcutaneous tumor. Occasionally, temperature differences among the three tumor thermistors were rather large (table 1). Distances of thermistors from tumor surface: T_1=20 mm, T_2= 10 mm, T_3=3 mm. Thickness of skin covering tumor=1 mm. Tumor weight at animal's death=38.3 g.

TABLE 1.—*Differences between highest and lowest temperatures recorded within the W256 from day of transplantation until the host's death*

No. of days	Time[a]	Average temperature differences measured by three thermistors in rat tumors					
		Rat No./tumor weight, g[b]				Controls, No.[c]	
		1/36.5	2/38.3	3/80.0	4/56.0	1	2
1	a.m.					1.4	1.0
	p.m.	2.7	1.7	2.6	1.7	1.7	1.7
2	a.m.	1.4	2.5	2.1	1.9	1.6	2.4
	p.m.	1.4	1.9	2.2	1.4	1.6	2.6
3	a.m.	2.5	1.9	2.5	2.0	1.8	1.7
	p.m.	1.1	1.3	2.2	1.7	2.2	2.4
4	a.m.	1.7	1.8	1.6	1.8	2.2	2.9
	p.m.	1.9	2.1	1.8	1.9	2.3	1.6
5	a.m.	1.7	1.9	2.1	2.1	2.3	2.2
	p.m.	0.6	2.6	2.0	1.7	1.9	2.2
6	a.m.	1.8	1.2	2.1	2.1	2.6	2.1
	p.m.	2.2	2.5	1.9	2.3	2.6	1.9
7	a.m.	2.5	2.0	1.5	2.3	2.5	2.7
	p.m.	2.4	2.1	1.9	1.6	2.6	1.6
8	a.m.	2.3	2.2	2.0	2.3	2.9	2.0
	p.m.	2.9	1.4	1.6	2.1	2.2	2.6
9	a.m.	2.6	1.3	1.6	1.6	3.1	2.3
	p.m.	1.7	2.3	2.0	1.6	3.1	2.5
10	a.m.	2.2	1.2	1.3	1.5	2.8	2.7
	p.m.	2.5	1.1	1.4	2.0	2.4	2.6
11	a.m.	1.9	1.0	1.6	1.7	2.9	3.7
	p.m.	2.1	1.7	1.4	1.2	2.8	1.9
12	a.m.	1.7	1.3	1.7	1.8	3.1	2.3
	p.m.	2.8	1.4	1.8	2.4	2.2	1.9
13	a.m.	2.0	1.5	2.0	2.7	2.7	2.1
	p.m.	2.2	1.5	1.3	Death	1.9	2.0
14	a.m.	2.5	1.3	2.3		2.7	2.3
	p.m.	2.3	2.3	2.0		2.9	2.2
15	a.m.	1.4	4.1	2.0		3.0	2.2
	p.m.	2.7	5.1	1.3		2.1	1.9
16	a.m.	2.7	Death	3.8		2.8	1.6
	p.m.	2.6		2.2		2.6	2.7
17	a.m.	2.9		0.2		3.1	2.5
	p.m.	Death		3.1		Killed	Killed
18	a.m.			4.4			
	p.m.			Death			

[a] Tumor was transplanted in the morning of day 1. a.m.=largest temperature difference measured between midnight and noon. p.m.=largest temperature difference recorded between noon and midnight.

[b] Tumor weight at the animal's death.

[c] Three thermistors were placed in the subcutaneous tissue of the lumbar region, no tumor.

vascular pedicle allowed mobilization without impairment of blood supply. During the determinations the animal was kept in the same cage and was free to move. The tumor temperature was recorded every 30 minutes.

The results of the three experiments show that in the abdominal location the average tumor temperature was 0.5–1.0°C higher than in the subcutaneous area, but temperature changes due to circadian rhythm and temperature gradients within the tumor remained unchanged.

Temperature Gradients Around Tumors

Temperature differences between the skin surface and the abdominal wall surface of the tumor were recorded in tumors grown at the end of vascular pedicles. Since these tumors were grown in a pouch of the subcutaneous tissue enveloped by a paraffin sack, the thermistors were placed between the paraffin and the skin or the paraffin and the abdominal wall. The tumor surface was therefore separated from the thermistor by a sheet of paraffin about 100 µm thick. Temperature was recorded in the anesthetized animals for periods of 20–40 minutes. The gradients observed in six experiments varied from 0.4 to 2.1°C (table 2), and as expected the colder temperatures were consistently registered by the skin-side thermistor. The temperature gradients around the tumor did not show any substantial difference from the gradients observed in the normal subcutaneous tissue or within the tumor.

Temperature Gradients Within Hyperthermic Tumors

The objective of these experiments was to assess the effect of hyperthermia on the existence and magnitude of temperature gradients within tumors.

Heat was applied to the skin overlaying the tumor until the temperature recorded by one of the thermistors reached the desired level. The energy input to the lamp was then regulated to maintain this level constantly for 30–60 minutes. The temperatures measured by the three thermistors embedded within the tumor were recorded before, during, and after the heat application until the tumor temperature had returned to basal levels.

The curves obtained in one experiment are shown in text-figure 3. Table 3 presents the summary of 10 experiments, where the highest gradients recorded before, during, and after heat application are presented. These gradients are compared with the thickness of the neoplastic tissue separating each thermistor from the skin surface of the tumor, closest to the heat source, from the abdominal wall surface, farthest from the heat source, and the thickness of the neoplastic tissue separating the thermistors from each other.

The nonuniformity of temperature that existed in normothermic tumors was exaggerated during hyperthermia. In 8 of 10 experiments, temperature gradients larger than 1°C were observed within tumors at locations only a few millimeters distant from each other. The time needed to reach the highest temperature also varied among the three thermistors within the same tumor. However, any change in the heat input occurring during hyperthermia was promptly reflected in the temperature recorded by each thermistor (text-fig. 3). Once the temperature gradients were stabilized,

TABLE 2.—*Maximal temperature gradients around a W256 during normothermia*

Tumor No./wt, g	Duration of monitoring, min	Maximum $T_{AB}-T_{SK}$,[a] °C
1/3.4	20	0.7
2/2.3	20	0.6
3/2.4	20	0.4
4/5.1	35	1.0
5/2.3	25	1.8
6/3.5	40	2.1

[a] T_{AB}=temperature recorded by a thermistor placed between the tumor and the abdominal wall. T_{SK}=temperature recorded by a thermistor placed between the tumor and the rat's skin.

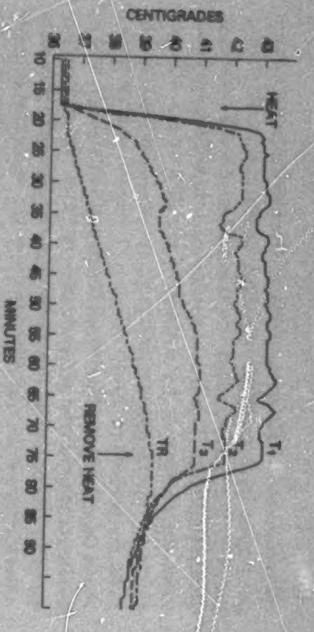

TEXT-FIGURE 3.—Temperature gradients of a 3.7-g W256 were measured first under physiologic conditions, then heat was applied to bring up and maintain the temperature of one thermistor at ≈43°C. During hyperthermia the temperature differences among the three thermistors became more accentuated. When heat was removed the gradients returned roughly to the starting levels within ≈1 hr. The times required to reach maximum temperatures were quite different among the three thermistors. *Note,* however, the prompt and simultaneous response of all three thermistors at changes of heat input. Distance of thermistors from skin surface of tumor: T_1=7 mm, T_2=3 mm, T_3=2 mm. T_R=rectal temperature.

they did not change appreciably whether the hyperthermia lasted 1 or 3 hours. Moreover, the correlation coefficients, calculated to assess the relationship between temperature changes and thickness of neoplastic tissue separating the thermistors from each other, or from the tumor surfaces, failed to show a consistent trend (table 3).

Text-figure 4 shows the curves obtained in one experiment when the tumor was in the abdominal cavity and heat was applied by a lamp placed 20 cm from the abdominal wall. Note that about a 4.5°C difference was observed between the recordings of two thermistors placed 1.3 cm apart in the 12.5-g tumor about 20 minutes after heating. When the heat was removed, the temperature gradients returned to about the levels prior to heating. This behavior was observed in three separate experiments, although the extent of temperature difference varied.

Influence of Blood Flow on Temperature Gradients of Normothermic and Hyperthermic Tumors

To evaluate changes in the temperature gradients produced by an increase or decrease of blood supply, we used in the first group of experiments normothermic tumors grown at the extremity of a vascular pedicle. The blood supply was measured as the volume of blood collected from the efferent tumor vein. Increase or decrease of blood supply was obtained by hypervolemia or hypovolemia induction in the host, respectively. The results of one of three experiments are shown in text-figure 5, where substantial changes in blood flow were followed by minimal changes in the temperature gradients within the tumor.

In the second group of experiments we used hyperthermic tumors. The energy input of the heat lamp was adjusted to bring the tumor temperature to 39–40°C as recorded by one thermistor; then the blood supply to the tumor was altered while the heat supply was kept constant. Text-figure 6 shows the results of one experiment where the application of heat produced increases of both volume and temperature of the tumor efferent blood. As the blood flow was stabilized at

TABLE 3.—*Tumor temperature gradients during hyperthermia and thickness of tumor tissue separating thermistors from the heat source*

Expt No.[a]	Tumor weight, g	Highest temperature, °C	Temperature gradients measured by thermistors T_1, T_2, and T_3 during hyperthermia[b]									Thickness of tumor tissue, mm[c]								
			Before heating			During heating			After heating			Between thermistors and skin surface			Between thermistors and abdominal surface[d]			Among thermistors within tumor		
			T_1-T_2	T_1-T_3	T_2-T_3	T_1-T_2	T_1-T_3	T_2-T_3	T_1-T_2	T_1-T_3	T_2-T_3	DS_1	DS_2	DS_3	DA_1	DA_2	DA_3	T_1-T_2	T_1-T_3	T_2-T
1	2.3	39.1	0.8	0.8	0	0.5	1.3	0.3	0.8	0.8	0	5	6	10	4	9	4	7	16	9
2	2.3	39.4	0.1	0.6	0.5	0.1	0.5	0.4	0	0.3	0.3	10	10	10	3	3	3	5	5	8
3	4.0	43.2	0.1	0.5	0.4	0.9	1.6	0.7	0.2	0.6	0.4	6	7	4	7	12	14	4	17	13
4	4.0	42.1	0.1	0.5	0.4	1.4	1.9	0.5	0	0.3	0.3	7	8	5	6	10	4	7	17	10
5	4.3	41.2	0.1	0.7	0.6	0.3	0.7	0.4	0.7	1.3	1.0	7	9	7	7	6	4	5	9	4
6	5.5	43.5	0.1	0.2	0.1	1.2	2.7	1.5	0.4	0.9	0.5	8	7	15	6	6	4	5	9	4
7	6.2	39.9	0.8	0.8	0	0.7	1.2	0.5	0.9	1.0	0.1	8	14	5	10	10	8	10	13	3
8	2.7	43.1	0.1	0.6	0.5	0.9	1.3	0.4	0.4	0.6	0.2	5	4	6	ND	ND	ND	9	19	10
9	3.7	43.5	0.1	0.2	0.1	1.2	2.5	1.3	0.1	0.4	0.3	2	3	7	10	9	9	13	20	7
10	4.5	43.0	0.5	1.4	0.1	1.2	1.8	0.6	1.5	1.5	0	10	10	10	ND	ND	ND	8	12	20

[a] Experiments 1–7: tumors grown at the extremity of a vascular pedicle; experiments 8–10: subcutaneously transplanted tumors.

[b] Base-line temperature was recorded by thermistors T_1, T_2, and T_3 for 30 min. Heat was applied until T_1 reached the highest temperature selected for the experiment (*see* column
Heat output of the lamp was regulated to keep T_1 at constant temperature. Heat was removed after steady state prevailed for about 15 min; then the tumor temperature was allowed stabilize and gradients were measured.

[c] At the end of the experiment the tumor was cut to expose position of thermistors. Distance of thermistor tip from the tumor surface in contact with skin (DS) or abdominal wall (D was measured by caliper (*see* fig. 2).

[d] ND=not determined.

the new level, hypovolemia was induced and a reduction of blood flow was obtained. Promptly, an increment of tumor temperature followed. When stabilization of this new condition was obtained, hypervolemia was induced and the tumor temperature subsequently decreased. During the modification of blood supply, the temperature gradients within the tumor persisted. The observations reported in text-figure 6 were consistently reproduced in six separate experiments performed under identical conditions.

The data obtained in the hyperthermic tumor experiments are reported in table 4. In the blood flow column three values are given for each experiment. The first one indicates the blood flow stabilized after the tumor temperature was brought to 39–40°C, the second value indicates reduction in the blood flow during hypovolemia, and the third value is the blood flow increment after hypervolemia. For each blood flow value the highest and lowest temperatures recorded by the thermistors embedded in the tumor are indicated in the adjacent columns. A change in blood flow produced a prompt change consistently in the local temperature of the tumor subjected to a constant heat input. The range of this change varied among tumors and also substantially varied within the same tumor. For instance, in the first experiment (table 4) a blood flow reduction of about 80% produced in the warmest area an increment of tumor temperature of 2.1°C, which was abolished by the subsequent increase in flood flow. In the coldest area of the tumor, however, the decreased blood flow produced a temperature increase of only 0.2°C, overcompensated for by the subsequent increase of blood flow that resulted in a 0.6°C drop in temperature.

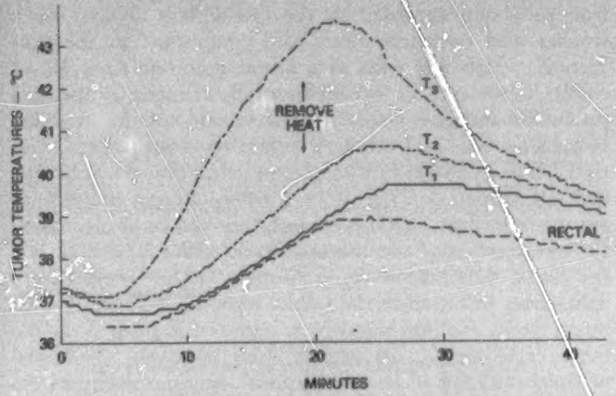

TEXT-FIGURE 4.—Temperature gradients of a 12.5-g W256 grown at the extremity of the ovarian pedicle of the rat and kept in the abdominal cavity. Heat was applied by a lamp located 20 cm away from the abdominal wall. *Note* that during hyperthermia the temperature differences among tumor thermistors became more accentuated. When heat was removed the gradients returned to about the initial levels. Distances of thermistors from the tumor surface: T_1=9 mm, T_2=9 mm, T_3=8 mm. Tumor size=2.5×3.0×1.8 cm.

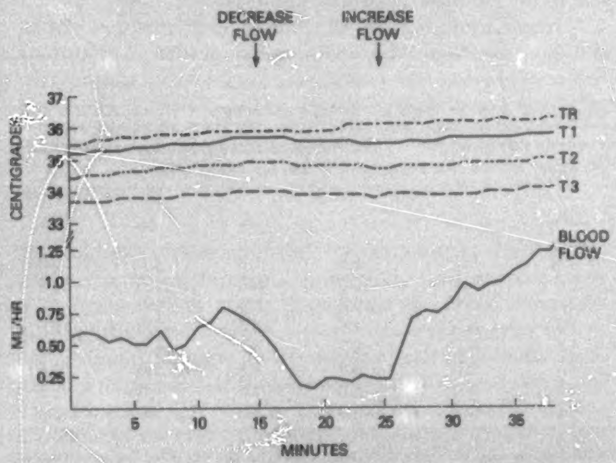

TEXT-FIGURE 5.—Relationship between changes in blood flow and temperature gradients within a 2.4-g normothermic tumor. The gradients showed minimal changes despite a doubling or a reduction to one-third of the basal tumor blood flow. T_1, T_2, and T_3 correspond to thermistors 1, 2, and 3.

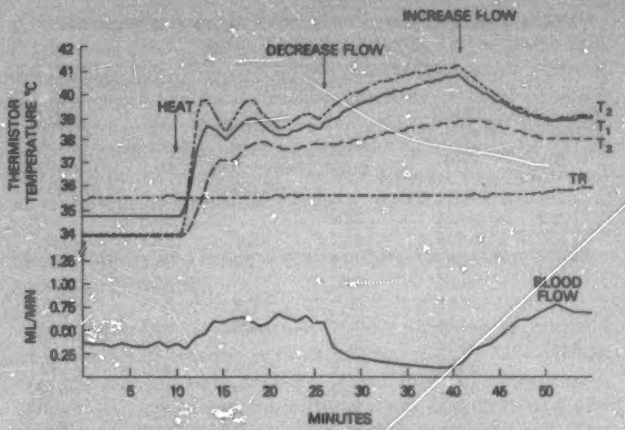

TEXT-FIGURE 6.—Relationship between blood flow changes and temperature gradients within hyperthermic tumors. Tumor temperature was increased to the desired level, then the power input to the lamp was kept constant, and changes in blood flow by hypovolemia or hypervolemia were produced. *Note* that application of heat sufficient to elevate tumor temperature to ≈39°C resulted in the increase of tumor blood supply. When a depression of blood supply was induced, the temperature of the tumor increased and the reverse was observed when the blood supply was enhanced. The temperature gradients, however, persisted throughout. T_1, T_2, and T_3 designate tumor thermistors. T_R = rectal temperature.

There was no reproducible pattern among several tumors in the modification of temperature gradients following blood supply changes. Despite the prompt temperature response to any modification in blood flow, very large blood flow changes were necessary to produce relatively modest temperature changes. This phenomenon indicates that conductive heat transfer in the tumor prevails over convective heat transfer. However, we could not establish an exact relationship between the extent of temperature changes in a tumor and a known change in blood supply.

Modification of Tumor Temperature Gradients by an Intra-arterial Pulse of Cold Serum

With these experiments we attempted to assess the effect on tumor temperature gradients of an abrupt modification in the temperature of the blood entering the tumor. The final objective was an evaluation of local tissue perfusion derived from the observed changes.

TABLE 4.—*Relationship between blood supply and temperature gradients within a tumor*

Expt No./ tumor wt, g	Blood flow, ml/ min[a]	Tumor temperatures and gradients, °C			
		Hottest area[b]	Difference after flow changes[c]	Coldest area[b]	Difference after flow changes[c]
1/2.3	0.618	39.0		38.5	
	0.108	41.1	+2.1	38.7	+0.2
	0.701	39.1	−2.0	38.1	−0.6
2/2.3	0.665	39.3		38.9	
	0.257	40.2	+0.9	39.8	+0.9
	0.731	39.4	−0.8	39.3	−0.5
3/2.8	0.810	38.9		38.3	
	0.170	41.9	+3.0	40.9	+2.6
	0.937	40.9	−1.0	40.0	−0.9
4/3.0	0.364	39.2		38.5	
	0.030	40.1	+0.9	39.2	+0.8
	0.406	39.4	−0.7	38.5	−0.7
5/3.5	0.583	40.2		37.0	
	0.208	42.9	+2.7	37.7	+0.7
	1.242	40.2	−2.7	37.5	−0.2
6/6.2	1.770	39.3		38.3	
	0.231	40.6	+1.3	39.6	+1.3
	1.780	40.1	−0.5	38.9	−0.7

[a] For each experiment three blood flow values are reported: when heat was applied to the tumor, when reduction in blood flow was induced, and when blood flow was returned to initial or higher levels.

[b] Temperatures measured when three different levels of blood supply to the tumor were kept constant for at least 15 min.

[c] Maximal temperature differences induced in tumors by variations in blood supply.

Normothermic Tumors

We used the preparation with a tumor growing at the extremity of the vascular pedicle and incorporating three thermistors. The rat was anesthetized, the abdominal cavity opened, and a catheter positioned in the left iliac artery and readied for the rapid injection of cold serum into the tumor afferent artery as described in "Materials and Methods" (fig. 1). Finally, the efferent vein of the tumor was cannulated, and the determination of blood flow was started.

After base-line values for tumor and host temperatures as well as for blood flow were established for 20–40 minutes, a pulse of cold serum was given and the temperature changes in the tumor and rectum were recorded every 30 seconds until approximate base-line values returned. Preliminary tests for duration, volume, and temperature of serum pulse showed that the best responses were obtained when volume was kept constant at 2 ml, the pulsed serum had the temperature of melting ice, and duration was 0.5–2 minutes.

Text-figure 7 shows the temperature gradients obtained from one experiment. The results of eight more experiments summarized in table 5 give the maximal temperature depressions produced by the cold pulse in three regions of the tumor containing the three thermistors as compared to the gradients measured in the rectum and in the tumor efferent blood of the same animal. Regardless of the temperature of the pulsed serum or the duration of the pulse, the temperature reduction recorded in the tumor was always much smaller and occurred much later than that in the host rectum, which was used as a physiologic reference. Blood supply to the tumors was substantially reduced by the cold pulse. For instance, in the case shown in text-figure 7 the blood flow was 21.7 ml/hr/g before the cold pulse, it was reduced to 1.6 ml/hr/g when blood temperature was lowest, and it returned to 23.2 ml/hr/g when efferent blood temperature reached 36°C. Although the cold pulse decreased the temperature of the tumor efferent blood by 2.3°C and the rectal temperature by 8.5°C, the largest temperature differences recorded in the tumor were 0.7, 0.7, and 0.4°C, respectively. Similar behavior is reported in table 5 for the other experiments. All tumors were relatively small and without evidence of necrosis around the thermistors as observed macroscopically at the end of each determination.

In three of the experiments a second pulse of cold plasma was injected about 10 minutes after the temperature depression of the first pulse was compensated. The range of temperature depression due to a second pulse was different from that obtained with the first stimulation, although the time required to reach the maximal temperature change was similar in most instances (table 6).

A major limitation in all these experiments was the inability to produce large temperature gradients in tumors,

TABLE 5.—*Temperature gradients in tumors receiving a pulse of cold serum in the afferent artery*

Expt. No./ tumor wt, g	Pulse, ia, of 2 ml cold serum		Maximal temperature depression in tumors produced by ia cold pulse, °C[a]					Times required to reach lowest temperatures, min[b]			
	Temperature, °C	Duration, min	ΔT_1	ΔT_2	ΔT_3	ΔT_R[c]	ΔT_{EB}[d]	t_1	t_2	t_3	t_R
1/2.3	1	1.0	0.2	0	0.1	2.0	0.7	3.0	1.0	1.0	1.0
2/2.2	1	0.6	0.2	0.2	0.2	2.5	1.8	10.0	10.0	10.0	1.5
3/2.1	1	0.6	0.4	0.2	0.4	2.4	2.2	9.0	9.0	7.0	2.0
4/4.2	1	1.0	1.0	0.4	0.8	1.8	ND	4.0	5.0	8.0	2.5
5/1.5	1	1.5	1.0	0.8	0.9	1.0	ND	6.5	6.5	6.0	3.5
6/2.4	10	2.0	0.4	0.2	0.1	5.7	0.6	3.5	3.5	3.0	0.5
7/2.4	10	1.0	0.8	0.7	0.5	8.5	2.4	4.0	3.0	4.0	1.5
8/2.3	10	2.0	0.3	0.5	0.4	1.2	1.5	3.0	4.0	4.0	2.0

[a] Differences between tumor temperatures observed during the last 5 min before pulse and the lowest temperature measured after pulse recorded by themistors T_1, T_2, T_3, T_R, and T_{EB}.

[b] t_1, t_2, t_3, and t_R are time differences measured by thermistors with corresponding symbols between end of cold pulse and time when lowest temperature was recorded.

[c] T_R=thermistor in the rectum.

[d] T_{EB}=thermistor in the tumor efferent blood. ND=not determined.

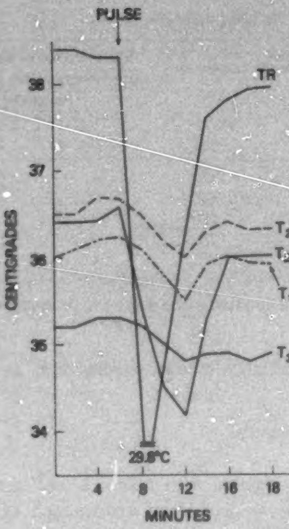

TEXT-FIGURE 7.—Temperature gradients measured by three thermistors (T_1, T_2, T_3) in a 2.4-g W256 receiving a pulse of cold (+1°C) serum in the tumor artery (*see* fig. 1). *Note* the extent of temperature depression obtained in the rectum (T_R) and efferent tumor blood (T_{EB}) compared with that registered within the tumor. Reduction of temperature in the tumor occurred later than in the rectum and efferent blood in all experiments. The shape of the temperature change curves varied from one tumor to another, but clear differences among the three thermistors were always maintained.

TABLE 6.—*Temperature gradients in tumors receiving two successive cold serum pulses in the afferent artery*

Expt No./tumor wt, g	Maximal temperature depression produced by cold serum, °C[a]				Time required to reach lowest tumor temperatures, min[b]			
	ΔT_1	ΔT_2	ΔT_3	ΔT_R	t_1	t_2	t_3	t_R
1/2.3	0.3	0.5	0.4	1.2	3.0	4.0	4.0	2.0
	0.2	0.3	0.3	0.6	2.0	4.0	4.0	2.0
2/2.4	0.8	0.7	0.5	8.5	4.0	3.0	4.0	1.5
	0.2	0.2	0.2	7.2	2.5	3.0	2.5	1.5
3/2.4	0.4	0.2	0.1	5.7	3.5	3.5	3.0	0.5
	0.5	0.3	0.3	4.9	3.5	3.5	3.5	0.5

[a] Differences between tumor temperatures were measured by thermistors T_1, T_2, T_3, and T_R during the last 5 min before pulse and the lowest temperature measured after pulse. T_R: thermistor measured rectal temperature for physiologic reference.

[b] Times elapsed between the end of cold pulse and lowest temperature recording.

comparable to those observed, for instance, in the rectum. Differences of fractions of a centrigrade are less convincing and more prone to errors than larger gradients. Notwithstanding this limitation, it is clear that a substantial reduction of blood temperature produced relatively small temperature depression and gradients in the tumor, as opposed to a substantial reduction in a normal organ like the rectum. In contrast, however, the tumor temperature gradients last longer.

Hyperthermic Tumors

In four additional experiments a pulse of cold serum was given to tumors kept at a temperature of 41–42°C. Hyperthermia was induced 10–15 minutes prior to the pulse and maintained until the end of the determination. A pulse of cold serum in the tumor artery, however, did not produce any appreciable change in the temperature levels and gradients within hyperthermic tumors. Again, the poor blood supply may be responsible for the limited importance of heat convection on tumor temperature.

Modification of Tumor Temperature Gradients by an External Coolant

To overcome the difficulty of obtaining a substantial temperature depression with an arterial pulse of cold serum, we used an external coolant in the following experiments. Tumors incorporating three thermistors and grown at the distal extremity of the vascular pedicle were utilized. The efferent tumor vein was cannulated for continuous measurement of blood flow, then the tumor was rapidly cooled with the ethanol procedure (*see* "Materials and Methods"). A thermistor in the rectal cavity registered the host temperature during the entire experiment. Text-figure 8 reports the data collected in one of five experiments, and table 7 summarizes the maximal temperature depression produced by the cold stimulus and the time required for the temperature to return to steady-state level.

The temperature gradients obtained with this procedure were larger than those obtained with the intra-arterial pulse of cold serum. Maximal depression of tumor temperature

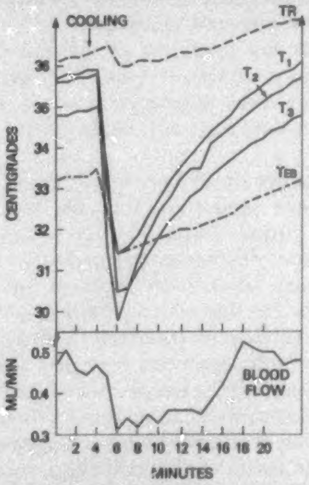

TEXT-FIGURE 8.—T_1, T_2, and T_3 are thermistors within the tumor, T_R in the rectum, and T_{EB} is the temperature of the tumor efferent blood. Temperature gradients within a 6.8-g W256 were obtained by ethanol cooling of the overlaying skin (*see* "Materials and Methods"). *Note* the rapid and extensive reduction of tumor temperature obtained with this procedure as compared with that obtained by the ia serum pulse (text-fig. 7). In this particular tumor the distances from the skin surface were T_1=3 mm, T_2=5 mm, and T_3=4 mm. In this tumor, as in others (table 7), there was no relationship between maximal temperature depression and the thickness of neoplastic tissue between the surface of the tumor facing the cooled skin and the thermistors. The shape of the curve representing the return of tissue temperature to original values was different for each thermistor. *Note* the substantial reduction of blood flow in the cooled tumor.

TABLE 7.—*Modification of tumor temperature by rapid cooling of the skin over the tumor*

Expt No./tumor wt, g	Maximal temperature depression produced by external cooling, °C[a, b]				Time required to return to basal temperatures, min[c]				Tumor tissue thickness separating thermistors from skin surface of tumor, mm[b, d]		
	ΔT_1	ΔT_2	ΔT_3	ΔT_{EB}	t_1	t_2	t_3	t_{EB}	T_1	T_2	T_3
1/10.6	6.4	4.0	3.6	ND	12	12	9	ND	14	16	16
2/2.3	3.3	1.4	2.9	1.3	15	13	12	14[e]	ND	8	8
3/6.8	4.5	6.0	4.5	2.0	20	19	17	20[e]	4	5	3
4/7.6	2.7	2.6	2.3	1.6	20	22	22	18	5	11	13
5/1.6	2.4	3.2	2.3	0.9	17	18	14	13	4	4	5

[a] Differences between temperatures registered by thermistors T_1, T_2, T_3, and T_{EB} 5 min before cooling and the lowest temperature measurement after cooling. T_{EB}=thermistor in the tumor efferent blood.

[b] ND=not determined.

[c] Times elapsed between lowest temperature measurements and return to basal temperatures after ethanol cooling; t_1, t_2, t_3, and t_{EB} are time differences measured in tumors and in tumor efferent blood, respectively.

[d] Skin thickness was ≈1.0 mm in all cases.

[e] In these cases the temperature did not return to basal levels but stabilized at slightly lower levels.

from the ethanol applications on the skin was obtained within 3.5 minutes on the average. This parameter was obviously influenced by the distance of the tumor thermistors from the skin surface where the cooling process was applied. However, since the coolant was evaporated in 2 minutes the rate of temperature return to the original levels was most probably related to the blood flow around the thermistors and was relatively independent from the thermistor-skin surface distance. The temperature reequilibration time, therefore, gives an indication of the local efficacy of the blood supply.

As expected, the curves representing the temperature reequilibration varied from one thermistor to another (text-fig. 8). The time required to compensate for each gradient within a tumor also presented substantial differences. For instance, in tumor 1 (table 7) it took 12 minutes to compensate a 6.4°C gradient as contrasted to a 4.0°C gradient measured in two separate regions by thermistors 1 and 2, respectively.

The temperature depression could not be related to the amount of tissue separating the cold source from each thermistor. In tumor 4 (table 7), for instance, almost the same temperature depression was measured by thermistors 1 and 2, although about twice as much tumor tissue separated thermistor 2 as that which separated thermistor 1 from the cooled skin surface. Alternatively, in tumor 2 thermistors 2 and 3 were both separated from the skin by a 8-mm thickness of tissue, and the temperature depression registered by thermistor 3 was about twice that of thermistor 2. In all cases, a reduction of efferent blood was produced by cooling the tumor. The range of this reduction varied from 25 to 40% of the precooling level.

Because the temperature depression was obtained in a few minutes and occurred simultaneously with a substantial reduction in blood flow, we concluded that differences in resumption of local perfusion were instrumental in determining the size of the temperature gradients observed among different areas of the same tumor. On the basis of this assumption, an estimate of local perfusion was obtained.

Estimation of Flow Distribution Within Tumors

The partition of blood supply within a tumor was estimated with the use of a mathematical model (*10*) that considers the rat as a system comprised of a tumor and normal tissues, represented by anatomically interconnected compartments. (For details, *see* "Appendix.") The tumor is divided into three compartments related to the three thermistors, and the temperature in each compartment is predicted as a function of time after a cold pulse of serum into the tumor artery or after the skin cooling by alcohol. The blood flow distribution into these three tissue compartments is estimated by fitting the model predictions with our data.

From the temperature drop values (table 5) after a pulse of cold serum, the flow distributions shown in table 8 were obtained. Text-figure 9 shows the comparison between the data for a 2.3-g tumor (tumor 8 in table 8) and the predictions of our model. The solid lines were obtained by assuming that 0, 90, and 10% of the afferent blood was flowing into each of the three compartments, respectively, and the dotted lines were obtained by assuming that the blood flow was uniform throughout the tumor. Visual comparison between temperature decrease and blood flow curves emphasize the nonuniform blood distribution for tumor 8 (text-fig. 9). Similar charts (not presented) were obtained for each of tumors 1–8 (table 8).

We calculated the blood flow distribution for tumors 8–10 (table 8) from the data on temperature drop subsequent to skin cooling (table 7). For example, for a 6.8-g tumor (tumor 10, table 8 and text-figure 10), the solid lines were calculated by assuming that the blood flow was distributed in the areas around the three thermistors as 50, 0, and 50% of the efferent tumor blood, respectively, whereas the dotted line was drawn by assuming uniform flow throughout the tumor. Again, the anisotropy of blood distribution around the thermistors is evident. The small differences in temperature prediction shown in text-figures 9 and 10 also emphasize that thermal diffusion and not convection is the major event in heat transfer within tumors.

DISCUSSION

The temperature gradients in the normal mammary gland of the virgin rat were comparable to those observed by Møller and Bojsen (*11*). The temperature difference within the gland was usually less than 1°C, without consist-

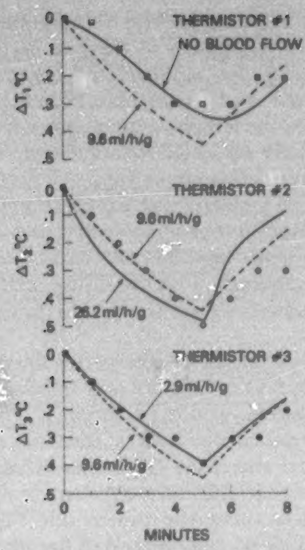

TEXT-FIGURE 9.—Comparison of mathematical model predictions with the experimental data (tumor 8, table 8). The points (□, ○, ●) on each of the three graphs refer to the tumor temperature decrease measured by thermistors 1, 2, and 3, respectively, following the injection of cold serum. ----, obtained by assuming uniform blood flow throughout the tumor, in this case 9.6 ml/hr/g. ——, obtained by assuming 0, 90% (26.2 ml/hr/g), and 10% (2.9 ml/hr/g) blood supply around thermistors 1, 2, and 3, resp. Similar curves were obtained for each tumor in table 8. Difference between experimental data and model predictions, with the assumption of uniform flow, was 0.023°C. Difference between experimental data and model predictions, with the assumption of nonuniform flow, was 0.020°C.

ent differences among glands. Temperature gradients within tumors were roughly similar to the gradients of the subcutaneous space where the tumors were transplanted. Both normal and neoplastic mammary tissues exhibited a clear circadian rhythm with the zenith at about midnight and nadir at about midday; the difference between the two could reach 3°C. It was surprising that both circadian rhythm and temperature gradients persisted in large tumors where thermistors were embedded in necrotic material. We have no explanation for this unexpected finding that was consistent in four separate experiments (table 1) and contrasted with previous observations (*11*).

Temperature gradients within the tumor increased under hyperthermic conditions. Since convective heat dissipation in the body is dependent on blood flow, and conductive heat transfer is determined by thermal conductivity of tissues, the increment of the measured temperature gradients suggests that convective heat transfer in tumors is inefficient.

In hyperthermic tumors an increase in blood flow cooled the tumor as expected. From the data of table 4 one can calculate that on the average an increase of 1 ml blood per gram of tissue per hour in the flow rate will cool the tumor by 0.16°C in the highest temperature regions. In the majority of tumors studied, the blood flow, measured by collecting the efferent blood from the tumor vein of tissue-isolated preparations, varied between 10 and 15 ml/hr/g. These volumes are three- to fivefold lower than the supply to a parenchymatous organ such as the liver (*12*). A doubling of tumor blood supply was the largest increment we could experimentally obtain by resorting to a hypervolemia level in the host that was outside physiologic limits and increased the arterial blood pressure by about 50 mm Hg. If a doubling of the blood flow to the tumor is the maximum possible

TABLE 8.—*Blood flow distribution within a tumor estimated from the temperature gradients induced by an intra-arterial cold serum pulse (tumors 1-8) or skin cooling by ethanol (tumors 9-12)*

Tumor No./ wt, g	Blood supply, ml/hr[a]	Blood flow, % of total supply estimated for each tumor area surrounding a thermistor[b]		
		T_1	T_2	T_3
1/2.3	11.0	90	0	10
2/2.2	14.3	33	33	33
3/2.1	17.6	10	0	90
4/4.2	44.5	90	0	10
5/1.5	41.2	90	0	10
6/2.4	18.5	90	0	10
7/2.4	29.5	70	30	0
8/2.3	22.1	0	90	10
9/2.3	34.5	0	90	10
10/6.8	48.9	50	0	50
11/7.6	50.9	20	30	50
12/1.6	30.5	50	0	50

[a] Measured by cannulation of the tumor efferent vein for tumors 1-8 (tissue-isolated preparations) and calculated for tumors 9-12 (sc implants). From previous determinations (7), the relationship between blood flow and tumor weight in W256 is: log(flow/weight) = 1.419−0.678 log weight.

[b] A mathematical model previously developed (*10*) was utilized to evaluate the distribution of blood in the areas around thermistors T_1, T_2, and T_3 incorporated by each tumor (*see* tables 5, 7).

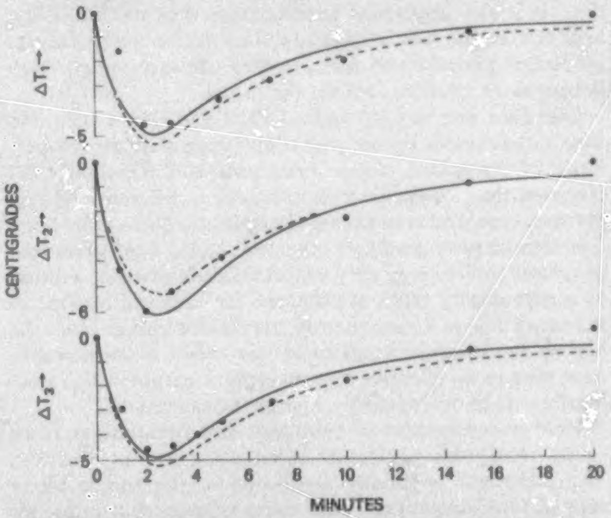

TEXT-FIGURE 10.—Comparison of mathematical model predictions with experimental data. *Each point* on the three graphs refers to the decrease in tumor temperatures as measured by thermistors 1, 2, and 3, resp., after the skin above the tumor was cooled. ----, was obtained by assuming uniform blood flow throughout the tumor, in this case 3.1 ml/hr/g. ——, were obtained by assuming 50% or 4.6 ml/hr/g) blood supply around thermistors 1, 2, and 3, resp. Difference between experimental data and model predictions, with the assumption of uniform flow, was 0.25°C. Difference between experimental data and model predictions, with the assumption of nonuniform blood flow, was 0.17°C.

increment that may be expected to occur in vivo, the efficiency of the tumor blood flow, both as a cooling or heat-carrying system, is rather low (*13, 14*).

Although the pulse of cold plasma substantially reduced the tumor blood flow and significantly decreased the temperature of tumor efferent blood, the reduction in tissue temperature was only a few tenths of a degree and with substantial anisotropy. The observation suggests that extensive arterial-venous shunts must exist which are able to exclude large sections of tumor tissue from efficient blood supply. Moreover, responses to subsequent pulses (table 6) indicate that the shunting varies with time and emphasize the importance of anisotropy in local blood distribution within tumors (*15, 16*).

The thermodilution experiments indicate that blood flow can be nearly zero in some region of a tumor and as much as threefold the average perfusion rate in other regions (table 8). Although the average perfusion rate decreases with the increase in tumor size, anisotropy of temperature distribution was quite evident in tumors of any size. Table 8 and text-figures 9 and 10 also indicate that a model utilizing homogeneous versus heterogeneous perfusion does not predict substantially different numerical values. This suggests that heat transfer in the tumor is dominated by conduction and not by convection. In a recent paper, Gibbs et al. (*17*) who explored temperature gradients within a tumor with a different method, reached a similar conclusion.

The size of temperature gradients observed in these experiments ~~caution against~~ the assumption that rapid and efficient heat distribution within the tumor can be achieved via the blood supply. Consequently, while it is more efficient to transfer heat to the tumor without relying solely on blood flow, it is also important to remember that the inefficient heat convection will help to maintain higher temperatures for longer periods, and will preserve the surprisingly high temperature gradients within the tumor.

Our data also caution against the belief that a temperature measurement in one region may represent the temperature of the whole tumor. Okamura and Reinhold (*18*) observed that for rat skin there is only a difference of 2°C between complete tolerance and maximum damage by heat. The temperature gradients observed during heat treatment of tumors in vivo may very well determine whether a lethal or a stimulatory effect is obtained for different regions of the same tumor. Consequently, the lowest rather than the highest temperature attained by the tumor is the determinant dose of an effective hyperthermic treatment; this dose hardly can be evaluated by a single measurement.

Heat-responsiveness of neoplastic cell populations is an easily predictable parameter in vitro but not in vivo (*19*). The difference is usually attributed to the tumor blood supply. Our data suggest that circumstances that influence heat conduction within the tumor or metabolism (*20*) control in vivo heat-responsiveness more effectively than events that influence heat convection.

APPENDIX

In general, two approaches have been followed to analyze the thermal dilution data (*21*). In the first one, it is assumed that after a cold serum pulse into a tumor, blood flow alone is responsible for the return to thermal equilibrium. This assumption is valid for well-perfused organs but fails for tumors with poor and anisotropic blood supply. In the second approach, the temperature changes are predicted by the bioheat transfer equation. Leaving aside the limitations of the bioheat transfer equation itself, this approach is useful only when applied to tissues with simple geometry. However, most tumors have complex geometry, are situated in a thermally asymmetric environment, and interact thermally with their surroundings. This condition is mathematically intractable; consequently, we resorted to the compartmental model.

The model was initially developed (*10*) to predict temperature distribution in tumors and normal tissue of rats during normothermia and hyperthermia. The model consists of nine compartments: three of them are constituted by the tissue around the three thermistors embedded in the tumor, one is the normal tissue adjacent to the tumor, one is the cooled skin above the tumor, one the skin on the adjacent normal tissue, one the rest of the skin, one the rest of the organism, and one is the blood pool. The temperature profile of each compartment is represented by a first-order ordinary differential equation, obtained by applying the general unsteady-state heat-balance equation: Net accumulation of thermal energy in each compartment=metabolic heat production+heat gained by conduction from interacting compartment(s)−heat lost to the perfusing blood−heat lost to the environment.

The detailed expression for each of the above heat-exchange terms and the values of the parameters incorporated into these terms for a tumor-bearing rat are given elsewhere (*22, 23*). During cooling by a cold pulse, the temperature of the tumor afferent blood is brought to the measured temperature, and during the application of alcohol to the skin, the skin above the tumor is brought to a low temperature. Upon substitution of experimentally obtained values for the various parameters and appropriate heat-exchange terms, the coupled set of ordinary differential equations is solved by digital computer, with the use of a fourth-order Runge-Kutte method to calculate the temperature distribution in each compartment.

REFERENCES

(*1*) Dickson JA. The effects of hyperthermia in animal tumour systems. Recent Results Cancer Res 1977; 59:43–111.

(*2*) Moricca G, Cavaliere R, Caputo A, Bigotti A, Colistro F. Hyperthermic treatment of tumours: Experimental and clinical applications. Recent Results Cancer Res 1977; 59:112–152.

(*3*) Yerushalmi A. Influence on metastatic spread of whole body or local tumor hyperthermia. Eur J Cancer 1976; 12:455–463.

(*4*) Dickson JA, Calderwood SK. Temperature range and selective sensitivity of tumors to hyperthermia: A critical review. Ann NY Acad Sci 1980; 335:180–205.

(*5*) Dickson, JA, Ellis HA. Stimulation of tumour cell dissemination by raised temperature (42°C) in rats with transplanted Yoshida tumours. Nature 1974; 248:354–358.

(*6*) Grantham FH, Hill DM, Rowland J, Gullino PM. Cage for continuous intravascular infusion of isotopes and drugs in small animals. J Natl Cancer Inst 1975; 55:203–205.

(*7*) Gullino PM. Techniques for the study of tumor physiopathology. Methods Cancer Res 1970; 5:45–91.

(8) Earle WR. A study of the Walker rat mammary carcinoma 256, in vivo and in vitro. Am J Cancer 1935; 24:566–612.

(9) Grantham FH, Hill DM, Gullino PM. Primary mammary tumors connected to the host by a single artery and vein. J Natl Cancer Inst 1973; 50:1381–1383.

(10) Jain RK. Temperature distribution in normal and neoplastic tissues during normothermia and hyperthermia. Ann NY Acad Sci 1980; 335:48–66.

(11) Møller U, Bojsen J. Heat transfer and blood flow in experimental tumors in rats compared with the circadian temperature rhythm of the body. Ann NY Acad Sci 1980; 335:22–34.

(12) Altman PL. In: Handbook of circulation. Dittmer DS, Grebe RM, eds. Philadelphia: Saunders, 1959:129.

(13) Song CW, Kang MS, Rhee JG, Levitt SH. The effect of hyperthermia on vascular function, pH, cell survival. Radiology 1980; 137:795–803.

(14) Jain RK, Grantham FH, Gullino PM. Blood flow and heat transfer in Walker 256 mammary carcinoma. JNCI 1979; 62:927–933.

(15) Endrich B, Reinhold HS, Gross JF, Intaglietta M. Tissue perfusion inhomogeneity during early tumor growth in rats. JNCI 1979; 62:387–395.

(16) Gautherie M. Thermopathology of breast cancer: Measurement and analysis of in vivo temperature and blood flow. Ann NY Acad Sci 1980; 335:383–415.

(17) Gibbs FA Jr, Peck JW, Dethlefsen LA. The importance of intratumor temperature uniformity in the study of radiosensitizing effects of hyperthermia in vivo. Radiat Res 1981; 87:187–197.

(18) Okumura Y, Reinhold HS. Heat sensitivity of rat skin. In: Streffer C, van Beuningen D, Dietzel F, et al, eds. Cancer therapy by hyperthermia and radiation. Baltimore: Urban & Schwarzenberg, 1978:220–221.

(19) Giovanella BC, Stehlin JS, Yim SO. Correlation of the thermosensitivity of cells to their malignant potential. Ann NY Acad Sci 1980; 335:206–214.

(20) Kang MS, Song CW. The effect of hyperthermia on cell survival in a mouse tumour without blood flow. Br J Radiol 1980; 53:606–607.

(21) Eberhart RC, Shitzer A, Hernandez EJ. Thermal dilution methods: Estimation of tissue blood flow and metabolism. Ann NY Acad Sci 1980; 335:107–132.

(22) Sien HP, Jain RK. Temperature distributions in normal and neoplastic tissues during hyperthermia: Lumped parameter analysis. J Thermal Biol 1979; 4:157–164.

(23) Chryanthopoulos GS, Jain RK. Thermal interactions between normal and neoplastic tissues in the rat, rabbit, swine, and dog during hyperthermia. Med Phys 1980; 7:529–536.

(24) Gullino PM, Grantham FH, Courtney AH. Utilization of oxygen by transplanted tumors in vivo. Cancer Res 1967; 27:1020–1030.

Correction

November 1981, vol 67, No. 5

In Letters to the Editor, "BCG and Cancer" (reply), by George W. Comstock, page 991, the references are incorrect. The following references are correct:

---

[1] Zbar B. Tumor regression mediated by *Mycobacterium bovis* (strain BCG). Natl Cancer Inst Monogr 1972; 35:341–344.

[2] Kendrick MA, Comstock GW. BCG vaccination and the subsequent development of cancer in humans. JNCI 1981; 66:431–437.

[3] Snider DE, Comstock GW, Martinez I, Caras GJ. Efficacy of BCG vaccination in prevention of cancer: An update: *Brief communication.* J Natl Cancer Inst 1978; 60:785–788.

[4] Skegg DC. BCG vaccination and the incidence of lymphomas and leukaemia. Int J Cancer 1978; 21:18–21.

Announcements

The Journal *will publish notices of major meetings dealing with cancer. Submission of notices 6 months in advance is requested to permit timely publication.*

Harvard Medical School Continuing Education Program

The following courses are being offered by the Department of Radiology, Brigham and Women's Hospital, and the Department of Continuing Education, Harvard Medical School:

Clinical Nuclear Medicine: 1982—Sixth Annual Postgraduate Course; AMA Category I Credit 26 hours; William D. Kaplan, M.D., Program Director; course date April 21–24, 1982.

Ultrasound for Clinicians—Seventh Annual Postgraduate Course; AMA Category I Credit 20 hours; Jason C. Birnholz, M.D., Program Director; course date May 3–5, 1982.

Cardiac Angiography 1982: Diagnostic and Therapeutic Coronary Arteriography—Annual Postgraduate Course; AMA Category I Credit 28 hours; David C. Levin, M.D., Program Director; course date May 24–27, 1982.

For additional information please contact the Department of Continuing Education, Harvard Medical School, 25 Shattuck Street, Boston, Massachusetts 02115 (telephone: 617-732-1525).

Aspirin Foundation of America

New Orleans, Louisiana, will be the site of this symposium to be held at the Tulane University School of Medicine on April 21–23, 1982. Participants will include 18 internationally recognized medical authorities who will take a new look at this versatile medication that continues to be cited in medical world literature for important new uses.

For additional information please contact Mr. Garrett Swenson, Chairman Symposium Committee, Aspirin Foundation of America, Inc., c/o American Home Products, 685 Third Avenue, New York, New York 10017 (telephone: 212-878-6150).

Cancer Management 1982

The Oncology Program of the University of Maryland School of Medicine and the American Cancer Society, Maryland Division, Inc., will present this course to be held at the Hyatt Regency, Baltimore, Maryland, on May 21–22, 1982.

For further information contact the Program of Continuing Education, University of Maryland School of Medicine, 10 South Pine Street, Baltimore, Maryland 21201 (telephone: 301-528-3956).

World Symposium on Asbestos

"Asbestos, Health, and Society" is the title of this symposium, sponsored by the Government of Canada, the Government of Quebec, and the Commission of the European Communities, to be held at the Sheraton Mt-Royal Hotel in Montreal, Canada, on May 24–27, 1982. The program has been designed to yield an exhaustive evaluation of the current asbestos situation, and to promote the free expression of the differing views held throughout the world on the subject.

For additional information please contact the Secretariat, World Symposium on Asbestos, 84 de Brésoles Street, Old Montreal, Quebec, Canada H2Y 1V5 (telephone: 514-845-6165; telex 05-24245).

First International Symposium on the Endocrine Lung in Health and Disease

The Veterans Administration Medical Center and the National Cancer Institute, in conjunction with George Washington University Medical Center, will conduct this conference to be held at the Hyatt Regency Capitol Hill hotel in Washington, D.C., on June 2–4, 1982. A panel of invited speakers will discuss the pulmonary endocrine cell, including anatomy, embryology, histochemistry, and the pathophysiology of its peptide products. Special sessions will be devoted to pulmonary endocrine tumors (small cell cancer and carcinoid).

For further information please contact Mr. Peter Petrossian, George Washington University Medical Center, Office of Continuing Medical Education, 2300 "K" Street, N.W., Washington, D.C. 20037 (telephone: 202-676-4285).

World Congress of Gastroenterology, Digestive Endoscopy, and Colo-Proctology

Stockholm, Sweden, will be the site of this meeting to be held on June 13–19, 1982. All information can be obtained from Stockholm Convention Bureau, Jakobs Torg 3, S-111 52 Stockholm, Sweden.

Annual Course in Advanced Immunology

The American Association of Immunologists will sponsor this course entitled "Regulatory Elements of the Immune System" to be held at Duke University, Durham, North Carolina, on June 15–24, 1982. Rapid advancements have led to an increased understanding of immune regulation and its application to the manipulation of responsiveness. This course will delve into these advances in immunobiology, immunogenetics, and molecular and clinical immunology. Topics will include immunoglobulin and MHC gene organization and control, regulation by interleukins, T and B cell clones and hybrids, effector mechanisms, and immunologic analysis and intervention in human disease.

To apply for the course, please submit a letter documenting your background in immunology and stating your reasons for wishing to attend, as well as current research/teaching activities and a brief c.v., no later than April 10, 1982, to: Dr. David W. Scott, AAI Course, Box 3010, Division of Immunology, Duke University Medical Center, Durham, North Carolina 27710.

First Conference on Radioprotectors and Anticarcinogens

This conference, sponsored by the National Bureau of Standards, National Cancer Institute, Federal Emergency Management Agency, Radiation Research Society, National Council on Radiation Protection and Measurements, and Commission of European Communities, will be held at the National Bureau of Standards, Gaithersburg, Maryland, on June 21–24, 1982. The conference will address the chemical, biochemical, and biological aspects of the effects of ionizing radiation and of chemical carcinogens and agents capable of altering these effects. The program will focus on the protection against acute (radiation sickness and lethality) and long-range (mutation and carcinogenesis) effects. In particular, it will address the relationships between protection from ionizing radiation and chemical carcinogens, pursue correlations of free-radical chemistry and the observed biological phenomena, and, finally, attempt to establish immunological, physiological, and nutritional criteria for "intrinsic resistance" toward radiation and chemical insults.

The conference will consist of 6 half-day sessions with 5–6 invited speakers per session, a panel discussion, and a poster session for contributed papers. Abstracts for posters will be required by May 1, 1982. For further information contact Ms. Kathy C. Stang, Materials Building B-348, National Bureau of Standards, Washington, D.C. 20234 (telephone: 301-921-3295 or Dr. M. G. Simic, 301-921-2374).

Design and Analysis of Scientific Experiments

The Massachusetts Institute of Technology will offer this one-week elementary course on July 12–17, 1982. Applications will be made to the physical, chemical, biological, medical, engineering, and industrial sciences, and to experimentation in psychology and economics. The course will be taught by Professors Harold Freeman and Paul Berger.

Further particulars may be obtained in writing to the Director of Summer Session, Room E19-356, Massachusetts Institute of Technology, Cambridge, Massachusetts 02139.

Veterinary Cancer Society

The executive committee of the Veterinary Cancer Society invites veterinarians and other health-related professionals to join our organization. The Veterinary Cancer Society is a non-profit educational organization whose objectives include promoting: 1) high standards of diagnosis, treatment, and prevention of animal cancers; 2) interdisciplinary research in neoplastic diseases of animals; 3) collection and dissemination of information about animal neoplasms; and 4) the design, implementation, and evaluation of studies of animal neoplasms, including cooperative clinical trials.

The Veterinary Cancer Society meets at least twice annually and publishes a quarterly newsletter. For the last two years we have cosponsored symposiums on clinical trial/protocol design at Purdue University.

Annual dues are currently $20. Interested persons should obtain an application for membership from Dr. Darryl N. Biery, Treasurer, Veterinary Cancer Society, University of Pennsylvania, School of Veterinary Medicine, Philadelphia, Pennsylvania 19104.

☆ U.S. GOVERNMENT PRINTING OFFICE: 1982-361-145/52

blank page

blank page

68/4

NEWARK PUBLIC LIBRARY
MAY 12 1982
U.S. GOVT. PUBS.
DEPOSITORY 376

JNCI

Journal of the National Cancer Institute

April 1982
Volume 68
Number 4

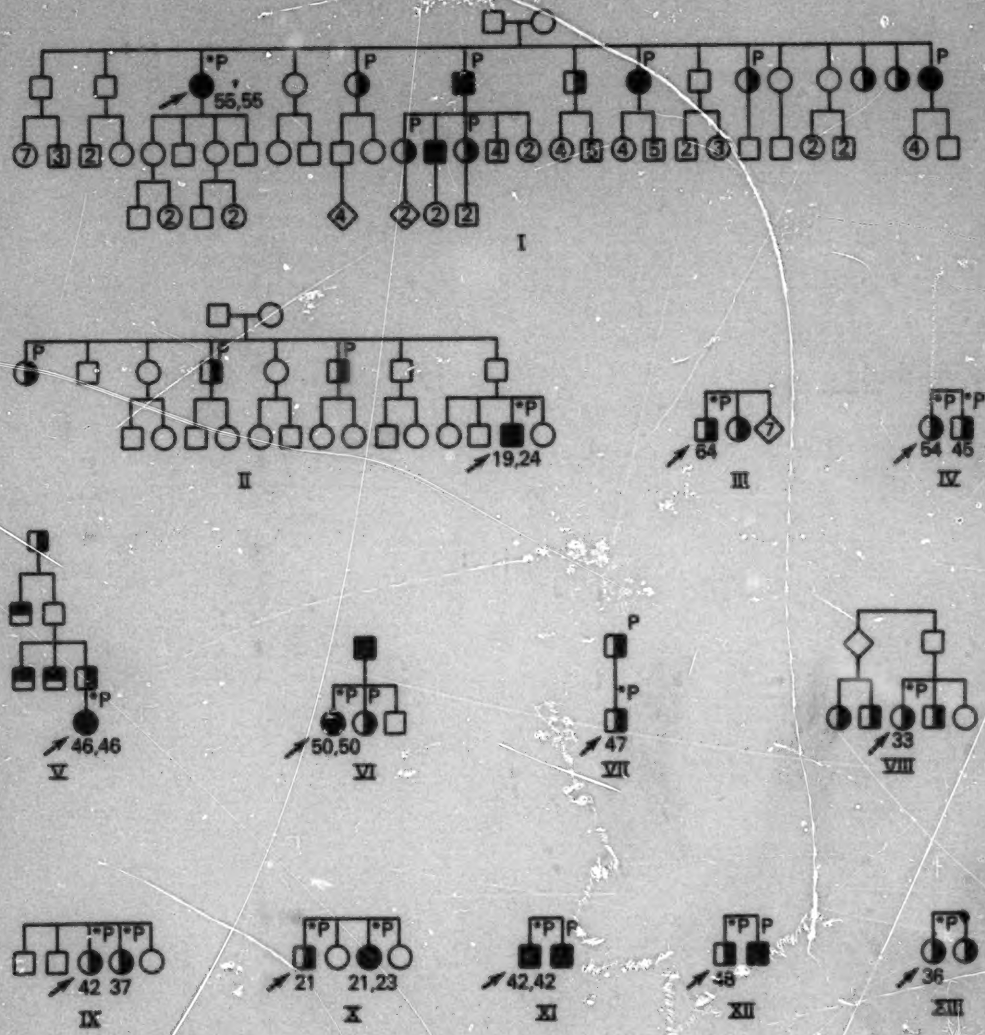
*P
55,55
P
P
P
P
P
P
7
3
2
2
4
2
2
4
4
2
3
2
2
4
4
5
2
3
2
2
4
I
P
P
P
P
*P
19,24
II
*P
7
64
III
*P
*P
54
45
IV
*P
46,46
V
*P
P
50,50
VI
P
*P
47
VII
*P
33
VIII
*P
*P
42
37
IX
*P
*P
21
21,23
X
*P
P
42,42
XI
*P
P
48
XII
*P
36
XIII

U.S. DEPARTMENT OF HEALTH AND HUMAN SERVICES Public Health Service National Institutes of Health

HE 20.3161:

The cover illustration depicts the pedigrees of 13 families showing carotid body tumors (see paper by Parry et al. on pages 573–578).

JNCI

Journal of the National Cancer Institute

April 198
Volume 68
Number 4

THE JOURNAL of the National Cancer Institute solicits manuscripts on original observations in laboratory and clinical research from all scientists. A manuscript is considered for publication with the understanding that it has not been published previously and is submitted exclusively to the Journal. Opinions expressed by the authors are not necessarily those of the publisher or its editors.

THE JOURNAL is published monthly (two volumes a year). The Secretary of Health and Human Services has determined that the publication of this periodical is necessary in the transaction of the public business required by law of this Department.

A MONOGRAPH SERIES covering proceedings of scientific meetings pertaining to cancer is also published. These books may be purchased from the Superintendent of Documents. Series subscriptions are not available and monographs are not included in a subscription to the Journal.

THE JOURNAL is for sale by the Superintendent of Documents, U.S. Government Printing Office, Washington, D.C. 20402. Price per copy, $6.00. Subscription price for two volumes per year in the United States, $65.00; foreign, $81.25. Payment is required in advance, and check or money order should be made payable to the Superintendent of Documents.

All inquiries regarding purchase of subscriptions or depository library distribution, including inquiries about missing issues and change of address, should be addressed to the Government Printing Office. The Government Printing Office requires payment in advance on all orders. Inquiries regarding missing issues or change of address for official subscriptions should be addressed to the Editorial Office, Room 850, Westwood Building, 5333 Westbard Avenue, Bethesda, Md. 20016.

VINCENT T. DEVITA, JR., *Director, National Cancer Institute*

BOARD OF EDITORS

PETER GREENWALD, *Editor in Chief*
ELIZABETH K. WEISBURGER, *Assistant Editor in Chief*
STUART A. AARONSON, *Associate Editor*
CHARLES H. EVANS, *Associate Editor*
MARY A. FINK, *Associate Editor*
JANET W. HARTLEY, *Associate Editor*
DONALD HENSON, *Associate Editor*
RONALD B. HERBERMAN, *Associate Editor*
GEORGE S. JOHNSON, *Associate Editor*
KURT W. KOHN, *Associate Editor*
ARTHUR S. LEVINE, *Associate Editor*
JOHN J. MULVIHILL, *Associate Editor*
ALAN S. RABSON, *Associate Editor*
RICHARD M. SIMON, *Associate Editor*

EDITORIAL STAFF

EDWIN A. HAUGH, *Managing Editor*
PAMELA T. ALLEN, *Assistant Managing Editor*
FLORENCE I. GREGORIC, *Monograph Editor*
Editors: DOROTHY D. KATZ, MERCEDES B. LA CHARITY,
I. AGNES REVESZ, JOAN O'BRIEN RODRIGUEZ,
CONSTANCE R. STONESTREET, and ANNA B. WITTIG

JNCI (NIH Publication No. 82-13)

U.S. DEPARTMENT OF HEALTH AND HUMAN SERVICES Public Health Service National Institutes of Health

Instructions to Authors

Text: Send one original and two copies. **Text-figures** (graphs, charts, and line drawings): Send one original and two copies. **Figures** (photomicrographs and photographs): Send three original glossy prints, unmounted. **Tables:** Send tabular material in typewritten form; do not submit tables as glossy prints to be photographed. The entire manuscript including footnotes, legends, and references must be typed double spaced. Single-spaced portions of a manuscript will be returned to the author for retyping. The mailing address is: Journal of the National Cancer Institute, Westwood Building, Room 850, 5333 Westbard Avenue, Bethesda, Maryland 20016.

Manuscripts should be accompanied by a covering letter from the author responsible for correspondence about the manuscript. The covering letter should contain a statement that the manuscript has been seen and approved by all authors and that all persons listed as authors have made significant (not merely administrative, technical, or supervisory) contributions to the content of the paper. The letter should also state that the manuscript or substantial portions thereof have not been previously published nor are they under consideration for publication in another journal.

Data too extensive for inclusion in a manuscript, but which may be of interest to other investigators, may be deposited with the National Auxiliary Publications Service (NAPS), c/o Microfiche Publications, P.O. Box 3513, Grand Central Station, New York, New York 10017. Authors using the NAPS facilities should indicate in a footnote how their additional data may be obtained.

TITLE: Be brief (no more than 14 words, if possible), but for indexing purposes include all key words. The annual subject index is prepared directly from the titles. Titles that form complete sentences are not acceptable. Do not use abbreviations or chemical formulas in titles.

BYLINE: Supply the complete first name, middle initial, and last name of each author. Avoid use of nicknames. Academic degree is optional; however, if a degree is provided for one author, it should be provided for all authors on a manuscript. Include the name of the institution, address, and zip code for each author. Indicate address for reprint requests in a footnote on the byline.

ACKNOWLEDGMENTS: Financial aid in support of research should be recognized in a footnote. Aid in technical fields, animal care, photography, stenography, and other areas may be mentioned in a separate footnote. Indicate the title (Dr., Mr., Mrs., Miss, Ms.) and affiliation of each person acknowledged.

ABSTRACT: Provide an abstract, 150 words or less, on a separate page. The abstract should describe only *results* of the work being reported. Speculation, historical background, or reference to published works will be deleted from abstracts. Any inbred strains, noninbred stocks, cell lines, or other living materials used in the work should be noted in the abstract.

TEXT: Avoid the use of laboratory jargon and abbreviations not in common usage. When possible, refrain from the use of abbreviations that form words (exceptions are PAGE, ALL). Whenever possible, write mathematical equations and chemical formulas on a single line; submit complicated chemical structures as artwork. Avoid repetition of data in the text when it is presented in tables or text-figures.

Use the following style sources: Webster's *Third New International Dictionary* and Dorland's *Illustrated Medical Dictionary* (25th ed) for spelling; *Council of Biology Editors Style Manual* (4th ed) for scientific abbreviations and symbols; *Government Printing Office Style Manual* for other abbreviations and symbols, punctuation, and hyphenation; *Biochemical Nomenclature and Related Documents* (IUB, 1976) for abbreviations of chemical substances; *Enzyme Nomenclature*, recommendations (1978) of the IUB for recommended names of enzymes and information on nomenclature of isozymes; *The Merck Index* (9th ed) for chemical compounds; "Standard Nomenclature for Inbred Strains of Mice: Seventh Listing" by Joan Staats (Cancer Res 1980;40: 2083–2128) for inbred mouse strains; "Standardized Nomenclature for Inbred Strains of Rats: Fourth Listing" by Joan Staats and Michael Festing (Transplantation 1973;16:221–245) for designations of inbred rat strains; *Animals for Research* (9th ed) prepared by the Institute of Laboratory Animal Resources, National Academy of Sciences, for designations of laboratory animal stocks and strains.

TABLES: Submit tabular material typed double spaced on a separate page. Computer print-outs of tables are acceptable only if they are double spaced and with satisfactory title, column headings, legends and other textual material. Provide headings for all columns of a table and indicate units of measurement where applicable.

TEXT-FIGURES: Refer to graphs, charts, and line drawings as text-figures. Make the abbreviations on text-figures identical to the abbreviations used in the text and legends. Symbols and lettering should be large enough to be legible if reduced. Glossy prints or original drawings in black ink are acceptable; orient vertically instead of horizontally.

FIGURES: Refer to photomicrographs and photographs as figures. Figures and their legends should fit a 7.5- by 9-inch dimension. Calculate that nine typewritten lines of legend will require 1 inch of vertical space. Type figure legends on a separate sheet and identify in the legend any lettering used on the figure. Trim photographs to show only important areas. Do not number face of photographs; use the back or overlay to indicate the top and number of each. Printed indicators may be included on photographs; do not use hand-drawn indicators. *Insert internal scale markers on all photomicrographs.* Color photographs must be grouped as a single plate. For color reproduction, submit both color transparencies and high-quality black and white reproductions. The need for color must be documented before it will be considered.

REFERENCES: Use any recent issue of the Journal as a style guide for reference lists. Number references in order of citation in both text and reference list. For periodicals, provide author(s), title of paper, journal, year, volume, and first and last page numbers. For books, give the author(s), title, name(s) of editor(s), location and name of publisher, year, pertinent chapter or section title, and page numbers. Follow *Index Medicus* for punctuation and abbreviations. Citations of papers in preparation or submitted for publication, unpublished observations, and personal communications should be noted parenthetically in the text. Do *not* include them in the reference list. The accuracy of all references is the responsibility of the authors and not of the editorial staff.

LETTERS TO THE EDITOR should pertain to recent articles in the Journal and should not contain new data unless relevant to the discussion of a particular paper. The authors addressed will be invited to reply to comments before correspondence is published. Letters will be edited by the Staff, subject to contributor approval.

FURTHER DETAILS on the preparation of manuscripts are set forth in the document "Uniform Requirements for Manuscripts Submitted to Biomedical Journals" prepared by the International Steering Committee of medical editors (*see* Am Rev Respir Dis 1979;119:3–10/Ann Intern Med 1979;90:95–99/Br Med J 1979;1:532–535/ or Lancet 1979;1:428–430).

UNITED STATES GOVERNMENT PRINTING OFFICE, WASHINGTON, D.C.: 1982

Table of Contents

Vol. 68, No. 4—April 1982

Investigations on Man

537 Oral contraceptive use and malignant melanoma — *Christopher Bain, Charles H. Hennekens, Frank E. Speizer, Bernard Rosner, Walter Willett, Charlene Belanger*

541 5-Fluorouracil, 1,3-bis(2-chloroethyl)-1-nitrosourea, and 1-(2-chloroethyl)-3-(4-methylcyclohexyl)-1-nitrosourea: Effect on the human granulopoietic system — *Hans-Peter Lohrmann, Karin A. Lepp, Wolfgang Schreml*

549 T_G cell involvement in the leukocyte adherence inhibition phenomenon — *S. G. Taylor IV, Patricia C. Saffold, Donald P. Braun, Jules E. Harris*

555 Interferon effect on cytotoxicity of peripheral blood and tumor-associated lymphocytes against human ovarian carcinoma cells — *Paola Allavena, Martino Introna, Cristiana Sessa, Costantino Mangioni, Alberto Mantovani*

563 Morphologic transformation and chromosomal changes induced by chemical carcinogens in skin fibroblasts from patients with familial adenomatosis coli — *Michiko Miyaki, Noriko Akamatsu, Tetsuo Ono, Akira Tonomura, Joji Utsunomiya*

573 Carotid body tumors in humans: Genetics and epidemiology — *Dilys M. Parry, Frederick P. Li, Louise C. Strong, J. Aidan Carney, David Schottenfeld, Ronald R. Reimer, Seymour Grufferman*

579 Lymphocyte fluorescence polarization changes after phytohemagglutinin stimulation in the diagnosis of colorectal carcinoma — *Glenn R. Hocking, Jennifer M. Rolland, Richard C. Nairn, Eric Pihl, Alan M. Cuthbertson, Edward S. R. Hughes, William R. Johnson*

585 Prevalence and correlates of anticipatory nausea and vomiting in chemotherapy patients — *Gary R. Morrow*

589 Retinoic acid-induced growth inhibition and morphologic differentiation of human neuroblastoma cells in vitro — *Neil Sidell*

Investigations on Nonhuman Systems

597 Gaseous formaldehyde and hydrogen chloride induction of nasal cancer in the rat — *Roy E. Albert, Arthur R. Sellakumar, Sidney Laskin, Marvin Kuschner, Norton Nelson, Carroll A. Snyder*

605 Enhancement of skin tumorigenesis by cigarette smoke condensate following β-irradiation in rats — *John F. McGregor (with revisions by D. K. Myers)*

613	Survival of mouse mammary gland transplants of normal, hyperplastic, and tumor tissues exposed to X-rays	*Leslie J. Faulkin, Dan J. Mitchell, Robert D. Cardiff, Marvin Goldman*
619	Bile acids: Effects on absorption of 1,2-dimethylhydrazine and 7,12-dimethylbenz[*a*]-anthracene in the colon of the rat and guinea pig	*Richard C. Rose, David L. Nahrwold*
623	Liver DNA bound in vivo with aflatoxin B_1 as a measure of hepatocarcinoma initiation in rainbow trout	*Mark Whitham, Joseph E. Nixon, R. O. Sinnhuber*
629	B16 melanoma cell variants: Irreversible inhibition of growth and induction of morphologic differentiation by anthracycline antibiotics	*Avraham Raz*
639	Differing stem cell self-renewal of lectin-separated murine bone marrow fractions	*Andrew L. Salner, Jane E. Obbagy, Samuel Hellman*
643	Immunologic relatedness of intracisternal A-particles in mouse embryos and neoplastic cell lines	*Thomas T. F. Huang, Jr., Patricia G. Calarco*
651	Methylazoxymethanol: Effect on the immune response of rats to human serum albumin	*Ahmed F. S. A. Habeeb, Alan M. Preston, Priscila Sanabria, Nelson Escobales*
657	Peptidoglycans extracted from gram-positive bacteria: Expression of antitumor activity according to peptide structure and route of injection	*Anne-François Goguel, Geneviève Lespinats, Charles Nauciel*
665	Rat hepatomas: Chemotherapy with Lycurim and Pyrazofurin	*May S. Lui, Robert C. Jackson, Ronald J. Harkrader, George Weber*
669	Liver tumors induced by a new beta-adrenoreceptor blocking agent in female rats	*Giovanni Ragnotti, Marco Presta, Laura Riboni, Teresa Zavanella*
673	Mechanisms of immunologic eradication of a syngeneic guinea pig tumor. I. Quantitative analysis of adoptive immunity	*Suyu Shu, James T. Hunter, Herbert J. Rapp, Leila S. Fonseca*
681	Esophageal carcinogenesis in F344 rats by nitrosomethylethylamines substituted in the ethyl group	*William Lijinsky, Joseph E. Saavedra, Melvin D. Reuber, Sandra S. Singer*
685	Induction and transplantation of murine skin cancers induced by methoxsalen plus ultraviolet (320–400 nm) radiation	*M. L. Kripke, W. L. Morison, J. A. Parrish*
691	Influences of age and anatomical site on ultraviolet carcinogenesis in BALB/c mice	*Peter Ebbesen, Margaret L. Kripke*

Announcements

695 American Cancer Society National Conference—The Primary Care Physician and Cancer

695 Eleventh Annual Meeting of the International Society for Experimental Hematology

695 Workshop on "Coagulation, Cancer, and Inflammation"

695 Approaches to the Management of Pain

695 Eighth Biannual Morris Hepatoma Symposium

695 Fourteenth Meeting of the International Society for Pediatric Oncology (SIOP)

695 Second International Congress of the T. and L. de Beaumont Bonelli Foundation for Cancer Research

695 Large Bowel Cancer: Biology and Control

blank page

Oral Contraceptive Use and Malignant Melanoma[1,2]

Christopher Bain, *M.B., B.S.*,[3,4] **Charles H. Hennekens**, *M.D.*,[3,5,6] **Frank E. Speizer**, *M.D.*,[3]
Bernard Rosner, *Ph.D.*,[3] **Walter Willett**, *M.D.*,[3] *and* **Charlene Belanger**, *M.A.*[3,7]

ABSTRACT—There was no overall relationship between a prior history of oral contraceptive (OC) use and the development of melanoma among 141 cases of nonfatal malignant melanoma and 2,820 age-matched controls drawn from respondents to a large postal survey of registered U.S. nurses; crude relative risk (RR) was 0.93 and 95% confidence limits (CL) were between 0.64 and 1.36. Adjustment for a number of additional variables did not alter this estimate materially. Duration of OC use and interval since first use were similarly unrelated to the occurrence of melanoma. For women diagnosed before age 40, there was a crude positive association of "ever" use of OC and melanoma (RR=1.78; 95% CL, 1.11–2.86). However, adjustment for geography and other variables diminished this association and rendered it statistically not significant (RR=1.43; 95% CL, 0.83–2.46). These data do not support the hypothesis that OC use is an independent risk factor for melanoma.—JNCI 1982; 68:537–539.

The possibility that OC use causes melanoma was first raised in a case report in 1968 (*1*). The findings of one prospective study of small sample size have provided some support for this correlation (*2*). Moreover, the hypothesis is consistent with existing biological knowledge. Specifically, OC use alters skin pigmentation in some women (*3*) and estrogen receptors have been identified in human melanomas (*4*, *5*), whereas injection of estrogen and progesterone into guinea pigs has been shown to increase melanocyte numbers and skin melanin content (*6*). This study examines the relationship of OC use with melanoma in case-control data.

METHODS

In 1976, questionnaires were mailed to all married female registered nurses 30–55 years of age who resided in 11 of the larger U.S. states and who were listed in the 1972 register of the American Nurses' Association. Of 172,413 nurses receiving questionnaires, 121,964 completed and returned them. Further details are given in a previous publication (*7*). Information was obtained about a history of any previous diagnosis of cancer, including specific type, and about current and past use of OC, including dates of starting and stopping each interval of use.

Among the respondents 142 reported a diagnosis of malignant or unspecified melanoma or malignant mole of the skin, generally without noting location, subsequent to 1960, when OC were first marketed commercially in the United States (*8*). A pathology report or a pathology note in the discharge summary was obtained for 85 cases, and the diagnosis was confirmed for 84 of them; the one uncertain diagnosis was excluded from all analyses. Thus the analyses were based on 141 cases of which 30 were described as the superficial spreading type, 1 as nodular, and the remainder as simply melanoma. For each case, 20 controls matched on year of birth were selected at random from the total group of respondents. OC use was defined as use at least 1 month prior to the date of diagnosis for each case, which was also used as the index date for her 20 controls; duration of use was the sum of all intervals of use prior to diagnosis. Where pertinent, additional variables were similarly related to date of diagnosis.

The strength of the association between OC use and melanoma was assessed by computing RR. These RR were adjusted for potential confounding variables by a multiple logistic regression procedure (*9*). For each RR, 95% CL were obtained (*10*); for the logit estimates, $\mathrm{CL}=e^{(\ln \mathrm{RR} \pm 1.96\ \mathrm{SE})}$ was applied.

RESULTS

There was no overall association between prior use of OC and a diagnosis of melanoma (RR=0.93; 95% CL, 0.64–1.36) (table 1). A logistic regression analysis adjusting for age at diagnosis, state of residence (grouped as Northern, Southern, or Central States), parity, age at first pregnancy, height, and prior hair dye use did not materially change this estimate for "ever" use of OC (RR=0.82; 95% CL, 0.53–1.27). These variables were included in the analyses because they either influence a woman's hormonal status (parity, age at first pregnancy) or demonstrated some association with a diagnosis of melanoma in crude analyses of these data. No information was collected on skin color.

The only significant predictor of increased risk in the logistic analysis was geography: The RR for those living in Southern States (Florida, Texas, and California) was 2.73 (1.63–4.59) compared with dwellers in Central States (New Jersey, Maryland, Pennsylvania, and Ohio). There was a

---

ABBREVIATIONS USED: CL=confidence limits; OC=oral contraceptive(s); RR=relative risk(s).

---

[1] Received February 4, 1981; revised August 21, 1981; accepted October 19, 1981.

[2] Supported by Public Health Service grants CA-16686 and CA-23645 from the National Cancer Institute.

[3] Channing Laboratory, Department of Medicine, Brigham and Women's Hospital and Harvard Medicine School, Boston, Mass. 02115.

[4] *Present address*: Department of Social and Preventive Medicine, University of Queensland Medical School, Brisbane, Australia.

[5] Recipient of Public Health Service Research Career Development Award HL-00286 from the National Heart and Lung Institute.

[6] *Address reprint requests to* Dr. Hennekens at Channing Laboratory, 180 Longwood Ave., Boston, Mass. 02115.

[7] We are indebted to the registered nurses who are participating in the study, and to the American Nurses' Association and the State Boards of Nursing for their help. We also thank Mr. David Dysert, Ms. Barbara Egan, and Ms. Inge Judge for assistance in parts of this research; Ms. Marion Garneau for performing the computer analyses; and Ms. Sherry Mayrent for editorial assistance.

TABLE 1.—*Crude and adjusted RR of melanoma among women who had, at any time, used OC, compared with those who never used OC*

Age at diagnosis, yr	No. of exposed cases	Crude RR (95% CL)	Adjusted RR (95% CL)
All women	41	0.93 (0.64–1.36)	0.82 (0.53–1.27)
<40	29	1.78 (1.11–2.86)	1.43 (0.83–2.46)
40–49	12	0.45 (0.23–0.86)	0.37 (0.17–0.79)

lesser excess risk for residents of Northern States (Connecticut, Massachusetts, Michigan, and New York), RR=1.84 (1.13–3.01).

There was no significant excess risk with increasing duration of use of OC (table 2). Again, this result was not altered by adjustment for all additional variables combined in logistic regression analysis. Similar results were obtained when the interval since the first use of OC was considered, and no consistent trend was evident when duration and interval were considered together.

Age-specific RR estimates (tables 1 and 2) indicate positive crude relationships with melanoma for women diagnosed before age 40 for "ever" use of OC and for 2 years or more of use. However, as shown in the tables, multivariate adjustment diminished the magnitude of these associations and rendered them statistically not significant. Among this subgroup of younger women, the strongest relationship with melanoma was for those who had used OC for more than 2 years and had started OC use at least 10 years prior to diagnosis, yielding RR=2.95 (1.16–7.49), based on 5 exposed cases. Again, the association was reduced in a logistic analysis, yielding RR=2.31 (0.77–6.94). Corresponding deficits of exposed cases existed among women diagnosed after age 40. As shown in table 3, the OC–melanoma association was significantly greater in women less than or equal to 39 years of age compared with those 40 and older ($P<0.001$ (*11*).

Restricting analysis of the relationship between OC use and melanoma to the 84 pathologically confirmed cases produced results similar to those obtained with the use of the entire data set. However, the statistical significance of the OC–melanoma associations among those with diagnoses at young ages were diminished or eliminated due to the smaller sample size.

Current or recent OC use did not exhibit different relationships with melanoma risk from those reported above for "ever" use.

DISCUSSION

The results of this study do not lend support to the general hypothesis that OC use predisposes to the development of malignant melanoma, although the adjusted RR of 0.82 (95% CL, 0.53–1.27) is compatible with up to a 27% excess risk among "ever" users of OC. The marginally significant crude association between OC use and melanoma among women diagnosed at younger ages decreases in strength and is no longer significant when the effects of other variables are controlled. The CL are wide, and a positive relationship cannot be excluded with certainty, particularly when considering the excess risk among younger women. As always, however, results of subgroup analyses should be interpreted cautiously, especially in view of the corresponding diminished risk among older women. The substantial decreases in RR among the younger women after adjustment for a few factors suggest that they may be even further diminished if more precise information had been obtained for other potentially confounding variables. These variables would include actual sun exposure, for which geography may be a crude marker (*12*), the use of protective sun screens and clothing, and skin color (*13–16*). In addition, because the etiology of the disease is so poorly understood, it is possible that other unknown sources of confounding might also have been present.

The lack of specific information on skin color merits comment. With the presumption that all cases were white, if blacks formed a substantial proportion of the control group and had used OC more than whites, a spurious lowering of the estimated risk could have occurred. However, a survey of the membership of the American Nurses' Association in 1974 recorded only 3.4% as black (American Nurses' Association: Unpublished data). With the use of this as the best estimate of the proportion of controls who were black, and with the extreme assumption that all had used OC, the overall RR for whites is still less than 1.0.

Because the study was based on responses to a postal questionnaire, the results concern only nonfatal cases of melanoma. This situation could lead to bias only if the fatality rates were different among users and nonusers of OC. In that regard, there is some evidence that hormonal factors may influence prognosis (*17–18*). In addition, most melanomas fall into one of two distinct histologic types [superficial spreading and nodular melanoma (*19*)], which could have different causes. Because nodular lesions have a worse prognosis (*19*) and are therefore likely to be underrepresented in our data, an association between OC use and fatal melanoma cannot be dismissed on the basis of the present findings. Various other sources of bias might exist in

TABLE 2.—*Crude and adjusted RR of melanoma among women using OC for various durations, compared with those who never used OC*

Age at diagnosis, yr	Duration of use, mo	No. of exposed cases	Crude RR (95% CL)	Adjusted RR (95% CL)
All women	1–24	18	0.83 (0.50–1.39)	0.84 (0.47–1.49)
	25+	23	1.04 (0.65–1.66)	0.83 (0.47–1.46)
<40	1–24	12	1.36 (0.71–2.60)	1.21 (0.59–2.48)
	25+	17	2.29 (1.30–4.02)	1.73 (0.88–3.39)
40–49	1–24	6	0.49 (0.21–1.15)	0.49 (0.18–1.30)
	25+	6	0.42 (0.18–0.98)	0.29 (0.11–0.81)

TABLE 3.—*Estimated RR of melanoma among younger and older women who had used OC previously compared with those who never used OC*

Age at diagnosis, yr	OC	Cases	Controls	RR
<40	+	29	394	1.78
	−	46	1,114	
40–49	+	12	413	0.45
	−	37	573	

this study (7, 20), but they are unlikely to have influenced the present findings.

The etiology of malignant melanoma remains poorly understood. Recent reviews have had nothing explicit to say about the risk factors other than that sun exposure is probably implicated (19, 21), and only a few small analytical studies have been reported previously (2, 13-15). The current study does not provide support for the existence of a causal association between OC use and melanoma, but it does not definitely exclude such a relationship, particularly among younger women and for fatal disease. Neither the current investigation nor the only other analytical study of OC use and melanoma reported to date (2) has specific information about sun exposure. Concurrent information on both variables will be necessary to reach more definitive conclusions about the part OC use may play in the development of melanoma. In addition, as the importance of dietary factors in the etiology and prevention of many cancers is becoming increasingly obvious (22-23), data on food consumption should be gathered to broaden our understanding of the causal pathways for melanoma and to allow study of interrelationships between OC use, diet, and melanoma.

In summary, the present study does not confirm previous suggestions of an overall association between OC use and melanoma, although it does raise the possibility that use of OC at younger ages for long periods may predispose to the development of this cancer. Further analytic studies of this relationship are needed that pay particular attention to histologic type of tumor (19, 24) and possibly to tumor site (2), as well as to potential confounding variables, especially to details of sun exposure and diet.

REFERENCES

(1) Ellerbroek WC. Oral contraceptives and malignant melanoma. JAMA 1968; 206:649-650.

(2) Beral V, Ramcharan S, Faris R. Malignant melanoma and oral contraceptive use among women in California. Br J Cancer 1977; 36:804-809.

(3) Jelinek JE. Cutaneous side effects of oral contraceptives. Arch Dermatol 1970; 101:181-186.

(4) Fisher RI, Neifeld JP, Lippman ME. Oestrogen receptors in human malignant melanoma. Lancet 1976; 2:337-339.

(5) Chaudhuri PK, Walker MJ, Briele HA, Beattie CW, Das Gupta TK. Incidence of estrogen receptor in benign nevi and human malignant melanoma. JAMA 1980; 244:791-793.

(6) Snell RS, Bischitz PG. The effect of large doses of estrogen and estrogen and progesterone on melanin pigmentation. J Invest Dermatol 1960; 35:73-82.

(7) Hennekens CH, Speizer FE, Rosner B, Bain CJ, Belanger C, Peto R. Use of permanent hair dyes and cancer among registered nurses. Lancet 1979; 1:1390-1393.

(8) Westoff CF, Ryder NB. Experience with oral contraception in the United States, 1960-1965. Clin Obstet Gynecol 1965; 11:734-752.

(9) Armitage P. Statistical methods in medical research. London: Blackwell, 1971.

(10) Miettinen OS. Estimability and estimation in case-referent studies. Am J Epidemiol 1976; 103:226-235.

(11) Woolf B. On estimating the relation between blood group and disease. Ann Hum Genet 1955; 19:251-253.

(12) Greenland S. The effect of misclassification in the presence of covariates. Am J Epidemiol 1980; 112:564-569.

(13) Gellin GA, Kopf AW, Garfinkel L. Malignant melanoma: A controlled study of possibly associated factors. Arch Dermatol 1969; 99:43-48.

(14) Lancester HO, Nelson J. Sunlight as a cause of melanoma: A clinical survey. Med J Aust 1957; 1:452-456.

(15) Klepp O, Magnus K. Some environmental and bodily characteristics of melanoma patients. A case-control study. Int J Cancer 1979; 23: 482-486.

(16) McCarthy WH, Black AL, Milton GW. Melanoma in New South Wales: An epidemiologic survey 1970-76. Cancer 1980; 46:427-432.

(17) Hersey P, Morgan G, Stone DE, McCarthy WH, Milton GW. Previous pregnancy as a protective factor against death from melanoma. Lancet 1977; 1:451-452.

(18) Rampen FH, Mulder JH. Malignant melanoma: An androgen-dependent tumour? Lancet 1980; 1:562-565.

(19) McGovern VJ. Aetiology of melanoma; classification and histological reporting; spontaneous regression; frozen section diagnosis. In: Milton GW, ed. Malignant melanoma of the skin and mucous membrane. New York: Churchill-Livingstone, 1977;1-25.

(20) Barton J, Bain C, Hennekens CH et al. Characteristics of respondents and non-respondents to a mailed questionnaire. Am J Public Health 1980; 70:823-825.

(21) Elwood JM, Lee JA. Recent data on the epidemiology of malignant melanoma. Semin Oncol 1975; 2:149-154.

(22) Doll R. The epidemiology of cancer. Cancer 1980; 45:2475-2485.

(23) Anonymous. Vitamin A and cancer. Lancet 1980; 1:575-576.

(24) McGovern VJ, Mihm MC, Bailly C, et al. The classification of malignant melanoma and its histologic reporting. Cancer 1973; 32: 1446-1457.

blank page

5-Fluorouracil, 1,3-Bis(2-chloroethyl)-1-nitrosourea, and 1-(2-Chloroethyl)-3-(4-methylcyclohexyl)-1-nitrosourea: Effect on the Human Granulopoietic System[1,2,3]

Hans-Peter Lohrmann,[4] Karin A. Lepp,[4] *and* Wolfgang Schreml[4,5]

ABSTRACT—The reaction pattern of the normal (nonleukemic) human granulopoietic system to single-agent treatment with 5-fluorouracil (FUra) and to a combination of FUra with two nitrosoureas, 1,3-bis(2-chloroethyl)-1-nitrosourea (BCNU) and 1-(2-chloroethyl)-3-(4-methylcyclohexyl)-1-nitrosourea (MeCCNU), was studied serially by morphologic and in vitro culture methods. The granulopoietic toxicity of FUra was acute and rapidly (by day 21) reversible. In contrast, the toxicity of the combination regimens was long lasting. Evidence exists that an early toxicity (that of FUra) and a delayed toxicity (that of the nitrosourea) were overlapping. Toxicity of BCNU and MeCCNU was most pronounced at the level of in vitro colony-forming units of the granulopoietic system (G-CFU$_C$). G-CFU$_C$ compartments of bone marrow and peripheral blood continued to be reduced in size at the time of recovery of the peripheral blood granulocyte count from nitrosourea-induced toxicity. This finding may be responsible for the cumulative toxicity to the human hematopoietic system that frequently has been observed after repeated administration of nitrosourea compounds.—JNCI 1982; 68:541–547.

Toxicity to the hematopoietic cell-renewal systems is a typical side effect of most cytotoxic drugs. For many of these drugs, this toxicity determines maximal tolerated doses and/or minimal time intervals between successive courses. For the majority of alkylating agents (with the exception of busulfan), antimetabolites, vinca alkaloids, and cytotoxic antibiotics, the cytotoxic drug-induced bone marrow failure is of short duration (*1*). However, the toxicity produced by the nitrosoureas does not fit this general pattern. A characteristic feature of the nitrosoureas is the long duration of hematotoxicity that follows single or short-term administration both in experimental animals (*2–12*) and humans (*13–20*). Studies in animal models have defined the reactions of the granulopoietic system at its different levels to nitrosoureas; similar data are not available for humans.

The increasing use of nitrosourea compounds in the treatment of human malignant diseases (*21, 22*) prompted us to study the effect of BCNU and MeCCNU on the human granulopoietic system. For clinical reasons, both drugs were administered in combination with FUra; therefore, the effect of FUra monotherapy on the human granulopoietic system also was studied. Our findings demonstrated that nitrosoureas depress the G-CFU$_c$ for a prolonged period of time. The observation that peripheral blood SNG recover in the presence of a continued depletion of the G-CFU$_c$ compartment may explain the cumulative toxicity frequently observed after repeated administration of nitrosoureas.

MATERIALS AND METHODS

Patients and treatment.—Twelve patients (ages 29–70 yr; median age, 64 yr) were treated with FUra for metastatic gastrointestinal tumors. The drug was given iv at a dose of 12.5 mg/kg body weight on each of 5 successive days.

As part of a clinical study on the effect of adjuvant chemotherapy for gastric cancer, 9 patients (ages 40–68 yr; median age, 62 yr) were treated with a combination of FUra (10 mg/kg, iv, on days 1–5) plus BCNU (40 mg/m^2 body surface area, iv, on days 1–5) after gastrectomy.

Twelve patients (ages 24–68 yr; median age, 55 yr) were treated with FUra (10 mg/kg, iv, on days 1–5), vincristine (1.4 mg/m^2, iv, on day 1), plus MeCCNU (175 mg/m^2, orally, on day 1) for various metastatic gastrointestinal tumors. MeCCNU was provided by the Investigational Drug Branch, Division of Cancer Treatment, National Cancer Institute, Bethesda, Md.

None of the patients had been pretreated with cytotoxic agents or radiotherapy before this study, and none had evidence of bone metastases as determined by X-rays, scintigrafy, and marrow aspirates. The patients had given informed consent, and they were aware that participation in the hematologic investigation program was not a prerequisite for treatment and that their participation could be stopped at any time during treatment.

Hematologic studies.—Bone marrow was aspirated from the posterior iliac crest after local anesthesia on day 0 (before drug administration) and, whenever possible, weekly thereafter during the first treatment course. The marrow (4–5 ml) was aspirated into a syringe containing 1 ml of sterile isotonic disodium EDTA solution. For preparation of marrow smears, approximately 1 ml of marrow was aspirated into a second EDTA-coated syringe after the position of the aspiration needle had been changed. Most aspirations were done by one of two physicians, and attempts were made to standardize as much as possible the variables of the aspiration technique (site and depth of aspiration, suction force,

---

Abbreviations used: BCNU=1,3-bis(2-chloroethyl)-1-nitrosourea; G-CFU$_c$=in vitro colony-forming units of the granulopoietic system; MeCCNU=1-(2-chloroethyl)-3-(4-methylcyclohexyl)-1-nitrosourea; SNG=segmented neutrophilic granulocytes.

---

[1] Received March 5, 1981; revised July 15, 1981; accepted September 25, 1981.

[2] Supported by the Deutsche Forschungsgemeinschaft (Sonderforschungsbereich 112, A6).

[3] Research procedures were in accord with the ethical standards of the Ethical Committee on Human Research, University of Ulm.

[4] Department of Internal Medicine, Division of Hematology–Oncology, University of Ulm, Steinhövelstrasse 9, D 7900 Ulm, Federal Republic of Germany.

[5] We gratefully acknowledge the excellent technical assistance of Mrs. Iris Repple and Ms. Felicitas Haber.

aspiration volume). Samples of venous peripheral blood were collected in heparinized syringes before each bone marrow aspiration.

The techniques of preparation of bone marrow and peripheral blood for G-CFU$_c$ cultures and the details of the culture technique were described in (*23, 24*). A single-layer agar (0.3%) culture was used; as a source of colony stimulating activity, 10% of human placenta-conditioned medium (*23*) was added. Cultures were set up in the presence of 15% fetal calf serum and were incubated for 10 days at 5% CO_2 in air in a humidified incubator. Colonies were defined as cell aggregates of more than 50 cells.

The details of the [^{3}H]thymidine suicide technique, performed to assess the proliferative activity of bone marrow G-CFU$_c$ after cytotoxic agent administration, were previously described (*25*). The "suicide fraction" indicates the percentage G-CFU$_c$ loss after in vitro incubation with radioactive [^{3}H]thymidine of high specific activity. The greater the suicide fraction, the greater was the proliferative activity of the G-CFU$_c$ population under study.

Morphologic evaluation of bone marrow smears.—Bone marrow differentials were obtained by differentiating at least 300 well-preserved bone marrow cells in at least 10 different parts of technically well-prepared Pappenheim-stained bone marrow smears. Erythrocyte:granulocyte ratios were calculated from the number of cells in the erythroid and granulocytic series. The proliferative granulocytic pool was defined as myeloblasts to myelocytes, and the maturing granulocytic pool as megamyelocytes to segmented neutrophils (*26*).

Estimation of bone marrow compartment sizes.—Any study of the effect of cytotoxic agents on human bone marrow is limited by the lack of methods to determine repeatedly at short intervals the human bone marrow compartment sizes. Both in vitro progenitor cell culture data and bone marrow differential counts provide relative data. Because marrow composition and bone marrow cellularity change at the same time after chemotherapy, such relative data provide rather limited information on the cytotoxic drug-induced changes of the bone marrow. This information is comparable to that provided by peripheral blood differential counts without knowledge of the absolute leukocyte counts.

In an effort to circumvent this methodologic problem, we assessed the usefulness of the bone marrow cell concentration of marrow aspirates, obtained under standardized conditions, as an index of the cellularity of human bone marrow. Although bone marrow aspirates do not always reflect accurately the marrow cellularity, some investigators have found the method to be of some value (*27, 28*). From our own experience with a rather large population of patients treated for primary breast cancer with adjuvant chemotherapy (*24*), we found the median bone marrow cell concentration of standard aspirates (corrected for the admixture of peripheral blood nucleated cells) to be a useful index of cytotoxic drug-induced changes in marrow cellularity (*29*). In the same patients, calculation of marrow cellularity from methyacrylate-imbedded sections of marrow spicules yielded comparable data (*30*). Thus we considered the bone marrow cell concentration of the aspirates times the relative number of cells in the marrow compartment under study as an index value for the compartment's size. These values were normalized, the pretreatment value being 100%. This method cannot provide exact data; however, from our experience we believe the time course of these compartment indices to be considerably more meaningful than that obtained only from the relative numbers of a given cell type.

Statistical anaylsis.—Statistical analysis was done by means of a program for a desk computer (model 983A; Hewlett-Packard Co., Palo Alto, Calif.) and the two-sided Mann-Whitney *U*-test.

RESULTS

Peripheral Blood SNG

Text-figure 1 shows the longitudinal changes of peripheral blood SNG after administration of the three drug regimens. Monotherapy with FUra caused a decline in blood granulocyte counts after day 5; nadirs were reached on day 21, and recovery to supranormal values were reached by day 28. After treatment with both nitrosourea-containing drug regimens, peripheral blood SNG similarly reached nadirs on day 21; however, in contrast to monotherapy with FUra, granulocyte counts recovered only gradually thereafter, and pretreatment values were not reached by day 35 and day 42 for MeCCNU and BCNU, respectively.

Peripheral Blood G-CFU$_c$

Chemotherapy-induced changes of the peripheral blood G-CFU$_c$ pool size (G-CFU$_c$/liter) are included in text-figure 1. After administration of FUra, a transient decrease occurred in the peripheral blood G-CFU$_c$ pool size; lowest values were reached between days 5 and 7 after treatment initiation. By day 14, recovery was apparent, and repletion of the peripheral blood G-CFU$_c$ pool was completed by day

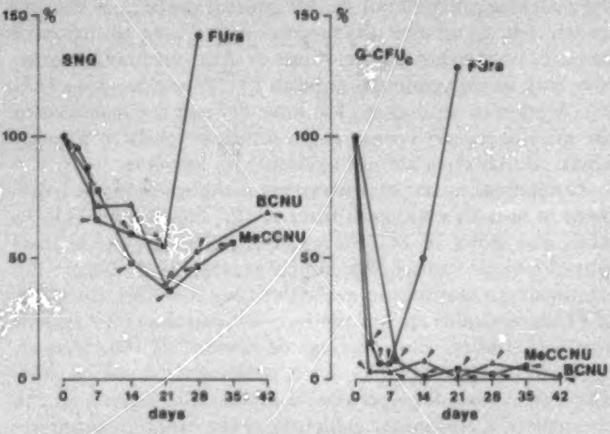

TEXT-FIGURE 1.—Time course of peripheral blood SNG/µl (*left panel*) and peripheral blood G-CFU$_c$/1 (*right panel*) after single-agent therapy with FUra (days 1–5), BCNU (days 1–5) + FUra (days 1–5), and MeCCNU (day 1) + FUra (days 1–5) + vincristine (day 1). Individual values at the different time points were normalized, the pretreatment value being 100%. Median values at the different time points are given. *Arrows* indicate values significantly ($P<0.05$) different from pretreatment values.

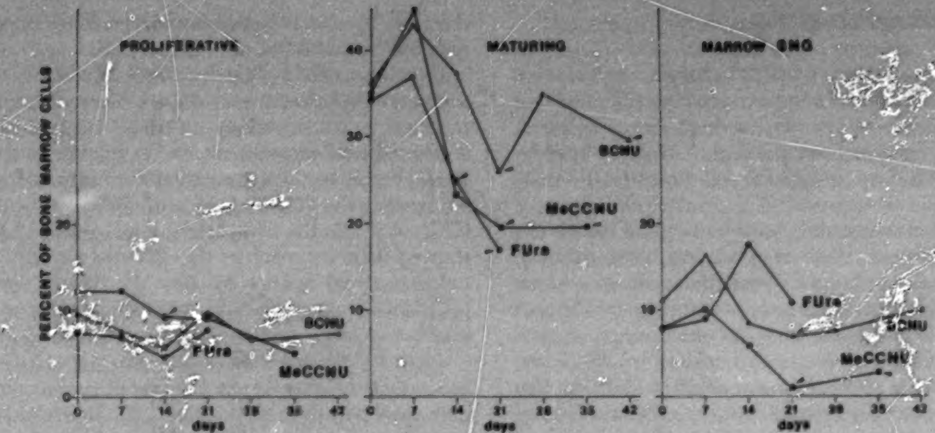

TEXT-FIGURE 2.—Bone marrow differential counts (median values) after treatment with FUra, BCNU + FUra, or MeCCNU + FUra + vincristine. *Proliferative*: proliferating granulocytic compartment (myeloblasts to myelocytes). *Maturing*: maturing granulocytic compartment (metamyelocytes to segmented neutrophils). *Marrow SNG*: segmented neutrophils. For further explanation, *see* legend to text-fig. 1.

21. After MeCCNU therapy, decreases in the peripheral blood G-CFU$_c$ pool size to near-zero values were recorded on days 14, 21, and 28 after chemotherapy; by day 35, there was no G-CFU$_c$ pool size recovery. Similarly, treatment with BCNU was followed by the almost complete disappearance of G-CFU$_c$ from the peripheral blood after day 3. As late as 42 days after treatment, no signs of recovery of the peripheral blood G-CFU$_c$ pool were evident.

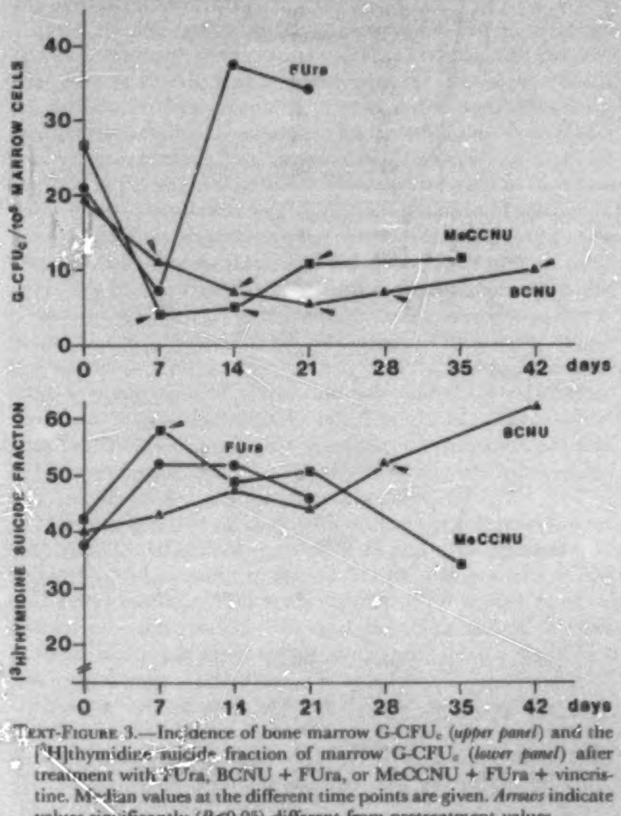

TEXT-FIGURE 3.—Incidence of bone marrow G-CFU$_c$ (*upper panel*) and the [^{3}H]thymidine suicide fraction of marrow G-CFU$_c$ (*lower panel*) after treatment with FUra, BCNU + FUra, or MeCCNU + FUra + vincristine. Median values at the different time points are given. *Arrows* indicate values significantly ($P<0.05$) different from pretreatment values.

Bone Marrow Differentials

The percentages of cells in the proliferating and maturing granulocytic pool and the percentages of bone marrow granulocytes, as derived from bone marrow differential counts, for the three treatment regimens are included in text-figure 2. The percentages of cells in the different granulopoietic compartments reflect not only size changes of these pools but also changes in the nongranulopoietic compartments (e.g., changes within the erythropoietic compartments). Therefore, no clear pattern can be derived from the data. Shortly after chemotherapy, however, a decrease apparently occurs in the relative number of cells in the proliferating granulocytic pool, concomitant with a relative increase of cells in the maturing granulocytic pool.

Incidence and Proliferative Activity of Bone Marrow G-CFU$_c$

Changes in the incidence of bone marrow G-CFU$_c$ (e.g., the number of G-CFU$_c$/10^5 bone marrow cells after administration of the three cytotoxic drug regimens) are shown in text-figure 3. After FUra monotherapy, a transient decrease occurred by day 7, with subsequent rebound to supranormal values by days 14 and 21. In contrast, the number of bone marrow G-CFU$_c$ remained considerably below pretreatment values after treatment with MeCCNU, and even more so after treatment with BCNU.

Included in text-figure 3 are the values for the [^{3}H]thymidine suicide fraction of bone marrow G-CFU$_c$ after cytotoxic drug treatment. After monotherapy with FUra, a small increase occurred in G-CFU$_c$ proliferative activity, but this increase was not statistically significant. Increased values for the proliferative activity of bone marrow G-CFU$_c$ after treatment with MeCCNU and BCNU were noted at some time points; again, these increases were not even marginally statistically significant. Because of the low absolute numbers of G-CFU$_c$ at these later time points after chemotherapy, statistical significance only can be expected when a clear-cut increase occurs in the proliferative activity.

Bone Marrow Compartment Sizes

Text-figure 4 shows the normalized changes with time of the different granulopoietic compartment sizes of the bone marrow after administration of the three drug regimens. Also included is a longitudinal assessment of the cellularity changes and normalized erythroid cell numbers of bone marrow.

After FUra monotherapy, bone marrow cellularity changed little during the first 14 days, but it increased to supranormal values by day 21. Erythroid cells showed an early decrease (day 7) and increases in numbers by days 14 and 21. Among the different granulopoietic marrow compartments, the G-CFU$_c$ were greatly depleted by day 7 and returned to somewhat supranormal values by day 21. The compartment of maturing granulocytic cells was smallest by day 14; by day 21, bone marrow SNG continued to be reduced in numbers.

Bone marrow cellularity after MeCCNU therapy was considerably below pretreatment values through day 21 but returned to pretreatment values by day 35. The number of erythroid cells showed two nadirs by days 7 and 21, respectively, but it returned to highly supranormal values by day 35. Among the granulopoietic compartments, the pool of G-CFU$_c$ was almost completely depleted by days 7 and 14, showed little recovery by day 21, and was still considerably below normal values by day 35. While the number of proliferating granulocytic cells was lowest on day 14, the number of bone marrow SNG reached its nadir by day 21.

After BCNU therapy, bone marrow cellularity reached low values on day 14, increased somewhat by day 21, but decreased again on days 28 and 42. Erythroid marrow cells

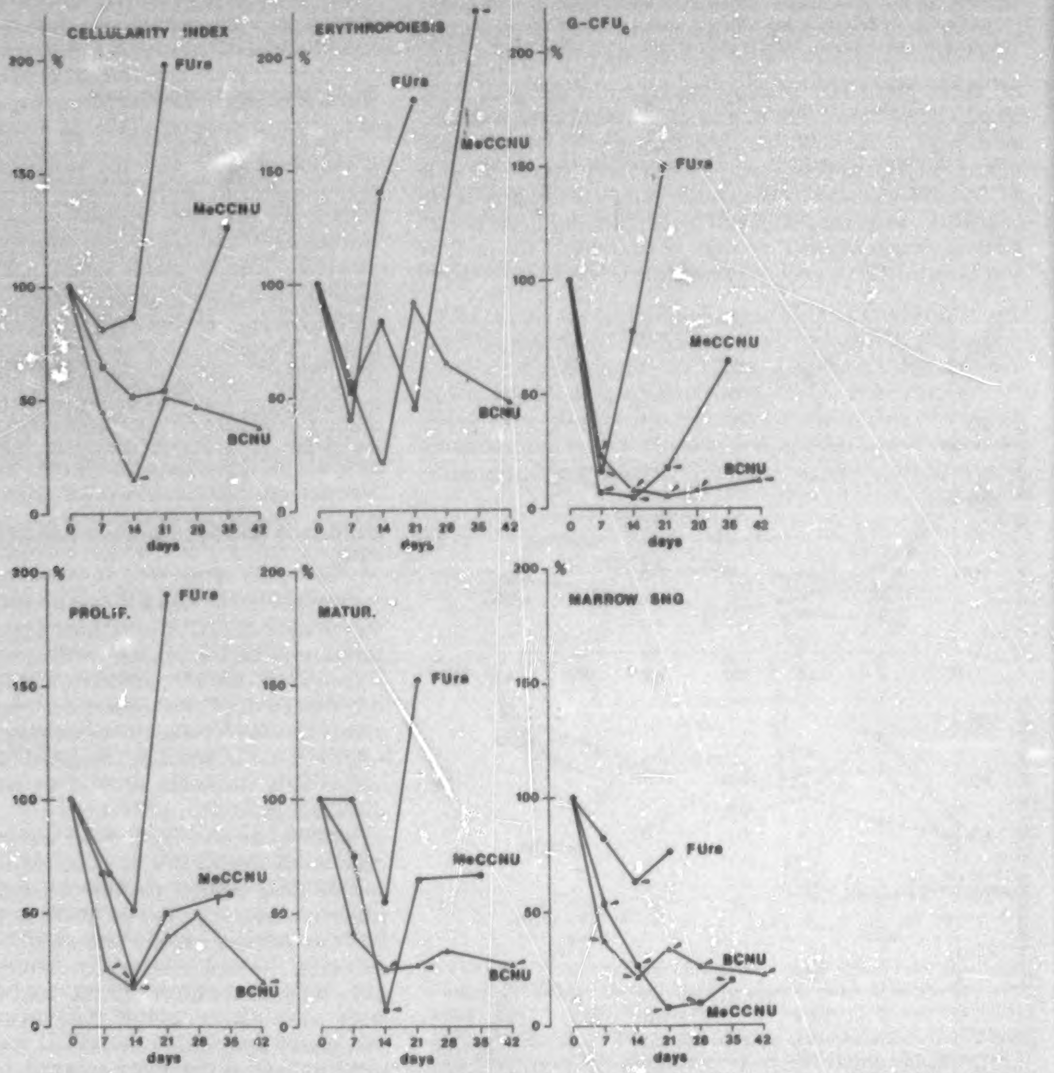

TEXT-FIGURE 4.—Bone marrow cellularity and bone marrow compartment sizes after treatment with FUra, BCNU + FUra, and MeCCNU + FUra + vincristine. Individual values were computed as described in "Materials and Methods" and normalized to the pretreatment value. Median values of the 3 treatment groups at the different time points are given. *Arrows* indicate values significantly different (P<0.05) from pretreatment values.

showed a similar reaction to the chemotherapy. All of the different granulopoietic compartments had decreased by days 7 and 14. By day 21, an abortive rise in the granulocytic proliferative and maturing pools was noted, followed by a second gradual decline. Definitive signs of recovery were not apparent as late as day 42 in any of the hematopoietic marrow compartments. At that time, the extent of recovery was smaller in the G-CFU$_c$ compartment than in the more mature granulocytic compartments.

DISCUSSION

The purpose of this study was to delineate the reaction pattern of a "normal" human granulopoietic system to three cytotoxic drug regimens, two of which contained nitrosourea compounds. However, the rather wide range of pretreatment values and the considerable variability of the changes observed in individual patients after chemotherapy raised the question whether these patients' granulopoietic systems were indeed normal. Disturbance of the hematopoietic system by tumors has been documented both clinically (*31*) and experimentally (*32-34*). Thus we cannot rule out that at least in some of the patients studied, the granulopoietic system was not in an undisturbed state. Nevertheless, the present study may reasonably well indicate the reaction pattern of the human granulopoietic system to the chemotherapy administered. To present the data in the most meaningful way, we chose to present the median rather than the mean values, thus correcting for some of the inhomogeneity in the patient populations under study.

Some of the variables that determine the toxicity of cytotoxic drugs on the granulopoietic system are well known: The dose of the drug is a major variable, but single doses act differently from repeated or split doses; similarly, drug combinations may exert toxicity different from that of the various components (*1*). Such variables may be studied easily in experimental animals. However, studies in humans only can be performed in the framework of an established or experimental treatment protocol, which sometimes may severely limit interpretation of the data. The value of such data lies in the fact that they refer to clinically relevant treatment schedules. For these reasons, the nitrosourea compounds were not given as single agents in the present study but rather in combination with a 5-day schedule of FUra. Also, a single dose of vincristine was added to the combination of FUra and MeCCNU. Thus the present study posed difficulties in defining the direct contribution of each of these cytotoxic drugs to the observed overall hematopoietic toxicity of the combination schedules.

The contribution of vincristine to the granulopoietic toxicity may be estimated from clinical and experimental observations. Vincristine is known for its low hematopoietic toxicity in humans. This is also true at the stem cell level in animal experiments (*35, 36*), and the same animal studies documented rapid hematopoietic recovery from vincristine-induced damage. Therefore, the conclusion is justified that vincristine contributed little if any to the early granulopoietic toxicity observed after treatment with a combination of vincristine, FUra, and MeCCNU, and that vincristine did not contribute to the late toxicity that occurred with this treatment schedule.

The extent and duration of the marrow toxicity exerted by the nitrosoureas alone may result from the differences in reaction pattern after FUra single-agent therapy and from that after FUra in combination with one of the nitrosoureas. A rather comprehensive picture of the cytotoxic drug-induced changes of the human granulopoietic system after administration of the three drug regimens may be drawn from the morphological differentiation of bone marrow and peripheral blood nucleated cells together with the culture of G-CFU$_c$. Our direct experimental data (text-fig. 1-3), and even more the results of our attempt at quantification of the size changes of the marrow compartments (text-fig. 4), indicate that granulopoietic toxicity is of immediate onset and of long duration after exposure to a combination of a 5-day schedule of FUra with either one of the two nitrosoureas (BCNU or MeCCNU). From comparison of this finding with the toxicity observed after single-agent therapy with FUra (repeated on 5 successive days), FUra apparently is responsible for part or all of the initial toxicity (days 0-21) observed after administration of the drug combinations. Our data do not permit us to exclude the possibility of a contribution from BCNU or MeCCNU to this initial toxicity. However, to ascertain whether such a contribution is involved, similar studies have to be performed after treatment with BCNU or MeCCNU alone. Our findings do permit us to attribute the delayed and long-lasting granulopoietic toxicity of the combination chemotherapy regimens solely to BCNU or MeCCNU. The abortive granulopoietic recovery noted on day 21 after treatment with FUra plus BCNU (text fig. 4) may reflect the overlap of the early FUra-induced toxicity and the delayed toxicity of the nitrosourea compound.

Our study demonstrated that the granulopoietic system depression is longer lasting after BCNU than after MeCCNU. However, this is not necessarily due to different properties of the two drugs, though BCNU may affect the cell cycle kinetics longer than does MeCCNU (*37, 38*). We gave MeCCNU as a single dose on day 1, whereas we gave BCNU in divided doses for 5 consecutive days. Animal studies on the changes with time in the hematopoietic stem cell compartments have been reported only after single doses of nitrosoureas (*2, 5, 8, 11, 12*) but not after repeated exposure to one of these compounds. Thus we can only speculate that greater damage to hematopoietic stem cells may result from split doses than from a single dose of BCNU.

Delayed hematopoietic toxicity of nitrosoureas has been reported in many experimental and clinical studies. Delayed recovery of pluripotent stem cells after nitrosourea exposure has been documented in experimental animals (*2, 8, 11, 12*). In mice, delayed recovery was accompanied by a low proliferative activity in those stem cells surviving BCNU treatment (*8*). The pattern of depletion and repletion of bone marrow G-CFU$_c$ appears to vary with the different species. Return of the G-CFU$_c$ compartment size to pretreatment values was reported to occur within 6 days in mice (*11, 12*), but normalization of the G-CFU$_c$ compartment in rats was seen only by day 21 (*5*). These and other data (*39, 40*) suggest a preferential kill of pluripotent stem cells by nitrosoureas. Bone marrow cellularity remained depressed for a prolonged period of time after nitrosoureas in both mice (*8*, *10*) and rats (*5*). The duration of nitrosourea-induced peripheral blood granulocytopenia may be dose-dependent (*3*). After treatment with methylnitrosourea (*10*), a second long-lasting neutropenia was observed after an initial short-lasting recovery of peripheral blood neutrophil counts. In humans, delayed leukopenia and granulocytopenia are well-known characteristic side effects of exposure to nitrosoureas (*13-20*); these effects were corroborated in the present study.

The causes of the delayed and long-lasting hematopoietic toxicity after nitrosourea exposure are a matter of discussion. Nitrosoureas preferentially kill pluripotent stem cells. Evidence exists that nitrosoureas preferentially damage the earliest pluripotent stem cells that are endowed with the greatest potential for proliferation and self-replication (*39*, *40*). Considerable time (which is determined by the proliferation kinetics of the granulocytic system) is required until the damage proceeds from the early stem cell level to the granulocyte compartments of bone marrow and blood. Because granulopoietic regeneration originates from pluripotent stem cells, their preferential damage may be responsible for the long duration of the granulopoietic toxicity caused by nitrosoureas.

Finally, nitrosoureas have been reported to induce a long-lasting reduction of the growth fraction of a proliferating cell population (*41*). This observation may provide an additional explanation for the long time required for hematopoietic reconstitution after nitrosourea treatment. It may also explain the failure of murine pluripotent hematopoietic stem cells (*8*) and human G-CFU$_c$ (text-fig. 3) to increase their proliferative activity early after administration of nitrosoureas to an extent similar to that reported after exposure to most other cytotoxic agents. The existence of long-lived metabolites has been suggested as a possible cause of the delayed hematopoietic toxicity of nitrosoureas (*22*). However, bone marrow transplanted within a few days after nitrosourea administration engrafts without any problems both in laboratory animals (*8*, *42*) and humans (*43*, *44*). This, in our opinion, refutes the hypothesis that the long-lived cytotoxic metabolites of nitrosoureas are responsible for their delayed hematotoxicity.

Regenerative rebound of bone marrow and peripheral blood G-CFU$_c$ frequently occurs during granulopoietic regeneration from cytotoxic drugs such as cyclophosphamide or methotrexate, particularly if the preceding cytotoxic drug-induced marrow hypoplasia was severe (*24*, *45*, *46*). No such rebound of bone marrow or peripheral blood G-CFU$_c$ occurred after exposure to the nitrosoureas. [We have also observed (unpublished data) that no rebound of G-CFU$_c$ occurred after repeated courses of nitrosoureas.] The failure of G-CFU$_c$ to regenerate with a rebound lends further support to the above suggestion that the proliferative activity of hematopoietic stem cells remains impaired over a prolonged period after exposure to nitrosoureas.

In clinical practice, the return of peripheral blood SNG from cytotoxic drug-induced depression toward normal is generally and tacitly assumed to indicate return of the granulopoietic compartments toward normal. We have previously demonstrated this assumption to be correct after cyclophosphamide-adriamycin "standard dose" combination chemotherapy (*24*), high-dose cyclophosphamide treatment (*45*), and high-dose methotrexate followed by citrovorum factor rescue (*46*). The present study indicates that recovery of human peripheral blood SNG counts occurs after nitrosourea treatment in spite of the continued depletion of the G-CFU$_c$ pool. A hypothetical explanation for this discrepancy may be a more rapid transit of cells through the depleted G-CFU$_c$ compartment. The slight increase in the proliferative activity of bone marrow G-CFU$_c$ at the time of peripheral blood SNG recovery after BCNU treatment (text-fig. 1, 3) is compatible with this interpretation. Granulocyte production may thus return to near-normal levels, while the progenitor cell compartment remains well below normal size. Furthermore, newly formed SNG apparently are released rapidly into the circulating blood rather than being retained in the bone marrow (text-fig. 2). This mechanism allows maintenance of near-normal peripheral blood SNG concentrations at the expense of a reduced bone marrow granulocyte storage pool.

It is well established clinical practice to readminister the nitrosourea as soon as the peripheral blood SNG count has returned to a normal level. However, repeated administration frequently has been observed to lead to cumulative toxicity (*16*, *19*, *20*). Our data allow a better understanding of this phenomenon: Apparently, in spite of the return of the peripheral blood SNG count to normal, a repeated nitrosourea dose will exert its toxicity on a G-CFU$_c$ pool that is still reduced in size. Conceivably, as in animal studies, the human pluripotent stem cell pool (at this time not accessible for quantiative analysis) undergoes changes that parallel those of the G-CFU$_c$ compartment. Thus the quantitative damage to the stem cell pool(s) will be greater after a second or third nitrosourea dose than after the first one. In addition, repeated exposure to nitrosoureas may lead to qualitative defects in hematopoietic stem cells. The repeated damage exerted by the drugs to the early pluripotent stem cells may lead to cumulative loss of proliferative capacity of the pluripotent stem cell compartment (*35*), curtailing this compartment's capacity to fulfill the demand for increased stem cell output into the hematopoietic cell lines during hematopoietic regeneration from nitrosourea-induced damage.

REFERENCES

(*1*) Lohrmann H-P, Schreml W. Cytotoxic drugs and the granulopoietic system. Berlin, Heidelberg, and New York: Springer, 1981.

(*2*) Blackett NM, Courtenay VD, Mayer SM. Differential sensitivity of colony-forming cells of hemopoietic tissue, Lewis lung carcinoma, and B16 melanoma to three nitrosoureas. Cancer Chemother Rep 1975; 59:929-933.

(*3*) Denine EP, Harrison SD, Peckham JC. Qualitative and quantitative toxicity of sublethal doses of methyl-CCNU in BDF$_1$ mice. Cancer Treat Rep 1977; 61:409-417.

(*4*) Fox PA, Panasci LC, Schein PS. Biological and biochemical properties of 1-(2-chloroethyl)-3-(β-D-glucopyranosyl)-1-nitrosourea (NSCD 254157), a nitrosourea with reduced bone marrow toxicity. Cancer Res 1977; 37:783-787.

(*5*) Haas RJ, Rohruber W, Netzel, B, Lau E. Effects of CCNU on hematopoiesis in rats. Cancer Treat Rep 1979; 63:377-383.

(*6*) Nagourney RA, Fox P, Schein PS. A comparison of the biological and biochemical properties of 1-(4-amino-2-methylpyrimidin-5-yl)methyl-3-(2-chloroethyl)-3-nitrosourea and 2-[3-(2-chloroethyl)-

3-nitrosoureido]-D-glucopyranose. Cancer Res 1978; 38:65–68.

(7) Panasci LC, Green D, Schein PS. Chlorozotocin. Mechanism of reduced bone marrow toxicity in mice. J Clin Invest 1979; 64:1103–1111.

(8) Pressler HD, Henderson ES. Effect of cytosine arabinoside and 1,3-bis(2-chloroethyl)-1-nitrosourea on hematopoietic precursors in the mouse. J Natl Cancer Inst 1971; 47:971–977.

(9) Reissman KR, Udupa KB, Kawada K. Effects of erythropoietin and androgens on erythroid stem cells after their selective suppression by BCNU. Blood 1974; 44:649–657.

(10) Seidel HJ. Hematologic effects of a single dose of methylnitrosourea. Exp Hematol 1977; 5:19–26.

(11) Udupa KB, Reissmann KR. Acceleration of granulopoietic recovery by androgenic steroids in mice made neutropenic by cytotoxic drugs. Cancer Res 1974; 34:2517–2520.

(12) Udupa KB, Reissmann KR. In vivo erythropoietin requirements of regenerating erythroid progenitors (BFU-e, CFU-e), in bone marrow of mice. Blood 1979; 53:1164–1171.

(13) Ahmann DL, Bisel HF, Hahn RG. A phase 2 evaluation of 1-(2-chloroethyl)-3-(4-methylcyclohexyl)-1-nitrosourea (NSC 95441) in patients with advanced breast cancer. Cancer Res 1974; 34:27–30.

(14) DeVita VT, Carbone PP, Owens AH, Gold GL, Krant MJ, Edmonson J. Clinical trials with 1,3-bis(2-chloroethyl)-1-nitrosourea, NSC-409962. Cancer Res 1965; 25:1876–1881.

(15) DeVita VT, Gold GL, Owens AH, Miller JM. Preliminary studies with 1,3-bis-(2-chloroethyl)-1-nitrosourea (BCNU). Proc Am Assoc Cancer Res 1964; 5:15.

(16) Fewer D, Wilson CB, Boldrey EB, Enot JK. Phase II study of 1-(2-chloroethyl)-3-cyclohexyl-1-nitrosourea (CCNU; NSC-79037) in the treatment of brain tumors. Cancer Chemother Rep 1972; 56:421–427.

(17) Hildebrand J, Badjou R, Collard-Ronge E, et al. Treatment of brain gliomas with high dose of CCNU and autologous bone marrow transplantation. Biomedicine 1980; 32:71–75.

(18) Moertel CG, Reitemeier RJ, Hahn RG. Therapy of advanced gastrointestinal cancer with 1-3-bis-(2-chloroethyl)-1-nitrosourea (BCNU). Clin Pharmacol Ther 1968; 9:652–656.

(19) Ward HW. Central nervous system tumors of childhood treated with CCNU, vincristine, and radiation. Med Pediatr Oncol 1978; 4:315–320.

(20) Young RG, Walker MD, Canellos GP, Schein PS, Chabner BA, DeVita VT. Initial clinical trials with Methyl-CCNU 1-(2-chloroethyl)-3-(4-methylcyclohexyl)-1-nitrosourea (MeCCNU). Cancer 1973; 31:1164–1169.

(21) Carter SK, Schabel FM, Broder LE, Johnston TP. 1,3-bis-(2-chloroethyl)-1-nitrosourea (BCNU) and other nitrosoureas in cancer treatment: A review. Adv Cancer Res 1972; 16:273–332.

(22) Oliverio VT. Pharmacology of the nitrosoureas: An overview. Cancer Treat Rep 1976; 60:703–707.

(23) Lohrmann, H–P, Hansi W, Heimpel H. Human placenta-conditioned medium for stimulation of human granulopoietic precursor cell (CFU-C) colony growth in vitro. Blut 1978; 36:81–88.

(24) Lohrmann H–P, Schreml W, Lang M, Betzler M, Fliedner TM, Heimpel H. Changes of granulopoiesis during and after adjuvant chemotherapy of breast cancer. Br J Haematol 1978; 40:369–381.

(25) Lohrmann H–P. Thymidine-suicide of human granulocytic progenitor cells (CFU-C). Biomedicine 1978; 28:319–323.

(26) Cronkite EP, Vincent PC. Granulocytopoiesis. Ser Hemat 1969; 4 (suppl II): 3–43.

(27) Blackett NM, Gordon MY. Observations on the distribution of granulocytic progenitor cells (CFU-C) in human bone marrow: The importance of the manner in which the results of in vitro cultures are reported: Reply. Br J Haematol 1978; 40:355–356.

(28) Coiffier B, Sicard B, Bryon PA, Germain D. Observations on human bone marrow granulocytic progenitor cell culture: A comparison of two ways to express results. Br J Haematol 1980; 44:335–337.

(29) Lohrmann H–P. Das Reaktionsmuster der normalen menschlichen Granulopoiese auf zytostatische Chemotherapie. Ph.D. thesis. Ulm: University of Ulm, 1979.

(30) Schreml W, Kubitza P, Lohrmann H–P. Attempt at quantification of the cytotoxic drug-induced changes of the human bone marrow compartments. Scand J Haematol, 1982. In press.

(31) Robinson WA. Granulocytosis in neoplasia. Ann NY Acad Sci 1974; 230:212–218.

(32) Keeb CR, Lala PK. Effects of Ehrlich ascites tumor transplantation in mice on the distribution of cells capable of forming hemopoietic colonies in vitro. Eur J Cancer 1978; 14:331–342.

(33) Lala PK. Hemopoietic stem cells in tumor bearing hosts. In: Cairnie AB, Lala PK, Osmond DG, eds. Stem cells of renewing cell populations. New York: Academic Press, 1976: 343–355.

(34) Reincke U, Burlington H, Carsten AL, Cronkite EP, Laissue JA. Hemopoietic effects in mice of a transplanted, granulocytosis-inducing tumor. Exp Hematol 1978; 6:421–430.

(35) Jenkins VK, Costanzi JJ, Ellis HN. Effects of single and combined chemotherapeutic agents on hemopoietic stem cells in mice. Am J Hematol 1976; 1:79–88.

(36) Smith WW, Wilson SM, Fred SS. Kinetics of stem cell depletion and proliferation: Effects of vinblastine and vincristine in normal and irradiated mice. J Natl Cancer Inst 1968; 40:847–854.

(37) Young RC. The effect of methyl CCNU (NSC-95441) on the cellular kinetics of normal and leukemic murine tissues in vivo. Cell Tissue Kinet 1973; 6:35–43.

(38) Young RC, DeVita VT. The effect of chemotherapy on the growth characteristics and cellular kinetics of leukemia L1210. Cancer Res 1970; 30:1789–1794.

(39) Botnick LE, Hannon EC, Hellman S. Nature of the hemopoietic stem cell compartment and its proliferative potential. Blood Cells 1979; 5:195–206.

(40) Trainor KJ, Morley AA. Screening of cytotoxic drugs for residual bone marrow damage. J Natl Cancer Inst 1976; 57:1237–1239.

(41) DeVita VT, Bray DA, Bostick F, Bagley CM. The effect of chemotherapy on the growth of leukemia L1210. II. Persistence of a nitrosourea-induced change in the growth characteristics of transplant generations. Cell Tissue Kinet 1972; 5:459–466.

(42) Stevens EE, Dicke KA. Bone marrow transfusion in mice treated with BCNU. Proc Am Ass Cancer Res 1976; 17:57.

(43) Graw RG Jr, Lohrmann HP, Bull MI, et al. Bone-marrow transplantation following combination chemotherapy immunosuppression (B.A.C.T.) in patients with acute leukemia. Transplant Proc 1974; 6:349–354.

(44) Weiner RS, Richman CM, Yankee RA, Parker L. Clinical results of autotransplantation after nitrosourea therapy. Exp Hematol 1979; 7 (suppl 5):384–388.

(45) Lohrmann H–P, Schreml W, Fliedner TM, Heimpel H. Reaction of human granulopoiesis to high-dose cyclophosphamide therapy. Blut 1979; 38:9–16.

(46) Schreml W, Lohrmann H–P. Effect of high-dose methotrexate with citrovorum factor on human granulopoiesis. Cancer Res 1979; 39:4195–4199.

blank page

T_G Cell Involvement in the Leukocyte Adherence Inhibition Phenomenon[1,2,3,4]

S. G. Taylor IV,[5] Patricia C. Saffold,[5] Donald P. Braun,[5] *and* Jules E. Harris[5,6]

ABSTRACT—Peripheral blood mononuclear cells (PBMC), T-cells, non-T-cells, T_G cells, and T_M cells were tested for leukocyte adherence inhibition (LAI) reactivity to purified protein derivative (PPD) in normal human volunteers to determine the reactive cell subfractions. T-cells were separated by sheep red blood cell rosetting and T_M and T_G cells by rosetting with anti-ox red blood cell (ORBC) IgM- and IgG-treated ORBC. Fresh PBMC, T-cells, and T_G cells gave positive LAI reactivity to PPD in PPD-positive donors only. PBMC that had undergone 24-hour incubation or extensive washing, non-T-cells, and T_M cells were unreactive. All cell subfractions were negative in PPD-negative donors. Indirect LAI assay was performed on the spent media from overnight incubation of unstimulated PBMC and also following a 1-hour incubation of the various cell subfractions obtained from a PPD-reactive donor with PPD. Positive reactions, indicating the release of an LAI factor (LAIF), were obtained with the spent media and with the T-cell and T_G cell subfractions following PPD stimulation, whereas non-T-cell and T_M cell subfractions yielded no reactivity. Incubation of sensitized T-cells with PPD in the presence of cycloheximide and preincubation of T-cells for 24 hours with cycloheximide before PPD exposure failed to inhibit LAI reactivity. These data suggest that T-cells, specifically T_G cells, can release LAIF upon specific antigen stimulation with PPD, whereas non-T-cell and T_M cell subpopulations fail to respond to the same stimulus. LAIF may also be released into the culture media with prolonged (overnight) incubation in artificial media or with extensive washing. Inhibition of protein synthesis during antigen exposure or up to 24 hours before antigen exposure does not appear to inhibit LAI reactivity.—JNCI 1982; 68:549–554.

The LAI assay has been identified as a simple and reliable test of cell-mediated tumor immunity (*1*). Recent studies have correlated positive LAI activity with delayed hypersensitivity reactivity (*2*) and with positive migration inhibition (*3*). Using the hemacytometer glass slide method of the LAI assay, several investigators have identified T-lymphocytes as the active cell population involved in the assay (*4–6*). Substantial evidence has also evolved that the phenomenon of LAI is mediated by a soluble factor (LAIF) (*4, 5, 7*). Using soluble supernatants, Koppi et al. (*8*) have demonstrated the production of a soluble factor (LAIF) by T-lymphocytes and the capacity of this factor to inhibit adherence of normal, nonimmune T- and B-cells, granulocytes, and glass-adherent monocytes.

Others have demonstrated the active participation of macrophages and monocytes armed with cytophilic antibody as a reactive cell population (*9, 10*); these results derive from a different assay technique in which the tube method was used and tests were done for leukocyte nonadherence. Evidence is now substantial that this test is not comparable to the slide method in several respects in addition to the active cell population involved. For instance, evidence for mediation by a soluble factor is lacking (*10*). The tube LAI assay appears more sensitive to antigen concentration and, in patients with advanced disease, may convert to negative while the slide assay remains positive (*10–14*). Immune memory appears to fatigue earlier by the tube method (*11, 13*).

In our evaluation of the slide method of LAI, we have used PPD as an antigen source for testing normal adults. We have confirmed T-lymphocytes to be the active cell population and have further demonstrated the T-cell subset possessing Fc receptors to IgG (T_G cells) as that fraction having persistent LAI activity to this stimulus.

MATERIALS AND METHODS

Healthy volunteers were used as the source for mononuclear cells. PPD was obtained from Connaught Medical Research Laboratories, Toronto, Canada (batch #24) and was diluted with PBS to an initial concentration of 1,000 µg/ml.

Slide LAI assay.—A modification of the method as originally described by Halliday and Miller (*1*) and Halliday (*7*) was used. Cell subfractions were suspended in RPMI-1640 medium at a concentration of 2×10^7 cells/ml, and 0.1 ml was added to plastic tissue culture tubes (Falcon Plastics, Oxnard, Calif). The cells were diluted with 0.05 ml of RPMI-1640 for the controls or with 0.05 ml of PPD diluted to the appropriate concentration in RPMI-1640 for the test samples. To each tube was added 0.05 ml of diluted, heat-inactivated human serum to yield a final concentration of 1×10^7 cells/ml in RPMI-1640 with 25% human serum. The human serum was obtained from a single donor and had been previously tested to exclude nonspecific adherence inhibition activity. All tests were performed with quadru-

---

ABBREVIATIONS USED: FCS=fetal calf serum; HBSS=Hanks' balanced salt solution; LAI=leukocyte adherence inhibition; LAIF=LAI factor; LSM=lymphocyte separation medium; ORBC=ox red blood cell(s); PBMC=peripheral blood mononuclear cell(s); PBS=phosphate-buffered saline; PPD=purified protein derivative; SRBC=sheep red blood cell(s).

---

[1] Received March 17, 1981; revised August 17, 1981; accepted November 27, 1981.

[2] Supported in part by Public Health Service grant CA-25793 from the National Cancer Institute.

[3] Presented in part at a meeting of the American Association for Cancer Research, San Diego, Calif., 1980.

[4] Research procedures were in accord with the ethical standards of the Investigational Review Board, Rush-Presbyterian-St. Luke's Medical Center, and of the Helsinki Declaration of 1975.

[5] Section of Medical Oncology, Department of Internal Medicine, Rush-Presbyterian-St. Luke's Medical Center, 1725 West Harrison St., Chicago, Ill. 60612.

[6] We gratefully acknowledge the technical assistance of Ms. Nadine M. Deak.

plicate samples. The samples were incubated at 37°C for 30 minutes with vigorous shaking every 10 minutes. A sample from each tube was placed on one hemacytometer slide and incubated in 5% CO_2 at 37°C with 100% humidity. After 60 minutes, eight predetermined 0.1×0.1-mm hemacytometer squares were counted in each slide. The cover slips were floated off, the slides were inverted twice in normal saline (once in each direction), a new cover slip was applied, and the same squares were counted again. The percentage cellular adherence (100×cells counted following washing/cells counted before washing) in each square was calculated and a mean plus or minus standard error determined for each sample. The significance of comparisons was determined by Student's *t*-test with $P<0.01$ indicating a positive reaction. All tubes were randomly coded before the first incubation by a nonparticipant in the experiment to prevent investigator bias. The samples were decoded at the time that statistical calculations were performed.

Indirect LAI assay.—PBMC subfractions were prepared as for the direct LAI test with the use of PPD-positive volunteers. These cell fractions were then incubated with or without PPD in the standard fashion except incubation time was increased to 60 minutes. The supernatants were removed and stored at 4°C overnight, with all samples subsequently tested on the same day. Aliquots of 0.1 ml supernatant were added to 0.1 ml of 2×10^6 PBMC collected from a PPD-negative donor and incubated at 37°C for 30 minutes with intermittent shaking. The cells were then placed on hemacytometer slides, and the LAI assay was performed in the usual manner (*8*).

Isolation of leukocyte subfractions.—Whole blood was aseptically collected in preservative-free heparinized tubes, diluted in HBSS, layered onto LSM, and centrifuged to obtain the PBMC layer. The PBMC have been found to contain between 5 and 15% contamination with granulocytes and monocytes (*15*). Residual red blood cells were lysed and platelets removed by slow centrifugation in 0.14 *M* NH_4Cl. Following two more washes, a portion of these cells was resuspended in HBSS, supplemented with 1% bovine serum albumin. We isolated T-cells by rosetting cells in the proportion of 5×10^6 cells (100 µl) with 300 µl of a 2% suspension of SRBC and 300 µl of heat-inactivated, SRBC-absorbed FCS. Tubes were incubated at 37°C for 5 minutes, centrifuged at 200×*g* for 5 minutes, and then incubated overnight at 4°C. The next day, pellets were gently resuspended, layered onto cold LSM, and centrifuged for 15 minutes at 1,600 rpm to obtain the T-cell-enriched and T-cell-depleted layers. The pellet that was enriched for T-cells was resuspended and washed in HBSS and then in 0.14 *M* NH_4Cl. Cells obtained by this method proved to be greater than 95% SRBC rosette-forming cells. Cells in the T-cell-depleted layer were not seen to rosette with sheep cells. A portion of these separate cell populations was tested for PPD reactivity in the LAI assay.

The remaining T-lymphocyte-enriched cells were incubated overnight in RPMI-1640 medium supplemented with 20% FCS and 0.6% gentamicin in a humidified atmosphere of 5% CO_2 in air. The next day, cells bearing receptors for the Fc portion of IgG or IgM were isolated by the ORBC-rosetting techniques of Moretta et al. (*16, 17*) and Ferrarini et al. (*18*). Fresh ORBC were washed in PBS, and a 5% ORBC suspension was prepared in PBS. Subagglutinating concentrations of rabbit anti-ORBC IgG or IgM were mixed with the 5% ORBC suspension and incubated for 1.5 hours at 37°C in the case of IgG or for 45 minutes at room temperature in the case of IgM. Each antibody-coated ORBC preparation was then washed twice with PBS and subsequently resuspended to a final concentration of 1% in HBSS. T_G and T_M rosettes were prepared by the addition of 100 µl of antibody-coated ORBC to each of the 1×10^6 T-cell preparations followed by centrifugation at 200×*g* for 5 minutes and incubation at 4°C for 30 minutes. Rosetting cells were isolated on cold LSM as described above for T-cells. LAI reactivity was assessed in cells enriched for T_G cells or T_M cells. The recovery of cells under these circumstances was about 25% of the initial T-cell-enriched population. For such cell fractionation, 250 ml of whole blood was required from individual donors. Eight volunteers who were reactive to PPD by delayed hypersensitivity skin testing were tested for LAI reactivity, and all were positive. Four

TABLE 1.—*LAI reactivity of cell populations separated by erythrocyte rosetting*

Cell population	Expt No.	Control[a]	PPD[a]	*P*-value[b]
PBMC	1	77.2±1.3	34.3±1.3	<0.001
	2	77.9±0.7	38.3±0.9	<0.001
	3	76.9±1.5	31.0±1.7	<0.001
	4	76.3±0.7	31.9±5.4	<0.001
	5	79.7±1.0	41.3±2.1	<0.001
	6	78.9±0.2	43.1±1.9	<0.001
T-cell-enriched	1	66.8±6.2	34.9±1.8	<0.001
	2	67.9±0.8	38.9±5.8	0.009
	3	77.8±2.5	38.9±4.3	0.002
	4	80.6±1.9	22.0±1.5	<0.001
	5	79.0±1.5	41.3±1.3	<0.001
	6	74.7±1.5	45.8±3.0	<0.001
Non-T-cell-enriched	1	76.9±2.2	73.3±1.0	NS
	2	66.6±1.2	70.2±0.2	NS
	3	77.6±2.0	79.1±1.6	NS
	4	78.9±1.9	78.6±1.2	NS
	5	78.7±1.4	79.7±1.2	NS
	6	76.5±2.4	76.5±1.9	NS

[a] Results are expressed as the mean percentage adherence of four assays ± the standard error.

[b] NS=not significant; all *P*-values >0.005.

TABLE 2.—*Direct LAI reactivity by T-cell subfractions in PPD-positive donors*[a]

Cell population	Expt No.	Control[b]	PPD[b]	*P*-value
PBMC	1	78.9±0.2	43.1±1.0	<0.001
	2	76.3±0.7	31.9±5.4	<0.001
	3	79.7±1.0	41.3±2.1	<0.001
T_G cells	1	78.8±1.4	57.7±0.5	<0.001
	2	72.9±1.6	39.5±3.6	0.001
	3	77.2±1.5	26.9±2.2	<0.001
T_M cells	1	80.9±1.7	77.5±2.2	0.044
	2	71.3±1.8	74.2±2.3	0.934
	3	79.7±1.2	77.5±1.4	0.128

[a] All subfractions were positively isolated with the use of IgG- and IgM-bound ORBC except for T_M cells in experiment 3, which were taken from the T-cells remaining after separation of T_G cells.

[b] Results are mean percentage adherent cells of four assays ± the standard error.

donors who were skin test-negative and nonreactive to PPD in the LAI assay were used as negative controls.

RESULTS

When tested with PPD across a wide range of concentrations, PBMC from skin test-positive donors gave consistently positive results by the LAI assay. No pattern of variation in the LAI reactivity across this range was apparent however, which is consistent with the observation that the LAI assay is a qualitative and not a quantitative assay (*7*). However, the upper and lower concentrations of 100 and 1 µg PPD/2×10⁶ cells gave somewhat variable results. Consequently, a concentration of 10 µg/2×10⁶ cells was used for subsequent experiments. On repeat testing over 1 year's time, no positive donor converted to negative.

Direct LAI With Various Cell Populations

Table 1 summarizes the effect on LAI responsiveness with the use of T-cell-enriched and T-cell-depleted cell populations in 6 donors with reactive PBMC. Whereas the T-cell-enriched cell subpopulation was consistently positive, the non-T-cell subset was always negative.

Further fractionation of T-cells into T_M and T_G cells demonstrated LAI reactivity by T_G cells only. The T_M-enriched subfraction was negative whether this subfraction was actively enriched for T_M cells by IgM-ORBC rosetting (table 2, expts 1 and 2) or whether it was the residual population remaining after T_G cell separation (table 2, expt 3).

LAI reactivity was tested in volunteers who were negative to PPD skin testing. Four donors were tested for LAI reactivity by their PMBC. Two were tested for T-cell reactivity and one for T_G and T_M cell reactivities (table 3). All tests were consistently negative, excluding the possibility that cell subfractionation techniques cause false-positive results.

An additional concern was that some cell separation techniques might impair the ability of the cell subfractions to respond to PPD in the LAI assay due to the nonspecific release of the active LAIF or due to impairment of its synthesis or secretion. Because isolation of either T_G or T_M cells requires six washes or more plus overnight incubation, separate experiments were performed to assess the effect on PBMC by either of these conditions. Table 4 demonstrates that neither extensive washing nor overnight incubation under conditions similar to those used for isolation of the T_G and T_M cell subpopulations affected normal adherence of PBMC to the glass hemacytometer slides, but both did prevent PBMC from specifically reacting to PPD. Thus although T_G and the total T-cell subpopulations are reactive following these procedures, PBMC failed to react. Overnight incubation of whole blood at 25°C with subsequent separation of PBMC resulted in normal reactivity, so that incubation in artificial media was required for loss of LAI response.

TABLE 3.—*LAI reactivity of PPD skin test-negative volunteers with the use of various blood mononuclear cell subpopulations*

Cell population	Expt No.	Control[a]	PPD[a]	*P*-value
PBMC	1	74.1±1.9	63.0±3.5	0.031
	2	72.2±1.5	77.9±0.6	0.995
	3	77.3±1.5	79.1±0.5	0.999
	4	74.9±0.4	75.6±2.3	0.701
T-cell-enriched	2	75.9±1.9	74.5±1.9	0.148
	4	77.2±1.7	76.8±1.8	0.884
Non-T-cell-enriched	2	73.0±2.0	74.0±2.7	0.433
	4	77.3±0.3	76.6±0.1	0.084
T_G-enriched	4	77.4±1.9	77.3±4.1	0.684
T_M-enriched	4	80.5±0.9	80.2±2.8	0.319

[a] Results are mean percentage adherent cells of four assays ± the standard error.

TABLE 4.—*LAI reactivity of PBMC from PPD-positive donors to PPD following exhaustive (six times) washing of cells and immediate testing or overnight incubation of cells*

Methodology	Expt No.	Control[a]	PPD[a]	*P*-value
Standard technique, day 1	1	77.2±1.3	34.3±1.3	<0.001
	2	77.9±0.7	38.3±0.9	<0.001
	3	79.0±1.0	34.5±2.0	<0.001
	4	79.7±1.0	41.0±1.4	<0.001
	5	76.0±1.0	38.9±1.7	<0.001
	6	75.6±1.6	37.6±1.8	<0.001
Washing six times, day 0	2	80.3±1.4	79.2±0.7	0.983
	3	77.2±1.0	80.1±1.3	0.069
Incubation for 24 hr, RPMI-1640 + 20% FCS	1	76.9±2.2	74.7±2.3	0.645
	2	72.8±3.0	70.9±3.8	0.131
	3	52.2±2.3	52.7±2.4	0.575
	4	81.2±1.5	80.7±2.1	0.759
Incubation for 24 hr, whole blood	5	76.8±4.1	25.4±1.8	<0.001
	6	78.1±1.7	28.0±2.7	0.002

[a] Results are mean percentage adherent cells of four assays ± the standard error.

To assess further the reason for loss of LAI reactivity of PBMC following overnight incubation in artificial media, we collected the supernatant of the incubated cells and assessed it for LAIF. Table 5 demonstrates that LAIF activity was present in the spent media, suggesting that overnight incubation led to nonspecific release of this factor into the media. Although the PBMC failed to react under these conditions, T-cells and T_G cells separated from these populations continued to maintain their specific LAI reactivity.

Indirect LAI of Various Cell Subpopulations

Results with the use of the indirect LAI assay confirmed the release of LAIF upon specific antigen challenge by PBMC, T-cells, and T_G cells but not by non-T-cells or T_M cells (table 6). Because of the presence of PPD in the supernatant used for the LAIF assay, it was important to use a PPD-negative donor for tests for LAIF. The negative

TABLE 5.—*Indirect LAI with the use of spent media from 24°C incubation of unstimulated PBMC, demonstrating the presence of an LAIF not present in the control media with 20% FCS*

Expt No.	Control[a]	Spent media[a]	*P*-value
1	72.8±3.0	42.2±1.9	<0.001
2	52.2±2.3	16.1±2.9	<0.001
3	67.9±0.8	18.1±1.1	<0.001

[a] Results are mean percentage adherent cells of four assays ± the standard error.

TABLE 6.—*Indirect LAI assay with the use of supernatants collected following incubation of PPD with various cell subfractions obtained from PPD-positive individuals*[a]

Cell population	Expt No.	Media control[b]	Supernatant of cultures[b]		P-value
			Without PPD[c]	With PPD	
PBMC	1	[illegible]6.3±1.5	77.8±1.4	33.7±2.8	<0.001
	2	76.2±2.6	ND	32.3±4.4	0.005
	3	76.6±1.7	78.7±1.9	47.9±0.9	<0.001
T-cells	2	76.2±2.6	ND	32.0±3.1	0.002
	3	76.3±1.7	81.4±0.6	25.8±2.6	0.001
Non-T-cells	2	76.2±2.6	ND	74.9±1.3	0.136
	3	76.6±1.7	ND	76.3±1.5	0.125
T_G cells	1	75.6±0.9	ND	46.5±1.3	<0.001
	2	76.2±2.6	ND	12.8±2.6	0.001
	3	76.6±1.7	79.6±0.3	24.6±1.5	<0.001
T_M cells	1	75.6±0.9	ND	74.7±3.8	0.406
	2	76.2±2.6	ND	75.6±1.1	0.193
	3	76.6±1.7	78.1±1.5	74.9±1.9	0.083

[a] PBMC from a PPD-negative donor were used for the LAI assay.

[b] Results are mean percentage adherent cells of four assays ± the standard error.

[c] ND=not determined.

donor was the donor in experiment 4 (table 3) whose cells were confirmed to be unresponsive to PPD by direct LAI assay, which was performed concomitantly with the indirect assay. For the control samples, the various cell subsets were incubated in the standard fashion with RPMI-1640 as medium controls; however, when sufficient cells were available, a second control with the use of supernatants from cell subsets incubated without PPD was also run.

The impact of cycloheximide treatment on LAI reactivity was assessed in various experiments. Incubation of 2×10^6 PBMC with up to 50 μg cycloheximide for 1 hour yielded 90% viability by trypan blue exclusion, whereas 100 μg cycloheximide resulted in a decrease to 60% viability. A 24-hour incubation with as little as 10 μg cycloheximide resulted in a decreased viability to 20–30% of cells. T-cell sensitivity to cycloheximide demonstrated the same pattern as PBMC.

To test the adequacy of protein inhibition by cycloheximide, we incubated PBMC from a normal volunteer in leucine-free RPMI-1640 with FCS and phytohemagglutinin at a concentration of 1:500 as a nonspecific mitogen; we used the method of Rosenberg and Levy (*19*). A 1-hour or a 24-hour incubation with as little as 10 μg cycloheximide/ml completely suppressed protein synthesis as evidenced by tritiated leucine uptake. No further suppression by 25- or 50-μg amounts was noted.

Table 7 displays the results of cycloheximide incubation on LAI reactivity. Cycloheximide at 25 μg does not affect the glass adherence of T-cells and has no impact on LAI response to concomitant exposure to PPD. Adding 50 μg cycloheximide to T-cells for 1 hour significantly reduced the glass adherence. Despite this reduction, the concomitant addition of PPD caused further specific LAI reactivity. In addition, incubation of T-cells with 10–50 μg of cycloheximide for 24 hours before PPD stimulation did not prevent glass adherence or the specific LAI reactivity to PPD.

DISCUSSION

Moretta et al., (*16, 17*) and Ferrarini et al. (*18*) have defined subsets of human T-cells on the basis of cell surface receptors for either the Fc portion of IgG (T_G cells) or the Fc portion of IgM (T_M cells). The method used involved enumeration by rosetting T-cells with ORBC coated with subagglutinating doses of either anti-bovine erythocyte IgM or IgG. T-cells rosetting with anti-ORBC were termed "T_G cells," and T-cells rosetting with anti-ORBC IgM were termed "T_M cells."

In a related set of experiments with pokeweed mitogen-stimulated B-cell production of intracytoplasmic antibody, it was established that T_M cells were helper cells and that the T_G cells were suppressor cells (*20*). It was found that up to 20% of human peripheral blood T-cells were T_G cells or suppressor cells, and the bulk of the remainder consisted of T_M cells or helper cells (*21*). The cells could be isolated and separated by differential centrifugation after rosetting with IgM- or IgG-coated ORBC. The two subsets were found to differ in their response to phytohemagglutinin. Subsequent work showed that T_M and T_G cells could also be distinguished on the basis of morphologic and histochemical characteristics (*22*).

That T_G and T_M cells truly represent suppressor and helper T-cells in the peripheral blood of humans has not been definitely established. Indeed, it appears that not all T-cells with a cell surface receptor for the Fc portion of IgG are suppressor cells. Antibody-dependent cellular cytotoxicity and natural killer cell activity have also been described with this subpopulation (*23, 24*). T_M cells may elicit suppression upon interaction with concanavalin A (*25*). Conversion of T_G cells to T_M cells on incubation or upon interaction with immune complexes has been reported (*26*). With these provisos, T_G and T_M determinations do permit separation of subpopulations of T-cells that appear to have distinct functions.

The results of our experiments support these cell separation techniques as yielding functionally distinct cell subsets and indicate that T_G cells, mononuclear cells with receptors for both SRBC and the Fc portion of immunoglobulin G, possess the unique property of specific LAI activity. Others have observed that a small percentage of monocytes may be

TABLE 7.—*Effect of cycloheximide treatment on LAI reactivity of T-cells from a PPD-sensitized donor to PPD*

Cycloheximide incubation time, hr	Cycloheximide, μg	Media control[a]	PPD, 10 μg[a]	Cycloheximide[a]	Cycloheximide + PPD[a]
1	10	85.2±1.5	48.6±2.7	83.7±1.3	43.4±3.1
	25	85.2±1.5	48.6±2.7	80.2±0.7	38.9±1.2
	50	85.2±1.5	48.6±2.7	50.5±2.1	16.8±2.1
	50	74.8±1.8	30.1±3.7	47.4±0.8	13.1±1.7
24	10	75.7±2.4	27.0±2.7	74.7±3.3	23.4±1.3
	10	79.1±1.3	43.9±2.0	73.3±1.6	46.4±4.1
	25	75.7±2.4	27.0±2.7	75.7±1.7	20.0±3.9
	25	79.1±1.3	43.9±2.0	76.2±0.5	44.5±1.8
	50	51.5±1.9		52.0±1.3	10.1±0.8
	50	52.9±1.7		49.2±1.1	11.9±2.6

[a] Results are mean percentage adherent cells ± the standard error.

necessary for LAI activity (*27*). Although small differences in the proportion of accessory cells in the various T-cell subpopulations may exist, the methods utilized for isolation of T-cells in these experiments yield less than 1% monocytes as assessed by latex ingestion and alpha napthylacetate esterase staining. Latex screening of T_G and T_M cells also demonstrates less than 0.1% contamination of these subfractions by monocytes. The fact that neither the non-T-cell nor the T_M cell subpopulations demonstrated LAI activity, with these subpopulations containing the same granulocyte and monocyte contaminants, makes it unlikely that these accessory cells are major participants in this LAI reactivity.

These experiments are consistent with the requirement of a secreted factor (LAIF) for inhibition of leukocyte glass adherence. We have shown that such a factor may be released into the media by overnight incubation in RPMI-1640 with 20% FCS and that exhaustive washing in HBSS or overnight incubation of cells in artificial media will cause a loss of the ability of PBMC to respond to antigen in the LAI assay, although normal glass adherence is not affected. Such a phenomenon seems most consistent with spontaneous release of LAIF by mechanical factors. It is also possible that the FCS may be responsible for the release of LAIF with overnight incubation in consideration of the observation that overnight incubation of unseparated whole blood did not impair LAI activity of PBMC. In any event, LAIF is demonstrable in the spent media after overnight incubation of PBMC; and, while the PBMC remain normally glass-adherent, they are unable to respond to specific antigen. We are unable to explain the observation that PBMC lose their ability to respond under these conditions, whereas T-cells, which constitute the majority of PBMC, will continue to respond under the same conditions when these cells are tested separately.

Specific release of LAIF by antigen challenge of sensitized cell subpopulations was demonstrated by the indirect LAI assay for T-cells as demonstrated by others (*5*, *6*, *8*). We have further characterized the cell subpopulation with this in vitro capacity to be erythrocyte rosette-positive and IgG Fc receptor-positive (T_G) cells. Several explanations for this difference between T_G and T_M cells are possible: T_G cells may bind LAIF more tightly, causing it to be resistant to release by the mechanical stresses and overnight incubation required in the isolation procedures, whereas non-T_G cells selectively lose this factor or the capacity to synthesize it. Thus this cell subpopulation may be the only one to have sufficient LAIF available for specific response to antigen in vitro. We have demonstrated that overnight incubation itself is not responsible for the lack of non-T-cells. Separation of T-cells from non-T-cells can be performed in 1 hour with the use of *Vibrio cholera* neuraminidase-treated SRBC. Separation and testing of T-cell and non-T-cell subfractions in 1 day with the use of this technique have not altered the LAI activity of the respective subfractions. An alternative possibility is that blocking factors may be released by some cell subsets, which then prevent specific LAI reactivity. These cell subsets with blocking activity may be selectively confined to non-T-cell and/or T_M cell subfractions. Active synthesis of LAIF may be a requirement, and only T_G cells may have this capacity. However, the continued LAI activity following 24-hour incubation with cycloheximide (an inhibitor of protein synthesis) argues against de novo protein synthesis as a requirement for specific LAI response by T-cells. Alternatively, a population of T_G cells may be truly distinctive in its ability to secrete LAIF in response to PPD as a specific antigen and thus be the major cell subset producing this lymphokine. Use of available monoclonal antibodies to define and isolate immunologically cell subsets may help to establish which of these several possibilities might explain the specificity of T_G cell LAI reactivity.

REFERENCES

(*1*) Halliday WJ, Miller S. Leukocyte adherence inhibition: A simple test for cell mediated tumor immunity and serum blocking factors. Int J Cancer 1972; 9:477–483.

(*2*) Burger DR, Vandenbark AA, Finke P, et al. Assessment of reactivity to tumor extracts by leukocyte adherence inhibition and dermal testing. J Natl Cancer Inst 1977; 59:317–323.

(*3*) Holt PG, Roberts LM, Fimmel PH, et al. The leukocyte adherence inhibition microtest: A rapid and sensitive procedure for the demonstration of cell mediated immunity in vitro. J Immunol Methods 1975; 8:277–288.

(*4*) Maluish AE, Halliday WJ. Quantitation of anti-tumor cell-mediated immunity by a lymphokine-dependent reaction using small volumes of blood. Cell Immunol 1975; 17:131–140.

(*5*) Creemers P. The role of leukocyte subpopulations in the indirect leukocyte adherence inhibition assay in the mammary tumor virus system. Eur J Immunol 1977; 7:48–53.

(*6*) Powell AE, Sloss AM, Smith RN. Leukocyte adherence inhibition: A specific assay of cell mediated immunity dependent on lymphokine-mediated collaboration between T lymphocytes. J Immunol 1978; 120:1957–1966.

(*7*) Halliday WJ. Leukocyte adherence inhibition and blocking factors in cancer. In: Bloom BR, Daniel JR, eds. In vitro methods in cell-mediated and tumor immunity. Vol 2. New York: Academic Press, 1976:547–554.

(*8*) Koppi TA, Maluish AE, Halliday WJ. Cellular mechanism of LAI. J Immunol 1979; 123:2255–2260.

(*9*) Grosser N, Marti JH, Procter JW, Thomson DM. Tube leukocyte adherence inhibition assay for the detection of antitumor immunity. I. Monocyte is the reactive cell. Int J Cancer 1976; 18:39–47.

(*10*) Marti JH, Grosser N, Thomson DM. Tube leukocyte adherence inhibition assay for the detection of antitumor immunity. II. Monocyte reacts with tumor antigens via cytophilic antitumor antibody. Int J Cancer 1976; 18:48–57.

(*11*) Flores M, Marti JH, Grosser N, MacFarlane JK, Thomson DM. An overview: Antitumor immunity in breast cancer assayed by tube leukocyte adherence inhibition. Cancer 1977; 39:494–505.

(*12*) Thomson DM, Tataryn DN, Schwartz R, MacFarlane JK. Abrogation of the phenomenon of leukocyte adherence inhibition by excess circulating tumor antigen. Cancer 1979; 15:1095–1106.

(*13*) Halliday WJ, Maluish AE, Stephenson PM, Davis NC. An evaluation of leukocyte adherence inhibition in the immunodiagnosis of colorectal cancer. Cancer Res 1977; 37:1962–1971.

(*14*) Maluish AE. Experiences with leukocyte adherence inhibition in human cancer. Cancer Res 1979; 39:644–648.

(*15*) Cobleigh MA, Braun DP, Harris JE. Age-dependent changes in human peripheral blood B-cells and T-cell subsets: Correlation with mitogen responsiveness. Clin Immunol Immunopathol 1978; 15:162–174.

(*16*) Moretta L, Ferrarini M, Durante ML, Mingari MC. Expression of a receptor for IgM by human T cells in vitro. Eur J Immunol 1975; 5:565–569.

(*17*) Moretta L, Ferrarini M, Mingari MC, Moretta A, Webb SR. Subpopulations of human T cells identified by receptors for immunoglobulins and mitogen responsiveness. J Immunol 1976; 117:2171–2174.

(*18*) Ferrarini M, Moretta L, Abrile R, Durante ML. Receptors for IgG. Molecules on human lymphocytes forming spontaneous rosettes with sheep red cells. Eur J Immunol 1975; 5:70–72.

(*19*) Rosenberg SA, Levy R. A rapid assay of cell-mediated immunity to soluble antigens based on the stimulation of protein synthesis. J Immunol 1972; 108:1080–1087.

(*20*) Moretta L, Webb SR, Grossie CE, Lydyard PM, Cooper MD. Functional analysis of two human T cell subpopulations: Help and suppression of B cell responses by T cells bearing receptors for IgM and IgG. J Exp Med 1977; 146:184–200.

(*21*) Moretta L, Mingari MC, Webb SR, et al. Imbalances in T cell subpopulations associated with immunodeficiency and autoimmune syndrome. Eur J Immunol 1977; 7:696–700.

(*22*) Grossi CE, Webb SR, Zicca A, et al. Morphological and histochemical analysis for two human T cell subpopulations bearing receptors for IgM and IgG. J Exp Med 1978; 147:1405–1417.

(*23*) West WH, Boozer RB, Herberman RB. Low affinity E-rosette formation by the human K cell. J Immunol 1978; 120:90–95.

(*24*) West WH, Cannon GB, Kay HD, Bonnard GD, Herberman RB. Natural cytotoxic reactivity of human lymphocytes against a myeloid cell line: Characterization of effector cells. J Immunol 1977; 118:355–361.

(*25*) Hayward AR, Layward L, Lydyard PM. Fc-receptor heterogeneity of human suppressor T cells. J Immunol 1978; 121:1–5.

(*26*) Pichler WJ, Lum L, Broder S. Fc-receptors on human T lymphocytes. I. Transition of Tgamma to Tmu cells. J Immunol 1978; 121:1540–1548.

(*27*) Maluish AE, Ames RS, McCoy JL. Monocyte requirements for production of human leukocyte adherence inhibition factor in response to PPD. Proc Am Assoc Cancer Res 1980; 21:248.

Interferon Effect on Cytotoxicity of Peripheral Blood and Tumor-Associated Lymphocytes Against Human Ovarian Carcinoma Cells[1,2,3]

Paola Allavena,[4] Martino Introna,[4] Cristiana Sessa,[5] Costantino Mangioni,[5] *and* Alberto Mantovani[4,6,7]

ABSTRACT—A study was done to investigate the tumoricidal activity of peripheral blood lymphocytes (PBL) and tumor-associated lymphoid cells (TAL) against freshly isolated tumor cells in human ovarian carcinoma. TAL and carcinoma cells were purified by density and velocity sedimentation on discontinuous Ficoll–Hypaque gradients and fetal bovine serum. Purified carcinoma cells from 23 ascitic and 3 solid tumors were used as targets in a 4- or a 20-hour ^{51}Cr release assay. K562 cells were used to measure natural killer (NK) activity. Freshly purified ovarian carcinoma cells were relatively resistant to lysis by normal unstimulated PBL. Cytolytic activity of ovarian cancer PBL and TAL did not exceed that of control PBL: Only one PBL preparation had high levels of cytotoxicity (36.2 and 42.9% specific lysis after 4 and 20 hr at an effector-to-target cell ratio of 50:1) against autologous cancer cells but not against allogeneic targets (<5% specific lysis). TAL and, to a lesser extent, ovarian cancer PBL showed impaired NK activity against K562 compared to the activity seen in controls. In vitro exposure to partially purified human fibroblast interferon (IFN) (1,000 U/ml for 1–18 hr) augmented NK activity against K562 of PBL and TAL. When ovarian carcinoma cells were used as targets, IFN enhanced the cytotoxicity of normal PBL in a 4- and 20-hour assay; stimulation by IFN was less frequently observed with ovarian cancer PBL and TAL in a 4-hour assay, but after 20 hours effector cells from tumor-bearing subjects showed IFN-boosted cytotoxicity against carcinoma cells similar to the degree of cytotoxicity seen in controls. IFN enhanced the cytotoxicity of PBL and TAL against both autologous and allogeneic carcinoma cells. Thus PBL and TAL are rarely cytotoxic against ^{51}Cr-labeled fresh autologous carcinoma cells, but in vitro exposure to IFN induced low levels of killing of ovarian tumor cells.—JNCI 1981; 68:555–562.

The in vitro cytotoxicity of lymphocytes has been considered one of the expressions of cell-mediated mechanisms of immune defense. For the evaluation of cell-mediated cytotoxicity against tumor cells in cancer patients, in vitro cultured cell lines have been extensively employed (*1*). Several methodologic factors, such as the susceptibility of cultured cells to NK cells (*2*), render the interpretation of the data on cytotoxicity against lines difficult.

Following a different experimental approach, in a series of studies freshly isolated, purified tumor cells, relatively resistant to NK lysis, were used in short-term ^{51}Cr release assays (*3–9*).

PBL from approximately 30% of cancer patients were cytotoxic against autologous tumor cells (*3–6*). In a recent study, in vitro exposure to IFN augmented lysis against allogeneic but not against autologous fresh cancer cells (*6*). Except for lung cancer, which has been studied extensively (*5, 6*), investigators using ^{51}Cr-labeled fresh solid tumor cells have studied heterogeneous series of neoplasms, mainly of mesenchymal origin (*3–6*). In the present study the cytotoxic activity of PBL and TAL was characterized in a homogeneous group of ovarian cancer patients with the use of freshly purified, ^{51}Cr-labeled carcinoma cells as targets.

MATERIALS AND METHODS

Human subjects.—Twenty-four patients with histologically confirmed ascites ovarian epithelial tumors admitted to the Department of Oncology, Clinic Ostetrica e Ginecologica, Università di Milano, formed the case list for this study (table 1). All patients had cancers classified as stages III and IV. Independent pathologists checked for the presence of tumor cells in ascitic fluids.

The control population consisted of 29 age-matched patients admitted to the same clinic for nonmalignant, noninfectious gynecologic disorders (e.g., benign ovarian cysts and myomas) and of 90 normal healthy adult volunteers.

Heparinized venous blood (10–50 ml) was obtained by venipuncture, and carcinomatous ascites was collected by paracentesis or at laparotomy. Solid tumor specimens were obtained during surgery.

PBL.—Blood was diluted 1:4 with PBS (Eurobio, Paris, France), and 40 ml was then placed on 10 ml Ficoll–Hypaque (Eurobio) for centrifugation at 400×*g* for 20 minutes at room temperature. Mononuclear cells were collected at the interface and washed with PBS, and 10–30×10^6 cells were incubated in 10–20 ml of RPMI-1640 medium supplemented with 20% FBS (Gibco-Biocult, Glasgow, Scotland) for 45 minutes at 37°C in plastic petri dishes (#3003; Falcon Plastics, Oxnard, Calif.). Nonadherent cells were collected, centrifuged at 400×*g* for 5 minutes, and finally resuspended in RPMI-1640 medium with 10% FBS or pooled human AB serum and 50 μg gentamicin/ml. Nonadherent cell preparations were only partially depleted of monocytes inasmuch as 2–4% of these cells as compared to 10–30% of the original mononuclear cell suspensions (*9*) were mononuclear phagocytes as assessed by morphology, avid uptake of neutral red,

---

Abbreviations used: A:T=attacker-to-target ratio(s); BME=Eagle's basal medium; FBS=fetal bovine serum; IFN=interferon; LU33=1 lytic U 33; NK=natural killer; PBL=peripheral blood lymphocytes; PBS=phosphate-buffered saline; RCI=relative cytotoxicity index; TAL=tumor-associated lymphoid cells.

[1] Received May 5, 1981; accepted October 22, 1981.

[2] Supported by finalized project "Control of neoplastic growth" from Consiglio Nazionale delle Ricerche, Rome, Italy (contract No. 79.00643.96); by an International Italy–Great Britain grant; and by Public Health Service grant 1-R01CA-26824 from the National Cancer Institute.

[3] Research procedures were in accord with the ethical standards of the Helsinki Declaration of 1975.

[4] Istituto di Ricerche Farmacologiche "Mario Negri," via Eritrea 62, 20157 Milan, Italy.

[5] Iª Clinica Ostetrica e Ginecologica, Università di Milano, via Commenda 12, 20122 Milan, Italy.

[6] *Address reprint requests to* Dr. Mantovani.

[7] We thank Dr. N. Colombo, Dr. P. Molina, and Dr. M. D'Incalci for invaluable help in collection of biologic samples.

TABLE 1.—*Characteristics of ovarian tumor cells used for cell-mediated cytolysis*

Target cell No.	Source	Histologic type	Grade	Stage	Spontaneous release at hr:[a] 4	20
1	Ascites	Serous	3	III	27	50
2	Ascites	Serous	2	III	17	36
3	Ascites	Serous	3	III	29	48
					21	41
4	Ascites	Serous	3	IV	43	47
6	Ascites	Endometrioid	4	IV	20	32
7	Ascites	Undifferentiated	4	III	32	47
8	Ascites	Endometrioid	3	IV	14	25
10	Ascites	Serous	3	IV	6	NT
11	Ascites	Serous	3	IV	19	29
12	Ascites	Serous	4	III	20, 24[b]	34, 41[b]
13	Ascites	Serous	3	III	31	34, 51[b]
14	Ascites	Serous	4	III	24	34, 32[b]
15	Ascites	Serous	3	IV	30	NT
16	Ascites	Serous	3	III	NT	48
	Solid	Serous			17	40
17	Ascites	Serous	1	III	33	32
	Solid	Serous			38	49
18	Ascites	Serous	3–4	III	40	46
19	Ascites	Serous	3	III	NT	41
20	Ascites	Serous	4	III	9	28
21	Ascites	Endometrioid	3	III	26	39
23	Ascites	Serous	4	IV	11	29
24	Ascites	Serous	2	III	29	47
25	Ascites	Endometrioid	2	IV	30	45
26	Solid	Serous	3	III	26	47
27	Ascites	Serous	3	IV	NT	49

[a] NT=not tested.

[b] Results of different experiments in which tumor cells from the same patient were tested.

and staining for nonspecific esterase.

TAL and ovarian carcinoma cells.—Enriched preparations of ovarian tumor cells and TAL were obtained by stepwise application of density and velocity sedimentation on discontinuous Ficoll–Hypaque or FBS gradients (*3, 4, 9*). Carcinomatous ascites was centrifuged at 400×*g* for 5 minutes. Cells were resuspended in PBS, and 20 ml of the cell suspension (1–5×10^6 cells/ml) was stratified on 10 ml Ficoll–Hypaque. The tubes (#25330; Corning Glass Works, Corning, N.Y.) were then centrifuged at 400×*g* for 20 minutes at room temperature and the mononuclear cell layer was aspirated. For removal of macrophages from ovarian ascites cell suspensions, mononuclear cells in serum-free medium (*9*) were incubated for 45 minutes at 37°C in plastic petri dishes. The procedure was repeated two to three times until contamination with mononuclear phagocytes, assessed by morphology and avid uptake of neutral red, was less than 5%. After being washed with 50 ml PBS, 10 ml of the mononuclear cell suspension (2×10^6/ml) was layered on discontinuous gradients consisting of 10 ml of 100% and 15 ml of 75% Ficoll–Hypaque. The tubes were centrifuged at 1,700 rpm for 10 minutes at room temperature. Lymphocyte-enriched suspensions were harvested at the 75–100% interface and tumor cells were found on top of the 75% fraction. The procedure was repeated once or twice if separation was not satisfactory. When separation of lymphocytes from tumor cells on discontinuous Ficoll–Hypaque gradients was not satisfactory, as judged by morphologic examination of Wright-stained smears, cell suspensions (10–20×10^6/10 ml PBS) were layered onto 10 ml fetal calf serum and incubated at room temperature for 60–90 minutes; tumor cells sedimented at the bottom of the discontinuous gradient, whereas cells with lymphoid morphology remained in the upper part of the gradient. The various phases of the separation procedure were monitored by morphologic examination of Wright-stained smears. Unseparated tumor cell suspensions and the purified lymphocytes or tumor cells were prepared with Papanicolaou's stain and occasionally examined by independent pathologists. Lymphoid cell and tumor cell suspensions were accepted for use when at least 95% (usually >98%) of the cells had the typical unequivocal morphology of the respective cell type. On the average, 50% of TAL had receptors for sheep erythrocytes and 18% for complement-coated zymosan (*9*). Less than 5% of the lymphoid cell suspensions belonged to the monocyte–macrophage lineage, as assessed by morphology, rapid uptake of neutral red, and nonspecific esterase staining, and work in progress shows that TAL have a significant blastogenic response to phytohemagglutinin. Primary ovarian carcinoma cultures with typical morphology and lack of contact inhibition could be established from purified tumor cells (*9*), but attempts to cultivate tumor cells from lymphocyte preparations consistently failed. Viability of enriched fractions always exceeded 90% and lymphocyte recovery ranged from 50 to 0.5×10^6 cells for different patients. When normal PBL were submitted to the same separation procedure used for ovarian tumors, NK activity was not significantly affected.

In addition to ovarian tumors, in 1 experiment TAL from a malignant effusion from a uterine carcinoma was employed (identified in the tables and text-figs.).

For the isolation of ovarian cells and tumor-associated lymphocytes from solid tumors, specimens were minced mechanically and then exposed for 45 minutes at 37°C to 0.3% collagenase (#40130; Sigma Chemical Co., St. Louis, Mo., or Worthington Biochemical Corp., Freehold, N.J.) in BME (Eurobio) containing 10 μg DNase/ml. After two washes with 50 ml BME, disaggregated cells were then treated as described above for the cellular preparations isolated from the ascitic fluids.

IFN.—Partially purified human fibroblast IFN (lot #45-10-9) was obtained from HEM Research Inc., Rockville, Md. Lymphoid cells ($1-5\times10^6$/ml) were cultured for 18 hours in the presence of 1,000 U IFN/ml in growth medium. Control lymphocytes were cultured alone. Lymphoid cells were washed with 50 ml PBS before their cytotoxic capacity was tested. In two experiments (*see* "Results") lymphocytes were exposed to IFN for shorter periods (1–6 hr) under the same conditions.

Target cells.—NK activity of PBL and TAL was measured with the use of K562 cells (*10*) as targets. K562 cells and freshly purified ovarian carcinoma cells ($1-5\times10^6$ cells in 1 ml growth medium) were incubated with 20–50 μCi of ^{51}Cr (Radiochemical Centre, Amersham, Buckinghamshire, England) at 37°C for 45 minutes. Labeled cells were washed twice with 50 ml of BME before use in cytolysis assays.

Cytotoxicity assay.—^{51}Cr-labeled tumor cells (10^4) were cultured in 0.2 ml RPMI-1640 medium with 10% serum in round-bottomed wells of MicroTest plates (Sterilin Ltd., Teddington, Middlesex, England). FBS was used in part of the experiments; after it became difficult to obtain, FBS was replaced with pooled human AB serum. Cytotoxicity data were similar in the two series of experiments. The routinely employed A:T was 25:1 or 50:1 for ovarian carcinoma cells. Lysis of K562 was routinely measured at A:T ranging from 6:1 to 50:1, but only data at A:T of 25:1 will be presented. Isotope release was determined after 4 and 20 hours of incubation, except for occasional experiments in which cytotoxicity was measured only at 20 hours. Isotope release was calculated as $(A/B)\times100$, where A is the isotope in the supernatant and B is the total incorporated radioactivity released by incubation with 1% sodium dodecyl sulfate in water. Specific lysis was calculated by subtraction of the spontaneous isotope release of tumor cells alone. Spontaneous ^{51}Cr release from ovarian carcinoma cells ranged from 6 to 43% after 4 hours of incubation and from 25 to 49% after 20 hours (table 1). In eight experiments, control cultures to which unlabeled ovarian carcinoma cells were added instead of lymphocytes were included; isotope release was not different from that of labeled target cells alone.

Statistical analysis.—At least three replicates per experimental group were employed throughout, and results of cytotoxicity tests were calculated as mean plus or minus the standard deviation; 4–6% increases in isotope release above base line were usually statistically significant at $P<0.05$ (Duncan's new multiple-range test).

In each NK experiment against K562, ovarian cancer lymphocytes were tested along with at least 3 control subjects. A semilog plot of the specific cytotoxicity data against the number of effector cells per sample was obtained; the number of effector cells required for 33% specific lysis was arbitrarily referred to as LU33. For each lymphoid cell preparation an RCI was calculated as: $\bar{X}_n$ LU33/t LU33, where $\bar{X}_n$ LU33 is the average LU33 value for control subjects tested concomitantly and t LU33 is the same for the test subject. Thus an RCI of 0.2 indicates that five times more test lymphocytes are required to obtain 33% lysis when compared to the amount of lymphocytes required by control effector cells. NK data were expressed also as RCI, because this procedure reduced the day-to-day coefficient of variation of the assay (*9, 11, 12*).

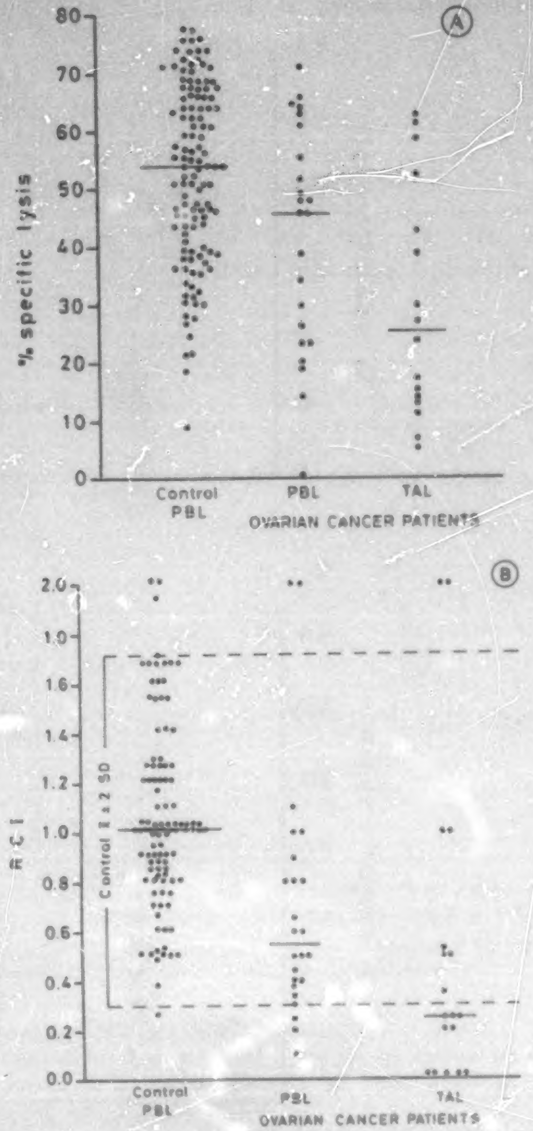

TEXT-FIGURE 1.—NK activity against K562 cells of PBL and TAL from ovarian cancer patients. Results are presented as percentage of specific lysis at an A:T of 25:1 (A) or as RCI (B). Cytotoxicity values from normal PBL were significantly higher than those for PBL ($P<0.01$) and TAL ($P<0.01$) from ovarian cancer patients.

RESULTS

In agreement with previous data (*9*), PBL and TAL from patients with ovarian tumors had impaired NK activity against K562 compared to the NK activity in control subjects. Cytotoxicity of TAL was lower than that of PBL from the same patients (text-fig. 1A, B).

Freshly isolated ovarian carcinoma cells were relatively resistant to lysis by unstimulated normal PBL (*9*). In only 5 of 35 experiments, significant lysis (>5% above background) was observed after 4 hours of culture. After 20 hours of interaction in 10 of 25 experiments, cytotoxicity was observed, the cytolysis values ranging from 5 to 27%. When PBL or TAL from ovarian cancer patients were tested against autologous or allogeneic tumor cells, on the whole the cytotoxicity of effector cells from tumor-bearing subjects was not greater or more frequently observed than that of control subjects (text-fig. 2A, B). Only PBL from 1 donor (of target cell #24) showed high levels of killing against autologous tumor cells, which clearly exceeded levels of killing of normal PBL: At an A:T of 50:1, specific lysis was 36.2% at 4 hours and 42.9% at 20 hours. The same PBL from the donor of target cell #24 were not cytotoxic against an allogeneic tumor (#4; specific lysis, 3.9% at 20 hr) nor were allogeneic ovarian cancer effectors lytic on #24 target cells. We could test PBL and cancer cells from the donor of

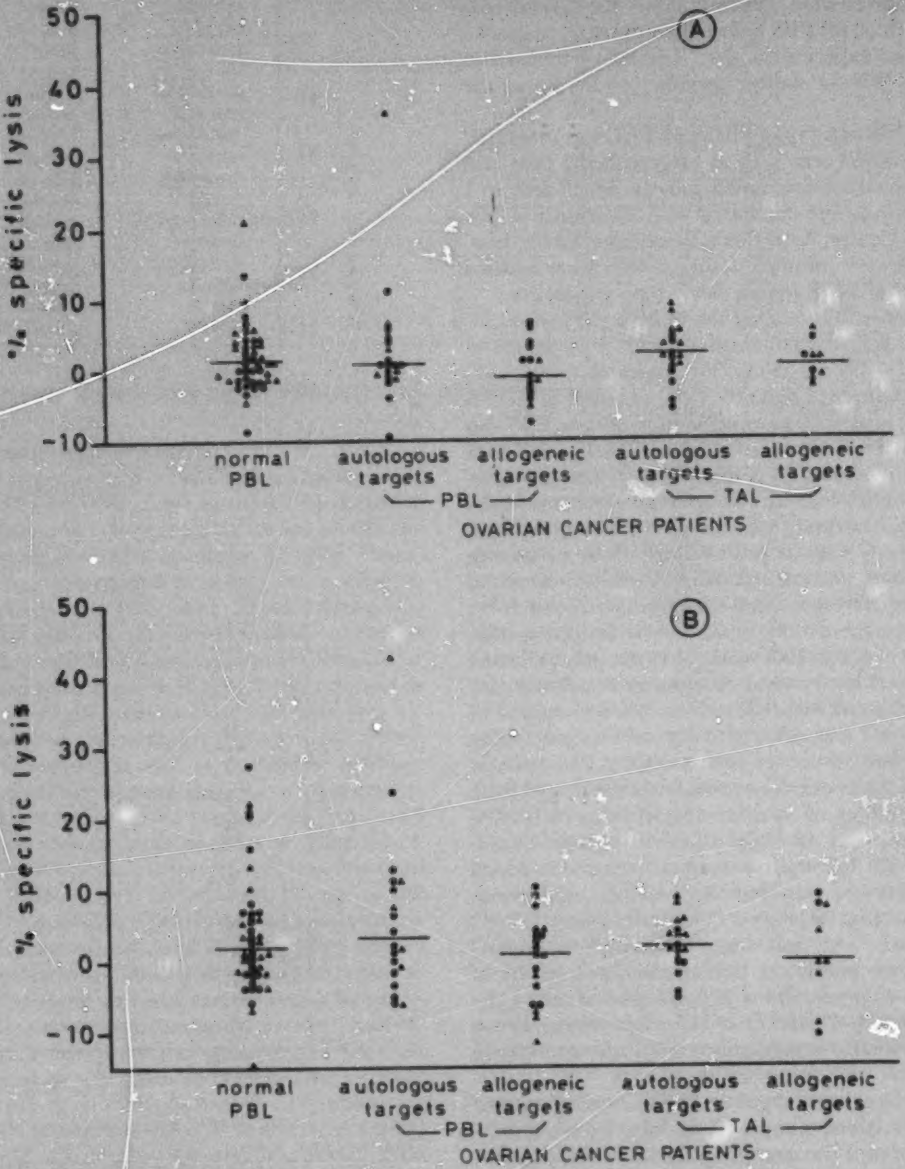

TEXT-FIGURE 2.—Cytotoxicity of PBL and TAL from ovarian cancer patients against autologous and allogeneic ovarian tumor cells. Cytolysis was measured in a 4-hr (A) and a 20-hr (B) assay with the use of an A:T of 25:1 (●) or 50:1 (▲). *Horizontal bars* indicate the medians.

target cell #24 only once.

In vitro exposure to IFN augments NK activity [reviewed in (*2*)]. It was therefore of interest to evaluate whether IFN-boosted effectors killed ovarian carcinoma cells, relatively resistant to base-line cytotoxicity of unstimulated effectors. Lysis of K562 cells was measured as a positive control for stimulation of NK activity by IFN. As shown in text-figure 3A, IFN (1,000 U/ml) enhance the NK activity against K562 of PBL from normal donors and of TAL and PBL from ovarian cancer patients (text-fig. 3B). Treatment with IFN did not always augment the cytotoxicity against K562. In fact, in 6 of 22 normal PBL and 7 of 26 ovarian cancer PBL and TAL, no increase in NK activity was observed. Inasmuch as only one exposure time (20 hr) and IFN concentration (1,000 U/ml) were used routinely, we cannot exclude that refractoriness of these preparations to IFN was related to these particular experimental conditions.

Results of cytotoxicity of ovarian carcinoma cells by IFN-stimulated effector cells are detailed in table 2, and the overall results are summarized in table 3. Against most carcinoma cells studied, IFN-treated normal PBL had significant cytolytic activity or, if unstimulated effectors already expressed some measurable cytolysis, this expression was enhanced after exposure to IFN. Stimulation of normal PBL cytotoxicity was already detectable after 4 hours of incubation (12/20 positive tests as compared to 12/19 at 20 hr) and absolute increases in lysis ranged from 5 to 40% with different targets (tables 2, 3). When PBL from ovarian cancer patients were used as effectors (table 2), stimulation of cytotoxic activity against autologous or allogeneic tumor cells was observed rarely at 4 hours; significant boosting was detected with 5 of 13 (autologous effectors) and 2 of 10 (allogeneic effectors) tumor cell preparations ($P<0.05$ vs. control PBL value; table 3). However, after a 20-hour assay, the cytolysis was significantly augmented in 8 of 14 carcinomas tested with autologous effectors and 4 of 11 tested with allogeneic PBL. In 3 (#8, 13, 18; table 2) of the 8 tests in which IFN-treated PBL caused more lysis than unstimulated effectors, cytotoxicity did not exceed isotope release of tumor cells alone, because untreated PBL had a significant "feeding" effect on targets abolished by IFN. When one considers the effects of IFN on cytotoxicity against autologous carcinoma cells, it is noteworthy that IFN decreased the tumoricidal activity of PBL from the donor of target cell #24 (from 42.9 to 31.1; 20 hr; table 2) whose effectors expressed appreciable levels of cytolysis against the autologous targets.

A limited number of TAL were tested for cytotoxicity against autologous or allogeneic tumor cells after exposure to IFN (table 2). Results were similar to those with PBL, and 5 of 9 and 3 of 5 tumor cell preparations tested with autologous and allogeneic effectors showed a significant augmentation of the cytotoxicity expressed by TAL after a 20-hour test.

DISCUSSION

Freshly isolated human ovarian carcinoma cells were relatively resistant to lysis by normal unstimulated PBL (*9*). Resistance to NK of tumor cells not cultured in vitro has also been observed with other human solid neoplasms and leukemias (*3–9*). However, in agreement with previous data (*9*) low, but significant, natural cytotoxicity against ovarian carcinoma cells was occasionally observed and was best observed after a 20-hour assay.

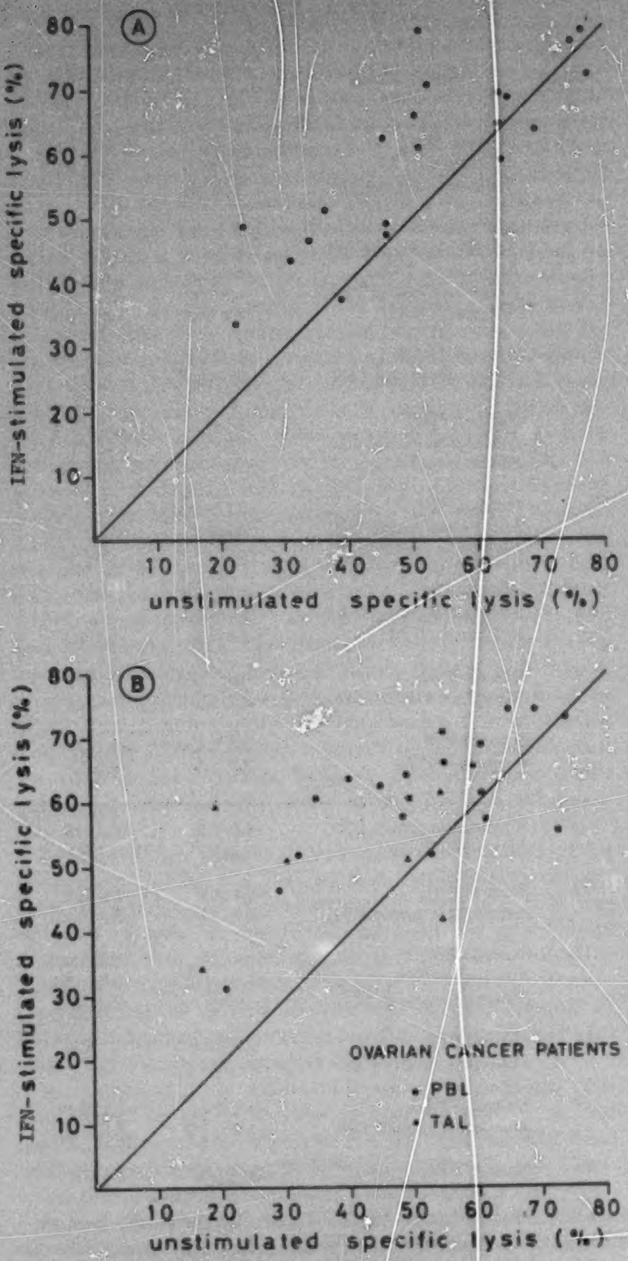

TEXT-FIGURE 3.—Effect of IFN on NK cytotoxicity against K562 cells of normal PBL (A) and ovarian cancer PBL and TAL (B).

In previous studies with different human tumors, in approximately 30% of the patients, evidence for cytotoxicity of PBL preferentially expressed against autologous tumor cells was obtained (*3–6*). In the present study only 1 subject had cytolytic activity against autologous tumor cells that clearly

best copy available

TABLE 2.—*Effect of IFN on cytotoxicity of PBL and TAL against fresh ovarian carcinoma cells*

Ovarian cancer cell No.	Effector cells[a]	Specific lysis without IFN/ Specific lysis with IFN	
		4 hr[b]	20 hr[b]
1	Normal PBL	1.4/3.8	−6.4/10.9[c]
	Autologous TAL	−1.7/4.5[c]	−4.9/0.3[c]
	Allogeneic cancer PBL	3.2/1.8	2.6/−1.4
3	Normal PBL	2.7/20.4[c]	2.1/44.9[c]
	Autologous cancer PBL	6.2/11.3[c]	7.2/12.1[c]
	Autologous TAL	4.0/7.3[c]	8.8/22.6[c]
	Allogeneic cancer PBL	−4.9/7.5[c]	−11.8/11.5[c]
	Allogeneic TAL	1.4/8.8[c]	−0.3/16.0[c]
4	Normal PBL	−2.8/5.3[c]	−3.2/5.7[c]
	Allogeneic cancer PBL	−4.5/6.1[c]	3.0/15.1[c]
6	Normal PBL	−4.0/5.6[c]	0.9/8.8[c]
	Autologous cancer PBL	−0.9/1.6	2.3/3.9
	Autologous TAL	−2.8/−1.2	1.8/4.2
7	Normal PBL	0.7/−0.1	7.2/13.2[c]
	Autologous cancer PBL	1.9/0.4	12.6/19.3[c]
	Allogeneic cancer PBL	−2.6/−1.4	4.4/−2.9
8	Normal PBL	−2.2/−1.2	−3.0/−1.1
	Autologous cancer PBL	−2.1/−1.6	−5.3/−0.7[c]
	Autologous TAL	−3.9/0.4[c]	−5.1/0.5[c]
10	Normal PBL	0.4/7.8[c]	NT
	Allogeneic cancer PBL	−2.2/0.4	NT
11	Normal PBL	−3.3/1.4[c]	−2.1/2.3[c]
	Allogeneic PBL	2.9/2.5	2.0/1.7
12	Normal PBL	1.1/7.5[c]	0.8/13.1[c]
	Autologous cancer PBL	2.9/5.9	−0.5/3.5[c]
	Allogeneic TAL	−1.4/3.7[c]	−0.1/8.9[c]
13	Normal PBL	−0.1/4.8[c]	5.4/5.6
	Autologous cancer PBL	−1.9/1.5	−5.8/1.3[c]
14	Normal PBL	−1.4/2.6[c]	2.0/13.8[c]
	Autologous TAL	−1.8/−2.9	0.3/−0.4
	Allogeneic cancer PBL	NT	0.8/10.4[c]
15	Normal PBL	7.6/18.5[c]	NT
	Allogeneic cancer PBL	5.9/7.5	NT
16[d]	Normal PBL	−2.2/0.6	−2.1/2.1[c]
	Autologous cancer PBL	−1.2/−1.9	−0.6/−0.9
17	Normal PBL	4.9/11.4[c]	6.8/7.4
	Autologous cancer PBL	−0.7/8.7[c]	11.4/10.9
	Allogeneic cancer PBL	5.2/2.7	−1.6/1.2
17[d]	Normal PBL	0.5/5.8[c]	0.7/−3.8
	Autologous cancer PBL	15.9/19.2	6.9/2.5
18	Normal PBL	−8.3/−7.8	−5.7/−3.0
	Autologous cancer PBL	−11.5/−8.5	−5.4/0.9[c]
	Allogeneic cancer PBL	−3.8/−12.3	2.9/−6.2
19	Normal PBL	NT	4.8/22.5[c]
	Autologous cancer PBL	NT	−3.0/6.7[c]
	Allogeneic cancer PBL	NT	7.0/7.0
20	Normal PBL	2.7/4.5	13/15.2
	Autologous cancer PBL	0.1/1.1	2.2/4.1
	Autologous TAL	−0.2/0.1	5.1/6.5
21	Normal PBL	−1.6/6.6[c]	6.4/11.4[c]
	Autologous cancer PBL	5.7/7.1	10.4/10.0
	Allogeneic TAL	4.3/8.5[c]	7.6/12.7[c]
23	Normal PBL	−0.5/1.6	−2.8/3.2[c]
	Autologous TAL	1.8/0.3	5.3/4.1
	Allogeneic TAL	1.5/−0.1	4.5/4.6
24	Normal PBL	22/15.8	21.6/24.6
	Autologous cancer PBL	36.2/24.3	42.9/31.1
	Autologous TAL	1.4/6.5[c]	7.7/12.4
25	Autologous TAL	0.9/6.9[c]	20.0/8.0
26	Normal PBL	13.5/24.2[c]	27.6/30.9
	Autologous cancer PBL	11.1/28.5[c]	24.1/35.4[c]
	Allogeneic cancer PBL[e]	1.9/0.1	9.5/12.2
	Allogeneic TAL[e]	1.3/3.6	8.5/5.2
27	Allogeneic cancer PBL	NT	−7.7/1.3[c]

[a] Effector cells were tested at an A:T of 50:1 or 25:1. Effector cells were exposed to IFN for 20 hr except for experiments with target #19 and 26 in which lymphocytes were incubated with IFN for 6 and 1 hr, respectively.

[b] Duration of the ^{51}Cr release assay. Release below that of tumor cells alone, −. NT=not tested.

[c] Lysis of lymphoid cells exposed to IFN significantly above that of unstimulated effectors ($P<0.05$).

[d] Carcinoma cells from solid primary tumor.

[e] Allogeneic cancer PBL and TAL were from a uterine tumor.

exceeded that of normal control PBL. Interestingly enough, PBL of this patient did not kill allogeneic carcinoma cells as usually observed in other human tumors with the use of a similar experimental approach (*3–6*). Several factors, in addition to a different immunobiology of the tumors studied, can account for the low frequency of reactivity of PBL against autologous ovarian carcinoma cells observed in the present investigation at variance with previous reports of other tumors. For instance the ovarian tumors considered in the present study were stage III or IV, because ovarian carcinoma is usually diagnosed very late, and autologous reactivity in other neoplasms was more frequently detected at early disease stages (*3, 4*). Moreover, weak reactivities may have been masked by the significant cytotoxicity observed occasionally with normal donor PBL.

Lymphoid cells isolated from ascites ovarian tumors did not show cytotoxicity against autologous or allogeneic ovarian carcinoma cells. Similarly, TAL from various human solid neoplasms did not kill tumor cells in a ^{51}Cr release assay, even when PBL from the same patient were reactive (*4, 5*). However, intratumor cytotoxic lymphocytes were found in nasopharyngeal carcinoma and in Burkitt's lymphoma (*4, 13*), and, using a visual microcytotoxicity assay, Werkmeister and co-workers (*14*) reported intratumor cytotoxicity in colorectal cancer even when PBL were not active. Although in the case of colorectal cancer the use of a visual microcytotoxicity assay (*14*) renders comparisons with these and previous data difficult, it is conceivable that

TABLE 3.—*Augmentation by IFN of cell-mediated lysis of fresh ovarian carcinoma cells*

Effector cells	Incubation time, hr	Tumor cells with stimulation of lysis/total	Absolute increase in lysis[a]
Normal PBL	4	12/20	7.6 (5–17)
	20	12/19	8.9 (5–42)
Patient PBL (autologous)	4	3/13[b]	10.3 (5–15)
	20	8/14[c]	6.7 (5–11)
Patient PBL (allogeneic)	4	2/10[b]	9.3 (6–12)
	20	4/21	11.3 (7–23)
Patient TAL (autologous)	4	3/9	5 (4–6)
	20	5/9[d]	6.8 (5–13)
Patient TAL (allogeneic)	4	3/5	5.3 (5–7)
	20	3/5	9.6 (5–16)

[a] Results are mean absolute increases in lysis (with ranges *in parentheses*) of IFN-stimulated effectors above unstimulated lymphocytes. Only experiments (*see* table 2) in which IFN caused a significant ($P<0.05$) augmentation of lysis were used to calculate the mean.

[b] $P<0.05$ compared to value of normal PBL tested at 4 hr; Fisher's exact test.

[c] With 3 tumor cell preparations (#8, 14, 18), isotope release of tumor cells with unstimulated effectors was significantly lower than that of tumor cells alone (table 2).

[d] Same as *footnote c* for two preparations (#1 and 8, table 2).

differences in the reactivity of intratumor lymphocytes are related to a different immunobiology of the neoplasms investigated.

Preliminary evidence for the presence of intratumor suppressor cells for lymphoproliferative responses (*15*) and for NK activity (*9, 16*) has been obtained in selected human neoplasms. The possible role of suppressor cells in the lack of cytotoxicity of TAL observed in this study and in other studies (*3–5*) remains to be elucidated.

Ovarian carcinoma cells were relatively resistant to lysis by normal unstimulated PBL (*9*). In agreement with previous preliminary data (*9*), in vitro exposure to IFN enhanced the cytotoxicity of normal PBL against freshly isolated ovarian tumor cells and this enhancement was observed in both a 4-hour and a 20-hour cytolysis assay. IFN also enhanced NK cytotoxicity against K562 of PBL and TAL from ovarian cancer patients, but stimulation of lysis of ovarian carcinoma cells in a 4-hour assay was observed less frequently with cancer effectors than with normal PBL. After 20 hours of interaction with targets, stimulation of lysis of fresh tumor cells was similar in frequency and magnitude to that observed with control PBL. It is tempting to speculate that the failure to find a consistent enhancement of lysis by IFN-treated tumor PBL and TAL after 4 hours of interaction with carcinoma cells is related to the impaired base-line NK activity of these effectors, which, according to this hypothesis, would require a longer interaction with the resistant target cells to reach the threshold of lysis.

Vánky et al. (*6*) have recently reported that IFN augmented the cytotoxicity of PBL from tumor-bearing patients against fresh cancer cells, provided the targets were from a different subject. On this basis they speculated that alloantigens are important in natural cytotoxicity under these conditions. Results reported here with a homogeneous series of ovarian cancer patients are clearly different from those of Vánky et al. (*6*). IFN-stimulated PBL or TAL from ovarian cancer patients were frequently cytotoxic against autologous tumor cells in a 20-hour assay. Both at 4 and 20 hours, no difference was observed in the cytotoxicity of ovarian cancer effector cells against autologous or allogeneic tumor cells, lymphoid cells from tumor-bearing patients being less reactive than normal PBL. Several factors, such as the different source of IFN, different preincubation time, and varying lengths of the assays, might partially account for the apparent discrepancy between results reported here with ovarian cancer and previous observations by Vánky et al. (*6*). For instance in our study, PBL or TAL were routinely exposed overnight to IFN before cytotoxicity was tested, whereas Vánky et al. (*6*) used a shorter preincubation. However, stimulation of cytolysis of autologous ovarian tumor cells was observed also in two experiments in which effectors were exposed to IFN for 1 or 6 hours (table 2) (target #26 and 19, respectively). Therefore, the apparent discrepancy between data reported here and previous data by Vánky et al. (*6*) possibly is related to differences in the immunobiology of the tumors investigated. In this context, it is of interest that mature NK cells were reported to kill allogeneic but not autologous fibroblasts; however, after stimulation, killing was detected against both autologous and allogeneic targets (*17*).

In some of the ovarian cancer patients, IFN enhanced the cytotoxicity of PBL and TAL against autologous carcinoma cells. In addition to stimulating NK lysis (*2*), IFN was reported to enhance specific T-cell-mediated cytotoxicity (*18*), and one might speculate that IFN-boosted cytolysis of autologous carcinoma cells is mediated by mature T-cells. Characterization of IFN-boosted effector cells capable of lysing autologous fresh ovarian carcinoma cells should elucidate the nature of this reactivity.

In conclusion, our results indicate that lymphoid cells from blood or ascites tumors of patients with advanced ovarian cancer, with impaired NK activity, usually have little cytotoxicity against freshly isolated autologous carcinoma cells, not exceeding that of PBL from control subjects; only in 1 of 24 patients did we observe appreciable killing of autologous, but not allogeneic, targets by PBL. Therefore, it is unlikely that lymphocyte-mediated cytotoxicity can act as a significant mechanism of restraint of the growth of these advanced neoplasms. In a few patients, in vitro exposure to IFN augmented the cytotoxicity of PBL and TAL against autologous or allogeneic fresh tumor cells. However, IFN-boosted cytolysis was usually low. Whether these levels of killing can have in vivo significance remains to be elucidated.

REFERENCES

(*1*) HELLSTRÖM KE, HELLSTRÖM I. Lymphocyte-mediated cytotoxicity and blocking serum activity to tumor antigens. Adv Immunol 1974; 18:209–215.

(2) Herberman RB, Djeu JY, Kay HD, et al. Natural killer cells: Characteristics and regulation of activity. Immunol Rev 1979; 44: 43–70.

(3) Vose BM, Vánky F, Klein E. Lymphocyte cytotoxicity against autologous tumour biopsy cells in humans. Int J Cancer 1977; 20: 512–519.

(4) Vose BM, Vánky F, Klein E. Human tumour–lymphocyte interaction in vitro. V. Comparison of the reactivity of tumour infiltrating blood and lymph-node lymphocytes with autologous tumour cells. Int J Cancer 1977; 24:895–902.

(5) Vose BM, Vánky F, Fopp M. Klein E. Restricted autologous lymphocytotoxicity in lung neoplasia. Br J Cancer 1978; 38:375–381.

(6) Vánky FT, Argov SA, Einhorn SA, Klein E. Role of alloantigens in natural killing. Allogeneic but not autologous tumor biopsy cells are sensitive for interferon-induced cytotoxicity of human blood lymphocytes. J Exp Med 1980; 151:1151–1165.

(7) Tötterman TH, Häyry P, Saksela E, Timonen T, Eklund B. Cytological and functional analysis of inflammatory infiltrates in human malignant tumors. II. Functional investigations of the infiltrating inflammatory cells. Eur J Immunol 1978; 8:872–875.

(8) Zarling JM, Eskra L, Borden EC, Horoszewicz J, Carter AW. Activation of human natural killer cells cytotoxic for human leukemia cells by purified interferon. J Immunol 1979; 123:63–70.

(9) Mantovani A, Allavena P, Sessa C, Bolis G, Mangioni C. Natural killer activity of lymphoid cells isolated from human ascitic ovarian tumors. Int J Cancer 1980; 25:573–582.

(10) Lozzio CB, Lozzio BB. *Brief communication*: Cytotoxicity of a factor isolated for human spleen. J Natl Cancer Inst 1973; 50:535–538.

(11) Fross HF, Baines MG. Spontaneous human lymphocyte-mediated cytotoxicity against tumour target cells. I. The effect of malignant disease. Int J Cancer 1976; 18:593–604.

(12) Santoli D, Trinchieri G, Moretta L, Zmijewski CM, Koprowski H. Spontaneous cell-mediated cytotoxicity in humans. Distribution and characterization of effector cells. Clin Exp Immunol 1978; 33: 309–318.

(13) Jondal M, Svedmyr E, Klein E, Singh S. Killer T cells in a Burkitt's lymphoma biopsy. Nature 1975; 255:405–407.

(14) Werkmeister JA, Phil E, Nind AP, Flannery GR, Nairn RC. Immunoreactivity by intrinsic lymphoid cells in colorectal carcinoma. Br J Cancer 1979; 40:839–847.

(15) Vose BM, Moore M. Suppressor cell activity of lymphocytes infiltrating human lung and breast tumours. Int J Cancer 1979; 24: 579–585.

(16) Eremin O. NK cell activity in the blood, tumor-draining lymph nodes and primary tumors of women with mammary carcinoma. In: Herberman RB, ed. Natural cell-mediated immunity against tumors. New York: Academic Press, 1980:1011–1029.

(17) Tarkkanen J, Timonen T, Saksela E. Induction of autologous reactivity of human NK cells. Scand J Immunol 1980; 11:383–390.

(18) Lindahl P, Leary P, Gresser I. Enhancement by interferon of the specific cytotoxicity of sensitized lymphocytes. Proc Natl Acad Sci USA 1972; 69:721–725.

Morphologic Transformation and Chromosomal Changes Induced by Chemical Carcinogens in Skin Fibroblasts From Patients With Familial Adenomatosis Coli[1,2]

Michiko Miyaki,[3] Noriko Akamatsu,[3] Tetsuo Ono,[3] Akira Tonomura,[4] *and* Joji Utsunomiya[5,6]

ABSTRACT—Skin fibroblasts from patients with familial adenomatosis coli (AC) and normal individuals were treated once with the carcinogen 4-nitroquinoline 1-oxide or *N*-methyl-*N'*-nitro-*N*-nitrosoguanidine and then passaged sequentially. Morphologically altered cells appeared in the cultures of carcinogen-treated AC fibroblasts at passages 6–8 (days 100–140) after treatment with the carcinogens, but carcinogen-treated normal cells and untreated AC and normal cells did not become altered even after cultivation for 25 passages. The cultures containing morphologically altered cells showed characteristics of transformed cells, such as a high frequency of colony formation in soft agarose, increased growth ability, and chromosomal abnormalities. The results suggest that AC patients have increased susceptibility to morphologic transformation and chromosomal changes induced by chemical carcinogens.—JNCI 1982; 68:563–571.

Individuals with familial AC, characterized by adenomatous polyps in the colon and rectum (*1*), have a high incidence of colon cancer and various other tumors, such as osteosarcoma (*2*), liposarcoma, and stomach cancer (*3*). Cultured skin fibroblasts from patients with this autosomal dominant trait have been reported to exhibit several growth abnormalities. The higher saturation density (*4, 5*), higher plating efficiency (*5, 6*), and lower serum requirement of AC fibroblasts (*4*) compared to those of cells from normal individuals suggested that AC fibroblasts partly resemble established cell lines. Different responses of AC and normal cells to a tumor promoter have also been reported by Kopelovich et al. (*7*) who demonstrated the acquisition of transplantability of AC fibroblasts into the anterior chamber of the eye of an athymic mouse after the fibroblasts were cultivated with TPA. The high susceptibility of AC fibroblasts to transformation by Kirsten MuSV (*8*) and pseudotypes of Moloney MuSV (*9*) indicates that these cells have a genetic factor similar to that in cells from other inherited high-risk groups of cancers, which have been reported to be susceptible to tumor viruses. In addition to the effect of virus, significant influences of physical and chemical carcinogens on genetic predisposition to cancer have been described in cases of some recessively inherited disorders. We have previously observed that skin fibroblasts from some individuals with manifest AC were more susceptible to the cytotoxicities of 4-NQO and mitomycin C than were cells from normal individuals, whereas the sensitivities of AC cells to MNNG and UV light were normal in regard to colony-forming ability (*5*). The present investigation was undertaken to examine the transformation of AC cells by these chemical carcinogens. This paper reports the morphologic transformation and chromosomal changes induced in AC fibroblasts by 4-NQO and MNNG.

MATERIALS AND METHODS

Fibroblasts were obtained by biopsy of skin from the left elbows of patients with familial AC and from normal individuals. The fibroblast AC(MS) was obtained from an AC patient (female, 45 yr old), and the fibroblast AC(YK) was obtained from a member of an AC family (male, 14 yr old). The normal cells, normal(MY) and normal(OK), were cultured from skin biopsy specimens obtained from normal individuals, a 29-year-old female and a 38-year-old female, respectively. Primary cultures were made by explantation, and cells were used at passage 10 after isolation. The cells were cultivated at 37°C in 5% CO_2 in air in EMEM (Nissui Seiyaku Co.) supplemented with 13% heat-inactivated (56°C, 30 min) FBS (GIBCO), 100 μg pyruvate/ml, 100 U penicillin G/ml, and 60 μg kanamycin/ml, and the medium was changed twice a week. When the cultures became confluent, the cells were detached from the glass dish by incubation with 0.016% Pronase E (Kaken Chemicals) and 0.02% EDTA at 25°C for 15 minutes. The cell suspension was centrifuged at 800 rpm for 5 minutes to remove Pronase, and then the cells were replated.

Transformation experiments were done by treatment of AC and normal cells for 1 hour with 4 or 8 *μM* 4-NQO or 40 *μM* MNNG in EMEM 24 hours after inoculation at a density of 2×10^6 cells/100-mm glass dish (6 dishes; 1.2×10^7 cells total for each experiment); the cells were then washed and cultivated in medium containing 13% FBS. The cultures were passaged successively at one-sixth the original cell density or at 5×10^6 cells/dish. At each passage, all cells from six dishes were combined and replated on the next six dishes. When morphologic alteration of the cells was observed or

ABBREVIATIONS USED: AC=adenomatosis coli; EMEM=Eagle's minimum essential medium; FBS=fetal bovine serum; MNNG=*N*-methyl-*N'*-nitro-*N*-nitrosoguanidine; MuSV=murine sarcoma virus; 4-NQO=4-nitroquinoline 1-oxide; TPA=12-*O*-tetradecanoylphorbol 13-acetate.

---

[1] Received May 14, 1981; accepted November 6, 1981.

[2] Supported in part by a Grant-in-Aid for Cancer Research from the Ministry of Education, Science and Culture, Japan.

[3] Department of Biochemistry, The Tokyo Metropolitan Institute of Medical Science, 3-18-22 Honkomagome, Bunkyoku, Tokyo 113, Japan.

[4] Department of Cytogenetics, Medical Research Institute, Tokyo Medical and Dental University, 1-5-45 Yushima, Bunkyoku, Tokyo 113.

[5] Department of Surgery and Polyposis Center, Tokyo Medical and Dental University.

[6] We are grateful to Dr. Makoto Umeda, Yokohama City University School of Medicine, for instruction in the method of preparation of chromosome specimens and for valuable discussion.

the cells had been passaged 10–14 times, the cultures were tested for colony formation in soft agarose and for their chromosome number.

Cytotoxicities of carcinogens were determined by measurement of the cell numbers 7 days after treatment of the cells with 4-NQO and MNNG.

We measured the saturation density 14 days after seeding 1×10^4 cells/cm^2. The medium containing 13% FBS was changed every 3 days.

Growth of cells in agarose was determined as follows: The cells were detached from dishes with Pronase and EDTA, washed, and suspended at 2×10^3/ml in 0.2% agarose containing 20% FBS, 100 μg pyruvate/ml, and 0.1% polypeptone. The suspensions (2.5 ml each) were layered on 0.5% agarose (10 ml) in 60-mm dishes, and colonies were counted after cultivation for 4–8 weeks. We used 8–16 agarose plates for each experiment.

Mitotic cells were counted after treatment of cells with 0.1 μg Colcemid/ml for 2 hours and preparation of chromosome specimens by the air-drying method with the use of acetic acid–methanol for fixation and Giemsa for staining.

RESULTS

The AC fibroblasts from patients with familial AC used in this study were highly sensitive to transformation by MuSV (9) and showed a 10–20% higher saturation density compared to that of normal cells (3), but their growth rate was similar to that of normal cells in medium containing 13% FBS. The AC and normal cells were all diploid at the beginning of the transformation experiments.

AC and normal fibroblasts were treated for 1 hour with 4-NQO or MNNG and then sequentially passaged at intervals of 2–3 weeks. The cumulative growth curves of 4-NQO-treated and solvent-treated cells are shown in text-figure 1. The growth of solvent-treated normal(MY) cells stopped at passage 18, and the growth rate of 4-NQO-treated normal cells decreased gradually from passage 20 after treatment with the carcinogen. In contrast, solvent-treated AC cells still proliferated at passage 20, and the growth rate of 8 *μM* 4-NQO-treated AC(MS) cells began to increase at passage 10 after treatment. This increase in growth rate was accompanied by transformation of the cells. Morphologically altered cells began to appear among the AC fibroblasts (fig. 1B) at passages 6–8 (days 100–140) after treatment with 8 *μM* 4-NQO. These altered cells were small and spindle shaped with a disorganized arrangement, and the proportion of altered cells increased during subsequent passages. Cells from all of the subculture dishes derived from 8 *μM* 4-NQO-treated AC(MS) cultures were morphologically changed. The morphologic alterations in the 4 *μM* 4-NQO-treated AC(MS) culture were less than those in the 8 *μM* 4-NQO-treated cells, and the cumulative growth rate did not change significantly.

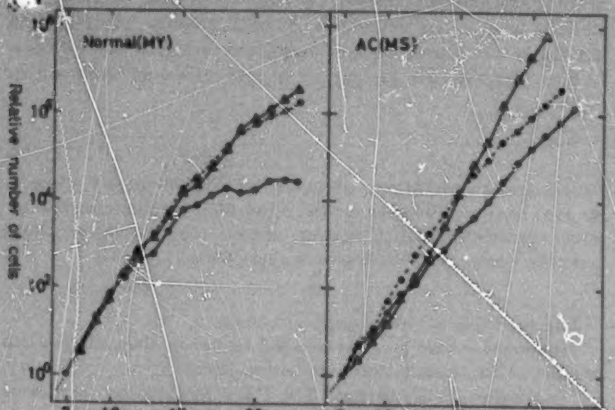

TEXT-FIGURE 1.—Cumulative growth curves of 4-NQO-treated normal and AC fibroblasts. The fibroblasts were treated with solvent or 4-NQO and then passaged at intervals of 2–3 wk. The number of cells per dish was measured at each passage, and the relative number of cells was plotted. ○——○, solvent. ●— —●, 4 *μM* 4-NQO. △——△, 8 *μM* 4-NQO-treated cells.

MNNG at 40 *μM* also induced morphologic changes in AC(MS) cells. However, neither carcinogen-treated normal cells nor solvent-treated cells (fig. 1A) became morphologically altered, even when cultivated for 25 passages in glass dishes.

The marked increase in colony-forming frequency (table 1) coincided with the morphologic alteration of the cells; e.g., after 10 passages the 8-*μM* 4-NQO-treated and the 40-*μM* MNNG-treated AC(MS) cells showed high efficiencies of colony formation in agarose, although their efficiencies at passage 3 were as low as those of solvent-treated cells. Colonies of MNNG-treated AC(MS) cells were larger (0.1–0.15 mm in diameter) than those of 4-NQO-treated AC(MS) cells (0.05–0.1 mm) (fig. 2).

The saturation density of carcinogen-treated AC(MS) cells was higher than that of solvent-treated cells (table 1). The proportion of mitotic cells in AC(MS) cultures treated with 8 *μM* 4-NQO or 40 *μM* MNNG was higher than that of normal cells in culture (table 1), and some of the round cells became detached from the dish during cultivation. Deep infolding of the nuclear membrane was also frequently observed in carcinogen-treated AC(MS) cells (table 1).

Chromosomal abnormalities appeared at the same time as the acquisition of colony-forming ability in soft agarose. The chromosomal aberrations are indicated in table 2. At metaphase, 44 and 35% of the 8 *μM* 4-NQO-treated and 40 *μM* MNNG-treated AC(MS) cells were hypotetraploid. The aneuploid cells in the carcinogen-treated AC(MS) cultures contained dicentric chromosomes at a frequency of 10–17% of the total mitotic cells (table 2), and the examples are shown in figure 3A and 3B. Metaphase cells in solvent-treated control cultures of this AC(MS) cell line contained no dicentric chromosomes (fig. 3D). The existence of these unusual chromosomes suggests that interchromosomal exchange occurred frequently in AC cells during long passages after treatment with carcinogens. The chromosomal change to aneuploidy and the appearance of an unusually large marker chromosome were also observed in another cell line, AC(YK) (table 2), although morphologic change of these cells was slight. In 4-*μM* 4-NQO-treated AC(YK) cells, 67% of the mitotic cells were hypotetraploid and 44% of the total mitotic cells contained an unusually large marker chromosome (fig. 3C). These AC(YK) cells exhibited tetraploidy

TABLE 1.—*Growth properties of carcinogen-treated normal and AC fibroblasts*[a]

Cells	Treatment	Cytotoxicity, percentage inhibition of cell growth[b]	No. of colonies in agarose per 5×10^5 cells inoculated[c]	Saturation density, ×10^4/cm^2[b]	Mitotic coefficient, %	Deep infolding of nuclear membrane, %
Normal(MY)	Solvent	0	0.3±0.4	1.9	0.10	0.05
Normal(MY)	4-NQO, 4 *µM*	43	1.2±0.7	2.3	0.65	0.33
Normal(MY)	4-NQO, 8 *µM*	66	1.1±0.8	2.9	1.36	0.37
Normal(MY)	MNNG, 40 *µM*	50	0.3±0.5	3.3	0.77	0.25
Normal(OK)	Solvent	0	0.3±0.4	2.2	0.39	0.16
Normal(OK)	4-NQO, 4 *µM*	63	0.4±0.7	2.1	0.40	0.27
AC(MS)	Solvent	0	0.8±0.4	2.5	0.28	0.09
AC(MS)	4-NQO, 4 *µM*	75	4.0±1.7	3.0	0.92	1.24
AC(MS)	4-NQO, 8 *µM*	87	24.2±5.3	4.0	3.99	9.95
AC(MS)	MNNG, 40 *µM*	56	27.0±6.7	7.9	2.50	5.19
AC(YK)	Solvent	0	1.1±0.3	3.1	0.58	0.22
AC(YK)	4-NQO, 4 *µM*	70	2.9±0.9	3.5	1.11	0.74

[a] Normal and AC fibroblasts were treated with carcinogen and then passaged. At passages 10–14 (days 140–200) after treatment of cells with carcinogen, the growth properties were measured as described in "Materials and Methods." The experiments for normal(MY) and AC(MS) were done with the use of glass dishes, and those for normal(OK) and AC(YK) were done with the use of plastic dishes. The mitotic coefficient and percentage deep infolding of the nuclear membrane were calculated from observations on 600–1,900 cells in each sample.

[b] Mean value obtained from two dishes.

[c] Means ± SE from 8 to 16 agarose plates.

TABLE 2.—*Chromosomal changes in carcinogen-treated normal and AC fibroblasts*[a]

Cells	Treatment	Chromosome No. of mitotic cells, %			Distribution of chromosome No. at near 4n[b]	Mitotic cells containing marker[c] chromosomes, %
		2n	Near 4n	>4n		
Normal(MY)	Solvent	100	0	0	—	0
Normal(MY)	4-NQO, 4 *µM*	97	3	0	—	0
Normal(MY)	4-NQO, 8 *µM*	54	46	0	90±2	1
Normal(MY)	MNNG, 40 *µM*	99	1	0	—	0
Normal(OK)	Solvent	100	0	0	—	0
Normal(OK)	4-NQO, 4 *µM*	98	2	0	—	0
AC(MS)	Solvent	100	0	0	—	1
AC(MS)	4-NQO, 4 *µM*	63	12	25	87±4	9
AC(MS)	4-NQO, 8 *µM*	21	44	35	79±5	10
AC(MS)	MNNG, 40 *µM*	44	35	21	81±5	17
AC(YK)	Solvent	76	24	0	90±2	0
AC(YK)	4-NQO, 4 *µM*	33	67	0	86±5	44

[a] Cultures of fibroblasts at passages 10–14 (days 140–200) after treatment with carcinogen or solvent were incubated with Colcemid. Chromosome specimens were prepared as described in "Materials and Methods." Chromosomal abnormalities were estimated from examination of 90–130 mitotic cells in each sample.

[b] Mean chromosome number obtained from 15 to 55 mitotic cells containing near-4n chromosomes in each sample (means ± SE).

[c] Dicentrics and an unusually large monocentric chromosome.

after treatment with solvent alone, but the chromosome number was nearly 92 and no marker chromosome was found in this control experiment (figs. 3E, 3F).

The normal cell lines [normal(MY) and normal(OK)] did not show any dicentric chromosomes, and almost all mitoses were diploid (table 2) except for those in the 8-*µM* 4-NQO-treated normal(MY) cell line. This cell line exhibited tetraploidy after treatment with 8 *µM* 4-NQO and subsequent culture, but the cells were not altered morphologically.

The experiments on AC(MS) and normal(MY) were attempted twice, and the transformation of AC(MS) cells and the unchanged morphology of normal(MY) cells were reproducible. The morphologically transformed AC(MS) cultures at passages 10–14 after treatment with 8 *µM* 4-NQO or 40 *µM* MNNG, however, did not form tumors in BALB/c nude mice when inoculated sc at 10^7 cells per mouse. These morphologically transformed cells continued to grow for 330 days (25 passages) after treatment with carcinogens. A colony in soft agarose obtained from the 120th day of culture of 40-*µM* MNNG-treated AC(MS) cells grew during a further 270 days in a liquid medium after a 60-day culture in agarose, but the growth rate gradually slowed down. The cells are still growing very slowly, and cloning of the transformed cells is in progress.

DISCUSSION

The increase in colony-forming efficiency in soft agarose has been widely used as a parameter of neoplastic transformation. The AC cells treated with 4-NQO and MNNG in the present experiment showed a high efficiency of growth in agarose, and the number of passages required for acquisition of the ability to grow in agar was consistent with that previously reported for transformation of human fibroblasts (*10*). The morphologically transformed cells also exhibited chromosomal aberrations, such as polyploidy, aneuploidy, and formation of dicentric chromosomes or abnormal marker chromosomes. However, the normal cell lines did not show morphological alteration during sequential passage after treatment with carcinogens. The structures of chromosomes in the normal cells were rather stable, since neither dicentric nor remarkably abnormal chromosomes were formed on carcinogen treatment and subsequent passages.

The chromosomal changes in human cells have been suggested to be correlated with the acquisition of other characteristics of cellular transformation (*11-13*). There are few reports on chemical transformation of human cells from normal tissues (*10, 11, 14*), and the low rate of transformation of human cells in culture has been considered to be due to the stability of chromosomes. It is significant that abnormal chromosomes were frequently observed in morphologically transformed AC cells in the present study. Some AC cells have been reported to exhibit frequent spontaneous reciprocal translocations between chromosomes (*15*), and epithelial cells from patients with Gardner's syndrome (*16*) showed increased tetraploidy during cultivation. Increased numbers of chromosomal breaks have been observed immediately after treatment of AC cells with MNNG (*17*). These observations and the present results suggest that AC is susceptible to chromosomal aberrations that might be correlated with the high risk of cancer for patients with AC and the high frequency of transformation of the fibroblasts by oncogenic viruses (*8, 9*), a tumor promoter (*7*), and chemical carcinogens (*18, 19*).

With respect to the mechanism of susceptibility of AC to chemical transformation, the difference in the extents of damage of AC and normal cells on 4-NQO treatment should be considered. Even when normal cells were treated with a concentration of 4-NQO higher than that causing damage of AC cells, they showed no morphologic alteration. In addition, untreated AC cells have a higher saturation density and longer life-span than untreated normal cells (text-fig. 1); the long life-span permits the cells before aging to undergo the many alterations required for neoplastic changes.

Recently, Rhim et al. (*19*) reported morphologic changes in AC fibroblasts when treated with MNNG for 7 days; however, the MNNG-treated cells produced no tumors in athymic nude mice (*19*). The AC cells morphologically transformed by 4-NQO (*18*) and MNNG in our experiments also did not form tumors in the subcutis of nude mice. The results of Rhim et al. and our results suggest that additional changes in carcinogen-treated AC cells are required for malignant transformation as described by Rhim et al. (*19*). Inoculation of AC cells treated with the tumor promoter TPA alone into the anterior chamber of the eye of a nude mouse produced a tumor (*7*). TPA enhanced the frequency of viral transformation of AC fibroblasts (*9*) and also increased the colony-forming frequency of the chemically transformed AC cells in soft agarose (data not shown). The tumorigenicity of AC cells treated with both carcinogen and TPA remains to be tested.

Although the tumorigenicity has not yet been confirmed, the morphologically altered AC fibroblasts possess the markers of transformation previously demonstrated in many cases of chemical transformation of other animal cells. Determination of the cellular factor that enhances the morphologic transformation of AC fibroblasts is required to elucidate the genetic factor in this syndrome.

REFERENCES

(*1*) Lockhart-Mummery JP, Dukes CE. Familial adenomatosis of colon and rectum, its relation to cancer. Lancet 1936; 1:586-589.

(*2*) Utsunomiya J, Nakamura T. The occult osteomatous changes in the mandible in patient with familial polyposis coli. Br J Surg 1975; 2: 45-51.

(*3*) Utsunomiya J, Maki T, Iwama T, et al. Gastric lesion of familial polyposis coli. Cancer 1974; 34:745-754.

(*4*) Pfeffer L, Lipkin M, Stutman O, Kopelovich L. Growth abnormalities of cultured human skin fibroblasts derived from individuals with hereditary adenomatosis of colon and rectum. J Cell Physiol 1976; 89:29-38.

(*5*) Miyaki M, Akamatsu N, Hirono U, et al. Characteristics of cultured fibroblasts of skin from patients with adenomatosis coli and Peutz-Jeghers' syndrome. In: Nagayo T, Mori W, eds. Gann Monograph on Cancer Research. Vol 25. Tokyo: Japan Scientific Societies Press, 1980:115-125.

(*6*) Kopelovich L. Phenotypic markers in human skin fibroblasts as possible diagnostic indices of hereditary adenomatosis of the colon and rectum. Cancer 1977; 40:2534-2541.

(*7*) Kopelovich L, Bias NE, Helson L. Tumour promoter alone induced neoplastic transformation of fibroblasts from humans genetically predisposed to cancer. Nature 1979; 282:619-621.

(*8*) Pfeffer LM, Kopelovich L. Differential genetic susceptibility of cultured human skin fibroblasts to transformation by Kirsten murine sarcoma virus. Cell 1977; 10:313-320.

(*9*) Miyaki M, Akamatsu N, Rokutanda M, et al. Increased sensitivity of fibroblasts of skin from patients with adenomatosis coli and Peutz-Jeghers' syndrome to transformation by murine sarcoma virus. Gan 1980; 71:797-803.

(*10*) Kakunaga T. Neoplastic transformation of human diploid fibroblast cells by chemical carcinogens. Proc Natl Acad Sci USA 1978; 75: 1334-1338.

(*11*) Benedict WF, Jones PA, Laug WE, Igel HJ, Freeman AE. Characterization of human cells transformed in vitro by urethane. Nature 1975; 256:322-324.

(*12*) Freeman AE, Lake RS, Igel HJ, et al. Heteroploid conversion of human skin cells by methylcholanthrene. Proc Natl Acad Sci USA 1977; 74:2451-2455.

(*13*) Cairns J. The origin of human cancers. Nature 1981; 289:353-357.

(*14*) Milo GE Jr, DiPaolo JA. Neoplastic transformation of human diploid cells in vitro after chemical carcinogen treatment. Nature 1978; 275:130-132.

(*15*) Sasaki MS. Fanconi's anemia, a condition possibly associated with a defective DNA repair. In: Hanawalt PC, Frieberg EC, Fox CF, eds. DNA repair mechanisms. New York: Academic Press, 1978:657-584.

(*16*) Danes BS. Increased tetraploidy: Cell-specific for the Gardner gene in the cultured cell. Cancer 1976; 38:1983-1988.

(*17*) Hori T, Murata M, Utsunomiya J. Chromosome aberrations induced by *N*-methyl-*N'*-nitro-*N*-nitrosoguanidine in cultured skin fibroblasts from patients with adenomatosis coli. Gan 1980; 71: 628-635.

(*18*) Miyaki M, Akamatsu N, Hirono U, Ono T, Tonomura A, Utsunomiya J. Transformation of fibroblasts from a patient with adenomatosis coli by treatment with a chemical carcinogen. Gan 1980; 71:741-742.

(*19*) Rhim JS, Huebner RJ, Arnstein P, Kopelovich L. Chemical transformation of cultured human skin fibroblasts derived from individuals with hereditary adenomatosis of colon and rectum. Int J Cancer 1980; 26:565-569.

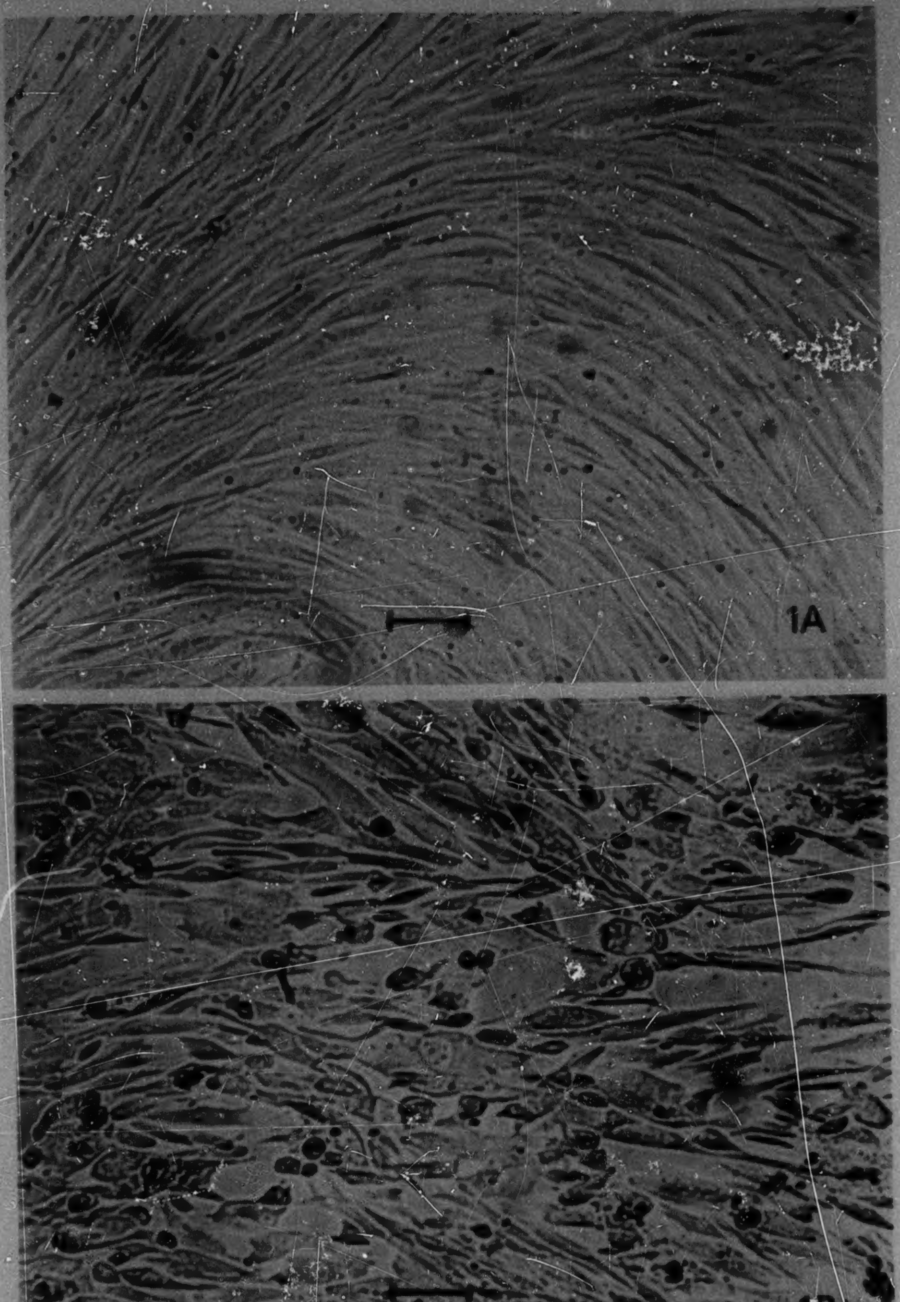

FIGURE 1.—Morphologic transformation of 4-NQO-treated AC fibroblasts. A) solvent-treated AC(MS) cells at passage 14 after treatment. B) 8 *μM* 4-NQO-treated AC(MS) cells at passage 10 after treatment. *Bars*=0.1 mm.

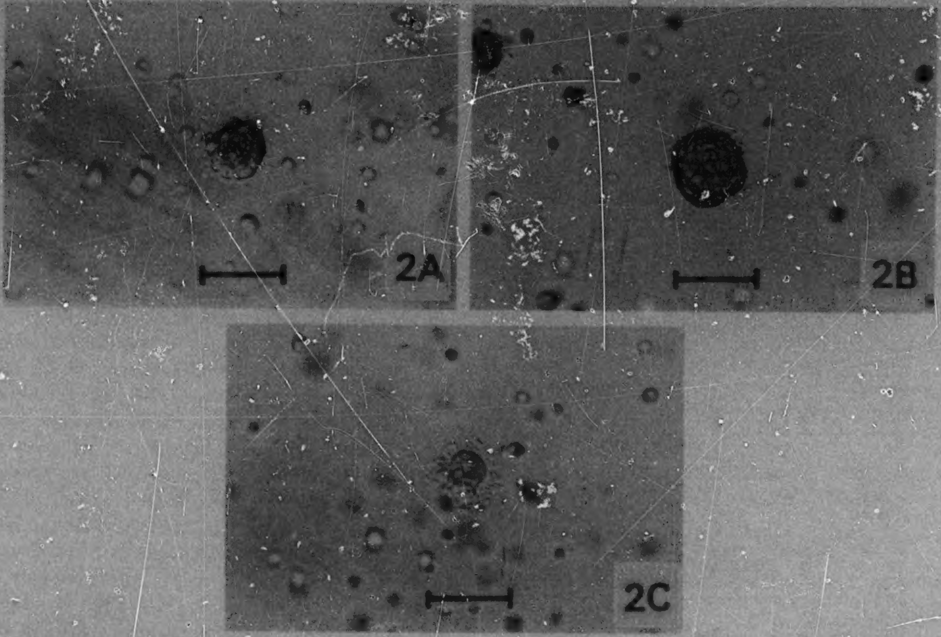

FIGURE 2.—Colonies of carcinogen-treated AC fibroblasts in soft agarose. Fibroblasts at passage 10 after treatment with carcinogen were plated on soft agarose and cultivated for 6 wk. A) 8 μM 4-NQO-treated AC(MS) cells. B) 40 μM MNNG-treated AC(MS) cells. C) Solvent-treated AC(MS) cells. *Bars*=0.1 mm.

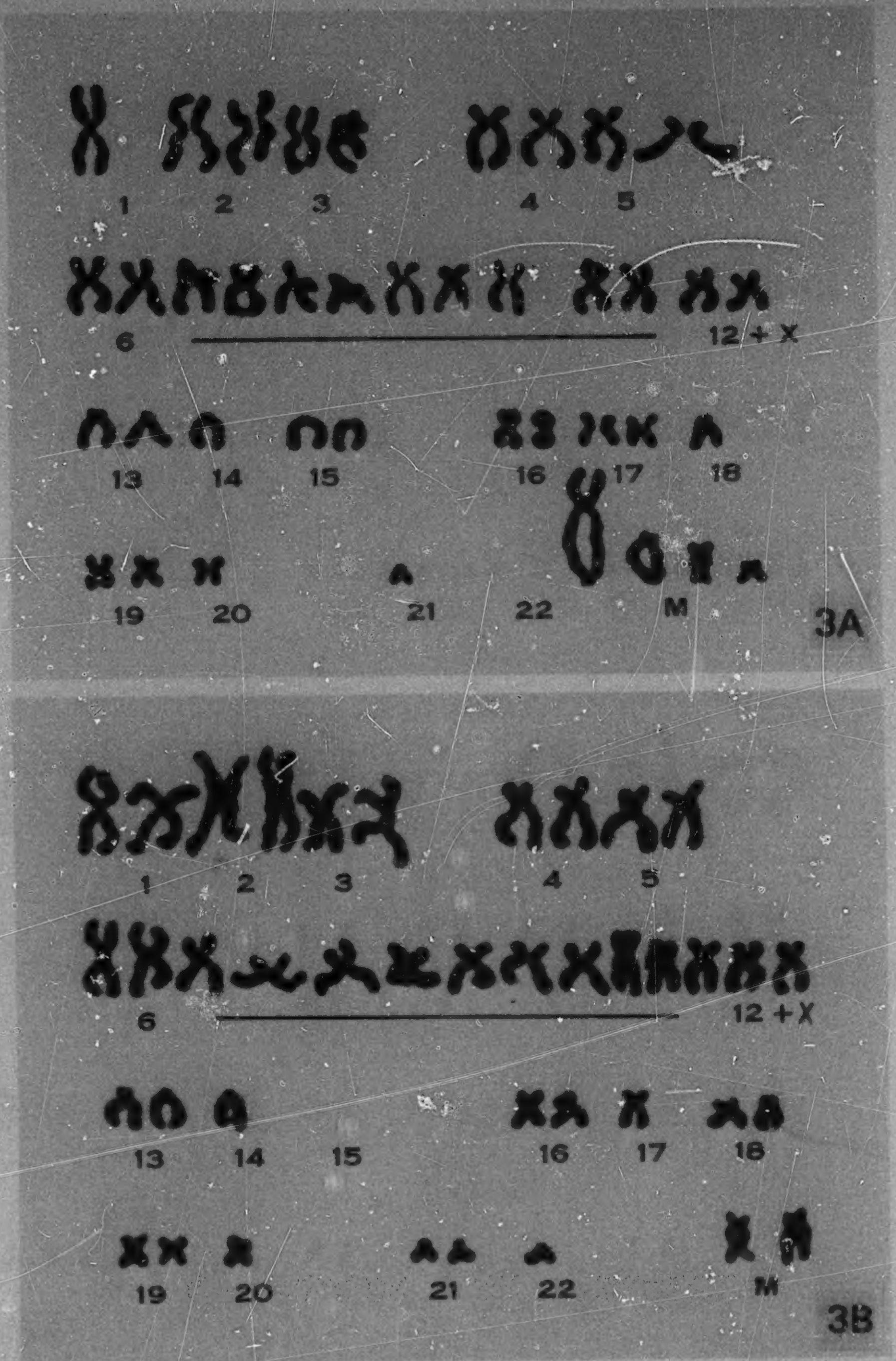
1
2
3
4
5
6
12 + X
13
14
15
16
17
18
19
20
21
22
M
3A
1
2
3
4
5
6
12 + X
13
14
15
16
17
18
19
20
21
22
M
3B

FIGURE 3.—Examples of mitoses showing dicentrics and unusually large monocentric marker chromosome. A) 8 μM 4-NQO-treated AC(MS) cells at passage 10 after treatment. B) 40 μM MNNG-treated AC(MS) cells at passage 10 after treatment. C) 4 μM 4-NQO-treated AC(YK) cells at passage 8 after treatment. D) Solvent-treated AC(MS) cells at passage 10 after treatment. E and F) Solvent-treated AC(YK) cells at passage 8 after treatment. M=marker chromosome.

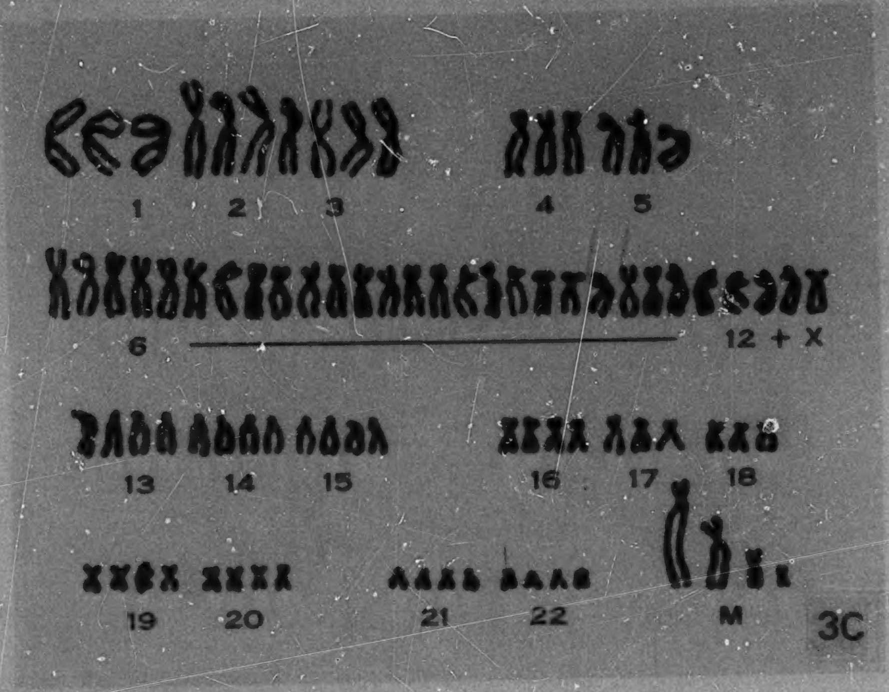
1
2
3
4
5
6
12 + X
13
14
15
16
17
18
19
20
21
22
M
3C

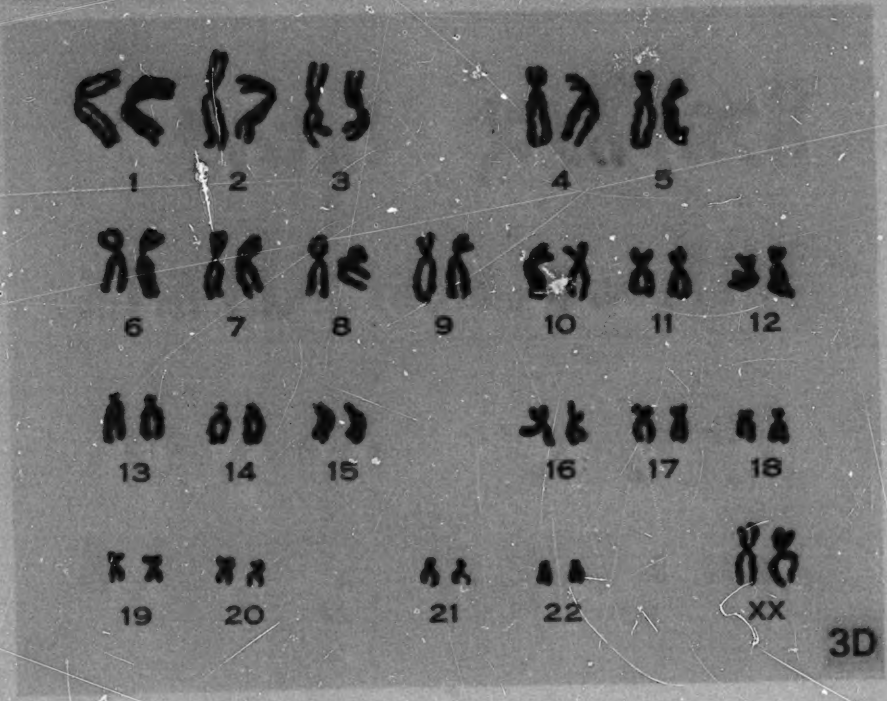
1
2
3
4
5
6
7
8
9
10
11
12
13
14
15
16
17
18
19
20
21
22
XX
3D

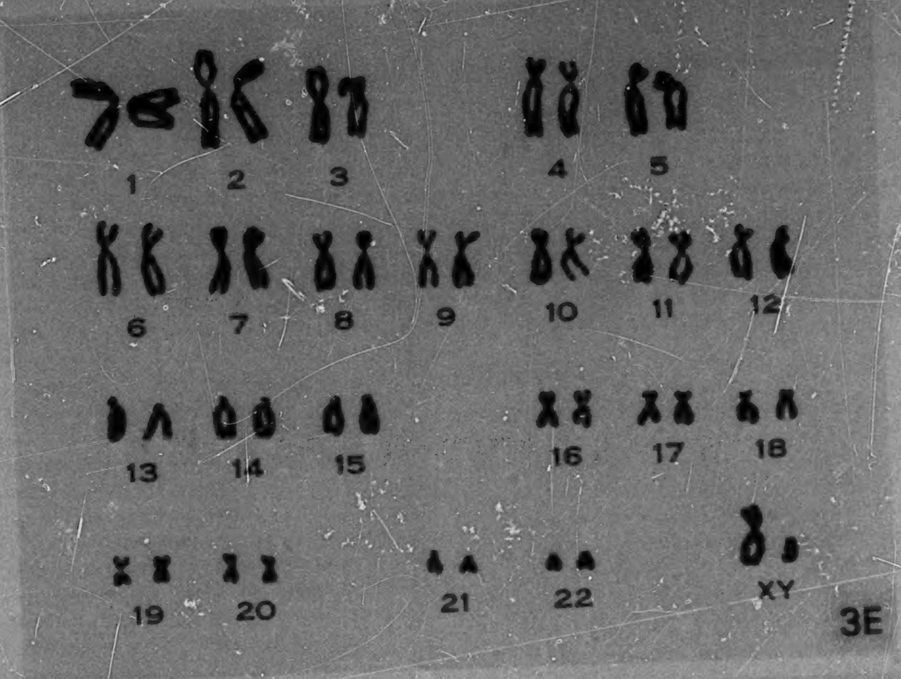
1
2
3
4
5
6
7
8
9
10
11
12
13
14
15
16
17
18
19
20
21
22
XY
3E

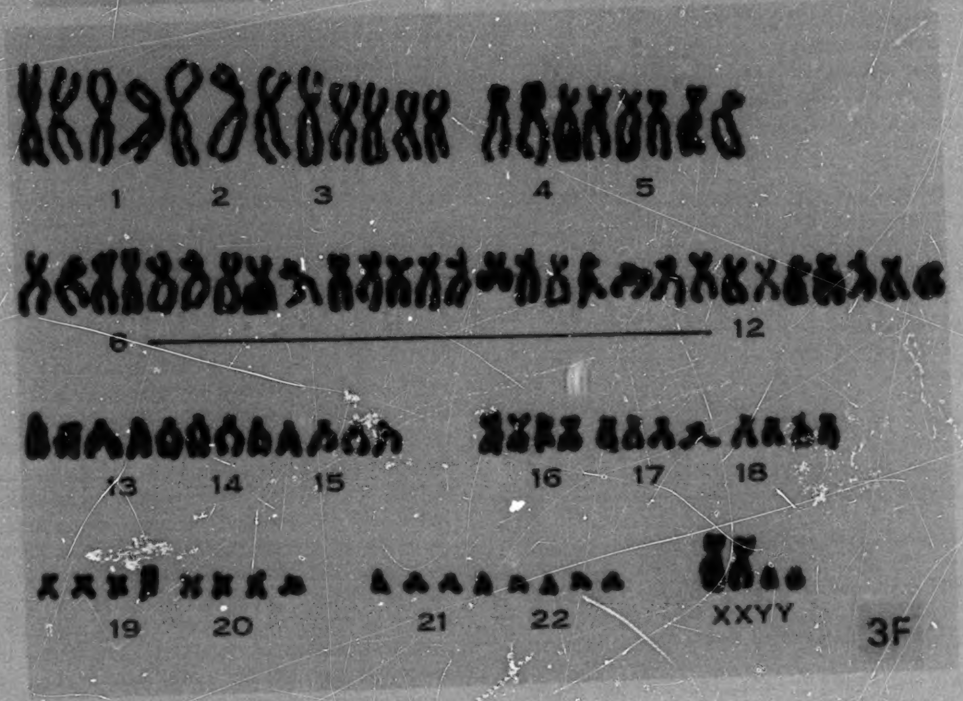
1
2
3
4
5
6
12
13
14
15
16
17
18
19
20
21
22
XXYY
3F

Carotid Body Tumors in Humans: Genetics and Epidemiology[1]

Dilys M. Parry,[2] Frederick P. Li,[2,3] Louise C. Strong,[4] J. Aidan Carney,[5] David Schottenfeld,[6] Ronald R. Reimer,[7,8] and Seymour Grufferman[9,10]

ABSTRACT—Genetic factors in the etiology of carotid body tumors (CBT) were sought in a medical record review of 222 histologically diagnosed cases at 12 U.S. medical centers. Patients in the series, which had a marked female predominance (146 females:76 males), usually developed tumors between the fourth and seventh decades of life (mean, 44.7 yr). In 16 patients who also had other extra-adrenal paragangliomas, suggesting a multiple primary tumor syndrome, CBT were diagnosed significantly earlier (mean, 35.4 yr; $P<0.01$). The occurrence of thyroid cancer in 5 other patients appeared to be excessive. Familial CBT was recognized in 16 patients from 13 affected families, including 9 newly ascertained kindreds. Compared with nonfamilial lesions, familial CBT tended to develop bilaterally (38% vs. 8% unilaterally) and at slightly earlier ages (41.6 vs. 44.9 yr). CBT was reported to occur in an autosomal dominant pattern in some families and within sibships in others; relatives were not examined for confirmation. The familial findings are generally consistent with a two-step mutation model of the development of hereditary and nonhereditary CBT; apparent deviations from the model might be clarified with additional data on this rare neoplasm.—JNCI 1982; 68:573–578.

The carotid bodies are paraganglia that probably develop from cells of the embryonic neural crest (*1*). Genetic etiology of CBT is suggested by familial occurrence of the neoplasm (*2*), and environmental influences are implied by the tumors' increased frequency at high altitudes (*3*). In this collaborative study, we examined hospital charts of 222 CBT patients to further clarify the etiologic role of host and environmental factors.

MATERIALS AND METHODS

The CCPDS is a program of uniform registration of patients at comprehensive cancer centers in the United States. In 1977, 10 member institutions of CCPDS, the National Cancer Institute, and the Cleveland Clinic Hospital agreed to provide hospital records for an epidemiologic study of patients with CBT (table 1). Because CBT is uncommon, the institutions were asked to retrieve data on all cases regardless of admission date. The wide variation among institutions in the cases contributed reflects differential case accrual as well as uneven success in chart retrieval. The records of 222 patients with CBT diagnosed through histologic examination were examined for sex, race, birthplace, birth date, past medical and family histories, date of onset of tumor manifestations, signs and symptoms at presentation with tumor, date of histologic diagnosis, extent of tumor, treatment, and outcome. Information concerning possible genetic or environmental risks was not uniformly recorded in the hospital charts.

Student's *t*-test was used to determine the statistical significance of the difference in mean ages. For patients with metachronous bilateral tumors, age at diagnosis was that for the first tumor. The chi-square test was used to evaluate differences in proportions of patients with bilateral tumors. The binomial proportion of females in a variety of tumor categories (total No. of females in category/total No. of patients in category) was compared to an expected proportion of 0.50 by means of the normal approximation (*4*). Data on many of the patients from the Mayo Clinic, Memorial Sloan-Kettering, and the Cleveland Clinic were included in previous articles (*5–9*).

RESULTS

The ages at diagnosis of CBT ranged from 11 to 83 years (mean, 44.7 yr; text-fig. 1). In most patients, the presenting sign was a slowly enlarging mass first noted an average of 5 years before histologic diagnosis (range, 0–47 yr). Unilateral CBT was diagnosed in 199 patients (90%) at an average age of 45.3 years and occurred with equal frequency in the left and right neck in both sexes. Bilateral tumors were diagnosed in 23 patients (10%) at an average age of 39.4 years, 6 years earlier than the age for unilateral tumor diagnosis ($P>0.05$).

Distribution of the 222 CBT patients by sex and race is shown in table 2. The proportion of females, 146 of 222 patients or 0.66, differed significantly from the expected value of 0.50 (table 3). Females predominated at all ages, particularly in the sixth and seventh decades of life (text-fig. 1). The excess of females was significant among patients

---

Abbreviations used: CBT=carotid body tumor(s); CCPDS=Centralized Cancer Patient Data System; PG=other extra-adrenal paraganglioma(s).

---

[1] Received June 4, 1981; revised October 23, 1981; accepted November 6, 1981.

[2] Clinical Epidemiology Branch, Division of Cancer Cause and Prevention, National Cancer Institute, Landow Building, Room 5A21, National Institutes of Health, Public Health Service, U.S. Department of Health and Human Services, Bethesda, Md. 20205.

[3] Division of Biostatistics and Epidemiology, Sidney Farber Cancer Institute, Harvard Medical School, Boston, Mass. 02115.

[4] Section of Medical Genetics, The University of Texas System Cancer Center, M. D. Anderson Hospital and Tumor Institute, Houston, Tex. 77030.

[5] Department of Surgical Pathology, Mayo Clinic and Mayo Foundation, Rochester, Minn. 55901.

[6] Department of Epidemiology and Preventative Medicine, Memorial Sloan-Kettering Cancer Center, New York, N.Y. 10021.

[7] Department of Epidemiology-Oncology, Cleveland Clinic Foundation, Cleveland, Ohio 44106.

[8] *Present address:* Centralized Cancer Patient Data System, Fred Hutchinson Cancer Research Center, Seattle, Wash. 98104.

[9] Department of Pediatrics and the Comprehensive Cancer Center, Duke University Medical Center, Durham, N.C. 27710.

[10] We thank our colleagues at the National Cancer Institute, Bethesda, Md.: Dr. Robert W. Miller and Dr. John J. Mulvihill for critical comments, Mr. Frank W. McKay and Ms. Margot Hanson for computer and statistical assistance, Ms. Wanda Wade for editorial assistance, and Ms. Toni Bredice for secretarial assistance.

TABLE 1.—*Centers contributing records of CBT patients*

Institution	No. of patients	Contributor
Cleveland Clinic Hospital	18	Ronald R. Reimer, *M.D.*
Duke University Comprehensive Cancer Center	8	Seymour Grufferman, *M.D.*
The Johns Hopkins Oncology Center	13	Raymond Seltser, *M.D.*
Mayo Clinic Comprehensive Cancer Center	116	J. Aidan Carney, *M.D., Ph.D.*
Memorial Sloan-Kettering Cancer Center	23	David Schottenfeld, *M.D.*
M. D. Anderson Hospital and Tumor Institute	8	Louise C. Strong, *M.D.*
National Cancer Institute	6	Dilys M. Parry, *Ph.D.*
Sidney Farber Cancer Institute	15	Frederick P. Li, *M.D.*
Ohio State University Comprehensive Cancer Center	4	Nancy Reiches, *Ph.D.*
Roswell Park Memorial Institute	2	Josef Vana, *M.D., Ph.D.*
University of California Cancer Research Institute at San Francisco	4	Calvin Zippin, *Ph.D.*
University of Wisconsin Clinical Cancer Center	5	John Crowley, *Ph.D.*
Total	222	

with unilateral tumors, but not among those with bilateral disease (table 3).

Malignant CBT, manifested as local invasion or metastasis, was found in only 9 patients, all with nonfamilial unilateral lesions: 4 had metastases to adjacent lymph nodes at the time of initial tumor excision, 4 had proved metastases in bone, and 1 had metastases in the lung. In these patients, the intervals between initial tumor diagnosis and metastatic disease ranged from 6.1 to 8.2 years.

Of 222 CBT patients, 37 (17%) developed other primary tumors (table 4). PG were diagnosed in 16 patients (#1–16), including 5 with bilateral CBT, and 4 with a third primary neoplasm. The PG occurred most frequently in the jugular body. The mean age at diagnosis of CBT in patients with PG was 35.4 years as compared with 45.4 years in patients without PG ($P<0.01$). The other 21 patients (#17–37) developed 26 additional tumors that were chiefly skin cancers and adenocarcinomas, including cancer of the thyroid gland in 5 females. The proportion of females among patients with PG did not differ significantly from 0.50, whereas females were in excess among patients with other primary tumors (table 3).

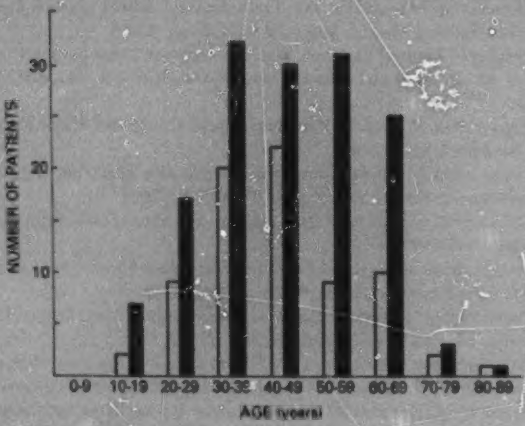

TEXT-FIGURE 1.—Age at diagnosis in 10-yr intervals for male and female CBT patients. □ = males, ■ = females.

Sixteen patients in this series (7%) were members of 13 families with CBT reported in 2 persons or more (text-fig. 2). Relatives were not clinically examined. A relative was considered to have had CBT only if this diagnosis was explicitly stated in the proband's chart. Families I–IV were reported previously (*6, 10, 11*); the remaining 9 were newly ascertained. Family IX was separately reported (*12*). Bilateral tumors were present in 6 of the 16 familial cases (38%) in our series, compared with 17 of 206 cases (8%) without a family history of CBT ($P<0.005$); 2 of the familial CBT cases also had PG. On the average, CBT was diagnosed 3 years earlier in familial than in nonfamilial cases (41.6 and 44.9 yr, respectively; $P>0.05$). There was no excess of females among the 16 histologically confirmed familial cases as compared to the significant female predominance among all nonfamilial cases (table 3). The lack of female predominance was also seen among all cases of CBT reported in the 13 families (22/45 affected individuals=0.49, $P>0.80$). CBT in multiple generations in 3 newly identified families (V–VII) involved vertical transmission through affected males. The 6 other new families were reported to have multiple affected siblings with apparently unaffected parents, including affected sib-pairs in family VIII who were first cousins.

Diverse medical conditions other than neoplasms were reported in individual CBT patients. Prior chronic cardiac or respiratory disorders were noted in 20 patients (table 5); this frequency (20/222 patients=9%) did not seem excessive for the patient age distribution, but the data may be incomplete and were not suitable for further analysis. Renal stones in 14 patients (6%) were of interest because hyperparathyroidism is associated with several neural crest tumors (*13, 14*). No other diseases were in striking excess. Most of the patients lived in the Midwestern or Northeastern United States and their histories showed no domicile at high altitudes, but their physicians may not have sought this information.

DISCUSSION

Epidemiology

This collaborative study confirmed previous reports that most CBT are unilateral without preference to side (*6*) and occur primarily during middle age (*6, 12, 15*). Although prolonged hypoxia resulting from chronic pulmonary dis-

TABLE 2.—*Sex and race of patients with CBT*

Race	Males	Females	Total
White	66	124	190
Black	1	13	14
Other[a]	2	1	3
Not specified	7	8	15
Total	76	146	222

[a] 1 Mexican, 1 Mestizo, 1 Oriental.

ease or high-altitude exposure was suggested previously as a cause of carotid body hyperplasia (*16, 17*) and neoplasia (*18*), evidence for it could not be obtained from our patients' fragmentary residential or medical histories. CBT were more frequent in women in this study, whereas diverse sex ratios were reported in smaller series in the literature (*6, 15, 19*). The twofold excess of women among nonfamilial cases in our study (137 females:69 males = 1.98) was less striking

TABLE 3.—*Proportion of females with CBT among different tumor categories*

Tumor category		Males	Females	Total	Proportion of females	Z^a	*P*-value[b]
No.	Type						
1	All tumors	76	146	222	0.66	4.63	<0.0001
2	Unilateral CBT	69	130	199	0.65	4.25	<0.0001
	Bilateral CBT	7	16	23	0.70	1.67	>0.09
3	CBT with PG	4	12	16	0.75	1.75	>0.08
	CBT with tumors other than PG	5	16	21	0.76	2.18	<0.03
	CBT without other tumors	67	118	185	0.64	3.68	<0.0002
4	Familial CBT	7	9	16	0.56	0.25	>0.80
	Nonfamilial CBT	69	137	206	0.67	4.67	<0.0001

[a] $Z=(|\hat{p}-p|-\frac{1}{2}n)/\sqrt{(pq/n)}$ where $\hat{p}$=females/total No. of patients, n=total, $p=\frac{1}{2}$, and $q=\frac{1}{2}$ (*4*).

[b] *P*-value: Determined for a two-tailed distribution.

TABLE 4.—*CBT patients with additional tumors*

Tumor category	Patient No. (reference)	Sex	Age at CBT diagnosis, yr	PG[a]	Other tumors[a,b] (No. of cases)
CBT with PG	1–5	♀	27, 36, 37, 46,[c,d,e] 48[c]	Jugular body	—
	6, 7	♂	21,[c] 35[c]	Jugular body	—
	8	♀	35	Jugular body, aortic arch body	—
	9, 10	♀	26, 36[c]	Vagal body	—
	11	♀	33[e]	Urinary bladder	—
	12 (*8*)	♀	39	Zuckerkandl bodies	—
CBT with PG and other tumors	13 (*9*)	♀	11	Thoracic sympathetic chain	Leiomyosarcomas, stomach; chondromas, lung
	14 (*9*)	♀	36	Jugular body	Leiomyosarcoma, urinary bladder
	15[f]	♂	36	Jugular body	Medullary carcinoma, thyroid gland
	16[f]	♂	59	Jugular body	Epidermoid carcinoma, lung
CBT with 2 cancers other than PG	17	♀	42	—	Follicular carcinoma, thyroid gland; endocarcinoma, endometrium
	18	♀	45	—	Cancer, NOS: skin and lower bowel
	19	♀	55	—	Malignant melanoma; sclerosing adenocarcinoma, thyroid gland
	20	♀	61	—	Adenocarcinoma, sigmoid colon; ductal carcinoma, breast
	21	♀	62	—	Epithelioma, cheek and nose; cancer, NOS: breast
CBT with 1 cancer other than PG	22–25	♀	44, 48, 61, 62	—	Scirrhous carcinoma, breast (2); cancer, NOS: breast (2)
	26–28	♀	34, 47, 75	—	Papillary and follicular carcinoma, thyroid gland (1); follicular carcinoma, thyroid gland (1); cancer, NOS: thyroid gland, (1)
	29, 30	♀	51, 72	—	Adenocarcinoma, endometrium
	31	♀	55	—	Large cell undifferentiated carcinoma, lung
	32	♀	60	—	Basal cell carcinoma, skin
	33, 34	♂	41, 55	—	Malignant lymphoma: nodular, well-differentiated lymphocytic type (1); diffuse histiocytic type (1)
	35	♂	32	—	Adenocarcinoma, colon
	36 (*6*)	♂	47	—	Squamous cell carcinoma, larynx
	37	♂	52	—	Cancer, NOS: skin

[a] —=none present.

[b] NOS=not otherwise specified.

[c] Bilateral CBT.

[d] Bilateral jugular body PG.

[e] Family history CBT.

[f] See table 5.

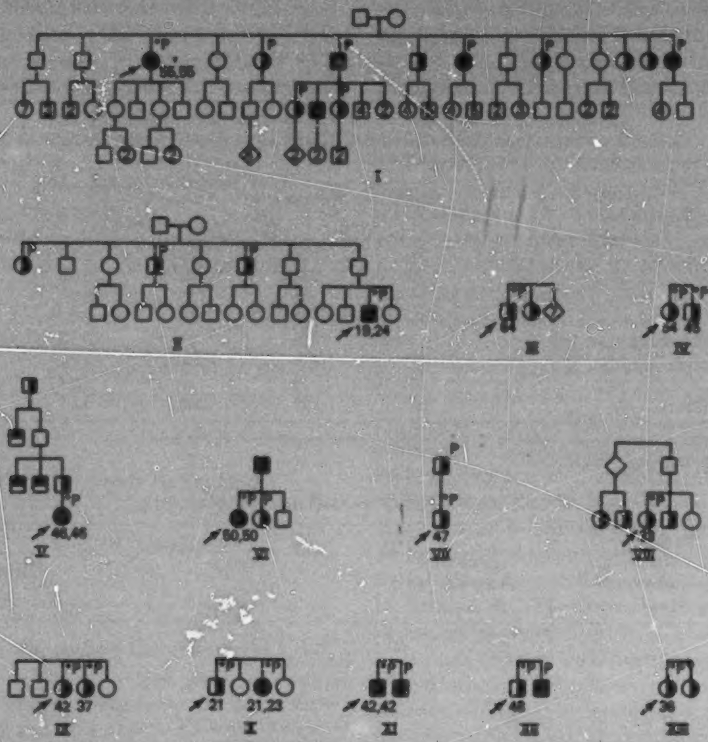

TEXT-FIGURE 2.—Pedigrees of 13 families with CBT. *Numbers under symbols* are ages in years at CBT diagnosis. The pedigrees of families I, II, and IX have been modified from the published versions (*2, 11, 12*). P = diagnosis by pathology; all others diagnosis by medical history only. □, ○ = unaffected males and females, respectively; ◧, ◐ = males and females, respectively, with unilateral CBT; ■, ● = males and females, respectively, with bilateral CBT; ⊟, ⊖ = tumor laterality not specified; ◇ = sex not specified; □, ○, ◇ with internal numbers = multiple siblings; * = patient in present series.

than the female predominance reported in residents at high altitudes in the Peruvian Andes (19 females:3 males), Mexico City (37 females:3 males), Bolivia (12 females:1 male), and Colorado (10 females:2 males) (*3, 20–22*). The female predominance consistently observed among the collaborating institutions suggests that females generally have increased susceptibility to CBT which may be further accentuated by prolonged hypoxia (*3, 16–18, 20–22*).

Multiple Primary Tumor Syndromes

Many of our patients developed multiple primary tumors. In particular, PG in 16 CBT patients cannot be explained by chance. Embryologically, all paraganglia including the carotid body are thought to develop from the neural crest (*23*). Concurrent development of these tumors in patients in this and previous reports (*6, 24–26*) may, therefore, be the consequence of a common susceptible progenitor cell (*23*). CBT have also been described in association with other disorders of neural crest-derived tissues, including pheochromocytoma and neurofibromatosis (*27, 28*). These conditions were not recorded in the present series; concurrence of CBT and PG in the absence of pheochromocytoma and neurofibromatosis may represent a distinct neuroendocrine syndrome.

Among our patients with CBT and PG, 4 had third primary tumors (table 4). Patient #13, who also had multiple birth defects, was 1 of 15 patients previously reported with this unusual tumor syndrome (*9*). The tumors in patient #14 may represent a variant of this disorder. In patient #15 medullary carcinoma of the thyroid gland, a tumor not described before with CBT, is a component of the neural crest-derived multiple endocrine neoplasia syndromes, types II and III. Epidermoid carcinoma of the lung in patient #16, a 59-year-old cigarette smoker, appears distinct from these genetically associated cancers.

The second primary tumors in CBT patients *without* PG included adenocarcinomas of the thyroid gland in 4 women and an unspecified thyroid cancer in a fifth (table 4). The thyroid cancers were not attributable to prior radiotherapy because only 1 of the women received such treatment. Biased ascertainment of conditions in structures in proximity to the carotid bodies might explain the finding. Concurrence of thyroid gland tumors with PG (including CBT) has been reported in other patients and in dogs (*3, 29, 30*). Among the other tumors found in CBT patients without PG, most were adenocarcinomas (breast, endometrium, and bowel) and skin cancers, the most common neoplasms in elderly women.

Genetic Implications

The aggregation of CBT in 13 families, including 9 newly ascertained kindreds, suggested that genetic factors were of

TABLE 5.—*Antecedent respiratory and cardiac diseases in CBT patients*

Patient No. (reference)	Sex	Age at CBT diagnosis, yr	Associated condition
			Pulmonary disease
15[a]	♂	36	Recurrent bacterial pneumonia
16[c]	♂	59	Chronic asthma, emphysema, tuberculosis
38, 39	♂	37, 68	Tuberculosis
40, 41 (*7*)	♂	48,[b] 58	Emphysema secondary to silicosis and to tracheal compression from massive goiter (1 each)
42	♀	37[c]	Lung abscess, lobectomy
43–46	♀	23, 26, 43, 45	Asthma
47–51	♀	32, 48, 56, 58, 65	Tuberculosis
			Cardiac disease
52	♂	44	Rheumatic heart disease, mitral stenosis, congestive heart failure
53	♀	24	Congenital aortic stenosis with aortic insufficiency
54	♀	36	Hypoplastic right ventricle, cyanosis, clubbing
55	♀	45	Rheumatic heart disease, aortic stenosis

[a] *See also* table 4.
[b] Bilateral CBT.
[c] Family history CBT.

etiologic importance in this rare neoplasm. As is characteristic of heritable tumors (*31*), the familial cases had a high frequency of bilateral and multifocal (CBT with PG) disease, an approximately equal sex ratio among affected individuals, and evidence of vertical transmission. In addition, patients with PG developed CBT at a relatively early age.

Knudson et al. (*31*) developed a two-step mutation hypothesis to explain the existence of hereditary and nonhereditary forms of several tumors. According to the hypothesis, in hereditary cases the first mutation is prezygotic and may be dominantly inherited; tumors develop only in rare somatic cells that sustain a postzygotic second mutation. In nonhereditary cases, tumors develop only when both mutations occur postzygotically in a single somatic cell line.

The two-step hypothesis was initially developed for retinoblastoma and other malignant embryonal tumors from a review of data on age at diagnosis, multiplicity of tumors, and familial tumor patterns (*31*). Similar data on CBT were collected in the present study. The predominance of bilateral and multifocal tumors within affected families and evidence of vertical transmission were consistent with a two-step mutation hypothesis. However, in contrast to expectations based on this model, ages at diagnosis of hereditary and nonhereditary CBT were not significantly different. This phenomenon had been observed previously for this tumor (*12*). Other aspects of our data also were not compatible with the simplest form of this hypothesis. Females predominated among patients with nonfamilial tumors, as compared with an expected frequency of 0.50 seen among familial cases in this series and in the literature (*2, 12*). Furthermore, female predominance approached significance in the combined category of nonfamilial bilateral and/or multifocal CBT (19 females/27 patients = 0.70; *P*>0.06). In the two-step hypothesis, nonfamilial bilateral or multifocal tumors are considered to result from new prezygotic heritable mutations and thus are expected to occur equally in both sexes. Finally, although consecutive affected generations were seen, the most frequent familial pattern was of multiple affected siblings with unaffected parents.

A consistent excess of females with CBT among institutions participating in this study suggested that the sex distributions of our patients reflected real differences in tumor susceptibility. The data on family history were much less reliable: Inasmuch as relatives were not examined, we likely underestimated the number of affected individuals within our families as well as the total frequency of familial disease. However, the familial patterns were similar to those described for 16 CBT families and for hereditary retinoblastoma (*2*). Retrospective family studies of both of these tumors suggested large numbers of asymptomatic gene carriers and apparent low gene penetrance. However, follow-up study of the progeny of familial and bilateral retinoblastoma probands indicated a highly penetrant autosomal dominant gene (*32*). Similar data on the progeny of CBT probands are not available.

Several explanations have been proposed for the departure of familial tumor patterns from that expected for autosomal dominant inheritance (*31*). Decreased gene penetrance could account for some unaffected gene carriers. Parental gonadal mosaicism could produce multiple affected siblings in the absence of an affected parent. Malignant embryonal tumors in distant relatives with unaffected common ancestors have been attributed to the lethality of the tumors in affected gene carriers and the survival advantage of the rare unaffected carrier. However, such selection is unlikely to be a significant factor in a benign tumor such as CBT that develops in middle age. This familial pattern could also result from cancer-associated chromosome deletions in offspring of balanced translocation carriers, as reported for familial Wilms' tumor and retinoblastoma (*33, 34*).

Hermann (*2*) applied the delayed mutation model of Auerbach (*35*) to explain the variety of familial patterns seen in both CBT and retinoblastoma. Both this and the two-step hypothesis of Knudson et al. (*31*) involve a two-phase mutational process, but the events involved in delayed mutation may relate only to the initial step of the Knudson hypothesis. In the Auerbach hypothesis, a labile genetic change (premutation) associated with a normal phenotype is transmitted through unaffected carriers. The premutated allele may revert to the normal allele or undergo further change (telomutation) associated with a high risk of a tumor phenotype. Telomutation in a germinal cell would produce affected offspring with unaffected parents and transmission of a highly penetrant autosomal dominant gene in subsequent generations. Telomutation in a target somatic cell would produce an affected individual who would transmit the premutated allele through unaffected carriers. Among 16 CBT pedigrees, Herrmann observed that the tumor frequency among offspring of affected females was lower than that predicted for autosomal dominant inheritance. Our additional pedigrees are noncontributory in this regard inasmuch as no affected woman had offspring. Preferential occurrence of somatic telomutation in affected women could account for the apparent lack of tumor in their progeny.

Data from the present study and the literature suggest that CBT occur in heritable and nonheritable forms. The familial form, like that of other hereditary tumors, is associated with a high frequency of bilaterality and tumors of other specific sites, occurs equally in both sexes, and is vertically transmitted in some families. The genetic etiology of CBT can be further clarified through clinical evaluation of obligate gene carriers and asymptomatic members of affected families to detect minimal or occult tumors, prospective study of progeny of affected individuals, and identification of markers of the CBT gene.

REFERENCES

(1) Le Douarin NM. Cell recognition based on natural morphological nuclear markers. Med Biol 1974; 52:281–319.

(2) Herrmann J. Delayed mutation model: Carotid body tumors and retinoblastoma. In: Mulvihill JJ, Miller RW, Fraumeni JF Jr, eds. Genetics of human cancer. New York: Raven Press, 1977:417–438.

(3) Saldana MJ, Salem LE, Travezan R. High altitude hypoxia and chemodectomas. Hum Pathol 1973; 4:251–263.

(4) Snedecor GW, Cochran WG. Statistical methods. 6th ed. Ames, Iowa: Iowa State Univ Press, 1967.

(5) Irons GB, Weiland LH, Warwick LB. Paragangliomas of the neck: Clinical and pathological analysis of 116 cases. Surg Clin North Am 1977; 57:575–583.

(6) Lack EE, Cubilla AL, Woodruff JM, Farr HW. Paragangliomas of the head and neck region. A clinical study of 69 patients. Cancer 1976; 39:397–409.

(7) Anderson R, Scarcella JV. Carotid body tumors. Am J Surg 1963; 106:856–859.

(8) Craig RW. Concurrent tumors of the left carotid body and both Zuckerkandl bodies. Arch Pathol 1934; 18:635–645.

(9) Carney JA. The triad of gastric epithelioid leiomyosarcoma, functioning extra-adrenal paraganglioma, and pulmonary chondroma. Cancer 1979; 43:374–382.

(10) Kroll AJ, Alexander B, Cochios F, Pechet L. Hereditary deficiencies of clotting factors VII and X associated with carotid-body tumors. N Engl J Med 1964; 270:6–13.

(11) Sugarbaker EV, Chretien PB, Jacobs JB. Bilateral familial carotid body tumors: Report of a patient with an occult contralateral tumor and postoperative hypertension. Ann Surg 1971; 174:242–247.

(12) Grufferman S, Gillman MW, Pasternak LR, Paterson CL, Young WG. Familial carotid body tumors: Case report and epidemiologic review. Cancer 1980; 46:2116–2122.

(13) Jackson CE, Frame B, Block MA. Prevalence of endocrine neoplasia syndromes in genetic studies of parathyroid tumors. In: Mulvihill JJ, Miller RW, Fraumeni JF Jr, eds. Genetics of human cancer. New York: Raven Press, 1977:205–208.

(14) Blacklock NJ. The pattern of urolithiasis in the Royal Navy. In: Hodgkinson A, Nordin BE, eds. Proceedings of the renal stone research symposium. London: Churchill, 1969:33–47.

(15) Oberman HA, Holtz F, Sheffer LA, Magielski JE. Chemodectomas (nonchromaffin paragangliomas) of the head and neck. Cancer 1968; 21:838–851.

(16) Lack EE. Carotid body hypertrophy in patients with cystic fibrosis and cyanotic congenital heart disease. Hum Pathol 1976; 8:39–47.

(17) Heath D. The carotid body in human cardiopulmonary disease. Pathol Microbiol 1973; 39:305–309.

(18) Chedid A, Jao W. Hereditary tumors of the carotid bodies and chronic obstructive pulmonary disease. Cancer 1974; 33:1635–1641.

(19) Shamblin WR, ReMine WH, Sheps SG, Harrison EG. Carotid body tumor (chemodectoma). Am J Surg 1971; 122:732–739.

(20) Krause-Senties LG. Tumores del cuerpo carotideo. Arch Invest Med (Mex) 1971; 2:25–30.

(21) Rios Dalenz J, Wayllace LZ. A clinical pathological study of 13 cases of carotid body tumors. Rev Med (La Paz) 1977; 1:7–14.

(22) Morfit HM, Swan H, Taylor ER. Carotid body tumors. Arch Surg 1953; 67:194–214.

(23) Bolande RP. The neurocristopathies. Hum Pathol 1974; 5:409–429.

(24) Nathanson SD, Gaylis H. Multicentric chemodectomata at high altitude. S Afr Med J 1974; 48:1715–1717.

(25) Bocian JJ, Tuschka OJ. Multicentric paragangliomas—vagal body and carotid body tumors. Calif Med 1958; 88:51–54.

(26) Lattes R. Nonchromaffin paraganglioma of ganglion nodosum, carotid body, and aortic arch bodies. Cancer 1950; 3:667–694.

(27) Sato T, Saito H, Yoshinaga K, Shibota Y, Sasano N. Concurrence of carotid body tumor and pheochomocytoma. Cancer 1974; 34:1787–1795.

(28) Melicow MM. One hundred cases of pheochromocytoma (107 tumors) at the Columbia-Presbyterian Medical Center, 1926–1976. Cancer 1977; 40:1987–2004.

(29) Albores-Saavedra J, Duran ME. Association of thyroid carcinoma and chemodectoma. Am J Surg 1968; 116:887–890.

(30) Hayes HM Jr, Fraumeni JF Jr. Chemodectomas in dogs: Epidemiologic comparisons with man. J Natl Cancer Inst 1974; 52:1455–1458.

(31) Knudson AG, Strong LC, Anderson DE. Heredity and cancer in man. Prog Med Genet 1973; 9:113–158.

(32) Schappert-Kimmijser J, Hemmes GD, Nijland R. The heredity of retinoblastoma. Ophthalmologica 1966; 151:197–213.

(33) Yunis JJ, Ramsay NK. Familial occurrence of the aniridia–Wilms tumor syndrome with the deletion 11p13–14.1. J Pediatr 1980; 96:1027–1030.

(34) Strong LC, Riccardi VM, Ferrell RE, Sparkes RS. Familial retinoblastoma and chromosome 13 deletion transmitted via an insertional translocation. Science 1981; 213:1501–1503.

(35) Auerbach C. A possible case of delayed mutation in man. Ann Hum Genet 1956; 20:266–269.

Lymphocyte Fluorescence Polarization Changes After Phytohemagglutinin Stimulation in the Diagnosis of Colorectal Carcinoma[1,2,3]

Glenn R. Hocking,[4] Jennifer M. Rolland,[4] Richard C. Nairn,[4,5] Eric Pihl,[4] Alan M. Cuthbertson,[6] Edward S. R. Hughes,[7] *and* William R. Johnson[7,8]

ABSTRACT—A lymphocyte fluorescence polarization test that measures reactivity to phytohemagglutinin (PHA) has permitted discrimination of a majority of patients with colorectal carcinoma from noncancer individuals. The test involves separation of two lymphocyte fractions from 20 ml venous blood on a modified leukocyte separation gradient, incubation with PHA for 45 minutes, addition of fluorescein diacetate, and analysis of change in fluorescence polarization. Of 19 colorectal patients tested preoperatively, 13 had a positive stimulation index, 3 a zero index, and 3 a negative index. Of 7 patients with other malignant neoplasms, a positive value was obtained in 6 and a negative value in 1. Of 14 patients with other diseases, a negative value was obtained in 9, zero in 3, and positive in 2. Of 31 normal donors a negative value was obtained in 27, zero in 2, and weak positive in 2. This rapid test promises to develop into a useful cancer-diagnostic method, and elucidation of its biological basis should identify a new cancer marker.—JNCI 1982; 68:579–583.

Fluorescent probes reveal early changes in lymphocytes after stimulation with antigen or mitogen (*1*), and this offers a feasible screening immunoassay procedure for diagnosing and monitoring of cancer patients. Kreutzmann et al. (*2*) and Pritchard et al. (*3*) reported fluorescent probe assays for lymphocyte response to short-term stimulation with PHA, which distinguished cancer patients from patients with other diseases and from healthy people. This assay is based on a method developed by Cercek and Cercek (*4*), in which decreased fluorescence polarization of intracellular fluorescein was shown by a fraction of normal donors' lymphocytes but not cancer patients' lymphocytes stimulated with PHA. Pritchard et al. (*3*) modified the technique to include separation of lymphocytes into two zones with the use of a Ficoll–Triosil gradient of carefully controlled density. For normal donors, the less dense fraction of lymphocytes responded to PHA better than the denser fraction, whereas the converse was found for cancer patients.

Our results from a preliminary series of cases provide confirmatory evidence of the usefulness of the double-zone fluorescence polarization technique in the detection of colorectal cancer.

MATERIALS AND METHODS

Patients and healthy donors.—Blood samples were obtained from 38 patients with histopathologically confirmed colorectal carcinoma (19 cases postoperative), and 7 patients with other cancers (1 case postoperative), as detailed in table 1, 14 patients with other diseases (table 2), and 31 healthy donors (table 3).

To satisfy ourselves about the objectivity of the tests, we examined "blind" without knowledge of the clinical status blood samples from all patients.

Blood lymphocyte separation.—Venous blood samples (20 ml) were collected from patients and control donors into three 10-ml "Vacutainer" tubes (#6484; Becton, Dickinson & Co., Waltham, Mass.) containing 143 IU lithium heparin. Up to three different blood samples were analyzed conveniently in 1 day. If necessary, blood was stored up to 24 hours at room temperature before use. Lymphocyte separation was performed essentially as described by Cercek and Cercek (*4*) and modified by Pritchard et al. (*3, 5*). Monocytes were removed by incubation with 0.1 g iron carbonyl powder, and lymphocytes were separated on a Ficoll 400 (Pharmacia, Piscataway N.J.)–Triosil 440 (Nyegaard & Co., Oslo, Norway) gradient (density, 1.081 g/cm^3 at 25°C; osmolality, 320 mosmol/kg) by centrifugation at 1,100×*g* at the interface for 25 minutes at 25°C. We divided the interface cells into two fractions by collecting 2 ml in an automatic pipette with the tip held approximately 2 mm above the cell layer (zone 1) and 2 ml with the tip held 2 mm below the cell layer (zone 2). Only occasionally did the interface cell layer appear as two distinct bands; whether or not this occurred, the same method of collection of the upper and lower zones was adopted for all blood samples. Usually, from a 20-ml blood sample, there were about 5–15×10^6 cells in zone 1 and 2–5×10^6 cells in zone 2. Because of the smaller cell numbers in zone 2, replicate experiments were not often feasible with this fraction. The cells of each zone were washed twice with 0.85% saline, once with DPBS (*6*) by centrifugation at 400×*g* for 5 minutes, and finally resuspended in DPBS at a concentration of 1–3×10^6 lymphocytes/ml.

Lymphocyte stimulation with PHA.—Aliquots (0.25 ml) of

ABBREVIATIONS USED: FDA=fluorescein diacetate; DPBS=Dulbecco's phosphate-buffered saline; PHA=phytohemagglutinin.

---

[1] Received June 9, 1981; accepted October 2, 1981.

[2] Supported by a grant from the Anti-Cancer Council of Victoria, Australia.

[3] Research procedures were in accord with the ethical standards of the Committee on Experimentation Involving Human Subjects, Monash University, and of the Helsinki Declaration of 1975.

[4] Department of Pathology and Immunology, Monash University, Alfred Hospital, Commercial Road, Prahran, Victoria, Australia 3181.

[5] *Address reprint requests to* Dr. Nairn.

[6] Cabrini Medical Centre, Malvern, Victoria, Australia 3144.

[7] Department of Surgery, Monash University.

[8] We thank Miss T. J. Brentnall for technical assistance and Dr. W. G. R. M. de Boer, Royal Southern Memorial Hospital, and Dr. M. Whiteside, Alfred Hospital, for the provision of blood samples.

lymphocytes from both zones were each incubated with 50 µl PHA (GIBCO, Grand Island, N.Y., reconstituted with distilled water, and diluted 1:5 with DPBS) at 37°C for 45 minutes.

FDA substrate solution.—A stock solution of 10 mg FDA/ml (Riedel-de Häen, Seelze-Hannover, Federal Republic of Germany) in Aristar grade glacial acetic acid (British Drug Houses, Poole, England) was prepared weekly. Fresh FDA substrate solution was made for each experiment by adding 10 µl FDA stock solution to 100 ml DPBS and by transferring 25 ml of this solution to 75 ml PBS to which 0.08 g NaCl and 0.03 g Na_2HPO_4 had been added. The substrate solution had a final osmolality of 330 mosmol/kg (pH 7.4) and was stored in a light-proof container at room temperature.

Fluorescence polarization measurement.—Control or PHA-stimulated cells were resuspended by drawing in and out three times a 21-gauge hypodermic needle attached to a 1-ml tuberculin syringe. Aliquots (0.25 ml) of the resuspended cells were mixed with 3 ml FDA substrate solution and transferred in a 1-cm quartz cuvette to a Perkin-Elmer MPF 44A spectrophotometer (Perkin Elmer Corp., Norwalk, Conn.). The spectrophotometer was used as described by Cercek and Cercek (*4*) except for the addition of a half wave plate (HNCP 37; Polaroid Corp., Cambridge, Mass.) in front of the excitation polarizer. Polarization values were determined (*4*) for zone 1 and 2 cells, unstimulated and PHA-stimulated, where possible in duplicate. The percentage reduction in mean polarization after PHA stimulation was calculated for zone 1 and 2 cells, and the difference between these (zone 2−zone 1=stimulation index) was determined for each case.

In table 3, results for normal individuals for whom repeat tests were made are shown. For cases #67 and 85, repeat values were obtained for two separations on the same day. For case #60, the stimulation indices were obtained for the same blood collection, one sample was separated and analyzed immediately, the other was separated and analyzed 24 hours later. Remaining repeat values were obtained for blood samples taken at intervals of 1 week to 6 months.

RESULTS

The correlation between stimulation index and clinical status is shown in text-figure 1. For colorectal carcinoma patients, preoperative blood samples from 13 of 19 cases gave a positive index, and 3 cases gave zero (table 1). The significance of the 3 false-negative cases is not known, but we are testing a larger series of patients to investigate the relationship between tumor stage, differentiation, and stimulation index. Of the 19 postoperative blood samples, the tumor recurrence in case #20 agrees with the positive index, while in case #22, the negative value may reflect successful treatment of a small recurrence detected 10 months previously. Three patients tested before and after surgical excision of tumor showed decreased values postoperatively. Eleven of 16 other cases tested postoperatively had a negative index, and the possible prediction of tumor recurrence by a positive index in cases #23 and 24 awaits further investigation and follow-up.

Of 7 patients with other cancers, 6 gave a positive index. We have no explanation for the negative value for case #45, but the possible effect of certain drugs on lymphocyte reactivity has not yet been established. Again, in case #44 the index decreased postoperatively.

In a small series of 14 patients with other diseases (table 2), there were two false-positives. One of these (case #46) is undiagnosed but is suspected of having a preclinical lymphoreticular cancer. The chronic inflammatory disease ulcerative colitis was associated with a negative index in 7 of

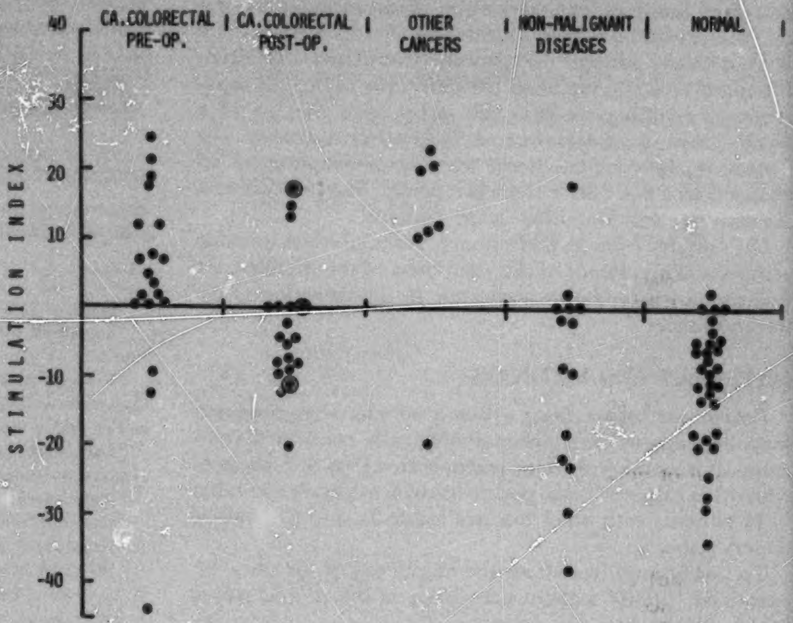

TEXT-FIGURE 1.—Fluorescence polarization changes after PHA stimulation: Stimulation indices for 38 patients with colorectal carcinoma (19 preoperative, 19 postoperative; ● recurrence confirmed), 7 patients with other cancers, 14 patients with other diseases, and 31 normal individuals.

TABLE 1.—*Cancer patients' responses to PHA*

Case No.	Age, yr	Sex	Diagnosis and blood samples[a]		Reduction in polarization after PHA stimulation, %		Stimulation index
					Zone 1	Zone 2	
1	74	♀	Colorectal carcinoma, preoperative		6.5	30.3	+23.8
2	75	♂	" " "		2.6	23.6	+21.0
3	72	♂	" " "		34.7	53.1	+18.4
4	65	♂	" " "		0	17.3	+17.3
5	57	♂	" " "		2.9	14.5	+11.6
6	72	♂	" " "		0	11.6	+11.6[b]
7	72	♂	" " "		6.3	13.5	+7.2
8	58	♂	" " "		9.4	16.0	+6.6
9	60	♂	" " "		0	6.6	+6.6
10	64	♀	" " "		6.9	10.7	+3.8
11	55	♀	" " "		0	3.3	+3.3
12	75	♀	" " "		0	1.1	+1.1
13	80	♀	" " "		4.1	4.9	+0.8
14	78	♀	" " "		0	0	0
15	55	♂	" " "		0	0	0
16	74	♂	" " "		0	0	0
17	61	♀	" " "		9.7	0	−9.7
18	67	♀	" " "		31.0	18.2	−12.8[c]
19	79	♂	" " "		44.6	0	−44.6
20	60	♀	" " 19 mo postoperative	R 18 mo postoperative	0	16	+16
21	73	♀	" " 14 mo "	" 12 mo "	0	0	0
22	41	♀	" " 24 mo "	" 14 mo[d] "	11.8	0	−11.8
23	54	♂	" " 15 mo "	NSR	0	14.4	+14.4
24	56	♀	" " 6 mo "	"	9.9	23.2	+13.3
25	47	♂	" " 6 days "	"	0	0	0
26	67	♂	" " 8 mo "	"	0	0	0
27	60	♀	" " 24 mo "	"	0	0	0
28	61	♀	" " 6 mo "	"	2.6	0	−2.6
29	64	♂	" " 28 mo "	"	4.6	0	−4.6
30	42	♂	" " 18 mo "	"	4.8	0	−4.8
31	58	♂	" " 4 mo "	"	5.8	0	−5.8
32	67	♂	" " 11 mo "	"	7.7	0	−7.7
33	57	♀	" " 32 mo "	"	8.4	0	−8.4
34	70	♀	" " 6 mo "	"	8.5	0	−8.5
35	64	♂	" " 3 mo "	"	20.9	12.2	−8.7
36	85	♀	" " 12 mo "	"	13.3	4.0	−9.3
37	74	♂	" " 48 mo "	"	12.3	0	−12.3
38	61	♀	" " 7 days "	"	33.3	12.7	−20.6
39	60	♂	Cancer of appendix, peritoneal dissemination		0	20.1	+20.1
40	86	♀	Cancer of esophagus, 4 days postoperative		11.4	32.1	+20.7
41	66	♀	Lymphocytic lymphoma		2.7	25.6	+22.9
42	51	♂	Hepatocellular carcinoma		0	11.9	+11.9
43	69	♂	Melanoma, lymph node 2°		4.8	16.2	+11.4
44	49	♂	Squamous cell carcinoma recurrence		0	10.7	+10.7[e]
45	24	♀	Osteosarcoma		19.9	0	−19.9

[a] R=recurrence; NSR=no sign of recurrence.

[b] Retested 3 mo post operation; stimulation index, −4.2.

[c] Retested 1 day post operation; stimulation index, −36.0.

[d] Radon implant 1 mo before test.

[e] Retested 1; 3 days post operation; stimulation index, 0 and, 0.

10 cases, a zero in 2 others, and a low positive in 1 other. Again, the possibility of preclinical cancer in this positive case will be followed up.

Testing of normal donors' blood lymphocytes (table 3) revealed a negative stimulation index in 27 of 31 cases and a zero value in 2 others. The two false-positive values were low, and for one of these retesting gave a negative index. None of the results seem to be age related, though the preponderance of young adults in our normal controls is a parameter that will be examined fully in our ensuing field trial of the test.

Polarization values obtained in a typical experiment are shown in table 4. In this experiment, duplicate unstimulated zone 1 polarization values differ by 2.3% from the mean. For the experiments of the present series, the variation of replicate polarization values from the mean was 0–9%, with an average variation of 3.2%. Only rarely was a variation greater than 9% obtained, and when this occurred, the experiment was regarded as technically unsatisfactory and was excluded.

TABLE 2.—*Noncancer patients' responses to PHA*

Case No.	Age, yr	Sex	Diagnosis	Reduction in polarization after PHA stimulation, %		Stimulation index
				Zone 1	Zone 2	
46	54	♀	Chronic neutropenia[a]	4.2	22.2	+18.0
47	28	♂	Ulcerative colitis	0	1.8	+1.8
48	66	♀	" "	0	0	0
49	56	♀	" "	0	0	0
50	29	♀	" "	1.8	0	−1.8
51	42	♀	" "	15.6	6.8	−8.8
52	55	♂	" "	9.2	0	−9.2
53	37	♀	" "	18.3	0	−18.3
54	30	♀	" "	25.9	2.5	−23.4
55	68	♀	" "	29.9	0	−29.9
56	39	♂	" "	48.3	9.9	−38.4
57	63	♀	Benign monoclonal paraproteinemia	0	0	0
58	54	♀	Diverticulosis	2.2	0	−2.2
59	63	♀	Mitral valve disease	22.0	0	−22.0

[a] Suspected preclinical lymphoreticular cancer.

DISCUSSION

A good correlation has been demonstrated between the results of the fluorescence polarization test and clinicopathologic diagnosis. Overall, there were only four false-negatives in 26 cases of cancer tested preoperatively, and four false-positives in 45 cases of nonmalignant disease or normal donors. Despite the lack of age matching in this preliminary series, the negative values of cancer patients tested postoperatively is a strong indication that the stimulation index is not age related. This conclusion is also supported by the results of Pritchard and co-workers (Personal communication).

The variation observed in repeat test results of individual normal donors is greater than that observed by Pritchard et al. (Personal communication), which may be due to relative technical inexperience with the method. Nevertheless, all the repeat values were negative. Conversion to negative or zero values 24 hours or more after tumor removal in the 3 cases tested suggests that absence of tumor cells restores normal lymphocyte reactivity. Presumably, the tumor exerts a direct or indirect effect on the blood lymphocytes which is detected by the probe assay. The possible diagnostic use of nonreversal to negative postoperatively indicating residual tumor is being explored, as is the use in follow-up testing of reversal of negative to positive values which indicate tumor recurrence. The nature of the tumor factor responsible for the effect on patients' lymphocytes is not yet known, but the technique should provide a means for its identification and thus of a new tumor marker.

Comparison of polarization values obtained for normal donors and cancer patients suggests that for samples from cancer patients, reactivity of zone 1 cells is decreased and for zone 2 cells is increased. Bater and Pritchard (*7*) found no difference in total cell number distribution on the gradient, between cancer patients and normal donors, which suggests that cancer is not associated simply with a shift in density of PHA-responding cells.

The cell type concerned in the observed fluorescence polarization changes has not yet been identified, and it may well be that more than one subclass participates in the response. Ørjasaeter et al. (*8*) reported that the responding cells in his lymphocyte fraction (density <1.077 g/cm^3) are the T-lymphocytes. In our own studies we have identified T-lymphocytes as the major component in both zones 1 and 2, whether from cancer or noncancer samples (Rolland JM, Nairn RC, Hocking GR, et al.: Manuscript in preparation). The indications so far are that the different behavior of the two zones and the difference between cancer and noncancer are likely to be functions of altered distribution and activity of T-cell subsets. Analysis of polarization changes in separated lymphocyte subpopulations requires larger volumes of blood than may reasonably be obtained from most patients studied. An alternative approach requiring smaller blood samples is suggested by the experiments of Udkoff et al. (*9*), who have distinguished a cell population showing decreased polarization by single cell flow cytometry. This system should permit elucidation of the major reactor cell type by correlation with surface markers and functional assays.

The changes in PHA-stimulated zone 1 lymphocytes detected by fluorescence polarization have been suggested to be due to mitochondrial changes (*10*). Whatever the explanation of the phenomenon, it has been confirmed as cancer

TABLE 3.—*Normal donors' responses to PHA*

Case No.	Age, yr	Sex	Reduction in polarization after PHA stimulation, %		Stimulation index[a]	
			Zone 1	Zone 2		
60	61	♂	34.2	0	−34.2	(−15.3)
61	24	♂	28.9	0	−28.9	
62	26	♂	27.6	0	−27.6	
63	24	♀	27.8	3.2	−24.6	
64	25	♀	20.5	0	−20.5	
65	24	♂	20.0	0	−20.0	(−4.2)
66	25	♂	19.0	0	−19.0	
67	24	♂	18.9	0	−18.9	(−16.8[b])
68	46	♂	29.7	11.3	−18.4	
69	35	♀	18.9	5.5	−13.4	
70	56	♂	13.3	0	−13.3	
71	21	♂	18.1	6.3	−11.8	
72	24	♂	11.4	0	−11.4	(−21.6)
73	29	♂	11.0	0	−11.0	
74	23	♀	13.8	3.7	−10.1	(−9.3, −21.3)
75	27	♂	9.1	0	−9.1	(−6.5)
76	25	♂	10.5	1.7	−8.8	
77	20	♀	33.3	24.6	−8.7	
78	25	♀	6.5	0	−6.5	
79	23	♀	47.0	41.0	−6.0	(−36.8)
80	22	♂	7.4	1.9	−5.5	
81	55	♂	5.1	0	−5.1	
82	26	♀	27.1	22.3	−4.8	
83	22	♀	6.7	2.0	−4.7	
84	24	♂	8.5	3.9	−4.6	
85	23	♂	3.8	0	−3.8	(−13.7[b], −16.1[b])
86	24	♀	3.3	1.4	−1.9	
87	30	♂	0	0	0	
88	37	♂	0	0	0	
89	25	♂	1.7	2.0	+0.3	(−12.8)
90	35	♂	0	1.7	+1.7	

[a] Repeat values are shown *in parentheses* in the order of testing.
[b] Repeat values on the same day.

TABLE 4.—*Sample experimental data*

Lymphocyte fluorescence polarization	Zone 1	Zone 2
Unstimulated	0.177	0.181
	0.169	
Mean	0.173	
PHA-stimulated	0.112	0.159
	0.117	
Mean	0.115	
Percent Reduction	33.5	12.2
Stimulation index = −21.3		

diagnostic by several others (*11–15*). Two groups (*16, 17*), however, were unable to distinguish cancer patients from normal subjects by this test. According to Cercek and collaborators in correspondence (*18–20*), this problem was attributable to "stray-light" artifacts in polarization measurements and an inability to isolate the density-specific lymphocyte subpopulation; however, this explanation is contested by Preece et al. (*21*) and Bagshawe et al. (*22*) in correspondence replies.

We believe that standardization and greater precision of several technical procedures should increase the reproducibility of this test. In particular, improvements could be made in standardization of collection and storage of blood samples, in separation of cell fractions, and in raw data analysis (by direct spectrophotometer–computer linkup). We are currently attempting to refine the test in these various ways to establish its potential for practical diagnosis of primary and recurrent cancer. The elucidation of the biological basis of such a diagnostic test is likely to yield a new cancer marker, and perhaps, of more fundamental significance, to lead to better understanding of cancer and lymphoid cell interactions.

REFERENCES

(*1*) NAIRN RC, ROLLAND JM. Fluorescent probes to detect lymphocyte activation. Clin Exp Immunol 1980; 39:1–13.

(*2*) KREUTZMANN H, FLIEDNER TM, GALLA HJ, SACKMAN E. Fluorescence-polarization changes in mononuclear blood leucocytes after PHA incubation: Differences in cells from patients with and without neoplasia. Br J Cancer 1978; 37:797–805.

(*3*) PRITCHARD JA, SUTHERLAND WH, SEAMAN JE, et al. Cancer-specific density changes in lymphocytes after stimulation with phytohaemagglutinin. Lancet 1978; 2:1275–1277.

(*4*) CERCEK L, CERCEK B. Application of the phenomenon of changes in the structuredness of cytoplasmic matrix (SCM) in the diagnosis of malignant disorders: A review. Eur J Cancer 1977; 13:903–915.

(*5*) PRITCHARD JA, SUTHERLAND WH. Lymphocyte response to antigen stimulation as measured by fluorescence polarization (SCM test). Br J Cancer 1978; 38:339–343.

(*6*) DULBECCO R, VOGT M. Plaque formation and isolation of pure lines with poliomyelitis viruses. J Exp Med 1954; 99:167–182.

(*7*) BATER AJ, PRITCHARD JA. Analysis of the lymphocyte separation technique used in the double-band SCM test. International Research Communication System—Medical Science 1980; 8:165.

(*8*) ØRJASAETER H, JORDFALD G, SVENDSEN I. Response of T lymphocytes to phytohaemagglutinin (PHA) and to cancer-tissue-associated antigens, measured by the intracellular fluorescence polarization technique (SCM test). Br J Cancer 1979; 40:628–633.

(*9*) UDKOFF R, CHAN S, NORMAN A. Identification of mitogen responding lymphocytes by fluorescence polarization. Cytometry 1981; 1:265–271.

(*10*) CERCEK L, CERCEK B. Involvement of mitochondria in changes of fluorescein excitation and emission polarization spectra in living cells. Biophys J 1979; 28:403–412.

(*11*) TAKAKU F, YAMANAKA T, HASHIMOTO Y. Usefulness of the SCM test in the diagnosis of gastric cancer. Br J Cancer 1977; 36:810–813.

(*12*) HASHIMOTO Y, YAMANAKA T, TAKAKU F. Differentiation between patients with malignant diseases and non-malignant diseases or healthy donors by changes of fluorescence polarization in the cytoplasm of circulating lymphocytes. Gan 1978; 69:145–149.

(*13*) HASHIMOTO Y, TAKAKU F, YAMANAKA T. Changes in structuredness of cytoplasmic matrix in single stimulated lymphocytes from healthy donors and patients with non-malignant and malignant diseases. Br J Cancer 1979; 40:156–160.

(*14*) STEWART S, PRITCHARD KI, MEAKIN JW, PRICE GB. A flow system adaption of the SCM test for detection of lymphocyte response in patients with recurrent breast cancer. Clin Immunol Immunopathol 1979; 13:171–181.

(*15*) SCHNUDA ND. Evaluation of fluorescence polarization of human blood lymphocytes (SCM test) in the diagnosis of cancer. Cancer 1980; 46:1164–1173.

(*16*) BALDING P, LIGHT PA, PREECE AW. Response of human lymphocytes to PHA and tumor-associated antigens as detected by fluorescence polarization. Br J Cancer 1980; 41:73–85.

(*17*) MITCHELL H, WOOD P, PENTYCROSS CR, ABEL E, BAGSHAWE KD. The SCM test for cancer. An evaluation in terms of lymphocytes from healthy donors and cancer patients. Br J Cancer 1980; 41:772–777.

(*18*) CERCEK B. Comments on "response of human lymphocytes to PHA and tumour-associated antigens as detected by fluorescence polarization." Br J Cancer 1980; 42:207–208.

(*19*) CERCEK L, PRITCHARD JA, SUTHERLAND WH. Comments on "response of human lymphocytes to PHA and tumour-associated antigens as detected by fluorescence polarization." Br J Cancer 1980; 42:208–209.

(*20*) CERCEK L, CERCEK B. Comments on "the SCM test for cancer. An evaluation in terms of lymphocytes from healthy donors and cancer patients." Br J Cancer 1980; 42:947–949.

(*21*) PREECE AW, LIGHT PA, BALDING P. Comments on "response of human lymphocytes to PHA and tumour-associated antigens as detected by fluorescence polarization." Br J Cancer 1980; 42:209–211.

(*22*) BAGSHAWE KD, PENTYCROSS CR, MITCHELL H. Comments on "the SCM test for cancer. An evaluation in terms of lymphocytes from healthy donors and cancer patients." Br J Cancer 1980; 42:949.

blank page

Prevalence and Correlates of Anticipatory Nausea and Vomiting in Chemotherapy Patients[1,2,3]

Gary R. Morrow[4,5]

ABSTRACT—Forty-seven of 225 (21%) consecutive cancer patients were found to experience nausea and/or vomiting prior to a chemotherapy treatment. Multivariate examination of demographic and clinical characteristics showed patients with anticipatory side effects to report more severe posttreatment emesis, to report their most severe posttreatment nausea as occurring later after treatment, and to be more likely to be taking cisplatin than patients without anticipatory side effects. Seventy percent of the patients with anticipatory nausea and/or vomiting attributed the side effects to a psychologic etiology.—JNCI 1982; 68:585–588.

In addition to causing marked disruption to the functioning of cancer patients in their daily activities, nausea and vomiting have been linked to such further treatment problems as postoperative wound dehiscence, dehydration, psychologic depression, and perhaps most importantly, risk of noncompliance with cancer therapy (*1, 2*). As cancer chemotherapeutic treatment regimens have become more complex with multidrug combinations and increasing dosages spread out over longer periods of time, potential problems resulting from nausea and vomiting side effects have become more prominent. Unfortunately (and unlike other situations resulting in these disagreeable side effects), symptom control by antiemetic medication may be incomplete (*3–5*).

Among the wide variations of nausea and vomiting behaviors associated with chemotherapeutic agents are those of patients who have been observed to show nausea and often vomiting in anticipation of chemotherapy treatments; although there have been anecdotal reports of chemotherapy-related ANV, the phenomenon has received little systematic study (*1, 6*). We examined both the incidence and potential correlates of ANV in chemotherapy patients.

METHODS

Subjects.—We studied 227 consecutive chemotherapy outpatients from three separate hospitals of The University of Rochester Cancer Center. All patients were assessed for ANV during their fourth treatment cycle. Clinical experience plus data from a pilot study indicated that patients who experience anticipatory side effects develop them prior to their fourth treatment course.

Data.—Potential correlates of ANV were examined from three general areas: demographic variables, clinical variables, and (for those patients experiencing ANV) self-reports of what they thought was causing the anticipatory side effects.

Demographic characteristics recorded were age, sex, marital status, race, and whether or not the patient had previous chemotherapy, radiotherapy, or surgery before entering their present course of treatment.

The type and number of drugs taken were recorded. A clinical judgment on potential emetic properties of each of 53 chemotherapeutic drugs in active use within the clinic was made before the study. An emetic score from 0 (no emetic property) to 4 (maximum emetic) was assigned each drug by the cancer center pharmacist and nurse clinician.

Pretreatment and posttreatment nausea and vomiting were assessed by a self-report questionnaire. As with other behaviors (*6–8*) both nausea and vomiting were seen as having three distinct topologic elements: frequency, severity, and duration. Questions were asked of each of these elements for nausea before treatment, vomiting before treatment, nausea after treatment, and vomiting after treatment. Frequency for each of the nausea and vomiting time frames was assessed by a four-point scale from "during or after every treatment" to "never." Patients were asked to fill in the number of hours that the nausea or vomiting generally lasted. The severity of the response was assessed on a six-point scale from "very mild" to "intolerable." A six-point scale from "during treatment" to "more than 24 hours after treatment" was scored when the nausea or vomiting was most severe.

Those patients found to experience nausea and/or vomiting before treatment were asked, "Why do you think you have the nausea and vomiting side effects in anticipation of treatment?" Their verbatim answers were recorded.

RESULTS

Prevalence

Of the first 227 patients, 2 refused the questionnaire. Thus a total of 225 responses were evaluable. Of the 225 patients, 47 (21%) reported experiencing ANV before a chemotherapy treatment.

ABBREVIATION USED: ANV=anticipatory nausea and/or vomiting.

---

[1] Received June 9, 1981; accepted November 6, 1981.

[2] Supported in part by Public Health Service grants R18CA-26832, R18CA-19681, and P30CA-11198 from the National Cancer Institute.

[3] Research procedures were in accord with the ethical standards of the Committee for the Protection of Human Subjects, University of Rochester.

[4] The University of Rochester Cancer Center and the Department of Psychiatry, University of Rochester School of Medicine and Dentistry, 300 Crittenden Blvd., Rochester, N.Y. 14642.

[5] Ms. Chris Morell provided invaluable technical assistance. Dr. Howard Iker and Dr. John Laughner, as well as Ms. Joan B. Morrow, provided helpful critiques. Mr. Charles L. M. Carnrike assisted in the data analyses. The help of Dr. James C. Arseneau, Dr. Robert F. Asbury, Dr. Richard F. Bakemeier, Dr. John M. Bennett, Dr. Laslo Boros, and Dr. Susan N. Rosenthal in implementing this study is greatfully acknowledged. Ms. Jacque Waight typed the manuscript.

Univariate Comparisons of Demographic and Clinical Characteristics

Univariate comparisons of potential differences between patients who experienced ANV and those who did not on demographic and clinical variables are shown in table 1. The group experiencing ANV was found to be significantly younger than those patients who did not (Student's t-test=−3.33; $P<0.001$). No statistically significant differences were found for sex, marital status, race, and whether or not the patient had previous chemotherapy, radiotherapy, or surgical treatment for their disease (χ^2_1s=0.01–1.46; P-values, not significant).

The taking of only two drugs (singularly or in combination) was found to be associated with patients experiencing ANV: dactinomycin (Fisher's exact probability test: $P<0.009$) and cisplatin (Fisher's exact probability test: $P<0.001$). Patients experiencing ANV took an average 2.5 (±1.1) chemotherapy agents as compared with an average of 2.0 (±1.0) chemotherapeutic agents for the group not experiencing ANV ($t=3.27$; $P<0.001$). The average emetic potential of drugs taken was found to be significantly higher ($t=2.56$; $P<0.01$) for the group experiencing ANV than for the patients not experiencing the phenomenon. No significant differences were found in susceptibility to motion sickness.

TABLE 1.—*Univariate comparisons between patients with and without anticipatory side effects*

Characteristics	Chemotherapy patients with ANV; total, 47[a]	Chemotherapy patients without ANV; total, 178	Significance[b]
Demographic			
Age, yr	52.2 (±14.3)[c]	59.6 (±13.4)[c]	0.001
Sex			
Male	12 (26%)	47 (26%)	NS
Female	35 (74%)	131 (74%)	
Marital status			
Married	36 (76%)	123 (70%)	
Divorced	3 (6%)	8 (4%)	NS
Widowed	4 (9%)	30 (16%)	
Never married	4 (9%)	17 (10%)	
Race			
Black	4 (9%)	5 (3%)	
White	43 (81%)	171 (96%)	NS
Other	— —	2 (1%)	
Previous treatment			
Chemotherapy	34%	37%	NS
Radiotherapy	34%	44%	NS
Surgery	26%	24%	NS
Clinical			
No. of drugs	2.5 (±1.1)[c]	2.0 (±1.0)[c]	0.001
Average emetic score of drugs: 0=none; 4=maximum	1.8 (±0.6)[c]	1.4 (±0.5)[c]	0.01
Susceptible to motion sickness	26%	16%	NS
Posttreatment nausea			
Frequency: 1=after every treatment; 5=never	2.3 (±1.4)[c]	3.7 (±1.6)[c]	0.001
Duration, hr	20.5 (±27.6)[c]	8.6 (±19.4)[c]	0.01
Severity: 1=very mild; 6=intolerable	2.8 (±1.5)[c]	1.3 (±1.6)[c]	0.001
When most severe	3.3 (±2.3)[c]	1.7 (±2.3)[c]	0.001
Posttreatment vomiting			
Frequency	2.9 (±1.6)[c]	4.3 (1.3)[c]	0.001
Duration	13.4 (±24.2)[c]	2.5 (±9.2)[c]	0.01
Severity	2.7 (±1.9)[c]	0.8 (±1.5)[c]	0.001
When most severe	2.5 (±2.4)[c]	0.7 (±1.6)[c]	0.001

[a] No data, —.
[b] NS=not significant.
[c] Mean plus or minus standard deviation.

Posttreatment nausea and posttreatment vomiting were found to be significantly more prevalent in patients with ANV. Patients experiencing ANV also experienced posttreatment nausea with significantly greater frequency than did chemotherapy patients not experiencing ANV ($t_{221}=-5.93$; $P<0.001$). When experienced, the posttreatment nausea was of longer duration (20.5±27.6 vs. 8.6±19.4 hr: $t_{221}=2.78$; $P<0.01$) and greater severity ($t_{221}=6.15$; $P<0.001$) for patients with ANV. The time when posttreatment nausea was most severe was significantly later after treatment for the patients with ANV (4–8 hr) than for other chemotherapy patients (0–4 hr) ($t_{221}=4.27$; $P<0.001$).

A similar pattern in posttreatment vomiting responses was found. Patients with ANV experienced posttreatment vomiting more frequently than did other chemotherapy patients ($t_{221}=-5.44$; $P<0.001$). The duration of posttreatment vomiting was longer (13.4 vs. 2.5 hr: $t_{221}=3.03$; $P<0.01$) and more variable (SD=24.2 vs. 9.2 hr: $F=6.98$; $P<0.001$) for patients experiencing ANV, as were both severity of vomiting ($t_{221}=7.01$; $P<0.001$) and when vomiting was the most severe ($t_{221}=4.71$; $P<0.05$).

Multivariate Comparisons of Patient Characteristics

Not surprisingly, several of the clinical characteristics were found highly intercorrelated. Thus several of the significant univariate comparisons may simply reflect redundant measurement.

To separate out the specific contributions the variables may have had toward ANV, we used two complementary multivariate approaches. The 13 variables found on univariate analysis to significantly differentiate the patients who experienced ANV from those who did not (those variables given in table 1 plus the taking of the two drugs either singly or in combination) were examined in a stepwise multiple regression in which the variables were regressed on the group membership.

Together, the 13 variables accounted for 28% of the variance in group membership. The three variables, self-report of severity of posttreatment vomiting, the taking of the drug cisplatin, and the time when the nausea was the worst, accounted for 26% of the total variance. The remaining 10 variables accounted for 2%.

Patients experiencing ANV might show a different pattern or combination of the characteristics examined than patients without the anticipatory side effects. A 2-group discriminant analysis examined the ability of the 13 characteristics to post hoc "predict" appropriate group membership. All 13 variables were allowed to enter into the prediction equation. A significant differentiation among the 2 groups was found ($\lambda=0.72$; $\chi^2=62.7$; $P<0.001$). Table 2 shows the efficiency with which the discriminant analysis correctly identified case membership for the group experiencing ANV and the group experiencing no ANV. Overall, an 80% accurate classification was achieved based on the 13 variables. Of the 45 patients experiencing ANV, 19 (42%) were correctly classified; of 45 patients, 26 (58%) were not. Of the 157 patients, 143 (91%) who did not experience ANV were correctly classified. Of the 157 patients, 14 (9%) were not. However, prediction of all patients not having ANV would give a 78% (157 of 202) accurate classification.

Physiologic Etiology

The treating oncologist for each patient with ANV was asked if the patient had any physiologic conditions such as *a*) mechanical obstruction of the gastrointestinal system by tumor, *b*) metabolic changes or imbalance, or *c*) brain metastases that would explain the side effects. None of the 47 patients had such a potential contributing factor.

Psychologic Etiology

Two of the patients with ANV reported past psychiatric treatment—in both cases, more than 4 years before being treated for cancer. Whereas an expected range of anxiety, depression, hostility, and other affective responses was shown and reported by patients experiencing ANV, the responses were predominantly reactive and not pathologic.

Patients experiencing ANV were asked, "Why do you think you have the nausea and vomiting side effects in anticipation of treatment?" Verbatim answers were classified into the three categories of "psychologic reasons," "treatment-related reasons," and "other reasons" as shown in table 3. Under psychologic reasons were placed responses that used the words "nervous," "anxious," "tension," "in my mind," "dread," and "no controls." Approximately 75% of 11 males and 75% of 36 females gave answers falling within this category. As can be seen in table 3, there were few differences in the percent of exact words used. Overall, for the combined sample, 33 (70%) of the 47 patients gave answers from which a psychologic etiology could be deduced. Three types of answers were classified into treatment-related reasons: "smell" (that patients appeared to notice in the treatment setting), "pills" (that were taken in preparation for the chemotherapy treatment), and, by 1 person, "distance" (the closer to the clinic the more the patient appeared to experience the side effects). Approximately 25% of the men and 10% of the women experiencing ANV gave a treatment-related reason. Inasmuch as the overall percentage of reasons given in this category was 13%, the numbers in each of the individual classifications are small. Overall, approximately 1 in 5 (17%) subjects gave the answer that they made "no sense" out of experiencing the anticipatory side effects. All of the patients giving this answer were female.

TABLE 2.—*Two-group discriminant analysis*

	Classified group		
	ANV	No ANV	Total
Actual group			
ANV	19	26	45[a]
No ANV	14	143	157[b]
Total	33	169	202

[a] Two patients with one missing variable.
[b] Twenty-five patients with one missing variable.

TABLE 3.—*Patient responses to question, "What do you think is causing the anticipatory nausea and vomiting?"*

Response	Males, *n* (% of 11)	Females, *n* (% of 36)	Total sample, *n* (% of 47)
Psychologic reasons			
Nervous	3 (27)	8 (20)	11 (23)
Anxious	2 (17)	6 (17)	8 (17)
Tension	0 (0)	3 (8)	3 (6)
In my mind	1 (9)	7 (19)	8 (17)
Dread	1 (9)	1 (3)	2 (2)
No control	1 (9)	0 (0)	1 (2)
Total	8 (73)	25 (69)	33 (70)
Treatment-related reasons			
Smell	3 (27)	1 (3)	4 (9)
Pills	0 (0)	1 (3)	1 (2)
Distance	0 (0)	1 (3)	1 (2)
Total	3 (27)	3 (9)	6 (13)
Other reasons			
It makes no sense	0 (0)	8 (22)	8 (17)
Total	0 (0)	8 (22)	8 (17)

DISCUSSION

Treatment-related variables were found to account for close to one-third of the variance associated with ANV. While an overall "hit rate" of 80% was found for separating patients who experienced the ANV behavior from those who did not on the basis of treatment variables, examination of these results shows significantly greater success in correctly identifying patients who *did not* have ANV rather than those who did. More pronounced side effects following chemotherapy treatment may be necessary but not sufficient for the development of ANV. Experiencing more pronounced side effects following chemotherapy treatment may facilitate or predispose the development of the anticipatory side effects.

The multivariate results require the usual cautious view given any results from multivariate techniques that maximize both true and error variance (*9*). The results require replication. The overall accuracy of approximately 80% (162 hits/202) may or may not prove clinically useful depending on the potential cost of missing a patient with ANV versus the consequences of incorrectly identifying a patient as having a probability of ANV when in fact he or she may not.

No consistent physiologic bases for ANV were found. Potential mechanical obstruction by tumor, gross metabolic changes, and brain metastases that may have influenced the neural strata involved in vomiting were not found. Patients in both groups represented a wide range of both diagnoses and treatment agents.

Patients' self-reported reasons for anticipatory side effects point to a major psychologic role in the phenomenon. And while anxiety and other reactive affective responses were noted, there did not appear to be common diagnosable psychopathology present in the patients with ANV. None of the patients reported nausea as a typical response to previous anxious experiences. Other converging lines of indirect evidence support a contention that ANV is a largely psychologic condition, perhaps the result of learning.

ANV develops only after several administrations of chemotherapeutic agents have been given. Clinical reports and data of this study support the notion that few instances of ANV are seen before a number of administrations of a given therapeutic agent(s), which would be consistent with the development of a learned psychologic response.

The nausea and vomiting seen in anticipation of treatment may be effected by a wide range of eliciting stimuli such as clinic sights and smells, stimuli usually associated with the treatment situation. Situations in which a response is elicited by a stimulus closely associated with a conditioned stimulus may be viewed within the learning theory explanation of stimulus generalization (*10*). The drug cisplatin has a noticeable metallic aftertaste; patients on the drug were found particularly prone to ANV. Children with leukemia have been found to develop a conditioned taste aversion to a distinctive flavored ice cream when it is paired with chemotherapy treatments (*11*).

If it is reasonable to view ANV as a behavioral phenomenon (most likely involving a form of conditioning), then treatment interventions based on learning theory principles may be considered applicable. Several techniques derived from learning theory have been applied to situations thought to be episodes of behaviorally conditioned vomiting. Among these techniques are those of positive practice and overcorrection (*12*), extinction (*13–15*), induced vomiting (*16*), contingent electric shock (*17*), and of perhaps greater efficacy, counter-conditioning procedures (*18–20*). Most of these studies were, unfortunately, single-case studies with little controlled methodology. The argument that these studies provide evidence that ANV is a conditioning phenomenon because conditioning-derived treatments have been shown effective is clearly circular. Nonetheless, the fact that such a wide range of behaviorally derived conditioning procedures has been found effective provides a degree of support for viewing ANV as a conditioned response. A randomized clinical trial examining the potential efficacy of behaviorally derived treatment interventions for the control of these anticipatory side effects is currently in progress (*21*).

REFERENCES

(*1*) Harris JG. Nausea, vomiting, and cancer treatment. CA 1978; 28: 194–201.

(*2*) Whitehead VM. Letter: Cancer treatment needs better antiemetics. N Engl J Med 1975; 293:199–200.

(*3*) Frytak S, Moertel CG, O'Fallon JR, et al. Delta-9-tetrahydrocannabinol as an antiemetic for patients receiving cancer chemotherapy. A comparison with prochlorperazine and a placebo. Ann Intern Med 1979; 91:825–830.

(*4*) Sallan SE, Cronin C, Zelen M, Zinberg NE. Antiemetics in patients receiving cancer chemotherapy. N Engl J Med 1980; 302:135–138.

(*5*) Frytak S, Moertel CG. Management of nausea and vomiting in the cancer patient. JAMA 1981; 245:393–396.

(*6*) Holland J. Psychological aspects of oncology. Med Clin North Am 1977; 61:737–748.

(*7*) Budzynski TH, Stoyva JM, Adler CS. Feedback induced muscle relaxation: Application to tension headaches. J Behav Ther Exp Psychiatry 1970; 1:205–211.

(*8*) Brown SL, Schwartz GE, Sweeney DR. Dissociation of self-reported and observed pleasure in depression. Psychosom Med 1978; 40: 536–548.

(*9*) Morrow GR. Clinical trials in psychosocial medicine: Methodologic and statistical considerations. Part III. Assessing measurement techniques in psychosocial oncology. Cancer Treat Rep 1980; 64:451-456.

(*10*) Marks MH. Learning: Processes. London: Macmillan, 1969.

(*11*) Bernstein IL. Learned taste aversions in children receiving chemotherapy. Science 1978; 200:1302–1303.

(*12*) Azrin NH, Wesolowski MD. Eliminating habitual vomiting in a retarded adult by positive practice and self-correction. J Behav Ther Exp Psychiatry 1975; 6:45–48.

(*13*) Wolf MM, Birnbauer JS, Williams T, Lawler J. A note on apparent extinction of the remitting behavior of a retarded child. In: Ullman LP, Krasner L, eds. Case studies in behavior modification. New York: Holt, Rinehart & Winston, 1965.

(*14*) Alferd GS, Blanchard EB, Buckley TM. Treatment of hysterical vomiting by modification of social contingencies: A case study. J Behav Ther Exp Psychiatry 1972; 3:209–212.

(*15*) Ingersoll B, Curry F. Rapid treatment of persistent vomiting in a 14-year-old female by shaping and time-out. J Behav Ther Exp Psychiatry 1977; 8:305–307.

(*16*) Spergel SM. Induced vomiting treatment of acute compulsive vomiting. J Behav Ther Exp Psychiatry 1975; 6:85–86.

(*17*) Joister RP, Cardron CJ, Worley L, Arthur D. Faradic therapy of chronic vomiting in infancy: A case study. J Behav Ther Exp Psychiatry 1975; 6:55–59.

(*18*) Mogan J, O'Brien JS. The counter-conditioning of a vomiting habit by sips of ginger ale. J Behav Ther Exp Psychiatry 1972; 3:135-137.

(*19*) Saunders DG. A case of motion sickness treated by systematic desensitization and in vivo relaxation. J Behav Ther Exp Pschiatry 1976; 7:381–382.

(*20*) Tasto DL, Chesney MA. The deconditioning of nausea and of crying by emotive imagery: A report of two cases. J Behav Ther Exp Psychiatry 1977; 8:139–142.

(*21*) Morrow GR. Behavioral treatment of anticipatory nausea and vomiting. Proc Am Soc Clin Oncol 1981; 22:396.

Retinoic Acid-Induced Growth Inhibition and Morphologic Differentiation of Human Neuroblastoma Cells In Vitro[1,2]

Neil Sidell[3,4]

ABSTRACT—Retinoic acid (RA) induced concentration-dependent morphologic differentiation and growth inhibition in the LA-N-1 human neuroblastoma cell line. Time course studies demonstrated a significant increase in the formation of long neurites in LA-N-1 cultures within 48 hours of RA addition; maximum expression of differentiation occurred at approximately 4 days. This differentiation profile corresponded to a detectable decrease in [^{3}H]thymidine incorporation at 48 hours and complete inhibition of cell growth after 3–4 days. The RA-induced morphologic differentiation and growth inhibition persisted despite removal of the drug. A soft agar assay system showed that RA also inhibited the ability of LA-N-1 cells to form anchorage-independent colonies and induced morphologic differentiation in colonies that did develop. These findings suggest that RA promoted the differentiation of LA-N-1 neuroblastoma cells, resulting in an altered expression of the malignant phenotype.—JNCI 1981; 68:589–596.

The role of vitamin A in the control of cellular differentiation of normal epithelial tissues has long been recognized. Recently, vitamin A and its derivatives (retinoids) have attracted wide attention as antipromoter agents in experimental carcinogenesis and by their ability to alter the expression, tumorigenicity, and growth of fully transformed cells in vitro (*1*). The direct growth-inhibitory effects of retinoids have been demonstrated on a variety of human cell types, including breast, cervical, lymphoblastic, and melanoma cell lines (*2*). Furthermore, retinoids have been shown to inhibit anchorage-independent growth and to stimulate melanogenesis of human melanoma cells in vitro (*3–5*). These effects on melanoma cells prompted this study of the effects of retinoids on human neuroblastoma, a tumor that originates, like melanoma, from tissue of the neurocrest (*6*). Here I report that RA can inhibit the growth, reduce the ability to form colonies in soft agar, and induce morphologic differentiation of a human neuroblastoma cell line. The results of this study support the concept that retinoids can promote the differentiation of certain neoplastic cell types.

MATERIALS AND METHODS

Cell cultures.—The LA-N-1 neuroblastoma cell line was a gift from Dr. Robert C. Seeger, Department of Pediatrics, School of Medicine, University of California at Los Angeles, Los Angeles, Calif. (*7*). These cells were maintained in RPMI-1640 medium (M.A. Bioproducts, Walkersville, Md.), supplemented with 10% heat-inactivated fetal calf serum, 50 IU penicillin/ml, 50 μg streptomycin/ml, and 1 μg Fungizone/ml (complete medium). Cells were grown in a humidified incubator at 37°C in a 5% CO_2 atmosphere. The cells were fed with media twice weekly and subcultured with the use of 0.025% trypsin in a Versene buffer consisting of 0.13 *M* NaCl, 5.4 m*M* EDTA–Na, 7 m*M* $NaHCO_3$, 1.0% glucose, and 2% antibiotic-antimycotic mixture (GIBCO, Santa Clara, Calif.).

Treatment of cells with RA.—*all-trans*-RA (Sigma Chemical Co., St. Louis, Mo.) was dissolved in ethyl alcohol or dimethyl sulfoxide to a concentration of 10^{-2} *M* and kept as stock solution up to 2 weeks at −70°C under nitrogen. For each experiment, RA was diluted from the stock solution directly into the growth medium so that the final solvent concentration was 0.1% (vol/vol). Control cultures contained 0.1% (vol/vol) solvent alone. This concentration did not affect the plating efficiency, growth, or cell morphology of LA-N-1 cells. For dose–response experiments, RA was diluted in solvent to obtain a series of tenfold decreasing concentrations from 10^{-2} to 10^{-6} *M* and then further diluted 1:1,000 into the culture medium.

Assays for inhibition of cell growth and DNA synthesis.—To examine the effects of RA on anchorage-dependent cell growth, we plated cells (10^5) in T-25 flasks (Falcon Plastics, Oxnard, Calif.) with 5 ml of culture medium. One day after plating, the culture medium was replaced with medium containing RA or with solvent control. The cultures were refed every 4th day with RA or solvent-containing medium until the day of counting, at which time the cells were detached with the trypsin–Versene buffer solution and counted with a hemacytometer. Cell viability was determined by trypan blue exclusion.

To determine the effects of RA on DNA synthesis, we plated 10^3 cells/well in quadruplicate wells of flat-bottom MicroTest plates (M.A. Bioproducts). Culture techniques and retinoid treatment were identical to those of the assay for growth inhibition. At various intervals after adding RA, the plates were pulsed with 0.5 μCi [^{3}H]thymidine/well. After 18 hours' additional incubation at 37°C, the cells were trypsinized and harvested on strips of fiberglass filter paper with the use of a multiple automated sample harvester (MASH-2; M.A. Bioproducts). They were then dried, and the individual samples were counted in a liquid scintillation counter.

LA-N-1 colony formation in soft agar.—The ability of LA-N-1 cells to form colonies in soft agar in the presence of RA

ABBREVIATIONS USED: RA=retinoic acid; CRABP=cellular RA-binding proteins.

---

[1] Received July 13, 1981; accepted October 28, 1981.

[2] Supported by Public Health Service young investigators research grant CA-25801 from the National Cancer Institute.

[3] Division of Surgical Oncology, UCLA School of Medicine, University of California at Los Angeles, Los Angeles, Calif. 90024.

[4] I am indebted to Dr. Jane E. Bottenstein for many helpful discussions and suggestions. I also gratefully acknowledge the technical assistance of Ms. Estela Famatiga and the editorial assistance of Ms. E. J. Shaw.

was determined by a modification of the method of Hamburger and Salmon (*8*). Cells (10^5) were suspended in 3 ml of 0.8% SeaPlaque Agar (FMC Corporation, Rockland, Maine) in complete medium containing RA or solvent control and overlaid onto 2 ml 1.5% agar:medium in 60-mm plastic petri dishes (Falcon Plastics). The plates were incubated at 37°C in a 5% CO_2 humidified atmosphere. Colonies consisting of at least 30 cells were counted after 10 days with the use of an inverted microscope.

Differentiation curve.—LA-N-1 cells were plated and treated with RA as in the cell growth inhibition assay. Starting with day 1 of RA administration, 200 cells/culture from at least three different regions were examined daily with a phase-contrast microscope. Cells were scored as morphologically differentiated if they possessed one or more processes at least twice as long as the soma diameter, according to the method of Sandquist et al. (*9*).

RESULTS

Dose-response relationship of RA-induced growth inhibition.—The dose-dependent effects of RA on the proliferation of LA-N-1 cells were assessed by cell counts after 7 days and by incorporation of [^{3}H]thymidine after 5 days. Text-figure 1 shows that cellular proliferation as assessed by both criteria was inhibited in a concentration-dependent manner over a range of 10^{-9} to 10^{-5} *M* RA. In these systems, 50% inhibition of cell growth and [^{3}H]thymidine incorporation was achieved with RA concentrations of 10^{-8} and 2×10^{-9} *M*, respectively. No decrease in the percentage of viable cells was detected in the treated cultures as compared to that of control cultures.

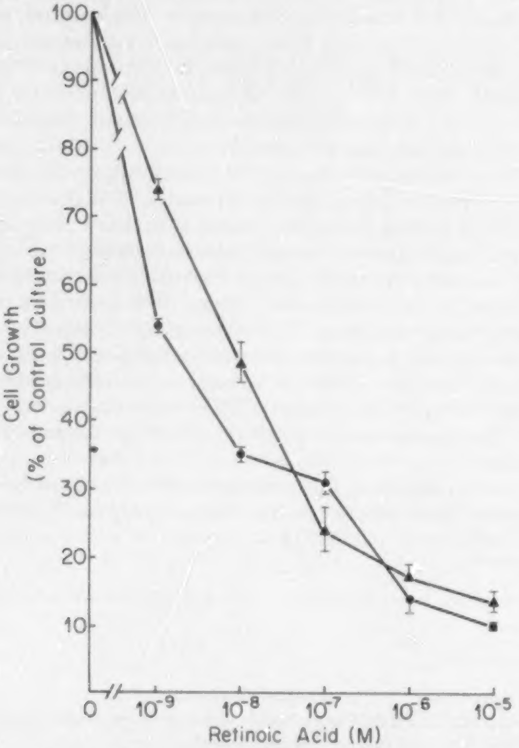

TEXT-FIGURE 1.—Dose-response curves showing effects of RA on LA-N-1 cell proliferation as assessed by viable cell counts (▲) after 7 days of treatment and by incorporation of [^{3}H]thymidine (●) after 5 days of treatment with RA. Values are the averages ± SE of triplicate and quadruplicate cultures, respectively, from two independent experiments.

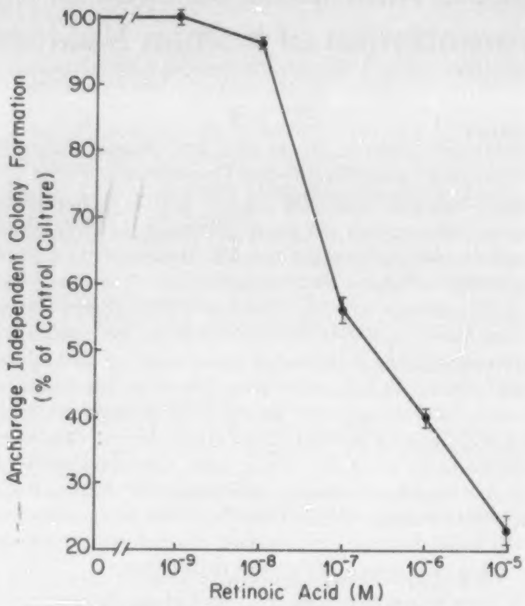

TEXT-FIGURE 2.—Dose-response curve of RA-induced inhibition of LA-N-1 colony formation in soft agar. Values are the averages ± SE of triplicate cultures from two independent experiments.

Recent studies of tumor growth in semisolid culture systems have suggested a correlation between anchorage-independent growth and tumorigenicity (*8*). In the present study, the ability of LA-N-1 cells to form colonies in soft agar in the presence of various concentrations of RA was determined (text-fig. 2). When 10^{-5} *M* RA was included in the agar culture, there was nearly an 80% reduction in the number of colonies that developed. This reduction was dose-dependent, with 50% inhibition occurring at approximately 4×10^{-7} *M* RA. Moreover, those colonies that developed in the presence of RA were smaller and showed extensive morphologic differentiation as evidenced by the presence of long, three-dimensional, neurite extensions (fig. 1).

Time course of RA-induced growth inhibition.—The growth curves of LA-N-1 cells in the absence and in the presence of 10^{-6} *M* RA are shown in text-figure 3. The number of viable cells in both the RA-treated and control cultures were similar for 48–72 hours. However, from 72–96 hours, cellular growth in the presence of RA was completely inhibited, with little change in cell count even after an additional 5-day incubation. This inhibition persisted for at least 8 days after the medium was replaced with control medium whether or not the cells were replated in fresh flasks (data not shown). Eventually, clusters of cells developed that had normal growth characteristics.

Text-figure 4 shows the daily [^{3}H]thymidine incorporation of the RA-treated and control cultures. Results were

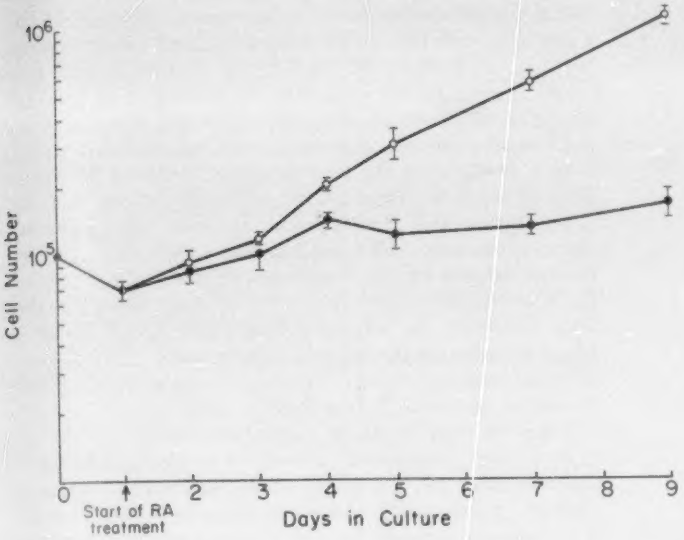

TEXT-FIGURE 3.—Time course of LA-N-1 cell growth in the absence (○) or presence (●) of 10^{-6} M RA. *Each point* represents the mean ± SE of triplicate flasks.

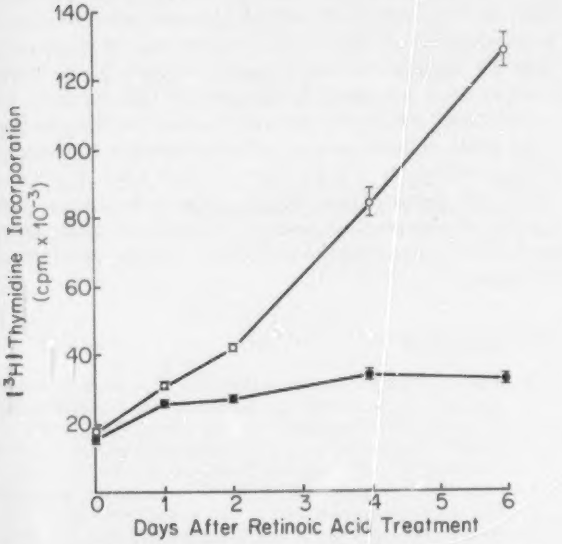

TEXT-FIGURE 4.—Time course of [^{3}H]thymidine incorporation by LA-N-1 cells in the absence (○) or presence (●) of 10^{-6} M RA. *Each point* represents the mean ± SE of quadruplicate samples.

analogous to those obtained by direct cell counts except that inhibition of the incorporated isotope could be detected earlier (within 24–48 hr) after the addition of 10^{-6} M RA.

RA-induced morphologic differentiation.—Treatment of LA-N-1 cells with RA caused a dramatic increase in morphologic differentiation as evidenced by the formation of long neurites (fig. 2). The RA concentration that caused maximum increase in the formation of neurites ranged from 10^{-5} to 10^{-6} M.

The time course of morphologic differentiation in the absence and presence of two concentrations of RA is shown in text-figure 5. In the presence of either 10^{-6} or 10^{-8} M RA, a significant increase in the percentage of differentiated cells could be detected within 48 hours; the maximum extent of differentiation occurred after approximately 4 days of treatment. However, treatment with 10^{-6} M RA produced a significantly greater percentage of differentiated cells than did 10^{-8} M RA. Moreover, at the lower concentration of RA, the processes were generally not as long as those formed in the presence of 10^{-6} M RA.

The morphologic differentiation induced by RA was retained by the LA-N-1 cells in the absence of the drug (fig. 2C). When RA was removed after 5–7 days of treatment at 10^{-5} to 10^{-6} M, most cells retained their long processes for at least 10 days. Furthermore, when RA-treated cells were replated with control medium, extensive differentiation remained apparent up to 7–10 days later. This long lag in reversibility of RA-induced morphologic differentiation parallels the persistent growth inhibition observed after removal of the drug.

DISCUSSION

The results of this study demonstrate that RA induces concentration-dependent growth inhibition and morphologic differentiation of the LA-N-1 human neuroblastoma cell line. RA was reported to affect a mouse teratocarcinoma cell line and a human promyelocytic leukemia cell line in a similar manner (*10, 11*). RA-induced inhibition of anchorage-dependent growth of LA-N-1 cells could be detected after 72 hours by cell counts but within 48 hours when assayed by incorporation of [^{3}H]thymidine. The elapsed time before reduction of [^{3}H]thymidine incorporation was observed corresponds to the time after RA treatment before an increase was seen in the morphologic differentiation of LA-N-1 cells. This correspondence is consistent with the reduced rate of DNA synthesis generally associated with a differentiation process (*12*) and supports the contention that true differentiation is occurring. Bottenstein (*13*) reported that morphologic differentiation of LA-N-1 cells also occurs when these cells are grown in serum-free, hormone-supplemented medium. However, no reduction in growth rate was

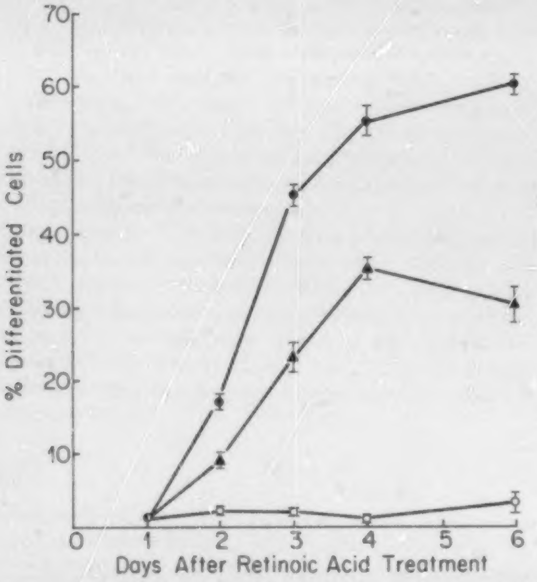

TEXT-FIGURE 5.—Time course of morphologic differentiation of LA-N-1 cells in the absence (○) or present of 10^{-5} *M* RA (●) and 10^{-6} *M* RA (▲). *Each point* represents the mean ± SE of values from triplicate flasks.

observed under those conditions. The fact that RA was added to the cultures 1 day after plating with no subsequent decrease in cell viability suggests that the effects in our study were not the result of the selection of more differentiated cells due to differences in cellular plating efficiency or RA cytotoxicity.

The growth-inhibitory activity of retinoids has been reported to be reversible in many tumor systems within 48 hours after removal of the drug (*2*, *14*). These reports contrast with the present data which demonstrated the relative irreversibility of RA-induced growth inhibition and morphologic differentiation of LA-N-1 cells. Nonreversible differentiation of human neuroblastoma cells was reported after treatment with cyclic AMP elevating agents (*15*); however, changes mediated by a variety of other agents and culturing in serum-free medium were found to be promptly reversible (*12*). Preliminary experiments indicate that the slow onset of growth of LA-N-1 cells after prolonged RA treatment (>7 days) may be due to a subpopulation of RA-resistant cells rather than to a slow reversibility of the entire population. Further studies are needed to clarify this point.

Recent reports indicate that retinoids can retard anchorage-independent growth of various histologic types of tumors (*3*, *16*). The present study extends these observations to human neuroblastoma by demonstrating that RA reduced the colony-forming ability of LA-N-1 cells in soft agar and promoted morphologic differentiation in colonies that did develop. To my knowledge, this is the first report of a system in which morphologic differentiation can be induced in suspension cultures of neuroblastoma cells. The implications of this RA-mediated phenomenon are presently unknown.

The mechanism(s) by which RA induces morphologic differentiation and exerts its antineoplastic effects on LA-N-1 and other cells has not yet been elucidated. One possibility could be suppression of the activity of endogenously produced growth factors in a manner analogous to retinoid-mediated blockage of the phenotypic cell transformation produced by sarcoma growth factor in rat fibroblasts (*17*). Such a mechanism has been proposed for the RA-induced differentiation of human HL-60 promelocytic leukemia cells (*11*). This or other mechanisms may involve direct interaction with nuclear DNA via binding to CRABP (*18*, *19*). Further support for this hypothesis will naturally depend on the detection of CRABP in LA-N-1 or other neuroblastoma cells. However, the relatively high content of CRABP in other neuroectoderm-derived tumors, such as melanoma (*20*) and retinoblastoma (*21*), make the presence of CRABP in human neuroblastoma a likely possibility.

Thus this report presents a new tumor model with which to study the differentiating activity of retinoids. This system becomes especially appealing when one considers the morphologic, biochemical, and electrophysiologic modes of differentiation that might be evaluated in neuroblastoma cells (*12*). Furthermore, the natural history of neuroblastoma, with its relatively high rate of spontaneous differentiation and regression in vivo (*22*), suggests that this tumor type may be among the most easily "triggered" to undergo maturational processes. In support of this concept, initial experiments testing the growth inhibitory effects of RA on eight other neuroblastoma cell lines indicated substantially greater sensitivity to RA treatment than that observed with other cell types. These results should encourage further studies of the possible role of retinoids as differentiating agents for controlling the malignant phenotype of this type of cancer.

REFERENCES

(*1*) MOORE T. Effects of vitamin A deficiency in animals: Pharmacology and toxicology of vitamin A. In: Sebrill WH, Harris RS, eds. The vitamins. Vol 1. New York: Academic Press, 1967:245–266.

(*2*) LOTAN R. Effects of vitamin A and its analogs (retinoids) on normal and neoplastic cells. Biochim Biophys Acta 1980; 605:33–91.

(*3*) MEYSKENS FL JR, SALMON SE. Inhibition of human melanoma colony formation by retinoids. Cancer Res 1979; 39:4055–4057.

(*4*) MEYSKENS FL JR, FULLER BB. Characterization of the effects of different retinoids on the growth and differentiation of a human melanoma cell line and selected subclones. Cancer Res 1980; 40:2194–2196.

(*5*) LOTAN R, LOTAN D. Stimulation of melanogenesis in a human melanoma cell line by retinoids. Cancer Res 1980; 40:3345–3350.

(*6*) BOTTENSTEIN J, MATHER J, SATO G. Growth of neuroepithelial-derived cell lines in serum-free hormone-supplemented media. Cold Spring Harbor Conf Cell Prolif 1979; 6:531–544.

(*7*) SEEGER RC, RAYNER SA, BANERJEE A, et al. Morphology, growth, chromosomal pattern, and fibrinolytic activity of two new human neuroblastoma cell lines. Cancer Res 1977; 37:1364–1371.

(*8*) HAMBURGER, A, SALMON SE. Primary bioassay of human tumor stem cells. Science 1977; 197:461–463.

(*9*) SANDQUIST D, WILLIAMS TH, SAHU SK, KATAOKA S. Morphological differentiation of a murine neuroblastoma clone in monolayer culture induced by dexamethasone. Exp Cell Res 1978; 113:375–381.

(*10*) LINDER S, KRONDAHL U, SENNERSTAM R, RINGERTZ NR. Retinoic acid-induced differentiation of F9 embryonal carcinoma cells. Exp Cell Res 1981; 132:453–460.

(*11*) BREITMAN RT, SELONIC SK, COLLINS SJ. Induction of differentiation of the human promyelocytic leukemia cell line (HL-60) by retinoic acid. Proc Natl Acad Sci USA 1980; 77:2936–2940.

(*12*) Bottenstein JE. Differentiated properties of neuronal cell lines. In: Sato GH, ed. Functionally differentiated cell lines. New York: Liss, 1982.

(*13*) ———. Serum-free culture of neuroblastoma cells. In: Evans AE, ed. Advances in neuroblastoma research. New York: Raven Press, 1980:161–170.

(*14*) Lacroix A, Lippman ME. Binding of retinoids to human breast cancer cell lines and their effects on cell growth. J Clin Invest 1980; 65:586–591.

(*15*) Prasad KN. Differentiation of neuroblastoma cells in culture. Biol Rev 1975; 50:129–165.

(*16*) Dion LD, Blalock JE, Gifford GE. Retinoic acid and the restoration of anchorage-dependent growth to transformed mammalian cells. Exp Cell Res 1978; 117:15–22.

(*17*) Todaro GJ, Delarco JE, Sporn MB. Retinoids block phenotypic cell transformation produced by sarcoma growth factor. Nature 1978; 276:272–274.

(*18*) Chytil F, Ong DE. Mediation of retinoic acid-induced growth and antitumour activity. Nature 1976; 260:49–51.

(*19*) Jetten A, Jetten ME. Possible role of retinoic acid binding protein in stimulation of differentiation of embryonal carcinoma cells by retinoids. Nature 1979; 278:180–182.

(*20*) Lotan R, Ong DE, Chytil F. Comparison of the level of cellular retinoid-binding proteins and susceptibility to retinoid-induced growth inhibition of various neoplastic cell lines. JNCI 1980; 64:1259–1262.

(*21*) Russel P, Wiggert B, Derr J, Albert D, Craft J, Chader G. Nuclear uptake of retinoids. Autoradiographic evidence in retinoblastoma cells in vitro. J Neurochem 1980; 34:1557–1560.

(*22*) Evans AE, Chatten J, D'Angio GJ, Gerson JM, Robinson J, Schnaufer L. A review of 17 IV-S neuroblastoma patients at the Children's Hospital of Philadelphia. Cancer 1980; 45:833–839.

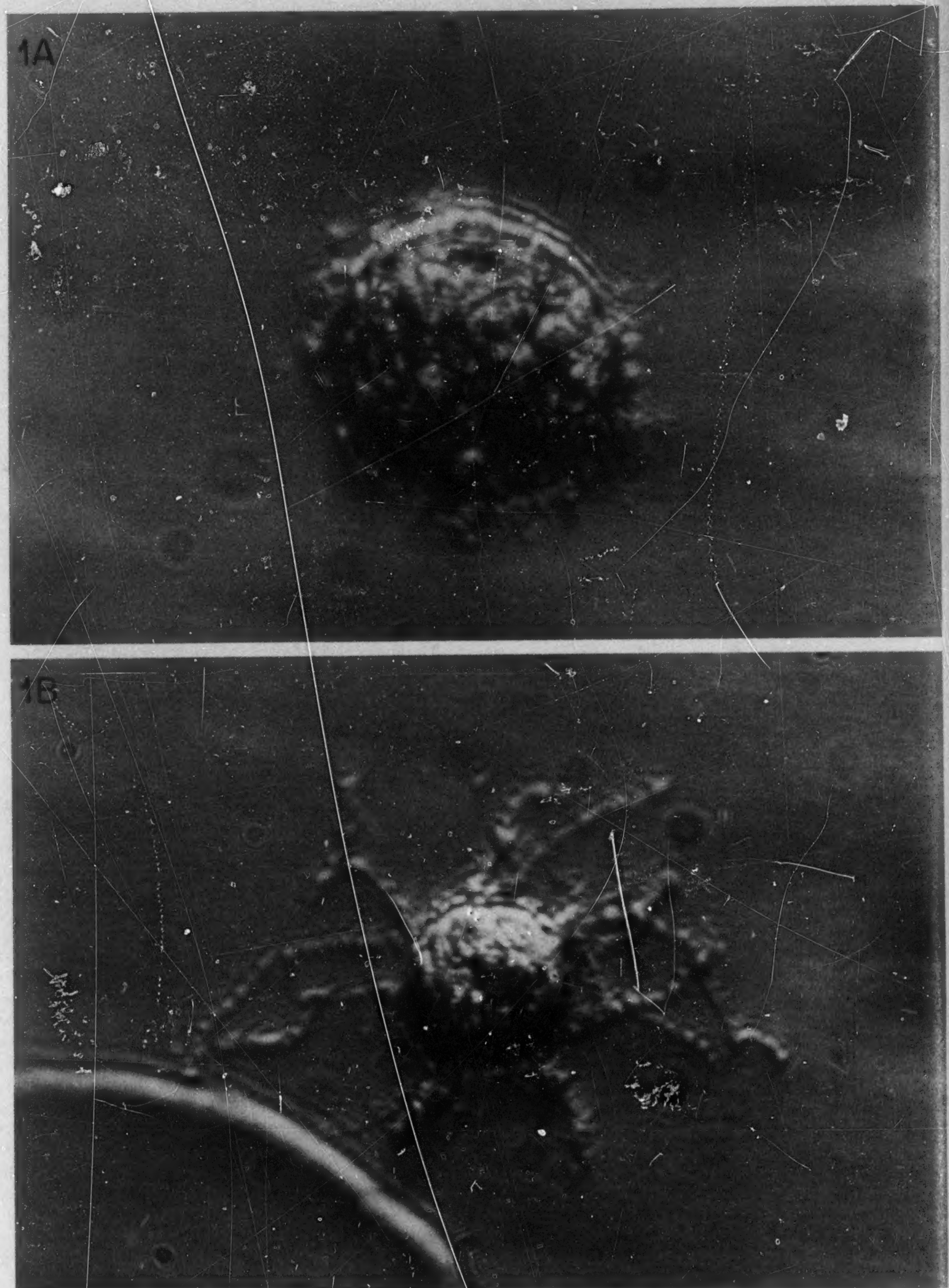

FIGURE 1.—RA-induced morphologic changes in LA-N-1 colonies grown in soft agar. 1A) typical colony after 10 days' growth in the absence of RA. 1B Colony after 10 days' growth in the presence of 10^{-6} *M* RA. Photographed under phase contrast with additional reflective light. × 100

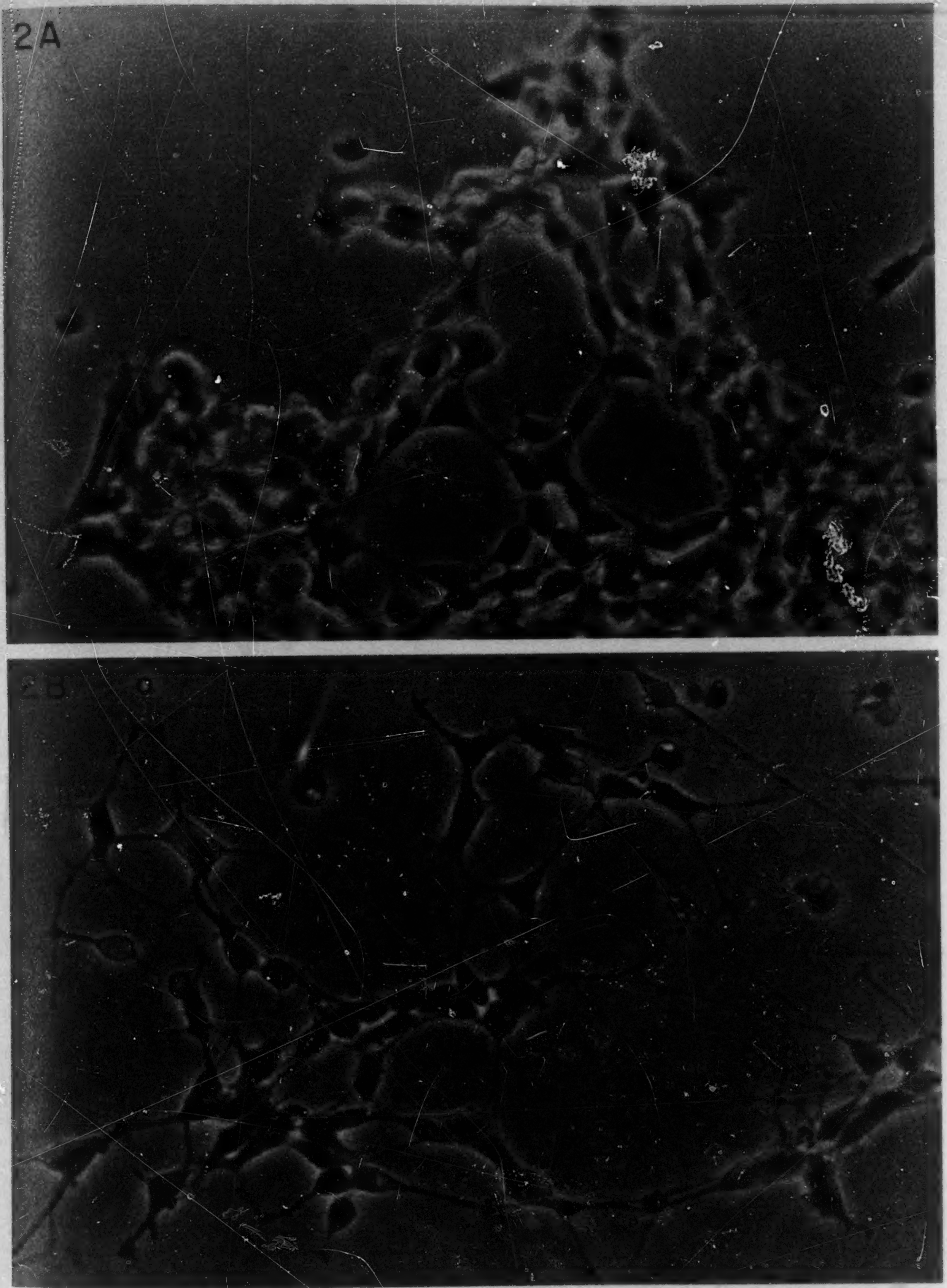

FIGURE 2.—RA-induced morphologic differentiation of LA-N-1 cells grown in monolayer. 2A) Control treated with solvent for 5 days. 2B) Cells cultured in the presence of 10^{-6} *M* RA for 5 days. 2C) Cells treated with 10^{-6} *M* RA for 8 days, replated, and cultured for 8 days in medium without RA. Photographed under phase contrast. × 500

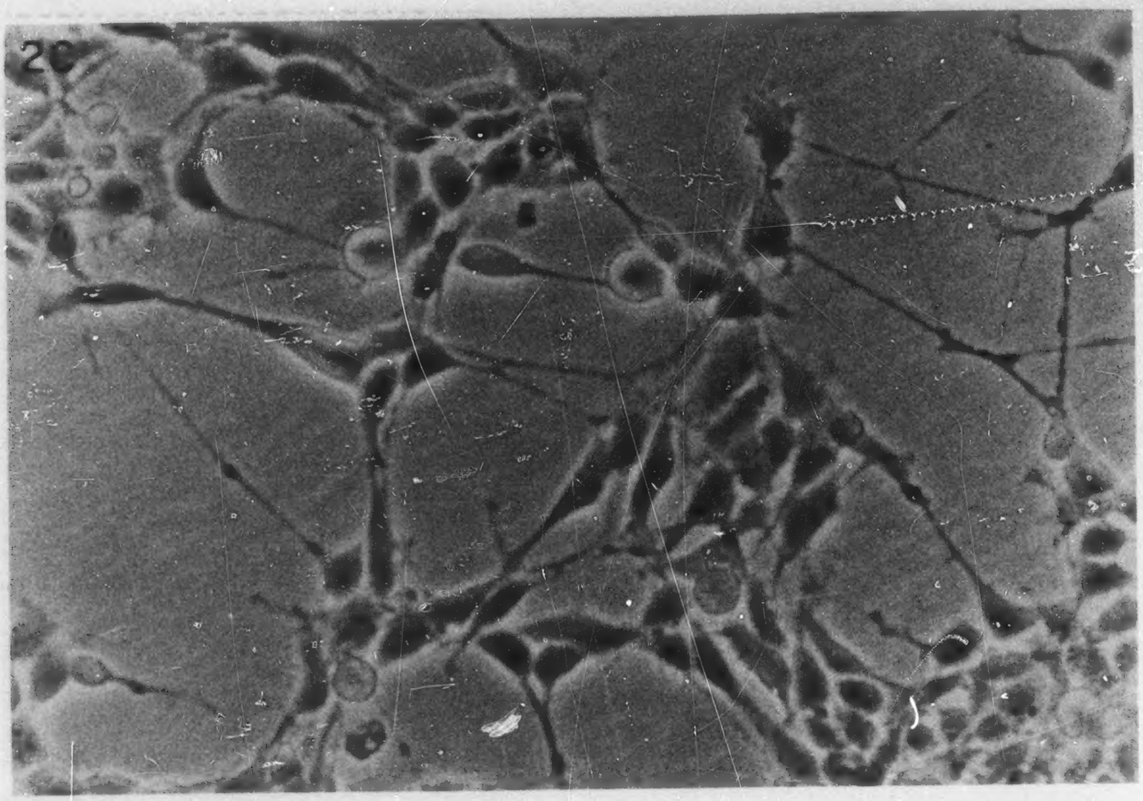
2C

Gaseous Formaldehyde and Hydrogen Chloride Induction of Nasal Cancer in the Rat[1,2]

Roy E. Albert,[3] Arthur R. Sellakumar,[3] Sidney Laskin,[3,4] Marvin Kuschner,[3] Norton Nelson,[3] and Carroll A. Snyder[3,5]

ABSTRACT—The carcinogenic response to the combined and separate exposures to formaldehyde (HCHO) and hydrochloric acid (HCl) was investigated in male inbred SD rats. The rats were exposed to gaseous HCHO, 14 ppm, and HCl, 10 ppm, in two experiments. In one experiment the gases were premixed at high concentrations before being diluted in the exposure chamber air to maximize the formation of the carcinogen bis(chloromethyl)ether (BCME). In the second experiment exposure was repeated to HCl and HCHO premixed at high concentrations, and not premixed (to minimize BCME formation), as well as to HCHO alone and HCl alone. The second experiment is being reported on at an interim stage. HCHO alone induced squamous carcinomas of the nasal cavity as did the combined exposures to HCHO and HCl. No carcinogenic response was observed with HCl alone. HCHO accounted for most, if not all, of the carcinogenic activity of the mixture of HCHO–HCl. JNCI 1982; 68:597–603.

The alpha halo ether BCME is a highly reactive industrial alkylating agent (*1*). Studies conducted in this laboratory have shown BCME to be carcinogenic in mice by skin painting (*2*), carcinogenic in rats by sc injection (*3*), and highly carcinogenic in the respiratory tract of rats by inhalation (*4, 5*). Subsequent epidemiologic investigations have shown that BCME is a human carcinogen (*6–8*). It breaks down to HCl and formaldehyde (HCHO). Recent studies have demonstrated that low levels of BCME may be formed by the gas-phase reaction of HCl and HCHO (*9*). Because of the potential hazard from the formation of BCME or other alkylating agents when significant quantities of HCHO and HCl are used in close proximity, a study was done to evaluate the effects of chronic inhalation exposure to a mixture of HCHO and HCl (experiment 1). A second study was done to repeat the combined exposure to HCHO and HCl and to examine the carcinogenic effects of each alone (experiment 2). The complete results of the first study and the preliminary results of the second study are reported here.

MATERIALS AND METHODS

Experiment 1.—Animals: Eight-week-old male inbred S-D rats (Blue Spruce Farms, Altamont, N.Y.) weighing 262±16.1 g were used. Purina Laboratory Chow (Ralston Purina Co., St. Louis, Mo.) and water were provided ad libitum except during exposure periods.

Gas exposure: A group of 99 rats were exposed to the mixture of HCl and HCHO. Groups of 50 air sham-exposed and 50 untreated rats were used as controls. HCHO vapor and HCl gas were mixed at high concentrations before introduction into the inhalation chambers to maximize the formation of BCME. HCHO vapor was entrained in air passing over a slurry of paraformaldehyde (purified trioxymethylene; Fisher Scientific Co., Fair Lawn, N.J.) in paraffin oil maintained at 75–90°C. The HCHO-laden air was directed into a 13.5-liter mixing vessel. HCl was simultaneously metered into the mixing vessel from a tank of compressed HCl 99.0% grade (Matheson Gas Products, East Rutherford, N.J.) with the use of a dual-syringe feed (Modern Metalcraft, Midland, Mich.). Make-up air was introduced into the mixing vessel from a compressed air tank (Linde, Division of Union Carbide Corp., New York, N.Y.) to yield an overall gas mixture flow rate of 4 liters/minute. The effluent from the mixing vessel passed directly into the air intake of the exposure chamber. Since the air flow through the exposure chamber was 300 liters/minute, there was a 75-fold dilution of the effluent from the mixing vessel.

Animal exposures took place in 1.3-m^3 exposure chambers, the details of which have been previously described (*10, 11*). Exposure chamber levels of HCHO and HCl were measured at 0.5-hour intervals, and levels of HCHO and HCl in the reaction vessel were measured twice daily. A chromotropic acid method was used for the analysis of HCHO (*12*), and HCl was measured by titration with sodium hydroxide. To determine BCME, we employed a trichlorophenol derivative technique followed by electron-capture gas chromatography analysis (*13*).

The rats were exposed to gases for 6 hours/day, 5 days/week for life. They were housed in suspended wire cages during nonexposure periods. All animals were observed daily, weighed monthly, and allowed to die naturally or were killed when moribund.

Necropsy and histologic samples: Complete necropsy was performed on each animal, and particular attention was given to the respiratory tract. In the HCHO–HCl-exposed group and the air sham-exposed group, the entire head was fixed in 10% neutral buffered Formalin and then decalcified.

ABBREVIATIONS USED: BCME=bis(chloromethyl) ether; CIIT=Chemical Industry Institute of Toxicology.

---

[1] Received May 13, 1981; accepted October 7, 1981.

[2] Supported by Public Health Service (PHS) contract N01CP-33260 from the Division of Cancer Cause and Prevention, National Cancer Institute (NCI); by PHS center grant ES-00260 and PHS grant ES-02270 from the National Institute of Environmental Health Sciences; and by PHS center grant CA-13343 and PHS grant CA-26724 from the NCI.

[3] New York University Medical Center, Institute of Environmental Medicine, 550 First Ave., New York, N.Y. 10016.

[4] Deceased 1976.

[5] We thank the following persons who participated in one or more phases of these studies: Mr. Stephen La Mendola, Dr. George M. Rusch, Dr. Gary Katz, Mr. Martin Erlichman, Mr. Daniel A. Isola, Dr. Virginia Cubberley, Mrs. Helen Ford, Mr. Robin Lindenboom, Mr. Frederick Fennikoh, Mr. Reade Moulton, Mr. Kenneth Magar, Mr. Gordon Cook, and Mrs. D. J. Natalizio.

The head was divided sagittally along the midline. Histologic slides were prepared from each side of the head to display the entire nasal cavity as viewed laterally from the midline, including the nasal turbinates, maxillary turbinates, and the endoturbinates. Histologic sections were also taken from the larynx, trachea, pulmonary lobes, liver, bladder, kidney, spleen, and other organs with gross pathologic alterations.

Experiment 2.—Animals: Nine-week-old male SD rats (Charles River CD) weighing 316±19 g were used. Animal care was the same as in experiment 1. One hundred rats were used in the following 5 treatment groups: *a*) combined exposure to HCHO and HCl where the two gases were premixed at high concentrations before dilution as in experiment 1; *b*) combined exposure to HCHO and HCl where the two gases were not premixed at high concentration but fed separately into the inlet air supply of the exposure chamber; *c*) HCHO alone; *d*) HCl alone; and *e*) air sham-exposed controls.

As in experiment 1, animal exposures were conducted in 1.3-m^3 exposure chambers. HCl and HCHO determinations were made every 0.5 hours during each 6-hour daily exposure. HCl levels were determined as in experiment 1. HCHO levels were determined by the chromotropic acid method used in experiment 1 or by use of an infrared gas analyzer (Miran IA; Foxboro Analytical, South Norwalk, Conn.) at a wavelength of 3.58 μm, calibrated by the chromotropic acid method. No BCME measurements have yet been made at this stage of the study.

Animal observations, weighings, killing, and autopsy procedures were done as in experiment 1, except for the preparation of the head. The decalcified head was cut vertically into four 5-mm-thick slabs, beginning just behind the nostrils and extending back as far as the orbits, including most of the nasal cavity. Histologic sections were obtained from the face of each slab. The tumor data reported here include only nasal lesions in rats that produced grossly evident nasal swelling as in figure 1. The complete pathology on all the animals will be presented in a subsequent report when the experiment is completed.

RESULTS

Experiment 1

The average measured gas concentrations in the exposure chamber over the entire experiment were 10.6 ppm HCl and 14.7 ppm HCHO. HCHO levels of 800–1,500 ppm and HCl levels of 5,000–8,000 ppm in the reaction vessel were found to be necessary to maintain the chamber concentrations at nominal levels of 10 ppm HCl and 14 ppm HCHO. To maintain the target level of HCl in the inhalation chambers, an excess had to be introduced to compensate for wall losses, presumably in the tubing and exposure chambers.

In the determination of BCME, the measured trichlorophenol adducts could have been formed from BCME or chloromethylal. The measured levels of trichlorophenol adducts therefore represent the upper limit of the BCME concentration. A total of 10 determinations were performed. Five determinations were performed 10 months after the exposures commenced, and five were performed 15 months after the exposures commenced. The BCME concentrations in the mixing vessel ranged from 8 to 179 ppb with an average of 75 ppb and a standard deviation of 64 ppb. The BCME levels in the exposure chamber were too low to measure but were estimated on the basis of a 75-fold dilution factor to average about 1.0 ppb.

The weight and mortality curves of the exposed animals are given in text-figures 1 and 2, respectively. In these figures, the air sham-exposed and colony controls are combined. The weight gains in the exposed group were substantially lower than that of the controls. Mortality was low up to 24 weeks, but it increased rapidly in the next 20 weeks and remained higher in the exposed group thereafter. As evidenced by gross and histologic examination, early deaths in both exposed and control rats were due to acute bronchopneumonia. Almost all animals dying later also had bronchiectasis and bronchopneumonia.

As shown in table 1, a high proportion of the exposed rats showed a squamous metaplasia of the nasal cavity that was not found in the control rats. There was also more epithelial hyperplasia and epithelial hyperplasia with atypia in the

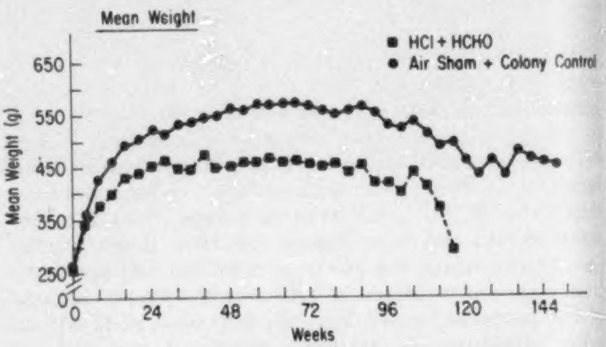

TEXT-FIGURE 1.—Growth of 99 rats receiving chronic exposure to the gaseous mixture of 14.7 ppm HCHO and 10.6 ppm of HCl compared to that of the combined group of 100 controls, 50 of which were air sham exposed and 50 of which were untreated (expt 1).

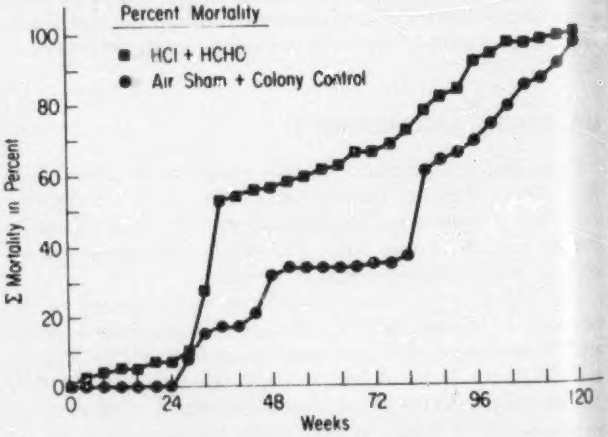

TEXT-FIGURE 2.—Mortality of rats following exposures to HCHO + HCl compared to mortality of the control groups (expt 2).

exposed group than in the controls. Many of the controls showed inflammation of the nasal mucosa, but the severity was much less marked than in the exposed rats. Mucosal changes in the larynx, trachea, and bronchi are shown in table 2. There was a substantial amount of hyperplasia of these mucosa in both exposed and control animals. In exposed rats, squamous metaplasia was more prominent in the nasal mucosa than in the laryngeal, tracheal, and bronchial mucosa.

Of the 99 animals, 28 developed tumors of the nose, 25 of which were squamous carcinomas and 3 of which were papillomas. The temporal pattern of the carcinoma occurrence is shown in the mortality-corrected cumulative incidence curve with respect to elapsed time after the onset of exposure (text-fig. 3). This mortality-corrected cumulative incidence was calculated by the life-table method which consists of calculating the fraction of animals that were alive in successive 4-week intervals and that die of nasal cancer and then obtaining the cumulative fraction of the animals not dying of nasal cancer. From this the cumulative fraction dying of nasal cancer is determined (*14*). The first carcinoma was seen at 223 days, and the mortality-corrected incidence rose steadily thereafter to a level of 77% at 720 days when there were only 3 animals alive. The cancers appeared invariably as a nasal swelling (fig. 1) and eventually caused dyspnea and wheezing. On gross examination, the tumors were opaque greyish-white masses which usually filled the nasal cavity and perforated the nasal bone, infiltrating the surrounding areas (fig. 2). Histologically, all the malignant tumors were squamous cell carcinomas, ranging from moderately to well-differentiated lesions (fig. 3). There were 2 animals dying at 552 and 560 days; both rats had nasal cancers with metastatic lesions in the lungs. In the exposed animals no primary tumors were observed in the larynx, trachea, or the lungs. No tumors were observed in the respiratory tracts of the controls. Nonrespiratory tract tumor incidences are shown in table 3.

TABLE 1.—*Lesions found in the nasal mucosa of rats exposed to premixed HCHO-HCl and in controls*[a]

Group	No. of rats examined	Rhinitis	Epithelial hyperplasia and hyperplasia with atypia	Squamous metaplasia	Squamous papilloma	Squamous cell carcinoma
Exposed rats	99	65	71	64	3	25
Controls	50	41	8	0	0	0

[a] Colony controls.

TABLE 2.—*Mucosal changes found in the laryngotracheobronchial tree in rats exposed to premixed HCHO and HCl and in controls*[a]

Observations	No. of exposed rats	No. of controls
Laryngeal	99	100
Hyperplasia	22	30
Hyperplasia with atypia	0	0
Squamous metaplasia	2	0
Tracheal	99	100
Hyperplasia	23	29
Hyperplasia with atypia	0	1
Squamous metaplasia	0	2
Bronchial	99	100
Hyperplasia	90	89
Hyperplasia with atypia	1	5
Squamous metaplasia	1	2

[a] Including air sham-exposed and colony controls.

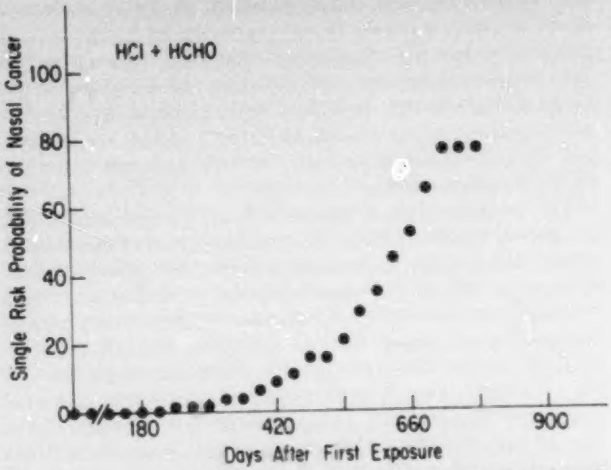

TEXT-FIGURE 3.—Mortality-corrected cumulative incidence of nasal carcinomas with time in 99 rats exposed to 14.7 ppm HCHO plus 10.6 ppm HCl for 6 hr/day, 5 days/wk, for life (expt 1).

TABLE 3.—*Tumors in organs other than the respiratory tract in rats exposed to premixed HCHO-HCl and in controls*

Groups	No. of rats examined	Total No. of tumors	No. of subcutaneous fibrosarcomas
Exposed rats	99	4[a]	3
Controls	100	15[b]	8

[a] Includes 1 pituitary adenoma.

[b] Includes 2 lymphomas, 3 pituitary adenomas, 1 adrenal cortical adenoma, and 1 hemangioma of the spleen.

Experiment 2

At this reporting the experiment has been in progress for 588 days (19.4 mo). Table 4 shows for the 5 treatment groups the average concentrations of HCHO and HCl, the number of exposures, the percent of survival at 588 days, and the number of nasal cancers. The concentrations of HCHO and HCl were very close to the target levels of 14 and 10 ppm, respectively. Although the exposures were nominally on a 5-day/week basis, there were no exposures on holidays, some shut down days for housekeeping, and occasional generation equipment failures. On the average, the exposures were done for two-thirds of each week, or 4.7 days/week, which was also the case in experiment 1. The animal weights are shown in text-figure 4. There was about a 14% depression in weight associated with the combined exposure to HCl and HCHO and about a 9% depression with HCHO exposure alone; there was no significant loss in the HCl-exposed group. The mortality curves for the various groups are shown in text-figure 5, and the survival at 588 days is given in table 4. HCl exposure had no effect on the mortality rate of 29%. A substantially higher mortality (45–49%) occurred in the combined HCHO and HCl exposures, and an intermediate mortality of 38% was seen after the HCHO exposure alone.

The number of nasal cancers in each group is also shown in table 4. As in experiment 1, on inspection of the rats, all of the histologically confirmed cancers were grossly evident as nasal swellings. No nasal swellings were seen that were not nasal cancers. All of the cancers except one were squamous cell carcinomas. The one exception was an adenocarcinoma which occurred in the combined nonpremixed HCHO–HCl group. There were 12 cancers in the combined premixed HCHO–HCl group, 6 cancers in the combined nonpremixed HCHO–HCl group, 10 cancers in the HCHO group and none in the HCl- or air sham-exposed groups.

The statistical comparisons of the cancer incidences are shown in table 5. The *P*-values by the Fisher's exact probability test for HCHO (P=0.001) and both combined HCHO–HCl exposure groups (P=0.016 and P=0.0002) were statistically significant in comparison with those of concurrent control groups and markedly so in comparison with those of the historical controls (P=10^{-8} to P=10^{-16}). There was no statistically significant difference between the cancer responses of the 2 combined HCHO–HCl groups (P=0.12). The mortality-corrected cumulative cancer incidence is shown in text-figure 6. Tumor formation began at 420 days and steadily increased thereafter; only 1 tumor, in the non-premixed HCHO–HCl group, appeared before 420 days. The 2 HCHO–HCl groups when combined had essentially the same slope as the HCHO group, with the premixed HCHO–HCl group having a somewhat higher slope than the HCHO group and the nonpremixed HCHO–HCl group having a somewhat lower slope than the HCHO group. The premixed HCHO–HCl group in experiment 2 had a substantially later time of onset than that in experiment 1 (420 compared to 240 days, respectively) so that the incidence at 600 days was about double that in experiment 1 compared to that in experiment 2 (35 vs. 17%).

TABLE 4.—*Results of experiment 2 after 588 days*

Treatment	Average concentration, ppm	No. of exposures	Mortality, %	No. of nasal cancers
Premixed				
HCHO	14.3			
+		374	49	12
HCl	10.0			
Not premixed				
HCHO	14.1			
+		378	45	6
HCl	9.5			
HCHO	14.2	382	38	10
HCl	10.2	382	29	0
Air sham-exposed	0	382	28	0

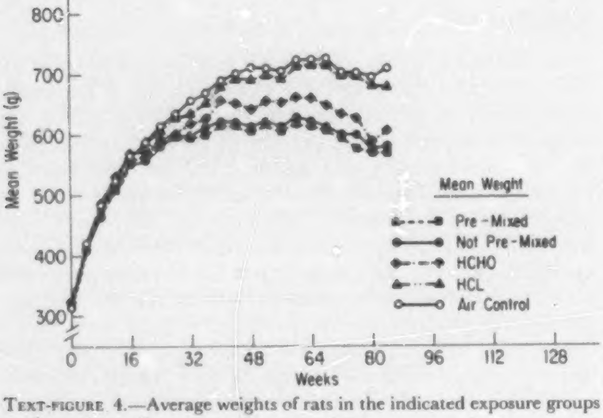

TEXT-FIGURE 4.—Average weights of rats in the indicated exposure groups of experiment 2.

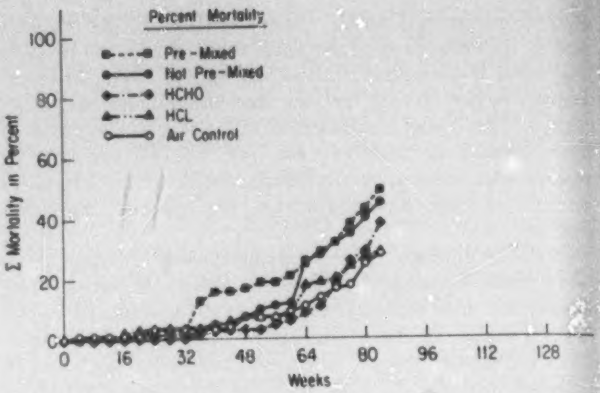

TEXT-FIGURE 5.—Cumulative mortality in the indicated exposure groups of experiment 2.

DISCUSSION

The results of the combined exposure to HCHO and HCl and HCHO alone are decisively positive for the induction of squamous carcinomas of the nasal cavity. It is clear that up to 84 weeks much of the carcinogenic response is from HCHO, since HCl exposure did not produce any cancers. The premixed HCHO–HCl and nonpremixed HCHO–HCl exposure groups were included in the experimental design to examine the possible effects of BCME arising from the interaction of HCl and HCHO. The introduction of HCl and HCHO separately into the exposure chambers caused these gases to interact at a 75-fold lower concentration than that under the premixed exposure conditions; presumably, there was a correspondingly lower concentration of BCME. With the measured level of BCME in the exposure chambers in experiment 1 at 1 ppb or less, it seems unlikely that BCME alone could contribute much to the tumorigenic response on the basis of the earlier BCME study (*4, 5*). Twenty days of exposure, 6 hours/day at 100 ppb (or a cumulative dose of 2,000-ppb exposure days), produced a 6% incidence of nasal cancer. In experiment 1 all the rats were dead by 100 weeks. With the BCME concentration estimated to be ≤1 ppb, the cumulative dose by 100 weeks

TABLE 5.—*Statistical tests (Fisher's exact probability test) on HCHO and HCl*[a]

Groups	Intrastudy comparisons, *P*-value	Historical comparisons, *P*-value
1 vs. 5	0.001	0.6×10^{-13}
2 vs. 3	0.12	—
2+3 vs. 5	0.0007	0.18×10^{-18}
2 vs. 5	0.016	0.11×10^{-7}
3 vs. 5	0.0002	0.14×10^{-15}

[a] Group 1—HCHO-exposed; group 2—HCHO+HCl—nonpremixed; group 3—HCHO+HCl—premixed; group 4—HCl; group 5—air sham-exposed.

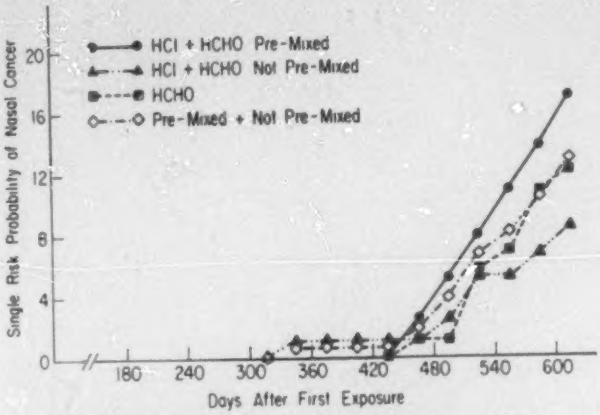

TEXT-FIGURE 6.—Mortality-corrected cumulative incidence of nasal carcinomas in the indicated exposure groups of experiment. 2

(5 exposures/wk) would have been ≤500-ppb exposure days. Even if the response were proportional to the cumulative dose, which is probably an upper limit, the incidence of nasal carcinomas would be only one-fourth of that observed with 20 exposures to 100 ppb of BCME or 1.5%. The observed nasal cancer incidence in experiment 1 was 25%. The protraction of the BCME exposure over 100 weeks in this experiment compared to 4 weeks in the earlier experiment might be expected to reduce the predicted nasal cancer incidence below 1.5% (*15*). BCME also induced esthesioneuroepitheliomas of the nasal mucosa in contrast to the squamous carcinomas observed in the experiments reported here. Supporting the lack of effect of BCME is the finding in experiment 2 that the tumorigenic responses are about the same for HCHO as occurred with the combination of the two HCHO-HCl groups (text-fig. 6). Nevertheless, in experiment 2 there was about twice the incidence of nasal cancers in the premixed HCHO-HCl group as in the nonpremixed HCHO-HCl group; this difference in tumor response was fairly unlikely on a chance basis (P=0.12). It remains to be seen whether the difference will continue through the rest of the experiment. If so, it may be that mixing the HCHO and HCl at high concentrations does produce an added carcinogenic effect, which, under the conditions of this experiment, counteracts a small suppressing effect of HCl on tumor formation by HCHO.

There are some differences between the carcinogenic responses to premixed HCHO and HCl in experiments 1 and 2. The Sprague-Dawley rats were obtained from different suppliers, and the animals in experiment 2 reached a higher plateau weight and had better survival and only about one-half the mortality-corrected nasal cancer incidence at 84 weeks (35 vs. 17%).

To our knowledge, the results of experiment 2 provide the first confirmation of the carcinogenic response to HCHO in the CIIT study (*16*). The conditions and responses in the two studies were strikingly similar. The exposure concentrations were the same at 14 ppm; both studies yielded squamous cell carcinomas of the nasal cavity. The rat strains, however, were different, the CIIT study involved F344 rats in contrast to the SD rats used here. At 18 months the studies were comparable with respect to the effect of HCHO on weight and mortality; rats in our study showed a 9% weight depression compared to 14% for the CIIT study, and the mortalities at 18 months were 26 and 20%, respectively. The carcinogenic response began earlier in the CIIT study (12 vs. 14 mo), and the number of rats dying of nasal cancer at 18 months was higher (19/100 in the CIIT study and 8/100 in our study). These differences may be due to the different strains of rats.

The results of experiment 2 do not decisively disprove the notion that the carcinogenic response to HCHO is a nonspecific response to irritation, but they do not support it either. The addition of the irritant HCl gas to HCHO did not enhance the carcinogenic response: The nonpremixed HCHO-HCl group had a somewhat lower response than the group exposed to HCHO alone, and the premixed HCHO-HCl group had a somewhat higher response. It is possible that the 14 ppm HCHO by itself was on a plateau of irritation response and that the HCl alone was not tested long enough or at a high enough concentration. A comparison of the nasal mucosal pathology in the various treatment groups will be reported later.

REFERENCES

(*1*) SUMMERS L. The α-halo ethers. Chem Rev 1955; 55:301-353.
(*2*) VAN DUUREN BL, GOLDSCHMIDT BM, KATZ C, LANGSETH L, MERCADO C, SIVAK A. Alpha-halo-ethers: A new type of alkylating carcinogen. Arch Environ Health 1976; 16:472-476.
(*3*) VAN DUUREN BL, SIVAK A, GOLDSCHMIDT BM, KATZ C, MELCHIONNE S. Carcinogenicity of halo-ethers. J Natl Cancer Inst 1969; 43:481-486.
(*4*) KUSCHNER M, LASKIN S, DREW RT, CAPPIELLO V, NELSON N. Tumors of the respiratory tract induced by inhalation of bis-(chloromethyl)ether. Arch Environ Health 1971; 23:135.
(*5*) ———. Inhalation carcinogenicity of alpha halo ethers. III. Lifetime and limited period inhalation studies with bis(chloromethyl)ether at 0.1 ppm. Arch Environ Health 1975; 30:73-77.
(*6*) FIGUEROA WG, RASZKOWSKI R, WEISS W. Lung cancer in chloromethyl methyl ether workers. N Engl J Med 1973; 288:1096-1097.
(*7*) NELSON N. The chloroethers—occupational carcinogens: A summary of laboratory and epidemiology studies. Ann NY Acad Sci 1976; 271:81-90.
(*8*) ALBERT RE, PASTERNACK BS, SHORE RE, LIPPMANN M, NELSON N, FERRIS B. Mortality patterns among workers exposed to chloromethyl ethers. Environ Health Perspect 1975; 11:209-214.
(*9*) FRANKEL LS, MCCALLUM KS, COLLIER L. Formation of bis-(chloromethyl)ether from formaldehyde and hydrogen chloride. Environ Sci Technol 1974; 8:356-359.
(*10*) DREW RT, LASKIN S. Environmental inhalation chambers. In: Gay WI, ed. Methods of animal experimentation. Vol 4. New York:

Academic Press, 1973:1–41.

(*11*) Laskin S, Kuschner M, Drew RT. Studies in pulmonary carcinogenesis. In: Hanna MG Jr, Nettesheim P, Gilbert JR, eds. Inhalation carcinogenesis. Springfield, Va: Clearinghouse for Federal Scientific and Technical Information, 1970: 321–351.

(*12*) Houle MJ, Long DE, Smette D. A simplex optimized colorimetric method for formaldehyde. Anal Lett 1970; 3:401–409.

(*13*) Solomon RA, Kallos GJ. Determination of chloromethyl methyl ether and bis(chloromethyl)ether in air at the part per billion level by gas-liquid chromatography. Anal Chem 1975; 47:955–958.

(*14*) Sachs R. Life table technique in the analysis of response-time data from laboratory experiments on animals. Toxicol Appl Pharmacol 1959; 1:203–227.

(*15*) Laskin S, Sellakumar AR, Kuschner M, et al. Inhalation carcinogenicity of epichlorohydrin in noninbred Sprague-Dawley rats. JNCI 1980; 65:751–757.

(*16*) Swenberg JA, Kerns WD, Mitchell RE, Gralla EJ, Pavkov KL. Induction of squamous cell carcinomas of the rat nasal cavity by inhalation exposure to formaldehyde vapor. Cancer Res 1980; 30: 3398–3402.

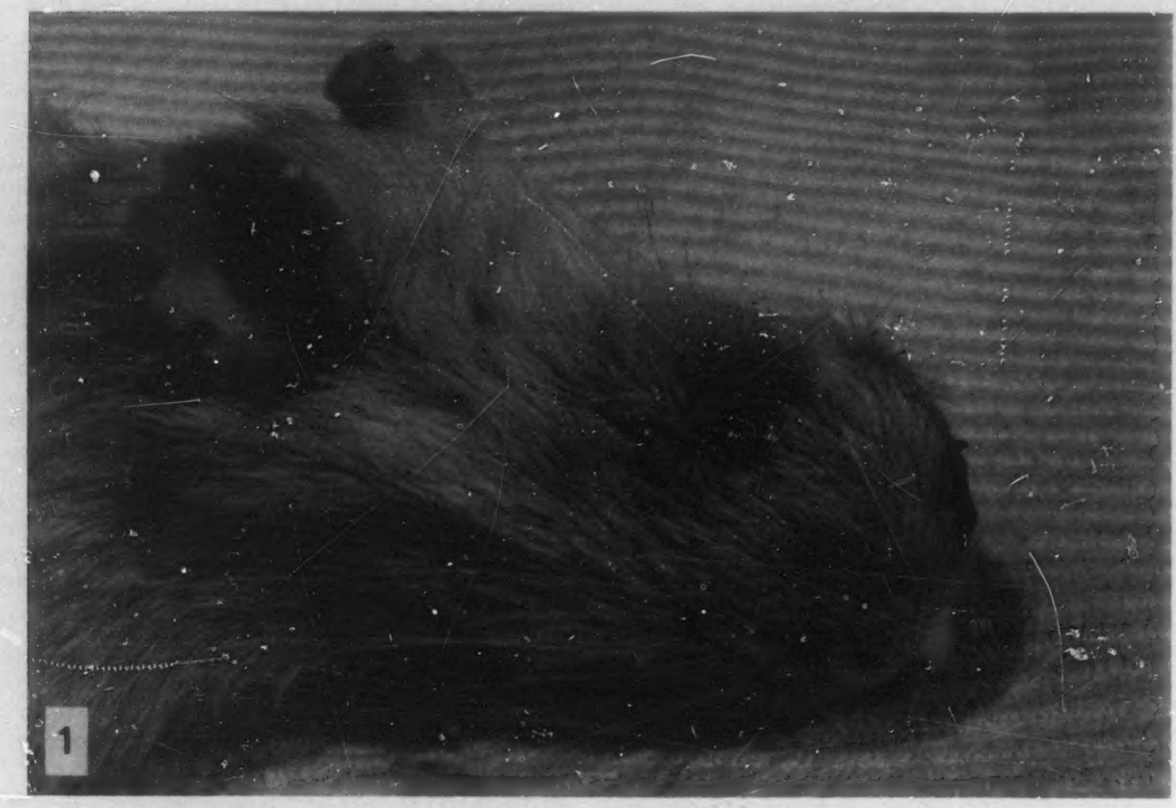

Figure 1.—Nasal carcinoma in a rat dying at 714 days after the start of the exposures to HCHO and HCl.

2

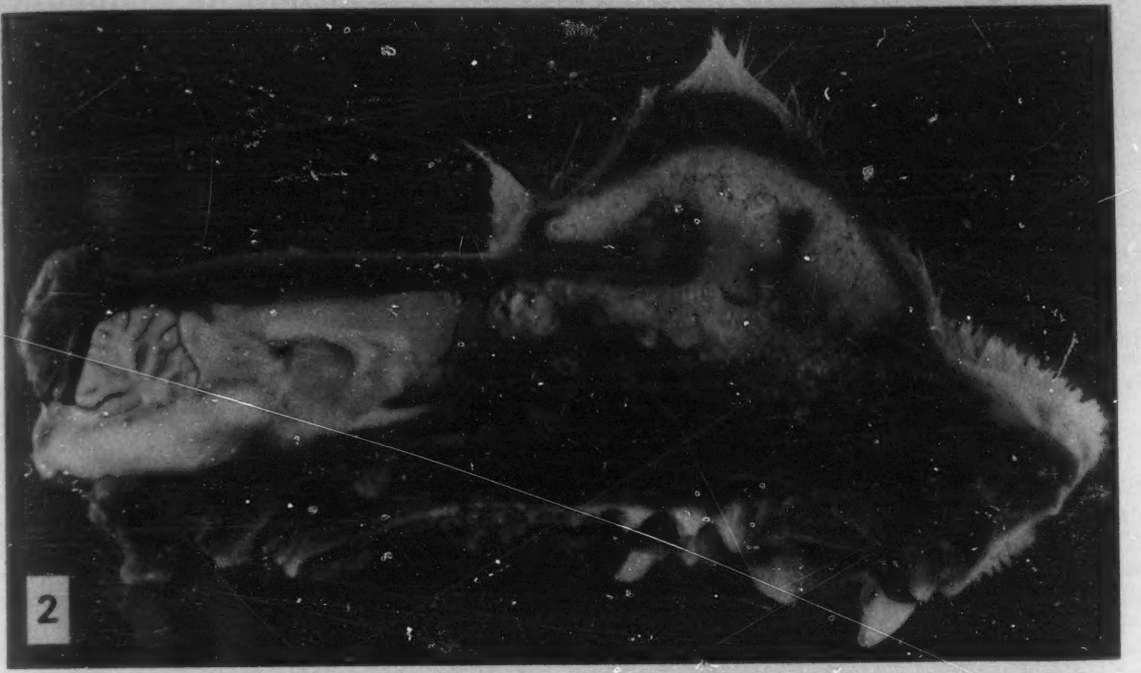

3

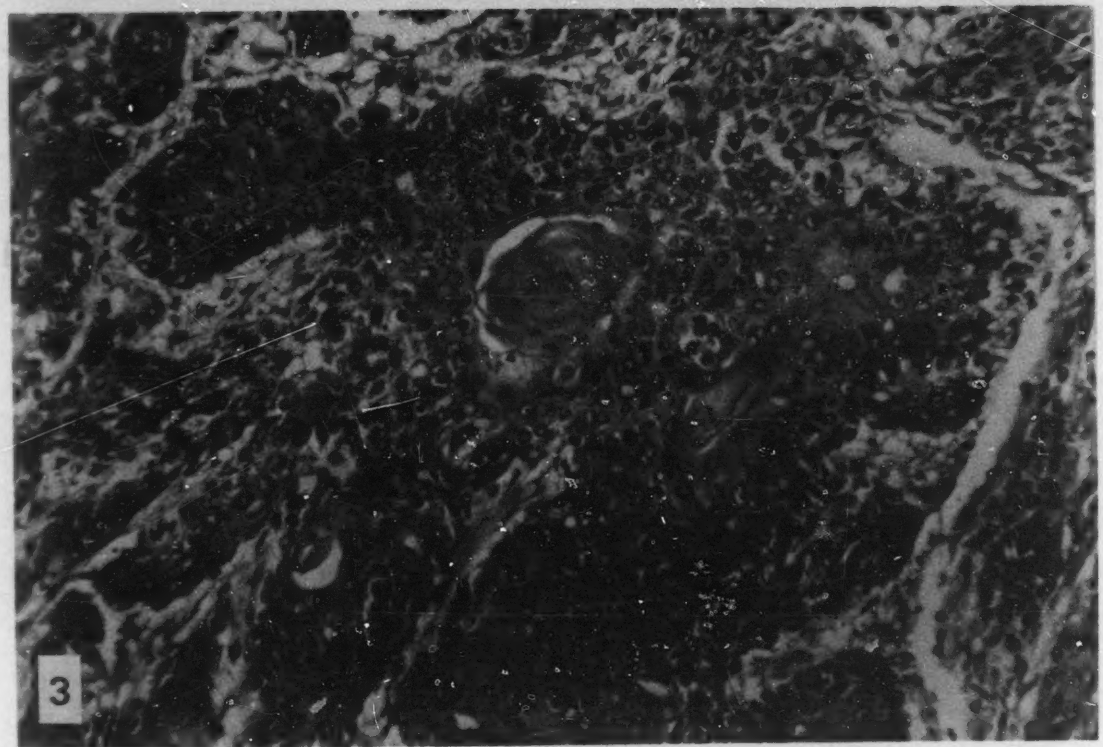

FIGURE 2.—Sagittal section through the skull of a rat with cancer. The grayish-white mass, a squamous cell carcinoma, fills a large portion of the nasal tract and perforates the nasal bone, infiltrating into the subcutaneous tissue.

FIGURE 3.—Detail of fig. 2 showing the invasive pattern of squamous cell carcinoma. Hematoxylin and eosin. × 220

blank page

Enhancement of Skin Tumorigenesis by Cigarette Smoke Condensate Following β-Irradiation in Rats[1,2,3]

John F. McGregor[4,5] (with revisions by D. K. Myers)[6,7]

ABSTRACT—The tumor-promoting ability of cigarette-smoke condensate (CSC) has been demonstrated in rat skin after β-irradiation. Skin tumors from male albino Charles River CD rats (outbred Sprague-Dawley descended) were classified into 2 groups: carcinomas and other noncarcinoma tumors. A statistically significant increase ($P<0.01$) in tumor yield occurred after CSC treatment that began 2 months after irradiation. This finding confirmed our previously published pilot observation. Extension of the pilot experiment to obtain data on carcinoma yield and an experiment to observe the effects of CSC treatment beginning immediately after irradiation were performed. When CSC treatment began immediately after irradiation, the yield of noncarcinoma tumors was significantly reduced ($P<0.01$), whereas the carcinoma yield increased but statistically not significantly ($P=0.12$). The increased yield of noncarcinoma tumors is attributed to a significant increase ($P<0.01$) of acute ulceration caused by CSC on recently irradiated skin. The increase in carcinoma yield resulted from an increase in the rate of conversion of noncarcinoma tumors to cancer. Carcinoma yield was also increased by CSC treatment beginning 2 months after irradiation, but the increase was not significant ($P=0.08$). The lack of statistical significance for the carcinoma yields in both experiments may be ascribed to the insufficient number of cancers produced by the treatments. The relative ratios of cancer yields (1.7 and 2.5) did not differ greatly from the 2.2 ratio for the increase of noncarcinoma tumors. The possible relevance of the findings to human carcinogenesis is discussed.—JNCI 1982; 68:605–611.

In a preliminary investigation we observed that CSC treatment of rat skin produced a significant threefold increase ($P<0.01$) in the number of skin tumors induced by β-radiation (*1*). This effect could be attributed to the tumor-promoting action of CSC because tumors were not produced by CSC treatment alone. The applications of CSC were begun 2 months after the irradiation (i.e., about halfway between exposure time and earliest appearance of tumors) when the epidermis presumably contains tumor cells well advanced toward neoplasia. The previous finding was particularly interesting because rat skin is well known for its refractoriness to carcinogenesis by coal tar (*2*) and carcinogenic hydrocarbons (*3*) and to the tumor-promoting action of croton oil (*4*). Thus it seemed important not only to confirm the pilot observation, with extension of the study into the cancerous phase, but also to assess the effect of CSC treatment beginning immediately after irradiation.

Although exposure to ionizing radiation is known to produce cancer in humans and animals, conflicting estimates of the cancer risk may be derived from various interpretations of synergism between ionizing radiation and other agents. For example, a significant increase in lung cancer deaths has been found among uranium miners who were exposed both to radon daughters and cigarette smoke (*5*), and the high yield of lung cancer among fluorspar miners may be related to exposure to radon daughters and to inhalation of mine dust (*6*). Because we are especially interested in the reasons for such increases in cancer incidence, a program was initiated to identify any kind of synergism between ionizing radiation and certain chemical carcinogens in the environment. The present results confirm the tumor-promoting ability of CSC in irradiated rat skin and also suggest that acute ulceration, as a consequence of CSC treatment, is capable of encouraging induced tumors to become malignant.

MATERIALS AND METHODS

Animals.—Male albino Charles River CD rats (outbred Sprague-Dawley descended) were chosen by reason of their susceptibility to skin tumor induction by ionizing radiation (*7*). We avoided using females because the production of mammary tumors could have complicated the interpretation of the results. The rats were about 42 days old when obtained from the supplier, housed 2 per suspended wire cage, and supplied Purina Laboratory Chow and water ad libitum. Gross health examinations and body weights provided evidence that the rats were in satisfactory condition for the treatments.

Radiation.—At about 63 days of age, deep anesthesia was induced in each rat with 62 mg pentobarbital/kg body weight, and the dorsal hair was removed with an Oster electric clipper (size 40 head). The age of 63 days corresponds approximately to the beginning (anagen) of the third hair growth cycle, as determined by the appearance of new hair growth in animals whose hair had been clipped a few days before the experiment started. The anesthetized rat

---

ABBREVIATIONS USED: AHH=aryl hydrocarbon hydroxylase; CMP=chronic murine pneumonia; CSC=cigarette smoke condensate.

---

[1] Received September 10, 1980; revised October 27, 1981; accepted November 6, 1981.

[2] Animals were maintained under the guidelines set forth by the Canadian Council on Animal Care.

[3] Dedicated to Dr. J. B. Newcombe, mentor and friend, who retired from Atomic Energy of Canada Limited in September 1979.

[4] Radiation Biology Branch, Atomic Energy of Canada Limited, Ontario, Canada.

[5] Deceased July 1980.

[6] *Address reprint requests to* Dr. Myers, Radiation Biology Branch, Health Sciences Division, Atomic Energy of Canada Limited, Chalk River Nuclear Laboratories, Chalk River, Ontario, Canada K0J 1J0.

[7] Thanks are expressed to Dr. F. G. Bock, Roswell Park Memorial Institute, for providing the cigarette smoke condensate and helpful advice; to Dr. N. J. Gragtmans, Dr. J. D. Childs, and Dr. M. C. Paterson of this branch for their constructive criticisms of the manuscript; to Mr. M. A. Jones for technical assistance; and to Mr. B. Ruhnke for performing the biopsies and for his excellent histologic examination.

was then placed inside a specially designed radiation chamber (*8*), and its back was superficially irradiated over a 5×3-cm area.

A flat source of strontium-90–yttrium-90 (140 mCi or 5.2 GBq) emitted β-particles of high energy (2.27 MeV), with a maximum penetration of about 10 mm in tissue. The dose rate at the surface of the skin was about 700 rad or 7 Gy/minute, and the dose measured at the undersurface of the skin was 60% of the surface dose, determined with lithium fluoride Teflon discs (*9*). A single surface dose of 1,600 rad (16 Gy) was used to produce skin tumors.

CSC.—The CSC was prepared from U.S. blended cigarettes (Orchard Park Laboratories, Orchard Park, Buffalo, N.Y.), and a supply on Dry Ice was received monthly. The frozen condensate was dissolved in reagent grade acetone on a 40% weight/volume basis. One application of acetone condensate on skin consisted of dipping a ⅞-inch artist's paint brush about ¼ inch into the material and brushing three downward strokes on shaved skin covering about 4×9 cm. Approximately 128 mg of CSC per application was deposited on the skin. Applications were performed three times a week for 18 months in one experiment and for 12 months in another.

Procedure and comments.—A total of 916 rats were used in two experiments with 10 test groups, of which 9 are shown in table 1. The remaining group served to test nicotine toxicity of CSC before beginning the experiment.

The first experiment was performed to assess the tumor-promoting action of CSC when its applications began immediately after irradiation, i.e., before the potential neoplastic tissue progressed toward neoplasia. The first application of CSC was completed within a few seconds after irradiation. This experiment also attempted to demonstrate that CSC alone (without irradiation) was a complete carcinogen in rat skin and to measure quantitatively the additive versus the synergistic effects. For this purpose, CSC applications were continued both in irradiated and nonirradiated animals for 18 months or about one-half of the maximum life-span of the rat. This time is equivalent to about 35 years in humans. The maximum incidence of bronchogenic carcinoma in human beings occurs after 30–35 years of smoking (*10*), also about one-half of the human life-span. The group sizes were 200 rats for the sequential treatment of radiation and CSC, 100 rats for radiation alone, 100 for CSC alone, and 100 for each of 2 untreated controls. In addition, a separate group of 100 rats received CSC for 12 months after the skin "barrier" (stratum corneum) was removed by a stripping technique, not only to facilitate CSC penetration to the basal layer of cells but also to stimulate cell division (*11*).

The second experiment repeated the pilot study (*1*), with the number of rats increased from 15 to 60 per group, a radiation and acetone control added, and the observation period increased from 8 to 14 months after irradiation. As before, CSC applications began 2 months after irradiation or about halfway through the latent period for first-appearing tumors, at which time the potential neoplastic skin would presumably contain foci of active and dormant tumor cells.

Tumors.—The skin was checked for tumors at monthly intervals from the time of irradiation. A tumor was recorded when it had reached the minimum size of 1 mm. Tumors that regressed from view were not included in the subsequent analysis. Skin tumors were divided into 2 groups: carcinomas and other noncarcinoma tumors. The term "papilloma" is frequently used to describe all types of benign tumors in rodent skin, but it is an imprecise description for most of the exophytic growths observed in the present work, where tumor morphology more often resembled keratoacanthomas than true papillomas (*1*). A detailed description of the morphology of radiation-induced epithelial skin tumors in rats has been given by Albert et al. (*7*). In the present study, all tumors except carcinomas were grouped together for purposes of statistical analysis. We have not attempted to classify them further because it is almost certain that all growths originated from the ectodermal epithelium; thus their exact histogenesis may be of little importance (*12*). Rats with apparent cancers were sedated 1 month after the appearance of cancer, and portions of the tumor were removed for histologic examination; thereafter, death was surgically induced and necropsy was performed to find visible tumors in the organs. Tissues were fixed in 10%

TABLE 1.—*Experimental regimen, survival, and tumor yields*

Treatment		Initial No. of rats	Duration of experiment, mo	Survival, %	Noncarcinoma tumors			Carcinomas		
First	Second				No.	Average	Ratio	No.	Average	Ratio
Expt 1. CSC applied immediately after irradiation										
Radiation	CSC	200	18	51	96	0.94	0.47	30	0.29	1.45
Radiation	None	100	18	35	70	2.00		7	0.20	
CSC	None	100	18	72	1	0.01		0		
Expt 2. CSC applied at 2 mo after irradiation										
Radiation	CSC	60	14	72	112	2.60	1.58	12	0.28	1.64
Radiation	None	60	14	60	59	1.64		6	0.17	
Controls and relevant tests										
Untreated control for irradiated phase		99	18	47	0			0		
Untreated control for CSC phase		100	18	76	0			0		
Radiation + acetone		60	6	95	30	0.53[a]				
CSC + stripping		100	18	78	6	0.08				

[a] Compared to 0.74 (difference statistically not significant) for experiment 2 when scored at 6 mo after irradiation.

buffered Formalin and then blocked in wax and stained with hematoxylin and eosin. Basal cell carcinomas and squamous cell carcinomas were identified. Since both of these tumor types are progressively invasive and grossly destructive to the skin, they were grouped together for the analyses in this work. Cancer was verified in a small number of tumors by rapid growth of tissue transplants in the flanks of weanling rats whose immunological system had been suppressed by whole-body irradiation and cortisone treatment (*13*).

RESULTS

In view of one report on the deaths of rats due to nicotine toxicity from CSC (*14*), 36 young rats were treated with CSC over a period of 3 weeks before the start of the experiment. The stratum corneum was first stripped from half this number of animals. No deaths or spastic convulsions were observed from the treatment.

Examination of the data for late deaths revealed that there were markedly fewer deaths among the animals in the CSC groups than among the other groups and that the increases in survival were statistically significant ($P \leq 0.02$) for two of three comparisons (table 2). Although the reason for this difference is not known, most of the deaths in the experiment could be attributed to CMP, a contagious syndrome with the probable etiology of a mycoplasma (*15*).

A comparison of mean tumor numbers at final scoring shows *a*) a reduction in yield of noncarcinoma tumors and an increase in carcinoma yield for CSC treatment beginning immediately after irradiation, and *b*) increases in yields of both carcinomas and other tumors for CSC treatment beginning 2 months following the irradiation (table 1). The data also show an increase in the number of tumors for the skin-stripping treatment, but in terms of absolute numbers this effect is not dramatic enough to be used in the analyses. There was a slight (not significant) reduction in tumor yield for acetone treatment after irradiation.

TABLE 2.—*Statistical comparisons of survival rates between groups with and without CSC treatment*

Treatment	Initial No. of rats	No. of rats dead	Survival, %	*P*-value[a]
Radiation dose response[b]				
800–12,800 rad	497	289	42	<0.01
Control	99	52	47	
CSC[c]				
Unstripped skin	100	28	72	
Stripped skin	100	22	78	
Combined treatments				
Expt 1[d]				
1,600 rad	100	65	35	0.015
1,600 rad + CSC	200	98	51	
Expt 2[e]				
1,600 rad	60	24	60	0.237
1,600 rad + CSC	20	17	72	

[a] χ^2 test.

[b] CMP "flared up" during this treatment at 14 mo of age for a period of [illegible] days, killing 22% of the animals.

[c] CMP occurred in ≈4% of the animals.

[d] CMP was first observed at 8 mo of age in 10% of the animals in the radiation group vs. 0.5% ($P<0.001$) in the radiation+CSC group.

[e] CMP was first observed at 7 mo of age in 27% of the animals in the radiation group vs. 14% ($P>0.05$).

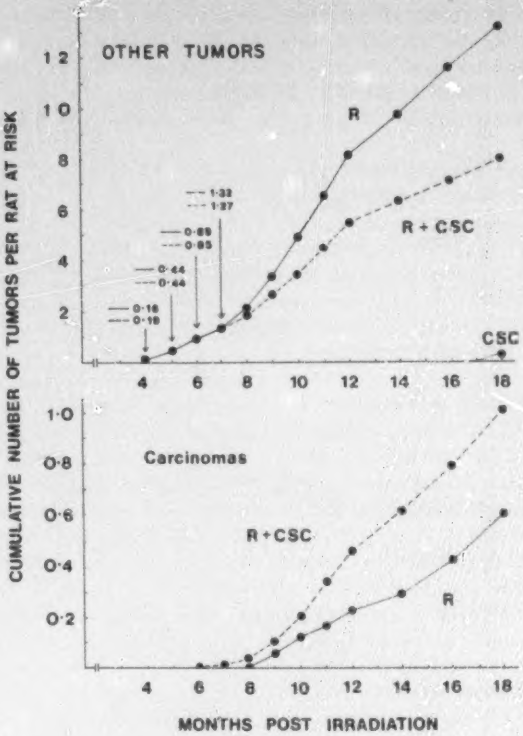

TEXT-FIGURE 1.—Cumulative incidence of tumors after CSC treatment beginning immediately after irradiation (R).

Tumor production is best interpreted by plotting the accumulated incidence of tumors per surviving animal against month of observation. For this, a life table method (*16*) of analysis provided incidence rates unbiased by loss of animals from premature deaths due to unrelated causes or killed because of unmistaken moribundity. The number of tumors scored at the end of 1 month was divided by the number of animals alive at the beginning of the month less half of those that died during the month, and the incidence rates of the successive months were serially accumulated. The clean separation of the curves for the two kinds of treatment make it more convincing that CSC did indeed increase tumor production in three of four comparisons (text-figs. 1, 2). The relative increases [(radiation+CSC): radiation alone] at the final month of analyses were 1.7-fold for carcinomas (text-fig. 1) and 2.2-fold for noncarcinoma tumors and 2.5-fold for carcinomas (text-fig. 2).

An additional benefit of the life table analysis is that it detects the earliest appearance of tumors, i.e., before they have advanced in growth to become recognizable cancers. The times of appearances of noncarcinoma tumors in both experiments, at about 3.5 and 4 months after irradiation, are in reasonable agreement. Carcinomas did not appear until 6–8 months after irradiation (text-figs. 1, 2).

Although the graphic presentations of tumor incidence increases in text-figures 1 and 2 are indicative of tumor-

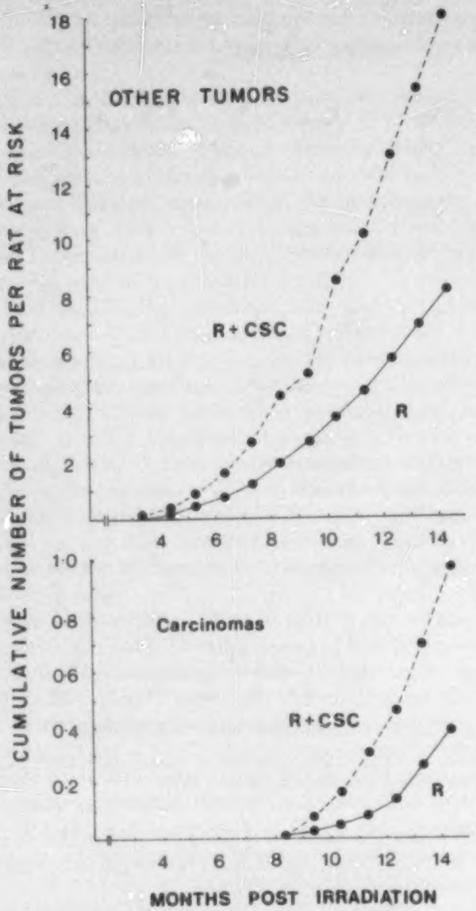

TEXT-FIGURE 2.—Cumulative incidence of tumors after CSC treatment beginning at 2 mo after irradiation (R).

promoting action by CSC, they do not provide the needed measure of confidence (*17*) to show a cause–effect relationship. Statistical significance, therefore, was assessed on the life table data at final analysis with a standard error of a difference test (*18*, *19*). A significant increase ($P<0.0001$) in yield of noncarcinoma tumors was obtained for CSC treatment beginning 2 months after irradiation, and nonsignificant ($P=0.125$, $P=0.079$) increases in carcinoma yields were obtained for the simultaneous and sequential treatments with CSC, respectively. This lack of statistical significance is very likely due to the insufficient numbers of cancers produced by the treatments (table 1), since their relative ratios do not differ greatly from that of the other tumors (text-fig. 2).

A skewed distribution is evident when the number of tumors per animal is plotted against percent of animals in each category (text-fig. 3). These data were also analyzed by a conventional chi-square contingency test for proportion of rats with multiple tumors, i.e., 2–12 tumors per rat. There were significantly more ($P=0.021$) multiple tumor bearers in the radiation and CSC group than in the radiation only group.

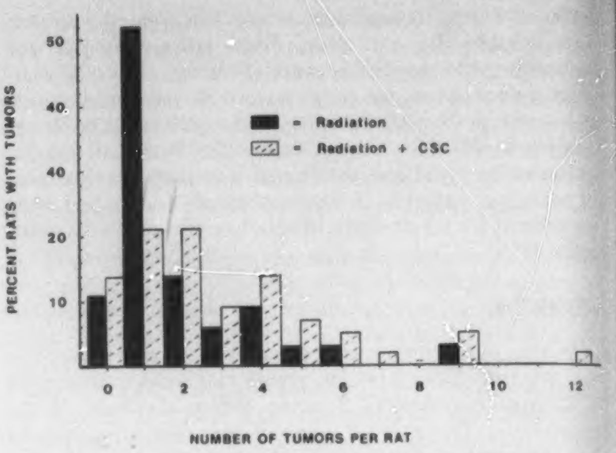

TEXT-FIGURE 3.—Distribution of tumors 12 mo after irradiation.

Although the standard error of the means provides an adequate approximation for tests of statistical significance in a variety of distributions markedly departing from normality (*20*), we decided that we should preclude possible bias from the use of a single statistical test with an alternative parametric test that avoids the requirements for tests involving *t*-distribution (*21*). Statistical significance, therefore, was also assessed on the proportions of rats with tumors with the use of a chi-square contingency test (*22*), and data were transformed by the method of Shellabarger (*23*). To compare the total number of tumors in each of 2 groups, the number of animals "at risk" was obtained by multiplying the number of animals in each group by the largest number of tumors observed on any animal in the comparison (*23*). The results of this contingency test ($P<0.001$ and $P\approx0.2$ for effects of CSC treatments on yield of noncarcinoma tumors and of carcinomas, respectively) were in reasonably good agreement with those based on the test of standard error of difference.

DISCUSSION

The results of the present study confirm the earlier observation of tumor-promoting action of CSC in rat skin when the cigarette tar was first applied 2 months after tumor induction by β-radiation (*1*). The present work entails four major points: *a*) the reduction in yield of noncarcinoma tumors for CSC treatment beginning immediately after irradiation, *b*) the later increase in carcinoma yield for the same treatment, *c*) the failure of CSC by itself to produce tumors, and *d*) the relevance of the present findings to human carcinogenesis.

The obvious explanation for the reduction in yield of noncarcinoma tumors would be a loss of potentially neoplastic tissue through death or sterilization of skin. Severe ulceration covered most of the irradiated skin area as a consequence of CSC applications beginning after irradiation, with a maximum effect of 50% rats with ulceration at 21 days, whereas only mild ulceration on only a portion of the irradiated area occurred for the radiation treatment alone, with a peak effect of 27% rats with ulceration at 16 days. Acute radiation exposures of 1,000 rad (10 Gy) or greater are generally required for the induction of skin cancer in both humans (*24*) and experimental animals (*25*), and such high levels of radiation usually lead to acute injury of skin including ulceration, the severity of which increases with dose. It must be emphasized that acute ulceration was not produced by CSC treatment alone or by CSC treatment beginning 2 months after irradiation, although a number of rats were observed with mild dermatitis in the CSC and radiation group. It is thus evident that degenerative changes from radiation were predominant in the skin immediately after exposure to 1,600 rad, demonstrated by greater susceptibility to destruction when CSC was applied, and presumably to injury by other agents.

Whereas the observed reduction of yield of noncarcinoma tumors may be attributed to a loss of potentially neoplastic tissue when CSC was applied immediately after irradiation, the increase in numbers of carcinomas in the same tissue is more difficult to explain. Carcinogenesis may be considered to occur in two stages (*26*), e.g., tumor initiation by β-radiation and tumor promotion by CSC. The modest increase in carcinoma yield with CSC applied immediately after irradiation must be attributed to a third factor and appears to be mostly due to an effect from acute ulceration, rather than to a promoter effect of CSC. This acute ulceration appears to have made the tissues more vulnerable to carcinogenesis. The results obtained with CSC applied immediately after irradiation are comparable in many ways to those observed after exposure of the skin to much higher doses of radiation alone (*7, 8*). In the second instance, more severe ulceration is associated with a suppression of tumor formation, probably due to elimination of the hair follicles in which many of the tumors originate (*7*), but the yield of carcinomas is not necessarily suppressed and may in fact be increased (*8*). The more severe skin damage at high radiation doses results in a shift from basal cell to squamous cell tumors (*7*). The effect of CSC applied immediately after irradiation may be equivalent, at least in part, to an increase in radiation dose.

That carcinomas were not produced in rat skin by CSC alone suggests, in light of the progress in understanding the activation process of polycyclic hydrocarbons since this work began in 1973, that rat skin may possibly be either deficient in appropriate enzymes for epoxidation of CSC hydrocarbons to form ultimate carcinogens or its detoxifying system is highly developed (*27*). It is well established that the tumor initiators in CSC are largely polycyclic aromatic hydrocarbons (*28*). Before this discovery, the earlier workers had demonstrated the refractoriness of rat skin to coal tar (*2, 29*). With the subsequent synthesis of hydrocarbon carcinogens, skin tumors were produced in the rat, but only after exceptionally long latent periods (*3, 30*). Although the refractoriness of rat skin would tend to favor a genetic interpretation, low penetration of the carcinogens because of their molecular size and thickness of skin may be responsible, in part, for the failure to produce skin tumors more readily (*31*). An attempt in the present study to increase penetration of CSC by stripping the stratum corneum (i.e., removing the dead surface layer of skin) once a month did provide some evidence of increased yield of papillomas, but this increase was not dramatic (table 1).

Although data from animal experiments cannot be used as a direct measure of the hazards in human beings, they have greatly increased our understanding of the mechanisms of carcinogenesis and confirmed the epidemiological evidence of cancer induction by occupational and environmental exposures.

In this study we have demonstrated for the first time a response of rat skin to a tumor-promoting agent. This finding is particularly interesting because croton oil, which is the most widely used promoting agent in testing polynuclear hydrocarbons for tumor-initiating activity, suffers from the shortcoming of being species-specific; i.e., it is effective in mouse skin but not in rat, guinea pig, or rabbit skin (*4*). CSC is primarily a tumor-promoting agent with weak carcinogenic activity in the mouse (*32*).

The presumptive role of acute ulceration to produce a higher rate of cancer raises the question of whether radiation followed by some other skin *irritant*, whether or not it is a promoting agent, would enhance carcinogenesis. For example, in chemical carcinogenesis, a synergistic effect occurred for skin tumors of mice first treated with 7,12-dimethylbenz[*a*]anthracene (initiator), then with croton oil, and later with turpentine, which is a skin irritant lacking promoter ability (*33*). More recently, in radiation carcinogenesis, a significant synergistic effect occurred in lung tumors in hamsters after sequential intratracheal instillations of polonium α-radiation and benzo[*a*]pyrene; however, most of this effect could be attributed to a potentiating effect of subsequent instillations of a seemingly innocuous agent, sodium chloride solution, on polonium carcinogenesis (*34*). Thus evidence is accumulating on the importance of a wide range of complex interactions between carcinogens, promoting agents (i.e., incomplete carcinogens), and noncarcinogens, in addition to simple synergism between two carcinogens. Further studies on these interactions are anticipated.

With regard to human carcinogenesis, a World Health Organization chronicle on smoking and disease (*35*) has described the isolation of an enzyme, AHH, from human tissues that metabolizes polycyclic hydrocarbons to form highly carcinogenic metabolites. The activity of this enzyme can be increased by exposure to cigarette smoke and also by taking various drugs in common use, but the extent of its inducibility in an assay with cultured lymphocytes from healthy persons fit a trimodal distribution, i.e., groups of individuals with low, intermediate, and high inducibility (*36*). These different levels of AHH activity have been demonstrated to be under genetic control (*36*). Individuals with genetically high AHH activity are regarded as being at a greater risk of developing lung cancer if they are heavy smokers compared with the risk of individuals with genetically low AHH activity, because those with high AHH activity produce more carcinogenic epoxides that those with low AHH activity (*37*). Some laboratories have experienced difficulty in confirming the reproducibility of the AHH assay and the trimodal distribution. However, animal experiments with inbred strains have demonstrated an association between the genetic locus for AHH and the increased susceptibility toward chemical tumorigenesis (*38*). Thus it is not unreasonable to speculate that cigarette-smoking uranium miners with low AHH activity would be less likely to develop lung cancer from cigarette smoking alone, than those with high AHH activity. The present work with rats has shown that although CSC failed to produce skin cancer, the skin was still susceptible to its tumor-promoting action on the development of radiation-induced tumors. It is possible that the tumor-promoting action of cigarette smoke might also occur in uranium miners with low AHH activity.

REFERENCES

(*1*) McGregor JF. Tumor-promoting activity of cigarette tar in rat skin exposed to radiation. J Natl Cancer Inst 1976; 56:429–430.

(*2*) Woglow WH. Experimental tar cancer. Arch Pathol Lab Med 1926; 2:533–576.

(*3*) Berenblum I. The carcinogenic action of 9,10-dimethyl-1,2-benzanthracene on the skin and subcutaneous tissues of the mouse, rabbit, rat, and guinea pig. J Natl Cancer Inst 1949; 10:167–174.

(*4*) Shubik P. Studies on the promoting phase in the stages of carcinogenesis in mice, rats, rabbits, and guinea pigs. Cancer Res 1950; 10:13–17.

(*5*) Archer VE, Gillam JD, Wagoner JK. Respiratory disease mortality among uranium miners. Ann NY Acad Sci 1976; 271:280–293.

(*6*) deVilliers AJ, Windish JP. Lung cancer in fluorspar mining community. I. Radiation, dust, and mortality experience. Br J Ind Med 1964; 21:94–109.

(*7*) Albert RE, Phillips ME, Bennett P, Burns F, Heimbach R. The morphology and growth characteristics of radiation-induced epithelial skin tumors in the rat. Cancer Res 1969; 29:658–668.

(*8*) McGregor JF. Association of malignancy with rapid growth in early lesions induced by irradiation of rat skin. JNCI 1979; 62:1043–1049.

(*9*) Cameron JR, Suntharalingam N, Kenney GN. Irradiation of TL standards, chapt 3.3. In: Thermoluminescent dosimetry. Madison, Wisc.: Univ Wisconsin Press, 1968:28.

(*10*) Wynder EL, Graham EA, Croninger AB. Experimental production of carcinoma with cigarette tar. Cancer Res 1953; 13:855–864.

(*11*) McGregor JF. Protection against acute radiation ulceration in healing rat epidermis. Radiat Res 1965; 25:164–170.

(*12*) Foulds L. Individual lesions of regional neoplasia. In: Neoplastic development. Vol 2. London, New York, and San Francisco: Academic Press, 1975:68–70.

(*13*) Toolan HW. Transplantable human neoplasms maintained in cortisone-treated laboratory animals: H.S. #1; H.Ep. #1; H.Ep. #2; H.Ep. #3; and H.Emb.Rh. #1. Cancer Res 1954; 14:660–666.

(*14*) McNally WD. The tar in cigarette smoke and its possible effects. Am J Cancer 1932; 16:1502–1514.

(*15*) Lindsey JR, Baker HJ, Overcash RG, Gassell GH, Hunt CE. Murine chronic respiratory disease. Am J Pathol 1971; 64:675–716.

(*16*) Sachs R. Life table technique in the analysis of response-time data from laboratory experiments on animals. Toxicol Appl Pharmacol 1959; 1:203–227.

(*17*) Interagency Regulatory Liaison Group, Work Group on Risk Assessment. Statistical analysis of results. Scientific bases for identification of potential carcinogens and estimation of risks. JNCI 1979; 63: 241–268.

(*18*) Muller HJ, Oster II, Zimmering S. Are chronic and acute gamma irradiation equally mutagenic in *Drosophila*? In: Sobels FH, ed. Repair from genetic radiation damage. New York and Toronto: MacMillan, 1963:275–304.

(*19*) Muller HJ. The standard error of the frequency of mutants some of which are of common origin. Records Genet Soc Am 1952; 21:52.

(*20*) Mantel N. Rapid estimation of standard errors of means for small samples. Am Statist 1951; 5:26–27.

(*21*) Siegel S. Choosing an appropriate statistical test. In: Nonparametric statistics. New York and London: McGraw-Hill, 1956:18–20.

(*22*) Snedecor GW. Enumeration data with more than one degree of freedom. In: Statistical methods. Ames, Iowa: Iowa State College Press, 1946:198–199.

(*23*) Shellabarger CJ. Mammary neoplastic response of Lewis and Sprague-Dawley female rats to 7,12-dimethylbenz(*a*)anthracene or X-ray. Cancer Res 1972; 32:883–885.

(*24*) Traenkle HL. X-ray induced skin cancer in man. Natl Cancer Inst Monogr 1963; 10:423–432.

(*25*) Glucksmann A. Carcinogenesis. In: Harris RJ, ed. Cellular basis and aetiology of late somatic effects of ionizing radiation. London and New York: Academic Press, 1963:121–133.

(*26*) Berenblum I. The cocarcinogenic action of croton resin. Cancer Res 1941; 24:44–48.

(*27*) Weisburger JH, Williams GM. Metabolism of chemical carcinogens. In: Becker FF, ed. Cancer 1. Etiology: Chemical and physical carcinogenesis. New York and London: Plenum Press, 1975:185–234.

(*28*) Wynder EL, Hoffmann D. Interpretations of experimental findings. In: Tobacco and tobacco smoke. New York and London: Academic Press, 1967:624–626.

(*29*) Watson AF. Comparative studies on carcinogenesis in rats. Am J Cancer 1935; 25:753–762.

(*30*) Oberling CH, Guérin M. Les réactions epithéliomateuses de la peau du rat après badigeonnage par le benzopyrène. Bull Assoc Fr Étude Cancer 1947; 34:30–42.

(*31*) Bock FG. Species differences in penetration and absorption of chemical carcinogens. Natl Cancer Inst Monogr 1963; 10:361–375.

(*32*) Van Duuren BL, Sivak A, Katz C, Melchionne S. Cigarette smoke carcinogenesis: Importance of tumor promoters. J Natl Cancer Inst 1971; 47:235–240.

(*33*) Boutwell RK. Some biological aspects of skin carcinogenesis. Prog Exp Tumor Res 1964; 4:207–250.

(*34*) Little JB, McGandy RB, Kennedy AR. Interactions between polonium-210 α-radiation, benzo(*a*)pyrene, and 0.9% NaCl solution instillations in the induction of experimental lung cancer. Cancer Res 1978; 38:1929–1935.

(*35*) Smoking and disease: The evidence reviewed. WHO Chron 1975; 29: 402–408.

(*36*) Kellermann G, Luyten-Kellermann M, Shaw CR. Genetic variation of aryl hydrocarbon hydroxylase in human lymphocytes. Am J Hum Genet 1973; 25:327–331.

(*37*) Kellermann G. Hereditary factors in human cancer. In: Hiatt HH, Watson JD, Winsten JA, eds. Origins of human cancer. Book B. Mechanisms of carcinogenesis. Cold Spring Harbor conferences on cell proliferation. Vol 4. Cold Spring Harbor, N.Y.: Cold Spring Harbor Laboratory, 1977:837–845.

(*38*) Kouri RE, Nebert DW. Genetic regulation of susceptibility to polycyclic hydrocarbon-induced tumors in the mouse. In: Hiatt HH, Watson JD, Winsten JA, eds. Origins of human cancer. Book B. Mechanisms of carcinogenesis. Cold Spring Harbor conferences on cell proliferation. Vol 4. Cold Spring Harbor, N.Y.: Cold Spring Harbor Laboratory, 1977:811–835.

APPENDIX: CLASSIFICATION OF SKIN TUMORS PRODUCED IN RATS BY β-RADIATION WITH OR WITHOUT CSC

N. J. Gragtmans, C.V.M., Radiation Biology Branch, Chalk River Nuclear Laboratories, Chalk River, Ontario, Canada

For the purpose of this report, epithelial tumors were classified on the basis of their behavior and morphology as either malignant or benign. Upon death of the animal, tumors were submitted for histologic evaluation.

Benign Epithelial Tumors

In general the nodules were well defined, firm, low, and broad based. They were usually keratinizing tumors, originating either from hair follicles or the basal cell layer of the epidermis. Hyperplasia of the follicular cells caused enlargement and fusion of many follicles into one mass. Benign epithelial tumors originating from the basal cell layer appeared as cauliflower-like growth with finger-like processes, made up of a connective tissue core covered by hyperplastic epithelium. However, in both cases the growth was outward, usually with little or no downward invasion. Initially, the mitotic rate of benign tumors was greater than differentiation and keratinization. However, in the later stages the rate of mitosis decreased, followed by differentiation and keratinization of the tumor cells, so that eventually most of the tumor was acellular and consisted of keratin.

Malignant Epithelial Tumors

Most of the tumors in the early stages resembled benign epithelial tumors, but with invasion of subjacent tissues the growth above the skin surface sloughed off, leaving a small ulcerating crater. The crater widened, continued to ulcerate, and frequently became necrotic and infected.

Identification of malignant and benign epithelial tumors is difficult in the early stages, because both seem to have a similar origin and resemble each other histologically. However, tumors were scored grossly when well developed, at which time size, shape, rate of growth, keratinization, sloughing, and ulceration were used as criteria for identification. Upon collection of the tumor, its classification was verified histologically.

Histologically malignant and benign epithelial tumors can easily be differentiated on the basis of keratinization, invasiveness, differentiation, and the frequency of mitotic figures. Malignant epithelial tumors were differentiated from dermally derived, upward-growing tumors (e.g., sebaceous tumors) simply by cell type and histologic arrangement.

blank page

Survival of Mouse Mammary Gland Transplants of Normal, Hyperplastic, and Tumor Tissues Exposed to X-Rays [1,2,3]

Leslie J. Faulkin,[4] Dan J. Mitchell,[4] Robert D. Cardiff,[5] *and* Marvin Goldman[6,7]

ABSTRACT—Mouse mammary tissues, including ducts, prelactating lobules, hyperplastic outgrowth lines, and tumors, were exposed to varying doses of X-rays and then transplanted to fat pads of nonirradiated BALB/c mice for study. Estimates of the dose of radiation that would allow survival of 50% of the transplants (SD_{50}) were made with the use of probit analysis. Nearly all duct and lobule transplants survived doses of X-rays from 0 to 800 rad. The survival rate declined rapidly following doses above 800 rad, and the calculated SD_{50} was 1,020 and 1,260 rad for mammary ducts and lobules, respectively. The three hyperplastic outgrowth lines tested gave very different results. Hyperplastic line Z5C$_1$ transplants had better than 90% survival at doses up to 1,200 rad and an SD_{50} between 1,200 and 1,600 rad. Hyperplastic line Z5D transplants had an SD_{50} of between 800 and 1,200 rad. Hyperplastic line D_1 transplants had a better than 90% survival following doses of 0–600 rad and an SD_{50} between 600 and 800 rad. The survival of tumor transplants was 100% following doses of X-rays up to 1,200 rad; the SD_{50} was in excess of 1,600 rad. The mouse mammary transplantation system can be used to study the direct effect of X-rays on normal, premalignant, and malignant mammary tissues and provides a basis for the study of the radiobiology of mammary tissues.—JNCI 1982; 68:613–618.

The mouse mammary gland was chosen as an animal model to systematically study the radiobiology of mammary glands. The mouse as an experimental model has several advantages: *a*) Mice have short life-spans and, consequently, they reach a tumor-bearing age in months rather than years; *b*) the existence of inbred strains of mice allows transplantation of syngeneic tissue; and *c*) lines of hyperplastic mammary tissue exist with defined characteristics of tumor incidence, morphology, and growth rate available for experimentation and comparison with those of normal tissue (*1–3*). The similarities between the hyperplastic lobuloalveolar lesions in the human mammary gland and those in the mouse mammary gland have been discussed earlier (*4*).

Reports in the literature of the effects of ionizing irradiation on the mouse mammary gland are restricted to the development of mammary tumors after whole-body irradiation. The incidence of mammary tumors, thymic lymphomas, and ovarian, pituitary, and harderian gland tumors was moderately increased following irradiation from an experimental nuclear explosion (*5*). Exposure to 8.8 rad each day for life resulted in mammary tumors in 47%, ovarian tumors in 88%, and lymphoid tumors in 36% of mice (*6*). The increase in mammary tumors following whole-body irradiation could be due to ovarian dysfunction rather than to a direct effect on the mammary gland.

Medina (*3*) has studied several lines of premalignant mammary tissue and reported that administering 450 rad of γ-radiation to the whole body of BALB/c mice bearing transplants of hyperplastic outgrowth lines increased the incidence of mammary tumors. Irradiation of hosts bearing D_1 outgrowth increased the tumor incidence from 4 to 23%. When the outgrowth line D_2 was used, the incidence rose from 45% for nonirradiated transplants to 61% for those transplants that were irradiated in the hosts. A second generation of transplants taken from the irradiated samples and placed in nonirradiated hosts had 0 and 39% tumor incidence for D_1 and D_2, respectively. These results again suggest that the increased tumor incidence could be due to the host's being irradiated rather than to a direct effect on the hyperplastic outgrowth.

Several studies of the survival of rat mammary gland cells following irradiation have been reported (*7–10*). In these studies the mammary glands were removed from rats exposed to whole-body irradiation and enzymatically dissociated into single cell suspensions. Then standard numbers of cells were inoculated into nonirradiated host rats. The transplanted cells were judged viable if one or more spheres of cells (or alveoli) were viable in the host 7 weeks later (*7*). A 50% brain homogenate was added to the mammary cell preparation at a 1:1 ratio to reduce the number of cells required for a successful transplant (*8*). No difference was found in the survival rate of irradiated cells from virgin donors as compared to that of cells from pregnant donors (*8*). The transplanted cells responded to the mammotropic hormones secreted by a pituitary tumor transplanted in the host rats and appeared normal in morphology (*7, 9*). The authors (*7, 9*) concluded that this is an effective way to study the direct effect of irradiation on the mammary gland.

The experiments in this paper, like those with the rat mammary gland, were designed to avoid the problem of whole-body irradiation by transplantation of samples immediately after exposure into nonirradiated hosts. The trans-

---

ABBREVIATION USED: SD_{50}=dose of radiation that would allow survival of 50% of the transplants.

---

[1] Received February 5, 1981; revised August 20, 1981; accepted November 19, 1981.

[2] Supported by Public Health Service grant R01CA-25915 from the National Cancer Institute.

[3] Animals were maintained under the guidelines set forth by the University of California.

[4] Department of Anatomy, School of Veterinary Medicine, University of California, Davis, Calif. 95616.

[5] Department of Pathology, School of Medicine, University of California, Davis.

[6] Department of Radiological Sciences, School of Veterinary Medicine, and Laboratory for Energy Related Health Research, University of California, Davis.

[7] We thank Ms. Judith E. Walls and Mr. Roy Kroll for their expert technical assistance and Dr. Leon S. Rosenblatt (Laboratory for Energy Related Health Research, University of California, Davis) for assistance with the statistical evaluations.

plants were placed in the inguinal mammary fat pads, which had been freed of host gland. The glands that grew from the transplant could be judged for viability and any change in morphology. By use of small samples of the gland that were excised from the donor with microdissection techniques, specific portions of the mammary gland, e.g., duct or alveoli, could be selected, and associated structures in the fat pad could be avoided. The direct selection of tissue also avoided the exposure of the transplanted cells to the enzymes used to dissociate the mammary cells in the rat experiments and similar ones in the mouse (*11*, *12*). It has been observed in the mouse that dissociation of the cells of the mammary glands of young females from a tumor-susceptible line prior to injection into the fat pad resulted in increased numbers of hyperplastic outgrowths from the transplanted cells (*11*). The transplants of dissociated cells of hyperplastic outgrowth lines developed an increased number of tumors (*12*).

The initial experiments reported here were designed to compare the survival of different types of mammary epithelium following exposure to graded doses of X-ray. The long-term goal is to use the mouse mammary gland transplant system for the study of the radiobiology of mammary tissue.

MATERIALS AND METHODS

Mice.—The BALB/c mice used in this study were either purchased from Simonsen Laboratories, Gilroy, Calif., or bred in our laboratory from strains supplied by Simonsen Laboratories. The mice were housed 5 to a cage, maintained in constant temperature-controlled (22°C) and light-controlled (12 hr) rooms, and given food and water ad libitum.

So that the problems associated with high doses of whole-body irradiation could be avoided, the mammary tissues in this study were irradiated in situ and then transplanted into nonirradiated syngeneic hosts. We prepared 3-week-old female host mice for transplantation by surgically removing the nipple and developing mammary ducts in both inguinal fat pads as previously described (*13*). Each mouse then received two transplants, one in each inguinal fat pad. The tissues were transplanted immediately following the host gland-clearing operation and within 2 hours of exposure of the donor tissues to X-rays.

At varying times following transplantation, ranging from 4 to 12 weeks, some host mice were killed and both inguinal fat pads and a sample of the host gland were removed, placed in fixative, and stained as wholemount preparations (*3*). The wholemount preparations were studied for growth and changes in morphology of the transplant. The transplant was determined to have grown if it had formed endbuds on ductal structures or more than doubled in size from the original transplant, and growth was used as a criterion of survival.

X-ray.—The mice bearing the donor tissues described below were exposed to whole-body X-rays from a 250-kV therapeutic machine. The machine was operated at 250 kV potential, with a current of 15 milliamperes and with the 0.25-mm copper and 1-mm aluminum filters in place. The animals were awake but restrained in a wooden box divided into stalls just large enough for a mouse. The box had a Lucite cover with air holes drilled in it. The target-to-subject distance was 50 cm, giving a dose rate of approximately 100 rad/minute. The Radocon meter was placed in an adjacent stall to monitor the amount of radiation during exposure.

Irradiated ducts.—A total of 150 mice were transplanted with 300 primary ducts from 5- to 6-week-old female mice. In addition to the nonirradiated control group, the donor animals were exposed to X-rays of 250, 600, 800, 1,000, 1,200, or 1,500 rad in a single exposure. The mice bearing the transplants were killed at 4, 6, or 8 weeks post implantation. With allowance made for a few intercurrent deaths and technical failures, the number of fat pads studied is shown in table 1.

Examination of the data for the initial groups in which irradiated ducts were studied led to several modifications of subsequent experiments. First, it was apparent that there were more low-dose groups than were necessary. The subsequent studies concentrated on doses in the range of 400–1,600 rad. Second, it was noted that the time in which the transplants were in the host may not have been long enough to give a reliable result. Consequently, the three time periods were increased to 4, 8, and 12 weeks rather than the 4, 6, and 8 weeks used in the study of the ducts. Increasing the time to 12 weeks emphasized the dramatic difference in apparent viability in the groups exposed to higher doses of irradiation.

Estimates of the SD_{50} were made by means of probit analysis (*14*). Data were insufficient in some groups to perform this analysis. The survival of a transplant is a quantal response; i.e., the transplant survived or it died. Linear regression analysis of log dose on probit of percent loss of transplants relative to that of controls was performed, and the SD_{50} was computed from the resultant linear equation. In the case of the duct transplants it was possible to compute 95% confidence intervals on the regression line, and from these intervals, the 95% confidence limits on the SD_{50} could be computed.

Irradiated lobules.—Lobules were obtained from the mammary fat pads of mice pregnant for 16–18 days. A donor mouse was irradiated with 0 (sham), 400, 800, or 1,200 rad of X-ray. A 1-mm^2 piece of lobule tissue was transplanted into each prepared inguinal fat pad of 15 host mice per dose for a total of 60 mice and 120 transplants. Five mice from each group were killed at 4, 8, and 12 weeks post transplantation for determination of survival rates.

Irradiated hyperplastic lines Z5C$_1$, Z5D, and D$_1$.—The hyperplastic outgrowth lines used in this study had relatively dense lobuloalveolar development and similar growth characteristics. The Z5C$_1$ and Z5D lines were developed in our laboratory from multiparous BALB/cfC3H mice. These hyperplastic lines are in the 14th generation and contain the mouse mammary tumor virus. These new lines were characterized elsewhere (*9*). The virus-free hyperplastic line studied was Medina's D$_1$ series developed in hormone-stimulated BALB/c mice. The D$_1$ hyperplastic outgrowth line has been well characterized and is currently in its 47th generation (*10*).

Both inguinal gland-free fat pads of 15 host mice were transplanted with irradiated hyperplastic tissues at each dose level of 0, 400, 800, and 1,200 rad per outgrowth line. An additional group given 600 rad was added to the D$_1$

study and another given 1,600 rad to the Z5C$_1$ and Z5D studies to identify the amount of radiation necessary to reduce the survival rate by 50%. A total of 150 transplants each for the Z5C$_1$ and Z5D lines and 120 transplants for the D$_1$ line were made. Five mice from each group were killed at 4, 8, and 12 weeks post transplantation for study. Some cages of mice were lost prior to completion of the experiment due to failure of the watering device in the cage.

Tumor.—The tumors used in this study were from the second generation passage of a single tumor that arose in a Z5C$_1$ transplant in generation 10. A single donor tumor for each group was irradiated with 0 (sham), 800, 1,200, or 1,600 rad of X-ray. The control group of tumors and the 800-rad-exposed group were transplanted into 14 gland-free fat pads of 7 host mice each, and the 1,200-rad-exposed and 1,600-rad-exposed groups were transplanted into 16 gland-free fat pads of 8 host mice for a total of 60 transplants. Initial tumor appearance was determined by twice weekly palpation of host animals. When the greatest single dimension of any tumor reached 20 mm, the tumor was surgically removed to prevent it from becoming life threatening and to allow the development of the contralateral transplant.

RESULTS

The viability of mouse mammary gland ducts 4, 6, or 8 weeks after transplantation is summarized in table 1. Viability of the transplants was judged by the examination of wholemount preparations for end-bud formation or an increase in the ducts present in the fat pad. The survival rate was very high for doses of radiation from 0 to 800 rad. At doses greater than 800 rad, the survival rate fell rapidly to 3 or 4% at 1,500 rad. The decrease in the survival rate was linear after 800 rad.

As presented in table 1, there were two replicates at 1,000 and 1,500 rad. An analysis of variance was performed to determine whether the replicates differed in the rate of survival at each of the termination times. Both effects were found to be insignificant (P>0.05), and the replicates were pooled for further analysis. Since very few transplants given 1,500 rad survived, visual inspection sufficed to determine that there was no essential difference between replicates given 1,500 rad. Survival of each group relative to that of controls was computed, and from these values the percent loss of survival was computed. The fit of the probit line to the data (for doses of ≥800 rad) was quite good. The correlation coefficient was 0.998 (P<0.01). The estimated SD$_{50}$ was 1,020 rad with 95% confidence limits of 790–1,070 rad.

The survival of transplants of lobules taken from a pregnant mouse that had been exposed to a single dose of radiation is shown in table 2. Using the criterion of increase in the size of the transplants, we were unable to correctly judge survival at 4 and 8 weeks post transplantation. In all of the irradiated groups, but not in the controls, the number of transplants that survived increased with time post transplantation. Among the transplants in the 800-rad-exposed group, 15% survived at 4 weeks, 50% at 8 weeks, and 90% at 12 weeks post transplantation. In the 1,200-rad-exposed group the survival percentages were 10, 20, and 63 at 4, 8, and 12 weeks after transplantation, respectively. The dissimilarity in the results for the different time periods made totaling the results inadvisable. Thus further analyses of these data were confined to the data obtained 12 weeks post transplantation. Only 2 of the radiation groups demonstrated a depression of the percent takes relative to those of the controls. Following exposure to 800 rad the survival was 90%, and at 1,200 rad the survival was 63% of that observed for the controls. Therefore, the SD$_{50}$ must be greater than 1,200 rad. Using all 3 radiation groups, we estimated the SD$_{50}$ from the probit analysis to be 1,260 rad. The fit of the probit line to these three data points was good (r=0.993), but the slope could not be shown to differ significantly from zero at the 5% level of significance. The 95% confidence limits would be extremely broad.

The viability of X-irradiated transplants of the established hyperplastic outgrowth lines was quite different for the lines tested. The results of the transplantation of Z5C$_1$ following various doses of X-ray are presented in table 3. Survival of all transplants was seen in the control group and in the 400-rad-exposed group at 4, 8, and 12 weeks after transplantation, and there appeared to be little heterogeneity in survival among the three time periods tested. Some transplants did not survive in the 800-rad-exposed group,

TABLE 1.—*Survival of mouse mammary gland duct transplants after a single dose of X-rays*

Dose, rad	Time after transplantation						Total		Percent of control
	4 wk		6 wk		8 wk				
	No. viable/ No. tspl[a]	Percent	No. viable/ No. tspl[a]	Percent	No. viable/ No. tspl[a]	Percent	No. viable/ No. tspl[a]	Percent	
0	16/16	100	16/18	89	21/22	95	53/56	94.6	100.0
250	10/10	100	10/10	100	11/12	92	31/32	96.9	102.4
600	2/4	50	3/6	50	7/8	88	12/18	66.7	70.5
800	8/10	80	8/10	80	9/10	90	25/30	83.3	88.0
1,000[b]	6/8	75	2/10	20	4/5	80	21/45	46.7	49.4
1,000	2/6	33	4/8	50	3/8	38			
1,200	2/6	33	1/8	12	2/8	25	5/22	22.7	24.0
1,500[b]	0/8	0	1/10	10	0/8	0	3/84	3.6	3.3
1,500	1/20	5	1/18	6	0/20	0			

[a] Number of transplants viable/number of transplants studied.

[b] No significant difference existed between the replicates, and the totals were combined.

but the survival rate was up to 97% following 1,200 rad for the total of all time groups. The survival rate dropped to a mere 3% when the dose of radiation was 1,600 rad. The data are not sufficient to do a probit analysis; the SD_{50} exceeded 1,200 rad and was less than 1,600 rad.

The survival of transplants of line Z5D is shown in table 4. There was very little heterogeneity of results in the various times post transplantation, and the results for the treatment groups were summed. The survival of the transplants in the control and 400-rad-exposed groups was 89%; it was 67% in the 800-rad-exposed groups. There were no surviving transplants in the 1,200-rad-exposed and 1,600-rad-exposed groups. For the Z5D hyperplastic outgrowth line, the SD_{50} was greater than 800 rad and less than 1,200 rad.

Transplants of irradiated D_1 hyperplastic outgrowth lines had a survival rate of 100% in the 0-rad-exposed group, 92% in the 400-rad-exposed group, and 90% in the 600-rad-exposed group (table 5). When the amount of X-ray given the donor was raised to 800 rad, the survival rate dropped to 2 of 30 transplants (or 7%), and only 2 of the 40 transplants exposed to 1,200 rad were viable. The SD_{50} was between 600 and 800 rad.

The viability of pieces of mammary tumor transplanted to the fat pad following irradiation is shown in table 6. The number of tumors that could be palpated of the total number of tumors transplanted are reported for radiation doses of 800, 1,200, or 1,600 rad as well as in the nonirradiated controls. In the control group, 6 of the 14 transplants were palpable 10 days after transplantation. The number of palpable tumors increased each period until all 14 were palpable 30 days after transplantation. When the transplanted pieces of tumor received 800 rad of X-ray, the first tumors were not palpable until 15 days after transplantation. The number of tumors increased to 12 of 14 transplants palpable 25 days after transplantation. The remaining 2 transplants did not develop into palpable tumors during the remaining 25 days of the experiment.

In the group exposed to 1,200 rad of radiation, the first palpable tumors occurred 20 days post transplantation. The number increased to 13 of 16 transplants palpable by 25 days after transplantation and continued to increase and reached 100% by 45 days after transplantation. The transplants that received 1,600 rad of X-ray were slower to develop the first palpable masses; by 25 days post transplantation, only 5 of the 16 transplants could be detected. The number palpable increased during each 5-day interval until 11 of 16 were detected by 40 days after transplantation. The maximum number of tumors developing in this group by 50 days post transplantation when the experiment was terminated was 11 tumors of 16 transplants (or 69%). The SD_{50} for tumor transplants was greater than 1,600 rad.

TABLE 2.—*Survival of lobule transplants from a pregnant mouse after a single dose of X-rays*

Dose, rad	Time after transplantation					
	4 wk		8 wk		12 wk	
	No. viable/No. tspl[a]	Percent	No. viable/No. tspl[a]	Percent	No. viable/No. tspl[a]	Percent
0	8/10	80	10/10	100	10/10	100
400	6/10	60	8/10	80	10/10	100
800	2/8	25	5/10	50	9/10	90
1,200	1/10	10	2/10	20	5/8	63

[a] Number of transplants viable/number of transplants studied.

TABLE 3.—*Survival of transplants of Z5C$_1$ line of hyperplastic mammary tissue after a single dose of X-rays*

Dose, rad	Time after transplantation						Total	
	4 wk		8 wk		12 wk			
	No. viable/No. tspl[a]	Percent	No. viable/No. tspl[a]	Percent	No. viable/No. tspl[a]	Percent	No. viable/No. tspl[a]	Percent
0	12/12	100	8/8	100	8/8	100	28/28	100
400	10/10	100	10/10	100	10/10	100	30/30	100
800	15/19	79	19/20	95	9/10	90	43/49	88
1,200	9/10	90	9/9	100	12/12	100	30/31	97
1,600	0/10	0	0/10	0	1/10	10	1/30	3

[a] Number of transplants viable/number of transplants studied.

TABLE 4.—*Survival of transplants of Z5D line of hyperplastic mammary tissue after a single dose of X-rays*

Dose, rad	Time after transplantation						Total	
	4 wk		8 wk		12 wk			
	No. viable/No. tspl[a]	Percent	No. viable/No. tspl[a]	Percent	No. viable/No. tspl[a]	Percent	No. viable/No. tspl[a]	Percent
0	8/8	100	10/12	83	7/8	88	25/28	89
400	8/10	80	7/8	88	10/10	100	25/28	89
800	5/10	50	7/8	88	ND		12/18	67
1,200	0/10	0	0/10	0	0/10	0	0/30	0
1,600	0/10	0	0/8	0	ND		0/18	0

[a] Number of transplants surviving/number of transplants studied. ND=not done.

TABLE 5.—*Survival of transplants of D_1 line of hyperplastic mammary tissue after a single dose of X-rays*

Dose, rad	Time after transplantation						Total	
	4 wk		8 wk		12 wk			
	No. viable/No. tspl[a]	Percent	No. viable/No. tspl[a]	Percent	No. viable/No. tspl[a]	Percent	No. viable/No. tspl[a]	Percent
0	10/10	100	10/10	100	12/12	100	32/32	100
400	8/8	100	7/8	88	7/8	88	22/24	92
600	10/10	100	8/10	80	9/10	90	27/30	90
800	0/10	0	2/10	20	0/10	0	2/30	7
1,200	0/10	0	0/10	0	2/20	10	2/40	5

[a] Number of transplants surviving/number of transplants studied.

TABLE 6.—*Viability of mammary tumor transplants exposed to a single dose of X-rays*

Dose, rad	Days post transplantation[a]							
	10	15	20	25	30	35	40	45
0	6/14 (43)	9/14 (64)	12/14 (86)	13/14 (93)	14/14 (100)			
800	0/14 (0)	2/14 (14)	10/14 (71)	12/14 (86)	12/14 (86)	12/14 (86)	12/14 (86)	12/14 (86)
1,200	0/16 (0)	0/16 (0)	9/16 (56)	13/16 (81)	14/16 (88)	14/16 (88)	15/15 (94)	16/16 (100)
1,600	0/16 (0)	0/16 (0)	0/16 (0)	5/16 (31)	7/16 (44)	10/16 (62)	11/16 (69)	11/16 (69)

[a] Results are numbers of tumors that could be palpated/total number of tumors transplanted (%).

TABLE 7.—*SD_{50} for normal, hyperplastic, and tumorous mammary gland transplants*

Tissue transplanted	SD_{50}, rad	95% confidence interval[a]
Normal mammary ducts	1,020	800–1,100
Normal lobules	1,260	—
$Z5C_1$ hyperplastic mammary line	1,200–1,600	—
Z5D hyperplastic mammary line	800–1,200	—
D_1 hyperplastic mammary line	600–800	—
Mammary tumor	1,600	—

[a] —=could not be calculated from the data.

DISCUSSION

The purpose of these experiments was to compare the effects of irradiation on normal, premalignant, and malignant mammary tissues. Using survival as the response criterion, we accomplished our purpose by establishing dose-response parameters for the various tissues. Wholemount preparations of the mammary outgrowths were used to judge survival, which was considered to be any increase in the size of the transplant. For comparison of one tissue with another, the SD_{50} was calculated or estimated from the data.

More than 90% of the nonirradiated normal duct and lobule transplants survived (tables 1, 2) and showed growth by the 4th week post transplantation. Increasing doses of radiation on the normal tissues resulted in fewer apparent survivors at 4 and 8 weeks post transplantation. The results when lobules were studied were dependent on the time that these transplants spent in the hosts; a higher proportion of survivors were usually detected at the later time points. We are studying the apparent retardation in growth rate with increased radiation dose and will report our findings later. The estimates of the SD_{50} for the two normal tissues were similar; the SD_{50} was about 1,020 rad for duct transplants and about 1,250 rad for lobule transplants (table 7). Nearly 100% of all duct and lobule transplants survived lower doses of radiation until a critical level was reached, followed by a steep decline in survival. These features also resemble the survival curves developed for normal rat mammary epithelium (*8*).

The premalignant mammary outgrowth lines used in these experiments are morphologically hyperplastic and were derived from hyperplastic alveolar nodules similar to nodules found in human mammary dysplasias (*4*). The radiosensitivity of the outgrowth lines studied has demonstrated a surprising diversity, although these lines are similar in morphology and growth rate. The $Z5C_1$ was much more radioresistant than were the normal tissues; the SD_{50} was between 1,200 and 1,600 rad. The Z5D line had an SD_{50} between 800 and 1,200 rad, like that of the normal tissues. By contrast, the D_1 tissue was more radiosensitive with an SD_{50} between 600 and 800 rad. The differences in the radiosensitivity of the three outgrowth lines probably reflect the biological variations in hyperplastic tissues. These observations emphasize our inability to generalize about the radiobiology of premalignant mammary tissue. Rather, the range of possible events will have to be defined by observations on a variety of hyperplastic lines. The D_1 outgrowth line is free of exogenous mammary tissue virus, and the $Z5C_1$ and Z5D lines are infected and express viral antigens (*1*). Although we do not believe that mammary tumor virus infection plays a role in the relative sensitivity of the mammary tissue, we are now examining additional outgrowth lines to study this possibility.

The tumor tissue appeared to be more radioresistant than either normal or premalignant mammary tissues. We were able to conduct the tumor experiments with fewer animals by palpating the fat pads to determine growth rather than periodically killing a number of animals. Consequently, the results of the tumor experiments are presented in a different format. However, a comparison of the tumor group 30 days post transplantation with a comparable normal or hyperplastic group 4 weeks post transplantation illustrates the differences. For example, 44% of the tumor transplants receiving 1,600 rad survived at 30 days after transplantation. No other group had significant survival at this level of radiation.

The experimental conditions described in this paper provide for the comparison of direct radiation effects on different types of mammary tissues. The use of the mammary transplantation system for the determination of the direct effect of X-rays on normal and premalignant mouse mammary tissues can provide the basis for the systematic study of the radiobiology of mammary tissues.

REFERENCES

(*1*) Ashley RL, Cardiff RD, Mitchell DJ, Faulkin LJ, Lund JK. Development and characterization of mouse hyperplastic mammary outgrowth lines from BALB/cfC3H hyperplastic alveolar nodules. Cancer Res 1980; 40:4232–4242.

(*2*) Medina D, DeOme KB. Effects of various oncogenic agents on tumor-producing capabilities of series D BALB/c mammary nodule outgrowth lines. J Natl Cancer Inst 1970; 45:353–363.

(*3*) Medina D. Preneoplastic lesions in mouse mammary tumorigenesis. Methods Cancer Res 1973; 7:1–53.

(*4*) Cardiff RD, Wellings SR, Faulkin LJ. Biology of breast preneoplasia Cancer 1977; 39:2734–2746.

(*5*) Furth J, Upton AC, Christenberry KW, Benedict WH, Moshman J. Some late effects in mice of ionizing radiation from an experimental nuclear detonation. Radiology 1954; 63;562–570.

(*6*) Lorenz E, Eschenbrenner AB, Heston WE, Uphoff D. Mammary-tumor incidence in female C3Hb mice following long-continued gamma irradiation. J Natl Cancer Inst 1951; 11:947–965.

(*7*) Gould MN, Biel WF, Clifton KH. Morphological and quantitative studies of gland formation from inocula of monodispersed rat mammary cells. Exp Cell Res 1977; 107:405–416.

(*8*) Gould MN, Clifton KH. The survival of mammary cells following irradiation in vivo: A directly generated single dose survival curve. Radiat Res 1977; 22:343–352.

(*9*) ———. The survival of rat mammary gland cells following irradiation in vivo under different endocrinological conditions. Int J Radiat Oncol Biol Phys 1978; 4:629–632.

(*10*) ———. Evidence for a unique in situ component of the repair of radiation damage. Radiat Res 1979; 77:149–155.

(*11*) DeOme KB, Miyamoto MJ, Osborn RC, Guzman RC, Lumb K. Detection of inapparent nodule-transformed cells in the mammary gland tissues of virgin female BALB/cfC3H mice. Cancer Res 1978; 38:2103–2111.

(*12*) Medina D, Shepherd F, Gropp T. Enhancement of the tumorigenicity of preneoplastic mammary nodule lines by enzymatic dissociation. J Natl Cancer Inst 1978; 60:1121–1126.

(*13*) DeOme KB, Faulkin LJ Jr, Bern HA, Blair PB. Development of mammary tumors from hyperplastic alveolar nodules transplanted into the gland-free mammary fat pads of female C3H mice. Cancer Res 1959; 19:515–520.

(*14*) Rosenblatt LS, Goldman M. The use of probit analysis to estimate dose effects on postirradiation leukocyte depressions. Health Phys 1967; 13:795–798.

Bile Acids: Effects on Absorption of 1,2-Dimethylhydrazine and 7,12-Dimethylbenz[*a*]anthracene in the Colon of the Rat and Guinea Pig[1,2]

Richard C. Rose, *Ph.D.*,[3,4] *and* **David L. Nahrwold**, *M.D.*[5]

ABSTRACT— The specific effects of bile acids as cocarcinogens were investigated. Absorptions of [^{14}C]7,12-dimethylbenz[a]anthracene, [^{14}C]dimethylhydrazine ([^{14}C]DMH), and [^{3}H]inulin from loops of colons from outbred Sprague-Dawley rats and Hartley guinea pigs were determined. In each animal absorption of one carcinogen and inulin was studied in one control loop and in an experimental loop containing either deoxycholic acid (DOC) or chenodeoxycholic acid (CDOC). DOC had a more pronounced effect on increasing loss of carcinogen from the intestinal lumen than did CDOC. This role of bile acids was consistent with their known effect of increasing intestinal permeability. Less carcinogen remained in the colon mucosa when DOC was present in the intestinal lumen. Although [^{14}C]DMH was absorbed more rapidly from the intestinal lumina of guinea pigs than from those of rats, the rat accumulated more of the carcinogen in the intestinal mucosa and liver.—JNCI 1982; 68:619–622.

Epidemiologic observations have provided correlations between dietary habits and the incidence of colorectal cancer in various populations (*1*). Dietary risk factors include high beef and fat consumption. Explanations for these findings have been sought in various animal models for carcinogenesis, including a DMH model in rats. These studies support the finding of carcinogenic effect of high-fat diets and suggest that consequent increased excretion of bile acids may contribute to colon tumor formation (*2–4*). An association has been noted between colon cancer incidence and elevated concentrations of fecal bile acids in humans (*5, 6*).

Despite the above observations, no specific effects of bile acids on the colon have been noted that account for their role as cocarcinogens. The possibility has not been tested that bile acids might alter uptake or metabolism of carcinogens by changing the structural and functional characteristics of the intestine through their detergent and other properties. Such a role might be possible in view of the known effects of bile acids on separating components of the epithelial cell membranes (*7, 8*) and disrupting the gastric mucosa (*9*) with consequent alterations in epithelial permeability properties.

This study was undertaken to determine whether bile acids increase absorption of a water-soluble carcinogen (DMH) and a carcinogen of low water solubility (DMBA). DMH is used as a substituted hydrazine representative of compounds known to be derived from rocket fuels, tobacco, and edible mushrooms (*10*). Entry of each carcinogen into an epithelium of the gastrointestinal tract must precede its carcinogenic action. Absorption of each carcinogen was compared with absorption of the biologically inert polysaccharide inulin. Results were obtained on rats, which are quite sensitive to the carcinogens used, and on guinea pigs, in which the carcinogens produce fewer tumors. The effect of a secondary bile acid (DOC), which is thought to be responsible for contributing to tumor formation (*11*), was compared with the effect of a primary bile acid (CDOC). In each animal, absorption of one carcinogen and inulin was studied in a control loop and in a paired experimental loop containing bile acid.

MATERIALS AND METHODS

Male outbred Sprague-Dawley rats weighing 300–350 g were obtained from Charles River Breeding Laboratories, Wilmington, Mass., and male Hartley guinea pigs weighing 500–600 g were obtained from Dutchland Laboratories, Denver, Pa. Both species were maintained on normal feed prepared by Charles River Breeding Laboratories.

Guinea pigs and rats were anesthetized with Penthrane (methoxyflurane). A midline abdominal incision was made and two adjacent colon segments were isolated with silk ties, with care being taken not to interrupt the blood supply to the isolated tissue. A small incision was made at each end of the segment and the loop was washed with warm, physiologic buffer. Tubing 3 cm in length was secured into each end of the loop and two ties were placed 3 cm apart to separate the loop into two approximately equal lengths. The bowel was replaced in the abdominal cavity, which was closed with the tubing ends exposed. Body temperature was maintained with a heat blanket and heat lamp. The proximal and distal loops were used alternately for exposure to bile acids.

The test solution in DMH studies was physiologic buffer with 1 µCi [^{14}C]DMH/ml (0.13 m*M*) and 10 µCi [^{3}H]inulin/ml. Experimental loops contained, in addition, 10 m*M* CDOC or DOC. Buffer consisted of 142 m*M* NaCl, 1.2 m*M* $MgCl_2$, 0.9 m*M* $CaCl_2$, 1.5 m*M* KH_2PO_4, and 4.2 m*M* K_2HPO_4 (pH 7.2). [^{14}C]DMH and [^{14}C]DMBA were pur-

---

ABBREVIATIONS USED: CDOC=chenodeoxycholic acid; DMBA=7,12-dimethylbenz[*a*]anthracene; DMH=1,2-dimethylhydrazine; DOC=deoxycholic acid.

---

[1] Received February 19, 1981; revised September 9, 1981; accepted November 18, 1981.

[2] Supported by Public Health Service grants 5P30CA-18450 from the National Cancer Institute (NCI) and 1R26CA-25878 from the National Large Bowel Cancer Project, NCI.

[3] Departments of Physiology and Surgery and the Specialized Cancer Research Center, The Milton S. Hershey Medical Center, The Pennsylvania State University, Hershey, Pa. 17033.

[4] *Address reprint requests to* Dr. Rose *at* Department of Surgery, The Milton S. Hershey Medical Center.

[5] Department of Surgery, The Milton S. Hershey Medical Center.

chased from New England Nuclear Corp, Boston, Mass.; both were at least 97% pure by the manufacturer's analysis.

Because of the low solubility of DMBA in buffer, this carcinogen was delivered as 1 µCi/ml (10 *µM*) in a 3% solution of methyl cellulose in buffer. The appropriate test solution (0.5 ml) was injected into each loop for a period of 10 minutes. The colon was removed and both loops were opened, rinsed briefly in cold buffer for removal of adherent radioactivity, and weighed. Tissues from DMH studies were extracted overnight in 0.1 *N* HNO_3, which was shown to remove at least 98% of both ^{3}H and ^{14}C activities. Tissues from DMBA studies were extracted first for 12 hours in acetonitrile to remove [^{14}C]DMBA and then in 0.1 *N* HNO_3 to remove [^{3}H]inulin. Aliquots of each sample were assayed for radioactivity with appropriate corrections made for counting efficiency. At the end of the test period, samples of liver (≈1 g) and blood (3 ml, by heart puncture) were obtained. Radioactivity was extracted by a method similar to that used for extraction of colon tissue. Statistical evaluations were made with Student's *t*-test.

RESULTS

The results (tables 1, 2) indicate that during the 10-minute test period approximately 94% of the inulin remained in the intestinal lumen of control loops during DMH studies and 86% remained during DMBA studies. This small difference, which is not statistically significant, might be attributed to the 3% methyl cellulose–buffer test solution used in DMBA studies. There was a tendency for increased loss of DMH, DMBA, and inulin from the lumen of loops that contained bile acids. This finding reached statistical significance only in DOC studies.

Tables 1 and 2 also show the amount of DMH, DMBA, and inulin extracted from the colon tissue calculated as a percentage of the total ^{14}C or ^{3}H injected into each intestinal loop. The results are also expressed on the basis of wet weight of each loop. Accumulation of DMH and DMBA in the tissues was reduced by DOC but usually not by CDOC. This result was generally true whether the percentage of DMBA and DMH in colon tissue was calculated on a per-loop basis or on the basis of wet weight of the intestinal tissue. The guinea pig absorbed DMH from control loops faster than the rat did ($P<0.01$) but accumulated less of the carcinogen in the colon tissue ($P<0.05$).

Limited information can be derived from the amounts of DMH extracted from liver and blood. Because liver and blood sample were common for control and bile acid loops, the most meaningful treatment of data is a comparison of [^{14}C]DMH and [^{3}H]inulin between rat and guinea pig. The data (table 3) indicate that the blood or liver [^{3}H]inulin did not differ significantly between animal species. However, rat blood had significantly less [^{14}C]DMH than did guinea pig blood, and rat liver accumulated significantly more [^{14}C]DMH than did guinea pig liver.

Bacterial dehydroxylation of CDOC into lithocholic acid and other compounds in the colon loops would make it difficult to separate the effect of CDOC from that of metabolites. The extent of metabolism in colon loops in vivo was evaluated by thin-layer chromatography (*12*). No significant modification of bile salts due to the action of colon bacteria was detected.

TABLE 1.—*Effect of CDOC and DOC on absorption of [^{14}C]DMBA and [^{3}H]inulin*[a]

Animal species	No. of animals	Bile acid	Inulin remaining, %	DMBA remaining, %	Inulin tissue, %	DMBA tissue, %	Percent inulin/g wet wt	Percent DMBA/g wet wt
Guinea pig	6	Control	89±4	71±2	4.5±0.9	13±1.3	7.6±1.5	23±3.8
		DOC	75±4[b]	67±5	2.8±0.4	7.4±0.8[c]	5.4±0.8	14±1.5[b]
Rat	8	Control	83±4	78±3	2.4±0.8	4.9±0.5	5.4±2.0	11±1.3
		DOC	75±4	66±3[b]	2.2±0.4	3.9±0.8	4.8±1.0	8.6±2
Guinea pig	6	Control	88±5	58±10	1.9±0.7	13.7±1.2	3.2±1.4	20±1.6
		CDOC	83±3	52±4	1.4±0.6	12.8±1.0	2.7±1.2	23±3.9
Rat	6	Control	98±5	73±4	1.5±0.1	8.4±1.5	4.4±0.1	20±4.4
		CDOC	85±4	62±4	1.8±0.3	6.1±1.2	5.7±1.7	17±4.4

[a] Values are means ± SE.
[b] Significantly different from control, $P<0.05$.
[c] Significantly different from control, $P<0.01$.

TABLE 2.—*Effect of CDOC and DOC on absorption of [^{14}C]DMH and [^{3}H]inulin*[a]

Animal species	No. of animals	Bile acid	Inulin remaining, %	DMH remaining, %	Inulin tissue, %	DMH tissue, %	Percent inulin/g wet wt	Percent DMH/g wet wt
Guinea pig	7	Control	101±5.2	36±2.3	1.2±0.2	7.6±0.7	2.2±0.4	15±2.1
		DOC	80±2.3[b]	28±3.7[c]	2.9±0.3[b]	4.3±0.4[b]	5.2±0.4[b]	8.1±1.0[c]
Rat	6	Control	97±3	63±2	1.0±0.2	9.9±1.3	2.3±0.5	24±3.2
		DOC	80±3[b]	45±4[c]	2.0±0.4	5.0±1.0[c]	5.4±1.0[c]	14.2±2.0[b]
Guinea pig	6	Control	92±8	30±4.2	1.0±0.2	7.8±1.0	1.7±0.3	14±2.6
		CDOC	81±6	28±3.9	2.8±0.6[c]	5.5±0.3[c]	4.4±1.0[c]	8.8±0.7
Rat	7	Control	87±2.6	58±3.8	2.4±0.8	10±1.7	5.6±1.9	24±3.9
		CDOC	85±2.1	53±4.1	4.0±0.8	9.1±0.7	10±2.2	24±3.1

[a] Values are means ± SE.
[b] Significantly different from control, $P<0.01$.
[c] Significantly different from control, $P<0.05$.

TABLE 3.—*Extractions of [^{3}H]inulin and [^{14}C]DMH from blood and liver*

Animal species	Blood[a]			Liver[b]		
	No. of animals	[^{3}H]inulin	[^{14}C]DMH	No. of animals	[^{3}H]inulin	[^{14}C]DMH
Guinea pig	9	313±61	1,555±133	8	311±64	1,273±215
Rat	10	467±133	931±151[c]	5	187±62	2,715±690[c]

[a] Values presented are cpm/ml, means ± SE.

[b] Values presented are cpm/g wet wt, means ± SE.

[c] $P<0.05$ between animal species.

DISCUSSION

Both epidemiologic observations and laboratory experiments have indicated that diets high in fat are associated with colon tumors. Inasmuch as the appearance of bile acids in the intestinal lumen is associated with increased tumor formation (*11*, *13*), it appeared that diets high in fat might result in tumors by causing release of bile into the intestine. We have evaluated the possibility that bile acids increase absorption of carcinogens in the colons of the rat and the guinea pig. Absorptions of a fat-soluble carcinogen (DMBA) and a water-soluble carcinogen (DMH) were studied. The hypothesis was evaluated in rats, which develop tumors in response to DMH and DMBA and in guinea pigs, which are less sensitive to these carcinogens. The secondary bile acid DOC resulted in increased loss of DMBA and DMH from the intestinal lumina of the guinea pig and the rat. This finding is indicative of an increase in permeability of the intestine, which probably results from dissolution of protein (*8*) or phospholipid (*7*) from the cell membrane. Loss of inulin from the lumen was also increased by DOC. This observation suggests that the effect of bile acids is not specific for carcinogens but generally reflects what is known about the actions of these detergents on biologic tissue (*14*, *15*) and about the resultant increased permeability to a large variety of compounds.

The amount of inulin found in the colon tissue was generally increased by bile acids in DMH studies, which indicates that increases in tissue permeability result in additional tissue spaces becoming available to inulin. The absence of this effect in DMBA studies suggests that the presence of 3% methyl cellulose protects the tissue against this alteration; the explanation for this protection is not apparent from the present studies.

While DOC increased the amount of inulin in colon tissue, it significantly reduced the amount of DMH and DMBA in tissue. No firm explanation can be given for this observation, but perhaps in loops having DOC rapid loss of carcinogen from the tissue occurs during the wash procedure due to damage of the mucosal cell membrane. Alternatively, it may be that DOC results in an increased rate of carcinogen transfer out of the tissue into the blood. The reason that carcinogen differs from inulin in this respect is of interest in the overall scheme of carcinogenesis and deserves further investigation.

Significantly less DMH was found in the colon mucosa of guinea pig intestine than in the mucosa of rat (table 2) despite the faster passage of DMH through the intestinal wall of guinea pig. This finding suggests that rat intestine specifically binds DMH during absorption. Rat liver also appears to bind DMH (or its ^{14}C-labeled metabolite) as indicated by more ^{14}C being present in rat liver than in guinea pig liver (table 3). Greater uptake of DMH by rat liver than by guinea pig liver would not be predicted in view of the faster absorption of DMH in guinea pigs and higher levels of DMH circulating in guinea pig blood. This finding suggests sequestering of DMH in rat liver, which correlates with metabolism of the carcinogen in this animal.

In conclusion, bile acids increase colon absorption of carcinogens through their well-documented effect of increasing intestinal permeability. An additional unexplained effect of the secondary bile acid DOC on increasing transport of carcinogen through the intestinal tissue is possible. More rapid circulation of carcinogen to the liver occurs with bile acids, and in rats conversion to the active metabolite follows. The present results appear to help explain the known effect of fecal bile acids on carcinogenesis in animals and humans. Higher levels of DMH in the liver and colon mucosa of the rat than of the guinea pig correlate with a greater rate of metabolism and binding in the rat. Although the present results show the role of bile acids on absorption of carcinogens, this role is not the only one bile acids play in carcinogenesis.

The concentration of bile acids used in the present study (10 m*M*) is higher than that normally found in the colon of humans or experimental animals. This concentration is approached, however, in the colons of certain patients (*16*) and in the study of Cohen et al. (*11*) on rats, in which it was seen that orally consumed bile acids enhance the formation of colon tumors in response to *N*-methyl-*N*-nitrosourea. In preliminary studies with the use of the protocol described above, we found that exposure of the colon mucosa to 1 m*M* DOC did not affect DMH absorption. It would be of interest to determine whether low concentrations of bile acids alter the colon properties when the exposure period is longer than the 10 minutes used in the present studies.

REFERENCES

(*1*) ARMSTRONG B, DOLL R. Environmental factors and the incidence and mortality from cancer in different countries with special reference to dietary practices. Int J Cancer 1975; 15:617–631.

(*2*) REDDY BS, NARISAWA T, WEISBURGER JH. Effect of a diet with high levels of protein and fat on colon carcinogenesis in F344 rats treated with 1,2-dimethylhydrazine. J Natl Cancer Inst 1976; 57:567–569.

(*3*) REDDY BS, NARISAWA T, VUKUSICH D, et al. Effect of quality and quantity of dietary fat and dimethylhydrazine in colon carcinogenesis in rats. Proc Soc Exp Biol Med 1976; 151:237–239.

(*4*) REDDY BS, WATANABE K, WEISBURGER J. Effect of high-fat diet on colon carcinogenesis in F344 rats treated with 1,2-dimethylhydrazine, methylazoxymethanol acetate, or methylnitrosourea. Cancer Res 1977; 37:4156–4159.

(*5*) HILL MJ, DRASAR BS, WILLIAMS RE, et al. Fecal bile acids and clostridia in patients with cancer of the large bowel. Lancet 1975; 1:535–539.

(*6*) REDDY BS, WYNDER EL. Metabolic epidemiology of colon cancer: Fecal bile acids and neutral sterols in colon cancer patients and patients with adenomatous polyps. Cancer 1977; 39:2533–2539.

(*7*) THOMAS AJ, NAHRWOLD DL, ROSE RC. Detergent action of sodium taurocholate on rat gastric mucosa. Biochim Biophys Acta 1972; 282:210–213.

(*8*) FRIZZELL RA, SCHULTZ SG. Effect of bile salts on transport across brush border of rabbit ileum. Biochim Biophys Acta 1970; 211: 589–592.

(*9*) Davenport HW. Destruction of the gastric mucosal barrier by detergents and urea. Gastroenterology 1968; 54:175–181.

(*10*) Toth B. The large bowel carcinogenic effects of hydrazines and related compounds occurring in nature and in the environment. Cancer 1977; 40:2427–2431.

(*11*) Cohen BI, Raicht RF, Deschner EE, Takahashi M, Sarwal AN, Fazzini E. Effect of cholic acid feeding on *N*-methyl-*N*-nitrosourea-induced colon tumors and cell kinetics in rats. JNCI 1980; 64:573–578.

(*12*) Hofmann AF. Thin-layer adsorption chromatography of free and conjugated bile acids on silicic acid. Lipid Res 1962; 3:127–128.

(*13*) Narisawa T, Magadia NE, Weisburger JH, Wynder EL. Promoting effect of bile acids on colon carcinogenesis after intrarectal instillation of *N*-methyl-N'-nitro-*N*-nitrosoguanidine in rats. J Natl Cancer Inst 1974; 53:1093–1097.

(*14*) Bright-Asare P, Binder HJ. Stimulation of colonic secretion of water and electrolytes by hydroxy fatty acids. Gastroenterology 1973; 64: 81–88.

(*15*) Dobbins JW, Binder HJ. Effect of bile salts and fatty acids on the colonic absorption of oxalate. Gastroenterology 1976; 70:1096–1100.

(*16*) Hofmann AF, Poley JR. Role of bile acid malabsorption in pathogenesis of diarrhea and steatorrhea in patients with ileal resection. I. Response to cholestyramine or replacement of dietary long chain triglyceride by medium chain triglyceride. Gastroenterology 1972; 62:918–934.

Liver DNA Bound In Vivo With Aflatoxin B$_1$ as a Measure of Hepatocarcinoma Initiation in Rainbow Trout [1,2,3]

Mark Whitham,[4,5] **Joseph E. Nixon,**[4,6] *and* **R. O. Sinnhuber**[4,7]

ABSTRACT—The in vivo binding of aflatoxin B$_1$ (AFB$_1$) to liver DNA was measured in rainbow trout subjected to various regimens and in coho salmon to determine if binding would correlate with tumor incidence and initiation of hepatocellular carcinoma. Establishment of time-course binding parameters showed no significant difference between 4, 12, 24, or 48 hours. Doses of 5, 25, 100, and 300 μg AFB$_1$/kg body weight produced an almost linear increase in binding with increasing dose. Compared to that of controls, AFB$_1$–DNA binding was twofold lower in β-naphthoflavone-treated trout and twentyfold lower in coho salmon. These two comparisons reflected a decrease in the effective activation and binding of AFB$_1$, correlated with tumor incidence, and are believed to correlate with a decrease in the initiation of hepatocellular carcinoma. AFB$_1$ binding was not significantly altered by dietary protein or cyclopropenoid fatty acids, which are thought to increase hepatocellular carcinoma incidence through promotional effects. The data were consistent with the view that in vivo binding of AFB$_1$ to liver DNA is a measure of cancer initiation by AFB$_1$ and correlated with the incidence of hepatocellular carcinoma in salmonid fish.—JNCI 1981; 68:623–628.

AFB$_1$ is a potent liver carcinogen in several animal species (*1*). Mt. Shasta strain rainbow trout (*Salmo gairdneri*) are extremely sensitive to the hepatocarcinogenic effects of AFB$_1$ and provide an excellent animal model for the study of this mycotoxin (*2*).

Biologic activation is required for the conversion of AFB$_1$ to metabolites that will bind nucleic acid (*3, 4*), reduce bacterial viability (*5–7*), cause mutagenesis (*8, 9*), and undergo detoxification to the 2,3-dihydro-2,3-dihydroxy-AFB$_1$ (*10*). In vivo macromolecular covalent binding of AFB$_1$ occurs to a much greater extent with nucleic acids than with protein (*11–13*) and has been suggested to be a better indicator of cancer initiation than binding to protein (*12*). Further evidence for the importance of nucleic acid binding is that phenobarbital treatment of rats decreases the incidence of AFB$_1$-induced hepatocarcinogenesis and decreases in vivo AFB$_1$ binding to DNA, while protein binding is unaffected (*12, 14*). Considerable indirect evidence has implicated AFB$_1$-2,3-oxide as the reactive species binding DNA and the nucleophilic N^7 position of guanine as the major site of attack (*9, 15–18*).

Many factors can significantly alter AFB$_1$-induced toxic and carcinogenic effects. Both the level and source of dietary protein affect hepatoma development in rats (*19, 20*) and rainbow trout (*21, 22*). The in vivo binding of AFB$_1$ to chromatin and DNA in low-protein-fed rats was lower than that in controls fed adequate protein (*23*). CPFA, naturally present in the seed oils of plants such as cotton and kapok, also markedly alter AFB$_1$-induced hepatocarcinogenesis (*24*). CPFA are carcinogenic when fed alone to trout (*24*) and act as powerful synergists that increase tumor incidence and growth when they are incorporated into rainbow trout diets with AFB$_1$ (*25–28*), aflatoxin M$_1$ (*29*), and aflatoxin Q$_1$ (*30*). In addition, CPFA alter lipid metabolism and produce extensive cell damage (*31, 32*). Drastic differences in the hepatocellular carcinoma incidence resulting from AFB$_1$ treatment occur in different species. The magnitude of AFB$_1$–nucleic acid binding in the rat, hamster, and mouse correlates well with the relative susceptibility of each species to AFB$_1$-induced hepatocarcinogenesis (*11, 13*).

Covalent binding to macromolecules in combination with toxicity studies provides a means for determining the formation and involvement of reactive metabolites in toxic responses such as cancer (*33*). For the assessment of relationships between the covalent binding of reactive metabolites to macromolecules and toxicities, the covalent binding should be determined when it is maximal (*33*). Alteration of cellular DNA is currently viewed by many investigators as the most attractive mechanism for initiation of carcinogenic processes by chemicals (*34*). In the case of AFB$_1$, the quantity of AFB$_1$–DNA adducts has been suggested as a measure of the activation of AFB$_1$ (*3, 4*) and possibly as an indication of the initiation of cancer (*12, 34*).

The purpose of this investigation was to determine whether in vivo binding of AFB$_1$ to salmonid liver DNA has application for prediction of tumor initiation. The relative binding was measured under specific protocols where initiation or promotional factors are thought to affect the tumor incidence. The following parameters were evaluated: *a*) the influence of source and level of dietary protein on AFB$_1$ binding in trout, *b*) the impact of CPFA on AFB$_1$ binding in trout, *c*) the comparison of AFB$_1$ binding in trout with

---

ABBREVIATIONS USED: AFB$_1$=aflatoxin B$_1$; AFM$_1$=aflatoxin M$_1$; CMC=carboxymethyl cellulose; CPFA=cyclopropenoid fatty acid(s); FPC=fish protein concentrate; MCA=3-methylcholanthrene; MFO=mixed-function oxidase.

---

[1] Received March 17, 1981; revised October 27, 1981; accepted November 6, 1981.

[2] Supported in part by Public Health Service grants ES00541, ES00550, and ES01926 from the National Institute of Environmental Health Science and CA20990 from the National Cancer Institute.

[3] Technical paper No. 5771, Oregon Agriculture Experiment Station. This paper represents part of the thesis research conducted at Oregon State University in partial fulfillment for the degree of Master of Science for M. W.

[4] Department of Food Science and Technology, Oregon State University, Corvallis, Oreg. 97331.

[5] *Present address:* James Ford Bell Technical Center, General Mills, 9000 Plymouth Ave., Minneapolis, Minn. 55427.

[6] *Address reprint requests to* Dr. Nixon.

[7] We thank Dr. George Bailey for his helpful discussions on DNA isolation and purification and Dr. Jerry Hendricks, Mr. John Casteel, Mr. Russell Zora, and Mr. Ted Will for their excellent assistance with the trout.

AFB_1 binding in the more resistant coho salmon (*Oncorhynchus kisutch*), and *d*) the effect of an enzyme inducer, β-naphthoflavone, on binding in trout.

TABLE 1.—*Protein diet composition*

Ingredient	40% protein	50% protein[a]	60% protein[a]	70% protein[a]
		Casein diet		
Casein	30.8	42.0	52.0	62.0
Gelatin	7.7	8.0	8.0	8.0
Dura-gel	6.0	6.0	6.0	6.0
Dextrin	15.3	15.9	6.5	0.0
α-Cell	10.7	4.1	6.5	6.0
Mineral mix[b]	4.0	4.0	4.0	4.0
CMC	1.0	1.0	1.0	1.0
Choline Cl_2	1.0	1.0	1.0	1.0
DL-Arginine	0.6	—	—	—
L-Cystine	0.2	—	—	—
DL-Methionine	0.4	—	—	—
DL-Tryptophane	0.3	—	—	—
Vitamin mix[b]	2.0	2.0	2.0	2.0
Salmon oil	20.0	15.0	12.0	9.0
Total	100.0	100.0	100.0	100.0
		FPC diet		
FPC	32.0	42.0	52.0	62.0
Gelatin	8.0	8.0	8.0	8.0
Dura-gel	0.0	0.0	0.0	0.0
Dextrin	21.3	21.9	12.5	6.0
α-Cell	12.2	6.6	9.0	8.5
Mineral mix	2.5	2.5	2.5	2.5
CMC	1.0	1.0	1.0	1.0
Choline Cl_2	1.0	1.0	1.0	1.0
Vitamin mix[b]	2.0	2.0	2.0	2.0
Salmon oil	20.0	15.0	12.0	9.0
Total	100.0	100.0	100.0	100.0

[a] *Dash* indicates that no amino acids were added to the diets.

[b] Composition described in *(2)*.

MATERIALS AND METHODS

$[^3H(G)]AFB_1$ (0.35–0.45 μCi/μg) was administered by ip injection at 50 μg AFB_1/kg body weight in 0.05–0.25 ml of 95% ethanol except where stated otherwise. We made injection solutions by mixing unlabeled AFB_1 (grade A; Calbiochem-Behring Corp., San Diego, Calif.) with $[^3H(G)]$-AFB_1 (15 Ci/mmol; Moravek Biochemicals, Brea, Calif.). $[^3H(G)]AFB_1$ was 98% radiochemically pure as determined by radiochromatography. Chemical purity of each AFB_1 shipment was confirmed by UV scanning and by thin-layer chromatography.

Animals and diets.—Mt. Shasta strain rainbow trout (*S. gairdneri*) eggs from our brood stock and coho salmon (*O. kisutch*) eggs obtained locally were hatched and reared at the Food Toxicology and Nutrition Laboratory, Oregon State University. Rainbow trout were fed Oregon Test Diet (*2*) in all experiments until the dietary changes indicated below were initiated or until AFB_1 treatment. Coho salmon in experiment 4 were fed Oregon Moist Pellet (*35*) until treatment with AFB_1.

Experiment 1 was conducted to follow the time-course binding in rainbow trout. Trout 10 months old and weighing approximately 45 g each were treated with AFB_1 (83 μg/kg body wt), fasted for 4, 12, 24, or 48 hours, and then killed. In experiment 2, the effect of AFB_1 dosage on total DNA binding was determined. Trout 11 months of age and weighing approximately 53 g each were administered AFB_1 at 5, 25, 100, or 300 μg/kg body weight, fasted for 24 hours, and then killed. Experiment 3 was done to determine the influence of both source and level of dietary protein on AFB_1 binding. Groups of trout 6 months old were fed 40, 50, 60, or 70% semipurified protein diets from two different protein sources, FPC or casein (table 1). After 5 months on these diets, trout weighing 58–71 g were treated with AFB_1, fasted for 24 hours, and then killed. In experiment 4, trout and coho salmon 13 months of age and weighing approximately 74 and 61 g, respectively, were studied to compare the DNA binding in different salmonid species. Both groups of fish were individually weighed and treated with AFB_1, fasted for 24 hours, and then killed. The influence of CPFA on AFB_1-DNA adduct formation was determined in experiment 5. Trout 14 months of age remaining from experiment 3 and weighing 95–145 g were used. These fish were fed 40 or 70% casein or FPC diet (table 1) for 7 months and were divided equally into two tanks for each diet. CPFA were incorporated into the diet at 100 ppm with the salmon oil in 1 group from each protein diet and fed from 23 to 32 days before AFB_1 treatment. The group not treated with CPFA represented the control. Each CPFA-fed group and its respective control were simultaneously administered AFB_1, fasted for 24 hours, and then killed. In experiment 6, the influence of β-naphthoflavone on AFB_1 binding was studied in 2 groups of trout 14 months of age and weighing 80–125 g. Trout were individually weighed and given ip injections of either β-naphthoflavone (Aldrich Chemical Co., Milwaukee, Wis.) at 100 mg/kg body weight in 0.27–0.43 ml of corn oil or with 0.3 ml of corn oil. Both groups were fasted exactly 4 days, treated with AFB_1, and then killed 24 hours later.

Extraction and purification of DNA.—Except for experiment 1, all fish were killed by a cranial blow 24 hours after injection with AFB_1. Livers were excised and immediately perfused with 0.9% NaCl and then nuclei were isolated according to the method of Hymer and Kuff (*36*). DNA was extracted from the final nuclear preparation and purified as described by Marmur (*37*) and modified by Croy and Wogan (*38*). The sequence of steps was extraction, precipitation, treatment with RNase, treatment with pronase, and precipitation. The purified DNA was hydrolyzed in 0.5 *N* perchloric acid at 80°C for 15 minutes (*11*).

Quantitative determinations.—Liver $[^3H(G)]AFB_1$ levels were determined by solubilization of 0.2-ml aliquots from whole-liver homogenates in 1 ml Soluene 350 (Packard Instrument Co., La Grange, Ill.) and counting in 10 ml Dimilume-30 (Packard Instrument Co.). Radioactivity of DNA hydrolysates was obtained by counting aliquots in Aquasol (New England Nuclear Corp., Boston, Mass.). Radioactivity was measured in a Beckman LS 7500 scintillation counter. A measure of covalent binding, AFB_1-DNA adduct formation, was calculated by the conversion of the radioactivity in the DNA hydrolysate to picomoles of AFB_1 and expressed as picomoles AFB_1 per milligram DNA. Variability of the DNA isolation and purification technique was analyzed by the measurement of the binding of three separate aliquots from the same whole-liver homogenate.

DNA hydrolysates were quantitated by the diphenylamine reaction (*39*), RNA contamination by the orcinol reaction (*40*), and protein contamination by the Lowry-Folin procedure (*41*). AFB$_1$ solutions were quantitated in 95% ethanol with the use of a molar extinction coefficient of E (362 nm)=21,800/cm. All colorimetric reactions and UV absorbance readings were determined in a Beckman Acta CIII spectrophotometer.

RESULTS

Effect of time and dose on binding of AFB$_1$ to trout liver DNA.—Covalent binding was maximal at 24 hours after AFB$_1$ administration; however, no significant difference was found between any of the sampling times over the period of 4–48 hours (table 2). An approximately linear increase in binding was obtained with increasing dose levels with a high correlation coefficient of binding for doses over the range 5–300 µg AFB$_1$/kg body weight (table 3).

Dietary protein effects on AFB$_1$ binding.—Binding of AFB$_1$ to trout liver DNA was significantly greater in fish fed 70% casein than in fish fed 70% FPC (table 4). However, binding in the fish fed 40, 50, and 60% casein was not significantly different from that in each corresponding group fed FPC. The 60% protein level from each source produced the greatest binding, but no significant differences were found between casein levels. The binding in the group fed 60% FPC was significantly greater than that in the groups fed either 50 or 70% FPC.

CPFA effect on AFB$_1$ binding to rainbow trout DNA.—Total AFB$_1$ in liver after 24 hours in trout maintained on 40 and 70% casein or FPC and fed 100 ppm CPFA for 23–32 days was not significantly different from that in controls not fed CPFA (table 5). AFB$_1$ binding to liver DNA in the CPFA-fed trout was not significantly different from that in controls either. Total liver AFB$_1$ tended to be higher and AFB$_1$ in DNA tended to be lower in the CPFA-fed trout.

TABLE 2.—*Effect of time after [^{3}H(G)]AFB$_1$ treatment on AFB$_1$ binding to trout liver DNA in vivo*

Hours after treatment	Binding, pmol AFB$_1$/mg DNA[a]
4	201±46.2
12	218±23.4
24	263±55.5
48	251±21.3

[a] Seven livers were pooled for each sample; n=3. Values are means ± SD. Values are not significantly different; P<0.05 (Student's t-test).

TABLE 3.—*Effect of [^{3}H(G)]AFB$_1$ dose on AFB$_1$ binding to trout liver DNA in vivo*

Dose, µg AFB$_1$/kg body wt	Binding, pmol AFB$_1$/mg DNA[a]
5	9.23±0.417
25	55.6±4.95
100	315±19.2
300	1,240±27.0

[a] At least 6 livers were pooled for each sample; n=3. Values are means ± SD. Correlation coefficient=0.9942; P>0.05.

TABLE 4.—*Effect of dietary protein on [^{3}H(G)]AFB$_1$ binding to trout liver DNA in vivo*

Protein source	Protein level, % of diet	Binding, pmol AFB$_1$/mg DNA[a]
Casein	40	258±43.2
Casein	50	253±34.7
Casein	60	329±36.6
Casein	70	299±10.0*
FPC	40	228±44.5
FPC	50	190±38.7†
FPC	60	309±56.3†,‡
FPC	70	189±42.1*,‡

[a] At least 5 livers were pooled for each sample; n=3. Values are means ± SD. *Same superscript symbols* represent significant difference; P<0.05 (Student's t-test).

TABLE 5.—*Effect of CPFA on [^{3}H(G)]AFB$_1$ binding to trout liver DNA in vivo*

Protein source	Protein level, %	Trout group	Liver levels, nmol AFB$_1$/g liver[a]	Binding, pmol AFB$_1$/mg DNA[a]
Casein	40	Control	2.72±0.12	275.0±13.6
Casein	40	CPFA fed	2.47±0.55	219.0±69.9
Casein	70	Control	2.57±0.30	283.0±62.3
Casein	70	CPFA fed	2.78±0.22	246.0±38.6
FPC	40	Control	2.30±0.18	270.0±33.6
FPC	40	CPFA fed	2.60±0.06	260.0±3.1
FPC	70	Control	1.83±0.39	210.0±46.7
FPC	70	CPFA fed	1.99±0.27	189.0±28.6

[a] At least 5 livers were pooled for each sample; n=3. Values are means ± SD. Values are not significantly different; P<0.05 (Student's t-test).

TABLE 6.—*Comparison of in vivo [^{3}H(G)]AFB$_1$ binding to DNA in rainbow trout and coho salmon livers*

Fish	Binding, pmol AFB$_1$/mg DNA[a]
Trout	243.0±85.9
Coho salmon	10.6±01.0

[a] At least 5 livers were pooled for each sample; n=3. Values are means ± SD. Values are significantly different; P<0.05 (Student's t-test).

Calculations were also performed from this study on the amount of AFB$_1$ present in liver tissue at 24 hours from 24 samples relative to the administered dose. Of the total administered [^{3}H(G)]AFB$_1$ dose, 15.4% (range: 10.7–21.5) was present in the liver and 3.1% (range: 2.3–5.0) was covalently bound to DNA. Approximately 20.4% (range: 15.0–25.3) of the total [^{3}H(G)]AFB$_1$ in the liver was bound to DNA.

AFB$_1$ binding to liver DNA in coho salmon and β-naphthoflavone-treated trout.—Table 6 shows the relative binding of AFB$_1$ to liver DNA in trout and coho salmon. Binding in coho salmon, which are less sensitive to AFB$_1$ carcinogenesis than trout, was approximately twentyfold lower than that in the trout. Table 7 shows the effect of pretreatment with 100 mg β-naphthoflavone/kg body weight 4 days before AFB$_1$ injection on [^{3}H(G)]AFB$_1$ binding in trout liver. Total label from [^{3}H(G)]AFB$_1$ in the liver was reduced twofold by β-

TABLE 7.—*Effect of β-naphthoflavone pretreatment on in vivo [^{3}H(G)]AFB$_1$ binding to trout liver DNA*

Treatment	Liver levels, nmol AFB$_1$/g liver[a]	Binding, pmol AFB$_1$/mg DNA[a]
Control	2.09±0.076*	162.0±18.2†
β-Naphthoflavone	0.941±0.148*	96.6±22.1†

[a] At least 5 livers were pooled for each sample; *n*=3. Values are means ± SD. *Same superscript symbols* indicate significant difference; *P*<0.05 (Student's *t*-test).

naphthoflavone, and binding to DNA was significantly reduced to 60% of that of the untreated controls. Variability of binding as a result of isolation procedures was determined in this experiment and calculated to be 1.2%.

DISCUSSION

Time-course and dose-response data are of critical importance for the determination of optimum conditions in binding studies and were obtained as essential information for use in subsequent experiments with rainbow trout. The measured binding of AFB$_1$ to rainbow trout liver DNA over the 48-hour period monitored was not significantly different (table 2). This observation is in marked contrast to that in the rat in which the maximum binding was from 2 to 6 hours followed by a rapid removal of bound AFB$_1$ between 6 and 24 hours (*11*). Two possible explanations for the difference are: *a*) Most of the binding occurs earlier than 4 hours after AFB$_1$ treatment and removal of adducts is extremely slow and *b*) excision repair or removal of bound AFB$_1$ occurs at a rate approximately equal to that of covalent binding to DNA, possibly due to slower absorption and metabolism of injected AFB$_1$ in trout at 10°C compared to rats at 37°C. If persistence of total DNA binding is an indicator of cancer initiation, the longer effective exposure time of rainbow trout, regardless of mechanism, would appear to place them at greater risk to the hepatocarcinogenic activity of AFB$_1$ than rats and could explain the extreme sensitivity of rainbow trout to the hepatocarcinogenic effects of AFB$_1$. From this experiment, a 24-hour sampling time was used in subsequent work to compare the effect of various parameters on binding. The approximately linear dose-binding data shown in table 3 indicate that binding sites for AFB$_1$ were not saturated in the dose range employed. The slightly upward trend of this curve could possibly indicate an inductive effect on the MFO system caused by increasing dosage, with greater activation and subsequent binding, or might indicate proportionally less loss of activated AFB$_1$ to detoxification reactions and binding to protein and RNA at higher doses.

Dietary protein of varied source and level has recently been observed to alter AFB$_1$-induced hepatocarcinogenesis in rainbow trout (*21, 22*). Increasing dietary protein in these studies increased AFB$_1$ tumor induction with both casein and FPC as a protein source. In addition, trout exposed to AFB$_1$ as embryos were observed to have a greater hepatoma incidence with increasing dietary protein levels (*22*); in that experiment, hepatomas were initiated in the embryos, so variable dietary protein in the growing trout affected tumor formation by altering promotional rather than initiating factors. These results are consistent with, and supported by, the lack of effect of variable dietary protein on AFB$_1$ binding in our study. Factors that influence only the promotional stages of tumor development should not influence the extent of initiation by chemical carcinogens (e.g., AFB$_1$ binding to critical sites on DNA). The significance of the differences in AFB$_1$ binding observed between 70% casein and 70% FPC treatments and between 60% FPC and 50 and 70% FPC treatments is not clear because the differences neither occurred in any pattern nor correlated with tumor incidence.

CPFA are far less carcinogenic than is AFB$_1$ in trout, but when fed in conjunction with AFB$_1$ (*25–28*) or fed to trout treated with AFB$_1$ as embryos (*42*), CPFA are potent synergists that greatly enhance tumor incidence and growth. In light of these biologic effects, CPFA may be classified primarily as tumor-promoting agents in the trout hepatocarcinoma model. Thus CPFA, as well as dietary protein, would not be expected to significantly increase initiating events. In fact, a slight reduction in AFB$_1$ binding to DNA with CPFA feeding was noted in this study and is in agreement with reduced AFB$_1$–DNA adduct formation by chronic CPFA treatment previously observed at this laboratory (Nixon JE: Unpublished data). In addition, recent studies (Taylor MJ, Bailey GS, Selivonchick DP: Unpublished data) showed that AFB$_1$ binding to DNA in intact isolated hepatocytes from CPFA-fed trout was reduced compared to that in controls. CPFA alteration of membrane structure may be responsible for reduced microsomal cytochrome P$_{450}$ and protein content and reduced MFO activity reported in CPFA-fed trout (*43–45*). Therefore, reduced microsomal activation presents an explanation for the slightly decreased in vivo AFB$_1$–DNA binding noted in this study. But while initial alkylation may be slightly decreased by dietary CPFA, promotion of these lesions by CPFA leads to a greatly elevated tumor response. At present, we have no explanation for the mild carcinogenic activity of CPFA when fed alone.

Rainbow trout exposed to AFB$_1$ as embryos are much more sensitive to hepatocarcinogenesis than coho salmon administered the identical embryo exposure and dietary regimen (Hendricks JD, Sinnhuber RO: Unpublished data). This observation suggests that differences in tumor-initiating events and not promotional factors may be responsible for the difference in hepatoma development in these two species. The twentyfold higher binding of AFB$_1$ in rainbow trout relative to the AFB$_1$ binding in coho salmon noted in this study (table 6) supports the hypothesis that binding can predict tumor initiation and incidence. However, conditions used in this study were those previously established for rainbow trout. Since relative to rainbow trout salmon grow poorly in captivity, data on time-course binding and on liver uptake and removal of AFB$_1$ in coho salmon would aid our understanding of the significance of this difference. However, in studies done to date (Loveland PM, Nixon JE, Hendricks JD, Sinnhuber RO: Unpublished data) in vitro metabolism of AFB$_1$ and MFO activities are generally lower in coho salmon than in trout. Faster DNA repair in coho than in trout would have explained the lower amount of AFB$_1$–DNA in coho than in trout, but we have no reason to believe that occurs.

Phenobarbital, an inducer of rat liver MFO activity, decreases in vivo AFB$_1$–nucleic acid binding and AFB$_1$-induced hepatocarcinogenesis in rats (*12, 14, 46*). Another MFO inducer, β-naphthoflavone, has been observed to dramatically increase MFO activity in rainbow trout (*47, 48*) and has been shown to provide tumor protection in some animal species (*49*). Recently, in our laboratory β-naphthoflavone was shown to protect against AFB$_1$-induced hepatocellular carcinoma (Hendricks JD, Nixon JE, Bailey GS, Sinnhuber RO: Unpublished data). Treatment with β-naphthoflavone, which is an MCA-type inducer (*47*), apparently increases overall AFB$_1$ metabolism, and detoxification reactions predominate over initiation events and result in tumor reduction (*49*). This observation is supported by the work of Gurtoo and Dahms (*50*) who have reported that several MFO enzymes are involved in AFB$_1$ metabolism and the enzymes react differently to MFO inducers and inhibitors. In vitro metabolism of AFB$_1$ to less toxic AFM$_1$ was stimulated while activation to AFB$_1$-2,3-oxide was inhibited by pretreatment of rats and mice with MCA. Thus if β-naphthoflavone reduces tumor incidence by decreasing initiation events in the trout system and AFB$_1$–DNA binding is an indicator of initiation., β-naphthoflavone should reduce AFB$_1$ binding. This view is supported by the fact that β-naphthoflavone treatment compared to treatment for controls did reduce AFB$_1$ binding by 40% in this study. In addition, the simultaneous twofold reduction in liver AFB$_1$ levels suggests that such treatment increased detoxification activity and enhanced conversion of AFB$_1$ to readily excretable metabolites. This view was further supported by recent work in our laboratory (Bailey GS, Taylor MJ, Selivonchick DP: Unpublished data) which showed that intact isolated hepatocytes from β-naphthoflavone-fed trout metabolized more AFB$_1$ and formed twentyfold more AFM$_1$, slightly more water-soluble metabolites, 70% less aflatoxicol, and 30-50% less AFB$_1$–DNA adducts than did hepatocytes from controls.

AFB$_1$–DNA adduct formation in the trout system under the conditions described in this paper seems to correlate well with the expected relative levels of binding, where promotional or initiating effects are the determining influence. When tumor development is attributed to promotional factors, such as dietary protein and CPFA, no relationship with DNA binding would be expected, and none was observed in this study. However, when the quantity of initiating events is presumed altered by a drug (β-naphthoflavone) or by species differences (coho salmon vs. trout), a positive relationship with DNA binding was expected and observed. Thus the data are consistent with the view that in vivo AFB$_1$–DNA binding is a measure of initiation of cancer by AFB$_1$ and correlates with the incidence of hepatocellular carcinoma in rainbow trout when promotional effects are not involved. Initiation as used in this discussion is the sum of activities involving AFB$_1$ that results in AFB$_1$–DNA adducts after 24 hours. The quantity of AFB$_1$ that was activated to AFB$_1$–2,3-oxide, that survived competing reactions to bind covalently to DNA, and that survived DNA repair to persist for 24 hours was used as a measure of initiation. That measure of initiation correlated well with carcinoma incidence. We realize that initiation is a complex process and mutagenic and carcinogenic activities correlate better with persistence of specific adducts than with total alkylation of DNA (*51*). However, total AFB$_1$–DNA adducts appear to be adequate for estimating initiation under in vivo conditions in the trout system and may be a useful assay for predicting tumor incidence.

AFB$_1$–DNA adducts in the trout system have been analyzed and were found to be remarkably similar to AFB$_1$–DNA adducts from rats (*52*). We are presently studying AFB$_1$–DNA adduct profiles in trout and salmon subjected to different nutritional, inducer, and inhibitor regimens to determine correlation of adduct profile and tumor incidence. Further study with coho salmon, a salmonid species resistant to AFB$_1$-induced hepatocarcinogenesis, and with MFO inducers such as β-naphthoflavone, which apparently alter initiation and detoxification pathways, could provide important information in understanding mechanisms of chemical carcinogenesis.

REFERENCES

(*1*) Wogan GN. Aflatoxin carcinogenesis. In: Busch H, ed. Methods in cancer research. Vol 7. New York: Academic Press, 1973:309–344.

(*2*) Sinnhuber RO, Wales JH, Hendricks JD, Putnam GB, Nixon JE, Pawlowski NE. Trout bioassay of mycotoxins. In: Rodricks JV, ed. Mycotoxins in human and animal health. Park Forest South, Ill: Pathotox Publishers, 1977:731–744.

(*3*) Garner RC. Microsome-dependent binding of aflatoxin B$_1$ to DNA, RNA, polyribonucleotides, and protein in vitro. Chem Biol Interact 1973; 6:125–129.

(*4*) Gurtoo HL, Bejba N. Hepatic microsomal mixed function oxygenase: Enzyme multiplicity for the metabolism of carcinogens to DNA-binding metabolites. Biochem Biophys Res Commun 1974; 61:735–742.

(*5*) Garner RC, Miller EC, Miller JA, Garner JV, Hanson RS. Formation of a factor lethal for *S. typhimurium* TA1530 and TA1531 on incubation of aflatoxin B$_1$ with rat liver microsomes. Biochem Biophys Res Commun 1971; 45:774–780.

(*6*) Garner RC, Miller EC, Miller JA. Liver microsomal metabolism of aflatoxin B$_1$ to a reactive derivative toxic to *Salmonella typhimurium* TA1530. Cancer Res 1972; 32:2058–2066.

(*7*) Schoenhard GL, Bishop PE, Lee DK, Sinnhuber RO. *Bacillus subtilis* GSY 1057 assay for aflatoxin B$_1$ activation by rainbow trout (*Salmo gairdneri*). J Assoc Off Anal Chem 1975; 58:1074–1076.

(*8*) Stott WT, Sinnhuber RO. Dietary protein levels and aflatoxin B$_1$ metabolism in rainbow trout (*Salmo gairdneri*). J Environ Pathol Toxicol 1978; 2:379–388.

(*9*) Stark AA, Essigmann JM, Demain AL, Skopek TR, Wogan GN. Aflatoxin B$_1$ mutagenesis, DNA binding, and adduct formation in *Salmonella typhimurium*. Proc Natl Acad Sci USA 1979; 76:1343–1347.

(*10*) Lin JK, Kennan KA, Miller EC, Miller JA. Reduced nicotinamide adenine dinucleotide phosphate-dependent formation of 2,3-dihydro-2,3-dihydroxy aflatoxin B$_1$ from aflatoxin B$_1$ by hepatic microsomes. Cancer Res 1978; 38:2424–2428.

(*11*) Garner RC, Wright CM. Binding of [^{14}C]aflatoxin B$_1$ to cellular macromolecules in the rat and hamster. Chem Biol Interact 1975; 11:123–131.

(*12*) Swenson DH, Lin JK, Miller EC, Miller JA. Aflatoxin B$_1$-2,3-oxide as a probable intermediate in the covalent binding of aflatoxins B$_1$ and B$_2$ to rat liver DNA and ribosomal RNA in vivo. Cancer Res 1977; 37:172–181.

(*13*) Ueno I, Friedman L, Stone CL. Species difference in the binding of aflatoxin B$_1$ to hepatic macromolecules. Toxicol Appl Pharmacol 1980; 52:177–180.

(*14*) Garner RC. Reduction in binding of [^{14}C]aflatoxin B$_1$ to rat liver macromolecules by phenobarbitone pretreatment. Biochem Pharmacol 1975; 24:1553–1556.

(*15*) Essigmann JM, Croy RG, Nadzan AM, et al. Structural identification of the major DNA adduct formed by aflatoxin B_1 in vitro. Proc Natl Acad Sci USA 1977; 74:1870–1874.

(*16*) Croy RG, Essigmann JM, Reinhold VN, Wogan GN. Identification of the principal aflatoxin B_1–DNA adduct formed in vivo in rat liver. Proc Natl Acad Sci USA 1978; 75:1745–1749.

(*17*) Fahmy MJ, Fahmy OG, Swenson DH. Aflatoxin B_1-2,3-dichloride as a model of the active metabolite of aflatoxin B_1 in mutagenesis and carcinogenesis. Cancer Res 1978; 38:2608–2616.

(*18*) Autrup H, Essigmann JM, Croy RG, Trump BF, Wogan GN, Harris CC. Metabolism of aflatoxin B_1 and identification of the major aflatoxin B_1–DNA adducts formed in cultured human bronchus and colon. Cancer Res 1979; 39:694–698.

(*19*) Madhavan TV, Gopalan C. Effect of dietary protein on aflatoxin liver injury in weanling rats. Arch Pathol 1965; 80:123–126.

(*20*) ———. The effect of dietary protein on carcinogenesis of aflatoxin. Arch Pathol 1968; 85:133–137.

(*21*) Lee DJ, Sinnhuber RO, Wales JH, Putnam GB. Effect of dietary protein on the response of rainbow trout (*Salmo gairdneri*) to aflatoxin B_1. J Natl Cancer Inst 1977; 60:317–320.

(*22*) Hendricks JD, Nixon JE, Loveland PM, Casteel JL, Sinnhuber RO. High dietary protein promotes embryo-induced aflatoxin carcinogenesis in rainbow trout. Fed Proc 1981; 40:948.

(*23*) Preston SR, Hayes JR, Campbell TC. The effect of protein deficiency on the in vivo binding of aflatoxin B_1 to rat liver macromolecules. Life Sci 1976; 19:1191–1198.

(*24*) Sinnhuber RO, Hendricks JD, Putnam GB. Sterculic acid, a naturally occurring cyclopropene fatty acid, a liver carcinogen to rainbow trout (*Salmo gairdneri*). Fed Proc 1976; 35:505.

(*25*) Sinnhuber RO, Wales JH, Lee DJ. Cyclopropenoids, cocarcinogens for aflatoxin-induced hepatoma in trout. Fed Proc 1966; 25:184.

(*26*) Lee DJ, Wales JH, Sinnhuber RO. A comparison of cyclopropenes and other possible promoting agents for aflatoxin-induced hepatoma in rainbow trout. Fed Proc 1976; 26:99.

(*27*) Sinnhuber RO, Lee DJ, Wales JH, Ayres JL. Dietary factors and hepatoma in rainbow trout (*Salmo gairdneri*). II. Cocarcinogenesis by cyclopropenoid fatty acids and the effect of gossypol and altered lipids on aflatoxin-induced liver cancer. J Natl Cancer Inst 1968; 41:1293–1301.

(*28*) Lee DJ, Wales JH, Sinnhuber RO. Synergism between cyclopropenoid fatty acids and chemical carcinogens in rainbow trout (*Salmo gairdneri*). Cancer Res 1968; 28:2312–2318.

(*29*) Sinnhuber RO, Lee DJ, Wales JH, Landers MK, Keyl AC. Hepatic carcinogenesis of aflatoxin M_1 in rainbow trout (*Salmo gairdneri*) and its enhancement by cyclopropene fatty acids. J Natl Cancer Inst 1974; 53:1285–1288.

(*30*) Hendricks JD, Sinnhuber RO, Nixon JE, Wales JH, Masri MS, Hsieh DP. Carcinogenic response of rainbow trout (*Salmo gairdneri*) to aflatoxin Q_1 and synergistic effect of cyclopropenoid fatty acids. JNCI 1980; 64:523–527.

(*31*) Roehm JN, Lee DJ, Politycka SD, Sinnhuber RO. The effect of sterculic acid on hepatic lipids of rainbow trout. Lipids 1970; 5:80–84.

(*32*) Struthers BJ, Wales JH, Lee DJ, Sinnhuber RO. Liver composition and histology of rainbow trout fed cyclopropenoid fatty acids. Exp Mol Pathol 1975; 23:164–170.

(*33*) Gillette JR. A perspective on the role of chemically reactive metabolites of foreign compounds in toxicity. I. Correlation of changes in covalent binding of reactivity metabolites with changes in the incidence and severity of toxicity. Biochem Pharmacol 1974; 23:2785–2794.

(*34*) Miller EC. Some current perspectives on chemical carcinogenesis in humans and experimental animals: Presidental address. Cancer Res 1978; 38:1479–1496.

(*35*) Crawford DL, Law DK, McKee TB, Westgate JW. Storage and nutritional characteristics of modified Oregon moist rations as an intermediate-moisture product. Prog Fish-Cult 1973; 35:33–38.

(*36*) Hymer WC, Kuff EL. Isolation of nuclei from mammalian tissues through use of Triton X-100. J Histochem Cytochem 1964; 12:359–363.

(*37*) Marmur J. A procedure for the isolation of deoxyribonucleic acid from micro-organisms. J Mol Biol 1961; 3:208–218.

(*38*) Croy RG, Wogan GN. Temporal patterns of covalent DNA adducts in rat liver after single and multiple doses of aflatoxin B_1. Cancer Res 1981; 41:197–203.

(*39*) Burton K. A study of the conditions and mechanisms of the diphenylamine reaction for the colorimetric estimation of deoxyribonculeic acid. Biochem J 1956; 62:315–323.

(*40*) Ceriotti G. Determination of nucleic acids in animal tissues. J Biol Chem 1955; 214:59–70.

(*41*) Lowry OH, Rosebrough HJ, Farr AL, Randall RJ. Protein measurement with the Folin phenol reagent. J Biol Chem 1951; 193:265–272.

(*42*) Hendricks JD. The use of rainbow trout (*Salmo gairdneri*) in carcinogen bioassay, with special emphasis on embryonic exposure. In: Dawe CJ, Harshbarger JC, Sugimura T, Takayama S, Kondo S, eds. The eleventh international symposium of the Princess Takamatsu Cancer Resarch Fund. Phyletic approaches to cancer. Tokyo: Japan Scientific Societies Press, 1981:227–240.

(*43*) Eisele TA, Nixon JE, Pawlowski NE, Sinnhuber RO. Effects of dietary cyclopropene fatty acids on the mixed function oxidase system of the rainbow trout. J Environ Pathol Toxicol 1978; 1:773–778.

(*44*) Loveland PM, Nixon JE, Pawlowski NE, et al. Aflatoxin B_1 and aflatoxicol metabolism in rainbow trout (*Salmo gairdneri*) and the effects of dietary cyclopropene. J Environ Pathol Toxicol 1979; 2:707–718.

(*45*) Selivonchick DP, Schaup HW. Characterization of liver microsomal proteins from rainbow trout (*Salmo gairdneri*) fed cyclopropenoid fatty acids. Fed Proc 1980; 39:644.

(*46*) McLean AE, Marshall A. Reduced carcinogenic effects of alfatoxin in rats given phenobarbitone. Br J Expt Pathol 1971; 52:322–329.

(*47*) Franklin RB, Elcombe CR, Vodicrik MJ, Lech JJ. Comparative aspects of the disposition and metabolism of xenobiotics in fish and mammals. Fed Proc 1980; 39:3144–3149.

(*48*) Haight LE, Nixon JE, Hendricks JD, Sinnhuber RO. Null effect of cruciferous vegetables on aflatoxin B_1 (AFB_1) induced carcinogenesis in rainbow trout. Fed Proc 1981; 40:948.

(*49*) Wattenberg LW. Effects of dietary constituents on the metabolism of chemical carcinogens. Cancer Res 1975; 35:3326–3331.

(*50*) Gurtoo HL, Dahms RP. Effects of inducers and inhibitors on the metabolism of aflatoxin B_1 by rat and mouse. Biochem Pharmacol 1979; 28:3441–3449.

(*51*) Singer B. Guest editorial. N-nitroso alkylating agents: Formation and persistence of alkyl derivatives in mammalian nucleic acids as contributing factors in carcinogenesis. JNCI 1979; 62:1329–1339.

(*52*) Croy RG, Nixon JE, Sinnhuber RO, Wogan GN. Investigation of covalent aflatoxin B_1–DNA adducts formed in vivo in rainbow trout (*Salmo gairdneri*) embryos and liver. Carcinogenesis 1980; 1:903–909.

B16 Melanoma Cell Variants: Irreversible Inhibition of Growth and Induction of Morphologic Differentiation by Anthracycline Antibiotics[1,2,3]

Avraham Raz[4,5]

ABSTRACT—The interaction of doxorubicin and *N*-trifluoroacetyladriamycin-14-valerate (AD32) with B16 melanoma cell variants that exhibit distinct metastatic properties was explored. The addition of the two drugs to cell monolayers at noncytolytic concentrations for 16 hours resulted in irreversible inhibition of proliferation of tumor cells and loss of their tumorigenicity after injection into inbred C57BL/6 mice. Cessation of melanoma cell proliferation was accompanied by cellular and nuclear hypertrophy and the development of axon-like processes. As assessed by drug-specific cytofluorescence, after 16-hour exposure of the cells to doxorubicin and AD32, the drugs were localized in the nuclei. Incubation of drug-treated cell monolayers for 6 additional days in drug-free culture medium led to the complete disappearance of nuclear stain. The highly metastatic B16-F10-B2 cell line was the most sensitive to the drugs' effects, whereas the other two malignant melanoma cell lines, although differing in their metastatic capabilities, exhibited similar sensitivities to the drugs' effects. Doxorubicin was notably more potent than AD32 in its growth inhibitory effect on the three tested melanoma cell variants. The possible mutagenic effect of anthracycline drugs on tumor cells was discussed.—JNCI 1982; 68:629–638.

Metastasis, the spread of neoplastic disease, is responsible for most therapeutic failures in clinical oncology. The metastatic process involves linked sequential steps in which neoplastic cells are detached from the primary tumor and disseminate to distant organs where they are arrested and divide to form new tumor foci. Despite the development of complex and aggressive therapeutic regimens, most deaths in cancer patients are due to the survival and growth of unique metastatic cells that are nonresponsive to the treatment [for reviews *see* (*1–3*)]. In the determination of the therapeutic schedule, the veracity of results from experimental tumor systems depends on the use of an appropriate biologic model (*4*). There would appear, then, to be a need for information on the susceptibility of tumor cell variants that exhibit distinct metastatic properties to anticancer drugs. The best characterized tumor system with regard to cellular properties and metastasis is the B16-F malignant melanoma series (*5*). It was shown that the parental B16 melanoma tumor is populated with cells that exhibit high and low metastatic potential as well as preferential metastasis to a particular organ (*5–8*).

Anthracycline antibiotics exhibit antineoplastic activity in experimental tumors (*9–12*) as well as in human malignant diseases (*13–15*). The doxorubicin and daunorubicin derivatives have been shown to intercalate with DNA, both via hydrophobic interactions between base pairs of the DNA and the glycon and by binding of the amino group of the sugar residues in the drug to the phosphate moiety of DNA (*16–18*). The development of different analogs like AD32, which exhibits a superior therapeutic activity in comparison to that of the two former molecules (*19*) but does not bind to calf thymus DNA (*20*) and does not exhibit drug-specific nuclear fluorescences in WI-38 fibroblasts (*21*), has promoted the idea that AD32 is metabolized to a nonfluorescence DNA-binding metabolite (*21, 22*).

In the present study we report that exposure of three B16 melanoma cell variants of different metastatic potential to doxorubicin and AD32 results in the irreversible inhibition of cell proliferation and is accompanied by a dramatic alteration in cell morphology.

MATERIALS AND METHODS

Anthracycline drugs.—Doxorubicin and AD32 were supplied by Dr. A. Mantovani (Istituto di Ricerche Farmacologiche Mario Negri, Milan, Italy).

Tumor cell variants.—The B16-F1 cell line (low incidence of lung colonization) was derived from pulmonary metastases produced by iv injection of B16 melanoma cells (*4*). The B16-F10 cell line (high incidence of lung colonization) was selected by successive passage of tumor colonies for ten in vivo–in vitro selections, as described previously (*4*). These 2 cell lines were supplied by Dr. I. J. Fidler (NCI-Frederick Cancer Research Facility, Frederick, Md.). The B16-F10-B2 (exhibiting preferential growth in the brain) is a variant cell line selected from the B16-F10 cell line after two in vivo–in vitro selection cycles of brain tumors, as described in detail previously (*7*).

Cell cultures.—All cultures were maintained on plastic plates in Dulbecco's modified Eagle's minimum essential medium supplemented with nonessential amino acids, L-glutamine, vitamins, antibiotics (Grand Island Biological

---

ABBREVIATIONS USED: AD32=*N*-trifluoroacetyladriamycin-14-valerate; cAMP=cyclic AMP; cEMEM=complete Eagle's minimum essential medium; PBS=phosphate-buffered saline [0.01 *M* phosphate buffer (pH 7.2)-0.154 *M* NaCl].

---

[1] Received April 3, 1981; revised August 13, 1981; accepted October 22, 1981.

[2] Supported by the Israel Cancer Research Fund (N.Y.) and the Sir Charles Clore Fellowship.

[3] Guidelines for the care and use of laboratory animals were followed as set forth by The Weizmann Institute of Science.

[4] Department of Cell Biology, The Weizmann Institute of Science, P. O. Box 26, Rehovot, Israel 76 100.

[5] I thank Professor M. Feldman for his interest during this work, Dr. R. Lotan and Dr. A. Ben-Zeev for their careful review of the manuscript, Mrs. M. Baer for her handling of the manuscript, and Mrs. R. Karkash for her excellent technical assistance.

Co., Grand Island, N.Y.), and 10% fetal bovine serum (Bio-Lab, Jerusalem, Israel) (cEMEM). Cell cultures were grown at 37°C in a humidified atmosphere containing 7% CO_2. To ensure reproducibility, we did all experiments with cultures from frozen stocks. For passage and enumeration, we harvested the tumor cells from cultures by overlaying the cells with a thin layer of 0.25% trypsin for 2 minutes. Cell counting was performed with the use of an electronic particle counter (Coulter counter, model ZBI; Coulter Electronics Inc., Hialeah, Fla.). Cell viability was assessed by trypan blue exclusion, and only suspensions with single cell viability above 95% were used in these studies.

Growth inhibition assay.—Cells were plated at 10^4 cells/dish (35 mm in diameter) in 1.5 ml cEMEM. After a phase of cell adherence (2–4 hr at 37°C), the anthracycline drugs were added; at various intervals the cultures were rinsed two times with PBS (pH 7.2), and fresh cEMEM was added to the cultures. The cells were detached and counted on day 7. The percentage of growth inhibition by each drug concentration was calculated from the 100% of drug-free control cultures. The experiments were preformed at least three times in triplicates.

Morphologic observations and intracellular distribution of anthracycline drugs.—Tumor cells (10^3) were plated in Lab-Tek tissue culture chamber slides (Lab-Tek Products, Naperville, Ill.) (phase microscopy) or on 25-mm-diameter cover slips that were placed in tissue culture dishes (fluorescence microscopy). Cell monolayers were fixed with 3% paraformaldehyde in PBS (pH 7.2) (60 min, 23°C). Before being washed three times with PBS, the cells were mounted in 90% glycerol in PBS, examined, and photographed with a Karl Zeiss microscope. Photomicrographs were taken on Kodak films (Plus-X, 32 ASA; Tri-X, 400 ASA).

RESULTS

Growth Inhibitory Effect of Doxorubicin and AD32 on B16 Melanoma Cell Variants

The melanoma cell variants B16-F1, B16-F10, and B16-F10-B2 were seeded (10^4 cells/plate) in cEMEM; 4 hours later, doxorubicin and AD32 were added at final concentrations ranging from 0.003 to 1.0 µg/ml. The cells were incubated with the drugs for 16 hours at 37°C, washed, and reincubated for 6 days in drug-free cEMEM. The relative sensitivities of the 3 tumor cell lines to the anthracycline drugs are presented in text-figure 1. The growth inhibition by doxorubicin and AD32 was concentration-dependent, and doxorubicin was notably more potent than AD32 in its effect on tumor cell growth (text-fig. 1).

Exposure of the 3 tumor cell lines for 16 hours to 1 µg/ml of either doxorubicin or AD32 markedly inhibited cell proliferation (85–95%). Cell viabilities at the end of the incubation were similar to those found in drug-free cultures. Furthermore, the number of cells in the complete growth-inhibited cultures was similar to the number of cells that were plated. These results suggest that the drug treatments were not lytic and that the observed growth inhibitory effects were probably due to an irreversible inhibition of tumor cell proliferation.

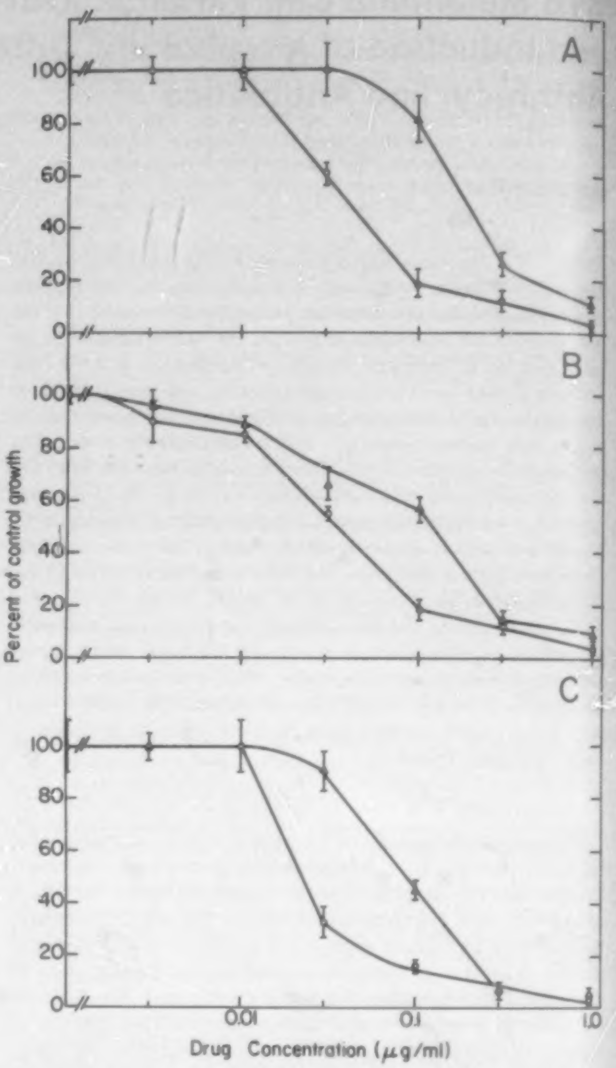

TEXT-FIGURE 1.—Effect of doxorubicin (○—○) and AD32 (△—△) on growth of B16-F1 (A), B16-F10 (B), and B16-F10-B2 (C). Cells were incubated with the various drug concentrations for 16 hr at 37°C, washed, and reincubated in drug-free cEMEM for 6 additional days. Cells were detached with 0.25% trypsin, and cell number was determined with a Coulter counter. *Each point* represents mean ± standard deviation calculated from triplicate experiments.

The concentration ratios of AD32 to doxorubicin required for 50% growth inhibition of B16-F1, B16-F10, and B16-F10-B2 were 4.8, 3.1, and 3.9, respectively, demonstrating the superior potency of doxorubicin to inhibit cell growth. The B16-F1 and B16-F10 exhibited similar sensitivity to the growth inhibition effect of the drugs, whereas the B16-F10-B2 cells were about 1.5–2 times more sensitive to the two antibiotic drugs as were the B16-F1 and B16-F10 melanoma cell lines.

The drug-treated B16-F1 melanoma cells could not escape from the arrest in cell division through weekly subculturing for a month; eventually, the cells produced intracellular vacuoles and died. Implantation sc of treated cells in syngenic C57BL/6 female mice (5×10^4 cells/mouse) failed to produce any detectable tumors after 3 months, whereas the control C57BL/6 female animals died within 30–35 days (10 mice/group).

Morphologic Changes of B16-F1 Melanoma Cells Induced by Doxorubicin and AD32

When B16-F1 melanoma cells were incubated for 16 hours with 0.1 μg doxorubicin/ml and 0.3 μg AD32/ml, most of the adherent cells lost their characteristic bipolar appearance (fig. 1A) and displayed exaggerated "dendrite"-like formation and an increase in size (figs. 1A, 1B). Further incubation of the 16-hour drug-treated monolayers in fresh cEMEM for 6 days led to dramatic morphologic alterations (figs. 2A–2E). The cells in the untreated cultures continued to proliferate normally and developed into large tumor cell colonies (fig. 2A); the melanoma cells in the drug-treated monolayers exhibited marked hypertrophy (figs. 2A, 2B). The cells were flattened extensively and full of filamentous elements; under these conditions cells occupied a substrate that was normally covered by 50–100 control cells (cf. fig. 2A with figs. 2B and 2C). In some cells binucleation could be observed (fig. 2B), suggesting that the cells can pass through one nuclear division with an impairment in cytokinesis. A completely different and striking morphologic alteration that the cells undergo in response to the drug treatment is presented in figures 3A and 3B. The cells developed enormously large axon-like processes that could exceed 250 μm in length (figs. 3A, 3B). Whether the cells extended these processes from the main cellular body or whether they migrated on the substrate leaving cytoplasmic tracks is still an open question.

Cytofluorescence Localization of Doxorubicin and AD32

One possible explanation for the mode by which the anthracycline antibiotics irreversibly inhibit melanoma cell proliferation is that the drugs bind and remain constantly within intracellular compartments, thus inducing permanent effects. To examine this possibility, we processed B16-F1 cells grown on glass cover slips for fluorescence visualization. Representative fluorescence and interference (Nomarski) photomicrographs of cells incubated for 16 hours with the drugs are shown in figs. 4A–4D. The cells were seeded at high densities so that a maximum number of cells could be photographed in one microscope field. Cells incubated with doxorubicin (figs. 4A, 4B) and AD32 (figs. 4C, 4D) exhibited the same basic pattern of cytofluorescence and nuclear localization. All the cells apparent to the Nomarski optics were fluorescent, indicating that all cells in the monolayer probably have an equal chance to be affected by the added drugs. After 6 days of incubation in drug-free cEMEM, no nuclear fluorescence could be detected in both doxorubicin- and AD32-treated cultures (figs. 5A, 5B), suggesting either that the drugs were metabolized to nonfluorescent derivative(s) or that they were extruded from the cells. Aside from the different concentrations of doxorubicin and AD32 needed to block melanoma cell proliferation, the drugs affected nuclear shape differently (*see* figs. 2A–2C, 5A–5D). Whereas the nuclei of doxorubicin-treated cells (fig. 2B; fig. 5A) were enlarged but remained spherical, the nuclei of AD32-treated cells underwent an enlargement that was accompanied by irregularity and development of lobes.

DISCUSSION

The two anthracycline antibiotics doxorubicin and AD32 irreversibly inhibited in a time- and dose-dependent manner the proliferation of B16 melanoma cells. Doxorubicin was notably more potent than AD32 in its growth inhibition effect on the three tested cell variants. The present study demonstrates in vitro heterogeneity in drug response among in vivo selected cell lines that exhibit distinct metastatic properties. Although the most metastatic B16 melanoma cell line B16-F10-B2 (*7*) was the most sensitive to the drug effect, one cannot conclude that susceptibility to the drugs correlates with the metastatic properties, since the other melanoma cell lines B16-F1 and B16-F10, while demonstrating marked differences in their metastatic behavior (*5, 32*), required similar drug concentrations to achieve 50% growth inhibition. Therefore, metastatic heterogeneity of tumor cells does not necessitate similar heterogeneity of other biologic parameters, i.e., susceptibility to cytotoxic drugs. Lotan and Nicolson (*24*) arrived at a similar conclusion when they found that various clones and cell lines of B16 melanoma are heterogeneous in the susceptibility to growth inhibition exerted by retinoic acid. Notwithstanding these biologic complexities, our study produced results that may contribute to the understanding of the mode of action of anticancer drugs on malignant cell variants selected from the same parental tumor.

The exact mechanism by which doxorubicin and AD32 irreversibly block cellular division of B16-F melanoma variants is not clear, and both drugs seem to exert their effect via similar mechanisms. Cells that were exposed for 16 hours to doxorubicin and AD32 exhibited marked nuclear fluorescence, which was abolished after washing and further incubation for 6 days in cEMEM. It is, however, possible that the permanent effect of the drugs is due to either a continuous presence of nonfluorescent metabolite(s), to the drugs being extruded after the cells were mutated to nondividers, or both. Indeed, anthracycline antibiotics were found to be mutagens in the Salmonella test (*25, 26*), to be able to transform cells in culture (*27*), and to induce tumors in rats (*27, 28*). Furthermore, an irreversible G_2 arrest of 70–90% of human lymphoma cells treated with doxorubicin was observed over a 72-hour period after drug removal (*29*).

The nuclear fluorescence observed in AD32-treated melanoma cells is in contrast to our previous report, where AD32-treated murine peritoneal macrophages showed mainly cytoplasmic fluorescence (*30*) as reported for WI-38 fibroblasts (*21*). Conceivably, the observed difference is due to the differences in cell types or to the capability of B16 melanoma cells to produce a fluorescent metabolite(s) from AD32 that has high affinity to the DNA. In a recent report, however, it was demonstrated that there is no clear correlation between cytofluorescence localization of a drug and its accumulation by intact L1210 cells or isolated nuclei (*31*).

The cessation of B16 melanoma cell proliferation is associated with a dramatic alteration in cell morphology. First, the cells lose their bipolar appearance, show exaggerated dendrite formation, and increase in size. Later, they followed two morphologic pathways: *a*) enormous increase in size (over fiftyfold to a hundredfold) and *b*) development of large axon-like processes possibly exceeding 250 μm. Cellular hypertrophy is a common consequence of treatment with agents inhibiting DNA synthesis (*32*). The observed morphologic changes reported here were regarded in neuroblastoma cells as evidence of cellular differentiation (*33, 34*) and in virus-transformed fibroblasts as acquisition of morphologic characteristics of nontransformed fibroblasts (*35*).

A wide variety of melanoma cells from diverse origins responded in vitro to changes in the intracellular levels of cyclic nucleotides by "morphologic differentiation." Melanocyte-stimulating hormone and cAMP caused Cloudman S91 melanoma cells to become flattened and more dendritic (*36*); the KHm-1 human melanoma cells altered their morphology in response to cAMP, to theophylline, or to incubation in serum-free medium (*37*). Cholera toxin and cAMP promote the formation and elongation of processes of Greene hamster melanoma cells (*38*). B16 melanoma cells treated with cAMP, phosphodiesterase inhibitors, and GTP responded in cessation of cell proliferation and altered morphology characteristic of the differentiated state (*39-41*). Thus melanoma cells are susceptible to morphologic differentiation in vitro; but whereas most of the above treatments induced reversible effects, the treatment of B16 melanoma cells with doxorubicin and AD32 induced irreversible cessation of cell proliferation and alteration of both cellular and nuclear morphology. Recently, doxorubicin was found to have significant therapeutic activity against various human melanoma xenografts in athymic mice (*42*).

On the basis of our results, B16 melanoma cells seem to be a highly suitable model system for the study of the mode of action of anthracycline antibiotics on neoplastic cells. Thus attempts to identify the molecular events accompanying the interaction of doxorubicin and AD32 with B16 melanoma are ongoing in our laboratory.

REFERENCES

(*1*) Fidler IJ, Gersten DM, Hart IR. The biology of cancer invasion and metastasis. Adv Cancer Res 1978; 28:149-250.

(*2*) Nicolson GL, Brunson KW, Fidler IJ. Specificity of arrest, survival and growth of selected metastatic variant cell lines. Cancer Res 1978; 38:4105-4115.

(*3*) Poste G, Fidler IJ. The pathogenesis of cancer metastasis. Nature 1980; 283:139-146.

(*4*) Fidler IJ. Tumor heterogeneity and the biology of cancer invasion and metastasis. Cancer Res 1978; 38:2651-2660.

(*5*) ———. Selection of successive tumour lines for metastasis. Nature [New Biol] 1973; 242:148-149.

(*6*) Brunson KW, Beattie G, Nicolson GL. Selection and altered tumour cell properties of brain-colonising metastatic melanoma. Nature 1978; 272:543-545.

(*7*) Raz A, Hart IR. Murine melanoma. A model for intracranial metastasis. Br J Cancer 1980; 42:331-334.

(*8*) Tao TW, Matter A, Vokel K, Burger MM. Liver-colonizing melanoma selected from B16 melanoma. Int J Cancer 1979; 23: 854-857.

(*9*) DiMarco A, Gaetani M, Dorigotti L, Soldati M, Bellini O. Daunomycin: A new antibiotic with antitumor activity. Cancer Chemother Rep 1964; 38:31-38.

(*10*) Silverstrini R, Lenaz L, DiFronzo G, Sanfilippo O. Correlations between cytotoxicity, biochemical effects, drug levels, and therapeutic effectiveness of daunomycin and adriamycin on sarcoma 180 ascites in mice. Cancer Res 1973; 33:2954-2958.

(*11*) Greco C, Calbresi F, Caputo M, Corsi A, Sacchi A, Zupi G. Adriamycin effect on the Lewis lung carcinoma, comparison between the original and its derivative subline. Eur J Cancer 1980; 16:1251-1255.

(*12*) Ohanian SH, Schalger SI, Goodman D. Analysis of intralesional adriamycin-induced regression of line-10 guinea-pig hepatoma. Cancer Immunol Immunother 1980; 8:179-187.

(*13*) Bonadonna G, Monfardini S, De Lena M, Fossati-Bellani F, Beretta G. Phase I and preliminary phase II evaluation of adriamycin (NSC 123127). Cancer Res 1970; 30:2572-2582.

(*14*) Middleman E, Luce J, Frei E III. Clinical trials with adriamycin. Cancer 1971; 28:844-851.

(*15*) Tan C, Hideco T, Yu KP, Murphy ML, Karnofsky D. Daunomycin, an antitumor antibiotic, in the treatment of neoplastic disease. Cancer 1967; 20:333-353.

(*16*) Calendi E, DiMarco A, Reggiani M, Scarpinato B, Valentini L. On physiocochemical interactions between daunomycin and nucleic acids. Biochim Biophys Acta 1965; 103:25-49.

(*17*) Chandra P. Role of chemical structure in biochemical activity of daunorubicin (NSC-82151) and adriamycin (NSC-123127) and some structural analogs: Macromolecular interactions and their biological consequences. Cancer Chemother Rep 1975; 6:115-122.

(*18*) DiMarco A. Adriamycin (NSC-123127): Mode and mechanism of action. Cancer Chemother Rep 1975; 6:91-106.

(*19*) Israel M, Modest EJ, Frei E III. *N*-Trifluoroacetyladriamycin-14-valerate, an analog with greater experimental antitumor activity and less toxicity than adriamycin. Cancer Res 1975; 35:1365-1368.

(*20*) Sengupta SK, Seshardri R, Modest EJ, Israel M. Comparative DNA-binding studies with adriamycin (ADR), *N*-trifluoroacetyladriamycin-14-valerate (AD32) and related compounds. Proc Am Assoc Cancer Res 1976; 17:108.

(*21*) Krishan A, Israel M, Modest EJ, Frei E III. Differences in cellular uptake and cytofluorescence of adriamycin and *N*-trifluoroacetyladriamycin-14-valerate. Cancer Res 1976; 36:2108-2110.

(*22*) Israel M, Karkowsky AM, Pegg WJ. Pharmacologic studies with radiolabeled *N*-trifluoroacetyladriamycin-14-valerate (AD32). Comparison of total anthracycline fluorescence and radioactivity in mouse serum and urine. Cancer Chemother Pharmacol 1980; 4: 79-82.

(*23*) Raz A, McLellan WL, Hart IR, et al. Cell surface properties of B16 melanoma variants with differing metastatic potential. Cancer Res 1980; 40:1645-1651.

(*24*) Lotan R, Nicolson GL. Heterogeneity in growth inhibition by *β*-transretinoic acid. Metastatic B16 melanoma clones and in vivo-selected cell variant lines. Cancer Res 1979; 39:4767-4771.

(*25*) Benedict WF, Baker MS, Haroun L, Choi E, Ames BN. Mutagenicity of cancer chemotherapeutic agents in the Salmonella/microsome test. Cancer Res 1977; 37:2209-2213.

(*26*) Seino Y, Nagao M, Yahagi T, Hoshi A, Kawachi T, Sugimura T. Mutagenicity of several classes of antitumor agents to *Salmonella typhimurium* TA98, TA100, and TA92. Cancer Res 1976; 38:2148-2156.

(*27*) Marquardt H, Philips FS, Sternberg SS. Tumorigenicity in vivo and induction of malignant transformation and mutagenesis in cell culture by adriamycin and daunomycin. Cancer Res 1976; 36: 2065-2069.

(*28*) Bertazzoli C, Chieli T, Solcia E. Different incidence of breast carcinomas or fibroadenomas in daunomycin or adriamycin treated rats. Experientia 1971; 27:1209-1210.

(*29*) Barlogie B, Drewinko B, Johnston DA, Freireich EJ. The effect of adriamycin on the cell cycle traverse of a human lymphoid cell line. Cancer Res 1976; 36:1975-1979.

(*30*) Facchinetti T, Raz A, Goldman R. A differential interaction of daunomycin, adriamycin and *N*-trifluoroacetyladriamycin-14-valerate with mouse peritoneal macrophages. Cancer Res 1978; 38: 3944-3949.

(*31*) Egorin MJ, Clawson RE, Choen JL, Ross LA, Bachur NR. Cytofluorescence localization of anthracycline antibiotics. Cancer Res

1980; 40:4669–4676.

(*32*) Cohen LS, Studzinki GP. Correlation between cell enlargement and nucleic acid and protein content of HeLa cells in unbalanced growth product by inhibitors of DNA synthesis. J Cell Physiol 1967; 69:331–340.

(*33*) Prasad KN, Hsie AW. Morphologic differentiation of mouse neuroblastoma cells induced in vitro by dibutyryl adenosine 3′:5′-cyclic monophosphate. Nature [New Biol] 1971; 233:141–142.

(*34*) Furmanski P, Silverman DJ, Ludin M. Expression of differentiated functions in mouse neuroblastoma mediated by dibutyryl cyclic adenosine monophosphate. Nature [New Biol] 1971; 233:413–415.

(*35*) Johnson GS, Pastan I. Role of 3′,5′-adenosine monophosphate in regulation of morphology and growth of transformed and normal fibroblasts. J Natl Cancer Inst 1972; 48:1377–1387.

(*36*) Pawelek J, Sanson M, Kah N, et al. Melanoma cells resistant to inhibition of growth by melanocyte stimulating hormones. Proc Natl Acad Sci USA 1975; 72:951–955.

(*37*) Kanzaki T, Hashimoto K, Bath DW. Human malignant melanoma in vivo and in vitro. J Natl Cancer Inst 1977; 59:775–779.

(*38*) DiPasquale AM, McGuire J, Moellmann G, Wasserman SJ. Microtubule assembly in cultivated Greene melanoma cells is stimulated by dibutyryl adenosine 3′:5′-cyclic monophosphate or cholera toxin. J Cell Biol 1976; 21:735–748.

(*39*) Kredier JW, Rosenthal M, Lengle N. *Brief communication:* Cyclic adenosine 3′,5′-monophosphate in the control of melanoma cell replication and differentiation. J Natl Cancer Inst 1973; 50:555–558.

(*40*) Kreider JW, Wade DR, Rosenthal M, Densley T. Maturation and differentiation of B16 melanoma cells induced by theophylline treatment. J Natl Cancer Inst 1975; 54:1457–1467.

(*41*) Giotta GJ, Smith JR, Nicolson GL. Guanosine 5′-triphosphate inhibits growth and stimulates differentiated functions in B16 melanoma cells. Exp Cell Res 1978; 112:385–393.

(*42*) Giuliani FC, Zirri KA, Kaplan NO. Therapeutic response of human tumor xenografts in athymic mice to doxorubicin. Cancer Res 1981; 41:325–335.

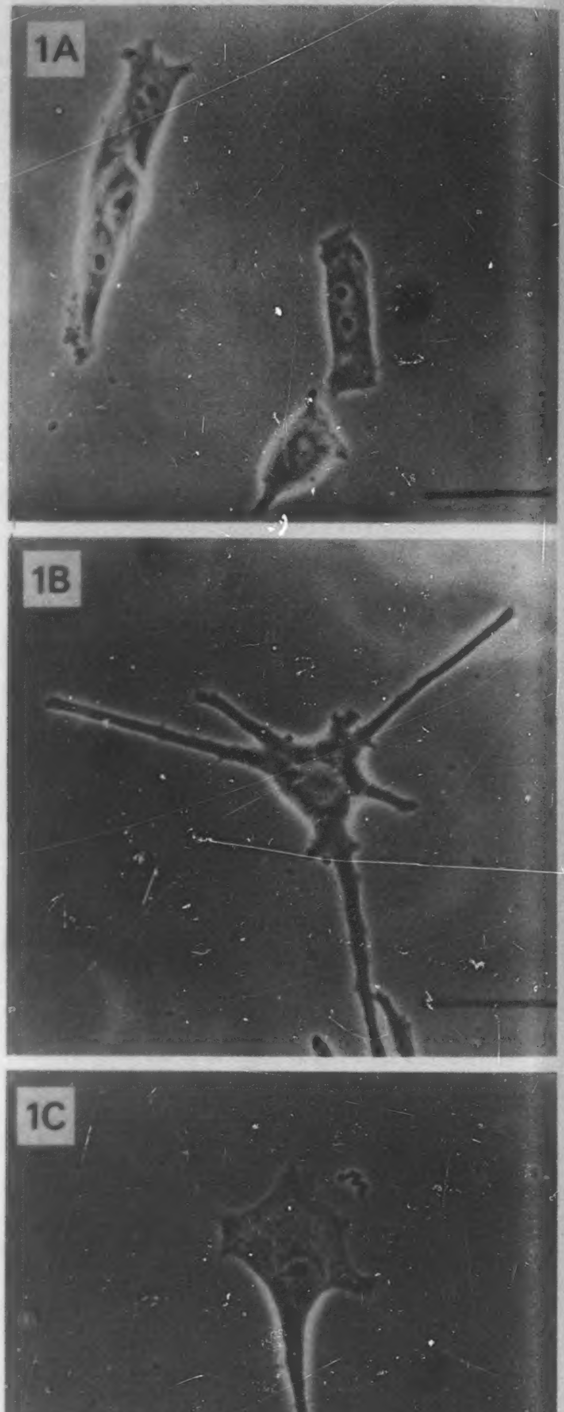

FIGURE 1.—Phase-contrast photomicrographs of B16-F1 melanoma cells. A) Control cells after 24 hr. B) Cells cultivated with 0.1 μg doxorubicin/ml for 16 hr. C) Cells cultivated with 0.3 μg AD32/ml for 16 hr. *Bar*=30 μm. × 250

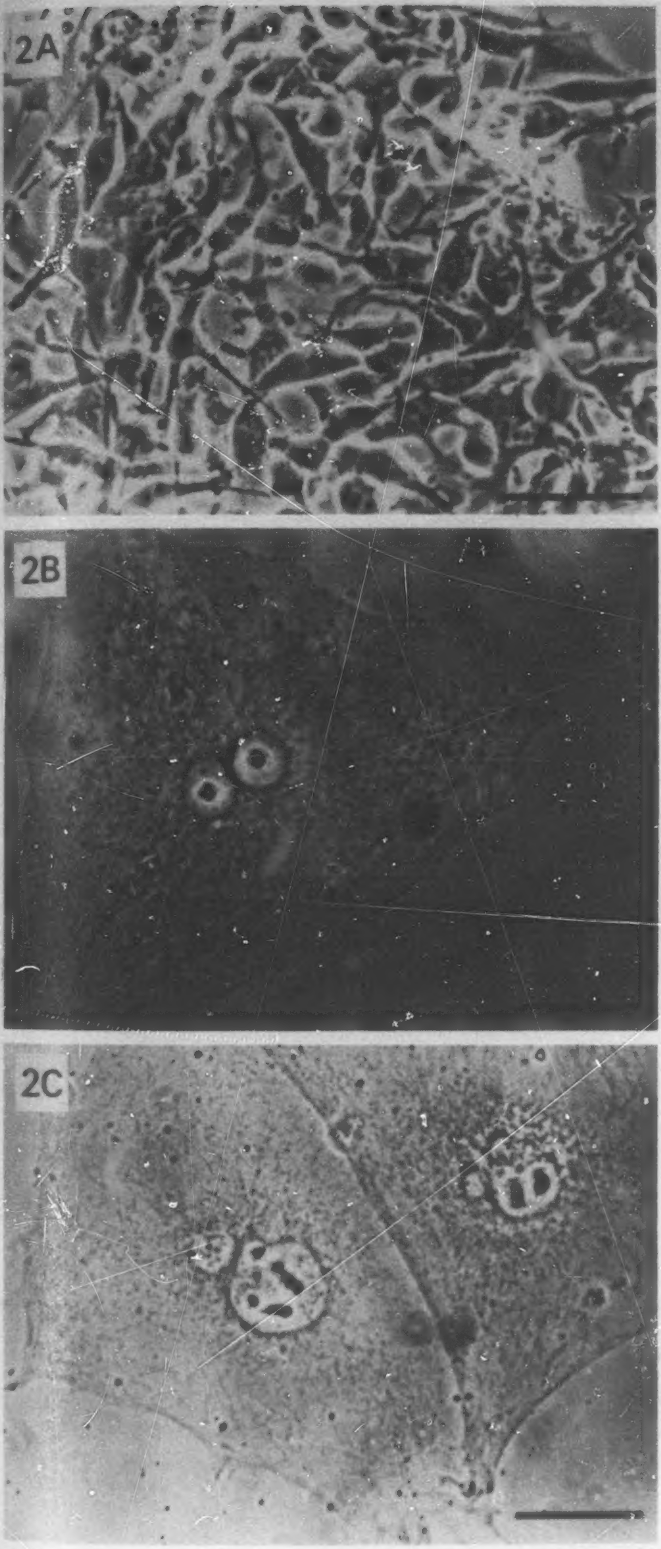

FIGURE 2.—Phase-contrast photomicrographs of B16-F1 melanoma cells. A) Control cells after 7 days in culture. B) Cells exposed to 0.1 μg doxorubicin/ml for 16 hr and then washed and reincubated until day 7. C) Same as fig. 2B but with 0.3 μg AD32/ml. *Bar*=30 μm. × 250.

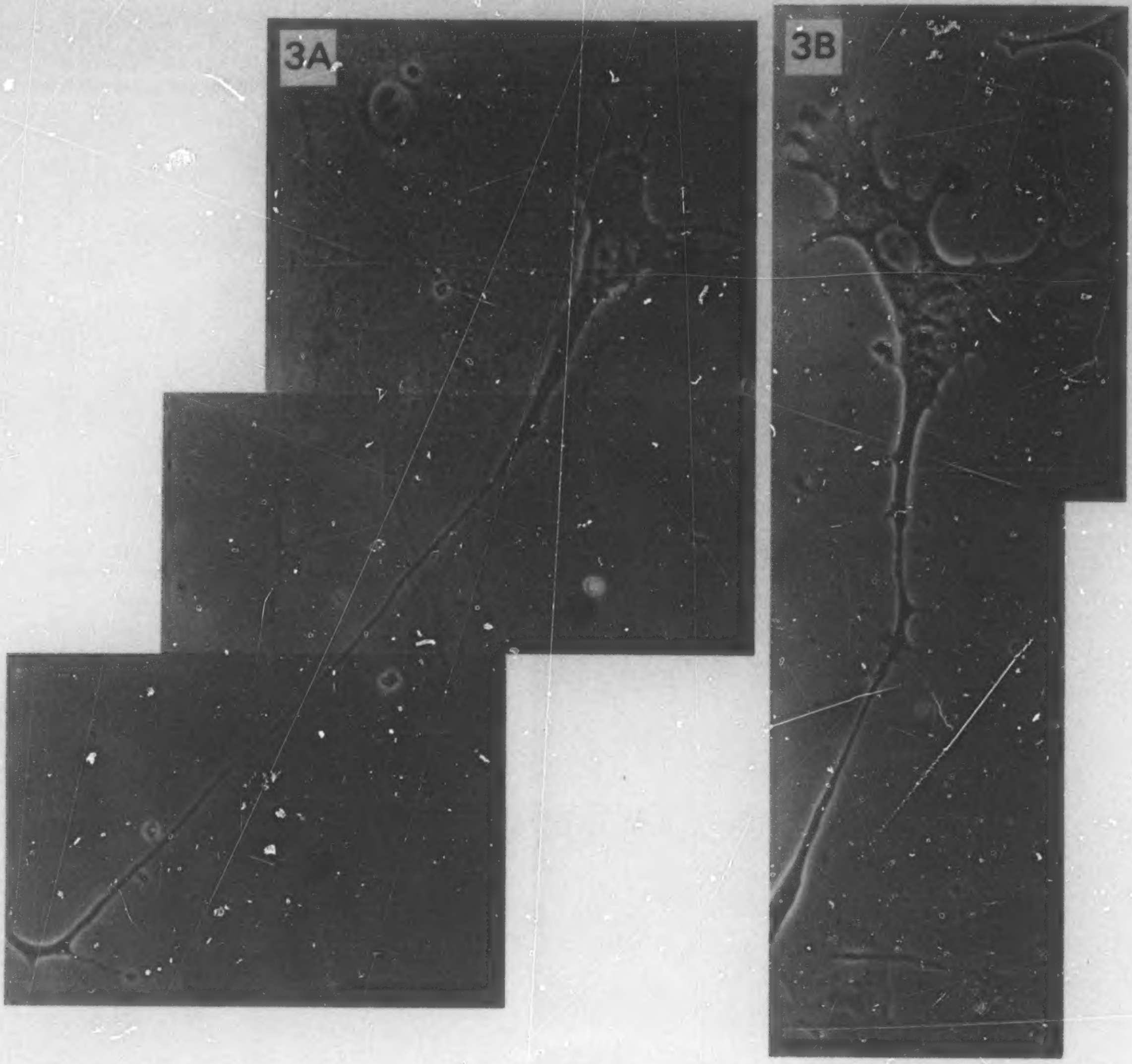

FIGURE 3.—Phase-contrast photomicrographs of B16-F1 melanoma cells exposed to 0.1 μg doxorubicin/ml (A) and to 0.3 μg AD32/ml (B). Details are given in the legend to fig. 2. *Bar*=30 μm. × 250

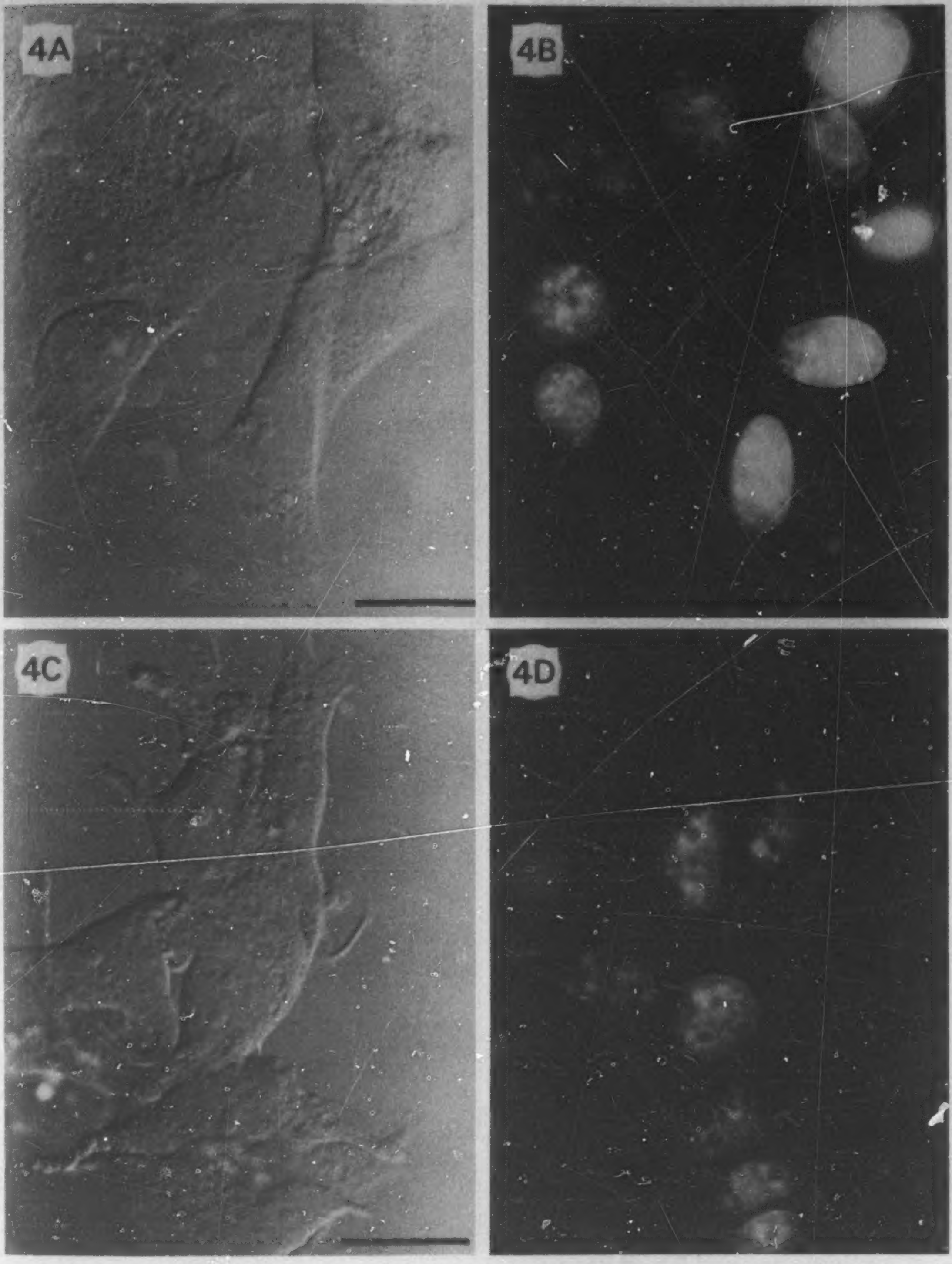

FIGURE 4.—Cytofluorescence localization of anthracycline antibiotics in B16-F1 melanoma cells. Cells grown on glass cover slips were exposed for 16 hr to 0.1 µg doxorubicin/ml (A, B) and to 0.3 µg AD32/ml (C, D). Cells were washed in PBS and fixed for 1 hr with 3% paraformaldehyde in PBS. Nomarski interference optics (A, C); fluorescence microscopy (B, D). *Bar*=72 µm. × 600

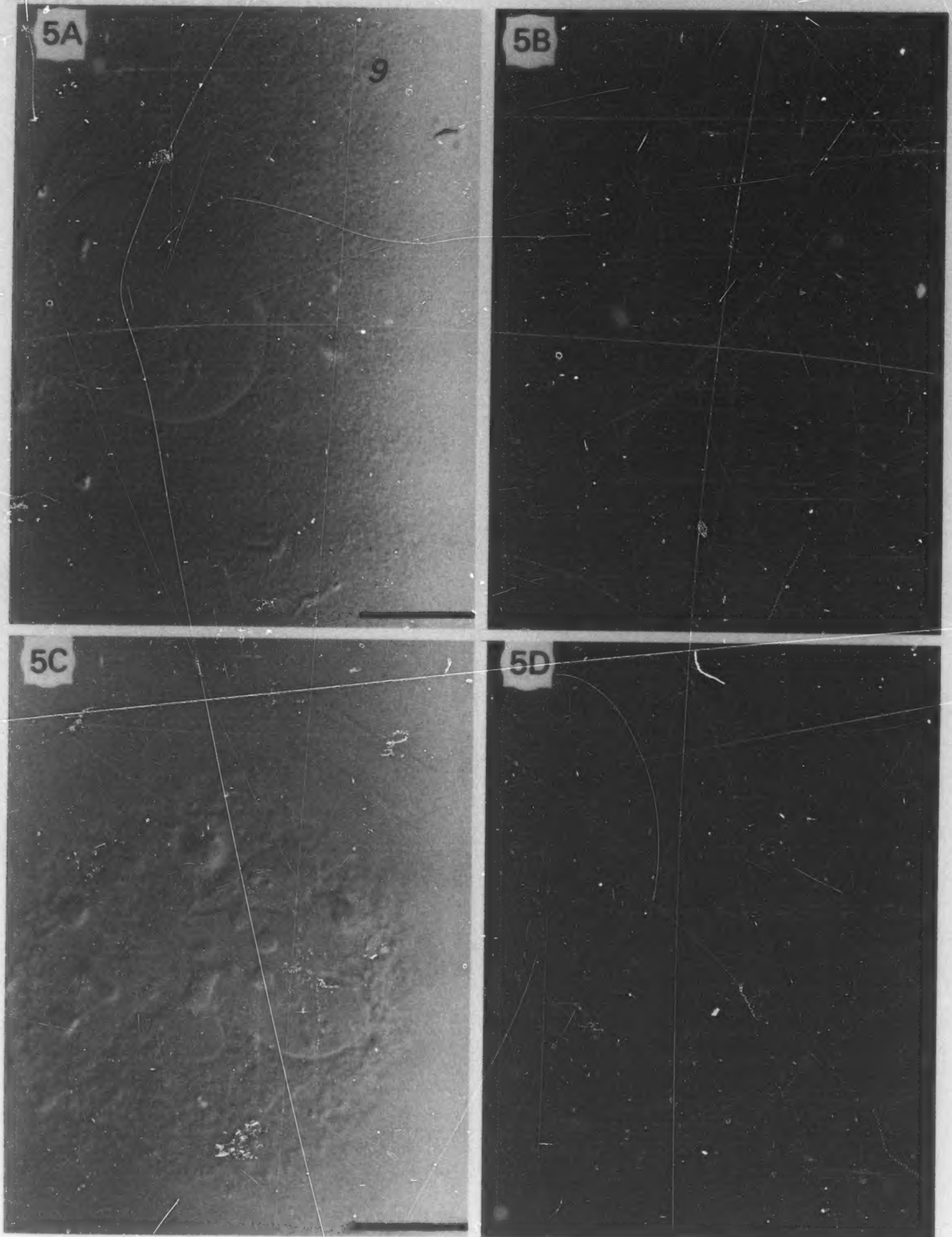

FIGURE 5.—Interference and fluorescence photomicrographs of B16-F1 melanoma cells cultivated on cover slips 6 days after drug removal. (For details see legends to figs. 4 and 3.) Doxorubicin-treated cells (A, B); AD32-treated cells (C, D). *Bar* = 72 μm. × 600

Differing Stem Cell Self-Renewal of Lectin-Separated Murine Bone Marrow Fractions[1,2,3]

Andrew L. Salner,[4] Jane E. Obbagy,[4] *and* Samuel Hellman[4]

ABSTRACT—The success of bone marrow transplantation depends not only on the engraftment of adequate numbers of hematopoietic stem cells but also on their self-renewal capacity, which must be sufficient to provide lifetime hematopoiesis. The lectin peanut agglutinin (PNA), when exposed to bone marrow, causes separation into two distinct fractions. The agglutinated fraction not only is enriched with colony-forming units—spleen but also is devoid of graft-versus-host (GVH) activity when injected into allogeneic lethally irradiated recipients, and therefore, it is considered to be an ideal source for bone marrow transplantation. The absence of GVH activity is presumably due to the separation of mature thymocytes into the nonagglutinated fraction and functionally immature thymocytes into the agglutinated fraction. Although there has been speculation that immature hematopoietic stem cells also selectively bind to PNA, other evidence suggests that the relationship of lectin binding specificity to level of maturity varies in different tissues. This study was performed to assess the self-renewal capacity of lectin-separated bone marrow stem cells. Results indicate that the self-renewal of the agglutinated fraction is significantly lower than that of the unfractionated bone marrow; such self-renewal of the nonagglutinated fraction is higher. This is further evidence for the heterogeneity of the stem cell pool. Stem cell enrichment should not be the goal in bone marrow transplantation; rather, the goal should be utilization of stem cells with the greatest self-renewal potential.—JNCI 1982; 68:639–641.

The stem cell compartment consists of a continuum of cells, with varying capacity for self-renewal and reciprocal likelihood for differentiation (*1, 2*). Under normal circumstances, the proliferative capacity of the bone marrow stem cell is not a limiting factor in animal survival. However, marrow aplasia can develop if the earliest stem cells are significantly reduced in number (*1–5*) or are required to proliferate extensively as in the case bone marrow transplantation (*6–10*).

Numerous techniques are currently under study to abrogate the GVH reaction frequently responsible for failure of survival following engraftment of allogeneic hematopoietic stem cells. One such technique entails the use of PNA, a lectin specific for membrane glycoproteins. Following exposure of murine bone marrow to this lectin, separation on a BSA gradient yields two distinct populations of cells: 1) the nonagglutinated fraction, containing mature thymocytes; and 2) the agglutinated fraction, which not only is devoid of GVH activity by virtue of its functionally immature thymocytes but also is enriched with CFU$_s$ (*11–14*). Therefore, the lectin-agglutinated fraction has been advocated as an ideal source of bone marrow for transplantation (*11–13*).

On the basis of the agglutination specificity of PNA to immature but not to mature thymocytes, it was speculated that a similar pattern of lectin separation of hematopoietic stem cells occurs (*12, 13, 15*). The lectin's binding characteristics, as a function of maturity and level of differentiation, have been studied for many different tissues. These data suggest that different tissues vary in their specificity, some with increasing and others with decreasing binding with level of differentiation (*13, 15–17*).

The present study was undertaken to investigate the self-renewal capacity of each of the fractions following lectin separation of bone marrow to determine *a*) whether PNA does separate stem cells on the basis of self-renewal potential and *b*) whether as a related observation certain membrane characteristics may change with maturity of stem cells.

MATERIALS AND METHODS

Donor and recipient animals were 8–12-week-old male inbred C3H/HeJ mice, with 20–26 g body weight (The Jackson Laboratory, Bar Harbor, Maine). Bone marrow cell suspensions were prepared by flushing the medullary cavity of the tibia and femur with PBS. The lectin agglutination, separation, and washing process was that described by Reisner et al. (*11*). A suspension of 3×10^8 bone marrow cells in 0.5 ml PBS were incubated with 0.3 ml PNA (Sigma Chemical Co., St. Louis, Mo.), 1 mg/ml for 5 minutes at room temperature. Rabbit erythrocytes, harvested from New Zealand White rabbits in Alsever's solution (GIBCO, Grand Island, N.Y.), were washed in PBS, and 1.8×10^8 erythrocytes in 0.3 ml PBS were added to the bone marrow–lectin mixture and incubated for an additional 2 minutes at room temperature. After the cells were layered onto a BSA gradient (5% wt/vol in PBS), the bottom (agglutinated) and top (nonagglutinated) fractions were harvested separately, and a third tube containing bone marrow cells not exposed to lectin (sham) was added to the experimental regimen. The 3 groups were washed sequentially with 0.2 *M* D-galactose (Sigma Chemical Co., St. Louis, Mo.) in PBS to bind irreversibly to lectin, lysing buffer (a solution of 155 m*M* ammonium chloride, 10 m*M* potassium bicarbonate, 0.01 m*M* EDTA in double-distilled water) to lyse the rabbit erythrocytes and PBS.

ABBREVIATIONS USED: BSA=bovine serum albumin; CFU$_s$=colony-forming units—spleen; GVH=graft versus host; PBS=phosphate-buffered saline; PNA=peanut agglutinin.

---

[1] Received April 9, 1981; revised October 19, 1981; accepted October 29, 1981.

[2] Supported in part by Public Health Service grants CA-12662 and CA-09221 from the National Cancer Institute.

[3] Animals were maintained under the guidelines set forth by the Harvard Medical School.

[4] Joint Center for Radiation Therapy, Department of Radiation Therapy, Harvard Medical School, 50 Binney St., Boston, Mass. 02115.

Cell counts, trypan blue viability, and differential cell counts were then performed, and the cells were injected into irradiated recipients. All irradiation was performed with a ^{137}Cs irradiator with opposing portals to a whole-body dose of 12.5 Gy in divided dose of 7.0 and 5.5 Gy, separated by 3 hours. This split-dose irradiation scheme has been developed in this laboratory to deliver a more marrow-toxic irradiation dose to prevent return of host marrow, while sparing the animal from gastrointestinal death.

In each experiment the cells of each of 4 groups (agglutinated, nonagglutinated, sham, and control) were injected into 8 animals for CFU_s determination 8 days later by the method of Till and McCulloch (*18*) and into 8 animals for transfer. Between 100 and 200 CFU_s were injected into each transfer animal. After a 14-day transfer time, bone marrow cells were harvested from the hindlimb and injected again into 8 animals per group for CFU_s determination.

The self-renewal capacity, R_s was determined by the ratio of CFU_s at the end of the 14-day transfer to the CFU_s initially seeding the hindlimb (*1*): $R_s = S_n/KS_i$, where S_i is the number of CFU_s injected, S_n is the number of CFU_s per hind limb at the end of the transfer, and K is a correction factor on the proportion of seeding stem cells that seed the hindlimb. Because the hindlimb has approximately 10% of the functional bone marrow, the factor is assumed to be 0.1. It is constant for every R_s determination, and therefore its actual value has no qualitative effect on the results decribed. There is in our experience a linear relationship that allows accurate comparison of R_s values over a broad range of injected CFU_s of 50–200, and animals given injections for transfer received CFU_s numbers within this range. Previous results have shown that R_s calculations can detect different self-renewal capacities under different physiologic and pharmacologic states (*1, 2, 19*). A low R_s means that there are few CFU_s harvested 14 days after transfer of 50–200 CFU_s, whereas a high R_s means that there are many.

RESULTS

Five separate experiments were analyzed for yield and CFU_s assay. In four of the five experiments, transfer was performed and R_s was calculated. To sample pure cell populations, numerous cells were left in the central portion of the BSA gradient because they were not in the well-demarcated agglutinated segment or in the narrow band of clearly nonagglutinated cells at the top of the tube. This technique following lectin separation and multiple serial washes resulted in 6.6% of the cells in the agglutinated fraction and 7.6% in the nonagglutinated fraction (table 1). These yields account for approximately 14% of the initial cells and CFU_s used. These fractions have been intentionally selected because they demonstrate the extremes of bound and unbound cells most likely to reveal any physiologic difference, including GVH activity. The yields are not particularly practical for transplantation, but they are representative of maximal separation of a functionally heterogeneous stem cell pool. Enrichment of CFU_s in the agglutinated fraction to a mean level of 119% of control, as opposed to a depression of the nonagglutinated fraction to a mean level of 73% of control (P=0.03), was noted. The mean relative enrichment of 1.83 was therefore seen. The CFU_s of the sham group was essentially equal to that of the control. Trypan blue viability of all fractions revealed 90% or more of each fraction's cells to be viable. Differential cell counts of each fraction revealed no significant difference in distribution of elements.

Table 2 demonstrates that similar S_i were used for transfer in all 4 groups. It also reveals the results of R_s from four different experiments. The mean percent control R_s of the agglutinated fraction was 66.8%, and that of the nonagglutinated fraction was 166% (P=0.01). The former was statistically different from the control, while the latter were not.

TABLE 1.—*Results of lectin separation: Yield, trypan blue viability, and CFU_s of bone marrow stem cells*[a]

Group	Yield, %[b]	Trypan blue viability, %	Total CFU_s	CFU_s/10^5	Control CFU_s/10^5, %
Agglutinated	6.6±1.5	90	2,454±525	15.5±1.0	119±5[c]
Nonagglutinated	7.6±1.6	95	1,537±298	9.2±1.4	73±13[c]
Sham	60.6±9.5	90	—	12.4±0.6	96±5
Control	—	95	—	13.0±0.7	—
Relative enrichment[d]				1.83±0.2	

[a] Results of five experiments are means ± SE.

[b] Percent of original cell pool prior to manipulation.

[c] P=0.03, determined by Student's t-test.

[d] Relative enrichment-agglutinated CFU_s/10^5 per nonagglutinated CFU_s/10^5

TABLE 2.—*Results of lectin separation: Self-renewal capacity of bone marrow stem cells*[a]

Group	No. of CFU_s		Self-renewal capacity	
	S_i[b]	S_n[c]	R_s	Control R_s[d]
Agglutinated	123±9	220±35	18.9±4.9	66.8±10.5
Nonagglutinated	176±23	795±128	45.1±5.2	166±13.6
Sham	122±6	291±68	24.5±7.6	84.5±17.5
Control	132±8	368±57	28.6±5.8	100

[a] Results of four experiments are means ± SE.

[b] S_i=No. of CFU_s injected in hindlimb.

[c] S_n=No. of CFU_s per hindlimb at end of transfer.

[d] P-values were determined by Student's t-test: agglutinated vs. nonagglutinated, 0.01; agglutinated vs. control, 0.05; nonagglutinated vs. control, 0.15; and sham vs. control, 0.55.

DISCUSSION

Peanut agglutinin, a lectin that is specific for D-galactosyl-β-(1→3)-*N*-acetyl-D-galactosamine, has demonstrated ability to separate thymocytes according to level of maturity (*11, 14*). The present study reveals significant CFU_s enrichment of the agglutinated fraction. Of great interest is the self-renewal of the agglutinated fraction, which is significantly below normal. In contrast, that of the nonagglutinated fraction is significantly above that of the agglutinated one.

These results indicate that lectins separate pluripotent stem cell fractions with differing proliferative potential. This finding is further evidence of the heterogeneity of the stem cell pool, with regard to self-renewal capacity (*1*). Stem cells progress from a state of great self-renewal potential to that of a lower self-renewal potential, concomitant with an increased proliferative activity and greater commitment to differentiation (*1*). This progression through the stem cell compartment appears to be irreversible. These data suggest that the progression is accompanied by changes in membrane characteristics responsible for differential agglutination by PNA of the more committed and therefore more proliferately active stem cells.

An intriguing alternative to explain the varying self-renewal is the conveyance of a higher self-renewal potential to the nonagglutinated fraction by the presence of mature thymocytes, and a lower self-renewal potential of the agglutinated fraction by the absence of mature thymocytes. While previous data in the literature have suggested a role for T-cells or regulatory cells in CFU$_s$ production (*20–22*), consistent data to support this have been lacking (*23*). A complex relationship may actually exist, with relative concentrations of T-cell and/or regulatory cell subtypes as the determining factor. Work is currently under way in this laboratory to investigate these possibilities. Even if this factor is in some way related to the varying self-renewal of the lectin fractions, the practical importance in bone marrow transplantation is still the lower self-renewal potential of the agglutinated fraction.

Stem cell enrichment is not an appropriately defined goal. This population is a continuum of cells, and what is sought is enrichment of those with the greatest proliferative capacity. Measure of stem cell numbers without regard to quality may, as in the case of PNA, be misleading. These data suggest that the use of the agglutinated fraction for bone marrow transplantation, despite its enrichment with CFU$_s$ and lack of GVH activity, may carry a significant risk of subsequent marrow failure.

REFERENCES

(*1*) Hellman S, Botnick LE, Hannon EC, Vigneulle RM. Proliferative capacity of murine hematopoietic stem cells. Proc Natl Acad Sci USA 1978; 75:490–494.

(*2*) Botnick LE, Hannon EC, Hellman. S. Nature of the hematopoietic stem cell compartment and its proliferative potential. Blood Cells 1979; 5:195–210.

(*3*) Morley A, Blake J. An animal model of chronic aplastic marrow failure: Late marrow failure after busulfan. Blood 1974; 44:49–56.

(*4*) Osband M, Cohen H, Cassady JR, Jaffe N. Severe and protracted bone marrow dysfunction following long term therapy with methyl-CCNU. Proc Am Soc Clin Oncol 1977; 18:303.

(*5*) Botnick LE, Hannon EC, Hellman S. Limited proliferation of stem cells surviving alkylating agents. Nature 1976; 262:68–70.

(*6*) Simonovitch L, McCulloch EA, Till JE. Decline in colony forming ability of marrow cells subjected to serial transplantation into irradiated mice. J Cell Comp Physiol 1964; 64:23–32.

(*7*) Cudkowicz G, Upton AC, Shearer GM. Lymphocyte content and proliferative capacity of serially transplanted mouse bone marrow. Nature 1964; 201:165–167.

(*8*) Metcalf D, Moore MA. Hematopoietic cells. In: Newberger A, Tatum EL, eds. Frontiers of biology. Amsterdam: North Holland. 1971:448–465.

(*9*) Harrison DE. Normal function of transplanted marrow cell lines from aged mice. J Gerontol 1975; 30:279–285.

(*10*) Reincke U, Burlington H, Cronkite EP, Hillman M, Laissue J. Selective damage to erythroblasts by ^{59}Fe. Blood 1975; 45:801–810.

(*11*) Reisner Y, Itzicovitch L, Mershorer A, Sharon N. Hematopoietic stem cell transplantation using mouse bone marrow and spleen cells fractionated by lectins. Proc Natl Acad Sci USA 1978; 75: 2933–2936.

(*12*) Reisner Y, Biniaminov M, Rosenthal E, Sharon N, Ramot B. Interaction of peanut agglutinin with normal human lymphocytes and with leukemic cells. Proc Natl Acad Sci USA 1979; 76:447–451.

(*13*) Reisner Y, Ikehara S, Hodes MZ, Good RA. Allogeneic hematopoietic stem cell transplantation using mouse spleen cells fractionated by lectins: In vitro study of cell fractions. Proc Natl Acad Sci USA 1980; 77:1164–1168.

(*14*) Reisner Y, Linker-Israeli M, Sharon N. Separation of mouse thymocytes into two subpopulations by the use of peanut agglutinin. Cell Immunol 1976; 25:129–134.

(*15*) Sharon N, Reisner Y. Lectin receptors as markers for lymphocyte subpopulations in mouse and man. In: Balaban M, ed. Molecular mechanisms of biological recognition. Amsterdam: Elsevier. 1979: 95–106.

(*16*) Newman RA, Klein PJ, Rudland PS. Binding of peanut lectin to breast epithelium, human carcinomas, and a cultured rat mammary stem cell: Use of the lectin as a marker of mammary differentiation. JNCI 1979; 63:1339–1346.

(*17*) Brown JC, Hunt RC. Lectins. Int Rev Cytol 1978; 52:277–349.

(*18*) Till JE, McCulloch EA. A direct measurement of the radiation sensitivity of normal mouse bone marrow cells. Radiat Res 1961; 14:213–222.

(*19*) Mauch P, Greenberger JS, Botnick, L, Hannon E, Hellman S. Evidence for structured variation in self-renewal capacity within long-term bone marrow cultures. Proc Natl Acad Sci USA 1980; 77:2927–2930.

(*20*) Goodman JW, Basford NL, Shinpock SG, Chambers ZE. An amplifier cell in hemopoiesis. Exp Hematol 1978; 6:151–160.

(*21*) Sharkis SJ, Wiktor-Jedrzejczak W, Ahmed A, Santos GW, McKee A, Sell KW. Antitheta-sensitive regulatory cell (TSRC) and hematopoiesis: Regulation of differentiation of transplanted stem cells in W/W$_v$ anemic and normal mice. Blood 1978; 52:802–817.

(*22*) Nathan DG, Chess L, Hillman DG, et al. Human erythroid burst-forming unit: T-cell requirement for proliferation in vitro. J Exp Med 1978; 147:324–339.

(*23*) Lipton JM, Reinherz EL, Kudisch M, Jackson PL, Schlossman SF, Nathan DG. Mature bone marrow erythroid burst-forming units do not require T-cells for induction of erythropoietin-dependent differentiation. J Exp Med 1980; 152:350–360.

blank page

Immunologic Relatedness of Intracisternal A-Particles in Mouse Embryos and Neoplastic Cell Lines[1,2,3]

Thomas T. F. Huang, Jr.,[4,5] *and* **Patricia G. Calarco**[4,6,7]

ABSTRACT—Murine intracisternal A-particles (IAP) are retroviruses expressed in large numbers in certain neoplastic cells and preimplantation mouse embryos. Immuno-electron microscopic detection of IAP-associated antigens in mouse rhabdomyosarcoma cells and early mouse embryos provides the first direct evidence that IAP produced by these two sources are serologically related. In both embryos and cells, data suggest that, after synthesis, IAP core protein rapidly associates with the endoplasmic reticulum. In addition, in embryos only, data confirm earlier observations that IAP-associated antigens are expressed on the cell surface. There is no evidence that the Golgi apparatus is involved in the processing of IAP antigens in either cell type.—JNCI 1982; 68:648–649.

Murine IAP are retrovirus particles that form by budding from the cytoplasm into the ER in certain neoplastic and normal cells of *Mus musculus* (*1*). For example, IAP occur in large numbers within plasmacytomas (*2*) and diverse tumors derived from all three germ layers (*3*). In contrast, IAP are rarely seen in normal adult tissues (*3*). However, IAP appear in large numbers during early preimplantation mouse embryogenesis, when their production is regulated as part of normal embryonic development (*4–7*). IAP appear between the two- and eight-cell stage but are diminished or absent in morulae and blastocysts. The appearance of IAP during early development has been noted also in two Asian mouse species, *M. pahari* and *M. cervicolor* (*8*).

Biochemical and serologic studies of IAP isolated from neoplastic sources (*9–11*) have demonstrated that IAP genetic information is endogenous to and highly reiterated within the *Mus* genome. There is also strong serologic evidence that IAP expressed in different neoplastic cells are related through a common core protein antigen (*12*). The relatedness of embryo IAP and IAP produced in tumor cells has not been determined. Because sufficient numbers of embryo IAP are difficult to obtain for making a biochemical comparison with IAP from neoplastic cells, we have undertaken a serologic approach using an antibody prepared against IAP purified from the MOPC 104E plasmacytoma (*13, 14*). We report here, using IEM techniques, that IAP produced in preimplantation mouse embryos are immunologically related to IAP produced in a neoplastic cell line.

MATERIALS AND METHODS

Embryos and culture.—Two-cell embryos were obtained from superovulated, pregnant female ICR mice (Simonsen Laboratories, Gilroy, Calif.) and cultured to the appropriate stages by the methods of Biggers and Stern (*15*). Zygotes were obtained from similar females a day earlier. Unfertilized eggs were obtained from superovulated, unmated females.

Antibodies.—The IAP used as the immunogen were prepared from MOPC 104E cells and provided to us by Dr. Nelson Wivel (NCI, Bethesda, Md.). One-dimensional gel analysis of these IAP revealed that they consisted primarily of a 73,000-dalton protein. Anti-IAP was prepared in rabbits by standard procedures and was characterized as follows [*see* (*13, 14*) for details]: Anti-IAP reacted as a single precipitin band against IAP in one-dimensional rocket electrophoresis. IIF and peroxidase–antiperoxidase staining of acetone-fixed cell lines demonstrated anti-IAP reactivity against cell lines producing IAP. In cell lines not producing IAP, no reactivity against other cellular components, e.g., ER, was observed. In addition, live embryos examined by IIF and immunoradiolabeling expressed IAP antigens on their cell surfaces whereas cell lines did not (*13*). In immunoprecipitation and gel analyses of labeled cell lines producing IAP, anti-IAP recognized primarily a protein of 73,000 daltons. Protein bands of 73,000, 69,000, and 67,000 daltons, which correlated with the stage-specific appearance of IAP, were also precipitated from labeled embryos (*14*). Absorption with the IAP immunogen removed the activity of the anti-IAP in all the assays described above. Goat anti-rabbit IgG conjugated to HRPO was obtained from Miles Chemical Co. (Elkhart, Ind.) and stored in frozen aliquots.

RMS cells and culture.—RMS cells (courtesy of Dr. John Dahlberg, NCI) were grown in four-well Lab-Tek chamber slides (Miles Chemical Co.) in Dulbecco's modified Eagle's minimum essential medium supplemented with 10% fetal calf serum. When cells were between 60 and 70% confluent, they were used in experiments.

IEM.—Tissues were fixed at room temperature. Embryo

ABBREVIATIONS USED: DAB=4-(dimethylamino)azobenzene; EM=electron microscopic; IEM=immuno-EM; ER=endoplamic reticulum; HRPO=horseradish peroxidase; IAP=intracisternal A-particle(s); IIF=indirect immunofluorescence; NCI=National Cancer Institute; NE=nuclear envelope; NRS=normal rabbit serum; PBS=phosphate-buffered saline; RMS=rhabdomyosarcoma cells.

---

[1] Received May 6, 1981; accepted October 8, 1981.

[2] Supported in part by Public Health Service grant HD-10884 from the National Institute of Child Health and Human Development and by grant 1-606 from the March of Dimes.

[3] Animals were maintained under the guidelines of the University of California at San Francisco.

[4] Department of Anatomy, School of Medicine, University of California at San Francisco, San Francisco, Calif. 94143.

[5] *Present address*: Department of Anatomy and Reproductive Biology, University of Hawaii Medical School, Honolulu, Hawaii 96822.

[6] *Address reprint requests to* Dr. Calarco.

[7] We gratefully acknowledge the technical assistance of Ms. Margaret Siebert and the photographic expertise of Mr. David Akers. We also thank Dr. A. Lopo and Dr. C. Banka for their helpful review of the manuscript.

zonae pellucidae were either digested with pronase (0.5%, 5 min in culture medium) or removed mechanically by extrusion through a small-bore micropipette. Embryos were then allowed to recover in culture medium for at least 2 hours. After being rinsed in Dulbecco's PBS, they were fixed in 0.05% glutaraldehyde in PBS (pH 7.0, 5–15 min) and then rinsed three times in PBS over 30 minutes. RMS cells were treated as monolayers in the chamber slides in which they were grown and processed as described above.

An indirect immunoperoxidase staining protocol was used as adapted from Willingham et al. (*16*). Antibody dilutions and rinses consisted of saponin buffer [Ca^{2+}- and Mg^{2+}-free Dulbecco's PBS plus 0.5% saponin (Sigma Chemical Co., St. Louis, Mo.), 1.0 m*M* ethyleneglycol-bis(β-aminoethyl ether)N,N'-tetraacetic acid, and 5.0 mg normal goat globulin/ml]. The normal goat globulin was prepared by the precipitation of normal goat serum twice with 50%-saturated ammonium sulfate. Embryos were treated as follows: 1) incubated in saponin buffer, 30 minutes; 2) incubated in first antibody (anti-IAP or NRS IgG at 0.05 mg/ml), 1.0 hours; 3) rinsed three times in saponin buffer, 1.0 hour total; 4) incubated in goat anti-rabbit IgG conjugated to HRPO (1/80 dilution), 1.0 hour; and 5) rinsed in saponin buffer, 1.0 hour. For development of the peroxidase reaction, cells or embryos were placed in 50 m*M* Tris buffer (pH 7.6, 15 min) containing 3,3'-diaminobenzidine (0.05 mg/ml) and hydrogen peroxide (0.02%). After being rinsed in 50 m*M* Tris buffer for 10 minutes, the reacted material was fixed secondarily for 15 minutes in 3.0% glutaraldehyde in 0.1 *M* phosphate buffer, containing 2.5% sucrose, then postfixed 15 minutes in 2% osmium tetroxide in 0.1 *M* phosphate buffer.

Fixed and reacted embryos were dehydrated in alcohol. After dehydration, the alcohol was exchanged with propylene oxide and then the embryos were embedded in Epon-Araldite. RMS cells were dehydrated in alcohol and infiltrated with Epon-Araldite directly (two changes over 24 hr at room temperature followed by a final change and subsequent hardening at 56°C for 48 hr). Thin sections were examined without being counterstained on a Hitachi HS-8 electron microscope.

RESULTS

The procedures for IEM examinations outlined here preserved sufficient ultrastructure for localization of IAP antigens in cell lines and embryos. In initial titration experiments, RMS cells were first fixed in 0.05% glutaraldehyde, and their membranes were then made permeable by treatment with 0.5% of the glycoside, saponin, which permitted antibody reagents to reach the ER. Other procedures such as primary fixation by 1.0% 1-ethyl-3(3-dimethylaminopropyl)-carbodiimide (Sigma Chemical Co.) together with 0.2% glutaraldehyde followed by saponin (*17*) did not allow antibody to penetrate into the matrix of the ER.

On comparison with the conventional preparation of embryos for EM examinations (*4*), our adapted procedure sufficiently preserved many cellular structures. We could resolve nuclei, mitochondria, fibrous material, ER, Golgi cisternae, and associated vesicles. However, artifacts such as whorled myelin-like structures and areas of apparent extraction were noted frequently. In general, preservation of unfertilized eggs, zygotes, and trophoblast cells was significantly improved when the primary fixation time was increased from 5 to 15 minutes.

RMS cells produced large numbers of IAP, and immunostaining of RMS cells with anti-IAP IgG was strong over the ER (fig. 1). Higher magnification allowed us to visualize discrete virions within the ER cisternae (fig. 2). Often the density of oxidized DAB obscured the virion's doughnut-like morphology, and the entire cisterna was darkened. In addition, limited areas of the nuclear envelope were lightly stained in regions near budding virions (fig. 2), whereas other areas of this membrane appeared free of reaction product. Occasionally, IAP were visible between the leaflets of the nuclear envelope (fig. 2). Neither Golgi cisternae nor associated vesicles showed staining (fig. 5). No IAP were observed free in the cytoplasm or budding from the plasma membrane. Control experiments with normal rabbit IgG showed no DAB deposits in the regions of IAP, ER, or in the nuclear envelope (figs. 3, 4).

If naturally occurring embryo IAP are related immunologically to the IAP produced by neoplastic cells, then embryo virions should also stain with our anti-IAP which was prepared against IAP from MOPC 104E. In fact, two- to eight-cell embryos demonstrated immunostaining for IAP antigens in regions where virions formed within the ER (figs. 6, 7). This immunostaining was often more diffuse than the staining seen in RMS cells, and there was some variation in the intensity with which individual IAP were stained. These IAP appeared to possess the small central core (≈30 nm) characteristic of small A-particles (*7*) or ε-particles (*18*). This may account for the observed staining differences because IAP from cell lines are exclusively of the "large A-type" with a central core of approximately 50 nm (*7*). Golgi regions did not exhibit reaction product (fig. 8), nor was there evidence of IAP antigen association with the nuclear envelope. Neither was there reaction product within ER cisternae of later embryo stages such as the blastocyst. Interestingly, IAP antigens were detected on the plasma membrane from the zygote to the eight-cell stage (fig. 6). Control experiments with NRS IgG revealed no staining over IAP, the ER, or the cell surface (fig. 9).

DISCUSSION

The results presented here outline a procedure for fixing embryos and cell lines and for making them permeable so that antigens within the ER could be localized. We have adapted the EGS[8] procedure introduced by Willingham et al. (*16*) to detect cytoplasmic antigens. Although the original method apparently cross-links the ER in a manner that prohibits antibody access to this compartment, a primary fixation in which more dilute aldehyde is used (Willingham MC: Personal communication) combined with increased concentrations of saponin results in satisfactory penetration of antibodies into the ER of cell lines grown as monolayers.

---

[8] 1-Ethyl-3-(3-dimethylaminopropyl)-carbodiimide-glutaraldehyde-saponin.

Using this modification, we report data here that provide direct evidence that IAP naturally expressed in mouse embryos are serologically related to those expressed in tumor cells.

Several investigations have helped to clarify the cellular events involved in retrovirus formation and maturation, at least in the C-virus system. The preponderance of avian C-type virus core polyprotein is synthesized on cytoplasmic rather than membrane-bound polyribosomes (*19*). Other studies in which temperature-sensitive murine leukemia viruses were used indicate that core polyproteins rapidly associate with the cytoplasmic face of the plasmalemma (*20, 21*). This association involves a stringent recognition event between the core polyprotein and the viral envelope gene product (*22*) that has previously integrated into the plasmalemma. Results from the IAP system are consistent with the C-virus model with two exceptions: Production of an IAP envelope gene product has never been reported, and the IAP core protein associates with the membrane of the ER rather than with the plasmalemma. In embryos, IAP antigens associate with and bud into the agranular ER at the two-cell stage before the association of ribosomes with the ER. This observation suggests that synthesis of IAP proteins also occurs on cytoplasmic (free) polyribosomes, although we have not been able to detect IAP antigen(s) in the cytoplasm before their incorporation into recognizable IAP. However, the 73,000-dalton IAP major core protein (p73) has been shown to be synthesized on membrane-bound ribosomes in MOPC 104E cells (*23*). One resolution of these observed differences may be that embryos synthesize IAP antigens in a different manner than do transformed cell lines. We do know that IAP antigens are expressed on the cell surface of embryos but not MOPC 104E cells (*13*).

In RMS cells, IAP antigens are localized primarily over the IAP and the ER cisternae and occasionally on the NE. This finding is consistent with results obtained from conventional EM studies that indicate that IAP form by budding into the ER, where they often remain attached (*24*). It is not surprising to observe the association of IAP antigens with the NE because the NE is considered to be derived from the ER (*25*). IAP have not been seen free in the cytoplasm or budding externally from IAP-producing neoplastic cells. In addition, we find no evidence that IAP antigens migrate to the Golgi region or to the surface of RMS cells. This observation is consistent with the observation by Kuff et al. (*12*) that IAP antigen is not found in the culture medium of neoplastic cells producing IAP. Moreover, IIF studies (*13*) do not detect IAP antigens on the surface of living, IAP-producing neoplastic cell lines.

However, our previous IIF work indicated that IAP-associated antigens *are* expressed on the surfaces of early embryos, in contrast to IAP antigen expression on IAP-producing neoplastic cells (*13*). The present study confirms these observations at the EM level. Because there is no evidence that the Golgi apparatus is involved in processing embryo IAP antigens, IAP antigens may be transported to the plasmalemma directly by the ER or they may enter from the cytoplasm without prior membrane association. This latter strategy is utilized by M13 coliphage procoat protein [*see* (*26*)].

Our previous work has shown that p73 is the major constituent of the immunogen used to prepare anti-IAP (*13*). With our anti-IAP, immunoprecipitation and gel analysis of early embryos reveal the p73 core antigen and two other antigens (67,000 and 69,000 daltons) that correlate directly with IAP presence (*14*). The IEM approach reported here may be detecting all three of these antigens. Surface labeling studies are in progress to determine which antigen(s) are expressed on the cell surface.

Although surface expression of the p73 core protein would be unusual, there are precedents for the surface expression of core protein antigens of other retroviruses (*27–29*). To account for this in molecular terms, Edwards and Fan (*30*) have studied Moloney murine leukemia virus-infected fibroblasts and present evidence for the synthesis of two primary translation products bearing core polyprotein antigen. One translation product, of 65,000 daltons, remains unglycosylated and is processed to form smaller mature virion core components. A second primary translation product of 75,000 daltons is glycosylated before its insertion into the cell surface. Although conjectural, the 75,000 component could contain a leader or signal sequence (*26, 31*) that determines radically different processing of otherwise similar information.

The biologic role, if any, for IAP information in the etiology of cancer or in the normal process of development remains conjectural. The IEM study reported here provides direct evidence that IAP from a neoplastic tissue are immunologically related to IAP appearing in normal development. This evidence increases the likelihood that more specific molecular probes derived from neoplastic cells, such as cloned nucleic acid sequences (*10, 11*), may be used to study further the processing of IAP information during normal development.

REFERENCES

(*1*) Dalton AJ, Heine UI, Melnick JL. Symposium: Characterization of oncornaviruses and related viruses—a report. J Natl Cancer Inst 1975; 55:941–943.

(*2*) Dalton AJ, Potter M, Merwin RM. Some ultrastructural characteristics of a series of primary and transplanted plasma-cell tumors of the mouse. J Natl Cancer Inst 1961; 26:1221–1267.

(*3*) Wivel NA, Smith GH. Distribution of intracisternal A-particles in a variety of normal and neoplastic tissues. Int J Cancer 1971; 7:167–175.

(*4*) Calarco PG, Brown EH. An ultrastructural and cytological study of preimplantation development of the mouse. J Exp Zool 1969; 171:253–284.

(*5*) Biczysko W, Pienkowski M, Solter D, Koprowski H. Virus particles in early mouse embryos. J Natl Cancer Inst 1971; 51:1041–1050.

(*6*) Calarco DG, Szollosi D. Intracisternal A particles in ova and preimplantation stage of the mouse. Nature [New Biol] 1973; 243:91–93.

(*7*) Chase DG, Pikó L. Expression of A- and C-type particles in early mouse embryos. J Natl Cancer Inst 1973; 51:1971–1975.

(*8*) Calarco PG, Callahan R, Yasamura T, Huang TT. Preimplantation mouse embryos of *Mus cervicolor* and *Mus pahari* express intracisternal A particles. J Cell Biol 1980; 87 (part 2):140A.

(*9*) Lueders KK, Kuff EL. Sequences associated with intracisternal A particles are reiterated in the mouse genome. Cell 1977; 12:963–972.

(*10*) Lueders KK, Kuff EL. Intracisternal A-particle genes: Identification in the genome of *Mus musculus* and comparison of multiple isolates from a mouse gene library. Proc Natl Acad Sci USA 1980; 77:

3571–3575.

(*11*) Ono M, Cole MD, White AT, Huang RC. Sequence organization of cloned intracisternal A particle genes. Cell 1980; 21:465–473.

(*12*) Kuff EL, Lueders KK, Ozer HL, Wivel NA. Some antigenic and structural properties of IAP occurring in mouse tumors. Proc Natl Acad Sci USA 1972; 69:218–222.

(*13*) Huang TT, Calarco PG. Evidence for the cell surface expression of intracisternal A particle antigens during early mouse development. Dev Biol 1981; 82:388–392.

(*14*) Huang TT Jr, Calarco PG. Immunoprecipitation of intracisternal A-particle-assocated antigens from preimplantation mouse embryos. JNCI 1981; 67:1129-1134.

(*15*) Biggers JD, Stern S. Metabolism of the preimplantation mouse embryo. Adv Reprod Physiol 1971; 6:1–59.

(*16*) Willingham MC, Yamada SS, Pastan I. Ultrastructural antibody localization of alpha2-macroglobulin in membrane-limited vesicles in cultured cells. Proc Natl Acad Sci USA 1978; 75:4359–4363.

(*17*) Willingham MC, Jay G, Pastan I. Localization of the ASV *src* gene product to the plasma membrane of transformed cells by electron microscopic immunocytochemistry. Cell 1979; 18:125–134.

(*18*) Yotsuyanagi Y, Szöllösi D. Embryo development and intracisternal particles in the mouse. Biol Cellulaire 1980; 39:201–204.

(*19*) Purchio AF, Jovanovich S, Erikson RL. Sites of synthesis of viral proteins in avian sarcoma virus-infected chicken cells. J Virol 1980; 35: 629–636.

(*20*) Yeger H, Kalnins VI, Stephenson JR. Type-C retrovirus maturation and assembly: Post-translational cleavage of the gag-gene coded precursor polypeptide occurs at the cell membrane. Virology 1978; 89:34–44.

(*21*) Yu AH, Soong MM, Wong PK. Maturation of Moloney murine leukemia virus. Virology 1979; 93:269–274.

(*22*) Witte ON, Baltimore D. Mechanism of formation of pseudotypes between vesicular stomatitis virus and murine leukemia virus. Cell 1977; 11:505–511.

(*23*) Lueders KK. In vitro synthesis of A-particle structural protein by membrane-bound polyribosomes. J Virol 1976; 18:1088–1094.

(*24*) Perk K, Dahlberg JE. Murine intracisternal A type particles fail to separate from the membrane of the endoplasmic reticulum. J Virol 1974; 14:1304–1306.

(*25*) Fawcett DW. The cell. Its organelles and inclusions. Philadelphia: Saunders, 1966.

(*26*) Wickner W. Assembly of proteins into membranes. Science 1980; 210: 861–868.

(*27*) Tung J-S, Yoshiki T, Fleissner E. A core polyprotein of murine leukemia virus on the surface of mouse leukemia cells. Cell 1976; 9: 573–578.

(*28*) Ledbetter JR, Nowinski RC, Emery S. Viral proteins expressed on the surface of murine leukemia cells. J Virol 1977; 22:65–73.

(*29*) Ledbetter J, Nowinski RC. Identification of the Gross cell surface antigen associated with murine leukemia cells. J Virol 1977; 23: 315–322.

(*30*) Edwards SA, Fan H. gag-Related polyproteins of Moloney murine leukemia virus: Evidence for independent synthesis of glycosylated and unglycosylated forms. J Virol 1979; 30:551–563.

(*31*) Blobel G, Dobberstein B. Transfer of proteins across membranes. J Cell Biol 1975; 67:835–851.

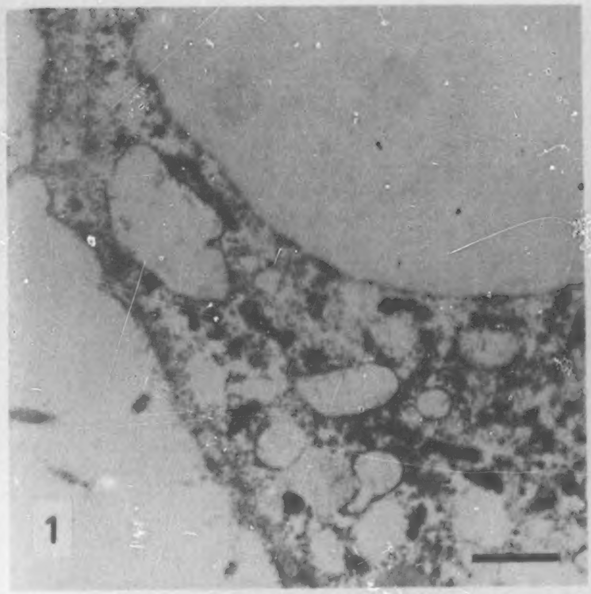

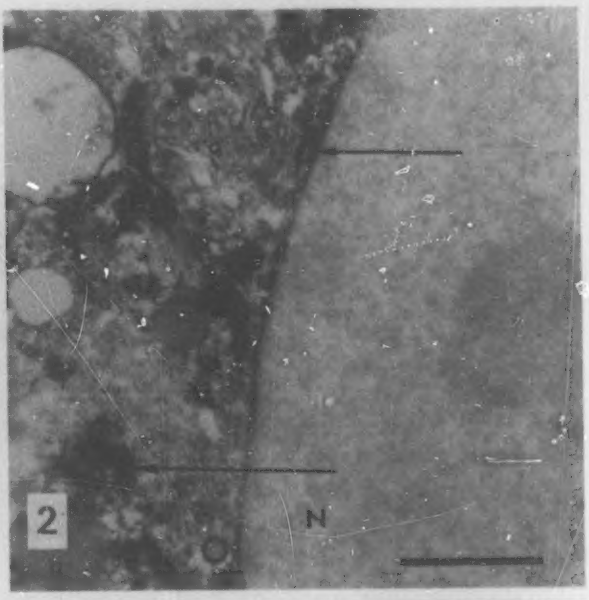

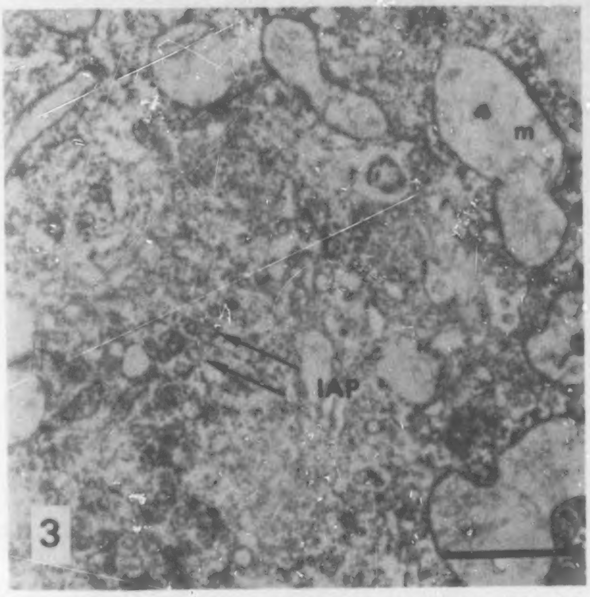

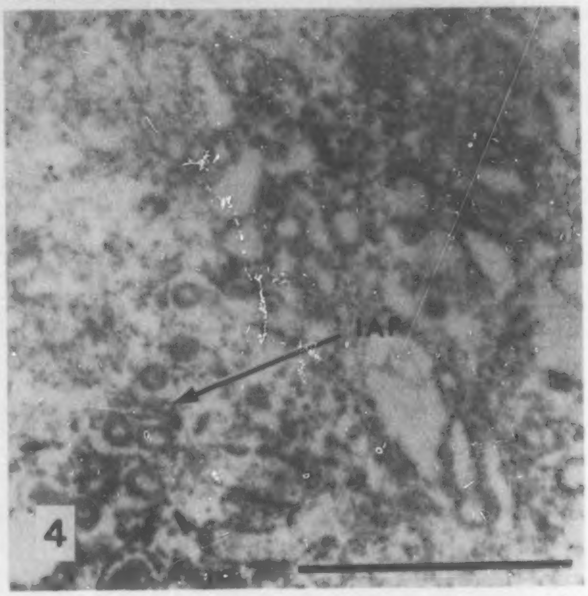

FIGURE 1.—RMS cells treated with anti-IAP IgG (described in "Materials and Methods"). Electron-dense reaction product can be seen over the ER cisternae. *Bar*=1 µm. × 12,500

FIGURE 2.—Higher magnification of RMS cell. Discrete virions are visible within ER cisternae (*lower arrow*) and occasionally between leaflets of NE (*upper arrow*). N=nucleus; li=lipid. *Bar*=1 µm. × 20,500

FIGURE 3.—RMS cell treated with NRS IgG. No reaction product is seen over the ER cisternae or IAP (*arrows*). m=mitochondrion. *Bar*=1 µm. × 18,200

FIGURE 4.—Higher magnification of a portion of fig. 3. No reaction product is visible. *Arrow* denotes IAP. *Bar*=1 µm. × 40,200

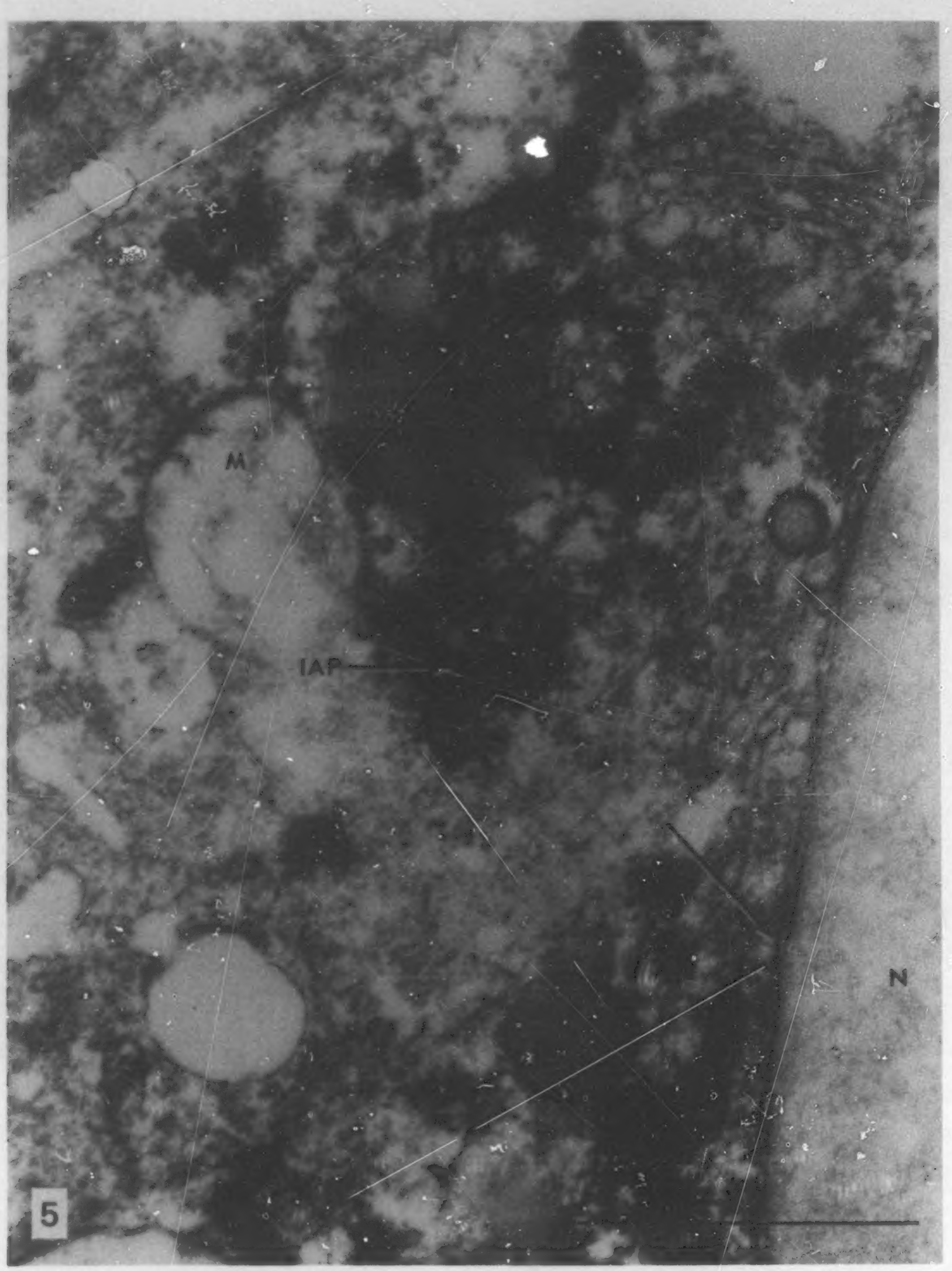

FIGURE 5.—Higher magnification of a portion of fig. 2, which is an RMS cell immunostained with anti-IAP IgG. Groups of IAP stain within the ER cisternae (*upper arrow*). Regions of the outer NE also stain (*lower arrow*). *Note* the cisternae (above *lower arrow*, near nucleus) that do not contain IAP an do not exhibit reaction product. Golgi regions (G) are also negative. N=nucleus; li=lipid; M=mitochondrion. *Bar*=1 μm. × 58,000

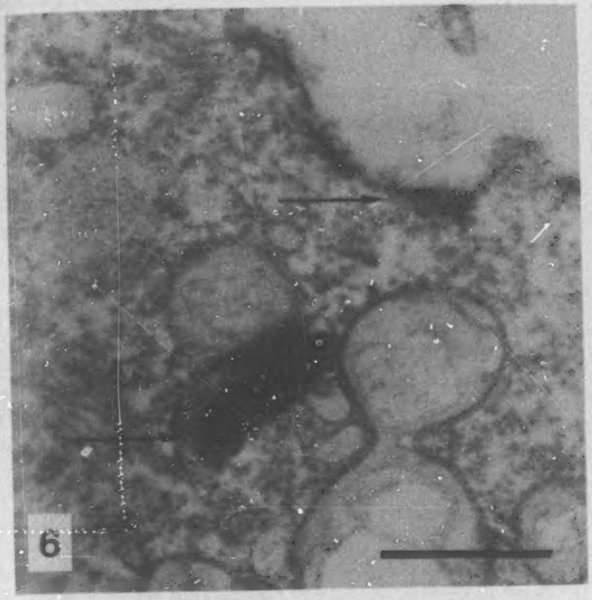

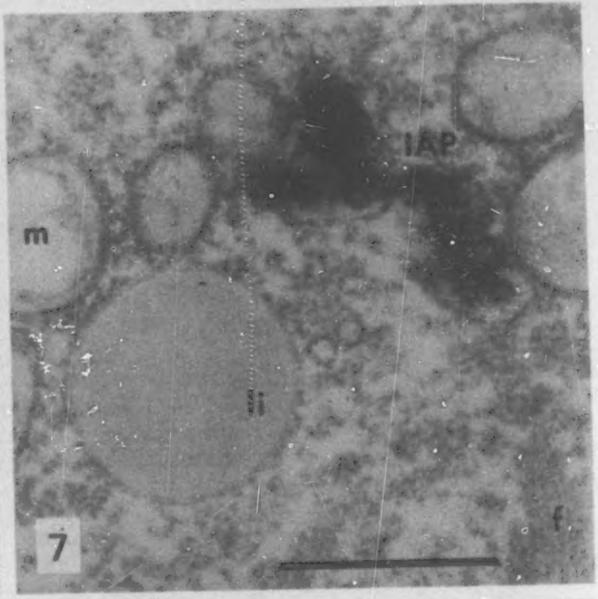

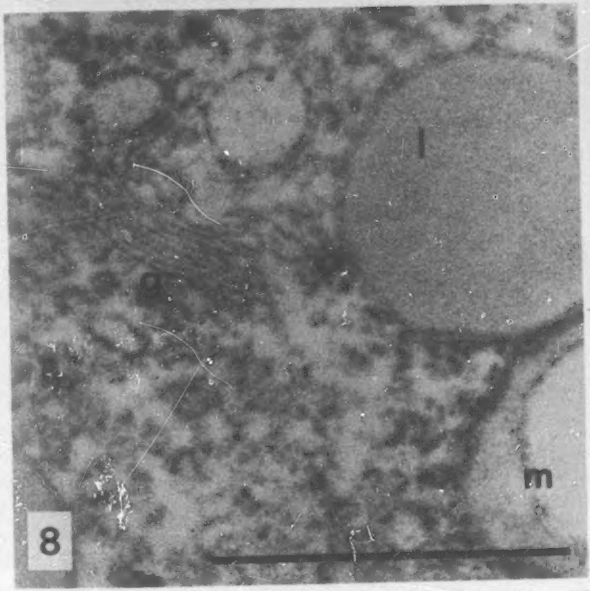

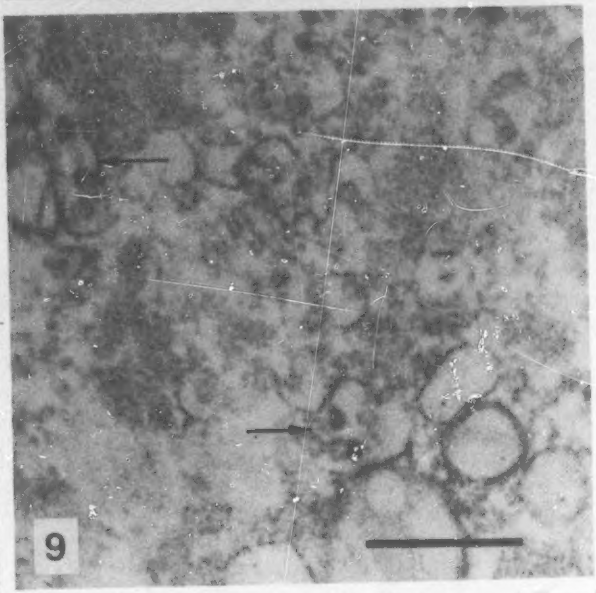

FIGURE 6.—BALB/c four- to eight-cell embryo immunostained with anti-IAP IgG (described in "Materials and Methods"). *Lower arrow* indicates IAP virions within ER. *Upper arrow* shows reaction product on cell surface of blastomere. *Bar*=1 µm. × 25,000

FIGURE 7.—BALB/c two-cell embryo immunostained with anti-IAP IgG. Filamentous material (f), lipid (li), and mitochondrion (m) are unstained. *Bar*=1 µm. × 32,400

FIGURE 8.—BALB/c two-cell blastomere treated with anti-IAP IgG. Golgi region (g) is negative. l=lipid; m=mitochondrion. *Bar*=1 µm. × 51,000

FIGURE 9.—BALB/c four-cell blastomere treated with NRS IgG. IAP virions within ER show no reaction product. Contrast has been somewhat enhanced photographically. *Bar*=1 µm. × 23,000

blank page

Methylazoxymethanol: Effect on the Immune Response of Rats to Human Serum Albumin[1,2,3]

Ahmed F. S. A. Habeeb,[4] Alan M. Preston,[4] Priscila Sanabria,[5] *and* Nelson Escobales[5]

ABSTRACT—Inbred male F344 rats treated with 20 mg methylazoxymethanol (MAM)/kg body weight showed minimal damage to DNA in bone marrow, spleen, and thymus and no suppression of the humoral immune response to human serum albumin (HSA). At high doses of MAM (40, 60, and 80 mg/kg), damage to DNA of bone marrow, spleen, and thymus was noted. The effect on the humoral immune responses was nonuniform. Some rats responded normally by eliciting precipitating antibodies, whereas others responded by synthesizing nonprecipitating antibodies at low levels. The production of nonprecipitating antibodies may indicate a restriction of the recognition of HSA antigenic determinants in rats given injections of MAM prior to immunization. The restriction may be a consequence of suppression or elimination of certain clones of lymphocytes responsible for recognition of certain antigenic determinants. This interference in some clones of lymphocytes would result in the synthesis of antibodies against one or two antigenic sites on the HSA and the concomitant inability of the produced antibodies to form complete lattice structure with antigen.—JNCI 1982; 68:651–656.

MAM, the aglycone moiety of the glycoside cycasin, has been found to be a potent carcinogen (*1*), mutagen (*2*), and hepatotoxin (*3*). Its tumorigenic effect has a broad spectrum. Neoplasms have been induced by MAM in the digestive tract (*4*), liver (*5*), lung (*6*), kidney (*7*), and brain (*8*) and in various species including rats (*9*), mice (*10*), guinea pigs (*11*), hamsters (*8*), and fish (*12*). In its manner of action, MAM belongs to the family of indirect-acting chemical carcinogens. The ultimate carcinogen generated from it is the highly reactive carbonium that alkylates guanine in several positions (N-7 and O-6 preferentially) (*13*).

Chemical carcinogens exert a variety of effects on the cells of the immune system (*14*). Several powerful carcinogens interfere with both cellular (*15*) and humoral (*16, 17*) immune responses. It is highly likely that the interactions of some chemical carcinogens with cells of the immune system result in the interruption of the function and ability of the immune system to respond to antigens without a neoplastic transformation having necessarily to occur.

However, if damaged, cells possess a mechanism for the repair and restoration of the integrity of the DNA molecule and the preservation of the fidelity of the transformation encoded in it (*18*). This DNA repair mechanism has been studied with the use of lymphocytes and has been found to be operative in them (*19*). This phenomenon suggests that chemical carcinogens can interact with the DNA of lymphoid cells and that the cells make an effort to repair the effects of this encounter.

The purpose of the investigation was to determine the effect of MAM at various doses on the humoral immune response of rats given injections of HSA and to determine the degree and rate of interaction of MAM with the DNA of the immunocompetent cells, as well as the rate of DNA repair synthesis.

MATERIALS AND METHODS

HSA, fatty acid-free, was supplied by Sigma Chemical Co. (St. Louis, Mo.). Bacto CFA was purchased from Difco Laboratories (Detroit, Mich.). MAM was supplied by Schwartz/Mann Div., Becton, Dickinson & Co. (Orangeburg, N.Y.), and [*methyl*-^{3}H]thymidine (sp act, 71.5 Ci/mmol) was purchased from ICN Pharmaceuticals Inc. (Cleveland, Ohio). Inbred male F344 rats were supplied by Charles River Breeding Laboratories (Wilmington, Mass.).

Immunoelectrophoresis.—Immunoelectrophoresis was performed on a projector slide cover glass 3¼×4 inches coated with a film of agarose [18 ml of 1.5% agarose in barbital buffer, μm = 0.05 (pH 8.4), containing 1:10,000 merthiolate]. Antisera from MAM-treated and immunized rats were placed in the central well and electrophoresed at 15 mA/plate for 90 minutes. Precipitin lines were allowed to develop for 24 hours after the addition of the antigen (HSA at 0.12 mg/ml) to the troughs. The plates were washed in saline, dried, and stained with Ponceau S (0.15% in trichloroacetic acid); they were then washed with 7% acetic acid and dried.

Double diffusion in agar.—Into a petri dish was poured 15 ml of 1% Noble agar in buffered saline (pH 7.2) containing 1:10,000 merthiolate. The agar was left to cool and aged for 1 day at room temperature. Wells were punched with a cork borer, the two central rows were filled with HSA solution, and the two peripheral rows were filled with 20 μl of antisera from MAM-treated and immunized rats. The dishes were placed in a moist atmosphere for 24 hours at room temperature for development of precipitin lines. This method afforded a rapid and sensitive method to screen numerous antisera for the appearance of anti-HSA antibodies from MAM-treated and immunized rats.

Quantitative precipitin test.—To 0.2 ml of a twofold increasing concentration of HSA in PBS was added 0.2 ml of antisera from MAM-treated and immunized rats. The mixtures were incubated at 40°C for 1 hour and then overnight at 4°C. The tubes were centrifuged and the precipitate was

---

ABBREVIATIONS USED: CFA=complete Freund's adjuvant; HSA=human serum albumin; MAM=methylazoxymethanol; PBS=phosphate-buffered saline.

---

[1] Received June 9, 1981; accepted November 19, 1981.

[2] Supported in part by Public Health Service grant 5-P30CA-16598-03 from the Puerto Rico Cancer Center–National Cancer Institute.

[3] Animals were maintained under the guidelines set forth in the "Guide for the Care and Use of Laboratory Animals" by the Institute of Laboratory Animal Resources, National Research Council.

[4] Department of Biochemistry and Nutrition, University of Puerto Rico, Medical Sciences Campus, G.P.O. Box 5067, San Juan, Puerto Rico 00936.

[5] Department of Physiology, University of Puerto Rico, Medical Sciences Campus.

washed twice with saline. The precipitate was dissolved in 0.2 ml 5% sodium dodecyl sulfate and 1 ml of water (*20*) and then mixed with 3 ml of reagent C of Lowry et al. (*21*). After the mixture stood for 20 minutes, 0.3 ml of Folin phenol reagent was added and the absorbance was read at 750 nm. The absorbance reading was converted to milligrams of antibody per sample by reference to a standard curve constructed by the subjection of known quantities of rabbit IgG to the same color reaction.

Preparation of Sepharose–HSA immunoabsorbent.—To quantitate the total antibody in the sera of MAM-injected and HSA-immunized rats and to detect nonprecipitating antibodies that would escape detection by the precipitin test, we used a Sepharose–HSA immunoabsorbent. We prepared the immunoabsorbent by conjugating HSA to activated Sepharose 4B. Sepharose 4B was activated by an acetonitrile solution of cyanogen bromide in 1 *M* Na_2CO_3 (*22*). To a solution (50 ml) of HSA in 0.1 *M* sodium phosphate buffer (pH 8; 3 mg/ml) was added 30 g of activated Sepharose, and the mixture was blended by gentle agitation for 18 hours at 4°C. The amount of protein conjugated was determined from the difference in concentration before and after reaction with activated Sepharose (determined from absorbance at 280 nm). After reaction, excess activated groups were blocked by mixing with gentle agitation the Sepharose cake with 50 ml of 0.5 *M* glycine in 0.1 *M* sodium phosphate buffer (pH 8) for 3 hours. The suspension was filtered and washed with 0.1 *M* sodium acetate, 2 *M* urea, 0.1 *M* $NaHCO_3$ (pH 10), water, and finally with PBS (pH 7.2). The Sepharose–HSA immunoabsorbent contained 3.25 mg HSA/ml packed immunoabsorbent.

Determination of antibody on Sepharose–HSA immunoabsorbent.—To 3 ml of packed immunoabsorbent in a glass column (1×20 cm) was added 0.15–0.3 ml of antiserum diluted with 2.5 ml PBS. The mixture was whirled thoroughly by a vortex mixer and then incubated at 4°C for 18 hours, after which the column was drained off and the immunoabsorbent was washed with PBS (pH 7.2; collecting 3.7 ml/tube) until absorbance reached 0.01. (This procedure required about 7–8 tubes.) Then the antibody was dissociated by the column's being washed with 5 *M* guanidine until absorbance was 0.01. The eluted antibody was monitored at 280 nm, and the pooled antibody was dialyzed twice against water and then against PBS. From the volume and the antibody content per milliliter [determined by the Lowry method; Lowry et al. (*21*)] the total amount of antibody per milliliter of antiserum was calculated.

Animal treatment and experimental protocol.—DNA repair studies: Male F344 rats weighing about 100 g received injections three times ip of 150 µCi [^{3}H]thymidine at 16, 4, and 0 hr before injection with MAM with the use of doses of 20, 40, or 60 mg/kg body weight. Animals were killed 2 per trial at 0, 2, and 18 hours after injection of MAM, and the femur, spleen, and thymus were dissected. Marrow was collected by aspiration of the femur with a syringe. Suspensions of spleen and thymus cells were obtained by means of the squash technique (*23*). DNA repair was monitored with the use of sedimentation techniques through 5–20% alkaline sucrose gradients in which DNA from cells lysed on the gradient permitted detection of DNA damage (*23*). From 0.1 to 0.3 ml of cells consisting of approximately 1 µg DNA that contained about 300–700 cpm was added to each gradient.

The lysed cells were centrifuged at 45,000×*g* in a type 40 rotor for 30 minutes at 20°C by means of a model L3-50 preparative ultracentrifuge (Beckman Instruments, Inc., Fullerton, Calif.). Fractions of 1.2 ml each were collected by means of a gradient fractionator (ISCO, Lincoln, Nebr.). In this method, the first fraction contained the 5% portion of the gradient. Bovine serum albumin was added to each fraction before precipitation with trichloroacetic acid. Each precipitate was solubilized (NCS solubilizer; Amersham/Searle Corp., Arlington Heights, Ill.) after which scintillation fluid was added (Aquasol II; New England Nuclear Corp., Boston, Mass.) and the radioactivity was determined in a liquid scintillation counter (Beckman Instruments, Inc.).

Immunologic studies: A group of male F344 rats were given injections ip of 0.1–0.3 ml MAM (7.0 mg/ml saline) so that each rat received 20 mg/kg body weight or saline alone (controls). Then after 0 hours, 2 hours, 12 hours, 24 hours, 3 days, and 7 days, a subgroup of 6 rats received injections im of 1 mg HSA emulsified in CFA (0.2 ml). Three weeks later a second injection of HSA (similar to the first) was given, and then the rats were bled (2 ml blood) through the heart 2 weeks later and thereafter at weekly intervals for 3 weeks. Other groups of rats received injections ip of MAM in saline so that the dose received was 40, 60, and 80 mg MAM/kg body weight. Control rats received saline alone. Then after 0 hours, 2 hours, 18 hours, 3 days, and 7 days, a subgroup of 4 rats received injections of 0.2 ml of HSA emulsified with CFA (containing 1 mg HSA). Three weeks later, the rats received a similar injection of HSA, and then 2 weeks after the second injection they were bled (2 ml blood) through the heart. The blood was collected in tubes treated with EDTA to prevent clotting. Plasma was decanted after centrifugation and preserved with merthiolate at 1:10,000. Controls were included consisting of rats immunized without prior MAM treatment and rats treated with MAM without immunization. To ascertain the immune responses of MAM-treated rats to injection of HSA, we determined the antibody both qualitatively by immunoelectrophoresis and double diffusion and quantitatively by the precipitin test and on an immunoabsorbent.

RESULTS

DNA Repair Studies

Damage to DNA was dose related, being minimal at 20 mg/kg and maximal at 60 mg/kg in all tissues studied (text-fig. 1). A low amount of damage was seen at zero time, maximum damage occurred after 2 hours, and some repair synthesis was noted after 18 hours (text-fig. 1). Some breakage was observed due to handling techniques as indicated by the height of the left-hand bar at zero time. The degree of this damage varied with individual tissues, being low with bone (6%) and higher with spleen (10–18%) and thymus (7–17%).

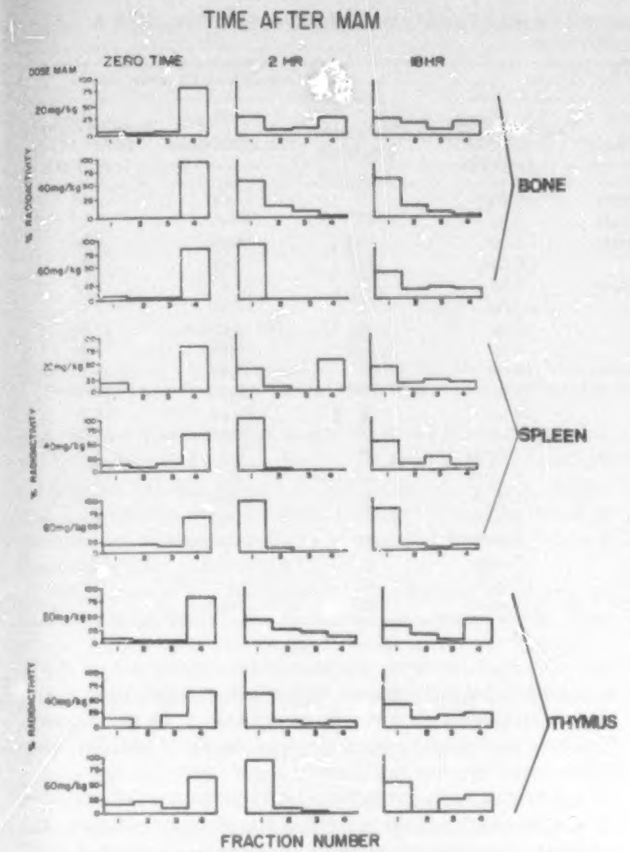

TEXT-FIGURE 1.—Effect of ip injections of MAM acetate at three dose levels (20, 40, and 60 mg/kg) on DNA of bone marrow, spleen, and thymus of rats killed at time of injection and 2 and 18 hr after injection with MAM. Histograms are based on sedimentation profiles of alkaline sucrose gradients from rats receiving 3 doses of 150 μCi each of [^{3}H]-thymidine 16, 4, and 0 hr before injection with MAM. The text-fig. was prepared so that the left-hand bar represents pooled samples of the lightest DNA fraction and each successive bar represents pooled samples of progressively heavier fractions.

Qualitative Determination of Antibody Response

All plasma from 20-mg/kg MAM-treated and HSA-immunized rats was screened for antibody by immunoelectrophoresis. However, this procedure was replaced by double diffusion in agar as a simple and rapid screening procedure for detecting precipitating antibody in rats immunized at 0 hours, 2 hours, 12 hours, 24 hours, 3 days, and 7 days after MAM treatment. Table 1 summarizes the responses of MAM-treated rats to immunization with HSA. All rats responded by production of antibodies. Table 2 shows the responses of rats given injections of MAM (40, 60, and 80 mg/kg body wt) prior to immunization by HSA as demonstrated by Ouchterlony. In the group of rats given injections of 40 mg MAM/kg body weight, all rats (that received injections of MAM 0, 2, and 18 hr before HSA immunization) responded by producing antibody. Conversely, plasma of some of the rats that were given injections of MAM 3 or 7 days before HSA immunization showed no precipitation in an Ouchterlony plate. This lack of precipitation may have been due either to absence of antibodies or to the presence of nonprecipitating antibodies.

In the group of 20 rats that were given injections of 60 mg MAM/kg body weight, 4 rats died (20%), 6 (30%) did not respond as shown by absence of precipitin lines, and 10 (50%) had precipitating antibodies. There was no apparent correlation between the formation of precipitin lines and the time between MAM injection and HSA immunization. In the group of 20 rats receiving injections of 80 mg MAM/kg prior to immunization, the mortality was considerable; 13 rats died (65%). In addition, 5 rats (25%) produced precipitating antibodies, whereas 2 (10%) produced nonprecipitating antibodies.

Quantitative Determination of Antibody Response

Because of the limited quantity of plasma from rats that were treated with 20 mg MAM/kg body weight, immune plasma from the first, second, and third bleedings of 2 rats was pooled and used for quantitative precipitin reaction (table 3). The value of antibody (mg/ml) plasma was that obtained at the equivalence point. The amount of antibody varied greatly among the individual rats in a given subgroup, which precluded any conclusion apart from the fact that MAM treatment (20 mg/kg body wt) prior to immu-

TABLE 1.—*Summary of the responses of rats to immunization by HSA after MAM injection (20 mg/kg body wt)*

Rat designation	Precipitin lines[a]	Interval between MAM and HSA
2	+++	0 hr
2^{x}	+++	0 hr
3^{x}	+++	0 hr
5^{x}	+++	0 hr
5	+++	0 hr
6^{x}	++	2 hr
6	+++	2 hr
7^{x}	+	2 hr
7	+	2 hr
8	++	2 hr
10	++	12 hr
10^{x}	+++	12 hr
12^{x}	+++	12 hr
12	++	12 hr
13^{x}	++	12 hr
13	+	12 hr
16	+	24 hr
16^{x}	+	24 hr
15	+++	24 hr
15^{x}	++	24 hr
17	++	24 hr
17^{x}	++	24 hr
19	+	3 days
19^{x}	+	3 days
21	+	3 days
21^{x}	+++	3 days
27	++	3 days
27^{x}	++	3 days
29	++	7 days
29^{x}	++	7 days
30	++	7 days
30^{x}	+++	7 days
31	+	7 days
31^{x}	++	7 days

[a] +=slight; ++=moderate; +++=notable.

TABLE 2.—*Summary of the responses of rats previously given injections of MAM (40, 60, and 80 mg/kg body wt) to immunization by HSA (shown by Ouchterlony)*

40 mg MAM/kg body wt			60 mg MAM/kg body wt			80 mg MAM/kg body wt		
Rat designation	Precipitin lines[a]	Interval between MAM and HSA	Rat designation	Precipitin lines[a]	Interval between MAM and HSA	Rat designation	Precipitin lines[a]	Interval between MAM and HSA
5	++	0 hr	9	No response	0 hr	13	Dead	0 hr
5$^{\times}$	+++	0 hr	9$^{\times}$	No response	0 hr	13$^{\times}$	Dead	0 hr
6	+++	0 hr	10	No response	0 hr	14	Dead	0 hr
6$^{\times}$	+++	0 hr	10$^{\times}$	++	0 hr	14$^{\times}$	Dead	0 hr
17	++	2 hr	21	No response	2 hr	25	++	2 hr
17$^{\times}$	+++	2 hr	21$^{\times}$	+++	2 hr	25$^{\times}$	Dead	2 hr
18	+++	2 hr	22	+++	2 hr	26	No response	2 hr
18$^{\times}$	+++	2 hr	22$^{\times}$	Dead	2 hr	26$^{\times}$	Dead	2 hr
29	++	18 hr	33	No response	18 hr	37	Dead	18 hr
29$^{\times}$	++	18 hr	33$^{\times}$	++	18 hr	37$^{\times}$	Dead	18 hr
30	++	18 hr	34$^{\times}$	++	18 hr	38	Dead	18 hr
30$^{\times}$	++	18 hr	34	+++	18 hr	38$^{\times}$	Dead	18 hr
41	+++	3 days	45	No response	3 days	50	++	3 days
41$^{\times}$	+++	3 days	46$^{\times}$	++	3 days	50$^{\times}$	++	3 days
42	No response	3 days	46	++	3 days	49	Dead	3 days
42$^{\times}$	No response	3 days	45$^{\times}$	Dead	3 days	49$^{\times}$	Dead	3 days
53$^{\times}$	No response	7 days	57	++	7 days	61	No response	7 days
53	+++	7 days	58	+++	7 days	61$^{\times}$	+	7 days
54$^{\times}$	+++	7 days	57$^{\times}$	Dead	7 days	62	+	7 days
54	+++	7 days	58$^{\times}$	Dead	7 days	62$^{\times}$	Dead	7 days

[a] +=slight; ++=moderate; +++=notable.

nization did not suppress the antibody response and was not affected whether MAM was given 0–7 days prior to immunization. If the values of the antibody of a subgroup are averaged (which represents 18 plasma samples from 6 rats and three bleedings), then there appears to be some potentiation of the humoral immune response by MAM; however, differences were not statistically significant.

TABLE 3.—*Amount of anti-HSA antibody in sera of rats immunized by HSA after MAM treatment (20 mg/kg body wt)*

Control—no MAM			MAM-treated		
Rat designation[a]	Antibody, mg/ml[b]	Interval between saline and HSA	Rat designation[a]	Antibody, mg/ml[b]	Interval between MAM and HSA
A	1.56	0 hr	D	1.8	0 hr
B	0.66 (1.01)	0 hr	E	1.3 (1.59)	0 hr
C	0.8	0 hr	F	1.68	0 hr
1	0.92	2 hr	4	1.9	2 hr
2	1.16 (1.26)	2 hr	5	0.46 (1.03)	2 hr
3	1.7	2 hr	6	0.74	2 hr
7	0.8	12 hr	10	2.76	12 hr
8	1.17 (1.13)	12 hr	11	1.0 (1.52)	12 hr
9	1.42	12 hr	12	0.8	12 hr
13	2.18	24 hr	16	1.32	24 hr
14	1.66 (1.67)	24 hr	17	3.8 (3.27)	24 hr
15	1.17	24 hr	18	4.7	24 hr
19	0.9	3 days	22	1.28	3 days
20	1.02 (1.03)	3 days	23	0.44 (1.75)	3 days
21	1.16	3 days	24	3.54	3 days
25	1.66	7 days	28	4.6	7 days
26	2.6 (1.94)	7 days	29	1.8 (2.69)	7 days
27	1.56	7 days	30	1.66	7 days

[a] Plasma from bleedings 1–3 and from 2 rats were pooled. A = rat 1 + 1$^{\times}$; B=4 + 4$^{\times}$; C = 9 + 9$^{\times}$; 1 = 18 + 18$^{\times}$; 2 = 20 + 20$^{\times}$; 3 = 14 + 14$^{\times}$; 7 = 22 + 22$^{\times}$; 8 = 23 + 23$^{\times}$; 9 = 24 + 24$^{\times}$; 13 = 26 + 26$^{\times}$; 14 = 28 + 28$^{\times}$; 15 = 25 + 25$^{\times}$; 19 = 32 + 32$^{\times}$; 20 = 36 + 36$^{\times}$; 21 = 37 + 37$^{\times}$; 25 = 39 + 39$^{\times}$; 26 = 44 + 44$^{\times}$; 27 = 42 + 42$^{\times}$. D = 2 + 2$^{\times}$; E = 5 + 5$^{\times}$; 4 = 6 + 6$^{\times}$; 5 = 7 + 7$^{\times}$; 6 = 8 + 8$^{\times}$; 10 = 10 + 10$^{\times}$; 11 = 12 + 12$^{\times}$; 12 = 13 + 13$^{\times}$; 16 = 15 + 15$^{\times}$; 17 = 16 + 16$^{\times}$; 18 = 17 + 17$^{\times}$; 22 = 21 + 21$^{\times}$; 23 = 27 + 27$^{\times}$; 24 = 19 + 19$^{\times}$; 28 = 29 + 29$^{\times}$; 29 = 30 + 30$^{\times}$; 30 = 31 + 31$^{\times}$.

[b] *Numbers in parentheses* are means of antibody level (mg/ml plasma) from a subgroup of rats.

In 19 rats (table 4) that received injections of 40, 60, and 80 mg MAM/kg body weight prior to immunization, the antibody level that gave precipitin lines in Ouchterlony was similar to the antibody level in the controls shown in table 3. However, 9 rats whose plasma did not give precipitin lines produced nonprecipitating antibodies that were trapped and recovered on the immunoabsorbent. The level of nonprecipitating antibodies in those 9 rats was quite variable. The variation did not seem to be dependent on the dose of MAM injected. Five rats produced a low level of nonprecipitating antibodies (0.33–0.89 mg antibody/ml plasma), while 4 rats had a higher level (1.08–2.88 mg antibody/ml plasma) that was of the same magnitude as that of the precipitating antibody produced in rats given 40, 60, and 80 mg MAM/kg body weight prior to immunization. It is evident that injection of MAM (at 40, 60, and 80 mg/kg) prior to immunization of rats with HSA evoked a variable spectrum of effects on the humoral immune response. In some rats the humoral immune response was unaffected and the rats responded by producing precipitating antibodies; other rats elicited nonprecipitating antibodies at a level similar to that of the controls, and still other rats had a depressed level of nonprecipitating antibodies.

DISCUSSION

MAM acetate can cause damage to DNA of the liver, kidney, and small intestine of rats (*24, 25*). Moreover, Damjanov et al. (*13*), using doses of 25 mg MAM/kg body weight, reported that after 14 days damage to liver DNA

TABLE 4.—*Determination of antibodies in rats given injections of MAM prior to immunization with HSA on sepharose-HSA immunoabsorbent*

40 mg MAM/kg body wt			60 mg MAM/kg body wt			80 mg MAM/kg body wt		
Rat serum pool	Antibody, mg/ml	Interval between MAM and HSA	Rat serum pool	Antibody, mg/ml[a]	Interval between MAM and HSA	Rat serum pool	Antibody, mg/ml[a]	Interval between MAM and HSA
5+6	1.04	0 hr	9+10	(2.1)	0 hr			
			21^x+22	2.43	2 hr	25	0.59	2 hr
			21	(0.89)		26	(1.08)	2 hr
29+30	3.07	18 hr	33	(0.52)	18 hr			
41+41^x	2.77	3 days	33^x+34	1.65	18 hr			
42	(0.33)	3 days	45	(0.40)	3 days	50+50^x	2.74	3 days
			46+46^x	1.8	3 days			
53+54	2.28	7 days	57+58	2.25	7 days	61	(0.64)	7 days
53^x	(2.88)	7 days						

[a] *Numbers in parentheses* indicate that the value was from rat that gave no precipitin lines in Ouchteriony.

had not been repaired. It is not surprising, therefore, that the equivalent and higher doses of MAM used in the present experiment caused damage to DNA in bone marrow, spleen, and thymus that persisted after 18 hours. That the repair in these tissues is dose related is also expected because it is well documented for other tissues (*13*).

Zedeck et al. (*26*) postulated that changes necessary for tumor growth occur soon after treatment with MAM. One of the purposes of the current study was to determine if MAM had a direct and immediate effect on immunocompetent cells. Although damage to the DNA of the bone marrow, spleen, and thymus of rats was noted, there was little humoral immunosuppression as measured by response to injection of HSA.

At low doses of MAM (20 mg/kg), there was no suppression of the immune response of rats against the injection of HSA. Conversely, with rats treated with high doses of MAM (40, 60, and 80 mg/kg body wt), the mortality increased with an increase in the doses of MAM. Moreover, the antibody responses of rats to HSA were not uniform; many animals that did not show precipitating antibodies responded by synthesizing nonprecipitating antibodies (at variable levels) that were detected by immunoabsorbents.

There is strong evidence that in cases in which nonprecipitating antibodies are produced as a result of antigenic stimulation by complex antigens, the antibodies are formed against one or two antigenic determinants that, on reaction with the antigen, will be incapable of forming a lattice structure necessary for precipitation. Thus guinea pig nonprecipitating antibodies against ovalbumin reacted with ovalbumin at a molar ratio of antibody:antigen of 1.5, which was less than 2.5 shown by antiovalbumin precipitating antibodies (*27, 28*). Similarly, Fab fragments derived from nonprecipitating antiovalbumin antibodies reacted with ovalbumin at a molar ratio of Fab:ovalbumin equals 2 compared to a ratio of 3.2 for Fab fragments derived from precipitating antiovalbumin antibody (*27, 28*). Nonprecipitating antibodies against cobrotoxin reacted at a molar ratio of antibody:antigen equals 0.79–0.97 compared to a value of 1.58–1.94 for precipitating antibodies (*29*). Recently, we showed that pigs elicited nonprecipitating antibodies against chicken egg white lysozyme during the period of immunization that was revealed on lysozyme immunoabsorbent column (*30*). Binding studies on both the nonprecipitating antibodies and Fab fragments derived from them indicated that the molar ratio of antibody or Fab:lysozyme equals 2 compared to a value of 3 for precipitating antibodies (*30*).

On the basis of these facts, we are proposing that nonprecipitating antibodies to HSA elicited in MAM-treated rats were produced as a consequence of a restriction in the recognition of some of the HSA antigenic determinants so that only one or two antigenic determinants were recognized by the rat's immune system. This limited recognition of HSA antigenic sites may indicate that certain clones of lymphocytes were either suppressed or eliminated as a result of MAM treatment. The outcome of these events would be the formation of antibodies against one or two antigenic determinants of HSA and their concomitant nonprecipitability. Of significance was the finding that MAM in high doses had a varied effect on the rat's humoral immune system so that some animals synthesized precipitating antibodies normally and others showed signs of restriction in their recognition of the antigenic determinants of a complex antigen resulting in the production of nonprecipitating antibodies at different levels. The use of immunoabsorbents was instrumental in trapping and detecting nonprecipitating antibodies. Except for the effects at high (approaching toxic) doses, it would appear that MAM does not inhibit the humoral immune responsiveness.

REFERENCES

(*1*) LAQUEUR GL, MICKELSEN O, WHITING MG, KURLAND LT. Carcinogenic properties of nuts from *Cycas circinalis* L. indigenous to Guam. J Natl Cancer Inst 1963; 31:919–951.

(*2*) GABRIDGE MG, DENUNZIO A, LEGATOR MS. Cycasin: Detection of associated mutagenic activity in vivo. Science 1969; 163:689–691.

(*3*) GANOTE GE, ROSENTHAL AS. Characteristic lesions of methylazoxymethanol induced liver damage. A comparative ultrastructural study with dimethylnitrosamine, hydrazine sulfate and carbon tetrachloride. Lab Invest 1968; 19:382–398.

(*4*) LAQUEUR GL, SPATZ M. Oncogenicity of cycasin and methylazoxymethanol. Gan Monogr Cancer Res 1975; 17:189–204.

(*5*) LAQUEUR GL, MATSUMOTO H. Neoplasms in female Fischer rats following intraperitoneal injection of methylazoxymethanol. J Natl Cancer Inst 1966; 37:217–232.

(*6*) HIRONO I, SHIBOYA C. High incidence of pulmonary tumors in dd mice by single injection of cycasin. Gan 1970; 61:403–407.

(*7*) ZEDECK MS, STERNBERG SS, MCGOWAN J, POYNTER RW. Methylazoxymethanol acetate: Induction of tumors and early effects on RNA synthesis. Fed Proc 1972; 31:1485–1492.

(*8*) SPATZ M. Toxic and carcinogenic alkylating agents from cycads. Ann NY Acad Sci 1969; 163:848–859.

(9) Laqueur GL, McDaniel EG, Matsumoto H. Tumor induction in germfree rats with methylazoxymethanol (MAM) and synthetic MAM acetate. J Natl Cancer Inst 1967; 39:355–371.

(10) O'Gara RN, Brown JM, Whiting MG. Induction of hepatic and renal tumors by the topical application of aqueous extract of cycad nut to artificial skin ulcers in mice. Fed Proc 1964; 23:1384.

(11) Spatz M. Carcinogenic effect of a cycad meal in guinea pigs. Fed Proc 1964; 23:1384–1385.

(12) Stanton MF. Hepatic neoplasms of aqueous fish to *Cycas circinalis.* Fed Proc 1966; 25:661.

(13) Damjanov I, Cox R, Sarma DS, Farber E. Patterns of damage and repair of liver DNA induced by carcinogenic methylating agents in vivo. Cancer Res 1973; 33:2122–2128.

(14) Prehn RT. Function of depressed immunologic reactivity during carcinogenesis. J Natl Cancer Inst 1963; 31:791–805.

(15) Outzen HC, Prehn RT. Alteration of cell mediated immunity in the mouse following administration of 4-nitroquinoline-1-oxide. Cancer Res 1973; 33:408–410.

(16) Stjernswärd J. Immunodepressive affect of 3-methylcholanthrene. Antibody formation at the cellular level and reaction against weak antigenic homografts. J Natl Cancer Inst 1965; 35:885–892.

(17) ———. Further immunological studies of chemical carcinogenesis. J Natl Cancer Inst 1967; 38:515–526.

(18) Howard-Flanders P. DNA repair and recombination. Br Med Bull 1973; 29:226–235.

(19) Liberman MW, Baney RN, Lee RE, Sell S, Farber E. Studies on DNA repair in human lymphocytes treated with proximate carcinogens and alkylating agents. Cancer Res 1971; 31:1297–1306.

(20) Habeeb AF, Atassi MZ. Immunochemistry of serum albumin. IV. Immunochemical cross reaction of fragments from the first, third and the last third of bovine serum albumin. Immunochemistry 1977; 14:449–457.

(21) Lowry OH, Rosebrough NJ, Farr AL, Randall RJ. Protein measurement with the Folin phenol reagent. J Biol Chem 1951; 193: 265–275.

(22) March SC, Parikh I, Cuatrecasas P. A simplified method for cyanogen bromide activation of agarose for affinity chromatography. Anal Biochem 1974; 60:149–152.

(23) Cox R, Damjanov I, Abanobi SE, Sarma DS. A method for measuring DNA damage and repair in liver in vivo. Cancer Res 1973; 33: 2114–2121.

(24) Zedeck MS, Sternberg SS, Poynter RW, McGowan J. Biochemical and pathological effects of methylazoxymethanol acetate, a potent carcinogen. Cancer Res 1970; 30:801–812.

(25) Kanagalingam K, Balis ME. In vivo repair of rat intestine DNA damage by alkylating agents. Cancer 1975; 36:2364–2372.

(26) Zedeck MS, Sternberg SS, Yataganas X, McGowan J. Early changes induced in rat liver by methylazoxymethanol acetate: Mitotic abnormalities and polyploidy. J Natl Cancer Inst 1974; 53: 719–724.

(27) Tamoto K, Nakamura J, Koyama J. Further studies on guinea pig non-precipitating antibodies to ovalbumin. J Biochem 1972; 72: 261–268.

(28) Tamoto K, Koyama J. Non-precipitating guinea pig antibodies as products of limited recognition of antigenic sites on the ovalbumin molecule. Immunology 1976; 31:67–77.

(29) Yang CC, Chang CC, Lin MF, Lee HY, Chuang LY. Purification and properties of non-precipitating antibodies to cobrotoxin. Int J Peptide Prot Res 1978; 12:303–310.

(30) Habeeb AF. Enzymic and immunochemical properties of lysozyme—Restriction of recognition of lysozyme antigenic determinants in pigs. Arch Biochem Biophys 1981; 212:618–628.

Peptidoglycans Extracted From Gram-Positive Bacteria: Expression of Antitumor Activity According to Peptide Structure and Route of Injection[1,2]

Anne-Françoise Goguel,[3] Geneviève Lespinats,[3] *and* Charles Nauciel[4]

ABSTRACT—The antitumor effect of peptidoglycans of various structures extracted from different gram-positive bacteria was studied, on chemically induced fibrosarcomas, in C3H/He, C57BL/6, and (C57BL/6 × C3H/He)F_1 mice. When given sc admixed with tumor cells, only some peptidoglycans (those extracted from *Bacillus megaterium* and *Staphylococcus aureus*) enhanced tumor resistance in syngeneic and semiallogeneic hosts, whereas other peptidoglycans (those extracted from *Micrococcus lysodeikticus* and *Corynebacterium poinsettiae*) possessed no antitumor effect. When tumor cells were given ip, administration of peptidoglycans by the same route was either without effect on tumor growth or it induced tumor enhancement. Enhancement could be observed with all of the peptidoglycans tested. The antitumor effect when given sc and the ability to stimulate the proliferation of B-lymphocytes were shared by the same two peptidoglycans, while the other two peptidoglycans were devoid of both activities. It appears that these biological activities depend on the structure of the peptide moiety of peptidoglycans and that mitogenic and antitumor responses are stimulated by similar structures. JNCI 1982; 68:657–663.

Whole bacteria have been widely used to increase tumor resistance. Most such studies have been done with BCG and *Corynebacterium parvum*, but other bacterial species, such as *Bordetella pertussis* (*1*), *Listeria monocytogenes* (*2*), *Streptococcus pyogenes* (*3*), *Brucella abortus* (*4*), and *Staphylococcus aureus* (*5*), have sometimes been used.

In view of obtaining reproducible results and to avoid undesirable side effects, many authors have investigated the possibility of using various bacterial extracts as efficient immunomodulators. Some fractions extracted from mycobacteria [mostly cell walls, interphase material extracted from mycobacteria, methanol-extracted residue from mycobacteria, and cord factor (*6–12*)] or from other bacteria [*Nocardia rubra* (*13, 14*) and *C. parvum* (*15*)] possess antitumor effects in several experimental models.

In a previous report (*16*), we described how the peptidoglycan extracted from the cell walls of *Bacillus megaterium* was able to inhibit the development of a chemically induced fibrosarcoma in rats. The peptidoglycan is the only cell wall polymer common to both gram-negative and gram-positive bacteria. This cell wall extract is a heteropolymer built of glycan strands interconnected through short peptide chains which are cross linked. The glycan moiety of the peptidoglycan is remarkably uniform throughout the bacterial world. It is made up of the repetition of *N*-acetylglucosamine and *N*-acetylmuramic acid connected by β-1,4 linking. The composition and structure of peptidoglycans seem rather constant among gram-negative bacteria, but variations are great among gram-positive bacteria. Among bacterial species, these variations can occur in the structure of the peptide chain and in the nature of the interpeptide bridge (*17*).

Previous studies have shown that bacterial peptidoglycans can exhibit adjuvant activity on cellular and humoral responses (*18, 19*) and can possess mitogenic effects (*20*). It was also established that variations in the structure of the peptide moiety are correlated with changes in the adjuvant and mitogenic properties of peptidoglycans. (Guenounou M, Goguel AF, Nauciel C: Submitted for publication).

The purpose of the present study is to evaluate whether the structure of the peptide moiety of peptidoglycan can also play a role in the stimulation of tumor resistance and whether we can establish a correlation among the different biological activities of a particular peptidoglycan.

MATERIALS AND METHODS

Mice.—Male and female inbred C3H/He, C57BL/6, and (C57BL/6 × C3H/He)F_1 (hereafter called B6C3F_1) mice, 2–6 months old, were obtained from the production colonies of the Institut de Recherches Scientifiques sur le Cancer and maintained in specific-pathogen-free conditions.

Bacterial components.—Peptidoglycans from various gram-positive bacteria were extracted according to the technique of Schleifer and Kandler (*21*) with slight modifications. The bacteria were disrupted by ultrasonic treatment, and the cell walls were collected by differential centrifugation and digested with trypsin (0.5 mg/ml) and ribonuclease (5 µg/ml) in 0.05 *M* phosphate buffer (pH 7.8) at 37°C for 16 hours. The cell-wall digest was then treated with 1% sodium dodecyl sulfate for 10 minutes in a boiling water bath and centrifuged at 12,000×*g* for 30 minutes. After centrifugation, the pellet was washed thoroughly with distilled water. Teichoic acid was extracted with 10% trichloroacetic acid at 4°C for 3 days, and the insoluble residue was washed three times in distilled water and lyophilized. The strains of bacteria that were so treated and the structure of the peptide moiety of their respective peptidoglycans are reported in table 1 (*17*). Soluble peptidoglycan was obtained from *B. megaterium* by treatment with egg-white lysozyme (Sigma

ABBREVIATIONS USED: EMEM=Eagle's minimum essential medium; [^{3}H]-dThd=tritiated thymidine; LPS=lipopolysaccharide; MST=mean survival time; PHA=phytohemagglutinin; SI=stimulation index.

---

[1] Received June 18, 1981; accepted November 2, 1981.

[2] Supported by a grant from the Centre National de la Recherche Scientifique, Programme Interdisciplinaire de Recherche sur les bases Scientifiques des Medicaments.

[3] Laboratoire d'Immunobiologie, Institut de Recherches Scientifiques sur le Cancer, BP 8, 94802 Villejuif Cedex, France.

[4] Laboratoire d'Immunochimie des Protéines, Institut Pasteur, 75015 Paris, France.

best copy available

TABLE 1.—*Peptide moiety structures of various peptidoglycans*

Bacteria (strain)	Peptide moiety structure
B. megaterium (ATCC 14581)	-LAla-DGlu ⌐msDAP[a]-DAla
S. aureus (strain Copenhagen)	-LAla-DGluNH$_2$ ⌐LLys-DAla
M. lysodeikticus (Institut Pasteur A 270)	-LAla-DGlu-Gly ⌐LLys-DAla
C. poinsettiae (NCPPB 846)	-Gly-DGlu ⌐LHSer-DAla

[a] *meso*-Diamino pimelic acid.

Chemical Co., St. Louis, Mo.) as previously described (*22*).

For each preparation, the chemical composition of the peptide moiety was checked by amino acid analysis. The expected ratios of amino acids in the various peptidoglycans were found, and only trace amounts of other amino acids were detected.

C. parvum.—A heat-killed suspension of *C. parvum* (2 mg Pasteur strain 4182/ml) was provided by Prof. R. Ducluzeau (Centre National de la Recherche Zoologique, Jouy-en-Josas, France).

Tumors.—Fibrosarcomas were originally induced in females by 2 mg 3-methylcholanthrene sc and were serially transplanted in syngeneic mice. Tumors from the 5th to 30th passages were used. They were removed aseptically and cut into small pieces. Tumor pieces were suspended in 0.25% trypsin in phosphate-buffered saline and stirred for 90 minutes at 37°C. After passage through sterile gauze, tumor cells were centrifuged and suspended in EMEM, and the number of viable cells was determined by trypan blue exclusion.

Tumor C3-9 was induced in C3H/He mice and tumor B6-2, in C57BL/6 mice; the number of tumor cells that induced 100% tumors in syngeneic mice were, respectively, 3×10^4 and 4×10^4 cells. In all experiments, these doses were used sc or ip in syngeneic and in semiallogeneic mice because no hybrid resistance was observed for these tumors.

In vivo test procedure.—Lyophilized peptidoglycans were suspended in EMEM, sterilized by heat in a boiling water bath, and redispersed by sonication before use. Tumor cells and peptidoglycans, at the desired concentrations, were mixed and immediately injected either sc or ip in a total volume of 0.1 ml. For mice inoculated sc, the tumor size was measured twice a week; for mice inoculated ip, mortality was recorded daily.

Mitogenic activity evaluation.—Mitogens used were PHA (HA 16; Burroughs-Wellcome Ltd., Beckenham, England) (final concentration, 1 μg/ml), LPS extracted from *Escherichia coli* 055:B5 (Difco Laboratories, Detroit, Mich.), and peptidoglycans (several concentrations).

Lymphocytes were cultured from spleens that were aseptically removed, minced with scissors, filtered through a 200-mesh stainless steel sieve, and then washed in EMEM. Single cell suspensions were prepared in RPMI-1640 medium supplemented with 10% complement-inactivated (56°C, 30 min) fetal calf serum (GIBCO, Grand Island, N.Y.), 2 m*M* glutamine (GIBCO), 100 U penicillin/ml, and 100 μg streptomycin/ml. Aliquots of 100 μl containing 2.5×10^5 spleen cells were placed in wells of Falcon #3040 MicroTest plates (Falcon Plastics, Oxnard, Calif.). To each well was added 100 μl of medium containing the mitogen at the desired concentration. All cultures were done in triplicate. The MicroTest plates were incubated at 37°C in a humidified atmosphere of 95% air–5% CO_2 for 24 hours, after which 1 μCi of [^{3}H]dThd (TMM 79 B; CEA, Gif-sur-Yvette, France; [*methyl*-^{3}H]dThd sp act: 25 Ci/m*M*) was added to each well. Cultures were harvested 18 hours later on glass fiber filters with a multiple sample collector (Skatron; Flow Laboratories, Inc., Ayrshire, Scotland). The glass fiber discs were then placed in toluene-based scintillation fluid (Lipoluma; Lumac, Basel, Switzerland), and the radioactivity was counted in an SL 30 Intertechnique scintillation spectrometer. The results are expressed as the mean net counts per minute. (Δ cpm = difference between responses in stimulated and unstimulated cultures; from 2 to 6×10^3 cpm were obtained in unstimulated cultures.) SI was calculated as the mean cpm in experimental culture/mean cpm in unstimulated culture.

Spleen cells were treated with anti-Thy 1.2 serum and complement. Anti-Thy 1.2 serum was prepared by the method of Reif and Allen (*23*). This antiserum killed 95% of thymocytes when it was diluted 1:10 and complement was present. Spleen cells (2.5×10^7 cells) were incubated on ice with 1 ml of diluted anti-Thy 1.2 serum for 60 minutes. The antiserum was then removed, and complement was added as 1 ml of fresh guinea pig serum diluted 1:10. After a further 30-minute incubation at 37°C, the cells were washed and adjusted to the desired concentration, and mitogenic activity was tested.

RESULTS

Local effects in mice administered particulate and soluble peptidoglycans sc.—When C3H/He mice were inoculated sc with peptidoglycan extracted from *B. megaterium* admixed with tumor cells, the peptidoglycan induced a delay in tumor appearance and a decrease in tumor take, as compared with tumor cell-inoculated controls. This effect was dose-dependent in the range of 5–500 μg peptidoglycan/animal (table 2). When injected at the same concentration and tested

TABLE 2.—*Inhibited tumor growth in C3H/He mice inoculated sc with peptidoglycans admixed with tumor cells*[a]

Peptidoglycan treatment	Dose, μg/mouse	Mean tumor diameter at day 20 ± SE, mm[b]	No. of tumor-free mice/No. tested
None	0	11.80±0.74	0/15
Particulate peptidoglycan[c]	5	7.10±1.33*	3/15
	50	4.0±0.85†	6/15
	500	0.47±0.26†	12/15
Soluble peptidoglycan[d]	50	4.87±0.82†	1/15
Whole *C. parvum*	5	1.60±0.64†	10/15
	50	0	15/15

[a] All mice were inoculated sc with 3×10^4 C3-9 tumor cells with or without admixed peptidoglycan or *C. parvum*.

[b] Probability was evaluated by Student's *t*-test. *=$P<0.01$; †=$P<0.001$.

[c] Particulate peptidoglycan was extracted from *B. megaterium*.

[d] Soluble peptidoglycan was obtained from *B. megaterium* peptidoglycan after lysozyme treatment.

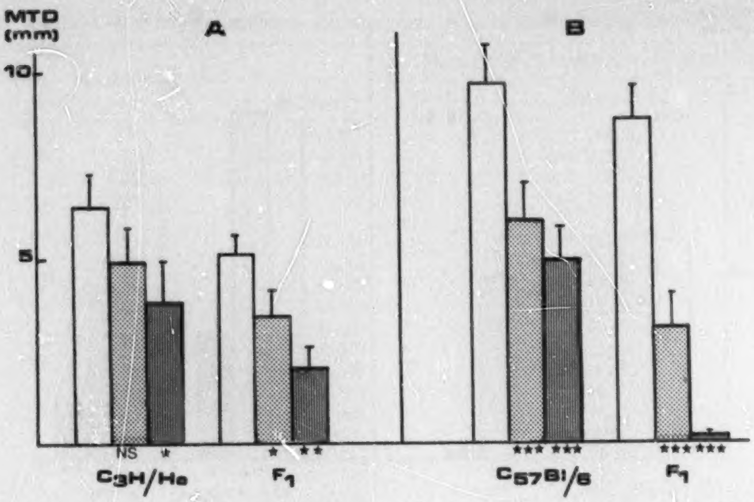

TEXT-FIGURE 1.—Local effect of sc heat-killed *S. aureus* and its peptidoglycan on A) C3-9 tumor growth and B) B6-2 tumor growth. F_1=B6C3F_1; MTD=mean tumor diameter measured 15 days after inoculation. □=tumor cells alone; ▨=tumor cells with 100 μg heat-killed *S. aureus*; ■=tumor cells with 100 μg peptidoglycan from *S. aureus*. Probability was evaluated by Student's *t*-test. *=$P<0.1$; **=$P<0.01$; ***=$P<0.001$; NS=not significant.

under the same conditions, whole heat-killed *C. parvum* was a more efficient antitumor agent than the peptidoglycan extracted from *B. megaterium* (table 2).

The peptidoglycan from *S. aureus* also inhibited tumor growth. The activities of purified peptidoglycan and whole cells were compared. Although peptidoglycan was more active than whole cells, the difference was not statistically significant (text-fig. 1). The effects of both preparations were more pronounced in F_1 mice than in syngeneic mice.

After solubilization by lysozyme treatment, the antitumor activity of peptidoglycan was decreased as compared with that of particulate peptidoglycan (table 2); although a significant decrease in the tumor growth rate was still observed, nearly all animals developed tumors. This indicated that the oligomeric form of peptidoglycan possessed some activity but was less efficient than the particulate and polymerized forms.

Comparative effects of peptidoglycans having different structures.—The local effect on tumor growth was tested after mice were inoculated sc with several peptidoglycans extracted from different bacteria. With C3-9 and B6-2 tumors, we found a reproducible difference between peptidoglycans. Those extracted from *B. megaterium* and *S. aureus* inhibited tumor growth, while peptidoglycans extracted from *Corynebacterium poinsettiae* and *Micrococcus lysodeikticus* were devoid of antitumor effect (text-figs. 2, 3).

Lack of direct cytotoxicity of peptidoglycans on tumor cells.—The addition of peptidoglycan to tumor cell cultures did not decrease their level of [^{3}H]dThd incorporation (table 3). Thus the effect of peptidoglycans on tumor growth cannot

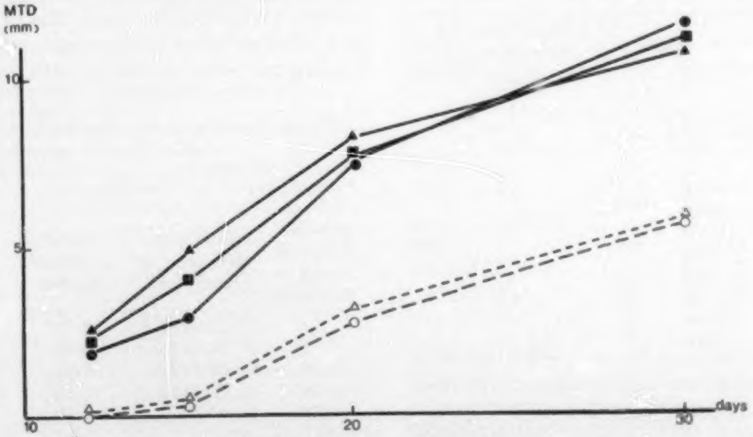

TEXT-FIGURE 2.—Effect of peptidoglycans having different structures on C3-9 tumor growth in C3H/He mice inoculated sc with 3×10^4 tumor cells alone (■) or admixed with 100 μg of peptidoglycan from *M. lysodeikticus* (▲), from *C. poinsettiae* (●), from *B. megaterium* (○), or from *S. aureus* (△). MTD=mean tumor diameter obtained from two identical experiments.

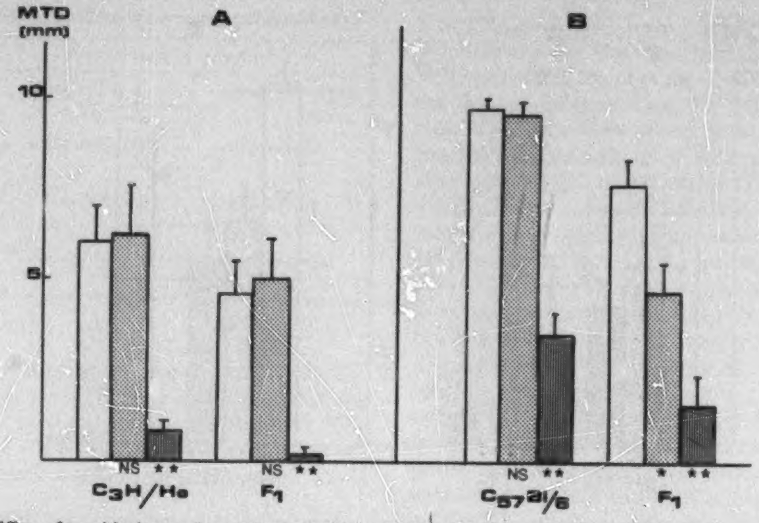

TEXT-FIGURE 3.—Effect of peptidoglycans from *S. aureus* or *M. lysodeikticus* on tumor growth. A) C3-9 tumor growth or B) B6-2 tumor growth. F_1=B6C3F_1; MTD=mean tumor diameter measured 15 days after injection and obtained from two identical experiments. □=tumor cells alone; ▨=tumor cells with 100 μg peptidoglycan from *M. lysodeikticus*; ▥=tumor cells with 100 μg peptidoglycan from *S. aureus*. Probability was evaluated by Student's *t*-test. ★=$P<0.02$; ★★=$P<0.001$; NS=not significant.

be related to a cytotoxic effect on tumor cells.

Local effects in mice administered peptidoglycans ip.—When C3H/He and B6C3F_1 mice were inoculated ip with admixed peptidoglycans and tumor cells, their MST was never extended and was often shortened. The absence of antitumor activity and occasional tumor enhancement were observed with all of the tested peptidoglycans, including those effective sc and those inactive (table 4). The same observations on tumor growth were made when peptidoglycan was administered in the range of 5–200 μg admixed with tumor cells (table 5). Results obtained when peptidoglycan was injected before tumor cells, at 2-day intervals from 12 to 1 days, have shown an absence of antitumor effect and an occasional tumor enhancement (data not shown).

TABLE 3.—*Lack of direct cytotoxicity of different peptidoglycans on C3-9 tumor cells*[a]

Bacterial peptidoglycan	Dose, μg/ml	[^{3}H]dThd incorporated, cpm × 10^{-3}
None	0	6.08
B. megaterium	50	11.08
	250	11.9
	500	15.1
S. aureus	50	8.9
	250	9.8
	500	10.2
C. poinsettiae	50	7.2
	250	8.1
	500	5.7
M. lysodeikticus	50	5.6
	250	8.7
	500	7.1

[a] Cytotoxicity was determined after 5×10^3 C3-9 tumor cells/well were incubated 48 hr at 37°C with the indicated concentrations of peptidoglycan. During the last 6 hr, 1 μCi [^{3}H]dThd/well was added. After the radioactive culture medium was removed, the cells were resuspended by trypsin treatment and harvested with a multiple sample collector on glass fiber filters. The incorporated radioactivity was then determined.

TABLE 4.—*Effect on C3-9 tumor growth in mice inoculated ip with different peptidoglycans*[a]

Treatment	MST±SE, days after inoculation	No. of survivors/total No.
None	44.8±6.0	1/8
Peptidoglycan		
B. megaterium	29.6±1.9[b]	0/10
S. aureus	35.9±1.5	0/10
M. lysodeikticus	34.9±3.4	0/10
C. poinsettiae	31.3±1.4[c]	0/10

[a] C3H/He mice were inoculated ip with 3×10^4 C3-9 tumor cells with or without 200 μg admixed peptidoglycan.

[b] $P<0.02$.

[c] $P<0.05$.

Mitogenic activity of peptidoglycans.—Mitogenic activity of peptidoglycans was tested on spleen cells from C3H/He, C57BL/6, and B6C3F_1 mice. The peptidoglycans that have an antitumor effect sc (*B. megaterium* and *S. aureus*) also have a mitogenic effect on spleen cells; the inactive peptidogly-

TABLE 5.—*Lack of dose-dependent response in syngeneic and semiallogeneic tumor rejections*[a]

Dose of *S. aureus* peptidoglycan injected ip, μg/animal	C3H/He		B6C3F_1	
	MST±SE, days after inoculation	No. of survivors/total No.	MST±SE, days after inoculation	No. of survivors/total No.
0	33.2±1.8	0/10	31.3±2.5	0/10
5	34.7±1.2	0/10	26.6±1.1[b]	0/10
10	35.8±2.0	0/10	32.5±1.1	0/10
50	32.6±2.2	1/10	28.5±1.3	0/10
200	33.2±1.7	1/10	27.0±1.2	0/10

[a] C3H/He and B6C3F_1 mice were inoculated ip with 3×10^4 C3-9 tumor cells with or without admixed peptidoglycan.

[b] $P<0.05$.

Table 6.—*Mitogenic activity of different peptidoglycans on spleen cells from various strains of mice*

Mitogen	Dose, μg/ml	Mean [^{3}H]dThd uptake ×10^{-3} cpm (SI)[a]		
		C3H/He	C57BL/6	B6C3F$_1$
LPS	1	5.3 (2.21)	15.8 (14.85)	8.6 (3.28)
	10	25.3 (6.77)	35.6 (32.14)	21.7 (6.75)
	50	51.8 (12.82)	67.2 (59.75)	57.6 (16.28)
	100	52.0 (12.88)	65.1 (57.94)	55.8 (15.79)
Peptidoglycan				
B. megaterium	1	0.8 (1.18)	0.5 (1.43)	−0.1 (0.97)
	10	5.1 (2.16)	2.1 (2.82)	2.5 (1.64)
	50	22.3 (6.08)	7.7 (7.75)	12.0 (4.17)
	100	28.1 (7.42)	8.4 (8.35)	13.0 (4.45)
S. aureus	1	1.7 (1.37)	0.2 (1.18)	−0.6 (0.83)
	10	6.5 (2.47)	1.1 (1.99)	1.7 (1.45)
	50	18.3 (5.18)	6.7 (6.83)	10.9 (3.88)
	100	23.1 (6.28)	6.2 (6.41)	12.7 (4.36)
C. poinsettiae	1	−0.8 (0.80)	−0.26(0.73)	−0.90(0.76)
	10	0.1 (1.01)	−0.21(0.77)	−0.70(0.82)
	50	5.75(2.29)	0.8 (1.69)	1.90(1.50)
	100	4.70(2.05)	0.4 (1.37)	0.2 (1.05)
M. lysodeikticus	1	−0.9 (0.78)	−0.2 (0.80)	−0.6 (0.82)
	10	0 (0.99)	0.1 (1.10)	−0.5 (0.84)
	50	2.80(1.64)	0.8 (0.70)	1.1 (1.27)
	100	3.40(1.76)	0.7 (1.58)	0.90(1.23)

[a] Data are mean net counts per min. Each value is the mean of triplicate wells counted in a representative experiment. SI was calculated with respect to controls.

cans (*C. poinsettiae* and *M. lysodeikticus*) have no significant mitogenic activity (table 6).

Peptidoglycans induced a proliferation of B-cells, because the elimination of T-cells by anti-Thy 1.2 serum and complement treatment did not modify the SI (table 7) and spleen cells from nude mice were stimulated by peptidoglycan (table 8). After solubilization of peptidoglycan by lysozyme treatment, the SI was dramatically decreased (table 9).

DISCUSSION

Bacterial extracts exhibiting antitumor activity were generally cell walls or cell wall components (*6–14*). However, some authors have reported that cell walls could be less active than whole cells (*7, 11, 15*). With *S. aureus*, the antitumor activities of whole bacteria and peptidoglycan were similar. This demonstrates that the peptidoglycan is an important stimulant for tumor resistance.

The antitumor activity of peptidoglycans extracted from four gram-positive bacteria were compared: Only some peptidoglycans (from *B. megaterium* and *S. aureus*) enhanced

Table 7.—*Mitogenic activity of peptidoglycans in the absence[a] of T-cells*

Mitogen	Dose, μg/ml	SI			
		C3H/He		B6C3F$_1$	
		Unfractionated cells	T-cell-depleted	Unfractionated cells	T-cell-depleted
PHA	1	5.75	1.57	13.62	1.40
LPS	50	10.22	12.72	20.82	29.90
Peptidoglycan					
B. megaterium	50	4.51	7.08	4.23	5.20
S. aureus	50	3.41	3.44	3.98	3.99
C. poinsettiae	50	1.71	1.64	1.18	1.25
M. lysodeikticus	50	1.08	1.50	1.0	0.66

[a] T-cells were removed by treatment with anti-Thy 1.2 serum plus complement.

Table 8.—*Mitogenic activity of peptidoglycans on spleen cells from nude mice*

Mitogen	SI	
	C57BL/6	C57BL/6, *nu/nu*[a]
LPS	69.04	28.18
Peptidoglycan		
B. megaterium	3.93	2.42
S. aureus	2.81	3.23

[a] Female *nu/nu* mice were derived from brother × sister matings (Institute de Recherches Scientifiques sur le Cancer).

Table 9.—*Mitogenic activity of particulate and soluble peptidoglycans*

Mitogen	Dose, μg/ml	SI		
		C3H/He	C57BL/6	B6C3F$_1$
LPS	50	16.31	69.04	17.99
Particulate[a] peptidoglycan	1	1.59	1.22	0.68
	10	3.64	1.91	1.47
	50	7.55	3.93	3.11
	100	8.23	4.73	3.82
Soluble[b] peptidoglycan	1	2.25	1.10	1.17
	10	2.22	0.88	0.79
	50	1.60	1.10	1.07
	100	1.96	1.01	0.66

[a] Particulate peptidoglycan was extracted from *B. megaterium*.

[b] Soluble peptidoglycan was obtained from *B. megaterium* peptidoglycan after lysozyme treatment.

tumor rejection when administered sc. The others (from *M. lysodeikticus* and *C. poinsettiae*) possessed no antitumor effects. Identical results were found with two fibrosarcomas, both poorly immunogenic. These two tumors showed no hybrid resistance; thus we checked the action of the different peptidoglycans in hybrid F_1 mice under the same conditions as in syngeneic parents. Peptidoglycan from *S. aureus* was even more effective in rejecting tumors in F_1 hosts than in the parents; peptidoglycan from *M. lysodeikticus* had no antitumor effect on C3-9 tumor and a weak effect on B6-2 tumor. These results show that the peptidoglycan structure is essential in determining (stimulating) tumor resistance.

As for other immunostimulants, the route of injection is important for the expression of antitumor activity (*10, 24–26*). When tested ip, all the peptidoglycans were inactive. The absence of an intraperitoneal effect with peptidoglycans could be explained by the following two reasons: first, by the nature of the tumor (*27*) because the tested fibrosarcomas were not ascites tumors but grew in a solid form likely to be insensitive to the intraperitoneal treatment with peptidoglycan. The second reason could be the lack of a lipid component in the cell walls of gram-positive bacteria. It is well established that BCG and *C. parvum* possess an antitumor effect when given ip and that the lipid components of their cell walls seem responsible, at least in part, for their activity (*28, 29*). Moreover, some lipids can amplify the antitumor activity of mycobacterial cell wall components, chemically defined, such as cord factor (*10, 14*).

We have shown that ip peptidoglycans either had no effect or had induced tumor enhancement. Enhancement could be observed with all of the tested peptidoglycans, whatever their activity sc. When given ip, the peptidoglycans were in close contact with numerous macrophages. It is known that stimulation of macrophages can induce the release of lysozyme (*30, 31*), which could rapidly destroy the peptidoglycans, and this might explain the absence of a dose effect when peptidoglycans were given ip. As with other immunostimulants, the mechanism of occasional tumor promotion could be due to the induction of suppressor cells (*32–34*) and to the release of prostaglandins (*35, 36*), but the reason why these suppressive mechanisms occur only in some instances remains unknown.

Studies with synthetic derivatives of peptidoglycan have established that the structure of the peptide moiety is critical in the expression of adjuvant and mitogenic activities (*37*), and this is especially true for the first two amino acids of the peptide chain (*37–39*). We have shown that the peptidoglycans for which the peptide sequence begins with –LAla–DGlu (as for *B. megaterium*) or –LAla–DGluNH$_2$ (as for *S. aureus*) possess mitogenic and antitumor activities; such peptidoglycans also present adjuvant activity (Guenounou M, Goguel AF, Nauciel C: Submitted for publication). When the first amino acid is a glycine (as for *C. poinsettiae*) or when the α-carboxyl group of D-glutamic acid is linked to a glycyl residue (as for *M. lysodeikticus*), adjuvant and mitogenic activities are not expressed.

Mitogenic and antitumor activities were reduced by lysozyme treatment; this suggests that the polymerization increases the activity of the molecule (*40*) and that these biological effects are not related to the presence of contaminants. Our results and those obtained by Guenounou have shown that some peptidoglycans were mitogenic for B-cells from several strains of mice, unrelated to the LPS response.

These findings raise the problem of whether or not a correlation could exist between adjuvant, B-cell mitogenic, and antitumor activities. A direct role for B-cells in tumor rejection seems rather unlikely, because these tumors were poorly immunogenic and the role of antitumor antibodies in tumor defense is far from proved. But the same structure could be necessary to induce adjuvant activity and B-cell proliferation and to stimulate the cells involved in tumor resistance.

REFERENCES

(*1*) Likhite VV. The delayed and lasting rejection of mammary adenocarcinoma cell tumors in DBA/2 mice with use of killed *Bordetella pertussis*. Cancer Res 1974; 34:1027–1030.

(*2*) Bast RC Jr, Zbar B, Mackaness GB, Rapp HJ. Antitumor activity of bacterial infection. I. Effect of *Listeria monocytogenes* on growth of a murine fibrosarcoma. J Natl Cancer Inst 1975; 54:749–756.

(*3*) Tsuruo T, Iida H, Tsukagoshi S, Sakurai Y. Suppression of Friend leukemia virus by Bacillus Calmette-Guérin and a streptococcal preparation OK-432. Int J Cancer 1980; 25:131–136.

(*4*) Martin A, Toujas L, Le Garrec Y, Dazord L, Amice J. Resistance to tumor graft in mice treated with inactivated *Brucella abortus* cultured in smooth or rough phase. JNCI 1979; 62:123–127.

(*5*) Minden P, McClatchy JK, Brunda MJ. Suppression and immunotherapy of the guinea pig line-10 hepatocarcinoma mediated by nonviable *Staphylococcus aureus*. JNCI 1978; 61:535–538.

(*6*) Chedid L, Lamensans A, Parant F, et al. Protective effect of delipidated mycobacterial cells and purified cell walls against Ehrlich carcinoma and a syngeneic lymphoid leukemia in mice. Cancer Res 1973; 33:2187–2195.

(*7*) Zbar B, Ribi E, Meyer T, Azuma I, Rapp HJ. Immunotherapy of cancer: Regression of established intradermal tumors after intralesional injection of mycobacterial cell walls attached to oil droplets. J Natl Cancer Inst 1974; 52:1571–1577.

(*8*) Lamensans A, Chedid L, Lederer E, et al. Enhancement of immunity against murine syngeneic tumors by a fraction extracted from nonpathogenic mycobacteria. Proc Natl Acad Sci USA 1975; 72:3656–3660.

(*9*) Ribi EE, Granger DL, Milner KC, Strain SM. *Brief communication*: Tumor regression caused by endotoxins and mycobacterial fractions. J Natl Cancer Inst 1975; 55:1253–1257.

(*10*) Leclerc C, Lamensans A, Chedid L, et al. Nonspecific immunoprevention of L1210 leukemia by cord factor (6-6′ dimycolate of trehalose) administered in a metabolizable oil. Cancer Immunol Immunother 1976; 1:227–232.

(*11*) Ribi EE, Toubiana R, Strain SM, et al. Further studies on the structural requirements of agents for immunotherapy of the guinea pig line-10 tumor. Cancer Immunol Immunother 1978; 3:171–177.

(*12*) McLaughlin CA, Schwartzman SM, Horner BL, et al. Regression of tumors in guinea pigs after treatment with synthetic muramyl dipeptides and trehalose dimycolate. Science 1980; 208:415–416.

(*13*) Ogura T, Namba N, Hirao F, Yamamura Y, Azuma I. Association of macrophage activation with antitumor effect on rat syngeneic fibrosarcoma by *Nocardia rubra* cell wall skeleton. Cancer Res 1979; 39:4706–4712.

(*14*) Pimm MV, Baldwin RW, Lederer E. Suppression of an ascitic rat hepatoma with cord factor and *Nocardia* cell wall skeleton in squalene emulsions. Eur J Cancer 1980; 16:1645–1647.

(*15*) Riveros-Moreno V, Bomford R, Scott MT. Antitumor activity of purified cell walls from *Corynebacterium parvum*. J Natl Cancer Inst 1978; 60:653–658.

(*16*) Nauciel C, Goguel AF. Inhibition of tumor growth by the peptidoglycan from *Bacillus megaterium*. J Natl Cancer Inst 1977; 59:1723–1726.

(*17*) Schleifer KH, Kandler O. Peptidoglycan types of bacterial cell walls and their taxonomic implications. Bacteriol Rev 1972; 36:407–477.

(*18*) Nauciel C, Fleck J, Martin JP, Mock M, Nguyen-Huy H. Adjuvant activity of bacterial peptidoglycans on the production of delayed hypersensitivity and on antibody response. Eur J Immunol 1974; 4:352–356.

(19) Nauciel C, Fleck J. Adjuvant activity of bacterial peptidoglycans. Z Immunitaetsforsch 1975; 149:349–353.

(20) Damais C, Bona C, Chedid L, Fleck J, Nauciel C, Martin JP. Mitogenic effect of bacterial peptidoglycans possessing adjuvant activity. *J* Immunol 1975; 115:268–271.

(21) Schleifer KH, Kandler O. Zur chemischen Zusammensetzung der Zellwand der Streptokokken. I. Die aminosäure Sequenz des Mureins von *Str. thermophilus* und *Str. faecalis.* Arch Mikrobiol 1967; 57: 335–364.

(22) Nguyen-Huy H, Nauciel C, Wermuth CG. Immunochemical study of the peptidoglycan of gram-negative bacteria. Eur J Biochem 1976; 66:79–84.

(23) Reif AE, Allen JM. The AKR thymic antigen and its distribution in leukemias and nervous tissues. J Exp Med 1964; 120:413–433.

(24) Cleveland RP, Meltzer MS, Zbar B. Tumor cytotoxicity in vitro by macrophages from mice infected with *Mycobacterium bovis* strain BCG. J Natl Cancer Inst 1974; 52:1887–1895.

(25) Ghaffar A, Cullen RT. In vitro antitumor effect of lymphoid cells from *Corynebacterium parvum*-treated mice: Effect of route of *C. parvum* administration. J Natl Cancer Inst 1977; 58:717–720.

(26) Di Luzio NR, McNamee R, Browder WI, Williams D. Glucan: Inhibition of tumor growth and enhancement of survival in four syngeneic murine tumor models. Cancer Treat Rep 1978; 62:1857–1866.

(27) Mazurek C, Chalvet H, Stiffel C, Biozzi G. Study of the mechanism of *Corynebacterium parvum* antitumor activity. I. Protective effect on the growth of two syngeneic tumours. Int J Cancer 1976; 17: 511–517.

(28) Baldwin RW, Pimm MV. BCG in tumor immunotherapy. Adv Cancer Res 1978; 28:91–147.

(29) Milas L, Scott MT. Antitumor activity of *Corynebacterium parvum.* Adv Cancer Res 1978; 26:257–306.

(30) Gordon S, Todd J, Cohn ZA. In vitro synthesis and secretion of lysozyme by mononuclear phagocytes. J Exp Med 1974; 139:1228–1248.

(31) Kokoshis PL, Di Luzio NR. Serum lysozyme: An index of macrophage function. J Reticuloendothel Soc 1979; 25:85–99.

(32) Kirchner H, Glaser M, Herberman RB. Suppression of cell-mediated tumour immunity by *Corynebacterium parvum.* Nature 1975; 257: 396–398.

(33) Kirchner H, Holden HT, Herberman RB. Splenic suppressor macrophages induced in mice by injection of *Corynebacterium parvum.* J Immunol 1975; 115:1212–1216.

(34) Klimpel GR, Henney CS. BCG-induced suppressor cells. I. Demonstration of a macrophage-like suppressor cell that inhibits cytotoxic T cell generation in vitro. J Immunol 1978; 120:563–569.

(35) Humes JL, Bonney RJ, Pelus L, et al. Macrophages synthesis and release prostaglandins in response to inflammatory stimuli. Nature 1977; 269:149–151.

(36) Grimm W, Seitz M, Kirchner H, Gemsa D. Prostaglandin synthesis in spleen cell cultures of mice injected with *Corynebacterium parvum.* Cell Immunol 1978; 40:419–426.

(37) Chedid L, Audibert F, Johnson AG. Biological activities of muramyl dipeptide, a synthetic glycopeptide analogous to bacterial immunoregulating agents. Prog Allergy 1978; 25:63–105.

(38) Ellouz F, Adam A, Ciorbaru R, Lederer E. Minimal structure requirements for adjuvant activity of bacterial peptidoglycan derivatives. Biochem Biophys Res Commun 1974; 59:1317–1325.

(39) Chedid L, Audibert F, Lefrancier P, Choay J, Lederer E. Modulation of the immune response by a synthetic adjuvant and analogs. Proc Natl Acad Sci USA 1976; 73:2472–2475.

(40) Takada H, Tsujimoto M, Kotani S, et al. Mitogenic effects of bacterial cell walls, their fragments and related synthetic compounds on thymocytes and splenocytes of guinea pigs. Infect Immun 1979; 25:645–652.

blank page

Rat Hepatomas: Chemotherapy With Lycurim and Pyrazofurin[1,2,3]

May S. Lui,[4] Robert C. Jackson,[4] Ronald J. Harkrader,[4] *and* George Weber[4,5]

ABSTRACT—Hepatoma 8999 was sensitive to Lycurim [1,4-di-(methylsulfonyloxy-ethylamino)-1,4-dideoxy-*ms*-erythritol] with a mean lethal dose (LD_{50}) of 8.1×10^{-8} *M* for a 6-hour treatment in vitro. The drug dose lethal to 10% of the rats with Lycurim (10 mg/kg) injected ip 12 times into hepatoma 8999-bearing BUF rats at 10-day intervals provided a mean increase in life-span (ILS) of 156%. The more rapidly growing, less differentiated hepatoma 3924A was tenfold less sensitive to Lycurim in vitro, and three treatments in vivo (10 mg/kg given every 8 days) gave an ILS of only 18% in ACI/N rats. Bacause hepatoma 8999 had a high adenosine kinase activity, the effect of Pyrazofurin (PF; 3-*β*-D-ribofuranosyl-4-hydroxypyrazole-5-carboxamide) was examined in vitro: The LD_{50} was 8.5×10^{-8} *M* in a 6-hour exposure. In hepatoma 3924A, with a fifteenfold lower adenosine kinase, the LD_{50} was 22-fold higher. Three treatments with PF (4 mg/kg given every 2 days) in hepatoma 8999 caused an 18% ILS and no host toxicity, but in hepatoma 3924A no significant ILS was observed. Lycurim combined with PF (0.05 *μM* each) in hepatoma 8999 cells in vitro provided synergistic kill, but Lycurim and PF (0.3 and 1 *μM*, respectively) in hepatoma 3924A cells yielded summation. When 10 rats with hepatoma 8999 were treated 15 times with the optimal dose of Lycurim (7.5 mg/kg every 10½ days), 1-year survivors numbered 7. Alternate doses of Lycurim (7.5 mg/kg) and PF (3 mg/kg) at 5-day intervals for 4 months to 10 rats gave an ILS of 152% with eight 1-year survivors and no host toxicity.—JNCI 1982; 68:665–668.

Hepatomas in general are extremely refractory to chemotherapy (*1, 2*), and slowly growing hepatomas are usually less responsive to chemotherapy than are rapidly growing hepatomas. This report presents chemotherapy studies with two transplanted rat hepatomas: the rapidly growing, poorly differentiated hepatoma 3924A and the more slowly growing, moderately differentiated hepatoma 8999. The investigation was done with two agents: the antimetabolite PF (3-*β*-D-ribofuranosyl-4-hydroxypyrazole-5-carboxamide; NSC-143095) and the bifunctional alkylating agent Lycurim [1,4-di-(methylsufonyloxy-ethylamino)-1,4-dideoxy-*ms*-erythritol; NSC-122402].

PF (*3, 4*) inhibits growth of transplantable tumors in mice and rats (*4, 5*). It is converted by the action of adenosine kinase (*6*) to its active form pyrazofurin 5′-monophosphate, an inhibitor of orotidylate decarboxylase (*4*). Previous work in this laboratory suggested that PF could be useful in anticancer combination chemotherapy (*7, 8*). Dix et al. (*6*) reported that after injection of PF into mice and rats, the concentration of PF nucleotides in the liver and kidney was almost an order of magnitude higher than that in any other tissues tested. This result affords the potential for exploitation for chemotherapy in those neoplasms of the kidney and liver that still possess sufficient differentiated function to cause extensive accumulation of the biologically active analog nucleotides.

Lycurim (*9*) has been shown to inhibit several experimental tumor systems (*10, 11*). Clinical trials in Hungary suggested that Lycurim had activity against chronic lymphocytic leukemia and some solid tumors (*12*). Earlier work (*13*) indicated that alkylating agents and antimetabolites may often be used effectively in combination (complementary inhibition).

The purpose of the present study was to determine the effect of Lycurim and PF alone and combined on rat hepatomas in vitro and in vivo. A preliminary account of some of these results was presented in (*14*).

MATERIALS AND METHODS

Tumors and animals.—The neoplasms were solid hepatomas 8999 and 3924A. Hepatoma 8999 is moderately differentiated and has a medium growth rate with a transplant interval of 3.5 months. Hepatoma 3924A is more rapidly growing and poorly differentiated and has a transplant interval of 3–4 weeks. The tumor-bearing rats were obtained from Dr. H. P. Morris, Howard University, Washington, D.C. The properties of these tumors were described in (*15*). Hepatoma 8999 was carried in inbred BUF rats and hepatoma 3924A in inbred ACI/N rats. Animals were kept in separate cages and given water and Purina Laboratory Chow ad libitum.

Transplantation.—Approximately 10^6 cells were transplanted sc into the right flank of male rats weighing 100 g. Chemotherapy was begun 2 days after inoculation for hepatoma 3924A and 3 days after inoculation for hepatoma 8999. Ten or more rats were in each treatment group.

Cell culture.—The hepatoma 3924A and 8999R lines were originated in this laboratory from the solid tumor forms of these hepatomas. Both cell lines were grown in monolayer cultures in McCoy's 5-A medium supplemented with 10% fetal calf serum, 100 U penicillin/ml, and 100 μg streptomycin/ml. Hepatoma 3924A was subcultured twice a week; hepatoma 8999R was subcultured at weekly intervals. The log phase doubling time was 15 hours for hepatoma 3924A and 40 hours for hepatoma 8999R (*16*).

For colony assays, cells were exposed to the drug for 6 hours, and then 500 cells were seeded into fresh medium. Colonies were counted after 7 days (3924A) or 8 days (8999R) as described in (*8*).

Drugs and supplies.—Lycurim was provided by Dr. S.

ABBREVIATIONS USED: ILS=increase in life-span; LD_{50}=mean lethal dose; PF=Pyrazofurin.

---

[1] Received June 23, 1981; accepted November 2, 1981.

[2] Supported by Public Health Service grants CA-13526 and CA-05034 from the National Cancer Institute.

[3] Animals were maintained under the guidelines set forth by the Indiana University School of Medicine Animal Welfare Committee.

[4] Laboratory for Experimental Oncology, Indiana University School of Medicine, 1100 West Michigan St., Indianapolis, Ind. 46223.

[5] *Address reprint requests to* Dr. Weber.

Eckhardt, National Oncology Institute, Budapest, Hungary. It was dissolved in distilled water immediately before injection because saline accelerated its rate of decomposition. PF was donated by Eli Lilly & Co., Indianapolis, Ind. It was dissolved in physiologic saline. Tissue culture supplies were purchased from Grand Island Biological Co., Grand Island, N.Y., or from Flow Laboratories, Inc., Rockville, Md.; reagent chemicals were from Sigma Chemical Co., St. Louis, Mo.

RESULTS

Cytotoxicity of Lycurim and PF as Single Drugs to Hepatoma Cells In Vitro

The survival curve of logarithmically growing cells treated with Lycurim shows that, at low concentrations of the drug, hepatoma 8999R cells were more sensitive than 3924A cells (text-fig. 1). Survival for both cell lines dropped sharply at Lycurim concentrations higher than 3×10^{-7} *M*.

The differential sensitivity of the two cell lines to PF was even more pronounced (text-fig. 2). Survival dropped sharply for hepatoma 8999R cells at PF concentrations higher than 3×10^{-8} *M*, whereas there was still 75% survival for hepatoma 3924A cells at 10^{-6} *M* PF. The LD_{50} values of Lycurim and PF after 6 hours' treatment are summarized in table 1.

Cytotoxicity of Lycurim and PF Combinations to Hepatoma Cells In Vitro

In hepatoma 8999R cells, Lycurim at 5×10^{-8} *M* gave 68% survival and PF at 5×10^{-8} *M* yielded 65% survival. The two agents together resulted in 29% survival when 44% was the value predicted by summation (table 2). Treatment of hepatoma 8999R cells with Lycurim (2×10^{-8} *M*) and PF (3×10^{-8} *M*) also provided synergistic cell kill with a survival of 44%

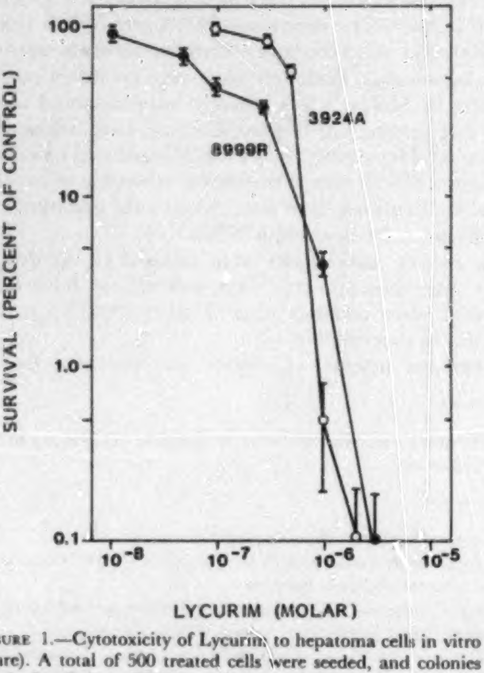

TEXT-FIGURE 1.—Cytotoxicity of Lycurim to hepatoma cells in vitro (6-hr exposure). A total of 500 treated cells were seeded, and colonies were counted after 7 days (3924A) or 8 days (8999R). *Vertical bars* indicate standard deviation.

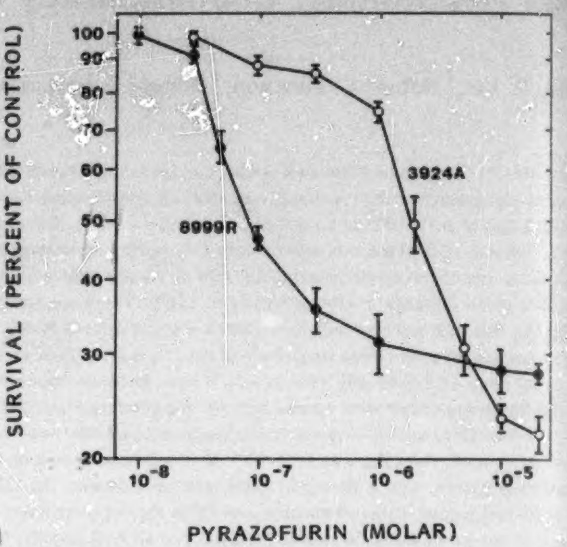

TEXT-FIGURE 2.—Cytotoxicity of PF to hepatoma cells in vitro (6-hr exposure). A total of 500 treated cells were seeded, and colonies were counted after 7 days (3924A) or 8 days (8999R). *Vertical bars* indicate standard deviation.

TABLE 1.—*LD_{50} values for 6-hour treatment as measured in colony assay*

Drugs	LD_{50} values for hepatoma cells	
	3924A	8999R
Lycurim	5.2×10^{-7} *M*	8.1×10^{-8} *M*
PF	1.9×10^{-6} *M*	8.5×10^{-8} *M*

TABLE 2.—*Cytotoxicity of Lycurim and PF combinations to hepatoma 8999R cells in vitro (6-hr treatment)*

Drugs (concentrations)	Measured colony count, % control	Predicted for summation[a]
Lycurim (2×10^{-8} *M*)	83	
PF (3×10^{-8} *M*)	92	
Lycurim (2×10^{-8} *M*) + PF (3×10^{-8} *M*)	44	76
Lycurim (5×10^{-8} *M*)	68	
PF (5×10^{-8} *M*)	65	
Lycurim (5×10^{-8} *M*) + PF (5×10^{-8} *M*)	29	44

[a] Assuming summation as defined by Webb (*17*).

By contrast, in hepatoma 3924A cells, the combinations of Lycurim and PF were only summative (table 3).

Chemotherapy of Hepatoma 8999 In Vivo

Table 4 compares the treatment of hepatoma 8999-bearing rats with different dosage levels of Lycurim and PF.

TABLE 3.—*Cytotoxicity of Lycurim and PF combinations to hepatoma 3924A cells in vitro (6-hr treatment)*

Drugs (concentrations)	Measured colony count, % control	Predicted for summation[a]
Lycurim (3×10^{-7} *M*)	84	
PF (1×10^{-6} *M*)	76	
Lycurim (3×10^{-7} *M*) + PF (1×10^{-6} *M*)	60	66
Lycurim (5×10^{-7} *M*)	56	
PF (2×10^{-6} *M*)	48	
Lycurim (5×10^{-7} *M*) + PF (2×10^{-6} *M*)	35	27

[a] Assuming summation as defined by Webb (*17*).

TABLE 4.—*Chemotherapy of hepatoma 8999 in vivo*

Treatment and dose regimen[a]	No. of toxic deaths/total No. of rats treated	ILS,[b] %	No. of 1-yr survivors/total No. of rats treated
Lycurim (15 mg/kg) given every 10 days (8 treatments)	8/10	38	1/10
Lycurim (12.5 mg/kg) given every 10 days (8 treatments)	8/10	125	0/10
Lycurim (10 mg/kg) given every 10½ days (15 treatments)	1/10	156	2/10
Lycurim (7.5 mg/kg) given every 10½ days (15 treatments)	0/10	164	7/10
Lycurim (10 mg/kg), single dose	2/10	38	0/10
PF (4 mg/kg) given every 2 days (3 treatments)	0/10	18	0/10
PF (6 mg/kg) given every 10 days (12 treatments)	1/10	17	0/10
Lycurim (7.5 mg/kg)+PF (3 mg/kg), single dose	2/10	30	0/10
Lycurim (7.5 mg/kg)+PF (3 mg/kg) given every 10½ days (15 treatments)	4/10	159	1/10
Lycurim (7.5 mg/kg)+PF[c] (3 mg/kg) given every 10½ days (15 treatments)	0/10	152	8/10

[a] Tumors were implanted at the same time, and rats were randomized between the groups. Treatment commenced 3 days after inoculation. Drugs were administered ip.

[b] Life-span of control rats was 124±18 days (mean ± SD for 30 rats). For calculation of ILS, 1-year survivors were counted as 365 days.

[c] PF doses were given 5 days after Lycurim.

Eight treatments with Lycurim at 15 mg/kg every 10 days or at 12.5 mg/kg every 10 days were very toxic to hepatoma 8999-bearing rats. Only 2 of 10 rats survived in each group with an ILS of 38 and 125%, respectively. Lycurim at 10 mg/kg was much less toxic. A single dose of Lycurim (10 mg/kg) yielded only a 38% ILS, whereas a similar dosage given every 10½ days (15 treatments) resulted in a 156% ILS with two 1-year survivors. The same schedule of Lycurim at 7.5 mg/kg produced no toxic death and increased the ILS to 164%, and there were seven 1-year survivors of 10 rats treated. Three treatments with PF at 4 mg/kg given every 2 days resulted in an 18% ILS in hepatoma 8999-bearing rats. Increasing the dose to 6 mg/kg given every 10 days (12 treatments) led to one toxic death with no increase in ILS. PF by itself resulted in no 1-year survivors.

Although neither Lycurim (7.5 mg/kg) nor PF (4 mg/kg) caused any toxic deaths when given alone, the combination was toxic in hepatoma 8999-bearing rats. Therefore, the dose of PF administered in combination with Lycurim was lowered to 3 mg/kg. A single dose of Lycurim (7.5 mg/kg) plus PF (3 mg/kg) yielded two toxic deaths among 10 rats treated. The ILS of 30% was observed with no long-term survivors. The same combination when given every 10½ days (15 treatments) was more effective with a 159% ILS and one 1-year survivor, although it increased the toxicity to the rats. The same dose when injected sequentially (PF given 5 days after Lycurim) did not further increase the ILS, but there were eight 1-year survivors among 10 rats treated. This schedule also reduced the toxicity of these drugs. Some of these data are presented in text-figure 3.

Chemotherapy of Hepatoma 3924A In Vivo

Lycurim at 10 mg/kg and 7.5 mg/kg yielded one toxic death among 10 rats treated. PF at 8 mg/kg also led to one toxic death. The two agents together were much more toxic than when they were used alone. Lycurim at 10 mg/kg with either 6 or 8 mg/kg PF was very toxic in ACI/N rats; among 10 rats in each group, there were five and seven toxic deaths, respectively. Lowering the dose of Lycurim in these combinations to 7.5 mg/kg reduced the number of toxic deaths to 1 and 2 rats, respectively.

Table 5 compares the treatment of hepatoma 3924A-bearing rats with different dosage levels and schedules of Lycurim and PF. Lycurim was less toxic in hepatoma 3924A-bearing rats than in hepatoma 8999-bearing rats. However, it was also less effective, resulting in only a 16–18% ILS. PF by itself was more toxic in tumor-bearing rats than in normal rats. Three treatments with PF at 6 mg/kg given every 2 days resulted in five toxic deaths and a 29% ILS. A single dose of Lycurim (10 mg/kg) and PF (4 mg/kg) resulted in three toxic deaths with a 12% ILS. A second treatment at the same dosage failed to improve survival among these rats.

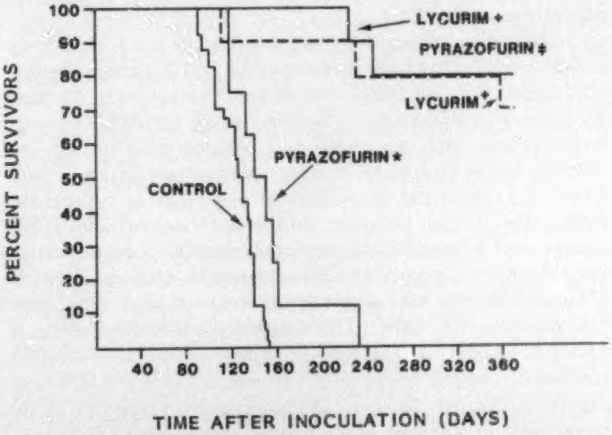

TEXT-FIGURE 3.—Chemotherapy of hepatoma 8999 in vivo. *=PF (4 mg/kg) given every 2 days (3 treatments). †=Lycurim (7.5 mg/kg) given every 10½ days (15 treatments). ‡=Lycurim (7.5 mg/kg)+PF given every 10½ days (16 treatments), with PF injected 5 days after Lycurim.

TABLE 5.—*Chemotherapy of hepatoma 3924A in vivo*

Treatment and dose regimen[a]	No. of toxic deaths/ total No. of rats treated	ILS,[b] %
Lycurim (10 mg/kg) given every 8 days (2 treatments)	0/10	18
Lycurim (15 mg/kg) given every 8 days (2 treatments)	1/10	16
Lycurim (20 mg/kg) given every 10 days (2 treatments)	7/10	13
PF (6 mg/kg) given every 2 days (3 treatments)	5/10	29
Lycurim (10 mg/kg)+PF (4 mg/kg) given every 10 days (2 treatments)	3/10	3
Lycurim (10 mg/kg)+PF (4 mg/kg), single dose	3/10	12

[a] Tumors were implanted at the same time, and rats were randomized between the groups. Treatment commenced 1 day after inoculation. Drugs were administered ip.

[b] Life-span of control rats was 36±4 days (mean ± SD) for 30 rats.

DISCUSSION

Because many of the enzymatic properties of hepatoma 8999 closely resemble those of moderately differentiated human hepatocellular carcinomas (*18*), we believe that this experimental system may provide a useful model for developing chemotherapy against the human disease. Lycurim, which in the optimal protocol gave 7 long-term survivors among 10 rats treated (when treatment was commenced 3 days following implantation), is the most effective single agent found so far for treatment of hepatoma 8999. Although rapidly growing tumors are frequently more responsive to alkylating agents than are more slowly growing neoplasms, hepatoma 3924A was less sensitive to Lycurim both in vitro and in vivo than was hepatoma 8999. The reason for this anomaly is not known.

Hepatoma 3924A was also much less sensitive in vitro to PF than was hepatoma 8999. This difference was probably a consequence of the higher adenosine kinase activity of hepatoma 8999 (*19*).

An effective strategy in combination chemotherapy is to utilize a cell cycle-phase-specific agent with a phase-nonspecific agent. For this reason we studied the action of PF and Lycurim in combination. The effect of an antimetabolite in combination with an agent that causes macromolecular damage has been termed "complementary inhibition." Sartorelli (*13*) reported a number of examples of synergistic interaction in vivo between antimetabolites and alkylating agents, and Schabel and Laster (*20*) described the potentiation of alkylating agents by 6-thioguanine. Our results with PF and Lycurim are unusual, however, in that synergism was obtained in vitro. This combination will provide a valuable model system for the study of the biochemical mechanism of the interaction between antimetabolites and alkylating agents. In vivo, the combination appears to be more toxic to the host animal than either agent used separately (tables 4, 5). This toxicity could be decreased by the administration of PF 5 days after Lycurim, and this combination gave a slightly better result than the best regimen of Lycurim alone. The 1-year survivors were tumor-free and appear to represent "cures." It is likely that this protocol is not yet optimal, and in future work we shall study the schedule dependence in greater detail. Important questions to be answered are to what extent may PF be replaced by other antimetabolites and Lycurim by other alkylating agents.

REFERENCES

(*1*) FALKSON G. Therapeutic approaches to hepatoma. Cancer Treat Rev 1975; 2:73–76.

(*2*) LOONEY WB, SCHAFFNER JG, TREFIL JS, KOVACS CJ, HOPKINS HA. Solid tumour models for the assessment of different treatment modalities. IV. The combined effects of radiation and 5-fluorouracil. Br J Cancer 1976; 34:254–261.

(*3*) GERZON K, WILLIAMS RH, HOEHN M, GORMAN M, DELONG DC. Pyrazomycin, a C-nucleoside with antiviral activity. In: Proceedings of the second international congress on heterocyclic chemistry, Montpelier, France, 1969:131.

(*4*) GUTOWSKI GE, SWEENEY MJ, DELONG DC, HAMILL RL, GERZON K. Biochemistry and biological effects of pyrazofurins (pyrazomycins): Initial clinical trial. Ann NY Acad Sci 1975; 255:544–551.

(*5*) SWEENEY MJ, DAVIS FA, GUTOWSKI GE, HAMILL RL, HOFFMAN DH, POORE GA. Experimental antitumor activity of pyrazomycin. Cancer Res 1973; 33:2619–2623.

(*6*) DIX DE, LEHMAN CP, JAKUBOWSKI A, MOYER JD, HANDSCHUMACHER RE. Pyrazofurin metabolism, enzyme inhibition, and resistance in L5178Y cells. Cancer Res 1979; 39:4485–4490.

(*7*) LUI MS, JACKSON RC, WEBER G. Enzyme pattern-directed chemotherapy; effects of antipyrimidine combinations on the ribonucleotide content of hepatomas. Biochem Pharmacol 1979; 28:1189–1195.

(*8*) OLAH E, LUI MS, TZENG DY, WEBER G. Phase and cell cycle specificity of Pyrazofurin action. Cancer Res 1980; 40:2869–2875.

(*9*) HORVATH T, VARGHA L. New alkylsulfonic acid esters with cytostatic activity. Acta Un Int Cancr 1964; 20:71–75.

(*10*) GOLDIN A, WOOD HB, ENGLE RR. Relation of structure of purine and pyrimidine nucleosides to antitumor activity. Cancer Chemother Rep 1968; 1 (part 2):1–272.

(*11*) SANDBERG J, GOLDIN A. Antileukemic action of a new sugar derivative dimethanesulfonate (NSC-122402) and related compounds in mice. Cancer Chemother Rep 1969; 53:367–376.

(*12*) HINDY I, SELLEI C, ECKHARDT S, SZENTKLARAY J, HARTAI F. Investigations with 1,4-bis-(2′-mesyloxyethylamino)-1,4-dideoxy-*meso*-erythritol (R-74). Neoplasma 1971; 18:277–282.

(*13*) SARTORELLI AC. Some approaches to the therapeutic exploitation of metabolic sites of vulnerability of neoplastic cells. Cancer Res 1969; 29:2292–2299.

(*14*) JACKSON RC, LUI MS, WEBER G. Experimental chemotherapy of rat hepatomas with Lycurim and Pyrazofurin. Proc Am Assoc Cancer Res 1981; 22:251.

(*15*) MORRIS HP, WAGNER BP. Induction and transplantation of rat hepatomas with different growth rate (including "minimal deviation" hepatomas). Methods Cancer Res 1968; 4:125–152.

(*16*) JACKSON RC, WILLIAMS JC, WEBER G. Enzyme pattern-directed chemotherapy: Synergistic interaction of 3-deazauridine with D-galactosamine. Cancer Treat Rep 1976; 60:835–843.

(*17*) WEBB JL. Enzyme and metabolic inhibitors. Vol 1. New York: Academic Press, 1963:507–512.

(*18*) WEBER G, MALT RA, GLOVER JL, WILLIAMS JC, PRAJDA N, WAGONER CD. Biochemical basis of malignancy in man. In: Davis W, Maltoni C, eds. Biological characterization of human tumours. Amsterdam: Excerpta Medica, 1976:60–72.

(*19*) JACKSON RC, MORRIS HP, WEBER G. Adenosine kinase and adenosine deaminase in rat hepatomas and kidney tumours. Br J Cancer 1978; 37:701–713.

(*20*) SCHABEL FM, LASTER WR. Therapeutic synergism (TS) of 6-thioguanine (6-TG) in combination with alkylating agents against leukemia L1210. Proc Am Assoc Cancer Res 1980; 21:271.

Liver Tumors Induced by a New Beta-Adrenoreceptor Blocking Agent in Female Rats[1,2,3]

Giovanni Ragnotti,[4] Marco Presta,[4] Laura Riboni,[4] *and* Teresa Zavanella[5,6]

ABSTRACT—A newly synthesized beta-adrenoreceptor blocking agent, DL-1-(2-nitro-3-methyl-phenoxy)-3-*tert*-butylamino-propan-2-ol (ZAMI 1305), administered intragastrically for 6 months induced hepatocellular carcinomas in female outbred Wistar rats in a dose-dependent fashion but was harmless to the livers of male outbred Wistar rats. Experiments with castrated animals confirmed the dependence of the carcinogenic effect of ZAMI 1305 on the hormonal status of the rat. When an isomer of ZAMI 1305, DL-1-(2-nitro-5-methyl-phenoxy)-3-*tert*-butylamino-propan-2-ol (ZAMI 1327), and DL-practolol, which have pharmacologic activities similar to those of ZAMI 1305, were administered by the same experimental technique as used for ZAMI 1305, no liver tumors appeared either in male or female rats.—JNCI 1982; 68: 669–672.

Tumor-promoting (*1*) or oncogenic (*2, 3*) activities of some beta-adrenoreceptor blocking agents have been reported. The suggestion that the oncogenic activity of these agents is related to their pharmacologic properties rather than to other mechanisms (*4*) is very disturbing from a clinical point of view. This suggestion seems to go along with the facts that those beta-blocking agents suspected to be oncogenic have rather different chemical structures and that a well-known hepatocarcinogen, 2-acetylaminofluorene (*5*), has been shown to have a beta-adrenoreceptor blocking activity (*6*).

Therefore, we investigated two newly synthesized molecules, ZAMI 1305 and ZAMI 1327, which have a comparable beta-adrenoreceptor blocking activity (*7*) and differ very slightly in their chemical structure (text-fig. 1), in their capacity to induce neoplastic transformation. Practolol, for which there are some indications of tumorigenicity in rodents (*3*), was included in the experiment for comparison.

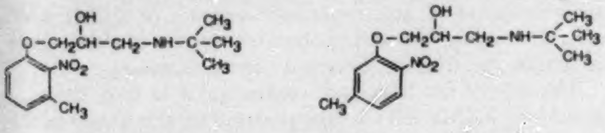
ZAMI 1305 ZAMI 1327

TEXT-FIGURE 1.—Chemical structure of ZAMI 1305 and ZAMI 1327.

MATERIALS AND METHODS

In a first experiment, outbred Wistar rats, 160 females and 160 males (Nossan, Correzzana, Italy) weighing 60–70 g each, were used. They were maintained on a complete standard diet of laboratory chow (Nossan) and water ad libitum. Constant temperature (22–24°C) and alternating periods of 12-hour dark and 12-hour light were also maintained. The animals were distributed at random into 8 groups for each sex (20 animals/group). One group was kept as a control, 1 group was treated with DL-practolol (300 mg/kg body wt/day), and the others were treated with ZAMI 1305 or ZAMI 1327 (25, 50, or 100 mg/kg body wt/day) for 6 months. ZAMI 1305, ZAMI 1327 (99.9% purity), and DL-practolol were gifts from Zambeletti S.p.A., Baranzate, Italy. The drugs, dissolved in 1% carboxymethylcellulose, were administered intragastrically (1 ml/100 g body wt). Control rats received the same volume of 1% carboxymethylcellulose. At the end of the treatment, surviving animals were bled to death and autopsied. Liver, lungs, and spleen were fixed in 12% neutral Formalin, and paraffin sections were stained with H & E.

In a second experiment, ZAMI 1305 was administered intragastrically at a dose of 100 mg/kg body weight/day to 16 castrated male rats treated im with 1 μg 17β-estradiol/day and 1 mg progesterone/day and to 14 ovariectomized female rats treated im with 100 μg testosterone/day. Hormone treatment was initiated immediately after surgery and continued throughout the experimental period. ZAMI 1305 administration was initiated 1 week after surgery. Controls were 11 male and 11 female intact rats treated with the same amount of ZAMI 1305. Some of the animals died or were killed after 2–5 weeks. The remaining animals were killed after 12 weeks. The animals were autopsied, livers were fixed in 12% Formalin, and paraffin sections were stained with H & E.

Liver lesions were histologically typed according to the classification of rat liver lesions suggested by the National Academy of Sciences (*8*).

RESULTS

Intact Animals

During the first month of treatment, 3–6 female rats treated with different doses of ZAMI 1305 (table 1) died with signs of hepatic failure. No other females died subsequently. No mortality was observed in male rats treated with ZAMI 1305 and in male and female rats treated with ZAMI 1327 and DL-practolol.

ABBREVIATIONS USED: H & E=hematoxylin and eosin; ZAMI 1305=DL-1-(2-nitro-3-methyl-phenoxy)-3-*tert*-butylamino-propan-2-ol; ZAMI 1327=DL-1-(2-nitro-5-methyl-phenoxy)-3-*tert*-butylamino-propan-2-ol.

---

[1] Received July 20, 1981; accepted October 22, 1981.

[2] Guidelines for the care and use of laboratory animals were followed as set forth by the International Commission on Laboratory Animals.

[3] Part of this work was presented to the Fifteenth Italian Congress of Pathology, Sorrento, October 16–20, 1979.

[4] Patologia Generale (EULO), Institute of Biomedical Sciences, Faculty of Medicine, University of Milan, via Valsabbina, 19, 25100 Brescia, Italy.

[5] Institute of Zoology, Faculty of Sciences, University of Milan, 20133 Milan, Italy.

[6] We thank Zambeletti S.p.A. (Baranzate, Italy) for financial support and Dr. P. Torchio (Zambeletti Research Laboratories) for laboratory assistance.

TABLE 1.—*Liver tumor prevalence in female rats treated with ZAMI 1305 for 6 months*

ZAMI 1305, mg/kg body wt/day	No. of surviving animals[a]	Relative liver wt, g/100 g body wt, mean ± SEM	No. of animals with: Neoplastic nodules (%)	Hepatocellular carcinoma (%)	Lung metastases
0	17	2.4 ± 0.1	0	0	0
25	17	3.5 ± 0.1[b]	7 (41)	1 (6)	0
50	18	4.3 ± 0.2[b]	13 (72)	5 (28)	0
100	14	6.5 ± 0.9[b]	12 (86)	9 (64)	4[c]

[a] No. of animals at start of experiment, 20. Rats that died during the experiment were excluded.

[b] Treated rats statistically different vs. the controls ($P<0.01$) as assessed by analysis of variance.

[c] Peritoneal spread was also present in 1 animal.

After 6 months, dose-related gross liver changes were present in female rats treated with ZAMI 1305. The liver was increased in weight (table 1) and there were whitish nodules of varying sizes (1–5 mm in diameter) at the capsular and cut surface, with hemorrhagic and cystic areas. Histologically, poorly differentiated to well-differentiated hepatocellular carcinomas (fig. 1), sometimes with areas with adenomatous patterns, were found in dose-dependent numbers (table 1). Lung metastases (figs. 2, 3) were present in 4 animals, and 1 animal also had peritoneal spread. Marked splenic enlargement, due to the presence of extensive foci of hematopoiesis, was observed in those females with large, metastatic tumors.

No liver changes were detected on gross and histologic examination in male rats given ZAMI 1305, in rats of either sex treated with ZAMI 1327 and DL-practolol, or in the controls.

Castrated Animals

To substantiate the role of the hormonal environment in liver carcinogenesis by ZAMI 1305, we administered the drug for a maximum of 3 months to 17β-estradiol–progesterone-treated castrated male rats and to testosterone-treated ovariectomized female rats. Histologic modifications of the livers of these animals were compared to those observed in male and female intact rats given the same dose of ZAMI 1305.

TABLE 2.—*Liver lesions in castrated male rats and ovariectomized female rats treated with ZAMI 1305[a] for 3 months*

Sex	Castrated or ovariectomized[b]	No. of animals	Oval cell hyperplasia	Clear cell foci	Neoplastic nodules
Male	No	5	0	1	0
Male	Yes	3	3	1	2
Female	No	3	3	2	3
Female	Yes	5	0	1	0

[a] All the animals were treated with 100 mg ZAMI 1305/kg body wt/day.

[b] Castrated males were treated im with 1 μg 17β-estradiol/day and 1 mg progesterone/day. Ovariectomized females were treated im with 100 μg testosterone/day.

The temporal sequence of early pathologic changes in the livers of castrated male and intact female rats mirrored that generally found after treatment with hepatic carcinogens (*8*). After 2–5 weeks of treatment, oval cell hyperplasia, tubular arrangement of the hepatocytes, and foci of acidophilic cells and of clear cells were found. After 3 months, neoplastic nodules (fig. 4) were present in most of the animals (table 2). In ovariectomized female and in intact male rats, small foci of clear cells or basophilic cells were occasionally detected.

DISCUSSION

Our results demonstrate that ZAMI 1305, a newly synthesized beta-adrenoreceptor blocking agent (*7*), when administered daily for 6 months, induces hepatocellular carcinomas in female outbred Wistar rats in a dose-dependent fashion but is ineffective in male outbred Wistar rats.

Other chemical carcinogens have been shown to have different oncogenic capacities in male and female rats (*9*). This difference has been ascribed either to a different metabolism of the molecules (*10, 11*) in the two sexes or to the sex-hormone status (*12, 13*). As for ZAMI 1305, its different oncogenic capacity in the two sexes does not seem to be related to a different metabolism of the molecule. We have in fact found (Presta M, Riboni L, Aletti MG: Unpublished data) that within month 1 of treatment the same metabolites of ZAMI 1305 (2-nitro-3-methyl-phenoxy-propan-1,2-diol, 2-nitro-3-methyl-phenoxy-ethyl-amino-propan-2-ol, and 2-amino-3-methyl-phenoxy-*tert*-butylamino-propan-2-ol) are found in the urine of rats of both sexes. However, Passetti et al. (*14*) reported an incapacity of female rats to metabolize ZAMI 1305 after a 6-month treatment, which could be due to a reduced capacity of the female neoplastic liver to metabolize this substance. An impaired capacity of hepatomas to metabolize foreign chemicals has in fact been reported (*15*).

Also, the *Salmonella*/microsome test of Ames (*16*) did not show evidence of any mutagenic activity of ZAMI 1305 after activation with microsomes from livers of either male or female rats (Sora S: Personal communication).

The role of the hormonal environment in liver carcinogenesis by ZAMI 1305 is substantiated by the results of the experiments with hormone-treated castrated animals. Surgery and hormone treatment in fact completely reverse the response to ZAMI 1305. After 3 months of treatment, neoplastic nodules were present in the livers of both intact female and 17β-estradiol–progesterone-treated castrated male rats, whereas only minor histologic alterations were observed in the livers of male and testosterone-treated ovariectomized female rats. Although we cannot exclude the possibility that a longer period of treatment or a different experimental scheme from the one adopted in this work could result in oncogenicity for ZAMI 1305 also in male rats, the data presented strongly suggest that the oncogenic effectiveness of ZAMI 1305 is related to the sex-hormone status of the animal.

No liver lesions were observed either in female or male rats after a 6-month treatment with DL-practolol and ZAMI 1327, an isomer of ZAMI 1305. However, in 2 of 5 female rats given ZAMI 1327 at a higher dose (400 mg/kg body wt/day) very small foci of basophilic cells were occasionally detected (Zavanella T: Unpublished observations).

As for the more general problem of the carcinogenic risk of beta-adrenoreceptor blocking agents, although our data failed to show evidence of tumor growth after administration of ZAMI 1327 and DL-practolol, the results obtained with ZAMI 1305 seem to indicate that, in agreement with previous reports (*3, 4*), this class of substances must be considered potentially oncogenic, at least under some defined conditions.

The study of the mechanism(s) underlying the observed different oncogenic capacities of ZAMI 1305 and ZAMI 1327, molecules having a similar pharmacologic activity (*7*) and differing very slightly in their chemical structures, should be elucidating if the suggested oncogenicity of beta-blockers is related to some specific characteristics of their chemical structures or to their pharmacologic activities.

REFERENCES

(*1*) Body H, Martin TL. The effect of propranolol on induction of rat liver tumors by a chemical carcinogen. Mol Pharmacol 1977; 13: 576–578.

(*2*) Paget GE. Carcinogenic action of pronethalol. Br Med J 1963; 16: 1266–1267.

(*3*) Food and Drug Administration. Status report on beta-blockers. FDA Drug Bull 1978; 8:13.

(*4*) Frishman W, Silverman R, Strom J, Elkayam U, Sonnenblick E. Clinical pharmacology of the new beta-adrenergic blocking drugs. Part 4. Adverse effects. Choosing a β-adrenoreceptor blocker. Am Heart J 1979; 98:256–262.

(*5*) Weisburger EK, Weisburger JH. Chemistry, carcinogenicity and metabolism of 2-fluorenamine and related compounds. Adv Cancer Res 1958; 5:331–431.

(*6*) Gurkalo VK, Pliss GB. The influence of chemical carcinogens on the physiological effects of adrenomimetics. Vopr Onkol 1978; 24: 49–53 (in Russian).

(*7*) Clavenna G, Visentin L, Romano A, Scrollini F. Attività beta-bloccante di due nuovi arilossi-alchil-amino-propanoli. In: Società Italiana di Farmacologia, ed. Atti del XIX Congresso della Società Italiana di Farmacologia. Ancona: Grafiche Bellomo, 1978:559.

(*8*) Institute of Laboratory Animal Resources, National Research Council, National Academy of Sciences. Histologic typing of liver tumors of the rat. JNCI 1980; 64:177–206.

(*9*) Toh YC. Physiological and biochemical reviews of sex differences and carcinogenesis with particular reference to the liver. Adv Cancer Res 1973; 18:155–209.

(*10*) Weisburger EK, Grantham PH, Weisburger JH. Differences in the metabolism of *N*-hydroxy-*N*-2-fluorenylacetamide in male and female rats. Biochemistry 1964; 3:808–812.

(*11*) DeBaun JR, Miller EC, Miller JA. *N*-Hydroxy-2-acetylaminofluorene sulfotransferase: Its probable role in carcinogenesis and in protein-(methion-S-yl) binding in rat liver. Cancer Res 1970; 30: 577–595.

(*12*) Firminger HI, Reuber MD. Influence of adrenocortical, androgenic, and anabolic hormones on the development of carcinoma and cirrhosis of the liver in A × C rats fed *N*-2-fluorenylacetamide. J Natl Cancer Inst 1961; 27:559–595.

(*13*) Morris HP, Firminger HI. Influence of sex and sex hormones on development of hepatomas and other hepatic lesions in strain A × C rats ingesting 2-diacetylaminofluorene. J Natl Cancer Inst 1956; 16:927–949.

(*14*) Passetti GL, Grassi F, Trebbi A. Metabolism of an aryloxy beta blocking drug. In: Frigerio A, ed. Recent developments in mass spectrometry in biochemistry and medicine. Vol 2. New York: Plenum, 1979:53–68.

(*15*) Adamson RH, Fouts JR. The metabolism of drugs by hepatic tumors. Cancer Res 1961; 21:667–671.

(*16*) Ames BN, Mccann J, Yamasaki E. Methods for detecting carcinogens and mutagens with the *Salmonella*/mammalian-microsome mutagenicity test. Mutat Res 1975; 31:347–364.

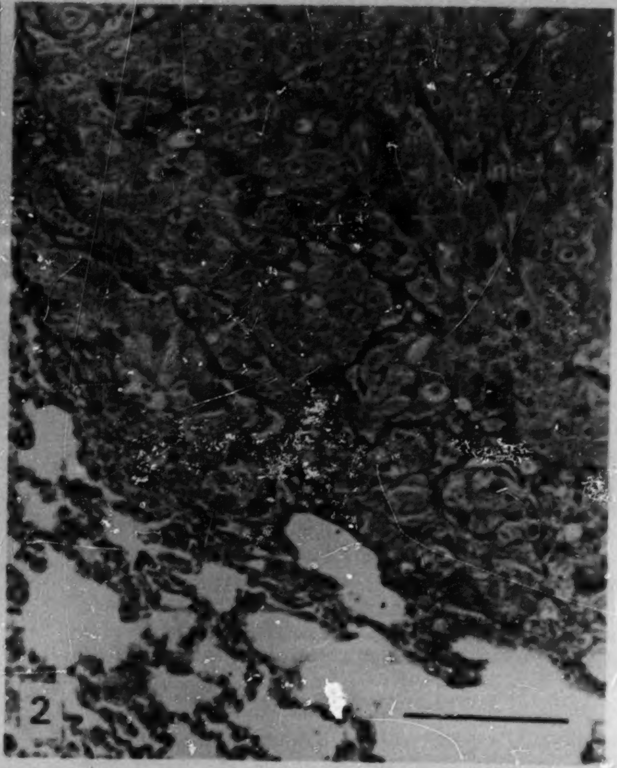

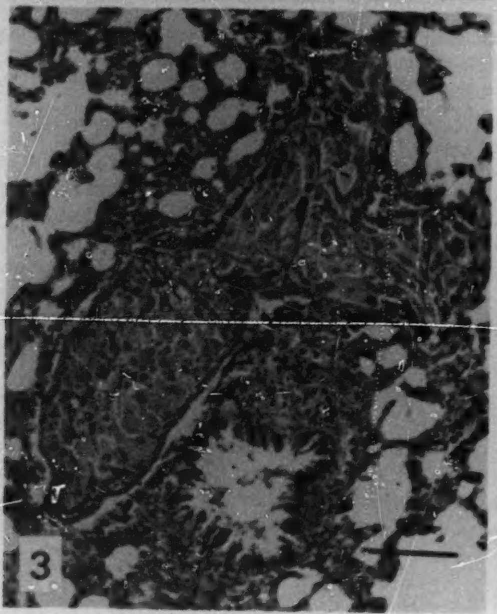

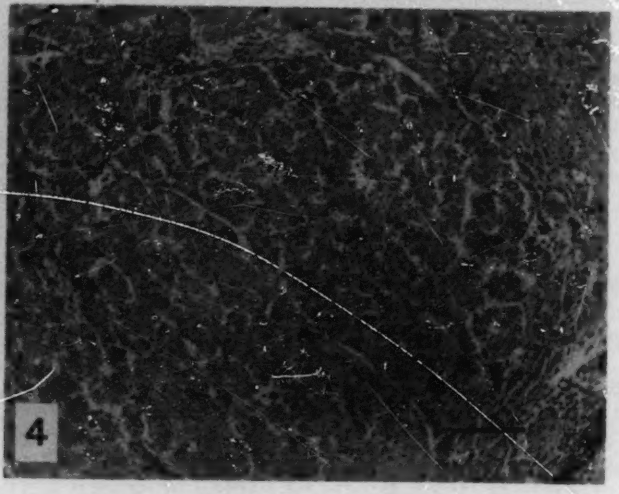

FIGURE 1.—Hepatocellular carcinoma in a female rat treated with 100 mg ZAMI 1305/kg body wt/day for 6 mo. H & E. *Bar*=0.1 mm. × 220

FIGURE 2.—Lung metastasis in a female rat treated as described in fig. 1. H & E. *Bar*=0.1 mm. × 240

FIGURE 3.—Tumor embolism in a pulmonary blood vessel of a female rat treated as described in fig. 1. H & E. *Bar*=0.1 mm. × 140

FIGURE 4.—Neoplastic nodule in the liver of a 17β-estradiol–progesterone-treated castrated male rat given ZAMI 1305 for 3 mo. H & E. *Bar*=0.1 mm. × 110

Mechanisms of Immunologic Eradication of a Syngeneic Guinea Pig Tumor. I. Quantitative Analysis of Adoptive Immunity[1,2]

Suyu Shu,[3,4] James T. Hunter,[3] Herbert J. Rapp,[3,5] *and* Leila S. Fonseca[3,6]

ABSTRACT—Adoptive immunity against a syngeneic hepatoma (line-10) of Sewall-Wright inbred strain 2 guinea pigs was analyzed by a two-dimensional titration of iv transferred immune lymphoid cells versus intradermal tumor challenges. Tumor resistance increased exponentially as a function of the number of immune lymphoid cells transferred. Within the tumor challenge doses analyzed, suppression of tumor growth mediated by the transferred immune lymphoid cells appeared to be independent of the primary immune response in the recipient. Quantitatively, rejection of a given number of tumor cells reflected the number of transferred immune cells and was independent of the presence of the same tumor at other skin sites. There was no evidence indicating that transferred immune cells were attracted specifically to the tumor inoculation site. The number of tumor cells that could be rejected at a skin site by adoptive immunity was greater than the estimated number of immune lymphoid cells present at the challenge site.—JNCI 1982; 68:673–680.

The adoptive transfer of specifically sensitized lymphoid cells is a potential means of specific cancer immunotherapy. Transfer to naive syngeneic animals of genetically compatible lymphoid cells specifically sensitized to tumor rejection antigens has prevented the growth of inoculated tumors, caused regression of established local tumors, and eradicated metastases (*1–4*). The requirement for syngeneic or autologous cells for adoptive immunity has limited the applicability of this approach in the treatment of humans with cancer (*5*). The recent development of in vitro methods that permit replication of T-lymphocytes (*6, 7*) that retain immunologic reactivity (*8–11*) has led to renewed interest in the use of adoptive immunity for cancer treatment.

Although previous studies have established its therapeutic efficacy, the mechanism of adoptive immunity against tumors remains an enigma. Direct killing of malignant cells by transferred immune lymphocytes has been postulated and generally accepted as an in vivo mechanism of tumor eradication since several types of neoplastic cells are lysed upon contact with immune lymphoid cells in vitro (*12–15*). In a previous study (*16*), we demonstrated that two major components of cell-mediated tumor immunity, in vitro cytotoxicity and adoptive immunity, reflected separate activities of two different lymphoid cell subpopulations. Two functionally distinct tumor-immune T-cell subpopulations were also identified in a rat Moloney sarcoma system (*17*). A subset of splenic T-cells associated with the elimination of the sarcoma in vivo was poorly tumor-cytotoxic in vitro, whereas the highly tumor-cytotoxic T-cell subset was tumor enhancing in vivo. In view of these findings, we have chosen adoptive transfer rather than an in vitro tumor cytotoxicity assay of undefined in vivo relevancy for mechanistic studies of tumor immunity. We now present the results of a study to elucidate some aspects of cellular mechanisms of adoptive immunity to the syngeneic line-10 hepatoma in strain 2 guinea pigs. This study was undertaken to analyze quantitatively the suppression of id implanted tumors in animals that were adoptively transferred iv with spleen cells from donors specifically immunized to the line-10 hepatoma.

MATERIALS AND METHODS

Guinea pigs.—Male Sewall-Wright inbred strain 2 guinea pigs 3–6 months old were obtained from the Small Animal Section, Veterinary Resources Branch, Division of Research Services, NIH, Bethesda, Md., and from the Division of Cancer Biology and Diagnosis Animal Holding Facility, NCI-Frederick Cancer Research Facility, Frederick, Md. Caged in groups of 6 or fewer, the animals were fed NIH guinea pig ration and given water ad libitum.

Tumor lines.—The line-10 hepatocellular carcinoma was originally induced in a male strain 2 guinea pig by feeding DENA in water. The tumor was converted to the ascites form and was passed ip in weanling strain 2 guinea pigs (*18, 19*). Inoculation of 10^6 viable ascites line-10 cells id in the side of the guinea pig led to progressive tumor growth, regional axillary lymph node metastases, and death in 60–90 days (*20*). At autopsy, a significant proportion of animals was found to have lung metastases (*21*). Another syngeneic DENA-induced hepatocellular carcinoma, line-1, was used for specificity control. Inoculation of 3×10^6 viable ascites line-1 cells id led to tumor growth for approximately 14 days which was followed by spontaneous regression (*18*). The line-10 and line-1 tumors each contained at least one distinct tumor-specific rejection antigen; both shared one or more embryonic antigens (*22, 23*). The ip passaged tumor lines were initiated periodically with ascites tumor cells stored in liquid nitrogen. The line-10 and line-1 tumor cells

---

ABBREVIATIONS USED: DENA=diethylnitrosamine; ED_{50}=number of immune lymphoid cells required to suppress the growth of tumors in 50% of guinea pigs; id=intradermal(ly); NIH=National Institutes of Health; RPMI-FBS=RPMI-1640 medium supplemented with 10% heat-inactivated fetal bovine serum (GIBCO, Grand Island, N.Y.), 50 U penicillin/ml, and 50 μg streptomycin/ml; TD_{50}=number of line-10 cells required to produce tumors in 50% of guinea pigs.

---

[1] Received July 28, 1981; accepted November 21, 1981.

[2] Animals were maintained under the guidelines set forth by the National Cancer Institute.

[3] Laboratory of Immunobiology, Division of Cancer Biology and Diagnosis, National Cancer Institute, National Institutes of Health, Public Health Service, U.S. Department of Health and Human Services, Bethesda, Md. 20205.

[4] *Address reprint requests to* Dr. Shu *at* Building 37, Room 2B16, National Institutes of Health, Bethesda, Md. 20205.

[5] Deceased September 25, 1981.

[6] Recipient of fellowship from Coordenacão de Aperfeicoamento de Pessoal de Nivel Superior (CAPES), Brazil.

used in experiments were in transplantation generations 12–20 and 90–100, respectively.

Immunization with line-10 or line-1 tumors.—Line-10-immune guinea pigs were produced by id inoculation into each animal of 0.2 ml of a vaccine consisting of 10^6 ascites line-10 cells admixed with 212 μg of cell walls from *Mycobacterium bovis* strain BCG (Phipps strain; Trudeau Institute, Saranac Lake, N.Y.) prepared as an emulsion with 3% mineral oil and 0.2% Tween in saline (*24, 25*). After 3–4 weeks, the animals received a series of 3–9 id weekly booster injections of 10^6 ascites line-10 cells in 0.1 ml of medium 199. Line-1-immune animals were produced by an initial id inoculation of 3×10^6 ascites line-1 cells. After a 4-week interval, the animals received 3–4 id booster injections of 3×10^6 ascites line-1 cells in a period of 6–8 weeks. Immune spleens were obtained from animals within 7–14 days after the last booster inoculations.

Preparation of nucleated spleen cell suspensions.—Guinea pigs were killed by cervical dislocation, and their spleens were removed aseptically. The organs were rinsed in RPMI-1640 medium and minced with scissors into pieces 1–4 mm in diameter. The minced tissue was forced through a 60-mesh stainless-steel wire screen and suspended in RPMI-1640 medium. The cell suspension was allowed to settle for approximately 1 minute, and three-fourths of the supernatant was decanted into a centrifuge tube. The remaining cell suspension containing cell aggregates and tissue debris was forced through a 22-gauge needle and was collected as described above. After centrifugation, erythrocytes were lysed by resuspension of the cell pellet in ammonium chloride–potassium lysing buffer (8.290 g NH_4Cl, 1.0 g $KHCO_3$, and 0.0372 g EDTA/liter, pH 7.4; Media Production Section, NIH, Bethesda, Md.). The cells were washed and resuspended in RPMI–FBS. The spleen cell suspension was depleted of plastic-adherent cells by incubation for 24 hours in plastic tissue culture dishes (#3025; Falcon Plastics, Oxnard, Calif.) in a 37°C humidified atmosphere consisting of 5% CO_2 in air.

Cell separation by Percoll gradient.—Percoll, a colloidal silica coated with povidone, was purchased from Pharmacia Chemicals, Uppsala, Sweden. Discontinous gradients were prepared by a modification of previously described methods (*26, 27*). A gradient was formed in a 12-ml plastic tube (#3033; Falcon Plastics) by layering 4 ml of the 35% Percoll solution on 3 ml of 50% Percoll. Approximately 200×10^6 viable spleen cells suspended in 2 ml of RPMI–FBS were layered over the gradient. The gradient was spun at 1,600 rpm ($400\times g$) in an International model PR-2 centrifuge for 30 minutes at room temperature. Cells were carefully removed from the gradient with a pipette and were washed three times with RPMI-1640 medium. Cells recovered in the interface between the 50 and 35% Percoll layers and above the 35% Percoll layer were designated as fractions I and II, respectively.

Adoptive transfer of immunity with spleen cells.—Spleen cells suspended in 2.0 ml of RPMI-1640 medium were transferred iv through the penile vein into normal strain 2 male guinea pigs anesthetized by inhalation of methoxyflurane (Metofane; Pitman-Moore, Inc., Washington Crossing, N.J.). Immediately thereafter, each animal was challenged id on the left side with ascites tumor cells in 0.1 ml medium 199. Challenged animals were observed for 4–6 weeks for evidence of progressive dermal tumor growth. To determine the quantitative relationship between the immune spleen cells transferred and the doses of tumor challenge that could be suppressed, we tested graded doses of immune spleen cells against graded doses of tumor cells. The ED$_{50}$ of immune spleen cells for a given tumor dose and the TD$_{50}$ of line-10 cells for a given immune spleen cell dose were computed by the Reed-Muench formula (*28*), and the standard error of each ED$_{50}$ or TD$_{50}$ was calculated by Pizzi's formula (*29*). Since the tumor challenge is an integral part of the adoptive transfer, we investigated its possible role in amplifying transferred immunity and/or stimulating host tumor immunity by giving a second id tumor challenge to those guinea pigs that had suppressed the growth of the first tumor challenges. The growth or lack of growth of the second challenge provided a means to evaluate quantitatively the immunogenicity of the first tumor challenge.

To estimate the proportion of iv transferred immune cells that accumulate and participate in specific tumor suppression at the site of challenge, we compared the number of immune cells transferred systemically and locally in the suppression of a given dose of tumor challenge. In the local adoptive transfer, tumor cells mixed with spleen cells at various ratios were suspended in RPMI-1640 medium. Immediately thereafter, 0.1 ml of the cell mixture was injected id into a normal guinea pig.

Irradiation of line-10 cells.—Line-10 cells were irradiated at a dose of 20,000 rad with a ^{60}Co γ-ray source (Gammacell 220). After irradiation, the viability of the cells was determined by trypan blue exclusion; no decrease in viability was observed after irradiation. To test whether irradiated cells were capable of growing progressively in strain 2 guinea pigs, we inoculated ip each weanling animal with 20×10^6 irradiated cells. No ascites tumors developed in the inoculated animals. A single, viable line-10 cell is capable of initiating fatal ascites tumor growth (Hunter JT: Unpublished data).

Analysis of results.—Log TD$_{50}$ and log ED$_{50}$ were calculated for tumor inoculation doses and transferred immune spleen cells, respectively, and were evaluated by regression analysis with a programmed calculator (HP-97; Hewlett-Packard Co., Corvallis, Oreg.). Significance of differences between the TD$_{50}$ or the ED$_{50}$ was estimated by Student's *t*-test.

RESULTS

Specificity of Adoptive Immunity

By active immunization, line-10 tumor has been shown to possess at least one tumor-specific rejection antigen distinct from that of other DENA-induced guinea pig hepatomas (*30*). Tumor-specific immunity to line-10 could be also transferred passively to normal recipients by intracardiac injection of mineral oil-induced immune peritoneal exudate cells (*1*). Although BCG cell wall was incorporated for initial immunization of guinea pigs to line-10, there was no evidence of tumor resistance in BCG-sensitized animals by either direct tumor challenge or adoptive transfer. Therefore, in this investigation we studied the specificity of adoptive immunity mediated by spleen cells from animals that had been immunized to the line-10 or the line-1 hepatoma. Table 1 summarizes the results of two experiments demonstrating that immune spleen cells transferred iv were capable of mediating specific suppression of the growth of id tumor challenges. The adoptive immunity against line-10 and line-1 was tumor line-specific; the growth of line-10 tumor was inhibited in animals given line-10 but not in those given line-1-immune spleen cells, whereas the growth of line-1 tumor was inhibited in animals given line-1 but not in those given line-10-immune spleen cells.

Quantitation of Adoptive Immunity by a Two-Dimensional Titration

Transferring 200×10⁶ immune spleen cells iv consistently suppressed the growth of 10^6 line-10 tumor cells given id. The quantitative relationship between the number of tumor cells that can be suppressed by a given number of immune spleen cells was established for line-10 by a two-dimensional titration in which the numbers of immune cells and line-10 tumor cells were varied. Over a large range of line-10 challenge doses (10^4–10^7 cells) tested, we found that the efficacy of the adoptive immunity increased with increasing numbers of transferred immune cells (table 2). The data in table 2 were based on determination of complete tumor suppression. In subsequent analyses, quantitative tumor resistance was estimated by comparison of the 50% end points.

TABLE 1.—*Specificity of adoptive transfer of immunity to guinea pig hepatomas*

Source of spleen cells[a]	Tumor incidence[b] in animals challenged with:	
	Line-10	Line-1[c]
Medium control	12/12	6/6
Normal animals	12/12	12/12
Line-10-immune animals	0/12	11/11
Line-1-immune animals	6/6	1/12

[a] Each guinea pig was given 200×10⁶ spleen cells iv in 4 ml medium 199 and was challenged id on the same day with 10^6 ascites line-10 or 3×10^6 ascites line-1 cells.

[b] No. of animals with tumor/No. tested 48 days after tumor challenge. Data were pooled from two experiments.

[c] Line-1 tumor normally grew id in medium control animals for ≈14 days before it spontaneously regressed. Immunity to line-1 was evaluated by the observation of a total lack of tumor growth.

TABLE 2.—*Quantitative analysis of adoptive transfer of tumor immunity in guinea pigs by a two-dimensional titration*[a]

No. of immune spleen cells transferred $\times10^{-6}$	Tumor incidence[b] after line-10 challenge dose of:				
	10^3	10^4	10^5	10^6	10^7
0	2/6	10/11	12/12	12/12	12/12
12.5		6/6			
25		1/10	9/11		
50		2/12	4/12	11/12	6/6
100		0/11	0/12	2/12	12/12
200				0/12	10/11
400					0/6

[a] Each guinea pig was given a suspension of immune spleen cells iv in 2 ml of RPMI-1640 medium and was challenged id on the same day with various numbers of ascites line-10 cells in 0.1 ml of medium 199.

[b] No. of animals with tumor/No. tested 38 days after challenge. Data were pooled from two independent experiments.

TABLE 3.—*Relationships between transferred immune spleen cells and line-10 tumor challenge doses in producing 50% end points*[a]

Part	Immune spleen cells $\times10^{-6}$	Log immune spleen cells (SE)	Line-10 dose	Log line-10 dose (SE)
I, TD_{50}	0		2.19×10^3	3.34 (0.27)
	25	7.40	$3.55\times10^{[illegible]}$	4.55 (0.22)
	50	7.70	$1.55\times10^{[illegible]}$	5.19 (0.25)
	100	8.00	2.50×10^6	6.40 (0.20)
	200	8.30	3.55×10^6	6.55 (0.19)
II, ED_{50}	19	7.28 (0.07)	10^4	4.00
	39	7.59 (0.07)	10^5	5.00
	72	7.86 (0.06)	10^6	6.00
	272	8.44 (0.09)	10^7	7.00

[a] TD_{50} and ED_{50} were calculated from data presented in table 2 according to the Reed-Muench formula. The TD_{50} in part I were calculated with fixed numbers of immune spleen cells, and the ED_{50} in part II, with fixed line-10 challenge doses.

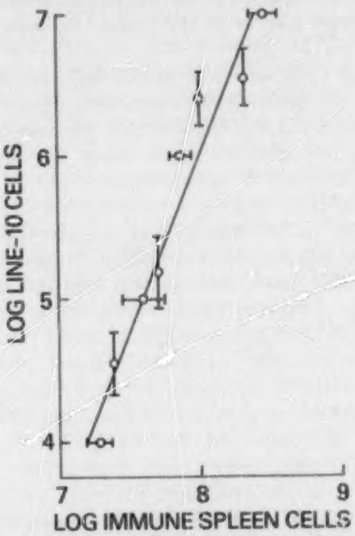

TEXT-FIGURE 1.—Logarithmic relationship between immune spleen cells and line-10 tumor challenge doses in producing 50% end points of tumor suppression in syngeneic recipients.

A summary of ED_{50} and TD_{50} determinations is shown in table 3. The 50% end points were computed from two directions: In part I, they were calculated as TD_{50}—numbers of tumor cells that would produce dermal tumors in 50% of animals receiving a given number of immune cells. In part II, they were calculated as ED_{50}—numbers of immune cells required to suppress the growth of a given tumor dose in 50% of the test animals. These values were then plotted logarithmically and analyzed by linear regression (text-fig. 1) The relationship can be illustrated by the linear first-order equation

$$y = 2.51x - 14.07.$$

In this equation, y is log tumor challenge dose, x is log immune cells, and the coefficient of determination of the regression line (r^2) is 0.95. The slope of the equation, 2.51, indicates that the efficacy of tumor suppression by adoptive immunity is an exponential function of increasing numbers of immune cells; i.e., a twofold increment in immune cells leads to an increased resistance of 5.62-fold in the tumor challenge dose.

Role of Host Systemic Immunity in the Rejection of Tumor by Adoptive Immunity

In adoptive transfer experiments, besides being an indicator for specificity and sensitivity of the test, tumor challenge might provide additional antigenic stimulation to the recipient. Therefore, tumor suppression might result from a combined effect of transferred immunity and host immune response. To study the role of host immunity in the rejection of tumor under the conditions of our system, we tested the tumor rejection capacity of guinea pigs in which a previous tumor challenge had been eliminated by adoptive immunity.

Guinea pigs that had been inoculated with various numbers of immune spleen cells were challenged on the same day with various doses of line-10 cells. Animals made tumor-free by adoptive transfer were tested 38 days later for evidence of heightened antitumor immunity. Two experiments illustrated in table 4 were designed to test whether rejection of 10^4 or 10^5 line-10 cells by adoptive immunity leads to an increased systemic immunity capable of rejecting 10^6 line-10 cells inoculated in the contralateral side. In control animals, each of which was given immune cells iv and challenged 38 days later with 10^6 line-10 cells, the ED_{50} of transferred immune spleen cells was 75×10^6. Animals rejecting an initial challenge of 10^4 or 10^5 line-10 cells did not show increased resistance to the second challenge of 10^6 line-10 cells, as judged by the ED_{50} of 72 and 76×10^6 immune spleen cells, respectively. The suppression of the growth of the second challenge reflected the numbers of immune spleen cells transferred and was independent of the rejection of a previous challenge. These findings thus suggest that rejection of 10^4 or 10^5 line-10 challenge by adoptive immunity did not depend on the host immune response to the tumor.

TABLE 4.—*Analysis of systemic tumor immunity in guinea pigs which previously rejected a line-10 tumor challenge*[a]

No. of immune spleen cells transferred on day 0 $\times 10^{-6}$	Tumor incidence[b] after 10^6 rechallenge when initial challenge was:		
	0	10^4	10^5
0	12/12		
25		9/9	2/2
50	6/6	8/10	7/8
100	1/6	2/11	3/12
ED_{50}	75×10^6	72×10^6	76×10^6

[a] Guinea pigs that had been inoculated iv with various numbers of immune spleen cells were challenged id on the same day with various doses of line-10 cells. At the 38th day, tumor-free animals, those which had rejected the day-0 line-10 challenge by adoptive immunity, were rechallenged id with 10^6 line-10 cells in the contralateral sides.

[b] No. of animals with tumor/No. tested 28 days after the second challenge. Data were pooled from two experiments.

Local Immune Stimulation and Tumor Rejection by Adoptive Immunity

Failure to demonstrate augmented host immunity after tumor rejection by adoptive immunity did not exclude the possible significance of a secondary local immune stimulation to tumor rejection. It was possible that the transferred immune cells were stimulated and proliferated at the site of tumor inoculation and that this was essential to initiate tumor suppression. To investigate this possibility, we determined by titration the number of immune spleen cells required to suppress a line-10 inoculum consisting of a mixture of live and irradiated cells. Irradiated line-10 cells are not tumorigeneic but retain tumor-specific rejection antigens (*30, 31*). Addition of irradiated cells to the tumor inoculum would provide more tumor-specific rejection antigen than that present in the inoculum with no irradiated cells. Experiments were done to determine the ED_{50} of immune spleen cells required to suppress a tumor inoculum consisting of live line-10 cells alone or of a mixture of live and irradiated line-10 cells. Table 5 shows that the ED_{50} of immune spleen cells in guinea pigs challenged with a mixture of 10^4 live and 99×10^4 irradiated line-10 cells was 18×10^6, whereas the ED_{50} of 25 and 71×10^6 were computed for guinea pigs challenged with 10^4 or 10^6 live line-10 cells, respectively. The ED_{50} of immune cells in animals challenged with 10^6 live cells and in those challenged with a mixture of 10^4 live and 99×10^4 irradiated line-10 cells (a total of 10^6 cells) were significantly different. This finding suggests that the irradiated tumor cells were not the targets for transferred immune cells. While the ED_{50} obtained when irradiated cells were added to live cells (18×10^6) was not significantly different from that obtained with live cells alone (25×10^6), the decrease in number of immune cells required to reject the tumor challenge containing irradiated cells suggested that antigenic stimulation at the local level might be important to tumor suppression.

TABLE 5.—*Influence of irradiated tumor cells on adoptive immunity to line-10 hepatoma in guinea pigs*[a]

No. of immune spleen cells transferred $\times 10^{-6}$	Tumor incidence[b] after line-10 challenge dose of:		
	Live cells		10^4 live cells plus 99×10^4 irradiated[c] cells
	10^6	10^4	
0	6/6	12/12	12/12
6.25		12/12	12/12
12.5		10/12	12/12
25	6/6	7/12	1/12
50	6/6	0/12	0/12
100	0/6	0/6	0/10
ED_{50}	71×10^6	25×10^6	18×10^6

[a] Each guinea pig was given immune spleen cells iv suspended in 2 ml of RPMI-1640 medium and was challenged id on the same day with ascites line-10 cells in 0.1 ml of medium 199.

[b] No. of animals with tumor/No. tested 38 days after challenge.

[c] 20,000 rad of γ-irradiation.

Biological Characteristics of Systemically Transferred Immunity

We estimated the proportion of transferred cells that found access to the challenge site and participated in tumor suppression. In preliminary experiments, we compared numbers of immune spleen cells (ED_{50}) required when administered iv and by direct mixing with tumor inoculum to achieve the same level of antitumor effect. However, comparison of the antitumor effect by different routes of administration was complicated by the fact that normal spleen cells suppressed tumor growth. This suppression as manifested by delayed appearance of palpable skin tumors was minimized by use of a population of effectors obtained from fractionation of spleen cells on a Percoll gradient. Spleen cell preparations contained approximately 50% lymphocytes. The viability by trypan blue exclusion was routinely 65-75%. Fraction I from the Percoll gradient contained 90% viable cells, although lymphocytes remained at 50%. Fraction II from the same Percoll gradient consisted of mostly dead cells (viability, <40%). The numbers of viable cells recovered in fractions I and II were 70 and 10% of the input, respectively.

Preliminary titrations indicated that the ED_{50} of unfractionated and fraction I immune spleen cells required for suppression of 10^5 line-10 cells by iv transfer were comparable. Therefore, local and systemic transfers of immunity were compared with fraction I of Percoll-fractionated immune spleen cells. The results (table 6) show that the ED_{50} of immune cells given iv was about 71 times greater than that obtained by direct mixing in the suppression of a line-10 challenge of 10^5 cells. This experiment was repeated once, and the ED_{50} computed for iv transfer was 36 times that for direct mixing (data not shown). These results suggest that there is no significant accumulation of iv transferred cells at the tumor inoculation site.

TABLE 6.—*Comparison of local and systemic adoptive immunity to a dermal line-10 challenge in guinea pigs*[a]

Spleen cells				
Mode of transfer[b]	Immune status	No. transferred × 10^{-6}	Tumor incidence[c]	ED_{50}
		0	6/6	
Local	Normal	2	6/6	
	Immune to line-1	2	6/6	
	Immune to line-10	2	1/6	1×10^6
	"	1	3/6	
	"	0.5	5/6	
	"	0.25	6/6	
Systemic	Immune to line-10	100	0/6	71×10^6
	"	50	6/6	
	"	25	6/6	
	"	12.5	5/6	

[a] Each guinea pig received a 10^5 line-10 id challenge in 0.1 ml of medium 199 on the day of adoptive transfer.

[b] Local was by direct mixing with line-10 cells before id inoculation; systemic was iv in 2 ml RPMI-1640 medium.

[c] No. of animals with tumor/No. tested 49 days after challenge.

TABLE 7.—*Expression of tumor immunity in skin of guinea pigs receiving immune lymphoid cells iv*[a]

Expt. No.	No. of immune spleen cells transferred × 10^{-6}	Tumor incidence[b] after No. of line-10 challenges × dose of:		
		1×10^6	10×10^6[c]	1×10^7
I	0	6/6	6/6	6/6
	100	0/6	1/5[d]	5/5
II	0	6/6	6/6	6/6
	100	0/6	1/6[e]	3/5

[a] Each guinea pig was given immune spleen cells iv in 2 ml of RPMI-1640 medium and was challenged id on the same day with ascites line-10 cells in 0.1 ml medium 199.

[b] No. of animals with tumor/No. tested.

[c] When multiple challenges were administered, the distance between the two sites was ≥25 mm.

[d] One animal had a static small papule at 14 days; 3 additional palpable tumors appeared at 28 days and persisted for the entire experimental period of 42 days.

[e] One animal developed 2 small papules that did not grow progressively but persisted throughout the experiment (42 days).

To test this further, we designed an experimental protocol in which the adoptively transferred immunity (100×10^6 immune spleen cells iv) was assessed by challenging the recipient with a single injection of 10^7 line-10 cells or with 10 injections of 10^6 line-10 cells spaced at least 25 mm apart from each other. The results of the two identically designed experiments I and II are shown in table 7. Challenge with 10^6 or 10^7 line-10 cells led to progressive tumor growth in all control animals (no immune cells transferred). Challenge with 10 injections of 10^6 line-10 cells at 10 separate sites in control animals was followed by tumor growth at all sites, except that 1 guinea pig of experiment I did not show a palpable tumor for 1 of the 10 challenges by the end of the experiment (42 days). In guinea pigs given 100×10^6 immune spleen cells iv, the growth of a 10^6 line-10 challenge was completely suppressed, whereas a 10^7 line-10 challenge at a single skin site grew in each of the 5 animals and in 3 of the 5 animals in experiments I and II, respectively. When 100×10^6 immune spleen cells were transferred iv, growth of the tumors at 10 challenge sites per recipient was suppressed in most animals. In experiment I, 1 guinea pig that was given immune cells and challenged at 10 skin sites had 1 small papule palpable at 14 days, and 3 additional tumors developed at day 28 and persisted until the end of the experiment (42 days). In experiment II, 1 animal that was given immune cells and challenged at 10 skin sites developed 2 small papules that did not grow progressively but did persist for the length of the experiment (42 days).

In a different experimental protocol, we further investigated the significance of attraction and accumulation of iv transferred immune cells in the area of dermal tumor challenge. This experiment was designed to test whether the presence of 10^7 line-10 cells in the skin could abrogate the antitumor activity to 10^6 line-10 cells inoculated adjacent to or distant from it. To avoid possible growth inhibition or enhancement of the 10^6 line-10 inoculations in animals that had extra tumor burden, we included groups of guinea pigs in which the inoculation sites of 10^7 line-10 cells were surgically excised 3 days after the onset of the experiment. Results show that suppression of the growth of 10^6 line-10 tumor cells by adoptive immunity was not influenced by the presence of 10^7 line-10 cells adjacent to it (table 8). These

TABLE 8.—*Lack of specific attraction at id tumor challenge site in guinea pigs given immune lymphoid cells iv*

No. of immune spleen cells transferred on day 0 ×10⁻⁶	Tumor incidence[a] when line-10 challenge doses were given on the:		
	Left flank[b]		Right flank: 10^6
	10^7	10^6	
0		6/6	6/6
100		0/5	1/5
0	6/6	6/6	6/6
100	5/5	0/5	1/5
0	SR[c]	6/6	6/6
100	SR[c]	0/5	0/5

[a] No. of animals with tumor/No. tested 35 days after challenge.

[b] When 2 injections per flank were given, the distance between inoculation sites was ≥25 mm.

[c] SR=surgically removed 3 days after challenge.

results suggest that the iv transferred cells were not attracted specifically to the tumor challenge skin site.

DISCUSSION

Impetus for the quantitative analysis of adoptive immunity reported here came from our previous study of interactions between immune lymphoid cells and line-10 targets (*16*). We found that immune cells that conveyed adoptive immunity possessed receptors for tumor-specific rejection antigens and reacted in vitro with cultured line-10 hepatoma cells, but such interactions did not lead to target cell destruction in vitro. In contrast, an immune lymphoid cell population mediating in vitro cytotoxicity failed to confer adoptive protection to line-10 challenge in vivo. The apparent discordance between the two observations led us to conclude that data from adoptive transfer may be required to form a basis for mechanistic studies of in vivo antitumor immunity. To facilitate studies on mechanisms of tumor immunity, we established quantitative relationships between effector cells and tumor targets in adoptive transfer experiments.

Results of two-dimensional titrations revealed that tumor rejection was an exponential function of immune lymphoid cell dose. The logarithmic values of the two variables were correlated linearly, with a slope of approximately 2.51. The exponential relationship between the numbers of immune lymphoid cells and the doses of tumor cells suppressed in adoptive immunity is of theoretical interest. The transferred immune cells may be restimulated and expanded, and/or the recipient may be immunized by the tumor challenge. Increasing tumor cell challenge doses would provide increased amount of antigen and perhaps a greater immune response. Thus the rejection of a higher dose tumor challenge would require proportionally fewer transferred immune cells. For this hypothesis to be validated, one must demonstrate that a secondary immune stimulation and/or the host primary immune response are important in the tumor suppression by adoptive immunity. A report by Alexander et al. (*32*) emphasized the role of the host immune response in tumor rejection by transferred immune lymphocytes in a rat fibrosarcoma model. We have taken a different approach and have examined whether heightened immunity existed in guinea pigs that had rejected a tumor challenge by adoptive immunity. The data presented in table 4 showed quantitatively that the ability of the guinea pig to suppress the growth of a second line-10 challenge (10^6 ascites tumor cells) was a function of transferred immune cells and was not influenced by tumor doses that had been previously . These data suggest that suppression of id line-10 rejected. These data suggest that suppression of id line-10 tumor challenges by the transferred immunity in guinea pigs was independent of development of systemic immunity in the recipients. However, we only examined the host response to 10^4 and 10^6 line-10 challenge doses. Our data do not exclude the possibility that greater systemic antitumor immunity is produced by higher challenge doses. The significance of the immunity developed in the recipient to the tumor eradication by adoptive immunity can be elucidated only py performing adoptive transfer in immunologically compromised hosts, since the immunity developed could be interpreted as a consequence rather than as a "cause" of the tumor rejection by adoptive immunity.

While development of systemic immunity did not seem to contribute to the tumor rejection in animals receiving immune cells at the doses of challenge cells tested, a local secondary immune stimulation at the tumor challenge site may be important in explaining the exponential relationship between immune lymphoid cells and tumor rejection. To test this possibility, we took advantage of the fact that irradiated line-10 cells are not tumorigeneic but retain their antigenicity (*30, 31*). Thus we analyzed quantitatively the rejection by adoptive immunity of a 10^4 line-10 cell inoculum in the presence of 99×10^4 irradiated tumor cells. Adding irradiated cells to the tumor inoculum was reported to be tumor enhancing, especially when the number of live tumor cells was relatively small (*33*). Indeed, we found that the mixtures of live and irradiated line-10 cells grew more rapidly than the same number of live cells alone. The enhancement was manifested by an earlier appearance of a palpable skin tumor. The numbers of immune cells required to suppress the growth of tumor challenges in 50% of the recipients with and without the presence of irradiated cells were 18 and 25×10^6, respectively (table 5). The difference between the numbers of immune cells required, however, is not statistically significant. Close scrutiny of experimental data revealed that animals receiving 25×10^6 immune spleen cells, either 1 of 12 or 7 of 12 developed palpable tumors after challenge with 10^4 line-10 cells admixed with 99×10^4 irradiated cells or with 10^4 line-10 cells alone, respectively. This difference could argue that increased antigenic stimulation did contribute to the tumor rejection. For the investigation of the role of antigenic stimulation at the tumor challenge site, a detailed quantitative analysis of the effect of various combinations of live and irradiated line-10 cells may be more revealing.

Much work has been done on mechanisms of passive transfer of delayed hypersensitivity reactions with radioactive isotope-labeled lymphoid cells. It is apparent that only a small proportion of the transferred cells is present in the reaction site at any particular time. It has thus been concluded that the transferred cells are not always attracted specifically nor are they required in large numbers at the site for a positive skin reaction (*34*). Our interest in studying the behavior of immune lymphoid cells after adoptive transfer was stimulated by the observation that, for the same level of tumor suppression, the number of immune lymphoid cells required when mixed directly with tumor cells was only a small fraction of the number needed when given iv. This observation suggests that iv transferred immune cells may not be always accessible to the tumor challenge site and that tumor rejection might be initiated by a small fraction of transferred immune cells.

To investigate more directly whether the transferred immune cells are specifically attracted to the tumor challenge site, we did the experiments described in tables 7 and 8. Our approach has the advantage of examining the overall biological effect of adoptive antitumor immunity and of avoiding pitfalls associated with radioactive isotope labeling [discussed extensively in (*35*)]. Our early experiments indicated that 100×10^6 immune spleen cells were sufficient to suppress the growth of 10^6 but not of 10^7 line-10 cells inoculated at a single skin site. If the limited capacity of the adoptive immunity to reject 10^7 line-10 cells is due to the lack of specific attraction at the challenge site rather than due to insufficient numbers of immune cells available in the recipient, one would expect that a total of 10^7 line-10 cells could be rejected, provided that they were divided into multiple small doses and inoculated at separate skin sites. Alternatively, if specific attraction of immune cells to the tumor challenge site played a significant role in the rejection of the tumor, one would expect that 10^6 line-10 cells would not be rejected when implanted next to a skin site where a large dose (10^7) of the same tumor cells was present. The results of the two types of experiments clearly demonstrated that transferred immune cells were not necessarily attracted specifically to the tumor inoculum.

It appears that expression of transferred immunity at separate skin sites was independent. Since multiple tumor challenges were spaced at least 25 mm apart from each other, these results did not exclude the possibility that specific attraction might have taken place near the challenge sites. For further documentation of this possibility, it will be necessary to perform adoptive transfer experiments with multiple tumor challenges separated by graduated distances.

As regards the distribution of transferred lymphoid cells in syngeneic recipients, previous studies showed that within 24 hours of transfer, more than 80% of the labeled cells were found in internal organs including liver, spleen, lung, and heart (*36*, *37*). Evidence also indicated that many of these cells were functionally damaged and therefore taken up by the reticuloendothelial system within hours of transfusion. A small proportion (1–2%) of transferred cells was present in the circulation at 24 hours, and this appeared to correlate well with the number of transferred cells detected in delayed hypersensitivity lesions (*36*). These findings and results of the present study indicate that the immune cells required to initiate tumor suppression at the skin site in our system must have been a minute fraction of the iv transferred cells. In the present study we observed that a 10^7 line-10 challenge dose was invariably rejected by 400×10^6 immune spleen cells. Our spleen cell suspension contained approximately 50% lymphocytes, of which probably less than 10% were specifically immune to the tumor. In the recipient, we may assume that less than 10% of the transferred cells were distributed in the skin. A 25-mm-diameter area represents approximately 2% of the skin of an adult guinea pig. If these estimations are valid, the number of immune cells required to initiate the suppression of a dose of 10^7 line-10 cells would be less than 0.04×10^6.

Certain conclusions can be drawn from this quantitative study of adoptive immunity: 1) The quantitative relationship between transferred immune lymphoid cells and tumor challenge doses is exponential; i.e., a twofold increase in immune cells leads to an increased resistance of 5.62-fold tumor challenge dose. 2) Within the line-10 challenge doses analyzed in this study, tumor suppression by adoptive immunity reflects the intrinsic characteristics of the immune cells and is independent of the development of a primary immune response in the recipient. 3) Success of tumor suppression is influenced not only by the total tumor burden but also by the distribution of the tumor in the recipient. 4) Lack of specific attraction of iv transferred immune lymphoid cells at the tumor challenge site suggests that only a small proportion of the transferred lymphoid cells participates in initiating tumor suppression.

REFERENCES

(*1*) Wepsic HT, Zbar B, Rapp HJ, Borsos T. Systemic transfer of tumor immunity: Delayed hypersensitivity and suppression of tumor growth. J Natl Cancer Inst 1970; 44:955–963.

(*2*) Borberg H, Oettgen HF, Chondry F, Beatti EJ Jr. Inhibition of established transplants of chemically induced sarcomas in syngeneic mice by lymphocytes from immunized donors. Int J Cancer 1972; 10:539–547.

(*3*) Fefer A. Immunotherapy and chemotherapy of Moloney sarcoma virus-induced tumors in mice. Cancer Res 1969; 29:2177–2183.

(*4*) Smith HG, Harmel RP, Hanna MG Jr, Zwilling BS, Zbar B, Rapp HJ. Regression of established intradermal tumors and lymph node metastases in guinea pigs after systemic transfer of immune lymphoid cells. J Natl Cancer Inst 1977; 58:1315–1322.

(*5*) Rosenberg SA, Terry WD. Passive immunotherapy of cancer in animals and man. Adv Cancer Res 1977; 25:323–388.

(*6*) Morgan DA, Ruscetti FW, Gallo R. Selective in vitro growth of T lymphocytes from normal human bone marrows. Science 1976; 193:1007–1008.

(*7*) Rosenberg SA, Spiess PJ, Schwarz S. In vitro growth of murine T cells. I. Production of factors necessary for T cell growth. J Immunol 1978; 121:1946–1950.

(*8*) Baker PE, Gillis S, Ferm MM, Smith KA. The effect of T cell growth factor on the generation of cytolytic T cells. J Immunol 1978; 121:2168–2173.

(*9*) Schendel DJ, Bonnard GD, Wank R, Dupont B. Proliferative and cytotoxic capacities of human cultured T cells. Transplant Proc 1978; 10:933–935.

(*10*) Tees R, Schreier MH. Selective reconstitution of nude mice with long-term cultured and cloned specific helper T cells. Nature 1980; 283:780–781.

(*11*) Cheever MA, Greenberg PD, Fefer A. Specific adoptive therapy of established leukemia with syngeneic lymphocytes sequentially immunized in vivo and nonspecifically expanded by culture with Interleukin 2. J Immunol 1981; 126:1318–1322.

(*12*) Burton RC, Warner NL. In vitro induction of tumor-specific immunity. IV. Specific adoptive immunotherapy with cytotoxic T cells induced in vitro to plasmacytoma antigens. Cancer Immunol Immunother 1977; 2:91–99.

(*13*) Chauvenet PH, McArthur CP, Smith RT. Demonstration in vitro of cytotoxic T cells with apparent specificity toward tumor-specific transplantation antigens on chemically induced tumors. J Immunol

1979; 123:2575–2581.

(*14*) Oehler JR, Herberman RB. Evidence for long-lasting tumor immunity in a syngeneic rat lymphoma model: Correlation of in vitro findings with in vivo observations. JNCI 1979; 62:525–529.

(*15*) Rosenau W, Morton DL. Tumor-specific inhibition of growth of methylcholanthrene-induced sarcomas in vivo and in vitro by sensitized isologous lymphoid cells. J Natl Cancer Inst 1966; 36: 825–836.

(*16*) Shu S, Steerenberg PA, Hunter JT, Evans CH, Rapp HJ. Adoptive immunity to the guinea pig line 10 hepatoma and the nature of in vitro lymphoid–tumor cell interactions. Cancer Res 1981; 41:3499–3506.

(*17*) Fernandez-Cruz E, Woda BA, Feldman JD. Elimination of syngeneic sarcomas in rats by a subset of T lymphocytes. J Exp Med 1980; 152:823–841.

(*18*) Churchill WH Jr, Rapp HJ, Kronman BS, Borsos T. Detection of antigens of a new diethylnitrosamine-induced transplantable hepatoma by delayed hypersensitivity. J Natl Cancer Inst 1968; 41: 13–29.

(*19*) Rapp HJ, Churchill WH Jr, Kronman BS, Rolley RT, Hammond WG, Borsos T. Antigenicity of a new diethylnitrosamine-induced transplantable guinea pig hepatoma: Pathology and formation of ascites variant. J Natl Cancer Inst 1968; 41:1–11.

(*20*) Zbar B, Bernstein ID, Rapp HJ. Suppression of tumor growth at the site of infection with living Bacillus Calmette-Guérin. J Natl Cancer Inst 1971; 46:831–839.

(*21*) Hunter JT, Ashely MP, Rapp HJ, Sukumar S, Zbar B. Pulmonary metastases in guinea pig as a consequence of dermal implantation of line-10 tumor cells. Cancer Immunol Immunother 1981; 11:39–44.

(*22*) Zbar B, Wepsic HT, Rapp HJ, Borsos T, Kronman BS, Churchill WH Jr. Antigenic specificity of hepatomas induced in strain-2 guinea pigs by diethylnitrosamine. J Natl Cancer Inst 1969; 43: 833–841.

(*23*) Borsos T, Richardson AK, Ohanian SH, Leonard EJ. Immunochemical detection of tumor-specific and embryonic antigens of diethylnitrosamine-induced guinea pig tumors. J Natl Cancer Inst 1973; 51:1955–1960.

(*24*) Zbar B, Rapp HJ, Ribi EE. *Brief communication:* Tumor suppression by cell walls of *Mycobacterium bovis* attached to oil droplets. J Natl Cancer Inst 1972; 48:831–835.

(*25*) Yarkoni E, Rapp HJ. Influence of oil concentration on the efficacy of tumor regression by emulsified components of mycobacteria. Cancer Res 1979; 39:535–537.

(*26*) Gutierrez C, Bernabe RR, Vega J, Kreisler M. Purification of human T and B cells by a discontinuous density gradient of percoll. J Immunol Methods 1979; 29:57–63.

(*27*) Ulmer AJ, Flad HD. Discontinuous density gradient separation of human mononuclear leucocytes using Percoll as gradient medium. J Immunol Methods 1979; 30:1–10.

(*28*) Davis BD, Dulbecco R, Eisen HN, Ginsberg HS, Wood WB. Computation of 50% endpoints (LD_{50} or ID_{50}) by method of Reed and Muench. In: McCarty M. Microbiology. 2d ed. New York: Harper, 1973:663–664.

(*29*) Pizzi M. Sampling variation of the fifty percent end-points, determined by the Reed-Muench (Behrens) method. Hum Biol 1950; 22:151–190.

(*30*) Bartlett GL, Zbar B. Tumor-specific vaccine containing *Mycobacterium bovis* and tumor cells: Safety and efficacy. J Natl Cancer Inst 1972; 48:1709–1726.

(*31*) Ashley MP, Zbar B, Hunter JH, Rapp HJ, Sugimoto T. Adjuvant-antigen requirements for active specific immunotherapy of microscopic metastases remaining after surgery. Cancer Res 1980; 40: 4197–4203.

(*32*) Alexander P, Delorme EJ, Hall JG. The effect of lymphoid cells from the lymph of specially immunized sheep on the growth of primary sarcomata in rats. Lancet 1966; 1:1186–1189.

(*33*) Révész L. Effect of lethally damaged tumor cells upon the development of admixed viable cells. J Natl Cancer Inst 1958; 20:1157–1186.

(*34*) Turk JL. Delayed hypersensitivity. Amsterdam: Elsevier/North-Holland, 1980.

(*35*) Ting C-C. Studies on the mechanisms for the induction of in vivo tumor immunity. II. Distribution and homing of cytotoxic effector and percursor cells. J Natl Cancer Inst 1978; 60:437–444.

(*36*) Turk JL. The passive transfer of delayed hypersensitivity in guinea pigs by the transfusion of isotopically-labelled lymphoid cells. Immunology 1962; 5:478–488.

(*37*) Mathisen DJ, Rosenberg SA. The in vivo distribution of transferred syngeneic, allogeneic, and xenogeneic lymphoid cells: Implication for the adoptive immunotherapy of tumors. J Immunol 1980; 124: 2295–2300.

Esophageal Carcinogenesis in F344 Rats by Nitrosomethylethylamines Substituted in the Ethyl Group[1,2,3]

William Lijinsky,[4] Joseph E. Saavedra,[4] Melvin D. Reuber,[4] *and* Sandra S. Singer[4]

ABSTRACT—The carcinogenic activity in male F344 rats of five nitrosomethylalkylamines related to nitrosomethylethylamine has been examined. All rats were tested by administration of controlled doses of the compounds in the drinking water. Nitrosomethylbenzylamine was the most potent carcinogen of the five, causing death of most animals with tumors of the upper gastrointestinal tract (mainly the esophagus) within 6 months after a total dose of 0.2 mmol. The remaining compounds, all of which can be considered true derivatives of nitrosomethylethylamine, were less potent than nitrosomethylbenzylamine but also induced a high incidence of tumors of the esophagus. Nitrosomethyl-2-phenylethylamine and nitrosomethylneopentylamine were of comparable potency, while nitrosomethyltrifluoroethylamine was considerably less potent, as measured by the time to death with esophageal tumors. Deuterium-labeled nitrosomethylethylamine, in which deuterium replaces hydrogen on the β-carbon atom of nitrosomethylethylamine, induced a high incidence of esophageal tumors as well as liver tumors after administration of identical doses. Reactions on the β-carbon atom of nitrosomethylethylamine might be important as well as oxidation at the α-carbon atoms in determining carcinogenic effects.—JNCI 1982; 68:681–684.

Nitrosomethylethylamine is something of an anomaly among simple aliphatic nitrosamines because it is so much less potent as a carcinogen than is nitrosodimethylamine or nitrosodiethylamine (*1*), although it is presumed to act as they do through oxidation to simple alkylating agents which alkylate nucleic acids, primarily DNA. The asymmetric NMEA would presumably give rise to both methylating and ethylating species. In addition, the activity of NMEA as a carcinogen is not congruent with another general rule proposed by Druckrey et al. (*1*) that asymmetric aliphatic nitrosamines have the esophagus as their target in the rat, whereas the symmetrical nitrosamines have the liver of the rat as their target; NMEA is primarily a liver carcinogen in the rat (*1*, *2*).

In the course of studies of the effect of deuterium substitution for hydrogen at various positions in the molecule of NMEA (*2*), we discovered that those deuterated derivatives with deuterium on the β-carbon of the ethyl group gave rise to a significant incidence of esophageal tumors as well as liver tumors. This led us to conclude that oxidation at the β-carbon plays a modifying role in carcinogenesis, as well as the usual oxidation at the α-carbon atoms which is commonly believed to be critical in activation of nitrosamines to their proximate carcinogenic forms. It seemed reasonable to pursue this by examining the effect of substitution of other atoms and groups at the β-carbon on the carcinogenicity of NMEA. A number of derivatives of this nitrosamine were prepared and administered to groups of rats by being dissolved in their drinking water at approximately equimolar doses. The time to death of tumor-bearing rats was then observed. The compounds tested included one with a single substituent, NMPA, and those with all three β-hydrogen atoms replaced, as in NMEA-d_3, NMFA, and NMNA. NMBA was included for comparison, although it is not strictly one of the compounds of this series. The structures of these compounds are shown in text-figure 1.

MATERIALS AND METHODS

Chemicals.—NMEA-d_3: NMEA-d_3 was prepared from acetyl-d_3 chloride, which was formed by heating 16 g (0.25 mol) of acetic acid-d_4 with 56 g (0.4 mol) of benzoyl chloride and distilling the resulting acetyl-d_3 chloride at 48°C. The yield was 12 g (68%). This product (8 g, 0.1 mol) was dissolved in benzene and cooled in ice, and dry methylamine gas was bubbled through the solution until the vapor above was alkaline. The reaction mixture was warmed to room temperature, and the methylamine hydrochloride was filtered off. Evaporation of the benzene left 5.6 g (73%) of *N*-methylacet[D_3]amide, which was spectroscopically identical with the undeuterated compound. This product (8.2 g, 0.11 mol) was dissolved in dry THF (50 ml) and added slowly to a suspension of aluminum lithium hydride (5.7 g, 0.15 mol) in dry THF. The mixture was boiled under reflux for 2 hours, and the excess hydride was destroyed by slow addition of 25 ml ethanol:water (1:1) followed by 25 ml water. The mixture was filtered, and 100 ml brine was added; the mixture was extracted with two treatments of 100 ml ethyl ether. The ethyl ether solution was extracted twice with 100 ml *N* HCl. The combined acid extracts were cooled in ice, 100 ml acetic acid was added, and then 30 g sodium nitrite was added slowly. After a 2-hour reaction, the pH was adjusted to 6, and the solution was extracted six times with 150 ml of methylene chloride. The methylene chloride solution was shaken three times with 150 ml 5% sodium hydroxide solution to destroy any nitrosamide present and was dried, and the methylene chloride was distilled off. The

---

ABBREVIATIONS USED: b=broad singlet(s); d=doublet; MS=mass spectrometry; m/z=mass/charge; NMBA=*N*-nitroso-*N*-methyl-*N*-benzylamine; NMEA=nitrosomethylamine(s); NMEA-d_3=*N*-nitroso-*N*-methyl-*N*-ethyl[2-D_3]amine; NMFA=*N*-nitroso-*N*-methyl-2,2,2-trifluoroethylamine; NMNA=*N*-nitroso-*N*-methyl-*N*-neopentylamine; NMPA=*N*-nitroso-*N*-methyl-*N*-2-phenylethylamine; q=quartet; s=singlet(s); THF=tetrahydrofuran.

---

[1] Received July 30, 1981; accepted November 27, 1981.

[2] Supported by Public Health Service contract N01CO-75380 from the Office of the Director, National Cancer Institute.

[3] Animals were maintained under the guidelines of the NCI-Frederick Cancer Research Facility.

[4] Chemical Carcinogenesis Program, NCI-Frederick Cancer Research Facility, P.O. Box B, Frederick, Md. 21701.

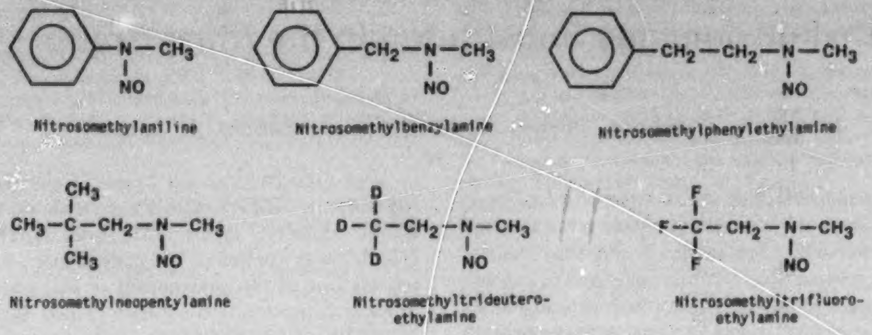

TEXT-FIGURE 1.—Structures of beta-substituted NMEA.

residual oil was distilled in vacuo, yielding 3.4 g (35%) of deuterated product (bp 60°C at 20 mm Hg). Analysis of the product by high-pressure liquid chromatography showed the presence of the nitrosamine and the absence of any significant impurity that could be the nitrosamide. By UV spectrophotometry, λ_{max}^{EtOH} (ϵ)=347 nm (94). MS was m/z, 91 (M^+, 100%), 90 (14), 79 (19), 61 (3), 60 (8), and 59 (18). IR spectrophotometry was 1,440, 1,460, and 1,040 cm^{-1} (N—N=O). NMR was δ 2.98, δ 3.68 (sharp s, 3H, $\underline{CH_3}$-two rotamers), δ 3.56, and δ 4.12 (b, 2H, —$\underline{CH_2}$-two rotamers).

NMBA and NMPA: NMBA and NMPA were prepared by addition of sodium nitrite to solutions of the secondary amines (Aldrich Chemical Co., Milwaukee, Wis.) in 2 *N* HCl, separation of the nitrosamine layers, and distillation of the nitrosoamines in vacuo. The purity of these compounds exceeded 99% by chromatography. Their physical characteristics and spectral properties have been described (*1*).

NMNA: Methylene chloride (200 ml) was cooled to 5°C and saturated with methylamine gas. A 1-*M* solution of 20 g (0.166 mol) trimethylacetyl chloride (Aldrich Chemical Co.) in methylene chloride was added dropwise. The ice bath was removed, and stirring was continued for 1 hour. The hydrochloride salt was removed by vacuum filtration. The filtrate was washed with 1 *N* hydrochloric acid, followed with aqueous sodium hydroxide and then with water. The solvent was removed on a rotary evaporator, and the product was recrystallized from petroleum ether:THF to give 15.34 g (80%) of white crystalline *N*-methyl-2,2-dimethylpropionamide. The mp was 39–90°C. NMR ($CDCl_3$) was δ 1.18 (s, 9H), δ 2.77 (d, 3H), and δ 6.0 (b, 1H).

A solution of 15 g (0.13 mol) of *N*-methyl-2,2-dimethylpropionamide in 130 ml of THF was reduced to *N*-methyl-*N*-neopentylamine in 76% yield with diborane·THF complex as described by Brown and Heim (*3*). The bp was 85–90°C [in the literature (*4*), 88–90°C]. The amine (7.5 g, 0.074 mol) was nitrosated as described by Büttner and Hünig (*5*). The nitrosamine was obtained in 88% yield. Its bp was 76–77°C at 14 mm Hg (in the literature, 76–77°C at 14 mm Hg). NMR ($CDCl_3$) was δ 0.92, δ 1.03 (s, 9H), δ 3.10 (s, 2.79H), δ 3.81 (s, 0.21H), δ 3.42 (s, 0.14), and δ 3.91 (s, 1.86H). By UV spectrophotometry, λ_{max}^{EtOH} (ϵ)=349 nm (85). MS was m/z, 130 (M^+, 29%), 115 (7), 85 (8), 74 (8), 73 (12), 70 (15), 57 (100), and 44 (60).

NMFA: *N*-Methyltrifluoroacetamide was prepared from trifluoroacetic anhydride and methylamine in a 94% yield as reported by Pailer and Huebsch (*6*). The mp was 48–49°C (in the literature, 48–49°C). NMR ($CDCl_3$) was δ 2.95 (d, 3H) and δ 6.46 (b, 1H).

Methyl-2,2,2-trifluoroethylamine hydrochloride was prepared in a 67% yield from the aluminum lithium hydride reduction of *N*-methyltrifluoroacetamide as described by Bissell and Finger (*7*). The mp was 218–221°C (in the literature, >200°C). NMR ($CDCl_3$) was δ 2.88 (s, 3H) and δ 3.98 (q, 2H).

Methyl-2,2,2-trifluoroethylamine hydrochloride (10 g, 0.075 mol) was nitrosated according to the procedure of Bissell and Finger (*7*). Distillation of the crude product at 1 atmosphere gave 7.1 g (76%) of pure NMFA. The bp was 135–136°C (in the literature, 131–133°C). IR spectrophotometry (film) was 1,475, 1,340, 1,216, 1,170, 833, and 754 cm^{-1}. NMR ($CDCl_3$) was δ 3.16 (s, 2.4H), δ 3.95 (s, 0.6H), δ 4.23 (q, 0.4H), and δ 4.80 (q, 1.6H). By UV spectrophotometry, $\lambda_{max}^{H_2O}$ (ϵ)=350 nm (75). MS was m/z, 142 (M^+, 100%), 110 (11), 83 (33), 73 (37), 69 (18), 59 (18), and 42 (81).

Animal treatments.—Each of the nitrosamines was administered to a group of 20 male F344 rats bred and housed in the barrier-maintained colony of the NCI-Frederick Cancer Research Facility. The animals, 7–8 weeks old at the beginning of the experiments, were housed 4/group in plastic cages with wire mesh bottoms and fed Rockland rat diet (Rockland, Inc., Gilbertsville, Pa.) in pellets ad libitum. As drinking water on each of 5 days of the week, 80 ml of a solution of the appropriate nitrosamine was supplied to each cage; on the remaining 2 days, the animals were given tap water ad libitum, with which they made up for any water deficit. No special group of untreated controls was part of this experiment; however, a continuous group of untreated animals is maintained in the facility, and their incidence of tumors did not differ from that reported for a large group of untreated Fischer 344 rats in various laboratories (*8*).

The period of animal treatment was originally planned for 30 weeks but was shortened in some regimens (such as with NMBA) because the animals began to die earlier. Similarly, we originally planned to supply all of the nitrosamines at equimolar doses, but we had to modify this because the selected concentration (0.34 m*M*) proved toxic with NMNA, NMBA, and NMPA. When the treatments ceased, the animals were allowed to die naturally (a few were killed when moribund) and were thoroughly necropsied; all major tissues and organs, as well as all lesions, were fixed for histopathologic examination.

RESULTS

The treatments given the groups of male rats, the duration of treatment, and the pattern of death of the animals are shown in table 1. Most of the rats died with tumors, usually of the types not found in untreated animals, and the number of each type of tumor induced by the various nitrosamines is shown in table 2.

For comparison, the results of the administration of the parent compound NMEA are given, although they were started 3 years earlier in rats of the same stock and have been reported previously (*2*). All groups of treated animals died at a more rapid rate than untreated rats, presumably because of the tumors induced. When this pattern of death is used as a criterion, although not as a quantitative measure, it appears that NMBA is the most potent carcinogen, since a relatively low dose of this compound led to the earliest deaths with esophageal tumors. NMPA is next in order of potency, followed by NMNA, NMFA, and NMEA and NMEA-d_3, which are about equal.

As might be expected, the lower dose of each nitrosamine that was administered at two doses was less effective than was the higher dose, although this difference was much more marked with NMFA than with NMPA. Although the lower dose of either NMPA or NMFA was 40% that of the higher one, there was very little difference in mortality between the 2 groups treated with different doses of NMPA, but there was a large difference between the 2 groups treated with different doses of NMFA.

Except with NMEA and NMEA-d_3, the tumors induced by the nitrosamines were all in the upper gastrointestinal tract. The tumor incidences in all of the groups were virtually 100%. NMEA induced almost exclusively liver tumors, while NMEA-d_3 induced a high incidence of esophageal tumors as well as liver tumors. Most of the treatments were so tumorigenic that few of the spontaneous tumors commonly found in untreated animals of this strain (*8*) were seen.

DISCUSSION

The mechanism of carcinogenesis by NMEA is not known, nor is it known for any N-nitroso compound, although it is suspected that oxidation of the molecule to an intermediate which, directly or indirectly, alkylates DNA at critical sites, is responsible. An explanation for the lesser activity of NMEA than of nitrosodimethylamine or nitrosodiethylamine might lie in the possibility of oxidation of NMEA to both a methylating and an ethylating agent, each of which might be formed in a lower concentration than if it were formed from the symmetrical compounds. Studies have not yet been done of the relative extents of methylation and ethylation of NMEA in vivo. One interpretation of our earlier results in which selectively deuterium-labeled NMEA were used is that ethylation is a more effective carcinogenic

TABLE 1.—*Survival of male rats treated with NMEA substituted on the β-carbon atom*

Compound	Concentration, mg/liter (m*M*)	Duration of treatment, wk	Total dose, mg (mmol)	No. of survivors at week															
				0	5	10	15	20	25	30	35	40	45	50	60	70	80	90	100
NMEA	30 (0.34)	30	90 (1.0)	20	20	20	20	20	20	20	20	20	18	17	14	5	1	0	
NMEA-d_3	31 (0.34)	30	93 (1.0)	20	20	20	20	20	20	20	19	19	18	17	12	9	3	0	
NMFA	62.5 (0.44)	28	175 (1.25)	20	20	20	20	20	18	15	11	6	2						
	25 (0.17)	30	75 (0.5)	20	20	20	20	20	20	20	20	19	19	19	19	17	15	11	9[a]
NMNA	22.5 (0.17)	22	50 (0.4)	20	17	17	17	15	14	11	6	2	0						
NMBA	13 (0.09)	22	29 (0.2)	20	17	17	17	15	9	4	0								
NMPA	28 (0.16)	28	78 (0.5)	20	20	20	20	20	19	11	3	0							
	9.5 (0.05)	33	31 (0.2)	20	20	20	20	19	19	16	7	2	0						

[a] Seven survivors were killed at 110 wk.

TABLE 2.—*Liver and upper GI[a] tract tumors in rats treated with substituted NMEA*

Compound	Concentration, mg/liter (m*M*)	Effective No. of animals	No. of tumor-bearing animals	No. of animals with tumors						
				Liver			Upper GI tract			
				Carcinoma	Hemangiosarcoma	Cholangiocarcinoma	Esophagus	Forestomach	Tongue	Nasal cavity
NMEA	30 (0.34)	20	14	9	1	0	1	0	0	4
NMEA-d_3	31 (0.34)	20	20	15	10	3	14	0	0	0
NMFA	62.5 (0.44)	20	19	0	0	0	19	7	4	0
	25 (0.17)	20	18	0	0	0	18	2	0	3
NMNA	22.5 (0.17)	17	16	0	0	0	16	0	0	0
NMBA	13 (0.09)	17	17	0	0	0	17	2	7	0
NMPA	28 (0.16)	20	19	0	0	0	19	9	0	0
	9.5 (0.05)	20	19	1	0	0	19	11	0	0

[a] Gastrointestinal.

event than is methylation (*2*). In those experiments in which the doses were 0.34 m*M*, few or no esophageal tumors were induced except by those derivatives with deuterium in the beta position of the ethyl group. Only at much higher doses, e.g., 1.5 m*M*, was a significant incidence of esophageal tumors (as well as liver tumors) induced by NMEA itself (*9*). This might lead to the conclusion that tumor induction in the esophagus is by some minor pathway that is only revealed at higher concentrations or when other pathways are overwhelmed.

This conclusion is, to some extent, borne out by the present experiments in which substitution on the β-carbon atom of the ethyl group of NMEA results in induction of tumors of the esophagus. The effect of substitution of deuterium at this position is to retard oxidation at the β-carbon. However, the presence of deuterium on the β-carbon atom of NMEA did not greatly affect the tendency of this compound to induce liver tumors in rats, since the survival and liver tumor incidence of the rats treated with NMEA or NMEA-d_3 did not differ much.

Deuterium labeling at the beta position of NMEA only slows down oxidation at that position, whereas substitution of three fluorine atoms or three methyl groups at that position can be expected to abolish oxidation. Consonant with this, NMFA and NMNA are both more potent esophageal carcinogens than is NMEA-d_3. Since NMNA is more effective than NMFA, it must be assumed that more is involved in the induction of esophageal tumors than the prevention of beta oxidation of the ethyl group, and this might affect the rate of alpha oxidation of the ethyl group. However, nitrosodiethylamine, which can undergo beta oxidation as easily as can NMEA, induces a high incidence of esophageal tumors in rats, even at low doses (*10*).

A reasonable conclusion might be that in the rat esophagus the profound effect of the NMEA substituted on the β-carbon atom might be due to production of a methylating agent by oxidation of the ethyl group at the alpha position. The nature of the substituent on the β-carbon could well determine the rate at which the methylating agent is produced in the esophagus, and hence the extent to which alkylation of DNA (or other critical macromolecule) occurs, and thereby its effectiveness in inducing esophageal tumors would be determined. This sequence has been suggested by some preliminary studies by D. P. Kleihues, University of Freiburg, Federal Republic of Germany, who has studied primarily NMBA. He found, as we report here, that NMBA is the most potent esophageal carcinogen among the nitrosamines examined in rats. The reason why none of these compounds induces liver tumors in rats might be related to an inability to oxidize the β-carbon atom of the ethyl group, although the reasons might be more complex. Certainly, nitrosodiethanolamine is purely a liver carcinogen in rats, but it is enormously weaker than is nitrosodiethylamine (*1*, *11*).

The failure of most of the beta-substituted NMEA to induce liver tumors in rats is surprising since the beta-substituted NMEA appear to methylate DNA in vivo as readily in rat liver as in the rat esophagus (*12*). Nitrosomethylcyclohexylamine, a potent esophageal carcinogen in rats (*13*, *14*), was shown to methylate DNA in the liver at the 7-position of guanine much more readily than it alkylated nucleic acids in the esophagus (*15*), but it did not give rise to liver tumors.

There is much less evidence that alkylation by the larger moiety of beta-substituted NMEA occurs, although in some studies oxidation of the methyl group to formaldehyde predominates over oxidation of the α-carbon of the larger group (*16*). However, oxidation to a methylating agent might well be the important reaction in carcinogenesis by these compounds in the esophagus. There are some exceptions to such a generalization, e.g., the carcinogenic action of nitrosomethylaniline. This compound is an esophageal carcinogen of reasonable potency in rats, although it is somewhat weaker than its analog nitrosomethylcyclohexylamine (*13*). Nitrosomethylaniline is not metabolized to a methylating agent, and it is difficult to conceive that it could be. Therefore, the mechanism of action of nitrosomethylaniline as an esophageal carcinogen in rats seems not to be through methylation of DNA in the esophagus. This observation suggests the possibility of alternative mechanisms by which the beta-substituted NMEA induce esophageal cancer in rats.

REFERENCES

(*1*) Druckrey H, Preussmann R, Ivankovic S, Schmähl D. Organotrope carcinogene Wirkungen bei 65 verschiedenen N-Nitroso-Verbindungen an BD-Ratten. Z Krebsforsch 1967; 69:103–201.

(*2*) Lijinsky W, Reuber MD. Carcinogenicity in rats of nitrosomethylethylamines labeled with deuterium in several positions. Cancer Res 1980; 40:19–21.

(*3*) Brown HC, Heim P. Diborane as a mild reducing agent for the conversion of primary, secondary and tertiary amides into the corresponding amines. J Am Chem Soc 1964; 86:3566–3567.

(*4*) Pine SH, Catto BA, Yamagishi FG. The Stevens rearrangements of *N,N,N*-trimethylneopentylammonium iodide. J Org Chem 1970; 35:3663–3666.

(*5*) Büttner G, Hünig S. Reaktion mit Hydroxyl-Ionen zu trans-α-Hydroxy-dialkyl-diazinen. Chem Ber 1971; 104:1088–1103.

(*6*) Pailer M, Huebsch WJ. Determination of primary and secondary amines as amides by means of gas chromatography on packed capillary columns. Monatsh Chem 1966; 97:1541–1543.

(*7*) Bissell ER, Finger M. Fluorine-containing nitrogen compounds. I. Trifluoroethylamines. J Org Chem 1959; 24:1256–1259.

(*8*) Goodman DG, Ward JM, Squire RA, Chu KC, Linhart MS. Neoplastic and nonneoplastic lesions in aging F344 rats. Toxicol Appl Pharmacol 1979; 48:237–248.

(*9*) Lijinsky W, Reuber MD. Comparative carcinogenicity of some aliphatic nitrosamines in Fischer rats. Cancer Lett 1981; 14:297–302.

(*10*) Lijinsky W, Reuber MD, Riggs CW. Dose-response studies in rats with nitrosodiethylamine. Cancer Res 1981; 41:4997–5003.

(*11*) Lijinsky W, Reuber MD, Manning WB. Potent carcinogenicity of nitrosodiethanolamine in Fischer 344 rats. Nature 1980; 288:309–310.

(*12*) Hodgson RM, Wiessler M, Kleihues P. Preferential methylation of target organ DNA by the oesophageal carcinogen *N*-nitrosomethylbenzylamine. Carcinogenesis 1980; 1:861–866.

(*13*) Goodall CM, Lijinsky W, Tomatis L, Wenyon CE. Toxicity and oncogenicity of nitrosomethylaniline and nitrosomethylcyclohexylamine. Toxicol Appl Pharmacol 1970; 17:426–432.

(*14*) Lijinsky W, Reuber MD. Carcinogenicity of deuterium-labeled *N*-nitroso-*N*-methylcyclohexylamine in rats. JNCI 1980; 64:1535–1536.

(*15*) Lijinsky W, Keefer L, Loo J, Ross AE. Studies of alkylation of nucleic acids in rats by cyclic nitrosamines. Cancer Res 1973; 33:1634–1641.

(*16*) Farrelly JG. A new assay for the microsomal metabolism of nitrosamines. Cancer Res 1980; 40:3241–3244.

Induction and Transplantation of Murine Skin Cancers Induced by Methoxsalen Plus Ultraviolet (320–400 nm) Radiation[1,2,3]

M. L. Kripke,[4] W. L. Morison,[4] *and* J. A. Parrish[5,6]

ABSTRACT—Properties of skin tumors resulting from treatment of mice with ip methoxsalen plus UVA (320–400 nm) radiation (PUVA) were compared to those of skin tumors induced by UVB (280–320 nm) radiation. Repeated treatment of C3H/HeN murine mammary tumor virus-negative ($C3H^-$) mice with PUVA produced both fibrosarcomas and squamous carcinomas that were indistinguishable morphologically from UVB-induced tumors. Fragments of 12 primary PUVA-induced tumors were transplanted into normal and immunosuppressed syngeneic recipients, and all grew progressively. In contrast, 19 primary tumors induced by repeated exposure of $C3H^-$ mice to UVB grew only in the immunosuppressed mice and not in the normal recipients. The growth of graded doses of cells from 5 PUVA-induced tumors was compared in normal and UVB-irradiated recipients. No preferential growth in UVB-irradiated mice was observed, even though this is characteristic of UVB-induced tumors. Thus PUVA-induced tumors do not appear to have the same antigenic properties as UVB-induced tumors.—JNCI 1982; 68:685–690.

The cutaneous responses to treatment with the chemical photosensitizer methoxsalen followed by exposure to UVA radiation (referred to by the acronym PUVA) are similar in many respects to those observed after exposure to UVB radiation. Both modalities produce erythema, increased pigmentation, epidermal hyperplasia, and cell injury (*1–4*). Furthermore, both UVB radiation and PUVA treatment (*5, 6*) are carcinogenic in mice. In humans, the carcinogenicity of these treatments has not been as firmly established, but UVB radiation is probably responsible for sunlight-induced skin cancer (*5*), and PUVA therapy is associated with a marked increase in the incidence of skin cancer in patients receiving this treatment for skin disease (*7*). Both types of treatment damage DNA directly, although the molecular lesions produced in DNA are quite different. Thymine dimers are probably the most important lesion induced by UVB radiation (*8*), whereas PUVA treatment produces monofunctional adducts and cross-links in DNA (*4*).

Because of the similarities in the biologic responses of skin to PUVA and UVB radiation, we were interested in comparing the antigenic properties of the tumors induced in mice by chronic treatment with these agents. Previous work has established that skin tumors induced in $C3H^-$ mice by UVB radiation have two unusual antigenic properties. 1) These tumors are highly antigenic, and most are rejected immunologically upon transplantation to normal syngeneic recipients (*9–11*). 2) These tumors will grow progressively in UVB-irradiated syngeneic mice because of the presence in the UVB-exposed animals of regulatory suppressor T-lymphocytes that specifically inhibit the immunologic rejection of these tumors (*12–14*). In these experiments, we have induced skin tumors in $C3H^-$ mice by repeated treatments with PUVA and have examined some of the antigenic properties of these tumors in transplantation tests. Specifically, we have compared the growth of fragments of primary PUVA-induced and UVB-induced tumors transplanted into normal and immunosuppressed syngeneic recipients. In addition, the growth of graded doses of cells from PUVA-induced tumors was compared in normal and UVB-irradiated hosts.

MATERIALS AND METHODS

Mice.—Specific-pathogen-free inbred female $C3H^-$ mice were supplied by the Animal Production Area of the NCI-Frederick Cancer Research Facility. They were housed 5 per cage in a room where ambient light was automatically regulated on a 12-hour light–dark cycle.

PUVA treatment.—Methoxsalen (Hoffmann-La Roche, Inc., Nutley, N.J.) was administered by ip injection of 0.5 ml of an 0.8-mg/ml solution of drug in saline containing 5 mg methylcellulose/ml. The solution was made up weekly and stored in dark bottles at 4°C. One hour after the injection of the drug, the mice were exposed to UVA radiation from a bank of 6 PUVA fluorescent bulbs (Sylvania, Danvers, Mass.) filtered through 0.5-mm Mylar to eliminate wavelengths shorter than 320 nm (*15*). The spectral irradiance of the source was measured with a cosine-corrected UV spectroradiometer system (International Light, Inc., Newburyport, Mass.), and measurements of the irradiance were made for the integrated 320- to 400-nm band with a WBS 350 SEE 400 detector. Over this wavelength range, the

ABBREVIATIONS USED: ATX=adult thymectomized X-irradiated; $C3H^-$=C3H/HeN murine mammary tumor virus-negative; PUVA=methoxsalen plus UVA radiation; UVA=ultraviolet, 320–400 nm; UVB=ultraviolet, 280–320 nm.

---

[1] Received August 24, 1981; accepted October 29, 1981.

[2] Supported by Public Health Service contract N01-CO-75380 from the Office of the Director, National Cancer Institute, with Litton Bionetics, Inc. The contents of this publication do not necessarily reflect the views or policies of the U.S. Department of Health and Human Services, nor does mention of trade names, commercial products, or organizations imply endorsement by the U.S. Government.

[3] Animals were maintained under the guidelines set forth by the National Institutes of Health Policy on Humane Care and Use of Animals and by the Animal Welfare Act in facilities accredited by the American Association for Accreditation of Laboratory Animal Care.

[4] Cancer Biology Program, NCI-Frederick Cancer Research Facility, P.O. Box B, Frederick, Md. 21701.

[5] Department of Dermatology, Harvard Medical School, Massachusetts General Hospital, Boston, Mass. 02114

[6] We thank Ms. Dolores Winterstein, Mr. Jeffrey Linebaugh, and Mr. Thomas Farris for their excellent technical assistance and Dr. Melvin Reuber for the histopathologic studies.

average incident dose rate was approximately 10 J/m^2/second.

The mice were housed on a shelf 20 cm below the fluorescent bulbs, and the cages were rotated systematically along the shelves before each treatment to compensate for the variations in irradiance along the length of the bulbs. The dorsal fur was removed from the animals with electric clippers (#40 blade) once per week, and the PUVA treatments were administered five times per week, beginning when the mice were 7 weeks of age. The animals were inspected once per week for tumor development, and the primary tumors were measured weekly. Upon reaching a size of approximately 10×10 mm in diameter, the tumors were removed for histologic examination and transplantation.

UVB treatment.—The mice were exposed to UVB radiation from a bank of FS40 sunlamps (Westinghouse, Bloomfield, N.J.) three times per week, as described previously (*10*). The average incident dose rate (non-cosine corrected) was 1 J/m^2/second, as measured by a Hewlitt-Packard radiant flux detector (model 8344A) with a sensitivity of 0.1 μV/μW/cm^2. Approximately 80% of this radiation is emitted in the wavelength range from 280 to 340 nm, with the peak emission at 313 nm. For tumor induction, each UVB treatment was of 10-minute duration; for tumor transplantation studies, the mice were treated for 60 minutes, three times per week, for at least 12 weeks.

Immunosuppression.—C3H$^-$ mice were immunosuppressed by thymectomy at 4–5 weeks of age, followed 2–4 weeks later by whole-body exposure to 450 R of X-radiation from a Philips MG301 X-ray unit. The mice were used in experiments 24 hours after X-irradiation and are referred to as ATX mice.

Tumor transplantation.—Tumors were removed aseptically and trimmed to remove necrotic areas and connective tissue. Fragments approximately 1 mm^3 in size were cut with a scalpel and implanted sc with a trocar through a small incision in the inguinal region of normal and ATX recipients.

Tumor cell suspensions were prepared from minced tumor tissue by digestion with collagenase, followed by incubation in DNase, as described by Peters et al. (*16*). This procedure resulted in single cell suspensions of greater than 90% viability, as judged by trypan blue exclusion. These suspensions were injected sc near the inguinal region of UVB-irradiated mice and age-matched unirradiated control animals. UV irradiation was not continued after the injection of the tumor cells. Recipient mice were examined weekly, and the tumors were measured in three perpendicular diameters.

Histologic examination.—Samples of the primary tumors were fixed in Bouin's solution, embedded, sectioned, and stained with hematoxylin and eosin. Diagnosis of histologic type was made on coded samples by a board-certified laboratory animal pathologist.

RESULTS

PUVA Carcinogenesis

Following ip injection with 0.4 mg methoxsalen, groups of 25 mice each were treated with three different doses of UVA radiation. The highest dose (9 kJ/m^2), which was delivered in 15-minute exposures, was below the minimum dose that produced visible phototoxicity in a 4-week pilot study. None of the animals in the carcinogenesis study exhibited any visible signs of phototoxic damage during the experiment. The life-table analysis of the rate of tumor induction by the three doses of PUVA is presented in text-figure 1. With these treatment regimens, the latent periods for tumor development were extremely long, but they appeared to be directly related to the dose of UVA radiation. Mice treated for 90 weeks with methoxsalen alone did not develop skin tumors, nor did mice treated with UVA alone. The total UVA doses given to the 2 UVA control groups were 3.1×10^3 kJ/m^2 over a 68-week period and 1.4×10^3 kJ/m^2 over a 90-week period, respectively.

The details of this experiment and the histologic types of the resulting tumors are summarized in table 1. All of the tumors developed on the backs of the animals; most were classified as fibrosarcomas, and a smaller number were squamous cell carcinomas. These results are reminiscent of the findings with chronic UVB irradiation in this mouse strain (*10*). In fact, when examined microscopically in a double-blind fashion, the tumors induced by PUVA were indistinguishable from those induced by UVB radiation. All mice treated with UVA alone survived for the duration of the study, except for a few animals that developed mammary adenocarcinomas at 1 year of age, a typical occurrence in females of this mouse strain. However, the longevity of the animals given ip injections five times per week with methoxsalen decreased sharply. Whether this decrease resulted from the toxicity of the solution, from the trauma of repeated injections, or both is not known.

Transplantation of Primary Tumors

Fragments of 12 of the 15 primary skin tumors that developed in the PUVA-treated mice were transplanted into

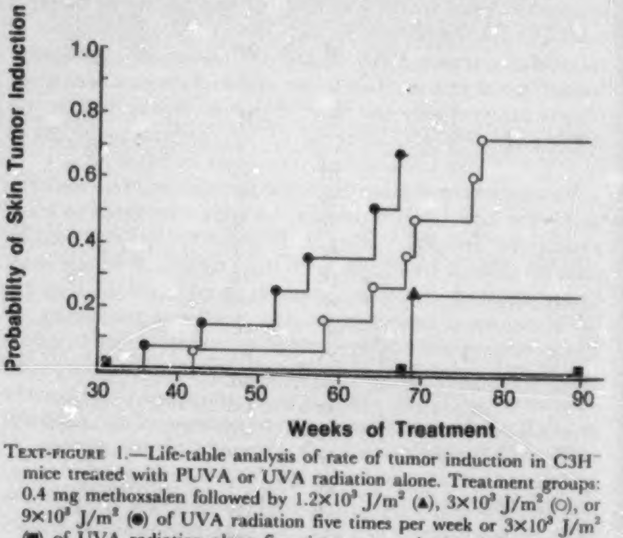

TEXT-FIGURE 1.—Life-table analysis of rate of tumor induction in C3H$^-$ mice treated with PUVA or UVA radiation alone. Treatment groups: 0.4 mg methoxsalen followed by 1.2×10^3 J/m^2 (▲), 3×10^3 J/m^2 (○), or 9×10^3 J/m^2 (●) of UVA radiation five times per week or 3×10^3 J/m^2 (■) of UVA radiation alone five times per week. Another group was treated with 9×10^3 J/m^2 of UVA radiation alone five times per week for 68 wk and developed no tumors.

TABLE 1.—*Skin tumor incidence in and survival of PUVA-treated mice*

No. of mice at start	Treatment[a]	No. of mice with skin tumors	No. of skin tumors	Histologic types of skin tumors: Carcinoma	Sarcoma	Other	Not examined	No. of mice without tumor	Mean survival time of tumor-free mice, wk	Longevity of mice, wk
25	UVA, 5 min	0	0	0	0	0	0	22[b]	97.0	97[c]
25	Methoxsalen	0	0	0	0	0	0	25	63.5	97[d]
25	Methoxsalen + UVA, 2 min	1	1	0	1	0	0	23[b]	50.3	96[d]
25	Methoxsalen + UVA, 5 min	7	7	2	4	0	1	18	51.2	90[d]
25	UVA, 15 min	0	0	0	0	0	0	25	75.0	75[c]
25	Methoxsalen + UVA, 15 min	6	7	1	4	0	2	19	46.6	75[d]

[a] UVA + Mylar, five exposures per week, 1 hr after methoxsalen injection; UVA dose rate, ≈10 J/m^2/sec. Methoxsalen = 0.5 ml ip (0.4 mg), five times per week. Mice were 7 wk old at the start of PUVA treatment.

[b] Remaining animals developed mammary adenocarcinoma and were excluded from survival data.

[c] Age of surviving mice at termination of study.

[d] Age of longest surviving mouse.

TABLE 2.—*Transplantation of primary skin tumors in normal and immunosuppressed syngeneic mice*

Carcinogen	No. of transplantable tumors/No. tested		No. of progressively growing implants/total implants (%)		Latent period, wk		Carcinomas: sarcomas
	Normal mice	ATX mice	Normal mice	ATX mice	Median	Range	
PUVA[a]	12/12	12/12	60/70 (86)	70/72 (97)	61	36–77	3:9
UVB[b]	0/19	19/19	0/94 (0)	75/93 (81)	47	36–61	1:18

[a] *See* table 1 for treatment schedule and doses.

[b] Mice were exposed for 10 min (0.6 kJ/m^2) three times per week to unfiltered FS40 sunlamps.

groups of 4–12 normal and immunosuppressed recipients. Three of the tumors were squamous carcinomas; the remainder were fibrosarcomas. As table 2 shows, all 12 tumors grew progressively in most recipients, regardless of whether they were immunosuppressed. At the same time, UVB-induced tumors with a similar range of latent periods were tested. As expected from previous studies (*9*, *10*), fragments of these UVB-induced primary tumors grew progressively only in the immunosuppressed mice and not in the normal recipients.

Growth of PUVA-Induced Tumors in UVB-Irradiated Mice

The experiment reported in table 2 demonstrated that tumors induced by PUVA do not exhibit the same high degree of antigenic strength as those induced by UVB radiation. However, this observation does not rule out the possibility that the PUVA-induced tumors might have antigens that are similar in specificity to those found on UVB-induced tumors, even though the magnitude of the primary immune response induced by these two sets of tumors differs. To test this possibility, we prepared cell suspensions of several of the PUVA-induced tumors and injected them sc into normal and UVB-irradiated mice. Mice exposed to UVB radiation for a 12-week period cannot reject UVB-induced tumors, but they exhibit resistance to the growth of syngeneic tumors induced by other carcinogens (*17*). This resistance appears to be caused by the development of a population of suppressor T-lymphocytes during UVB irradiation that recognizes antigens present on UVB-induced tumors and inhibits the immune response against these antigens (*12–14*). Thus preferential growth of the PUVA-induced tumors in UVB-irradiated mice, relative to their growth in untreated animals, would imply antigenic similarity between these tumors and tumors induced by UVB radiation.

Several such experiments are illustrated in text-figures 2 and 3 and in table 3. Ten independent experiments with five different PUVA-induced tumors were performed. In no instance was the incidence of a PUVA-induced tumor significantly higher in UVB-irradiated mice than in age-matched, untreated recipients. This was true even though in 5 of the experiments the PUVA-induced tumors developed more rapidly and/or with a higher frequency in ATX mice than in normal animals (e.g., *see* text-figs. 2, 3). In

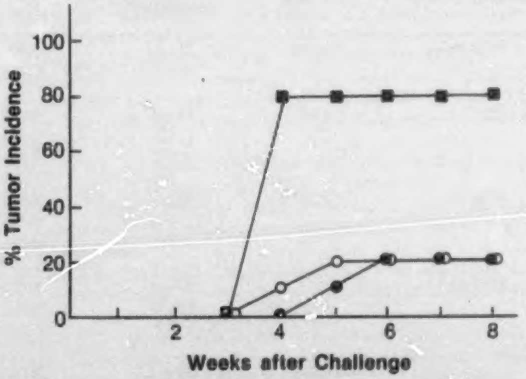

TEXT-FIGURE 2.—Tumor incidence following challenge with cell suspension of PUVA-induced fibrosarcoma P-327. ●=5×10^5 cells injected sc into 10 normal mice; ○=10 mice pretreated with UVB radiation for 12 wk; ■=5 mice immunosuppressed by adult thymectomy and sublethal (450 R) X-irradiation.

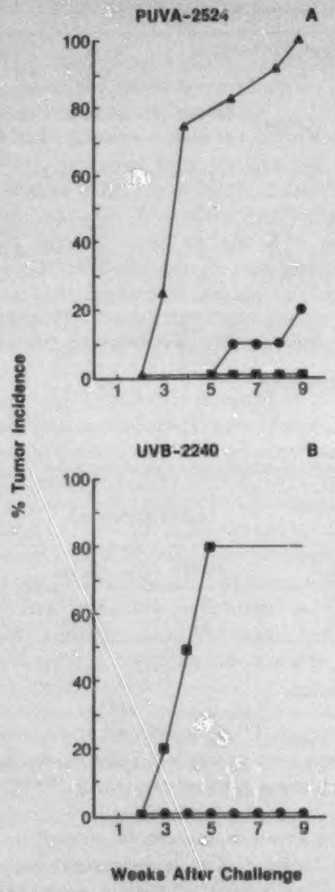

TEXT-FIGURE 3.—Tumor incidence following challenge with cell suspensions of PUVA-induced fibrosarcoma (PUVA-2524) and UVB-induced fibrosarcoma (UVB-2240). Challenge dose of 5×10^4 cells of PUVA-2524 (A) and 2×10^6 cells of UVB-2240 (B) injected sc. Treatment groups: 10 normal mice (●), 10 mice pretreated with UVB radiation for 12 wk (■), and 9 mice immunosuppressed by adult thymectomy and sublethal (450 R) X-irradiation (▲).

contrast, a cell suspension of a UVB-induced fibrosarcoma, also prepared by collagenase digestion, grew progressively in most UVB-irradiated mice but not in the normal recipients (text-fig. 3B).

DISCUSSION

These studies demonstrate that repeated treatment of C3H⁻ mice over a long period of time with doses of PUVA that were insufficient to produce visual evidence of phototoxicity leads to the development of skin cancers. On the basis of the examination of tissue sections with a light microscope, these skin cancers are morphologically indistinguishable from those induced in this mouse strain by UVB radiation. Both squamous cell carcinomas and fibrosarcomas are produced by the PUVA treatment. Despite the morphologic similarity between PUVA-induced and UVB-induced tumors and despite the many similarities in the biologic effects of these two treatments, the PUVA-induced tumors do not exhibit the same behavior in transplantation tests as that normally observed with UVB-induced tumors.

Upon transplantation of tissue fragments from primary tumors, the UVB-induced skin cancers generally are rejected immunologically by normal syngeneic recipients (*9–11*). In contrast, all of the PUVA-induced tumors grew progressively in normal recipients. Thus by the criterion of the ability to induce complete immunologic rejection in unimmunized syngeneic hosts, the UVB-induced tumors as a group are highly antigenic, but the PUVA-induced tumors are not. It has been reported that, in chemical carcinogenesis, the antigenic strength of tumors induced in mice by 3-methylcholanthrene is directly related to the dose of the carcinogen (*18*). Thus it is possible that had higher, photo-

TABLE 3.—*Growth of PUVA-induced fibrosarcomas in UVB-irradiated mice*

Challenge tumor	Cell dose	Treatment of recipients[a]	Cumulative tumor incidence[b] at wk 1	2	3	4	5	6	Percent final incidence at wk 12
P-2524	6×10^4	None	0/9	0/9	0/9	7/9	7/9	7/9	78
		UVB	0/10	1/10	2/10	5/10	7/10	7/10	70
P-2524	1×10^4	None	0/10	0/10	0/10	1/10	1/10	2/10	20
		UVB	0/10	0/10	0/10	0/10	0/10	0/10	0
		ATX	0/5	0/5	1/5	2/5	3/5	3/5	60
P-2210	1×10^5	None	0/10	0/10	5/10	8/10	10/10		100
		UVB	0/10	0/10	3/10	9/10	10/10		100
		ATX	0/5	0/5	2/5	3/5	5/5		100
P-2523	2×10^5	None	0/10	6/10	8/10	8/10	8/10	8/10	80
		UVB	0/10	3/10	5/10	6/10	6/10	6/10	60
		ATX	5/10	10/10					100
	2×10^4	None	0/10	0/10	1/10	1/10	1/10	1/10	10
		UVB	0/10	0/10	0/10	0/10	0/10	0/10	0
		ATX	0/10	0/10	1/10	3/10	3/10	3/10	30

[a] UVB = 3.6 kJ/m^2, three times per week for 12 wk from unfiltered FS40 sunlamps. ATX=adult thymectomy and 450 R X-radiation.
[b] No. of mice with tumor/No. challenged.

toxic doses of PUVA been used, the resulting tumors might have been more highly antigenic. However, this possibility seems unlikely since there was no indication that tumors induced by the highest doses of PUVA differed as a group from those induced by the lower doses. Furthermore, in UVB carcinogenesis, the proportion of highly antigenic (regressor) tumors does not change as a function of either latency or carcinogen dose (*19*). In the experiments performed in this study (table 2), the doses of UVB and PUVA were comparable, in that neither agent produced visible acute phototoxic effects and both induced skin cancers with approximately the same range of latent periods. Even under these conditions of similar carcinogenicity, the antigenic strength of the resulting tumors differed dramatically for the two agents.

The PUVA-induced and UVB-induced tumors also differed in their ability to exhibit preferential growth in UVB-irradiated mice, relative to that in normal recipients. This behavior is characteristic of both progressor and regressor UVB-induced tumors (*19*). Most or all fragments of regressor tumors regress when transplanted into normal recipients and grow progressively when transplanted into UVB-irradiated mice. To evaluate progressor UVB-induced tumors, one must compare the rates of tumor growth in normal and UVB-irradiated mice or inject a dose of cells in a single cell suspension that is low enough to produce tumors in fewer than 100% of the normal recipients. When tested in this way, none of the PUVA-induced tumors grew more rapidly or at a higher incidence in UVB-treated hosts than in unirradiated mice. In several instances, the PUVA-induced tumors grew at a submaximal rate in the normal recipients and were capable of exhibiting enhanced growth in immunosuppressed mice. Even under these conditions, no enhancement was observed in the UVB-irradiated recipients. The finding that enhanced growth of UVB-induced tumors is mediated by the presence of immunologic regulatory suppressor cells that are specific for UVB-induced tumors as a group (*12–14*) suggests two possible interpretations. Either the PUVA-induced tumors are devoid of detectable tumor-specific transplantation antigens, or their antigens differ in specificity from those exhibited by UVB-induced tumors. It seems unlikely that the PUVA-induced tumors would be completely nonimmunogenic, because some of them grew to a greater extent in immunosuppressed mice than in normal animals when tested at a limiting dose. However, a formal demonstration that this differential growth is immunologically mediated or that these tumors can immunize against subsequent tumor challenge has not yet been made. Regardless of which interpretation is correct, these results demonstrate that, by this criterion also, PUVA-induced tumors differ from UVB-induced tumors in their transplantation properties.

Two implications can be drawn from this study and, although speculative, deserve consideration. The first relates to the development of nonmelanoma skin cancer in humans undergoing PUVA therapy (*7*) and the observation that these lesions are morphologically similar to sunlight-induced skin cancer (*20*). It could be assumed that PUVA-associated tumors in humans will follow the same relatively benign course and have a low metastatic potential as do sunlight-induced skin cancers. However, although certainly there are differences in skin carcinogenesis between humans and mice with PUVA and UVB, the relevant conclusion to be drawn from the animal experiments is that the morphologic similarity of skin cancers induced by these two agents is not necessarily an indicator of similarity in biologic behavior.

The second implication is related to the origin and nature of tumor-specific transplantation antigens. It is not clear why PUVA treatment induces tumors that have such different antigenic characteristics from those induced by UVB radiation. Although the difference in antigenic strength might be explained by differences in the immunosuppressive properties of UVB and PUVA treatments (*21*), this hypothesis does not account for the apparent difference in specificity between the sets of tumors induced by the two agents. Since the major difference between treatment of mice with PUVA or UVB is the nature of the molecular lesion produced in DNA, this raises the possibility that a particular carcinogen may induce a unique set of tumor-specific antigens, based on the site and/or nature of the initial lesion that it produces in DNA. Although this possibility is highly speculative, recent work suggesting that tumors induced in vitro in epidermal cell cultures by a single dose of UVB radiation may have the same antigenic characteristics as those induced by UV irradiation in vivo (*22*) makes it an intriguing hypothesis for further consideration.

REFERENCES

(*1*) Hausser KW, Vahle W. Sunburn and suntanning. In: Urbach F, ed. Biologic effects of ultraviolet radiation. New York: Pergamon Press, 1969:3–21.

(*2*) Rauth AM. Effects of UV light on mammalian cells in culture. Curr Top Radiat Res 1970; 6:193–248.

(*3*) Pathak MA, Kramer DM, Fitzpatrick TB. Photobiology and photochemistry of furocoumarins (psoralens). In: Pathak MA, Harber LC, Seiji M, Kukita A, eds. Sunlight and man. Tokyo: Univ Tokyo Press, 1974:335–368.

(*4*) Song P-S, Tapley KJ Jr. Photochemistry and photobiology of psoralens. Photochem Photobiol 1979; 29:1177–1197.

(*5*) Epstein JH. Photocarcinogenesis: A review. Natl Cancer Inst Monogr 1978; 50:13–26.

(*6*) Griffin AC. Methoxsalen in ultraviolet carcinogenesis in the mouse. J Invest Dermatol 1959; 32:367–372.

(*7*) Stern RS, Thibodeau LA, Kleinerman RA, et al. Risk of cutaneous carcinoma in patients treated with oral methoxsalen photochemotherapy for psoriasis. N Engl J Med 1979; 300:809–813.

(*8*) Smith KC. Molecular changes in the nucleic acids produced by ultraviolet and visible radiation. In: Pathak MA, Harber LC, Seiji M, Kukita A, eds. Sunlight and man. Tokyo: Univ Tokyo Press, 1974:57–66.

(*9*) Kripke ML. Antigenicity of murine skin tumors induced by ultraviolet light. J Natl Cancer Inst 1974; 53:1333–1336.

(*10*) ———. Latency, histology and antigenicity of tumors induced by ultraviolet light in three inbred mouse strains. Cancer Res 1977; 37:1395–1400.

(*11*) Daynes RA, Spellman CW, Woodward JG, Stewart DA. Studies into the transplantation biology of ultraviolet light-induced tumors. Transplantation 1977; 23:343–348.

(*12*) Fisher MS, Kripke ML. Systemic alteration induced in mice by ultraviolet light irradiation and its relationship to ultraviolet carcinogenesis. Proc Natl Acad Sci USA 1977; 74:1688–1692.

(*13*) ———. Further studies on the tumor-specific suppressor cells induced by ultraviolet radiation. J Immunol 1978; 121:1139–1144.

(*14*) Daynes RA, Spellman CW. Evidence for the generation of suppressor cells by ultraviolet radiation. Cell Immunol 1977; 31:182–187.

(*15*) DE FABO EE, KRIPKE ML. Wavelength dependence and dose-rate independence of UV radiation-induced immunologic unresponsiveness of mice to a UV-induced fibrosarcoma. Photochem Photobiol 1980; 32:183-188.

(*16*) PETERS LC, BRANDHORST JA, HANNA MG JR. Preparation of immunotherapeutic autologous tumor cell vaccines from solid tumors. Cancer Res 1979; 39:1353-1360.

(*17*) KRIPKE ML, THORN RM, LILL PH, CIVIN CI, PAZMIÑO NH, FISHER MS. Further characterization of immunologic unresponsiveness induced in mice by UV radiation: Growth and induction of non-UV-induced tumors in UV-irradiated mice. Transplantation 1979; 28:212-217.

(*18*) PREHN RT. Relationship of tumor immunogenicity to concentration of the oncogen. J Natl Cancer Inst 1975; 55:189-190.

(*19*) KRIPKE ML. Immunologic mechanisms in UV radiation carcinogenesis. Adv Cancer Res 1981; 34:69-106.

(*20*) ROENIGK HH JR, CARO WA. Skin cancer in the PUVA-48 cooperative study. J Am Acad Dermatol 1981; 4:319-324.

(*21*) KRIPKE ML, MORISON WL, PARRISH JA. Differences in the immunologic reactivity of mice treated with UVB or methoxsalen plus UVA radiation. J Invest Dermatol 1981; 76:445-448.

(*22*) ANANTHASWAMY HW, KRIPKE ML. In vitro transformation of primary cultures of neonatal BALB/c mouse epidermal cells with ultraviolet-B radiation. Cancer Res 1981; 41:2882-2890.

Influences of Age and Anatomical Site on Ultraviolet Carcinogenesis in BALB/c Mice[1,2,3]

Peter Ebbesen[4] *and* **Margaret L. Kripke**[5,6]

ABSTRACT—Young adult BALB/c mice were more susceptible to the induction of skin tumors from FS40 sunlamps than were 18-month-old animals. The relative contributions of tissue and host factors to this difference in susceptibility to carcinogenesis were analyzed by reciprocal grafting of skin between young and old animals, followed by repeated exposures of the grafts to UV radiation. More tumors developed in ear skin grafted to the middorsum of young recipients than in that of old recipients, regardless of the age of the skin donor. These ear skin grafts were more susceptible to tumor induction than were comparable grafts of back skin. When large areas of dorsal skin (16 cm^2) were grafted to young adult mice, very old skin (>2 yr) was more susceptible to tumor induction than skin that was 1 year old at the start of irradiation.—JNCI 1982; 68:691–694.

The incidence of nonmelanoma skin cancer in humans increases markedly with increasing age in susceptible populations. Furthermore, these skin cancers frequently occur on parts of the body that are the most heavily exposed to solar radiation (*1*). These observations have been interpreted as indicating that sunlight-induced skin cancer results from the progressive accumulation of actinic damage on sun-exposed parts of the body (*2*). However, the contribution of other factors, such as differences in the intrinsic susceptibility of skin from different sites or of different ages to carcinogenesis or age-dependent differences in host defense mechanisms, has not been ruled out.

To explore some of these possibilities, we have used the system of experimental UV carcinogenesis in inbred mice (*3*). Previous work with chemical carcinogens showed that one can analyze the contributions of various host and tissue properties to carcinogenesis by grafting skin of different sources onto syngeneic recipients and studying the development of tumors in the grafted skin (*4, 5*). In these experiments, we have used this approach to separate the factors of cumulative UV dose, tissue age and site, and host influences to determine whether the skin obtained from mice of different ages possesses intrinsic differences that affect its photocarcinogenic response. In addition, we compared the relative susceptibility to UV carcinogenesis of ear skin and back skin by grafting these tissues onto the backs of syngeneic mice and by exposing the grafts to UV radiation.

MATERIALS AND METHODS

Animals.—Specific-pathogen-free BALB/cAnN mice were supplied by the NCI-Frederick Cancer Research Facility's Animal Production Area. They were given free access to water (10–12 ppm chlorine) and Purina Mouse Chow, except during UV exposure, and were housed in rooms where ambient light was automatically regulated on a 12-hour light–dark cycle.

Skin grafts.—Skin removed from the backs of donor mice was scraped with a scalpel to remove subcutaneous fat and connective tissue. A cork borer was used to cut uniform circular grafts 1.5 cm in diameter. Ear skin was prepared by separation of the anterior and posterior ear surfaces and by removal of the cartilage layer. Both surfaces were used as grafts. The recipients were anesthetized with Diabutal, and graft beds the size of the grafts were cut with scissors in the dorsal skin down to the pannicular layer. The grafts were held in place with four sutures and covered with adhesive bandages for 6 days. Each animal received one graft of ear skin and one graft of back skin. In half of the mice, the ear graft was placed anterior to the back skin graft; in the other half, the position of the grafts was reversed. In one experiment, large squares of back skin (16 cm^2) were grafted onto the recipients. These were held in place with wound clips. To prevent tumors from developing in the recipient mice outside of the graft area, we removed the ears of the recipients. We removed only the fur on the grafted skin before UV exposure.

UV irradiation.—The mice were shaved once a week with electric clippers and were exposed three times per week (Monday, Wednesday, and Friday) to a bank of six FS40 sunlamps (Westinghouse, Bloomfield, N.J.). For the first 8 weeks, the animals were given 30-minute exposures; thereafter, each treatment consisted of a 60-minute exposure. In experiments with the small grafts, UV irradiation began 3 months after grafting; in the experiment with 16-cm^2 grafts, UV treatment was started 10 months after grafting.

The mice were housed on shelves 20 cm below the sunlamps, and the cages were rotated systematically along the shelf before each UV exposure to ensure uniform irradiation over the course of the experiment. The average dose rate of the light source was approximately 2 J/m^2/second, as measured with a non-cosine-correcting Hewlett-Packard radiant flux detector (model 8344A), with a sensitivity of 0.1 μV/μW/cm^2. Approximately 80% of the total energy of the

---

[1] Received August 28, 1981; accepted December 11, 1981.

[2] Supported by Public Health Service (PHS) contract N01CO-75380 from the Office of the Director, National Cancer Institute (NCI), with Litton Bionetics, Inc. (M. L. K.); and by PHS grant 1-R01CA-26109-02 (P. E.) from the NCI. The contents of this publication do not necessarily reflect the views or policies of the U.S. Department of Health and Human Services, nor does mention of trade names, commercial products, or organizations imply endorsement by the U.S. Government.

[3] Animals were maintained under the guidelines set forth by the National Institutes of Health Policy on Humane Care and Use of Animals and by the Animal Welfare Act in facilities accredited by the American Association for Accreditation of Laboratory Animal Care.

[4] Institute of Cancer Research, Aarhus DK-8000, Denmark.

[5] Cancer Biology Program, NCI-Frederick Cancer Research Facility, P.O. Box B, Frederick, Md. 21701.

[6] *Address reprint requests to* Dr. Kripke.

sunlamps is emitted in the wavelength range from 280 to 340 nm, with a peak emission at 313 nm. The mice were irradiated through wire cage tops that reduced the irradiance by a factor of 2.

The mice were examined weekly for tumor development, and each tumor was measured weekly. The time of tumor appearance was determined retrospectively as the week at which a progressively growing lesion reached a size of 4×4 mm in diameter. When a tumor reached the size of approximately 10×10 mm, the animal was killed and the tumor was fixed in Bouin's solution, sectioned, and stained with hematoxylin and eosin for microscopic evaluation. Only 1 tumor-bearing mouse died before the tumor tissue could be prepared for histologic analysis; all other tumors were evaluated microscopically.

Statistical tests.—The method of Kaplan and Meier (*6*) was used to describe the patterns of tumor development in the carcinogenesis studies. This is a life-table analysis and thus takes into account animals that die before developing a tumor. The results were expressed as the probability that an animal has a tumor as the function of the duration of the experiment. Differences between treatment groups were tested with a censored rank order test according to the method of Breslow (*7*).

RESULTS

Tumor Induction in Young and Old Mice

In the first experiment, the rate of tumor induction in ungrafted skin by UV radiation was compared in young and old BALB/c male mice. The "young" mice were 4–5 weeks old at the time of their first exposure to UV radiation; the "old" mice were 18 months old at the initiation of treatment. Cages of young and old mice were alternated on each shelf of the irradiator to minimize the possibility of inadvertently introducing differences in the exposure of the 2 groups to UV radiation.

As is illustrated in text-figure 1, tumor development began earlier in the young mice than in the older animals, and the patterns of tumor development differed significantly for the 2 groups ($P=0.026$). Thus when mice are given equivalent doses of UV radiation, the younger animals are more susceptible to the carcinogenic effects of UV radiation than are the older mice in that the latent period is shortened. However, by 32 weeks of irradiation, the incidence of tumors was the same in both groups. Most tumors in both groups were squamous cell carcinomas and fibrosarcomas that arose on the ears. No differences were noted between the 2 groups in the proportion of tumors of these two histologic types.

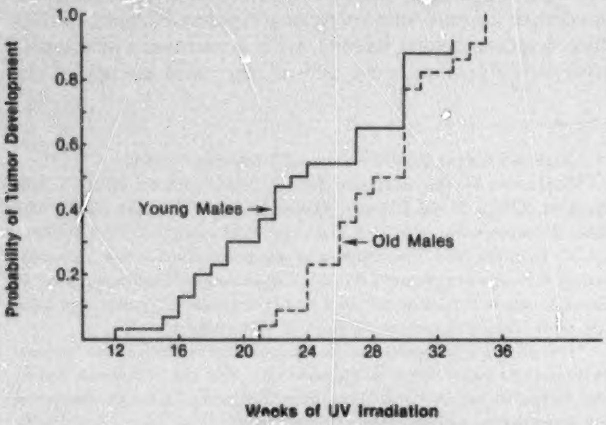

TEXT-FIGURE 1.—Probability of skin cancer development in BALB/c male mice exposed to FS40 sunlamp irradiation three times per week. The young mice (No.=30) were 4 wk old, and the old mice (No.=22) were 18 mo old at the start of the UV treatment. The probability of no difference between these groups is <3%, as determined by a two-tailed *t*-test.

Tumor Induction in Grafted Skin

To determine whether the increased susceptibility of young mice to UV carcinogenesis was an inherent property of the skin, we measured the rate of tumor development for young ear and back skin grafted to young recipients and compared it with that of young ear and back skin grafted to older mice. We performed an analogous experiment with skin from old donors. In this experiment, female mice were used throughout to minimize the problem of damage to grafts caused by fighting among the males. In addition, 4-week-old animals could not be used as graft recipients because of their small size and relative frailty, so the grafting was performed on mice that were 10–12 weeks old. UV irradiation commenced 12 weeks after grafting, so that at the start of UV exposure the young mice were 22–24 weeks old and the old mice were 70 weeks old. Tumor incidence data were collected until week 37 of the UV irradiation, which was the time when the older mice reached approximately 2 years of age.

The tumor incidence data obtained with the ear skin grafts are summarized in table 1. The rate of tumor development was not affected by the grafting procedure. Ear tumors developed on the young mice (group 1) at the same rate as tumors arose on the young ear skin grafted to young recipients (group 2), and tumors appeared on the ears of old mice (group 4) at the same rate as they developed in old ear skin grafted to old recipients (group 5) ($P>0.1$ for both comparisons). Again, the young mice developed tumors more rapidly than the old mice, although this difference was smaller than in the previous experiment (group 1 vs. 4, $P=0.035$; groups 1 and 2 vs. 4 and 5, $P=0.007$). This increased susceptibility to tumor development was not an intrinsic property of the ear skin, however. When young ear skin was grafted to old recipients (group 6), the pattern of tumor development resembled that observed with old skin (groups 4 and 5). Conversely, old skin grafted to young recipients (group 3) assumed the characteristics of young skin with regard to tumor induction (groups 1 and 2). There were no detectable differences in the patterns of tumor induction among groups 1, 2, and 3 or among groups 4, 5, and 6 ($P<0.1$ for all comparisons). However, tumor development differed significantly in old skin grafted to young recipients (group 3) and old skin grafted to old recipients (group 5, $P=0.05$) and in the reverse situation of young skin grafted to old mice (group 6) versus young skin grafted to young recipients (group 2; $P=0.004$). Thus the pattern of tumor development in the grafted ear skin resembled that

TABLE 1.—*Development of UV-induced tumors in grafts of young or old ear skin*

Group No.	Graft	Host[a]	No. of mice at start of UV treatment	No. of mice that died tumor-free	No. of tumor-bearing mice	Tumor incidence, %[b]	Average latency, wk[c]
1	None	Young	40	0	28	70	31
2	Young	Young	41	0	30	73	33
3	Old	Young	40	0	32	80	32
4	None	Old	29	4	16	55	35
5	Old	Old	30	4	16	53	36
6	Young	Old	32	4	15	47	35

[a] Young=20-22 wk at start of UV treatment; old=70 wk at start of UV treatment. All mice were BALB/c females.

[b] Number of mice that developed tumors in 37 wk/number at start of UV treatment.

[c] Week at which the probability of tumor development first equalled or exceeded 0.5.

observed in the recipients and did not resemble the pattern exhibited by the graft donors.

In this experiment, the mice had been grafted with both ear skin and circular pieces of dorsal skin, 1.5 cm in diameter. In spite of the fact that the ear and back skin grafts were approximately the same size and received equivalent exposures to UV radiation, tumors developed in only two of the back skin grafts. In both cases, tumors had appeared earlier in the grafted ear skin. In all groups, tumors appeared only at sites that were exposed directly to UV radiation, i.e., the ears on ungrafted mice and the shaved graft sites of the grafted animals.

In the final experiment, we attempted to compare the susceptibility of adult and senescent mouse skin to photocarcinogenesis. In this instance, large (16 cm^2) squares of back skin were grafted from 10- or 60-week-old female donors onto 10-week-old female recipients. UV irradiation was initiated 45 weeks later, so that the "adult" skin was approximately 1 year old at this time and the senescent skin was 2 years old. During the next 6 months of UV treatment and observation, 4 of the 106 ungrafted adult mice developed back tumors (text-fig. 2). The grafting of skin of the same age as the skin of these animals did not affect this pattern of tumor induction (5 of 91 mice developed skin cancers). However, tumor development was markedly enhanced in the senescent skin (17 of 77 mice developed cancers in the grafted skin). Tumors occurred only on the shaved dorsum of these animals since their ears had been removed prior to irradiation. No differences in the histologic types or proportion of different tumor types were noted among the groups. The ratio of carcinomas:sarcomas was between 3 and 4:1 in all groups.

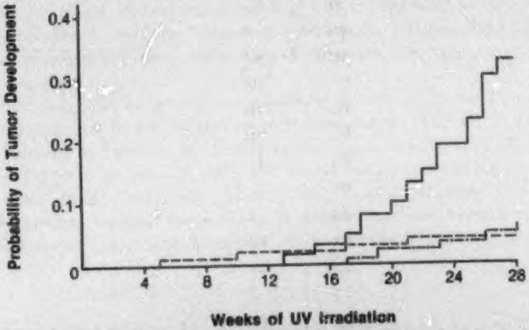

TEXT-FIGURE 2.—Probability of cancer development in grafted back skin of female BALB/c mice. Ungrafted, 12-mo-old mice (- - - -) (No.=106 at start of UV treatment); mice grafted with 12-mo-old skin (-·-·-) (No.=91 at start of UV treatment); mice grafted with 24-mo-old skin (——) (No.=77 at start of UV treatment). The probability of no difference between the rate of cancer development in old skin versus each of the other groups is <0.1% as determined by a two-tailed t-test.

DISCUSSION

These studies indicate that young mice, between the ages of 1 and 6 months, are more susceptible than 18-month-old mice to photocarcinogenesis. This finding agrees with the experiment reported by Blum et al (*8*) in which tumors appeared more readily on the ears of 2- to 3-month-old haired albino mice than on the ears of mice that were 10 months old at the start of irradiation. Forbes et al. (*9*), who compared photocarcinogenesis in hairless mice, made a similar observation, namely, that mice 6 weeks old at the beginning of UV treatment developed tumors more rapidly than 16-week-old animals. The grafting experiment (table 1) suggests, in addition, that this difference is not attributable to some inherent characteristic of the skin but, rather, depends on certain physiologic factors in the host that change as a function of age. This result raises the interesting possibility that during the first half of the life-span of the animals, the age of the host at the time of the first UV exposures may be a determining factor in UV carcinogenesis.

When large grafts were used as a target for UV carcinogenesis, the skin from very old (>2 yr) mice appeared to be more susceptible to transformation than skins from adult animals (text-fig. 2). This was an intrinsic property of the skin since the recipients were all from the same age group. The difference between this result and the result obtained with the small grafts could be due to the very advanced age of the skin used for large grafts; alternatively, the size of the graft could be a determining factor in whether host or tissue influences dominate a given situation. With large grafts, the expression of any host influences might be minimized.

The sources of these differences in host factors and skin properties are not known, but there are many possible candidates for such an effect. For example, the ability to repair certain types of UV-induced damage in DNA changes with age in BALB/c mice (*10*), the proliferative response of epidermal cells to UV radiation differs in animals of different ages (*11*), the activity of various host defense mechanisms changes with age (*12*), and in human skin the mechanical and optical properties change with age (*13*). Regardless of the underlying mechanisms, it is clear that the total cumulative dose of UV radiation and genetic susceptibility are not the only determining factors in photocarcinogenesis. Under conditions in which genetic background, total UV dose, and time for tumor development remained constant, age-dependent host factors and skin properties that influence photocarcinogenesis can be detected. In the study comparing grafted ears and small back-skin grafts, most tumors developed in the ear grafts. Of 93 grafted tumor-bearing mice, all developed tumors on the grafted ear skin, and only 2 of these animals subsequently developed tumors on the grafted back skin as well. Thus the greater susceptibility of ears to photocarcinogenesis relative to back skin in this strain does not result from greater exposure of the ears to UV radiation, as might be expected because of their position relative to the back. Instead, this high frequency of tumor development seems to reflect the fact that ear skin is intrinsically more susceptible to the carcinogenic effects of UV radiation than back skin, most likely because of differences in the optical properties of ears and back skin, resulting from differences in pelage and in thickness of the stratum corneum.

Thus, although UV dose and genetic background clearly influence photocarcinogenesis both in humans (*1*) and experimental animals (*3*), these studies show that other intrinsic properties of the target tissue and age-dependent properties of the host also play a role in the development of UV-induced skin cancers. These findings, coupled with those of Forbes et al. (*9*) demonstrating that photocarcinogenesis also is influenced by the pattern of UV dose delivery, emphasize the complexity of this tumor system and illustrate the difficulties underlying calculations of estimated risks for human photocarcinogenesis.

REFERENCES

(*1*) Urbach F. Geographic pathology of skin cancer. In: Urbach F, ed. The biologic effects of ultraviolet radiation, Oxford: Pergamon Press, 1969:635–650.

(*2*) Fears TR, Scotto J, Schneiderman MA. Mathematical models of age and ultraviolet effects on the incidence of skin cancer among whites in the United States. Am J Epidemiol 1977; 105:420–427.

(*3*) Kripke ML. Latency, histology, and antigenicity of tumors induced by ultraviolet light in three inbred mouse strains. Cancer Res 1977; 37:1395–1400.

(*4*) Ebbesen P. Ageing increases susceptibility of mouse skin to DMBA carcinogenesis independent of general immune status. Science 1974; 183:217–218.

(*5*) Lappé MA. Evidence for the antigenicity of papillomas induced by 3-methylcholanthrene. J Natl Cancer Inst 1968; 40:823–846.

(*6*) Kaplan EL, Meier P. Nonparametric estimation from incomplete observations. J Am Stat Assoc 1958; 53:457–481.

(*7*) Breslow N. A generalized Kruskal-Wallis test for comparing k samples to unequal censorship. Biometrika 1970; 57:579.

(*8*) Blum HF, Grady HG, Kirby-Smith JS. Relationships between dosage and rate of tumor induction by ultraviolet radiation. J Natl Cancer Inst 1942; 3:91–97.

(*9*) Forbes PD, Davies RE, Urbach F. Aging, environmental influences, and photocarcinogenesis. J Invest Dermatol 1979; 73:131–134.

(*10*) Ananthaswamy HN, Fisher MS. Photoreactivation of ultraviolet radiation-induced pyrimidine dimers in neonatal BALB/c mouse skin. Cancer Res 1981; 41:1829–1833.

(*11*) Grekin DA, Epstein JH. Effects of age on acute UVB-induced skin responses. Proc Am Soc Photobiol 1981; 9:75

(*12*) Makinodon T. Mechanism, prevention and restoration of immunologic aging. Birth Defects 1978; 14:197–212.

(*13*) Daly CH, Odland GF. Age-related changes in the mechanical properties of human skin. J Invest Dermatol 1979, 73:84–87.

Announcements

The Journal *will publish notices of major meetings dealing with cancer. Submission of notices 6 months in advance is requested to permit timely publication.*

American Cancer Society National Conference—The Primary Care Physician and Cancer

The American Cancer Society, in cooperation with the American Academy of Family Physicians, will sponsor this conference to be held at the Hyatt Regency Washington on Capitol Hill, Washington, D. C., on June 24–26, 1982. The objective of this conference is to provide an increased understanding by the primary care physician of the wide range of medical and psychosocial problems of the cancer patient. The multidisciplinary approach to managing these problems will be stressed.

Attendance is open to members and students of the medical and health-related professions. There is no registration fee; advance registration is requested. For additional information please write to Dr. Nicholas G. Bottiglieri, American Cancer Society Conference, The Primary Care Physician and Cancer, 777 Third Avenue, New York, New York 10017.

Eleventh Annual Meeting of the International Society for Experimental Hematology

Baltimore, Maryland, will be the site of this meeting to be held on August 12–15, 1982. For additional information please contact Dr. Lyle R. Heim, Department of Pediatrics, Texas Tech University, School of Medicine, 4800 Alberta Avenue, El Paso, Texas 79905.

Workshop on "Coagulation, Cancer and Inflammation"

The National Heart, Lung, and Blood Institute, the National Cancer Institute, and the National Institute of Arthritis, Diabetes, and Digestive and Kidney Diseases will sponsor this workshop to be held at the Airlie House, Airlie, Virginia, on September 8–10, 1982. This workshop will address the roles of the coagulation and fibrinolytic pathways, the monocyte and macrophage, and the integrated interactions between fluid phase molecules and cells in the pathobiology of thrombotic disease, cancer, and inflammation.

Those who wish to attend the workshop should notify the National Heart, Lung, and Blood Institute in writing by July 1, 1982, and indicate their specialty and specific research interests. Applicants will be notified of their acceptance by July 15, 1982. For further details or to apply for the conference, please contact Dr. Anne P. Ball, Division of Blood Diseases and Resources, National Heart, Lung, and Blood Institute, Federal Building, Room 5A12, Bethesda, Maryland 20205 (telephone: 301-496-5911).

Approaches to the Management of Pain

The Bay Area Tumor Institute and the East Bay Cancer Program will co-sponsor this conference to be held at Goodman's Hall, 10 Jack London Square, Oakland, California, on September 9, 1982. The conference will deal with the multidisciplinary approach to the management of pain.

For additional information contact Ms. Despina C. M. Johnson, Program Manager, 2844 Summit Street, Suite 204, Oakland, California 94609 (telephone: 415-465-8570).

Eighth Biannual Morris Hepatoma Symposium

This Satellite Symposium of the Thirteenth International Cancer Congress will be held at the Westin Hotel, Fifth Avenue at Westlake, Seattle, Washington, on September 16, 1982.

Additional information may be obtained from Dr. Wayne E. Criss, Morris Hepatoma Program Director, Cancer Center, Howard University, Washington, D. C. 20060 (telephone: 202-636-6351/52).

Fourteenth Meeting of the International Society for Pediatric Oncology (SIOP)

Berne, Switzerland, will be the site of this meeting to be held at the Department of Pediatrics, Inselspital, Berne, on September 21–25, 1982. "New Modes of Therapy and Supportive Care" will be the main theme of the meeting. Reports on current trials and a pathologists' meeting will be included.

For further information please write to Dr. Hans P. Wagner, c/o SPOG, Institute for Clinical and Experimental Cancer Research, Tiefenauspital, 3004 Berne, Switzerland.

Second International Congress of the T. and L. de Beaumont Bonelli Foundation for Cancer Research

"The Role of Viruses in Human Cancer" is the subject of this conference to be held in the Royal Palace, Naples, Italy, on September 23–26, 1982. The purpose of the conference is to provide current results and perspectives in main areas in which viruses have been potentially associated with human malignancies.

Additional information may be obtained from Dr. Errico di Lorenzo, Organizing Secretary, V.le Elena, 80122 Naples, Italy.

Large Bowel Cancer: Biology and Control

An exhibit and brochure, prepared by the National Large Bowel Cancer Project, is available for distribution through the American College of Surgeons. "Finding the Cause," "Current Management," and "Toward the Solution" are the topic areas of this three-panel exhibit and 36-page brochure that are particularly suited for teaching seminars, national meetings, and workshops on cancer of the large bowel.

The exhibit and brochures can be obtained separately or together. There is no fee for either, except for shipping charges. For further information, please contact Ms. Irene J. Diament, Administrative Assistant, Cancer Department, American College of Surgeons, Chicago, Illinois 60611 (telephone: 312-664-4050).

U.S. GOVERNMENT PRINTING OFFICE: 1982-311-216/53

blank page

JNCI (NIH Publication No. 82-13)

68/5

JNCI

Journal of the National Cancer Institute
May 1982
Volume 68
Number 5

NEWARK PUBLIC LIBRARY
JUN 10 1982
U. S. ... S.
D...

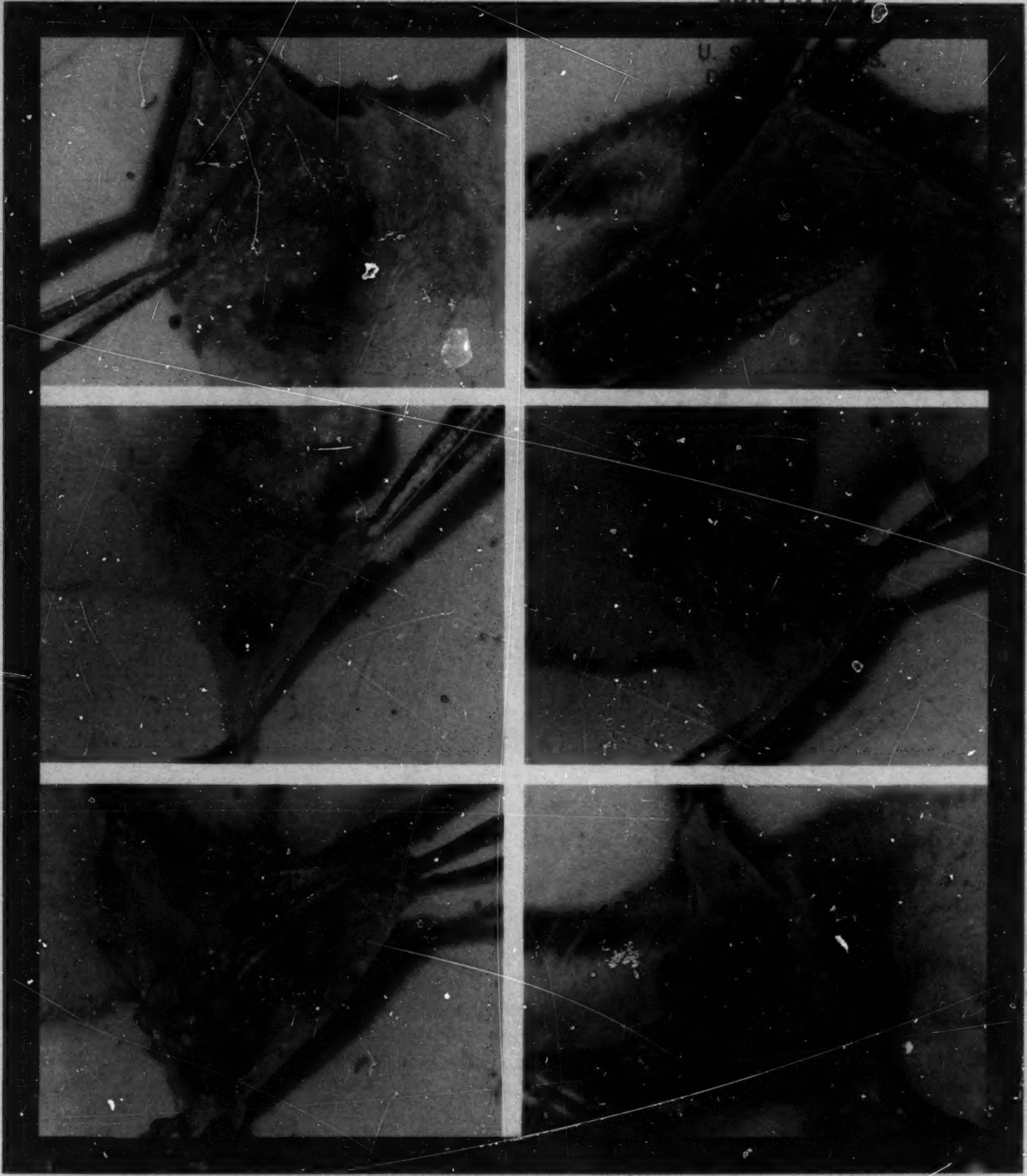

U.S. DEPARTMENT OF HEALTH AND HUMAN SERVICES Public Health Service National Institutes of Health

HE 20. 3161:

The photographs on the cover suggest inhibition by vitamin E of cancer induced by 7,12-dimethylbenz[*a*]anthracene (DMBA) in the buccal pouches of Syrian golden hamsters. Photographs on the *left* show effects of DMBA painting at 10, 12, and 14 weeks; those on the *right* show effects of DMBA plus vitamin E treatment. This study by Shklar (*see* paper on pages 791–797) is one of a growing number of investigations on inhibition of carcinogenesis by micronutrients or their analogues.

JNCI

Journal of the National Cancer Institute

May 1982
Volume 68
Number 5

THE JOURNAL of the National Cancer Institute solicits manuscripts on original observations in laboratory and clinical research from all scientists. A manuscript is considered for publication with the understanding that it has not been published previously and is submitted exclusively to the Journal. Opinions expressed by the authors are not necessarily those of the publisher or its editors.

THE JOURNAL is published monthly (two volumes a year). The Secretary of Health and Human Services has determined that the publication of this periodical is necessary in the transaction of the public business required by law of this Department.

A MONOGRAPH SERIES covering proceedings of scientific meetings pertaining to cancer is also published. These books may be purchased from the Superintendent of Documents. Series subscriptions are not available and monographs are not included in a subscription to the Journal.

THE JOURNAL is for sale by the Superintendent of Documents, U.S. Government Printing Office, Washington, D.C. 20402. Price per copy, $7.00. Subscription price for two volumes per year in the United States, $70.00; foreign, $87.50. Payment is required in advance, and check or money order should be made payable to the Superintendent of Documents.

All inquiries regarding purchase of subscriptions or depository library distribution, including inquiries about missing issues and change of address, should be addressed to the Government Printing Office. The Government Printing Office requires payment in advance on all orders. Inquiries regarding missing issues or change of address for official subscriptions should be addressed to the Editorial Office, Room 850, Westwood Building, 5333 Westbard Avenue, Bethesda, Md. 20016.

VINCENT T. DEVITA, JR., *Director, National Cancer Institute*

BOARD OF EDITORS

PETER GREENWALD, *Editor in Chief*

ELIZABETH K. WEISBURGER, *Assistant Editor in Chief*

STUART A. AARONSON, *Associate Editor*

CHARLES H. EVANS, *Associate Editor*

MARY A. FINK, *Associate Editor*

JANET W. HARTLEY, *Associate Editor*

DONALD HENSON, *Associate Editor*

RONALD B. HERBERMAN, *Associate Editor*

GEORGE S. JOHNSON, *Associate Editor*

KURT W. KOHN, *Associate Editor*

ARTHUR S. LEVINE, *Associate Editor*

JOHN J. MULVIHILL, *Associate Editor*

ALAN S. RABSON, *Associate Editor*

RICHARD M. SIMON, *Associate Editor*

EDITORIAL STAFF

EDWIN A. HAUGH, *Managing Editor*

PAMELA T. ALLEN, *Assistant Managing Editor*

FLORENCE I. GREGORIC, *Monograph Editor*

Editors: DOROTHY D. KATZ, MERCEDES B. LA CHARITY, I. AGNES REVESZ, JOAN O'BRIEN RODRIGUEZ, CONSTANCE R. STONESTREET, and ANNA B. WITTIG

JNCI (NIH Publication No. 82-13)

U.S. DEPARTMENT OF HEALTH AND HUMAN SERVICES Public Health Service National Institutes of Health

Instructions to Authors

Text: Send one original and two copies. **Text-figures** (graphs, charts, and line drawings): Send one original and two copies. **Figures** (photomicrographs and photographs): Send three original glossy prints, unmounted. **Tables:** Send tabular material in typewritten form; do not submit tables as glossy prints to be photographed. The entire manuscript including footnotes, legends, and references must be typed double spaced. Single-spaced portions of a manuscript will be returned to the author for retyping. The mailing address is: Journal of the National Cancer Institute, Westwood Building, Room 850, 5333 Westbard Avenue, Bethesda, Maryland 20016.

Manuscripts should be accompanied by a covering letter from the author responsible for correspondence about the manuscript. The covering letter should contain a statement that the manuscript has been seen and approved by all authors and that all persons listed as authors have made significant (not merely administrative, technical, or supervisory) contributions to the content of the paper. The letter should also state that the manuscript or substantial portions thereof have not been previously published nor are they under consideration for publication in another journal.

Data too extensive for inclusion in a manuscript, but which may be of interest to other investigators, may be deposited with the National Auxiliary Publications Service (NAPS), c/o Microfiche Publications, P.O. Box 3513, Grand Central Station, New York, New York 10017. Authors using the NAPS facilities should indicate in a footnote how their additional data may be obtained.

TITLE: Be brief (no more than 14 words, if possible), but for indexing purposes include all key words. The annual subject index is prepared directly from the titles. Titles that form complete sentences are not acceptable. Do not use abbreviations or chemical formulas in titles.

BYLINE: Supply the complete first name, middle initial, and last name of each author. Avoid use of nicknames. Academic degree is optional; however, if a degree is provided for one author, it should be provided for all authors on a manuscript. Include the name of the institution, address, and zip code for each author. Indicate address for reprint requests in a footnote on the byline.

ACKNOWLEDGMENTS: Financial aid in support of research should be recognized in a footnote. Aid in technical fields, animal care, photography, stenography, and other areas may be mentioned in a separate footnote. Indicate the title (Dr., Mr., Mrs., Miss, Ms.) and affiliation of each person acknowledged.

ABSTRACT: Provide an abstract, 150 words or less, on a separate page. The abstract should describe only *results* of the work being reported. Speculation, historical background, or reference to published works will be deleted from abstracts. Any inbred strains, noninbred stocks, cell lines, or other living materials used in the work should be noted in the abstract.

TEXT: Avoid the use of laboratory jargon and abbreviations not in common usage. When possible, refrain from the use of abbreviations that form words (exceptions are PAGE, ALL). Whenever possible, write mathematical equations and chemical formulas on a single line; submit complicated chemical structures as artwork. Avoid repetition of data in the text when it is presented in tables or text-figures.

Use the following style sources: Webster's *Third New International Dictionary* and Dorland's *Illustrated Medical Dictionary* (25th ed) for spelling; *Council of Biology Editors Style Manual* (4th ed) for scientific abbreviations and symbols: *Government Printing Office Style Manual* for other abbreviations and symbols, punctuation, and hyphenation; *Biochemical Nomenclature and Related Documents* (IUB, 1978) for abbreviations of chemical substances; *Enzyme Nomenclature*, recommendations (1978) of the IUB for recommended names of enzymes and information on nomenclature of isozymes; *The Merck Index* (9th ed) for chemical compounds; "Standard Nomenclature for Inbred Strains of Mice: Seventh Listing" by Joan Staats (Cancer Res 1980;40: 2083–2128) for inbred mouse strains; "Standardized Nomenclature for Inbred Strains of Rats: Fourth Listing" by Joan Staats and Michael Festing (Transplantation 1973;16:221–245) for designations of inbred rat strains; *Animals for Research* (9th ed) prepared by the Institute of Laboratory Animal Resources, National Academy of Sciences, for designations of laboratory animal stocks and strains.

TABLES: Submit tabular material typed double spaced on a separate page. Computer print-outs of tables are acceptable only if they are double spaced and with satisfactory title, column headings, legends and other textual material. Provide headings for all columns of a table and indicate units of measurement where applicable.

TEXT-FIGURES: Refer to graphs, charts, and line drawings as text-figures. Make the abbreviations on text-figures identical to the abbreviations used in the text and legends. Symbols and lettering should be large enough to be legible if reduced. Glossy prints or original drawings in black ink are acceptable; orient vertically instead of horizontally.

FIGURES: Refer to photomicrographs and photographs as figures. Figures and their legends should fit a 7.5- by 9-inch dimension. Calculate that nine typewritten lines of legend will require 1 inch of vertical space. Type figure legends on a separate sheet and identify in the legend any lettering used on the figure. Trim photographs to show only important areas. Do not number face of photographs; use the back or overlay to indicate the top and number of each. Printed indicators may be included on photographs; do not use hand-drawn indicators. *Insert internal scale markers on all photomicrographs.* Color photographs must be grouped as a single plate. For color reproduction, submit both color transparencies and high-quality black and white reproductions. The need for color must be documented before it will be considered.

REFERENCES: Use any recent issue of the Journal as a style guide for reference lists. Number references in order of citation in both text and reference list. For periodicals, provide author(s), title of paper, journal, year, volume, and first and last page numbers. For books, give the author(s), title, name(s) of editor(s), location and name of publisher, year, pertinent chapter or section title, and page numbers. Follow *Index Medicus* for punctuation and abbreviations. Citations of papers in preparation or submitted for publication, unpublished observations, and personal communications should be noted parenthetically in the text. Do *not* include them in the reference list. The accuracy of all references is the responsibility of the authors and not of the editorial staff.

LETTERS TO THE EDITOR should pertain to recent articles in the Journal and should not contain new data unless relevant to the discussion of a particular paper. The authors addressed will be invited to reply to comments before correspondence is published. Letters will be edited by the Staff, subject to contributor approval.

FURTHER DETAILS on the preparation of manuscripts are set forth in the document "Uniform Requirements for Manuscripts Submitted to Biomedical Journals" prepared by the International Steering Committee of medical editors (*see* Am Rev Respir Dis 1979;119:3–10/Ann Intern Med 1979;90:95–99/Br Med J 1979;1:532–535/ or Lancet 1979;1:428–430).

UNITED STATES GOVERNMENT PRINTING OFFICE, WASHINGTON, D.C.: 1982

Table of Contents

Vol. 68, No. 5—May 1982

Investigations on Man

697	Heterogeneous response to X-ray and ultraviolet light irradiations of cultured skin fibroblasts in two families with Gardner's syndrome	*Timothy J. Kinsella, John B. Little, John Nove, Ralph R. Weichselbaum, Frederick P. Li, Robert J. Meyer, David J. Marchetto, W. Bradford Patterson*
703	Systemic administration of human leukocyte interferon to melanoma patients. I. Effects on natural killer function and cell populations	*Sidney H. Golub, Fred Dorey, Dean Hara, Donald L. Morton, Martyn W. Burk*
711	Systemic administration of human leukocyte interferon to melanoma patients. II. Cellular events associated with changes in natural killer cytotoxicity	*Sidney H. Golub, Paula D'Amore, Marcia Rainey*
719	Characterization of a monoclonal antibody reactive with a subset of human breast tumors	*Dorothy Yuan, Fred J. Hendler, Ellen S. Vitetta*
729	Epidemiologic and age-dependent data on multiple myeloma in Austria	*Heinz Ludwig, Elke Fritz, Hans P. Friedl*
735	Generation of suppressor cells for natural killer activity in cancer patients after surgery	*Atsushi Uchida, Roland Kolb, Michael Micksche*
743	Measurement of cancer incidence in the United States: Sources and uses of data	*E. Robert Greenberg, Theodore Colton, Curtis Bagne*
751	Degrees of malignancy in human primary central nervous system tumors: Ornithine decarboxylase levels as better indicators than adenosylmethionine decarboxylase levels	*Giuseppe Scalabrino, Daniela Modena, Maria Elena Ferioli, Mirella Puerari, Giovanni Luccarelli*
755	An increased risk for lung cancer mortality associated with sugarcane farming	*Henry Rothschild, James J. Mulvey*
761	A 94,000-dalton glycoprotein expressed by human melanoma and carcinoma cells	*Kohzoh Imai, Barry S. Wilson, Aldo Bigotti, Pier G. Natali, Soldano Ferrone*
771	Isolation, culture, and transplantation of human hepatocytes	*S. C. Strom, R. L. Jirtle, R. S. Jones, D. L. Novicki, M. R. Rosenberg, A. Novotny, G. Irons, J. R. McLain, G. Michalopoulos*
779	Mitogen-induced blastogenesis and receptor mobility inhibition by breast cancer serum with elevated orosomucoid (α_1-acid glycoprotein) levels	*David A. Cheresh, John A. Distasio, Charles L. Vogel, Diana M. Lopez*

Investigations on Nonhuman Systems

785 Zinc deficiency, alcohol, and a retinoid: Association with esophageal cancer in rats — *Gamal N. Gabrial, Thomas F. Schrager, Paul M. Newberne*

791 Oral mucosal carcinogenesis in hamsters: Inhibition by vitamin E — *Gerald Shklar*

799 Thy-1 antigen on normal and neoplastic rat mammary tissues: Changes in location and amount of antigen during differentiation of cultured stem cells — *Philip S. Rudland, Michael J. Warburton, Paul Monaghan, Mary A. Ritter*

813 Surgical resection of the rat colon: Effects on carcinogenesis by 1,2-dimethylhydrazine — *C. A. Rubio, G. Nylander*

817 Intracerebral adoptive immunotherapy of a murine lymphoma antigenically altered by drug treatment in vivo — *L. Romani, M. C. Fioretti, R. Bianchi, B. Nardelli, E. Bonmassar*

823 Combined treatments with vitamin A and 5-fluorouracil and the growth of allotransplantable and syngeneic tumors in mice — *Yoshifumi Tomita, Kunisuke Himeno, Kikuo Nomoto, Hideya Endo, Tomio Hirohata*

829 Comparative tumor-initiating activity of complex mixtures from environmental particulate emissions on SENCAR mouse skin — *Stephen Nesnow, Larry L. Triplett, Thomas J. Slaga*

835 Moloney murine sarcoma virus tumors in CBA/J mice: Chemopreventive and chemotherapeutic actions of supplemental β-carotene — *Eli Seifter, Giuseppe Rettura, Jacques Padawer, Stanley M. Levenson*

841 Nonimmunogenic radiation-induced lymphoma: Immunity induction by a somatic cell hybrid — *Eitan Yefenof, Mira Goldapfel, Rosalie Ber*

851 Purification and transplantation of hepatocytes from livers of carcinogen-treated rats — *Steven B. Miller, Theresa P. Pretlow, Joe A. Scott, Thomas G. Pretlow II*

859 Malignant fibrous histiocytomas induced by 4-(hydroxyamino)quinoline 1-oxide in rats — *Yoichi Konishi, Hiroshi Maruyama, Yoshio Mii, Yoshizumi Miyauchi, Yoshihiko Yokose, Kenji Masuhara*

867 Prostate adenocarcinoma in rats: Induction by 3,2′-dimethyl-4-aminobiphenyl — *Shoichi Katayama, Emerich Fiala, Bandaru S. Reddy, Abraham Rivenson, Jerald Silverman, Gary M. Williams, John H. Weisburger*

875 Comparison of in vitro and in vivo effects of thymidine on L1210 leukemia in mice — *Daniel S. Zaharko, Lori M. Ramonas*

Announcements

881 Gordon Research Conference

881 Seventh European Symposium on Hormones and Cell Regulation

881 Southeastern Cancer Research Association Meeting

881 Seventh International Symposium of the World Association of Veterinary Microbiologists, Immunologists, and Specialists in Infectious Diseases

881 Chemotherapy Foundation Symposium V

881 Harvard Medical School Continuing Education Program

881 NIH Consensus Development Panel Statement Available

882 Availability of Serum Panels

882 Scientists Center for Animal Welfare Invites New Applications

882 Disposal of Laboratory Wastes Project

blank page

Heterogeneous Response to X-Ray and Ultraviolet Light Irradiations of Cultured Skin Fibroblasts in Two Families With Gardner's Syndrome[1,2]

Timothy J. Kinsella,[3,4] John B. Little,[3] John Nove,[3] Ralph R. Weichselbaum,[3] Frederick P. Li,[5,6] Robert J. Meyer,[5] David J. Marchetto,[7] *and* W. Bradford Patterson[7]

ABSTRACT—A heterogeneous response to X-ray and far UV (254 nm) light irradiations was found in cultured skin fibroblast lines from 2 separate families with Gardner's syndrome. When compared to 2 normal control cultures and cultures from 2 patients with nonfamilial colon cancer, cultures from 4 clinically affected members of family 1 showed increased sensitivity to the lethal effects of both X-ray and UV light irradiations. These cell lines also showed a delayed pattern of X-ray potentially lethal damage repair (PLDR) and absent UV PLDR. In contrast, cultures from 3 members of family 2 (2 of whom were clinically affected) showed a normal response of survival and PLDR to both X-ray and UV light irradiations. Thus increased sensitivity of cultured skin fibroblasts to X-ray and UV light irradiations was not a consistent in vitro finding in patients with Gardner's syndrome. However, in families with Gardner's syndrome who demonstrate in vitro radiosensitivity, additional studies are needed to assess the usefulness of these techniques in detecting affected individuals prior to the development of colon carcinoma and other manifestations.—JNCI 1982; 68:697–701.

Gardner's syndrome is an autosomal dominant disease characterized by multiple adenomatous polyps of the colon and rectum, associated with osteomas and soft tissue tumors (*1–4*). Affected individuals are markedly predisposed to colon adenocarcinomas. Polyps usually appear during the 2d to 3d decade of life and gradually increase in number over the next 10–15 years. Colonic adenocarcinomas develop at this stage and may be multifocal. Prophylactic removal of the colon is the recommended treatment prior to cancer development.

In vitro sensitivity of cultured skin fibroblasts to X-ray or UV light irradiation has been reported in several genetic diseases with an increased frequency of spontaneous and radiation-induced cancers. These diseases include autosomal recessive disorders such as XP (*5, 6*), AT (*6, 7*), and autosomal dominant retinoblastoma (*8*). A specific DNA repair defect has been identified in XP to explain the phenotypic manifestation of sun sensitivity and the increased frequency of skin cancer (*9*). The increased sensitivity of AT and retinoblastoma may also reflect a DNA repair defect associated with carcinogenesis.

On the basis of the in vitro observation by Danes (*10*) and Kopelvich et al. (*11*), we questioned whether a DNA repair defect might play a role in the cancer development with Gardner's syndrome. Because of the technical difficulties in establishing cell lines from colon epithelium, we chose to measure radiation damage and repair in cultured skin fibroblast lines.

We previously reported an increased sensitivity to both X-ray and UV light irradiations of the cultured skin fibroblasts from 2 affected members of a family with Gardner's syndrome (*12*). This report presents further observations of X-ray and UV light irradiation sensitivity in other members of the previously reported family as well as in a second family with Gardner's syndrome.

MATERIALS AND METHODS

Patients.—A medical history and physical examination were performed on each study patient from families 1 and 2. Special attention was directed toward examination of the skeleton, skin, and subcutaneous tissue. Pertinent diagnostic studies included sigmoidoscopy (with biopsy of polyps), upper gastrointestinal and colon X-rays (with contrast), and plain bone X-rays when appropriate. A pedigree from each family was constructed by interview with the study patients and other family members.

Fibroblast lines.—A 3.0-mm punch biopsy specimen of the skin was obtained from each patient in families 1 and 2 and established in culture in our laboratory and at Meloy Laboratories Inc., Springfield, Va. Control skin fibroblast lines were established in our laboratory from 2 normal donors and 2 patients with sporadic, nonfamilial colon cancer. Skin fibroblast lines from a patient with XP and one with AT were obtained from the American Type Culture Collection, Rockville, Md.

All cell strains were grown in Eagle's minimum essential medium (F-15; GIBCO, Grand Island, N.Y.) supplemented with 15% fetal bovine serum (M.A. Bioproducts, Walkersville, Md.), 50 mg gentamycin/ml (Schering, Bloomfield, N.J.), and 0.9 g of D-glucose and 0.66 mg of sodium pyru-

---

ABBREVIATIONS USED: AT=ataxia telangiectasia; CNS=central nervous system; PLDR=potentially lethal damage repair(s); RF=recovery factors; XP=xeroderma pigmentosum.

---

[1] Received January 12, 1981; revised November 19, 1981; accepted November 27, 1981.

[2] Supported by in part Public Health Service (PHS) grant CA-11751 from the National Cancer Institute and by PHS grant ES-00002 from the National Institute of Environmental Health Science.

[3] Laboratory of Radiobiology, Harvard University School of Public Health, Boston, Mass. 02115.

[4] *Address reprint requests to* Dr. Kinsella, Building 10, Room B3-B38, Radiation Oncology Branch, Division of Cancer Treatment, National Cancer Institute, National Institutes of Health, Bethesda, Md. 20205.

[5] Division of Medical Oncology, Sidney Farber Cancer Institute, Harvard Medical School, Boston, Mass. 02115.

[6] Clinical Epidemiology Branch, Division of Cancer Cause and Prevention, National Cancer Institute.

[7] Division of Cancer Control, Sidney Farber Cancer Institute.

vate/liter. They were maintained in T-75 flasks (Falcon Plastics, Oxnard, Calif.) in a 5% CO_2–95% air atmosphere at 37°C. The cells were passaged weekly by exposure to 0.25% trypsin in calcium- and magnesium-free Earle's balanced salt solution, usually at a 1:4 dilution. Cell strains were tested prior to passage 15. Gardner's syndrome, AT, XP, and control cells were studied at similar passage levels.

X-ray and UV light irradiations.—X-ray and UV light survival studies were performed by a standard colony formation assay. Cells were detached from the stock cultures with 0.25% trypsin, suspended, and reseeded into 100-mm petri dishes (Falcon Plastics) in numbers calculated to yield approximately 50 macroscopic colonies per dish when the plating efficiency and lethality from X-ray or UV light irradiation were accounted for. Triplicate dishes were seeded for each dose point. The dishes were returned to the incubator and irradiated 18–20 hours later at ambient temperature. X-rays were delivered from a General Electric Maximar unit operating at 220 kV potential and 15 mA with a half-value layer of 0.5 mm of copper. The X-ray dose rate was 80 rad/minute as measured by a condenser ionization chamber (Victoreen Instrument Div., Sheller-Globe Corp., Cleveland, Ohio). UV light (254 nm) exposures were done in a specially constructed irradiator consisting of a bank of five germicidal lamps. The UV dose rate was 0.35 J/m^2 as measured by a germicidal photometer (IL 254; International Light, Inc., Newburyport, Mass.).

After irradiation, the cultures were returned to the incubator, the medium was renewed at 5 days, and the cells were fixed and stained after 14 days. Macroscopic colonies of at least 50 cells were scored as survivors. A minimum of four dose points were used for each survival curve determination. The D_0 (the inverse of the slope) of the survival curve was determined from a least-square regression analysis of the individual data points. For UV survival curves, the D_0 was determined for the first (sensitive) component. The results presented in the text-figures and tables represent data pooled from three to five separate experiments.

Measurement of PLDR.—For measurements of the capacity of cells to repair potentially lethal damage, cultures were allowed to reach the confluent, density-inhibited phase of growth. The culture medium was then renewed daily for 3 days, and the experiment was performed on the 4th day. Replicate cultures were irradiated with a single dose of either X-ray or UV light and returned to the incubator. UV-irradiated cultures were overlaid with their own medium. At varying times thereafter, single dishes were removed, trypsinized, and seeded with fresh medium into three 100-mm petri dishes (Falcon Plastics) at low density to score for colony-forming ability as described above. An RF for X-ray and UV PLDR was calculated by the ratio of surviving colonies at the time of maximal repair (4–6 hr for X-ray PLDR and 24–30 hr for UV PLDR in normal controls) to surviving colonies at time 0.

Chromosomes from phytohemagglutinin-stimulated peripheral leukocytes from each Gardner's patient were analyzed with both C- and G-banding at the Cytogenetics Laboratory, Biotech Research Laboratories, Rockville, Md.

RESULTS

The sensitivities to X-ray and UV light irradiations and the ability to repair potentially lethal damage of cultured skin fibroblasts from the 2 Gardner's syndrome families were compared to those of 2 normal controls, 2 patients with nonfamilial colon cancer, and 1 patient each with AT and XP. A description of the non-Gardner's cell lines is presented in table 1.

The results for cultured skin fibroblasts from 4 clinically affected members of family 1 are outlined in table 2. All cell lines were found to be sensitive to the lethal effects of both X-ray and UV light irradiations. The X-ray D_0's were intermediate to those of the normal controls and sporadic colon cancer patients (D_0=135–160 rad) and AT patients (D_0=46 rad). Similarly, the UV D_0's for this family were intermediate to those of both controls ($D_0 \simeq 2.5$–3.0 J/m^2) and the XP patients ($D_0 \simeq 0.8$ J/m^2). A comparison of the mean D_0 of the 4 control cell lines with that of the 4 cell lines from family 1 by the generalized Wilcoxon test (*13*) showed a significant difference for both X-irradiation (148.8±11.1 vs. 107±6.7 rad; $P<0.01$) and UV light irradiation (2.83±0.24 vs. 1.35±0.13 J/m^2; $P<0.01$). Cell survival curves for both X-ray and UV light irradiations showed small and variable shoulders with the extrapolation numbers ranging from 1.0 to 1.8 (text-fig. 1).

To further investigate our observation of increased sensitivity to irradiation, we studied the PLDR in these cell lines. When normal human skin fibroblasts are irradiated with either X-ray or UV light while in the density-inhibited stationary phase of growth and later subcultured to a low density to stimulate cell proliferation, cell survival is enhanced (*14*). The maximum enhancement occurs within 6 hours for X-ray PLDR and within 24–30 hours for UV PLDR. AT cell lines are deficient in X-ray PLDR, and XP cell lines are deficient in UV PLDR (*6*).

As previously described by Little (*15*), PLDR is associated

TABLE 1.—*Characteristics of the non-Gardner's cell lines*

Cell strain	Disease	Age, yr	Average plating efficiency, %	X-ray D_0, rad	UV D_0, J/m^2	PLDR RF[a]	
						X-ray	UV
AG 1522	Normal	Newborn	15.0	145	2.8	4.3	3.5
B-797	Normal	18	18.0	135	2.5	5.2	4.0
B-813	Sporadic colon cancer	38	14.0	160	3.0	4.1	2.6
B-814	Sporadic colon cancer	63	12.5	155	3.0	3.8	2.5
CRL 1343	AT	7	3.0	46	2.9	1.2	3.2
CRL 1223	XP (Group A)	7	10.0	160	0.8	4.6	0.8

[a] Calculated at 4–6 hr after X-ray irradiation and 24–30 hr after UV irradiation.

TABLE 2.—*Clinical and experimental findings in family 1 with Gardner's syndrome*[a]

Cell line	Age, yr	Clinical characteristics	Average plating efficiency, %	X-ray D_0, rad	UV D_0, J/m^2	PLDR RF[b] X-ray, delayed pattern	PLDR RF[b] UV
2938[c]	51	Proband; symptomatic; polyps and fibromas; colon cancer with liver metastases found at exploration	9	102	1.2	1.2	0.4
2974[c]	26	Daughter of proband; asymptomatic; polyps, total colectomy; no cancer found	11	101	1.4	1.5	0.6
3052	50	Sister of proband; asymptomatic; polyps only; total colectomy, no colon cancer; right breast cancer at age 45 yr	16	115	1.3	2.1	1.0
3056	16	Son of proband; asymptomatic; polyps only; total colectomy, no colon cancer	18	110	1.5	1.8	0.3

[a] Seven other family members affected with: colon cancer, colon polyps, and skin cysts (1 member), colon cancer and colon polyps (2 members), colon cancer (polyp status unknown) (1 member), and skin cysts (2 members).

[b] Calculated at 4–6 hr after X-ray irradiation and 24–30 hr after UV irradiation.

[c] Previously reported (*12*).

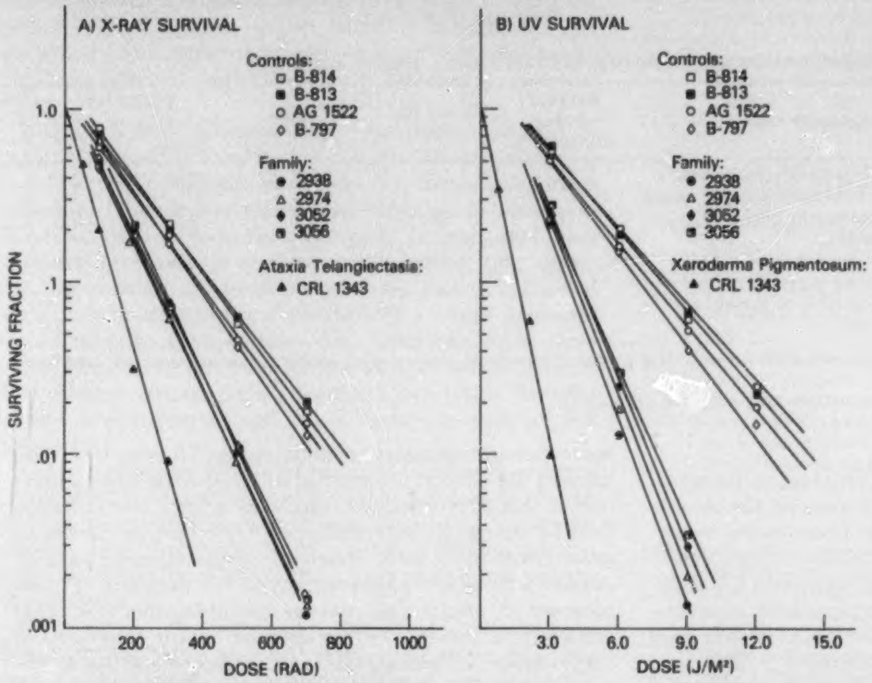

TEXT-FIGURE 1.—The X-ray A) and UV light B) survival curves of skin fibroblast lines from 4 members of family 1, 4 controls, and an AT (X-ray) or XP (UV) cell line.

with a change in the slope of the curve. An appropriate comparison of PLDR can be made by comparison at survival enhancement at similar levels of survival. To reduce the surviving cell population to 1% to quantitate PLDR, we used the following radiation doses: family 1 cell lines, 500 rad and 6.0 J/m^2; family 2 cell lines, normal control, and nonfamilial colon cancer lines, 700 rad and 12.0 J/m^2; an AT cell line, 300 rad and 12.0 J/m^2; and an XP cell line, 700 rad and 2.0 J/m^2.

We found no PLDR to UV light in any cell line (RF <1.0) from family 1 (text-fig. 2). A consistent delayed pattern of PLDR was noted to X-ray irradiation in these cell lines. A survival enhancement was not evident until 6–8 hours after irradiation, and the RF were lower than those of controls (RF=1.2–2.1 compared to 3.8–5.2) (text-fig. 2). The 2 nonfamilial colon cancer fibroblast lines showed a normal PLDR to both X-ray and UV irradiations.

Three members of family 2 have been studied of whom 2 are clinically affected with Gardner's syndrome. The patient from whom cell line 3090 was obtained appeared to be unaffected clinically but at age 17 might not have developed any phenotypic manifestations. However, all skin fibroblast lines tested in vitro showed a normal cell survival (D_0) and a normal pattern of PLDR after both X-ray and UV light irradiations (table 3).

Karyotyping of peripheral leukocytes was done on all Gardner's syndrome patients whose skin fibroblasts were tested. All leukocytes had a normal diploid pattern to C- and G-banding (Kinsella TJ, Little JB, Nove J, et al.: Unpublished data).

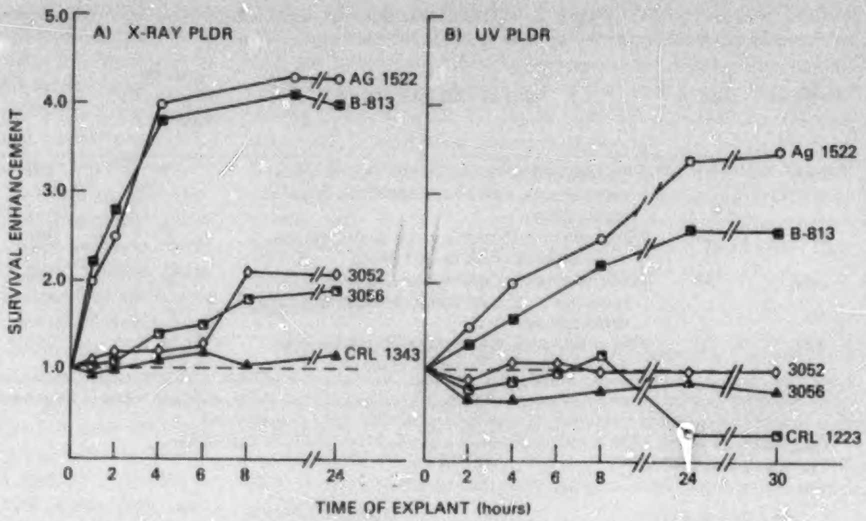

TEXT-FIGURE 2.—Patterns of PLDR for X-ray A) and UV light B) irradiations for cell lines from 2 members of family 1 (3052 and 3056), 2 control lines (AG 1522 and B-813), and either an AT line (CRL 1343) or an XP line (CRL 1223).

TABLE 3.—*Clinical and experimental findings in family 2 with Gardner's syndrome*[a]

Cell line	Age, yr	Clinical characteristics	Average plating efficiency, %	X-ray D_0, rad	UV D_0, J/m^2	PLDR RF[b]	
						X-ray	UV
3103	23	Daughter of proband; symptomatic; polyps, lipomas, fibromas; total colectomy; no cancer	15	135	2.5	6.4	2.8
3091	19	Son of proband; symptomatic; polyps only; colectomy recommended	12	152	2.7	5.2	3.1
3090	17	Son of proband; asymptomatic; no polyps; a single lipoma removed at age 12; normal physical examination now; no osteomas; under close follow-up	24	135	2.5	4.0	5.1

[a] Twelve other family members affected with: colon cancer and colon polyps (3 members), colon cancer (polyp status unknown) (2 members), and colon polyps (7 members).

[b] Calculated at 4–6 hr after X-ray irradiation and 24–30 hr after UV irradiation.

DISCUSSION

We have demonstrated a discordant response to the lethal effects of X-ray and far UV light in cultured skin fibroblasts in 2 families with Gardner's syndrome. In an earlier investigation of radiation sensitivity in 2 clinically affected members of family 1, increased sensitivity to X-ray and UV light irradiations and defective PLDR were postulated to represent a DNA repair defect responsible for the neoplastic and other manifestations of Gardner's syndrome (*12*). The normal response to both X-ray and UV light irradiations in the clinically affected members of family 2 does not support this hypothesis. The explanation for this difference in in vitro radiation sensitivity is unknown, and additional studies are needed. We cannot detect any difference in the phenotypic expression of Gardner's syndrome between families 1 and 2. Soft tissue benign tumors (lipomas, fibromas, and sebaceous cysts) occur throughout both family pedigrees. There were no reports in either family of skin carcinoma or of skin intolerance to therapeutic irradiation.

Increased sensitivity to X-irradiation of cultured skin fibroblasts has been found in other autosomal dominant diseases both with and without a cancer predisposition [familial retinoblastoma (*10*) and Huntington's chorea (*16*), respectively]. In retinoblastoma, there appears to be a difference in the in vitro radiosensitivity between patients with sporadic and hereditary retinoblastoma. These in vitro data support the clinical observation of an increase of secondary cancer (usually osteogenic sarcoma) within the radiation field for hereditary retinoblastoma (*17*). Further studies on radiosensitivity in some D-deletion retinoblastoma patients suggest a locus for radiosensitivity in the long arm of chromosome 13, adjacent to that for retinoblastoma (*19*). Theoretically, a patient with a deletion in the long arm of chromosome 13 encompassing both loci would be at the greatest risk of radiation-induced cancer. Chromosome analysis in both families affected with Gardner's syndrome revealed no chromosomal abnormalities.

Increased radiosensitivity is also reported in cultured skin fibroblasts (*16*) and in Epstein–Barr virus-transformed lymphocytes (*18*) from Huntington's chorea patients and some at-risk family members. Again, the radiosensitivity is postulated to reflect a defective DNA repair based on similar pathologic features of CNS neuronal degeneration found in another disorder of radiosensitivity, AT (*20*). No CNS degeneration occurs in patients with Gardner's syndrome, but in Turcot's syndrome, a presumed autosomal recessive polyposis disease, CNS tumors (usually gliomas) are a clinical manifestation (*21, 22*).

XP is the best characterized DNA repair-deficient human disease. Patients affected with this autosomal recessive disease develop sunlight-induced skin cancer with a frequency approximating 100% by age 20 (*11*). Cultured skin fibroblasts are sensitive to UV light irradiation and are usually unable to repair potentially lethal damage (*7*). A variable defect in the pyrimidine dimer excision repair pathway is demonstrated in most patients. However, cultured cells from some patients are proficient in excision repair but defective in postreplication repair (*23*). These cells also show a normal PLDR to UV light. This heterogeneity in in vitro testing of DNA repair of skin fibroblasts from XP patients may suggest a comparable explanation for the different findings in the 2 study families with Gardner's syndrome.

Danes and Krush (*24*) reported increased tetraploidy in short-term cultures that contain both skin epithelial cells and fibroblasts in 28 patients affected with Gardner's syndrome. In addition, tetraploidy was present in skin epithelial cell and fibroblast cultures in 19 of 50 family members at risk. Cultured skin fibroblasts alone did not show increased skin tetraploidy in affected patients or in family members at risk. However, another group failed to substantiate the usefulness of this short-term epithelial cell culture assay in detecting affected individuals with Gardner's syndrome (*25*).

Kopelvich and colleagues have extensively used skin fibroblast cultures to investigate a possible DNA repair defect in patients with polyposis syndromes that include Gardner's syndrome. They report several abnormalities in some skin fibroblast cultures from these polyposis patients, including increased susceptibility to viral transformation (*26*), defective organization of the fibroblast actin matrix (*27*), and malignant transformation through only a tumor promoter (*7*). The authors argue that skin fibroblasts from these polyposis patients are already initiated to carcinogenesis. The clinical phenotype of Gardner's syndrome includes benign and malignant soft tissue tumors to support this argument.

Colon epithelium cells from patients with Gardner's syndrome show increased tetraploidy (*28*) and abnormal growth kinetics by tritiated thymidine incorporation (*29*). At the present time, further in vitro testing is limited by the technical difficulty of establishing long-term bowel epithelium cultures.

In summary, the increased sensitivity of cultured skin fibroblasts to X-ray and UV light irradiations does not appear to be a consistent in vitro marker of gene carriers of Gardner's syndrome. However, the possibility should be considered that radiosensitivity segregates with a Gardner's syndrome gene in some affected families and is useful in identification of high-risk persons in those kindreds.

REFERENCES

(*1*) Gardner EJ. Follow-up study of a family group exhibiting dominant inheritance for a syndrome including intestinal polyps, osteomas, fibromas and epidermal cysts. Am J Human Genet 1962; 14:376–390.

(*2*) Bussey HJ. Familial polyposis coli: Family studies, histopathology, differential diagnosis, and results of treatment. Baltimore: The Johns Hopkins Univ Press, 1975:59–63.

(*3*) Pavlides GP, Milligan FD, Clarke DN, et al. Hereditary polyposis coli I: The diagnostic value of colonoscopy, barium enema, and fetal occult blood. Cancer 1977; 40:2632–2639.

(*4*) Asman HB, Peirce ER. Familial multiple polypsis. A statistical study of a large Kentucky kindred. Cancer 1970; 25:972–981.

(*5*) Cleaver, JE. DNA repair with purines and pyrimidines in radiation and carcinogen-damaged normal and xeroderma pigmentosum cells. Cancer Res 1973; 33:362–369.

(*6*) Weichselbaum RR, Nove J, Little JB. Deficient recovery from potentially lethal radiation damage in ataxia telangiectasia and xeroderma pigmentosum. Nature 1978; 271:261–262.

(*7*) Paterson MC, Smith BP, Lohman PH, Anderson AR, Fishman L. Defective excision repair of gamma ray-damaged DNA in human (ataxia telangiectasia) fibroblasts. Nature 1976; 260:444–446.

(*8*) Weichselbaum RR, Nove J, Little JB. X-ray sensitivity of diploid fibroblasts from patients with hereditary and sporadic retinoblastoma. Proc Natl Acad Sci USA 1978; 75:3962–3964.

(*9*) Robbins JH, Kraemer KH, Lutzner MA, Festoff BW, Coion HG. Xeroderma pigmentosum: An inherited disease with sun sensitivity, multiple cutaneous neoplasms, and abnormal DNA repair. Ann Intern Med 1974; 80:221–248.

(*10*) Danes BS. Increased in vitro tetraploidy: Tissue specific within the heritable colorectal cancer syndromes with polyposis coli. Cancer 1978; 41:2330–2334.

(*11*) Kopelvich L, Bias NE, Helsom L. Tumour promotion alone induces neoplastic transformation of fibroblasts from humans genetically predisposed to cancer. Nature 1979; 282:619–621.

(*12*) Little JB, Nove J, Weichselbaum RR. Abnormal sensitivity of diploid skin fibroblasts from a family with Gardner's syndrome to the lethal effects of X-irradiation, ultraviolet light and mitomycin-C. Mutat Res 1980; 70:241–250.

(*13*) Wilcoxon F. Individual comparisons by ranking methods. Biometrics 1945; 1:80–88.

(*14*) Little JB. Repair of sublethal and potentially lethal radiation damage in plateau phase cultures of human cells. Nature 1969; 224: 804–806.

(*15*) ———. Factor influencing the repair of potentially lethal radiation damage in growth-inhibited human cells. Radiat Res 1973; 62: 311–323.

(*16*) Arlett CF, Muriel WJ. Radiosensitivity in Hungtington's chorea cell strains: A possible preclinical diagnosis. Heredity 1979; 42:276–278.

(*17*) Sagerman RH, Cassady JR, Tretter P, Ellsworth RM. Radiation-induced neoplasm following external beam therapy for children with retinoblastoma. Am J Roentgenol 1969; 105:529–535.

(*18*) Moshell AN, Tarone RE, Barrett SF, Robbins JH. Radiosensitivity in Huntington's disease: Implications for pathogenesis and presymptomatic diagnosis. Lancet 1980; 1:9–11.

(*19*) Nove J, Little JB, Weichselbaum RR, Nichols WW, Hoffman E. Retinoblastoma, chromosome 13, and in vitro cellular radiosensitivity. Cytogenet Cell Genet 1979; 24:176–184.

(*20*) Kramer KH. Progressive degenerative diseases associated with defective DNA repair: Xeroderma pigmentosum and ataxia telangiectasia. In: Nichols WW, Murphy DG, eds. DNA repair processes. Miami: Symposia Specialists Inc., 1977: 37–71.

(*21*) Bauchman FA, List CF. Williams JR. The glioma-polyposis syndrome. N Engl J Med 1969; 281:1345–1348.

(*22*) Turcot J, Despress JP, St Pierre F. Malignant tumors of the central nervous system associated with familial polyposis of the colon: Report of two cases. Dis Colon Rectum 1959; 2:465–468.

(*23*) Setlow RB. Repair deficient human disorders and cancer. Nature 1978; 271:713–717.

(*24*) Danes BS, Krush AJ. The Gardner syndrome: A family study in cell culture. J Natl Cancer Inst 1977; 58:771–775.

(*25*) Delhaney J, Pritchard MB, Bussey HJ, Morson BC. Tetraploid fibroblasts and familial polyposis coli. Lancet 1980; 1:1365.

(*26*) Pfeffer L, Kopelvich L. Differential genetic susceptibility of cultured human skin fibroblasts to transformation by Kirsten murine sarcoma virus. Cell 1977; 10:313–320.

(*27*) Kopelvich L, Conlon S, Pollack R. Defective organization of actin in cultured skin fibroblasts from patients with inherited adenocarcinoma. Proc Natl Acad Sci USA 1979; 74:3019–3022.

(*28*) Danes BS. Increased tetraploidy: Cell-specific for the Gardner gene in the cultured cell. Cancer 1976; 38:1983–1988.

(*29*) Deschner E, Lewis CM, Lipkin M. In vitro study of human rectal epithelial cells. I. Atypical zone of H^3-thymidine incorporation in mucosa of mutliple polyposis. J Clin Invest 1963; 42:1922–1928.

blank page

Systemic Administration of Human Leukocyte Interferon to Melanoma Patients. I. Effects on Natural Killer Function and Cell Populations[1,2,3]

Sidney H. Golub,[4] Fred Dorey,[5] Dean Hara,[4] Donald L. Morton,[4] *and* Martyn W. Burk[4,6]

ABSTRACT—Natural killer (NK) cytotoxicity was assessed against K562 targets in 14 melanoma patients who received daily im doses of human leukocyte interferon (IFN) for 42 consecutive days. The most common pattern of NK activity was a decline from pretreatment levels 1 day after initiation of treatment, followed by increasing cytotoxicity with peak activity at day 7 and a subsequent gradual decline to pretreatment levels during the remaining weeks of treatment. This pattern was particularly apparent in patients who received 3×10^6 or 9×10^6 U IFN/day, while patients who received 1×10^6 U IFN/day tended to lack the decline at day 1 and maintained the elevated NK activity past day 7. Changes in NK activity could not be related to changes in absolute lymphocyte counts; to proportions of cells bearing membrane receptors for sheep red blood cells, of cells bearing membrane receptors for erythrocyte–antibody–complement, or of cells bearing FCγ receptor; or to clinical response to IFN.—JNCI 1982; 68: 703–710.

Considerable interest has focused recently on the use of IFN as an antineoplastic agent in humans (*1–3*). Thus far, IFN has not been used extensively for patients with metastatic malignant melanoma. We are participating in a multiinstitutional trial sponsored by the American Cancer Society to investigate the possible therapeutic benefit of human leukocyte IFN (IFN-α) for the treatment of malignant melanoma. Clinical results of this trial will be reported separately. This report will focus on the effects of IFN on NK activity and cell surface markers. Systemic administration of IFN to cancer patients results in a marked increase in NK activity shortly after first administration (*4, 5*). We investigated the effect of daily doses of IFN given over a 42-day period. The purpose of these studies was to determine how long and at what level elevated NK activity could be maintained.

NK activity in these patients is of interest for several reasons. First, NK cells are cytotoxic to tumor cells and may contribute to the host defenses against the neoplastic disease. Whether the therapeutic benefits of IFN are due to elevated NK activity or to some other mechanism such as direct antineoplastic effects, is difficult to determine. However, NK activity is an easy and convenient means to measure the biologic activity of IFN. Thus measurement of NK activity in a systematic fashion following administration of IFN may prove useful in the adjustment of dosage and time schedules for the use of this agent.

MATERIALS AND METHODS

Patients.—Sixteen patients with metastatic malignant melanoma were entered into the study. Patients had metastases to subcutaneous tissues and/or lungs. The patients received daily doses of 1×10^6 U, 3×10^6 U, or 9×10^6 U IFN for 42 consecutive days. The IFN was human leukocyte IFN (IFN-α) provided by the American Cancer Society as part of a multiinstitutional trial. The patients were randomly assigned dosage, and the IFN was administered by im injection. Toxicity and therapeutic benefit is the subject of a separate report (*6*). The present report focuses solely on immunologic effects in the first 16 patients treated.

Preparation of PBL.—PBL were obtained daily for 2 days before initiation of IFN treatment, daily for 3 days after initiation of treatment, and weekly thereafter. PBL were prepared on standard Ficoll-Hypaque gradients and tested immediately after preparation. Samples were also cryopreserved as described previously (*7*) for future analysis. All results reported in this study utilized freshly prepared cells and not cryopreserved cells.

Cytotoxicity assay.—NK cytotoxicity was measured against K562 myeloid leukemia cells. In some experiments, additional targets were included. These included the human melanoma cell line UCLA-SO-M14 (henceforth termed "M14"), which is generally resistant to NK cytotoxicity in a 4-hour assay but is sensitive in long-term (>18 hr) cytotoxicity tests (*8*). We have also used M14 cells coated with rabbit anti-M14 IgG to measure ADCC. Also tested were L14 cells, an EBV-transformed B-lymphoblastoid cell line derived from the peripheral blood of the donor of the M14 line. For all cytotoxicity assays a microcytotoxicity ^{51}Cr release assay was used as described previously (*9*). E:T were 100:1, 50:1, 25:1, and 12.5:1 with all targets. Results are expressed as percent cytotoxicity calculated by the formula: Percent cytotoxicity=(cpm released in test−spontaneous release)/(total release−spontaneous release)×100. Spontaneous release was determined in the wells containing targets

---

ABBREVIATIONS USED: ADCC=antibody-dependent cellular cytotoxicity; RBC=red blood cell(s); EAγ=ox RBC coated with IgG to detect Fcγ receptor cells; EAC=erythrocyte-antibody-complement; EBV=Epstein-Barr virus; E:T=effector-to-target cell ratio(s); IFN=interferon; NK=natural killer; PBL=peripheral blood lymphocyte(s); *r*=correlation coefficient; WBC=white blood cell(s).

---

[1] Received May 26, 1981; accepted November 19, 1981.

[2] Supported in part by Public Health Service grant CA-17013 from the National Cancer Institute.

[3] Research procedures were in accord with the ethical standards of the Human Subjects Protection Committee, UCLA School of Medicine.

[4] Division of Oncology, Department of Surgery, UCLA School of Medicine, University of California at Los Angeles, Los Angeles, Calif. 90024.

[5] Department of Biomathematics, UCLA School of Medicine.

[6] The authors thank Edythe Garvey, *R.N.*, and Robin Bowker, *M.T.*, for their assistance.

without added lymphocytes, and total release was calculated from wells containing targets and 5% Nonidet P40 detergent. All tests were performed in RPMI-1640 medium, supplemented with antibiotics and 10% pooled human AB serum. One lot of serum was used, and this lot had been screened and showed no activity in ADCC and no augmentation or diminution of NK cytotoxicity when compared to other serum supplements. Fetal bovine serum was not used because we had shown previously that it can induce NK-like cytotoxicity (*8*). To assure ourselves that the cytotoxicity assay was working properly each day, we thawed a sample of cryopreserved PBL from a single batch from 1 donor and tested it during each experiment. These data were used simply as a quality control on the cytotoxicity test and as a means of searching for systematic variations, such as those due to day of the week, in the assay system.

Cell surface markers.—Each patient's PBL samples were tested for the proportion of cells bearing the receptor for sheep RBC (rosette-forming cells) characteristic of T-cells, for the proportion of cells binding ox RBC coated with rabbit IgG to detect Fcγ receptor cells (EAγ rosette-forming cells), and for the proportion of cells binding sheep RBC coated with rabbit IgM and DBA/2 mouse complement to detect complement receptor cells (EAC rosette-forming cells). Total WBC counts and differentials were also performed. The technique of rosette formation and further details of the reagents used were detailed in (*10*). The healthy control donors were also tested sequentially for their proportion of cells bearing membrane receptors for EAγ (rosette-forming cells). Previous studies in this laboratory with both cancer patients and controls (*11–13*) showed no significant changes over time in the proportion of cells bearing membrane receptors for sheep RBC or EAC rosette-forming cells and therefore these assays were not repeated with this group of control donors.

RESULTS

Changes in NK Activity of IFN-Treated Patients and Controls

When all 14 IFN-treated patients were considered as a group, regardless of dose of IFN administered, a consistent pattern of increased cytotoxicity against K562 targets was seen. This pattern is shown in text-figure 1 for all four E:T tested. Typically, cytotoxicity declined after 24 hours of treatment, then increased steadily until day 7 of treatment, and then returned to pretreatment levels for the duration of treatment. This is illustrated with a representative patient in text-figure 2. This patient showed a striking increase in NK cytotoxicity against K562 targets during week 1 of treatment, then a decline toward pretreatment levels during the subsequent period of IFN treatment, and a further decline after treatment was completed. This pattern was seen at all four E:T tested; however, only the lowest ratio showing the greatest increase is shown in text-figure 2. Also illustrated in text-figure 2 is the small standard error for any single ^{51}Cr release assay. This pattern was followed by most of the individuals tested (*see* also table 2). At day 7, 81% of the patients had higher NK activity than at the pretreatment samplings ($P<0.01$; Wilcoxon rank sum test), whereas 56% were elevated at day 21.

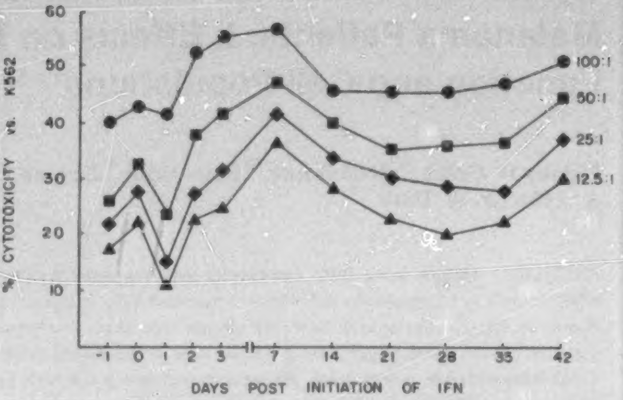

TEXT-FIGURE 1.—NK cytotoxicity vs. K562 targets of 14 IFN-treated melanoma patients. Four E:T were tested. All results are the average percentages of cytotoxicity for the patients tested at each time point.

The different levels of NK activity at days 0 and 7 are shown in text-figure 3. The increased cytotoxicity is detected in parallel at all E:T tested. The fact that IFN-activated NK is detected equivalently at all ratios allowed us to reduce the data to a single number by simply averaging the percent lysis of all 4 doses. The results in text-figure 3 show that we are testing in the linear portion of the cytotoxicity dose-response curve at both days 0 and 7. Therefore, any of the four ratios could be used for analysis. We chose to incorporate all the information into one value by using the mean of the four ratios. This mean cytotoxicity was then compared to the pretreatment values (average of the mean cytotoxicity of days −1 and 0), and the net change in cytotoxicity was determined. This analysis confirmed our observation that peak cytotoxicity was expressed on day 7 of treatment (table 1). In fact, the day 7 values were the only statistically significant increases in NK cytotoxicity ($P<0.05$; both the paired *t*-test and Wilcoxon signed rank test).

In addition to the average change in NK activity, we determined the proportion of patients with elevated or

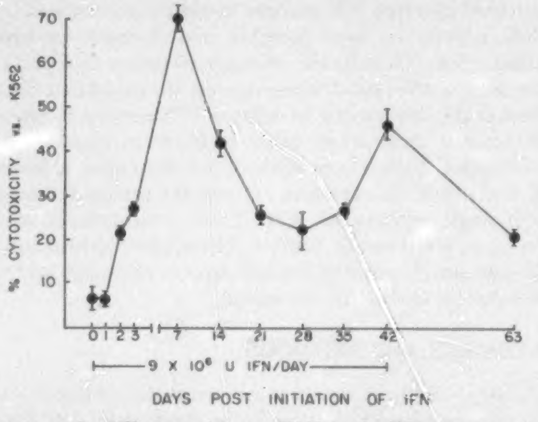

TEXT-FIGURE 2.—NK cytotoxicity vs. K562 in the ^{51}Cr release assay for patient #1. *Vertical bars* indicate standard error of the mean for cytotoxicity of the 12.5:1 E:T.

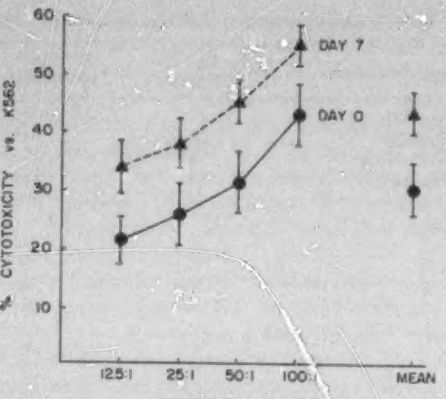

Text-figure 3.—Average NK cytotoxicity for all 14 patients at days 0 and 7 of treatment. *Horizontal axis* also shows mean of four ratios. *Vertical bars* indicate standard error of the mean.

Table 2.—*NK activity of individual patients at selected time points*

Patient No.	IFN dose, U/day	Mean[a] percent NK cytotoxicity at day:[b] Pretreatment[c]	1	7	21	35
1	9×10^6	23	17	73	29	34
2	1×10^6	37	27	50	32	51
3	3×10^6	58	19	58	44	51
4	1×10^6	13	22	43	44	17
5	9×10^6	29	21	36	23	19
6	3×10^6	29	NT	44	22	22
7	3×10^6	32	19	37	27	25
8	9×10^6	52	42	59	54	36
9	1×10^6	29	33	38	35	52
10	1×10^3	14	11	31	33	29
11	3×10^6	13	14	35	28	NT
12	9×10^6	26	13	23	23	12
13	1×10^6	21	25	45	37	27
14	9×10^6	36	13	34	17	27
15	3×10^6	10	24	34	43	29
16	1×10^6	8	24	16	20	NT
No. increased[d]/No. tested:			6/15	13/16[e]	9/16	7/14
		Days	2	14	28	42
No. increased[d]/No. tested:			8/14	10/15	9/15	9/14
		Day	3			
No. increased[d]/No. tested:			9/15			

[a] Mean of four E:T.
[b] NT=not tested.
[c] Average of day −1 and day 0.
[d] Compared to pretreatment.
[e] $P<0.01$ by Wilcoxon rank sum test. All other time points not statistically significant.

diminished NK activity at each time point. These data are shown in table 2 where the pretreatment values for 16 patients are listed. For clarity, NK results are shown only at selected posttreatment time points, but the proportion of patients increasing at each of the remaining time points is given at the bottom of table 2. This type of analysis confirms that increased NK activation is seen at day 7, inasmuch as 13 of 16 patients displayed increased NK activity on day 7 relative to pretreatment values ($P<0.01$; Wilcoxon signed rank test). In seven of nine sampling periods during IFN treatment, more than one-half of the patients showed increased NK activity. This would be a very unlikely finding if IFN had no effect on NK. The sole time point where less than one-half of the patients had increased NK activity was 24 hours after initiation of treatment (9 of 15 declined). This phenomenon is discussed below.

We examined the data to determine if any correlation existed between initial NK activity and subsequent NK activity. There was only a weak correlation between pretreatment values and the day 7 values ($r=0.35$; Pearson coefficient of correlation). The correlation between initial values and peak response was even less ($r=0.17$). Although we could not detect an obvious correlation between initial level and response to IFN, we cannot rule out the possibility that high initial values (e.g., patient #3, table 2) be precluded from a response because of some type of saturation of the NK system.

We also studied 4 healthy donors sequentially to determine what changes in NK activity might occur without IFN administration. These 4 donors were sampled at the same intervals as the patients and were studied concurrently with the patients. The results (table 1) show that the controls failed to demonstrate any increase in NK cytotoxicity. Thus a reasonable conclusion is that the consistent and significant

Table 1.—*NK cytotoxicity and changes in cytotoxicity with time in IFN-treated patients and controls*

Day of treatment	Patients No. tested	Mean NK ± SE[a]	Change ± SE[b]	Controls No. tested	Mean NK ± SE[a]	Change ± SE[b]
−1	12	25.8±4.3	—	4	44.1±3.2	—
0	14	30.3±4.5	—	4	29.5±2.2	—
1	13	21.0±2.4	−7.0±3.7	4	23.5±2.1	−13.3±0.7[c]
2	12	32.5±5.8	+3.8±5.0	4	27.6±7.8	−9.2±6.4
3	12	35.3±4.0	+7.7±5.0	4	25.6±4.1	−11.2±2.3
7	14	43.1±3.5	+15.3±3.7[c]	4	35.5±8.4	−1.3±7.6
14	13	35.0±2.9	+6.6±4.2	4	25.8±8.7	−11.0±8.7
21	14	31.8±2.7	+3.9±3.7	4	34.1±8.1	−2.7±7.0
28	13	32.4±3.4	+3.5±4.3	3	28.2±5.0	−6.8±5.0
35	13	30.0±3.9	+1.0±3.8	4	40.2±7.3	+3.4±6.5
42	13	36.7±4.9		3	23.7±1.4	−11.3±1.4

[a] Mean of average NK; 4 doses.
[b] Mean (day of test) − mean (day −1 + day 0)/2.
[c] $P<0.05$; paired *t*-test or Wilcoxon signed rank test.

increase in NK activity in the patients was a result of the IFN treatment.

One interesting feature noted in both controls and patients was a decline in NK activity 24 hours after the first dose of IFN. The finding of such a decline in the immediate posttreatment period in the patients is not surprising; Kariniemi et al. (*14*) noted a similar phenomenon in IFN-treated healthy subjects. However, the similar decline in our untreated controls suggested that in some cases a decline in NK activity is unrelated to IFN treatment. We considered the possibility of a systematic error inherent in our NK assay. Because all patients and controls were entered into the study on a Monday (day −1), days 1 and 7 would always be on a Wednesday and Tuesday, respectively. If the test conditions tended to be poor on Wednesdays, we would see an artifactual decline in NK activity. Conversely, an increase in cytotoxicity at day 7 could be due to an abnormally sensitive NK assay system on Tuesdays. Considering the number of variables involved in the assay (e.g., lymphocyte preparation, tissue culture, and radiolabeling of K562), this possibility had to be considered. As part of this study, we had routinely tested aliquots of a single batch of cryopreserved PBL from 1 donor. We previously showed that cryopreserved PBL give highly reproducible results in immunologic assays (*7*) and retain activity in NK assays (*15*), although at a somewhat decreased level. When we analyzed these daily controls, no significant differences by day of the week were seen (table 3). Thus a systematic error in the NK assay was an unlikely explanation for either the decline in NK seen at day 1 or the increase at day 7. In fact, the increase at day 7 was particularly striking when compared to the results of other assays done on Tuesdays (days 0, 14, 21, 28, 35, and 42) in that this comparison has the fewest possible technical variables. We also arranged the control standard NK results according to the simultaneously tested patient samples. In this calculation, each time a patient was tested at a particular time point the simultaneous frozen standard result was also recorded at that time point. These results, also shown in table 3, indicate considerable stability in the NK assay. Whereas variation in the ^{51}Cr release assay on a day-to-day basis remains a problem with studies such as this, the assay appeared to have sufficient reproducibility to expose a strong trend such as the one seen in our group of patients.

NK Activity Against Targets Other Than K562

Preliminary studies have been initiated to determine if the IFN-augmented cytotoxicity is confined to K562 or can be detected against other targets as well. Thus far we have only studied 3 patients, all of whom showed marked increases against K562. However, when tested against the NK-resistant M14 melanoma target, none of the 3 patients showed any increased cytotoxicity after IFN treatment. Cytotoxicity, before and after IFN administration, never exceeded 5% lysis. One patient was also tested for ADCC against M14 targets coated with rabbit anti-M14 IgG. The activity of ADCC paralleled NK activity with an increase from 25% (E:T, 100:1) at day 0 to 45% at day 7. Therefore, the M14 targets were susceptible to lysis in ADCC, and activity of ADCC also appeared to respond to IFN treatment. The 3d patient was tested against an EBV-transformed B-cell line (L14) modestly susceptible to NK killing. Activity against the L14 increased from a pretreatment value of 7% to a peak of 47% during IFN treatment. Thus our preliminary results suggested that IFN-activated cytotoxicity can be detected against targets besides K562, such as L14 or IgG-coated M14, but not against all targets because untreated M14 cells remained resistant.

TABLE 3.—*NK assay variability with one cryopreserved sample*

Sample tested on:	Sample No. tested	Average[a] percent cytotoxicity ± SE
Monday	10	26±3
Tuesday	23	26±3
Wednesday	9	25±3
Thursday	14	29±3
Friday	14	21±3
Day		
−1	10	24±4
0	10	30±6
1	10	24±3
2	10	29±4
3	11	23±3
7	10	28±5
14	11	25±4
21	11	22±3
28	10	25±4
35	10	32±5
42	10	35±4

[a] Each sample was tested at four E:T and the results are expressed as the means of the four ratios. Results are expressed as the averages of these individual means.

Effect of Dose of IFN Administered on NK

NK activity was evaluated according to the dose of IFN administered to the patients. The results, expressed as net changes in mean percent cytotoxicity, are shown in table 4. Although the size of these groups was too small to justify meaningful statistical comparisons, some observations could be made. The lowest dose used (1×10^6 U IFN/day) was as effective in elevating NK activity as the higher doses (3×10^6 or 9×10^6 U IFN/day), and this low dose may even have been more effective in maintaining the elevated NK activity after week 1 of treatment. Of the 3 patients who failed to

TABLE 4.—*Change in average NK cytotoxicity by dose of IFN administered*

Day of treatment	Mean change ± SE at IFN/dose of:		
	1×10^6 U/day tested on 5 patients	3×10^6 U/day tested on 4 patients	9×10^6 U/day tested on 5 patients
1	+1.6±3.5	−17.3±12.0	−9.3±3.8
2	+4.7±2.8	−3.6±16.8	+7.6±7.9
3	+5.1±4.9	+16.5±19.5	+4.4±4.4
7	+19.4±3.3[a]	+11.3±5.3	+14.6±9.3
14	+18.3±7.1	−1.3±8.8	+3.7±4.7
21	+14.1±6.0	−2.1±6.2	−1.4±5.2
28	+16.0±6.1	−7.5±6.0	−2.4±5.3
35	+13.5±4.0	−6.4±1.1	−6.9±5.5
42	+21.4±2.8	−4.6±3.3	+1.5±9.2

[a] $P<0.05$; paired *t*-test or Wilcoxon signed rank test.

show any increase in NK, 2 were treated with 9×10^6 U IFN/day and 1 was treated with 3×10^6 U IFN/day. In contrast, the higher doses seem more likely to induce a sharp drop in activity at 24 hours, followed by a distinct rise during week 1. Of the 5 patients who did not decline at day 1, 3 were treated with 1×10^6 U IFN/day and 2 received 3×10^6 U IFN/day. Therefore, the lowest dose of IFN used in this study appeared to be sufficient for maximal activation of NK. This, of course, does not mean that therapeutic effects will be similarly affected.

Although NK activity did not show an obvious IFN dose-dependent response, the decline in circulating leukocytes did (table 5). The leukopenic effects of IFN were most apparent with the higher doses administered. This suppression was confined to the granulocytes because the proportion of lymphocytes rose during treatment (table 5), and absolute lymphocyte counts were not significantly affected (table 5; text-fig. 4).

Effect of Time Interval Between IFN Administration and Sampling on NK Activity

Other studies in humans have indicated that peak NK activity is detected 12–48 hours after first administration of IFN (*4, 5*). We had intended to do all sampling at 24 hours after the previous IFN dose, and this procedure was followed during the first 3 days while the patients were hospitalized (days 1, 2, and 3 of treatment). For subsequent treatments, the patients administered the IFN themselves. In many cases, the patients chose to administer the agent the morning before the clinic visit. Thus in about one-half of the samples the IFN was administered from 1 to 5 hours before PBL samples were obtained, whereas in the others the IFN was given 12–24 hours before sampling. We have compared the cytotoxicity according to this interval, and the results are given in text-figure 5. No statistically significant differences could be detected between the shorter or longer time intervals at any of the four treatment points analyzed. Later treatment points (days 35 and 42) had too few samples with the short intervals to allow for comparison, and the early treatment points (days 1, 2, and 3) were uniformly tested at 24 hours post IFN. Thus we could not find any substantial difference in NK activity during the later treatment periods (1–4 wk of treatment) between those who received IFN less than 5 or more than 12 hours before sampling. However, in three of the four time points in text-figure 5 (days 7, 14, and 28), the longer interval results were higher. Therefore, we may have slightly underestimated the NK activity in some patients. All patients are now carefully instructed to administer the IFN at the designated time of day, and further studies will have greater uniformity in this respect. Irrespective of time intervals between dose and sampling, the longer periods of IFN treatment (14–28 days) displayed lower NK activity than did the peak period (7 days). Therefore, it is unlikely that the later period of declining NK is associated with a change in the kinetics of NK activation. We also obtained repetitive samples from patients late in the course of treatment when NK activity had declined. These samples, obtained over a 12-hour period following the next dose of IFN, also remained low in NK activity (data not shown).

TABLE 5.—*Dose effect of IFN on WBC counts and percent lymphocytes*

Day of treatment	Average total WBC (average percent lymphocytes)[a] at IFN dose of:		
	1×10^6 U/day tested on 5 patients	3×10^6 U/day tested on 4 patients	9×10^6 U/day tested on 5 patients
−1	7,450 (23.5)	4,050 (21.8)	5,950 (29.3)
0	7,700 (20.3)	NT	5,150 (35.5)
1	5,600 (22.2)	5,325 (20.8)	4,425 (22.3)
2	5,900 (41.0)	3,000 (36.5)	4,540 (30.8)
3	3,667 (50.5)	NT	3,333 (51.3)
7	4,940 (41.0)	3,425 (50.0)	2,500 (50.8)
14	4,375 (42.0)	3,450 (41.5)	2,960 (60.2)
21	4,820 (36.0)	3,050 (46.0)	2,925 (46.8)
28	4,900 (33.4)	2,667 (53.0)	2,360 (51.8)
35	5,220 (30.2)	3,033 (48.0)	2,700 (49.2)
42	5,020 (34.6)	2,833 (36.0)	2,740 (47.6)

[a] NT=none (or only 1) tested.

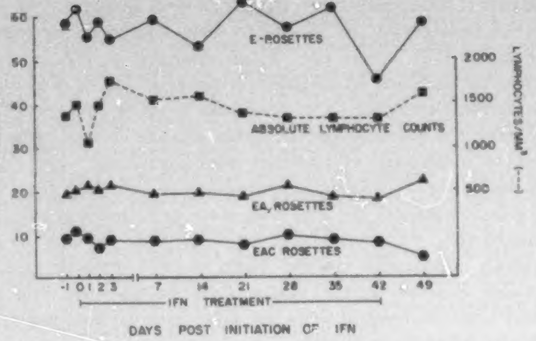

TEXT-FIGURE 4.—Cell populations during IFN treatment. *Each point* represents average of all patients tested. E=RBC.

Changes in Cell Populations During IFN Treatment

We have monitored the ability of PBL from these patients to form sheep RBC, EAγ, and EAC rosettes during IFN

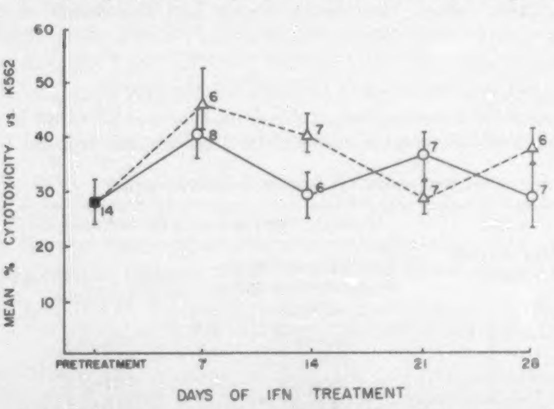

TEXT-FIGURE 5.—Effect on NK activity of time interval between IFN administration and sampling. *Vertical axis* shows mean of four ratios averaged for group of patients. Samples drawn 12–24 hr after previous IFN dose (△—△) are compared to samples drawn 1–5 hr after previous dose (○—○). *Vertical bars* indicate standard error of the mean. *Numbers adjacent to symbols* indicate number of patients tested.

treatment. The results are shown in text-figure 4. No substantial changes in the ability to form rosettes were associated with IFN treatment. Thus changes in NK activity cannot be ascribed to changes in proportions of T-cells, of complement receptor cells, or of cells bearing Fcγ receptors. Although the average rosette values did not change, possibly separate subgroups of patients were simultaneously rising and declining. However, examination of the data from the individual patients showed that most were quite stable. No characteristic patterns could be identified for any of the subgroups separated on the basis of IFN dose or clinical response. Similar stable results (data not shown) were obtained with sequential tests for EAγ (rosette-forming cells) with the 4 healthy controls.

Also shown in text-figure 4 is the absolute lymphocyte counts. Except for a brief period of variability immediately after the start of IFN treatment, total lymphocyte numbers were also remarkably stable. Thus changes in NK activity on a per-cell basis can also be taken as estimates of total NK activity. No noteworthy changes in lymphocyte numbers or populations (as measured by these three rosette assays) could be detected during IFN treatment.

Correlation of NK Activity to Clinical Response

Five patients (2 given high dose; 2, intermediate; 1, low dose) were considered to have had some benefit from IFN therapy as shown by either regression of established lesions or stabilization of previously rapidly growing tumors. Conversely, 4 patients (1 given high dose; 1, intermediate; 2, low dose) had more rapid tumor growth while on treatment. NK activity for these 2 subgroups is compared in table 6. Both groups responded to IFN treatment with equivalent increases in average NK cytotoxicity. All 4 patients who did poorly and 4 of 5 patients who did well had NK activity elevated at day 7 when compared to NK activity at day 0. The only discernible difference between these groups is the somewhat lower initial pretreatment cytotoxicity for the patients who had continued rapid disease progression ("nonresponders"). The 2 groups were comparable in other pretreatment values; the nonresponders had an average absolute lymphocyte count of 1,395/mm^3, 60.5% sheep RBC rosettes, and 19% EAγ rosettes, whereas the "responders" had pretreatment values of 1,316 lymphocytes/mm^3, 53.8% sheep RBC rosettes, and 16.8% EAγ rosettes. Whether pretreatment NK cytotoxicity will be a useful discriminant for predicting who will respond to IFN therapy obviously cannot be determined from this small sampling, although it does appear to warrant further examination. Even those patients who had very poor clinical responses to IFN did demonstrate increased NK responses.

TABLE 6.—*NK activity by clinical status*

Day of treatment	Average mean percent cytotoxicity ± SE	
	Clinical improvement or stabilization in 5 patients	Disease progression in 4 patients
−1	28.8±6.7	16.2±4.4
0	30.6±9.4	19.4±8.8
1	19.9±3.6	21.7±2.8
2	26.2±2.2	19.6±7.5
3	29.8±3.3	31.6±5.7
7	47.3±8.0	35.7±7.3
14	40.7±4.2	26.9±4.0
21	32.6±3.5	30.7±4.9
28	36.4±5.1	24.4±11.0

DISCUSSION

We aimed to define the parameters of changes in NK activity in a relatively homogeneous patient group treated with human leukocyte IFN. Our results indicate that systemic administration of an IFN-containing preparation regularly and reproducibly increased NK activity of PBL. There are several features of the pattern of NK cytotoxicity in these patients that may help to define some of the biologic properties of these agents. The general pattern we observed was a transient decline at 24 hours, followed by a gradual increase until peak cytotoxicity is reached about day 7 of treatment. Subsequently, NK activity tended to decline toward pretreatment values.

Our conclusion as to the pattern of NK response is based on two separate types of statistical analysis. We compared the mean response of all patients at each time point to their mean pretreatment response by the paired *t*-test (table 1). This analysis would smooth out some of the variation inherent in any repetitive testing of individuals and should provide a clearer picture of the underlying kinetics of the response to IFN. It will also provide an estimate of the magnitude of change. We also analyzed for the proportion of patients who increased at each time point over their individual pretreatment base-line values by the Wilcoxon rank sum test (table 1). This type of analysis is less sensitive to a few extreme responses. However, it does not provide an estimate of the magnitude of the changes. Both types of analysis, as well as inspection of each patient's results, lead to the conclusion that a common pattern of NK responses exists in most of these patients.

The initial decline at 24 hours following IFN treatment has also been described by Kariniemi et al. (*14*) in normal volunteers who received IFN and by Einhorn et al. (*16*) at 6 hours following treatment in cancer patients. Some caution is required in interpreting this decline because we observed a similar decline in normal controls who did not receive IFN (table 1). Since this decline in NK activity could not be related to any systematic error in the NK assay (table 2), it may be related to repetitive venipuncture or other hard-to-define variables. Our observation that the decline in NK activity at 24 hours was most pronounced among the patients who received the highest IFN doses does indicate that at least a component of this decline may be a real consequence of IFN treatment. The reasons for this decline are unclear, although redistribution of NK cells seems the best available explanation (*14*).

Time of peak NK activity was 7 days following initiation of treatment in our study, which is later than in other published observations of NK activity in IFN-treated cancer patients. Einhorn et al. (*4*), using single doses or daily doses (*16*) of 3×10^6 U IFN, found peak NK activity at 12–24 hours after initiation of IFN treatment. Similar results were reported by Huddlestone et al. (*5*) in a small series of patients who received 10×10^6 U IFN, whereas Kariniemi et al. (*14*) found no augmentation within 5 days in normal volunteers who received 3×10^6 U. Differences in purity of the IFN used and differences in the immune status of the individuals treated probably cause some of the differences in kinetics among the various studies. Our results are most similar to the results in normal healthy subjects (*14*), except that we find a significant increase in NK activity. The similarity of our results and those in IFN-treated healthy subjects probably reflects the relatively small impairment in immune status in stage III melanoma patients (*17*). All in vivo studies show agreement that systemic administration results in a less rapid increase in NK activity than can be achieved by the in vitro exposure of lymphocytes to IFN (*18*). This implies the existence of control mechanisms in addition to the direct interaction of IFN with NK cells, and this possibility is addressed in (*19*).

We observed that continued daily doses of IFN generally failed to maintain NK cytotoxicity at the elevated level after peak activity was reached on day 7 of treatment. This return to pretreatment NK activity is not due to any detectable change in kinetics of response, because samples obtained 1–5 hours or 12–24 hours after IFN administration were equivalently low in cytotoxicity (text-fig. 5). This observation is somewhat different than the results of Einhorn et al. (*16*), who found that long-term daily administration of 3×10^6 U IFN resulted in continued elevated NK activity. We observed a similar maintenance of high NK cytotoxicity in our lowest-dose group (1×10^6 U/day) (table 3), and therefore small differences in purity or dosage may explain this discrepancy. Also, we evaluated the patients weekly for 7 weeks and did note a slight but statistically insignificant increase in week 7 of treatment, whereas Einhorn et al. (*16*) measured NK activity at 3-month intervals. Thus a pattern of declining NK in the immediate weeks following initiation of treatment with a return to elevated NK activity upon longer treatment would be consistent with both sets of results. This finding suggests a cycling of NK activity, which may indicate an effect of IFN on NK precursors. This possibility is discussed more thoroughly in (*19*).

Our results (text-fig. 5) indicate that IFN administration is not associated with any significant change in the proportion of cells bearing the membrane receptors for sheep RBC or EAC or of cells bearing Fcγ receptors (EAγ). Thus changes in NK activity cannot be associated with any redistribution of cell types as measured with these assays. The lack of change in proportion of Fcγ receptor cells is interesting in light of observations on increased expression of Fcγ receptors when cells are treated in vitro with IFN (*20, 21*). Although it is possible that the Fcγ receptor cells are expressing more receptors per cell in the IFN-treated patients, both studies cited above showed enhanced Fcγ receptor expression by increases in the proportion of cells bearing membrane receptors for EAγ. Our failure to detect any such change in these patients again points out the difference between the in vitro and in vivo immunologic effects of IFN.

Finally, we had hoped that the effects of IFN on NK activity would be a useful indicator of those patients obtaining clinical benefit from this agent. This does not appear to be the case, because both clinical responders and nonresponders showed equivalent increases in NK activity (table 6). However, those patients who had some clinical benefit from IFN did appear to have higher pretreatment levels of NK activity. This may be related to a greater tumor burden in the poor responders; NK activity has been reported to be suppressed in patients with large tumor burdens (*22, 23*). A larger series of patients will have to be studied to determine if pretreatment NK level will predict response to IFN treatment with any accuracy. The variability of both NK assays and of NK activity in the population probably will preclude actually selecting patients for treatment on this basis, but further investigation in this area may help determine the basis of IFN action in the cancer patient.

REFERENCES

(*1*) Strander H. Interferons: Antineoplastic drugs? Blut 1977; 35:279–299.

(*2*) Merigan TC, Sikora K, Breeden JH, Levy R, Rosenberg SA. Preliminary observations on the effect of human leukocyte interferon in non-Hodgkin's lymphoma. N Engl J Med 1978; 299:1449–1453.

(*3*) Gutterman JU, Blumenschein GR, Alexanian R, et al. Leukocyte interferon-induced tumor regression in human metastatic breast cancer, multiple myeloma, and malignant lymphoma. Ann Intern Med 1980; 93:399–406.

(*4*) Einhorn S, Blomgren H, Strander H. Interferon and spontaneous cytotoxicity in man. II. Studies in patients receiving exogenous leukocyte interferon. Acta Med Scand 1978; 204:477–483.

(*5*) Huddlestone JR, Merigan TO Jr, Oldstone MB. Induction and kinetics of natural killer cells in humans following interferon therapy. Nature 1979; 282:417–420.

(*6*) Krown SE, Burk M, Kirkwood JM, Kerr D, et al. Human leukocyte interferon (HuLeIf) in malignant melanoma (MM): Preliminary report of the American Cancer Society clinical trial. Proc Am Assoc Cancer Res 1981; 22:158.

(*7*) Golub SH, Sulit HL, Morton DL. The use of viable frozen lymphocytes for studies in human tumor immunology. Transplantation 1975; 19:195–202.

(*8*) Golub SH, Golightly MG, Zielske JV. "NK-like" cytotoxicity of human lymphocytes cultured in media containing fetal bovine serum. Int J Cancer 1979; 24:273–283.

(*9*) Seeley JK, Golub SH. Studies on cytotoxicity generated in human mixed lymphocyte cultures. I. Time course and target spectrum of several distinct concomitant cytotoxic activities. J Immunol 1978; 120:1415–1422.

(*10*) Golightly MG, Golub SH. The in vitro culture characteristics and requirements for expression of receptors for IgM on human peripheral blood lymphocytes. Clin Exp Immunol 1980; 39:222–232.

(*11*) Golub SH, Forsythe AB, Morton DL. Sequential examination of lymphocyte proliferative capacity in patients with malignant melanoma receiving BCG immunotherapy. Int J Cancer 1977; 19:18–26.

(*12*) Golub SH, Holmes EC. In vitro assay of immunocompetence in patients with lung cancer treated with levamisole. Cancer Immunol Immunother 1979; 7:143–149.

(*13*) Roth JA, Golub SH, Cukingnan RA, Brazier J, Morton DL. Cell-mediated immunity is depressed following cardiopulmonary bypass. Ann Thorac Surg 1981; 31:350–356.

(*14*) Kariniemi AL, Timonen T, Kousa M. Effect of leukocyte interferon on natural killer cells in healthy volunteers. Scand J Immunol 1980; 12:371–374.

(*15*) Callery CD, Golightly M, Sidell N, Golub SH. Lymphocyte surface markers and cytotoxicity following cryopreservation. J Immunol Methods 1980; 35:213–223.

(*16*) Einhorn S, Blomgren H, Strander H. Interferon and spontaneous cytotoxicity in man. V. Enhancement of spontaneous cytotoxicity in patients receiving human leukocyte interferon. Int J Cancer 1980; 26:419–428.

(*17*) Golub SH, Rangel DM, Morton DL. In vitro assessment of immunocompetence in patients with malignant melanoma. Int J Cancer 1977; 20:873–880.

(*18*) Silva A, Bonavida B, Targan S. Mode of action of interferon-mediated modulation of natural killer cytotoxic activity: Recruitment of pre-NK cells and enhanced kinetics of lysis. J Immunol 1980; 125:479–484.

(*19*) Golub SH, D'Amore P, Rainey M. Systemic administration of human leukocyte interferon to melanoma patients. II. Cellular events associated with changes in natural killer cytotoxicity. JNCI 1982; 68:711–717.

(*20*) Itoh K, Inoue M, Kataoka S, Kumagai K. Differential effect of interferon on expression of IgG- and IgM-Fc receptors on human lymphocytes. J Immunol 1980; 124:2589–2595.

(*21*) Fridman WH, Gresser I, Bandu MT, Aquet M, Neauport-Sautes C. Interferon enhances the expression of Fcγ receptors. J Immunol 1980; 124:2436–2441.

(*22*) Pross HF, Baines MG. Spontaneous human lymphocyte-mediated cytotoxicity against tumor target cells. I. The effect of malignant disease. Int J Cancer 1976; 18:593–604.

(*23*) Takasugi M, Ramseyer A, Takasugi J. Decline of natural nonselective cell-mediated cytotoxicity in patients with tumor progression. Cancer Res 1977; 37:413–418.

Systemic Administration of Human Leukocyte Interferon to Melanoma Patients. II. Cellular Events Associated With Changes in Natural Killer Cytotoxicity[1,2,3]

Sidney H. Golub,[4] **Paula D'Amore,**[4,5] *and* **Marcia Rainey,**[4,6]

ABSTRACT—Treatment of patients with malignant melanoma with daily doses of human leukocyte interferon (IFN) resulted in natural killer (NK) cytotoxicity that increased during the 1st week of treatment and subsequently declined to pretreatment levels despite continued IFN administration; events involved in these changes were examined. The increased cytotoxicity was associated with an increased number of cells able to bind K562 targets and an increased proportion of cells able to mediate cytolysis of K562 targets. The period of increasing NK activity was also associated with an increased ability to generate in vitro cytotoxic effectors against K562 targets by stimulation with allogeneic lymphoblastoid cells. The responding cells in this system were depleted of NK activity by adherence to immune complexes. These results suggested that increased NK activity during week 1 of in vivo treatment was associated with augmentation of the development of NK cells from noncytotoxic precursors in addition to direct effects on NK cells. In contrast, the decline in NK activity appeared to be primarily a direct effect on NK cells, because these cells could no longer be augmented in vitro by additional IFN. The refractory state to IFN augmentation of cytotoxicity was limited to the period of IFN treatment in vivo, and responsiveness to IFN was promptly regained upon cessation of treatment. No evidence for the development of suppressor cells of NK effector function could be obtained.—JNCI 1982; 68:711–717.

The preceding paper in this series (*1*) described a consistent pattern of changes in NK activity after the systemic administration of human leukocyte IFN to patients with metastatic malignant melanoma. The administration of IFN is associated with an increase in circulating NK activity, which usually peaks by day 7 of continuous treatment. After the achievement of elevated levels of NK cytotoxicity, patients tend to display declining NK activity despite continued treatment with IFN. In the studies reported in this paper, we have addressed two questions: *a*) What are the events associated with the increase in NK activity early during IFN treatment and *b*) what are the events associated with the subsequent decline in NK cytotoxicity?

Increases in NK cytotoxicity either could be the result of direct activation of mature NK cells by IFN (*2, 3*) or could include activation of precursor cells not previously capable of mediating cytolysis. We have attempted to address this question by an analysis of the target-binding cells during the course of IFN treatment and by analyzing the ability of NK-depleted cell populations to generate anti-K562 killer cells.

Several possible explanations for the decline in NK cytotoxicity following IFN treatment can be envisioned. The pool of precursor cells, presumably located in the bone marrow, may become exhausted; the activated NK cells may redistribute from the circulating compartment and therefore may no longer be detectable in the peripheral blood; the cells may become refractory to further IFN stimulation; or suppressive mechanisms, including suppressor cells, may become activated. The first two possibilities, redistribution of cells or exhaustion of bone marrow precursors, are difficult to test in the human and therefore we have concentrated on the other two possibilities: resistance to further IFN activation and development of suppressor cells.

Our results thus far indicate that the early phases of increased NK activity following IFN treatment are associated with increases in both the number of cells able to mediate NK lysis and the number of TBC. Furthermore, IFN treatment also appears to be associated with an augmented response to alloantigen-induced NK activity. Thus our data are consistent with increases in both NK precursors and mature NK cells following IFN treatment. The subsequent decline in NK activity is associated with increased resistance of cells to in vitro activation by IFN. However, we could find no evidence for the development of suppressor cells to NK activity.

MATERIALS AND METHODS

Preparation of lymphocyte samples.—The patient population tested was described in the previous paper in this series (*1*). PBL samples were prepared by standard Ficoll-Hypaque density gradient centrifugation procedures and were cryopreserved as previously described (*4*). Cryopreserved cells were used, in general, when we subjected cells to identical manipulations and the cells were drawn from the same patient at different time points during treatment. Cryopreserved cells were used for all studies in this report except the sequential analysis of TBC and of cytotoxic cells in the single cell assay and in some of the in vitro activation with IFN experiments. Previous studies in our laboratory have shown that cryopreserved cells retain NK cytotoxicity, al-

---

ABBREVIATIONS USED: CML=cell-mediated lympholysis; RBC=red blood cell(s); EAγ=ox RBC coated with IgG to detect Fcγ receptor cells; E:T=effector-to-target cell ratios; IFN=interferon; MLC=mixed lymphocyte culture; NK=natural killer(s); PBL=peripheral blood lymphocyte(s); TBC=target-binding cell(s).

---

[1] Received May 26, 1981; accepted September 18, 1981.

[2] Supported in part by Public Health Service grant CA-17013 from the National Cancer Institute.

[3] Research procedures were in accord with the ethical standards of the Human Subjects Protection Committee, UCLA School of Medicine.

[4] Division of Oncology, Department of Surgery, UCLA School of Medicine, University of California at Los Angeles, Los Angeles, Calif. 90024.

[5] Department of Pathology, UCLA School of Medicine.

[6] The interferon used for treating the patients was provided by the American Cancer Society.

though it is uniformly at a predictably diminished level of activity (*5*).

Cytotoxicity assays.—NK cytotoxicity was measured against K562 targets by the standard ^{51}Cr release assay described in the preceding paper. With freshly prepared PBL, the assay was tested at four serial dilutions yielding E:T from 100:1 to 12.5:1, and the results were expressed as the means of all four ratios. With cryopreserved lymphocytes, cell recovery generally allowed testing only at the 100:1 ratio. In addition to the ^{51}Cr release assay, we have used the single cell binding and lysis assay developed by Grimm and Bonavida (*6*) and modified for human NK assessment by Targan and Dorey (*3*). Equal numbers (2.5×10^5) of PBL and target cells were mixed in 0.1 ml, incubated for 10 minutes at 37°C, and centrifuged for 10 minutes at 1,200×*g*. Warm (37°C) 1% agarose solution (100 µl) was added to each tube and gently mixed with the cells. The cell suspension was then spread onto a glass slide coated with 2% agar. When the agarose had solidified, one set of slides was read for binding cells, and another set was incubated for 3 hours at 37°C. This set was then stained for 6 minutes in trypan blue, washed in RPMI-1640 medium for 10 minutes, and fixed in Formalin for scoring of dead targets. Each set was done in duplicate, and 300 PBL were scored on each slide. Results never varied more than 1% from one slide to its duplicate. For the studies on the characteristics of the killer cells, at least 100 binding cells were scored in the lysis assay. Results in this assay were expressed as either percentage of PBL binding K562 in the binding assay or percentage of total PBL with bound and dead K562 as determined by trypan blue staining in the lysis assay.

The human leukocyte IFN (IFN-α) used in vitro was generously provided by Dr. M. Krim, Sloan Kettering Institute, and was used in vitro at a dose of 100 U/ml. Cells were pretreated for 60 minutes in 1 ml and washed prior to testing. Indomethacin (Sigma Chemical Co., St. Louis, Mo.) was used at 1×10^{-5} *M* and was included in the cytotoxicity assay for the 4-hour duration of the test.

Induction of NK-like cytotoxicity by stimulation with allogeneic lymphoblastoid cell line cells.—PBL were depleted of anti-K562 cytotoxic NK cells by passage over monolayers of EAγ according to the method of Kedar et al. (*7*). These monolayers were constructed with the use of sheep RBC and rabbit anti-sheep RBC IgG. The NK-depleted PBL were then assayed in MLC-CML assays as previously described (*5*). The cells were stimulated in vitro with irradiated allogeneic lymphoblastoid cell line cells, and separate MicroTest plates were assayed for [^{3}H]thymidine incorporation (MLC) and cytotoxicity against K562 targets (CML) after 6 days of incubation. The efficacy of the monolayers of EAγ was routinely checked by loss of activity in NK assays and depletion of EAγ (rosette-forming cells).

Depletion of adherent cells.—Adherent cells were depleted by passage over Sephadex G10 columns. PBL, 5–10 million, were passed over a G10 1-ml column (Pharmacia Fine Chemicals, Piscataway, N.J.) in a 5-ml disposable sterile syringe. The cells were allowed to incubate for 30 minutes on the beads before elution with 10 volumes of media. Efficacy of removal of adherent cells was confirmed by loss of cells staining for nonspecific esterase. Passage of PBL over nylon fiber columns was accomplished by the same technique with the use of columns packed with 100 mg of scrubbed nylon fiber (Fenwal Laboratories, Deerfield, Ill.).

RESULTS

Quantitation of TBC and NK Cells

We analyzed 4 patients with repeated assays of the number of K562 binding cells and K562 killing cells in the single cell assay system. The results for binding cells are seen in text-figure 1, and the results for lytic cells are shown in text-figure 2. Both results were given as the proportion of cells either binding or killing when compared to total PBL. Both binders and killers increased early during IFN treatment. Peak activity was found during week 1, usually at day 7, and closely paralleled the increased activity noted in the ^{51}Cr release assay, as described in the previous paper of this series (*1*).

After the achievement of peak levels of TBC or killer cells, the proportion of cells active in both these assays declined despite continued administration of IFN. The proportion of binding and killing cells after peak activity returned toward pretreatment levels but remained slightly elevated. This was also consistent with the ^{51}Cr release results as detailed in tables 1 and 2 in the previous paper in this series (*1*).

Some of the characteristics of the binding and killing cells are illustrated in table 1 in this paper. In these studies, cryopreserved PBL were used from an IFN-treated patient who showed a typical pattern of NK activity in ^{51}Cr release assays against K562, with peak activity on day 7. In contrast to results with the other 4 patients (text-fig. 1), no appreciable increase in K562 binding cells was seen after IFN treatment with this patient. However, the proportion of lytic cells approximately doubled in the samples drawn 2 or 7 days after the initiation of IFN treatment and then declined to below the pretreatment value after 35 days of treatment. Binding and killing cells were also assessed with the NK-resistant M14 melanoma targets. These targets have been shown to be resistant to lysis by either normal or IFN-

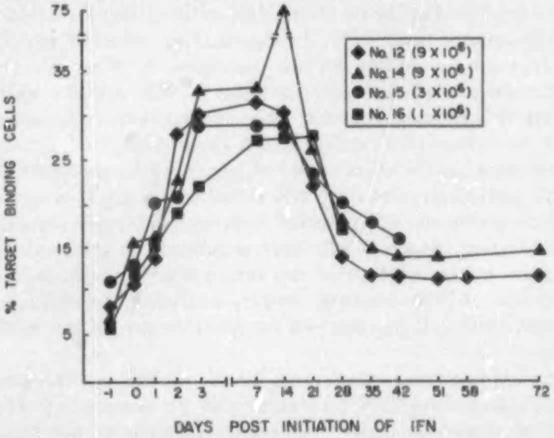

TEXT-FIGURE 1.—Proportion of K562 TBC (*vertical axis*) is shown as a function of days of IFN treatment (*horizontal axis*). *In upper right box:* Four patients' entry numbers and dose of IFN used in vivo.

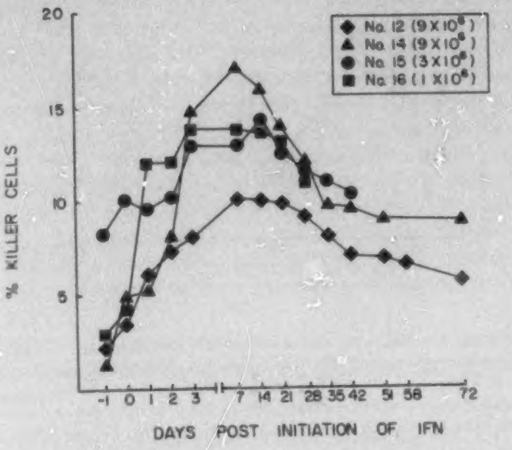

TEXT-FIGURE 2.—Proportion of NK cells in IFN-treated patients. Proportion of PBL lysing K562 targets was measured (*vertical axis*). *In upper right box:* Four patients' entry numbers and dose of IFN used in vivo.

activated NK cells. Although as many M14 binders as K562 binders could be detected, the proportion of M14 killers was consistently very low both before and during IFN treatment. Thus the increased cytotoxicity appeared to be limited to NK-sensitive targets.

Depletion of the Fcγ receptor cells on EAγ monolayers resulted in a 60%- to 90%-depletion of EAγ rosette-forming cells. While this procedure resulted in only a partial depletion of K562 or M14 binding cells, it did substantially reduce the proportion of lytic cells. Approximately 80% of the killer cells were removed by passage over EAγ monolayers. Thus effectors obtained either before or during IFN treatment were predominantly Fcγ receptor-bearing cells. However, a population of Fcγ receptor-negative, nonlytic target-binding cells could also be detected. Passage of the PBL over nylon fiber columns to deplete B-cells and monocytes resulted in an enrichment for both binders and killers (table 1). In this case, we did observe the more typical increase in K562 binders early during IFN treatment and a subsequent decline. The increase in binders was accompanied by a parallel increase in the proportion of binders that killed the targets. The fact that the proportion of K562 binding and killing cells increased in day 2 and day 7 nylon nonadherent cells indicated that this elevation was not simply due to increased "stickiness" of cells from IFN-treated patients. Similarly, the lack of change in M14 binders argues against any nonspecific surface change. Also, nylon fiber fractionation reduced the proportion of Fcγ receptor cells while increasing NK activity. Presumably, NK inactive monocytes were removed on the columns.

In Vitro Generation of NK-Like Cytotoxicity From PBL of IFN-Treated Patients

Because the TBC data indicated an increase in the number of TBC after the initiation of IFN treatment, we considered the possibility that IFN treatment increases the number of NK precursors in the peripheral blood. To determine if there is any increase in the number or activity of NK inactive precursors of NK cells during IFN treatment, we attempted to generate NK activity in vitro. Cryopreserved PBL from various points during treatment were depleted of NK activity by passage over EAγ monolayers. The nonadherent cells were then stimulated in Microwell plates with allogeneic lymphoblastoid cell line cells. After 6 days of culture, sets of Microwell plates were assayed for proliferation and other sets were assayed for cytotoxic activity against K562 targets. The results of a representative experiment of this type are given in text-figure 3. The ability to generate NK activity in vitro shows a similar time course as the original NK activity as detected in the peripheral blood. No differences in proliferative activity were observed at any point during treatment, although differences were detected in cytotoxicity. Nonstimulated control PBL showed no cytotoxicity. In four such series of experiments with the use of FBL from 4 IFN-treated patients, increased anti-K562 cy-

TABLE 1.—*Single cell NK assays with PBL from IFN patient #13*

Parameters	Single cell NK assays with PBL drawn on day:[a]			
	0	2	7	35
Percent ^{51}Cr release assays[b]	21	31	45	27
Unfractionated cells				
Percent K562 binding cells[c]	8	10	9	3
Percent K562 killers[d]	24	36	40	9
Total percent NK cells vs. K562[e]	1.9	3.6	3.6	0.3
Percent M14 binding cells[c]	12	10	13	10
Percent M14 killers[d]	10	6	7	2
Total percent NK cells vs. M14[e]	1.2	0.6	0.9	0.2
Percent EAγ rosette-forming cells	18	29	33	24
Monolayer cells depleted of EAγ				
Percent K562 binding cells[c]	4	7	8	1
Percent K562 killers[d]	6	7	8	4
Total percent NK cells vs. K562[e]	0.2	0.5	0.6	0.1
Percent M14 binding cells[c]	6	5	6	4
Percent M14 killers[d]	0	2	2	0
Total percent NK cells vs. M14[e]	0	0.1	0.1	0
Percent EAγ rosette-forming cells	7	3	8	2
Nylon fiber column-passed cells				
Percent K562 binding cells[c]	13	14	19	12
Percent K562 killers[d]	28	40	40	13
Total percent NK cells vs. K562[e]	3.6	5.6	7.6	1.6
Percent M14 binding cells[c]	18	13	20	15
Percent M14 killers[d]	4	3	4	1
Total percent NK cells vs. M14[e]	0.7	0.4	0.8	0.2
Percent EAγ rosette-forming cells	10	11	6	7

[a] Cryopreserved PBL drawn at indicated days during treatment with 1×10^6 U IFN/day.

[b] Mean percent cytotoxicity (4 ratios) vs. K562 as determined with daily assays of fresh PBL.

[c] Proportion of PBL that bound target; 300 PBL counted.

[d] Proportion of PBL with bound trypan blue-stained targets; 100 target-binding PBL counted.

[e] Product of percent binders and percent killers.

totoxicity could be generated from PBL drawn at the time of peak NK activity (2 patients) or at times just preceding peak NK activity (2 patients, including the one in text-fig. 3). These data supported, although did not directly prove, the concept that IFN treatment is associated with increase in NK precursors.

Effect of In Vitro Addition of IFN to PBL From IFN-Treated Patients

We next considered the possible explanations for a decline in NK activity following the achievement of peak levels of NK activity. One possibility is that the mature NK cells, or other IFN-responsive cells, become refractory to further IFN activation. We have examined this by comparing PBL from various time points during treatment for NK activity with and without the addition of a 60-minute pretreatment with 100 U IFN. Results for a typical experiment of this type are shown in text-figure 4, where cryopreserved PBL from 1 patient was tested in simultaneous assays with and without pretreatment with IFN. In this patient, IFN augmented anti-K562 NK activity of PBL obtained before treatment, early during treatment, or after the termination of treatment. In contrast, samples obtained from the period of peak NK activity through most of the rest of the treatment period were unresponsive to IFN. Similar results have been obtained with freshly prepared PBL tested with and without IFN in each repetitive test.

The results with 10 patients tested with 100 U IFN in vitro are summarized in text-figure 5. The results were expressed as average increase in cytotoxicity associated with pretreatment with IFN (percent cytotoxicity in presence of IFN minus percent cytotoxicity in absence of IFN). The results were accumulated into five time periods. The first was the pretreatment period, followed by three treatment periods comprising: the first three samplings (days 1, 2, and 3), the next three sampling periods during treatment (days 7, 14, and 21), and the last three treatment periods (days 28, 35, and 42). The final samplings were those after termination of treatment. When summarized in this fashion, it was apparent that pretreatment samples were regularly associated with increased NK activity with an average increase of 8.4%. Results from the earliest time periods were quite similar (average increase, 7.1%), but the response to IFN markedly diminished in subsequent samplings (<1% average increase). However, when the patients completed the course of IFN treatment, responsiveness in vitro to IFN activation of NK activity returned (average increase, 9.7%). The effect of time on in vitro response to IFN was statistically significant as determined by analysis of variance ($P<0.05$). Also, in vitro activation by IFN was statistically significant for the entire group of 69 lymphocyte samples tested from

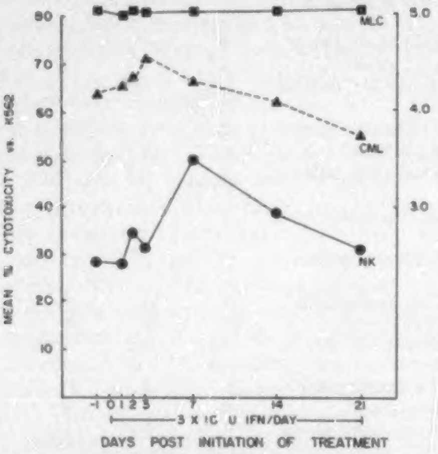

TEXT-FIGURE 3.—NK and MLC-CML responses of PBL from patient #2. PBL were drawn at various times during treatment with 3×10^6 U IFN/day and were tested for NK activity. Cryopreserved samples were then depleted of Fcγ receptor cells and stimulated for 6 days in vitro with irradiated allogeneic lymphoblasts. One set of wells were assayed for [^{3}H]thymidine incorporation, and results are expressed as $\log_{10}$ cpm/1×10^6 PBL (*right vertical axis*) and are designated MLC. Other Microwell plates were assayed for cytotoxicity vs. K562 (CML). Both CML and NK results are mean cytotoxicity percentages of four E:T (*left vertical axis*). Cytotoxicity of Fcγ-depleted cells (without stimulation) did not exceed 1% for any sample at the highest of the four E:T.

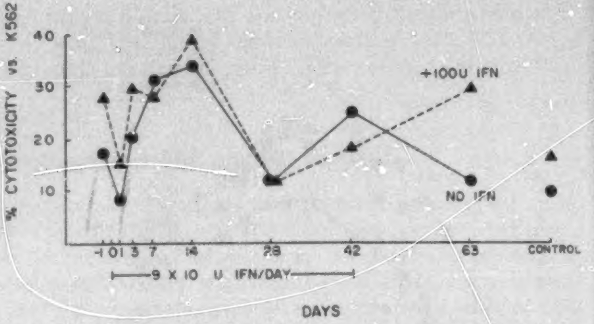

TEXT-FIGURE 4.—NK, with and without IFN pretreatment, of PBL from IFN-treated patient #1. Results are mean cytotoxicity percentages of four E:T (*vertical axis*) of PBL drawn at various times during treatment (*horizontal axis*). Control indicates PBL from a healthy donor. Cells were tested after incubation for 60 min in media with no IFN or 100 U IFN.

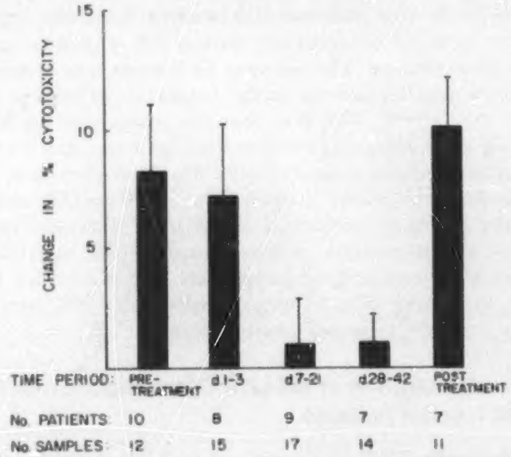

TEXT-FIGURE 5.—Summary of in vitro IFN activation of NK. Results are cytotoxicity changes calculated as percent cytotoxicity with IFN − percent cytotoxicity without IFN. Results are averaged within time periods according to the number of patients, rather than number of samples, tested. *Vertical bars* indicate standard error. Days, d.

these patients ($P<0.01$; paired t-test). This simply indicated that our IFN was active for in vitro augmentation of NK cytotoxicity. We also tried treatment with IFN dosages of 10, 333, or 1,000 U and pretreatment periods of 24 hours. Neither different IFN dosages nor longer treatment could induce greater NK activity from PBL drawn late in the course of IFN treatment (data not shown). Thus these results showed that lymphocytes from the period of peak NK cytotoxicity through subsequent declining NK cytotoxicity were less responsive to IFN in vitro for the development of increased NK activity. The response returned to normal, or even above normal, levels following termination of IFN treatment.

Lack of Adherent Suppressor Cells for NK Effector Function

We considered the possibility that declining NK activity was due to an adherent suppressor cell, particularly a prostaglandin-secreting suppressor cell. To examine this possibility, we tested PBL for cytotoxicity before and after removal of adherent cells by passage over Sephadex G10 columns. The results of a typical experiment are given in text-figure 6. Removal of G10-adherent cells had a slight enhancing effect on most PBL samples from normal donors, as illustrated with the control donor tested simultaneously with the patient samples in text-figure 7. However, removal of G10-adherent cells from the patient's PBL did not restore NK activity in PBL samples drawn past the peak of in vivo induced NK activity.

An alternative approach to searching for an adherent suppressor cell is shown in text-figure 7. In these experiments, 1×10^{-5} *M* indomethacin was added to abrogate the synthesis of prostaglandins. As shown in text-figure 7, indomethacin had a slight enhancing effect on NK activity of either the control lymphocytes or the IFN-treated patient lymphocytes. However, neither indomethacin alone nor indomethacin and IFN restored activity from postpeak low NK samples. This was best illustrated with the day 42 sample (text-fig. 7) where activity had declined to below pretreatment levels and could not be restored with IFN, indomethacin, or a mixture of IFN and indomethacin. These results, in combination with the G10 column fractionation experiments, failed to provide any evidence for a G10-adherent, indomethacin-sensitive suppressor cell contributing to the decline in NK activity during later periods of IFN systemic treatment.

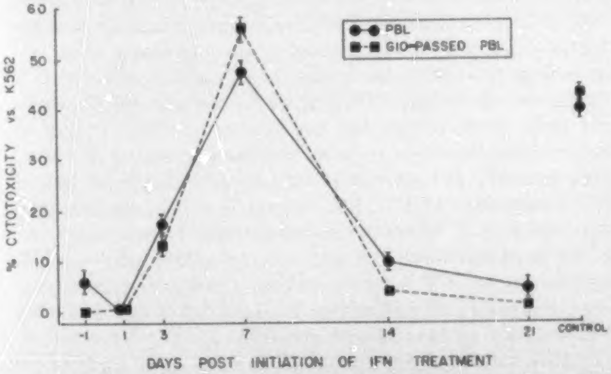

TEXT-FIGURE 6.—Effect of passage of PBL over G10 columns on NK cytotoxicity. PBL were drawn from patient #11 (3×10^6 U IFN/day). PBL and G10-passed PBL were tested at 100:1 vs. K562 (*vertical axis*), as were identically treated PBL from a healthy control donor. *Vertical bars* indicate standard error of the mean.

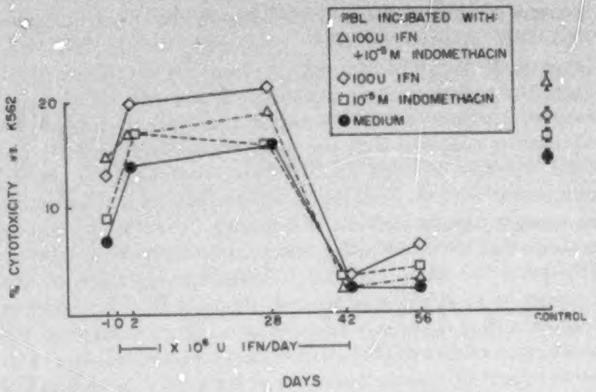

TEXT-FIGURE 7.—Effect of IFN, indomethacin, or IFN + indomethacin on NK of PBL from patient #10 (1×10^6 U IFN/day). For clarity, standard errors are given only with PBL from healthy control donor. *Vertical bars* indicate standard error of the mean.

DISCUSSION

We studied the events involved in the increasing NK cytotoxicity noted during week 1 of treatment of patients with human leukocyte IFN and the events involved in the subsequent decline in NK activity despite continued IFN treatment.

In vitro treatment of lymphocytes with IFN requires only a short period of treatment to augment NK cytotoxicity (*8*, *9*), whereas in vivo treatment of patients results in increases of NK cytotoxicity, which are detectable only after 2–7 days after initiation of treatment. Since im injection of leukocyte IFN results in detectable circulating levels within hours after administration (*10*), one would expect increased NK cytotoxicity promptly after initiation of IFN therapy if direct interaction between IFN and NK cells was the sole mechanism involved in augmenting cytotoxicity. Instead, the delayed time course of increased NK cytotoxicity in these patients suggested an increase in the development of NK cells from noncytotoxic precursors. To test this possibility, we examined the proportion of cells binding to K562 targets. Sequential studies of 4 patients clearly indicated an increased number of TBC shortly after the initiation of IFN treatment (text-fig. 1). Furthermore, there is also a parallel increase in the proportion of lymphoid cells that are actually mediating cytolysis of the K562 targets (text-fig. 2; table 1). If we assume that the lineage of NK cells involves differentiation of nonbinding, noncytotoxic precursors into binding cells ("pre-NK" cells) and then into mature binding and killing NK cells, our data would be consistent with the construct of an increase in the number of pre-NK cells and an increase in the development throughout this pathway, that is, an increase in the number of pre-NK cells and an increase in mature NK cells. In vitro studies have indicated that IFN appears to affect primarily mature NK cells, because depletion of NK cells on immune complexes abrogates the ability to augment cytotoxicity with IFN (*2*) and in vitro treatment with IFN does not increase the proportion of binding cells but only the proportion of killing cells and their kinetics of lysis (*3*, *9*). Our results are in partial agreement with those of the in vitro studies; we observed an increase in the proportion of lytic cells (text-fig. 2), and all activity was localized to Fcγ receptor-bearing cells (table 1). However, we also observed a consistent increase in the proportion of K562 binding cells (text-fig. 1). This increase indicates that there is a substantial difference between the short-term effects of IFN on NK cells in vitro and the long-term effects of repeated treatment with IFN in vivo. Thus the in vitro models appear to be quite useful for the examination of the effects of IFN on mature NK cells but fail to reveal the possible effects of IFN on precursors of NK cells. The increase in TBC found after systemic administration of IFN argued for an increased recruitment of NK cells from a noncytotoxic pool. These results are somewhat in contrast to the failure to find increased binding cells in mice treated with tilorone, an IFN inducer (*11*). Possibly, IFN and IFN inducers do not have identical effects on the NK system.

Since we do not have reliable phenotypic or functional markers for noncytotoxic, nonbinding NK precursors, it is difficult to test the hypothesis generated from these results that IFN administration promotes differentiation into NK cells. In an attempt to deal with this question, we turned to the in vitro generation of "NK-like" cytotoxicity. This type of cytotoxicity, which mimics NK cytotoxicity in specificity, can be generated by in vitro stimulation of lymphocytes in MLC with allogeneic or autologous lymphoblastoid cell line cells (*12*, *13*). If we make the assumption that the in vivo differentiation of NK cells from their precursors is similar to the in vitro generation of NK-like cytotoxicity, we can use this model to approach this problem. Our results, illustrated in text-figure 3, demonstrate an increase in MLC-generated anti-K562 cytotoxicity from PBL samples from periods of increasing NK activity in vivo. The NK-like cytotoxicity was generated from noncytotoxic cells; the PBL were first depleted of NK activity by passage over monolayers of EAγ. These results are quite similar to the increased cytotoxicity detected in CML assays when IFN is added to the MLC in vitro (*14*). However, we added no exogenous IFN in these cultures, and our results therefore reflect the increased ability to generate cytotoxic effectors, particularly against K562 targets, from PBL from patients treated with IFN. Although these results are certainly not a direct test of NK precursor activity, since we have no direct proof that the "NK-like" cytotoxicity is identical to standard NK cytotoxicity, these data are consistent with our hypothesis that IFN treatment augments the generation of NK cells from noncytotoxic precursors in vivo. As such, IFN may prove to be an extremely interesting agent for the study of the development and lineage of NK cells.

That continued IFN treatment failed to maintain NK activity at high levels was of considerable interest. Instead, NK activity declined following the peak attained in week 1 of treatment toward pretreatment NK levels. Our data strongly suggest that one major explanation for this phenomenon is the development of a refractory state to further IFN augmentation of NK cytotoxicity (text-figs. 4, 5). We found that PBL obtained before treatment, early during IFN treatment, or after completion of IFN treatment had NK activities that could be readily boosted in vitro by the pretreatment of cells with 100 U IFN for 60 minutes. However, PBL drawn from 1 week of treatment through 6 weeks of treatment showed little augmentation of NK cytotoxicity by in vitro pretreatment with IFN. These experiments were performed with pretreatment of PBL with IFN followed by washing of the pretreated PBL to eliminate IFN effects on target cells (*15*). Einhorn et al. (*16*) has also noted a diminished capacity of lymphocytes from IFN-treated patients to respond to IFN in vitro. Their results, in combination with ours, suggest that repeated doses of IFN will not have the ability to maintain high levels of NK cytotoxicity as cells become refractory to IFN stimulation. Our preliminary results (Golub S: Unpublished data) suggest that this refractory state extends to other forms of augmentation of NK cytotoxicity, because cells refractory to human leukocyte IFN (IFN-α) augmentation of NK cytotoxicity are also resistant to boosting by fibroblast IFN (IFN-β). The implications of these findings for proper dose and timing of IFN treatment are not clear; it is yet to be established that activation of NK cells is a crucial component of any antitumor effects of IFN. However, these results do suggest that alternative schedules, such as short treatment periods interrupted by rest periods, should be considered. This would be especially true if the refractory state associated with NK cytotoxicity can also be extended to other IFN-mediated biologic changes.

We also considered the possibility of the development of suppressor cells as an explanation of the declining NK activity seen after week 1 of IFN treatment. We attempted to find G10-adherent suppressor cells such as have been described in mouse cells exposed to carrageenan (*17*) or *Corynebacterium parvum* (*18*). Adherent cells have also been shown to inhibit spontaneous cytotoxicity against human tumor targets (*19*) and are required for the mitogen-induced suppression of human NK (*20*). Prostaglandins, a well-known secretion product of macrophages, can also suppress NK (*21*). Therefore, we considered the possibility that adherent cells, perhaps by means of prostaglandin secretion, were responsible for the decline in NK activity late in IFN treatment. As shown in text-figure 6, removal of G10-adherent cells failed to prevent the decline in NK activity or restore responsiveness to IFN. Similarly, removal of nylon-adherent cells did not restore activity of PBL drawn late in IFN treatment (table 1). Thus we could not demonstrate the participation of adherent suppressor cells. Furthermore, the addition of indomethacin had no appreciable effect on NK or response to IFN in vitro, making a prostaglandin-secreting suppressor cell unlikely to be involved in the declining NK activity in this system (text-fig. 7). We have yet to examine T-cell subpopulations that may show suppressive activity on NK function, and there is certainly the possibility of suppressor cells for the generation of NK activity from their noncytotoxic precursors. DeBoer et al. (*22*) have identified a human T-cell subpopulation that can suppress NK cell function, and Nair and Schwartz (*23*) have shown that concanavalin A-activated lymphocytes can suppress human NK activity. Non-T-lymphoid cells have been described to inhibit human K-cell function (*24*), and thus there is considerable precedent for the concept of lymphocyte regulation of human NK function. However, the addition of NK-depleted PBL from IFN-treated patients to fresh normal PBL failed to suppress NK activity of the normal PBL (Golub S: Unpublished observations), again indicating the lack of suppressors in this system for NK effector function. The possible contribution of suppressor cells for the development and expression of NK cytotoxicity is currently under study.

We would attribute the increase in NK activity demonstrated in patients treated with IFN to augmentation of NK cytotoxicity by mature NK cells and by the recruitment of noncytotoxic cells into the pool of available effector cells. The subsequent decline in NK cytotoxicity appears to be predominantly due to the inability of IFN to augment NK cytotoxicity from cells already pretreated in vivo with IFN. Other factors that may affect the regulation of NK cytotoxicity in vivo, such as redistribution of NK cells or effects on bone marrow precursor cells, must also be considered in discerning the systemic effects of this agent on the NK system.

REFERENCES

(*1*) Golub SH, Dorey F, Hara D, Morton DL, Burk MW. Systemic administration of human leukocyte interferon to melanoma patients. I. Effects on natural killer function and cell populations. JNCI 1982; 68:703–710.

(*2*) Zarling JM, Eskra L, Borden EC, Horoszewicz J, Carter JM. Activation of human natural killer cells cytotoxic for human leukemia cells by purified interferon. J Immunol 1979; 132:63–70.

(*3*) Targan S, Dorey F. Interferon activation of "pre-spontaneous killer" (pre-SK) cells and alteration in kinetics of lysis of both "pre-SK" and active SK cells. J Immunol 1980; 124:2157–2161.

(*4*) Golub SH, Sulit HL, Morton DL. The use of viable frozen lymphocytes for studies in human tumor immunology. Transplantation 1975; 19:195–202.

(*5*) Callery CD, Golightly M, Sidell N, Golub SH. Lymphocyte surface markers and cytotoxicity following cryopreservation. J Immunol Methods 1980; 35:213–223.

(*6*) Grimm E, Bonavida B. Mechanism of cell-mediated cytotoxicity at the single cell level. I. Estimation of cytolytic T lymphocyte frequency and relative lytic efficiency. J Immunol 1979; 123:2861–2869.

(*7*) Kedar E, Ortiz de Landazuri M, Bonavida B. Cellular immunoadsorbents: A simplified technique for separation of lymphoid cell populations. J Immunol 1974; 112:1231–1243.

(*8*) Djeu JY, Heinbaugh JA, Holden HT, Herberman RB. Augmentation of mouse natural killer cell activity by interferon and interferon inducers. J Immunol 1978; 122:175–181.

(*9*) Silva A, Bonavida B, Targan S. Mode of action of interferon-mediated modulation of natural killer cytotoxic activity: Recruitment of pre-NK cells and enhanced kinetics of lysis. J Immunol 1980; 125:479–484.

(*10*) Cantell K, Pyhala L, Strander H. Circulating human interferon after intramuscular injection into animals and man. J Gen Virol 1974; 22:453–458.

(*11*) Roder JC, Kiesslin GR, Biberfeld P, Andersson B. Target effector interaction in the natural killer (NK) cell system. II. Isolation of NK cells and studies on the mechanism of killing. J Immunol 1978; 121:2509–2515.

(*12*) Svedmyr EA, Deinhardt F, Klein G. Sensitivity of different target cells to the killing action of peripheral lymphocytes stimulated by autologous lymphoblastoid cell lines. Int J Cancer 1974; 13:891–903.

(*13*) Jondal M, Targan S. In vitro induction of cytotoxic effector cells with spontaneous killer cell specificity. J Exp Med 1978; 147:1621–1636.

(*14*) Zarling JM, Sosman J, Eskra L, Borden EC, Horoszewicz JS, Carter WA. Enhancement of T cell cytotoxic response by purified human fibroblast interferon. J Immunol 1978; 121:2002–2004.

(*15*) Trinchieri G, Santoli D. Anti-viral activity induced by culturing lymphocytes with tumor-derived or virus-transformed cells. J Exp Med 1978; 147:1314–1333.

(*16*) Einhorn S, Blomgren H, Strander H. Interferon and spontaneous cytotoxicity in man. V. Enhancement of spontaneous cytotoxicity in patients receiving human leukocyte interferon. Int J Cancer 1980; 26:419–428.

(*17*) Cudkowicz G, Hochman PS. Carageenan-induced decline of natural killer activity. I. In vitro activation of adherent non-T-suppressor cells. Cell Immunol 1980; 53:395–404.

(*18*) Lotsova E. *C. parvum*-mediated suppression of the phenomenon of natural killing and its analysis. In: Herberman R, ed. Natural cell-mediated cytotoxicity against tumors. New York: Academic Press, 1980:735–752.

(*19*) Schulof RS, Michitsch RW, Livingston PO, Gupta S. Monocyte-mediated suppression of lymphocyte cytotoxic activity for cultured autologous melanoma cells. Cell Immunol 1981; 57:529–532.

(*20*) Hofman F, Rand N, Fahey JF. Adherent cell requirement for PWM-stimulated factor suppression of natural killer cytotoxicity. Cell Immunol 1981; 58:356–365.

(*21*) Droller MJ, Schneider MU, Perlmann P. A possible role of prostaglandins in the inhibition of natural and antibody-dependent cell-mediated cytotoxicity against tumor cells. Cell Immunol 1978; 39:165–177.

(*22*) DeBoer KP, Kleinman R, Teodorescu M. Identification and separation by bacterial adherence of human lymphocytes that suppress natural cytotoxicity. J Immunol 1981; 126:276–281.

(*23*) Nair MP, Schwartz SA. Suppression of natural killer activity and antibody-dependent cellular cytotoxicity by cultured human lymphocytes. J Immunol 1981; 126:2221–2229.

(*24*) Pollack SB, Emmons SL. Inhibition of human killer cells by autologous lymphocytes. J Immunol 1979; 122:718–722.

blank page

Characterization of a Monoclonal Antibody Reactive With a Subset of Human Breast Tumors[1,2,3]

Dorothy Yuan,[4] Fred J. Hendler,[5,6] *and* Ellen S. Vitetta[4,7]

ABSTRACT—Fusion of spleen cells, from mice immunized against the human hormone-dependent breast cancer cell line ZR-75-1, with murine myeloma cells resulted in the establishment of a hybridoma cell line, HY59-H10 (H59). The purified monoclonal IgM produced by the hybridoma reacts with the most differentiated human breast tumor cell lines but not with cells derived from normal breast secretions or with numerous other malignant cell lines. Of 106 biopsy specimens examined, H59 bound to 54% of malignant breast specimens, to 83% of fibroadenomas, and to 82% of specimens containing fibrocystic disease. Binding could not be detected in uninvolved breast tissue.—JNCI 1982; 68:719–728.

Cells from human breast tumors may have distinct antigens that can elicit specific antibody and cell-mediated responses in patients with breast carcinoma (*1–3*). However, due to the complexity of the immune response, the specificities of the antisera have been difficult to assess (*4*). For a critical analysis of tumor-specific antigens, it would be advantageous to use a panel of monoclonal antibodies such as those that can be generated by somatic cell hybridization between myeloma cells and spleen cells obtained from immunized animals (*5*). This approach has been used to successfully generate monoclonal antibodies against human malignant cells (*6–9*). Our paper describes the characterization of the first of a series of monoclonal antibodies that we have generated against a malignant hormone-dependent human breast cell line, ZR-75-1 (*10*). This antibody is reactive with a distinct subset of well-differentiated human breast cancer cell lines, human breast carcinoma, and benign breast disease tissue but does not have activity against cells that bear HLA determinants, oncofetal antigens, CEA, or with the breast antigen detected by anti-murine GP52 sera (*11*). The antibody may, therefore, be recognizing a more differentiated breast cancer. Recently, a number of monoclonal antibodies against human breast tumor cells have also been described by other investigators (*12, 13*). None of those antibodies, however, have characteristics similar to those of the antibody described herein.

MATERIALS AND METHODS

Cell line used for immunization.—The ZR-75-1 cells, a line of human breast cancer cells, were selected as the source of antigen. The cell line was derived from metastatic breast cancer cells isolated from the ascitic fluid of a postmenopausal woman with metastatic infiltrating ductal carcinoma of the breast (*10*). The cells, which have been in continuous culture for 5 years, have epithelial morphology as determined by light and electron microscopy, have a human chromosomal karyotype, and are not a HeLa cell contaminant as determined by chromosomal banding and glucose 6-phosphate dehydrogenase isozyme analysis (*10*). These cells have retained estrogen, progesterone, androgen, glucocorticoid, and insulin receptors (*14, 15*). They do not produce the milk proteins casein and α-lactalbumin (*10*) but do make CEA (*16*).

Cultured cell lines.—Table 1 lists the cultured cell lines used in this study. ZR-75-1 cells were grown in Richter's improved minimum essential medium containing 10% calf serum, 10^{-8} *M* β-estradiol, 10^{-8} *M* insulin, 62 mg penicillin/liter, and 130 mg streptomycin/liter to maximize growth. The media for the other breast cell lines were similar in that calf serum and, where appropriate, hormones were substituted for FCS. Cells were removed from culture flasks by means of a rubber policeman. Cell aggregates were dissociated by passage through successively smaller-gauge needles. The resulting cell suspension contained more than 70% single cells. Alternatively, cells were removed by incubation for 5 minutes at 37°C in 1 m*M* EDTA.

ABBREVIATIONS USED: CEA=carcinoembryonic antigen; DMEM=Dulbecco's modified Eagle's minimum essential medium; FACS=fluorescence-activated cell sorter; FCS=fetal calf serum; GAM=goat anti-mouse immunoglobulin; H & E=hematoxylin and eosin; IP=immunoperoxidase; NCI=National Cancer Institute; PAGE=polyacrylamide gel electrophoresis; P=patient group; PBS=phosphate-buffered saline; RAκ=rabbit anti-mouse κ; RAλ=rabbit anti-mouse λ; RAμ=rabbit anti-mouse μ; FITC-RAμ=fluorescinated RAμ; RIA=radioimmunoassay; SDS=sodium dodecyl sulfate; UTHSCD=The University of Texas Health Science Center at Dallas.

---

[1] Received May 26, 1981; accepted November 19, 1981.

[2] Supported by Public Health Service grant CA-23115 from the National Cancer Institute (NCI); by the Ira Kassanoff Fund, The Blanche Mary Taxis Foundation; and by a Biomedical Research Support grant from The University of Texas Health Science Center at Dallas (UTHSCD).

[3] Research procedures were in accord with the ethical standards of the Institutional Review Committee of UTHSCD.

[4] Department of Microbiology, The University of Texas Health Science Center at Dallas, 5323 Harry Hines Boulevard, Dallas, Tex. 75235.

[5] Department of Internal Medicine, UTHSCD.

[6] *Address reprint requests to* Dr. Hendler.

[7] We thank the following for providing us with cells: the NCI Breast Cancer Task Force Cell Culture Bank (Dr. C. B. Piczak, NCI, and Dr. E. Jensen, Mason Research Institute, Rockville, Md.); Dr. M. E. Lippman and Dr. W. R. Kidwell, NCI; Dr. R. G. Smith, Department of Medicine, and Dr. P. MacDonald and Dr. J. C. Porter, Department of Obstetrics, Gynecology, and Physiology, UTHSCD. We also thank Ms. E. Carlton, Ms. L. Trahan, Dr. D. Richardson, Ms. J. Tseng, and Mr. D. R. Quick, UTHSCD, for expert technical assistance; and Ms. G. A. Cheek and Ms. D. Marcoulides, UTHSCD, for secretarial assistance. We are also grateful to Dr. E. P. Frenkel, Department of Internal Medicine, and Dr. Fred Silva, Department of Pathology, UTHSCD, and Dr. William Kingsley, Department of Pathology, Baylor Medical Center, Dallas, Tex., for their review of the scientific data. We are especially indebted to Dr. Jonathan W. Uhr, Department of Microbiology, UTHSCD, for his constant support and advice and his assistance with the manuscript.

TABLE 1.—*Cells used for panel testing*

Designation	Cell Type	Original investigator (reference)
Cultured breast cell lines		
ZR-75-1[a]	Breast cancer, infiltrating ductal	Engel LW, et al. (*12*)
MCF-7[a]	Breast cancer, infiltrating ductal	Soule HD, et al. (*29*)
MCF-7[a,b]	Breast cancer, infiltrating ductal	Soule HD, et al. (*29*)
MDA-MB-231[b]	Breast cancer	Cailleau R, et al. (*30*)
BT20[b]	Breast cancer, infiltrating ductal	Lasfargues EY, et al. (*31*)
T47D[b]	Breast cancer, infiltrating ductal	Kaydar I, et al. (*32*)
HBL 100[b]	Normal breast	Gattney EV (*33*)
WRK-1[c]	DMBA rat mammary tumor	Kidwell WR, et al. (*34*)
Cultured carcinoma cell lines[d]		
#50	Squamous carcinoma; cervix	Porter JC, et al. (*35*)
#6	Squamous carcinoma; colon	Porter JC (unpublished data)
#117	Adenocarcinoma; ovary	Porter JC (unpublished data)
#296	Adenocarcinoma; endometrium	Kurameto H, et al. (*36*)
#194	Choriocarcinoma; trophoblast	Patillo RA, Gey GO (*37*)
#253	Adenocarcinoma, endometrium	Porter JC, Gal D (manuscript in preparation)
#265	Adenocarcinoma; endometrium	Porter JC (unpublished data)
#168	Squamous carcinoma; cervix	Porter JC (unpublished data)
#230	Squamous carcinoma; cervix	Porter JC (unpublished data)
#110	Undifferentiated carcinoma; ovary	Porter JC (unpublished data)
Lymphocytic cell lines		
NALL-1[e]	Non-B-, Non-T-cell lymphocytic leukemia	Miyoshi I, et al. (*28*)
NALM-1[e]	Pre-B-cell leukemia	Minowada J, et al. (*38*)
SMS-JiGi[e]	B-lymphoblastoid (Epstein-Barr virus transformed)	Smith RG (unpublished data)
BCL_1	Murine B-cell leukemia	Slavin S, Strober S (*39*)
Neuronal cell lines[e]		
U251-MG	Glioma	Ponten J (*40*)
SMS-KAN	Neuroblastoma	Biedler JL (*41*)
SH-SY-5Y	Neuroblastoma	Ross RA, et al. (*42*)
Melanocyte-melanoma cell lines[e]		
U1 I	Normal melanocytes	Meyskens FL, et al. (*43*)
M1RW	Melanoma	Meyskens FL, Fuller BB (*44*)
Noncultured cells		
Human amnion	Normal	Porter JC (unpublished data)
Peripheral blood lymphocytes	Normal	Donor: Yuan D Donor: Vitetta ES

[a] Obtained from Dr. M. E. Lippman, NCI.
[b] Obtained from the NCI Breast Cancer Task Force Cell Culture Bank [Dr. C. B. Piczak (NCI) and Dr. E. Jensen (Mason Research Institute)].
[c] Obtained from Dr. W. R. Kidwell, NCI.
[d] Obtained from Dr. J. C. Porter, UTHSCD.
[e] Obtained from Dr. R. G. Smith, UTHSCD.

Animals.—Female BALB/c mice (6–8 wk old) obtained from Cumberland Farms, Clinton, Tenn., were immunized ip with 10^6 ZR-75-1 cells three times at 2-week intervals and challenged iv with the same cell dose 3 days before being killed.

Cell fusion.—Spleen cells from immunized animals were fused with P_3×63 Ag 8 myeloma cells (*17*), according to the methods described by Kennett (*18*). Splenocytes and myeloma cells were mixed and incubated at a ratio of 5:1 in the presence of 33% polyethylene glycol 1000 (J. T. Baker Chemical Co., Phillipsburg, N.J.) in serum-free DMEM (GIBCO, Grand Island, N.Y.). Cells were diluted in DMEM containing hypoxanthine, aminopterin, and thymidine (Sigma Chemical Co., St. Louis, Mo.) (*19*) and seeded in 96-well plates (Linbro Scientific Inc., Hamden, Conn.) at 5×10^4 myeloma cells/well. Visible colonies appeared 10–14 days after hybridization.

RIA.—Hybridoma secretions were screened by an indirect RIA modified from the methods described by Segal and Klinman (*20*). Target cells (10^5/well), briefly fixed with 0.125% glutaraldehyde, were incubated with secretions for at least 3 hours. After washing with PBS (pH 7.3) containing 5% horse serum, approximately 50,000 cpm (1×10^7 cpm/µg) ^{125}I-labeled affinity-purified GAM were added. After 3 hours of incubation, cells were washed with 0.5% Nonidet P40 in 0.15 *M* NaCl–0.01 *M* Tris (pH 8) and air dried. The wells were cut with a hot wire device and counted in a gamma counter (model #1195; Nuclear Chicago Tractor Analytic; Amersham/Searle Corp., Arlington Heights, Ill.). Direct binding with ^{125}I-labeled IgM purified from hybridoma ascites fluid was performed in a similar manner.

Radiolabeling of hybridoma secretions.—Hybridoma cells (10^7) were cultured for 6–8 hours at 10^6 cells/ml in leucine-free Eagle's minimum essential medium (GIBCO) supplemented with 10% FCS, glutamine, antibiotics, and 1 mCi [^{3}H]-leucine (134 Ci/mmol; Amersham/Searle Corp.). Cells were removed by centrifugation, and aliquots of the dialyzed supernatants were treated with various antibodies and *Staphlococcus aureus* (*21*). Immune complexes were eluted in 1% SDS containing 8 *M* urea, and the eluates were analyzed by PAGE [7.5% polyacrylamide gels containing SDS (SDS-PAGE)] (*21*). Gels were fractionated with a gel slicer (Hoefer Scientific Instruments, San Francisco, Calif.). The slices were treated with 0.2% SDS for 24 hours, scintillation cocktail was added (Redi-Solv.; Beckman Instruments, Inc., Fullerton, Calif.), and the samples were counted in a scintillation counter (model #LS 330; Beckman Instruments, Inc.).

Radioiodination of antibodies.—Affinity-purified GAM or purified hybridoma IgM were labeled with $Na^{125}I$ by lactoperoxidase catalyzed iodination (*22*). Fifty μg protein in 100 μl PBS was incubated with 1 mCi $Na^{125}I$ (Amersham/Searle Corp.), 5 μg lactoperoxidase (Sigma Chemical Co.), and 5 μl 0.03% H_2O_2 for 2 minutes at 24°C. The reaction was terminated by the addition of 1 ml PBS, and the sample was exhaustively dialyzed against PBS. An equal volume of FCS was added after 1 hour of dialysis to retard degradation of the iodinated protein.

Antisera.—Each of the affinity-purified antibodies has been characterized as described below or in the indicated reference:

1) RAM (*23*).

2) RAμ (*23*).

3) GAM: This antiserum (*24*) was affinity purified on Sepharose-mouse IgG. It had reactivity against γ-, κ-, and λ-chains.

4) RAκ: TEPC-15 and other murine myeloma proteins were obtained from Litton Bionetics, Kensington, Md. A New Zealand White rabbit was immunized with 100 μg TEPC-15 (α,κ) in complete Freund's adjuvant. Four weeks later and at 2- to 20-week intervals thereafter, the rabbit was given booster injections of 25 μg TEPC-15 in incomplete adjuvant. The resulting serum contained antibodies to murine α-, κ-, and λ-immunoglobulin chains, as assessed by indirect precipitation of a panel of ^{125}I-labeled myeloma proteins. The serum was affinity purified on Sepharose bound to MOPC-21 (γ,κ) and absorbed sequentially with Sepharose bound to MOPC-104E (μ,λ) and MOPC-315 (α,λ). The resulting affinity-purified antibody was concentrated to 1.0 mg/ml by negative-pressure dialysis and was stored at −70°C. As determined by RIA, the antibody was specific for κ [positive reaction with RPC-5 (γ,κ), MOPC-21 (γ,κ), TEPC-183 (μ,κ), and TEPC-15 (α,κ)] and negative for λ, α, and μ [as determined by RIA with the use of MOPC-315 (α,λ), and MOPC-104E (μ,λ)].

5) RAλ: In a procedure similar to that described in category 4 above, a rabbit anti-RPC-20 (free λ-chain) was affinity purified on Sepharose-MOPC-104E (μ,λ) and absorbed with Sepharose bound to TEPC-15 (α,κ), TEPC-183 (μ,κ), and MOPC-21 (γ,κ). The anti-λ-antibodies were shown to be specific by indirect precipitation in which the same panel of myeloma proteins, described in category 4 above, was used.

Immunofluorescence staining.—Cell suspensions either were stained directly or were fixed first with 4% paraformaldehyde for 15 minutes. Balanced salt solution containing 0.2% sodium azide was used for all washes, and cells were maintained at 4°C. Aliquots of cells were incubated with various concentrations of primary antibodies at 5×10^6 cells/ml for 20 minutes. After washing, the cells were stained with the secondary antibody FITC-RAμ (*25*) for 10 minutes. Analysis on the FACS was performed as described in (*26*).

Patient tissue specimens.—Tumor tissues obtained from patients undergoing breast biopsy or mastectomy were frozen in liquid nitrogen. Cryosections (6–8 μm) were prepared from the frozen samples in a cryostat. Representative sections of each tumor were stained with H & E, and the presence of tumor cells was confirmed. Cryosections were fixed in 50% acetone-PBS, washed with PBS, and dried. The area of the slide containing the section was covered with 100 μl ^{125}I-labeled H59 IgM or an irrelevant hybridoma antibody, ^{125}I-labeled BCL_1 IgM (*27*). Sections were incubated for 3 hours at 24°C and washed with PBS-FCS (5%). The sections were exposed to X-ray film (Kodak X-Omatic) for 16 hours before development of the film.

RESULTS

Selection of hybridomas.—In a hybridization of splenocytes from a mouse immunized with ZR-75-1 cells, approximately 80% of the seeded wells contained clones that survived the selection medium. Of these, 20 clones secreted antibodies that bound to the human breast tumor cells used for immunization. Only one hybridoma, H59, did not bind to the discriminator cell line NALL-1 (*28*) used to detect antibodies against "common" human cell surface antigens. This hybridoma was further cloned by limiting dilution and has been maintained for more than 8 months in tissue culture without loss of secretory ability.

Analysis of secreted antibodies.—H59 cells were labeled with $[^3H]$leucine, and an aliquot of the dialyzed secretion was analyzed by SDS-PAGE (without immunoprecipitation). The remainder of the secretion was immunoprecipitated with antisera directed against mouse immunoglobulin, κ-chain, λ-chain, and μ-chain (RAM, RAκ, RAλ, and RAμ). Analysis of the immunoprecipitates by SDS-PAGE (not shown) indicated that the clone was secreting IgM_κ, as well as the immunoglobulin of the parent myeloma line ($IgG_{1\kappa}$). The IgM_κ does not bind to protein A.

Purification and characterization of the monoclonal antibody from H59 cells.—The cells from clone H59 were injected into mineral oil-primed (0.2 ml/mouse) BALB/c mice. The globulin from the ascitic fluid generated in this manner was prepared by (50%) ammonium sulfate precipitation, and the dissolved precipitate was fractionated on an AcA 34 Biogel (LKB Instruments, Rockville, Md.) column equilibrated in Tris-buffered saline (pH 7) to separate IgM and IgG. The fractions containing IgM were pooled and concentrated by lyophilization. The purified IgM was radiolabeled by iodination and immunoprecipitated by the same panel of antibodies used for the $[^3H]$leucine-labeled secretion. SDS-PAGE analysis of the labeled IgM and immunoprecipitation analysis confirmed the purity of the preparation and that the H59 was an IgM_κ antibody.

Binding of ZR-75-1 cells.—To demonstrate the ability of the purified IgM to specifically bind to ZR-75-1 cells, the purified IgM was used to stain fixed ZR-75-1 cells by indirect immunofluorescence. Fluorescinated affinity-purified RAμ was used as a secondary reagent, and the cells were analyzed on the FACS. As indicated by the plot of scatter and fluorescence intensity for each cell, (fig. 1A), the cells were highly heterogeneous in size. Some of the heterogeneity may be attributed to multinucleated cells and small cell clumps. Nevertheless, from a plot of cell number versus fluorescence intensity derived from figure 1A, we calculate that more than 78% of the population were bound by antibody under saturating conditions. The nonspecific binding (fig. 1B), as determined by the percentage of cells stained in the absence of primary antibody or in the presence of the nonspecific antibody BCL$_1$ IgM, was less than 10%.

When viable (instead of fixed) ZR-75-1 cells were used for staining, higher concentrations of antibody were needed for saturation, and a lower percentage (net, 53%) of the cells were stained (text-fig. 1). All dead cells in the preparation, as determined by scatter characteristics, were excluded in the analysis.

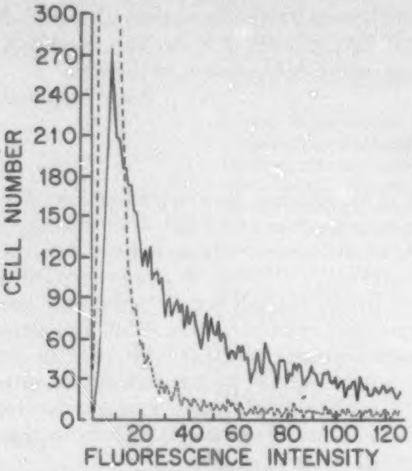

TEXT-FIGURE 1.—FACS profile of fixed ZR-75-1 cells stained with ^{125}I-labeled H59. Approximately 1×10^6 paraformaldehyde-fixed ZR-75 cells were incubated with A) 2 μg H59 or B) no antibody for 20 min at 4°C. After washing, cells were stained with 5 μg FITC-RAμ for 10 min and again washed. The light scatter and fluorescence intensity of each cell is represented by a dot.

Testing of H59 binding to normal and malignant cells.—The above results had established that the antibody produced by clone H59 binds to ZR-75-1 cells but not to another human cell line, NALL-1. The next step was to test more extensively the activity of H59.

Either ^{125}I-labeled IgM from clone H59 or an irrelevant monoclonal ^{125}I-labeled IgM was incubated with a number of cell lines fixed in the same manner as were the ZR-75-1 cells (text-fig. 2; table 1). Of the 6 human breast cancer cell lines tested (MCF-7* are MCF-7 cells obtained from a second source), only 3 reacted with the IgM secreted by H59. Most importantly, the monoclonal IgM does not bind to a breast cell line derived from normal human breast secretions, HBL-100, or to a 7,12-dimethylbenz[*a*]anthracene-induced rat mammary cancer cell line, WRK-1.

In addition, the antibody was tested against a panel of carcinomas. With the exception of the carcinomas derived from endometrial cells, which were moderately positive, all others bound background levels of radioactivity.

Binding to cell lines of lymphoid, melanocytic, and neuronal origin, as well as to a few cell types not maintained in culture, was evaluated. All of these lines with the exception of a glioma cell line demonstrated negligible binding.

Reactivity of H59 IgM with fresh tumor tissue.—A method was devised for autoradiographic labeling of patient tumors (*see*

TEXT-FIGURE 2.—Binding of H59 IgM to breast cell lines and other cell types. Fixed cells (1×10^5) from each cell line were incubated with 50,000 cpm of either ^{125}I-labeled H59 IgM (●) or with a control, ^{125}I-labeled BCL$_1$ IgM (△). The amount of radioactivity bound by each cell type after extensive washing was determined by direct counting in the gamma counter. *See* table 1 for listing of cells used.

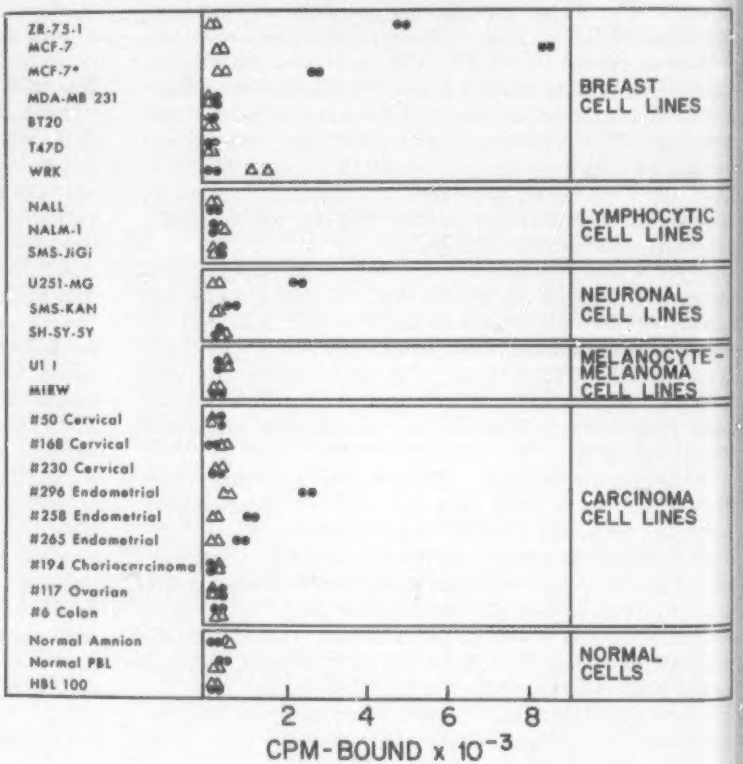

TABLE 2.—*Labeling of tissue sections by H59 IgM*

Pathologic diagnosis	Tumors tested, total No.	H59-binding tumors	Percent positive
Breast carcinoma	71	38	54
Fibroadenoma	11	9	84
Fibrocystic disease	24	20	83
Total	106	67	63

"Materials and Methods"). To ascertain the validity of the method, we stained cryosections of ZR-75-1 and T47D cell pellets. As seen in figure 2 (*left panel*) the reactive cell line ZR-75-1 was uniformly labeled with ^{125}I-labeled H59 IgM (100%), and the nonreactive cell line T47D showed only background staining; the control antibody ^{125}I-labeled BCL$_1$ IgM (*right panel*) did not bind to any of the sections. To determine the sensitivity of this method, we prepared cryosections of cell pellets from mixtures of T47D cells containing decreasing percentages of ZR-75 cells (fig. 2). It is apparent that autoradiography can specifically detect 1% positive cells in a mixed population. The sensitivity of this method has been compared with that of IP staining in which adjacent cryosections of the same cell pellet were used. The sensitivities appear to be within the same order of magnitude. Autoradiography offered the advantage of allowing the simultaneous processing of a large number of specimens without laborious examination of individual slides.

The cryosections obtained from a total of 106 breast biopsy specimens were evaluated by means of autoradiography. Figure 3 shows the autoradiographic staining of representative cryosections. Cryosections from some specimens diagnosed as infiltrating intraductal breast carcinoma stained as extensively as did ZR-75-1 cells (P-6), whereas other sections stained with less uniformity but contained regions of intense antibody binding (P-2, P-5). There are also sections of tumors from many patients with intraductal carcinoma that did not stain significantly above the background (P-3). A cryosection from noninvolved breast tissue obtained from a patient with a highly reactive tumor (not shown) did not react with the antibody. Included in figure 3 are also the cryosections of patients with fibrocystic disease (P-1) and fibroadenoma (P-7). These sections also stained with the H59 antibody. However, the pattern of labeling is different from that seen in carcinoma sections.

Figure 4 compares the pattern of autoradiographic labeling with cells that can be detected in the sections by H & E staining. The areas of H59 binding can be directly correlated with regions of tumor cells, and regions to which the antibody does not bind are associated with an absence of tumor cells. The correlates of binding to fibroadenomas and fibrocystic diseased tissue are also associated with regions of increased cellular density. Table 2 shows the cumulative results of all breast tissue sections we have analyzed. H59 antibody binds to 54% of tissue sections from patients with pathologically documented breast cancer. It binds to 84% of fibroadenomas and 82% of fibrocystic diseased tissue.

DISCUSSION

We have established the hybridoma cell line H59, resulting from the fusion of spleen cells, from a mouse immunized against a human breast cancer cell line, with a murine myeloma cell. The purified monoclonal IgM antibody produced by this hybridoma reacts with a restricted subset of human breast cancer cells.

H59 is reactive with the cell lines ZR-75-1 and MCF-7 which are derived from human infiltrating intraductal breast cancer tissue. These cell lines have maintained a well-differentiated glandular morphology and contain estrogen as well as other hormone receptors (*14*). H59 binds less well to a second clone of MCF-7 cells, MCF-7*, which are known to have fewer estrogen receptors (*45*). The antibody does not react with T47D, a cell line with trace amounts of estrogen receptor and high progesterone receptor (*45*) or with cell lines having no estrogen receptor. It does not bind nonhuman mammary cancer cells known to have mouse mammary tumor virus (*46*). It does not bind cell line HBL-100 which may be derived from normal human mammary secretions. Thus H59 binds to the most differentiated of human breast cancer tissue culture cells.

H59 was tested against a variety of normal and neoplastic cell lines to establish its specificity for breast cell carcinomas. The results of the tests indicate that the reactivity of the H59 IgM is highly restricted for the following reasons: 1) The antibody does not seem to detect the oncofetal antigen shared by normal fetal brain tissue and some breast tumor cells (*47*), inasmuch as both the MBA-MB 231 and BT 20 cell lines have been shown to express oncofetal antigens (*4*, *48*), and the H59 IgM does not react with these lines. 2) The antigen recognized by H59 is probably not the CEA (*49*) present on many colon carcinomas and some normal tissues, since H59 does not bind to BT 20 cells, which have been shown to express this antigen (*48*). H59 also does not bind to a number of adenocarcinoma cells, including colon carcinoma cells which most probably express the CEA. Furthermore, H59 does not bind to ^{125}I-labeled CEA (Roche Laboratories, Nutley, N.J.) (Yuan D, Vitetta ES; Unpublished observations). 3) H59 IgM does not recognize an antigen that shares determinants with the GP52 viral antigen (*50*) because T47D cells, which express the viral antigen (*46*), are negative with H59. Moreover, GP52 found in breast tumor cells is an intracellular antigen (*11*), whereas H59 antigen apparently is expressed on the cell surface. Preliminary biochemical characterization of the H59 antigen indicates that it constitutes two monomers of approximately 30,000 daltons with isoelectric points ranging between pH 5.5 and 6 (*51*). H59 antibody has some reactivity with adenocarcinoma cells derived from endometrial tissues and with the glioma cell line. The reactivity may be due either to cross-reactivity or to a limited expression of the antigen. Therefore, we conclude that the reactivity of H59 antibody is highly, although not exclusively, restricted to human breast tumor cells.

To test the ability of H59 antibody to bind tissue sections from breast cancers, we developed a rapid, reproducible radioautographic assay. Mesa-Tajada et al. (*11*) and Schlom et al. (*12*) have used IP staining as a means of determining breast specimen reactivity. Although our method necessitates the use of radiolabeled antibodies that have a defined half-life, it has several advantages: 1) It is simpler inasmuch as it is a direct rather than an indirect immunoassay; 2) it is less prone to artifacts associated with the secondary antibody, the IP technique, or the diaminobenzidine color reactions; and 3) evaluation of samples is more rapid. The assay has been quantified, and it appears to be as sensitive as the IP assay.

With the radioautographic assay we have determined that H59 reacts with a majority of human breast cancer tissue specimens. It also binds to an even greater proportion of fibrocystic diseased tissues and fibroadenomas. Binding studies with other monoclonal antibodies (Hendler FJ, Yuan D, Vitetta ES; manuscript in preparation) show that the tissue specimens that do not bind to H59 do bind to other monoclonal antibodies with broader reactivity for breast carcinomas.

We postulate that H59 may be reacting with a differentiation antigen restricted to a subset of more differentiated breast cancers. The evidence in support of this hypothesis is that H59 binds only to the most differentiated human breast cancer cell lines, to the majority of abnormal tissue from patients with fibrocystic disease and fibroadenomas (which are both benign hyperplasias of breast tissue), and to only a portion of human breast cancer tissues. This putative surface antigen may be coexpressed with the intracellular estrogen receptor because our panel test suggests that H59 reacts only with estrogen receptor-positive cell lines. Studies are in progress to analyze the possible relationship of H59 binding and the presence of estrogen receptor in patient samples. If one assumes that breast cancers that have retained differentiation antigens have a better prognosis, as is the case with estrogen receptor-positive cancers (*52*), the presence of H59 antigen in a tumor might have important clinical implications.

REFERENCES

(*1*) Sheikh KM, Quismorio FP, Friou GJ, Lee Y-T. Ductular carcinoma of the breast: Serum antibodies to tumor-associated antigens. Cancer 1979; 44:2083–2089.

(*2*) Hollinshead AC, Jaffurs WT, Alpert LK, Harris JE, Herberman RB. Isolation and identification of soluble skin-reactive membrane antigens of malignant and normal human breast cells. Cancer Res 1974; 34:2961–2968.

(*3*) Avis F, Avis I, Newsome JF, Haughton G. Antigenic cross-reactivity between adenocarcinoma of the breast and fibrocystic disease of the breast. J Natl Cancer Inst 1976; 56:17–25.

(*4*) Husuchi M, Robinson DS, Cailleau R, Irie RF, Morton DL. A serologic study of cultured breast cancer cell lines: Lack of antibody response to tumour specific membrane antigens in patients. Clin Exp Immunol 1980; 39:90–96.

(*5*) Kohler G, Milstein C. Continuous cultures of fused cells secreting antibody of predefined specificity. Nature 1975; 256:495–497.

(*6*) Herlyn M, Steplewski Z, Herlyn D, Koprowski H. Colorectal carcinoma-specific antigen: Detection by means of monoclonal antibodies. Proc Natl Acad Sci USA 1979; 76:1438–1442.

(*7*) Kennett RH, Gilbert F. Hybrid myelomas producing antibodies against a human neuroblastoma antigen present on fetal brain. Science 1979; 203:1120–1121.

(*8*) Koprowski H, Steplewski Z, Herlyn D, Herlyn M. Study of antibodies against human melanoma produced by somatic cell hybrids. Proc Nat Acad Sci USA 1978; 75:3405–3409.

(*9*) Nadler LM, Stashenko P, Hardy R, Schlossman SF. A monoclonal antibody defining a lymphoma associated antigen in man. J Immunol 1980; 125:570–577.

(*10*) Engel LW, Young NA, Tralka TS, Lippman ME, O'Brien SJ, Joyce MJ. Establishment and characterization of three new continuous cell lines derived from human breast carcinomas. Cancer Res 1978; 38:3352–3364.

(*11*) Mesa-Tejada R, Keydar I, Ramanarayanen M, Ohno T, Feroglio C, Spiegelman S. Detection in human breast carcinomas of an antigen immunologically related to a group-specific antigen of mouse mammary tumor virus. Proc Natl Acad Sci USA 1978; 75: 1529–1535.

(*12*) Schlom J, Wunderlich D, Teramoto YA. Generation of human monoclonal antibodies reactive with human mammary carcinoma cells. Proc Natl Acad Sci USA 1980; 77:6841–6845.

(*13*) Colcher D, Hand PH, Schlom J. A spectrum of monoclonal antibodies reactive with human mammary tumor cells. Proc Natl Acad Sci USA 1981; 78:3199–3203.

(*14*) Lippman ME, Osborne CK, Knazek R, Young N. In vitro model systems for the study of hormone-dependent human breast cancer. N Engl J Med 1977; 296:154–159.

(*15*) Osborne CK, Monaco ME, Lippman ME, Kahn CR. Correlation among insulin binding, degradation, and biological activity in human breast cancer cells in long-term tissue culture. Cancer Res 1978; 38:94–102.

(*16*) Neuwald PD, Anderson C, Salivar WO, et al. Expression of oncodevelopmental gene products by human tumor cells in culture. JNCI 1980; 64:447–459.

(*17*) Svasti Y, Milstein C. The complete amino acid sequence of a mouse K light chain. Biochem J 1972; 128:427–444.

(*18*) Kennett RH. Cell fusion. Methods Enzymol 1978; 58:345–359.

(*19*) Littlefield JW. Selection of hybrids from matings of fibroblasts in vitro and their presumed recombinants. Science 1964; 145:709–710.

(*20*) Segal GP, Klinman NR. Defining the heterogeneity of anti-tumor antibody responses. J Immunol 1976; 116:1539–1546.

(*21*) Vitetta ES, Yuan D, Krolick K, et al. Characterization of the spontaneous murine B cell leukemia (BCL_1). III. Evidence for monoclonality using an anti-idiotype antibody. J Immunol 1979; 122:1649–1654.

(*22*) Marchalonis JJ. An enzymatic method for the trace iodination of immunoglobulins and other proteins. Biochem J 1969; 113:299–305.

(*23*) Isakson PC, Krolick KA, Uhr JW, Vitetta ES. The effect of anti-immunoglobulin antibodies on the in vitro proliferation and differentiation of normal and neoplastic murine B cells. J Immunol 1980; 125:886–892.

(*24*) Vitetta ES, Uhr JW, Boyse EA. Isolation and characterization of H-2 and TL alloantigens from the surface of mouse lymphocytes. Cell Immunol 1972; 4:187–191.

(*25*) Ligler FS, Vitetta ES, Uhr JW. Cell surface immunoglobulin. XXII. Reappearance of surface IgM and IgD on murine splenocytes after removal by capping. J Immunol 1977; 119:1545–1546.

(*26*) Ligler FS, Smith RG, Kettman JR, et al. Detection of tumor cells in the peripheral blood of nonleukemic patients with B-cell lymphoma: Analysis of "clonal excess." Blood 1980; 55:792–801.

(*27*) Krolick KA, Villemez C, Isakson PC, Uhr JW, Vitetta ES. Selective killing of normal and neoplastic B cells by antibodies coupled to the A chain of ricin. Proc Natl Acad Sci USA 1980; 77: 5419–5423.

(*28*) Miyoshi I, Hiraki S, Tsubota T, Kubonishi I, Kimura I, Masuji H. Human B cell, T cell and null cell leukaemic lines derived from acute lymphoblastic leukaemia. Nature 1977; 267:843–844.

(*29*) Soule HD, Vasquez J, Long A, Albert S, Brennan MD. A human cell line from pleural effusion derived from a breast carcinoma. J Natl Cancer Inst 1973; 51:1409–1416.

(*30*) Cailleau R, Young R, Olivé M, Reeves WJ Jr. Breast tumor cell lines from pleural effusions. J Natl Cancer Inst 1974; 53:661–674.

(*31*) Lasfargues EY, Cantinho WG, Moore DH. Heterotransplantation of a human breast carcinoma cell line. Cancer Res 1972; 32:2365–2368.

(*32*) Keydar I, Chen L, Karby S, et al. Establishment and characterization of a cell line of human breast carcinoma origin. Eur J Cancer 1979; 15:659–670.

(*33*) Gaffney EV, Pigott DA, Grimaldi MA. Human serum and the growth of human mammary cells. JNCI 1979; 63:913–918.

(*34*) Kidwell WR, Monaco ME, Wicha MS, Smith GS. Unsaturated fatty acid requirements for growth and survival of a rat mammary tumor cell line. Cancer Res 1978; 38:4091–4100.

(35) Porter JC, Nalick RH, Vellios F, Neaves WB, MacDonald PC. New tissue culture cell lines derived from human squamous cell carcinoma of the cervix and vagina. Am J Obstet Gynecol 1978; 130:487–496.

(36) Kuramoto H, Tamura S, Notake Y. Establishment of a cell line of human endometrial adenocarcinoma in vitro. Am J Obstet Gynecol 1972; 114:1012–1019.

(37) Pattillo RA, Gey GO. The establishment of a cell line of human hormone-synthesizing trophoblastic cells in vitro. Cancer Res 1968; 28:1231–1236.

(38) Minowada J, Koshiba H, Janossy G, Greaves MF, Bollum FJ. A Ph1 chromosome positive human leukemia cell line (NACM-I) with pre-B cell characteristics. Leuk Res 1979; 3:261–266.

(39) Slavin S, Strober S. Spontaneous murine B cell leukaemia. Nature 1977; 272:624–625.

(40) Ponten J. Neoplastic human glia cells in culture. In: Fogh J, ed. Human tumor cells in vitro. New York: Plenum Press, 1980:175–206.

(41) Biedler JL, Ross RA, Shanoke S, Spengler BA. Human neuroblastoma cytogenetics: Search for significance of homogeneously staining regions and double minute chromosomes. In: Evans AE, ed. Advances in neuroblastoma research. New York: Raven Press, 1980:81–96.

(42) Ross RA, Joh TH, Reis DJ, Spengler BA, Biedler JL. Neurotransmitter-synthesizing enzyme in human neuroblastoma cells: Relationship to morphological diversity. In: Evans AE, ed. Advances in neuroblastoma research. New York: Raven Press, 1980:151–160.

(43) Meyskens FL Jr, Berglund EB, Saxe, DF, et al. Biological and biochemical properties of a human uveal melanocyte-derived cell line. In Vitro 1980; 16:775–780.

(44) Meyskens FL Jr, Fuller BB. Characterization of the effects of different retinoids on the growth and differentiation of a human melanoma cell line and selected subclones. Cancer Res 1980; 40: 2194–2196.

(45) Horwitz KB, Zava DT, Thilagar AK, Jensen EM, McQuire WL. Steroid receptor analyses of nine human breast cancer cell lines. Cancer Res 1978; 38:2434–2437.

(46) Spiegelman L, Keydar I, Mesa-Tejada R, et al. Possible diagnostic implications of a mammary tumor virus related protein in human breast cancer. Cancer 1980; 46:879–892.

(47) Irie RF, Irie K, Morton DL. A membrane antigen common to human cancer and fetal brain tissues. Cancer Res 1976; 36:3510–3517.

(48) Hurlimann J, Dayal R. Antigens of a human breast carcinoma cell line (BT 20). I. Synthesis of serum proteins, membrane-associated antigens, and oncofetal-associated antigens. JNCI 1978; 61:677–685.

(49) Gold P, Freedman SO. Specific carcinoembryonic antigens of the human digestive system. J Exp Med 1965; 122:467–481.

(50) Ritzi E, Martin DS, Stolfi RL, Spiegelman S. Plasma levels of a viral protein as a diagnostic signal for the presence of mammary tumor: The effect of tumor removal. J Exp Med 1977; 145:999–1013.

(51) Hendler FJ, Yuan D, Vitetta ES. Characterization of a monoclonal antibody to human breast cancer cells. Trans Assoc Am Physicians. In press.

(52) Knight WA, Livingston RB, Gregory EJ, McGuire WL. Estrogen receptor as an independent prognostic factor for early recurrence in breast cancer. Cancer Res 1977; 37:4669–4671.

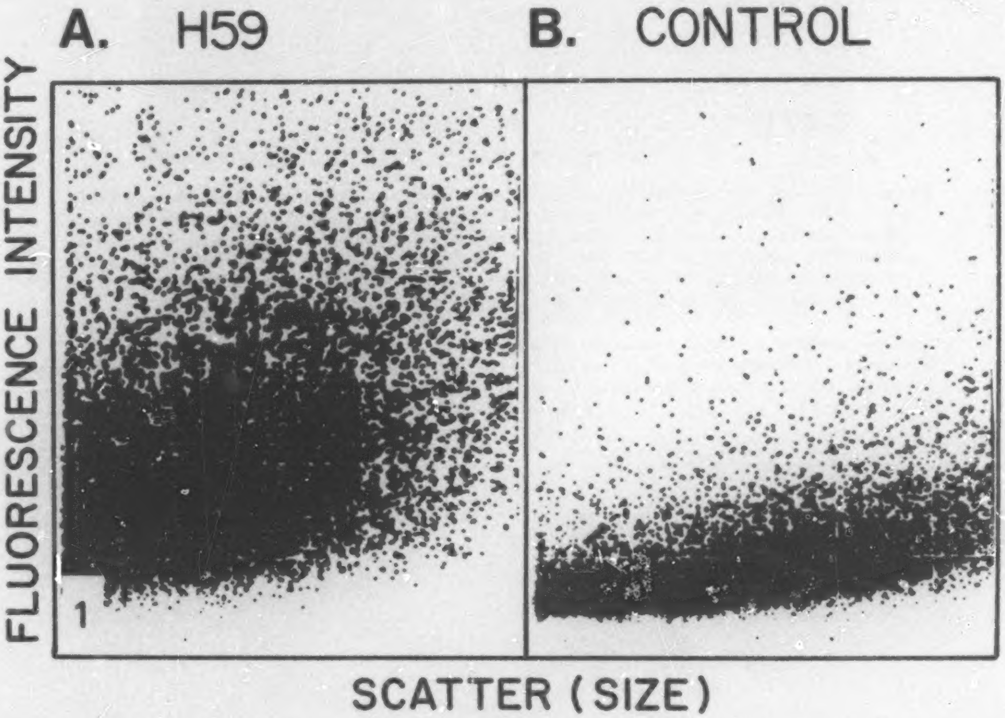

Figure 1.—FACS analysis of freshly prepared ZR-75-1 cells. Cultured ZR-75-1 cells were removed from culture flasks with 0.01 *M* EDTA. After washing, $\approx 5\times10^5$ cells were stained with either 10 μg H59 (——) or an irrelevant hybridoma antibody, BCL$_1$ IgM (- - -), for 20 min at 4°C. Cells were then washed and stained with 10 μg FITC-RAμ for 10 min at 4°C. The plot of cell number vs. fluorescence intensity was derived by FACS analysis. The percentage of positively stained cells was calculated by determining the number of cells in channels 10–127.

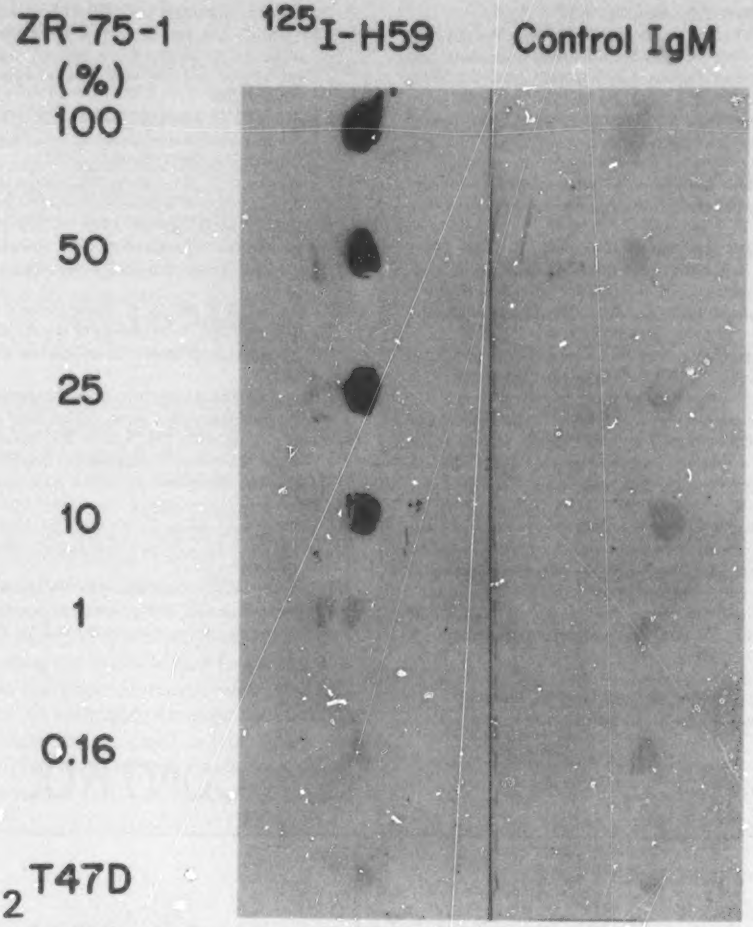

FIGURE 2.—Binding of ^{125}I-labeled H59 to cryosections of cultured cell lines. Cultured ZR-75-1 and T47D cells were harvested and resuspended as single cell suspensions. Varying proportions of cells from each cell line were mixed, centrifuged, and the pellets frozen and sectioned. The cryosections were fixed in acetone-PBS and incubated with either ^{125}I-labeled H59 or ^{125}I-labeled control IgM (BCL$_1$ IgM) (100,000 cpm/section) for 3 hr at 24°C. After four washes with PBS containing 5% serum, the sections were dried and exposed to X-ray film for 16 hr before development of the film.

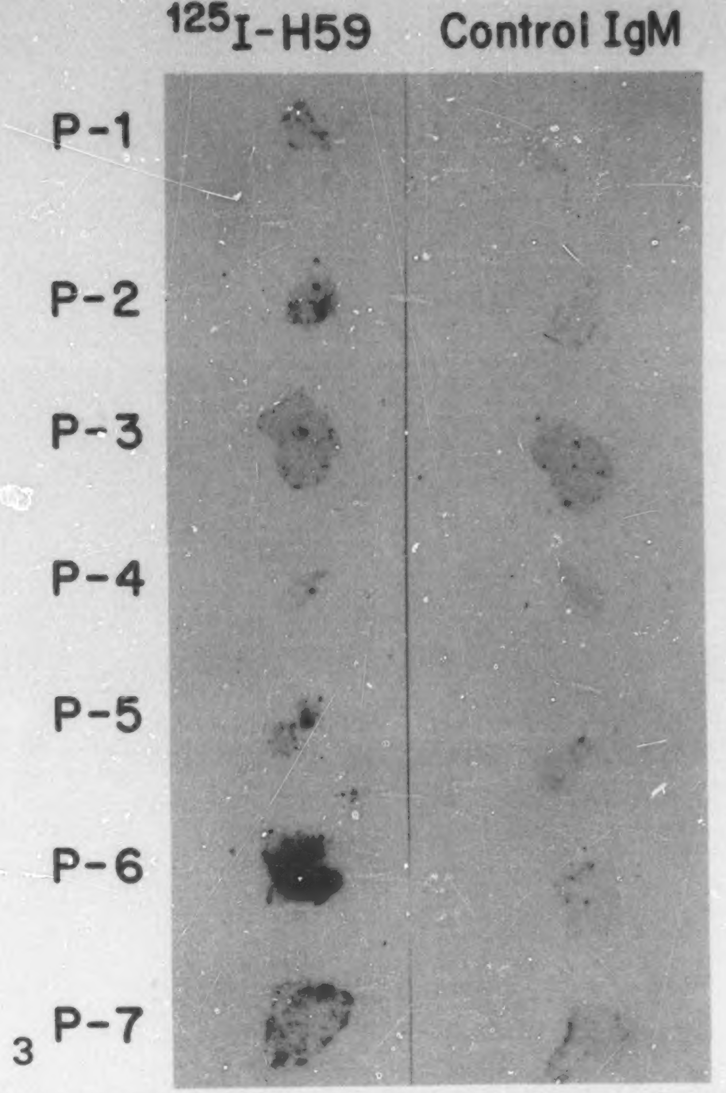

FIGURE 3.—Binding of ^{125}I-labeled H59 to cryosections of excised tumors. Tumors were frozen, sectioned, and stained as in fig. 2. Histologic diagnosis was as follows: P-1, fibrocystic disease; P-2, intraductal carcinoma; P-3, intraductal carcinoma; P-4, fat necrosis; P-5, intraductal carcinoma; P-6, intraductal carcinoma and fibrocystic disease; and P-7, fibroadenoma.

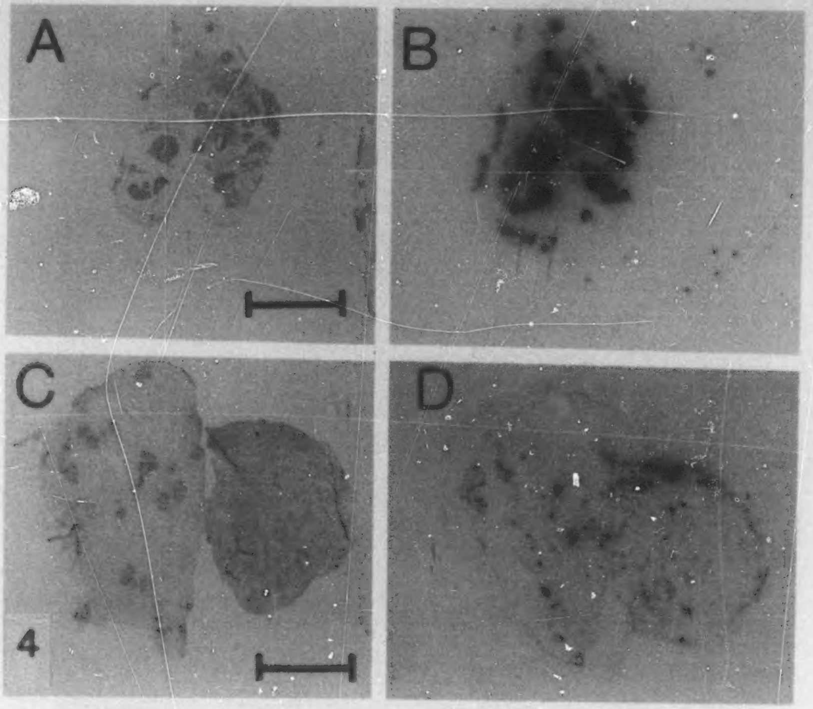

FIGURE 4.—Comparison of cryosections for ^{125}I-labeled H59 binding and histopathology. Cryosections from patients with intraductal carcinoma (4A, 4B) or fibrocystic disease and fibroadenoma (4C, 4D) were either stained with ^{125}I-labeled H59 (4B, 4D) or stained with H & E (4A, 4C). Areas of intense staining by both methods represent malignant cells. *Bar* = 5 mm.

Epidemiologic and Age-Dependent Data on Multiple Myeloma in Austria[1,2]

Heinz Ludwig,[3,4,5] Elke Fritz,[3,4] *and* Hans P. Friedl[6]

ABSTRACT—The mortality rates for multiple myeloma showed an increasing trend between 1969 and 1979, when multiple myeloma accounted for 6‰ of the reported cancer deaths in Austria. The median age at diagnosis was relatively high: 68.5 years for males and 69.0 years for females. The age-corrected male:female ratio of 1.23:1 indicated a higher incidence of multiple myeloma in males. Age-standardized (standard population for Europe) incidence rates amounted to 1.5/100,000 male inhabitants and 1.2/100,000 female inhabitants/year. In a subsample of patients with multiple myeloma, the paraprotein types as well as the κ:λ ratio resembled the frequency distribution of normal immunoglobulins. There were no age-related differences for the stages of the disease and the poor risk factors at diagnosis for patients 65 years old or younger or for those over 65 years of age at diagnosis. Survival rates were significantly higher for younger patients than for older ones, with a 50% survival time of 45 and 26 months, respectively. The differences resulted solely from the dissimilar general life expectancies in both groups, and survival rates with strict regard to multiple myeloma proved to be identical in younger and older patients.—JNCI 1982; 68:729–733.

Studies on the epidemiology of multiple myeloma already were done in the early 1940's, but data have become more reliable only after the accuracy and ease of diagnosis had been improved by the introduction of paper and later of immune electrophoresis (*1*). Data dealing with the sexual and ethnic distribution of myeloma patients as well as the overall incidence of myeloma are now available for several countries. So far no epidemiologic survey has been published for Austria, a country with an age distribution typical for central Europe, namely, a large percentage of elderly inhabitants. With this report we aim to close this information gap on the incidence of and mortality from multiple myeloma in Austria and investigate the influence of age at the time of diagnosis on the clinical course of the disease.

MATERIALS AND METHODS

Population.—At the end of 1979 Austria had 7.4 million inhabitants (47.2% males and 52.8% females) who were almost exclusively Caucasians. The average life expectancy at birth was 66.6 years for males and 73.7 years for females. Of the total population, 29.6% were younger than 20 years. As in other European countries, a relatively large portion, 18.5% of the total population, were over 60 years old.

Cancer registry.—Since 1970 the cancer registry of the Austrian Central Statistical Bureau requires notification of all new cases of cancer by all hospitals, all departments of radiology, and all institutes of pathology, thus covering the total population. The data used in this paper include incidence rates and death rates for multiple myeloma (code 203) from 1969 through 1979 as well as other cancers categorized under "neoplasms of lymphatic and hemopoietic tissues" (codes 202, 204, 205, 206, and 207) according to the International Statistical Classification of Diseases, Injuries, and Causes of Death (*2*) and general population statistics.

Hospital patients.—Between 1970 and 1980, 134 patients with multiple myeloma were treated as inpatients at the Department of Medicine II, University of Vienna. In 128 cases sufficient data were available to analyze the age distribution at the onset of the disease, and in 114 cases it was possible to study the distribution of paraprotein types and the survival times. Myeloma cases were staged in 70 patients at the time of diagnosis according to the staging system of Durie and Salmon (*3*). Seventeen of these patients received an identical first course of polychemotherapy consisting of melphalan (0.5 mg/kg body wt), cyclophosphamide (15 mg/kg body wt), vincristine (1.4 mg/m^2), and prednisone (40 mg on days 1–7 and 20 mg on days 8–14). Selected clinical parameters and laboratory findings were compared for early versus late age of manifestation.

Statistical evaluation.—The crude statistical data were converted into age-specific incidence and mortality rates. For comparisons those values were age standardized with the use of the standard population for Europe published in 1976 (*4*). For the examination of the significance of trends, the sign-trend test by Cox and Stuart (*5*) was applied. Survival rates were calculated from the observed survival times according to the life table method (*6*). For comparisons of survival by the log rank test (*7*), four additional life table graphs were established: *P* for the entire population of patients with multiple myeloma, *G* for the entire reference population, *GY* for the reference population 65 years of age or younger, and *GO* for the reference population over 65 years of age.

The general life expectancies *G*, *GY*, and *GO* refer strictly to the observed groups; i.e., for each patient sex and age at diagnosis were entered into the probability rates, and the weighed probabilities were calculated for 7 consecutive years. For each group and each relevant point in time t, the number of expected deaths E was calculated by age and sex standardization of the general mortality by means of the following formulas: $E_Y(t) = (p_P(t) - p_G(t) + p_{GY}(t)) \times N_Y(t)$ and $E_O(t) = (p_P(t) - p_G)t) + p_{GO}(t)) \times N_O(t)$, where p stands for probability of death and N_Y and N_O denote the

---

[1] Received June 4, 1981; accepted December 29, 1981.

[2] Supported by Austrian research grant 3997.

[3] Department of Medicine II, University of Vienna, Garnisongasse 13, 1090 Vienna, Austria.

[4] Ludwig Boltzmann Institute of Gerontology, Garnisongasse 13, 1090 Vienna, Austria.

[5] *Address reprint requests to* Dr. Ludwig at Department of Medicine II, University of Vienna.

[6] Austrian Central Statistical Bureau, Neue Hofburg, 1014 Vienna, Austria.

number at risk in the specific group of patients. Significances according to the log rank test and for the evaluation of clinical parameters were evaluated by the chi-square test.

RESULTS

For 1969 and 1979 the exact number of reported deaths from multiple myeloma, Hodgkin's disease, and other lymphoreticular cancers are given in table 1. During that decade the mortality rate for multiple myeloma and other lymphoreticular neoplasms increased slowly, whereas the death rates for Hodgkin's disease decreased. Text-figure 1 shows the statistically significant time trends expressed as mortality per 100,000 members of a European standard population. Neither the percentage of multiple myeloma from all deaths caused by lymphoreticular cancers (range: 13.6–17.2%) nor the proportion of cancer deaths due to multiple myeloma (range: 4.4–6.2‰) varied systematically over the observed period of time.

The incidence of multiple myeloma in Austria was of the same magnitude as the mortality and in 1979 accounted for 139 (13.5%) of the 1,026 cases registered as lymphoreticular cancers. For multiple myeloma the age distribution at diagnosis was slightly skewed to the right with a median of 68.9 years of age (68.5 yr for males and 69.0 yr for females). The 6th and 7th decades of life contained the peak incidence, considerably fewer patients were over 80 years of age at diagnosis, and multiple myeloma rarely occurred below the age of 40. The age pattern remained constant with an almost identical median for each year between 1970 and 1979.

The age-specific incidence rates per 100,000 inhabitants for 1979 are presented in text-figure 2. Age-standardized incidence rates from 1970 to 1979 for males and females separately are shown in text-figure 3. After 1975 the sex ratio remained rather constant (males:females=1.23±0.08:1), and the curves seemed to have stabilized into a steadily increasing frequency of newly registered myeloma cases as opposed to the probable random variations during the first 5 years of compulsory notification of cancers to the cancer registry. When the average age-standardized incidence for 1975–79 (1.5/100,000 persons and year for males and 1.2/100,000 persons and year for females) was compared to the incidence rates for 16 other European countries reported in 1979 (*4*), Austria was located in the 13th and 12th place for males and females, respectively, following Yugoslavia and the German Democratic Republic and preceding Poland (text-fig. 4).

Analysis of the 134 patients diagnosed and treated at the Department of Medicine II, University of Vienna, between 1970 and 1979 yielded an age distribution very similar to that of the myeloma patients registered for all of Austria. The median age at manifestation was also very close to the respective parameter of the total population, namely, 68.2 years. Apart from small random variations, the ratio of patients 65 or younger to those 65 or older was constant throughout the observed decade.

TABLE 1.—*Deaths from multiple myeloma, Hodgkin's disease, and other lymphoreticular cancers in Austria: 1969 and 1979*

Cancer	No. of deaths (%)	
	1969	1979
Multiple myeloma	109 (13.6)	166 (15.6)
Hodgkin's disease	123 (15.4)	115 (10.8)
Non-Hodgkin's lymphomas and leukemias	568 (71.0)	783 (73.6)
Total	800 (100)	1,064 (100)

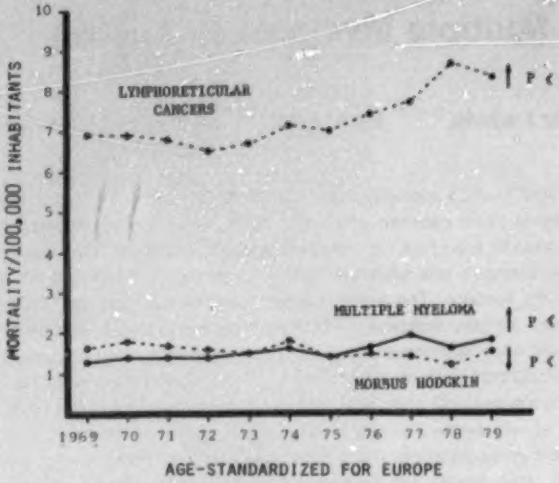

TEXT-FIGURE 1.—Age-standardized mortality rates (European standard population) for multiple myeloma, Hodgkin's disease, and other lymphoreticular cancers for the decade between 1969 and 1979.

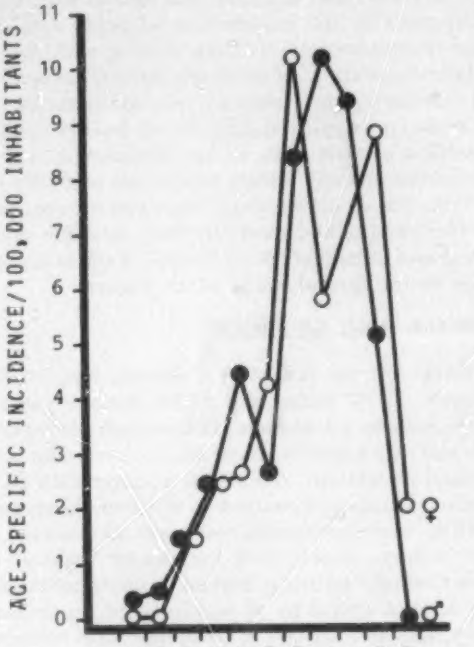

TEXT-FIGURE 2.—Age-specific incidence rates for multiple myeloma per 100,000 male or female inhabitants of Austria in 1979 show peak incidences in the 7th and 8th decades of life.

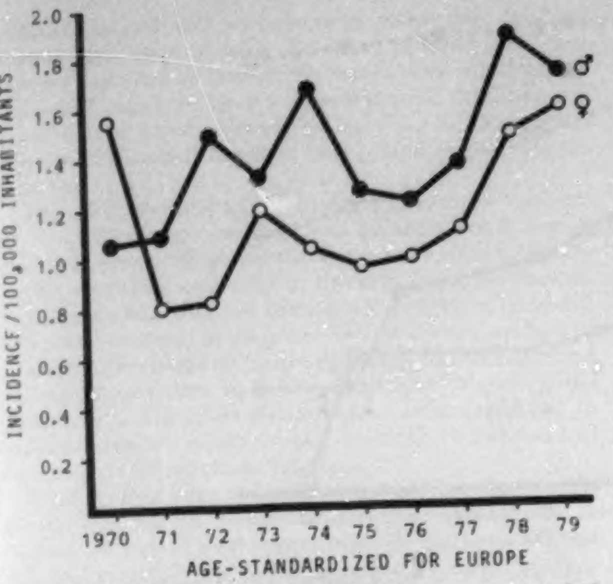

TEXT-FIGURE 3.—Time trends of standardized incidence rates (standard population for Europe) per 100,000 male or female inhabitants of Austria between 1970 and 1979.

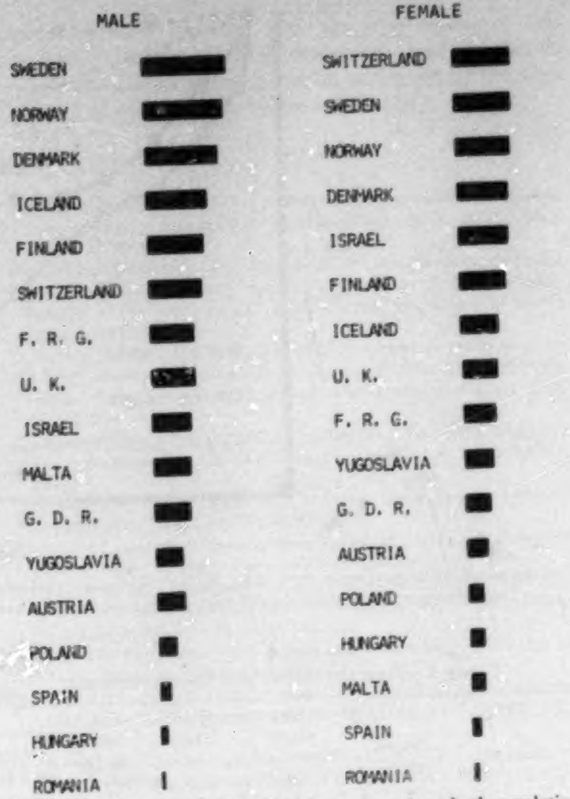

TEXT-FIGURE 4.—Age-standardized incidence rates (standard population for Europe) reported for various European countries and Israel.

The frequencies of the various paraprotein types were determined in a group of 114 patients. Text-figure 5 shows that the results followed the frequency distribution pattern of normal immunoglobulins (*8*) as expected from a representative sample of multiple myeloma cases. In the total group of patients, the κ:λ ratio of 2.43:1 was comparable to that from other countries (*9–11*).

According to age at the manifestation of disease, the patients were divided into 2 groups of 65 years or younger and over 65 years, and the younger and the older age groups were compared. There was no difference with regard to the different stages of the disease at diagnosis, nor did the poor risk factors differ between either group at the threshold shown (table 2) or at other clinically relevant limits (creatinine, 1.4 mg/100 ml; calcium, 10.5 mg/100 ml; hemoglobin, 12.0 g/100 ml).

Although during the 1970's therapy of multiple myeloma was extended by the introduction of polychemotherapy regimens, at every particular point of time all patients, regardless of their age, received the same treatment. When high-dose intermittent polychemotherapy was instituted for all patients, 17 had not been treated previously, and those patients were selected to study drug tolerance. As shown in table 3, the cytostatic drug tolerance was markedly reduced in the group of older patients. After the first course of polychemotherapy, the lowest number of leukocytes was only 1,200 in the older patients compared to 4,700 in the younger ones. Considering the small sample size, the individual variations were too great to allow for a statistical confirmation of the observed differences.

Comparing the survival rates for the 2 age groups, we found that survival in younger patients was significantly ($P<0.00001$) higher than that in older ones. However, the general life expectancy of the 2 groups also differed greatly (text-fig. 6). If this fact was taken into account by the inclusion of the age group-specific death rates into the statistical evaluation, the age-related differences in survival rates vanished completely. For the younger patient group, the age group-specific expected 50% survival time of 45.4

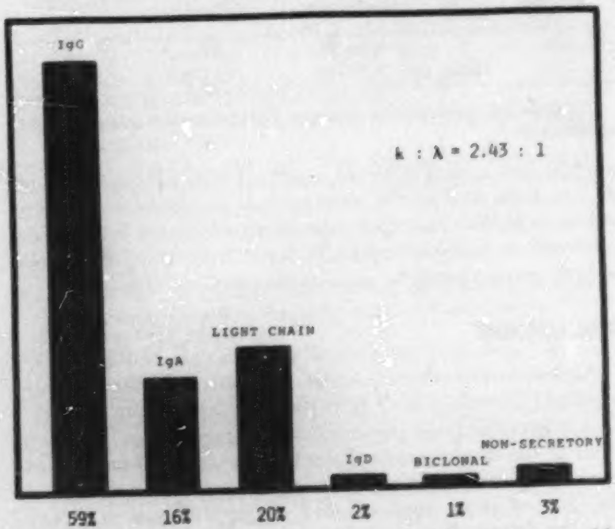

TEXT-FIGURE 5.—Distribution of paraprotein types in 114 patients with multiple myeloma.

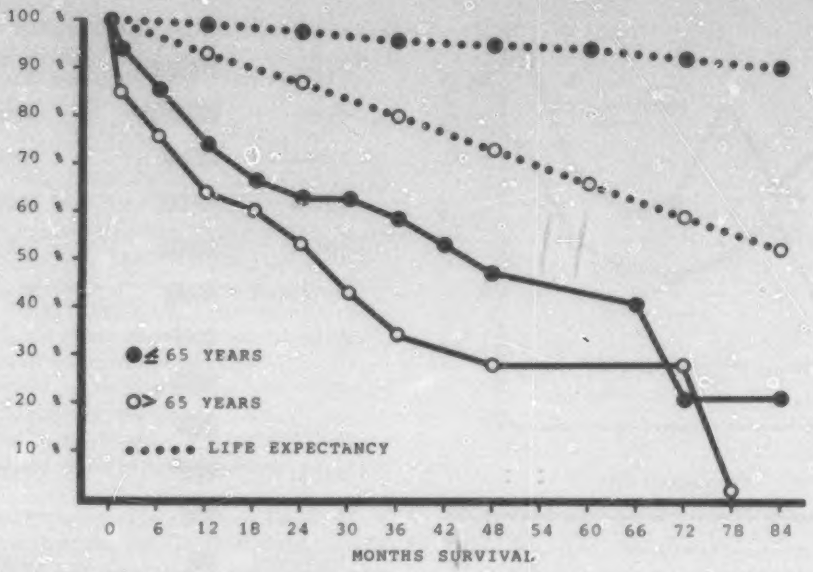

TEXT-FIGURE 6.—Survival rates (——), are higher in younger patients than in those over 65 yr of age at diagnosis, but the diverse life expectancies (····) completely accounted for the differences in survival rates between the 2 age groups.

TABLE 2.—*Poor risk factors and age at diagnosis*[a]

Age, yr	No. of cases	Percentages at stage			Creatinine >2.0 mg/100 ml	Calcium >12.5 mg/100 ml	Hemoglobin <8.5 g/100 ml
		I	II	III			
≤65	31	16	26	58	16	10	10
>65	39	10	23	67	18	10	10
Total	70	13	24	63	17	10	10

[a] Differences are not significant statistically.

TABLE 3.—*Nadir after chemotherapy*[a]

Age, yr	No. of cases	Leukocytes	Platelets	Hemoglobin
≤65	9	5.2×10^3	2.97×10^5	12.3
>65	8	1.7×10^3	1.45×10^5	10.1

[a] Values are expressed as medians. Differences are not significant statistically.

months was matched by an observed 50% survival time of 44.7 months, and for the older patient group the equivalent values were 28.5 and 25.8 months, respectively. With strict reference to multiple myeloma, the complete survival rates of both groups could be considered identical ($P=0.7$).

DISCUSSION

As observed in other countries, mortality rates for multiple myeloma increased in Austria over the last decade (*12, 13*). This observation can possibly be explained by an improvement of the diagnostic facilities because medical services in Austria are covered by a social health insurance system, and the cost of more sophisticated diagnostic tests is not a limiting factor. But since it is not possible to verify the diagnostic exactness of all death certificates in the country, the question as to whether the number of myeloma cases has actually increased must remain unanswered.

The median age at diagnosis was higher than that in most other countries (*14, 15*); however, it was comparable to that reported for Sweden in 1970 (*16*) and remained stable during the observed period of time. The reason for the elevated age level could be differences in the population characteristics. A relatively large segment of the Austrian population is over 60 years old, and the total population is stagnant; i.e., the number of inhabitants remained constant, and their age distribution did not change significantly between 1969 and 1979. This and the fact that medical services are not only free and easily available but also well established and familiar to old people could account for the high median age of myeloma patients.

When the age-specific incidence rates are compared to those of other countries (*12, 17*), the figures are below the expected level. Even though notification of cancer cases is compulsory, the cancer registry has been in operation only since 1970, and complete recording of data apparently has not as yet been achieved.

In most countries the sex ratio for multiple myeloma incidence is in favor of males (*18, 19*). The same holds true for Austria, where the disease is more frequent in men than in women, but the difference is not outstandingly high.

Age-standardized incidence rates for males and females fluctuated widely during 1970–74 and showed an increasing trend and a stable male:female ratio between 1975 and 1979. The differences in the curve patterns between the early and late 1970's could be random because other published data (*12*) show variations in the same order of magnitude. Conversely, it is possible that at the very beginning of compulsory cancer registration larger centers complied more quickly and the rural population of Austria could possibly be under-represented in those figures. To avoid a possible bias, we used only the more recent data for comparison with those of other European countries. The fact that our data are comparatively recent does not influence the results, however, since a control showed that the combined figures for the decade or even the incidence rates between 1970 and 1972 would have placed Austria into the same rank.

The north-south gradient in the incidence of multiple myeloma in Europe could at least partially result from a diverse quality of diagnosis and registration. In the Scandinavian countries, especially in Sweden, extensive research and documentation have been conducted for a relatively long time, whereas in countries with a lower standard of living, e.g., Romania or Spain, the diagnostic facilities and the reporting system may be less efficient. However, the possibility of a true genetic difference in susceptibility to multiple myeloma similar to that reported for Negroes and Caucasians (*12*) cannot be ruled out.

Since no data were available on the distribution of paraprotein types in the myeloma cases documented for all of Austria, we used as a subsample multiple myeloma patients who had been diagnosed and treated at the Department of Medicine II, University of Vienna, during the relevant period of time. That patient group was very similar to the collective myeloma population of Austria in respect to age distribution and median age at diagnosis. As expected, the frequency distribution of paraprotein types as well as the κ:λ ratio of all secretory myelomas closely resembled the characteristics of normal immunoglobulins and were comparable to other published data (*20*).

Because of the generally late onset of multiple myeloma and the consequently high median age of the patients, there seemed to be an interesting opportunity to investigate the influence of age on the course of the disease. At the time of diagnosis we found no age-related differences regarding the stage of the disease and the poor risk factors. The early progression of the disease appears to be very similar in younger and older patients, and the diagnosis seems to be made at equivalent stages of tumor development. In 2 small groups of patients under identical therapy, age-dependent differences were observed in the sensitivity of bone marrow cells to cytostatic drugs. Besides an intrinsic decrease in cytostatic drug tolerance of bone marrow cells in the aged, the retarded restoration due to an age-related deficit in the hematopoietic microenvironment (*21*) could explain those results.

In accordance with the results published for the U.S. Southwest (*22*), survival rates were higher for younger patients than for patients over 65 years of age. Although this finding is statistically highly significant and clinically relevant, it does not permit the conclusion that the course of the disease is accelerated in old age. There are vast differences in the general life expectancies of the 2 age groups apart from their malignant affliction, and survival with strict regard to multiple myeloma does not show any age-related differences. While the incidence rates of multiple myeloma correlate strongly with age, the course of this cancer does not seem to be age-dependent, and the shorter survival rates of older patients can be explained by the high risk of general multiple morbidity in old age.

REFERENCES

(*1*) Ritzmann SE, Loukas D, Sakai H, Daniels JC, Levin WC. Idiopathic (asymptomatic) monoclonal gammopathies. Arch Intern Med 1975; 135:95–106.
(*2*) World Health Organization. Manual of the international statistical classification of diseases, injuries, and causes of death. Eighth revision of the international list of diseases and causes of death. Geneva: WHO, 1967.
(*3*) Durie BG, Salmon SE. A clinical staging system for multiple myeloma: Correlation of measured myeloma cell mass with presenting clinical features, response to treatment, and survival. Cancer 1975; 36:842–854.
(*4*) Waterhouse JA, Muir C, Correa P, Powell J. Cancer incidence in five continents. Vol III. IARC publication No. 15. Lyon: IARC, 1976.
(*5*) Cox DR, Stuart A. Quick sign tests for trend in location and dispersion. Biometrika 1955; 42:80–95.
(*6*) Kaplan EL, Meier P. Nonparametric estimation from incomplete observations. J Am Stat Assoc 1958; 53:457–481.
(*7*) Peto R, Pike MC, Armitage P, et al. Design and analysis of randomised clinical trials requiring prolonged observation of each patient. Br J Cancer 1977; 34:585–612; 35:1–39.
(*8*) Stiehm ER, Fudenberg HH. Serum levels of immune globulins in health and disease. Pediatrics 1966; 37:715–727.
(*9*) Pick AI, Shoenfeld Y, Frohlichmann R, Weiss H, Vana D, Schreibman S. Plasma cell dyscrasia: Analysis of 423 patients. JAMA 1979; 241:2275–2278.
(*10*) Pruzanski W. Clinical manifestation of multiple myeloma: Relation to class and type M component. Can Med Assoc J 1976; 114:896–897.
(*11*) Lin KT. Myeloma proteins in adult Chinese patients. Chin J Microbiol 1977; 10:28–36.
(*12*) Blattner WA. Epidemiology of multiple myeloma and related plasma cell disorders: An analytic review. In: Potter M, ed. Progress in myeloma. New York: Elsevier/North-Holland, 1980:1–65.
(*13*) Stalsberg H. Lymphoreticular tumors in Norway and in other European countries. J Natl Cancer Inst 1973; 50:1685–1702.
(*14*) Farhangi M, Osserman EF. Biology, clinical patterns, and treatment of multiple myeloma and related plasma-cell dyscrasias. In: Twomey MB, Good RA, eds. The immunopathology of lymphoreticular neoplasms. London: Plenum Medical Book Co., 1978:641–718.
(*15*) Talerman A. Clinico-pathological study of multiple myeloma in Jamaica. Br J Cancer 1969; 23:285–293.
(*16*) Waldenström J. Diagnosis and treatment of multiple myeloma. New York: Grune, 1970.
(*17*) Linos A, Kyle RA, O'Fallon WM, Kurland LT. Incidence and secular trend of multiple myeloma in Olmsted County, Minnesota: 1965–77. JNCI 1981; 66:17–20.
(*18*) Isobe T, Osserman EF. Pathologic conditions associated with plasma cell dyscrasias: A study of 806 cases. Ann NY Acad Sci 1971; 190:507–518.
(*19*) Medical Research Council's Working Party on Leukaemia in Adults. Prognostic features in the third MRC myelomatosis trial. Br J Cancer 1980; 42:831–840.
(*20*) Kyle RA. Multiple myeloma: Review of 869 cases. Mayo Clin Proc 1975; 50:29–40.
(*21*) Wolf NS. The hemopoietic microenvironment. In: Lajtha LG, ed. Clinics in hematology. Vol 8/2. London: Saunders, 1979:469–500.
(*22*) Alexanian R, Balcerzak S, Bonnet JD, et al. Prognostic factors in multiple myeloma. Cancer 1975; 36:1192–1201.

blank page

Generation of Suppressor Cells for Natural Killer Activity in Cancer Patients After Surgery[1,2]

Atsushi Uchida,[3] **Roland Kolb,**[4] *and* **Michael Micksche**[3]

ABSTRACT—Natural killer (NK) cell activity was examined in breast cancer patients before and after surgery, and the cells involved in the postoperative depression of cytotoxicity were characterized. NK activity against K562 target cells determined in a 4-hour ^{51}Cr release assay of blood lymphocytes from preoperative patients was comparable to that of normal donors. After surgery the patients showed a decrease in NK activity but not in number of large granular lymphocytes in the effector cell population. When blood mononuclear cells from postoperative patients were depleted of monocytes by adherence to a serum-coated plastic dish and a Sephadex G10 column and then cultured for 24 hours, they showed an increase in NK activity. Furthermore, adherent blood cells of postoperative patients, but not of normal donors or preoperative patients, suppressed the lytic function of NK cells of normal individuals. Twenty-four-hour preculture of suppressor and effector cells was required for suppression of cytotoxicity. Neither postoperative sera nor culture supernatants of suppressor monocytes and effector cells suppressed NK activity. In contrast, the lymphoproliferative response to mitogen was not affected by surgery, and postoperative blood monocytes did not inhibit the mitogenic response of normal lymphocytes. The results suggest that the appearance of suppressor monocytes in the circulation could be one cause of depression of NK activity in postoperative cancer patients.—JNCI 1982; 68:735–741.

Lymphoid cells from normal individuals display a spontaneous cytotoxicity against a variety of tumor cells and some normal target cells (*1, 2*). The effector cells are designated NK cells and are thought to play an important role in host resistance against tumors, virus-infected cells, and microbes (*1*). Recently, human NK cell activity has been demonstrated to be exerted by a morphologic subpopulation of lymphoid cells, LGL (*3, 4*), although the proportion of active NK cells among LGL is not yet determined.

It has been demonstrated that NK activity is depressed in tumor-bearing animals (*5*). Pronounced reduction of NK activity is documented in patients with advanced cancer (*6, 7*) but not in patients with regionally-locally controlled tumors (*8*). The existence of cells and factors regulating the level of NK activity both in vivo and in vitro is suggested by experimental evidence: Interferon enhances the activity of NK cells (*9, 10*). Prostaglandins have both an inhibitory effect (*11, 12*) and a stimulatory effect on NK cells (*12*). NK activity of mouse spleen cells can be suppressed by spleen cells of mice exhibiting low cytotoxicity as the result of young age or of experimental treatments (*13–16*). In humans, carcinomatous pleural effusions are found to contain suppressor monocyte-macrophages, which could be one cause of the lack of NK activity in the effusion of cancer patients (*17*).

Trauma is often accompanied by a loss of immunocompetency. Shortly after major surgery, patients were found to have impaired cell-mediated immunity, such as anergy to skin test antigens (*18*) and depression of lymphoproliferative response to mitogens and antigens (*19*). Recently, suppressor cells were demonstrated to be responsible for the depression of mitogenic response after thermal injury (*20*) and of mixed lymphocyte reactions after surgical trauma (*21*). In addition, the incidence of tumor take and spontaneous metastases has been shown to increase when tumor-injected animals are subjected to surgery (*22*).

NK cells seem to be more effective in dealing with a small number of tumor cells than in dealing with a large tumor cell load (*1*). Recent evidence in experimental animal models has suggested that NK cells are important in host defense against circulating tumor cells and therefore can prevent the development of tumor cells into metastases (*23–27*). It is important to know whether the level of NK activity is depressed in cancer patients after surgery, since surgical manipulation of cancer patients is known to result in an abrupt appearance of malignant cells in the circulation and an increased incidence of tumor metastases (*28, 29*). The present study was designed to investigate the effect of surgery on NK activity (especially its regulatory mechanism) of patients with breast cancer.

MATERIALS AND METHODS

Patients.—Peripheral blood was obtained from 21 patients with breast carcinoma of stage I or II. The patients, ranging in age from 30 to 65 years, had never been given any anticancer agent at the time of the study. All patients underwent modified radical mastectomy including prophylactic lymph node dissection. Controls were peripheral blood specimens from 21 healthy females whose ages were roughly matched with those of the patients.

Cell preparation and separation.—Effector cells were prepared as described elsewhere (*7, 17, 30*). Lymphocyte-rich mononuclear cells were isolated from heparinized peripheral blood by centrifugation on a Ficoll-Hypaque gradient (sp gr, 1.077; Nyegaard & Co., Oslo, Norway). The cells in the interface were collected, washed, and resuspended in RPMI-1640 tissue culture medium supplemented with 25 m*M* HEPES,[5] 2 m*M* L-glutamine, 100 U penicillin/ml, 100 μg

---

ABBREVIATIONS USED: FCS=fetal calf serum; LGL=large granular lymphocyte(s); NK=natural killer; PHA-P=phytohemagglutinin-P.

---

[1] Received July 2, 1981; accepted November 19, 1981.

[2] Research procedures were in accord with the ethical standards of the Helsinki Declaration of 1975.

[3] Institute for Cancer Research, University of Vienna, Borschkegasse 8a, A-1090 Vienna, Austria.

[4] First Department of Surgery, University of Vienna, A-1097 Vienna, Austria.

[5] 4-(2-Hydroxyethyl)-1-piperazine ethanesulfonic acid.

streptomycin/ml, and 10% heat-inactivated FCS (Gibco Biocult, Glasgow, Scotland) (referred to as "complete medium"). The mononuclear cells were then incubated in a 75-cm^2 plastic dish (Falcon Plastics, Oxnard, Calif.), which had been coated overnight with heat-inactivated FCS, for 60 minutes at 37°C. After incubation, the nonadherent cell suspensions were removed and the dish was washed three times with cold medium. The adherent cells were then removed from the dish by incubation for 15 minutes at 4°C with phosphate-buffered saline containing 0.2% EDTA and 5% heat-inactivated FCS and by vigorous washing with a pipette. They were then resuspended in complete medium. The recovery of the adherent cells containing more than 93% monocytes as judged by nonspecific esterase staining and morphology was 5-10% for normal donors and 10-15% for preoperative and postoperative cancer patients of the original number of cells placed on the dish. This fraction is hereafter referred to as "monocytes." The nonadherent cells were washed, resuspended in complete medium, and passed through a Sephadex G10 column to remove further contaminating monocytes. The recovery of the G10-nonadherent cells containing more than 99% lymphocytes as judged by nonspecific esterase staining and morphology was 65-90% of the original input. The fraction is hereafter referred to as "lymphocytes." Every fraction was more than 95% viable according to trypan blue dye exclusion.

Target cells.—The K562 human myeloid leukemia cell line (*31*) was used as targets as previously described (*7, 17*). Target cells were labeled by addition of 100 μCi $Na_2{}^{51}CrO_4$ (sp act, 100-350 μCi/μg Cr; Radiochemical Centre, Amersham, Buckinghamshire, England), incubated for 1 hour at 37°C, washed, and resuspended at a concentration of 1×10^5/ml in complete medium.

Cytotoxicity assay.—A 4-hour ^{51}Cr release assay was performed as described elsewhere (*7, 17*). We added 100 μl labeled target cells (1×10^4) and 100 μl effector cells at different numbers to wells of round-bottomed microtiter plates (Linbro Scientific Inc., New Haven, Conn.). Each plate was centrifuged and incubated for 4 hours at 37°C in a humidified atmosphere of 5% CO_2 in air. Samples were harvested by the transfer of 100 μl of supernatant from each well to vials, and the activity was counted in an auto-gamma scintillation counter. Spontaneous ^{51}Cr release was determined in wells containing target cells and medium, and maximum release was determined by addition of Triton X-100. The percentage of cytotoxicity for each assay was calculated by the following formula for triplicate samples: Percent cytotoxicity=[(experimental release − spontaneous release)/(maximum release − spontaneous release)]×100. The ranges of spontaneous and maximum release were 3-12% and 80-95% of the total isotope count added, respectively.

Suppressor assay for NK activity.—Effector cells at a concentration of 1×10^6/ml in complete medium were precultured for 24 hours in a 17×100-mm plastic tube (Falcon Plastics) in a humidified atmosphere of 5% CO_2 in air in the presence or absence of different numbers of cells used as suppressors as previously described (*17*). After culture, the tube was centrifuged at 200×*g* for 10 minutes, and the supernatant was removed and stored at −70°C. The cells were washed three times, resuspended in complete medium, and tested for cytotoxicity as described above. Inhibition of cytotoxicity was expressed as the percentage of suppression obtained from the following formula: Percent suppression=[1−(percent cytotoxicity in the presence of suppressor cells)/(percent cytotoxicity in the absence of suppressor cells)]×100.

Proliferative response to mitogen.—Mononuclear cells (1×10^5) were cultured in 200 μl complete medium in microtiter culture wells (Falcon Plastics) with an optimal dose of 15 μg PHA-P/ml (Difco Laboratories, Detroit, Mich.) and 5×10^{-5} *M* 2-mercaptoethanol for 72 hours in a humidified 5% CO_2 atmosphere (*17, 30*). Then 1 μCi [^{3}H]thymidine (5 Ci/mmol; Radiochemical Centre) was added to each well for the last 6 hours of the culture, and the incorporation of thymidine into DNA was measured in a liquid scintillation counter. Results were expressed as mean Δcpm in triplicate wells, where Δcpm was the difference between the cpm of stimulated and unstimulated cultures.

Suppressor assay for mitogenic response.—Monocytes (2×10^4) in 100 μl complete medium were mixed with the same volume of 1×10^5 responding cells and cocultured as described above. Inhibition of proliferative response to mitogen was expressed as the percentage of suppression obtained from the following formula: Percent suppression=[1−(Δcpm in the presence of suppressor cells)/(Δcpm in the absence of suppressor cells)]×100.

Statistical analysis.—The results were evaluated for statistical significance by Student's *t*-test.

RESULTS

Cytotoxicity against K562 cells of peripheral blood mononuclear cells of patients with stage I or II breast cancer was comparable to that of age-matched normal donors (table 1). At 1-2 weeks after surgery, blood mononuclear cells of cancer patients showed a decrease in cytotoxicity at effector-to-target cell ratios of 10:1-40:1. Significant reduction of NK activity was observed in 16 of 21 patients after surgery and was not related to the stage of disease and length of anesthesia administration (data not shown). Kinetic studies showed that the depression of cytotoxicity in cancer patients became noticeable 2-3 days after surgery and lasted over 2 weeks, while normal donors tested on the same day that patients were tested showed relatively constant levels of NK

TABLE 1.—*Effects of surgery on NK activity, number of LGL, and mitogenic response in cancer patients*[a]

Subject	Percent LGL[b]	Percent cytotoxicity to K562 cells at:			[^{3}H]thymidine uptake in response to PHA-P, Δcpm
		10:1[c]	20:1[c]	40:1[c]	
Cancer patients					
Before surgery	19±2	31±2	44±2	57±3	46,932±4,882
After surgery[d]	18±2	11±2[e]	20±3[e]	28±3[e]	43,268±5,563
Normal donors	21±2	34±2	49±2	64±3	50,874±4,607

[a] Results are expressed as means ± SE of 21 individuals.
[b] Percentage of LGL was determined by Giemsa staining.
[c] Effector-to-target cell ratio.
[d] Seven to 14 days after surgery.
[e] Value is significantly lower than that before surgery ($P<0.05$).

activity (daily variance being usually <10% cytotoxicity) (data not shown). In contrast, no significant differences were observed in the frequency of LGL in blood lymphocytes of normal individuals and preoperative and postoperative cancer patients. The number of LGL-binding K562 cells was also not affected by surgery (data not shown). While the NK cells are not synonymous with or equivalent in number to LGL, up to 70% of LGL have been demonstrated to be able to function as NK cells against highly sensitive target cells (Herberman RB: Personal communication). These results suggest that surgery may be followed by a reduction in the lytic activity but not in the number of NK cells in the peripheral blood of cancer patients.

However, no significant differences were seen in lymphoproliferative responses to PHA-P of normal donors and cancer patients before and 7–14 days after surgery.

For the detection of cells involved in the depression of NK activity in postoperative cancer patients, blood mononuclear cells were depleted of monocytes by adherence to a serum-coated plastic dish and a Sephadex G10 column. The mere removal of monocytes caused no enhancement of cytotoxicity against K562 cells (table 2). When these monocyte-depleted cells from postoperative patients were cultured for 24 hours in complete medium, they showed a significant increase in NK activity. In contrast, blood mononuclear cells of preoperative patients and normal individuals showed no such increase. The removal of monocytes from 24-hour-cultured mononuclear cells resulted in no increase in cytotoxicity. These results suggest that the peripheral blood of postoperative cancer patients contains potentially cytotoxic cells, which are functionally suppressed by monocytes and can recover their lytic function after a 24-hour in vitro culture in the absence of suppressor monocytes.

TABLE 2.—*Recovery from suppression of NK activity in postoperative cancer patients*

Subject No.	Operation[a]	Percent cytotoxicity at effector-to-target ratio of 20:1				
		Unseparated		Monocyte depleted before culture		Monocyte depleted after culture: Cultured
		Fresh	Cultured	Fresh	Cultured	
Cancer patients						
#1	−	43	41	48	45	44
	+	17[b]	16	19	34[c]	15
#2	−	36	30	31	32	33
	+	9[b]	12	8	23[c]	9
#3	−	52	60	60	55	53
	+	31[b]	32	35	53[c]	27
#4	−	38	43	37	35	42
	+	12[b]	10	15	30[c]	11
#5	−	58	56	67	63	55
	+	35[b]	31	32	53[c]	33
#6	−	44	35	44	37	39
	+	22[b]	16	26	44[c]	18
#7	−	45	53	52	46	49
	+	48	44	52	49	40
Normal individuals						
#8	None	59	60	56	58	63
#9	None	38	30	47	38	41
#10	None	43	44	47	45	46
#11	None	51	60	61	59	49
#12	None	54	58	50	60	55

[a] Blood mononuclear cells from normal donors and preoperative (−) and postoperative (+) cancer patients were cultured for 24 hr in complete medium. Monocytes were removed either before or after culture.

[b] Value is significantly lower than that of preoperation ($P<0.05$).

[c] Value is significantly higher than that of corresponding cells ($P<0.05$).

TABLE 3.—*Effect of monocytes on NK activity*[a]

Normal lymphocytes precultured with:	Effector:target	Suppressor:effector[b]	Percent cytotoxicity against K562 cells	Percent suppression[b]
Medium	10:1	—	43	—
	20:1	—	57	—
	40:1	—	72	—
Normal monocytes	20:1	0.1:1	59	−4
	20:1	0.2:1	54	5
	20:1	0.5:1	51	11
	20:1	1:1	58	2
Preoperative monocytes	20:1	0.1:1	55	4
	20.1	0.2:1	60	−5
	20:1	0.5:1	52	9
	20:1	1:1	53	7
Postoperative monocytes	20:1	0.1:1	40	30[c]
	20:1	0.2:1	34	40[c]
	20:1	0.5:1	32	44[c]
	20:1	1:1	29	49[c]

[a] Blood lymphocytes of a normal individual were precultured with or without blood monocytes of a normal donor, a preoperative patient, or a postoperative patient for 24 hr, then washed, and tested.

[b] —, no suppressor cells were present.

[c] Value is significant ($P<0.05$). Similar results were obtained in four different experiments.

For confirmation of the above suggestion, functional

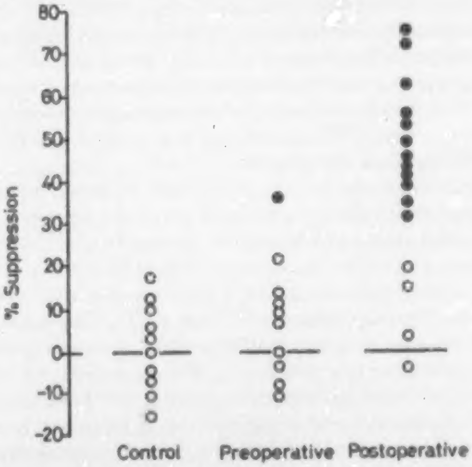

TEXT-FIGURE 1.—Suppression of NK activity by monocytes. Blood lymphocytes of normal donors were precultured for 24 hr with or without 20% blood monocytes from normal donors or preoperative or postoperative cancer patients, washed, and tested for cytotoxicity against K562 cells at an effector-to-target ratio of 20:1. Percentage of suppression was calculated as described in "Materials and Methods" and evaluated for statistical significance (●: $P<0.05$; ○: $P>0.05$).

TABLE 4.—*Effects of preincubation on suppressor activity of postoperative monocytes*[a, b]

Expt No.	Addition of monocytes	Without preincubation		Preincubated at 4°C		Preincubated at 37°C	
		Cytotoxicity, %	Suppression, %	Cytotoxicity, %	Suppression, %	Cytotoxicity, %	Suppression, %
1	−	53	—	57	—	51	—
	+	55	−4	52	9	23	55[c]
2	−	40	—	43	—	48	—
	+	36	10	37	14	24	48[c]
3	−	47	—	50	—	51	—
	+	52	−11	54	−8	34	33[c]
4	−	77	—	73	—	72	—
	+	70	9	67	8	47	35[c]
5	−	33	—	31	—	39	—
	+	28	15	35	−13	11	72[c]

[a] Normal lymphocytes were preincubated for 24 hr with or without 20% postoperative monocytes, either at 4°C or 37°C, washed, and tested for cytotoxicity against K562 cells at a lymphocyte-to-target cell ratio of 20:1.

[b] −, monocytes were not added, no suppressor cells were present; +, monocytes were added.

[c] Value is significant ($P<0.05$).

blood NK cells of normal controls were precultured for 24 hours with or without blood monocytes of postoperative patients showing a reduction of NK activity after surgery, then washed, and tested. As previously reported (*17, 32*), NK activity and compositions of 24-hour-cultured mononuclear cells were similar to those of freshly drawn cells (data not shown). Results of a representative experiment are shown in table 3. Blood monocytes did not lyse K562 cells in this assay (data not shown). NK activity of normal lymphocytes was suppressed by postoperative blood monocytes, whereas monocytes from preoperative patients or normal donors did not inhibit cytotoxicity. Monocyte-mediated suppression of NK activity was noticeable at a suppressor-to-effector cell ratio of 0.1:1 and peaked at 0.2:1–1:1. The recovery of viable cells cocultured with monocytes was comparable to that of viable cells cultured alone (data not shown), indicating that monocytes are not toxic to lymphocytes. Significant suppression of NK activity of normal lymphocytes by postoperative monocytes was observed at a suppressor-to-effector ratio of 0.2:1 in 12 of 16 patients showing postoperative reduction of NK activity (text-fig. 1). In contrast, blood monocytes of postoperative patients showing no depressed NK activity after surgery did not inhibit cytotoxicity (data not shown).

To ascertain whether the preculture of suppressor monocytes and NK cells is required for the suppression of NK activity, we tested postoperative monocytes for the activity suppressing the lytic function of NK cells with or without preincubation with fivefold the number of normal lymphocytes for 24 hours either at 4°C or 37°C. The addition of monocytes to a mixture of effector and target cells did not inhibit NK activity (table 4). Preincubation of normal lymphocytes with postoperative monocytes for 24 hours at 37°C suppressed cytotoxicity, whereas preincubation at 4°C did not. The presence of 24-hour-cultured monocytes only during a cytotoxicity assay also gave no inhibition of NK activity (data not shown). The results suggest that 24-hour contact of suppressor monocytes and NK effector cells prior to a cytotoxicity assay is necessary for suppression of NK activity.

The possibility that suppressor substances are secreted by suppressor monocytes was examined. Normal lymphocytes were precultured for 24 hours in complete medium, postoperative sera, supernatants produced by 24-hour cultures of postoperative monocytes, or supernatants from 24-hour cultures of postoperative monocytes and normal lymphocytes. They were then washed and tested for NK activity. Neither culture supernatant nor serum suppressed NK activity, whereas monocytes did suppress cytotoxicity (table 5). The presence of indomethacin, an inhibitor of prostaglandin synthesis, during the preculture and cytotoxicity assay failed to abrogate the monocyte-mediated suppression of NK activity (data not shown). The results suggest that suppressor–effector cell interaction is necessary for the suppression of NK activity.

TABLE 5.—*Effects of serum and supernatants of monocyte culture on NK activity*[a]

Expt No.	Percent cytotoxicity against K562 cells of lymphocytes cultured with:				
	Medium	Monocytes	Serum	Monocyte culture supernatants	Monocyte-lymphocyte culture supernatants
1	41	15[b]	39	43	37
2	62	36[b]	56	59	61
3	59	26[b]	61	56	55
4	72	47[b]	68	71	69
5	36	20[b]	37	32	35
6	51	34[b]	47	53	48

[a] Normal blood lymphocytes were precultured for 24 hr with 20% monocytes, 20% serum, or 24-hr culture supernatants of monocytes with or without lymphocytes from postoperative patients, then washed, and tested for cytotoxicity at an effector-to-target cell ratio of 20:1.

[b] Value is significantly lower compared to that in other groups ($P<0.05$).

So that we could ascertain whether postoperative blood monocytes suppress the mitogenic response, normal lymphocytes were stimulated with PHA-P in the presence or absence of postoperative monocytes. Monocytes did not inhibit lymphoproliferative response, whereas they suppressed NK activity (table 6). Increasing numbers of monocytes also failed to inhibit mitogenic response (data not shown).

TABLE 6.—*Effects of monocytes from postoperative patients on PHA-P response and NK activity*[a]

Expt No.	[^{3}H]thymidine incorporation in response to PHA-P, Δcpm[b]		Percent suppression	Percent cytotoxicity against K562 cells at effector-to-target cell ratio of 20:1		Percent suppression
	Normal lymphocytes	Postoperative monocytes added		Normal lymphocytes	Postoperative monocytes added	
1	52,083±3,947	48,451±3,656	7	62	36	42[c]
2	36,820±815	37,926±746	−3	52	14	75[d]
3	76,197±2,841	72,845±3,721	5	44	26	41[c]
4	62,037±3,593	56,734±2,914	9	39	11	69[c]
5	43,949±1,658	46,503±2,715	−6	59	26	53[c]

[a] Lymphocyte-rich mononuclear cells from normal individuals were tested for mitogenic response and NK activity in the presence or absence of 20% monocytes from postoperative cancer patients.

[b] Results are expressed as means ± SD.

[c] Value is significant ($P<0.05$).

DISCUSSION

The present study has demonstrated that the activity of NK cells decreases after removal of tumors from patients with stage I or II breast cancer. The findings are of practical interest, since evidence is increasing that NK cells may play an important role in host resistance against circulating tumor cells and therefore inhibit the development of tumor cells into metastases: In mice with high NK activity, iv injected tumor cells are rapidly eliminated (*33*). A close correlation is demonstrated between levels of host natural cytotoxicity and/or NK activity and capacity to eliminate blood-borne tumor cells (*24*). Low NK activity was associated with increased incidence of metastases in 3-week-old nude mice (*25*). Tumor cells modified to be sensitive to NK lysis by in vitro culture demonstrated in vivo an increased growth rate, faster induction time, and an increased metastatic capability in beige mice showing impaired NK activity compared to the NK activity in control mice (*26, 27*). In addition, surgical manipulation of cancer patients is known to result in an abrupt appearance of tumor cells in the circulation of these patients and to be correlated with an increased incidence of metastases (*28, 29*). Our findings of the postoperative reduction in NK activity in cancer patients could be one mechanism by which tumor metastases are enhanced after surgery. The findings, however, somewhat differ from other observations that after surgery NK activity specifically directed toward melanoma cells increased in patients with stage I malignant melanoma but decreased in patients with stage II malignant melanoma (*34*). The discrepancy may be explained by differences in the disease, surgical procedure, and cytotoxicity assay.

One mechanism of the lack of NK activity has been shown to be the presence of suppressor cells in the spleens of *Corynebacterium parvum*-injected, bone marrow-tolerant, infant, carrageenan-treated, hydrocortisone-treated, or adriamycin-treated mice (*13–16*). NK suppressor cells induced by hydrocortisone or carrageenan were found to be macrophage-like, and those from infant or irradiated mice were found to be null cells (*14*). We have found that blood monocytes from postoperative cancer patients can suppress the activity of functional NK cells and are responsible for the depression of NK activity in these patients. The findings are in agreement with those of previous reports that adherent blood cells of some cancer patients (*35*) or monocyte-macrophages of malignant pleural effusions of lung cancer patients (*17*) have suppressor activity for NK cells.

The mechanism by which suppressor cells inhibit NK activity is not clear. The present study demonstrates that 24-hour contact of suppressor monocytes and NK effector cells is required for suppression of NK activity. This observation is in contrast with that of other reports that suppression results from the mere addition of suppressor cells to a mixture of effector and target cells in mouse models (*14*) but is in keeping with our previous findings in humans (*17*) and the findings of others in mice (*36*) of a requirement for prolonged contact of suppressor and effector cells prior to a cytotoxicity assay. It has been shown that 24-hour culture of lymphocytes results in induction of interferon and enhancement of NK activity (*37*). However, it seems unlikely that postoperative monocytes inhibit culture-induced activation of NK cells rather than suppress NK activity, since no significant difference was observed in NK activities of fresh and 24-hour-cultured lymphocytes and culture supernatants contained no detectable amount of interferon (data not shown), as previously observed (*17, 32*). These differing results may be based on the method of culture

There is evidence that suppressor substances are involved in the suppression of NK activity. Sera from mice contain inhibitors of both NK activity and antibody-dependent cellular cytotoxicity (*38*). Culture supernatants of suppressor cells from hydrocortisone-treated mouse spleens inhibit NK activity (*39*). NK activity is suppressed by prostaglandins (*11, 12*). In contrast, blood monocytes from postoperative cancer patients suppressed NK activity by direct interaction with NK cells and independently of prostaglandin induction. Our findings confirm those of previous reports that suppression of NK activity by adherent cells from the peripheral blood (*35*) and pleural effusions (*17*) of cancer patients is not lowered by indomethacin.

We have demonstrated that functionally suppressed NK cells can recover their lytic function when these cells are first depleted of suppressor monocytes and then cultured for 24 hours. The mere removal of monocytes from blood mononuclear cells caused no enhancement of NK activity. This observation is in agreement with the findings of others (*40*) and with our previous observations (*7, 17, 32*) but differs from the observation in another report (*41*) that NK activity is enhanced after the removal of adherent cells. Possibly, the discrepancy is based on the details of removal of monocytes.

In the present study, cancer patients 7-14 days after surgery showed no decrease in lymphoproliferative response to mitogen, and their blood monocytes did not suppress mitogenic response. However, some patients tested on the 2d postoperative day showed depression of mitogen reactivity but had no mitogenic suppressor cells in their circulation (data not shown).

Why suppressor monocytes appear in the circulation of cancer patients after surgery is not clarified in the present study. Neither depression of NK activity nor development of NK suppressor cells was observed in patients with nonneoplastic disease after surgery or in cancer patients who received extensive anesthesia but did not have their tumors removed (Uchida A: Manuscript in preparation). Possibly suppressor monocytes are released from the tumor site at the time of surgical resection, since surgical manipulation of cancer patients is known to result in an abrupt appearance of viable tumor cells in the peripheral blood (*28*). Further studies on the regulatory function of monocytes within the site of breast tumors may support the above suggestion.

REFERENCES

(*1*) Herberman RB, Holden HT. Natural cell-mediated immunity. Adv Cancer Res 1978; 27:305-377.

(*2*) Kiessling R, Wigzell H. An analysis of the murine NK cells as to structure, function, and biological relevance. Immunol Rev 1979; 44:165-208.

(*3*) Timonen T, Saksela E, Ranki A, Häyry P. Fractionation, morphological and functional characterization of effector cells responsible for human natural killer activity against cell-line targets. Cell Immunol 1979; 48:133-148.

(*4*) Timonen T, Saksela E. Isolation of human NK cells by density gradient centrifugation. J Immunol Methods 1980; 36:285-291.

(*5*) Herberman RB, Nunn ME, Lavrin DH. Natural cytotoxic reactivity of mouse lymphoid cells against syngeneic and allogeneic tumors. I. Distribution of reactivity and specificity. Int J Cancer 1975; 16:216-229.

(*6*) Pross HF, Baines MG. Spontaneous human lymphocyte-mediated cytotoxicity against tumor target cells. I. The effect of malignant disease. Int J Cancer 1976; 18:593-604.

(*7*) Uchida A, Michsche M. Natural killer cells in carcinomatous pleural effusions. Cancer Immunol Immunother 1981; 11:131-138.

(*8*) Takasugi M, Ramseyer A, Takasugi J. Decline of natural nonselective cell-mediated cytotoxicity in patients with tumor progression. Cancer Res 1977; 37:413-418.

(*9*) Gidlund M, Örn A, Wigzell H, Senik A, Gresser I. Enhanced NK cell activity in mice injected with interferon and interferon inducers. Nature 1978; 273:759-761.

(*10*) Djeu JY, Heinbaugh JA, Holden HT, Herberman RB. Augmentation of mouse natural killer cell activity by interferon and interferon inducers. J Immunol 1979; 122:175-181.

(*11*) Droller MJ, Schneider MU, Perlman P. A possible role of prostaglandins in the inhibition of natural and antibody-dependent cell-mediated cytotoxicity against tumors. Cell Immunol 1978; 39:165-177.

(*12*) Kendall RA, Targan S. The dual effect of prostaglandin and ethanol on the natural killer cytolytic process effector activation and natural killer cell target cell conjugate lytic inhibition. J Immunol 1980; 125:2770-2777.

(*13*) Hochman PS, Cudkowicz G, Dausset J. Decline of natural killer cell activity in sublethally irradiated mice. JNCI 1978; 61:265-268.

(*14*) Cudkowicz G, Hochman PS. Regulation of natural killer activity by macrophage-like and other type of suppressor cells. In: Siskind GW, Litwin SD, Weksler ME, eds. Developmental immunology. London: Grune, 1979:1-21.

(*15*) Savary CA, Lotozova E. Suppression of natural killer cell activity by splenocytes from *Corynebacterium parvum*-injected, bone marrow-tolerant, and infant mice. J Immunol 1978; 120:239-243.

(*16*) Santoni A, Riccardi C, Sorci V, Herberman RB. Effects of adriamycin on the activity of mouse natural killer cells. J Immunol 1980; 124:2329-2335.

(*17*) Uchida A, Micksche M. Suppressor cells for natural killer activity in carcinomatous pleural effusions of cancer patients. Cancer Immunol Immunother 1981; 11:255-263.

(*18*) Pietsch JB, Meakins JL, Maclean LD. The delayed hypersensitivity response: Application in clinical surgery. Surgery 1977; 82:349-355.

(*19*) Salo M. Effect of anesthesia and surgery on the number of and mitogen-induced transformation of T- and B-lymphocytes. Ann Clin Res 1978; 10:1-13.

(*20*) Miller CL, Baker CC. Changes in lymphocyte activity after thermal injury. J Clin Invest 1979; 63:202-210.

(*21*) Wang BS, Heacock EH, Wu AV, Mannick JA. Generation of suppressor cells in mice after surgical trauma. J Clin Invest 1980; 66:200-209.

(*22*) Saba TM, Antikatzides TG. Decreased resistance to intravenous tumour-cell challenge during reticuloendothelial depression following surgery. Br J Cancer 1976; 34:381-389.

(*23*) Gorelik E, Fogel M, Feldman M, Segal S. Differences in resistance of metastatic tumor cells and cells from local tumor growth to cytotoxicity of natural killer cells. JNCI 1979; 63:1397-1404.

(*24*) Hanna N, Fidler IJ. Role of natural killer cells in the destruction of circulating tumor emboli. JNCI 1980; 65:801-809.

(*25*) Hanna N. Expression of metastatic potential of tumor cells in young nude mice is correlated with low levels of natural killer cell-mediated cytotoxicity. Int J Cancer 1980; 26:675-680.

(*26*) Talmadge JE, Meyers KM, Prieur DJ, Starkey JR. Role of NK cells in tumour growth and metastasis in beige mice. Nature 1980; 284:622-624.

(*27*) ———. Role of natural killer cells in tumor growth and metastasis: C57BL/6 normal and beige mice. JNCI 1980; 65:929-935.

(*28*) Roberts S, Long L, Jonassen O, McGrath R, McGraw E, Cole WH. The isolation of cancer cells from the blood streams during uterine curettage. Surg Gynecol Obstet 1960; 111:3-11.

(*29*) El Rifi K, Bacon B, Methigan J, Hope E, Cole WH. Increased incidence of pulmonary metastases after celiotomy: Counteraction by heparin. Arch Surg 1965; 91:625-634.

(*30*) Uchida A, Hoshino T. Reduction of suppressor cells in cancer patients treated with OK-432 immunotherapy. Int J Cancer 1980; 26:401-404.

(*31*) Lozzio CB, Lozzio BB. Human chronic myelogenous leukemia cell-line with positive Philadelphia chromosome. Blood 1975; 45:321-334.

(*32*) Uchida A, Micksche M. In vitro augmentation of natural killing activity by OK-432. Int J Immunopharmacol 1981; 3:365-375.

(*33*) Riccardi C, Puccetti P, Santoni A, Herberman RB. Rapid in vivo assay of mouse natural killer cell activity. JNCI 1979; 63:1041-1045.

(*34*) Hersey P, Edwards A, McCarthy WH. Tumor-related changes in natural killer cell activity in melanoma patients. Influence of stage of disease, tumor thickness and age of patients. Int J Cancer 1980; 25:187-194.

(*35*) Vose BM. Natural killers in human cancer: Activity of tumor-infiltrating and draining node lymphocytes. In: Herberman RB, ed. Natural cell-mediated immunity against tumors. New York: Academic Press, 1980:1081-1097.

(*36*) Brunda MJ, Taramelli D, Holden HT, Varesio L. Effects of resting and activated macrophages on natural killer cell activity and lymphoproliferation. Proc Am Assoc Cancer Res 1981; 22:310.

(*37*) Reynolds CW, Brunda MJ, Holden HT, Herberman RB. Role of macrophages in in vitro augmentation of rat, mouse, and human natural killer activities. JNCI 1981; 66:837-842.

(*38*) Nair PN, Fernandes G, Onoe K, Day NK, Good RA. Inhibition of effector cell functions in natural killer cell activity (NK) and antibody-dependent cellular cytotoxicity (ADCC) in mice by normal and cancer sera. Int J Cancer 1980; 25:667-677.

(39) Hochman PS, Cudkowicz G. Suppression of natural cytotoxicity by spleens of hydrocortisone-treated mice. J Immunol 1979; 123:968-976.

(40) de Vries JE, Mendelsohn J, Bont WS. Requirement for monocytes in the spontaneous cytotoxic effects of human lymphocytes against non-lymphoid target cells. Nature 1980; 283:574-576.

(41) Saksela E, Timonen T, Ranki A, Häyry P. Morphological and functional characterization of isolated effector cells responsible for human natural killer activity to fetal fibroblasts and to cultured cell line targets. Immunol Rev 1979; 44:71-123.

blank page

Measurement of Cancer Incidence in the United States: Sources and Uses of Data[1,2]

E. Robert Greenberg, *M.D.*,[3] **Theodore Colton**, *Sc.D.*,[4] *and* **Curtis Bagne**, *Ph.D.*[5,6]

ABSTRACT—Since 1937, investigators have compiled a vast amount of information on cancer incidence in the United States. Three national cancer surveys were conducted in 1937, 1947, and 1969–71; each used somewhat different methods but covered populations who overlapped greatly. Concurrently, population-based tumor registries were developed that were capable of measuring cancer incidence. Since 1973, the Surveillance, Epidemiology, and End Results Program, an amalgam of such registries, has generated cancer incidence data for the United States. Available data provide a rough measure of the size of the cancer problem and may help those who direct prevention programs and those who plan studies of cancer etiology. Because the completeness and validity of existing incidence data are not known with certainty, comparisons among these incidence rates require cautious interpretation.—JNCI 1982; 68:743–750.

The rate of cancer occurrence receives extraordinary attention in the United States. Witness, for example, the controversy that erupted after publication of an article claiming that the U.S. cancer incidence may be increasing (*1*). The article received coverage on the television evening news, became the subject of debate in Congress, and was cited by the White House Council on Environmental Quality as evidence that factors causing cancer are on the increase and that chemical carcinogens may require tighter regulations (*2*). Subsequently, a number of epidemiologists and other scientists strongly objected to the methods of analysis and the conclusions of the article (*3, 4*). The controversy pointed out the great importance placed on cancer incidence figures by elected officials and by the general public.

Scientists working in cancer research often have reason to cite cancer incidence rates. Many scientists, however, seem unaware of how these rates are generated, their validity, and their proper interpretation. In this paper, we review the sources of U.S. cancer incidence information and indicate some of the uses and limitations of these data. The basis for the paper is a 2-year study that we and our colleagues conducted to evaluate current and potential methods of determining cancer incidence in the United States. The detailed reports of the evaluation are available from the National Technical Information Service (*5, 6*).

HISTORICAL BACKGROUND: THE NATIONAL CANCER SURVEYS

Until the late 1930's there were no sources of cancer incidence data for the U.S. population. Mortality figures provided the only population-based information on cancer occurrence, and these, supplemented with reports of hospital case series, were used to support estimates of the scope of the cancer problem. In fact, the literature of that era reveals little concern with the rate of new cancer occurrence in the population, i.e., cancer incidence. The proportion of the population affected with cancer, i.e., cancer prevalence, was used as an indicator of the burden of cancer morbidity and appears to have been of greater initial interest than incidence. The first large survey done by the NCI reflected this concern with existing rather than new cancer cases.

Begun in 1937, the study covered 10 metropolitan areas (Atlanta, Ga.; Birmingham, Ala.; Chicago, Ill.; Dallas–Fort Worth, Tex.; Denver, Colo.; Detroit, Mich.; New Orleans, La.; Philadelphia, Pa.; Pittsburgh, Pa.; and San Francisco, Calif.) and included a population of 13 million, roughly 10% of the total U.S. population. Areas were chosen so that the distribution of the population among three regions—the North, the South, and the West—was proportionate to that of all cities of 100,000 population or larger. They were not meant to be representative of the U.S. population but were, instead, restricted to metropolitan regions with a central city population of more than 100,000 where one could expect better diagnostic information and greater cooperation of the local medical community (*7*).

The NCI staff surveyed each area for 1 year (either 1937, 1938, or 1939) and tried to identify all existing and newly diagnosed cases of cancer (except for leukemia and Hodgkin's disease) and to obtain detailed medical data for each case. The notion of using household interview surveys was rejected because cancer patients and their families seemed unable to give accurate information on primary site, histology, and other clinical information. Further, an appreciable number of persons at that time were not aware that their physicians had diagnosed a cancer in them or, if they knew, might not be willing to disclose this information. The NCI investigators thus chose to survey sources of medical care as a way to identify cancer cases and to obtain more reliable and comprehensive clinical information.

All physicians, hospitals, and clinics in the area received, by mail, forms that requested information on each cancer

---

ABBREVIATIONS USED: DCO=death certificate only; EREP=End Results Evaluation Program; MC=microscopically confirmed; NCI=National Cancer Institute; NSD=nonspecific diagnoses; SEER=Surveillance, Epidemiology, and End Results; TNCS=Third National Cancer Survey.

---

[1] Received July 8, 1981; accepted December 8, 1981.

[2] Supported in part by Public Health Service (PHS) contract N01CP-71047 from the Division of Cancer Cause and Prevention, National Cancer Institute (NCI), and by PHS grant 5P30CA-23108-03 from the NCI.

[3] Norris Cotton Cancer Center, Dartmouth-Hitchcock Medical Center, Hanover, N.H. 03755.

[4] Boston University School of Public Health, Boston, Mass. 02118.

[5] Lafayette Clinic, Detroit, Mich. 48233.

[6] We gratefully acknowledge the assistance of members of the NCI Biometry Branch and of personnel with the Surveillance, Epidemiology, and End Results Program registries, many of whom helped us gather information. Susan Vogt and Emily Fayen participated in the original evaluation. Philip Cole, Dwight Janerich, and O. Ross McIntyre provided helpful suggestions to us while we were writing the manuscript.

patient including name, date of diagnosis, type of treatment, current vital status, and method of confirmation of diagnosis. If requested, the field staff visited physicians' offices to abstract the required data. Physicians who did not return their forms promptly were contacted directly; only about 2% of physicians refused to participate. Staff also searched death certificates to identify cancer deaths and check the completeness of case finding.

Initial reports from this first survey, commonly called the Ten Cities Survey of 1937, focused on the mortality and prevalence of cancer in each area, as well as percent distributions of cases (both residents and nonresidents of the areas) by primary site, race, and sex. Incident cases were reported in terms of new cases per reported death, or when actual incidence rates were cited, the crude rates were reported (*8–17*). In 1944 and again in 1949, Dorn (*18, 19*) summarized the survey findings by presenting age-, race-, sex-, and site-specific incidence rates.

The second national survey occurred in 1947–48 and covered the same 10 metropolitan areas (with the exception of Fort Worth). Similar methods of case identification and data collection were used, but attention was focused on incident, resident cases. This time leukemia and Hodgkin's disease were included. Results from the survey, after adjustment for inclusion and coding discrepancies to make them consistent with those of the earlier survey, were published in another series of reports (*20–29*). A final summary report described variations in cancer incidence by age, sex, race, geographic region, marital status, and primary site. It also reported intercity variations, trends in cancer morbidity, associations of cancer incidence with income class, stage of disease at diagnosis, comparison of death certificates with case reports, and interpretation of the age-incidence curve (*7*).

The populations studied in the two Ten Cities Surveys were not highly representative of the total U.S. population with regard to cancer occurrence. In 1950, for example, cancer mortality for the populations covered in the Ten Cities Survey was about 10% higher than that for the total U.S. population (*30*) and indicated that cancer occurred less frequently in rural areas. This notion was supported by a survey in the rural state of Iowa.

The Iowa study of 1950 employed the same techniques as those used in the Ten Cities Surveys. Only 6.8% of the population of Iowa at that time lived in cities of 100,000 or more. Comparison of age-adjusted incidence rates for Iowa with those for the 10 metropolitan areas showed Iowa to have cancer rates 14% lower for males and 8% lower for females. Checks on internal consistency and comparison with mortality figures indicated that the lower incidence rates were real and not explained by selective migration of ill persons to urban areas or by differences in diagnostic levels (*31*).

Twenty-one years elapsed between completion of the second Ten Cities Survey and the TNCS of 1969–71. The organizers of the TNCS wished to assess trends in cancer morbidity from 1937 to 1971 and to achieve broader coverage of the U.S. population. Seven of the original 10 cities continued in the TNCS. Coverage of six of these was enlarged to include entire standard metropolitan statistical areas as defined by the U.S. Department of Commerce. The staff surveyed the entire State of Colorado, instead of Denver alone. Addition of Iowa increased coverage of the rural and farm population and permitted comparison with the 1950 results. Chicago, included in the original studies, was replaced by another northern metropolitan area, Minneapolis–St. Paul, Minn. Philadephia was not resurveyed because of administrative difficulties, and, in New Orleans, the medical community did not seem receptive to a survey by a Federal Agency.

Data collection methods used in the TNCS differed from those of past surveys. Rather than relying on direct reporting by physicians, TNCS field staff visited hospitals, clinics, radiation therapy centers, pathology laboratories, and physicians' offices to abstract the needed information directly from patient records. To maximize data completeness and accuracy, staff searched multiple sources for missed cases and used rigorous quality-control procedures.

The staff of the TNCS found information on 181,027 new cases of cancer among residents of the survey areas. A summary report on the TNCS presented variation of incidence rates by race, by sex, and for different primary sites and histologic types (*32*). A series of advanced reports gave incidence data for the individual survey areas (*33–42*). An analysis of trends in cancer incidence from 1937 to 1969 was published and took into some account the changes in the covered geographic areas (*43*). Data on hospitalization and payments to hospitals were also reported (*44*), as were detailed analyses of incidence rates for individual anatomic sites (*45–49*).

INDIVIDUAL TUMOR REGISTRIES

Independent of the conduct of the three national cancer surveys, local population-based tumor registries developed and proliferated. New York State began an incidence-reporting registry in 1940 (*50*), and Connecticut organized its registry in 1941 with data complete back to 1935 (*51*). These two registries became the reference points for U.S. cancer incidence data during the interval between the national surveys of 1947 and 1969–71.

Many other large tumor registries arose during the 1950's, often by amalgamation of local hospital registries. Their general purpose was to monitor cancer treatment and outcome with the intent of improving patient care. A number of these registries joined in 1956 into the EREP, which measured survival of cancer patients (*52*). Because some of the registries in EREP covered all the hospitals in a defined geographic area, they were also used to generate incidence data. Additional population-based registries sprang up under the Regional Medical Program in the 1960's, again with the purpose of improving medical care. Data from several of these registries were published in the three editions of "Cancer Incidence in Five Continents" (*53–55*) and were used to compare incidence rates among distinct geographic areas in the United States and other countries.

THE SEER PROGRAM

The National Cancer Act of 1971 became law days before the end of the reporting period for the TNCS. The political activity and hearings around this legislation emphasized the need for statistics to plan and evaluate the expanding cancer program and called into question the adequacy of the ad hoc National Cancer Surveys.

Even before the TNCS had commenced, NCI officials had decided that it would be the last survey of its kind in the United States. A major drawback to the periodic morbidity survey was the extensive time required to plan the survey, secure the cooperation of the medical communities, and recruit and train staff. When to this planning and start-up time was added the 3-year reporting period plus another year or 2 for analysis and dismantling of the survey, it became clear that a series of decennial surveys would require nearly continuous effort. Also, a continuous registry system appeared capable of providing the survival data then obtained from the EREP (*56*).

In 1971 NCI appointed an Ad Hoc Advisory Committee on Population-Based Epidemiology Research Centers to assess the potential contributions of participants in the TNCS and the EREP to a broadened program of cancer epidemiology. In its report the Committee affirmed a need for cancer incidence data and recommended that NCI "develop a coordinated program of cancer surveillance, descriptive epidemiology and end-results evaluation." It stated, however, that "NCI research and program goals do not presently require, or even suggest an ultimate need for, the establishment of a large scale, broadly-based national program of cancer registration" (*57*).

In 1973 the NCI established the SEER Program. SEER initially included eight population-based tumor registries that had participated in either the TNCS or the EREP or in both. The program now includes nine registries in the United States and one in Puerto Rico; each registry determines the incidence of cancer and the survival of all cancer patients resident within its geographic bounds. The basis for the selection of participant registries has been their demonstrated ability to operate and maintain a population-based cancer-reporting system and the unique population subgroups that they cover (*58*).

The nine U.S. registries cover a population of about 20 million individuals located in diverse areas of the country (table 1). Each registry annually reports every new case of disease that meets criteria for patient residence and date of diagnosis.

The SEER data set consists primarily of demographic and follow-up information about the patient, and a description of the neoplasm and is presented below:

- Basic identification:
  - SEER participant
  - Case No. and check digit
  - Type of reporting source
- Demographic information:
  - Place of residence at diagnosis
  - Residence summary
  - Place of birth
  - Year of birth
  - Age at diagnosis
  - Race–ethnicity
  - Sex
  - Marital status at diagnosis
- Description of this neoplasm:
  - Date of diagnosis
  - Sequence No.
  - Primary site
  - Laterality
  - Multiplicity within primary site
  - Histologic type
  - Diagnostic confirmation
  - Extent of disease
- Therapy:
  - Date cancer-directed therapy started
  - First course of cancer-directed therapy

TABLE 1.—*SEER Program registries in the United States*

Registry	Year of first reporting	Reporting area	Land area, square mile	Population,[a] × 10^3	Population density, per square mile
San Francisco–Oakland, Calif.	1973	5 counties (Alameda, Contra Costa, Marin, San Francisco, and San Mateo)	2,480	3,110	1,254
Connecticut	1973	Entire state	4,862	3,032	624
Atlanta, Ga.	1976	5 counties (Clayton, Cobb, De Kalb, Fulton, and Gwinnett)[b]	1,728	1,390	812
Hawaii	1973	Entire state	6,425	769	120
Iowa	1973	Entire state	55,941	2,824	51
New Orleans, La.[c]	1974	3 parishes (Jefferson, Orleans, and St. Bernard)	1,080	982	909
Detroit, Mich.	1973	3 counties (Macomb, Oakland, and Wayne)	1,952	4,200	2,152
New Mexico[d]	1973	Entire state	121,412	1,016	8
Utah	1973	Entire state	82,096	1,059	13
Seattle, Wash.	1974	13 counties (Clallam, Grays Harbor, Island, Jefferson, King, Kitsap, Mason, Pierce, San Juan, Skagit, Snohomish, Thurston, and Whatcom)	17,691	2,303	130

[a] Based on 1970 Census of the Population.

[b] Ten rural counties added with data back to 1978: Glascock, Greene, Hancock, Jasper, Jefferson, Morgan, Putnam, Taliaferro, Warren, and Washington.

[c] Withdrawn from the program in 1981. Last data were from 1978.

[d] The New Mexico Registry also collects data from the predominantly Indian population of Northwestern Arizona.

Follow-up information:
  Date of last follow-up or of death
  Follow-up status
  Cause of death
  International Classification of Diseases code used for cause of death

Information on environmental and occupational exposures and family histories is not included because it is not reliably documented in the medical records that serve as the basis for case reporting. Names of patients, hospitals, and physicians are not identified in data submitted to NCI to help maintain the privacy of individuals.

Registry staff identify cases primarily through searches of hospital discharge lists, pathology report forms, and radiation therapy records. The approach to searching for cases varies among registries. Most registries use their employees to perform this task, but some, such as the one in Connecticut, rely on employees of the local hospitals to find cases. In several states, but not all, state law or health department regulation requires physicians and hospitals to report new cases of cancer to the registry.

In 1978 the SEER Program published its first report on cancer incidence covering 1973–76. The data consisted of age-adjusted rates for 20 common cancer sites, presented by year of diagnosis, race, sex, and tumor registry area (*58*). The SEER Program has also published detailed age-, sex-, and race-specific cancer incidence figures for each registry for 1973–77 (*59*).

ASSESSING THE QUALITY OF REPORTED DATA

Despite the abundance of reported cancer incidence data for the United States, only limited information exists on the validity of these figures, largely because there have been no standards against which a particular set of incidence data could be compared to determine its completeness and diagnostic accuracy. There are, however, three figures that may serve as crude indicators of data quality. These are the proportion of cases known by DCO, the percent MC, and the proportion of cases with NSD. The DCO figures indicate completeness of registration. The MC and NSD figures indicate the accuracy of diagnostic information.

The DCO figure is the proportion of registered cases for which the only information about the diagnosis of cancer comes from a death certificate. Two types of patients contribute to this figure: 1) patients, such as those not hospitalized, for whom death certificates provide the only documentation of cancer and 2) deceased patients whose cancer diagnosis is recorded in a medical record that has been overlooked by the case-finding personnel of the registry. When a case of cancer is identified through review of death certificates, registry staff usually contact the certifying physician or hospital where death occurred to obtain records with additional diagnostic information. Only if none are found does the case count as DCO. Thus a low DCO figure may indicate thorough follow-back of information in addition to complete case finding.

Completeness of registration and the DCO figure partly depend on the way cancer patients obtain medical care. Those who receive all their care in out-of-state hospitals (which often are not covered by a registry) are not reported as cases unless they die and have a cancer noted on the death certificate. Those who lack ready access to medical care may suffer with undiagnosed cancer until it, or another condition, causes their death. Increased accessibility and use of medical care thus will result in more cases reported and a lower DCO figure. The elderly, in particular, have had a substantial increase in their use of medical services since the mid-1960's. As a result, one might expect more of their cancers to be diagnosed and reported. In part because of these reasons, some authors recommend that data on people over 65 should be excluded from analyses of temporal trends in cancer incidence and mortality (*4, 60*).

The proportion of cases for whom cancer has been histologically or cytologically confirmed makes up the MC measure and reflects the accuracy of diagnostic information in the registry. For primary cancer arising in the liver, pancreas, brain, or other inaccessible organs, an MC diagnosis provides reassurance that cancer is actually present and that it is primary and not metastatic to these sites. Of course, microscopic confirmation reflects not only the quality of diagnostic information but also the accessibility of medical services.

The NSD figure is the proportion of cases reported as primary cancers of the liver, bone, and "other or unspecified" sites. In the United States, primary cancers of the liver and bones are rare, although metastases to these sites are frequent. Some patients initially thought to have cancers arising in the liver or bone will, on closer study, be found to have cancers that have metastasized to these organs. Similarly, cancers of unknown or unspecified primary sites will be seen more frequently when diagnostic searches are less vigorous. The NSD measure is not a good indicator of data quality for purposes of comparing data from the United States with those from different countries, because in many countries primary liver cancer is much more common than it is in the United States.

Table 2 lists these three indicators of data completeness and quality for the three national cancer surveys and for the SEER Program (1973–77). The DCO proportion has decreased from nearly 16% in the first Ten Cities Survey to 1.4% in the SEER Program (range 1.0–3.0% for the U.S. registries) (*59*). As noted above, the lower DCO figures for recent data partly reflect greater access to care by the elderly and vigorous follow-back of death certificates in addition to improved case finding. The percent of MC tumors has increased to a high of 92.2% (range, 88.9–96.8%) in the

TABLE 2.—*Indicators of validity for major U.S. cancer incidence data sources*

Source	DCO, %[a]	MC, %[b]	NSD, %[c]
Ten Cities Survey of 1937–39[d]	15.9	63.9[e]	NA[f]
Ten Cities Survey of 1947–48	13.6	64.7	7.3
TNCS of 1969–71	2.1	90.1	4.5
SEER Program of 1973–77	1.4	92.2	4.5

[a] Percent of all cases with information only from a death certificate.

[b] Percent of all cases histologically or cytologically confirmed.

[c] Percent of all cases classed as bone, liver, or "other and unspecified" primary sites.

[d] Leukemia and Hodgkin's disease were not included.

[e] Estimate based on data in (6) (includes skin cancers).

[f] Data not available.

SEER Program, whereas the proportion of tumors in the liver, brain, and other and unspecified categories has declined from 7.3% in 1947–48 to 4.5% now. To the extent that these indicators reflect differences in overall data validity and not changes in use of medical services, there appears to have been a steady improvement in the quality of incidence data collected nationally. While it is encouraging that recent data seem more accurate than those collected previously, one must be impressed by the difficulty of making comparisons among incidence rates from four programs whose data differ so widely in quality.

USES OF INCIDENCE DATA

How may one use and interpret the information that has been collected on U.S. cancer incidence? A frequent use is to indicate the overall size of the cancer problem in the United States. The American Cancer Society for a number of years has published these figures based on the New York and Connecticut Tumor Registries, the TNCS, and the SEER Program (*61*). These numbers serve to educate the public, to aid those who determine government policy, and, in conjunction with mortality data, to assess the burden of cancer on various segments of the U.S. population.

A criticism of the use of NCI data for this purpose has been that the data were inaccurate because they came from a population not representative of the entire U.S. population (*3*). The population covered by the SEER Program is, in fact, on the average somewhat younger and better educated and has a higher mean family income than the total U.S. population. In addition, persons living on farms and rural blacks are underrepresented and urban blacks are overrepresented. Despite these differences, the cancer mortality experience of the SEER Program-covered population is quite similar to that of the total U.S. population (*4*). Moreover, the issue of whether the SEER Program-covered population is representative of the entire U.S. population is of relatively little scientific importance. A population not entirely representative can still produce reasonably accurate and reliable estimates of incidence if one knows the nature and extent to which the population differs from the total U.S. population and if one uses appropriate methods of statistical adjustment. There also is no apparent need for great accuracy of these cancer morbidity figures. National estimates of cancer incidence that are slightly off the mark neither greatly misinform the public nor distort the ability of Congress to determine how much money it wishes to allocate for cancer research.

Another use of national cancer incidence data is to identify demographic groups who have exceptionally high or low risk of cancer. Such information helps physicians advise persons of their risk of cancer and helps target programs for early detection and prevention. The observation that malignant melanoma incidence was high among whites in New Mexico, for example, led to efforts to educate physicians and the public about melanoma recognition and treatment (*62*). Knowledge about high- and low-risk groups may also lead to etiologic hypotheses that can be tested through specific epidemiologic studies. For these purposes, data generally are more valuable if they come from clearly defined demographic groups in restricted geographic areas rather than from a cross section of the U.S. population. Under the first approach, subjects are identified who can later be traced and enrolled in detailed etiologic or follow-up studies. The information collected under the second approach comes from individuals who may be scattered throughout the country and cannot feasibly be enrolled in such studies.

A further use of national cancer incidence rates is to identify time trends in the occurrences of specific tumors. The SEER Program was initially envisioned as a cancer surveillance system (*4*), capable of detecting increases in the incidence of common cancers and the appearance of unusual new cancer types, such as angiosarcoma of the liver that occurs in workers exposed to vinyl chloride (*63*). In theory, incidence is preferable to mortality for surveillance data because case-fatality rates change over time and because increased incidence may not be rapidly reflected by increased mortality for those cancers that are not quickly fatal. The superiority of incidence data is unproved, however, and some authors believe that mortality data are more reliable indicators of cancer trends (*3, 4*). Perhaps the experience of the SEER Program over the coming years will provide evidence for or against the value of national cancer incidence surveillance.

Members of the public look at cancer incidence surveillance as a way to detect geographic "hot spots," i.e., places with exceptionally high rates. Often their concern is with environmental pollution from chemical wastes concentrated in a small space, such as occurred at Love Canal, N.Y. (*64*). This type of geographic surveillance poses some practical difficulties. First, if one surveys many geographic areas and many specific cancer types, some areas will be noted to have statistically significant high incidence rates due purely to chance and to the multitude of place–cancer combinations examined. Second, the population in an area may not be large enough to reveal, with statistical significance, a substantial increase in cancer incidence because most cancers occur relatively rarely and most environmental carcinogens appear to cause an increase in only one or a few cancer types. For example, 23 years of data were available from the roughly 4,900 residents of the Love Canal area, but these numbers would not have been sufficient to detect a 50% increase in the incidence of most cancers had such occurred (*64*). Third, not all inhabitants of an area are actually exposed to the environmental contaminant of interest (because they are recent immigrants or because the contaminant is not distributed throughout the area). The presence of these persons dilutes the measured effect of the contaminant and lessens the likelihood of detecting an increase in incidence. Lastly, identification of a "hot" area does not ensure that a previously unsuspected etiologic factor will be found responsible for the increased incidence. Sometimes the increase is largely due to factors already known to cause cancer, such as asbestos exposure in the shipbuilding industry (*65*), and often, despite myriad suspicions, no satisfactory explanation can be established. These practical difficulties and the potential to generate unfounded fears (or inappropriate reassurances) may explain why many epidemiologists lack enthusiasm for this type of small-area geographic surveillance.

best copy available

PROBLEMS IN THE INTERPRETATION OF CANCER INCIDENCE DATA

Interpretation of cancer incidence estimates poses several problems for the users of these data. First, cancer incidence rates may not accurately reflect a population's exposure to the causes of cancer because the rates are measures of clinically detected disease only. Cancer incidence is a function of three separate rates: *a*) the rate of cancer initiation (due to the accumulated factors that cause cancer), *b*) the rate which persons transit from initiation to recognition of the cancer (due to biologic factors promoting tumor growth and sociologic factors influencing tumor detection), and *c*) the rate at which persons with occult cancer are removed from the population by death. An increase over time in the incidence rate of cancer may thus be due to many factors, of which increased carcinogenesis is only one. An increased rate of cancer detection, a reduction in the relative rate at which people with cancer leave the population (due to migration or death from other causes), or a reduction in factors that retard cancer growth will also cause the measured incidence rate to rise. The first possibility requires careful consideration. An abrupt rise (≈15%) in breast cancer incidence was reported in 1974 following publicity given this disease after its diagnosis in Mrs. Ford and Mrs. Rockefeller (*58*). Part of the increased incidence was likely due to increased detection by women practicing self-examination and by physicians performing more screening examinations. Changes in diagnostic criteria (vide infra) may also have occurred. Whatever the explanation, by 1976 the rates had returned nearly to 1973 levels (*58*). Since the early 1970's the NCI Cancer Control Program, the American Cancer Society, and state and local health agencies have mounted large-scale projects to promote screening and early self-recognition of cancer. Many of these efforts have been directed at the populations covered by the SEER Program and have probably inflated the SEER Program-measured cancer incidence rates apart from any real increase in cancer onset.

Current and past U.S. cancer incidence data are based principally on the diagnoses recorded by physicians in the hospital record. This information is not standardized and will vary according to physician preferences for particular diagnoses. The basis for the determination of what actually is cancer has changed with time, especially for lesions of "borderline" invasiveness. For example, papillary tumors of the urinary bladder that were once classified as benign transitional cell papilloma are now usually diagnosed as grade I transitional cell carcinoma. More subtle shifts in diagnostic criteria may have occurred for cancers of other sites such as the endometrium, prostate gland, and breast. Changes such as these may underlie observed temporal or geographic differences in incidence.

Another difficulty with interpreatation of incidence rates is the variable levels of completeness of data from different sources. Despite intense efforts to find all new cases of cancers, some cancer patients are always missed due to migration from the coverage area to an uncovered hospital or because of oversights by data collection staff. The completeness of case identification appears to vary considerably for data collected at different times or at different places, which may account totally or partly for reported differences in incidence rates. Thus in comparing two incidence rates, one needs to know the level of completeness of the two data sets, but such figures are hard to come by. Although the DCO figure provides a crude basis for comparing completeness, it is an imperfect measure. As noted above, the DCO figure is affected by the accessibility of medical care, and differences in medical care use may confound inferences based on the DCO figure.

The data in cancer surveys and tumor registries are often based on limited diagnostic information. Among all lung cancer cases included in the TNCS, for example, 40% lacked a specific histologic diagnosis and 16% had not been confirmed as cancer by microscopic examination (*32*). For cancers of less accessible sites such as the pancreas, stomach, and brain, specific diagnoses are frequently not available in the patients' records. One therefore should not try to extract detailed diagnostic information from cancer incidence rates and may have to use data grouped by major anatomic site and with numerous diagnoses of unspecified histology.

Comparability of two sets of incidence data may also be compromised by variable inaccuracies in the census population estimates used to calculate incidence rates. Inaccuracies in census counts have ranged from 2½% to nearly 10% for age, race, and sex subgroups of the U.S. population, and greater degrees of inaccuracies may pertain for geographic subgroups of the U.S. population (*66*). Incidence rates for intercensal years require estimations of population that may be more imprecise. Thus the user of cancer incidence rates should bear in mind that small variations between two incidence rates may be due to differential inaccuracies in the population denominators and not to true differences in the occurrence rate of cancer. This caveat, of course, also pertains to analyses of mortality rates.

So that comparisons can be made, most U.S. cancer incidence rates are published as summary estimates that are "age standardized." This procedure reduces the effects of differing age structures in the population rates compared, but it does not eliminate them. In fact, the choice of a standard population can affect the results of comparison (*60*), and age-standardized rates that use recent U.S. census figures as a standard are heavily weighted by data from the very elderly. This group is less likely to be diagnosed accurately and has greatly increased its use of medical care over the past two decades. Preferred alternatives are to examine age- and sex-specific data or to use a truncated summary measure based on data from those under age 65.

CONCLUSIONS

Investigators have generated a vast amount of information on cancer incidence in the United States. Available data span almost 45 years and cover many different geographic populations in the United States. The groups included have been and continue to be predominantly urban, but most of the larger demographic segments of the population are now representd to some extent.

The existing data may prove useful to physicians in advising patients about cancer risk and in targeting prevention efforts. The data contribute to estimates of overall cancer morbidity, figures useful for public planning. Examination of cancer incidence rates for different populations can also lead to hypotheses about cancer cause.

Because cancer incidence rates have been generated with the use of differing methods of case ascertainment and because detection of cancer varies by year and region, rates must be compared cautiously. Comparisons of data may be affected by variable inaccuracies in census data, by the partial lack of standardization of pathologic diagnoses, and by distortions introduced by "age standardization." Despite these limitations, cancer incidence data, when paired with mortality data, provide a resource of readily available information on cancer occurrence in the United States.

REFERENCES

(*1*) Pollack ES, Horm JW. Trends in cancer incidence and mortality in the United States, 1969–76. JNCI 1980; 64:1091–1103.

(*2*) Toxic Substances Strategy Committee. Toxic chemicals and public protection. A report to the President. Washington, D.C.: U.S. Govt Print Off, May 1980.

(*3*) Smith RJ. Government says cancer rate is increasing. Science 1980; 209:998–1002.

(*4*) Doll R, Peto R. The causes of cancer: Quantitative estimates of avoidable risks of cancer in the United States today. JNCI 1981; 66:1191–1308.

(*5*) Bagne C, Fayen E, Greenberg ER, Vogt S, Colton T. Evaluation of the Surveillance, Epidemiology, and End Results Program of the National Cancer Institute. Springfield, Va.: Natl Technical Information Service, 1980 (NTIS accession No. PB-80-105182).

(*6*) Greenberg ER, Colton T, Bagne C, Fayen EG. Alternative methods for determining cancer incidence and survival in the United States. Springfield, Va.: Natl Technical Information Service, 1981 (NTIS accession No. PB-81-124752).

(*7*) Dorn HF, Cutler SJ. Morbidity from cancer in the United States: Parts I and II. DHEW Public Health Serv Mongr 56. Washington, D.C.: U.S. Govt Print Off, 1959.

(*8*) Mountain JW, Dorn HF, Boone BR. The incidence of cancer in Atlanta, Ga., and surrounding counties. Public Health Rep 1939; 54:1255–1273.

(*9*) Dorn HF. The incidence of cancer in Cook County, Illinois, 1937. Public Health Rep 1940; 55:628–650.

(*10*) McDowell AJ. The incidence of cancer in Pittsburgh and Allegheny County, Pennsylvania, 1937. Public Health Rep 1940; 55:1419–1451.

(*11*) ———. The incidence of cancer in Detroit and Wayne County, Michigan, 1937. Public Health Rep 1941; 56:703–739.

(*12*) ———. The incidence of cancer in New Orleans, La., 1937. Public Health Rep 1941; 56:1141–1170.

(*13*) ———. The incidence of cancer in Dallas and Fort Worth, Texas, and surrounding counties, 1938. Public Health Rep 1942; 57:125–139.

(*14*) Sommers HJ. The incidence of cancer in Birmingham and Jefferson County, Alabama, 1938. Public Health Rep 1942; 57:377–397.

(*15*) ———. The incidence of cancer in San Francisco and Alameda Counties, California, 1938. Public Health Rep 1942; 57:1566–1586.

(*16*) ———. The incidence of cancer in Philadelphia, Pa., 1938. Public Health Rep 1942; 57:1843–1857.

(*17*) ———. The incidence of cancer in Denver, Colorado, 1939. Public Health Rep 1942; 57:1971–1986.

(*18*) Dorn HF. Illness from cancer in the United States. Public Health Rep 1944; 59:33–48; 65–77; 97–115.

(*19*) ———. Morbidity from cancer. J Washington Acad Sci 1949; 39:117–119.

(*20*) Cutler SJ. Cancer illness among residents in Atlanta, Georgia, 1947. Washington, D.C.: U.S. Govt Print Off, 1950 (PHS publication No. 13).

(*21*) Grodowitz W. Cancer illness among residents of San Francisco and Alameda Counties, California, 1947. Washington, D.C.: U.S. Govt Print Off, 1950 (PHS publication No. 65).

(*22*) Warran II. Cancer illness among residents of New Orleans, Louisiana, 1947. Washington, D.C.: U.S. Govt Print Off, 1950 (PHS publication No. 67).

(*23*) Marcus SC. Cancer illness among residents of Denver, Colorado, 1947. Washington, D.C.: U.S. Govt Print Off, 1952 (PHS publication No. 112).

(*24*) Cutler SJ. Cancer illness among residents of Pittsburgh, Pennsylvania, 1947. Washington, D.C.: U.S. Govt Print Off, 1952 (PHS publication No. 126).

(*25*) ———. Cancer illness among residents of Chicago, Illinois, 1947. Washington, D.C.: U.S. Govt Print Off, 1952 (PHS publication No. 152).

(*26*) Marcus SC. Cancer illness among residents of Dallas, Texas, 1948. Washington, D.C.: U.S. Govt Print Off, 1952 (PHS publication No. 178).

(*27*) ———. Cancer illness among residents of Birmingham, Alabama, 1948. Washington, D.C.: U.S. Govt Print Off, 1952 (PHS publication No. 216).

(*28*) Cutler SJ, Rowan JC. Cancer illness among residents of Detroit, Michigan, 1948. Washington, D.C.: U.S. Govt Print Off, 1952 (PHS publication No. 217).

(*29*) Cutler SJ, Marcus SC. Cancer illness among residents of Philadelphia, Pennsylvania, 1948. Washington, D.C.: U.S. Govt Print Off, 1952 (PHS publication No. 244).

(*30*) Spiegelman M. Demographic differentials in cancer mortality in urban and rural areas of the United States, 1940. U.S. Public Health Service, Vital Statistics, Special Reports 33, No. 14. Washington, D.C.: U.S. Govt Print Off, 1952.

(*31*) Haenszel W, Marcus SC, Zimmerer EG. Cancer morbidity in urban and rural Iowa. DHEW Public Health Monogr 37. Washington, D.C.: U.S. Govt Print Off, 1956.

(*32*) Cutler SJ, Young JL Jr. Third National Cancer Survey: Incidence data. Natl Cancer Inst Monogr 1975; 41:1–454.

(*33*) Biometry Branch (National Cancer Institute). The Third National Cancer Survey advanced three year report, 1969–1971 incidence (excluding carcinoma in situ). Bethesda, Md.: National Institutes of Health, 1974 [DHEW publication No. (NIH)74–637].

(*34*) Medical Association of Georgia and Biometry Branch (National Cancer Institute). Cancer in the Atlanta metropolitan area, the Third National Cancer Survey advanced three year report, 1969–1971 incidence (excluding carcinoma in situ). Bethesda, Md.: National Institutes of Health, 1974 [DHEW publication No. (NIH)75-638].

(*35*) Department of Public Health and Epidemiology (University of Alabama School of Medicine) and Biometry Branch (National Cancer Institute). Cancer in the Birmingham metropolitan area, the Third National Cancer Survey advanced three year report, 1969–1971 incidence (excluding carcinoma in situ). Bethesda, Md.: National Institutes of Health, 1974 [DHEW publication No. (NIH)75-639].

(*36*) Colorado Central Cancer Registry (Colorado Department of Health) and Biometry Branch (National Cancer Institute). Cancer in Colorado, the Third National Cancer Survey advanced three year report, 1969–1971 incidence (excluding carcinoma in situ). Bethesda, Md.: National Institutes of Health, 1974 [DHEW publication No. (NIH)75-640].

(*37*) University of Texas Southwestern Medical School and Biometry Branch (National Cancer Institute). Cancer in the Dallas–Fort Worth metropolitan area, the Third National Cancer Survey advanced three year report, 1969–1971 incidence (excluding carcinoma in situ). Bethesda, Md.: National Institutes of Health, 1974 [DHEW publication No. (NIH)75-641].

(*38*) Michigan Cancer Foundation and Biometry Branch (National Cancer Institute). Cancer in the Detroit metropolitan area, the Third National Cancer Survey avanced three year report, 1969–1971 incidence (excluding carcinoma in situ). Bethesda, Md.: National Institutes of Health, 1974 [DHEW publication No. (NIH)75-642].

(*39*) Cancer Epidemiology Research Center (Department of Preventive Medicine, University of Iowa Hospitals) and Biometry Branch (National Cancer Institute). Cancer in Iowa, the Third National Cancer Survey advanced three year report, 1969–1971 incidence (excluding carcinoma in situ). Bethesda, Md.: National Institutes of Health, 1974 [DHEW publication No. (NIH)74-643].

(*40*) Division of Epidemiology (School of Public Health, University of Minnesota) and Biometry Branch (National Cancer Institute).

Cancer in the Minneapolis-St. Paul metropolitan area, the Third National Cancer Survey advanced three year report, 1969-1971 incidence (excluding carcinoma in situ). Bethesda, Md.: National Institutes of Health, 1974 [DHEW publication No. (NIH)75-644].

(41) Cooperative Health Survey (Department of Biostatistics, University of Pittsburgh) and Biometry Branch (National Cancer Institute). Cancer in the Pittsburgh metropolitan area, the Third National Cancer Survey advanced three year report, 1969-1971 incidence (excluding carcinoma in situ). Bethesda, Md.: National Institutes of Health, 1974 [DHEW publication No. (NIH)74-645].

(42) California Tumor Registry (San Francisco Bay Area Resource for Cancer Epidemiology, State of California, Department of Health) and Biometry Branch (National Cancer Institute). Cancer in the San Francisco Bay area, the Third National Cancer Survey advanced three year report, 1969-1971 incidence (excluding carcinoma in situ). Bethesda, Md.: National Institutes of Health, 1974 [DHEW publication No. (NIH)74-646].

(43) Cutler SJ, Devesa S. Trends in cancer incidence and mortality in the U.S.A. In: Doll R, Vodapza I, eds. Host environmental interactions in the etiology of cancer in man. Lyon: IARC, 1973:15-34.

(44) Scotto J, Chiazze L Jr. Third National Cancer Survey: Hospitalizations and payments to hospitals. Washington, D.C.: U.S. Govt Print Off, 1976 [DHEW publication No. (NIH)76-1094].

(45) Weiss NS, Young JL Jr, Roth GJ. Marital status and incidence of ovarian cancer: The U.S. Third National Cancer Survey, 1969-1971. J Natl Cancer Inst 1977; 58:913-915.

(46) Scotto J, Fraumeni JF Jr, Lee JA. Melanomas of the eyes and other noncutaneous sites: Epidemiologic aspects. J Natl Cancer Inst 1976; 56:489-491.

(47) Scotto J, Kopf A, Urbach F. Nonmelanoma skin cancer among whites in four areas of the United States. Cancer 1974; 34:1333-1338.

(48) Scotto J, Fears TR, Cori GB. Measurements of ultraviolet radiation in the United States and comparisons with skin cancer data. Bethesda, Md.: National Institutes of Health, 1975 [DHEW publication No. (NIH)76-1029].

(49) Fears TR, Scotto J, Schneiderman MA. Skin cancer, melanoma, and sunlight. Am J Public Health 1976; 66:461-464.

(50) Greenwald P, Burnett WS, Kirmss V, Brennan K, Nasca, PC. Cancer incidence and mortality in New York State (exclusive of New York City). New York: Bureau of Cancer Control, New York State Department of Health, 1976.

(51) Connelly RR, Campbell PC, Eisenberg H. Central Registry of cancer cases in Connecticut. Public Health Rep 1968; 83:386-390.

(52) Cutler SJ, Latourette HB. A national cooperative program for the evaluation of end results in cancer. J Natl Cancer Inst 1959; 22:633-646.

(53) International Union Against Cancer. Cancer incidence in five continents: A technical report. Vol I. In: Doll R, Payne P, Waterhouse J, eds. Berlin, Heidelberg, and New York: Springer-Verlag, 1966.

(54) ———. Cancer incidence in five continents: A technical report. Vol II. In: Doll R, Muir C, Waterhouse J, eds. Berlin, Heidelberg, and New York: Springer-Verlag, 1970.

(55) ———. Cancer incidence in five continents: A technical report. Vol III. In: Waterhouse J, Muir C, Correa P, Powell J, eds. Lyon: IARC, 1976.

(56) Haenszel W. The United States network of cancer registries. In: Grundmann E, Pedersen E, eds. Cancer registry. New York: Springer-Verlag, 1975.

(57) Ad Hoc Advisory Committee on Population-Based Epidemiology Resource Centers. Report. Bethesda, Md.: National Cancer Institute, Nov 1971.

(58) Young JL Jr, Asire AJ, Pollack ES, eds. SEER Program: Cancer incidence and mortality in the United States, 1973-1976. Washington, D.C.: U.S. Govt Print Off, 1978 [DHEW publication No. (NIH)78-1837].

(59) Young JL Jr, Percy CL, Asire AJ, eds. Surveillance, epidemiology, and end results: Incidence and mortality data, 1973-77. Natl Cancer Inst Monogr 1981; 57:1-1082.

(60) Doll R, Cook P. Summarising indices for comparison of cancer incidence data. Int J Cancer 1967; 2:269-279.

(61) 1977 cancer facts and figures. New York: American Cancer Society, 1976.

(62) Redman JC. Prevention of malignant melanoma—New Mexico joins Australia (letter). Australas J Dermatol 1977; 18:145-147.

(63) Creech JL, Johnson MN. Angiosarcoma in the manufacture of polyvinyl chloride. J Occup Med 1974; 16:150-151.

(64) Janerich DT, Burnett WS, Feck G, et al. Cancer incidence in the Love Canal area. Science 1981; 212:1402-1407.

(65) Blot WJ, Harrington JM, Toledo A, Hoover R, Heath CW, Fraumeni JF Jr. Lung cancer and World War II shipyard employment. N Engl J Med 1978; 299:620-624.

(66) Siegel JS. Estimates of coverage of the population by sex, race, and age in the 1970 census. Demography 1974; 11:1-23.

Degrees of Malignancy in Human Primary Central Nervous System Tumors: Ornithine Decarboxylase Levels as Better Indicators Than Adenosylmethionine Decarboxylase Levels[1,2,3,4]

Giuseppe Scalabrino,[5] Daniela Modena,[5] Maria Elena Ferioli,[5] Mirella Puerari,[5] *and* Giovanni Luccarelli[6,7]

ABSTRACT—The levels of activity of ornithine decarboxylase (ODC) and adenosylmethionine decarboxylase (AMD) were measured in various types of primary human tumors of the central nervous system (CNS) and whenever possible were related to the malignancy of the tumor graded according to histopathologic criteria. In astrocytomas ODC levels increased linearly and progressively from infratentorial pilocytic astrocytoma (grade I) to glioblastoma multiforme (grade IV) and correlated well with the degree of histologic malignancy of the tumor. AMD activity levels, however, correlated with tumor malignancy only up to grade III astrocytoma. Medulloblastomas exhibited an unusual dichotomy with regard to the levels of polyamine biosynthetic decarboxylases (PBD): Medulloblastomas had the highest ODC activities of all the CNS tumors tested but had low AMD activities. In tumors of neuroepithelial tissue ODC level increases and, when present, AMD level increases were not due to proliferation of new blood vessels, because CNS hemangioblastomas had very low levels of both PBD activities. No significant differences in either of the PBD levels were observed among the several variants of meningiomas tested, the meningotheliomatous, the transitional, and the fibrous meningiomas. However, atypical forms of meningioma, i.e., those with mitotic figures, whatever the histologic variants, had higher levels of ODC, but not of AMD, than the typical forms, i.e., those without mitotic figures.—JNCI 1982; 68:751–754.

There is mounting interest in a variety of biochemical and/or immunologic molecules as potential markers for human CNS tumors. These molecules can be detected in neoplastic cells from which they may leak out into the CSF and be detected there (*1–3*). Polyamines for example are considered despite some limitations as helpful markers in the diagnosis of human brain tumors and in the evaluation of the degree of tumor malignancy and of effectiveness of therapy (*1, 4–6*).

High levels of putrescine and spermidine have been found in the CSF of patients with different kinds of untreated malignant brain tumors, whereas the polyamine contents in the CSF of cancer patients after clinical improvement declined nearly to the levels seen in reference patients with various nonneoplastic neurologic diseases (*7*). Further studies of Marton and co-workers (*8, 9*) emphasized that the elevations of putrescine and spermidine levels in CSF of patients with medulloblastoma correlated well with the progression of this tumor, whereas such a correlation was not always found in CSF of patients with glioblastoma multiforme or with anaplastic astrocytoma (*10*). Marton and co-workers (*11*) proposed a tentative explanation for the difference between the two types of tumor patients, those with medulloblastomas and those with supratentorial malignant gliomas.

The limited data available thus far on the polyamine contents of human brain neoplastic tissues agree in indicating that these tumors are generally characterized by putrescine concentrations higher than those of the normal human brain (*12, 13*). Furthermore, the extent of this putrescine elevation was found to be a reliable indicator of the degree of malignancy of brain neoplasms, according to conventional histopathologic criteria (*13*).

A previous study in our laboratory (*14*) demonstrated that the extent of the increases in the activities of ODC (EC 4.1.1.17) and AMD (EC 4.1.1.50) in the epidermis of human epitheliomas was directly proportional to the neoplasm's growth rate and therefore correlated well with the tumor's malignancy. To establish whether such a correlation exists between increases in these enzyme levels and the degree of growth rate and malignancy of the neoplasm in human organ tumors other than those of the skin, we determined the PBD levels in various types of human primary CNS tumors. Whenever possible, we studied tumors with well-defined grades of growth rate and malignancy according to conventional histopathologic criteria.

MATERIALS AND METHODS

Patients.—None of the cancer patients from whom the neoplastic tissues were obtained had received any antineoplastic therapy before neurosurgery nor did they have any other diseases. The mean ages for each patient group were: infratentorial pilocytic astrocytomas (grade I), 23 years; supratentorial astrocytomas (grade II), 26 years; supratentorial astrocytomas (grade III), 39 years; glioblastomas multiforme (grade IV), 57 years; medulloblastomas, 10 years; transitional meningiomas, 54 years; meningotheliomatous meningiomas, 53 years; fibrous meningiomas, 56 years; and hemangioblastomas, 56 years. Although we also measured

---

Abbreviations used: AMD=adenosylmethionine decarboxylase; CNS=central nervous system; CSF=cerebrospinal fluid; ODC=L-ornithine decarboxylase; PBD=polyamine biosynthetic decarboxylases.

---

[1] Received July 13, 1981; accepted November 27, 1981.

[2] Supported by grant 80.01479.96 of the Finalized Project "Control of Tumor Growth," Consiglio Nazionale delle Richerche (CNR), Rome, Italy.

[3] A preliminary report of this study has been presented at the Seventh International Congress of Neurological Surgery, Munich, July 12–18, 1981.

[4] Research procedures were in accord with the ethical standards of the Helsinki Declaration of 1975.

[5] Institute of General Pathology and CNR Center for Research in Cell Pathology, University of Milan, Via Mangiagalli 31, 20133 Milan, Italy.

[6] Neurological Institute "C. Besta," 20133 Milan, Italy.

[7] We thank Professor G. Morello, Professor F. Pluchino, and Dr. M. Fornari, Neurological Institute "C. Besta," for advice and practical aid in the various phases of this work.

the levels of PBD activities in samples of human brain tissue taken from patient with nonneoplastic neurologic diseases (results not reported here), we do not believe it is correct to consider these values as normal control values. For obvious ethical reasons it is impossible to obtain fresh samples of normal human brain, i.e., tissues that are not autopsy specimens.

Human primary CNS tumors.—The neoplasms employed in this study were localized in different areas of the human CNS and were obtained by neurosurgical procedures from patients under general anesthesia. None of the neoplasms had any macroscopic necrotic areas or ulcerations. The excised neoplastic tissues were immediately cut into two pieces. The first and larger piece was quickly frozen in liquid nitrogen and used immediately for the enzyme assays. The second and smaller piece was fixed in Formalin, embedded in paraffin, and processed for the usual histologic examination to ascertain the type of neoplasm and the degree of its malignancy. The 5-µm sections cut from every specimen were stained routinely with hematoxylin and eosin and with Masson's trichrome stain. Glioma tumor specimens were routinely stained with Mallory's phosphotungstic acid-hematoxylin and with Cajal-Holzer stain. Sections from medulloblastomas were stained by the Bielschowsky method for reticulum impregnation. Histopathologic diagnosis for each neoplastic specimen was made without any information on the results of the enzyme assays. The histopathologic diagnosis and the grading of the neoplasms were made according to the principles of the WHO classification recently summarized by Zülch (*15*). For the astrocytomas and the meningiomas only, we followed an additional criterion of classification proposed by Rubinstein (*16, 17*). Neoplastic tissue samples that showed marked histopathologic heterogeneity, marked edema, or reactive changes were excluded. Metastases to the brain from extraneural neoplasms were deliberately excluded from our research, because they do not reflect the neoplastic transformation of any CNS structure and because they are frequently made up of mixtures of normal cells and neoplastic cells.

Chemicals.—L-[1-^{14}C]ornithine (60 mCi/mmol) and *S*-adenosyl-L-[carboxyl-^{14}C]methionine (60 mCi/mmol) were purchased from the Radiochemical Centre, Amersham, Buckinghamshire, England. All other chemicals were of the highest grade of purity available commercially.

Enzyme assays.—The activity of ODC was assayed as previously described (*14*), with the only difference being that the labeled L-ornithine in each incubation mixture was 0.2 µCi. Putrescine-activated AMD activity was assayed as described by Jänne and Williams-Ashman (*18*). Assays were always done in duplicate. The incubation was done as previously described (*14*). Samples were counted in a Tri-Carb liquid scintillation spectrometer (model 3365; Packard Instrument Co., La Grange, Ill.). Counting efficiency was determined by both internal and external standardizations and was 80±5% by both methods. The amount of $^{14}CO_2$ liberated from tubes containing heat-inactivated enzyme or water was subtracted from all other samples before the correction for protein content. When the lowest activities were measured, the cpm values were as follows: 200 cpm with a blank value of 60 cpm for ODC and 350 cpm with a blank value of 40 cpm for AMD. Protein content was determined by the method of Geiger and Bessman (*19*), with bovine serum albumin as standard. The protein content of each assay tube ranged from 2 to 3 mg in the ODC assay and from 1 to 1.5 mg in the AMD assay.

Differences in enzyme activity levels were analyzed by Student's *t*-test.

RESULTS

Table 1 presents the levels of ODC and AMD activities observed in some types of human brain neuroepithelial tumors. The level of ODC activity in the astrocytoma group progressively and significantly increased from infratentorial pilocytic astrocytoma to supratentorial glioblastoma multiforme through supratentorial astrocytomas of grades II and III. The increase appeared to be directly proportional to the degree of neoplastic dedifferentiation, as indicated by the histopathologic criteria for the malignancy for these types of tumors. Furthermore, if one adopts Rubinstein's suggestion (*16*), dividing the astrocytomas regardless of their localization into 2 groups, the first of which includes the benign and differentiated forms (grades I and II astrocytomas) and the second of which includes the malignant and dedifferentiated forms (grade III astrocytoma and glioblastoma multiforme), one can observe that the value of ODC activity for dedifferentiated astrocytomas was nearly six times that of differentiated astrocytomas. It can also be seen that medulloblastoma, a brain tumor highly malignant in its clinical course, had the highest level of ODC activity among all the human CNS tumors of any histogenetic origin tested by us.

When we consider the activity levels of the other PBD AMD in the same types of brain tumors, we can see that this enzymatic activity progressively and significantly increased from the infratentorial pilocytic grade I astrocytoma to the supratentorial grade III astrocytoma, so that it, as well as ODC, followed quite well the degree of histopathologic malignancy of the tumor. However, it can also be seen that there was no further increase in AMD activity between supratentorial grade III astrocytoma and glioblastoma multiforme. Therefore, the increase in AMD activity from infratentorial pilocytic astrocytoma (grade I) to glioblastoma multiforme (grade IV) was not complete similar to that in ODC activity. The AMD activity level in the dedifferentiated astrocytomas, as compared with that in the differentiated astrocytomas, was about twofold and consequently its increase was of a lesser magnitude than that of the ODC activity (table 1).

The surprising finding is, however, that medulloblastomas showed a clear dichotomy between the levels of the two PBD activities, revealing the highest ODC level and the lowest AMD level in any of the human brain tumors of neuroepithelial tissue we tested (table 1). It seems noteworthy that the AMD activity level of the medulloblastomas (all of which originated in the cerebellum) was very close to that of the infratentorial pilocytic astrocytomas (all of which were also localized in the cerebellum), despite the great difference between the degrees of malignancy of these two types of tumors.

TABLE 1.—*Activities of ODC and AMD in different primary human neuroepithelial tumors*

Code	Tumor type	Tumor grade	No. of patients	Enzyme activities, pmol $^{14}CO_2$/mg protein/30 min[a]	
				ODC	AMD
A	Infratentorial pilocytic astrocytoma	I	10	1.4±0.21	24.4±4.69
B	Supratentorial astrocytoma	II	5	5.9±0.49	38.3±6.56
C	Supratentorial astrocytoma	III	5	10.7±1.77	58.1±7.67
D	Supratentorial glioblastoma multiforme	IV	20	19.5±2.79	56.3±7.62
A+B	Differentiated astrocytomas	I-II	15	2.8±0.60	30.5±4.70
C+D	Dedifferentiated astrocytomas	III-IV	25	17.8±2.43	56.6±6.27
E	Medulloblastoma		6	54.5±8.84	21.6±4.17

Statistical comparison[b]

Code	ODC P-value	AMD P-valu
A vs. B	<0.001	<0.05
A vs. C	<0.001	<0.01
A vs. D	<0.001	<0.01
A vs. E	<0.001	NS
B vs. C	<0.05	<0.05
B vs. D	<0.05	<0.05
C vs. D	<0.05	NS
D vs. E	<0.01	<0.05
A+B vs. C+D	<0.001	<0.01

[a] Results are means ± SE.

[b] Evaluated by Student's *t*-test. NS=not significant.

Inasmuch as the vascular component usually represents a very large part of the tumor bulk in human CNS tumors, particularly in astrocytomas and medulloblastomas (*20, 21*), we measured the levels of PBD activities in hemangioblastomas, human brain tumors of vascular origin. We wished to ascertain whether the enhancements in PBD activities that we saw in astrocytomas and medulloblastomas might be at least in part related to increased formation of new blood vessels in the neoplastic tissues. This we found was not to be the case, and the data in table 2 show that hemangioblastomas of the human CNS had very low levels of PBD activities.

TABLE 2.—*Activities of ODC and AMD in various human brain blood vessel and meningeal tissue tumors*

Code	Tumor type	No. of patients	Enzyme activities, pmol $^{14}CO_2$/mg protein/30 min[a]	
			ODC	AMD
A	Hemangioblastoma	4	0.8±0.12	3.3±0.87
B	Meningeal tumors:			
	Fibrous meningioma	6	6.0±1.33	60.4±8.52
	Meningotheliomatous meningioma	16	8.7±1.45	56.1±7.60
	Transitional meningioma	8	5.6±1.19	45.8±6.16
C	Typical meningiomas	20	6.2±1.05	51.8±5.22
D	Atypical meningiomas	10	11.6±1.68	61.7±6.81

Statistical comparison[b]

Code	ODC P-value[c]	AMD P-value[c]
C vs. D	<0.05	NS

[a] Results are means ± SE.

[b] Evaluated by Student's *t*-test. NS=not significant.

[c] No other statistically significant differences were found within the meningioma group.

Table 2 shows that the levels of ODC and AMD activities were not significantly different in the three types of human meningiomas, the transitional, the meningotheliomatous, and the fibrous meningioma. Nevertheless, if we accept the suggestion of Rubinstein (*17*) to divide the meningiomas into atypical and typical forms on the basis of the presence or absence of mitotic figures regardless of histologic variants, we observe that ODC levels in the atypical forms were nearly double those of the typical forms, without significant corresponding differences between the AMD levels.

DISCUSSION

The present study stresses that in different types of human brain neoplasms the extent of ODC enhancement and in some types also the extent of AMD enhancement are correlated with the growth rate and the degree of dedifferentiation of the tumor as determined by histopathologic criteria. The progressive increase in ODC activity is particularly striking in the different grades of astrocytomas and in glioblastoma multiforme, whereas the progressive increase in AMD activity is clearly demonstrated only from astrocytoma grades I to III. It is well known that the neoplastic growth rate is much slower in low-grade, well-differentiated astrocytomas than in the high-grade, malignant gliomas, including glioblastoma multiforme (*22*). Within the astrocytoma group, the size of the ODC increase is also directly proportional to the number of cells engaged in DNA synthesis, which has been demonstrated to be greater in high-grade astrocytomas and in glioblastoma multiforme than in low-grade astrocytomas (*23*). Like the activity of ODC, the activities of other enzymes, such as hexokinase, glucose-6-phosphate dehydrogenase, and phosphogluconate dehydrogenase, have been demonstrated to increase linearly in proportion to the degree of neoplastic dedifferentiation in astrocytomas of grades I to IV, which includes glioblastoma multiforme (*24*).

Our measurements of the levels of ODC activity in astrocytomas and in glioblastoma multiforme indirectly agree with and complement the results provided by Harik and Sutton (*13*), who reported that putrescine content is higher in high-grade astrocytomas than in low-grade astrocytomas. It is well known that only ODC makes putrescine in eukaryotic cells (*25*). Our results showing that infratentorial astrocytomas have much lower ODC levels than supratentorial astrocytomas are once again in agreement with those of Harik and Sutton (*13*), who demonstrated that infratentorial astrocytomas have lower putrescine levels than the supratentorial ones.

Furthermore, our results supplement those of Harik and Sutton (*13*), since we determined the levels of PBD activities in medulloblastomas, which was not included in their study. Medulloblastomas show a very peculiar dichotomy between these two enzyme levels, with striking ODC enhancement not accompanied by a similar change in AMD activity. At present, it is exceedingly difficult to account for this phenomenon. This finding seems to us to be of great interest and quite new in human oncology, since to the best of our knowledge it is the first report of a human tumor with a very high ODC level in combination with a low AMD level. A similar dichotomy has already been reported for rat hepatomas with different growth rates (*26*) and for mouse skin tumors (*27*).

Again, our results also extend those of Harik and Sutton (*13*) for meningiomas, since we have differentiated some histologic types of these tumors, albeit without observing any significant difference in the levels of either ODC or AMD activities among the morphologic variants. However, the incidence of mitotic figures in tumors of meningeal tissues has been claimed by Crompton and Gautier-Smith (*28*) to be an important criterion in the assessment of the likelihood of recurrence and a rough indicator for rapid growth. Similarly, we can state that in meningiomas the ODC but not the AMD level increase is related to the neoplastic growth rate, since we demonstrated that the atypical forms have higher levels only of ODC than the typical forms.

Although it is always difficult to draw conclusions in oncology from merely quantitative studies, the results of the present study, together with those of a previous study (*14*) on the levels of PBD activities in different human tumors of the brain and the skin, indicate that assays of these enzyme levels in tissue specimens obtained after the surgical removal of the neoplasms may frequently be a useful tool for the evaluation of the grade of growth rate and malignancy of human neoplasms.

REFERENCES

(*1*) Seidenfeld J, Marton LJ. Biochemical markers of central nervous system tumors measured in cerebrospinal fluid and their potential use in diagnosis and patient management: A review. JNCI 1979; 63:919–931.

(*2*) de Tribolet N, Carrel S. Human glioma tumour-associated antigens. Cancer Immunol Immunother 1980; 9:207–211.

(*3*) Wikstrand CJ, Bigner DD. Immunobiologic aspects of the brain and human gliomas. Am J Pathol 1980; 98:515–567.

(*4*) Marton LJ. Polyamines and brain tumors. Natl Cancer Inst Monogr 1977; 46:127–131.

(*5*) ———. Polyamines and brain tumors: Relationship to patient monitoring and therapy. Adv Polyamine Res 1981; 3:425–430.

(*6*) ———. CSF polyamines. Potential as brain tumor markers. Arch Neurol 1981; 38:73–74.

(*7*) Marton LJ, Heby O, Levin VA, Lubich WP, Crafts DC, Wilson CB. The relationship of polyamines in cerebrospinal fluid to the presence of central nervous system tumors. Cancer Res 1976; 36:973–977.

(*8*) Marton LJ, Edwards MS, Levin VA, Lubich WP, Wilson CB. Predictive value of cerebrospinal fluid polyamines in medulloblastoma. Cancer Res 1979; 39:993–997.

(*9*) ———. CSF polyamines: A new and important means of monitoring patients with medulloblastoma. Cancer 1981; 47:757–760.

(*10*) Fulton DS, Levin VA, Lubich WP, Wilson CB, Marton LJ. Cerebrospinal fluid polyamines in patients with glioblastoma multiforme and anaplastic astrocytoma. Cancer Res 1980; 40:3293–3296.

(*11*) Pierangeli E, Levin VA, Seidenfeld J, Marton LJ. Putrescine diffusion in cat brain and capillary permeability in rat brain: Relation to CSF putrescine levels in brain tumor patients. Eur J Cancer 1981; 17:143–147.

(*12*) Kremzner LT, Barrett RE, Terrano MJ. Polyamine metabolism in the central and peripheral nervous system. Ann NY Acad Sci 1970; 171:735–748.

(*13*) Harik SI, Sutton CH. Putrescine as a biochemical marker of malignant brain tumors. Cancer Res 1979; 39:5010–5015.

(*14*) Scalabrino G, Pigatto P, Ferioli ME, Modena D, Puerari M, Carù A. Levels of activity of the polyamine biosynthetic decarboxylases as indicators of degree of malignancy of human cutaneous epitheliomas. J Invest Dermatol 1980; 74:122–124.

(*15*) Zülch KJ. Principles of the new World Health Organization (WHO) classification of brain tumors. Neuroradiology 1980; 19:59–66.

(*16*) Rubinstein LJ. Tumors of the central nervous system. In: Atlas of tumor pathology, 2d series, fascicle 6. Washington, D.C.: Armed Forces Institute of Pathology, 1972:19–85.

(*17*) ———. Tumors of the central nervous system. In: Atlas of tumor pathology, 2d series, fascicle 6. Washington, D.C.: Armed Forces Institute of Pathology, 1972:169–190.

(*18*) Jänne J, Williams-Ashman HG. Dissociation of putrescine-activated decarboxylation of s-adenosyl-L-methionine from the enzymic synthesis of spermidine and spermine by purified prostatic enzyme preparations. Biochem Biophys Res Commun 1971; 42:222–229.

(*19*) Geiger PJ, Bessman SP. Protein determination by Lowry's method in the presence of sulfhydryl reagents. Anal Biochem 1972; 49:467–473.

(*20*) Waggener JD, Beggs JL. Vasculature of neural neoplasms. Adv Neurol 1976; 15:27–49.

(*21*) Leestma JE. Brain tumors. Am J Pathol 1980; 100:242–316.

(*22*) Steel GG. Growth kinetics of brain tumours. In: Thomas DG, Graham DI, eds. Brain tumours. London: Butterworth, 1980:10–20.

(*23*) Hoshino T, Nomura K, Wilson CB, Knebel KD, Gray JW. The distribution of nuclear DNA from human brain-tumor cells. J Neurosurg 1978; 49:13–21.

(*24*) Timperley WR. Glycolysis in neuroectodermal tumours. In: Thomas DG, Graham DI, eds. Brain tumours. London: Butterworth, 1980:145–167.

(*25*) Morris DR. Section introduction: Biosynthesis of polyamines. Adv Polyamine Res 1978; 1:13–15.

(*26*) Williams-Ashman HG, Coppoc GL, Weber G. Imbalance in ornithine metabolism in hepatomas of different growth rates as expressed in formation of putrescine, spermidine, and spermine. Cancer Res 1972; 32:1924–1932.

(*27*) O'Brien TC, Simsiman RC, Boutwell RK. Induction of the polyamine-biosynthetic enzymes in mouse epidermis and their specificity for tumor promotion. Cancer Res 1975; 35:2426–2433.

(*28*) Crompton MR, Gautier-Smith PC. The prediction of recurrence in meningiomas. J Neurol Neurosurg Psychiat 1970; 33:80–87.

An Increased Risk for Lung Cancer Mortality Associated With Sugarcane Farming[1,2,3]

Henry Rothschild[4] *and* **James J. Mulvey**[4,5]

ABSTRACT—In a study to determine putative occupation-related factors responsible for the excessive mortality due to lung cancer in southern Louisiana, the next-of-kin were interviewed of 284 of 400 persons (71%) randomly sampled from a total of 815 persons who died of lung cancer during 1971 through 1977 and had lived in any of 10 parishes (counties) of southern Louisiana. Of the decedents, 108 (38%) had been employed for at least 6 months as sugarcane farm workers at some time during their lives. Logistic regression analysis indicated this industrial involvement differed significantly ($P<0.0001$) from that of a control group, consisting of persons who had died of any cause other than lung cancer and who were matched for year of death, age, sex, race, and parish of residence; only 58 (20%) matched controls had had sugarcane farm employment (odds ratio=2.4; 95% confidence interval, 2.0–2.9). Employment in other industries or tobacco consumption could not account for the elevated risk of lung cancer mortality associated with sugarcane farming. After adjustment for smoking, the relative risk estimate of lung cancer mortality for sugarcane farm workers was 2.4 (95% confidence limits, 1.7–3.6). The sugarcane farmers who died with lung cancer had worked for longer periods in the sugarcane farm industry than did those sugarcane farmers in whom lung cancer did not develop ($P=0.006$). No specific histopathologic cell type was noted to be increased in persons who had been employed in sugarcane farming; however, 2 sugarcane farmers had had mesotheliomas.—JNCI 1982; 68:755–760.

As has long been recognized, persons in certain occupations have an increased risk for lung cancer compared with the risk of the general population (*1–9*). One of the many industries suggested to be associated with increased risk for lung cancer, for example, is shipbuilding (*8, 9*), which has been a predominant industry in Louisiana for several decades (*10*). In the course of a study on the familial aggregation of lung cancer, we noted that an unusually large number of persons who died with lung cancer had been sugarcane farmers (*11*). Coincidently, the parishes involved in sugarcane production were located in southern Louisiana, an area with excessive mortality due to lung cancer (*12*). To further investigate the validity of this observation, we conducted a matched-pair case-control study of lung cancer mortality in 10 parishes of southern Louisiana.

MATERIALS AND METHODS

A computerized listing of deaths in the 10 rural, southern Louisiana parishes (East Feliciana, Iberia, Lafourche, Pointe Coupee, St. Bernard, St. Helena, St. James, St. John, St. Martin, and West Feliciana) used in our previous studies (*12, 13*) was provided by the Office of Public Health Statistics, Louisiana Health and Human Resources Administration. Four parishes (Lafourche, Iberia, St. Bernard, and St. Martin) ranked in the highest 3% for all counties of the United States for lung cancer mortality among white men during 1950–69 (*14*).

To augment the limited data on the death certificates, we randomly selected 400 of the 815 persons who died in the 10 target parishes during 1971 through 1977 and had lung cancer listed as the cause of death (ICD codes 162 through 163) (*15*). The cause of death was verified for this sample by medical or pathologic records. A computer program matched each of these decedents for sex, race, age at death within 10 years, year of death, and parish of usual residence with a person who died of any cause other than lung cancer. In the case of multiple matches, the control whose age was closest to the case's age was selected. The controls included 13 persons whose deaths were attributed to other neoplasms.

We were able to interview the nearest living relative of 284 matched case and control pairs; 78% were spouses and 22% were first-degree relatives. The interviews were done by persons trained in interviewing techniques and with the knowledge of each person's case or control status. By means of a structured questionnaire, detailed employment histories, including specific information about the duties performed and materials handled for all jobs held 6 months or longer, were obtained. These jobs were classified according to the SICM (*16*). Closed-format questions inquiring whether the decedent had ever been employed in the sugarcane and/or shipbuilding industries were included. The occupational section of each questionnaire was concluded by a review with each respondent of a checklist of industries of "usual" employment. The smoking information obtained for each decedent included: whether a nonsmoker, smoker, or ex-smoker; cigarette, cigar, or pipe smoker; the average amount smoked per day; the total number of years smoked; and the years smoking started and/or stopped.

Estimates of the RR (odds ratios) of employment on lung cancer were calculated for each of 15 industrial categories and for various parameters: age of death (≤63, >63 yr), race (white, black), sex (male, female), and smoking status (ever smoker, never smoker) (*17*). Using logistic regression, we tested for interactions of the RR for employment in sugarcane farm or shipbuilding industries with the various parameters (*18*). The covariates and risk indicators were regressed

---

Abbreviations used: ICD=International Classification of Diseases; RR=relative risk(s): SICM=Standard Industrial Classification Manual.

---

[1] Received July 28, 1981; accepted December 29, 1981.

[2] Supported in part as a special project of the Council for Tobacco Research-USA, Inc.

[3] Research procedures were in accord with the ethical standards of the Institutional Review Board, Louisiana State University Medical Center.

[4] Department of Medicine, Louisiana State University Medical Center, New Orleans, La. 70112.

[5] We thank Dr. Frances Mather, Dr. A. Wouter Voors, Mr. Wee Lock Ooi, Mr. Thomas Ballinger, Ms. Sherolyn Weed, Ms. Virginia Howard, and Ms. Kathleen Corcoran for their collaboration.

upon the outcome variable (disease status) with the use of both a retrospective and prospective representation of these data (*19*). Dummy variables were used in the completed program to calculate the logistic coefficients.

Sequential deletions of terms were made to obtain a final well-fitting model. The decision to delete parameters was based on the *t*-tests for significance of each parameter estimate, on the changes in the value of the log likelihood, and on the goodness of fit of the models compared with the observed stratified odds ratios. The log linear model was used to test for specific three-way interactions (*20*). When effect modification was absent, summary RR point and interval estimates were calculated by the Mantel-Haenszel method (*21*).

Methods for histopathologic slide ascertainment and classification have been described previously (*13*). All available original histopathologic slides of the cases were reviewed separately by two pathologists who later conferred without knowledge of prior diagnosis to decide on the final histopathologic classification. Multiple sections of tissue were usually available. The World Health Organization classification of lung cancer (*22*) was used to categorize the tumors, with one modification; i.e., the group of small cell anaplastic carcinomas was not further divided into subcategories.

RESULTS

Table 1 shows the estimated RR for the usual industrial classifications and selected subdivisions for the 284 persons who had died of lung cancer and their controls. Shipbuilding, the usual industry of 13 cases and 9 controls, was the industry of employment for 6 months or more of 48 cases and 40 controls (odd ratio=1.2). Using the logistic method revealed an interaction term between shipbuilding as the usual industry of employment and sex, males having an odds ratio of 1.7 and females having one of 0.3. However, the small sample size for this group precluded any further analysis.

TABLE 1.—*Estimated RR for the usual industry of employment*[a]

Industry (SICM classification)	Cases	Controls	Odds ratio (95% confidence interval)[b]
Agriculture (0100–0132, 0134–0783)	25	24	1.1 (0.6, 1.9)
Sugarcane farming (0133)	45	24	2.3 (1.8, 3.0)[c]
Forestry (0800–0851)	1	2	0.5 (0.1, 5.3)
Fishing (0900–0971)	6	7	0.9 (0.3, 2.6)
Mining (1000–1499)	18	13	1.4 (0.7, 2.9)
Construction (1500–1799)	24	24	1.0 (0.7, 1.4)[d]
Nondurable goods (2000–2399, and 3000–3299)	20	16	1.3 (0.6, 2.5)
Lumber (2400–2799)	5	8	0.6 (0.2, 1.9)
Petrochemical (2800–2999)	7	11	0.6 (0.2, 1.6)
Metal (3300–3728, and 3740–3999)	7	11	0.6 (0.2, 1.6)
Shipbuilding (3730–3732)	13	9	1.5 (0.6, 3.5)
Transportation (4000–4971)	27	42	0.6 (0.4, 1.0)
Wholesale–retail (5000–5999)	25	30	0.8 (0.5, 1.4)
Personal services (6000–6799, 8000–8091, 9100–9721)	44	46	1.0 (0.6, 1.5)
Professional–government (7000–7999, 8100–8999)	17	17	1.0 (0.7, 1.4)[d]
Total	284	284	

[a] Industry in which the decedent had worked for the longest period of time.
[b] Test-based 95% confidence interval except where noted (*23*).
[c] $P<0.001$.
[d] Taylor series 95% confidence interval (*24*).

TABLE 2.—*Comparison of percentage distribution of usual industry of employment between those ever and never employed in sugarcane farming*[a]

Usual industry of employment (SICM classification)	Ever employed in sugarcane-farming industry[b]	
	Yes, %	No, %
Agriculture, general farm[c] (0100–0783)	17.5	5.0
Sugarcane farming (0133)	41.6	0
Forestry (0800–0851)	0	0.8
Fishing (0900–0971)	1.2	2.7
Mining (1000–1499)	3.0	6.5
Construction (1500–1799)	6.0	9.5
Nondurable goods (2000–2399, 3000–3299)	5.4	6.5
Lumber (2400–2799)	1.2	2.7
Petrochemical (2800–2999)	0	4.5
Metal (3300–3728, and 3740–3999)	1.8	3.7
Shipbuilding (3730–3732)	3.0	4.2
Transportation (4000–4971)	3.6	15.7
Wholesale–retail (5000–5999)	3.0	12.4
Personal services (6000–6799, 8000–8091, 9100–9721)	11.5	17.7
Professional–government (7000–7999, 8100–8999)	1.2	8.0

[a] For ≥6 mo.
[b] Includes both cases and controls.
[c] Farmers who grew a variety of crops including sugarcane were included in this category.

Sugarcane farming was the usual industry of 45 (16%) cases and 24 (8%) controls (odds ratio=2.3; 95% confidence interval, 1.8–3.0). Furthermore, 108 (38%) lung cancer cases and 58 controls (20%) (odds ratio=2.4; 95% confidence interval, 2.0–2.9) had "ever" (≥6 mo) been employed in this industry; many persons had worked for several months during the harvest and planting seasons each year.

Because the major findings of this study pertained to sugarcane farm employment, subsequent analysis focused on estimation of the RR of lung cancer mortality for cases having ever had a sugarcane farm occupation. Logistic analysis indicated that employment in shipbuilding for 6 months or more was not confounding the observed association between sugarcane farming and increased lung cancer mortality. Four cases and 1 control had shipbuilding as their usual occupation and sugarcane farming as a secondary occupation (table 2). Most (59%) who worked as sugarcane farmers for 6 months or more were categorized as having "farming" as their usual employment. Using the logistic method, we found that employment in other industries did not confound the association between increased lung cancer mortality and sugarcane farming.

Although based on relatively small numbers, the increased risk for lung cancer mortality of sugarcane farmers could not be accounted for by cigarette smoking (table 3). No significant heterogeneity was found between the odds ratios of smokers and nonsmokers with the use of a log linear model to detect a three-way interaction term (likelihood

TABLE 3.—*RR for ever employed in sugarcane farming according to smoking category*

Smoking category (No.)	Case or control	Employment in sugarcane farming[a]			Odds ratio (95% confidence interval)[b]
		Yes	No	Total	
Nonsmoker (75)	Cases	3	10	13	0.9 (0.2, 3.9)
	Controls	15	47	62	
	Total	18	57		
Smoker[c] (493)	Cases	105	166	271	2.6 (1.8, 4.0)
	Controls	43	179	222	
	Total	148	345		

[a] For ≥6 mo.
[b] Test-based 95% confidence interval (*23*).
[c] Includes cigarette, cigar, and pipe smokers.

ratio chi square, 1.85; *P*=0.17). Decedents for whom cigarette pack-year data were available were classified as "moderate" smokers (≤40 pack-yr) and "heavy" smokers (>40 pack-yr). No significant heterogeneity in the RR for lung cancer was found for moderate smoking sugarcane farmers (odds ratio=1.7) and heavy smoking sugarcane farmers (odds ratio=2.7). The summary RR for sugarcane farmers adjusted for smoking was 2.4 (95% confidence interval, 1.7–3.6). Matching in the analysis was not retained because of the dearth of nonsmoking discordant pairs for persons employed in sugarcane farming.

The odds ratios for sugarcane farmers were increased irrespective of race, sex, or age (table 4). Smoking was not a confounding variable because the smoking-adjusted odds ratios for these indicators did not differ significantly from the crude odds ratios. Calculation of a summary RR estimate was indicated by the lack of heterogeneity between the odds ratios of the categorical variables. When smoking, age, race, sex, and usual industry were simultaneously taken into account in the logistic model, the adjusted summary RR estimate for lung cancer mortality was 2.8.

TABLE 4.—*Estimated RR for sugarcane farming according to race, sex, and age category adjusted for smoking*

Variable (No.)	Case or control	Employment in sugarcane farming[a]		Odds ratio (95% confidence interval)[b]	Smoking-adjusted odds ratio (95% confidence interval)[c]
		Yes	No		
Race					
White (480)	Case	78	162	2.6 (1.7, 3.9)	2.8 (1.7, 4.4)
	Control	38	202		
Nonwhite (88)	Case	30	14	2.6 (1.1, 6.1)	2.3 (0.9, 5.7)
	Control	20	24		
Sex					
Male (488)	Case	95	149	2.3 (1.6, 3.4)	2.5 (1.6, 3.7)
	Control	53	191		
Female (80)	Case	13	27	3.4 (1.1, 10.3)	2.7 (0.8, 8.9)
	Control	5	35		
Age, yr					
≤63 (270)	Case	47	86	2.0 (1.2, 3.5)	1.9 (1.1, 3.4)
	Control	29	108		
>63 (298)	Case	61	90	2.8 (1.7, 4.6)	3.1 (1.8, 5.4)
	Control	29	118		

[a] For ≥6 mo.
[b] Test-based 95% confidence interval (*23*).
[c] *See* (*21*).

TABLE 5.—*Logistic regression fit for lung cancer mortality data*

Covariate	Logistic coefficient[a]	Standard error	Coefficient:standard error	*P*-value
Smoking	1.005	0.170	5.907	0.00001
Sugarcane	0.458	0.101	4.554	0.00001
Shipbuilding-sex	0.357	0.130	2.746	0.007

[a] The odds ratio = exp (2×logistic coefficient).

The persons who died of lung cancer were employed longer in the sugarcane industry (28.4 yr) than the controls who had worked in that industry (20.7 yr). A two-tailed *t*-test to compare cases and controls for differences in length of employment showed that the 95% confidence interval for this difference in mean number of years of sugarcane farm employment was 2.1–13.2 years.

The results of a retrospective approach of regression on sugarcane employment as the outcome variable were consistent with those of the prospective approach to modeling. The final well-fitting logistic regression model of the prospective representation of these data suggested that the odds in favor of lung cancer mortality were influenced by smoking, sugarcane farming, and a shipbuilding–sex interaction (table 5). The goodness-of-fit chi-square *P*-value for this model was 0.77.

A review of specific histologic types of lung cancers revealed no predominant cell type associated with sugarcane farm employment. Of the 284 decedents with lung cancer, pathologic material was obtained for 205 cases (72%) (table 6). Squamous cell carcinoma and small cell anaplastic carcinoma were the most common tumor types, closely followed in frequency by adenocarcinoma. Analysis of these data indicated that the distribution of histopathologic types was not significantly different for persons employed in sugarcane farming compared with those never employed in this industry.

TABLE 6.—*Histologic types of lung cancers in 205 cases*

Tumor type	Sugarcane farm employment,[a] No. (%)	No sugarcane farm employment, No. (%)
Squamous cell	26 (32.5)	39 (31.2)
Small cell anaplastic	17 (21.3)	26 (20.8)
Adenocarcinoma	15 (18.8)	23 (18.4)
Bronchiolo-alveolar	1 (1.3)	1 (0.8)
Large cell	8 (10.0)	24 (19.2)
Combined, squamous cell and adenocarcinoma	1 (1.3)	1 (0.8)
Cancer, not otherwise specified	10 (12.5)	9 (7.2)
Mesothelioma	2 (2.5)	0 (0.0)
Small cell anaplastic and squamous cell	0 (0)	1 (0.8)
Small cell and large cell anaplastic	0 (0)	1 (0.8)
Total	80 (100.2)	125 (100)

[a] For ≥6 mo.

DISCUSSION

The relationship between sugarcane farming and lung cancer was not anticipated and is being reported because a positive association was observed. This is an instance for which the causal hypothesis was generated by the data rather than the investigator. Therefore, this positive association requires cautious interpretation until the work has been reproduced in another investigation.

No association between sugarcane farm industry employment and lung cancer mortality has been reported previously. Several reasons may contribute to the discrepancy between our findings and previous studies in Louisiana, which used death certificate listings only to obtain the usual occupation of decedents (*9, 25*). On many of the death certificate listings, a sugarcane farmer was reported as "farmer," with no indication of the type of crop he was engaged in producing. Also, women living on farms were often reported as "housewives" on the death certificates, but the interviews revealed that many of these women had

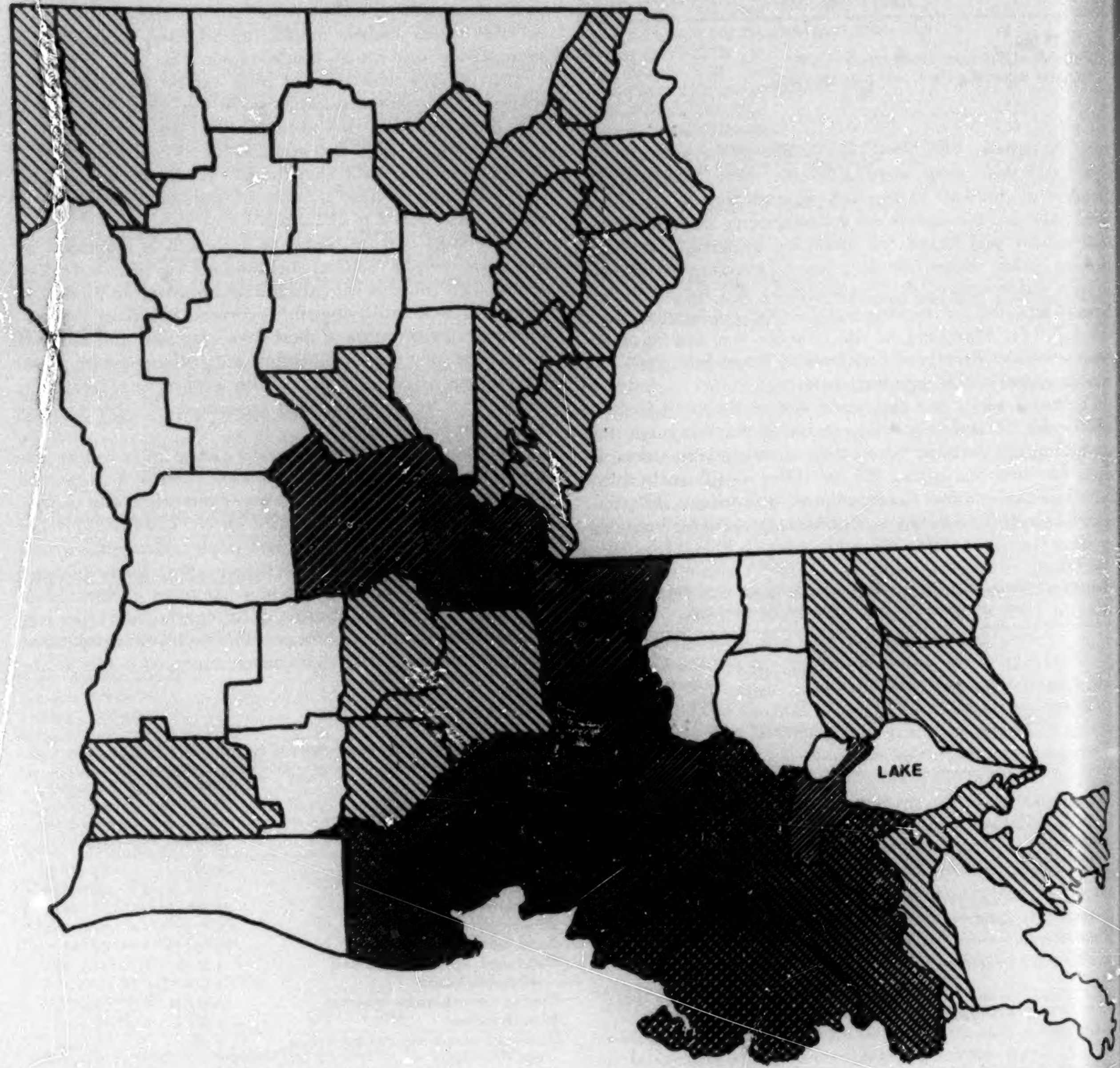

TEXT-FIGURE 1.—A map of the parishes (counties) of Louisiana showing those where sugarcane is produced and those in the top quarter for age-adjusted mortality due to lung cancer for white men (1967–76) (*12*). ▩, Parishes in the top quarter of lung cancer mortality. ▨, Parishes growing sugarcane for sugar production.

worked in the fields planting and harvesting sugarcane.

We were unable to estimate the percentage of the work force of the target parishes or of Louisiana involved in sugarcane farming because accurate employment figures were not available for the years prior to 1970. Thus we are unable to calculate the incidence of lung cancer for persons working in this industry.

Many of the parishes in Louisiana that grow sugarcane have high mortality due to lung cancer (*12*) (text-fig. 1). In the continental United States, sugarcane production is a major industry in only two other states: Florida and Texas. Two of the three sugarcane-growing counties of Florida (Indian River and Palm Beach) but none of three counties in Texas have a high mortality due to lung cancer (*14*). In Texas, however, sugarcane farming was started only after 1970 (Jones JP: Personal communication). Thus sufficient time may not have elapsed for the disease to be manifested.

Several hypotheses may explain the association between increased lung cancer mortality and sugarcane farming. It may be related to the manner in which the sugarcane is harvested. When mechanized sugarcane harvesting equipment was introduced during the 1930's and 1940's, burning of the cane to remove excess leafage became common practice. Harvesting the cane is done in three steps: 1) The cane plant is cut down; 2) a short time later the cane rows are fired and the excess leafage is burned away, leaving the cane stalk; and 3) the stalks are transported to the sugarmills for processing into raw sugar. The burning of the cane rows greatly increases airborne suspended particles that may act as an irritant to the respiratory tract tissue. This irritation could promote increased susceptibility to other carcinogens. The burning process may also convert chemicals used in the production of sugarcane to substances with carcinogenic potential. Comparison of the lung cancer mortality for countries involved in sugarcane production or those that do or do not practice burning is difficult at this time because of the unreliable county-specific mortality statistics for many of these countries.

The association could be a noncausal relationship reflecting an association of both employment and mortality with some as yet unidentified factor. Many of the workers in sugarcane farm occupations are of low socioeconomic level, which may implicate such factors as nutrition, sanitation, housing, and access to health care (*26*). Perhaps not coincidently some of the herbicides, plant-growth regulators, and insecticides used in the Louisiana sugarcane industry contained arsenic or chlorinated hydrocarbons, chemicals that have been identified with increased risk of cancer in humans (*27*).

Although most of the persons in our study employed in sugarcane farm occupations were growers and field laborers, 34 of the field laborers had at some time worked as bagasse handlers (21 cases and 13 controls). Bagasse is the sugarcane plant residue left after the juice has been extracted. Bagassosis, a relatively benign occupational respiratory disease, has been described in persons exposed to moldy bagasse (*28*) and has been associated with inhalation of spores of *Thermoactinomyces vulgaris* (*29*). This exposure might suggest an association with a microbial contamination of the products of the sugarcane industry.

Although no consistent histopathologic tumor type was associated with sugarcane farm employment, in our study population we found 2 sugarcane farmers who had no discernible exposure to asbestos but had mesotheliomas. Mesothelioma, a rare tumor associated with asbestos exposure, was reported in 5 patients in India who were occupationally exposed to sugarcane rather than to asbestos (*30*).

Both the use of next-of-kin interviews with nonblinded interviewers to obtain information concerning diseased persons and the retrospective design of this study impose restrictions on the investigator's ability to make definitive statements regarding disease–smoking–occupation interactions. Therefore, the results of this study should be considered with respect to its design and the inherent biases. Although epidemiology is not a precise method, when applied properly, it can be a valuable tool to provide direction in our search for potential health hazards.

REFERENCES

(*1*) Seaton A. Occupational pulmonary neoplasms. In: Morgan WK, Seaton A, eds. Occupational lung disease. Philadelphia: Saunders, 1977:357–384.

(*2*) Wagoner JK, Archer VE, Carroll BE, Holaday DA, Lawrence PA. Cancer mortality patterns among U.S. uranium miners and millers, 1950 through 1962. J Natl Cancer Inst 1964; 32:787–801.

(*3*) Selikoff IJ, Hammond C, Churg J. Asbestos exposure, smoking, and neoplasia. JAMA 1968; 204:106–112.

(*4*) Koskela R-S, Hernberg S, Karva R, Jarvinen E, Nurinen M. A mortality study of foundry workers. Scand J Work Environ Health 1976; 2 (suppl 1):78–89.

(*5*) Monson RR, Nakano KK. Mortality among rubber workers. I. White male union employees in Akron, Ohio. Am J Epidemiol 1976; 103:284–296.

(*6*) Gibson ES, Martin RH, Lockington JN. Lung cancer mortality in a steel foundry. J Occup Med 1977; 19:807–812.

(*7*) Selikoff IJ, Hammond EC. Asbestos-associated disease in United States shipyards. CA 1978; 28.87–99.

(*8*) Blot WJ, Harrington JM, Toledo A, Hoover R, Heath CW, Fraumeni JF Jr. Lung cancer after employment in shipyards during World War II. N Engl J Med 1978; 299:620–624.

(*9*) Gottlieb MS, Stedman RB. Lung cancer in shipbuilding and related industries in Louisiana. South Med J 1979; 2:1099–1101.

(*10*) U.S. Department of Commerce, Social and Economics Statistics Administration. County business patterns, Louisiana, 1973. Bureau of Census publication CBP-73-20.

(*11*) Ooi WL, Mulvey JJ, Chen VW, Wilson AF, Corcoran KA, Rothschild H. Familial aggregation of lung cancer. Clin Res 1981; 29:315A.

(*12*) Rothschild H, Voors AW, Weed SG, Vial LJ, Welsh RA, Johnson WD. Trends in respiratory system cancer mortality in Louisiana: Geographic distribution in 1950–1969 and 1967–1976 compared. Am J Pub Health 1979: 69:380–381.

(*13*) Rothschild H, Buechner H, Welsh R, Vial LJ, Weinberg R. Histological typing of lung cancer in Louisiana. Cancer. In press.

(*14*) Mason TJ, McKay FW. U.S. cancer mortality by county; 1950–1969. Washington, D.C.: U.S. Govt Print Off, 1974 [DHEW publication No. (NIH)74-615].

(*15*) National Center for Health Statistics. International Classification of Diseases. Eighth revision. Washington, D.C.: U.S. Govt Print Off, 1967 (PHS publication No. 1693).

(*16*) Executive Office of the President, Office of Management and Budget. Standard industrial classification manual. Washington, D.C.: U.S. Govt Print Off, 1972.

(*17*) Fleiss JL. Statistical methods for rates and proportions. New York: Wiley, 1973:53–66, 109–129.

(*18*) Prentice R. Use of the logistic model in retrospective studies. Biometrics 1976; 32:599–606.

(*19*) Breslow N, Powers W. Are there two logistic models of restrospective studies? Biometrics 1978; 34:100–105.

(20) Bishop YM. Discrete multivariate analysis. Cambridge, Mass.: MIT Press, 1975:551.

(21) Mantel N, Haenszel W. Statistical aspects of the analysis of data from retrospective studies of disease. J Natl Cancer Inst 1959; 22:719–748.

(22) Kreyberg L, Liebow AA, Uehlinger EA. Histological typing of lung tumors in histological classification of tumors #1. Geneva: WHO, 1967.

(23) Miettinen OS. Sample interval estimation of risk ratio. Am J Epidemiol 1974; 100:515–516.

(24) Woolfe B. On estimating the relation between blood group and disease. Ann Hum Genet 1954; 19:251–253.

(25) Gottlieb MS, Pickle LW, Blot WJ, Fraumeni JF Jr. Lung cancer in Louisiana: Death certificate analysis. JNCI 1979; 63:1131–1137.

(26) Brown SM, Selvin S, Winkelstein W. The association of econom status with the occurrence of lung cancer. Cancer 1975; 36:1903-1911.

(27) Tomatis L, Agthe C, Bartsch H, et al. Evaluation of the carcinogenicity of chemicals: A review of the International Agency f Research on Cancer Monograph Program (1971 to 1977). Cancer Res 1978; 38:877–885.

(28) Hearn CE. Bagassosis: An epidemiological, environmental, and clinical survey. Br J Industr Med 1968; 25:267–282.

(29) Seabury J, Salvaggio J, Buechner H, Kundar VG. Bagassosis. III. Isolation of thermophilic and mesophilic actinomycetes and fung from moldy bagasse. Proc Soc Exp Biol Med 1968; 129:351-360.

(30) Das DB, Fletcher AG, Doedhare SG. Mesothelioma in an agricultural community of India: A clinicopathological study. Aust NZ J Surg 1976; 46:218–226.

A 94,000-Dalton Glycoprotein Expressed by Human Melanoma and Carcinoma Cells[1,2]

Kohzoh Imai,[3,4] Barry S. Wilson,[3,5] Aldo Bigotti,[6] Pier G. Natali,[6] *and* Soldano Ferrone[3,7,8]

ABSTRACT—The IgG2a monoclonal antibody (MoAb) 376.96S, secreted by a hybridoma derived from a mouse immunized with cultured human melanoma cells COLO 38, reacts with a single 94,000-dalton glycoprotein that is peripherally associated with the plasma cell membrane of cultured melanoma cells. Indirect immunofluorescence analysis with cryostat thin sections of human tissues showed that this antigen is absent from a large variety of normal tissues but is readily detectable on melanomas, nevi, and several different carcinomas. The MoAb 376.96S binds with cultured melanoma and carcinoma cell lines to a similar extent and can mediate both complement-dependent and cell-dependent lysis of these cells. The 94,000-dalton glycoprotein detected by MoAb 376.96S is distinct in its tissue distribution, antigenicity, and molecular profile from several structures previously identified with monoclonal antibodies that have similar molecular weights. JNCI—1982; 68:761–769.

Melanoma represents one type of human tumor in which the hybridoma technique has been successfully used to develop MoAb to tumor-associated antigens (*1–9*). Several of the melanoma-associated antigens identified with MoAb have apparent MM in the range of 95,000. Woodbury et al. (*2*) and Dippold et al. (*4*) have defined single-chain membrane-bound antigens with the apparent MM of 97,000 and 95,000 daltons, respectively. Mitchell et al. (*6*) have described a 95,000-dalton melanoma-associated antigen which is associated with three additional components with MM of 11,600, 29,000, and 26,000 daltons respectively, and Wilson et al. (*9*) have identified a 94,000-dalton glycopolypeptide which is associated with 75,000-, 70,000-, and 25,000-dalton structures. In this study we describe a new 94,000-dalton glycoprotein that is expressed by melanoma and carcinoma cells and is distinct from similar MM glycoproteins identified with monoclonal antibodies in terms of tissue distribution, antigenicity, and molecular profile.

MATERIALS AND METHODS

Monoclonal antibodies.—The MoAb 376.96S and 345.134 are secreted by hybridomas constructed with the murine myeloma cell line Sp2/0-Ag14 and splenocytes from BALB/c mice immunized with cultured human melanoma cells COLO 38, according to the procedures we have described elsewhere (*5*). The MoAb 345.134 identifies a membrane-bound antigen which is expressed by human melanoma cells but is undetectable on melanocytes. This antigen, which is expressed on a large variety of normal and malignant cells, consists of an 85,000-dalton glycoprotein linked to a 30,000-dalton polypeptide by disulfide bonds. The serologic and immunochemical characterization of the MoAb 345.134 was described elsewhere (*10*). The MoAb 465.12S was prepared with the use of splenocytes from a mouse immunized with cultured human melanoma cells M21. The MoAb 465.12S reacts with a cytoplasmic antigen expressed in human melanoma cells, but is undetectable in melanocytes. This antigen, which is expressed in epithelial cells from several organs and in a variety of tumors, consists of four glycopolypeptides with MM of 94,000, 75,000, 70,000, and 25,000 daltons, respectively. The method of preparation as well as the serologic and immunochemical characterization of this antibody have been described elsewhere (*11*). The hybridomas secreting these monoclonal antibodies have been subcloned and have been propagated in vitro and in vivo for about 1 year. Immunodiffusion analysis with rabbit anti-mouse Ig antisera (Litton Bionetics Inc., Kensington, Md.) indicated that both antibodies were of the IgG2a subclass. The MoAb I_{12} to a 95,000-dalton membrane antigen (*4*) was provided by Dr. W. Dippold, Dr. K. Lloyd, and Dr. L. Old of the Sloan-Kettering Institute, New York, N.Y.

Conventional xenoantisera.—FITC-labeled rabbit anti-mouse IgG1 and IgG2a antisera were purchased from Meloy Laboratories Inc., (Springfield, Va.). Both reagents have a fluorescein-to-protein ratio of 3 and have been used at a protein concentration of 1.5 mg/ml. Before use, one volume of each antiserum was sequentially incubated at 4°C for 60 minutes with one volume of packed ABRh$^+$ erythrocytes and of packed cultured human melanoma cells M10 to absorb contaminating antibodies that may cause false-positive reactions. The adsorbed FITC-labeled reagents did not stain cultured cell lines or tissue substrates.

Cultured human cell lines.—Human cells in long-term culture were maintained in RPMI-1640 medium containing 10% calf serum. A confluent monolayer of melanoma cells (BwV)

ABBREVIATIONS USED: ADCC=antibody-dependent cell-mediated cytotoxicity; FITC=fluorescein isothiocyanate; IIF=indirect immunofluorescence; MoAb=monoclonal antibody (antibodies); MM=molecular mass(es); PBS=phosphate-buffered saline; SDS-PAGE=sodium dodecyl sulfate polyacrylamide gel electrophoresis; SpA=purified protein A from *Staphylococcus aureus.*

---

[1] Received August 4, 1981; accepted December 22, 1981.

[2] Supported in part by grant 81013296 from the Consiglio Nazionale delle Ricerche, Rome, Italy; by Public Health Service (PHS) grant AI-13154 from the National Institute of Allergy and Infectious Diseases; and by PHS grants CA-32619, CA-32609, CA-32634, and CA-32635 from the National Cancer Institute.

[3] Department of Pathology and Surgery, Columbia University, 630 West 168th St., New York, N.Y. 10032.

[4] Visiting investigator from the Department of Internal Medicine, Sapporo Medical College, Sapporo, Japan.

[5] Recipient of a special fellowship from the Leukemia Society of America.

[6] Regina Elena Cancer Institute, Rome, Italy.

[7] *Address reprint requests to* Dr. Ferrone.

[8] We acknowledge the excellent technical assistance of Ms. M. R. Nictora and the secretarial assistance of Ms. Ellen Schmeding.

or a suspension of melanoma cells (COLO 38, M21) in a T-25 flask (Falcon Plastics, Cockeysville, Md.) were intrinsically radiolabeled with 2 mCi D-[6-^{3}H(N)]glucosamine hydrochloride, 30 mCi/mmol (New England Nuclear Corp., Boston, Mass.), according to the method described by Duksin and Bornstein (*12*) or they were surface labeled with ^{125}I by the Iodogen method of Salisbury and Graham (*13*). The cells were solubilized with Nonidet P40 detergent in PBS containing 10 *μM* of the proteolytic inhibitor phenylmethylsulfonyl fluoride. The resulting extract was cleared by centrifugation at 7,000×*g* and stored at −20°C. Cell extracts obtained with 3 *M* KCl or urea were dialyzed against PBS (pH 7.0) prior to use.

Tissue specimens.—Tissues were obtained surgically from untreated patients and from patients undergoing different therapeutic regimens. Normal tissues were obtained from sites directly adjacent to neoplastic lesions. Tissue specimens were snap-frozen in liquid nitrogen, and two consecutive cryostat sections of 4-μm thickness were obtained from each frozen tissue: One section was stained with toluidine blue (0.1% in FBS) and the other section was fixed for 10 minutes in cold absolute acetone and then used in the IIF test. Absolute acetone was chosen over other fixatives because it retained the most detail after fluorescent staining.

Binding assays, complement-dependent and cell-dependent cytotoxicity assays.—IIF assay was performed as described in (*8*). Acetone-fixed 4-μm cryostat sections of surgically removed tissues were overlayed with 5 *μg* MoAb 376.96S/ml for 30 minutes at 25°C. After washing for 5 minutes in cold PBS, we applied FITC rabbit anti-mouse Ig antiserum for an additional 30 minutes. After a final wash with cold PBS, the sections were mounted in PBS-buffered glycerol and observed with a Leitz Ortholux II fluorescence microscope equipped for phase-contrast microscopy and with epillumination. We used the distinct bright green fluorescent staining of the plasma membrane as a criterion of positive reactions of tissue sections with monoclonal antibodies. As a control, we tested unreactive tissue sections with concentrated, 20-μg/ml solutions, and diluted 0.5-μg/ml solutions of monoclonal antibodies to avoid false-negative reactions attributable to either a low concentration of the monoclonal antibodies or to a prozone-like effect (*14*). The specificity of fluorescent staining was controlled by testing tissue sections with myeloma protein secreted by the murine myeloma cells P3-X63-Ag8 and with culture supernatants of the hybridomas 376.96S from which the monoclonal antibodies had been removed by adsorption at 4°C with one volume of cultured human melanoma cells M10. The efficiency of adsorption was confirmed by the failure of the adsorbed culture supernatant to stain cultured human melanoma cells.

We performed the ^{125}I-labeled SpA radioimmunometric assay in microtiter plates as described elsewhere (*15*). The complement-dependent cytotoxicity test was done as an eosin-exclusion test with the use of rabbit serum as a complement source (*16*).

ADCC assay was performed in 96-well Microtiter plates (Cooke Laboratory Products Div., Dynatech Laboratories, Inc., Alexandria, Va.) with murine splenocytes as effectors (*17*). The percentage of specific ^{51}Cr release from the cells was used as a measure of lysis and was calculated as follows: % ADCC = $(A-B)-(C-B)/(T-B)-(C-B)\times 100$, where A=mean cpm of test samples, B=mean cpm of counter background, C=mean cpm of antibody-free control in the presence of effector cells, and T=mean cpm of total amount of ^{51}Cr incorporated into the target cells. We performed all test combinations in triplicate; the spontaneous or background leakage of ^{51}Cr from the target cells ranged from 13 to 21% of the total incorporated radiolabel.

Indirect immunoprecipitation, sequential immunoprecipitation SDS–PAGE.—Indirect immunoprecipitation and sequential immunoprecipitation were performed as described previously (*18*) except that protein A–Sepharose 4B was used in place of the Formalin-fixed bacteria and preclearing of the NP-40 detergent cell extract was not necessary. SDS–PAGE was performed in 90×1.5-mm slab gels containing an acrylamide gradient of 5–12.5% and the SDS buffer system of Laemmli (*19*). The gels containing [^{3}H]glucosamine-labeled antigens were processed for fluorography as described by Bonner and Laskey (*20*). Rabbit phosphorylase a (MM 94,000), bovine serum albumin (MM 68,000), ovalbumin (MM 44,000), carbonic anhydrase (MM 29,000) and whale myoglobin HM 17,000 were used as standards.

RESULTS

Structural Profile of the Antigen Recognized by MoAb 376.96S

Indirect immunoprecipitation of [^{3}H]glucosamine-labeled BwV or COLO 38 melanoma cell extracts with MoAb 376.96S revealed a single component having an apparent MM of 94,000 daltons (fig. 1). A component with the same apparent MM was also immunoprecipitated from ^{125}I-labeled COLO 38 melanoma cells, which indicated the existence of both carbohydrate and protein moieties in this molecule. In addition, a 94,000-dalton molecule was immunoprecipitated by the MoAb 376.96S from the urinary bladder carcinoma cell lines MANO and T24 and the prostate carcinoma line H494 but not from the cultured B-lymphoid cell Raji and the cultured T-lymphoid cell 1301 (fig. 1). The apparent MM of the 94,000-dalton antigen did not change when SDS–PAGE was performed in the absence of 2-mercaptoethanol. The molecule could be readily solubilized under mildly dissociating conditions (10 m*M* phosphate buffer, 3 *M* KCl, 0.1 *M* urea) and in the absence of detergents.

The structure recognized by the MoAb 376.96S is antigenically unrelated to the 94,000-dalton component identi-

TABLE 1.—*Reactivity of MoAb 376.96S with normal human tissues assessed by IIF assay*

Reactivity	Normal tissues
Negative	Brain cortex, colon, endometrium, fat tissue, gallbladder, kidney, lung, lymph node, mammary gland, skin from perineum, spleen, sympathetic ganglia, testis, thymus, urinary bladder, rectum
Very weakly stained	Stomach epithelium, limited areas of the epidermal basal layer from skin of the neck and abdomen.

fied by the MoAb 465.12S, since in sequential immunodepletion experiments neither of the antibodies was able to deplete the 94,000-dalton structure detected by the other antibody (fig. 2). Also, immunodepletion experiments performed with a limited amount of the MoAb I_{12}, provided by Dr. Dippold and colleagues, Sloan-Kettering Institute, New York, N.Y., indicate that this monoclonal antibody and the MoAb 376.96S recognize antigenically distinct structures (fig. 3).

Pattern of Reactivity of MoAb 376.96S With Surgically Removed Normal and Tumor Tissues

The results of the screening of MoAb 376.96S on fresh normal and tumor tissues by IIF are summarized in table 1. The MoAb 376.96S failed to stain a variety of normal tissue sections except sections of stomach epithelium and limited areas of the epidermal basal layer from the skin of the neck and the abdomen. The staining of the tissues was very faint, barely detectable with the oil-immersion objective of the fluorescence microscope. Among benign lesions of the skin, the MoAb 376.96S stained a high proportion of intradermal nevi (3 of 6 cases) and compound nevi (5 of 8 cases), whereas 6 cases of blue nevi and 6 cases of pigmented skin lesions (sebaceous warts, sclerosing angioma, and keratoacanthoma) were negative. Conversely, the incidence and the intensity of staining were found to be highly increased when pathologic lesions and tumors were tested with the MoAb 376.96S (table 2). The most reactive group with the monoclonal antibody was the melanoma group, where 83% (15 of 18 cases) of primary lesions arising from the superficial spreading, malignant lentigo, and nodular type lesions exhibited bright green fluorescence of the plasma membrane (fig. 4).

The monoclonal antibody stained only 65% of metastatic melanomas (13 of 20 cases), and the fluorescence was less bright than that found in primary tumors. The staining pattern observed in both primary and metastatic melanomas was independent of melanin content and showed a high degree of heterogeneity within each lesion as it ranged from negative reactions to very bright staining. A high percentage of skin carcinomas (6 of 12 cases of basal cell and squamous cell carcinomas) were reactive in the IIF test and were most noted for a great variation in staining intensity among the various specimens. For tumors other than those from the skin, the MoAb 376.96S was reactive with 22% of the breast carcinomas (10 of 45 cases) including infiltrating ductal, medullary, lobular type, and their metastases, and with one case each of rectum adenocarcinoma, glioblastoma, transitional cell carcinoma of the urinary bladder, and liver adenoma. In these cases, most of the tumor tissues tested showed a variable degree of staining in which only some areas of the tumor cell plasma membranes were brightly stained.

TABLE 2.—*Reactivity of MoAb 376.96S with human tumor tissues assessed by IIF assay*

Tumors	No. positive/No. tested
Primary melanoma	15/18
Metastatic melanoma	13/20
Skin basal cell and squamous cell carcinoma	6/12
Breast adenocarcinoma	10/45
Gastrointestinal tract adenocarcinoma	1/9
Mixed brain tumors	1/9
Urinary bladder transitional cell carcinoma	1/2
Liver adenoma	1/1
Thyroid adenocarcinoma	0/4
Parotid Wharthin's tumor	0/3
Gallbladder adenocarcinoma	0/3
Lung adenocarcinoma and squamous cell carcinoma	0/3
Sarcoma	0/3
Seminoma	0/2
Ovarial adenocarcinoma	0/2
Uterine adenocarcinoma	0/2

TABLE 3.—*Reactivity of a panel of human cell lines in ^{125}I-labeled SpA radioimmunometric binding assay with MoAb 376.96S*

Cell type	Cell line	^{125}I-labeled SpA-bound MoAb 376.96S, cpm
Melanoma	B0649	7,900
	BW5	5,000
	COLO 38	6,400
	M14	9,500
	M16	10,400
	M21	3,500
Carcinoma		
Breast	ALAB496	6,000
Breast	BT-20	2,500
Breast	Hs578T	3,400
Cervix	D98	<500
Colon	HT29	6,400
Lung	A549	10,500
Prostate	H494	25,000
Prostate	DU-145	4,000
Urinary bladder	EJ	5,400
Urinary bladder	Hu456	4,800
Urinary bladder	MANO	8,300
Urinary bladder	T24	4,200
Lymphoid		
T-type	1301	<500
B-type	Daudi	<500
B-type	Raji	<500
B-type	WI-L2	<500
Myeloid	K562	<500

Serologic Reactivity of the MoAb 376.96S With Cultured Human Cell Lines

The MoAb 376.96S was tested in a ^{125}I-labeled radioimmunometric binding assay to compare the level of the 94,000-dalton glycoprotein expressed by different types of cultured human cell lines (table 3). The MoAb 376.96S bound in considerable amounts to most of the melanoma cell lines and also reacted with 9 of 10 carcinoma cell lines, but it was unreactive with cultured lymphoid cells. The prostate carcinoma line H494 was unusual in that it expressed more than double the level of antigen detectable on the next most reactive carcinoma or melanoma cell line. The same pattern of reaction of the MoAb 376.96S was also obtained in the adsorption test and in the indirect immunofluorescence assay with staining detectable at the plasma membrane but not in cytoplasm of the cultured cells.

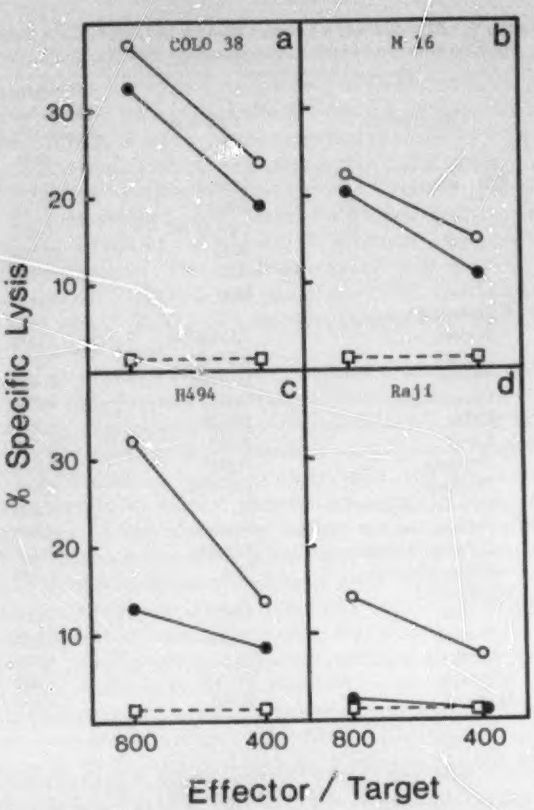

TEXT-FIGURE 1.—Antibody-mediated cell-dependent lysis of various cell lines with the MoAb 376.96S and mouse splenocytes. Microtiter plates (96 wells) containing 4×10^3 ^{51}Cr-labeled melanoma cells (COLO 38 and M16), prostate carcinoma cells (H494), and the B-lymphoid cells (Raji) were first incubated with MoAb 376.96S (●——●), 345.134S (○——○), or Sp2-O myeloma supernatant (□---□) prior to addition of murine C3H/HeN splenocytes. After 18 hr of incubation, the supernatants were harvested and counted in a gamma counter, and the percent of ^{51}Cr release was determined.

The MoAb 376.96S mediates complement-dependent and cell-dependent lysis of cultured melanoma and carcinoma cells; results of representative experiments are shown in text-figure 1. In contrast, the antibody does not mediate immune lysis of cultured lymphoid cells. They are, however, susceptible to complement-dependent and cell-dependent lysis mediated by the MoAb 345.134 which recognizes an antigenic structure unrelated to that identified by the MoAb 376.96S.

DISCUSSION

We described a 94,000-dalton plasma membrane glycoprotein absent from the large majority of normal human tissues but readily detectable in human melanomas and lesions of the skin and in some breast carcinomas; some rare positive cases were noted for tumors of the brain and gastrointestinal tract. Immunochemical analysis with cultured melanoma and carcinoma cell lines indicates that the 94,000-dalton structure is not disulfide-bridged in its native state and is peripheral rather than integral in its association with the plasma cell membrane. The second conclusion is based on the ability to solubilize the 94,000-dalton component from melanoma cells in the absence of detergents. Serologic analysis with cultured human cell lines showed that MoAb 376.96S can mediate complement-dependent and cell-dependent cytotoxicity in a fashion that parallels the cell surface expression of the 94,000-dalton target antigen.

The size and tissue distribution of the glycoprotein detected by MoAb 376.96S are similar to those of the antigens described by Brown et al. (*21*) and Dippold et al. (*4*). However, as shown here, the monoclonal antibody provided by Dr. Dippold and his colleagues reacts with a molecule different than the one detected by our monoclonal antibody. The apparent molecular weight of the structure detected by Dr. Dippold's antibody is slightly lower than that of our 94,000-dalton structure. As yet, we cannot assess the relationship between our reagent and the one reported by Brown et al. (*21*) since the reagent has not been made available to us. Exchange of monoclonal antibodies through workshops sponsored by the National Institutes of Health will greatly benefit these types of comparative analyses. The 94,000-dalton structure identified by the MoAb 376.96S also differs from that described by Mitchell et al. (*6*) since the latter is not detectable on nevi (*22*) and carcinoma cells and is associated with three other glycopolypeptides. Finally, the 94,000-dalton structure detected by MoAb 376.96S differs in tissue distribution and in antigenic and molecular profile from the cytoplasmic antigen identified by our MoAb 465.12 (*9*).

The MoAb 376.96 could mediate complement-dependent and cell-dependent lysis of both melanoma and carcinoma cells. The MoAb 225.28S to a high-molecular-weight melanoma-associated antigen could mediate cell-dependent lysis but not complement-dependent lysis of melanoma cells (Imai K, Pellegrino MA, Wilson BS, Ferrone S: Submitted for publication), even though it is of the same IgG subclass as the MoAb 376.96S (IgG2a) and the corresponding target antigen is expressed at a level similar to that of the target antigen recognized by the MoAb 376.96S. These results indicate that factors other than antigen density and antibody subclass play a crucial role in the outcome of immune lytic reactions. This contention is also supported by the finding that a significant increase in the extent of immune lysis mediated by the MoAb 376.96 can occur when melanoma cells are treated with low concentrations of puromycin which do not effect the level of expression of the 94,000-dalton target structure (Imai K, Ferrone S: Unpublished observations).

The 94,000-dalton glycoprotein described in this study shares several features with other membrane-bound and cytoplasmic antigens we have identified in human melanoma cells with monoclonal antibodies. These include a high-molecular-weight membrane-bound antigen (*9*), an 85,000-dalton membrane-bound glycoprotein (*10*), a four chain cytoplasmic antigen (*9*), and Ia antigens (*23*) which are the human counterparts of the murine I-E subregion antigens (*24*). The 94,000-dalton glycoprotein described in this study, the high molecular weight antigen, the 85,000-dalton antigen, and the cytoplasmic antigen are similar in their distribution on cells of the melanocyte lineage since they are not detectable on melanocytes but are expressed by nevi and melanoma cells (*9*). Conversely, Ia antigens have a more restricted distribution since they are detectable only on melanocytes which have undergone malignant transformation (*8*). Additional common features of the 94,000-dalton glycoprotein and the other markers we have identified are 1) presence in both primary and metastatic lesions (*8, 9*), and 2) heterogeneous expression within cells of a single melanoma lesion and/or among different lesions (*8, 9*). The second finding raises the possibility that a successful application of monoclonal antibodies to tumor-associated antigens in the area of radioimaging and immunotherapy may require the use of a cocktail of monoclonal antibodies to distinct tumor-associated antigens to detect or eliminate tumor cells with little or no expression of a given determinant.

REFERENCES

(*1*) Koprowski H, Steplewski A, Herlyn D, Herlyn M. Study of antibodies against human melanoma produced by somatic cell hybrids. Proc Natl Acad Sci USA 1978; 75:3405-3409.

(*2*) Woodbury RG, Brown JP, Yeh MY, Hellström I, Hellström KE. Identification of a cell surface protein, p97, in human melanomas and certain other neoplasms. Proc Natl Acad Sci USA 1980; 77:2183-2187.

(*3*) Carrel S, Accolla RS, Carmagnola AL, Mach JP. Common human melanoma-associated antigen(s) detected by monoclonal antibodies. Cancer Res 1980; 40:2523-2528.

(*4*) Dippold WG, Lloyd KO, Li LT, Ikeda H, Oettgen HF, Old LJ. Cell surface antigens of human malignant melanoma: Definition of six antigenic systems with mouse monoclonal antibodies. Proc Natl Acad Sci USA 1980; 77:6114-6118.

(*5*) Imai K, Molinaro GA, Ferrone S. Monoclonal antibodies to human melanoma-associated antigens. Transplant Proc 1980; 12:380-383.

(*6*) Mitchell KF, Fuhrer JP, Steplewski Z, Koprowski H. Biochemical characterization of human melanoma cell surfaces: Dissection with monoclonal antibodies. Proc Natl Acad Sci USA 1980; 77:7287-7291.

(*7*) Imai K, Ng AK, Ferrone S. Characterization of monoclonal antibodies to human melanoma-associated antigens. JNCI 1981; 66:489-496.

(*8*) Natali PG, Imai K, Wilson BS, et al. Structural properties and tissue distribution of the antigen recognized by the monoclonal antibody 653.40S to human melanoma cells. JNCI 1981; 67:591-601.

(*9*) Wilson BS, Imai K, Natali PG, Ferrone S. Distribution and molecular characterization of a cell-surface and a cytoplasmic antigen detectable in human melanoma cells with monoclonal antibodies. Int J Cancer 1981; 28:293.

(*10*) Imai K, Natali PG, Kay NE, Wilson BS, Ferrone S. Tissue distribution and molecular profile of a differentiation antigen detected by a monoclonal antibody (345.134S) produced against human melanoma cells. Cancer Immunol Immunother. In press.

(*11*) Natali PG, Wilson BS, Imai K, Bigotti A, Ferrone S. Tissue distribution, molecular profile and shedding of a cytoplasmic antigen identified by the monoclonal antibody 465.12S to human melanoma cells. Cancer Res. In press.

(*12*) Duksin D, Bornstein P. Impaired conversion of procollagen to collagen by fibroblasts and bone treated with tunicamycin, an inhibitor of protein glycosylation. J Biol Chem 1976; 252:955-962.

(*13*) Salisbury JG, Graham JM. Cell-surface radioiodination with the sparingly soluble catalyst Iodogen. Differences between dividing and nondividing rodent thymocytes. Biochem J 1981; 194:351-355.

(*14*) Linder E, Mieltimen A. Prozone effect in indirect immunofluorescence. Scand J Immunol 1976; 5:513-519.

(*15*) McCabe RP, Quaranta V, Frugis L, Ferrone S, Reisfeld RA. A radioimmunometric antibody-binding assay for the evaluation of xenoantisera to melanoma-associated antigens. JNCI 1979; 62:455-463.

(*16*) Ferrone S, Pellegrino MA. Cytotoxic antibodies to cultured melanoma cells in the sera of melanoma patients. J Natl Cancer Inst 1977; 58:1201-1204.

(*17*) Imai K, Ng AK, Glassy MA, Ferrone S. ADCC of cultured human melanoma cells: Analysis with monoclonal antibodies to human melanoma associated antigens. Scand J Immunol. In press.

(*18*) Allison JP, Belvedere M, Reisfeld RA, Pellegrino MA, Ferrone S. Serologic and immunochemical characterization of HLA-A9 xenoantisera. J Immunol 1978; 121:579-585.

(*19*) Laemmli UK. Cleavage of structural proteins during the assembly of the head of bacteriophage T4. Nature 1970; 227:680-685.

(*20*) Bonner WM, Laskey RA. A film detection method for tritium-labelled proteins and nucleic acids in polyacrylamide gels. Eur J Biochem 1974; 46:83-88.

(*21*) Brown JP, Woodbury RG, Hart CE, Hellström I, Hellström KE. Quantitative analysis of melanoma-associated antigen p97 in normal and neoplastic tissues. Proc Natl Acad Sci USA 1981; 78:539-543.

(*22*) Herlyn M, Clark WH, Mastrangelo MJ, et al. Specific immunoreactivity of hybridoma-secreted monoclonal anti-melanoma antibodies to cultured cells and freshly derived human cells. Cancer Res 1980; 40:3602-3609.

(*23*) Wilson BS, Indiveri F, Pellegrino MA, Ferrone S. DR (Ia-like) antigens on human melanoma cells: Serological detection and immunological characterization. J Exp Med 1979; 149:658-688.

(*24*) Ferrone S, Allison JP, Pellegrino MA. Human DR (Ia-like) antigens: Biological and molecular profile. Contemp Top Mol Immunol 1978; 7:239-281.

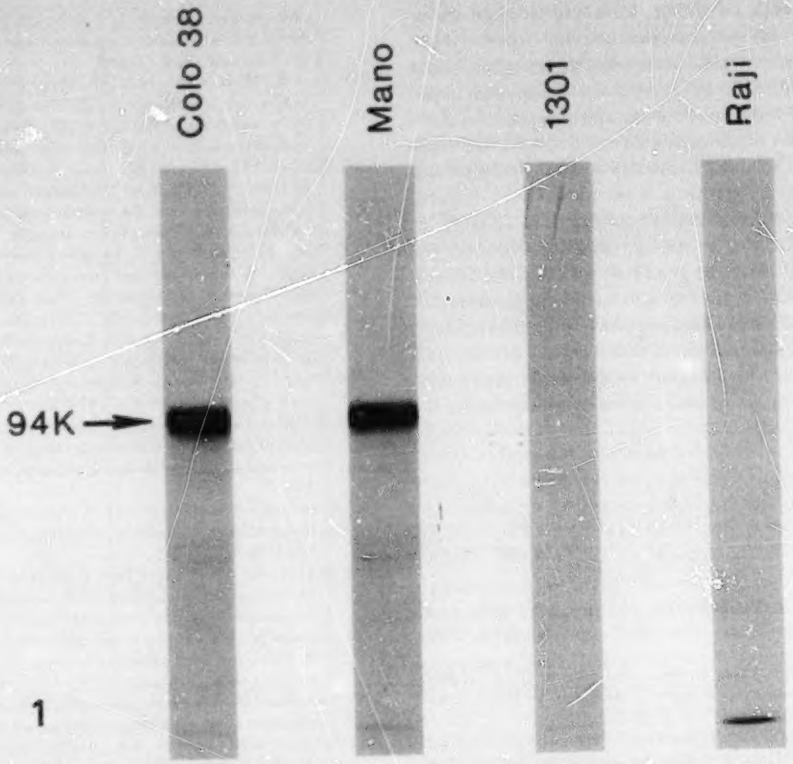

FIGURE 1.—Immunochemical analysis of 94,000-dalton antigens detected by MoAb 376.96S from various cultured cell lines. D-[6-^{3}H(N)]glucosamin hydrochloride-labeled antigens from a cultured melanoma cell line (COLO 38), a cultured bladder carcinoma cell line (MANO), a cultured T-lymphoid cell line (1301), and a cultured B-lymphoid cell line (Raji) were immunoprecipitated by reaction with the MoAb 376.96S and were subjected to SDS-PAGE under reducing conditions (2% 2-mercaptoethanol). The gel was processed by fluorography and exposed to Kodak XR-OMAT film.

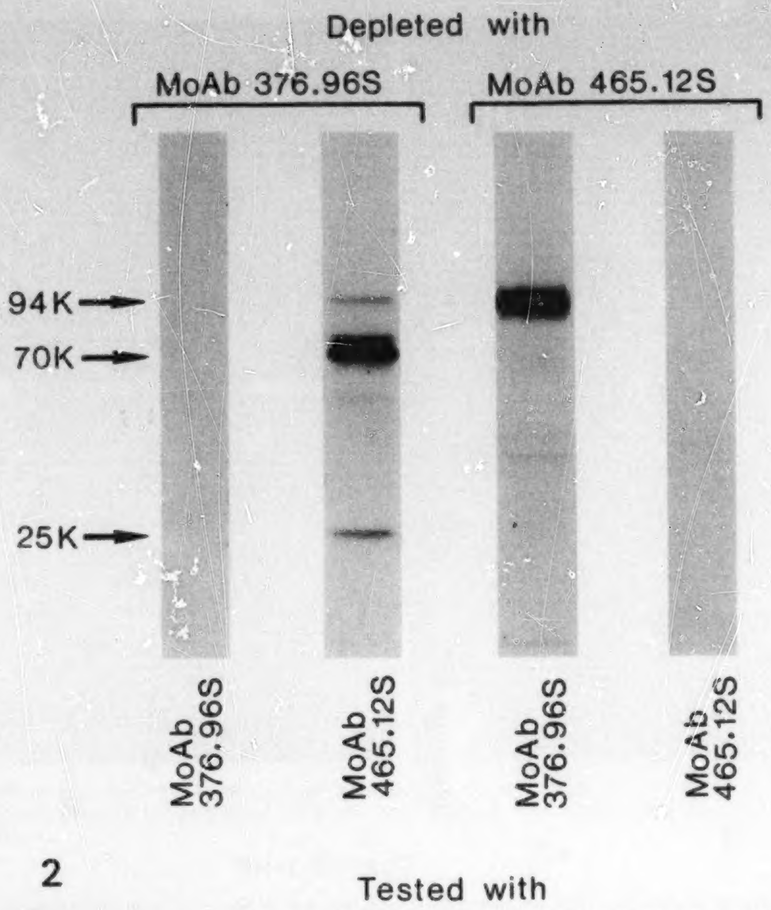
Depleted with
MoAb 376.96S
MoAb 465.12S
94K
70K
25K
MoAb 376.96S
MoAb 465.12S
MoAb 376.96S
MoAb 465.12S
Tested with

2

FIGURE 2.—Relationship between the antigenic structures detected by MoAb 376.96S and MoAb 465.12S. A D-[6-^{3}H(N)]glucosamine hydrochloride-labeled BwV melanoma NP40 cell extract was exhaustively immunodepleted by sequential reaction with MoAb 376.96S or MoAb 465.12S. The remaining labeled antigens were split into 2 groups and immunoprecipitated by both monoclonal antibodies and then subjected to SDS-PAGE under reducing conditions (2% 2-mercaptoethanol). The gel was processed for fluorography and exposed to Kodak XR-OMAT film.

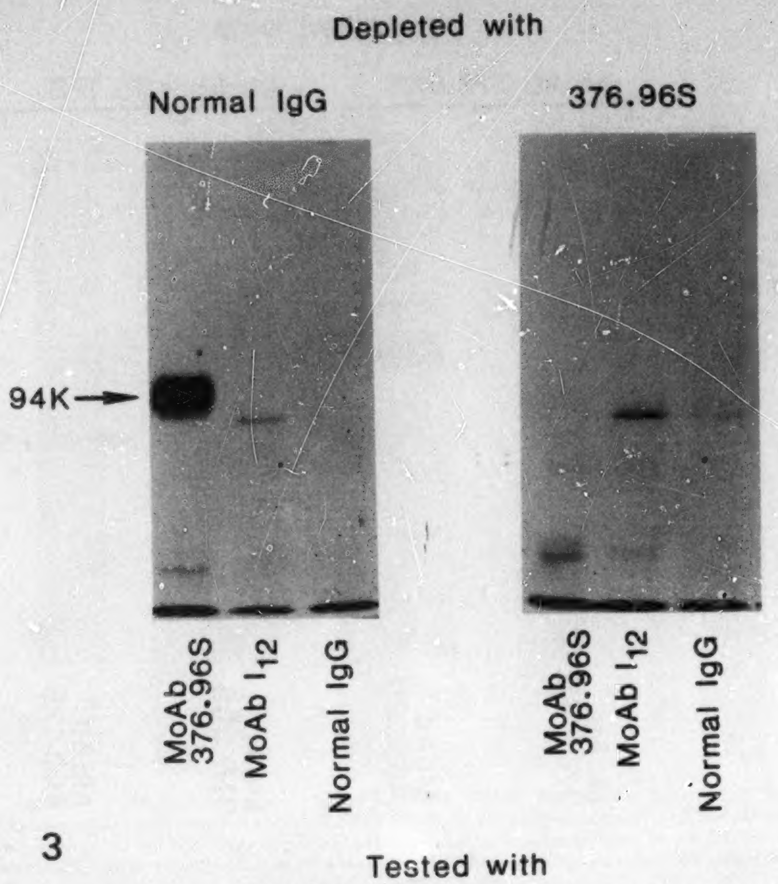
Depleted with
Normal IgG
376.96S
94K
MoAb 376.96S
MoAb I_{12}
Normal IgG
MoAb 376.96S
MoAb I_{12}
Normal IgG
Tested with

3

FIGURE 3.—Relationship between the antigenic structure detected by MoAb 376.96S and the MoAb I_{12}. A D-[6-^{3}H(N)]glucosamine hydrochloride-labeled BwV melanoma NP40 extract was exhaustively immunodepleted by sequential reaction with normal human IgG–Sepharose 4B or Sepharose 4B loaded with MoAb I_{12}. The remaining labeled antigens were then immunoprecipitated with normal human IgG or the xenoantibodies and subjected to SDS-PAGE under reducing conditions (2% 2-mercaptoethanol). The gel was processed by fluorography and then exposed to Kodak XR-OMAT film.

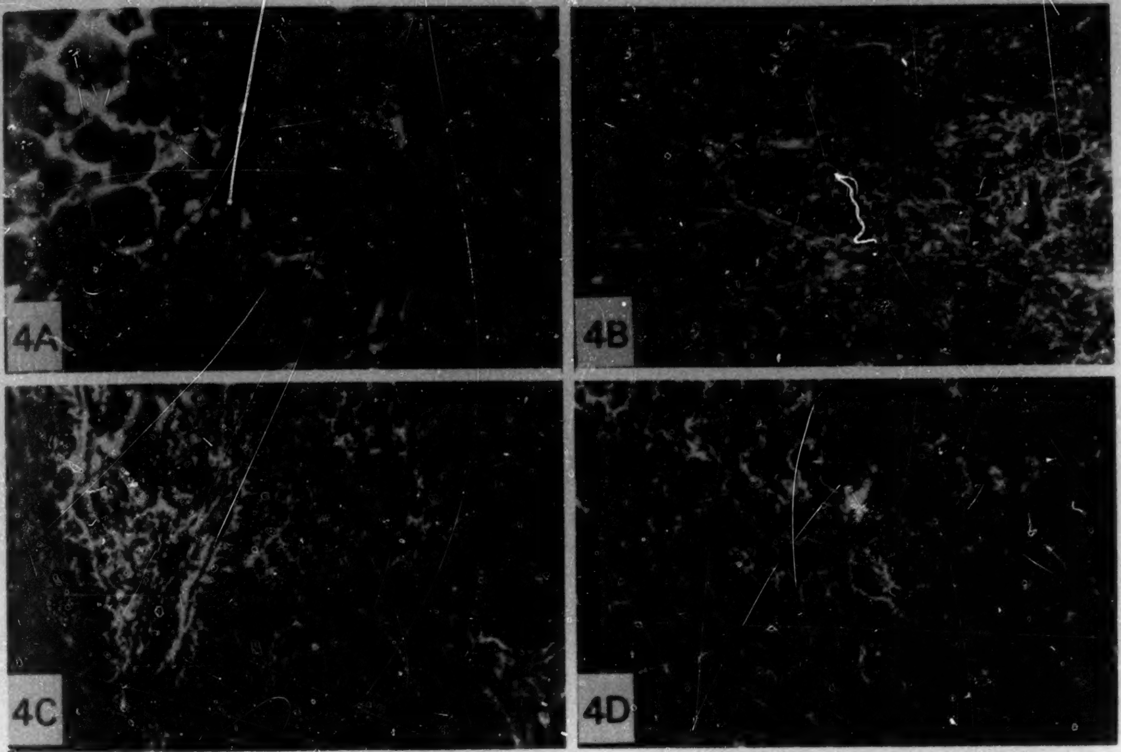

Figure 4.—Indirect immunofluorescent staining of cryostat thin sections (4μm) of various human tumors by the MoAb 376.96S. Malignant lentigo A), nodular melanoma B), infiltrating ductal breast carcinoma C), and skin basal cell carcinoma D) all exhibited a smooth staining of the plasma membrane. A) ×1,000. B), C), D) ×400.

blank page

Isolation, Culture, and Transplantation of Human Hepatocytes[1,2,3]

S. C. Strom[4,5] R. L. Jirtle,[6] R. S. Jones,[7] D. L. Novicki,[4] M. R. Rosenberg,[4] A. Novotny,[4] G. Irons,[4]
J. R. McLain,[6] *and* G. Michalopoulos[4,8,9]

ABSTRACT—The in situ two-step collagenase perfusion technique used for the isolation of hepatocytes from rat liver was adapted into a procedure applicable to pieces of human liver obtainable from surgical procedures. Human hepatocytes obtained by this method were maintained in primary culture for 10 days. The cellular changes observed at the light microscopic and electron microscopic levels are described. The changes in microsomal enzymes as a function of the age of the cultures were also measured. Exposure of the human hepatocytes to procarcinogens known to be metabolized by rodent liver resulted in unscheduled DNA synthesis. The isolated hepatocytes were also transplanted into two-thirds partially hepatectomized athymic nude mice. The transplanted cells formed nodules with characteristic hepatic architecture. These studies demonstrate that hepatocytes obtained from human liver by the described modified collagenase technique can be used for in vitro studies in chemical carcinogenesis.—JNCI 1982; 68:771–778.

The technique of the two-step in situ collagenase perfusion, originally introduced by Berry and Friend (*1*) and modified by Seglen (*2*), is a widely used method for obtaining viable dispersed hepatocytes from adult rat liver. The perfusate is introduced through vascular pathways, and the completion of the procedure results in dissociated liver tissue that can be further dispersed into isolated hepatocytes by simple mechanical means. The isolated hepatocytes can be used in vitro either as a suspension (*2*) or in primary culture (*3-6*). Additionally, the liver cells can be transplanted into syngeneic recipient animals (*7-9*). The main advantage of this collagenase dissociation procedure is that it results in a large number of cells with excellent viability. Thus multiple replicate samples from a single liver can be utilized for a variety of applications.

Studies utilizing a large number of intact human hepatocytes have thus far been limited because of the inability to adapt the in situ collagenase perfusion technique to human liver. The difficulties have been mainly technical, since large quantities of collagenase and perfusate are required to scale up this technique for the human liver. In previous reports fragments of human liver tissue from needle biopsies have been placed in explant culture (*10*). However, the small sample size severely restricts the experimentations that can be performed, and multiple replicate samples cannot be obtained. Primary cultures of adult human hepatocytes, analogous to those of adult rat hepatocytes, would require a large number of viable cells. Establishment of the methods for such primary cultures would be applicable to experimental studies involving a variety of disciplines. Primary cultures of human hepatocytes can be of use in studies related to the effects of chemical carcinogens on human tissues and the interspecies comparisons between, for example, humans and rodents. They may provide the ideal substrate for the culture of the various hepatitis viruses. They could also be used in the studies of intermediary human hepatic metabolism and physiology.

We (*7*) and others (*8*) have recently described systems of transplantation of adult rat parenchymal hepatocytes. After transplantation the hepatocytes proliferate and become organized into a structure that is similar to the one found in the liver. We have used this transplantation system to quantify the effects of genotoxic agents on rat hepatocytes (*11*) and to investigate the mechanism of liver regeneration (*12*). If adult human hepatocytes could be stimulated to proliferate when transplanted into athymic nude mice, the probability of cell survival and neoplastic transformation after cellular exposure to genotoxic agents could be quantified in a manner similar to that developed for rat hepatocytes.

In this report we describe a modified version of the in situ collagenase perfusion technique that can be applied to fragments of human liver tissue. This approach obviates the logistic difficulties in the use of an intact human liver. The method uses quantities of collagenase and perfusate, for example, that are on a scale analogous to the one used in the in situ perfusions of rat liver. We further describe properties of these isolated human hepatocytes in terms of their morphology in primary culture, their microsomal enzyme levels, and the UDS measured when these hepatocytes are exposed to procarcinogens. The morphology of human hepatocytes transplanted into nude mice is also described.

MATERIALS AND METHODS

Materials.—Collagenase II was obtained from Worthington Biochemical Corp. (Freehold, N.J.) from lots that were

ABBREVIATIONS USED: BP=benzo[*a*]pyrene; 2-FAA=*N*-2-fluorenylacetamide; RER=rough endoplasmic reticulum; SER=smooth endoplasmic reticulum; UDS=unscheduled DNA synthesis.

---

[1] Received September 17, 1981; accepted December 11, 1981.

[2] Supported in part by Public Health Service grants R01CA-30241 and R01CA-25951A from the National Cancer Institute and by donations from Dupont Chemical Company to Duke University.

[3] Research procedures were in accord with the ethical standards of the Human Research Ethics Committee, Duke University, and of the Helsinki Declaration of 1975.

[4] Department of Pathology, Duke University Medical Center, Durham, N.C. 27710.

[5] Salary support by National Institutes of Health–National Cancer Institute research service award CA-06743.

[6] Department of Radiology, Duke University Medical Center.

[7] Department of Surgery, Duke University Medical Center.

[8] *Address reprint requests to* Dr. Michalopoulos, Box 3432, Department of Pathology, Duke University Medical Center, Durham, N.C. 27710.

[9] We thank Mr. Henry Estrada for his assistance with the electron microscopy procedures.

tested in terms of their capacity to produce viable hepatocytes from adult rat liver. Tissue culture media were obtained from Grand Island Biological Co. (Grand Island, N.Y.). Athymic nude mice were obtained from Charles River Breeding Laboratories (Wilmington, Mass.). Chemicals were purchased from Sigma Chemical Co. (St. Louis, Mo.) unless otherwise specified.

Perfusion technique.—Pieces of canine liver were obtained from dogs used for a variety of experiments not directly involving the liver. Hepatic tissue was removed within 5 minutes after cessation of cardiac function. The perfusions of canine liver fragments were performed to define the conditions that would allow perfusions of fragments of human liver. The conditions described below for the fragments of human liver reflect the accumulated experience with multiple perfusions of canine liver fragments. Human hepatic tissue fragments were obtained from discarded surgical material removed from two patients during scheduled surgical procedures.

In the first case a right lobectomy was performed for the removal of a solitary neoplastic lesion metastatic from colon adenocarcinoma in a 62-year-old white female. In the second case a right lobectomy was performed in a 14-year-old male for the removal of a lesion later diagnosed as fibromyxosarcoma. In both cases the right lobe of the liver was brought for pathologic examination within 20 minutes after ligation of the right portal vein and hepatic artery branches. The location of the neoplastic lesion was identified, and sections were taken to establish histopathologic diagnosis. The diameter of the neoplastic lesion by gross criteria did not exceed 5 cm. Hepatic tissue was removed from the periphery of the discarded material and at a distance of at least 5 cm from the periphery of the neoplastic lesion. Care was taken to ensure that the removed pieces were surrounded by a hepatic capsule on all sides except for one cut surface. The thickness between the edge of the capsule and the exposed cut surface did not exceed 2 cm. The largest of the liver pieces did not exceed 3.5 cm in width. The weight range for the pieces was between 6 and 12 g. The tissue pieces were placed in ice-cold saline and transported to the perfusion site. Plastic polyethylene catheters (18-gauge or smaller) were inserted into every vascular orifice that could be identified on the cut surface (from 3 to 5/piece). The tissue pieces were then perfused with a calcium-free buffer. One liter of the buffer contained potassium chloride (0.5 g), sodium chloride (8.3 g), and HEPES[10] buffer (2.4 g) (*13*). The pH of the buffer had been previously adjusted to 7.4 with sodium hydroxide. The flow rate was adjusted to 14 ml/minute/catheter. The perfusate was allowed to drain and was not recirculated. After 20 minutes the perfusion buffer was changed to one of identical composition to that described above with the addition of calcium chloride ($CaCl_2 \cdot 2H_2O$) at a concentration of 74 mg/liter and collagenase at a concentration of 0.5 mg/ml of buffer. The collagenase solution was perfused at an identical rate and for the same time as those used for the calcium-free buffer. The perfusion buffers were delivered to the hepatic fragments at a temperature of 37°C. The temperature at the delivery site (one of the blanched areas) was measured with a thermistor probe connected to a digital thermocouple thermometer (model bat 8; Bailey Instruments Co., Inc., Saddle Brook, N.J.). Previous experience with the canine liver and with rat liver perfusions indicated that there is at least a temperature loss of 5°C along 40 mm of silicone tubing (≈3–5 mm in diameter). For these perfusions (and for all rat liver perfusions in our laboratory), the perfusate container is maintained at 42°C so that a delivery temperature of 37°C to the liver is maintained.

As soon as the perfusion was started, it was observed that wedge-shaped areas on the surface of each liver piece began to blanch (fig. 1). The blanched areas covered approximately 70% of the surface of each fragment. At the end of the perfusion process, the liver pieces (blanched and nonblanched areas) were minced with a scissors into fragments less than 1 mm in diameter. The resultant minced material was filtered through a nylon mesh filter (150-μm pore size). The cellular suspension was washed in ice-cold calcium-free buffer and centrifuged for 2 minutes at 50×*g*. The washing procedure was repeated three times. The total yield of isolated hepatocytes was approximately 50×10^6 cells/g of liver. A viability test of trypan blue exclusion indicated that more than 70% of the hepatocytes excluded the dye.

Culture methods.—The isolated hepatocytes were suspended in minimum essential medium with Earle's salts supplemented with insulin (10^{-7} *M*), fetal bovine serum (10%), and gentamicin (50 μg/ml). The cells were inoculated into collagen-coated (*5, 14*) 60-mm-diameter tissue culture plates at a density of 3.5×10^6 cells/plate. Although previous studies (*14*) have shown that higher levels of cytochrome P_{450} can be maintained in hepatocytes on collagen gels, collagen-coated substrates as compared to collagen gels can be more easily used for autoradiography and were the substrate of choice in these studies. The medium (5 ml/plate) was changed 4 hours after hepatocyte inoculation and every 24 hours thereafter. Phase-contrast microscopy of the cells at days 1–5 indicated that less than 3% of the cells were nonparenchymal, in agreement with previous reports (*2*). We calculated the percent of attached cells by dividing the measured DNA content of the cells attached to the plates at various time points by that of the total DNA in the initial inoculated sample. The DNA content was measured according to the method of Setaro and Morley (*15*).

Measurement of microsomal enzymes.—Cytochrome P_{450} and cytochrome *b*5 were measured according to the method of Omura and Sato (*16*). NADPH–cytochrome *c* reductase was measured according to the method of Phillips and Langdon (*17*).

Measurement of UDS.—Autoradiographies were performed for the measurement of UDS according to the method of Williams (*18*) and Probst et al. (*19*). Hepatocytes were cultured in collagen-coated eight-chamber slides (Lab-Tek Products, Div. Miles Laboratories Inc., Naperville, Ill.). These slides allow comparison of replicate (eight) cultures, on the same microscope slide with each culture exposed to different procarcinogens. After exposure of each chamber culture for 20 hours (from 4 to 24 hr in culture age) to medium supplemented with [^{3}H]thymidine (10 μCi/ml) and with solvent (control) or a specific concentration of procarcinogen, the chamber walls were removed, and the slides were extensively washed and finally coated under safe lights with a thin layer of undiluted Kodak NTB-3 emulsion. The slides were kept in the dark at room temperature for 10 days. They were subsequently developed and stained with hematoxylin and eosin.

---

[10] 4-(2-Hydroxyethyl)-1-piperazine ethanesulfonic acid.

Electron microscopic procedures.—The specimens were fixed in the plate in 4% glutaraldehyde (buffered with 0.1 *M* sodium cacodylate), postfixed in 1% osmium tetroxide, and stained with uranyl acetate. Cells were embedded in Epon and lifted off the plate. Sections were taken through the Epon-embedded cells. The final sections (500–600 Å thick) were stained with 4% acetate and Reynold's stain.

Transplantation into nude mice.—The methods for transplantation were similar to those previously described for rats (*7*), except for the omission of brain homogenate. Human hepatocytes (5×10^5) were injected into the interscapular fat pads of athymic nude mice. The nude mice had been subjected to a two-thirds partial hepatectomy 1 hour prior to hepatocyte injection. The animals were killed 20 days after transplantation, and the fat pads were removed and processed as previously described (*7*).

RESULTS

Of the cells inoculated into collagen-coated plates, 42% remained attached after 24 hours and two medium changes. These results are comparable to those seen for rat hepatocytes (*3-6*). Examination of the cultured hepatocyte monolayers by phase-contrast microscopy at 4 hours after inoculation showed that the hepatocytes had attached to the collagen substrate in small groups composed of two or three cells, but they still had a rounded contour. At 24 hours after inoculation, most cells had spread out and formed a continuous monolayer (fig. 2). Each cell had a refractile, round nucleus with a prominent nucleolus. The cytoplasm had a fine granularity with the occasional appearance of small refractile droplets, probably of lipid origin. The epithelial morphology of the cells was maintained for at least 10 days in culture. As with primary cultures of rat hepatocytes, no evidence of hepatocellular growth was observed.

Samples of the monolayer cultures were taken at day 1 and processed for electron microscopy. A typical appearance of a human hepatocyte in culture on day 1 is shown in figure 4. Large numbers of oblong mitochondria, RER, and prominent SER were seen. Desmosomes were noted in the opposing surfaces of adjacent hepatocytes. Structures analogous to bile canaliculi were not noted. These structures have been shown to be maintained in rat hepatocytes when cultured on floating collagen membranes, but not when cultured on a rigid substrate (*20*). Large numbers of vesicles of SER were seen in the hepatocytes from the first case, especially at day 1. Such a change is classically induced experimentally with phenobarbital, but it can also be induced by large number of drugs, toxins, and nutritional disorders. The medications given to patient #1 preoperatively included 5-fluorouracil, diazepam, and acetaminophen. In electron microscopic studies of needle biopsy specimens from human liver, a similar increase in SER was noticed in patients given diazepam (*21*). Such a change was not seen in hepatocytes obtained from patient #2.

TABLE 1.—*Microsomal enzyme levels as a function of time in culture*[a]

Time in culture, days	Cytochrome P_{450}	Cytochrome *b*5	NADPH-cytochrome *c* reductase
		Case 1	
0	1,380 (100)	2,354 (100)	0.279 (100)
1	785 (58)	963 (41)	0.247 (89)
4	758 (55)	617 (26)	0.352 (126)
		Case 2	
0	970 (100)	392 (100)	0.177 (100)
1	670 (69)	474 (121)	0.235 (133)
4	541 (56)	276 (70)	0.148 (84)

[a] The absolute values indicate picomoles of cytochrome per milligram of microsomal protein or units of reductase per milligram of microsomal protein. *Numbers in parentheses* are percentages of the values measured in the human hepatocytes immediately after the collagenase perfusion (time 0 sample).

Monolayer cultures from both cases were also processed for measurements of microsomal enzymes. The data shown in table 1 express the measured values of the indicated parameters in absolute numbers as well as percentages of the values seen in the isolated hepatocytes immediately after the perfusion. For both cases as an average, the cytochrome P_{450} levels after 24 hours in culture were approximately 60% of those for cells immediately after perfusion. Furthermore, the cytochrome P_{450} levels declined only slightly between days 1 and 4 in culture.

UDS was measured in autoradiographs performed as described in "Materials and Methods." The procarcinogens used were chosen from compounds that are known to be metabolized and result in UDS in primary cultures of rat hepatocytes (*19*). The data obtained are shown separately for the two cases in table 2.

TABLE 2.—*UDS induced in cultures of human hepatocytes by procarcinogens*[a]

Carcinogen, dose	Grains/nucleus, mean±SE[b]	
	Case 1	Case 2
Control	8.4±0.5	11.82±1.1
Diethylnitrosamine, m*M*		
5	13.9±1.1[c]	14.8±0.6, NS
15	17.7±1.5[c]	16.0±1.1[c]
25	16.5±1.2[c]	19.9±1.1[c]
Dimethylnitrosamine, m*M*		
1	11.3±0.8[c]	18.5±1.1[c]
5	11.1±0.6[c]	15.9±1.1[c]
15	18.0±1.5[c]	11.6±0.6, NS
2-FAA, μ*M*		
1	16.8±0.8[c]	17.6±1.0[c]
10	19.0±1.4[c]	20.1±1.3[c]
100	27.2±11.1[c]	19.7±1.2[c]
BP, μ*M*		
1	9.8±0.7, NS	13.1±1.0, NS
10	13.1±1.2[c]	14.4±1.2, NS
100	11.3±1.2[d]	16.2±1.0[d]

[a] Freshly isolated hepatocytes were exposed to the indicated concentration of carcinogen plus 10 μCi [^{3}H]thymidine/ml for 20 hr.

[b] NS=not significantly different from control. Statistical analysis was performed with the use of Student's *t*-test.

[c] Significantly different from control at $P<0.01$.

[d] $P<0.02$.

When human hepatocytes were injected into the intercapsular fat pads of two-thirds hepatectomized athymic nude mice, hepatocyte nodule formation was observed (fig. 3). The cells maintained a morphologic appearance characteristic of hepatocytes, and the nodule formation was analogous to that seen when rat hepatocytes are transplanted into either syngeneic recipient animals (*7*) or athymic nude mice (Michalopoulos G, Strom SC, Jirtle RL: Unpublished data).

DISCUSSION

Quantitative analysis of the effects of chemical carcinogens on cells or tissues of human origin is essential for ultimate assessment of carcinogenic risk in humans and for interspecies comparisons between humans and other species mostly applied in assaying carcinogenicity (rodents). Studies pursuing this approach have been previously presented with replicating cell lines (*22*) or strains of human fibroblasts alone (*23*) or in combination with hepatocytes (*24*). Analogous studies have been extensively conducted in organ cultures of human bronchus (*25*). These studies have demonstrated the capacity of the human bronchus to provide metabolic activation for a wide variety of carcinogens previously recognized as respiratory carcinogens for the rodents.

Studies with human hepatocytes have lagged due to the lack of a feasible technique that can be applied to human liver and result in large numbers of viable hepatocytes, in a way analogous to the case of the two-step collagenase perfusion extensively characterized for rat liver (*2*). The results shown in the present report demonstrate that with use of the modified in situ collagenase perfusion technique, large numbers of viable adult hepatocytes can be obtained that are suitable for primary culture and transplantation into athymic nude mice. The results presented here are not a comprehensive analysis of all the possible studies that could be performed to fully characterize the morphological and biochemical properties of human hepatocytes in primary culture or in transplantation. To our knowledge, however, this is the first incidence where large numbers of viable hepatocytes have been isolated and replicate samples analyzed from a single piece of human liver. The data presented also demonstrate the feasibility of adapting to human hepatocytes the techniques developed for culturing and transplanting rat hepatocytes.

The technique of collagenase perfusion, as described in this report, can be scaled and adjusted for liver fragments of different sizes. In previous studies with dog liver (Michalopoulos G, Strom SC, Jirtle RL: Unpublished results), we observed the highest yield of viable hepatocytes when the fragments were perfused at a flow rate of 14 ml/minute/catheter. We consider it an essential point of the technique to perfuse fragments surrounded entirely by the hepatic capsule with only one cut surface. This configuration forces the perfusate to flow back through the cut surface and perfuse areas whose vascularity is dependent on the vessels of the cut surface. Hepatic tissue sufficiently viable to be amenable to the described procedure can be obtained from organ donors or from scheduled hepatic resections. Hepatic lobectomy (right or left lobe) is frequently performed to remove solitary metastatic lesions resulting from primary neoplasms already resected in the past. For reasons relating to easy hemostasis and tumor containment, it is preferrable to remove the whole lobe that contains the tumor rather than to just enucleate the tumor with a rim of hepatic tissue. Since the remaining liver lobe regenerates to reconstitute total hepatic mass within 10 days, the size of liver tissue removed (when at least one lobe remains) is not of critical importance. The resulting specimen brought into the surgical pathology laboratory usually contains more hepatic tissue than needed for the establishment of diagnosis. The residual excess tissue (normally discarded) can be utilized for the procedure presented in this report. The uniqueness of this procedure is that it applies to larger fragments of hepatic tissue, so that numbers of hepatocytes sufficient for multiple replicate experimental points can be obtained. Previous procedures applicable to needle biopsies or small wedge biopsies (*9*) have already been described.

The main limitations of those systems were that the resulting number of hepatocytes were too small and the viability was not high enough. Most important, however, is the fact that the small wedge or needle biopsy procedures did not utilize hepatic tissue that would be otherwise discarded, but rather they were applicable to hepatic tissue fragments that, in most instances, need to be processed in toto for diagnostic purposes. Such pieces are not routinely available for research purposes due to restrictions justafiably imposed by ethics committees. Such restrictions, however, usually do not apply to tissue that will definitely be otherwise discarded and is not of diagnostic use. This technique, with the details presented in "Materials and Methods," was so far successful in both of the only two instances that we applied it for the purposes of this report.

The measurement of UDS by autoradiography as described by Williams (*18*) is particularly suitable for human hepatocytes in that it can be adapted for use with small samples. Each of the chambers of an eight-chamber slide has an area of 1 cm^2, which allows up to 100,000 hepatocytes to be individually evaluated by counting of the grains per nucleus as previously described (*17, 18*).

The results obtained from the studies with UDS (table 2) indicate that the hepatocytes can metabolize the procarcinogens to active genotoxic metabolites which then react with DNA. The UDS assay used indicates the amount of DNA synthesis that takes place to fill the gaps generated during the excision repair process. 2-FAA was a good inducer of UDS in both cases. Nitrosamines also induced UDS in both cases. In both cases, lesser degrees of UDS were seen with BP than with 2-FAA at equivalent concentrations. Although it is premature to generalize from these two cases, the observed rank order of maximal induced UDS for the fou carcinogens (2-FAA>nitrosamines>BP) correlates well with the observed rank described in rat hepatocyte monolayer systems by Williams (*18*), by Tong et al. (*26*), and by u (*27*). More cases are necessary to give us an estimate of the range of variation of these responses in the human population. The preliminary results of this report do point out however, interesting similarities between rat and human hepatocytes in terms of their responses to these carcinogens.

Differences in the degree of response to the same concentrations of chemicals were seen between the two cases (e.g. dimethylnitrosamine). These differences may reflect patterns of expression of hepatic microsomal or cytosol enzym activities that are known to be affected by drugs, nutrients, sex, and age. All four of these factors differed in these two cases. An increase in membranes and vesicles of SER was seen in the first case. This change has been described (*21*) in patients after prolonged use of Valium (diazepam), as in this case. This change is also reflected in the higher levels of cytochrome P_{450} complex seen in the hepatocytes of the first case (table 1). The decrease in cytochrome P_{450} levels seen is analogous to that described for the rat hepatocytes (*14*). The decrease in cytochrome P_{450}, however, is much less in the cultures of human hepatocytes. At day 4 in culture, in both cases, more than 50% of the cytochrome P_{450} is still maintained. In similar cultures of rat hepatocytes, less than 10% of the original value of cytochrome P_{450} is still maintained at day 4. The reasons for these differences are not clear at the present time.

We have previously demonstrated that when rat hepatocytes are transplanted into syngeneic hosts, liver nodules develop with a characteristic hepatocyte histologic architecture (*7*). We have also shown that the nodules of hepatocytes at the site of transplantation arise as a result of clonal proliferation of hepatocytes. Analogous proliferation of cells is not seen in primary cultures. We have utilized the transplantation system to quantify the effects of ionizing radiation on the clonogenic survival of parenchymal rat hepatocytes (*11*). This assay system also enables the clonogenic survival of rat hepatocytes to be estimated after an in vitro exposure to mutagenic and carcinogenic compounds. Because of the results in figure 3, this in vivo clonogenic assay system may also be adapted for use with human hepatocytes. The transplantation of human hepatocytes into athymic nude mice, in a manner similar to that developed for rat hepatocytes, also may enable us to estimate the genotoxic effects of mutagenic and carcinogenic agents that are metabolized by the human liver. Full characterization of this system, in a way analogous to that of the rat system, will be attempted in future studies.

In conclusion, we have developed a modified version of the in situ collagenase perfusion technique that can be used to enzymatically disperse hepatocytes from pieces of human liver. These hepatocytes can be used for primary culture or transplantation. The studies with cytochrome P_{450} and UDS indicate that despite differences in sex, age, and exposure to drugs, common trends may be seen in human hepatocytes. These trends, in the case of cytochrome P_{450}, may be different than those seen with the rat. Accumulation of experience with a larger number of cases will allow comprehensive analysis of these trends and differences. These studies indicate that the collagenase perfusion technique presented in this report can result in production of large numbers of human hepatocytes from which replicate samples can be obtained for meaningful studies.

NOTE ADDED IN PROOF

Since this paper was accepted for publication, a similar technique for perfusing hepatic fragments was described by Reese and Byard (In Vitro 1981; 17:935–940).

REFERENCES

(*1*) Berry MN, Friend DS. High yield preparation of isolated rat liver parenchymal cells. J Cell Biol 1969; 43:506–520.

(*2*) Seglen PO. Preparation of isolated rat liver cells. Methods Cell Biol 1976; 18:29–83.

(*3*) Bissel DM. Study of hepatocyte function in cell cultures. Prog Liver Dis 1976; 5:69–82.

(*4*) Bonney RS, Becker JE, Walker PR, Potter VR. Primary monolayer cultures of adult rat liver parenchymal cells suitable for study of regulation of enzyme synthesis. In Vitro 1974; 9:399–413.

(*5*) Michalopoulos G, Pitot HC. Primary culture of parenchymal liver cells on collagen membranes. Exp Cell Res 1975; 94:70–78.

(*6*) Laishes BA, Williams GM. Conditions affecting primary cell cultures of functional adult rat hepatocytes. In Vitro 1976; 12:821–832.

(*7*) Jirtle RL, Biles C, Michalopoulos G. Morphologic and histochemical analysis of hepatocytes transplanted into syngeneic hosts. Am J Pathol 1980; 101:115–123.

(*8*) Mito M, Ebata H, Kusano M, Onishi T, Saito T, Sakamoto S. Morphology and function of isolated hepatocytes transplanted into rat spleen. Transplantation 1979; 28:499–505.

(*9*) Laishes BA, Farber E. Transfer of viable putative preneoplastic hepatocytes to the livers of syngeneic host rats. JNCI 1978; 61:507–512.

(*10*) Guillouzo A, Oudea P, LeGuilly Y, Oudea MC, Lenoir P, Bourel M. An ultrastructural study of primary cultures of adult human liver tissue. Exp Mol Pathol 1972; 16:1–15.

(*11*) Jirtle RL, Michalopoulos G, McLain JR, Crowley J. Transplantation system for determining clonogenic survival of parenchymal hepatocytes exposed to ionizing radiation. Cancer Res 1981; 41:3512–3518.

(*12*) Jirtle RL, McLain JR, Michalopoulos G. Effects of hepatectomy on transplanted hepatocytes. Proc Am Assoc Cancer Res 1981; 22:abstract No. 557.

(*13*) Deschenes J, Valet JP, Marceau N. Hepatocytes from newborn and weanling rats in monolayer culture. In Vitro 1980; 16:722–730.

(*14*) Michalopoulos G, Russell F, Biles C. Primary cultures of hepatocytes on human fibroblasts. In Vitro 1979; 15:796–806.

(*15*) Setaro F, Morley C. A modified fluorometric method for the determination of microgram quantities of DNA from cells or tissue cultures. Anal Biochem 1976; 71:313–317.

(*16*) Omura T, Sato R. The carbon-monoxide binding pigment of liver microsomes. J Biol Chem 1964; 239:2370–2378.

(*17*) Phillips AH, Langdon RG. Hepatic triphosphopyridin nucleotide cytochrome *c* reductase: Isolation, characterization and kinetic studies. J Biol Chem 1964; 237:2652–2660.

(*18*) Williams GM. Detection of chemical carcinogens by unscheduled DNA synthesis in rat liver primary cell cultures. Cancer Res 1977; 37:1845–1851.

(*19*) Probst GS, McMahoy RE, Hill LE, Thompson CZ, Epp JK, Neal SB. Chemically induced unscheduled DNA synthesis in primary rat hepatocyte cultures. Environ Mutagen 1981; 3:11–32.

(*20*) Sattler CA, Michalopoulos G, Sattler GL, Pitot HC. Ultrastructure of adult rat hepatocytes cultured on floating collagen membranes. Cancer Res 1978; 38:1539–1549.

(*21*) Jezequel AM, Koch M, Orlandi FA. Morphometric study of the endoplasmic reticulum in human hepatocytes. Gut 1974; 15:737–747.

(*22*) Skopek RT, Liber HL, Peyman BW, Thilly WG. Isolation of a human lymphoblastoid cell line heterozygous at the thymidine-kinase locus: A possibility for a rapid human cell mutation assay. Biochem Biophys Res Commun 1978; 84:411–416.

(*23*) Albertini RJ, DeMars R. Diploid azaguanine resistant mutants of cultured human fibroblasts. Science 1970; 169:482–485.

(*24*) Michalopoulos G, Strom SC, Kligerman AD, Iron GP, Novicki DL. Mutagenesis induced by procarcinogens at the hypoxanthine-guanine phosphoribosyl transferase locus of human fibroblasts co-cultured with rat hepatocytes. Cancer Res 1981; 411:1873–1878.

(*25*) Harris CC, Frank AL, van Haaften C, et al. Binding of ^{3}H-benzo(*a*)pyrene to DNA in cultured human bronchus. Cancer Res 1976; 36:1011–1018.

(*26*) Tong C, Laspia MF, Telang S, Williams GM. The use of adult rat liver cultures in the detection of the genotoxicity of various polycyclic aromatic hydrocarbons. Environ Mutagen 1981; 3:477–487.

(*27*) Strom SG, Kligerman AD, Michalopoulos G. Comparisons of the effects of chemical carcinogens in mixed cultures of rat hepatocytes and human fibroblasts. Carcinogenesis 1981; 2:709–715.

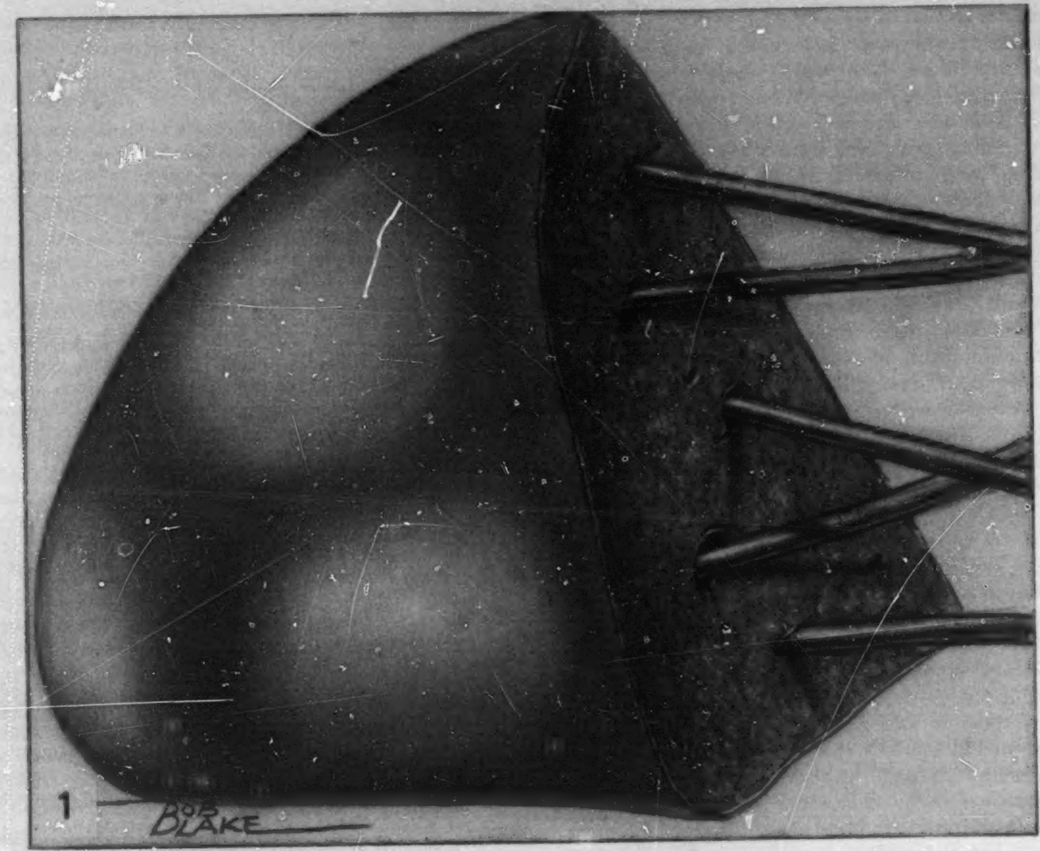

FIGURE 1.—Schematic drawing of an idealized piece of human liver during the perfusion process. Blanched areas on the surface indicate areas perfused by the catheterized vessels. *Note* the presence of only one cut surface.

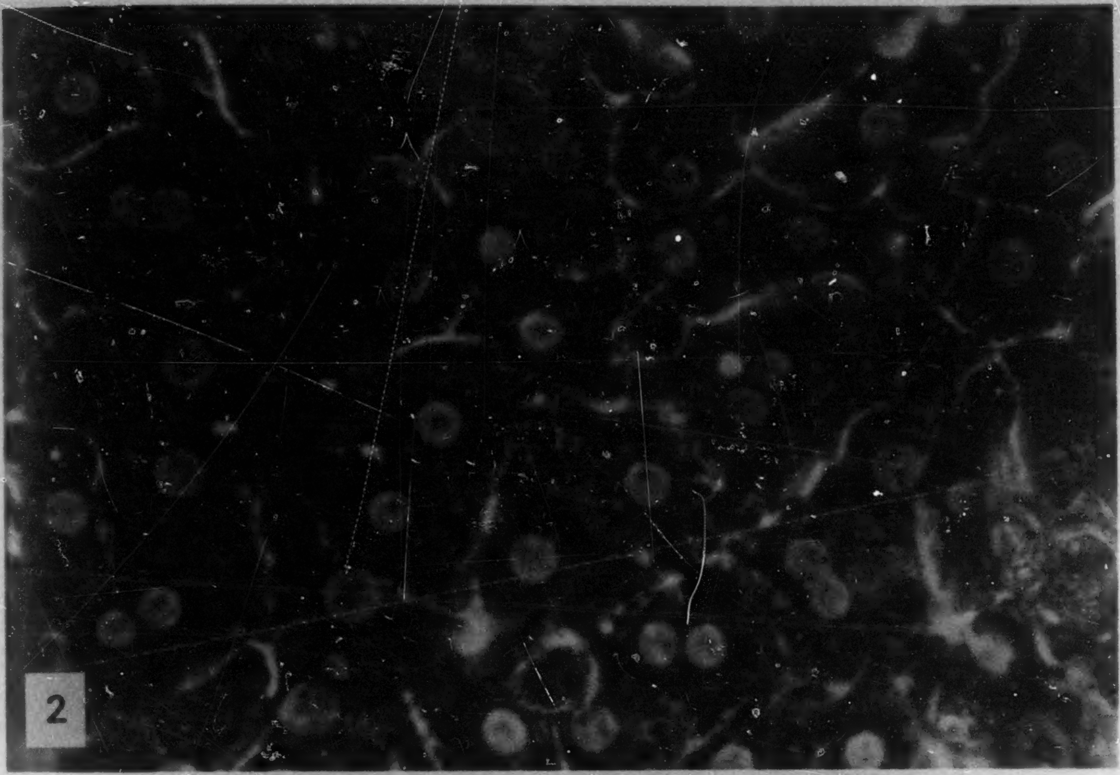

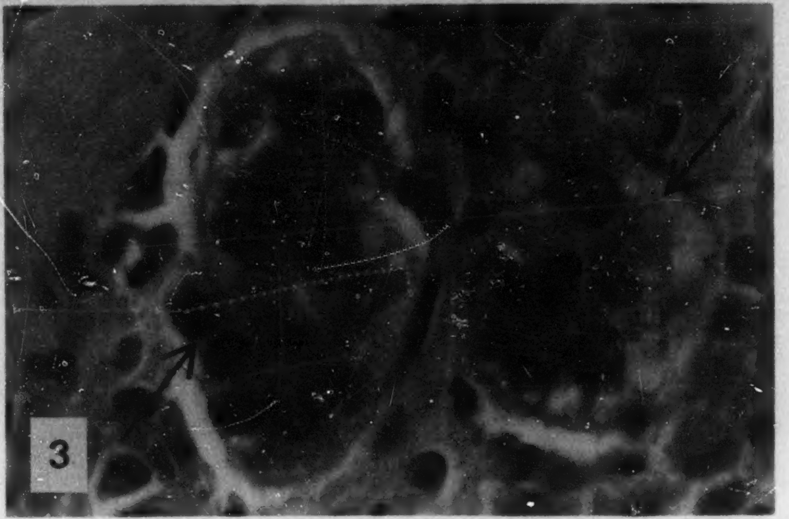

FIGURE 2.—Phase-contrast photomicrographs of human hepatocytes at 24 hr in primary culture. × 100

FIGURE 3.—Clusters of human hepatocytes (*arrows*) 20 days after transplantation into athymic nude mice. Cells were injected 1 hr after the mice were subjected to a two-thirds partial hepatectomy. Sections were stained with hematoxylin and eosin. × 400

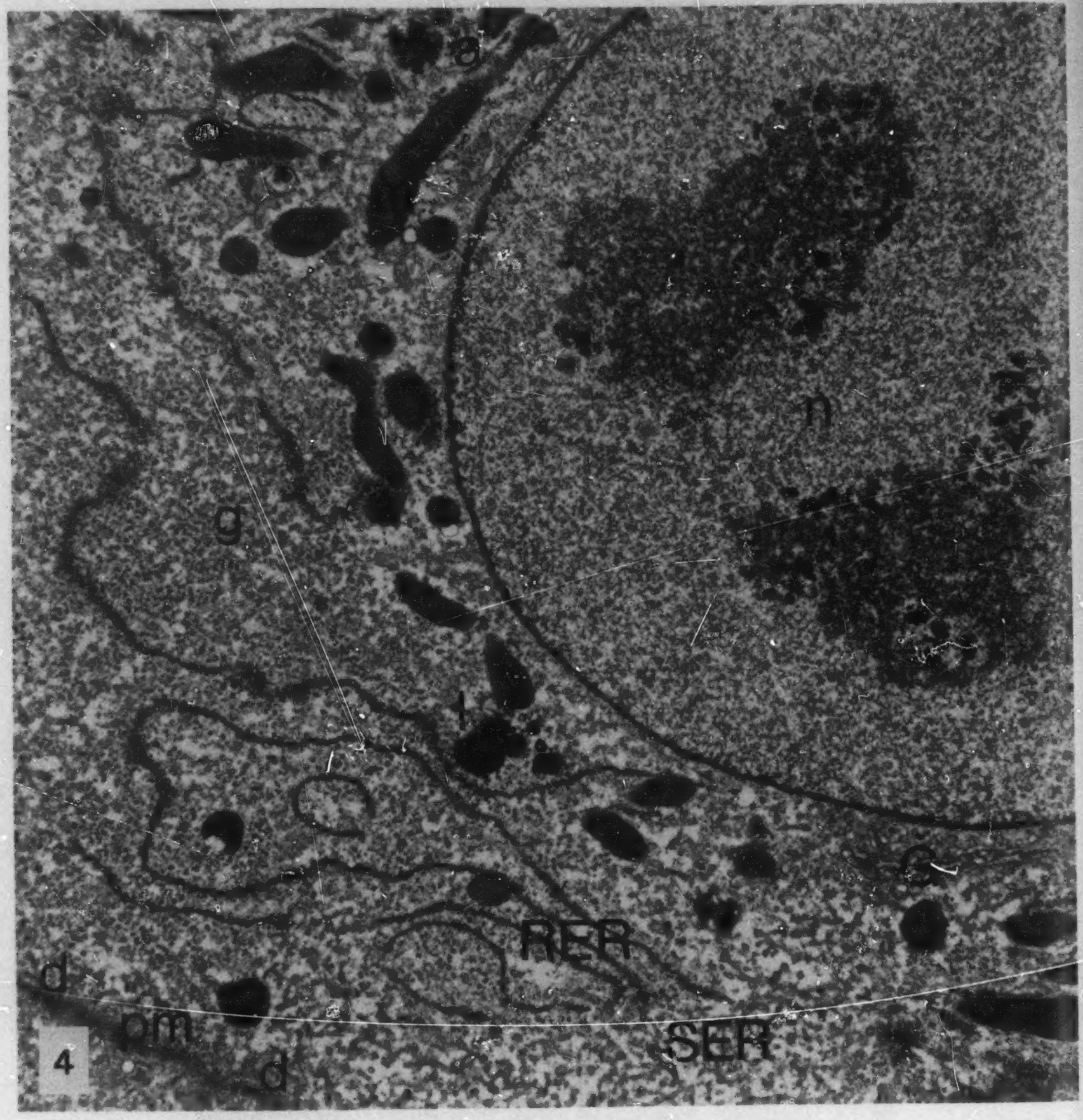

FIGURE 4.—Electron micrograph of a human hepatocyte at 1 day in culture. n=nucleus; m=mitochondrion; g=glycogen granules; G=Golgi apparatus; l=lipid droplets; pm=plasma membrane; a=autophagosome; d=desmosome. × 5,800

Mitogen-Induced Blastogenesis and Receptor Mobility Inhibition by Breast Cancer Serum With Elevated Orosomucoid (α_1-Acid Glycoprotein) Levels [1,2,3]

David A. Cheresh,[4] **John A. Distasio,**[4,5,6] **Charles L. Vogel,**[5] *and* **Diana M. Lopez**[4,5,7]

ABSTRACT—Sera from cancer patients have been shown to suppress normal lymphoid cell responsiveness in vitro. In the present study, sera from breast cancer patients were demonstrated to be inhibitory to the concanavalin A (Con A)-, *Proteus vulgaris*-derived phytohemagglutinin-, and pokeweed mitogen-induced blastogenic responses of normal lymphoid cells. Orosomucoid (OR) (α_1-acid glycoprotein), an acute-phase reactant, was elevated in these sera, and a positive correlation existed between the OR level in the sera and its immunosuppressive capacity. When normal lymphoid cells were reacted in fluorescein isothiocyanate-labeled Con A, cells that had been preincubated in breast cancer sera known to contain an elevated level of OR showed a significant decrease in Con A receptor mobility as compared to the receptor mobility of the same lymphoid cells preincubated in normal sera. Thus a component(s) from the sera of breast cancer patients had the capacity to inhibit lymphocyte activation. This inhibition might have resulted from an interaction of OR with the cell membrane.—JNCI 1982; 68:779–783.

That breast cancer patients are immunologically compromised is well documented (*1–4*). Numerous studies have demonstrated reduced immune function, particularly in the patient with advanced-stage disease. Lymphoid cells from breast cancer patients have been shown to be deficient in their ability to serve as effector cells in cytotoxic reactions, to undergo blast transformation, and to mediate delayed-type hypersensitivity reactions (*1–4*).

We have recently reported that lymphoid cells from breast cancer patients with metastatic disease responded poorly in a Con A-induced blastogenic assay, as compared to cells of normal donors. With the use of the competitive inhibitor α-methyl-D-mannoside, we could maximize the difference in blastogenic response between lymphoid cells from healthy donors and lymphoid cells from cancer patients with early- as well as late-stage disease (*5*). Our study suggested that a membrane alteration on the lymphoid cells from these patients might affect Con A binding or Con A receptor affinity. In ^{125}I-labeled Con A binding studies, we were unable to detect an alteration in the average number of Con A receptors or the average receptor affinity for Con A on lymphocytes from metastatic breast cancer patients. Moreover, using FITC-labeled anti-Con A, we were unable to detect a difference in the number of cells capable of binding Con A (Schilder RJ, Distasio JA: Unpublished results).

In the present study, we investigated the possibility that a factor in sera from breast cancer patients may interact with lymphocyte membranes and alter their capacity to be stimulated by mitogen. Numerous reports in the literature have demonstrated the immunosuppressive potential of sera from cancer patients (*6–9*). The serum factor OR (α_1-acid glycoprotein) is a constituent of normal serum which is elevated in the acute phase of inflammation, neoplasia, rheumatoid arthritis, and pregnancy (*10, 11*). When OR is added to normal lymphoid cells in culture, it is capable of inhibiting mitogen-induced blast transformation, mixed lymphocyte responses, and cytotoxic reactions (*12, 13*). OR is a glycoprotein (mol wt, 41,000), 42% of which is carbohydrate. It has a high (10–12%) sialic acid content (*14*) and is composed of 181 amino acids, which have significant sequence homology to the constant and variable portions of immunoglobulin (*15*). OR has been shown to be associated with the membranes of lymphocytes, monocytes, and granulocytes (*16*). While liver is the primary site of OR synthesis and secretion, a recent study indicates that OR is also secreted by T-lymphocytes (*16*). Thus it seems plausible that OR may serve as an immunoregulatory molecule.

In the present study, we examined the effects of sera from metastatic breast cancer patients on the activation of lymphoid cells from normal donors. We show a positive correlation between the OR level and the immunosuppressive potential of the sera. We also demonstrate that breast cancer patients' sera known to have an elevated level of OR are capable of inhibiting Con A receptor mobility. These findings indicate that a lymphocyte membrane alteration is induced by the serum of the breast cancer patient and that OR may be the responsible factor.

ABBREVIATIONS USED: Con A=concanavalin A; FITC=fluorescein isothiocyanate; HBSS$^-$=Hanks' balanced salt solution without Ca^{2+} or Mg^{2+}; LSM=Lymphocyte Separation Medium; OR=orosomucoid; PBS=phosphate-buffered saline; PHA=phytohemagglutinin; PHA-P=PHA isolated from *Proteus vulgaris*; PWM=pokeweed mitogen; *r*=correlation coefficients.

---

[1] Received October 30, 1981; accepted January 26, 1982.

[2] Supported by a grant from the Women's Cancer Association of the University of Miami.

[3] Research procedures were in accord with the ethical standards of the Human Assurance Committee, University of Miami School of Medicine.

[4] Department of Microbiology D4-4, University of Miami School of Medicine, Miami, Fla.

[5] Department of Oncology D8-4, University of Miami School of Medicine.

[6] *Address reprint requests to* Dr. Distasio at the Department of Microbiology D4-4, University of Miami School of Medicine, P.O. Box 016960, Miami, Fla. 33101.

[7] We thank Ms. Dawn East and Ms. Margaret Szaro (University of Miami Hospitals and Clinics) for identifying suitable patients for our study, confirming clinical characteristics of patients, and obtaining the blood; and Dr. Karl Schmid (Department of Biochemistry, School of Medicine, Boston University, Boston Mass.) for providing the purified orosomucoid that was used as the standard in this study. We give special thanks to Mrs. Frances Susi for typing the manuscript.

MATERIALS AND METHODS

Patient population.—Sera were collected from 25 women with metastatic breast cancer. The following staging procedures were done for each woman before she was entered into this study: complete medical history, physical examination, and blood and platelet counts; liver function tests; plasma carcinoembryonic antigen assay; chest X-ray; liver and bone radionuclide scans; and confirmatory bone X-rays of bone scan-positive areas. All of the patients were shown to have local, regional, or distant metastases. No patient receiving systemic therapy for cancer within the past year was entered into the study. Excluded from the study were patients who had received radiation therapy and patients with a history of diabetes mellitus, alcoholism, rheumatoid arthritis, or any other chronic condition. The mean age of the patients was 58.0 years (range, 30–77 yr). Sera were collected from 28 healthy women for use in control assays. The mean age of the normal donors was 52.3 years (range, 23–70 yr).

Collection of sera.—Blood was obtained by venipuncture and was allowed to clot for 2 hours at room temperature. The sera were separated from the clots by centrifugation at 1,000×*g* for 15 minutes. The sera were allowed to stand at room temperature for 24 hours, which inactivated complement, and the complement-inactivated sera were then stored at 4°C until use.

Quantitation of serum OR.—Serum levels of OR were determined by the Mancini single radial immunodiffusion method (*17*). Goat anti-OR (Miles Laboratories, Inc., Elkhart, Ind.) was diluted 1:5 with PBS (pH 7.4). The diluted antibody was prewarmed to 50°C and mixed with equal parts of 2% agarose (liquefied) in a 0.1-*M* sodium barbital buffer (pH 8.4). The agarose-antibody solution was thoroughly mixed and poured between glass plates spaced 1 mm apart. After solidification, one glass plate was removed, and wells (2 mm in diameter) were punched in the gel. Diluted sera or solutions of OR standards (0.0625–1.0 mg/ml) were added in 3-µl amounts to triplicate wells, and diffusion was at room temperature in a humidified chamber for 48 hours. Precipitated rings were measured with calipers. Serum OR levels were compared to an OR standard curve that had been plotted as the diameter (mm) of the precipitin band as a function of the log of the OR concentration. OR used as the standard in this assay was provided by Dr. Karl Schmid, Boston University, Boston, Mass.

Isolation of mononuclear cells.—Peripheral blood mononuclear cells were obtained from healthy individuals with type O blood. Blood was obtained by venipuncture into syringes containing sufficient heparin (The Upjohn Co., Kalamazoo, Mich.) to yield a final concentration of 10 U/ml blood. Blood was diluted with an equal volume of sterile saline. Mononuclear cells were isolated by discontinuous density gradient centrifugation with LSM (Litton Bionetics Inc., Kensington, Md.). Diluted blood (20 ml) was layered over 15 ml of LSM. The gradients were spun at 400×*g* for 40 minutes at 19°C. Mononuclear cells were recovered from the interface and were washed three times with RPMI-1640 medium (GIBCO, Grand Island, N.Y.) supplemented with 100 U penicillin/ml and 50 µg streptomycin/ml (Associated Biomedic Systems, Inc., Buffalo, N.Y.). Washed cells were pelleted by centrifugation for 10 minutes at 25°C. Cells were resuspended appropriately for each assay as described below.

Blastogenesis assay.—Triplicate cultures were initiated in #3040 microtiter plates (Falcon Plastics, Los Angeles, Calif.) by the addition of 0.01 ml of each of the following solutions to each well of the plate: 0.5 mg Con A/ml (Calbiochem-Behring Corp., Los Angeles, Calif.), 0.1 mg PHA-P/ml (Difco Laboratories, Detroit, Mich.), or 0.5 mg PWM/ml (GIBCO). For control cultures, 0.01 ml of growth medium was added in place of mitogen. An additional 0.19 ml of growth medium supplemented with 10% human serum and containing 1×10^5 mononuclear cells was dispensed per well, and cultures were incubated for 72 hours in a 5% CO_2 humidified atmosphere. Eighteen hours before being harvested, cultures were pulsed with 0.01 ml of [^{3}H]thymidine solution (50 µCi/ml). A Skatron cell harvester (Flow Laboratories, Inc., Rockville, Md.) was used, and cells were collected on #78-105-05 glass fiber filter paper (Flow Laboratories, Inc.) and washed. Filter paper disks containing [^{3}H]DNA were placed in polyethylene vials with 5 ml of a scintillation cocktail of toluene containing 5 g 2,5-diphenyloxazole/liter and 0.2 g 1,4-bis[2-(5-phenyloxazolyl)] benzene/liter (Yorktown, Inc., Hackensack, N.J.). Vials were enumerated in a Tri-Carb liquid scintillation counter (model 3330; Packard Instrument Co., La Grange, Ill.). Data are presented as counts per minute of experimental cultures with mitogen less counts per minute of control cultures without mitogen.

Con A receptor mobility.—Mononuclear cells (2×10^6 cells) from a normal individual were incubated for 1 hour at 37°C in the presence of 0.2 ml of serum from a normal donor or breast cancer patient. The cells were washed once with HBSS$^-$. The cell pellet was resuspended in 0.2 ml FITC-Con A (Miles Laboratories, Inc.) (15 µg/ml) in HBSS$^-$. The incubation was done for 15 minutes in a 37°C water bath, after which time 0.2 ml of a 4% paraformaldehyde solution was added, thereby fixing the cells. We had previously determined that 15 minutes at 37°C was the optimal time for the fluorescent cells to demonstrate maximal capping under the conditions of this assay. After fixation, the cells were washed with PBS containing 1 mg bovine serum albumin/ml. Cells were then placed on a slide, and the number of cells with rings, patches, and caps was determined with a Nikon Optiphot microscope equipped with epifluorescence. Each slide was examined blindly, and a minimum of 200 cells/slide were counted. A cell was considered capped when the fluorescence was distributed uniformly over no more than one-third of the cell membrane. Cells with uropod formation were not counted.

Statistical analysis.—Data were analyzed by Student's *t*-test for unpaired random variables. A *P*-value of less than 0.05 was considered significant, and *r* were calculated by linear regression analysis.

RESULTS

Individual blastogenic responses of healthy donors' lymphoid cells incubated in the presence of sera from normal individuals (n=14) or sera from breast cancer patients (n=15) (hereafter called normal sera and breast cancer sera, respectively) were determined (text-fig. 1). The mean plus

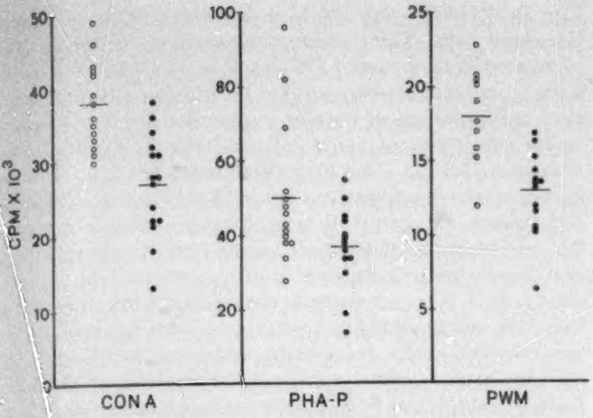

TEXT-FIGURE 1.—Effect of normal or breast cancer sera on the Con A-, PHA-P-, and PWM-induced blastogenic response of normal lymphoid cells. ○=blastogenic response of lymphoid cells incubated in normal sera; ●=blastogenic response of lymphoid cells incubated in breast cancer sera. *Bars* represent mean blastogenic response in counts per minute. Effects of each serum tested were determined on lymphoid cells from 1 of 4 healthy donors. For additional experimental details, *see* "Materials and Methods."

or minus standard error for each response is recorded in table 1. In the presence of breast cancer sera, the mean Con A, PHA-P, and PWM mitogenic responses were inhibited approximately 29% ($P<0.001$), 26% ($P<0.05$), and 27% ($P<0.001$), respectively.

The serum OR concentrations of normal donors and breast cancer patients are compared in text-figure 2. In normal sera ($n=28$), the mean OR level was 0.77 mg/ml (range, 0.5–1.26 mg/ml). In the breast cancer sera ($n=25$), the mean OR level was 1.47 mg/ml (range, 0.64–2.65 mg/ml). Statistical analysis revealed that the breast cancer sera contained significantly elevated levels of OR ($P<0.001$).

The correlation between the breast cancer serum OR level and its immunosuppressive capacity appears in text-figure 3. In each experiment the blastogenic responses of lymphocytes from healthy donors in the presence of serum from each patient was compared to the response in the presence of serum from a normal donor. The percentage of the blastogenic response of healthy donor's lymphocytes in the presence of breast cancer sera ($n=12$) as compared to the response in the presence of normal sera ($n=12$) is reported on the ordinate. The OR level of each breast cancer patient's serum is reported on the abscissa. The OR level of the cancer sera is negatively correlated with its capacity to support blast transformation. The r of the Con A-, PHA-P-, and PWM-induced blastogenic responses were −0.70, −0.63, and −0.53, respectively.

Normal donors' lymphocytes were preincubated in the presence of sera from breast cancer patients known to have elevated concentrations of OR or in the presence of sera from normal individuals and then tested for Con A receptor mobility. The total number of cells demonstrating ring, patch, and cap fluorescence is shown in table 2. The normal sera ($n=6$) used in these studies had a mean OR level ± SE of 0.70 mg/ml±0.04, whereas the breast cancer sera ($n=6$) had a mean OR level ± SE of 1.96 mg/ml±0.19. When normal donors' lymphocytes were preincubated in breast cancer sera, the total number of cells bearing ring fluorescence was significantly increased ($P<0.05$), and the total number of cells with caps was significantly decreased ($P<0.001$) as compared to normal donors' lymphocytes preincubated in normal donor sera. The number of cells showing patched fluorescence remained unchanged ($P>0.05$). These same sera were tested for their ability to support blast transformation in the presence of Con A, PHA-P, and PWM. Preincubation of lymphocytes from healthy donors in breast cancer sera resulted in a mean

TABLE 1—*Blastogenic responses of lymphoid cells incubated in normal or breast cancer sera*[a]

Mitogen	Mean cpm ± SE of cells incubated in:		Percent of normal response
	Normal sera	Breast cancer sera	
Con A	38,271±1,542	27,120±1,789	71
PHA-P	50,346±5,157	37,345±2,734	74
PWM	17,956±912	13,033±733	73

[a] Statistical analysis was performed by Student's t-test. Mean cpm of normal donors' lymphocytes incubated in breast cancer sera ($n=14$) were compared to the mean cpm of normal donors' lymphocytes incubated in sera from normal individuals ($n=14$). The Con A, PHA-P, and PWM blastogenic responses were significantly decreased ($P<0.001$, <0.05, and <0.001, respectively) when cells were incubated in breast cancer sera as compared to cells preincubated in normal sera.

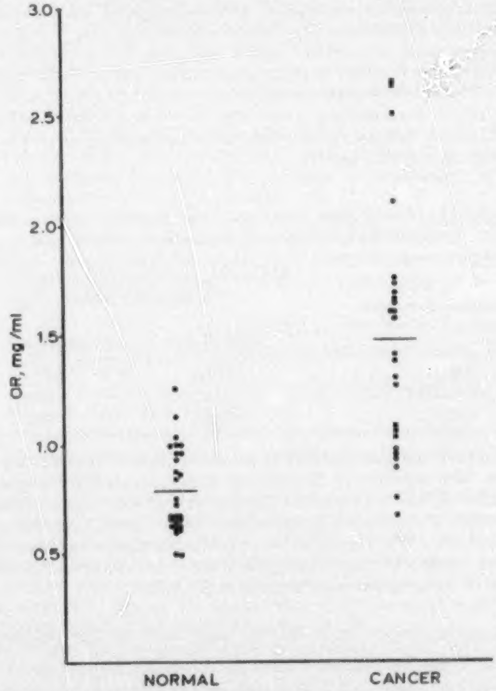

TEXT-FIGURE 2.—Serum OR levels of metastatic breast cancer patients and normal donors. *Bars* represent mean OR concentration (mg/ml). Mean OR concentration in normal sera ($n=28$) is 0.77 mg/ml, and in breast cancer sera ($n=25$) it is 1.47 mg/ml. For experimental details, *see* "Materials and Methods."

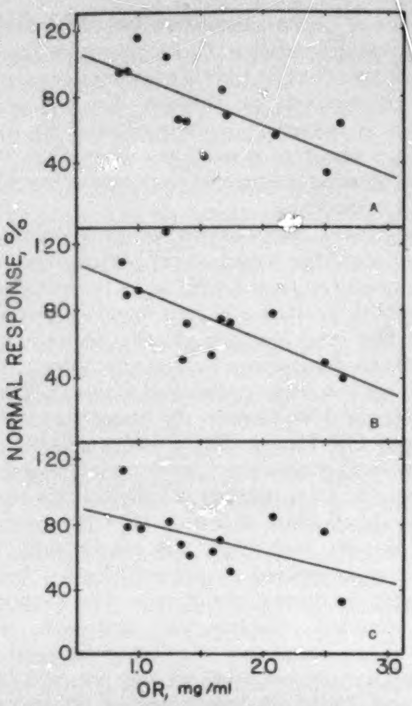

TEXT-FIGURE 3.—Effect of OR concentration of breast cancer sera on the Con A-, PHA-P-, and PWM-induced (A, B, and C, respectively) blastogenic response of normal lymphoid cells. *Each point* represents the percent blastogenic response of normal lymphoid cells incubated in serum from a breast cancer patient as compared to those cells incubated in serum from a matched normal donor, as a function of the OR concentration (mg/ml) of each cancer serum tested. The *r* of Con A, PHA-P, and PWM responses are −0.70, −0.63, and −0.53, respectively. The effects of each serum tested were determined with lymphoid cells from 1 of 4 healthy donors. For additional experimental details, *see* "Materials and Methods."

TABLE 2.—*Con A ring, patch, and cap fluorescence in normal donors' lymphocytes incubated with normal or breast cancer sera*[a]

Flourescence type	Mean No. of fluorescent cells/200 cells ± SE after incubation with:	
	Normal sera	Breast cancer sera
Rings	131±4	146±5
Patches	34±2	35±4
Caps	34±2	19±2

[a] Statistical analysis was performed by Student's *t*-test. In each comparison, the number of fluorescent lymphocytes/200 lymphocytes preincubated in the presence of breast cancer sera was compared to the number of fluorescent lymphocytes/200 lymphocytes preincubated in normal sera. When lymphocytes were preincubated in breast cancer sera, the number of rings was significantly increased ($P<0.05$), and the number of caps significantly decreased ($P<0.001$).

blastogenic response of 56, 65, and 68% of the response in the presence of normal sera, respectively.

DISCUSSION

In the present study we demonstrated that sera from metastatic breast cancer patients are capable of inhibiting Con A-, PHA-P-, and PWM-induced activation of normal lymphoid cells. These reduced blastogenic responses were correlated with elevated OR levels in the sera of patients with metastatic breast cancer. OR is an acute-phase reactant, a component of normal serum that becomes elevated under conditions of acute inflammation, pregnancy, and neoplasia (*10, 11*). This glycoprotein has been shown to be highly immunosuppressive when added to human lymphoid cells grown in vitro. OR was shown to inhibit mitogen-induced blast transformation, mixed lymphocyte responses, and T-cell rosette formation in the presence of sheep erythrocytes (*13*). A recent study in the murine system has shown that OR, when added to lymphocyte cultures, inhibits the induction of antibody-secreting cells and development of cell-mediated lympholysis against allogeneic target cells. Bennett and Schmid (*12*) implicated the carbohydrate portion of the molecule as being instrumental in its immunosuppressive capability

Experiments by Chiu et al. (*13*) demonstrated that human lymphocytes preincubated in OR and subsequently washed were inhibited in their capacity to be stimulated by mitogen. These investigators suggested that OR may inhibit lymphocyte activation by interacting with the cell surface. More recently, Gahmberg and Andersson (*16*) demonstrated that F(ab)'$_2$ anti-OR was able to bind to the membranes of lymphocytes, granulocytes, and monocytes. Work in our laboratory supports the concept that OR is capable of associating with membranes. We have shown that this glycoprotein interacts with synthetic phospholipid vesicles and is capable of displacing a membrane-bound anionic probe (Cheresh DA, Haynes DH, Distasio JA: Submitted for publication). Our results suggest that OR affects the net charge on the polar head region of the phospholipid membrane. Moreover, addition of pure OR to lymphoid cells in culture results in an inhibition of mitogen-induced activation as well as of receptor mobility. These experiments suggest that OR at elevated concentrations is capable of interacting with the lymphoid cell membrane and/or of modulating cellular mechanisms known to be associated with lymphocyte activation.

Receptor mobility as measured by Con A capping occurs in two stages. First, the ligand receptor complexes passively aggregate into multiple patches of variable size, and second, the patches aggregate into a single mass or a cap. Only the second stage is energy-dependent (*18*). The formation of patches is attributed to the ability of the ligand to cross-link receptors (*18*). Our results indicate that both stages in Con A receptor redistribution are affected, since we see a significantly greater number of cells with ring fluorescence in the breast cancer serum-treated lymphocytes as well as a significant decrease in the number of cells that demonstrate capped fluorescence. Therefore, it does not appear that normal lymphoid cells preincubated in breast cancer serum are simply metabolically inhibited, since ring-to-patch formation, which occurs spontaneously, is also inhibited.

Other studies have demonstrated that individuals known to have suppressed lymphoid function demonstrate reduced receptor capping. Markedly reduced Con A capping has been demonstrated as a function of age in humans (*19*). It is also well documented that lymphocytes from aged individuals respond poorly in mitogen-induced blastogenesis (*20, 21*). Similar findings have been reported in the aged rat, in which reduced receptor mobility of three lymphoid surface proteins was shown (*22*). Immune hyporesponsiveness was shown to correlate with age in these animals (*23*). An interesting note is that certain drugs that impede membrane receptor mobility are also very inhibitory to cell proliferation. Cytochalasin B, a drug known to perturb submembrane microfilaments, is inhibitory to cell proliferation (*24*) and has been shown to inhibit redistribution of membrane-bound ligands (*25*). Local anesthetics and tranquilizers have been shown to inhibit PHA-induced lymphocyte transformation (*26*) as well as inhibit membrane receptor redistribution (*27*). These agents prevent membrane depolarization (*28, 29*), which is a necessary step in lymphocyte activation and has been shown to occur within the first few minutes after mitogen binding (*30, 31*).

In this study we have demonstrated a correlation between the OR level and the inhibitory effects of breast cancer serum on mitogen-induced blastogenesis of normal lymphoid cells. Other serum components may play an immunosuppressive role. Previous studies have demonstrated various serum proteins known to be immunosuppressive, e.g., α-fetoprotein (*32*), C-reactive protein (*33*), and immunoregulatory α-globulin (*34*), are elevated in cancer patients. Elevation of any of these factors may affect the inhibitory capability of a patient's serum. However, in parallel work in which we added OR to normal human lymphocyte cultures, we were able to demonstrate a similar pattern of immunosuppression as that found with breast cancer serum containing elevated levels of OR. Therefore, OR must be considered as an additional serum protein that can influence lymphocyte responsiveness.

REFERENCES

(*1*) Stein JA, Adler A, Shlomo BE, Maor M. Immunocompetence, immunosuppression, and human breast cancer. Cancer 1976; 38:1171–1187.

(*2*) Nemoto T, Han T, Minowada J, Angkur V, Chamberlain A, Dao TL. Cell-mediated immune status of breast cancer patients: Evaluation by skin tests, lymphocyte stimulation, and counts of rosette-forming cells. J Natl Cancer Inst 1974; 53:641–645.

(*3*) Weese JL, Oldham RK, Tormey DC, et al. Immunologic monitoring in carcinoma of the breast. Surg Gynecol Obstet 1977; 145:209-218.

(*4*) Wanebo HJ, Thaler HT, Hansen JA, et al. Immunologic reactivity in patients with primary breast cancer. Cancer 1978; 41:84–94.

(*5*) DiStasio JA, Cheresh DA, Schilder RJ, Vogel CL, Silverman MA, Lopez DM. Maximizing differences in the concanavalin A-induced blastogenic responses of lymphocytes from breast cancer patients and controls by the use of α-methyl-D-mannoside. JNCI 1982; 68:69–74.

(*6*) Israël L, Edelstein R. In vivo and in vitro studies on nonspecific blocking factors of host origin in cancer patients. Isr J Med Sci 1978; 14:105–130.

(*7*) Whitehead RH, Bolton PM, Newcombe RG. Is there a factor in sera from cancer patients that inhibits lymphocyte response to phytohemagglutinin? Eur J Cancer 1974; 10:815–818.

(*8*) Suciu-Foca N, Buda J, McManus J, Thiem T, Reemtsma K. Impaired responsiveness of lymphocytes and serum-inhibitory factors in patients with cancer. Cancer Res 1973; 33:2373–2377.

(*9*) Nair PN, Fernandes G, Onoé K, Day NK, Good RA. Inhibition of effector cell functions in natural killer cell activity (NK) and antibody-dependent cellular cytotoxicity (ADCC) in mice by normal and cancer sera. Int J Cancer 1980; 25:667–677.

(*10*) Schmid K. α_1-Acid glycoprotein. In: Putnam FW, ed. The plasma proteins. New York: Academic Press, 1975:183–228.

(*11*) Bachus H. Serum glycoproteins and malignant neoplastic disorders. CRC Crit Rev Clin Lab Sci 1977; 8:333–362.

(*12*) Bennett M, Schmid K. Immunosuppression by human plasma α_1-acid glycoprotein: Importance of the carbohydrate moiety. Proc Natl Acad Sci USA 1980: 77:6109–6113.

(*13*) Chiu KM, Mortensen RF, Osmand AP, Gewurz H. Interactions of α_1-acid glycoprotein with the immune system. 1. Purification and effects upon lymphocyte responsiveness. Immunology 1977; 32:997–1005.

(*14*) Emura J, Ikenaka T, Collins JH, Schmid K. The constant and variable regions of the carboxy-terminal CNBr fragment of α_1-acid glycoprotein. J Biol Chem 1971; 246:7821–7823.

(*15*) Schmid K, Emura J, Schmid MF, Stevens RL, Nimberg RB. Sequence comparison of human plasma α_1-acid glycoprotein and the immunoglobulins. Int J Pept Protein Res 1978; 11:42–48.

(*16*) Gahmberg CG, Andersson LC. Leukocyte surface origin of human α_1-acid glycoprotein (orosomucoid). J Exp Med 1978; 148:507–521.

(*17*) Mancini G, Carbonara AO, Heremans JF. Immunochemical quantitation of antigens by single radial immunodiffusion. Immunochemistry 1965; 2:235–254.

(*18*) Unanue ER, Karnovsky MJ, Engers HD. Ligand-induced movement of lymphocyte membrane macromolecules. J Exp Med 1973; 137:675–689.

(*19*) Noronha AB, Antel JP, Roos RP, Arnason BG. Changes in concanavalin A capping of human lymphocytes with age. Mech Ageing Dev 1980; 12:331–337.

(*20*) Hallgren HM, Kersey JH, Dubey DP, Yunis EJ. Lymphocyte subsets and integrated immune function in aging humans. Clin Immunol Immunopathol 1978; 10:65–78.

(*21*) Hallgren HM, Buckley CE III, Gilbertsen VA, Yunis EJ. Lymphocyte PHA responsiveness, immunoglobulins and autoantibodies in aging humans. J Immunol 1973; 111:1101–1107.

(*22*) Gilman SC, Woda BA, Feldman JD. T lymphocytes of young and aged rats. J Immunol 1981; 127:149–153.

(*23*) Scott M, Bolla R, Denckla WD. Age-related changes in immune function of rats and the effect of long-term hypophysectomy. Mech Ageing Dev 1979; 11:127–136.

(*24*) Yoshinaga M, Yoshinaga A, Waksman BH. Regulation of lymphocyte responses in vitro: Potentiation and inhibition of rat lymphocyte responses to antigen and mitogens by cytochalasin B. Proc Natl Acad Sci USA 1972; 69:3251–3255.

(*25*) DePetris S. Inhibition and reversal of capping by cytochalasin B, vinblastine and colchicine. Nature 1974; 250:54–56.

(*26*) Cullen BF, Chretien PB, Leventhal BG. The effect of lignocaine on PHA-stimulated human lymphocyte transformation. Br J Anaesth 1972; 44:1247–1252.

(*27*) Ryan GB, Unanue ER, Karnovsky MJ. Inhibition of surface capping macromolecules by local anesthetics and tranquilizers. Nature 1974; 250:56–57.

(*28*) Shanes AM. Mechanism of change in permeability in living membranes. Nature 1980; 188:1209–1210.

(*29*) Blaustein MP, Goldman DE. Action of anionic and cationic nerve-blocking agents: Experiment and interpretation. Science 1966; 153:429–432.

(*30*) Allwood G, Asherson GL, Davey MJ, Goodford PJ. The early uptake of radioactive calcium by human lymphocytes treated with phytohaemmaglutinin. Immunology 1971; 21:509–516.

(*31*) Whitney RB, Sutherland RM. Enhanced uptake of calcium by transforming lymphocytes. Cell Immunol 1972; 5:137–147.

(*32*) Murgita RA, Tomasi TB. Suppression of the immune response by α-fetoprotein. J Exp Med 1975; 141:269–286.

(*33*) Mortensen RF, Osmand AP, Gewurz H. Effects of C-reactive protein on the lymphoid system. I. Binding to thymus-dependent lymphocytes and alteration of their functions. J Exp Med 1975; 141:821–839.

(*34*) Cooperband SR, Davis RC, Schmid K, Mannick JA. Competitive blockade of lymphocyte stimulation by a serum immunoregulatory alpha globulin (IRA). Transplant Proc 1969; 1:516–523.

blank page

Zinc Deficiency, Alcohol, and a Retinoid: Association With Esophageal Cancer in Rats[1,2,3]

Gamal N. Gabrial,[4] Thomas F. Schrager,[4] and Paul M. Newberne[4,5]

ABSTRACT—Groups of Charles River Sprague-Dawley male rats were given intragastric intubations of methylbenzylnitrosamine after receiving one of the following diets for 4 weeks: control, zinc-deficient, or zinc-deficient diet plus 4% ethanol in the drinking water. One zinc-deficient group was zinc repleted after the dosing period; the other group, zinc-deficient plus 4% ethanol, received 13-*cis*-retinoic acid (13-*cis*-RA) after the dosing period. Zinc deficiency significantly enhanced esophageal tumor incidence; the addition of ethanol further enhanced tumor incidence. Zinc repletion reduced tumor incidence, whereas the addition of 13-*cis*-RA enhanced tumor incidence.—JNCI 1982; 68:785–789.

A previous study in this laboratory showed that zinc deficiency (7 ppm in the diet) enhanced the incidence and reduced the lag time for the induction of esophageal tumors in rats by MBN (*1*). A more recent study showed that chronic alcohol consumption also had an enhancing effect on MBN esophageal carcinogenesis (*2*). These results are consistent with epidemiologic findings that link both of these factors to increased risk of the disease in certain parts of the world (*3–6*). Nevertheless, neither of these factors is consistently linked to the disease worldwide, which suggests that more complex interactions of additional factors may be involved in the etiology of this neoplasm.

This study was undertaken to further examine the effects of zinc deficiency on MBN-induced esophageal carcinogenesis alone and in combination with chronic alcohol consumption. In addition, we examined the effects of the synthetic retinoid 13-*cis*-RA on the tumor growth phase of animals exposed to both zinc deficiency and chronic alcohol consumption. To more closely pinpoint the effects of zinc deficiency on the MBN carcinogenic process, we repleted one deficient group with zinc after the carcinogen-dosing period to separate the effects exerted by zinc deficiency during the initiation period from those exerted over the entire course of carcinogenesis.

MATERIALS AND METHODS

Experimental animals.—Weanling male outbred Sprague-Dawley rats (Charles River Breeding Laboratories, Wilmington, Mass.) were housed in plastic cages as described previously (*1*). After an appropriate adjustment period, they were started on the diet listed in table 1. The protein source was C-1 assay protein isolated from soybean (The Skidmore Co., Cincinnati, Ohio). We reduced the zinc content of the soybean protein isolate by washing the isolate several times with a solution of the tetrasodium salt of EDTA (pH 4.3). The basal zinc-free diet, mixed in our laboratory, contained about 2 ppm zinc. After zinc carbonate was added, the control diet contained 50 ppm of zinc and the zinc-deficient diet contained 7 ppm. All animals were fed ad libitum. They were given free access to either deionized water or deionized water containing 4% ethanol. After the rats had been on their respective diets for 4 weeks, MBN was administered intragastrically, at the rate of 2 mg/kg body weight, twice weekly for 4 weeks. One group of rats receiving control diet received no MBN. At the end of the MBN-dosing period, one zinc-deficient group was switched to control diet (zinc repletion; group 4), and another group receiving zinc-deficient diet plus 4% alcohol was provided a dietary supplement of 67 μg 13-*cis*-RA/g diet (group 6). These dietary regimens were maintained for 29 weeks until the termination of the experiment. At this point all animals were killed and complete autopsies were performed. The number and distribution of animals are shown in table 2. All animals were weighed weekly; growth rates are shown in text-figure 1.

Hair.—Hair was sheared with an electric clipper from the dorsal skin over the point of the shoulders at the start of the experiment, immediately before MBN dosing and 1 month after the end of MBN dosing. Hair samples (≈30 mg) were analyzed for zinc and copper contents according to the methods of Kopito (*7*) and McBean et al. (*8*).

Blood.—Blood samples were taken by orbital puncture at the beginning of the study, immediately before carcinogen dosing, at the end of the carcinogen-dosing period, and 1 month after the end of dosing. All containers and glassware used were cleaned with nitric acid. Serum copper and zinc were determined by direct aspiration of 1:8 dilutions of serum in deionized water into the atomic absorption spectrophotometer (*9*).

Microsomal enzyme assays.—At the end of the study, liver samples from selected animals in each group were assayed for activity of two microsomal enzymes, PNA and aryl hydrocarbon hydroxylase, according to procedures standard to this laboratory (*10*).

RESULTS

Serum zinc and copper levels.—Serum zinc and copper levels

Abbreviations used: 13-*cis*-RA=13-*cis*-retinoic acid; MBN=methylbenzylnitrosamine; PNA=*p*-nitroanisoledemethylase.

---

[1] Received December 4, 1980; revised October 5, 1981; approved December 3, 1981.

[2] Supported in part by Public Health Service (PHS) grant ES-00597 from the National Institute of Environmental Health Sciences, by PHS grant CA-25382 from the National Cancer Institute, and by Hoffmann-LaRoche Inc., Nutley, N.J.

[3] Animals were maintained under the guidelines set forth in the "Guide for the Care and Use of Laboratory Animals" by the Institute of Laboratory Animal Resources, National Research Council.

[4] Animal Pathology Laboratory, Department of Nutrition and Food Science, Massachusetts Institute of Technology, Cambridge, Mass. 02139.

[5] *Address reprint requests to* Dr. Newberne.

remained stable throughout the experiment in the 2 control diet groups (with or without MBN) (table 3). There was a significant drop in serum zinc levels after 1 month on the zinc-deficient diet for groups 3–6. These levels remained low except in the zinc-repleted group (group 4) in which zinc levels returned to normal within 1 month after repletion. Alcohol consumption or 13-*cis*-RA had no effect on serum zinc levels beyond that exerted by the zinc deficiency.

Copper levels approached a significant increase (P=0.05) in the zinc-deficient group after 1 month. Copper serum levels increased significantly after 3 months in the zinc-deficient plus alcohol group and after 2 months in the zinc-deficient plus alcohol plus 13-*cis*-RA group.

Hair zinc and copper levels.—Hair zinc levels remained constant in both control diet groups, with or without MBN (table 4). In the 4 zinc-deficient groups, zinc levels dropped significantly after 1 month. Zinc levels in the repletion group (group 4) remained low 1 month after repletion. Copper levels remained constant throughout the experiment in all groups.

Body weight.—There was no significant difference between the 2 control diet groups with or without MBN (text-fig. 1). The weights of the zinc-deficient groups decreased significantly during weeks 3 and 4. This was also the time at which other symptoms of zinc deficiency began to appear, such as alopecia, coarse fur, and dermatitis. The zinc-deficient plus alcohol group (group 5) weighed less than the zinc-deficient group; addition of 13-*cis*-RA had no effect on growth. Upon repletion with zinc, group 4 quickly began to gain weight approaching that of the controls.

TABLE 1.—*Composition of the basal zinc-free diet*

Component	Amount fed, g/100 g
Soybean protein	30.0
Methionine	0.7
Corn starch	26.5
Sucrose	27.0
Cellulose fiber	5.0
Mazola corn oil	5.0
Mineral mix[a]	3.5
Vitamin mix[b]	2.0
Choline chloride	0.3
Vitamin B_{12} (μg)	5.0

[a] Composition of mineral mix in grams: $CaCO_3$, 190.5; $CaHPO_4$, 144.1; K_2HPO, 403.8; $MgCO_3$, 73.2; $MgSO_4 \cdot 7H_2O$, 191.7; $FeSO_4 \cdot 7H_2O$, 17.4; $MnSO_4 \cdot H_2O$, 15.4; KI, 0.02; $CuSO_4 \cdot 5H_2O$, 1.96; NaF, 0.22; NaCl, 82.4; $NaCO_3$, 40.6; $Cu_2(SO_4) \cdot H_2O$, 0.009; $NaSeO_3$, 0.02; glucose, 1,041.

[b] Composition of vitamin mix in grams: menadione, 0.1; riboflavine, 0.4; thiamine HCl, 0.8; pyridoxine, 0.8; calcium pantothenate, 2; folic acid, 1; nicotinic acid, 5; inositol, 25; Roche A & D mix (500/50), 6; *dl*-α-tocopherol acetate (500 U/g), 22.5; sucrose, 1,941.

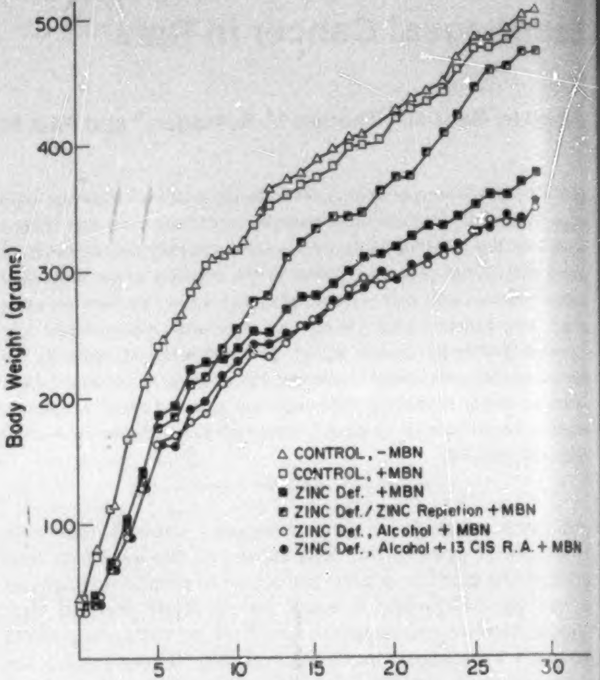

TEXT-FIGURE 1.—Growth curves of different dietary groups. Weights of zinc-deficient groups are significantly less ($P<0.001$) than those of controls after 3 wk. Weight of zinc-deficient, zinc-repleted group is no longer significantly less than weights of controls after 15 wk.

Microsomal enzyme activity.—There was little variation in PNA activity among the various groups except for a slight increase (on a milligram per microsomal protein basis) in the zinc-deficient group receiving MBN, alcohol, and 13-*cis*-RA. The zinc-deficient group that was returned to control diet after MBN treatment (group 4) had the highest total liver PNA activity.

Tumorigenesis studies.—Zinc deficiency significantly enhanced MBN-induced esophageal tumor incidence as com-

TABLE 2.—*Animal groups, treatment, and tumor incidence*[a]

Group No.	Total No. of rats	Dietary zinc, ppm	MBN[b]	4% ethyl alcohol in drinking water	13-*cis*-RA[c]	No. of rats with tumors/ No. of survivors (%)	Total No. of tumors	Average No. of tumors per rat
1	12	60	−	−	−	0/12 (—)	0	0.00
2	40	60	+	−	−	14/35 (40.0)	63	4.5
3	40	7	+	−	−	25/33 (75.7)	76	3.04
4[d]	40	7 (60)	+	−	−	18/35 (51.4)	87	4.83
5	40	7	+	+	−	29/34 (85.3)	99	3.41
6	40	7	+	+	+	33/35 (94.3)	76	2.30

[a] The + and − signs mean presence or absence of diet component.

[b] 2 mg/kg body wt, twice weekly, 8 doses.

[c] 13-*cis*-RA (67 μg/g) was added to the diet at the end of dosing.

[d] Returned to control diet, 60 ppm zinc, at end of MBN administration. Groups 3, 5, and 6 were significantly different from group 2, $P<0.005$. Groups 3 and 4 were significantly different, $P<0.05$.

TABLE 3.—*Serum zinc and copper concentrations during carcinogenesis*[a]

Group No.	Dietary zinc, ppm	MBN	Ethyl alcohol	13-*cis*-RA	Time of measurement	Serum concentrations, μg/100 ml ± SE	
						Zinc	Copper
1	60	–	–	–	Initial	116.1±7.4	109.3±5.9
					1 mo	—	—
					2 mo	—	—
					3 mo	119.4±7.3	112.2±4.9
2	60	+	–	–	Initial	115.5±9.3	109.4±12.9
					1 mo	117.9±8.1	110.9±12.4
					2 mo	129.8±8.3	120.9±11.5
					3 mo	128.1±10.7	120.8±6.8
3	7	+	–	–	Initial	115.5±7.2	107.6±11.0
					1 mo	63.4±9.6[b]	131.2±7.6
					2 mo	74.1±9.9[b]	124.8±12.5
					3 mo	80.5±6.5[b]	128.6±11.9
4[c]	7 (60)	+	–	–	Initial	114.6±6.8	106.8±11.3
					1 mo	59.9±7.2[b]	117.8±12.6
					2 mo	75.3±5.8[b]	126.9±12.5
					3 mo	110.4±10.4	120.5±9.5
5	7	+	+	–	Initial	113.4±6.4	107±11.1
					1 mo	—	—
					2 mo	65.9±8.5[b]	113.8±11.9
					3 mo	77.6±7.7[b]	146.2±18.1[d]
6	7	+	+	+	Initial	113.9±6.4	108±10.3
					1 mo	—	—
					2 mo	64.6±9.2[b]	156±21.3[d]
					3 mo	76.7±12.3[b]	157±9.10[d]

[a] The + and – signs mean presence or absence of diet component.
[b] Significantly different from base-line levels, $P<0.001$.
[c] Returned to 60 ppm zinc after completion of MBN administration.
[d] Significantly different from base-line levels, $P<0.001$.

TABLE 4.—*Hair-zinc and copper concentrations during carcinogenesis*[a]

Group No.	Dietary zinc, ppm	MBN	Ethyl alcohol	13-*cis*-RA	Time of measurement	Concentrations, ppm ± SE	
						Zinc	Copper
1	60	–	–	–	Initial	228.1±21.1	20.7±3.7
					1 mo	—	—
					3 mo	215.7±18.8	20.0±4.3
2	60	+	–	–	Initial	228.3±12.5	21.0±2.8
					1 mo	210.0±39.0	20.5±4.4
					3 mo	201.2±18.8	22.2±5.1
3	7	+	–	–	Initial	231.5±13.1	20.3±3.1
					1 mo	175.7±26.8[c]	—
					3 mo	182.7±18.4[c]	21.4±3.9
4[b]	7 (60)	+	–	–	Initial	228.7±20.1	20.8±2.4
					1 mo	281.9±24.1[c]	20.7±3.5
					3 mo	187.6±12.6[c]	22.8±6.3
5	7	+	+	–	Initial	230.4±9.6	20.7±2.8
					1 mo	—	—
					3 mo	177.3±12.0[c]	22.4±6.9
6	7	+	+	+	Initial	229.7±17.6	19.3±4.6
					1 mo	—	—
					3 mo	180.0±13.9[c]	18.6±1.8

[a] The + and – signs mean presence or absence of diet component.
[b] Returned to 60 ppm zinc after completion of MBN administration.
[c] Significantly different from base-line levels, $P<0.001$.

pared with that among rats on control diet (75.7 vs. 40%, $P<0.005$). The addition of alcohol to the zinc-deficient diet (group 5) further enhanced tumor incidence (85.3%), although this increase was not statistically significant ($P=0.05$). Addition of 13-*cis*-RA to the diet (group 6) at the end of carcinogen treatment enhanced tumor incidence even further. Again, this enhancement was not significantly different ($P=0.05$) from the tumor level produced by zinc-deficient diet alone. Morphologically, tumors in the 13-*cis*-RA group tended to coalesce, which made counting of the individual tumors difficult. When a zinc-deficient dietary group was switched to a control diet (group 4) after the end of carcinogen treatment and was continued on control diet for 21 weeks until the end of the experiment, at week 29, a significantly reduced tumor incidence from the level of the zinc-deficient group was observed (75.7 vs. 51%, $P<0.05$).

DISCUSSION

The dramatic fluctuations in esophageal cancer incidence from one geographic area of the world to another provide a unique opportunity to identify factors associated with increased risk of the disease and to test these factors experimentally. Although this epidemiologic approach has linked a number of environmental agents to the risk of this neoplasm, none of the factors shows a consistent association to increased worldwide esophageal cancer mortality (*11*). Therefore, more complex interactions of a number of factors may impinge on the etiology of esophageal cancer.

As shown in table 2, additional factors can modify the enhancing effects of zinc deficiency on MBN esophageal carcinogenesis. Zinc deficiency alone (group 3) significantly enhanced tumor incidence, comparable to what was found in an earlier study (*1*) (75.7% in zinc-deficient group vs. 40% in the control diet group, compared to 79% in the zinc-deficient group vs. 29% in the control diet group in the previous study). This similarity is noteworthy since in the previous study animals on control diet were pair-fed to zinc-deficient animals, whereas in this study all groups received food ad libitum. Pair-feeding was used in the earlier study to document the effects of zinc independently of food intake and reduced growth. As shown in text-figure 1, zinc-deficient animals experienced a reduced growth rate compared to that in rats receiving control diet ad libitum. Reduced growth rate is accompanied by a reduction in food intake.

Comparison of these studies suggests that what little effect, if any, results from reduced food intake and reduced growth is a reduction in tumor incidence. This observation has been substantiated in a more recent study (Schrager TF, Newberne PM: Unpublished data) and is consistent with the hypothesis that reduced calorie intake may reduce tumor production. These findings confirm that the enhancement of tumor incidence resulting from a zinc-deficient diet is not due to the reduction in growth rate; on the contrary, this reduction might understate slightly the significance of the effect of zinc deficiency on tumor incidence.

Although it has not been established that defects in the immune system can enhance carcinogenesis, this possibility exists and the role of zinc in the immune system should be considered. Zinc deficiency causes atrophy of lymphoid tissues and can lead to derangements in both humoral and cellular immunity (*12*, *13*). This relationship requires further investigation.

To determine more clearly the effect of zinc deficiency on the initiation phase of carcinogenesis, we placed group 4 rats on a zinc-deficient diet before and during carcinogen treatment and then returned them to a control (zinc-sufficient) diet for the remaining 21 weeks of the experiment. This protocol would also indirectly indicate the effects of zinc deficiency on the tumor growth phase. The tumor growth effect was of interest in light of previous findings by McQuitty et al. (*14*), Duncan and co-workers (*15*), and DeWys and Pories (*16*) that zinc deficiency can inhibit the growth of a variety of tumors. If this were the case in the MBN–esophageal tumor model, it would mean that zinc deficiency enhancement must occur during the initiation phase. Therefore, if we eliminated the deficiency during tumor growth, maximum tumor production would occur. Instead of maximum tumor production, we observed the opposite effect. Zinc repletion reduced tumor incidence to a level approaching that in animals receiving control diet throughout the experiment (51% tumors on zinc repletion vs. 40% on control diet). This finding suggests that zinc deficiency during the tumor growth phase of MBN-induced esophageal cancer, rather than inhibiting tumor growth, provides a major enhancement to tumor incidence, as evidenced by comparison of the zinc-repleted rats (group 4) with the rats (group 2) that received zinc-deficient diet during both initiation and promotion (51 vs. 75.7%, respectively). Whether this effect of zinc deficiency during tumor growth occurs only in combination with zinc deficiency during tumor initiation or would occur if applied during tumor growth alone has not been determined and requires further study.

The enhancement of esophageal tumor growth by zinc deficiency, in contrast to an inhibition of tumor growth in other tissues that have been studied, parallels the difference in the generalized response to zinc deficiency of esophageal epithelium compared to other tissues. This finding suggests a possible mechanism by which zinc deficiency might enhance esophageal tumor incidence. Whereas most other tissues exhibit a hypoplastic response to zinc deficiency and show tumor inhibition, the esophageal epithelium exhibits a hyperplasia and parakeratosis (*17–20*), conditions that might enhance the susceptibility of this tissue to initiation by chemical carcinogenesis and promote the subsequent growth of tumors (*21*, *22*).

The addition of chronic alcohol consumption to the zinc-deficient diet (group 5) further enhanced tumor incidence (85.3 vs. 75.7%). Although this level was not significantly different from the tumor level in the zinc-deficient group, this degree of enhancement has been observed in two other experiments, indicating a consistent trend. Whether alcohol exerts an effect on MBN carcinogenesis through a pathway similar to the pathway of zinc deficiency has not been determined. There are a number of possible mechanisms for the action of alcohol. Karatsume and co-workers (*23*) found that among a number of solvents, ethanol was most effective in enhancing the penetration of benzo[*a*]pyrene and other polycyclic hydrocarbons into the esophageal mucosa. Furthermore, alcohol can alter the activity of mixed function oxidases (*24*, *25*), a group of enzymes involved in the metabolism of most carcinogens, including nitrosamines. An alteration in the activity of these enzymes could affect the ultimate amount of carcinogens produced. In addition, a prolonged exposure to ethanol can dehydrate and irritate such tissues as the esophageal epithelium (*8*) and cause esophagitis and other disturbances in the integrity of this protective barrier, such as hyperplasia (*11*) and other conditions that might enhance susceptibility of the esophageal epithelium to chemical carcinogens. Another possibility is that chronic alcohol consumption causes nutritional deficiencies or imbalances, either by replacing nutrient-rich calories of food with nutrient-free calories of alcohol, or by increasing the excretion of nutrients from the body. These nutritional disturbances may then alter the organism's response to carcinogenic exposure (*11*). Studies by Vallee and co-workers (*26*) showed that cirrhotic alcoholics had reduced serum zinc levels and hyperzincuria. Sullivan and Lankford (*27*) found increased zincuria in 50% of noncirrhotic alcoholics. Flynn and co-workers (*28*) found significantly lower plasma zinc levels in alcoholic pregnant women than in nonalcoholic pregnant women. Wang and Pierson (*29*) found that plasma zinc levels dropped significantly after 14 weeks in rats consuming 20% alcohol. If such an effect of alcohol on zinc status does exist, it suggests a connection between these two factors in the etiology of esophageal cancer.

The addition of 13-*cis*-RA to the zinc-deficient diet plus ethanol group (group 6) during the tumor growth period further enhanced tumor incidence. Although the level of enhancement in this group was not statistically significant compared to that in the zinc-deficient diet plus alcohol group, this same effect has been observed in an additional study (the results of which are in preparation or in press) and indicates a trend. On the basis of studies in our laboratory showing a protective effect of 13-*cis*-RA on bladder tumor incidence (Newberne PM: Unpublished observation) and other studies showing similar effects (*30*), this enhancement is somewhat unexpected. Whether this enhancement is specific to MBN esophageal carcinogenesis or is the result of an interaction between the synthetic retinoid and zinc deficiency and/or chronic alcohol consumption is unclear and requires further investigation.

REFERENCES

(*1*) Fong LY, Sivak A, Newberne PM. Zinc deficiency and methylbenzylnitrosamine-induced esophageal cancer in rats. JNCI 1978; 61: 145–150.

(*2*) Gabrial GN, Newberne PM. Zinc deficiency, alcohol and esophageal cancer. In: Hemphill DD, ed. Trace substances in environmental health—XIII. Columbia: Univ Missouri Press, 1979:315–324.

(*3*) Rothman KJ. Alcohol. In: Fraumeni JF Jr, ed. Persons at high risk of cancer. New York: Academic Press, 1975:142–143.

(*4*) Lin HJ, Chan WC, Fong YY, Newberne PM. Zinc levels in serum, hair and tumors from patients with esophageal cancer. Nutr Rep Int 1977; 15:635–643.

(*5*) Fong L, Lin HJ, Chan WC, Newberne PM. Zinc and copper concentrations in tissues from esophageal cancer patients and animals. In: Hemphill DD, ed. Trace substances in environmental health—XI. Columbia: Univ Missouri Press, 1977:184–192.

(*6*) Mobarhan S, Dowlatshahi K, Diba YY. Hair zinc levels from a normal population of northeast Iran with a high incidence of esophageal carcinoma. Am J Clin Nutr 1980; 33:940.

(*7*) Kopito L. Atomic absorption spectroscopy in clinical chemistry. Pittsburgh: Fischer Scientific Co., 1970.

(*8*) McBean LD, Mahloudji M, Reinhold JG. Correlation of zinc concentration in human plasma and hair. Am J Clin Nutr 1971; 24:506–509.

(*9*) Monivcilgnic B, Betonje B, Shah BG. Effects of the matrix of the standard on results of atomic absorption spectrophotometry of zinc in serum. Clin Chem 1971; 21:588–590.

(*10*) Newberne PM, Weigert J, Kula N. Effects of dietary fat on hepatic mixed-function oxidases and hepatocellular carcinoma induced by aflatoxin B_1 in rats. Cancer Res 1979; 39:3986–3991.

(*11*) Warwick GP, Harrington JS. Some aspects of epidemiology and etiology of esophageal cancer. Adv Cancer Res 1973; 17:82–215.

(*12*) Dreizes S. Nutrition and the immune response—a review. Int J Vitam Nutr Res 1978; 49:220–228.

(*13*) Biesel WR. Malnutrition and the immune response. In: Neuberger A, Jukes TH, eds. Biochemistry of nutrition. Vol I. Baltimore: Univ Park Press, 1979:1–19.

(*14*) McQuitty JT, DeWys WD, Monaco L, et al. Inhibition of tumor growth by dietary zinc deficiency. Cancer Res 1970; 30:1387–1390.

(*15*) Duncan JR, Dreosti IE, Albrecht CF. Zinc intake and growth of a transplanted hepatoma induced by 3′-methyl-4-dimethylaminoazobenzene in rats. J Natl Cancer Inst 1974; 53:277–278.

(*16*) DeWys W, Pories W. Inhibition of a spectrum of animal tumors by dietary zinc deficiency. J Natl Cancer Inst 1972; 48:375–381.

(*17*) Follis RH Jr, Day HG, McCollum EV. Histological studies of the tissues of rats fed a diet extremely low in zinc. J Nutr 1941; 22:223–234.

(*18*) Barney GH, Orgebin-Crist MC, Macapinlac MP. Genesis of esophageal parakeratosis and histologic changes in the testes of the zinc-deficient rat and their reversal by zinc repletion. J Nutr 1968; 95: 526–534.

(*19*) Hurley LS. Zinc deficiency in the developing rat. Am J Clin Nutr 1969; 22:1332–1339.

(*20*) Diamond I, Swenerton H, Hurley LS. Testicular and esophageal lesions in zinc-deficient rats and their reversibility. J Nutr 1971; 101:77–84.

(*21*) Warwick GP. Effect of the cell cycle on carcinogenesis. Fed Proc 1971; 30:1760–1765.

(*22*) Berg JW. Worldwide variation in cancer incidence as clues to cancer origin. In: Hiatt HH, Watson JD, Winstein JA, eds. Origins of human cancer. Book A. Vol 4. New York: Cold Spring Harbor Laboratory, 1977:15–19.

(*23*) Karatsume M, Koholi S, Horie A. Test of alcoholic beverages and ethanol solutions for carcinogenicity and tumor-promoting activity. Gan 1971; 62:395–405.

(*24*) Capel ID, Williams DC. The effect of long-term ethanol intake on the hepatic carcinogen metabolizing enzyme systems of mice. Int Res Commun Syst Med Sci 1978; 6:297.

(*25*) Rubin E, Lieber CS. Hepatic microsomal enzymes in man and rat: Induction and inhibition by ethanol. Science 1968; 162:690–691.

(*26*) Vallee BC, Wacker WE, Bartholomay AF, Robin ED. Zinc metabolism in hepatic dysfunction. I. Serum zinc concentrations in Laennec's cirrhosis and their validation by sequential analysis. N Engl J Med 1956; 255:403–408.

(*27*) Sullivan JF, Lankford HG. Urinary excretion of zinc in alcoholism and postalcoholic cirrhosis. Am J Clin Nutr 1962; 10:153–157.

(*28*) Flynn A, Martier SS, Sokol RJ, Miller SI, Golden NL, Del Villano BC. Zinc status of pregnant alcoholic women: A determinant of fetal outcome. Lancet 1981; 2:572–575.

(*29*) Wang J, Pierson RN. Distribution of zinc in skeletal muscle and liver tissue in normal and dietary controlled alcoholic rats. J Lab Clin Med 1975; 85:50–58.

(*30*) Sporn MB. Retinoids and carcinogenesis. Nutr Rev 1977; 35:65–69.

blank page

Oral Mucosal Carcinogenesis in Hamsters: Inhibition by Vitamin E[1,2]

Gerald Shklar, *D.D.S., M.S.*[3]

ABSTRACT—Eighty young adult male and female Syrian golden hamsters (*Mesocricetus auratus*) were divided into 4 equal experimental groups. In group 1 animals the left buccal pouch was painted three times weekly with a 0.5% solution of 7,12-dimethylbenz[*a*]anthracene (DMBA) in heavy mineral oil. In group 2 animals the left buccal pouch was similarly painted with DMBA, but the animals also received orally 10 mg vitamin E (*dl*-α-tocopherol) in peanut oil twice weekly on alternate days with the DMBA painting. Group 1 animals received a similar amount of peanut oil vehicle, group 3 animals received only vitamin E (vitamin E controls) in peanut oil, and group 4 animals served as untreated controls receiving only peanut oil. Four animals in each group (2 males and 2 females) were killed at 8, 10, 12, 14, and 16 weeks. Buccal pouches were photographed and excised, and tumors were noted and measured in the left buccal pouches. In group 2 animals receiving vitamin E, tumor formation was significantly delayed, so that by 14–16 weeks there were fewer tumors and their average size was smaller than that of tumors in group 1 animals that were painted with DMBA but received no vitamin E supplement. In group 2 there was also less invasion of underlying tissues and less surface necrosis.—JNCI 1982; 68:791–797.

There has been renewed interest recently in nutritional supplements as cancer chemopreventive agents (*1*). Inhibition of tumor growth by retinoids has been reported in a variety of experimental tumor systems, including carcinomas of the bladder (*2, 3*), skin (*4*), lung (*5*), and breast (*6*). Recently, these findings were confirmed in two oral mucosal tumor systems: 1) the hamster buccal pouch painted with DMBA in oil (*7*) and 2) the hamster tongue painted with DMBA in acetone (*8, 9*). Vitamin E (α-tocopherol) has received some renewed interest in recent years and has been accepted as an essential nutrient for humans (*10*), although its physiologic role has not been significantly clarified and its relation to pathologic states remains controversial. A major function of vitamin E in animals appears to be that of an antioxidant, inhibiting both enzymatic and nonenzymatic lipid peroxidation and preventing the spread of peroxidation through lipids, perhaps in membranes (*11–14*).

The relationship of vitamin E to experimental tumors had been reported in early studies with contradictory results. Davidson (*15*) in 1934 found a delay in skin carcinogenesis in mice on a diet high in vitamin E. Telford (*16*) in 1949 found that vitamin E supplements increased the percentage of lung tumors in a tumor strain of mouse and that vitamin E deficiency resulted in decreased numbers of tumors.

More recently, Harman (*17*) reported that dietary vitamin E inhibited dibenzanthracene-induced tumors. Slaga and Bracken (*18*) found that vitamin E and other antioxidants were effective inhibitors of DMBA-induced tumor initiation and attributed their activity to their ability to prevent the in vivo activation of polycyclic aromatic hydrocarbons to carcinogen epoxides or other intermediates. Cook and McNamara (*19*) found that mice receiving a diet with a high vitamin E content developed fewer adenomas and fewer invasive carcinomas of the colon than mice receiving dimethylhydrazine and a normal diet.

The hamster buccal pouch tumor system is an excellent model for oral epidermoid carcinoma and has been shown in numerous studies to be a reliable experimental system, with consistent time patterns of tumor development as well as the preceding precancerous leukoplakic lesions (*20*). Dysplastic leukoplakic lesions develop at 6–8 weeks, carcinoma in situ at 8–10 weeks, frank epidermoid carcinomas at 10–12 weeks, and large verrucous and invasive carcinomas at 12–14 weeks. It was decided that a study of the effect of vitamin E on hamster buccal pouch carcinogenesis could effectively confirm some of the recent reports on the role of vitamin E as a possible tumor inhibitor.

A chemical carcinogenesis system such as the hamster buccal pouch offers a more reliable indication of tumor retardation or prevention than do systems that use transplanted tumors. The oral chemical carcinogenesis system more closely approximates the human cancer situation, with a relatively long latent period, slow growth, carcinoma rather than sarcoma development, noninbred host, and the presence of viruses uncommon. In contrast, transplantation models use inbred hosts, the tumors are predominantly sarcomas or leukemia in an advanced stage of progression with no latent period, the tumors grow rapidly, and passenger viruses are common (*21*). Furthermore, there are no spontaneously arising tumors of the hamster buccal pouch that could complicate the interpretation of tumor development stimulated by the chemical carcinogen.

MATERIALS AND METHODS

Eighty young adult male and female noninbred Syrian golden hamsters (*Mesocricetus auratus*) 4–6 weeks of age served as experimental animals. They were obtained from Charles River Breeding Laboratories, Wilmington, Mass. The animals were housed 5 per plastic cage with wood chips for bedding. The environment was controlled with an alternating 12-hour light–dark cycle. Water and laboratory chow (Rat Chow 5012; Ralston Purina Co., St. Louis, Mo.) were

---

ABBREVIATION USED: DMBA=7,12-dimethylbenz[*a*]anthracene; H & E = hematoxylin and eosin.

---

[1] Received March 18, 1981; revised November 20, 1981; accepted December 11, 1981.

[2] Animals were maintained under the guidelines set forth by Harvard University.

[3] Department of Oral Medicine and Oral Pathology, Harvard School of Dental Medicine, 188 Longwood Ave., Boston, Mass. 02115.

TABLE 1.—*Gross pathology, number, and size of tumors at death*

No. of weeks after start of experiment	Group 1 (DMBA)			Group 2 (DMBA + vitamin E)			Group 3 (vitamin E)			Group 4 (untreated)		
	Pathology	Average tumor No.	Average tumor diameter, mm	Pathology	Average tumor No.	Average tumor diameter, mm	Pathology	Average tumor No.	Average tumor diameter, mm	Pathology	Average tumor No.	Average tumor diameter, mm
8	Leukoplakia	0	—	Erythema	0	—	Normal mucosa	0	—	Normal mucosa	0	—
10	Tumors	3	3	Leukoplakia	0	—	Normal mucosa	0	—	Normal mucosa	0	—
12	Tumors	6	5	Tumors	4	3	Normal mucosa	0	—	Normal mucosa	0	—
14	Tumors	9	7	Tumors	7	4	Normal mucosa	0	—	Normal mucosa	0	—
16	Tumors	14	8	Tumors	8	7	Normal mucosa	0	—	Normal mucosa	0	—

available ad libitum. The hamsters were divided into 4 equal groups of 20 (10 males and 10 females) and were treated as follows: group 1—DMBA painted; group 2—DMBA painted and vitamin E administered; group 3—vitamin E administered; and group 4—untreated controls.

DMBA (Sigma Chemical Co., St. Louis, Mo.) in a 0.5% solution in heavy mineral oil (U.S.P.) was painted on the left buccal pouch mucosa three times per week. Vitamin E (DL-α-tocopherol; Sigma Chemical Co.) was dissolved in peanut oil and administered by mouth with a thin pipette twice weekly in a dose of 10 mg (4 drops of a 50-mg vitamin E solution/ml). Vitamin E was offered on alternate days with the DMBA painting. Both group 1 animals (DMBA) and group 4 animals (untreated controls) received 4 drops of peanut oil on a schedule similar to that of vitamin E to control for the vitamin E vehicle.

Two male and 2 female animals in each group were killed at 8, 10, 12, 14, and 16 weeks after the initiation of the experiment. Buccal pouches were photographed, dissected, fixed in 10% Formalin, sectioned in paraffin, and stained with H & E for microscopic study. Major organs (liver, kidneys, spleen, heart, and lungs) were also removed at autopsy, fixed in 10% Formalin, and prepared for microscopic evaluation. Grossly observed buccal pouch tumors were counted, and the figures were used for statistical analysis. Student's *t*-test for paired data was used to determine level of significance. Diameters of tumors were also measured.

RESULTS

Gross observations.—Both the appearance of leukoplakia and the development of visible tumors in the left pouches of the group 2 animals (DMBA + vitamin E) were significantly delayed as compared to those seen in group 1 animals (DMBA) (table 1, text-fig. 1). Tumors at all stages of development in group 2 animals tended to be smaller than those in group 1 animals and their numbers were fewer (figs. 1-6). No abnormalities were noted in group 3 and group 4 control animals. No significant changes were observed in liver, kidneys, spleen, heart, and lungs at autopsy in animals in any of the 4 groups. Two animals in group 1 with extensive large tumors of the left buccal pouch mucosa at 16 weeks appeared to have some tumor extension into the cervical region, with fixation of the buccal pouch to the underlying tissue.

Statistical analysis.—In each of the 4 groups studied, 4 animals were randomly killed at 8, 10, 12, 14, and 16 weeks after the start of the experiment. Determination of statistical results was based on the gross observation of the number of tumors in the left buccal pouches of animals killed from 8 to 16 weeks in each of the 2 groups. The mean and standard deviation were calculated for each group. Student's *t*-test for paired data was used to determine the level of statistical significance between groups, and the *P*-values are indicated. The mean value and standard deviation for group 1 were 32±18.7, and the values for group 2 were 19±14.0. There was a statistically significant difference ($P \leq 0.01$) in tumor numbers between groups 1 and 2.

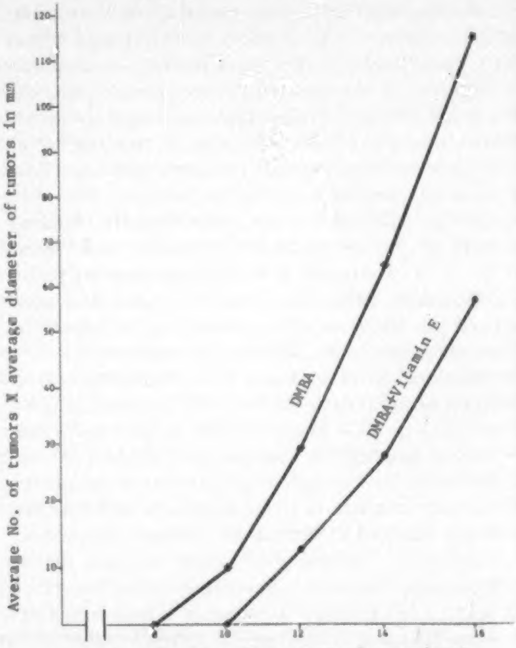

TEXT-FIGURE 1.—Expression of buccal pouch tumor involvement. Average tumor number and size in animals from group 1 (DMBA) and group 2 (DMBA+vitamin E) from 8 and 10 wk, respectively.

Microscopic observations.—In group 1 animals the left buccal pouches demonstrated hyperkeratosis and dysplasia at 8 weeks, areas of carcinoma in situ and small papillary carcinomas at 10 weeks, larger papillary and invasive carcinomas at 12 weeks, and more extensive lesions at 14 weeks with extensive inflammatory infiltrate beneath the carcinomas and surface necrosis. At 16 weeks the large carcinomas were often confluent, and there were extensive surface necrosis and deep invasion into underlying tissues.

In group 2 animals, the left buccal pouches demonstrated similar pathology, but with a delay in development of lesions, so that buccal pouch mucosa appeared relatively free of dysplastic changes at 8 weeks, although some hyperkeratosis was observed as well as lymphocytic infiltration of underlying corium (figs. 7, 8).

At 16 weeks, there were fewer tumors, individual tumors tended to be smaller than those in the group 1 animals, and there was less surface necrosis. Less evidence was observed of deep extension into underlying tissue (figs. 9, 10).

DISCUSSION

The experimental results confirm previous preliminary findings in other experimental tumor systems that vitamin E is capable of delaying tumor formation or retarding carcinogenesis. The hamster buccal pouch model offers reliable data on tumor development, and the tumors can be observed, studied, and measured at various stages. The observations are somewhat comparable to those with retinoids and with immunoenhancing agents (*22*) such as bacillus Calmette-Guerin (*23*) and levamisole (*24*). There is some suggestion that retinoids may also retard carcinogenesis by serving to enhance the organism's immune response, since stimulation of cell-mediated immunity by retinoids has been demonstrated in both mice (*25*) and hamsters (*26*). Perhaps vitamin E functions in a similar manner, although antioxidant action suggests a more obvious role in delaying chemical carcinogenesis by preventing the formation of proximal carcinogens, now considered to be the diol epoxides (*27*).

Another possible role could relate to the finding that vitamin E has a stimulatory effect on the microsomal hydroxylation of drugs in livers of experimental rats. Since liver microsomes catalyze the hydroxylation of carcinogenic hydrocarbons, this might in some way also inhibit the development of proximal carcinogens (*28*).

The minimum nutritional requirement of α-tocopherol for adult humans appears to be in the range of 5–7 mg/day, and the average intake in the United States is 7–9 mg/day (*29*). Recommended dietary allowance is currently 8–10 mg/day.

Vitamin E is adequately absorbed in the gastrointestinal tract so that it can be administered orally (*30*).

REFERENCES

(*1*) Bollag W. Prophylaxis of chemically-induced benign and malignant epithelial tumors by vitamin A acid (retinoic acid). Eur J Cancer 1972; 8:689–693.

(*2*) Sporn MB, Squire RA, Brown CC, Smith JM, Wenk ML, Springer S. 13-*cis*-Retinoic acid: Inhibition of bladder carcinogenesis in the rat. Science 1977; 195:487–489.

(*3*) Sporn MB. Retinoids and carcinogenesis. Nutr Rev 1977; 35:65–69.

(*4*) Bollag W Therapeutic effects of an aromatic retinoic acid analog on chemically induced skin papillomas and carcinomas of mice. Eur J Cancer 1974; 10:731–737.

(*5*) Saffiotti U, Montesano R, Sellakumar AR, Borg SA. Experimental cancer of the lung. Inhibition by vitamin A of the induction of tracheobronchial squamous metaplasia and squamous cell tumors. Cancer 1967; 20:857–864.

(*6*) Moon RC, Grubbs CJ, Sporn MB. Inhibition of 7,12-dimethylbenz(*a*)anthracene-induced mammary carcinogenesis by retinyl acetate. Cancer Res 1976; 36:2626–2630.

(*7*) Shklar G, Schwartz J, Grau D, Trickler D, Wallace K. Inhibition of hamster buccal pouch carcinogenesis by 13-*cis*-retinoic acid. Oral Surg 1980; 50:45–52.

(*8*) Shklar G, Marefat P, Kornhauser A, Trickler D, Wallace K. Retinoid inhibition of lingual carcinogenesis. Oral Surg 1980; 49: 325–332.

(*9*) Shklar G, Flynn E, Szabo G, Marefat P. Retinoid inhibition of experimental lingual carcinogenesis: Ultrastructural observations. JNCI 1980; 65:1307–1316.

(*10*) Bieri JG, Farrell PM. Vitamin E. Vitam Horm 1976; 34:31–75.

(*11*) Tappel AL. Vitamin E and free radical peroxidation of lipids. Ann NY Acad Sci USA 1972; 230:12–28.

(*12*) Tinberg HM, Barber AA. Studies on vitamin E action: Peroxidation inhibition in structural protein-lipid micelle complexes derived from rat liver microsomal membranes. J Nutr 1970; 100:413–418.

(*13*) Molenaar I, Vos J, Jager C, Hommes FA. The influence of vitamin E deficiency on biological membranes; an ultrastructural study on the intestinal epithelial cells on ducklings. Nutr Metab 1970; 12: 358–362.

(*14*) McCay PB, Poyer JL, Pfeifer PM, May HE, Gilliam HE. A function of α tocopherol: Stabilization of the microsomal membrane from radical attack during TPNH-dependent oxidations. Lipids 1971; 6:297–306.

(*15*) Davidson JR. An attempt to inhibit the development of tar-carcinomata in mice. Can Med Assoc J 1934; 31:486–487.

(*16*) Telford IR. The effects of hypo- and hyper-vitaminosis E in lung tumor growth in mice. Ann NY Acad Sci 1949; 52:132–134.

(*17*) Harman D. Dibenzanthracene-induced cancer. Inhibition effect of dietary vitamin E. Clin Res 1969; 17:125–129.

(*18*) Slaga TJ, Bracken WM. The effects of antioxidants on skin tumor initiation and aryl hydrocarbon hydroxylase. Cancer Res 1977; 37: 1631–1635.

(*19*) Cook MG, McNamara P. Effect of dietary vitamin E on dimethylhydrazine-induced colonic tumors in mice. Cancer Res 1980; 40: 1329–1332.

(*20*) Shklar G. Experimental oral pathology in the Syrian hamster. Prog Exp Tumor Res 1972; 16:518–538.

(*21*) Bartlett GL, Krieder JW, Parnell DM. Immunotherapy of cancer in animals: Models or muddles. J Natl Cancer Inst 1979; 56:207–210.

(*22*) Shklar G, Eisenberg E, Flynn E. Immunoenhancing agents and experimental leukoplakia and carcinoma of the hamster buccal pouch. Prog Exp Tumor Res 1979; 24:269–282.

(*23*) Giunta JJ, Reif AE, Shklar G. Bacillus Calmette-Guerin and antilymphocyte serum in carcinogenesis. Effects on hamster buccal pouch. Arch Pathol Lab Med 1974; 98:237–240.

(*24*) Eisenberg E, Shklar G. Levamisole and hamster pouch carcinogenesis. Oral Surg 1977; 43:562–571.

(*25*) Dennert G, Lotan R. Effects of retinoic acid on the immune system: Stimulation of T killer cell induction. Eur J Immunol 1978; 8:23–29.

(*26*) Sonis ST, Shklar G. Preliminary immunologic studies on retinoid inhibition of experimental carcinogenesis. J Oral Med. 1981; 36: 117–119.

(*27*) Osborne MR. Diolepoxides—the key to hydrocarbon carcinogenesis. Trends Biochem Sci 1979; 4:210–213.

(*28*) Carpenter MP. Vitamin E and microsomal drug hydroxylations. Ann NY Acad Sci 1972; 230:81–92.

(*29*) Horwitt MK. Therapeutic uses of vitamin E in medicine. Nutr Rev 1980; 38:105–113.

(*30*) Losowsky MS, Kelleher J, Walker BE, Davies T, Smith CL. Intake and absorption of tocopherol. Ann NY Acad Sci 1972; 203: 212–222.

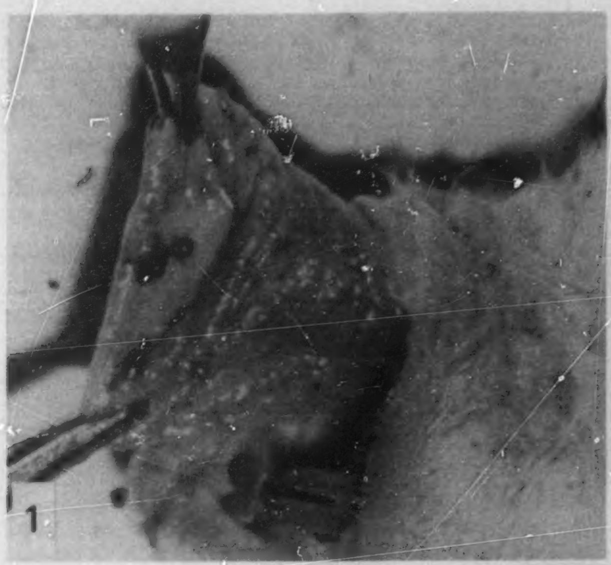

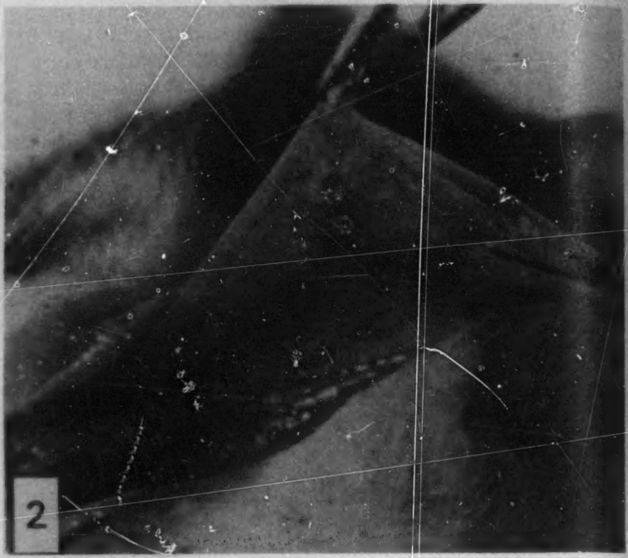

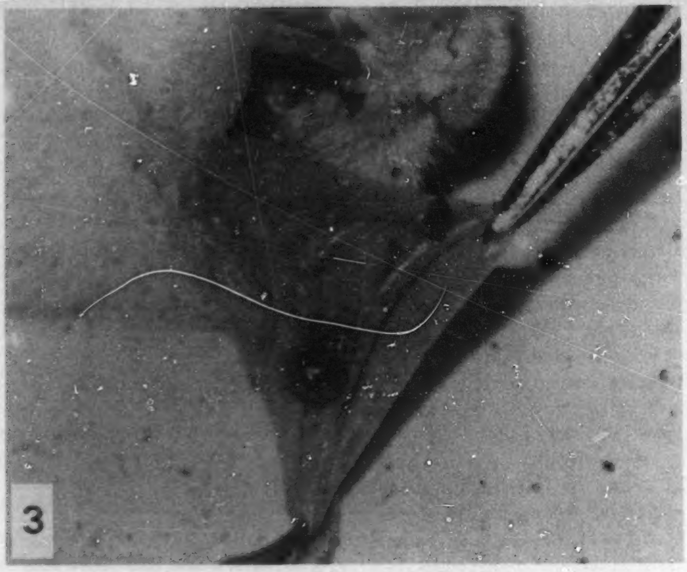

FIGURE 1.—Left buccal pouch of group 1 (DMBA) hamster at 10 wk. *Note* several small tumors.
FIGURE 2.—Left buccal pouch of group 2 (DMBA+vitamin E) animal at 10 wk. *Note* leukoplakia and several small erosions.
FIGURE 3.—Left buccal pouch of group 1 animal at 12 wk. Several moderately sized tumors are evident.

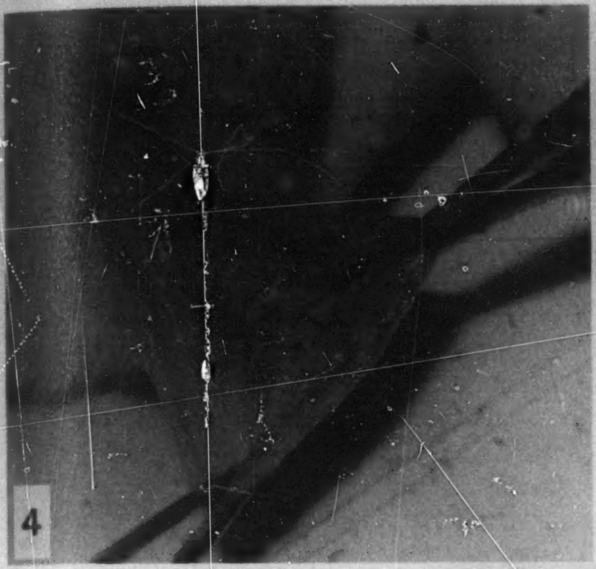

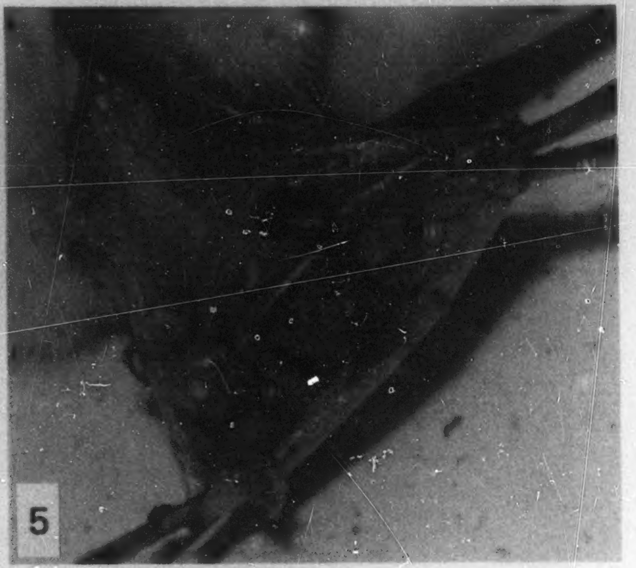

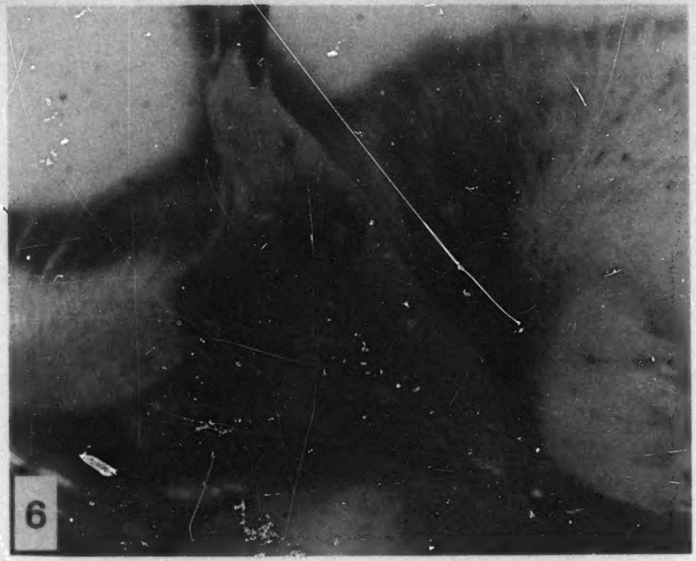

FIGURE 4.—Left buccal pouch of group 2 animal at 12 wk. *Note* 2 small tumors.

FIGURE 5.—Left buccal pouch of a group 1 animal at 14 wk. *Note* numerous large tumors and several small tumors.

FIGURE 6.—Left buccal pouch of group 2 animal at 14 wk; 2 moderately sized tumors are apparent.

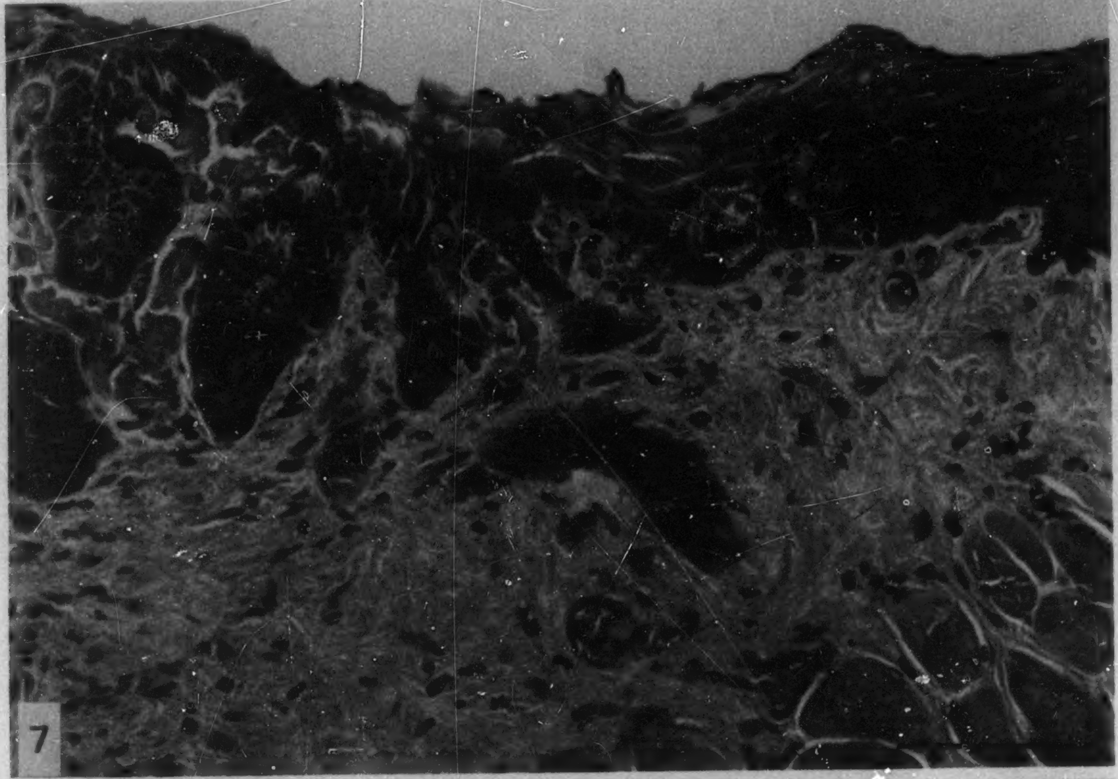

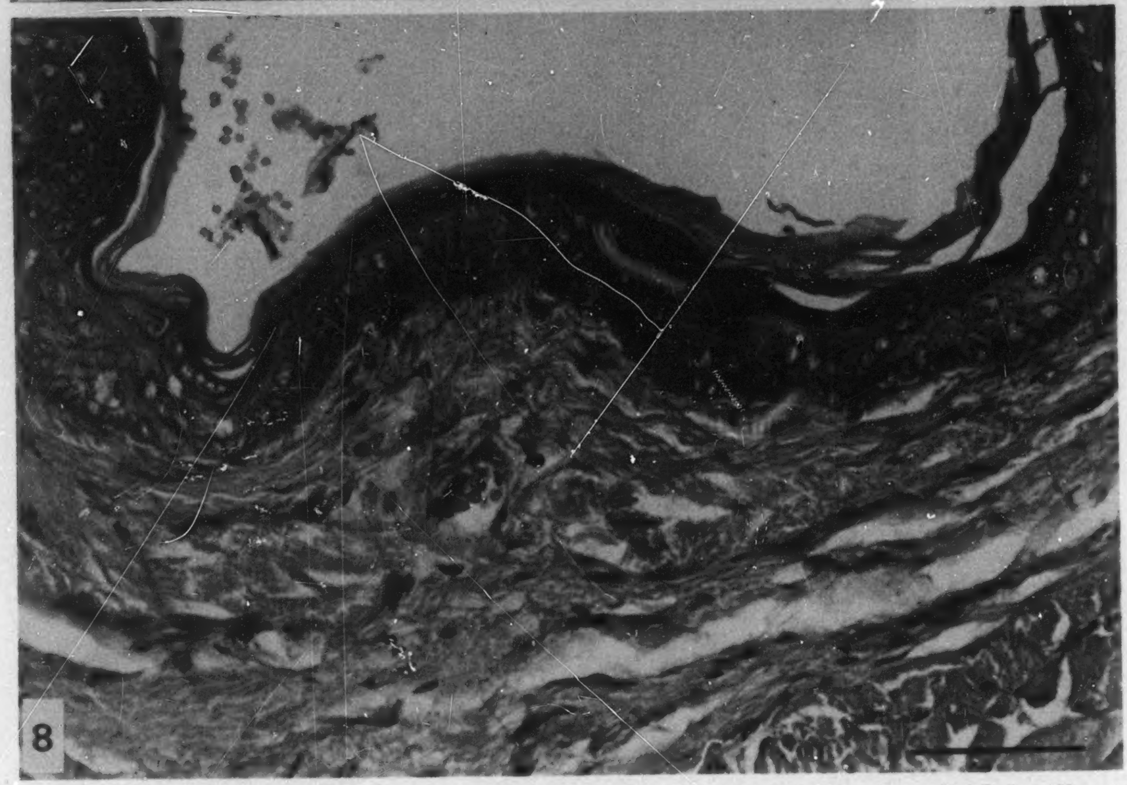

FIGURE 7.—Left buccal pouch mucosa of group 1 animal at 8 wk showing an area of dysplasia and early carcinoma. H & E. *Bar*=100 µm. × 250
FIGURE 8.—Left buccal pouch mucosa of group 2 animal at 8 wk showing hyperkeratosis. H & E. *Bar*=100 µm. × 250

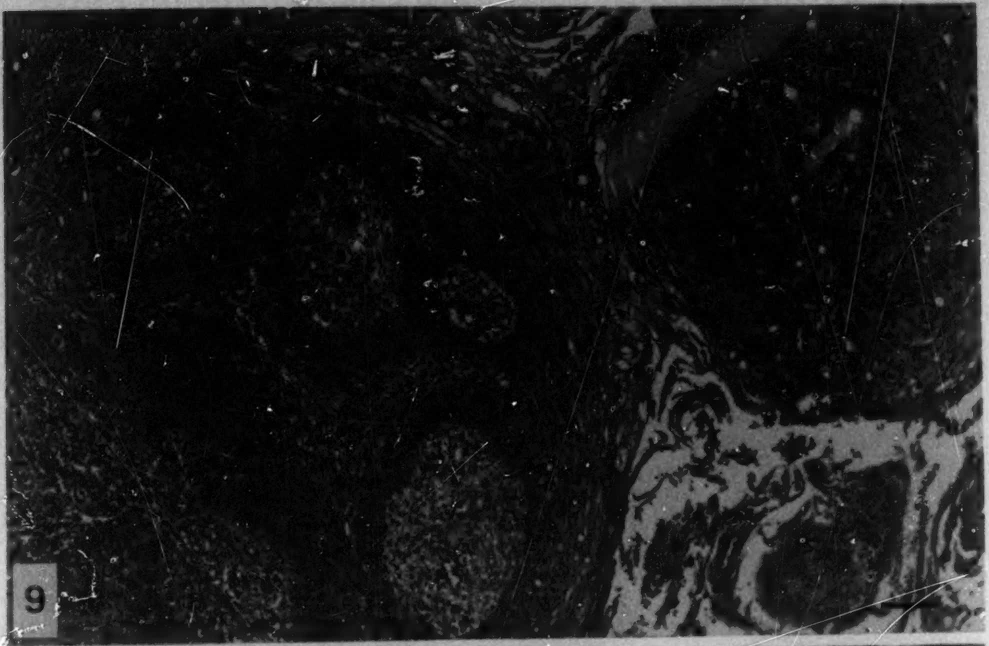

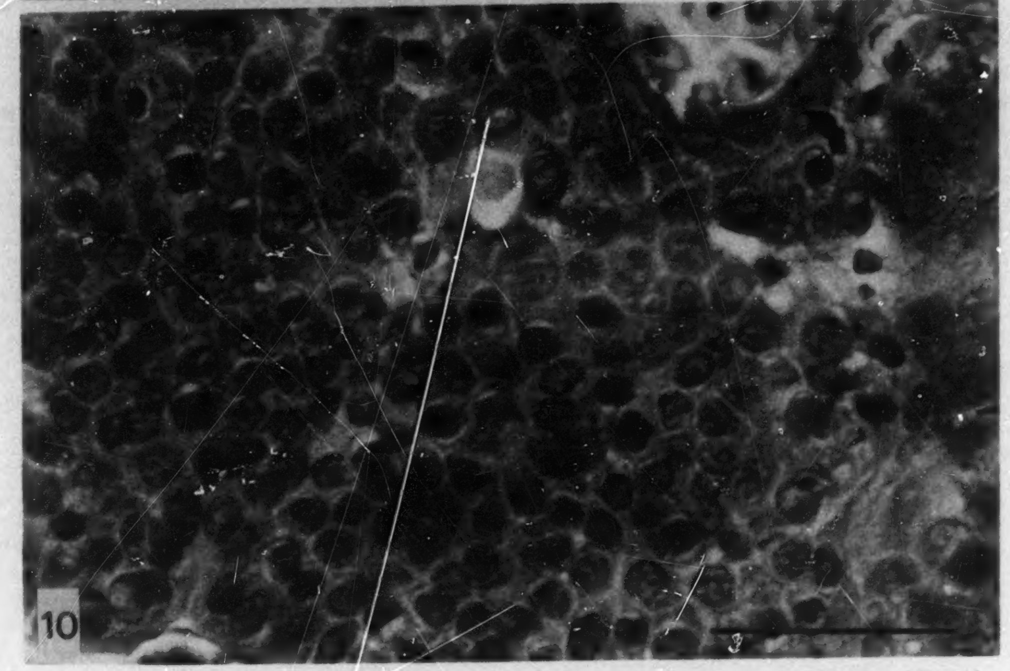

FIGURE 9.—Tumor of left buccal pouch in group 2 animal at 12 wk with the pathology of a well-differentiated papillary epidermoid carcinoma. H & E. *Bar*=100 µm. × 80

FIGURE 10.—High-power view of fig. 1 showing large hyperchromatic nuclei and numerous mitoses. H & E. *Bar*=100 µm. × 350

blank page

Thy-1 Antigen on Normal and Neoplastic Rat Mammary Tissues: Changes in Location and Amount of Antigen During Differentiation of Cultured Stem Cells[1,2]

Philip S. Rudland,[3] Michael J. Warburton,[3] Paul Monaghan,[3] *and* **Mary A. Ritter[4,5]**

ABSTRACT—With the use of immunofluorescent and immunocytochemical techniques on histologic sections of mammary glands from inbred WF rats, the thymocyte differentiation antigen (Thy-1) was identified partially on and immediately adjacent to the myoepithelial cells of ducts and alveoli. This antigen was absent from epithelial cells lining such structures. Some fibroblastic cells external to these structures also bore Thy-1. During glandular development the intensity of fluorescence due to the binding of Thy-1 antibodies increased as the myoepithelial cells matured. Similarly, mammary adenocarcinomas induced by 7,12-dimethylbenz[*a*]anthracene (DMBA) and *N*-methyl-*N*-nitrosourea contained elongated, presumptive myoepithelial cells that demonstrated varying degrees of Thy-1 immunofluorescence. This phenomenon was qualitatively mimicked by cultured cell lines from normal and DMBA-induced tumors. Elongated myoepithelial-like and fibroblast-like cells possessed Thy-1, whereas the cuboidal epithelial cell lines failed to express this antigen on the cell surface. Measurement of the relative number of Thy-1 molecules per cell by antiserum absorption techniques suggested that a neoplastic stem cell line, rat mammary (Rama) 25, contained about 3×10^5 Thy-1 molecules per cell in a form not directly accessible at the cell surface to anti-Thy-1 antibodies; the number of cryptic Thy-1 molecules was reduced when this cell line differentiated to alveolar-like cells in culture. However, when this cell line differentiated to myoepithelial-like cells, approximately 5×10^6 molecules per cell were exposed to anti-Thy-1 antibodies with a concomitant reduction of the cryptic pool. Morphologic maturation of elongated, myoepithelial-like cell line variants was also accompanied by increased surface Thy-1 fluorescence. Thus some of the myoepithelial cells in normal glands and tumors may arise by differentiation of epithelial stem cells and a spectrum of maturation states of the myoepithelial cell may exist as monitored by cellular morphology and surface Thy-1 expression.—JNCI 1982; 68:799–811.

The epithelial component of an adult female rat mammary gland consists of two structures, ducts and alveoli. Each structure contains a central lumen surrounded by lining epithelial cells, which are in turn surrounded by elongated, contractile myoepithelial cells. The cells lining the alveoli secrete milk-specific products during pregnancy and lactation (*1*). Recent in vitro (*2*) and in vivo (*3*) studies have raised the possibility that mammary epithelial development can take place by processes similar to those encountered in the hematopoietic system (*4–6*). In hematopoiesis all blood cells are formed by cell proliferation and differentiation from a population of pluripotent stem cells, whereas in the mammary system an epithelial stem cell line (Rama 25) has been cloned from an adenocarcinoma that can proliferate and differentiate to form the other two major epithelial cell classes: alveolar-like and myoepithelial-like cells. The cell surface differentiation antigen Thy-1 has been of considerable use as a marker in mapping hematopoietic development in the rat (*7–11*), and recent experiments suggest that Thy-1 may act as an adhesive molecule involved in cell positioning and migration (*12, 13*). Since Thy-1 is also present on mouse mammary tissue (*14*) and some rat mammary cell lines (*15*), this molecule may also be important in rat mammary differentiation. We now report on the appearance of Thy-1 during normal and neoplastic rat mammary development in vivo and in cloned cell lines in vitro. This work establishes the validity of Thy-1 in cloned cell lines in vitro as an experimental system for the investigation of the role of Thy-1 in mammary cell differentiation and has enabled us to make quantitative studies of both cryptic and cell surface Thy-1 in mammary stem and myoepithelial cells, respectively.

MATERIALS AND METHODS

Source and preparation of tissue and tumors.—ICRF inbred WF rats were used. We induced tumors in 50-day-old females by feeding them either 20 mg DMBA/100 g in corn oil (15 mg/ml) by a stomach tube (*16*) or by giving them two injections iv (separated by a month) of 5 mg MNU/100 g in 20 mg Earle's salts/ml (pH 6.0) (*17*); tumors developed within 2 or 3 months, respectively, and more than 90% were mammary adenocarcinomas (*18*). Sarcomas were produced by sc injection of 10^6 polyomavirus-transformed rat fibroblasts and harvested after 1 month. All tumors were excised at about 1 cm in diameter before they became necrotic. For normal tissues, female rats of varying ages were killed and the lower pairs of mammary glands routinely removed. The other mammary glands gave essentially the same histologic

---

ABBREVIATIONS USED: CM=conditioned medium; DMBA=7,12-dimethylbenz[*a*]anthracene; DMEM=Dulbecco's modified Eagle's minimum essential medium; DMSO=dimethyl sulfoxide; FCS=fetal calf serum; FITC=fluorescein isothiocyanate; ICRF=Imperial Cancer Research Fund; MNU=*N*-methyl-*N*-nitrosourea; PBS=phosphate-buffered saline.

---

[1] Received May 13, 1981; revised October 13, 1981; accepted November 27, 1981.

[2] Guidelines for the care and use of laboratory animals were followed as set forth by the Ludwig Institute for Cancer Research, Royal Marsden Hospital.

[3] Ludwig Institute for Cancer Research (London Branch), Royal Marsden Hospital, Sutton, Surrey, SM2 5PX, England.

[4] Imperial Cancer Research Fund (ICRF), P.O. Box 123, Lincoln's Inn Fields, London, WC2A 3PX, England.

[5] We thank Miss Mary Oliver, Mrs. Ruth Thompson, and Mrs. Carol Sauvage (ICRF) and Mr. D. Winslow and Mrs. Diana Mitchell (Ludwig Institute for Cancer Research) for expert technical assistance and Dr. R. C. Hallowes (ICRF) and Dr. B. Gusterson and Professor A. M. Neville (Ludwig Institute for Cancer Research) for valuable advice.

appearance. All tumors and tissues were cut into slices, which were then fixed in 5% glacial acetic acid–95% absolute ethanol (4°C), embedded in polyester wax (37°C), sectioned at 2½ and 5 µm, and stored at 4°C (*19*). For immunocytochemical localization of myosin and type IV collagen, pieces from parallel glands were fixed for 1 day in Methacarn (10% acetic acid, 30% chloroform, and 60% methanol) before being embedded in paraffin wax and sectioned.

Isolation and growth of cell lines.—The isolation of the rat mammary cloned cell lines Rama 25, Rama 27, and Rama 29 has been described previously (*2-4*). These and the remaining lines used are documented in table 1. The new cuboidal clonal cell lines Rama 41 (*20*), Rama 75, and Rama 102 from normal rudimentary glands of 7-day-old female ICRF WF rats were obtained from primary cultures of mammary epithelial cells (*21*) growing in Ham's nutrient mixture F-12 that had been exposed for 1 day to confluent cultures of Rama 29 (CM) and that had been reinforced with 10–30 ng epidermal growth factor/ml, 50 ng hydrocortisone/ml, 50 ng insulin/ml, and 10% FCS. Cell transfers, removal of contaminating fibroblasts, and single cell cloning procedures were performed as described previously (*2*). The single cell cloned lines Rama 29T and Rama 259 are variants of Rama 29 and Rama 25, respectively, selected independently for crisscross morphology and high proliferation rates and ability to grow in medium containing 1.8% DMSO. Rama 300 was obtained by single cell cloning of the fast-sticking cell fraction (*21*) of a DMBA-induced mammary carcinoma. Rama 500, Rama 502, and Rama 503 were single cell clones of "floaters" obtained when medium containing confluent cultures of Rama 25 cells was replated (*5*). Cell lines were all grown in DMEM, 10% FCS, 50 ng hydrocortisone/ml, and 50 ng insulin/ml, except the following lines: Rama 41 (DMEM was replaced by 100% CM) and Rama 75 and Rama 102 (DMEM was replaced by 50% CM and 50% DMEM). All cells were maintained at 37°C in 10% CO_2 in air. We obtained cuboidal cell cultures of Rama 25, Rama 41, Rama 75, Rama 102, and Rama 259 by harvesting subconfluent (≈1.5×10^6 cells/9-cm dish) cultures between fixed passage numbers (e.g., for Rama 25 cells; only those between passage 25 and 28 were used), the dilution factor on each passage being 8. "Droplet" and "doming" (*22*) cultures were obtained by the following procedure: Rama 25 and Rama 75 cells were plated at 2×10^5 cells per 9-cm dish and grown to confluence for 5 days in DMEM, 10% FCS, 50 ng hydrocortisone/ml, and 50 ng insulin/ml. The medium was then replaced by a similar medium containing 500 ng prolactin/ml, and a further change to medium containing 250 m*M* DMSO was made 2 days later. All cultures were harvested after 2 days' exposure to DMSO. These cultures were considered to contain alveolar-like cells (*3, 23*). Rama 259 did not form domes under these conditions. Lump structures (*5*) that inhibited dome formation occurred in high-passaged (passage 29 or 30) cultures of Rama 25 and Rama 75 (passages 15 and 16). Cultures in which both structures were required were used at passage 28 or 29 (Rama 25) or passage 14 or 15 (Rama 75), and cultures in which only droplet cells and domes were required were used at passage numbers below these. Cultures for immunofluorescence were grown on plastic cover slips (*2*), washed twice with PBS, and then fixed, usually for 2 hours in 95% ethanol at 4°C. Although mammary epithelial cells did not grow well on glass cover slips, these were required when acetone alone was used as a fixative. After 2 hours the cover slips were transferred to 70% ethanol at 4°C before use, preferably on the same day.

Antisera.—Four anti-Thy-1 antisera were used in each experiment reported. The first antiserum, from Dr. R. J. Morris, was an F(ab')$_2$ preparation of a rabbit antiserum to pure rat brain Thy-1. It contained three known specificities: Thy-1.1 alloantigen, 8%; rat-mouse cross-reacting Thy-1 xenoantigen, 41%; and rat-specific Thy-1 xenoantigen, 51%

TABLE 1.—*Fluorescence intensities of Thy-1 antiserum bound to different cultured cells*

Cultured cell line					Observed changes	
Rama No.	Source	Morphology	Probable cell type	Surface Thy-1[a]	Morphologic	Surface Thy-1[a]
25	Tumor epithelium	Cuboidal	Epithelial[b]	–	Elongated Droplet	++ –
75	Normal epithelium	Cuboidal	Epithelial[c]	–	Elongated Droplet	++ –
259	Rama 25	Cuboidal	Epithelial[c]	–	Elongated	+
102	Normal epithelium	Cuboidal	Epithelial[c]	–	Elongated	++
41	Normal epithelium	Cuboidal	Epithelial[b]	–	None	
29	Rama 25	Elongated	Myoepithelial[b]	++	None	
29T	Rama 29	Elongated	Myoepithelial[c]	++++	None	
500	Rama 25	Elongated	Myoepithelial[c]	++	None	
502	Rama 25	Elongated	Myoepithelial[c]	+++	None	
503	Rama 25	Elongated	Myoepithelial[c]	+	None	
27	Normal stroma	Elongated	Fibroblastic[b]	++	None	
300	Tumor stroma	Elongated	Fibroblastic[c]	++	None	

[a] Cells were scored for fluorescence intensity on a scale from zero (–) to maximum (++++) from four fields from four cover slips and the mean was recorded.

[b] On the basis of electron microscopic and biochemical evidence (*3, 5*).

[c] On the basis of light microscopic evidence only, and similarity in behavior to characterized cells.

(*24*). It was either conjugated directly to FITC (ratio of *F*-value to *P*-value=1.7) or used in the indirect immunofluorescence assay with $F(ab')_2$-sheep anti-rabbit $F(ab')_2$-FITC or goat anti-rabbit immunoglobulin-FITC as the second antibody. The second antiserum from Dr. A. F. Williams was the $F(ab')_2$ preparation of a monoclonal anti-Thy 1.1 antiserum (*25*). The two alloantisera anti-Thy 1.1 (C3H anti-AKR) and anti-Thy 1.2 (AKR anti-C3H) were purchased from Nordic Immunological Laboratories. All three mouse antisera were used in combination with FITC-labeled goat anti-mouse immunoglobulin (Nordic Immunological Laboratories). Pure rat brain Thy-1, antisera to myosin, and type IV collagen were kindly given by Dr. R. J. Morris, Dr. M. J. Owen (*26*), and Dr. L. A. Liotta (*27*), respectively.

Immunofluorescence and immunocytochemistry.—Tissue sections were dewaxed (*19*), followed by two 10-minute washes in isotonic PBS. Cultured cells on cover slips were rinsed twice with PBS. Specimens were then incubated for 30 minutes at room temperature with 10–20 µl of the following concentrations of antisera: 75 µg FITC-labeled $F(ab')_2$ rabbit anti-rat Thy-1/ml, 37 µg unconjugated rabbit anti-rat Thy-1/ml, 10 µg monoclonal anti-Thy 1.1/ml, and 1:5 dilutions of anti-Thy 1.1 and anti-Thy 1.2 alloantisera. Specimens were then rinsed for 20 minutes two times in PBS, and those not exposed to the FITC-conjugated antiserum were further incubated for 30 minutes with 10–20 µl of either FITC-sheep anti-rabbit $F(ab')_2$ (60 µg/ml) or FITC-goat anti-rabbit immunoglobulin (1:10) or FITC-goat anti-mouse immunoglobulin (1:5) as appropriate, followed by further 20-minute washes (two times) with PBS. Tissues were mounted in PBS-glycerol (9:1) (pH 8.2). Fluorescence was examined with a Zeiss RA microscope equipped with epi-illumination optics. Photography was done on Ilford HP5 film with the use of an exposure time of 1 or 2 minutes. For the identification of the location of Thy-1-positive structures in relation to the basement membrane, parallel sections were incubated with 1:100 antiserum to type IV collagen and visualized with rhodamine-conjugated sheep anti-rabbit $F(ab')_2$ serum (*27*). Immunocytochemistry was performed as for the indirect immunofluorescence assays with 100 µl of 75 µg FITC-labeled $F(ab')_2$ rabbit anti-rat Thy-1/ml. The sections were then incubated wtih 100 µl of 1:50 dilution of alkaline phosphatase conjugated to goat anti-rabbit IgG. The alkaline phosphatase was localized as a red color by incubation with Fast Red TR Base and naphthol AS-B1 phosphoric acid (*28*). Sections were then counterstained with Mayer's hemalum and mounted in buffered glycerinated gelatin. Immunocytochemical localization of myoepithelial cells and basement membranes with the use of 1:100 dilutions of antisera to myosin (*26*) and type IV collagen (*27*) was done as for the Thy-1 antigen (Warburton MJ, Mitchell D, Rudland PS: Manuscript in preparation).

Thy-1 antigen was also localized on lactating glands by an indirect immunoperoxidase technique at the ultrastructural level. Lobuloalveolar units were dissected out with a minimum of adherent stroma and incubated in 100 µl of the monoclonal anti-Thy 1.1 serum as before for 2 hours. The specimen was washed for 15 minutes in PBS and then incubated for a further 2 hours in 100 µl of 1:10 dilution of a sheep anti-mouse serum conjugated with horseradish peroxidase (*28*). The specimen was washed for a further 15 minutes in PBS and then incubated for 5 minutes in PBS containing 0.05% (wt/vol) 3,3′-diaminobenzidine (Sigma Chemical Co.) and 0.06% (vol/vol) hydrogen peroxide. All incubations were performed at room temperature. The tissue was then fixed for 2 hours in 2% (wt/vol) glutaraldehyde and post-fixed overnight in 1% (wt/vol) osmium tetroxide at 4°C. Both fixatives were phosphate buffered (0.05 *M*; pH 7.2–7.4) and their osmolarity was adjusted to 350 mosmol by addition of sucrose. The tissue was dehydrated in a series of graded ethanols and embedded, via propylene oxide, in Epon-Araldite resin. The resin blocks were polymerized at 60°C for 48 hours. Sections for light microscopy were stained with toluidine blue in 1% borax, and ultrathin sections were cut with a diamond knife on a Reichert OM U4 microtome. Without being stained, ultrathin sections were examined directly in a Philips EM 400 transmission electron microscope at 60 kV.

Specificity of Thy-1 immunofluorescence and immunochemical localization.—The specificity of the fluorescence for Thy-1 was demonstrated by abrogation of FITC fluorescence on tissue sections and cells in culture by prior incubation of the anti-Thy-1 antiserum with *a*) a threefold molar excess of pure Thy-1 antigen (overnight, 4°C) or by *b*) rat thymocytes (10^8/100 µg $F(ab')_2$; 1 hr at 4°C). No immunofluorescence was seen when the FITC-labeled or rhodamine-conjugated $F(ab')_2$-sheep anti-rabbit $F(ab')_2$, FITC-$F(ab')_2$ goat anti-rabbit immunoglobulin, or FITC-goat anti-mouse immunoglobulin were used in the absence of Thy-1 antibodies. Controls for all antisera used were included in every experiment. The rabbit anti-rat Thy-1, monoclonal anti-Thy 1.1, and anti-Thy 1.1 alloantisera all gave the same pattern of specific immunofluorescence on tissue sections and cell lines (all rats are Thy 1.1 in type). The anti-Thy 1.2 alloantiserum gave no specific immunofluorescence. The specificity of Thy-1 immunocytochemical localization was demonstrated by abrogation of red coloration due to alkaline phosphatase activity by prior incubation of the rabbit anti-Thy-1 serum with the pure Thy-1 antigen.

Quantitative absorptions and radioactive binding assays.—The assays were done as described by Morris and Williams (*29*). Eighty microliters of 0.283 µg $F(ab')_2$ or Fab anti-Thy 1.1 antiserum/ml was absorbed at 0°C for 1 hour with treble dilutions of measured numbers of cells (in 80 µl medium). The absorbed sera were removed, after centrifugation at 12,000×*g* for 1 minute, and their remaining activity was assessed by incubation with 1×10^7 glutaraldehyde-fixed adult rat thymocytes for 1 hour at 0°C. Binding of antiserum to these target cells was determined in a subsequent incubation with ^{125}I-labeled rabbit anti-mouse immunoglobulin, and the ^{125}I that was bound was measured in a gamma counter (LKB Instruments, Inc.). For detergent extraction, 60 µl of cells (3×10^8/ml) was mixed with an equal volume of 4% Triton X-100 and kept at 0°C in PBS for 45 minutes. Sixty microliters of 30% bovine serum albumin was then added to reduce the action of the detergent, and treble dilutions of cells were set up for absorption with the monoclonal anti-Thy-1 antiserum. Controls containing the same number of cells were processed in parallel, with the use of 60 µl PBS to replace the detergent. In addition, absorptions were set up with treble dilutions of detergent-containing buffer plus antibody but *no* cells to control for the possible effect of detergent in the binding assay.

RESULTS

Thy-1 on Tissue Sections

In the normal mammary gland from 7-day-old females, ductal myoepithelial cells, identified as elongated cells just internal to the basement membrane (*30*), showed no Thy-1-positive staining (table 2). The basement membrane was visualized by antitype IV collagen immunofluorescence or by silver staining for reticulin (not shown). By day 25 of development, areas near the basement membrane and/or myoepithelial cells were weakly positive and from day 45 onward these areas showed an increase in Thy-1 immunofluorescence (table 2) (figs. 1A–1D). From that time onward myoepithelial cells could be detected in similar positions in alveolar buds and alveoli (*31*). Myoepithelial cell and/or basement membrane areas in ducts from the glands of pregnant and lactating animals were strongly Thy-1-positive. At these later stages in development, the straplike myoepithelial cells producing a basket-like pattern round the alveolar lumina were also strongly positive (not shown). Additional Thy-1-positive cell types were probably fibroblasts [elongated cells external to the basement membrane (*30*)] and fat cells (fig. 1C). Ductal and secretory alveolar epithelial cells were always Thy-1 negative. All small blood vessels were Thy-1 positive; the antigen appeared to be on the vascular basement membrane (figs. 1A–1D).

The DMBA- and MNU-induced mammary adenocarcinomas consisted in part of circular structures composed of cuboidal epithelial cells, sometimes surrounded by a layer or layers of Thy-1-positive elongated cells (figs. 1E, 1G, 1I). In addition, finger-like processes of blocks of elongated cells penetrated through the more differentiated areas of the tumors, and these processes contained cells of varying degrees of Thy-1 positivity (fig. 1G). The general pattern of staining was also observed in the Rama 25-induced tumors (not shown). Blood vessels (with the exception of major arteries) within these neoplastic tissues were Thy-1 positive with a location similar to that of normal tissues (fig. 1H). In the sarcoma tissue, derived from polyomavirus-transformed rat fibroblasts, only occasional streaks of Thy-1-positive immunofluorescence were seen, mainly associated with capillaries and nerves (fig. 1F).

TABLE 2.—*Fluorescence intensities of Thy-1 antiserum bound to sections of mammary glands at different stages in development*

Developmental stage of mammary tissue[a]	Epithelium[b]	Myoepithelium[c]
Day 7	–	–
Day 25	–	±
Day 42	–	+
Day 75	–	+
Day 100	–	+
Day 13 of pregnancy	–	++
Day 9 of lactation	–	++
DMBA-induced tumors	–	+
MNU-induced tumors	–	+

[a] Tissue was from female rat. Only mammary parenchyma was considered: Nearly all capillaries, fibroblasts, and fat cells in stroma were also positive.

[b] Epithelium was always zero (–).

[c] Fluorescence intensity was recorded near (i.e., on and/or adjacent to) myoepithelial cells on the scale of zero (–) to maximum (++); ± indicates that some of the areas have positive fluorescence (+) and others have no fluorescence on the same tissue section. Six areas of each section were examined from four sections of each stage.

The localization of Thy-1 in the myoepithelial cell areas was examined in more detail with the use of an immunocytochemical technique. In the parenchyma of the normal rat mammary gland from 40-day-old female rats, Thy-1 was located in two positions and in differing concentrations: weakly on the myoepithelial cells and strongly in the region immediately adjacent to the myoepithelial cells and distal from the epithelial cells lining the ducts (figs. 2A–2D). The position of the myoepithelial cells in parallel glands was confirmed by their immunocytochemical localization with antimyosin serum (fig. 2E) (*26*) and antiprekeratin serum (not shown) (Warburton MJ, Mitchell D, Rudland PS: Manuscript in preparation). The strongly Thy-1-positive region immediately adjacent to the myoepithelial cells seemed to occur in the region of the basement membrane as visualized by immunocytochemical localization of type IV collagen in parallel glands (fig. 2F) (*27*). Thy-1 was not seen in the intercellular ground substance external to the basement membrane (fig. 2B). These results were confirmed by visualization of monoclonal antibodies to Thy-1 at the ultrastructural level in mammary glands from lactating rats. Thy-1 was predominantly in the lamina densa of the basement membrane as well as on the occasional mesenchymal cell external to the basement membrane (fig. 3). However, its distribution along the basement membrane varied. The intensity of stain was greatest when opposite a Thy-1-bearing mesenchymal cell and was gradually reduced on either side. This changed distribution of Thy-1 in the basement membrane could occur over the distance of a single myoepithelial cell (fig. 3). In these lactating glands the alveoli were so distended that the myoepithelial cells were forced apart, exposing flattened epithelial cells to the basement membrane. The basement membrane in these positions could also contain Thy-1 (not shown).

Distribution of Thy-1 on Cultured Cell Lines

All elongated (myoepithelial-like) cell lines were Thy-1 positive. This was true for lines derived from both tumor (figs. 4G–4I) and normal tissue (not shown), as well as for elongated cells developing in cultures of a cuboidal cell line (figs. 4D–4F; 5A–5F). Thus both the dual converter (e.g., Rama 75; figs. 5A–5C) and the monoconverter (e.g., Rama 102; figs. 5D–5F) cuboidal epithelial cell lines derived from normal glands yielded Thy-1-positive elongated cells. All cuboidal cell lines (figs. 4A–4C; 5A–5F) and their droplet and doming cultures (figs. 5G–5I) were Thy-1-negative (table 1). The intensity of Thy-1 immunofluorescence on myoepithelial-like cells varied from subline to subline, the more bipolar being more positive. This was demonstrated in the elongated series of cells cloned initially from Rama 25: Rama 29, Rama 29T, Rama 500, Rama 502, and Rama 503 (table 1). The cells of both fibroblastic cell lines (Rama

27 and Rama 300; figs. 4J–4L) gave positive staining. The fluorescence associated with Thy-1 circumscribes the cells and the antigen is probably mainly localized in their plasma membranes.

Eight different fixatives were tested: 70% ethanol (4°C), 95% ethanol (4°C), 95% ethanol–5% glacial acetic acid (4°C), 100% methanol (4°C), 75% acetone–25% methanol (−20°C), 100% acetone (−20°C), 2% paraformaldehyde (4°C), and 95% ethanol after a 5-minute treatment of the cells with 200 µg disodium EDTA/ml. All but two gave comparable levels of positive staining on Rama 27 and Rama 29 cells on cover slips. Those pretreated with EDTA appeared to be brighter, presumably owing to rounding up of the cells. However, morphologic information is lost by this shape change. One hundred percent acetone also gave slightly brighter immunofluorescent staining, but this was the direct result of a higher background.

Organized cellular structures in Rama 25 and Rama 75 cultures were also studied. The domes that occur in droplet cultures were Thy-1 negative (figs. 5G–5I). In contrast, the lumps and ridges produced predominantly by elongated cells showed positive Thy-1 immunofluorescence on these elongated cells (figs. 5J–5L).

Quantitative Studies of Thy-1 on Cell Lines

The relative amounts of surface Thy-1 were measured on Rama 25 (epithelial stem cell), Rama 29 (myoepithelial-like cells), and Rama 27 (fibroblastic cells) subconfluent cell cultures. Rama 27 and Rama 29 gave consistent results requiring $1.3\pm0.1\times10^4$ and $0.92\pm0.04\times10^4$ cells, respectively, to give 50% absorption of 20 µl monoclonal anti-Thy-1 antibody at 0.283 µg/ml: $4.3\pm0.6\times10^4$ rat thymocytes gave 50% absorption (text-fig. 1A). Thus Rama 27 cells bore 3.3 times and Rama 29 bore 4.7 times more cell surface Thy-1 molecules than did rat thymocytes, which have been shown to carry approximately 1×10^6 molecules of Thy-1 per cell (*25*). Rama 25 cuboidal cell cultures gave variable results, ranging from no absorption at all to 50% absorption with 40×10^4 cells/20 µl antiserum (text-fig. 1B), which represented a range of less than 10^4 to 1×10^5 Thy-1 molecules/cell. This variation correlated with the passage number of the cultures—the greater the passage number and hence the associated spontaneous conversion to Thy-1-positive elongated cells, the greater the absorptive capacity. Confluent cultures of Rama 25 cells grown in DMSO, hydrocortisone, insulin, and prolactin to produce droplet cells and domes gave 50% absorption values ranging from 9×10^4 to 2×10^6 cells. However, these cultures were maintained considerably longer than the subcultures of Rama 25 cuboidal cells and would therefore be expected to produce relatively more spontaneous conversions to elongated cells.

Treatment with the detergent Triton X-100 did not increase the amount of detectable Thy-1 in Rama 27, Rama 29, and rat thymocytes. However, 5 of 5 experiments with untreated Rama 25 and 3 of 5 experiments with DMSO- and hormone-treated Rama 25 Triton extracts showed greater absorption than did the experiment with whole cells [Rama 25, whole: Triton extract=1.3 to 1.4; Rama 25 plus DMSO, whole: Triton extract=1.1 to 1.3 (text-figs. 1B, 1C)]. Thus the number of cryptic (not detectable at surface of whole cells) Thy-1 molecules per cell was approximately 3×10^5 for Rama 25 and from 0 to 8×10^4 for Rama 25 droplet cells with DMSO and hormones. The appearance of the cryptic antigen within Rama 25 cells was not an artifact of the detergent treatment for the following reasons: 1)

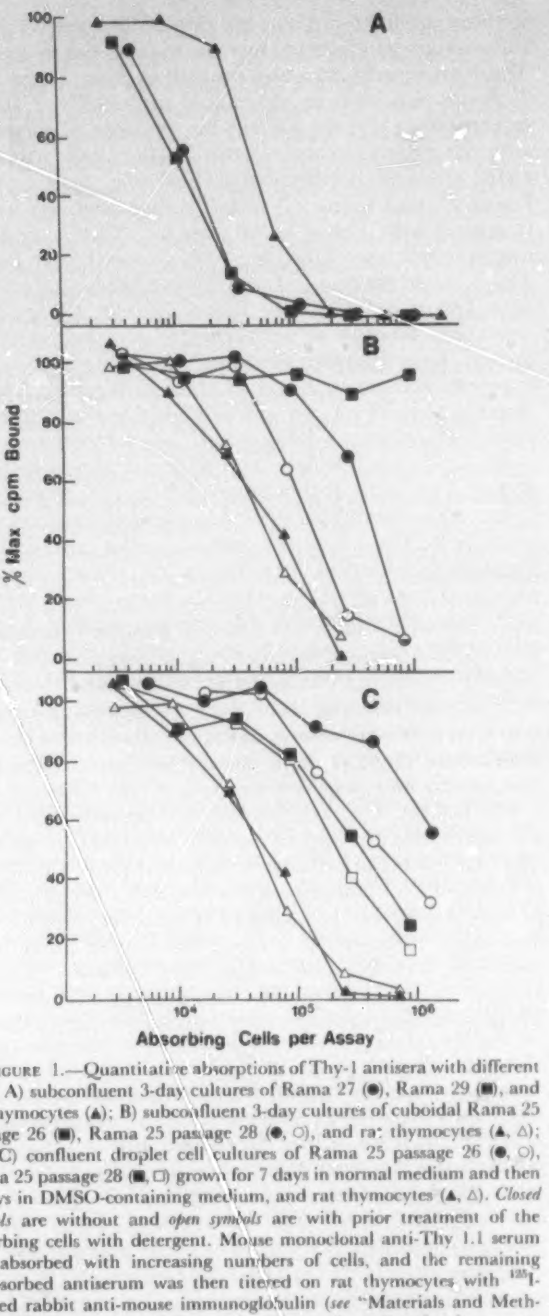

TEXT-FIGURE 1.—Quantitative absorptions of Thy-1 antisera with different cells: A) subconfluent 3-day cultures of Rama 27 (●), Rama 29 (■), and rat thymocytes (▲); B) subconfluent 3-day cultures of cuboidal Rama 25 passage 26 (■), Rama 25 passage 28 (●, ○), and rat thymocytes (▲, △); and C) confluent droplet cell cultures of Rama 25 passage 26 (●, ○), Rama 25 passage 28 (■, □) grown for 7 days in normal medium and then 2 days in DMSO-containing medium, and rat thymocytes (▲, △). *Closed symbols* are without and *open symbols* are with prior treatment of the absorbing cells with detergent. Mouse monoclonal anti-Thy 1.1 serum was absorbed with increasing numbers of cells, and the remaining unabsorbed antiserum was then titered on rat thymocytes with ^{125}I-labeled rabbit anti-mouse immunoglobulin (*see* "Materials and Methods"). The percentage of the maximum cpm bound to the thymocytes was followed as a function of increasing numbers of absorbing cells. Max=maximum.

Treatment of the original binding buffers with Triton X-100 without cells failed to increase the amount of detectable Thy-1 over the background controls without Triton X-100. 2) Some cells with no detectable surface Thy-1 [e.g., rat erythrocytes (*32*)] did not exhibit increases after treatment with the detergent (not shown). 3) Other cells with appreciable amounts of cell surface Thy-1 (e.g., rat thymocytes, Rama 29, and Rama 27) failed to show any increase after treatment with Triton X-100 (text-fig. 1B, 1C). 4) Absorption of monoclonal Thy-1 antibody first with pure rat brain Thy-1, as detailed in "Materials and Methods," and then with Triton X-100-treated Rama 25 cells still yielded no detectable binding of antibodies to rat thymocytes (not shown). Thus detergent treatment did not interfere with the apparent amount of Thy-1 in those cells with or without demonstrable Thy-1 nor with antibody–antigen complexes. Finally, fluorescently labeled anti-Thy-1 serum was added to Rama 25 cells that had been made completely permeable in and fixed with 75% acetone–25% methanol at −20°C. Under these conditions weak fluorescence specifically associated with Thy-1 was seen over the entire cells, unlike the fluorescence observed with Rama 29 cultures that completely circumscribed the cells. These results are consistent with those obtained with the detergent-treated Rama 25 cells in that Thy-1 was detected at lower levels and in this case with a cellular distribution different from that observed in Rama 29 cells.

DISCUSSION

Using immunologic detection methods, we have studied the appearance of the Thy-1 antigen in the development of rat mammary tissue in two systems, in vivo (tissue sections) and in vitro (cloned cell lines). Myoepithelial cells in vivo were Thy-1 positive, although most of the antigen seemed to reside in the region of the basement membrane. This topologic association was confirmed at the ultrastructural level. The epithelium lining the lumina in both ducts and alveoli apparently lacked the antigen. The intensity of the myoepithelial Thy-1 immunofluorescence, and hence probably the amount of antigen present, increased with the development of the gland, from being negative in rats at day 7 to being strongly positive in rats at age 45 days, with a further increase during pregnancy and lactation. Inasmuch as the first mammary myoepithelial cells (elongated cells with myofilaments) appear before birth (*33, 34*), these early cells must either bear low amounts of Thy-1 antigen (not detectable by immunofluorescence) or totally lack Thy-1 antigen. This pattern of Thy-1 distribution and its increase upon maturation of the myoepithelial cells are also seen in the cloned cell lines, although the quantitative comparison with the change in vivo cannot be made as yet. All cuboidal cell lines and their droplet (alveolar-like) derivatives lack surface Thy-1. In contrast, all cloned elongated (myoepithelial-like) cell lines, as well as elongated cells developing within stem cell cultures, are Thy-1 positive, and the more mature (bipolar) elongated cell lines bear more antigen. Thus the Thy-1 antigen provides a good qualitative cell marker with which to study rat myoepithelial cell differentiation in vitro and possibly in vivo, although for the in vivo study our observation that some fibroblasts are Thy-1 positive and that the bulk of the antigen on or adjacent to myoepithelial cells is asymmetrically distributed necessitates the use of additional markers (e.g., antitype IV collagen and antimyosin antibodies) to distinguish these two cell types (*35*). These results are similar to those in the brain where Thy-1 increases approximately twentyfold during the first 3 postnatal weeks and has a predominantly neuronal distribution (*36, 37*). This cellular distribution is also mimicked by some of the rat cell lines that express other neuronal characteristics, whereas cell lines with clearly glial properties are negative for Thy-1 (*24*). However, in the brain there is a general quantitative difference with the in vivo situation since none of the central nervous system-derived lines approach the level of antigen found in adult rat brain (*24*). In the mammary gland we are unable to assess accurately the amount of antigen present on myoepithelial cells because the myoepithelial cells cannot be purified directly. However, a comparison of the relative intensities of anti-Thy-1 fluorescence on mature myoepithelial cells in vivo and elongated myoepithelial-like cells in vitro suggests that these intensities are more comparable than those on neuronal cells in vivo and in vitro. This finding may perhaps be due to the higher numbers (approximately three times) of Thy-1 molecules per cell on cultured, elongated, myoepithelial-like cells than on the neuronal cell lines carrying the maximum observed numbers of Thy-1 molecules (*24*).

Myoepithelial cells are also known to exist in DMBA-induced adenocarcinomas (*38*) and we can detect Thy-1-positive elongated cells, presumed to be myoepithelial cells, round the outside of some circular arrays of cuboidal cells. However, the positive identification of myoepithelial cells in the tumors is much more difficult to establish than in normal glands since the position of myoepithelial cells in the tumors with respect to the basement membrane is often difficult to ascertain. There exists a whole class of rather elongated cells that infiltrate the well-differentiated areas of the tumors in finger-like processes often, where extensive enough, giving rise to apparently sarcomatous areas (*6*). Many of the cells within these areas also stain with Thy-1 antiserum to varying degrees. Whether they are myoepithelial cells showing varying degrees of expression of Thy-1 antigen, fibroblasts, lymphoid, or mast cells (*7*) is uncertain. Many of these cells, however, may be myoepithelial since similar blocks of elongated cells have been produced in tumors formed by our rat mammary cuboidal cells in nude mice; and some of them were identified as of rat rather than of mouse origin (*2, 20*).

Recent studies of mouse thymocyte development have indicated that cells first acquire intracellular and/or cryptic Thy-1 at a stage prior to the one when the antigen is exposed at the cell surface (*39*). In addition, the mammary stem cell line Rama 25 may contain cytoplasmic Thy-1 (*15*). However, this finding was based on immunofluorescence after acetone fixation, a system where we find that the high background obscures specific cytoplasmic immunofluorescence. We have, therefore, used more sensitive assays (quantitative absorptions and radioimmune binding assays) both to detect and quantitate surface (whole cells) versus surface plus possible intracellular (detergent extracts of cells) Thy-

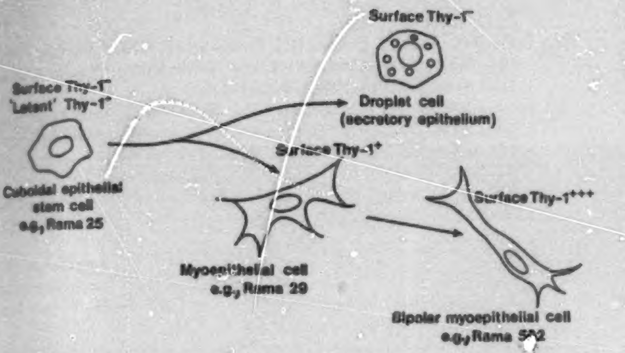

TEXT-FIGURE 2.—Schematic summary of the differentiation of mammary epithelial cells. Cuboidal epithelial stem cells with no detectable surface Thy-1 (Thy-1^-) but with latent Thy-1 (Thy-1^+) or cryptic Thy-1 differentiate to either droplet cells with no detectable Thy-1 (Thy-1^-) and reduced cryptic Thy-1 or to elongated, myoepthelial-like cells with surface Thy-1 (Thy-1^+) and then to bipolar myoepithelial-like cells with additional surface Thy-1 (Thy-1^{+++}), as recorded in table 1.

1. We find that subconfluent cultures of mammary epithelial stem cells (Rama 25) contain an average of 3×10^5 molecules of cryptic Thy-1 per cell. Rama 25 cultures treated with DMSO (droplet cells) contain appreciably less (0–8×10^4 molecules of cryptic Thy-1). The lower number of cryptic Thy-1 molecules per cell in the DMSO-treated Rama 25 cells possibly reflects the lower percentage of stem cells within these cultures rather than a smaller number of cryptic antigens per cell. The exact location of this cryptic Thy-1 is unknown, although by analogy with the mouse prothymocyte it could be intracellular and its correct glycosylation may be a prerequisite for exposure on the cell surface (*39, 40*). The differentiation of mammary epithelial cells (text-fig. 2) therefore involves a series of steps whereby a population of surface Thy-1-negative stem cells, at least some of which contain a pool of intracellular Thy-1, gives rise to either Thy-1-negative secretory or to surface Thy-1-positive myoepithelial cells that bear increasing numbers of Thy-1 molecules as differentiation proceeds.

Although Thy-1 provides an excellent marker molecule in certain differentiating systems, little is known of its function. It may play a role in the formation of domes in a subline of Rama 25 (*41*). This suggestion was based on the findings that Thy-1 could be detected on the surface of incipient domes (particularly at cell junctions); that, with fixatives allowing free access of the antibodies to the interior of cells, the cells showed enhanced cytoplasmic fluorescence, particularly in doming regions; and that antibodies to Thy-1 could specifically block formation of domes. We have been unable to repeat all three findings satisfactorily when using xenogeneic, allogeneic, and monoclonal antibodies to Thy 1.1 on Rama 25 cultures. However, using low protein concentrations, particularly with the monoclonal antibodies, we can observe fluorescence, especially round heterogeneities in the cell monolayer, e.g., cell junctions, domes (droplet cells), lumps, and ridges (elongated and/or myoepithelial cells). However, this fluorescence is abolished only by preabsorption of the antibodies with thymocytes and/or pure Thy-1 in the cases of ridges and lumps (figs. 5G–5L). Anti-Thy 1.1 antibodies at high concentrations can block dome formation, but this blockage could also be achieved with similar concentrations of anti-Thy 1.2 antisera that failed to show specific binding at any concentration tested. Since the original authors (*41*) used different sources of xenogeneic and monoclonal antibodies to Thy 1.1 than those used here, we cannot exclude the possibility that the reported fluorescence observed in domes with these antibodies and the prevention of formation of domes by the monoclonal antibodies (*41*) are unique for this collection of Thy-1 antisera. However, the same group (*42*) have recently reported that the antidoming effect of their monoclonal antibodies was not removed by absorption to Thy 1.1-positive cells and was therefore unrelated to Thy-1.

In the mouse brain Thy-1 has been found in association with synaptic complexes, suggesting that it may be involved in cell to cell interaction of the neuronal elements (*43*). Recently, in the rat Thy-1 antigen has also been found in regions associated with the basement membrane surrounding some blood vessels, including the postcapillary venules in lymph node, and on interstitial connective tissue on the dermis and lamina propria. Thy-1 may, therefore, function in mediating selective adhesion of cells to connective tissue substrates and hence could be involved in controlling migration and in homing of lymphocytes during recirculation (*8, 12, 13*). In regard to the mammary gland, Radnor (*44*) has suggested that contact of mammary epithelial cells with the basement membrane may result in production of myoepithelial cells in early developmental stages. We have found that increased synthesis of some of the major constituents of basement membranes, type IV collagen and fibronectin, occurs with concomitant expression of cell surface Thy-1 molecules in cell lines cloned from Rama 25, which are intermediate in morphology between cuboidal and fully elongated forms (Warburton MJ, Ritter M, Rudland PS: Unpublished results). This finding and our observations of extracellular Thy-1 in the region of the basement membrane raise the possibility that interactions between basement membrane components and cell surface Thy-1 may be involved in controlling subsequent myoepithelial cell development and/or positioning within the mammary gland.

REFERENCES

(*1*) RAYNAUD A. The mammary gland: Morphogenesis, structure, and growth. In: Kon SK, Cowie AT. Milk: The mammary gland and its secretions. New York: Academic Press, 1961:3–46.

(*2*) BENNETT DC, PEACHEY LA, DURBIN H, RUDLAND PS. A possible mammary stem cell line. Cell 1978; 15:283–298.

(*3*) RUDLAND PS, BENNETT DC, WARBURTON MJ. Hormonal control of growth and differentiation of cultured mammary gland epithelial cells. In: Ross R, Sato GH, eds. Hormones and cell culture: Cold Spring Harbor Conference on Cell Proliferation, Cold Spring Harbor, N.Y.: Cold Spring Harbor Laboratory, 1979; 6:677–699.

(*4*) ———. Growth and differentiation of cultured rat mammary epithelial cells. In: Iacobelli S, King RJ, Linder HR, Lippman ME, eds. Proceedings of the First International Congress on Hormones and Cancer. New York: Raven Press, 1980:255–270.

(*5*) RUDLAND PS, BENNETT DC, RITTER MA, NEWMAN RA, WARBURTON MJ. Differentiation of a rat mammary stem cell line in culture. In: Jimenez de Asua L, Levi Montalcini R, Shields R, Iacobelli S, eds. Control mechanisms in animal cells. New York: Raven Press, 1980:341–365.

(*6*) RUDLAND PS, ORMEROD EJ, PATERSON FC. Stem cells in rat mammary development and cancer: A review. J R Soc Med 1980; 73:437–442.

(7) Ritter MA, Gordon LK, Goldschneider I. Distribution and identity of Thy-1 bearing cells during ontogeny in rat hemopoietic and lymphoid tissues. J Immunol 1978; 121:2463–2471.

(8) Ritter MA. The differential expression of Thy-1 antigen on cell surfaces and extracellular matrix during lymphopoiesis. In: Horton J, ed. Development and differentiation of vertebrate lymphocytes. Amsterdam: Elsevier/North Holland, 1980:75–86.

(9) Goldschneider I, Gordon LK, Morris RJ. Demonstration of Thy-1 antigen on pluripotent hemopoietic stem cells in the rat. J Exp Med 1978; 148:1351–1366.

(10) Crawford JM, Goldschneider I. Thy-1 antigen and B lymphocyte differentiation in the rat. J Immunol 1980; 124:969–976.

(11) Hunt SV. The presence of Thy-1 on the surface of rat lymphoid stem cells and colony-forming units. Eur J Immunol 1979; 9:853–859.

(12) Ritter MA, Morris RJ. Thy-1 antigen: Selective association in lymphoid organs with the vascular basement membrane involved in lymphocyte recirculation. Immunology 1980; 39:85–91.

(13) Morris RJ, Ritter MA. Association of Thy-1 cell surface differentiation antigen with certain connective tissues in vivo. Cell Tissue Res 1980; 206:459–475.

(14) Hilgers J, Haverman J, Nusse R, et al. Immunologic, virologic, and genetic aspects of mammary tumor virus-induced cell-surface antigens: Presence of these antigens and the Thy-1.2 antigen on murine mammary gland and tumor cells. J Natl Cancer Inst 1975; 54:1323–1333.

(15) Lennon VA, Unger M, Dulbecco R. Thy-1: A differentiation marker of potential mammary myoepithelial cells in vitro. Proc Natl Acad Sci USA 1978; 75:6093–6097.

(16) Huggins C, Briziarelli G, Sutton H. Rapid induction of mammary carcinoma in the rat and the influence of hormones on the tumors. J Exp Med 1959; 109:25–42.

(17) Gullino P, Pettigrew HM, Grantham FH. Nitrosomethylurea as mammary gland carcinogen in rats. J Natl Cancer Inst 1975; 54:401–414.

(18) Williams JC, Gusterson B, Humphreys J, et al. *N*-Methy-*N*-nitrosourea-induced rat mammary tumors. Hormone responsiveness but lack of spontaneous metastases. JNCI 1980; 66:147–155.

(19) Lebacq AM, Ritter MA. B-cell precursors in early chicken embryos. Immunology 1977; 37:123–134.

(20) Bennett DC. Rat mammary lines: Their isolation and characterisation. Ph.D. thesis. London: London University, 1979.

(21) Rudland PS, Hallowes RC, Durbin H, Lewis D. Mitogenic activity of pituitary hormones on cell cultures of normal and carcinogen-induced tumor epithelium from rat mammary glands. J Cell Biol 1977; 73:561–577.

(22) McGrath CM. Cell organization and responsiveness to hormones in vitro: Genesis of domes in mammary cultures. Am J Zool 1975; 15:231–236.

(23) Newman RA, Klein PJ, Rudland PS. Binding of peanut lectin to breast epithelium, human carcinomas, and a cultured rat mammary stem cell: Use of the lectin as a marker of mammary differentiation. JNCI 1979; 63:1339–1346.

(24) Morris RJ, Mancini PE, Pfeiffer SE. Thy-1 cell surface antigen on cloned nerve cell lines of the rat and mouse: Amount, location, and origin of the antigen in the cells. Brain Res 1980; 182:119–135.

(25) Mason DW, Williams AF. The kinetics of antibody binding to membrane antigens in solution and at the cell surface. Biochem J 1980; 187:1–20.

(26) Owen MJ, Auger J, Barber BH, Edwards AJ, Walsh FS, Crumpton MJ. Actin may be present on the lymphocyte cell surface. Proc Natl Acad Sci USA 1978; 75:4484–4488.

(27) Liotta LA, Wicha MS, Foidart JM, Rennard SI, Garbisa S, Kidwell WR. Hormonal requirement for basement membrane collagen deposition by cultured rat mammary epithelium. Lab Invest 1979; 41:511–518.

(28) Avrameas S. Immunoenzyme techniques: Enzymes as markers for the localization of antigens and antibodies. Int Rev Cytol 1970; 27:349–383.

(29) Morris RJ, Williams AF. Antigens on mouse and rat thymocytes recognized by rabbit antiserum against rat brain: The quantitative analysis of a xenogeneic antiserum. Eur J Immunol 1975; 5:274–281.

(30) Hamperl H. The myoepithelia. Curr Top Pathol 1970; 53:161–220.

(31) Russo J, Wilgus C, Russo IH. Susceptibility of the mammary gland to carcinogenesis. Am J Pathol 1979; 96:721–736.

(32) Ritter MA, Morris RJ, Goldschneider I. Hidden Thy-1 in a subpopulation of mouse bone marrow cells. Immunology 1980; 39:375–384.

(33) Salazar H, Tobon H. Morphological changes in the mammary gland during development, pregnancy and lactation. In: Josimovich JB, Reynolds M, Cobo E, eds. Lactogenic hormones, fetal nutrition and lactation. New York: Wiley, 1974:221–227.

(34) Schlotke B. Histochemische Untersuchungen zur Rolle der myoepithelzellen (MEZ) bei der morphogenese von mammaturmoren der Hündin. Zentrabl Veterinaermed [A] 1976; 23:661–669.

(35) Warburton MJ, Head LP, Rudland PS. Redistribution of fibronectin and cytoskeletal proteins during the differentiation of rat mammary tumor cells in vitro. Expt Cell Res 1980; 132:57–66.

(36) Douglas T. Occurrence of a theta-like antigen in rats. J Exp Med 1972; 136:1054–1062.

(37) Acton RT, Pfeiffer SE. Distribution of Thy-1 differentiation alloantigen in the rat nervous system and in a cell line derived from a rat peripheral neurinoma. Dev Neurosci 1978; 1:110–117.

(38) Young S, Hallowes RC. Tumours of the mammary gland. In: Turusov VS, ed. Pathology of tumours in laboratory animals. Vol 6. Tumours of the rat. Lyon: IARC Press, 1973:31–74.

(39) Trowbridge IS, Hyman R, Mazauskas C. The synthesis and properties of T25 glycoprotein in Thy-1 negative mutant lymphoma cells. Cell 1978; 14:21–32.

(40) Trowbridge IS, Hyman R, Ferson T, Mazauskas C. Expression of Thy-1 glycoprotein in lectin-resistant lymphoma cell lines. Eur J Immunol 1978; 8:716–723.

(41) Dulbecco R, Bologna M, Unger M. Role of the Thy-1 antigen in the in vitro differentiation of a rat mammary cell line. Proc Natl Acad Sci USA 1979; 76:1848–1852.

(42) Dulbecco R, Unger M, Bologna M, Battifora H, Syka P, Okada S. Cross reactivity between Thy-1 and a component of intermediate filaments demonstrated using a monoclonal antibody. Nature 1981; 292:772–774.

(43) Acton RT, Addis J, Carl GF, McClain LD, Bridges WF. Association of Thy-1 differentiation alloantigen with synaptic complexes isolated from mouse brain. Proc Natl Acad Sci USA 1978; 75:3283–3287.

(44) Radnor CJ. Myoepithelial cell differentiation in rat mammary glands. J Anat 1972; 111:381–398.

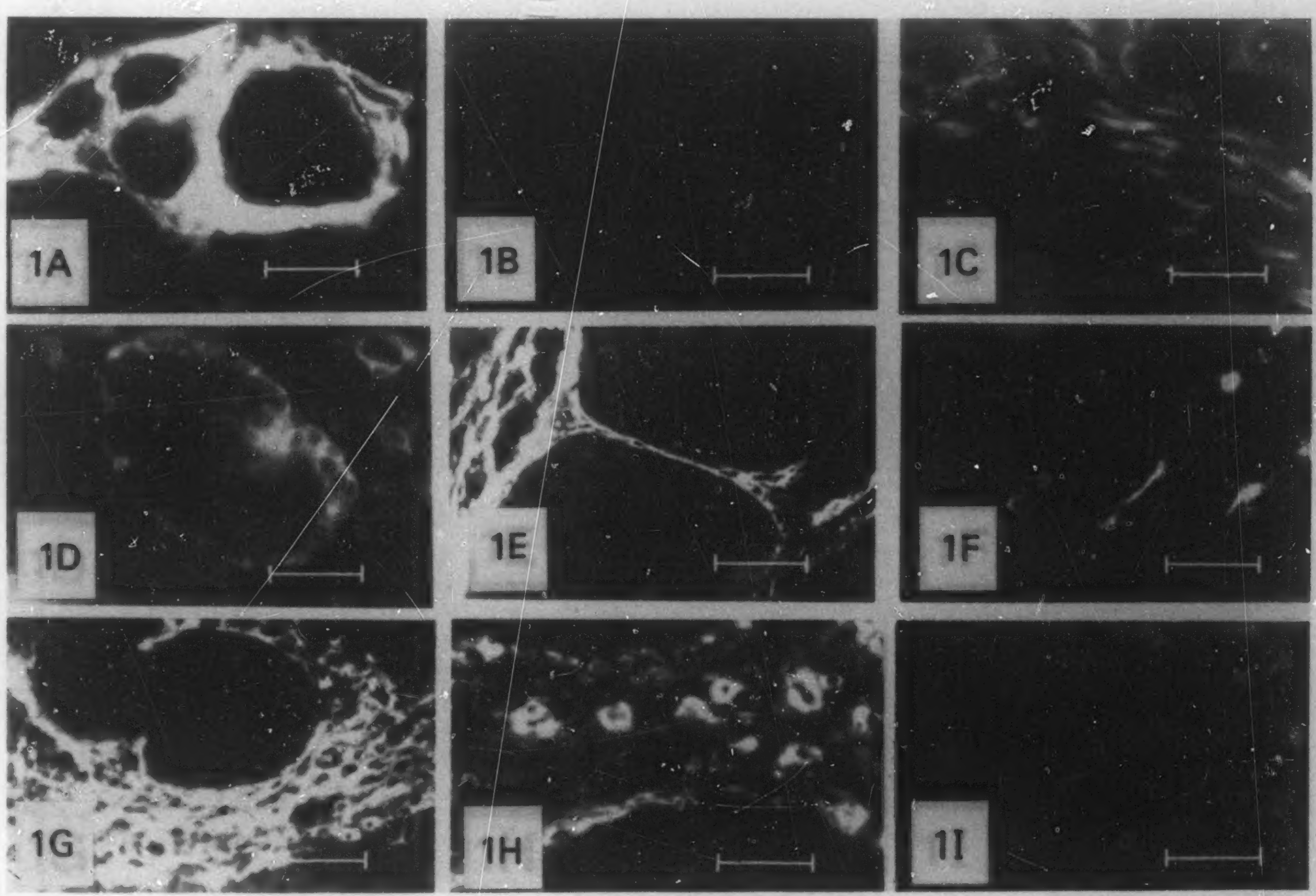

FIGURE 1.—Binding of fluorescently labeled antisera to histologic sections of glandular material. Histologic sections from: A–D) mammary glands of 45- to 50-day-old female rats, E) MNU-induced tumors, F) polyomavirus-transformed cell-induced tumors, and G–I) DMBA-induced tumors. The sections were stained with rabbit anti-Thy-1 and then the antibodies were visualized indirectly with FITC–sheep anti-rabbit serum, except for sections shown in figs. 1B and 1I, which were initially stained with rabbit-anti-Thy-1 preabsorbed with purified Thy-1, and for sections in fig. 1D, which were stained with Thy-1 monoclonal antibodies and visualized with goat anti-mouse serum. Sections were viewed by fluorescence optics and identical exposure times of 1 min were used for all photographs. A–D, H: *bar*=30 μm. E–I: *bar*=60 μm

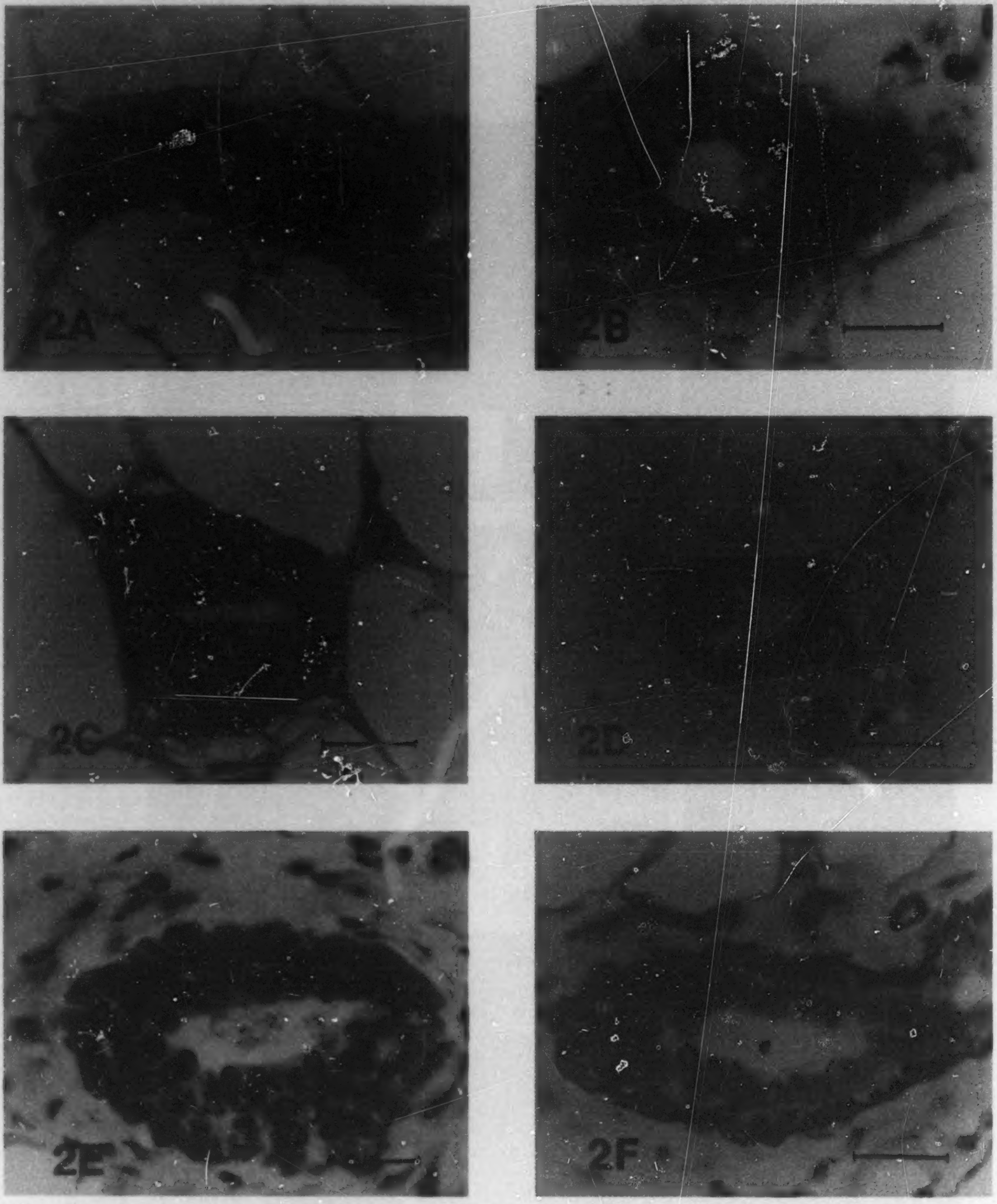

FIGURE 2.—Immunocytochemical localization of Thy-1 in mammary gland from 40-day-old rats. Immunocytochemical sections stained with: A–C) rabb anti-Thy-1, D) anti-Thy-1 preabsorbed with purified Thy-1, E) antimyosin, and F) antitype IV collagen. The antibodies are visualized indirectly by th development of a red coloration with alkaline phosphatase conjugated to goat anti-rabbit serum. Nuclei are stained with Mayer's blue hemalum (s "Materials and Methods"). The maximum distribution of Thy-1 varied from A) a narrow band through B) a broader band to C) a broad ban enveloping fibroblast-like cells and small capillaries. A, C–F: *bar*=30 µm. B: *bar*=25 µm

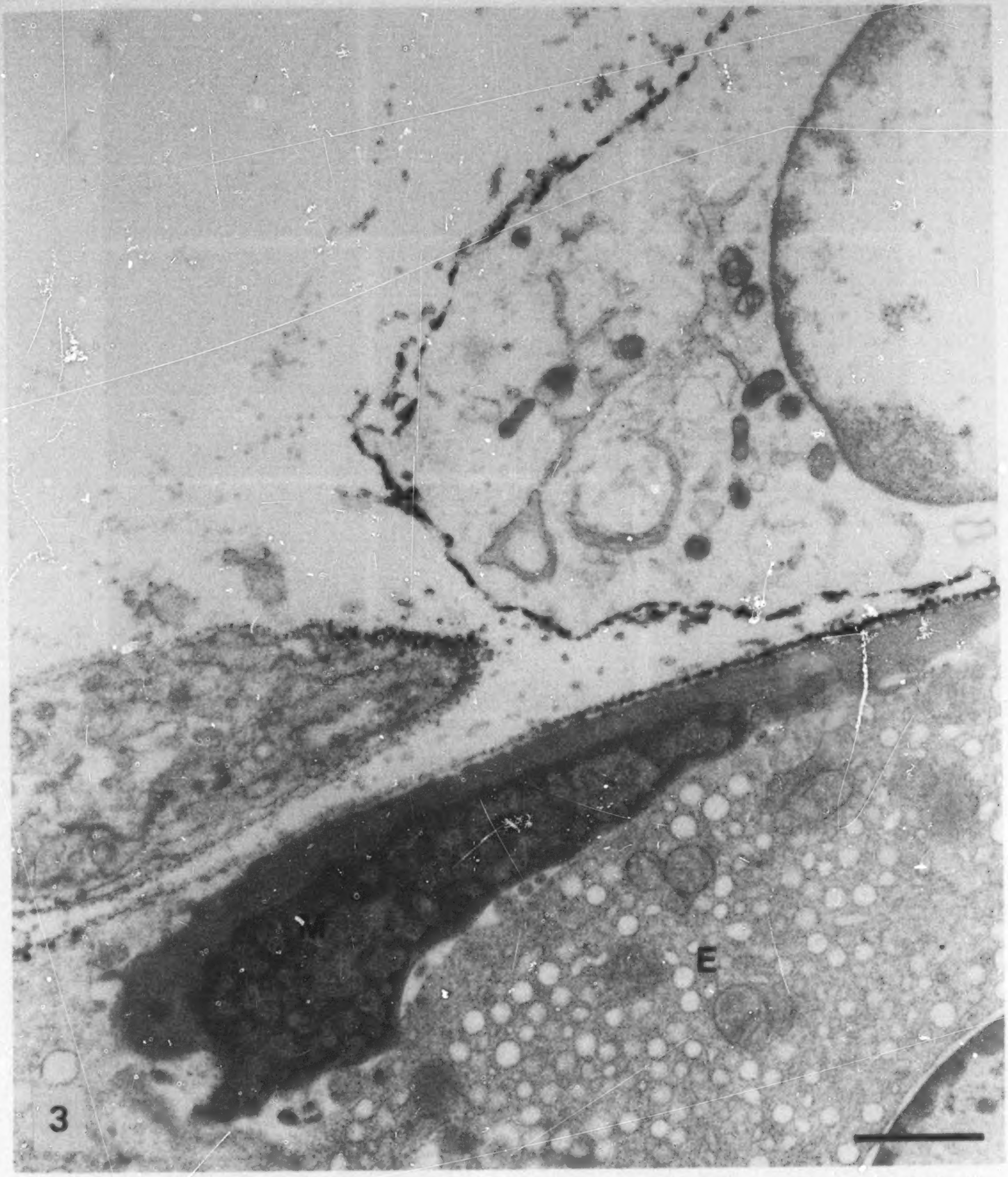

FIGURE 3.—Ultrastructural immunocytochemical localization of Thy-1 in mammary glands of lactating rats: Tissues are stained with monoclonal antibodies to Thy 1.1. The antibodies were visualized indirectly by the development of a brown coloration with horseradish peroxidase conjugated to sheep anti-mouse serum. Ultrathin sections were cut and viewed directly in the electron microscope (see "Materials and Methods"). The section shows an epithelial (E) and myoepithelial cell (M) within and 2 mesenchymal cells external to the basement membrane of the mammary gland from a lactating rat. Thy-1 is present in the lamina densa of the basement membrane adjacent to part of the myoepithelial cell and on the plasma membrane of the larger of the 2 mesenchymal cells. Bar=1 μm

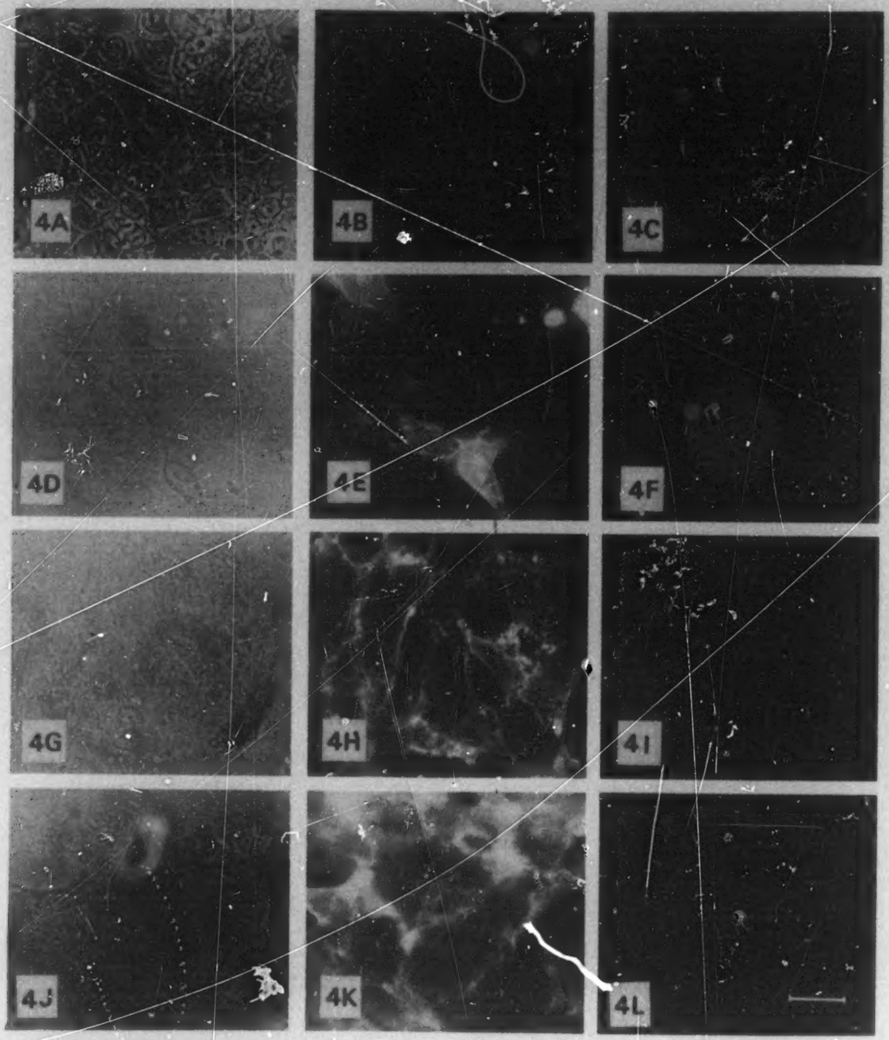

FIGURE 4.—Binding of fluorescently labeled Thy-1 antiserum to cell lines from DMBA-induced tumors: A–C) cultures of Rama 25 cuboidal cells, D–F) elongated cells formed in Rama 25 cultures, G–I) cultures of myoepithelial-like Rama 29 cells, and J–L) cultures of stroma-derived Rama 300 cells. *First two photographs in each vertical column* show the same field stained with FITC-conjugated Thy-1 antiserum viewed by phase-contrast and fluorescence optics. *Last photograph in each vertical column* shows a duplicate culture stained with FITC-conjugated Thy-1 antiserum preabsorbed with rat thymocytes, viewed by fluorescence optics. Identical illuminations and exposure times of 1 min were used for all eight fluorescence photographs. A–L: *Bar*=25 µm

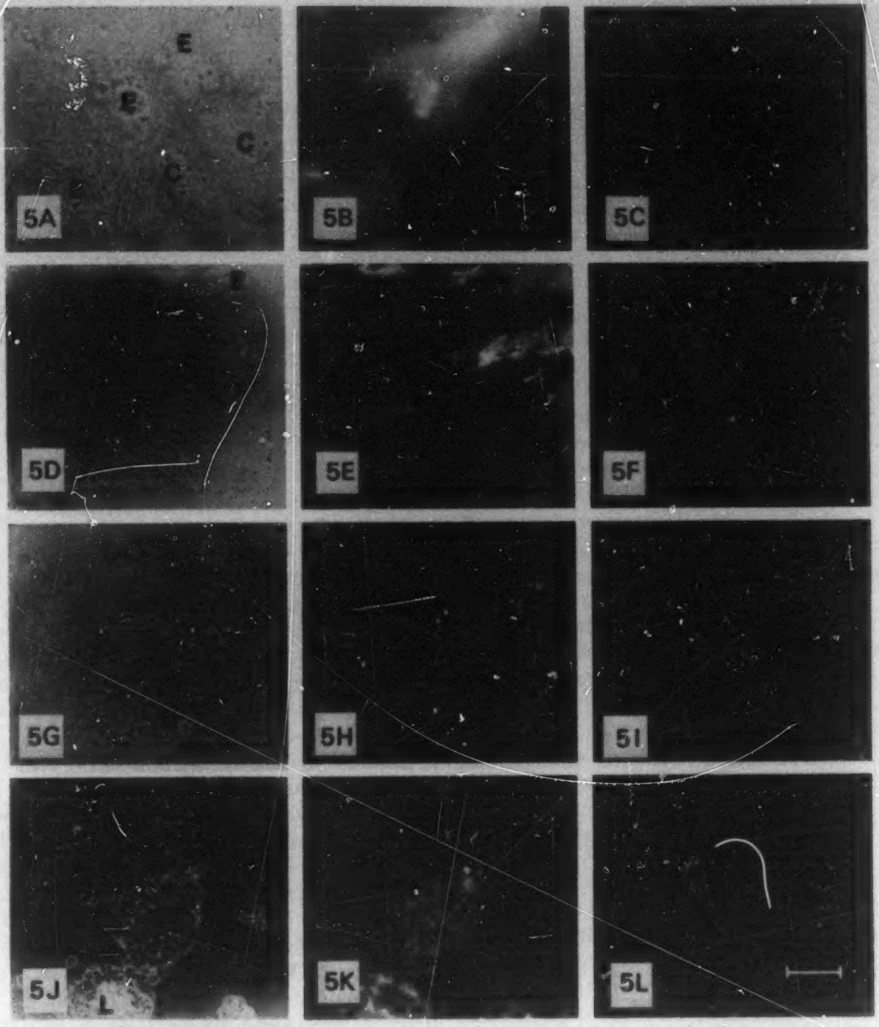

FIGURE 5.—Binding of fluorescently labeled Thy-1 antiserum to cuboidal epithelial cell line containing elongated cell converts and structures: Epithelial cultures from normal glands of: A–C) dually converting Rama 75 cells showing both cuboidal ("C" label on fig.) and elongated ("E" label on fig.) morphologies and D–F) singly converting Rama 102 cells showing both cuboidal and elongated morphologies. Structures formed in confluent Rama 25 cultures are: G–I) a dome ("DO" label on fig.) in droplet cells and J–L) lumps ("L" label on fig). *First two photographs in each vertical column* show the same field stained with FITC-conjugated Thy-1 antiserum viewed by phase-contrast and fluorescence optics. *Last photograph in each vertical column* shows a duplicate culture stained with FITC-conjugated Thy-1 antiserum preabsorbed with thymocytes as before. Exposure times as for fig. 1. A–L: *Bar*=25 μm

blank page

Surgical Resection of the Rat Colon: Effects on Carcinogenesis by 1,2-Dimethylhydrazine[1,2,3]

C. A. Rubio, *M.D., F.I.A.C.,*[4] *and* G. Nylander, *M.D.*[5,6]

ABSTRACT—Following a 3-month treatment with 1,2-dimethylhydrazine (DMH) given weekly (sc), outbred Sprague-Dawley rats were subjected to partial resection of the transverse colon. After surgery, DMH treatment was continued for 6 months, after which the rats were killed. At autopsy, 63% of the tumors were found in the transverse colon. By contrast, only 29% of the tumors found in the "sham-operated" control animals occurred in the transverse colon. Surgical trauma in the colon mucosa subjected to the action of carcinogenic agents appeared to promote the conditions suitable for the development of tumors in that organ.—JNCI 1982; 68:813–815.

The 5-year survival following "curative" resection for carcinoma of the colon and rectum is about 45% (*1*). The reasons for the failure to obtain permanent cures in the remaining cases are local recurrence, regional recurrence, and/or distant metastases.

The reported incidence of recurrence at the anastomotic site following surgery for colorectal tumors varies widely. Olson et al. (*2*) reported an incidence of 1.4%; Cass et al. (*3*), of 3%; Southwick et al. (*4*) and Goligher et al. (*5*), of 10%; Beal and Cornell (*6*), of 15%; and Welch and Donaldson (*7*), of 33%. The true mechanism responsible for the development of local recurrences at the suture line remains unknown; Morgan and Lloyd-Davis (*8*), Goligher et al. (*9*), Southwick and Cole (*10*), and Cole (*11*) believe that local recurrences at or near the suture line following resection for cancer of the colon are the result of implantation of cancer cells from the tumor into the suture line during surgery (text-fig. 1). On the basis of this theory, several intraoperative treatments have been proposed for destruction of the cells desquamating from the tumor. The use of these procedures, however, has not resulted in lower numbers of anastomotic recurrences as reported in well-documented studies (*10*). Thus the results of intraoperative procedures, aimed at preventing recurrences by sterilizing tumor cells, have been contradictory.

The cause of recurrence at colon anastomotic sites in humans is also thought to be due to microscopic cancer cells left in the tissues adjacent to but outside the line of anastomosis. After surgery these nests of cancer cells may grow and invade the anastomosis from the outside.

We reported an increased incidence of experimentally induced colon tumors in animals previously subjected to colon surgery (*12*, *13*). In those experiments, segments of colon were excised and retransplanted in the abdominal wall by the method of Thiry-Vella. In light of these results we investigated whether a minor surgical trauma in the colon mucosa subjected to the action of a carcinogen could promote the development of tumors at the site of surgery.

MATERIALS AND METHODS

Thirty-six male outbred Sprague-Dawley rats (Anticimex, Stockholm, Sweden) averaging 200 g in weight were studied. Of the 36 rats, 26 received sc 21 mg DMH/kg body weight suspended in 1 ml EDTA solution (as stabilizing agent), once a week for 3 months.

At 3 months, 16 of the 26 rats were subjected to partial resection of the transverse colon (the transverse colon is herein considered 4 cm distal to the hepatic flexure). The resection was done approximately 2 cm distal to the hepatic flexure. The animals were anesthetized with mebumal–ether, and a ring of about 2 mm in width of transverse colon was removed and fixed in 10% neutral Formalin for histologic examination. An end-to-end anastomosis of the transverse colon was done with the use of a chromic catgut.

The remaining 10 animals were "sham operated." (The transverse colon was massaged for 5 min but no resection was done.) One week after the operation, the treatment with weekly injections of DMH was continued for another 27 weeks.

The remaining 10 of the 36 rats received sc injections of EDTA once a week for 3 months. After 3 months the animals were operated on under mebumal–ether anesthesia, and a 2-mm-wide segment of the transverse colon was removed. The weekly sc injection of EDTA was continued after the surgery until the end of week 27.

At the end of the observation period all animals were killed, and the presence of tumors in the various colon segments was noted.

RESULTS

All 26 animals receiving DMH developed colon tumors (tables 1, 2). None of the operated rats receiving vehicle developed tumors. In the 16 operated animals receiving DMH, 24 tumors developed in the colon and/or rectum (i.e., 1.5 tumors/animal; table 1). In the sham-operated group of animals receiving DMH, 14 tumors developed (i.e., 1.4 tumors/animal; table 2). The highest number of tumors found in the group treated with DMH and partial resection was 2 tumors/animal. A similar result was obtained in sham-operated animals receiving DMH.

ABBREVIATION USED: DMH=1,2-dimethylhydrazine.

---

[1] Received June 3, 1981; accepted December 3, 1981.

[2] Supported by grants from the Swedish Cancer Society, from the Cancer Society of Stockholm, and from the Karolinska Institute.

[3] Guidelines for the care and use of laboratory animals were followed as set forth by the Department of Pathology, Karolinska Sjukhuset.

[4] Department of Pathology, Karolinska Sjukhuset, Box 60500, Stockholm, Sweden S-104 01.

[5] Department of Surgery, Karolinska Sjukhuset.

[6] We gratefully acknowledge the technical assistance of Bengt Walin, Maggie Sveander, and Marie-Louise Alun.

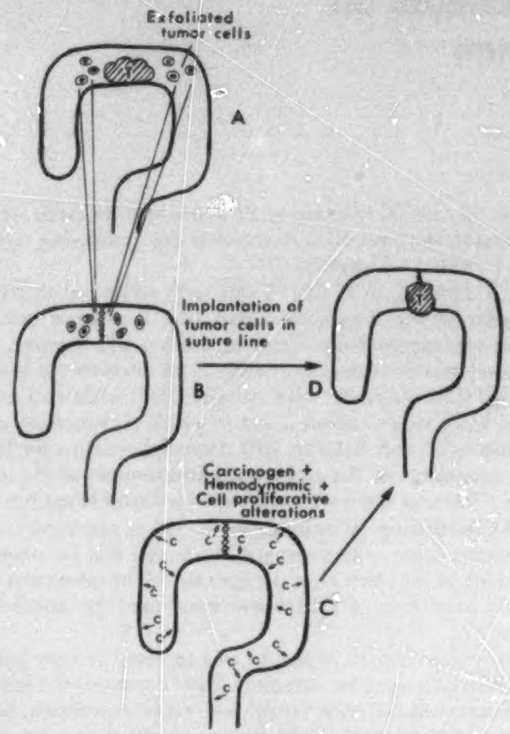
Exfoliated tumor cells
A
Implantation of tumor cells in suture line
B
D
Carcinogen + Hemodynamic + Cell proliferative alterations
C

TEXT-FIGURE 1.—Local recurrence of cancer at or near the suture line following resection of colon for cancer is believed to be due to implantation of exfoliating tumor cells (A) in the suture line (B). The alternative mechanism is proposed: DMH (and probably environmental colonotropic carcinogens) induces cellular aberrations in the colon mucosa. Partial colon resection promotes at the anastomotic site a mechanism of repair, which is achieved by colon cells having aberrations (C). Aberrant cells may incite malignant transformation (D) during the process of local repair in the colon mucosa.

Of the 24 tumors in animals treated with DMH and partial resection of the colon, 63% were found in the transverse colon. In the sham-operated animals, only 29% of the 14 tumors were located in the transverse colon. The difference between these 2 groups was significant (*P*<0.001).

The histologic examination of resected colon segments obtained at surgery 3 months after the initiation of the DMH treatment revealed normal histology only. No signs of atypical epithelium or tumors could be found in these segments.

TABLE 1.—*Number of tumors in the colon and rectum in 16 rats treated with DMH*[a]

Type of tumor	No. of tumors				
	Ascending colon	Transverse colon	Descending colon	Rectum	Total
Invasive adenocarcinoma	1	9	6	1	17
Adenoma	1	6	0	0	7
Total	2	15	6	1	24

[a] Rats were treated with DMH for 3 mo and then operated on, with minimal resection of the transverse colon. DMH treatment was continued after the operation for an additional 3 mo. Results were obtained after 6 mo of DMH treatment.

TABLE 2.—*Number of tumors in the colon and rectum in 10 rats treated with DMH*[a]

Type of tumor	No. of tumors				
	Ascending colon	Transverse colon	Descending colon	Rectum	Total
Invasive adenocarcinoma	4	3	4	0	11
Adenoma	1	1	1	0	3
Total	5	4	5	0	14

[a] Rats were treated with DMH for 3 mo and then sham operated. DMH treatment was continued after the operation for an additional 3 mo. Results were obtained after 6 mo of DHM treatment.

Of the 24 tumors found in the operated group and receiving DMH, 7 were tubular adenomas with varying degrees of epithelial atypia and the remaining 17 were invasive adenocarcinomas. Of the 15 tumors found in the transverse colon, 6 were adenomas and the remaining 9 were invasive adenocarcinomas. Of the 14 tumors found in the 10 sham-operated rats receiving DMH, 3 were tubular adenomas with varying degrees of epithelial atypia and the remaining 11 were invasive adenocarcinomas. Of the 4 tumors found in the transverse colon, 1 was an adenoma and the rest were invasive adenocarcinomas.

DISCUSSION

Protracted treatment of rodents with colonotropic carcinogens induces colon tumors (*14*). These tumors are usually circumscribed, and their histologic features vary from tubular adenoma to nonmucus- and mucus-producing invasive adenocarcinomas. The development of circumscribed lesions indicates that those experimental tumors are local manifestations of an ongoing cancer process taking place in the colon mucosa as a whole. The causes of the local tumor development remain obscure.

Partial colon resection can induce, at anastomosis and near anastomosis, hemodynamic and cell proliferative mechanisms of repair. Under normal conditions, complete healing would be achieved some time after the operation. In our experimental model the carcinogenic substance may have induced aberrations in the epithelial cells, thus interfering with the normal mechansisms of repair. Those epithelial aberrations may have triggered the mechanism(s) leading to malignant transformation.

While the tumor incidence was high in the transverse colons of operated animals, a parallel decrease in tumor incidence was observed in the distal colons of these animals. The causes for this phenomenon remain obscure.

No special markers were used to indicate the site of anastomosis during the operation. This procedure was followed to avoid difficulties in interpretation of final results due to the possible association between foreign bodies, carcinogens, and tumor development. Thus identification of the anastomotic suture line in the transverse colon at autopsy has been difficult. Therefore, whether the tumor developed primarily at or near the anastomotic suture line is not known.

Oscarson et al. (*15*) and Williamson et al. (*16*) demonstrated in rats that the resection of the small bowel increased the incidence of experimental colon tumors. Compensatory hyperplasia in the colon was considered to be a predisposing factor to the development of neoplasia in the residual adapted bowel. In those experiments, extensive resection of the small intestine and large bowel was done, with the colon carcinogen being injected almost simultaneously (*15, 16*). By contrast, in our model only a minimal segment of the colon was resected at the time that the mucosa was probably saturated with the carcinogen (after 3-mo treatment). Although marked compensatory mucosal hyperplasia as shown after extensive bowel resection (*15, 16*) probably did not occur in our model, the possibility of minimal local hyperplasia preceding tumor formation could not be ruled out.

Our results indicate: *a*) that the local tumors may develop following resection of the transverse colon in the absence of previously exfoliated tumor cells and *b*) that surgical trauma in the colon mucosa subjected to the action of carcinogenic agents may promote conditions suitable for development of tumors.

REFERENCES

(*1*) Carter SK. Guest editorial. Large-bowel cancer—the current status of treatment. J Natl Cancer Inst 1976; 56:3–10.

(*2*) Olson RM, Perencevich NP, Malcolm AW, Chaffey JT, Wilson RE. Patterns of recurrence following curative resection of adenocarcinoma of the colon and rectum. Cancer 1980; 45:2969–2974.

(*3*) Cass AW, Million RR, Pfaff WW. Patterns of recurrence following surgery alone for adenocarcinoma of the colon and rectum. Cancer 1976; 37:2861–2865.

(*4*) Southwick HW, Harridge WH, Cole WH. Recurrence at the suture line following resection for carcinoma of the colon; incidence following preventive measures. Am J Surg 1962; 130:86–95.

(*5*) Goligher JC, Dukes CE, Bussey HJ. Local recurrence after sphincter-saving excisions for carcinoma of the rectum and rectosigmoid. Br J Surg 1951; 39:199–209.

(*6*) Beal JM, Cornell GN. A study of the problem of recurrence of carcinoma at the anastomotic site following resection of the colon for carcinoma. Ann Surg 1956; 143:1–11.

(*7*) Welch JP, Donaldson GA. Detection and treatment of recurrent cancer of the colon and rectum. Am J Surg 1978; 135:505–510.

(*8*) Morgan CN, Lloyd-Davis OV. The comparative results and treatment for cancer of the rectum. Postgrad Med J 1959; 26:135–138.

(*9*) Goligher JC, Dukes CE, Bussey HJ. Preservation of the anal sphincters in the radical treatment of rectal cancer. Ann Roy Coll Surg Engl 1958; 22:311–317.

(*10*) Southwick HW, Cole WH. Prophylactic and adjuvant measures in the treatment of carcinoma of the colon. In: Turell R, ed. Diseases of the colon and anorectum. Philadelphia: Saunders, 1969:453.

(*11*) Cole WH. The mechanisms of spread of cancer. Surgery 1973; 137: 853–871.

(*12*) Rubio CA, Nylander G, Santos M. Experimental colon cancer in the absence of intestinal contents in Sprague-Dawley rats. JNCI 1980; 64:569–572.

(*13*) Rubio CA, Nylander G. Further studies on the carcinogenesis of the colon of the rat with special reference to the absence of intestinal contents. Cancer 1981; 48:951–953.

(*14*) LaMont JT, O'Gorman TA. Experimental colon cancer. Gastroenterology 1978; 75:1157–1169.

(*15*) Oscarson JE, Veen HF, Ross JS, Malt RA. Ileal resection potentiates 1,2-dimethylhydrazine-induced colonic carcinogenesis. Ann Surg 1979; 189:503–508.

(*16*) Williamson RC, Bauer FL, Terpstra OT, Ross JS, Malt RA. Contrasting effects of subtotal enteric bypass, enterectomy, and colectomy on azoxymethane-induced intestinal carcinogenesis. Cancer Res 1980; 40:538–543.

Intracerebral Adoptive Immunotherapy of a Murine Lymphoma Antigenically Altered by Drug Treatment in Vivo[1,2,3]

L. Romani,[4] M. C. Fioretti,[4] R. Bianchi,[4] B. Nardelli,[4] *and* E. Bonmassar[4,5]

ABSTRACT—Intracerebral tumor neutralization assay and adoptive immunotherapy with in vitro sensitized lymphocytes were done in immunodepressed mice challenged intracerebrally with L5178Y/DTIC lymphoma, a tumor subline antigenically altered by treatment with 5-(3,3-dimethyl-1-triazenyl)-1H-imidazole-4-carboxamide (DTIC) in vivo. Primary cytotoxic T-lymphocytes (CTL) were generated in vitro against L5178Y/DTIC cells with the use of splenocytes of histocompatible (BALB/cCr × DBA/2Cr)F_1 donors. The extent of antitumor activity of CTL was evaluated by the measurement of tumor cell proliferation in the brain, as judged by the ^{125}I-labeled 2'-deoxyuridine uptake values and by survival times of recipient mice. The results of the experiments showed: *a*) CTL were highly effective in inhibiting tumor growth when they were injected along with L5178Y/DTIC tumor cells in a Winn-type neutralization assay; *b*) the tumor inhibition mediated by CTL was specific, since no antilymphoma effects were detected when CTL sensitized against L5178Y/DTIC line were admixed with the parental L5178Y tumor or with other unrelated lymphoma cells; and *c*) local adoptive immunotherapy with CTL given on day 1, 3, or 5 after the intracerebral challenge with L5178Y/DTIC lymphoma substantially impaired tumor cell proliferation and significantly increased survival times of recipient leukemic mice.—JNCI 1982; 68:817–822.

The possibility of increasing antitumor responses by enhancing the immunogenic strength of cancer cells following treatment of tumor-bearing hosts was previously demonstrated (*1, 2*). Both in vivo and in vitro treatments of murine lymphoma cells with an antineoplastic agent (i.e., DTIC) (*3, 4*) have been found to increase markedly tumor cell immunogenicity. The new transplantation antigens detectable in DTIC-treated tumor cells, referred to as DMTA (*5*), were found to elicit specific transplantation resistance (*6*) and cell-mediated cytotoxic responses by sensitization in vivo (*7*) and by a primary (*8*) or secondary (*9*) response in vitro.

It has been established that immunogenic tumors can be treated successfully with adoptive transfer of in vivo sensitized lymphocytes (*10, 11*). More recently, it has been shown that in vitro generated CTL are also effective against murine neoplasias in a Winn assay-type model (*12, 13*) or in immuno-chemotherapy protocols (*13*). In addition, nonimmune spleen cells produced minimal (*14*) or no antitumor effects (*15*).

In the present study the therapeutic efficacy of primary CTL sensitized against DMTA was evaluated with the use of an ic tumor model. A Winn-type neutralization assay and adoptive immunotherapy were performed on the brain.

The brain is an immunologically privileged site (*16*), although a weak allograft response can be demonstrated in the brain against histoincompatible normal (*17*) or tumor cells (*18*). Therefore, the transfer of sensitized lymphocytes could supplement the brain with immunocompetent cells capable of impairing the progressive growth of an immunogenic tumor inoculated in this organ.

Our results showed that local adoptive immunotherapy can be successfully applied in the brain when the target lymphoma cells were rendered highly immunogenic after DTIC treatment in vivo.

MATERIALS AND METHODS

Animals.—(BALB/cCr × DBA/2Cr)F_1 (CD2F_1; *H-2^d/H-2^d*) and (C57BL/6Cr × DBA/2Cr)F_1 (BD2F_1; *H-2^b/H-2^d*) mice were obtained from the National Cancer Institute, Bethesda, Md. Both sexes of mice ranging in age from 2 to 4 months were used.

Tumors.—Chemically induced ascitic leukemia L5178Y (*19*) of DBA/2 origin and Rauscher virus-induced leukemia RBL-5 of C57BL/6 origin (*20*) were maintained in histocompatible mice by weekly ip injection of 10^6–10^7 cells. Lymphoma L5178Y/DTIC was obtained by DTIC treatment of the original line L5178Y, as previously described (*21*), and was routinely maintained in CD2F_1 mice immunosuppressed with cyclophosphamide (180 mg/kg ip) 6 hours before challenge.

In vitro sensitization.—The in vitro primary cytotoxic lymphocytes were obtained as previously described in detail (*8*); 35×10^6 viable "responder" CD2F_1 spleen cells were cocultured with 8.7×10^5 irradiated (5,000 rad in vitro delivered by ^{60}Co irradiator; HOT SPOT MKIV, United Kingdom Atomic Energy Authority, Horwell, England) L5178Y/-DTIC "sensitizer" tumor cells (responder:sensitizer ratio of 40:1) in 25-cm^2 tissue culture flasks (Costar, Cambridge, Mass.) in a final volume of 20 ml of enriched RPMI-1640 medium (*8*). The cultures were incubated in an upright

---

ABBREVIATIONS USED: CNS=central nervous system; CTL=cytotoxic T-lymphocyte(s); DMTA=drug-mediated tumor antigen(s); DTIC=5-(3,3-dimethyl-1-triazenyl)-1H-imidazole-4-carboxamide; ic=intracerebral (intracerebrally); [^{125}I]dUrd=^{125}I-labeled 2'-deoxyuridine.

---

[1] Received June 18, 1981; accepted November 27, 1981.

[2] Supported by Progetto Finalizzato "Controllo della Crescita Neoplastica," contract No. 81.01364.96/115.1803 (Consiglio Nazionale delle Ricerche, Rome).

[3] Animals were maintained under the guidelines set forth in the "Guide for the Care and Use of Laboratory Animals" by the Institute of Laboratory Animal Resources, National Research Council.

[4] Institute of Pharmacology, University of Perugia, Via del Giochetto, Perugia 06100, Italy.

[5] We thank Dr. J. Mayo, Mr. C. Reeder, and Dr. V. L. Narayanan, National Cancer Institute, Bethesda, Md., for supplying many of the animals and drugs that we used. We are also grateful to Mr. Mario Andrielli, Institute of Pharmacology, University of Perugia, for his expert technical assistance.

position at 37°C in a 5% CO_2-humidified atmosphere. On the 5th day, the lymphoid cells were harvested, pooled, and centrifuged for 10 minutes at 200×*g*. A viable cell count was performed and CTL were divided into two fractions, one of which was assayed by the ^{51}Cr release assay in vitro and the other by the neutralization assay and immunotherapy experiments.

^{51}Cr release microcytotoxicity assay.—Mixtures of 10^4 labeled target cells and 2×10^6 cytotoxic "attacker" lymphocytes, in a final volume of 0.2 ml, were incubated for 4 hours at 37°C in a 5% CO_2 atmosphere with the use of U-shaped 96-well microtiter plates (C.A. Greiner and Söhne, Nürtingen, Federal Republic of Germany). At the end of the incubation period, the plates were centrifuged (800×*g* for 10 min), and 0.1 ml of the supernatant was counted in a γ-scintillation counter (model 5142; Packard Instrument Co., Downers Grove, Ill.). Experimental results were expressed as the percentage of specific lysis calculated as previously described (*8*).

Intracranial transplantation procedure.—The ic inoculum procedure was previously described (*18*). Tumor cells were suspended in a volume of 0.03 ml of RPMI-1640 medium and injected under sterile conditions through the center-middle area of the frontal bone to a 2-mm depth with the use of a 0.1-ml glass microsyringe (Hamilton Co., Reno, Nev.) and a 27-gauge disposable needle.

Evaluation of lymphoma cell growth at the brain level.—The growth of the lymphoma cells injected ic was monitored with a radioisotopic technique detailed elsewhere (*22*). 5-Fluoro-2′-deoxyuridine (25 μg) and [^{125}I]dUrd (0.5 μCi) were admixed and injected ic in a total volume of 0.03 ml of RPMI-1640 medium. Three hours later, the brains were removed and soaked in 95% ethyl alcohol for 3 days according to Bennett's technique (*23*) or collected 24 hours after [^{125}I]dUrd administration without ethanol extraction. The radioactivity was read in a γ-scintillation counter and expressed as the geometric mean of the percent of [^{125}I]dUrd uptake with respect to the amount of labeled compound injected. The survival times were also recorded by observation of mice for at least 60 days after ic injection, and tumor growth was documented by macroscopic observation at autopsy.

Tumor neutralization assay.—A modified Winn assay was employed. A mixture of a graded number of CTL and tumor cells at various ratios (CTL:tumor cells=100:1, 50:1, and 25:1) was immediately injected ic in a total volume of 0.03 ml of RPMI-1640 medium. The tumor growth rate was assessed as described above.

Adoptive immunotherapy.—Groups of 6–8 mice were inoculated ic with lymphoma cells at the desired concentration. At different days after challenge, 10^7 CTL were injected ic. The results were expressed as in the Winn assay experiments.

Irradiation of mice.—Mice were irradiated at room temperature with a ^{60}Co irradiator delivering γ-rays at 900 rad/minute.

Statistical analysis.—Differences in survival times were analyzed according to the Mann-Whitney *U* test. Data concerning [^{125}I]dUrd uptake were statistically evaluated with the use of Student's *t*-test calculated on the logs of the original cpm.

RESULTS

Intracerebral Growth of L5178Y/DTIC Lymphom Cells

Intact or immunodepressed (400 rad) CD2F$_1$ mice wer given ic injections of 10^6 cells of the L5178Y/DTIC sublin The growth of tumor cells was monitored on days 5, 6, and 11 after challenge by measurement of the [^{125}I]dUr uptake in the brain. Additional groups of mice not subjecte to the [^{125}I]dUrd uptake test were utilized for surviva studies.

The results in text-figure 1 indicate that the immunogeni line grew progressively in intact or immunodepressed host until day 5 after challenge. Later, tumor cell proliferatio declined in nonimmunodepressed recipients, whereas [^{125}I]-dUrd increased markedly in the brains of irradiated mice Mortality data confirm that lethal tumor growth occurre in immunodepressed hosts, whereas L5178Y/DTIC lym phoma cells were rejected in intact recipients.

Intracerebral Tumor Neutralization Assay

Spleen cells of CD2F$_1$ donors were cocultured in vitr with irradiated L5178Y or L5178Y/DTIC tumor cells. Under optimal experimental conditions, immune lymphocyte were markedly cytotoxic against L5178Y/DTIC but n against L5178Y cells, in accord with results of previou studies (*8*).

The antitumor effects of anti-L5178Y/DTIC lymphocyte were evaluated in irradiated CD2F$_1$ mice by ic injection o a mixture of CTL and 10^6 L5178Y/DTIC lymphoma cell at CTL:tumor ratios of 100:1, 50:1, and 25:1. A portion o sensitized lymphocytes was also assayed by the ^{51}Cr releas test at different CTL:target cell ratios. The extent of tumo growth was evaluated on day 7 after injection, with the us

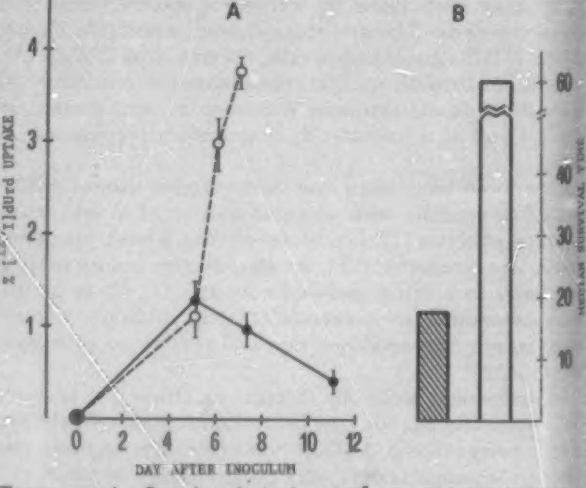

TEXT-FIGURE 1.—Growth and rejection of 10^6 cells of L5178Y/DTIC lym-phoma in the brains of CD2F$_1$ mice. [^{125}I]dUrd uptake values (A) in the brains of intact (●——●) or irradiated (400 rad; ○- - - -○) mice o survival times (B) of intact (▨) or irradiated (☐) recipients. Backgroun [^{125}I]dUrd uptake (i.e., isotope uptake in the brains of nonleukemic mice) did not exceed 0.20% in either intact or irradiated mice.

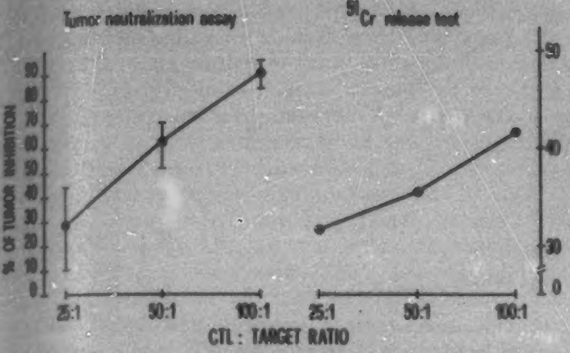

TEXT-FIGURE 2.—Winn-type neutralizing activity (ic) and in vitro cytolytic effects of CTL against L5178Y/DTIC lymphoma cells. Graded numbers of CTL admixed with 10^5 L5178Y/DTIC cells were inoculated ic into irradiated (400 rad) CD2F$_1$ mice. Tumor growth was evaluated by the [^{125}I]dUrd uptake in the brain tested on day 7 after challenge. The percentage (geometric mean) of isotope uptake in the brains of mice inoculated with lymphoma cells alone or CTL alone was 3.87 (mean + SE, 4.52; mean − SE, 3.27) or 0.19 (mean + SE, 0.26; mean − SE, 0.13), respectively.

of the [^{125}I]dUrd uptake technique. Tumor cell proliferation was markedly impaired (text-fig. 2) when CTL were admixed with lymphoma cells at CTL:tumor cell ratios of 100:1 and 50:1. At a ratio of 25:1 tumor growth was not significantly inhibited. A parallel study with the ^{51}Cr release test also pointed out that marked cytolytic activity against the DTIC lymphoma subline was provided by the CTL used for the tumor neutralization assay (text-fig. 2).

A mixture of CTL against L5178Y/DTIC and 10^5 L5178Y/DTIC tumor cells at a CTL:tumor ratio of 100:1 was injected ic into immunodepressed CD2F$_1$ mice. Two additional groups of intact or immunodepressed hosts were inoculated ic with 10^5 cells of the same lymphoma line. The [^{125}I]dUrd uptake test was performed on day 7 after injection, and the mortality of the recipient mice was recorded in a parallel experiment (text-fig. 3). Tumor cell proliferation was markedly impaired when CTL were admixed with the lymphoma, as judged by the [^{125}I]dUrd uptake values. Comparable inhibition of tumor growth was also found in nonimmunodepressed recipients. No intact animals challenged with DTIC lymphoma cells died, whereas all irradiated hosts died with evidence of ic leukemia growth. However, if they were inoculated with tumor cells admixed with specifically sensitized CTL, immunodepressed recipients survived beyond the 60-day observation period. In contrast, lethal tumor growth occurred in irradiated mice when given injections of L5178Y/DTIC cells along with fresh nonsensitized CD2F$_1$ splenocytes. A similar result was obtained with normal splenocytes cultivated without antigenic stimulus for 5 days, which actually facilitated tumor growth to some extent (data not shown).

Requirement of Viable CTL for Tumor Neutralization

CTL generated in vitro against L5178Y/DTIC subline were exposed to 10,000 rad or disrupted by freezing-thawing four times. The viability after treatments, judged by the trypan blue exclusion test, was unchanged in irradiated cells, whereas it was markedly reduced (ranging from 4 to 8%) in frozen and thawed CTL. Irradiated or frozen-thawed CTL were incapable of lysing L5178/DTIC cells (table 1) or of protecting mice inoculated ic with the same lymphoma in a Winn-type neutralization test (table 1).

Specificity of CTL for Tumor Neutralization

Splenocytes from CD2F$_1$ donors were sensitized in vitro against L5178Y/DTIC or allogeneic RBL-5 tumor cells. Anti-RBL-5 or anti-L5178Y/DTIC lymphocytes were admixed with L5178Y/DTIC cells (CTL:tumor ratio of 100:1) and inoculated ic into irradiated (400 rad) CD2F$_1$ hosts. We completed the experiment by admixing CTL sensitized against L5178Y/DTIC or RBL-5 lines with RBL-5 cells (CTL:tumor ratio of 100:1) and injecting the mixture into the brains of immunodepressed (400 rad) BD2F$_1$ recipients.

The results, expressed as percentages of tumor inhibition measured on day 7 after challenge, show that CTL anti-RBL-5 were unable to prevent tumor growth of the DTIC subline. In turn, CTL anti-L5178Y/DTIC did not impair the proliferation of RBL-5 cells. On the contrary, specifically immune CTL were highly effective in inhibiting the lymphoma cells used for in vitro sensitization (text-fig. 4).

When effector cells were tested against the parental L5178Y line or against the *H-2*-compatible but antigenically unrelated LSTRA lymphoma, no significant impairment of tumor cell proliferation was observed. (*See* legend to text-fig. 4.)

Adoptive Immunotherapy in the Brain

Adoptive immunotherapy with CTL sensitized against L5178Y/DTIC was performed with the use of immunodepressed CD2F$_1$ mice that were given ic injections of 10^5 cells

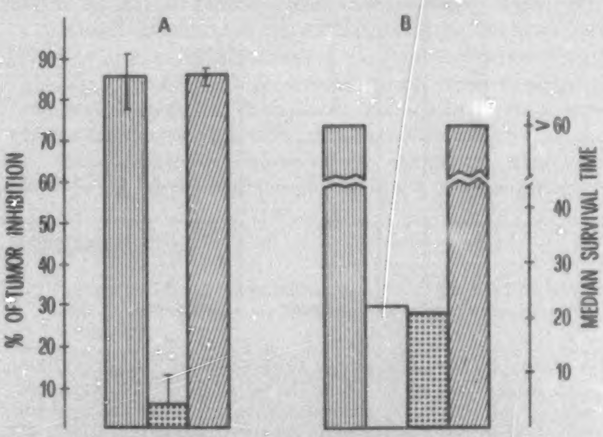

TEXT-FIGURE 3.—Winn-type neutralization assay in mice challenged ic with 10^5 cells of L5178Y/DTIC lymphoma. Inhibition of brain [^{125}I]-dUrd uptake (A) or median survival times (B) of *a*) immunodepressed mice inoculated with lymphoma cells admixed with 10^7 CTL (▥); *b*) immunodepressed mice inoculated with lymphoma cells admixed with 10^7 fresh, nonsensitized splenocytes (▦); *c*) immunodepressed mice challenged with lymphoma cells alone [percentage (geometric mean) of [^{125}I]dUrd uptake 7 days after tumor challenge, 3.00 (mean + SE, 3.27; mean − SE, 2.42)] and median survival time (□); and *d*) nonimmunodepressed mice inoculated with lymphoma cells alone (▨).

of L5178Y/DTIC lymphoma. The animals were inoculated ic with 10^7 CTL 1, 3, or 5 days later. Then 7 days after tumor challenge the extent of brain [^{125}I]dUrd uptake was measured. Tumor growth was significantly impaired (text-fig. 5A) in all cases, although the efficiency of CTL-mediated inhibition of L5178Y/DTIC lymphoma decreased progressively with the time elapsing between tumor challenge and adoptive transfer. No effect was detected with the use of fresh or in vitro cultured nonsensitized spleen cells (data not shown).

TABLE 1.—*Effect of different treatments of CTL on their antitumor activity in the Winn-type neutralization assay*

Type of CTL used[a]	Percent [^{125}I]dUrd uptake[b]	P[c]	Percent specific lysis[d]	Mortality data	
				MST[e]	D/T[f]
No CTL	1.71 (2.23–1.32)			18	6/6
Untreated CTL	0.17 (0.24–0.12)	<0.01	49.0±0.7	>60	0/6
FT-CTL	3.13 (3.88–2.52)	NS	7.3±1.0	19	6/6
X-CTL	1.68 (2.07–1.36)	NS	11.4±0.3	19	6/6

[a] CTL sensitized in vitro against L5178Y/DTIC tumor cells were admixed with 10^5 cells of the same lymphoma (CTL:tumor ratio of 100:1) and injected ic into immunodepressed CD2F$_1$ mice. FT-CTL=CTL disrupted by freezing-thawing four times. X-CTL=CTL inactivated by exposure to 10,000 rad in vitro.

[b] The [^{125}I]dUrd was given ic on day 7 after tumor challenge. The [^{125}I]dUrd uptake of background untreated brains was 0.15 (0.18–0.12), and no significant [^{125}I]dUrd uptake increase was found in the brains of mice inoculated with CTL, FT-CTL, or X-CTL alone. *Numbers in parentheses* indicate geometric mean + SE and geometric mean − SE, respectively.

[c] Probability values were calculated according to Student's *t*-test, in which the uptake values found in mice challenged with lymphoma cells alone (i.e., no CTL) were compared with those found in mice inoculated with CTL plus tumor cells. NS=not significant.

[d] Attacker:target cell ratio of 100:1. Values are expressed as arithmetic mean percent ± SE.

[e] Median survival time in days.

[f] No. of dead mice/total No. of mice tested.

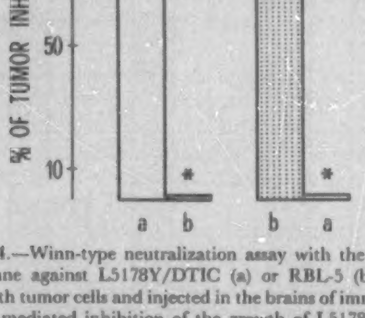

TEXT-FIGURE 4.—Winn-type neutralization assay with the use of CD2F$_1$ CTL immune against L5178Y/DTIC (a) or RBL-5 (b) lymphomas, admixed with tumor cells and injected in the brains of immunodepressed mice: CTL-mediated inhibition of the growth of L5178Y/DTIC (10^5) cells inoculated into CD2F$_1$ brain (A) or of RBL-5 (5×10^3) cells inoculated into BD2F$_1$ brain (B). The ic growth of L5178Y/DTIC and RBL-5 tumor cells, in terms of percent (geometric mean) [^{125}I]dUrd uptake 7 days after tumor challenge, was 2.80 (mean + SE, 3.92; mean − SE, 2.01) and 4.37 (mean + SE, 5.47; mean − SE, 3.50), respectively. In this experiment CTL anti-L5178Y/DTIC lymphoma did not show antitumor activity when it was admixed with the parental L5178Y line or unrelated LSTRA lymphoma and inoculated at CTL:tumor ratio of 100:1 into CD2F$_1$ recipients. The percent of tumor inhibition did not exceed 10% in both cases and was not statistically significant. *P<0.01.

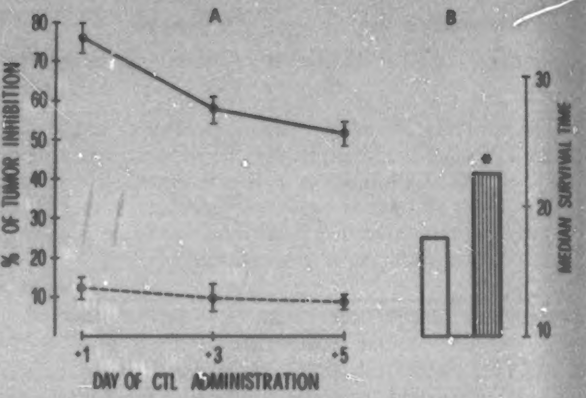

TEXT-FIGURE 5.—Adoptive immunotherapy with CTL, sensitized in vitro against L5178Y/DTIC lymphoma, at various days after ic tumor injection. A) Inhibition of brain [^{125}I]dUrd uptake (7 days after tumor challenge) in immunodepressed CD2F$_1$ mice inoculated ic with 10^5 L5178Y/DTIC cells (●——●) or 5×10^2 L5178Y parental line (●- - -●) and with CTL (CTL:tumor cell ratio of 100:1). B) Median survival times of irradiated mice given L5178Y/DTIC lymphoma (□) or L5178Y/DTIC plus CTL 3 days after tumor challenge (▥). *P<0.05; probability was calculated according to the Mann-Whitney *U* test, in which mortality data on mice inoculated with tumor cells alone were compared with those on leukemic recipients treated with CTL 3 days after tumor challenge. The percent inhibition of L5178Y/DTIC tumor growth provided by fresh, nonsensitized lymphocytes [injected 1 (+1), 3 (+3), or 5 (+5) days after tumor challenge] was −43, −26, and −17, respectively, the negative values indicating tumor growth enhancement. Median survival time of mice treated 3 days after tumor challenge with nonsensitized lymphocytes was not significantly different from that of untreated mice.

The effectiveness of CTL against L5178Y/DTIC was also confirmed in mortality studies conducted in parallel. The results (text-fig. 5B) show that recipient mice challenged with L5178Y/DTIC and inoculated ic with CTL 3 days after tumor challenge survived significantly longer than untreated controls.

No therapeutic effect of anti-L5178Y/DTIC CTL was detected in the same immunotherapy model when the L5178Y parental line was used for tumor challenge, as evident by the percentages of tumor inhibition (text-fig. 5A). Moreover, the life-spans of animals inoculated ic with the parental line and treated with CTL were not prolonged (data not shown).

DISCUSSION

The present study points out that the ic growth of a murine lymphoma rendered immunogenic by pharmacologic manipulation can be impaired by an ic transfer of CTL sensitized in vitro against the same tumor.

A number of studies performed in our laboratory (*1*, *3*, *6*, *8*) and elsewhere (*2*, *7*) provided convincing evidence that drug treatment of tumor-bearing hosts leads to a substantial increase of tumor immunogenicity, in terms of either greater density of preexisting tumor-associated transplantation antigens (*24*) or generation of novel antigenic determinants [DMTA (*5*)]. The immunogenic strength of murine lymphoma lines treated for serial transplant generations with DTIC appears to be extremely great, being comparable to that of *H-2* incompatible leukemias (*25, 26*).

The present investigation showed that the L5178Y/DTIC subline can be rejected in the brains of nonirradiated CD2F$_1$ recipients (text-fig. 1B), whereas lethal lymphoma growth occurs in immunodepressed hosts. These data provide additional emphasis on the extremely high levels of L5178Y/DTIC immunogenicity, since weak allograft responsiveness (*18, 27*) and essentially no natural resistance (*28*) are detectable in the mouse brain.

The growth rate of L5178Y/DTIC was also tested in the brains of either intact or irradiated mice (text-fig. 1A) with the use of ic uptake of [^{125}I]dUrd. A similar technique was developed by Shapiro (*29*), using the labeled DNA precursor [^{3}H]thymidine. There is a large consensus that both techniques provide reliable methods for estimating cell proliferation (i.e., DNA synthesis) of either normal (*30*) or tumor tissues (*31*).

The adoptive transfer of in vitro specifically sensitized CTL for immunotherapy of experimental tumors has been tested by various investigators (*12, 13*). The results of these studies showed that CTL alone can provide limited therapeutic effects, although CTL combined with chemotherapy gives a stronger protection (*32*).

The tumor model adopted in the present investigation appears to be quite different from models described in the literature for localized or generalized tumor growth outside the CNS. The inoculation of lymphoma cells ic is followed by a rapid and relatively localized growth in mouse brain, leading to early death of the host (*18*). Histologic observations conducted on the host harboring the L5178Y/DTIC growth show that lymphoma cells infiltrate a large zone of the hemisphere where the tumor was injected (data not shown). However, the autopsy conducted on animals that died following ic tumor inoculation did not reveal extensive leukemia growth in the peripheral organs such as spleen, liver, or lungs, similar to that detected in mice dying with generalized lymphoma. Therefore, presumably, in the present study most mice succumbed to localized leukemia growth in the CNS.

The Winn assay-type experimental results (text-figs. 2–4) are consistent with the hypothesis that specific cytotoxicity against L5178Y/DTIC cells can take place in the brain environment, when in vitro generated CTL are in close contact with target lymphoma cells. This phenomenon was evident either in terms of inhibition of [^{125}I]dUrd uptake in the brain (text-figs. 2, 3A, 4) or in terms of protection from lethal leukemia growth (text-fig. 3B). However, nonsensitized lymphocytes, obtained fresh or obtained after culture of splenocytes without antigenic stimulus, did not impair the ic lymphoma growth (text-fig. 3).

The requirement for viable lymphocytes was confirmed by data given in table 1. Moreover, the specificity of CTL was demonstrated by the following observations: *a*) failure of anti-L5178Y/DTIC CTL to afford protection against the *H-2*-unrelated RBL-5 lymphoma (text-fig. 4); *b*) failure of the same CTL to impair the growth of the parental L5178Y line or of the *H-2*-identical but etiologically unrelated Moloney leukemia virus-induced LSTRA line (*see* legend to text-fig. 4); and *c*) failure of anti-RBL-5 CTL to inhibit the ic growth of the L5178Y/DTIC subline (text-fig. 4). All these data are consistent with those of previous in vitro cytotoxicity studies, which favored the hypothesis of the presence of membrane antigens on L5178Y/DTIC cells not detectable in the line of origin [i.e., DMTA (*8*)] and non-cross-reactive with those of other lymphomas homozygous for the same *H-2* haplotype or differing with regard to the *H-2* complex (*33*).

Having demonstrated that the brain environment does not impair the antilymphoma effectiveness of CTL, we took a further step to test whether CTL when transferred directly into the brain parenchyma could be used for immunotherapy protocols. The results shown in text-figure 5 provided evidence that CTL can be considered of therapeutic value in this experimental design, as shown by the significant reduction of lymphoma cell growth and increase in the lifespan of treated recipients over that of untreated controls. The decline of CTL-mediated protection with increasing time between tumor challenge and CTL transfer is not unexpected since lymphoma cell multiplication within the CNS produces a rapid increase in the number of target cells, thus reducing the effector-to-target cell ratio.

Studies not illustrated in the present communication showed that ^{51}Cr-prelabeled CTL diffuse within the brain early after cell transfer ic. This result would account for the effectiveness of effector lymphocytes even when injected 3 days after tumor challenge, i.e., when lymphoma cells extensively infiltrate the brain parenchyma. In fact, CTL diffusion appears to be a prerequisite for the cell-to-cell contact needed for killer lymphocytes to mediate cytotoxic effects against neoplastic cells in tumor-bearing hosts (*34*).

It is well known that the CNS infiltration by leukemia cells is a serious complication of the lymphomatous disease (*35–37*). Therefore, the present approach seems to open up new perspectives for therapeutic application, when lymphoma cells, possessing a high density of either spontaneous or drug-mediated transplantation antigen(s), cross the blood-brain barrier and invade the brain compartment.

REFERENCES

(*1*) Fioretti MC. Immunopharmacology of 5-(3,3-dimethyl-1-triazeno)-imidazole-4-carboxamide (DTIC). Pharmacol Res Commun 1975; 7:481–491.

(*2*) Nicolin A, Vadlamudi S, Goldin A. Antigenicity of L1210 leukemia sublines induced by drugs. Cancer Res 1972; 32:653–657.

(*3*) Bonmassar E, Bonmassar A, Vadlamudi S, Goldin A. Immunological alteration of leukemic cells in vivo after treatment with an antitumor drug. Proc Natl Acad Sci USA 1970; 66:1066–1074.

(*4*) Contessa AR, Giampietri A, Bonmassar A, Goldin A. Increased immunogenicity of L1210 leukemia following short-term exposure to 5-(3,3-dimethyl-1-triazeno)-imidazole-4-carboxamide (DTIC) in vivo or in vitro. Cancer Immunol Immunother 1979; 7:71–76.

(*5*) Houchens DP, Bonmassar E, Gaston MR, Kende M, Goldin A. Drug-mediated immunogenic changes of virus-induced leukemia in vivo. Cancer Res 1976; 36:1347–1352.

(*6*) Fioretti MC, Santoni A, Romani L, et al. Transplantation resistance of syngeneic mice against a drug-treated lymphoma derived from non-immunogenic tumor line. Fed Proc 1977; 36:1260.

(7) Nicolin A, Bini A, Coronetti E, Goldin A. Cellular immune response to a drug-treated L5178Y lymphoma subline. Nature 1974; 251:654–655.

(8) Romani L, Fioretti MC, Bonmassar E. In vitro generation of primary cytotoxic lymphocytes against L5178Y leukemia antigenically altered by 5-(3,3-dimethyl-1-triazeno)-imidazole-4-carboxamide in vivo. Transplantation 1979; 28:218–222.

(9) Santoni A, Kinney Y, Goldin A. Secondary cytotoxic response in vitro against Moloney lymphoma cells antigenically altered by drug treatment in vivo. J Natl Cancer Inst 1978; 60:109–112.

(10) Rosenberg SA, Terry WD. Passive immunotherapy of cancer in animals and man. Adv Cancer Res 1977; 25:347–382.

(11) Gorczynski RM. Evidence for in vivo protection against murine sarcoma virus-induced tumors by T-lymphocytes from immune animals. J Immunol 1974; 112:533–539.

(12) Burton CR, Warner NL. In vitro induction of tumor-specific immunity. IV. Specific adoptive immunotherapy with cytotoxic T-cells induced in vitro to plasmacytoma antigens. Cancer Immunol Immunother 1977; 2:91–99.

(13) Kedar E, Schwartzbach M, Hefetz S, Raanan Z. In vitro induction of cell-mediated immunity to murine leukemia cells. V. Adoptive immunotherapy of leukemia in mice with lymphocytes sensitized in vitro to leukemic cells. Cancer Immunol Immunother 1978; 4:151–159.

(14) Cheever MA, Greenberg PD, Fefer A. Therapy of leukemia by non-immune syngeneic spleen cells. J Immunol 1980; 124:2137–2142.

(15) Vadlamudi S, Padarathsingh SM, Bonmassar E, Goldin A. Effect of combination treatment with cyclophosphamide and isogeneic or allogeneic (L1210) mice. Int J Cancer 1971; 7:160–168.

(16) White RJ. Experimental transplantation of the brain. In: Rapaport F, Dausset J, eds. Human transplantation. New York: Grune, 1968:692–709.

(17) Raju S, Grogan JB. Immunologic study of the brain as a privileged site. Transplant Proc 1977; 9:1187–1191.

(18) Fioretti MC, Circolo A, Bianchi R, Merletti-Rivosecchi P, Bonmassar E. Immunochemotherapy studies with murine lymphoma cells growing in mouse brain. I. Studies with tumor-associated histocompatibility antigens. Cancer Immunol Immunother 1980; 9:145–156.

(19) Alexander P, Connell DI, Mikulska ZB. Treatment of murine leukemia with spleen cells or sera from allogeneic mice immunized against the tumor. Cancer Res 1966; 26:1508–1515.

(20) Herberman RB, Aoki I, Nunn M, et al. Specificity of ^{51}Cr-release cytotoxicity of lymphocytes immune to murine sarcoma virus. J Natl Cancer Inst 1974; 53:1103–1111.

(21) Nicolin A, Spreafico F, Bonmassar E, Goldin A. Antigenic changes of L5178Y lymphoma after treatment with 5-(3,3-dimethyl-1-triazeno)imidazole-4-carboxamide in vivo. J Natl Cancer Inst 1976; 56:89–93.

(22) Hofer KB, Hughes L. Incorporation of iododeoxyuridine-^{125}I into DNA of L1210 leukemia cells during tumor development. Cancer Res 1970; 30:236–243.

(23) Bennett M. Rejection of marrow allografts: Importance of *H-2* homozygosity of donor cells. Transplantation 1972; 14:289–298.

(24) Fuji H, Mihich E, Pressman D. Differential tumor immunogenicity of L1210 and its sublines. I. Effect of an increased antigen density on tumor cell surfaces on primary B-cell responses in vitro. J Immunol 1977; 119:983–986.

(25) Riccardi C, Fioretti MC, Giampietri A, Puccetti P, Goldin A. Growth and rejection patterns of murine lymphoma cells antigenically altered following drug treatment in vivo. Transplantation 1978; 25:63–68.

(26) Fioretti MC, Riccardi C. Rejection of drug-treated tumor cells in the peritoneal cavity of mice. Pharmacol Res Commun 1975; 7:387–393.

(27) Hasek M, Chutna J, Sladecek M. Immunological tolerance and tumour allografts in the brain. Nature 1977; 268:68–69.

(28) Circolo A, Bianchi R, Nardelli B, Rivosecchi-Merletti P, Bonmassar E. Mouse brain: An immunologically privileged site for natural resistance against lymphoma cells. J Immunol. In press.

(29) Shapiro WR. The effect of chemotherapeutic agents on the incorporation of DNA precursor by experimental brain tumors. Cancer Res 1972; 32:2178–2185.

(30) Menconi E, Neri M, Sorci V, Frati L. The use of ^{125}I-iododeoxyuridine for semi-microevaluation of human lymphocyte response to phytohemagglutinin in vitro. J Immunol Methods 1978; 22:191–196.

(31) Bonmassar E, Houchens DP, Fioretti MC, Goldin A. Uptake of 5-iododeoxyuridine as a measure of tumor growth and tumor inhibition. Chemotherapy 1975; 21:321–329.

(32) Kedar E, Raanan M, Schwartzbach M. In vitro induction of cell-mediated immunity to murine leukemia cells. VI. Adoptive immunotherapy in combination with chemotherapy of leukemia in mice, using lymphocytes sensitized in vitro to leukemia cells. Cancer Immunol Immunother 1978; 4:161–169.

(33) Taramelli D, Romani L, Bonmassar A, Fioretti MC, Goldin A. Expression of normal histocompatibility antigens in murine lymphomas treated with 5-(3,3-dimethyl-1-triazeno)-imidazole-4-carboxamide (DTIC) in vivo. Eur J Cancer 1981; 17:411–420.

(34) Mathisen DJ, Rosenberg SA. The in vivo distribution of transferred syngeneic, allogeneic and xenogeneic lymphoid cells: Implication for the adoptive immunotherapy of tumors. J Immunol 1980; 124:2295–2300.

(35) Thomas LB, Chirigos MA, Humphreys SR, Goldin A. Pathology of the spread of L1210 leukemia in the central nervous system of mice and effect of treatment with Cytoxan. J Natl Cancer Inst 1962; 28:1355–1389.

(36) Moore EW, Thomas LB, Shaw RK, Freireich EJ. The central nervous system in acute leukemia. AMA Arch Intern Med 1960; 105:451–468.

(37) Posner JB, Shapiro WR. Brain tumor: Current status of treatment and its complications. Arch Neurol 1976; 32:781–784.

Combined Treatments With Vitamin A and 5-Fluorouracil and the Growth of Allotransplantable and Syngeneic Tumors in Mice[1,2,3]

Yoshifumi Tomita,[4] Kunisuke Himeno,[5] Kikuo Nomoto,[5] Hideya Endo,[6] and Tomio Hirohata[4,7]

ABSTRACT—The combined effect of retinol palmitate (RP) and 5-fluorouracil (FUra) was examined with the use of allotransplantable and syngeneic murine tumor systems. The ip combined administration of RP (5,000 IU/kg/day) and FUra (5 mg/kg/day, 20 mg/kg/day, or 20 mg/kg/every 3d day) suppressed the tumor growth in ICR/JCL mice given sc inoculations of 5×10^6 allotransplantable sarcoma 180 cells and prolonged the survival time of mice inoculated ip with 10^7 tumor cells, as compared with the survival time of mice given the single administration of either RP or FUra. Similar results were obtained when BALB/c mice were inoculated sc with a syngeneic BALB/c Meth A fibrosarcoma and treated with RP (5,000 IU/kg/day) and FUra (20 mg/kg/every 3d day). The growth of Meth A implanted on day 10, as a rechallenge, was significantly suppressed in the group pretreated with RP alone or both RP and FUra for 9 days from day 1. The growth of Meth 1, another syngeneic tumor of BALB/c origin, inoculated on day 10 as a rechallenge tumor was unaffected by the treatment with RP and/or FUra. An immune response to tumor-specific antigens seemed to be involved in the combined effects of these two drugs.—JNCI 1982; 68:823–827.

The combined therapy of anticancer drugs and polyenes such as vitamin A is reportedly effective for some types of human cancer (*1–3*). Animal experiments showed that the effects of anticancer drugs together with relatively high doses ($\approx 10^5$–10^6 IU/kg) of vitamin A were positive (*4–8*). Similar effects were observed in in vitro experiments, and labilizing of the cell membrane by the polyenes was given as an explanation (*9–11*). However, the actual effectiveness of the combination therapy and the related mechanisms remain open to question.

We attempted to elucidate the effectiveness and the mechanism of the combined treatment of vitamin A and FUra on an allotransplantable murine tumor system and on a syngeneic murine tumor system.

MATERIALS AND METHODS

Animals.—Female mice of a noninbred ICR/JCL stock and a BALB/c strain from CLEA Japan Inc. (Tokyo, Japan) and Shizuoka Laboratory Animal Center (Shizuoka, Japan), respectively, were kept on the basal diet CE-II (CLEA Japan Inc.) and used for experiments when they had reached 8 weeks of age.

Tumors.—Allotransplantable S180 was maintained by weekly passage in the peritoneal cavities of ICR mice. Fibrosarcomas of BALB/c origin, Meth A and Meth 1, were maintained also by peritoneal passage in BALB/c mice. After being washed with Hanks' balanced salt solution, the tumor cells harvested at 5–7 days after implantation were used for the experiments.

Drugs.—Chocola-A (RP) purchased from Eisai Co. (Tokyo) was used as vitamin A. FUra was obtained from Kyowa Hakko Kogyo Co. (Tokyo). RP and FUra were dissolved in phosphate-buffered saline (0.8% NaCl–0.02% KCl–0.11% Na_2HPO_4–0.02% KH_2PO_4) and a 5% glucose solution, respectively, before injection (0.2 ml/mouse).

Assay of antitumor activity in vivo.—ICR mice were inoculated ip with 10^7 S180 cells (for the ascites form) or sc with 5×10^6 S180 cells (for the solid form). BALB/c mice were inoculated sc with 10^7 Meth A cells. These mice were given ip various doses of RP and/or FUra from day 1 after the tumor implantation. The controls were given solvents only. Each group included 10 mice. The day of tumor inoculation was referred to as day 0, unless otherwise stated in the text. Antitumor activity of the drugs was evaluated according to tumor growth for the solid type and survival time for the ascites type.

Assay for the growth of rechallenged tumors in a syngeneic tumor system.—BALB/c mice were inoculated sc in the dorsum with 10^7 cells of Meth A on day 0 and thereafter were given ip RP and/or FUra until day 9. These same mice were rechallenged sc with 10^7 cells of Meth A in the right flank on day 10. For the comparison of the growth of Meth A and Meth 1 tumors, 10^7 cells of Meth 1 were rechallenged sc on day 10 in the left flank. The growth of the rechallenged tumor was measured at the day indicated in the text-figures.

RESULTS

Effect of a single administration of RP and FUra on tumor growth.—Preliminary experiments were done to determine appropriate doses of RP and FUra for the combined treat-

---

ABBREVIATIONS USED: FUra=5-fluorouracil; RP=retinol palmitate; S180=sarcoma 180; TSA=tumor-specific antigen.

---

[1] Received July 14, 1981; accepted December 15, 1981.

[2] Supported in part by a Grant-in-Aid for scientific research from the Ministry of Education, Science and Culture, Japan.

[3] Animals were maintained under the guidelines set forth in the "Guide for the Care and Use of Laboratory Animals" by the Institute of Laboratory Animal Resources, National Research Council.

[4] Department of Public Health, School of Medicine, Kurume University, 67, Asahi-machi, Kurume City 830, Japan.

[5] Department of Immunology, Cancer Research Institute, Faculty of Medicine, Kyushu University, Fukuoka 812, Japan.

[6] Department of Biochemistry, Cancer Research Institute, Faculty of Medicine, Kyushu University.

[7] We thank Mr. M. Fujiki for excellent technical assistance and Dr. M. Ohara for comments on the manuscript.

ment. The survival time and tumor growth were measured in ICR mice inoculated sc or ip with S180 cells and then given ip various doses of RP or FUra alone. The survival time of mice was not definitely altered by the RP administration of 5,000, 12,500, or 25,000 IU/kg/day. Tumors continued to grow progressively in mice treated with 5,000 IU RP/kg/day. Although administration of 25,000 or 125,000 IU RP/kg/day resulted in regression of the tumor growth after day 14, all mice in these groups died by day 20. RP in a dose of less than 5,000 IU/kg/day affected neither the survival time nor the tumor growth.

FUra administration of 5 mg/kg/day, 20 mg/kg/day, or 20 mg/kg/every 3d day prolonged the survival time of mice and to some extent suppressed the tumor growth. The lifespan of the mice was shortened when FUra at a dose of 80 mg/kg was given every 3d day.

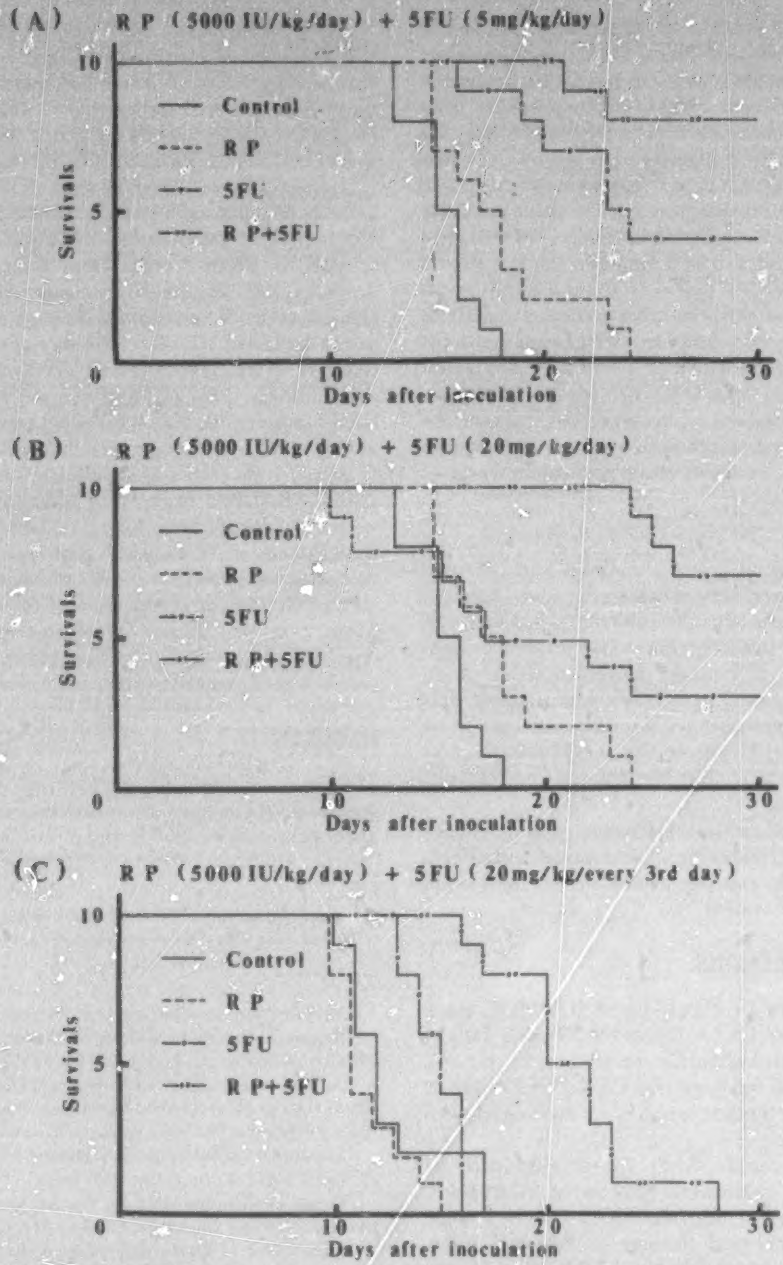

TEXT-FIGURE 1.—Combined effect of RP and FUra (5FU) on the survival time of mice inoculated with S180. ICR mice were inoculated ip with 10^7 S18 cells on day 0 and then ip with (A) 5,000 IU RP/kg/day and 5 mg FUra/kg/day, (B) 5,000 IU RP/kg/day and 20 mg FUra/kg/day, or (C) 5,000 IU RP/kg/day and 20 mg FUra/kg/every 3d day from day 1.

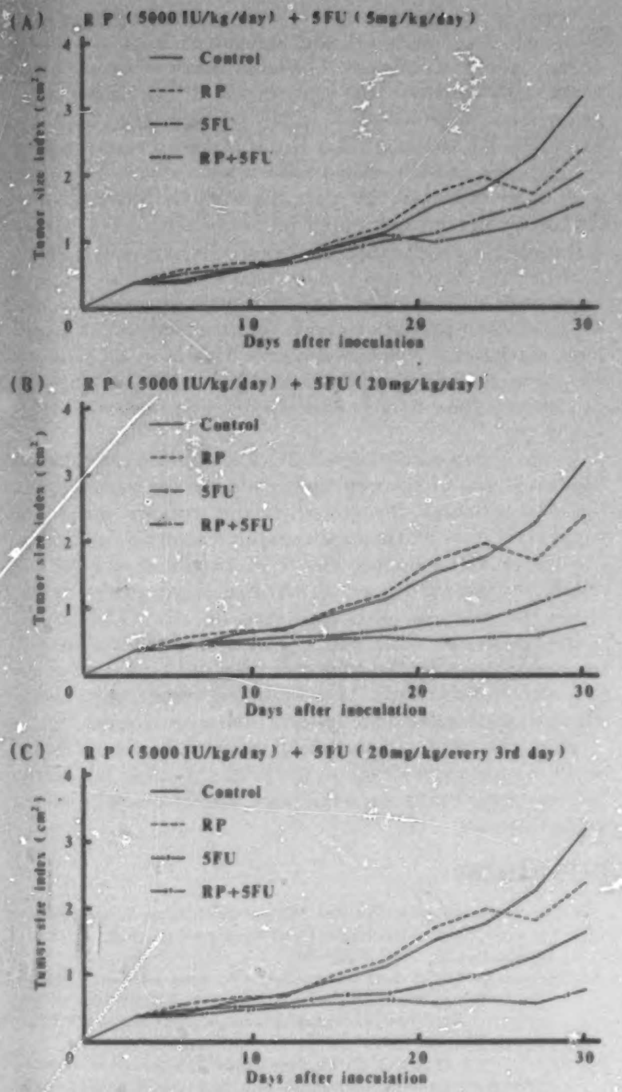

TEXT-FIGURE 2.—Combined effect of RP and FUra (5FU) on the growth of allotransplantable S180. ICR mice were inoculated sc with 5×10⁶ S180 cells on day 0 and treated as stated in the legend of text-fig. 1.

A similar relation between the dose of RP or FUra and their effect on the survival time and the tumor growth was observed in BALB/c mice inoculated with the syngeneic Meth A tumor. Therefore, doses of 5,000 IU RP/kg/day and 5 mg FUra/kg/day, 20 mg FUra/kg/day, or 20 mg FUra/kg/every 3d day were used for the following experiment.

Combined treatment in an allotransplantable S180 system.—ICR mice were inoculated ip or sc with S180 cells on day 0 and then were given RP and/or FUra from day 1. The survival time of mice was prolonged with both FUra alone and the combined treatment. The combined treatment was significantly superior to treatment with FUra alone in every protocol tested (text-fig. 1). The tumor growth was suppressed most effectively with the combined treatment, particularly at 2 weeks or later after tumor transplantation (text-fig. 2). The enhancing effect of RP on the antitumor activity of FUra was clearly shown in the protocol of 5,000 IU RP/kg/day and 20 mg FUra/kg/every 3d day (text-fig. 2C).

Combined treatment in a syngeneic tumor system.—BALB/c mice were inoculated sc with syngeneic Meth A tumor cells on day 0, and the ip treatment was started from day 1. The protocol of 5,000 IU RP/kg/day and 20 mg FUra/kg/every 3d day was used in this system. The tumor growth was not significantly affected by RP alone but was to some extent suppressed by FUra alone (text-fig. 3). The combined treatment exhibited a definite suppressive effect on the tumor growth. The suppression became distinct 12 days or later after tumor inoculation.

Growth of rechallenged tumors in BALB/c mice pretreated with RP and FUra.—BALB/c mice were inoculated sc with Meth A tumor cells as a primary challenge on day 0, given 5,000 IU RP/kg/day and/or 20 mg FUra/kg/every 3d day from days 1 to 9, and transplanted with Meth A or Meth 1 tumor cells as the rechallenge on day 10. The growth of the rechallenged Meth A tumor was enhanced with FUra alone, while it was suppressed by treatment with RP alone or a combined treatment with these drugs (text-fig. 4A). The growth of Meth 1, another syngeneic tumor of BALB/c origin, as a rechallenge was not influenced by the treatment

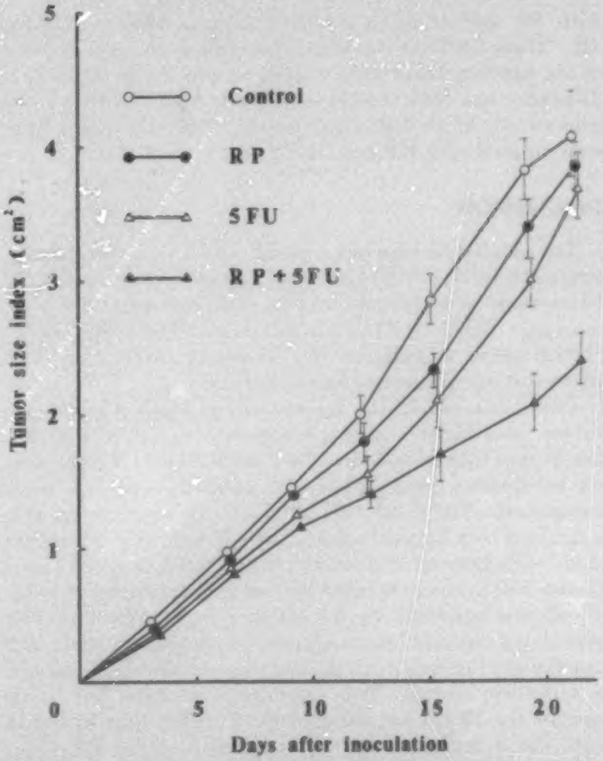

TEXT-FIGURE 3.—Effects of RP and FUra (5FU) given concomitantly on the growth of a syngeneic Meth A tumor. BALB/c mice were implanted sc with 10⁷ Meth A cells on day 0 and given ip 5,000 IU RP/kg/day and 20 mg FUra/kg/every 3d day from day 1. *Vertical bars* show standard errors of the means.

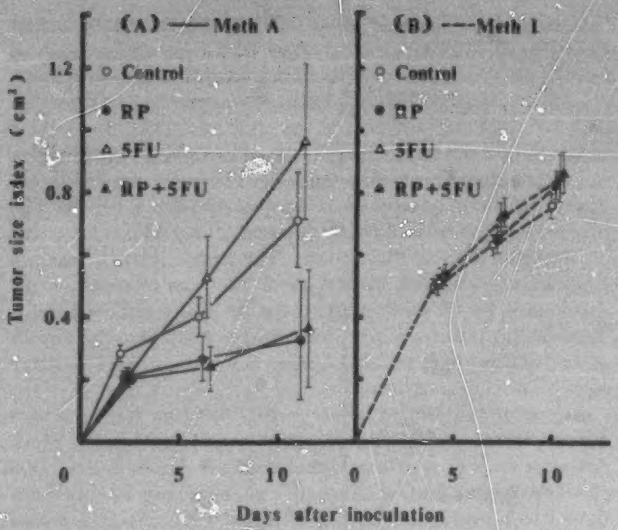

TEXT-FIGURE 4.—Suppression of the growth of syngeneic tumors given as a rechallenge in BALB/c mice pretreated with RP and FUra (5FU). BALB/c mice implanted sc with Meth A were given RP and FUra ip in a procedure similar to that described in the legend of text-fig. 3, except that the administration was continued until day 9. The mice were rechallenged with 10^7 cells of (A) Meth A or (B) Meth 1 on day 10. *Vertical bars* show standard errors of the means.

with RP and/or FUra in Meth A-primed hosts (text-fig. 4B). These findings remained the same even with excision of the primary inoculated tumors on day 9. No significant difference was observed between Meth A and Meth 1 in the growth of the rechallenged tumor when unprimed mice were treated with RP and/or FUra.

DISCUSSION

The combined treatment of RP and FUra was demonstrated to be more effective than a single administration of FUra alone in allotransplantable and syngeneic tumor systems (text-figs. 1–3). Thus a relatively low dose of RP (5×10^5 IU/kg) seems to enhance the antitumor activity of FUra when it is administered simultaneously.

The system of BALB/c mice as a host, Meth A as a target tumor, and Meth 1 as a TSA-uncross tumor of BALB/c origin was thus assumed to be a useful tool for analyzing the mechanism responsible for the combined effects of these compounds. The combined effect of anticancer drugs and vitamin A may be partly due to the adjuvanticity of vitamin A (*12–15*). Dennert and Lotan (*16*), Dennert et al. (*17*), and Glaser and Lotan (*18*) reported that the generation of killer T-cells was enhanced by treatment with vitamin A in allogeneic or syngeneic tumor systems. In the present study, RP augmented the resistance against the rechallenged tumor in a syngeneic system. This augmentation appeared to be specific for TSA, since the growth of a TSA-uncross tumor with the rechallenge was not suppressed by the RP treatment (text-fig. 4). The enhanced immune response to TSA with RP may play some role in the antitumor effect of the combined treatment. The extent of the immunologic contribution was not determined.

Other investigators ascribed the combined effect of polyenes including vitamin A and anticancer drugs to the labilizing activity of polyenes. The labilization of the cell membrane may facilitate the penetration of anticancer drug into cells, as suggested from in vitro experiments (*9–11, 19*). However, RP did not affect the viability of tumor cells i the presence of FUra in vitro (data not shown). This resul is in agreement with the data reported by Akiyama et a (*9*), who observed that either retinol or retinal but not R enhanced the direct cytotoxic action of fusidic acid on HeL cells in vitro. If RP was metabolized to retinol or retinal i vivo, such a direct effect would contribute to the in viv suppression of primary tumors, together with the immunologic mechanism mentioned above. However, no direct effect seemed to be operative since the combined effect appeared later than 10 days after the first administration (text-figs. 2, 3).

In the group administered FUra alone, the rechallenge Meth A tumor grew more rapidly than in the controls (text-fig. 4A), although the growth of the primary tumor wa suppressed with FUra alone compared with findings in th controls or RP alone (text-figs. 2, 3). Inasmuch as grow another syngeneic tumor of BALB/c origin (Meth 1) w much the same in all groups (text-fig. 4B), TSA-specifi nonresponsiveness but not a general immunosuppressio may be induced by the administration of FUra alone in th presence of tumor cells. The combined treatment protecte the host against the TSA-specific nonresponsiveness.

Thus vitamin A may be useful not only to potentiate th effect of anticancer drugs on the primary tumor but also t prevent recurrences or metastases after treatment of th primary tumor.

REFERENCES

(*1*) CERNI C, KOKRON O, MICKSCHE M. Aspects of chemo-immunotherap in a controlled clinical study for treatment of bronchogeneic cance Chemotherapy 1976; 8:287–293.

(*2*) HOEFER-JANKER H, KHAZNE F, SCHEEF W. Erste klinische Erfahrungen mit subtoxischen Vitamin A Dosen im Rahmen der radiologischen und zytostatischen Tumortherapie. Krebsarzt 1969; 4:203-207.

(*3*) KOMIYAMA S, HIROTO I, RYU S, NAKASHIMA T, KUWANO M, ENDO H Synergistic combination therapy of 5-fluorouracil, vitamin A an cobalt-60 radiation upon head and neck tumors. Oncology 1978 35:253–257.

(*4*) CAMERON I, GRUBBS B, ROGERS W. High-dose methylprednisolon vitamin A, and vitamin C in rats bearing the rapidly growin Morris 7777 hepatoma. Cancer Treat Rep 1979; 63:477–483.

(*5*) COHEN MH, CARBONE PP. Enhancement of the antitumor effects o 1,3-bis(2-chloroethyl)-1-nitrosourea and cyclophosphamide by vitamin A. J Natl Cancer Inst 1972; 48:921–926.

(*6*) NATHANSON L, MADDOCK CL, HALL TC. Exploratory studies o vitamin A and cyclophosphamide in tumor-bearing mice. J Cli Pharmacol 1969; 9:359–373.

(*7*) Prutkin L. Antitumor activity of vitamin A acid and fluorouracil use in combination on the skin tumor, keratoacanthoma. Cancer Re 1973; 33:128–133.

(*8*) TANI E, MORIMURA T, KABA K, ITAGAKI T. Preliminary study of th effects of vitamin A on antineoplastic activities of chemotherapeuti agents in glioma. Neurol Med Chir (Tokyo) 1980; 20:665–677.

(*9*) AKIYAMA S, KOMIYAMA S, KUWANO M. Synergistic effect of vitami A and fusidic acid on HeLa cells in vitro. Gan 1979; 70:709–713.

(*10*) MEDOFF G, SCHLESSINGER D, KOBAYASHI GS. *Brief communication:* Polyene potentiation of antitumor agents. J Natl Cancer Inst 1973 50:1047–1050.

(*11*) KUWANO M, KAMIYA T, ENDO H, KOMIYAMA S. Potentiation of 5 fluorouracil, chromomycin A3, and bleomycin by amphotericin B or polymyxin B in transformed fibroblastic cells. Antimicrob Agents Chemother 1973; 3:580–584.

(12) Lotan R. Effects of vitamin A and its analogs (retinoids) on normal and neoplastic cells. Biochim Biophys Acta 1980; 605:33–91.

(13) Dresser DW. Adjuvanticity of vitamin A. Nature 1968; 217:527–529.

(14) Felix EL, Loyd B, Cohen MH. Inhibition of the growth and development of a transplantable murine melanoma by vitamin A. Science 1975; 189:886–888.

(15) Jurin M, Tannock IF. Influence of vitamin A on immunological response. Immunology 1972; 23:283–287.

(16) Dennert G, Lotan R. Effects of retinoic acid on the immune system: Stimulation of T killer cell induction. Eur J Immunol 1978; 8:23–29.

(17) Dennert G, Crowley C, Kouba J, Lotan R. Retinoic acid stimulation of the induction of mouse killer T-cells in allogeneic and syngeneic systems. JNCI 1979; 62:89–94.

(18) Glaser M, Lotan R. Augmentation of specific tumor immunity against a syngeneic SV40-induced sarcoma in mice by retinoic acid. Cell Immunol 1979; 45:175–181.

(19) Kuwano M, Akiyama S, Endo H, Kohga M. Potentiation of fusidic acid and lentinan effects upon normal and transformed fibroblastic cells by amphotericin B. Biochem Biophys Res Commun 1972; 49: 1241–1248.

blank page

Comparative Tumor-Initiating Activity of Complex Mixtures From Environmental Particulate Emissions on SENCAR Mouse Skin[1,2,3,4,5]

Stephen Nesnow,[6] **Larry L. Triplett,**[7] *and* **Thomas J. Slaga**[7,8]

ABSTRACT—The value of the SENCAR mouse for testing tumorigenic properties of complex mixtures on mouse skin was studied. Seven complex mixtures were obtained as dichloromethane extracts of collected particulate emissions from three diesel-fueled automobiles, a heavy-duty diesel engine, a nonleaded gasoline-fueled automobile, a coke oven battery, and a roofing tar pot. These emissions were applied topically at multiple doses to both male and female SENCAR mice that were subsequently promoted with 12-*O*-tetradecanoylphorbol 13-acetate. Two statistical analyses were applied to the data to rank the samples and to provide 95% confidence intervals. One analysis used tumor multiplicity data, applied them to a nonlinear Poisson model, and the second analysis used tumor incidence data and applied them to a log-probit model. Both analyses ranked the complex mixtures in similar order. Benzo[*a*]pyrene content alone could not account for all the tumorigenic activity in each complex mixture, indicating that other components also contribute to the overall tumorigenic activity.—JNCI 1982; 68:829–834.

SENCAR mice, a relatively new type of highly sensitive animals bred with the selective pressure of DMBA–TPA two-stage carcinogenesis (*3*), have demonstrated their capability in mechanistic studies of chemical carcinogens. Recent works by Slaga et al. (*4*), Iyer et al. (*5*), DiGiovanni et al. (*6*), and Hennings et al. (*7*) reveal the increased sensitivity of the SENCAR mouse to polycyclic aromatic hydrocarbons and their derivatives. To date the SENCAR mouse system has not been used extensively in the analysis of complex mixtures, although mouse skin tumorigenesis with the use of other mouse strains has been applied to the bioassay of complex mixtures including cigarette smoke condensate and its components (*8–11*) and combustion emission samples from gasoline (*12–17*) and diesel engines (*18, 19*). Previous reports by Kotin et al. (*18*) and by Mittler and Nicholson (*13*) presented conflicting results on the mouse skin tumorigenicity of diesel exhaust components. Similar studies with gasoline exhaust revealed a positive tumorigenic response from applications of condensates and extracts to mouse skin (*12–17*). Some of these studies used exhaust condensates, which combined the volatile and particulate phases of the emission samples, and most studies used different strains of mice. The purpose of this study was to compare tumorigenic effects of organic substances associated with the particulate phase of emission samples with the use of the same mouse stock (SENCAR) and by means of similar collection and chemical isolation procedures for all samples. A variety of sources was examined including diesel and gasoline vehicle emissions and roofing tar and coke oven emissions.

The results indicate that this mouse stock is particularly well suited for the analysis of complex environmental mixtures in addition to its demonstrated capability with pure agents.

MATERIALS AND METHODS

Sample generation and isolation.—The sample generation, isolation, and characterization have been previously described by Huisingh et al. (*20*). Diesel sample A was obtained from a preproduction 1973 Datsun-Nissan 220C vehicle; diesel sample B, from a 1978 Oldsmobile 350 vehicle; diesel sample C, from a prototype Volkswagen turbocharged Rabbit vehicle; diesel sample D from a 1972 heavy-duty Caterpillar 3304 engine; and gasoline sample, from a 1977 Ford Mustang II-302 vehicle, with catalyst and emission controls, with the use of unleaded gasoline. The vehicles were mounted on a chassis dynamometer with a repeated highway fuel economy cycle of 10.24 miles, an average speed of 48 miles/hour, and a running time of 12.75 minutes. The heavy-duty Caterpillar 3304 engine was mounted on an engine dynamometer at 2,200 rpm steady state with an 85-pound load. The diesel engines were fueled with the same batch of No. 2 diesel fuel. Particulate samples were collected by means of a dilution tunnel in which the hot exhaust was diluted, cooled, and filtered through Pallflex Teflon-coated Fiberglas filters. Particulate coke oven samples were col-

---

ABBREVIATIONS USED: BP=benzo[*a*]pyrene; DMBA=7,12-dimethylbenz[*a*]anthracene; TID_{50}=tumor-initiating dose that produced tumors in 50% of the survivors over acetone–TPA-treated controls; TPA=12-*O*-tetradecanoylphorbol 13-acetate.

---

[1] Received July 21, 1981; accepted January 7, 1982.

[2] Supported by the U.S. Environmental Protection Agency, contract 79D-X0526, under interagency agreement 40-728-78 with the U.S. Department of Energy through the Office of Health and Environmental Research, U.S. Department of Energy, under contract 7405 eng-26 with Union Carbide Corporation.

[3] This report has been reviewed by the Health Effects Research Laboratory, U.S. Environmental Protection Agency, and approved for publication. Approval does not signify that the contents necessarily reflect the views and policies of the U.S. Environmental Protection Agency, nor does mention of trade names or commercial products constitute endorsement or recommendation for use.

[4] Preliminary accounts of this work have been previously reported (*1, 2*).

[5] Animals were maintained under the guidelines set forth by the Oak Ridge National Laboratory.

[6] Carcinogenesis and Metabolism Branch (MD-68), Genetic Toxicology Division, Health Effects Research Laboratory, U.S. Environmental Protection Agency, Research Triangle Park, N.C. 27711.

[7] Biology Division, Oak Ridge National Laboratory, Oak Ridge, Tenn. 37830.

[8] We thank the following people from the U.S. Environmental Protection Agency, Research Triangle Park, N.C.: Dr. R. L. Bradow, Mr. R. H. Jungers, Dr. B. D. Harris, Mr. T. O. Vaughan, and Dr. R. B. Zweidinger for the sample isolation, characterization, and handling; Mr. A. Stead, Dr. J. Creason, and Dr. V. Hasselblad for the statistical calculations; and Ms. Carol Evans for the computer programming.

lected from the top of the coke oven battery at Republic Steel, Gadsden, Ala., with the use of a massive air volume sampler. Because of local wind conditions, an unknown portion of the emission sample may have been from the urban environment. The roofing tar emission sample was collected by means of a conventional tar pot with an external propane burner. Pine pitch (tar) was heated to 182–193°C, and particulate emissions were collected with the use of a 1.8-m stack extension and Teflon socks in a baghouse.

The diesel, gasoline, coke oven, and roofing tar emission samples were Soxhlet extracted with dichloromethane, which was then removed by evaporation under dry nitrogen. The BP analysis was performed according to the method of Swanson et al. (*21*).

Animals.—The SENCAR mouse stock, selected for its increased sensitivity to carcinogenesis (*3*), was used. These mice were derived by breeding Charles River CD-1 mice with male skin tumor-sensitive mice that were originally derived from Rockland mice. Mice were selected for sensitivity to the DMBA–TPA two-stage system of tumorigenesis for eight generations. These mice were initially obtained from Dr. R. Boutwell (McArdle Laboratory for Cancer Research, University of Wisconsin, Madison, Wis.) and are now raised at the Oak Ridge National Laboratory.

Chemicals.—TPA was obtained from Dr. P. Borchert (University of Minnesota, Minneapolis, Minn.), and BP was obtained from Aldrich Chemical Co. (Milwaukee, Wis.) All the agents were prepared under yellow light immediately before use.

Tumor experiments.—Studies used eighty 7- to 9-week-old mice per treatment group (40 of each sex). Animals were housed in plastic cages (10/cage) with hardwood chip bedding, fed Purina Laboratory Chow and water ad libitum, and maintained at 22–23°C with 10 changes of air per hour. Animals were treated and housed under yellow light for the complete experiment. All mice were shaved with surgical clippers 2 days before the initial treatment, and only those mice in the resting phase of the hair cycle were used. All samples at all doses were applied as a single topical treatment, in 0.2 ml of spectral quality acetone except for the 10-mg dose, which was administered in five daily doses of 2 mg. One week after treatment, the tumor promotor TPA (2.0 µg in 0.2 ml acetone) was topically administered twice weekly. Skin tumor formation was recorded weekly, and papillomas greater than 2 mm in diameter were included in the cumulative total if they persisted for 1 week or longer. Both the number of mice with tumors and the number of tumors per mouse were determined and recorded weekly. Papillomas were removed randomly for histologic verification.

Statistical analyses.—Analyses were done on tumor scorings performed 24–26 weeks after initiation. Two types of statistical analyses were performed. For tumor incidence data, a probit model was fitted with the use of log dose as the regression and with the assumption that some spontaneous tumors do occur in the TPA controls (*22*). The probit formula used is $P = \beta_0 + (1-\beta_0)\,\phi\,(\beta_1 + \beta_2 \ln x)$, where P is the probit proportion, x is the dose applied, and ϕ is the standard normal cumulative distribution function. The model parameters β_0, β_1, and β_2 were estimated from the raw data by maximum likelihood methods (*22*). The TID_{50} was then directly estimated as a function of these fitted parameters, and 95% confidence intervals were constructed with the use of the asymptotic variance of these parameter estimates.

The tumor multiplicity data at each dose for individual animals were analyzed by a nonlinear Poisson model with a background correction term (*23*): $\lambda_i = \beta_0 + e^{\beta_1 + \beta_2 \ln (x_i)}$ where λ_i is the number of papillomas per mouse, x_i is the dose, β_0 is the background activity, and β_1 and β_2 are the model parameters that jointly determine the increase in tumor multiplicity with increasing dose. Using maximum likelihood methods (*23*), we estimated the model parameters from the raw data and used them to calculate the number of excess papillomas per mouse over backgrond at a dose of 1 mg. Asymptotic 95% confidence intervals for these activities were obtained by means of the variance–covariance matrix estimated during the model-fitting process.

RESULTS

The complex mixture emission samples that were bioassayed for tumor-initiating activity were all dichloromethane extracts of particulate emissions. The collection devices differed depending on the type of emission source. The diesel and gasoline particulate samples were collected on Teflon-coated Fiberglas filters after the exhaust was cooled and diluted with ambient air. The coke oven particulate sample was collected by electrostatic precipitation, and the roofing tar sample was collected by filtration of the cooled emission through a Teflon sock.

Each particle type contained a different amount of organic extractable material (table 1) (*20*). The organic extractable material ranged from 7 to 8% for diesel sample A and coke oven to more than 99% for roofing tar, which was essentially all organic-soluble. BP content per milligram of extract also varied widely, from 0.0002 to 0.11%. BP content per milligram particle ranged from 0.4 to 889 ng BP/mg particle.

Tumor formation after application of diesel sample A began after a 7- to 8-week latent period and reached a plateau at approximately week 20 (text-fig. 1) for both tumor multiplicity (papillomas per mouse) and tumor incidence (percent mice with papillomas), except for the tumor incidence in the animals treated with 10 mg of extract which

TABLE 1.—*Analysis of organic extractable material in complex mixture samples*

Sample	Extractable, %[a]	BP, ng/mg extract[b]	BP, ng/mg particle[b]
Diesel A	8	1,173	96.2
Diesel B	17	2	0.4
Diesel C	18	26	4.6
Diesel D	27	2	0.5
Gasoline	43	103	44.1
Roofing tar	>99	889	889
Coke oven	7	478	31.5

[a] Material was extracted by dichloromethane with the use of a Soxhlet apparatus.

[b] BP analysis was performed according to the procedure of Swanson et al. (*21*) and has been previously reported by Huisingh et al. (*20*).

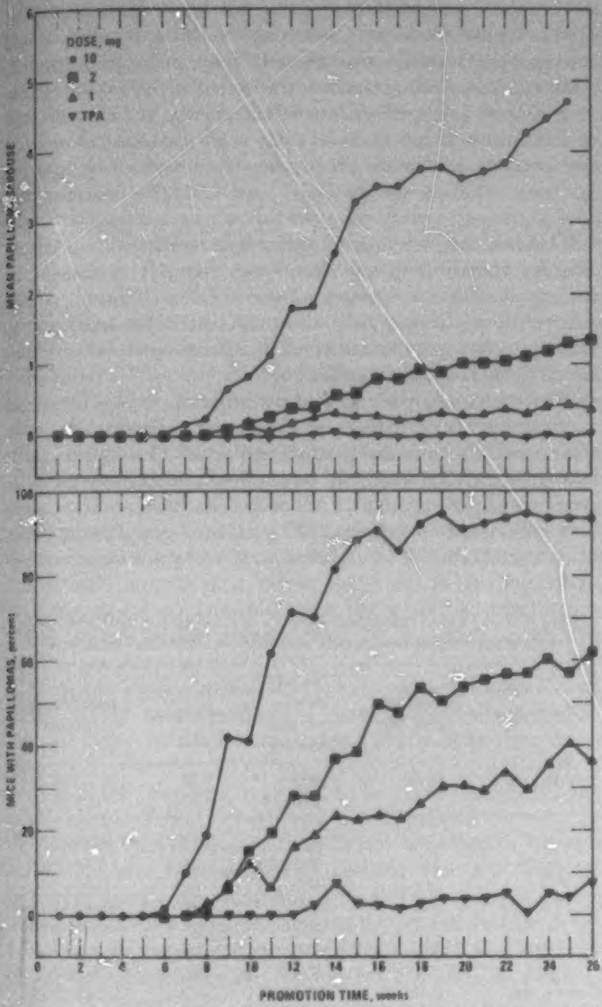

TEXT-FIGURE 1.—Tumor initiation by diesel sample A and TPA control group. TPA control animals were treated first with 0.2 ml acetone and then twice weekly with 2 μg TPA. Each group initially consisted of 40 male and 40 female SENCAR mice.

continued to increase. With BP, plateaus were reached at weeks 22–23 (text-fig. 2). In both examples, tumor formation expressed either as papillomas per mouse or percent of mice with papillomas was dependent on dose. Tumor latency also seemed to be dependent on the dose applied. At the highest dose tested, diesel sample A and BP elicited tumors in 90% or more of the animals treated.

In all experimental groups, survival was quite high, for 96% of the test groups experienced 90% or greater survival and 38% of the test groups had 100% survival (tables 2, 3). The four diesel samples ranged in activity from 0 to 5.7 papillomas/mouse (table 2). Diesel samples A and C gave a dose-related response in both papillomas per mouse and percent of mice with papillomas. Maximal response in diesel sample B was at the 2.0-mg dose with the higher dose giving a lower tumor response, this possibly a result of a toxic effect. Diesel sample D at several doses produced more tumors than did acetone and TPA treatment in controls (table 3); however, no dose response was evident. The gasoline sample, like diesel samples B and C, produced a weak response.

The roofing tar and coke oven samples produced dose-related, strong tumor responses. At the highest dose tested (10.0 mg/mouse), papillomas per mouse were 5.7–7.7 with practically every animal bearing tumors (table 3). BP elicited the greatest number of papillomas per mouse, 10.2 at approximately 1% the dose of the roofing tar or coke oven samples. Again, a clear dose response was evident at the four doses of BP tested. The formation of tumors in mice treated with acetone and promoted twice weekly with TPA was extremely low, 0.08 and 0.05 papilloma/mouse in male and female animals, respectively. Mice initiated with up to 100.92 μg of BP followed by promotion with acetone did not develop tumors (data not shown).

DISCUSSION

The results presented confirm and expand the earlier observations of Kotin et al. (*18*) on diesel exhaust components and clearly indicate the tumorigenic potential of these

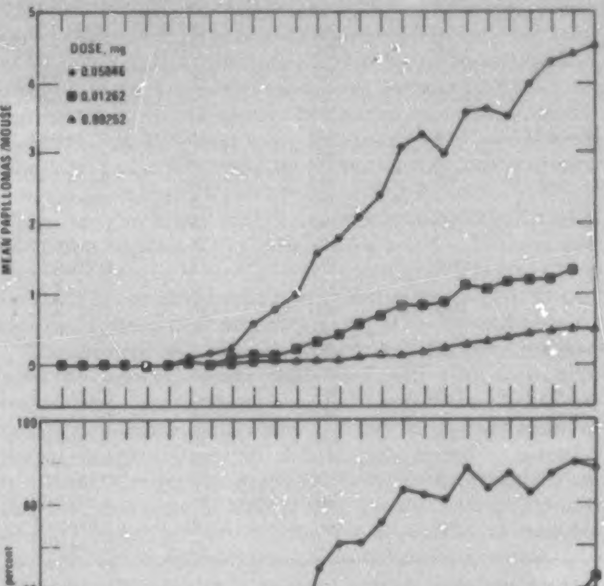

TEXT-FIGURE 2.—Tumor initiation by BP. Each group initially consisted of 40 male and 40 female SENCAR mice.

TABLE 2.—*Tumor-initiating activity of diesel and gasoline particulate emission extracts on SENCAR mouse skin*

Sample	Initiating dose, mg	No. of survivors[a] and their sex	Mice with papillomas, %	Papillomas/ mouse[b]
Diesel A	0.1	37♂	0	0
		39♀	3	0.03±0.16
	0.5	38♂	26	0.34±0.63
		39♀	23	0.39±0.85
	1.0	40♂	33	0.38±0.59
		38♀	39	0.53±0.76
	2.0	35♂	66	1.1±1.2
		40♀	58	1.6±1.9
	10.0	38♂	90	5.5±3.3
		37♀	97	5.7±3.7
Diesel B	0.1	40♂	13	0.13±0.34
		40♀	15	0.18±0.45
	1.0	39♂	26	0.36±0.71
		40♀	18	0.25±0.59
	2.0	40♂	20	0.35±1.15
		40♀	40	0.40±0.50
	10.0	39♂	21	0.21±0.41
		39♀	10	0.13±0.41
Diesel C	0.1	40♂	18	0.16±0.39
		37♀	14	0.14±0.36
	0.5	37♂	14	0.14±0.35
		40♀	5	0.05±0.22
	1.0	38♂	21	0.21±0.41
		39♀	18	0.26±0.50
	2.0	38♂	21	0.24±0.49
		35♀	14	0.17±0.45
	10.0	38♂	24	0.34±0.67
		38♀	42	0.47±0.60
Diesel D	0.1	39♂	10	0.15±0.48
		38♀	0	0
	0.5	39♂	10	0.13±0.41
		38♀	8	0.08±0.27
	1.0	39♂	15	0.15±0.36
		40♀	5	0.05±0.22
	2.0	38♂	11	0.11±0.31
		39♀	5	0.05±0.22
	10.0	40♂	10	0.10±0.31
		39♀	5	0.06±0.22
Gasoline	0.10	39♂	5	0.05±0.22
		39♀	13	0.23±0.67
	0.50	39♂	13	0.15±0.43
		38♀	18	0.24±0.54
	1.0	40♂	18	0.18±0.39
		40♀	10	0.13±0.40
	2.0	37♂	22	0.24±0.50
		39♀	21	0.23±0.49
	3.0	34♂	18	0.24±0.51
		40♀	23	0.28±0.56

[a] Each test group initially consisted of 40 male or female mice. Scoring of tumor data was performed 24–26 wk after initiation.

[b] Values are means ± SD for replicate samples of papillomas per mouse based on individual animal determinations. Number of replicates is the corresponding number of mice surviving for that test group.

materials. The four diesel samples varied widely in the tumorigenic responses they produced. Since the fuel, driving cycle, and collection and extraction procedures used in the production of the light-duty diesel samples A–C were similar, the differences in tumor responses are most likely because of differences in engine design and operating characteristics. It is not unlikely that different gasoline samples would also give a range of tumor responses had they been evaluated. Thus comparisons can be made only on a sample-by-sample basis, and conclusions cannot be generalized to encompass one entire class of technology. Three different types of emission sources were used in this study. The diesel and gasoline samples are collected from combustion sources, whereas coke oven emissions are from the pyrolytic conversion of coal and roofing tar emissions from the evaporation of pine pitch. It has been recently reported that the volatile components of roofing tar pitches from asphalt or coal tar are also carcinogenic on CD-1 and C3H/HeJ mouse skin (*24*).

The complex mixture samples seem to segregate into two activity classes of mouse skin "tumorigens": *a*) those producing maximal responses of greater than 5 papillomas/mouse (diesel sample A, roofing tar, and coke oven) and *b*) those producing responses of 0.2–0.5 papillomas/mouse (diesel samples B–D and gasoline).

The tumor multiplicity data were analyzed by means of a nonlinear model based on the Poisson distribution with correction for the background response. This model gave excess (over TPA control) tumor multiplicity activities in papillomas per mouse at 1 mg of extract, a convenient term for comparison of samples. The predicted activities at 1 mg of extract (table 4) correlated well with the observed re-

TABLE 3.—*Tumor-initiating activity of roofing tar and coke oven particulate emission extracts and BP on SENCAR mouse skin*

Sample	Initiating dose, mg	No. of survivors[a] and their sex	Mice with papillomas, %	Papillomas/ mouse[b]
Roofing tar	0.10	40♂	10	0.13±0.40
		39♀	15	0.21±0.52
	0.50	40♂	28	0.35±0.66
		39♀	13	0.15±0.43
	1.0	39♂	38	0.41±0.56
		40♀	45	0.80±1.10
	2.0	39♂	36	0.62±1.18
		38♀	37	0.45±0.69
	10.0	39♂	100	6.4±4.4
		40♀	95	5.7±4.1
Coke oven	0.10	40♂	13	0.13±0.33
		40♀	10	0.30±0.82
	0.50	40♂	73	1.8±1.5
		40♀	70	1.8±1.6
	1.0	37♂	95	2.6±2.3
		39♀	72	2.0±2.1
	2.0	39♂	95	4.0±3.0
		38♀	90	3.5±2.9
	10.0	39♂	100	7.1±4.3
		40♀	100	7.7±5.3
BP	0.00252	40♂	45	0.50±0.60
		39♀	31	0.44±0.75
	0.01262	40♂	73	1.8±1.6
		37♀	57	1.1±1.1
	0.05046	39♂	100	5.8±2.9
		40♀	75	2.8±2.8
	0.10092	38♂	95	10.2±5.8
		39♀	97	7.9±5.6
TPA[c]	0	37♂	8	0.08±0.28
		39♀	5	0.05±0.22

[a] Each test group initially consisted of 40 male or 40 female mice. Scoring of tumor data was performed 24–26 wk after initiation.

[b] Values are means ± SD for replicate samples of papillomas per mouse based on individual animal determinations. Number of replicates is the corresponding number of mice surviving for that test group.

[c] TPA-treated mice received 0.2 ml of actone and 1 wk later began a treatment schedule of 2 μg TPA two times weekly.

sponse at that dose (tables 2, 3) for those samples in which the calculated model adequately fit the observed data. With the use of this method for comparison, the complex mixture samples ranked in the order: coke oven>diesel A≧roofing tar≧diesel C = gasoline. Other distribution models (e.g., negative binomial) have also been successfully applied to the analysis of tumor multiplicity data from mouse skin experiments (*25*).

A comparison of the samples by tumor incidence was performed by means of the log-probit model with a nonzero background (*22*), and the results are described in table 5. The log-probit model considers mice on an individual basis and groups them into 1) mice with no tumors and 2) mice with 1 or more tumors. The samples are ranked by the calculated TID_{50}. All samples except diesel sample B, diesel sample D, and gasoline had data that spanned the 50% tumor incidence value; therefore, log-probit calculations for these samples reflect the observed tumor incidences. The calculated results show that the BP treatment is more active than, and statistically different ($P=0.05$) from, the coke oven, which is more active than, and statistically different from, diesel sample A or roofing tar. (These samples are statistically equivalent.) When subjected to the log-probit analysis, diesel samples B–D and the gasoline sample gave TID_{50} values much greater than 10 mg with wide 95% confidence intervals.

Both the tumor multiplicity and tumor incidence data gave similar rankings for the most active samples, even though different statistical models were used in their analyses.

Mouse skin has been reported to be quite sensitive to the tumorigenic effects of polycyclic aromatic hydrocarbons (*3–7*). The SENCAR mouse is exquisitely sensitive to BP as a tumor initiator because 4–9 μg applied once and followed by twice weekly applications of 2 μg TPA will produce a 50% papilloma incidence, depending on sex (tables 3, 5). However, the tumor data presented in tables 2 and 3 cannot be explained solely by the BP content (*see* table 1), because there is no significant relationship between TID_{50} (or mean papillomas per mouse) and BP content in each complex mixture. The coke oven sample produced 2.0–2.6 papillomas/mouse at 1 mg of extract. The BP content in 1 mg of coke oven extract is 478 ng, a dose that would produce less than 0.5 papilloma/mouse when applied to SENCAR mice. The diesel C sample contains 2 ng BP/mg extract, a dose that would produce only a background response; yet 1 mg of diesel sample C produces 0.21–0.26 papilloma/mouse. Diesel sample A contains the largest amount of BP—1,170 ng/mg of extract. Tumors obtained at the 10-mg extract dose (11.7 μg BP) level were approximately 5 or 6/mouse. Similar doses of BP (12.62 μg) produced only 1 or 2 tumors/mouse. Therefore, BP can be accounting for only 20–30% of the activity seen, and other components of the mixture seem to be playing a role in its tumorigenic activity. For example, β-propiolactone, a mouse skin tumorigen (*26*), has been detected in diesel exhaust particulate samples (*27*). Cocarcinogenic effects may also play a role in the overall activity.

TABLE 4.—*Comparison of predicted tumor multiplicity based on a nonlinear Poisson model*[a]

Sample	Excess papillomas per mouse at 1 mg of extract	Sex of mice	95% confidence intervals
Coke oven	2.2[b]	♂	2.0–2.4
	2.0[b]	♀	1.9–2.2
Diesel A	0.49[b]	♂	0.38–0.63
	0.68[b]	♀	0.57–0.79
Roofing tar	0.38[b]	♂	0.30–0.49
	0.44[b]	♀	0.35–0.55
Diesel C	0.21	♂	0.14–0.3
	0.17	♀	0.11–0.25
Gasoline	0.17	♂	0.12–0.24

[a] Predicted excess (over TPA controls) papillomas per mouse at 1 mg of extract were calculated on a UNIVAC 1100 computer with the use of the nonlinear Poisson model as described in "Materials and Methods." Calculations are shown only for those experimental groups for which the calculated model adequately fits the observed data at all dose levels.

[b] The distribution of tumors at some dose levels was not Poisson because the variances exceeded the means.

TABLE 5.—*Comparison of tumor incidence based on log-probit analysis*[a]

Sample	TID_{50}, mg[b]	Sex of mice	95% confidence intervals
BP	0.0036	♂	0.0021–0.0062
	0.0091	♀	0.0057–0.015
Coke oven	0.30	♂	0.22–0.40
	0.42	♀	0.31–0.58
Diesel A	1.6	♂	1.2–2.2
	1.5	♀	1.1–1.9
Roofing tar	1.8	♂	1.2–2.7
	2.1	♀	1.5–2.8

[a] Log-probit analysis with a nonzero background was performed according to Hasselblad et al. (22) on a UNIVAC 1100 computer as described in "Materials and Methods."

[b] Diesel samples B–D and gasoline produced TID_{50} values >10 mg with large 95% confidence intervals and are not listed.

The identity of substances present in these complex mixtures is currently under study and will yield important information regarding their active components. SENCAR mouse skin seems particularly well suited for evaluation of the tumorigenic potential of both pure agents or complex mixtures. The results presented here further substantiate this fact and provide information on the relative tumorigenicity based on tumor initiation of a series of complex mixtures obtained from combustion, pyrolytic, and evaporative sources.

REFERENCES

(*1*) SLAGA TJ, TRIPLETT LL, NESNOW S. Mutagenic and carcinogenic potency of extracts of diesel and related environmental emission: Two-stage carcinogenesis in skin tumor sensitive mice (SENCAR). In: Pepelko WE, Danner RM, Clarke NS, eds. Health effects of diesel engine emissions. Proceedings of an international symposium. Vol 2. Washington, D.C: U.S. Govt Print Off. 1980: 874–897 (EPA publication No. EPA-600/9-80-057B).

(*2*) NESNOW S, TRIPLETT LL, SLAGA TJ. Tumorigenesis of diesel exhaust, gasoline exhaust and related emission extracts on SENCAR mouse skin. In: Waters M, Sandhu SS. Lewtas J, Claxton L, Nesnow S, eds. Short-term bioassays in the analysis of complex environmental mixtures, II. New York: Plenum Press. 1981:277–297.

(*3*) BOUTWELL RK. Some biological aspects of skin carcinogenesis. Prog Exp Tumor Res 1964; 4:207–250.

(*4*) Slaga TJ, Gleason GL, Mills G, et al. Comparison of the skin tumor-initiating activities of dihydrodiols and diol-epoxides of various polycylic aromatic hydrocarbons. Cancer Res 1980; 40:1981-1984.

(*5*) Iyer RP, Lyga JW, Secrist JA III, Daub GH, Slaga TJ. Comparative tumor-initiating activity of methylated benzo(*a*)pyrene derivatives in mouse skin. Cancer Res 1980; 40:1073-1076.

(*6*) DiGiovanni J, Slaga TJ, Boutwell RK. Comparison of the tumor-initiating activity of 7,12-dimethylbenz(*a*)anthracene and benzo(*a*)pyrene in female SENCAR and CD-1 mice. Carcinogenesis 1980; 1:381-389.

(*7*) Hennings H, Devor D, Wenk ML, et al. Comparison of two stage epidermal carcinogenesis initiated by 7,12-dimethylbenz-(*a*)anthracene or *N*-methyl-*N'*-nitro-*N*-nitrosoguanidine in newborn and adult SENCAR and BALB/c mice. Cancer Res 1981; 41:773-779.

(*8*) Homburger F, Treger A, Baker JR. Mouse-skin painting with smoke condensates from cigarettes made of pipe, cigar, and cigarette tobaccos. J Natl Cancer Inst 1963; 31:1445-1459.

(*9*) Wynder EL, Hoffmann D, eds. Tobacco and tobacco smoke. New York: Academic Press, 1967:135-315.

(*10*) Van Duuren BL, Sivak A, Katz C, Melchionne S. Cigarette smoke carcinogenesis: Importance of tumor promoters. J Natl Cancer Inst 1971; 47:235-240.

(*11*) Gori GB, ed. Towards less hazardous cigarettes; the first set of experimental cigarettes. Washington, D.C.: U.S. Govt Print Off, 1977 [DHEW publication No. (NIH)76-905].

(*12*) Kotin P, Falk HL, Thomas M. Aromatic hydrocarbons. II. Presence in the particulate phase of gasoline-engine exhausts and the carcinogenicity of exhaust extracts. AMA Arch Ind Hyg Occup Med 1954; 9:164-177.

(*13*) Mittler S, Nicholson S. Carcinogenicity of atmospheric pollutants. Ind Med Surg 1957; 26:135-138.

(*14*) Hoffmann D, Wynder EL. Studies on gasoline engine exhaust. J Air Pollut Control Assoc 1963; 13:322-327.

(*15*) Hoffmann D, Theisz E, Wynder EL. Studies on the carcinogenicity of gasoline exhaust. J Air Pollut Control Assoc 1965; 15:162-165.

(*16*) Brune HF. Experimental results with percutaneous applications of automobile exhaust condensates in mice. In: Mohr U, Schmahl D, Tomatis L, Davis W, eds. Air pollution and cancer in man. Lyon: IARC, 1977:41-47 (IARC Scientific Publication No. 16).

(*17*) Misfeld J, Timm J. The tu[illegible]r-producing effect of automobile exhaust condensate and fraction[illegible]hereof. Part III. Mathematical-statistical evaluation of the test r[illegible]lts. J Environ Pathol Toxicol 1978; 1:747-772.

(*18*) Kotin P, Falk HL, Thomas M. Aromatic hydrocarbons. III. Presence in the particulate phase of diesel-engine exhausts and the carcinogenicity of exhaust extracts. AMA Arch Ind Health 1955; 11:11[illegible]-120.

(*19*) Misfeld J. The tumor-producing effects of automobile exhaust condensate and of diesel exhaust condensate: Mathematical-statistical evaluation of test results. In: Pepelko WE, Danner RM, Clarke NA, eds. Health effects of diesel engine emissions. Proceedings of an international symposium. Vol 2. Washington, D.C.: U.S. Govt Print Off, 1980:1012-1025 (EPA publication No. EPA/9-80-057B).

(*20*) Huisingh JL, Bradow RL, Jungers RH, et al. Mutagenic and carcinogenic potency of extracts of diesel and related environmental emissions; study design, sample generation, collection, and preparation. In: Pepelko WE, Danner RM, Clarke NA, eds. Health effects of diesel engine emission. Proceedings of an International symposium. Vol 2. Washington, D.C.: U.S. Govt Print Off, 1980:788-800 (EPA publication No. EPA-600/9-80-057B).

(*21*) Swanson P, Morris C, Hedgecoke R, Jungers R, Thompson R, Bumgarner J. A rapid analytical procedure for the analysis of benzo(*a*)pyrene in environmental samples. Trends Fluorescence 1978; 1:22-27.

(*22*) Hasselblad V, Stead AG, Creason JP. Multiple probit analysis with a nonzero background. Biometrics 1980; 36:659-663.

(*23*) Stead AG, Hasselblad V, Creason JP, Claxton L. Modeling the Ames test. Mutat Res 1981; 85:13-27.

(*24*) Thayer PS, Menzies KT, Von Thuna P, Niemeier RW. Carcinogenicity to mouse skin of volatile components of roofing asphalts and pitches. Proc Am Assoc Cancer Res 1981; 22:136.

(*25*) Drinkwater NR, Klotz JH. Statistical methods for the analysis of tumor multiplicity data. Cancer Res 1981; 41:113-119.

(*26*) Slaga TJ, Bowden GT, Shapas BG, Boutwell RK. Macromolecular synthesis following single application of alkylating agents used as initiators of mouse skin tumorigenesis. Cancer Res 1971; 33:769-776.

(*27*) Menster M, Sharkey AG Jr. Chemical characterization of diesel exhaust particulates. Oak Ridge, Tenn.: ERDA Technical Information center, 1977:1-47 (PERC/RI-77/5).

Moloney Murine Sarcoma Virus Tumors in CBA/J Mice: Chemopreventive and Chemotherapeutic Actions of Supplemental β-Carotene[1,2,3,4]

Eli Seifter, *Ph.D.*,[5,6] **Giuseppe Rettura**, *Ph.D.*,[6] **Jacques Padawer**, *Ph.D.*,[7] *and* **Stanley M. Levenson**, *M.D.*[6]

ABSTRACT—Decreased tumor frequency, increased latent period, and increased rate of tumor regression were observed in male inbred CBA/J mice fed supplemental β-carotene before and/or after they were inoculated with the Moloney sarcoma virus. When β-carotene feeding was begun after tumors were already present, it markedly increased the rate of tumor regression. β-Carotene minimized the virus-induced thymus gland involution that accompanies tumor growth, and this action on the thymus gland was believed to underlie part of β-carotene's antitumor activity. The basal diet, a standard commercial mouse chow containing more vitamin A than the National Research Council recommends as a daily allowance for rodents, supported normal growth, reproduction, and longevity of normal mice. The work reported here is the first demonstration of the antitumor action of β-carotene in mice inoculated with an oncogenic virus.—JNCI 1982; 68:835–840.

β-Carotene, a dietary precursor of vitamin A, is currently the subject of much interest as a possible tumor preventive agent (*1*). Epidemiologic data have shown that populations with low serum vitamin A contents are at higher risk for tumor development than are those with normal or high serum vitamin A levels (*2*). This finding has led to suggestions that supplemental vitamin A might have beneficial effects in lowering tumor incidence of populations at high tumor risk. However, the possibility that prophylactic use of vitamin A could induce clinically significant vitamin A toxicity has caused workers to explore alternative vitamin A-like dietary tumor preventive agents. Recent examinations of epidemiologic data show that populations ingesting foods rich in β-carotene are at lower tumor risk than are those on a low carotene diet (*3*). Because β-carotene has minimal toxicity, the concept of using β-carotene for tumor chemoprevention is attractive. The present study[8] was done to determine whether supplemental β-carotene is effective for tumor prevention and therapy in a tumor system that is responsive to supplemental vitamin A.

MATERIALS AND METHODS

Three experiments were conducted to examine the influence of supplemental β-carotene on tumor incidence and growth due to the M-MuSV tumor virus: In the first two, supplemental β-carotene feeding was begun before tumor inoculation, whereas in the third, β-carotene supplementation was begun after the tumor had developed. A fourth experiment was done to obtain data on the influence of supplemental β-carotene on the thymic status of normal and virus-inoculated mice, because these findings might contribute to understanding the mechanisms of antitumor action of β-carotene.

Animals, housing, and diets.—Five-week-old male inbred CBA/J mice were purchased from The Jackson Laboratory, Bar Harbor, Maine, and maintained in our laboratory for 1 week before use in any experiment. Two or 3 days after their arrival in our laboratory, the animals were examined, weighed, and allocated randomly to cages housing 5 mice each. Shoe box-type cages of opaque polyethylene with the dimensions of 5×8×12 inches and with a 3-mesh galvanized wire top were used. The mice were housed in a room with a 12-hour day–night cycle, temperature of 25°C, and relative humidity of about 35%.

The powdered laboratory chow (Teklad, Inc., Monmouth, Ill.) that served as the basal or control ration for the mice contained 6,190 IU vitamin A palmitate/kg and 4.3 mg β-carotene (equivalent to 7,167 IU vitamin A)/kg; the total (13,357 IU/kg diet) is well above the National Research Council recommended daily requirement of vitamin A for normal rodents, which averages 6,000 IU/kg diet for growth, pregnancy, lactation, and longevity. Therefore, the basal control diet is *not* deficient in vitamin A. Rodents fed this diet have normal levels of serum vitamin A of 62±3 μg/dl (*4*).

Experimental diets contained additional β-carotene (90 or 120 mg/kg powdered chow). These values were chosen because 90 mg β-carotene is equivalent to 150,000 U vitamin A (IU=0.62 μg β-carotene), the level of dietary vitamin A supplementation that we used earlier and found effective against M-MuSV (*5, 6*).

M-MuSV.—The virus (M-MuSV) used in these experiments was originally obtained from Dr. J. B. Moloney,

---

ABBREVIATION USED: M-MuSV=Moloney murine sarcoma virus.

---

[1] Received July 22, 1981; accepted December 3, 1981.

[2] Supported in part by the Army Research contract DADA 17-70-C and by Public Health Service grant 5-K06GM-14208 from the National Institute of General Medical Sciences.

[3] A portion of this work was presented at the 175th national meeting of the American Chemical Society held March 13–17, 1978, in Anaheim, California.

[4] Animals were maintained under the guidelines set forth by the Albert Einstein College of Medicine and in the "Guide for the Care and Use of Laboratory Animals" by the Institute of Laboratory Animal Resources, National Research Council.

[5] Department of Biochemistry, Albert Einstein College of Medicine, Yeshiva University, Bronx, N.Y. 10461.

[6] Department of Surgery, Albert Einstein College of Medicine.

[7] Department of Anatomy, Albert Einstein College of Medicine.

[8] The concept presented in the present report, i.e., the use of β-carotene for tumor chemoprevention and for tumor chemotherapy, was first proposed by us in an application to the National Institutes of Health in 1974 (NIH grant application CA 16818-01, pp. 28, 38, and 40).

National Cancer Institute, and was designated as lot #206. For use as an inoculum, the virus was passed through CBA/J mice from which the tumors were harvested and treated for extraction of the virus. The virus was reconstituted with a phosphate-saline buffer so that virus recovered from 1 g of tumor was present in 1 ml of suspension, yielding 1 g eq/ml. In the present experiments, the virus was used in tenfold (10^{-1} g eq/ml) or hundredfold (10^{-2} g eq/ml) dilutions. Inoculations consisted of im injections of 0.1 ml of virus suspension in the inner aspect of the left thigh. Tumors were graded on a scale of 1–4, as described by Blumenshein and Moloney (*7*).

Lymphocyte count.—Mice were killed in an ether chamber, and thymus glands were removed and weighed to the nearest milligram on a Roller-Smith tissue balance. Derived statistics are reported to 0.1 mg.

Thymic lymphocytes were counted in samples prepared by mincing the thymus gland of each animal in 6 ml buffer (medium 199 with Hanks' salts; GIBCO, Grand Island, N.Y.); the homogenate was then passed through a No. 100 stainless steel screen. The residue was washed twice with 1.5-ml portions of buffer, and the final volume was adjusted to 10 ml. The cell suspension was mixed thoroughly, and 0.1 ml was further diluted to 2 ml with buffer. An aliquot of this suspension was then placed in a Neubauer hemacytometer (American Optical Corp., Buffalo, N.Y.), and lymphocytes were counted independently by two observers.[9]

Experiments.—Experiments on the thymotropic action of β-carotene were begun in 1974 (*8*). The experiments with virus were done in the spring of 1975 and the fall of 1977 (*9*).

Experiment 1: Four groups of CBA/J mice (10 mice/group) were established and housed as described. Two of the groups were fed the basal ration, and 2 received the basal ration supplemented with 90 mg β-carotene/kg diet. After 3 days, half the animals (1 group of controls and 1 group of β-carotene-supplemented mice) were inoculated with 0.1 ml of a virus suspension containing 0.1 eq of the virus present in 1 g tumor/ml (10^{-1} g eq/ml), and the other half were inoculated with 0.1 ml of the virus solution diluted 1:10 with buffer (10^{-2} g eq/ml).

Experiment 2: This experiment was conducted several weeks later than experiment 1. Not only was a different shipment of mice used, but the β-carotene supplements were also increased to 120 mg/kg diet. Other conditions were similar to those of experiment 1.

Experiment 3: The purpose of this experiment was to determine if supplemental β-carotene fed to mice only after M-MuSV tumors had appeared would influence tumor growth. Twenty male CBA/J mice were inoculated with 0.2 ml of a 10^{-1} g eq preparation. By day 7, these mice had a mean tumor score of 2. At this time, half the mice were started on the β-carotene-supplemented ration, while the other half were continued on the basal ration.

Experiment 4: The purpose of this experiment was to determine the effect of supplemental β-carotene on the thymus glands of normal mice and mice inoculated with M-MuSV.

Four groups of mice were established, each of which consisted of 6 mice/cage and 4 cages/group. Group 1 received the control ration and no virus inoculation; group 2 received the control ration plus M-MuSV (10^{-1} g eq/ml); group 3 was β-carotene supplemented (90 mg/kg diet) but not virus inoculated; and group 4 was β-carotene supplemented and M-MuSV inoculated (10^{-1} g eq/ml). Virus was inoculated 3 days after the mice started their respective diets. On days 1, 2, 3, 7, and 17 post inoculation, mice of one cage in each group were weighed before being killed, and their thymus glands were studied.

RESULTS

Influence of β-Carotene Supplementation on M-MuSV Tumors

Tumor incidence was reduced when mice were fed β-carotene supplements before and after their inoculation with either the higher or lower inoculum of M-MuSV ($P<0.005$ and <0.009, respectively, table 1). Supplemental β-carotene increased the latent period for tumor development for animals receiving either the higher virus inoculum ($P<0.005$ in experiment 1 and <0.01 in experiment 2) or the more dilute inoculum ($P<0.008$ in experiment 1 and <0.05 in experiment 2, table 2).

Supplemental β-carotene slowed the daily increment of tumor progression. For the higher dose inoculum, the tumor growth increments were 0.25 score U/day; β-carotene lowered these values to 0.13 U/day in experiment 1 and to 0.19 U/day in experiment 2. Similarly for the lower virus inoculum, the daily increments were lowered from 0.25 to 0.09 U/day by β-carotene in experiment 1 and from 0.19 to 0.09 U/day in experiment 2 (table 3; text-fig. 1).

When tumors developed in the β-carotene-supplemented mice, the tumors were present for a shorter time than if the mice were β-carotene unsupplemented (table 3). The shortened time resulted from lengthened latent periods and more rapid tumor regression (tables 3, 4; text-fig. 1). Mean tumor size was dependent on inoculum size; smaller inocula produced tumors of smaller mean size. Mean tumor size was reduced by β-carotene supplementation, which had an effect similar to that of reducing the inoculum size by one log unit.

Because of the large inoculum size used, tumor progression was most rapid in experiment 3, and tumor regression did not occur in control animals during the period of observation

TABLE 1.—*Tumor incidence (experiments 1 and 2)*

M-MuSV inoculum, g eq/ml	Diet	CBA/J mice[a]		χ^2_1	P
		Tumor-bearing	Tumor-free		
10^{-1}	Control	20	0		
	β-Carotene supplemented	13	7	8.48	<0.005
10^{-2}	Control	17	3		
	β-Carotene supplemented	9	11	7.03	<0.009

[a] Mice are classified as tumor "takes" or "no takes."

---

[9] We are indebted to Dr. Achilles Demetriou and Dr. Anton Schittek (Department of Surgery, Albert Einstein College of Medicine) who contributed to this aspect of the experiment.

TABLE 2.—*Supplemental β-carotene and latent period of M-MuSV tumors in CBA/J mice*

M-MuSV inoculum, g eq/ml	Diet	Experiment 1			Experiment 2		
		Latent period, days[a]	No. of mice with tumor/No. inoculated	P[b]	Latent period, days[a]	No. of mice with tumor/No. inoculated	P[b]
10^{-1}	Control	5.8±0.3	10/10	<0.005	6.1±0.2	10/10	<0.01
	β-Carotene supplemented	8.3±0.6	8/10		7.1±0.2	5/10	
10^{-2}	Control	7.1±0.4	9/10	<0.008	7.9±0.3	8/10	<0.05
	β-Carotene supplemented	10.5±0.8	4/10		9.8±1.0	4/10	

[a] Mean ± SEM.
[b] Analyzed by Student's *t*-test for small samples.

(text-fig. 2). Tumor regression was rapid in the β-carotene-supplemented groups, and no mouse died. The experiment was concluded after regression had occurred in all of the β-carotene-supplemented mice (38 days). By that time, 3 of 10 control mice with grade 4 tumors had died between days 28 and 30.

Influence of β-Carotene Supplementation on the Thymus Glands of Normal and M-MuSV-Inoculated Mice

After 3 days of β-carotene supplementation (table 5), the size of the thymus glands increased ($P<0.001$) and the numbers of small lymphocytes in the gland increased by more than 50% ($P<0.001$). Inoculation with M-MuSV caused a rapid and progressive loss in thymus mass due to the decrease in the numbers of small thymic lymphocytes (50% in 7 days, $P<0.001$). Supplemental β-carotene largely prevented this: The decrease in these mice was 27%; this difference is statistically significant ($P<0.005$).

DISCUSSION

The experiments reported here clearly establish prophylactic and therapeutic actions of supplemental β-carotene given to CBA/J mice inoculated with M-MuSV: 1) β-Carotene supplementation begun before M-MuSV inoculation and continued throughout the experiment lowered tumor incidence, decreased tumor scores, and decreased the time required for tumor regression. 2) β-carotene supplementation begun after classification of tumors as grade 2 in mice receiving large inocula of M-MuSV hastened regression. 3) Administration of β-carotene to normal mice caused increases in thymus weights and in the numbers of small thymic lymphocytes, with no other obvious changes in the gross appearance of the thymus glands. Supplemental β-carotene begun before M-MuSV inoculation partially prevented the thymic involution that otherwise occurred in mice inoculated with M-MuSV.

Comparison of these results with those we have reported for supplemental vitamin A shows that the qualitative and quantitative anti-M-MuSV tumor activities of β-carotene

TABLE 3.—*Supplemental β-carotene and tumor persistence[a] in M-MuSV-inoculated CBA/J mice*

Parameter	Experiment 1				Experiment 2			
	10^{-1} g eq M-MuSV/ml		10^{-2} g eq M-MuSV/ml		10^{-1} g eq M-MuSV/ml		10^{-2} g eq M-MuSV/ml	
	Control diet	β-Carotene-supplemented diet	Control diet	β-Carotene-supplemented diet	Control diet	β-Carotene-supplemented diet	Control diet	β-Carotene-supplemented diet
Days palpable tumor was present	18	9	6	5	10	8	9	6
	19	4	18	6	21	5	9	8
	10	5	7	8	8	7	4	3
	22	3	10	3	14	9	6	5
	11	9	17		19	4	11	
	11	12	18		11		5	
	9	8	18		7		15	
	10	7	7		9		9	
	10		17		10			
	9				15			
x̄	12.9	7.1	12.7	5.5	12.3	6.6	8.5	5.5
SE	±1.5	±1.1	±2.1	±1.0	±1.5	±0.9	±1.0	±1.0
P[b]	<0.01		<0.03		<0.03		<0.1	
No. of mice with tumor/No. inoculated	10/10	8/10	9/10	4/10	10/10	5/10	8/10	4/10

[a] Tumors were graded from 1 to 4.
[b] Analyzed by Student's *t*-test for small samples.

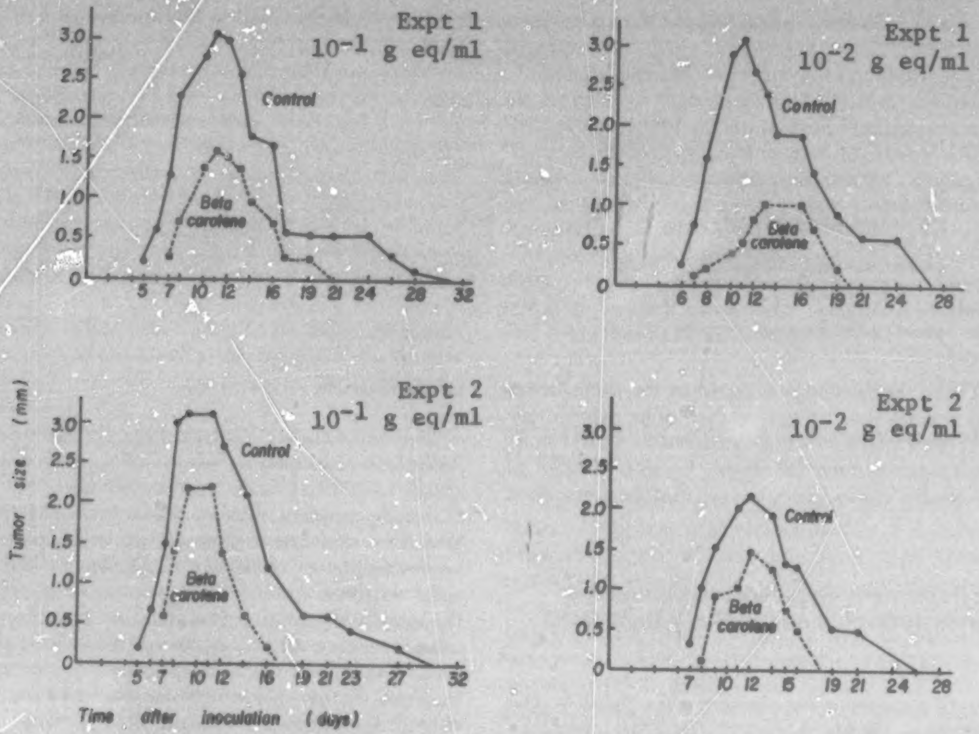

TEXT-FIGURE 1.—Mean tumor scores for mice in expt 1 and 2. All mice received 0.1 ml of indicated M-MuSV inoculum. Mice were fed a diet containing 90 mg β-carotene/kg in expt 1 and 120 mg β-carotene/kg in expt 2.

are similar to those of vitamin A. Similarly, we have found in other experiments that supplemental β-carotene, like vitamin A, inhibits the development and growth of cancer in C3H mice inoculated with syngeneic C3HBA (breast adenocarcinoma) cells (*9*).

Spontaneous resistance of M-MuSV in syngeneic BALB/c mice is strongly dependent on lymphocytes, particularly on T-lymphocyte activity (*10*). Similarly, work from our laboratory has shown that resistance to M-MuSV tumor growth in CBA/J mice is strongly decreased by agents or conditions that inhibit lymphocyte activity, such as antilymphocytic serum, thymectomy, cortisone or ACTH administration, or burns or other physical stress, whereas resistance is increased greatly by thymic hormones, vitamin A, or other agents that induce lymphopoiesis or prevent injury-induced lymphopenia (*11–13*).

Along with the increase in thymus cellularity, Cohen and Cohen (*14*) have shown the development in vitamin A-supplemented mice inoculated with sheep red blood cells of an increase in the number of splenic antibody-producing cells. Not only Floershein and Bollag (*15*), but also Rettura et al. (*16*) have shown that supplemental vitamin A speeds the rejection of skin allografts by mice.

We have called those actions of vitamin A that increase the numbers of thymus gland lymphocytes and the numbers of circulating lymphocytes the thymotropic and lympho-

TABLE 4.—*Supplemental β-carotene and tumor regression*[a] *in M-MuSV-inoculated CBA/J mice*

Parameter	Experiment 1				Experiment 2			
	10^{-1} g eq M-MuSV/ml		10^{-2} g eq M-MuSV/ml		10^{-1} g eq M-MuSV/ml		10^{-2} g eq M-MuSV/ml	
	Control diet	β-Carotene-supplemented diet	Control diet	β-Carotene-supplemented diet	Control diet	β-Carotene-supplemented diet	Control diet	β-Carotene-supplemented diet
No. of mice with tumor/No. inoculated	10/10	8/10	9/10	4/10	10/10	5/10	8/10	4/10
$\bar{x}$ of tumor regression	7.1	3.4	6.8	2.0	7.0	3.2	5.1	2.8
±SE	1.1	1.2	0.9	0.0	0.9	0.4	0.6	0.5
P^b	<0.02		<0.006		<0.005		<0.01	

[a] Mean tumor regression is expressed in days from midpoint of maximum tumor size.
[b] Analyzed by Student's *t*-test for small samples.

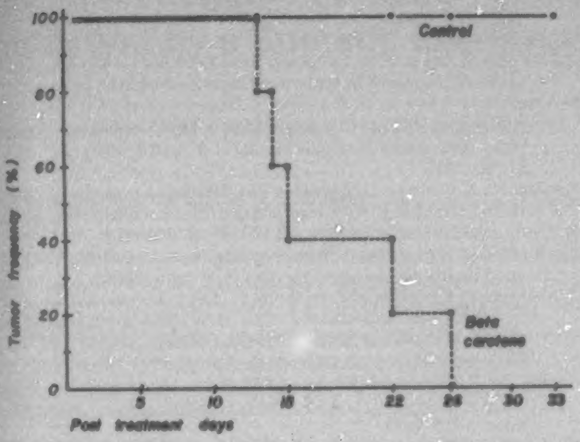

TEXT-FIGURE 2.—Persistence of tumors in mice in expt 3. Animals fed β-carotene-supplemented chow began their diet on the 7th day after inoculation.

poietic actions of supplemental vitamin A (*17–19*). We have correlated these actions of supplemental vitamin A with the development of increased immune competence, particularly of cell-mediated reactions such as those that accompany skin rejection (*16*), immunization to poxvirus vaccine (*20*), or regression of M-MuSV tumors and decreased rates of tumor take when transplanted tumor inocula are from nonviral, immunogenic tumors (*21*). Similarly, we have found that β-carotene supplementation promotes allograft rejection (*22*) and induces a modest increase in peripheral blood lymphocytes (*23, 24*).

We have called the thymic involution which occurs after M-MuSV inoculation a stressful action of the virus because it resembles the thymic involution reported to occur after a large number of physical, chemical, or pathogenic stressors have been applied (*25*). We have reported that supplemental vitamin A moderates the thymic effects of these stressors and have referred to this response as the anti-stress action of vitamin A (*26*). In the present study it is clear that β-carotene is also an antistress (antitumor) agent, thus extending our findings regarding the influence of β-carotene in suppressing stress responses in physically injured or chemically poisoned rodents.

Cohen et al. (*27*) have shown that elective operation trauma (general anesthesia) induces relative lymphopenia and diminished lymphocyte transformation (in vitro). These inhibitions of immune phenomena were prevented when dietary vitamin A supplements were fed to patients and are thus related to our findings in rodents.

Recently, Medawar and Hunt (*28*) have pointed out that the immunity-promoting action of vitamin A is probably through its actions on the cellularity of thymus glands and that this action is probably critical for the antitumor action of the vitamin. This view (*28*) is similar to the one we have expressed earlier (*5, 17, 29–31*). Similarly, Lotan and Dennert (*32*) and Lotan (*33*) have related the thymic effects of vitamin A to the enhancement of the tumor immunity by vitamin A.

The data do not permit us to determine if the actions of β-carotene reported here require that it be converted to vitamin A; the experiments were not designed to adduce this specific point. The important effects of β-carotene which we have described as shown by the thymus, the white blood cells, and the control of the tumor growth are produced by amounts of β-carotene that do not, in our experience, lead to any signs of vitamin A toxicity. We speculate that, as a consequence of their concentration in certain organs, tissues, and body fluids other than blood plasma, such as lymph (*34*), vitamin A and β-carotene influence the growth and maturation of cells that regulate various immune functions, such as thymus function, and thereby moderate tumor growth.

TABLE 5.—*Supplemental β-carotene and thumus gland effects on M-MuSV-inoculated CBA/J mice*

Treatment groups	Days on diet/days postinoculation					
	3/0		6/3		10/7	
	Thymus weight,[a] mg	TTL[b]$\times10^{-6}$	Thymus weight,[a] mg	TTL[b]$\times10^{-6}$	Thymus weight,[a] mg	TTL[b]$\times10^{-6}$
A, Control diet	46.8±1.0	33.3±0.9	45.5±1.0	35.0±1.1	45.8±1.3	31.3±1.2
B, Control diet and M-MuSV inoculated	47.5±1.1	32.4±1.0	31.5±1.4	15.0±1.2	25.0±1.3	11.5±1.2
C, β-Carotene-supplemented diet	56.0±1.6	55.8±2.0	53.9±1.9	54.1±0.9	54.7±2.1	52.6±1.5
D, β-Carotene supplemented diet and M-MuSV inoculated	55.2±0.8	54.9±2.4	40.3±1.0	24.9±1.2	40.2±2.2	38.3±1.5
	P[c]					
A vs. B	NS	NS	<0.005	<0.001	<0.001	<0.001
A vs. C	<0.001	<0.001	<0.002	<0.001	<0.005	<0.001
A vs. D	<0.001	<0.001	<0.05	<0.01	NS	<0.01
B vs. D	<0.001	<0.001	<0.005	<0.001	<0.001	<0.001
C vs. D	NS	NS	<0.005	<0.001	<0.001	<0.001

[a] Values are means ± SEM.
[b] TTL=total thymic lymphocytes. Values are means ± SE.
[c] Determined by the variance analysis and the Newman-Keuls test. NS=not significant.

REFERENCES

(*1*) Editorial. Vitamin A, retinol, carotene, and cancer prevention. Br Med J 1980; 281.

(*2*) Bjelke E. Dietary vitamin A and human lung cancer. Int J Cancer 1975; 15:561–565.

(*3*) Peto R, Doll R, Buckley JD, Sporn MB. Can dietary beta-carotene materially reduce human cancer rates? Nature 1981; 290:201–208.

(*4*) Seifter E, Crowley L, Rettura G, et al. Influence of vitamin A on wound healing in rats with femoral fracture. Ann Surg 1975; 181:836–841.

(*5*) Seifter E, Zisblatt M, Levine N, Rettura G. Inhibitory action of vitamin A on a murine sarcoma. Life Sci 1973; 13:945–951.

(*6*) Rettura G, Schittek A, Hardy M, Levenson SM, Demetriou A, Seifter E. *Brief communication:* Antitumor action of vitamin A in mice inoculated with adenocarcinoma cells. J Natl Cancer Inst 1975; 54:1489–1491.

(*7*) Blumenschein GR, Moloney JB. Quantitative dose-response relationships of murine sarcoma virus (Moloney) in BALB/c mice. J Natl Cancer Inst 1969; 42:123–133.

(*8*) Rettura G, Schittek A, Demetriou A, Seifter E. Protection against thymic involution by β-carotene. The 170th national meeting of the American Chemical Society, Division of Agricultural and Food Chemistry, Chicago, Ill., Aug. 24–29, 1975. Abstract No. 59.

(*9*) Seifter E, Rettura G. β-carotene inhibits tumor growth in mice. The 175th national meeting of the American Chemical Society, Division of Agricultural and Food Chemistry, Anaheim, Calif., March 13–17, 1978. Abstract No. 45.

(*10*) Hardy MA, Zisblatt M, Levine N, Goldstein AL, Lilly F, White A. Reversal by thymosin of increased susceptibility of immunosuppressed mice to Moloney sarcoma virus. Transplant Proc 1971; 3:926–928.

(*11*) Rettura G, Seifter J, Zisblatt M, Levenson SM, Levine N, Seifter E. *Brief communication:* Metyrapone-inhibited oncogenesis in mice inoculated with a murine sarcoma virus. J Natl Cancer Inst 1973; 51:1983–1985.

(*12*) Seifter E, Rettura G, Demetriou AA, Levenson S, Rahman S, Seifter J. Inhibition of murine sarcoma development by deoxycorticosterone acetate. J Natl Cancer Inst 1974; 53:1809–1812.

(*13*) Seifter E, Rettura G, Levenson SM, Appleman M, Seifter J. Aspirin inhibits a murine viral infection. Life Sci 1975; 16:629–633.

(*14*) Cohen BE, Cohen IK. Vitamin A: Adjuvant and steroid antagonist in the immune response. J Immunol 1973; 111:1376–1380.

(*15*) Floersheim GL, Bollag W. Accelerated rejection of skin homografts by vitamin A acid. Transplantation 1972; 14:564–567.

(*16*) Rettura G, Levenson SM, Schittek A, Seifter E. Vitamin A action on oncogenesis and graft rejection. Surg Forum 1975; 26:301–303.

(*17*) Seifter E, Rettura G, Seifter J, Davidson H, Levenson SM. Thymotropic action of vitamin A. Fed Proc 1973; 32:947.

(*18*) Seifter E, Rettura G. Vitamin A in animal tumor therapy: Adrenolytic, thymotropic and lymphopoietic actions. Cancer Cytol 1977; 17:21–22.

(*19*) Seifter E, Barbul A, Levenson SM, Rettura G. Lymphopoietic action of vitamin A in tumor-bearing mice. Fed Proc 1978; 37:335.

(*20*) Seifter E, Rettura G, Padawer J, Demetriou AA, Levenson SM. Antipyretic and antiviral action of vitamin A in Moloney sarcoma virus- and poxvirus-inoculated mice. J Natl Cancer Inst 1976; 57:355–359.

(*21*) Seifter E, Rettura G, Levenson SM. Decreased resistance of C3H/HeHa mice to C3HBA tumor transplants: Increased resistance due to supplemental vitamin A. JNCI 1981; 67:467–472.

(*22*) Rettura G, Stratford F, Levenson SM, Seifter E. Enhanced graft rejection due to beta-carotene. Fed Proc 1981; 40:860.

(*23*) Seifter E, Levenson SM, Rettura G. The lymphopoietic action of vitamin A and beta-carotene. The 181st national meeting of the American Chemical Society, Division of Agricultural and Food Chemistry, Atlanta, Ga., March 29–April 3, 1981. Abstract No. 13.

(*24*) Seifter E, Rettura G, Levenson SM. A common mechanism for the tumor inhibitory actions of vitamin A and arginine. J Maine Med Assoc 1979; 70:287.

(*25*) Selye H. Thymus and adrenals in the response of the organism to injuries and intoxications. Br J Exp Pathol 1936; 17:234–248.

(*26*) Rettura G, Levenson SM, Rahman S, Seifter E. Anti-viral action of vitamin A in BALB/c mice. Fed Proc 1974; 33:687.

(*27*) Cohen BE, Gill G, Cullen PR, Morris PJ. Reversal of postoperative immunosuppression in man by vitamin A. Surg Gynecol Obstet 1979; 149:658–662.

(*28*) Medawar PB, Hunt R. Anti-cancer action of retinoids. Immunology 1981; 42:349–353.

(*29*) Rettura G, Barbul A, Levenson SM, Seifter E. Increased survival in mice with C3H breast adenocarcinoma after tumor excision and vitamin A supplementation. Surg Forum 1978; 29:170–172.

(*30*) Barbul A, Thysen B, Rettura G, Levenson SM, Seifter E. White cell involvement in inflammatory wound healing and immune actions of vitamin A. J Parent Enter Nutr 1978; 2:129–140.

(*31*) Seifter E, Rettura G, Levenson SM, Critselis A. Mechanism of action of vitamin A in immunogenic tumor systems. In: Siegenthaler W, Lüthy R. Current chemotherapy. Proceedings of the tenth international congress of chemotherapy, Zurich, Switzerland, September 1977. Washington, D.C.: Am Soc Microbiol, 1978:1290–1292.

(*32*) Lotan R, Dennert G. Stimulatory effects of vitamin A analogs on induction of cell-mediated cytotoxicity in vivo. Cancer Res 1979; 39:55–58.

(*33*) Lotan R. Effects of vitamin A and its analogs (retinoids) on normal and neoplastic cells. Biochim Biophys Acta 1980; 605:33–91.

(*34*) Seifter E, Rettura G, Levenson SM. Carotenoids and cell-mediated immune responses. In: Charalambous G, Inglett G, eds. Quality of foods and beverages: Recent developments in chemistry and technology. New York: Academic Press, 1981:335–347.

Nonimmunogenic Radiation-Induced Lymphoma: Immunity Induction by a Somatic Cell Hybrid[1,2,3]

Eitan Yefenof,[4] Mira Goldapfel,[4] *and* Rosalie Ber[5]

ABSTRACT—The cell line designated PIR-2 is a nonimmunogenic X-ray-induced thymoma of C57BL/6 origin that is unable to induce antitumor immunity in syngeneic lymphocytes in vitro and in mice in vivo. Fusion of PIR-2 with an allogeneic "universal fuser" A9HT (clone 3c) resulted in the establishment of a somatic cell hybrid designated A9/PIR. C57BL/6 lymphocytes sensitized in vitro with A9/PIR could lyse parental PIR-2 cells, as well as other syngeneic tumors. However, immunization of mice with the hybrid significantly enhanced PIR-2 tumor takes while it partially protected the animals against a challenge with unrelated syngeneic tumors. The results imply that somatic cell hybridization can increase the immunogenicity of an otherwise nonimmunogenic tumor. However, in view of the enhancing effects of hybrid preimmunization on parental tumor cell growth, the possible application of this approach for immunotherapy is questionable.—JNCI 1982; 68: 841–849.

Adult C57BL/6 mice exposed to fractionated irradiation or inoculated intrathymically with RadLV develop a high incidence of lymphatic leukemias after a latent period of 3–6 months (*1*). Previous studies in our laboratory have demonstrated that RadLV-induced thymomas may elicit syngeneic antitumor cell-mediated immunity in vitro, which is induced by and is directed at virus-associated antigens expressed on the tumor cell membrane (*2, 3*). In contrast, X-ray-induced primary thymomas do not express virus-related antigenicity and are not immunogenic in vitro.

Since it has recently been reported that rejection of a nonimmunogenic murine lymphoma could be induced by immunization with somatic cell hybrids (*4*), we decided to investigate whether host immune unresponsiveness toward X-ray-induced tumors could be overcome after immunization with a hybrid between a radiogenic leukemia and an allogeneic cell.

MATERIALS AND METHODS

Animals.—Female inbred C57BL/6 mice 5–6 weeks old at the start of the experiments were used. The mice were obtained from the animal facilities of the Hebrew University-Hadassah Medical Center, Jerusalem.

Antisera.—Anti-H-2^b and anti-H-2^k alloantisera were produced by immunizing BALB/c mice with pooled spleen, kidney, and liver cell suspensions from C57BL/6 and C3H mice, respectively, at biweekly intervals over 20 weeks. Rat anti-RadLV was the gift of Dr. M. Haas, Salk Institute, La Jolla, Calif., and was prepared as described earlier (*5*). Goat anti-Rauscher gp70 and anti-p30 antibodies were provided by Dr. E. M. Fenyo, Karolinska Institute, Stockholm, and were prepared as described elsewhere (*6*). Anti-Thy 1.2 monoclonal antibody was the gift of Dr. P. Lake, University College, London, and was prepared as described in (*7*).

Cell lines.—EL-4 is a 7,12-dimethylbenz[*a*]anthracene-induced T-cell lymphoma of C57BL/6 origin (*8*), 136.5 is a RadLV-induced C57BL/6 thymoma (*9*), YBA is a Moloney virus-induced T-cell lymphoma of CBA ($H\text{-}2^k$) origin (*4*), and PIR-2 is a cell line established in our laboratory from an X-ray-induced C57BL/6 thymoma. PIR-2 cells survive perfectly in a medium supplemented with HAT but expire within 24–48 hours when subjected to 100 μM ouabain. The cell lines were grown in RPMI-1640 medium containing 10% FCS and antibiotics. A9HT (clone 3c) is a "universal fuser" derived from L-cells of C3H ($H\text{-}2^k$) origin. The isolation of this double mutant cell line, containing both dominant and recessive mutations, has been described elsewhere (*10*). The cells were routinely cultivated as monolayer cultures in DMEM supplemented with 7% FCS. To minimize reversion, we routinely added 50 µg 6-thioguanine/ml and 3 mM ouabain to the medium. A9HT cells cannot survive in medium containing HAT.

Fusion and selection of hybrids.—A subconfluent monolayer of A9HT cells in a 250-ml flask was rinsed twice with cold, serum-free, alkaline RPMI-1640, after which 1,000 hemagglutinating units of UV light-inactivated Sendai virus in 2 ml PBS was added and absorbed on ice for 30 minutes.

Twice-rinsed PIR-2 cells, (10^7) in 0.5 ml PBS were added to the monolayer. The flask was left on ice for 30 minutes and then transferred to 37°C for 60 minutes, when 20 ml DMEM supplemented with 10% FCS was added. The growth medium was supplemented with HAT-O 24 hours later.

Most of the cells expired within 72 hours, but a few survivors began to multiply after 7–10 days, and 3 weeks later these cells grew into colonies. The mass hybrid culture designated A9/PIR was not cloned. The cells grew as an easily detachable monolayer, which could be subcultured without trypsinization.

Chromosome analysis.—Cells in exponential phase were in-

ABBREVIATIONS USED: C'=complement; CI=cytotoxicity index; DMEM=Dulbecco's modified Earle's medium; FCS=fetal calf serum; HAT=hypoxanthine, aminopterin, and thymidine; HAT-O=HAT and 0.5 mM ouabain; MLTC=mixed lymphocyte-tumor culture; MuLV= murine leukemia virus; PBS=phosphate-buffered saline; RadLV=radiation leukemia virus; SR=specific release; TSA=tumor-specific antigen.

---

[1] Received July 28, 1981; accepted November 12, 1981.

[2] Supported in part by the Israel Cancer Research Fund; by the Leukemia Research Foundation, Inc., Chicago, Ill.; by Mr. and Mrs. Stewart Resnick, Los Angeles, Calif.; and by the Dr. "I" Fund, New York, N.Y.

[3] Animals were maintained under the guidelines set forth by The Hebrew University-Hadassah Medical School.

[4] The Lautenberg Center for General and Tumor Immunology, The Hebrew University-Hadassah Medical School, Jerusalem 91010, Israel.

[5] Faculty of Medicine, Technion-Israel Institute of Technology, Haifa 31096, Israel.

cubated with 0.3 μg Colcemid/ml (GIBCO, Grand Island, N.Y.) for 1 hour at 37°C, resuspended in a hypotonic 0.075-*M* potassium chloride solution for 20 minutes, and fixed in freshly prepared methanol:acetic acid 3:1 solution. Metaphase spreads were prepared by dropping the solution on chilled wet slides and staining with Giemsa (Fisher Scientific Co., Fair Lawn, N. J.) diluted 1:15 in 0.15 *M* phosphate buffer (pH 8.0). Metaphases were examined by high-power light microscopy, and the modal number of biarmed and total chromosomes was calculated on the basis of 10–20 metaphases.

Complement-dependent microcytotoxicity assay.—With the use of an automatic Hamilton syringe, aliquots of 3-μl antiserum dilutions containing 10^3 target cells were placed into rings of a microtray (Hamax, Moss, Norway) covered with paraffin oil. After 20 minutes of incubation at 4°C, 1 μl of rabbit C' diluted 1:6 was added to each ring, and the trays were incubated for another 45 minutes at 37°C. Subsequently, 1 μl of 0.4% trypan blue was added to each ring, and the proportion of living cells was determined under the light microscope. CI was calculated according to the formula: CI=% living cells in control−% living cells in test sample/% living cells in control.

Immunization.—Tumor cells (30×10^6) in a total volume of 0.2 ml, irradiated with 9,000 rad, were inoculated sc to both flanks of C57BL/6 mice.

Tumor cell challenge.—Various numbers of viable tumor cells were inoculated sc into control or preimmunized C57BL/6 mice 2 weeks after immunization.

MLTC.—Splenocytes from normal animals or animals that were preimmunized (primed) 10–14 days earlier were mixed in tissue culture flasks with irradiated (9,000 rad) tumor cells at a 10:1 responder:stimulator ratio under conditions described elsewhere (*11*). Mixed cultures were incubated for 6 days in a humidified atmosphere with 5% CO_2 at 37°C.

Lymphocyte-mediated cytotoxicity assay.—Following 6 days of incubation, mixed cultures were harvested and their cytotoxic activity was determined with the use of the 5-hour incubation $Na_2{}^{51}CrO_4$ release assay as described elsewhere (*12*). Percentage ^{51}Cr SR was calculated according to the formula: SR%=(release in test−spontaneous release/maximal release−spontaneous release)×100.

RESULTS

Chromosome analysis of parental and hybrid cell lines.—Typical metaphase plates of PIR-2, A9HT, and A9/PIR are shown in figures 1, 2, and 3, and the results obtained with 10–20 different metaphases of each line are summarized in table 1. The modal chromosome number of A9HT was 51 (range 45–57) with a mean of 22 biarmed chromosomes which served as markers for this cell line. Ten metaphases of PIR-2 showed 41 acrocentric chromosomes apparently due to a trisomy in chromosome 15, which is a common feature of murine T-cell lymphomas (*13*). A9/PIR had a mode of 82 chromosomes of which 21 were biarmed.

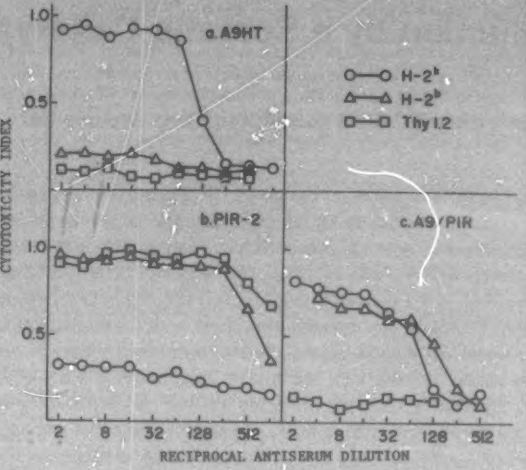

TEXT-FIGURE 1.—Expression of H-2 and Thy 1.2 alloantigens on parental and hybrid cells determined by C'-dependent microcytotoxicity assay. The initial antiserum dilutions were: anti-H-2^b, 1:10; anti-Thy 1.2, 1:1,000.

Membrane characteristics of parental and hybrid cell lines.—A9HT and PIR-2 expressed the *H-2^k* and *H-2^b* haplotypes, respectively (text-fig. 1). PIR-2 expressed the T-cell marker Thy 1.2 as well. Both *H-2^k* and *H-2^b* were expressed on the A9/PIR hybrid, whereas Thy 1.2 was not expressed. PIR-2 did not express virus-associated antigens on the cell membrane (text-fig. 2), whereas A9HT reacted with anti-gp70, p30, and RadLV antisera. The expression of virus-associated antigens was retained in the A9/PIR hybrid (text-fig. 2). The characteristics of the hybrid compared with those of the parental cell lines are summarized in table 1.

Inhibition of tumor growth in preimmunized recipients.—All C57BL/6 animals (5 of 5) developed tumors and subsequently succumbed when inoculated with 10^5 EL-4, 136.5, or PIR-2 cells (table 2). PIR-2 tumor growth was somewhat delayed when compared to EL-4 and 136.5 tumor growth; palpable tumors appeared later and the mice survived longer.

C57BL/6 mice could be partially protected against a challenge of 10^5 EL-4 or 136.5 cells if they were preimmunized with either EL-4 or 136.5 (table 2). Under such circumstances some of the animals remained tumor-free,

TABLE 1.—*Characteristics of parental and hybrid cell lines*[a]

Cell line	Survival in HAT-O	Adherence	No. of chromosomes (range)	No. of biarmed chromosomes (range)	H-2^b	H-2^k	Thy 1.2	gp70	p30	RadLV
A9HT	−	+++	51 (45–57)	22 (17–25)	−	+	−	+	+	+
PIR-2	−	−	41	0	+	−	+	−	−	−
A9HT/PIR	+	+	82 (72–87)	21 (18–23)	+	+	−	+	+	+

[a] +=positive, +++=notable, −=negative.

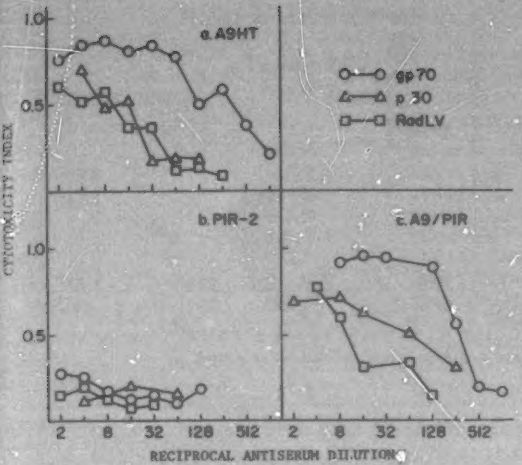

TEXT-FIGURE 2.—Expression of MuLV-associated antigens on parental and hybrid cells determined by C′-dependent microcytotoxicity assay. The initial antiserum dilutions were: anti-gp70 and p30, 1:50; anti-RadLV, 1:5.

and tumor takes in the rest were significantly delayed. However, mice preimmunized with EL-4 or 136.5 were not protected against a challenge with PIR-2 cells. Immunization with PIR-2 cells did not inhibit tumor growth after challenge with either EL-4, 136.5, or PIR-2 itself.

Effect of irradiation on tumor takes.—EL-4 tumor growth was significantly enhanced in C57BL/6 animals that had been exposed to 400 rad whole-body irradiation 24 hours before challenge (table 3). Preirradiation of PIR-2 recipients had no effect on tumor appearance or survival.

Generation of antitumor cytotoxicity in vitro.—We have previously shown (*2*) that generation of cytotoxicity in C57BL/6 lymphocytes responding to syngeneic RadLV-induced tumors is dependent on preimmunization of the responder cell donor with the appropriate tumor cells. In vitro sensitization of C57BL/6 splenocytes with either 136.5 or EL-4 cells after in vivo priming resulted in the generation of cytotoxicity

TABLE 3.—*Takes of EL-4 and PIR-2 tumors in sublethally irradiated C57BL/6 mice*

Pretreatment, rad[a], [b]	Challenge[c]	Tumor takes, No./total	Tumor appearance after challenge, mean days (range)[c]	Survival time after challenge, mean days (range)[d]	Significance level of survival[b], [e]
—	EL-4	6/6	11.0 (9–13)	23.5 (20–27)	—
—	PIR-2	5/6	20.0 (18–24)	36.0 (33–39)	—
400	EL-4	6/6	8.0 (5–10)	17.2 (14–21)	$P<0.005$
400	PIR-2	6/6	20.3 (17–24)	35.7 (32–38)	NS

[a] Whole-body irradiation 24 hr before challenge.

[b] —=controls.

[c] Viable cells (10^5) injected sc.

[d] Tumor-free mice were excluded.

[e] Evaluated by Student's *t*-test. NS=not significant.

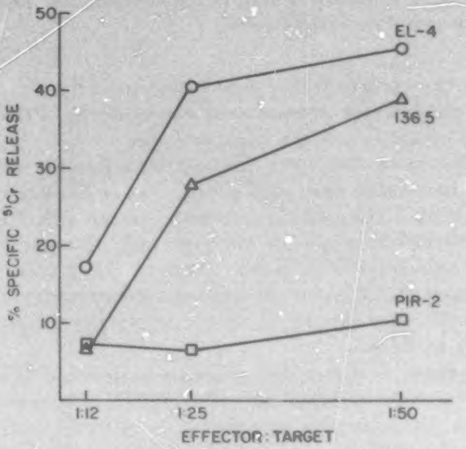

TEXT-FIGURE 3.—Generation of antitumor cytotoxicity in syngeneic lymphocytes. EL-4-, 136.5-, and PIR-2-primed C57BL/6 splenocytes were cocultivated with the corresponding tumor cells. Cytotoxicity was determined with the use of ^{51}Cr-labeled EL-4, 136.5, and PIR-2, respectively.

TABLE 2.—*Protection of tumor growth in syngeneic mice by preimmunization with different cell lines*

Immunization[a], [b]	Challenge[c]	Tumor takes, No./total	Tumor appearance after challenge, mean days (range)[d]	Survival time after challenge, mean days (range)[d]	Significance level of survival[b], [e]
—	EL-4	5/5	8.8 (7–11)	23.6 (21–26)	—
—	136.5	5/5	11.6 (11–13)	23.4 (22–25)	—
—	PIR-2	5/5	18.6 (17–20)	36.4 (35–38)	—
EL-4	EL-4	2/5	17.0 (16–18)	36.0 (33–39)	$P<0.005$
EL-4	136.5	2/5	15.0 (29–31)	31.0 (29–33)	$P<0.005$
EL-4	PIR-2	5/5	22.8 (16–20)	35.6 (31–40)	NS
136.5	EL-4	3/5	16.0 (15–18)	32.3 (31–34)	$P<0.001$
136.5	136.5	4/5	14.2 (12–17)	29.5 (28–32)	$P<0.001$
136.5	PIR-2	5/5	20.2 (17–22)	34.8 (33–36)	NS
PIR-2	EL-4	5/5	8.8 (8–10)	21.2 (20–23)	NS
PIR-2	136.5	5/5	10.8 (10–12)	22.2 (20–23)	NS
PIR-2	PIR-2	5/5	19.8 (19–20)	35.2 (31–37)	NS

[a] Heavily irradiated cells (2×10^7) injected sc.

[b] —=controls.

[c] Viable cells (10^5) injected sc.

[d] Tumor-free mice were excluded.

[e] Evaluated by Student's *t*-test. NS=not significant.

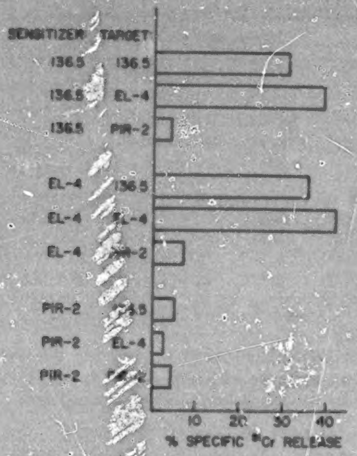

TEXT-FIGURE 4.—Cytotoxic activity of 136.5-primed lymphocytes sensitized in vitro with syngeneic tumors.

toward the corresponding tumor line (text-fig. 3). In contrast, lymphocytes primed and sensitized by PIR-2 cells showed no antitumor cytotoxic activity.

Lymphocytes that were 136.5 primed became cytotoxic when sensitized in vitro with either 136.5 or EL-4 cells (text-fig. 4). Both 136.5 and EL-4 targets, but not PIR-2 targets, were susceptible to lysis by cytotoxic cells obtained from in vitro stimulation with either 136.5 or EL-4 cells. When splenocytes of 136.5-primed animals were cocultivated with PIR-2 cells, they showed no cytotoxic activity toward PIR-2, 136.5, or EL-4.

Text-figure 5 shows the cytotoxic activity of C57BL/6 lymphocytes cocultivated with the A9/PIR hybrid or parental lines. Lymphocytes stimulated by A9/PIR could efficiently lyse PIR-2 as well as EL-4 targets. Considerable cytotoxic activity was also observed against YBA cells which share the *H-2*^{k} haplotype with A9HT. C57BL/6 splenocytes

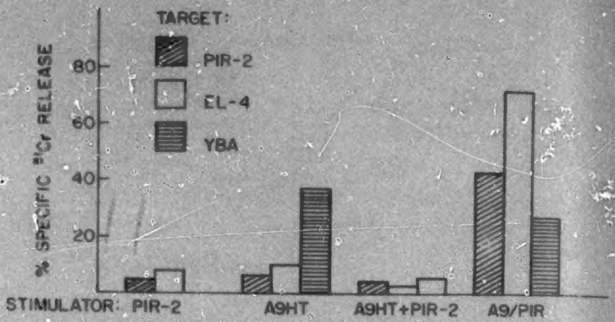

TEXT-FIGURE 5.—Cytotoxic activity of C57BL/6 lymphocytes stimulated in vitro with parental and hybrid cell lines.

sensitized by A9HT cells were cytotoxic toward YBA targets but not to EL-4 or PIR-2 targets. Sensitization with PIR-2 or with a mixture of PIR-2 and A9HT cells did not result in generation of cytotoxicity.

Effect of immunization with A9/PIR on tumor growth.—All control C57BL/6 animals (100%) developed tumors and subsequently died when inoculated sc with either 10^4, 10^5, 10^6 EL-4 cells (table 4, text-fig. 6). When the mice were preimmunized with A9/PIR cells, a partial protection against EL-4 tumor growth was observed; some animals remained tumor-free, and in the rest tumor development and death were significantly delayed. Preimmunization with A9HT, PIR-2, or a mixture of A9HT and PIR-2 cells was not protective. Similar results were obtained with C57BL/6 animals challenged with 136.5 cells (results not shown).

However, A9/PIR preimmunized mice inoculated with PIR-2 cells showed enhancement of tumor growth and animal death (table 5, text-fig. 7). The enhancing effect was significant when 10^5 and 10^6 PIR-2 cells were inoculated, whereas tumors in A9/PIR immunized animals challenged with 10^4 or 10^7 cells did not develop faster than tumors in control mice. The protective effect against EL-4 and the

TABLE 4.—*Effect of immunization by hybrid and parental cell lines on EL-4 tumor growth*

Immunization[a]	No. of EL-4 cells inoculated sc[b]	Tumor takes, No./total	Palpable tumor first detected, mean days ± SE (range)[c]	Tumor diameter, mean mm ± SE (range)[d]	Survival days of tumor-bearing mice, mean ± SE (range)[e]	Significance level of survival[a,f]
—	10^4	8/8	10.6±0.6 (8–13)	14.1±1.7 (8–21)	24.8±0.7 (22–27)	—
A9/PIR	10^4	5/8	12.6±1.2 (9–15)	11.6±3.2 (1–20)	29.2±1.5 (24–33)	$P<0.025$
A9HT+PIR-2	10^4	8/8	9.8±0.8 (8–13)	15.2±2.0 (8–22)	24.1±0.9 (21–26)	NS
A9HT	10^4	8/8	10.2±0.6 (8–12)	14.2±1.7 (7–20)	24.6±1.1 (21–28)	NS
PIR-2	10^4	8/8	9.8±0.3 (9–11)	14.7±2.0 (6–20)	23.3±1.2 (21–29)	NS
—	10^5	8/8	9.5±0.5 (8–10)	15.6±1.8 (10–23)	21.4±0.5 (20–24)	—
A9/PIR	10^5	4/8	11.5±1.2 (9–15)	10.7±3.9 (2–21)	41.8±4.4 (32–53)	$P<0.001$
A9HT+PIR-2	10^5	8/8	8.9±0.5 (7–11)	14.5±1.9 (9–23)	22.0±0.3 (21–23)	NS
A9HT	10^5	7/7	9.7±0.6 (8–12)	15.4±2.1 (7–22)	22.0±0.5 (19–23)	NS
PIR-2	10^5	7/7	8.6±0.4 (7–10)	15.9±2.3 (8–24)	22.0±0.5 (20–23)	NS
—	10^6	7/7	9.0±0.6 (7–11)	17.3±1.9 (11–25)	21.1±0.6 (18–22)	—
A9/PIR	10^6	6/8	12.2±0.6 (10–14)	12.6±2.9 (2–22)	29.7±2.9 (22–37)	$P<0.01$
A9HT+PIR-2	10^6	7/7	8.9±0.5 (7–10)	18.0±2.0 (10–24)	21.6±0.8 (19–24)	NS

[a] —=controls.
[b] 13 days after immunization.
[c] Days after EL-4 inoculation; tumor-free mice were excluded.
[d] Measured on tumor-bearing animals at day 17 after EL-4 inoculation.
[e] Days after EL-4 inoculation.
[f] Evaluated by Student's *t*-test; tumor-free mice were excluded. NS=not significant.

TABLE 5.—*Effect of immunization by hybrid and parental cell lines on PIR-2 tumor growth*

Immunization[a]	No. of PIR-2 cells inoculated sc[b]	Tumor takes No./total	Palpable tumor first detected, mean days ± SE (range)[c]	Tumor diameter, mean mm ± SE (range)[d]	Survival days of tumor-bearing mice, mean ± SE (range)[e]	Significance level of survival[a, f]
—	10^4	5/8	24.2±1.2 (21–28)	6.8±1.7 (2–9)	35.2±1.1 (33–39)	—
A9/PIR	10^4	6/8	18.5±0.9 (16–21)	14.6±1.6 (11–19)	33.5±0.9 (30–36)	NS
A9HT+PIR-2	10^4	6/8	23.9±1.3 (20–27)	7.3±1.2 (3–10)	36.7±1.3 (32–40)	NS
A9HT	10^4	4/8	23.2±2.0 (19–28)	6.7±2.1 (2–12)	34.7±1.2 (32–38)	NS
PIR-2	10^4	5/8	24.0±1.1 (21–27)	5.8±1.3 (3–10)	35.8±1.4 (33–40)	NS
—	10^5	6/7	26.0±1.5 (21–30)	6.5±2.1 (1–14)	40.7±1.6 (34–45)	—
A9/PIR	10^5	7/7	17.0±1.0 (14–21)	17.0	25.9±2.1 (21–34)	$P<0.001$
A9HT+PIR-2	10^5	7/7	25.3±1.3 (20–29)	7.3±1.8 (2–15)	39.1±1.4 (35–44)	NS
A9HT	10^5	7/7	25.3±1.7 (18–31)	6.7±1.7 (2–13)	39.9±1.7 (34–45)	NS
PIR-2	10^5	6/6	25.2±1.6 (20–30)	7.3±2.1 (1–15)	37.8±2.0 (31–44)	NS
—	10^6	7/7	18.0±1.6 (13–25)	12.0±1.8 (5–17)	38.1±1.6 (32–43)	—
A9/PIR	10^6	7/7	13.6±1.0 (11–17)	16.7±1.7 (12–19)	29.7±1.8 (21–35)	$P<0.005$
A9HT+PIR-2	10^6	6/6	17.7±1.3 (15–23)	8.6±1.1 (6–11)	37.5±1.5 (34–42)	NS

[a] —=controls.

[b] 13 days after immunization.

[c] Days after PIR-2 inoculation; tumor-free mice were exluded.

[d] Measured on tumor-bearing animals alive at day 30 after PIR-2 inoculation.

[e] Days after PIR-2 inoculation.

[f] Evaluated by Student's *t*-test; tumor-free mice were excluded. NS=not significant.

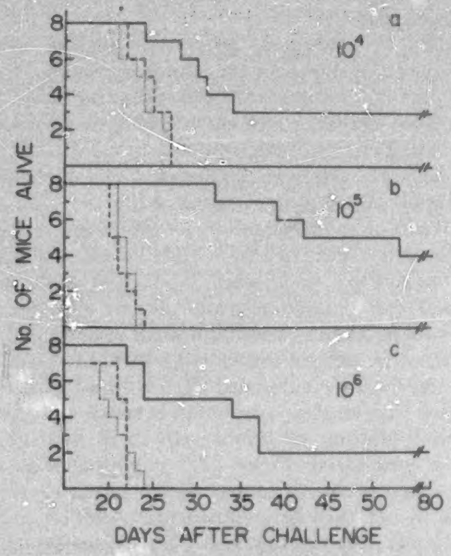

TEXT-FIGURE 6.—Survival of C57BL/6 mice preimmunized with parental or hybrid cells and challenged with EL-4. ·········, nonimmunized (control) mice; ------------, mice preimmunized with A9HT+PIR-2 cells; ————, mice preimmunized with A9/PIR-2 cells.

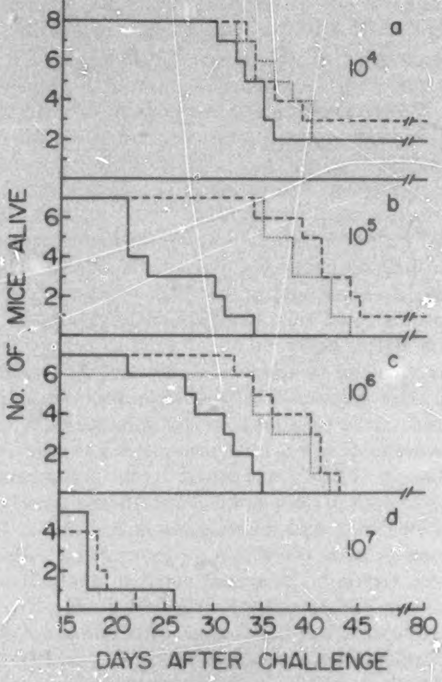

TEXT-FIGURE 7.—Survival of C57BL/6 mice preimmunized with parental or hybrid cells and challenged with PIR-2. ·········, nonimmunized (control) mice; ------------, mice preimmunized with A9HT+PIR-2 cells; ————, mice preimmunized with A9/PIR hybrid cells.

enhancement of PIR-2 tumor growth were optimal when the A9/PIR immunized mice were challenged with 10^5 cells.

DISCUSSION

The demonstration that many experimental tumors can elicit immune responses in syngeneic hosts raised the possibility of immunologic intervention in the process of neoplasia (*14, 15*). The relevance of this approach, however, had been disputed in view of recent studies that suggest that spontaneously arising tumors are, in most cases, nonimmunogenic (*16, 17*). In fact, experiments that clearly demonstrate specific antitumor immunity have been mainly restricted to virally and chemically induced laboratory tumors (*18, 19*).

Klein and Klein (*20*) have proposed that immune surveillance against virus-induced tumors involves preselection of immune response genes favoring rejection responses directed against virus-associated antigens. The nonrejectabil-

best copy available

ity of spontaneous tumors may thus be attributed to the lack of such immune response gene preselection. According to this view, antigenic modification of the tumor cell membrane might prove useful in overcoming the genetically determined immune unresponsiveness of the host. Indeed, it has been shown that viral xenogenization (*21, 22*), chemical modification (*23*), and somatic cell hybridization (*4*) could significantly increase the immunogenicity of otherwise weakly immunogenic tumors.

In a previous study (*2*) we investigated the in vitro induction of cell-mediated immunity against radiation- and RadLV-induced leukemias. It was found that generation of cytotoxic T-cells against syngeneic RadLV-infected tumors required preimmunization (priming) of the responding lymphocyte donor with the corresponding tumor cells. The cytotoxic response was induced by and directed at virus-associated antigens expressed on the tumor cell membrane. X-ray-induced tumors did not express virus antigenicity and were therefore resistant to cytotoxicity.

We have established several cell lines, derived from X-ray-induced thymomas of C57BL/6 origin, that remained virus-negative during propagation in vitro. The characteristics of one cell line, designated PIR-2, are documented in the present study. PIR-2 expressed the serologically defined H-2^b alloantigens, as well as the T-cell marker Thy 1.2. It does not react with anti-RadLV, anti-gp70, and anti-p30 antisera. In vivo priming and subsequent in vitro sensitization of C57BL/6 lymphocytes with PIR-2 do not result in the generation of anti-PIR-2 cytotoxic cells. With the use of the same procedure, 136.5 and EL-4 tumor lines, known to express C-type virus antigenicity (*2, 9*), could efficiently induce antitumor cytotoxic responses. Furthermore, cytotoxic lymphocytes generated against 136.5 or EL-4 lyse both 136.5 and EL-4 tumors but not PIR-2 targets, and neither of the lines is lysed by 136.5-primed lymphocytes cocultivated with PIR-2 cells.

Immunogenicity of tumors in vivo can be evaluated by the antitumor protective effect of preimmunization with inactivated tumor cells and by the enhancement of tumor growth in animals whose immune system has been impaired by irradiation. PIR-2 was found to be nonimmunogenic according to both of these criteria. Immunization of C57BL/6 mice with PIR-2 had no effect on either PIR-2, EL-4, or 136.5 tumor growth, whereas mice immunized with EL-4 or 136.5 were partially protected against a challenge with either EL-4 or 136.5, but not with PIR-2 cells. Exposure of mice to 400 rad whole-body irradiation enhanced the takes of EL-4 tumors, whereas there was no effect on PIR-2 tumor growth.

It was therefore of interest to determine whether the PIR-2 thymoma could be rendered immunogenic after hybridization with an allogeneic tumor cell. For this purpose, PIR-2 cells were fused with the universal fuser A9HT, and establishment of the A9/PIR somatic cell hybrid was confirmed by chromosome analysis and the coexpression of H-2^b and H-2^k alloantigens. The MuLV-related antigens present on A9HT were fully expressed on the hybrid. In contrast, the Thy 1.2 antigen of PIR-2 was not detected in A9/PIR.

We initially investigated the ability of A9/PIR to induce cytotoxic responses in vitro. When C57BL/6 lymphocytes were sensitized with irradiated A9/PIR cells, cytotoxic lymphocytes capable of lysing PIR-2, EL-4, and YBA (that share the *H-2^k* haplotype with A9HT) were generated. YBA cells were used as targets for detection of anti-*H-2^k* allocytotoxicity since A9HT cells could not be efficiently labeled by $Na_2{}^{51}CrO_4$; background isotope release exceeded 40% during the cytolysis assay (5 hr). Cocultivation of C57BL/6 lymphocytes with A9HT or a mixture of A9HT + PIR-2 did not result in generation of anti-PIR-2 cytotoxicity. It thus appears that after hybridization with A9HT, PIR-2 acquired the ability to stimulate cytotoxic lymphocytes capable of recognizing and lysing parental PIR-2 cells. The generation of cytotoxicity by the A9/PIR hybrid did not require preimmunization of the responding lymphocyte donor. Several possibilities may account for this observation: *1*) Low expression of a putative TSA on PIR-2 is increased after hybridization to a level sufficient for stimulation of cytotoxic lymphocytes; *2*) the allogeneic A9HT cell membrane acts as an adjuvant for the TSA of PIR-2; *3*) the responding lymphocytes are stimulated by a modified TSA expressed on the hybrid and can still recognize original, nonimmunogenic TSA on parental PIR-2 cells, bringing about their lysis.

Cytotoxic lymphocytes generated against syngeneic MuLV-infected tumor cells are mainly stimulated by virus-modified self H-2 antigens (*24–26*). Since both MuLV and H-2^b antigens are expressed on A9/PIR, it is conceivable that the anti-EL-4 cytotoxic response of C57BL/6 lymphocytes sensitized by the hybrid is directed against the MuLV-H-2^b complex also expressed on EL-4 (*2*).

After the in vitro investigation we proceeded to study the immunogenicity of the hybrid in vivo. For this purpose, A9/PIR-preimmunized mice were inoculated with different numbers of viable tumor cells, and the rate of tumor growth was evaluated. Preimmunization with the hybrid had a protective effect against a challenge with EL-4 and 136.5, while it significantly enhanced PIR-2 tumor growth. This observation implies that correlation between cytotoxicity in vitro and inhibition of tumor growth in vivo obviously cannot be postulated. Prehn (*27*) suggested that a weak immune reaction may stimulate tumor growth rather than inhibit it. It can thus be assumed that A9/PIR induced a weak immune response against TSA expressed on PIR-2 resulting in stimulation of PIR-2 tumor growth. In contrast, the virus-related anti-EL-4 and 136.5 response generated by the hybrid is stronger and therefore sufficient to inhibit tumor growth.

The effectiveness of immunization with A9/PIR on both EL-4 and PIR-2 takes was dependent on the dose of inoculated viable tumor cells. An optimal inhibition and enhancement of EL-4 and PIR-2, respectively, was achieved when the animals were challenged with 10^6 cells. Preimmunization with the hybrid was less effective when larger or smaller doses of tumor cells were injected, suggesting that a very high or low tumor inoculum may more easily escape the impact of a preexisting immune response.

In conclusion, our results clearly demonstrate that a nonimmunogenic tumor modified by somatic cell hybridization can be rendered immunogenic. However, a possible application of this approach for immunotherapy is questionable in view of the stimulatory effects of hybrid preimmunization on parental tumor cell growth.

REFERENCES

(*1*) Haran-Ghera N, Peled A. Induction of leukemia in mice by irradiation and by radiation leukemia virus variants. Adv Cancer Res 1979; 30:45–87.

(*2*) Yefenof E, Tcharkirov R, Kedar E. In vitro generation of cytotoxic lymphocytes against radiation- and radiation leukemia virus-induced tumors. I. Role of viral antigenicity. Cancer Immunol Immunother 1980; 8:171–178.

(*3*) Yefenof E, Meidav A, Kedar E. In vitro generation of cytotoxic lymphocytes against radiation and radiation leukemia virus-induced tumors. III. Suppression of antitumor immunity in vitro by lymphocytes of mice undergoing radiation leukemia virus-induced leukemogenesis. J Exp Med 1980; 152:1473–1483.

(*4*) Klein G, Klein E. Induction of tumor cell rejection in the low responsive YAC lymphoma strain A host combination by immunization with somatic cell hybrids. Eur J Cancer 1979; 15:551–557.

(*5*) Haas M. Transient virus expression during murine leukemia induction by X-irradiation. J Natl Cancer Inst 1977; 58:251–257.

(*6*) Fenyö EM, Yefenof E, Klein E, Klein G. Immunization of mice with syngeneic Moloney lymphoma cells induces separate antibodies against virion envelope glycoprotein and virus induced cell surface antigens. J Exp Med 1977; 146:1521–1535.

(*7*) Lake P, Clark EA, Khorshid M, Sunshine G. Production and characterization of cytotoxic Thy-1 antibody secreting hybrid cell lines. Detection of T cell subsets. Eur J Immunol 1979; 9:875–886.

(*8*) Gorer PA. Studies in antibody response of mice to tumour inoculation. Br J Cancer 1950; 4:372–379.

(*9*) Haas M. Continuous production of radiation leukemia virus in C57BL thymoma tissue culture lines: Purification of the leukemogenic virus. Cell 1974; 1:79–83.

(*10*) Ber R, Wiener F, Fenyö EM. Proof of in vivo fusions of murine tumor cells with host cells by universal fusers. J Natl Cancer Inst 1978; 60:931–933.

(*11*) Kedar E, Schwartzbach M, Hefetz S, Raanan Z. Adoptive immunotherapy of leukemia in mice with lymphocytes sensitized in vitro to leukemia cells. Cancer Immunol Immunother 1978; 4:151–159.

(*12*) Kedar E, Unger E, Schwartzbach M. Optimization of tissue culture conditions for the generation of cytotoxic lymphocytes. J Immunol Methods 1976; 13:1–19.

(*13*) Spira J, Wiener F, Ohno S, Klein G. Is trisomy cause or consequence of murine T cell leukemia development? Studies on Robertsonian translocation mice. Proc Nat Acad Sci USA 1979; 76:6619–6621.

(*14*) Rosenberg SA, Terry WO. Passive immunotherapy of cancer in animals and man. Adv Cancer Res 1977; 25:323–388.

(*15*) Weiss DW. Tumor antigenicity and approaches to tumor immunotherapy. Berlin, Heidelberg, and New York: Springer-Verlag, 1980.

(*16*) Hewitt HB, Blake RR, Walder AS. A critique of the evidence for active host defence against cancer, based on personal studies of 27 murine tumours of spontaneous origin. Br J Cancer 1976; 33:241–259.

(*17*) Weiss DW. The questionable immunogenicity of certain neoplasms. Cancer Immunol Immunother 1977; 2:11–19.

(*18*) Baldwin RW. Immunological aspects of chemical carcinogenesis. Adv Cancer Res 1973; 18:1–75.

(*19*) Klein G. Immunological surveillance against neoplasia. Harvey Lect 1975; 69:71–102.

(*20*) Klein E, Klein G. Immune surveillance against virus-induced tumors and nonrejectability of spontaneous tumors: Contrasting consequences of host versus tumor evolution. Proc Natl Acad Sci USA 1977; 74:2121–2125.

(*21*) Kobayashi H, Takeichi N, Kuzumaki N. Xenogenization of tumor cells. In: Xenogenization of lymphocytes, erythroblasts and tumor cells. Hokkaido Univ Med Libr Ser. Vol 10. Sapporo, Japan: Hokkaido Univ School of Medicine, 1978:117–168.

(*22*) Kuzumaki N, Kobayashi H. Reduced transplantability of syngeneic mouse tumors superinfected with membrane viruses in *nu/nu* mice. Transplantation 1976; 22:545–550.

(*23*) Galili N, Naor D, Asjo B, Klein G. Induction of immune responsiveness in a genetically low-responsive tumor-host combination by chemical modification of the immunogen. Eur J Immunol 1976; 6:473–476.

(*24*) Shellam GR, Knight RA, Mitchison NA, Gorczynski RM, Maoz A. The specificity of effector T-cells activated by tumors induced by murine oncornaviruses. Transplant Rev 1976; 29:249–276.

(*25*) Levy JP, Leclerc JC. The murine sarcoma virus induced tumor: Exception or general model in tumor immunology? Adv Cancer Res 1977; 24:1–66.

(*26*) Zarling DA, Keshet I, Watson A, Bach FH. Association of mouse major histocompatibility and Rauscher murine leukemia virus envelope glycoprotein antigens on leukemia cells and their recognition by syngeneic virus immune cytotoxic T-lymphocytes. Scand J Immunol 1978; 8:497–508.

(*27*) Prehn RT. Do tumors grow because of the immune response of the host? Transplant Rev 1976; 28:34–42.

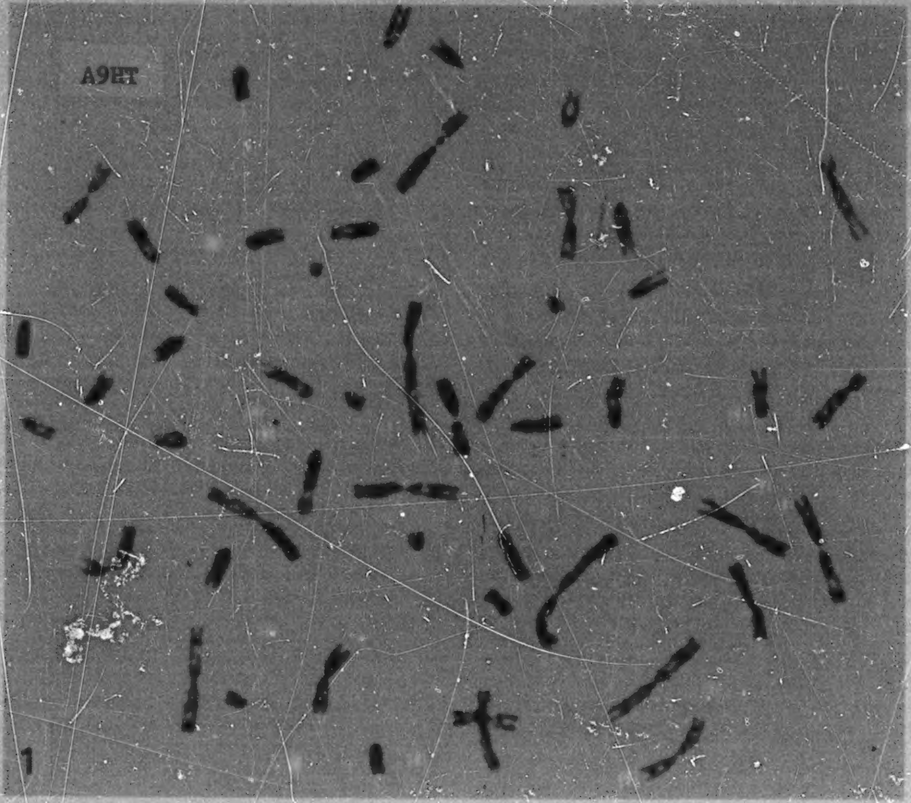

FIGURE 1.—Typical metaphase plate of the A9HT allogeneic universal fuser (30 acrocentric and 21 biarmed chromosomes).

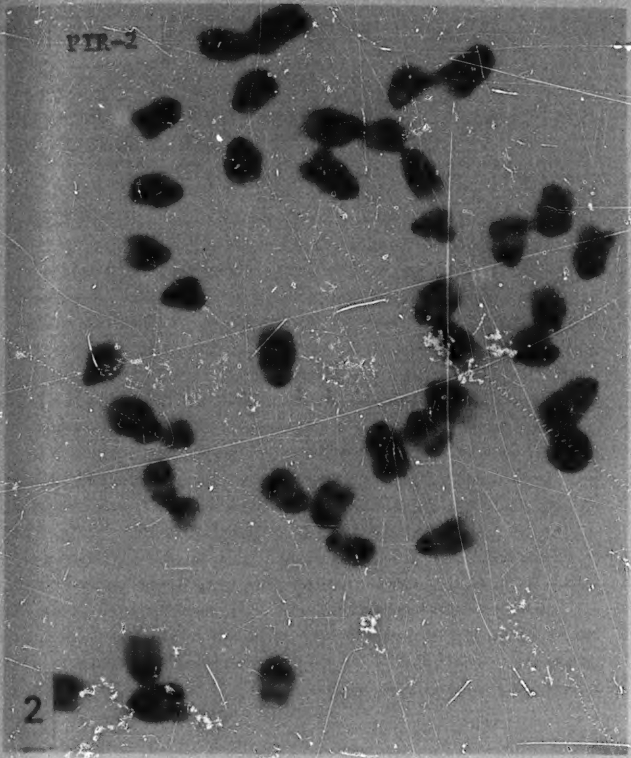

FIGURE 2.—Typical metaphase plate of the PIR-2 cell line (41 acrocentric chromosomes).

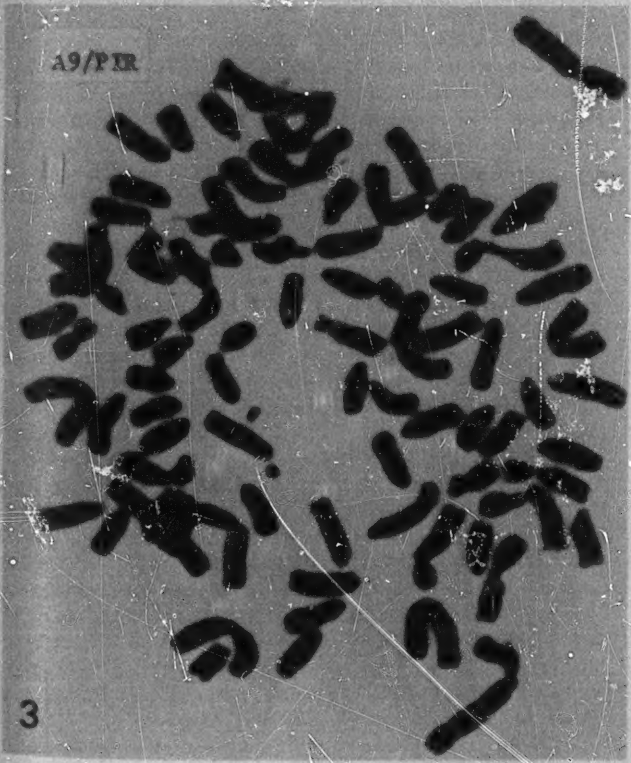

FIGURE 3.—Typical metaphase plate of the somatic cell hybrid A9/PIR (58 acrocentric and 22 biarmed chromosomes).

Purification and Transplantation of Hepatocytes From Livers of Carcinogen-Treated Rats[1,2,3]

Steven B. Miller,[4] Theresa P. Pretlow,[4,5] Joe A. Scott,[4] *and* Thomas G. Pretlow II[6,7]

ABSTRACT—Young adult male F344 rats were given 90 ppm diethylnitrosamine in drinking water for 5 weeks. Cells were obtained in suspension from the livers of these animals by in situ perfusion of collagenase. Cells were separated in a 2.7–16% (wt/wt) continuous gradient of Ficoll in tissue culture medium in the Sorvall TZ-28 reorienting zonal rotor for 10 minutes at 4°C with a centrifugal force of 12×*g* at the sample–gradient interface (26×*g* at the gradient–cushion interface). Up to half a billion liver cells were separated without exceeding the band capacity. In all experiments the purest fractions contained more than 90% hepatocytes. After centrifugation, 72.4±6.6% of the purified hepatocytes had histochemically demonstrable γ-glutamyl transpeptidase (GGT). When purified hepatocytes were injected into the mesenteric veins of rats given a diet containing 0.02% (wt/wt) *N*-2-fluorenylacetamide for 7 days and subjected to partial hepatectomy, all rats that received these cells developed foci that exhibited histochemically demonstrable GGT. Hepatocytes with histochemically demonstrable GGT make up all or part of what previously has been referred to as "liver colony-forming units." With the TZ-28 reorienting zonal rotor, these cells can be purified in biochemically preparative quantities.—JNCI 1982; 68:851–857.

The process of carcinogenesis involves at least two stages: initiation, which is irreversible and takes place over a short period of time, and promotion, which is at least partially reversible and takes place over an extended period of time [recently reviewed in (*1–5*)]. Although it is still useful to talk about the stages of initiation and promotion, it is now widely recognized that carcinogenesis is a multistep process (*1–3*). In hepatocarcinogenesis, enzyme-altered foci occur soon after the administration of carcinogens and long before carcinomas appear (*4–7*). In a recent review, Miller and Miller (*3*) stated: "The evidence suggests that these foci of hepatic cells are precursors of hepatic tumors, but whether or not some of the cells in these foci are neoplastic has not been determined." We do not know how closely any of the phenotypes of these enzyme-altered foci is linked to malignant transformation.

The purification of subpopulations of cells with defined rates of sedimentation from the livers of animals exposed to carcinogens makes available subpopulations with a limited range of phenotypic characteristics that can be readily determined. The orthotopic grafting of these phenotypically characterized subpopulations would permit their biologic activity to be tested, i.e., their ability to generate enzyme-altered foci and/or carcinomas in suitably prepared hosts. Recently, a technique (*8, 9*) has been developed for the transplantation of precursor cells during hepatocarcinogenesis into syngeneic host rats. We now report our use of this technique to test the ability of purified, enzyme-altered hepatocytes to form enzyme-altered colonies in the livers of syngeneic hosts. The method used for cell separation will permit the purification of as many as a half a billion liver cells in a single, 10-minute centrifugation.

MATERIALS AND METHODS

Animals.—Male F344 rats were obtained from animals bred and maintained in the University of Alabama in Birmingham animal facility from a strain originally obtained from the Charles River Breeding Laboratories (Wilmington, Mass.). The animals were housed at a maximum of 4 per cage and maintained on a 12-hour light cycle with free access to tap water. They were fed a standard laboratory diet (Wayne Lab-Blox-8604-00; Professional Animal Diet, Wayne Pet Food Co., Vinemont, Ala.) ad libitum.

Diet.—At 90–110 g, donor rats were continued on the standard laboratory pellets, but 60 (*10*) or 90 ppm DENA (Eastman Kodak Co., Rochester, N.Y.) was added to their drinking water. The animals received the DENA for 5 weeks ± 3 days. Fresh DENA in water was prepared and changed twice a week. The carcinogen was removed and replaced with tap water 72 hours prior to killing.

Rats that were to receive transplanted liver cells were allowed to achieve a weight of 150–250 g. Seven days prior to receiving transplanted cells, the host animals were placed on a 0.02% (wt/wt) 2-FAA diet (Bio-Serv Inc., Little Silver, N.J.) as used by Laishes and Rolfe (*9*). The transplantation of cells and partial hepatectomy were accomplished during the same laparotomy. Seven days after partial hepatectomy and injections of cells, the 2-FAA was discontinued, and the standard laboratory pellets were reinstituted.

ABBREVIATIONS USED: DENA=diethylnitrosamine; EGTA=ethyleneglycol-bis(β-aminoethyl ether)*N*,*N*′-tetraacetic acid; 2-FAA=*N*-2-fluorenylacetamide; GGT=γ-glutamyl transpeptidase; JMEM=Joklik's modification of Eagle's minimum essential medium.

---

[1] Received July 30, 1981; accepted December 11, 1981.

[2] Supported by Public Health Service grants CA-13148 and CA-23922 from the National Cancer Institute and by grant CD-142 from the American Cancer Society.

[3] Animals were maintained under the guidelines set forth by the University of Alabama in Birmingham.

[4] Department of Pathology, University of Alabama in Birmingham, Birmingham, Ala. 35294.

[5] *Address reprint requests to* Dr. Pretlow.

[6] Department of Pathology and Department of Biochemistry, University of Alabama in Birmingham.

[7] We thank Dr. George Michalopoulos, Duke University School of Medicine, Durham, N.C., for his advice regarding the preparation of liver cells in suspension and the use of collagen membranes to assess the viability of liver cells; and Mrs. Katherine Sexton, University of Alabama in Birmingham, for her excellent assistance in the preparation of this manuscript.

Suspensions of cells.—For each experiment 1–6 rats were used as donors. Suspensions of liver cells were prepared by a modification of the method of Berry and Friend (*11*). The animals were anesthetized with ether, the abdomen was opened, and the vena cava was entered inferior to the liver with an 18-gauge angiocatheter. A clamp was placed on the vena cava superior to the liver. Both the portal vein and hepatic artery were incised for drainage. With a peristaltic pump, the liver was perfused at a rate of 20 ml/minute with 50 ml of 5 m*M* EGTA (Sigma Chemical Co., St. Louis, Mo.) in JMEM (Grand Island Biological Co., Grand Island, N.Y.) followed by 250 ml of 0.05% collagenase (Worthington type I; Worthington Diagnostics Div., Millipore Corp., Freehold, N.J.) in JMEM at room temperature. Following perfusion, the liver was excised, weighed, minced to fragments of approximately 3 mm in greatest dimension, and incubated at 37°C in 20 ml of the described collagenase solution for 20 minutes. The liver fragments were then dispersed mechanically. The cells were centrifuged at 97×*g* for 7.5 minutes at 4°C, resuspended in cold 10% horse serum in JMEM, filtered through 40-µm Nitex (TETKO Inc., Elmsford, N.Y.), and counted with hemacytometer chambers. We assessed cell viability by observing the ability of cells to exclude trypan blue. In some experiments, the ability of liver cells to attach to collagen membranes was assessed.

Cell separation.—Liver cells were separated with a TZ-28 reorienting zonal rotor (Dupont Instruments, Sorvall Operations, Newtown, Conn.) in a Sorvall RC-5B refrigerated centrifuge (Dupont Instruments). Speed was monitored with a Sorvall Portac (Dupont Instruments). The cushion, gradient, and sample were loaded dynamically, while the speed of the rotor was 500 rpm. The 60-ml cushion was made of equal parts of a 32.8% (wt/vol) solution of sodium metrizoate (Hypaque; Nyegaard & Co., Oslo, Norway) and a 10% (wt/wt) solution of Ficoll (polysucrose; average mol wt, 400,000; Pharmacia Fine Chemicals, Piscataway, N.J.) in JMEM. A continuous Ficoll gradient was formed with a two-chambered gradient generator as previously described by Pretlow et al. (*12*) and later modified by Green et al. (*13*). The 1,250-ml gradient used in our experiments varied from 2.7% (wt/wt) Ficoll at the sample–gradient interface, 4.2 cm from the center of revolution, to 16% (wt/wt) Ficoll at the gradient–cushion interface, 9.3 cm from the center of revolution. The gradient was allowed to equilibrate in the rotor for 90 minutes at 4°C prior to use. When less than half a billion cells were separated, a 16-ml sample was used. When more than half a billion cells were separated, a 50-ml sample was used. The sample was dynamically loaded with a syringe in 10–30 seconds. The cells were sedimented at 500 rpm for 10 minutes at 4°C with a centrifugal force of 12×*g* at the sample–gradient interface. After centrifugation, the rotor was slowly decelerated over 10–15 minutes.

Gradient fractions.—We unloaded the gradient statically by siphoning 40-ml fractions at a rate of 40 ml/minute. Cell counts were performed on all fractions with hemacytometer chambers. Multiple sets of permanent slides were prepared from the starting sample and from each fraction with a Cytocentrifuge (Shandon Southern Instruments Inc., Sewickley, Pa.). The slides were stained in parallel with Wright-Giemsa stain and for GGT as described by Rutenberg et al. (*14*) and modified by Jacobs et al. (*15*). Differential counts of 500 cells were performed on each fraction. To confirm the linearity of the gradient, we measured refractive indices with the Abbe-3L refractometer (#33-45-58-01; Bausch & Lomb Inc., Rochester, N.Y.).

Transplantation of cells.—The four purest fractions (fractions 12–15) of hepatocytes from the separation of a half a billion liver cells were pooled in a 250-ml centrifuge tube and diluted with 100 ml of JMEM to decrease the viscosity. The cells were centrifuged at 97×*g* for 7.5 minutes at 4°C and resuspended in JMEM at a concentration of 1×10^6 cells/ml. The viabilities of the cell suspensions were estimated, and slides were prepared and stained as previously described. Cells were transplanted by the method of Laishes and Rolfe (*9*). On the 7th day of 2-FAA feeding, the host rats were anesthetized with ether, a midline abdominal incision was made, and a partial hepatectomy was performed by the method of Higgins and Anderson (*16*). A small loop of intestine was gently removed from the abdominal cavity. A mesenteric vein was isolated, and 1 ml of the cell suspension was infused through a 26-gauge needle over 20–30 seconds. The needle was withdrawn, and a small piece of Gelfoam (The Upjohn Co., Kalamazoo, Mich.) was gently held on the injection site until hemostasis was achieved. The loop of intestine was placed back into the abdominal cavity, and the abdomen was closed. On the 10th day after transplantation of cells, the host rats were killed by prolonged exposure to ether. The animals were weighed, and the livers were excised. Multiple slices of liver were taken for frozen sections. Two contiguous sections were taken from each slice to be stained for GGT activity and with hematoxylin and eosin.

RESULTS

Starting sample.—Animals that received 90 ppm DENA had a greater proportion of hepatocytes with histochemically demonstrable GGT than animals that received 60 ppm DENA and were used for all separation and transplantation experiments. We obtained an average of 355.3±65.3 million cells per liver; 87.7±4.8% of the cells excluded trypan blue. The starting sample suspensions of cells contained 52.4±12.0% hepatocytes, 32.1±7.8% other nucleated cells, and 15.5±5.2% erythrocytes as determined by morphologic evaluation of Wright-Giemsa-stained preparations. Similar preparations are illustrated in an earlier report (*15*). When stained for GGT, 68.4±10.3% of the hepatocytes exhibited activity. Of the nonhepatocytes, 3.8±1.7% had histochemically demonstrable GGT. These have been termed "type II cells," are probably oval cells, and were illustrated in a color plate published previously (*15*).

Rotor separation.—Between 188 and 517 million liver cells were separated without exceeding the band capacity. In those experiments when band capacity was not exceeded, the total recovery of cells was 93.8±2.5% of the cells introduced into the rotor. In all experiments, fractions were obtained that had more than 90% hepatocytes. When more than half a billion cells were introduced into the rotor, both the purity and the total recovery of cells decreased. The recovery from gradient centrifugations of 1.0, 1.5, and 2.4 billion cells was 77.9, 73.2, and 63.8%, respectively.

When 188–517 million liver cells were separated, the fractions containing the purest hepatocytes were located between fractions 4 and 15. In these fractions, 93.2±1.3% of the nucleated cells were hepatocytes. Up to fraction 20, over 80% of the cells were hepatocytes (text-fig. 1). When both 1.0 (not shown in text-fig. 1) and 1.5 billion cells were separated, it appeared that the gradient had been overloaded. As discussed previously (*12*), when the band capacity of a gradient is exceeded, cells sediment farther, i.e., to fractions containing more rapidly sedimenting cells. In the experiments in which we exceeded the band capacity, there was a broadening of the curves (text-fig. 1) with a shift of cells that sediment slowly under ideal conditions into fractions that ordinarily contain highly purified hepatocytes. With the overloading of the gradient and the loss of ideal conditions, there was a loss of purity in those fractions of rapidly sedimenting cells that previously contained mostly hepatocytes. The gradient was grossly overloaded when 2.4 billion cells were sedimented. The modal population of hepatocytes was shifted all the way down to fraction 11. There were 6 million nucleated cells in fraction 11 that were not hepatocytes, and they represented 10.2% of the nucleated cells in that fraction.

When estimated by dye exclusion, viability of hepatocytes in fractions 5-24 was always greater than 75%. Similar results were obtained when viability was assessed by attachment to collagen membranes at 24 hours. This observation is consistent with previous reports comparing these two methods (*17*). The large population of hepatocytes seen at the top of the gradient was mostly nonviable. This finding is consistent with the observation that dead cells sediment much less rapidly than viable cells (*12*). It is important to note that hepatocytes with and without GGT sediment similarly (text-fig. 2).

Transplantation of cells.—The combined and concentrated four purest fractions (fractions 12-15) of hepatocytes contained a sample for injection with 97.4±1.4% hepatocytes (excluding erythrocytes). After the cells had been washed, counted, and concentrated, the viability of the injected cells was 55.0±3.0%. The decreased viability resulted from the repeated centrifugations used to concentrate the cells. Frozen sections of all livers taken at the time of partial hepatectomy showed that there was almost no histochemically demonstrable GGT (fig. 1). As early as 4 days after injection, we were able to see periportal foci of cells with GGT. Twelve animals from three separate experiments survived until they were killed 10 days after transplantation. Livers from all 12 had numerous colonies with histochemically demonstrable GGT. The foci (fig. 2) appeared to be composed of hepatocytes (fig. 3). Control rats undergoing the same regimen as the hosts but without receiving the injection of cells failed

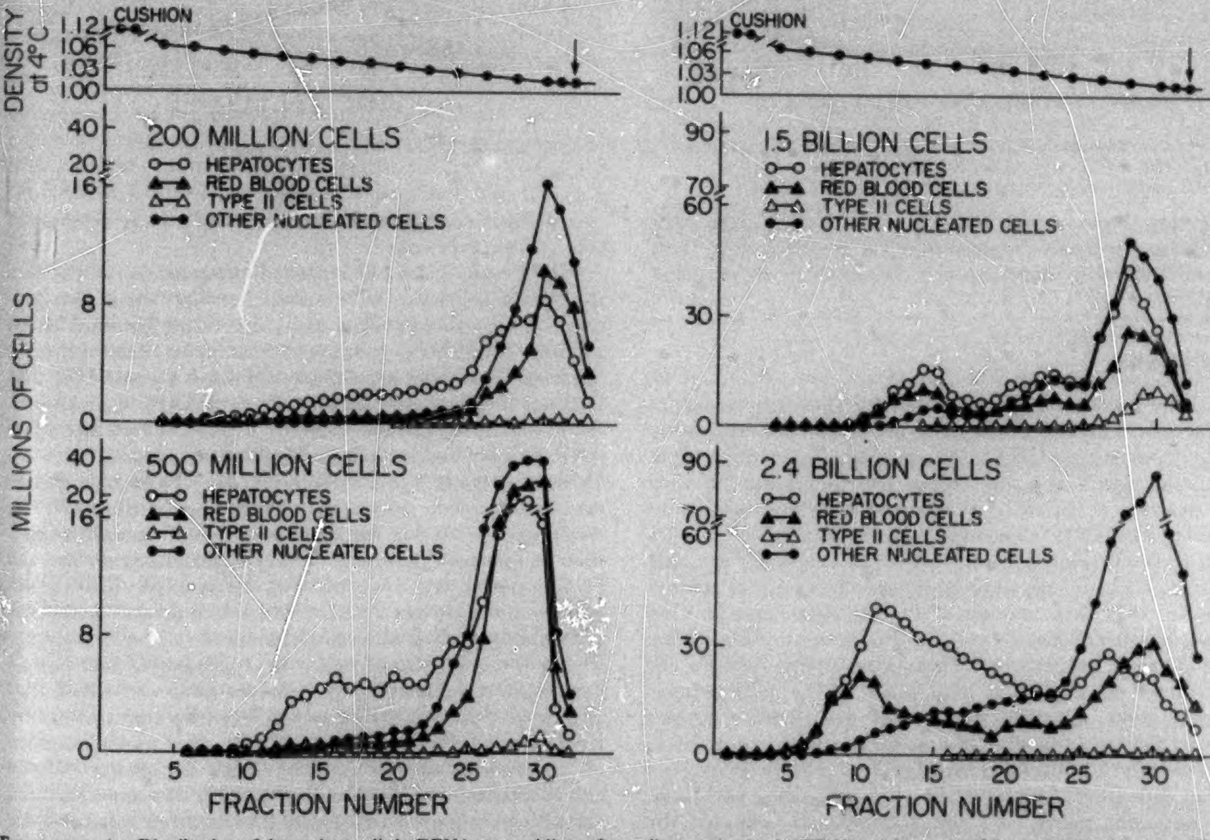

TEXT-FIGURE 1.—Distribution of the various cells in DENA-exposed liver after sedimentation in the TZ-28 zonal rotor at 4°C for 10 min with a centrifugal force of 12×*g* at the sample-gradient interface. Differential counts of 500 cells were performed on Wright-Giemsa-stained slides of each fraction. *Arrows* mark the sample-gradient interface on the density plots.

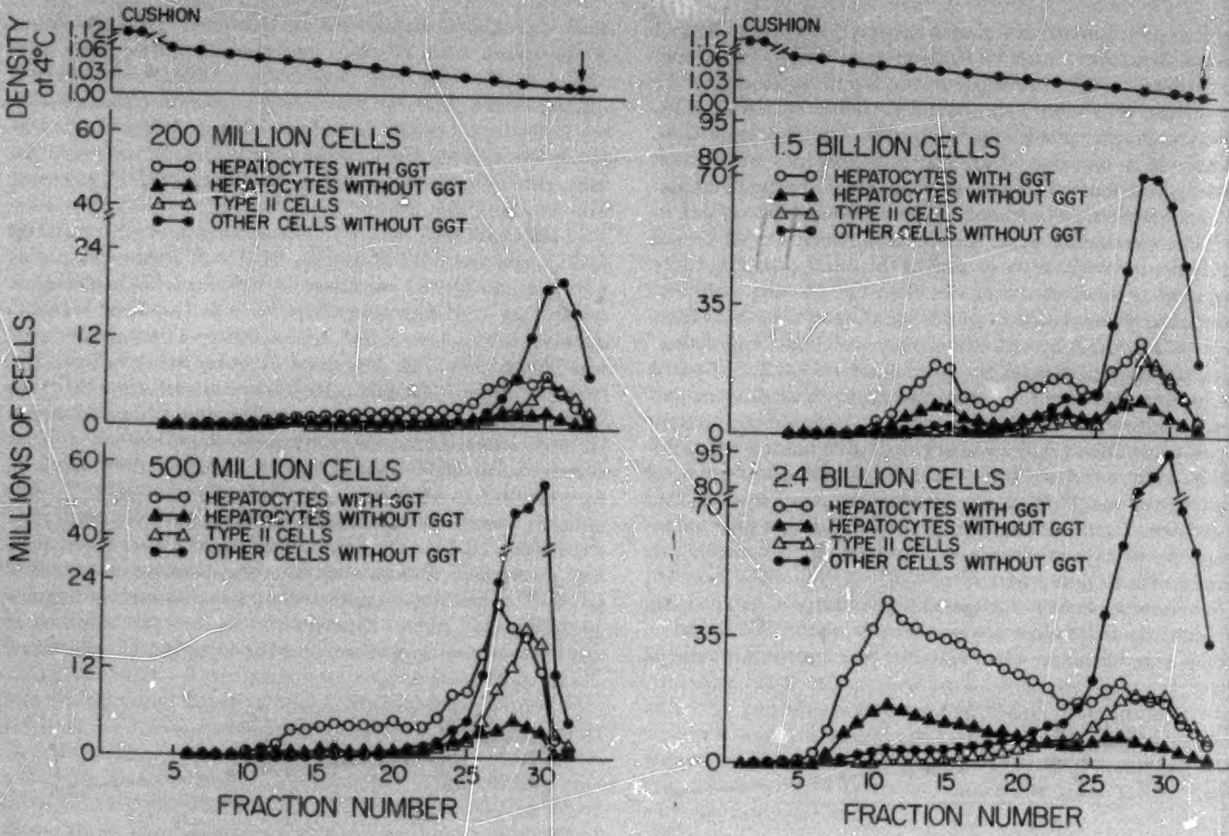

TEXT-FIGURE 2.—Distribution of the various cells based on GGT-stained slides of the same fractions illustrated in text-fig. 1.

to develop the same type of foci with GGT. Occasional cells with histochemically demonstrable GGT were seen in these control rats; this observation is discussed in more detail later.

DISCUSSION

Laishes and Rolfe (*9*) demonstrated that the transplantation of initiated liver cells gave rise to foci with histochemically demonstrable GGT and to hepatocellular carcinomas. The most significant correlation they found was between the number of viable cells injected and the number of colonies with GGT that were formed. Since they used a heterogeneous population of liver cells, they were not able to identify which cells were responsible for the liver colony-forming units they measured in their assay system. Our recipient rats developed colonies that were similar, but we used purified hepatocytes. These experiments provide the first direct proof that at least some of the liver colony-forming units described by Laishes and Rolfe (*9*) were derived from enzyme-altered hepatocytes. It does not, however, exclude additional types of cells as possible precursors of foci with GGT. Our work, like that of Laishes and Rolfe (*9*), does not prove "... that the injected cells are the progenitors of GT(+) colony cells"; exploration on that subject awaits the use of appropriate markers such as "... definitive cytogenetic markers to follow the progeny of colony precursor cells ..." (*9*).

While many have minimized the importance of the fact that 0.02% 2-FAA in the employed semisynthetic diet produces a variable but often easily detectable increase in the activity of GGT in rat livers, this point deserves some discussion. In citing a publication from his group (*18*) that includes the feeding of 0.02% 2-FAA (2-AAF) in a semisynthetic diet to F344 rats, Farber (*1*) states: "The dietary 2-AAF does not induce foci under these conditions, when fed for up to 4 weeks[16] [our reference (*18*)]." In fact, when one examines the data presented in chart 6 by Tsuda et al. (*18*), there is an increase in the number of hepatic foci with GGT that Tsuda et al. (*18*) term "a very slight increase when the feeding period was 4 weeks." On the average, this increase appears to be greater than threefold. Laishes and Rolfe (*19*) have discussed their observation that cells with GGT appear during the treatment of rats with 0.02% 2-FAA and partial hepatectomy as used by us; however, cells with GGT that appear on this diet are clearly different in size and nature from cells in colonies obtained 10 days after transplantation of hepatocytes with GGT. The "resolving power" of the image analyzer used by Tsuda et al. (*18*) was such that "the actual minimum size of a lesion that could be measured by this method was 0.2 mm in diameter." This threshold in size would exclude most of the cells with GGT in the livers of animals maintained on 0.02% 2-FAA without transplanted hepatocytes with GGT while including the majority of colonies arising from hepatocytes with GGT infused via the mesenteric veins as performed in our experiments.

In our experiments, we separated 12 times more liver cells than have been separated with other methods of velocity sedimentation (*20*) while maintaining equal purity of hepatocytes. The large numbers of purified hepatocytes can now be further purified into different subpopulations by additional, sequential techniques such as free-flow electrophoresis (*21*) and adherence chromatography. We would also like to separate the hepatocytes with GGT from the hepatocytes without this enzyme. Enzyme-altered hepatocytes have lost the ability to store iron (*6, 22*). Williams (*6*) has suggested that the administration of an iron overload to rats treated with carcinogens might alter the physical properties of the hepatocytes that accumulate iron and facilitate the use of physical methods for the purification of the enzyme-altered hepatocytes that do not accumulate iron.

We also observed a large population of nonviable hepatocytes at the top of the gradient. We suspect that, as a result of the carcinogen feeding, these hepatocytes are much more fragile than nonaltered hepatocytes. This view is supported by the fact that when normal liver cells are subjected to similar velocity sedimentations, this population is not seen (*20, 23*). The carcinogen regimen received by the animals to be used as donors was similar to that used previously (*10, 22*) except that we used 90 ppm DENA instead of 40 or 60 ppm DENA to obtain a larger proportion of hepatocytes with GGT. It provided large numbers of enzyme-altered hepatocytes while there was only minimal oval cell proliferation (*10, 22*). Three rats were observed over a period of several months after treatment with 90 ppm DENA. All 3 were killed when moribund and had multiple hepatomas. Two of these 3 animals had pulmonary metastases.

Reorienting gradient zonal centrifugation provides a method by which large quantities of cells and subcellular particles can be purified (*24*). In addition to the rotor's large capacity, the rotor offers the advantage that direct comparison has shown that a larger proportion of the cells from the starting sample are recovered from this rotor than can be recovered after isokinetic sedimentation (*13, 25*). The superior recovery of cells from the rotor results from its unique design that eliminates the wall effect seen with parallel-walled tubes (*12*).

In recent years this rotor has been used for the isolation of yeast in various phases of the cell cycle (*26*), calf thymus nuclei (*27*), rabbit renin granules (*28*), human blood and marrow cells (*29*), mouse ascitic tumor cells (*13, 30*), human tonsillar cells (*25*), and rat hepatocytes (*23*). Both Wells et al. (*29*) and Daugherty et al. (*25*) were able to culture their cells after they were purified in this rotor. When implanted into mice, separated malignant cells retained the capacity to form tumors (*13*). The large capacity and high recovery reported by these investigators suggested that this rotor can provide an effective means for purification of sufficient numbers of enzyme-altered hepatocytes to permit a detailed analysis of their biochemical and biologic characteristics. If one considers the large numbers of cells needed for many liver cell assays (*31, 32*), including our own, this rotor will facilitate studies that were not previously possible with purified enzyme-altered hepatocytes.

REFERENCES

(*1*) Farber E. The genesis of cancer with chemicals. Arch Pathol Lab Med 1980; 104:499–502.

(*2*) Pitot HC, Sirica AE. The stages of initiation and promotion in hepatocarcinogenesis. Biochim Biophys Acta 1980; 605:191–215.

(*3*) Miller EC, Miller JA. Mechanisms of chemical carcinogenesis. Cancer 1981; 47:1055–1064.

(*4*) Kitagawa T. Histochemical analysis of hyperplastic lesions and hepatomas of the liver of rats fed 2-fluorenylacetamide. Gan 1971; 62:207–216.

(*5*) Fiala S, Fiala ES. Activation by chemical carcinogens of γ-glutamyl transpeptidase in rat and mouse liver. J Natl Cancer Inst 1973; 51: 151–158.

(*6*) Williams GM. Functional markers and growth behavior of preneoplastic hepatocytes. Cancer Res 1976; 36:2540–2543.

(*7*) Shinozuka H, Lombardi B. Synergistic effect of a choline-devoid diet and phenobarbital in promoting the emergence of foci of γ-glutamyltranspeptidase-positive hepatocytes in the liver of carcinogen-treated rats. Cancer Res 1980; 40:3846–3849.

(*8*) Laishes BA, Farber E. Transfer of viable putative preneoplastic hepatocytes to the livers of syngeneic host rats. JNCI 1978; 61:507–512.

(*9*) Laishes BA, Rolfe PB. Quantitative assessment of liver colony formation and hepatocellular carcinoma incidence in rats receiving intravenous injections of isogeneic liver cells isolated during hepatocarcinogenesis. Cancer Res 1980; 40:4133–4143.

(*10*) Becker FF, Sell S. Differences in serum α-fetoprotein concentrations during the carcinogenic sequences resulting from exposure to diethylnitrosamine or acetylaminofluorene. Cancer Res 1979; 39:1437–1442.

(*11*) Berry MN, Friend DS. High-yield preparation of isolated rat liver parenchymal cells. J Cell Biol 1969; 43:506–520.

(*12*) Pretlow TG II, Weir EE, Zettergren JG. Problems connected with the separation of different kinds of cells. In: Richter GW, Epstein MA, eds. International review of experimental pathology. Vol 14. New York: Academic Press, 1975:91–204.

(*13*) Green CL, Pretlow TP, Tucker KA, et al. Large-capacity separation of malignant cells and lymphocytes from the Furth mast cell tumor in a reorienting zonal rotor. Cancer Res 1980; 40:1791–1796.

(*14*) Rutenburg AM, Kim H, Fischbein JW, Hanker JS, Wasserkrug HL, Seligman AM. Histochemical and ultrastructural demonstration of γ-glutamyl transpeptidase activity. J Histochem Cytochem 1969; 17:517–526.

(*15*) Jacobs JM, Pretlow TP, Fausto N, Pitts AM, Pretlow TG II. Separation of two populations of cells with gamma-glutamyl transpeptidase from carcinogen-treated rat liver. JNCI 1981; 66:967–973.

(*16*) Higgins GM, Anderson RM. Experimental pathology of the liver. I. Restoration of the liver of the white rat following partial surgical removal. Arch Pathol 1931; 12:186–202.

(*17*) Michalopoulos G, Pitot HC. Primary culture of parenchymal liver cells on collagen membranes. Exp Cell Res 1975; 94:70–78.

(*18*) Tsuda H, Lee G, Farber E. Induction of resistant hepatocytes as a new principle for a possible short-term in vivo test for carcinogens. Cancer Res 1980; 40:1157–1164.

(*19*) Laishes BA, Rolfe PB. Search for endogenous liver colony-forming units in F344 rats given a two-thirds hepatectomy during short-term feeding of 2-acetylaminofluorene. Cancer Res 1981; 41:1731–1741.

(*20*) Pretlow TG II, Williams EE. Separation of hepatocytes from suspensions of mouse liver cells using programmed gradient sedimentation in gradients of Ficoll in tissue culture medium. Anal Biochem 1973; 55:114–122.

(*21*) Pretlow TG II, Pretlow TP. Cell electrophoresis. In: Bourne GH, Danielli JF, eds. International review of cytology. Vol 61. New York: Academic Press, 1979:85–128.

(*22*) Williams GM, Yamamoto RS. Absence of stainable iron from preneoplastic and neoplastic lesions in rat liver with 8-hydroxyquinoline-induced siderosis. J Natl Cancer Inst 1972; 49:685–692.

(23) Pretlow TP, Dinwiddie WC Jr, Gorman SG, Pretlow TG II. Large-scale purification of hepatocytes in a reorienting zonal rotor. Fed Proc 1980; 39:284.

(24) Wells JR, Gross DM, Sheeler P. A large capacity re-orienting density gradient zonal centrifuge rotor. Lab Pract 1970; 19:497–499.

(25) Daugherty DF, Scott JA, Pretlow TG II. The separation of human palatine tonsillar cells in the reorienting gradient zonal rotor: A large-capacity enrichment of plasma cells. Clin Exp Immunol 1980; 42:370–377.

(26) Wells JR, James TW. Cell cycle analysis by culture fractionation. Exp Cell Res 1972; 75:465–474.

(27) Nixon JC, McCarty KS Jr, McCarty KS Sr. The use of a reorienting density-gradient rotor with continuous sample flow for the isolation of calf thymus nuclei. Anal Biochem 1973; 55:132–142.

(28) Gross DM, Barajas L. The large-scale isolation of renin-containing granules from rabbit renal cortex by zonal centrifugation. J Lab Clin Med 1975; 85:467–477.

(29) Wells JR, Opelz G, Cline MJ. Characterization of functionally distinct lymphoid and myeloid cells from human blood and bone marrow. II. Separation by velocity sedimentation. J Immunol Methods 1977; 18:79–93.

(30) Childress WJ, Freedman RI, Koprowski C, Doolittle MH, Sheeler P, Oppenheimer SB. Surface characteristics of separated subpopulations of mouse teratocarcinoma cells. Exp Cell Res 1979; 122:39–45.

(31) Atryzek V, Tamaoki T, Fausto N. Changes in polysomal polyadenylated RNA and α-fetoprotein messenger RNA during hepatocarcinogenesis. Cancer Res 1980; 40:3713–3718.

(32) Castle T, Kreamer W, Liu DS, Richardson A. Characterization of RNA synthesis by isolated hepatocytes in suspension. Arch Biochem Biophys 1979; 195:423–437.

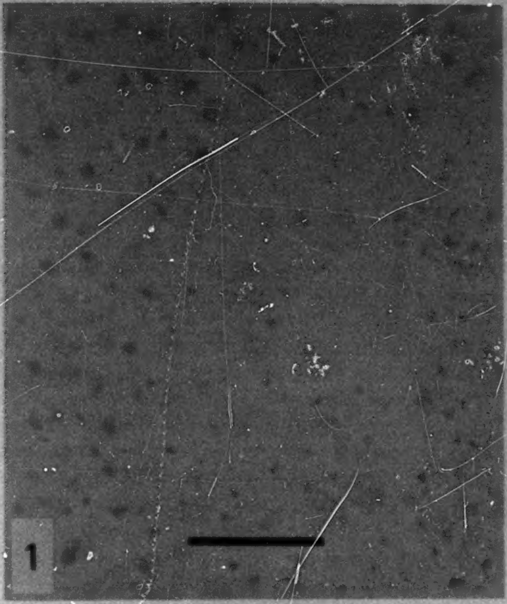

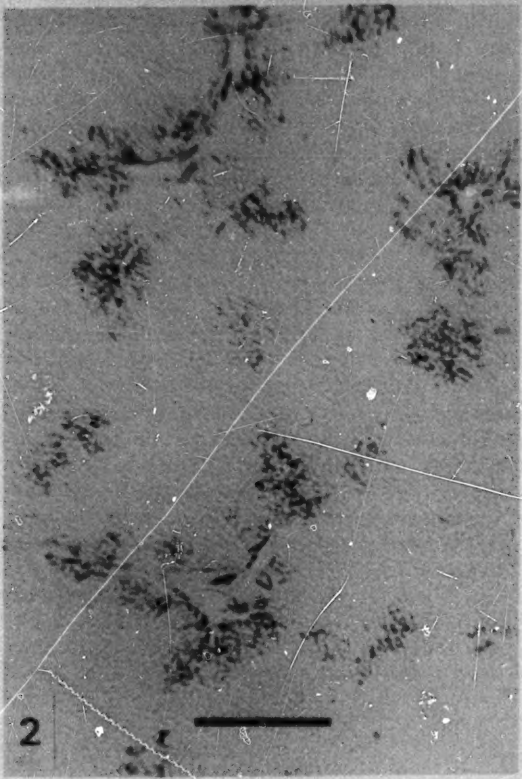

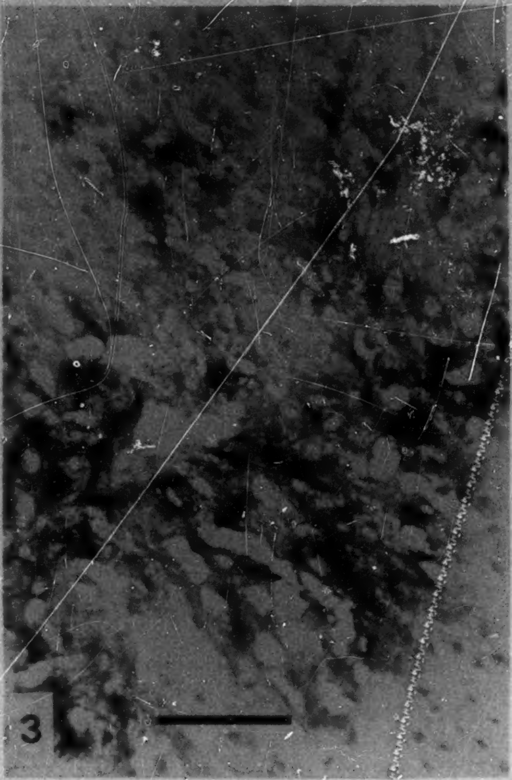

FIGURE 1.—Frozen section of liver from a host rat on 2-FAA for 7 days removed at the time of partial hepatectomy and the transplantation of cells. Stained for GGT and counterstained with methyl green. *Bar*=60 µm. × 330

FIGURE 2.—Frozen section of liver from a host rat 10 days after the transplantation of purified hepatocytes. *Note* numerous foci with histochemically demonstrable GGT. *Bar*=450 µm. × 45

FIGURE 3.—Higher magnification of the section of liver from a host rat 10 days after the transplantation of hepatocytes. *Bar*=75 µm. × 270

Malignant Fibrous Histiocytomas Induced by 4-(Hydroxyamino)quinoline 1-Oxide in Rats[1,2]

Yoichi Konishi,[3] Hiroshi Maruyama,[3] Yoshio Mii,[4] Yoshizumi Miyauchi,[4] Yoshihiko Yokose,[3] *and* **Kenji Masuhara[4]**

ABSTRACT—Subcutaneous and bone malignant fibrous histiocytomas (MFH) were induced in high incidence in rats by 4-(hydroxyamino)-quinoline 1-oxide (4-HAQO). Subcutaneous MFH were induced locally by repeated weekly injections of 1 mg 4-HAQO/rat for 4 weeks. Between 16 and 48 weeks after the final treatment, 13/15 (87%) male noninbred Wistar rats developed tumors. The histologic subtypes of these tumors were as follows: 11 fibrous, 1 myxoid, and 1 giant cell. Bone MFH were induced between 18 and 25 weeks by implantation of 4-HAQO (8 mg/rat) into the bone marrow of the tibia in 12/14 (86%) male noninbred Fischer 344 rats. The histologic subtypes of these tumors were as follows: 6 fibrous, 4 myxoid, and 2 giant cell. Morphologically, these MFH appeared similar to human MFH.—JNCI 1982; 68:859–865.

Since the early description of MFH by O'Brien and Stout (*1*), this type of malignant neoplasm has remained controversial because of its uncertain histogenesis. In 1978, Weiss and Enzinger (*2*) described MFH to be primitive, pleomorphic sarcomas showing partial fibroblastic and histiocytic differentiation, as indicated by collagen production and occasional phagocytosis, and reported that MFH could be distinguished from pleomorphic variants of liposarcomas, fibrosarcomas, or rhabdomyosarcomas. Subsequently, histologic features of MFH permitting differential diagnosis from other tumors have been reported (*3, 4*). It is now evident that MFH develop in soft tissues in various sites of the body, including bone (*5*), that they are the most common soft tissue sarcoma of late adult life, and that the prognosis is poor (*6–8*). It is obvious that an animal model of human MFH is needed for the study of the pathogenesis of this malignant neoplasm. It has been reported that subcutaneous MFH was induced in rats by potential carcinogens and by some plant extracts and their tannin-containing fractions (*9*), and experimental approach to fibrous histiocytoma in syngeneic mice inoculated with transformed bone marrow macrophages has been reported (*10*). However, these reports do not constitute an animal model of MFH since the former experimental approach involved multiple injections of carcinogens for a long time, and the latter one was a mixture of in vitro and in vivo systems. This paper communicates briefly the induction of subcutaneous and bone MFH by 4-HAQO in rats.

MATERIALS AND METHODS

Fifty-nine, 6-week-old, approximately 180-g male noninbred Wistar rats (Kiwa Animal Farm, Wakayama, Japan) or Fischer 344 rats (Nippon Charles River Animal Farm, Tokyo, Japan) were used. 4-HAQO (Nakarai Chemical, Ltd., Kyoto, Japan) was dissolved in 40% DMSO at 2 mg/ml and was injected into the subcutaneous dorsal tissue at 1 mg/rat once a week for 4 weeks. Injections were made in the same subcutaneous area that had been marked at the time of the first injection. 4-HAQO, a yellow powder, was inserted into the bone marrow of the left tibia as follows: Rats were anesthetized with ether. The front of the tibia about 1 cm distal from the knee joint was exposed surgically, the periosteum and the cortical bone were incised, and 8 mg 4-HAQO/rat was inserted aseptically with a small curet. A sham operation was made in the same way in some rats, except that 4-HAQO was not inserted.

The experimental groups were as follows: Group 1 Wistar rats received 4 sc injections of 0.5 ml 40% DMSO/rat; group 2 Wistar rats received 4 sc injections of 4-HAQO; group 3 Fischer 344 rats were subjected to the sham operation; and group 4 Fischer 344 rats received the surgically implanted 4-HAQO. All rats were housed in wire cages in an air-conditioned room at 24°C and were given Oriental MF diet (Oriental Yeast Co., Ltd., Tokyo, Japan) and water ad libitum. The initial and effective numbers of rats and the times of sacrifice are shown in table 1.

Complete autopsies with careful macroscopic examinations were performed. Subcutaneous and bone tumors, subcutaneous tissue at the site of injections, visible pathologic regions, and major internal organs such as lung, liver, pancreas, kidney, and spleen were fixed in 10% buffered Formalin or Bouin's solution. Bones were decalcified as described by Plank and Rychlo (*11*). All tissues were embedded in paraffin, sectioned, and stained with H & E. Special stains such as periodic acid–Schiff, alcian blue, azan Mallory, and Van Gieson's stains were used when necessary.

For electron microscopic studies, small pieces of tumor tissues were fixed in 2.5% glutaraldehyde in 0.1 *M* phosphate buffer for 2 hours, washed three times with 0.1 *M* phosphate buffer containing 0.25 *M* sucrose, and again fixed in 1% osmium tetroxide in 0.1 *M* phosphate buffer for 1 hour. The samples were then dehydrated in a graded series of alcohols and embedded in Epon-812. Ultrathin sections made with an LKB-8800 ultramicrotome were first examined with toluidine blue staining by light microscopy and were then stained with uranyl acetate and lead citrate and examined

---

ABBREVIATIONS USED: DMSO=dimethyl sulfoxide; 4-HAQO=4-(hydroxyamino)quinoline 1-oxide; H & E=hematoxylin and eosin; MFH=malignant fibrous histiocytoma(s).

---

[1] Received August 20, 1981; accepted December 11, 1981.

[2] Supported in part by Grant-in-Aid 401057 for Cancer Research from the Ministry of Education, Science and Culture of Japan.

[3] Department of Oncological Pathology, Cancer Center, Nara Medical University, 840 Shijo-cho, Kashihara, Nara 634, Japan.

[4] Department of Orthopedic Surgery, Nara Medical University.

TABLE 1.—*Tumor incidence and size in 4-HAQO-treated rats*

Group No.	No. of rats		Tumor incidence[b] (%)	Rat No. with tumors	Time killed, wk	Tumor size,[c] cm
	Initial	Effective[a]				
1	12	12	0/12 (0)	—	50	—
2	20	15	13/15 (87)	25938	22	5.1×4.7
				25944	26	7.5×7.0
				25946	28	10.5×8.8
				25950	30	9.0×6.5
				26945	32	11.0×6.4
				25941	33	3.5×3.0
				25043	43	11.5×9.3
				25951	43	5.5×5.0
				25937	48	9.0×7.0
				25936	48	8.5×6.0
				25953	48	5.0×3.5
				25940	50	4.5×2.0
				25949	50	2.5×1.8
3	13	13	0/13 (0)	—	40	—
4	14	14	12/14 (86)	79072	20	5.6×6.0
				79075	20	3.0×3.8
				79137	22	5.0×1.0
				79073	24	4.0×5.0
				79136	24	1.5×2.4
				79076	26	4.9×5.6
				79080	26	4.4×5.0
				79134	26	3.0×4.2
				79077	27	2.8×3.7
				79078	27	3.6×6.0
				79079	27	2.1×3.4
				79133	31	4.0×6.8

[a] Based on histologic examinations.
[b] No. of rats with tumor/No. of treated rats.
[c] Tumor size was measured when rats were killed and is expressed as diameter × depth.

with a JEOL electron microscope (model 100-C; Nippon Densi Co. Ltd., Tokyo, Japan).

RESULTS

Tumor Incidence

The initial and effective number of rats, the incidence of tumors, the time of sacrifice, and tumor size are shown in table 1. Five rats from group 2 died of pneumonia, and no tumors were found in those rats. Subcutaneous tumors were induced in 13/15 (87%) group 2 rats, and bone tumors were found in 12/14 (86%) group 4 rats. No tumors of other sites were found in rats from groups 2 and 4, and no tumors developed in rats from groups 1 and 3. The tumors in group 2 rats appeared between weeks 16 and 48, and tumors in group 4 rats appeared between weeks 18 and 25. The tumors grew rapidly after they became visible or palpable.

Pathology

Tumors in group 2 rats were located in the subcutaneous tissue at the injection site, whereas tumors in group 4 rats were in the tibial bone (fig. 1). Some large bone tumors showed invasion to the cortical bone and periosseous soft tissue. Tumors in rats from groups 2 and 4 appeared similar. They were hard, and their cut surfaces were lobulated and grayish white or yellowish white. Some tumors had a diffuse or partly jelly-like appearance. Inguinal lymph node and/or lung metastases were observed in 2 rats from group 4. Tumors in rats from groups 2 and 4 had essentially the same histologic pleomorphic appearance. These tumors were classified according to the description of Weiss and Enzinger (*2*), as shown in table 2.

Fibrous MFH consisting of spindle cells grew in focal areas with a storiform (matting-like) arrangement (figs. 2, 3). Osteoid reaction in the tumor was seen in a group 4 rat, but tumor osteoid was not seen. Variants of this type showed pleomorphism with bizarre tumor giant cells, Touton or epulis giant cells, and/or xanthomatous cells. Mitotic figures were frequent. The predominant feature of the giant-cell type was the presence of bizarre tumor giant cells and epulis giant cells. Storiform arrangement was not predominant (figs. 4–6). Mitotic figures were frequent. The myxoid type exhibited diffuse myxomatous change, staining with alcian blue, and contained bizarre tumor giant cells (figs. 7, 8). This type of MFH rarely had a storiform arrangement. Various extents of lymphocyte infiltration were seen in these types of tumor. The fibrous type was found in 11/13 (84%) group 2 rats and in 6/12 (50%) group 4 rats. Metastases were fibrous-type MFH. Electron microscopic examination showed that the tumors consisted of three major cell types: fibroblast-like cells, histiocyte-like cells, and undifferentiated cells (fig. 9). Collagen fibers were seen in the interstitial spaces, but bundle formation was not seen. Fibroblast-like cells, which were frequently seen in fiber-proliferating areas, were spindle shaped, elongated, or polygonal. Their nuclei were smooth surfaced, and their cytoplasm contained a dilated rough endoplasmic reticulum and microfilaments

TABLE 2.—*Histologic analysis of 4-HAQO-induced subcutaneous and bone tumors*

Group No.	Rat No. with tumors	Histologic subtype	Histologic analysis[a]						
			Storiform pattern	Tumor giant cells	Touton-type giant cells	Epulis-type giant cells	Xan-thoma-tous cells	Myxoid area	Metastasis
2	25938	Fibrous	++	+	+	−	−	−	−
	25944	Fibrous	+	+	+	+	−	+	−
	25946	Fibrous	+	+	−	+	+	+	−
	25950	Fibrous	+	+	−	+	−	+	−
	25945	Myxoid	−	+	−	+	+	++	−
	25941	Giant cell	−	+	+	++	−	−	−
	25943	Fibrous	+	++	+	+	−	+	−
	25951	Fibrous	+	+	−	+	−	+	−
	25937	Fibrous	++	++	++	++	−	−	−
	25936	Fibrous	+	++	+	+	−	−	−
	25953	Fibrous	++	+	−	+	−	−	−
	25940	Fibrous	++	+	−	+	−	−	−
	25949	Fibrous	++	+	−	+	−	−	−
4	79072	Myxoid	−	+	+	−	−	++	−
	79075	Myxoid	+	+	−	−	−	++	−
	79137	Fibrous	+	+	−	−	+	−	−
	79073	Giant cell	+	+	++	+	−	−	−
	79136	Fibrous	+	+	−	−	−	−	−
	79076	Fibrous	+	+	−	+	−	−	Lung, ILD[b]
	79080	Giant cell	+	+	−	++	+	−	−
	79134	Fibrous	+	+	+	+	−	−	−
	79077	Fibrous	++	+	−	+	+	+	Lung
	79078	Myxoid	−	+	−	−	−	++	−
	79079	Fibrous	+	+	−	−	−	−	−
	79133	Myxoid	−	++	+	−	+	++	−

[a] −=not seen; +=moderate; ++=frequent.

[b] ILD=inguinal lymph node.

with focal densities. Histiocyte-like cells were rounded, their nuclei were indented with a clear nucleolus, and their cytoplasm contained many lysosomes, small vacuoles, and pinocytotic vesicles. The surface of these cells had many microvilli. Undifferentiated cells were relatively small and round. Their round nuclei contained dispersed chromatin, their cytoplasmic organelles were poorly developed, and their nuclear:cytoplasmic ratio was high. Intermediate-type cells, which could not be distinguished from fibroblast-like or histiocyte-like cells, multinucleated giant cells, and xanthomatous cells, were also observed.

DISCUSSION

In the present work, we induced MFH in subcutaneous tissue and bone marrow by treating rats with 4-HAQO. This compound is a reduction product (*12*) of the carcinogen 4-nitroquinoline 1-oxide (*13*), which was shown to induce subcutaneous tumors on local application (*14–16*), mesodermal cancers on ip injection (*17*), and pancreatic tumors on iv injection (*18, 19*). Previously, the subcutaneous sarcomas induced by 4-HAQO were described as fibrosarcomas (*15*). However, the experiment was performed in the early 1960's, when the entity of MFH had not yet been described. Since then there has been much recent progress in histologic diagnosis of MFH, and as a result, it is controversial whether these sarcomas are MFH.

Subtypes of MFH in human cases have been classified on the basis of criteria suggested by Kempson and Kyriakos (*20*) and Weiss and Enzinger (*2*). Enjoji et al. (*7*) divided MFH into four types—common, myxoid, xanthogranulomatous, and giant cell— and further divided the common type into predominantly pleomorphic and predominantly storiform subtypes. Kearney et al. (*21*) divided MFH into four types—fibrous, giant cell, myxoid, and inflamamtory.

In the present work, rat subcutaneous and bone tumors were diagnosed as MFH and were classified into three major subtypes: fibrous, giant cell, and myxoid. Indeed, it was difficult to distinguish the different subtypes because mixtures with components of the various cell types occur in varying proportions; nevertheless, a type of MFH is predominantly fibrous and occurs frequently. Spontaneous MFH in rats has been reported (*22*), but rat MFH is different from its human counterpart; however, in the present experiment we could observe subtypes of MFH which are classifiable in humans. Furthermore, the cell populations observed electron microscopically in rat MFH may corresponded to those observed in human MFH (*23, 24*).

In the present work, subcutaneous and bone MFH were induced by 4-HAQO, a suggestion that chemical carcinogens may be important in the development of human MFH. Further experiments are required on the induction of MFH with other carcinogens in various animal species. Spontaneous subcutaneous tumors occur in laboratory animals in long-term feeding experiments, and spontaneous MFH have been reported only in rats (*22, 25, 26*) and in dogs and cats (*27*). In this connection, histologic re-evaluation of spontaneous tumors in laboratory animals may be required. Nevertheless, induction of subcutaneous and bone MFH by 4-HAQO in rats provides a useful experimental model for studying the histogenesis and characteristic growth behavior of MFH.

REFERENCES

(*1*) O'Brien JE, Stout AP. Malignant fibrous xanthomas. Cancer 1964; 17:1445–1458.

(*2*) Weiss WS, Enzinger FM. Malignant fibrous histiocytoma. Cancer 1978; 41:2250–2266.

(*3*) Shimoda T, Yamashita H, Furusato M, et al. Liposarcoma. A light and electron microscopic study with comments on their relation to malignant fibrous histiocytoma and angiosarcoma. Acta Pathol Jpn 1980; 30:779–797.

(*4*) Ushijome S, Hirota T. Malignant fibrous histiocytoma—with special reference to its differential diagnosis. Acta Pathol Jpn 1980; 30:799–813.

(*5*) Feldman F, Lattes R. Primary malignant fibrous histiocytoma (fibrous xanthoma) of bone. Skeletal Radiol 1977; 1:145–160.

(*6*) Hajdu SI. Tumors of fibrous tissue. In: Hajdu SI, ed. Pathology of soft tissue tumors. Philadelphia: Lea & Febiger, 1979:57–164.

(*7*) Enjoji M, Hashimoto H, Tsuneyoshi M, Iwasaki H. Malignant fibrous histiocytoma. A clinicopathologic study of 130 cases. Acta Pathol Jpn 1980; 30:727–741.

(*8*) McCarthy EF, Matsuno T, Dorfman HD. Malignant fibrous histiocytoma of bone: A study of 35 cases. Hum Pathol 1979; 10:57–70.

(*9*) Prodhan SN, Chung EB, Ghosh B, Paul BD, Kapadia GJ. Potential carcinogens. I. Carcinogenicity of some plant extracts and their tannin-containing fractions in rats. J Natl Cancer Inst 1976; 52:1579–1582.

(*10*) Yumoto T, Morimoto K. Experimental approach to fibrous histiocytoma. Acta Pathol Jpn 1980; 30:767–778.

(*11*) Plank J, Rychlo A. A method for quick decalcification. Zentralbl Pathol Anat 1952; 89:252–254.

(*12*) Ochiai E, Ohta A, Nomura H. Polarization of heterocyclic rings with aromatic character. CXVIII. 4-Hydroxyaminoquinoline-*N*-oxide. Chem Pharm Bull (Tokyo) 1957; 5:310–313.

(*13*) Nakahara W, Fukuoka F, Sugimura T. Carcinogenic action of 4-nitroquinoline-*N*-oxide. Gan 1957; 48:129–137.

(*14*) Shirasu Y. Comparative carcinogenicity of 4-nitroquinoline-1-oxide and 4-hydroxyaminoquinoline 1-oxide in 3 strains of mice. Proc Soc Exp Biol Med 1965; 118:812–814.

(*15*) Endo H, Kume F. Comparative studies on the biological actions of 4-nitroquinoline 1-oxide and its reduced compound, 4-hydroxyaminoquinoline 1-oxide. Gan 1963; 54:443–453.

(*16*) ———. Induction of sarcoma in rats by a single injection of 4-hydroxyaminoquinoline 1-oxide. Gan 1965; 56:261–265.

(*17*) Shurgin A, Becker FF. Sequential events in induction of sarcomas by 4-hydroxyaminoquinoline 1-oxide; fibroplasia, a premalignant phase. J Natl Cancer Inst 1974; 53:159–164.

(*18*) Hayashi Y, Hasegawa T. Experimental pancreatic tumor in rats after intravenous injection of 4-hydroxyaminoquinoline 1-oxide. Gan 1971; 62:329–330.

(*19*) Konishi Y, Denda A, Inui S, Takahashi S, Kondo H. Pancreatic carcinoma induced by 4-hydroxyaminoquinoline 1-oxide after partial pancreatectomy and splenectomy in rats. Gan 1976; 67:919–920.

(*20*) Kempson RL, Kyriakos M. Fibroxanthosarcoma of the soft tissue: A type of malignant fibrous histiocytoma. Cancer 1972; 29:961–976.

(*21*) Kearney MM, Soule EH, Ivins JC. Malignant fibrous histiocytoma. A retrospective study of 167 cases. Cancer 1980; 45:167–178.

(*22*) Ward JM, Kulwich BA, Reznik G, Berman JJ. Malignant fibrous histiocytoma. An unusual neoplasm of soft tissue origin in the rat that is different from the human counterpart. Arch Pathol Lab Med 1981; 105:313–316.

(*23*) Taxy JB, Battifora H. Malignant fibrous histiocytoma. An electron microscopic study. Cancer 1977; 40:254–267.

(*24*) Fu YS, Gabbiani G, Kaye GI, Lattes R. Malignant soft tissue tumors of probable histiocytic origin (malignant fibrous histiocytomas): General considerations and electron microscopic and tissue culture studies. Cancer 1975; 35:176–198.

(*25*) Greaves P, Faccini JM. Spontaneous fibrous histiocytic neoplasms in rats. Br J Cancer 1981; 43:402–411.

(*26*) Goodman DG, Ward JM, Squire RA, et al. Neoplastic and nonneoplastic lesions in aging Osborne-Mendel rats. Toxicol Appl Pharmacol 1980; 55:433–447.

(*27*) Gleiser CA, Raulston GL, Jardine JE, Gray KN. Malignant fibrous histiocytoma in dogs and cats. Vet Pathol 1979; 16:199–208.

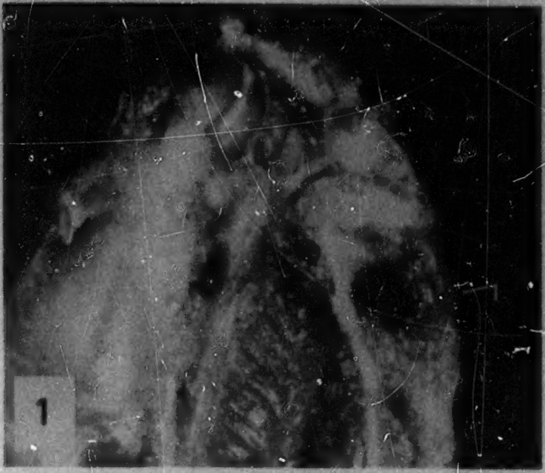

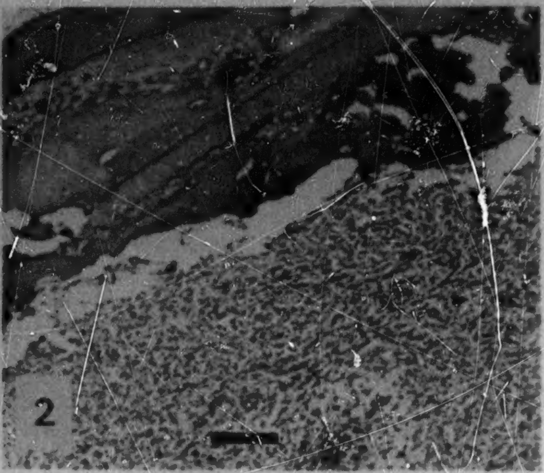

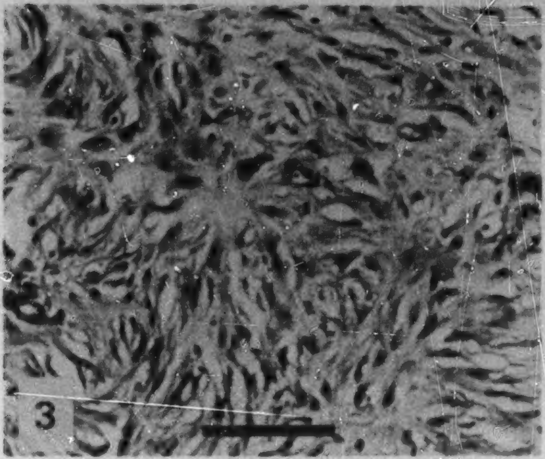

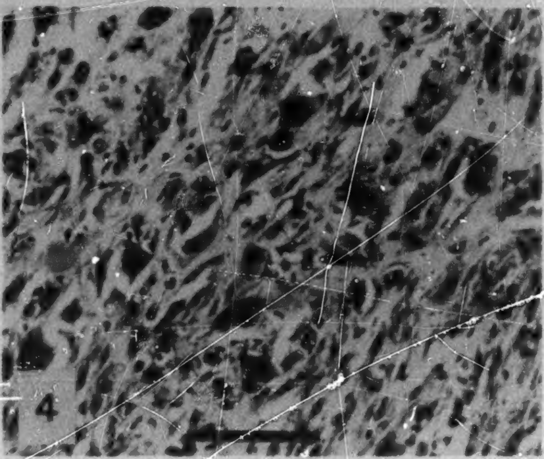

FIGURE 1.—Macroscopic view of tumor in the left tibia of rat #79137 given 4-HAQO. *Note* tumor development in the bone.

FIGURE 2.—Histology of fibrous type MFH in the left tibia of rat #79079 given 4-HAQO. *Note* tumor development in the bone marrow. H & E. *Bar*=200 µm. × 100

FIGURE 3.—Histology of fibrous type MFH in rat #79077 given 4-HAQO. *Note* storiform arrangement. H & E. *Bar*=200 µm. × 200

FIGURE 4.—Histology of giant-cell type of MFH in rat #79080 given 4-HAQO. *Note* numerous giant cells. H & E. *Bar*=200 µm. × 200

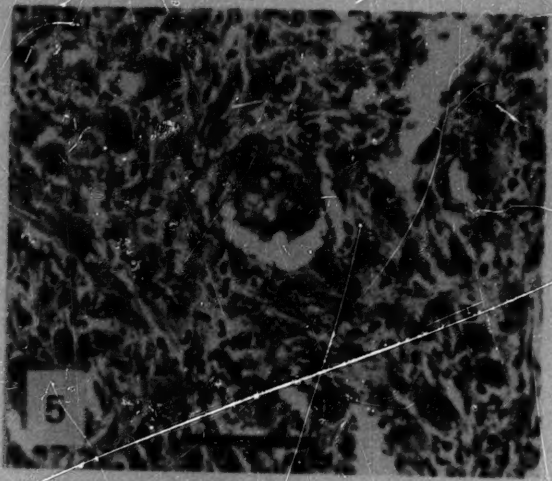

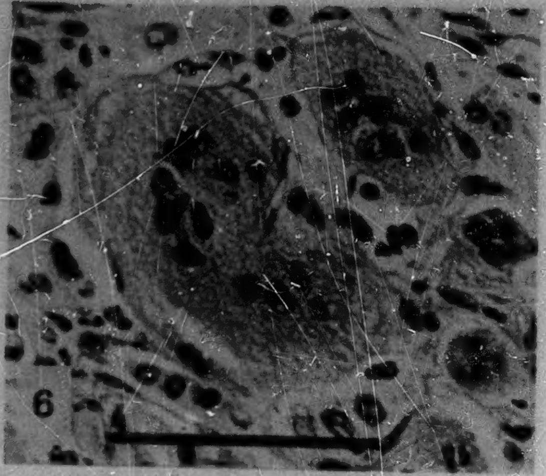

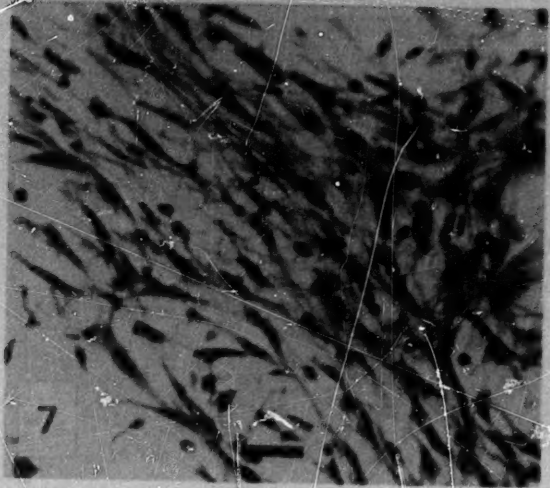

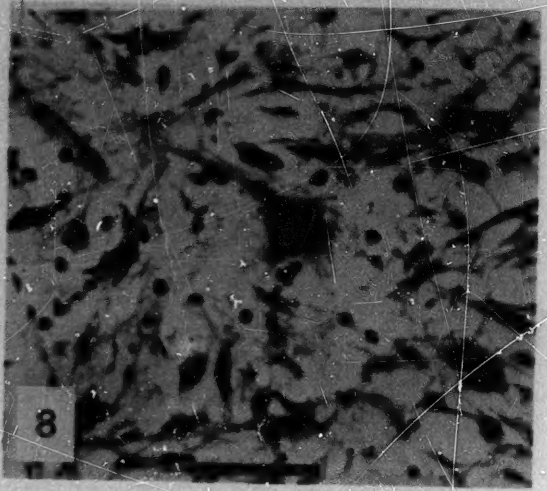

FIGURE 5.—Histology of giant-cell type of MFH in rat #79080 given 4-HAQO. *Note* xanthomatous cell. H & E. *Bar*=200 µm. × 200

FIGURE 6.—Histology of giant-cell type of MFH in rat #79080 given 4-HAQO. *Note* epulis giant cells. H & E. *Bar*=200 µm. × 400

FIGURE 7.—Histology of myxoid type of MFH in rat #25945 given 4-HAQO. H & E. *Bar*=200 µm. × 100

FIGURE 8.—Histology of myxoid type of MFH in rat #25945 given 4-HAQO. *Note* bizarre tumor cells. H & E. *Bar*=200 µm. × 200

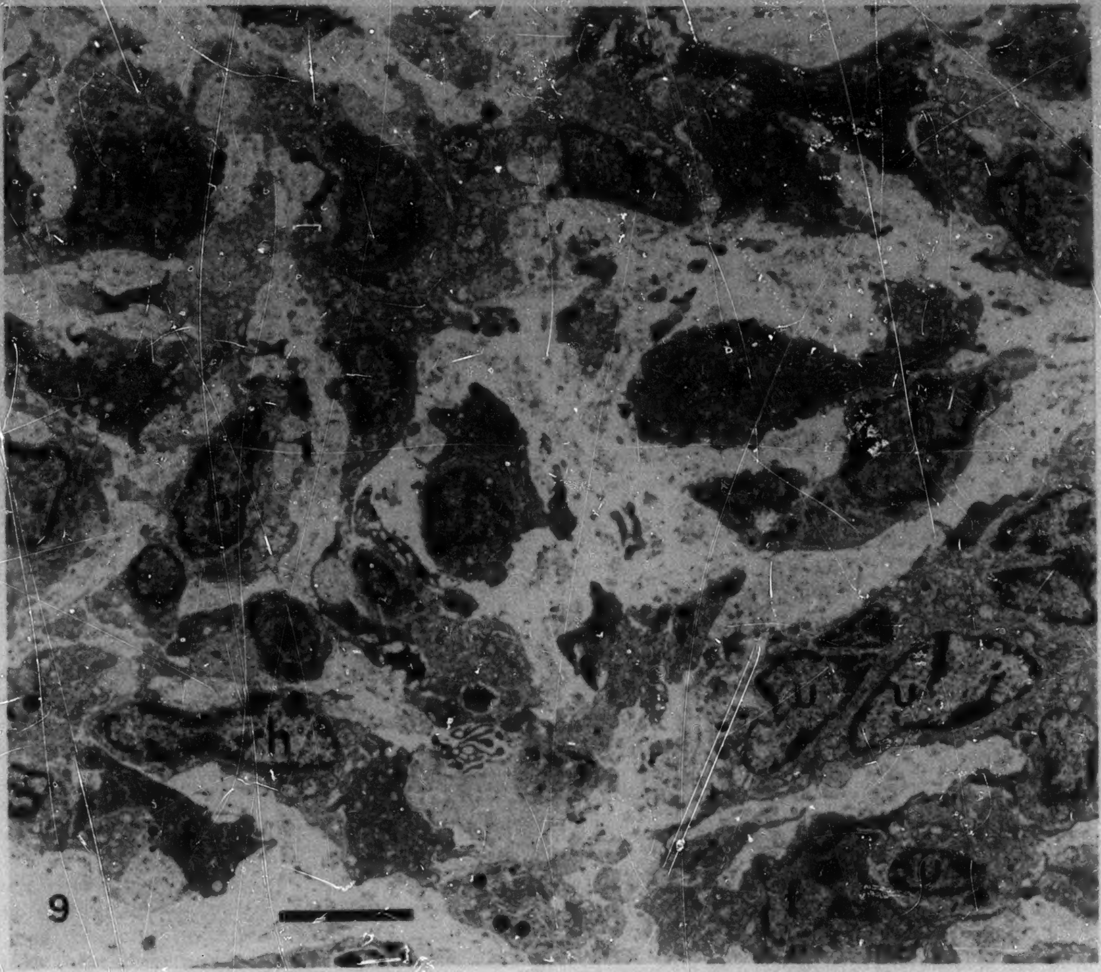

9

FIGURE 9.—Electron microscopic view of MFH with fibroblast-like cells, histiocyte-like cells, and undifferentiated cells in rat #79079 given 4-HAQO. f=fibroblast-like cell; h=histiocyte-like cell; u=undifferentiated cell. *Bar*=5.0 μm. × 1,600

Prostate Adenocarcinoma in Rats: Induction by 3,2′-Dimethyl-4-aminobiphenyl [1,2,3,4]

Shoichi Katayama,[5,6] **Emerich Fiala,**[5] **Bandaru S. Reddy,**[5] **Abraham Rivenson,**[5] **Jerald Silverman,**[5]
Gary M. Williams,[5] *and* **John H. Weisburger**[5,7,8]

ABSTRACT—Five experiments designed for various purposes [mainly for the study of colon carcinogenesis in inbred F344 male rats given sc injections of 3,2′-dimethyl-4-aminobiphenyl (DMAB)] were reviewed as to the production and presence of neoplastic lesions of the prostate gland. The overall incidence of prostate proliferative lesions among 293 animals exposed to DMAB was 32% (95 animals). Early in situ carcinomas were present in 66 animals, larger intra-acinar carcinomas in situ in 28, and invasive carcinoma in 1. None of the control animals in these studies exhibited prostate neoplasms. The conclusion, therefore, is that DMAB can induce adenocarcinomas in the rat prostate gland. JNCI 1982; 68:867–873.

Chemical carcinogens with an organotropism for almost every organ of the rodent have been identified, and with the use of these chemicals, organ site models for cancer induction have been developed. A notable exception is the prostate gland. Although many attempts have been made to induce cancer in this organ, there are no reliable means for chemically inducing prostate adenocarcinomas through systemic action (*1–18*). A naturally occurring prostate carcinoma in rats more than 30 months old of the ACI–Segaloff strain was described in detail in (*19*).

Chemicals that have induced prostate carcinoma in rats and mice include benzo[*a*]pyrene (*1*) and 3-methylcholanthrene (*2–4*). However, the prostate gland had to be exposed directly to these chemicals by insertion of a carcinogen-containing pellet (*2–4*) or by direct injection of a carcinogen (*1–3*). The tumors induced were, in most cases, squamous cell carcinomas which are quite rare in humans. Recently, Pour (*20*) reported squamous carcinomas induced through the systemic action of *N*-nitrosobis(2-oxopropyl)amine in MRC rats. Prostate tumors have also been produced by X-irradiation (*6, 7*).

Among the derivatives of 4-aminobiphenyl, DMAB has been known to be a multipotential carcinogen for the large and small intestine, mammary gland, ear duct, salivary gland, and urinary bladder of the rat, either by sc injection or oral administration (*21–28*). In a study on the effects of disulfiram on the carcinogenicity of DMAB in rats and hamsters, we noted a small number of in situ carcinomas in the prostate glands of rats, but not in hamsters, exposed to DMAB (*29*).

One reason for performing studies with DMAB at our institute is the close chemical similarity of this synthetic carcinogen to certain mutagens isolated from cooked meat or fish (*30–33*). There is an association, in turn, between the incidence of cancer of the colon, breast, and prostate gland in meat-eating populations. Vegetarian populations, such as Seven-Day Adventists, have a much lower incidence of these diseases (*34, 35*). It is of great interest, therefore, that the synthetic chemical DMAB should be able to induce in rats the three types of cancer which appear to exhibit certain parallel characteristics in geographic pathology.

Consequently, all ongoing studies with DMAB at this institute were carefully evaluated for the occurrence of prostate lesions, including one experiment designed and conducted to validate and extend the findings of Fingerhut and Veenema (*5*) in inducing prostate carcinoma. In this report, we describe the effects of DMAB on the prostate glands of rats in five separate experiments.

MATERIALS AND METHODS

This report records procedures and findings for five experiments performed at the Naylor Dana Institute (*26–29*). Although the experiments had different purposes, the animals used were from the same strain of inbred rats, CDF (F-344)/CrlBR, and were from the same source (Charles River Breeding Laboratories, Inc., Portage, Mich., or Kingston, N.Y.), except for experiment III in which germfree F344 rats (from Charles River Breeding Laboratories stock bred in our institute) were used. In each experiment, the carcin-

---

ABBREVIATIONS USED: DMAB=3,2′-dimethyl-4-aminobiphenyl; DMBA=7,12-dimethylbenz[*a*]anthracene; H & E=hematoxylin and eosin; NCI=National Cancer Institute; NMU=*N*-nitroso-*N*-methylurea.

---

[1] Received August 8, 1981; accepted December 11, 1981.

[2] Supported by Public Health Service (PHS) grant CA-12376 from the National Cancer Institute (NCI); by PHS contracts CP-33208 and CP-85659 from the Division of Cancer Cause and Prevention, NCI; and by PHS grant CA-15400 from NCI through the National Large Bowel Cancer Project.

[3] This report is dedicated to the founder of the American Health Foundation, Dr. Ernst L. Wynder, on the occasion of the 10th anniversary of the Naylor Dana Institute for Disease Prevention.

[4] Animals were maintained under the guidelines set forth by the American Association for Accreditation of Laboratory Animal Care.

[5] American Health Foundation, Naylor Dana Institute for Disease Prevention, Valhalla, N.Y. 10595.

[6] *Present address:* Department of Pathology, Osaka University Medical School, Osaka, Japan.

[7] *Address reprint requests to* Dr. John H. Weisburger.

[8] We thank the staff of the Research Animal Facility for animal care and treatment, Miss Carol Meyer for preparation of histologic materials, and Mrs. L. Stempel for editorial support.

ogen was DMAB (Ash-Stevens, Inc., Detroit, Mich.; or the Extramural and Intramural Carcinogenesis Programs, NCI, through the carcinogen repository, Illinois Institute of Technology, Chicago, Ill.). The DMAB was dissolved in corn oil and injected sc once a week. The basal diet was NIH-07 (Zeigler Bros., Gardeners, Pa.) in experiment IV; Purina Laboratory Chow (Ralston Purina Co., St. Louis, Mo.) in experiment I; and a powdered semipurified diet, AIN-76, with different fat or fiber contents (Bioserve, Inc., Frenchtown, N.J.), in experiments II, III, and V (table 1).

Experiment I, March 1976–June 1977.—Seventy-five F344 male rats were divided into 3 groups: 30 were treated with DMAB only, 30 had DMAB and disulfiram in the diet, and the appropriate controls (*29*). DMAB, 20 mg/kg body weight, was injected sc once a week for 37 weeks. From the starting group of 60 DMAB-exposed rats, 46 were available for study. Total experiment period was 68 weeks.

Experiment II, April 1978–February 1979.—Sixty-three F344 male rats were initially used and were divided into 5 groups (*27*). Injections of 50 mg DMAB/kg body weight once a week for 20 weeks were given to 48 rats that were on either a low-fat (5% beef tallow in a semipurified diet) or a high-fat diet (20% beef tallow in a semi-purified diet). Among the DMAB-treated animals, 44 were available for evaluation. Total experiment period was 42 weeks.

Experiment III, April 1978–April 1979.—The animals in this experiment were germfree F344 rats, a line maintained in our institute since 1976 (*26, 27*). Injections of 50 mg DMAB/kg body weight once a week for 20 weeks were given to 77 rats that were on either the low-fat or high-fat diet as described above; 6 rats served as vehicle controls. Of the DMAB-treated rats, 68 were examined in this study (table 1). Total experiment period was 50 weeks.

Experiment IV, February 1979–April 1980.—Of the 189 F344 male rats in this experiment (*28*) 135, on either 15% wheat bran in the control diet or 15% citrus pulp in the control diet, were given injections of 50 mg DMAB/kg body weight once a week for 20 weeks. Fifty-four controls and sentinels for health testing were on either the basal control diet or one of the fiber diets. Total experiment period was 60 weeks.

Experiment V, August 1978–April 1980.—This experiment was designed to extend the findings in (*5*). When groups of gonadectomized male rats were given iv injections of 10 mg DMBA, as in (*5*), most died. Therefore, larger groups of gonadectomized rats were given three iv injections of 5 mg DMBA every 2 weeks and then were held as described in table 1. Other groups were given iv injections of 2 mg MNU, a mammary carcinogen (cf. *36*), and thus reasoned to be a putative prostate carcinogen. For the same reason, DMAB, a carcinogen active on the colon and breast of the rat, was administered as described below.

Fifty-one F344 male rats were divided into 4 groups. At 90 days of age, 48 rats were orchiectomized. One month later, injections of 20 mg DMAB/kg body weight once a week for 40 weeks were given to 42 of the castrated animals that were on either a low-fat (5% lard in a semipurified diet) or high-fat diet (33% lard in a semipurified diet). The remaining castrates served as vehicle controls or untreated

TABLE 1.—*Carcinogenicity of DMAB in rat prostate gland*[a]

Experiment (reference)	No. of animals examined	No. of animals with change: Early (small) carcinoma in situ (%)	Carcinoma in situ (%)	Invasive adenocarcinoma	Single DMAB dose, mg/kg body wt/wk (No. of wk)	Average cumulative dose DMAB/animal, mg	Total experiment period, No. of wk
Expt I (*29*)							
DMAB alone	21	3	3	0	20 (42)	289	68
DMAB+disulfiram	25	2	5	0	20 (42)	241	68
Expt II[b] (*27*)							
DMAB+low fat	23	1	0	1	50 (20)	292	42
DMAB+high fat	21	4	0	0	50 (20)	296	42
Expt III[b,c] (*26, 27*)							
DMAB+low fat	37	3	1	0	50 (20)	259	50
DMAB+high fat	31	3	1	0	50 (20)	260	50
Expt IV (*28*)							
DMAB alone	44	17	3	0	50 (20)	275	60
DMAB+wheat bran	45	16	9	0	50 (20)	272	60
DMAB+citrus pulp	46	17	6	0	50 (20)	266	60
Total	293	66 (23)	28 (10)	1			
Expt V[d] (unpublished data)							
DMAB+low fat	21	0	0	0	20 (40)	256	86
DMAB+high fat	21	0	0	0	20 (40)	260	86
Control[e]	144	0	0	0	0	0	42–86
Control[f]	30	1	3	0	0	0	82

[a] Data from 5 experiments, with diverse-specific aims, that were performed at our institute, March 1976 through April 1980.

[b] Low fat diet: 5% beef tallow; high fat diet: 20% beef tallow.

[c] Germfree F344 strain maintained at our institute were used. (For details, *see* text.)

[d] All animals were castrated at 90 days of age, according to procedure of Fingerhut and Veenema (*5*). Low fat diet: 5% lard; high fat diet: 33% lard.

[e] Vehicle controls and untreated animals of all experiments. The longest experiment with normal rats lasted 68 wk.

[f] Control group of experiment performed in 1980–81, extending over 82 wk.

controls. Total experiment period was 86 weeks—the longest of the five experiments.

Tissue processing, all experiments.—At the end of each experiment, all survivors were killed with CO_2 and then necropsied. During the experiments, animals that appeared moribund were killed. All available prostate tissues were submitted to histologic examination in 10% buffered Formalin. The samples were trimmed in a sagittal plane to include the urinary bladder and dorsal and ventral lobes of the prostate gland in one histologic piece. After paraffin embedding, four to five sections at various levels were cut and stained with H & E.

RESULTS

DMAB is known to induce cancer of the colon and breast. In our institute, we have used DMAB to study the pathogenesis of colon and breast cancer and the influence of a number of modifying elements, such as the enzyme inhibitor disulfiram, or certain nutritional components, such as fat or fiber (*26-29*). In connection with the first of these tests involving disulfiram, the inadvertent observation was made that male rats that were given 20 mg DMAB/kg body weight (expt I) for 37 weeks and held for a total of 68 weeks exhibited in situ carcinomas of variable size in the prostate gland. For this reason, we reviewed specifically the prostate tissue sections and data obtained in the remainder of the experiments with DMAB (which were originally designed to provide information on the pathogenesis of colon cancer) and performed a detailed microscopic study.

In all five experiments, no obvious manifestation of disease in the prostate gland was apparent. Of the five experiments, four involved normal rats, whereas the fifth experiment used male rats that were gonadectomized at age 90 days. Microscopically, neoplastic lesions in prostate tissues were seen in nongonadectomized F344 rats treated in experiments I–IV with DMAB. Although the weekly dose was different in the four experiments (20 or 50 mg/kg), the total dose administered in all four experiments was of the same order of magnitude (241–296 mg DMAB). The amount of carcinogen did not seem to influence greatly the overall yield of prostate tumors. However, the length of the observation period apparently did affect the total tumor yield which was higher in the more extended periods, especially in experiment IV. In summary: In all four experiments, 33% of the animals had various degrees of carcinoma development in situ; in experiment II, 1 invasive adenocarcinoma developed; in experiment IV, the yield of carcinoma lesions in situ was as high as 60%; the modifiers (specifically disulfiram), fats or fiber levels, or germfree status had no obvious effect.

All lesions were located in the ventral lobe of the prostate gland. The microscopic alterations in affected prostate tissues included an overgrowth of the epithelial lining of the acini which "piled up" and formed secondary micro-acini that assumed the well-known cribriform pattern. This pattern occurred even in the smallest incipient lesions (figs. 1, 2). Cytologically, the overgrown cells were obviously dysplastic, with vesiculated nuclei containing one or two relatively distinctive nucleoli (fig. 2).

No notable morphologic differences in the prostate neoplasms were observed among the experiments, except in the size of the lesion. In more advanced cases, proliferating epithelial cells occupied almost the entire space of one or several acini (figs. 3, 4) but without obvious invasion into the adjacent tissue. In some cases the neoplasms were multifocal but, even so, they were confined to the ventral lobes. Secretory products were observed in the neoplastic acini. In one rat from experiment II, an overt tumor of the prostate gland was present. Grossly, it was a firm yellow mass, 1.5×0.9×0.6 cm, which presented on the left dorsal lobe of the prostate gland. Histologic examination revealed this tumor to be an invasive adenocarcinoma (figs. 5, 6).

In gonadectomized rats from experiment V, no gross or microscopically visible lesions were observed in prostate tissues, even though the experiment was extended to 86 weeks. This finding was not only true for the carcinogen DMAB (table 1) but also for NMU and DMBA (data not given). With DMBA, we encountered high mortality within weeks after injection of the carcinogen at the level used by Fingerhut and Veenema (10 mg) and also at 5 mg. Thus it seems quite clear that three kinds of carcinogens, which are thought to have an effect on the prostate gland, failed to be active in gonadectomized rats. Dr. R. Kroes (personal communication) also could not reproduce the original results of Fingerhut and Veenema (*5*).

DISCUSSION

This report provides an extension of an inadvertent observation made during an experiment for the study of the pathogensis of cancer at important sites in humans (large bowel and breast) as induced in rats by the chemical carcinogen DMAB. A gross enlargement of the prostate gland led to a detailed study of microscopically visible lesions in all prostate tissues in experiments performed at this institute on F344 male rats given DMAB. We found that this chemical administered once a week by sc injection could, through systemic action, induce lesions in the prostate gland, specifically in the ventral part of the gland, that ranged from minute carcinomas in situ, with an incidence up to 38%, to large carcinomas in situ, with an incidence up to 20%. There also was 1 invasive adenocarcinoma. Metastases were not seen. More tumors were seen in the tissues of the groups used in the longer experiments. A recent paper (*37*) dealt with the spontaneous prostate adenocarcinoma incidence in control and certain treated F344 rats, approximately 2 years of age or older, in the NCI bioassay program.[8] In this population of old rats, less than 1% had adenocarcinoma, and an average of about 3.6% had adenoma. However, in certain participating laboratories, an incidence as high as 15% was noted. Nonetheless, the DMAB model described herein provides a means to obtain higher yields of prostate adenocarcinoma in a shorter time under highly controlled conditions.

---

[8] In a more recent experiment involving normal, nongonadectomized F344 rats and extending over 82 wk, an untreated control group of 30 rats had 3 animals with carcinoma in situ and 1 animal with an early (small) carcinoma in situ (table 1, footnote *f*).

We are reporting these findings at this time because DMAB is the first available systemically acting chemical that reliably induces prostate adenocarcinoma. Modification of the experiment protocols may lead to improved yields, especially of the more advanced lesions. Such studies are currently planned and in part have been initiated at this institute, particularly since DMAB has a structure similar to certain naturally occuring dietary compounds suspected of being associated etiologically with the development of cancer in the colon, breast, and prostate gland (*32–44*).

It will be important to study the underlying endocrine situation, inasmuch as prostate cancer is likely under endocrine control, as is breast cancer and, therefore, possibly is subject to dietary modulation (*36, 45–48*). The model described should be useful to study systematically the modifying factors, such as diet and the endocrine elements, under highly controlled conditions. Thus, as in the case of breast cancer (*36*), such model studies can provide background information on the pathogenesis and etiology of prostate carcinoma in humans (*36, 49*).

REFERENCES

(*1*) Moore RA, Melchionna RH. Production of tumors of the prostate of the white rat with 1,2-benzpyrene. Am J Cancer 1937; 30:731–741.

(*2*) Dunning WF, Curtis MR, Segaloff A. Methylcholanthrene squamous cell carcinoma of the rat prostate with skeletal metastases, and failure of the rat liver to respond to the same carcinogen. Cancer Res 1946; 6:256–262.

(*3*) Horning ES, Dmochowski L. Induction of prostate tumours in mice. Br J Cancer 1947; 1:59–63.

(*4*) Mirand EA, Staubitz WJ. Prostatic neoplasms of the Wistar rat induced with 20-methylcholanthrene. Proc Soc Exp Biol Med 1956; 93:457–462

(*5*) Fingerhut B, Veenema RJ. An animal model for the study of prostatic adenocarcinoma. Invest Urol 1977; 15:42–48.

(*6*) Hirose F, Takizawa S, Watanabe H, Takeichi N. Development of adenocarcinoma of the prostate in ICR mice locally irradiated with X-rays. Gan 1976; 67:407.

(*7*) Brown CE, Warren S. Carcinoma of the prostate in irradiated parabiotic rats. Cancer Res 1978; 38:159–162.

(*8*) Horning ES. The effects of castration and stilboestroal on prostatic tumours in mice. Br J Cancer 1949; 3:211–230.

(*9*) Noble RL. The development of prostatic adenocarcinoma in Nb rats following prolonged sex hormone administration. Cancer Res 1977; 37:1929–1933.

(*10*) Rivenson A, Silverman J. The prostatic carcinoma in laboratory animals: A bibliographic survey from 1900 to 1977. Invest Urol 1979; 16:468–472.

(*11*) Coffey DS, Isaacs JT, Weisman RM. Animal models for the study of prostatic cancer. In: Murphy GP, ed. Prostatic cancer. Littleton, Mass.: PSG Pub, 1979:89–109.

(*12*) Isaacs JT, Coffey DS. Animal models in the study of prostate cancer. Cancer Detect Prev 1979; 2;587–599.

(*13*) Pollard M. Spontaneous prostate adenocarcinomas in aged germfree Wistar rats. J Natl Cancer Inst 1973; 51:1235–1241.

(*14*) Shain SA, McCullough B, Segaloff A. Spontaneous adenocarcinomas of the ventral prostate of aged A×C rats. J Natl Cancer Inst 1975; 55:177–180.

(*15*) Noble RL. Sex steroids as a cause of adenocarcinoma of the dorsal prostate in Nb rats and their influence on the growth of transplants. Oncology 1977; 34:120–138.

(*16*) Sato G, Desmond W, Kelly J. Human prostatic tumors in conditioned animals and culture. Cancer Chemother Rep 1975; 59:47–49.

(*17*) Shimosato Y, Kameya T, Nagai K, et al. Transplantation of human tumors in nude mice. J Natl Cancer Inst 1976: 56:1251–1260.

(*18*) Okada K, Schroeder FJ, Jellinhaus W, Wullstein HK, Heinemeyer HM. Human prostatic adenoma and carcinoma: Transplantation of cultured cells and primary tissue fragments in nude mice. Invest Urol 1976; 13:395–403.

(*19*) Ward JM, Reznik G, Stinson SF, Lattuada CP, Longfellow DG, Cameron TP. Histogenesis and morphology of naturally occurring prostatic carcinoma in the ACI/segHapBR rat. Lab Invest 1980; 43:517–522.

([illegible]) Pour PM. A new prostatic cancer model: Systemic induction of prostatic cancer in rats by a nitrosamine. Cancer Lett 1981; 13:303–308.

(*21*) Walpole AL, Williams MH, Roberts DC. Bladder tumours induced in rats of two strains with 3,1′-dimethyl-4-aminodiphenyl. Br J Cancer 1955; 9:170–176.

(*22*) Spjut HJ, Noall MW. Experimental induction of tumors of the large bowel of rats. A review of the experience with 3,2′-dimethyl-4-aminobiphenyl. Cancer 1971; 28:29–37.

(*23*) Clayson D, Garner R. Carcinogenic aromatic amines and related compounds, chapt 8. In: Searle CE, ed. Chemical carcinogens. Washington, D.C.: American Chemical Soc Monogr 173. 1976:366–461.

(*24*) Bralow SP, Weisburger JH. Experimental carcinogenesis in the digestive organs. Clin Gastroenterol 1976; 5:527–542.

(*25*) Arcos JC, Argus MF. Chemical induction of cancer: Structural bases and biological mechanisms. Vol IIB. New York: Academic Press; 1974.

(*26*) Reddy BS, Watanabe K. Effect of intestinal microflora on 3,2′-dimethyl-4-aminobiphenyl-induced carcinogenesis in F344 rats. JNCI 1978; 61:1269–1271.

(*27*) Reddy BS, Ohmori T. Effect of intestinal microflora and dietary fat on 3,2′-dimethyl-4-aminobiphenyl-induced colon carcinogenesis in F344 rats. Cancer Res 1981; 41:1363–1367.

(*28*) Reddy BS, Mori H. Effect of dietary wheat bran and dehydrated citrus fiber on 3,2′-dimethyl-4-aminobiphenyl-induced intestinal carcinogenesis in F344 rats. Carcinogenesis 1981; 2:21–25.

(*29*) Fiala E, Weisburger JH, Katayama S, Chandrasekaran V, Williams GM. The effect of disulfiram on the carcinogenicity of 3,2′-dimethyl-4-aminobiphenyl in Syrian golden hamsters and rats. Carcinogenesis 1981; 10:965–969.

(*30*) Sugimura T, Kawachi T, Nagao M, Yahagi T. Mutagens in food as causes of cancer. In: Newell GR, Ellison NM, eds. Nutrition and cancer: Etiology and treatment. New York: Raven, 1981:59–71.

(*31*) Shelby MD, Matsushima T. Meeting report: Mutagens and carcinogens in the diet and digestive tract. Mutat Res 1981; 85:177–183.

(*32*) Weisburger JH, Reddy BS, Hill P, Cohen LA, Wynder EL, Spingarn NE. Nutrition and cancer—on the mechanisms bearing on causes of cancer of the colon, breast, prostate, and stomach. Bull NY Acad Med 1980; 56(8):673–696.

(*33*) Weisburger JH, Spingarn NE, Wang YY, Vuolo LL. An assessment of the role of mutagens and endogenous factors in larger bowel cancer. Cancer Bull 1981; 33:124–129.

(*34*) Cairns J, Lyon JL, Skolnick M, eds. Banbury report 4. Cancer incidence in defined populations. Cold Spring Harbor, NY: Cold Spring Harbor Laboratory, 1980.

(*35*) Reddy BS, Sharma C, Darby L, Laakso K, Wynder EL. Metabolic epidemiology of large bowel cancer. Fecal mutagens in high- and low-risk population for colon cancer. A preliminary report. Mutat Res 1980; 72:511–522.

(*36*) Reddy BS, Cohen LA, McCoy GD, Hill P, Weisburger JH, Wynder EL. Nutrition and its relationship to cancer. Adv Cancer Res 1980; 32:237–345.

(*37*) Reznik G, Hamlin MH, Ward JM, Stimson SF. Prostatic hyperplasias and neoplasia in aging F344 rats. Prostate 1981; 2:261–268.

(*38*) Wynder EL, Mabuchi K, Whittemore WF Jr. Epidemiology of cancer of the prostate. Cancer 1971; 26:344–360.

(*39*) Franks LM. Etiology, epidemiology, and pathology of prostatic cancer. Cancer 1973; 32:1092–1095.

(*40*) Edwards CN, Steinthorsson E, Nicholson D. An autopsy study of latent prostatic cancer. Cancer 1953; 6:531–554.

(41) Karube K. Study of latent carcinoma of the prostate in the Japanese based on necropsy material. Tohoku J Exp Med 1961; 74:265–285.

(42) Akazaki K, Stemmermann GN. Comparative study of latent carcinoma of the prostate among Japanese in Japan and Hawaii. J Natl Cancer Inst 1973; 50:1137–1142.

(43) Hirayama T. Diet and cancer. Nutr Cancer 1979; 1:67–81.

(44) Holman CD, James IR, Segal MR, Armstrong BK. Recent trends in mortality from prostate cancer in male populations of Australia and England and Wales. Br J Cancer 1981; 44:340–348.

(45) Pollard M, Chang C, Burleson G. Investigations on prostate adenocarcinomas in rats. Cancer Treat Rep 1977; 61:153–156.

(46) Isaacs JT, Heston WD, Weissman RM, Coffey DS. Animal models of the hormone-sensitive and -insensitive prostatic adenocarcinomas, Dunning R-3327-H, R-3327-H1 and R-3327-AT. Cancer Res 1978; 38:4353–4359.

(47) Heston WD, Menon M, Tananis C, Walsh PC. Androgen, estrogen and progesterone receptors of the R3327H Copenhagen rat prostatic tumor. Cancer Lett 1979; 6:45–50.

(48) Drago JR, Goldman LB, Mauer RE, Eckels DD, Gershwin ME. Histology, histochemistry, and acid phosphatase of Noble (Nb) rat prostate adenocarcinomas and treatment of an androgen-dependent Nb rat prostate adenocarcinoma. JNCI 1980; 64:931–937.

(49) Doll R, Peto R. The causes of cancer: Quantitative estimates of avoidable risks of cancer in the United States today. JNCI 1981; 66:1191–1308.

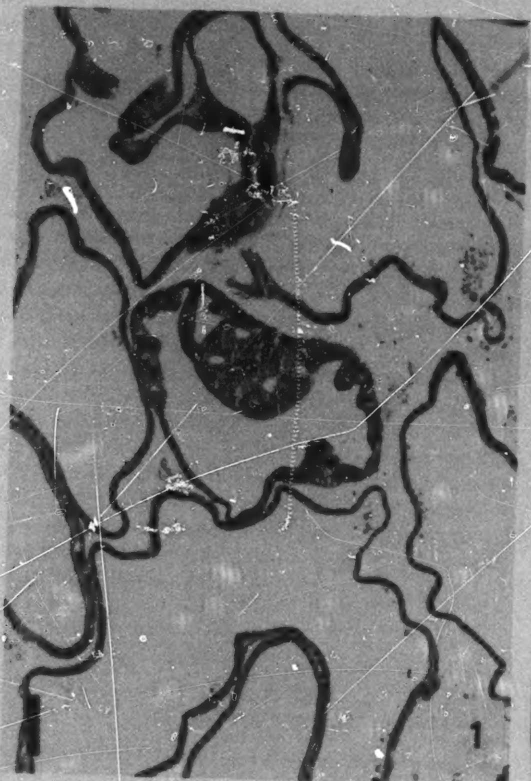

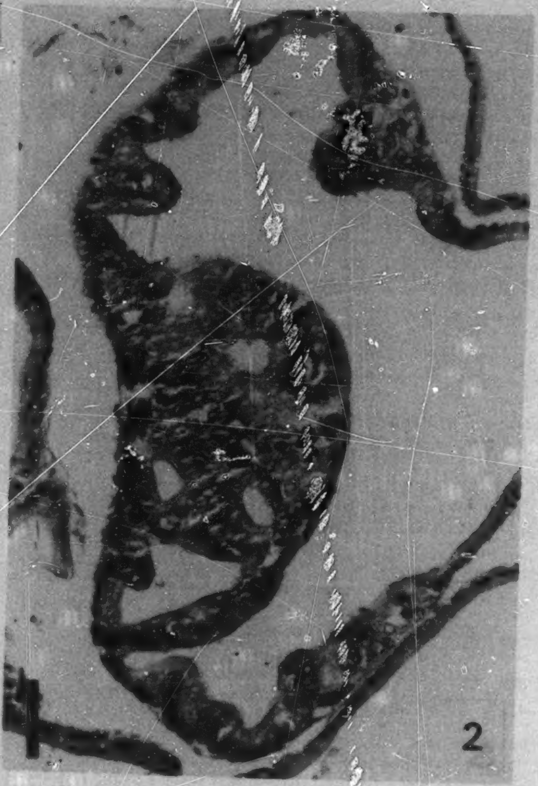

FIGURE 1.—Proliferative lesion of the prostate gland involving a single acinus. Cells are arranged in a cribriform pattern (DMAB + wheat bran diet, expt IV). H & E. *Bar*=100 µm. × 90

FIGURE 2.—Higher magnification of fig. 1. Compare the thickness and proliferation of neoplastic epithelium with the surrounding normal epithelia. H & E. *Bar*=50 µm. × 228

FIGURE 3.—Carcinoma in situ involving several acini. A cribiform pattern of the cells is prominent (DMAB alone, expt I). H & E. *Bar*=300 µm. × 36. (Reprinted with the permission of Rivenson A, Silverman J. Prostatic cancer in laboratory animals. In Rose D, ed. Endocrinology of cancer. Vol III. Cleveland and Boca Raton: CRC Press, 1982:1.)

FIGURE 4.—Higher magnification of fig. 3. Secretory products are present in the acini. A few mitoses are also seen. H & E. *Bar*=50 µm. × 228

FIGURE 5.—A well-differentiated adenocarcinoma of the prostate gland invading into the dorsal lobe (DMAB + low fat diet, expt II). H & E. *Bar*=300 µm. × 36

FIGURE 6.—Higher magnification of fig. 5. The neoplastic acini are irregular in structure, and cells display numerous mitotic figures. H & E. *Bar*=50 µm. × 228

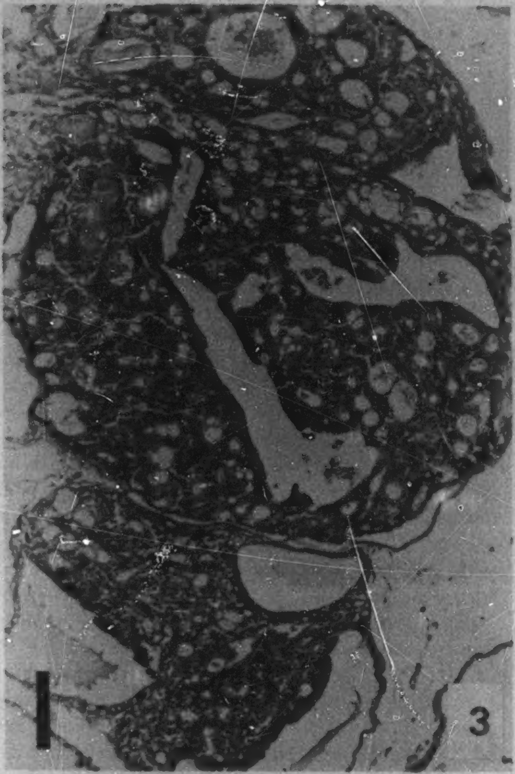
3

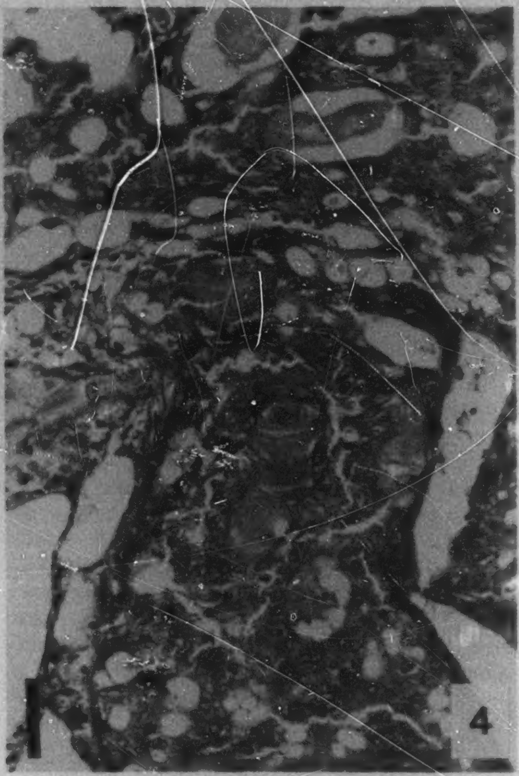
4

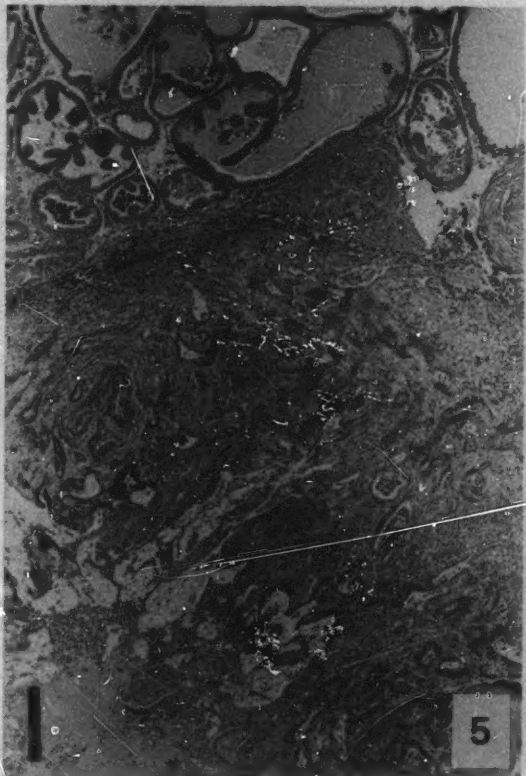
5

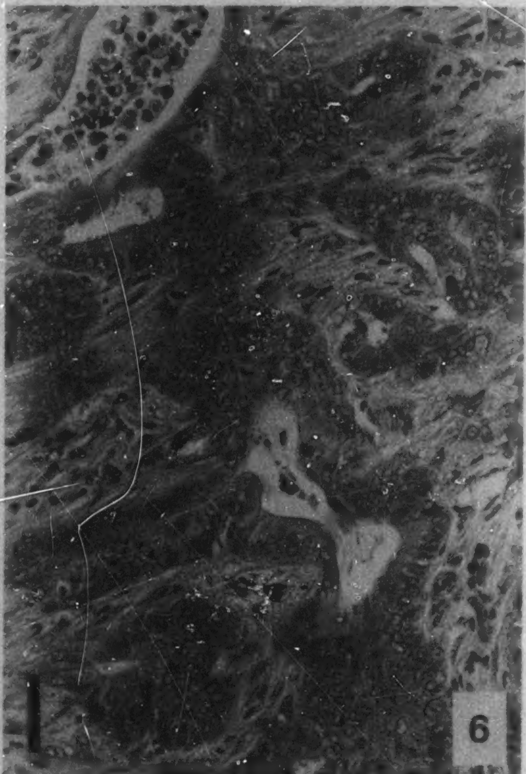
6

Comparison of In Vitro and In Vivo Effects of Thymidine on L1210 Leukemia in Mice[1]

Daniel S. Zaharko[2,3] *and* **Lori M. Ramonas**[2,4,5]

ABSTRACT—Previous investigators have shown that L1210 leukemia in vitro growth can be inhibited by thymidine (dThd) by exposure for 24 hours to dThd concentrations as low as 0.1 m*M*. These experiments were conducted in an attempt to determine why dThd, although effective as a cytostatic agent against L1210 in vitro, is ineffective against L1210 in (BALB/c×DBA/2)F_1 ($CD2F_1$) mice. Systematic variations of dThd concentration and exposure times were examined in both a growth-inhibition assay and a soft agar cloning assay in vitro. The growth of cells exposed to 0.1–1.0 m*M* dThd for 15 hours was inhibited dramatically during exposure, but growth recovered to control rate rapidly when dThd was washed off the cells. With 96 hours of exposure to 1.0 m*M* dThd, growth rate did not return to control rate up to 120 hours after washing. Cloning efficiency was reduced to less than 1% of control by prior 96-hour exposure of L1210 cells to more than 0.5 m*M* dThd. Concentrations of deoxycytidine (dCyd) of 1.0 μM partially reversed cytotoxicity caused by dThd greater than 0.1 m*M*, and 10 μM dCyd completely reversed this cytotoxicity. In vivo plasma dThd concentrations during ip injections of 3,600 mg dThd/kg body weight every 8 hours for 4 days (approximately lethal dose for 10% of animals treated) ranged from 10 to 0.1 m*M*, but these concentrations were ineffective in prolonging survival time of L1210-bearing mice. Plasma concentrations of dCyd prior to dThd exposure were less than 1.0 μM. Following injection of dThd (3,600 mg/kg body wt), plasma dCyd was 2.8±0.5 μM (normal mice) and 6.1±0.5 μM (L1210-bearing mice). Thus the rise of dCyd in plasma following dThd administration in vivo prevented the cytotoxicity of dThd seen in vitro from being manifested in vivo in $CD2F_1$ mice.—JNCI 1982; 68:875–880.

Early reports in the literature indicate that dThd inhibits DNA synthesis (*1*) and acts as a cell-synchronizing agent (*2*). The biochemical mechanisms for these actions have been intensively studied over the intervening years and have been well summarized in a recent publication (*3*). Text-figure 1 illustrates that dThd exerts its inhibitory actions on cell functions by being converted to TTP which controls a variety of enzyme activities. The generally accepted mechanism for inhibition by dThd of cell growth is a block of the ribonucleotide reductase at the level of deoxyribopyrimidylate production (*4*). This inhibitory action can be reversed by providing dCyd (*5*). Recently, on the basis of in vitro studies and human xenograph studies in athymic mice, it was suggested that dThd might be a selective antitumor agent if high plasma concentrations (millimolar or greater) are sustained in vivo (*6, 7*). Subsequent reports, however, indicate that dThd used alone is not very useful as an antitumor agent in vivo in a variety of tumor systems (*8–11*). For the L1210 mouse leukemia in particular, it has been demonstrated that complete growth inhibition in vitro can be achieved by millimolar concentrations of dThd (*12*). However, in vivo, at doses that should have resulted in millimolar concentrations in the plasma of mice bearing ascites L1210 leukemia, no increase in life-span of the mice was observed (*9*).

In this article we confirm this anomaly and explore further the pharmacokinetic and biochemical reasons for the discrepancy between the in vitro and in vivo effects of dThd on the L1210 leukemia.

MATERIALS AND METHODS

Animals and tumors.—(BALB/c × DBA/2)F_1 (hereafter called $CD2F_1$) mice, 20–25 g, were used in all studies. L1210 mouse leukemia was maintained by ip passage and transplanted by iv injection into the tail veins of mice for in vivo experimental studies. Trypan blue exclusion was used to determine the number of viable cells injected. For in vitro studies these same L1210 mouse leukemia cells were grown in suspension culture at 37°C in RPMI-1630 medium supplemented with 20% heat-inactivated horse serum, L-glutamine (1, m*M*), 2-mercaptoethanol (50 μM), penicillin, and streptomycin. dCyd in this supplemented media, as measured by HPLC, was less than 1 μM. The number of cells used in the colony survival or in the growth assay was determined with a Coulter counter, and the viability (trypan blue, periodic checks) was greater than 90%.

Cultures used to measure the growth inhibition by dThd were maintained in an exponential growth phase at densities between 0.3 and 1.8×10^6 cells/ml. Control doubling time in this medium under these conditions is 24 hours.

The method of Chu and Fisher (*13*) for colony survival in soft agar was used to determine the viability of cells after dThd treatment in vitro. The percent colony formation of control cells was 50±4 (SD). The evaluation of antitumor activity in vivo followed the techniques of Schabel et al. (*14*). Animals dying of drug toxicity were not used in scoring the median survival day.

dThd and dCyd.—These substances were obtained from Sigma Chemical Co., St. Louis, Mo. To administer the large quantities of dThd required, we injected all in vivo doses ip in a volume of 0.1 ml/g of mouse. This solution was made

---

ABBREVIATIONS USED: Cyd=cytidine; dCyd=deoxycytidine; dThd=thymidine; EMEM=Eagle's minimum essential medium; DMEM=Dulbecco's modified EMEM; HPLC=high-pressure liquid chromatography; psi=pounds per square inch.

---

[1] Received August 31, 1981; accepted January 11, 1982.

[2] Laboratory of Chemical Pharmacology, Division of Cancer Treatment, National Cancer Institute, National Institutes of Health, Public Health Service, U.S. Department of Health and Human Services, Bethesda, Md. 20205.

[3] *Address reprint requests to* Dr. Zaharko at Building 37, Room 5D11, National Institutes of Health, Bethesda, Md. 20205.

[4] *Present address:* Congressional Science Fellow, 1131 Longworth House Office Building, D.C. 20515.

[5] We acknowledge the technical assistance of Susan Arnold, Ernestine Gregory, Concepcion Muneses, and Edward Walsh.

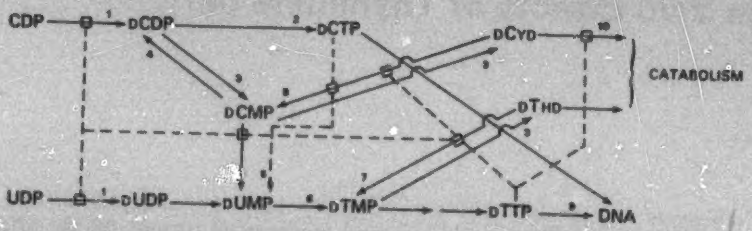

TEXT-FIGURE 1.—Biochemical pathways involved in deoxyprimidine metabolism. Enzymes known to be involved are: 1, ribonucleoside diphosphate reductase; 2, nucleoside diphosphokinase; 3, nucleoside dephosphorylase; 4, deoxycytidylate kinase; 5, deoxycytidylate deaminase; 6, dThd synthetase; 7, dThd kinase; 8, dCyd kinase; 9, DNA polymerase; 10 Cyd deaminase. -□-, inhibition; ••••, stimulation.

isotonic by adding the appropriate amounts of NaCl to the aqueous dThd solution. dThd was dissolved in DMEM for the in vivo infusion studies.

Chromatography.—A liquid chromatographic technique used for the measurement of nucleosides (*15*) was adapted to HPLC to resolve and quantitate dThd and dCyd from other UV-absorbing plasma and tissue components. The stainless steel column was 25 cm long × 4 mm in internal diameter and was packed with Aminex A-8 cation-exchange resin, particle size 7±1.0 μm (Bio-Rad Laboratories, Richmond, Calif.). The eluent was $(NH_4)_2CO_3$ adjusted with NH_4OH to pH 9.95 (to resolve Cyd from dCyd) or to pH 9.75 (to measure low dThd plasma concentrations). Ambient temperatures of 25°C and a flow rate of 0.2 ml/minute resulted in a pressure that fluctuated around 1,000 psi, depending on the age of the prefilter (Rheodyne, 2 μm) and precolumn (5 cm × 2 mm, A-8 Aminex), which were changed when the pressure exceeded 3,000 psi. The flow was maintained constant, independent of pressure by an Altex 110A solvent-metering pump. Peak heights were measured at 254 or 270 nm in an 8-μl flow cell with a Schoeffel SF770 spectrophotometer and quantitated with a Shimadzu C-E 1B data processor. Peak heights were proportional to the quantities of dThd and dCyd in the solution that was injected. Standard curves were linear in the utilized range. With the volumes of injections used, dThd below 1 μM was undetectable, and dCyd below 0.5 μM was undetectable. The plasma dThd peak was confirmed by its comigration with standard dThd on the A-8 Aminex column. Also, the postulated plasma dThd peak was collected and rerun on a Rheodyne RP-8, 25 cm × 4-mm stainless steel column eluted with 0.005 M NH_4 acetate (pH=4.9), 95:5 with acetonitrile (eluent flow, 1.0 ml/min). This peak from the A-8 column coeluted with a standard dThd on the RP-8 column. The dCyd peaks from plasma and spleen extracts were also confirmed by their comigration in the above two chromatographic systems with a standard dCyd. In addition, with the use of a stop-flow technique on the A-8 column, a standard dCyd peak's UV spectrum was scanned between 200 and 300 nm with a Schoeffel SF 770 coupled with an MM 700 memory module and matched that of the scan of peaks with dCyd retention times in plasma and spleen extracts. These findings, coupled with the observation that Cyd and dCyd are cleanly resolved in the above two systems, give us some confidence that we are indeed measuring changes in dCyd following the administration of high doses of dThd to mice.

Sample preparation.—Blood was collected by decapitation of the mice anesthetized a few minutes earlier with 80 mg pentobarbital/kg body weight. Spleens were removed just prior to decapitation and quickly frozen by clamping between two aluminum blocks kept in Dry Ice between each clamping. The blood was centrifuged (1,500×*g* for 15 min), and the plasma was collected and frozen. Three volumes of methanol were added to each thawed volume of plasma. The precipitate was spun at 12,000×*g* in an Eppendorf centrifuge and discarded; the supernatant was dried at 50°C under slight vacuum to create an airflow. The dried supernatant was made up with the eluting buffer to half the volume of the original plasma volume used. A precipitate formed, which was centrifuged (12,000×*g*), and an aliquot of the supernatant was used to inject into the HPLC chromatographic column. The frozen spleen was processed in the same manner except 3.5 ml methanol/g spleen was used and the initial step was to blend with a Tekmar homogenizer with microprobe. The methanol-dried fraction was made up in 0.7 ml eluting buffer/g spleen weight. Calculations for concentrations per milliliter of plasma or per gram wet weight of spleen were made. Recoveries were 95±5% for dThd and 80±5% for dCyd when these substances were added to plasma and then extracted.

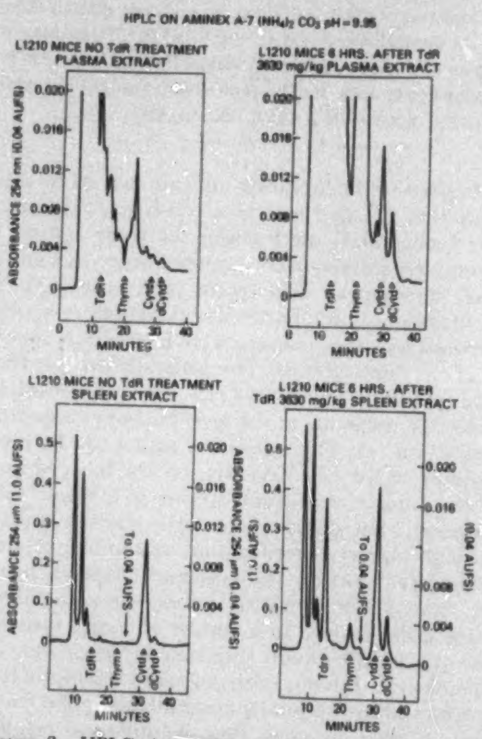

TEXT-FIGURE 2.—HPLC chromatographs of plasma and spleen extracts from mice. Aminex A-8 column eluted with $(NH_4)_2CO_3$ (pH=9.95) at 25°C; flow rate, 0.2 ml/min. AUFS=absorption units full scale; TdR=dThd; Thym=thymine; Cytd=Cyd; dCytd=dCyd.

RESULTS

Text-figure 2 illustrates typical HPLC chromatograms of plasma and spleen extracts from mice. All subsequent quantitative calculations are made from such typical chromatograms.

In Vivo Plasma Kinetics

Text-figure 3 illustrates results of plasma concentrations of dThd in mice following single doses that ranged in toxicity from nonlethal to lethal. Note the change in half-life as doses progress from nonlethal to lethal. On the basis of these data, we chose a dose around 3,600 mg/kg body weight for subsequent therapeutic tests. The assumption was that this dose, if repeated every 8 hours, would sustain a plasma concentration of dThd between 0.1 and 10 m*M* during the major portion of the dosing interval.

Text-figure 4 data confirm this assumption when the dosing period was 4 days. A critical dThd concentration of above 0.1 m*M* was selected because of previous reports (*12, 16*) that maximal growth suppression of L1210 in vitro was achieved above concentrations of 0.1 m*M* when growth inhibition was measured during exposure to dThd.

In Vitro Cytostatic and Cytotoxic Response

We confirmed this above finding of growth inhibition with our L1210 leukemia cells. Growth of these cells during 96 hours of exposure to dThd was one-tenth or less that of controls when dThd concentrations were 0.1 m*M* or greater. In addition, we collected data (text-fig. 5) illustrating that after the dThd is washed off, L1210 cells may recover rapidly from their growth inhibiton. The time of exposure to dThd as well as the concentration is important in the determination of the degree of inhibition and the time to recovery.

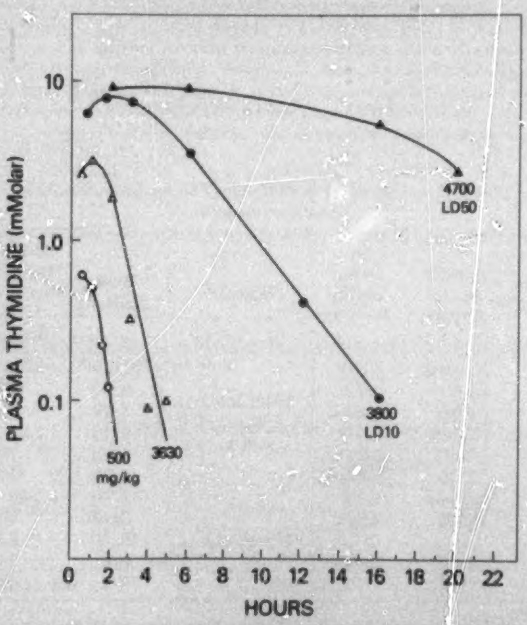

TEXT-FIGURE 3.—Plasma dThd of CD2F$_1$ mice following a single ip dose of dThd in a volume of 0.1 ml/g body wt. *Each point* represents an HPLC analysis of a pooled plasma extract from 3 mice. LD10=10% lethality; LD50=50% lethality.

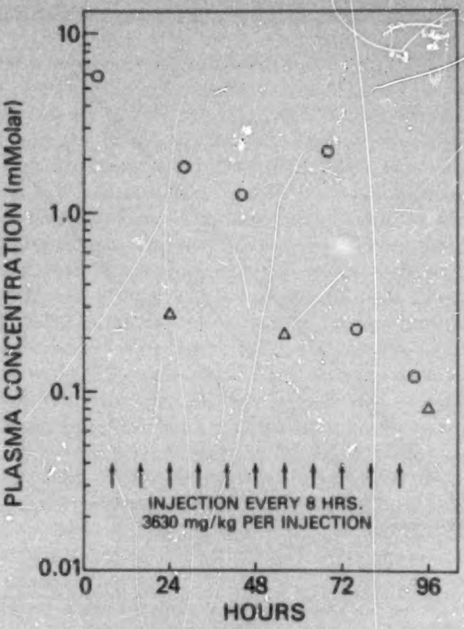

TEXT-FIGURE 4.—Plasma dThd of CD2F$_1$ mice following multiple ip doses of dThd in a volume of 0.1 ml/g body wt. *Each point* represents an HPLC analysis of a pooled extract from 3 mice. ○=4 hr after injection. △=8 hr after injection. The first injection was at zero hour.

To determine to what extent this inhibitory effect of dThd was cytotoxic, we then conducted a colony survival assay of L1210 following a 4-day exposure to various concentrations of dThd. Text-figure 6 illustrates two findings. First, dThd indeed is cytotoxic to L1210 cells and results in a 3-log cell kill at a concentration of 1.0 m*M* maintained for 4 days prior to cloning. Concentrations below 0.1 m*M* are, however, only slightly cytotoxic, and concentrations between 0.1 and 1.0 m*M* are intermediate in toxicity. Second, if present during the dThd exposure at the proper concentration, dCyd can reverse the cytotoxicity. The proper concentration for 1 m*M* dThd appears to be between 5 and 10 μM dCyd.

In Vivo Therapeutic Response

Our first in vivo therapeutic experiment was designed to determine whether single doses of dThd could affect the growth of L1210 in vivo. Table 1 presents data that indicate neither dThd administration twice a day nor three times a day for 4 days slows the growth of L1210 in vivo as determined by the survival time of mice. Notice also the wide range of toxicities seen on the same schedule, which indicates perhaps a variable pharmacokinetic behavior of dThd in individual mice. Because of the rapidly changing plasma concentrations resulting from such single doses and the earlier in vitro findings indicating that sustained high dThd concentrations were necessary to maintain inhibition of growth or result in cytotoxicity in vitro, we conducted an in

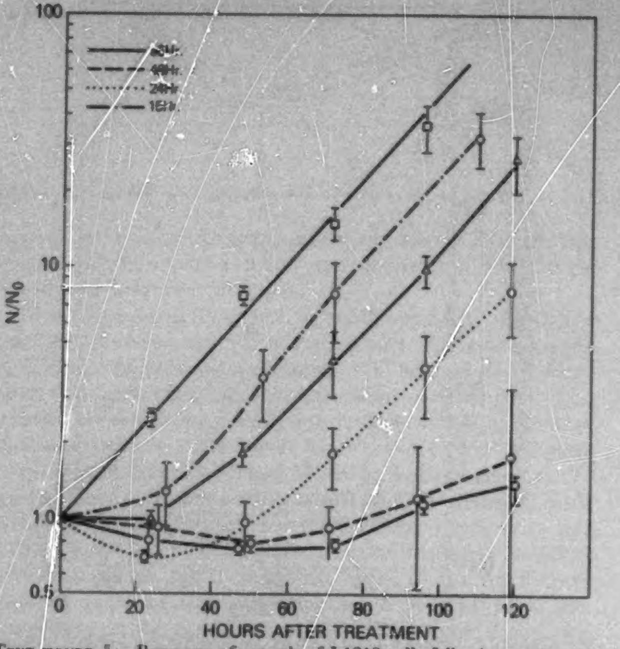

TEXT-FIGURE 5.—Recovery of growth of L1210 cells following treatment with dThd. Cells were suspended at a density of 1×10^6 cells/ml and grown for various times (15, 24, 48, and 96 hr) in normal or dThd-containing media. They were then all washed three times in fresh normal medium and reincubated in fresh normal medium at a density of 2.5×10^5 cells/ml. dThd treatment: ○=1 m*M*; △=0.1 m*M*; □=no dThd. N/NO=No. of cells in drug-treated tubes/No. of cells in control tubes.

vivo experiment in which we infused dThd ip for 4 days. We monitored the plasma dThd by daily sampling tail vein blood.

Table 2 presents these data. Control animals that died of tumor died mainly between days 7 and 8. Animals that died of dThd toxicity died much earlier (day 1, 2, or 3) and had plasma dThd concentrations around 10 m*M*. dThd-infused animals that died of tumor had plasma dThd concentrations around 1.0–2.0 m*M* for each of the 4 days of infusion. This difference between plasma steady-state dThd concentrations in mice manifesting drug toxicity and in mice dying of tumor verifies the variable pharmacokinetic behavior of dThd in individual mice. Similar results indicating the lack of antitumor action at maximally tolerable dThd infusions have been obtained in a different mouse strain [(C57BL × DBA)F_1 (BDF_1)] with L1210 in independent studies in another laboratory (*16*). These in vivo data indicated that the resistance of L1210 in vivo to dThd under these dose schedules was more likely due to a biochemical reason rather than to a pharmacokinetic one.

Text-figure 6 presents data indicating that dCyd between 5 and 10 µ*M* is necessary to reverse the cytotoxicity of dThd in an in vitro colony survival assay. We therefore looked in vivo at dCyd concentrations in normal animals and L1210-bearing animals receiving high doses of dThd.

Plasma and Spleen dCyd

Our first experiment was to determine the recovery of added dCyd (1×10^{-5} *M*) from normal, dThd-untreated mouse blood at 0 and 37°C. The recovery of dCyd was consistently 75% even with incubation times up to 2 hours at 37°C. This phenomenon indicates that the CDF_1 mouse strain lacks significant deaminase activity in the blood in

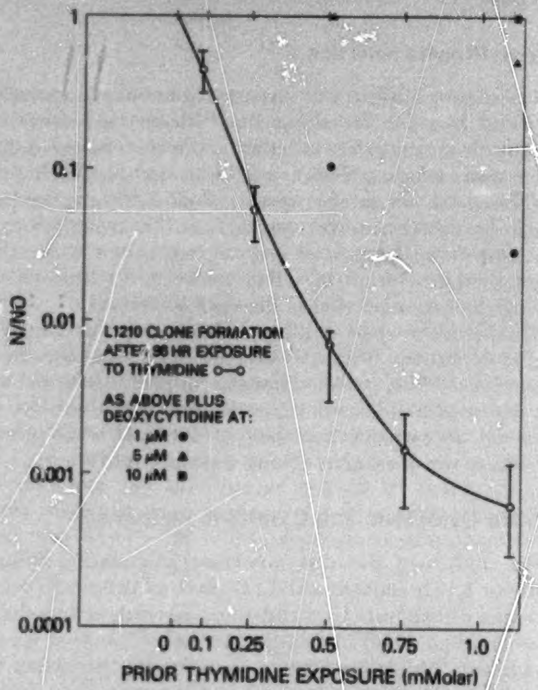

TEXT-FIGURE 6.—Colony survival assay of L1210 cells after 96 hr of exposure to various concentrations of dThd and dCyd. Cells were exposed at a density of 1×10^6 cells/ml. The culture medium was changed daily, and the cells were washed three times prior to seeding in soft agar at three densities (10^2, 10^3, and 10^4 cells/ml). Visible colonies were counted after 10 days and again after 14 days of incubation at 37°C. Agreement between these two counts was excellent. N/NO=No. of colonies in drug-treated tubes/No. of colonies in control tubes.

TABLE 1.—*Antitumor activity of dThd on L1210-bearing and normal mice*

Expt No.	Experimental group[a]	Dose,[b] mg/kg body wt	Schedule[c]	Toxic deaths[d]	Median survival day, nontoxic deaths
1	Normal	3,500	hQ 8 hr×2 on days 1, 2, 3, and 4	1/10	>30
	L1210	3,500		0/10	7.5
	L1210	Saline		1/10	7.5
2	Normal	3,800		8/10	>30
	L1210	3,800		5/10	7.5
	L1210	Saline		1/10	7.5
3	Normal	3,630	Q 8 hr×12	2/20	>30
	L1210	3,630		3/14	8.5
				10/20	8.5
	L1210	Saline		0/8	7.0
				0/4	8.5

[a] L1210 given iv 1×10^4 cells; treatment was started 24 hr later.

[b] Dose for each injection, delivered ip in a volume of 0.1 ml/g of mouse.

[c] Q=quantity of dose indicated.

[d] No. of mice that died/total No. of mice given injections.

contrast to that of another strain (BDF_1) (*16*).

Table 3 indicates that after dThd treatment the plasma dCyd concentration rises in both normal and L1210-bearing mice. The plasmas of L1210 mice after dThd treatment have a higher concentration of dCyd than those of normal mice, and this difference is statistically significant ($P<0.01$). Recall that a dCyd concentration of 5 μM or above is sufficient to reverse the cytotoxic response of dThd measured in the colony survival assay in vitro.

There is also a statistically significant difference ($P<0.001$) between the plasma dThd concentration of normal dThd-treated mice and L1210 dThd-treated mice. It appears from these data and the plasma dThd data presented in table 2 that some L1210 mice are unable to clear dThd from their blood as rapidly as most normal mice.

A regression analysis was run between all the plasma dThd and simultaneous dCyd concentrations from multiple injection experiments in which mice were killed for blood from 2 to 24 hours after a dThd injection ip of 3,600 mg/kg body weight. We analyzed 37 samples, 3 pooled mice/sample. The regression equation for dCyd on dThd is $Y=0.0023X+1.33\ \mu M$ with a standard error of Y on X of ±1.5 and a correlation coefficient of 0.70. Thus higher dThd concentrations extracellularly in vivo are roughly related to higher dCyd concentrations extracellularly. This correlation could theoretically result because of a rise in TTP intracellularly, which would influence the balance among dCyd nucleotide production, utilization, and degradation (*see* text-fig. 1).

Table 3 also presents data from the spleens of mice. Note the higher dCyd in L1210 mice. L1210 grows extensively in the spleens of these mice.

TABLE 2.—*dThd infusion of L1210-bearing and normal mice*

Experimental group	Infusion[a]	No. of animals	Day of death: Due to tumor	Day of death: Drug toxicity	Plasma dThd, mM 24–96 hr
Normal	dThd	4	—	—	2.59±0.26
L1210	EMEM	12	7, 7, 8, 8, 8, 7, 7, 6, 7, 7, 8, 8	—	—
L1210	dThd	19	8, 8, 8, 9, 9, 7, 7	2, 2, 2, 2, 2, 2, 2, 3, 1, 3, 2	1.99±0.20 nontoxic 9.39±2.81 toxic

[a] 200 mg dThd/kg/hr in MEM or EMEM alone for 96 hr, ip infusion; 45 mg dThd/ml of infusion fluid.

DISCUSSION

These studies set out to further our understanding of the action of dThd alone by comparison of its in vitro and in vivo effects on L1210. Because of the rapid clearance of dThd from the body, we thought that it should be established that the lack of an antitumor effect was not attributable to a pharmacokinetic problem of inability to sustain plasma concentrations. We have shown that both concentration and exposure time are important. These data suggest that even with frequent single high doses of dThd, concentrations in the millimolar range are difficult to sustain in plasma. Even in those cases in which the maximal tolerable concentration of dThd was administered by injection or infusion to L1210-bearing mice, no demonstrable cytotoxic or cytostatic effect on L1210 growth was evident. It is evident, though, that much variability exists from individual mouse to mouse in the manner in which dThd is cleared from the blood. Note the variable toxicity with similar doses in table 1 and the relationship of plasma concentration with toxicity in table 2 and text-figure 3. The intolerable dThd plasma concentration in $CD2F_1$ mice is somewhere between 2 and 10 mM if sustained. We have discussed this toxicity in more detail in an earlier publication (*17*).

Our observation of consistent recovery of dCyd from blood incubated at 37°C for prolonged periods indicates the lack of a deaminase for dCyd in the blood of these mice.

The observation of a rise in dCyd in mouse plasma after dThd administration, particularly the higher levels in L1210-bearing mice compared to the levels in normal mice, was at first somewhat puzzling. Cyd deaminase, for which dCyd is a good substrate, is present in high activities in mouse liver, kidney, and leukemic mouse spleen (*18–21*). These high enzyme activities might be expected to maintain the low dCyd concentrations that we find in normal mice and result in even lower levels in L1210-bearing mice, which we observed. There are various conflicting reports of the inhibition by TTP of Cyd deaminase, depending on the source of enzyme (*18–20*). The enzyme from leukemic mouse spleen has been reported not to be inhibited by concentrations of TTP up to 3 mM. Therefore, we expected a fall in dCyd after excess dThd because of the well-documented inhibition of the only known source for de novo production of deoxynucleotides, ribonucleotide reductase, by TTP and the lack of inhibition of the deaminase primarily responsible for catabolic removal of dCyd. However, deoxycytidylate deaminase is potently inhibited by TTP at concentrations as low as 0.2 mM (*21*). We therefore speculate that the

TABLE 3.—*dThd and dCyd concentrations in plasmas and spleens from normal and L1210-bearing animals*[a]

Animal type	No treatment				dThd treatment[b]			
	Plasma		Spleen		Plasma		Spleen	
	dThd	dCyd	dThd	dCyd	dThd	dCyd	dThd	dCyd
Normal	<1	0.9±0.1	<5	<2.5	435±136	2.8±0.8	1,380±283	27±4
L1210[c]	<1	0.6±0.1	<5	<2.5	1,381±116	6.1±0.5	2,726±1,253	47±9

[a] Values are micromolar±SEM. Six or more mice per mean value.

[b] 3,600 mg dThd/kg injected ip 6 hr prior to killing. Volume, 0.1 mg/g of mouse.

[c] L1210 cells (1×10^{4}) injected 6 days prior to killing.

interplay between formation of the dCyd nucleotides and their removal by deaminases and dephosphorylases intracellularly must be affected by the extracellular supply of both dThd and dCyd. There must be a response to this interplay of enzymes (*see* text-fig. 1) in various organs in vivo that results in a rise in plasma dCyd, and thus we speculate a maintenance of the dCyd nucleotides intracellularly in L1210. These data support the concept that in vivo L1210 cells use circulating plasma dCyd and/or dThd to form their dThd and dCyd nucleotides.

However, since there is no external source of dCyd in vitro, unless supplied, the excess production of TTP from excess dCyd does result in a depletion of dCyd nucleotides and hence inhibition of DNA synthesis, which the cells can apparently tolerate for only a finite time before death occurs.

The potential of dThd as a single therapeutic agent is not encouraging (*22*). However, because of its unique characteristics in modulation of biochemical pathways involved in DNA synthesis and its potential in combination chemotherapy, dThd needs continued study. Initial studies of dThd in combination with methotrexate (*9*), 5-fluorouracil (*23*), and β-cytosine arabinoside (*24*) suggest that further exploration of this mode of use may be fruitful. Further understanding of the subtle mechanism of action of dThd in vivo may be helpful in this regard.

These studies also indicate that caution should be exercised when extrapolating from in vitro drug effects to anticipated in vivo drug effects.

REFERENCES

(*1*) Xeros N. Deoxyriboside control and sychronisation of mitosis. Nature 1962; 194:682–683.

(*2*) Bootsma D, Budke L, Vos O. Studies on synchronous division of tissue culture cells initiated by excess thymidine. Exp Cell Res 1964; 33:301–309.

(*3*) Reynold EC, Harris AW, Finch LR. Deoxyribonucleoside triphosphate pools and differential thymidine sensitivities of cultured mouse lymphoma and myeloma cells. Biochim Biophys Acta 1979; 561:110–123.

(*4*) Reichard P, Canellakis ZN, Canellakis ES. Studies on a possible regulatory mechanism for the biosynthesis of deoxyribonucleic acid. J Biol Chem 1961; 236:2514–2519.

(*5*) Schachtschabel DO, Lazarus H, Farber S, Foley GE. Sensitivity of cultured human lymphoblasts (CCRF-CEM) to inhibition by thymidine. Exp Cell Res 1966; 43:512–514.

(*6*) Lee S, Giovanella BC, Stehlin JS Jr. Selective lethal effect of thymidine on human and mouse tumor cells. J Cell Physiol 1977; 92:401–405.

(*7*) ———. Effect of excess thymidine on the growth of human melanoma cells transplanted in thymus deficient nude mice. Cancer Lett 1977; 3:209–214.

(*8*) Tattersall MH, Brown B, Frei E. The reversal of methotrexate toxicity by thymidine with maintenance of antitumour effects. Nature 1975; 253:198–200.

(*9*) Semon JH, Grindey GB. Potentiation of the antitumor activity of methotrexate by concurrent infusion of thymidine. Cancer Res 1978; 38:2905–2911.

(*10*) Howell SB, Jenkins RS, Streifel J. Activity of thymidine as a chemotherapeutic agent against human tumor xenografts in nude mice. Cancer Res 1979; 39:3875–3880.

(*11*) Chiuten DF, Wiernik PH, Zaharko DS, Edwards L. Clinical Phase I–II and pharmacokinetic study of high-dose thymidine given by continuous intravenous infusion. Cancer Res 1980; 40:818–822.

(*12*) Lowe JK, Grindey GB. Inhibition of growth rate and deoxynucleoside triphosphate concentrations in cultured leukemia L1210 cells. Mol Pharmacol 1976; 12:177–184.

(*13*) Chu MY, Fisher GA. Incorporation of cytosine-^{3}H arabinoside and its effects on the murine leukemia cells (L5178Y). Biochem Pharmacol 1968; 17:753–767.

(*14*) Schabel FM, Griswold DP, Laster WR, Corbett TH, Lloyd HH. Quantitative evaluation of anticancer agent activity in experimental animals. Pharmacol Ther, Part A 1977; 1:411–435.

(*15*) Singhal RP. Ion-exclusion chromatography: Analysis and isolation of nucleic acid components and influence of separation parameters. Arch Biochem Biophys 1972; 152:800–810.

(*16*) Egan EM, Sargent L, Rosowsky A, Kufe W. Rescue of thymidine cytotoxicity in L1210 ascites by elevated endogenous levels of deoxycytidine. Cancer Treat Rep 1981; 65:853–860.

(*17*) Herman EH, Jordan W, Ardalan B, Zaharko DS, Bolten BJ, Cooney DA. Toxicologic effects of a high dose of thymidine in mice. Toxicol Appl Pharmacol 1980; 56:443–446.

(*18*) Ipata PL, Gercignani G. Cytosine and cytidine deaminase from yeast. Methods Enzymol 1978; 51:394–401.

(*19*) Wentworth OF, Wolfender R. Cytidine deaminases (*E. coli* and *H. liver*). Methods Enzymol 1978; 51:402–407.

(*20*) Rothman IK, Malathi VG, Silber R. Cytidine deaminase from leukemia mouse spleen. Methods Enzymol 51:408–412.

(*21*) Maley GF. Deoxycytidylate deaminase from T2-infected *Escherichia coli*. Methods Enzymol 1978; 51:412–418.

(*22*) Bruno S, Poster DS, Bono VH, MacDonald JS, Kubota TT. High-dose thymidine in clinical oncology. Cancer Treat Rep 1981; 65:57–64.

(*23*) Martin D, Stolfi R. Thymidine enhancement of antitumor activity of 5-fluorouracil against advanced murine breast carcinoma. Proc Am Assoc Cancer Res 1977; 18:126.

(*24*) Danhauser LL, Rustum YM. Effect of thymidine on the toxicity, antitumor activity, and metabolism of 1,β,D-arabinofuranosylcytosine in rats bearing a chemically induced colon carcinoma. Cancer Res 1980; 40:1274–1280.

Announcements

The Journal will publish notices of major meetings dealing with cancer. Submission of notices 6 months in advance is requested to permit timely publication.

Gordon Research Conference

"Statistics in Chemistry and Chemical Engineering" is the subject of this conference to be held at the New Hampton School, New Hampton, New Hampshire, on August 2–6, 1982. Participants will discuss new developments in statistical methodology and new applications of statistics in chemistry-related areas.

Requests for applications to the conference, or additional information, should be addressed to Dr. Alexander M. Cruickshank, Director, Gordon Research Conferences, Pastore Chemical Laboratory, University of Rhode Island, Kingston, Rhode Island 02881 (telephone: 401-783-4011).

Seventh European Symposium on Hormones and Cell Regulation

Sainte-Odile (near Strasbourg), France, will be the site of this symposium to be held on October 4–7, 1982. The main topics of this conference are: synthesis of peptides and precursors; steroid action and gene expression; germ cell development; regulatory peptides in reproduction; insulin action; arachidonic acid cascade; cyclic nucleotide metabolism; and bioenergetics and calcium distribution.

The general attendance is limited to 120 persons on a first-come first-registered basis. Participants may present posters related to the topics of the conference. For detailed information on the program and registration, please write to Dr. R. Denton, Department of Biochemistry, University of Bristol Medical School, Bristol BS8 1TD, Great Britain (U.K.).

Southeastern Cancer Research Association Meeting

The Southeastern Section of the American Association for Cancer Research (Southeastern Cancer Research Association) will meet at the Quality Inn, Gatlinburg, Tennessee, on October 14–15, 1982. The meeting format will include scientific presentations from Association members and a special symposium entitled "Growth Factors, Viruses, and Protein Phosphorylation."

The meeting is open to all medical researchers and scientists. For additional information, please contact Dr. Wayne E. Criss, Cancer Center, Howard University, Washington, D.C. 20059.

Seventh International Symposium of the World Association of Veterinary Microbiologists, Immunologists, and Specialists in Infectious Diseases

Barcelona, Spain, will be the site of this meeting entitled "Infectious Diseases of the Gastro-Intestinal Tract in Bovine and Porcine Species" to be held on October 18–21, 1982.

For additional information, please write to Dr. Juan Plana Duran, Gran Via de les Corts Catalanes, 794 bajos (Chaflán Lepanto), Barcelona 13, Spain.

Chemotherapy Foundation Symposium V

The Division of Medical Oncology of the Department of Medicine, the Department of Neoplastic Diseases, and the Page and William Black Post-Graduate School of Medicine of the Mount Sinai School of Medicine will present this symposium entitled "Innovative Cancer Chemotherapy—Tomorrow" to be held at the Barbizon Plaza Hotel in New York City, on November 10–12, 1982. Dr. Ezra M. Greenspan is chairman of the meeting which will also cover recent developments in chemoimmunotherapy and biological response modifiers.

Symposium registrants are eligible for AMA Category I credits. For information on registration, please write to the Director, the Page and William Black Post-Graduate School of Medicine, Mount Sinai School of Medicine, Annenberg 5-206, 1 Gustave Levy Place, New York, New York 10029 (telephone: 212-650-6772).

Harvard Medical School Continuing Education Program

The following courses are being offered by the Department of Radiology, Brigham and Women's Hospital, and the Department of Continuing Education, Harvard Medical School:

Computed Tomography—Fifth Annual Postgraduate Course; AMA Category I credit: 28 hours; Steven E. Seltzer, M.D., Program Director; course date September 19–23, 1982.

Chest Disease—Eighth Annual Postgraduate Course; AMA Category I credit: 30 hours; Peter G. Herman, M.D., Program Director; course date October 18–22, 1982.

Angiography, Interventional Radiology, and the New Imaging Modalities—Twelfth Annual Postgraduate Course; AMA Category I credit: 28 hours; Michael A. Bettmann, M.D., Program Director; course date October 25–28, 1982.

For additional information please contact the Department of Continuing Education, Harvard Medical School, 25 Shattuck Street, Boston, Massachusetts 02115 (telephone: 617-732-1525).

NIH Consensus Development Panel Statement Available

A National Institutes of Health Consensus Development Panel has issued a report on the safety and efficacy of CT scanning of the brain. This consensus statement on "Computed Tomographic Scanning of the Brain" is now available for the medical community and the public from the Office for Medical Applications of Research, National Institutes of Health. Free, single copies may be obtained from Mr. Michael Bernstein, Office for Medical Applications of Research, Building 1, Room 216, National Institutes of Health, Bethesda, Maryland 20205.

Availability of Serum Panels

A variety of serum components (e.g., peptide hormones, viral antigens, isoenzymes, glycoproteins, antibodies, immune complexes, tumor-associated antigens, carbohydrates, phospholipids, nucleosides, etc.) have been reported to be uniquely present, or present in elevated or decreased quantities, in the sera of cancer patients, as compared to other patients or to normal individuals. The National Cancer Institute is interested in evaluating assays that have potential for the immunodiagnosis of cancer. Coded serum panels are available to evaluate assays which have given preliminary indications of discrimination between cancer patients and controls. Promising results on this coded panel may provide the basis for further support in development of the immunoassay.

Preliminary data documenting a useful test and request for a coded serum panel to evaluate it should be sent to: Immunodiagnosis Serum Panels, Building 31, Room 3A10, National Cancer Institute, National Institutes of Health, Bethesda, Maryland 20205.

Scientists Center for Animal Welfare Invites New Applications

The Scientists Center for Animal Welfare invites science writers to apply for awards of $500 each for articles on any topic relating to the use of live animals in biomedical experimentation or scientific education. Awards will be made in each of two categories: articles already published and articles being prepared for publication. Applications must contain the following information:

a) Name, address, phone number, affiliation
b) Copy of the published article or an outline of the proposed article
c) Date (or estimated date) of publication, and name of magazine, journal, or newspaper
d) Estimated length of proposed article
e) Samples of previously published work (submit at least two)

Awards will be based not only on the published article, or outline of the proposed article, but also on the quality of samples of previously published work. (Samples do not have to be on the subject of animal experimentation.) The purpose of the Scientists Center journalism stipends is to encourage the publication of thoughtful, thoroughly researched articles on issues surrounding the use of animals in biomedical research in the public press or in scientific journals.

The deadline for receipt of applications is September 30, 1982. The award date is November 1, 1982. Please send completed applications to: Ms. Marcia R. Feinleib, Scientists Center for Animal Welfare, Suite 221, 11325 Seven Locks Road, Potomac, Maryland 20854 (telephone: 301-983-0544).

Disposal of Laboratory Wastes Project

The International Agency for Research on Cancer, with the financial support of the Office of Safety of the National Cancer Institute of the United States, initiated a project in 1979 to evaluate methods for the disposal of laboratory wastes contaminated with chemical carcinogens. The aim of the project is to devise chemical degradation techniques for the disposal of wastes when incineration facilities are not available, and to publish these techniques in a series of manuals. The wastes include aqueous solutions and organic solvents, solid wastes, animal litter, carcasses, and contents of petri dishes. Consideration is also given to effective methods for decontaminating equipment and laboratory space, i.e., in case of accidental spills. The methods devised should be simple, practical, and inexpensive.

The approach of this program is described in *IARC Internal Technical Report No. 79/002* and *IARC Scientific Publications No. 37 and 43*, the first volumes issued in this series. The project comprises: bibliographical searches for existing methods and information about chemical reactions of the compounds that could be utilized for devising methods; investigation of new methods; and validation of any proposed methods through collaborative testing. The "decontaminated" waste arising from a given technique will also be tested for mutagenicity to ensure that the procedure does result in a detoxified product. The documents are finalized by a committee drawn from the collaborating group.

Scientists interested in this project are invited to participate. Collaboration can consist of submitting proposals, elaborations of methods, and validation of methods in inter-laboratory collaborative tests. For further information write to Dr. M. Castegnaro, International Agency for Research on Cancer, 150 Cours Albert Thomas, 69372 Lyon Cédex 2, France.

blank page

blank page

JNCI (NIH Publication No. 82-13)

68/6

JNCI

Journal of the National Cancer Institute

June 1982
Volume 68
Number 6

KD
15.
9.2
7.7
7.2
6.2
1
2
3
4
5

JUN 15 1982
U. S. GOVT. PUBS.
DEPOSITORY 376

U.S. DEPARTMENT OF HEALTH AND HUMAN SERVICES Public Health Service National Institutes of Health

HE 20. 3161:

This month's cover shows electrophoretic separation on agarose gels of DNA fragments containing mouse mammary tumor virus sequences. Mammary tumor DNA from high-expressor and low-expressor mice were analyzed with the use of restriction endonuclease mapping procedures. *Arrows* identify fragments containing endogenous provirus sequences and give their sizes in kilo bases (Kb). Additional bands arise from proviruses acquired during exogenous infection (*see* paper by Altrock et al. on pages 1037–1041).

JNCI

Journal of the National
Cancer Institute

June 1982
Volume 68
Number 6

THE JOURNAL of the National Cancer Institute solicits manuscripts on original observations in laboratory and clinical research from all scientists. A manuscript is considered for publication with the understanding that it has not been published previously and is submitted exclusively to the Journal. Opinions expressed by the authors are not necessarily those of the publisher or its editors.

THE JOURNAL is published monthly (two volumes a year). The Secretary of Health and Human Services has determined that the publication of this periodical is necessary in the transaction of the public business required by law of this Department.

A MONOGRAPH SERIES covering proceedings of scientific meetings pertaining to cancer is also published. These books may be purchased from the Superintendent of Documents. Series subscriptions are not available and monographs are not included in a subscription to the Journal.

THE JOURNAL is for sale by the Superintendent of Documents, U.S. Government Printing Office, Washington, D.C. 20402. Price per copy, $7.00. Subscription price for two volumes per year in the United States, $70.00; foreign, $87.50. Payment is required in advance, and check or money order should be made payable to the Superintendent of Documents.

All inquiries regarding purchase of subscriptions or depository library distribution, including inquiries about missing issues and change of address, should be addressed to the Government Printing Office. The Government Printing Office requires payment in advance on all orders. Inquiries regarding missing issues or change of address for official subscriptions should be addressed to the Editorial Office, Room 850, Westwood Building, 5333 Westbard Avenue, Bethesda, Md. 20816.

VINCENT T. DEVITA, JR., *Director, National Cancer Institute*

BOARD OF EDITORS

PETER GREENWALD, *Editor in Chief*

ELIZABETH K. WEISBURGER, *Assistant Editor in Chief*

STUART A. AARONSON, *Associate Editor*

CHARLES H. EVANS, *Associate Editor*

MARY A. FINK, *Associate Editor*

JANET W. HARTLEY, *Associate Editor*

DONALD HENSON, *Associate Editor*

RONALD B. HERBERMAN, *Associate Editor*

GEORGE S. JOHNSON, *Associate Editor*

KURT W. KOHN, *Associate Editor*

ARTHUR S. LEVINE, *Associate Editor*

JOHN J. MULVIHILL, *Associate Editor*

ALAN S. RABSON, *Associate Editor*

RICHARD M. SIMON, *Associate Editor*

EDITORIAL STAFF

EDWIN A. HAUGH, *Managing Editor*

PAMELA T. ALLEN, *Assistant Managing Editor*

FLORENCE I. GREGORIC, *Monograph Editor*

Editors: DOROTHY D. KATZ, MERCEDES B. LA CHARITY,
I. AGNES REVESZ, JOAN O'BRIEN RODRIGUEZ,
CONSTANCE R. STONESTREET, and ANNA B. WITTIG

JNCI (NIH Publication No. 82-13)

U.S. DEPARTMENT OF HEALTH AND HUMAN SERVICES   Public Health Service   National Institutes of Health

Instructions to Authors

Text: Send one original and two copies. **Text-figures** (graphs, charts, and line drawings): Send one original and two copies. **Figures** (photomicrographs and photographs): Send three original glossy prints, unmounted. **Tables:** Send tabular material in typewritten form; do not submit tables as glossy prints to be photographed. The entire manuscript including footnotes, legends, and references must be typed double spaced. Single-spaced portions of a manuscript will be returned to the author for retyping. The mailing address is: Journal of the National Cancer Institute, Westwood Building, Room 850, 5333 Westbard Avenue, Bethesda, Maryland 20816.

Manuscripts should be accompanied by a covering letter from the author responsible for correspondence about the manuscript. The covering letter should contain a statement that the manuscript has been seen and approved by all authors and that all persons listed as authors have made significant (not merely administrative, technical, or supervisory) contributions to the content of the paper. The letter should also state that the manuscript or substantial portions thereof have not been previously published nor are they under consideration for publication in another journal.

Data too extensive for inclusion in a manuscript, but which may be of interest to other investigators, may be deposited with the National Auxiliary Publications Service (NAPS), c/o Microfiche Publications, P.O. Box 3513, Grand Central Station, New York, New York 10017. Authors using the NAPS facilities should indicate in a footnote how their additional data may be obtained.

TITLE: Be brief (no more than 14 words, if possible), but for indexing purposes include all key words. The annual subject index is prepared directly from the titles. Titles that form complete sentences are not acceptable. Do not use abbreviations or chemical formulas in titles.

BYLINE: Supply the complete first name, middle initial, and last name of each author. Avoid use of nicknames. Academic degree is optional; however, if a degree is provided for one author, it should be provided for all authors on a manuscript. Include the name of the institution, address, and zip code for each author. Indicate address for reprint requests in a footnote on the byline.

ACKNOWLEDGMENTS: Financial aid in support of research should be recognized in a footnote. Aid in technical fields, animal care, photography, stenography, and other areas may be mentioned in a separate footnote. Indicate the title (Dr., Mr., Mrs., Miss, Ms.) and affiliation of each person acknowledged.

ABSTRACT: Provide an abstract, 150 words or less, on a separate page. The abstract should describe only *results* of the work being reported. Speculation, historical background, or reference to published works will be deleted from abstracts. Any inbred strains, noninbred stocks, cell lines, or other living materials used in the work should be noted in the abstract.

TEXT: Avoid the use of laboratory jargon and abbreviations not in common usage. When possible, refrain from the use of abbreviations that form words (exceptions are PAGE, ALL). Whenever possible, write mathematical equations and chemical formulas on a single line; submit complicated chemical structures as artwork. Avoid repetition of data in the text when it is presented in tables or text-figures.

Use the following style sources: Webster's *Third New International Dictionary* and Dorland's *Illustrated Medical Dictionary* (25th ed) for spelling; *Council of Biology Editors Style Manual* (4th ed) for scientific abbreviations and symbols: *Government Printing Office Style Manual* for other abbreviations and symbols, punctuation, and hyphenation; *Biochemical Nomenclature and Related Documents* (IUB, 1978) for abbreviations of chemical substances; *Enzyme Nomenclature*, recommendations (1978) of the IUB for recommended names of enzymes and information on nomenclature of isozymes; *The Merck Index* (9th ed) for chemical compounds; "Standard Nomenclature for Inbred Strains of Mice: Seventh Listing" by Joan Staats (Cancer Res 1980;40: 2083–2128) for inbred mouse strains; "Standardized Nomenclature for Inbred Strains of Rats: Fourth Listing" by Joan Staats and Michael Festing (Transplantation 1973;16:221–245) for designations of inbred rat strains; *Animals for Research* (9th ed) prepared by the Institute of Laboratory Animal Resources, National Academy of Sciences, for designations of laboratory animal stocks and strains.

TABLES: Submit tabular material typed double spaced on a separate page. Computer print-outs of tables are acceptable only if they are double spaced and with satisfactory title, column headings, legends and other textual material. Provide headings for all columns of a table and indicate units of measurement where applicable.

TEXT-FIGURES: Refer to graphs, charts, and line drawings as text-figures. Make the abbreviations on text-figures identical to the abbreviations used in the text and legends. Symbols and lettering should be large enough to be legible if reduced. Glossy prints or original drawings in black ink are acceptable; orient vertically instead of horizontally.

FIGURES: Refer to photomicrographs and photographs as figures. Figures and their legends should fit a 7.5- by 9-inch dimension. Calculate that nine typewritten lines of legend will require 1 inch of vertical space. Type figure legends on a separate sheet and identify in the legend any lettering used on the figure. Trim photographs to show only important areas. Do not number face of photographs; use the back or overlay to indicate the top and number of each. Printed indicators may be included on photographs; do not use hand-drawn indicators. *Insert internal scale markers on all photomicrographs.* Color photographs must be grouped as a single plate. For color reproduction, submit both color transparencies and high-quality black and white reproductions. The need for color must be documented before it will be considered.

REFERENCES: Use any recent issue of the Journal as a style guide for reference lists. Number references in order of citation in both text and reference list. For periodicals, provide author(s), title of paper, journal, year, volume, and first and last page numbers. For books, give the author(s), title, name(s) of editor(s), location and name of publisher, year, pertinent chapter or section title, and page numbers. Follow *Index Medicus* for punctuation and abbreviations. Citations of papers in preparation or submitted for publication, unpublished observations, and personal communications should be noted parenthetically in the text. Do *not* include them in the reference list. The accuracy of all references is the responsibility of the authors and not of the editorial staff.

LETTERS TO THE EDITOR should pertain to recent articles in the Journal and should not contain new data unless relevant to the discussion of a particular paper. The authors addressed will be invited to reply to comments before correspondence is published. Letters will be edited by the Staff, subject to contributor approval.

FURTHER DETAILS on the preparation of manuscripts are set forth in the document "Uniform Requirements for Manuscripts Submitted to Biomedical Journals" prepared by the International Steering Committee of medical editors (*see* Am Rev Respir Dis 1979;119:3–10/Ann Intern Med 1979;90:95–99/Br Med J 1979;1:532–535/ or Lancet 1979;1:428–430).

UNITED STATES GOVERNMENT PRINTING OFFICE, WASHINGTON, D.C.: 1982

Table of Contents

Vol. 68, No. 6—June 1982

Letters to the Editor

883 Cartesian reductionism and cancer — *Harry Rubin*

884 Spontaneous liver tumors in laboratory rats — *Morris Pollard*

Investigations on Man

885 Breast cancer and serum cholesterol — *Robert A. Hiatt, Gary D. Friedman, Richard D. Bawol, Hans K. Ury*

891 Carcinomas of the cervix and corpus uteri in humans: Stage-dependent blood levels of substance(s) immunologically cross-reactive with insulin — *K. Pavelić, M. Bolanča, N. Veček, J. Pavelić, T. Marotti, S. Vuk-Pavlović*

895 A quest for the mechanism of "spontaneous" malignant transformation in culture with associated advances in culture technology — *Katherine K. Sanford, Virginia J. Evans*

915 Cancer incidence in humans: Relationship to plasma lipids and relative weight — *R. B. Wallace, C. Rost, L. F. Burmeister, P. R. Pomrehn*

919 High cloning efficiency of human lymphoid cells in agarose without feeder layers — *Kathleen N. Ayres*

925 Mortality among workers in a nickel refinery and alloy manufacturing plant in West Virginia — *Philip E. Enterline, Gary M. Marsh*

935 Cell-mediated immunity to mouse mammary tumor virus antigens by patients with hyperplastic benign breast disease — *C. B. Cannon, S. H. Barsky, T. C. Alford, L. F. Jerome, V. Tinley, J. L. McCoy, J. H. Dean*

945 Effect of enzymatic disaggregation on proliferation of human tumor cells in soft agar — *Anne W. Hamburger, Christine P. White, Kathleen Tencer*

Investigations on Nonhuman Systems

951 Diverse xenotropic virus expressions in two NZB mouse breeding lines that differ in chromosome breakage — *Carmen Bernard, Ingrid Emerit*

957 Phenotypic stability of murine tumor cells in vitro and in vivo — *James Varani, Edmund J. Lovett*

963	Development of resistance to MOPC-315 plasmacytoma after intralesional and intraperitoneal melphalan therapy of tumor-bearing BALB/c mice. I. Enhancement of in vivo rejection responses by combined chemotherapy–immunotherapy	*Aliza Adler, Irit Altbaum*
971	Hematopoietic precursor cells in mice treated with 4-demethoxydaunorubicin and doxorubicin	*Giulio Massa, Giuseppe Bogliolo, Francesco D'Amore, Carlo Muzzulini, Riccardo Ghio, Ivo Pannacciulli*
977	Inheritance of cellular resistance to the antitumor agent ICRF 159 in somatic cell hybrids	*David H. Eagar, Andrew M. Creighton*
981	Further studies on the relationship between allotransplantability and the presence of the cell surface glycoprotein epiglycanin in the TA3-MM mouse mammary carcinoma ascites cell	*Scott C. Miller, John F. Codington, George Klein*
989	Carcinogenesis by isomers of *N*-nitroso-3,5-dimethylpiperidine	*W. Lijinsky, M. D. Reuber, Sandra S. Singer, George M. Singer*
993	Effect of 7,12-dimethylbenz[*a*]anthracene on production and action of gamma interferon	*Karen A. Golemboski, Debra K. D. DeLor, Uldis N. Streips, Gerald Sonnenfeld*
997	Murine tumor necrosis-inducing factor: Purification and effects on myelomonocytic leukemia cells	*Saul Green, Areta Dobrjansky, Mary Ann Chiasson*
1005	Surface antigen expressed in hematopoietic cells derived from *Fv-4*^{r} mouse strains	*Hiroshi Yoshikura, Takeshi Odaka*
1011	2′-Deoxycoformycin-induced hemolysis in the mouse	*Ellen Spremulli, Gerald W. Crabtree, Daniel L. Dexter, Israel Diamond, Paul Calabresi*
1015	Carcinogen-induced DNA damage and cellular alterations in F344 rat colon organ cultures	*Nitin T. Telang, Gary M. Williams*
1023	Cross-resistance of cultured murine leukemia vincristine-resistant P388 cells to vinblastine, vindesine, and bis(*N*-ethylidene vindesine) disulfide, disulfate	*Lee J. Wilkoff, Elizabeth A. Dulmadge*
1027	Intracellular adriamycin levels and cytotoxicity in adriamycin-sensitive and adriamycin-resistant P388 mouse leukemia cells	*Ram Ganapathi, William Reiter, Awtar Krishan*
1033	Thermotolerance in the murine jejunum	*Kurt J. Henle*
1037	Detection of acquired provirus sequences in mammary tumors from low-expressor, low-risk mice	*Bruce W. Altrock, Robert D. Cardiff, John P. Puma, Judi K. Lund*

Announcements

1043 Ions, Cell Proliferation, and Cancer Symposium

1043 Laser, Microwaves, Ultraviolet, and Ultrasound: Biophysical and Biological Basis, Applications, and Hazards in Medicine in Industry Program

1043 Fourth Annual Pharmacy Symposium on Cancer Chemotherapy

1043 A New Organization—American College of Epidemiology

1043 Annual Meeting of the American College of Epidemiology

1043 International Cancer Symposium

1043 Symposium on Application of Biological Markers to Carcinogen Testing

1044 A New Journal—Survey of Immunologic Research

1044 Eighth FDA Science Symposium

blank page

Letters to the Editor

Cartesian Reductionism and Cancer

Sɪʀ: The guest editorial by Straus[1] uses much of the same evidence cited in my own editorial[2] a year earlier but draws the opposite conclusion, namely, that somatic mutation (or some variant thereof) is the origin of most cancer. The fact that the same evidence can be used to support such divergent views illustrates the futility of a point-by-point rebuttal, tempting as that might be. There was, however, one result that I emphasized in my analysis which is notable by its omission in Straus' editorial. The application of 3-methylcholanthrene to single prostatic fibroblasts results in malignant transformation in some of the descendents of up to 100% of the cells.[3] A similar result was recently reported when a combination of X-rays and a promoting agent was used to initiate transformation.[4] These findings illustrate the extreme susceptibility of inheritable properties of animal cells subjected to perturbing effects, most particularly when the cells are already perturbed by being in culture. They supplement many other observations that show the prevalence of heritable but not primarily genetic changes in cultured cells, including those that occur in early passages of cells explanted from embryos which lead eventually to cell lines,[5] or senescence[6] and the non-Mendelian mosaic pattern of resistance to 5-bromo-2′-deoxyuridine in populations of cells maintained in the presence of the drug.[7] While these regimens may ultimately alter the genome, this is likely to result from a complex evolution of the relationship between the genome and other affected parts of the cell, which brings me to my major point. The relationship between genes and the rest of the cell is reciprocal, not unidirectional, and represents a continuing dialogue. It is no longer productive of anything but polemics to vest exclusive rights for the heritable behavior of the cell in any single component. The cell is the minimal reproductive and functional unit of life, and the imposition of new external conditions, including carcinogens, probably results in a response of the cell as a whole. This can lead to a new state of equilibrium among all the coordinated parts of the cell, which may or may not be heritable. That the genome of the cell will respond as an integral part of the adjustment of the whole unit seems inevitable. This appears to be inherent in some of the diverse conditions known to cause genetic transpositions: the stationary growth state in bacteria, growth of *Drosophila* cells in culture, temperature changes in *Antirrhinum*.[8] None of these seem likely to act directly on DNA.

I believe the reason we keep returning to altered DNA as our model for carcinogenesis is that it is the only *established*, molecularly defined mechanism for determining heredity. This confining behavior is reminiscent of the old story of the fellow looking under a lamppost for a coin lost elsewhere because there was light where he searched. We act confidently as if the malignant transformation were the prototype of a precise mutational event, despite our knowledge that it is chiefly an unpredictably imprecise loss of the organized behavior of the cell, characterized by pleomorphism and an instability leading progressively downhill to autonomy[9]—a sort of biological entropy. There is an appropriate level at which to consider this disorganization, and it has to do with the influences that impose order on the enormous inhomogeneity of the cell. About these we know almost nothing apart from the dictum that all organization arises from preexisting organization.[10] The approach to this level transcends but also incorporates the usual mechanistic assumptions that underlie the purely physicochemical approach of present-day biology. This was recognized long ago by Niels Bohr in his concern that the methods commonly used to study life destroy or distort its defining attribute and thus lead to a type of biological indeterminacy.[11] This view has been elaborated in particular by Elsasser, also a theoretical physicist, who emphasizes the need to face the *irreducible* complexity of living things.[12] Therefore, the proper study of organisms may involve a "renunciation of [mechanistic] knowledge" similar to that which was, paradoxically, necessary to broaden and deepen our understanding of the physical universe.[11] Until we learn to think and then to work in this broadened context, we will continue to promulgate new hypotheses of carcinogenesis—in the same old reductionist way—whenever the last one begins to fade and another bandwagon comes on the scene. To restrict the pattern of our thought to the mold of conventional Cartesian reductionism is to exclude the possibility of the breakthrough to organismic thinking required to penetrate the intellectual morass of carcinogenesis.

Hᴀʀʀʏ Rᴜʙɪɴ
Department of Molecular Biology
University of California, Berkeley
Berkeley, California 94720

---

[1] Sᴛʀᴀᴜs DS. Somatic mutation, cellular differentiation and cancer causation. JNCI 1981; 67:233–240.

[2] Rᴜʙɪɴ H. Is somatic mutation the major mechanism of malignant transformation? JNCI 1980; 64:995–1000.

[3] Mᴏɴᴅᴀʟ S, Hᴇɪᴅᴇʟʙᴇʀɢᴇʀ C. In vitro malignant transformation by methylcholanthrene of the progeny of single cells derived from C3H mouse prostate. Proc Natl Acad Sci USA 1970; 65:219–229.

[4] Kᴇɴɴᴇᴅʏ AR, Lɪᴛᴛʟᴇ JB. High efficiency, kinetics and numerology of transformation by radiation in vitro. In: Burchenal J, Oettgen H, eds. Cancer: Achievements, challenges, and prospects for the 1980's. Vol I. New York: Grune, 1980.

[5] Tᴏᴅᴀʀᴏ G, Gʀᴇᴇɴ H. Quantitative studies of the growth of mouse embryo cells in culture and their development into established lines. J Cell Biol 1963; 17:299–313.

[6] Hᴀʏғʟɪᴄᴋ L, Mᴏᴏʀʜᴇᴀᴅ P. The serial cultivation of human diploid cell strains. Exp Cell Res 1961; 25:585–621.

[7] Hᴀʀʀɪs M, Cᴏʟʟɪᴇʀ K. Phenotypic evolution of cells resistant to bromodeoxyuridine. Proc Natl Acad Sci USA 1980; 77:4206–4210.

[8] Cᴀɪʀɴs J. The origin of human cancers. Nature 1981; 289:353–357.

[9] Fᴏᴜʟᴅs L. Neoplastic development. Vol I. New York: Academic Press, 1969.

[10] Wᴇɪss P. The science of life. Mount Kisco, N.Y.: Futura, 1973.

[11] Bᴏʜʀ N. Light and life. Nature 1933; 131:421–423, 457–459.

[12] Eʟsᴀssᴇʀ W. The chief abstractions of biology. Amsterdam and New York: Elsevier/North-Holland, 1973.

Spontaneous Liver Tumors in Laboratory Rats

SIR: I refer to the report by Ogawa et al. in the August 1981 issue of JNCI.[1] The authors note that spontaneous liver tumors are rare in laboratory rats. I call their attention to a report on a high incidence of liver tumors that occurred spontaneously in aged germfree male and female Wistar rats.[2] Laboratory rats are not usually maintained for over 30 months, which may explain the low incidence of liver tumors reported by investigators. In more recent examinations, γ-glutamyl transpeptidase-positive foci have been observed in the livers of younger Wistar, Sprague-Dawley, and ACI rats. A possible explanation for the rare occurrence of spontaneously occurring liver tumors in laboratory rats may be that the tumors are slow-growing or that the "carcinogenic" agent(s) are of such low levels that over 30 months is required for them to develop into clearly defined liver tumors. Their etiology (etiologies) may be related to contaminants in the diets that were consumed by the rats. This possibility raises the important problem of interpreting the development in experimental rats of spontaneously developing tumors, which would be accelerated and enhanced if, in the course of bioassay procedures, the rats were administered promotional agents and not initiating agents.

MORRIS POLLARD
Lobund Laboratory
University of Notre Dame
Notre Dame, Indiana 46556

---

[1] OGAWA K, ONOÉ T, TAKEUCHI M. Spontaneous occurrence of γ-glutamyl transpeptidase-positive hepatocytic foci in 105-week-old Wistar and 72-week-old Fischer 344 male rats. JNCI 1981; 67:407–412.

[2] POLLARD M, LUCKERT PH. Spontaneous liver tumors in aged germfree Wistar rats. Lab Anim Sci 1979; 29:74–77.

Breast Cancer and Serum Cholesterol [1,2,3]

Robert A. Hiatt,[4] **Gary D. Friedman,**[4] **Richard D. Bawol,**[4] *and* **Hans K. Ury**[4,5]

ABSTRACT—Recent studies have suggested a role for dietary fat in the etiology of breast cancer. The relation of serum cholesterol and other serum lipid measures to breast cancer incidence was investigated in a cohort of 95,179 women who had multiphasic health checkups from 1964 through 1972. Through 1977, 1,035 new breast cancer cases occurred in over 752,000 person-years of follow-up. Age-adjusted incidence rates were 1.45, 1.37, 1.31, and 1.40/1,000 person-years from the lowest to the highest quartile of serum cholesterol level, respectively. Similarly, no statistically significant relation was detected between β-lipoprotein or total lipids and breast cancer. The sample size was sufficiently large to have detected a relative risk of 1.4 or larger with a probability of 99.9% at the 0.05 level of significance. The expected relation of breast cancer to established risk factors was confirmed by univariate analysis, and serum cholesterol and breast cancer were not associated after simultaneous consideration of nine other risk factors by multivariate analysis. These data suggest that the postulated causal relation between dietary fat and breast cancer does not act via an effect on circulating lipid levels.—JNCI 1982; 68:885-889.

A role for dietary fat in the etiology of breast cancer has been suggested by several lines of evidence. Internationally, breast cancer incidence is directly correlated with levels of affluence and industrialization (*1*); moreover, in populations, the highest socioeconomic class has had twice the risk of that of the lowest class (*2*). The search for etiologic factors associated with economic development and higher social position has led to extensive studies of the role of reproductive behavior and attendant hormonal influences (*3*). Recently, more attention is being paid to the etiologic role of dietary constituents (*4*). Dietary fat and breast cancer mortality have been directly correlated in human population studies (*5*) and in case-control studies in which women with breast cancer reported a higher intake of nutrients, especially of total and saturated fats, than did controls (*6*). The dietary fat hypothesis receives support also from animal studies in which rats fed a high-fat diet had a substantially higher incidence of mammary tumors than control rats fed a low-fat diet (*7*). Although it has not been shown consistently that serum cholesterol and dietary fat intake are related in cross-sectional studies, a recent prospective study detected a positive association (*8*). Moreover, serum cholesterol is also strongly correlated with dietary fat in comparisons of different populations (*9*). Thus it has been hypothesized that serum cholesterol levels might predict risk of breast cancer. To examine this hypothesis, we measured the incidence of breast cancer in a cohort of over 95,000 women who were characterized by their levels of serum cholesterol and other blood lipid measures.

SUBJECTS AND METHODS

Cohort at risk.—The population at risk of cancer consisted of women members of the KFHP. These women were 15 years of age and over and had undergone at least one MHC in the period 1964 through 1972. Variables of interest, which were collected by questionnaire and laboratory testing at the time of the MHC, were used to characterize women at the beginning of their follow-up period. These included basic demographic information, reproductive histories, use of exogenous estrogen, smoking and alcohol consumption history, previous breast symptoms and operations, diagnostic X-ray films of the chest, mammography, weight, height, and serum cholesterol, total lipid, and β-lipoprotein levels. Serum cholesterol was measured by an Auto-Analyzer (Technicon Co., White Plains, N.Y.) until the end of 1968 and by an Autochemist (AGA Corp., Stockholm, Sweden) from 1969 through 1972. Total lipids and β-lipoprotein were measured only by the Autochemist from 1969 through 1972. The frequency distributions of cholesterol levels and the age-specific mean levels of cholesterol were similar for both methods. The overall mean for women was 229.9 mg/dl by the Auto-Analyzer and 229.8 mg/dl by the Autochemist.

Detection of the occurrence of breast cancer.—Cases of breast cancer in this group of women were identified from two sources. The first source was a computer file of all KFHP hospital discharges in northern California from 1971 through 1977. This file included patients discharged from KFHP hospitals in the five San Francisco Bay area counties (Alameda, San Francisco, Marin, Contra Costa, and San Mateo) plus Solano, Sacramento, and Santa Clara counties. Although only the first three primary discharge diagnoses were sought, it would be unlikely for any newly developed cancer of the breast to be missed by this method of ascertainment. The second source was a manual review of disease indexes for the years 1960 through 1970 in all KFHP hospitals in northern California. The California Tumor Registry, which covers only the five San Francisco Bay area counties and which overlaps the KFHP files for the years 1969 through 1977, provided a partial check on the completeness of the KFHP records. When we cross-matched the

---

ABBREVIATIONS USED: KFHP=Kaiser Foundation Health Plan; MHC=multiphasic health checkup; RR=relative risk(s); SMSA=standard metropolitan statistical area; TNCS=Third National Cancer Survey.

---

[1] Received March 26, 1981; revised December 31, 1981; accepted January 15, 1982.

[2] Supported by Public Health Service contract N01CB-84238 from the Division of Cancer Biology and Diagnosis, National Cancer Institute.

[3] Research procedures were in accord with the ethical standards of the Institutional Review Board (for the Protection of Human Subjects), the Kaiser-Permanente Medical Care Program.

[4] Department of Medical Methods Research, Kaiser-Permanente Medical Care Program, 3451 Piedmont Ave., Oakland, Calif. 94611.

[5] We thank Ms. Beverly Whitmarsh and Mr. Kenneth Weaver for technical assistance and Mr. Abraham B. Siegelaub for help with the statistical analysis. The support and encouragement of Dr. Elizabeth Anderson, Project Officer, National Cancer Institute, are gratefully acknowledged.

KFHP hospital discharge file with the tumor registry file for KFHP members, we detected only 26 (2.5%) additional documented breast cancers.

All medical records of persons with breast cancer detected in this manner were reviewed to confirm the diagnosis and record the date of diagnosis. A file of all detected breast cancer cases from the years 1960 through 1977 was created and cross-matched with the file of women who had had an MHC during the period 1964 through 1972. All persons with a diagnosis of breast cancer before and up to 6 months after their first MHC were excluded, leaving a cohort of 95,179 women who were 15 years and older without a history of breast cancer and who had had an MHC. From 1964 to December 31, 1977, breast cancer developed in 1,035 of these women.

Determination of the duration of follow-up.—Because of unequal follow-up periods, we used person-years of exposure to determine rates. Follow-up always began at the date of a woman's first MHC and ended with the diagnosis of cancer, the end of the study, or when she was lost to follow-up due to termination of membership. If she terminated membership and there was no termination date on file, loss to follow-up was estimated to occur at a point halfway between the year of the last MHC and December 31, 1977. This method for estimating the end of follow-up was required for 19.2% of the subjects.

If a woman left the KFHP and subsequently developed breast cancer, this breast cancer would not have been detected; however, she was not considered at risk after leaving the KFHP. If she had gone to an outside facility for diagnosis and treatment while still a KFHP member, she would probably have had the diagnosis recorded on her next KFHP hospitalization. We therefore were confident that we had reasonably complete ascertainment of breast cancers that occurred while women were still members of the KFHP.

Statistical analysis.—Breast cancer incidence rates were calculated in relation to each independent variable of interest. Rates were age adjusted by the direct method with the use of total population as the standard. A standard z-statistic was used for two-sided tests of significance between the rates for dichotomous variables with the use of the variance of the age-adjusted rate given by Chiang (*10*). For ordered qualitative variables and continuous variables, grouped into ordered categories, possible trends were examined by the calculation of the Mantel extension chi-square and the slope coefficient (*11*).

To ensure that some relation between cholesterol and breast cancer was not obscured by confounding factors, we performed multivariate analysis employing Cox's proportional hazards model (*12*) programmed for the Statistical Analysis System (*13*). This procedure allows for the differing length of follow-up of the subjects. Only women at least 30 years of age were included in this analysis, since risk is so low below that age. The 8% of women who were neither white nor black were excluded. Moreover, because of the unacceptable number of unknown values, women who had their first MHC in 1964 were eliminated from these analyses. After the above exclusions, 50,000 women without breast cancer remained in the cohort. Because the additional statistical benefit of including more than about 5 noncases to 1 case is small (*14*), we randomly selected women without breast cancer in a ratio of 5:1 to cases. We excluded 3% of the cohort with more than three unknown values, which left 714 cases and 3,675 noncases for the multivariate analysis.

Multivariate analysis was also performed by multiple logistic regression analysis as programmed by Brand and Sholtz [described in Rosenman et al. (*15*)]. Although this analysis does not take length of follow-up into account, results of the two multivariate analyses were essentially identical; only those based on the Cox model are presented.

The extremely large number of breast cancer cases in this study make it highly probable that an association with serum cholesterol would be observed and be statistically significant at the 0.05 level, if such an association truly existed. Of 1,035 breast cancer cases, 948 were among 87,354 women (869,602 years of follow-up) with known age and cholesterol values. When cholesterol concentrations are separated into low (<220 mg/dl) and high (≥220 mg/dl) levels, there is a 75% chance of detecting an RR as small as 1.2 and an almost certain probability (99.9%) of detecting an RR of 1.4 or larger. Although there is no direct way to calculate the statistical power of our multivariate analysis, 714 breast cancer cases is a very large number in comparison to the number in other cohort studies.

RESULTS

Incidence of breast cancer.—Breast cancer incidence in the entire cohort was 1.38/1,000 person-years of follow-up. Age-specific rates (table 1) revealed a direct relation to age, with the highest rates in the group over 70 years of age. The mean person-years of follow-up was 7.9. The age-specific rates were similar to those reported by the TNCS for the San Francisco SMSA (*16*).

Serum lipids.—The incidence of breast cancer was neither directly nor inversely associated with the level of serum cholesterol measured at the first MHC. When cholesterol concentrations were separated into low (<220 mg/dl) and high (≥220 mg/dl) levels, a slight and nonsignificant negative association was noted for the age-adjusted rates (1.39/1,000 person-yr vs. 1.35/1,000 person-yr, respectively). When women were classified by quartiles of cholesterol

TABLE 1.—*Age-specific breast cancer incidence per 1,000 person-years of follow-up in a cohort of 95,179 women who had an MHC before diagnosis of cancer*

Age groups, yr	No. of cancers, age at diagnosis	No. of persons at risk, age at entry	No. of person-years at risk in age group	Rate per 1,000 person-yr	Annual rate per 1,000 women from TNCS[a]
15–39	64	48,137	266,159	0.24	0.15
40–49	275	20,874	170,388	1.61	1.49
50–59	342	15,934	164,239	2.08	2.14
60–69	238	8,168	104,529	2.28	2.58
≥70	116	2,066	46,465	2.50	2.99
Total	1,035	95,179	751,780	1.38	1.40[b]

[a] San Francisco–Oakland SMSA for women, all races, age ≥15 yr.

[b] Age adjusted by direct method. Standard=person-yr in MHC cohort.

TABLE 2.—*Breast cancer incidence per 1,000 person-years of follow-up by serum cholesterol, β-lipoprotein, and total lipids determined at MHC before diagnosis of cancer*

Cholesterol, mg/100 ml	No. of cancers	Person-yr of follow-up	Age-adjusted rate[a]
<194	183	187,928	1.45
195–219	211	163,186	1.37
220–244	201	142,195	1.31
>245	353	196,293	1.40
Total[b]	948	689,602	1.37

β-lipoprotein, U	No. of cancers	Person-yr of follow-up	Age-adjusted rate[a]
<13.9	54	43,318	1.74
14.0–16.9	57	35,449	1.72
17.0–20.9	58	38,028	1.40
>21.0	119	44,179	2.24
Total	288	160,974	1.79

Total lipids, mg/100 ml	No. of cancers	Person-yr of follow-up	Age-adjusted rate[a]
<0.79	57	41,449	1.83
0.80–1.09	74	40,362	1.90
1.10–1.49	59	35,743	1.50
>1.50	81	34,571	1.96
Total	271	152,125	1.78

[a] Age-adjusted=direct method with total study group with data for the variable used as standard.

[b] Figures are based on cohort of 87,354 women with known cholesterol values.

level, the hypothesized trend of increasing incidence with increasing cholesterol was not seen (table 2). Instead, rates decreased from the lowest to the 220- to 224-mg/dl level and increased for the ≥245-mg/dl level. The same general pattern was seen for β-lipoprotein and total lipids. In 10-year age-specific groups, breast cancer incidence showed no consistent trend for any of the three lipid measures, indicating that no relation existed for women in either the premenopausal or postmenopausal age groups. The subset of women who had β-lipoprotein and total lipids measured at their first MHC during the period from 1969 through 1972 had a total incidence higher than that in the total cohort (1.79 and 1.78/1,000 person-yr, respectively). This difference is only partially explained by the greater age of this subcohort.

Known risk factors.—The incidence of breast cancer was found to increase with the highest educational level attained (P=0.001), which we used as a measure of socioeconomic status. Breast cancer was more common among white women (1.46/1,000 person-yr) than black women (0.98/1,000 person-yr, P<0.001) or Asian women (0.87/1,000 person-yr, P=0.002). We did not have specific information about breast cancer in family members, but breast cancer did occur more commonly in women with a history of any cancer in mothers or sisters (P=0.045). We noted a slightly increased risk of breast cancer among women never married versus those ever married, but the difference was not significant.

Breast cancer incidence generally decreased with increasing age of menarche after age 13 years (P=0.008). Women with menopause before age 40 years had substantially less risk of breast cancer than those with later menopause. Rates generally increased with menopausal age (P=0.016), but the trend was not steady. We did not have data on the age at first pregnancy but, as expected, parity was inversely related to breast cancer risk (P=0.012).

We found an inverted U-shaped relation between the Quetelet index of body mass (weight/height^2 × 100) and breast cancer rates. Breast cancer was less common in the most lean and the most obese than in the women in the middle range in this cohort. Daily alcohol consumption was directly related to breast cancer risk in an uneven trend from no drinks through one to two and three to five drinks to over five drinks per day (P=0.016). The rate was nonsignificantly higher in smokers than in nonsmokers but was significantly higher in ex-smokers than current smokers (P=0.008).

A history of at least one chest X-ray examination and a history of nipple discharge were not significantly related to breast cancer rates. However, the rates were higher in women who had a history of any breast operation (P<0.001) and in those who had any abnormality on mammography (P=0.043). The last two variables probably reflect the presence of benign breast disease. The use of birth control pills, of pills to control menstrual periods, and of any "hormones" in the year before the MHC had no significant relation to breast cancer rates.

Multivariate.—When 10 covariables and breast cancer were analyzed together, the results (table 3) still failed to show any significant relation between cholesterol and breast cancer. That is, no hidden association of cholesterol and breast cancer incidence was uncovered by simultaneous consideration of nine other variables that either were known risk factors or (in the case of smoking) were associated with breast cancer in our study population in the univariate analysis. The variables with most effect in this analysis can be assessed by a comparison of the adjusted RR and the significance probabilities. Thus being of older age, of lower

TABLE 3.—*Results of multivariate analysis of risk factors for breast cancer in women age 30 years and over*

Variable	Significance, P	Adjusted RR	95% confidence limits	RR associated with:
Age	<0.001	1.28	1.15, 1.41	10-yr increase
Parity	0.003	0.93	0.89, 0.98	Each additional birth
Race	0.008	1.45	1.10, 1.90	White vs. black
Menopause	0.018	0.76	0.61, 0.95	Yes vs. no at MHC
Age at menarche	0.032	0.95	0.90, 0.99	1-yr increase
Education	0.144	1.05	0.98, 1.11	Completion increased one level[a]
Quetelet index	0.194	1.07	0.96, 1.20	One unit increase, pounds/inch^2 × 100
Smoker	0.234	1.10	0.94, 1.29	Current or ex-smoker vs. never smoked
Cholesterol	0.337	1.01	0.99, 1.03	10-mg/dl increase
Alcohol	0.639	0.96	0.80, 1.14	Current use, yes vs. no

[a] Levels = elementary, high school, 2 yr of college, 3–4 yr of college, and postgraduate.

parity, white, premenopausal (at any given age), and of a younger age at menarche were significantly related to breast cancer with a probability of 5% or less that the association occurred by chance. The level of highest education, body mass, smoking status, alcohol consumption, and cholesterol level were not significantly associated with breast cancer. The same analysis was performed for women according to whether they said they were premenopausal or postmenopausal at the time of their first MHC. In both analyses, cholesterol remained unrelated to breast cancer incidence with the adjusted RR for an increase of 10 mg/dl close to 1.0 for both groups.

DISCUSSION

The principal finding of this study was that no direct relation exists between the result of a single serum cholesterol determination and the subsequent development of breast cancer in women. Similarly, no direct relation was seen between total serum lipids or β-lipoprotein, which is highly correlated with cholesterol, and breast cancer in this cohort. This conclusion was based on the absence of any observed dose-response relation between women characterized by the quartile of their blood lipid levels and their subsequent development of breast cancer. The meaning of the pattern of observed rates is not known and is compatible with either random fluctuation in rates or increased risk for women at either extreme of serum cholesterol level. A simple dichotomization of cholesterol revealed a small and nonsignificant negative association of cholesterol level with breast cancer. Multivariate analysis indicated no relation between serum cholesterol and breast cancer with simultaneous consideration of nine other possible risk factors.

Our findings are consistent with previous reports of higher breast cancer risk with increasing age (*3, 17*), with higher educational level representing socioeconomic status (*2*), in white versus black or yellow races (*17*), with reproductive variables of lower age of menarche and higher age of menopause, with lower parity (*3, 17*), with indicators of benign breast disease (*17*), and in women who have never married (*16*). We found no increased risk in women who had taken estrogens to control menstrual periods or to control birth (*17*). As a proxy for family history of breast cancer (*17*), we found that there was also increased risk with a family history of any cancer in mothers and sisters. We did not confirm previous reports on increased risk in women with greater body mass (*18*), although this relation has not been consistently found (*17*).

Univariate analysis suggested that alcohol consumption was associated with increased risk of breast cancer. This same relation has been noted by Williams and Horm (*19*) in a case-control study based on the TNCS, and a possible etiologic role for alcohol has been discussed by Williams (*20*). In our multivariate analysis where the alcohol variable was dichotomized, we did not confirm an independent effect of alcohol. Analyses are under way to examine this relation further.

Current smokers were at slightly but not significantly greater risk than nonsmokers. However, ex-smokers had a significantly greater risk than either nonsmokers or current smokers, possibly related to differences in socioeconomic status (*21*).

The results of the present study are consistent with and enlarge upon other recent studies of the relation of serum cholesterol to subsequent development of breast cancer in follow-up studies. Kark and co-workers (*22*) reported a slight negative association between serum cholesterol and breast cancer in a prospective study in Evans County, Georgia. However, their results were based on only 7 cases of breast cancer. Williams and co-workers (*23*) found a small but insignificant negative correlation between serum cholesterol and breast cancer in the Framingham study based on 75 breast cancer cases that occurred over an 18-year period; in Tecumseh, Michigan, Higgins found no relation between base-line cholesterol or triglyceride levels and the incidence of breast cancer that developed in 65 women over a 13- to 20-year period (Higgins M: Unpublished data).

Case-control studies of women *after* the diagnosis of breast cancer have yielded conflicting results (*24–29*), although most suggest that serum lipids (*24–27*) and urinary cholesterol (*28*) are higher in women with breast cancer than in various other groups. Concerning the possible etiologic relation of serum cholesterol to cancer, however, these studies have shortcomings in their choice of controls and their inability to determine whether the high cholesterol level or the cancer was primary. Even with prospective studies that determine cholesterol before the diagnosis of cancer, the metabolic influence of subclinical cancer on cholesterol must be considered, since investigators have found that the inverse association between serum cholesterol and cancer mortality may hold for only 2–7 years of follow-up (*30, 31*). That is, subclinical cancer may have some effect on cholesterol level. Because, in the present study, the mean time to diagnosis of breast cancer was 7.9 years (range, 1–13 yr) and in the Framingham study cancer incidence was measured over an 18-year period, we would expect this potential effect to be minimal. However, further work that examines time to diagnosis in the relation of serum cholesterol and cancer is needed.

Although it does not disprove the hypothesis that high dietary fat is an etiologic factor in breast cancer, our study adds to a growing body of negative data. Hill and co-workers (*32*) as well as Wynder and associates (*4*) have proposed plausible biological explanations of how dietary fat might be tied to breast cancer, but prospective human epidemiologic evidence from Evans County (*22*), Framingham (*23*), Tecumseh (Higgins M: Unpublished data, 1980), and the current KFHP population does not support a role for serum cholesterol in this disease. The data by Rost and co-workers from the Lipid Research Clinic in Iowa (*33*) suggest a conflicting finding, but details of this study are not yet published. It should also be appreciated that the animal work by Carroll and Khor (*7*) showed an increasing incidence of mammary tumors with increasing vegetable fats rather than animal fats in the diet.

The relation between cancer and serum cholesterol that seems better supported is an inverse one for all cancers together and for colon cancer in men specifically. The analyses of this relation in the large prospective studies of coronary heart disease (*23, 30, 34–37*) are limited in that they usually deal only with men and that they include insufficient cases of the less common cancers to draw reliable conclusions.

The inverse overall association of cholesterol and cancer remains unexplained. The effect of competing mortality from diseases in which cholesterol is a risk factor (e.g., coronary heart disease) has been suggested (*23*). However, Kark and co-workers (*22*) excluded persons who died of cardiovascular disease and found that the inverse relationship was enhanced for men but not for women. Other hypotheses that consider increased membrane permeability to carcinogens, reduced ability of lymphocytes to detect and kill tumor cells, and other pathophysical mechanisms in which cholesterol may play a role (*23*) need further study.

In conclusion, we were unable to find any direct association between serum cholesterol and breast cancer incidence in a cohort of over 95,000 women in the KFHP. Similarly, in about one-fourth of this cohort, we found no relation of serum β-lipoprotein or total lipids to breast cancer. The lack of association between serum cholesterol and breast cancer was evident throughout both univariate and multivariate analyses, in which most other known risk factors for breast cancer behaved as expected on the basis of previous knowledge. Our findings suggest that dietary fat intake, if related to increased breast cancer risk, is related through some other metabolic pathway than through an elevation of the serum lipids measured in this study.

REFERENCES

(*1*) Doll R, Muir P, Waterhouse J, eds. Cancer incidence in five continents. Vol 2. Berlin: Springer-Verlag, 1970.

(*2*) Graham S, Levin M, Lilienfeld AM. The socioeconomic distribution of cancer of various sites in Buffalo, N.Y., 1948–1952. Cancer 1960; 13:180–191.

(*3*) MacMahon B, Cole P, Brown J. Etiology of human breast cancer: A review. J Natl Cancer Inst 1973; 50:21–42.

(*4*) Wynder EL, MacCornack F, Hill P, Cohen LA, Chan P, Weisburger JH. Nutrition and the etiology and prevention of breast cancer. Cancer Detect Prev 1976; 1:293–310.

(*5*) Drasar BS, Irving D. Environmental factors and cancer of the colon and breast. Br J Cancer 1973; 27:167–172.

(*6*) Miller AB, Kelly A, Choi NW, et al. A study of diet and breast cancer. Am J Epidemiol 1978; 107:499–509.

(*7*) Carroll KK, Khor HT. Effects of level and type of dietary fat on incidence of mammary tumors induced in female Sprague-Dawley rats by 7,12-dimethylbenzanthracene. Lipids 1971; 6:415–420.

(*8*) Shekelle RB, Shryock AMacM, Paul O, et al. Diet, serum cholesterol, and death from coronary heart disease: The Western Electric study. N Engl J Med 1981; 304:65–70.

(*9*) Keys AB. Seven countries: A multivariate analysis of death and coronary heart disease. Cambridge, Mass.: Harvard Univ Press, 1980.

(*10*) Chiang CL. Standard error of the age-adjusted death rate. In: Vital statistics special reports. Selected studies. Vol 47. Washington, D.C.: U.S. Govt Print Off, 1961:273–285.

(*11*) Mantel N. Chi-square tests with one degree of freedom: Extensions of the Mantel-Haenszel procedure. J Am Stat Assoc 1963; 58:690–700.

(*12*) Cox DR. Regression models and life-tables. J R Stat Soc 1972; 34:187–220.

(*13*) Harrell F. The PHGLM procedure. In: Reinhardt PS, ed. SAS supplementary library user's guide. 1980 ed. Raleigh, N.C.: SAS Institute, Inc., 1980:119–131.

(*14*) Lubin JH. Some efficiency comments on group size in study design. Am J Epidemiol 1980; 111:453–457.

(*15*) Rosenman RH, Brand RJ, Sholtz RI, Friedman M. Multivariate prediction of coronary heart disease during 8.5 year follow-up in the Western Collaborative Group Study. Am J Cardiol 1976; 37:903–910.

(*16*) Cutler SJ, Young JL Jr, eds. Third National Cancer Survey: Incidence data. Natl Cancer Inst Monogr 1975; 41:1–454.

(*17*) Kelsey JL. A review of the epidemiology of human breast cancer. Epidemiol Rev 1979; 1:74–109.

(*18*) De Waard F. Breast cancer incidence and nutritional status with particular reference to body weight and height. Cancer Res 1975; 35:3351–3356.

(*19*) Williams RR, Horm JW. Association of cancer sites with tobacco and alcohol consumption and socioeconomic status of patients: Interview study from the Third National Cancer Survey. J Natl Cancer Inst 1977; 58:525–547.

(*20*) Williams RR. Breast and thyroid cancer and malignant melanoma promoted by alcohol-induced pituitary secretion of prolactin, T.S.H., and M.S.H. Lancet 1976; 1:996–999.

(*21*) Friedman GD, Siegelaub AB, Dales LG, Seltzer CC. Characteristics predictive of coronary heart disease in ex-smokers before they stopped smoking: Comparison with persistent smokers and nonsmokers. J Chronic Dis 1979; 32:175–190.

(*22*) Kark JD, Smith AH, Hames CG. The relationship of serum cholesterol to the incidence of cancer in Evans County, Georgia. J Chronic Dis 1980; 33:311–322.

(*23*) Williams RR, Sorlie PD, Feinleib M, McNamara PM, Kannel WB, Dawber TR. Cancer incidence by levels of cholesterol. JAMA 1981; 245:247–252.

(*24*) Basu TK, Williams DC. Plasma and body lipids in patients with carcinoma of the breast. Oncology 1975; 31:172–176.

(*25*) Smethurst M, Basu TK, Williams DC. Levels of cholesterol, 11-hydroxycorticosteroids and progesterone in plasma from postmenopausal women with breast cancer. Eur J Cancer 1975; 11:751–755.

(*26*) Feldman EB, Carter AC. Circulating lipids and lipoproteins in women with metastatic breast carcinoma. Endocrinology 1971; 33:8–13.

(*27*) Barclay M, Escher GC, Kaufman RJ, Terebus-Kekish O, Greene EM, Skipski VP. Serum lipoproteins and human neoplastic disease. Clin Chim Acta 1964; 10:39–47.

(*28*) Acevedo HF, Campbell EA, Frich JC Jr, Dugan PJ, Saier EL, Merkow LP. Urinary cholesterol. VI. Its excretion in women with inoperable inflammatory carcinoma of the breast. Cancer 1974; 34:1727–1736.

(*29*) Nydegger UE, Butler RE. Serum lipoprotein levels in patients with cancer. Cancer Res 1972; 32:1756–1760.

(*30*) Cambien F, Ducimetiere P, Richard J. Total serum cholesterol and cancer mortality in a middle-aged male population. Am J Epidemiol 1980; 112:388–394.

(*31*) Rose G, Shipley MJ. Plasma lipids and mortality: A source of error. Lancet 1980; 1:523–525.

(*32*) Hill MJ, Goddard P, Williams RE. Gut bacteria and aetiology of cancer of the breast. Lancet 1971; 2:472–473.

(*33*) Rost C, Wallace RB, Burmeister LF, Pomrehn PR. Lipids and ponderosity as predictors of cancer incidence: The Lipid Research Clinic (LRC). Abstracts of the twenty-first conference on cardiovascular disease epidemiology, March 27–29, 1981, Washington, D.C. Cardiovasc Epidemiol Newslett 1981; 30:22.

(*34*) Rose G, Blackburn H, Keys A, et al. Colon cancer and blood-cholesterol. Lancet 1974; 1:181–183.

(*35*) Kagan A, McGee DL, Yano K, Rhoads GG, Nomura A. Serum cholesterol and mortality in a Japanese-American population: The Honolulu Heart Program. Am J Epidemiol 1981; 114:11–20.

(*36*) Kozarevic DJ, McGee D, Vojvodic N, et al. Serum cholesterol and mortality: The Yugoslavia Cardiovascular Disease Study. Am J Epidemiol 1981; 114:21–28.

(*37*) Garcia-Palmieri MR, Sorlie PD, Costas R Jr, Havlik RJ. An apparent inverse relationship between serum cholesterol and cancer mortality in Puerto Rico. Am J Epidemiol 1981; 114:29–40.

blank page

Carcinomas of the Cervix and Corpus Uteri in Humans: Stage-Dependent Blood Levels of Substance(s) Immunologically Cross-Reactive With Insulin[1,2]

K. Pavelić,[3] M. Bolanča,[4] N. Veček,[4] J. Pavelić,[3] T. Marotti,[3] *and* S. Vuk-Pavlović[5]

ABSTRACT—Inasmuch as the elevated levels of substance(s) immunologically cross-reactive with insulin (SICRI) in a diabetic woman with carcinoma of the corpus uteri decreased following the surgical removal of the uterus and ovaries, 80 women with cervical carcinomas of various stages and 70 women with carcinomas of the corpus uteri of various stages were screened for the levels of SICRI and C-peptide. The levels of SICRI in the second, third, and fourth stages of the cancers were elevated (up to six times above the normal levels of immunoreactive insulin) and stage-dependent. The levels of C-peptide, which are related to the insulin-secreting activity of pancreatic β-cells, were normal and independent of the stage of cancer.—JNCI 1982; 68:891–894.

Recently, we screened patients with Hodgkin's (*1*) and non-Hodgkin's lymphomas (Pavelić K, Vuk-Pavlović S: Submitted for publication) for the levels of SICRI and of C-peptide in non-Hodgkin's lymphoma. We found that the levels of SICRI in blood depend on the stage of Hodgkin's disease and are significantly higher in the relapse phase than in the remission phase of non-Hodgkin's lymphomas [(*1*); Pavelić K, Vuk-Pavlović S: Submitted for publication]. Our preliminary results with mice suggest that SICRI is produced by the tumors themselves and that it stimulates tumor proliferation (*2*). Therefore, the ability of a clinician to control and modulate blood levels of SICRI in cancers might be relevant.

We found high levels of SICRI in the blood and tumor tissue in a diabetic patient with carcinoma of the corpus uteri. After surgery SICRI decreased sharply, but glucose levels remained unaffected. This finding precipitated the screening of SICRI in the blood of 150 women with cervical carcinomas or carcinomas of the corpus uteri, i.e., solid tumors. The mean levels of blood SICRI were elevated in all stages of the disease and were higher in the patients with a more progressive disease.

MATERIALS AND METHODS

Blood was drawn from hospitalized patients before breakfast. It was immediately refrigerated at 4°C, and the clot was removed by centrifugation. Glucose levels in sera were measured immediately thereafter according to (*3*). The levels of SICRI in sera, in trypsinized tumor cells, and in normal uterine and renal cells (*4*) were determined by the insulin-specific RIA (*5*) with the use of radioiodinated porcine and crystalline rat insulin standards (Sorin, Sallugia, Italy). The levels of C-peptide were measured by the RIA (Byk-Mallinckrodt, Dietzenbach, Federal Republic of Germany) according to (*6*). If RIA determinations were not performed on the same day that the blood was drawn, sera were frozen immediately after clot removal and kept at −20°C (not longer than 15 days). On several occasions, RIA determinations in fresh control sera were compared with the respective values obtained with the same sera frozen for 15 days and no difference was noted.

The full RIA titration of SICRI was performed and the dilution–activity lines were parallel to those obtained with the insulin standard in the sera of 2 patients.

The results were statistically evaluated by the χ^2 test with the use of a computer program (*7*).

RESULTS

Patient #1 (76 yr old) was admitted to the clinic on October 23, 1979, for postmenopausal uterine bleeding lasting 5 months. For the last 20 years, she had suffered from hypertension. She had geriatric diabetes, which was controlled by diet only, 1 year before the admission to the hospital. The histologic examination of the material obtained by a fractional curettage demonstrated an adenocarcinoma of the corporeal endometrium. Phytohemagglutinin-stimulated blastic transformation of the patient's lymphocytes (*8*) yielded an index of 29, in contrast to 80 found in healthy controls. (These indices are the ratios of [^{3}H]thymidine incorporated by the phytohemagglutinin-stimulated cells vs. those incorporated by the nonstimulated cells.) The granulocyte inhibition test (*9*) to tuberculin (purified protein derivative) gave an index of 140 in comparison to 80 in normal controls. The concentration of IgM in blood was 640 mg/liter (normal values: 700–2,800); the concentrations of IgG and IgA were normal. These results together with the histologic findings prompted surgical removal of the uterus and adnexa.

The uterus was slightly enlarged, but there were no macroscopic changes in the ovaries. Metastases were not found in the abdominal cavity and organs therein. The histopathologic examination of the uterus confirmed the preoperative diagnosis of an endometrial adenocarcinoma.

ABBREVIATIONS USED: RIA=radioimmunoassay(s); SICRI=substance(s) immunologically cross-reactive with insulin.

---

[1] Received April 28, 1981; revised November 20, 1981; accepted December 11, 1981.

[2] Research procedures were in accord with the ethical standards of the Helsinki Declaration of 1975.

[3] Department of Experimental Biology and Medicine, Rugjer Bošković Institute, Bijenička 54, 41001 Zagreb, Croatia, Yugoslavia.

[4] Department of Gynecology and Obstetrics, Medical School, University of Zagreb, Petrova 13, 41000 Zagreb, Croatia, Yugoslavia.

[5] *Address reprint requests to* Dr. Vuk-Pavlović, Institute of Immunology, Rockefellerova 2, 41000 Zagreb, Croatia, Yugoslavia.

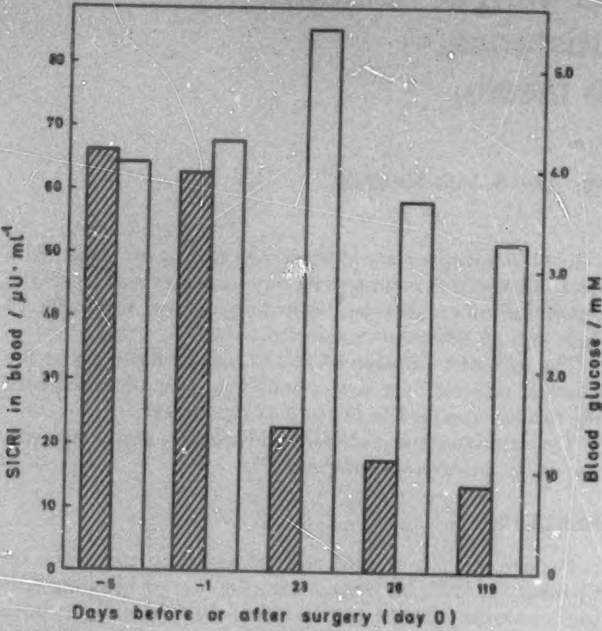

TEXT-FIGURE 1.—Levels of SICRI (▨) and glucose (☐) in blood of diabetic patient #1 with adenocarcinoma of corpus uteri, before and after surgery. Blood was drawn before breakfast.

The tumor penetrated the myometrium to a depth of 8 mm. A fortnight later a dose of 2,500 rad of radioactive cesium was applied for 48 hours in the vagina. Six months after therapy the patient felt well, and the gynecologic examination showed no pathologic changes. The immune status was normal.

The serum levels of SICRI and glucose (text-fig. 1) were determined on two occasions before and three occasions after surgery. As can be seen in text-figure 1, high preoperative levels of SICRI, determined by insulin-specific RIA, decreased dramatically following surgical treatment. The elevated preoperative blood glucose levels, however, were not influenced significantly by the sharp decrease of SICRI showing that this tumor-associated substance(s), found in the diabetic patient, does not exert the same physiologic effects as insulin.

We incubated the patient's serum with [^{125}I]insulin for 3 days and chromatographed it on a Sephadex G-50 column (1×60 cm) equilibrated with water (*10*). A single peak at $V_e:V_t$=0.53 was obtained indicating that during incubation degradation of radioiodinated insulin did not occur. (V_e and V_t denote the elution volume and the total volume of the gel measured by ^{125}I-labeled Na, respectively.) An identically treated sample of normal serum also gave a single peak with the ratio $V_e:V_t$=0.58, showing that the apparent molecular

TABLE 1.—*Significance of differences between blood SICRI levels in patients with various stages of cervical carcinomas and carcinomas of the corpus uteri evaluated by the χ^2 test*[a]

Stage of cervical carcinoma or carcinoma of the corpus uteri	Significance of difference		
	IV	III	II
I	$P<0.01$	$P<0.01$	NS
II	$P<0.01$	NS	
III	NS		

[a] Data displayed in text-fig. 2a (carcinomas of corpus uteri) and text-fig. 2b (cervical carcinomas) were evaluated separately; the significances of the differences between stages of cancer were the same in both groups. NS=not significant.

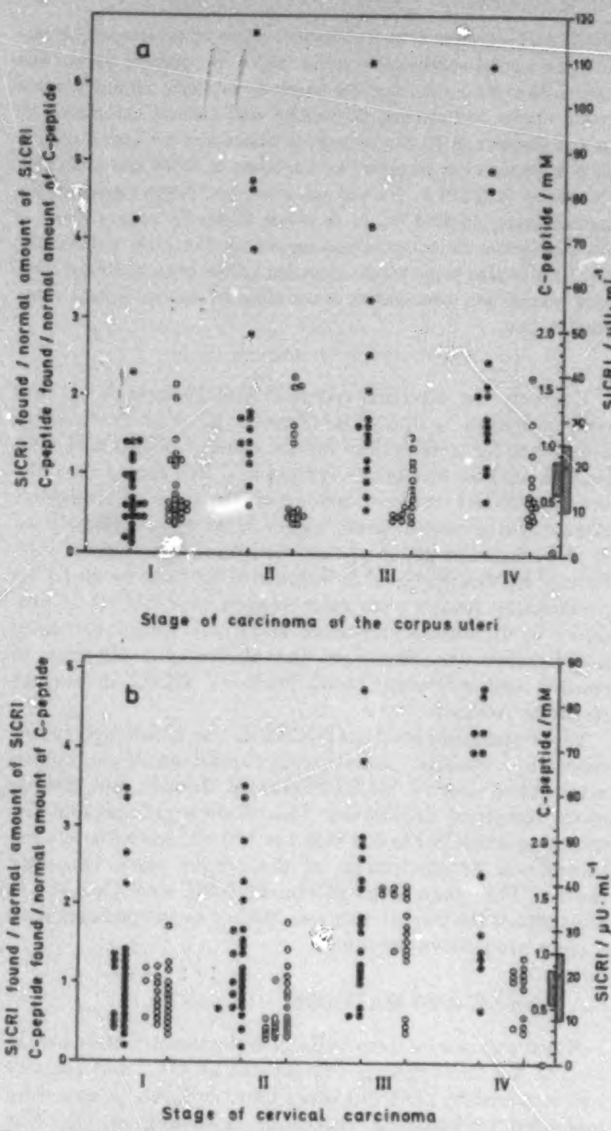

TEXT-FIGURE 2.—Preoperative levels of SICRI (●) and C-peptide (○) in the blood of 70 patients with carcinomas of the corpus uteri (a) and 80 patients with cervical carcinomas (b). *Left ordinate* displays the normalized scale both for SICRI and C-peptide. *Scales on the right ordinate* display the absolute concentrations where the *shaded areas* denote the mean ranges of minimal and maximal values of C-peptide and insulin detected by the respective RIA in 200 normal persons. Blood was drawn before breakfast. The ages of 131 of 150 patients were between 50 and 80 yr. Two were older (the oldest being 84 yr) and 17 younger (the youngest being 20 yr). No correlation was found between the patients' ages and blood levels of SICRI and C-peptide.

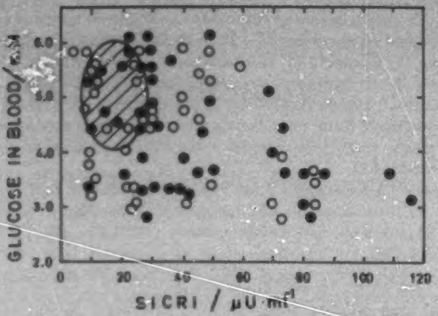

TEXT-FIGURE 3.—Correlation of levels of SICRI and glucose in the blood of 82 patients with carcinomas of the corpus uteri (●) and cervical carcinomas (○). Only the patients from text-fig. 2 for whom both SICRI and glucose were measured in the same sample of blood are represented. *Data points within the shaded area* represent patients with normal levels of both SICRI and glucose.

weight of SICRI is not altered by binding to other macromolecules.

We determined the intracellular SICRI levels in the tumor itself and in pieces of normal uteri and normal kidneys as references. SICRI (35 μU/g of tumor tissue) was compared with 1.5±0.5 and 0.7±0.5 μU/g found in the uteri and in the kidneys, respectively.

These results prompted a survey of 70 nondiabetic patients with various stages of carcinomas of the corpus uteri and 80 nondiabetic patients with various stages of cervical carcinomas for the levels of SICRI and of C-peptide. This peptide (a cleaved part of the proinsulin molecule) reflects the blood levels of insulin. The results are presented in text-figure 2, and the levels of significance of the differences between groups are tabulated in table 1. While the differences in SICRI levels were significant between stages I and III, I and IV, and II and IV in both cancers, there was no difference between the corresponding C-peptide levels (text-fig. 2).

For 82 patients we have data on the levels of glucose in the same samples of blood in which SICRI and C-peptide were measured. The correlation of SICRI and blood glucose is shown in text-figure 3.

DISCUSSION

From the data presented in text-figures 1–3, we conclude that: 1) Blood SICRI levels are not paralleled by the C-peptide levels; 2) SICRI is closely associated with and probably secreted by the tumor, since it is high in the blood of a diabetic tumor-bearing patient before surgery and decreases following surgery and since its intracellular levels are more than 20 times higher in the tumor than in the normal uteri; and 3) only very high levels of SICRI induce hypoglycemia (text-fig. 3). Moreover, the present results demonstrate elevated and stage-dependent levels of SICRI in patients with cervical carcinomas and carcinomas of the corpus uteri as detected by RIA specific for pancreatic insulin (text-fig. 2); i.e., the more progressive the disease, the higher the blood level of SICRI.

Similarly, elevated levels of insulin-like substances have also been noted in patients with fibrosarcoma (*11*), adenocarcinoma (*12*), cervical carcinoma where hypoglycemia also was noticed (*4*), renal adenocarcinoma (*13*), Hodgkin's disease (*1*), and non-Hodgkin's lymphoma (Pavelić K, Vuk-Pavlović S: Submitted for publication). Also, a large body of evidence for the existence and function of tumor-associated SICRI has been accumulated in our work with murine tumors under a variety of experimental in vivo (*2*) and in vitro (*14*) conditions. From these experiments, we know that SICRI-secreting tumors grow faster (*2, 15, 16*). There are, however, tumors not associated with elevated SICRI. Recently, we screened 24 patients with tumors of the ovaries and found no change in the blood-immunoreactive insulin levels (Sekelji B, Grgurević M, Pavelić K: Unpublished data).

The present findings raise the question about the molecular identity and origin of SICRI associated with tumors. The results of the Sephadex G-50 gel filtration of sera preincubated with the radioiodinated insulin (*see* "Results") demonstrate that RIA-detectable entities are neither the products of insulin degradation nor insulin bound to macromolecular carriers. Also, SICRI most probably is secreted by the tumor tissue, at least in diabetic tumor-bearing patients [(*13*); this work] and in mice with alloxan-induced diabetes (*2*). This SICRI secretion by the tumor tissue has been proved in vitro directly in murine mammary aplastic carcinoma (*14*).

Concentrations of SICRI and C-peptide in peripheral blood are correlated (*17*) and result from the balance of secretion rates and respective clearance rates. It is known that the normal clearance rates of insulin are larger than those of C-peptide (*17*). From a study of nondiabetic, nonobese patients, Horwitz et al. (*17*) obtained the relation [insulin] = 0.39 [C-peptide] − 0.78 in the peripheral blood. By use of this empirical equation, it is easy to show that under normal conditions the concentrations of peripheral C-peptide will always rise faster than those of pancreatic insulin.

In the present paper, we demonstrate the opposite effect; i.e., peripheral levels of SICRI rise much faster than C-peptide levels and SICRI concentrations depend on the stage of cancer, whereas those of C-peptide do not (text-fig. 2). Thus SICRI is probably not generated by proinsulin splitting. Inasmuch as the high level of SICRI in blood is not necessarily accompanied by hypoglycemia (text-fig. 3), it might be identical to proinsulin; the increased levels of this molecule, however, would also increase the level of RIA-detectable C-peptide (*18*).

Theoretically, there are various explanations for the elevated levels of SICRI in diabetics and nondiabetics where the corresponding changes of C-peptide levels do not take place. One is that insulin has a clearance rate much lower than normal. However, insulin turnover rates in insulin-dependent tumors are higher than normal (*19*), which refutes this idea.

The alternative explanation is based on the assumption that tumor tissue secretes SICRI. Several facts support this hypothesis: 1) high preoperative and low postoperative levels of SICRI in diabetic patient #1; 2) the lack of correlation of SICRI and blood sugar levels in patient #1 (text-fig. 1) and the apparently weak correlation in a population of nondiabetic patients (text-fig. 3), showing that the elevated levels of SICRI are not necessarily followed by hypoglycemia; and 3) the lack of correlation between the stage of tumor-dependent SICRI levels and the independent levels of C-peptide.

The idea of ectopic production of insulin and insulin-like molecules is theoretically less unfamiliar if one knows that molecules functionally and immunologically related to insulin are found in various cells and tissues, even in the microbial world [(*10*) and references therein].

REFERENCES

(*1*) Pavelić K, Pekić B, Slijepčević M, Popović M. Insulin levels in Hodgkin's disease. Br J Haematol 1980; 46:133–135.

(*2*) Pavelić K. Aplastic carcinoma in diabetic mice: Hyperglycemia-suppressed proliferation rate and insulin synthesis by tumor cells. JNCI 1979; 62:139–141.

(*3*) Hyvarinen A, Nikkila EA. Specific determination of blood glucose with *o*-toluidine. Clin Chim Acta 1962; 7:140–143.

(*4*) Kiang DT, Bauer GE, Kennedy BJ. Immunoassayable insulin in carcinoma of the cervix associated with hypoglycemia. Cancer 1972; 31:801–805.

(*5*) Morgan CR, Lazarow A. Immunoassay of insulin, two antibody system. Plasma insulin levels of normal, subdiabetic and diabetic rats. Diabetes 1963; 12:115–121.

(*6*) Heding LG. Radioimmunological determination of human C-peptide in serum. Diabetologia 1975; 11:541–548.

(*7*) Davies RG. Program No. 32.: Computer programming in quantitative biology. London and New York: Academic Press, 1971:312–318.

(*8*) Thorpe PE, Knight CS. Microplate culture of mouse lymph node cells. I. Quantitation of responses to allogeneic lymphocytes, endotoxin and phytomitogens. J Immunol Methods 1974; 5:387–404.

(*9*) Søberg M, Bendixen G. Human lymphocyte migration as a parameter of hypersensitivity. Acta Med Scand 1967; 181:247–256.

(*10*) Le Roith D, Shiloach J, Roth J, Lesniak MA. Evolutionary origins of vertebrate hormones: Substances similar to mammalian insulins are native to unicellular eukaryotes. Proc Natl Acad Sci USA 1980; 77:6184–6188.

(*11*) Plovnick H, Ruderman NM, Aoki T, Chideckel EW, Poffenbarger PL. Non-β-cell tumor hypoglycemia associated with increased nonsuppressible insulin-like protein (NSILP). Am J Med 1979; 66:154–159.

(*12*) Shames JM, Dhurandhar NR, Blackard WG. Insulin-secreting bronchial carcinoid tumor with widespread metastases. Am J Med 1968; 44:632–637.

(*13*) Pavelić K, Popović M. Insulin and glucagon secretion by renal adenocarcinoma. Cancer 1981; 48:98–100.

(*14*) Pavelić K, Ferle-Vidović A, Osmak M, Vuk-Pavlović S. Synthesis of immunoreactive insulin in vitro by aplastic mammary carcinoma preconditioned in diabetic mice. JNCI 1981; 67:687–688.

(*15*) Pavelić K, Slijepčević M, Pavelić J, et al. Growth and treatment of Ehrlich tumor in alloxan-diabetic mice. Cancer Res 1979; 39:1807–1813.

(*16*) Pavelić K. Growth of a methylcholanthrene-induced fibrosarcoma in mice with diabetes mellitus. Eur J Cancer 1980; 16:279–284.

(*17*) Horwitz DL, Starr JI, Mako ME, Blackard WG, Rubenstein AH. Proinsulin, insulin, and C-peptide concentrations in human portal and peripheral blood. J Clin Invest 1975; 55:1278–1283.

(*18*) Melani F, Rubenstein AH, Oyer PE, Steiner DF. Identification of proinsulin and C-peptide in human serum by a specific immunoassay. Proc Natl Acad Sci USA 1970; 67:148–155.

(*19*) Woods M. Hormonal control of metabolism in cancer. In: Wright E, ed. Control mechanisms in respiration and fermentation. New York: Roland Press, 1963:253–264.

A Quest for the Mechanism of "Spontaneous" Malignant Transformation in Culture With Associated Advances in Culture Technology[1,2]

Katherine K. Sanford[3] *and* **Virginia J. Evans**[4]

ABSTRACT—The discovery of "spontaneous" malignant transformation of mouse cells in culture raised questions answerable only by obtaining a better control of culture conditions through technologic advances. One of these advances was the introduction of cellophane and later glass as a substrate to replace the plasma clot matrix, widely used in tissue culture at that time. Removal of cells from plasma clot and culture under cellophane or on glass not only increased cell yield but also allowed the manipulation of individual cells in suspension. Other advances included the design and technology of three-dimensional substrate cultures, the establishment for the first time of clonal cell populations from single isolated cells, the development of instrumentation and quantitative techniques for measuring cell proliferation, the introduction of the suspension culture of cells of "fixed tissue" origin, and the formulation of serum-free, antibiotic-free, chemically characterized culture media that could support the continuous proliferation of numerous cell lines from different tissues and species. These technologic advances promoted the application of microbial techniques to vertebrate tissue cells, marked the beginning of modern quantitative cell culture, and provided the tools for recent developments in virology, vaccine production, genetics, molecular biology, and other areas of biomedical research. These technologic advances were associated with a quest for an explanation of spontaneous malignant transformation. In this quest it was found that normal tissue cells of various rodent species after prolonged culture in the absence of added carcinogens or viruses and even in serum-free, chemically defined medium undergo malignant transformation. Certain differences between the normal cell and its malignant derivative were identified, and their reliability as in vitro criteria of malignancy was shown. Certain observations support the hypothesis that aberrant methylation of nucleic acids may be a chemical event in carcinogenesis, and methyltransferases were discovered in all RNA retroviruses examined. Three environmental agents were found to enhance or induce malignant transformation: the type of serum used, molecular oxygen, and repeated exposure to low-intensity fluorescent light. All three agents produce chromosomal DNA damage. Experimental results indicate that the DNA damage produced by light results directly or indirectly from the intracellular generation of hydrogen peroxide and/or the derivative free hydroxyl radical. Thus the malignant transformation of rodent cells is not spontaneous but is induced by specific environmental agents that produce chromosomal DNA damage. The progression to malignancy in mouse cells and the susceptibility of human cells to malignant transformation appear to be associated with an impaired capacity to repair the DNA damage produced by these environmental agents.—JNCI 1982; 68:895–913.

The discovery years ago of the "spontaneous" neoplastic or malignant transformation of normal cells in culture raised a number of questions fundamental to the problem of cancer; this discovery led to a long quest for elucidation of mechanisms, possible contributing factors, and associated cellular lesions. An important element in this quest was the need to fashion tissue culture into a precise quantitative tool. One of the outstanding pioneers in cell culture was Wilton R. Earle who, with his co-workers in the Tissue Culture Section of NCI, advanced cell culture technology and increased our knowledge of malignant transformation. The Tissue Culture Section was initially headed by Dr. Earle and subsequently by Dr. Virginia J. Evans and later by Dr. Katherine K. Sanford. In this report, we summarize the activities of this Section and have attached a bibliography to document the contributions of the individual members of the staff and collaborating scientists.

ADVANCES IN CELL CULTURE TECHNOLOGY

Before his studies at NCI, Dr. Earle had been attempting to control the environment of mammalian cells in culture. Among his contributions, he showed that short exposure of leukocytes or chick fibroblasts to light in the visible range caused cell degeneration, especially in the presence of photosensitizing substances from red blood cells (*1–4*); improved the techniques of both hanging-drop cover slip and Carrel flask culture by introducing means for adjustment of pH, oxygen, and carbon dioxide (*5, 6*); devised a simple press for mincing soft tissues (*7*); formulated an isotonic balanced saline solution, Earle's saline, (*6*); and introduced the use of HS as a supplement to chick embryo extract and chicken plasma clot and showed that this medium could support the continued proliferation of epithelial cells from rat mammary carcinoma (*8–10*). He found that thin, strip-shaped explants for both initiation and subculture provided an increased cell yield as compared with the 1- to 2-mm^2 explant in use at that time (*11*). An approximately direct relationship between explant size and area of outgrowth was observed, as was a minimal size that failed to grow because of some factor(s) other than exhaustion of the medium (*12*).

Abbreviations used: AMV=avian myeloblastosis virus; Ara-C=β-cytosine arabinoside; BP=benzo[*a*]pyrene; FBS=fetal bovine serum; HS=horse serum; MCA=3-methylcholanthrene; MuMTV=murine mammary tumor virus; NCI=National Cancer Institute; P_{O_2}=partial pressure of oxygen; RAV-1=Rous-associated leukemia virus; RSV=Rous sarcoma virus.

---

[1] Received June 15, 1981; revised December 2, 1981; accepted December 22, 1981.

[2] Animals were maintained under the guidelines of the National Cancer Institute.

[3] Laboratory of Cellular and Molecular Biology, Division of Cancer Cause and Prevention, Building 37, Room 2D02, National Cancer Institute, National Institutes of Health, Public Health Service, U.S. Department of Health and Human Services, Bethesda, Md. 20205.

[4] Biomedical Research Institute, Rockville, Md. 20852.

Replacement of the Plasma Clot and Development of Three-Dimensional Mass Cultures

Our discovery of malignant transformation of mouse cells in culture raised a question as to whether the transformation is spontaneous, i.e., resulting from intrinsic instability of cells or induced by some environmental factor(s). Therefore, research efforts were directed toward developing a chemically characterized culture medium that eliminated any unidentified chemical carcinogens, hormones, or viruses which might be introduced through the biologic culture medium of chick embryo extract, HS, and chicken plasma that were used in all of our experiments. The chemically undefined plasma clot was replaced with a sheet of perforated cellophane, an inert defined material. The cellophane sheet provided a luxuriance of cell growth superior to that obtained in plasma clot or glass-substrate explant cultures (*13–17*). Cultures of increasingly larger surface area were grown (*18*), including cell types of biomedical importance such as human skin epithelium, bone, and cornea for preservation and transplantation (*19–29*), human endocrine tissue for hormone production (*30*), and human cells in nonhuman serum for potential use in vaccine production (*31*). The cellophane sheet also allowed the ready dispersal of cells for development of single cell clones and cell suspensions that could be inoculated on glass substrate and quantified for growth experiments (*32, 33*). By use of a massive inoculum, dispersed cells from chick embryo tissue could be seeded onto glass flasks (*33*). Two types of three-dimensional substrate cultures were developed: one with multifolded perforated cellophane sheets as substrate and the other with pyrex glass helices through the interstices of which the nutrient fluid was mechanically circulated (*34*). These three-dimensional substrate cultures yielded even greater amounts of living cells than were produced on two-dimensional substrates and were forerunners of present-day commercial vessels used for bulk production of substrate-dependent cells (*35*).

Development of a Cloning Procedure

Purity of cell type can be attained only by the isolation and growth of single tissue cells. In the late 1940's, the inability to grow single cells resulted from inadequate culture media and incomplete knowledge of the physiologic requirements of small numbers of cells. Whereas a large clump of tissue cells could adapt a reasonable volume of culture medium, one cell grown in an identical volume was unable to adjust the fluid sufficiently for survival and proliferation. A procedure was therefore developed for isolating single cells in glass capillary tube segments by which the rapid diffusion of metabolites was restricted and the culture medium was thus conditioned. Under these conditions, single isolated mammalian tissue cells for the first time were grown into clonal populations (*36*). The first cloned line NCTC 929L, derived from strain L, is widely used in many areas of research. This capillary cloning procedure, later modified and simplified (*37, 38*), provides greater assurance than plating methods that the clonal population is indeed derived from one cell. To preclude possible contamination of clones with cells from chick embryo extract, a procedure was developed for extract filtration (*39*). The capillary cloning procedure was successfully applied to many other cell types of chicken, mouse, or human origin such as cells from the liver, the parotid gland, subcutaneous connective tissue, or mammary carcinoma (*40–46*). This precise cloning technique led to the development of other cloning procedures and the application of bacteriologic plating methods to mammalian tissue cells.

Quantification of Cell Proliferation and Development of Suspension Cultures

For further development of a chemically defined culture medium, a quantitative growth assay was required to evaluate nutritional factors influencing cell proliferation (*47*). Methods and instrumentation were designed for the preparation of replicate cultures from sieved, mechanically stirred cell suspensions (*48–51*) and for quantification of proliferation rates by enumeration of isolated cell nuclei (*52*). So that cells would not be lost during quantitative nutrient fluid renewal, a new culture vessel was designed, the T-flask, with a conical tip into which dislodged cells could settle during slow centrifugation (*53*). A modification of this flask for use with high-resolution photomicrography was subsequently developed (*54*). Rubber stoppers for these flasks, shown to be toxic to cells and perhaps even carcinogenic, were replaced with silicone stoppers designed by Earle and fabricated to his specifications (*55*).

Studies on the influence of inoculum size showed that cell population density per unit volume of culture medium is a major factor affecting rates of cell proliferation (*56*). Established cell lines such as NCTC clone 929L were found to proliferate at equivalent rates on glass and cellophane substrate (*57*). The influence of motion of the medium on cell proliferation was then explored by a comprehensive study of rate of roller tube rotation on cell yield (*58*). At the highest speed of rotation, 2,400 revolutions per hour, individual cells were free floating and proliferating at a high rate. This study demonstrated for the first time that "fixed-tissue" mammalian cells that have undergone malignant transformation can proliferate as a free-floating suspension in rapidly agitated fluid medium (*59*). The Brunswick-type rotary mechanical shaker designed for the antibiotics industry was then redesigned and successfully used for large-scale, batch-type culture of mammalian cells in suspension (*60–62*). The dynamics of cell proliferation in the suspension culture, glycolytic rates under different culture conditions, and chemical alterations of the medium were analyzed in efforts to devise culture conditions that would enhance cell yield (*62–66*). From these batch-type, suspension cultures and the large-scale, surface substrate cultures, adequate numbers of cells were obtained for analyses of biochemical properties including enzyme patterns. These characterizations were essential for identifying the type of cells in culture and for determining the extent to which the cells maintain differentiated function and structure during continuous culture.

Development of Chemically Defined Culture Media

By 1950, two chemically defined media had been reported that supported outgrowth and limited survival of avian embryonic tissue. However, in neither of these did mammalian NCTC clone 929L cells proliferate as determined by our quantitative assay (*67*). In our development of a chemically defined medium, two approaches were used: analytic and synthetic combined with depletion techniques (*68*). NCTC clone 929L served as the assay cells. Both the serum and embryo extract components of the medium were fractionated separately and analyzed chemically (*69–71*). Two fractions, the ultrafiltrate of embryo extract and the large molecular protein fraction of HS, together yielded cell numbers approaching those obtained with complete medium (*72*). Further fractionation of the serum proteins yielded globulin fractions I and III that could be substituted for the large molecular fraction of HS in a protein-free basal medium (*73*). Because all protein fractions stimulated growth, it appeared that the proteins might be serving a physical protective role in the medium; therefore, some large molecular polymers were tested in a protein-free basal medium, but none of these supported maximum growth (*74*). During the course of these analytic studies, whole-egg ultrafiltrate was found to be an effective substitute for chick embryo extract ultrafiltrate (*75*). Our synthetic approach was to add defined components to the protein fraction of HS and/or the ultrafiltrate of chick embryo extract (*76*). These supplements included an amino acid mixture formulated from chromatographic analyses of the free and conjugated amino acids in the complex biologic medium (*69, 70*); Earle's saline formed the diluent, and vitamins with certain other components from mixture 199 of Morgan et al. (*77*) were tested in groups (*78*). By 1954, fractionations, analyses of these fractions, and exploratory nutritional experiments made possible the formulation of a chemically defined medium, later designated NCTC-109; in January 1955 a line of NCTC clone 929L, designated NCTC 2071, was initiated in this serum-, protein-, and antibiotic-free medium, cultured continuously for 24 years thereafter (*79–81*), and found on subculture to proliferate reproducibly from a lower inoculum size than was possible with NCTC clone 929L in serum–embryo extract medium (*56, 82*). This medium and the synthetic medium 858 of Healy et al. (*83*) were the first chemically defined media to support proliferation of an established mammalian cell line; these two media differ qualitatively and quantitatively in numerous components.

Some 30 additional cell lines from five species including man, monkey, hamster, rat, and mouse were adapted by gradual serum depletion to serum-free, chemically characterized medium NCTC-135 (differing from NCTC-109 in lacking cysteine) (*84–92*). The successful growth of cells in chemically defined medium could result from adaptation or from the selective multiplication of variants or mutants of the original cells. However, certain lines retained some functional differentiation and showed no more alterations than were observed in cells explanted from in vivo to serum-containing medium. In fact, analyses of numerous cell lines adapted to continuous growth in serum-free chemically defined medium showed, with few exceptions, enzyme profiles similar to those in serum-containing medium (*93*). Furthermore, normal embryo cells from mouse and rat tissues could be explanted directly to chemically defined medium and grown continuously thereafter in the absence of serum or exogenous protein (*94–96*).

Fischer (*97*) and Eagle (*98*) identified, in short-term studies, the essential amino acids, and Eagle (*99*) identified the essential vitamins for cell survival and proliferation. However, these essential components were always identified in a medium containing dialyzed serum which can prevent the development and manifestation of certain nutritional deficiencies (*100*). By use of serum-free, protein-free, chemically defined medium, we disclosed some additional requirements for long-term proliferation. Biotin was shown for the first time to be a requirement for continued proliferation (*101*); vitamin B_{12} and inositol were required by certain cell lines but were not required by others (*91, 100–102*). An interrelationship between folic acid concentration, vitamin B_{12}, and nucleic acid synthesis in murine cells was established and analyzed (*103–107*). We showed for the first time that the nonessential amino acids are required for maintaining a high rate of cell proliferation in the absence of serum protein (*100, 108, 109*). Galactose could be substituted for glucose in cultures of mouse and human cells, but cell yield was reduced (*110*). In efforts to simplify and improve the growth-promoting properties of the medium, individual components and groups of components were evaluated by quantitative growth assays (*101, 109, 111–114*). Simpler media such as NCTC-126 and NCTC-163 were formulated, all components of which served some function or were necessary for cell survival, maximum proliferation, or prevention of cell fragility (*84, 92, 101, 115, 116*). Recently, the new NCTC formulation 168 was developed for human skin epithelial cells, a cell type of importance for carcinogenesis studies (*117*).

The successful growth of cells in serum-free, chemically defined medium can be attributed to several factors including the commercial availability of high-quality chemicals, instrumentation for obtaining pure water, and equipment and procedures to ensure chemically clean glassware (*55*). Earle developed, for the early carcinogen studies (*9*), a method and apparatus for the cleaning of glassware by digestion of organic residues with hot sulfuric–nitric acid in steam-jacketed Duriron kettles (*118*). He introduced, for heat sterilization, the use of Patapar wrapping paper, a vegetable parchment that minimizes the release of volatile toxic substances. Since house-generated steam usually contains toxic substances to prevent oxidation of pipes, Earle designed and had fabricated stainless-steel-clad autoclaves with self-contained indirect distilled water steam generators. No antibiotics were introduced into the cell cultures because they prevent ready detection of microbial contaminants that complicate interpretation of nutritional and biochemical data.

To facilitate culturing of cells in chemically defined media and to enhance usefulness of the cells, we examined commercially prepared powdered NCTC media and procedures for cryopreservation of cells. Critical evaluation of the ball-milled, powdered media with no added serum revealed deficiencies that limited their usefulness as serum-free media in certain nutritional and biochemical studies (*119*). Classical procedures for cryopreservation in liquid nitrogen were successfully adapted for cells grown in chemically defined medium (*120*). We were thus in a position to suspend life processes at any stage of culture and store the cells for later retrieval and study.

Not only have chemically defined media been useful for growing cells in stationary culture, but they are also useful for growing cells in agitated fluid suspension. However, a supplement of 0.12% methylcellulose (Dow type MC, 10–15 centipoises), a chemically characterized nutritionally inert polymer, was essential to prevent deterioration of cells by mechanical stresses imposed on them as a result of rapid fluid agitation (*121*, *122*). With this supplement, malignant cell lines, adapted to chemically defined medium, produced consistently high cell yields (*115*, *122*, *123*). Normal lines, such as LLC MK_2 derived from monkey kidney, failed to grow (*124*). The observations that methylcellulose substitutes for serum in agitated suspension culture and also promotes survival and proliferation of fragile cells grown in chemically defined medium in stationary culture (*125*) suggest that one role of the large serum protein molecules is to provide physical protection to cells during mechanical stress.

Analysis of the Role of Serum and Introduction of a Serum Substitute

Although we have shown that serum is not an absolute requirement for in vitro survival and proliferation, it facilitates initiation of cell lines and promotes cell proliferation. However, serum is not only a depot for bound nutrients such as trace elements, vitamins, and cofactors, but it is also a source of chemical variability and can introduce adventitious microbial contaminants such as mycoplasma as well as hormones, antibodies, enzymes, or cytotoxic factors (*126–128*). Diverse effects of serum on cells have been noted. For example, the addition of serum to chemically defined medium reversibly altered certain isozyme patterns of three lines of human epithelial-like cells (*129*). NCTC clone 929L cells, after their adaptation to a chemically defined medium, showed altered morphology, increased adhesion to glass substrate with reduced intercellular cohesion, and greatly decreased rates of cell migration (*130*) as revealed by time-lapse microcinematography (*131*). These changes could be reversed by addition of serum to the cultures (*130*). In addition, when added immediately after X-irradiation, serum modified the irradiation response of cultures by speeding their recovery (*132*). Addition of serum proteins to a chemically defined medium deficient in certain vitamins and amino acids prevented the development and manifestation of the nutritional deficiencies (*100*).

A low-molecular-weight (mol wt, <1,500), heat-stable growth factor from Bacto-peptone could substitute for serum and sustain continuous growth of a number of serum-dependent mammalian cell lines. Although the chemical nature of the biologically active component(s) is not yet firmly established, this factor is autoclavable and nonantigenic and may be of considerable value for vaccines and other biologics in obviating problems with viruses and other unknown components of serum (*133–135*). In addition, this factor shortens the time required for adaptation of cells from serum-supplemented medium to continuous growth in protein-free, chemically defined medium (*127*, *136*).

Identification of Serum Type, Visible Light, and Oxygen as Factors Influencing Chromosomal Stability and Cell Proliferation

The type of serum supplement was found to influence karyotypic stability. The chromosomes of mouse cells grown in HS-supplemented medium as compared with FBS-supplemented medium were more unstable, shifting rapidly from the diploid number and altering in morphology as a result of chromatid breaks and rearrangements (*137–142*). These observations suggest that HS produces chromatid breaks at a faster rate than FBS and/or FBS protects against chromatid breakage. In a recent study (*143*), the large molecule fraction of HS (excluded volume from Sephadex G-25) produced alterations in chromosome number and structure; also, HS caused chromatid breaks at or near the centromere as well as caused terminal chromatid exchanges resulting from breaks in the centromeric areas.

Another factor influencing karyotypic stability was found to be the oxygen concentration in the gas phase of the culture. Oxygen dissolved in the culture medium is essential for maintaining a normal respiration rate, but the Po_2 must not be damaging to the cell. The gas phase in most cell cultures is either residual air or an air:CO_2 mixture (18–20% O_2). Decreasing the oxygen concentration in mass culture from atmospheric (18%) to 1% decreased the number of chromosomal aberrations and the rate of shift from diploidy (*144–146*). In fact, 18% O_2 may be a factor in the evolution of heteroploidy and long-term cell lines (*147*, *148*). Lowering the oxygen concentration in the gas phase to 0–1% also enhanced survival and growth of single cells, whether malignant or normal, in a variety of culture media compared for their effectiveness in promoting clonal growth (*148*, *149*). The cytotoxicity or clonal growth inhibition produced by atmospheric oxygen could not be alleviated by addition of the reducing agents cysteine or thioglycollate (*150*). The oxygen sensitivity of freshly explanted mouse embryo cells or low-passage human diploid fibroblasts was greater than that of long-term heteroploid cell lines that had been continuously propagated at and adapted to the high oxygen level. Whereas a low oxygen level enhanced clonal growth, no difference in cell yield or glycolytic activity was observed between cultures at higher inoculum sizes as used routinely for mass culture that were gassed with 18% (atmospheric) O_2 (growth medium Po_2, ≈120 mm Hg) and those gassed with 1% O_2 (growth medium Po_2, ≈40–60 mm Hg). A Po_2 of 40–60 mm Hg is comparable to physiologic values of intercellular fluids in vivo. In mass culture, the respiratory activities of the many cells may adjust the growth medium Po_2 to the lower more physiologic concentration (*151*). In contrast to fibroblasts, epithelial cells in mass culture require the higher oxygen concentration for optimal growth (*152*).

Shielding cultures from room lights during routine handling also reduced the incidence of abnormal chromosomes including minutes and metacentrics that result from chromatid breaks and exchanges (*144*, *146*). Further studies showed that a single 3- to 20-hour exposure to low-intensity, cool-white fluorescent light (4.6 W/m^2) at 37°C produces chromatid breaks and exchanges in both mouse and human cells (*153*, *154*). The effective wavelength (405 nm) is in the visible range (*155*). The light-induced chromatid damage is enhanced by oxygen and can be almost completely prevented by the addition of catalase or glutathione with ascorbic acid to the culture medium during light exposure; superoxide dismutase has no effect (*153, 154*). These observations implicate H_2O_2 produced in the illuminated culture medium or in the cell as a causative agent. Light and oxygen in the presence of riboflavine, tyrosine, and L-tryptophan generate clastogenic (chromosome-breaking) amounts of H_2O_2 in the culture medium (*155, 156*). However, cells washed free of medium and illuminated in saline for 3 hours show chromosome damage to the same extent as cells illuminated in culture medium (*154, 155*). Furthermore, mannitol, a scavenger of ·OH significantly decreases the light-induced damage (*154*). Thus both H_2O_2 and the derivative ·OH generated within the cell during light exposure are agents that directly or indirectly cause the chromatid damage. Sodium selenite added to the cultures also significantly decreases the damage in a dose-related manner and may be necessary to maintain sufficient activity of glutathione peroxidase, a selenoenzyme that catalyzes the decomposition of H_2O_2 (*154*). Survival of cells in mass culture after exposure to visible light depends on the medium used and the cell type. Epithelial cells grown in medium NCTC-168 are more resistant to cytocidal effects of light than are fibroblasts (*157*). Light-induced cytocidal effects can be prevented by the use of tinted flasks (Taylor WG, Camalier RF: Unpublished observations).

Visible light in the presence of oxygen was found to have several other effects on cells in culture. Twenty-hour exposure at 37°C of mouse and human cells to low-intensity (4.6 W/m^2) fluorescent light produces DNA-protein cross-links. The effective wavelength(s) is in the visible region of the spectrum, 450–490 nm. The cross-linkage is medium mediated, proportional to the intensity of fluorescent light, enhanced by oxygen, decreased at high cell density, and insensitive to catalase. This linkage removed by digestion with *Tritirachium album* Limber proteinase K is between DNA and protein. These lesions are usually repaired within 24 hours. Light-induced cross-links were probably not discovered previously because the light was administered at high intensity under nonphysiologic conditions of low temperature and nutrient-deficient medium. Light causes more strand breaks than cross-links. Under nonphysiologic conditions, breaks predominate, whereas under physiologic conditions, breaks are repaired more rapidly than cross-links. Consequently, cross-links predominate, and this damage at the molecular level may lead to important biologic aberrations such as mutations, chromosome damage, and malignant transformation (*158, 159*).

Another effect of low-intensity light (6–9 W/m^2) was the enhancement of proliferation rate and life-span of human diploid fibroblasts. Whereas long exposure (>8 hr) of cells and medium to light produces toxic and/or growth-inhibitory photoproducts, especially for low-density cell populations, short exposures (3–4 hr) reproducibly enhance the proliferation rate in a reversible manner and significantly extend the life-span. This reversible response is mediated by a substance(s) generated by light exposure of culture medium (*160, 161*). Light produces some mitogenic substance(s) in certain components of the chemically defined medium (Parshad R, Sanford KK: Unpublished observations).

SPONTANEOUS MALIGNANT TRANSFORMATION IN CULTURE

Earle's primary research objective was to elucidate the mechanism of carcinogen-induced malignant transformation of mouse cells in culture. Even before his studies at NCI, he performed exploratory experiments to select a suitable tissue and carcinogen dose and to develop procedures for documenting morphologic changes (*162–165*). In assessing the neoplastic potential of tissue culture cells implanted in vivo, he observed that tumor cells exhibit more invasive, rapid growth and less necrosis at the intramuscular than at the subcutaneous site (*166*) and that carcinoma cells may initially give rise to tumors in vivo typical of the parent tumor but later, despite epithelial architecture, give rise to tumors simulating fibrosarcoma (*167, 168*). He documented a gradual morphologic alteration in carcinogen-treated cultures of mouse cells that resembled the morphology of cultured cells derived from a carcinogen-induced rat tumor (*169*).

Discovery of Spontaneous Neoplastic Transformation in Culture

In 1940 at NCI, Earle initiated a line of cells from normal subcutaneous connective tissue of a strain C3H mouse; when the morphology of the cells had stabilized, cultures were exposed to the carcinogen 20-methylcholanthrene, i.e., MCA, for periods ranging from 6 days to more than a year; untreated cultures were also maintained. Assays for malignant neoplastic transformation were made by im implantation of the cultured cells into C3H mice. Morphologic and growth changes associated with carcinogen dosage and similar to those reported earlier were observed (*9*). Furthermore, morphology was documented photographically with the unique cine- and still-microphotographic instrumentation he designed (*170, 171*). These morphologic alterations stabilized and persisted for years (*172–175*). Cells were first implanted in mice after 500 days in culture and 25 days after removal from the carcinogen (*176*). Sarcomas developed from the implanted cells irrespective of carcinogen dosage (*177*). One of the malignant cell lines, designated strain L and exposed for 111 days to MCA, was cultured continuously for 8 years, at which time a clonal population was derived, as noted earlier (*36*). The control untreated cultures also gave rise to tumors. This observation was interpreted as resulting from a possible contamination with the carcinogen, although alternative explanations were proposed (*176, 178*). The sarcomas originating from the cultured cells were shown to possess a metabolism characteristic of that of malignant tumors (*179*). The Golgi and mitochondria of the carcinogen-treated cells and derivative tumors showed few changes from those of untreated control cells (*180*).

With the passage of time, a progressive decrease occurred in vitro in the capacity of the mouse cell strains, including

NCTC clone 929L, to give rise to sarcomas when the cells were injected into animals of the inbred strain of origin (*181*), and the extent of vascular reaction elicited by each cell strain in transparent chambers in vivo varied with percentage of tumors produced (*182*). The decrease in tumorigenicity of NCTC clone 929L was subsequently shown to result from an immunologic incompatibility between the cells and mice of the inbred strain of origin (*183*). It is of interest that when NCTC clone 929L was later adapted to serum-free, protein-free, chemically defined medium, the cells gave rise to sarcomas in approximately 90% of animals inoculated. This marked increase in tumor-producing capacity could result from antigenic alterations or alterations in biosynthetic capacities that enhance transplantability of the cultured cells (*101, 184*). The results of these carcinogen experiments and those of Dr. George Gey, The Johns Hopkins Medical School, on rat fibroblasts (*185*) showed clearly that carcinogenesis can occur in vitro. However, it was still uncertain whether the neoplastic transformation of the mouse cells was induced or spontaneous.

In a subsequent study additional lines of mouse cells underwent neoplastic transformation in the absence of added carcinogen, and trace levels of MCA did not enhance the incidence. These results led to the conclusion that neoplastic transformation is a reproducible response of strain C3H mouse fibroblasts to the culture conditions used (*186*). Further studies showed that cell lines derived from a wide variety of normal tissues, including liver, kidney, epidermis, parotid gland, subcutaneous connective tissue, and skeletal muscle of different mouse and rat strains as well as cells from Syrian and Chinese hamsters, regularly undergo neoplastic transformation during long-term culture (*40, 94, 95, 137, 187–192*). Tumors arising from implants of the cultured cells were indistinguishable from many anaplastic sarcomas and carcinomas of in vivo origin. To date, two mammalian species, guinea pig and human, appear resitant to both spontaneous transformation in culture and foreign-body carcinogenesis (*193*).

Clonal Analysis of Neoplastic Transformation

With the development of a cloning procedure, two questions concerning neoplastic transformation in culture could be answered. 1) Is this a bona fide cell transformation or is it a selective process by which latent tumor cells in the tissue explant overgrow normal tissue components? 2) Would the change occur simultaneously or would it occur randomly in parallel cell lines grown from a single cell either in plasma clot matrix or with cellophane substrate but under otherwise similar culture conditions? A clone was developed from C3H mouse connective tissue. Parenthetically, the only relationship between this clone and clone NCTC 929L is that both were derived from C3H mice. During an 18-month study of 17 parallel lines of this clone, 8 failed to produce tumors in syngeneic hosts whereas 9 became tumorigenic. Clearly, from a single cell in culture, neoplastic cells arose by the process of transformation and not by selective overgrowth. The transformations appeared randomly, suggestive of mutational events (*187*). We continued two of the cell lines, one tumorigenic and the other nontumorigenic, for a comparative study of their properties in an effort to identify "markers" of neoplastic transformation. Nontumorigenic or nonneoplastic cells will be referred to henceforth in this paper as "normal." The normal line subsequently became transformed and gave rise to a low incidence of sarcomas. Markers of neoplastic transformation will be considered later.

Induction of Neoplastic Transformation by Viruses and Chemical Carcinogens

Because of the erratic nature of spontaneous neoplastic transformation in long-term culture, we attempted to induce a rapid and controlled transformation, preferably in a clonal population, before spontaneous transformation occurred. Our objective was to obtain paired normal and derivative neoplastic cell populations for comparative study. Two tumor viruses were examined as possible inducing agents, RSV and polyomavirus. The first step with RSV was to resolve the controversy concerning the specific tissue cell, monocyte or fibroblast, that becomes infected and transformed in vivo by RSV. Our studies showed that the fibroblast from subcutaneous connective tissue is the cell susceptible to infection. However, under our culture conditions, morphologic alterations were not induced. Furthermore, the lack of inbred chickens for assay of tumorigenicity and the rapidity with which the virus induces tumors in host tissues precluded adequate in vivo testing of the cultures (*194, 195*). Malignant transformations were produced repeatedly by polyomavirus in a clone of epithelial-like cells from C3H mouse parotid gland. However, soon after the virus-induced transformation, all control untreated cultures underwent spontaneous transformation (*40*). In Syrian hamster embryo cells, reputedly more stable than mouse cells in culture, malignant transformations could be induced by high-titered polyomavirus under certain conditions, but the transformations were not rapid nor entirely reproducible. In addition, hamster embryo cells did not exhibit a finite lifespan as previously postulated, and all hamster lines underwent spontaneous transformation (*190*). Although RSV continued replication in Rous sarcoma cells in culture, efforts to produce MuMTV at high titer in mouse mammary carcinoma cells were less successful. Cells were established in culture from spontaneous, primary, and transplanted C3H mouse mammary carcinomas known to contain MuMTV. Although the tumor cell lines continued to grow autonomously when implanted in vivo, MuMTV disappeared from the cells with prolonged culture. Continued virus replication in the cell was apparently not required for maintenance of the neoplastic state (*196*). Furthermore, high-titered and reproducible virus preparations could not be obtained from these cultures.

Chemical carcinogens, tested as inducing agents, produced malignant transformations in some Syrian hamster embryo cell lines, with the response neither rapid nor completely reproducible. Carcinogen treatment of mouse, rat, and Chinese hamster cell lines did not induce transformation nor enhance the spontaneous change as judged by tumorigenicity of the cells in syngeneic hosts (*192*). Cultures of human epithelial cells actively metabolized the environmentally ubiquitous carcinogen BP (*197*). At low noncytotoxic concentrations, BP formed adducts to cellular DNA. Because these adducts persisted for at least 7 days, they may accumulate with prolonged BP exposure. This finding suggests that chronic low-level exposure of human skin epithelium to BP may lead to an accumulation of DNA damage (*198*). For this reason, the culture of human skin epithelial cells under controlled conditions is important for in vitro carcinogenesis studies. However, human cells are less suitable for in vivo assays of tumorigenicity and have been less well characterized than cells from inbred rodents such as the mouse.

Because the induction of malignant transformation by tumor viruses or chemical carcinogens in rodent cells was not rapid nor always reproducible and was usually complicated by the almost simultaneous and/or erratic spontaneous transformation of control cultures, we continued our efforts to identify and control environmental factors that might influence or cause spontaneous transformations. One advantage of studying spontaneous in contrast to induced transformants is that responses to the exogenous inducing agents that are unrelated to malignant transformation are absent; thus properties uniquely associated with malignant transformation can be more readily identified.

Hypotheses Concerning the Etiology of Spontaneous Neoplastic Transformation

Intermittent anaerobiosis and cell crowding as causative factors.—Several hypotheses concerning the etiology of so-called spontaneous malignant transformation have been proposed through the years (*184*). Intermittent anaerobiosis was postulated as a condition that could induce malignant transformation. However, we observed no influence of anaerobic treatment on time or incidence of malignant conversion in two independent studies on lines of mouse cells (*199, 200*). Subsequently, certain observations suggested that the transformation in mouse cells is associated with activation of endogenous viruses of the murine leukemia–sarcoma complex; attempts to demonstrate such an incontrovertible association have been unsuccessful (*201–203*). An influence of high cell density on acquisition of neoplastic potential has also been reported. Some of our experimental observations prompted us to reassess this concept. Normal rat embryo cells maintained for approximately 3 years with regular medium renewals but with limited or no subculturing formed densely multilayered sheets in vitro but did not grow as sarcomas in vivo. In contrast, cells initiated from the same embryo cell suspension but maintained at a lower population density by repeated subculture became tumorigenic (*95*). In our reassessment of the postulate that high cell density with extensive cell–cell contact promotes malignant transformation whereas low cell density with limited cell–cell contact prevents transformation, we found that manipulation of inoculum size to maximize or minimize cell contact did not reproducibly influence malignant transformation. We concluded that serial culture of cells at low population density with limited cell–cell contact was insufficient to prevent transformation and that deliberate selection of colonies or cultures of well-spread, cytologically normal cells was necessary to maintain a normal cell population. Contrariwise, serial culture of cells at high density conferred a growth advantage to malignant cells which, in contrast to normal cells, are usually less anchorage-dependent and thus capable in crowded culture of proliferation in multilayers (*204*).

The aberrant methylation hypothesis of malignant transformation.—The observation that certain tumor tissue extracts have a greater methylating capacity than do extracts of normal tissue cells led to the concept that altered nucleic acid methylation may be the initiating or necessary chemical event in at least some types of malignant transformation (*205*). This hypothesis was evaluated in a more rigidly controlled biologic system than that used previously. Mouse cells transformed spontaneously in culture in the absence of exogenous virus or chemical carcinogen and the normal cells from which they arose were compared under the same culture conditions and after the same period in vitro; both cell populations also grew at the same rate in culture. The malignant cell extracts had a greater methylating capacity than did extracts of the normal cells (*206, 207*). A consistent but small difference between tRNA methylation was also observed in the paired lines (*208*). These results are consistent with the aberrant methylation hypothesis. No difference was observed between the paired cell lines in methylation of satellite DNA; both heavy- and light-strand DNA had essentially equal amounts of 5-methylcytosine despite a 1.5-fold higher cytosine content in the heavy strand (*209*). The biologic function of methylcytosine in mammalian cell DNA is still unclear. Although methylcytosine was known to be present in nuclear and mitochondrial DNA, it was shown for the first time to occur also in rat liver microsomal DNA, which has distinctly different properties from those of mitochondrial and nuclear DNA (*210*). A qualitative difference was observed between the methylase activities of normal and malignant mouse mammary tissue, but the normal lactating tissue extracts had a greater capacity to methylate RNA than did the tumor tissue extracts (*211*). These conclusions are consistent with the aberrant methylation hypothesis, with the reservation that aberrant does not imply hypermethylation.

In these studies, support for the methylation hypothesis was provided by the discovery of methyltransferases in all RNA tumor viruses examined. These viruses included AMV (*212*), RSV (*213*), RAV-1 (*213*), MuMTV (*211*), and, in addition, intracisternal A-particles which have several biochemical properties of RNA tumor viruses (*214*). These A-particles, found consistently in tumors and embryo cells but not in adult tissues, are frequently associated with C-type particles; however, they are neither infective nor apparent precursors of immature forms of C-particles (*215*). The column chromatographic procedure developed for methylase assay facilitates identification, purification, and characterization of these enzymes (*216*). An N^2-guanine methyltransferase was partially purified from chick embryo cells (*217*), purified 120-fold from AMV, and characterized (*218*). Six methylases, indistinguishable from cellular enzymes and not found in other RNA tumor viruses, were associated with the intracisternal A-particles; five were found in the nucleoprotein core, possibly having been packaged in the core during viral synthesis (*214*). N^2-guanine RNA methyltransferase was integrally associated with both

MuMTV and its putative nucleoprotein core, the intracytoplasmic A-particle (*211*). In AMV, the methylase is not a core component, is possibly of cellular origin, and may have a function in the virus life cycle (*219, 220*). N^2-guanine RNA methyltransferase is also associated with RSV and RAV-1, and an additional purine methylase N^1-adenine RNA methyltransferase was found in RSV but not in AMV or RAV-1. Although all examined RNA tumor viruses alter methylation of nucleic acids, it is still uncertain whether these methylations are primary or causal, secondary, or concomitant to malignant transformation (*221*).

Elimination of Suspect Causative Agents in Malignant Transformation

Our primary objective in developing a chemically characterized culture medium was to determine whether cells grown in this better defined environment still undergo malignant transformation. Five lines of C3H mouse cells (*96, 222*) and three lines of rat embryo cells (*95*) were initiated and maintained continuously in serum- and protein-free, chemically defined medium; all mouse lines transformed after prolonged culture, but the rat cells remained normal for years. In four of the mouse lines, cells in primary culture grew as sarcomas even before they could be subcultured. Also, normal mouse tissue cells underwent malignant transformation when explanted into Millipore diffusion chambers inserted ip into C3H mice and maintained in the same chamber without the mitotic stimulation associated with subculturing (*223*). The transformed mouse lines with one exception were found to be free of known murine viruses (*96, 222*). The experiments with mouse cells in chemically defined medium ruled out exogenous viruses, known chemical carcinogens, and hormones as the causative agents of these transformations. The results also supported the concept of spontaneous change.

Influence of Type of Serum on Malignant Transformation

The first evidence that these transformations were not strictly spontaneous but could be induced or influenced by environmental factors was the discovery that the type of serum added to the medium accelerated and increased the frequency of malignant transformation. C3H mouse cells cultured in chemically defined medium supplemented with gelding HS became transformed after short culture periods ranging from 3 to 6 months, whereas cells cultured with FBS became transformed after more variable and considerably longer periods extending to more than 2 years (*224*). These observations were, in general, confirmed in a number of studies and also were verified in cells from other mouse strains (*94, 137, 138, 189, 222*). Of types of serum tested, including fetal horse, stallion, mare, early fetal bovine, bovine calf, and adult bovine, the most active in promoting transformation were stallion, gelding horse, and bovine calf; however, FBS reproducibly delayed or inhibited transformation (*139, 140, 225*). Cells exposed to HS for as little as 15 days became transformed even when subsequently grown in FBS; in fact, the longer the culture was exposed to HS before it was transferred to FBS, the shorter was the time required for its transformation (*226*). Thus some carcinogenic factor(s) in HS appears to initiate malignant transformation. This factor(s) is apparently heat-stable (*126*). FBS added to culture medium supplemented with HS or bovine calf serum delayed or prevented the malignant transformation that occurred in the absence of FBS (*226, 227*). Therefore, some influence in FBS appears to protect against such transformation. Efforts to identify and characterize the active factors in HS and FBS were unsuccessful in that none of the isolated serum fractions or combinations of fractions reproducibly controlled the malignant transformation (*139, 143, 203, 228*). However, as noted earlier, the type of serum that increased the frequency of transformation also caused karyotypic instability. Conceivably, an environmental factor that produces karyotypic instability of cultured cells may also induce carcinogenesis in vitro. In support of this concept, we note that the more stable the karyotype, the less frequent the occurrence of malignant transformation among cells from different species (*229, 230*). The two other environmental factors producing karyotypic instability, atmospheric oxygen and visible light, were examined as possible causative agents.

Light and Oxygen as Causative Agents in Malignant Transformation of Mouse Cells

Repeated exposure of mouse cells to visible light and atmospheric oxygen was found to enhance or induce malignant transformation. Cell lines initiated from different pools of C3H mouse embryos were divided into sublines maintained either shielded from light or repeatedly exposed to low-intensity light (4.6 W/m^2); cultures were gassed with either atmospheric (18%) or 0–1% O_2. Five of seven lines became tumorigenic during the test period. In two of these lines, tumors developed only from the light-exposed cells; in another, the transformation occurred earlier in the light-exposed cells, and in the remaining two, tumor latent periods in syngeneic hosts were significantly shorter in the cultures exposed to light or gassed with atmospheric oxygen (*144*). The so-called spontaneous transformations of mouse cells even in serum-free, chemically defined medium (*96, 222*) were apparently produced by the repeated exposure of cells to room lights and by continuous exposure to a high concentration of oxygen in the culture medium.

When we analyzed the chromosomes of tumors arising from implanted tissue culture cells, we observed a wide and characteristic distribution of chromosome numbers and types similar to that observed in the precursor culture cells; this observation indicated that most of the karyotypically diverse cells in culture were malignant and capable of continued progressive growth in vivo (*231*). Neither could a common pattern of chromosomal constitution characterize the tumors, nor could any specific chromosomal aberration be correlated with the onset of malignant transformation of mouse cells in vitro, although the incidence of abnormal chromosomes tended to increase at about the time of malignant transformation (*139, 141, 222, 232*). Chromosomes of rat cells were more stable, but some alterations occurred long before malignant transformation; no chromosomal alteration or pattern of chromosomal change characterized the malignant as compared with the normal rat cell populations (*95*). Nevertheless, the apparent association between karyotypic instability and accelerated malignant transformation induced by serum, visible light, and atmospheric oxygen suggests that agents in culture that damage chromosomal DNA may also initiate carcinogenesis (*144*).

Enhanced Susceptibility to Chromosome Damage in Relation to Malignant Transformation

As mentioned earlier, repeated exposure to visible light in the presence of atmospheric oxygen causes chromosomal aberrations and also enhances malignant transformation of mouse cells in culture (*144*). However, some cell lines developed chromosomal aberrations and transformed even when shielded from light and cultured at a low oxygen concentration. These observations suggest that additional factors, extrinsic and/or intrinsic, operate in malignant transformation. Extrinsic factors may include other as yet unidentified chemical agents in the culture environment or fluctuations in the oxygen concentration of the medium. Although cultures were gassed with 0-1% O_2, the cells received unavoidable brief exposures to atmospheric oxygen during culture manipulations. One intrinsic factor is the increased susceptibility of malignant mouse cells to light-induced chromatid damage, which was determined experimentally by the enumeration of chromatid breaks and exchanges after a single 20-hour exposure to low-intensity (4.6 W/m^2) fluorescent light. The frequency of light-induced chromatid breaks and exchanges was significantly higher in the malignant cells than in their normal precursors, and this increase was associated with their spontaneous neoplastic transformation (*233*).

In contrast to mouse cells, human cells from normal donors do not develop the increased susceptibility to light-induced chromatid breaks during culture. Human cells are also transformed with difficulty by carcinogenic agents, maintain a stable karyotype, and have not with one possible exception (*234*) been reported to undergo spontaneous transformation in culture. After a period of culture, however, human tumor cells, human cells transformed in culture by chemical carcinogens to malignant cells, and cells from donors genetically predisposed to a high risk of cancer (xeroderma pigmentosum and ataxia telangiectasia) show an increase in susceptibility as compared with the susceptibility among their normal counterparts or cells from normal donors [(*235*); Parshad R, Sanford KK, Jones GM: Unpublished observations]. Thus malignant transformation in human cells, as in mouse cells, is apparently associated with an increased susceptibility to light-induced chromosomal DNA damage. This increased susceptibility as discussed later results from deficiencies in the repair of DNA damage; in fact, the loss of DNA repair capacity may be an essential step in the progression to malignant neoplastic state.

MARKERS OF NEOPLASTIC TRANSFORMATION IN CULTURE

A major objective of this laboratory was the establishment of differences at the cellular and molecular level between the normal cell in culture and its malignant derivative. Cellular changes rigidly associated with malignant transformation could provide in vitro criteria of transformation and be useful in designing strategies for cancer treatment. Three approaches to meet this objective were used. In the first, a clonal population of fibroblasts from adult mouse connective tissue was observed during neoplastic transformation and was examined for morphologic and physiologic alterations. In the second approach, a transformation system was developed with a well-characterized, metabolically active, highly differentiated cell type, e.g., the liver parenchymal cell, and any alterations in differentiated properties associated with transformation were elucidated. In the third approach, normal and neoplastic cell pairs of common origin, some from the same cell, were compared; such pairs were frequently taken from frozen stocks that had been cryopreserved at various stages of in vitro life. In these studies, cells from inbred animals were used primarily to facilitate the in vivo assay for malignant transformation.

The In Vivo Assay for Malignant Transformation

The distinguishing feature of malignant neoplastic cells is their capacity for uncontrolled invasive growth leading to destruction of normal tissues, sometimes metastasis formation, and ultimate death of the affected animal. In view of this definition, our conclusive test for malignant transformation of cells in culture was the demonstration of their capacity to grow as malignant neoplasms when implanted into compatible hosts. The implantation of cells in vivo presents certain difficulties, particularly those related to histoincompatibility, a result of antigenic changes in the cultured cells or of genetic drift in the recipient animals. Therefore, implants are commonly made in X-irradiated or immunosuppressed animals (*183*), the nude mouse, or immunologically privileged sites such as the anterior chamber of the mouse eye (*94*) and the hamster cheek pouch. The in vivo assay not only is time consuming but also requires large numbers of cells. Furthermore, results are difficult to interpret, especially if they are negative. Therefore, reliable criteria of malignancy are needed that correlate with tumorigenicity in vivo and that directly apply to cells in culture. Such criteria might also provide insight into the progression of cellular and molecular events in malignant transformation.

Clonal Analysis of Cellular Changes in Malignant Transformation

The cells of the first carcinogenesis experiments were heterogeneous populations of fibroblasts from connective tissue. With the introduction of cloning, a better controlled cell system was obtained inasmuch as normal and neoplastic cells were both derived in culture from the same cell. However, as noted earlier, the normal cells ultimately became transformed and produced a low incidence of sarcoma. Cells of the "high" and "low" tumorigenic lines were found to be antigenic to mice of the inbred strain of origin and to cross-react with each other and also with the unrelated NCTC clone 929L cells (*44, 236*). Apparently, these two unrelated clones of C3H mouse cells, NCTC clone 929L and both lines of the second clone, had acquired the same new transplantation antigen(s) after their neoplastic transformation in culture. Although both high and low lines had become antigenic to the C3H mouse and both proliferated at the same rate in vitro, their proliferation rates in vivo differed widely. The difference in tumor production by the two lines resulted from the more rapid proliferation in vivo of the high tumorigenic line to establish a critical tumor mass before host immunity developed (*236*).

A clonal analysis of each line showed that cells of the low tumorigenic line differed from those of the high tumorigenic line in heritable characteristics including a lower rate of glycolysis, lower activities of the enzymes metabolizing glucose oxidatively, longer tumor latency in vivo, and reduced capacity to induce a vascular response in the host (*44, 86, 237–240*). The type of culture medium in which the cells had been grown influenced their transplantability and tumorigenic potential in syngeneic hosts (*44*). Growth of the low-line cells in mice for one generation significantly increased their tumorigenic potential, and this increase was shown to result from an enhanced resistance to the immunity induced by the cells (*241*). Hereditary alterations in enzyme activities and morphology were demonstrated within a clone derived from one of the high-line tumors (*46, 242, 243*). All these lines and clones showed marked karyotypic alterations (*244*). This genetic instability can account for the morphologic and biochemical alterations and the acquisition of neoplastic potential observed in these cells during continuous culture.

Characterization of Differentiated Cells in Continuous Culture

The large-scale suspension and surface–substrate cultures produced adequate masses of cells for analyses of biochemical properties. Our objectives were to identify cells in culture as to type and tissue of origin, to determine whether they maintained differentiated function and structure, and to establish any effects of medium or growth conditions on biochemical behavior. A cell line of particular interest for characterization was derived in 1948 from the liver of a 2-day-old C3H mouse (*42, 245*). In contrast to 10 murine fibroblast lines that were negative for glycogen, this line and a derivative clone stored glycogen even after 12 years in culture (*246–248*). After prolonged culture in vitro and an extended latent period in vivo, the clonal derivative produced tumors resembling anaplastic carcinomas of hepatic origin (*188*). The cells could then be grown in agitated fluid suspension for such characterizations as growth kinetics, glycolysis, glutamine effects on metabolism, and yields of α-keto and certain amino acids in the depleted medium (*249–251*). The liver cells, after years of culture and malignant transformation, maintained certain differentiated properties of the tissue of origin. These properties included a high arginase activity, which was considerably higher than that observed in six lines of mouse fibroblasts of connective tissue origin or in HeLa and was about 75% of that in mouse liver, high rhodanese (thiosulfate sulfurtransferase) activity, and detectable activity of four steroid reductases characteristic of liver parenchymal cells (*46, 84, 248, 252*). β-D-Glucuronidase activity was greater in the cultured cells than in the intact liver (*253*). The cells were deficient, however, in activities of catalase and uricase (urate oxidase) (*254*). Certain enzyme activities such as catalase and alkaline phosphatase declined during culture of all cell lines examined, regardless of the tissue of origin, whereas high acid phosphatase was maintained during serial culture of cells of adult, neonatal, or embryonic origin (*93, 138*).

Four additional studies indicated that structural or functional differentiation can be maintained during prolonged culture of other cell types. In the first study, well-differentiated murine mammary carcinoma maintained differentiated architecture and the characteristic high arginase activity after 1.5 years and 35 transplant generations in vitro (*45*). However, other murine neoplasms including mammary carcinoma, hepatoma, melanoma, and thyroid carcinoma, when continuously cultured in vitro, produced tumors in vivo resembling sarcoma (*45, 167, 168, 255*). In vivo transplantation of mammary and pulmonary carcinomas has also led to "sarcomatous" change. Either malignant epithelial cells during prolonged culture lose their differentiated morphology, or the stromal tissue of the original tumor undergoes malignant transformation in vitro. Our experiments provided evidence for both concepts. A clonal analysis showed that cell lines from certain mammary carcinomas can assume fibroblast-like morphology in vitro and lose arginase activity, but they retain in vivo properties of anaplastic carcinoma, i.e., cyst formation. Also, by growing tumor transplants in a hybrid host to replace the original stroma with hybrid cells, we showed that stromal tissue in culture can undergo malignant transformation (*45*). In a second study, cultures of human hydatid mole continued to secrete gonadotropic hormone in large amounts for periods exceeding 1 year (*30*); in a third study, cells of a murine melanoma continued to produce melanin for more than a year while rapidly proliferating in culture (*255*). Finally, in the fourth study, C3H mouse fibroblasts, human epithelial cells, and monkey kidney cells, as expected, remained immunologically species-specific after years of proliferation in culture (*115*). However, many cell lines after prolonged culture lose certain differentiated properties of the tissue of origin (*93, 248*). Although this loss of differentiated properties may be associated with random mutation, induced changes in DNA, or quantitative changes in enzyme activities, it has not been rigidly correlated with the onset of malignant transformation.

Comparison of Paired Normal and Malignant Cell Populations

In this approach to determine markers of neoplastic transformation, we looked for differences between populations of normal cells and their malignant derivatives. For this purpose we developed cell lines, normal and spontaneously transformed tumorigenic, both from a common cell pool or even from the same cell to minimize differences in tissue or cell type. Cell populations cryopreserved before and after spontaneous malignant transformation also served as paired cell lines.

We found that several properties postulated as markers of malignant transformation cannot be applied with confidence to all cell systems because the markers were not reliable when tested on these more biologically controlled paired cells. These properties include agglutinability by certain plant lectins (*256*), loss of contact inhibition or density-dependent inhibition of growth with "piling-up" of cells (*184, 257, 258*), acquisition of infinite growth potential (*257*), capacity to grow in low serum concentration (*259*), exaggerated incidence of surface microvilli, blebs, and ruffles (*260*), disorganized or decreased numbers of microtubules (*261*), production of plasminogen activator (*262*), thickening of ruthenium red-staining coat (*263*), and resistance to the cytotoxic effect of 7,12-dimethylbenz[*a*]anthracene (*264*). Multilayering or piling-up of cells may be more influenced by cell type, culture density, age of culture, type of culture medium, and frequency of medium renewal than by the malignant or normal state of the cells. For example, carcinoma cells can show monolayer growth, whereas normal embryo cells can grow in multilayers (*33, 138, 184, 230, 232, 257, 258, 265*). An enhanced growth rate and saturation density are observed in malignant as compared with normal cells under certain conditions in short-term culture. However, similar growth properties can develop in long-term normal cell lines. Therefore, these criteria are not applicable to all cell systems (*259, 265, 266*). Although we observed no conspicuous increase in aerobic glycolysis with malignant transformation, an enhanced anaerobic glycolysis was usually observed in both virus-induced and spontaneously transformed malignant cells as compared with their nontumorigenic counterparts (*86, 138, 204, 265, 267*). We also found that fetal antigens can be re-expressed in adult cells during culture and may be associated with their spontaneous malignant transformation (*268*).

Criteria for Identification of Malignant Cells in Culture

Cytology and colony morphology.—Cytologic criteria of cancer as applied to tissue or exfoliated cells in vivo prompted us to examine the cytology and colony morphology of the paired cell lines as well as to follow changes occurring during malignant transformation of mouse, rat, and hamster cells in culture. Certain changes that were detected more readily with the light microscope than with the electron microscope (*269*) correlated with the onset of tumorigenicity or neoplastic potential and provided criteria for identification of malignant cells in culture, applicable to spontaneous, virus-induced, and chemically induced transformations of fibroblasts or epithelial cells (*262*). These criteria included increased cytoplasmic basophilia, reduced spreading of cytoplasm on a solid surface substrate, random orientation, increased separation of cells, cell underlap or crisscross growth, heterogeneity in cell size and shape, nuclear abnormalities, increased nuclear:cytoplasmic ratio, increased nucleolar size and number, and tendency of cells to form cords or clumps. Criteria were applied to two types of stained preparations: 24- to 48-hour outgrowths of cells migrating from small clumps inoculated on cover glasses and colonies arising from proliferation of trypsinized single cell suspensions plated in plastic flasks (*270, 271*). Although no single morphologic feature could always be associated with malignant transformation, combinations of features showed a high correlation with tumorigenicity. Cytologic diagnoses were consistent with results of in vivo assays in 92% of the numerous cultures examined (*138, 143, 191, 192, 204,* [illegible]*, 257, 259, 265, 272–274*). The reproducibility of the changes, even within populations derived from one cell in culture, and their regular association with malignant transformation suggest that morphologic changes are direct manifestations of the malignant transformation.

Reduced cytoplasmic spreading, measurable as a decrease in mean projected area of attached cells, was successfully used to assay the transition of rodent cells from normal to tumorigenic (*275*). A comparison of seven pairs of malignant and normal cell lines examined under identical culture conditions provided quantitative evidence that a decrease in projected area of cell and nucleus and a decrease in dry mass of lamellar cytoplasm (the thin peripheral cytoplasm of cells adherent to solid substrate) characterize the malignant cell (*276*). With reduced cytoplasmic spreading, the surface:volume ratio of the cell also decreases, and this decrease may affect exchange of nutrients and metabolites (*230*). This reduced spreading could result from deficiencies in elaboration of plasma membrane with associated lamellar cytoplasm or from cytoskeletal alterations.

The reduction in surface area of malignant cells might be illusory especially if residual cytoplasm and cell membrane were stored in the form of microvilli or other cell surface projections not visible by the light microscope (*259, 275*). In fact, an exaggerated incidence of microvilli and other cell surface projections has been reported as characteristic of tumor cells. For the comparison of the topography of populations of asynchronously dividing normal and malignant cells unperturbed by disruptive synchronization methods, it was first necessary to establish whether the paired normal and malignant cells undergo predictable changes in surface morphology as they progress through the cell cycle. No influence of cell cycle on surface topography was observed. Furthermore, our scanning electron microscopy studies revealed no increased incidence of cell surface projections including microvilli, blebs, and ruffles on the malignant cells as compared with their normal counterparts, both derived in culture from the same cell (*260, 277, 278*). These findings support the concept that the malignant cell as compared with its normal precursor has a decreased surface area relative to mass resulting from a decreased elaboration of plasma membrane and associated lamellar cytoplasm.

The reduced cytoplasmic spreading and rounding of transformed cells leading to an apparent increase in nuclear:cytoplasmic ratio and basophilia could also result from alterations in distribution or amount of cytoskeletal components including microtubules and microfilament bundles (stress fibers or actin cables). An examination of normal and malignant cells of the paired lines by polarizing microscopy of living cells and by indirect immunofluorescence microscopy of the fixed cells treated with antibody against tubulin (microtubule protein) or actin revealed no disorganization or decrease in numbers of microtubules in the malignant cells. However, when these cells were compared with their normal counterparts, the malignant cells appeared to have thinner and fewer actin cables when examined by both polarizing and indirect immunofluorescence microscopy (*261*).

Another criterion of malignant transformation, in addition to decreased cytoplasmic spreading, is the loss of parallel orientation of cells. The orientation of cells is determined by their direction of locomotion, which was analyzed by microcinematography of paired normal and malignant cells derived in culture from the same cell and filmed under identical culture conditions. Individual normal cells during sequential 2.5-hour periods tended to maintain the same direction of locomotion, whereas the malignant cells had a random pattern of locomotion; the malignant cells also showed a higher rate of locomotion. This random pattern and loss of parallel orientation may result from the decreased amount of lamellar cytoplasm (consequently fewer attachment sites to substrate), fewer actin cables, and higher migration rate (*279*).

Loss of anchorage dependence.—Malignant cells frequently show a progression of morphologic changes from decreased cytoplasmic spreading on surface substrate to rounding, ultimate detachment, and growth in suspension. This loss of substrate or anchorage dependence has been measured by the capacity of cells to divide and form colonies in a semisolid matrix such as agar (*280*), agarose, or methylcellulose. This assay was used successfully to discriminate between paired normal and malignant rodent cell lines of fibroblast origin; growth in agarose correlated with tumorigenicity in vivo (*273*).

Growth in agarose as a selective assay for malignant cells emphasizes the importance of loss of anchorage dependence for growth of cells as cancer in vivo (*273*). In the in vivo assay, if suspensions of trypsinized cells are injected, those cells that are anchorage-dependent may not have adequate or suitable substrate on which to attach and grow. Boone (*281*) presented some evidence that substrate-dependent, presumably normal cells implanted in vivo attached to a solid substrate (polycarbonate plates or glass beads) continue to grow and produce tumors. Tests of this concept with paired normal and malignant cell lines showed that some cells, nontumorigenic when implanted in suspension, were tumorigenic when implanted attached to polycarbonate plates or glass helices. The transplantability of malignant cells implanted on solid substrate was also enhanced. The plate implant test proved to be one of the most sensitive bioassays for the malignancy of cultured cells (*282*).

Reduced anchorage dependence rather than loss of "contact-inhibition of mitosis" probably accounts for the changed growth pattern observed in certain malignant transformations in culture. Cessation of growth in confluent monolayers of normal cells is usually interpreted as the result of contact inhibition of mitosis. An alternative interpretation is that cell crowding inhibits division of anchorage-dependent normal cells by limiting the area of solid substrate available for cell attachment, spreading, and mitotic division. Because malignant cells are less anchorage- or substrate-dependent, they can continue proliferating under conditions of limited or unavailable solid substrate (*138, 230, 257, 258*).

Susceptibility to killing by activated macrophages.—Numerous studies have shown that activated mouse peritoneal macrophages selectively kill tumor cells in vitro in a reaction that requires close apposition or direct contact between the target cell and the macrophage. We found that the macrophage reaction also discriminates between normal and malignant cells of paired lines derived in vitro from the same cell or cell pool (*204, 283*). The reaction can be visualized in a confluent layer of target cells as a clearing or plaque overlying a small area of attached macrophages (*284*) and can be quantified as released label from tritiated thymidine-prelabeled target cells (*285*). The dynamics of both the macrophage reaction and the cytotoxic T-lymphocyte reaction with tumor cells were analyzed by microcinematography. The translational movement of activated macrophages on a layer of tumor cells was up to five times the rate observed on normal cells. The macrophage–tumor cell interaction was characterized by repeated, relatively short contacts, inducing cytostasis or killing of the tumor cell, but similar repeated contacts with normal cells did not lead to cell destruction (*286*). The capacity of a single immune cytotoxic T-lymphocyte to lyse more than one allogeneic target cell was also clearly demonstrated (*287*). The mechanism to account for the specific killing of tumor cells by activated macrophages is still unknown. Some evidence supports the concept that H_2O_2 formed and released by the macrophage on contact is the mediator of this cytotoxicity (*288*).

The increased sensitivity of malignant cells to chromatid damage by H_2O_2 and its derivative ·OH could result from loss or inactivation of cellular defense enzymes such as catalase or glutathione peroxidase that destroy H_2O_2. However, these enzyme activities were similar in paired normal and malignant cell populations (*235, 289*). Another possibility is that the susceptible cells have an impaired capacity to repair the DNA damage produced by H_2O_2 and its derivative ·OH.

Deficiency in DNA Repair Capacity

As noted earlier, mouse cells spontaneously transformed in culture, human tumor cells (Parshad R, Sanford KK, Jones GM: Unpublished observations), and human cells transformed in culture by chemical carcinogens show an increased incidence of chromatid breaks after exposure to fluorescent light when these cells are compared with their normal counterparts (*233, 235*). Chromatid breaks represent unrepaired DNA double-strand breaks, and their increased incidence reflects an impaired DNA repair capacity. The extent of DNA repair is also influenced by the stage of the cell cycle at the time of exposure to the damaging agent [(*289*); Parshad R, Sanford KK, Jones GM, Tarone RE: Manuscript in preparation]. Malignant mouse and human cells were susceptible to chromatid breaks when these cells were exposed to light during late S–G_2, whereas their normal counterparts were not. Addition of a known inhibitor of DNA repair, caffeine, during late S–G_2 light exposure had no effect on the frequency of chromatid breaks in the malignant cells, but caffeine significantly increased chromatid breakage in the normal cells. These results suggest that normal mouse and human cells have a caffeine-sensitive mechanism(s) for repair of DNA strand breaks resulting from light exposure during late S–G_2, whereas this mechanism(s) is absent or deficient in the malignant cells.

In additional experiments, mouse and human cells were exposed to light during G_1 and subsequently treated with caffeine. The cytogenetic findings are consistent with the concept that the malignant mouse cells, which are normally less efficient in excision repair than human cells, are also deficient in replication repair; in contrast, when compared with their normal counterparts, the malignant human cells are deficient in excision repair of G_1 light-induced DNA damage [(*289*); Parshad R, Sanford KK, Jones GM, Tarone RE: Manuscript in preparation]. However, the deficiency in the human cells is compensated by effective replication repair during the subsequent S-period. Thus two basic defects in malignant mouse and human cells were disclosed by the analysis of responses to damage inflicted at different stages of the cell cycle.

Since light-induced damage is mediated through the intracellular generation of H_2O_2 and its derivative ·OH (*153*, *154*), both of which are produced during X-irradiation, we also compared the incidence of chromatid breaks following X-irradiation during G_2 in the lin[illegible]ormal human fibroblasts KD and its malignant derivative HUT-14 (Parshad R, Gantt R, Sanford KK, Jones GM, Tarone RE: Submitted for publication). In this unique study, the extent of chromatid damage was quantitatively determined after X-radiation was applied exclusively in the G_2 period of the cell cycle or within 1.5 hours of metaphase. The malignant cells showed significantly more chromatid breaks and gaps than their normal counterparts. Exposure of cells to inhibitors of DNA repair, caffeine and Ara-C, immediately after their irradiation significantly increased the X-ray-induced chromatid damage in the normal cells but had little influence on the malignant cells. These results suggest that the DNA damage induced by X-ray during G_2 in the normal KD cells is repaired to a large extent by a mechanism(s) sensitive to both caffeine and Ara-C, whereas the malignant derivatives are totally defective in this mechanism(s). In additional studies (Parshad R, Sanford KK, Jones GM: Unpublished observations), all human tumor cell lines examined showed a defect in repair of X-irradiation-induced chromosomal DNA damage inflicted during the G_2 period of the cell cycle. No such defect was observed in a comparable number of fibroblast lines from normal, healthy donors. These findings with X-irradiation confirm and extend our previous observations of deficiencies in malignant cells of both mouse and human origin in the repair of light-induced chromosomal DNA damage inflicted during late S–G_2.

A MECHANISM OF SPONTANEOUS MALIGNANT TRANSFORMATION IN CULTURE

From our experimental findings, we conclude that the so-called spontaneous malignant transformation of mouse cells in culture is not spontaneous but is induced by specifically identifiable environmental factors. These factors include a chemical component(s) in serum, visible light, and high concentration of oxygen. These factors also cause chromosomal DNA damage. The light-induced chromosomal damage results from unrepaired DNA double-strand breaks produced directly or indirectly. We found that, as compared with normal cultures or cells from normal human donors, mouse and human cells following their malignant transformation in culture and human tumor cells have lost their capacity to repair this type of DNA damage. These findings support the concept that DNA damage and deficient DNA repair are implicated in the process of malignant transformation. Possibly unrepaired DNA damage at specific gene loci leads to the activation of cellular genes for transformation.

The light-induced DNA damage results from the intracellular generation of H_2O_2 and the derivative ·OH. Under physiologic conditions, these products are normal metabolites whose levels are regulated in vivo by defense enzymes and by the vascular control of oxygen supply to the tissues. However, these products are potentially dangerous (*290*), and it has been suggested that spontaneous human cancer may arise from DNA damage caused by their excessive endogenous production (*291*). We postulate that mouse cells that have an exceedingly low catalase activity are particularly susceptible to malignant transformation in culture because they are repeatedly exposed to visible light, continuously subjected to nonphysiologic high concentrations of oxygen in the culture medium, and eventually acquire a deficiency in repair of the DNA damage produced by these environmental agents.

REFERENCES

(*1*) Earle WR. Degeneration in vitro of leucocytes and connective tissue cells under the influences of light. Proc Soc Exp Biol Med 1927; 24:611–64.

(*2*) ———. Studies upon the effect of light on blood and tissue cells. I. The action of light on white blood cells in vitro. J Exp Med 1928; 48:457–473.

(*3*) ———. Studies upon the effect of light on blood and tissue cells. II. The action of light on erythrocytes in vitro. J Exp Med 1928; 48:667–681.

(*4*) ———. A simple apparatus and method for the injection of early chick embryo. Elisha Mitchell Soc J 1924; 40:171–175.

(*5*) ———. A technique for adjustment of pH of hanging drop tissue cultures. Pub Health Rep 1931; 46:1998–2008.

(*6*) ———. A technique for the adjustment of oxygen and carbon dioxide tensions, and hydrogen ion concentration in tissue cultures planted in Carrel flasks. Arch Exp Zellforsch 1934; 16:116–138.

(*7*) ———. A simple press for mincing soft tissues. Arch Exp Zellforsch 1932; 13:510–511.

(*8*) ———. A study of the Walker rat mammary carcinoma 256, in vivo and in vitro. Am J Cancer 1935; 24:566–612.

(*9*) ———. Production of malignancy in vitro. IV. The mouse fibroblast cultures and changes seen in the living cells. J Natl Cancer Inst 1943; 4:165–212.

(*10*) Schilling EL, Sanford KK. Preparation of chicken plasma without the use of anticoagulants. Procedure 30441. TCA Manual 1975; 1:63–66.

(*11*) ———. Use of strip-shaped explants in tissue cultures. Arch Pathol 1939; 27:88–94.

(*12*) Earle WR, Thompson JW. The influence of the size of the explant upon cultures of chick fibroblasts in vitro. Pub Health Rep 1930; 45:2672–2698.

(*13*) Evans VJ, Earle WR. The use of perforated cellophane for the growth of cells in tissue culture. J Natl Cancer Inst 1947; 8:103–119.

(*14*) ———. The use of perforated cellophane for the growth of cells in tissue culture. Acta Un Int Cancr 1948; 6:625–627.

(*15*) Earle WR, Evans VJ, Edward MF, Duchesne E. Influence of perforation design on growth of tissue cells under perforated cellophane sheets in vitro. J Natl Cancer Inst 1949; 10:291–295.

(*16*) Schilling EL, Earle WR, Evans VJ. Use of perforated cellophane substrate in slide preparation tissue cultures. J Natl Cancer Inst 1950; 10:883–891.

(17) Price FM, Handleman SL. The preparation and use of perforated cellophane for tissue culture. Procedure 21684. TCA Manual 1975; 1:59–60.

(18) Earle WR, Evans VJ, Schilling EL. Extension of cellophane substrate procedure to growth of in vitro cultures of large areas. J Natl Cancer Inst 1950; 10:943–967.

(19) Perry VP, Evans VJ, Earle WR, Hyatt GW. Tissue culture. Transplant Bull 1955; 2:60–61.

(20) Bassett CA, Evans VJ, Campbell DH, Earle WR. Characteristics and potentials of long-term cultures of human skin. Plast Reconstr Surg 1956; 17:421–429.

(21) Perry VP, Evans VJ, Hyatt GW, Earle WR, Draheim JW. Storage. Transplant Bull 1956; 3:50–52.

(22) Perry VP, Evans VJ, Earle WR, Hyatt GW, Bedell WC. Long-term tissue culture of human skin. Am J Hyg 1956; 63:52–58.

(23) Bassett CA, Campbell DH, Evans VJ, Earle WR. The cytotoxic activity of rabbit immune globulin prepared from tissue cultures of human skin and whole human placenta. J Immunol 1957; 78:79–93.

(24) Perry VP, Evans VJ, Young JM, Earle WR, Hyatt GW. Some recent studies with tissue culture as related to tissue transplantation. Transplant Bull 1957; 4:28–30.

(25) Algire GH, Borders ML, Evans VJ. Studies of heterografts in diffusion chambers in mice. J Natl Cancer Inst 1958; 20:1187–1201.

(26) Pappas AM, Evans VJ, Hyatt GW, Earle WR. Acceleration of skin defect closure. Surg Gynecol Obstet 1961; 113:681–686.

(27) Draheim JW, McPherson SD, Evans VJ, Perry VP, Earle WR. Tissue culture viability of preserved cornea. Transplant Bull 1955; 2:145.

(28) McPherson SD Jr, Draheim JW, Evans VJ, Perry VP, Earle WR. The viability of fresh and frozen cornea as determined in tissue culture. Am J Ophthalmol 1956; 41:513–519.

(29) Draheim JW, McPherson SD, Evans VJ, Earle WR. Further studies on the viability of frozen corneas as determined in tissue culture. Am J Ophthalmol 1957; 44:182–188.

(30) Waltz HK, Tullner WW, Evans VJ, Hertz R, Earle WR. Gonadotrophic hormone secretion from hydatid mole grown in tissue culture. J Natl Cancer Inst 1954; 14:1173–1185.

(31) Perry VP, Evans VJ, Earle WR. The cultivation of large cultures of HeLa cells in horse serum. Science 1955; 121:805

(32) Shannon JE Jr, Earle WR. Qualitative comparison of the growth of chick-heart and strain L fibroblasts planted as suspensions on pyrex glass and perforated cellophane substrates. J Natl Cancer Inst 1951; 12:155–177.

(33) Shannon JE Jr, Earle WR, Waltz HK. Massive tissue cultures prepared from whole chick embryos planted as a cell suspension on glass substrate. J Natl Cancer Inst 1952; 13:349–363.

(34) Earle WR, Schilling EL, Shannon JE Jr. Growth of animal tissue cells on three-dimensional substrates. J Natl Cancer Inst 1951; 12:179–193.

(35) Taylor WG, Evans VJ, Fox CH, Camalier RF, Sanford KK. Evaluation of the dyna-cell vessel for bulk production of substrate-dependent cells. Biotechnol Bioeng 1975; 17:1847–1851.

(36) Sanford KK, Earle WR, Likely GD. The growth in vitro of single isolated tissue cells. J Natl Cancer Inst 1948; 9:229–246.

(37) Sanford KK, Covalesky AB, Dupree LT, Earle WR. Cloning of mammalian cells by a simplified capillary technique. Exp Cell Res 1961; 23:361–372.

(38) Sanford KK. Animal cells: Capillary techniques. In: Kruse PF, Patterson MK, eds. Tissue culture: Methods and applications. New York: Academic Press, 1973:237–242.

(39) Bryant JC, Earle WR, Peppers EV. The effect of ultracentrifugation and hyaluronidase on the filtrability of chick-embryo extract for tissue culture. J Natl Cancer Inst 1953; 14:189–225.

(40) Sanford KK, Dunn TB, Covalesky AB, Dupree LT, Earle WR. Polyoma virus and production of malignancy in vitro. J Natl Cancer Inst 1961; 26:331–357.

(41) Likely GD, Sanford KK, Earle WR. Further studies on the proliferation in vitro of single isolated tissue cells. J Natl Cancer Inst 1952; 13:177–184.

(42) Hobbs GL, Sanford KK, Evans VJ, Earle WR. Establishment of a clone of mouse liver cells from a single isolated cell. J Natl Cancer Inst 1957; 18:701–707.

(43) Perry VP, Sanford KK, Evans VJ, Hyatt GW, Earle WR. Establishment of clones of epithelial cells from human skin. J Natl Cancer Inst 1957; 18:709–717.

(44) Sanford KK, Merwin RM, Hobbs GL, Young JM, Earle WR. Clonal analysis of variant cell lines transformed to malignant cells in tissue culture. J Natl Cancer Inst 1959; 23:1035–1059.

(45) Sanford KK, Dunn TB, Westfall BB, Covalesky AB, Dupree LT, Earle WR. Sarcomatous change and maintenance of differentiation in long-term cultures of mouse mammary carcinoma. J Natl Cancer Inst 1961; 26:1139–1183.

(46) Sanford KK, Westfall BB, Chu EH, et al. Alterations in morphology, arginase, and β-glucuronidase within a clone of mouse tumor cells in vitro. J Natl Cancer Inst 1961; 26:1193–1219.

(47) Earle WR. Recent advances in tissue culture and concluding remarks. In: Green JW, ed. New developments in tissue culture. New Brunswick, N.J.: Rutgers Univ Press, 1962:1–22.

(48) Evans VJ, Earle WR, Sanford KK, Shannon JE, Waltz HK. The preparation and handling of replicate tissue cultures for quantitative studies. J Natl Cancer Inst 1951; 11:907–927.

(49) Taylor WG, Price FM, Dworkin RA, Evans VJ. A simple device for planting replicate mammalian cell cultures. In Vitro 1972; 7:295–299.

(50) Evans VJ, Taylor WG. Monolayer cultures. In: Kruse PF, Patterson MK, eds. Tissue culture: Methods and applications. New York: Academic Press, 1973:211–216.

(51) Taylor WG, Evans VJ. Preparation and use of replicate mammalian cell cultures. In: Prescott DM, ed. Methods Cell Biol 1974; 8:47–73.

(52) Sanford KK, Earle WR, Evans VJ, Waltz HK, Shannon JE. The measurement of proliferation in tissue cultures by enumeration of cell nuclei. J Natl Cancer Inst 1951; 11:773–795.

(53) Earle WR, Highhouse F. Culture flasks for use with plane surface substrate tissue cultures. J Natl Cancer Inst 1954; 14:841–851.

(54) Fox CH, Chaconas PG, Sanford KK. An improved culture flask for photographic and visual observation of living cell cultures. J Microsc 1976; 107:79–83.

(55) Price FM, Sanford KK. Cleaning and preparation of glassware for cell culture. Procedure 10311. TCA Manual 1976; 2:379–382.

(56) Earle WR, Sanford KK, Evans VJ, Waltz HK, Shannon JE Jr. The influence of inoculum size on proliferation in tissue cultures. J Natl Cancer Inst 1951; 12:133–153.

(57) Earle WR, Evans VJ, Sanford KK, Shannon JE Jr, Waltz HK. Influence of glass and cellophane substrates on proliferation of strain L cells in tissue culture. J Natl Cancer Inst 1951; 12:563–567.

(58) Earle WR, Schilling EL, Bryant JC. Influence of tube rotation velocity on proliferation of strain L cells in surface substrate roller-tube cultures. J Natl Cancer Inst 1954; 14:853–864.

(59) Earle WR, Schilling EL, Bryant JC, Evans VJ. The growth of pure strain L cells in fluid-suspension cultures. J Natl Cancer Inst 1954; 14:1159–1171.

(60) Earle WR, Bryant JC, Schilling EL. Certain factors limiting the size of the tissue culture and the development of massive cultures. Ann NY Acad Sci 1954; 58:1000–1011.

(61) Earle WR, Bryant JC, Schilling EL, Evans VJ. Growth of cell suspensions in tissue culture. Ann NY Acad Sci 1956; 63:666–682.

(62) Westfall BB, Peppers EV, Bryant JC, Schilling EL, Earle WR. Effect on the medium of growth of clone NCTC 929 cells as suspensions in agitated flasks with simple fluid addition. J Natl Cancer Inst 1958; 21:429–435.

(63) Westfall BB, Peppers EV, Earle WR. The change in concentration of certain constituents of the medium during growth of the strain HeLa cells. Am J Hyg 1955; 61:326–333.

(64) Bryant JC, Schilling EL, Earle WR. Massive fluid-suspension cultures of certain mammalian tissue cells. I. General characteristics of growth and trends of population. J Natl Cancer Inst 1958; 21:331–348.

(65) ———. Massive fluid-suspension cultures of certain mammalian tissue cells. II. Glucose utilization and cell proliferation. J Natl Cancer Inst 1958; 21:349–364.

(66) Earle WR. Long-term cultivation of animal tissue cells in large cultures. Fed Proc 1958; 17:967–974.

(67) Evans VJ, Shannon JE Jr, Bryant JC, Waltz HK, Earle WR, Sanford KK. A quantitative study of the effect of certain chemically defined media on the proliferation in vitro of strain L cells from the mouse. J Natl Cancer Inst 1953; 13:773–783.

(68) Evans VJ. Probable future trends in the nutrition of tissue cultures. J Natl Cancer Inst 1957; 19:539–553.

(69) Westfall BB, Peppers EV, Sanford KK, Earle WR. The amino acid content of the ultrafiltrate from horse serum. J Natl Cancer Inst 1954; 15:27–35.

(70) Westfall BB, Peppers EV, Earle WR. The free and combined amino acids in the protein-free ultrafiltrates from whole chick-embryo extracts. J Natl Cancer Inst 1954; 15:433–438.

(71) ———. α-Keto acids in tissue culture. I. The concentration of pyruvic and α-ketoglutaric acids in the ultrafiltrates from horse serum and chick-embryo extract. J Natl Cancer Inst 1955; 16:337–347.

(72) Sanford KK, Waltz HK, Shannon JE Jr, Earle WR, Evans VJ. The effects of ultrafiltrates and residues of horse serum and chick-embryo extract on proliferation of cells in vitro. J Natl Cancer Inst 1952; 13:121–137.

(73) Sanford KK, Westfall BB, Fioramonti MC, et al. The effect of serum fractions on the proliferation of strain L mouse cells in vitro. J Natl Cancer Inst 1955; 16:789–802.

(74) Evans VJ, Bryant JC, Sanford KK, Earle WR. Studies of certain defined media for testing proliferation in replicate tissue cultures. Ann NY Acad Sci 1954; 58:1012–1020.

(75) Evans VJ, Bryant JC, McQuilkin WT, et al. Studies of nutrient media for tissue cells in vitro. III. Whole egg extract ultrafiltrate for long-term cultivation of strain L cells. Cancer Res 1957; 17:317–324.

(76) Sanford KK, Leadbetter PA, Bryant JC, Baker WP, Evans VJ, Earle WR. The effects of amino acids as supplements to fractions of serum and embryo extract on the proliferation of cells in vitro. J Natl Cancer Inst 1953; 14:513–518.

(77) Morgan JF, Morton HJ, Parker RC. Nutrition of animal cells in tissue culture. I. Initial studies in synthetic medium. Proc Soc Exp Biol Med 1950; 73:1–8.

(78) Fioramonti MC, Bryant JC, McQuilkin WT, Evans VJ, Sanford KK, Earle WR. The effect of horse serum residue and chemically defined supplements on proliferation of strain L clone 929 cells from the mouse. Cancer Res 1955; 15:763–766.

(79) Evans VJ, Bryant JC, Fioramonti MC, McQuilkin WT, Sanford KK, Earle WR. Studies of nutrient media for tissue cells in vitro. I. A protein-free chemically defined medium for cultivation of strain L cells. Cancer Res 1956; 16:77–86.

(80) Evans VJ, Bryant JC, McQuilkin WT, et al. Studies of nutrient media for tissue cells in vitro. II. An improved protein-free chemically defined medium for long-term cultivation of strain L-929 cells. Cancer Res 1956; 16:87–94.

(81) McQuilkin WT, Evans VJ, Earle WR. The adaptation of additional lines of NCTC clone 929 (strain L) cells to chemically defined protein-free medium NCTC 109. J Natl Cancer Inst 1957; 19:885–907.

(82) Fioramonti MC, Evans VJ, Earle WR. The effect of inoculum size on proliferation of NCTC strain 2071, the chemically defined medium strain of NCTC clone 929 (strain L). J Natl Cancer Inst 1958; 21:579–583.

(83) Healy G, Fisher D, Parker RC. Nutrition of animal cells. I. Synthetic medium No. 858. Proc Soc Exp Biol Med 1955; 89:71–77.

(84) Sanford KK. Growth and characterization of mammalian tissue cells in chemically defined medium. In: Proceedings of the symposium on the characterization and uses of human diploid cell strains. Opatija, Ljubljana: Institute of Immunology, 1963:195–208.

(85) Evans VJ, Kerr HA, McQuilkin WT, Earle WR, Hull RN. Growth in vitro of a long-term strain of monkey kidney cells in medium NCTC 109 free of any added protein. Am J Hyg 1959; 70:297–302.

(86) Sanford KK, Woods MW, Scott DB, Kerr HA. Stability in vitro of diverse capacities for tumor production and glucose metabolism in three murine clones derived from the same cell. J Natl Cancer Inst 1969; 42:945–952.

(87) Bakken PC, Evans VJ, Earle WR, Stevenson RE. Establishment of a strain of human skin cells on chemically defined medium NCTC 109. Am J Hyg 1961; 73:96–104.

(88) Evans VJ, LaRock JF, Yosida TH, Potter M. A new tissue culture isolation and explantation of the P388 lymphocytic neoplasm in a chemically characterized medium. Exp Cell Res 1963; 32:212–217.

(89) Evans VJ, Bryant JC, Kerr HA, Schilling EL. Chemically defined media for the cultivation of long-term cell strains from four mammalian species. Exp Cell Res 1964; 36:439–474.

(90) Den Beste HE, Fjelde A, Jackson JL, Andresen WF, Kerr HA, Evans VJ. Adaptation, growth, and chromosomal analysis of HEp-2 cells in chemically defined medium. J Natl Cancer Inst 1966; 36:1075–1088.

(91) Price FM, Kerr HA, Andresen WF, Bryant JC, Evans VJ. Some in vitro requirements of cells of C3H mouse, Chinese hamster, green monkey, and human origin. J Natl Cancer Inst 1966; 37:601–617.

(92) Evans VJ, Sanford KK. Development of defined media for studies on malignant transformation in culture. In: Katsuta H, ed. Nutritional requirements of cultured cells. Tokyo: Japan Sci Soc Press; Baltimore: Univ Park Press, 1978:149–194.

(93) Westfall BB. Biochemical taxonomic enzymology of certain cell strains in vitro. Natl Cancer Inst Monogr 1967; 26:229–246.

(94) Evans VJ, Parker GA, Dunn TB. Neoplastic transformations in C3H mouse embryonic tissue in vitro determined by intraocular growth. I. Cells from chemically defined medium with and without serum supplement. J Natl Cancer Inst 1964; 32:89–121.

(95) Jackson JL, Sanford KK, Dunn TB. Neoplastic conversion and chromosomal characteristics of rat embryo cells in vitro. J Natl Cancer Inst 1970; 45:11–23.

(96) Andresen WF, Price FM, Jackson JL, Dunn TB, Evans VJ. Characterization and spontaneous neoplastic transformation of mouse embryo cells isolated and continuously cultured in vitro in chemically defined medium NCTC 135. J Natl Cancer Inst 1967; 38:169–183.

(97) Fischer A. On the protein metabolism of tissue cells in vitro. J Natl Cancer Inst 1953; 13:1399–1423.

(98) Eagle H. The specific amino acid requirements of mammalian cells (strain L) in tissue culture. J Biochem 1955; 214:839–852.

(99) ———. Nutrition needs of mammalian cells in tissue culture. Science 1955; 122:501–504.

(100) Dupree LT, Sanford KK, Westfall BB, Covalesky AB. Influence of serum protein on determination of nutritional requirements of cells in culture. Exp Cell Res 1962; 28:381–405.

(101) Sanford KK, Dupree LT, Covalesky AB. Biotin, B12 and other vitamin requirements of a strain of mammalian cells grown in chemically defined medium. Exp Cell Res 1963; 31:345–375.

(102) Sanford KK, Dupree LT. Activity of vitamin B12 in mammalian cells in tissue culture. Ann NY Acad Sci 1964; 112:823–830.

(103) Price FM, Rotherham J, Evans VJ. Pyrimidine nucleoside requirements of a neoplastic C3H mouse cell strain. J Natl Cancer Inst 1967; 39:529–538.

(104) Rotherham J, Price FM, Evans VJ. Some aspects of the role of folic acid in nucleic acid synthesis in a neoplastic C3H mouse cell strain. J Natl Cancer Inst 1968; 41:781–788.

(105) Price FM, Rotherham J, Evans VJ. Some aspects of the role of vitamin B_{12} in nucleic acid synthesis in a neoplastic C3H mouse cell strain. I. Growth studies. J Natl Cancer Inst 1970; 44:85–90.

(106) Rotherham J, Price FM, Evans VJ. Some aspects of the role of vitamin B_{12} in nucleic acid synthesis in a neoplastic C3H mouse cell strain. II. Incorporation of precursors. J Natl Cancer Inst 1970; 44:91–97.

(107) Rotherham J, Price FM, Otani TT, Evans VJ. Some aspects of the role of vitamin B_{12} and folic acid in DNA-thymidine synthesis in a neoplastic C3H mouse cell strain. J Natl Cancer Inst 1971; 47:277–287.

(108) Sanford KK, McQuilkin WT, Fioramonti MC, Evans VJ, Earle WR. Study of amino acid requirements for increase in cell population of NCTC clone 929 (strain L). J Natl Cancer Inst 1958; 20:775–785.

(*109*) Evans VJ, Fioramonti MC, Sanford KK, Earle WR, Westfall BB. Studies of nutrient media for tissue cells in vitro. IV. The effect of amino acid mixtures on the proliferation of the long-term strain 2071 of NCTC clone 929 of strain L cells. Am J Hyg 1958; 66:66–76.

(*110*) Robinson EA, Kalckar HM, Troedsson H, Sanford KK. Metabolic inhibition of mammalian uridine diphosphate galactose 4-epimerase in cell cultures and in tumor cells. J Biol Chem 1966; 241:2737–2745.

(*111*) Peppers EV, Fioramonti MC, Westfall BB, Evans VJ, Earle WR. Effect of lack of glutamine on subline 2071 mouse cells. J Natl Cancer Inst 1956; 21:611–620.

(*112*) Evans VJ, Fioramonti MC, Earle WR. Studies of nutrient media for tissue cells in vitro. V. The effect of the coenzymes of medium NCTC 109 on the proliferation of NCTC strain 2071 and NCTC strain 2937. Am J Hyg 1959; 70:28–33.

(*113*) Evans VJ, Fioramonti MC, Randolph LK, Earle WR. Studies of nutrient media for tissue cells in vitro. VI. The effect of nucleic acid derivatives mixture of medium NCTC 109 on NCTC strain 2071 and NCTC strain 2981. Am J Hyg 1960; 71:168–175.

(*114*) Fioramonti MC, Evans VJ, Mantel N, Earle WR. Studies of nutrient media for tissue cells in vitro. VII. The effect of the glucuronic acid mixture of NCTC 109 on the proliferation of NCTC strain 2071 and NCTC strain 3145. Am J Hyg 1960; 72:204–210.

(*115*) Evans VJ, Bryant JC. Advances in tissue culture at the National Cancer Institute in the USA. In: Ramakrishnan CV, ed. Tissue culture. The Hague: W. Junk, 1965:145–167.

(*116*) Price FM, Evans VJ. Preparation of medium NCTC 163. Procedure 35714. TCA Manual 1977; 3:497–501.

(*117*) Price FM, Camalier RF, Gantt R, Taylor WG, Smith GH, Sanford KK. A new culture medium for human skin epithelial cells. In Vitro 1980; 16:147–158.

(*118*) Earle WR. Production of malignancy in vitro. I. Method of cleaning glassware. J Natl Cancer Inst 1943; 4:131–133.

(*119*) Sanford KK, Hoemann RE, Bryant JC, Shannon JE, Evans VJ. Premixed powders for protein-free cell culture media: A quantitative evaluation. J Natl Cancer Inst 1968; 40:895–905.

(*120*) Evans VJ, Montes de Oca H, Bryant JC, Schilling EL, Shannon JE. Recovery from liquid-nitrogen temperature of established cell lines frozen in chemically defined medium. J Natl Cancer Inst 1962; 29:749–757.

(*121*) Bryant JC, Schilling EL, Earle WR, Evans VJ. Massive fluid-suspension cultures of certain mammalian tissue cells. III. Exploratory supplementation experiments with chemically defined medium NCTC 109. J Natl Cancer Inst 1960; 24:859–871.

(*122*) Bryant JC. Mammalian cells in chemically defined media in suspension cultures. Ann NY Acad Sci 1966; 139:143–161.

(*123*) Bryant JC, Evans VJ, Schilling EL, Earle WR. Effect of chemically defined medium NCTC 109 supplemented with Methocel and of silicone coating the flasks on strain 2071 cells in suspension cultures. J Natl Cancer Inst 1961; 26:239–252.

(*124*) Bryant JC. Glucose and lactic acid trends in suspension cultures of two established mammalian cell strains in chemically defined media. Biotechnol Bioeng 1970; 12:429–464.

(*125*) ———. Methylcellulose effect on cell proliferation and glucose utilization in chemically defined medium in large stationary cultures. Biotechnol Bioeng 1969; 11:155–179.

(*126*) Sanford KK, Burris JF, Handleman SR. Chemical analyses of sera influencing neoplastic transformation in vitro. J Natl Cancer Inst 1972; 49:1553–1561.

(*127*) Taylor WG. "Feeding the baby"—serum and other supplements to chemically defined medium. J Natl Cancer Inst 1974; 53:1449–1457.

(*128*) Fox CH, Sanford KK. Chemical analysis of mammalian sera commonly used as supplements for tissue culture media. Procedure 94121. TCA Manual 1975; 1:233–237.

(*129*) German JL III, Evans VJ, Cortner JA, Westfall BB. Characterization of three human cell lines by chromosomal complement and by certain biochemical parameters. Reversible alteration of isozyme patterns by different media. J Natl Cancer Inst 1964; 32:681–707.

(*130*) McQuilkin WT, Earle WR. Cinemicrographic analysis of cell populations in vitro. J Natl Cancer Inst 1962; 28:763–799.

(*131*) Earle WR. General design of a comparative microcinematographic equipment for tissue culture. In: Rose GG, ed. Cinemicrography in cell biology. New York: Academic Press, 1963:27–52.

(*132*) Montes de Oca H, Schilling EL, Bryant JC, Evans VJ, Earle WR. Serum action on radiation response in tissue culture. J Natl Cancer Inst 1963; 30:57–66.

(*133*) Taylor WG, Taylor MJ, Lewis NJ, Pumper RW. Studies on a serum substitute for mammalian cells in culture. I. Biological efficacy of whole and fractionated peptone dialysate. Proc Soc Exp Biol Med 1972; 139:96–99.

(*134*) Taylor WG, Dworkin RA, Pumper RW, Evans VJ. Biological efficacy of several commercially available peptones for mammalian cells in culture. Exp Cell Res 1972; 74:275–279.

(*135*) Taylor WG, Evans VJ, Pumper RW. Studies on a serum substitute for mammalian cells in culture. II. Analyses of fractionated peptone dialysate and the use of glycine peptides. In Vitro 1974; 9:278–285.

(*136*) Taylor WG, Parshad R. Peptones as serum substitutes for mammalian cells in culture. Methods Cell Biol 1977; 15:421–434.

(*137*) Parshad R, Sanford KK. Search for genetic influences on neoplastic transformation and chromosomal stability of mouse cells cultured in medium supplemented with horse or fetal bovine serum. J Natl Cancer Inst 1972; 49:1155–1163.

(*138*) Sanford KK, Barker BE, Parshad R, et al. Neoplastic conversion in vitro of mouse cells: Cytologic, chromosomal, enzymatic, glycolytic, and growth properties. J Natl Cancer Inst 1970; 45:1071–1096.

(*139*) Parshad R, Sanford KK. Effect of horse serum, fetal calf serum, calf serum, bovine serum, and fetuin on neoplastic conversion and chromosomes of mouse embryo cells in vitro. J Natl Cancer Inst 1968; 41:767–779.

(*140*) Mitchell JT, Andresen WF, Evans VJ. Comparative effects of horse, calf, and fetal serums on chromosomal characteristics and neoplastic conversion of mouse embryo cells in vitro. J Natl Cancer Inst 1969; 42:709–721.

(*141*) Evans VJ, Jackson JL, Andresen WF, Mitchell JT. Chromosomal characteristics and neoplastic transformation of C3H mouse embryo cells in vitro in horse and fetal calf serum. J Natl Cancer Inst 1967; 38:761–769.

(*142*) Parshad R, Sanford KK. Effect of horse serum and fetal calf serum on stability of chromosomes in mouse embryo cells in vitro. J Natl Cancer Inst 1967; 39:145–152.

(*143*) Sanford KK, Parshad R, Handleman SL, Price FM, Gantt RR, Evans VJ. Serum-induced chromosome damage and neoplastic transformation of mouse cells in vitro. In Vitro 1979; 15:448–496.

(*144*) Sanford KK, Parshad R, Jones G, Handleman S, Garrison C, Price F. Role of photosensitization and oxygen in chromosome stability and "spontaneous" malignant transformation in culture. JNCI 1979; 63:1245–1255.

(*145*) Parshad R, Sanford KK. Oxygen supply and stability of chromosomes in mouse embryo cells in vitro. J Natl Cancer Inst 1971; 47:1033–1035.

(*146*) Parshad R, Sanford KK, Jones GM, Price FM, Taylor WG. Oxygen and light effects on chromosomal aberrations in mouse cells in vitro. Exp Cell Res 1977; 104:199–205.

(*147*) Sanford KK. Evidence for oncogenic properties of heteroploid cell lines. Natl Cancer Inst Monogr 1968; 29:283–287.

(*148*) Taylor WG, Richter A, Evans VJ, Sanford KK. Influence of oxygen and pH on plating efficiency and colony development of WI-38 and Vero cells. Exp Cell Res 1974; 86:152–156.

(*149*) Richter A, Sanford KK, Evans VJ. Influence of oxygen and culture media on plating efficiency of some mammalian tissue cells. J Natl Cancer Inst 1972; 49:1705–1712.

(*150*) Taylor WG, Sanford KK, Richter A, Hursey ML, Evans VJ. Effect of reducing agents and oxygen on plating efficiency of some mammalian cells in culture. J Natl Cancer Inst 1974; 52:763–767.

(*151*) Taylor WG, Camalier RF, Sanford KK. Density-dependent effects of oxygen on the growth of mammalian fibroblasts in culture. J Cell Physiol 1978; 95:33–40.

(*152*) Taylor WG, Camalier RF. Modulation of epithelial cell proliferation in culture by dissolved oxygen. J Cell Physiol 1982; 111:21–27.

(153) Parshad R, Sanford KK, Jones GM, Tarone RE. Fluorescent light-induced chromosome damage and its prevention in mouse cells in culture. Proc Natl Acad Sci USA 1978; 75:1830–1833.

(154) Parshad R, Taylor WG, Sanford KK, Camalier RF, Gantt R, Tarone RE. Fluorescent light-induced chromosome damage in human IMR-90 fibroblasts: Role of hydrogen peroxide and related free radicals. Mutat Res 1980; 73:115–124.

(155) Parshad R, Sanford KK, Taylor WG, Tarone RE, Jones GM, Baeck AE. Effect of intensity and wavelength of fluorescent light on chromosome damage in cultured mouse cells. Photochem Photobiol 1979; 29:971–975.

(156) Taylor WG, Camalier RF, Taylor MJ. A spectrophotometric assay for hydrogen peroxide in tissue culture medium. Procedure 74252. TCA Manual 1979; 5:1081–1086.

(157) Taylor WG, Camalier RF, Baeck AE, Gantt R. Type-specific cell killing and DNA strand breaks after exposure to visible light or hydrogen peroxide. J Cell Biol 1979; 83:111.

(158) Gantt R, Parshad R, Ewig RA, et al. Fluorescent light-induced DNA crosslinkage and chromatid breaks in mouse cells in culture. Proc Natl Acad Sci USA 1978; 75:3809–3812.

(159) Gantt R, Jones GM, Stephens EV, Baeck AE, Sanford KK. Visible light-induced DNA crosslinks in cultured mouse and human cells. Biochim Biophys Acta 1979; 565:231–240.

(160) Parshad R, Sanford KK. Proliferative response of human diploid fibroblasts to intermittent light exposure. J Cell Physiol 1977; 92:481–486.

(161) ———. Intermittent exposure to fluorescent light extends lifespan of human diploid fibroblasts in culture. Nature 1977; 268: 736–737.

(162) Earle WR, Voegtlin C. The mode of action of methylcholanthrene on cultures of normal tissues. Am J Cancer 1938; 34:373–390.

(163) Earle WR. A simple photoelectric exposure meter for use in photomicrography. J Biol Photogr Assoc 1938; 7:54–58.

(164) Lillie RD, Earle WR. Iron hematoxylins containing ferric and ferrous iron. Am J Pathol 1939; 15:765–770.

(165) Earle WR. Procedure for the fixation, staining, and mounting of whole mounts from tissue cultures grown in Carrel D 3.5 flasks. J Natl Cancer Inst 1947; 8:83–89.

(166) Earle WR, Voegtlin C. A comparison of the growth of the Jensen rat sarcoma in subcutaneous and intramuscular transplants. Natl Inst Health Bull 1935; 164:47–58.

(167) ———. A further study of the Walker rat mammary carcinoma Nr. 256 in vitro. Arch Exp Zellforsch 1937; 20:140–155.

(168) ———. Walker 256 rat mammary carcinoma in vitro. Arch Pathol 1939; 27:80–87.

(169) ———. A further study of the mode of action of methylcholanthrene on normal tissue cultures. Pub Health Rep 1940; 55:303–322.

(170) Earle WR. Production of malignancy in vitro. II. Photomicrographic equipment. J Natl Cancer Inst 1943; 4:135–145.

(171) Earle WR, Crisp LR. Production of malignancy in vitro. III. Microcinematographic equipment. J Natl Cancer Inst 1943; 4:147–164.

(172) Earle WR, Schilling EL, Shelton E. Production of malignancy in vitro. IX. Description of cells at the fluid interface of the culture. J Natl Cancer Inst 1950; 10:865–881.

(173) ———. Production of malignancy in vitro. X. Continued description of cells at the glass interface of the cultures. J Natl Cancer Inst 1950; 10:1067–1103.

(174) Shelton E, Earle WR. Production of malignancy in vitro. XIII. Behavior of recovery cultures. J Natl Cancer Inst 1951; 11:817–837.

(175) Earle WR. Some morphologic variations of certain cells under controlled experimental conditions. Natl Cancer Inst Monogr 1962; 7:213–236.

(176) Earle WR, Nettleship A. Production of malignancy in vitro. V. Results of injections of cultures into mice. J Natl Cancer Inst 1943; 4:213–227.

(177) Nettleship A, Earle WR. Production of malignancy in vitro. VI. Pathology of tumors produced. J Natl Cancer Inst 1943; 4:229–248.

(178) Earle WR. A summary of certain data on the production of malignancy in vitro. In: The American Association for the Advancement of Science research conference on cancer. Vol 24. Gibson Island, Md., 1944. Washington, D.C.: AAAS, 1945:139–153.

(179) Burk D, Earle WR, Winzler RJ. Production of malignancy in vitro. VII. Metabolism and biotin vitamer content of tumors produced. J Natl Cancer Inst 1944; 4:363–372.

(180) Dalton AJ, Earle WR. Production of malignancy in vitro. VIII. Observations on the mitochondria and Golgi material. J Natl Cancer Inst 1944; 4:539–554.

(181) Earle WR, Shelton E, Schilling EL. Production of malignancy in vitro. XI. Further results from reinjection of in vitro cell strains into strain C3H mice. J Natl Cancer Inst 1950; 10:1105–1113.

(182) Algire GH, Chalkley HW, Earle WR. Vascular reactions of normal and malignant tissues in vivo. III. Vascular reactions of mice to fibroblasts treated in vitro with methylcholanthrene. J Natl Cancer Inst 1950; 11:555–579.

(183) Sanford KK, Hobbs GL, Earle WR. The tumor-producing capacity of strain L mouse cells after ten years in vitro. Cancer Res 1956; 16:162–166.

(184) Sanford KK. Malignant transformation of cells in vitro. Int Rev Cytol 1965; 18:249–311.

(185) Gey GO. Cytological and cultural observations on transplantable rat sarcomata produced by the inoculation of altered normal cells maintained in continuous culture. Cancer Res 1941; 1:737.

(186) Sanford KK, Earle WR, Shelton E, et al. Production of malignancy in vitro. XII. Further transformations of mouse fibroblasts to sarcomatous cells. J Natl Cancer Inst 1950; 11:351–375.

(187) Sanford KK, Likely GD, Earle WR. The development of variations in transplantability and morphology within a clone of mouse fibroblasts transformed to sarcoma-producing cells in vitro. J Natl Cancer Inst 1954; 15:215–237.

(188) Evans VJ, Hawkins NM, Westfall BB, Earle WR. Studies on culture lines derived from mouse liver parenchymatous cells grown in long-term tissue culture. Cancer Res 1958; 18:261–266.

(189) Andresen WF, Evans VJ, Price FM, Dunn TB. Neoplastic transformations in cells explanted from the kidneys of 3-day-old C3H mice. J Natl Cancer Inst 1966; 36:953–963.

(190) Sanford KK, Hoemann RE. Neoplastic transformation of mouse and hamster cells in vitro with and without polyoma virus. J Natl Cancer Inst 1967; 39:691–703.

(191) Barker BE, Sanford KK. Cytologic manifestations of neoplastic transformation in vitro. J Natl Cancer Inst 1970; 44:39–63.

(192) Sanford KK, Handleman SL, Fox CH, et al. Effects of chemical carcinogens on neoplastic transformation and morphology of cells in culture. J Natl Cancer Inst 1974; 53:1647–1659.

(193) Brand KG. Foreign body induced sarcomas. In: Becker FF, ed. Cancer. 1. A comprehensive treatise. New York: Plenum Press, 1975:485–511.

(194) Sanford KK, Likely GD, Bryan WR, Earle WR. The infection of cells in tissue culture with Rous sarcoma virus. J Natl Cancer Inst 1952; 12:1317–1343.

(195) ———. The infection of cells in tissue culture with Rous sarcoma virus. In: Proceedings of the second national cancer conference. Vol 2. Cincinnati, Ohio, March 3–5, 1952. New York: American Cancer Society, 1952:1376–1384.

(196) Sanford KK, Andervont HB, Hobbs GL, Earle WR. Maintenance of the mammary-tumor agent in long-term cultures of mouse mammary carcinoma. J Natl Cancer Inst 1961; 26:1185–1191.

(197) Fox CH, Selkirk JK, Price FM, Croy RG, Sanford KK, Cottler-Fox M. Metabolism of benzo(*a*)pyrene by human epithelial cells in vitro. Cancer Res 1975; 35:3551–3557.

(198) Camalier RF, Gantt R, Price FM, et al. Effect of visible light on benzo(*a*)pyrene binding to DNA of cultured human skin epithelial cells. Cancer Res 1981; 41:1789–1793.

(199) Sanford KK. An attempt to induce malignant transformation of cells in vitro by intermittent anaerobiosis. J Natl Cancer Inst 1965; 35:719–725.

(200) Sanford KK, Parshad R. Oxygen supply and neoplastic conversion of mouse embryo cells in vitro. J Natl Cancer Inst 1968; 41:1389–1394.

(201) Hall WT, Andresen WF, Sanford KK, Evans VJ, Hartley JW. Virus particles and murine leukemia virus complement-fixing antigen in neoplastic and nonneoplastic cell lines. Science 1967; 156:85–88.

(*202*) Hall WT, Andresen WF, Evans VJ. In vitro and in vivo observations on a murine C-type virus. J Virol 1967; 1:1238–1254.

(*203*) Sanford KK, Handleman SL, Hartley JW, Jackson JL, Gantt RR. "Spontaneous" neoplastic transformation in vitro: Influence of endogenous murine leukemia virus and serum fractions. J Natl Cancer Inst 1972; 49:1177–1189.

(*204*) Taylor WG, Camalier RF, Tucker RW, Sanford KK. Population density as a factor in the evolution of neoplastic cell lines. Cancer Res 1978; 38:3840–3846.

(*205*) Srinivasan PR, Borek E. Enzymatic alteration of nucleic acid structure. Science 1964; 145:548–553.

(*206*) Gantt RR, Evans VJ. Comparison of soluble RNA methylase capacity in paired neoplastic and nonneoplastic cell lines in vitro. Cancer Res 1969; 29:536–541.

(*207*) Gantt RR. In vitro transfer RNA methylation in paired neoplastic and nonneoplastic cell cultures. Cancer Res 1971; 31:609–612.

(*208*) Quinn CE, Gantt RR, Evans VJ. Comparison of methyl-labeled tRNA in a neoplastic cell line with a paired nonneoplastic control. Exp Mol Pathol 1970; 13:231–241.

(*209*) Gantt R, Montes de Oca F, Evans VJ. Methylation of satellite deoxyribonucleic acid in mouse neoplastic and non-neoplastic cell cultures. In Vitro 1973; 8:288–294.

(*210*) Gantt R, Schneider WC. Presence of 5-methylcytosine in rat liver mitochondrial and microsomal DNA. Dev Neurosci 1979; 5:465–471.

(*211*) Gantt R, Smith GH, Julian BT. Virion-associated and cellular RNA methylase activity in normal and neoplastic mammary tissue from mammary tumor virus-infected and -uninfected mice. Cancer Res 1975; 35:1847–1853.

(*212*) Gantt RR, Stromberg KJ, Montes de Oca F. A specific RNA methylase associated with avian myeloblastosis virus. Nature 1971; 234:35–37.

(*213*) Gantt RR, Smith GH, Julian BT. Base specific methylase activity in RNA tumor viruses: Avian leukosis virion-associated RNA methylase(s). Virology 1973; 52:584–586.

(*214*) Chepelinsky AB, Gantt R, Wivel N. Presence of RNA methylases in intracisternal A particles purified from a mouse plasma cell tumor. Eur J Biochem 1980; 103:339–347.

(*215*) Hall WT, Hartley JW, Sanford KK. Characteristics of and relationship between C particles and intracisternal A particles in cloned cell strains. J Virol 1968; 2:238–247.

(*216*) Gantt RR, Julian BT. A rapid column chromatographic procedure for the assay of RNA methyltransferases. Anal Biochem 1973; 54:283–285.

(*217*) Izzo P, Gantt R. Partial purification and characterization of an N^2-guanine RNA methyltransferase from chicken embryos. Biochemistry 1977; 16:3576–3581.

(*218*) Taylor MT, Gantt R. Partial purification of a ribonucleic acid N^2-guanine methyltransferase associated with avian myeloblastosis virus. Biochemistry 1979; 18:5253–5258.

(*219*) Stromberg K, Gantt RR, Wilson SH. Structural studies on avian myeloblastosis virus: Conditions for isolation and biochemical characteristics of the core component. Biochem Biophys Acta 1973; 304:1–11.

(*220*) Gantt RR, Stromberg KJ, Julian BT. Absence of ribonucleic acid methylase in the avian myeloblastosis virus core. J Virol 1972; 9:1057–1058.

(*221*) Gantt RR. Is aberrant nucleic acid methylation related to malignant transformation? J Natl Cancer Inst 1974; 53:1505–1508.

(*222*) Evans VJ, Andresen WF. Spontaneous neoplastic transformations in C3H mouse cells in vitro. In: Katsuta H, ed. Cancer cells in culture. Tokyo: Univ Tokyo Press; Baltimore: Univ Park Press, 1968:263–280.

(*223*) Shelton E, Evans VJ, Parker GA. Malignant transformation of mouse connective tissue grown in diffusion chambers. J Natl Cancer Inst 1963; 30:377–391.

(*224*) Evans VJ, Andresen WF. Effect of serum on spontaneous neoplastic transformation in vitro. J Natl Cancer Inst 1966; 37:247–249.

(*225*) Evans VJ, Price FM, Sanford KK, Kerr HA, Handleman SL. Comparative effects of mare, stallion, gelding horse, and fetal bovine sera on neoplastic transformation in vitro. J Natl Cancer Inst 1972; 49:505–511.

(*226*) Andresen WF, Jackson JL, Mitchell JT, Evans VJ. Effects of changing horse and fetal calf serum supplements on neoplastic conversion and chromosomal characteristics of mouse embryo cells in vitro. J Natl Cancer Inst 1969; 43:377–383.

(*227*) Sanford KK, Jackson JL, Parshad R, Gantt RR. Evidence for an inhibiting influence of fetal bovine serum on "spontaneous" neoplastic transformation in vitro. J Natl Cancer Inst 1972; 49:513–518.

(*228*) Price FM, Gantt RR, Evans VJ. Effect of fractions of horse and fetal bovine serum on neoplastic conversion of C3H mouse cells in tissue culture. In Vitro 1971; 6:437–440.

(*229*) Sanford KK, Parshad R, Gantt R. Light and oxygen effects on chromosomes, DNA and neoplastic transformation of cells in culture. In: Katsuta H, ed. Nutritional requirements of cultured cells. Tokyo: Japan Sci Soc Press; Baltimore: Univ Park Press, 1978:117–148.

(*230*) Sanford KK. "Spontaneous" neoplastic transformation in vitro. In: Clark RL, Cumley RW, McCay JE, Copeland MM, eds. Oncology. Chicago: Year Book Med Publ, 1970:76–82.

(*231*) Parshad R, Sanford KK. Chromosomal analysis of tumors derived from mouse cells after neoplastic conversion in vitro in various serum-supplemented media. J Natl Cancer Inst 1969; 43:71–76.

(*232*) Sanford KK. "Spontaneous" neoplastic transformation of cells in vitro: Some facts and theories. Natl Cancer Inst Monogr 1967; 26:387–418.

(*233*) Parshad R, Sanford KK, Tarone RE, Jones GM, Baeck AE. Increased susceptibility of mouse cells to fluorescent light-induced chromosome damage after long-term culture and malignant transformation. Cancer Res 1979; 39:929–933.

(*234*) Nakagomi O, Ishida N. Establishment of a cell line from a human fetal liver and its xenotransplantation to nude mice. Gan 1980; 71:213–219.

(*235*) Parshad R, Gantt R, Sanford KK, Jones GM, Camalier RF. Light-induced chromatid damage in human skin fibroblasts in culture in relation to their neoplastic potential. Int J Cancer 1981; 28:335–340.

(*236*) Sanford KK, Merwin RM, Hobbs GL, Fioramonti MC, Earle WR. Studies on the difference in sarcoma-producing capacity of two lines of mouse cells derived in vitro from one cell. J Natl Cancer Inst 1958; 20:121–145.

(*237*) Sanford KK, Westfall BB, Woods MW, Earle WR. Metabolic variations within a clone of mouse fibroblasts transformed to neoplastic cells in vitro. Acta Un Int Cancr 1959; 15:675–679.

(*238*) Woods MW, Sanford KK, Burk D, Earle WR. Glycolytic properties of high and low sarcoma-producing lines and clones of mouse tissue-culture cells. J Natl Cancer Inst 1959; 23:1079–1088.

(*239*) Scott DB, Pakoskey AM, Sanford KK. Analysis of enzymatic activities of clones derived from variant cell lines transformed to malignant cells in tissue culture. J Natl Cancer Inst 1960; 25:1365–1379.

(*240*) Sanford KK, Westfall BB. Growth and glucose metabolism of high and low tumor-producing clones under aerobic and anaerobic conditions in vitro. J Natl Cancer Inst 1969; 42:953–959.

(*241*) Sanford KK, Merwin RM, Hobbs GL, Earle WR. Influence of animal passage on a line of tissue-culture cells. J Natl Cancer Inst 1959; 23:1061–1077.

(*242*) Sanford KK. Clonal studies on normal cells and on their neoplastic transformation in vitro. Cancer Res 1957; 18:747–752.

(*243*) Sanford KK, Westfall BB. Alterations in vitro within a clone of mouse tumor cells. Pathol Biol 1961; 9:545–548.

(*244*) Chu EH, Sanford KK, Earle WR. Comparative chromosomal studies on mammalian cells in culture. II. Mouse sarcoma-producing cell strains and their derivatives. J Natl Cancer Inst 1958; 21:729–751.

(*245*) Evans VJ, Earle WR, Wilson EP, Waltz HK, Mackey CJ. The growth in vitro of massive cultures of liver cells. J Natl Cancer Inst 1952; 12:1245–1265.

(*246*) Westfall BB, Evans VJ, Shannon JE Jr, Earle WR. The glycogen content of cell suspensions prepared from massive tissue culture: Comparison of cells derived from mouse connective tissue and mouse liver. J Natl Cancer Inst 1953; 14:655–664.

(*247*) Peppers EV, Westfall BB, Earle WR. Glycogen content of cell suspensions prepared from massive tissue culture. II. Comparison of fourteen cell strains after long cultivation in vitro. J Natl Cancer

Inst 1959; 23:823–831.

(248) Westfall BB. Characterization of cells in tissue culture. Natl Cancer Inst Monogr 1962; 7:147–158.

(249) Westfall BB, Evans VJ, Peppers EV, et al. Observations on the metabolic behavior of a clone of mouse liver cells grown in agitated fluid suspension. Cancer Res 1958; 18:947–951.

(250) Westfall BB, Peppers EV, Earle WR. α-Keto acids in tissue culture. II. Studies on the used medium. J Natl Cancer Inst 1960; 24:417–423.

(251) Westfall BB, Evans VJ, Peppers EV, Hawkins NM, Earle WR. Effect of glutamine on the growth and metabolism of liver cells in vitro. J Natl Cancer Inst 1956; 17:131–138.

(252) Westfall BB, Peppers EV, Evans VJ, et al. The arginase and rhodanese activities of certain cell strains after long cultivation in vitro. J Biophys Biochem Cytol 1958; 4:567–570.

(253) Kuff EL, Evans VJ. β-Glucuronidase activities of cultured cells derived from C3H mouse liver. J Natl Cancer Inst 1961; 27:667–678.

(254) Peppers EV, Westfall BB, Kerr HA, Earle WR. Note on the catalase activity of several mammalian cell strains after long cultivation in vitro. J Natl Cancer Inst 1960; 25:1065–1068.

(255) Sanford KK, Likely GD, Evans VJ, Mackey CJ, Earle WR. The production of sarcomas from cultured tissues of hepatoma, melanoma, and thyroid tumors. J Natl Cancer Inst 1952; 12:1057–1077.

(256) Gantt RR, Martin JR, Evans VJ. Agglutination of in vitro cultured neoplastic and non-neoplastic cell lines by a wheat germ agglutinin. J Natl Cancer Inst 1969; 42:369–373.

(257) Sanford KK. Biologic manifestations of oncogenesis in vitro: A critique. J Natl Cancer Inst 1974; 53:1481–1485.

(258) ———. "Indicators" of neoplastic conversion in vitro. In: Katsuta H, ed. Cancer cells in culture. Tokyo: Univ Tokyo Press; Baltimore: Univ Park Press, 1968:281–289.

(259) Sanford KK, Handleman SL, Jones GM. Morphology and serum dependence of cloned cell lines undergoing spontaneous malignant transformation in culture. Cancer Res 1977; 37:821–830.

(260) Wetzel B, Sanford KK, Fox CH, Jones GM, Westbrook EW, Tarone RE. Topography of nonneoplastic and neoplastic cells of common origin. Cancer Res 1977; 37:831–842.

(261) Tucker RW, Sanford KK, Frankel R. Tubulin and actin in paired nonneoplastic and spontaneously transformed neoplastic cell lines in vitro: Fluorescent antibody studies. Cell 1978; 13:629–642.

(262) Montesano R, Drevon C, Kuroki T, et al. Test for malignant transformation of rat liver cells in culture: Cytology, growth in soft agar, and production of plasminogen activator. J Natl Cancer Inst 1977; 59:1651–1658.

(263) Sanford KK, Hall WT, Hobbs BA, Hursey ML. Ruthenium red-staining coat of paired neoplastic and nonneoplastic mouse cell lines in culture. J Natl Cancer Inst 1976; 56:1031–1033.

(264) Evans VJ, Price FM, Kerr HA, Montes de Oca H. Effect of 7,12-dimethylbenz[*a*]anthracene on non-neoplastic and neoplastic rodent cells in culture. J Natl Cancer Inst 1970; 45:429–441.

(265) Sanford KK, Barker BE, Woods MW, Parshad R, Law LW. Search for "indicators" of neoplastic conversion in vitro. J Natl Cancer Inst 1967; 39:705–733.

(266) Sanford K. Discussion: The use of three-dimensional matrix tissue culture for bioassay of cancer. Recent Results Cancer Res 1969; 17:163–167.

(267) Sanford KK, Westfall BB, Jackson JL. Glucolysis during culture of neoplastic and non-neoplastic murine cell lines under aerobic and anaerobic conditions. J Natl Cancer Inst 1970; 44:611–614.

(268) Ting CC, Sanford KK, Price FM. Expression of fetal antigens in fetal and adult cells during long-term culture. In Vitro 1977; 14:207–211.

(269) Cornell R. Spontaneous neoplastic transformation in vitro: Ultrastructure of transformed cell strains and tumors produced by injection of cell strains. J Natl Cancer Inst 1969; 43:891–906.

(270) Fox CH, Cottler-Fox M, Sanford KK. Rapid staining and preservation of cells grown in plastic tissue culture flasks. Stain Technol 1974; 49:105–107.

(271) Fox CH. Staining cultures of cells. Procedure 60117. TCA Manual 1977; 3:583–586.

(272) Farnes P, Price FM, Barker BE, Evans VJ. Histochemical studies of mouse embryo cell lines. I. Properties of cells cultivated in medium containing fetal calf or horse serum. J Natl Cancer Inst 1968; 40:283–294.

(273) Tucker RW, Sanford KK, Handleman SL, Jones GM. Colony morphology and growth in agarose as tests for spontaneous neoplastic transformation in vitro. Cancer Res 1977; 37:1571–1579.

(274) Handleman SL, Sanford KK, Tarone R, Parshad R. The cytology of spontaneous neoplastic transformation in culture. In Vitro 1977; 13:526–536.

(275) Fox CH, Dvorak JA, Sanford KK. Cytometric analysis of neoplastic transformation of vertebrate cell populations. Cancer Res 1976; 36:1556–1561.

(276) Fox CH, Caspersson T, Kudynowski J, Sanford KK, Tarone RE. Morphometric analysis of neoplastic transformation in rodent fibroblast cell lines. Cancer Res 1977; 37:892–897.

(277) Wetzel B, Jones GM, Sanford KK. Cell cycle and topography in non-synchronized monolayers: The use of autoradiography and time-lapse for more rigorous SEM studies. Scan Electron Microsc 1977; 1:545–552.

(278) Wetzel B, Kendig EM, Jones GM, Sanford KK. A systematic scanning electron microscope (SEM) analysis of mitotic cell populations in monolayer culture. Scan Electron Microsc 1978; 2:1–10.

(279) Sanford KK, Jones GM, Tarone RE, Fox CH. Direction of locomotion in clones of nonneoplastic fibroblasts and their neoplastic derivatives. Exp Cell Res 1977; 109:454–459.

(280) MacPherson I, Montagnier L. Agar suspension culture for the selective assay of cells transformed by polyoma virus. Virology 1964; 23:291–294.

(281) Boone CW. Malignant hemangioendotheliomas produced by subcutaneous inoculation of Balb/3T3 cells attached to glass beads. Science 1975; 188:68–70.

(282) Sanford KK, Boone CW, Merwin RM, Jones GM, Garrison CU. The plate-implant as a bioassay for the neoplastic potential of cultured cells. Int J Cancer 1980; 25:509–516.

(283) Tucker RW, Meltzer MS, Sanford KK. Susceptibility to killing by BCG-activated macrophages associated with "spontaneous" neoplastic transformation in culture. Int J Cancer 1981; 27:555–562.

(284) Tucker RW, Sanford KK. BCG-activated macrophages in an in vitro assay for neoplastic cells. Procedure 73439. TCA Manual 1978; 4:841–844.

(285) Meltzer MS, Tucker RW, Sanford KK, Leonard EJ. Interaction of BCG-activated macrophages with neoplastic and nonneoplastic cell lines in vitro: Quantitation of the cytotoxic reaction by release of tritiated thymidine from prelabeled target cells. J Natl Cancer Inst 1975; 54:1177–1184.

(286) Meltzer MS, Tucker RW, Breuer AC. Interaction of BCG-activated macrophages with neoplastic and nonneoplastic cell lines in vitro: Cinemicrographic analysis. Cell Immunol 1975; 17:30–42.

(287) Rothstein TL, Mage M, Jones G, McHugh LL. Cytotoxic T-lymphocyte sequential killing of immobilized allogeneic tumor target cells measured by time-lapse microcinematography. J Immunol 1978; 121:1652–1656.

(288) Nathan CF, Silverstein SC, Brukner LH, Cohn ZA. Extracellular cytolysis by activated macrophages and granulocytes. II. Hydrogen peroxide as a mediator of cytotoxicity. J Exp Med 1979; 149:100–113.

(289) Parshad R, Sanford KK, Jones GM, Tarone RE, Hoffman HA, Grier AH. Susceptibility to fluorescent light-induced chromatid breaks associated with DNA repair deficiency and malignant transformation in culture. Cancer Res 1980; 40:4415–4419.

(290) Chance B, Sies H, Boveris A. Hydroperoxide metabolism in mammalian organs. Physiol Rev 1979; 59:527–605.

(291) Totter JR. Spontaneous cancer and its possible relationship to oxygen metabolism. Proc Natl Acad Sci USA 1980; 77:1763–1767.

blank page

Cancer Incidence in Humans: Relationship to Plasma Lipids and Relative Weight [1, 2, 3]

R. B. Wallace,[4] C. Rost,[4] L. F. Burmeister,[4] *and* P. R. Pomrehn[4]

ABSTRACT—Surveillance was done on cancers in subjects in rural Iowa for 6 years after they participated in a cardiovascular risk factor-screening program. Among 5,565 men and women 20–94 years old at screening, 131 persons were identified as having cancers. Each cancer patient was matched to a control without cancer, and differences in antecedent plasma cholesterol and triglyceride levels and relative weight were sought. Mean relative weight at screening was lower among cancer patients of both sexes than among controls. Plasma cholesterol levels were lower among male patients and higher among female patients than among controls, with the differences more prominent for those less than 60 years old at screening. In males, the lower cholesterol levels occurred only in those with neoplasms developing within 24 months of screening. The higher cholesterol levels among female patients with cancers limited to gonadal hormone-related sites were not time-dependent. Triglyceride levels were not significantly different between cancer patients and controls in any analytic group, but triglyceride levels did closely parallel cholesterol alterations. A minimum of 1% of the cohort had diagnosed cancers before the screening program.—JNCI 1982; 68:915–918.

The risk of developing coronary heart disease is clearly related to antecedent blood cholesterol levels. Interest in the predictive value of cholesterol levels for cancer incidence has arisen for several reasons: to identify for preventive purposes groups at high risk of cancer, to search for clues to cancer causation and pathology, and to evaluate the concern that the manipulation of blood lipid levels to decrease the risk of one disease may unfavorably alter the risk of another disease.

Several investigators (*1–10*) have explored the cancer–cholesterol relationship mostly focusing on mortality and using populations originally involved in the study of cardiovascular disease. These populations varied in age, sex, and racial distributions. The studies also varied in method of subject ascertainment, in length of follow-up, in emphasis on cancer incidence versus mortality, and in attention given to specific cancer sites. Here we report the relationship between the levels of plasma lipids and relative weight and the cancer incidences in a rural Iowa population.

METHODS

The subjects, 20–94 years old, were residents of Cedar County, Iowa, and participants in one of 10 collaborative LRC population studies supported by the National Heart, Lung, and Blood Institute, Bethesda, Md. All persons were studied by standardized procedures previously described (*11*). After a community publicity and information effort, we ascertained and enumerated the subjects by using current telephone directories. Eligible subjects, 25–59 years of age, were then invited to one of nine community screening clinics where, after an overnight fast, blood was drawn for plasma cholesterol and triglyceride determinations by standard LRC methods (*12*). Height and weight (without coats and shoes) were measured, and the patients' histories were obtained, though the occurrences of prior cancers were not specifically queried. Persons less than 25 and more than 59 years old, not specifically invited but attending the screening clinics in response to publicity, were treated in the same manner and included in this report if they met county residency requirements. Overall, 70% of enumerated persons participated in the screening activity. All were white.

Subjects were initially screened between July 1973 and December 1975. Beginning in 1973, a statewide cancer incidence registry was established in Iowa as part of the Surveillance, Epidemiology, and End Results Program of the National Cancer Institute (*13*). The registry records all incident cancers except nonmelanoma skin tumors and registration is thought to be more than 99% complete. Participants in the LRC survey were linked by name, address, sex, and birthdate to subjects in the cancer registry files through January 1980, an average of nearly 6 years of follow-up. Mortality surveillance was maintained by linkage with statewide death record computer tapes and surveillance of local obituary notices. A 15% random sample of the cohort is being followed annually by active surveillance for another study, revealing that, as of 1980, 96% of the living study subjects were still within the State, thus assuring nearly complete follow-up. No attempt was made to ascertain the status of subjects leaving the State.

The State of Iowa also had complete ascertainment of incident cancers in 1969–71 as part of the Third National Cancer Survey (*14*). Our study cohort was also linked to this data base in a manner similar to that reported above to detect participants with cancers diagnosed 1969–71, prior to lipid study.

Each subject with neoplasm developing after lipid screening was matched to another control member of the cohort not known to have a cancer or to have died at the time of the primary tumor occurrence. Controls were matched to cases by age within 1 year, by sex, by community screening site, and by nearest date of screening. In no instance did a significant difference in mean years of education or distri-

---

ABBREVIATION USED: LRC=Lipid Research Clinic.

---

[1] Received July 30, 1981; accepted January 22, 1982.

[2] Supported by Public Health Service (PHS) contract NIH-NHLI-72-2913 from the Lipid Research Clinics Program, National Heart, Lung, and Blood Institute, and PHS contract N01CP-43200 from the Division of Cancer Cause and Prevention, National Cancer Institute.

[3] Research procedures were in accord with the ethical standards of the Committee on Human Experimentation, University of Iowa College of Medicine.

[4] Department of Preventive Medicine and Environmental Health, College of Medicine, The University of Iowa, Iowa City, Iowa 52242.

bution of occupations occur between any case and control analytic group. Those persons with documented cancers occurring prior to the screening activity were matched to a control subject in the same manner as above. Two subjects with separate cancers occurring both before and after lipid screening were excluded from analysis. Means of lipid levels and relative weight (expressed at the Quetelet Index: wt/ht^2×1,000) were compared with the use of paired t-tests.

RESULTS

On linking study subjects to the 1969–71 cancer register, 17 men and 37 women were found to have documented cancers prior to lipid screening. In general their lipid levels were higher than those of the matched controls, but significantly so only for cholesterol levels in men. Sex-specific relative weights were similar between these patients and controls. The subjects with cancers occurring before screening were excluded from further analysis.

Table 1 shows the age and sex distributions of the study cohort at the time of lipid measurement and the number of incident cancers over the surveillance interval. A total of 131 cancers were detected after lipid screening from a total of 5,565 persons. The distribution of neoplasms by site is shown in table 2.

Table 3 shows the overall sex-specific mean lipid levels and relative weight for the 131 persons with incident cancers and for their matched controls. Male patients had lower mean cholesterol and triglyceride levels and female patients higher lipid levels than did their respective controls, but none of the differences was significant. Examination of subjects according to age at screening revealed that the magnitude of the sex-specific lipid differences persisted for those less than 60 years of age, with a mean cholesterol level in female cancer patients significantly higher than that in the controls (table 3). Also, in the younger age group, the mean relative weight of the cancer patients was significantly lower in both sexes. Differences in mean lipid levels and relative weight were generally diminished or absent in the older age group. In these and subsequent analyses, no significant patient–control differences in mean triglyceride levels were found in any analytic category, though these levels in general paralleled cholesterol levels.

Table 1.—*Age and sex distributions of the study cohort and number of incident cancers*

Age group, yr	Males No.	Males Incident cancers	Females No.	Females Incident cancers
20–29	305	1	351	1
30–39	519	4	620	8
40–49	565	6	678	9
50–59	619	15	694	19
60–69	353	20	425	15
70–79	130	12	221	12
80–89	27	2	53	6
90–99	1	0	4	1
Total	2,519	60	3,046	71

Table 2.—*Number of cancer patients according to anatomic site of neoplasms*

Tumor site	No. of patients
Breast	32
Prostate gland	16
Colon	13
Bone marrow	8
Uterine cervix	7
Kidney	6
Lung	6
Lymph nodes	6
Ovary	5
Rectum	5
Brain	4
Bladder	3
Larynx	3
Thyroid gland	3
Uterine corpus	3
Uterus	3
Pancreas	2
Other of unknown origin	6
Total	131

Table 4 shows mean lipid levels and relative weight according to the interval between screening and cancer occurrence. The lower cholesterol levels for male cases seen in table 3 were also present for those with cancer occurring within 24 months of screening, but this difference diminished in subjects with cancer onset more than 24 months after screening. In contrast, the elevated mean cholesterol levels in female cases persisted and were not related to the interval between screening and disease onset. In all categories, cancer patients had a lower mean relative weight than did controls, with differences being significant for the longer screening interval.

Table 3.—*Mean plasma cholesterol and triglyceride levels and relative weight among cancer patients and matched controls*

Analytic category (No. of subjects)	Mean plasma cholesterol mg/dl±SE		Mean plasma triglyceride mg/dl±SE		Mean relative weight±SE	
	Cases	Controls	Cases	Controls	Cases	Controls
All males (60)	200.9±3.8	209.7±4.9	127.5±7.9	136.2±9.5	26.34±0.43	27.30±0.55
All females (71)	228.7±3.9	218.0±4.4	127.8±6.7	120.8±7.1	25.75±0.48	27.14±0.59
Subjects ≤59 yr old						
Males (26)	201.9±6.3	209.2±7.0	128.8±13.8	129.3±14.6	25.77±0.61[a]	27.72±0.79
Females (37)	225.7±5.7[a]	207.0±5.6	112.4±7.6	106.0±8.5	24.59±0.60[a]	27.32±0.81
Subjects ≥60 yr old						
Males (34)	203.4±4.6	210.1±6.9	126.6±9.3	141.4±12.6	26.84±0.59	27.09±0.78
Females (34)	232.1±5.4	230.3±6.2	144.5±10.7	137.3±10.9	27.06±0.68	26.94±0.8

[a] $P<0.05$.

TABLE 4.—*Mean plasma cholesterol and triglyceride levels and relative weight according to interval between screening and cancer incidence*

Analytic category (No. of subjects)	Mean plasma cholesterol, mg/dl±SE		Mean plasma triglyceride, mg/dl±SE		Mean relative weight±SE	
	Cases	Controls	Cases	Controls	Cases	Controls
Subjects with cancers occurring ≤24 mo after screening						
Males (24)	199.4±4.9	211.5±6.1	108.7±7.9	136.9±16.6	27.10±0.71	27.37±0.93
Females (29)	221.9±5.2	210.6±8.0	130.1±12.3	108.1±7.9	25.86±0.78	26.51±0.80
Subjects with cancers occurring >24 mo after screening						
Males (36)	205.0±5.4	208.5±7.3	140.2±11.7	135.8±11.5	25.90±0.53[a]	27.37±0.70
Females (42)	233.5±5.5	223.0±4.9	126.2±7.7	129.3±10.3	25.67±0.61[a]	27.55±0.83

[a] $P<0.05$.

TABLE 5.—*Mean lipid levels and relative weight for cases and controls according to specific cancer sites or site groups*

Specific cancer sites or site group (No. of subjects)	Mean plasma cholesterol mg/dl±SE		Mean plasma triglyceride mg/dl±SE		Mean relative weight±SE	
	Cases	Controls	Cases	Controls	Cases	Controls
Colon-rectum (18)						
Males (8)	218.0±11.9	218.3±15.1	107.0±0.9	108.4±11.5	27.86±0.87	26.99±2.02
Females (10)	223.0±3.9	225.1±7.3	107.9±6.3	133.7±22.7	26.36±1.60	27.87±0.47
Female hormone related (40)[a]	232.3±5.6[b]	217.1±5.3	133.3±10.1	125.9±9.6	25.38±0.65	27.68±0.85
Smoking related[c] (12)	206.2±9.4[b]	218.5±11.6	106.4±10.3	117.9±13.7	25.58±1.2	30.02±1.7[b]
Prostate gland (16)	206.1±7.3	202.5±8.8	131.5±14.7	147.2±22.5	26.83±0.77	25.79±0.78

[a] Includes 32 patients with breast cancer, 3 patients with uterine corpus cancer, and 5 patients with ovarian cancer.

[b] $P<0.05$.

[c] Includes 6 patients with lung cancer, 3 patients with laryngeal cancer, and 3 patients with bladder cancer, all but 1 in males.

Though the number of cancers at specific organ sites was limited, some specific sites and site groups were examined (table 5). No significant differences in mean lipid levels or relative weight were seen between cases and controls for colon-rectal or prostate cancers. Women with gonadal hormone-related cancers (breast, uterine corpus, and ovary) had a significantly higher mean cholesterol level than the controls. The 32 subjects with breast cancer had a mean cholesterol level 11 mg/dl higher than that of their controls, a marginally significant difference ($P<0.06$). Subjects with smoking-related cancers (11 males out of 12 subjects) had a significantly lower mean cholesterol level and relative weight.

DISCUSSION

As noted above, there are several important reasons for exploring the association of blood lipid levels with the subsequent development of cancer. Our findings agree with earlier published reports in some respects but differ in other respects.

None of the prior studies available to us explored blood triglyceride levels. We found no statistically significant relationship of triglyceride to cancer incidence in any analytic category, perhaps in part due to the number of study subjects and to the greater variance of such levels. However, mean triglyceride levels tended to vary in the same direction as that of the cholesterol levels, and further exploration of triglyceride alterations may be of value.

Males with cancers occurring after lipid screening had a mean plasma cholesterol level about 10 mg/dl lower than that of the matched controls, a finding most prominent for men under 60 years of age at the time of screening but less so for the older age group. Similar findings for incident cancers among males were reported in the Framingham (*5*) and Evans County studies (*4*), but neither study reported separately results for various age groups. Possibly, blood cholesterol is differentially predictive for cancer at different age groups as it is for coronary heart disease. Other available studies (*3*, *6–10*) focused solely on mortality.

We found no significant alteration in cholesterol levels associated with colon-rectal or prostate cancers, but the number of subjects was small. Williams et al. (*5*) and Rose et al. (*2*) have reported that cholesterol levels are significantly and inversely associated with the development of colon cancer, but evidence exists that these levels are related to tumor staging and may not necessarily precede tumor development (*15*). When smoking-related cancers (lung, laryngeal, esophageal, and bladder) were considered together, the mean cholesterol level was significantly lower than that among controls.

In our study, female cancer patients had mean cholesterol levels generally higher than those of their matched controls. The mean cholesterol level was 18.7 mg/dl higher among cancer patients less than 60 years of age at screening ($P<0.05$) but only 2 mg/dl higher (not significant) for those 60 years and older when compared to the mean cholesterol level of their respective controls. The Framingham (*5*) and Evans County (*4*) studies evaluated women and found no important or significant cholesterol–cancer association. To our knowledge no other study has reported age-specific differentials in this association among women and, as in studies of males, the suggestion arises that cholesterol–cancer relationships are age-dependent. The elevated cholesterol levels in younger female patients were limited to patients with cancers at the hormone-related sites: breast, uterine corpus, and ovary. Mean differences in cholesterol levels between female patients and controls, excluding patients with cancers at these hormone-related sites, were negligible (results not shown). The higher mean cholesterol levels for the 32 breast cancer patients alone were only marginally significant, and results from other studies with reference to breast cancer are conflicting. Boyd in (*16*) reported findings similar to our own, whereas Friedman (*17*) reported no association between cholesterol levels and breast cancer incidence. Kark et al. (*4*) reported a small but insignificant decrease in cholesterol levels in breast cancer patients in Evans County. Dyer et al. (*7*) reported a significantly higher mean cholesterol level among women dying of breast cancer than among women alive 5 years after lipid screening. Cholesterol levels have also been inversely related to breast cancer survival (*18*). In our study mean cholesterol levels were higher among patients with breast cancer and other hormone-related cancers, though the mean relative weight was lower when compared to that of controls. Clearly, this issue requires further exploration.

For the entire population and for each sex, we found a lower mean relative weight at screening in those destined to develop neoplasms regardless of the blood-cholesterol associations. This finding has been described previously in reference to the natural history and metabolic consequences of cancer (*19*). For investigators exploring the causal significance of lipid-cancer associations, taking ponderosity into account seems important.

Some methodologic findings emerged in describing the lipid-cancer relationships. Several populations, including our own, were originally used for the study of cardiovascular disease. Hence we did not ask our subjects at screening whether they had had a previous cancer. By retrospective linkage with the tumor registry, we discovered that, at a minimum, 1% of our subjects had a documented cancer before the cohort was assembled. Not knowing this could lead to misclassification of subjects and could alter the study findings. However, for middle-aged cohorts, the likelihood of prior cancers is probably small.

We found lower mean cholesterol levels among male cases to be prominent only among those cases occurring within 24 months of screening, which has been suggested previously by Rose et al. (*20*) who dealt with early versus late cancer mortality in men. The Paris study also showed that cancer-associated cholesterol differentials gradually disappeared with increasing survival interval after incidence (*3*). However, in Evans County, patients with cancer emerging within 12 months of screening had slightly higher mean cholesterol levels than did the general population, in contrast to the lower cholesterol levels seen in subjects with cancers emerging more than 12 months after screening. In our study, the positive cholesterol-cancer association in women did not diminish with increasing interval between screening and disease incidence. This sex-specific difference may reflect differential cancer sites, clinical stage, or biologic impact on the host. No other studies were available to contrast this observation.

Our report was not intended to explore further the biologic meaning of the lipid-cancer associations. Exploring causal mechanisms for the emerging associations in this study may require knowledge of environmental variables such as diet, caloric expenditure, and alcohol and tobacco use—data not available for most of our cohort. A search for pathophysiologic explanations for such associations would require exploration of lipid effects on competing causes of morbidity and mortality and would require separate consideration of each anatomic site and histologic type of neoplasm, inasmuch as the biology of each may be quite different. Ultimately, however, the exploration of the blood lipid-cancer associations and their causal importance in populations is important for understanding lipid-related summary risk status and the effects of specific lipid interventions.

REFERENCES

(*1*) Westlund K, Nicolaysen R. Ten-year mortality and morbidity related to serum cholesterol. Scand J Clin Lab Invest [Suppl] 1972; 30:127.

(*2*) Rose G, Blackburn H, Keys A, et al. Colon cancer and blood-cholesterol. Lancet 1974; 1:181-183.

(*3*) Cambien F, Ducimetiere P, Richard J. Total serum cholesterol and cancer mortality in a middle-aged male population. Am J Epidemiol 1980; 112:388-394.

(*4*) Kark JD, Smith AH, Hames CG. The relationship of serum cholesterol to the incidence of cancer in Evans County, Georgia. J Chronic Dis 1980; 33:311-322.

(*5*) Williams RR, Sorlie PD, Feinlieb M, McNamara PM, Kannel WB, Dawber TR. Cancer incidence by levels of cholesterol. JAMA 1981; 245:247-252.

(*6*) Yaari S, Goldbourt U, Even-Zohar S, Neufeld HN. Associations of serum high density lipoprotein and total cholesterol with total, cardiovascular, and cancer mortality in a 7-year prospective study of 10,000 men. Lancet 1981; 1:1011-1015.

(*7*) Dyer AR, Stamler J, Paul O, et al. Serum cholesterol and risk of death from cancer and other causes in three Chicago epidemiologic studies. J Chronic Dis 1981; 34:249-260.

(*8*) Kagan A, McGee DL, Yano K, Rhoads GG, Nomura A. Serum cholesterol and mortality in a Japanese-American population. Am J Epidemiol 1981; 114:11-20.

(*9*) Kozarevic DJ, McGee D, Vojvodic N, et al. Serum cholesterol and mortality. Am J Epidemiol 1981; 114:21-28.

(*10*) Garcia-Palmieri MR, Sorlie PD, Costas R Jr, Havlik RJ. An apparent inverse correlation between serum cholesterol and cancer mortality in Puerto Rico. Am J Epidemiol 1981; 114:29-40.

(*11*) The Lipid Research Clinics Programs Epidemiology Committee. Plasma lipid distributions in selected North American populations: The Lipid Research Clinics Program prevalence study. Circulation 1979; 60:427-439.

(*12*) Lipid Research Clinics Program. Manual of laboratory operation. Vol. 1. Lipid and lipoprotein analysis. Washington, D.C.: U.S. Govt Print Off, 1974 [DHEW publication No. (NIH)75-628].

(*13*) Young JL Jr, Asire AJ, Pollack ES. Cancer incidence and mortality in the United States, 1973-1976. Washington, D.C.: U.S. Govt Print Off, 1978 [DHEW publication No. (NIH)78-1837].

(*14*) Culter SJ, Scotto J, Devesa SS, Connelly RR. Third National Cancer Survey—an overview of available information. J Natl Cancer Inst 1974; 53:1565-1575.

(*15*) Miller SR, Tartter PI, Papatestas AE, Slater G, Aufses AH Jr. Serum cholesterol and human colon cancer. JNCI 1981; 67:297-300.

(*16*) Anonymous. Breast cancer foreshadowed with lipids. Oncology Times 1980 June II:18.

(*17*) Friedman GA. Serum cholesterol and breast cancer incidence in 95,000 members of the Kaiser Foundation Health Plan. National Cancer Institute, Breast Cancer Task Force, Intercom 1980 Sept 9:12.

(*18*) Tartter PI, Papatestas AE, Ioannovich J, Mulvihill MN, Lesnick G, Aufses AH. Cholesterol and obesity as prognostic factors in breast cancer. Cancer 1981; 47:2222-2227.

(*19*) Costa G, Donaldson S. The nutritional effects of cancer and its treatment. Nutr Cancer 1980; 2:22-29.

(*20*) Rose G, Shipley MJ. Plasma lipids and mortality: A source of error. Lancet 1980; 1:523-526.

High Cloning Efficiency of Human Lymphoid Cells in Agarose Without Feeder Layers[1,2]

Kathleen N. Ayres[3,4,5]

ABSTRACT—A protocol has been developed that consistently gives high cloning efficiencies for human lymphoid cell lines (lymphoblastoid and lymphoma) in agarose without the use of feeder layers. This procedure utilizes a cloning medium that contains horse serum, α-ketoglutarate or oxalacetate, and high levels of glutamine.—JNCI 1982; 68:919–923.

Cloning assays have become vital for the measurement of cellular mutation, transformation, and survival after treatment with various drugs or DNA-damaging agents and for the selection of somatic cell hybrids after cell fusion. Human lymphoid lines have long been used for these assays because they are easy to maintain in suspension culture, retain a near-diploid karyotype, and unlike human fibroblasts have an unlimited life-span (*1*). The purpose of this article is to report a protocol for cloning human lymphoid cells. The protocol does not use time-consuming feeder layers and, for the cell line Raji, has given cloning efficiencies as high as 83% (*2*), with 50% being obtained routinely. Furthermore, the optimized cloning medium contains much less FCS (0–5%) than that used previously, a definite advantage if one considers the present exorbitant price of FCS.

Our goal was to find a system that could be used for the isolation of drug-resistant cell clones and hybrid cell clones as well as for survival curves and mutation assays. Since we wanted to be sure that all the cells in the clone were derived from a single cell, we opted for growth in agarose (*3–5*) rather than growth in mitrotiter plates (*6*). Cloning in agarose has the disadvantage that it may select for certain cell types (*4*). Conversely, the microtiter method is more likely to allow metabolic cooperation between cells when more than one cell is seeded per well, thus yielding misleading survival curves. In addition, analysis of microtiter plating experiments can involve statistical methods that are less direct than those required by agarose cloning.

MATERIALS AND METHODS

Cells.—Cultures of L33-6-1 [a lymphoblastoid line isolated from a patient with infectious mononucleosis by Dr. P. R. Glade and subcloned by Sato et al. (*7*)], Raji [a Burkitt's lymphoma-derived cell line established by Pulvertaft (*8*)], and HH-4 [a lymphoblastoid line derived from WI-L2 by Skopek et al. (*9*) and originally isolated from a patient with spherocytosis] were provided by Dr. J. Littlefield (The Johns Hopkins University, Baltimore, Md.), Dr. P. Gerber (National Institutes of Health, Bethesda, Md.), and Dr. W. G. Thilly, respectively. Using the procedure of DelGiudice and Hopps as described by McGarrity (*10*), Bioassay Systems (Cambridge, Mass.) found these cultures to be free from mycoplasma contamination. The cells were routinely grown in RPMI-1640 medium, without antibiotics, supplemented with 17% FCS and 2, 4, or 6 m*M* glutamine as dictated by the experimental conditions. Once a week, the stock cultures were diluted to 0.4×10^6 cells/ml with fresh medium and then incubated at 37°C in a humidified atmosphere of 95% air and 5% CO$_2$.

Cloning.—Our cloning protocol is a modification of the cloning method of Sato et al. (*7*) with the omission of the feeder layer and the substitution of Sea Plaque agarose (Marine Colloids, Inc., Rockland, Maine; control lot #12978), which gels at a lower temperature (<30°C) than the Seakem agarose (36°C) originally used by Sato et al. (*7*). Seventeen days before a cloning experiment, a stationary culture (7-day culture) was diluted to 0.4×10^6 cells/ml. It was diluted in a similar fashion again on the 7th, 14th, 15th, and 16th days of culture and cloned in agarose on the 17th day. For plating of the cells, a 2.5-ml bottom layer of a 0.24% agarose–medium mixture was poured per 60-mm culture dish, and the dishes were incubated in a cold room at 0–4°C for 15 minutes. The dishes were then either used directly or stored (≤1 wk) until the day of use. To obtain the 0.24% agarose, 0.24 g of agarose was added to 10 ml of 0.9% saline and autoclaved for 15 minutes at 120°C. The agarose–saline mixture was immediately diluted tenfold with warm medium in a water bath (35–36°C). On the day of plating, 0.2 ml of medium containing the desired number of cells was mixed with 2.0 ml of a 0.22% agarose–medium mixture and poured gently over the bottom layers. The 2.0-ml aliquots were mixed with the cells in blood-dilution tubes in a water bath (35–36°C). The plates were again placed at 0–4°C for 15 minutes and subsequently incubated at 36–37°C at 90–100% humidity and 6.0–6.5% CO$_2$ for 1 month. Once the plates are poured, they should not be agitated because this agitation will interfere with the gelling process. After plating, random dishes could be selected and scanned at 100–200× to make sure that the cells plated were single

---

Abbreviations used: FCS=fetal calf serum (sera); HAT=hypoxanthine, aminopterin, thymidine; HS=horse serum (sera).

---

[1] Received August 4, 1981; accepted January 28, 1982.

[2] Supported by Public Health Service (PHS) contract N01CP-85669 from the Division of Cancer Cause and Prevention, National Cancer Institute; and by pathobiology postdoctoral traineeship PHS 5-T32GM-07190-04-0011.

[3] Department of Microbiology, The University of Chicago, 920 East 58th St., Chicago, Ill. 60637.

[4] *Address reprint requests to*: Dr. Bernard S. Strauss, Department of Microbiology, The University of Chicago, 920 East 58th St., Chicago, Ill. 60637.

[5] I thank Dr. W. G. Thilly (Massachusetts Institute of Technology, Cambridge, Mass.), who suggested that α-ketoglutarate might improve cloning efficiencies of lymphoid cells. I acknowledge Dr. Bernard Strauss (The University of Chicago) who extended the hospitality of his laboratory for the duration of this work. I also thank Ms. M. Chambers and Mrs. B. Neal, The University of Chicago, for technical assistance.

cells and not clusters of cells. Each dish was fed 0.5 ml of cloning medium the following day and at weekly intervals thereafter. Colonies were visible at 2 weeks and scoreable between 3 and 4 weeks (depending on the cell line). Colonies could then be isolated with the use of a Pasteur pipette and dispersed into 0.5 ml of medium in blood-dilution tubes.

Materials.—All sera used for cloning and general stock maintenance were heat inactivated at 56°C for 30 minutes. The FCS, premium HS, and RPMI-1640 (without glutamine) were obtained from Kansas City Biological, Inc., Lenexa, Kan. α-Ketoglutarate, α-ketobutyrate, oxalacetate, and sodium pyruvate were obtained from Sigma Chemical Co., St. Louis, Mo., whereas the glutamine was obtained from Grand Island Biological Co., Grand Island, N.Y., and the β-mercaptoethanol was from Eastman Kodak Co., Rochester, N.Y. We made a 0.2-*M* stock of glutamine and 0.1-*M* stocks of α-ketoglutarate, α-ketobutyrate, oxalacetate, and sodium pyruvate by dissolving these compounds in RPMI-1640 medium and adjusting the pH to 7.2. Aliquots of these stocks were kept frozen and added to the medium on the day of use. For these experiments, cells were plated in 60-mm Corning tissue culture dishes (Corning Glass Works, Corning, N.Y.) at 100 cells/dish.

RESULTS

First attempts to clone these lymphoid cells with the use of the standard growth medium (17% FCS in RPMI-1640 medium containing 2 m*M* glutamine) produced cloning efficiencies of approximately 5% for Raji and 0.1% for L33-6-1. We then found that logarithmic cells produced higher cloning efficiencies than cells from a stationary culture, and we devised a dilution scheme that yielded a high number of cells in logarithmic growth. All of the experiments discussed in this paper have used this dilution scheme. Variations may also succeed, but if the cells are diluted too frequently without being allowed to go through a stationary phase, some lymphoid cultures die out and, in particular, Raji and L33-6-1 do not give high cloning efficiencies. The dilution scheme described in "Materials and Methods" gave the highest cloning efficiencies in our laboratory. In the experiments reported here, we also carefully controlled factors such as the agarose lot, pH, CO_2 concentration, and humidity.

Table 1 shows the cloning efficiencies obtained after growth in standard working medium plus 2 m*M* glutamine, followed by plating in various supplemented media. The results in table 1 are typical of those obtained in several similar experiments. The highest cloning efficiencies were obtained in media that contained either 15% HS and no FCS (medium D) or a mixture of 10% HS and 5% FCS (media C, H, I, J, and A). A comparison of media A, B, and C, which were identical with the exception of the molarity of glutamine, showed that the highest molarities of glutamine produced the highest cloning efficiencies. The results for media A, F, H, and I suggested that α-ketoglutarate, oxalacetate, and sodium pyruvate each yielded a significant increase in the number of clones (compared to medium F which contained none of these ingredients). α-Ketobutyrate (not a tricarboxylic acid cycle intermediate) may have produced some increase in the number of clones compared to the number produced in medium F, but the clones were often diffuse and difficult to count as well as being quite small (*see* fig. 1). Colonies that grew up in the presence of α-ketoglutarate or oxalacetate (tricarboxylic acid cycle intermediates) tended to appear more rapidly and produce more uniformly sized colonies than colonies that grew up in media without one of these supplements.

The cloning efficiencies depicted in table 1 were obtained after growth of the stock cells in RPMI-1640 supplemented with 17% FCS and 2 m*M* glutamine. Table 2 gives cloning efficiencies for a similar experiment in which 6 m*M* glutamine was substituted for the 2 m*M* glutamine during the growth of stock cells. The results in table 2 are typical of those obtained in several similar experiments. All of the supplemented media tested in table 2 gave higher cloning efficiencies than their counterparts in table 1. Further improvements may possibly be obtainable by adjustment of

TABLE 1.—*Cloning efficiencies of Raji and L33-6-1 in agarose with various cloning media, after growth in 2 mM glutamine*

Supplement	Cloning efficiencies with cloning medium[a]									
	A	B	C	D	E	F	G	H	I	J
FCS, %	5	5	5	0	15	5	5	5	5	5
HS, %	10	10	10	15	0	10	10	10	10	10
Glutamine, m*M*	4	2	6	4	4	4	4	4	4	4
α-Ketoglutarate, m*M*	1	1	1	1	1	0	0	0	0	1
α-Ketobutyrate, m*M*	0	0	0	0	0	0	1	0	0	1
Pyruvate, m*M*	0	0	0	0	0	0	0	0	1	1
Oxalacetate, m*M*	0	0	0	0	0	0	0	1	0	1
Raji cloning efficiency, %[b]	[illegible]	24±1	32±1	33±1	14±1	21±1	26±1	33±1	28±1	28±1
L33-6-1 cloning efficiency, %[b]	14±1	13±1	23±1	24±1	10±1	11±1	16±1	21±1	14±1	14±1

[a] Medium for both growth and cloning was RPMI-1640 (without glutamine), which was made up from powder and adjusted to pH 7.2. Various cloning media (A–J) were obtained by the addition to RPMI-1640 of the supplements listed in the left-hand column, where the units are % and m*M*. All FCS was from lot #308385 (Kansas City Biological, Inc.), and all HS was from lot #26079 (Kansas City Biological, Inc.). Before plating, both Raji and L33-6-1 were grown in RPMI-1640 plus 17% FCS and 2 m*M* glutamine and were kept in logarithmic growth by adherence to the dilution schedule described in "Materials and Methods."

[b] Cloning efficiencies were calculated from the average number of colonies counted on ten 60-mm plates for both Raji and L33-6-1 after plating Raji at 100 cells/dish and L33-6-1 at 200 cells/dish in each of the above media. Uncertainties quoted are standard deviations calculated from the numbers of clones. To minimize systematic errors in the comparison, we obtained the results simultaneously in one large experiment using common parental cell stocks.

TABLE 2.—*Cloning efficiencies of Raji in agarose with various cloning media, after growth in 6 mM glutamine*

Supplement	Cloning efficiencies with cloning medium[a]						
	K	L	M	N	O	P	Q
FCS, % (lot)	5 (#308385)	5 (#30004)	0	5 (#308385)	5 (#308407)	5 (#308385)	5 (#308385)
HS, %	10	10	15	10	10	10	10
Glutamine, m*M*	6	6	6	6	6	6	6
α-Ketoglutarate, m*M*	1	1	1	1	1	0	0
Pyruvate, m*M*	0	0	0	0	0	0	1
Oxalacetate, m*M*	0	0	0	1	0	1	0
Raji cloning efficiency, %[b]	45±2	47±2	51±2	46±2	39±2	48±2	40±2

[a] Conditions were the same as those in table 1 with the exception that three different lots of FCS were used (lot numbers are identified in the table) and that before plating, Raji was grown in RPMI-1640 plus 17% FCS and 6 m*M* glutamine. Cells were kept in logarithmic growth prior to plating by following the dilution schedule described in "Materials and Methods."

[b] Cloning efficiencies were calculated from the average number of colonies counted on ten 60-mm plates after plating Raji at 100 cells/plate in each medium. Uncertainties quoted are standard deviations calculated from the numbers of clones. To minimize systematic errors in the comparison, we obtained the results simultaneously in one large experiment using common parental cell stocks.

the glutamine supplement to the specific needs of individual cell lines.

When media K, L, M, and O were compared, 15% HS again produced the highest cloning efficiency, whereas cloning efficiencies of the other three media varied with the FCS lot. When the mixture of 5% FCS and 10% HS was used for cloning, we repeatedly observed this differential in cloning potential among lots of the FCS. The variability between lots of HS was not as great, perhaps because the HS was obtained from a single donor herd.

Although the differences in cloning efficiency produced by the addition of sodium pyruvate versus α-ketoglutarate are not large in table 2, they seem to be larger than those in table 1. In addition, visual inspection of colony growth showed that α-ketoglutarate and oxalacetate produced firm, rapidly appearing, rapidly growing colonies, whereas sodium pyruvate did not (*see* fig. 1). In addition to the experiments represented in the tables, we performed a separate set of experiments suggested by the results of Broome and Jeng (*11*), who reported that a thiol such as β-mercaptoethanol could have growth-promoting activity for lymphoid cells. Unfortunately, we found no beneficial effect from the addition of β-mercaptoethanol. At 5×10^{-5} *M* β-mercaptoethanol, the plating efficiencies of both Raji and L33-6-1 were almost identical between control and β-mercaptoethanol plates.

In summary, the cloning efficiencies that we have been able to obtain using either 15% HS or 10% HS and 5% FCS plus additional supplements of α-ketoglutarate or oxalacetate and 6 m*M* glutamine have been much higher than those obtained previously. We have obtained routine cloning efficiencies of 50% for Raji (range=45–83%) (*2*), of 20% for L33-6-1 (range=10–35%), and of 35% for HH-4 (range=15–50%).

DISCUSSION

Although some consider cloning of cells to be more art than science, large increases in cloning efficiencies may be obtained for a number of cell lines if important parameters are systematically optimized. We found the single most important factor to be the substitution of HS for the FCS that had been used previously. Components of HS have been found essential for colony formation of mouse primitive red blood cells as well (*12*). However, the combination of 5% FCS and 10% HS seemed to give more repeatedly reliable results inasmuch as the plates tended to become acidic less rapidly. Acidity makes the agarose less firm, and the clones become unscoreable. Hence our preferred cloning medium composition is 10% HS, 5% FCS, 6 m*M* glutamine, and 1 m*M* α-ketoglutarate or 1 m*M* oxalacetate in a base of RPMI-1640.

This procedure has allowed the cloning of lymphoblastoid (L33-6-1 and HH-4) as well as lymphoma (Raji) cell lines. At present, we have no data on the cloning efficiencies of recently isolated lymphoid cell lines. However, many lymphoid lines that tend to clump in stationary phase can still be cloned by means of this procedure, because the dilution scheme establishes logarithmic growth where the clumps of cells are usually smaller and dispersible by gentle shaking. We have not determined whether α-ketoglutarate and oxalacetate promote cloning because they are intermediates in the tricarboxylic acid cycle or because they can ultimately be converted to glutamine. They may exert their activity because of their interaction with serum components, as demonstrated by McKeehan and McKeehan (*13*). However, α-ketobutyrate (not a tricarboxylic acid cycle intermediate) is not as effective as are α-ketoglutarate and oxalacetate in enhancing size and discreteness of clones. Glutamine has been shown to be a major source of energy for some cells in culture, including lymphoma cells (*14–16*). However, we have obtained the glutamine enhancement of cloning with both lymphoma and lymphoblastoid cells.

We have used this protocol to obtain dose-response curves to 6-thioguanine, ouabain, diphtheria toxin, and neocarzinostatin and to obtain survival curves after treatment with methyl methanesulfonate, *N*-methyl-*N'*-nitro-*N*-nitrosoguanidine, and *N*-acetoxy-2-acetylaminofluorene. This protocol has also been used for selection of hybrid cells with the use of both the HAT-selection system of Littlefield (*17*) and the HAT–ouabain-selection system (*18, 19*).

REFERENCES

(*1*) NILSSON K, PONTÉN J. Classification and biological nature of established human hematopoietic cell lines. Int J Cancer 1975; 15:321–341.

(2) Tatsumi K, Bose KK, Ayres K, Strauss BS. Repair of neocarzinostatin-induced deoxyribonucleic acid damage in human lymphoblastoid cells: Possible involvement of apurinic/apyrimidinic sites as intermediates. Biochemistry 1980; 19:4767–4772.

(3) Macpherson I, Montagnier L. Agar suspension culture for the selective assay of cells transformed by polyoma virus. Virology 1964; 23:291–294.

(4) Macpherson I. Soft agar techniques. In: Kruse PF Jr, Patterson MK, eds. Tissue culture: Methods and applications. New York: Academic Press, 1973:276–280.

(5) Iscove NN, Schreier MH. Clonal growth of cells in semisolid or viscous medium. In: Lefkovits I, Pernis B, eds. Immunological methods. New York: Academic Press, 1979:379–385.

(6) Kraemer KH, Waters HL, Buchanan JK. Survival of human lymphoblastoid cells after DNA damage measured by growth in microtiter wells. Mutat Res 1980; 72:285–294.

(7) Sato K, Slesinski RS, Littlefield JW. Chemical mutagenesis at the phosphoribosyltransferase locus in cultured human lymphoblasts. Proc Natl Acad Sci USA 1972; 69:1244–1248.

(8) Pulvertaft RJ. A study of malignant tumours in Nigeria by short-term tissue culture. J Clin Pathol 1965; 18:261–273.

(9) Skopek TR, Liber HL, Penman BW, Thilly WG. Isolation of a human lymphoblastoid line heterozygous at the thymidine kinase locus: Possibility for a rapid human cell mutation assay. Biochem Biophys Res Commun 1978; 84:411–416.

(10) McGarrity GJ. Detection of contamination. In: Jakoby WB, Pastan IH, eds. Methods in enzymology: Cell culture. Vol 58. New York: Academic Press, 1979:18–29 (*See*, especially, pp 24, 25).

(11) Broome JD, Jeng MW. Promotion of replication in lymphoid cells by specific thiols and disulfides in vitro. Effects on mouse lymphoma cells in comparison with splenic lymphocytes. J Exp Med 1973; 138:574–592.

(12) Iscove NN, Schreier M. Analysis of the serum requirement for colony formation by primitive red cell precursors in culture. In: Basel Institute for Immunology annual report. Basel: Basel Institute for Immunology, 1979:94.

(13) McKeehan WL, McKeehan KA. Serum factors modify the cellular requirement for Ca^{2+}, K^+, Mg^{2+}, phosphate ions, and 2-oxocarboxylic acids for multiplication of normal human fibroblasts. Proc Natl Acad Sci USA 1980; 77:3417–3421.

(14) Lavietes BB, Regan DH, Demopoulos HB. Glutamate oxidation in 6C3HED lymphoma: Effects of L-asparaginase on sensitive and resistant lines. Proc Natl Acad Sci USA 1974; 71:3993–3997.

(15) Reitzer LJ, Wice BM, Kennell D. Evidence that glutamine, not sugar, is the major energy source for cultured HeLa cells. J Biol Chem 1979; 254:2669–2676.

(16) Zielke HR, Sumbilla CM, Sevdalian DA, Hawkins RL, Ozand PT. Lactate: A major product of glutamine metabolism by human diploid fibroblasts. J Cell Physiol 1980; 104:433–441.

(17) Littlefield JW. Selection of hybrids from matings of fibroblasts in vitro and their presumed recombinants. Science 1964; 145:709–710.

(18) Baker RM, Brunette DM, Mankovitz R, et al. Ouabain-resistant mutants of mouse and hamster cells in culture. Cell 1974; 1:9–21.

(19) Corsaro CM, Migeon BR. Gene expression in euploid human hybrid cells: Ouabain resistance is codominant. Somat Cell Genet 1978; 4:531–540.

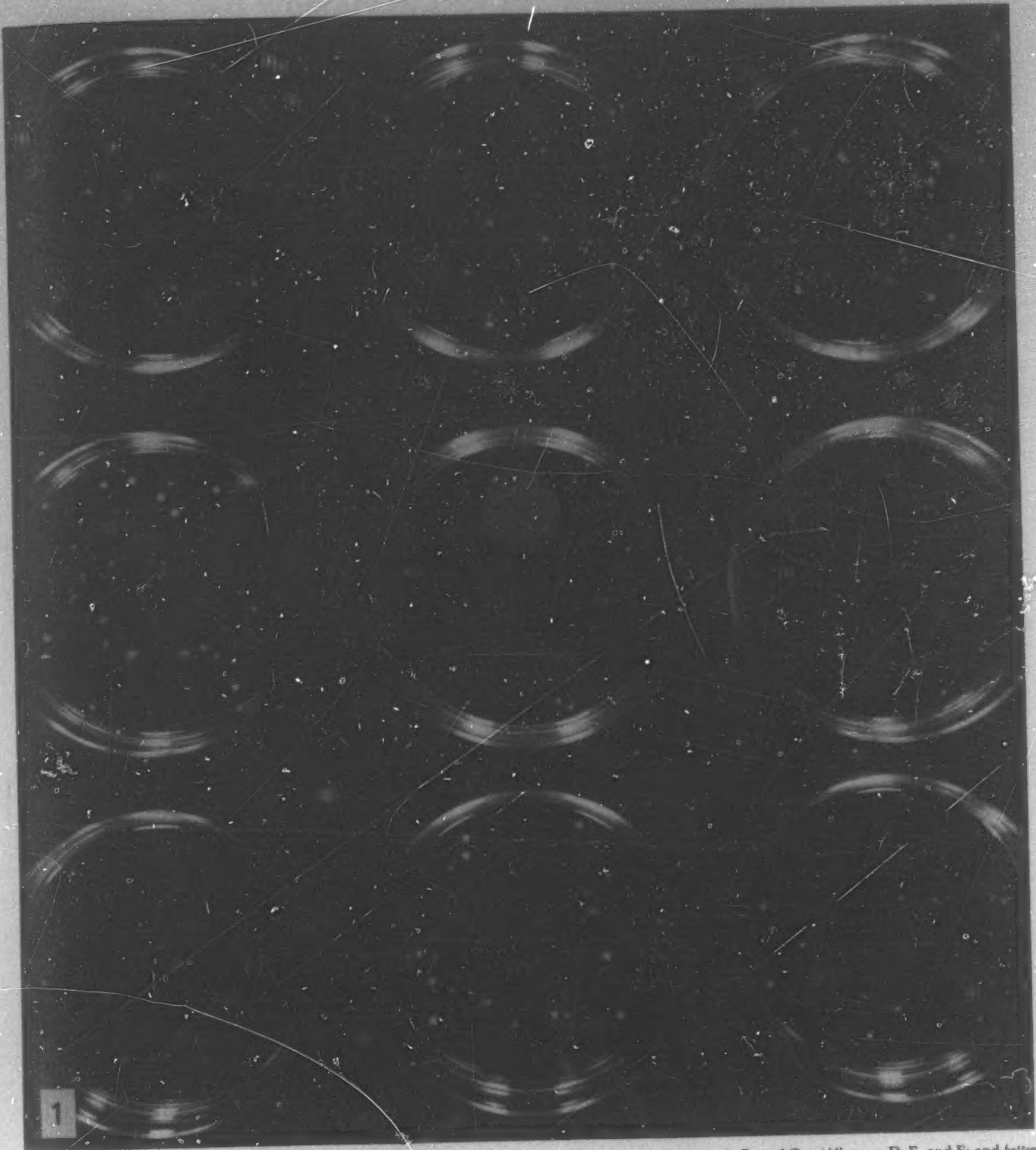

FIGURE 1.—Selected Raji dishes used for the data in table 1. Media used were (from *left* to *right*): *top row*—A, B, and C; *middle row*—D, E, and F; and *bottom row*—G, H, and I. Medium components are specified in table 1.

blank page

Mortality Among Workers in a Nickel Refinery and Alloy Manufacturing Plant in West Virginia[1, 2]

Philip E. Enterline, *Ph.D.*,[3] *and* **Gary M. Marsh**, *Ph.D.*[3, 4]

ABSTRACT—Workers from a nickel refinery at Huntington, W. Va., which received a nickel matte from smelters in Ontario, Canada, during 1922–47 were studied for excesses in sinonasal and lung cancers. Other workers who were in a nickel alloy production plant operated in conjunction with the refinery but who did not work in the refinery were also studied. Evidence is presented on the existence of a nasal cancer hazard and possibly a lung cancer hazard among workers employed in the nickel refinery. Two of these workers developed a sinonasal cancer. Evidence of a respiratory cancer hazard in other parts of the plant before or after 1947 is weak, and the observed results could be due to chance variations from the mortality experience of the standard reference populations. Among nonrefinery workers hired while the nickel refinery was in operation, 2 employees had a probable sinonasal cancer. The first employee worked in a high-temperature conversion process where nickel carbonate was decomposed to nickel oxide, and the second employee is believed to have done maintenance work in the plant where this process was used. For both cohorts combined there were slight overall excesses in lung, stomach, and prostate cancers with some evidence of a dose-response relationship for these cancers.—JNCI 1982; 68:925–933.

Nickel has been mined and smelted in the Sudbury region of Ontario, Canada, since the last century. A copper–nickel matte—essentially a mixture of Cu_2S and Ni_3S_2—was shipped from that area to nickel refineries in various parts of the world. Epidemiologic studies at four of these refineries (Clydach, Wales; Kristiansand, Norway; and Port Colborne and Copper Cliff, Canada) have shown an excess in cancers of the lung and nasal sinuses [(*1–3*); Sutherland RB: Mortality among sinter plant workers. Toronto: Report of the Division of Industrial Hygiene, Ontario Department of Health, 1969].

Matte from one Sudbury smelter was also shipped to a nickel refinery at Huntington, W. Va. The refinery, owned by INCO Limited, was operated in conjunction with the manufacture of wrought forms of nickel-containing alloys. The refinery consisted of two departments: 1) calcining and 2) melting and casting.

The calcining department operated from 1922 to 1947. There, high copper–nickel matte from Sudbury was crushed, ground, and oxidized at 1,200°C in four gas-fired calciners to produce copper–nickel oxide suitable for the manufacture of Monel alloy. Four more calcining furnaces were built early in 1941 to oxidize low copper–nickel matte produced mainly in New Caledonia from oxide nickel ore, although some was also received from Sudbury. The calcining department also reduced nickel oxide from Canada to nickel metal and occasionally decomposed copper–nickel carbonate from the plant's pickling operations to copper–nickel oxides. Concentrations of total particulates were very high where the matte was crushed, ground, and handled (50–500 mg/m^3), whereas concentrations around the calciners were much lower (10–20 mg/m^3). Concentrations of airborne nickel in these areas were estimated to range from 20 to 350 mg Ni/m^3 and from 5 to 15 mg Ni/m^3, respectively (International Nickel Co., Ltd.: Nickel and its inorganic compounds. Report submitted to the National Institute for Occupational Safety and Health, Oct. 1976).

The melting and casting department operated gas-fired open-hearth furnaces and electric arc furnaces to melt various nickel-containing alloys and cast them into ingots. These ingots were then forged, rolled, drawn, or otherwise worked into various wrought forms of nickel-containing alloys.

This is a report of an investigation of the mortality experience of workers employed for 1 year or more in the refinery at the Huntington plant. The investigation was undertaken to ascertain whether these workers experienced an increased incidence of cancers of the lung and nasal sinuses as did refinery workers elsewhere who oxidized nickel matte in dusty environments. This report also describes the mortality experience of other workers who were employed at the Huntington plant and who were exposed to airborne nickel in various forms but who either did not work in the refinery or worked there for less than a year. This part of the study was undertaken to investigate whether an increased incidence of respiratory cancer was associated with the manufacture of wrought forms of nickel-containing alloys.

MATERIALS AND METHODS

Since the calciners at Huntington were torn down near the end of 1947, we decided to examine the company rolls as of January 1, 1948. Some 1,855 men on the payrolls that day had been hired before 1947 and had thus accumulated at least 1 year's service while the calciners were still in

---

Abbreviations used: ICD=International Statistical Classification of Diseases, Injuries, and Causes of Death; SMR=standardized mortality ratio(s).

---

[1] Received August 12, 1981; accepted January 28, 1982.

[2] Supported by a contract between Huntington Alloys, Inc., a subsidiary of INCO Limited, and the University of Pittsburgh.

[3] Department of Biostatistics, Graduate School of Public Health, University of Pittsburgh, Pittsburgh, Pa. 15261.

[4] We gratefully acknowledge the assistance and patience of Mr. Fred Hardwick and other employees of Huntington Alloys, Inc., Huntington, W. Va., and the technical and editorial assistance provided by Dr. J. Stuart Warner of INCO Limited, Toronto, Canada. Ms. Michele LaValley, Mrs. Vanessa Gleason, and Mr. Donald Fisherowski assisted in the data processing operations, and Miss Mary Preininger provided the computer programming support. We are also deeply appreciative of the late Mr. Kenneth Wassam for his dedication and enthusiasm while serving as project director in the early phases of this study.

operation. This group included active employees, service and disability pensioners, and employees who were laid off as of January 1, 1948, but who were recalled sometime during the year 1948. The completeness of the company files for active employees was verified by a comparison of names obtained from personnel records of men who worked a year or more with names that appeared on the quarterly social security tax return the company had filed with the U.S. Internal Revenue Service for the first quarter of 1948 and the first quarter of 1949. No names were missing in the personnel records. This verification process was fully described elsewhere (4).

This group of 1,855 men was further subdivided with respect to exposure to the calcining operations. Personnel records indicated that 109 of these men had worked in the calcining department for a year or more. In addition, 157 men had worked a year or more in the melting and casting department. Since this department was physically adjacent to and shared seniority with the calcining department, many of these men probably were exposed at some time to the calcining operations, although their personnel records do not explicitly show this. For the purpose of this investigation all 266 refinery workers were considered as having been exposed to calcining operations, and the combined operations will be referred to simply as "refinery."

Of the remaining 1,589 men hired before 1947, some 137 had worked in either the calcining or melting and casting departments but for less than 1 year. Thus 1,452 or 91.4% of these men had never worked in the refinery and were not exposed to the calcining operations. This group of 1,589 men will be referred to as "nonrefinery workers."

The total of 1,855 workers were followed for deaths from January 1, 1948, through December 31, 1977, with results as shown in table 1. The vital status of 1,657 or 89.3% of the study members was known from plant records, either because they were still employed, had died while employed, or had retired under pension plans in which they were, in effect, followed by the company. The vital status of all but 10 of the remaining study population was determined through various follow-up resources including the Social Security Administration, the U.S. Postal Service, the Veterans Administration, and direct telephone inquiries. Overall, 99.4% of these workers were traced and of the 791 who were known to have died, death certificates were obtained for 789 or 99.7%. All death certificates were coded by an independent nosologist to the Seventh Revision of the ICD.

An additional group of 1,354 male employees who worked for a year or more during 1948–59 but who could not have been exposed to the calcining operations was identified in the company's personnel records. All but 9 of these men were hired after 1947, i.e., after the calciners had been removed. Nine of them had been hired in 1947, but their positions were such that they would have had no opportunity for exposure to the calcining operations. While this group had no exposure to the calcining operations, it did share some of the exposures of the refinery group inasmuch as some of these men worked for a year or more in the melting and casting department. This group will be referred to as "hired after 1946."

TABLE 1.—*Follow-up results for male nickel workers who were on the company payrolls January 1, 1948, and who had worked a year or more*

Vital status as of 12/31/77	No.	Percent[a]
Alive	1,054	56.8
Dead	791	42.6
Death certificate found	789	(99.7)
No death certificate found	2	(0.3)
Lost to follow-up	10	0.6
Total	1,855	100.0

[a] *Numbers in parentheses* are not part of the overall total of 1,855 but are subgroups of the 791 deaths.

The completeness of this group has not been verified, but the fact that no names were missing from files for men hired earlier suggests that this cohort was probably fully identified. These men were also followed for deaths through 1977 with results as shown in table 2. The vital status of 777 or 57.4% of the group hired after 1946 was known from plant records, whereas the vital status for all but 9 of the remaining study members was determined through the same tracing resources used with the first cohort. As in the first cohort, over 99% were traced. For the 94 study members who died, 97.9% of the death certificates have been located. All death certificates were coded by an independent nosologist to the Seventh Revision of the ICD. For both cohorts, observed numbers of deaths were compared to numbers expected based on the mortality experience of the U.S. white male population. For the computation of the expected numbers, person-years of observation were allocated to 5-year age and calendar time categories and multiplied by corresponding cause-specific U.S. death rates (5). To adjust for geographic variations in mortality, we also computed expected numbers of deaths based on the white male population of the 6-county area surrounding the Huntington plant from which the work force was largely drawn (Cabell, Wayne, Mason, Putnam, and Lincoln Counties, W. Va., and Lawrence County, Ohio). The local mortality rates are available for cancer for the years 1950–77, but for other causes of death rates are available only for the years 1962–77. Where appropriate, U.S. and local death rates were adjusted to the Seventh Revision of the ICD through the application of comparability ratios published by the U.S. Public Health Service (6). Ratios of observed-to-expected numbers of deaths were expressed as SMR, which are estimates in percentage form of rate ratios for nickel workers compared to those for the standard population, adjusted for age and calendar time to the person-years distribution of the employment group of interest. If one assumes that the observed

TABLE 2.—*Follow-up results for male nickel workers who were hired after 1946 and who had worked a year or more*

Vital status as of 12/31/77	No.	Percent[a]
Alive	1,251	92.4
Dead	94	6.9
Death certificate found	92	(97.9)
No death certificate found	2	(2.1)
Lost to follow-up	9	0.7
Total	1,354	100.0

[a] *Numbers in parentheses* are not part of the overall total of 1,354 but are subgroups of the 94 deaths.

TABLE 3.—*Observed and expected deaths and SMR*[a] *for 3 groups of male nickel workers employed a year or more*

Cause of death (ICD Seventh Revision codes)	Hired before 1947						Hired after 1946[d]		
	Refinery[b]			Nonrefinery[c]					
	Observed	Expected	SMR	Observed	Expected	SMR	Observed	Expected	SMR
All causes	113	108.02	104.6	678	795.94	85.2[e]	94	129.46	72.6[e]
All malignant neoplasms (140–205)	29	21.47	135.0	141	150.50	93.7	21	22.75	92.3
Digestive (150–159)	7	6.34	110.4	37	46.57	79.4	6	5.21	115.1
Respiratory (160–164)	10	7.18	139.2	49	46.62	105.1	10	7.68	130.2
Larynx (161)	0	0.35	—	2	2.36	84.7	0	0.30	—
Bronchus, trachea, lung (162–163)	8	6.75	118.5	47	43.69	107.6	10	7.27	137.6
Other (residual)	2	0.08	2,443.5[e]	0	0.56	—	0	0.11	—
Genitourinary (177–181)	3	2.63	114.1	21	21.62	97.1	1	1.75	57.1
Leukemias–lymphomas (200–205)	3	2.02	148.2	14	13.75	101.8	3	3.33	90.0
Other malignant neoplasms (residual)	6	3.30	181.8	20	21.95	91.1	1	1.66	60.1
Stroke (330–334)	12	7.40	162.1	66	66.69	99.0	5	4.32	115.7
All heart disease (400–440)	41	47.57	86.2	319	355.66	89.7	28	42.32	66.2[f]
Nonmalignant respiratory disease (470–527)	8	6.01[f]	133.2	25	45.81	54.6[e]	2	4.77	42.0
Influenza and pneumonia (480–493)	4	2.35	170.4	11	19.58	56.2	0	2.28	—
Other (residual)	4	3.66	109.3	14	26.22	53.4[f]	2	2.48	80.6
All external causes (800–998)	10	8.00	125.0	29	50.12	57.9[e]	16	31.40	51.0[e]
All other causes (residual)	13	17.57	73.9	96	127.11	77.1[e]	20	23.56	84.9
Unknown causes (included in "all causes" only)	0			2			2		

[a] Expected deaths are based on total U.S. white male mortality rates.
[b] Number at risk: 266. Person-years at risk: 6,738.9.
[c] Number at risk: 1,589. Person-years at risk: 39,380.9.
[d] Number at risk: 1,354. Person-years at risk: 31,203.8.
[e] $P<0.01$.
[f] $P<0.05$.

number of deaths follows a Poisson distribution, confidence intervals can be placed on the SMR and significant deviations of the SMR from 100, indicating deficit and excess mortality risks, can be identified (*7*).

RESULTS

Table 3 shows the mortality experience of the following 3 groups of workers compared to that expected based on the total U.S. white male mortality experience: 1) those hired before 1947 who worked a year or more in the refinery, 2) those hired before 1947 who worked a year or more but not a year or more in the refinery (nonrefinery), and 3) those who were hired after 1946—too recently to have worked a year or more in the refinery. Among refinery workers (as defined) SMR were elevated for nearly every cause shown. A notable exception is the category "all heart disease" where a 13.8% deficit in deaths was observed. The excess in respiratory cancer is mainly due to the two deaths in the "other [respiratory cancer] (residual)" category. Both of these deaths were from sinonasal cancers, and the excess is statistically significant. One of these men worked at the calciner from 1941 to 1944. The personnel records of the other show that he worked in the melting and casting department.[6] As indicated above, however, since seniority was in the combined departments, the second man possibly spent some time at the calciner. The excess in nonmalignant respiratory disease among refinery workers is of interest due to the high dust levels in matte crushing, grinding, and handling. This excess is mainly due to influenza and pneumonia, however, and may not be due to work in the refinery. Curiously, there is no large excess in lung cancer among these refinery workers.

Among workers who were employed before 1947 and who did not work a year or more in the refinery, table 3 shows that there was a statistically significant deficit for "all causes." For individual causes SMR were somewhat lower than those for refinery workers and were generally not in excess. For nonmalignant respiratory disease there was a significant deficit in mortality. Under coding rules in effect for the Seventh Revision of the ICD, there were no deaths codable to sinonasal cancer. However, 2 deaths were noted with a known clinical diagnosis of sinus cancer. For one of these the death certificate diagnosis was listed as "carcinoma of ethmoid." Under the Seventh Revision of the ICD this death was to be coded to bone cancer. It is of interest, however, that under the Eighth Revision of the ICD this death would have been coded to sinonasal cancer. For the other death, the death certificate diagnosis was "cancer of the left maxillary." Under both the Seventh and Eighth Revisions of the ICD, this death would be coded to bone cancer. Biopsies on these two cases showed that they were probably carcinomas. The pathologist believed that they both fit a category known as "Schminke tumors"—a nasopharyngeal cancer. Richard Doll (personal communication to J. S. Warner, Oct. 8, 1980) reviewed these two cases and believed that they were compatible with a diagnosis of poorly differentiated squamous cancer of the nasal sinuses. One of the sinonasal (nasopharyngeal?) cancers among men who were employed before 1947 and who did not work a year or more in the refinery was in a man who worked in an acid-reclaim plant where copper-nickel carbonates were precipitated from pickling solutions and decomposed to copper–nickel oxide at about 1,000°C. The other was in a millwright in the polishing mill adjacent to the acid-reclaim process. It is believed that this worker did maintenance work in the acid-reclaim plant.

---

[6] During 1914–19 this man worked as a heel finisher in a shoe factory. Shoe factory workers appear to have an increased incidence of nasal cancer (*8*).

Among workers hired after 1946 table 3 shows that the SMR were generally low. There have been no deaths from sinonasal cancer among these workers. There was a slight excess in digestive and lung cancer deaths, however, and in deaths from stroke. The pattern of mortality among these workers is similar to that among refinery workers.

Table 4 summarizes some of the information available on the sinonasal cancers. Included here are estimates of nickel exposure. These will be discussed below.

In the calculation of the SMR for table 3, the expected number of deaths was derived from the experience of the entire white male population of the United States. The population in the Huntington, W. Va., area has a mortality experience differing somewhat from that of the entire United States, and some of the excesses and deficits in SMR shown in table 3 are due to this difference.

Table 5 shows how SMR differ if based on U.S. death rates, State of West Virginia death rates, and death rates for the counties in the Huntington area. Generally, local rates are higher than U.S. death rates so that the workers' mortality appears more favorable when a local comparison group is used. SMR for respiratory cancer and for stroke are lower, and the excess shown in table 3 among workers hired after 1946 disappears. However, a slight excess emerges in the cause-of-death category "leukemias–lymphomas." Use of local rates for comparison is probably the more valid, and these rates will be used where cancer SMR are calculated in the tables that follow.

Table 6 is similar to table 3 except that in table 6 only cancer mortality is shown and only those cohort members who lived 20 years or more after first exposure are examined. Also, local death rates are used in the calculation of expected deaths rather than U.S. rates. The period 20 years since first exposure is of particular interest since if carcinogens were in the environment of the plant, they probably would not produce a detectable cancer excess until this period had expired.

Table 6 shows a 40.5% excess in overall cancer mortality among the refinery workers. Only the excess for the category "other respiratory cancer" is statistically significant, however, which is due to the two sinonasal cancers discussed previously. Lung cancer does not show an important excess. For nonrefinery workers hired before 1947, SMR are only slightly elevated, but there is no important excess in respiratory cancer. Workers hired after 1946 have a low overall death rate for "all cancer" and for most sites. For all 3 groups mortality from leukemia–lymphoma is elevated, although in two instances numbers of deaths are very small. Generally, the picture we see here is a cancer death rate receding from somewhat elevated rates apparently associated with work in the old refinery.

Table 7 shows for both cohorts combined the relationship between respiratory cancer deaths and interval from onset of employment and duration of employment. The interval from onset of employment and possibly the duration of employment show some direct relationship to respiratory

TABLE 4.—*Deaths probably due to sinonasal cancer*

Date of hire	Dates at refinery	Work history	Date of death	Death certificate diagnosis	Cumulative nickel exposure,[a] mg Ni/m^3 mo		Average nickel exposure,[a] first 20 yr, mg Ni/m^3
					Overall	First 20 yr	
1924	None	1924–55—polisher, maintenance mechanic, and millwright; 1955–68—maintenance (melting and casting department); 1968—retired	1976	Carcinoma of ethmoid	53.1	7.2	0.03
1928	1929–48	1928—sheetmill and mechanical departments; 1929–33—millwright (melting and casting department); 1933–48—laborer (yard department) and ladleman (melting and casting department); 1948—retired	1964	Cancer of right maxillary and ethmoid sinus	56.7	56.7	0.24
1940	None	1940–76—laborer, pickler helper, millwright helper, pickler, furnace operator in acid reclaim, and leader in acid reclaim; 1976—retired	1977	Cancer of left maxillary	67.4	40.2	0.20
1941	1941–44	1941–44—laborer (calcining department); 1944–46—on leave; 1946–49—laborer, floorman, paperman, and pickler helper (sheetmill department); 1949—laborer (melting and casting department); 1949–55—laborer, shearman, heater helper, billy rollman, and floorman (sheetmill department); 1955–64—laborer (steel shop); 1964–66—laborer (pipe shop); 1966–67—laborer (melting and casting department); 1967–68—helper (mechanical maintenance); 1968—retired	1969	Cancer of left ethmoid and nose	208.3	199.6	0.94

[a] Estimates are based on current measurements and historic midget impinger counts.

TABLE 5.—*Observed deaths and SMR based on three standard populations for 2 groups of male nickel workers employed a year or more*

Cause of death[a]	Hired before 1947				Hired after 1946			
		SMR				SMR		
	Observed	U.S.	State	County[b]	Observed	U.S.	State	County[b]
All causes, 1960–77	596	90.5[c]	82.0[d]	84.1[d]	83	73.0[d]	57.6[d]	60.6[d]
Stroke (330–334)	54	98.8	88.8	83.2	5	126.2	86.2	76.8
All heart disease (400–440)	278	94.2	86.4[c]	90.7	25	63.0	51.4[d]	55.4[d]
Nonmalignant respiratory disease (470–527)	25	58.5[d]	43.8[d]	44.9[d]	2	46.1	28.9	32.9
All external causes (800–998)	25	74.0	59.1[d]	65.7[c]	12	50.5[c]	35.9[d]	39.2[d]
All malignant neoplasms (140–205), 1950–77	170	98.9	103.2	103.5	21	92.3	85.1	81.8
Digestive (150–159)	44	83.2	93.2	100.6	6	115.1	116.5	123.3
Respiratory (160–164)	59	109.7	106.6	101.4	10	130.2	110.1	93.2
Genitourinary (177–181)	24	99.0	109.6	107.9	1	57.1	56.8	52.4
Leukemias–lymphomas (200–205)	17	107.7	118.1	130.6	3	90.0	92.6	108.1
Other malignant neoplasms (residual)	26	103.0	100.8	96.2	1	20.9	18.4	18.6

[a] *Numbers in parentheses* refer to ICD Seventh Revision codes.

[b] White male population of Cabell, Wayne, Mason, Putnam, and Lincoln Counties (W. Va.) and Lawrence County (Ohio).

[c] $P<0.05$.

[d] $P<0.01$.

TABLE 6.—*Observed and expected deaths from malignant neoplasms and SMR[a] for 3 groups of male nickel workers employed a year or more, 20 years or more after first exposure*

Cause of death (ICD Seventh Revision codes)	Hired before 1947						Hired after 1946[b]		
	Refinery[c]			Nonrefinery[d]					
	Observed	Expected	SMR	Observed	Expected	SMR	Observed	Expected	SMR
All malignant neoplasms (140–205)	27	19.22	140.5	133	131.24	101.3	9	12.80	70.3
Digestive (150–159)	7	4.74	147.7	32	35.06	91.3	2	2.46	81.2
Respiratory (160–164)	10	7.55	132.4	49	46.62	105.1	4	6.26	63.9
Larynx (161)	0	0.28	—	2	1.86	107.8	0	0.13	—
Bronchus, trachea, lung (162–163)	8	7.14	112.0	47	43.89	107.1	4	6.07	65.9
Other (residual)	2	0.12	1,643.9[e]	0	0.87	—	0	0.07	—
Genitourinary (177–181)	3	2.35	127.6	20	18.61	107.5	1	0.97	103.1
Leukemias–lymphomas (200–205)	3	1.45	206.9	14	10.13	138.2	2	0.97	206.0
Other malignant neoplasms (residual)	4	3.13	127.8	18	20.83	86.4	0	1.12	—

[a] Expected deaths are based on death rate for white males from local six-county area.

[b] Number at risk: 1,287. Person-years at risk: 6,359.7.

[c] Number at risk: 259. Person-years at risk: 4,501.4.

[d] Number at risk: 1,533. Person-years at risk: 27,227.8.

[e] $P<0.05$.

cancer mortality. None of the SMR are statistically significant, however. These findings were consistent for both the refinery and nonrefinery workers when analyzed separately.

Table 8 shows estimates of nickel exposure made by the company for each department. These estimates are intended to represent average airborne concentrations of nickel in all forms over an 8-hour shift. Estimates have been derived by the use of limited historical sample data obtained by the midget impinger–particle counting technique and converted to modern gravimetric expression. In addition, data derived from several hundred recent gravimetric samples were used to estimate historic exposures. Whenever possible and/or applicable, the modern data were adjusted on the basis of a knowledge of process changes and environmental controls that were implemented over the years. The unadjusted extrapolation of modern sample data to historical exposures is imperfect, but it can be assumed that the historical exposures were the same or, in most cases, of greater magnitude. Substances to which workers were exposed in addition to nickel were those commonly contained in the alloys and processing. Some of these materials were chromium, iron, copper, grinding dust, solvents, and acid mists. The historical data indicate very high levels of dust at the calciner, but it was not possible to determine the various components of the dust or to identify all the species of nickel. However, the calciner is the only area where a significant exposure to nickel subsulfide, a potent nickel carcinogen in animals, would be likely.

Using the departmental exposure estimates shown in table 8, one can calculate for each worker an estimate of his cumulative and average nickel exposure based on departmental assignments, as shown in personnel records, and relate this exposure to his mortality experience. Table 9 shows SMR for respiratory cancer by a time-weighted cumulative measure of nickel exposure for each of the 3 groups of workers shown in tables 3 and 6. As in table 6, expected respiratory cancer deaths are based on the local mortality experience.

TABLE 7.—*Observed and expected respiratory cancer deaths and SMR*[a] *by interval from onset of employment and duration of employment for all male nickel workers employed a year or more*

Interval from onset of employment, yr	Parameter	Duration of employment, yr				Total
		<20	20–29	30–39	≥40	
<20	Observed deaths	6	—	—	—	6
	Expected deaths	8.53				8.53
	SMR	70.3				70.3
20–29	Observed deaths	2	16	—	—	18
	Expected deaths	6.31	14.73			21.04
	SMR	31.7	108.6			85.6
30–39	Observed deaths	2	10	17	—	29
	Expected deaths	3.07	7.74	14.26		25.07
	SMR	65.1	129.1	119.2		115.7
≥40	Observed deaths	2	3	6	5	16
	Expected deaths	0.81	1.84	7.06	4.58	14.29
	SMR	247.1	162.8	85.0	109.3	112.0
Total	Observed deaths	12	29	23	5	69
	Expected deaths	18.73	24.31	21.32	4.58	68.84
	SMR	64.1	119.3	107.9	109.3	100.1

[a] Expected deaths are based on death rates for white males from local six-county area.

TABLE 8.—*Historic*[a] *nickel exposure by department*

Department	Exposure, mg Ni/m^3
Acid reclaim	0.02
Blacksmith shop	0.02
Carpenter shop[b]	0.02
Chipping and hammer	0.75[c]
Cold drawing (acid reclaim 1970 on)	0.10[c]
Combustion[b]	0.05
Electrical[b]	0.10
Extrusion	0.20[c]
General offices[b]	0.01
Heat treatment	0.02
Machine shop	0.03[c]
Mechanical[b]	0.01
Melting and casting	0.25[c]
Merchant mill	0.30[c]
Night superintendent[b]	0.01
Pipe shop[b]	0.08
Polishing	0.10[c]
Primary mill	0.06
Reduction pilot plant	0.02
Refinery	5.00[c]
Research and development[b]	0.05
Roll grinding	0.03
Roll turning	0.03
Sheet mill (acid reclaim to 1970)	0.20[c]
Shipping	0.01
Standards or industrial engineering[b]	0.01
Steel shop[b]	0.12
Stocks	0.01
Stores	0.01
Strip mill	0.20[c]
Transportation[b]	0.01
Vacuum melting	0.15
Welding products	0.02
Yard[b]	0.10
Warehouse	0.01
Watchman[b]	0.01
Inspection (unassigned)[b]	0.05

[a] Based on current measurements except as noted.

[b] Plant-wide work assignment.

[c] Based on historic midget impinger counts.

Table 9 shows some trends in respiratory cancer mortality related to exposure. However, these trends are not consistent. Refinery workers at the highest exposure level have the greatest respiratory cancer excess, but for nonrefinery workers at this exposure level there is a deficit. The four cancer cases described in table 4 did not have unusually high nickel exposures. Three would fall in the exposure group 50–99 mg Ni/m^3 months, whereas one would fall in the highest grouping 200 or more. Only the two sinonasal cancers among refinery workers are included in table 9, and the presence of these cancers does not greatly affect the trends shown.

One problem with table 9 is that for those who died exposures are counted up to the time of death. Exposures during some period before a death from respiratory cancer would probably have little to do with the respiratory cancer and should, therefore, be excluded. In addition, respiratory cancer deaths could have been included that occurred within 20 years of hire, and as noted in table 6, these deaths probably would be unrelated to exposure at the plant due to long latent period for this type of cancer. These two problems are partly corrected in table 10 where only exposure during the first 20 years from date of hire is related to mortality 20 years or more after date of hire. The dose-response relationship is somewhat weaker here in contrast to that seen in table 9. Removal of the two sinonasal cancers has little effect on the relationships shown in tables 9 and 10 so that there is apparently a slight direct relationship between nickel exposure and lung cancer. This relationship is probably not simply the result of confounding due to combining unlike subgroups because there is some evidence for a direct relationship in the 3 subgroups.

If exposure groups in table 10 (r=0.53) are recombined as shown in table 11, a much stronger relationship emerges (r=0.79). We do not know whether this is an artifact because these exposure categories were deliberately chosen from those in table 10 to produce a stronger relationship. The relationship shown here and in tables 9 and 10 holds when rates are adjusted by the direct method, so it is not an artifact resulting from use of an indirect adjustment method. Even in the highest exposure category, however, the SMR is not greatly elevated, and none of the SMR are statistically significant. The linear regression equations derived from data in tables 10 and 11 are very similar. For table 10 the regression equation is $y=101.66+0.11x$, whereas for table 11 it is $y=96.27+0.12x$. Thus, if this represents an underlying relationship, it is not much affected by regrouping as in table 11. This model predicts very little response at zero dose. A better fitting model ($r=0.99$) for the data in table 11 is a logarithmic model of the form $y=a+b \ln x$; however, this model is not appropriate for predicting response at zero dose.

One question that might be raised about table 11 is whether the nonrefinery group may show a dose-response relationship because of some brief exposure in the refinery. Of the total 1,589 men in the nonrefinery group, 138 actually worked briefly in the refinery (<1 yr). However, the respiratory cancer death rate in this group of 138 men was not excessive (SMR=74.9). Thus the inclusion of this small group of men with the nonrefinery group is not the reason for the dose-response relationship shown in table 11.

Probably a more important question is whether the dose-response relationship shown in table 11 is peculiar to respiratory cancer or applies to several or all causes of death. If several causes of death are involved, particularly deaths other than cancer deaths, then evidence that nickel is related

TABLE 9.—*Observed and expected deaths from respiratory cancer and SMR[a] for 3 groups of male nickel workers by cumulative nickel exposure*

Cumulative nickel exposure, mg Ni/m³ mo	Hired before 1347						Hired after 1946			All workers		
	Refinery			Nonrefinery								
	Observed	Expected	SMR	Observed	Expected	SMR	Observed	Expected	SMR	Observed	Expected	SMR
<10	0	0.05	—	7	11.48	61.0	3	4.92	61.0	10	16.45	60.8
10–24	0	0.33	—	4	8.18	48.9	4	2.49	160.5	8	11.00	72.7
25–49	0	0.76	—	16	11.99	133.5	3	2.19	136.8	19	14.94	127.2
50–99	3	2.48	121.2	14	10.78	129.9	0	0.92	—	17	14.18	119.9
100–199	2	1.80	111.1	5	3.94	126.8	0	0.19	—	7	5.93	118.0
≥200	5	2.67	187.6	3	3.75	79.9	0	0.04	—	8	6.46	123.8

[a] Expected deaths are based on death rates for white male population from local six-county area.

TABLE 10.—*Observed and expected deaths from respiratory cancer and SMR[a] for 3 groups of male nickel workers 20 years after first exposure by cumulative nickel exposure up to 20 years from onset of exposure*

Cumulative nickel exposure, mg Ni/m³ mo[b]	Hired before 1947						Hired after 1946			All workers		
	Refinery			Nonrefinery								
	Observed	Expected	SMR	Observed	Expected	SMR	Observed	Expected	SMR	Observed	Expected	SMR
<10 (4.20)	0	0.04	—	10	13.22	75.6	1	2.70	37.1	11	15.96	68.9
10–24 (18.89)	0	0.34	—	15	13.26	113.2	3	1.66	181.1	18	15.26	117.9
25–49 (39.03)	0	1.00	—	10	10.35	96.6	0	1.24	—	10	12.59	79.5
50–99 (64.37)	4	3.08	129.8	10	4.43	225.8[c]	0	0.53	—	14	8.04	174.1
100–199 (160.91)	2	0.61	330.2	4	5.35	74.8	0	0.14	—	6	6.10	98.4
≥200 (563.80)	4	2.48	161.1	None at risk			None at risk			4	2.48	161.1

[a] Expected deaths are based on death rates for white male population from local six-county area.
[b] *Numbers in parentheses* are arithmetic means of worker exposure.
[c] $P<0.05$.

TABLE 11.—*Observed and expected deaths from respiratory cancer and SMR[a] for 3 groups of male nickel workers 20 years after first exposure by cumulative nickel exposure up to 20 years from onset of exposure*

Cumulative nickel exposure, mg Ni/m³ mo[b]	Hired before 1947						Hired after 1946			All workers		
	Refinery			Nonrefinery								
	Observed	Expected	SMR	Observed	Expected	SMR	Observed	Expected	SMR	Observed	Expected	SMR
<10 (4.20)	0	0.04	—	10	13.22	75.6	1	2.70	37.1	11	15.96	68.9
10–49 (27.50)	0	1.34	—	25	23.63	105.8	3	2.90	103.4	28	27.87	100.5
50–199 (99.53)	6	3.69	162.6	14	9.78	143.1	0	0.67	—	20	14.14	141.4
≥200 (563.80)	4	2.48	161.1	None at risk			None at risk			4	2.48	161.1

[a] Expected deaths are based on death rates for white male population from local six-county area.
[b] *Numbers in parentheses* are arithmetic means of worker exposure.

TABLE 12.—*Observed and expected deaths and SMR*[a] *for all male nickel workers employed a year or more 20 years after first exposure by cumulative nickel exposure up to 20 years from onset of exposure, selected causes of death*

Cause of death (ICD Seventh Revision codes)	Cumulative nickel exposure, mg Ni/m^3 mo											
	<10			10–49			50–199			≥200		
	Observed	Expected	SMR	Observed	Expected	SMR	Observed	Expected	SMR	Observed	Expected	SMR
All causes	190	230.30	82.5[b]	335	374.30	89.5	223	217.35	102.6	34	32.88	103.4
All malignant neoplasms (140–205)	29	42.96	67.5[c]	78	74.00	105.4	52	39.88	130.4	10	6.44	155.2
Digestive (150–159)	6	11.03	54.4	17	18.87	90.1	14	10.76	130.1	4	1.60	249.6
Stomach	1	2.14	46.7	4	3.59	111.4	5	2.10	238.1	0	0.30	—
Colorectal	1	4.44	22.5	5	7.52	66.5	4	4.25	94.1	1	0.62	161.3
Other (residual)	4	4.44	90.1	8	7.77	102.9	5	4.41	113.4	3	0.68	441.2
Respiratory (160–164)	11	15.97	68.9	28	27.83	100.6	20	14.14	141.4	4	2.48	161.1
Genitourinary (177–181)	5	5.79	86.4	10	9.71	103.0	9	5.62	160.1	0	0.82	—
Prostate gland (177)	4	3.55	112.7	6	5.67	105.8	7	3.52	198.9	0	0.43	—
Other (residual)	1	2.72	36.8	4	4.66	85.8	2	2.63	76.0	0	0.39	—
Other (residual)	7	10.17	68.8	23	17.56	131.0	9	9.36	96.2	2	1.54	129.9
Stroke (330–334)	18	19.85	90.7	30	30.36	98.8	29	18.77	154.5[c]	2	2.43	82.2
All heart disease (400–440)	89	102.89	86.5	152	170.79	89.0	95	98.34	96.6	14	14.80	94.6
Nonmalignant respiratory disease (470–527)	11	13.27	82.9	12	22.64	53.0[c]	9	13.01	69.2	2	1.92	103.9
All other causes (residual)	43	50.47	85.2	63	83.33	75.6[c]	38	45.35	83.8	6	7.09	84.6

[a] Expected deaths for cancer are based on death rates for white male population from local six-county areas; all others are based on death rates for U.S. white males.

[b] $P<0.01$.

[c] $P<0.05$.

to respiratory cancer in this instance would be weakened. Table 12 shows for both cohorts of nickel workers SMR by dose for several causes of death. There is a weak dose-response relationship for all causes of death, which, however, is primarily due to a direct relationship between dose and cancer deaths. Other major causes of death categories do not show any marked relationship to dose. Within the cancer category the relationship is with digestive, respiratory, and genitourinary cancers. Further subdivision of the categories "digestive and genitourinary" shows that there are slight excesses in stomach and prostate cancers and that these cancers are related to dose. Colorectal cancer was not in excess but was also dose related. The high SMR (441.2) for other digestive cancers in the highest dose category was due to two cancers in the cause-of-death category "cancer of the liver and biliary passages." One was a cancer of the gall-bladder, and one was a malignant hepatoma. Both men with these cancers had worked at the calciner. Overall, however, this cause-of-death category was not in excess (observed, 4; expected, 4.2). A Russian study has implicated nickel in stomach cancer, and a recent study of nickel platers suggests a stomach cancer excess (*9, 10*). A statistically significant prostate cancer excess has been reported for workers at mines, mills, and a smelter in the Sudbury area of Ontario (*11*). We do not know of any other studies reporting colorectal or liver cancer in nickel workers, and perhaps our observations on these cancers are unimportant.

DISCUSSION

The discovery of sinonasal cancer among nickel refinery workers at Huntington, W. Va., is important, particularly in light of similar findings in other studies. While only one sinonasal cancer was clearly related to actual nickel refining (calcining), given the small number (109) of workers in that operation the relative risk there was very high. Other studies have suggested that furnace work in nickel refineries carries a high risk of producing sinonasal cancer [(*1–3*); Sutherland RB: Mortality among sinter plant workers. Toronto: Report of the Division of Industrial Hygiene, Ontario Department of Health, 1969]. There is evidence here that sinonasal cancer patients had worked in acid reclaim, a high-temperature decomposition process, and these findings may support that theory. The actual nickel exposure of the sinonasal cancer patients was not unusually high.

For lung cancer there was no marked overall excess, which is an unexpected finding in view of an excess reported in other studies. It would seem that if exposure to nickel or its compounds produced sinonasal cancer at the Huntington refinery, a greater excess in lung cancer should have appeared. Nickel exposures may have been considerably lower at Huntington than in other studies, however. It has been noted that dust concentrations around the calciners were much lower than those at Clydach, Port Colborne, or Copper Cliff (International Nickel Co., Ltd.: Nickel and its inorganic compounds. Report submitted to the National Institute for Occupational Safety and Health, Oct. 1976), which may in part account for the lack of any large excess. It is also possible that lower or different exposures are involved in sinonasal cancer than in lung cancer. However, the fact that there is some evidence of a dose-response relationship for lung cancer suggests that even at these lower exposure levels, some causal relation between lung cancer and nickel exposure may have been present. The problem may be simply one of detecting an excess at these lower exposure levels. Stomach and prostate cancers have been reported in excess in other studies, and it may be significant that in this study these cancers are slightly in excess and appear to be dose related.

REFERENCES

(1) Doll R, Mathews JD, Morgan LG. Cancers of the lung and nasal sinuses in nickel workers: A reassessment of the period of risk. Br J Ind Med 1977; 34:102–105.

(2) Pedersen E, Andersen A, Hogetveit A. Second study of the incidence and mortality of cancer of respiratory organs among workers at a nickel refinery. Ann Clin Lab Sci 1978; 8:503–504.

(3) Mastromatteo E. Nickel: A review of its occupational health aspects. J Occup Med 1967; 9:127–136.

(4) Marsh GM, Enterline PE. A method for verifying the completeness of cohorts used in occupational mortality studies. J Occup Med 1979; 21:665–670.

(5) Marsh GM, Preininger M. OCMAP: A user-oriented occupational cohort mortality analysis program. Am Statistician 1980; 34:245–246.

(6) National Office of Vital Statistics, U.S. Dept of Health, Education, and Welfare, Public Health Service. Comparability of mortality statistics—special reports—selected studies. Washington, D.C.: U.S. Govt Print Off, vol 51, No. 4 (March 1965); series 2, No. 66 (1975).

(7) Bailar JC III, Ederer F. Significance factors for the ratio of a Poisson variable to its expectation. Biometrics 1964; 20:639–643.

(8) Acheson ED. Occupationally induced diseases. Prev Med 1976; 5:309–311.

(9) Saknyn AV, Shabynina N. Some statistical data on carcinogenous hazards for workers engaged in the production of nickel from oxidized ores. Gig Tr Prof Zabol 1970; 14:10 (in Russian).

(10) Burges DC. Mortality study of nickel platers. In: Brown SS, Sunderman FW, eds. Nickel toxicology. London: Academic Press, 1980:15–18.

(11) Shannon HS, Cecutti AG, Julian JA, Muir DC, Roberts RS. Mortality studies in Ontario nickel workers—the Falconbridge project. In: Brown SS, Sunderman FW, eds. Nickel toxicology. London: Academic Press, 1980:23–26.

best copy available

blank page

Cell-Mediated Immunity to Mouse Mammary Tumor Virus Antigens by Patients With Hyperplastic Benign Breast Disease[1,2,3]

G. B. Cannon,[4] S. H. Barsky,[5] T. C. Alford,[6] L. F. Jerome,[4] V. Tinley,[6] J. L. McCoy,[7,8] *and* J. H. Dean[4,9]

ABSTRACT—Peripheral blood leukocytes of patients with preoperative breast cancer, benign breast disease, and benign gynecologic disorders and normal healthy females were tested, as blind coded specimens, with murine mammary tumor virus (MuMTV) antigens in the direct and indirect leukocyte migration inhibition (LMI) assays. The incidence of reactivity by patients with breast cancer was low. (From 5 to 35% breast cancer patients reacted, depending on which group of control individuals they were compared to and what antigen was used.) Nonparametric analyses showed no differences between control groups (normal donors and patients with gynecologic disorders) and breast cancer patients with either assay. However, there was a significant difference between benign breast disease patients with hyperplasia and 1) benign breast disease patients without hyperplasia ($P<0.03$) and 2) patients with gynecologic disorders ($P<0.04$) in the direct assay when it was performed blindly with the gp52 antigen. Patients with hyperplasia (benign breast disease as well as breast cancer) had a higher incidence of enhanced migration in the indirect test than breast disease patients without hyperplasia. The enhanced migration to the MuMTV was correlated to enhanced migration to a 3-*M* KCl extract of the breast cancer cell line MCF-7 in simultaneous tests. Thus the LMI assays with MuMTV antigens do not appear valuable in breast cancer diagnosis, but they may help to identify a small group of benign breast disease patients whose breast pathology is thought to be associated with a high risk for developing breast cancer.—JNCI 1982; 68:935–943.

The MuMTV has been shown to have some immunologic relationship to human breast cancer. Antibodies to the glycoprotein coat (gp52) of the MuMTV were found to bind to breast tumor tissue and not to normal tissue (*1*), and IgG in the sera of breast cancer patients bound to MuMTV-infected cells (*2, 3*). IgG binding to MuMTV was seen more frequently with sera from breast cancer patients than with sera from patients with benign breast disease or from normal individuals (*4*). Leukocytes from postoperative breast cancer patients were also found to react to MuMTV in the LMI assay (*5, 6*).

Although the basis for the development of breast cancer-associated reactivity against MuMTV antigens is unclear, it seemed possible that detection of such activity might be useful for early diagnosis of cancer or for detection of groups of women at high risk of developing breast cancer. The present study was set up to evaluate the possible application of the LMI assay with MuMTV antigens in the diagnosis of breast cancer. Preoperative patients with breast disease as well as normal hospital workers and preoperative patients with a variety of benign gynecologic diseases were tested in the direct and indirect LMI assays. Since a considerable portion of patients with benign breast disease were found to be reactive, their lesions were classified according to the degree of hyperplasia, and this information was compared with the LMI results to determine whether LMI reactivity was associated with a particular type of benign breast disease.

MATERIALS AND METHODS

Source of leukocytes.—Leukocytes were obtained from heparinized whole-blood samples that were sent under code from the George Washington University Hospital, Washington, D.C. All blood donors were from this hospital and included patients just prior to biopsy for evaluation of breast disease (and subsequently shown to have either breast cancer or benign breast disease), patients with benign gynecologic disorders, and normal female hospital personnel. The mean ages in years and age ranges for each of these groups were as follows: breast cancer patients, 56.5 (24–85); patients with benign breast disease, 41 (19–76); patients with gynecologic disorders, 41 (26–57); and normal female hospital personnel, 33 (21–64).

Pathology.—All breast biopsy specimens had been previously processed for routine light microscopy. This procedure included extensive sectioning of each biopsy specimen, fixation in 10% buffered Formalin, dehydration in a series of graded alcohols (70–100%) and xylol, paraffin embedding, 6-μm cryostat sectioning, and staining with hematoxylin and eosin.

Histologic sections of all the biopsy specimens of the

ABBREVIATIONS USED: HAN=hyperplastic alveolar nodules; LMI=leukocyte migration inhibition; MI=migration index (indices); MuMTV=murine mammary tumor virus; PAGE=polyacrylamide gel electrophoresis; PBS=phosphate-buffered saline; PMN=polymorphonuclear; PPD=purified protein derivative.

---

[1] Received August 21, 1981; accepted January 15, 1982.

[2] Supported by Public Health Service contract N01CB-74087-S from the Breast Cancer Task Force, Division of Cancer Biology and Diagnosis, National Cancer Institute.

[3] Research procedures were in accord with the Office of Human Research, George Washington University.

[4] Immunotoxicology Section, Litton Bionetics, Inc., 5516 Nicholson Lane, Kensington, Md. 20795.

[5] Laboratory of Pathology, Division of Cancer Biology and Diagnosis, National Cancer Institute, National Institutes of Health, Public Health Service, U.S. Department of Health and Human Services, Bethesda, Md. 20205.

[6] Department of Surgery, George Washington University Medical Center, Washington, D.C. 20006.

[7] Laboratory of Immunodiagnosis, Division of Cancer Biology and Diagnosis, National Cancer Institute.

[8] *Present address:* Carcinogenesis Testing Program, Toxicology Branch, Division of Cancer Cause and Prevention, National Cancer Institute.

[9] *Present address:* National Institute of Environmental Health Sciences, National Institutes of Health, Research Triangle Park, N.C. 27709.

benign breast lesions were reevaluated without knowledge of the LMI results. The sections were classified into categories 0 through 5 according to the magnitude of proliferation of epithelial cells. The categories were: 0) fat or stroma, occasional cysts; 1) prominent cysts, apocrine metaplasia, focal adenosis; 2) prominent sclerosing adenosis, crowding of ducts and acini, prominent apocrine metaplasia, but no intraductal proliferation; 3) intraductal proliferation either in the form of papillomatosis or hyperplasia; 4) intraductal papilloma; and 5) extremely atypical hyperplasia. A number of the cases had more than one biopsy more than 1 month apart; these were consistently placed in the same category, and the reader was unaware that there was a previous biopsy and what the classification of the biopsy specimen was.

Antigens.—MuMTV, purified from the supernatant of the mouse mammary tumor tissue-cultured cell line MM5 by density gradient sedimentation, was obtained from the NCI-Frederick Cancer Research Facility, Frederick, Md. The gp52 was supplied by Dr. Wade Parks, University of Miami School of Medicine, Miami, Fla., by a method previously described (*7*).

The MCF-7 antigen was a 3-*M* KCl extract prepared from a large pool of this human breast cancer-derived cell line by a method described previously (*8*).

Direct LMI assay.—The direct LMI assay measures the capacity of the test individual's lymphocytes to produce a lymphokine in response to the antigens and also the capacity of their PMN cells to respond to the lymphokine by inhibition of migration. The procedure has been described previously (*8*). Leukocytes were separated from red blood cells by gravity sedimentation of heparinized whole blood on Plasmagel and incubated with the antigen (25 μg MuMTV, 50 μg MCF-7, or 0.5–1 μg gp52) at 37°C for 45 minutes. They were then drawn into 25-μl capillary pipettes, which were then centrifuged, cut, and placed in Sterilin chambers to which McCoy's 5-A medium, supplemented with 10% fetal bovine serum and 100 μg gentamicin/ml, had been added. After the mixture was incubated for 18–24 hours, the circles of migration (×20) were projected onto paper with an inverted microscope, drawn, and later measured by planimetry. The data were expressed as an MI, which is the mean migration area of four replicates in the presence of antigen divided by the mean migration area of four replicates in the absence of antigen.

Indirect LMI assay.—The indirect LMI assay measures the capacity of the test individual's lymphocytes to produce a lymphokine in response to the antigen. Lymphokine production is then measured by a test of the culture supernatant for inhibition or enhancement of migration of a normal donor's PMN cells. The procedure was described previously by McCoy et al. (*9*). Mononuclear cells were separated from whole blood by Ficoll–Hypaque (lymphocyte-separating medium; Litton Bionetics, Inc., Kensington, Md.) flotation. Cells were washed with PBS, concentrated by centrifugation, and adjusted to a concentration of 1×10^{6} cells in RPMI-1640 medium with 1% human serum (blood group AB), glutamine, gentamicin, and HEPES[10] buffer, and 0.1 ml was dispensed into microtubes (Bel-Art Products, Pequannock, N.J.). Antigen (25 μg MuMTV or 50 g MCF-7) was added in a 0.1-ml volume. Control tubes contained 0.1 ml medium without antigen in addition to the cells. Tubes were incubated for 2–6 hours and centrifuged for 5–10 minutes at 200×*g*, and the supernatants were removed. Fresh medium (0.2 ml) was added to each tube, and the cells were resuspended and incubated at 37°C for 24 hours. The supernatant containing the lymphokine was removed, stored at −70°C for 1–2 weeks, and then assayed on the donors' PMN cells. The PMN cells were obtained from heparinized blood by a two-step procedure. Whole blood was layered onto Plasmagel and incubated for 45–60 minutes at 37°C. The fluid layer was removed, diluted with PBS up to 40 ml, and underlaid with 10 ml Ficoll–Hypaque. After centrifugation at 400×*g* for 30 minutes, the PMN cells were located in the pellet. After resuspension and washing once, the PMN cells were resuspended in agarose at 1×10^{8}/ml and dispensed by droplets into flat-bottom wells of microtiter plates. When the agarose solidified after 1–2 minutes, 0.1 ml of tenfold dilutions of the supernatant to be tested diluted was added to each well. After the mixture containing PMN cells and supernatant was incubated, at 37°C for 18–24 hours in a 5% CO_2 incubator, inner and outer circles were traced from projections of a microscope with a 10× lens. The net area of migration was then calculated. The MI was the mean of the replicates for the experimental group divided by the mean of the replicates for the control culture supernatant.

Statistical analysis.—MI of the various clinical groups were compared by the Wilcoxon rank sum test, or the proportions of reactive individuals in the various groups were compared by chi-square analysis.

To define reactive individuals, we used cutoffs based on the MI of 3 groups of control individuals. The cutoff was set at the lower tenth percentile of the results of the control group so that 10% or less of the MI values of the control group would fall below it. The 3 groups of controls were: 1) the normal donors, 2) the patients with preoperative gynecologic diseases, and 3) the preoperative patients in the combined benign breast disease categories 0, 1, and 2 (i.e., the group lacking intraductal proliferation). Thus it was possible to determine the reactivity of cancer or benign breast disease patients relative to that of the 3 groups of controls.

RESULTS

Direct LMI Assay With gp52 Antigen

Blind study.—The direct LMI assay was performed on 85 individuals by a technician who had no knowledge of the diagnosis of any of the individuals. One of us reevaluated the histologic slides of all the patients with benign breast disease without any knowledge of the test results. Text-figure 1 is a scattergram of the MI of the patients and controls and is based on the reevaluated pathology. By the Wilcoxon rank sum test, the MI of the patients with benign breast disease in category 3 were significantly different from those of the patients with gynecologic disorders ($P<0.04$) and the

---

[10] 4-(2-Hydroxyethyl)-1-piperazine ethanesulfonic acid.

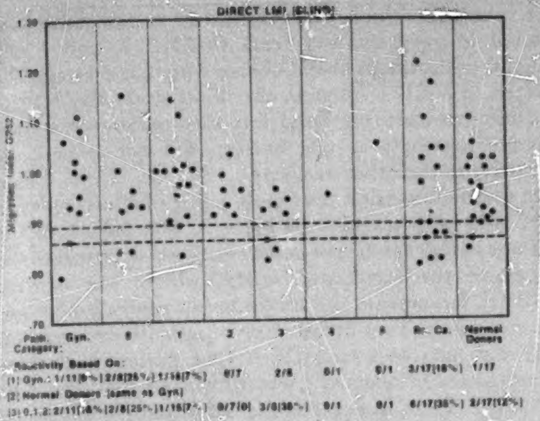

TEXT-FIGURE 1.—Scattergram of MI of patients with gynecologic disorders, patients with benign breast disease in categories 0 through 5 (as described in "Materials and Methods"), breast cancer patients, and normal donors tested blindly with gp52 in the direct LMI assay. - - -, the cutoffs based on the normal donors or control patients with gynecologic disorders (*lower line*) or on the reactivity of patients with benign breast disease in categories 0, 1, or 2 (*upper line*). Along the *abscissa* are indicated the No. of individuals below each cutoff/total No. tested (% positive).

patients with benign breast disease in combined categories 0, 1, and 2 ($P<0.03$). None of the results obtained from the patients in the other groups were significantly different from those obtained from any of the control groups. The cutoff for the normal donors and the patients with gynecologic disorders was the same (0.86), and it was used to evaluate the proportion of reactive individuals among the patients with benign breast disease in the other categories. Breast cancer patient reactivity was 3 of 17 (18%) as compared to an overall reactivity of 5 of 40 (13%) among the patients with benign breast disease. Two of 8 (25%) patients with benign breast disease in categories 0 and 3 reacted as compared to 1 of 15 (7%) of the patients with benign breast disease in category 1 and none of the patients with benign breast disease in categories 2, 4, and 5. If the lower tenth percentile of the MI of the patients with combined categories 0, 1, and 2 benign breast disease with the least hyperplasia was used as a cutoff (0.89), 3 of 8 (38%) of the patients with benign breast disease in category 3 and 6 of 17 (35%) of the breast cancer patients reacted. None of these proportions were significantly different by chi-square analysis.

Double-blind study.—Another group of 102 individuals was assyed in the direct LMI test with the gp52 antigen, and the assay was performed double blindly; i.e., the technician performed the first part of the assay, and one of us drew the circles of migration and performed the planimetry measurements. Both individuals had no knowledge of the diagnosis of any of the test subjects. Again, the slides of the benign breast disease patients were reevaluated without any knowledge of the test results. The results are shown in text-figure 2. None of the groups were significantly different from each other when evaluated by the Wilcoxon rank sum test. Cutoffs of the 3 groups of controls were also used to evaluate the results. On the basis of the cutoff of 0.91 for the patients with gynecologic disorders, the normal donors' and the breast cancer patients' reactivities were similar (13%). Two of 12 (17%) patients with benign breast disease in category 0 and 2 of 17 patients with benign breast disease in category 1 were reactive, as compared to none of the patients with benign breast disease in categories 2, 3, 4, and 5. When an even more conservative cutoff (0.83) was set, based on the normal donor's reactivity, most individuals in all patient groups were unreactive or had very little reactivity (8% for patients with benign breast disease in category 1 and 7% for breast cancer patients). When the MI of the patients with benign breast disease in combined categories 0, 1, and 2 were used to set the cutoff (0.93), 2 of 5 of the patients with category 3 benign breast disease and 4 of 15 (27%) of the breast cancer patients reacted; however, 2 of 14 (14%) of the patients with gynecologic disorders and 2 of 16 (13%) of the normal donors reacted. None of these proportions differed by chi-square analysis.

Blind and double-blind studies combined.—If the results of blind studies were combined and analyzed relative to the benign breast disease (categories 0, 1, and 2) cutoff, 5 of 13 (38%) patients with benign breast disease in category 3 and 10 of 32 (31%) breast cancer patients reacted. By chi-square analysis, the reactivity of patients with benign breast disease in category 3 and the reactivity of the breast cancer patients were significantly different from the reactivities of patients with benign breast disease in categories 0, 1, and 2 ($P<0.05$), but neither differed significantly from the reactivities of the patients with gynecologic disorders or the normal donors.

Direct LMI Assay With MuMTV

Blind study.—Many of the individuals tested with gp52 were also tested with MuMTV. None of the groups differed significantly from each other by the Wilcoxon rank sum test. Again, the cutoffs for the normal donors and the patients with gynecologic disorders were more conservative (0.84 and 0.85, respectively), and only 4 of 44 (9%) benign breast disease patients reacted as compared to 3 of 21 (14%) breast cancer patients. With the cutoff for the patients with benign breast disease (categories 0, 1, and 2), 1 of 5 patients

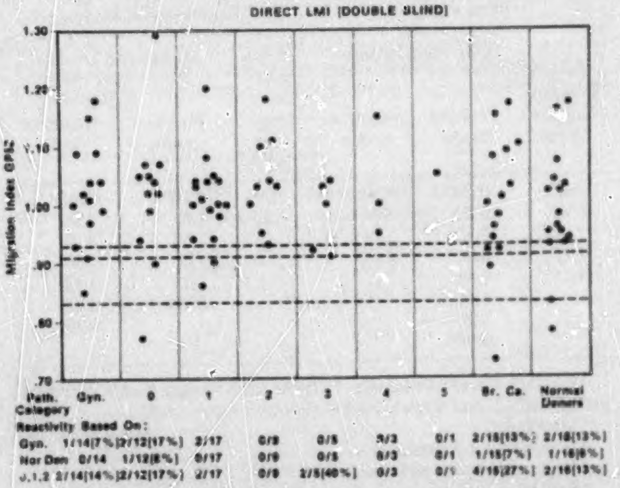

TEXT-FIGURE 2.—Scattergram of MI of patients as in text-fig. 1, but these individuals were tested double blindly. Nor Don=normal donors.

with benign breast disease in category 3, 1 of 2 patients with benign breast disease in category 4, and 4 of 21 (19%) breast cancer patients reacted.

Double-blind study.—None of the groups reacted in the double-blind study with MuMTV with the use of any of the cutoffs. All groups were similar by the Wilcoxon rank sum test. Thus in this series of tests, the intact virus antigen did not discriminate preoperative breast cancer reactivity from that of any of the control groups.

Breast cancer reactivity to gp52 relative to histology of the breast tumors.—At least half of the reactive breast cancer patients had infiltrating lesions and at least one positive lymph node—4 of 6 in the blind study and 2 of 4 in the double-blind study (table 1). Among patients with invasive cancer but negative lymph nodes, only 1 of 4 in the blind study and 2 of 7 in the double-blind study reacted if the cutoffs for the patients with benign breast disease in categories 0, 1, and 2 were used for the evaluation. Only 1 of 7 patients with in situ lesions reacted. The patient with the highest index (1.21) had an in situ lesion associated with hyperplasia.

Direct LMI With gp52 and MCF-7 in Paired Experiments

Many patients tested with gp52 were tested simultaneously with MCF-7. The blind and double-blind tests were analyzed separately. The lower tenth percentile of MI for the patients with benign breast disease in categories 0, 1, and 2 combined was used as a cutoff for each antigen. These data are shown in text-figure 3 (A–C) and are summarized in table 2. In the blind study, the MI of all groups of patients were positively correlated to these two antigens but were only significantly correlated with MI of the normal individuals and the patients with benign breast disease in categories 0, 1, and 2 combined. Four of 6 breast cancer patients who reacted to gp52 did not react to MCF-7, and 1 of the patients with benign breast disease who reacted to gp52 also reacted to MCF-7. Thus in the blind study the MI to the two antigens were correlated, but often patients who showed positive reactivity to one antigen did not show positive reactivity to the other antigen.

In the double-blind tests, only a few patients tested with gp52 were also tested with MCF-7. The MI of all tested patients except the breast cancer patients were combined to determine the correlation index, which was significant ($P<0.01$). In contrast, the MI for breast cancer patients were not correlated. Two breast cancer patients who reacted to gp52 did not react to MCF-7. One patient with benign breast disease in category 1 who reacted to gp52 also reacted to MCF-7. Thus, in general, the MI of individuals tested in either the blind or double-blind studies were correlated, with the possible exception of those of the breast cancer patients.

TABLE 1.—*MI of patients with breast cancer, categorized by histology of lesions in direct LMI assay with gp52*

MI					
Blind study			Double-blind study		
In situ invasion: Negative node	Infiltrating invasion: Positive node	Infiltrating invasion: Negative node	In situ invasion: Negative node	Infiltrating invasion: Positive node	Infiltrating invasion: Negative node
0.81[a]	**0.84**[a]	**0.82**[a]	0.94	**0.[illegible]**[a]	**0.92**[a]
0.92	**0.86**[a]	1.04	1.00	1.01	0.96
1.04	**0.87**[a]	1.04		1.08	1.03
1.17	**0.87**[a]	0.98[b]		1.09	1.08
1.21[c]	0.89			1.17	1.15
	0.91			**0.73**[a,d]	1.13[e]
	1.02				**0.89**[a,f]
	0.97[f]				

[a] Positive MI are boldface. Patients with benign breast disease in categories 0, 1, and 2 were used to determine the cutoff.

[b] Medullary.

[c] In situ with hyperplasia.

[d] Inflammatory or metastatic.

[e] Colloid.

[f] Tubular.

Indirect LMI Assay With MuMTV Antigen

Migration inhibition.—The indirect LMI assay was performed on 213 individuals with MuMTV as the antigen, and three dilutions of the supernatants were tested for lymphokine. To evaluate the data for evidence of a migration inhibitory lymphokine, we compared the lowest indices obtained for each individual at any of the three dilutions among the various patient and control groups. As in the direct assay, all these blood samples were tested blindly. In addition, usually a different technician than the one who set up the assay and drew the circles measured the circles, so the test was usually double blind. Again, the histologic slides of all the patients with benign breast disease were reevaluated without any knowledge of the test results. Cutoffs were set at the lower tenth percentile of the same 3 groups of control individuals used in the direct LMI analysis. The least reactive control group was the patients with gynecologic disorders, and the cutoff based on their reactivity was 0.91. With this cutoff, 17 of 49 (35%) breast cancer patients, 35 of 83 (42%) benign breast disease patients, and 13 of 42 (30%) normal donors reacted. Patients with benign breast disease in categories 0, 1, and 4 were particularly reactive at 44, 48, and 67%, respectively. With the normal donors' MI used to calculate the cutoff, only 9 of 49 (18%) breast cancer patients reacted as compared to 8 of 25 patients with benign breast disease in category 0 and 11 of 33 (33%) patients with benign breast disease in category 1. When the MI of patients with benign breast disease in categories 0, 1, and 2 were combined to form the cutoff, the breast cancer reactivity was very low (6%). None of the groups differed from each other by the Wilcoxon rank sum test. Thus the indirect LMI assay with the MuMTV antigen failed to discriminate among the groups when the lowest MI were compared among the various groups.

Migration enhancement.—A lymphokine that causes enhanced migration of granulocytes has been described (*10*). Therefore, these same data were evaluated for the possible presence of such a lymphokine. To evaluate whether any test group had increased migration, we compared the high-

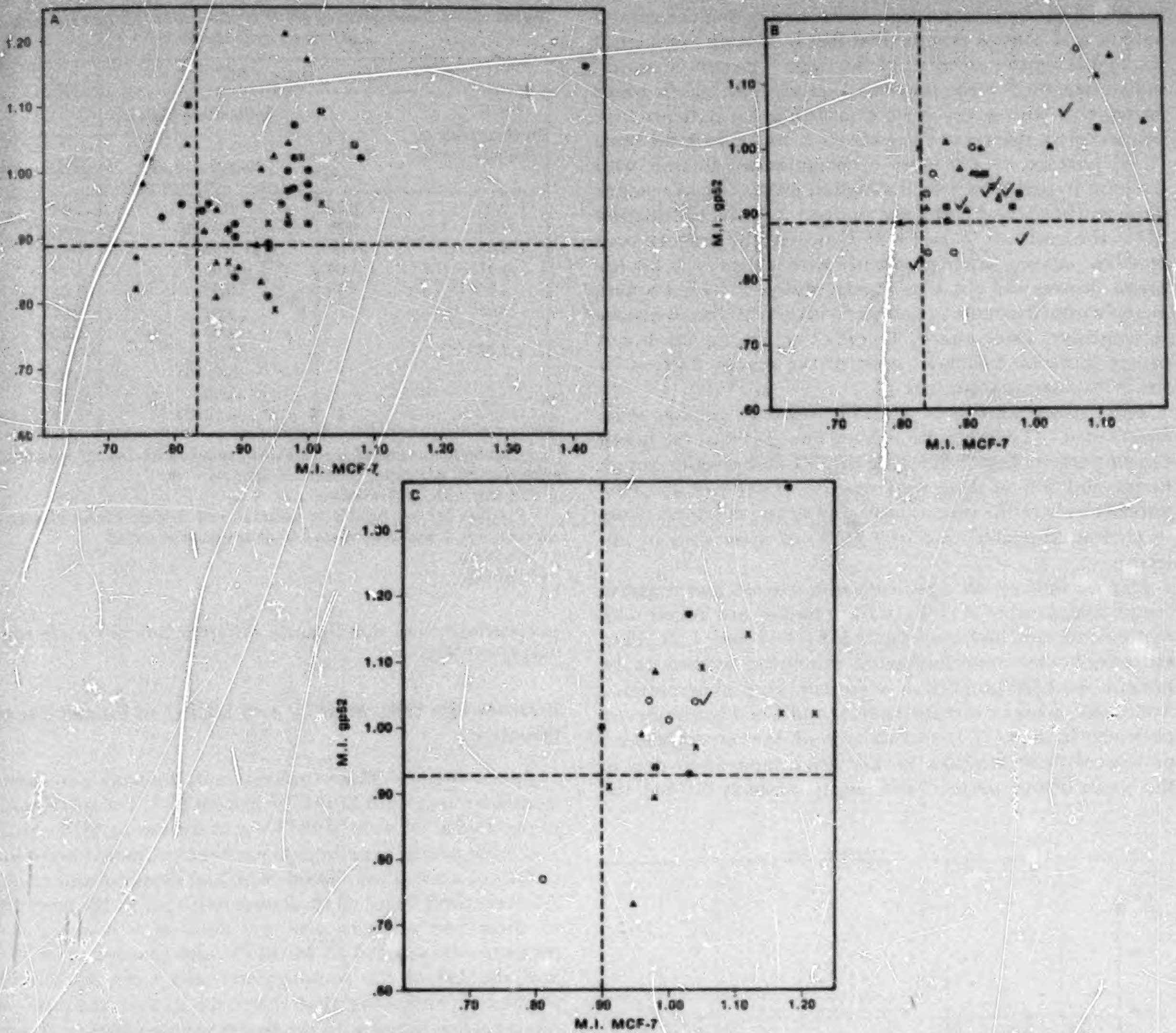

TEXT-FIGURE 3.—Correlation diagram of MI of test individuals assayed simultaneously with gp52 and MCF-7 when the assay was performed blindly. A) Normal donors (●), breast cancer patients (▲), and patients with gynecologic disorders (x). B) Patients with benign breast disease in categories 0 (○), 1 (▲), 2 (■), 3 (√), and 4 (4). C) Assay was performed double blindly. Normal donors (●), breast cancer patients (▲), patients with gynecologic disorders (x), and patients with benign breast disease in categories 0 (○), 2 (■), and 3 (√).

TABLE 2.—*Simultaneous reactivity[a] to gp52 and MCF-7 based on blind tests*

Individuals tested	Reactivity to both antigens[b]	Reactivity to gp52 only[b]	Reactivity to MCF-7 only[b]	Nonreactivity to both antigens[c]	r[d]
Breast cancer patients	2/16	4/16	2/16	8/16	+0.507
Normal females	0/30	3/30	4/30	23/30	+0.512[e]
Patients with gynecologic disorders	0/6	2/6	0/6	4/6	+0.577
Patients with benign breast disease					
Category 0	0/6	2/6	0/6	4/6	+0.661[e]
Category 1	0/13	1/13	1/13	11/13	+0.661[e]
Category 2	0/7	0/7	0/7	7/7	+0.661[e]
Category 3	0/7	2/7	0/7	5/7	+0.479

[a] Benign breast disease patients in categories 0, 1, and 2 were used to determine the cutoff.
[b] No. of persons reactive/total No. of persons tested.
[c] No. of persons nonreactive/total No. of persons tested.
[d] Correlation coefficient.
[e] $P<0.01$.

est MI of all three supernatant dilutions among the various patient and control groups (text-fig. 4). Cutoffs were set at the higher tenth percentile of the same 3 groups of control individuals used in the previous analysis. The cutoffs based on patients with gynecologic disorders or on patients with benign breast disease in categories 0, 1, and 2 were the same (1.19) (text-fig. 4). Category 3 benign breast disease, with the most hyperplasia, had the highest proportion of reactive patients (33%), and 2 of these patients had the two highest MI in the study—1.53 and 1.59. However, the proportion of reactive patients among patients with category 3 benign breast disease was not significantly different by chi-square analysis from that among patients with benign breast disease in combined categories 0, 1, and 2 or among the breast cancer patients. Similarly, none of the groups differed by the Wilcoxon rank sum test.

Breast cancer reactivity to MuMTV relative to histology of the breast tumors.—Lowest indices: Very few (4/49) of the breast cancer patients had infiltrating tumors and positive lymph nodes, and 50% of these were reactive. Twelve of 35 (34%) patients with infiltrating tumors and negative lymph nodes reacted as compared to 3 of 8 (38%) of those with in situ lesions.

Highest indices: all 3 patients who reacted had negative lymph nodes (table 3). Two of these had in situ lesions with hyperplasia and had quite high MI—1.31 and 1.36. Thus the lymphokine that facilitated migration seemed to be present in a high proportion of patients with hyperplasia—3 of 8 benign breast disease patients and 2 of 4 breast cancer patients. In fact, if the reactivity of the breast disease patients with hyperplasia (5/13) was compared to that of the breast disease patients without hyperplasia (8/104), the proportions were significantly different by chi-square analysis ($P<0.005$).

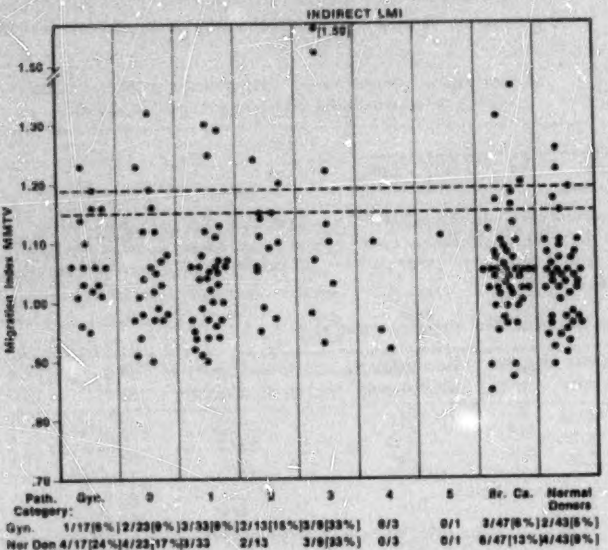

TEXT-FIGURE 4.—Scattergram of highest indirect LMI MI of the same patients as in text-fig. 1. - - -, cutoffs based on the normal donors (*lower line*) or on patients with gynecologic disorders (*upper line*) or patients with benign breast disease in categories 0, 1, and 2 (*upper line*). Along the *abscissa* are indicated the No. of individuals above each cutoff/total No. tested (% positive). Nor Don=normal donors.

TABLE 3.—*Classification of MI of breast cancer patients in indirect LMI assay with MuMTV*

Highest MI[a]			
	Infiltrating invasion		
In situ invasion: Negative node	Positive node	Negative node	Negative node
0.99	0.85	0.87	1.06
1.04	0.99	1 (0.89)	2 (1.07)
1.05	1.02	0.95	2 (1.08)
1.17	1.06	0.96	1.09
1.05[b]	1.13	0.97	2 (1.10)
1.05[b]		0.99	1.18
1.31[b, c]		1.00	**1.20**[c]
1.36[b, c]		1.01	0.96[d]
		3 (1.02)	1.02[d]
		1.03	1.05[e]
		5 (1.05)	1.12[e]

[a] *Numbers in parentheses* are MI preceded by No. of individuals with that MI when No. of individuals is >1.

[b] In situ with hyperplasia.

[c] Positive MI are boldface; patients with benign breast disease in categories 0, 1, and 2 were used to determine the cutoff.

[d] Comedo.

[e] Tubular.

Indirect LMI With MuMTV and MCF-7 in Paired Experiments

Lowest indices.—Many patients and controls were tested simultaneously with MuMTV and MCF-7. The relationship of the lowest MI with MuMTV and the lowest MI to MCF-7 in these paired experiments has been evaluated according to tests of normal individuals who had simultaneous results. A lower cutoff based on the lowest tenth percentile reactivity to these two antigens was set. Four of 6 breast cancer patients who reacted to MuMTV also reacted to MCF-7, and the MI of the simultaneous tests were significantly correlated, indicating that reactivity to two antigens was related when tested with the breast cancer patients. Among patients with benign breast disease in categories 0 and 1, a lower proportion who reacted to MuMTV also reacted to MCF-7—2 of 5 and 1 of 6, respectively. In patients with category 2 benign breast disease, both patients who reacted to MuMTV also reacted to MCF-7, and in the normal individuals all 3 patients who reacted to MuMTV did not react to MCF-7. The MCF-7 and MuMTV MI were not significantly correlated in any subject other than the breast cancer patients, and in benign breast disease of category 0 there was a negative correlation or discordance.

Highest indices.—The highest MI to MuMTV and MCF-7 in simultaneous tests were evaluated in text-figure 5 and summarized in table 4. The MI to the two antigens were correlated in all types of test individuals and significantly so in all but the patients with gynecologic disorders and patients with benign breast disease in category 2. At least half of the patients who reacted to MuMTV also reacted to MCF-7. Seven of 9 breast cancer patients who reacted to MCF-7 did not react to MuMTV. The 2 patients with

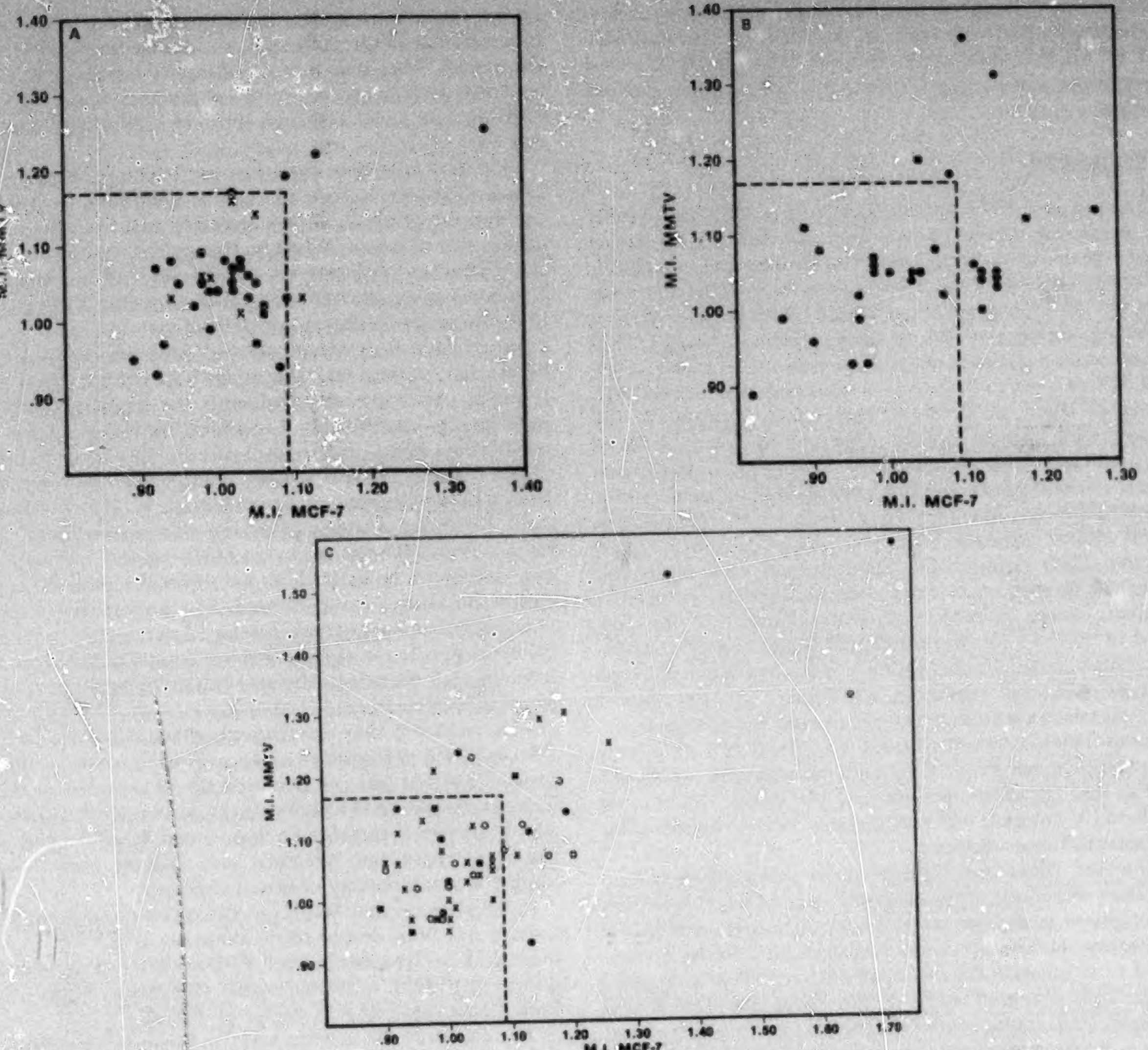

TEXT-FIGURE 5.—Correlation diagram of highest MI of test individuals assayed simultaneously with MuMTV and MCF-7 in the indirect assay. A) Normal donors (●) and patients with gynecologic disorders (x). B) Breast cancer patients (●). C) Patients with benign breast disease in categories 0 (○), 1 (x), 2 (■), and 3 (●).

TABLE 4.—*Simultaneous LMI reactivity[a] to MCF-7 and MuMTV based on highest MI*

Individuals tested	Reactivity to both antigens[b]	Reactivity to MuMTV only[b]	Reactivity to MCF-7 only[b]	Nonreactivity to both antigens[c]	r^d
Breast cancer patients	2/31 (6)	2/31 (6)	9/31 (29)	18/31 (58)	+0.515[e]
Normal females	2/30 (7)	1/30 (3)	0/30 (0)	27/30 (90)	+0.597[e]
Patients with gynecologic disorders	0	0	1/8 (13)	7/8 (88)	+0.095
Patients with benign breast disease					
Category 0	2/13 (15)	1/13 (8)	3/13 (23)	7/13 (54)	+0.775[e]
Category 1	3/25 (15)	1/25 (4)	1/25 (4)	20/25 (80)	+0.574[e]
Category 2	1/8 (13)	1/8 (13)	1/8 (13)	5/8 (63)	+0.469
Category 3	2/7 (29)	0/7 (0)	2/7 (29)	3/7 (43)	+0.881[e]

[a] Patients with breast disease in categories 0, 1, and 2 were used to determine the cutoff.
[b] No. of persons reactive/total No. of persons tested (%).
[c] No. of persons nonreactive/total No. of persons tested (%).
[d] Correlation coefficient.
[e] Significant at $P<0.01$.

benign breast disease in category 3 and the 2 breast cancer patients who had very high MI to MuMTV also had high MI to MCF-7, indicating that the response to the viral antigen was similar to a response to a breast tumor-derived antigen.

DISCUSSION

The purpose of the present study was to evaluate whether the previously observed reactivity of MuMTV in breast cancer patients could be applied to breast cancer diagnosis (*5, 6*). In these previous studies, most of the patients were postoperative breast cancer or benign breast disease patients, and these studies were not performed blindly. About 65% of breast cancer patients reacted to gp52 in our laboratory, and 31% reacted to MuMMV-containing milk in the laboratory of Black et al. (*11*). The results obtained in the present study would appear to be in contrast to those of these previous studies in that 31% of the preoperative breast cancer patients reacted with the use of our least conservative cutoff. However, Zachrau et al. (*12*) tested preoperative breast cancer patients with gp55, and only 1 of 12 (8%) reacted. Their criterion for reactivity was an index of less than 0.80. By this conservative criterion, a similar proportion of breast cancer patients in our double-blind study reacted, i.e., 1 of 15 (7%). On the whole, the breast cancer patients' reactivities to gp52 and MuMTV were low among preoperative breast cancer patients, and their reactivities did not differ significantly from those of two sets of control patients (normal female hospital workers and preoperative patients with benign gynecologic diseases). Consequently, we do not believe that the direct or indirect LMI assays with the use of MuMTV antigens and peripheral blood can be useful for diagnosis of breast cancer.

However, there were differences in antigen preparation and assay technique in the experiments in Black's laboratory as compared to the preparation and technique used in our laboratory: 1) The gp55 was obtained by PAGE as compared to sequential ion-exchange and gel chromatography for the gp52 prepared by Dr. Parks; 2) the MuMMTV was obtained from mouse milk as compared to the supernatant from a mouse mammary tumor tissue-cultured cell line; 3) leukocytes were prepared by gravity sedimentation in the plasma and lysing of the erythrocytes with sodium chloride and distilled water as compared to gravity sedimentation in Plasmagel which augmented erythrocyte sedimentation; and 4) the assay was performed in Sykes Moore as compared to Sterilin chambers which are disposable.

The postoperative breast cancer reactivity to MuMTV was observed more frequently in women with in situ lesions than in women with invasive cancers (*11*). The incidence of reactivity that we observed previously was high in cancer patients without lymph node involvement (68% or 13/19) as compared to that in patients with invasive cancer with lymph nodes positive for tumor (45% or 5/11), except for women with invasive cancer who had been frequently skin tested with allogeneic breast-tumor-derived antigens (13/15, 87%) (Cannon GB, McCoy JL: Unpublished observations). In the present study with the direct and indirect tests, 33–50% of the patients with preoperative cancers with positive lymph nodes were reactive when the patients with benign breast disease in categories 0, 1, and 2 were used to determine the cutoff. The incidence of reactivity among the cancer patients with negative lymph nodes was lower—4 of 18 (22%) in the direct test and 15 of 43 (35%) in the indirect test.

One may speculate that the reactivity in the peripheral blood of patients harboring a tumor is different from that in the peripheral blood of postoperative patients who are relatively free of tumor. Possibly, the reactive lymphocytes are sequestered at the tumor site or otherwise inhibited, in stage I patients more than in stage II patients, and the pattern becomes reversed after mastectomy.

In our pathologic reevaluation of our preoperative benign breast disease patients, the category with the highest reactivity in the direct test and with the highest MI in the indirect test was category 3 in which the intraductal proliferation was either in the form of papillomatosis or hyperplasia. In retrospective studies involving reexamination of benign breast disease pathology, Black et al. (*13*) and Kodlin et al. (*14*) have shown a gradation of benign breast disease lesions, from normal to an atypia consistent with in situ carcinoma, to be related to an upward trend for breast cancer incidence. Davis et al. (*15*) reported that patients with epithelial hyperplasia developed mammary carcinoma 2.5 times as often as did the general female population, and patients with fibrocystic disease with no hyperplasia had 1.2 times the expected rate of mammary cancer. Monson et al. (*16*) have shown that women with chronic mastitis were at 2.5 times the risk of normal women for developing breast cancer and that this risk persisted for 30 years after biopsy. The association of reactivity to the viral antigens with the type of benign breast disease that is considered to be at high risk from pathologic evidence may provide some further insight into the biology of breast cancer.

A lymphokine that facilitates enhanced migration of leukocytes has been described by Weisbart et al. (*10*). It was produced by lymphocytes of PPD-sensitive donors in response to PPD. It was heat-stable, dialyzable, and distinct from leukocyte inhibitory factor by PAGE.

The ability of the indirect assay to measure a lymphokine that was measured by facilitation of normal donors' PMN cells to migrate was observed in 2 breast cancer patients with in situ carcinoma with hyperplasia, as well as in 3 benign breast disease patients with hyperplasia. This increased migration was also observed in 1 patient with breast cancer in situ with hyperplasia in the direct test. Previously, we have observed this increased or enhanced migration in first-degree relatives at high risk for melanoma and colon cancer in families with a high incidence of melanoma and colon cancer (Cannon GB, Dean JH, Greene MH, Blattner WA: Unpublished observations). These family members were tested in the direct agarose LMI test with melanoma-derived and colon cancer-derived extracts.

The increased or enhanced migration to MuMTV that we observed also occurred in simultaneous tests with MCF-7 as the antigen. Thus the antigens may be similar in these two materials and, in fact, MCF-7 has been implicated as containing a virus (*17*). Black et al. (*18*) have found correlations of LMI with gp55 and cryostats of in situ breast carcinomas and have suggested the immunologic relationship of these two materials. However, Zachrau et al. (*12*) did not find as much correlation in reactivity to MCF-7 and the in situ breast cryostats as they did with MCF-7 and gp55 or gp55 and the in situ breast cryostats in postoperative patients. They also found very low reactivity to both MuMTV and MCF-7 in preoperative patients.

Jenson et al. (*19*) have described a form of benign breast disease, characterized by atypical lobules, which was found more frequently in cancer-associated breasts (containing cancer or contralateral to cancer) than in breasts examined during random routine autopsies. The lesions showed variable degrees of epithelial hyperplasia, forming a gradation between normal epithelium and carcinoma in situ. Jenson et al. suggest that these lesions may be homologous to HAN that are abundant in mouse strains having a high incidence of mammary cancer. Wsi-zen et al. (*20*) have observed an increased or enhanced migration of macrophages in mice tested in LMI tests with cryostat sections of HAN that have formed tumors. They state that a substance produced by these early tumor cells may enhance macrophages or other inflammatory cells and drive them out of the area and suggest that the tumor would have a more favorable environment in which to develop. These authors attribute the enhanced migration to the tissue source, rather than to the leukocyte donor. However, the enhanced migration in patients with hyperplasia is interesting. These patients may have a tissue similar to the HAN present in their bodies at the time of the blood donation.

The identification of a subset of benign breast disease patients, who are at a higher risk pathologically with a functional immune response to MuMTV, seems to point to a possible association of virus recognition with early breast cancer.

REFERENCES

(*1*) Mesa-Tejada R, Keydar I, Ramanarayanan M, Ohno T, Fenoglio C, Spiegelman S. Detection in human breast carcinoma of an antigen immunologically related to a group-specific antigen of mouse mammary tumor virus. Proc Natl Acad Sci USA 1978; 75:1529–1533.

(*2*) Hoshino M, Dmochowski L. Electron microscope study of antigens in cells of mouse mammary tumor cell lines by peroxidase-labeled antibodies in sera of mammary-tumor-bearing mice and of patients with breast cancer. Cancer Res 1973; 33:2551–2558.

(*3*) Müller M, Zotter S, Kemmer C. Specificity of human antibodies to intracytoplasmic type-A particles of the murine mammary tumor virus. J Natl Cancer Inst 1976; 56:295–303.

(*4*) Witkin SS, Sarbor NH, Kinne DW, Good RA, Day NK. Antibodies reactive with mouse mammary tumor virus in sera of breast cancer patients. Int J Cancer 1980; 25:721–725.

(*5*) Black MM, Moore DH, Shore B, Zacharau RE, Leis HP Jr. Effect of murine milk samples and human breast tissues on human leukocyte migration indices. Cancer Res 1974; 34:1054–1060.

(*6*) McCoy JL, Dean JH, Cannon GB, et al. Leukocyte migration inhibition and lymphocyte blastogenesis responses in breast carcinoma patients to mouse mammary tumor virus and to viron gp52 antigen and Rauscher murine leukemia virus–Kirsten sarcoma virus gp69/71 antigen. J Natl Cancer Inst 1978; 60:1259–1267.

(*7*) Parks WP, Howk RS, Scolnick EM, Oroszlan S, Gilden RV. Immunochemical characterization of two major polypeptides from murine mammary tumor virus. J Virol 1974; 13:1200–1210.

(*8*) McCoy JL, Jerome LF, Anderson C, et al. Leukocyte migration inhibition of soluble extracts of MCF-7 tissue culture cell line derived from breast carcinoma. J Natl Cancer Inst 1976; 57:1045–1049.

(*9*) McCoy JL, Dean JH, Herberman RB. Direct and indirect agarose microdroplet migration inhibition assays for detection of cell mediated immunity to human tumor associated antigens. In: Bloom RB, David JR, eds. In vitro methods in cell-mediated and tumor immunity. New York; Academic Press, 1976:621–628.

(*10*) Weisbart RH, Bluestone R, Goldberg LS, Pearson CM. Migration enhancement factor: A new lymphokine. Proc Natl Acad Sci USA 1974; 71:875–879.

(*11*) Black MM, Zacharau RE, Shore B, Leis HP Jr. Biological considerations of tumor-specific and virus-associated antigens of human breast cancers. Cancer Res 1976; 36:769–774.

(*12*) Zachrau RE, Black MM, Dion AS, Shore B, Williams CJ, Leis HP Jr. Specificity of the simultaneous cell-mediated immune reactivity to RIII murine mammary tumor virus glycoprotein 55 and human breast cancer tissues. Cancer Res 1978; 38:3414–3420.

(*13*) Black MM, Barclay TH, Cutler SJ, Hankey BF, Asire AJ. Association of atypical characteristics of benign breast lesions with subsequent risk of breast cancer. Cancer 1972; 29:338–343.

(*14*) Kodlin D, Winger EE, Morgenstern NL, Chen V. Chronic mastopathy and breast cancer, a follow-up study. Cancer 1977; 39:2603–2607.

(*15*) Davis HH, Simons M, Davis JB. Cystic disease of the breast: Relationship to carcinoma. Cancer 1964; 17:957–978.

(*16*) Monson RR, Yen S, Macmahon B, Warren S. Chronic mastites and carcinoma of the breast. Lancet 1976; 2:224–226.

(*17*) McGrath CM, Grant PM, Soule HD, Glancy T, Rich MA. Replication of oncovirus-like particles in human breast carcinoma cell line, MCF-7. Nature 1974; 252:247–250.

(*18*) Black MM, Zachrau RE, Dion AS, et al. Cellular hypersensitivity to gp 55 of RIII-murine mammary tumor virus and gp 55-like protein of human breast cancers. Cancer Res 1976; 36:4137–4142.

(*19*) Jensen HM, Rice JR, Wellings SR. Preneoplastic lesions in the human breast. Science 1976; 191:295–297.

(*20*) Wei-zen W, Miller FR, Blazor BA, Medina D, Heppner G. Opposing effects of cryostat sections of preneoplastic and neoplastic mouse mammary lesions on in vitro migration of peritoneal exudate cells. J Immunol 1979; 122:2059–2067.

blank page

Effect of Enzymatic Disaggregation on Proliferation of Human Tumor Cells in Soft Agar[1,2]

Anne W. Hamburger,[3] Christine P. White,[3] and Kathleen Tencer[3,4]

ABSTRACT—Cell suspensions were prepared by either mechanical or enzymatic disaggregation methods from biopsy specimens from 54 patients with various tumors. The biologic activities of cells derived from the two suspensions were then examined. Biopsy specimens of solid tumors were minced, and one-half of each specimen was further processed by being teased with needles, whereas the other half was exposed to a combination of collagenase, hyaluronidase, and DNase. The enzymatic disaggregation method yielded fewer cells per gram of tissue than the mechanical method. However, the percentage of dye-excluding cells was increased by the enzymatic procedure in 93% of the cases. Cells obtained by enzymatic means also had higher cloning efficiencies than those obtained by mincing. The histologic types of cells present in the initial cell suspensions were the same for cells obtained by the enzymatic or mechanical disaggregation methods. The number of colonies obtained was linearly related to the number of cells plated in both cases. The tritiated thymidine suicide indices (estimates of the percentage of cells in the S-phase of the cell cycle) were the same for the two cell populations obtained by the two methods. The results indicate that cells obtained from solid tumors by enzymatic dissociation methods did not differ significantly from cells obtained by the more conventional mechanical techniques. However, cell viabilities and cloning efficiencies were significantly improved by the enzymatic technique.—JNCI 1982; 68:945–949.

A method of cloning human tumor cells in soft agar has recently been developed (*1*, *2*). This technique appears to be suitable for culture of a variety of neoplasms of different histopathologies (*3*, *4*). The cell colonies retain many of the histologic, histochemical, functional, and immunologic properties of the tumor of origin. This system proved to be useful in elucidating biophysical and biologic properties of CFC from patients with a variety of neoplasms (*5*). This assay is also being used for testing of in vitro sensitivity of human tumor cells to anticancer drugs and for screening of new anticancer agents (*6*).

Cloning efficiencies of cells from many cancer patients are low in the soft agar system. In addition, only 25% of tumors yield enough cells to permit drug sensitivity testing (*7*). Improvements in disaggregating solid tumors should increase both cloning efficiencies and cell yield. We have previously used mechanical techniques to disrupt solid tumors (*1*, *3*), but the resultant debris, clumping, physical damage, and low yield resulted in suboptimal cloning efficiencies. Although collagenase has been reported to be effective in disrupting lung tumors, sarcomas, and melanomas (*8*), we sought a method that utilizes a combination of enzymes to maximize cell yields for many tumor types.

Enzymatic disaggregation techniques may cause subtle, hard-to-control changes in cells, such as membrane alterations, protein loss, altered metabolism, and changes in antigenicity and drug sensitivity (*9–12*). It is therefore of utmost importance to compare rigorously the biologic activities of cells obtained by either mechanical or enzymatic means from the same tumor. We have found that a combination of enzymes enhanced cloning efficiencies of tumor cells without changing several other biologic properties. The results of this study indicate that cells obtained by enzymatic dissociation techniques from solid tumors are acceptable for use in agar cloning assays.

MATERIALS AND METHODS

Collection and treatment of cells.—Tumor cells were obtained from biopsy specimens of solid tumors from 54 patients with various neoplasms. The cancerous nature of the specimens was confirmed by a clinical pathologist. Appropriate informed consent was obtained from all the patients. We obtained tumor nodules after surgery and removed all fat and necrotic and connective tissues. The tumors were then cut into two pieces of approximately equal size and similar gross morphology and were weighed. One piece of each tumor was disaggregated mechanically, and the other piece was disaggregated enzymatically. Mechanically dissociated tumors were minced with scalpels and teased apart with 22-gauge needles. Cells released into the media were filtered through 22-μm Nitex gauze for removal of cell clumps and were washed twice in HBSS (GIBCO, Grand Island, N.Y.) with 10% heat-inactivated FCS (Reheis Chemical Co., Kankakee, Ill.). Viable nucleated cell counts were determined in a hemacytometer with the use of erythrosin B. The second piece of tumor tissue was similarly minced into 3- to 6-mm pieces and then removed to a 25-ml trypsinizing flask and resuspended in enzyme solution. We used various combinations and sequences of enzymes initially, and later we used the following mixture: Approximately 1 g of tissue was resuspended in 7 ml collagenase (1,800 U/ml collagenase type I; Sigma Chemical Co., St. Louis, Mo.), 7 ml hyaluronidase (type I 1,220 U/ml; Sigma Chemical Co.), and 0.02% DNase (38,800 Kunitz U/mg protein). All the enzymes were prepared in HBSS and stored in aliquots at −40°C. Tissue pieces were incubated in a shaking water

---

Abbreviations used: CFC=colony-forming cells; FCS=fetal calf serum; HBSS=Hanks' balanced salt solution; [^{3}H]dThd=tritiated thymidine.

---

[1] Received September 17, 1981; accepted February 12, 1982.

[2] Supported in part by Public Health Service grants CA-26008 and CA-28669 from the National Cancer Institute.

[3] Cell Culture Department, American Type Culture Collection, 12301 Parklawn Dr., Rockville, Md. 20852.

[4] We thank Dr. Juan Posada and Dr. Philip Schein, Georgetown University School of Medicine, Washington, D.C., and Dr. Charles Currier, Washington Hospital Center, Washington, D.C., for providing the specimens used in these studies. We also thank Mrs. Shirley Umali and Ms. Shirley Mazur for preparation of the manuscript.

bath at 37°C for 1.5–3 hours. We stopped treatment when only a few pieces of tissue were left in the suspension. Cells freed from the tissues were washed and filtered as described for mechanically released cells. We performed differential counts on slides prepared with a cytocentrifuge and stained by the Papanicolaou (*13*) and Wright-Giemsa methods and we assayed for nonspecific esterase-activity (*14*).

Culture assay for CFC.—Cells were cultured as described by us earlier (*1, 2*). Underlayers (1 ml), containing enriched McCoy's 5-A medium in 0.5% Bacto-agar (Difco Laboratories, Detroit, Mich.), were prepared in plastic petri dishes 35 mm in diameter. Conditioned medium was not included. Cells to be tested were suspended in 0.3% agar in enriched CMRL 1066 medium (GIBCO) with 15% horse serum (Flow Laboratories Inc., Springfield, Va.). Each culture received 5×10^5 cells in 1 ml of agar–medium mixture. Cultures were incubated at 37°C in a humidified incubator with a 7.5% CO_2 atmosphere.

Scoring of cultures.—Cultures were examined with a Zeiss inverted-phase microscope at 100 and 160× magnification for the presence of clumps immediately after plating, and those containing clumps were discarded. Final colony counts of coded plates were made between 10 and 21 days after plating; aggregates of 30 cells or more were considered colonies. The 0.3% agar layer that contained the colonies was fixed and dried onto microscope slides as described (*15*). Slides were stained with Papanicolaou stain for examination of morphology. The presence of peroxidase, nonspecific esterase, and periodic acid–Schiff and mucicarmine reactivities was also determined (*13, 14*).

Determination of the proportion of cells in DNA synthesis by [^{3}H]dThd suicide test.—The [^{3}H]dThd suicide method was used for estimation of the proportion of CFC in the DNA synthetic S-phase of the cell cycle (*16*). Samples of 2×10^6 cells suspended in HBSS and 10% heat-inactivated, dialyzed FCS were added to 1.0 ml of HBSS containing 40 μCi of [^{3}H]- dThd (23 Ci/mmol; Amersham/Searle Corp., Arlington Heights Ill.). Control samples were added to HBSS alone. Cell suspensions were incubated for 30 minutes at 37°C and washed twice with 20 ml of cold HBSS containing 100 μg unlabeled thymidine/ml and 10% FCS. Each suicide and control suspension was cultured in four replicate plates at a concentration of 5×10^5 cells per plate.

Statistical analysis.—Statistical significance of the differences between samples was determined by Student's *t*-test. Four or five plates were scored per point. The effect of each disaggregation method on each dependent variable, such as percentage of dye-excluding cells, was determined by a two-way analysis of variance. Statistical significance was determined at the 5% level.

RESULTS

Cell yields.—The total number of cells released from tumor specimens by either mechanical or enzymatic means was extremely variable for all tumor types (table 1). However, the median yields of cells obtained by mechanical procedures were greater than the median yields obtained by enzymatic procedures for breast, colon, and kidney tumors. The median cell yields by the two methods were not significantly different for lung or ovarian tumors or for melanomas.

Proportion of viable cells.—The percentage of dye-excluding cells was variable for all disease types (table 1). In general, the proportion of viable cells obtained by enzymatic methods was higher than that obtained by mechanical methods for all disease types except melanoma. The median yield of viable cells per gram of tissue was slightly greater when ovarian, lung, and kidney tumors were enzymatically dissociated and slightly lower when colon or melanoma tumors were enzymatically dissociated compared to the yields of mechanical disaggregation.

Clonogenicity.—Cloning efficiencies were variable within the same disease type (table 1). However, the median cloning efficiencies of cells released enzymatically from tumors of all disease types tested was higher than that of the mechanically released cells. Neither the kinetics of colony growth nor the size of individual colonies formed was consistently different

TABLE 1.—*Effect of enzymatic and mechanical disaggregation procedures on cell yield, viability, and cloning efficiencies*

Disease type	Disaggregation method[a]	No. of samples	No. of cells/g tumor tissue, $\times10^{-6}$		Cell viability, %		No. of viable cells/g tumor tissue, $\times10^{-6}$		No. of colonies, 5×10^5 cells	
			Median	Range	Median	Range	Median	Range	Median	Range
Adenocarcinoma										
Ovary	E	9	26	3–89	50	1–70	3	1–20	32	0–224
	M	6	19	2–69	15	1–20	1	0.4–5	0	0–80
Breast	E	20	8	4–36	74	12–93	5	2–15	24	0–308
	M	16	15	2–173	8	0–89	5	0–30	0	0–168
Lung	E	9	39	6–160	70	5–100	8	2–35	60	0–117
	M	8	32	2–204	3	1–24	2	0–15	3	0–30
Colon	E	7	13	4–76	73	11–89	4	2–11	48	0–256
	M	6	39	15–198	36	20–62	43	5–96	8	0–48
Kidney	E	3	6	6–6.6	44	40–50	17	3–28	3	0–6
	M	3	44	16–73	8	6–10	3	1–4	0	
Melanoma	E	3	86	12–183	50	38–74	43	9–70	340	324–516
	M	2	85	49–140	41	12–70	53	6–100	176	136–210
Miscellaneous tumors	E	3	4	1.4–12	70	5–73	3	1–8	81	0–200
Mesothelioma testicular fibrosarcoma	M	2	12	10–15	19	12–26	2.7	1.2–3.9	0	

[a] E=enzymatic disaggregation; M=mechanical disaggregation.

TABLE 2.—*Morphologic analysis of cells released by enzymatic or mechanical means*

Disease type	No. of samples	Disaggregation method[a]	Percentage[b] ± SE			
			Released tumor cells	Macrophages	Lymphocytes	Granulocytes
Adenocarcinoma						
Colon	6	E	96±2	2±1	1±1	1±1
	6	M	94±2	1±1	1±1	2±2
Breast	8	E	90±2	2±1	3±1	3±1
	8	M	92±2	3±1	2±1	3±1
Lung	5	E	90±3	1±1	3±1	3±1
	5	M	88±2	4±1	2±1	3±1
Melanoma	3	E	91±1	4±1	1±1	3±1
	2	M	92±2	1±1	4±2	3±1

[a] E=enzymatic disaggregation; M=mechanical disaggregation.

[b] Percentages of cell types for each tumor were based on two slides, 500 cells/slide.

for cells obtained by enzymatic or mechanical dissociation techniques.

There was considerable heterogeneity in cloning efficiencies, cell viabilities, and cell yields for the group as a whole. Due to the large variability in the data, and the relatively small number of samples in different disease categories, differences between cells derived by enzymatic means and those derived by mincing were often of borderline significance. However, for all disease types, cloning efficiencies of cells prepared enzymatically were greater than cloning efficiencies of cells obtained by mincing from the same tumor in 28 cases. No differences in cloning efficiencies of cells obtained by the two methods were observed in 14 instances. In only 3 cases were cloning efficiencies of cells derived from minced tissue greater than cloning efficiencies of cells obtained enzymatically from the same tumor. Similarly, the percentage of viable cells obtained enzymatically was greater than the percentage of viable cells obtained mechanically from the same tumor in 42 cases. In only 3 cases was the percentage of viable cells observed greater from mechanically dissociated cells than from enzymatically dissociated cells from the same tumor. In 27 cases, more cells were obtained per gram of tissue from the same tumor by mechanical methods. In 20 cases, more cells were obtained enzymatically. In 25 cases the yield of viable cells per gram of tissue was greater when enzymatic dissociation methods were used. In 6 cases no differences in yields of viable cells were observed. In 15 cases, the yield of viable cells per gram of tissue was greater when mechanical methods were used compared to that obtained by the enzymatic method.

Cytology of released cells.—To determine if mechanical and enzymatic procedures released morphologically different populations of cells, we examined the cytologic profile of the suspensions (table 2). Tumor cells comprised the majority of cells for all disease categories as determined by morphologic analysis. There were no significant differences in the median numbers of tumor cells from suspensions obtained by either mechanical or enzymatic methods. Variable and low numbers of macrophages, lymphocytes, and granulocytes were observed. We did not observe any difference in the number of cell types between enzymatically or mechanically prepared cell suspensions.

Relationship between number of cells plated and colony formation.—Text-figure 1 shows the relationship between the number of cells plated and the number of colonies formed from cells obtained from a patient with adenocarcinoma of the colon. The results from 3 other patients with adenocarcinoma of the colon, lung, and breast were qualitatively similar, although the actual number of colonies varied. A linear relationship was observed between the number of nucleated cells plated (up to 5×10^5 cells) and the number of colonies formed among cells obtained by either mechanical or enzymatic methods. The nonlinearity observed above 5×10^5 cells per plate may have been due to depletion of nutrients or to the toxic effects of cell crowding. However, significantly more colonies were formed at each cell concentration tested when cells were obtained by enzymatic methods.

Proliferative state of tumor cells obtained by different disaggregation methods.—Because enzymatic treatment of tumor cells may alter the cell cycle properties (*17, 18*), we examined whether

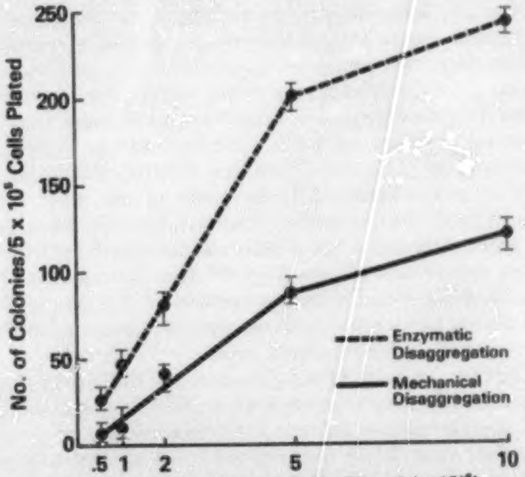

TEXT-FIGURE 1.—Relationship between colony formation and the number of nucleated cells plated. Pieces of a tumor from a patient with adenocarcinoma of the colon were disaggregated by either enzymatic or mechanical methods, and the cells were plated at the concentrations indicated.

Table 3.—*Effect of [^{3}H]dThd on colony formation by cells obtained by enzymatic or mechanical disaggregation*

Expt No.	Tumor type	Disaggregation method*	No. of colonies/5×10^5 cells±SE	Survival of CFC, %
1	Ovarian, adenocarcinoma	E	88±12	7
		M	52±12	4
2	Breast, adenocarcinoma	E	84±8	31
		M	65±6	28
3	Breast, adenocarcinoma	E	20±8	150
		M	12±5	183
4	Melanoma	E	516±20	140
		M	36±8	144
5	Colon, adenocarcinoma	E	448±47	37
		M	48±9	16
6	Colon, adenocarcinoma	E	288±24	12
		M	60±7	10
7	Colon, adenocarcinoma	E	200±30	10
		M	84±8	7

*E=enzymatic disaggregation; M=mechanical disaggregation.

the number of cells in the S-phase of the cell cycle was different for cells obtained by either enzymatic or mechanical means. Incubation of cells with high-specific-activity [^{3}H]dThd decreased colony formation in 5 cases and increased colony formation in 2 cases (table 3). The survival of CFC obtained by enzymatic means was not significantly different than that observed with cells obtained by mechanical disruption.

DISCUSSION

The mechanical disaggregation methods routinely used to produce cell suspensions for clonogenic assays of human tumor cells do not yield large numbers of viable cells, and cloning efficiencies are often low. An enzymatic disaggregation technique that would increase both cell yield and cloning efficiency would be desirable. However, before a new disaggregation procedure is employed, it is necessary to compare it with the proven technique to determine the similarity between the cell suspensions. We therefore divided tumors into two pieces of approximately equal size and similar gross morphology for direct comparison of the effect of the two disaggregation methods on the same tumor. A potential problem with this approach has been noted by Slocum et al. (*17*), who found that cloning efficiencies may vary in anatomically different parts of the same tumor. Cowan et al. (*18*), however, observed that cells from different parts of the same tumor have similar cloning efficiencies. Direct comparison of cells from the same tumor may therefore be more useful than comparison of the effects of the two disaggregation methods on separate groups of different tumors of the same histologic type.

The heterogeneity of our data makes it difficult to predict whether enzymatic treatment would be superior to mechanical disaggregation for an individual tumor of a given histologic type. More samples would be needed to predict with greater certainty the optimal method for disaggregation of an individual tumor. In general, enzymatic procedures appeared superior for all tumor types tested except for melanoma. For example, the fraction of cells able to exclude dye was significantly greater for the enzymatically released suspensions in 42 of 45 tumors tested. In addition, a slightly greater yield of viable cells per gram of tissue was noted for lung, ovarian, and kidney tumors. We have found that it is preferable to work with cell suspensions of high viability, and that cell suspensions that contain large numbers of dead cells and debris do not grow well (*3*). Theoretically, it is possible to remove dead cells from mechanically prepared suspensions. Our attempts to selectively remove dead cells by centrifugation through FCS, Ficoll–Hypaque, or Percoll have not significantly enriched the suspensions for viable cells. Slocum et al. (*19*) reported similar results.

Cloning efficiency provides a more useful estimate of the cells' proliferative ability than does dye exclusion. Cloning efficiencies of tumor cells obtained by enzymatic treatment were equal to or greater than that observed for mechanically disaggregated cells in 42 of 45 cases. These data agree with those in an initial report by Pavelic et al. (*8*) but vary from their later report for lung tumors and melanoma (*19*). Our number of cases for these disease types is small, and it is possible that in a larger population significant differences would not be observed. Because cloning efficiencies of tumor cells were significantly increased in cell suspensions obtained by enzymatic means, this method may be of use to investigators studying biologic properties or drug sensitivities of CFC.

The two dispersion methods may release different populations of cells. Tumors contain many nontumor cells, including macrophages and lymphocytes. We have shown that macrophages influence survival of clonogenic cells (*3*). Morphologic and histochemical analyses did not indicate significant differences in the cytologic profile of cells obtained by the two dissociation methods. The low percentage of tumor-infiltrating macrophages observed in these studies differs from the findings of Gauci and Alexander (*20*). They observed that the macrophage content of tumors ranged from 0 to 30%, although the majority of tumors contained less than 10% macrophages. However, our results are similar to those reported by Slocum et al. (*19*), who found a median of 7% macrophage–monocytes in their preparations. These differences may be due to the fact that the method of Gauci and Alexander (*20*) involved the use of a macrophage-specific heteroantibody rather than the histochemical method used in this study.

Enzyme treatment may also alter the cycling characteristics of tumor cells (*21, 22*). We estimated the proportion of cells in the S-phase of the cell cycle by [^{3}H]dThd suicide techniques. The fraction of cells in the S-phase was not significantly different for cells obtained by the two methods from the same patient. The increase in colony formation in 2 cases observed after exposure to [^{3}H]dThd has been observed previously (*3*), and it may relate to recruitment of clonogenic cells from a G_0 state to a cycling state. However, the effects of cell cycle-specific drugs on CFC obtained by the two disaggregation techniques should not be significantly different because the suicide indices were not significantly different.

In summary, both the viabilities and the cloning efficiencies of cells obtained by enzymatic methods were higher than those of cells obtained by mechanical disaggregation. Neither the cytologic profile nor the fraction of cells in the

S-phase of the cell cycle was significantly different for cells obtained from the same patient by the two methods. The results indicate that the enzymatic procedure did not damage the functional activity of tumor cells. Preliminary experience with drug tests in cells from a small number of patients suggests that cells obtained by enzymatic procedures may be useful in the study of drug sensitivities of clonogenic cells. Data on many patients are required to verify this result. In addition, clinical observations must be made to determine if cells obtained enzymatically may be used for prediction of the patient's clinical response.

REFERENCES

(*1*) Hamburger AW, Salmon SE. Primary bioassay of human tumor stem cells. Science 1977; 197:461–463.

(*2*) ——— Primary bioassay of human myeloma stem cells. J Clin Invest 1977; 60:846–854.

(*3*) Hamburger AW, Salmon SE, Kim MB, et al. Direct cloning of human ovarian carcinoma cells in agar. Cancer Res 1978; 38:3438–3444.

(*4*) Buick RN, Stanisic TH, Fry SE, Salmon SE, Trent JM, Krasnovich P. Development of an agar–methyl cellulose clonogenic assay for cells in transitional cell carcinoma in the human bladder. Cancer Res 1979; 39:5051–5056.

(*5*) Hamburger AW, Kim MB, Salmon SE. The nature of cells generating human myeloma colonies in vitro. J Cell Physiol 1979; 98:371–376.

(*6*) Salmon SE, Hamburger AW, Soehnlen BJ, Durie BG, Alberts DS, Moon TE. Quantitation of differential sensitivity of human tumor stem cells to anticancer drugs. N Engl J Med 1978; 298:1321–1327.

(*7*) Von Hoff DD, Casper J, Bradley E, Sandbach S, Jones D, Makuch R. Association between human tumor colony-forming assay results and response of an individual patient's tumor to chemotherapy. Am J Med 1981; 70:1027–1032.

(*8*) Pavelic ZP, Slocum HK, Rustum YM, Creaven PJ, Karakousis C, Takita H. Colony growth in soft agar of human melanoma, sarcoma, and lung carcinoma cells disaggregated by mechanical and enzymatic methods. Cancer Res 1980; 40:2160–2163.

(*9*) Waymouth C. To disaggregate or not to disaggregate: Injury and cell disaggregation, transient or permanent? In Vitro 1974; 10:97–111.

(*10*) Twentyman PR. An artefact in clonogenic assays of bleomycin cytotoxicity. Br J Cancer 1977; 36:642–644.

(*11*) Penning JJ, LeVan JH. Modified enzymatic technique for production of cell suspensions of a murine fibrosarcoma. JNCI 1981; 66:85–87.

(*12*) Barranco SC, Bolton WE, Novak JK. Time-dependent changes in drug sensitivity expressed by mammalian cells after exposure to trypsin. JNCI 1980; 64:913–916.

(*13*) Luna AL ed: Manual of histologic staining methods. New York: McGraw-Hill, 1968:162–165.

(*14*) Williams W, Beutler E, Erslev A, Rundles RW. Hematology. New York: McGraw-Hill, 1977:1627–1638.

(*15*) Salmon SE, Buick RN. Preparation of permanent slides of intact soft-agar colony cultures of hematopoietic and tumor stem cells. Cancer Res 1979; 39:1133–1336.

(*16*) Iscove N, Till J., McCulloch E. The proliferative state of mouse granulopoietic progenitor cells. Proc Soc Exp Biol Med 1970; 134:33–37.

(*17*) Slocum HK, Pavelic LP, Rustum VM, Karakousis C, Takita H, Creaven PJ. Is there anatomical segregation of important cell populations in human solid tumors? Proc Am Assoc Cancer Res 1981; 22:154.

(*18*) Cowan JD, McCracken JD, Von Hoff DD. Multiple drug sensitivity concordance in the human tumor cloning system. Proc Am Assoc Cancer Res 1981; 22:350.

(*19*) Slocum HK, Pavelic ZP, Rustum YM, et al. Characterization of cells obtained by mechanical and enzymatic means from human melanoma sarcoma, and lung tumors. Cancer Res 1981; 41:1428–1434.

(*20*) Gauci R, Alexander P. The macrophage content of some human tumors. Cancer Lett 1975; 1:29–32.

(*21*) Barendsen GW. Analysis of tumour responses by excision and in vitro assay of cellular clonogenic capacity. Br J Cancer 1980; 41:209–216.

(*22*) Rasey JS, Nelson NJ. Effect of tumor disaggregation on results of in vitro cell survival assay after in vivo treatment of the EMT-6 tumor: X-rays, cyclophosphamide and bleomycin. In Vitro 1980; 16:547–553.

blank page

Diverse Xenotropic Virus Expressions in Two NZB Mouse Breeding Lines That Differ in Chromosome Breakage[1,2]

Carmen Bernard[3] *and* Ingrid Emerit[4,5]

ABSTRACT—Two breeding lines of the NZB/Bl mouse strain, which was originated from Bielschowsky's stock and maintained as a conventional inbred colony since 1963, were developed by selective matings according to chromosome breakage incidence in bone marrow cells. These breeding lines were used because they represent an interesting experimental model, since they differ in the manifestations of the autoimmune process and the incidence of lymphomas. The present study showed that embryos from both breeding lines differed in the expression of the xenotropic type C RNA virus, characteristic of NZB mice. All 17 cultures initiated with embryos from the line showing high chromosome breakage (HB) had positive reverse transcriptase (RT) reactions after cocultivation with an indicator cell line (SIRC). On the contrary, only 3 of the 22 embryos from the line showing low chromosome breakage (LB) had RT activity at late passages (7–10). The chromosome studies done on these embryo cultures showed highly significant differences in the chromosome breakage incidence for the 2 breeding lines [10.6 and 20.5% of cells with aberrations for LB and HB embryos, respectively ($P<0.001$)].—JNCI 1982; 68:951–958.

NZB mice spontaneously develop an autoimmune syndrome similar to human lupus erythematosus with immune complex nephritis and antinuclear and antinucleic acid antibodies, as well as Coombs' positive hemolytic anemia. If the mice do not succumb to the nephritis and anemia, they frequently die of lymphoid neoplasia of the immunoblastic type (*1*). In 1972, we demonstrated an important increase in chromosomal breakages in bone marrow cells from NZB mice of our strain (*2*). Other colonies have mosaicism for spleen cell euploidy and aneuploidy involving specific chromosomes (*3–5*). The chromosome instability is correlated with the presence of a clastogenic agent in the sera of these mice (*6*). By selective matings founded on chromosome breakage frequencies in bone marrow, 2 NZB lines could be developed: an HB line and an LB line (*7*). Comparative studies of HB and LB mice showed significant differences in the incidence of lymphomas and other neoplasias. The conversion of the Coombs' test was also significantly more frequent and occurred earlier in HB mice than in LB mice (*7*). The data of the present study indicate that the 2 NZB lines differ also in endogenous virus expression.

MATERIALS AND METHODS

Animals.—The NZB/Bl mouse strain originated from Bielschowsky's stock and had been maintained as a conventional inbred colony in Paris since 1963. From the selection period on, the animals were no longer bred by brother × sister matings but between litters so as to assure the mating of extremes. Animals with chromosome breakage figures under 10% are LB animals; those with chromosome breakage figures over 30% are HB animals. Both percentages are statistically different for 50 mitoses studied. The proportion of LB and HB animals in the 2 breeding lines, developed by selective matings according to chromosome breakage incidences in bone marrow cells, is shown in table 1. Since the cytogenetic study of generation F7 of the LB line has shown normal values in 98% of the females, the chromosome breakage incidence of the females was not controlled before the mating from generation 8 on. In 14.3% of the males, increased chromosome breakage had to be expected (table 1) and for this reason the breakage rate was established for all males used for the continuation of the LB line. The 4 males used for the production of the LB litters had chromosome breakage figures between 0 and 6.3%. The animals belonged to filial generations 7–10 and were 5–7 months old when they were mated. Three litters from HB parents and 4 litters from LB parents were delivered by cesarean section at days 16–17 of gestation. The LB litters consisted of 9, 10, and 8 embryos (litters 1, 2, and 4, respectively), except for litter 3 consisting only of 3 embryos, from which 1 did not give successful cultures. The number of fetuses in the 3 HB litters was 8, 10, and 12, respectively, from which 6 were taken at random for the cultures.

Cell cultures.—Primary cell cultures were derived by trypsinization from single embryos after removal of the head, limbs, tail, and abdominal organs. The cells were grown in RPMI-1620 medium supplemented with 20% heat-inactivated fetal bovine serum containing antibiotics. When confluent, each monolayer was transferred by treatment with 0.25% trypsin. Passages of embryonic fibroblasts were done at 5-day intervals.

To enhance potential recovery of endogenous xenotropic virus, we cocultivated embryonic cells with susceptible heterologous cells. At the first passage of embryonic cells, one of the cultures was grown in the presence of rabbit corneal

---

ABBREVIATIONS USED: HB=high chromosome breakage; LB=low or normal chromosome breakage; RSV=Rous sarcoma virus; RT=reverse transcriptase; TCA=trichloroacetic acid.

---

[1] Received February 10, 1981; revised November 30, 1981; accepted December 22, 1981.

[2] Supported in part by Action Thématique Programmée from Centre National de la Recherche Scientifique and by a research grant from Groupements des Entreprises Françaises dans la Lutte contre le Cancer.

[3] Laboratoire d'Hématologie Expérimentale, Centre Hayem, Hôpital Saint-Louis, 2 place du Dr. Fournier, 75475 Paris Cédex 10, France.

[4] *Address reprint requests to* Dr. Emerit *at* Laboratoire de Cytogénétique Expérimentale, Institut Biomédical des Cordeliers, 15 rue de l'Ecole de Médecine, 75006 Paris, France.

[5] We thank Miss L. Cernjavski for her excellent technical assistance.

TABLE 1.—*Stage of the selective breeding when this study was done*[a]

Breeding line	Sex	Generation							
		F_0	F_1	F_2	F_3	F_4	F_5	F_6	F_7
LB	♂	28.6	54.9	65.2	68.4	84.0	64.0	73.5	85.7
	♀	30.8	65.2	66.7	63.8	71.2	67.0	85.7	98.0
Total studied		87	100	150	137	116	84	76	69
HB	♂	20.0	35.0	37.0	26.4	30.0	36.0	0	—
	♀	17.3	59.4	47.6	28.6	29.0	32.5	17.9	—
Total studied		87	72	174	152	102	68	47	—

[a] The figures represent percentages of animals in the 2 populations: For the LB line this proportion increased from 28.6 to 85.7%; for the HB line, the proportion of animals with HB figures could not be increased beyond generation 5. *Dash* indicates not done.

cell lines SIRC. These cocultures were done at a ratio of 3×10^6 NZB embryonic cells to 10^6 SIRC cells and were transferred at a split ratio of 2:1 every 2d day.

Virologic studies.—a) RT assays: The cocultures between NZB and SIRC cells were checked for the presence of extracellular C-type viruses by RT assay performed on the culture fluids.

Medium from each tissue culture was clarified by centrifugation at 10,000×*g* for 10 minutes. Of the clarified supernatant, 15 ml was then loaded onto an 8-ml cushion of 20% glycerol in 0.05 *M* Tris-HCl (pH 8) and 0.10 *M* NaCl and spun at 105,000×*g* for 90 minutes at 4°C. The viral pellet was resuspended in 50 µl of the above buffer containing 1 m*M* 1,4-dithiothreitol and 0.1% Triton X-100 or 0.05% Nonidet P40. Of this virus suspension, 20 µl was added to 50 µl of a reaction mixture containing 50 m*M* Tris-HCl (pH 8), 50 m*M* KCl, 0.5 m*M* $MnCl_2$, 1 m*M* 1,4-dithiothreitol, 0.04 A_{260} U of polydeoxyadenylate:deoxythymidylate (12:18), and 3×10^{-6} *M* [^{3}H]TTP (sp act, 40–50 Ci/mmol). After 30 minutes' incubation at 37°C, the reaction was arrested with chilled saturated pyrophosphate and 10% TCA. The acid-precipitable fractions were collected on Millipore membranes (450 nm), washed with 5% TCA, and enumerated in a Packard liquid scintillation counter. Twenty microliters of pelleted virus used in the reaction mixture corresponded to virus produced by 2×10^6 cocultured cells: results were considered negative when about 0.2 pmol of [^{3}H]dTMP (<10,000 cpm) was incorporated into acid-precipitable nucleotides.

b) Determination of host range: The virus particles recovered by ultracentrifugation from the cocultures of HB embryos were inoculated onto mouse cells of the N- or B-type to determine whether the virus from our strain has a xenotropic host range as described by Levy and Pincus (*8*).

Chromosome studies.—The chromosome analysis for the establishment of the chromosome breakage incidence in the parent animals was done on bone marrow cells. The mitoses were arrested in metaphase by ip injection of 0.01 ml colchicine/g body weight (0.24% solution), 2 hours before one femur bone was removed from the animal under general anesthesia. The bone marrow was washed out of the femur with a syringe and needle. After hypotonic pretreatment (75 m*M* KCl) for 20 minutes, the cells were fixed in ethyl alcohol to glacial acetic acid at 3:1. Slides were air dried and stained with Giemsa. The chromosomes were scored for aberrations under the microscope on coded slides. Gaps and breaks of one or both chromatids, acentric fragments, dots, and structurally rearranged chromosomes were noted. The aberration rate was calculated from a total of 50 mitoses.

For chromosome studies in fibroblast cultures from NZB embryos, colchicine was added to the culture medium after a cultivation of 24 hours for the last 3 hours. The cultures were studied at passage 1 or 2. After trypsinization, the cells were exposed to the same procedure as described above for bone marrow, except that iced wet slides were used for spreading of the mitoses instead of dry slides prewarmed in a flame.

RESULTS

Host range of virus.—The virus recovered by ultracentrifugation from the cocultures was not infectious for mouse cells but grew readily in a mink cell line, thus indicating a xenotropic host range. This experiment was done with virus particles from three different cocultures.

Virus production.—As seen from table 2, the virus assays in the culture media from 17 cocultures of NZB/Hb embryos were positive from the fourth subcultivation on. In 3 embryos, positive results were obtained even at passage 2. The enzyme levels reached very high titers from passage 4 on, and in 7 of the 17 embryos the RT values measured were higher than 20 pmol of incorporated [^{3}H]dTMP/2×10^6 cocultivated cells.

Among the 22 embryos from the NZB/Lb substrain, only 3 had positive RT reactions at late passages (7–10). Two of these belonged to litter 2 that differed from the 3 other litters by the low number of fetuses. The RT levels did not exceed 0.5 pmol of [^{3}H]dTMP incorporation.

Chromosome studies.—Chromosome analysis could be done in 21 of the 22 LB embryo cultures. In embryo #5 the number of mitoses available was too low. No increase in the aberration rate was found in 10 embryo cultures (47.6%); the remaining had "intermediate" breakage frequencies (11–29%). No LB embryo had HB aberration rates i.e., higher than 30%.

The proportion of animals with normal and intermediate breakage rates varied according to litters. In 1 litter, all fetuses had normal values. This litter was derived from the male with the lowest aberration rate (0%) and belonged to filial generation 10.

In 4 of the 17 HB embryo cultures, chromosome analysis could not be done because of lack of mitoses. Among the 13 cultures studied, 3 had aberration rates higher than 30%, 8 had intermediate breakage figures, and only 2 had normal values.

The mean of mitoses with aberrations was 10.6% for LB

TABLE 2.—*Incidence of chromosome abnormality and retrovirus production in embryo cells derived from 2 breeding lines of the NZB mouse strain*

Breeding line	Generation	Litter No.	Embryo No.	Percent of mitoses with chromosome aberrations[a]	Total chromosome aberrations/100 mitoses[a]	RT assays in cell media[b] at passages No.:		
						1–3	4–6	7–10
LB	F_7	1	1	16.0	22.0	–	–	–
			2	11.1	13.3	–	–	+
			3	14.0	14.0	–	–	–
			4	29.7	45.9	–	–	–
			5	ND	ND	–	–	–
			6	22.5	22.5	–	–	–
LB	F_7	2	7	16.7	19.0	–	–	++
			8	15.2	17.4	–	–	++
LB	F_8	3	9	2.0	4.0	–	–	–
			10	6.9	6.9	–	–	–
			11	20.5	26.7	–	–	–
			12	17.8	20.0	–	–	–
			13	28.9	46.7	–	–	–
			14	12.8	29.8	–	–	–
LB	F_{10}	4	15	5.9	9.1	–	–	–
			16	0	0	–	–	–
			17	0	0	–	–	–
			18	0	0	–	–	–
			19	6.3	6.3	–	–	–
			20	5.6	5.6	–	–	–
			21	3.1	3.1	–	–	–
			22	4.8	4.8	–	–	–
HB	F_{10}	5	23	35.5	48.4	++	++	++
			24	17.4	19.6	+	++	++
			25	30.0	35.0	–	+	++
			26	ND	ND	+	+	++
			27	ND	ND	–	+++	+++
			28	42.1	47.4	–	+	+++
HB	F_{10}	6	29	9.1	9.1	–	+	+
			30	12.1	12.1	–	+	+
			31	6.3	6.3	–	+	+
			32	22.7	25.0	–	+	+
			33	27.5	32.5	–	+++	+++
			34	12.5	17.9	–	+	+
HB	F_{10}	7	25	26.0	30.0	–	+++	+++
			36	18.5	27.8	–	+++	+++
			37	ND	ND	–	+++	+++
			38	18.0	24.0	–	++++	++++
			39	ND	ND	–	+	+++

[a] ND: not done.

[b] RT results are in cpm (*see* "Materials and Methods"); –: <10,000 cpm; +: 11,000–50,000 cpm; ++: 50,000–100,000 cpm; +++: 100,000–400,000 cpm; ++++: 400,000–800,000 cpm.

embryo cultures and 20.5% for HB embryo cultures ($P<0.001$). The total of aberrations per 100 cells also differed significantly for LB and HB embryo cultures (14.1 and 25.0%, respectively).

The aberrations consisted of gaps and breaks of one or both chromatids, telomeric extrusions, fragments, dots, exchange figures, and structurally rearranged chromosomes. Pulverization of single chromosomes and fragmentation of the whole metaphase plate as described previously (*6*) were observed in HB embryo cultures.

DISCUSSION

Increased chromosome breakage and rearrangement are observed in fibroblast cultures from NZB embryos (*5, 9*) and in "direct" chromosome preparations from bone marrow cells of adult NZB mice (*2*). This chromosome breakage characteristic could be used as the basis of a selection experiment that resulted in the separation of a line with LB incidence. The proportion of animals with HB and LB rates in the progeny depended on the phenotype of the parents (*7*). Comparative studies of the 2 lines showed that the selection on the basis of chromosome breakage rates had influenced also the pathologic manifestations of the NZB mouse disease. Malignant lymphomas occurred in 14.1% of NZB mice from the HB line, while the incidence was only 4.2% in the LB line ($P<0.01$). The conversion of the Coombs' test was also significantly different for both breeding lines. From the HB line 60% of males and nearly 70% of females were Coombs' test-positive at the age of 6 months compared to only 3–4% of the LB mice. The data of the present study show also significant differences for the expression of the xenotropic type C RNA virus of NZB mice (*8*).

The enzyme RT is common to all mammalian type C RNA viruses. These viruses need RT for their integration in the genome of the host as DNA provirus. NZB embryo cultures usually do not yield this enzyme at detectable levels, and cocultivation with susceptible cells is necessary to enhance the possibility of detecting low levels of virus production. This finding was also the case in the present study, in which an SIRC cell line was used as an indicator. All embryo cultures from the HB line gave positive RT assays of high titer. The virus recovered by ultracentrifugation of the cocultures was shown to have a xenotropic host range similar to that of the virus described by Levy and Pincus (*8*) in their NZB colony. A treatment with 5-iodo-2′-deoxyuridine for eventual induction of an NZB-X2, as described by Elder et al. (*10*), was not done either in HB or in LB cells. Only 3 of the 22 cocultures initiated from embryos of the LB line displayed enzyme activity at late passages. Of these 3 embryos, 2 were unique since they belonged to litter 2 with only 3 fetuses. We may conclude that the selection has also influenced the virus production and that the LB line releases only exceptionally the NZB virus at detectable levels. More sensitive assays might give positive results for the presence of the NZB virus. This possibility does not preclude the interest of this study in the intention to show differences between the 2 breeding lines. That these differences in virus expression exist could be shown in a significant way.

NZB mice are supposed to lack normal restriction of complete xenotropic virus expression and to release spontaneously this endogenous virus. Two independently segregating autosomal dominant genes (*11*) or rather one single autosomal dominant gene (*12, 13*) is involved in the genetic regulation of virus expression. The results of studies on reciprocal crosses and back-crosses between animals of both breeding lines agree with regard to the dominance of the breakage characteristic and these studies reach the same conclusion as the studies on virus expression (*14*). Mutation at virus suppressor loci was suggested as the cause for the spontaneous virus release in NZB mice (*11*). Thus, beside the possibility of having selected a line on the basis of virus infectivity, selection based on virus restriction has to be considered.

In general there was a good correlation between virus recovery and chromosome aberration rate. The earliest RT assays were observed for litter 5, which was comprised also of the 3 embryos with the highest aberration rates and 2 cultures of bad growth. Litter 6, comprised of 2 embryos with normal and 2 embryos with near-normal values (12.1 and 12.5%, respectively), gave positive results only in later passages not exceeding 50,000 cpm. Possibly, the 2 embryos from litter 6 with normal cytogenetic results (9.1 and 6.3%) would have shown higher aberration rates at later passages when the RT assays became positive. The discrepancy between considerably increased breakage rates and negative RT assays in 2 of the LB embryos (#4 and 13) is more difficult to explain, but the number of discordant results is too small to change the conclusion.

Damaging properties of both DNA and RNA viruses to the chromosomes are well known [*for review see* Nichols (*15*)]. The effect of the avian oncoviruses in mammalian systems has been intensively studied. Using rat fibroblasts, Nichols and co-workers (*16*) found chromosome aberrations after the cells were infected with RSV. Increased breakage was also observed by Kato (*17*) with RSV in Chinese hamster cells. Chromosome abnormalities were regularly observed in sarcomas induced by RSV (*18, 19*) and the type of aberrations, especially minute fragments and "pulverizations," is quite similar to that observed in the NZB cultures.

If a causal relationship between chromosome damage and virus release is presumed, the question remains whether the virus is also responsible for the development of tumors and autoimmune reactions. The oncogenic properties of xenotropic viruses are not confirmed, and recent evidence suggests that most endogenous type C viruses are not transforming agents but are inherited in the host to function in other biologic processes (*20*). Autoimmune reactions were found to be independent of xenotropic virus in the NZB mice studied by Datta and Schwartz (*11*).

Another possibility would be that the chromosome aberrations themselves, secondary to somatic mutation, are responsible for the development of cancer and autoimmune reactions in this strain. The eventual role of chromosome instability at the origin of cancer and abnormal immune reactions has been proposed already by other authors (*21, 22*).

Further work is necessary for a better understanding of the interrelationship between viruses, chromosome damage, and pathologic manifestations of NZB mouse disease. The 2 NZB mouse breeding lines differing in these parameters may be useful as an experimental model.

REFERENCES

(*1*) Talal N. Autoimmunity and lymphoid malignancy in New Zealand black mice. Prog Clin Immunol 1974; 2:101–120.

(*2*) Halpern B, Emerit J, Housset E, Feingold J. Possible autoimmune processes related to chromosomal abnormality (breakage) in NZB mice. Nature [New Biol] 1972; 235:214–215.

(*3*) Fialkow PJ, Paton GR, East J. Chromosomal abnormality in spleens of New Zealand black mice, a strain characterized by autoimmunity and malignancy. Proc Natl Acad Sci USA 1973; 70:1094–1098.

(*4*) Fialkow PJ, Bryant JI, Friedman JM. Specificity of acquired chromosome abnormality in New Zealand black mice. Int J Cancer 1978; 21:505–510.

(*5*) Lerner RA, Jensen F, Kennel SJ, Dixon FJ, Desroches G, Francke U. Karyotypic, virologic and immunologic analysis of two continuous lymphocyte lines established from New Zealand black mice: Possible relationship of chromosomal mosaicism to autoimmunity. Proc Natl Acad Sci USA 1972; 69:2965–2969.

(*6*) Emerit, I, Levy A, de Vaux Saint Cyr C. Chromosome damaging agent of low molecular weight in the serum of New Zealand black mice. Cytogenet Cell Genet 1980; 26:41–48.

(*7*) Emerit I, Feingold J, Levy A, Martin E, Housset E. Tumor incidence and development of autoimmune hemolytic anemia in two breeding lines of the NZB mouse strain that differ in chromosome breakage. JNCI 1980; 64:513–517.

(*8*) Levy JA, Pincus T. Demonstration of biological activity of a murine leukemia virus of New Zealand black mice. Science 1970; 170:326–327.

(*9*) Emerit I, Bernard C, Housset E. Chromosome breakage and xenotropic C-type virus in embryonic cultures from New Zealand black mice. Cytogenet Cell Genet 1979; 23:264–273.

(*10*) Elder JH, Gautsch JW, Jensen FC, et al. Differential expression of two distinct xenotropic viruses in NZB mice. Clin Immunol Immunopathol 1980; 15:493–501.

(*11*) Datta KS, Schwartz RS. Genetics of expression of xenotropic virus and autoimmunity in NZB mice. Nature 1976; 263:412–414.

(*12*) Stephenson JR, Aaronson SA. Demonstration of a genetic factor influencing spontaneous release of a xenotropic virus of mouse cells. Proc Natl Acad Sci USA 1974; 71:4925–4929.

(*13*) Levy JA, Joyner J, Nayar KT, Kouri RE. Genetics of xenotropic virus expression in mice. I. Evidence for a single locus regulating spontaneous production of infectious virus in crosses involving NZB/BINJ and 129/J strains of mice. J Virol 1979; 30:754–758.

(*14*) Levy A, Emerit I, Feingold J. Chromosomal instability of NZB mice, a dominant trait. Biomedicine. In press.

(*15*) Nichols WW. Viruses and chromosomes. In: Busch H, ed. The cell nucleus.Vol 2. New York: Academic Press, 1974:437–458.

(*16*) Nichols WW, Levan A, Heneen WK, Peluse M. Synergism of the Schmidt-Ruppin strain of the Rous sarcoma virus and cytidine triphosphate in the induction of chromosome breaks in human cultured leukocytes. Heriditas 1965; 54:213–236.

(*17*) Kato R. The chromosomes of forty-two primary Rous sarcomas of the Chinese hamster. Hereditas 1968; 59:63–66.

(*18*) Mark J. Double minutes: A chromosomal aberration in Rous sarcomas in mice. Hereditas 1966; 57:1–22.

(*19*) Mitelman F. The chromosomes of fifty primary Rous rat sarcomas. Hereditas 1971; 69:155–186.

(*20*) Levy JA. Are type C viruses transforming agents? Biomedicine 1981; 34:4–8.

(*21*) German J. Genes which increase chromosomal instability in somatic cells and predispose to cancer. Prog Med Genet 1972; 8:61–101.

(*22*) Fialkow PK. Autoimmunity and chromosomal aberration. Am J Hum Genet 1966; 18:93–97.

blank page

Phenotypic Stability of Murine Tumor Cells In Vitro and In Vivo[1,2,3]

James Varani[4] *and* **Edmund J. Lovett**[4]

ABSTRACT—Murine fibrosarcoma cells that vary in their transplantability in syngeneic mice were isolated from a heterogeneous parent tumor (induced in a female C57BL/6 inbred mouse) and maintained in culture by serial passage. Several biologic properties that discriminate between the high- and low-transplantable lines (including adhesiveness, motility, and levels of chymotrypsin-like esterase activity), as well as properties that do not separate these lines (e.g., in vitro growth rates and levels of protease and glycosidase activities), were measured at periodic intervals over 2 years. Ability to induce primary tumors and to induce metastases from these tumors were evaluated at the same intervals. The high- and low-transplantable lines were also transplanted into syngeneic mice at tumorigenic doses. Isolates from primary and metastatic tumors induced in the animals were reestablished in culture and examined for the various characteristics at passages 5, 10, 20, and 30. The properties of the cells maintained continually in culture remained stable throughout the 2-year observation period. Tumor isolates showed some evidence of modulation immediately after reestablishment in culture, but by passage 10 they appeared to be identical to the prototype parent lines. These data show that the fibrosarcoma cells do not undergo continual phenotypic "drift" as has been suggested to occur with other tumor lines maintained by serial passage in animals or in culture.—JNCI 1982; 68:957–962.

Recent investigations in several laboratories have revealed that uncloned tumors are heterogeneous entities comprised of several distinct subpopulations (*1–7*). Many of these heterogeneous tumors are being used in efforts to determine which of their properties contribute to cancer. It is essential, therefore, to determine exactly how stable these tumor populations are, particularly since many phenotypic alterations are known to occur in tumor cells maintained in culture or in animals over a long period of time (*8–12*). The only way that the stability of particular cell populations can be verified is by maintaining the cells in culture or in animals for extended periods and examining them periodically with regard to specific characteristics. This report addresses the question of tumor cell stability in one model system.

MATERIALS AND METHODS

Tumor cells.—Two populations of fibrosarcoma cells isolated from a 3-methylcholanthrene-induced tumor in a female C57BL/6 inbred mouse (The Jackson Laboratory, Bar Harbor, Maine) were used in this study. These two populations represent prototype "high-transplantable" and "low-transplantable" lines of cells. A description of the isolation procedures used to obtain these cells has been presented in our recent reports (*6, 7*). A number of additional lines with characteristics similar to those of these prototype lines have also been isolated (*6, 7, 13–15*).

The prototype high-transplantable line was isolated from a pulmonary metastasis in a C57BL/6 mouse that was given an injection of 1×10^5 parent cells in the right rear footpad 30 days earlier. The prototype low-transplantable line was isolated from the parent cells by adapting the cells to grow in medium supplemented with 10% normal human serum in place of 10% FCS. After passage of the cells in human serum-containing medium for 3 months, they were returned to medium with FCS and maintained ever since. After establishment in culture, both lines were cloned. Cloning was accomplished by seeding dishes 35 mm in diameter with small numbers of cells (≈100 cells/dish) and by isolating individual colonies by scraping with a glass needle. Colonies isolated in this manner were subcloned two additional times in the same manner. The cells were then diluted and added to microtiter wells in 50-μl volumes. The wells were subsequently examined under phase-contrast microscopy, and those wells containing only a single colony were noted. The cells harvested from such wells were assumed to be clonally derived.

In addition to the two prototype lines, six isolates were established in culture from primary tumors or metastatic tumors that developed in syngeneic mice after injection with either of the two prototype lines. After establishment in culture, the six isolates as well as the two prototype lines were maintained under identical conditions which included growth on medium 199 supplemented with 10% FCS. We purchased the cell culture media and the reagents used throughout this study from GIBCO, Grand Island, N.Y. FCS was obtained from the Kansas City Biological Co., Lenexa, Kans. We used cell culture plastic ware from a number of commercial sources; none of them proved to be superior to the others. The cells were grown at 37°C in 5% CO_2 atmosphere. All cell lines were determined to be free of mycoplasma contamination by culture on mycoplasma agar and in mycoplasma broth.

Experimental protocol.—The two prototype lines were established simultaneously between January and May 1977 and were maintained by serial passage in culture. They were subcultured at a 1:4 split ratio on a 3- to 5-day schedule. Each line was periodically examined with regard to several biologic properties over the ensuing 2 years. On two occasions (at ≈1 yr and 1.5 yr after the start of the experiment) cells of each line were removed from the freezer and compared with the cells maintained in culture. The tumor isolates were also maintained in culture by serial passage and examined at passages 5, 10, 20, and 30.

ABBREVIATION USED: FCS=fetal calf serum.

---

[1] Received June 3, 1981; revised December 16, 1981; accepted January 15, 1982.

[2] Supported by Public Health Service grants CA-29550 and CA-29551 from the National Cancer Institute.

[3] Animals were maintained under the guidelines set forth by the University of Michigan.

[4] Department of Pathology, The University of Michigan Medical School, Box MC45, 1335 East Catherine St., Ann Arbor, Mich. 48109.

The properties examined included growth kinetics, adhesiveness (as determined by resistance to trypsin-mediated release from plastic dishes), motility, and various hydrolytic enzyme levels. Growth kinetics were determined by adding 1×10^5 cells to dishes 35 mm in diameter in 2 ml of growth medium. At daily intervals fresh medium was added, and the cells were harvested by trypsinization and enumerated with the use of an electronic particle counter (model ZB; Coulter Electronics, Garden Grove, Calif.).

For the determination of adhesiveness, 1×10^5 cells were added to the 35-mm dishes and allowed to grow for 18 hours. The dishes were then washed twice with phosphate-buffered saline and treated with a solution of 0.25% trypsin (1:250; Difco Laboratories, Detroit, Mich.). The plates were rotated at 50 r/min at room temperature, and samples of the supernatant were taken at 1-minute intervals. After 10 minutes, all cells that were still attached were removed by vigorous trituration. Cells were enumerated with an electronic particle counter, and the percentage of cells detached at each time period was determined. The procedure has been described in detail in a recent report (*13*).

We determined cell motility with the use of an agarose assay as described previously (*16*). A single-cell suspension was prepared and centrifuged into a pellet. The pellet was resuspended in growth medium containing 0.2% Seaplaque agarose (Marine Colloids, Inc., Rockland, Maine). Drops of 5-μl size containing about 1×10^5 cells were added to wells of a microtiter plate. After the drops had solidified, they were overlayered with growth medium. The plates were then incubated at 37°C for 18 hours. Cell migration was determined at this time by measuring the distance between the edge of the agarose drop and the leading edge of the migrating cells.

We measured hydrolytic enzyme activities, i.e., nonspecific protease activity, β-glucosaminidase activity, and chymotrypsin-like esterase activity. Hemoglobin hydrolysis was used as a measure of nonspecific protease activity. It was measured by a highly sensitive solid-phase assay as described in a previous report (*17*). The substrate was dried onto the surface of microtiter wells at 10 μg/well. Viable tumor cells, 5×10^6/well, were added in a 200-μl volume, and the assay was run for 1 hour at 37°C. Trypsin (type I, twice crystallized from bovine pancreas; Sigma Chemical Co., St. Louis, Mo.) was used as a control enzyme.

Glucosaminidase activity was measured with the use of a standard colorimetric assay (*18*) with *p*-nitrophenyl-*N*-acetyl-D-glucosaminide as the substrate. For this assay and the chymotrypsin-like esterase assay, we prepared cell extracts by homogenization and three cycles of freeze-thawing in 0.1% Triton X-100 detergent. The extracts were diluted to contain 1 mg protein/ml. Cell extract protein (50 μg) was incubated with the substrate for 30 minutes at 37°C. Jack Bean β-*N*-acetylglucosaminidase (Sigma Chemical Co., St. Louis, Mo.) was routinely used as control enzyme for these studies.

The substrate *N*-acetyl-DL-phenylalanine-β-naphthyl ester was used as the substrate for the chymotrypsin-like esterase activity (*19*). This substrate is susceptible to chymotrypsin-like enzymes and is also hydrolyzed by a number of nonproteolytic esterases. Extract protein (100 μg) was incubated at 37°C for 45 minutes with the substrate. Chymotrypsin (type II, crystallized three times from bovine pancreas) was used as control. With each of the three enzyme assays, the linear portion of the curve was determined with respect to enzyme concentration at a given point in time and with respect to time at a given enzyme concentration. Concentrations of the viable tumor cells or tumor cell extracts were chosen to fit within the linear portion of the curve. The substrates and control enzyme preparations used in these assays were obtained from Sigma Chemical Co.

In addition to examination of these in vitro characteristics, in vivo behavior of the cell lines was characterized at periodic intervals. This involved determining the transplantability or the percentage of syngeneic mice that developed primary tumors after injection of 1×10^5 cells in the right hind footpad, and the metastatic potential or the percentage of injected animals that developed metastatic tumors in the lungs and the number of lung tumors per animal. We used 4- to 6-week-old, inbred female C57BL/6 mice in these experiments. The high- and low-transplantable lines at a given passage level were compared to one another on the same day. Animals chosen at random from the common stock were used with both groups. Thus, although different batches of animals were used to compare the groups from passage to passage, animals from the same batch were used with both prototype lines at a given passage.

RESULTS

Stability of the Prototype Lines

The two prototype lines exhibited several biologic differences when they were initially isolated and tested as described in our recent reports (*6, 7, 13–15, 20*). There were differences in adhesiveness, motility, and levels of several hydrolytic enzyme activities. There were also differences between these lines in ability to induce tumors when transplanted into syngeneic mice and in the tumors' ability to spontaneously metastasize.

The same characteristics that were initially examined in the two prototype lines were followed over a 2-year period during which time both cell populations were maintained under standard conditions (as defined in "Materials and Methods"). The results of the various in vitro assays performed as shown in text-figures 1–4. Growth curves shown in text-figure 1 indicate little variation in the high-transplantable line over the period of observation. Similarly, the growth rate of the low-transplantable line showed little variation over the same period, although the saturation density was somewhat higher in the later passages. Adhesiveness, as indicated by sensitivity to trypsin-mediated release from the surfaces of plastic culture dishes, and motility are shown in text-figures 2 and 3. Both characteristics were stable in the two lines over the 2-year observation period. The high-transplantable cells were always more adhesive and more motile than the low-transplantable cells. Enzyme activities are shown in text-figure 4. We previously reported (*6, 7*) that the high-transplantable cells had higher levels of glucosaminidase activity than the low-transplantable cells. However, after several passages under standard conditions, the levels of glucosaminidase activity in the high-transplantable cells fell and the levels in the low-transplantable cells rose. Activities in both cell lines reached similar levels by passage 20 and have remained relatively stable ever since. Although protease activity was not routinely measured during the initial phase of this study, when this activity was measured starting at passage 30, there was no significant difference between the lines and no evidence of modulation with time in culture with either line. In contrast, the *N*-acetyl-DL-phenylalanine-β-naphthyl esterase activity was greater in the low-transplantable cells than in the high-transplantable cells at the time of isolation and remained so throughout the observation period. There was no evidence of modulation of the activity in either line.

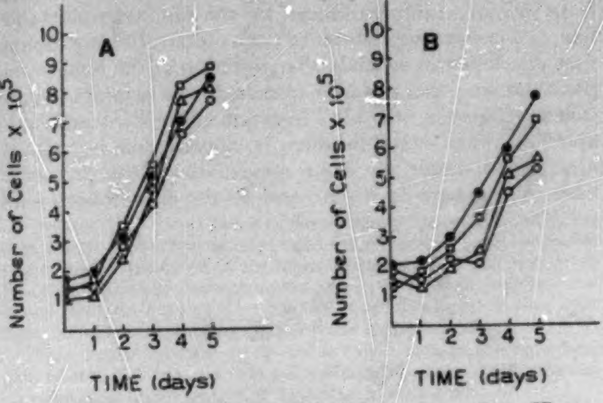

TEXT-FIGURE 1—In vitro growth rates of the prototype lines. SE were <10% of the mean values. A) High-transplantable line. B) Low-transplantable line. ○—○, passage 60; △—△, passage 120; □—□, passage 180; ●—●, passage 240.

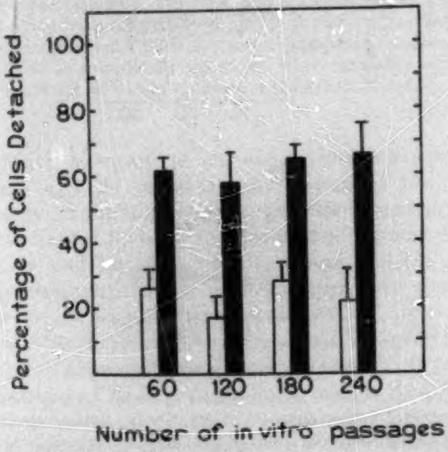

TEXT-FIGURE 2—Trypsin-mediated detachment of the prototype lines. Cells were plated at 1×10^6 cells/ml in 35-mm culture dishes at time 0 and assayed for sensitivity to trypsin-mediated detachment 18 hr later (*13*). The assay involves sampling at 2-min intervals over 10 min, although only 1 time point (at 5 min) is shown. Values are means ± SEM of the percentage of released cells from triplicate plates. The *t*-test was used to evaluate the significance of the difference between the high- and low-transplantable lines at each passage. $P\leq0.05$ for the differences. □, High-transplantable line; ■, low-transplantable line.

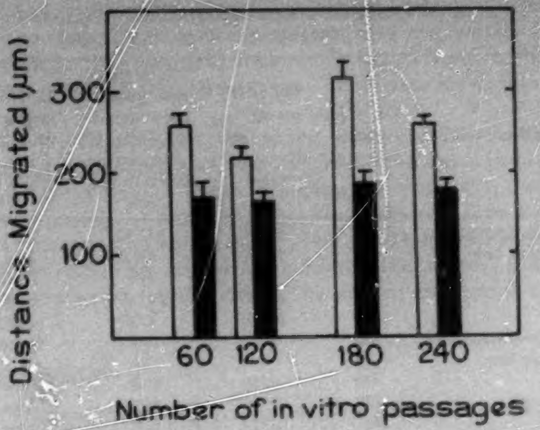

TEXT-FIGURE 3.—Motility of the prototype lines was assayed with the use of the agarose procedure (*16*). □, High-transplantable line; ■, low-transplantable line. Values are the average distances ± SEM from the leading edge to the edge of the agarose drop on 4 sides of each of 4 drops. Significance of the difference between the high- and low-transplantable lines at each passage was evaluated by Student's *t*-test. $P<0.001$ for all the differences.

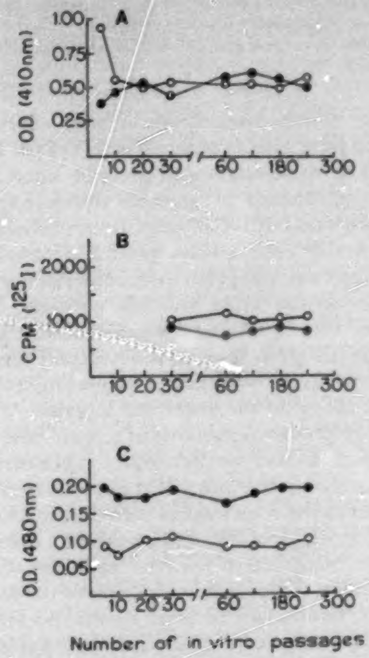

TEXT-FIGURE 4.—Enzyme activity assays of the prototype lines were done as described in "Materials and Methods" and in previous publications (*17–19*). A) Glucosaminidase activity. B) Protease activity. C) Chymotrypsin-like esterase activity. ○—○, High-transplantable line; ●—●, low-transplantable line. The glucosaminidase and chymotrypsin-like esterase values are averages of triplicate samples. SE were <10% of the means. Protease values are averages of 4 samples; standard errors were <15% of the means. Student's *t*-test was used to evaluate the significance of the differences between the high- and low-transplantable lines at each passage. The differences in the chymotrypsin-like esterase activity were significant at all passages ($P\leq0.05$). The other enzyme activities were not significantly different between the two prototype lines. O. D.=optical density.

TABLE 1.—*Transplantability and metastasis formation by the prototype lines*

Cell population	No. of in vitro passages	No. of tumors/No. of mice given injections[a, b]	No. of mice with pulmonary metastases/No. of mice with primary tumors[b, c]	No. of metastases/mouse, mean ± SEM[b, c]
High-transplantable line	10	30/30	11/30	2±1
	30	20/20	4/20	5±3
	60	8/8[d]	2/8	5±4
	120	18/20	11/18	6±4
	240	20/20	7/20	4±3
Low-transplantable line	10	2/10	0/2	None
	30	—	—	—
	60	5/30	0/5	None
	120	7/25[d]	0/7	None
	240	5/20	0/5	None

[a] Each animal received 1×10^5 viable tumor cells in the right hind footpad. All animals were examined at 3- to 5-day intervals and were scored as negative if there was no evidence of tumor growth 35 days after injection (*6*).

[b] —=not measured.

[c] Animals were killed with ether after 35 days, and their lungs were examined for metastatic tumor nodules after inflation with india ink (*21*).

[d] Significance levels were determined by a chi-square test. When the passage 60 high-transplantable line was compared with the passage 120 low-transplantable line (the 2 groups with the smallest difference), the *P*-value was <0.01.

In addition to measuring these in vitro characteristics, both cell lines were also compared with regard to various parameters of in vivo behavior at periodic intervals. Table 1 shows the percentage of animals developing primary tumors after injection of 1×10^5 cells. It can be seen that the high-transplantable cells always produced tumors in virtually 100% of the animals given injections. Ability to induce tumors was somewhat more variable with the low-transplantable cells, but in all cases a substantially lower percentage of animals given injections developed tumors. Furthermore, there was no evidence of increasing transplantability over the course of the observation period.

In addition to producing tumors at a high rate, the high-transplantable cells also spontaneously metastasized from the primary tumors to the lungs of the tumor-bearing mice. The rate of spontaneous metastasis varied from a low of 20% at passage 30, to a high of 61% at passage 120. Overall, lung metastases were identified in 35 of the 96 animals (36%) that developed primary tumors after injection of the high-transplantable cells. In contrast to these results, no lung metastases were identified in any of the animals that developed primary tumors after injection of the low-transplantable cells (table 1).

On two separate occasions, stock cultures of each line that had been frozen during the initial phase of the study were removed from the freezer and established in culture. They were then injected into syngeneic mice (1×10^5 cells in the right rear footpad) and compared to the lines maintained continually in culture. The prototype lines had been in culture for periods of approximately 1 and 1.5 years at the time when the comparisons were made. The lines reestablished from frozen stocks maintained their distinctive features with regard to in vivo behavior. On both occasions the high-transplantable line formed tumors in 100% of the animals given injections and spontaneously metastasized in 35–50% of the tumor-bearing animals. The low-transplantable line, however, only formed tumors in 4 out of 16 animals on the first occasion and in 2 out of 20 animals on the second. No evidence of metastases was observed in any of the 6 tumor-bearing animals or in the 30 non-tumor-bearing animals.

Stability of Isolates Derived From the High- and Low-Transplantable Line-Induced Tumors

To further assess the stability of these cell lines, we established tumors in C57BL/6 mice and subsequently reestablished them in culture. Two isolates were obtained from primary tumors induced by the high-transplantable line, two isolates were obtained from metastatic lung tumors that developed in animals after injection of the high-transplantable line, and two were obtained from primary tumors that developed in mice after injection of the low-transplantable line. After reestablishment in culture, each isolate was maintained under the same conditions as the prototype lines. At passages 5, 10, 20, and 30 the new isolates were

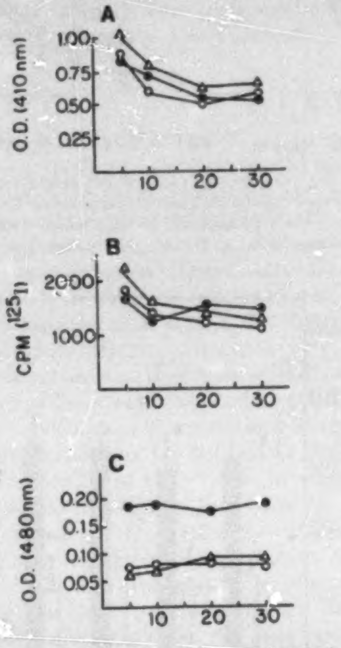

TEXT-FIGURE 5.—Enzyme activity assays of tumor isolates were done as described in previous reports (*17–19*). O—O, Isolates obtained from primary tumors that developed in animals given injections of the high-transplantable line; Δ—Δ, isolates obtained from metastatic lung tumors that developed in animals given injections of the high-transplantable line; ●—●, isolates obtained from primary tumors that developed in animals given injections of the low-transplantable line. SE were routinely <10% of the mean values in all three procedures. Differences between the isolates derived from tumors induced by the high-transplantable line and isolates derived from the low-transplantable line in chymotrypsin-like esterase activity were calculated by the Student's *t*-test and were found to be significant $P \leq 0.05$ O. D.=optical density.

TABLE 2.—*Transplantability and metastasis formation by six tumor isolates*

Tumor isolate[a]	No. of in vitro passages	No. of tumors/No. of mice given injections[b]	No. of mice with pulmonary metastases/No. of mice with primary tumors[c]	No. of metastases/mouse, mean±SEM[c]
1	5	10/10	4/10	2±1
	10	20/20	7/20	4±1
	20	20/20	5/20	1±1
2	5	8/8[d]	5/8	2±2
	10	20/20	8/20	2±1
	20	20/20	6/20	2±2
3	5	20/20	9/20	5±1
	10	19/20	8/19	4±3
	20	20/20	6/20	4±3
4	5	20/20	15/20	7±2
	10	20/20	4/20	5±1
	20	20/20	9/20	5±1
5	5	9/20[d]	1/9	None
	10	5/20[d]	0/5	None
	20	4/20[d]	0/4	None
6	5	2/6[d]	0/2	None
	10	8/20	0/8	None
	20	4/20	0/5	None

[a] Isolates 1 and 2 were obtained from primary tumors induced by the high-transplantable line. Isolates 3 and 4 were obtained from metastatic tumors which developed in the lungs of animals that had been given injections of the high-transplantable cells in the footpad. Isolates 5 and 6 were obtained from primary tumors which developed in mice after injection with the low-transplantable cells in the footpad.

[b] Each mouse received 1×10^5 viable tumor cells in the right hind footpad at 3- to 5-day intervals and was scored as negative if there was no evidence of tumor growth 35 days after injection (*6*).

[c] Mice were killed with ether after 35 days, and their lungs were examined for metastatic tumor nodules after inflation with india ink (*21*).

[d] Significance levels were determined by a chi-square test. Each of the values obtained with the low-transplantable isolates was compared with the value obtained with the high-transplantable isolate 2 at passage 5. Since fewer animals were used in this group than in the other groups, values that are statistically significant when compared to this group will also be statistically significant when compared to the other groups. $P\leq0.05$ for all values obtained with isolates 5 and 6.

examined with regard to the same characteristics as the prototype lines. In summary, by passage 5 the in vitro growth rates of the isolates were very similar to those of the prototype lines. Likewise, there was no difference in adhesiveness or motility between the tumor isolates and the respective prototype lines. Similar results were obtained at passages 10, 20, and 30 (data not shown).

Remarkable differences were observed, however, between the tumor isolates and the prototype lines with regard to enzyme levels. The tumor isolates had higher levels of protease and glycosidase activities at passage 5 than did the prototype lines. The chymotrypsin-like esterase activity was slightly elevated in the isolates. Of those isolates derived from the high-transplantable line, the metastatic tumor isolates had higher levels of activity than did the primary tumor isolates. By passage 10 the differences between the various isolates and the parent lines were reduced, and by passage 20 and subsequent passages the differences were gone. From that point on, all isolates and both prototype lines had similar levels of protease and glycosidase activities; the low-transplantable prototype line and the isolates derived from that line still had much higher levels of the chymotrypsin-like esterase activity. These data are shown in text-figure 5.

The six isolates were also tested with regard to in vivo behavior at passages 5, 10, and 20. The overall data obtained at passage 5 show a slight trend toward increasing transplantability in the recent isolates. However, even this slight trend disappeared by the later passages. Thus with regard to in vivo behavior the isolates resembled the prototype lines from which they were derived. The in vivo data are shown in table 2.

DISCUSSION

This report addresses the problem of tumor line stability: Are the numerous subpopulations of tumor cells that can be isolated from uncloned tumors stable or are they continually undergoing phenotypic alteration? This question is important for at least two reasons. First, many heterogeneous tumor models are being used in efforts to determine what particular phenotypic characteristics contribute to cancer (*5–7, 13–15, 20, 22–25*), and the results of such studies would not be valid if the populations used were in a continual state of change. Second, it has been suggested that variant tumor populations arise early in the course of tumor development and that it is specific subpopulations that give rise to metastases (*2, 3*). The ability to prove or disprove such a theory requires the existence of clones of metastatic and nonmetastatic cells stable enough to be examined after isolation.

The results presented in this report show that in at least one model system a number of phenotypic characteristics are stable in tumor cell lines maintained continually in culture for a long period of time (≤2 yr) or passed through syngeneic animals and reestablished in culture. In terms of in vitro growth rates, adhesiveness, motility, and chymotrypsin-like esterase activity, there was no evidence of modulation in either of the prototype lines examined. Furthermore, there was no evidence of modulation in the degree of transplantability or in the frequency of spontaneous metastasis formation with either line. It should be noted that since metastasis formation is to a large extent a function of primary tumor transplantability and growth kinetics, the lack of change in the rates of metastasis formation probably reflects the lack of change in transplantability.

These results show that at least with regard to the properties examined here, the populations generated from the parent tumor are not undergoing constant phenotypic drift simply as a result of in vitro or in vivo maintenance. Furthermore, they add strength to our previous findings of a strong correlation between adhesiveness and transplantability and the lack of correlation between in vitro growth rates and transplantability (*6, 7, 13–15*).

In contrast to these results, the protease and glycosidase activities did show evidence of modulation. When the conditions under which the cells were maintained were altered [i.e., going from medium with human serum to medium with FCS (*6*) and going from culture to primary tumors to metastatic tumors to culture (*7*)], the enzyme activities varied. Since the activities could be manipulated in a predictable way depending on the conditions of maintenance, this suggests that environmental pressures induced the expression of different levels of enzyme activity in a given cell population. Alternatively, it is possible that the environmental pressures selected for preexisting subpopulations that had arisen during the course of tumor growth. With the presently available data it is impossible to definitively choose between these two explanations. Whatever the reason for the modulation of these enzyme activities, once the cells were adapted to culture and maintained under standard conditions, the enzyme activities were as stable as the other properties that were examined.

It is difficult to know how general the findings are that were made with this fibrosarcoma model until similar studies are done with cell lines derived from a number of other tumors. To date not enough systems have been investigated thoroughly, probably because of the time involved in such studies. In a model that has been observed over a period of years, Sanford et al. (*26, 27*) identified stable differences in anaerobic energy metabolism in variants derived from transformed mouse fibroblasts; the differences were associated with stable differences in transplantability. A recent study by Chambers et al. (*28*) also suggested that tumor cell lines could remain stable for a prolonged period of time in vitro. Their study, however, spanned only a 3- to 4-month period, and it is not known whether these lines will demonstrate the same properties after they are maintained for a longer period of time.

In summary, these results do not suggest that tumor progression does not occur; it clearly does occur (*29*). Furthermore, these results do not conflict with the recent evidence presented by Poste, Doll, and Fidler (*30*) who showed that while individual clones that form an established tumor line may be unstable, the overall population comprised of these clones is very stable.

REFERENCES

(*1*) Fidler IJ. Selection of successive tumour lines for metastases. Nature 1973; 242:148–149.

(*2*) Fidler IJ, Kripke ML. Metastasis results from preexisting variant cells within a malignant tumor. Science 1977; 197:893–895.

(*3*) Kripke ML, Gruys E, Fidler IJ. Metastatic heterogeneity of cells from an ultraviolet light-induced murine fibrosarcoma of recent origin. Cancer Res 1978; 38:2962–2967.

(*4*) Heppner GH, Dexter DL, DeNucci T, Miller FR, Calabresi P. Heterogeneity in drug sensitivity among tumor cell subpopulations of a single mammary tumor. Cancer Res 1978; 38:3758–3763.

(*5*) Briles EB, Kornfeld S. Isolation and metastatic properties of detachment variants of B16 melanoma cells. J Natl Cancer Inst 1978; 60:1217–1222.

(*6*) Varani J, Orr W, Ward PA. Comparison of subpopulations of tumor cells with altered migratory activity, attachment characteristics, enzyme levels and in vivo behavior. Eur J Cancer 1979; 15:585–592.

(*7*) ———. Hydrolytic enzyme activities, migratory activity and in vivo growth and metastatic potential of recent tumor isolates. Cancer Res 1979; 39:2376–2380.

(*8*) Augusti-Tocco G, Sato G. Establishment of clonal lines of neurons from mouse neuroblastoma. Proc Natl Acad Sci USA 1969; 64:311–315.

(*9*) Sanford KK, Likely GD, Earle WR. The development of variations in transplantability and morphology within a clone of mouse fibroblasts transformed to sarcoma-producing cells in vitro. J Natl Cancer Inst 1954; 15:215–237.

(*10*) Todaro GJ, Green H. Quantitative studies on the growth of mouse embryo cells in culture and their development into established lines. J Cell Biol 1963; 17:299–313.

(*11*) Foley GE, Handler AH, Lynch PM, Wolman SR, Stulberg CS, Eagle H. Loss of neoplastic properties in vitro. II. Observations on KB sublines. Cancer Res 1965; 25:1254–1261.

(*12*) Foley GE, Drolet BP. Loss of neoplastic properties in vitro. I. Observations with S-180 cell lines. Cancer Res 1964; 24:1461–1467.

(*13*) Varani J, Orr W, Ward PA. Adhesive characteristics of tumor cell variants of high and low tumorigenic potential. JNCI 1980; 64:1173–1178.

(*14*) Varani J, Lovett EJ, Elgebaly S, Lundy J, Ward PA. In vitro and in vivo adherence of tumor cell variants correlated with tumor formation. Am J Pathol 1980; 101:345–352.

(*15*) Varani J, Lovett EJ, Elgebaly S, Lundy J. Characteristics of tumor cell clones with varying malignant potential. In: Hellman K, ed. Metastasis; clinical and experimental aspects. The Hague: Nijhoff, 1981.

(*16*) Varani J, Orr W, Ward PA. A comparison of the migration patterns of normal and malignant cells in two assay systems. Am J Pathol 1978; 90:159–172.

(*17*) Varani J, Johnson K, Kaplan J. Development of a solid-phase assay for measurement of proteolytic enzyme activity. Anal Biochem 1980; 107:377–384.

(*18*) Bosmann HB, Lockwood T, Morgan HR. Surface biochemical changes accompanying primary infection with Rous sarcoma virus. Exp Cell Res 1974; 83:25–30.

(*19*) Cohen W, Erlanger BF. Studies on the reactivity of diethylphosphorylchymotrypsin. J Am Chem Soc 1960; 82:3928–3934.

(*20*) Orr FW, Varani J, Delikatny J, Jain N, Ward PA. Comparison of the chemotactic responsiveness of two fibrosarcoma subpopulations of differing malignancy. Am J Pathol 1981; 102:160–167.

(*21*) Wexler H. Accurate identification of experimental pulmonary metastases. J Natl Cancer Inst 1966; 36:641–645.

(*22*) Fidler IJ. Biological behavior of malignant melanoma cells correlated to their survival in vivo. Cancer Res 1975; 35:218–224.

(*23*) Fidler IJ, Nicolson GL. Tumor cell and host properties affecting the implantation and survival of blood-borne metastatic variants of B16 melanoma. Isr J Med Sci 1978; 14:38–50.

(*24*) Nicolson GL, Winkelhake JL. Organ specificity of blood-borne metastases as determined by cell adhesion. Nature 1975; 255:230–232.

(*25*) Winkelhake JL, Nicolson GL. Determination of adhesive properties of variant metastatic melanoma cells to BALB/3T3 cells and their virus-transformed derivatives by a monolayer attachment assay. J Natl Cancer Inst 1976; 56:285–291.

(*26*) Sanford KK, Wood MW, McNair Scott DB, Kerr HA. Stability in vitro of diverse capacities for tumor production and glucose metabolism in three murine clones derived form the same cell. J Natl Cancer Inst 1969; 42:945–952.

(*27*) Wood MW, Sanford KK, Burk D, Earle WR. Glycolytic properties of high and low sarcoma-producing lines and clones of mouse tissue-culture cells. J Natl Cancer Inst 1959; 23:1079–1088.

(*28*) Chambers AF, Hill RP, Ling V. Tumor heterogeneity and stability of the metastatic phenotype of mouse KHT sarcoma cells. Cancer Res 1981; 41:1368–1372.

(*29*) Nowell PC. The clonal evolution of tumor cell populations. Science 1976; 194:23–28.

(*30*) Poste G, Doll J, Fidler IJ. Interactions among clonal subpopulations affect stability of the metastatic phenotype in polyclonal populations of B16 melanoma cells. Proc Natl Acad Sci USA 1981; 78:6226–6230.

Development of Resistance to MOPC-315 Plasmacytoma After Intralesional and Intraperitoneal Melphalan Therapy of Tumor-Bearing BALB/c Mice. I. Enhancement of In Vivo Rejection Responses by Combined Chemotherapy–Immunotherapy[1,2]

Aliza Adler, *Ph.D.*,[3,4] *and* **Irit Altbaum**, *M.Sc.*[5,6]

ABSTRACT—Experimental and clinical evidence indicates that some chemotherapeutic agents may enhance tumor cell immunogenicity. This study was undertaken to test the possibility that melphalan [L-phenylalanine mustard (L-PAM)]—a clinically useful drug—can modulate tumor cells in vivo and in vitro in a syngeneic experimental system of MOPC-315 plasmacytoma in BALB/c mice and that this modulation can be expressed in vivo by enhanced tumor resistance. Tumor-bearing mice were treated with L-PAM intralesionally and ip by a split-course chemotherapy to avoid excessive toxicity of the drug. As a result of this treatment, about 60% of the mice had complete tumor regression; of these, 40–60% were resistant to viable tumor cell challenge and were designated as "cured-immune." Immunogenicity of irradiated MOPC-315 was tested in BALB/c mice; significant protection against tumor cell challenge was not achieved. In vitro L-PAM-treated MOPC-315 cells induced a measurable but weak antitumor response. Combination of both therapeutic approaches, i.e., chemotherapy and active immunization by L-PAM-treated tumor cells, was attempted with the use of various schedules. Immunotherapy given after L-PAM-induced tumor regression significantly enhanced in vivo antitumor response to challenge by 10^4 and 10^5 viable MOPC-315 tumor cells. When immunotherapy was attempted before chemotherapy in the presence of actively growing though still occult tumor, it reduced the chemotherapy cure rate and resulted in a low rate of tumor resistance. Addition of BCG did not remarkably affect the results. The findings point to the importance of timing of active immunization relative to tumor load and chemotherapy. The implication is that chemotherapy-induced regression is mediated by host immune mechanisms in this experimental model.—JNCI 1982; 68:963–969.

Experimental evidence indicates that host antitumor mechanisms are activated under conditions of tumor regression caused by chemotherapeutic agents. Development of resistance to viable tumor cell challenge was demonstrated in several experimental models, e.g., in mice bearing plasmacytomas after cure by aniline mustard (*1–4*) or by cyclophosphamide (*5, 6*) and in guinea pigs with hepatomas after intralesional adriamycin (*7*), L-PAM, or 1,3-bis(2-chloroethyl)-1-nitrosourea (*8*).

Of the various treatment modalities employed in clinical and experimental cancers, chemotherapy and immunotherapy are directed toward control of systemic disease and, theoretically, should complement each other. Although chemotherapy frequently partially controls the disease by significantly reducing the tumor burden, it rarely affects cure, whereas immunotherapy at its best was shown only to affect minimal residual disease (*9, 10*). A combination of the two modalities should entail the possibility of an additive effect of the enhancement of tumor cell immunogenicity by chemotherapy and the stimulation of relevant host antitumor response by immunotherapy.

An investigation of chemical modulation of tumor cells with respect to their expression of tumor-associated antigens was reported (*11*); also investigated were alkylating agents (*12*), some of which are employed in clinical chemotherapy (*13–16*).

It was suggested that the mechanism of action of chemotherapeutic agents on tumor cells both in vivo and in vitro is either that the agent directly modulates the tumor cell (*12, 14*) or the drug acts indirectly as a hapten and forms a tumor-associated protein–hapten conjugate, thus enhancing the immunogenicity of the carrier protein (*15, 16*).

The selection of L-PAM for this investigation was based on the following considerations: *1*) L-PAM has haptenic activity and can induce a specific antitumor response after active immunization by the tumor–protein–L-PAM conjugate (*16, 17*); *2*) the direct action of L-PAM on tumor cells permits effective intratumoral therapy, which ensures maximal contact between the drug and tumor cells in vivo; *3*) indirect evidence indicates that such in vivo contact may have a late systemic antitumor effect in human melanoma, for regional perfusion with L-PAM resulted in some instances in disappearance of distant lesions (*18*); *4*) L-PAM is widely employed in clinical cancer therapy for multiple myeloma, melanoma, breast cancer, ovarian cancer, and other cancers.

We found the experimental model of the mouse plasma-

ABBREVIATIONS USED: [^{3}H]dThd=[^{3}H]thymidine; LD$_{50}$=median lethal dose; L-PAM=L-phenylalanine mustard (melphalan); PBS=phosphate-buffered saline.

---

[1] Received June 4, 1981; revised November 23, 1981; accepted December 31, 1981.

[2] Supported by a research grant from Tel-Aviv University Research Authority.

[3] Tumor Immunology Unit, Institute of Oncology, Beilinson Medical Center, Petah Tiqva, Israel, and Tel-Aviv University Sackler School of Medicine, Tel-Aviv, Israel.

[4] *Address reprint requests to* Dr. Adler at the Beilinson Medical Center.

[5] Tumor Immunology Section, Institute of Oncology, Rokach Hospital, Tel-Aviv.

[6] We thank Professor S. Ben-Efraim, Department of Human Microbiology, Sackler School of Medicine, Tel-Aviv University, for his interest and advice.

cytoma suitable for this study because of its responsiveness to L-PAM therapy both by intralesional and systemic administrations and because of the indication that tumor regression caused by this treatment is accompanied by development of in vivo tumor resistance (*19*).

One of the main objectives of this investigation was to establish optimal sequences and schedules for combined chemotherapy–immunotherapy to achieve the highest cure rate and to induce strong tumor resistance. This first part of the study deals with development of methods for in vivo chemotherapy and active immunization by in vitro L-PAM-treated tumor cells and with the combination of the two methods. The ultimate goal of this ongoing work is to identify the immune mechanisms involved in tumor rejection after L-PAM therapy and to apply the knowledge gained for selective stimulation of such responses.

MATERIALS AND METHODS

Animals.—Male inbred BALB/c mice, 6–8 weeks old and weighing approximately 20 g, were obtained from The Weizmann Institute, Rehovot, Israel, and used throughout this study.

Tumor cells.—Mineral oil-induced MOPC-315 plasmacytoma, originally developed by Potter and Walters (*3*), was obtained from Dr. D. Givol, The Weizmann Institute, and maintained in vivo by serial sc inoculation into syngeneic BALB/c mice. The cells were irradiated by tele-cobalt at 3,000 and 6,000 rad.

L-PAM.—L-PAM was obtained as dry powder from Wellcome Foundation Ltd., London, England. It was diluted in an acid-alcohol solution and in a diluent supplied by Wellcome. We used 0.2 ml of L-PAM in an appropriate concentration for intratumoral or ip injection in tumor-bearing mice.

In vitro L-PAM treatment of tumor cells was performed as follows: A single cell suspension of 10^6 tumor cells in 2.5 ml PBS containing 25 µg of L-PAM was incubated in a shaker bath for 30 minutes at 37°C in 50-ml plastic tubes. The tumor cells were then washed twice in 50 ml PBS and tested for viability by trypan blue before immunization.

Immunization.—Immunization was performed with single cell suspensions obtained from in vivo grown ascites MOPC-315 tumor. This preparation had a high viability count compared to the approximately 50% viability of the suspension prepared from the subcutaneous tumor nodule (table 1). Immunization was done by sc injection of irradiated or L-PAM-treated cells, given twice at weekly intervals. Unless otherwise specified, 10^6 MOPC-315 cells were used as the immunizing inoculum.

BCG.—The (freeze-dried) BCG vaccine used for admixture with tumor cells for sc immunization as well as for intratumoral injection was from Glaxo Laboratories (Greenford, Middlesex, England) and contained approximately 10^6 viable organisms/0.1 ml.

Viable tumor cell challenge.—After the LD_{50} of tumor cells was established (10^2 tumor cells in repeated experiments), a dose of 10^4 viable tumor cells was chosen for challenge inasmuch as this dose gave a reproducible 100% tumor take. Thus a tumor cell challenge of 10^4 cells was used in most experiments, unless otherwise specified.

RESULTS

Tumor Take and Mortality

To establish the biologic behavior of MOPC-315 plasmacytoma in BALB/c mice in terms of tumor take and subsequent mortality, we titrated the tumor cells obtained from in vivo passage by sc injection of various tumor cell concentrations. The results of three such experiments are presented in text-figure 1, where 8 mice were used for each tumor cell concentration in each experiment. Palpable nodules (0.5–0.8 mm in diameter) became manifest in some mice at 10–16 days. Subsequently, all mice showed tumor takes and died within 30–35 days when tumors as large as 2.5–3 cm were present. No spontaneous tumor regressions were observed. The LD_{50} fell between 10 and 10^2 tumor cells, and a 10^4-cell dose showed 100% take in all experiments as calculated from curves shown in text-figure 1.

Effect of BCG on Tumor Take and Mortality

We tested the possible effect of BCG on tumor take and on mortality of BALB/c mice inoculated with MOPC-315. Three schedules of BCG administration were tested: *1*) systemic pretreatment of mice by subcutaneous BCG on day 14 before tumor inoculation; *2*) admixture of BCG with viable tumor cells before inoculation; and *3*) intratumoral BCG injection. The results of experiments with the use of schedules *1* and *2* are shown in text-figures 2 and 3.

There were some delays in tumor take and prolongation of survival but no tumor regressions or cures were seen in mice given injections of BCG before tumor inoculation and those given injections of the BCG–tumor cell mixture, as compared to non-BCG-treated tumor-inoculated mice. Direct intratumoral BCG injection of small, medium-sized, or large tumors had no effect on further tumor progression or survival. No tumor regressions were observed after intratumoral BCG injection (results not shown). We concluded that the MOPC-315 tumor is only weakly responsive to BCG-mediated antitumor effector mechanisms.

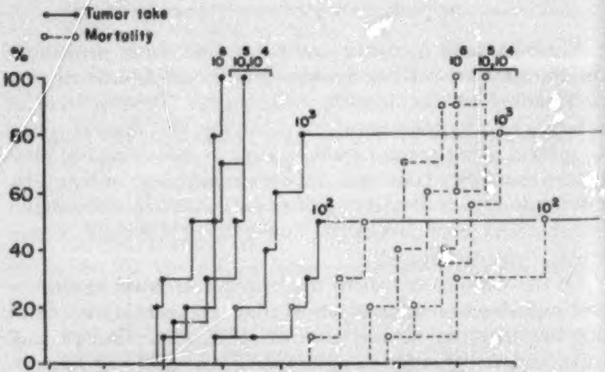

TEXT-FIGURE 1.—Tumor take and mortality of BALB/c mice after sc injection of MOPC-315 in various concentrations. Pooled data of three consecutive experiments are shown; 24 mice were used for each cell concentration.

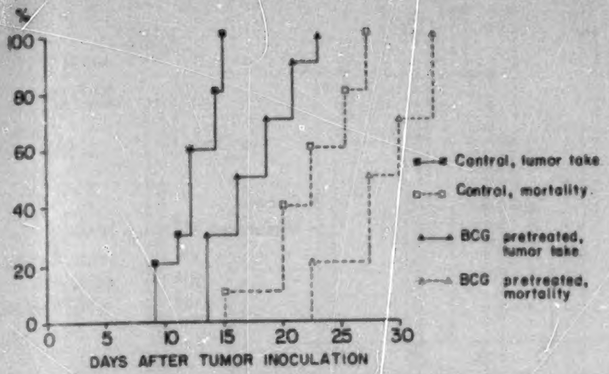

TEXT-FIGURE 2.—Tumor take and mortality of BALB/c mice after sc injection of 10^4 tumor cells in normal (control) mice and in mice pretreated on day 14 with sc BCG (10^8 viable organisms/mouse). Pooled data of three experiments are shown; 18 mice were in each group.

Immunogenicity of MOPC-315 Tumor Cells

The accepted procedure for testing the immunogenicity of a given tumor in a syngeneic system is to either excise the local tumor or actively immunize animals with irradiated tumor cells (alone or admixed with BCG) and to look for protection against viable tumor cell challenge in surgically cured or preimmunized animals. Both approaches were tried in the MOPC-315 plasmacytoma in BALB/c mice with negative results. The subcutaneous tumor nodule, even if excised early (at a diameter of 0.5–0.8-mm), regrew at the site of surgery and the tumor took at distant sites upon viable tumor cell challenge. Thus surgical cure was not achieved.

Active immunization by means of irradiated tumor cells (treated with 3,000 and 6,000 rad) given alone or admixed with BCG was attempted by the sc route on days 1 and 7 followed on day 21 by viable tumor cell challenge. No protection against challenge with 10^4 viable tumor cells was achieved (text-fig. 4). When immunized mice were challenged with 10^3 tumor cells, tumor take was similar to that in nonimmunized mice (results not shown).

These studies indicate that the MOPC-315 plasmacytoma is a nonimmunogenic or weakly immunogenic tumor and that different approaches are needed to elicit tumor rejection.

Active Immunization by In Vitro L-PAM-Treated MOPC-315 Cells

We performed a pilot experiment to establish the optimal conditions for in vitro treatment of tumor cells by L-PAM. Viable tumor cells were exposed to decreasing concentrations of L-PAM from 1,000 to 1 μg L-PAM/10^6 tumor cells for 30 minutes at 37°C. The effect of these drug concentrations on [^{3}H]dThd uptake, trypan blue staining, and tumorigenicity of treated MOPC-315 cells was examined. Results of two experiments are presented in table 1.

The lowest L-PAM concentration that completely abolished tumorigenicity was 25 μg/10^6 tumor cells, while cells treated with 5 μg L-PAM gave 40 to 60% tumor take, and those treated with 1 μg showed 100% take. No correlation was found between tumor take by L-PAM-treated cells and reduction in [^{3}H]dThd incorporation; [^{3}H]dThd was reduced at a similar rate at all L-PAM concentrations except 1 μg. Thus [^{3}H]dThd incorporation cannot serve as a sensitive index of tumorigenicity.

Vital staining by trypan blue was tested as an indicator of membrane damage and not of tumorigenicity. Concentrations of 100 μg L-PAM/10^6 tumor cells and above significantly reduced trypan blue-negative cells, whereas lower concentrations did not affect cell viability. Therefore, all experiments of active immunization were performed with tumor cells treated with 25 μg L-PAM, a concentration answering the criteria of minimal cell membrane damage, yet rendering the cell nontumorigenic.

The diluent used for the L-PAM concentration of 1,000 μg completely abolished [^{3}H]dThd uptake and reduced cell viability by trypan blue criterion, whereas the tumorigenicity of MOPC-315 cells was unaffected (100% take), even showing enhanced tumor growth. This finding indicates that while the diluent may cause transient cell damage with

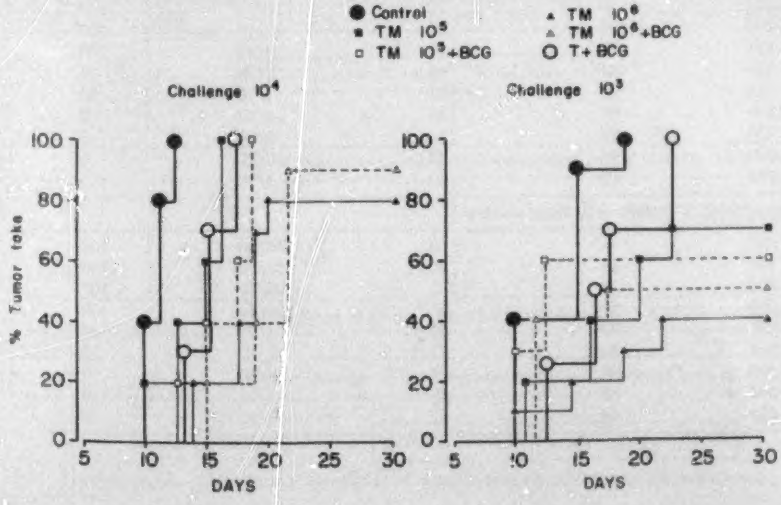

TEXT-FIGURE 3.—Tumor take in BALB/c mice preimmunized by in vitro L-PAM-treated tumor cells (TM) upon challenge of 10^4 and 10^3 viable MOPC-315 cells. Immunization was done by 10^5 and 10^6 cells (TM) with or without admixture of BCG. Control mice were inoculated with viable 10^4 and 10^3 MOPC-315 cells (T) alone (●——●) or admixed with BCG (○——○). Pooled data of two experiments are shown, 20 mice were in each group.

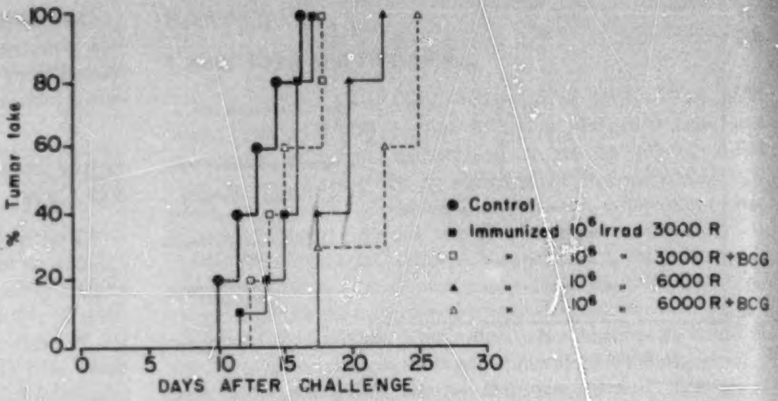

TEXT-FIGURE 4.—Tumor cell challenge in mice preimmunized with 10^6 MOPC-315 tumor cells irradiated with 3,000 and 6,000 rad (R) with or without admixture of BCG on days 1 and 7. Challenge dose of 10^4 MOPC-315 cells was given on day 21.

in vivo tumor cell recovery, treatment with L-PAM causes irreversible cell death.

We performed active immunization by sc injection of 10^5 and 10^6 L-PAM-treated cells on days 1 and 7 followed on day 21 by viable tumor cell challenge. This experiment was repeated twice, with and without admixture of BCG, with 20 mice in each treatment group (text-fig. 3). Minimal protection by immunization could be detected when mice were challenged with 10^4 viable cells. With a lower dose of 10^3 viable cells, a significant proportion of animals showed tumor resistance. When survivors of the 10^3-cell challenge were rechallenged with 10^4 viable cells, all were found to be resistant. Thus challenging preimmunized animals with a low dose of viable tumor cells has a boosting effect on in vivo tumor resistance. The immunizing dose of 10^6 L-PAM-treated MOPC-315 cells resulted in a rate of protection higher than that of the 10^5 cell dose. While some tumor protection was achieved by active immunization with L-PAM-treated cells, this schedule of immunization shows low efficacy in the MOPC-315 plasmacytoma in BALB/c mice. Addition of BCG to the tumor cell vaccine did not enhance tumor resistance.

Intratumoral and Systemic Therapy of Established Tumors With L-PAM

A pilot study showed that tumoricidal doses of L-PAM are toxic to BALB/c mice. For active tumor regression, intralesional or ip doses of 500–600 μg L-PAM/mouse are needed (25–30 mg/kg body wt). These doses caused 40–50% mortality of mice due to toxicity. Since lower doses of L-PAM did not cause complete tumor regression, a split-course

TABLE 1.—*Effect of various concentrations of L-PAM on MOPC-315 cells in vitro on [³H]dThd incorporation, trypan blue staining and tumorigenicity*

L-PAM concentration/10^6 cells, μg	[³H]dThd cpm	[³H]dThd Suppression, %	Trypan blue viability, %	Tumor take No. of tumors/No. of mice inoculated	Tumor take Percent
Experiment 1 (tumor cells from subcutaneous nodule)					
0	12,414	—[a]	50	10/10	100
0, diluent for 5 μg	7,582	39	50	10/10	100
0, diluent for 1,000 μg	163	99	10	10/10	100[b]
1	1,422	88	47	10/10	100
5	229	98	49	6/10	60
10	214	98	51	2/10	20
25	205	98	48	0/10	0
100	230	98	25	0/10	0
500	220	98	16	0/10	0
1,000	180	99	10	0/10	0
Experiment 2 (tumor cells from ascites)					
0	20,013	—[a]	95	10/10	100
0, diluent for 5 μg	12,400	38	90	10/10	100
0, diluent for 1,000 μg	250	99	25	10/10	100[b]
1	4,030	80	91	10/10	100
5	260	99	89	4/10	40
10	251	99	87	1/10	10
25	250	99	85	0/10	0
100	203	99	29	0/10	0
1,000	200	99	12	0/10	0

[a] — = not measured.

[b] Enhanced tumor growth.

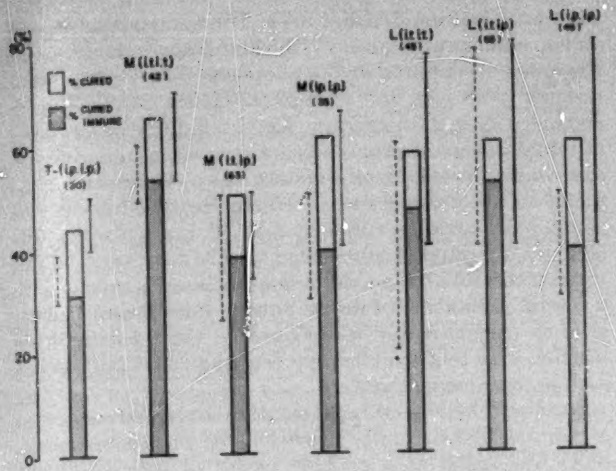

Text-figure 5.—Percentages of L-PAM-cured and "cured-immune" mice (resistant to 10^4 tumor cell challenge). Various schedules of chemotherapy are presented for medium-sized (M) and large (L) tumors: Split-course of L-PAM was given intratumorally (i.t.), ip (i.p.), and in combination; mice in the T-group were inoculated with tumor on day 7 but remained clinically tumor-free. ——=range of results from several experiments for percentage of cure; -----=percent of antitumor response. *Numbers in parentheses* represent total numbers of mice pooled from several experiments for each schedule.

therapy was devised: Tumor-bearing mice were treated with 200–300 μg (10–15 mg/kg body wt) L-PAM on day 1; after 2–3 days they were treated with higher doses of 400–500 μg (20–25 mg/kg body wt). This schedule reduced mortality due to toxicity and achieved a high proportion of tumor regressions.

We experimented with various routes of L-PAM administration (text-fig. 5). In all six experiments L-PAM treatment resulted in complete tumor regression in 43–64% of mice and in partial regression or no effect in the remaining 36–57% of mice. Repeated L-PAM administration did not significantly improve the cure rate achieved by one split-course chemotherapy, which indicates tumor cell resistance to chemotherapy in a certain proportion of animals. Increased toxicity was observed after repeated L-PAM treatments.

Rapid development of subcutaneous tumor nodules from small (0.5 cm) to medium-sized (0.5–0.9 cm) and large (1–1.5 cm) nodules precludes accumulation of sizable groups of animals carrying small tumors. Therefore, most experiments were performed with medium-sized and large tumors.

The rate of cure (complete regression) by different routes of L-PAM administration was quite similar in all groups (text-fig. 5). Cured mice were challenged by 10^4 viable MOPC-315 cells and those showing resistance to challenge were designated "cured-immune." The proportion of "cured-immune" mice was highest with medium-sized tumors treated with intralesional L-PAM and similar in large tumors treated with intralesional or intralesional followed by ip L-PAM. In both the medium-sized and large tumor groups L-PAM administered ip (i.p., i.p.; text-fig. 5) resulted in lower tumor resistance.

On the basis of these data most experiments were performed with mice bearing medium-sized and large tumors and were inoculated with L-PAM first intratumorally and then ip (i.t., i.p.; text-fig. 5). Mice given injections of tumor and drug treated on day 7 before tumor development (T-; text-fig. 5) with ip L-PAM (i.p., i.p.; text-fig. 5) showed low cure rates as well as low tumor resistance in cured animals. Thus prophylactic systemic chemotherapy was less effective than active chemotherapy of tumor-bearing animals in the MOPC-315 plasmacytoma system, indicating that in vivo antitumor responses are related to the size of the tumor and its biologic activity and that these may be implicated in mediating cure by chemotherapy.

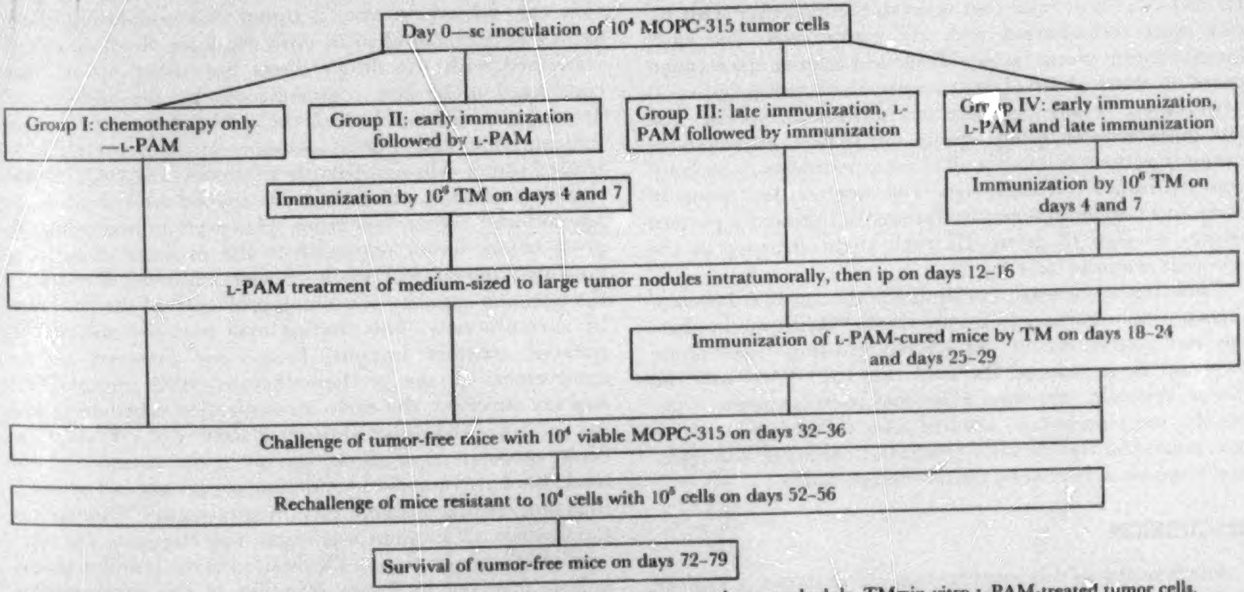
Day 0—sc inoculation of 10^4 MOPC-315 tumor cells
Group I: chemotherapy only —L-PAM
Group II: early immunization followed by L-PAM
Group III: late immunization, L-PAM followed by immunization
Group IV: early immunization, L-PAM and late immunization
Immunization by 10^6 TM on days 4 and 7
Immunization by 10^6 TM on days 4 and 7
L-PAM treatment of medium-sized to large tumor nodules intratumorally, then ip on days 12–16
Immunization of L-PAM-cured mice by TM on days 18–24 and days 25–29
Challenge of tumor-free mice with 10^4 viable MOPC-315 on days 32–36
Rechallenge of mice resistant to 10^4 cells with 10^5 cells on days 52–56
Survival of tumor-free mice on days 72–79

Text-figure 6.—Schematic presentation of combination chemotherapy–immunotherapy schedule. TM=in vitro L-PAM-treated tumor cells.

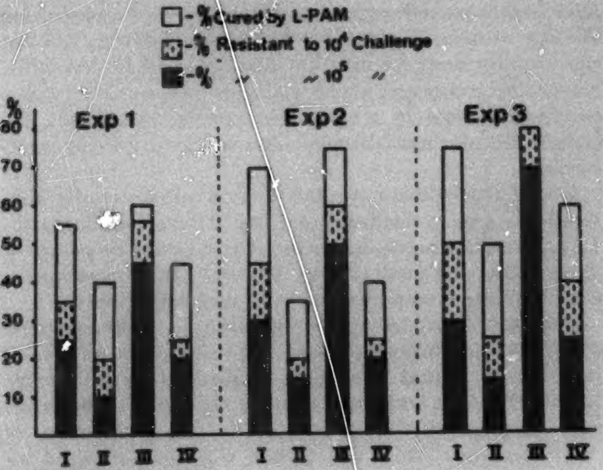

TEXT-FIGURE 7.—Combined treatment by chemotherapy–immunotherapy. For group designation *see* text-fig. 6. Data of three separate experiments are shown. There were 20 mice per experiment for each treatment group.

Combined Chemotherapy–Immunotherapy

Results presented so far show that *a*) 60–70% of tumor-bearing mice can be cured by L-PAM treatment under optimal conditions with 50–60% of these mice developing tumor resistance to viable tumor cell challenge and *b*) active specific immunization of healthy mice by means of in vitro L-PAM-treated cells induces a weak but measurable rejection response. It follows that combination of the two approaches may further enhance the in vivo antitumor response.

We explored various combined chemotherapy–immunotherapy schedules. A schematic design of the experiments is presented in text-figure 6.

All 4 treatment groups were challenged with 10^4 viable tumor cells 2 weeks after the last immunization of groups III and IV. Those mice that rejected the challenge with 10^4 cells were rechallenged with 10^5 viable cells. The early immunization group (group II) showed inferior results compared to those of the chemotherapy alone group (group I) with respect to both cure rate and antitumor response. The late immunization group (group III) showed an enhanced tumor rejection response in all three experiments to both 10^4 and 10^5 tumor cell challenge. The combination group of early and late immunizations (group IV) showed a pattern similar to that of group III with slight increase in the rejection response (text-fig. 7).

These results indicate that timing of the combined chemotherapy–immunotherapy is important. When immunotherapy was applied during the actively growing tumor phase in group II, it reduced the cure rate by L-PAM and the tumor rejection response following chemotherapy. Conversely, immunotherapy applied after L-PAM-induced tumor regression significantly ($P<0.001$) enhanced the rejection response achieved by chemotherapy alone.

DISCUSSION

The first part of this investigation was designed to explore and optimize methods and treatment schedules for MOPC-315 tumor-bearing BALB/c mice. The approach was based on two main assumptions: *1*) Chemotherapy-induced tumor regression is followed by development of in vivo tumor rejection responses and *2*) these responses can be further enhanced by immunotherapy. Results of different schedules of L-PAM chemotherapy indicate that when tumor regression was achieved, cured animals had a demonstrable capacity to reject viable tumor cell challenge. While 50–70% of the mice could be cured by L-PAM, the remaining 30–50% did not respond to repeated L-PAM treatment. In this respect, the BALB/c model resembles human tumors with a certain proportion of tumor-bearing mice showing resistance to chemotherapy. Consequently, the question arises whether cure by chemotherapy is mediated by host factors such as immune mechanisms.

Irradiated MOPC-315 cells tested by active immunization of normal BALB/c mice proved to be nonimmunogenic. BCG was tested as a possible means of stimulating the antitumor responses in this experimental model without demonstrable effect. Thus enhancing the immunogenicity of MOPC-315 cells became the major issue of the investigation.

In vitro exposure of MOPC-315 cells to L-PAM was tried as a means of possible modulation of tumor cells. The technique was based on known data from the literature (*15–17*) that L-PAM can act as a hapten and thus it can enhance tumor-associated antigen recognition. Immunoprophylaxis by means of L-PAM-treated cells induced a slight in vivo antitumor response. With schedules of optimal L-PAM regimens worked out to achieve cure and an indication at hand that in vitro L-PAM-treated tumor cells can immunize mice against viable tumor cell challenge, we directed our main efforts toward the combination of the two treatment modalities to achieve the enhancement of antitumor responses.

We built the experimental design of the combined chemotherapy–immunotherapy on the assumption that intratumoral injection of L-PAM followed by systemic administration can achieve in vivo a tumor cell-modulating effect similar to that found in in vitro exposure. Such an effect, combined with the drug's direct antitumor action, was considered to be best complemented by the addition of active immunization. Indeed, the results of the experiments indicate that active immunization by in vitro L-PAM-treated tumor cells significantly enhances in vivo antitumor responses when immunotherapy is applied after chemotherapy-induced tumor regression. However, immunotherapy given before tumor regression in the presence of actively growing—though still occult—tumors, caused a decrease in the rejection capacity of animals and lowered the cure rate by chemotherapy. This finding may partially answer the question whether immune factors are involved in the achievement of cure by chemotherapy. Were immune factors not involved, the early immunization schedule would not influence the direct antitumor activity of L-PAM. One could speculate that immunization in the presence of actively growing tumors can stimulate suppressor cell activity, thus diminishing immune antitumor responses, whereas immunization after tumor regression may stimulate the relevant antitumor responses. Elucidation of the immune mechanisms involved in tumor rejection in this experimental model is the main object of ongoing investigations.

REFERENCES

(1) Whisson ME, Connors TA. Cure of mice bearing advanced plasma cell tumours with aniline mustard. Nature 1965; 206:689–691.

(2) McCoy JL, Dean JH, Law LW. Immunogenicity, antigenicity and mechanisms of tumor rejection of mineral oil-induced plasmacytomas in syngeneic BALB/c mice. Int J Cancer 1970; 6:422–430.

(3) Potter M, Walters JL. Effect of intraperitoneal pristane on established immunity to the Adj-PC-5 plasmacytoma. J Natl Cancer Inst 1973; 51:875–881.

(4) Padarathsing ML, Dean JH, McCoy JL, Lewis DD, Northing JW. Restorative effects of levamisol on cell-mediated immune responses following chemotherapy with aniline mustard in mice bearing ADJ-PC5 plasmacytoma. Cancer Treat Rep 1978; 62:1627–1635.

(5) Lubet RA, Carlson DE. Tumor immunity against MOPC 104E: Effects of different therapeutic regimens. Cancer Immunol Immunother 1977; 2:267–270.

(6) Lubet RA, Carlson DE. Immunity against MOPC 104E plasmacytoma: Effects of tumor size and time post therapy on in vivo tumor immunity. J Natl Cancer Inst 1978; 60:1107–1111.

(7) Ohanian SH, Schlager SI, Goodman D. Analysis of the intralesional adriamycin-induced regression of primary and metastatic growth of line-10 guinea pig hepatoma. Cancer Immunol Immunother 1980; 8:179–187.

(8) Ohanian SH, Yarkoni E, Hunter JT, et al. Local chemotherapy of a metastasizing guinea pig tumor. In: Day SB, Myers WP, Stanley P, eds. Cancer invasion and metastasis: Biological mechanisms and therapy. Progress in cancer research and therapy. Vol 5. New York: Raven Press, 1977:473.

(9) Mathé G. Systemic active immunotherapy is shifting from the Middle Ages to a Renaissance period. I. The multiplication of randomized trials showing significant effect of active immunotherapy on residual minimal disease (Editorial). Cancer Immunol Immunother 1978; 5:149–152.

(10) Hanna MG, Brandhorst LC, Peters LC. Active specific immunotherapy of residual micro-metastasis. An evaluation of sources, doses and ratios of BCG with tumor cells. Cancer Immunol Immunother 1979; 7:165–173.

(11) Staab HJ, Anderer FA. Immunogenicity of tumours modified with various chemicals. Br J Cancer 1977; 35:395–402.

(12) Palmer WN, Swanson TL, Moore GE, Hyde PM. Immunogenicity of tumors alkylated with cyclohexyl-, benzyl-, or 2,4-dinitrophenylmethacrylate. Ann NY Acad Sci 1976; 277:412–427.

(13) Borsos T, Bast RC, Ohanian SH, Segerling M, Zbar B, Rapp HJ. Induction of tumor immunity of intratumoral chemotherapy. Ann NY Acad Sci 1976; 276:565–572.

(14) Contessa AN, Giampietri A, Bonmasser A, Goldin A. Increased immunogenicity of L1210 leukemia after short-term exposure to 5-(3,3′-dimethyl-1-triazeno)-imidazole-4-carboxamide (DTIC) in vivo and in vitro. Cancer Immunol Immunother 1979; 7:71–76.

(15) Arai K, Wallace HW, Blakemore WS. Haptenic activity of L-phenylalanine mustard. Cancer Res 1973; 33:1905–1913.

(16) ———. Immunotherapy of cancer with L-phenylalanine mustard as a hapten. Cancer Res 1973; 33:1914–1920.

(17) Arai K, Spencer JS, Wallace HW. Effect of hapten plus anti-hapten tumor serum treatment on established rat fibrosarcoma. Cancer Res 1979; 39:6–16.

(18) Wagner DE. Regional chemotherapy. In: Blakemore WS, Radin IS, eds. Current perspectives in cancer therapy. Scranton, Pa.: Harper & Row, 1968:52–57.

(19) Adler A, Ben Efraim S. Tumor-associated immune responses in BALB/c mice bearing MOPC 315 plasmacytoma following intralesional chemotherapy by melphalan. 4th international congress of immunology, Paris: 1980, Abstract No. 10.4.01.

blank page

Hematopoietic Precursor Cells in Mice Treated With 4-Demethoxydaunorubicin and Doxorubicin[1,2]

Giulio Massa,[3] Giuseppe Bogliolo,[3] Francesco D'Amore,[3] Carlo Muzzulini,[3] Riccardo Ghio,[3] *and* Ivo Pannacciulli[3,4]

ABSTRACT—The hematologic toxicity of 4-demethoxydaunorubicin (4-dmDNR), a new anthracycline more potent and less cardiotoxic than doxorubicin (Dx), was studied. Dose-survival curves of bone marrow hematopoietic precursor cells (HPC) in situ were determined with the use of (C57BL × C3H)F_1 mice and with assays of colony-forming units—spleen, culture, and erythroid—by in vivo and in vitro methods. Time response of HPC was followed in mice treated at days 0, 2, and 5 with 0.75 mg 4-dmDNR/kg or 4.5 mg Dx/kg and in mice receiving 2.23 mg 4-dmDNR/kg or 3.96 mg Dx/kg twice a week for 4 weeks. The dose-survival curves of HPC for 4-dmDNR were exponential. Slight differences in sensitivity among assayed populations were seen. Although the doses of 4-dmDNR required to reduce the survival of HPC to 37% were similar or lower than those of Dx, following intermittent treatment with doses of 4-dmDNR with the same optimal antitumor activity as with Dx, 4-dmDNR seemed to have a lesser effect on hematopoietic progenitors and a greater effect on peripheral blood cells than did Dx. However, during prolonged administration 4-dmDNR appeared to be toxic at every hematopoietic level.—JNCI 1982; 68:971–976.

Researching on Dx analogues with a better toxic: therapeutic ratio, Arcamone et al. (*1, 2*) prepared and studied 4-dmDNR ($C_{26}H_{27}NO_9CHl$; mol wt, 533.97). In mice 4-dmDNR revealed a greater potency than did Dx and proved effective also after oral administration. The toxicity pattern was similar to that induced by Dx, although with a lower cardiotoxicity in mice and rabbits. When given iv to mice, 4-dmDNR caused ventricular lesions only at doses that proved to be lethal. Although antitumoral activity and general toxicity were similar to those of Dx, the lower myocardiotoxicity made 4-dmDNR an interesting candidate for clinical studies. Therefore, we deemed worthwhile a study of the myelotoxic activity of 4-dmDNR for further information about the potential usefulness of the drug.

We performed such an evaluation by assaying the dose and time response of HPC in animals treated with a single or repeated administration of 4-dmDNR and by comparing the results with those obtained in similar experiments with Dx. This approach is justified by the useful role of hematopoietic assays in the prediction of clinical marrow toxicity of new anticancer chemotherapeutic agents (*3*).

MATERIALS AND METHODS

Mice.—(C57BL × C3H)F_1 mice, 2–3 months old, of both sexes were used as donors and recipients of bone marrow cells. Recipient mice were irradiated with a Theratron Junior cobalt-60 unit device (80 rad/min; total dose delivered, 900 rad).

Drugs.—Dx was supplied by Farmitalia Carlo Erba (Milan, Italy) in the form of a red powder. It was stored in the dark in a desiccator at 4°C and immediately before use was dissolved in normal saline (0.9% NaCl) at the working concentration. The 4-dmDNR (IMI30, batch PB 950/68), also supplied by Farmitalia Carlo Erba in the form of a powder, was stored and diluted in the same way. Structure, molecular weight, and biologic and pharmacologic activities of 4-dmDNR have been studied (*1, 2*). Since iv administration seemed preferable for anthracyclines (*4*), both Dx and 4-dmDNR were injected into tail veins of mice.

Experimental design and rationale of adopted schedules.—Experiment A, dose-survival curves of bone marrow HPC in mice treated wtih 4-dmDNR or Dx: Five groups of 5 normal mice each received iv 1.2, 1.7, 2.9, 4.7, and 7.9 mg of the drug/kg body weight, respectively. Each dose was 5:3 of the previous one. We selected the dose range taking into account that, by previous toxicologic experiences, the LD_{50} of 4-dmDNR in the mouse at 3 months after a single iv dose is about 4.9 mg/kg body weight (*5*). Five other groups of normal mice, matched for number, sex, age, and body weight, received injections with increasing doses of Dx (2.7, 4.5, 6.8, 11.5, and 19.0 mg/kg body wt, respectively). Again, each dose was 5:3 of the previous one. The LD_{50} of Dx in the mouse at 3 months after iv injection of a single dose was 11.76 mg/kg body weight (*6*). This experimental design was aimed at an evaluation of the shape and slope of HPC survival curves obtained with 4-dmDNR, which allowed us to investigate the sensitivity of each HPC population tested with the drug. Moreover, by calculating on the obtained curves the doses of 4-dmDNR and Dx that reduced the surviving fraction of the population assayed to 37% of the normal value (D37), we were able to compare the hematologic toxicity of 4-dmDNR to that of Dx. Twenty-four hours after injection, VPRC, total leukocyte count, and the number of reticulocytes per 100 RBC in orbital sinus blood were determined: soon after, the mice were killed by cervical dislocation. Both

---

ABBREVIATIONS USED: CFU=colony-forming unit(s); CFU_c=CFU—culture; CFU_e=CFU—erythroid; CFU_s=CFU—spleen; D37=reduction to 37% of normal value; 4-dmDNR=4-demethoxydaunorubicin; Dx=doxorubicin; HPC=hematopoietic precursor cells; LD_{50}=dose required to kill 50% of animals; *r*=regression coefficient; RBC=red blood cells; VPRC=volume of packed RBC; WBC=white blood cells.

---

[1] Received July 15, 1981; revised December 7, 1981; accepted January 26, 1982.

[2] Supported in part by contract 15/79.00653.96/115.4751 from the Consiglio Nazionale delle Ricerche, Rome.

[3] Istituto Scientifico di Medicina Interna, Cattedra di Patologia Speciale Medica RR, University of Genoa, Viale Benedetto XV 6, 16132 Genoa, Italy.

[4] We thank Professor Anna M. Casazza for helpful criticism and Ms. B. Johnston for editing and preparing the manuscript.

femurs were removed, bone marrow cellularity was checked, and bone marrow suspension was prepared. Controls that received injections with saline were subjected to equal checks.

Experiment B, time response of bone marrow HPC in mice treated with repeated doses of 4-dmDNR or Dx: In this recovery experiment, aimed to assess the effects of the drugs at varying times, a repeated treatment schedule (administration of the drug at days 0, 2, and 5) used in tests of antitumoral activity of anthracyclines was applied. In C3H mice inoculated with Gross leukemia cells this schedule was the best for Dx to develop its antileukemic activity, and it was also satisfactory for 4-dmDNR (*7*). We selected the doses of 4-dmDNR and Dx, taking into account that the above referred experiment and similar experiments on the effects of 4-demethoxy derivatives of anthracyclines against mouse tumors (*2, 5, 7, 8*) have shown that the optimal antitumor dose of 4-dmDNR is four to six times lower than that of Dx. According to this rationale, 2 groups of 40 normal mice each respectively received iv 0.75 mg 4-dmDNR/kg and 4.5 mg Dx/kg, at days 0, 2, and 5. At days 2, 3, 5, 6, 8, and 9, treated mice (5) for each group and saline-treated controls (5) were killed soon after determination of the aforementioned peripheral blood counts; assays of HPC were performed on bone marrow suspensions.

Experiment C, time response of bone marrow HPC in mice treated with 4-dmDNR or Dx for several weeks: The main problem with prolonged treatment with anthracyclines is cardiotoxicity. With this experiment we aimed to evaluate hematologic changes in mice treated for several weeks with doses of and a schedule of 4-dmDNR or Dx known to induce cardiotoxicity of a comparable degree. In mice, ventricular lesions of a significant degree have been observed after a cumulative dose of 10 mg 4-dmDNR; comparable effects have been obtained with a cumulative dose of 25-30 mg Dx (*5*). These cumulative doses were adopted in this study. Moreover, the drugs were administered according to a schedule modeled on those proposed for the study of anthracycline cardiotoxicity (*5*). The doses and the treatment schedule were therefore as follows: two administrations per week of 1.23 mg 4-dmDNR/kg body weight or of 3.96 mg Dx/kg body weight for 2 weeks, 1 week interval, and then two administrations of the same dose per week for 2 additional weeks. No study of specific toxicity apart from hematologic toxicity was made. At the end of weeks 2, 3, 4, and 5 the determinations on peripheral blood and bone marrow reported in experiments A and B were performed on 5 treated mice of each group and on 5 saline-treated controls.

Collection, preparation, and counts of samples.—Bone marrow collection and preparation of bone marrow monodispersed cell suspensions were accomplished with the usual techniques (*9*). The peripheral blood counts were done by conventional methods (*10*).

Assays for HPC.—A first aliquot of the cell suspension (obtained from femurs) was assayed for its CFU_s content according to the transplant method (*11*). Nine mice, irradiated as reported above, were used as recipients for each suspension, i.e., for the bone marrow of each donor mouse. A total of 0.5 ml of cell suspension, in medium diluted to contain 4×10^4 bone marrow cells, was injected into tail vessels. The host mice were killed with ether 9 days after injection, and their spleens were excised and fixed in Tellyesniczky's fluid. The number of visible colonies was then counted: The mean number of colonies in each spleen was calculated, and the total number of CFU_s per femur plus or minus the standard error was determined. A second aliquot of the cell suspension was assayed for its content of CFU_c according to the in vitro method of Bradley and Metcalf (*9*). One milliliter of agar medium (α-medium) containing 1×10^5 bone marrow nucleated cells and 20% horse serum was pipetted into triplicate 35-mm Falcon petri dishes over 0.1 ml of colony-stimulating factor prepared from an extract of the uterine membrane of a pregnant mouse. After 7 days of incubation, we examined cultures by using an inverted microscope. The number of colonies that contained more than 50 cells was recorded, and the mean number of CFU_c per femur plus or minus the standard error was calculated. A third aliquot of the same cell suspension was assayed for its CFU_e content according to the in vitro method of Iscove et al. (*12*). Nucleated, 1×10^5 bone marrow cells were plated into duplicate 35-mm Falcon petri dishes with a 1-ml mixture of 0.8% methylcellulose–30% horse serum, and 0.25 U erythropoietin was prepared by use of plasma from phenylhydrazine-treated sheep. Only those colonies that contained more than 8 cells, as revealed by the inverted microscope after 3 days, were scored; the mean number of CFU_e plus or minus the standard error per femur was then determined.

Statistical methods.—Single data points after treatment with 4-dmDNR or Dx, and in controls, were examined by the same assays on the same day to eliminate possible day-to-day variance of the assays. In time-response experiments, the values of both groups were compared between themselves and/or with control values by Student's *t*-test. Survival fractions were calculated on the absolute number of surviving HPC per femur. In charts, the contents of CFU_s, CFU_c, and CFU_e per femur were normalized to those found for the corresponding controls treated with 0.9% NaCl solution. The linear *r*-value between drug doses and survival fractions and its significance were evaluated. On the dose-survival curves D37 was calculated. The analysis of variance among sensitivities to each drug of each population assayed was calculated (variance ratio F and its significance) (*13*).

RESULTS

Lethal toxicity.—In experiment A the mice were killed 24 hours after drug injection, thus preventing the possibility for evaluation of any lethality on the part of either drug. In preliminary experiments the survival rate during 10 days after treatment with three doses at days 0, 2, and 5 was 10 of 10 for animals treated with 0.75 mg 4-dmDNR/kg body weight and for animals treated with 4.5 mg Dx/kg body weight. During the 5 weeks of experiment C, no spontaneous death of 4-dmDNR-treated or Dx-treated mice was observed. Signs of general toxicity were not relevant.

Changes in peripheral blood cells, in bone marrow cellularity, and in HPC 24 hours after 4-dmDNR or Dx single injection.—The results are shown in table 1 and text-figure 1. In 4-dmDNR- and Dx-treated mice the dose-survival curves within the dose range here selected were described by a single simple

TABLE 1.—*Effects of 4-dmDNR and Dx on peripheral blood cells and bone marrow cellularity in mice*[a]

Parameter	Values in untreated mice	Treatment of mice with 4-dmDNR, mg/kg body wt, for dose-survival curve					Treatment of mice with Dx, mg/kg body wt, for dose-survival curve				
		1.2	1.7	2.9	4.7	7.9	2.7	4.5	6.8	11.5	19.0
VPRC, %	44±0.8	44±0.5	43±0.2	42±0.7	42±0.9	41±0.5^{b}	43±0.6	44±0.4	38±0.6^{b}	39±0.3^{b}	39±0.4^{b}
WBC ×10^{9}/liter	4.0±0.2	4.4±0.2	3.8±0.2	3.3±0.4^{b,c}	2.3±0.4^{b,c}	1.2±0.5^{b,c}	5.0±0.4	4.9±0.3	3.8±0.4	2.8±0.3^{b}	1.3±0.2^{b}
Reticulocytes ×100 RBC	27±3.0	17±2.1^{c}	13±3.1^{b,c}	10±1.2^{b,c}	7±1.5^{b,c}	3±0.8^{b,c}	24±1.5	22±2.1^{b}	18±2.0^{b}	16±1.7^{b}	10±2.1^{b}
Bone marrow cells ×10^{6}	13.5	12.1	10.7	7.9	5.0	2.5	10.6	10.[illegible]	7.7	9.2	7.0

[a] Values are means ± SE.

[b] Values are significantly different ($P<0.05$) from those found in untreated mice.

[c] Values are significantly different ($P<0.05$) from those found in Dx-treated mice.

exponential for every cell population checked (for each curve r, $P<0.01$). With comparison by analysis of variance of the slopes of the survival curves for 4-dmDNR, CFU$_s$ appeared significantly ($P<0.01$) more sensitive than did CFU$_c$ and CFU$_e$ were significantly ($P<0.01$) more sensitive than were CFU$_s$. CFU$_s$, CFU$_c$, and CFU$_e$ were more sensitive ($P<0.01$) than were bone marrow cells, WBC, and reticulocytes. The dose-survival curve of bone marrow cellularity indicated a higher sensitivity ($P<0.01$) than did WBC.

The D37's for each curve and the ratios D37 DX:D37 4-dmDNR are reported in table 2. In each cell population assayed, except for CFUc and CFUe, the D37's for mice treated with 4-dmDNR appeared lower than the D37's for mice treated with DX. For each drug, the D37's for WBC, reticulocytes, and bone marrow cellularity were much higher than the D37's for HPC. However, at relatively low doses, lower than 4.7 mg of the drug/kg body weight (i.e., the approximate LD$_{50}$), 4-dmDNR appeared to affect hematopoietic stem cells less than did Dx administered in doses that gave the same degree of leukocyte reduction.

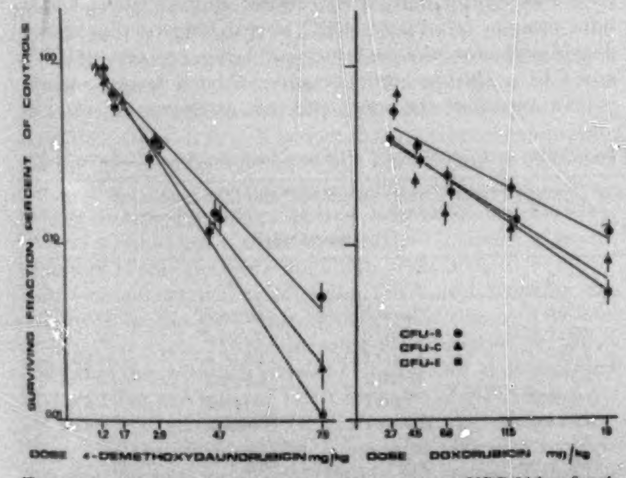

TEXT-FIGURE 1.—Dose-survival curves of bone marrow HPC 24 hr after 4-dmDNR and Dx single injection. For each experimental point: *vertical bars*, means ± SE. The r's—4-dmDNR: CFU$_s$ $r=-0.992$ ($P<0.01$); CFU$_c$ $r=-0.999$ ($P<0.01$); CFU$_e$ $r=-0.970$ ($P<0.01$). The r's—Dx: CFU$_s$ $r=-0.947$ ($P<0.01$); CFU$_c$ $r=-0.842$ ($P<0.01$); CFU$_e$ $r=-0.994$ ($P<0.01$).

Effects on peripheral blood cells, bone marrow cellularity, and HPC by an intermittent treatment schedule with 4-dmDNR or Dx.—The sequence of changes in peripheral blood cell levels, bone marrow cellularity, and bone marrow CFU$_s$, CFU$_c$, and CFU$_e$ during the following intermittent administration of 4-dmDNR is reported alongside the sequence for Dx-treated mice in text-figure 2 and table 3. Following the first two doses of 4-dmDNR, the reduction in WBC, peripheral blood reticulocytes, and bone marrow cellularity was severe.

TABLE 2.—*D37's for peripheral blood cells, bone marrow cellularity, and bone marrow HPC after 4-dDNR and Dx*[a] *administration*

CFU and cells	D37		D37 Dx:D37 4-dmDNR
	4-dmDNR	Dx	
CFU$_s$	2.91	5.13	1.76
CFU$_c$	2.71	2.65	0.98
CFU$_e$	2.66	2.88	1.08
WBC	5.72	15.29	2.66
Reticulocytes	3.06	19.02	6.21
Bone marrow cells	4.85	33.45	6.89

[a] In doses of mg/kg body wt.

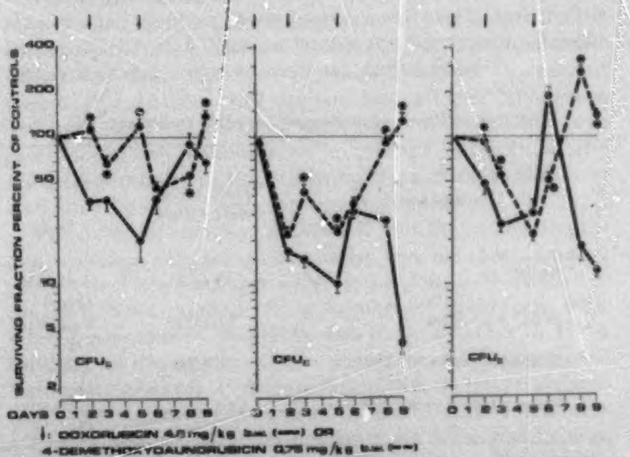

TEXT-FIGURE 2.—Fractional survival of CFU as a function of time during and after an intermittent treatment schedule with Dx and 4-dmDNR. For each experimental point: *vertical bars*, means ± SE. Values marked with an *asterisk* are significantly different ($P<0.05$) from the corresponding values (●) of Dx-treated animals. Body weight=b.w.

TABLE 3.—*Effects of an intermittent schedule with 4-dmDNR and DX on peripheral blood cells and bone marrow cellularity*[a]

Parameter	Values in untreated mice	Drug	Effects of intermittent 4-dmDNR[b] and Dx[c] schedule: Treatment day 2	3	5	6	8	9
VPRC, %	44±0.8	4-dmDNR	43±0.4	37±0.5[d]	39±1.1[d]	39±0.6[d]	41±0.7[d]	40±1.2[d]
		Dx	41±2.4	44±1.2	45±1.7	42±0.6	40±0.6	41±1.2
WBC ×10^9/liter	5.0±0.2	4-dmDNR	4.7±0.3	2.7±0.1[d,e]	5.0±0.2[e]	3.1±0.1[d,e]	6.1±0.1[d,e]	5.8±0.1[d,e]
		Dx	5.5±0.3	4.3±0.7	4.0±0.1[d]	5.4±0.8	3.4±0.2[d]	3.9±0.2[d]
Reticulocytes ×100 RBC	27±3.0	4-dmDNR	11±1.2[d,e]	10±2.1[d,e]	2±0.4[d,e]	8±1.1[d,e]	23±2.3[e]	45±3.0[d,e]
		Dx	22±2.1	23±1.8	30±1.5	34±1.7	32±0.9	31±1.9[d]
Bone marrow cells ×10^6	13.5	4-dmDNR	9.5	6.5	5.4	3.0	9.0	8.4
		Dx	8.0	7.3	9.2	11.2	10.0	6.0

[a] Values are means ± SE.
[b] 0.75 mg/kg body wt.
[c] 4.5 mg/kg body wt.
[d] Values are significantly different ($P<0.05$) from those found in untreated mice.
[e] Values are significantly different ($P<0.05$) from those found in Dx-treated mice.

However, the administration of the third dose of the drug did not interfere with the recovery of these cells for which the levels at the end of the observation period were higher than or equal to normal. Following 4-dmDNR administration, there was a reduction in bone marrow CFU_c, CFU_e and, to a much lower degree, CFU_s. A recovery followed that caused all tested cell populations to overshoot normal values. Within the time limits of this experiment, the recovery from 4-dmDNR damage was not followed by a secondary fall, and thus at the end of the observation period the 4-dmDNR-treated mice had a higher than normal endowment of hematopoietic progenitors.

In Dx-treated mice the reduction in bone marrow cellularity, WBC, and reticulocytes was less severe and that of HPC more severe than that observed in mice treated with 4-dmDNR. The recovery of CFU_c was abortive, that of CFU_e was short lived, and that of CFU_s just reached normal values. Moreover, a secondary fall of HPC followed the initial recovery.

On the whole, in comparison of intermittent treatments with 4-dmDNR or Dx at doses that in previous experiments showed an optimal antitumor activity, 4-dmDNR seemed to have a severe effect on bone marrow cellularity and peripheral blood cells but to relatively spare CFU_s, thus allowing a full recovery of HPC. However, Dx appeared to affect peripheral blood cells and bone marrow cellularity to a lesser degree, but it depleted bone marrow content of progenitors. The short observation time did not allow us to study the possible late consequences of these effects.

Effects on peripheral blood cell levels, bone marrow cellularity, and HPC bone marrow content by prolonged treatment twice a week with 4-dmDNR.—As shown in text-figure 3 and table 4, during prolonged biweekly treatment 4-dmDNR severely reduced bone marrow cellularity and WBC and particularly the reticulocyte level in peripheral blood. The hematopoietic progenitor content in the bone marrow also appeared progressively depleted. After week 4, despite the continued 4-dmDNR administration, there was a recovery of CFU_s to normal values and of CFU_c to subnormal values. Only CFU_e stayed at very low levels. In comparison, Dx, administered with a similar schedule at a cumulative dose that gave comparable cardiotoxic effects, did not affect CFU_s, bone marrow cellularity, WBC, or reticulocytes to a similar degree and allowed a prompter and better recovery of CFU_c and CFU_e. During administration of both drugs, erythropoiesis appeared the most affected, as shown by the low

TABLE 4.—*Effects of prolonged biweekly treatment with 4-dmDNR and DX on peripheral blood cells and bone marrow cellularity*[a]

Parameter	Values in untreated mice	Drug	Effects of prolonged twice a week 4-dmDNR[b] and DX[c] treatment: Treatment week 2	3	4	5
VPRC, %	44±0.8	4-dDNR	32±0.4[d]	36±0.8[d]	32±0.5[d]	28±1.4[d]
		Dx	29±0.6[d]	35±0.3[d]	32±0.6[d]	30±0.5[d]
WBC ×10^9/liter	5.0±0.2	4-dDNR	2.5±0.2[d,e]	4.7±0.1	4.8±0.5	3.1±0.3[d,e]
		Dx	5.1±0.2	4.9±0.2	4.5±0.3	4.3±0.2
Reticulocytes ×100 RBC	27±3.0	4-dDNR	3±0.2[d,e]	5±0.7[d,e]	3±0.9[d]	2±0.4[d]
		Dx	6.3±1.4[d]	12.3±3.1[d]	8.6±2.4[d]	6.3±1.3[d]
Bone marrow cells ×10^6	13.5	4-dDNR	1.4	6.2	2.0	10.0
		Dx	10.6	4.6	6.0	14.6

[a] Values are means ± SE.
[b] 1.23 mg/kg body wt.
[c] 3.96 mg/kg body wt.
[d] Values are significantly different ($P<0.05$) from those found in untreated mice.
[e] Values are significantly different ($P<0.05$) from those found in Dx-treated mice.

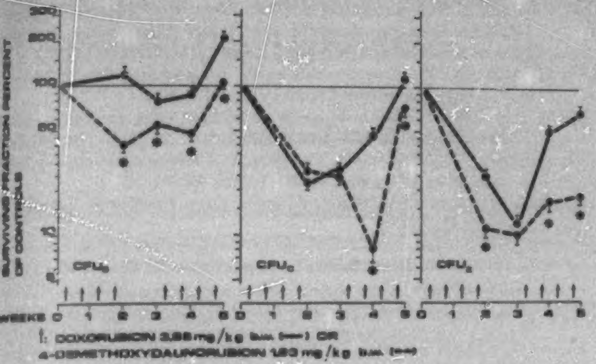

TEXT-FIGURE 3.—Fractional survival of CFU as a function of time during biweekly treatment with Dx and 4-dmDNR. For each experimental point: *vertical bars*, means ± SE. Values marked with an *asterisk* are significantly different ($P<0.05$) from the corresponding values (●) of Dx-treated animals. Body weight=b.w.

values attained by CFU$_e$ and reticulocytes. The minor changes in WBC in Dx-treated mice and their early recovery in 4-dmDNR-treated animals do not reflect the severe involvement of CFU$_c$. On the whole, with the adopted schedule of prolonged administration, 4-dmDNR appeared to be toxic at every hematopoietic level.

DISCUSSION

The results here reported show that, like other anthracyclines (*14–18*), 24 hours after injection, 4-dmDNR in a single dose causes a dose-related reduction in bone marrow hematopoietic progenitors, either pluripotential (CFU$_s$) or committed to myeloid (CFU$_c$) or erythroid (CFU$_e$) differentiation. The 24-hour dose-survival curves show a "shoulder" portion, probably pointing to efficiency of cell repair of sublethal damage induced by low doses of the drug. The remaining portion fits a single exponential shape, confirming that 4-dmDNR, like Dx and other anthracyclines (*14, 15*), acts on HPC, which are in all phases of the cell cycle. There are significant differences among the slopes of the survival curves for each HPC population assayed. However, these differences, although statistically significant, are rather slight. It is well known that pluripotent stem cells (CFU$_s$) are mainly resting while committed progenitors (CFU$_c$ and CFU$_e$) are actively proliferating in normal mice (*19*). It is therefore intriguing that 4-dmDNR, like Dx (*14*), induces a reduction of mainly resting CFU$_s$ almost as severe as that of highly proliferating CFU$_c$ and CFU$_e$.

Anthracyclines act by affecting DNA and arresting the cell cycle in G_2 (*20*), thus killing cells that are in the proliferative cycle. Although some data support the possibility that the cytotoxic activity of 4-dmDNR is determined by inhibition not only of DNA but also of RNA synthesis (*21*), on the whole 4-dmDNR shares this cycle dependency. To explain the effect on CFU$_s$, one must take into account that changes in bone marrow progenitor content following anticancer drug administration, while a good index of drug myelotoxicity, are due to such a complex interplay of frequently counteracting factors that a satisfactory analysis based on a single property of each progenitor population is hindered. Moreover, a major role could be played by pharmacokinetics. Experiences in tumor-bearing mice have shown high levels of 4-dmDNR in different tissues for 24–48 hours after iv injection (*22*). In this period, resting cells may be recruited to compensate for the initial damage by the drug and thus may become more sensitive to its toxic effect. Similar considerations may help to explain the erratic discrepancies between changes in HPC, bone marrow cellularity, and peripheral blood cells observed in dose-related and time-related experiments. Every proliferating phase of the hematopoietic lines may be differently affected by cycle-dependent cytotoxic drugs, and every line may develop its own compensative reactions, thus concealing part of the damage. A tentative analysis of these changes is beyond the limits of this discussion.

The 4-dmDNR is a derivative of daunorubicin, and the effects of 4-dmDNR should be better compared with those of daunorubicin. However, Dx is by far a more versatile and diffuse antitumor agent than daunorubicin, and a comparison with Dx therefore has a greater significance. The differences between 4-dmDNR and Dx on hematopoietic precursor cells are better evaluated when one takes into account that Dx is less "potent" than 4-dmDNR; i.e., Dx has the same antitumoral activity as 4-dmDNR at doses four to five times higher. However, the doses of 4-dmDNR required to reduce to 37% the survival of CFU$_s$, CFU$_c$, and CFU$_e$ are 1.76, 0.98, and 1.08 times, respectively, those of Dx. Moreover, at low single doses 4-dmDNR produces the same or a higher degree of leukopenia and bone marrow cellularity reduction than dose Dx, but 4-dmDNR induces a significantly lower reduction in HPC. It seems that at these doses the hematopoietic suppression caused by the drug does not affect the earlier phases of hematopoiesis. Consequently, in comparison with Dx, in single low doses the new anthracycline would have a lower impact on bone marrow and allow a quicker and more complete recovery. At higher doses Dx and 4-dmDNR either have a similar effect on HPC or Dx is less toxic than 4-dmDNR.

The time-related analysis of toxic effects of 4-dmDNR also showed that low, repeated doses of the drug affected the earlier phases of hematopoiesis (i.e., the HPC compartment) less than did low, repeated doses of Dx with a comparable antileukemic activity and a lower leukopenic action. Moreover, the injurious effect of 4-dmDNR was more transitory, followed by a prompt recovery of the affected populations, thus allowing the animal to maintain its full potential for bone marrow regeneration.

The different effects of 4-dmDNR and Dx on hematopoietic cells are intriguing, but there are no clear data to explain it. Other authors who have extensively studied 4-dmDNR have pointed out a number of differences with related compounds, probably due to an increase in DNA binding, an increase in cellular uptake, or a different distribution in tissues (*5*). Uptake of 4-dmDNR by mouse embryo fibroblasts is greater than that of Dx, and 4-dmDNR induces a higher number of DNA breaks in CCRF-CEM cells in vitro (*5*). Which, if any, of these differences accounts for the observed differences remains to be defined by further studies.

The 4-dmDNR administered for a long period of time shows generally a severe toxicity on HPC that is matched by a similarly severe effect on bone marrow cellularity, WBC, and reticulocytes. However, at the end of the administration period, the hematopoietic precursors begin to recover, except for the erythroid line, which stays severely depleted. These data indicate a cumulative hematologic toxicity of repeated doses of the drug that is only partially compensated for by the hematopoietic system. In this experiment the myelotoxic activity of 4-dmDNR was also compared with that of Dx at cumulative doses of the two drugs with comparable cardiotoxicity. The 4-dmDNR showed a more severe hematologic toxicity than did Dx, but again one must take into account that a 3:2 dosage ratio was applied in this experiment, whereas the optimal antitumoral ratio is 4:5 (*2, 5, 7, 8*).

In conclusion, the new anthracycline derivative 4-dmDNR induces a dose-related reduction in HPC with slightly different effects with respect to the population assayed, has relatively little effect on HPC at low doses, but has a relatively severe cumulative effect. If 4-dmDNR were to be applied clinically, these results would suggest that single, relatively low doses could be well tolerated and could be repeated at short intervals for a few times. However, the cumulative toxicity cautions against prolonged administration.

REFERENCES

(*1*) Arcamone F, Bernardi L, Giardino P, et al. Synthesis and antitumor activity of 4-demethoxydaunorubicin, 4-demethoxy-7,9-diepidaunorubicin, and their beta anomers. Cancer Treat Rep 1976; 60:829–834.

(*2*) Arcamone F. Doxorubicin. Anticancer antibiotics. New York: Academic Press, 1981.

(*3*) Marsh JC. The effects of cancer chemotherapeutic agents on normal hematopoietic precursor cells: A review. Cancer Res 1976; 36:1853–1882.

(*4*) Lenaz L, Di Marco A. On the reported lack of effectiveness of daunomycin (NSC-82151) and adriamycin (NSC-123127) on solid tumors. Cancer Chemother Rep 1972; 56:431–432.

(*5*) Casazza AM, Di Marco A, Bonadonna G, et al. Effects on modifications in position 4 of the chromophore or in position 4′ of the aminosugar on the antitumor activity and toxicity of daunorubicin and doxorubicin. In: Crooke ST, Reich SD, eds. Anthracyclines. New York: Academic Press, 1980:403–430.

(*6*) Arcamone F, Di Marco A, Casazza AM. Chemistry and pharmacology of new antitumor anthracyclines. In: Humezawa H, ed. Advances in cancer chemotherapy. Tokyo: Japan Science Society Press and Baltimore: Univ Park Press, 1978:297–312.

(*7*) Casazza AM. Preclinical studies for the evaluation of new anthracycline analogs. Chemioter Oncol 1978; 4:310–326.

(*8*) ——— Experimental evaluation of anthracycline analogs. Cancer Treat Rep 1979; 63:835–844.

(*9*) Bradley TR, Metcalf D. The growth of mouse bone marrow cells in vitro. Aust J Exp Biol Med Sci 1966; 44:287–300.

(*10*) Dacie JV, Lewis SM. Practical haematology. Edinburgh: Churchill-Livingstone, 1975.

(*11*) Till JE, McCulloch EA. A direct measurement of the radiation sensitivity of normal mouse bone marrow cells. Radiat Res 1961; 14:213–222.

(*12*) Iscove NN, Sieber F, Winterhalter KH. Erythroid colony formation in cultures of mouse and human bone marrow: Analysis of the requirement for erythropoietin by gel filtration and affinity chromatography on agarose–concanavalin A. J Cell Physiol 1973; 83:305–320.

(*13*) Bliss CI. Statistics in biology. New York: McGraw-Hill, 1970.

(*14*) Razek A, Valeriote F, Vietti T. Survival of hematopoietic and leukemic colony-forming cells in vivo following the administration of daunorubicin or adriamycin. Cancer Res 1972; 32:1496–1500.

(*15*) Marsh JC. Comparison of the sensitivities of human, canine, and murine hematopoietic precursor cells to adriamycin and *N*-trifluoroacetyladriamycin-14-valerate. Cancer Res 1979; 39:360–364.

(*16*) Blackett NM, Marsh JC, Gordon MY, Okell SF, Aguado M. Simultaneous assay by six methods of the effect on hemopoietic precursor cells of adriamycin, methyl CCNU, ^{60}Co rays, vinblastine and cytosine arabinoside. Exp Hematol 1978; 6:2–8.

(*17*) Buick RN, Messner HA, Till JE, McCulloch EA. Cytotoxicity of adriamycin and daunorubicin for normal and leukemia progenitor cells of man. JNCI 1979; 62:249–255.

(*18*) Huybrechts M, Symann M, Trouett A. Effects of daunorubicin and doxorubicin, free and associated with DNA, on hemopoietic stem cells. Cancer Res 1979; 39:3738–3743.

(*19*) Lajtha LG. Haemopoietic stem cells. Br J Haematol 1975; 29:529–535.

(*20*) Barlogie B, Drewinko B, Johnston DA, Freireich EJ. The effect of adriamycin on the cell cycle traverse of a human lymphoid cell line. Cancer Res 1976; 36:1975–1981.

(*21*) Supino R, Necco A, Dasdia T, Casazza AM, Di Marco A. Relationship between effects on nucleic acid synthesis in cell cultures and cytotoxicity of 4-demethoxy derivatives of daunorubicin and adriamycin. Cancer Res 1977; 37:4523–4528.

(*22*) Formelli F, Di Marco A, Casazza AM, Pratesi G, Supino R, Mariani A. Biological properties of 4-demethoxydaunorubicin: In vivo and in vitro studies. In: Siegenthaler A, Luthy R, eds. Current chemotherapy. Proceedings of the tenth international congress of chemotherapy, Zurich, September 18–23, 1977. Washington, D.C.: American Society of Microbiology, 1978:1240–1242.

Inheritance of Cellular Resistance to the Antitumor Agent ICRF 159 in Somatic Cell Hybrids[1]

David H. Edgar[2] *and* **Andrew M. Creighton**[3]

ABSTRACT—Two independently derived sublines of Syrian hamster BHK 21S cells that demonstrate resistance to the antitumor agent ICRF 159 (NSC-129943) were fused to sensitive cells in both intraspecific and interspecific crosses, and the responses of the resultant hybrids to the drug were determined. In intraspecific hybrids from crosses involving either of the sublines, resistance to ICRF 159 was expressed codominantly with the hybrid response being halfway between the parental responses. In interspecific hybrids from crosses with sensitive mouse cells, resistance was also expressed but to a lesser extent than in the intraspecific hybrids. However, subsequent passaging of an interspecific hybrid resulted in an increase in the degree of resistance, which appeared to be accompanied by a loss of telocentric mouse chromosomes. The results suggested that resistance in these lines was due to an alteration in the cellular target involved in the response to ICRF 159.—JNCI 1982; 68:977–980.

Drug resistance as displayed by somatic cells in culture can serve as a model system for the study of the changes that may accompany the emergence of drug-resistant cell populations during the chemotherapy of malignant disease and can allow for an examination of the genetic nature of the cellular events that lead to these changes. For such an examination the technique of somatic cell hybridization has been widely employed and the degree to which drug resistance is expressed in hybrids between sensitive and resistant cells has been observed to be dependent on the particular agent involved (*1*). Such variations appear to be attributable to differences in the molecular mechanisms underlying the acquisition of resistance. The level of expression of resistance in such hybrids may therefore provide clues to the mechanisms involved in cases where the molecular basis of cytotoxicity is unknown.

ICRF 159 is one of a series of bisdioxopiperazine derivatives that were originally synthesized as potential intracellularly activated chelating agents (*2*) and were shown to be active against experimental tumors in mice and rats (*3*). It has subsequently been developed as a drug for the treatment of human neoplastic disease (*4*, *5*) and more recently has found some application in the treatment of severe psoriasis (*6*).

At the cellular level, ICRF 159 has been shown to cause abnormal chromosome condensation when present at the G_2–M phase of the cell cycle (*7*), the phase at which ICRF 159 has also been shown to exert its maximum lethality as assessed by impairment of reproductive integrity (*8*). Binding studies with radioactively labeled ICRF 159 (*9*) failed to show an association with any cellular macromolecules, and the molecular mechanism(s) underlying the agent's cellular effects, including the putative role of chelation, remains unclear.

We are investigating the nature of ICRF 159-induced resistance in cultured cell lines as part of a study of the mechanism of action of this class of drugs. ICRF 159-resistant sublines of Syrian hamster cells have been isolated, following continuous culture of the parent cells in vitro in relatively low concentrations of the drug (*10*, *11*). These sublines were shown to have little or no significant cross-resistance to a wide variety of agents with known mechanisms of action and to be similar to the parent line with respect to uptake of [^{14}C]ICRF 159. Further, stable inheritance of resistance in the absence of the agent suggested that the resistant lines may have arisen by somatic mutation.

We now report the results of somatic cell hybridization experiments. These results show that resistance to ICRF 159 in these two Syrian hamster sublines is due to alterations at the genetic level and give some indication of the possible nature of these changes.

MATERIALS AND METHODS

Cell culture.—Cell culture was done in an LEEC incubator in a water-saturated atmosphere of 10% CO_2 in air at 37°C. Cells were grown routinely as monolayers on plastic petri dishes (diameter, 50 mm; A/S Nunc, Roskilde, Denmark) in DMEM supplemented with 10% FCS, which was obtained from Gibco Europe Ltd., Glasgow, Scotland. Hybrid selection was performed with essentially the culture system described by Littlefield (*12*). We used HAT (DMEM with 10% FCS to which 15 μg/ml hypoxanthine, 0.45 μg/ml aminopterin, and 10 μg/ml thymidine were added).

BHK 21S/TK$^-$ was a subline of BHK 21S (*13*), which we selected for its ability to grow in medium supplemented with 30 μg 5-bromo-2′-deoxyuridine/ml by gradually increasing the concentration of the agent in the medium and by subsequent cloning. The TK-deficient nature of the subclone was confirmed by its inability to grow in HAT. BS/159-1/HGPRT$^-$ and BS/159-4/HGPRT$^-$ were the two sublines of ICRF 159-resistant BHK 21S cells, BS/159-1 and BS/159-4, respectively, whose independent isolations

---

ABBREVIATIONS USED: DMEM=Dulbecco's modified Eagle's minimum essential medium; FCS=fetal calf serum; HAT=DMEM with 10% FCS and containing 15 μg hypoxanthine/ml, 0.45 μg aminopterin/ml, and 10 μg thymidine/ml; HGPRT=hypoxanthine-guanine phosphoribosyl transferase; ID_{50}=dose causing 50% inhibition; PEG=polyethylene glycol; RI_{50}=ID_{50} (resistant)/ID_{50} (sensitive); TK=thymidine kinase.

---

[1] Received July 21, 1981; revised December 15, 1981; accepted January 26, 1982.

[2] Department of Immunology, Agricultural Research Council Institute of Animal Physiology, Babraham, Cambridge CB2 4AT, England.

[3] *Address reprint requests to* Dr. Creighton *at* Cellular Pharmacology and Antitumour Chemistry Laboratory, Imperial Cancer Research Fund, Lincoln's Inn Fields, London WC2A 3PX, England.

have been described previously (*10, 11*) and which had been further selected for deficiency in HGPRT by having been cloned in 10 µg 6-thioguanine/ml and by having been tested for sensitivity to HAT. The 3T3/TK⁻ mouse cells were a line of Swiss 3T3 cells that were deficient in the enzyme TK, that were able to grow in the presence of 5-bromo-2′-deoxyuridine (30 µg/ml), and that were sensitive to HAT. They were obtained from Dr. K. Quade, Department of Tumour Virology, Imperial Cancer Research Fund Laboratories, London, England.

Cell fusion.—Cell monolayers were harvested with trypsin (0.25% wt/vol), washed twice with phosphate-buffered saline, and suspended in DMEM. Cell fusion was performed in suspension with the use of PEG of molecular weight 6,000 as the fusogen. We mixed 10^6 cells of each parental type and centrifuged them at 1,000 rpm in an M. S. E. Bench Top Centrifuge (Measuring Scientific Equipment Co., Crawley, England) for 5 minutes. The pellet was washed twice with DMEM and resuspended in 50% (wt/vol) PEG (6,000 mol wt) in DMEM at 37°C. After 1 minute the volume was slowly diluted to 10 ml by the addition of DMEM at 37°C. Aliquots of 1 ml were then transferred to petri dishes containing 5 ml DMEM with 10% FCS. We renewed the medium after 3 hours to remove the residual PEG; 24 hours later this medium was replaced by HAT, which was renewed after 3 days. After 6–7 days, we picked out putative hybrid clones by using cloning rings.

ICRF 159.—ICRF 159 [(±)1,2-bis(3,5-dioxopiperazin-1-yl)propane, Razoxane; NSC-129943] was synthesized in these laboratories and was dissolved in 0.9% (wt/vol) saline before administration.

Analysis of drug response.—To assess the effect of ICRF 159 on the reproductive integrity of cells, we did colony-forming survival assays by using a range of concentrations of the agent. We seeded 400 cells into each dish and added the drug 3 hours later. After 6 days without medium renewal, the number of colonies containing 50 or more apparently normal cells was counted after they were fixed and stained with Leishman's stain. Although the drug was present throughout this period, its concentration would have fallen fairly rapidly, with a half-life of about 12 hours under the conditions of the incubation. Each dose was administered to triplicate dishes, each experiment was done three times, and the mean values were obtained. ID_{50} for a cell type was the dose required to reduce the colony-forming ability of the cells by 50% relative to the colony-forming ability of untreated control cultures, and RI_{50} was the ratio of ID_{50} for a resistant cell population compared with the ID_{50} for the sensitive cell line.

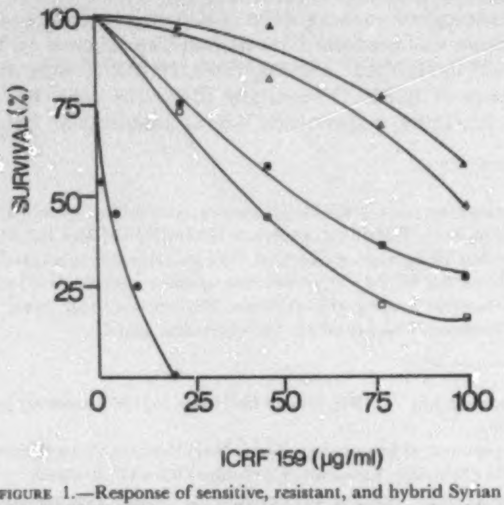

TEXT-FIGURE 1.—Response of sensitive, resistant, and hybrid Syrian hamster cells to ICRF 159 in colony-forming survival assays. Sensitive BHK 21S/TK⁻ (●), hybrid C2 (□), hybrid D2 (■), resistant BS/159-1/HGPRT⁻ (△), and resistant BS/159-4/HGPRT⁻ (▲).

TABLE 1.—*ICRF 159 ID_{50} values for sensitive and resistant Syrian hamster cells and intraspecific hybrids*

Cell type	ICRF 159 ID_{50} mean values[a]
BHK 21S/TK⁻	2.0 (1.8, 2.5, 1.7)
BS/159-1/HGPRT⁻	102 (98, 109, 99)
BS/159-4/HGPRT⁻	110 (112, 115, 103)
Hybrid C1	43 (36, 48, 45)
Hybrid C2	41 (39, 44, 40)
Hybrid C3	49 (49, 50, 51)
Hybrid D1	51 (48, 55, 50)
Hybrid D2	52 (59, 47, 50)
Hybrid D3	53 (44, 60, 55)

[a] Doses were administered at µg/ml. Mean values, calculated from the three experimental values shown *in parentheses*, are given.

Chromosome spreads.—To examine the chromosome complements of the various cell types, we treated the cells in monolayer with 0.1 µg vinblastine sulfate/ml (Sigma Chemical Co., London, England) for 2 hours, harvested them with trypsin (0.25%), made them swell using 0.07 *M* KCl for 12 minutes, and fixed them with 3:1 methanol:acetic acid before dropping them onto slides. Chromosome preparations were stained with 2% Giemsa for 10 minutes.

RESULTS

Expression of Resistance to ICRF 159 in Intraspecific Hybrids

To study the mode of inheritance of resistance to ICRF 159 in cell fusion experiments, we had to introduce additional markers (HGPRT⁻ and TK⁻) into the parental cell lines as described in "Materials and Methods." The introduction of these markers did not, however, result in any detectable alteration in the responses to ICRF 159.

Three clones each were picked out from intraspecific crosses between BHK 21S/TK⁻ and BS/159-1/HGPRT⁻ (C1-3) and BS/159-4/HGPRT⁻ (D1-3). The hybrid nature of the clones was confirmed by examination of their chromosome complements (mean values of 80–85 compared with ≈41 for the parent cells). Control fusions of each of the parents with itself failed to yield any colonies.

We then performed colony-forming assays, six subcultures (≈20 generations) post fusion, using a range of concentrations of ICRF 159. Text-figure 1 shows the responses of the parent cells and one representative hybrid from each of the two crosses (C2 and D2), and table 1 summarizes the ID_{50} values for all cells involved. The responses of the hybrid clones can be seen to be intermediate between those of the relevant parents, with the hybrid ID_{50} values being approx-

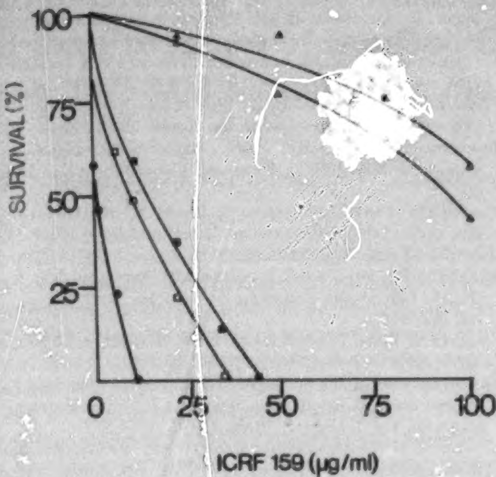

TEXT-FIGURE 2.—Effect of ICRF 159 on the colony-forming ability of mouse $3T3/TK^-$ cells (●), the drug-resistant Syrian hamster cells $BS/159\text{-}1/HGPRT^-$ (△) and $BS/159\text{-}4/HGPRT^-$ (▲), and interspecific cell hybrids A1 (□) and B1 (■).

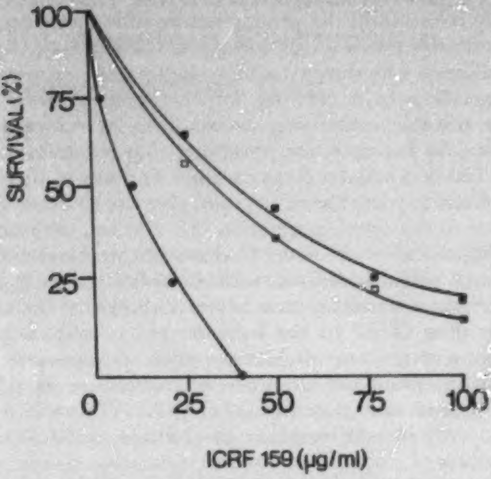

TEXT-FIGURE 3.—Colony-forming survival response of interspecific hybrid A2 to ICRF 159-treated subcultures (six) after cells were cloned (●) and after a further 18 subcultures in either normal medium (□) or in HAT (■).

imately halfway between the parental values. Therefore, resistance to ICRF 159 in both $BS/159\text{-}1/HGPRT^-$ and $BS/159\text{-}4/HGPRT^-$ was expressed codominantly in hybrids with the sensitive parent line.

Expression of Resistance to ICRF 159 in Interspecific Hybrids

To examine the possibility that resistance to ICRF 159 in the 2 lines described was due to alteration at the genetic level, we fused both to the ICRF 159-sensitive mouse cell line $3T3/TK^-$. A previous report (*14*) showed that for hybrids from crosses between mouse and Syrian hamster cells mouse chromosomes were preferentially lost upon serial subculture of the hybrid clones. Therefore, we wished to investigate the effect of altering the relative gene dosage on response to ICRF 159.

Three clones were picked out from each of the two crosses and were designated A1–3 ($3T3/TK^-$ × $BS/159\text{-}1/HGPRT^-$) and B1–3 ($3T3/TK^-$ × $BS/159\text{-}4/HGPRT^-$). The mean chromosome numbers of the hybrid clones lay in the range of about 100–120, being approximately the sum of the parental complements. The hybrid nature of these clones was further confirmed by the presence of both the submetacentric and metacentric chromosomes characteristic of the parent hamster cells in addition to the telocentric chromosomes characteristic of the parent mouse cells.

TABLE 2.—*ICRF 159 ID_{50} values for sensitive mouse cells, resistant Syrian hamster cells, and interspecific hybrids*

Cell type	ICRF 159 ID_{50} mean values[a]
$3T3/TK^-$	0.9 (0.8, 0.8, 1.1)
$BS/159\text{-}1/HGPRT^-$	102 (98, 109, 99)
$BS/159\text{-}4/HGPRT^-$	110 (112, 115, 103)
Hybrid A1	9.9 (9.3, 10.3, 10.1)
Hybrid A2	10.1 (10.6, 10.0, 9.7)
Hybrid A3	9.8 (8,9, 9.9, 10.6)
Hybrid B1	12.4 (10.9, 12.2, 14.1)
Hybrid B2	11.8 (9.9, 12.1, 13.4)
Hybrid B3	12.0 (11.8, 13.2, 11.0)

[a] Doses were administered at µg/ml. Mean values were calculated from the three experimental values shown *in parentheses*.

The parental responses to ICRF 159 with those of two representative hybrids (A1 and B1) in colony-forming survival assays are shown in text-figure 2, and the ID_{50} values for parents and hybrids are listed in table 2. One can see that resistance to ICRF 159 is still expressed in the hybrids, though to a lesser extent than in the intraspecific hybrids described above.

The effect of serial subculture on the response of hybrid A2 to ICRF 159 was then investigated. Text-figure 3 shows the response in colony-forming assays of A2 at subculture 6 after cloning (A2/6) and after a further 18 subcultures in either DMEM with 10% FCS (A2/24) or in HAT (A2/24/HAT). The response of A2 to ICRF 159 was altered with time in culture with an approximately fourfold increase in the ID_{50} value. The morphologies and population-doubling times of A2/24 and A2/24/HAT did not differ significantly from those of A2/6, but the mean chromosome numbers had dropped from 105 to 83 and 87, respectively. Although a full karyotypic analysis was not attempted, the reduction of metacentric (positive hamster) chromosomes from a mean of 30 to 25 and 26, respectively, suggested that the differences may be more attributable to telocentric mouse chromosome loss.

DISCUSSION

The genetic origins of various drug-resistant cellular phenotypes in vitro have been established by application of a variety of criteria such as stable inheritance, altered gene products, and the mapping of drug resistance to a particular chromosome (*15*). In such mapping, the preferential loss of, for example, human chromosomes in human–mouse somatic cell hybrids (*16*) has proved to be valuable. In this report we have used mouse–hamster hybrids, which had been shown previously (*14*) to lose mouse chromosomes preferentially to establish the genetic nature of hamster cell variants resistant to the antitumor agent ICRF 159.

Resistance was shown to be codominantly expressed in intraspecific hybrids (text-fig. 1). This result provides clues to the possible underlying mechanisms of resistance. It excludes, for example, the possibility that resistance is due to the loss of a cellular function since mutants of this type, when fused to parent sensitive cells, give rise to hybrids also sensitive to the agent in question (*17*, *18*); i.e., the resistant phenotype is then recessive. Codominant expression of resistance is often associated with an alteration in a drug-specific target, resulting in a lowered affinity of the target for the drug. Thus in the hybrids that possess both the sensitive and resistant targets the level of response to the agent is intermediate. Examples of this nature have been demonstrated with alteration of (Na, K)-ATPase (*19*) and tubulin (*20*) in cells resistant to ouabain and Colcemid, respectively.

Since resistance to ICRF 159 is not the result of impaired drug uptake (*10*), we suggest that it may be the result of an alteration in a target molecule involved in response to the agent. This putative target is presumably involved in normal cell cycle traverse control, since it has been shown (*21*) that the cytotoxic action of ICRF 159 is closely related to a characteristic perturbation of the cell cycle.

The results of the interspecific hybridization experiments show that the previously demonstrated (*14*) preferential loss of mouse chromosomes by the 24th subculture results in an increase in the level of resistance to ICRF 159 (text-fig. 3). The underexpression of resistance in the early stages (text-fig. 2) could be explained if preferential expression of the mouse drug-specific target was postulated. This kind of preferential expression occurs in one of three enzymes, lactate dehydrogenase, viewed in such hybrids (*14*). The subsequent increase in the RI_{50} of hybrid A2 could well be a reflection of an increase in the ratio of resistant hamster targets to sensitive mouse targets, which is in turn due to an increase in the ratio of hamster to mouse chromosomes coding for the targets. We are currently attempting to isolate human cell lines resistant to ICRF 159, with the intention of extending this analysis to the mapping of resistance to a single human chromosome in human-rodent hybrids.

REFERENCES

(*1*) Harris M. Phenotypic expression of drug resistance in hybrid cells. J Natl Cancer Inst 1973; 50:423–429.

(*2*) Creighton AM. Bisdiketopiperazines: A new class of antitumor agent. In: Umezawa H, ed. Progress in antimicrobial anticancer chemotherapy (proceedings of the 6th International Congress for Chemotherapy). Vol 1. Baltimore: University Park Press, 1970:167–169.

(*3*) Creighton AM, Hellmann K, Whitecross S. Antitumour activity in a series of bisdiketopiperazines. Nature 1969; 222:384–385.

(*4*) Bakowski MT. ICRF 159, (±)1,2-bis(3,5-dioxopiperazin-1-yl)propane NSC-129943; Razoxane. Cancer Treat Rev 1976; 3:95–107.

(*5*) Poster DS, Penta J, Marsoni S, Bruno S, MacDonald JS. Bisdiketopiperazine derivatives in clinical oncology: ICRF-159. Cancer Clin Trials 1980; 3:315–320.

(*6*) Atherton DJ, Wells RS, Laurent MR, Williams YF. Razoxane (ICRF 159) in the treatment of psoriasis. Br J Dermatol 1980; 102:307–317.

(*7*) Sharpe HB, Field EO, Hellmann K. Mode of action of the cytostatic agent ICRF 159. Nature 1970; 226:524–526.

(*8*) Creighton AM. The effects of ICRF 159 on synchronised L-cells at various stages of the cell cycle. Abstracts. XIth International Cancer Congress. Vol 3. Florence, Italy: UICC, 1974:423.

(*9*) Dawson KM. Studies on the stability and cellular distribution of dioxopiperazines in cultured BHK-21S cells. Biochem Pharmacol 1975; 24:2249–2253.

(*10*) White K. Studies on the mechanism of cellular resistance to the antitumour agent ICRF 159. Ph.D. thesis. London: University of London, 1979.

(*11*) White K, Creighton AM. Studies of resistance to ICRF 159 in cell line BS/159-1. Br J Cancer 1977; 36:421.

(*12*) Littlefield JW. Selection of hybrids from matings of fibroblasts in vitro and their presumed recombinants. Science 1964; 145:709–710.

(*13*) Capstick PB, Garland AJ, Masters RC, Chapman WG. Some functional and morphological alterations occurring during and after the adaptation of BHK 21 clone 13 cells to suspension culture. Exp Cell Res 1966; 44:119–128.

(*14*) Migeon BR. Hybridization of somatic cells derived from mouse and Syrian hamster: Evolution of karyotype and enzyme studies. Biochem Genet 1968; 1:305–322.

(*15*) Siminovitch L. On the nature of hereditable variation in cultured somatic cells. Cell 1976; 7:1–11.

(*16*) Weiss MC, Green H. Human–mouse hybrid cell lines containing partial complements of human chromosomes and functioning human genes. Proc Natl Acad Sci USA 1967; 58:1104–1111.

(*17*) de Saint Vincent RB, Buttin G. Studies on 1-β-D-arabinofuranosyl cytosine-resistant mutants of Chinese hamster fibroblasts. Somatic Cell Genet 1979; 5:67–82.

(*18*) Chasin LA. Non-linkage of induced mutations in Chinese hamster cells. Nature [New Biol] 1972; 240:50–52.

(*19*) Corsaro CM, Migeon BR. Gene expression in euploid human hybrid cells: Ouabain resistance is codominant. Somatic Cell Genet 1978; 4:531–540.

(*20*) Ling V, Aubin JE, Chase A, Sarangi, F. Mutants of Chinese hamster ovary (CHO) cells with altered colcemid-binding affinity. Cell 1979; 18:423–430.

(*21*) Edgar DH, Creighton AM. ICRF 159-induced cell cycle perturbation in vitro: Its relationship to inhibition of colony-forming ability. Br J Cancer 1981; 44:236–240.

Further Studies on the Relationship Between Allotransplantability and the Presence of the Cell Surface Glycoprotein Epiglycanin in the TA3-MM Mouse Mammary Carcinoma Ascites Cell[1,2,3]

Scott C. Miller,[4] **John F. Codington,**[5,6] *and* **George Klein**[7,8]

ABSTRACT—The loss of strain specificity in the TA3-St mammary carcinoma ascites cell during passage in ascites form in diseased syngeneic strain A mice was confirmed by the observation that TA3-MM/2 ascites cells were capable of progressive growth in 7 foreign mouse strains. Support for the hypothesis that allotransplantability in the TA3-MM lines may be due to masking of cell surface histocompatibility H-2^{a} antigens by large glycoprotein (epiglycanin) molecules was obtained from the finding that the capacity of the TA3-MM/2 ascites cell to absorb anti-H-2^{a} antibody was several times less than that of the parent TA3-St ascites cell, although it was greater than the capacity of the non-strain-specific TA3-Ha line. Further support for the location of epiglycanin molecules at the cell surface was obtained by transmission electron-microscopic observation of a high concentration of filamentous structures, usually 20–40 nm long, but often extending to 200–300 nm length at the TA3-MM/2 cell surface. Similar structures were also observed at the TA3-Ha cell surface but were not observed at the surface of the TA3-St ascites cell, a cell known to contain no detectable epiglycanin. Epiglycanin molecules, obtained by two different methods from TA3-MM/1, TA3-MM/2, and TA3-Ha ascites cells, were shown to be similar with respect to their capacities to inhibit the binding of ^{125}I-labeled epiglycanin to its antibody, induced in the rabbit by TA3-Ha ascites cells in a radioimmunoassay.—JNCI 1982; 68:981–988.

Two transitions from strain specificity to nonstrain specificity in the spontaneously derived TA3 mammary carcinoma ascites tumor have been reported (*1–3*). The first transition was observed in the strain-specific ascites subline TA3-Ha, which became allotransplantable during "routine" passage(s) in A/HeHa mice (*1*). Although the circumstances of this event or series of events were not reported, loss of strain specificity presumably occurred between in vivo passages 200 and 300 (*1*). In an effort to explain loss of strain specificity in physicochemical and morphologic terms, a wide variety of experimental procedures have been performed (*4–12*). As a result of this work, a mechanism to explain allotransplantability in the TA3-Ha ascites cell, namely, masking of cell surface histocompatability H-2^{a} antigens by large, endogenous glycoprotein (epiglycanin) molecules, has been suggested (*5, 12–15*).

A more recent event resulting in loss of strain specificity occurred in a second strain-specific subline, TA3-St, of the same tumor. In this instance, however, ascites cells were injected into A/HeHa mice infected with pneumonia-producing microorganism (*2, 3*). Within a single passage in vivo, lectin-binding sites were observed on the cell surface (*2, 3*). This phenomenon is characteristic of the new allotransplantable line and absent from the parent strain-specific line. From the new TA3-MM line, the two sublines TA3-MM/1 and TA3-MM/2 were established and differed somewhat in the composition of their cell surface glycoproteins (*2*).

The two independently derived allotransplantable lines TA3-Ha and TA3-MM differed markedly from each other in certain properties, such as cell size and chromosome numbers (*2, 3*). The common feature of the two cell lines, however, was an abundance of the large endogenous cell surface glycoprotein epiglycanin. In this paper, surface characteristics of the TA3-MM/2 subline are compared to those of the TA3-Ha and TA3-St ascites cells as observed by high-resolution transmission electron microscopy. In addition, we compared the capacity of the three cell lines to absorb antibodies to the H-2^{a} antigen and compared structural features of epiglycanin samples isolated from the two TA3-MM sublines with those of TA3-Ha epiglycanin by means of a recently described radioimmunoassay (*16*) with the use of an antibody to TA3-Ha epiglycanin.

MATERIALS AND METHODS

Cells.—The origin and characteristics of the TA3-St and TA3-Ha ascites cells have previously been described (*1, 3*). The TA3 tumor arose spontaneously as a mammary carcinoma in a female A/HeHa mouse. The two ascites sublines TA3-St and TA3-Ha were strain-specific, but after more than 200 passages in ascites form the TA3-Ha ascites cells lost their strain specificity, whereas TA3-St ascites cells remained strain-specific for more than 600 passages in ascites form in healthy strain A mice. The transition of the TA3-St ascites cell into the TA3-MM cell (*2, 3*) occurred during the passage of the TA3-St ascites cells (passage 321) into A/HeHa mice with an acute respiratory disease (*3*). Two variants, TA3-MM/1 and TA3-MM/2, which differed slightly in cell surface chemical composition, were established (*2, 3*). Cell lines were maintained by weekly passage

---

[1] Received July 30, 1981; revised January 22, 1982; accepted February 12, 1982.

[2] Supported by Public Health Service (PHS) grants CA-08418, CA-18600, and 5-R01CA-14054 from the National Cancer Institute; by PHS grant DE-04931 from the National Institute of Dental Research; and by contract EY76CO20119 from the U.S. Department of Energy.

[3] Animals were maintained under the guidelines set forth in the "Guide for the Care and Use of Laboratory Animals" by the Institute of Laboratory Animal Resources, National Research Council.

[4] Radiobiology Division, Department of Pharmacology, College of Medicine, University of Utah, Salt Lake City, Utah 84112.

[5] Laboratory for Carbohydrate Research, Department of Biological Chemistry and Department of Medicine, Harvard Medical School, Massachusetts General Hospital, Boston, Mass. 02114.

[6] *Address reprint requests to* Dr. Codington.

[7] Department of Tumor Biology, Karolinska Institutet Medical School, S 104 01 Stockholm 60, Sweden.

[8] We thank Ms. Mary Beth Bowman, Ms. Heidi Rowland, Mrs. Cyla Silber, and Ms. Mary McDonough for their technical assistance.

in A/HeJ mice (The Jackson Laboratory, Bar Harbor, Maine) with ip inocula of 10^5 TA3-MM/1, TA3-MM/2, or TA3-Ha and 10^6 TA3-St ascites cells. After 7 days, cells were collected by transperitoneal aspiration, as previously described (*3, 4*).

Electron microscopy.—The cells were prepared for electron microscopy on the day of harvest. Because the appearance of filamentous material at the cell surface by electron microscopy depends on the methods of fixation and staining, similar procedures were used on the cells in this study as were previously used (*11*). Washed cells were fixed in suspension in 2% glutaraldehyde in 0.1 *M* sodium cadodylate buffer and post-fixed for 1 hour in 1% osmium tetroxide in the same buffer. The cells were dehydrated in ethanol and embedded in Spurr's low-viscosity plastic (*17*). The sections cut for electron microscopy were stained with uranyl acetate and lead citrate and examined on a JEOL 100S electron microscope.

Allograft experiments.—Both syngeneic (A/Sn) and allogeneic (A.SW, A.CA, A.BY, C57BL/6, C3H, CBA, and DBA/2) mice were bred and housed at the Department of Tumor Biology, Karolinska Institutet Medical School, Stockholm, Sweden. Mice were given ip inoculations of 10^6 TA3-St or TA3-MM/2 cells or 10^5 TA3-Ha cells. The day of death was recorded in each case, and each mouse was examined to determine if death was attributable to tumor growth.

Absorption of anti-H^{a} *antibody.*—Seven serial dilutions (4.0–6.2×10^4 cells) and controls of each cell line in triplicates were incubated at 37°C for 45 minutes with A.CA anti-H-2^a antiserum (diluted 1:8 with RPMI-1640 medium containing 10% calf serum). After centrifugation, an aliquot of each supernatant was tested. The amount of absorbed antibody was calculated from the cytotoxic action in the presence of guinea pig complement against normal A/Sn lymph node cells as target cells (*18*). Comparison of the absorptive capacity of the three cell lines for a single pool of antiserum, expressed as the ratio of bound to free antibody $[(100-P):P]$ was calculated according to the method of Reif (*19*). A G-value was calculated (*19*), and its reciprocal 1/G was used as a measure of the absorptive capacity of the different cell lines.

Inhibitory activities by radioimmunoassay.—The induction and characteristics of an antibody to epiglycanin are described elsewhere (*16*). Experiments for comparison of the inhibitory activities of analogous fractions of epiglycanin from TA3-MM/1, TA3-MM/2, and TA3-Ha ascites cells were performed by a radioimmunoassay (*16*). After the incubation of the inhibitor (the substance containing the antigenic determinant) and the anti-epiglycanin antiserum, the mixture was incubated with [^{125}I]epiglycanin. Activity was measured by the amount of sample required to inhibit 50% of the binding of the radiolabeled epiglycanin with the antibody.

RESULTS

Comparative Morphology of TA3-MM/2, TA3-Ha, and TA3-St Cells

Viewed by low-power transmission electron microscopy, the TA3-MM/2 (fig. 1), TA3-Ha (fig. 2), and TA3-St ascites cells (fig. 3) are generally spherical when fixed in suspension. All are characterized by cell surface projections and microvilli. At the surfaces of the TA3-MM/2 and TA3-Ha cells, the microvilli are numerous and usually straight and appear to be rigid as they extend from the cell body. On the TA3-St cell the microextensions are often curved and extend from a more irregular cell surface (fig. 3).

Cells from each of the three sublines (figs. 1–3) possess large pleomorphic eccentrically located nuclei with moderate amounts of clumpy heterochromatin. The nucleoli are usually large, and sometimes several nucleoli are seen in a nucleus. Mitochondria and some rough endoplasmic reticulum are distributed throughout the cytoplasm. A Golgi complex is usually seen near the cell center, and free ribosomes are abundant in the cytoplasm. Intracisternal virus particles and virus particles budding from the plasma membrane are seen in the cells of all three cell lines.

Comparative Studies of the Filamentous Material at the Surfaces of the TA3-MM/2, TA3-Ha, and TA3-St Cells

No morphologically distinct coat is seen at the surface of the strain-specific TA3-St cells (fig. 4). In contrast, a distinct coat is evident at the surface of similarly prepared non-strain-specific TA3-Ha ascites cells (fig. 5). This cell surface coat appears as a meshwork of fine filamentous material and usually extends to a distance of 30–50 nm or more from the plasma membrane. The cell coat is particularly evident on the microvilli of this cell.

Morphologically distinct filamentous structures are also present at the surface of the TA3-MM/2 ascites cell (fig. 6). These structures resemble the material at the surface of the TA3-Ha ascites cells (fig. 5). However, the filamentous material of the TA3-MM/2 surface is usually not as thick as that seen at the surface of the TA3-Ha cell. As for the TA3-Ha cell, the filamentous material usually extends from 20 to 40 nm from the plasma membrane and the surface coat is most conspicuous on the microvilli. Virus particles budding from the surface of TA3-MM/2 cells (fig. 7), like those budding from TA3-Ha cells (*11*), have a coat at their surfaces similar in appearance to that seen on the plasma cell membrane. In areas of high microvilli density, numerous long and very thin filamentous structures are seen bridging adjacent microvilli (fig. 8). These structures have a low electron density and often extend to 300 nm in length.

Transplantability

The TA3-MM/2 ascites cell, as well as the TA3-Ha cell, exhibited the capacity to grow progressively in ascites form in 7 foreign mouse strains and in the syngeneic strain A mouse (table 1). By contrast, the TA3-St ascites cell continued to exhibit strain-specific characteristics and grew only in the syngeneic strain A mouse.

Absorptive Capacities

The relative amounts of anti-H-2^a antibody absorbed by the TA3-MM/2, TA3-Ha, and TA3-St ascites cells are illustrated in text-figure 1. The TA3-MM/2 cells absorbed

Table 1.—*Transplantation characteristics of TA3 sublines inoculated ip with 1×10⁶ ascites cells in mice*[a]

Cell sublines	Syngeneic mice, A/Sn	Allogeneic mice						
		A.SW	A.CA	A.BY	C57BL/6	C3H	CBA	DBA/2
TA3-St	2/2	0/2	0/2	0/2	0/2	0/2	0/2	0/2
TA3-Ha[b]	4/4	4/4	4/4		3/4		4/4	4/4
TA3-MM/2	2/2	2/2	2/2	2/2	2/2	2/2	2/2	2/2

[a] Data are reported as the number of mice dead of progressively growing tumors within 30 days per the number of mice given inoculations.

[b] The inoculum (ip) was 1×10^5 cells/mouse.

an amount of antibody intermediate between that of the non-strain-specific TA3-Ha and the strain-specific TA3-St cells.

Radioimmunoassay

The capacities of epiglycanin fractions from the TA3-MM/1 and TA3-MM/2 ascites cells to inhibit the binding of [^{125}I]epiglycanin (from TA3-Ha cells) with the antibody to epiglycanin (from TA3-Ha cells) (*16*) are compared with those of similar fractions of epiglycanin isolated from the TA3-Ha ascites cell (table 2). Material cleaved from either TA3-MM/1 or TA3-MM/2 cells by proteolysis (*2*) and purified by gel filtration (fraction A) exhibited approximately the same level of activity as a fraction isolated in the same way from TA3-Ha ascites cells. A fraction shed from proliferating TA3-MM/2 cells into the ascitic fluid of syngeneic hosts and purified by gel filtration (fraction II) (*2*) exhibited somewhat greater inhibitory activity than its TA3-Ha counterpart. In each sample except one, removal of sialic acid residues with neuraminidase significantly increased the inhibitory activity.

DISCUSSION

The qualitative loss in strain specificity (table 1) that occurred in the strain-specific TA3-St ascites cell to produce the new subline TA3-MM was accompanied by both chemical and morphologic changes. Comparison of electron micrographs of the TA3-MM/2 with those of the TA3-Ha and TA3-St cell lines is made in figures 1–8. The surface of the TA3-MM/2 variant cell (fig. 1) is replete with long extended microvilli and resembles the surface of the non-strain-specific TA3-Ha cell (fig. 2) far more than it does the surface of the parent TA3-St cell (fig. 3), which is characterized by irregular ridges and folds. The TA3-MM/2 cell was found to possess a surface coat (fig. 6) with the notable appearance of filamentous material similar to that found at the surface of the TA3-Ha ascites cell (fig. 5) (*11*).

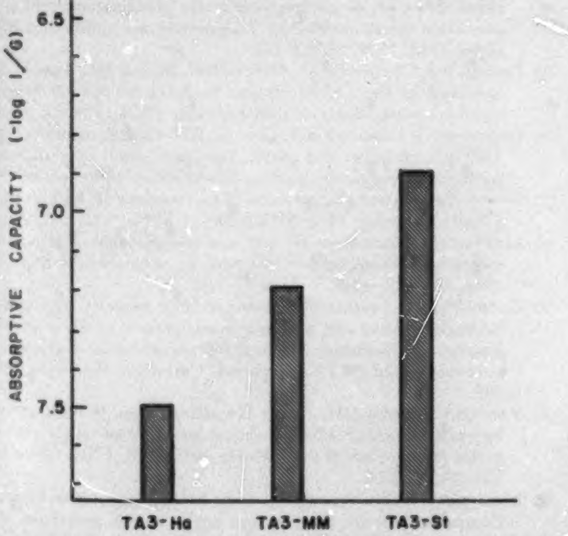

Text-figure 1.—Absorptive capacities for anti-H-2^a antibody for TA3-Ha, TA3-MM/2, and TA3-St ascites cells. Values are calculated for 1/G according to Reif (*19*) and indicate the amount of antibody bound/cell when 50% of the cytotoxic activity of the antibody was bound.

The presence of filaments (often 300 nm long) at the surface of the TA3-MM/2 cell (fig. 8) was only observed in areas in which microvilli existed in close proximity. Similar structures were seen on the surface of the TA3-Ha cell (not shown) (*11*). The existence of these filaments is probably explained by the stability afforded by the microvilli, which may serve as anchors for the thin structures, rather than by a greater abundance of this material in these areas. The appearance of the filaments depends on the details of the fixation procedure (*11*) and requires fixing first with glutaraldehyde and then with osmium tetroxide. It is probable that the long strands seen at the TA3-MM/2 cell surface (fig. 8) are composed of epiglycanin molecules, which, after glutaraldehyde fixing, exist as aggregates of sufficient diameter and electron density to be visible by electron microscopy. Isolated molecules of epiglycanin from either the TA3-MM/2 or TA3-Ha cells appear as long, thin rods, extending to approximately 500 nm (*2*). The physical characteristics of the isolated material are thus consistent with

Table 2.—*Amounts of comparable neuraminidase-treated and untreated fractions from TA3-MM/1, TA3-MM/2, and TA3-Ha ascites cells required to inhibit the reaction: [^{125}I]epiglycanin + anti-epiglycanin antibody*[a]

Inhibitor	Amount of cell fractions required for 50% inhibition, ng					
	TA3-MM/1		TA3-MM/2		TA3-Ha	
	U	N	U	N	U	N
Fraction A, P-100 column[b]	1.5	0.5	1.2	1.2	1.5	0.3
Fraction II, Sepharose 4B column[c]			0.6	0.2	2.0	0.5

[a] U = untreated ascites cell fractions; N = neuraminidase-treated ascites cell fractions.

[b] Cleaved from viable cells by incubation with L-1-tosylamido-2-phenylethyl-chloromethylketone-trypsin (18 μg/ml) at 4°C (*2*).

[c] Shed from proliferating cells in vivo into the ascitic fluid of A/HeJ mice bearing the tumor (*2*).

those of the material seen by transmission electron microscopy at the surfaces of the two allotransplantable lines. The absence of epiglycanin at the TA3-St cell surface may explain our inability to see by electron microscopy any such material at the surface of this cell.

The TA3-MM/2 ascites cell appears to be as allotransplantable as the TA3-Ha cell (table 1). It is tempting to suggest that the capacity of TA3-MM/2 ascites cells to grow progressively in ascites form in mice of foreign strains is due to masking of surface histocompatability H-2^a antigens by epiglycanin molecules. It was suggested that this protective effect in the TA3-Ha ascites cell was due mainly to a physical or steric effect (*13–15*), a suggestion consistent with the size and shape (*2, 6*) and the high concentration of epiglycanin molecules at the TA3-Ha cell surface (*2, 8, 14*). With regard to the allotransplantability of the TA3-MM/2, however, other factors may be important. Although the TA3-MM/1 line possesses approximately the same number of epiglycanin molecules per cell as the TA3-Ha ascites cell (4×10^6), the TA3-MM/2 cell appears to have only 30–40% of this number (*2*). The lower capacity of the TA3-MM/2 ascites cell to absorb anti-H-2^a antibody than the TA3-Ha cell (text-fig. 1) is consistent with this observation. Thus the degree of allotransplantability of the TA3-MM/2 line does not appear to be as proportionate to the epiglycanin concentration as is the in vitro absorptive capacity for anti-H-2^a antibody.

Fraction II from the TA3-MM/2 cell was found to be somewhat more active as an inhibitor in the radioimmunoassay than the comparable fraction from the TA3-Ha cell (table 2). This is of interest since epiglycanin from the TA3-MM/2 cell differed in carbohydrate composition from that of the other two lines, there being a greater proportion of *N*-acetylglucosamine residues and a smaller proportion of the major carbohydrate chains, a disaccharide of a galactose residue attached by a β-linkage at position 3 of *N*-acetylgalactosamine (*8*). Since we have demonstrated that the carbohydrate moiety in epiglycanin is involved as the antigenic determinant for this antibody (*16*), the results in the radioimmunoassay suggest that epiglycanin from the TA3-MM/2 cell probably possesses at least as many antigenic structures as those of the TA3-Ha or TA3-MM/1 cells. It is not known, however, whether or not the carbohydrate composition of epiglycanin has any direct influence on the allotransplantability of the cell.

In a series of TA3-Ha/A.CA hybrid cell lines, a direct relationship appeared to exist between the degree of allotransplantability and epiglycanin concentration (*12*) with some minor exceptions. For example, the TA3-Ha/A.CA/6 line was highly allotransplantable, yet it possessed a low concentration of epiglycanin (*12*). Its concentration of cell surface sialic acid, however, was relatively large (570 μg/10^9 cells), approximately the same as that of the TA3-Ha ascites cell (*20*). The TA3-MM/2 line possesses twice this concentration of sialic acid (*2*). Although it has been observed that cell surface sialic acid does not affect the absorptive capacity (*13*), and in general, allotransplantability is neither proportional to the amount nor to the composition of sialic acid (*20*), a combination of factors, among them the very high concentration of sialic acid, may serve to increase the allotransplantability of the TA3-MM/2 cell.

Due to the complexity of the macromolecular structures at the cell surface and their yet poorly understood interrelationships, as well as to the probable influences of other parameters such as cell morphology and physiology, it is difficult to establish a direct relationship between structure and function in cell surface glycoproteins. Nevertheless, the present studies have shown that at least in two TA3 ascites tumor lines, the TA3-MM/2 and TA3-Ha lines that had independent origins as ascites cells and are different from each other in many important cell characteristics (*2, 3*), the presence of the endogenous large cell surface glycoprotein epiglycanin is associated with allotransplantability. It is not known whether or not the presence of this glycoprotein at the cell surface actually determines or directly influences the morphology of the TA3-MM/2 and TA3-Ha cell surfaces that is manifested in numerous long and regularly spaced microvilli (figs. 1, 2). Nevertheless, the possibility that this characteristic topography of the two lines directly influences transplantation characteristics must be considered. A suggestion has been made that allotransplantability in the TA3-Ha ascites cell was due to interference in the immune response by blocking factors composed of epiglycanin and antibody (*21*). This hypothesis was based on the finding that epiglycanin shed from proliferating ascites cells was present in the serum (*21*). The most plausible explanation for allotransplantability in these cell lines, however, remains that of histocompatability (H-2) antigen masking by cell surface epiglycanin molecules. The results presented in this report are consistent with this hypothesis.

REFERENCES

(*1*) Hauschka TS, Weiss L, Holdridge BA, Cudney TL, Zumpft M, Planinsek JA. Karyotypic and surface features of murine TA3 carcinoma cells during immunoselection in mice and rats. J Natl Cancer Inst 1971; 47:343–359.

(*2*) Codington JF, Cooper AG, Miller DK, et al. Isolation and partial characterization of an epiglycanin-like glycoprotein from a new non-strain-specific subline of TA3 murine mammary adenocarcinoma. JNCI 1979; 63:153–161.

(*3*) Cooper AG, Codington JF, Miller DK, Brown MC. Loss of strain specificity of the TA3-St subline: Evidence for the role of epiglycanin in mouse allogeneic tumor growth. JNCI 1979; 63:163–169.

(*4*) Codington JF, Sanford BH, Jeanloz RW. Glycoprotein coat of the TA3 cell. Isolation and partial characterization of a sialic acid-containing glycoprotein fraction. Biochemistry 1972; 11:2559–2564.

(*5*) ——— Cell-surface glycoproteins of two sublines of the TA3 tumor. J Natl Cancer Inst 1973; 51:585–591.

(*6*) Slayter HS, Codington JF. Size and configuration of glycoprotein fragments cleaved from tumor cells by proteolysis. J Biol Chem 1973; 248:3405–3410.

(*7*) Codington JF, Linsley KB, Jeanloz RW, Irimura T, Osawa T. Immunochemical and chemical investigations of the structure of glycoprotein fragments obtained from epiglycanin, a glycoprotein at the surface of the TA3 cancer cell. Carbohydr Res 1975; 40:171–182.

(*8*) Van Den Eijnden DH, Evans NA, Codington JF, Reinhold V, Silber C, Jeanloz RW. Chemical structure of epiglycanin, the major glycoprotein of the TA3-Ha ascites cell. J Biol Chem 1979; 254:12153–12159.

(*9*) Matsumoto I, Codington JF, Jahnke MR, Jeanloz RW, Osawa T. Comparative lectin binding and agglutination properties of the strain-specific, TA3-St, and the non-strain specific TA3-Ha, murine mammary carcinoma ascites sublines. Further studies of receptors in epiglycanin. Carbohydr Res 1980; 80:179–189.

(*10*) Codington JF, Cooper AG, Brown MC, Jeanloz RW. Evidence that the major cell surface glycoprotein of the TA3-Ha carcinoma contains the *Vicia graminea* receptor sites. Biochemistry 1975; 14:855–859.

(*11*) Miller SC, Hay ED, Codington JF. Ultrastructural and histochemical differences in cell surface properties of strain-specific and nonstrain-specific TA3 adenocarcinoma cells. J Cell Biol 1977; 72:511–529.

(*12*) Codington JF, Klein G, Cooper AG, Lee N, Brown MC, Jeanloz RW. Further studies on the relationship between large glycoprotein molecules and allotransplantability in the TA3 tumor of the mouse: Studies on segregating TA3-Ha hybrids. J Natl Cancer Inst 1978; 60:811–818.

(*13*) Sanford BH, Codington JF, Jeanloz RW, Palmer PD. Transplantability and antigenicity of two sublines of the TA3 tumor. J Immunol 1973; 110:1233–1237.

(*14*) Codington JF. Masking of cell surface antigens on cancer cells. In: Cellular membranes and tumor cell behavior. Baltimore: Williams & Wilkins, 1975:395–419.

(*15*) ———. The masking of cancer cell surface antigens. In: Waters H, ed. Handbook of cancer immunology. Vol 8. New York: Garland STPM Press, 1981:171–203.

(*16*) Codington JF, Bhavanandan VP, Silber C, Jeanloz RW, Bloch KJ. The characteristics of an antibody to epiglycanin, a glycoprotein of the TA3-Ha mouse tumor cell. In: Yamakawa T, Osawa T, Handa S, eds. Glycoconjugates. Tokyo: Japan Sci Soc Press, 1981:310–311.

(*17*) Spurr AR. A low-viscosity epoxy resin embedding medium for electron microscopy. J Ultrastruct Res 1969; 26:31–43.

(*18*) Klein G, Gars U, Harris H. Isoantigen expression in hybrid mouse cells. Exp Cell Res 1970; 62:149–160.

(*19*) Reif AE. An experimental test of two general relationships to describe the adsorption of antibodies by cells and tissues. Immunochemistry 1966; 3:267–278.

(*20*) Codington JF, Klein G, Silber C, Linsley KB, Jeanloz RW. Variations in the sialic acid compositions in glycoproteins of mouse ascites tumor cell surfaces. Biochemistry 1979; 18:2145–2149.

(*21*) Cooper AG, Codington JF, Brown MC. In vivo release of glycoprotein I from the Ha subline of TA3 murine tumor into ascites fluid and serum. Proc Natl Acad Sci USA 1974; 71:1224–1228.

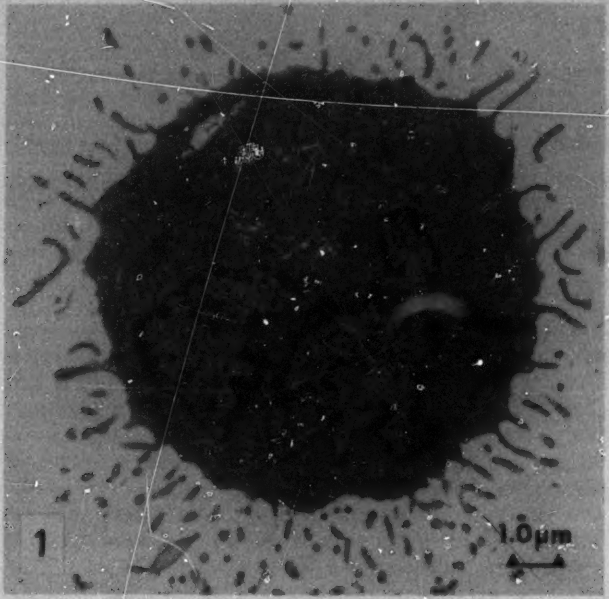

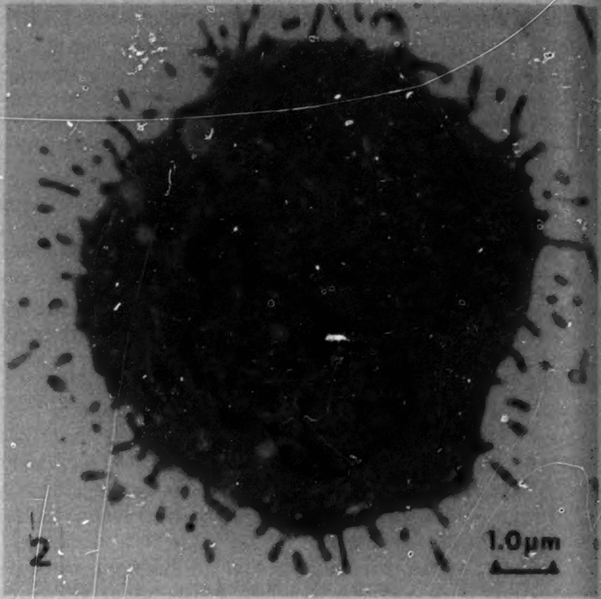

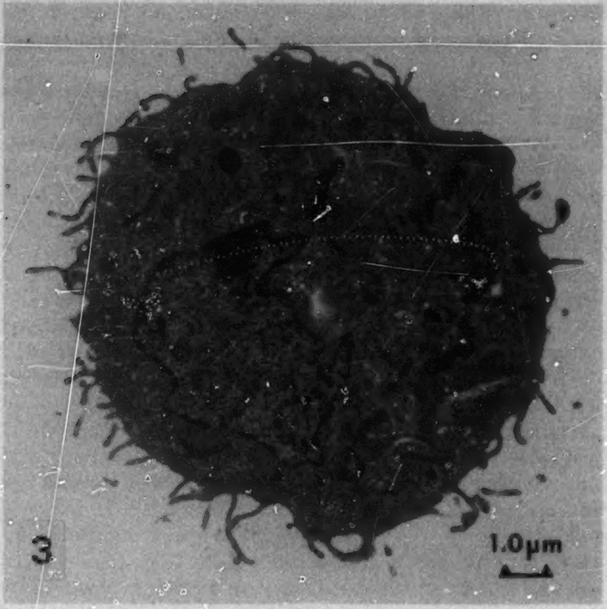

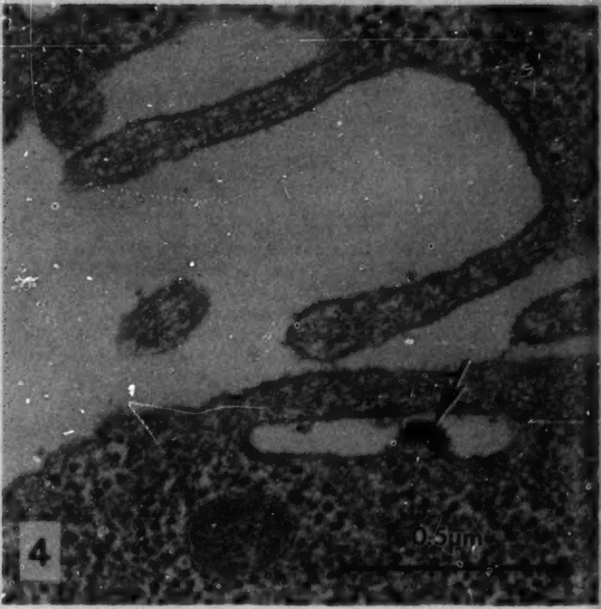

FIGURE 1.—Low-power electron micrograph of non-strain-specific TA3-MM/2 mammary carcinoma ascites cell fixed in suspension. × 7,000

FIGURE 2.—Low-power electron micrograph of non-strain-specific TA3-Ha mammary carcinoma ascites cell fixed in suspension. × 8,900

FIGURE 3.—Low-power electron micrograph of strain-specific TA3-St mammary carcinoma ascites cell fixed in suspension. × 6,000

FIGURE 4.—High-power electron micrograph showing surface characteristics of strain-specific TA3-St cells. Very little cell coat (glycocalyx) is evident on the cell surface. *Arrow* indicates a virus particle budding from the cell surface. × 66,400

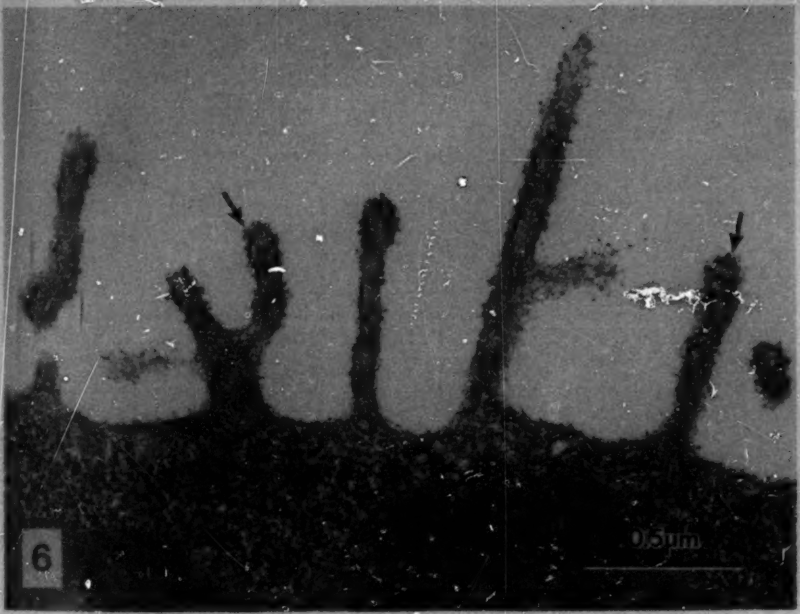

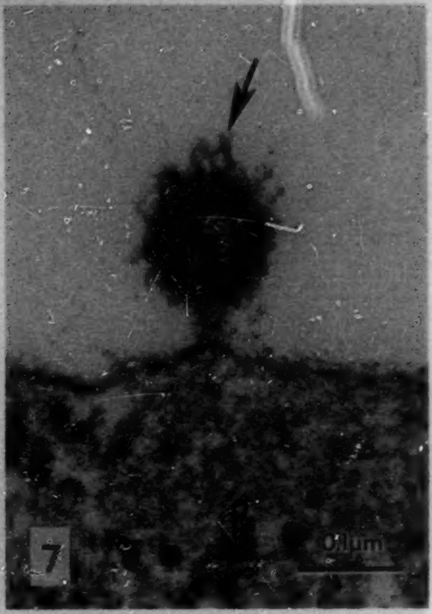

FIGURE 5.—*Arrows* indicate an extensively fuzzy or filamentous-looking cell surface on non-strain-specific TA3-Ha cells. × 56,000

FIGURE 6.—A morphologically distinct cell surface coat (*arrows*) is also evident on non-strain-specific TA3-MM/2 cells, but is less extensive than that seen on the TA3-Ha cell (fig. 5). × 47,200

FIGURE 7.—*Arrow* indicates a virus particle with a surface coat, budding from the cell surface of a TA3-MM/2 cell. × 150,000

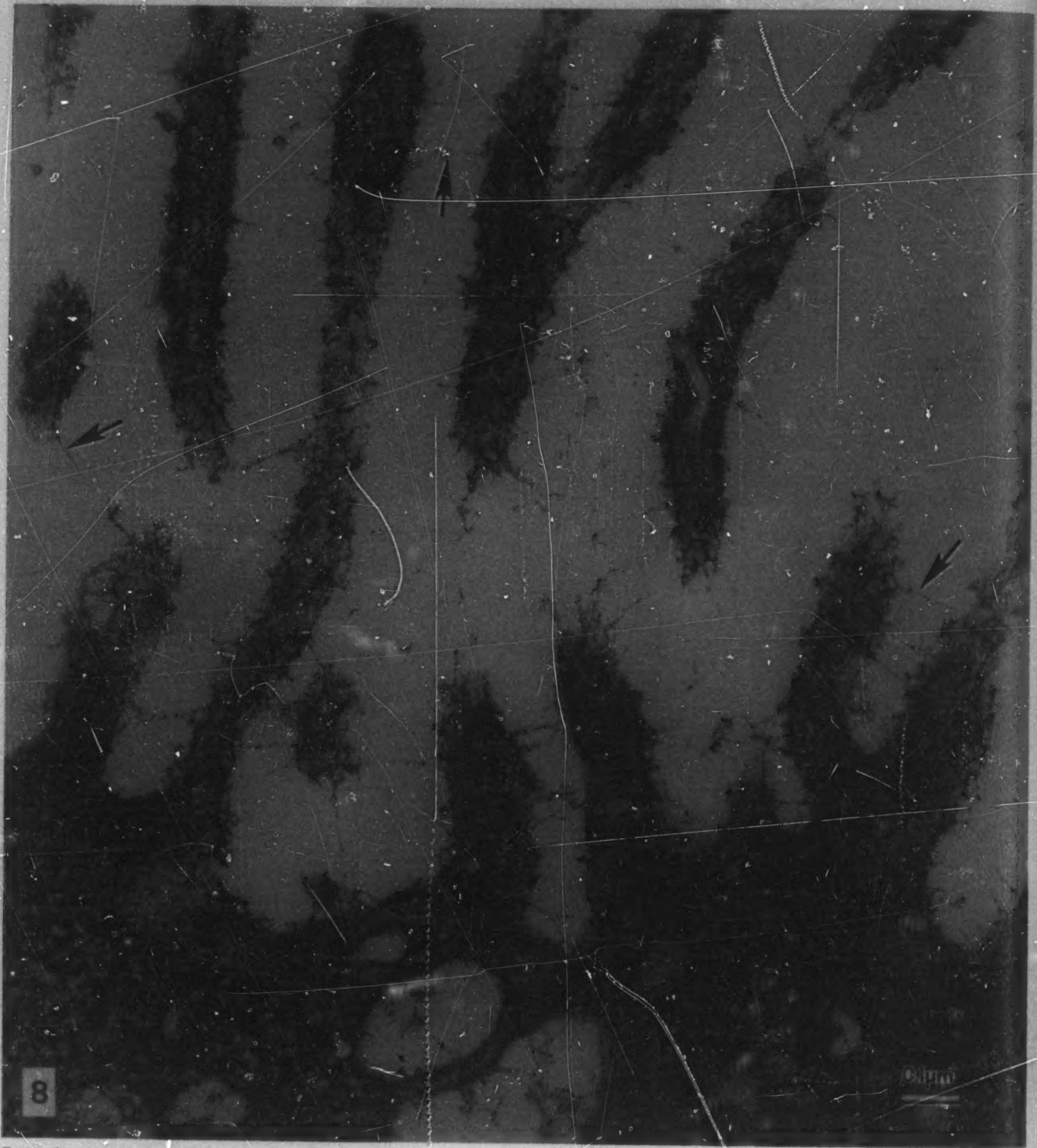

FIGURE 8.—*Arrows* indicate the long, thin filamentous structures that are often seen bridging adjacent microvilli on non-strain-specific TA3-MM/2 cells. × 103,000

Carcinogenesis by Isomers of *N*-Nitroso-3,5-dimethylpiperidine [1,2,3]

W. Lijinsky,[4] M. D. Reuber,[4] Sandra S. Singer,[4] *and* George M. Singer[4]

ABSTRACT—The *cis*- and *trans*-isomers of *N*-nitroso-3,5-dimethylpiperidine were administered separately in drinking water solution to groups of 20 female F344 rats for 50 weeks. The concentrations of the solutions were 0.72 m*M* for the *cis*-isomer and 0.14 m*M* for the *trans*-isomer. In both groups the animals died with tumors of the upper gastrointestinal (GI) tract, mainly carcinomas of the esophagus, at about the same time. A third group of animals was given a mixture of the two isomers in the ratio of 5 *cis*:1 *trans*, and these animals died more rapidly with the same upper GI tumors. The *trans*-isomer appeared to be a more potent carcinogen than the *cis*-isomer. The 3,5-dimethyl derivative is a less potent carcinogen than nitrosopiperidine.—JNCI 1982; 68:989–991.

The great increase in carcinogenicity of NM when substituted with methyl groups in the beta positions (*1*) was ascribed to changes in the conformation of the molecule because of the two methyl groups. The *trans*-isomer of DMNM was considerably more potent than the *cis*-isomer in rats (*2*). It was of interest to know whether this effect was similar for other cyclic nitrosamines and, to this end, a similar study was undertaken of the analogous DMNP.

Initially, DMNP was prepared as a mixture of isomers by reduction of 3,5-lutidine with either Adams' catalyst and hydrogen or sodium and ethanol followed by nitrosation. By analogy with the NM, DMNP was expected to be more carcinogenic than NP. DMNP was, therefore, administered to noninbred Sprague-Dawley rats at a lower dose than that of NP. In fact, DMNP proves to be less carcinogenic than its parent, and the incidence of tumors was small. Consequently, another experiment was undertaken in F344 rats and involved administration of higher doses of DMNP alongside its two isomers, comprising the mixture, at comparable doses.

MATERIALS AND METHODS

DMNP.—This compound was prepared by catalytic reduction of 3,4-lutidine and was resolved into the *cis*- and *trans*-isomers as previously described (*3*). Their structures were ascertained by NMR spectrometry, as follows:

Cis.—NMR ($CDCl_3$): 0.95 δ (d, 3H, *syn*-3-Me, $J_{\text{Me-3ax}}$ = 6.34 Hz), 1.03 (d, 3H, *anti*-5-Me, $J_{\text{Me-5ax}}$ = 6.37), 2.00 (ddd, 1H, *syn*-2-ax-H, J_{gem} = −12.81, $J_{\text{2ax-3ax}}$ = 11.66, $J_{\text{2ax-6ax}}$ = 0.87), 3.17 (ddd, 1H, *anti*-6-ax-H, J_{gem} = −12.70, $J_{\text{6ax-5ax}}$ = 11.75), 4.64 (ddd, 1H, *anti*-6-eq-H, J_{gem} = −12.70, $J_{\text{6eq-5ax}}$ = 4.49, $J_{\text{6eq-2eq}}$ = 1.7), 5.00 (ddd, 1H, *syn*-2-eq-H, J_{gem} = −12.81, $J_{\text{2eq-3ax}}$ = 4.10, $J_{\text{2eq-6eq}}$ = 1.7).[5]

Trans.—0.89 δ (d, 3H, *syn*-3-Me, $J_{\text{Me-3H}}$ = 6.79 Hz), 1.00 (d, 3H, *anti*-5-Me, $J_{\text{Me-5H}}$ = 6.85), 1.57 (t, 2H, 4-H, $J_{\text{4H-3H}}$ = $J_{\text{4H-5H}}$ = 5.74), 1.7–2.35 (m, 2H, 3-H and 5-H), 3.40 (dd, 1H, *anti*-6-"axial"-H, J_{gem} = −13.23, $J_{\text{6H-5H}}$ = 6.98), 3.80 (dd, 1H, *syn*-2-axial-H, J_{gem} = −12.97, $J_{\text{2H-3H}}$ = 6.66), 3.84 (dd, 1H, *anti*-6-axial-H, J_{gem} = −13.23, $J_{\text{6H-5H}}$ = 4.40), 4.21 (dd, 1H, *syn*-2-"eq"-H, J_{gem} = −12.97, $J_{\text{2H-3H}}$ = 4.32).[6]

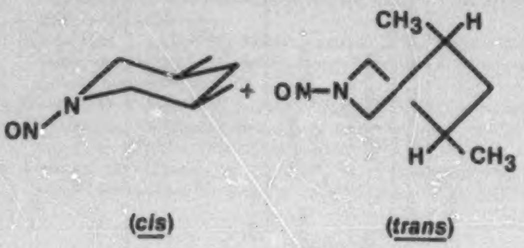

TEXT-FIGURE 1.—DMNP.

Animal treatments.—Groups of 20 female F344 rats, 7–8 weeks old at the beginning of treatment, were housed 4/cage and given Rockland rat diet ad libitum. DMNP and its two isomers were dissolved in water, at the concentrations shown in table 1, and administered as drinking water solutions to the rats at the rate of 80 ml/cage/day (20 ml/rat) on each of 5 days a week; on the remaining 2 days tap water was given ad libitum. The rats were allowed to die naturally and were carefully necropsied. All lesions and major organs and tissues were fixed for histologic examination.

RESULTS AND DISCUSSION

In table 1 the results of treating F344 rats with DMNP or its *cis*- and *trans*-isomers are shown. The survival of the treated animals is given together with the numbers of animals with tumors of the upper GI tract. These tumors are rarely, if ever, seen in the untreated control rats continuously maintained in our colony.

Administration of a 0.88-m*M* solution of the mixture of isomers of DMNP (82% *cis*-isomer, 16% *trans*-isomer) to F344 rats for 50 weeks (a total dose of 4.4 mmol/rat) resulted in the death of all of the animals with tumors by 82 weeks. An equimolar concentration of NP given for only 28 weeks (a total dose of 2.5 mmol) resulted in the death of all of the animals with tumors by the 36th week of the experiment (*4*). In both cases, the cause of death was principally basal cell carcinomas of the esophagus (table 1). Thus it appears

---

ABBREVIATIONS USED: DMNM=*N*-nitroso-2,6-dimethylmorpholine; DMNP=*N*-nitroso-3,5-dimethylpiperidine; GI=gastrointestinal; NM=nitrosomorpholine(s); NMR=nuclear magnetic resonance; NP=nitrosopiperidine(s).

---

[1] Received July 30, 1981; accepted January 15, 1982.

[2] Supported by Public Health Service contract N01CO-75380 from the Office of the Director, National Cancer Institute.

[3] Animals were maintained under the guidelines set forth by the NCI-Frederick Cancer Research Facility.

[4] Chemical Carcinogenesis Program, NCI-Frederick Cancer Research Facility, Frederick, Md. 21701.

[5] d=doublet.

[6] t=triplet; m=unresolved multiplet.

TABLE 1.—*Survival and tumor incidence in female rats treated with DMNP and its cis- and trans-isomers*

Compound	Concentration of compound in water, mg/liter (m*M*)	Length of treatment, wk	Total dose, mg (mmol)	No. of animals at wk												No. of animals with upper GI tumors	No. of rats with tumors of:					
																	Esophagus		Forestomach		Tongue	
				0	10	20	30	40	50	60	70	80	90	100	110		Carcinomas	Total	Carcinomas	Total	Carcinomas	Total
DMNP (mixture of 5 *cis*-isomer:1 *trans*-isomer	124 (0.88)	50	620 (4.4)	20	20	20	20	20	18	11	4	1[a]				16	9	16	0	4	—	—
Cis-isomer	102 (0.72)	50	510 (3.6)	20	20	20	20	20	20	19	18	15	10	8	3[b]	17	14	17	5	8	5	6
Trans-isomer	20 (0.14)	50	100 (0.7)	20	20	19	19	19	19	18	16	13	10	4	2[b]	18	13	14	3	6	5	8

[a] Died at 82 wk.
[b] Killed at 115 wk.

that the presence of the two methyl groups in both beta positions of NP reduced the carcinogenic potency considerably; the same conclusion was drawn from the experiment in Sprague-Dawley rats, although in this case the dose was lower and the treatment period was shorter (40 wk), but the number of rats with tumors of the esophagus and forestomach was small—only 4 of 15 animals. This phenomenon is the opposite of the effect of analogous methyl substitution in NM. Introduction of the methyl groups into NM resulted in a large increase in carcinogenic potency and also produced a change in the affected organ—induction of esophageal tumors instead of the liver tumors produced by NM (*1*).

The groups of rats treated with the *cis*- and *trans*-isomers of DMNP separately also died with esophageal tumors, and the survival of both groups was comparable, even though the dose of the *trans*-isomer was only one-fifth of the *cis*-isomer. Since the incidence of tumors induced was very similar, it can be concluded that the two treatments were equally effective and that, therefore, the *trans*-isomer is a more potent carcinogen than the *cis*-isomer. This finding is analogous to the finding with DMNM, the *trans*-isomer of which was considerably more effective than the *cis*-isomer in inducing esophageal tumors in rats. In these experiments, both the *cis*- and *trans*-isomers of DMNP apparently contributed to the carcinogenic effect, since the treatment with the mixture was more effective than the treatment with either isomer alone; the dose of the mixture was the sum of the doses of each isomer.

The results of a number of previous chronic tests of methyl-substituted cyclic nitrosamines in rats led to the suggestion that a rigid "chair" conformation was favorable for the induction of esophageal tumors. In this conformation, removal of the alpha axial protons is facilitated by stereoelectronic support of the carbanion by the π-system of the N-nitroso function (*5, 6*).

However, this hypothesis is not satisfactory since, in both DMNP and DMNM (*1*), the *trans*-dimethyl groups force a distortion of the chair conformation. The ring is twisted so that both methyl groups can be pseudoequatorial and A(1, 3) interactions can be minimized. A consequence of this distortion is that all four alpha protons become approximately stereochemically equivalent.

In both instances, all four alpha protons of the *trans*-dimethyl isomers are exchanged by methanolic 40% sodium deuteroxide, but those of the piperidine are exchanged much more slowly than those of the morpholine. Under the same conditions, 2 hours at 50°C, only the axial alpha protons of the *cis*-isomer of the morpholine are exchanged, but no exchange can be demonstrated in the *cis*-isomer of DMNP even after 16 hours. The most important effect of the altered conformation induced by the *trans* dimethyl groups may be to render the alpha protons more susceptible to base abstraction. Thus doubling the number of chemically reactive sites may contribute to the observed increase in carcinogenicity in rats compared with the carcinogenicity of the *cis*-isomers.

The lessening of the carcinogenicity of DMNP compared with that of NP supports our observation that the relative carcinogenic potency of NP is inversely related to their octanol–water partition coefficients (*7*).

It is likely that the critical activation of DMNP occurs in the esophagus, since in mutagenesis studies in *Salmonella typhimurium* with a rat liver microsomal preparation for activation, there was no detectable quantitative difference in activity between the *cis*- and *trans*-isomers (*8*).

REFERENCES

(*1*) Lijinsky W, Taylor HW. Increased carcinogenicity of 2,6-dimethylnitrosomorpholine compared with nitrosomorpholine in rats. Cancer Res 1975; 35:2123–2125.

(*2*) Lijinsky W, Reuber MD. Comparison of carcinogenesis by two isomers of nitroso-2,6-dimethylmorpholine. Carcinogenesis 1980; 1:501–503.

(*3*) Singer SS, Singer GM. Isolation of gram quantities of configurational isomers of cyclic nitrosamines by preparative liquid chromatography. J Liquid Chromatogr 1979; 2:1219–1228.

(*4*) Kupper R, Reuber MD, Blackwell BN, Lijinsky W, Koepke SR, Michejda CJ. Carcinogenicity of the isomeric *N*-nitroso-Δ^3- and *N*-nitroso-Δ^2-piperidines in rats and the in vivo isomerization of the Δ^3- to the Δ^2-isomer. Carcinogenesis 1980; 1:753–757.

(*5*) Lyle RE, Saavedra JE, Lyle GG, et al. Conformational stereochemistry in electrophilic reactions with cyclic anions. Tetrahedron Lett 1976; 4431–4434.

(*6*) Singer GM, Lijinsky W. Relative extents of hydrogen–deuterium exchange of nitrosamines: Relevance to biological isotope studies. Cancer Lett 1979; 8:29–34.

(*7*) Singer GM, Taylor HW, Lijinsky W. Liposolubility as an aspect of nitrosamine carcinogenicity: Quantitative correlations and qualitative observations. Chem Biol Interact 1978; 19:133–142.

(*8*) Andrews AW, Lijinsky W. Mutagenicity of 45 nitrosamines in *Salmonella typhimurium*. Teratog Carcinog Mutagen 1980; 1:295–303.

blank page

Effect of 7,12-Dimethylbenz[*a*]anthracene on Production and Action of Gamma Interferon[1,2,3]

Karen A. Golemboski,[4,5] Debra K. D. DeLor,[4] Uldis N. Streips,[4] and Gerald Sonnenfeld[4,6,7]

ABSTRACT—Spleens were removed from Swiss Webster mice, and cultures of spleen cells were prepared. Gamma (type II immune) interferon (IFN) production was induced in these cells by addition of the purified protein form of phytohemagglutinin (PHA-P) to the cultures. When 7,12-dimethylbenz[a]anthracene (DMBA) was added to the cultures either before or after addition of PHA-P, the production of gamma IFN was inhibited. The degree of inhibition was greater when the cells were treated with DMBA before addition of PHA-P. In experiments to determine the effects of DMBA on the antivirus activity of previously prepared gamma IFN preparations, DMBA was either added to target cells before the addition of exogenous gamma IFN or mixed together with exogenous gamma IFN. In both cases, the antivirus activity of this exogenous gamma IFN was not affected. These data suggest that DMBA treatment can inhibit the production but not the antivirus activity of murine gamma IFN.—JNCI 1982; 68:993–996.

The production of rat and mouse fibroblast (alpha–beta) IFN in tissue culture has been shown to be inhibited by pretreatment of the cultures with various carcinogens (*1–5*). These carcinogens include benzo[*a*]pyrene, aflatoxin B_1, 2-aminofluorene, chloroacetaldehyde, and DMBA (*1–5*). Weakly carcinogenic analogues of these chemicals had no effect on alpha–beta IFN induction. In these experiments a wide variety of alpha–beta IFN inducers were used, including viruses and polyriboinosinic-polyribocytidylic acid (*1–5*). The carcinogen treatment had no effect on virus replication or on the viability of the cell cultures.

An additional class of IFN has also been described (*6*). Gamma (type II immune) IFN is a lymphokine produced by lymphoid cells as part of a cell-mediated immune response (*6–8*). The present study was done to determine if the production and action of gamma IFN could also be affected by treatment of cells with the potent carcinogen DMBA.

The results of these experiments suggest that the production of gamma IFN by mouse spleen cells was inhibited by pretreatment of the cells with DMBA. In addition, gamma IFN production was also inhibited, but to a lesser extent, when DMBA treatment was withheld until after the cells were stimulated to produce IFN. Addition of DMBA to target cells prior to or together with addition of exogenous gamma IFN did not affect the antivirus activity of the IFN.

MATERIALS AND METHODS

Mice.—Female Swiss Webster mice 6–8 weeks old were obtained from Laboratory Supply Co., Indianapolis, Ind. These mice are potent producers of gamma IFN (*9*).

Chemicals.—DMBA was obtained from Eastman Organic Chemicals, Rochester, N.Y. DMSO and acetone were obtained from J. T. Baker Chemical Co., Phillipsburg, N.J. Ethanol was obtained from Aaper Alcohol and Chemical Co., Louisville, Ky.

Gamma IFN production.—Production experiments: Gamma IFN was produced by stimulation of murine spleen cells with PHA-P (Difco Laboratories, Inc., Detroit, Mich.) (*10*). Cultures of 5×10^6 spleen cells were prepared in 1 ml of RPMI-1640 medium (GIBCO, Grand Island, N.Y.) supplemented with 1% fetal bovine serum and 5×10^{-5} M 2-mercaptoethanol. Cell viability (live cells/total cells) was determined by trypan blue dye exclusion. PHA-P (34 μg) was added to each culture, and the cultures were allowed to incubate at 37°C for 3 days in 5% CO_2. Culture supernatants were harvested and contained the gamma IFN activities. This IFN has been shown to be gamma IFN because of its pH 2 sensitivity, 56°C resistance, and anti-alpha–beta IFN serum resistance (*7*).

Action experiments: Pools of murine gamma IFN were produced by tuberculin (Jensen-Salsbery Laboratories, Kansas City, Mo.) challenge of mice sensitized previously with *Mycobacterium bovis* strain BCG (*7*). The IFN activity was in the serum.

IFN assay.—Antivirus titers were determined by plaque reduction on mouse L-929 cells with the use of the Indiana strain of vesicular stomatitis virus (*11*). The antivirus titer corresponded to the reciprocal of the greatest dilution of test sample that reduced virus plaques by 50%. In this assay, one IFN antivirus unit equals 0.88 NIH G-002-904-511 reference units.

Statistical analysis.—The data were analyzed by means of Student's *t*-test.

ABBREVIATIONS USED: DMBA=7,12-dimethylbenz[*a*]anthracene; DMSO=dimethyl sulfoxide; IFN=interferon(s); PHA-P=purified protein form of phytohemagglutinin.

---

[1] Received August 5, 1981; accepted February 5, 1982.

[2] Supported in part with Federal funds from the Environmental Protection Agency under grant R-807619. The contents do not necessarily reflect the views and policies of the Environmental Protection Agency, nor does mention of trade names or commercial products constitute endorsement or recommendation for use.

[3] Animals were maintained under the guidelines set forth by the University of Louisville School of Medicine accredited by the American Association for Accreditation of Laboratory Animal Care.

[4] Department of Microbiology and Immunology, University of Louisville School of Medicine, Louisville, Ky. 40292.

[5] Recipient of a University Fellowship from the Graduate School of the University of Louisville.

[6] *Address reprint requests to* Dr. Sonnenfeld.

[7] We gratefully acknowledge the assistance of Ms. Virginia Black in the preparation of this manuscript.

RESULTS

Effect of DMBA on the Viability of Spleen Cells

DMBA was dissolved in DMSO. DMSO was an acceptable solvent because it did not affect the viability of the spleen cells as determined by trypan blue dye exclusion (text-figs. 1, 2). Ethanol and acetone were not useful as solvents because they were toxic to the cells in the concentrations required (data not shown). Lower concentrations of DMBA had little effect on the viability of the cells, whether or not they were added before or after stimulation of gamma IFN production with PHA-P (text-figs. 1, 2). High concentrations of DMBA decreased viability of the spleen cells by a small amount at the commencement of the culture (text-figs. 1, 2). A minimal effect was observed on the viability of the cells at the termination of the culture, the time of maximal gamma IFN production (text-figs. 1, 2).

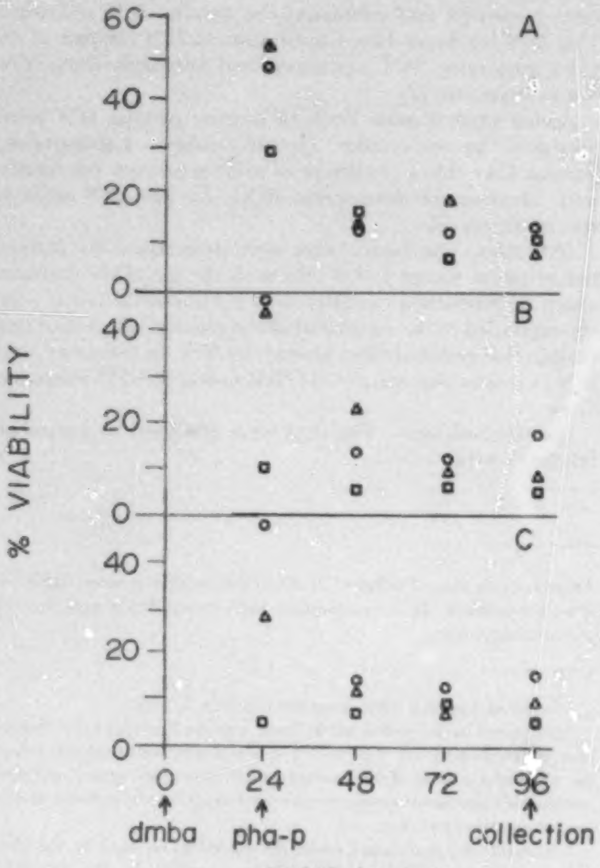

TEXT-FIGURE 1.—Effect on viability of spleen cells of addition of DMBA 24 hr prior to stimulation of cultures with PHA-P. ○=PHA-P only added; △=PHA-P and DMSO only added; □=PHA-P+DMBA in DMSO added. 1A) 8 μM DMBA in 0.2% DMSO. 1B) 40 μM DMBA in 1% DMSO. 1C) 80 μM DMBA in 2% DMSO. Viabilities at the commencement of cultures were 90–95%. Viabilities were determined by counting 200 cells and by determining the number of viable (nonstaining) cells per total cells counted at each time interval.

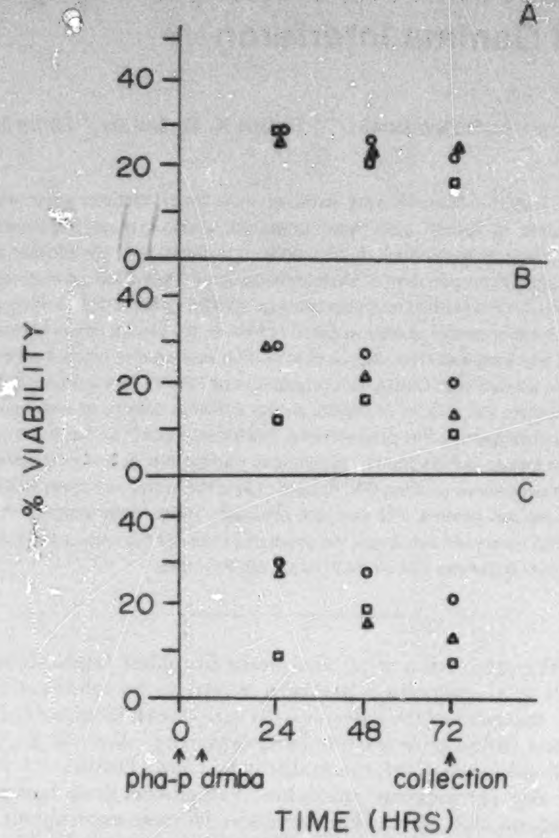

TEXT-FIGURE 2.—Effect on viability of spleen cells of addition of DMBA 4–5 hr after stimulation of cultures with PHA-P. ○=PHA-P only added; △=PHA-P and DMSO only added; □=PHA-P+DMBA in 0.2% DMSO added. 2A) 8 μM DMBA in 0.2% DMSO. 2B) 40 μM DMBA in 1% DMSO. 2C) 80 μM DMBA in 2% DMSO. Initial viabilities and determination of viabilities are as described in text-fig. 1.

Effect of DMBA on Gamma IFN Production

Various concentrations of DMBA were added to cultures of spleen cells. Twenty-four hours later, the DMBA was removed, cells were washed, and 34 μg of PHA-P was added to the cultures to induce gamma IFN. Three days later, the culture supernatants were harvested and assayed for antivirus activity. Since the IFN assay is a titration, a decrease of 50% or greater (or a 100% increase) in antivirus titer was required for the chemical treatment to be judged to have a reliable effect on IFN induction (*4*). No conclusions can be reached on a dose-response correlation from these data. DMBA pretreatment significantly decreased the production of gamma IFN (table 1).

PHA-P (34 μg) was added to cultures of spleen cells. Four to five hours later, several concentrations of DMBA were added to the cultures. The cultures were incubated for 3 days, and then supernatants were harvested and assayed for antivirus activity. This DMBA treatment also inhibited the production of gamma IFN (table 2).

TABLE 1.—*Effect of DMBA treatment of spleen cells 24 hours prior to addition of PHA-P on gamma IFN induction*

Treatment of cells	No. of expt	Anti-virus titer ± SD	Change, %[a]	P[b]
PHA-P + 0.2% DMSO	8	42±20	—	—
PHA-P + 0.2% DMSO + 8 μM DMBA	8	21±14	−50	<0.02
PHA-P + 1% DMSO	8	37±25	—	—
PHA-P + 1% DMSO + 40 μM DMBA	8	7±4	−81	<0.02
PHA-P + 2% DMSO	8	42±32	—	—
PHA-P + 2% DMSO + 80 μM DMBA	8	7±4	−83	<0.02

[a] Percent change as compared to cells treated with equivalent volume of DMSO. Minus indicates decrease.

[b] *P*-value as compared to cells treated with equivalent volume of DMSO.

Effect of DMBA Treatment on the Antivirus Action of IFN

L-929 cells were used as the target cells for the assay of IFN activity. L-929 cells were treated with various concentrations of DMBA. No effect of DMBA on the viability of the L-929 cells was observed with the use of trypan blue dye exclusion (text-fig. 3). In addition, no effect on cell viability was observed when DMBA was mixed with gamma IFN and applied to L-929 cells (text-fig. 3).

L-929 cells were treated with various concentrations of DMBA. Twenty-four hours later, the DMBA was removed, and the cells were washed twice with medium. Exogenous gamma IFN was added to the L-929 cells, and the IFN assay was performed as described above. No effect of DMBA treatment on the antivirus action of gamma IFN was observed (table 3).

Various concentrations of DMBA were mixed with gamma IFN preparations. The preparations were then applied to L-929 cells, and the IFN assay was done as described above. No effect of DMBA addition on the antivirus activity of the gamma IFN was observed (table 4).

TABLE 2.—*Effect of DMBA treatment of spleen cells 4–5 hours after addition of PHA-P on gamma IFN induction*

Treatment of cells	No. of expt	Anti-virus titer ± SD	Change, %[a]	P[b]
PHA-P + 0.2% DMSO	9	185±75	—	—
PHA-P + 0.2% DMSO + 8 μM DMBA	9	140±89	−24	NS
PHA-P + 1% DMSO	9	147±76	—	—
PHA-P + 1% DMSO + 40 μM DMBA	9	66±50	−55	<0.02
PHA-P + 2% DMSO	9	16±37	—	—
PHA-P + 2% DMSO + 80 μM DMBA	9	17±10	−72	<0.02

[a] Percent change as compared to cells treated with equivalent volume of DMSO. Minus indicates decrease.

[b] *P*-value as compared to cells treated with equivalent volume of DMSO. NS = not significant.

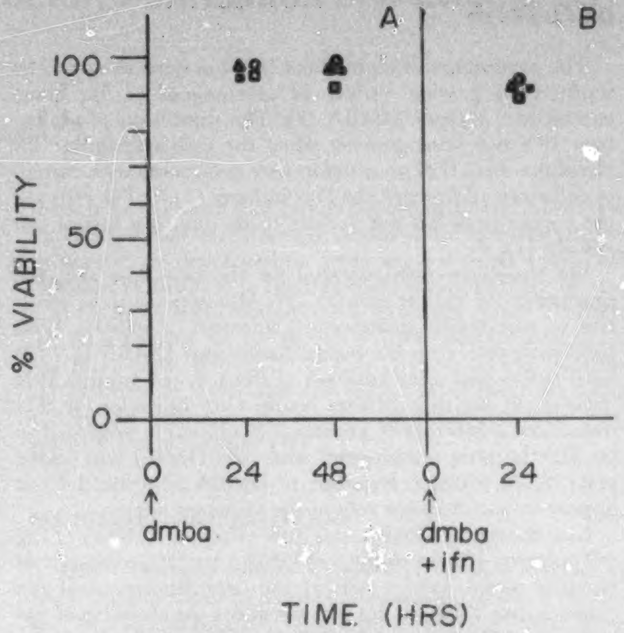

TEXT-FIGURE 3.—Effect on viability of L-929 cells of addition of DMBA. ○=gamma IFN only added; △=gamma IFN and 2% DMSO; □=gamma IFN and 80 μM DMBA in 2% DMSO; ■=40 μM DMBA in 1% DMSO. 3A) Addition of DMBA 24 hr prior to addition of gamma IFN. 3B) Simultaneous addition of DMBA and gamma IFN. Initial viabilities and determination of viabilities are as described in text-fig. 1.

TABLE 3.—*Effect of DMBA treatment of L-929 cells on the antivirus activity of exogenous gamma IFN*

Treatment of cells	No. of expt	Antivirus titer ± SD	Change, %[a]	P[b]
Gamma IFN + 2% DMSO	8	5,715±2,729	—	—
Gamma IFN + 1% DMSO + 40 μM DMBA	8	8,775±5,561	+53	NS
Gamma IFN + 2% DMSO + 80 μM DMBA	8	7,712±3,074	+35	NS

[a] Percent change as compared to gamma IFN + DMSO treatment of cells. Plus indicates increase.

[b] *P*-value is compared to gamma IFN + DMSO treatment of cells. NS = not significant.

TABLE 4.—*Effect of simultaneous addition of DMBA and gamma IFN to L-929 cells on antivirus activity*

Treatment of cells	No. of expt	Antivirus titer ± SD	Change, %[a]	P[b]
Gamma IFN + 2% DMSO	6	1,063±333	—	—
Gamma IFN + 1% DMSO + 40 μM DMBA	6	1,526±774	+44	NS
Gamma IFN + 2% DMSO + 80 μM DMBA	6	1,341±437	+26	NS

[a] Percent change as compared to gamma IFN + DMSO treatment of cells. Plus indicates increase.

[b] *P*-value is compared to gamma IFN + DMSO treatment of cells. NS = not significant.

DISCUSSION

The production of alpha-beta IFN has been shown to be sensitive to a wide variety of carcinogens (*1-5*). These carcinogens include DMBA (*3*). The inhibition of alpha-beta IFN has been greatest when the cells responsible for the alpha-beta IFN production were pretreated with carcinogen before addition of the IFN inducer (*1-5*). The effect of the carcinogens did not appear to be due to a loss of cell viability (*3, 4*).

We have now demonstrated for the first time that the production of murine gamma IFN also appears to be sensitive to carcinogen treatment. Treatment of gamma IFN-producing cells with the potent carcinogen DMBA (*12, 13*) both before and after addition of PHA-P, the gamma IFN inducer, to the cell cultures resulted in inhibition of IFN induction. Inhibition of gamma IFN induction appeared to be slightly more pronounced when the DMBA was added prior to the inducer, but time of DMBA addition did not appear to play a major role in the observed effect.

Low dosages of DMBA had little effect on viability of the cell cultures. Higher dosages of DMBA partly decreased the viability of the spleen cells at the commencement of the cultures, but they did not greatly affect the viability of the cultures at the termination of the cultures when gamma IFN production was highest. Loss of cell viability, therefore, does not appear to play a major role in the effect of DMBA on gamma IFN production; however, selective loss of viability of gamma IFN-producing cells in cultures treated with high concentrations of DMBA may make some contribution to the drop in gamma IFN production, especially since DMBA treatment could have had its greatest effect on rapidly dividing cells. In addition, although no gross effects were observed on viability as determined by trypan blue dye exclusion, effects on macromolecular synthesis could have occurred. The simultaneous addition of DMBA and PHA-P to cells could have had effects on cell protein, DNA, or RNA synthesis that could have resulted in decreased gamma IFN production. Experiments to further study the mechanism of the effects of DMBA on gamma IFN induction are in progress.

Since the IFN assay is a titration, there is a twofold variability in results. Therefore, only 50% decreases can be taken as being reliable decreases from control value. It is not yet clear if any correlation can be made between dose of DMBA used and amount of decrease in gamma IFN titer greater than 50%.

DMBA treatment of cells with dosages that affect IFN induction (*3*) did not appear to significantly affect the antivirus activity of exogenously added gamma IFN. In addition, mixing DMBA directly with gamma IFN did not affect antivirus activity. Therefore, DMBA does not appear to have a direct degradative effect on gamma IFN production; i.e. DMBA-treated cells do not degrade gamma IFN, and DMBA does not inactivate gamma IFN. The exact mechanism of the effects of DMBA on IFN induction will be the subject of further study in our laboratory.

REFERENCES

(*1*) De Maeyer E, De Maeyer-Guignard J. Inhibition by 3-methylcholanthrene of interferon formation in rat-embryo cells infected with Sindbis virus. J Natl Cancer Inst 1964; 32:1317-1331.

(*2*) De Maeyer-Guignard J, De Maeyer E. Effect of carcinogenic and noncarcinogenic hydrocarbons on interferon synthesis and virus plaque development. J Natl Cancer Inst 1965; 34:265-276.

(*3*) Hahon N, Booth JA, Stewart JD. Aflatoxin inhibition of viral interferon induction. Antimicrob Agents Chemother 1979; 16:277-282.

(*4*) Barnes MC, Streips UN, Sonnenfeld G. Effect of carcinogens and analogs on interferon induction. Oncology 1981; 38:98-101.

(*5*) Sonnenfeld G, Barnes MC, Schooler J, Streips UN. Inhibition of interferon induction as a screen for the carcinogenic potential of chemicals. In: Khan A, Hill NO, Dorn GL, eds. Interferon: Properties and clinical uses. Dallas: Leland Fikes Foundation Press, 1980:589-598.

(*6*) Salvin SB, Youngner JS, Lederer WH. Migration inhibitory factor and interferon in the circulation of mice with delayed hypersensitivity. Infect Immun 1973; 7:68-75.

(*7*) Youngner JS, Salvin SB. Production and properties of migration inhibitory factor and interferon in the circulation of mice with delayed hypersensitivity. J Immunol 1973; 111:1914-1922.

(*8*) Sonnenfeld G, Mandel AD, Merigan TC. In vitro production and cellular origin of murine type II interferon. Immunology 1979; 36:883-890.

(*9*) Sonnenfeld G, Harned CL, Thaniyavarn S, Huff T, Mandel AD, Nerland DE. Type II interferon induction and passive transfer depress the murine cytochrome P-450 drug metabolism system. Antimicrob Agents Chemother 1980; 17:969-972.

(*10*) Epstein LB, Cline MJ, Merigan TC. The interaction of human macrophages and lymphocytes in the phytohemagglutinin-stimulated production of interferon. J Clin Invest 1971; 50:744-753.

(*11*) Brodeur BR, Weinstein Y, Melmon KL, Merigan TC. Reciprocal changes in interferon production and immune responses of mouse spleen cells fractionated over columns of insolubilized conjugates of histamine. Cell Immunol 1977; 29:363-372.

(*12*) Pienta RJ. A hamster embryo cell model system for identifying carcinogens. In: Griffin AC, Shaw CR, eds. Carcinogens: Identification and mechanisms of action. New York: Raven Press, 1979:121-141.

(*13*) McCann JE, Ames BN. The *Salmonella*/microsome mutagenicity test: Predictive value for animals carcinogenicity. In: Hiatt HH, Watson JD, Winston JA, eds. Origins of human cancer. Book C. Human risk assessment. Cold Spring Harbor, N.Y.: Cold Spring Harbor Laboratory, 1977:1431-1450.

Murine Tumor Necrosis-Inducing Factor: Purification and Effects on Myelomonocytic Leukemia Cells[1,2,3]

Saul Green,[4,5] **Areta Dobrjansky,**[4] *and* **Mary Ann Chiasson**[4,6]

ABSTRACT—The tumor necrosis-inducing factor (TNF) found in sera of *Corynebacterium parvum*-treated, endotoxin-stressed BALB/C and outbred albino CD®-1 mice has been purified to a single band of protein by polyacrylamide gel electrophoresis after identification and removal of contaminating albumin and transferrin. This purified TNF has a molecular weight of 140,000, is glycoprotein in nature, and migrates on free electrophoresis as an α_2-globulin. TNF activity was continuously monitored during purification by bioassy in vitro (tumor cell lysis) and was confirmed by demonstration of induction of tumor necrosis in vivo. A single target tumor cell line, murine myelomonocytic leukemia (WEHI/3), was used in both assays. In the in vivo assay, controls were heat-inactivated samples of TNF. As additional controls, a line of TNF-resistant WEHI/3 cells was used in the in vitro assay. Results from in vivo radiolabeling of TNF-sensitive and TNF-resistant cells indicated a difference between their cytoplasmic peptide profiles. Optimal TNF production was not altered in *C. parvum*-endotoxin-treated mice by treatment with silica, a substance that is specifically toxic for macrophages. Exposure of mice to 650 rad whole-body radiation, which is not markedly damaging to macrophage elements in the reticuloendothelial system, completely abrogated the ability of the mice to produce TNF after *C. parvum*-endotoxin treatment. These findings suggest that in the sera of *C. parvum*-endotoxin-treated mice the protein that induces necrosis in tumors may not be of macrophage origin—JNCI 1982; 68:997–1003.

Numerous substances that exercise control over growth and proliferation of malignant cells exist in the sera of animals. Research in our laboratory on *C. parvum*-treated, endotoxin-stressed mice has focused on an activity in the sera that induced necrosis in transplanted tumors (*1*). This in vivo activity was ascribed to a substance designated as TNF.

Partial purification of TNF was initially accomplished by Green et al. (*2*). A fraction enriched in antitumor activity ($B_{1\text{-}4}$) contained glycoprotein and migrated on free electrophoresis as an α_2-globulin and on nondenaturing PAG with a retardation factor of 0.35–0.50. TNF had an apparent molecular weight of about 140,000 and contained trace amounts of galactosamine, sialic acid, glucose, and fructose. It did not contain DNA, RNA, or evidence of activity by the following enzymes: acid phosphatase, alkaline phosphatase, β-glucuronidase, glucosidase, α-galactosidase, DNAase, neuraminidase, lysozyme, or nonspecific esterases. Fraction $B_{1\text{-}4}$ could be distinguished from certain lymphokines by several physical properties: stability to heating at 56°C; loss of activity after heating at 70°C; insensitivity to the action of trypsin, chymotrypsin, or neuraminidase; and lack of cytotoxicity for normal fibroblasts in cuture.

Fraction $B_{1\text{-}4}$ contained four proteins (*2*), was able to induce necrosis in tumors in vivo, and was cytotoxic for mouse L-cells in vitro. Inasmuch as the cytotoxic effects of TNF were measured in two tumor cell lines, and because there is no evidence that induction of tumor necrosis in vivo and lysis of cells in culture are mediated by the same effector substance, we developed an assay using a single tumor cell line that is sensitive to the cytotoxic action of TNF in vivo and in vitro—a myelomonocytic leukemia called "WEHI/3." As a control, we developed a TNF-resistant line of the WEHI/3 cells (R-WEHI/3). Use of these cells to measure the activity of TNF and the adoption of more stringent criteria for defining TNF activity have facilitated the final purification of murine TNF.

MATERIALS AND METHODS

Mice.—Outbred albino female CD®-1 mice (30–40 g), from Charles River Breeding Laboratories, North Wilmington, Mass., and BALB/c female mice (18–20 g), bred in our own breeding facility, were used in this study.

C. parvum.—Formalin-killed *C. parvum* strain CN-6134 was obtained from Burroughs-Wellcome Co., Research Triangle Park, N.C.

Endotoxin.—*Escherichia coli* 0127:B8, lot #568487, was obtained from Difco Laboratories, Detroit, Mich.

Silica suspensions.—Quartz particles (0.5–1.0 μm in diameter) were separated from amorphous silica preparations (Sigma Chemical Co., St. Louis, Mo.) by differential centrifugation in 0.9% NaCl. Particle size was estimated by microscopic examination. The weight of the material in suspension was determined by passing a known volume of the suspension through a preweighed 0.45-μ Millipore filter

---

ABBREVIATIONS USED: EMEM=Eagle's minimum essential medium; LD_{100}=lethal dose—100%; MCA=3-methylcholanthrene; PAG=polyacrylamide gel(s); PAGE=PAG electrophoresis; PCA=perchloric acid; SDS=sodium dodecyl sulfate; TNF=tumor necrosis-inducing factor; R=TNF-restant; S=TNF-sensitive; TNS=TNF-rich serum.

---

[1] Received August 12, 1981; accepted January 15, 1982.

[2] Supported by Public Health Service grants CA-08748 and CA-23906 from the National Cancer Institute and by grants from the Martin Elk League for Cancer Research, from the Fuller Foundation Inc., from the Harriet Ames Charitable Fund, and from the Pat Gibbs Cancer Fund.

[3] Animals were maintained under the guidelines set forth by the Sloan-Kettering Institute for Cancer Research.

[4] Memorial Sloan-Kettering Cancer Center, 1275 York Ave., New York, N.Y. 10021.

[5] *Address reprint requests to* Dr. Green at 345 East 68th St., New York, N.Y. 10021.

[6] We gratefully acknowledge the skilled assistance of Dr. Paul J. Higgins in performing the immunochemical and electrophoretic analyses and of Mr. Alan Alfieri in performing the radiation experiments. We thank Dr. Jerome S. Nisselbaum for his assistance in preparing the manuscript and Mr. Abraham P. Abraham for typing the manuscript.

and by drying the filter disk and reweighing it. All silica suspensions were autoclaved before use.

Whole-body radiation.—Seven days before the start of treatment with *C. parvum* (*2*), whole-body radiation at a dose rate of 122 rad/minute was given to CD®-1 mice by means of a ^{137}Cs Gammacel unit (Atomic Energy of Canada, Ltd., Ottawa, Canada). Total dose was 650 rad (*3*) for each mouse in this study.

Preparation of TNF (fraction B_{1-4}).—Glassware and solutions (where appropriate) were autoclaved at 120°C for 40 minutes. Plastics were gas sterilized with ethylene oxide for 3 hours at 120°C or were soaked in Cidex (Scientific Products, Division of American Hospital Supply Corp., McGaw Park, Ill.) for 24 hours.

TNS was prepared from *C. parvum*–endotoxin-treated mice (*2*). Partial purification of TNF from aliquots of 100 ml sterile mouse sera (200 CD®-1 mice) was accomplished by ammonium sulfate fractionation and Sephacryl-S 200 superfine gel filtration. Pooled fractions (G-200 II) were filter sterilized, concentrated by lyophilization, dialyzed free of salt, and stored frozen at −20°C. Aliquots of approximately 4 mg G-200 II protein/ml were dialyzed against Tris–glycine buffer (pH 8.6) (*4*) for 24 hours and placed on 15 ml preparative PAG in a modified Canalco electrophoresis apparatus (Miles Laboratories, Inc., Elkhart, Ind.) (*2*). Electrophoresis at 4°C was for 16 hours at 6 mA/PAG. Proteins were localized by staining one PAG with 0.02% G-250 Coomassie blue dye in 4% PCA (*5*). The TNF-containing segment, with its characteristic four-band pattern (*2*), was used as a reference, and corresponding segments containing these proteins were sliced out of the remaining unstained PAG. Proteins were extracted from the PAG by homogenization in 0.9% NaCl with the use of a Polytron (Brinkmann Instruments, Inc., Great Neck, N.Y.). The pooled supernatants were freed of PAG particles by centrifugation and filtration through 0.45-μ Millipore filters, and the supernatants were concentrated by lyophilization. This preparation was called "fraction B_{1-4}." Protein was determined by the method of Lowry et al (*6*).

WEHI/3 cells.—WEHI/3 tumor cells growing in tissue culture (*7*) were adapted to growth in mice as follows: Cells (10^7) were injected into the peritoneal cavity of each of ten 6- to 8-week-old BALB/c female mice. After 14 days the ascitic fluid containing the tumor cells was aspirated and the washed cells were counted. Viable cells (10^7; trypan blue exclusion) in 0.5 ml sterile EMEM were reinjected ip into each of 5 BALB/c mice. Cells were maintained by weekly ip transplants.

Solid WEHI/3 tumors were raised in mice by injection of 10^6 viable cells, in 0.05 ml EMEM, into the shaved ventral skin of syngeneic BALB/c mice. Well-defined tumors (0.6–0.8 cm in diameter) resulted in 6–8 days. These tumors did not regress spontaneously and if left untreated were lethal in 4–6 weeks.

WEHI/3 tumor cells were propagated in 25-cm^2 Falcon culture flasks after inoculation of 3×10^4 cells in 5.0 ml EMEM containing 10% fetal calf serum, 2 m*M* glutamine, 100 U penicillin/ml, and 100 μg streptomycin/ml. Incubation was at 37°C in 95% air–5% CO_2. Doubling time was from 14 to 16 hours. The cells were loosely adherent and were completely recovered by gentle agitation of the flasks and the medium. The growth rate of these cells in culture was not affected by as much as 100 μg of *E. coli* endotoxin/ml medium.

R-WEHI/3 cells.—In vitro-propagated WEHI/3 cells were selected for TNF resistance, over a 6-week period, by growth in culture medium containing progressively greater concentrations of TNF (100–500 μg G-200 fraction/ml medium). Cells were considered R to a particular concentration of TNF when the growth rate in TNF was the same as that in the control flasks. R-WEHI/3 cells were routinely propagated in medium containing 100 μg TNF. Full sensitivity to TNF could be restored by passaging R-WEHI/3 cells in TNF-free medium for at least 20 days (five passages).

TNF purification.—Methods used for final purification of TNF activity from fraction B_{1-4} are described later in the text.

TNF bioassay.—In vivo activity of TNF was determined in BALB/c mice bearing 7-day intradermal transplants of WEHI/3 tumor cells, as previously described for MCA-induced fibrosarcomas in (*1*).

TNF assay in vitro.—Triplicate determination of cell viability (trypan blue exclusion) was done with the use of WEHI/3 populations exposed to graded amounts of TNF-containing fractions. After 72 hours of incubation at 37°C in a moist air–CO_2 atmosphere, cells were fully suspended in the medium by gentle agitation, and the viable cells were counted. Differences giving a probability of less than 1% ($P\leq0.01$) by Student's *t*-test for small samples were considered significant. A typical effect of graded doses of TNF on S-WEHI/3 and R-WEHI/3 cells is shown in text-figure 1.

TNF criteria.—We define TNF as the substance that conforms to the following criteria: 1) No TNF sample shall contain more than 1.0 μg endotoxin/ml as measured by the Limulus assay (*8*) (assay kit from M.A. Bioproducts, Walk-

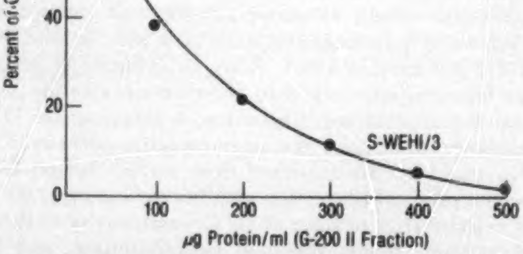

TEXT-FIGURE 1.—Growth of cultured S-WEHI/3 cells and R-WEHI/3 cells as a function of the protein concentration of TNF (fraction G-200 II) in the culture medium. Each sample of TNF was added to duplicate culture flasks after they were inoculated with 0.6–0.7×10^4 cells. Viable cells were counted after 72-hr incubation. Experiment was performed three times. Results are reported as percentages of control value; no count varied from the mean by more than ±5%.

ersville, Md.). 2) An iv injection of twice the concentration of the test sample that induces necrosis (*2*) in an intradermal WEHI/3 tumor in 24 hours must result in complete tumor regression in at least 50% of the mice. 3) The dose of TNF that is lethal for tumor cells must show no toxicity for the tumor-bearing host. 4) A dose-related inhibition of S-WEHI/3 cell growth in culture must be demonstrable. 5) No growth inhibition in R-WEHI/3 cells must result after incubation with five times the LD_{100} dose of TNF for S-WEHI/3 cells. 6) No inhibition of growth in culture of normal mouse fibroblasts must result after incubation with five times the LD_{100} dose of TNF for S-WEHI/3 cells.

Immunodiffusion.—Double diffusion was done on prepunched Immuo-Tec agarose plates (Calbiochem-Behring Corp., Los Angeles, Calif.) according to the method of Ouchterlony (*9*).

Immunoelectrophoretic analysis.—Electrophoresis was done in 1.0% agarose (wt/vol) slabs with the use of Beckman B-2 buffer (pH 8.6) at 20 mA/200 V for 1.0 hour (*10*). On completion of the electrophoretic separation, antisera troughs were filled with 50 µl of the selected antiserum, and the precipitin patterns were developed for 48 hours at 37°C. After incubation, the agarose slab was dialyzed against 0.15 *M* NaCl for 24 hours before the precipitin patterns were stained with 0.5% Amido Black 10B in 7% acetic acid.

Single radial immunodiffusion analysis.—For quantification of serum proteins at stages of TNF purification, 50–200 µl rabbit antisera to the proteins identified by immunoelectrophoresis were incorporated in 2.5 ml of 1% (wt/vol) agarose in Beckman B-2 buffer (pH 8.6) (*11, 12*). For regression analysis of protein concentrations of the test samples, antigen wells were cut and filled with 4 µl of the unknown samples; precipitin disks were measured after incubation of the agarose plates at 37°C. The specificities of these antisera were ascertained by immunoelectrophoresis, immunodiffusion, and radial immunoprecipitation (*10*).

Metabolic labeling and SDS–PAGE of WEHI/3 cellular protein.—Three days after passage, ^{3}H-labeled amino acids (5 µCi/ml of medium; New England Nuclear Corp., Boston, Mass.) were added to each WEHI/3 cell culture to obtain metabolically labeled proteins. The cells were harvested after 4 days and were washed once by centrifugation in growth medium and twice in phosphate-buffered saline. Cell pellets were lysed in 1 ml of 0.01 *M* Tris–HCl/0.5% Nonidet NP-40 (pH 7.5) (Shell Chemical Corp., New York, N.Y.). Protein determinations were by Bio-rad assay (*13*). ^{3}H-labeled amino acid-labeled WEHI/3 cellular protein (100 µg) was separated in 7.5% SDS-PAG slabs (*14*). The radioactive peptides were visualized by En^{3}Hance (New England Nuclear Corp.) treatment and autoradiography on X-Omat R film (Eastman Kodak Co., Rochester, N.Y.), followed by densitometry of the individual fluorographs.

RESULTS

Identification of Proteins in Fraction B_{1-4}

Immunoelectrophoretic and agar gel double-diffusion analysis of fraction B_{1-4} suggeted the presence of transferrin, α_2-globulin, and several polymeric forms of albumin. The presence of albumin and transferrin was confirmed by means of monospecific antisera to these mouse proteins.

An explanation for the presence of several forms of albumin in the B_{1-4} fraction of TNF was sought. Mouse albumin was purified from fraction G-200 II by preparative PAGE (*2*). PAG disks containing albumin were identified with the use of antimouse albumin by double diffusion. The protein was extracted from the PAG, and aliquots of the extract were subjected to several increasing cycles of freeze-drying and re-solution. When aliquots of these samples were run on PAGE, the stained PAG showed the presence of multiple forms of polymerized albumin. Thus the albumin in fraction B_{1-4} represents one or more of these polymeric forms.

Albumin, transferrin, and TNF were next located in preparative PAG containing an aliquot of the B_{1-4} fraction. In figure 1, the typically stained four-band TNF pattern (A, F) can be seen between disks 7 and 11. Albumin (B, C) was found in disks 10–15. Transferrin (D) was distributed between disks 10 and 11. TNF activity (E), identified with S-WEHI/3 and R-WEHI/3 cells in vitro, was found in disks 7–9. No TNF activity was found in disks 10–20. Thus the antitumor activity of the B_{1-4} fraction does not co-migrate with the proteins albumin and transferrin. Total protein in the B_{1-4} fraction used in this experiment was 5.3 mg/ml. Concentrations of albumin and of transferrin, determined by radial immunodiffusion (*11, 12*), were 1.05 and 2.65, respectively.

During these experiments we noted the presence of a cytotoxic substance for WEHI/3 cells in incompletely dialyzed extracts of blank PAG. This substance did not induce necrosis in tumors in vivo and could be completely removed by prolonged dialysis. Unfortunately, such prolonged dialysis caused a marked reduction in the TNF activity of the protein mixtures. To produce TNF free of albumin, transferrin, and this unidentified cytotoxic substance, we developed an alternative to the slicing and homogenization procedure.

Figure 1, E, shows that disk 8 contained a high titer of TNF activity but no albumin or transferrin. This disk was 4.6 cm from the origin. Accordingly, PAG 4.6 cm long were prepared. Aliquots of G-200 II in 0.12 *M* sucrose were layered on each "short" PAG, and electrophoresis was performed as previously described. After 16 hours the upper chamber of the apparatus was removed and, while keeping the PAG tubes in place, a presterilized dialysis bag containing 5.0 ml of sterile electrophoresis buffer was attached to the bottom of each PAG tube by a rubber O-ring. The apparatus was reassembled, placed in an ice-water bath, and electrophoresis was continued for 3 hours at 9 mA/PAG. The dialysis bags were removed from the PAG tubes, and their contents were pooled, concentrated, and dialyzed against 0.9% NaCl until free of buffer salts. The product was sterilized by filtration.

Figure 2 shows that the protein collected from the dialysis bags (called β-fraction) moved as a single band on nondenaturing PAG (C), migrated 4.6 cm from the origin, and gave a positive test for glycoproteins with periodic acid–Schiff stain (D) (*15*). No serum albumin or transferrin was detectable in this sample. This purified protein preparation migrated in free electrophoresis as an α_2-globulin, contained less than 1.0 µg/ml endotoxin (Limulus assay kit), and had a molecular weight of 140,000 as estimated by the method of Andrews (*16*). For each 24 mg of fraction G-200 II that was applied to 12 short PAG and collected by electrophoresis into dialysis bags, the protein yield was about 3.5 mg.

Text-figure 2 shows the relationship between the amount of protein in the partially purified fractions from TNS and the cytotoxic activity for S-WEHI/3 cells in culture. On the basis of the amount of protein needed to produce a reduction of 50% in the number of viable cells (*see* "Materials and Methods"), purified TNF (β-fraction) from the short PAG was about 50 times more active than the original TNS. R-WEHI/3 cells showed no inhibition from 500 μg of this purified TNF. In addition to producing lysis of WEHI/3 cells in vitro, an iv injection of 1.0 mg of this protein given to each of 7 BALB/c mice bearing intradermal WEHI/3 tumors resulted in a "+++" necrosis in each of the tumors.

The fact that WEHI/3 cells became resistant to TNF when they were grown in its presence led us to search for differences between the S-WEHI/3 and R-WEHI/3 cells. Comparison of the cytoplasmic proteins by PAGE showed a general similarity between them. However, densitometer tracings of the S-WEHI/3 and R-WEHI/3 peptides, made radioactive in vivo and identified by fluorography after SDS-PAGE separation (*see* "Materials Methods"), showed noticeable differences in the 17K and 70K regions. These observations indicate that the peptides contributing to peak complexity in these regions, as well as their relative concentrations, were different.

Role of Macrophage in TNF Production

The possibility that TNF might be of macrophage origin was suggested (*17*). During the preparation of TNS for purification of TNF, we examined the proposed role of the macrophage in TNF production in mice. We gave mice injections of crystalline silica (SiO_2), an agent specifically toxic for macrophages (*18-20*). Preliminary tests showed substantial macrophage destruction in the fluid of the peritoneal cavity of th[illegible]reated mice after 3 daily ip injections (1.0 mg injection/mouse). Microscopic examination of spleen, liver, kidney, and lung sections showed silica widely distributed throughout the body tissue 5 days after administration. At this time and for 15 additional days silica-treated mice failed to clear iv-injected colloidal carbon particles.

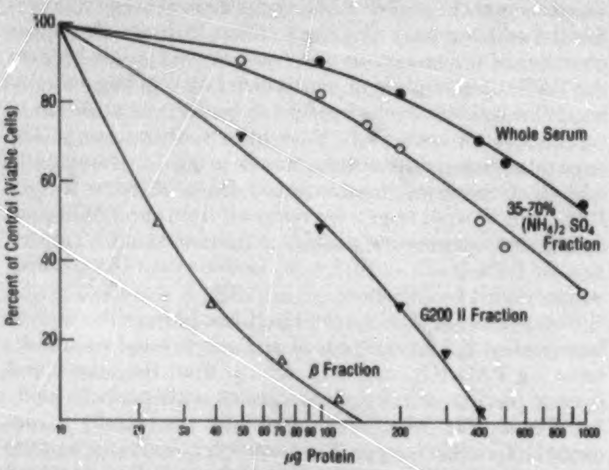

TEXT-FIGURE 2.—Growth inhibition of S-WEHI/3 cells by fractions from TNS during purification of TNF. Samples tested were whole TNS, the 35–70% ammonium sulfate insoluble fraction, the G-200 II fraction from the S-200 gel column, and fraction β from short PAG.

TABLE 1.—*Effect of silica treatment or whole-body radiation on TNS[a] production in* C. parvum*-treated endotoxin-stressed CD®-1 mice*

Treatment[b] with:	Tumor necrosis activity in sera[c] of: Untreated mice	Silica-treated mice[d]	Whole-body irradiated mice[e]
0.9% NaCl	3/3 (−)	8/8 (−)	3/3 (−)
C. parvum alone	3/3 (−)	5/5 (−)	7/7 (−)
Endotoxin alone	3/3 (−)	3/3 (−)	4/4 (−)
C. parvum–endotoxin	8/8 (+++)	9/9 (+++)	8/8 (−)

[a] TNS was produced by method of Green et al. (*2*).

[b] By iv injection.

[c] TNF activity was determined by in vivo assay with intradermal WEHI/3 tumors as targets. (−) = no activity; (+++) = necrosis over 75% of tumor surface area in all mice 24 hr after iv injection of TNS.

[d] Treatment with silica was by daily ip injection of a suspension in 0.9% NaCl of 1.0 mg silica/ml/mouse beginning 7 days before start of *C. parvum* treatment.

[e] Whole-body radiation was delivered (as described in "Materials and Methods") 7 days before iv injection of *C. parvum*.

Silica particles (0.5–1.0 μm in diameter) were suspended in saline (to a concentration of 2.0 mg/ml) and autoclaved. For 7 days, we gave daily ip injections of 0.5 ml of the suspension to each of 25 CD®-1 female mice. This silica dose did not cause the mice to lose weight or to show signs of toxicity. We then gave the mice iv injections of *C. parvum*, followed in 7 days by endotoxin. This treatment with *C. parvum* and endotoxin normally results in the appearance of TNF in the circulation (*2*).

For the purposes of comparison a second group of mice were given 650 rad whole-body radiation 7 days before injection of *C. parvum*. At this level of radiation, there is widespread destruction of the host's blood-forming cells, with subsequent transient immunoincompetence. Circulating T-cells and B-cells were significantly reduced, but the function of fixed and circulating macrophages was only temporarily impaired (*3*).

Table 1 shows that the TNF-forming capacity of silica-treated mice was not impaired; mice that received whole-body radiation failed to respond to the priming effect of treatment with *C. parvum* and endotoxin. Although one cannot rule out the possibility that some residual macrophage helper activity remains in silica-treated mice, our findings suggest that TNF production is not primarily a macrophage function.

DISCUSSION

The activity of TNF was previously measured by an in vivo assay that depended on the induction of necrosis in intradermal MCA-induced tumors or by an in vitro assay that relied on the cytotoxicity of the sample for L-cells in culture. In the in vivo assay, false-positive results can occur from contamination of samples with bacterial endotoxin. In the in vitro assay, growth inhibition or lysis of L-cells in culture can be precipitated by a variety of lymphotoxins that do not prossess necrosis-inducing activity in vivo. Also, a lack of specificity is possible when two distinctly different tumor cell lines are used as targets (*1*, *2*).

During the course of our studies on the purification and mechanism of action of TNF, development of a more specific bioassay was considered. Our finding that WEHI/3 cells were S in vivo and in vitro, and that a line of these cells could be made specifically R in vitro, allowed the development of such a bioassay. In addition, more stringent criteria were applied to the definition of the term "TNF activity." The application of these constraints and the development of a new procedure that permitted the removal of TNF from PAG free of contamination by albumin, transferrin, or the cytotoxic PAG component resulted in the preparation of purified TNF.

In confirmation of our earlier findings (*2*) the product, which showed a single band of protein after electrophoresis on nondenaturing PAG, is an α_2-globulin that stains as a glycoprotein, has a molecular weight of 140,000 and is inactivated when heated at 70°C for 1 hour.

The cellular mechanism of TNF resistance or sensitivity is unknown. The noticeable differences we found between the peptide patterns of S-WEHI/3 cells and R-WEHI/3 cell derivatives suggest that resistance may be related to changes in several cellular peptides. Inasmuch as metabolic labeling of WEHI/3 cellular protein with ^{3}H-labeled amino acids was done in the presence of complete growth medium containing cold amino acids, the labeled bands, located by densitometer scanning, represent major and probably rapidly "turning over" protein species. Whether one or more of these changes, either qualitatively or quantitatively, results in the conference of resistance is not known. The present findings suggest that a reasonable approach to the identification of potential TNF-binding moieties would reside in a rigorous evaluation of the peptides in the approximately 17K and 70K regions.

Sera from mice made hypersensitive to endotoxin by pretreatment with *C. parvum* contain interferon, migration inhibition factor, lymphoid differentiating factor, cytotoxic activity for cultures of some tumor cell lines (but not normal cell lines), and in vivo tumor necrosis-inducing activity (*2*, *21–24*). The cytotoxic and the necrotizing activities in TNS have frequently been attributed to a single endogenous factor of putative macrophage origin (*17*). A serum factor that is cytotoxic for L-cells in culture and that probably is of macrophage origin has been identified by a number of investigators (*25–28*). This substance has a molecular weight of about 50,000 and is electrophoretically heterogeneous. A cytolytic substance elaborated in vitro by endotoxin-stimulated macrophages did not induce tumor necrosis in vivo (Alexander P: Personal communication; Mannel, DN: Personal communication). Thus the possibility exists that the macrophage-derived cytotoxin contaminates the TNS and creates confusion when the in vitro assay for TNF with L-cells is used. Recently, Kull and Cuatrecasas (*29*) examined the ability of partially purified factors from TNS to induce tumor necrosis and regression in vivo. Their study clearly showed that multiple forms of cytotoxic activity were separated on gel filtration. Those proteins with molecular weights of 50,000 (or below) and 225,000 failed to induce tumor necrosis in vivo. Only the protein in the 150,000-molecular-weight range induced tumor necrosis and regression in vivo. Kull and Cuatrecasas concluded that the cytotoxic and necrotizing activities in murine tumor necrosis serum were separate and distinct entities.

Our present data support the concept that the factor in mouse serum that induces tumor necrosis in vivo is not of macrophage origin. The results of our experiments in which an acute subversion of in vivo macrophages was accomplished by injection of silica (*30–34*) showed no alteration of the TNF-forming ability of the *C. parvum*-treated, endotoxin-stressed mice. In contrast, exposure of mice to 650 rad whole-body radiation, which results in the drastic depletion of lymphoid system cells but produces only a transient decrease in the population of fixed and circulating macrophages (*3*), completely eliminated the TNF-producing capacity of the *C. parvum*-treated, endotoxin-stressed mice.

We recognize that depleting the macrophage population with silica in vivo does not result in the abrogation of all the helper activity functions of activated macrophages (*34*). However, because silica is selectively toxic for macrophages in vivo (*30*, *31*), our finding that a marked reduction in macrophage activity is without influence on the production of TNF supports the concept that TNF is not a macrophage product.

REFERENCES

(*1*) Carswell EA, Old LJ, Kassel RL, Green S, Fiore N, Williamson B. An endotoxin-induced serum factor that causes necrosis of tumors. Proc Natl Acad Sci USA 1975; 72:3666–3670.

(*2*) Green S, Dobrjansky A, Carswell EA, et al. Partial purification of a serum factor that causes necrosis of tumors. Proc Natl Acad Sci USA 1976; 73:381–385.

(*3*) International Atomic Energy Agency. Manual on radiation haematology. Vienna: International Atomic Energy Agency, 1971:147–15 (Technical Report Series 123).

(*4*) Ornstein L. Disc electrophoresis. I. Background and theory. Ann NY Acad Sci 1964; 121:321–349.

(*5*) Holbrook IB, Leaver AG. A procedure to increase the sensitivity of staining by Coomassie Brilliant Blue G 250. Anal Biochem 1976; 75:634–636.

(*6*) Lowry OH, Rosebrough NJ, Farr AL, Randall RJ. Protein measurement with the Folin phenol reagent. J Biol Chem 1951; 193:265–275.

(*7*) Ralph P, Nakoinz I. Direct toxic effects of immunopotentiators on monocytic, myelomonocytic, and histocytic or macrophage tumor cells in culture. Cancer Res 1977; 37:546–550.

(*8*) Levin J, Tomasulo PA, Oser RS. Detection of endotoxin in human blood and demonstration of an inhibitor. J Lab Clin Med 1970; 75:903–911.

(*9*) Ouchterlony O. Antigen antibody reactions in gels Acta Pathol Microbiol Scand 1949; 26:507–518.

(*10*) Borenfreund E, Higgins PJ, Bendich A. In vivo–in vitro rat liver carcinogenesis: Modifications in protein synthesis and ultrastructure. Ann NY Acad Sci 1980; 349:357–372.

(*11*) Mancini G, Carbonara AO, Hermano JF. Immunochemical quantitation of antigens by single radial immunodiffusion. Immunochemistry 1965; 2:235–254.

(*12*) Tong C, Stonehill EH, Higgins PJ, Bendich A. Differential association of fetal antigen with hepatoma tissue grown in vivo and in vitro. Eur J Cancer 1978; 14:147–152.

(*13*) Bradford MM. A rapid and sensitive method for the quantitation of microgram quantities of protein utilizing the principle of protein-dye binding. Anal Biochem 1976; 72:248–254.

(*14*) Loemmuli UK. Cleavage of structural proteins during the assembly of the head of bacteriophage T 4. Nature 1970; 227:680–685.

(*15*) Zacharius RM, Zell TE, Morrison JH, Woodlock JJ. Glycoprotein staining following electrophoresis on acrylamide gels. Anal Biochem 1969; 30:148–152.

(16) Andrews P. The gel filtration behavior of proteins related to their molecular weights over a wide range. Biochem J 1965; 96:595–606.

(17) Old LJ. Tumor necrosis factor. Clin Bull 1976; 6:118–120.

(18) Keller R. Abrogation of antitumor effects of *Corynebacterium parvum* and BCG by antimacrophage agents: *Brief communication.* J Natl Cancer Inst 1977; 59:1751–1953.

(19) Lotzova E, Cudkovicz G. Abrogation of resistance to bone marrow grafts by silica particles. J Immunol 1974; 113:798–803.

(20) van Loveren H, Snoek M, Den Otter W. Effects of silica on macrophages and lymphocytes. J Reticuloendothel Soc 1977; 22:523–531.

(21) Younger JS, Salvin SB. Properties of migration inhibitory factory and interferon in the circulation of mice with delayed hypersensitivity. J Immunol 1973; 111:1914–1922.

(22) Hoffman MK, Oettgen HF, Old LJ, Mittler RS, Hammerling U. Induction and immunologic properties of tumor necrosis factor. J Reticuloendothel Soc 1978; 23:307–311.

(23) Helson LS, Green S, Carswell EA, Old LJ. Effect of tumour necrosis factor on cultured human melanoma cells. Nature 1975; 258:731–732.

(24) Helson L, Helson C, Green S. Effects of murine tumor necrosis factor on heterotransplanted human tumors. Exp Cell Biol 1979; 47:53–60.

(25) Currie GA, Basham C. Activated macrophages release a factor which lyses malignant cells but not normal cells. J Exp Med 1975; 142:1600–1605.

(26) Matthews N, Watkins JF. Tumour necrosis factor from the rabbit. I. Mode of action, specificity and physiochemical properties. Br J Cancer 1978; 38:302–309.

(27) Ruff MR, Gifford GE. Purification and physiochemical characterization of rabbit tumor necrosis factor. J Immunol 1980; 125:1671–1677.

(28) Männel DN, Meltzer MS, Mergenhagan SE. Generation and characterization of a lipopolysaccharide-induced and serum-derived cytotoxic factor for tumor cells. Infect Immun 1980; 28:204–211.

(29) Kull FC, Cuatrecasas P. Preliminary characterization of the tumor cell cytotoxin in tumor necrosis serum. J Immunol 1981; 126:1279–1283.

(30) Vigliani EC, Pernis B. The pathogenesis of silicosis: A review. Bull Hyg 1961; 36:1–9.

(31) ———. Immunological aspects of silicosis. Adv Tuberc Res 1963; 12:230–282.

(32) Kessel RW, Monaco L, Marchiso MA. The specificity of the cytotoxic action of silica; a study in vitro. Br J Exp Pathol 1963; 44:351–364.

(33) Mims CA. The peritoneal macrophages of mice. Br J Exp Pathol 1964; 45:37–43.

(34) Hatch RF, Kindsvatter VH. Lung retention of quartz dust smaller than one half micron. J Industr Hyg 1947; 29:342–346.

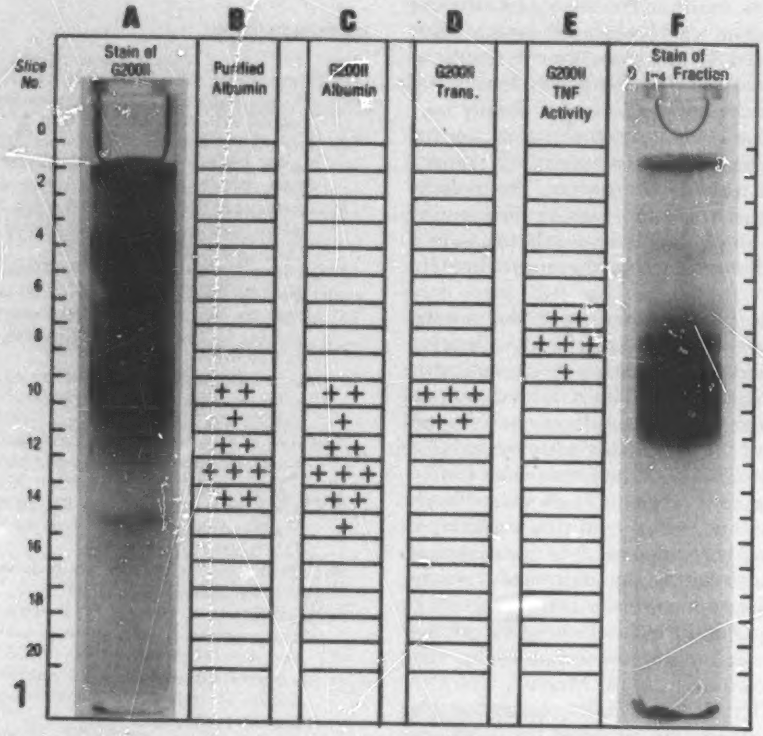

FIGURE 1.—PAGE of TNF fraction G-200 II, staining of fractions G-200 II and B_{1-4}, and identification of protein components in PAG disks by immunodiffusion. A, F: Preparative PAG (*2*) stained for protein with G-250 Coomassie blue dye in 4% PCA. B: Presence of albumin in disks cut from a PAG on which purified albumin was run. C: Location of albumin in disks cut from a PAG on which G-200 II was run. D: Location of transferrin in disks cut from a PAG on which G-200 II was run. E: Location of TNF activity in disks cut from a PAG on which G-200 II was run. +, ++, and +++ indicate the relative antigen concentration present in the disks as inferred by the shape of the precipitin line, its sharpness, and the rate and distance of migration on Ouchterlony plates.

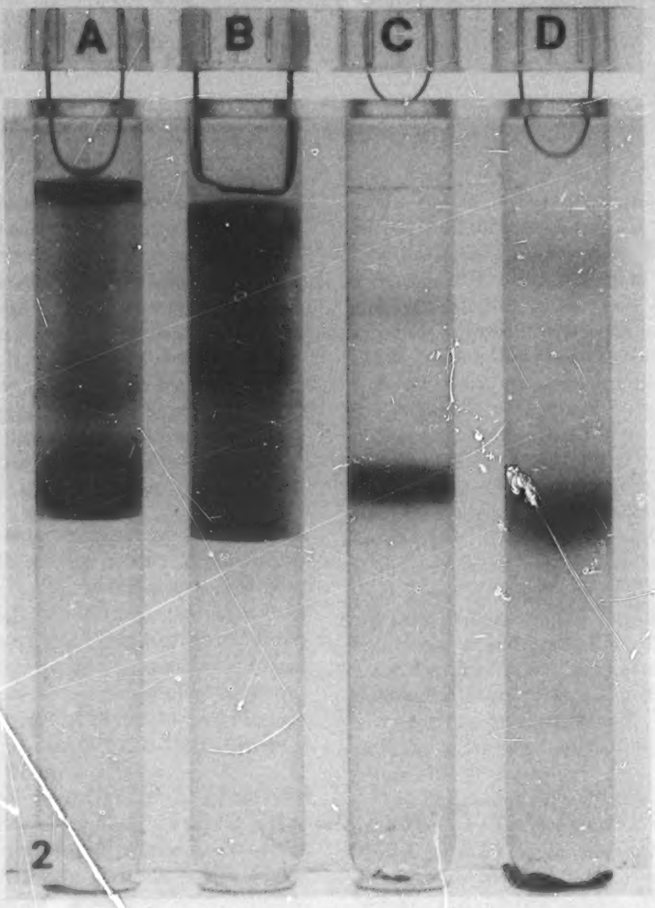

FIGURE 2.—Purification of TNF by modified PAGE. All PAG were stained with 0.02% G-250 Coomassie blue dye in 4% PCA and washed with 7% acetic acid. A: A short PAG (4.6 cm) showing G-200 II after electrophoresis for 16 hr at 6 mA/PAG. B: A short PAG showing protein that remained after second electrophoresis at 9 mA for 3 hr. C: A 10-cm PAG on which the concentrate of TNF electrophoresed from B was run. D: A 10-cm PAG on which the concentrated purified TNF protein was run, followed by stain for glycoprotein with periodic acid–Schiff reagent (*15*).

blank page

Surface Antigen Expressed in Hematopoietic Cells Derived From *Fv-4*^{r} Mouse Strains[1,2]

Hiroshi Yoshikura[3,4] *and* Takeshi Odaka[3,5]

ABSTRACT—*Fv-4* locus controls the susceptibility of mice to ecotropic murine leukemia virus (MuLV). Antiserum against *Fv-4*$^{r/s}$ mice with BALB/c background was raised in inbred BALB/c mice. In the complement-dependent cytotoxicity test, the antiserum killed the hematopoietic cells derived from *Fv-4*$^{r/-}$ mice but not those from *Fv-4*$^{s/s}$ mice, and the genetic cross experiments located the locus controlling the expression of the target molecule of the antibody in the close vicinity of *Fv-4*. In addition, the antigenic expression of the exogenously infecting MuLV suppressed the expression of the target molecule of the antiserum. The expressions of these two antigens appear to compete with each other on the cell surface. JNCI 1982; 68:1005–1009.

The presence of *Fv-4* locus was indicated by the isolation of a mouse strain from a ddY mouse colony in Shizuoka, Japan, which was resistant to N-, B-, or NB-tropic ecotropic MuLV (*1*). The resistance allele (*Fv-4*^{r}) was dominant over the sensitive (*Fv-4*^{s}) allele, and the gene segregated independently of *Fv-1* or *Fv-2* (*1*). The introduction of *Fv-4*^{r} in AKR mice completely suppressed expression of endogenous MuLV as well as the development of thymus leukemia (*2*). A gene quite similar to *Fv-4*^{r} was widely distributed in wild mice in Asia and the United States (*3, 4*).

Fv-4w^{r}, wild mouse-derived *Fv-4*^{r}-like gene, which was recently suggested to be identical to *Fv-4*^{r} (*5*), was introduced in BALB/c mice to obtain the partially congenic strain BALB/c-*Fv-4w*$^{r/r}$ (C4W) (*5*). Because the *Fv-4*^{r} restriction was suggested to exist at the level of virus penetration of the cells (*6*), and the resistance was dominant, we suspected the existence of specific cell surface antigen in *Fv-4*^{r} mouse hematopoietic cells. To detect such antigen, we raised antibody against *Fv-4*$^{r/s}$ mouse spleen cells in BALB/c mice. This report deals with the detection of mouse *Fv-4*^{r}-specific cell surface antigen by means of a cytotoxicity test in which anti-C4W serum was used.

MATERIALS AND METHODS

Mice.—Inbred BALB/c mice were maintained in our Institute. The C4W strain has BALB/c mouse genetic background and harbors the *Fv-4*^{r} gene derived from an Fu mouse, a wild mouse trapped in Fussa in the Tokyo area. An (Fu × BALB/c)F$_2$ mouse with *Fv-4*$^{r/s}$ genotype was successively backcrossed with BALB/c mice with *Fv-4*$^{r/s}$ genotype (*5*), and the C4W mouse was established from the offspring of brother-sister matings of the seventh backcross generation. For the preparation of immunizing spleen cells, we took mice of the 11th backcross generation that were not used for mating. Mice used for genetic analysis were of the 10th and 11th backcross generations (F$_2$N$_{10}$ and F$_2$N$_{11}$).

Target of cytotoxicity test.—A spleen tumor appeared in a male *Fv-4*$^{r/r}$ mouse of the FRG strain [previously designated as G strain (*1*), which was derived from a ddY laboratory mouse colony in Shizuoka, Japan] 146 days after a single ip dose of 7,12-dimethylbenz[*a*]anthracene (*2*). The tumor was subcutaneously transplanted four times and then cultured in vitro. After examination of the culture (with fluorescent antibody technique and anti-Thy-1.2), T. Kuhara of this Institute suggested that cell line BS(43), established by T. Odaka, was a T-cell line (unpublished data).

Preparation of antiserum against Fv-4$^{r/-}$ *mouse spleen cells.*—An (Fu × BALB/c)F$_2$ mouse with *Fv-4*$^{r/s}$ genotype was serially backcrossed with BALB/c mice. The spleen cells from mice of the 11th backcross generation were pooled and used as immunogen. Inasmuch as the *Fv-4* genotype of each donor was not determined, the immunogen was derived from both *Fv-4*$^{r/s}$ and *Fv-4*$^{s/s}$ mice. The antibody was raised in 7 BALB/c female mice. At weekly intervals, the BALB/c mice were given ip injections of the cells at a dose equivalent to the cells of 1 spleen per mouse. Cytotoxicity to BS(43) cells was tested at intervals. The cytotoxic titer began to increase after four injections, and after five injections, 6 of 7 mice developed high cytotoxic titers that remained unchanged after further immunizations. The remaining mouse did not develop cytotoxic activity in the serum even after eight injections.

The following experiments were performed with pooled sera from the 6 mice that had each received five injections. Antisera: Anti-Thy-1.2 monoclonal antibody (product of hybridoma cell line F7D5) was purchased from Dainihon Seiyaku Co., Osaka, Japan. We prepared anti-Hax by giving iv injections of SIRC cells infected with Harvey murine sarcoma virus enveloped in xenotropic MuLV NZB-IU-1 (*7*) to rabbits, as described by Morse et al (*8*). We obtained antiserum against ecotropic MuLV by injecting iv undisrupted ecotropic anti-FN-2 (*9*) into the rabbits. Ecotropic

---

ABBREVIATIONS USED: anti-FN-2=antiserum against Friend murine leukemia virus; anti-Hax=antiserum against xenotropic murine leukemia virus; anti-Thy-1.2=monoclonal antibody against Thy-1.2; MuLV=murine leukemia virus; F-MuLV=Friend MuLV; PFU=plaque-forming units.

---

[1] Received August 12, 1981; accepted December 22, 1981.

[2] Supported in part by a grant from the Japanese Ministry of Education, Science and Culture, Japan.

[3] Department of Genetics, The Institute of Medical Science, The University of Tokyo, P.O. Takanawa, Tokyo 108, Japan.

[4] *Address reprints requests to* Dr. Yoshikura *at his present address*: Department of Microbiology, Faculty of Medicine, The University of Tokyo, P.O. Hongo, Tokyo 113, Japan.

[5] We thank Dr. H. Ikeda, Department of Genetics, University of Tokyo, for preparing the anti-C4W serum with which the preliminary phase of the study was performed. We also thank Miss Sachiko Tejima and Miss Michiko Yamashita for technical assistance, and Dr. J. Yokota (on leave from Gumma University Medical School) for checking some of the cytotoxicity data.

MuLV was neutralized by anti-FN-2 but not by anti-Hax. Cells infected with ecotropic MuLV were specifically killed by anti-FN-2 in the presence of complement. Anti-Hax neutralized xenotropic virus preferentially and killed all the mouse hematopoietic cells so far tested in the presence of complement, as in (*8*).

Cytotoxicity test: The complement-dependent cytotoxicity test was performed essentially in the same manner as described in (*10, 11*). Heat-inactivated antiserum was serially diluted twofold in culture medium in the multiwell tray (Flow Laboratories, Inc., Rockville, Md.) by means of the Titertek multichannel pipette (Flow Laboratories, Inc.). Each well contained 50 µl diluted serum; fresh rabbit serum in a volume of 2 µl was added as a source of complement to each well; 10 µl cell suspension (≈5×10^5 cells/ml) was then added. The trays were incubated for 40 minutes at 37°C. The percentage of killed cells was determined by the trypan blue dye-exclusion test.

Preparation of cells for absorption of antiserum was essentially in the same manner as described in (*11*). Mice, 5–6 weeks old, were killed, and cells either from the spleen or the thymus were suspended in McCoy's 5-A medium supplemented with 7.5% heat-inactivated fetal calf serum; the cells were washed once with the medium. Cell concentration was adjusted, and the cell suspension was centrifuged to obtain a cell pellet. Anti-C4W serum, fiftyfold to a hundredfold diluted in a volume of 100 µl, was added to the tube containing the cell pellet. The cells were then suspended and incubated at 4°C for 40 minutes. The tubes containing the cells and the antiserum were centrifuged, and the supernatants were used for the cytotoxicity assay of BS(43) cells. In the linkage test (text-fig. 1), the cell number was constantly 5×10^7 cells.

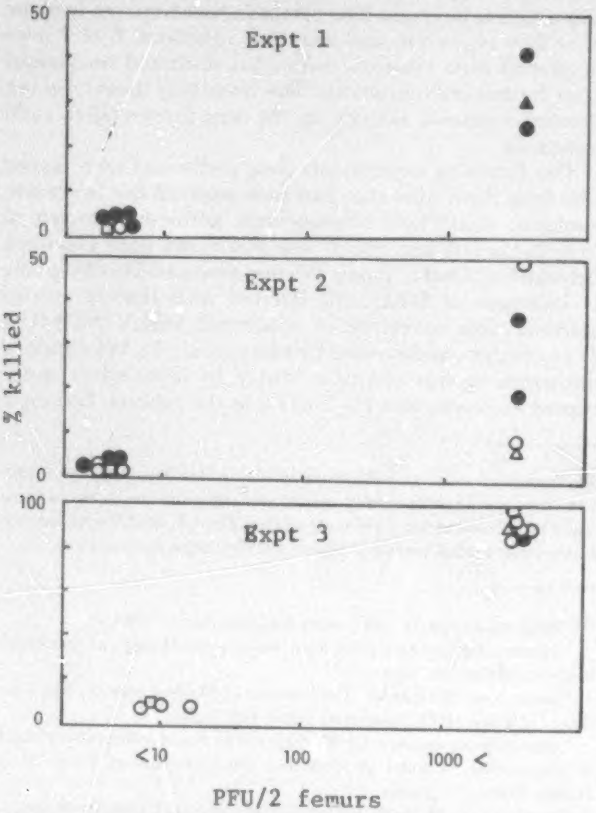

TEXT-FIGURE 1.—Correlation between MuLV and the capacity of spleen cells to absorb anti-C4W antibody. PFU/2 femurs of the mice (*abscissa*) were plotted against the cytotoxicity of the serum absorbed by the spleen cells (*ordinate*). Cells were derived from male (●) and female (○) *Fv-4*$^{r/s}$ × BALB/c backcrossed mice, from male (▲) and female (△) BALB/c mice, and from female (□) C4W mice.

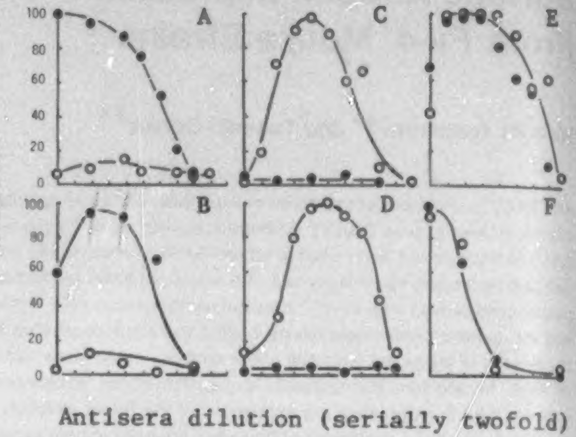

TEXT-FIGURE 2.—Complement-dependent cytotoxicity tests with BS(43) cells and F-MuLV-infected BS(43) cells. Tests were performed with anti-C4W serum (2A, 2B), anti-FN-2 (2C, 2D), anti-Hax (2E), and anti-Thy-1.2 (2F). Antisera were diluted serially twofold (from *left* to *right* in text-fig.). Highest dose was 1:30 for anti-C4W serum, 1:4 for anti-FN-2, 1:4 for anti-Hax, and 1:200,000 for anti-Thy-1.2. ● =BS(43) cells and ○ =F-MuLV-fected BS(43) cells.

RESULTS

Anti-C4W serum cytotoxic activity in BS(43) cells and absorption by mouse spleen cells.—Antiserum against *Fv-4*$^{r/-}$ mouse spleen cells (anti-C4W serum) was tested for complement-dependent cytotoxicity in various cell lines: F-MuLV-derived line 745a of DBA/2 mouse origin (*12*), line T3K of DDD mouse origin (*13*), and F-MuLV-transformed nonproducer line FVTCT of BALB/c origin (*14*) were negative; mouse mammary tumor-derived line FM3A (*15*) and AKR mouse thymoma-derived line AKSL2 (*16*) were also negative. The cell line that was sensitive to the antibody was BS(43) (text-fig. 2), a line derived from an FRG mouse with *Fv-4*$^{r/r}$ genotype.

Presence of the target molecule of the cytotoxic antibody was determined by the absorption test in C4W (*Fv-4*$^{r/r}$) and BALB/c (*FV-4*$^{s/s}$) mouse spleen cells. As shown in text-figure 3A, C4W spleen cells absorbed the activity much more efficiently than did BALB/c cells, indicating that the target molecule of the cytotoxic antibody was present more abundantly in the *Fv-4*$^{r/r}$ mice than in *Fv-4*$^{s/s}$ mice. However, we do not know whether a small number of the target molecules were present in BALB/c mouse cells, inasmuch as the majority of BALB/c cells absorbed the cytotoxic activity. Lack of preferential absorption by male mouse cells, relative to female cells, indicated the absence of antibody against the male antigen in the serum. Text-figure 3B shows two independent absorption experiments performed with thymus and spleen cells from C4W and BALB/c mice. The efficiency of absorption was almost identical for thymus and spleen cells, indicating that the expression of the anti-C4W target did not vary in these two cell types.

By means of the absorption test, we determined the presence of the anti-C4W target in various mouse strains. Among the mice tested, FRG ($Fv\text{-}4^{r/r}$), and its F_1 hybrid derived from cross-breeding with AKR ($Fv\text{-}4^{r/s}$), and (C57BL × Hz-IV)F_1-derived W(Hz) ($Fv\text{-}4^{r/r}$) absorbed the cytotoxic activity efficiently, whereas NFS, C57BL/6, DBA/2, DDD, DDDFv^r, and NZB mice (all $Fv\text{-}4^{s/s}$) did not.

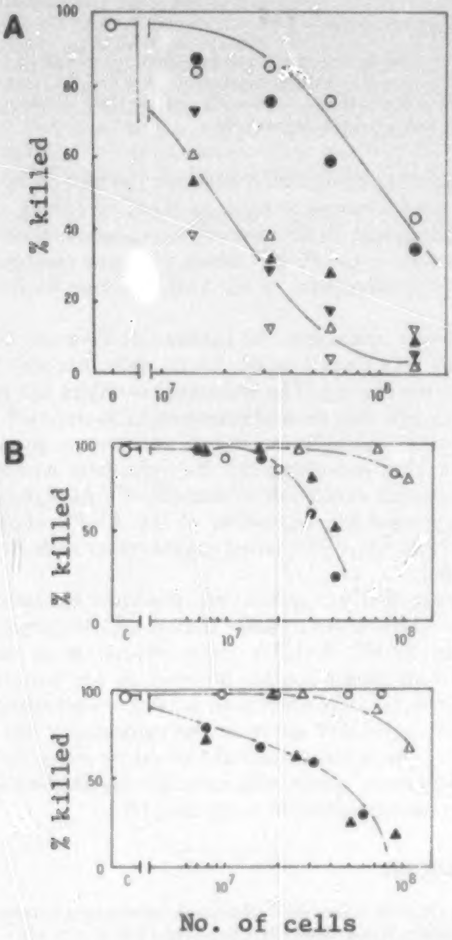

TEXT-FIGURE 3.—Absorption of anti-C4W antibody by BALB/c and C4W mouse cells. 3A) Anti-C4W serum diluted a hundredfold was absorbed by the indicated number of spleen cells and was assayed for cytotoxicity in BS(43) cells. (Percentages of cells killed were not corrected in any of the experiments reported in this paper.) Cells were derived from male (●) and female (○) BALB/c mice and from 2 male (▲, ▼) and 2 female (△, ▽) C4W mice. 3B) Two independent absorption experiments with thymus and spleen cells from C4W and BALB/c mice. Anti-C4W serum diluted fiftyfold was absorbed by thymus and spleen cells and was assayed for cytotoxicity in BS(43) cells. Cells were from the thymuses (●) and spleens (▲) of male C4W mice and from the thymuses (○) and spleens (△) of female BALB/c mice.

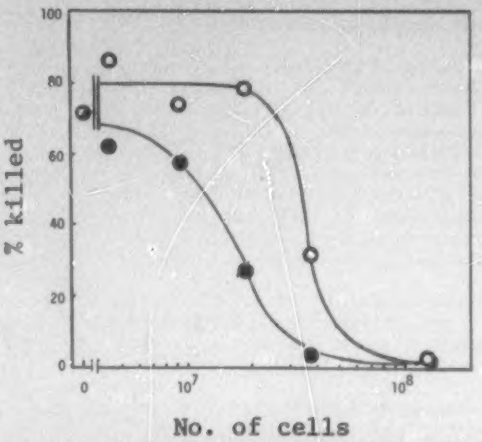

TEXT-FIGURE 4.—Absorption of anti-C4W serum by BS(43) cells and F-MuLV-infected cells. The hundredfold diluted anti-C4W serum was absorbed in the same manner as in text-fig. 3, and the absorbed serum was tested for complement-dependent cytotoxicity in BS(43) cells. ● = absorbed by BS (43) cells and ○ = absorbed by F-MuLV-infected BS(43) cells.

Genetic analysis.—To correlate the presence of the anti-C4W target and the *Fv-4* genotype (sensitivity to NB-tropic F-MuLV), linkage between the two markers was tested in ($Fv\text{-}4^{r/s}$ × BALB/c) backcrossed mice (text-fig. 1). The spleens were removed under anesthesia, and the cells were used for the absorption test: 100 µl anti-C4W serum diluted a hundredfold was absorbed by 5×10^7 cells for 40 minutes (accidentally 90 min in expt 2). The splenectomized mice were given injections of NB-tropic F-MuLV (2×10^4 PFU of XC plaque-forming MuLV and 2×10^3 spleen focus-forming units/mouse). After 10–12 days, the bone marrow cells were collected and plated on the C-182 sarcoma-negative, leukemia-positive mouse cells. The virus producers were detected by the UV-XC assay (*17*). In these experiments, we found a perfect correlation between the two markers; i.e., all of the 12 virus-susceptible mice failed to absorb the activity efficiently, whereas all of the 14 resistant mice absorbed the activity.

Suppresion of anti-C4W target by exogenous MuLV infection.—Although the above experiments suggested a close association between the *Fv-4* locus and susceptibility to anti-C4W cytotoxic antibody, we cannot state whether the antigen recognized by the antiserum was the product of the *Fv-4* locus or a product coded by an unrelated gene closely linked to *Fv-4*. We therefore examined the effect of exogenous MuLV infection on the expression of this antigen. Because the *Fv-4* locus regulates the susceptibility of mice to MuLV, a modification of the target cells could modify the expression of the antigen. F-MuLV-infected BS(43) cells were prepared by co-culturing the cells with mouse lung fibroblast line FV131 which produces F-MuLV (*18*). Although $Fv\text{-}4^{r/r}$ mouse-derived cells are relatively resistant to MuLV (*19*), the infection was established after 2–3 weeks of co-culture. The floating BS(43) cells were freed of the glass-adherent FV131 cells; the infected BS(43) cells were indistinguishable morphologically from the parental BS(43) cells. Text-figure 2 shows the results of the cytotoxicity tests with these two BS(43) cell lines. F-MuLV infection caused the cells to be

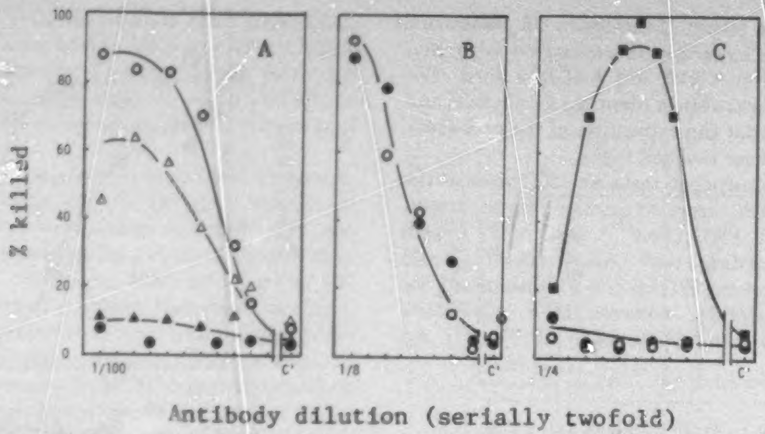

TEXT-FIGURE 5.—Cytotoxicity tests with thymus and bone marrow cells as targets. Antisera were diluted serially twofold (from *left* to *right* in text-fig.). C′ = complement without antisera. 5A) Complement-dependent cytotoxicity of anti-C4W serum. ● = BALB/c thymus cells, ▲ = BALB/c bone marrow cells, ○ = C4W thymus cells, and △ = C4W bone marrow cells. 5B) Cytotoxicity of anti-Hax. ● = BALB/c thymus cells and ○ = C4W thymus cells. 5C) Cytotoxicity of anti-FN-2. ■ = F-MuLV-infected BS(43) cells, ● = BALB/c thymus cells, and ○ = C4W thymus cells.

sensitive to anti-FN-2 and rendered the cells resistant to the anti-C4W serum. The infected BS(43) cells remained as sensitive as the uninfected BS(43) cells to anti-Hax or to anti-Thy-1.2. The absorption test indicated that the number of expressed anti-C4W targets was reduced in the infected cells (text-fig. 4).

Thymus and bone marrow cells as targets.—Cytotoxicity test were performed with thymus and bone marrow cells. C4W-derived thymus or bone marrow cells were sensitive to anti-C4W serum, whereas BALB/c-derived cells were completely resistant. Thymus cells were relatively more sensitive than were the bone marrow cells (text-fig. 5A). Anti-Hax, killed equally thymus cells of C4W and BALB/c origins (text-fig. 5B). Anti-FN-2, which killed ecotropic MuLV-infected cells, failed to kill the thymus cells of both origins (text-fig. 5C). These experiments indicated that the anti-C4W target was expressed on the C4W mouse cell surface, but not on the BALB/c mouse cell surface, and that the anti-C4W target and the antiserum against ecotropic MuLV did not cross-react. We also noticed that thymus or bone marrow cells were more sensitive (approximately tenfold) to the anti-C4W serum than were the BS(43) cells (text-figs. 2, 5A). The greater sensitivity probably was not due to a higher expression of the antigen, because about the same number of thymus or spleen cells and BS(43) cells were required for absorption (text-figs. 3, 4).

DISCUSSION

Antibody against spleen cells derived from $Fv\text{-}4^{r/o}$ mice with BALB/c genetic background (anti-C4W antibody) was raised in BALB/c mice. The antibody killed, in the presence of complement, the hematopoietic cells derived from $Fv\text{-}4^{r/-}$ mice but not those from $Fv\text{-}4^{o/o}$ mice. The genetic cross experiments indicated that the *Fv-4* locus and the locus controlling the presence of the anti-C4W target are located very close to each other. If the following considerations are taken into account, these two loci could be the same: When the target cells were infected with F-MuLV, the expression of the anti-C4W target was reduced to an undetectable level, suggesting competition between the anti-C4W target and the MuLV-coded antigen in their expression on the BS(43) cell surface. In de novo infection, therefore, the C4W target present on the $Fv\text{-}4^{r/-}$ mouse cells may competitively interfere with adsorption of the MuLV virions by the virus receptor.

This theory agrees with the previous observation that the level of the *Fv-4* control on the MuLV infection may be the virus penetration (*6*). The situation resembles the case of C/E avian cells that showed resistance to subgroup E avian leukosis viruses (*20*). However, two phenomena apparently contradict this hypothesis: *a*) No infectious endogenous MuLV has been isolated so far from $Fv\text{-}4^{r/-}$ mice; inversely, $Fv\text{-}4^{r}$ suppressed the expression of the AKR endogenous MuLV (*2*). *b*) Anti-FN-2 failed to cross-react with the anti-C4W target.

Numerous BALB/c spleen cells absorbed the anti-C4W antibody, which could indicate that anti-C4W targets were present in $Fv\text{-}4^{o/o}$ BALB/c mice though in a reduced amount. This interpretation, however, is not tenable, because *a*) BALB/c cells when used as targets were completely resistant to anti-C4W serum in the cytotoxicity test (text-fig. 5A); *b*) the immunoglobulin could be nonspecifically absorbed by many spleen cells, especially by phagocytic cells that have immunoglobulin receptors (*21*).

REFERENCES

(*1*) SUZUKI S. *Fv-4*: A new gene affecting the splenomegaly induction by Friend leukemia virus. Jpn J Exp Med 1975; 45:473–478.

(*2*) ODAKA T, IKEDA H, AKATSUKA T. Restricted expression of endogenous N-tropic XC-positive leukemia virus in hybrids between G and AKR mice: An effect of the *Fv-4^r* gene. Int J Cancer 1980; 25:757–762.

(*3*) ODAKA T, IKEDA H, MORIWAKI K, MATSUZAWA A, MIZUNO M, KONDO K. Genetic resistance in Japanese wild mice (*Mus musculus molossinus*) to an NB-tropic Friend murine leukemia virus. JNCI 1978; 61:1301–1306.

(*4*) GARDNER MB, RASHEED S, PAL BK, ESTES JD, O'BRIEN SJ. *Akvr-1*, a dominant murine leukemia restriction gene, is polymorphic in leukemia-prone wild mice. Proc Natl Acad Sci USA 1980; 77:531–535.

(5) Odaka T, Ikeda H, Yoshikura H, Moriwaki K, Suzuki S. *Fv-4*: Gene controlling resistance to NB-tropic Friend murine leukemia virus. Distribution in wild mice, introduction into genetic background of BALB/c mice, and mapping of chromosomes. JNCI 1981; 67:1123–1127.

(6) Yoshikura H, Naito Y, Moriwaki K. Unstable resistance of G mouse fibroblasts to ecotropic murine leukemia virus infection. J Virol 1979; 29:1078–1086.

(7) Hartley JW, Rowe WP. Naturally occurring murine leukemia viruses in wild mice: Characterization of a new "amphotropic" class. J Virol 1976; 19:19–25.

(8) Morse HC III, Chused TM, Boehm-Truitt M, Mathieson BJ, Sharrow SO, Hartley JW. XenCSA: Cell surface antigens related to the major glycoproteins (gp70) of xenotropic murine leukemia viruses. J Immunol 1979; 122:443–454.

(9) Yoshikura H, Yoshida M. Intracellular restriction of ecotropic murine leukemia virus in rat NRK cells and its abolishment by adaptation. J Virol 1978; 27:612–618.

(10) Boyse EA, Old LJ, Chouroulinkov I. Cytotoxic test for demonstration of mouse antibody. Methods Med Res 1964; 10:39–47.

(11) Risser R. Friend erythroleukemia antigen. A viral antigen specified by spleen focus-forming virus and differentiation antigen controlled by the *Fv-4* locus. J Exp Med 1979; 149:1152–1167.

(12) Friend C, Scher W, Holland JG, Sato T. Hemoglobin synthesis in murine virus-induced leukemic cells in vitro: Stimulation of erythroid differentiation by dimethyl sulfoxide. Proc Natl Acad Sci USA 1971; 68:378–382.

(13) Ikawa Y, Yoshida M. Erythroblastosis-inducing RNA sequences in Friend leukemia virus (FLV) of various sources. In: Ikawa Y, Odaka T, eds. Oncogenic viruses and host cell genes. New York: Academic Press, 1979:163–172.

(14) Fieldsteel AH, Kurahara CK, Dawson PJ. Friend virus-induced reticulum cell sarcomas grown in vitro: Further evidence for the absence of Friend virus. Cancer Res 1969; 29:1846–1850.

(15) Nakano, N. Establishment of cell lines in vitro from mammary ascites tumor of mouse and biological properties of the established lines in a serum containing medium. Tohoku J Exp Med 1966; 88:69–84.

(16) Stockert E, DeLeo AB, O'Donnell PV, Obata Y, Old LJ. G(AKSL2): A new cell surface antigen of the mouse related to the dualtropic mink cell focus-inducing class of murine leukemia virus detected by naturally occurring antibody. J Exp Med 1979; 149:200–215.

(17) Rowe WP, Pugh WE, Hartley JW. Plaque assay techniques for murine leukemia viruses. Virology 1970; 42:1136–1139.

(18) Yoshikura H, Hirokawa Y, Yamada M, Sugano H. Production of Friend leukemia virus in a mouse lung cell line. Jpn J Med Sci Biol 1967; 20:225–236.

(19) Kai K, Ikeda H, Yuasa Y, Suzuki S, Odaka T. Mouse strain resistant to N-, B- and NB-tropic murine leukemia viruses. J Virol 1976; 20:436–440.

(20) Pani PK. Inter-relationship between genes controlling endogenous virus expression and those controlling susceptibility to exogenous RNA tumour viruses: Evidence for linkage between the group specific antigen and tumour virus *e* loci. J Gen Virol 1977; 38:61–74.

(21) Stanworth DR, Turner MW. Immunochemical analysis of immunoglobulins and their sub-units. In: Weir, DM, ed. Handbook of experimental immunology. Oxford: Blackwell, 1978:6.84–6.86.

blank page

2′-Deoxycoformycin-Induced Hemolysis in the Mouse[1,2,3]

Ellen Spremulli, *M.D.,*[4,5,6] **Gerald W. Crabtree,** *Ph.D.,*[5] **Daniel L. Dexter,** *Ph.D.,*[4,5]
Israel Diamond, *M.D.,*[5,7] *and* **Paul Calabresi,** *M.D.*[4,5]

ABSTRACT—2′-Deoxycoformycin (dCF), a tight-binding inhibitor of adenosine deaminase, has recently been entered into clinical trials. Toxicity has included lymphopenia, seizures, coma, conjunctivitis, renal failure, and hemolysis. Mice treated with dCF on a variety of schedules exhibited massive hemolysis. Hemolysis was brief, lasting about 20 hours, and did not recur upon readministration of the drug unless readministration was delayed for at least 6 days after initial exposure, which suggests that a sensitive subpopulation of cells was selectively destroyed. Splenectomy failed to protect the animals from dCF-induced hemolysis. Administration of adenosine or 2′-deoxyadenosine without dCF did not cause hemolysis, and use of these two agents with dCF did not potentiate the observed hemolysis. ATP and dATP levels were measured in erythrocytes, and changes in levels of these nucleotides did not correspond with the development of hemolysis.—JNCI 1982; 68:1011–1014.

Recently, dCF, a tight-binding inhibitor of AdoDA (*1*), has been entered into phase I and II clinical trials. Responses have been observed in patients with mycosis fungoides and T-cell acute lymphoblastic leukemia (*2–4*). Although in initial trials the drug was well tolerated (*5*), significantly more drug toxicity was encountered in recent clinical studies. Toxic manifestations included serositis, lethargy, seizures, coma, renal failure, conjunctivitis, and hemolysis (*2–4, 6*).

Recently, Smith et al. (*7*) reported that dCF at an ip dose of 10 mg/kg in mice caused hemolysis. In the present report, we confirm their findings and present additional data that may help elucidate the mechanism responsible for the hemolysis.

MATERIALS AND METHODS

Inbred BALB/c, (C57BL × DBA/2)F_1 (BDF_1), and C57BL/6 male and female mice and outbred Swiss male and female mice were purchased from Cumberland View Farms, Clinton, Tenn. Animals were housed in the Roger Williams General Hospital Animal Care Facility (Providence, R.I.).

Obtained from Dr. John Douros (National Cancer Institute, Bethesda, Md.), dCF was dissolved in 0.9% NaCl before use. Because of the unexpected nature of the toxicity encountered, some duplicate experiments were done with the use of dCF from different lot numbers. Identity of the compound as dCF was confirmed by HPLC and by a test for AdoDA inhibition with the use of the method of Chassin et al. (*8*). Ado and dAdo were purchased from Sigma Chemical Company, St. Louis, Mo.

Splenectomy was performed on mice under ether anesthesia through a left subcostal incision. The spleen was mobilized and bluntly dissected from the pancreas, and the wound was closed with clips. Animals were rested at least 10 days after splenectomy before treatment was begun. Complete splenectomy was verified by autopsy.

The urine was examined for hemosiderin by the ferric ferrocyanide stain. Urine from several mice was pooled and centrifuged, and the sediment was stained with 2% potassium ferrocyanide and 1% hydrochloric acid.

Hemoglobin electrophoresis was performed on pooled urine specimens with the use of blood from a single mouse as a control. The hemolyzed mouse red blood cells and urine were applied to Titan III cellulose acetate plates and subjected to electrophoresis for 20 minutes at 350 V. Subsequently, the plates were stained, cleared, and scanned at 525 nm.

We treated 5 mice with 20 mg dCF/kg as a single ip dose, and we determined osmotic fragility 8 hours later using an osmotic fragility kit (Becton, Dickinson & Co., Rutherford, N.J.). For these studies, blood was incubated for 20 minutes in concentrations of saline varying from 0 to 0.85% and the concentration at which hemolysis began was recorded. The amount of hemolysis was quantitated by measurement of absorbance at 540 nm.

Pooled urine samples from mice treated with 15 mg dCF/kg were submitted to the Boston Medical Center Laboratory, Boston, Mass., and assayed for myoglobin.

We prepared blood from individual mice for HPLC by extracting 2 ml of blood with 20% perchloric acid, neutralizing the extract with potassium hydroxide, and freezing the supernatant. Levels of ATP and dATP were determined by HPLC with the use of a Varian LCS-1000 equipped with a Whatman Partisil-10 SAX column (4.6 mm×25 cm; Whatman, Inc., Clifton, N.J.). The conditions used for HPLC analysis were as described by Crabtree et al. (*9*) with detection at 254 nm.

Doses of dCF ranged from 1 to 20 mg/kg. A variety of schedules was used including a single ip or sc dose only or two doses daily, three doses daily, one dose daily for 5 days,

---

ABBREVIATIONS USED: Ado=adenosine; AdoDA=Ado deaminase (EC 3.5.4.4); dAdo=2′-deoxyadenosine; dCF=2′-deoxycoformycin: Pentostatin, (*R*)-3-(2-deoxy-*β*-D-*erythro*-pentofuranosyl)-3,6,7,8-tetrahydroimidazo [4,5-*d*][1,3]diazepin-8-ol; HPLC=high-performance liquid chromatography.

---

[1] Received August 20, 1981; accepted January 26, 1982.

[2] Supported by Public Health Service grants CA-13943-07 and CA-26218-02 from the National Cancer Institute.

[3] Guidelines for the care and use of laboratory animals were followed as set forth by The Roger Williams General Hospital and the National Research Council.

[4] Department of Medicine, Roger Williams General Hospital, 825 Chalkstone Ave., Providence, R.I. 02908.

[5] Division of Biology and Medicine, Brown University, Providence, R.I. 02912.

[6] *Address reprint requests to* Dr. Spremulli, Department of Medicine, Roger Williams General Hospital.

[7] Department of Pathology, Roger Williams General Hospital.

and one dose followed by a second dose either 3, 4, 5, 6, 7, 8, or 9 days later given either ip or sc. In addition, some animals were treated by continuous infusion over 24 hours with doses ranging from 1 to 20 mg/kg.

We accomplished continuous infusion by inserting PE10 polyethylene tubing into the lateral tail vein of the mouse. A volume of 5 ml was delivered during 24 hours by a Harvard Infusion Pump.

Ado and dAdo were dissolved in physiologic saline and administered ip or by continuous infusion both alone and in combination with dCF. Doses used included 400 mg/kg ip one time, one dose of 400 mg/kg ip daily for 3 days, and 1,000 mg/kg by continuous infusion during 24 hours.

RESULTS

Doses of dCF equal to or greater than 10 mg/kg ip or sc caused massive hemoglobinuria in some animals (table 1). Not all animals developed hemolysis; some animals that did not demonstrate hemoglobinuria on initial exposure to the drug did develop hemolysis when they were reexposed to the drug at a later date. Hemolysis occurred in both male and female animals and in several different types of mice including BDF$_1$, BALB/c, Swiss, and C57BL/6. This effect was observed with all four different lot numbers of dCF examined.

Table 1 shows the hematocrit fall observed after dCF treatment. The decrease in hematocrit was quite dramatic in some of these animals and was accompanied by visible hemoglobinemia. The observation of hemoglobinuria always correlated with a fall in hematocrit of at least 8% below that of control animals.

Hemoglobinuria, when observed, started at approximately 11 hours after an ip or sc dose of dCF and was brief; the urine generally cleared by hour 30. The animals appeared clinically healthy despite the hemoglobinuria. The identity of hemoglobin in the urine was verified by hemoglobin electrophoresis in which mouse blood was used as the standard. Tests for myoglobin and bilirubin were negative.

TABLE 1.—*Occurrence of hemoglobinuria and changes in hematocrit with increasing doses of dCF*[a]

dCF dose, mg/kg	No. of mice with hemoglobinuria/total mice	Average hematocrit, mean ± SD	
		20 hr	50 hr
None (control)	0/10	47±2.1	50±2.3
1	0/10	46.4±2.7	48.8±3.1
4	0/10	44.8±3.0	40.6±2.6
8	0/10	43.8±1.6	38.8±1.7
10	5/10	40±2.4^{b}	34.8±3.6^{b}
		43±2.7^{c}	45.5±3.1^{c}
15	5/10	35.6±2.7^{b}	31.4±2.9^{b}
		ND	41.3±.58^{c}
20	5/10	32.4±1.7^{b}	29.4±1.8^{b}
		ND	36.5±3.0^{c}

[a] Groups of 10 female BDF$_1$ mice were treated with dCF and observed for the development of hemoglobinuria. Serial hematocrits were determined at the times indicated. Each mouse received a single ip injection. ND=not determined.

[b] With hemoglobinuria.

[c] Without hemoglobinuria.

Slides of the peripheral blood before and during the episodes of hemolysis failed to show burr cells or fragmented cells; however, multiple spherocytes were seen. Ferric ferrocyanide stain of urine sediment was negative. No changes in osmotic fragility of mouse erythrocytes were observed following dCF treatment (data not shown).

Autopsies were done on 6 mice during the episodes of hemoglobinuria; the kidneys showed no evidence of hemoglobinuric nephropathy.

Splenectomized and control BDF$_1$ female mice were given a single ip injection of dCF and observed for 72 hours. Splenectomy failed to prevent hemolysis as manifested by hemoglobinuria, hemoglobinemia, and a fall in hematocrit, which occurred between hours 10 and 15 in both groups. Spherocytes were observed in approximately equal numbers in the peripheral blood of both splenectomized and control animals.

Animals developing hemoglobinuria after an ip dose of 15 mg dCF/kg were challenged with a second dose at varying intervals. The interval between the first and second challenge ranged from 24 hours to 10 days. None of the animals that received a second dose of dCF less than 6 days after the initial treatment redeveloped hemoglobinuria. Some animals rechallenged 6 or more days after initial treatment redeveloped hemoglobinuria, which suggests that a sensitive cell population was selectively destroyed.

The following results were obtained after the specified treatments: *a*) Ten female BDF$_1$ mice were given 15 mg dCF/kg ip daily for 5 days starting on day 1. On day 2 all 10 mice had hemoglobinuria; however, by 48 hours the urine appeared normal in all these animals and remained so throughout the rest of the injection period and for a 10-day observation period thereafter. b) Four BALB/c females were given 15 mg dCF/kg ip daily for 2 days; at 24 hours 3 of 4 had hemoglobinuria, which cleared by hour 30 and did not recur despite the second injection of dCF at hour 24. *c*) Four BALB/c females were treated with 15 mg dCF/kg at hours 0 and 48. All 4 mice developed hemoglobinuria, which cleared before hour 48 and did not recur during a 4-day observation period. *d*) Five female BALB/c mice received 15 mg dCF/kg ip on day 1 through day 4; all 5 had a temporary period of hemoglobinuria, which cleared by hour 35 and did not recur. *e*) Six Swiss female mice treated with 15 mg dCF/kg ip on day 1 developed hemoglobinuria, which recurred when the second challenge was given on day 6.

When dCF was administered by 24-hour infusion, none of the animals developed hemoglobinuria. In these experiments, dCF doses ranged from 1 to 20 mg/kg, and at least 3 mice were used in each group.

Mice infused with 2,500 mg/kg of Ado or dAdo alone over 24 hours did not develop hemoglobinuria. When mice were treated with 1 mg dCF/kg ip and 1 hour later were infused with either Ado or dAdo (2,500 mg/kg) over 24 hours, the treatment was lethal; but immediately before the mice died, hemoglobinuria was not observed. Several other experiments were conducted in mice treated with combinations of dCF and either Ado or dAdo (*see* table 2). Animals receiving 1 mg dCF/kg ip followed by a 24-hour infusion of either Ado or dAdo (1,000 mg/kg) did not develop hemo-

TABLE 2.—*Hematocrit changes observed in mice treated with dCF, Ado, or dAdo*[a]

Dose, mg/kg			No. of mice per group	Mean hematocrit ± SD, after drug (hr)		
DCF	Ado	dAdo		DCF	Ado	dAdo
—	—	—	4	50±4.1 (0)	49±2.8 (16)	43±4.4 (48)
15	—	—	10	47±4.3 (0)	32±3.3 (30)	27±5.8 (48)
—	400	—	5	49±5.6 (24)	51±4.1 (40)	
—	—	400	5	42±3.9 (24)	47±4.1 (40)	
2	400	—	5	41±3.4 (24)	45±3.7 (40)	
2	—	400	5	42±3.3 (24)	49±4.4 (40)	
4	1,000*	—	2	43 (40)		
4	—	1,000*	1	49 (35)		
6	1,000*	—	2	35 (24)	35 (48)	
6[b]	400[b]	—	7	49±4.0 (0)	42±2.6 (26)	45±3.2 (48)

[a] Female BDF_1 mice were treated with dCF either as a single agent or in combination with Ado or dAdo. Hematocrits were determined at various intervals. Drugs were given either ip or by continuous infusion (*) over 24 hr. Where injections were repeated, the second injections were given 24 hr later. *Dash* indicates none given.

[b] Given two times.

globinuria. Additional studies were performed in which 4 mg dCF/kg was given ip and 1 hour later the mouse was infused with either Ado or dAdo (1,000 mg/kg) for 24 hours. Although hematocrit decreased slightly, gross hemolysis was not evident. Further experiments were conducted in which 6 mg dCF/kg was administered ip daily for 4 days; on day 2, 400 mg Ado/kg was injected ip daily for 3 days. In this group of 7 animals, none developed obvious hemoglobinuria. Serial hematocrits are recorded in table 2.

Table 3 shows the nucleotide levels of erythrocytes 18 hours after mice were treated with dCF, Ado, dAdo, or a combination of dCF and either Ado or dAdo. ATP levels did not change appreciably when mice were treated with either Ado or dAdo (400 mg/kg) or with 1 mg dCF/kg. Doses of 10 or 20 mg dCF/kg resulted in a greater than 50% decrease in ATP levels. Treatment with 1 mg dCF/kg followed by either Ado or dAdo (400 mg/kg) resulted in similar decreases in ATP levels. Measurable levels of dATP were seen with either high-dose dCF or low-dose dCF and either Ado or dAdo. ADP levels were not appreciably different from those of controls in any treatment group.

TABLE 3.—*Nucleotide profiles of mouse erythrocytes 18 hours after treatment with dCF, Ado, or dAdo*[a]

Treatment (mg/kg)	Nucleotide levels, nmol/ml packed cells			
	ADP	dADP	ATP	dATP
Saline control	81±19	—	977±64	—
Ado (400)	94±12	—	937±68	—
dAdo (400)	112±43	—	1,073±208	—
dCF (1)	82±14	—	900±145	—
dCF (10)	48±14	7±7	293±3	21±8
dCF (20)	80±27	—	441±12	27±9
dCF (1)+Ado (400)	61±16	31±13	330±45	35±13
dCF (1)+dAdo (400)	64±10	22±3	338±15	196±35
dCF (10)+Ado (400)	44±9	tr	212±22	49±11
dCF (10)+dAdo (400)	39±9	14±6	133±5	104±14
dCF (1)+dAdo (200)	66±8	14±2	580±21	177±64

[a] Mice were treated ip with a single dose of dCF, Ado, dAdo, or with dCF followed 1 hr later by either Ado or dAdo. Nucleotide profiles were determined on erythrocytes 18 hr after treatment. Results are expressed as averages (with ranges) of determinations from 2 separate animals per treatment; tr=trace.

DISCUSSION

The drug dCF is a new antineoplastic agent that has recently been investigated in phase I and II clinical studies. Interest in this drug originated from its potential use *a*) as a single agent against T-cell leukemias and lymphomas and *b*) in combination with Ado analogs against a variety of solid human tumors. Clinical trials are being conducted on dCF at the Roger Williams Cancer Center and toxicity has been observed (*3*). The study reported here is part of our overall program to investigate the effects of dCF on cultured cells and in rodents to elucidate more fully the mechanisms of dCF-induced toxicity.

The doses of dCF used in this study were higher than those used by most previous investigators. Agarwal (*10*) examined AdoDA inhibition in mouse tissue after doses of dCF as high as 10 mg/kg ip and obtained complete inhibition of AdoDA in all tissues examined; lower doses (0.2 mg/kg, ip), even when given repeatedly, failed to completely inhibit AdoDA activity in spleen and small intestine.

In contrast to AdoDA-deficient children who are not anemic, patients with markedly increased AdoDA have been reported to have a hemolytic anemia (*11*). Patients with this disorder have 45- to 70-fold increases in erythrocyte AdoDA activity. The authors (*11*) postulated that the low ATP levels found in these erythrocytes are responsible for the hemolytic anemia.

Yu et al. (*12*) incubated human leukemia tumor cells in vitro with dCF and dAdo and found a marked rise in dATP and a decrease in ATP and GTP. One patient with T-cell leukemia was treated with dCF, and the concentrations of dATP, ATP, and GTP were monitored via HPLC in leukemia cells. Concentrations of dATP rose while those of ATP fell.

Siaw et al. (*6*) reported decreased erythrocyte ATP levels in a patient who developed hemolysis after treatment with dCF. This patient had a marked fall in erythrocyte ATP as well as an increase in dATP and inhibition of *S*-adenosyl-L-homocysteine hydrolase. The decrease in ATP occurred over 11 days; hemolysis was observed at about this time. Smith et al. (*7*) have reported that ATP levels fall in mouse erythrocytes after dCF treatment. Our results are consistent with their data in that we also observed a decrease in erythrocyte ATP after dCF.

An unexpected finding in our studies was the low ATP levels in animals that received both dCF and Ado; Siaw et al. (*6*) suggested that dCF might interfere with ATP generation. The decreases in ATP that we observed do not correlate with hemolysis, since mice given 1 mg dCF/kg and 400 mg/kg of either Ado or dAdo had profound falls in ATP levels without changes in hematocrit.

In contrast to our finding are the findings of Smith et al. (*7*) who reported that the ip injection of Ado in dCF-treated mice increased the occurrence of hemolysis. The explanation for this difference in toxicity between our two laboratories is unclear at present but may reflect differences in toxicity encountered by various clinical investigators (*2–6*). The important point is that massive transient hemolysis in mice has been documented by two laboratories.

Possible explanations for the massive hemolysis observed have been examined. First, dCF-induced changes in Ado and ATP metabolism might affect the erythrocyte membrane. These changes could lead to alterations in the surface properties of the cell, which are detectable by the spleen. The data presented above do not support this hypothesis, since splenectomized animals demonstrated hemolysis. In addition, careful examination of peripheral blood smears at hourly intervals from the time of drug injection until the onset of hemolysis revealed some spherocytes but very few burr cells or cell fragments.

Another possible explanation could be that high circulating levels of Ado or dAdo result in intracellular changes in the corresponding nucleotide since the nucleoside transport system of erythrocytes is very efficient (*13*). However, no hemolysis was observed when mice were infused with Ado or dAdo after pretreatment with dCF at a concentration just below that known to cause hemolysis when used alone (*see* table 2).

Our data support the hypothesis that a sensitive subpopulation of cells is destroyed by exposure to dCF and that it takes about 6 days for this cell population to be reestablished. We are presently examining old and young murine erythrocytes for their susceptibility to dCF-induced hemolysis.

Clinical trials have used doses of dCF ranging from 4 to 160 mg/m^2 either as an iv push or as an infusion. Initial reports of toxicity in clinical trials were limited to lymphopenia and elevated serum uric acid levels (*5*). As more patients have been treated with dCF, a wider range of toxicities has been reported, including massive hemolysis (*4*, *6*). Although toxicity seen in an animal may or may not occur in patients, the hemolysis observed in these preclinical investigations should alert the clinical investigator to the possibility that hemolysis may complicate treatment.

REFERENCES

(*1*) Calabresi P, Parks RE Jr. Chemotherapy of neoplastic diseases. Antiproliferative agents and drugs used for immunosuppression. In: Gilman AG, Goodman LS, Gilman A, eds. The pharmacological basis of therapeutics. 6th ed. New York: Macmillan Publishing Co., 1980:1249–1313.

(*2*) Benjamin RS, Plunket W, Keating MJ, et al. Phase I and biochemical pharmacological studies of deoxycoformycin. Proc Am Soc Clin Oncol 1980; 21:337.

(*3*) Cummings FJ, Crabtree GW, Spremulli E, Rogler-Brown T, Parks RE Jr., Calabresi P. Studies with 2′-deoxycoformycin in man and subhuman primates. Proc Am Soc Clin Oncol 1980; 21:332.

(*4*) Kufe D, Major P, Agarwal R, Reinherz E, Frei E III. Phase I–II trial of deoxycoformycin (dCF) in T-cell malignancies. Proc Am Soc Clin Oncol 1980; 21:328.

(*5*) Smyth JF, Chassin MM, Harrap KR, Adamson RH, Johns DG. 2′-Deoxycoformycin (dCF): Phase I trial and clinical pharmacology. Proc Am Assoc Cancer Res 1979; 20:47.

(*6*) Siaw MF, Mitchell BS, Koller CA, Coleman MS, Hutton JJ. ATP depletion as a consequence of adenosine deaminase inhibition in man. Proc Natl Acad Sci USA 1980; 77:6157–6161.

(*7*) Smith CM, Belch A, Henderson JF. Hemolysis in mice treated with deoxycoformycin, an inhibitor of adenosine deaminase. Biochem Pharmacol 1980; 29:1209–1210.

(*8*) Chassin MM, Adamson RH, Zaharevitz DW, Johns DG. Enzyme inhibition titration assay for 2′-deoxycoformycin and its application to the study of the relationship between drug concentration and tissue adenosine deaminase in dogs and rats. Biochem Pharmacol 1979; 28:1849–1855.

(*9*) Crabtree GW, Nelson JA, Parks RE Jr. Failure of 6-ThioGMP to inhibit guanylate kinase in intact cells. Biochem Pharmacol 1977; 26:1577–1584.

(*10*) Agarwal RP. Deoxycoformycin toxicity in mice after long term treatment. Cancer Chemother 1980; 5:83–87.

(*11*) Valentine WN, Paglia DE, Tartaglia AP, Gilsanz F. Hereditary hemolytic anemia with increased red cell adenosine deaminase (45- to 70-fold) and decreased adenosine triphosphate. Science 1977; 195:783–784.

(*12*) Yu AL, Bakay B, Kuno FH, Nyhan WL. Effects of 2′-deoxycoformycin on the metabolism of purines and the survival of malignant cells in a patient with T cell leukemia. Cancer Res 1981; 41:2677–2682.

(*13*) Oliver JM, Paterson AR. Nucleoside transport. I. A mediated process in human erythrocytes. Can J Biochem 1971; 49:262–270.

Carcinogen-Induced DNA Damage and Cellular Alterations in F344 Rat Colon Organ Cultures [1,2,3]

Nitin T. Telang [4,5] *and* **Gary M. Williams** [4,6,7]

ABSTRACT—Optimized culture conditions were used to achieve prolonged survival of colon mucosa from conventional inbred F344 strain rats. Up to 21 days in culture, a high percentage of explants had viable mucosa with intact crypt columns and maintained active replicative DNA synthesis in the proliferative zone of the crypts. An acute 4-hour in vitro exposure to 0.5 m*M* of the colon-selective carcinogens 1,2-dimethylhydrazine dihydrochloride (DMH) and *N*-methyl-*N'*-nitro-*N*-nitrosoguanidine (MNNG) produced 26 and 78% suppressions of replicative DNA synthesis, respectively, whereas the same exposure to the liver carcinogen dimethylnitrosamine produced only a 5% suppression. The thymidine-labeling index of DMH-exposed cells was lower than that of control cells at 1 day and then increased above the control values 7–21 days later. MNNG exposure produced pronounced morphologic changes in the crypt columns. MNNG-exposed cultures that were transplanted into the mammary fat pads of syngeneic female rats produced hypercellular cysts different from those formed by nonexposed fragments. These findings indicate that the acute and persistent effects of colon carcinogens can be studied directly on the target tissue in organ culture.—JNCI 1982; 68:1015–1022.

Techniques for organ culture of rodent colon fragments (*1–6*) now permit maintenance of this tissue in a defined environment for a variety of studies. Such organ culture systems have been used to demonstrate the metabolism of carcinogens by the cultured mucosal epithelium by 1) the determination of the binding of metabolites to DNA or the production of metabolites (*7, 8*) as well as by 2) the examination of carcinogen-induced modulation in cell replication (*1*) and in DNA synthesis (*3, 9, 10*). Although in vitro malignant transformation in mouse mammary gland organ cultures (*11*) and in explant cultures of human pancreatic duct (*12*) has been documented, neoplastic alteration of colon mucosa by in vitro exposure to colon-selective carcinogens has not yet been demonstrated. In the present study, acute and persistent effects of the colon-selective procarcinogen DMH, the liver carcinogen DMN, and the direct-acting carcinogen MNNG, which also produces colon tumors, were examined in a rat colon organ culture system. Transplantation of exposured fragments into the mammary fat pad was used to evaluate the nature of the morphologic alterations in carcinogen-exposed organ cultures.

MATERIALS AND METHODS

Animals.—Eight- to 10-week-old conventional male inbred F344 rats were used in all the organ culture experiments. As a prerequisite for organ culture, the animals were maintained on an antibiotic treatment of 0.08 mg neomycin sulfate/day and 200 U Mycostatin/day in the drinking water for 3–4 days before culture (*5*). The animals were killed by CO_2 asphyxiation, and the descending colons were collected in sterile Hanks' buffered salt solution. The organ cultures were initiated within 0.5 hour of procuring the tissues.

Organ cultures.—The basic organ culture technique used was similar to that of Shamsuddin et al. (*4*), as previously described (*5*). Full-thickness tissue fragments were attached by their serosal side to Metricel GA-4 filters (0.8 μm pore size) and were cultured in 60-mm bacteriological petri plates (Falcon Plastics, Oxnard, Calif.) in 5 ml of WME (*13*). The medium was supplemented with 10% calf serum, 1 mU insulin/ml and 1 μ*M* dexamethasone. The antibiotics Mycostatin (100 U/ml) and gentamicin (100 μg/ml) were also included in the complete WME. The organ cultures were maintained at 37°C in an atmosphere of 95% O_2:5% CO_2 and were rocked at 10 cycles/minute to achieve intermittent exposure of the tissue to the gas and liquid phases. Routinely, the culture medium was replenished every 24 hours during the 1st week and every 48 hours thereafter.

Biochemical studies.—The interaction of carcinogens with the mucosal epithelium was assessed in short-term organ cultures by examination of the modulation in replicative DNA synthesis. After a 24-hour preincubation, the cultures were exposed to 0.5 m*M* DMN (Eastman Kodak Co., Rochester, N.Y.), DMH (*sym*-dimethylhydrazine dihydrochloride; Aldrich Chemical Co., Milwaukee, Wisc.), or to MNNG (Sigma Chemical Co., St. Louis, Mo.) for 4 hours; this dose was the maximally effective sublethal dose of DMN and MNNG. These cultures together with parallel solvent-exposed controls were then incubated with 10 μCi $[^3H]$-

---

Abbreviations used: AOM=azoxymethane; DMH=1,2-dimethylhydrazine dihydrochloride; DMN=dimethylnitrosamine; dThd=thymidine; $[^3H]$dThd=tritiated dThd; H & E=hematoxylin and eosin; LI=labeling index; MAM=methylazoxymethanol; MNNG=*N*-methyl-*N'*-nitro-*N*-nitrosoguanidine; PAS=periodic acid–Schiff; SSC=standard saline citrate buffer (15 m*M* sodium chloride and 1 m*M* sodium citrate); WME=Williams' medium E.

---

[1] Received September 4, 1981; accepted January 26, 1982.

[2] Supported by Public Health Service contract N01CP-75952 from the Division of Cancer Cause and Prevention, National Cancer Institute.

[3] Animals were maintained under the guidelines of the National Research Council.

[4] Division of Pathology and Toxicology, Naylor Dana Institute for Disease Prevention, American Health Foundation, Dana Rd., Valhalla, N.Y. 10595.

[5] *Present address:* Division of Molecular Virology, Sloan-Kettering Institute for Cancer Research, 1275 York Ave., New York, N.Y. 10021.

[6] *Address reprint requests to* Dr. Williams.

[7] We thank Ms. Sondra Solomon and Ms. Maritza Cotto for excellent technical assistance, Mr. C. Q. Wong for photography, and Mrs. N. McNeilly for preparing the manuscript. This publication is dedicated to the founder of the American Health Foundation, Dr. Ernst L. Wynder, on the occasion of the 10th anniversary of the Naylor Dana Institute for Disease Prevention.

dThd/ml (45–50 Ci/mmol; New England Nuclear Corp., Boston, Mass.) for 18–20 hours to label all the cells that entered S-phase during this interval.

The mucosal cells from these cultures were dissociated from the underlying stromal tissue by incubation of the fragments in 0.25% Pronase (Calbiochem-Behring Corp., San Diego, Calif.) for 25–30 minutes at 37°C. The cells detached after gentle scraping with a rubber policeman were recovered by centrifugation of the medium (800–1,000 rpm/10 min). The resulting pellet was used for DNA extraction essentially according to the method of Marmur (*14*), with minor modifications that have been found effective for DNA isolation from mammary gland organ cultures (*15, 16*). The mucosal cells were resuspended in SSC and were lysed in the presence of 1% sodium dodecyl sulfate by alternate freezing and thawing. The resulting lysate was extracted once with chloroform–isoamyl alcohol (24:1), and the aqueous fraction was submitted to incubation with RNase (500 µg/ml for 1 hr at 37°C) and subsequently with Pronase (500 µg/ml for 1 hr at 37°C). After another extraction with chloroform–isoamyl alcohol and centrifugation, the DNA from the aqueous phase was precipiated by the addition of 2 volumes of cold ethanol. The precipitate was dissolved in SSC, and 100-µl aliquots of the sample were taken for the determination of DNA-bound dThd radioactivity. The DNA content of the sample was determined by measurement of the absorbance at 260 nm and also by the ethidium bromide fluorescence assay of Beers and Whitliff (*17*).

Morphologic studies.—The cellular effects of DMH, DMN, and MNNG were examined in the organ cultures after a 4-hour exposure to the carcinogens. These carcinogen-exposed cultures together with the solvent-exposed controls were maintained in WME. Two hours before the harvest at the designated times, the organ cultures were incubated with 10 µCi [^{3}H]dThd/ml and fixed in 10% buffered Formalin. The paraffin sections of the fragments were submitted to standard emulsion autoradiographic procedures (*5, 18*). Only the longitudinally sectioned, intact crypt columns that had at least two labeled nuclei with at least five grains per nucleus were included in [^{3}H]dThd LI determinations. These were then compared with nonexposed controls to determine carcinogen-induced proliferative alterations.

Transplantation studies.—For these experiments, the colon organ cultures from female rats were exposed to 0.5 m*M* MNNG for 4 hours and were maintained in culture for 7 days before transplantation into the mammary parenchyma-free fat pads of syngeneic recipients of the same sex. The technique used for surgical removal of the mammary parenchyma from the recipients was similar to that described by DeOme et al. (*19*), Haslam and Bern (*20*), and Richards and Nandi (*21*). The transplantation was done contralaterally such that a single recipient was implanted with an MNNG-exposed fragment and a fragment from the solvent-exposed control group. The recipient animals were maintained on normal diet and were killed 3 and 6 months after transplantation. The histologic nature of the cellular outgrowths was assessed from the histopathologic examination of the fat pads after being stained with H & E. The functional integrity of the outgrowths was determined by the presence of PAS-positive material.

RESULTS

Colon Organ Cultures

Consistent with the previous observations of Reiss and Williams (*5*), the culture conditions that supported prolonged survival of colon mucosa from the conventional mouse or the germfree rat were found to be equally conducive for maintenance of tissue from the conventional rat. Seventy-seven percent of fragments displayed intact crypt columns at 21 days in culture, and the surviving crypt columns showed persistent DNA synthesis in the crypts (table 1). During the initial phases of culture, the fragments frequently possessed shallow crypt columns, but in 14- and 21-day cultures, the surviving crypt columns were of normal height and had a normal cell number, thus resembling the day-1 cultures. The average number of cells ± SD per crypt column at days 1, 7, 14, and 21 were 37±4, 25±6, 36±5, and 39±3, respectively. The progressive increase in [^{3}H]dThd LI (table 1) was essentially similar to the increase reported by others (*6*).

Autoradiographic examination of explants pulsed with [^{3}H]dThd revealed that the mucosal cells in the lower third (normal proliferative zone) of the crypt column incorporated the radioisotope (figs. 1, 2). This pattern of labeling was consistently observed throughout the duration of culture.

In Vitro Effects of Carcinogens

The interaction of DMN, DMH, or MNNG with mucosal cell DNA was examined by evaluating the effect on DNA synthesis after an acute exposure of the cultures to the carcinogens. A 4-hour exposure to equimolar concentrations of the colon carcinogens DMN (activation-dependent) or MNNG (activation-independent) produced a 26–34% and a 74–78% suppression of incorporation of [^{3}H]dThd, respectively, in replicate experiments over the next 20 hours (table 2). In contrast, a similar exposure to the activation-dependent liver carcinogen DMN resulted in only a 5% suppression. The inhibition of replicative DNA synthesis by DMH but not by DMN is consistent with a selective ability of the colon mucosal epithelium to metabolize the colon carcinogen.

The differential susceptibility of mucosal cells to effects of DMN, DMH, and MNNG, as seen by the reduction in DNA-associated [^{3}H]dThd radioactivity (table 2), was also

TABLE 1.—*Condition of mucosal epithelium of rat colon in organ culture*

Culture duration, days[a]	Survival[b]	Average percent [^{3}H]dThd LI[c] ± SD
1	8/8 (100)	6.0±1.5
2	8/8 (100)	8.5±0.4
7	15/16 (94)	9.7±0.4
14	13/15 (87)	19.0±7
21	17/22 (77)	18.0±6

[a] Explant cultures were maintained in serum-supplemented WME. After requisite times, cultures were labeled with 10 µCi [^{3}H]dThd/ml for 2 hr before being harvested.

[b] No. of fragments with intact crypt columns open to the luminal surface/No. of fragments cultured (%).

[c] (No. of labeled cells/total No. of crypt cells) × 100, as determined in three separate experiments.

manifested as reduced [^{3}H]dThd LI ± SD immediately after carcinogen exposure. Thus the percent [^{3}H]dThd LI ± SD at 20 hours after DMH and MNNG exposure was found to be 6±2 and 3±1%, respectively. In contrast, DMN exposure did not result in any reduction, with the percent [^{3}H]dThd LI ± SD being 11±2%, which was comparable to the control value of 10±2%.

Continued maintenance of cultures exposed to DMH or MNNG resulted in a marked enhancement in the LI within 7 days, with the percent [^{3}H]dThd LI ± SD of 14±2 and 18±1%, respectively. The morphologic abnormalities in these cultures included shortening of the crypt columns, with DNA-synthesizing cells extending up the crypts into nonproliferative regions (figs. 3, 4). In contrast, DMN exposure did not produce any change in the [^{3}H]dThd LI or in the morphology of the crypt columns as compared to the LI or the morphology of the controls.

Examination of cultures exposed to DMH and MNNG and maintained for 14 or 21 days revealed significant morphologic changes in surviving crypt columns. Although DMH exposure induced progressive enhancement in the percent [^{3}H]dThd LI ± SD from 14±2% at 7 days to 30±4% at 21 days, this modulation in DNA synthetic activity was not accompanied by morphologic changes other than by shortened crypts. In contrast, MNNG exposure resulted in progessively increased atypical changes, such as shortened crypt columns, crypts showing hypercellularity, and epithelial cells showing loss of polarity (fig. 5). These crypts displayed increased mitotic activity (table 3).

TABLE 2.—*Effect of carcinogens on DNA synthesis in [^{3}H]dThd-labeled rat colon organ cultures*[a]

Carcinogen	Radioactivity in tissue homogenate					
	Experiment I			Experiment II		
	cpm/100 μl supernatant fraction[b]	cpm/μg DNA[c]	Inhibition, % of control	cpm/100 μl supernatant fraction[b]	cpm/μg DNA[c]	Inhibition, % of control
None	7,700	611	0	7,780	617	0
DMN	6,316	579	5	6,350	582	6
DMH	5,802	453	26	5,200	406	34
MNNG	2,627	138	78	2,770	145	74

[a] After an initial 24 hr preincubation, cultures were exposed to 0.5 m*M* DMN, DMH, or MNNG for 4 hr. Carcinogens were aspirated, and [^{3}H]dThd was added to the cultures for 18–20 hr. Mucosal epithelial cells were dissociated, and DNA was extracted as detailed in "Materials and Methods."

[b] Radioactivity was determined in the ethanol-precipitable supernatant fraction of the mucosal cell lysate which had been digested with RNase and Pronase.

[c] DNA content was quantitated from the OD at 260 nm and by the ethidium bromide fluorescence assay.

TABLE 3.—*Acute cellular effects of MNNG on rat colon mucosa in organ culture*[a]

Culture duration after carcinogen exposure, days	Incidence[b] of:			
	Atypical crypt columns[c]		Fragments with mitotic cells	
	DMSO	MNNG	DMSO	MNNG
1	0/8	7/8 (87)	0/8 (0)	0/8 (0)
7	0/16	14/16 (87)	0/16 (0)	4/16 (25)
14	0/24	16/18 (88)	3/24 (12)	7/18 (39)

[a] Explant cultures were exposed to 0.5 m*M* MNNG or to the solvent dimethyl sulfoxide (DMSO) for 4 hr and were subsequently maintained in serum-supplemented WME.

[b] Data for No. of cultures with characteristic/No. of cultures examined (%) were pooled from two separate experiments having a range of variation of <5%.

[c] These shallow crypts had DNA-synthesizing and dividing cells in the nonproliferative regions, and columns showed hypercellularity and loss of polarity.

TABLE 4.—*Fate of MNNG-exposed colon organ cultures transplanted into mammary fat pads*[a]

Treatment group	No. of fat pads examined	Fate of implants[b]		
		Resorbed	Persisting with single-layered epithelium	Persisting with hypercellular epithelium
DMSO, controls	14	8	6	0
MNNG-exposed	12	2	0	10

[a] After a 4-hr exposure to 0.5 m*M* MNNG or to the solvent dimethyl sulfoxide (DMSO), the cultures were maintained for 7 days in WME. Fragments were transplanted into inguinal mammary fat pads contralaterally.

[b] Grafts were recovered 3 mo after transplantation.

Transplantation Studies

Because only MNNG produced persistent atypical changes in mucosal crypts, to assess the nature of these cellular alterations we exposed cultures to MNNG and transplanted them into the parenchyma-free mammary fat pads of syngeneic female recipients. The extent of survival and the morphologic appearance of the colon mucosa from MNNG-exposed explants were compared to those of parallel controls that had been transplanted contralaterally into the same recipients. The MNNG-exposed transplants showed a higher incidence of survival than the controls (table 4). The control transplants that survived beyond 3 months in this heterotopic site formed hollow cysts that were lined by a single layer of columnar epithelium (fig. 6). In contrast, the cysts formed from MNNG-exposed implants had intact crypt columns as well as hyperplastic and dysplastic mucosal glands (figs. 7–9). Generally, the cysts formed by the control transplants were smaller in size than cysts from MNNG-exposed transplants. Functional integrity of the mucosal epithelium in both control and exposed explants was evident from the PAS-positive material, both on the cell surfaces and in the lumina of the cysts.

DISCUSSION

Prolonged in vitro maintenance of colon mucosa from conventional rats has been reported by several groups (*2, 4–6*). However, morphologic integrity of the mucosal epithelium in most of these cultures (*2, 4, 6*) was found to be drastically altered as early as 14 days after the initiation of cultures, and the mucosal epithelium was seen as a single layer of surface epithelium without any crypts. In contrast, Reiss and Williams (*5*) have reported a high incidence of intact crypt columns in colon organ cultures from conventional mice and germfree rats up to 35 days. Using descending colons from the conventional rat and the supportive culture conditions that were identified by Reiss and Williams (*5*), we achieved consistent long-term survival of intact crypt columns for a period of at least 21 days in the present study. Moreover, the pattern of DNA synthesis in these explant cultures was similar to that occurring in vivo (*22–26*). Thus the present results confirm our previous preliminary observations (*10*) in which the degree of preservation of the colon mucosal epithelium was compared in the cultures from the conventional mouse and rat. The preservation of intact crypt columns in the mucosal epithelium is an important prerequisite for experiments in which the effects of carcinogens on the pattern of DNA synthesis in crypt columns are to be examined. Thus the results on long-term survival of intact crypt columns (table 1) demonstrate that specific modifications in the experimental system, such as pretreatment of the animals with antibiotics, the use of Metricel filters as a substrate, and the presence of dexamethasone in an enriched culture medium, are useful for the long-term maintenance of morphologically normal colon mucosa.

The differential susceptibility of mucosal epithelium to in vitro carcinogen exposure was evident from the extent of suppression of [^{3}H]dThd incorporation into cellular DNA and also from the kinetics of increase in [^{3}H]dThd LI after carcinogen exposure. Thus the colon-selective, activation-dependent carcinogen DMH and the direct-acting agent MNNG produced greater suppression of [^{3}H]dThd incorporation than did the metabolism-dependent liver carcinogen DMN. Furthermore, the severity of suppression of DNA synthesis and its subsequent rebound was more pronounced after DMH exposure than after DMN exposure. The inhibition of replicative DNA synthesis produced by DMH and the subsequent time-dependent reversal of this inhibitory effect, as seen in the present study, are consistent with the response induced by DMH and a form of its metabolite, MAM acetate, in rabbit colon organ cultures (*3*). Carcinogen-selective inhibition of replicative DNA synthesis by DMH and by MAM acetate but not by benzo[*a*]pyrene has also been observed in explant cultures of human colon (*27*). An essentially similar inhibition in the level of replicative DNA synthesis in vivo was reported in the rat colon after a single intrarectal instillation of DMH (*28*) or after a single iv infusion of MAM acetate (*29*). In mouse colon, Chan et al. (*30*) found a rapid reduction in the number of DNA-synthesizing cells after exposure to DMH. These studies, which indicate an interaction of the carcinogens with DNA, are consistent with other in vivo studies in which DMH has been shown to form adducts in colon DNA (*31, 32*). Likewise, exposure of colon organ cultures to radiolabeled procarcinogen has resulted in the association of radioactivity with cellular DNA (*2, 10*) or in the formation of carcinogen–DNA adducts (*6*). These in vitro studies therefore are suggestive of an intrinsic carcinogen-metabolizing capacity of the colon with generation of DNA-damaging metabolites.

The increased DNA synthesis in crypts of carcinogen-exposed fragments maintained beyond the acute exposure has not been observed in other organ colon studies, although return toward normal levels of DNA synthesis has been reported (*3, 27*). The increase found in the present study is qualitatively similar to the increase found in in vivo studies (*28, 29*) and could represent either an expansion of the stem cell population or a loss of some of the upper differentiated, nonproliferative cell compartment in the shortened crypts, resulting in a greater relative number of the stem cells.

Induction of morphologic abnormalities in rat colon after repeated injections of AOM has been reported by Shamsuddin and Trump (*33*), with the predominant atypical lesion being mucous cell hyperplasia. In a subsequent report (*34*), these investigators examined the effect of in vitro exposure to MNNG of colon organ cultures from rats pre-exposed in vivo to four weekly doses of AOM. These investigators observed focal areas of hypercellularity, loss of polarity, and anaplasia at 1 and 2 weeks after MNNG exposure. The total time required for the morphologic expression of carcinogen-induced changes was about 10 weeks. In the present experiments, a single in vitro exposure to MNNG produced a molecular defect within 24 hours of carcinogen exposure, and the resulting morphologic lesions showed a time-dependent increase at 7 and 14 days of culture. The occurrence of morphologic changes in the crypts of cultures exposed to a single dose of MNNG and the time-dependent increase in the incidence of these morphologic lesions reflects a high degree of sensitivity of the present experimental system.

Inasmuch as an acute exposure to DMH (*35*), to its proximate metabolite MAM acetate (*36*), or to MNNG (*37*) has been shown to produce malignant conversion of colon epithelium, the inhibition of replicative DNA synthesis by a single exposure to DMH or to MNNG, the induction of persistent cell proliferation in nonproliferative regions of the crypt columns, and the production of atypical crypt columns after carcinogen exposure, as observed in the present experiments, are suggestive of a relevant alteration in the target tissue after in vitro exposure to the carcinogens.

The enhanced cellularity in MNNG-exposed transplants probably reflects the cellular expression of a carcinogen-induced molecular change which enables the mucosal epithelium to proliferate in a heterotopic site. Although transplants of rodent colon adenocarcinoma are known to exhibit progressive growth (*38–40*), normal colon mucosa, when transplanted, has shown only a limited growth potential. Thus Fergusson and Parrott (*41*) have demonstrated the survival of fetal mouse colon up to 2 months, whereas fragments of adult mouse small intestine were reported to survive for about 1 month (*42*). In a recent report, Valerio et al. (*43*) have described the survival of human xenografts of colon in nude mice. From among the various sites of transplantation that were tested, such as renal subcapsular, intrapertoneal, and subcutaneous, only the last-mentioned site supported the prolonged survival of colon transplants for about 3 months. The rat mammary fat pad as a site of transplantation has been used extensively for examination of malignant transformation in mammary tissue (*20, 21*). However, little evidence is available on the ability of mammary fat pads to support the growth of nonmammary tissue. Williams et al. (*44, 45*) and Jirtle et al. (*46*) have demonstrated that liver tissue can survive in this transplantation site. Consistent with all these observations, in the present study prolonged survival of colon fragments was obtained, and in addition, a difference in the nature of outgrowths from MNNG-exposed fragments, compared to the nature of the outgrowths from nonexposed fragments, indicates that mammary fat pad transplantation could be a useful assay system for analysis of the effects of carcinogens and promoters on colon cultures.

REFERENCES

(*1*) Defries EA, Franks LM. An organ culture method for adult colon from germfree and conventional mice: Effects of donor age and carcinogen treatment on epithelial mitotic activity. J Natl Cancer Inst 1977; 58:1323–1328.

(*2*) Autrup H, Stoner GD, Jackson F, Harris CC, Shamsuddin AK. Explant culture of rat colon: A model system for studying metabolism of chemical carcinogens. In Vitro 1978; 14:268–277.

(*3*) Mak KM, Chang WW. Inhibition of DNA synthesis by 1,2-dimethylhydrazine and methylazoxymethanol acetate in rabbit colon mucosa in organ culture. JNCI 1978; 61:799–805.

(*4*) Shamsuddin AK, Barrett LA, Autrup H, Harris CC, Trump BF. Long-term organ culture of adult rat colon. Pathol Res Pract 1978; 163:362–372.

(*5*) Reiss B, Williams GM. Conditions affecting prolonged maintenance of mouse and rat colon in organ culture. In Vitro 1979; 15:877–890.

(*6*) Schiff LJ, Moore SJ. Organ culture of adult rat colonic mucosa on fibrin foam. In Vitro 1980; 16:893–906.

(*7*) Autrup H, Harris CC, Fugaro S, Selkirk JK. Effect of various chemicals on the metabolism of benzo(*a*)pyrene by cultured rat colon. Chem Biol Interact 1977; 18:337–347.

(*8*) Autrup H, Schwartz RD, Essigmann JM, Smith L, Trump BF, Harris CC. Metabolism of aflatoxin B_1, benzo(*a*)pyrene, and 1,2-dimethylhydrazine by cultured rat and human colon. Teratog Carcinog Mutagen 1980; 1:3–13.

(*9*) Reiss B, Williams GM. Induction of DNA repair and suppression of DNA synthesis by carcinogens in colon organ culture. Fed Proc 1978; 37:479.

(*10*) Telang NT, Reiss B, Fiala ES, Reddy BS, Williams GM. Response of rodent colon in organ culture to 1,2-dimethylhydrazine. Proc Am Assoc Cancer Res 1980; 21:103.

(*11*) Telang NT, Banerjee MR, Iyer AP, Kundu AB. Neoplastic transformation of epithelial cells in whole mammary gland in vitro. Proc Natl Acad Sci USA 1979; 76:5886–5890.

(*12*) Parsa J, Marsh WH, Sutton AL, Butt KM. Effects of dimethylnitrosamine on organ-cultured adult human pancreas. Am J Pathol 1981; 102:403–411.

(*13*) Williams GM, Gunn JM. Long-term cell cultures of adult rat liver epithelial cells. Exp Cell Res 1974; 89:139–142.

(*14*) Marmur J. A procedure for the isolation of deoxyribonucleic acid from microorganisms. J Mol Biol 1961; 3:208–218.

(*15*) Bodell WJ, Banerjee MR. DNA repair in normal and preneoplastic mammary tissue. Cancer Res 1978; 38:736–740.

(*16*) Kundu AB, Telang NT, Banerjee MR. Binding of 7,12-dimethylbenz[*a*]anthracene to BALB/c mouse mammary gland DNA in organ culture. JNCI 1978; 61:465–469.

(*17*) Beers PC, Whitliff JL. Measurements of DNA and RNA in mammary gland homogenates by the ethidium bromide technique. Anal Biochem 1975; 63:433–441.

(*18*) Williams GM. Detection of chemical carcinogens by unscheduled DNA synthesis in rat liver primary cell cultures. Cancer Res 1977; 37:1845–1851.

(*19*) DeOme KB, Faulkin LJ Jr, Bern HA, Blair PB. Development of mammary tumors from hyperplastic alveolar nodules transplanted into gland-free mammary fat pads of female C3H mice. Cancer Res 1959; 19:515–520.

(*20*) Haslam SZ, Bern HA. Histopathogenesis of 7,12-dimethylbenz(*a*)anthracene-induced rat mammary tumors. Proc Natl Acad Sci USA 1977; 74:4020–4024.

(*21*) Richards J, Nandi S. Neoplastic transformation of rat mammary cells exposed to DMBA or NMU in cell culture. Proc. Natl Acad Sci USA 1978; 75:3836–3840.

(*22*) Bertalanffy FD. Mitotic rates and renewal times of the digestive tract epithelium in the rat. Acta Anat (Basel) 1960; 40:130–148.

(*23*) Cairnie AB, Lamerton LF, Steel GG. Cell proliferation studies in the intestinal epithelium of the rat. I. Determination of kinetic parameters. Exp Cell Res 1965; 39:528–538.

(*24*) Lipkin M. Phase 1 and phase 2 proliferative lesions of colonic epithelial cells in diseases leading to colonic cancer. Cancer 1974; 34:878–888.

(*25*) Messier B, Leblond CP. Cell proliferation and migration as revealed by radioautography after injection of thymidine-H^3 into male rats and mice. Am J Anat 1960; 106:247–285.

(*26*) Rijke RP, Plaisier HM, Langendoen NJ. Epithelial cell kinetics in the descending colon of the rat. Virchows Arch B [Cell Pathol] 1979; 30:85–94.

(*27*) Mak KM, Slater GI, Hoff MB. Inhibition of DNA synthesis by carcinogens in human colon mucosa in organ culture. JNCI 1979; 63: 1305–1312.

(*28*) DeRubertis FR, Craven PA. Early alterations in rat colonic mucosal cyclic nucleotide metabolism and protein kinase activity induced by 1,2-dimethylhydrazine. Cancer Res 1980; 40:4589–4598.

(*29*) Zedeck MS, Grab DJ, Sternberg SS. Differences in the acute response of the various segments of rat intestine to treatment with the intestinal carcinogen, methylazoxymethanol acetate. Cancer Res 1977; 37:32–36.

(*30*) Chan PC, Cohen LA, Weisburger JH. Early effects of a single intrarectal dose of 1,2-dimethylhydrazine in mice. Cancer Res 1976; 36:13–17.

(*31*) Hawks A, Magee PN. The alkylation of nucleic acids of rat and mouse in vivo by the carcinogen 1,2-dimethylhydrazine. Br J Cancer 1974; 30:440–447.

(*32*) Swenberg JA, Cooper HK, Bucheler J, Kleihues P. 1,2-dimethylhydrazine-induced methylation of DNA bases in variour rat organs and the effect of pretreatment with disulfiram. Cancer Res 1979; 39:465–467.

(*33*) Shamsuddin AK, Trump BF. Colon epithelium. II. In vivo studies of colon carcinogenesis. Light microscopic, histochemical, and ultrastructural studies of histogenesis of azoxymethane-induced colon carcinomas in Fischer 344 rats. JNCI 1981; 66:389–401.

(*34*) Shamsuddin AK, Trump BF. Colon epithelium. III. In vitro studies of colon carcinogenesis in Fischer 344 rats. *N*-Methyl-*N*′-nitro-*N*-nitrosoguanidine-induced changes in colon epithelium in explant culture. JNCI 1981; 66:403–411.

(*35*) Schiller CM, Curley WH, McConnell EF. Induction of colon tumors by a single oral dose of 1,2-dimethylhydrazine. Cancer Lett 1980; 11:75–79.

(*36*) Zedeck MS, Sternberg SS. *Brief communication*: A model system for studies of colon carcinogenesis: Tumor induction by a single injection of methylazoxymethanol acetate. J Natl Cancer Inst 1974; 53:1419–1421.

(*37*) Narisawa T, Nakano H, Hayakawa M, Sato T, Sakuma A. Tumors of the colon and rectum induced by *N*-methyl-*N*′-nitro-*N*-nitrosoguanidine. In: Nakahara W, Takayama S, Sugimura T, Odashima S, eds. Topics in chemical carcinogenesis. Baltimore: Univ Park Press, 1972:145–158.

(*38*) Ward JM, Yamamoto RS, Weisburger JH, Benjamin T. *Brief communication*: Transplantation of chemically induced metastatic mucinous adenocarcinomas of the jejunum and colon in rats. J Natl Cancer Inst 1973; 51:1997–1999.

(*39*) McCall DC, Cole JW. Transplantation of chemically-induced adenocarcinomas of the colun in an inbred strain of rats. Cancer 1974; 33:1021–1026.

(*40*) Corbett TH, Griswold DP, Roberts BJ, Peckham JC, Schabel FM. Tumor induction relationships in development of transplantable cancer of the colon in mice for chemotherapy assays, with a note on carcinogenic structure. Cancer Res 1975; 35:2434–2439.

(*41*) Ferguson A, Parrott DM. Growth and development of antigen-free grafts of fetal mouse intestine. J Pathol 1972; 106:95.

(*42*) Rowinski J, Kaminski M. Transplanted mucosa of mouse small intestine as a model for cell proliferation studies. Gastroenterology 1973; 65:642.

(*43*) Valerio MG, Fineman EL, Bowman RL, et al. Long-term survival of normal adult human tissues as xenografts in congenitally athymic nude mice. JNCI 1981; 66:849–858.

(*44*) Williams GM, Klaiber M, Farber E. Differences in growth of transplants of liver, liver hyperplastic nodules and hepatocellular carcinomas in the mammary fat pad. Am J Pathol 1977; 89:379-388.

(45) Williams GM, Hirota N, Rice JM. The resistance of spontaneous mouse hepatocellular neoplasms to iron accumulation during rapid iron loading by parenteral administration and their transplantability. Am J Pathol 1979; 94:65-72.

(46) Jirtle RL, Biles C, Michalopoulos G. Morphologic and histochemical analysis of hepatocytes transplanted into syngeneic hosts. Am Assoc Pathol 1980; 101:115-125.

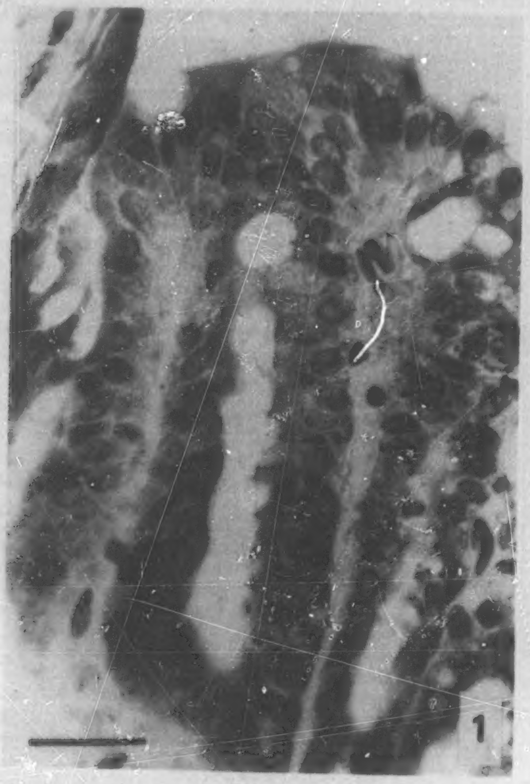

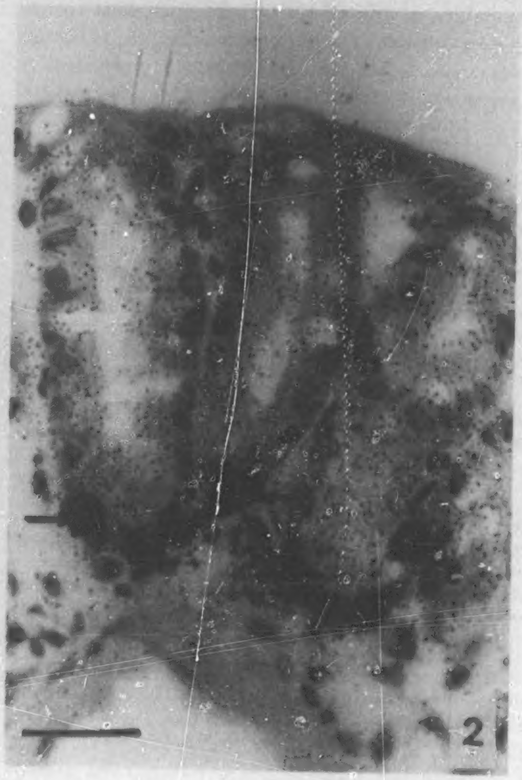

Figure 1.—Autoradiograph of rat colon cultured 2 days and pulsed with [^{3}H]dThd for 2 hr before harvest. Labeled cells are present in the lower third of the crypt columns. H & E. *Bar* = 30μ. × 576

Figure 2.—Autoradiograph of rat colon cultured 7 days and pulsed with [^{3}H]dThd for 2 hr before harvest. Labeled cells (*arrow*) are still confined to the lower third of the columns. H & E. *Bar* = 30μ. × 576

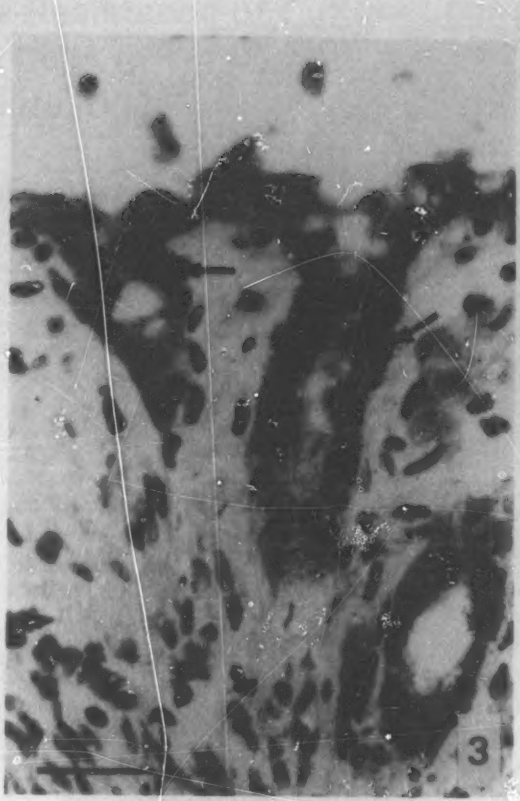

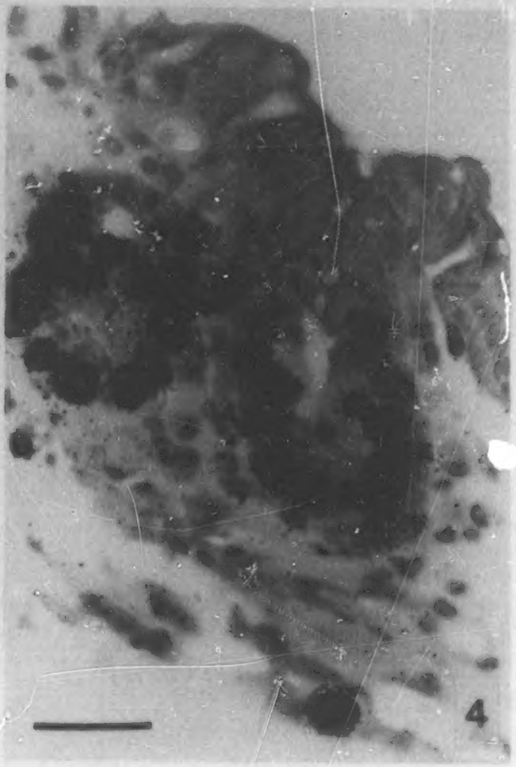

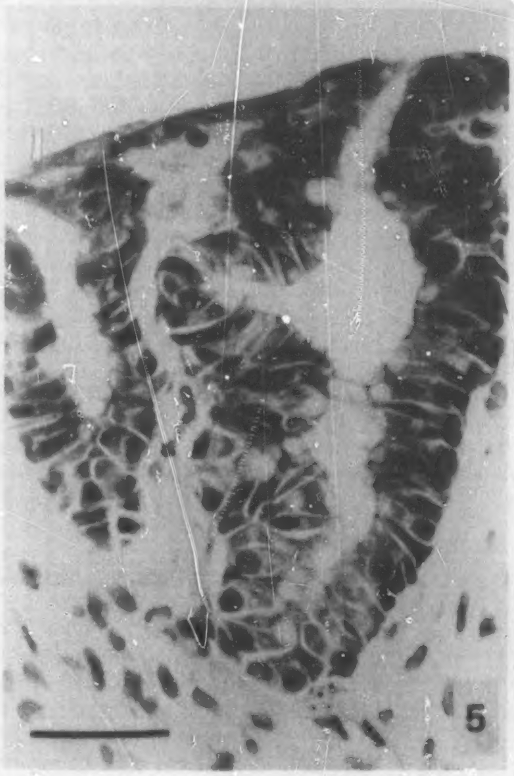

FIGURE 3.—Autoradiograph of DMH-exposed rat colon cultured 7 days and pulsed with [^{3}H]dThd for 2 hr before harvest. Crypt columns are shortened, and labeled cells are present in the upper portions of the crypt (*arrowheads*). H & E. *Bar* = 30μ. × 576

FIGURE 4.—Autoradiograph of an MNNG-exposed rat colon cultured 7 days and pulsed with [^{3}H]dThd for 2 hr before harvest. Crypts are distorted and labeled cells are present in the base as well as midsection of the crypt column. H & E. *Bar* = 30μ. × 576

FIGURE 5.—MNNG-exposed rat colon culture harvested 14 days after MNNG exposure. Atypical crypt column displays hypercellularity of mucosal epithelium and loss of polarity of cells. H & E. *Bar* = 35μ. × 576

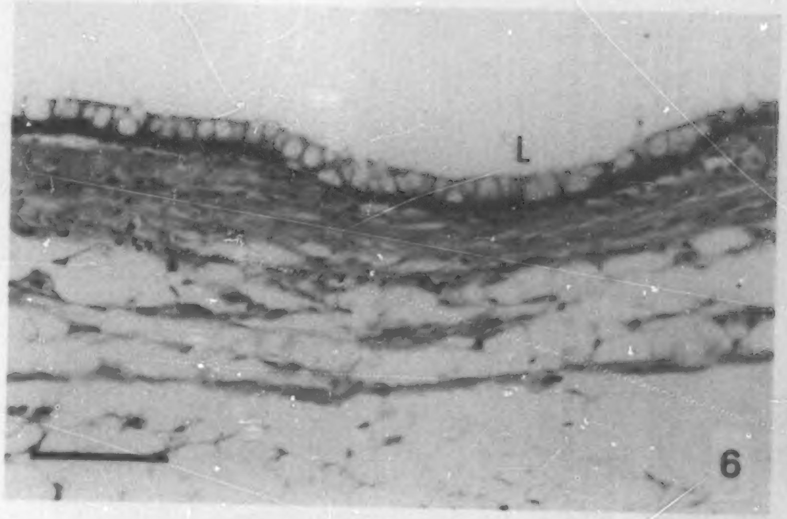

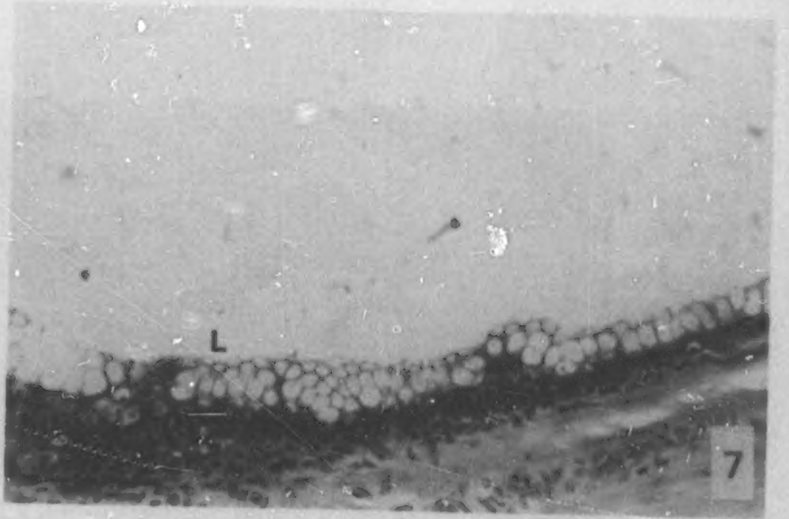

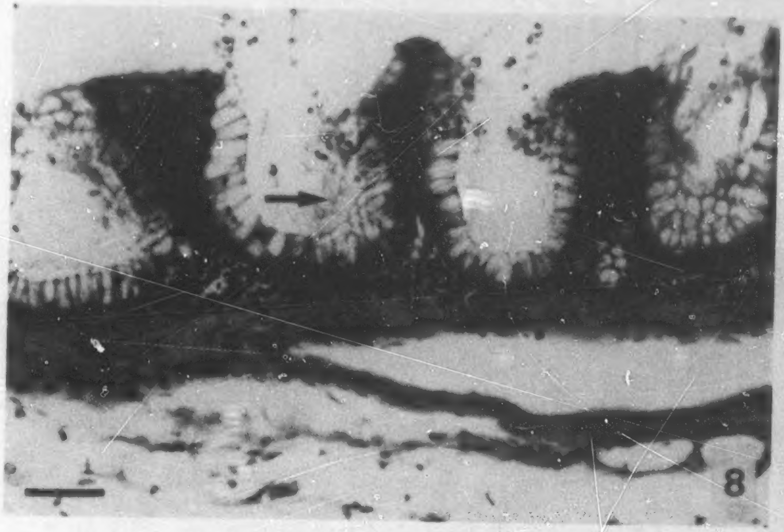

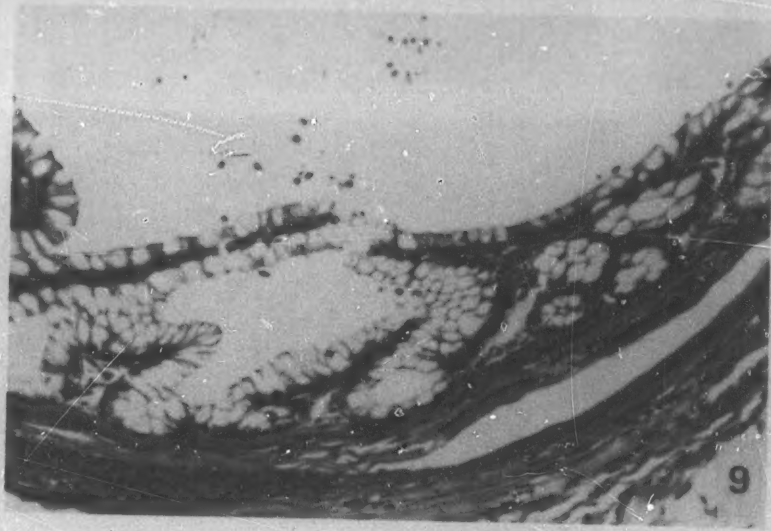

FIGURE 6.—Transplanted fragment of control 1-wk culture of rat colon at 3 mo after transplantation. Single layer of columnar epithelium lines the lumen (L) of a cystic structure. H & E. *Bar* = 130μ. × 150

FIGURE 7.—Transplanted fragment of MNNG-exposed 1-wk culture of rat colon at 4 mo after transplantation. Hyperplastic epithelium lines the cystic structure, and PAS-positive sections are abundant in the lumen (L). PAS. *Bar* = 130μ. × 150

FIGURE 8.—Transplanted fragment of MNNG-exposed 1-wk culture of rat colon at 5 mo after transplantation. Hyperactive mucosal glands have secreted PAS-positive material into the lumina of the crypt columns (*arrow*). PAS. *Bar* = 45μ. × 250

FIGURE 9.—Transplanted fragment of MNNG-exposed 1-wk culture of rat colon at 6 mo after transplantation. Hypercellular mucosal epithelium is present in dysplastic crypts. H & E. *Bar* = 45μ. × 250

Cross-Resistance of Cultured Murine Leukemia Vincristine-Resistant P388 Cells to Vinblastine, Vindesine, and Bis(*N*-ethylidene vindesine) Disulfide, Disulfate[1,2,3]

Lee J. Wilkoff[4] *and* **Elizabeth A. Dulmadge**[4,5]

ABSTRACT—Cultured P388 leukemia cells derived from vincristine (VCR)-resistant cell populations developed in vivo in (C57BL × DBA/2)F_1 mice (P388/VCR) were cross-resistant to vinblastine (VLB), vindesine (VDS), and bis(*N*-ethylidene vindesine)disulfide, disulfate (bis-VDS). Cross-resistance was a function of concentration and time of exposure. Cultured P388/VCR cells were more sensitive to $6.1\times10^{-5}M$ bis-VDS than to $6.1\times10^{-5}M$ VDS or to $6.1\times10^{-5}M$ VLB. Cultured P388 cells derived from VCR-sensitive P388 leukemia passaged in vivo (P388/0) were significantly more sensitive to VDS and bis-VDS than to VLB. This degree of difference in sensitivity was also a function of concentration and time of exposure.—JNCI 1982; 68:1023–1026.

VDS and bis-VDS are synthetic vinca alkaloids that are derivatives of VLB (*1, 2*). These agents have been developed in an attempt to produce an effective chemotherapeutic agent with less neurotoxicity than that of VCR and with less hematologic toxicity than that of VLB (*1–3*). VDS has been reported to have pharmacokinetic properties different from those of VCR and VLB (*1, 4*). However, VDS and bis-VDS have similar molecular structures, bind to tubulin, and have a similar spectrum of responses in experimental animal tumor systems (*1, 2, 4, 5*).

VDS has been shown to be an active agent for treatment of childhood acute lymphocytic leukemia in relapse (*6*). However, the problem of the degree of cross-resistance between VCR and VDS has not been resolved (*3*). Although Mathé et al. (*7*) and Tan (*8*) have reported that patients considered to be resistant to VCR responded to treatment with VDS, Krivit et al. (*3*) presented evidence of clinical cross-resistance between VCR and VDS in patients with acute lymphocytic leukemia. Schabel et al. (*9*) showed that P388 tumors resistant to VCR (P388/VCR) were resistant to treatment with VCR and VDS and were partially resistant to VLB and bis-VDS. To determine if the target tumor cells of P388 murine tumors, independent of host factors, are resistant to VLB, VDS, and bis-VDS, we compared the sensitivity of cultured P388/VCR and P388/0 cells to the three agents. Preliminary results of these studies were recently reported (*10*).

MATERIALS AND METHODS

The P388/VCR tumor was developed by treatment of (C57BL × DBA/2)F_1 (BD$2F_1$) mice bearing the P388 ascites tumor with 1 mg VCR/kg body weight on days 1, 5, and 9 after ip implantation of 10^6 or 10^7 P388 cells as previously described (*11*). Proliferating cultured P388/0 cells were developed from sensitive cell populations passaged in vivo in BD$2F_1$ mice, and cultured P388/VCR cells were established from resistant cell populations developed after the 16th in vivo passage (*11*).

The P388/0 and P388/VCR cells were propagated in DMEM (*12*) supplemented with 10% horse serum and 2-mercaptoethanol (*13*) as previously described (*11*). Under these conditions the leukemia cell populations exponentially proliferated with doubling times (mean±SD) of 14.2±2.0 hours for P388/0 and 16.5±1.9 hours for P388/VCR between cell densities of 5.0×10^4 and 1.0×10^6 cells/ml. At the time of these studies, the P388/VCR cell line had completed approximately 1,600 doublings of the population in culture.

The effect of VLB, VDS, or bis-VDS on the viability of proliferating cell populations was determined by initiating cultures at a cell density of 10^5 cells/ml in a total volume of 100 ml medium in spinner flasks 48 hours prior to the addition of drug. The spinner cultures were incubated at 37°C on a magnetic stirrer. Proliferating cell populations were exposed to selected drug concentrations for 1, 2, 4, 6, or 24 hours, and the number of surviving cells was determined by colony formation in semisolid medium.

The semisolid medium used was DMEM supplemented with 20% horse serum, 50 μM 2-mercaptoethanol, 100 mg sodium pyruvate/liter of medium, and a final concentration of 0.15% agarose type II (Sigma Chemical Co., St. Louis, Mo.). Cells from the drug-treated P388 cultures were seeded at 10,000, 1,000, and 100 cells/tube in quadruplicate, and the cells from the control cultures were seeded at 100 cells/tube in a series of eight tubes. The tubes were incubated for 10–12 days in 5% CO_2 atmosphere. Only colonies with 50 or more cells were counted (*14*). Colony formation efficiencies of control cultures were 66±3.1% for P388/0 and 82.1±1.7% for P388/VCR.

VLB, VDS, and bis-VDS were dissolved in sterile, dis-

ABBREVIATIONS USED: bis-VDS=bis(*N*-ethylidene vindesine)disulfide, disulfate; DMEM=Dulbecco's modified Eagle's minimum essential medium; P388/0=P388 leukemia sensitive to vincristine; P388/VCR=P388 leukemia resistant to vincristine; TMC=theoretical maximum concentration(s); VCR=vincristine; VDS=vindesine; VLB=vinblastine.

---

[1] Received September 4, 1981; approved January 15, 1982.

[2] Supported by Public Health Service contract N01CM-97309 from the Division of Cancer Treatment, National Cancer Institute.

[3] Animals were maintained under the guidelines set forth by the Southern Research Institute.

[4] Cell Biology Division, Kettering-Meyer Laboratory, Southern Research Institute, P.O. Box 3307-A, Birmingham, Ala. 35255.

[5] We thank Dr. H. E. Skipper and Dr. F. M. Schabel, Jr., for their helpful discussions and encouragment, Mr. John A. Burdeshaw for statistical analysis of the data, Dr. W. R. Laster and Mrs. Mary Trader for providing the P388 leukemia and vincristine-resistant P388 tumors, and Mrs. Carol S. Eldridge for the excellent technical assistance.

tilled, and deionized water and diluted with cell culture medium to predetermined concentrations.

The sensitivities of cultured P388/VCR and P388/0 cell populations were compared by chi-square analysis. The standard errors of the ratios of surviving fractions of P388/VCR and P388/0 cell populations were calculated as described by Kendall and Stuart (*15*).

The in vitro concentrations of the agents used in this study can be compared with the estimated TMC that can be obtained in the body fluids of mice, with the assumption of rapid, equal distribution in all fluids following the administration of a drug dose lethal to 10% of the mice (*16*). The TMC for VLB is 8.0 μg/ml, for VDS 2.6 μg/ml, and for bis-VDS 2.0 μg/ml.

RESULTS AND DISCUSSION

When proliferating P388/0 cell populations were exposed to VLB, VDS, and bis-VDS for periods up to 6 hours, the results indicated that VDS was the most cytotoxic and VLB was the least cytotoxic of the three agents (table 1). For instance, there was no detectable decrease in viability of the cell populations exposed to 8.0 μg VLB/ml throughout 6 hours. However, P388/0 cell populations exposed to 2.0 μg bis-VDS/ml for 6 hours exhibited a 2.2 $\log_{10}$ reduction in viability, and when these populations were exposed to 2.6 μg VDS/ml for 6 hours, a 2.4 $\log_{10}$ reduction in viability was detected. When the exposure period was increased to 24 hours, a maximum degree in reduction of viability of the cell populations (3.7 $\log_{10}$ reduction in viability) was observed for all three agents at these concentrations.

Cultured P388/VCR cells treated with VLB, VDS, or bis-VDS exhibited cross-resistance to the vinca alkaloids (table 1). When the sensitivity of P388/VCR cells is compared with that of P388/0 cells to the three agents after a 24-hour exposure period, it is evident that the surviving fractions of the P388/VCR cells treated with VLB, VDS, or bis-VDS were significantly greater than the surviving fractions of the P388/0 cells treated with the same agents. Furthermore, when the sensitivities of P388/VCR and P388/0 cell populations are compared to VDS and bis-VDS as a function of time, it is apparent that at each time interval the surviving fractions of the P388/VCR cells treated with 0.26 or 2.6 μg VDS/ml or 2.0 μg bis-VDS/ml were significantly greater than the surviving fractions of the P388/0 cells.

In another series of experiments we compared the sensitivities of P388/VCR and P388/0 cells to equimolar concentrations of VLB, VDS, and bis-VDS after a 6-hour exposure period (table 2). Cross-resistance to VLB was demonstrated at concentrations of 6.1×10^{-6} and 6.1×10^{-5} *M* when the surviving fractions of the P388/VCR cell

TABLE 1.—*Sensitivity of cultured P388/VCR and P388/0 cells to VLB, VDS and bis-VDS*[a]

Agent	Dose, μg/ml	Exposure period, hr	S_f[b] P388/VCR	S_f[b] P388/0	S_f P388/VCR:S_f P388/0 ±SE[c]	*P*-value[d]
VLB	0.8	1	400/400	400/400	1.0±0.0	NS
		2	400/400	400/400	1.0±0.0	NS
		4	400/400	400/400	1.0±0.0	NS
		6	400/400	400/400	1.0±0.0	NS
		24	268/400	660/40,000	40.6±2.1	<0.001
	8.0	1	400/400	400/400	1.0±0.0	NS
		2	400/400	400/400	1.0±0.0	NS
		4	400/400	400/400	1.0±0.0	NS
		6	400/400	400/400	1.0±0.0	NS
		24	292/400	8/40,000	3,650±1,295	<0.001
VSD	0.26	1	400/400	244/400	1.54±0.07	<0.001
		2	400/400	100/400	4.00±0.35	<0.001
		4	400/400	164/4,000	24.4±1.9	<0.001
		6	400/400	624/40,000	64.1±2.5	<0.001
		24	212/400	8/40,000	2,650±945	<0.001
	2.6	1	400/400	528/4,000	7.6±0.3	<0.001
		2	400/400	232/4,000	17.2±1.1	<0.001
		4	400/400	208/40,000	192±13	<0.001
		6	400/400	136/40,000	294±25	<0.001
		24	216/400	8/40,000	2,700±963	<0.001
bis-VDS	0.2	1	400/400	400/400	1.0±0.0	NS
		2	400/400	400/400	1.0±0.0	NS
		4	400/400	400/400	1.0±0.0	NS
		6	400/400	400/400	1.0±0.0	NS
		24	400/400	560/40,000	71.4±3.0	<0.001
	2.0	1	400/400	144/400	2.78±0.19	<0.001
		2	400/400	288/4,000	13.9±0.8	<0.001
		4	400/400	356/40,000	112±6	<0.001
		6	400/400	216/40,000	185±13	<0.001
		24	228/400	8/40,000	2,850±1,015	<0.001

[a] Proliferating cells were exposed to drugs, and the number of cells surviving drug treatment was estimated by assay in semisolid medium as described in "Materials and Methods."

[b] S_f=surviving fraction.

[c] Standard error of the ratio was estimated as described in (*15*).

[d] S_f's for each exposure period were compared with the use of chi-square analysis. NS=not significant.

populations were compared to the surviving fractions of the P388/0 cell populations. Cross-resistance to VDS and bis-VDS was detected at concentrations between 6.1×10^{-7} and 6.1×10^{-5} *M*. The data also indicate that cultured P388/VCR cells were more sensitive to 6.1×10^{-5} *M* bis-VDS than to 6.1×10^{-5} *M* VDS or VLB. In addition, we observed that at these equimolar concentrations, the P388/0 cell populations were significantly more sensitive to the VLB analogues than to VLB.

Cultured P388/VCR cell populations are not only cross-resistant to VLB, VDS, and bis-VDS (tables 1, 2) but also to adriamycin, adriamycin analogues (except cinerubin A), and actinomycin D (*11*), and are partially cross-resistant to VP16-213, a semisynthetic podophyllotoxin (*17*). Cultured P388/VCR cell populations were relatively sensitive to VP16-213 concentrations of 6.1×10^{-6} and 6.1×10^{-5} *M* (*17*). These VP16-213 concentrations (3.6 and 36.0 μg/ml) are physiologically attainable, since the TMC for VP16-213 is approximately 42 μg/ml (*17*). Although treatment of P388/VCR cell populations with 6.1×10^{-5} *M* (111 μg/ml) of bis-VDS for 6 hours resulted in a 1.2 $\log_{10}$ reduction in viability of the cell population, this concentration is relatively high since the TMC for this agent is 2.0 μg/ml (table 2).

Resistance and cross-resistance of cultured P388 cells to the vinca alkaloids was a function of concentration and time of exposure (table 1) (*11, 17*). Hill and Whelan (*18*) in a preliminary report indicated that cultured leukemia L5178Y cell populations resistant to VCR (L5178Y/VCR) are cross-resistant to VDS, and L5178Y cells resistant to VDS (L5178Y/VDS) are cross-resistant to VCR. They also reported that the presence or absence of cross-resistance appeared to be dose-dependent. Furthermore, they reported that both L5178Y/VCR and L5178Y/VDS cells were cross-resistant to VLB, adriamycin, and 4-epiadriamycin, and partially cross-resistant to actinomycin D.

Sweeney et al. (*19*) have reported that exposure of cultured Chinese hamster ovary cells to 2.8×10^{-8} *M* VDS, 8.3×10^{-8} *M* VLB, or 2.4×10^{-8} *M* VCR for 5 hours resulted in 40–50% accumulation of cells in mitosis. Although we did not determine accumulation of cells in mitosis, the results in table 2 indicate that 6.1×10^{-7} *M* VLB or VDS will produce 0.2 to 1.7 $\log_{10}$ reduction in viability of the P388/0 cell populations. We had previously reported that exposure of P388/0 cells to 6.1×10^{-8} or 6.1×10^{-7} *M* VCR for 6 hours would result in an 0.8 or 1.4 $\log_{10}$ reduction in viability of the P388/0 cell populations (*11*). The data reported by Sweeney et al. (*19*) with the use of 40–50% accumulation of mitotic cells as an end point, indicate that Chinese hamster ovary cells are less sensitive to VLB than to VDS or VCR (*19*). The data in table 2 and previously reported results with VCR (*11*), with the use of surviving cells in semisolid medium as an end point, indicate that P388/0 cells are also less sensitive to VLB than to VDS or VCR. Howard et al. (*20*) reported that the degree of mitotic arrest seen with the vinca alkaloids may depend on the cultured cell lines used. Their experiments with cultured leukemia L1210 cells showed that although VDS was the most effective agent in inhibiting cell proliferation and arresting cells in mitosis, VCR was less effective than VLB. Howard et al. (*20*) also reported evidence indicating that VDS had a greater effect than VLB or VCR on cyclic nucleotide metabolism in

TABLE 2.—*Sensitivity of cultured P388/VCR and P388/0 cells to various concentrations of VLB, VDS, and bis-VDS during a 6-hr exposure period*[a]

Drug concentration, *M*	VLB				VDS				bis-VDS			
	S_f[b]		S_f P388/VCR: S_f P388/0 ± SE[c]	*P*-value[d]	S_f[b]		S_f P388/VCR:S_f P388/0 ± SE[c]	*P*-value[d]	S_f[b]		S_f P388/VCR: S_f P388/0 ± SE[c]	*P*-value[d]
	P388/VCR	P388/0			P388/VCR	P388/0			P388/VCR	P388/0		
6.1×10^{-7}	252/400	252/400	1.0±0.1	NS	332/400	656/40,000	50.6±2.3	<0.001	284/400	620/4,000	4.6±0.2	<0.001
6.1×10^{-6}	352/400	292/4,000	12.1±0.7	<0.001	304/400	52/40,000	585±83	<0.001	184/400	86/40,000	214±26	<0.001
6.1×10^{-5}	308/400	200/4,000	15.4±1.1	<0.001	264/400	4/40,000	6,600±3,308	<0.001	224/4,000	4/40,000	460±282	<0.001

[a] Proliferating cells were exposed to drugs for 6 hr, and the number of cells surviving drug treatment was estimated by assay in semisolid medium as described in "Materials and Methods."

[b] S_f=surviving fraction.

[c] Standard error of the ratio was estimated as described in (*15*).

[d] S_f's for each exposure period were compared with the use of chi-square analysis. NS=not significant.

L1210 cells.

Our observation of cross-resistance of cultured P388/VCR cells to VLB, VDS, and bis-VDS (tables 1, 2) is in agreement with the cross-resistance observed by Schabel et al. (*9*) for the in vivo passaged P388/VCR tumor, and indicates that cross-resistance is a function of the cellular properties of the P388/VCR cells and independent of any host factors. The cause of resistance and cross-resistance to the vinca alkaloids has not been defined. Reports have indicated that several factors may be involved, such as decreased drug transport across cell membranes (*21-24*), decreased drug retention by cells (*21, 24-29*), decreased binding affinities to target macromolecules (*24, 30*), altered intracellular distribution (*24, 25, 30*), and changes in cell membrane structure (*31, 32*). Because VLB and VDS are agents of clinical interest and because bis-VDS may have potential clinical utility, this cell culture system should provide an experimental model for investigation of the cause of resistance and cross-resistance to the vinca alkaloids.

REFERENCES

(*1*) Dyke RW, Nelson RL. Phase I anti-cancer agents. Vindesine (desacetyl vinblastine amide sulfate). Cancer Treat Rev 1977; 4:135-142.

(*2*) Gerzon K. Dimeric catharanthus alkaloids. In: Cassady JM, Douros JD, eds. Medicinal chemistry: A series of monographs. New York: Academic Press, 1980:271-317.

(*3*) Krivit W, Anderson J, Chilcote R, Pyesmany A, Chard R, Hammond D. A study of the cross-resistance of vincristine and vindesine in reinduction therapy for acute lymphocytic leukemia in relapse. Am J Pediatr Hematol Oncol 1980; 2:217-221.

(*4*) Owellen RJ, Root MA, Hains FO. Pharmacokinetics of vindesine and vincristine in humans. Cancer Res 1977; 37:2603-2607.

(*5*) Owellen RJ, Hartke CA, Dickerson RM, Hains FO. Inhibition of tubulin-microtubule polymerization by drugs of the vinca alkaloid class. Cancer Res 1976; 36:1499-1502.

(*6*) Krivit W, Hammond D. A phase II study by the children's cancer study group. In: Siegenthaler W, Luthy R, eds. Current chemotherapy. Proceedings of the 10th International Congress of Chemotherapy. Washington, D.C.: Am Soc Microbiol, 1978:1331-1334.

(*7*) Mathé G, Misset JL, De Vassal F, et al. Phase II clinical trial with vindesine for remission induction in acute leukemia, blastic crisis of chronic myeloid leukemia, lymphosarcoma, and Hodgkin's disease: Absence of cross-resistance with vincristine. Cancer Treat Rep 1978; 62:805-808.

(*8*) Tan C. Clinical and pharmacokinetic studies of vindesine in 50 children with malignant diseases. In: Siegenthaler W, Luthy R, eds. Current chemotherapy. Proceedings of the 10th International Congress of Chemotherapy. Washington, D. C. : Am Soc Microbiol, 1978:1326-1328.

(*9*) Schabel FM Jr, Skipper HE, Trader MW, Laster WR Jr, Corbett TH, Griswold DP Jr. Concepts for controlling drug-resistant tumor cells. In: Mouridsen HT, Palshof T, eds. Breast cancer. Experimental and clinical aspects. Oxford: Pergamon Press, 1980:199-211.

(*10*) Wilkoff LJ, Dulmadge EA. Cultured leukemia P388 cells resistant to vincristine (P388/VCR); cross-resistance to vinblastine (NSC-49842), vindesine (NSC-245467), and bis-(*N*-ethylidene vindesine)-disulfide, disulfate (NSC-277096). Proc Am Assoc Cancer Res 1981; 22:239.

(*11*) ———Resistance and cross-resistance of cultured leukemia P388 cells to vincristine adriamycin, adriamycin analogs, and actinomycin D. JNCI 1978; 61:1521-1524.

(*12*) Morton HJ. A survey of commercially available tissue culture media. In Vitro 1970; 6:89-108.

(*13*) Broome JD, Jeng MW. Growth stimulation of mouse leukemia cells by thiols and disulfides in vitro. J. Natl Cancer Inst 1972; 49:579-581.

(*14*) Courtenay VD. A soft agar colony assay for Lewis lung tumour and B16 melanoma taken directly from the mouse. Br J Cancer 1976; 34:39-45.

(*15*) Kendall MG, Stuart A. The advanced theory of statistics. Vol 1. London: Griffin, 1963:232.

(*16*) Schabel FM Jr, Skipper HE, Trader MW, Wilcox WS. Experimental evaluation of potential anticancer agents. XIX. Sensitivity of nondividing leukemia cell populations to certain classes of drugs in vitro. Cancer Chemother Rep 1965; 48:17-30.

(*17*) Wilkoff LJ, Dulmadge EA. Partial cross-resistance of cultured murine leukemia vincristine-resistant P388 cells to 4'-demethylepipodophyllotoxin ethylidene-β-D-glucoside. Proc Soc Exp Biol Med 1980; 164:51-56.

(*18*) Hill BT, Whelan RD. In vitro isolation and characterization of lines of L5178Y lymphoblasts resistant to vincristine or vindesine. Proc Am Assoc Cancer Res 1981; 22:261.

(*19*) Sweeney MJ, Boder GB, Cullinan GJ, et al. Antitumor activity of deacetyl vinblastine amide sulfate (vindesine) in rodents and mitotic accumulation studies in culture. Cancer Res 1978; 38:2886-2891.

(*20*) Howard SM, Theologides A, Sheppard JR. Comparative effects of vindesine, vinblastine, and vincristine on mitotic arrest and hormonal response of L1210 leukemia cells. Cancer Res 1980; 40:2695-2700.

(*21*) Brockman RW, Yagisawa Y, Ling V, et al. Modes of acquiring resistance to chemotherapeutic agents. In: Siegenthaler W, Luthy R, eds. Current chemotherapy. Proceedings of the 10th International Congress of Chemotherapy. Washington, D.C.: Am Soc Microbiol, 1978:97-102.

(*22*) Biedler LJ, Riehm H. Cellular resistance to actinomycin D in Chinese hamster cells in vitro: Cross-resistance, radioautographic and cytogenetic studies. Cancer Res 1970; 30:1174-1184.

(*23*) Riehm H, Biedler JL. Cellular resistance to daunomycin in Chinese hamster cells in vitro. Cancer Res 1971; 31:409-412.

(*24*) DiMarco A. Mechanism of action and mechanisms of resistance to antineoplastic agents that bind to DNA. In: Schabel FM Jr, ed. Fundamentals in cancer chemotherapy. Basel: Karger, 1978:216-227.

(*25*) Danø K. Experimentally developed cellular resistance to daunomycin. Acta Pathol Microbiol Scand A (Suppl N) 1976; 256:11-80.

(*26*) Kessel D, Wodinsky J. Uptake in vivo and in vitro of actinomycin D by mouse leukemias as factors in survival. Biochem Pharmacol 1968; 17:161-164.

(*27*) Kessel D, Botterill V, Wodinsky I. Uptake and retention of daunomycin by mouse leukemic cells as factors in drug response. Cancer Res 1968; 28:938-941.

(*28*) Skovsgaard T. Mechanism of cross-resistance between vincristine and daunorubicin in Ehrlich ascites tumor cells. Cancer Res 1978; 38:4722-4727.

(*29*) Inaba M, Kobayashi H, Sakura Y, Johnson RK. Active efflux of daunorubicin and adriamycin in sensitive and resistant sublines of P388 leukemia. Cancer Res 1979; 39:2200-2203.

(*30*) Schwartz HS, Kanter AM. Cell interactions: Determinants of selective toxicity of adriamycin (NSC-123127) and daunorubicin (NSC-82151). Cancer Chemotherap Rep 1975; 6(part 3):107-113.

(*31*) Bosmann BH, Kessel D. Altered glycosidase levels in drug resistant mouse leukemias. Mol Pharmacol 1970; 6:345-349.

(*32*) Bosmann BH. Mechanisms of cellular drug resistance. Nature 1971; 233:566-569.

Intracellular Adriamycin Levels and Cytotoxicity in Adriamycin-Sensitive and Adriamycin-Resistant P388 Mouse Leukemia Cells[1,2,3,4]

Ram Ganapathi,[5,6] **William Reiter,**[5,7] *and* **Awtar Krishan**[5]

ABSTRACT—Adriamycin (ADR) (NSC-123127) uptake and retention in ADR-sensitive P388 leukemia (P388/S) and ADR-resistant P388 leukemia (P388/R) cells were compared by fluorometry and laser flow cytometry (FCM) and were correlated with cytotoxic effects. Drug levels in P388/R cells treated in vitro with ADR (1–10 μg/ml) were twofold to fourfold lower than were levels in similarly treated P388/S cells. FCM analysis of P388/S and P388/R cells exposed in vitro to ADR showed qualitative and quantitative differences in ADR fluorescence profiles of drug-treated cells (1–5 μg/ml) but not of the isolated nuclei (0.5–10 μg/ml). Drug-induced perturbations in cell cycle traverse and chromosome aberrations were seen in P388/S but not in P388/R cells treated with 0.5–5 μg ADR/ml in vitro or 4–8 mg ADR/kg in vivo. The role of FCM in rapidly comparing and quantitating cellular ADR fluorescence profiles of ADR-sensitive and ADR-resistant tumors was demonstrated.—JNCI 1982; 68:1027–1032.

The rapid emergence of drug-resistant tumor clones continues to be a serious challenge in cancer chemotherapy. A number of biochemical and pharmacological studies have suggested that alterations in intracellular drug transport and retention, metabolic pathways, and target enzyme production may be responsible for drug resistance at the cellular level (*1–4*).

ADR and DAU are important anthracycline antibiotics with clinical activity against a wide variety of human cancers (*5, 6*). A number of recent studies on ADR- and DAU-resistant Ehrlich ascites (*7, 8*) and P388 mouse tumors (*9–11*) have suggested that anthracycline resistance is due to the reduced intracellular drug uptake and an enhanced drug efflux mechanism (*7, 8, 12, 13*).

Tumor cell populations are highly heterogeneous and contain subpopulations that differ in their response to the cytotoxic action of anthracyclines. Thus an assay system that will analyze drug uptake and retention in individual tumor cells (compared to conventional procedures for drug quantitation in cell homogenates) would be ideal for studying patterns of drug resistance at the cellular level. Some of our recent studies on detection and quantitation of cellular anthracycline content by direct laser excitation of individual cells have demonstrated the feasibility of this methodology for the study of anthracycline uptake and retention in tumor cell populations (*14*).

In the present study, we have compared intracellular ADR transport and retention by fluorometric and FCM methods in P388/S and resistant P388/R leukemia cells. We have also compared intracellular ADR levels with ADR-induced effects on cell cycle traverse, cytotoxicity, and induction of chromosome aberrations.

MATERIALS AND METHODS

P388/S and P388/R mouse leukemia cell lines (*9*) were obtained from Dr. Randall K. Johnson, Arthur D. Little, Inc., Cambridge, Mass. P388/S and P388/R tumor cells were maintained in female DBA/2 mice by weekly ip transplantation. Ascites from the ADR-sensitive and ADR-resistant tumors were also established as suspension cultures in RPMI-1640 tissue culture medium (Grand Island Biological Co., Grand Island, N.Y.) supplemented with 10% FCS (Flow Laboratories, Inc., McLean, Va.), 10 μm 2-mercaptoethanol, and the antibiotics penicillin and streptomycin.

Suspension cultures of P388/S and P388/R cells were exposed to ADR (0.1–5.0 μg/ml) for 24 hours, and cell counts were determined by trypan blue dye exclusion. Cultures treated with ADR (0.01–5.0 μg/ml) for 3 hours were centrifuged, washed twice in drug-free media, and plated (5×10^4 cells/plate) in 35×10-mm petri dishes with RPMI-1640 supplemented with 20% FCS, 10 μm 2-mercaptoethanol, and 0.3% agar. For continuous drug exposure, cells were plated with ADR (0.01–5.0 μg/ml) as above. After 8 days of incubation in a humidified 5% CO_2 atmosphere, colonies (>50 cells) in untreated control and ADR-treated plates were counted under an inverted tissue culture microscope. Plating efficiency of control P388/S and P388/R cells under these conditions was 16 and 4%, respectively.

P388/S and P388/R tumor cells (2×10^6/ml) from DBA/2 donors were suspended in Eagle's minimum essential

---

ABBREVIATIONS USED: ADR=adriamycin; DAU=daunomycin; FCM=flow cytometry; FCS=fetal calf serum; P388/R=ADR-resistant P388 leukemia; P388/S=ADR-sensitive P388 leukemia.

---

[1] Received September 4, 1981; accepted January 15, 1982.

[2] Supported by Public Health Service grants CA-14395 and CA-29360 from the National Cancer Institute.

[3] A preliminary report of this work was presented at the seventy-first annual meeting of the American Association for Cancer Research held May 28–31, 1980, in San Diego, California.

[4] Animals were maintained under the guidelines of the National Research Council.

[5] Comprehensive Cancer Center for the State of Florida and Department of Oncology, R-71, University of Miami School of Medicine, P.O. Box 016960, Miami, Fla. 33101.

[6] *Address reprint requests to* Dr. Ganapathi at his *present address:* Department of Molecular and Cellular Biology, Research Division, Cleveland Clinic Foundation, 9500 Euclid Ave., Cleveland, Ohio 44106.

[7] *Present address:* Department of Internal Medicine, University of Miami School of Medicine.

medium supplemented with 10% FCS and incubated with ADR (1.0 and 10 μg/ml) at 37°C. Aliquots of 2×10^6 cells were removed at various times (30 min–4 hr), centrifuged, washed twice in 10 ml of cold 0.85% sodium chloride, and extracted with 50% ethanol–0.3 *N* hydrochloric acid and centrifuged (*15*). ADR fluorescence in the supernatant was determined at excitation and emission wavelengths of 470 and 585 nm, respectively, in an Aminco-Bowman Spectrophotofluorometer (American Instrument Co., Silver Spring, Md.). ADR content was computed from standard curves prepared with ADR hydrochloride (NSC-123127).

Female DBA/2 mice implanted with 10^6 P388/S and P388/R cells were treated ip on day 5 with 4 or 8 mg ADR/kg in 0.85% sodium chloride. Mice (2/group) were killed 1–4 hours after treatment, and intracellular ADR fluorescence was determined in duplicate P388/S and P388/R samples as outlined before.

In vitro cultures of ADR-sensitive and ADR-resistant tumor cells were incubated with 1.0 and 5 μg ADR/ml in RPMI-1640 supplemented with 10% FCS. Aliquots of cells after 1 and 3 hours of incubation were centrifuged at 80×*g* in a refrigerated centrifuge, resuspended in cold drug-free medium, and analyzed for intracellular ADR fluorescence by FCM (*14*). In this procedure, single cells in a sheath flow were excited by a monochromatic, 488-nm laser beam, and the light scatter or fluorescence emission was quantitated and scaled in a pulse-height analyzer. Intracellular ADR fluorescence was analyzed in a Coulter Electronics TPS-1 LL cell sorter (Coulter Electronics, Inc., Hialeah, Fla.) equipped with a Spectraphysics model 164-08 laser tuned to deliver 1.5 W at 488 nm. Data were collected on a TPS-1 data analysis module connected to a Hewlett-Packard 9845A desk-top computer. ADR-treated P388/S and P388/R cells (in vivo) were stained with propidium iodide–hypotonic citrate (*16*) and were analyzed for cell cycle distribution by FCM. Details of our procedures for laser excitation of intracellular ADR fluorescence, cell cycle analysis, standardization of instrumentation, and data analysis have been described (*14*).

Nuclear isolation was achieved by a 15-minute exposure of cells to 0.03% Nonidet P40 (Bethesda Research Laboratories, Inc., Gaithersburg, Md.) in Hanks' balanced salt solution. This procedure resulted in cell lysis and release of nuclei, which were washed twice and recovered by centrifugation at 200×*g*. Isolated nuclei were incubated at 37°C with ADR (0.5, 1.0, and 10 μg/ml). Nuclei were recovered by centrifugation, washed twice, and analyzed for ADR content by fluorimetry (after 50% ethanol–0.3 *N* hydrochloric acid extraction) and FCM.

For cytogenetic analysis, log-phase cultures (10^6 cells/ml) of P388/S and P388/R cells were treated with ADR (0.1, 1.0, and 5.0 μg/ml) for 6–8 hours. Then, 0.05 μg vinblastine sulfate (Eli Lilly & Co., Indianapolis, Ind.)/ml was added to the cultures for 2–4 hours before termination of the incubation. Cells were centrifuged and washed in Hanks' balanced salt solution, exposed to 0.075 *M* potassium chloride for 10 minutes at room temperature for hypotonic swelling, and then fixed in methanol–acetic acid (3:1 vol/vol) for 1 hour. Air-dried smears were stained with carbol fuchsin and analyzed for chromosome damage.

RESULTS

The effect of ADR on proliferation of P388/S and P388/R cells in suspension culture and as colonies in soft agar is shown in table 1. In suspension cultures of P388/R cells exposed to ADR (0.1–5.0 μg/ml) for 24 hours, no significant decrease in cell count (except at 5.0 μg/ml) was noted in contrast to markedly (drug concentration-dependent) reduced counts in P388/S cells. In the soft-agar assay, P388/S cells exposed to 0.01 μg ADR/ml for 3 hours (or continuously for 8 days) had only 8–10% (of control) colonies; however, P388/R had 100% (of control). No colonies were seen in P388/S cells exposed to higher concentrations of ADR (0.1–5.0 μg/ml) for 3 hours or continuously. In contrast, in P388/R cells exposed to 0.1 μg ADR/ml for 3 hours or continuously, the number of colonies counted were 88 and 64% of the control, respectively. Exposure of P388/R cells to 1.0 μg ADR/ml for 3 hours reduced the number of colonies to 18% of the control, whereas after exposure for 8 days (in soft agar), no colonies were seen. At a higher concentration of 5.0 μg ADR/ml, no colony growth was observed in P388/R treated for 3 hours or continuously. From these data, P388/R cells clearly demonstrated resistance to the cytotoxic effects of ADR in both the trypan blue dye exclusion procedure and the soft-agar colony-forming assay.

The uptake and intracellular retention of ADR (determined by fluorometric methods) by P388/S and P388/R cells treated in vitro with 1 and 10 μg ADR/ml are shown in text-figure 1. Differences in uptake were evident by the 1st hour of incubation and reached maximum values after 4 hours. Intracellular ADR levels in P388/S cells between 1 and 4 hours of incubation were twofold to fourfold higher than intracellular ADR levels in P388/R cells. In P388/S and P388/R cells treated in vivo with 4 and 8 mg ADR/kg, drug uptake and subsequent retention by P388/S cells were twofold to fourfold higher than were uptake and retention by similarly treated P388/R cells (table 2).

TABLE 1.—*Effect of ADR on growth and colony-forming ability of P388/S and P388/R cells*

ADR concentration, μg/ml	Cell counts[a]		Colony assay[b]			
			P388/S		P388/R	
	P388/S[c]	P388/R	3 hr[d]	Continuously	3 hr	Continuously
0.01	—	—	10	8	100	100
0.1	38	118	2	0	88	64
1.0	13	98	0	0	18	0
5.0	0	50	0	0	0	0

[a] Cultures in triplicate were treated with ADR for 24 hr, and trypan blue dye-excluding cells were counted in a hemacytometer. —=not done.

[b] P388/S and P388/R cells were treated with ADR for 3 hr or continuously for 8 days and plated as outlined in "Materials and Methods."

[c] Number of dye-excluding cells in treated populations is expressed as a percentage of untreated controls.

[d] Number of colonies (>50 cells) after 8 days of incubation is expressed as a percentage of control.

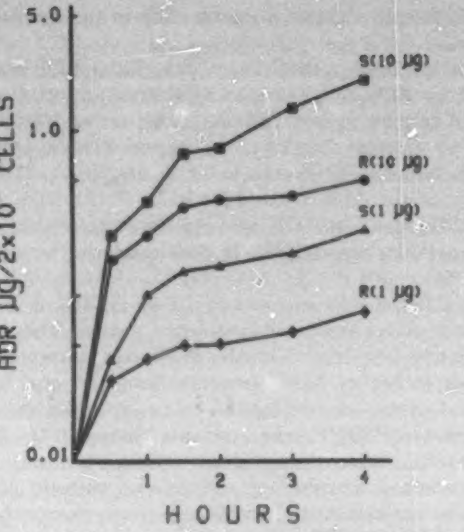

TEXT-FIGURE 1.—ADR uptake and retention profiles of P388/S (S; ▲, ■) and P388/R (R; ♦, ●) cells in vitro in the presence of 1 and 10 µg ADR/ml. Cellular ADR content was determined as outlined in "Materials and Methods." Each value represents the mean of three separate determinations; SD <10%.

Cellular drug fluorescence profiles of P388/S and P388/R cells incubated with ADR and analyzed by FCM are shown in text-figure 2. In cells treated with 1 µg ADR/ml and analyzed after 1 hour (text-fig. 2A), weak fluorescent signals could be detected in both P388/S and P388/R, and the peak of fluorescence distribution was at channel 15. In P388/S and P388/R cells, 72 and 18% of the population, respectively, could be detected (between channels 10 and 128) on the basis of their drug fluorescence. After 3 hours of incubation with 1 µg ADR/ml (text-fig. 2B), drug fluorescence in P388/S cells was twofold higher (fluorescent peak shifted from channel 15 to 30) than was fluorescence in P388/R (no major shift in fluorescent peak). In the drug-sensitive population, nearly 100% of the cells could be detected on the basis of ADR fluorescence as compared to only 25% of the cells in the drug-resistant subline.

Text-figure 2C shows the cellular drug fluorescence profiles of P388/S and P388/R cells treated with 5 µg ADR/ml for 1 hour. In both populations, approximately 80% of the cells could be detected by their fluorescence. However, in the ADR-sensitive population, cells were twofold more fluorescent (peak, channel 30) than cells in the ADR-resistant population (peak, channel 15). After 3 hours of incubation with 5 µg ADR/ml (text-fig. 2D), 100% of the P388/S cells could be detected by their fluorescence as compared to only 74% of similarly treated P388/R. Further, P388/S cells treated with ADR for 3 hours were threefold more fluorescent (peak, channel 100) than were P388/S cells treated with the same dose of ADR but for 1 hour (peak, channel 30). In contrast, P388/R cells treated with ADR for 3 hours

TABLE 2.—*ADR levels in P388/S and P388/R cells treated in vivo*[a]

Time, hr[b]	ADR concentration, µg/5×10^6 cells, after mice were treated with:			
	4 mg ADR/kg body wt		8 mg ADR/kg body wt	
	P388/S	P388/R	P388/S	P388/R
1	0.61±0.03	0.32±0.10	1.55±0.02	0.37±0.03
2	0.67±0.10	0.18±0.02	0.99±0.05	0.27±0.01
4	0.44±0.06	0.23±0.06	0.79±0.05	0.3±0.01

[a] Female DBA/2 mice were implanted ip with 1×10^6 P388/S or P388/R cells on day 0. On day 5, mice were treated ip with ADR in 0.85% sodium chloride.

[b] Tumor cells were retrieved at times indicated and analyzed as outlined in "Materials and Methods."

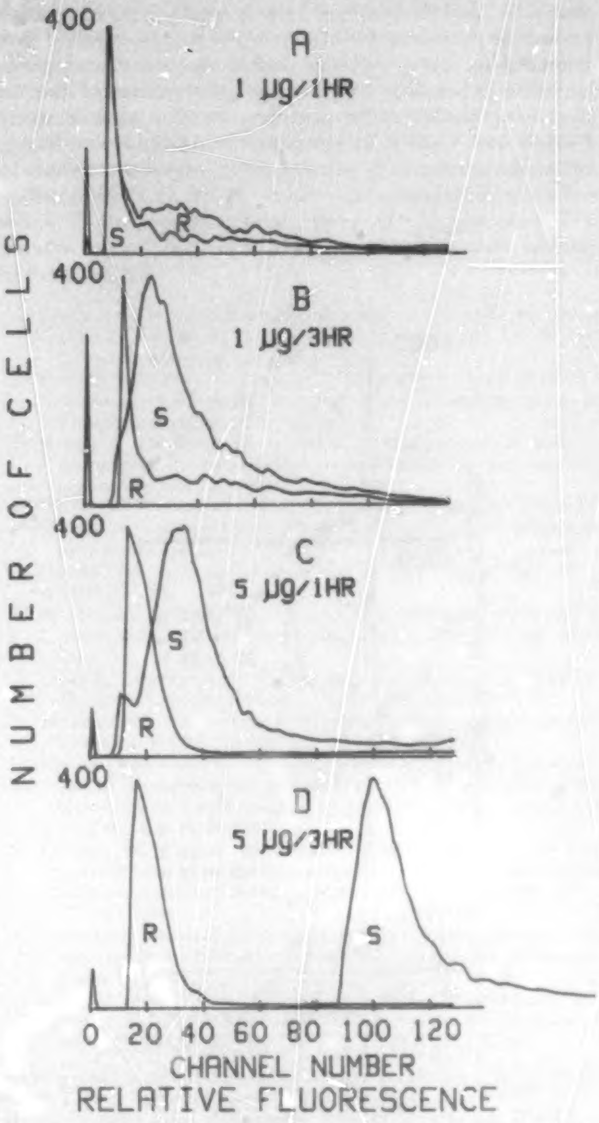

TEXT-FIGURE 2.—ADR fluorescence profiles of sensitive (S) and resistant (R) cells treated in vitro with 1 µg ADR/ml for 1 and 3 hr (A and B, respectively) and with 5 µg ADR/ml for 1 and 3 hr (C and D, respectively). Fluorescence amplification used was 50. Photomultiplier high-voltage setting was 500, and laser output at 488 nm was 0.75 W.

(peak, channel 20) showed only a marginal increase in the amount of cellular ADR fluorescence as compared to P388/R cells treated with the same dose of ADR but for 1 hour (peak, channel 15).

ADR-induced perturbations in cell cycle traverse were studied in P388/S and P388/R tumor cells from mice treated with 4 mg ADR/kg. As shown in text-figure 3, after 12 hours of drug treatment, accumulation of cells in the S-phase and G_2 phase was seen in P388/S (text-fig. 3B) but not in P388/R (text-fig. 3C) cells, for which the distribution was similar to that of an untreated control (text-fig. 3A).

In an earlier study (*17*), we reported that human lymphoblasts CCRF-CEM, human peripheral blood mononuclear cells, and P388 mouse leukemia cells exposed to ADR in vitro or in vivo and subsequently stained with the DNA-intercalating dye propidium iodide show a concentration and time-dependent reduction in fluorescence of the nuclear-propidium iodide complex. In the present study, P388/S and P388/R cells exposed to ADR in vivo (8 mg/kg) were subsequently stained with propidium iodide for cell cycle distribution analysis by FCM. In P388/S cells, a 15% reduction in the peak channel of propidium iodide nuclear fluorescence was seen after 4–8 hours, whereas P388/R cells showed no peak shift in the nuclear fluorescence.

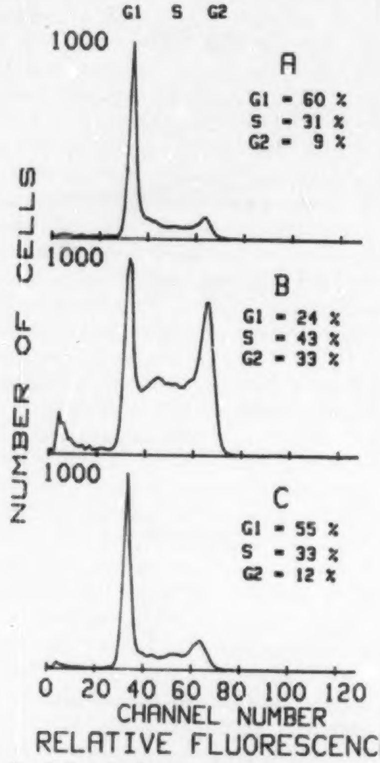

TEXT-FIGURE 3.—Cell cycle phase distributions of 12-hour, untreated control P388/S cells (A) and of ADR-treated (4 mg/kg) P388/S (B) and P388/R (C) cells 12 hr after treatment in vivo. DNA distribution histograms of 12-hr control P388/R cells were similar to the histogram 3A, except for an 8% decrease in the proportion of S-phase cells and a corresponding increase in cells with G_1 DNA content. Day 5 tumor-bearing mice were treated ip with drug, and retrieved tumor cells were analyzed by FCM after being stained with propidium iodide.

To test the hypothesis that intracellular ADR fluorescence between ADR-sensitive and ADR-resistant cells was related to differences in intracellular transport and retention and not to nuclear binding, we exposed isolated nuclei of P388/S and P388/R cells to 0.5, 1, and 10 µg ADR/ml and analyzed the ADR-treated nuclei by fluorimetry and FCM. No differences in ADR nuclear fluorescence were seen between P388/S and P388/R cells analyzed by either technique.

In P388/S cells exposed to 0.1 µg ADR/ml for 8 hours, mitotic plates were rare, and when present, they contained primarily fragmented and agglutinated chromosomes. Exposure to higher ADR concentrations (1.0 and 5.0 µg/ml) caused chromosomal agglutination and pulverization. In contrast in P388/R cells, concentrations of 0.1, 1.0, and 5.0 µg ADR/ml had no significant effect on mitotic index or chromosome morphology. Occasional mitotic plates containing agglutinated chromosomes were observed only at a dose of 5.0 µg ADR/ml.

DISCUSSION

Various mechanisms by which cells resist the cytotoxic effects of the anthracycline antibiotics DAU and ADR have been suggested (*3, 7, 8, 12, 13, 18, 19*). Studies on mouse tumor cells resistant to DAU and ADR have suggested specific mechanisms for drug resistance (*7, 8, 12, 13, 19*).

Fluorometric data from the present study show that intracellular uptake and retention of ADR were twofold to fourfold lower in the ADR-resistant cells than in the ADR-sensitive cells similarly treated. These results agree with those of earlier reported studies on ADR- and DAU-resistant mouse tumors (*7, 8, 12*). Comparison of drug uptake profiles (text-fig. 1) shows that, although intracellular ADR levels in P388/S and P388/R cells were similar after 30 minutes of incubation, on continued incubation, P388/S cells accumulated significantly more ADR than did P388/R cells. A 10-fold increase in extracellular ADR concentration resulted in an 8-fold increase in intracellular ADR levels in P388/S cells in contrast to a 5-fold intracellular increase of ADR by the P388/R population. Comparison of the in vivo ADR uptake profiles confirmed the in vitro differences in ADR uptake and retention by the P388/S and the P388/R cells. These results suggest that the salient difference between ADR-sensitive and ADR-resistant cells is the reduced ability of the ADR-resistant cells to transport and accumulate ADR.

Results from the FCM analysis of ADR fluorescence (text-fig. 2) in the P388/S and P388/R cells confirmed the in vitro fluorometric studies and further showed qualitative and quantitative differences in ADR uptake patterns between the two cell types. When P388/S cells were exposed to 1 and 5 µg ADR/ml, nearly every cell in the population was fluorescent after 3 hours, and the mean peak value of the fluorescence was much higher than that of P388/R cells similarly treated. In the P388/R population, the number of cells detectable was threefold higher in cultures exposed to 5 µg ADR/ml than in cultures treated with 1 µg ADR/ml, but the amount of cellular ADR fluorescence did not signif-

best copy available

icantly increase with the increase in ADR concentration. Unlike the ADR-sensitive population, the ADR-resistant cells showed no significant increase in the percentage of cells detectable by FCM with continued incubation (1 vs. 3 hr) with ADR. These results suggest that, in contrast to ADR-resistant cells, ADR transport and accumulation by the ADR-sensitive cells are more rapid and concentration-dependent.

Low intracellular ADR levels and possibly reduced ADR retention have been suggested as mechanisms for resistance to the cytotoxic effects of ADR (*7, 8, 12, 13*). Our studies by dye exclusion and soft-agar colony assay (table 1) indicate that P388/R cells are a hundredfold more resistant than P388/S cells to the cytotoxic effects of ADR. In a previous study (*12*), the basis of which was an in vivo bioassay, P388/R cells were shown to be 800-fold more resistant than were their ADR-sensitive counterparts. This quantitative discrepancy in resistance is probably due to the 1-hour drug exposure in the Inaba and Johnson study (*12*) in contrast to the 3-hour exposure in the present study. A number of other studies (*4, 14, 20*) and the one being reported here indicate that ADR is slowly transported across the cell membrane, and near steady-state levels of ADR are achieved in 2-4 hours. Our results indicate that on prolonged ADR exposure, cytotoxic ADR levels are also accumulated by P388/R cells and are expressed as decreases in colony-forming ability. Resistance to the cytotoxic effects of ADR in P388/R cells were further evident in the lack of ADR-induced cell cycle perturbations (text-fig. 3) and in chromosome damage. In contrast, P388/S cells showed the classical, concentration-dependent effect of ADR on cell cycle traverse, chromosome damage and cytotoxicity (*4, 21-23*).

Cytotoxic effects of ADR are suggested to occur after intercalation of the drug with DNA (*18, 24*). In the present study, fluorometric and FCM analyses of isolated nuclei from P388/S and P388/R cells incubated with ADR (0.5-10 μg/ml) showed no differences between the two cell types in the amount of nucleus-associated drug. Further, unlike the qualitative and quantitative differences seen in the cellular ADR fluorescence profiles of live cells (text-fig. 2) analyzed by FCM, no differences in nucleus-associated ADR were seen when ADR-treated isolated nuclei of P388/S and P388/R cells were analyzed. This result agrees with that of a study on the binding of DAU (0.05 and 0.1 μg/ml) to isolated nuclei of ADR-sensitive and ADR-resistant P388 cells (*12*). Reports on nuclear binding of DAU in DAU-sensitive and DAU-resistant Ehrlich ascites cells have been variable (*25, 26*). Dano (*25*) reported no significant difference in DAU binding in isolated nuclei of wild-type DAU-sensitive (near tetraploid) and in DAU-resistant (hyperdiploid) Ehrlich ascites tumor cells. Similarly, in comparing DAU binding in cell homogenates of DAU-sensitive and DAU-resistant Ehrlich ascites cells, Skovsgaard (*8*) found no differences at steady-state DAU concentrations at or below 1.0 μg/ml. Enhanced DAU binding in wild-type DAU-sensitive cells at higher steady-state DAU concentrations was suggested to be due to ploidy differences (*8*). In a recent study on DAU-sensitive and DAU-resistant Ehrlich ascites cells, Londos-Gagliardi et al. (*26*) using cell fractionation techniques reported nuclear-associated DAU levels in the DAU-resistant cells to be slightly lower than levels in the DAU-sensitive cells. However, when nuclear-DAU levels were expressed as a ratio of cellular DNA content, DAU levels in the DAU-resistant population were twofold to fourfold lower than levels in the DAU-sensitive cells. Possible reasons for this difference were not discussed, but differences in ploidy may be a plausible reason. In the present study, ploidy of P388/S and P388/R cells was similar, with a modal chromosome number of 40. Similarities in DNA content between the two cell types was further confirmed on analysis by FCM of propidium iodide-stained nuclei.

In conclusion, this study demonstrates that in P388/R cells cellular accumulation of ADR was twofold to fourfold lower than levels accumulated in P388/S cells. In the soft-agar colony assay, P388/R cells were a hundredfold more resistant to the cytotoxic effects of ADR than were P388/S cells. In contrast to P388/S, no dose-dependent effect of ADR on drug-induced cell cycle perturbations and chromosome damage was seen in P388/R. Resistance to ADR in P388/R was not due to reduced drug binding to the nucleus.

REFERENCES

(*1*) Brockman RW. Mechanisms of resistance. In: Sartorelli AC, Johns DG, eds., Handbook of experimental pharmacology. Vol 38. Part 1. Berlin: Springer-Verlag, 1975; 352-410.

(*2*) Inaba M, Fujikura R, Sakurai Y. Comparative study of in vivo development of resistance to various classes of antitumor agents in P388 leukemia. Gan 1979; 70:607-613.

(*3*) Kessel D, Botterill V, Wodinsky I. Uptake and retention of daunomycin by mouse leukemic cells as factors in drug response. Cancer Res 1968; 28:938-941.

(*4*) Yesair DW, Thayer PS, McNitt S, Teague K. Comparative uptake, metabolism and retention of anthracyclines by tumors growing in vitro and in vivo. Eur J Cancer 1980; 16:901-907.

(*5*) Carter SK. Adriamycin—a review. J Natl Cancer Inst 1975; 55:1265-1274.

(*6*) Skovsgaard T, Nissen NI. Adriamycin, an antitumor antibiotic: A review with special reference to daunomycin. Dan Med Bull 1975; 22:61-73.

(*7*) Dano K. Experimentally developed cellular resistance to daunomycin. Acta Pathol Microbiol Scand [A] 1976; suppl 256:11-80.

(*8*) Skovsgaard T. Mechanisms of resistance to daunorubicin in Ehrlich ascites tumor cells. Cancer Res 1978; 38:1785-1791.

(*9*) Johnson RK, Ovejera AA, Goldin A. Activity of anthracyclines against an adriamycin (NSC-123127)-resistant subline of P388 leukemia with special emphasis on cinerubin A (NSC-18334). Cancer Treat Rep 1976; 60:99-102.

(*10*) Johnson RK, Chitnis MP, Embrey WM, Gregory EB. In vivo characteristics of resistance and cross-resistance of an adriamycin-resistant subline of P388 leukemia. Cancer Treat Rep 1978; 62:1535-1547.

(*11*) Wilkoff LJ, Dulmadge EA. Resistance and cross-resistance of cultured leukemia P388 cells to vincristine, adriamycin, adriamycin analogs, and actinomycin D. JNCI 1978; 61:1521-1524.

(*12*) Inaba M, Johnson RK. Uptake and retention of adriamycin and daunorubicin by sensitive and anthracycline resistant sublines of P388 leukemia. Biochem Pharmacol 1978; 27:2123-2130.

(*13*) Inaba M, Kobayashi H, Sakurai Y, Johnson RK. Active efflux of daunorubicin and adriamycin in sensitive and resistant sublines of P388 leukemia. Cancer Res 1979; 39:2200-2203.

(*14*) Krishan A, Ganapathi R. Laser flow cytometric studies on the intracellular fluorescence of anthracyclines. Cancer Res 1980; 40:3895-3900.

(*15*) Bachur NR, Moore AL, Bernstein JG, Liu A. Tissue distribution and disposition of daunomycin (NSC-82151) in mice: Fluorometric and isotopic methods. Cancer Chemother Rep 1970; 54:89–94.

(*16*) Krishan A. Rapid flow cytofluorometric analysis of mammalian cell cycle by propidium iodide staining. J Cell Biol 1975; 66:188–193.

(*17*) Krishan A, Ganapathi RN, Israel M. Effect of adriamycin and analogs on the nuclear fluorescence of propidium iodide-stained cells. Cancer Res 1978; 38:3656–3662.

(*18*) Di Marco A. Mechanism of action and mechanism of resistance to antineoplastic agents that bind to DNA. Antibiot Chemother 1978; 23:216–227.

(*19*) Skovsgaard T. Mechanisms of cross-resistance between vincristine and daunorubicin in Ehrlich ascites tumor cells. Cancer Res 1978; 38:4722–4727.

(*20*) Meriwether WD, Bachur NR. Inhibition of DNA and RNA metabolism by daunorubicin and adriamycin in L1210 mouse leukemia. Cancer Res 1972; 32:1137–1142.

(*21*) Barranco SC. Review of the survival and cell kinetic effects of adriamycin (NSC-123127) on mammalian cells. Cancer Chemother Rep 1975; 6:147–152.

(*22*) Krishan A, Frei E III. Effect of adriamycin on the cell cycle traverse and kinetics of cultured human lymphoblasts. Cancer Res 1976; 36:143–150.

(*23*) Vig BK. Chromosome aberrations induced in human leukocytes by the antileukemic antibiotic adriamycin. Cancer Res 1971; 31:32–38.

(*24*) Schwartz HS, Schioppacassi G, Kanter PM. Mechanisms of selectivity of intercalating agents. Antibiot Chemother 1978; 23:247–254.

(*25*) Dano K. Active outward transport of daunomycin in resistant Ehrlich ascites tumor cells. Biochim Biophys Acta 1973; 323:466–483.

(*26*) Londos-Gagliardi D, Aubel-Sadron G, Maral R, Trouet A. Subcellular localization of daunorubicin in sensitive and resistant Ehrlich ascites tumor cells. Eur J Cancer 1980; 16:849–854.

Thermotolerance in the Murine Jejunum[1,2]

Kurt J. Henle[3,4,5]

ABSTRACT—The heat sensitivity of the murine jejunum from C3H/HeJ mice and its capacity to develop thermotolerance were measured. Exteriorized loops of murine jejunum were heated in water baths at temperatures of 43–46°C for various times. Animal mortality was used to calculate the median lethal dose by day 7 ($LD_{50/7}$) in minutes as a function of temperature. The $LD_{50/7}$ value was independent of the length of the intestinal loop, the presence of serum in the heating medium, prior starvation of animals, and fluid replacement post heating. The time–temperature plot for the $LD_{50/7}$ values had an exponential slope constant of $-0.71\,°C^{-1}$, similar to that for other normal tissues. A heat treatment of 5 minutes at 45°C increased the $LD_{50/7}$ (total time at 45°C) from 5.9 minutes to 13.0 and 15.6 minutes for 1- and 3-day fractionation intervals, respectively. Death after intestinal heating was associated with septicemia and reached a peak on days 2 and 3 post hyperthermia. Gentamicin (0.1 mg/mouse/day) increased the $LD_{50/7}$ at 45°C from 5.9 to 9.6; however, septicemia was still noted in dying, gentamicin-treated mice. Additional antibiotics did not further increase the $LD_{50/7}$. Heat fractionation with gentamicin increased the $LD_{50/7}$ (total time at 45°C) to 23.0 and 12.5 minutes at 45°C for 1- and 3-day intervals, respectively. These data suggest that thermotolerance plays a significant role in the intestinal heat response, but that the heat damage to intestinal barriers against bacterial septicemia may be superimposed on the cellular damage to the crypt–villus system.—JNCI 1982; 68:1033–1036.

Hyperthermia is currently used on an experimental basis for the treatment of human cancers (*1*). Although the role of hyperthermia in the clinic is generally that of an adjuvant to either radiation or chemotherapy, more data are needed on the effects of hyperthermia alone in both normal and malignant tissues. In addition, the degree to which thermotolerance can be induced in various tissues must be known before the effects of fractionated hyperthermia can be assessed.

When compared to other normal tissues such as skin (*2*), the small intestine is one of the more radiation-sensitive tissues and also appears highly sensitive to hyperthermia. The purpose of this study was the quantitation of both the heat sensitivity of the murine small intestine and the development of thermotolerance in this tissue as indicated by animal lethality.

MATERIALS AND METHODS

Mice (C3H/HeJ) were purchased from The Jackson Laboratory, housed without special provisions, and used for experiments in a body weight range of 21–23 g at approximately 8 weeks of age. The mice were anesthetized ip with pentobarbital sodium (66 mg Nembutal/kg body wt; Abbott Laboratories), and a loop of jejunum (3.5 cm, unless otherwise noted) immediately distal to the ligament of Treitz was exteriorized through a 1-cm abdominal incision. The apex of this loop was marked with a loose suture through the mesenteric membrane and around the intestinal section. This suture was used both as the support for a 0.8-g weight that prevented flotation of the intestinal loop and as the identification of the same intestinal segment in the fractionation experiments. Neither the suture nor the weight appeared to constrict blood vessels. The exteriorized loops were covered with saline-saturated cotton gauze until 4 mice were prepared for simultaneous heat treatments (total preparation time: 10 min).

A picture of the experimental setup for heating the intestinal loops has been published previously in (*2*). A glass pan is covered by a plastic platform that contains four holes 1 cm in diameter. The glass pan is seated inside a 38-liter precision-controlled water bath (±0.05°C), and the heating medium for the intestinal loops is circulated by a pump through a stainless steel heat exchanger inside the bath and horizontally across the glass pan at a maximum flow rate of 3.4 liters/minute. The temperature gradients in the glass pan have been reported under these experimental conditions (*2*) and are insignificant at a depth of more than 2 mm below the air–fluid interphase. Since approximately 90% of the intestinal loop is more than 2 mm deep in the heating medium (maximum depth, 1.3 cm), heating is virtually uniform. The measured temperature transient in the intestinal lumen following immersion was equivalent to a lag time of 0.3 minute at 45°C, i.e., the difference between the total heating time and biologically equivalent time at constant temperature (*3*). Temperature gradients across the intestine were not detected in measurements under thermal equilibrium conditions (5 min after immersion). The temperature of the heating medium and rectal temperatures were monitored continuously (model 423; Yellow Springs Instrument Co.); core temperatures remained below 39.5°C at all times. Immediately before immersion of exteriorized intestinal loops, the temperature of the heating medium was raised 0.2°C above the target temperature to compensate for the cooling of the medium when the platform support was placed onto the glass pan.

Each experimental point on the graphs represents at least 8 animals with approximately equal numbers of males and

---

ABBREVIATION USED: $LD_{50/7}$=median lethal dose by day 7.

---

[1] Received September 17, 1981; accepted February 14, 1982.

[2] Supported by American Cancer Society grant PDT-28 and by Public Health Service grant CA-27817 from the National Cancer Institute.

[3] Department of Radiology, University of Utah Medical Center, Salt Lake City, Utah 84132.

[4] *Address reprint requests to* Dr. Henle at his *present address*: Department of Medicine, University of Arkansas for Medical Sciences; and Veterans Administration Medical Center (151/7), 300 East Roosevelt Rd., Little Rock, Ark. 72206.

[5] I am grateful to Dr. J. W. Peck and Dr. L. A. Dethlefsen for critical review of this manuscript and to Mr. W. L. Kershisnik for excellent technical assistance.

females. Both males and females showed a similar heat sensitivity (*see* SE of $LD_{50/7}$ in table 1), although a detailed study on the effect of animal sex on heat sensitivity was not performed. Survival data are analyzed by linear regression with the use of probits (*4*).

RESULTS

Initial experiments were designed for identification of significant treatment variables for the heating of the exteriorized jejunal loops. In these experiments the $LD_{50/7}$ value at 45°C was determined with the use of: *a*) variable lengths of intestinal loop (3.5 vs. 6.5 cm); *b*) different heating media (McCoy's 5-A medium with and without 10% fetal bovine serum and Dulbecco's saline with and without penicillin-streptomycin antibiotics); *c*) varying intestinal content (24-hr prior starvation vs. free access to food until the experiment); and *d*) fluid replacement to counteract potential dehydration of the animal. [Ringer's saline (1 ml) was injected ip three times per day during the 3 days after the heat treatment. The fluid replacement eliminated the 7–8% weight loss that was normally observed.]

None of the above-listed variables had a statistically significant effect on the $LD_{50/7}$ at 45°C. Therefore, the results from all of these experiments were pooled in text-figure 1. An independent repeat experiment, with the use of the treatment conditions used for the remainder of the experiments (3.5-cm loop, Dulbecco's saline as heating medium, free access to food before heating, and no fluid replacement post heating), is shown separately by the solid symbols in text-figure 1. The inset of the graph shows the same data as probits versus natural logarithm of the heating time at 45°C; the calculated $LD_{50/7}$ value was 5.9 minutes (table 1).

The time of animal death after a single heat treatment peaked on the 2d day post heating, and more than 90% of the animals died within 5 days. Less than 3% of the animals died later than 7 days post heating. After fractionated hyperthermia, deaths peaked 1 day after the last treatment with no additional deaths after 4 days.

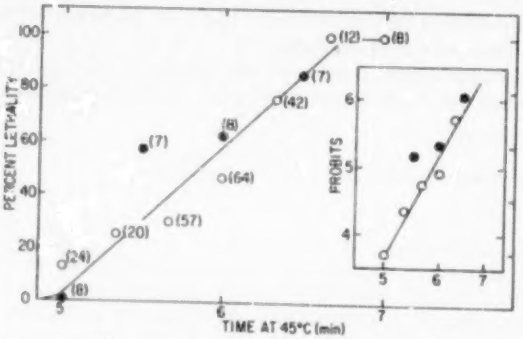

TEXT-FIGURE 1.—Hyperthermia dose response for the exteriorized murine jejunum. Lethality within 7 days is plotted as a function of heating time at 45°C. The number of animals used for each datum is given *in parentheses*. *Inset* shows the same data when lethality is converted to probits and plotted against the natural logarithm of the heating time. ○, composite of several experiments with different heating media, fluid replacement after hyperthermia, and prior starvation (*see* text). ●, results of an independent repeat experiment; lines were fitted by eye; calculated values are given in table 1.

TABLE 1.—*$LD_{50/7}$*

Text-figure	Temperature, °C	t[a]	$LD_{50/7}$ ± SE[b]
1	45	—	5.9±0.1
2A	43	—	29.4±0.5
	44	—	12.8±0.2
	45	—	5.8±0.1
	46	—	3.6±0.1
2B	43	—	37.6±0.6
	44	—	16.8±0.2
	45	—	9.6±0.2
	46	—	4.6±0.3
4A	45	0	5.9±0.2
		1	13.0±0.1
		3	15.6±0.9
4B	45	0	9.7±0.1
		1	23.0±0.5
		3	12.5±0.8

[a] Days after an initial treatment of 5 min at 45°C before reheating.

[b] Calculated values (min) of $LD_{50/7}$ and standard error of the mean with the use of *(4)*.

Cultures of cardiac blood from mice 2 days after lethal hyperthermia showed high levels of *Pseudomonas aeruginosa*. Gentamicin (0.1 mg/mouse/day) given ip (Garamycin; Schering Corp.) in two fractions daily during each of the first 3 days after hyperthermia increased the $LD_{50/7}$ at 45°C from 5.9 to 9.7 minutes (table 1, text-fig. 2). A similar increase in the $LD_{50/7}$ was measured in the temperature range of 43–46°C when mice were maintained on gentamicin. Lower temperatures were not included in this study since heating times in excess of 45 minutes required additional anesthesia. Cardiac blood cultures from mice on gentamicin 2 days after 10 minutes at 45°C to the jejunum showed the presence of *Moraxella*, but additional antibiotics (carbenicillin, ampicillin, and polymixin B) alone or in combination with gentamicin did not further increase the $LD_{50/7}$ at 45°C. The independent repeat experiment with gentamicin showed a reduced protective effect of the antibiotic (text-fig. 3) and blood cultures at this time detected the presence of some *P. aeruginosa*.

The increase in the $LD_{50/7}$ expressed as the total heating time with fractionated hyperthermia is shown in text-figure 4 with and without gentamicin. The intestinal loops were heated for 5 minutes at 45°C and reheated 0, 1, 3, or 5 days later with variable heating times at 45°C. (For the day-0 interval, 5 min at 45°C was followed by 3 min at 37°C before reheating.) Without gentamicin, the $LD_{50/7}$ increased from 5.9 to 13.0 and 15.6 at 45°C for the 1- and 3-day fractionation intervals, respectively (table 1, text-fig. 4A). Data for the 5-day fractionation interval are not shown since these experiments were complicated by the formation of intestinal adhesions. During exteriorization the breaking of these adhesions was accompanied by bleeding, and death after the second heat treatment could not be separated clearly from the effects of that mechanical trauma. Although the data for the 5-day fractionation interval had much scatter, the fractionation response resembled that of the 1-day fractionation interval.

Thermotolerance in the murine jejunum showed different kinetics in control and gentamicin-maintained mice. With gentamicin, the 1-day fractionation interval showed a higher level of thermotolerance than the 3-day interval, with $LD_{50/7}$ values of 23.0 and 12.5 minutes at 45°C, respectively (text-fig. 4B, table 1).

The temperature dependence of the $LD_{50/7}$ for single heat treatments with and without gentamicin is shown in text-figure 3. The time-temperature relationship shows a constant exponential slope with an average of $-0.71°C^{-1}$ without and with gentamicin, but with gentamicin the curve is shifted 0.2-0.5°C toward higher temperatures. Intestinal cross sections from non-gentamicin-treated mice 2 or 3 days after 6 minutes at 45°C showed no significant reduction in the number of regenerating crypts; however, gentamicin-maintained mice after intestinal hyperthermia of 9, 9.5, and 10 minutes at 45°C showed progressive but anisotropic destruction of crypts 2 days post heating. Crypt survival was not quantitated because of the nonuniform distribution of surviving crypts.

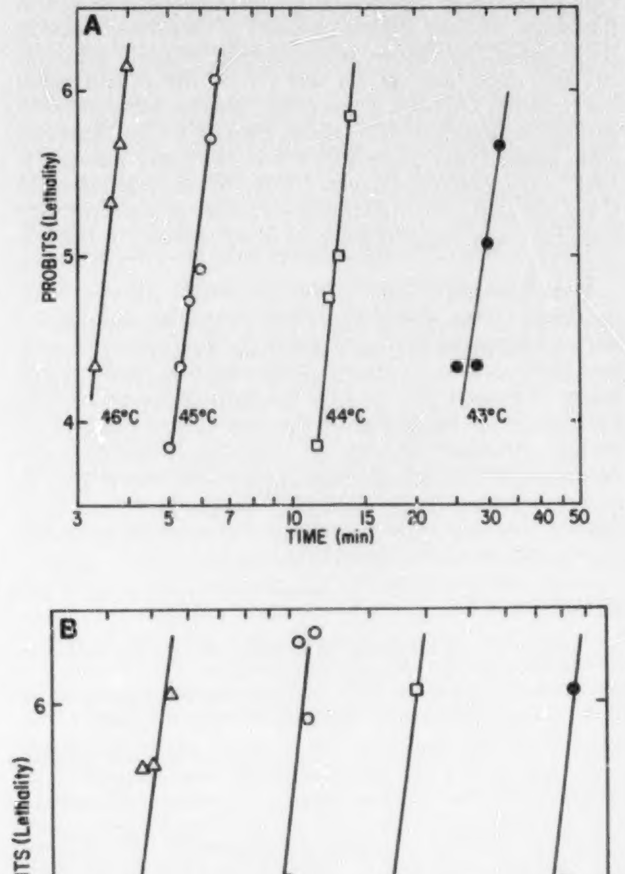

TEXT-FIGURE 2.—Hyperthermia dose response for exteriorized murine jejunum at temperatures of 43-46°C. Each experimental point represents 8-10 mice. The calculated $LD_{50/7}$ values are listed in table 1. A) Without gentamicin maintenance. B) With gentamicin maintenance over 3 days post hyperthermia (*see* text).

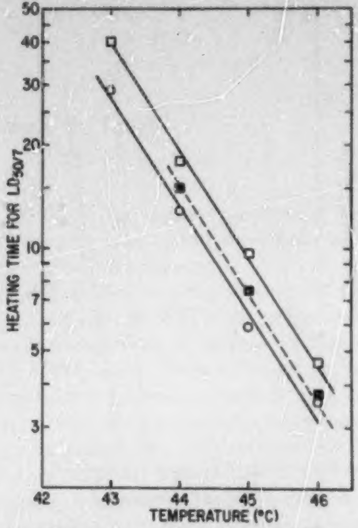

TEXT-FIGURE 3.—Time-temperature plot of the $LD_{50/7}$ with and without gentamicin. ○, data without gentamicin. □, data with gentamicin. ■, data of the independent gentamicin repeat experiment in which blood cultures revealed some *P. aeruginosa*.

DISCUSSION

The slope on the time-temperature curve in text-figure 3 is similar to that for other tissues (*2*). However, the heating time of the exteriorized jejunum required to kill 50% of the animals is only half of that required for 50% necrosis of rat skin and mouse ear, tail, or leg (*2*), even after gentamicin protection. Although it is difficult to compare heat sensitivity in different tissues when different experimental end points are used, the observations in this study suggest, nevertheless, that the small intestine is more heat-sensitive than skin. The measured $LD_{50/7}$ without gentamicin maintenance probably does not reflect cell killing of crypt stem cells, but rather the massive breakdown of barriers against bacterial invasion. Alternatively, the $LD_{50/7}$ with gentamicin maintenance appears to be associated with heat-induced killing of crypt stem cells. Crypt stem cell survival was not quantitated due to the asymmetry of surviving cells. Similar asymmetry was reported for intestinal sections treated with combined heat and radiation (*5*, *6*). Higher crypt survival near the mesenteric side has been attributed to temperature gradients of the order of 1°C in the exteriorized intestinal loop, presumably due to cooling by circulating blood (*7*). In our system we could not measure any temperature gradients in the intestinal segments immersed 1 cm in the heating medium, and this result agrees with that in (*5*).

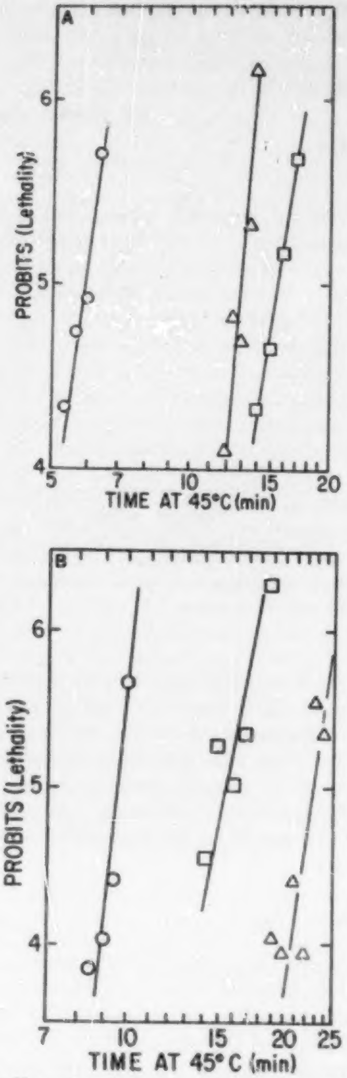

TEXT-FIGURE 4.—Hyperthermia fractionation response (45°C) of exteriorized murine jejunum. Jejunal segments were heated for 5 min at 45°C on day 0 and reheated 0 (○), 1 (△), or 3 days (□) after initial hyperthermia. The plotted heating time is the total time at 45°C in the two fractions. A) Without gentamicin maintenance. B) With gentamicin during the fractionation interval and for 3 days after the second fraction.

Furthermore, the rapid temperature transients upon immersion (3) suggest that large temperature gradients do not exist at thermal equilibrium. It appears more likely that hyperthermia causes multiple nutrient and pH gradients across the intestine. Such gradients may be aggravated by general anesthesia. Relevant physiologic data are not available.

When hyperthermia was applied to the same intestinal segment in two fractions, the total $LD_{50/7}$ was increased. This observation suggests that thermotolerance had developed in the jejunum after the initial heat treatment of 5 minutes at 45°C. However, the relative contributions to the increased $LD_{50/7}$ by thermotolerance, as defined in vitro (*8*), and by repair of heat damage are unknown. Therefore, we cannot compare the magnitude of thermotolerance in vivo with that of thermotolerance in vitro, where tolerance is defined in terms of the ratio of slopes on hyperthermia survival curves (*8*). Furthermore, if thermotolerance in vivo is expressed in terms of a ratio of LD_{50} values, the magnitude of the ratio depends on the specific formulation of the ratio (*9*). However, the time course of thermotolerance is independent of the definition of a thermotolerance ratio. With the use of the simplest form of a thermotolerance ratio (i.e., total $LD_{50/7}$ fractionated/$LD_{50/7}$ single heating), the data in this study indicate different kinetics of thermotolerance in the presence and absence of gentamicin. Without gentamicin, this ratio becomes 2.2 and 2.7 for the 1- and 3-day fractionation intervals, respectively, whereas with gentamicin maintenance the ratio rises to 2.4 with a 1-day fractionation interval and declines to 1.3 for the 3-day interval. A peak in thermotolerance with a 1-day fractionation interval is similar to the thermotolerance kinetics in vitro (*8*) and resembles those kinetics observed in mouse feet (*9*, *10*) and skin (*11*).

Thermotolerance kinetics for the murine jejunum with gentamicin may, therefore, reflect a cellular survival response, whereas without gentamicin the fractionation results could be based on an altered physiology that would retard bacterial invasion into the heat-traumatized jejunal section. Detailed histologic studies of the jejunal heat response to support this conjecture are not available. In any case, the data for mice without gentamicin show that measurements of heat sensitivity and thermotolerance in vivo include features that may be separate from, and not predictable by, in vitro cell survival experiments.

REFERENCES

(*1*) MILDER JW, ed. Conference on hyperthermia in cancer treatment. Cancer Res 1979; 39:2232–2340.

(*2*) HENLE KJ, DETHLEFSEN LA. Time-temperature relationships for heat-induced killing of mammalian cells. Ann NY Acad Sci 1980; 335:234–253.

(*3*) HENLE KJ, ROTIROTI JL. Time-temperature conversions in biological applications of hyperthermia. Radiat Res 1980; 82:138–145.

(*4*) FINNEY DJ. Probit analysis. 3d ed. London: Cambridge Univ Press, 1971.

(*5*) MERINO OR, PETERS LJ, MASON KA, WITHERS HR. Effect of hyperthermia on the radiation response of the mouse jejunum. Int J Radiat Oncol Biol Phys 1978; 4:407–414.

(*6*) HUME SP, MARIGOLD JC, FIELD SB. The effect of local hyperthermia on the small intestine of mouse. Br J Radiol 1979; 52:657–662.

(*7*) HUME SP, ROBINSON JE, HAND JW. The influence of blood flow on temperature distribution in the exteriorized mouse intestine during treatment by hyperthermia. Br J Radiol 1979; 52:219–222.

(*8*) HENLE KJ, DETHLEFSEN LA. Heat fractionation and thermotolerance: A review. Cancer Res 1978; 38:1843–1851.

(*9*) RICE LC, URANO M, MAHER J. The kinetics of thermotolerance in the mouse foot. Radiat Res 1981; 89:291–297.

(*10*) HENLE KJ. Discussion. Ann NY Acad Sci 1980; 335:279–280.

(*11*) FIELD SB, ANDERSON RL. Thermotolerance: A review of observations and possible mechanisms. Natl Cancer Inst Monogr. In press.

Detection of Acquired Provirus Sequences in Mammary Tumors From Low-Expressor, Low-Risk Mice[1,2,3]

Bruce W. Altrock,[4,5] Robert D. Cardiff,[4,6] John P. Puma,[4] *and* **Judi K. Lund[4]**

ABSTRACT—Murine mammary tumor virus (MuMTV) provirus sequences in the DNA from early-occurring (average age 10 mo) and late occurring (age >20 mo) tumors in BALB/cfC3H mice were analyzed by Eco RI restriction endonuclease mapping procedures. All early tumors were MuMTV antigen-positive mammary adenocarcinomas that contained the 0.92- and 4.0-kilo base (kb) exogenous C3H MuMTV-specific Pst I restriction endonuclease fragments. All but 1 of the late mammary adenocarcinomas had MuMTV antigens detected by peroxidase antiperoxidase staining, and all contained the 0.92- and 4.0-kb exogenous virus Pst I fragments. Three late nonmammary tumors lacked both MuMTV antigens and acquired provirus sequences. Greater numbers of MuMTV sequences were detected in both early and late-arising mammary tumors by Eco RI restriction endonuclease mapping than were detected in tissues from uninfected BALB/c mice. However, neither the number nor the location of MuMTV proviruses correlated with tumor latent period.—JNCI 1982; 68:1037–1041.

Exogenous MuMTV are highly oncogenic for the mammary epithelium of susceptible strains of mice and generally produce tumors with a mean latent period of 12 months or less (*1–4*). The presence of exogenous C3H MuMTV provirus sequences in BALB/cfC3H tumor tissue has been confirmed by the detection of exogenous MuMTV-specific 0.92- and 4.0-kb Pst I restriction endonuclease fragments by Southern blot analysis (*5*). However, the presence of exogenous MuMTV was not sufficient for neoplastic transformation to occur, since the same provirus sequences were detected in the normal lactating BALB/cfC3H mammary glands of infected females (*5*). Endogenous forms of MuMTV have also been detected in normal and neoplastic tissue of all inbred strains of mice (*6*). These endogenous proviruses apparently lack the highly oncogenic character of the exogenous MuMTV and can be distinguished from exogenous MuMTV proviruses by their restriction endonuclease maps (*5–7*). Endogenous MuMTV have been associated with mammary tumors that occur late in life (*8*). To date, exogenous MuMTV has not been associated with tumors occurring after prolonged latent periods (≥18 mo).

Recently, we have reported studies of tumor risk and latency in exogenously infected BALB/cfC3H mice (*1*). Two subpopulations of MuMTV-infected mice were identified in those studies; one group developed 100% tumors by 17 months of age with a mean age of detection of 10 months (high risk), whereas the other group did not develop tumors earlier than 20.5 months of age and exhibited only a 15% tumor incidence at 24 months (low risk). Although both groups expressed MuMTV antigens in their milk, the levels in the milk of high-risk mice were at least 33 times higher than those observed in the milk of low-risk mice. On the basis of the data available at that time, it was not known whether the tumors arising in both high-risk and low-risk mice possessed exogenous MuMTV sequences. The possibility existed that the tumors occurring in the low-risk BALB/cfC3H mice may have involved only endogenous MuMTV provirus information.

In the present studies we compared the morphology, virus antigenicity, and the MuMTV provirus sequences associated with mammary tumors arising in high-risk and low-risk BALB/cfC3H mice. Tumors observed in both groups were predominantly adenocarcinomas and contained viral antigens. Adenocarcinomas from high-risk and low-risk mice contained both exogenous and endogenous MuMTV provirus sequences and had comparable numbers of MuMTV provirus copies. Therefore, the acquisition of exogenous MuMTV proviruses may have been necessary, but was not sufficient, to ensure early tumor development.

MATERIALS AND METHODS

Mice and virus.—BALB/c and BALB/cfC3H mice were from Simonsen Laboratories, Gilroy, Calif. MuMTV virus from the Mm5mt/cl cell line was obtained from NCI-Frederick Cancer Research Facility, Frederick, Md., through the Biological Carcinogenesis Branch, National Cancer Institute.

PAP staining.—Paraffin-embedded tissues were sectioned at 5 μm, mounted on glass slides, and incubated at 56°C overnight. After dewaxing, we immersed the sections in absolute methanol containing 0.3% H_2O_2 for 3 minutes. After washing in 0.01 *M* PBS (pH 7.4), the sections were incubated with nonimmune goat serum diluted 1:10 for 30 minutes. Subsequently, we applied the following antisera sequence: rabbit anti-MuMTV, 1:500; goat anti-rabbit, 1:40; and rabbit PAP, 1:50. Each step lasted 30 minutes and was followed by a wash in PBS. The immune complex was detected with 3-amino-9-carbazole. We counterstained

---

ABBREVIATIONS USED: DTT=DL-dithiothreitol; kb=kilo base; MuMTV=murine mammary tumor virus(es); PAP=peroxidase antiperoxidase; PBS=phosphate-buffered saline; [^{32}P]cDNA=^{32}P-labeled complementary DNA; SDS=sodium dodecyl sulfate; SSC=sodium chloride and sodium citrate solution.

---

[1] Received October 27, 1981; accepted February 5, 1982.

[2] Supported by Public Health Service (PHS) contract N01CP-61013 from the Division of Cancer Cause and Prevention, National Cancer Institute (NCI); and by PHS training grant CA-05245 from the NCI.

[3] Animals were maintained under the guidelines set forth in the "Guide for the Care and Use of Laboratory Animals" by the Institute of Laboratory Animal Resources, National Research Council; and by the American Association for the Accreditation of Laboratory Animal Care.

[4] Department of Pathology, School of Medicine, University of California, Davis, Davis, Calif. 95616.

[5] *Present address:* Applied Molecular Genetics, Inc., 1892 Oak Terrace Lane, Newbury, Calif. 91320.

[6] *Address reprint requests to* Dr. Cardiff.

the sections in Mayer's hematoxylin and mounted with Kaiser's glycerol gelatin (*9, 10*). Two investigators (R.D.C. and J.K.L.) viewed one or two PAP-stained sections of each tumor independently and recorded the percentage of MuMTV antigen-positive cells.

Nucleic acid extraction.—Tissues were minced, suspended in extraction buffer [10 m*M* Tris-HCl (pH 8.0), 10 m*M* NaCl, 10 m*M* EDTA], and disrupted with a dounce homogenizer. The homogenate was passed through cheesecloth. Proteinase K (500 µg/ml) and SDS (0.5%) were added to the filtrate. We incubated the mixtures at 43°C overnight and then extracted them twice with equal volumes of buffer-saturated phenol (*11*). The extracts were dialyzed exhaustively against 5 m*M* Tris-HCl (pH 8.0), 10 m*M* NaCl, and 0.1 m*M* EDTA.

Viral RNA was obtained by phenol extraction of SDS-disrupted proteinase K-digested virus. The RNA was disaggregated into 35S subunits by being heated at 90°C for 3 minutes and then by centrifugation in a 5-20% sucrose gradient. Material that sedimented at 20-35S was pooled, precipitated with ethanol, and dissolved in 10 m*M* Tris-HCl (pH 8.0), 50 m*M* KCl, and 1 m*M* EDTA.

Preparation of MuMTV [^{32}P]cDNA.—MuMTV-specific [^{32}P]cDNA was prepared in a 50-µl reaction mixture that contained 50 m*M* Tris-HCl (pH 8.1), 75 m*M* KCl, 10 m*M* MgCl$_2$, 2 m*M* DTT, 0.2 m*M* of each dGTP, dCTP, and dTTP, 100-200 µCi [α-^{32}P]dATP (2,000 Ci/mmol; New England Nuclear Corp. Boston, Mass.), 25 µg actinomycin D/ml, 0.5 µg MuMTV 20-35S RNA, 500 µg calf DNA primers (*12*), and 50 U of avian myeloblastosis virus reverse transcriptase (provided by Dr. J. Beard, Life Sciences Inc., St. Petersburg, Fla., through the Biological Carcinogenesis Branch, National Cancer Institute). The mixture was incubated at 37°C for 30 minutes. The reaction was stopped by the addition of EDTA, SDS, and NaOH to final concentrations of 50 m*M*, 0.5% and 0.3 *M*, respectively. The mixture was incubated at 65°C for 3-4 hours to hydrolyze the viral RNA, then neutralized with HCl, and passed over a column of Sephadex G-50. The [^{32}P]cDNA eluted in the void volume and was precipitated with ethanol and dissolved in 5 m*M* Tris-HCl (pH 8.0), 10 m*M* NaCl, and 0.1 m*M* EDTA.

Enzyme digests and blotting—Restriction endonucleases were purchased from New England BioLabs, Beverly, Mass. Digestion mixtures contained 5-20 µg cellular DNA and 1 µg λ-DNA in a solution of 50 m*M* Tris-HCl (pH 7.4), 50 m*M* NaCl, 5 m*M* MgCl$_2$, 5 m*M* DTT, and 50 µg lysozyme/ml. The reactions were incubated at 37°C and stopped by addition of EDTA, and the reaction products were electrophoresed in 1% agarose gels. We stained the gels with ethidium bromide and verified the completeness of digestion by the λ-DNA pattern. The transfer of DNA fragments from the agarose gels to nitrocellulose filters (Schleicher & Schuell, Inc. Keene, N.H.) was done as described by Southern (*13*). The filters were baked at 80°C in vacuo for 2-4 hours and then prehybridized for 6-18 hours at 37°C in annealing mix containing 3× SSC (0.45 *M* NaCl, 0.045 *M* sodium citrate), 40% (vol/vol) deionized formamide, 200 µg yeast RNA/ml, 50 µg sheared calf thymus DNA/ml, 1 m*M* EDTA, and 3× Denhardt's buffer (0.6% each of bovine serum albumin, polyvinyl pyrrolidone, and Ficoll) (*14*). Hybridizations were performed by incubating the filters (250 cm^2) with 2×10^6 cpm [^{32}P]cDNA in 2 ml annealing mix at 37°C for 4 days. Unhybridized cDNA was removed from the filters by being washed three or four times in 200-ml changes of buffer (2× SSC, 0.1% SDS, 5 ml saturated sodium pyrophosphate/liter) at 23°C, by being washed once in buffer for 0.5-1 hour at 65°C, and then by being washed once in 0.1× buffer at room temperature. The filters were air dried and then exposed at −70°C for 1-14 days to Kodak X-R5 X-OMAT film in the presence of Dupont Cronex intensifying screens.

RESULTS

Tumor morphology and antigenicity.—Tumors arising in high-expressor, high-risk mice (mean latent period, 10 mo) were all identified as adenocarcinomas according to the classification of Dunn (*15*) and contained MuMTV antigens detectable by PAP staining (table 1). By comparison 9 of 12 (75%) tumors arising in old ($\geq$20.5 mo) low-expressor, low-risk mice were adenocarcinomas. All but 1 of the adenocarcinomas from low-risk mice had detectable MuMTV antigens. The level and distribution of detectable virus antigen were similar in tumors from high- and low-risk mice. The 3 nonmammary tumors from low-risk mice lacked detectable MuMTV antigens.

Pst I restriction endonuclease mapping.—The DNA extracted from tumors of 18 high- and low-expressor mice were digested with the Pst I restriction endonuclease and analyzed by the Southern blotting procedure with the use of [^{32}P]-labeled C3H MuMTV cDNA (fig. 1) (*14, 16*). The DNA from all tumors of high-expressor mice contained the 0.92- and 4.0-kb Pst I restriction endonuclease fragments characteristic of exogenous C3H MuMTV as well as the 0.77-, 1.4-, 1.7-, 4.8-, and 5.1-kb fragments of the endogenous BALB/c proviruses. The DNA from most mammary tumors of low-expressor mice also contained these exogenous and endogenous MuMTV Pst I fragments. One exception to this observation was the Pst I map of a late-arising (28 mo of age) MuMTV antigen-negative, low-expressor tumor ZII (table 1), which lacked the 4.8-kb endogenous provirus fragment. The DNA from the 3 nonmammary tumors from low-expressor mice contained only the endogenous BALB/c MuMTV provirus fragments.

Eco RI restriction endonuclease mapping.—Because Pst I maps of tumor DNA from high- and low-expressor mice were the same, we investigated next the possible differences in provirus numbers and sites of integration in low- and high-expressor tumors with the use of Eco RI restriction endonuclease (fig. 2). This enzyme cuts each MuMTV provirus once producing 4.0- and 6.1-kb MuMTV fragments coupled to their adjacent host cellular sequences (*17*). In BALB/c mouse spleen DNA, 5 Eco RI bands of 6.2, 7.2, 7.7, 9.2, and 15.0 kb were detected and represented endogenous MuMTV provirus sequences (*8*). Tumor cells that were infected with exogenous MuMTV acquired additional integrated provirus sequences, which could be detected as additional bands in Eco RI maps of cellular DNA (*5*). Tumors from high-expressor BALB/cfC3H mice evaluated by this procedure had from one to six additional Eco RI bands. This finding was consistent with the acquisition of exogenous MuMTV

TABLE 1.—*PAP and restriction endonuclease mapping data for high- and low-expressor BALB/cfC3H mice*

Animal No.[a, b]	Tumor type	PAP staining[c]	Exogenous MuMTV Pst I fragments, 0.92 and 4.0 kb	Additional MuMTV[d] Eco RI, fragments
High-expressor mice				
3013	Adenocarcinoma	++	+	1
3016	Adenocarcinoma	+++	+	5
3018	Adenocarcinoma	++	+	4
3047	Adenocarcinoma	++	+	4
3525	Adenocarcinoma	+	+	3
3687	Adenocarcinoma	+	+	2
3799	Adenocarcinoma	+	+	2
3800	Adenocarcinoma	+	+	6
Low-expressor mice				
3317	Adenocarcinoma	+	+	1
3348	Adenocarcinoma	+++	+	4
3434	Adenocarcinoma	+++	+	2
3441	Adenocarcinoma	+++	+	6
3443	Adenocarcinoma	+++	+	4
87A	Adenocarcinoma	++	+	6
87B	Adenocarcinoma	++	+	4
ZII	Adenocarcinoma	−	+	6
3081	Sarcoma	−	−	0
3366	Undifferentiated cancer	−	−	0
3373	Lymphoma	−	−	0

[a] Tumors 87A and 87B were from the same animal.

[b] Tumor from animal #ZII lacked the 7.2-kb endogenous MuMTV fragment.

[c] PAP grading system: ± = 0–1% positive cells, + = 1–25% positive cells, ++ = 25–50% positive cells, and +++ = 50–100% positive cells.

[d] The 6.2-, 7.2-, 7.7-, 9.2-, and 15.0-kb endogenous MuMTV fragments are not included. The 0.92- and 4.0-kb endogenous MuMTV Pst I fragments are included for low-expressor mice.

proviruses reported to occur in these animals (*5*). In general, high- and low-expressor mammary tumors contained equivalent numbers of integrated MuMTV proviruses. All of the mammary tumors from low-expressor mice had from 1 to 6 additional Eco RI MuMTV fragments. All but animal ZII also had the expected endogenous provirus fragments. The ZII tumor DNA lacked the 7.2-kb endogenous fragment normally detected in BALB/c DNA. The nonmammary tumors from low-expressor animals that lacked MuMTV antigens and the 0.92- and 4.0-kb Pst I exogenous MuMTV fragment also lacked additional Eco RI fragments.

DISCUSSION

Most female BALB/c mice infected with C3H MuMTV by foster nursing or by injection develop mammary tumors early in life (mean latent period, 10 mo) (*1–4*). However, some exposed individuals do not develop tumors before 20 months of age, if at all. Our early studies demonstrated a relationship between the levels of milk MuMTV antigen expression in individual females and their respective tumor latent periods (*1*). Females with large amounts of milk MuMTV antigens (≥100 μg/ml; high expressors) developed early tumors, whereas those with low milk MuMTV levels (≤3 μg/ml; low expressors) either did not develop tumors or developed them late in life (15% by 24 mo of age). Although the milk from unexposed BALB/c animals did not contain detectable MuMTV antigens, we could not exclude the possibility that the antigen detected in low-expressor milk was from a derepressed, endogenous MuMTV provirus. Such endogenous MuMTV expression may also have played a role in tumor development in these animals (*8*).

We compared the morphologic and viral antigenic features of tumors from both high- and low-expressor mice. Mammary adenocarcinomas that arose in both high- and low-expressor mice (with one exception) were MuMTV antigen-positive. Though some nonmammary tumors did arise in the low-expressor population, these lacked PAP-detectable MuMTV antigens. Therefore, the morphologic and antigenic criteria used did not distinguish between high- and low-expressor mammary tumors.

Next we examined these tumors for the presence of exogenous MuMTV-specific Pst I restriction endonuclease fragments. All of the mammary adenocarcinomas found in high- and low-expressor females contained the Pst I 0.92- and 4.0-kb fragments characteristic of exogenous C3H MuMTV provirus (*5*). These fragments have not been observed in the liver, lactating mammary gland, hyperplastic outgrowths or tumors from our BALB/c colony. Therefore, we interpret their presence to indicate infection of the tissue by exogenous MuMTV (*5, 19*). The 3 MuMTV antigen-negative nonmammary tumors from low-expressor mice contained endogenous BALB/c MuMTV provirus DNA but lacked the 0.92- and 4.0-kb exogenous provirus fragments. These data indicate that the late-arising mammary adenocarcinomas from low-expressor mice were infected with exogenous MuMTV and expressed viral antigens in a manner comparable to that of high-expressor tumors.

We next compared the number and location of MuMTV sequences in tumors from both MuMTV expression groups. Mammary tumors from both high and low expressors contained additional copies of MuMTV genes as detected by Eco RI restriction endonuclease mapping. The numbers of additional MuMTV Eco RI fragments varied from one to six among the individual tumors tested. However, the number of additional fragments did not correlate with tumor latency. No C3H MuMTV host Eco RI fragments were detected, which were common throughout the high- or low-expressor mammary tumors studied. A unique situation was observed in the MuMTV antigen-negative mammary adenocarcinoma (animal #ZII) which contained the 0.92- and 4.0-kb exogenous MuMTV Pst I fragments and had six additional MuMTV Eco RI fragments but lacked one of the endogenous BALB/c MuMTV Eco RI fragments. Understanding the mechanism of this genetic rearrangement and its consequences will require further study.

The increased numbers of MuMTV provirus sequences detected in both low- and high-expressor mammary tumors is consistent with MuMTV involvement in tumor development in both groups of mice. However, no evidence of a correlation between MuMTV copy number or location and latent period (expressor status) was obtained. Although these studies exclude the hypothesis that the MuMTV found in low-expressor mice was exclusively endogenous virus, they do not provide a clear explanation for the prolonged latent period and low tumor incidence in low-expressor animals. Explanation of these concurrent phenomena awaits further study.

REFERENCES

(*1*) Altrock BW, Cardiff RD. Mouse mammary tumor virus infections: Viral expression and tumor risk. JNCI 1979; 63:1075–1080.

(*2*) Bentvelzen P. The biology of the mouse mammary tumor virus. Int Rev Exp Pathol 1972; 22:259–297.

(*3*) Moore DH, Holben JA, Charney J. Biological characteristics of some mouse mammary tumor viruses. J Natl Cancer Inst 1976; 57:889–896.

(*4*) Noon MC, Wolford RG, Parks WP. Expression of mouse mammary tumor viral polypeptides in milks and tissues. J Immunol 1975; 115:653–658.

(*5*) Cohen JC, Shank PR, Morris VL, Cardiff R, Varmus HE. Integration of the DNA of mouse mammary tumor virus in virus-infected normal and neoplastic tissue of the mouse. Cell 1979; 16:333–345.

(*6*) Morris VL, Madeiros E, Ringold GM, Bishop MJ, Varmus HE. Comparison of mouse mammary tumor virus specific DNA in inbred wild and Asian mice, and in tumors and normal organs from inbred mice. J Mol Biol 1977; 114:73–91.

(*7*) Arthur LO, Altrock BW, Schochetman G. Type-specific determinants on proteins of an endogenous CeH mouse mammary tumor virus (MMTV) distinguish this virus from highly oncogenic exogenous MMTVs. Virology 1981; 110:270–280.

(*8*) Bentvelzen P, Brinkhog J, Haaijman JJ. Genetic control of endogenous murine mammary tumor virus reinvestigated. Eur J Cancer 1978; 14:1137–1147.

(*9*) St George JA, Cardiff RD, Young LJ, Faulkin LJ. The immunochemical distribution of mouse mammary tumor virus antigen in BALB/cfC3H mammary epithelium. JNCI 1979; 63:813–820.

(*10*) Taylor CP. Immunoperoxidase techniques. Arch Pathol Lab Med 1978; 102:113–121.

(*11*) Gross-Bellard M, Oudet P, Chambon P. Isolation of high molecular weight DNA from mammalian cells. Eur J Biochem 1973; 36:32–38.

(*12*) Taylor JM, Illmensee R, Summers J. Efficient transcription of RNA into DNA by avian sarcoma virus polymerase. Biochim Biophys Acta 1976; 442:324–330.

(*13*) Southern EM. Detection of specific sequences among DNA fragments separated by gel electrophoresis. J Mol Biol 1975; 98:503–517.

(*14*) Denhardt DT. A membrane filter technique for the detection of complementary DNA. Biochem Biophys Res Commun 1966; 23:641–646.

(*15*) Dunn TB. Morphology of mammary tumors in mice, In: Homburger F, ed. The physiopathology of cancer. New York: Harper, 1959:38–84.

(*16*) Fanning TG, Puma JP, Cardiff RD. Selective amplification of mouse mammary tumor virus in mammary tumors of GR mice. J Virol 1980; 36:109–114.

(*17*) Cohen JC, Varmus HE. Endogenous mammary tumour virus DNA varies among wild mice and segregates during inbreeding. Nature 1979; 278:418–423.

(*18*) Cohen JC, Majors JE, Varmus HE. Organization of mouse mammary tumor virus specific DNA endogenous to BALB/c mice. J Virol 1979; 32:483–496.

(*19*) Ashley RL, Cardiff RD, Fanning TG. Reevaluation of the effect of mouse mammary tumor virus infection on the BALB/c mouse hyperplastic outgrowth. JNCI 1980; 65:977–986.

1

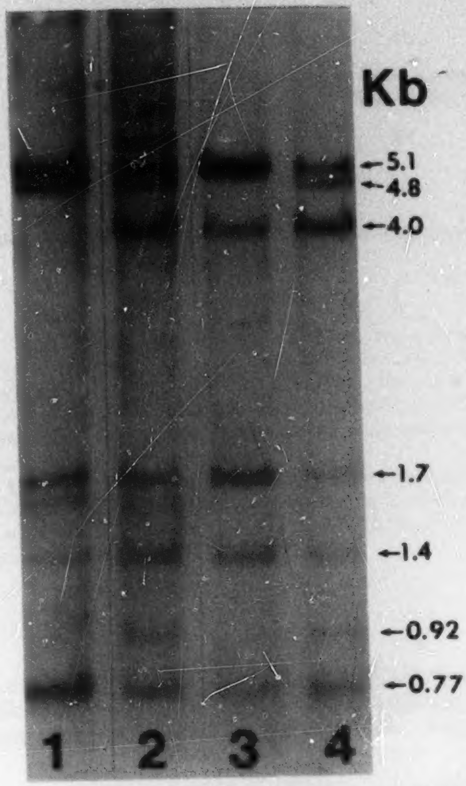

FIGURE 1.—Demonstration that the acquired proviruses in both high- and low-expressor DNA are exogenous MuMTV. Samples were digested with Pst I and analyzed as described in "Materials and Methods." The examples shown are: lane 1, BALB/c spleen; lane 2, low-expressor tumor 87B; lane 3, low-expressor tumor ZII; lane 4, high-expressor tumor 3525. *Numbers on the right* indicate the sizes of the fragments. The 0.92- and 4.0-kb fragments are characteristic of the presence of the exogenous C3H MuMTV (*5*).

2

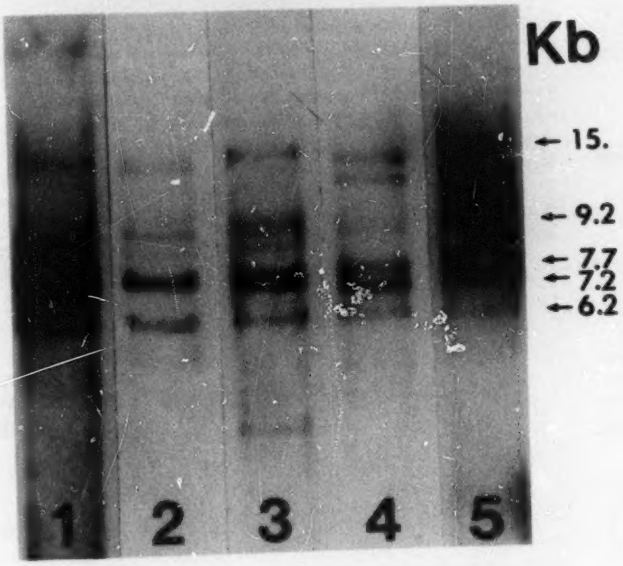

FIGURE 2.—Detection of acquired MuMTV proviruses in high-expressor and low-expressor tumor DNA. Samples are digested with Eco RI and analyzed as described in "Materials and Methods." The examples shown are: lane 1, BALB/c spleen; lane 2, low-expressor tumor ZII; lane 3, low-expressor tumor 3443; lane 4, high-expressor tumor 3800; lane 5, lymphoma 3373. *Arrows* identify fragments containing endogenous provirus sequences and give their sizes in kb.

blank page

Announcements

The Journal *will publish notices of major meetings dealing with cancer. Submission of notices 6 months in advance is requested to permit timely publication.*

Ions, Cell Proliferation, and Cancer Symposium

The National Cancer Institute and the W. Alton Jones Cell Science Center will sponsor this symposium to be held in Lake Placid, New York, on July 14–16, 1982. Subjects will include the roles of sodium potassium, calcium, and magnesium, pH, cyclic nucleotides and calcium-binding proteins in a wide variety of proliferating systems and in cancer development.

Information on speakers, submission of posters, registration, and accommodations may be obtained by writing to Dr. W. L. McKeehan, W. Alton Jones Cell Science Center, Old Barn Road, Lake Placid, New York 12946 (telephone: 518-523-2427).

Laser, Microwaves, Ultraviolet, and Ultrasound: Biophysical and Biological Basis, Applications, and Hazards in Medicine and Industry Program

The Massachusetts Institute of Technology Department of Mechanical Engineering and the Harvard-MIT Division of Health Science Technology will sponsor this program to be held at the Massachusetts Institute of Technology, Cambridge, Massachusetts, on August 9–13, 1982. The course will emphasize practical considerations in safe and effective use of these modalities in medical and industrial practice, e.g., methods and instrumentation for power measurement, calibration, dosimetry, compliance with Federal and State regulations, etc.

For additional information, please contact the Director of Summer Sessions, Room E19-356, Massachusetts Institute of Technology, Cambridge, Massachusetts 02139.

Fourth Annual Pharmacy Symposium on Cancer Chemotherapy

Houston, Texas, will be the site of this meeting to be held at the Shamrock Hilton Hotel on September 12–14, 1982. The symposium will include sessions on cancer research status; patient psychotherapeutic management; hyperthermia; breast cancer update; DES daughters; and chemotherapy exposure risk. Workshop topics will include a patient panel, reconstructive surgery, death and dying, and bone marrow transplants. A seven-hour course entitled "Oncology Pharmacy: A Basic Course," designed for the new practitioner in oncology pharmacy, will also be held.

For additional information please contact Ms. Sharon Bronson, Department of Pharmacy, M. D. Anderson Hospital and Tumor Institute, 6723 Bertner Avenue, Houston, Texas 77030 (telephone: 713-792-3870).

A New Organization—American College of Epidemiology

A new organization for professional epidemiologists has been founded. The American College of Epidemiology is reviewing applications from individuals who have qualifying training and experience in epidemiology and who have made significant contributions to the study or practice of epidemiology. Membership categories include: Fellow, Associate, Affiliate, and International Fellow.

Dr. Abraham Lilienfeld was elected President of the College. Other Officers include Dr. Dwight Janerich, Vice-President; Dr. Curtis Mettlin, Secretary; Dr. Jess Kraus, Treasurer, and Dr. Jennifer Kelsey, Chairman of Membership Committee.

The goals of the College include the certification of epidemiologists who are trained and accomplished in the practice of their discipline, stimulating of education programs in epidemiology, and providing a forum for discussion of issues confronting the practice of epidemiology.

Persons interested in the programs of the American College of Epidemiology or in membership may obtain additional information from Dr. Curtis Mettlin, Secretary, American College of Epidemiology, ℅ Roswell Park Memorial Institute, 666 Elm Street, Buffalo, New York 14263.

Annual Meeting of the American College of Epidemiology

Chicago, Illinois, will be the site of this meeting to be held at the O'Hare Inn, September 30–October 1, 1982. For further details please contact Dr. Curtis Mettlin, Secretary, American College of Epidemiology, Roswell Park Memorial Institute, 666 Elm Street, Buffalo, New York 14263.

International Cancer Symposium

ITR Biomedical Research of the University of Illinois, International Committee, and the Illinois Cancer Council will sponsor this symposium entitled "Cancer: Etiology and Prevention" to be held at the Pick Congress Hotel, Chicago, Illinois, on October 4–6, 1982.

The scientific program will emphasize research on the genetic characteristics of cancer at the cellular level, immunologic factors in susceptibility, and methods of chemo- and immunoprevention. Special sessions on reconciling the divergent points of view on the use of BCG as an immunoprophylactic agent are planned. All papers by invitation only.

The program will be of particular interest to experimental oncologists, clinicians, immunologists, radiologists, pathologists, oncology nurses, and those involved in cancer control. For further information please contact Dr. Ray G. Crispen, ITR Biomedical Research, University of Illinois, 904 W. Adams Street, Chicago, Illinois 60607.

Symposium on Application of Biological Markers to Carcinogen Testing

The U. S. Environmental Protection Agency will sponsor this symposium to be held at the Holiday Inn, Bethesda, Maryland, on November 15–19, 1982. This symposium will discuss the current status of biochemical and immunologicl markers to carcinogenicity with three main objectives: to review and update specific markers, to identify data gaps, and to recommend research goals. Sessions will encompass in vivo and in vitro systems, enzymes, oncofetal antigens and hormones, monoclonal antibodies, viruses, and DNA-adducts. Abstracts for poster sessions will be accepted until October 15, 1982.

For additional details please contact Ms. Claire M. Wilson, Associated Universities, Inc., Suite 603, 1717 Massachusetts Avenue, N. W., Washington, D. C. 20036 (telephone: 202-462-4475).

A New Journal—Survey of Immunologic Research

S. Karger Publishers announces the newest source of information for immunologists entitled *Survey of Immunologic Research*. This new journal began publication in April. It will provide scientists involved in immunology with an interpretative synthesis of selected topics drawn from the vast array of literature produced each year.

For further information or for sample copies please contact Mr. Paul Clark, S. Karger Publishers, Inc., 150 Fifth Avenue, Suite 1105, New York, New York 10011 (telephone: 212-924-9222).

Eighth FDA Science Symposium

"Recent Advances in Analytical Methodology in the Life Sciences" is the subject of this symposium to be held at the Uniformed Services University of the Health Sciences, 4301 Jones Bridge Road, Bethesda, Maryland, on August 16–18, 1982. The symposium will focus on recent advances being made in areas of analytical methodology—chemical, physical, instrumental, biochemical, physiological, etc.

Attendance is open to all interested parties and there is no registration fee. Interested investigators are invited to submit symposium-related abstracts which may be presented during the poster session. Poster abstracts should be transmittted for consideration no later than July 2, 1982.

For further information please contact Dr. Constantine Zervos, Office of Health Affairs (HFY-31), Food and Drug Administration, 5600 Fishers Lane, Rockville, Maryland 20857 (telephone: 301/443-4490).

☆ U.S. GOVERNMENT PRINTING OFFICE: 1982-361-145/55

blank page

JNCI (NIH Publication No. 82-13)

All issues available have been filmed. Unfortunately, any scattered missing issues are no longer available.

69/1

JNCI

Journal of the National Cancer Institute

July 1982
Volume 69
Number 1

NEWARK PUBLIC LIBRARY
SEP 22 1982
U. S. GOVT. PUBS.
DEPOSITORY 376

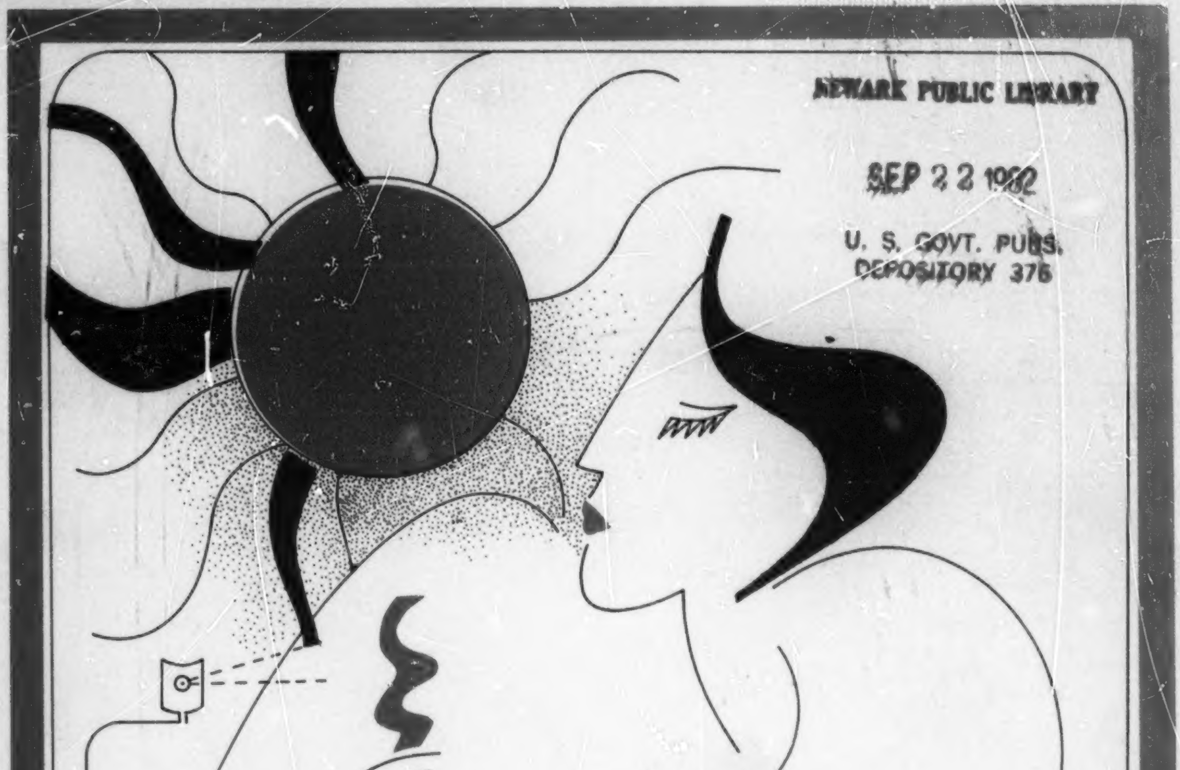

U.S. DEPARTMENT OF HEALTH AND HUMAN SERVICES Public Health Service National Institutes of Health

HE 20.3161:

JNCI Journal of the National Cancer Institute Volume 69 Number 1 pp. 1-318 July 1982

The cover design is an impression of the participants in photochemical reactions, and possibly in photochemical toxicity effects—the host, the light, and synthetic or natural chemicals. Featured in this issue are the proceedings of the Seventh Food and Drug Administration Science Symposium on Photochemical Toxicity, March 17–18, 1981 (*see* proceedings on pages 143–316). [Graphics by Ms. Betty Hebb, Medical Arts and Photography Branch, National Institutes of Health]

JNCI

Journal of the National
Cancer Institute

July 1982
Volume 69
Number 1

THE JOURNAL of the National Cancer Institute solicits manuscripts on original observations in laboratory and clinical research from all scientists. A manuscript is considered for publication with the understanding that it has not been published previously and is submitted exclusively to the Journal. Opinions expressed by the authors are not necessarily those of the publisher or its editors.

THE JOURNAL is published monthly (two volumes a year). The Secretary of Health and Human Services has determined that the publication of this periodical is necessary in the transaction of the public business required by law of this Department.

A MONOGRAPH SERIES covering proceedings of scientific meetings pertaining to cancer is also published. These books may be purchased from the Superintendent of Documents. Series subscriptions are not available and monographs are not included in a subscription to the Journal.

THE JOURNAL is for sale by the Superintendent of Documents, U.S. Government Printing Office, Washington, D.C. 20402. Price per copy, $7.00. Subscription price for two volumes per year in the United States, $70.00; foreign, $87.50. Payment is required in advance, and check or money order should be made payable to the Superintendent of Documents.

All inquiries regarding purchase of subscriptions or depository library distribution, including inquiries about missing issues and change of address, should be addressed to the Government Printing Office. The Government Printing Office requires payment in advance on all orders. Inquiries regarding missing issues or change of address for official subscriptions should be addressed to the Editorial Office, Room 850, Westwood Building, 5333 Westbard Avenue, Bethesda, Md. 20816.

VINCENT T. DEVITA, JR., *Director, National Cancer Institute*

BOARD OF EDITORS

PETER GREENWALD, *Editor in Chief*

ELIZABETH K. WEISBURGER, *Assistant Editor in Chief*

STUART A. AARONSON, *Associate Editor*

CHARLES H. EVANS, *Associate Editor*

MARY A. FINK, *Associate Editor*

JANET W. HARTLEY, *Associate Editor*

DONALD HENSON, *Associate Editor*

RONALD B. HERBERMAN, *Associate Editor*

GEORGE S. JOHNSON, *Associate Editor*

KURT W. KOHN, *Associate Editor*

ARTHUR S. LEVINE, *Associate Editor*

JOHN J. MULVIHILL, *Associate Editor*

ALAN S. RABSON, *Associate Editor*

RICHARD M. SIMON, *Associate Editor*

EDITORIAL STAFF

EDWIN A. HAUGH, *Managing Editor*

PAMELA T. ALLEN, *Assistant Managing Editor*

FLORENCE I. GREGORIC, *Monograph Editor*

Editors: DOROTHY D. KATZ, MERCEDES B. LA CHARITY, I. AGNES REVESZ, JOAN O'BRIEN RODRIGUEZ, CONSTANCE R. STONESTREET, and ANNA B. WITTIG

JNCI (NIH Publication No. 82-13)

U.S. DEPARTMENT OF HEALTH AND HUMAN SERVICES   Public Health Service   National Institutes of Health

Instructions to Authors

Text: Send one original and two copies. **Text-figures** (graphs, charts, and line drawings): Send one original and two copies. **Figures** (photomicrographs and photographs): Send three original glossy prints, unmounted. **Tables:** Send tabular material in typewritten form; do not submit tables as glossy prints to be photographed. The entire manuscript including footnotes, legends, and references must be typed double spaced. Single-spaced portions of a manuscript will be returned to the author for retyping. The mailing address is: Journal of the National Cancer Institute, Westwood Building, Room 850, 5333 Westbard Avenue, Bethesda, Maryland 20816.

Manuscripts should be accompanied by a covering letter from the author responsible for correspondence about the manuscript. The covering letter should contain a statement that the manuscript has been seen and approved by all authors and that all persons listed as authors have made significant (not merely administrative, technical, or supervisory) contributions to the content of the paper. The letter should also state that the manuscript or substantial portions thereof have not been previously published nor are they under consideration for publication in another journal.

Data too extensive for inclusion in a manuscript, but which may be of interest to other investigators, may be deposited with the National Auxiliary Publications Service (NAPS), c/o Microfiche Publications, P.O. Box 3513, Grand Central Station, New York, New York 10017. Authors using the NAPS facilities should indicate in a footnote how their additional data may be obtained.

Approximately one-half of all manuscripts submitted to the Journal are accepted for publication. Publication of manuscripts is contingent on transfer of copyright to the Journal. Forms for this purpose will be sent to authors when a manuscript has been approved for publication. All material published in the Journal is in the public domain; therefore, permission to reproduce any portions is not necessary. As a matter of courtesy, communication should be made to the author(s) concerned.

TITLE: Be brief (no more than 14 words, if possible), but for indexing purposes include all key words. The annual subject index is prepared directly from the titles. Titles that form complete sentences are not acceptable. Do not use abbreviations or chemical formulas in titles.

BYLINE: Supply the complete first name, middle initial, and last name of each author. Avoid use of nicknames. Academic degree is optional; however, if a degree is provided for one author, it should be provided for all authors on a manuscript. Include the name of the institution, address, and zip code for each author. Indicate address for reprint requests in a footnote on the byline.

ACKNOWLEDGMENTS: Financial aid in support of research should be recognized in a footnote. Aid in technical fields, animal care, photography, stenography, and other areas may be mentioned in a separate footnote. Indicate the title (Dr., Mr., Mrs., Miss, Ms.) and affiliation of each person acknowledged.

ABSTRACT: Provide an abstract, 150 words or less, on a separate page. The abstract should describe only *results* of the work being reported. Speculation, historical background, or reference to published works will be deleted from abstracts. Any inbred strains, noninbred stocks, cell lines, or other living materials used in the work should be noted in the abstract.

TEXT: Avoid the use of laboratory jargon and abbreviations not in common usage. When possible, refrain from the use of abbreviations that form words (exceptions are PAGE, ALL). Whenever possible, write mathematical equations and chemical formulas on a single line; submit complicated chemical structures as artwork. Avoid repetition of data in the text when it is presented in tables or text-figures.

Use the following style sources: Webster's *Third New International Dictionary* and Dorland's *Illustrated Medical Dictionary* (25th ed) for spelling; *Council of Biology Editors Style Manual* (4th ed) for scientific abbreviations and symbols; *Government Printing Office Style Manual* for other abbreviations and symbols, punctuation, and hyphenation; *Biochemical Nomenclature and Related Documents* (IUB, 1978) for abbreviations of chemical substances; *Enzyme Nomenclature*, recommendations (1978) of the IUB for recommended names of enzymes and information on nomenclature of isozymes; *The Merck Index* (9th ed) for chemical compounds; "Standard Nomenclature for Inbred Strains of Mice: Seventh Listing" by Joan Staats (Cancer Res 1980;40:2083-2128) for inbred mouse strains; "Standardized Nomenclature for Inbred Strains of Rats: Fourth Listing" by Joan Staats and Michael Festing (Transplantation 1973;16:221-245) for designations of inbred rat strains; *Animals for Research* (9th ed) prepared by the Institute of Laboratory Animal Resources, National Academy of Sciences, for designations of laboratory animal stocks and strains.

TABLES: Submit tabular material typed double spaced on a separate page. Computer print-outs of tables are acceptable only if they are double spaced and with satisfactory title, column headings, legends and other textual material. Provide headings for all columns of a table and indicate units of measurement where applicable.

TEXT-FIGURES: Refer to graphs, charts, and line drawings as text-figures. Make the abbreviations on text-figures identical to the abbreviations used in the text and legends. Symbols and lettering should be large enough to be legible if reduced. Glossy prints or original drawings in black ink are acceptable; orient vertically instead of horizontally.

FIGURES: Refer to photomicrographs and photographs as figures. Figures and their legends should fit a 7.5- by 9-inch dimension. Calculate that nine typewritten lines of legend will require 1 inch of vertical space. Type figure legends on a separate sheet and identify in the legend any lettering used on the figure. Trim photographs to show only important areas. Do not number face of photographs; use the back or overlay to indicate the top and number of each. Printed indicators may be included on photographs; do not use hand-drawn indicators. *Insert internal scale markers on all photomicrographs.* Color photographs must be grouped as a single plate. For color reproduction, submit both color transparencies and high-quality black and white reproductions. The need for color must be documented before it will be considered.

REFERENCES: Use any recent issue of the Journal as a style guide for reference lists. Number references in order of citation in both text and reference list. For periodicals, provide author(s), title of paper, journal, year, volume, and first and last page numbers. For books, give the author(s), title, name(s) of editor(s), location and name of publisher, year, pertinent chapter or section title, and page numbers. Follow *Index Medicus* for punctuation and abbreviations. Citations of papers in preparation or submitted for publication, unpublished observations, and personal communications should be noted parenthetically in the text. Do *not* include them in the reference list. The accuracy of all references is the responsibility of the authors and not of the editorial staff.

LETTERS TO THE EDITOR should pertain to recent articles in the Journal and should not contain new data unless relevant to the discussion of a particular paper. The authors addressed will be invited to reply to comments before correspondence is published. Letters will be edited by the Staff, subject to contributor approval.

FURTHER DETAILS on the preparation of manuscripts are set forth in the document "Uniform Requirements for Manuscripts Submitted to Biomedical Journals" prepared by the International Steering Committee of medical editors (*see* Am Rev Respir Dis 1979;119:3-10/Ann Intern Med 1979;90:95-99/Br Med J 1979;1:532-535/ or Lancet 1979;1:428-430).

UNITED STATES GOVERNMENT PRINTING OFFICE, WASHINGTON, D.C.: 1982

Table of Contents

Vol. 69, No. 1—July 1982

Investigations on Man

1 T-Lymphocyte and B-lymphocyte subpopulations infiltrating human mammary carcinomas — *Oleg Eremin, Robin R. A. Coombs, Terence D. Prospero, David Plumb*

9 Methionine regulation of *N*-5-methyltetrahydrofolate:homocysteine methyltransferase and its influence on the growth and protein synthesis in normal, neoplastic, and transformed cells in culture — *Jadwiga W. Tautt, Elżbieta L. Anuszewska, Jadwiga H. Koziorowska*

15 DNA distribution in human colon carcinomas and its relationship to clinical behavior — *R. C. Wolley, K. Schreiber, L. G. Koss, M. Karas, A. Sherman*

23 Circulating immune complex levels in patients with gestational trophoblastic neoplasia — *Anthony A. Rayner, Ross Berkowitz, Glenn Steele, Jr., Peter H. Schur, Mary L. Rodrick, Donald P. Goldstein, Paul J. Harte, Richard E. Wilson, Norman Zamcheck, Alelia E. Munroe*

Investigations on Nonhuman Systems

27 Decrease of tumor growth in mice after intravenous thymosin-treated bone marrow cell injection — *Didier Cupissol, Augustin Rey, Allan L. Goldstein, Bernard Serrou*

33 Relationship between xenotransplantability and cell surface properties of ascites sublines of a rat mammary adenocarcinoma — *Susan C. Howard, Steven R. Hull, John W. Huggins, Coralie A. Carothers Carraway, Kermit L. Carraway*

41 Steroid hormone receptors in the rat mammary adenocarcinoma induced by *N*-hydroxy-*N*-2-fluorenylacetamide — *Sara Antonia Li, Danuta Malejka-Giganti, Jonathan J. Li*

47 Platinum-complexed antitumor immunoglobulins that specifically inhibit DNA synthesis of mouse tumor cells — *Esther Hurwitz, Rina Kashi, Meir Wilchek*

53 Differences in spleen suppressor cell content in rats with progressing and regressing tumors — *Michael A. Hollingsworth, Donald L. Evans*

59 Gastrin protection against chemically induced gastric adenocarcinomas in Wistar rats: Histopathology of the glandular stomach and incidence of gastric adenocarcinoma — *Massaharu Tatsuta, Hisako Yamamura, Haruo Taniguchi, Hiroshi Tamura*

67 Subcutaneously injected radiolabeled liposomes: Transport to the lymph nodes in mice *Vasily I. Kaledin, Nellie A. Matienko, Valery P. Nikolin, Yevgeny V. Gruntenko, Vladimir G. Budker, Tamara E. Vakhrusheva*

73 Prophylactic and therapeutic actions of supplemental β-carotene in mice inoculated with C3HBA adenocarcinoma cells: Lack of therapeutic action of supplemental ascorbic acid *Giuseppe Rettura, Francis Stratford, Stanley M. Levenson, Eli Seifter*

79 Flow cytometric analysis of R3327 rat prostate adenocarcinoma grown in vivo and in vitro *Alice J. Claflin, Alan Pollack, Theodore Malinin, Norman L. Block, George L. Irvin*

89 Depression of natural antitumor resistance of C57BL/6 mice by leukemogenic doses of radiation and restoration of resistance by transfer of bone marrow or spleen cells from normal, but not beige, syngeneic mice *E. Gorelik, R. B. Herberman*

95 Spontaneous occurrence of atypical hyperplasia and adenocarcinoma of the uterus in androgen-sterilized SD rats *Shinichi Morikawa, Souei Sekiya, Masabumi Naitoh, Hiroshi Iwasawa, Bin Takeda, Hiroyoshi Takamizawa*

103 Combined inhibitors of carcinogenesis: Effect on azoxymethane-induced intestinal cancer in rats *Norman D. Nigro, Arthur W. Bull, Paulette S. Wilson, Barbara K. Soullier, Majid A. Alousi*

109 Generation of long-term T-lymphoid cell lines with specific cytotoxic reactivity for a syngeneic murine lymphoma *Timothy J. Eberlein, Maury Rosenstein, Paul J. Spiess, Steven A. Rosenberg*

117 Pathogenesis of lesions induced in rat lung by chronic tobacco smoke inhalation *Carol A. Heckman, Walden E. Dalbey*

131 Noncytolytic extraction of murine tumor-specific transplantation antigens with the nonionic detergent octyl-β-D-glucopyranoside *Stephen J. LeGrue, Catherine M. Macek, Barry D. Kahan*

137 Use of young nude mice for selection of subpopulations of cells with increased metastatic potential from nonsyngeneic neoplasms *Vincent A. Pollack, Isaiah J. Fidler*

Photochemical Toxicity——Proceedings of the seventh in the series of Food and Drug Administration Science Symposia

---

Introduction

151 Photochemical toxicity: Toxic, allergic, and carcinogenic aspects with emphasis on predicting effects in humans—an introduction *F. Alan Andersen*

Basic chemistry, physics, and biology relating to photosensitization

155 Optical radiation measurements: Instrumentation and sources of error *Robert J. Landry, F. Alan Andersen*

163 Molecular aspects of drug photosensitivity with special emphasis on psoralen photosensitization reaction *Madhu A. Pathak*

171 Immunosuppressive effects of ultraviolet (280–320 nm) radiation and psoralen plus ultraviolet (320–400 nm) radiation in mice *Margaret L. Kripke*

Cellular assay systems

177 Cell damage by near ultraviolet radiation: Role of DNA-protein cross-links *A. Eisenstark, S. Kovacs, J. Terry*

183 Tumor virus induction and host cell capacity inactivation: Possible in vitro tests for photosensitizing chemicals *L. E. Bockstahler, T. P. Coohill, C. D. Lytle, S. P. Moore, J. M. Cantwell, B. J. Schmidt*

189 Comparative photobiology of psoralens *M. J. Ashwood-Smith, A. T. Natarajan, G. A. Poulton*

199 Genotoxic effects of sunlight-activated waste water in cultured mammalian cells *Gary F. Strniste, David J. Chen, Richard T. Okinaka*

205 Interaction of oxygen and oxy-radicals with carotenoids *Norman I. Krinsky, Susan M. Deneke*

211 A method to quantify the potency of photosensitizers that modify cell membranes *John P. Pooler, Dennis P. Valenzeno*

Experimental animal systems

219 In vitro assay of the effects of psoralens plus ultraviolet radiation on human lymphoid cells *Kenneth H. Kraemer*

229 Modification of photocarcinogenesis by chemical agents *Frederick Urbach, P. Donald Forbes, Ronald E. Davies*

237 Current status of predictive animal models for drug photoallergy and their correlation with drug photoallergy in humans *Leonard C. Harber, Robert B. Armstrong, Hideyuki Ichikawa*

245 Toxic effect of ultraviolet light on melanocytes: Use of animal models in pigment research *George Szabo, Frederick B. Blog, Andrija Kornhauser*

Animal photochemical toxicity effects

253 Toxicologic aspects of photosensitization in livestock *A. Earl Johnson*

259 Chemical and biochemical aspects of photosensitization in livestock and poultry *G. Wayne Ivie*

Human photochemical toxicity effects

265 Chemical phototoxicity in humans *John H. Epstein*

269 Human models for identification of photosensitizing chemicals *Albert M. Kligman, Kays H. Kaidbey*

READEX

274 Therapeutic in vivo photochemistry: Photochemical toxicity studies in humans — *John A. Parrish*

279 Photosensitization by porphyrins and prevention of photosensitization by carotenoids — *Micheline M. Mathews-Roth*

287 Ocular phototoxicity and psoralen plus ultraviolet radiation (320–400 nm) therapy: An experimental and clinical evaluation — *Sidney Lerman*

Summary and conclusions

305 Concluding remarks — *Constantine Zervos*

307 Registrants

Correction

317 June 1981, Vol 66, No. 6 pages 1203 and 1233: The Causes of Cancer: Quantitative Estimates of Avoidable Risks of Cancer in the United States Today — *Richard Doll, Richard Peto*

Announcements

317 Second International Congress on Hormones and Cancer

317 Workshop Conference on Diet and Cancer

317 Annual Symposium on Diagnostic Imaging

317 Fourth International Symposium on Nasopharyngeal Carcinoma

317 Fifth Annual Bristol-Myers Symposium on Cancer Research

317 Twenty-Sixth Annual Clinical Conference

318 European Organization for Research on Treatment of Cancer Symposium

318 Thirtieth Annual Scientific Meeting of the American Society of Cytology

318 Sixteenth Midyear Topical Symposium of the Health Physics Society

318 Urological Cancer Symposium

T-Lymphocyte and B-Lymphocyte Subpopulations Infiltrating Human Mammary Carcinomas[1,2]

Oleg Eremin,[3,4] Robin R. A. Coombs,[3] Terence D. Prospero,[3] *and* David Plumb[3,5]

ABSTRACT—Both T- and B-lymphocytes were found in human primary mammary carcinomas and were distributed in widely varying amounts, but in most tumors, T-lymphocytes predominated. A small percentage of the T-lymphocytes expressed receptors for the Fc portion of IgG (FcγR), but very few had receptors for C3 ($C3^+$) (comparable to the findings in blood). A prominent subset of lymphocytes had FcγR and were $C3^+$, and most of these were surface immunoglobulin (sIg)-bearing cells. The majority of lymphocytes from this subset were Fc^+ $C3^+$, and only a small percentage were Fc^+ $C3^-$ (in contrast to the findings in blood). IgD and IgM were the predominant classes of immunoglobulin found on the B-lymphocytes. The different preparative techniques did not result in a selective loss of lymphocyte subsets, but collagenase digestion did lead to a loss of expression of the C3 receptor on the lymphocyte surface, which was recoverable when lymphocytes were reincubated at 37°C. No evidence was found for blocking of the C3 receptor by immune complexes with activated complement—JNCI 1982; 69:1–8.

The presence of lymphocytes within human solid tumors has been well documented histologically [for review, *see* (*1*)]. A prominent host infiltrative response has been found to be associated in many different types of solid tumors with an improved prognosis (*2–12*), suggesting a possible beneficial host antitumor response. The precise functions in vivo of these tumor-infiltrating lymphocytes, however, and in particular their possible role in controlling local growth and preventing metastatic tumor spread, are poorly defined.

We are in the process of investigating the immunologic reactivity and antitumor activity of lymphocytes within human mammary carcinomas. An integral part of our study is the characterization of the different lymphocyte subsets infiltrating these tumors, such knowledge forming an important background for the understanding of the various functional properties of these lymphocytes.

Although various groups of workers have published data on lymphocyte subsets infiltrating different human solid tumors (*13–19*), in most of these investigations various lymphocyte subsets were either incompletely characterized or not studied at all, and very few dealt comprehensively with malignant growths of the breast. In this publication we present our detailed findings on the T- and B-lymphocyte subpopulations infiltrating human mammary carcinomas and describe some of the artifactual alterations of lymphocyte receptors encountered with the enzymatic technique used to isolate the lymphocytes from the tumors. Our findings reveal a pattern of lymphocyte subsets, different in certain aspects, from the pattern previously described for lymphocytes in blood (*20*). Our results suggest a possible selective migration into and/or retention within these primary tumors of specific lymphocyte subsets (with specific functional properties, *see* "Discussion"), thus offering a possible explanation for "tumor escape" from immune defense mechanisms.

MATERIALS AND METHODS

Clinical material.—Patients were women between 40 and 70 years of age with a clinical stage I or II mammary carcinoma (confined to the breast and axilla) and who were undergoing mastectomy and axillary clearance as a potentially curative procedure. Lymph nodes were obtained from the axillary contents of the radical mastectomy specimens. Tonsils were obtained from patients undergoing tonsillectomy for recurring bouts of tonsillitis, which was quiescent at the time of surgery.

Tumor-derived lymphocyte preparations.—Mechanical disaggregation: The breast tumor specimen was obtained sterilely at surgery from the excised biopsy sample which had been sent for the frozen section biopsy examination. The tumor specimen (half of the excised growth) was cleared of fat and fascia and was washed in TCM consisting of RPMI-1640 medium with 10% heat-inactivated FCS, 25 m*M* HEPES[6] (pH 7.2), 0.7 g sodium bicarbonate/liter, 100 μg streptomycin/liter, and 100,000 IU penicillin G/liter. The specimen was then carefully cut (size 10 scalpel blades) into small, thin slices while it was in a small pot filled with TCM. Cells spilled out from the tissue slices during this procedure, and the cell-enriched supernatant was removed, filtered through sterile gauze layers for removal of residual stromal fragments, and then washed five times in TCM. This technique usually produced a low yield of viable cells.

Enzymatic digestion: The small, chopped-up tumor pieces were incubated in collagenase (type I; Sigma London Chemical Co. Ltd., London, England) at 37°C for 11–14 hours. (The enzyme solution was prepared by dissolving 300 U

ABBREVIATIONS USED: $C3^+$=C3 receptor bearing; $C3^-$=lacking a receptor for C3; DARR=direct antiglobulin rosetting reaction; Fc^+=Fc receptor bearing; Fc^-=lacking a receptor for Fc; FcγR=receptor for Fc portion of IgG; FcμR=receptor for Fc portion of IgM; FCS=fetal calf serum; FITC=fluorescein isothiocyanate; K=killer; NK=natural killer; ORBC=ox red blood cells; sIg=surface immunoglobulin; SRBC=sheep red blood cells; T^+=rosetting with SRBC; T^-=lacking a receptor for SRBC; TCM=tissue culture medium; Tγ=T-lymphocytes with FcγR; Tμ=T-lymphocytes with FcμR.

---

[1] Received January 26, 1981; revised January 5, 1982; accepted February 5, 1982.

[2] Supported by a grant from the Cancer Research Campaign (England).

[3] Department of Pathology, Division of Immunology, University of Cambridge, Addenbrooke's Hospital, Hills Road, Cambridge, CB2 2QQ, England.

[4] *Address reprint requests to* Dr. Eremin at his *present address*: Department of Clinical Surgery, University of Edinburgh, The Royal Infirmary, Edinburgh, EH3 9YW, Scotland.

[5] We thank Dr. A. R. Bradwell, Department of Experimental Pathology, Immuno-diagnostics Research Laboratory, Birmingham, England.

[6] 4-(2-Hydroxyethyl)-1-piperazine ethanesulfonic acid.

collagenase/ml in protein-free TCM; this solution was filter sterilized and stored at −30°C.) The prolonged incubation of the tumor pieces produced a thick cell suspension, which was washed six times with TCM and passed through sterile gauze layers for removal of residual stromal fragments and debris. This procedure usually yielded a substantial number of viable cells ($5–50\times10^6$) which was primarily dependent on the size of the tumor specimen to be processed. The lymphocytes were isolated from such enzyme preparations by separation on Sephadex G-10 columns (*see* below). Lymphocyte numbers, viability, and contamination by macrophages and/or tumor cells were reassessed in the column eluate.

Non-tumor-derived lymphocyte preparations.—Blood: Venous blood from healthy adult volunteers was collected by venipuncture into syringes containing preservative-free heparin (30 IU/ml). Lymphocytes were isolated from the heparinized blood on a Ficoll-Hypaque gradient, washed, and suspended in TCM. Monocytes and polymorphonuclear leukocytes were removed from the mononuclear cell suspensiosns by incubation with carbonyl iron (37°C for 1 hr), and the phagocytic cells were removed with a strong magnet.

Lymph nodes and tonsils: Lymphocytes were isolated from the axillary lymph nodes and tonsils as previously described (*20*), and the phagocytic cells were removed as above.

So that the effect of collagenase digestion on lymphocyte viability and cell surface markers could be assessed, various lymphocyte preparations (1×10^7 blood, tonsil, or lymph node cells) were incubated with 15 ml collagenase type I (Sigma London Chemical Co. Ltd.) at 37°C for varying periods (30 min–24 hr). A previous study had revealed that separation of lymphocytes on Sephadex G-10 columns did not result in a selective loss of lymphocyte subsets (*21*).

Cell viability and morphology.—The viability of the cells in the various lymphocyte preparations was ascertained by phase-contrast microscopy, and the morphology of the cells (rosetted and nonrosetted) was determined by examination of wet slides of the mononuclear cell suspensions stained with toluidine blue, by cytocentrifuge preparations, and by dried smears fixed with methanol and stained with May-Grünwald-Giemsa and Sudan black.

Sephadex G-10 columns.—Sephadex G-10 columns, as described previously (*21, 22*), were used to isolate lymphocytes from enzymatically digested tumor cell preparations—the much larger macrophages and tumor cells being entrapped on the column. Occasionally, cell suspensions obtained by mechanical disaggregation were similarly separated.

Surface markers.—The various lymphocyte subsets were determined by the use of lymphocyte markers; this methodology has been outlined previously (*20*). The thymus-derived T-lymphocyte population was detected by the nonspecific SRBC-rosetting reaction (*23*). The T-lymphocyte subset with FcμR was determined by rosette formation with ORBC coated with a subagglutinating dose of rabbit IgM anti-ORBC antibody. Because of the as yet unexplained inhibitory effect of RPMI-1640 medium on the expression of FcμR on human lymphocytes [(*24*); Eremin O, Plumb D: Unpublished observations], both indicator cells and lymphocytes were finally resuspended in medium 199 (GIBCO) containing 10% heat-inactivated FCS, 100 μg streptomycin/liter, and 100,000 IU penicillin G/liter.

The sIg-bearing B-lymphocyte population and the various subpopulations bearing different classes of immunoglobulins (IgG, IgA, IgM, and IgD) were determined by the DARR as described by Coombs et al. (*25*). The same technique was used to couple sheep anti-human C3 and sheep anti-human C4 antibody to ORBC for use as indicator cells in detecting complement components on the lymphocyte surface.

The FcγR-bearing lymphocyte subset was detected by opsonic adherence of ORBC coated with a subagglutinating and an optimal dose of rabbit IgG anti-ORBC antibody (*26*). Complement receptor-bearing lymphocytes were estimated by rosette formation with ORBC sensitized with a subagglutinating and an optimal dose of rabbit IgM anti-ORBC antibody and C5-deficient mouse complement (*20*). Mixed rosetting reactions in which FITC-labeled indicator SRBC and/or ORBC were used have been outlined (*20*).

The class-specific sheep anti-human immunoglobulins and anti-human complement components (purified C3 and C4) were prepared at the Immuno-diagnostics Research Laboratory. The specificities of the immunoglobulin class-specific sheep antisera were characterized by reverse passive hemagglutination of indicator cells (ORBC linked with sheep antisera) with purified human immunoglobulins (*27*).

Statistical analysis.—Where relevant, the significance of a particular lymphocyte subset value was assessed by a one-way analysis of variance.

RESULTS

Non-Tumor-Derived Lymphocyte Preparations

Untreated.—Lymphocytes isolated from the blood of healthy controls and from tumor-free axillary lymph nodes and tonsils were 98% viable and free of contaminating phagocytic cells (≤3%).

Treated.—Incubation of blood lymphocytes at 37°C with collagenase for short periods (1–4 hr) resulted in minimal cell losses, but incubation for long periods (15–24 hr) resulted in substantial cells losses (30–50%). The final cell suspensions, however, were composed of viable lymphocytes (95%). It is obviously not possible in these experiments to reproduce exactly the conditions under which the tumor is digested by the collagenase. Minimal cell losses occurred during incubation of the various lymphocyte preparations in TCM at 37°C for 2–3 days. Lymphocyte suspensions were also passed through Sephadex G-10 columns, and a high percentage (>75%) of viable cells was recovered (*21*).

Tumor-Derived Lymphocyte Preparations

Mechanical disaggregation.—A variable but usually low yield ($<2\times10^6$) of viable cells (tumor cells, macrophages, and lymphocytes) and a correspondingly lower yield ($<1\times10^6$) of lymphocytes were obtained by this technique; however, most of the cells were necrotic and fragmented. Occasionally, mechanical disaggregation of tumors did produce substantial numbers of viable cells ($5–15\times10^6$) and lymphocytes ($2–10\times10^6$). In some instances the cell mixture was purified on Sephadex G-10 columns.

Enzymatic digestion.—Incubation with collagenase yielded a substantially larger number (5–50×10^6) of viable cells (tumor cells, macrophages, and lymphocytes) from the tumor specimens. The total number of cells obtained from any specimen was determined primarily by the size of the tumor sample processed. The number of lymphocytes, relative to the other nonlymphoid cells (1:10–1:1) and in absolute terms (1×10^6–22×10^6), varied markedly from specimen to specimen. Breast tumors with a histologically recognizable and prominent lymphocytic infiltrate yielded the most lymphocytes when enzymatically digested. With many specimens the tumor-infiltrating lymphocytes were isolated from the tumor cell preparations by passage through Sephadex G-10 columns. An average of 44% (30–57%) of the tumor-infiltrating lymphocytes was recovered from the column in the eluate, and an average of 85% (76–94%) of the mononuclear cells eluted from the column was lymphocytes.

Lymphocyte Subpopulations Found in Human Mammary Carcinomas

Table 1 depicts the various lymphocyte subsets found in cell preparations obtained by different preparative techniques from human primary breast cancers. Comparable percentages of rosetting lymphocytes were obtained when both mechanical and enzymatic dispersion techniques were used on the same specimen, provided mechanical disaggregation yielded at least 10^6 viable lymphocytes. With lower yields of viable lymphocytes, discrepancies occurred between the techniques, suggesting that representative lymphocyte subpopulations were not being released from the tumor by the nonenzymatic method (data not shown). Rosetting reactions, depicted in table 1, were only done with lymphocytes prepared by mechanical disaggregation in which at least 10^6 viable lymphocytes were isolated.

The T-lymphocytes were the predominant lymphocyte subpopulation in each preparative group; however, the proportion varied widely among the different preparations, and in a few suspensions, it was less than the B-lymphocyte subset. The percentages of T-lymphocytes in the different cell preparations were comparable. Similarly, the sIg-bearing B-lymphocyte population was comparable in all preparative groups, although again like the T-lymphocyte subset above, the sIg-bearing B-lymphocyte population showed wide biological fluctuations.

The FcγR-bearing lymphocyte subset in the lymphocyte population isolated by collagenase digestion plus Sephadex G-10 passage, however, was just significantly lower ($P<0.05$) when compared with the subsets obtained by the other two preparative techniques. The higher percentages in the other 2 groups were probably due to prominent monocyte-macrophage contamination, which made accurate determination of the numbers of Fc^+ lymphocytes difficult and was not due to selective retention of the subsets on Sephadex G-10 columns (*21*, *22*).

The complement receptor-bearing lymphocyte subset was quite low in the cell preparations obtained by prolonged preincubation with collagenase. The lymphocytes obtained from breast tumors by mechanical disaggregation, however, had a significant percentage of $C3^+$ lymphocytes. This receptor expression suggested either that the collagenase treatment could selectively modify or remove the C3 receptor on the lymphocyte surface or that enzymatic digestion (with its much larger yield of lymphocytes) was freeing lymphocytes from within the tumor substances in which C3 receptors were blocked possibly by complement-containing immune complexes (*see* "Removal of C3 Receptor From Cell Surface by Preincubation of Lymphocytes With Collagenase").

The "null" cell population (lacking sIg and a receptor for SRBC), although higher than that normally found in lymphocyte suspensions from non-tumor-derived lymphoid compartments (*20*, *28*), was still on average low. Less than 10% of the total lymphocytes were isolated from the growths.

A substantial number (20–70%) of the nonlymphoid cells (predominantly macrophages and possibly some tumor cells) possessed FcγR and carried sIg—probably cytophilically acquired. These cells, characterized by morphology and in some instances by staining reactions with Sudan black, were excluded, as far as possible, from the determinations of the appropriate lymphocyte subpopulations. Also, a variable but at times a significant number (0–33%) of the nonlymphoid cells (macrophages) expressed receptors for C3, and these were also excluded from the determinations of the $C3^+$ lymphocyte subpopulations.

TABLE 1.—*T- and B-lymphocyte subpopulations infiltrating human mammary carcinomas*

Preparative technique	Rosetting lymphocyte subset[a]			
	T-rosettes	Fc rosettes	C3 rosettes	sIg rosettes
Collagenase digestion, *n*=20	64±18 (37–80)	22±10 (7–37)	4±5 (0–14)[b]	29±10 (14–45)
Collagenase digestion + Sephadex G-10, *n*=23	58±12 (34–83)	16±6 (10–30)[c]	5±5 (0–10)[b]	34±13 (12–57)
Mechanical disaggregation, *n*=11[d]	55±17 (24–77)	23±9 (13–36)	24±15 (5–60)	36±18 (9–68)

[a] Results are expressed as mean percentages ± standard deviations (ranges).

[b] Collagenase used in the preparative technique removed the C3 receptor, resulting in a very low C3-rosetting lymphocyte subset ($P<0.00001$; *see* tables 2, 3).

[c] This Fc-rosetting lymphocyte subset was just significantly lower ($P<0.05$) when compared with the other two Fc-rosetting subsets. The higher percentages were probably due to prominent monocyte–macrophage contamination in the other 2 groups, which made accurate determination of the numbers of Fc^+ lymphocytes difficult and was not due to selective retention of the subsets on Sephadex G-10 columns (*21*, *22*).

[d] Three samples of tumor-infiltrating lymphocytes were further purified with an additional passage through Sephadex G-10 columns. Lymphocyte preparations were used for rosetting reactions only when ≥1×10^6 viable lymphocytes were isolated by the preparative technique.

TABLE 2.—*Complement components C3 and C4 on tumor-infiltrating lymphocytes*

Breast tumor specimen	Rosetting lymphocytes detected by:[a]			
	Anti-C3		Anti-C4	
	Mechanical disaggregation	Collagenase digestion + Sephadex G-10	Mechanical disaggregation	Collagenase digestion + Sephadex G-10
1	11	1	14	1
2	9	4	24	12
3	10	1	20	1
4	10	14	16	21
5	47	5	36	2
6	11	1	14	1
7	6	4	2	2
8	30	16 (2)	27	15 (7)
9	—	8 (1)	—	18 (2)
10	—	3 (0)	—	23 (8)
Mean ± SD (range)	16±15 (2–47)	6±6 (1–16)	18±12 (2–36)	7±8 (1–21)

[a] Results are expressed as percentages of lymphocytes with C3 and C4 on their cell surface (percentages after incubation in TCM at 37°C for 48 hr). —=not done.

C3 and C4 on Lymphocytes Isolated From Human Mammary Carcinomas

Table 2 reveals the presence of C3 and C4 on human tumor-infiltrating lymphocytes, as detected by rosette formation with sheep anti-human C3- and C4-coated ORBC, and their subsequent loss from the lymphocyte surface after incubation at 37°C for 48 hours in the absence of active complement. The highest percentage of rosettes was seen with lymphocytes obtained by mechanical disaggregation, and reduced percentages of rosettes were found with lymphocytes obtained by collagenase pretreatment. These data, therefore, suggest that receptor blockade was not the reason for the low levels of $C3^+$ lymphocytes found in enzymatic preparations of breast tumors.

The significance of the complement components C3 and C4 on tumor-infiltrating lymphocytes is uncertain. Surgical manipulation and trauma and contamination by blood and tissue fluids, with resultant activation of the complement cascade, may explain the presence of C3 and C4 on the isolated lymphocytes, even when mechanical disaggregation was done in the presence of EDTA, which prevents activation of complement.

Removal of C3 Receptor From Cell Surface by Preincubation of Lymphocytes With Collagenase

For the assessment of the effect of collagenase digestion on tumor-derived lymphocyte surface markers, lymphocytes from blood, tonsil, and lymph node were used as models. Table 3 shows that pretreatment of human lymphocytes with collagenase can result in the loss or possible modification of certain lymphocyte surface receptors, particularly when enzymatic digestion is prolonged. The receptor for SRBC (T-lymphocyte marker) on lymphocytes from tonsil and lymph node was susceptible, even when the incubation periods were short. Blood lymphocytes, contrariwise, required prolonged incubation with collagenase to strip off the receptor.

By the DARR assay, however, sIg was resistant to even prolonged (16 hr) collagenase treatment. The B-lymphocyte population isolated from breast tumors was therefore accurately enumerated. The null cell values in each tumor lymphocyte preparative group were low (*see* table 1), although the null cell values were higher than the values found in non-tumor-derived lymphocyte sources (*20*, *28*). Such values suggest that the enzymatic technique used for the isolation of tumor-infiltrating lymphocytes did not result in artifactual T-lymphocyte values.

The FcγR on lymphocytes from tumor-draining lymph

TABLE 3.—*Effect of collagenase digestion on non-tumor-derived lymphocyte surface receptors*

Lymphocytes[a]			Lymphocyte rosettes[b]			
Source	Incubation, hr	Treatment[c]	T	Fc	C3	sIg
Blood	4	TCM	66	32	13	30
		Collagenase	70	34	4	26
		Reincubation	72	31	17	27
Blood	16	TCM	60	27	23	36
		Collagenase	13	7	1	34
		Reincubation	63	23	24	33
Tonsil	4	TCM	52	45	67	50
		Collagenase	12	1	7	48
		Reincubation	46	7	40	58
Tonsil	16	TCM	60	12	40	38
		Collagenase	32	1	5	42
		Reincubation	55	1	25	44
Lymph node	4	TCM	40	30	58	62
		Collagenase	42	1	1	57
		Reincubation	43	7	40	60
Lymph node	16	TCM	51	29	60	47
		Collagenase	10	1	2	49
		Reincubation	42	6	47	43

[a] Six representative lymphocyte preparations are shown, although in each group five specimens were processed (*see* "Materials and Methods").

[b] Results are expressed as percentages for individual samples.

[c] Incubation of 10^7 lymphocytes was at 37°C for 4–16 hr in 15 ml TCM or collagenase (*see* "Materials and Methods"). After incubation with collagenase, lymphocytes were washed three times in TCM, and some cells were further incubated in TCM at 37°C for 48 hr (reincubation).

nodes and tonsils was highly susceptible to enzymatic digestion. The Fc receptor on blood lymphocytes, however, was resistant to collagenase digestion, although prolonged digestion (16 hr) was usually detrimental to a variable degree. Subsequent incubation in TCM at 37°C for 24–48 hours resulted in the full reexpression of the FcγR on blood lymphocytes but led to only a partial and much-reduced reexpression on lymphocytes from nodes and tonsils.

The C3 receptor on all the lymphocytes tested (irrespective of the lymphoid source) was highly susceptible to pretreatment with the collagenase used to isolate cells from breast tumors. In some instances, enzymatic digestion at 37°C for only 30 minutes resulted in significantly reduced detection of C3$^+$ lymphocytes (data not shown). Subsequent incubation at 37°C resulted in reexpression of the C3 receptor, presumably due to resynthesis of the receptor on the cell surface. This reexpression on blood lymphocytes was again complete after 24–48 hours, whereas with tonsil and lymph node lymphocytes, reexpression was substantial but was often incomplete, and the C3 receptors formed weak rosettes.

Effect of Incubation on Surface Receptors of Lymphocytes

Simple incubation (TCM, 37°C, 48 hr) of lymphocytes isolated from different lymphoid sources (non-tumor derived: blood, lymph node, and tonsil; tumor derived: enzymatically digested with collagenase) further exemplified the differential expression of certain receptors on lymphocytes from different lymphoid compartments.

Non-tumor derived.—No selective loss of T-lymphocyte (SRBC-rosetting) or B-lymphocyte (sIg-bearing) subpopulations occurred during the incubation. Examination of lymph node and tonsil lymphocytes, however, revealed reduced populations of cells expressing the FcγR on the cell membrane. Preincubation of blood lymphocytes, however, did not alter the percentage of FcγR-bearing lymphocytes. This difference probably explains the inability of lymph node and tonsil lymphocytes to reexpress fully the FcγR after pretreatment with collagenase and subsequent incubation in TCM (*see* table 3).

The percentage of measurable C3$^+$ tonsil lymphocytes tended to fall and the rosettes were weaker with reincubated lymphocytes, whereas the C3$^+$ lymph node lymphocyte subset was unchanged (3/5 specimens) or it increased (2/5 specimens). Incubation of blood lymphocytes resulted, in all instances (5 samples), in a prominent increase of the C3$^+$ subpopulation. The increase (blood, lymph node), however, was due to the incomplete expression of FcμR when incubation was with TCM containing RPMI-1640 medium at 37°C for 48 hours.

The FcμR-bearing lymphocyte subset was substantial (20–43%) in all lymphoid compartments studied. These maximal levels were only detected after the lymphocytes were incubated at 37°C and the rosetting assay was performed with the lymphocytes and indicator cells suspended in medium 199.

TABLE 4.—*T^+ Fc^+ ($T\gamma$) subsets of tumor-infiltrating lymphocytes*

Breast tumor specimen	Preparative technique	Mixed rosetting reactions[a]		
		T-rosettes, T^+ Fc^-	Mixed rosettes, T^+ Fc^+	Fc rosettes, T^- Fc^+
1	Mechanical disaggregation	55	5	45
	Collagenase digestion + Sephadex G-10	57	8	35
2	Mechanical disaggregation	88	2	10
	Collagenase digestion + Sephadex G-10	92	1	7
3	Mechanical disaggregation	85	5	15
	Collagenase digestion + Sephadex G-10	77	7	16
4	Collagenase digestion + Sephadex G-10	70	4	26
	Collagenase digestion and reincubation[b]	74	8	18

[a] Results are expressed as percentages of total rosettes counted. FITC-labeled indicator SRBC or ORBC were used (*20*).

[b] Tumor-infiltrating lymphocytes, isolated from collagenase-digested tumor and Sephadex G-10-passaged cells, were incubated in TCM at 37°C for 48 hr.

Tumor derived.—When lymphocytes isolated from breast tumors were incubated in TCM at 37°C for 48 hours, the previously low percentage of C3$^+$ lymphocytes was replaced by a substantially increased number of lymphocytes rosetting with the IgM complement-coated ORBC. Part of the increase was due to the expression of FcμR on the tumor-infiltrating T-lymphocytes (confirmed by rosetting with ORBC coated with rabbit IgM anti-ORBC and by mixed rosetting assays); maximal expression was not influenced by the diluent in which lymphocytes and indicator cells were suspended. The remainder of the rosette increase was due to the reexpression of C3 receptors on the lymphocyte surface. These findings substantiate further that the C3 receptors were degraded or removed from the lymphocyte cell surface by enzymatic digestion during cell preparations. This reexpression of the C3 receptor, in association with the lack of alteration of the FcγR during incubation, is comparable to the findings with blood lymphocytes (*see* "Non-tumor derived") and is indirect evidence that the tumor-infiltrative

TABLE 5.—*sIg^+ and Fc^+ subsets of tumor-infiltrating lymphocytes*

Breast tumor specimen	Preparative technique	Mixed rosetting reactions[a]		
		Immunoglobulin rosettes, sIg^+ Fc^-	Mixed rosettes, sIg^+ Fc^+	Fc rosettes, sIg^- Fc^+
1	Mechanical disaggregation	26	66	8
	Collagenase digestion + Sephadex G-10	37	60	3
2	Collagenase digestion + Sephadex G-10	60	36	4
	Collagenase digestion and reincubation[b]	58	34	8

[a] Results are expressed as percentages of total rosettes counted. FITC-labeled indicator ORBC were used (*20*).

[b] Tumor-infiltrating lymphocytes were isolated from collagenase-digested tumors, passaged through Sephadex G10 columns, and were reincubated in TCM at 37°C for 48 hr.

TABLE 6.—*T^+ $C3^+$ and $T\mu$ subsets of tumor-infiltrating lymphocytes*

Breast tumor specimen	Preparative technique	Mixed rosetting reactions[a]		
		T-rosettes, T^+ $C3^-$	Mixed rosettes, T^+ $C3^+$	C3 rosettes, T^- $C3^+$
1	Mechanical disaggregation	48	2	50
2	Mechanical disaggregation	88	0	12
3	Mechanical disaggregation	78	0	22
	Collagenase digestion and reincubation	55	29[b]	17
4	Collagenase digestion and reincubation	47	33[b]	20

[a] Results are expressed as percentages of total rosettes counted. FITC-labeled indicator SRBC or ORBC were used (*20*).

[b] Tumor-infiltrating lymphocytes were isolated from collagenase-digested tumors and were incubated in TCM at 37°C for 48 hr. The resultant $T\mu$ lymphocytes rosetted with IgM-complement-coated indicator cells as well as with IgM-coated ORBC controls.

TABLE 7.—*Fc^+ and $C3^+$ subsets of tumor-infiltrating lymphocytes*

Breast tumor specimen	Preparative technique	Mixed rosetting reactions[a]		
		Fc rosettes, Fc^+ $C3^-$	Mixed rosettes, Fc^+ $C3^+$	C3 rosettes, Fc^- $C3^+$
1	Mechanical disaggregation	20	63	17
2	Mechanical disaggregation	17	73	10
3	Collagenase digestion and reincubation[b]	22	60	18
4	Collagenase digestion and reincubation[b]	15	43	32

[a] Results are expressed as percentages of total rosettes counted. FITC-labeled indicator ORBC were used (*20*).

[b] Tumor-infiltrating lymphocytes were isolated from collagenase-digested tumors, passaged through Sephadex G-10 columns, and were reincubated in TCM at 37°C for 48 hr.

lymphocyte originates from the intravascular compartment within the mammary tumor.

Characterization of Different T- and B-Lymphocyte Subsets by Mixed Rosetting Reactions on Tumor-Infiltrating Lymphocytes

Mixed rosetting reactions (table 4) showed that only a small number of the tumor-infiltrating T-lymphocytes had FcγR, i.e., were Tγ; most Fc^+ lymphocytes were sIg-bearing B-cells (*see* table 5). This finding was not altered by the preparative technique used (table 4).

Table 6 shows that there were virtually no T^+ $C3^+$ lymphocytes within breast carcinomas. Successful determinations of $C3^+$ lymphocytes could be done only with lymphocytes prepared by mechanical disaggregation of the tumor because enzyme treatment removed the C3 receptor and reincubation, even in RPMI-1640 medium, permitted expression of FcμR, albeit less readily than if the reincubation was in medium 199. The data in table 7 show that in both types of lymphocyte suspensions, prepared either by mechanical disaggregation or by collagenase digestion and Sephadex G-10 separation with reincubation in TCM at 37°C for 48 hours, most of the Fc^+ lymphocytes were also $C3^+$. However, a small percentage (low absolute number) was Fc^+ $C3^-$ lymphocytes, but this percentage was less than the level previously found for blood (*20*), suggesting a selective migration into and a retention and/or proliferation within the mammary tumor of various lymphocyte subsets.

Most of the tumor-derived lymphocytes with FcγR were determined by mixed rosetting assays to belong to the sIg-bearing B-lymphocyte subpopulation. This data is presented in table 5.

Classes of Immunoglobulins Present on Tumor-Infiltrating Lymphocytes

As can be seen from table 8, the spectrum of immunoglobulin classes present on lymphocytes isolated by enzymatic digestion or mechanical disaggregation from breast cancers was similar: IgD and IgM were predominant. The elevated level of IgG-bearing cells in cell suspensions from mechanically disaggregated tumors was probably due to absorbed or cytophilically acquired immunoglobulin because a variable but small number of macrophages was present in the cell suspensions not preincubated at 37°C before the rosetting assay was performed. However, no statistically significant differences were detected when the relevant immunoglobulin class-specific rosettes of the two different preparative groups were compared.

DISCUSSION

The present study has shown that both T-lymphocyte subsets and sIg-bearing B-lymphocyte subsets infiltrate human primary mammary carcinomas. A wide range of values was determined for both the T- and B-lymphocyte populations, but T-lymphocytes were predominant in most specimens studied. This pattern was seen in all the tumor-derived

TABLE 8.—*Classes of immunoglobulins on the surface of tumor-infiltrating lymphocytes*

Preparative technique	Lymphocyte rosettes[a]				
	sIg[b]	IgG	IgM	IgA	IgD
Collagenase digestion + Sephadex G-10, *n*=8	34±14 (12–56)	8±6 (2–17)	16±15 (4–50)	8±6 (1–20)	15±10 (2–25)
Mechanical disaggregation, *n*=4	30±8 (22–35)	12±4 (7–13)[c]	12±6 (7–18)	6±4 (2–11)	17±9 (5–25)

[a] Results are expressed as mean percentages ± standard deviations (ranges). No statistically significant differences were detected by a comparison of the relevant immunoglobulin class-specific rosettes of the 2 preparative groups.

[b] The sIg is expressed as total immunoglobulin.

[c] Cell suspensions obtained from mechanically disaggregated tumors were not preincubated at 37°C before the rosetting assays were performed, which may account for the elevated levels of IgG-bearing lymphocytes detected.

lymphocyte preparations, irrespective of the techniques used for isolation of the tumor-infiltrating lymphocytes. The findings presented in this paper not only confirm some of the published data on T- and/or B-lymphocyte subpopulations infiltrating different types of human solid tumors (*15–18, 29–33*) but also document much more fully and define more precisely the various lymphocyte subpopulations found in malignant growths of the breast.

Mechanical disaggregation, because of its low yield of viable cells, was generally found to be an unsatisfactory technique for isolating tumor-infiltrating lymphocytes from breast tumor specimens. Most cancers were scirrhous and were associated with a prominent stromal reaction; as such, they required enzymatic digestion with collagenase. Häyry and Tötterman (*17*), for humans, and Russell et al. (*34*), for mice, similarly found collagenase to be a satisfactory enzyme for preparation of cell suspensions from solid tumors.

The preparative techniques used in the present investigation did not appear to destroy tumor-infiltrating lymphocyte subsets selectively, but collagenase digestion did alter and probably removed the C3 receptor on lymphocyte surfaces. Continued incubation at 37°C for 48 hours usually resulted in reexpression of C3 on the lymphocyte surface, and although the complement components C3 and C4 were detected on the surface of a variable percentage of the tumor-infiltrating lymphocytes, our inability to detect the C3 receptor (by the rosette assay) on lymphocytes isolated from enzymatically digested tumor specimens was not due to receptor blockade. Pretreatment of non-tumor-derived lymphocytes (e.g., from blood, lymph node, or tonsil) with collagenase type I (Sigma London Chemical Co. Ltd.) did lead to differential losses of the various lymphocyte surface receptors, particularly when incubation was prolonged, and the C3 receptor was especially susceptible.

The C3$^+$ lymphocyte subset therefore was quite prominent among the tumor-infiltrating lymphocytes. Most of the C3$^+$ lymphocytes within the mammary tumors were shown by mixed rosetting reactions to be a subset of the sIg-bearing B-lymphocyte population. Complement receptor-bearing cells infiltrating human cancers have also been described by Claudy et al. (*29*), for skin tumors, and by Catalona et al. (*35*), for bladder neoplasms, but we were unable to find reports in the literature of such lymphocyte subsets infiltration mammary carcinomas. Our investigations have also revealed the presence of tumor-associated immunoglobulin (Eremin O, Plumb D: Unpublished observations) suggesting an in situ antitumor humoral response. The specificity and beneficial (or otherwise) effect of such a response, however, remain to be carefully evaluated.

Fc lymphocyte subsets obtained from breast cancer tissue did not appear to have collagenase-digestable Fc receptors. Although Fc$^+$ subsets were prominent, far fewer Fc$^+$ cells were found in tissue digests than were found in the blood of patients with breast cancers (*20*). In 1979, Vose and Moore (*19*) also described Fc$^+$ lymphocytes infiltrating mammary carcinomas. They, as well as Häyry and Tötterman (*17*), have found FcγR lymphocytes infiltrating a variety of human solid tumors (*16, 17, 19*). In the present study, we further characterized this lymphocyte subset by mixed rosette assays, which revealed that most FcγR lymphocytes belonged to the sIg-bearing population and were Fc$^+$ C3$^+$ cells; a smaller percentage was Fc$^+$ C3$^-$. This Fc$^+$ C3$^-$ tumor-derived subset was much smaller than an identical subset previously found in lymphocyte preparations from blood (*20*). This result, when compared to our previous findings (*36*), suggested a paucity of killer K-lymphocytes and NK lymphocytes infiltrated mammary carcinomas. This lack of K-cell and NK cell cytotoxicities was confirmed by the findings of a concurrent study (*37*), which establishes the importance of the present data and their notable correlation with some of the functional studies done to date. Lack of appropriate cytotoxic cells within breast tumors, although appropriate cytotoxic cells are present in significant numbers in the blood of breast tumor patients, may be partly responsible for continued tumor growth. The T-lymphocyte population isolated from the breast tumors was found in the small number of samples tested to have a small subset of Tγ and a much larger subset of Tμ lymphocytes. The range of Tγ levels is comparable to that of Tγ levels found in blood (Eremin O, Plumb D: Unpublished data), but a larger series of samples is necessary to confirm the lower range of Tμ levels found within tumors compared to the range of Tμ levels detected in blood (Eremin O, Plumb D: Unpublished data). Thus lymphocyte subsets in which both the T-suppressor and the T-helper cells are found (*38*) are present within human mammary tumors. Because of some Fc receptor overlap between helper and suppressor populations and because of the ease with which receptors are modulated on the T-lymphocyte surface, a rigid functional classification based on the reactivities of IgG and IgM receptors on T-lymphocytes may not be correct in some instances.

Bustamante et al. (*32*) and De Panfilis et al. (*33*) described some of the classes of immunoglobulins found on B-lymphocytes infiltrating skin cancers. Their findings are at variance with our data. In our study, IgD and IgM were the predominant classes detected. However, differences may exist between the different pathologic types of solid growths. This intertumor difference is partly suggested by the total absence of IgM-bearing lymphocytes infiltrating malignant melanoma (*32*) and their obvious presence in tumor infiltrates of carcinoma of the breast (*39*).

From the specimens used in the study, no obvious correlation between various tumor parameters (e.g., size, grade of malignancy, or spread to lymph nodes) and the spectrum of lymphocyte subsets was detected. All the data presented, however, were obtained from clinically localized malignant growths—breast tumors with or without metastatic spread to axillary nodes. Metastatic spread of tumor to the regional lymph nodes had no obvious effect on rosetting patterns detected, a finding similar to that described previously for lymphocyte subpopulations of tumor-draining lymph nodes (*20*).

Lymphocytes infiltrating mammary carcinomas presumably migrate into the tumor cell milieu from the intravascular compartment of the tumor, but factors responsible for such cell fluxes are as yet poorly defined (*40–42*). Differential alterations of surface marker profiles for tumor-derived and non-tumor-derived lymphocytes, obtained after digestion with collagenase and/or incubation for prolonged periods at 37°C, suggest that tumor-infiltrating lymphocytes probably originate from the circulating intravascular compartment.

REFERENCES

(*1*) Underwood JC. Lymphoreticular infiltration in human tumors: Prognostic and biological implications: A review. Br J Cancer 1974; 30:538–548.

(*2*) Berg JW. Inflammation and prognosis in breast cancer. A search for host resistance. Cancer 1979; 12:714–720.

(*3*) Anastassiades OT, Pryce ON. Immunological significance of the morphological changes in lymph nodes draining breast cancer. Br J Cancer 1966; 20:239–249.

(*4*) Hamlin IM. Possible host resistance in carcinoma of the breast: A histological study. Br J Cancer 1968; 22:383–401.

(*5*) Hawley PR, Westerholm P, Morston BC. Pathology and prognosis of carcinoma of the stomach. Br J Surg 1970; 57:876–883.

(*6*) Bennett SH, Futrell J, Roth JA, Hoye RC, Ketcham AS. Prognostic significance of histologic host response in cancer of the larynx or hypopharynx. Cancer 1971; 28:1255–1265.

(*7*) Lauder I, Aherne W. The significance of lymphocytic infiltration in neuroblastoma. Br J Cancer 1972; 26:321–330.

(*8*) Fisher ER, Gregario RM, Fisher B, Redmond C, Vellios F, Sommers SC. The pathology of invasive breast cancer. Cancer 1975; 36:1–85.

(*9*) Murray D, Hreno A, Dutton J, Hampson LG. Prognosis in colon cancer: A pathological reassessment. Arch Surg 1975; 110:908–915.

(*10*) Di Paola M, Bertolotti A, Colizza S, Coli M. Histology of bronchial carcinoma and regional lymph nodes as putative immune response of the host to the tumor. J Thorac Cardiovasc Surg 1977; 73:531–537.

(*11*) Sala O, Ferlito A. Morphological observations of immunobiology of laryngeal cancer. Evaluation of the defensive activity of immunocompetent cells present in tumor stroma. Acta Otolaryngol (Stockh) 1976; 81;353–363.

(*12*) Watt AG, House AK. Colonic carcinoma. A quantitative assessment of lymphocyte infiltration at the periphery of colonic tumors related to prognosis. Cancer 1978; 41:279–282.

(*13*) Nind AP, Nairn RC, Rolland JM, Guli EP, Hughes ES. Lymphocytic anergy in patients with carcinoma. Br J Cancer 1973; 28:108–117.

(*14*) Yata J, Desgranges C, De-Thé G, et al. Nasopharyngeal carcinoma. VII. B and T lymphocytes in the circulating blood and in tumor tissue. Biomedicine 1974; 21:244–250.

(*15*) Jondal M, Klein G. Classification of lymphocytes in nasopharyngeal carcinoma (NPC) biopsies. Biomedicine 1975; 23:163–165.

(*16*) Vose BM, Vánky F, Klein E. Human tumor–lymphocyte interaction in vitro. V. Comparison of the reactivity of tumor-infiltrating, blood and lymph-node lymphocytes with autologous tumor cells. Int J Cancer 1977; 20:895–902.

(*17*) Häyry P, Tötterman TH. Cytological and functional analysis of inflammatory infiltrates in human malignant tumors. I. Composition of the inflammatory infiltrates. Eur J Immunol 1978; 8:866–871.

(*18*) Svennevig JL, Close O, Harboe M, Svaar H. Characterization of lymphocytes isolated from non-lymphoid human malignant tumors. Scand J Immunol 1978; 7:487–493.

(*19*) Vose BM, Moore M. Suppressor cell activity of lymphocytes infiltrating human lung and breast tumors. Int J Cancer 1979; 24:579–585.

(*20*) Eremin O, Plumb D, Coombs RR. T and B lymphocyte populations in human normal lymph node, regional tumor lymph node and inflammatory lymph node. Int Arch Allergy Appl Immunol 1976; 52:277–290.

(*21*) Kanski A, Spencer J, Eremin O. Sephadex G-10 columns do not retain selectively T and B lymphocyte subpopulations. J Immunol Methods 1981; 42:147–156.

(*22*) Eremin O, Wilson A, Coombs RR, Ashby J, Plumb D. Antibody-dependent cellular cytotoxicity in the guinea pig. The role of the Kurloff cell. Cell Immunol 1980; 55:312–327.

(*23*) Brown G, Greaves MF. Enumeration of absolute numbers of T and B lymphocytes in human blood. Scand J Immunol 1974; 3:161–169.

(*24*) Moretta L, Ferrarini M, Durante LM, Mingari MC. Expression of a receptor for IgM by human T cells in vitro. Eur J Immunol 1975; 5:565–569.

(*25*) Coombs RR, Wilson AB, Eremin O, et al. Comparison of the direct antiglobulin rosetting reaction with the mixed antiglobulin rosetting reaction for the detection of immunoglobulin on lymphocytes. J Immunol Methods 1977; 18:45–54.

(*26*) Hallberg T, Gurner BW, Coombs RR. Opsonic adherence of sensitized ox red blood cells to human lymphocytes as measured by rosette formation. Int Arch Allergy Appl Immunol 1973; 44:500–510.

(*27*) Coombs RR, Edebo L, Feinstein A, Gurner BW. The class of antibodies sensitizing bacteria measured by mixed reverse passive antiglobulin haemagglutination (MrPAH). Immunology 1978; 34:1037–1044.

(*28*) Eremin O, Roberts P, Plumb D, Stephens JP. Human regional tumor lymph nodes: Alterations of micro-architecture and lymphocyte subpopulations. Br J Cancer 1980; 41:62–72.

(*29*) Claudy AL, Viac J, Schmitt D, Alaris A, Thivolet J. Identification of mononuclear cells infiltrating basal cell carcinomas. Acta Derm Venereol (Stockh) 1976; 56:361–365.

(*30*) Husby G, Hoagland PM, Strickland RG, Williams RC Jr. Tissue T and B cell infiltration of primary and metastatic cancer. J Clin Invest 1976; 57:1471–1482.

(*31*) Schoorl R, Riviere AB, Borne AE, Feltkamp-Vroom TM. Identification of T and B lymphocytes in human breast cancer with immunohistochemical techniques. Am J Pathol 1976; 84:529–544.

(*32*) Bustamante R, Schmitt D, Pillet C, Thivolet J. Immunoglobulin-producing cells in the inflammatory infiltrate of cutaneous tumors. Immunocytologic identification in situ. J Invest Dermatol 1977; 68:346–349.

(*33*) De Panfilis G, Colli V, Manfredi G, et al. In situ identification of mononuclear cells infiltrating cutaneous carcinoma: An immunohistochemical study. Acta Derm Venereol (Stockh) 1979; 59:219–222.

(*34*) Russell SW, Doe WF, Hoskins RG, Cochrane CG. Inflammatory cells in solid murine neoplasms. I. Tumor disaggregation and identification of constituent inflammatory cells. Int J Cancer 1976; 18:322–330.

(*35*) Catalona WJ, Mann R, Nime F, et al. Identification of complement-receptor lymphocytes (B cells) in lymph nodes and tumor infiltrates. J Urol 1975; 114:915–921.

(*36*) Eremin O, Kraft D, Coombs RR, Franks D, Ashby J, Plumb D. Surface characteristics of the human K (killer) lymphocyte. Int Arch Allergy Appl Immunol 1977; 55:112–125.

(*37*) Eremin O, Coombs RR, Ashby J. Lymphocytes infiltrating human breast cancers lack K cell activity and show low levels of NK cell activity. Br J Cancer 1981; 44:166–176.

(*38*) Moretta L, Mingari MC, Moretta A, Romanzi CA. Immunoregulatory subpopulations of human T lymphocytes. Biomedicine 1979; 30:4–8.

(*39*) Richters A, Kaspersky CH. Surface immunoglobulin positive lymphocytes in human breast cancer tissue and homolateral axillary lymph nodes. Cancer 1975; 35:129–133.

(*40*) Emeson EE. Migratory behavior of lymphocytes with specific reactivity to alloantigens. J Exp Med 1978; 147:13–18.

(*41*) Haskill JS, Parthenais E. Immunologic factors influencing the intra-tumor localization of ADCC effector cells. J Immunol 1978; 120:1813–1817.

(*42*) Radov LA, Haskill JS, Korn JH, Fett JW. Correlation between tumor-specific systemic and in situ immunity as manifested by the delayed hypersensitivity response. JNCI 1979; 62:103–108.

Methionine Regulation of *N*-5-Methyltetrahydrofolate:Homocysteine Methyltransferase and Its Influence on the Growth and Protein Synthesis in Normal, Neoplastic, and Transformed Cells in Culture[1,2]

Jadwiga W. Tautt,[3] Elżbieta L. Anuszewska,[3] *and* **Jadwiga H. Koziorowska[3]**

ABSTRACT—Normal human embryonic fibroblasts (CLV-58) and normal embryonic rat fibroblasts (REF) revealed equal growth in media containing 0.2 m*M* DL-homocysteine thiolactone (HOM) or in methionine (METH) enriched with 1.5 μ*M* cyanocobalamin and 0.1 m*M* folic acid, whereas L 5178Y lymphoblasts and transformed rat fibroblasts (REF-S) showed more or less acute need for exogenous METH. In normal cells general protein synthesis remained unimpaired during 24 hours after substitution of METH by HOM. In L 5178Y and REF-S cells, however, protein synthesis was significantly inhibited. Measurements of *N*-5-methyltetrahydrofolate:homocysteine methyltransferase revealed a two- to threefold increase of enzyme activity in normal cells grown on HOM and in L 5178Y and REF-S cells grown on HOM with added METH. HeLa cells showed variability in growth pattern, in general protein synthesis response, and in inducibility of methyltransferase upon substitution of METH by HOM.—JNCI 1982; 69:9–14.

The enzymatic biosynthesis of METH, its mechanism, and regulation have been the subject of many studies. In animal tissues the final methyl transfer reaction that converts HOM to METH is catalyzed by mTHF:HOMmTase (EC 2.1.1.5). Due to the activity of this enzyme, METH requirements of whole animals (*1*) and cells cultured in vitro (*2*) can be met by nutrients that contain HOM, folic acid, and vitamin B_{12} without added METH.

In the course of the search for metabolic differences between normal and neoplastic cells, it was demonstrated that eight cell lines derived from normal tissues show equal growth in medium that contains either METH or HOM (*3–8*). This was not the case with FL amnion cells (*4*); however, these cells are heteroploid and exhibit HeLa cell markers. The findings presented in the above studies as well as in the studies of Chello and Bertino (*9*) also show that Walker carcinosarcoma 256, mouse 5178Y lymphoma, mouse lymphatic leukemia L 1210, P 1815 mastocytoma, human monocytic leukemia J 111, human lymphoblastic leukemia CCRF-HSB-2, lung adenocarcinoma A-549, and two human virus-transformed cell lines all exhibit absolute METH requirement for cell growth in culture. These observations are in contrast with the earlier results (*2, 10*) that indicate that HEP-2 and HeLa cells exhibit comparable growth on METH and HOM. It is difficult to establish the validity of these experiments because the authors used undialyzed serum in their experiments that could have provided sufficient amounts of METH for cell growth. Recently, Kreis and Goodenow (*8*) concluded that a general discrimination between benign and malignant tissue on the grounds of capability of a nutritional replacement of METH by HOM is not applicable for human neoplastic cells. They found that three cell lines derived from human tumors including HeLa cells showed comparable growth in both kinds of media. In recent studies we have demonstrated that cells from methylcholanthrene-induced unpassaged rat sarcomas behave similarly in METH-deprived culture medium and in medium without METH but supplemented with HOM, folic acid, and vitamin B_{12} (*11*).

The activity of mTHF:HOMmTase was shown to be dependent on the level of vitamin B_{12} (*12, 13*), folic acid (*14*), and METH (*13, 15*). Studies of Kamely et al. (*3*) demonstrated that in BHK cells mTHF:HOMmTase activity increased 2.5- to 4.0-fold over the highest levels obtained in the presence of METH, B_{12}, and folic acid when HOM was substituted for METH in the growth medium. This enzyme activity increase was blocked by puromycin. BHK cells showed equal growth in medium that contained either METH or HOM. Taylor and Hanna (*16*) have analyzed the effects of cyanocobalamin, L-METH, folic acid, DL-mTHF and other nutrients on mTHF:HOMmTase in CHO cells and their mutants. The mutants were distinguished from CHO cells by their incapability to grow and survive when HOM was substituted for METH. The authors concluded that the level of mTHF:HOMmTase induced by high medium folate concentrations is a critical determinant of CHO cell survival in METH-free media.

In the present study we attempted to determine biochemical events that correlate with METH auxotrophy of cells in culture. For this purpose we analyzed the effects of METH depletion or decrease and HOM addition on the growth of normal, transformed, and neoplastic cells in culture. We also determined the response of general protein synthesis to these media changes and measured the levels of mTHF:HOMmTase in cell extracts. Since the increase of mTase activity upon METH substitution by HOM requires concomitant protein synthesis (*3*), we have assumed that substitution of METH by HOM may lead to impairment of protein synthesis in certain cells, diminishing the enzy-

---

ABBREVIATIONS USED: BHK=baby hamster kidney; CHO=Chinese hamster ovary; EMEM=Eagle's minimum essential medium; HOM=homocysteine; METH=methionine; mTase=methyltransferase; mTHF=*N*-5-methyltetrahydrofolate; PBS=phosphate-buffered saline; REF=rat embryonic fibroblast; REF-S=transformed rat fibroblast.

[1] Received April 15, 1981; revised November 12, 1981; accepted November 19, 1981.

[2] Supported by the Polish National Cancer Program PR-6, Warsaw, Poland.

[3] Institute for Drug Research and Control, 00-725 Warsaw, Chełmska 30/34, Poland.

matic formation of METH to amounts that are insufficient for the growth and survival of these cells.

MATERIALS AND METHODS

Cell lines.—HeLa and L 5178Y cells were cultivated in our laboratory for several years. Normal human CLV-58 cell line was obtained by standard methods. REF were derived from 19-day-old embryos of Sprague-Dawley rats. REF-S cells were spontaneously transformed counterparts of REF cells. In a series of experiments we ascertained that the cells produced fibrosarcomas in 100 percent of animals when inoculated into newborn Sprague-Dawley rats.

Culture methods.—All cells, with the exception of L 5178Y lymphoblasts, were grown routinely in flasks in commercially available EMEM 1959. L 5178Y cells were cultured in suspension in Fischer's medium without stirring. The media were reinforced with 10 or 8% calf serum, respectively, previously dialyzed for 24 hours at 4°C against three changes of a solution containing 8 g NaCl, 0.4 g KCl, 1 g glucose, and 0.35 g $NaHCO_3$ per liter and supplemented with 100 µg streptomycin sulfate/ml and 100 U penicillin G/ml. The dialyzed calf serum was analyzed by a microbiological method using Leuconostoc mesenteroides P 60 to ascertain its METH contribution to the media. Only a trace amount of METH was found in the dialyzed serum. For three passages prior to the experiments all cell types were cultivated in media enriched with 1.5 µ*M* cyanocobalamin and then harvested, washed, and transferred into experimental media. During the course of the studies, the cells were repeatedly checked by the method of Chen (*17*) to assure that they were free of Mycoplasma contamination.

Experimental media.—The basic experimental media consisted of EMEM and Fischer's medium without METH and folic acid. During the experiments, 0.2 m*M* DL-homocysteine thiolactone was added to the media enriched with 1.5 µ*M* cyanocobalamin and 0.1 m*M* folic acid. All media were reinforced with dialyzed calf serum, 10 or 8% respectively, and with different amounts of METH where indicated.

Growth rate and viability.—Growth rate was assessed every 24 hours during 3 days by determination of cell numbers. Triplicate cell counts, in agreement within ±10%, were averaged to plot the cell growth pattern. The data presented in the text are means from 5–6 studies performed for each type of culture. Viability of the cells was checked by the trypan blue exclusion test.

Enzyme preparation and assay.—All cells, with the exception of L 5178Y cells, were released from the surface by trypsin. Trypsinization was stopped by addition of the serum-containing medium. All cells were washed twice in PBS (pH 7.2), suspended in phosphate buffer (pH 7.4) that contained 0.01 *M* of reduced glutathione, and disrupted in a sonic oscillator (MSE-MK 2; MSE, 25–28 Buckingham Gate, London S.W.1. England). The debris was removed by centrifugation at 20,000×*g* for 30 minutes and the supernatant was assayed for mTHF:HOMmTase activity. Protein concentration was measured by the method of Lowry et al. (*18*) in each sample.

The activity of mTHF:HOMmTase was determined by measurement of [^{14}C]METH formation from [5-^{14}C]mTHF as described by Kamely et al. (*3*). A standard reaction mixture contained in a total volume of 0.200 ml was 100 m*M* phosphate buffer (pH 7.4), 125 m*M* 2-mercaptoethanol (Fluka, Buchs, Switzerland), 250 µ*M* (−)-s-adenosyl-L-methionine iodide (Calbiochem-Behring Corp., La Jolla, Calif.), 50 µ*M* cyano-B_{12} (Sigma Chemical Co., London, England), 250 µ*M* DL-HOM (Serva Feinbiochemica GmbH, Heidelberg, Federal Republic of Germany) prepared just before use from the thiolactone derivative, 100 n*M* [5-^{14}C]mTHF (sp act, 57 mCi/m*M*; Amersham International Ltd., Amersham, England), and 100 µl of cell extract. The reaction mixtures were incubated for 1 hour at 37°C and the reaction terminated by addition of 0.8 ml of ice cold water. The mixtures were passed through a Dowex 1-Cl (SERVA) column, that retained [5-^{14}C]mTHF and washed with an additional 1.0 ml water. The [^{14}C]METH thus formed was measured in the pooled effluent by counting an aliquot in a toluene-Triton-X-100-2,5-diphenyloxazole, (PPO) and 1,4-bis[2-(5-phenyloxazolyl)]benzene (POPOP) solution with a liquid scintillation spectrometer (LS 3150 P; Beckman Instruments Inc., Cedar Grove, N.J.). Specific activities were expressed in nmoles of METH formed per milligram protein per hour at 37°C and were the average of three determinations with a variation of less than 10%.

Determination of protein synthesis.—For studies of protein synthesis a number of parallel cultures were seeded at 1–2×10^4 cells per flask and grown in 2 ml of experimental culture medium. At definite time intervals, every monolayer culture was labeled for 30 minutes with 1 µCi of L-[^{3}H]-valine/ml (sp act, 2 Ci/mmol; Amersham International Ltd.). We stopped incorporation by decanting the pulsing medium, washing the cultures five times with cold Earle's salt solution, and dissolving the cells in 0.5 ml of 1 *N* NaOH. After 20 minutes at 37°C, 1 ml of 20% trichloroacetic acid was added to precipitate the cell protein. The precipitate was collected on Millipore filters (Millipore Corp., Bedford, Mass.) and counted in a toluene-based scintillation fluid. L 5178Y cells were centrifuged at 120×*g* for 10 minutes, washed three times, dried, and processed as indicated above. The radioactivity of all samples was measured with a Beckman LS 3150 P liquid scintillation spectrometer.

RESULTS

All cell types were studied several times in the course of

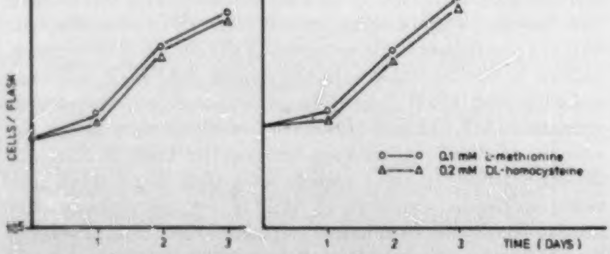

TEXT-FIGURE 1.—Growth of REF and CLV-58 cells in media containing L-METH, or DL-HOM without METH. *Abscissa:* time in days after inoculation. *Ordinates:* cell growth as evaluated by number of cells per flask.

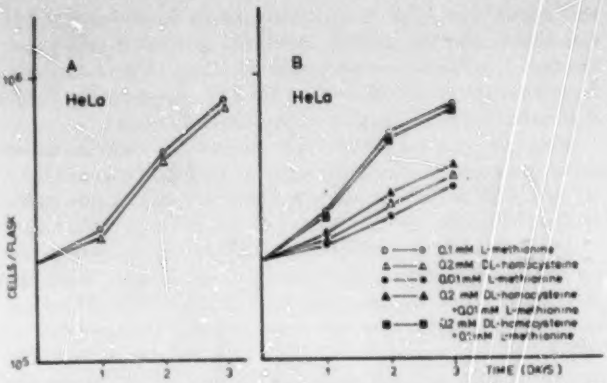

TEXT-FIGURE 2.—Variations in the growth pattern of HeLa cells. A) Growth of HeLa cells in media containing L-METH or DL-HOM without METH, or B) in the same media and in media with DL-HOM and L-METH added at indicated concentrations. *Ordinates and abscissa* are as in text-fig. 1.

TABLE 1.—*mTHF:HOMmTase activities in various cell types*

Cell line[a]	METH formed/mg of protein/hr, nmole ± SE[b]
CLV-58	24.5±4.9
REF	54.8±0.3
REF-S	32.0±6.2
HeLa	38.8±7.8–48.8±8.8
L 5178Y	15.0±3.1

[a] Cells were grown in the basic media containing 0.2 mM DL-HOM, 1.5 μM cyanocobalamin, and 0.1 mM folic acid.

[b] Mean values of 5–6 measurements.

passaging. The CLV-58 normal human embryonic fibroblasts and REF showed unimpaired growth independently of the passage level investigated (from 5 to 20 for CLV-58 cells and from 4 to 10 for REF cells) in the medium devoid of METH but supplemented with HOM and enriched with cyanocobalamin and folic acid (text-fig. 1). In contrast to the earlier findings (*8*), HeLa cells revealed varied responses to substitution of METH by HOM. In successive sets of experiments performed at intervals of several weeks, the cells showed either unimpaired rate of growth on HOM (text-fig. 2A) or their growth on day 3 decreased to about 50% of the control level (text-fig. 2B). The decrease in growth rate could be reversed and brought back to control levels in the presence of 0.1 mM METH. L 5178Y cells (text-fig. 3) revealed the reported inability of growth (*3*) on HOM unless it was enriched with 0.1 mM METH. Text-figure 3

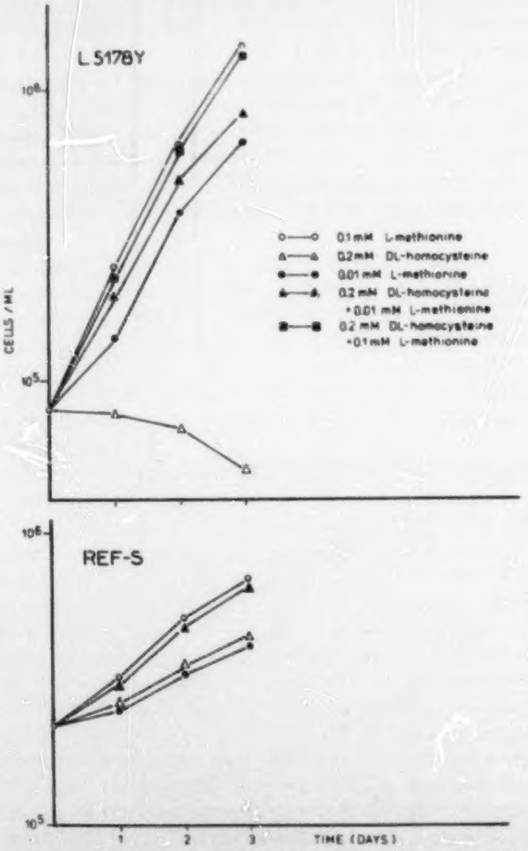

TEXT-FIGURE 3.—Growth of REF-S and L 5178Y cells in media containing L-METH, or DL-HOM without METH, or DL-HOM and L-METH. *Ordinates:* cell growth as evaluated by the number of cells per flask for REF-S cells or by the number of cells per ml for L 5178Y cells. *Abscissa:* time after inoculation.

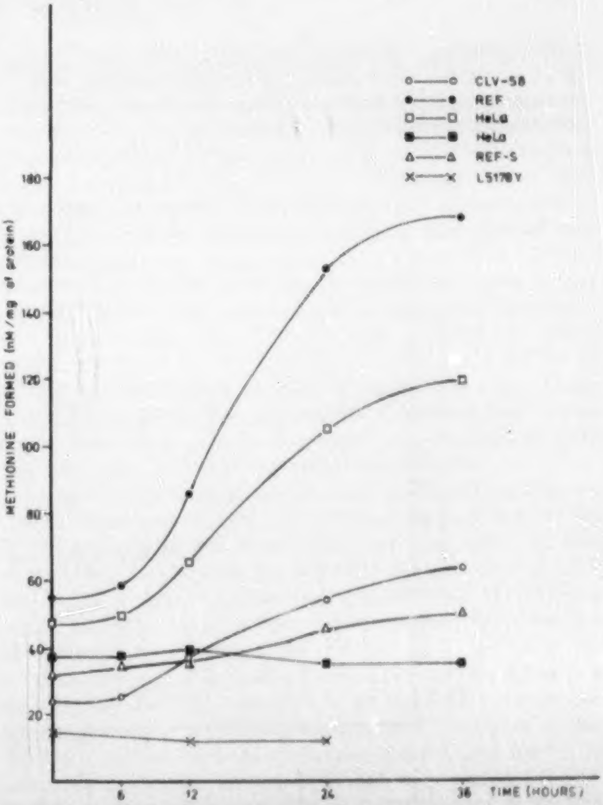

TEXT-FIGURE 4.—mTase activity in cell extracts after refeeding with METH-deficient medium. Cells were grown in media supplemented with 0.1 mM folic acid, 0.2 mM DL-HOM, and 1.5 μM cyanocobalamin.

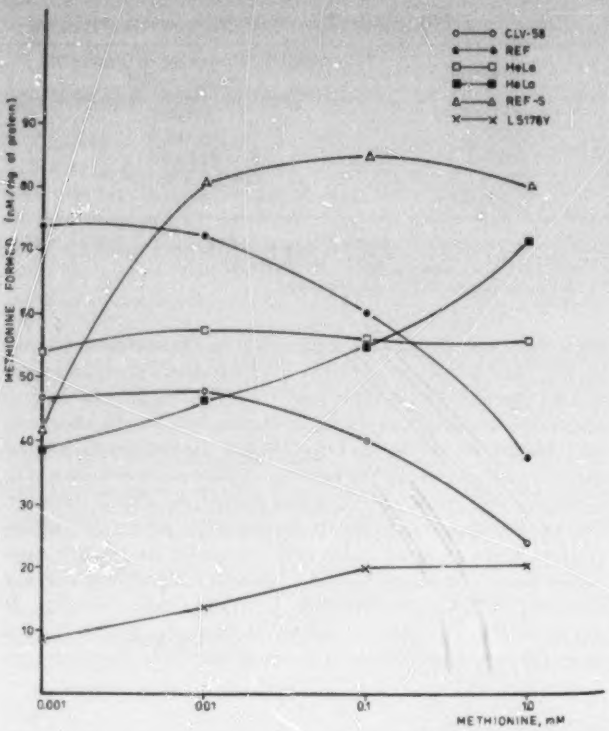

TEXT-FIGURE 5.—Effect of METH concentration on the specific activities of mTase. Cultures were inoculated for 24 hr in EMEM or Fischer's medium containing DL-HOM and various amounts of L-METH and then assayed for enzyme-specific activities.

also shows that REF-S, grown in media in which METH was substituted by HOM, exhibited growth impairment: On day 3, growth rate decreased to about 60% of controls. A concentration of 0.01 mM of METH improved the REF-S growth rate to reach that of the control cultures.

Measurements of mTHF:HOMmTase activity.—Specific activity of the enzyme was twice as great in REF than in CLV-58 and REF-S cells in analogous culture conditions (table 1). L 5178Y cells showed rather low specific enzyme activity.

After substitution of HOM for METH, the enzyme activity remained at about the same level for 6 hours in all the cell cultures (text-fig. 4), then in REF and CLV-58 cells it increased threefold over the next 30 hours as compared to zero time. In contrast, in L 5178Y cells enzyme activity did not show any increase during 24 hours. At 36 hours the mTHF:HOMmTase activity was not measured in L 5178Y cells because of a gradual loss of cell viability under these culture conditions. REF-S cells showed a rather small but significant ($P<0.05$) increase of specific enzyme activity.

The experiments performed at different time intervals revealed that in HeLa cells the specific activity of mTHF:HOMmTase remained unchanged or increased to a value 2.5 times higher than that at zero time.

Text-figure 5 shows that increase of the METH levels from 0.001 mM to 0.1 mM in the HOM-containing medium raised B_{12}-mTase activity in REF-S and L 5178Y cells twofold. However, the optimal level of METH for a twofold increase in L 5178Y cells was ten times higher than that in REF-S cells. In contrast, supplementation of the media with increasing amounts of METH led to a gradual repression of the enzyme activity in normal CLV-58 and REF cells. Text-figure 5 also shows that in HeLa cells METH either did not

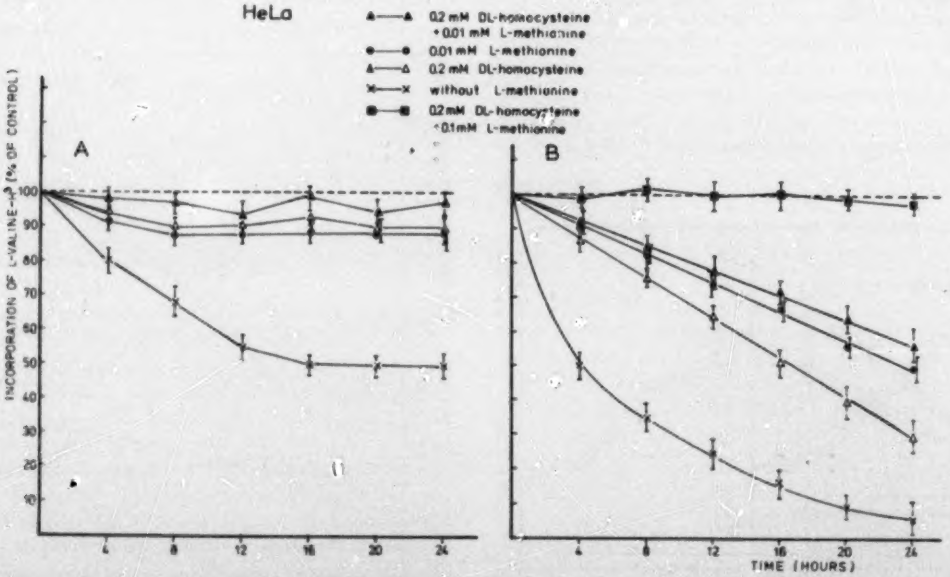

TEXT-FIGURE 6.—Variability in the response of general protein synthesis in HeLa cells. A) Protein synthesis in HeLa cells cultured in EMEM without L-METH and in EMEM with 0.2 mM DL-HOM without METH. B) Protein synthesis in HeLa cells cultured under the same conditions as in panel A and additionally in EMEM containing 0.2 mM DL-HOM and 0.01 mM or 0.1 mM METH. Protein synthesis was measured by [^{3}H]valine incorporation. Synthesis is expressed as percentage of control value; each point is the mean of triplicate aliquots.

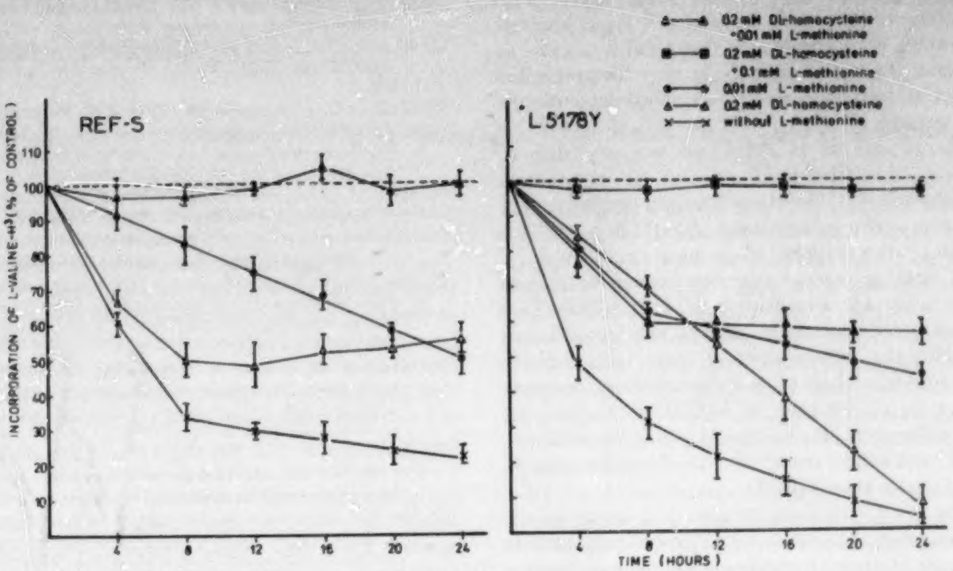

TEXT-FIGURE 7.—Protein synthesis in REF-S and L 5178Y cells cultured in EMEM or in Fischer's medium without L-METH, or in EMEM with 0.2 m*M* DL-HOM without L-METH, or DL-HOM and L-METH, respectively, at the concentrations indicated. Experiments were performed and the synthesis was estimated as indicated in text-fig. 6.

influence enzyme activity or with increasing levels raised it progressively.

Measurements of protein synthesis.—We performed these experiments to determine whether or not cell growth response differences that were due to changes in the media content were correlated with differences in the protein synthesis response.

After METH was substituted for HOM, protein synthesis in HeLa cells either remained unimpaired (text-fig. 6A), or was significantly inhibited ($P<0.001$) (text-fig. 6B). In this series of experiments as much as 0.1 m*M* METH was needed to prevent inhibition of protein synthesis. It is evident from text-figure 6 that the protein synthesis response to exogenous METH deprivation also showed a significant ($P<0.01$) degree of variation.

Inhibition of protein synthesis in REF-S cells was noticeable already 4 hours after METH deprivation, and it declined to 20% of the control level at zero time after 24 hours (text-fig. 7). Substitution of METH by HOM caused the level of protein synthesis to fall about 60% of the control level at zero time in 24 hours. When cells were incubated in medium with 0.01 m*M* METH, the valine incorporation declined to levels similar to those observed in medium with HOM but without METH. However, in the presence of HOM and 0.01 m*M* METH, protein synthesis was unaffected. In L 5178Y cells the inhibition of valine incorporation was complete after 24 hours both in medium without METH and in medium without METH but containing HOM. In cells that were cultivated on HOM, ten times as much 0.1 m*M* METH was needed to restore protein synthesis.

In both types of normal cells, CLV-58 and REF, grown in medium devoid of METH, protein synthesis remained unaffected for the period of 24 hours.

DISCUSSION

Conflicting views have been presented to explain differences in the capacity of mammalian cells to grow in culture media that contain HOM instead of METH. Ashe et al. (*4*) demonstrated that adult normal cell extracts have a higher proportion, about 75%, of their total mTHF:HOMmTase in the holoenzyme form, whereas all neoplastic cell and embryonic cell extracts have less than 45% of their enzyme in this form. On the basis of this evidence, they claimed that neoplastic cells may have one or more defects that prevent them from using HOM in place of METH for growth and survival. Other studies (*7*) indicate, however, that neoplastic and transformed cells, although they are METH auxotrophs, do synthesize METH endogenously from mTHF at rates that are at least as high as in normal cells. These findings led the authors to conclude that there was one or more specific functions in neoplastic and transformed cells that can only be fulfilled by exogenous METH.

In our studies normal human and rat fibroblasts did not change their growth rate upon replacement of METH by HOM and supplementation of medium with folic acid and vitamin B_{12}. In the presence of HOM the growth of REF-S and L 5178Y cells remained unimpaired when METH was added to the medium. HeLa cells were either dependent or independent of exogenous METH.

Measurement of mTHF:HOMmTase activity showed a two- to threefold increase in CLV-58 and REF upon substitution of METH by HOM, whereas in L 5178Y cells and REF-S a similar increase in enzyme activity occurred only when the cells were grown on HOM with added METH. HeLa cells showed a twofold increase of enzyme activity in some experiments in the absence, and in others, exclusively in the presence of METH. From a comparison of experimental conditions under which various cell types showed unimpaired growth with conditions that enable a two- to threefold increase of enzyme activity, it may be concluded that this enzyme activity increase was a critical determinant of unimpaired growth.

The increase of mTHF:HOMmTase activity due to METH removal from the medium can be completely blocked by puromycin (*3*). From our findings on the protein synthesis response to the substitution of METH by HOM, it is evident that impairment of protein synthesis in L 5178Y, REF-S, and, in certain experiments, in HeLa cells could interfere with an increase of mTHF:HOMmTase activity and with the formation of METH in sufficient amounts to fulfill the requirement of these cells for this amino acid. Since this kind of protein synthesis response paralleled the type of response to METH-starvation, we conclude that differences in the sensitivity of protein synthesis to METH-starvation could account for differences in cell growth and survival on HOM.

These findings do not explain the cause or causes of the observed differences in the sensitivity of protein synthesis to METH-starvation. Protein synthesis does not reach its maximum rate until a certain intracellular concentration of amino acids is reached (*19*). As shown by Eagle et al. (*20*), the concentration of amino acids varies with the extracellular amino acid level and also with the specific acid and cell line. METH is not only an essential amino acid for protein formation, but it is also required for methylation of DNA, RNA, and proteins. In the absence of exogenous METH, complete ribosomes are not formed as a consequence of a lack of methyl groups required for ribosome synthesis from newly made 45 S precursor RNA (*21*, *22*). Different rates of protein synthesis shutdown in different cell lines could then result either from different rates of METH depletion or from variability in the rate of disappearance of methyl groups required for the initiation of protein synthesis.

HeLa cells showed varied responses to METH-depletion or METH-substitution. Since our experimental procedures were reproducible and since we can exclude the possibility of contamination of HeLa cells with some other cells in the course of passaging, the simplest explanation is that the cultures contained subpopulations differing in their metabolic features.

Preferential selection or overgrowth of one or another subpopulation at the time of the experiment could account for the observed variations. It has been reported that metastatic ability and tumorigenicity of HEp-3 cells (*23*) disappear during prolonged passage in culture. If this were true of HeLa cells and some other tumor derived-cells maintained in tissue culture for long periods of time, then the conclusions of Kreis and Goodenow (*8*) on the impossibility of general discrimination between benign and neoplastic cells on the ground of their METH requirement should be revised.

REFERENCES

(*1*) Du Vigneaud V, Ressler C, Rachele Jr. The biological synthesis of labile methyl groups. Science 1950; 112:267–271.

(*2*) Mangum JH, North JA. Vitamin B_{12}-dependent methionine biosynthesis in HEp-2 cells. Biochem Biophys Res Commun 1968; 23:105–110.

(*3*) Kamely D, Littlefield JW, Erbe RW. Regulation of 5-methyltetrahydrofolate homocysteine methyltransferase activity by methionine, vitamin B_{12} and folate in cultured baby hamster kidney cells. Proc Natl Acad Sci USA 1973; 70:2585–2589.

(*4*) Ashe H, Clark BR, Chu F, Hardy DN, Halpern BC, Smith RA. N^5-methyltetrahydrofolate homocysteine methyl-transferase activity in extracts from normal, malignant and embryonic tissue culture cells. Biochem Biophys Res Commun 1974; 57:417–425.

(*5*) Halpern BC, Clark BR, Hardy DN, Halpern RM, Smith RA. The effect of replacement of methionine by homocysteine on survival of malignant and normal adult mammalian cells in culture. Proc Natl Acad Sci USA 1974; 71:1133–1136.

(*6*) Halpern BC, Ezzell R, Hardy DN, et al. Effect of methionine replacement by homocysteine in cultures containing both malignant rat breast cell carcinoma Walker 256 cells and normal adult rat liver fibroblasts. In Vitro 1975; 11:14–19.

(*7*) Hoffman RM, Erbe RW. High in vitro rate of methionine biosynthesis in transformed human and malignant rat cells auxotrophic for methionine. Proc Natl Acad Sci USA 1976; 73:1523–1527.

(*8*) Kreis W, Goodenow M. Methionine requirement and replacement by homocysteine in tissue cultures of selected rodent and human malignant and normal cells. Cancer Res 1978; 38:2259–2262.

(*9*) Chello PL, Bertino JR. Dependence of 5-methyltetrahydrofolate utilization by L 5178Y murine leukemia cells in vitro on the presence of hydroxycobalamin and transcobalamin II. Cancer Res 1973; 35:1898–1904.

(*10*) Mangum JH, Murray BK, North JA. Vitamin B_{12}-dependent methionine biosynthesis in cultured mammalian cells. Biochemistry 1969; 8:3496–3499.

(*11*) Koziorowska J, Pieńkowska K, Tautt J. Dependence on exogenous methionine of rat sarcoma and murine leukemic cells in culture. Arch Immunol Ther Exp 1980; 28:709–716.

(*12*) Dickerman HW, Redfield BG, Bieri JG, Weissbach H. The role of vitamin B_{12} in methionine biosynthesis in avian liver. J Biol Chem 1964; 239:2545–2552.

(*13*) Kutzbach C, Galloway E, Stockstad EL. Influence of vitamin B_{12} and methionine on levels of folic acid compounds and folate enzymes in rat liver. Proc Soc Exp Biol Med 1967; 124:801–805.

(*14*) Weissbach H, Taylor RT. Roles of vitamin B_{12} and folic acid in methionine synthesis. Vitam Horm 1970; 28:415–440.

(*15*) Finkelstein JD, Kyle WE, Harris BJ. Methionine metabolism in mammals. Regulation of homocysteine methyltransferase in rat tissue. Arch Biochem Biophys 1971; 146:84–92.

(*16*) Taylor RT, Hanna ML. Folate-dependent enzymes in cultured Chinese hamster ovary cells: Induction of 5-methyltetrahydrofolate homocysteine cobalamin methyltransferase by folate and methionine. Arch Biochem Biophys 1975; 171:507–520.

(*17*) Chen TR. In situ detection of mycoplasma contamination in cell cultures by fluorescent Hoechst 33258 stain. Exp Cell Res 1977; 104:255–262.

(*18*) Lowry OH, Rosebrough NJ, Farr AL, Randall KJ. Protein measurement with the Folin phenol reagent. J Biol Chem 1951; 193:265–275.

(*19*) Griffiths JB. The effect of cell population density on nutrient uptake and cell metabolism: A comparative study of human diploid and heteroploid cell lines. J Cell Sci 1972; 10:515–524.

(*20*) Eagle H, Piez KA, Levy M. The intracellular amino acid concentrations required for protein synthesis in cultured human cells. J Biol Chem 1961; 236:2039–2042.

(*21*) Vaugham MH Jr, Soeiro R, Warner JR, Darnell JE. The effects of methionine deprivation on ribosome synthesis in HeLa cells. Proc Natl Acad Sci USA 1967; 58:1527–1534.

(*22*) Vaugham MH Jr, Pawłowski PJ, Forchhammer J. Initiation of protein synthesis in HeLa cells deprived of single essential amino acids. Proc Natl Acad Sci USA 1971; 68:2057–2061.

(*23*) Ossowski L, Reich E. Loss of malignancy during serial passage of human carcinoma in culture and discordance between malignancy and transformation parameters. Cancer Res 1980; 40:2310–2315.

DNA Distribution in Human Colon Carcinomas and Its Relationship to Clinical Behavior[1,2]

R. C. Wolley, *Ph.D.*,[3,4] **K. Schreiber**, *M.D.*,[3] **L. G. Koss**, *M.D.*,[3,5] **M. Karas**, *M.D.*,[3] *and* **A. Sherman**, *M.S.*[3]

ABSTRACT—Striking differences in outcome of surgically treated colon adenocarcinomas were observed in 33 patients according to the DNA distribution patterns in tumor nuclei, measured by flow cytometry. As discussed and defined in the text and confirmed by appropriate control studies, the tumors were classified into 2 groups: predominantly diploid (20 tumors) and predominantly nondiploid (13 tumors). During the follow-up period of 3–5 years, 12 of the 13 patients with "nondiploid" tumors died of disease within 4–34 months, and the 1 patient still alive after 59 months has extensive metastases. Only 6 of the 20 patients with "diploid" tumors died of disease, sometimes after a slow, protracted clinical course. There were 14 patients with no evidence of disease for periods ranging from 30 to 60 months; 1 of these patients died of other causes. Histologic grading and Dukes' staging appeared to play a relatively limited role in the outcome, although lymph node metastases and vascular invasion were more often observed in the nondiploid tumors. These observations suggest that the determination of DNA distribution in colon carcinomas may prove to be of prognostic value.—JNCI 1982; 69:15–22.

The determination of nuclear DNA content, hence, in the broader sense, ploidy of large numbers of cells, has been facilitated by flow cytometry (*1–3*). This method is based on rapid measurements of fluorescence of specific dyes that bind stoichiometrically to double-stranded DNA. To perform the measurements accurately and avoid errors due to cell fragmentation and clumping, one must prepare a suspension of single cells; these cells must be stained with pure dyes of documented value and examined with an instrument with an appropriate wavelength.

In reference to solid epithelial human tumors, there are several significant problems with this approach. Because the cells in such tumors are bound to each other by desmosomes and other types of cell junctions (*4*), the preparation of a monocellular cell suspension must rely either on mechanical shearing of tumor fragments or on the use of proteolytic enzymes or on a combination of the two methods (*5, 6*). All of these agents and procedures cause varying degrees of damage to the cells (*7*). An alternate approach to the question of DNA distribution in human tumors is stripping the nuclei of their cytoplasm (*8, 9*). A suspension of intact, cleanly isolated nuclei obviates clumping that is commonly present in suspensions of cells derived from solid tumors. It is evident that the method used for nuclear isolation must be shown to preserve the DNA content in control studies.

Regardless of the method of preparation, samples of human solid tumors will contain a variable proportion of benign cells derived from blood vessels or connective tissue as well as an admixture of inflammatory cells. The DNA content alone is not sufficient for identification of such cells and for determination of their impact on the results of DNA measurements in tumors. For this reason, other control studies are necessary. The most secure way for one to determine the identity of cells or nuclei is based on morphologic criteria in smears (*10*). Such preparations may be stained by the Feulgen method. The measurement of the density of the Feulgen stain by means of a cytophotometer in a statistically valid sample gives rise to accurate histograms of the DNA distribution in a population of cells (*11*). Unfortunately, the time required for such studies is exceedingly long; thus the method does not lend itself to rapid determinations of clinical value. However, the method may be used on selected samples for the control of data obtained by flow cytometry.

In this paper we report a prospective study on the significance of the DNA distribution, determined by flow cytometry, in nuclei isolated from 33 colon carcinomas and appropriate controls. The method of preparation of the material and the resulting DNA distributions were controlled by the approaches described below. The DNA distributions of the tumors were compared with histologic grading and pathologic staging, and their prognostic value was judged by 3–5 years' follow-up of the patients.

MATERIALS AND METHODS

Samples.—In 1976 and 1977, samples of tissues were obtained from 33 fresh surgical resection specimens of colon carcinoma. Portions of grossly nonnecrotic tissue weighing approximately 2 g each were excised from tumors. Samples of colon epithelium of similar weight, taken from the margin of the surgical specimen showing no gross or histologic abnormalities, were used as controls. The benign epithelium was carefully separated from the muscle by a razor blade.

Preparation of suspension of nuclei.—Nuclei were isolated with the use of citrate buffer as previously described (*9*). The tissue samples were finely minced with scissors, incubated in a homogenization flask with 50 ml of CASC at room temperature for 30 minutes with constant agitation with the use of a magnetic stirrer, and then homogenized for 4 minutes with the use of a VirTis tissue homogenizer (setting #7).

ABBREVIATIONS USED: AO=acridine orange; CASC=0.09 *M* citric acid and 0.01 *M* sodium citrate; OD=optical density; PI=propidium iodide; TKM=0.05 *M* Tris, 0.02 *M* KCl, and 0.005 *M* $MgCl_2$ at pH 7.2.

---

[1] Received July 27, 1981; revised October 22, 1981; accepted Feburary 8, 1982.

[2] Research procedures were in accord with the ethical standards of the Institutional Review Board for the Protection of Human Subjects, Montefiore Hospital and Medical Center.

[3] Department of Pathology, Montefiore Hospital and Medical Center, Albert Einstein College of Medicine, Bronx, N.Y. 10467.

[4] *Present address:* Ortho Diagnostics, Westwood, Mass. 02090.

[5] *Address reprint requests to* Dr. Koss, Montefiore Hospital and Medical Center, 111 East 210th St., Bronx, N.Y. 10467.

This homogenate was cooled and filtered through eight layers of gauze for removal of any remaining tissue fragments, and the filtrate was centrifuged at 220×*g* for 10 minutes. The crude sediment containing nuclei was washed twice by resuspension in cold CASC, followed by centrifugation. The resulting suspension of nuclei was kept at 4°C until used. Aliquots of this nuclear suspension were checked by microscopic examination with the use of phase contrast and, after Papanicolaou staining, bright-field microscopy. Without exception, the preparations revealed well-preserved nuclei with only occasional wisps of cytoplasm attached. The nuclei to be analyzed by flow cytometry were washed several times in TKM, counted, and diluted to a concentration of 2×10^5/ml.

Normal human lymphocytes.—Normal, unstimulated human lymphocytes were used for control of staining and instrument adjustment and calibration. The lymphocytes were isolated from samples of peripheral blood from normal blood donors. Citrated blood, 1 ml, was diluted with 3 ml of normal saline and layered on 10 ml of Ficoll–Hypaque (Ortho Diagnostics, Raritan, N.J.) in a 15-ml centrifuge tube. The sample was centrifuged for 30 minutes at 400×*g*. The top cell band, consisting of approximately 90% lymphocytes, was removed with a Pasteur pipette and washed twice in phosphate buffer (pH 7.2) by centrifugation for 10 minutes at 220×*g*. The lymphocytes were either used immediately or frozen in phosphate buffer with 1% sucrose added for future use.

Staining.—Aliquots of nuclei isolated from all 33 tumor and benign control specimens were stained with the metachromatic dye AO (Sigma Chemical Co., St. Louis, Mo.) purified by the method of Zanker (*12*). One milliliter of AO solution (8.5×10^{-6} g/ml in TKM) was mixed with 1 ml of TKM containing 2×10^5 nuclei and allowed to equilibrate for 5 minutes (*13*). Measurements of green fluorescence at a wavelength of 530 nm corresponding to double-stranded DNA content (*14*) were made within 10 minutes of staining. During the latter part of this study, aliquots of 11 tumors and benign samples were also stained with PI (Calbiochem-Behring Corp., La Jolla, Calif.). Nuclei (1×10^5) in TKM were centrifuged for 10 minutes at 220×*g* and then resuspended in 1 ml of 0.1% sodium citrate containing 0.05 mg PI/ml (*15*). The suspensions of nuclei in PI were allowed to stand for 15 minutes at 4°C, and the DNA distributions were determined by measurement of the intensity of red fluorescence at 600 nm.

The DNA histograms generated by the two fluorochromes were compared and were in most instances identical. The small differences in the histograms that occurred in some cases were attributed to different aliquots of the nuclear samples used in these studies. In no case was the interpretation of the basic DNA distribution patterns affected by the choice of fluorochrome.

Measurements of fluorescence.—All counts and fluorescence measurements were made with the use of a Cytofluorograf system consisting of a Cytograf model 6300A, Cytofluorograf model 4802A, and a Multichannel Distribution Analyzer model 2100 (Ortho Instruments, Westwood, Mass.). After being stained as described, the nuclei were resuspended by being syringed twice with the use of a disposable tuberculin syringe fitted with a 25-gauge needle, and then they were analyzed immediately. We have found that this procedure results in a monodispersed sample, effectively disrupting any possible aggregates of nuclei that may form during centrifugation and staining (*16*). Before use with colon nuclei, the adjustment of the instrument and the quality of the batch of stains to be used were checked by generation of a DNA histogram of unstimulated lymphocytes. With an appropriate instrument setting and adequate stain, a histogram with a tight peak in the diploid range was generated.

The measurements of the nuclei of colon origin were conducted as follows: For each sample the benign control was studied first. Fluorescence intensity and light scatter were measured simultaneously. Light scatter provided information on the size of the particles and allowed us to exclude from the DNA histogram most of the debris, identified as small particles of lower fluorescence intensity than the diploid nuclei. It must be assumed that in every histogram some debris could not be differentiated from isolated nuclei. We analyzed each tumor immediately after its benign control had been analyzed without changing the setting of the instrument. We determined the reproducibility of results by generating, for each sample, a minimum of three histograms with AO and three with PI, when used. Each histogram was based on the measurement of 10^4 nuclei. Results were recorded as 100-channel histograms of fluorescence (text-fig. 1).

Control studies.—DNA content of isolated nuclei: To determine whether the steps used in nuclear isolation affected the DNA content of the sample, we compared the DNA content of two aliquots of the same tumor by the method of Savitzky and Stand (*13*).[6] In one aliquot (0.84 g in wet wt), the DNA was determined directly in the tissue. From the other tissue aliquot (0.86 g in wet wt), the nuclei were isolated as described, and their DNA content was determined. The DNA content, calculated per gram of wet tissue, was 11.6 mg for the whole tissue and 14.4 mg for the isolated nuclei. Thus the DNA content of the nuclei was not reduced by the citrate buffer isolation method.

Cytophotometry of Feulgen-stained samples.—After completion of the study of the 33 original tumors and controls that comprise this report, it became apparent that yet another method of determining the accuracy of the flow cytometric results was desirable. For this reason 2 additional colon tumors and benign controls were studied by flow cytometry and by measurement of Feulgen absorption. These flow cytometric histograms were generated on a recently acquired minicomputer (MINC 11; Digital Equipment Corp., Maynard, Mass.) interfaced with the Cytofluorograf. Smears of aliquots of nuclei isolated from the 2 colon tumors and their controls were fixed in 2% buffered formaldehyde for 12 hours and stained with Feulgen (*11*). The DNA content of 200 sequential nuclei from each of the samples was determined by quantitation of Feulgen absorption with the use of a high-resolution photometric system consisting of a Zeiss Universal Scanning microphotometer on line with a PDP-12 computer (*17*). The nuclei were scanned with a stepsize of 0.5 μm at a wavelength of 560 nm. Each nucleus was photographed at the time of scanning to facilitate subsequent identification. The raw data were measurements of the light transmission through a 0.8-μm effective aperture in the object plane. After the data were rescaled so that the minimum transmission in the background was assigned the value of 190, the OD was then calculated from the Beer-Lambert Law; $OD = -\log(t/t_0)$, where t is the local transmission value and t_0 is the background transmission value taken to be 200. This OD value was scaled up by a factor of 100 for convenience, since the values were then represented as integers.

---

[6] We thank Dr. Simon Neubort, Department of Radiology (Radiobiology), Albert Einstein College of Medicine, for his contribution to this study.

After the transformation of the image from transmission to OD values, the area and integrated OD of the nucleus were calculated and stored. After an entire sample had been run, OD distributions, which correspond to DNA distributions, were collected and plotted. All of the data were visually correlated with individual nuclei that were classified as either of benign or of malignant type on the basis of well-defined morphologic characterization of the nucleus (such as shape, chromatin pattern, size, and number of nucleoli) routinely used to distinguish between normal and malignant cells (*10*). The histograms of the control benign samples were based on the 200 nuclei (text-figs. 2, 3). Two histograms of the malignant samples were obtained: the first based on the 200 nuclei (text-figs. 2B, 3B) and the second after exclusion of morphologically benign or questionable nuclei (text-fig. 3C).

Pathologic evaluation and follow-up of patients.—Histologic grade, the presence of vascular invasion, lymph node metastases, and Dukes' stage were determined for each tumor. The modified Dukes' system (*18*) used classified tumors confined to mucosa and submucosa as A, invading muscularis as B, invading periserosal fat with or without metastasis to regional lymph nodes as C, and presenting distant metastases as D. The results of follow-up of the patients were obtained from the Tumor Registry at Montefiore Hospital and Medical Center by direct communication with individual physicians and, in some cases, by postmortem examination.

RESULTS

Flow Cytometry

The histograms of the DNA distribution of the 33 control samples of nuclei isolated from benign colon epithelium were typical of those of a cycling, nonsynchronized cell population (text-figs. 1A, 1C). The large peak in the diploid

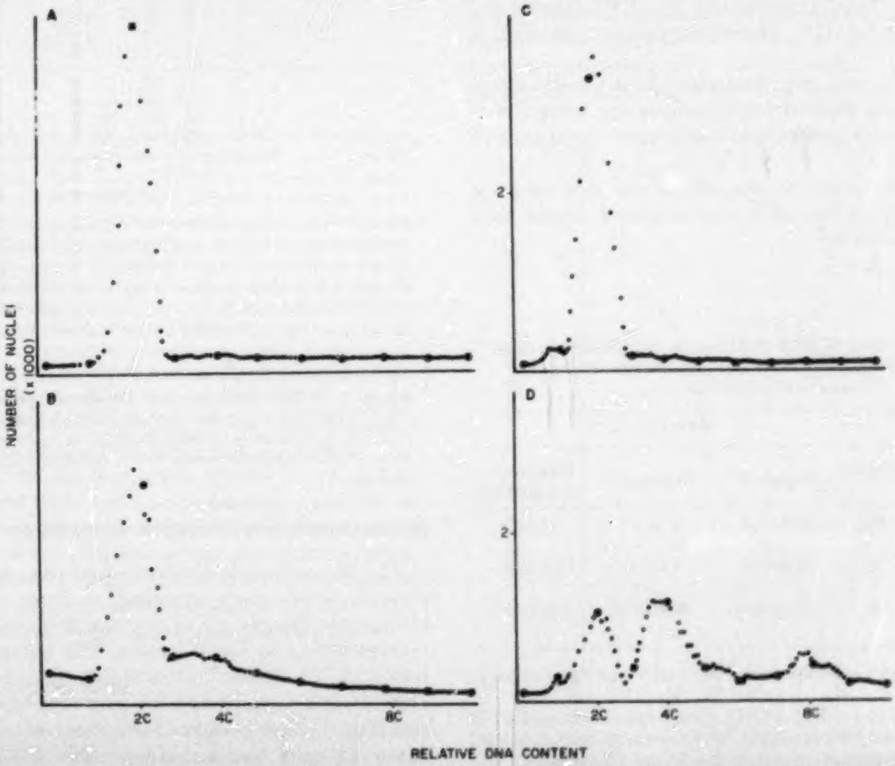

TEXT-FIGURE 1.—Histograms based on the measurement of the fluorescence intensity of 10,000 PI-stained nuclei. A and C: Typical histograms for nuclei obtained from benign colon epithelium showing a diploid cell population. Most of the nuclei represent cells isolated during the G_0 and G_1 phases of the cycle, with a small S-phase and G_2 phase group. A is the control for B, and C is the control for D. B: Histogram obtained from a grade II, Dukes' B-tumor is typical of histograms on patients who showed no evidence of disease 3–5 yr after surgery. Bulk of the nuclear sample is in the diploid region, although a secondary near-triploid population of nuclei is present. D: Histogram of a grade II Dukes' C-tumor removed from a patient who developed recurrent disease. There are three distinct peaks: one in the diploid region, one dominant peak in the tetraploid region, and one in the octaploid region. In the absence of a dominant peak in the diploid region, the tumor was classified as nondiploid.

range represented cells in G_0 and G_1 stages of the cell cycle. A small peak formed by nuclei with twice the DNA content (tetraploid or 4C) corresponded to cells in G_2, and the nuclei with intermediate DNA content presumably corresponded to cells in S-phase. Table 1 shows that there was little variation among the benign samples.

The histograms of DNA distribution of the 33 tumor samples could be divided into 2 groups (table 1). In the first group composed of 20 samples, the overall histogram patterns were roughly similar to those obtained with the benign samples (text-fig. 1B). Most nuclei (mean of 86.4% ± SD of 6.4%) formed only one major peak centered around the 2C region of the histogram, while the remainder of the nuclei were distributed between 2C and 8C. The broad configuration of the principal peak clearly indicated that the DNA content was much more variable than that in the benign controls. This group of tumors was classed as "predominantly diploid" with the clear understanding that this term indicated an approximation of the DNA content and did not exclude the possibility that subpopulations of hypodiploid, hyperdiploid, or even triploid nuclei may also be present within the peak.

In the 13 remaining tumors, the proportion of nuclei in the 2C region was significantly smaller (mean of 37.9% ± SD of 15.5%). The tumor histograms displayed a variety of patterns forming major peaks in the 3C or 4C regions and even beyond (text-fig. 1D). These tumors were classified as "nondiploid."

Using Student's *t*-test, we determined that the difference in the proportion of diploid nuclei among the benign samples and the 2 tumor groups was statistically significant ($P < 0.001$).

No attempts were made to identify the stages of cell cycle in tumor cells. We believe that such attempts would have been highly speculative.

Table 1.—*Summary of DNA distribution data based on flow cytometry of 33 colon carcinomas and suitable controls, as described in text*[a]

Samples	No. of samples	Means ± SD, %		
		Region 2C	Region 3C	Region 4C and greater
Benign controls[b]	33	93.8±3.6	2.7±1.8	3.5±2.3
Tumors[c]				
Predominantly diploid	20	86.4±6.4	5.3±2.2	8.4±6.0
Predominantly nondiploid	13	37.9±15.5	36.6±29.5	25.9±18.7

[a] Each measurement of 10,000 nuclei was performed three times or more.

[b] Benign control samples had a DNA distribution characteristic of that of a cycling normal cell population, with most of the cells in the 2C region and a small proportion of cells in the 3C and 4C regions.

[c] On the basis of their DNA distributions, the colon carcinomas were divided into 2 groups: 1 group of 20 tumors with the majority of nuclei in the diploid range and the other group with a majority of nuclei in greater than the diploid range. The tumor nuclei in the diploid region did not form sharp peaks as seen in control samples but rather had a broad distribution of cells of similar, but not necessarily identical, DNA content.

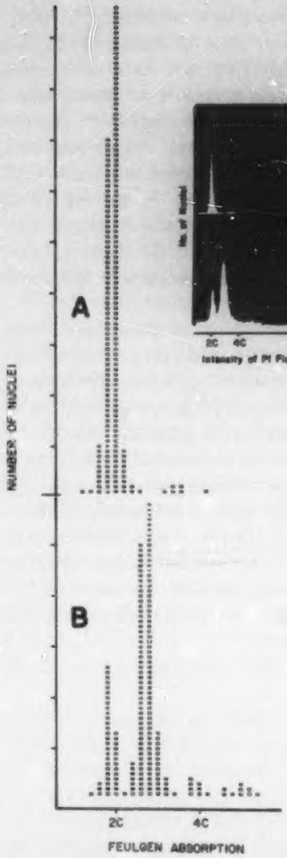

Text-figure 2.—Comparison of DNA histograms of nuclei determined by measurement of Feulgen absorption by high-resolution cytophotometry of 200 nuclei in a control sample of benign epithelium (A) and a corresponding colon carcinoma (B), with measurement of DNA content of 10,000 nuclei from each of the same samples by flow cytometry (*inset*). In spite of the differences in the numbers of nuclei measured, the histograms obtained by the two methods of DNA quantitation are very similar. Control sample shows a typical diploid cell population (A and *top inset*). Tumor shows two peaks: one in the diploid region and one in the triploid region. In this case all of the tumor nuclei studied by the Feulgen method were visually classified as malignant, indicating that a proportion of malignant cells were diploid in a tumor classified as nondiploid.

Measurements of Feulgen Absorption

The histograms of Feulgen absorption of the two control samples were nearly identical to those obtained by flow cytometry: Nearly all of the nuclei formed a single peak corresponding to the 2C value. The remaining nuclei with higher DNA content presumably represented replicating cells (cf. text-figs. 2A and 3A with text-figs. 1A and 1C and top insets). The Feulgen histograms of nuclei from the 2 tumor samples had a more variable DNA content, which indicated cell populations of variable ploidies, and were virtually identical with histograms generated by flow cytometry (cf. text-figs. 2B and 3B with bottom insets). By visual inspection of photographs taken of each nucleus in the Feulgen-stained smears, none of the nuclei in the control samples were classified as malignant. In the first tumor

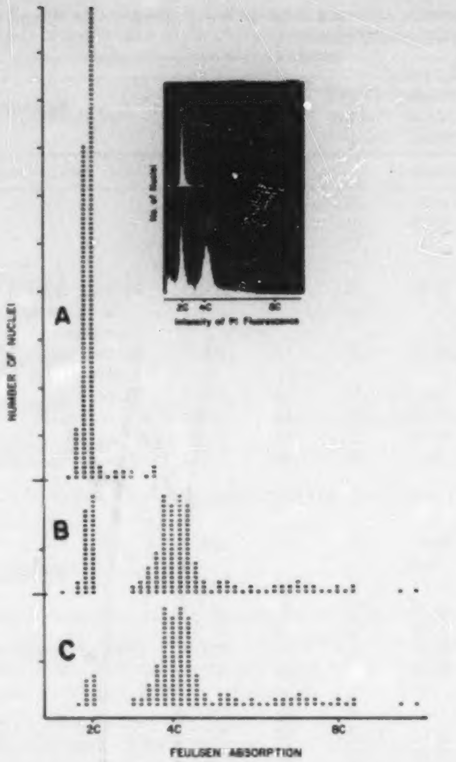

TEXT-FIGURE 3.—Comparison of DNA histograms of nuclei derived from a benign control sample (A) and colon carcinoma (B and C) by the Feulgen method and by flow cytometry of the same samples (*inset*). Histogram B was based on 200 sequential nuclei derived from the tumor. A very similar distribution of DNA content is present in the tumor histogram generated by flow cytometry (*inset, bottom*). Tumor was classified as nondiploid. After visual elimination of morphologically benign or questionable nuclei, histogram C was constructed, which shows that the tumor contained a significant population of nuclei of malignant origin in the diploid region and in the tetraploid region.

sample, all of the nuclei had malignant characteristics, regardless of DNA content. In the second tumor, benign and malignant nuclei were present. Those nuclei visually classified as benign or questionable were all diploid and were eliminated from the histogram shown in text-figure 3C, which is based only on nuclei *positively identified as malignant.* There was a proportion of nuclei with morphologic characteristics of cancer that fell within the diploid range. Furthermore, the basic configuration of the two histograms (text-figs. 3B, 3C) has remained similar, even after the elimination of presumably benign or questionable nuclei.

Pathologic and Clinical Data

Table 2 lists the principal clinical and pathologic data on the 33 patients studied. The tumors among these patients were divided into the 2 groups: predominantly diploid and predominantly nondiploid. Table 3 compares the flow cytometric classification of the colon tumors to conventional methods of tumor evaluation. Among the 20 patients in the diploid category, there were 2 tumors of grade I, 16 tumors of grade II, and 2 tumors of grade III. In the nondiploid tumor group there were 2 tumors of grade I, 7 tumors of grade II, and 4 tumors of grade III. There was evidence of lymph node metastases in 8 of 20 tumors in the diploid group and 10 of 13 tumors in the nondiploid group. Definite evidence of vascular invasion by tumor was observed in 4 of 20 diploid and 9 of 12 nondiploid tumors. Correlation with Dukes' classification showed that the diploid tumors were divided between Dukes' B- and C-classifications (7 and 10, respectively) with 1 tumor classified as Dukes' A and 2 as Dukes' D. Only 2 of the 13 nondiploid tumors were classified as Dukes' B with the other 11 classified as Dukes' C. Correlation of patient follow-up with the 2 tumor groups showed that 14 of the 20 patients with diploid tumors remained free of disease and 6 died of recurrent disease. Of the 13 patients with nondiploid tumors, all had recurrences of disease within 2 years and only 1 survived with metastatic disease beyond 3 years. The differences are reflected in the life-table analysis (text-fig. 4).

The patients in the nondiploid category, with one exception, died of disease within a short period of time, ranging from 4 to 34 months after surgery, with an average survival of 17.7 months. The sole survivor of 59 months has extensive liver metastases.

In the diploid group, 2 patients with known liver metastases at initial surgery survived 34 and 45 months, respectively. There were also 3 patients with lymph node metastases who remained free of disease, although 2 of them died of unrelated causes after 30–34 months of follow-up. The average survival time of the 5 patients who died of disease

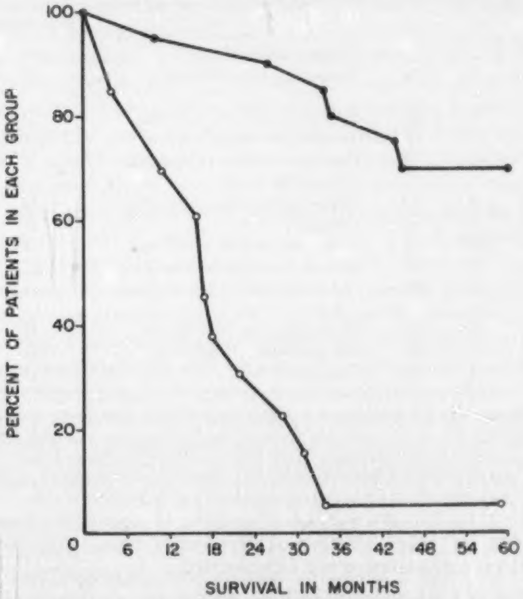

TEXT-FIGURE 4.—Survival of patients with diploid tumors (●) and nondiploid tumors (○). At the end of 24 mo of follow-up, >90% of the patients with diploid tumors were alive, compared with <25% of patients with nondiploid tumors. After 5 yr of follow-up, 13 of the 20 patients (65%) with diploid tumors were alive with no evidence of disease (1 of them died of unrelated cause without evidence of disease); only 1 of the 13 patients in the nondiploid group (7.5%) was still alive with extensive metastases, 59 mo after surgery.

TABLE 2.—*Correlation between the DNA distribution of 33 colon carcinomas with clinical follow-up, histologic grading, lymph node metastases, vascular invasion, and Dukes' classification*[a]

Patient No.	Sex	Age, yr	Location and size of tumor	Grade	Vascular invasion	Lymph node metastases[b]	Dukes' stage	Follow-up in mo	Results[c]	Remarks[d]
				Predominantly diploid tumors						
1	♂	84	Rectosigmoid, 4.5×3.5×2 cm	II	No	0/5	B	53	NED	
5	♀	56	Rectosigmoid, 3×3×1 cm	II	Probable	0/16	B	47	NED	
8	♀	71	Ascending colon and cecum, 5×3×2.5 cm	II	Probable	1/8	C	53	NED	
9	♂	60	Sigmoid colon, 4×4.3 cm	II	No	0/20	C	48	NED	Patient treated presently for malignant lymphoma
10	♀	70	Cecum and ascending colon, 2.5×3 cm	II	Yes	0/26	B	45	NED	Second tumor. First tumor occurred in 7/74.
11	♀	64	Sigmoid colon, 6×6 cm	II	Probable	1/6	D	34	DOD	FUra
12	♀	78	Sigmoid colon, 3.5×3.8×0.8 cm	II	No	0/27	B	44	NED	
13	♀	69	Cecum, 7×2×2 cm	II	Probable	0/12	C	42	NED	FUra
14	♀	51	Transverse colon, 8×8 cm	II	Yes	No	D	45	DOD	Tumor thrombus portal vein
16	♂	76	Ascending colon, largest of 6 polypoid masses, 6×5×3.5 cm	I	No	0/32	A	36	NED	
19	♀	73	Sigmoid colon, 10 cm in diameter	II	Yes	Multiple	C	52	NED	
21	♀	58	Sigmoid colon, 6.5×7 cm	III	No	0/17	B	46	NED	
22	♀	76	Descending colon, 2×3.5 cm	II	Yes	4/16	C	10	DOD	
24	♀	83	Ascending colon, 3×2.5 cm	II	Probable	6/18	C	35	DOD	
25	♂	86	Right colon, 5.5×4.5 cm	III	No	6/25	C	30	NED	Died of cardiac arrest
26	♀	61	Sigmoid colon, 5.5 cm in diameter	II	Not clear	0/12	C	48	NED	
28	♀	82	Rectosigmoid, 3.5×3×1 cm	II	No	2/9	C	26	DOD	
29	♀	76	Sigmoid colon, 6.5×5×1.5 cm	II	No	0/15	B	60	NED	
30	♀	64	Sigmoid colon, 5×5 cm	I	No	0/16	B	60	NED	
31	♂	81	Cecum, 8.5 cm in diameter	II	Probable	1/14	C	44	DOD	Mestatases to lungs
				Predominantly nondiploid tumors						
2	♀	68	Cecum, 10×8×3 cm	II	Yes	4/22	C	28	DOD	
3	♀	62	Sigmoid colon, 5×4 cm	I	No	0/5	B	59	EOD	Alive with liver metastases—FUra
4	♀	68	Sigmoid colon, 4.2×2.5 cm	II	Yes	8/14	C	17	DOD	
6	♂	87	Transverse colon, 8×3 cm	III	Yes	6/11	C	17	DOD	
7	♂	79	Cecum and ascending colon, 6.2×3.5×3 cm	II	Probable	8/9	C	4	DOD	
15	♂	70	Descending colon, 2×5 cm	II	No	4/16	C	34	DOD	
17	♀	82	Cecum, 7×3 cm	II	Yes	6/8	C	18	DOD	
18	♀	74	Left colon, 4.2×3.1×0.5 cm	III	Yes	7/20	C	11	DOD	
20	♀	76	Sigmoid colon, 2.5×1×0.8 cm	III	Yes	0/17	B	22	DOD	FUra
23	♀	82	Sigmoid colon, 4 cm in diameter	I	Yes	7/13	C	4	DOD	FUra
27	♀	73	Sigmoid colon, 3.2×2.2 cm	II	Probable	0/23	C	11	DOD	
32	♂	84	Sigmoid colon, 5×6.5 cm	III	Yes	5/10	C	31	DOD	
33	♂	63	Cecum, 6×4 cm	II	Yes	2/20	C	16	DOD	FUra

[a] There was no significant correlation between histologic grade and DNA distribution except for the grade III tumors of which 4 of 6 were nondiploid. All of the patients with nondiploid tumors had either lymph node or vascular involvement, and all but 1 died of disease within <3 yr. Comparison of Dukes' staging with DNA distribution shows that the nondiploid tumors generally had a higher stage than the diploid tumors. Yet most patients with diploid patterns remained free of disease regardless of Dukes' stage. Furthermore, the progression of disease was very slow in some patients with diploid tumors (patients 11 and 14).

[b] No. of lymph nodes with cancer/total No. of lymph nodes found.

[c] NED=no evidence of disease. DOD=dead of disease. EOD=evidence of disease.

[d] FUra=patient treated with 5-fluorouracil.

TABLE 3.—*Summary of table 2 showing comparison of the flow cytometric classification of the colon tumors with conventional methods of tumor evaluation*[a]

Pathologic classification	Total No. of samples	Predominant ploidy	
		Diploid	Nondiploid
Dukes' classification			
A	1	1	0
B	9	7	2
C	21	10	11
D	2	2	0
Histologic grades			
I	4	2	2
II	23	16	7
III	6	2	4
Lymph node metastases	18	8	10
Vascular invasion	13	4	9

[a] For discussion, *see* table 2, footnote *a*.

was 31.8 months, nearly twice as long as that for the nondiploid group.

DISCUSSION

Behavior patterns, hence prognosis of carcinoma of the colon, one of the most frequent malignant tumors observed today, has been studied by Dukes who has introduced the commonly accepted system of staging (*19*). This system provided broad prognostic statistical guidelines based on gross findings and histologic evidence. Histologic grading, also proposed by Dukes (*20*), is a highly subjective exercise that reflects the pathologist's training, competence, and ability.

The purpose of the research described in this paper is to base the prognosis of colon cancer on objective, machine-generated criteria. Initial attempts to determine the prognostic value of ploidy of various human cancers were made with the use of Feulgen stain and chromosome counts (*21–23*). In reference to carcinomas of the uterine cervix and the endometrium (*24*) and the breast (*25*), Atkin concluded that tumors of predominantly diploid pattern generally had a better prognosis than aneuploid neoplasm. Since the development of flow cytometry, the ploidies of a variety of solid human tumors have been determined (*26–33*). These studies have confirmed the abnormalities in DNA distribution in various forms of human cancer. However, because of insufficient length of follow-up, the prognostic significance of the flow cytometric observations has not been previously established (*34*).

Flow cytometry offers the advantage of a large data base to establish the ploidy of human cancer for purposes of diagnosis and prognosis. Unfortunately, the preparation of cell suspensions by mechanical shearing or proteolytic enzymes often results in cell destruction or insufficient dispersion of cells (*7*). In the case of colon tissues, it proved impossible to obtain a suspension of intact, single cells. For this reason, this research was based on the study of isolated nuclei, as also used by Vindeløv et al. (*32*). The main disadvantage of this approach is the inability to study metabolic events in the cytoplasm. The method of nuclear isolation described in this study is a modification of that used by Skerrow and Matoltsy (*35*) for isolation of desmosomes from epidermis. Fortuitously, this modified method results in a suspension of intact nuclei of remarkable purity and has been extensively tested on tissues and cells from the uterine cervix, lung, colon, and liver (*9*). The comparison of the DNA content of the isolated nuclei with intact tissues, described in this paper, proved that the DNA recovery is high. Nuclei prepared by this method do not have to be fixed or analyzed immediately because the low pH of the solution used for nuclear isolation inhibits the action of endonucleases (*36*). We have found this method reproducible and reliable with a variety of tumors. Thus, if generally accepted, this method may prove to be a common denominator for the study of DNA content of various human and experimental neoplasms.

Flow cytometry has one more inherent weakness, i.e., the inability to identify in flow the nature of the particles generating the signals. Suspension of nuclei, even though derived from clearly cancerous tissue, may consist of an admixture of nuclei of benign cells, vascular connective tissue, and hematogenous origin. For this reason, a cytophotometric control study of Feulgen-stained nuclei was performed. The fact that the DNA histograms generated by flow cytometry and by Feulgen absorption of epithelial nuclei were remarkably similar (text-figs. 2, 3) suggests that nuclei of nonepithelial cells had little if any effect on the results. With the use of visual criteria, this study also confirms the presence of malignant cell nuclei within the diploid range (text-figs. 2B, 3C). This possibility has been suggested by others who found that the large population of diploid nuclei in colon tumors cannot be explained by contamination with normal cells (*37, 38*).

Interpretation of DNA histograms generated by flow cytometry for a cycling diploid cell population, such as stimulated lymphocytes or cells in tissue culture, is relatively simple, and several methods of calculating the proportions of cells in different stages of the cell cycle are available (*39, 40*). However, determining the cell cycle stages in a complex cell population of unknown ploidy, such as one derived from human cancer, is much more difficult, if not impossible, with the technology available to us in 1976 and 1977 when this study was performed. The state of the cell cycle can be surmised or guessed for such histograms as shown in text-figures 1–3 only if one assumes that the ploidy of the cells is known and constant and all the cells are cycling normally.

For this reason, the tumors were assessed in reference to DNA content of nuclei, and the possible implications of cell dynamics or ploidy were disregarded pending further research. Fortuitously, the colon tumors had two predominant DNA distribution patterns: one predominantly diploid and the other nondiploid as already defined. Since the inception of this study, others have reported similar observations without indicating their possible prognostic value (*37, 38*). It appears from our follow-up data that these 2 groups of tumors have a strikingly different behavior pattern. The diploid group appears to be much less aggressive even in the presence of known metastases. The nondiploid tumors lead to rapid dissemination of the disease and patients' death within a short period of time, which strongly suggests a correlation between ploidy of colon tumors and prognosis as has been noted for some other human tumors (*24, 25*). Thus the results suggest that biologic factors of either tumor aggressiveness or patients' resistance to disease are somehow reflected in the DNA distributions. Obviously, the results of this report based on the small group of patients must be confirmed by additional data.

REFERENCES

(*1*) Sugarbaker EV, Thornthwaite JT, Temple WT, Ketcham AS. Flow cytometry: General principles and applications to selected studies in tumor biology. Int Adv Surg Oncol 1979; 2:125–153.

(*2*) Marx JL. Lasers in biomedicine: Analyzing and sorting cells. Science 1975; 23:821–823.

(*3*) Wolley RC, Kawamoto K, Herz F, Hirano A, Koss LG. Flow cytometry of human brain tumors. Prog Neuropathol 1979; 4:267–276.

(*4*) Koss LG, Dembitzer HM, Herz F, Herzig N, Schreiber K, Wolley RC. The monodisperse cell sample: Problems and possible solutions. In: Wied GL, Bahr GF, Bartels PH, eds. Proceedings of the international conference on automation of uterine cancer cytology. Chicago: Tutorials of Cytology, 1976; 5:4–59.

(*5*) Tucker JH, Gresham GA. Preparation of cervical scrape material for automatic screening. Br J Obstet Gynaecol 1971; 78:947–953.

(*6*) Waymouth C. To disaggregate or not to disaggregate. Injury and cell disaggregation, transient or permanent? In Vitro 1974; 10:97–111.

(*7*) Wolley RC, Herz F, Dembitzer HM, Schreiber K, Koss LG. The monodisperse cervical smear. Quantitative analysis of cell dispersion and loss with enzymatic and chemical agents. Anal Quant Cytol 1979; 1:43–49.

(*8*) Farsund T. Preparation of bladder mucosa cells for micro-flow fluorometry. Virchows Arch [Cell Pathol] 1974; 16:35–38.

(*9*) Koss LG, Wolley RC, Schreiber K, Mendecki J. Flow-microfluorometric analysis of nuclei isolated from various normal and malignant human epithelial tissues. J Histochem Cytochem 1977; 25:565–572.

(*10*) Koss LG. Diagnostic cytology and its histopathologic bases. 3d ed. Philadelphia: Lippincott, 1979.

(*11*) Gaub J, Auer G, Zetterberg A. Quantitative cytochemical aspects of a combined Feulgen-Naphthol yellow S staining procedure for the simultaneous determination of nuclear and cytoplasmic proteins and DNA in mammalian cells. Exp Cell Res 1975; 92:323–332.

(*12*) Zanker VB. Methoden und Ergebnisse der Farbstoffreinigung. Gang der Reinigung eines Farbstoffes, demonstriert am Beispiel des Acridin-orange. Acta Histochem (Jena) 1973; 13:281–289.

(*13*) Savitzky JP, Stand F. A method for the preparation of mammalian deoxyribonucleic acid. Biochim Biophys Acta 1966; 114:419–420.

(*14*) Darzynkiewicz Z, Traganos F, Sharpless T, Melamed MR. Lymphocyte stimulation: A rapid multiparameter analysis. Proc Natl Acad Sci USA 1976; 73:2881–2884.

(*15*) Krishan A. Rapid flow cytofluorometric analysis of mammalian cell cycle by propidium iodide staining. J Cell Biol 1975; 66:188–193.

(*16*) Wolley RC, Herz F, Dembitzer HM, Schreiber K, Koss LG. The use of a slide spinner in the analysis of cell dispersion. J Histochem Cytochem 1976; 24:11–15.

(*17*) Koss LG, Bartels PH, Bibbo M, Freed SZ, Taylor J, Wied GL. Computer discrimination between benign and malignant urothelial cells. Acta Cytol (Baltimore) 1975; 19:378–391.

(*18*) Asher VB, Coller FA. The prognostic significance of direct extension of carcinoma of the colon and rectum. Ann Surg 1954; 139:846–855.

(*19*) Dukes CE. The classification of cancer of the rectum. J Pathol Bacteriol 1932; 35:323–332.

(*20*) ———. The surgical pathology of rectal carcinoma. J Clin Pathol 1949; 2:95–98.

(*21*) Atkin NB. The relationship between the deoxyribonucleic acid content and ploidy in human tumors. Cytogenetics 1962; 1:113–122.

(*22*) Bohm N, Sandritter W. DNA in human tumors: A cytophotometric study. Pathology 1975; 60:152–219.

(*23*) Nasiell M, Kato H, Auer G, Zetterberg A, Roger V, Karlen L. Cytomorphologic grading and Feulgen DNA analysis of metaplastic and neoplastic bronchial cells. Cancer 1978; 41:1511–1521.

(*24*) Atkin NB. Nuclear size in carcinoma of the cervix: Its relationship to DNA content and to prognosis. Cancer 1964; 17:1391–1399.

(*25*) ———. Modal deoxyribonucleic acid value and survival in carcinoma of the breast. Br Med J 1972; 1:271–272.

(*26*) Barlogie B, Göhde W, Johnston DA, et al. Determination of ploidy and proliferative characteristics of human solid tumors by pulse cytophotometry. Cancer Res 1978; 38:3333–3339.

(*27*) Bichel P, Frederiksen P, Kjaer T, Thommesen P, Vindeløv LL. Flow microfluorometry and transrectal fine-needle biopsy in the classification of human prostatic carcinoma. Cancer 1977; 40:1206–1211.

(*28*) Frederiksen P, Reske-Nielsen E, Bichel P. Flow cytometry in tumours of the brain. Acta Neuropathol (Berl) 1978; 46:65–68.

(*29*) Kawamoto K, Herz F, Wolley RC, Hirano A, Kajikawa H, Koss LG. Flow cytometric analysis of the DNA distribution in human brain tumors. Acta Neuropathol (Berl) 1979; 46:39–44.

(*30*) Schumann J, Göhde W, Zante J. Aneuploidies in solid human tumors. In: Lutz D, ed. Pulse cytophotometry III. 3d ed. Ghent: European Press Medikon, 1978:447–457.

(*31*) Vindeløv LL, Hansen HH, Christensen IJ, et al. Clonal heterogeneity of small cell anaplastic carcinoma of the lung demonstrated by flow cytometric DNA analysis. Cancer Res 1980; 40:4295–4300.

(*32*) Vindeløv LL. Flow microfluorometric analysis of nuclear DNA in cells from solid tumors and cell suspensions. Virchows Arch [Cell Pathol] 1977; 24:227–242.

(*33*) Tribukait B, Esposti PL. Quantitative flow-microfluorometric analysis of the DNA in cells from neoplasms of the urinary bladder: Correlation of aneuploidy with histological grading and the cytological findings. Urol Res 1978; 6:201–205.

(*34*) Laerum OD, Farsund T. Clinical application of flow cytometry: A review. Cytometry 1981; 2:1–13.

(*35*) Skerrow CJ, Matoltsy G. Isolation of epidermal desmosomes. J Cell Biol 1974; 63:515–521.

(*36*) Taylor CW, Yeoman LC, Daskal I, Busch H. Two-dimensional electrophoresis of proteins of citric acid nuclei prepared with aid of a Tissumizer. Exp Cell Res 1973; 82:215–226.

(*37*) Petersen SE, Lorentzen M, Bichel P. A mosaic subpopulation structure of human colorectal carcinomas demonstrated by flow cytometry. In: Laerum OD, Lindmo T, Thorud E, eds. Flow cytometry IV. Oslo, Bergen, and Trondheim: Universitetsforlaget, 1980:412–416.

(*38*) Barlogie B, Drewinko B, Schumann J, et al. Cellular DNA content as a marker of neoplasia in man. Am J Med 1980; 69:195–203.

(*39*) Dean PN, Jett JH. Mathematical analysis of DNA distributions derived from flow microfluorometry. J Cell Biol 1974; 60:523–527.

(*40*) Fried J, Perez AG, Clarkson BD. Flow cytofluorometric analysis of cell cycle distributions using propidium iodide properties of the method and mathematical analysis of the data. J Cell Biol 1976; 71:172–181.

Circulating Immune Complex Levels in Patients With Gestational Trophoblastic Neoplasia[1, 2]

Anthony A. Rayner, *M.D.,*[3] **Ross Berkowitz**, *M.D.,*[4,5] **Glenn Steele, Jr.**, *M.D., F.A.C.S.,*[3,6] **Peter H. Schur**, *M.D., F.A.C.P.,*[7] **Mary L. Rodrick**, *Ph.D.,*[3] **Donald P. Goldstein**, *M.D.,*[4,5] **Paul J. Harte**, *M.B., F.R.C.S.(I),*[3] **Richard E. Wilson**, *M.D., F.A.C.S.,*[3] **Norman Zamcheck**, *M.D.,*[8] *and* **Alelia E. Munroe**, *B.S.*[3]

ABSTRACT—The clinical course, human chorionic gonadotropin (HCG) levels, and serial circulating immune complex (CIC) levels in 21 patients with gestational trophoblastic neoplasia (GTN) were correlated for the evaluation of the relationship between CIC levels and trophoblastic tumor burden. CIC levels were normal in 18 of 21 patients at the time of presentation, and 2 of the 3 patients who presented with elevated CIC levels had significant comorbid disease (toxemia and hepatitis). Nine patients were followed into gonadotropin remission, and all 9 developed an increase in CIC levels at the time of remission. It was concluded that CIC, at least as measured by two antigen-nonspecific techniques, is generally not elevated at initial presentation in the patient with GTN; this lack of an elevation is probably due to marked tumor antigen excess. Thus the in vivo importance of CIC as a "blocker" of host antitumor response at this stage is doubtful. After effective treatment as HCG levels return to normal, the demonstrated elevation in serial levels of CIC may reflect a return of adequate host immune response at a time of minimal tumor burden.—JNCI 1982; 69:23–26.

We and other investigators have reported increased levels of CIC in patients with cancer (*1–3*). Clinical monitoring of CIC has been proposed as a marker for tumor prognosis, response to therapy, and recurrence (*4–6*). Nevertheless, the clinical usefulness of antigen-nonspecific immune complex assays in a variety of patients with different tumor diagnoses continues to be disputed (*7*). We have recently selected a group of patients with GTN to assess the potential clinical value of serial CIC monitoring. We believe that these patients would most likely reflect clinically significant CIC changes, because their tumors are uniquely responsive to chemotherapy (even when presenting with widespread metastases) (*8*), because they can be followed to complete remission in a relatively short period of time, and because GTN regularly and predictably secretes HCG that can be used as a sensitive and specific quantitation of trophoblastic tumor (*9*).

The current study was undertaken for assessment of CIC levels in patients with HM with the use of two antigen-nonspecific CIC assay techniques: the PEG turbidity assay and the C1q binding assay. Serial levels of CIC and HCG were measured in patients with molar pregnancy for determination of the relationship between CIC and trophoblastic tumor burden.

MATERIALS AND METHODS

Twenty-one patients who presented to the New England Trophoblastic Disease Center from January 1980 to March 1981 with histologically confirmed HM were included in this study. The mean age of these patients was 25.6 years with a range of 17–38 years. Thirteen patients presented with molar pregnancy in situ, and 8 were referred with persistent postevacuation trophoblastic disease.

All serum samples were obtained from the patients in the morning after an overnight fast and used immediately for the HCG assay or stored at −70°C for subsequent CIC determinations. Serial samples on individual patients for the two antigen-nonspecific CIC assays were thawed only once with parallel assays performed on the same day.

Serum HCG levels were determined by the beta subunit radioimmunoassay method originally described by Vaitukaitis and associates (*10*) and modified by Kosasa and coworkers (*11*). This assay is specific for HCG and has a sensitivity of 10 mIU/ml. Patients were considered in remission after three consecutive normal weekly HCG levels (*8*).

Two antigen-nonspecific CIC assays were performed. C1q binding of CIC was determined by the method of Nydegger et al. (*12*), modified by Zubler et al. (*13*). Radiolabeled C1q was added to EDTA-treated serum samples, and bound C1q was then precipitated with PEG. The upper limit of normal for this assay in our laboratory is 23 μg aggregated human globulin equivalents per milliliter (*14*). The PEG turbidity assay for CIC has been previously reported in detail from our laboratory (*1, 15*). We have recently modified this PEG turbidity technique by using a final serum dilution of 1:10 in borate buffer (0.1 *M*, pH 8.4) containing PEG 6000 at a final concentration of 3.75% (wt/vol). After 2 hours of

---

ABBREVIATIONS USED: C1q=subcomponent q of the first component of complement; CIC=circulating immune complex(es); GTN=gestational trophoblastic neoplasia; HCG=human chorionic gonadotropin; HM=hydatidiform mole; OD=optical density; PEG=polyethylene glycol.

---

[1] Received October 6, 1981; accepted February 12, 1982.

[2] Supported in part by the Brigham Surgical Group, Inc.; by Public Health Service grants CA-22513 and CA-04486 from the National Cancer Institute (NCI); and by National Research Service Award ST32CA-09280 from the NCI.

[3] Department of Surgery, Brigham and Women's Hospital, Harvard Medical School, 75 Francis St., Boston, Mass. 02115.

[4] Department of Gynecology and Obstetrics, Brigham and Women's Hospital, Harvard Medical School.

[5] New England Trophoblastic Disease Center, Brigham and Women's Hospital, Harvard Medical School.

[6] *Address reprint requests to* Dr. Steele.

[7] Department of Rheumatology and Immunology, Brigham and Women's Hospital, Harvard Medical School.

[8] Mallory Gastrointestinal Research Laboratory, Boston City Hospital, Boston, Mass. 02118.

incubation at 20°C, samples are read on a Perkin-Elmer double-beam spectrophotometer (Perkin-Elmer Corp., Oak Brook, Ill.). Increase in turbidity due to insolubilization of CIC by PEG is reported as ΔOD units × 10^{-3}. Values greater than 280 represented two standard deviations from our pooled normal human serum controls (*1*).

RESULTS

CIC levels by both the PEG and the C1q binding assays were normal in 18 of 21 GTN patients at the time of their presentation for treatment. The median initial CIC value was 203 ΔOD U × 10^{-3}. Two of 3 patients who presented with elevated CIC levels in the PEG assay also had elevations by C1q binding. These 2 patients had significant comorbid disease at time of presentation—1 with toxemia and the other with hepatitis.

Serial CIC and HCG levels were measured on a median of five samples per patient (range, 2–11). Nine patients were followed into gonadotropin remission, and all 9 demonstrated an increase in their serial CIC levels by the PEG turbidity assay at the time of remission (text-fig. 1). The clinical, gonadotropin, and PEG–CIC course in a patient cured by molar evacuation is summarized in text-figure 2.

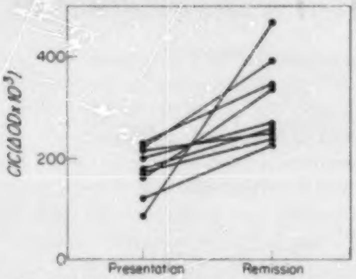

TEXT-FIGURE 1.—CIC levels at time of presentation and remission for the 9 patients entering gonadotropin remission.

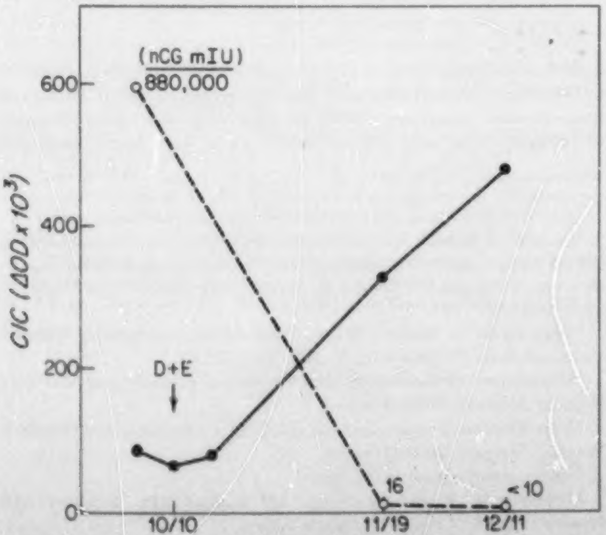

TEXT-FIGURE 2.—Serial HCG (hCG) and CIC values in a patient cured by molar evacuation.

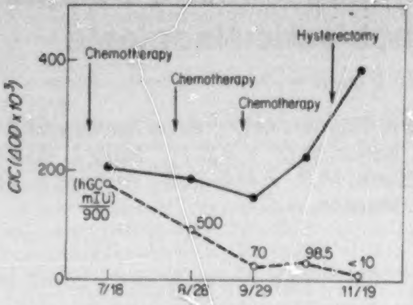

TEXT-FIGURE 3.—Serial HCG (hCG) and CIC values in a patient requiring multiple courses of chemotherapy and hysterectomy to induce remission.

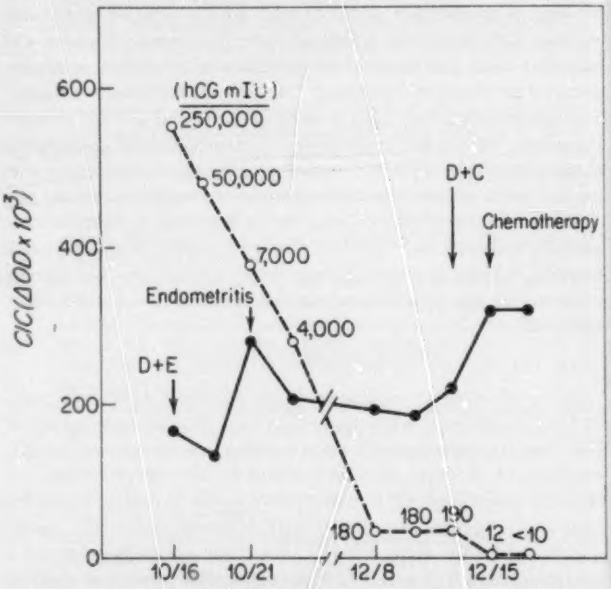

TEXT-FIGURE 4.—Serial HCG (hCG) and CIC values in a patient who was sustaining intercurrent infection and was eventually cured by additional surgery and chemotherapy.

Elevations in serial CIC levels were observed only in patients at the time of gonadotropin remission or in patients with comorbid disease. Text-figure 3 depicts the course of a patient with nonmetastatic trophoblastic disease who required chemotherapy and eventual hysterectomy for induction of tumor remission. Despite an early dramatic fall in HCG level, CIC did not rise until a minimal tumor burden was achieved as indicated by HCG values approaching normal. During episodes of comorbid illness, CIC elevations (presumably not related to changes in tumor burden) were observed. Text-figure 4 demonstrates the effect of infection on CIC levels in a patient who developed endometritis during treatment. Despite dramatic reduction in tumor bulk, quantitated by HCG decrease, patients who did not enter gonadotropin remission did not develop increases in serial CIC values. Text-figure 5 summarizes the course of such a patient who was initially treated by molar evacuation and then chemotherapy for persistent trophoblastic disease.

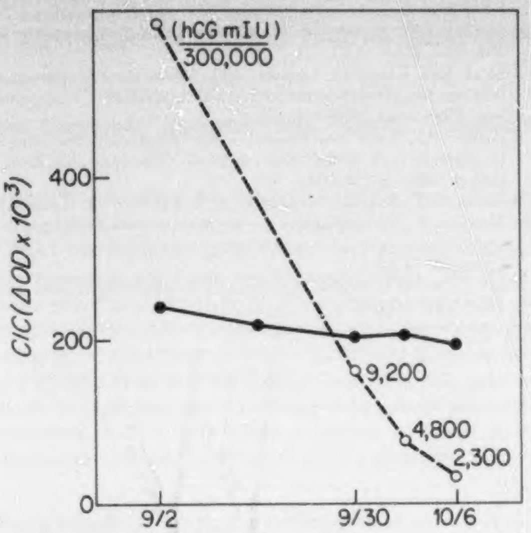

TEXT-FIGURE 5.—Serial HCG (hCG) and CIC values in a patient who, following molar evacuation, had not yet entered remission.

DISCUSSION

Molar pregnancy is an excellent clinical model for assessment of the potential relationship between CIC and tumor burden. The amount of viable trophoblastic tumor is sensitively and specifically quantitated by the serum level of HCG. Because trophoblastic tumors are exquisitely responsive to therapy, patients may be followed from presentation with bulk disease until they achieve complete gonadotropin remission in a relatively short period of time. In addition, patients with molar gestation are generally young and free of significant comorbid disease.

In this study, 18 of 21 patients with molar pregnancy had normal CIC levels at presentation as measured by two antigen-nonspecific assays. Two of the 3 patients who presented with elevated CIC levels had a significant comorbid disease—toxemia and hepatitis. Nine patients were followed until they achieved gonadotropin remission, and all 9 developed elevation of serial CIC levels at the time of documented remission. In all of the other patients, CIC values were elevated only when comorbid disease such as endometritis was present.

Three general problems must be considered when CIC is evaluated in any patient with neoplastic disease. First, CIC levels must be measured serially in individual patients who have a well-defined tumor course. Variation in the kinetics of CIC formation, elimination, and detectability may lead to a wide range of "normal" values. Attempts to define arbitrary normal and abnormal CIC values, in contrast to using the patient as her own control in serial studies, will bias against finding any significant biologic effect. Thus, although all of the patients developed increased levels of serial CIC at the time of gonadotropin remission, individual remission CIC values were above our own normal range in only 4 of the cured patients. The elevations in CIC in the other 5 patients would not have been detectable with the use of single serum samples, regardless of the antigen-nonspecific assay used.

Second, comorbid disease must be carefully considered when CIC data are analyzed. Elevated CIC levels were presumably due to comorbid disease in 3 patients—2 at presentation and 1 during the course of therapy.

Third, the measurement of CIC with any antigen-nonspecific assay will depend on the capability of the particular methodology applied. In this group of patients, the PEG turbidity assay detected elevated CIC levels more frequently than did the C1q binding assay. Although the PEG turbidity assay can detect CIC containing all immunoglobulin classes, C1q binding can only measure CIC containing immunoglobulin capable of binding complement (*1*).

It is interesting to speculate why patients with molar pregnancies develop elevated CIC levels only at the time they enter gonadotropin remission. Since HM is unique among human tumors in possessing a full complement of paternal chromosomes (*16*), these tumors may appropriately be regarded as allogeneic tissue and should provide a major antigenic challenge to the host immune system. At the time of presentation, patients may have such a large tumor burden that circulating antigen is in great excess. In previous work, we have shown that the PEG-CIC assay is not capable of accurately quantitating model complexes in extremes of antigen excess (*11*). The reduced tumor burden in these patients near the time of remission may provide a more suitable antigen:antibody ratio for CIC formation and detection, due either to a decrease in circulating antigen load by effective therapy or to an increase in host antibody production after a temporary period of immune incompetence.

The increased levels of CIC at the time of gonadotropin remission in these patients may signify a vigorous host immune response at a time of minimal tumor burden. Further investigation is warranted to isolate and analyze the contents of these immune complexes and to delineate the serial course of CIC values in cured patients followed longer after gonadotropin remission.

REFERENCES

(*1*) RAYNER AA, STEELE GD JR, RODRICK ML, et al. Application of polyethylene glycol turbidity assay to detection of circulating immune complexes in cancer patients. Am J Surg 1981; 141:460–464.

(*2*) ROSSEN RD, REISBERG MA, HERSH EM, GUTTERMAN JU. The C1q binding test for soluble immune complexes: Clinical correlations obtained in patients with cancer. J Natl Cancer Inst 1977; 58:1205–1215.

(*3*) THEOFILOPOULOS AN, ANDREWS BS, URIST MM, MORTON DL, DIXON FJ. The nature of immune complexes in human cancer sera. J Immunol 1977; 119:657–663.

(*4*) GUPTA RK, GOLUB SH, MORTON DL. Correlation between tumor burden and anticomplementary activity in sera from cancer patients. Cancer Immunol Immunother 1979; 6:63–71.

(*5*) HOFFKEN K, MEREDITH ID, ROBINS RA, BALDWIN RW, DAVIES CJ, BLAMEY RW. Circulating immune complexes in patients with breast cancer. Br Med J 1977; 2:218–220.

(*6*) STEELE G JR, SONIS S, STELOS P, et al. Circulating immune complexes in patients following clinically curative resection of colorectal cancer. Surgery 1978; 83:648–654.

(*7*) HERBERMAN RB, BORDES M, LAMBERT PH, et al. Report on international comparative evaluation of possible value of assays for immune complexes for diagnosis of human breast cancer. Int J Cancer

1981; 27:569–576.

(*8*) Goldstein DP, Berkowitz RS. Management of gestational trophoblastic neoplasms. Curr Probl Obstet Gynecol 1980; 3:1–42.

(*9*) Kim W, Takahashi T, Nisselbaum JS, Lewis JL Jr. Heterotransplantation of human choriocarcinoma in nude mice. I. Morphologic and biologic characteristics. Gynecol Oncol 1978; 6:165–182.

(*10*) Vaitukaitis JL, Braunstein GD, Ross GT. A radioimmunoassay which specifically measures human chorionic gonadotropin in the presence of human luteinizing hormone. Am J Obstet Gynecol 1972; 113:751–758.

(*11*) Kosasa TS, Levesque LA, Goldstein DP, Taymor ML. Early detection of implantation using a radioimmunoassay specific for human chorionic gonadotropin. J Clin Endocrinol Metab 1973; 36:622–624.

(*12*) Nydegger V, Gerber H, Lambert PH, Miescher PA. Detection de complexes antigene-anticorps circulants par precipitation a l'aide de C1q et de polyethylene-glycol. Schweiz Med Wochenschr 1974; 104:126–127.

(*13*) Zubler RH, Lange G, Lambert PH, Miescher PA. Detection of immune complexes in unheated sera by a modified ^{125}I-C1q binding test. J Immunol 1976; 116:232–235.

(*14*) Kammer GM, Soter NA, Schur PH. Circulating immune complexes in patients with necrotizing vasculitis. Clin Immunol Immunopathol 1980; 15:658–672.

(*15*) Rodrick ML, Rayner AA, Steele GD Jr, Finn D, Verhare M, Munroe A. An evaluation of two antigen nonspecific assays for circulating immune complexes using a model system. J Clin Lab Immunol. In press.

(*16*) Kajii T, Ohama K. Androgenetic origin of hydatidiform mole. Nature 1977; 268:633–634.

Decrease of Tumor Growth in Mice After Intravenous Thymosin-Treated Bone Marrow Cell Injection[1,2]

Didier Cupissol,[3] Augustin Rey,[3] Allan L. Goldstein,[4] *and* Bernard Serrou[3,5]

ABSTRACT—The effect of iv injection in C57BL/6 mice of 3×10^7 bone marrow cells preincubated in either thymosin fraction V or thymosin α-1 was evaluated on the growth of a 3-methylcholanthrene-induced transplantable tumor in a syngeneic system. The effect was then compared to that elicited by theophylline or levamisole, which both demonstrated thymosin-like action in vitro. The results showed significantly retarded tumor growth ($P<0.001$) and prolonged survival time ($P<0.001$) when thymosin fraction V was used. The same results were obtained with thymosin α-1 with use of the same protocol but only one-twentieth of the concentration of fraction V. Theophylline and levamisole demonstrated no antitumor effect.—JNCI 1982; 69:27–31.

Recent studies suggest the presence of an immune imbalance in both tumor-bearing animals (*1*) and in cancer patients (*2, 3*). This imbalance is characterized by an increased level of immune complexes (*4, 5*) and by the presence of suppressor cells (*6–11*). Two phases are distinguishable in this imbalance: an early phase after tumor implantation characterized by the presence of tumor-inhibiting lymphocytes and a later phase characterized by the presence of tumor-enhancing lymphocytes that possess in vitro cytotoxicity for target cells (*12*). Moreover, Small and Trainin (*13*) have shown that tumor-inhibiting sensitized lymphocytes are not observed when tumor-enhancing lymphocytes are present. The concept of immune balance still contains many unknowns with regard to its regulation of and action on lymphocyte differentiation and maturation (*3*). Among these unknowns are thymosin (*14*), thymic factor (*15*), factor thymique serique (FTS) (*16, 17*), and thymic humoral factor (THF) (*18*).

Ahmed et al. (*19*) and Goldstein et al. (*20, 21*) have shown that the thymic extract thymosin fraction V can elicit differentiation of bone marrow lymphocytes into T-lymphocytes. Thymosin fraction V includes thymosin α-1 and other subfractions involved in the differentiation and maturation of helper, cytotoxic, and suppressor cells (*19, 22, 23*). Recent experimental and clinical results suggest that substances such as thymosin can restore immune balance and simultaneously modulate the amplitude of the immune reaction and the suppressor activity (*10, 11, 23, 24*). Within this context, some investigators have shown that T-lymphocytes may facilitate growth of murine syngeneic tumors (*25*). The same phenomenon was observed for cells that were autosensitized in vitro beforehand (*26*). Since these lymphocytes arose from the thymic cortex and were identified as suppressor cells, they may be found to facilitate tumor growth (*25*).

Consequently, it seemed reasonable to evaluate the effect of a thymic factor, such as thymosin, on the modulation of tumor growth by T-lymphocytes. We confirmed the previous findings of Umiel and Trainin (*25*) who described a T-lymphocyte population that enhanced tumor growth. We found this population sensitive to both cortisone and irradiation (*10*). These lymphocytes lost their tumor growth-enhancing potential when they were preincubated in a thymic factor (*27*) other than thymosin and not only significantly reduced tumor growth but also reduced the number of pulmonary metastases. These results seemed sufficiently encouraging to warrant evaluation of the thymosin effect on bone marrow cells injected into mice with MCA-induced tumors. We chose the bone marrow cell model because it is directly applicable to the situation in cancer patients and because the known regulatory role of bone marrow and null cells (*28, 29*). In addition, it was of interest to compare these results with those obtained with levamisole and theophylline (*30–32*) which show similar effects in vitro on lymphocyte differentiation as those observed for thymosin (*11*).

Our results show that bone marrow cells from normal syngeneic mice do not stimulate tumor growth and that bone marrow cells preincubated with thymosin significantly inhibit local syngeneic tumor growth.

MATERIALS AND METHODS

Tumor system.—The animals used were 12-week-old C57BL/6 male mice. The left hindlimb was injected with 2×10^6 viable tumor cells from an MCA-induced transplantable tumor maintained in our laboratory. This tumor is lethal at 31±1.7 days, is weakly immunogenic in vitro, and is unable to induce T-cell cytotoxicity, killer, or NK activities (*33*). However, in vivo immunization can be induced by either amputation 14 days after tumor implantation or ip injection of irradiated tumor cells.

We evaluated the following criteria: tumor weight, tumor volume, and mean survival time. Tumor weight and volume were evaluated on days 7, 14, 21, and 28 after iv injection of bone marrow cells. We injected a large number of viable tumor cells (2×10^6) to parallel the human situation where the tumor mass is often substantial at the time of diagnosis.

ABBREVIATIONS USED: A-RFC=autorosette-forming cells. MCA=3-methylcholanthrene; NK=natural killer.

---

[1] Received March 4, 1980; revised December 10, 1981; accepted February 9, 1982.

[2] Supported by grants ATP 43-76-75 from the Institut National de la Santé et de la Recherche Médicale (INSERM), by grant 76-1-1766 from the Délégation Générale à la Recherche Scientifique et Technique, and by the Association pour le Développement de la Recherche Contre le Cancer. Villejuif, France.

[3] Laboratoire d'Immunopharmacologie des Tumeurs, INSERM U 236 and ERA-CNRS No. 844, Centre Paul Lamarque, Hôpital Saint-Éloi, BP 5054, 34033 Montpellier Cedex, France.

[4] Department of Biochemistry, George Washington University Medical Center, Washington D.C. 20037.

[5] We thank Mrs. C. Esteve, Mr. C. Gondral, and Mr. A. Sautou for their expert technical assistance and Mrs. F. Benavenq for typing the manuscript.

TABLE 1.—*MCA-induced transplantable tumor growth decreased by thymosin-preincubated bone marrow cells when injected on the day of tumor implantation in syngeneic mice*[a]

Group No.—treatment	Mean ± SD					
	Tumor weight, mg, on the following days after tumor implantation:			Tumor volume, cm^3, on the following days after tumor implantation:		
	7[b]	14[c]	21[d]	6[e]	14[f]	21[g]
1—control medium	1.17±0.19	4.70±0.05	9.97±0.05	1.40±0.10	4.75±0.05	9.75±0.25
2—bone marrow cells alone	1.21±0.05	4.68±0.49	10.2±0.18	1.40±0.05	4.82±0.05	9.63±0.16
3—bone marrow cells + thymosin fraction V	0.88±0.07	3.64±0.05	4.5±0.3	0.98±0.05	3.71±0.10	4.59±0.05
4—bone marrow cells + thymosin α-1	0.94±0.05	3.64±0.05	5.3±0.35	1.07±0.08	3.96±0.05	4.88±0.05
5—bone marrow cells + levamisole	1.64±0.27	4.70±0.09	10.0±0.05	1.52±0.05	4.28±0.01	8.90±0.1
6—bone marrow cells + theophylline	1.64±0.06	4.78±0.08	13.2±1.55	1.59±0.02	4.44±0.14	9.65±0.05

[a] There were 30 mice in each group. Bone marrow cells were injected iv on the day of tumor implantation. Data were analyzed by the chi-square method.

[b] $P<0.05$ for the group comparisons: 1 vs. 3, 4, 5, and 6; 2 vs. 3, 4, 5, and 6; 3 vs. 4, 5, and 6.

[c] $P<0.05$ for the group comparisons: 1 vs. 3, 4, and 6; 2 vs. 5 and 6; 3 vs. 5 and 6; 4 vs. 5 and 6.

[d] $P<0.05$ for the group comparisons: 1 vs. 2, 3, 4, 5, and 6; 2 vs. 3, 4, 5, and 6; 3 vs. 4, 5, and 6; 4 vs. 5 and 6.

[e] $P<0.05$ for the group comparisons: 1 vs. 4, 5, and 6; 2 vs. 3, 4, 5, and 6; 3 vs. 4, 5, and 6; 4 vs. 5, and 6.

[f] $P<0.05$ for the group comparisons: 1 vs. 2, 3, 4, 5, and 6; 2 vs. 3, 4, 5, and 6; 3 vs. 4, 5, and 6; 4 vs. 5 and 6.

[g] $P<0.05$ for the group comparisons: 1 vs. 3, 4, 5, and 6; 2 vs. 4, 5, and 6; 3 vs. 4, 5, and 6; 4 vs. 5 and 6.

Bone marrow cells.—We obtained bone marrow from 12-week-old normal syngeneic mice by flushing the femur with RPMI-1640 medium (Gibco-Biocult, Glasgow, Scotland). Cells were then counted, viability was evaluated by trypan blue exclusion, and 3×10^7 bone marrow cells in 0.2 ml RPMI-1640 were injected iv either on the day of tumor implantation or 10 days after tumor implantation.

Drugs.—We used concentrations of 400 μg/ml/2×10^6 bone marrow cells for thymosin fraction V (lot C 100496) and 20 μg/ml/10^6 cells for pure thymosin α-1 (lot 160486). Theophylline (Bruneau Pharmaceutical Co., Paris, France) was employed at 200 μg/ml/2×10^6 cells and levamisole (Specia Pharmaceutical Co., Paris, France) at 200 μg/ml/2×10^6 cells. For all drugs, incubation time was 1 hour at 37°C. The dose retained for experimentation was that which in our experience yielded the maximum increase in vitro of A-RFC in the immunodepressed patient (A-RFC, <15%) with advanced solid tumor (*34*, *35*).

Experimental groups.—Each group contained 30 mice. Each experiment was repeated four times. In the first part of the study, experimental groups received normal syngeneic bone marrow cells pretreated with different drugs and injected iv on the day of tumor implantation. In the second part of the study, experimental groups received normal syngeneic bone marrow cells pretreated with the same drugs at the same concentrations as in the first part but injected iv 10 days after tumor implantation.

RESULTS

Experimental groups receiving normal syngeneic bone marrow cells pretreated with drugs and injected iv on the day of tumor implantation.—Animals given injections of 3×10^7 normal bone marrow cells (group 2) demonstrated no tumor growth inhibition (table 1). Tumor growth was similar to that of the control animals which did not receive bone marrow cells (group 1). On day 7, tumor weight and volume decreased significantly in animals given injections of thymosin fraction V- or thymosin α-1-preincubated bone marrow cells (groups 3 and 4) compared to animals that received untreated bone marrow cells (group 2). This difference persisted and became more accentuated on days 14 and 21.

Animals receiving bone marrow cells pretreated with levamisole or theophylline (groups 5 and 6) demonstrated

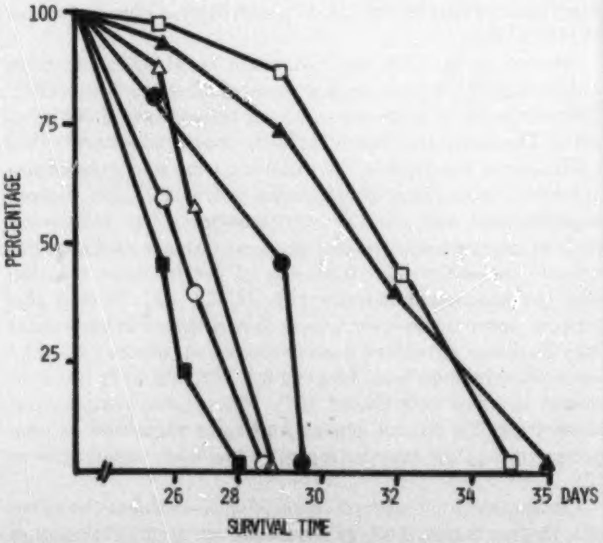

TEXT-FIGURE 1.—Thymosin-preincubated syngeneic bone marrow cells increase survival time in mice when injected iv on the day of tumor implantation. ■, Controls; ○, bone marrow cells alone; □, bone marrow cells + thymosin fraction V; ▲, bone marrow cells + thymosin α-1; ●, bone marrow cells + levamisole; △, bone marrow cells + theophylline.

TABLE 2.—*MCA-induced transplantable tumor growth decreased by thymosin-preincubated bone marrow cells when injected 10 days after tumor implantation in syngeneic mice*[a]

Group No.—treatment	Mean ± SD							
	Tumor weight, mg, on the following days after tumor implantation:				Tumor volume, cm^3, on the following days after tumor implantation:			
	17[b]	24[c]	31	38	17[d]	24[e]	31	38
1—control medium	4.70±0.10	10.70±0.08	NS	NS	4.30±0.05	10.40±0.5	NS	NS
2—bone marrow cells alone	4.60±0.05	10.50±0.10	NS	NS	4.26±0.10	10.30±0.5	NS	NS
3—bone marrow cells + thymosin fraction V	2.18±0.09	4.07±0.12	6.8±0.31	9.3±0.04	2.20±0.10	4.25±0.5	7.1±0.13	9.8±0.1
4—bone marrow cells + thymosin α-1	2.30±0.08	3.90±0.12	7.2±0.50	10±0.04	2.30±0.07	4.35±0.5	6.5±0.1	9±0.2
5—bone marrow cells + levamisole	4.52±0.05	10.50±0.05	12.8±0.05	NS	4.08±0.03	14.06±0.3	13.1±0.05	NS
6—bone marrow cells + theophylline	4.60±0.08	14.05±0.08	14.9±0.09	NS	4.19±0.04	16.35±0.5	15.1±0.8	NS

[a] There were 30 mice in each group. Bone marrow cells were injected iv 10 days after tumor implantation. NS=no survival. Data were analyzed by the chi-square method.

[b] $P<0.05$ for the group comparisons: 1 vs. 2, 3, and 4; 2 vs. 3, 4, and 5; 3 vs. 4, and 5; 4 vs. 5.

[c] $P<0.05$ for the group comparisons: 1 vs. 2, 3, and 5; 2 vs. 3, 4, and 5; 3 vs. 4 and 5; 4 vs. 5.

[d] $P<0.05$ for the group comparisons: 1 vs. 2, 3, and 4; 2 vs. 3, 4, and 5; 3 vs. 4 and 5; 4 vs. 5.

[e] $P<0.05$ for the group comparisons: 1 vs. 2, 3, 4, and 5; 2 vs. 4 and 5; 3 vs. 4 and 5.

an enhancing effect (significant weight difference on day 7, then a slight difference on days 14, 21, or 28) compared to that seen in control group 2 and in the groups treated with the thymosin plus bone-marrow cells (groups 3 and 4; table 1).

We found significant differences in survival times in favor of animals in groups 3 and 4 compared with groups that received levamisole- or theophylline-pretreated cells (groups 5 and 6) (text-fig. 1). There was no significant difference in survival times between the groups receiving thymosin fraction V and thymosin α-1.

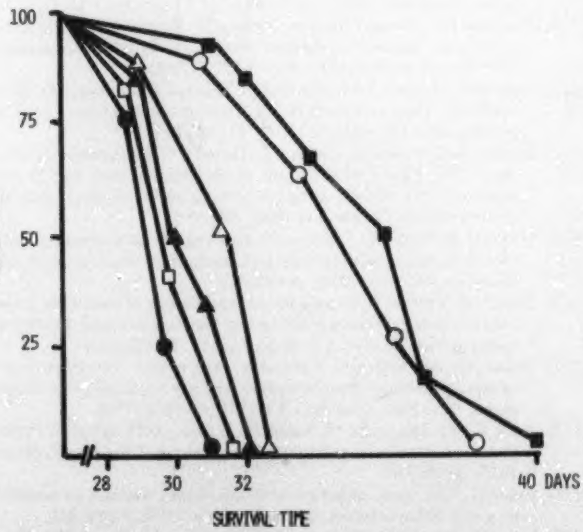

TEXT-FIGURE 2.—Thymosin-preincubated syngeneic bone marrow cells increase survival time in mice when injected iv 10 days after tumor implantation. ●, Controls; ▲, bone marrow cells alone; ■, bone marrow cells + thymosin fraction V; ○, bone marrow cells + thymosin α-1; △, bone marrow cells + levamisole; □, bone marrow cells + theophylline.

Experimental groups receiving normal syngeneic bone marrow cells pretreated with drugs and injected iv 10 days after tumor implantation.—Tumor growth was similar in mice given injections of 3×10^7 normal bone marrow cells (group 2) whether injected on the day of tumor implantation or 10 days after implantation (tables 1, 2). Theophylline effects were not significant (groups 5 and 6). In contrast, thymosin fraction V and thymosin α-1 (groups 3 and 4) yielded significantly different results compared to those obtained from all the other groups. The difference was not so pronounced on day 17 as on day 24 after tumor implantation (table 2). By days 31 and 38 after tumor implantation, only those animals survived that had received cells pretreated with thymosin fraction V or thymosin α-1. This difference was clearly significant ($P<0.001$; text-fig. 2).

DISCUSSION

The results show that normal bone marrow cells from syngeneic animals pretreated with thymosin were able to retard tumor growth and to increase survival times of animals with MCA-induced transplantable tumors. Theophylline and levamisole showed no significant effect compared to that shown by control groups. These results confirm and expand upon data of Umiel and Trainin (*25*) who showed earlier that lymphocytes from syngeneic normal and tumor-bearing mice were able to stimulate 3LL tumor growth. In our previous studies splenocytes and thymocytes pretreated with thymosin fraction V retarded tumor growth and reduced the number of pulmonary metastases due to Lewis tumor (*10, 11*). The results parallel those obtained with other types of thymic factors in different models by Ban An Khaw and Rule (*36*) and by Cupissol et al. (*27*) and are superior to results obtained with the iv injections of thymosin alone in the same model (Cupissol, Rey, Favier et al.: In preparation).

The tumor system employed here has been characterized in the authors' laboratory (*33*) and has never demonstrated T-cell-specific cytotoxicity after mixed lymphocyte culture, antibody-dependent cell-mediated cytotoxicity or NK activities. Nevertheless, immune complexes are present during tumor growth and increase over time (*5*), and weak in vivo immunity can be obtained by tumor amputation or injection of in vitro irradiated cells, which was demonstrated with the use of the Winn assay (*33*).

We show here that tumor growth was not accelerated after iv injection of normal bone marrow cells. This was not the case for injected splenocytes and thymocytes from tumor-bearing animals or even normal lymphocytes, a T-dependent phenomenon (*9*, *10*, *26*). Thymosin not only overcame lymphocyte-induced facilitated tumor growth, but also impeded it. Bone marrow cells did not facilitate tumor growth, which may suggest that in contrast with the results presented by Duwe and Singhal (*28*), there was no suppressor cell activity expressed by bone marrow cells, at least not in our model. In contrast, bone marrow cells preincubated with thymosin retarded tumor growth as do thymocytes or splenocytes under the same conditions (*10*). This action may imply that the target cell is an immature suppressor T-cell, not yet expressing suppressor activity (*37*). In the present system, it is impossible to determine if the point of impact for thymosin involves NK cells known to be present in bone marrow. Preliminary results suggest that NK cells are not involved in this mechanism and that the thymosin effect disappears after anti-Lyt 1 antiserum treatment.

Only thymosin fraction V and thymosin α-1 were active in restarting tumor growth and increasing survival time; Levamisole and theophylline were not. We have shown that these four substances in vitro raise the number of A-RFC (*34*, *35*) in healthy and tumor-bearing patients with decreased or normal A-RFC levels (*38*). These cells correspond to a T-lymphocyte theophylline-resistant (*29*, *30*) nonsuppressor subpopulation, probably an immature T-cell subpopulation (*39*). However, we have shown that theophylline, levamisole, and thymosin can modulate induction and expression of suppressor cells induced by concanavalin A (*24*) as well as suppressor activity in patients with solid tumors (*11*). These results agree with those published by Patt et al. (*40*).

However, with the exception of thymosin fraction V and thymosin α-1, in vitro results did not correlate with in vivo animal observations for the experimental system employed or with the results of Webb et al. (*32*) for theophylline. This observation suggests that in vitro tests are not suitable for the evaluation of the immunorestorative or immunostimulatory potential of a given drug (*10*, *34*). In addition, although the thymosin fraction V and thymosin α-1 results can be paralleled, the α-1 concentration employed was 20 times less than the concentration of fraction V. It might be of interest to evaluate the effects of other subfractions, especially those of the small peptides (*23*).

The results presented take on greater significance when they are considered in the light of potential clinical application. It is striking that all the results are statistically significant when the small number of cells employed is considered. Furthermore, the results were the same with bone marrow cells injected immediately after tumor implantation and with those given 10 days later, i.e., when tumor evolution is considerably advanced. This point should be stressed since it can be compared to the human situation where diagnosis is often made after significant tumor evolution has occurred. This technique presents definite advantages since to obtain the same antitumor effect as with other methods, only a small number of bone marrow cells are necessary and much less thymosin is needed than that required for iv injection or other routes of administration (*40*, *41*). Our model can be integrated with cancer patient treatment by the introduction of autologous bone marrow cell injection after high-dose chemotherapy (*42*). We are presently evaluating this possibility.

REFERENCES

(*1*) Prehn RT, Lappé MA. An immunostimulation theory of tumor development. Transplant Rev 1971; 7:26–54.

(*2*) Herberman RB. Cell-mediated immunity to tumor cells. Adv Cancer Res 1974; 19:207–263.

(*3*) Serrou B, Gauci L, Caraux J, Cupissol D, Thierry C, Esteve C. Immune imbelance in cancer patients. Recent Results Cancer Res 1980; 75:41–46.

(*4*) Baldwin RW, Price MR, Rebius RA. Blocking of lymphocyte cytotoxicity for rat hepatoma cells by tumor specific antigen-antibody complexes. Nature [New Biol] 1972; 238:185–187.

(*5*) Gauci L, Caraux J, Serrou B. Immune complexes in the context of the immune response in cancer patients. In: Serrou B, Rosenfeld C eds. Human cancer immunology. Amsterdam and New York: Elsevier/North-Holland 1981; 37–38.

(*6*) Broder J, Muul L, Waldmann TA. Suppressor cells in neoplastic disease. JNCI 1978; 61:5–11.

(*7*) Kirchner H, Chused TM, Herberman RB, Holden HT, Lavrin DH. Evidence of suppressor cell activity in spleens of mice bearing primary tumors induced by Moloney sarcoma virus. J Exp Med 1974; 139:1473–1487.

(*8*) Raov S, Bennett JA, Shen FW, Gershon RK, Mitchell MS. Antigen–antibody complexes generate Lyt 1 inducers of suppressor cells. J Immunol 1980; 125:63–67.

(*9*) Reinisch CL, Andrew SL, Schlossman SF. Suppressor cell regulation of immune response to tumors: Abrogation by adult thymectomy. Proc Natl Acad Sci USA 1977; 74:2989–2992.

(*10*) Serrou B, Rosenfeld C, Caraux J, Thierry C, Cupissol D, Goldstein AL. Thymosin modulation of suppressor function in mice and in man. Ann NY Acad Sci 1979; 332:35–100.

(*11*) Serrou B, Cupissol D, Caraux J, Thierry C, Rosenfeld C, Goldstein AL. Ability of thymosin to decrease in vivo and in vitro suppressor cell activity in tumor bearing mice and cancer patients. Recent Results Cancer Res 1980; 75:110–114.

(*12*) Gabizon A, Small M, Trainin N. Kinetics of the response of spleen cells from tumor-bearing animals in an in vivo tumor neutralization assay. Int J Cancer 1976; 18:813–819.

(*13*) Small M, Trainin N. Separation of populations of sensitized lymphoid cells into fractions inhibiting and fractions enhancing syngeneic tumor growth in vivo. J Immunol 1976; 117:292–297.

(*14*) Goldstein AL, Guha A, Zatz MM, Hardy MA, White A. Purification and biological activity of thymosin, a hormone of the thymus gland. Proc Natl Acad Sci USA 1972; 69:1800–1803.

(*15*) Aiuti F, Schirrmacher U, Ammirati I, Fiorilli H. Effect of thymus factor on human precursor T lymphocytes. Clin Exp Immunol 1975; 20:499–503.

(*16*) Bach JF. The mode of action of thymic hormones and its relevance to T-cell differentiation. Transplant Proc 1976; 8:243–248.

(*17*) Bach JF, Bach MA, Charreire J, Dardenne M, Pleau JM. Mechanism of action and biological significance of thymic factor. Ann NY Acad Sci 1979; 332:23–32.

(*18*) Trainin N, Rotter U, Yakino Y, et al. Biochemical and biological properties of THF in animal and human models. Ann NY Acad

Sci 1979; 332:9–25.

(*19*) Ahmed A, Wong M, Thurman GB, et al. T-lymphocyte maturation: Cell surface markers and immune function induced by T-lymphocyte cell-free products and thymosin polypeptides. Ann NY Acad Sci 1979; 332:81–94.

(*20*) Goldstein AL, Thurman GB, Rossio JL, Costanzi JJ. Immunologic reconstitution of patients with primary immunodeficiency diseases and cancer after treatment with thymosin. Transplant Proc 1977; 9:1141–1144.

(*21*) Goldstein AL, Thurman GB, Low TL, Rossio JL, Trivers GE. Hormonal influences on the reticuloendothelial system: Current status of the role of thymosin in the regulation and modulation of immunity. J Reticuloendothel Soc 1978; 23:253–266.

(*22*) Goldstein AL, Low TL, McAdoo M, et al. Thymosin alpha 1: Isolation and sequence analysis of an immunologically active thymic polypeptide. Proc Natl Acad Sci USA 1977; 74:725–729.

(*23*) Low TL, Thurman GB, Chincarini C, et al. Current status of thymosin research. Evidence for the existence of a family of thymic factors that control T cell maturation. Ann NY Acad Sci 1979; 332:33–41.

(*24*) Serrou B, Goldstein AL, Caraux J. Regulation of human suppressor cell function by thymosin. Biomedicine 1979; 31:89–93.

(*25*) Umiel T, Trainin N. Immunological enhancement of tumor growth by syngeneic thymus-derived lymhocytes. Transplantation 1974; 18:244–250.

(*26*) Ilfeld D, Carnaud C, Cohen IR, Trainin N. In vitro cytotoxicity and in vivo tumor enhancement induced by mouse spleen cells auto-sensitized in vitro. Int J Cancer 1973; 12:213–222.

(*27*) Cupissol D, Touraine JL, Serrou B. Ability of lymphocytes treated with thymic factor to decrease lung metastasis in tumor bearing mice. Thymus 1981; 3:9–16.

(*28*) Duwe AK, Singhal SK. The immunoregulatory role of bone marrow. I. Suppression of the induction of antibody responses to T-dependent and T-independent antigens by cells in the bone marrow. Cell Immunol 1979; 43:362–371.

(*29*) Rucheton M, Thierry C, Cupissol D, Rosenfeld C, Serrou B. Suppressor activity of the human ALL null cell line Reh. A tool for the study of suppressor cell mechanism. Cancer Immunol Immunother 1981. In press.

(*30*) Howard AR, Graham L. E-rosette formation by foetal liver and spleen cells incubated with theophylline. Clin Exp Immunol 1976; 23:279–284.

(*31*) Limatibul S, Shore A, Dosch HM, Gelfand EW. Theophylline modulation of E-rosette formation: An indicator of T-cell maturation. Clin Exp Immunol 1978; 33:503–513.

(*32*) Webb D, Brown W, Plescia OJ. Antitumor effects of polynucleotides and theophylline. Cancer Res 1972; 32:1814–1819.

(*33*) Reme T, Gauci L, Serrou B. Antigénicité des tumeurs chimio-induites chez la souris. II. Nature et spécificité de la réponse immune secondaire in vitro en culture mixte leucocytes-cellules tumorales. Ann Immunol (Paris) 1978; 129C:766.

(*34*) Caraux J, Goldstein AL, Esteve C, Serrou B. Thymosin alpha 1 restores the depressed binding of autologous erythrocytes by T-cells from cancer patients. Biomedicine 1979; 31:88–89.

(*35*) Thierry C, Esteve C, Caraux J, Goldstein AL, Serrou B. Immunopharmacology of autologous-rosette forming T-cells in humans. Tenth Annual Meeting of the Scandinavian Society for Immunology. Scand J Immunol 1979; 10:382.

(*36*) Ban An Khaw, Rule AH. Immunotherapy of the Dunning leukaemia with thymic extracts. Br J Cancer 1973; 28:288–292.

(*37*) Uytdehaag F, Heijnen CJ, Ballieux RE. Regulation of in vitro antibody synthesis in man: Role of T cell derived antigen specific suppressor factors. In: Serrou B, Rosenfeld C, eds. New trends in human immunology and cancer immunotherapy. Paris and London: Doin-Saunders, 1980:601–603.

(*38*) Caraux J, Thierry C, Serrou B. Human autologous rosettes. II. Prognostic significance of variations in autologous rosette-forming cells in the peripheral blood of cancer patients. JNCI 1979; 63:593–597.

(*39*) Caraux J, Thierry C, Esteve C, Flores G, Lodise R, Serrou B. Human autologous rosettes. I. Mechanism of binding of autologous erythrocytes by T-cells. Cell Immunol 1979; 45:36–48.

(*40*) Patt Y, Hersh E, Adebite M, Goldman R, Mavligit G. In vivo and in vitro clinical studies of immune modulation by thymus hormones. Ann NY Acad Sci 1979; 332:160–171.

(*41*) Cohen MH, Chretien PB, Ihde DC, et al. Thymosin fraction V and intensive combination chemotherapy. JAMA 1979; 241:1813–1816.

(*42*) Gorin MC, Miller JY, Salomon C, et al. Immunocompetence following autologous bone marrow transplantation. Exp Hematol 1975; 7:327–346.

blank page

Relationship Between Xenotransplantability and Cell Surface Properties of Ascites Sublines of a Rat Mammary Adenocarcinoma[1,2,3,4]

Susan C. Howard,[5] Steven R. Hull,[6] John W. Huggins,[5] Coralie A. Carothers Carraway,[7] *and* Kermit L. Carraway[8,9]

ABSTRACT—Cell surface properties of several ascites sublines of the 13762 rat mammary adenocarcinoma were compared in an effort to understand factors important to the xenotransplantability of these tumors into C57BL/6J mice. MAT-C, MAT-C1, and MAT-cMR6-S ascites sublines were xenotransplantable; MAT-B1, MAT-C2, and MAT-MR2-S were not. All of these sublines contained a large mucin-type sialoglycoprotein (ASGP-1) as a major cell surface component. MAT-B1 and MAT-cMR6-S ASGP-1 molecules were sulfated, but MAT-C1 and MAT-MR2-S incorporated little sulfate. The major oligosaccharide of MAT-C1 ASGP-1, a disialo-oligosaccharide, was present in very low amounts in the other sublines. ASGP-1 was detected readily in the plasma of animals with MAT-C1 or MAT-MR2-S tumors, but it was not detected readily in animals with MAT-B1 or MAT-cMR6-S tumors. Thus none of these significant features of ASGP-1 that differed among the sublines correlated with xenotransplantation. However, both MAT-C1 and MAT-cMR6-S sublines had branched cell surface microvilli. Moreover, MAT-C grown in mice after xenotransplantation had extensive, branched microvilli, even though only about 10% of the population of the cells grown in the rat had them. These results suggest that the branched microvilli may provide a protective mechanism, possibly by acting as a barrier to the approach of cytotoxic cells.—JNCI 1982; 69:33–40.

The cell surface is believed to play an important role in allowing tumors to escape immune destruction by the host (*1*). Two hypotheses have been advanced to account for the allotransplantability and xenotransplantability of the Ha subline of the TA3 mouse mammary tumor and the failure of the St subline to transplant into foreign strains and species. The first hypothesis is that the presence of a major sialoglycoprotein, called "epiglycanin," on the Ha subline masks H-2 surface antigens necessary for recognition (*2, 3*). The St subline does not contain significant amounts of epiglycanin (*4*). The second hypothesis is that shed cell surface components, including epiglycanin, interact with components of the immune system to block tumor cell destruction (*5*).

However, our recent studies on xenotransplantation of sublines of the 13762 rat mammary adenocarcinoma suggest that neither of these hypotheses can completely explain tumor cell survival in a foreign host. Both the xenotransplantable MAT-C1 and nonxenotransplantable MAT-B1 ascites sublines have a major cell surface sialoglycoprotein (ASGP-1) that represents 0.5% of the total cellular protein (*6, 7*). The rates of shedding of the glycoprotein and its fragments are similar for the two sublines (*8*). These results suggest that other factors are important in allowing the escape of the tumors from immune surveillance. Among the parameters previously shown to differ between the xenotransplantable and nonxenotransplantable sublines are cell surface morphology (*9*), cell surface receptor mobility (*9, 10*), and size and composition of sialoglycoprotein (*11*). Examination of several new sublines indicates that of these parameters morphology is most closely correlated with xenotransplantation.

MATERIALS AND METHODS

Materials.—D-[1-^{3}H]glucosamine HCl (2–6 Ci/nmol) and [^{35}S]sulfate (100 mCi/nmol) were from Amersham/Searle Corp.; Instagel was from Packard Instrument Co.; CsCl (99.99%) was a product of Varlacoid; guanidine hydrochloride (grade I) was from Sigma Chemical Co.; peanut lectin was from Miles-Yeda, Ltd.; NS-ST X-ray film was from Eastman Kodak Co.

Ascites cells were maintained as previously described (*6*). Passage and cloning of MR cells were performed as previously described (*12*).

General methods.—FITC–Con A lectin receptor redistribution (*9, 10*), D-[1-^{3}H]glucosamine and [^{35}S]sulfate incorporation in vivo (*6, 11*), ASGP-1 purification and isopyknic density gradient centrifugation in CsCl with 4 *M* guanidine hydrochloride (*6*), alkaline borohydride elimination (*6*), Biogel P-4 chromatography (*6*), and ion exchange (*11*) were

---

ABBREVIATIONS USED: Con A=concanavalin A; FITC=fluorescein isothiocyanate; PNA=peanut agglutinin; SDS=sodium dodecyl sulfate.

---

[1] Received October 7, 1980; revised November 24, 1981; accepted February 22, 1982.

[2] Supported by Public Health Service (PHS) grants GM-25818 and GM-30295 from the National Institute of General Medical Sciences; by PHS grants CA-19985, CA-25173, and CA-31695 from the National Cancer Institute; and by the Oklahoma Agriculture Experiment Station.

[3] A nomenclature was developed for the new sublines that would be descriptive of their origin. The "MR" designation indicates the cultured line of MAT-B cells from Mason Research Institute, Worcester, Mass. A prefix "c" is used for clones of the cultured line. The term "MAT" indicates cells grown as ascites tumors (mammary ascites tumor). The "S" is included to indicate those sublines that developed sialoglycoprotein during ascites passage [*see* (*12*)].

[4] This is journal article J-3780 of the Oklahoma Agriculture Experiment Station. The research was conducted in cooperation with the U.S. Department of Agriculture Agricultural Research Service, Southern Region.

[5] Department of Biochemistry, Oklahoma State University, Stillwater, Okla. 74078.

[6] Department of Biochemistry, University of Miami School of Medicine, Miami, Fla. 33101.

[7] Department of Oncology, University of Miami School of Medicine.

[8] *Address reprint requests to* Dr. K. L. Carraway, Department of Anatomy (R-124), University of Miami School of Medicine, Miami, Fla. 33101.

[9] We thank Mrs. Charlene Bymaster for technical assistance.

performed as previously described. Scanning electron microscopy was done as described previously (*9*), except that osmication was performed at 4°C for 15 minutes.

Xenotransplantation.—For each tumor line tested, C57BL/6J female mice were given injections of 1×10^6 tumor cells suspended in 0.25 ml of 0.9% NaCl (pH 7.4) (*7*). Controls received injections of 0.25 ml 0.9% NaCl.

Detection of ASGP-1 in blood plasma.—Ascites tumor-bearing rats were anesthetized with diethyl ether and decapitated by means of a guillotine. Blood was collected in a potassium oxalate-coated beaker, poured into potassium oxalate-coated Corex tubes, and centrifuged at 500×*g* for 2 minutes for cell removal. Plasma was treated with an equal volume of 5% 2-mercaptoethanol and 2% SDS in a boiling water bath for 5 minutes before electrophoresis on a 4.5–15% acrylamide gradient gel slab (*6*). The slab was stained with ^{125}I-labeled PNA and dried for autoradiography (*13*).

RESULTS

Morphology, Receptor Mobility, and Xenotransplantability of New Sublines

Text-figure 1 shows the derivation of the tumor sublines examined. Some properties of the MAT-B, MAT-B1, and MAT-C1 sublines were reported previously (*7–10*). The MAT-C1 subline exhibited highly branched microvilli and restricted Con A receptor mobility and was xenotransplantable. The MAT-B and MAT-B1 cells had a more normal surface architecture with unbranched, curved microvilli, ruffles, and ridges. Their Con A receptors were highly mobile, and the cells were not xenotransplantable. Most (90%) of the MAT-C cells had short, straight microvilli and intermediate receptor mobility and were xenotransplantable. About 10% of the population had branched microvilli (*9*).

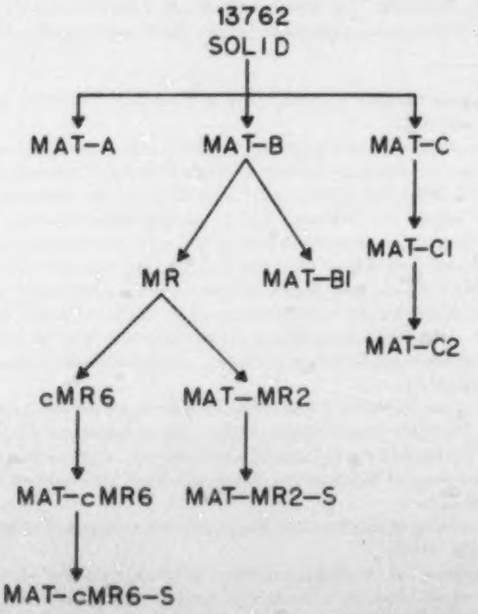

TEXT-FIGURE 1.—Lineage of the 13762 mammary adenocarcinoma sublines.

TABLE 1.—*Xenotransplantability of 13762 ascites sublines into C57BL/6J mice*

Injection	No. of mice killed/total No. of mice[a]
Saline	0/9
MAT-B1	0/8
MAT-MR2-S	0/8
MAT-cMR6-S	6/8
MAT-C2	0/8
MAT-C1[b]	8/10
MAT-C3	0/10

[a] Numbers were identical for a 30- or 90-day period.
[b] See (7).

The new sublines were obtained from a variant (MR) of MAT-B adapted to cell culture by Dr. Erling Jensen, Mason Research Institute. MR cells were cloned (*12*), and one of the clones (cMR6) was injected into rats to give an ascites tumor line (MAT-cMR6). After about 18 passages of these ascites cells, the major sialoglycoprotein ASGP-1 appeared abruptly (*12*). These cells were called MAT-cMR6-S (*8*). Likewise, the uncloned MR cells were injected into animals to give the MAT-MR2 (an earlier passage was designated MAT-MR1) and passaged until ASGP-1 appeared at about passage 19 to give the MAT-MR2-S subline (*8*). The properties of these two variants at subsequent passages have been compared to those of MAT-B1 and MAT-C1.

The morphology of the MR cells injected into animals changed at each successive stage noted above. The MR cells (cloned or uncloned) had fewer prominent microvilli than the ascites cells derived from them (fig. 1). The most dramatic difference, however, occurred at the stage of the appearance of ASGP-1 when the MAT-cMR6-S cells exhibited branched microvilli, but the MAT-MR2-S cells did not (figs. 1C, 1F).

Treatment of the MAT-cMR6-S and MAT-MR2-S cells with fluorescent Con A did not show the dramatic differences in Con A receptor mobility previously observed between MAT-B1 and MAT-C1 cells. Neither of the new sublines underwent the extensive capping that occurred with MAT-B1 cells, although MAT-MR2-S cells did undergo a limited capping reaction. Limited receptor mobility was also observed for MAT-cMR6-S cells, but microscopic examination suggested that the effect was due to clustering of the branched microvilli rather than to the typical capping response observed with MAT-B1 cells. Thus the branched MAT-cMR6-S microvilli appear to be stabilized and to have relatively immobile Con A receptors, as previously observed for MAT-C1 microvilli. The mobility observed may be due to the apparent lower density of microvilli on MAT-cMR6-S cells than on MAT-C1 cells.

The xenotransplantability of the new sublines was tested by the injection of the sublines into C57BL/6J mice (*7*). The MAT-cMR6-S cells were approximately as efficient in killing the mice (table 1) as were the previously tested MAT-C1 cells (*7*), but none of the other sublines were active (table 1).

Sialoglycoprotein of the New Sublines

Since MAT-B1 and MAT-C1 sublines differed in oligosaccharide composition (*6*) and sulfation (*11*) of ASGP-1, the glycoprotein was isolated from each of the new sublines after double labeling with [^{3}H]glucosamine and [^{35}S]sulfate. Density gradient profiles in CsCl/4 *M* guanidine hydrochloride showed more ^{35}S label in ASGP-1 from MAT-cMR6-S (text-fig. 2) than from MAT-MR2-S (text-fig. 3).

Oligosaccharides were isolated from ASGP-1 of MAT-cMR6-S and MAT-MR2-S by alkaline borohydride treatment and fractionated on Biogel P-4. The profiles of oligosaccharides for MAT-cMR6-S (text-fig. 4) were more similar to those for MAT-B1 (*6, 11*) than to those for MAT-C1. In particular, the MAT-cMR6-S profiles showed a reduced peak II oligosaccharide characteristic of MAT-B1 ASGP-1. The oligosaccharide profile for MAT-MR2-S ASGP-1 was simpler than any observed previously.

For additional characterization, the major oligosaccharide peaks of the new sublines were further fractionated by DEAE-Sephadex chromatography, as described previously for MAT-B1 oligosaccharides (*1*). Text-figure 5 shows the column profiles of the oligosaccharides from MAT-cMR6-S on DEAE-Sephadex. The results were similar to those obtained with MAT-B1 (*11*). MAT-C1 oligosaccharides were also fractionated by sequential Biogel P-4 and DEAE-Sephadex chromatography. The DEAE-Sephadex chromatography and gas chromatography analyses of the oligosaccharide carbohydrate compositions indicated that component II-3, the acidic fraction of II from Biogel P-4, contained two sialic acid residues, two galactose, and one glucosamine per one galactosaminitol. Component II-3 had the same composition as the acidic oligosaccharide from epiglycanin of TA3-Ha mammary adenocarcinoma cells (*14*). Component III-2, the intermediate peak from DEAE-Sephadex chromatography of peak III from Biogel P-4, contained one sialic acid, one galactose, and one glucosamine per one galactosaminitol. Further structural analyses of these oligosaccharides are in progress.

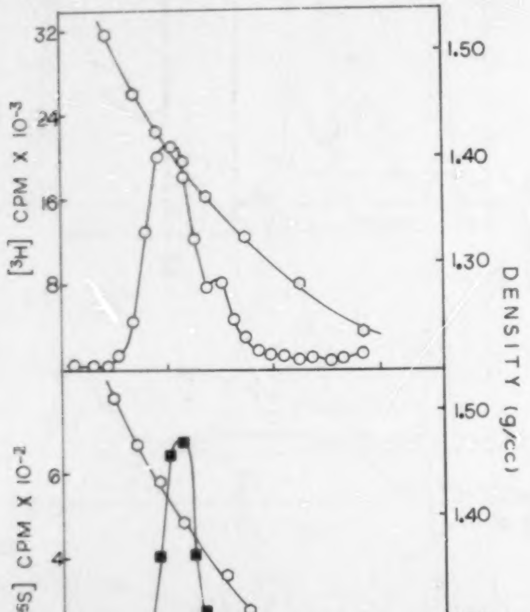

TEXT-FIGURE 2.—Density gradient centrifugation of [^{3}H]glucosamine (*top*) and [^{35}S]SO_4^{-2}-labeled (*bottom*) MAT-cMR6-S membrane vesicles in CsCl gradients containing 4 *M* guanidine hydrochloride (○, ■). Density (○). MAT=ascites, MR=cultured, c=cloned, and S=sialoglycoprotein.

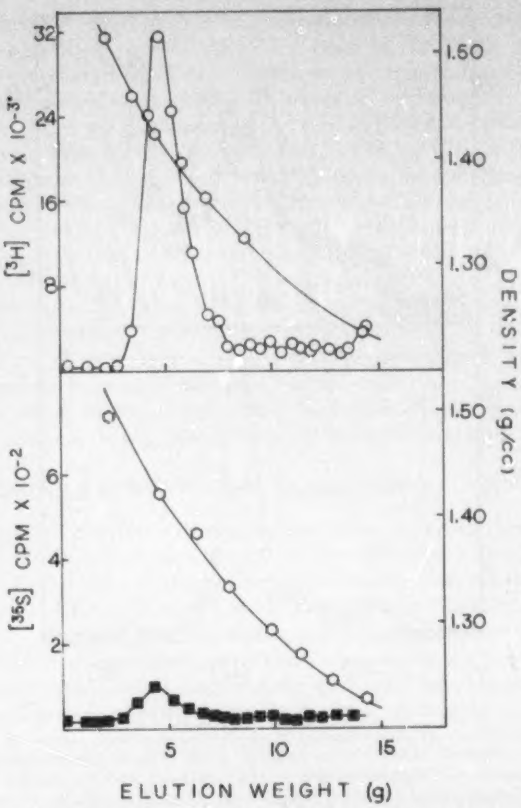

TEXT-FIGURE 3.—Density gradient centrifugation of [^{3}H]glucosamine (○) and [^{35}S]SO_4^{-2}-labeled (■) MAT-MR2-S membrane vesicles in CsCl gradients containing 4 *M* guanidine hydrochloride. Density (○).

Table 2 shows the fraction of metabolically incorporated glucosamine in these two oligosaccharides from three sublines—MAT-B1, MAT-C1, and MAT-cMR6-S. There appeared to be no obvious relationship between the content of a particular sialo-oligosaccharide and xenotransplantability. This finding was consistent with results of analyses of whole-cell sialic acid, which also did not show any correlation with xenotransplantability (data not shown).

ASGP-1 in Plasma

The rates of shedding in vitro were essentially the same for MAT-B1 and MAT-C1 sublines, but there was a 2.5-fold greater amount of soluble ASGP-1 in MAT-C1 ascitic

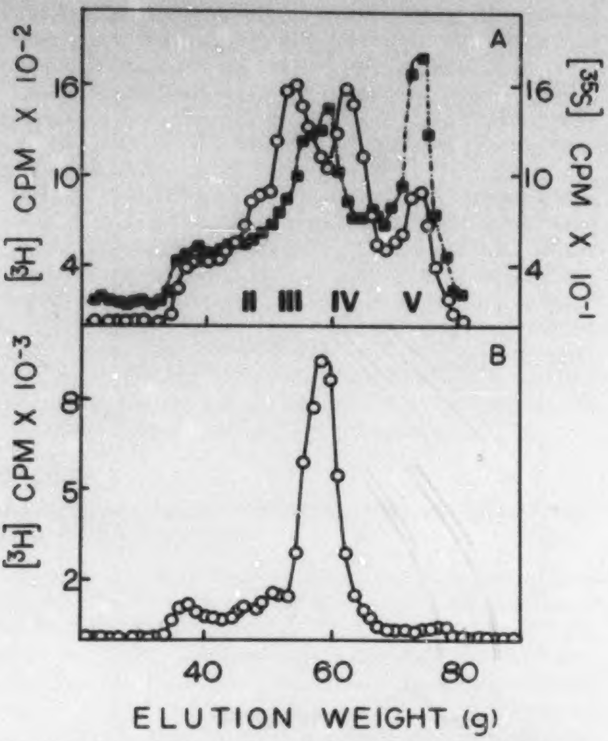

TEXT-FIGURE 4.—Gel filtration on Biogel P-4 of oligosaccharides from new sublines. A) Oligosaccharides of MAT-cMR6-S ASGP-1 labeled with [^{3}H]glucosamine (○) and [^{35}S]sulfate (■). B) Oligosaccharides of MAT-MR2-S (○) labeled with [^{14}C]glucosamine. The samples were mixed, alkaline borohydride treated (1.0 *M* $NaBH_4$, 0.05 *M* NaOH, 16 hr, 45°C), neutralized with acetic acid, and chromatographed on a Biogel P-4 column (200–400 mesh, 0.9×113 cm) equilibrated with 1.0 *M* pyridine acetate (pH 6.0). *Roman numerals* refer to the peaks with *open circles* in A.

fluid (*8*). Since antigens in blood may act as part of blocking factors to abrogate immune destruction of tumors, we assayed blood plasma for soluble ASGP-1 using radiolabeled PNA, which has been shown to bind specifically to ASGP-1 (*12*, *13*), on SDS electrophoresis gels of plasma from animals with the different ascites sublines. PNA was observed to bind to all of the sublines tested by fluorescence microscopy with the use of FITC–PNA (*15*) and to bind to the ASGP-1 molecules of all the sublines with the use of ^{125}I-labeled PNA overlays on SDS–polyacrylamide gel electrophoresis of the whole cells (*13*). Thus it can be used to estimate ASGP-1 in cells, tissues, or fluids, regardless of degree of sialylation, but it is only semiquantitative (*13*). Figure 2 shows that there were negligible amounts of plasma ASGP-1 in animals with MAT-B1 (nontransplantable) and MAT-cMR6-S (transplantable) tumors compared to those with MAT-C1 (transplantable) and MAT-MR2-S (nontransplantable) tumors. Thus there was no correlation between the amount of soluble ASGP-1 in the circulation and xenotransplantability of the tumor. The most reasonable explanation for these results is that ASGP-1 was cleared from the circulation.

Cell Surface Changes in a Variant of MAT-C1 Cells

During the course of passage of MAT-C1 cells over more than 4 years, we have noted one instance in which the tumor spontaneously changed to a new form. The morphology of the new variant, named "MAT-C2," was substantially different from that of MAT-C1. The cells did not exhibit the extensively branched microvilli of MAT-C1 cells. The predominant morphology was similar to that shown by MAT-

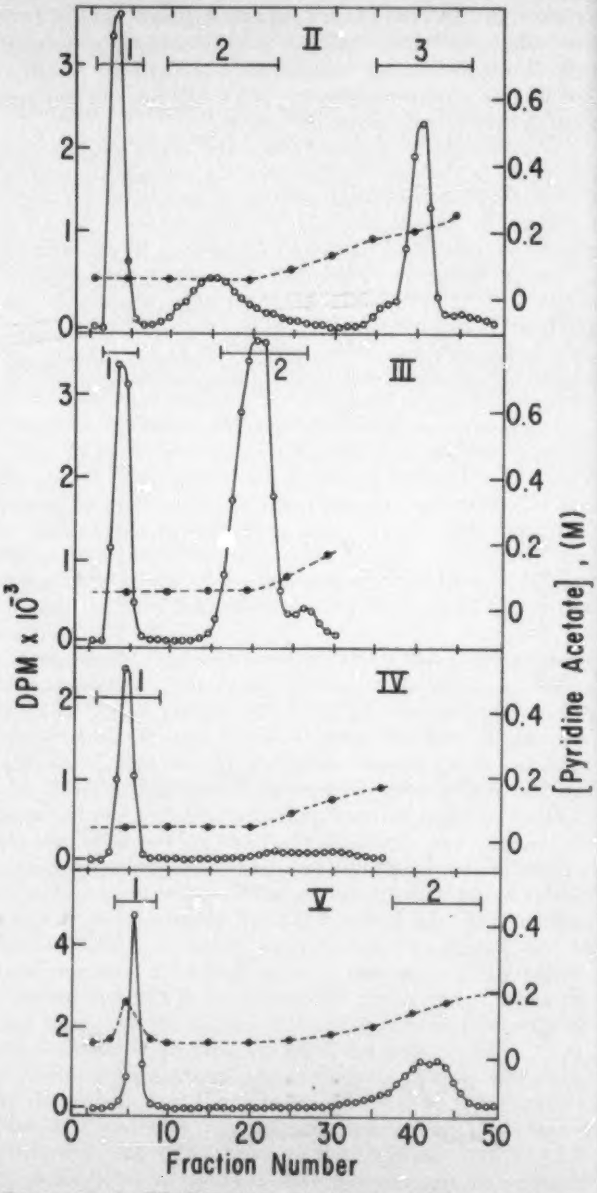

TEXT-FIGURE 5.—DEAE–Sephadex fractionation of oligosaccharides from MAT-cMR6-S. *Roman numerals* refer to fractions from text-fig. 4A. *Brackets* indicate isolated fractions used for further analyses and indicate the designations used for oligosaccharides. Thus II-3 is the oligosaccharide eluted at about fraction 40 from the column whose profile is shown in the *top graph*.

TABLE 2.—*Distribution of labeled glucosamine in oligosaccharide fractions from different sublines*

Subline	Total glucosamine, %	
	II-3	III-2
MAT-B1	12	29
MAT-C1	27	28
MAT-cMR6-S	5	22

MR2-S in figure 1. The MAT-C2 oligosaccharide pattern was simple, resembling that of MAT-MR2-S, although slightly shifted. The change in morphology and oligosaccharide was accompanied by a loss of xenotransplantability (table 1). Concomitant with these changes, a bacterial infection was discovered in the animal colony used for passage of the cells. The infectious agent was not identified specifically, although two isolates of *Staphylococcus* were obtained from the animals. The infection was eliminated by quarantine and antibiotic treatment. Passage of MAT-C2 cells was continued in the healthy animals. Over about 25 passages the ASGP-1 reverted to an oligosaccharide profile on Biogel P-4 resembling that for MAT-C1 (text-fig. 6). These cells were designated MAT-C3. They were not xenotransplantable, and few of them contained branched microvilli.

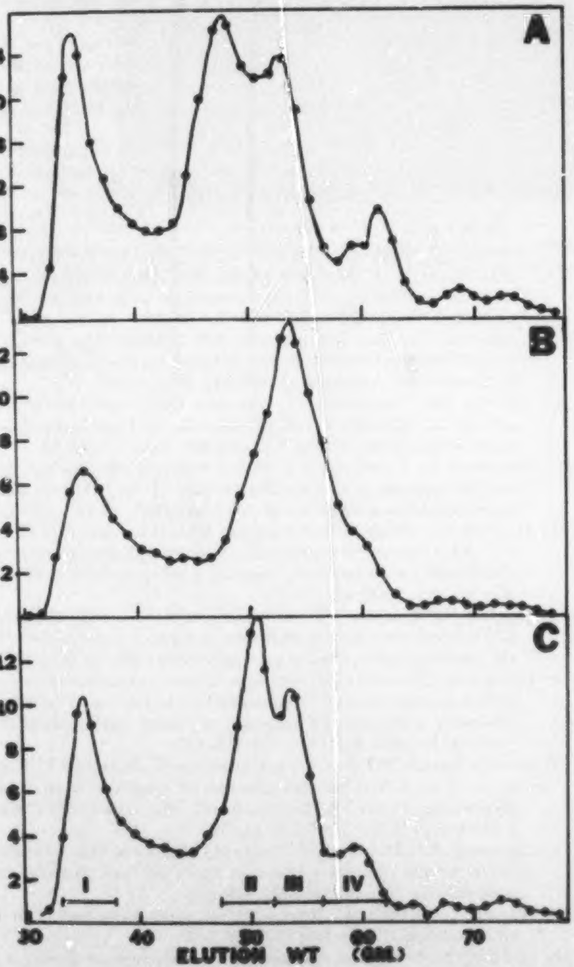

TEXT-FIGURE 6.—Gel filtration of oligosaccharides from MAT-C1 (A), MAT-C2 (B), and MAT-C3 (C) on Biogel P-4.

To determine the reason for the shift in Biogel P-4 profiles in going from MAT-C1 to MAT-C2 to MAT-C3, we fractionated the oligosaccharides by DEAE-Sephadex chromatography. The ratios of neutral oligosaccharides to monosialo- to disialo-oligosaccharides were determined for each subline from the glucosamine labeling. For MAT-C1 the ratio was 1:5:5. For MAT-C2 the ratio was 1:2:2. For MAT-C3 the ratio was 1:5:6. Thus the change in pattern appears to result primarily from a change in sialylation, MAT-C2 having a much smaller amount of sialylated oligosaccharides compared to neutral oligosaccharides than the other sublines. Whether there were other changes in these oligosaccharides (e.g., fucosylation) remains to be investigated.

Morphology of MAT-C Cells Grown in Mice

MAT-C cells were heterogeneous when grown in the rat. About 10% of the population had extensive, branched microvilli, but the remainder had short, straight microvilli (*9*). When MAT-C cells were transplanted into mice and isolated shortly before the death of the animal, most of the cells (>80%) had branched microvilli. These results suggested a selection mechanism favoring the cells with branched microvilli and provided support for the concept that morphology is important for survival of tumor cells in the foreign species.

DISCUSSION

In previous studies a number of differences have been noted between MAT-B1 and MAT-C1 ascites sublines of the 13762 rat mammary adenocarcinoma that might be related to their differences in xenotransplantability. Several new sublines, obtained by ascites passage of a cultured subline of the tumor (*12*), have been examined in an attempt to understand the reason for the xenotransplantability difference.

One difference of particular interest between the sublines was the sialic acid content of the major sialoglycoprotein ASGP-1. MAT-C1 ASGP-1 had a threefold higher content of sialic acid than MAT-B1 ASGP-1. The difference was primarily due to a larger amount of disialohexasaccharide on the MAT-C1 ASGP-1. However, the amount of disialohexasaccharide did not correlate with xenotransplantability (table 2), since the new subline MAT-cMR6-S, which was xenotransplantable, had a low content of disialohexasaccharide. Moreover, in the change from MAT-C1 to MAT-C2 to MAT-C3 cells, there was a loss and then a reappearance of the disialohexasaccharide with a loss but not a reappearance of xenotransplantability.

These changes in oligosaccharide during and after an infection of the animals suggest that a selection process was occurring in response to the changing immunologic status of the animal. The simplest explanation is that cells with highly sialated ASGP-1 were favored in the healthy animals, whereas cells with more poorly sialated ASGP-1 were favored in the infected animals.

TABLE 3.—*Properties of ascites sublines*

Property	MAT-B1	MAT-C1	MAT-cMR6-S	MAT-MR2-S	MAT-C2[a]
Xenotransplantation	−	+	+	−	−
Branched microvilli	−	+	+	−	−
ASGP-1 sulfation	+	−	+	−	ND
Receptor redistribution	+++	−	+	+	ND
Plasma ASGP-1	−	+	−	+++	+

[a] Symbols indicate relative amounts of plasma ASGP-1 cells showing redistribution. −=0; +=0.25; +++=1. ND=not determined.

The absence of sulfate (*11*) is also not required for xenotransplantation, as indicated by results with the MAT-cMR6-S subline (table 3). Likewise, extensive receptor redistribution (*8, 10*) is not necessary for prevention of xenotransplantation, and the blood plasma concentration of soluble ASGP-1 appears unrelated. The only parameter for the sublines studied that correlated with xenotransplantability was cell morphology. However, the results should not be construed to indicate that morphology is the only important factor. Other parameters not evaluated in this work may also be important. Moreover, xenotransplantation may depend on a combination of cell surface parameters including those above, none of which is absolutely essential.

If morphology can play a role in aiding tumor cells to escape immunologic defense mechanisms, it is instructive to consider possible contributions of the branched microvilli to tumor cell survival. If the mechanisms for killing tumor cells involve cell-to-cell contact, the branched microvilli provide a formidable physical barrier to a close encounter. Whereas unbranched microvilli may interdigitate and facilitate cell-to-cell interactions, no interdigitation appears feasible with the branched structures on these cells. The structure and stability of the branched microvilli (*10, 16*) mitigate against deformation, which may be an important consideration to immune destruction (*17*). Moreover, the increased surface area permitted by the branched microvilli could increase the amount of sialoglycoprotein available at the cell periphery because of the increased depth of the sialoglycoprotein layer, effectively enhancing the cell surface charge density. Mobility of antigens on microvilli of some cells appears to be restricted (*18*). In MAT-C1 cells mobility of cell surface antigens (*9*), as well as Con A-binding molecules (*9, 10*), is restricted. If antigen mobility is a prerequisite for immune killing (*19, 20*), this restriction might aid in tumor cell survival. Clearly, there are a number of ways in which morphology can contribute to tumor cell survival. The significance of these possibilities is being evaluated by further experimentation.

The correlation of morphology and xenotransplantation should not suggest that the presence of ASGP-1 or the glycoprotein shedding is unimportant to tumor cell survival. These factors may contribute to survival of the tumors in syngeneic or allogeneic hosts. The cells probably develop a battery of survival mechanisms against host defenses which can be used individually or collectively against different levels of host defense mechanisms.

REFERENCES

(*1*) Nicolson GL, Poste G. The cancer cell: Dynamic aspects and modifications in cell-surface organization (part 2). N Engl J Med 1976; 295:253–258.

(*2*) Miller SC, Hay ED, Codington JF. Ultrastructural and histochemical differences in cell surface properties of strain-specific and nonstrain-specific TA3 adenocarcinoma cells. J Cell Biol 1977; 72:511–529.

(*3*) Sanford BH, Codington JF, Jeanloz RW, Palmer PD. Transplantability and antigenicity of two sublines of the TA3 tumor. J Immunol 1973; 110:1233–1237.

(*4*) Codington JF, Cooper AG, Brown MC, Jeanloz RW. Evidence that the major cell surface glycoprotein of the TA3-Ha carcinoma contains the *Vicia graminea* receptor sites. Biochemistry 1975; 14:855–859.

(*5*) Cooper AG, Codington JF, Brown MC. In vivo release of glycoprotein I from the Ha subline of TA3 murine tumor into ascites fluid and serum. Proc Natl Acad Sci USA 1974; 71:1224–1228.

(*6*) Sherblom AP, Buck RL, Carraway KL. Purification of the major sialoglycoproteins of 13762 MAT-B1 and MAT-C1 rat ascites mammary adenocarcinoma cells by density gradient centrifugation in cesium chloride and guanidine hydrochloride. J Biol Chem 1980; 255:783–790.

(*7*) Sherblom AP, Huggins JW, Chesnut RW, Ownby CL, Dermer GB, Carraway KL. Cell surface properties of ascites sublines of the 13762 rat mammary adenocarcinoma. Relationship of the major sialoglycoprotein to xenotransplantability. Exp Cell Res 1980; 126:417–426.

(*8*) Howard SC, Sherblom AP, Huggins JW, Carraway CA, Carraway KL. Shedding of the major plasma membrane sialoglycoprotein from the surface of 13762 rat ascites mammary adenocarcinoma cells. Arch Biochem Biophys 1981; 207:40–50.

(*9*) Carraway KL, Doss RC, Huggins JW, Chesnut RW, Carraway CA. Effects of cytoskeletal perturbant drugs on ecto-5′-nucleotidase, a concanavalin A receptor. J Cell Biol 1979; 83:529–543.

(*10*) Huggins JW, Trenbeath TP, Yeltman DR, Carraway KL. Restricted concanavalin A redistribution on the branched microvilli of an ascites tumor subline. Exp Cell Res 1980; 127:37–46.

(*11*) Sherblom AP, Carraway KL. Sulfate incorporation into the major sialoglycoprotein of the MAT-B1 subline of the 13762 rat ascites mammary adenocarcinoma. Biochemistry 1980; 19:1213–1219.

(*12*) Howard SC, Sherblom AP, Chesnut RW, Carraway CA, Carraway KL. Changes in expression of a major sialoglycoprotein associated with ascites forms of a mammary adenocarcinoma. Biochim Biophys Acta 1980; 631:79–89.

(*13*) Huggins JW, Trenbeath TP, Sherblom AP, Howard SC, Carraway KL. Glycoprotein differences in solid and ascites forms of the 13762 rat mammary adenocarcinoma. Cancer Res 1980; 40:1873–1878.

(*14*) Helm RM, Carraway KL. Evidence for the association of two cell surface glycoproteins of 13762 mammary ascites tumor cells. Concanavalin A-induced redistribution of peanut agglutinin-binding proteins. Exp Cell Res 1981; 135:418–424.

(*15*) van den Eijnden DH, Evans NA, Codington JF, Reinhold V, Silber C, Jeanloz RW. Chemical structure of epiglycanin, the major glycoprotein of the TA3-Ha ascites cell. The carbohydrate chain. J Biol Chem 1979; 254:12,153–12,159.

(*16*) Carraway KL, Huggins JW, Cerra RF, Yeltman DR, Carraway CA. α-Actinin-containing branched microvilli from an ascites adenocarcinoma. Nature 1980; 285:508–510.

(*17*) Weiss L. Guest editorial: Neuraminidase, sialic acids, and cell interactions. J Natl Cancer Inst 1973; 50:3–19.

(*18*) de Petris S. Preferential distribution of surface immunoglobulins on microvilli. Nature 1978; 272:66–68.

(*19*) Bourguignon LY, Hyman R, Trowbridge I, Singer SJ. Participation of histocompatibility antigens in capping of molecularly independent cell surface components by their specific antibodies. Proc Natl Acad Sci USA 1978; 75:2406–2410.

(20) Geiger B, Rosenthal KL, Klein J, Zinkernagel RM, Singer SJ. Selective and unidirectional membrane redistribution of an H-2 antigen with an antibody-clustered viral antigen: Relationship to mechanisms of cytotoxic T-cell interactions. Proc Natl Acad Sci USA 1979; 76:4603–4607.

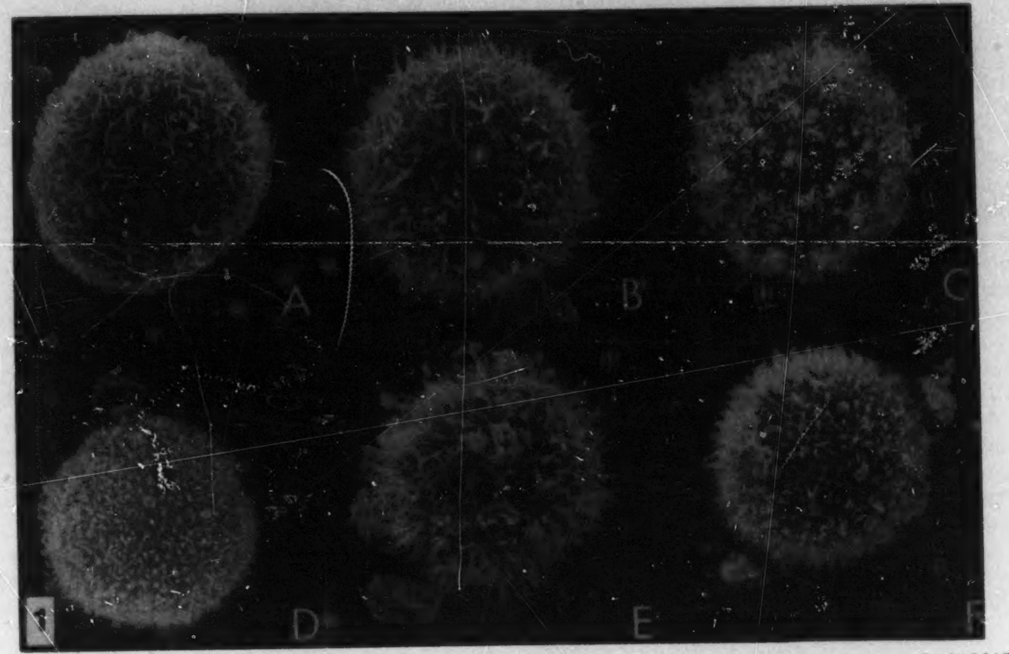

Figure 1.—Scanning electron micrographs showing the progressive morphologic changes as cultured cells adapt to ascites growth. A) MAT-cMR6 (MR clone 6) in vitro, passage 4. B) MAT-cMR6, ascites passage 3. C) MAT-cMR6-S, ascites passage 22, after development of ASGP-1. D) MR (uncloned) in vitro. E) MAT-MR2, ascites passage 13. F) MAT-MR2-S, ascites passage 28, after development of the glycoprotein. A, B, D, and E: × 2,700. C and F: × 2,400.

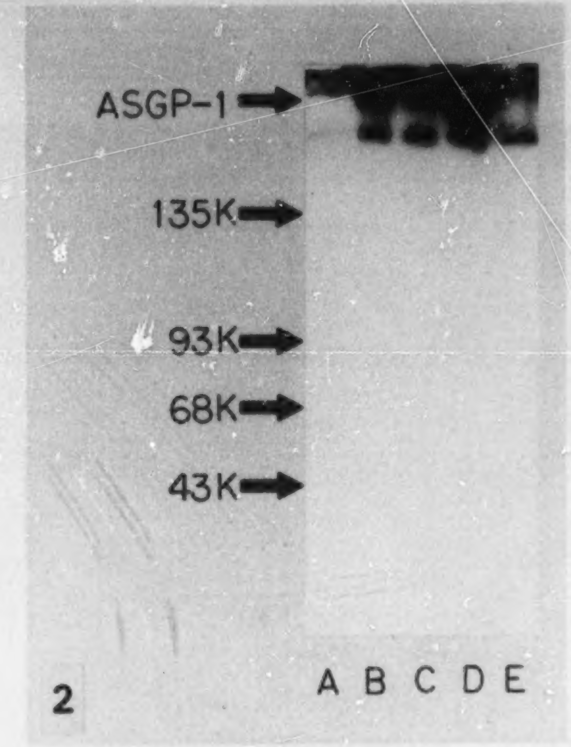

FIGURE 2.—ASGP-1 in blood plasma of ascites tumor-bearing rats detected by ^{125}I-labeled PNA binding. Plasma was treated with an equal volume of solubilizing mixture, and 160 µg protein/well was electrophoresed on a 4.5–15% acrylamide gradient slab. ^{125}I-labeled PNA staining and autoradiography were performed as previously described (*6*). Ascites sublines shown are: MAT-B1 (A), MAT-C1 (B), MAT-C2 (C), MAT-MR2-S (D), and MAT-cMR6-S (E).

Steroid Hormone Receptors in the Rat Mammary Adenocarcinoma Induced by *N*-Hydroxy-*N*-2-fluorenylacetamide [1,2,3,4]

Sara Antonia Li, [5,6] **Danuta Malejka-Giganti,** [7] *and* **Jonathan J. Li** [5,8]

ABSTRACT—The steroid hormone receptors in *N*-2-fluorenylacetamide (2-FAA)- and *N*-hydroxy-2-FAA-induced mammary adenocarcinomas in outbred Sprague-Dawley rats were analyzed. Both 8S and 4S estrogen-binding components have been detected in cytosols of these tumors following sucrose gradient sedimentation in low salt. Competitive binding analyses of this binder indicated a specificity profile expected of an estrogen receptor. Both androgen and progesterone receptors were also present in the cytosols of these mammary tumors. While the androgen receptor sedimented in the 8S region of the gradient, the progestin binder appeared only as a 4S moiety under similar conditions. The relative concentrations of these receptors (expressed in fmol/mg protein ± SE) were: 17β-estradiol (28.6±4.1) > 5α-dihydrotestosterone (8.5±2.2) > progesterone (5.0±1.3). The progesterone receptor was increased at least eightfold in the mammary adenocarcinomas from ovariectomized rats that were treated with diethylstilbestrol for 6 days. Binding equilibrium data indicated $K_a=1.2\text{-}1.8\times10^9\ M^{-1}$ for the above cytoplasmic hormone receptor complexes (K_a, association constant). Although cytosols prepered from lactating mammary gland contained appreciable quantities of glucocorticoid receptor, only trace amounts were found in the mammary adenocarcinoma.—JNCI 1982; 69:41–45.

2-FAA and *N*-hydroxy-2-FAA administered systemically are mammary gland carcinogens in female Sprague-Dawley rats (*1, 2*). A single dose of *N*-hydroxy-2-FAA administered topically or ip also yields a high tumor incidence in the mammary gland of these rats (*3, 4*).

The presence of steroid hormone receptors in certain endocrine tumors has been used as an indicator of the hormone responsiveness of these tumors (*5–8*). Analyses of steroid hormone receptors in human breast cancers and in experimental mammary tumors show a multiplicity and varying amounts of these receptors (*8–16*). The DMBA-induced mammary adenocarcinoma in the rat is the most extensively studied experimental model; receptors for estrogen, progesterone, androgen, glucocorticoid, and prolactin have been characterized (*10–15*). However, the composition of steroid hormone receptors in 2-FAA- or *N*-hydroxy-2-FAA-induced mammary adenocarcinoma has not been studied. The present investigation was undertaken to characterize the steroid hormone receptors in 2-FAA- and *N*-hydroxy-2-FAA-induced mammary carcinomas in outbred Sprague-Dawley rats and to compare the levels of hormone receptors found in these mammary tumors with those found in lactating mammary glands of rats of the same strain.

MATERIALS AND METHODS

Animals, compounds, and treatment.—Four-week-old female outbred Sprague-Dawley rats (Holtzman Co., Madison, Wis.), housed individually, were fed a semisynthetic diet containing 20% casein (*17*). 2-FAA (mp 196°C and *N*-hydroxy-2-FAA (mp 150–151°C) were prepared as previously described (*1, 3*) and shown to be authentic by UV and infrared spectra as well as by thin-layer chromatography. The compounds were dispersed in 7% gum arabic in 0.15 *M* NaCl at a concentration of 10 mg/ml. The suspended compounds were injected ip three times weekly for 4 weeks at a dose level of 0.01 mmol/100 g body weight (*2*). After the treatment was completed, the animals were weighed and examined for tumors once weekly. The earliest mammary tumors were palpable at about 3.3 or 1.9 months after treatment with 2-FAA or *N*-hydroxy-2-FAA, respectively, had ceased. Rats bearing mammary tumors of sufficient sizes (1–2 cm^3) were ovariectomized 48 hours before use. Since a preliminary study indicated similar characteristics and levels of steroid receptors in both 2-FAA- and *N*-hydroxy-2-FAA-induced mammary adenocarcinomas, all data presented herein were obtained from mammary tumors induced by *N*-hydroxy-2-FAA. Groups of ovariectomized rats bearing mammary tumors were treated for 6 days with a single DES pellet (20 mg) implanted sc in each rat as previously described (*18*). The pellet was removed 48 hours before the excision of tumors. Samples of all mammary

---

ABBREVIATIONS USED: DC=dextran-coated charcoal; DES=diethylstilbestrol; 5α-DHT=5α-dihydrotestosterone (17β-hydroxy-5α-androstan-3-one); DMBA=7,12-dimethylbenz[*a*]anthracene; 2-FAA=*N*-2-fluorenylacetamide; K_a=association constant; MER-25=ethamoxytriphetol, 1-[*p*-(2-diethylaminoethoxy)phenyl]-1-phenyl-2-(*p*-methoxyphenyl)ethanol; MNU=*N*-methyl-*N*-nitrosourea; mp=melting point; R 5020=17,21-dimethyl-19-nor-pregna-4,9-diene-3,20-dione (Promegestone); TEDT=10 m*M* Tris-HCl–1.5 m*M* EDTA–1 m*M* dithiothreitol.

---

[1] Received April 8, 1981; revised January 14, 1982; accepted February 9, 1982.

[2] Supported by Public Health Service grants CA-22008 and CA-28000 from the National Cancer Institute and by grants from the U.S. Veterans Administration.

[3] Presented in part at the 69th Annual Meeting of the American Association for Cancer Research, Washington, D.C., April 5–8, 1978.

[4] Animals were maintained under the guidelines set forth by the Veterans Administration Medical Center. The animal facility has been approved by the American Association for Accreditation of Laboratory Animal Care.

[5] Medical Research Laboratories, Building 49, Veterans Administration Medical Center, 54th St. and 48th Ave., South, Minneapolis, Minn. 55417, and Department of Urologic Surgery, University of Minnesota Medical School, Minneapolis, Minn. 55455.

[6] *Address reprint request to* Dr. S. A. Li *at* the Medical Research Laboratories, Veterans Administration Medical Center.

[7] Laboratory for Cancer Research, Veterans Administration Medical Center, Minneapolis, Minn. 55417, and Department of Laboratory Medicine and Pathology, University of Minnesota Medical School, Minneapolis, Minn. 55455.

[8] We are grateful to Mr. Terry L. Cuthbertson for his excellent technical assistance and Dr. Robert E. Rydell for histologic examination of mammary tumors. We also thank Ms. Debra Romero for secretarial assistance.

tumors were fixed in buffered Formalin and then sectioned. The 5- to 6-μm-thick sections were stained routinely with hematoxylin and eosin for histologic examination. Of the carcinogen-induced mammary tumors, 65% were adenocarcinomas. The mammary fibroadenomas and adenomas were not included in the steroid receptor analyses presented herein. Lactating rats were decapitated on days 13–14 of lactation. The mammary tissues of lactating rats and mammary adenocarcinomas were excised and placed in cold 0.15 *M* NaCl in TEDT buffer (pH 7.4).

Receptor analyses.—Tumor samples were separated from necrotic or hemorrhagic regions, and all tissues studied were trimmed of fat and connective tissue. The normal and tumor tissues were minced, rinsed, and then homogenized on ice in 2 volumes of either TEDT buffer or TEDT buffer containing 10% glycerol, depending on the hormone binder to be examined (*19*). A Polytron-type PT-10 homogenizer (Kinematica GMBH, Lucerne, Switzerland) was used for the disruption of the mammary glands and tumors at four 3-second bursts and at a rheostat setting of 3.0. Homogenates were then centrifuged at 100,000×*g* for 1 hr at 4°C in a Spinco L2-65B ultracentrifuge. Supernatant fractions were passed through Millipore filters (Millex, 0.45 μm; Millipore Corp., Bedford, Mass.) to remove lipid and particulate matter (*18, 19*). Aliquots of the filtered cytosols containing approximately 17 mg protein/ml were incubated with the appropriate radioactive steroid at 2.5–10 n*M* 17β-[2,4,6,7-^{3}H]estradiol (105 Ci/mmol), [1,2,6,7-^{3}H]progesterone (103 Ci/mmol), [17α-*methyl*-^{3}H]R 5020 (86 Ci/mmol), 5α-[1,2,6,7-^{3}H]DHT (80 Ci/mmol), or [6,7-^{3}H]dexamethasone (38 Ci/mmol) (New England Nuclear Corp., Boston, Mass.) alone or in combination with the corresponding radioinert hormone at one hundredfold-excess concentrations. Antiestrogens when used in competitive binding assays were incubated at five hundredfold-excess concentrations. Following the 90-minute incubation period, cytosols were assessed for radioactivity and then treated with DC to separate unbound steroids as described previously (*18, 19*). DC treatment was for 12 minutes for progestin binding and 1 hour for estrogen, androgen, and glucocorticoid binding. Preliminary experiments indicated that these time periods were sufficient for optimal removal of unbound hormone and some of the hormone from lower affinity binding components. The labeled cytosols were layered on 4.6-ml linear 5–20% sucrose gradients prepared in TEDT buffer with the use of a Buchler gradient former. The samples were centrifuged for 17 hours at 39,000 rpm in a Spinco SW50.1 rotor at 4°C. Gradient tubes were pierced and nine-drop fractions were collected in scintillation vials. Radioactivity sampling and measurements have been reported earlier (*20*). Catalase (11.3S), bovine serum albumin (4.6S), ovalbumin (3.7S), γ-globulin (7.0S), and myoglobin (2.0S) served as sedimentation standards. We calculated sedimentation coefficients of the radioactive peaks by using the method of Martin and Ames (*21*). We determined protein concentration of the cytosols by the method of Lowry et al. (*22*), using bovine serum albumin as a standard.

Scatchard analyses (*23*) of binding affinities for estrogen, androgen, and progestin binders were performed at cytosol protein concentrations of 4–6 mg/ml. Aliquots of these appropriately diluted cytosols were incubated with varying concentrations (1–12 n*M*) of labeled hormones for 22 hours on ice with constant agitation to attain equilibrium according to the method of Ellis and Ringhold (*24*). We subtracted nonspecific binding from these data, using corresponding nonlabeled hormones at one hundredfold excess at each concentration. These data were corrected for background (cytosol without added radioactivity). Scatchard plots were subjected to linear regression analysis with the use of an HP-97 Hewlett programmable calculator.

RESULTS

Estrogen binding in mammary adenocarcinoma and in lactating mammary gland.—Estrogen binding in cytosols of either 2-FAA- or *N*-hydroxy-2-FAA-induced mammary carcinomas exhibited a discrete 8S binding component and a smaller 4S binding moiety (text-fig. 1). The size of the 4S component varied and was absent in some of the mammary tumor cytosol preparations. The 8S peak was completely abolished by either one hundredfold-excess nonlabeled 17β-estradiol or DES, whereas the 4S peak was only partially inhibited. The lactating mammary gland also contained a similar cytosolic 8S plus 4S estrogen binder. The specificity of the estrogen receptor in both these tissues was demonstrated by the inability of corticosteroids as well as androgen and progesterone to compete with the radiolabeled 17β-estradiol for binding (table 1). Both nafoxidine hydrochloride (U-11100A)—1-[2-[*p*-(3,4-dihydro-6-methoxy-2-phenyl-1-

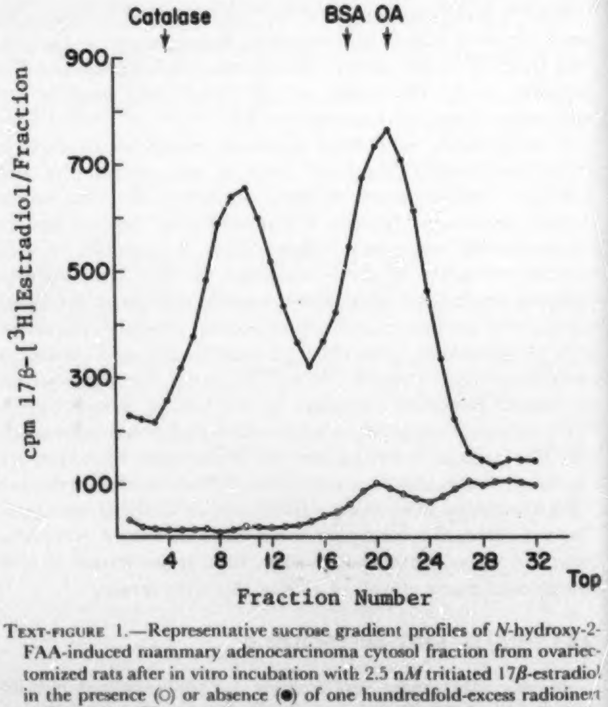

Text-figure 1.—Representative sucrose gradient profiles of *N*-hydroxy-2-FAA-induced mammary adenocarcinoma cytosol fraction from ovariectomized rats after in vitro incubation with 2.5 n*M* tritiated 17β-estradiol in the presence (○) or absence (●) of one hundredfold-excess radioinert 17β-estradiol. The cytosols were then treated with DC for 1 hr. Each 5–20% sucrose gradient contained 0.3 ml cytosol. Protein concentration of the cytosol was 18.5 mg/ml. Catalase, bovine serum albumin (BSA), and ovalbumin (OA) are indicated as sedimentation markers.

TABLE 1.—*Effect of various steroids on the binding of labeled 17β-estradiol to the cytosols of N-hydroxy-2-FAA-induced mammary adenocarcinoma and mammary gland of lactating rats*

Nonlabeled steroid[a]	Percent inhibition[b]	
	Adenocarcinoma	Mammary gland
17β-Estradiol	86	83
DES	79	75
Ethinylestradiol	83	73
Progesterone	0	3
5α-DHT	0	9
Hydrocortisone	0	5
Aldosterone	0	2
Enclomiphene citrate[c]	57	48
Nafoxidine HCl	73	54
MER-25	26	38

[a] Aliquots of mammary adenocarcinoma or mammary gland cytosol (16 mg protein/ml) were incubated at 0–3°C in a total vol of 0.5 ml with 2.5 n*M* tritiated 17β-estradiol alone or in combination with competing nonradioactive steroids (2.5×10^{-7} *M*) for 90 min. Free hormone was removed by DC absorption (1 hr).

[b] Radiolabeled 17β-estradiol concentration in these cytosols, without competitor, corresponded to 0% inhibition. Values are based on the mean of triplicate determinations in separate experiments.

[c] Radioinert antiestrogens were used at 12.5×10^{-7} *M*.

naphthyl)phenoxy]ethyl]pyrrolidine hydrochloride—and enclomiphene citrate—1-[*p*-(β-diethylaminoethoxy)phenyl]-1,2-diphenyl-2-chlorethylene monocitrate—were effective competitors at five hundredfold-excess concentrations. However, MER-25 exhibited notably less reduction of the labeled 17β-estradiol at this concentration.

Scatchard analyses and estrogen receptor concentration.—Cytosol fractions of mammary adenocarcinoma induced by *N*-hydroxy-2-FAA were incubated with varying concentrations (1–12 n*M*) of radioactive 17β-estradiol at 0–3°C. A Scatchard plot of the data showed a single class of high-affinity, low-capacity binding sites with a K_a of 1.3×10^9 M^{-1} similar to that found for lactating mammary gland (2.0×10^9 M^{-1}) (text-fig. 2). The amount of cytoplasmic estrogen receptor found in *N*-hydroxy-2-FAA-induced mammary adenocarcinoma (table 2) was almost twice the level found in 13- to 14-day lactating mammary glands.

Progestin receptor and induction by estrogen.—The concentration of specific progestin binding was low in the mammary adenocarcinoma of ovariectomized rats (table 2). When a 20-mg DES pellet was implanted for 6 days in ovariectomized rats bearing mammary adenocarcinomas, we found an eightfold increase in specific progestin binder (table 2), using [^{3}H]R 5020 as ligand. Competition for the progesterone receptor was essentially complete (>90%) in the presence of either one hundredfold-excess radioinert progesterone or R 5020. Binding specificity was assessed by the low level (<7%) of competition by either 17β-estradiol, hydrocortisone, or triamcinolone acetonide—9-fluoro-11β,21-dihydroxy-16α,17-[1-methylethylidenebis(oxy)]pregna-1,4-diene-3,20-dione. However, 5α-DHT partially inhibited (49%) the labeled R 5020 or progesterone binding at the same concentration. Under conditions of the receptor assay, serum derived from either untreated or DES-treated rats exhibited little specific progestin binding with the use of tritiated R 5020. Therefore, it was unlikely that the 4S progesterone

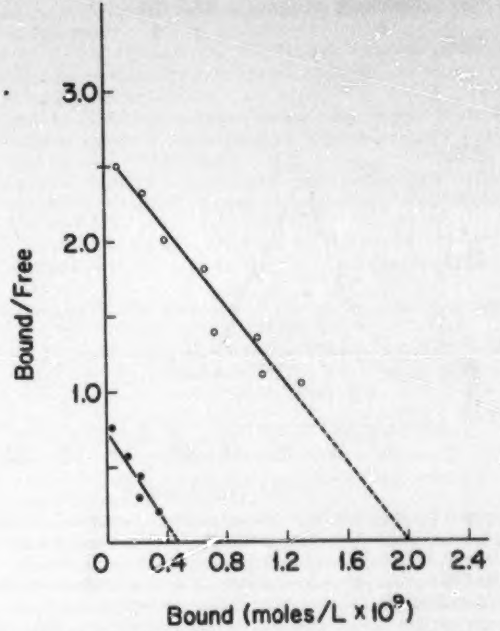

TEXT-FIGURE 2.—Scatchard analyses of specific cytoplasmic estrogen receptor in *N*-hydroxy-2-FAA-induced mammary adenocarcinoma (○) and lactating mammary gland (●). Incubations were done at 1–10 n*M* for 22 hr at 3°C to attain equilibrium and then treated with DC (1 hr). Nonspecific binding was subtracted from these data with the use of nonlabeled 17β-estradiol at one hundredfold-excess concentration at each data point. Protein concentration was 9.0 mg/ml for *N*-hydroxy-2-FAA-induced mammary tumor and 9.5 mg/ml for lactating mammary gland. L=liter.

TABLE 2.—*Association constants, sedimentation values, and concentration of steroid hormone receptors in N-hydroxy-2-FAA-induced mammary adenocarcinoma*[a]

Receptor, ligand	Sedimentation values, cytosol[b]	K_a, 10^9 M^{-1} [c]	Receptor levels in mammary gland, fmol/mg cytosol protein[d]	
			Tumor	Lactating[e]
17β-Estradiol	8	1.4	28.6±4.1 (13)	16.5±1.7 (5)[f]
5α-DHT	8	1.2	8.5±2.2 (5)	ND (4)
R 5020	4	1.7	5.0±1.3 (5)	17.1±5.8 (4)[g]
	4[h]	1.8	38.7±12.5 (8)	
Triamcinolone acetonide	ND		ND (6)	49.3±2.5 (4)

[a] ND=not detectable.

[b] Sedimented in low-salt medium. Sedimentation values were determined according to the method of Martin and Ames (*21*) with the use of five standards.

[c] Calculated from Scatchard plots. Protein concentration ranged from 4 to 6 mg/ml. Data represent the means of three separate determinations at 0–3°C.

[d] Values are means ± SEM. No. of individual determinations indicated *in parentheses*.

[e] Determinations were performed on cytosols derived from 13- to 14-day lactating rats.

[f] $P<0.01$, compared with value for the tumor.

[g] $P<0.05$, compared with value for the tumor.

[h] Ovariectomized rats were treated for 6 days with a 20-mg DES pellet implanted sc. Pellets were removed 48 hr before excision of tumors.

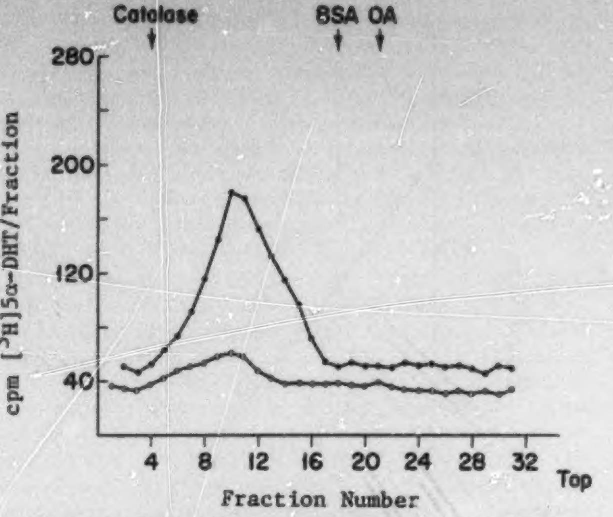

TEXT-FIGURE 3.—Representative sucrose gradient patterns of cytosolic androgen receptor in *N*-hydroxy-2-FAA-induced mammary adenocarcinoma from 48-hr ovariectomized rats. Incubations were done at 2.5 n*M* [^{3}H]5α-DHT alone (●) or in combination with one hundredfold-excess radioinert 5α-DHT (○). Following DC treatment (1 hr), aliquots of 0.3 ml were applied to each gradient. Protein concentration was 17.8 mg/ml. Catalase, bovine serum albumin (BSA), and ovalbumin (OA) served as sedimentation coefficient standards, as previously indicated.

receptor observed in mammary tumor cytosols of estrogen-treated rats was due to appreciable binding of this radiolabeled ligand to serum proteins. Scatchard analyses of the progesterone receptor (table 2) indicated that the affinity constant for this binder was in the same range as that for the estrogen receptor in the mammary tumor. The amount of progesterone receptor in lactating mammary glands significantly exceeded the level in *N*-hydroxy-2-FAA-induced mammary tumors.

Androgen binding in mammary adenocarcinoma.—Specific androgen binding was determined in cytosols of *N*-hydroxy-2-FAA-induced mammary adenocarcinomas. Following sucrose gradient centrifugation, a single 8S component was observed with the use of labeled 5α-DHT (text-fig. 3). Competition performed at one hundredfold-excess unlabeled 5α-DHT was appreciable (72%). In contrast, adrenocorticoids and DES did not exhibit significant competition for the 8S androgen receptor, whereas 17β-estradiol partially inhibited (51%) the binding of radioactive androgen to the receptor at one hundredfold-excess concentration. The amount of specific androgen binding in cytosols of lactating mammary glands, however, was undetectable.

Comparison of glucocorticoid binding in the lactating mammary gland and mammary tumor.—Although mammary gland cytosols of the 13-day lactating rats contained appreciable quantities of 8S glucocorticoid receptor (table 2) confirming a previous report (*13*), cytosols of mammary adenocarcinomas induced with *N*-hydroxy-2-FAA contained no detectable amounts of glucocorticoid binding.

DISCUSSION

The presence of estrogen, progesterone, androgen, and glucocorticoid receptors in human breast cancer cells is well documented (*5, 8, 9, 11*), and the use of multiple receptor assays in the evaluation of these tumors to predict response to hormone therapy is gaining appreciation. Of the carcinogen-induced rat mammary adenocarcinomas examined for steroid receptors, variable quantities of estrogen, progesterone, and glucocorticoid receptors have been described (*10, 11, 13, 14*). Recently, androgen receptors have also been shown in DMBA- and MNU-induced rat mammary tumors (*15, 16*). The level of steroid receptors in normal mammary gland as well as in chemically induced mammary carcinomas is highly dependent on the endocrine state of the animal. Under comparable conditions, the concentration of estrogen receptor in lactating mammary glands of ovariectomized rats found in the present study is similar to values previously reported (*8, 25–27*). Moreover, the amounts of both progesterone and glucocorticoid receptors in these mammary tissue cytosols are within the same range described elsewhere (*8, 28*). Between *N*-hydroxy-2-FAA-induced mammary tumors and other chemically induced mammary adenocarcinomas there are both similarities and differences in steroid receptor concentrations. The level of cytosolic estrogen receptor in *N*-hydroxy-2-FAA-induced mammary tumors is comparable to the levels of 8S plus 4S receptors found in either DMBA- or MNU-induced mammary carcinomas (*16, 29–31*) but nearly twelvefold higher than the level found in R3230AC transplantable rat mammary tumors (*30*). Since the quantity of progesterone receptor in various carcinogen-induced mammary carcinomas has been shown to be highly sensitive to either ovariectomy or hypophysectomy (*16, 29, 32*), the low level of progestin binder in *N*-hydroxy-2-FAA-induced mammary adenocarcinomas determined in this study may be expected. A nearly eightfold increase in specific R 5020 binding was obtained in *N*-hydroxy-2-FAA-induced mammary tumors in estrogen-primed animals. Increases in progesterone receptor have been demonstrated previously in DMBA-induced mammary carcinomas after estrogen treatment (*32, 33*). However, the level of androgen binder in *N*-hydroxy-2-FAA-induced mammary adenocarcinomas is markedly higher than the nil levels found in lactating mammary glands and twice the level seen in MNU-induced mammary tumors (*16*) but considerably lower than the level of 7S binder in DMBA-induced mammary carcinomas (*15*). The most striking difference between *N*-hydroxy-2-FAA-induced mammary tumors and other chemically induced tumors of the mammary gland is the absence of significant amounts of glucocorticoid receptor compared to the presence of high levels of 7–8S binder in both DMBA-induced mammary tumors and R3230AC transplantable mammary neoplasms (*8, 13*), as well as in lactating mammary glands. As a result of these findings, the *N*-hydroxy-2-FAA-induced mammary adenocarcinoma appears to be useful in delineating receptor interactions of certain hormonal agents, such as synthetic progestins in which glucocorticoid binding would interfere.

REFERENCES

(*1*) MILLER EC, MILLER JA, HARTMAN HA. *N*-Hydroxy-2-acetylaminofluorene: A metabolite of 2-acetylaminofluorene with increased carcinogenic activity in the rat. Cancer Res 1961; 21:815–824.

(*2*) GUTMANN HR, LEAF DS, YOST Y, RYDELL RE, CHEN CC. Structure-activity relationships of *N*-acylarylhydroxylamines in the rat. Cancer Res 1970; 30:1485–1498.

(*3*) Malejka-Giganti D, Rydell RE, Gutmann HR. Mammary carcinogenesis in the rat by topical application of fluorenylhydroxamic acids and their acetates. Cancer Res 1977; 37:111–117.

(*4*) Malejka-Giganti D. Activation of certain N-arylacetamides and N-arylacetohydroxamic acids in relation to mammary gland tumorigenesis in the rat. Natl Cancer Inst Monogr 1981; 58:69–77.

(*5*) Jensen EV, Smith S, DeSombre ER. Hormone dependency in breast cancer. J Steroid Biochem 1976; 7:911–917.

(*6*) Ekman P, Snochowski M, Zetterberg A, Högberg B, Gustafsson J-Å. Steroid receptor content in human prostatic carcinoma and response to endocrine therapy. Cancer 1979; 44:1173–1181.

(*7*) Creasman WT, McCarty KS Sr, Barton TK, McCarty KS Jr. Clinical correlates of estrogen- and progesterone-binding proteins in human endometrial adenocarcinoma. Obstet Gynecol 1980; 55:363–370.

(*8*) Wittliff JL, Mehta RG, Boyd PA, Goral JE. Steroid-binding proteins of the mammary gland and their clinical significance in breast cancer. J Toxicol Environ Health 1976; suppl 1:231–256.

(*9*) Allegra JC, Lippman ME, Thompson EB, et al. Relationship between the progesterone, androgen, and glucocorticoid receptor and response rate to endocrine therapy in metastatic breast cancer. Cancer Res 1979; 39:1973–1979.

(*10*) McGuire WL, Julian JA. Comparison of macromolecular binding of estradiol in hormone-dependent and hormone-independent rat mammary carcinoma. Cancer Res 1971; 31:1440–1445.

(*11*) Terenius L. Estrogen and progesterone binders in human and rat mammary carcinoma. Eur J Cancer 1973; 9:291–294.

(*12*) Kelly PA, Bradley C, Shiu RP, Meites J, Friesen HG. Prolactin binding to rat mammary tumor tissue. Proc Soc Exp Biol Med 1974; 146:816–819.

(*13*) Goral JE, Wittliff JL. Comparison of glucocorticoid-binding proteins in normal and neoplastic mammary tissues of the rat. Biochemistry 1975; 14:2944–2952.

(*14*) ———. Characteristics of progesterone-binding components in neoplastic mammary tissues of the rat. Cancer Res 1976; 36:1886–1893.

(*15*) Ip MM, Milholland RJ, Kim U, Rosen F. Characterization of androgen receptors in 7,12-dimethylbenz(a)anthracene-induced and transplantable rat mammary tumors. Cancer Res 1978; 38:2879–2885.

(*16*) Arafah BM, Gullino PM, Manni A, Pearson OH. Effect of ovariectomy on hormone receptors and growth of *N*-nitrosomethylurea-induced mammary tumors in the rat. Cancer Res 1980; 40:4628–4630.

(*17*) King CM, Gutmann HR. The action of the carcinogen *N*-(2-fluorenyl)acetamide on rat liver catalase and arginase in vivo. Cancer Res 1964; 24:770–779.

(*18*) Li JJ, Cuthbertson TL, Li SA. Inhibition of estrogen tumorigenesis in the Syrian golden hamster kidney by antiestrogens. JNCI 1980; 64:795–800.

(*19*) Li JJ, Li SA, Cuthbertson TL. Nuclear retention of all steroid hormone receptor classes in the hamster renal carcinoma. Cancer Res 1979; 39:2647–2651.

(*20*) Li SA, Li JJ. Estrogen-induced progesterone receptor in the Syrian hamster kidney. I. Modulation by antiestrogens and androgens. Endocrinology 1978; 103:2119–2128.

(*21*) Martin RG, Ames BN. A method for determining the sedimentation behavior of enzymes: Application to proteins. J Biol Chem 1961; 236:1372–1379.

(*22*) Lowry OH, Rosebrough NJ, Farr AL, Randall RJ. Protein measurement with Folin phenol reagent. J Biol Chem 1951; 193:265–275.

(*23*) Scatchard G. The attraction of proteins for small molecules and ions. Ann NY Acad Sci 1949; 51:660–672.

(*24*) Ellis DJ, Ringhold HJ. The uterine estrogen receptor: A physicochemical study. In: McKerns KW, ed. The sex steroids. New York: Appleton-Century-Crofts and Meredith Corp., 1971:73–106.

(*25*) Moore BP, Forsyth IA. Influence of local vascularity on hormone receptors in mammary gland. Nature 1980; 284:77–78.

(*26*) Bohnet HG, Gómez F, Friesen HG. Prolactin and estrogen binding sites in the mammary gland of the lactating and non-lactating rat. Endocrinology 1977; 101:1111–1121.

(*27*) Leung BS, Jack WM, Reiney CG. Estrogen receptor in mammary glands and uterus of rats during pregnancy, lactation and involution. J Steroid Biochem 1976; 7:89–95.

(*28*) Haslam SZ, Shyamala G. Progesterone receptors in normal mammary gland: Receptor modulations in relation to differentiation. J Cell Biol 1980; 86:730–737.

(*29*) Arafah BM, Manni A, Pearson OH. Effect of hypophysectomy and hormone replacement on hormone receptor levels and the growth of 7,12-dimethylbenz(*a*)anthracene-induced mammary tumors in the rat. Endocrinology 1980; 107:1364–1369.

(*30*) McGuire WL, Julian JA, Chamness GC. A dissociation between ovarian dependent growth and estrogen sensitivity in mammary carcinoma. Endocrinology 1971; 89:969–973.

(*31*) Hawkins RA, Hill A, Freedman B, et al. Oestrogen receptor activity and endocrine status in DMBA-induced rat mammary tumours. Eur J Cancer 1977; 13:223–228.

(*32*) Koenders AJ, Geurts-Moespot A, Zolingen SJ, Benraad TJ. Progesterone and estradiol receptors in DMBA-induced mammary tumors before and after ovariectomy and after subsequent estradiol administration. In: McGuire WL, Raymond JD, Baulieu EE, eds. Progesterone receptors in normal and neoplastic tissues. New York: Raven Press, 1977:71–84.

(*33*) Asselin J, Kelly PA, Caron MG, Labrie F. Control of hormone receptor levels and growth of 7,12-dimethylbenz(*a*)anthracene-induced mammary tumors by estrogens, progesterone and prolactin. Endocrinology 1977; 101:666–671.

blank page

Platinum-Complexed Antitumor Immunoglobulins That Specifically Inhibit DNA Synthesis of Mouse Tumor Cells[1,2,3]

Esther Hurwitz,[4] **Rina Kashi,**[4] *and* **Meir Wilchek**[4,5]

ABSTRACT—Platinum salts were complexed with antitumor reactive immunoglobulins (Ig). The Pt-complexed antitumor Ig retained their specific antibody binding activity. The inhibition of DNA synthesis by Pt salts (K_2 $PtCl_4$ and *cis*-diamminedichloroplatinum II) and Pt–Ig complexes was studied in 2 tumor cell lines of mice. The Pt–Ig complexes were much more effective inhibitors of DNA synthesis when complexed with Ig, which had binding affinity toward the test tumor cells.—JNCI 1982; 69:47–51.

Platinum-containing complexes in general and *cis*-DDP in particular are effective antitumor agents (*1*, *2*). The therapeutic effectivity of such complexes was demonstrated in various experimental animal models (*3–5*). Furthermore, *cis*-DDP is now widely used clinically and is considered to be an effective drug against metastatic testicular and ovarian carcinoma.

The major drawback of *cis*-DDP, as with many other anticancer agents, is its high degree of toxicity (*6*, *7*). Other Pt complexes such as condensation products with various amides, mainly the nucleic acid bases uracil and thymine (Pt blues) or Pt complexes with diaminocyclohexanes have been developed. Many such cis-diaminoplatinum derivatives exhibited antitumor activity in vivo and were less toxic (*8*, *9*).

Antitumor antibodies have been used by us and others as carriers of a number of chemotherapeutic agents in an attempt to increase the chemotherapeutic agents' specificity toward the tumor cells and thereby reduce the agents' general toxicity (*10–12*). When applied in vivo in some tumor systems (*12*) mixtures of antitumor antibodies and drugs were more effective than either of them separately.

We have tested the use of antitumor Ig as Pt carriers to tumor cell-reactive Ig and used them as inhibitors of DNA synthesis in vitro. Similar complexes have been prepared by others (*13*), but they were used only in crystallographic studies.

Pt–Ig complexes with specificity toward a particular tumor cell were found to be more efficient in inhibiting DNA synthesis by that cell than was Pt complexed to normal Ig or to serum albumin. In 1 tumor cell line in which the Pt salts K_2PtCl_4 and *cis*-DDP inhibited DNA synthesis, only at high concentrations, Pt–antitumor Ig was a much more effective inhibitor.

MATERIALS AND METHODS

Tumor cells.—Two types of tumor cells were used: *a*) Moloney virus-induced lymphoma or YAC cells (*14*) maintained in vivo in inbred A/J male mice and *b*) a B-cell leukemia, 38C13, produced in inbred C3HeB mice by induction with 7,12-dimethylbenz[*a*]anthracene (*15*). For the experiments the tumor cells were kept in culture in RPMI-1640 medium containing 10% FCS and glutamine antibiotics, and, in the case of 38C13 cells (*16*), 5×10^{-5} M β-mercaptoethanol.

Ig.—Anti-YAC was produced in goats by injection of a soluble papain digest of the YAC cell membrane as described previously (11). These antibodies were preferentially more cytotoxic to YAC cells, but they were not specific in their binding capacity. The anti-38C13 was produced by Dr. J. Haimovich when goats received injections of a 38C13 cell surface IgM. In each case the Ig fraction was precipitated from the antisera by ammonium sulfate at 33% saturation. A mouse-specific anti-YAC IgM was produced from a hybridoma line according to (*17*). The IgM was precipitated from mouse ascitic fluid by ammonium sulfate at 45% saturation.

The Ig–Pt complex preparation.—The Pt–Ig complex was prepared by the reaction of 10 mg Ig at a concentration of 50 mg/ml PBS [0.15 M NaCl–0.01 M phosphate (pH 7.2)] with 0.3 mg K_2PtCl_4 (Ventron Corp., Danvers, Mass.) at a concentration of 6 mg/ml in 0.1 M phosphate buffer (pH 6.4) for 2–3 hours at room temperature. The resulting material was applied to a Biogel P-60 column (Bio-Rad Laboratories, Richmond, Calif.) run in 0.1 M phosphate buffer at pH 6.4 for the separation of bound from free Pt (text-fig. 1). The amount of complexed Pt was assayed *a*) by a combination of ion exchange, resin-loaded papers, and X-rays spectrography (performed by Mr. L. E. Weeks, Monsanto Co., St. Louis, Mo.) (*18*) and *b*) by the unbound Pt determined spectrophotometrically (*19*); the complexed Pt was obtained from the difference between the total and the unbound Pt. Free Pt was separated from bound Pt by ultrafiltration through conical membranes (Centriflo; Amicon, Oosterhout, Holland).

Evaluation of antitumor activity.—Inhibition of DNA synthe-

ABBREVIATIONS USED: *cis*-DDP=*cis*-diamminoplatinum dihalides; dThd=thymidine; FCS=fetal calf serum; HSA=human serum albumin; Ig=immunoglobulin(s); NGIg=normal goat Ig; PBS=phosphate-buffered saline; TCA=trichloroacetic acid.

---

[1] Received May 13, 1981; revised January 3, 1982; accepted February 5, 1982.

[2] Department of Chemical Immunology, The Weizmann Institute of Science, Rehovot 76100, Israel.

[3] Guidelines for the care and use of laboratory animals were followed as set forth by the Weizmann Institute of Science.

[4] Department of Biophysics, The Weizmann Institute of Science.

[5] We thank Dr. J. Haimovich, Tel-Aviv University, Tel-Aviv, Israel, for the 38C13 cell line, for the goat antiserum to the surface IgM, and for the [^{3}H]IgM 38. We appreciate the Physical Sciences Center, Monsanto Co., St. Louis, Mo., for assaying the platinum content of some of the platinum-immunoglobulin complexes.

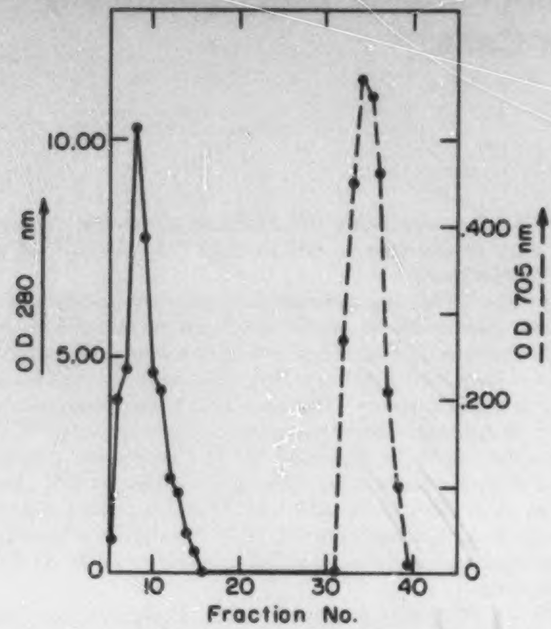

TEXT-FIGURE 1.—Fractionation of Pt-goat anti-YAC Ig for the separation from unbound Pt. After Pt was complexed with Ig, the material was applied to a column of Biogel P-60 (16×2 cm; Bio-Rad Laboratories) developed in 0.1 *M* phosphate buffer at pH 6.4. Fractions of 1 ml were collected. The Ig–Pt was determined by absorbance at 280 nm (——). Aliquots of the unbound Pt were analyzed spectrophotometrically by absorbance at 705 nm (- - -). OD=optical density.

sis by K_2PtCl_4, *cis*-diamminedichloroplatinum II (Bristol, Syracuse, N.Y.), and the Ig–Pt complexes was determined by a method similar to the one in (*10*). The tumor cells ranging from 1×10^4 to 5×10^5/ml were suspended in their suitable growth media (RPMI-1640 containing 10% FCS. The cells were dispensed in 100-µl aliquots into the wells of Microtiter plates (MicroTest II 3040; Falcon Plastics, Oxnard, Calif.). The Pt compounds were added to the cells in 50-µl amounts. The plates were incubated for 2–3 hours at 37°C in a humidified atmosphere of 5% CO_2 in air. At that time, 10 µl of 0.3 µCi [*methyl*-^{3}H]dThd (6.25 Ci/mmol; Nuclear Research, Be'ér-Sheva, Israel) was added to each well, and the plate was incubated for 20 hours as above. The [*methyl*-^{3}H]dThd incorporation was close to linear at this period of incubation. The reaction was terminated by TCA precipitation as described in (*10*).

The antibody activity.—The antibody activity of the Ig–Pt complexes was determined by one of the three following methods: *a*) complement-mediated lysis—tumor cells, 5×10^5/ml, in 50 µl RPMI-1640 plus 10% FCS were mixed with the 50 µl of antibody solutions, incubated for 40 minutes at room temperature, centrifuged, and washed. Fresh guinea pig serum, diluted 1:5, was added to cells (100 µl/tube). After 1 hour of incubation at 37°C, the number of dead or damaged cells was counted by trypan blue staining. *b*) Indirect binding assay—antibody solutions diluted in PBS (50 µl) were added to 5×10^5 YAC cells in 100 µl RPMI-1640 for 1 hour at room temperature. After two washings, ^{125}I-labeled goat anti-mouse (Fab')$_2$ (*16*) (^{125}I-labeled goat anti-mouse antibodies were separated from unbound ^{125}I by gel filtration on Sephadex G-25) was added and allowed to stand for another hour at room temperature. After an additional two washings of the cells, the contents in the wells were cut and enumerated in a gamma counter. *c*) Direct binding to radiolabeled antibody—the surface IgM of leukemia 38C13 was labeled by [^{3}H]leucine. Dilutions of the antibodies were made in normal goat serum, and 50-µl aliquots were mixed with 50 µl of ^{3}H-labeled IgM 38 (40,000 cpm) (*20*). After 30 minutes at room temperature, rabbit anti-goat serum was added and kept overnight at 4°C. After centrifugation the precipitate was dissolved in 1 *M* NaOH, transferred into scintillation fluid, and counted.

RESULTS

Complexes of Pt were prepared with several Ig, such as NGIg, goat anti-YAC Ig, goat anti-38C13 Ig, mouse anti-YAC monoclonal IgM, and HSA. The concentration of the reactants and the incubation time were varied in the differ-

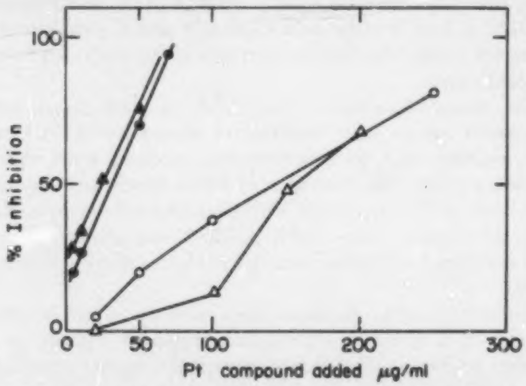

TEXT-FIGURE 2.—Inhibition of DNA synthesis by Pt salts. The inhibition of DNA synthesis by the platinates (*cis*-Pt and K_2PtCl_4) was measured by the platinates' effects on the incorporation of [*methyl*-^{3}H]dThd. YAC cells (10^5/well) (●, ▲) or leukemia 38C13 cells (2×10^4/well) (○, △) were incubated with Pt salts for 2–3 hr at 37°C, after which [*methyl*-^{3}H]dThd was added; incubations were continued overnight. The reaction was terminated by TCA precipitation.

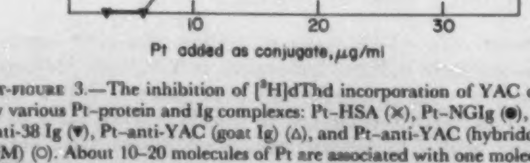

TEXT-FIGURE 3.—The inhibition of [^{3}H]dThd incorporation of YAC cells by various Pt–protein and Ig complexes: Pt–HSA (×), Pt–NGIg (●), Pt–anti-38 Ig (▼), Pt–anti-YAC (goat Ig) (△), and Pt–anti-YAC (hybridoma IgM) (○). About 10–20 molecules of Pt are associated with one molecule of Ig or HSA.

ent preparations. The coupling procedure described in "Materials and Methods" was the most efficient as judged by the resulting inhibition of [*methyl*-^{3}H]dThd uptake in vitro. Use of Ig concentrations lower than 50 mg/ml resulted in a reduction of Pt complexed to the Ig, whereas concentration of the platinate being increased during the reaction caused precipitation. The suitable length of incubation was from 2 to 3 hours, inasmuch as prolongation of the reaction time resulted in precipitation. Some precipitation also occurred upon freezing and thawing. The amount of Pt complexed to the Ig was determined by either one of the following procedures: 1) X-ray spectrography performed directly on the samples (*18*) and 2) spectrophotometric (*19*) assay of the unbound Pt subtracted from the total. This method could not be used directly because the presence of protein interfered with the color reaction. Between 2 and 10 mol of Pt were bound per mole Ig in the different preparations.

Inhibition of DNA synthesis as measured by uptake of [*methyl*-^{3}H]dThd was used as a criterium of activity of the Pt complexes. As shown in text-figure 2, both the platinate K_2PtCl_4 and the *cis*-$(NH_3)_2PtCl_2$ similarly inhibited the uptake of [*methyl*-^{3}H]dThd by YAC cells in culture. The B-leukemia cells (38C13) were inhibited by the platinate and *cis*-DDP only at much higher concentrations than were the YAC cells.

The inhibition of the Pt-Ig complexes is depicted in text-figures 3 and 4. The degree of inhibition varied somewhat with the different preparations. However, with all the preparations of antitumor reactive Ig-Pt complexes, the inhibition was stronger than could be accounted for by the amount of Pt bound to the Ig as compared to both Pt salt and *cis*-DDP. An inhibitory activity was observed also by Pt complexed to nonspecific proteins such as normal Ig and HSA but with concentrations higher than those of Pt bound to the cell reactive Ig (text-figs. 3, 4). In the B-cell leukemia 38C13, DNA synthesis was inhibited by the Pt salts, K_2PtCl_4 and *cis*-DDP, at concentrations above 50 μg/ml. Pt complexed to antibodies (anti-YAC), which were strongly reactive with the tumor cells, were effective inhibitors. Antibodies directed against the specific surface IgM of 38C13 cells (idiotypic antibodies), although capable of attaching to the cells at specific sites, were not as effective as the anti-YAC Ig that was as reactive with these tumor cells as with the YAC cell toward which it was directed originally. Perhaps the anti-YAC IgG was more effective due to its ability to attach to many sites, as seen by fluorescence studies. The inhibitions by the Pt-Ig conjugates were not reversible over 48 hours. In both systems the immune Ig by itself had no effect on the dThd incorporation.

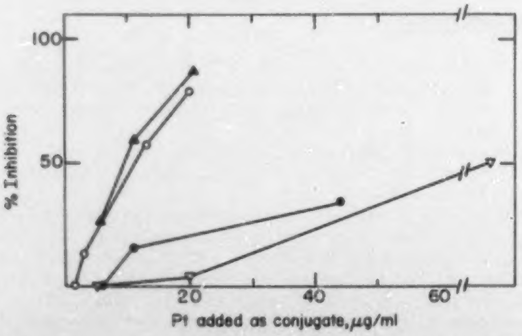

TEXT-FIGURE 4.—The inhibition of [^{3}H]dThd incorporation of leukemia 38C13 cells, by various Pt-Ig preparations: Pt-anti-YAC Ig, preparation 1 (▲); Pt-anti-YAC Ig, preparation 2 (○); Pt-anti-38 Ig (●); and Pt-NGIg (▽). About 10-12 molecules of Pt are associated with one molecule of Ig.

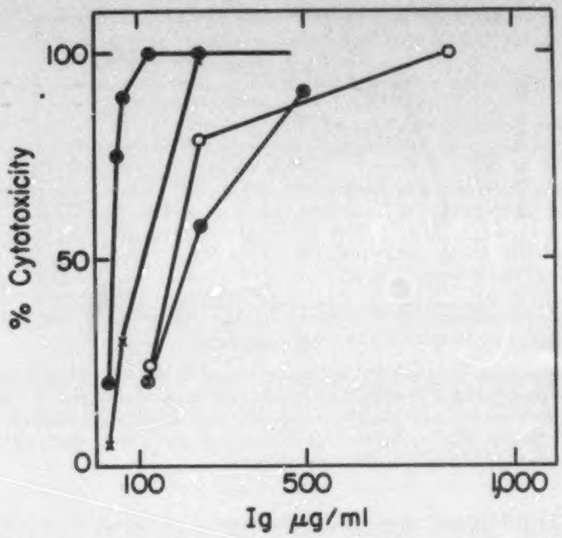

TEXT-FIGURE 5.—Antibody activity of Pt-anti-YAC complexes measured by complement-mediated cytotoxicity. Complement-mediated lysis of YAC cells was measured by incubation of YAC cells (5×10^5) with dilutions of anti-YAC, goat Ig, or Pt-anti-YAC complexes. Anti-YAC Ig, preparation 1 (×); anti-YAC Ig, preparation 2 (●); Pt-anti-YAC, preparation 1 (○); and Pt-anti-YAC, preparation 2 (⊛).

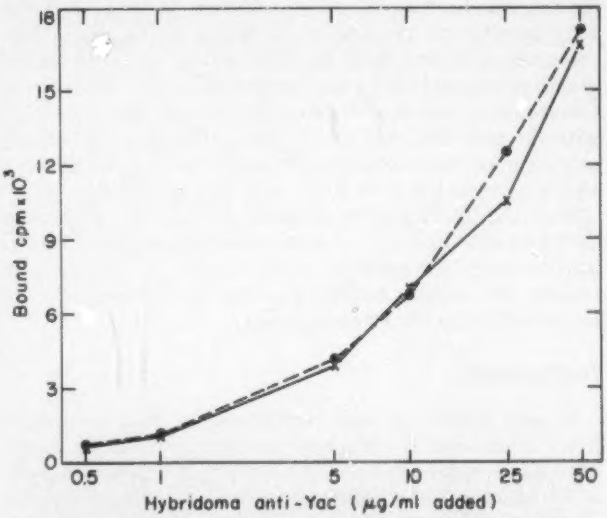

TEXT-FIGURE 6.—Antibody binding activity of Pt-anti-YAC IgM complexes. Antibody binding activity of a hybridoma anti-YAC IgM to YAC Formalin-fixed cells (10^5/well) was measured after its complexing with Pt. Binding activity was measured indirectly with ^{125}I-labeled goat anti-mouse $(Fab')_2$. Mouse anti-YAC IgM (●- - -●), Pt-mouse anti-YAC (x—x).

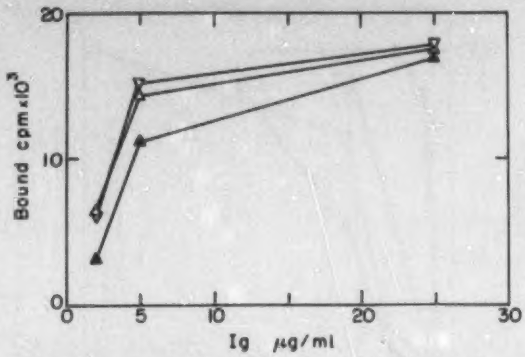

TEXT-FIGURE 7.—Antibody binding activity of Pt–anti-38 complexes. Antigen binding of Pt complexed anti-38 goat Ig was measured by a direct binding assay with the use of the ^{3}H-labeled antigen, surface IgM of leukemia 38C13 cells. Goat anti-38 Ig (▽); Pt–anti-38 Ig, preparation 1 (△); and Pt–anti-38 Ig, preparation 2 (▲).

Complement-mediated cytotoxicity by some Pt-antitumor Ig preparations was considerably diminished (text-fig. 5). While with one preparation 55% of the original activity was still maintained, in another preparation the activity dropped to 20% of the original. The decrease in complement activity may be related to the amount of Pt bound to the antibody or to the occupation by Pt of a complement site. To test whether Pt complexing affected the antibody binding capacity, the binding of antibodies to the tumor cells was assayed indirectly in the YAC system with ^{125}I-labeled goat anti-mouse (Fab′)$_2$ as a second antibody. As shown in text-figure 6, identical binding curves were obtained both with the anti-YAC and the Pt–anti-YAC; thus the binding of the hybridoma antibody IgM anti-YAC was not affected by its complexing with Pt. In the B-cell leukemia 38C13 system, the binding of Pt–anti-38 IgM idiotypic antibodies to ^{3}H-labeled IgM (*20*) was not markedly reduced by the attachment of the antibody to Pt (text-fig. 7). Thus in both systems the antigen binding capacity of the antibody was not modified by the Pt complexing.

DISCUSSION

In this study we have demonstrated that complexes formed between Pt salts and antibodies retain both the antibody activity and the DNA synthesis inhibitory activity of Pt. Moreover, the inhibitory activity was enhanced with Pt–Ig complexes in which the Ig possessed high binding affinity toward the tumor cells. The complexes between Ig and Pt were formed simply by incubation of Pt salt with the antibodies for a few hours at room temperature.

Complexes between proteins including Ig and Pt have been previously used in X-ray crystallography (*13*). In these studies the native crystal was soaked in the Pt salt. X-ray crystallography showed that Ig have six high-affinity sites and some additional low-affinity sites (*13*). The present results, which indicate an occupancy of 2–10 Pt sites, agree with those of the crystallographic studies, although we have prepared the Pt–Ig complexes in aqueous solutions.

The antigen binding capacity of the antitumor Ig is almost fully retained (text-figs. 6, 7), whereas the complement-fixing ability of these antibodies is reduced to about 20–50% of the original in different preparations (text-fig. 5). The reduction of the complement-fixing ability can be attributed to the binding of Pt to portions of the Fc receptor, thereby perhaps blocking the complement recognition site in this part of the molecule.

The mechanism of the enhanced Pt activity when bound to specific antibody has not been elucidated; yet one can speculate that for Pt to interact with DNA (*21*, *22*) it has to penetrate the cell nucleus. The antibodies may bring the Pt to the cell surface and promote the internalization of the metal through their own binding to the antigen(s) toward which they are directed. Hurwitz et al. (*23*) have previously shown that daunorubicin, which also exerts its activity in the cell nucleus, when bound covalently to antitumor antibodies can penetrate the cell in the bound form and localize in or on the cell nucleus. Another possibility is that DNA found on the surface of tumor cells, due to its higher affinity to Pt, may cause removal of Pt from the antibody–Pt complex. Still a third possibility exists in which Pt is dissociated from its antibody complex on the cell surface and enters the cell via channels for ions opened through cell stimulation by specific antibodies. Studies to determine the exact localization and mode of action of antibody–Pt complexes are now in progress.

The mechanism of the Pt antitumor activity is not fully established. In vitro Pt was shown to interact with DNA (*24*). Several in vivo studies suggested an involvement of the immune system in the promotion of Pt action (*24–26*). Immunodepressing compounds such as hydrocortisone were shown to decrease Pt potency, while immunostimulants such as zymosan were shown to increase it.

Our findings show that Pt bound to tumor cell reactive antibodies is more efficient in the inhibition of DNA synthesis than is Pt bound to normal or nonspecific Ig or than is Pt salts. An explanation is that when under an in vivo environment Pt may attach to tumor cell-surface antibodies and thereby promote its deliverance to the pertinent cells. By this view one may also explain the therapeutic efficacy of Pt doses below the cytotoxic concentrations to the tumor cells in vitro and in vivo (*27*). In vivo explorations of the effectivity of Pt–immune Ig complexes are now in progress.

REFERENCES

(*1*) ROSENBERG B, VANCAMP L, TROSKO JE. Platinum compounds: A new class of potent antitumour agents. Nature 1969; 222:385–386.

(*2*) LEH FK, WOLF W. Platinum complexes: A new class of antineoplastic agents. J Pharm Sci 1976; 65:315–328.

(*3*) ROSENBERG B, VANCAMP L. The successful regression of large solid sarcoma 180 tumors by platinum compounds. Cancer Res 1970; 30:1799–1802.

(*4*) KOCIBA RJ, SLEIGHT SD, ROSENBERG G. Inhibition of Dunning ascites leukemia and Walter 256 carcinoma with *cis*-diamminedichloroplatinum. Cancer Chemother Rep 1970; 54 (part 1):325–328.

(*5*) TALLEY RW. Chemotherapy of a mouse reticulum cell sarcoma with platinum salts. Proc Am Assoc Cancer Res 1970; 11:78.

(*6*) AGGARWAL SK, BROOMHEAD JA, FAIRLIE DP, WHITEHOUSE MW. Platinum drug: Combined anti-lymphoproliferative and nephrotoxicity assays in rats. Cancer Chemother Pharmacol 1980; 4:249–258.

(*7*) KHAN A, HILL JM. Inhibition of lymphocyte blastogenesis by platinum compounds. J Surg Oncol 1971; 3:565–567.

(*8*) Davidson JP, Faber PJ, Fisher RG Jr, Mansy S, et al. Platinum-pyrimidine blues and related complexes: A new class of potent antitumor agents. Cancer Chemother Rep 1975; 59 (part 1):287–300.

(*9*) Speer RJ, Ridgway H, Hall LM, et al. Coordination complexes of platinum as antitumor agents. Cancer Chemother Rep 1975; 59:629–641.

(*10*) Hurwitz E, Levy R, Maron R, Wilchek M, Arnon R, Sela M. The covalent binding of daunomycin and adriamycin to antibodies with retention of both drug and antibody activity. Cancer Res 1975; 35:1175–1181

(*11*) Hurwitz E, Maron R, Bernstein A, Wilchek M, Sela M, Arnon R. The effect in vivo of chemotherapeutic drug-antibody conjugates in two murine experimental tumor systems. Int J Cancer 1978; 21:747–755.

(*12*) O'Neill GJ. The use of antibody as drug carriers. In: Gregoriadis G, ed. Drug carriers in biology and medicine. New York: Academic Press, 1979:23–43.

(*13*) Colman RM, Diesenhofer J, Huber R, Palm W. Structure of the human antibody molecule Kol (immunoglobulin G1): An electron density map at 5 Å resolution. J Mol Biol 1976; 100:257–282.

(*14*) Klein E, Klein G. Antigenic properties of lymphomas induced by Moloney agent. J Natl Cancer Inst 1964; 32:547–568.

(*15*) Haran-Ghera N, Peled A. Thymus and bone marrow derived lymphatic leukaemia in mice. Nature 1973; 24:396–398.

(*16*) Bergman Y, Haimovich J. Characterization of a carcinogen-induced murine B lymphocyte cell line of C3H/eB origin. Eur J Immunol 1977; 7:413–417.

(*17*) Köhler G, Milstein C. Derivation of specific antibody producing tissue culture and tumor lines by cell fusion. J Immunol 1976; 6:511–519.

(*18*) Campbell WJ, Spano EF, Green TE. Micro and trace analysis by a combination of ion exchange resin-loaded papers and X-ray spectrography. Anal Chem 1966; 38:987–996.

(*19*) Golla ED, Ayres GH. Spectrophotometric determination of platinum with *O*-phenylenedianine. Talanta 1972; 20:199–210.

(*20*) Eshhar Z, Blatt C, Bergman Y, Haimovich J. Induction of secretion of IgM from cells of B cell line 38c 13 by somatic cell hybridization. J Immunol 1979; 122:2430–2434.

(*21*) Howle JA, Gale GR. *cis*-Dichlorodiammineplatinum II persistent and selective inhibition of deoxyribonucleic acid synthesis in vivo. Biochem Pharmacol 1970; 19:2757–2762.

(*22*) Roberts JJ, Pascoe JM. Cross-linking of complementary strands of DNA in mammalian cells by antitumour platinum compounds. Nature 1972; 235:282–284

(*23*) Hurwitz E, Maron R, Arnon R, Wilchek M, Sela M. Daunomycin-immunoglobulin conjugates, uptake and activity in vitro. Eur J Cancer 1978; 14:1213–1220.

(*24*) Roberts JJ, Thompson AJ. Mechanism of action of antitumor platinum compounds. In: Cohn W, ed. Progress in nucleic acid research and molecular biology. New York: Academic Press, 1979:71–134.

(*25*) Rosenberg B. Enhanced antigenicity as a possible mode of action of platinum antitumor drugs. In: Advances in antimicrobial and antineoplastic chemotherapy. Vol 2. Baltimore: Univ Park Press, 1972:101–102.

(*26*) Conran PB, Rosenberg B. The role of host defence in the regression of sarcoma-180 in mice treated with *cis*-dichlorodiamineplatinum II. In: Advances in antimicrobial and antineoplastic chemotherapy. Vol 2. Baltimore: Univ Park Press, 1972:235–236.

(*27*) Rosenberg B. Possible mechanisms for the antitumor activity of platinum coordination complexes. Cancer Chemother Rep 1975; 59:589–598.

blank page

Differences in Spleen Suppressor Cell Content in Rats With Progressing and Regressing Tumors[1,2,3]

Michael A. Hollingsworth[4] *and* **Donald L. Evans**[4]

ABSTRACT—Young New Zealand Black rats (<35 wk old) developed progressively growing tumors when given injections of cells from a syngeneic 3-methylcholanthrene (MCA)-induced fibrosarcoma. Spontaneous tumor regression occurred in animals more than 10 months of age. Compared to the responses of spleen cells from age-matched controls, spleen cells from rats in which tumor progression was present (progressor rats) showed decreased proliferative responses to concanavalin (Con A), phytohemagglutinin (PHA), and syngeneic MCA tumor cells. Spleen cells from rats in which the tumors had regressed (regressor rats), however, produced significant increases in proliferative responses when compared with the responses of spleen cells from age-matched controls and from progressor rats. Cell-mixing experiments implicated the presence of two spleen suppressor cell populations in progressor rats, one of which was not present in regressor rats. The unique suppressor cell found in progressor rats appeared to be specific for tumor cell-induced proliferative responses. Spleen cells from both progressor and regressor rats produced similar suppressive effects in the PHA and Con A responses of normal cells.—JNCI 1982; 69:53–58.

Spleen cells from certain tumor-bearing animals (*1*, *2*) and peripheral blood lymphocytes from some humans with malignant tumors (*3*) have decreased proliferative responses to Con A and PHA. These diminished responses have been attributed to suppressor cells (*1–3*). Suppressor cells from tumor-bearing animals were effective inhibitors of tumor-specific and alloreactive cytotoxic T-lymphocytes (*4–7*), lymphoma cell proliferation (*8*), mixed leukocyte culture responses (*4*, *9*, *10*), lymphoproliferative responses to tumor-associated antigens (*11*), graft-versus-host reactions (*12*), and host resistance to syngeneic tumors (*13*).

In other work, whole-body irradiation inactivated a spleen-seeking suppressor cell in MC1315 tumor-bearing BALB/c mice. Tumors in these animals subsequently regressed (*14*). Reports on the effects of splenectomy of tumor-bearing animals indicated equivocal results demonstrating inhibition (*15–18*), enhancement (*19*, *20*), or no effect on tumor growth (*21–23*).

We previously reported (*24*) an age-related increase in natural immunity to a syngeneic MCA-induced fibrosarcoma in New Zealand Black rats. Inoculation of tumor cells into these animals was followed by growth of palpable tumors that spontaneously regressed in animals 12–16 months of age. Tumors in younger animals did not regress. We also characterized variations in the proliferative response to PHA, Con A, and irradiated syngeneic MCA tumor cells in aging normal NBR rats. In younger animals (<52 wk old), ADH cells generated the highest Con A responses, whereas NA cells produced the highest PHA responses. The proliferative response of Unf cells by younger animals was low, possibly because of a naturally occurring suppressor cell. [*See* (*24*) for discussion.] The Con A and PHA responses of older animals did not differ significantly between NA and ADH fractions (*24*).

Observation of these age-related variations necessitated the use of age-matched sets of animals in tests to compare the responses of spleen cells from rats in which tumor progression was present (rat progressors, tumor progressors) and from rats in which the tumors had regressed (rat regressors, tumor regressors) with the responses of cells from normal controls. In the present work, spleen cells derived from MCA tumor progressors were shown to have decreased proliferative responses to Con A, PHA, and irradiated MCA tumor cells (MLTC assay) as compared to the responses of age-matched normal rats. Spleen cells from tumor progressors suppressed (in vitro) normal spleen cell proliferation responses to mitogens and tumor cells. Spleen cells from tumor regressors, however, showed no decreased reactivity to mitogens. They had greater than normal proliferative reactivity to MCA cells, and in the cell transfer experiments they did not suppress normal spleen cell responses to tumor cells, but instead enhanced the normal cells' proliferative capacity. Spleen cells from regressor rats (like those from progressor rats) were capable of suppressing the mitogen responsiveness of normal spleen cells.

MATERIALS AND METHODS

Animals.—Inbred syngeneic New Zealand Black rats (NBR Pl/Cr) were obtained from a breeding colony maintained at the Bowman Gray School of Medicine, Winston-Salem, N.C., and from the National Cancer Institute rat breeding facility at Charles River Breeding Laboratories, Inc., Wilmington, Mass.

Tumors.—The tumors used for animal injections and in the MLTC assays were derived from MCA-induced fibrosarcomas in NBR rats (*25*). MCA tumor cells were myco-

---

ABBREVIATIONS USED: ADH=nylon wool-adherent; Con A=concanavalin A; [^{3}H]dThd=tritiated thymidine; MCA=3-methylcholanthrene; MLTC=mixed leukocyte tumor cell; NA=nylon wool-nonadherent; PHA=phytohemagglutinin; Unf=unfractionated.

---

[1] Received May 28, 1981; revised January 6, 1982; accepted February 5, 1982.

[2] Supported in part by grants from the Ruth Diehl Foundation, from the Gaston County Cancer Society, and by grant IM 220 from the American Cancer Society.

[3] Animals were maintained under the guidelines set forth by the Bowman Gray School of Medicine, American Association for Accreditation of Laboratory Animal Care.

[4] Department of Microbiology and Immunology, Bowman Gray School of Medicine, Wake Forest University, 300 South Hawthorne Rd., Winston-Salem, N.C. 27103

TABLE 1.—*Proliferative responses to Con A, PHA, and irradiated MCA tumor cells by spleen cells from tumor progressors and normal NBR rats*

Spleen cells[a]	$[^3H]$dThd incorporation, cpm[b]			
	Unstimulated[c]	Con A-stimulated[d]	PHA-stimulated[d]	MCA-stimulated[d]
Normal Unf	798±294	6,486±1,626	9,297±2,592	11,283±3,904
Progressor Unf	450±116	1,825±1,754[e]	4,533±1,505[e]	3,312±2,228[e]
Normal NA	7,742±939	27,498±5,170	62,061±18,079	25,452±3,466
Progressor NA	2,390±892	2,437±1,635[e]	6,271±138[e]	10,277±3,372[e]
Normal ADH	2,061±1,242	65,148±19,092	20,389±5,970	26,445±434
Progressor ADH	1,924±1,113	1,885±1,891[e]	2,358±31[e]	10,297±1,524[e]
None[f]	125±68	386±85	506±38	4,577±3,209

[a] Spleen cells were Unf or were separated over nylon wool columns into NA and ADH populations. These results represent 9 independent experiments on rats 6–25 wk of age.

[b] Values are means ± SD.

[c] No stimulation of spleen cells by mitogens or tumor cells during 4 days of cultivation.

[d] Spleen cells were stimulated as indicated with Con A, PHA, or irradiated MCA tumor cells after 4 days of cultivation.

[e] Significantly different from normal ($P<0.01$).

[f] From cultures containing only RPMI-1640 medium, Con A, PHA, or irradiated MCA tumor cells.

plasma-free and negative for retroviruses. Tumor cells were passaged continuously in vitro in Dulbecco's modified Eagle's minimum essential medium, containing 10% fetal bovine serum and 50 μg gentamycin sulfate/ml (Garamycin; Schering Corporation, Kenilworth, N.J.), and the cells were buffered with sodium bicarbonate. MCA tumor cells, 5×10^6, were injected sc into young animals (aged <8 mo) to generate tumor progressors and into older animals (aged >12 mo) which subsequently developed into spontaneous tumor regressors (*24*). Tumor progressors were used in those experiments after tumor volume had reached at least 1×10^5 mm^3. Tumor regressors were used only after the tumors had completely regressed. We did not detect tumor cells in the spleens of tumor progressors or tumor regressors.

Spleen cell preparation.—Rats were exsanguinated, their spleens were aseptically removed, and single cell suspensions were obtained by pressing the spleen tissue through a 200-gauge, stainless steel mesh, tissue sieve. RPMI-1640 medium (KC Biologicals, Lenexa, Kans.) was supplemented with 10% fetal bovine serum (KC Biologicals), 25 m*M* HEPES[5] buffer, 5×10^5 2-mercaptoethanol (Calbiochem-Behring Corp., San Diego, Calif.), and nutrients [1% each of L-glutamine and other nonessential amino acids, essential amino acids, vitamins, and sodium pyruvate (Flow Laboratories, Inc., Rockville, Md.)]. Cell suspensions were pelleted (300×*g*) and depleted of erythrocytes by resuspension in Tris-ammonium chloride [9 parts 0.155 *M* NH_4Cl_3:1 part 0.170 *M* Tris (pH 7.2)].

Cells were washed and resuspended, viable cell counts were made, and cells were resuspended in RPMI-1640 medium at 5×10^6 cells/ml. These cells were designated as Unf.

Nylon wool fractionation.—Cells were fractionated over a nylon wool column (*26*). NA (T-cell-enriched) and ADH (B-cell and macrophage-enriched) cells were obtained. The Unf, NA, and ADH populations were each resuspended (5×10^6 cells/ml) in supplemented RPMI-1640 medium for use in the MLTC and mitogen-induced blastogenesis assays.

Mitogen-induced blastogenesis.—Mitogen-induced blastogenesis was performed with the use of Con A (Calbiochem-Behring Corp.) and PHA (Burroughs-Wellcome Co., Research Triangle Park, N.C.). Spleen cells, 5×10^5, were added to optimal mitogen amounts (1 μg Con A or 0.6 μg PHA) in a final volume of 200 μl RPMI-1640 medium. Triplicate cultures were incubated in microtiter plates (Costar, Data Packaging Corp., Cambridge, Mass.) and labeled with 2 μCi $[^3H]$dThd (ICN Pharmaceuticals, Inc., Irvine, Calif.) on day 4. Cultures were harvested 18 hours later by means of a microharvester (Bellco Glass, Inc., Vineland, N.J.). Samples were counted in a scintillation counter (model LS-233; Beckman Instruments, Inc., Fullerton. Calif.)

Tumor-induced blastogenesis.—Spleen cells were tested for proliferative responses to MCA tumor cells in MLTC cultures. Spleen cells, 5×10^5, were mixed with 1.25×10^4 irradiated (10,000 rad) MCA tumor cells. The cultures were incubated, labeled with $[^3H]$dThd, and harvested as described under "*Mitogen-induced blastogenesis.*"

Spleen cell reconstitutions.—NA and ADH cells from progressor or regressor rats were mixed at the indicated ratios with NA and ADH cells from normal age-matched rats (at ratios of 90% normal cells mixed with 10% tumor progressor or tumor regressor cells and 70% normal cells mixed with 30% tumor progressor or regressor cells). The mixed cells, 5×10^6, were then tested in the mitogen-induced blastogenesis and tumor cell-induced blastogenesis assays described above.

Statistical analysis.—The data were analyzed with the use of Student's *t*-test for comparison of two mean values.

RESULTS

Mitogen responses of normal, tumor progressor, and tumor regressor spleen cells.—Data in table 1 show that Unf, NA, and ADH spleen cells from rats bearing progressive MCA tumors had significantly decreased proliferative responses to Con A and PHA, as compared to the responses of age-matched controls. The Con A responses by regressor Unf and NA cells were often greater than the responses of normal cells but were not highly statistically significant ($P<0.1$) (table 2). Regressor ADH spleen cell responses to Con A and regressor NA and ADH responses to PHA were significantly greater than

---

[5] 4-(2-Hydroxyethyl)-1-piperazine ethanesulfonic acid.

TABLE 2.—*Proliferative responses to Con A, PHA, and irradiated MCA tumor cells by spleen cells from tumor regressors and normal NBR rats*

Spleen cell[a]	$[^3H]$dThd incorporation, cpm[b]			
	Unstimulated[c]	Con A-stimulated[d]	PHA-stimulated[d]	MCA-stimulated[d]
Normal Unf	2,794±470	71,440±8,227	78,376±10,000	7,346±1,514
Regressor Unf	2,170±992	75,589±8,144	50,931±13,862[e]	18,116±1,737[e]
Normal NA	1,176±275	38,179±2,038	34,814±2,038	18,359±3,950
Regressor NA	1,155±127	39,040±243	48,146±1,197[e]	32,266±3,685[e]
Normal ADH	952±89	39,717±12,177	51,030±3,822	12,407±1,557
Regressor ADH	1,507±489	71,313±2,100[e]	86,710±3,229[e]	20,003±4,355[e]
None[f]	238±108	205±22	351±23	2,391±501

[a] Spleen cells were Unf or were separated oven nylon wool columns into NA and ADH populations.

[b] Values are means ± SD.

[c] No stimulation of spleen cells by mitogens or tumor cells during 4 days of cultivation.

[d] Spleen cells were stimulated as indicated with Con A, PHA, or irradiated MCA tumor cells after 4 days of cultivation.

[e] Significantly different from normal ($P<0.05$).

[f] From cultures containing only RPMI-1640 medium plus Con A, PHA, or irradiated MCA tumor cells.

were the responses of normal spleen cell controls (table 2). Regressor Unf cell responses to PHA were variable: The responses of cells from 2 regressor rats were significantly increased, the responses of cells from another animal were not significantly different from normal, and there were three instances of significantly decreased responses, an example of which is presented in table 2.

MLTC responses.—In table 1 the proliferative responses of spleen cells from tumor progressors and age-matched normal NBR rats to irradiated syngeneic MCA tumor cells are shown. The responses of all fractions (Unf, NA, and ADH) of spleen cells from progressor rats were significantly less than those of the age-matched normal animals. The MLTC responses of regressor Unf, NA, and ADH cells (table 2) were significantly greater (6 experiments) than the responses of comparable normal cells.

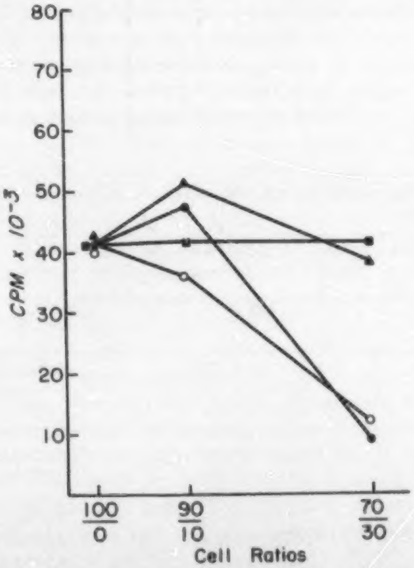

TEXT-FIGURE 1.—Normal ADH spleen cells were tested for Con A responsiveness in reconstitution assays. Different ratios of normal and tumor-bearing nylon wool fractionated spleen cells were tested. Normal and test cells (5×10^5 total cells) were mixed in cultures that consisted of 90%:10% and 70%:30% (normal cells:test cells) ratios, respectively. Mixtures were normal ADH + normal ADH control (■), normal ADH + normal NA (▲), normal ADH + tumor progressor ADH (○), and normal ADH + tumor progressor NA (●).

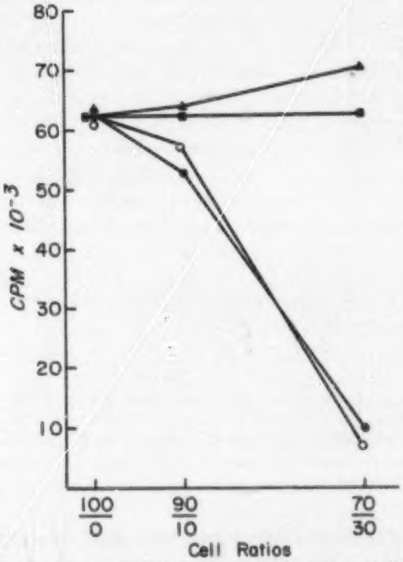

TEXT-FIGURE 2.—Determination of normal NA spleen cell responses to PHA after reconstitution (as described in text-fig. 1) with normal NA cells (■), normal ADH cells (▲), tumor progressor NA cells (○), and tumor progressor ADH cells (●).

Reconstitution experiments.—We next determined the regulatory effects of spleen cells from progressor and regressor rats by mixing spleen cells from those animals with normal rat spleen cells. Text-figure 1 shows the effect of mixing NA or ADH tumor progressor spleen cells with age-matched (15 wk) normal ADH spleen cells. [These cells were tested because they produced the highest responses to Con A (table 1)]. The addition of progressor ADH cells and of certain proportions (30%) of progressor NA cells to normal ADH cells produced a significant decrease in the proliferative responses, as compared to the values obtained after mixing different ratios of only normal cells. The same effects (significant decreases) were observed when fractionated progressor spleen cells were mixed with NA cells from normal animals and then stimulated with PHA (text-fig. 2). The addition of either progressor NA or progressor ADH cells to normal spleen cells caused a reduction in the normal proliferative responses.

The responses of normal spleen cells obtained from young (13-wk-old) animals to irradiated MCA cells were similar for both NA and ADH cells (table 1). The addition of progressor NA or progressor ADH cells to normal NA cells (text-fig. 3) or to normal ADH cells (text-fig. 4) produced significantly suppressed MLTC proliferative responses by the normal cells.

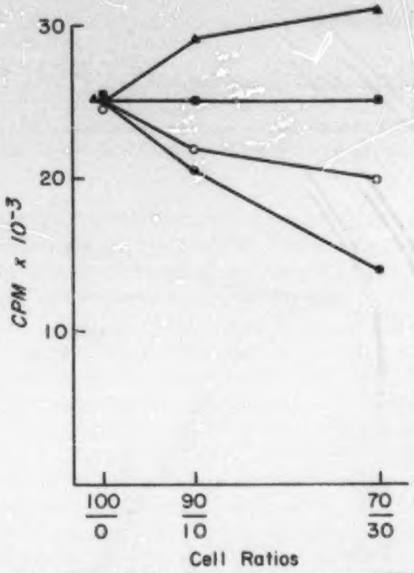

TEXT-FIGURE 3.—Normal NA spleen cell responses to MCA tumor cells (MLTC assay) after reconstitution with normal NA cells (■), normal ADH cells (▲), tumor progressor NA cells (○), and tumor-bearing ADH cells (●).

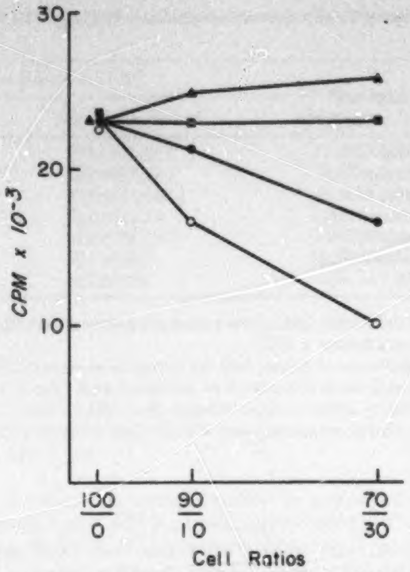

TEXT-FIGURE 4.—Normal ADH spleen cell responses to MCA tumor cells (MLTC assay) after reconstitutions with normal ADH cells (■), normal NA cells (▲), tumor progressor ADH cells (○), and tumor progressor NA cells (●).

Effects of regressor spleen cells on normal proliferative responses.—Table 3 shows the effects of mixing regressor spleen cells with normal cells on the proliferative responses to Con A and PHA. The addition of regressor NA cells to normal ADH cells produced a reduction in the Con A and PHA

TABLE 3.—*Effects of tumor regressor spleen cells on proliferative responses of normal rat spleen cells to Con A, PHA, and irradiated syngeneic MCA tumor cells*

Mixture				[^{3}H]dThd incorporation, cpm,[a] after stimulation with:		
Normal cells, %		Regressor cells, %		Con A	PHA	MCA tumor cells
NA	ADH	NA	ADH			
100[b]				38,179±3,973	34,814±2,038	21,083±4,120
90	10			35,498±2,475	38,542±3,725	19,755±958
70	30			36,448±2,939	46,520±2,606	14,504±2,039
90			10	14,699±9,133[c]	36,601±3,155	29,755±7,432[c]
70			30	10,717±2,066[c]	5,641±2,186[c]	30,138±4,811[c]
90		10		51,287±20,047	27,589±3,294	30,865±4,099[c]
70		30		57,590±12,878[c]	34,497±3,884	31,418±7,651[c]
	100			39,717±12,177	57,030±3,822	7,033±1,594
10	90			43,302±11,008	57,022±6,654	4,346±158
30	70			38,449±1,365	54,484±1,097	5,977±3,148
	90	10		30,217±2,445	11,243±2,163[c]	12,921±2,912[c]
	70	30		20,387±2,800[c]	11,909±1,893[c]	18,220±2,651[c]
	90		10	9,414±1,566[c]	66,727±2,271	6,554±4,009
	70		30	13,855±9,934[c]	6,420±2,446[c]	6,162±867

[a] Values are means ± SD.
[b] No. of cells treated: 5×10^5.
[c] Significantly different from normal control ($P<0.05$).

proliferation responses of normal ADH cells (as compared to the responses in cultures containing only normal cells that were separated and remixed). Regressor NA cells produced a significant increase in the normal NA Con A response. Regressor ADH cells suppressed the normal NA and normal ADH response to both Con A and PHA.

The remixing of normal NA cells with normal ADH cells in the MLTC assay produced a decrease in the normal NA tumor cell-induced proliferative response (table 3). In similar experiments the presence of normal NA cells had little effect on normal ADH cell mitogen-induced proliferative responses. However, the addition of regressor NA spleen cells or regressor ADH spleen cells to either normal NA or normal ADH cells caused a significant increase in all normal proliferative responses to MCA cells (table 3).

DISCUSSION

We have previously shown (*24*) that NBR rats demonstrated an age-related change in susceptibility to progressive growth of a syngeneic MCA-induced fibrosarcoma. In that study we found that relatively young animals had a high incidence (>90%) of progressive tumor growth, whereas older animals had a decreased incidence of progressive tumor takes (20%) and increased incidences of regressing tumors (40%) and no tumor takes (40%).

Several investigators have previously shown decreased proliferative responses to Con A and PHA by lymphoid cells obtained from animals bearing progressively growing tumors (*1-3, 12*). We have confirmed these observations (table 1) and extended them by showing a decreased in vitro proliferative response to syngeneic MCA-induced fibrosarcoma cells in animals with progressively growing tumors (table 1). We have also shown that spontaneous regressor animals produce proliferative responses to mitogens and tumor cells that are generally greater than the responses of normal and progressor spleen cells (table 2).

The lower proliferative responses observed in progressor animals may be caused by suppressor cells (*1-12*). An alternate explanation would be that progressor animals contain fewer mitogen and tumor-reactive cells (*1*). Spleen cells from normal young animals of many different rat strains (including NBR) possess an ADH cell, the removal of which results in enhanced mitogen-induced cellular proliferation by NA cells (*1, 2, 5, 24, 27-29*). In the present study, suppressor cells from progressor rats were identified by means of reconstitution experiments. These experiments indicated that both NA and ADH spleen cells from progressor animals suppress normal spleen cell proliferative responses to Con A (text-fig. 1), PHA (text-fig. 2), and MCA tumor cells (text-figs. 3, 4). Suppression produced by tumor progressor spleen cells appears nonspecific inasmuch as it affects both mitogen and tumor cell-induced proliferative responses.

Compared to progressor rats, regressor rats had greater than normal mitogen and tumor cell-induced proliferation responses. Regressor NA spleen cell responses to PHA and to syngeneic tumor cells (table 2), and regressor ADH responses to Con A, PHA, and tumor cells (table 2), were significantly higher than were the equivalent normal spleen cell responses. When regressor spleen cells were mixed with normal spleen cells and tested in proliferation assays (table 3), regressor ADH cells suppressed normal NA and normal ADH spleen cell responses to both Con A and PHA. ADH cells from age-matched normal controls were not suppressive in similar mixing experiments. Unlike progressor NA cells, regressor NA cells enhanced the response of normal NA cells to Con A (table 3).

In general, the suppression of normal mitogen responses by regressor NA and ADH cells was similar to that caused by the same spleen cell fractions of progressor spleen cells. These data suggest that both progressive tumor growth and development of tumor immunity (regression) occur coincidentally with the generation of spleen cells that suppress normal Con A and PHA responses. The suppressive effects were greater in the progressor and regressor ADH spleen cells than in NA cells (text-fig. 2; table 3), as evidenced by the degree of suppresion exhibited by these ADH cells after mixing with normal cells.

Other investigations of rat spleen cell proliferative responses indicated that macrophages and/or prostaglandins mediate suppression (*1, 2, 4, 5, 10, 12, 16, 27*). We have previously shown (Evans DL, Hooper CJ, Johnson K: Submitted for publication) that nylon wool did not completely separate T-cells from B-cells and macrophages. NA cells contained low numbers of macrophages (3%), and ADH cells likewise contained T-cells (13%). The suppressive effect on mitogen responsiveness of cells present in progressor and regressor ADH fractions could be due to macrophages. We recently reported that Percoll density gradient centrifugation of NA and ADH cells produced enriched populations of both NA and ADH suppressor cells (*30*; Evans DL, Hooper CJ, Johnson K: Submitted for publication). The ADH suppressor cell produced significant reduction of PHA responses. This cell has a density of 1.055-1.065 g/ml and by morphological and biochemical (nonspecific, esterase-positive) criteria appears to be a macrophage. However, the NA suppression of the PHA response probably was due to a T-cell (identified by means of a monoclonal anti-T-cell antibody) of density 1.07-1.09 g/ml (*30*; Evans DL, Hooper CJ, Johnson K: Submitted for publication). Both T-cells and macrophages in normal rat spleens thus are capable of suppressing mitogen responses.

Perhaps the most important result of the cell mixing experiments was obtained when comparisons were made between the activities of regressor and progressor cells in the MLTC assays. When added to normal NA or normal ADH cells, both regressor NA and regressor ADH spleen cells produced an enhancement of the normal spleen cell responses to MCA tumor cells (table 3). Similar experiments with progressor spleen cell fractions demonstrated suppressive activities (text-figs. 3, 4) of these equivalent spleen fractions.

It is evident from these studies that more than one type of suppression is produced by spleen cells from rat progressors and regressors. Spleen cells from tumor progressor animals contain at least two suppressor populations (functions): the suppression of the normal rat mitogen and MLTC proliferative responses. Regressor spleen cells likewise have mitogen suppression activities but lack the ability to suppress normal cell responses to syngeneic tumor cells. This differential in suppresor cell function may be of considerable importance in the development of tumor immunity. Studies are currently in progress to specifically identify these different suppressor cell populations and to determine if tumor immunity in our model system is produced by a qualitative or quantitative change in these regulating cells.

REFERENCES

(*1*) Kruisbeek AM, van Hees M. Role of macrophages in the tumor-induced suppression of mitogen responses in rats. J Natl Cancer Inst 1977; 58:1653–1660.

(*2*) Kruisbeek AM, Zijlstra J, Zurcher C. Tumor-induced changes in T cell mitogen responses in rats: Suppression of spleen and blood lymphocyte responses and enhancement of thymocyte responses. Eur J Immunol 1978; 8:200–206.

(*3*) Zembala M, Mytar B, Popiela T, et al. Depressed in vitro peripheral blood lymphocyte response to mitogens in cancer patients: The role of suppressor cells. Int J Cancer 1977; 19:605–613.

(*4*) Bluestone JA, Lopez C. Suppression of the immune response in tumor-bearing mice. II. Characterizations of adherent suppressor cells. JNCI 1979; 63:1221–1227.

(*5*) Weiss N, Fitch FN. Macrophages suppress CTL generation in rat mixed leukocyte cultures. J Immunol 1977; 199:510–516.

(*6*) Glaser M, Kirchner H, Holden HT, Herberman RB. *Brief communication:* Inhibition of cell-mediated cytotoxicity against tumor-associated antigens by suppressor cells from tumor-bearing mice. J Natl Cancer Inst 1976; 56:865–867.

(*7*) Takei F, Levy JG, Kilburn DG. In vitro induction of cytotoxicity against syngeneic mastocytoma and its suppression by spleen and thymus cells from tumor-bearing mice. J Immunol 1976; 116:288–293.

(*8*) Kirchner H, Muchmore AV, Chused TM, et al. Inhibition of proliferation of lymphoma cells and T lymphocytes by suppressor cells from spleens of tumor-bearing mice. J Immunol 1975; 114:206–210.

(*9*) Argyris BF. Factors affecting suppressor cell activity in tumor-allosensitized mice. JNCI 1980; 64:959–966.

(*10*) Connolly KM, Elgert KD. Reversal of macrophage augmented MLR reactivity by tumor-induced splenic suppressor T cells and their soluble factors. Cell Immunol 1979; 44:99–108.

(*11*) Glaser M, Kirchner H, Herberman RB. Inhibition of in vitro lymphoproliferative responses to tumor-associated antigens by suppressor cells from rats bearing progressive growing Gross leukemia virus-induced tumors. Int J Cancer 1975; 16:384–393.

(*12*) Anaclerio A, Moras ML, Conti G, Mistrello G, Spreafico F. Suppression of mitogen responses and graft-versus-host reaction by splenocytes from mice bearing Lewis lung carcinoma. JNCI 1978; 61:471–475.

(*13*) Treves AJ, Carnaud C, Trainin N, et al. Enhancing T lymphocytes from tumor-bearing mice suppress host resistance to a syngeneic tumor. Eur J Immunol 1975; 4:722–727.

(*14*) Enker WE, Jacobitz JL. In vivo splenic irradiation eradicates suppressor T cells causing the regression and inhibition of established tumor. Int J Cancer 1980; 25:819–825.

(*15*) Chang RW, Turk JL. Increased resistance in splenectomized mice to a methylcholanthrene-induced tumour. Br J Cancer 1977; 35:768–776.

(*16*) Yamagishi H, Pellis NR, Kahan BD. Effect of splenectomy upon tumor growth. Characterization of splenic tumor-enhancing cells in vivo. Surgery 1980; 87:655–661.

(*17*) Milas L, Mujagić H. The effect of splenectomy on fibrosarcoma metastasis in lungs of mice. Int J Cancer 1973; 11:186–190.

(*18*) Ferrer JF. Enhancement of the growth of sarcoma 180 in splenectomized and sham-operated AKR in mice. Transplantation 1968; 6:160–166.

(*19*) Gershon RK, Carter RL. Factors controlling concomitant immunity in tumor-bearing hamsters: Effects of prior splenectomy and tumor removal. J Natl Cancer Inst 1969; 43:533–543.

(*20*) Faraci RP, Marrone JC, Lesser GR, Ketcham AS. The effect of splenectomy on tumor immunity and the metastatic spread of a murine reticulum cell sarcoma. Panminerva Med 1975; 17:59–64.

(*21*) Fisher MS, Kripke ML. Further studies on the tumor specific suppressor cells induced by ultraviolet radiation. J Immunol 1978; 121:1139–1144.

(*22*) Whitney RB, Pope BL, Levy JG. Immune competence and immunosuppressive factors in splenectomized tumor-bearing mice. Cell Immunol 1977; 28:15–21.

(*23*) Yamagishi H, Pellis NR, Kahan BD. Surgical immunodepression: Role of splenic suppressor cells. Surg Forum, 1978; 29:465–468.

(*24*) Hollingsworth MA, Barrowclough J, Evans DL. Age-related increases in mitogenic responses and natural immunity to a syngeneic fibrosarcoma in rats. Mech Ageing Dev 1981; 17:95–106.

(*25*) Evans DL. Oncofetal antigens in chemical and viral-induced tumors. J Reticuloendothel Soc 1976; 20:117–126.

(*26*) Julius M, Simpson E, Herzenberg L. A rapid method for the isolation of functional thymus-derived murine lymphocytes. Eur J Immunol 1973; 3:645–649.

(*27*) Folch H, Yoshinaga M, Waksman BH. Regulation of lymphocyte responses in vitro. III. Inhibition by adherent cells of the T-lymphocyte response to phytohemagglutinin. J Immunol 1973; 110:835–839.

(*28*) DeKruyff RH, Kim YT, Siskind GW, Weksler ME. Age related changes in the in vitro immune response: Increased suppressor activity in immature and aged mice. J Immunol 1980; 125:142–147.

(*29*) Skowron-Cendrzak A, Ptak W. Suppression of local graft-versus-host reactions by mouse foetal and newborn spleen cells. Eur J Immunol 1976; 6:451–452.

(*30*) Evans DL, Hooper CJ, Johnson K, McGee M. Cell requirements for optimum proliferative responses of rat spleen cells. Immunobiology, 1981; 159:366–381.

Gastrin Protection Against Chemically Induced Gastric Adenocarcinomas in Wistar Rats: Histopathology of the Glandular Stomach and Incidence of Gastric Adenocarcinoma[1,2]

Masaharu Tatsuta, *M.D.*,[3] **Hisako Yamamura**, *B.S.*,[3] **Haruo Taniguchi**, *M.D.*,[4] *and* **Hiroshi Tamura**, *M.D.*[3]

ABSTRACT—The effects of gastrin on the histopathology of the glandular stomach and on the incidence of gastric carcinoma induced by *N*-methyl-*N'*-nitro-*N*-nitrosoguanidine (MNNG) were investigated in inbred Wistar (W) rats. Prolonged administration of gastrin after treatment with MNNG significantly reduced the incidence of adenocarcinomas of the glandular stomach. In addition, atypical glandular proliferations were significantly less frequent and were smaller, and the incidence of marked mucosal atrophy was significantly reduced in both the antral and oxyntic gland mucosae. Both atypical glandular hyperplasia and mucosal atrophy are precursors of gastric cancers; prolonged administration of gastrin to rats after treatment with MNNG suppressed development of precursors of gastric cancer and so prevented development of gastric cancers.—JNCI 1982; 69:59–66.

Prolonged administration of gastrin to rats after treatment with MNNG significantly reduced the incidence of adenocarcinoma of the glandular stomach (*1*, *2*). It has also been reported (*3*) that hypergastrinemia in the rat after a Billroth II antral implant operation exerted a protective effect against experimental gastric carcinogenesis in that portion of the stomach remaining. Gastrin exerts a trophic influence on the gastric mucosa (*4*) and stimulates both gastric acid secretion and mucosal blood flow. These actions could decrease the suspectibility of gastric mucosa to carcinogenesis, but the exact mechanism of gastrin's effect is unknown.

In the present study, we examined gastrin's effects on the histopathology of the glandular stomach and on development of gastric adenocarcinomas by injecting gastrin in depot form into rats that had been treated with MNNG.

MATERIALS AND METHODS

Young male W inbred rats of about the same age (6 wk old) and initially weighing 100–150 g were given drinking water containing 50 µg MNNG/ml (Wako Pure Chemical Industries, Ltd., Osaka) for 25 weeks. The MNNG solution was given to rats every other day from bottles covered with aluminum foil or painted a dark color. From week 26 the rats were given ordinary tap water and divided randomly into 3 groups. Group 1 (18 rats) received no treatment; group 2 (10 rats) was given the vehicle olive oil only (0.5 ml/rat); group 3 (20 rats) was given 300 µg tetragastrin (C-terminal tetrapeptide of gastrin; Nissui Pharmaceutical Co. Ltd., Tokyo, Japan) per day as a suspension in 0.5 ml olive oil/rat. From the beginning of week 26 to the end of week 29, the rats in groups 2 and 3 were given one injection a day; then from week 30 to the end of the experiment, they were given one injection every other day. All injections were given sc between 2 and 3 p.m. at a different site each time.

Animals that survived for more than week 35 were included in the effective numbers. Rats were killed when they became moribund, and those that died or were killed during the experimental period were autopsied. The stomach was fixed with a 10% neutralized Formalin solution for histologic examination. Tissues were embedded in paraffin and stained with H & E.

Histologically, adenocarcinomas were defined as lesions in which neoplastic glands had penetrated the muscularis mucosa to involve the submucosa and occasionally such deeper layers as the muscle coat, serosa, and peritoneal tissues. Cancers of the glandular stomach were classified as follows (*2*):

1) Highly differentiated adenocarcinoma: Adenocarcinoma showing atypical glandular structure with a tubular or papillary pattern and an arrangement of cells comparable to that enclosing normal gastrointestinal crypts, but adenocarcinoma in which these glands involved the muscularis mucosa (fig. 1A).
2) Well-differentiated adenocarcinomas: *a*) common type—less highly differentiated glands, consisting of disorderly masses of atypical cells containing a small amount of intracellular mucin (fig. 1B); *b*) mucinous carcinoma—active mucin secretion, often resulting in mucinous nodules with a large amount of extracellular mucin, with only a few isolated groups of tumor cells (fig. 1C).
3) Poorly differentiated adenocarcinomas: *a*) Anaplastic carcinoma—highly anaplastic cells scattered individually without any typical glandular or tubular differentiation; *b*) signet-ring cell carcinoma—tumor cells with large amounts of intracellular mucin, giving the cells a signet-ring appearance (fig. 1D).

A lesion in which the constituent cells of the gland stained hyperchromatically, the course and the size of the glands were irregular, and the nuclei were pleomorphic was called "atypical glandular hyperplasia" when it was confined to the mucosa with no penetration through the muscularis mucosa. Atypical glandular hyperplasia was classified into three grades according to severity: 1) mild—slight, irregular glandular proliferation with little or no cellular atypism resulting from a response to injury of the mucosa caused by

---

ABBREVIATIONS USED: H & E=hematoxylin and eosin; MNNG=*N*-methyl-*N'*-nitro-*N*-nitrosoguanidine.

---

[1] Received July 2, 1981; revised February 3, 1982; accepted February 17, 1982.

[2] Animals were maintained under the guidelines set forth by The Center for Adult Diseases, Osaka.

[3] Department of Gastrointestinal Oncology, The Center for Adult Diseases, Osaka, 3-3, Nakamichi 1-chome, Higashinari-ku, Osaka 537, Japan.

[4] Department of Pathology, The Center for Adult Diseases, Osaka.

TABLE 1.—*Incidence of gastric cancer in MNNG-treated rats*

Group No. and treatment	No. of effective rats	No. (%) of rats with gastric cancer
1. MNNG alone[a]	14	14 (100)
2. MNNG + olive oil[b]	9	9 (100)
3. MNNG + tetragastrin[c]	17	8 (47.1)[d]

[a] 50 μg MNNG/ml was given in the drinking water for 25 wk.

[b] 0.5 ml of olive oil was administered to rats after exposure to 50 μg MNNG/ml for 25 wk.

[c] 300 μg of tetragastrin in depot form was administered to rats after exposure to 50 μg MNNG/ml for 25 wk.

[d] Differences between values for groups 1 and 3 and values for groups 2 and 3 were statistically significant ($P<0.05$; $P<0.01$).

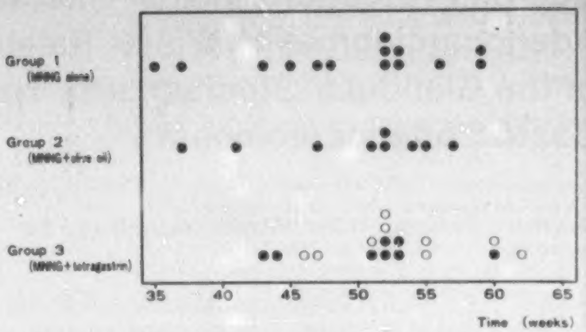

TEXT-FIGURE 1.—Incidence of gastric cancers in the glandular stomach of MNNG-treated rats after 35 experimental wk. For explanation of treatment, *see* table 1. ○=no tumor; ●=adenocarcinoma.

the carcinogen (figs. 2, 3); 2) moderate—moderately irregular glandular proliferation with cellular atypism (fig. 4); and 3) severe—marked irregular epithelial proliferation with remarkable cellular and structural atypism limited to the glandular epithelium (fig. 5). The severe grade type can be equated with intramucosal carcinoma in the human stomach.

Mucosal atrophy of the antral mucosa was classified as follows: 1) mild atrophy—little or no change in the antral mucosal gland, but sometimes superficial inflammatory infiltration, edema, and epithelial damage apparent; 2) mild atrophy with overgrowth of foveolar layer—irregular overgrowth of the tubules of the superficial zone of epithelium with a variable degree of cystic changes and nearly always many glands of the deep zone remaining, which, however, show mild atrophic change; 3) moderate atrophy—marked disappearance of the antral mucosal glands; and 4) severe—usually complete disappearance of antral mucosal glands.

The height of the fundic mucosa was estimated in the central portion of the anterior and posterior walls on histologic sections cut at right angles to the surface of the mucosa. The mean of six readings, three from each portion of the anterior and posterior walls, was taken for each stomach.

The results were analyzed by the chi-square test (*5*) or Fisher's exact probability test (*6*). "Significant" indicates a calculated *P*-value of less than 0.05.

RESULTS

Incidence of gastric cancers.—The incidence of gastric cancer in each group is summarized in table 1 and text-figure 1. Among rat groups 1, 2, and 3, a total of 4, 1, and 3 rats, respectively, died before week 35 either of respiratory infection or of wasting. No tumors were found in any of these animals, which were excluded from the effective numbers.

All rats examined in group 1 (treated with MNNG alone) and in group 2 (treated with MNNG and then olive oil) had gastric cancers. The incidence of gastric cancer in group 3 (treated with MNNG and then tetragastrin) was significantly less than that in groups 1 and 2. All tumors were found in the antrum in all groups.

No gastric cancer was found in 5 rats treated with MNNG and killed at week 25.

Histologic types of adenocarcinomas.—Table 2 shows the distribution of the histologic types of adenocarcinoma among 14 group 1 rats, 9 group 2 rats, and 13 group 3 rats. Histologically, all experimentally induced tumors in the glandular stomach were adenocarcinomas. Highly differentiated adenocarcinomas were found in all rats in group 1 and in group 2. In group 3 the incidence of highly differentiated adenocarcinomas was only 37.5%, the other tumors being adenocarcinomas with little or no glandular structure. A signet-ring cell carcinoma was seen in 1 group 3 rat (12.5%). The differences between the incidences of highly differentiated adenocarcinoma in groups 1 and 3 and in groups 2 and 3 were statistically significant.

Histopathology of oxyntic gland mucosa.—The effects of tetragastrin on the oxyntic gland mucosa are summarized in tables 3 and 4. Differences were significant between the control groups (groups 1, 2, and 4) and the tetragastrin-treated group (group 3), with respect to the height of the oxyntic gland mucosa and the incidence of atypical glandular hyperplasia. In group 1 and in group 2, mucosal atrophy was remarkable in the oxyntic gland area, but

TABLE 2.—*Histologic types of adenocarcinomas in glandular stomach of MNNG-treated rats*

Group No. and treatment[a]	No. of effective rats	No. of rats with adenocarcinoma	No. (%) of rats with highly differentiated adenocarcinoma	No. (%) of rats with well-differentiated adenocarcinoma of:		No. (%) of rats with poorly differentiated	
				Common type	Mucinous type	Signet-ring cell carcinoma	Anaplastic carcinoma
1. MNNG alone	14	14	14 (100)	0	0	0	0
2. MNNG + olive oil	9	9	9 (100)	0	0	0	0
3. MNNG + tetragastrin	13	8	3 (37.5)[b]	3 (37.5)	1 (12.5)	1 (12.5)	0

[a] For explanation of treatment, *see* table 1.

[b] Differences between the incidences of highly differentiated adenocarcinomas in groups 1 and 3 and incidences in groups 2 and 3 were statistically significant ($P<0.005$; $P<0.01$).

TABLE 3.—*Mucosal height of the oxyntic gland area in MNNG-treated rats*

Group No. and treatment[a]	Mucosal height in mm, mean ± SE
1. MNNG alone	0.42±0.02
2. MNNG + olive oil	0.43±0.02
3. MNNG + tetragastrin	0.73±0.02[b]
4. No treatment	0.65±0.03[c]

[a] For explanation of treatment, *see* table 1. No treatment: Rats were given ordinary tap water throughout the experimental period and killed at wk 52.

[b] Differences between values in groups 1 and 3 and values in groups 2 and 3 were statistically significant ($P<0.001$; $P<0.001$).

[c] Differences between values in groups 1 and 4 and values in groups 2 and 4 were statistically significant ($P<0.001$).

administration of tetragastrin after treatment with MNNG for 25 weeks resulted in a significant increase in the height of the fundic mucosa in group 3. Atypical glandular hyperplasia was found in groups 1, 2, and 3 less frequently and was less marked in oxyntic gland mucosa than that in the antral gland mucosa. No severe or moderate atypical glandular hyperplasia was seen in the oxyntic mucosa in any of the groups, and mild atypical glandular hyperplasia was found less frequently in group 3 rats than in the control groups 1 and 2.

Histopathology of antral gland mucosa.—The effects of tetragastrin on the antral mucosa are summarized in tables 5 and 6. Mucosal atrophy was marked in the antral mucosa in group 1 treated with MNNG only and in group 2 treated with MNNG and then olive oil. In group 3 treated with MNNG and then tetragastrin, the incidence of mucosal atrophy of moderate or severe grade was less frequent. The differences between the incidences of marked mucosal atrophy in groups 1 and 3 were statistically significant. Atypical glandular hyperplasias of various grades were frequent in the antrums of groups 1 and 2. Prolonged administration of tetragastrin after MNNG treatment in group 3 significantly decreased the incidences of atypical glandular hyperplasias of moderate or severe grade in the antral mucosa. The incidence of mild atypical glandular hyperplasia was also decreased by tetragastrin treatment: The differences between the values in groups 2 and 3 were statistically significant, but those between the values in groups 1 and 3 were not.

TABLE 4.—*Incidence of atypical glandular hyperplasia in oxyntic gland mucosa of MNNG-treated rats*

Group No. and treatment[a]	No. of effective rats	No. (%) of rats with atypical glandular hyperplasia		
		Mild	Moderate	Severe
1. MNNG alone	14	7 (50.0)	0	0
2. MNNG + olive oil	9	5 (55.6)	0	0
3. MNNG + tetragastrin	17	1 (5.9)[b]	0	0

[a] For explanation of treatment, *see* table 1.

[b] Differences between values in groups 1 and 3 and values in groups 2 and 3 were statistically significant ($P<0.02$; $P<0.01$).

DISCUSSION

In 1967 Sugimura and Fujimura (*7*) reported that when MNNG was given to rats in their drinking water, adenocarcinomas of the glandular stomach developed at a high incidence within 1 year. Gastric acid secretion decreased during cancer development in rats treated in this way, as it does during development of gastric cancer in humans (*8*). These findings suggested that MNNG may be useful in studies of the pathogenesis and pathophysiology of gastric cancer.

The sequential morphologic changes in the stomach during carcinogenesis were investigated in rats (*8–11*), hamsters (*12*), and dogs (*13–15*) to elucidate precursors of gastric carcinoma. In rats, Saito et al. (*9*) showed the following

TABLE 6.—*Incidence of atypical glandular hyperplasia in antral mucosa of MNNG-treated rats*

Group No. and treatment[a]	No. of effective rats	No. (%) of rats with atypical glandular hyperplasia		
		Mild	Moderate	Severe
1. MNNG alone	14	7 (50.0)	9 (64.3)	8 (57.1)
2. MNNG + olive oil	9	6 (66.7)	6 (66.7)	7 (77.8)
3. MNNG + tetragastrin	17	3 (17.3)[b]	3 (17.6)[c]	2 (11.8)[d]

[a] For explanation of treatment, *see* table 1.

[b] Differences between values in groups 2 and 3 were statistically significant ($P<0.02$), but differences between values of groups 1 and 3 were not.

[c] Differences between values in groups 1 and 3 and values in groups 2 and 3 were statistically significant ($P<0.05$; $P<0.02$).

[d] Differences between values in groups 1 and 3 and values in groups 2 and 3 were statistically significant ($P<0.02$; $P<0.002$).

TABLE 5.—*Incidence of mucosal atrophy in antral mucosae of MNNG-treated rats*

Group No. and treatment[a]	No. of effective rats	No. (%) of rats with:			
		Mild atrophy with overgrowth of foveolar layer	Mild atrophy	Moderate atrophy	Severe atrophy
1. MNNG alone	14	3 (21.4)	0	5 (35.7)	6 (42.9)
2. MNNG + olive oil	9	1 (11.2)	0	4 (44.4)	4 (44.4)
3. MNNG + tetragastrin	17	4 (23.5)	7 (41.2)	5 (29.4)	1 (5.9)

[a] For explanation of treatment, *see* table 1. For comparison of the incidence of moderate and severe atrophy in groups 1 and 3, the chi-square test was used. For this analysis the four grades of the mucosal atrophy were contracted to two, namely, mild atrophy with and without overgrowth of foveolar layer versus moderate and severe atrophy. The differences in groups 1 and 3 were statistically significant, but differences between those in groups 2 and 3 were not significant.

changes: first erosion and shallow ulcer formation, then regenerative glandular hyperplasia following adenomatous hyperplasia, and finally development of adenocarcinoma. Bralow et al. (*8*) reported that histologic changes occurred in rats within 3 days of exposure and consisted of submucosal edema, eosinophilic infiltration, and an increase in the lamina propria. By the 28th week, a marked increase in the thickness of the lamina propria, pinching of the basal portion of the glands, and formation of microcysts were observed, but no mucosal ulceration, glandular atypism, or significant areas of mucosal atrophy were seen. However, at week 52 of treatment with MNNG, extensive changes were found in the mucosa with areas of atrophy, glandular atypism, intestinal metaplasia, and microcyst formation.

Gastric atrophy may be a precursor of gastric cancer induced by MNNG in rat stomach, because the main site of development of both atrophy and tumor formation in rats treated with MNNG appears to be the antrum. Mucosal atrophy involved the antral mucosa more than the fundal area (*8*, *10*). Mucosal atrophy resulted from injury to the generative cell zone by MNNG (*11*), and it was the end result of erosion or superficial erosive changes.

Glandular atypism or atypical glands may also be precursors of gastric cancer in rats. Shirai (*10*) reported that the appearance of atypical glands and sometimes glandular hyperplasia in the pyloric mucosa were important early changes in carcinogenesis of the glandular stomach of the rat. The atypical glands that developed after week 16 often invaded the submucosa. This appearance of atypical glands showing submucosal growth seemed to be the initial carcinogenic change in the gastric mucosa. Saito et al. (*9*) reported that after atrophy and erosion of the mucosa, regenerative glandular hyperplasia (i.e., irregular glandular proliferation) developed at the margin of the erosions in weeks 3–5 and that these lesions persisted for the rest of the experiment. This type of proliferation is considered to be a reaction to injury of the mucosa caused by MNNG, but the possibility that it is an initial step in cancer development cannot be disregarded.

In dogs (*14*), about half of the experimentally induced gastric cancers developed from an active or a healed ulcer. In rats, erosion and/or ulceration of the mucosa acquired importance as a chance for carcinogenesis during repetition of mucosal damage and repair (*9*). However, in our study and the study of Shirai (*10*) there were few erosions, because the concentration of the carcinogen was low. Therefore, we conclude that erosion is not necessary for MNNG gastric carcinogenesis in rats.

Human cancers frequently originate from areas of intestinal metaplasia in the stomach. Moreover, intestinal metaplasia is often observed in countries where stomach cancer is common (*16*). There are many reports of a close correlation between intestinal metaplasia and adenocarcinoma of the stomach, especially carcinoma of the well-differentiated type (*17*, *18*). During gastric carcinogenesis of the glandular stomach of the rat, intestinal metaplasia has been detected (*15*, *19*). However, in the present study no intestinal metaplasia was observed, so our experiment provides no information on the relationship between intestinal metaplasia and development of MNNG-induced gastric cancer.

The present results show that administration of tetragastrin in depot form after MNNG treatment for 25 weeks reduced the incidence of gastric cancer in the glandular stomach of the rat. Moreover, gastrin suppressed the development of mucosal atrophy and atypical glandular hyperplasia, which are considered precursors of gastric cancer in rats. Therefore, gastrin most likely suppresses development of precursors of gastric cancer and so prevents the development of gastric cancer.

Gastrin exerts a trophic influence on the gastric mucosa and stimulates gastric acid secretion and mucosal blood flow. These actions may be related to the reduced incidence of gastric cancer, but the exact mechanism of the effect of gastrin is unknown and needs further study.

REFERENCES

(*1*) Tatsuta M, Itoh T, Okuda S, Taniguchi H, Tamura H. Effect of prolonged administration of gastrin on experimental carcinogenesis in rat stomach induced by *N*-methyl-*N'*-nitro-*N*-nitrosoguanidine. Cancer Res 1977; 37:1808–1810.

(*2*) Tatsuta M, Itoh T, Okuda S, et al. Effects of gastrin and histamine on gastric carcinogenesis induced in rats by *N*-methyl-*N'*-nitro-*N*-nitrosoguanidine. Eur J Cancer 1980; 16:631–638.

(*3*) Deveney CW, Freeman H, Way LW. Experimental gastric carcinogenesis in rat. Effect of hypergastrinemia and acid secretion. Am J Surg 1980; 139:49–54.

(*4*) Johnson LR. The trophic action of gastrointestinal hormones. Gastroenterology 1976; 70:278–288.

(*5*) Siegel S. Nonparametric statistics for the behavioral sciences. New York: McGraw-Hill, 1956.

(*6*) Snedecor GW, Cochran WG. Statistical methods. Ames, Iowa: Iowa State Univ Press, 1967.

(*7*) Sugimura T, Fujimura S. Tumour production in glandular stomach of rats by *N*-methyl-*N'*-nitro-*N*-nitrosoguanidine. Nature 1967; 216:943–944.

(*8*) Bralow SP, Gruenstein M, Meranze DR, Bonakdarpour A, Shimkin MB. Adenocarcinoma of glandular stomach and duodenum in Wistar rats ingesting *N*-methyl-*N'*-nitro-*N*-nitrosoguanidine. Histopathology and associated secretory changes. Cancer Res 1970; 30:1215–1225.

(*9*) Saito T, Inokuchi K, Takayama S, Sugimura T. Sequential morphological changes in *N*-methyl-*N'*-nitro-*N*-nitrosoguanidine carcinogenesis in the glandular stomach of rats. J Natl Cancer Inst 1970; 44:769–783.

(*10*) Shirai T. Periodical observations of the glandular stomach in rats treated with *N*-methyl-*N'*-nitro-*N*-nitrosoguanidine. Nagoya Med J 1974; 19:155–167.

(*11*) Takabayashi S, Uchida Y, Kotake Y. Morphogenesis of adenocarcinoma induced by *N*-methyl-*N'*-nitro-*N*-nitrosoguanidine in the rat stomach. In: Pfeiffer CJ, ed. Gastric cancer. New York: Witzstrock, 1979:255–276.

(*12*) Kogure K, Sasadaira H, Kawachi T, et al. Further studies on induction of stomach cancer in hamsters by *N*-methyl-*N'*-nitro-*N*-nitrosoguanidine. Br J Cancer 1974; 29:1932–1942.

(*13*) Shimasato Y, Tanaka N, Kogure K, Fujimura S, Kawachi T, Sugimura T. Histopathology of tumors of canine alimentary tract produced by *N*-methyl-*N'*-nitro-*N*-nitrosoguanidine, with particular reference to gastric carcinomas. J Natl Cancer Inst 1971; 47:1053–1070.

(*14*) Saito T, Sasaki O, Matsukuchi T, Iwamatsu M, Inokuchi K. Experimental gastric cancer: Pathogenesis and clinicohistopathologic correlation. In: Herfarth C, Schlag P, eds. Gastric cancer. Berlin: Springer-Verlag, 1979:22–31.

(*15*) Sugimura T, Kawachi T. Experimental induction of gastric cancer. In: Pfeiffer CJ, ed. Gastric cancer. New York: Witzstock, 1979:231–254.

(*16*) Correa P, Cuello C, Duque E. Carcinoma and intestinal metaplasia of the stomach in Colombian migrants. J Natl Cancer Inst 1970; 44:297-306.

(*17*) NAKAMURA K, SUGANO H, TAKAGI K, KUMAKURA K. Carcinoma of the stomach in incipient phase; its histogenesis and histological appearances. Gan 1968; 59:251-258.

(*18*) JÄRVI O, LAUREN P. On the role of heterotopia of the intestinal epithelium in the pathogenesis of gastric cancer. Acta Pathol Microbiol Scand 1964; 29:26-44.

(*19*) MATSUKURA N, KAWACHI T, SASAJIMA K, SANO T, SUGIMURA T, HIROTA T. Induction of intestinal metaplasia in the stomachs of rats by *N*-methyl-*N'*-nitro-*N*-nitrosoguanidine. JNCI 1978; 61:141-144.

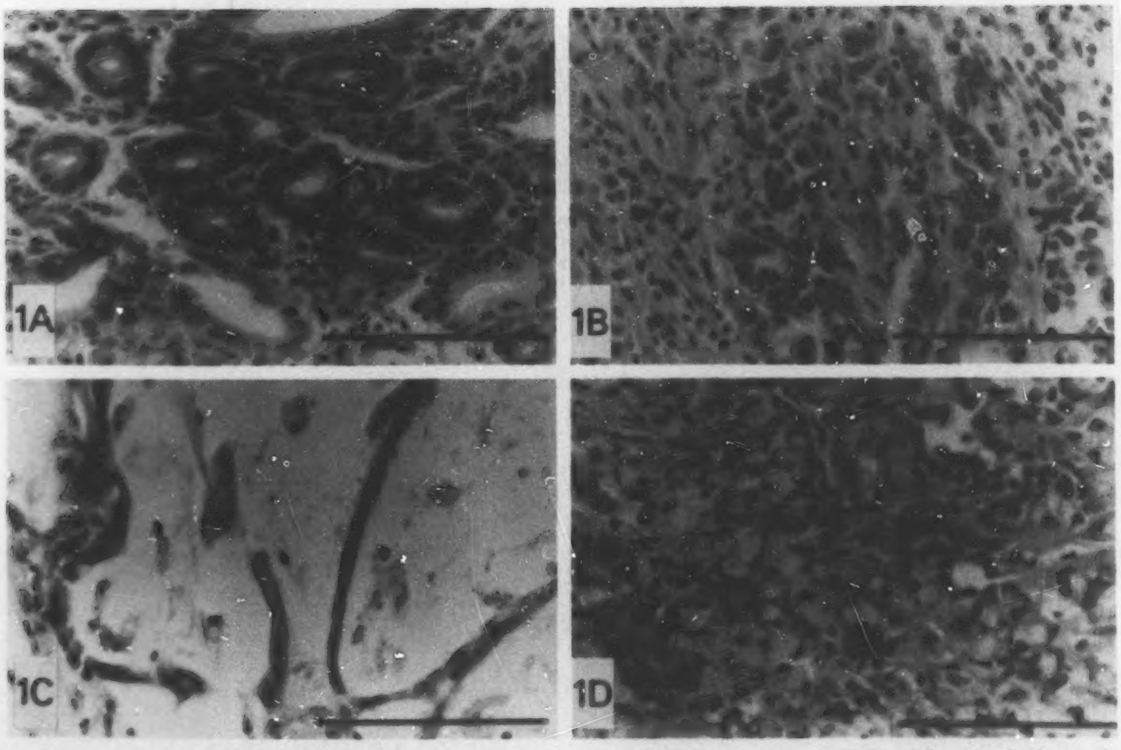

FIGURE 1.—Histologic classification of adenocarcinomas in the glandular stomach of MNNG-treated rats. A) Highly differentiated adenocarcinoma. B) Common type of well-differentiated adenocarcinoma. C) Mucinous well-differentiated adenocarcinoma. D) Signet-ring cell carcinoma of poorly differentiated adenocarcinoma. H & E. *Bars*=0.1 mm. × 400

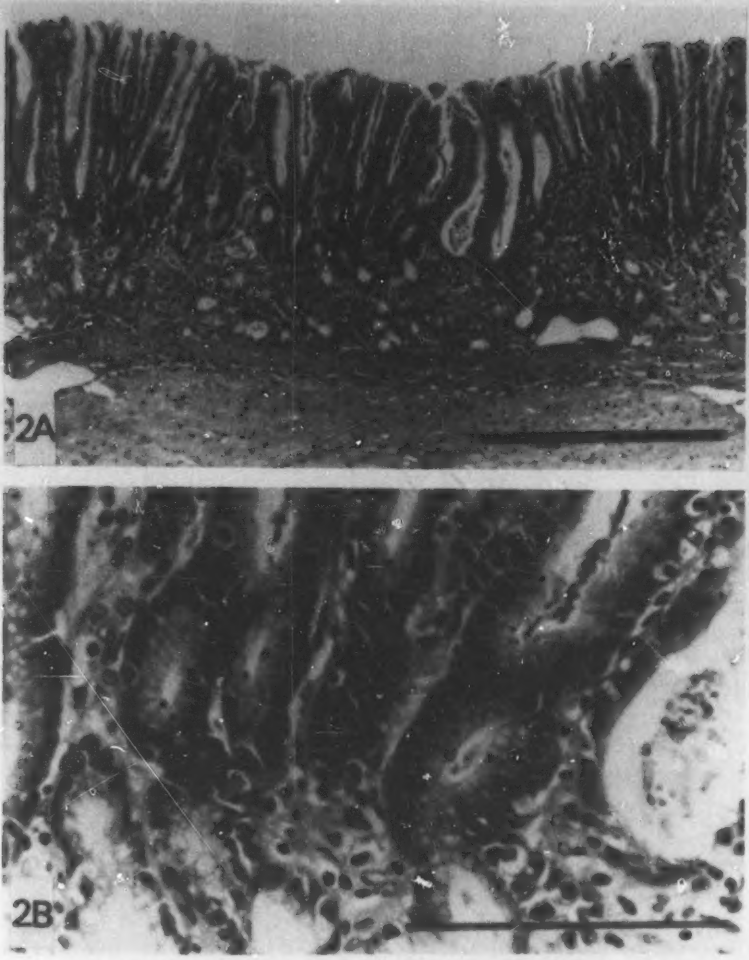

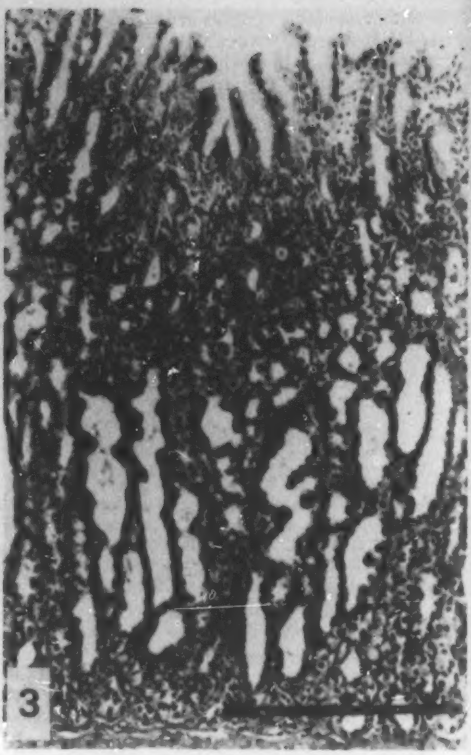

FIGURE 2.—Mild atypical glandular hyperplasia in the pyloric gland mucosa in rat of control group 1 treated with MNNG alone for 25 wk. *Note* slight, irregular glandular proliferation with little or no cellular atypism. H & E. A) *Bar*=0.3 mm. × 100. B) *Bar*=0.1 mm. × 400

FIGURE 3.—Mild atypical glandular hyperplasia in the oxyntic gland mucosa in rat of control group 1. H & E. *Bar*=0.2 mm. × 100

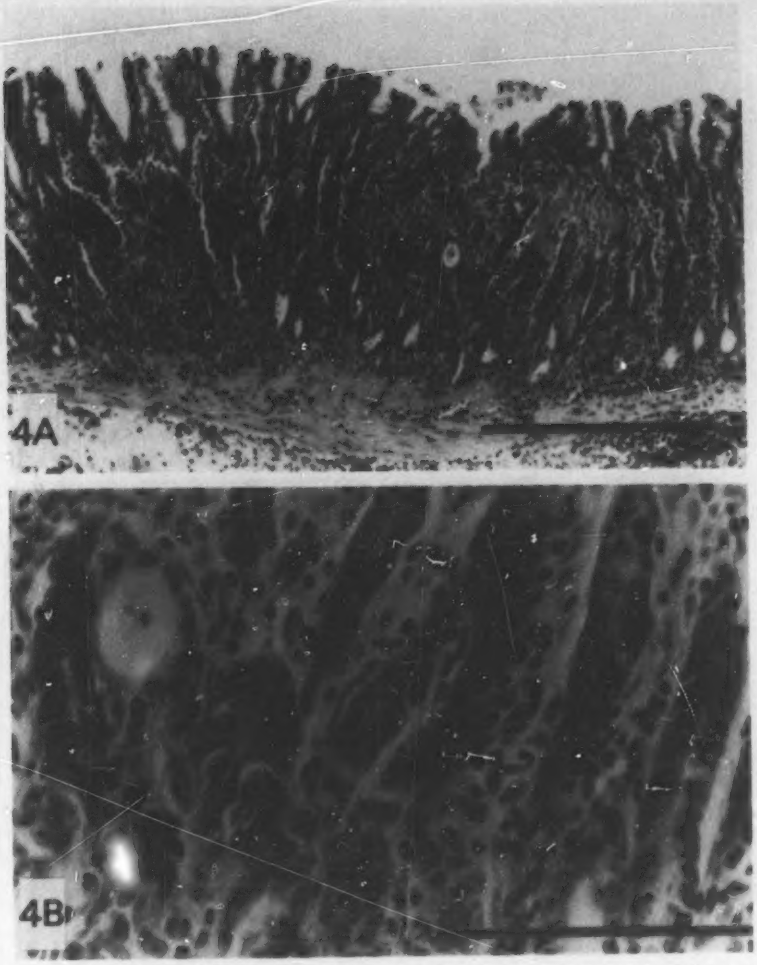

FIGURE 4.—Moderate atypical glandular hyperplasia in the pyloric gland mucosa in rat of control group 1. *Note* moderate, irregular glandular proliferation with cellular atypism. H & E. A) *Bar*=0.3 mm. × 100. B) *Bar*=0.1 mm. × 400

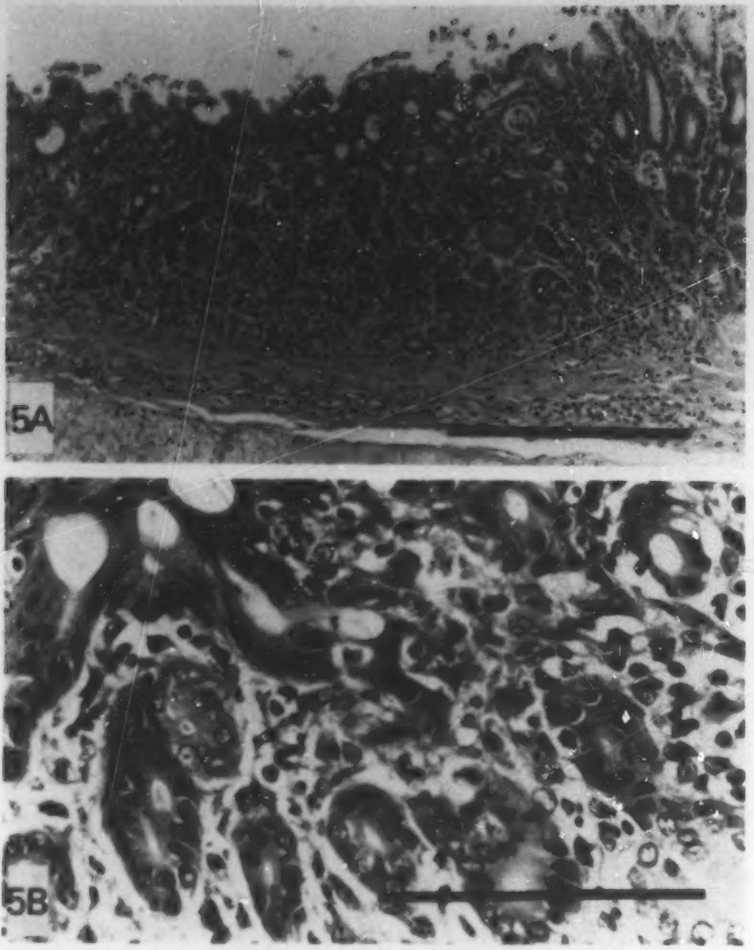

FIGURE 5.—Severe atypical glandular hyperplasia in the pyloric gland mucosa in rat of control group 1. *Note* marked, irregular epithelial proliferation, with marked cellular and structural atypism, which is confined to the mucosa with no penetration through the muscularis mucosa. H & E. A) *Bar*=0.3 mm. × 100. B) *Bar*=0.1 mm. × 400

Subcutaneously Injected Radiolabeled Liposomes: Transport to the Lymph Nodes in Mice [1,2]

Vasily I. Kaledin, [3] **Nellie A. Matienko,** [3] **Valery P. Nikolin,** [3] **Yevgeny V. Gruntenko,** [3] **Vladimir G. Budker,** [4] *and* **Tamara E. Vakhrusheva** [4,5]

ABSTRACT—Male A/He mice were given sc injections in the feet with $[3,5,3'\text{-}^{125}I]$triiodothyronine, $[^{125}I]T_3$, either in the free state or encapsulated within sonicated phosphatidylcholine liposomes. Radioactivity was recovered from the injection site, the popliteal lymph nodes (LN), blood, liver, lungs, and spleen at various times (5 min to 6 hr) after injection. The highest level of radioactivity was found in the popliteal LN of mice given liposome-encapsulated (LE) $[^{125}I]T_3$: For more than 3 hours after the injection, radioactivity was fivefold to fiftyfold higher there than that in all the other organs including the popliteal LN of mice given injections of free $[^{125}I]T_3$. The results demonstrated that sc injected liposomes enter the lymphatic pathways and reach the draining LN. Thus local administration of LE antitumor drugs into the sites of a malignant tumor before its excision might be useful in preventing postoperative metastases to the draining LN.—JNCI 1982; 69:67–71.

In a previous paper (*1*), we suggested that liposomes, when administered into a lymphatic vessel, can reach the regional LN and remain there as corpuscular bodies. We attempted to use this approach to deliver antitumor agents to LN with tumor metastases (*2*). The available model, i.e., mice with metastatic tumors in the popliteal LN, however, was not suitable for the direct injection of drug-containing liposomes into a lymphatic vessel. In view of the known high permeability of the endothelial walls of lymph capillaries to particulate and colloid material (*3*), we injected LE antitumor agents, *cis*-diamminedichloroplatinum(II) or hydrocortisone, sc into mouse feet with primary tumors with the expectation that some portion of the drug-carrying liposomes would enter the lymphatic channels and, ultimately, the metastatically affected popliteal LN. Although the results indicated that when this mode of administration was used, the drug exerted an antimetastatic effect in the LE but not in the free form (*1, 2*) and thus lent credibility to our assumption, experiments were needed to demonstrate that liposomes injected into tissues do enter the lymphatic vessels and reach the draining LN. To our knowledge, only a few reports in the literature deal with this problem (*4, 5*). If our assumptions are correct, the interstitial administration of drug-containing liposomes into a tumor site would ensure the entrance of the drug into the whole set of draining LN to which the metastatic cells can spread. This route of administration would eliminate the need for the difficult and often impracticable method of direct injection of liposomes into each lymphatic vessel leading to the regional LN.

This study was designed to trace the distribution of radioactivity in the draining LN and other organs of mice after sc injection into the feet of LE or free radiolabel. The results demonstrated that in mice given injections of LE $[^{125}I]T_3$, the amount of radioactivity per gram of tissue in the popliteal LN was over tenfold higher than that in other organs and that in the popliteal LN of control mice given free $[^{125}I]T_3$.

MATERIALS AND METHODS

Mice.—Male 10-week-old inbred A/HeJ mice were used that were bred in the vivarium of the Institute of Cytology and Genetics of the Siberian Branch of the U.S.S.R. Academy of Sciences. The animals were kept in metal cages and had free access to food and water.

Liposomes.—Liposomes were prepared from egg yolk phosphatidylcholine as previously described (*2*). We prepared an emulsion with 30 mg of the lipid in 1.5 ml of a 0.14-*M* NaCl solution containing 2 mCi $[^{125}I]T_3$ (sp act, 1 Ci/mmol); Radiochemical Centre, Amersham, Buckinghamshire, England). The mixture was sonicated (22 kHz and 0.16 amp.) five times for 1 minute with 0.5-minute intervals at 0°C. Nonencapsulated $[^{125}I]T_3$ was removed from the liposomes by gel filtration through a Sephadex G-50 column (Pharmacia Chemicals, Uppsala, Sweden). The average size of liposomal vesicles prepared in this manner has been shown to be 430±17 Å (*2*). Approximately 1.5% of the original radioactivity was entrapped within the liposomes. The radioactivity of 1 ml of the liposome suspension containing 20 mg phosphatidylcholine was about 4.0×10^7 cpm. The label remained vesicle bound after incubation of the labeled liposomes for 3 hours at 25°C. The liposome suspension was diluted with saline to a final concentration of about 3 mg of the lipid per ml (6.15×10^6 cpm). A solution of free $[^{125}I]T_3$ at the same concentration was used in the control experiments.

Treatment.—Mice received 0.1 ml sc injections of the liposome suspension or a solution of free $[^{125}I]T_3$ into the region of the plantar aponeurosis (0.05 ml into each foot). The total dose of radioactivity was 6.15×10^5 cpm per mouse. The mice were decapitated at fixed times, and blood samples were collected. The popliteal LN were dissected, and the

ABBREVIATIONS USED: $[^{125}I]T_3$=$[^{125}I]$3,5,3′-triiodothyronine; LE=liposome-encapsulated; LN=lymph node(s).

---

[1] Received July 21, 1981; accepted January 19, 1982.

[2] Animals were maintained under the guidelines set forth by the Institute of Cytology and Genetics, Siberian Branch of the U.S.S.R. Academy of Sciences.

[3] Institute of Cytology and Genetics, Siberian Branch of the U.S.S.R. Academy of Sciences, Novosibirsk, 90, U.S.S.R.

[4] Institute of Organic Chemistry, Siberian Branch of the U.S.S.R. Academy of Sciences.

[5] We thank Miss A. Fadeeva for translating this manuscript from Russian into English.

feet were amputated above the ankle joint. In some experimental groups, the liver, lungs, and spleen were removed and weighed. Radioactivity was registered in a counter (Minigamma model; LKB Producter AB., Bromma, Sweden). The sum of counts of both feet and that of both popliteal LN of each mouse were determined. For calculation of the amount of radioactivity per gram of tissue, the weight of the popliteal LN was taken as 2 mg (1 mg for each node). The data were tested by Student's *t*-test for statistical significance.

RESULTS

Recovery of Radioactivity From the Injection Site, Popliteal LN, and Blood

Injection site.—The patterns of radioactivity recovered from the feet after injection of free or LE [^{125}I]T$_3$ varied considerably (text-fig. 1A, 1B). Free [^{125}I]T$_3$ was removed rapidly from the injection site; the feet retained only 30% of the label 15 minutes after injection and virtually none 1.5 hours after injection. Half-time of the label removal was estimated to be 10 minutes (text-fig. 1B). LE [^{125}I]T$_3$ remained longer at the injection site; 15 minutes after injection more than 90% of the label was still in the feet and at 1.5 hours as much as 40% of the radioactivity could still be recovered from the injection site. The half-life of the [^{125}I]T$_3$ removal from the feet was 80 minutes (test-fig. 1B).

Popliteal LN.—In mice treated with free [^{125}I]T$_3$, the popliteal LN showed the highest radioactivity (0.24% of the total amount administered) 5 minutes after the injection (text-fig. 2). The radioactivity level subsequently decreased, and it reached the base value at 1.5 hours. In mice inoculated with LE [^{125}I]T$_3$, the radioactivity recovered from the LN 5 minutes after injection was fivefold higher than that in control mice. The level of nodal radioactivity in these mice rose during the next 25 minutes and reached maximum value (1.34% of the injected dose) at 30 minutes. Radioactivity decreased steadily thereafter, and at 3 hours it approached the 0.27% level which was the highest level in controls given free [^{125}I]T$_3$.

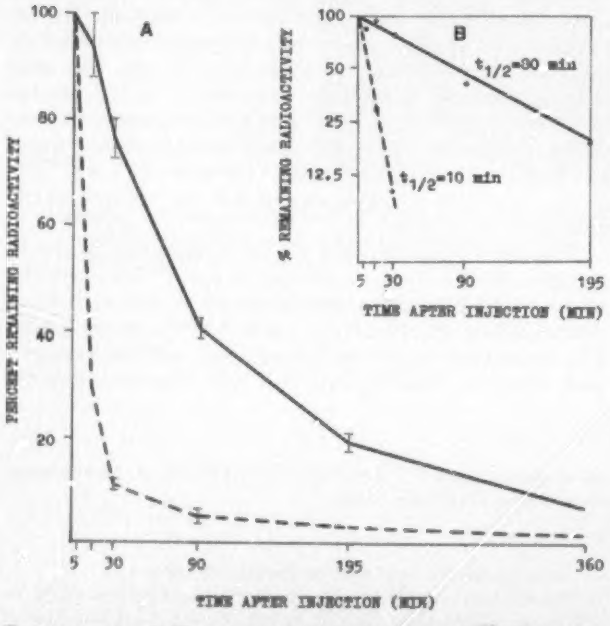

TEXT-FIGURE 1.—A) Time course of the disappearance of [^{125}I]T$_3$ from the injection site. ——, LE [^{125}I]T$_3$; ----, free [^{125}I]T$_3$. A total of 0.05 ml of a liposome suspension containing 6.15×10^{6} cpm [^{125}I]T$_3$/ml or the same amount of free [^{125}I]T$_3$ was injected into each mouse foot. *Each point* represents the sum of counts in both feet (mean ± SE) of 4-6 animals. B) Apparent half-life (t$_{1/2}$) of radioactivity removal from the injection site in experimental and control mice. Values are taken from the experiment presented in A.

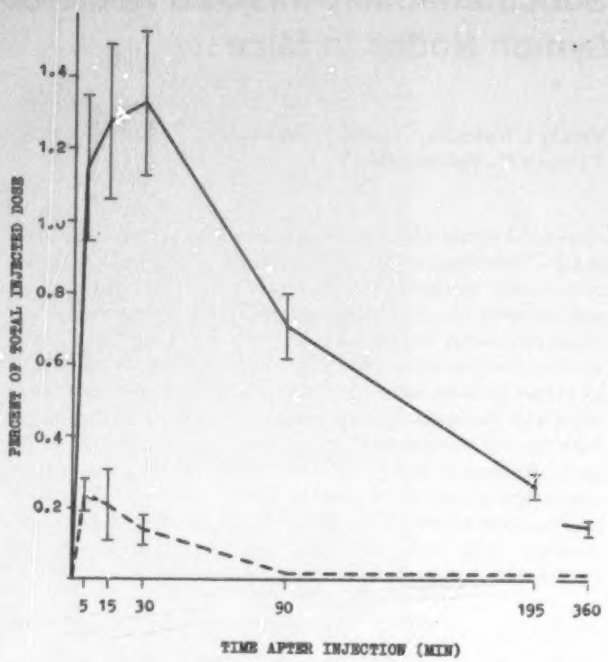

TEXT-FIGURE 2.—Radioactivity recovered from the popliteal LN of mice given sc injections of [^{125}I]T$_3$ into the feet. ——, LE [^{125}I]T$_3$; ----, free [^{125}I]T$_3$. For details *see* text-fig. 1.

Whole blood.—The recovery rates of free or LE [^{125}I]T$_3$ from the whole blood of experimental and control mice are presented in text-figure 3. Radioactivity rapidly appeared in the blood of mice given free [^{125}I]T$_3$. The recovery rate reached a maximum level 15 minutes after injection, but it decreased by half at 3 hours. In contrast, LE [^{125}I]T$_3$ entered the bloodstream much more slowly; however, after it reached a blood radioactivity level of about half of the highest control level, it remained fairly constant throughout the experiment.

Relative Radioactivities in the Blood, Popliteal LN, and Other Organs

Data for radioactivities in the blood, popliteal LN, liver, lungs, and spleen, calculated per gram of tissue (relative radioactivity) at various times after administration of LE or free [^{125}I]T$_3$, are summarized in table 1. The highest level of relative radioactivity was observed in the popliteal LN of mice given LE $[^{125}I]T_3$; for over 3 hours after injection, radioactivity was fivefold to fiftyfold higher than that in any other organs of the experimental or control mice.

Results were significantly different for the group that received free $[^{125}I]T_3$. In this group, the radioactivity of the popliteal LN exceeded that of the blood by eighteenfold at 5 minutes and fivefold at 30 minutes after injection. However, at 1.5 hours, there was no difference in radioactive label concentration between the LN and the blood. Relative radioactivity in the liver, lungs, and spleen was at about the same level as that of the blood. Similarly, in the group given LE $[^{125}I]T_3$, the concentration of the isotope in the organs was not appreciably higher than that in the blood. Thus even in the liver, an organ outstanding in its capacity to sequester liposomes, label concentration was only three to four times higher than that in the blood.

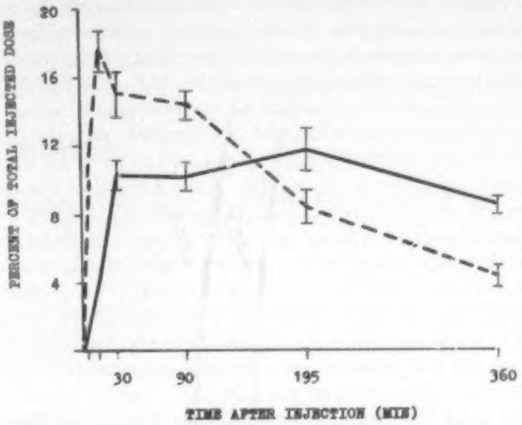

TEXT-FIGURE 3.—Radioactivity recovered from the whole blood of mice after sc injection of $[^{125}I]T_3$ as described in legend of text-fig. 1. ——, LE $[^{125}I]T_3$; ----, free $[^{125}I]T_3$. The experimentally obtained counts were adjusted to 1.6 ml, the average total blood volume of a mouse (7% of body wt.).

DISCUSSION

The results indicate that after sc injection into the feet of mice, free $[^{125}I]T_3$ is rapidly removed from the injected site. The early appearance of radioactivity in the blood indicates that free $[^{125}I]T_3$ passes easily through the capillary walls and is carried away by the bloodstream. A portion of the injected $[^{125}I]T_3$ penetrates the lymphatic capillaries, but because blood flows much faster than lymph, the major bulk of the hormone is removed with the circulating blood and only a small portion passes through the regional LN with the lymph. Thus from 5 to 15 minutes after injection of free $[^{125}I]T_3$, 50% of the isotope was removed from the feet, whereas not more than 0.25% of it was present in the popliteal LN. LE $[^{125}I]T_3$ was removed from the injection site almost tenfold more slowly than the free label. Radioactivity appeared in the blood later and in smaller amounts in these mice than in those given free $[^{125}I]T_3$. In contrast, the label was found early and in high quantities in the draining LN. During the same 10 minutes (5–15 min after injection), in mice given LE $[^{125}I]T_3$, approximately 6% of

TABLE 1.—*Relative radioactivities in the blood, popliteal LN, and other organs of mice given injections of* $[^{125}I]T_3$^{a}

Organ or tissue	$[^{125}I]T_3$	Relative radioactivities at times after injection, min					
		5	15	30	90	195	360
		Radioactivities expressed as cpm×10^3/g of wet tissue, mean ± SE					
Blood	Free	38.6±4.01	66.3±4.97	56.6±4.14	54.3±2.92	32.1±3.84	16.5±1.96
	LE	3.1±0.12^{b}	15.5±2.43^{b}	39.2±2.78^{c}	38.4±2.93^{c}	44.7±4.65	32.2±2.28^{b}
Popliteal LN	Free	726.0±194.00	651.8±306.00	285.5±101.00	55.0±7.05	73.5±36.95	92.6±73.90
	LE	3,543.9±649.10^{c}	3,9389±712.00^{c}	4,107.7±630.80^{b}	2,169.2±286.15^{b}	815.4±92.85^{b}	458.2±39.92^{c}
Liver	Free	—	—	—	67.3±4.95	38.8±4.60	17.3±2.48
	LE	—	—	—	178.8±9.01^{b}	144.0±4.49^{b}	108.8±4.03^{b}
Lungs	Free	—	—	—	55.0±6.40	38.0±8.30	17.1±1.95
	LE	—	—	—	71.8±10.20	52.3±4.49	59.0±4.89^{b}
Spleen	Free	—	—	—	40.4±6.50	29.9±7.10	18.9±[illegible].90
	LE	—	—	—	52.1±1.62	37.8±2.71	37.9±3.45^{d}
		Radioactivities expressed as % of injected dose/g tissue, mean±SE					
Blood	Free	6.3±0.65	10.8±0.81	9.2±0.67	8.8±0.47	5.2±0.62	2.7±0.32
	LE	0.5±0.02^{b}	2.5±0.40^{b}	6.4±0.45^{c}	6.2±0.48^{c}	7.3±0.76	5.2±0.37^{b}
Popliteal LN	Free	118.1±31.54	106.0±49.76	46.4±16.42	8.9±1.15	12.0±6.00	15.1±12.02
	LE	576.2±105.54^{b}	640.5±115.77^{c}	667.9±102.57^{b}	352.7±46.53^{b}	132.6±15.10^{b}	74.5±6.49^{c}
Liver	Free	—	—	—	10.9±0.81	6.3±0.75	2.8±0.40
	LE	—	—	—	29.1±1.46^{b}	23.4±0.73^{b}	17.7±0.66^{b}
Lungs	Free	—	—	—	8.9±1.04	6.2±1.35	2.8±0.32
	LE	—	—	—	11.7±1.66	8.5±0.73	9.6±0.80^{b}
Spleen	Free	—	—	—	6.6±1.06	4.9±1.15	3.1±0.94
	LE	—	—	—	8.5±0.26	6.1±0.44	6.2±0.56^{d}

[a] A total of 0.05 ml of a liposome suspension containing $[^{125}I]T_3$ (6.15×10^6 cpm/ml) or the same amount of free $[^{125}I]T_3$ was injected into each mouse foot in groups of 4–6 mice. —=not measured.

[b] Significantly different from control, $P<0.001$.

[c] Significantly different from control, $P<0.01$.

[d] Significantly different from control, $P<0.05$.

the label was removed and about a quarter of this quantity was recovered from the popliteal LN. At an earlier time 5 minutes after injection, almost half of the isotope removed from the feet was present in the LN. These results, along with data in the literature (*4, 6–8*), demonstrate that liposomes, like particulate matter and colloids (*3*), are absorbed from tissues predominantly, if not exclusively, by lymphatic capillaries rather than by blood capillaries; hence the lymphatic system is presumably the sole pathway through which liposomes are transported from the injection site.

Obviously, the passage of liposomes along this pathway is slow, and their concentration is high as long as they remain at the injection site. Consequently, the high radioactivity recovered from the popliteal LN of mice given injections of LE $[^{125}I]T_3$ might have been due merely to the passage of lymph carrying large amounts of labeled liposomes through the LN. Was this the only reason for the high recovery rate, or were the liposomes in some way retained by the nodes? The observation that the radioactivity level in the LN of mice given LE $[^{125}I]T_3$ kept rising for at least 30 minutes after injection favors the idea of liposome retention. However, as shown in table 1, the group given injections of LE $[^{125}I]T_3$ had more than three times higher radioactivity in the liver compared with that in the blood, whereas the group that received free $[^{125}I]T_3$ exhibited no difference in the relative radioactivities in the liver and blood. The liver is known to be the major organ site where the iv injected liposomes are accumulated (*9, 10*). Hence, although the administration route we employed precluded a direct entry of the liposomes into the blood, a certain proportion of them still gained access to the general circulation. This phenomenon may be attributed either 1) to the ability of a certain proportion of liposomes to pass unhampered through the LN or 2) to the clogging of lymphatic sinuses by liposomal vesicles and the entrance of others into the general circulation through pathways that bypass the obstructed LN.

If the second assumption were true, the relationship between label concentration in the LN and the dose of inoculated liposomes would not be linear. To test this assumption, we performed an experiment in which we injected into the feet of mice a liposome suspension diluted threefold, sixfold, and twelvefold with saline. The radioactivity recovered from the popliteal LN of these mice was directly related to the dose of liposomes injected; as a result, the percentage of radioactivity in the LN was consistently the same at all doses employed (table 2). The results of this experiment indicate that sonicated liposomes do not obstruct mechanically the lymphatic sinuses in the LN. Instead, the movement of the liposomes in the LN is decelerated by the slowing of the lymph flow and by the multiple collisions of liposomal vesicles with the nodal reticulum meshwork. Because there are lymph-borne metastasizing tumor cells anchored in areas where liposomes pass through the LN, contact with these cells is inevitable. Direct contact with tumor cells is crucial for the tumoricidal effectiveness of drug-containing liposomes (*2, 11, 12*).

TABLE 2.—*Radioactivity recovered from the popliteal LN of mice that received different doses of LE $[^{125}I]T_3$ sc in the feet*[a]

Time after injection, min	Percentage of radioactivity recovered after liposome dose of:[b]			
	0.025	0.05	0.1	0.3
15	1.51	1.07	1.01	1.28
30	1.64	1.34	1.66	1.34

[a] Data are expressed as percentage of the injected dose (mean of 4 mice).

[b] Dose is expressed as mg of lipid per mouse.

It was shown that "solid" liposomes, liposomes prepared from lipids whose temperature of phase transition is above body temperature, fuse poorly, if at all, with cells, and the agent encapsulated in them is delivered to the cells mainly by phagocytosis of liposomal vesicles (*13–15*). Solid liposomes presumably can exert an antimetastatic effect on phagocytizing tumor cells only. It is unlikely that the phagocytic activity of tumor cells would be higher than that of macrophages; thus macrophages in the LN should be more vulnerable to the action of solid liposomes than tumor cells. Liposomes prepared from lipids whose point of phase transition is below body temperature ("fluid" liposomes) can fuse with both normal and malignant cells (*13–15*). Consequently, the cytotoxic action of drugs entrapped in fluid liposomes on tumor cells which they encounter as they traverse the lymphatic sinuses is surely not weaker than that exerted on normal cells of the LN.

Both solid and fluid stable liposomes that do not interact with cells in the LN, apparently pass through LN and ultimately enter the bloodstream. Entrance of undegraded liposomes absorbed by lymphatic capillaries from the abdominal cavity into the blood is now well documented (*7, 8*). Hence, when stable liposomes are used as drug vehicles, only a portion of the drug reaching an LN can exert its cytotoxic action. Fluid liposomes from biogenic lipids, which do not contain cholesterol, are unstable in body fluids (*7, 16*). The longer such liposomes stay in an LN, the larger is the number of vesicles destroyed that are not fused with cells and not subjected to phagocytosis; moreover, the released drug has a chance to exert its cytotoxic action in the LN before it enters the general circulation. Therefore, there are grounds for the assumption that it is precisely the unstable fluid liposomes that would affect metastatic growth spreading by the lymphatic pathways more efficiently than the stable liposomes. This phenomenon is apparent when a LE drug is administered directly into a lymphatic vessel. With regard to the local injection of liposomes into tissues, the question may be raised whether unstable liposomes are less effective than stable ones, since a portion of the unstable vesicles is possibly degraded before entering the lymphatic vessels. However, this theory may not be the case: Liposomes devoid of cholesterol are unstable in body fluid only but not in saline (*7*) in which they are suspended and remain long enough at the injection site. Further experiments are needed to clarify this point. Experiments are also needed to determine the differential characteristics of the lymphatic absorption of injected unilamellar and multilamellar liposomes from the tissue and their passage through LN.

Tumor sites are drained by a network of lymphatic vessels and numerous LN, and none is secure against metastatic spread. To be reasonably certain that metastatic spread is prevented, one has to deliver an antitumor agent to each draining LN. In the case of even a superficial cancerous growth (e.g., mammary tumor), the direct administration of an antitumor agent into each lymphatic vessel is a formidable task. It can be done, however, by the local injection of the LE drug into tissues in the region where the tumor is located. The present work, along with results previously published (*4*, *5*), demonstrates that this approach provides a high concentration of the drug in the draining LN and, as has been demonstrated in our previous paper (*2*), a strong antimetastatic action. Our results support the idea that liposomes could be used as vehicles of choice for transport of scintigraphic agents (*4*) and X-ray contrast media to the lymphatic pathways in indirect lymphography.

REFERENCES

(*1*) Kaledin VI, Matienko NA, Budker VG, Nikolin VP, Gruntenko YV. The inhibitory effect of liposome-encapsulated *cis*-diamminedichloroplatinum(II) on tumor metastases in the lymph nodes in mice. Proc Acad Sci USSR 1978; 242:473–476 (in Russian).

(*2*) Kaledin VI, Matienko NA, Nikolin VP, Gruntenko YV, Budker VG. Intralymphatic administration of liposome-encapsulated drugs to mice: Possibility for suppression of the growth of tumor metastases in the lymph nodes. JNCI 1981; 66:881–887.

(*3*) Zhdanov DA. General anatomy and physiology of the lymphatic system. Mikhailov VP, ed. Leningrad: Medgis, 1952:5–42 (in Russian).

(*4*) Richardson VJ, Osborne MP, Jeyasingh K, Ryman BE, Burn J. Differential localization of [^{99m}Tc]technetium-labeled liposomes in normal and tumour-bearing lymph nodes of the rat. Br J Cancer 1978; 38:177.

(*5*) Segal AW, Gregoriadis D, Black CD. Clin Sci Molec Med 1975; 49:99–106 (cited by: Gregoriadis D. Targeting of drugs. Nature 1977; 265:407–411).

(*6*) McDougall IR, Dunnick JK, Goris ML, Kriss JP. In vivo distribution of vesicles loaded with radiopharmaceuticals: A study of different routes of administration. J Nucl Med 1975; 16:488–491.

(*7*) Kirby C, Clarke J, Gregoriadis G. Effect of the cholesterol content of small unilamellar liposomes on their stability in vivo and in vitro. Biochem J 1980; 186:591–598.

(*8*) Parker RJ, Hartman KD, Sieber SM. Lymphatic absorption and tissue disposition of liposome-entrapped [^{14}C]adriamycin following intraperitoneal administration to rats. Cancer Res 1981; 41:1311–1317.

(*9*) Tyrrell DA, Heath TD, Colley CM, Ryman BE. New aspects of liposomes. Biochim Biophys Acta 1976; 457:259–302.

(*10*) Hinkle GH, Born GS, Kessler WV, Shaw SM. Preferential localization of radiolabeled liposomes in liver. J Pharm Sci 1978; 67:795–798.

(*11*) Fendler JH, Romero A. Liposomes as drug carriers. Life Sci 1977; 20:1109–1120.

(*12*) Richardson VJ, Ryman BE, Jewkes RF, Jeyasingh K, Tattersall MN. Tissues distribution and tumor localization of ^{99m}Technetium labeled liposomes in cancer patients. Br J Cancer 1979; 40:35–43.

(*13*) Poste G, Papahadjopoulos D. Lipid vesicles as carriers for introducing materials into cultured cells: Influence of vesicle lipid composition on mechanism(s) of vesicle incorporation into cells. Proc Natl Acad Sci USA 1976; 73:1603–1607.

(*14*) Papahadjopoulos D, Poste G. Studies on membrane fusion with natural and model membranes. Methods Membr Biol 1979; 10:1–121.

(*15*) Margolis LB. Lipid–cell interactions as a model of cellular membrane interactions. In: Turakulov YaKh, ed. Proceedings of the symposium on lipids of biological membranes, Tashkent, U.S.S.R. Oct 15–19, 1980. Tashkent, U.S.S.R.: Uzbek Acad Sci 1980:11–12 (in Russian).

(*16*) Davis C, Gregoriadis G. The effect of lipid composition on the stability of liposomes in vivo. Biochem Soc Trans 1979; 7:680–682.

blank page

Prophylactic and Therapeutic Actions of Supplemental β-Carotene in Mice Inoculated With C3HBA Adenocarcinoma Cells: Lack of Therapeutic Action of Supplemental Ascorbic Acid[1,2,3,4]

Giuseppe Rettura, *Ph.D.*,[5] **Francis Stratford**, *M.D.*,[5] **Stanley M. Levenson**, *M.D.*,[5] *and* **Eli Seifter**, *Ph.D.*[5,6]

ABSTRACT—Decreased tumor incidence, increased latent period, and increased survival time were observed in C3H/HeJ mice fed supplemental β-carotene for 3 days and then inoculated with 10^4 C3HBA (syngeneic) tumor cells. In addition, C3H/HeJ, C3H/He, and CBA/J mice, fed supplemental β-carotene beginning immediately after they were inoculated with 2×10^5 C3HBA tumor cells, showed decreased tumor growth and increased survival time. When β-carotene was fed to mice in which palpable tumors were already present, it similarly slowed tumor growth and extended animal survival time. Ascorbic acid supplementation (5 g/kg diet), introduced into the experiment as a possible synergist for β-carotene's antitumor action, was without therapeutic action when tested in the presence or absence of β-carotene supplements. The basal diet, a standard commercial mouse chow, contains more vitamin A than the National Research Council's recommended dietary allowance for normal rodents and supports normal growth, reproduction, and longevity of normal mice. The work reported here is the first demonstration of the antitumor action of β-carotene in animals with a transplanted tumor.—JNCI 1982; 69:73–77.

Previous work from our laboratory showed that supplemental vitamin A in nontoxic amounts has both tumor preventive and therapeutic actions in C3H and CBA mice inoculated with C3HBA adenocarcinoma cells (*1*, *2*). Additionally, we showed that supplemental vitamin A has similar prophylactic and therapeutic action in two other animal tumor model systems—MuSV and BW10232 (*3*, *4*). Because dietary carotenes are the usual source of vitamin A for herbivores and omnivores such as mice, and because we have shown recently that supplemental β-carotene has marked tumor preventive and therapeutic actions in mice inoculated with an oncogenic virus (M-MuSV), we tested the action of β-carotene in a nonviral transplantable tumor system that responds to vitamin A.

MATERIALS AND METHODS

Animals.—Inbred female C3H/HeJ and male CBA/J mice were obtained at 5 weeks of age from The Jackson Laboratory, Bar Harbor, Maine. Female C3H/He mice of similar age were obtained from the Charles River Breeding Laboratories, Wilmington, Mass. The animals were examined, weighed, and allocated randomly to cages housing 5 mice/cage in a room with a 12-hour day-night cycle, at a temperature of 25°C and relative humidity of about 35%. C3H mice were used in experiments 1, 2, and 5, and CBA mice were used in experiments 3 and 4.

Diets.—In experiments 1 and 2 the mice were maintained on a powdered laboratory chow (Teklad, Inc., Monmouth, Ill.) which served as the basal or control ration. It contains 6,190 IU vitamin A palmitate/kg diet and 4.3 mg β-carotene (equivalent to 7,167 IU vitamin A); the total 13,357-IU/kg diet is well above the National Research Council's recommended dietary allowance of vitamin A, which averages 6,000 IU/kg diet for normal growth, pregnancy, lactation, and longevity of normal rodents. The basal control diet is, therefore, not deficient in vitamin A.

We prepared two experimental diets from the basal diet. One was made by addition of an alcoholic solution of vitamin A palmitate (150,000 IU/kg diet); the other was made by the addition of an alcoholic solution of 90 mg β-carotene/kg diet.

In experiments 3 and 4, in place of Teklad as the control or basal chow, Purina Laboratory Chow (#5001) was used (Ralston Purina Co., St. Louis, Mo.). It contains considerably more vitamin A (15,000 IU/kg) than the Teklad product; in addition, it contains 6.5 mg β-carotene/kg diet.

Tumors.—Adenocarcinoma C3HBA (*5*) was obtained from The Jackson Laboratory as a transplant in young C3H/HeJ female mice. The inocula were prepared from solid tumors 1.2 cm in diameter. The tumor tissue was gently minced in a cold phosphate-buffered saline solution containing penicillin and streptomycin and filtered through a wire screen. The residue was discarded, and the filtrate was centrifuged for 10 minutes at 1,800×*g*. The supernatant was discarded and the precipitate was suspended in cold buffer. To count the viable cells, we stained an aliquot of the suspension with 0.4% trypan blue. The concentration of cells was adjusted with buffer so that a 0.1-ml suspension contained 1×10^6 viable cells. Mice received tumor cells sc in

---

ABBREVIATIONS USED: AA=ascorbic acid; ANOVA=analysis of variance; M-MuSV=Moloney murine sarcoma virus; TD_{50}=minimum inoculum dose required to produce tumors in 50% of the animals; TD_{100}=minimum inoculum dose required to produce tumors in 100% of the animals.

---

[1] Received August 12, 1981; accepted January 28, 1982.

[2] Supported in part by the Army Research contract DADA 17-70-C; by Public Health Service grant 5-K06GM-14208 from the National Institute of General Medical Sciences; and by research funds of the Department of Surgery, Albert Einstein College of Medicine, Yeshiva University, Bronx, N.Y.

[3] Presented in part at the 175th national meeting of the American Chemical Society, Anaheim, Calif., March 13–17 1978, and at the 72d annual meeting of the American Society of Biological Chemists, St. Louis, Mo., May 31–June 4, 1981.

[4] Animals were maintained under the guidelines set forth in the "Guide for the Care and Use of Laboratory Animals" by the Institute of Laboratory Animal Resources, National Research Council.

[5] Department of Surgery, Albert Einstein College of Medicine, Yeshiva University, Bronx, N.Y. 10461.

[6] Department of Biochemistry, Albert Einstein College of Medicine, Yeshiva University.

an area of the nipple line, approximately 1.3 cm above the right inguinal lymph node.

In experiments 1 and 2, female C3H/HeJ mice were used; in experiments 3 and 4, male CBA/J mice were used as recipients. Inocula for these experiments were prepared by passing the C3HBA tumor through CBA hosts, harvesting the tumors, and then preparing the inocula as described above. In experiment 5, we used C3H/He female mice from the Charles River Breeding Laboratories. Inoculation was sc in the outer surface of the thigh.

In all cases inoculum sites were gently palpated daily to determine the date of tumor appearance. After a tumor appeared, its size was estimated daily with the use of a caliper with millimeter divisions. Tumor size was recorded as the average of the major and minor diameters of the generally ovate tumor. Latency was recorded as the number of days required for the development of a palpable tumor. The latent period is a measure of tumor resistance; i.e., the longer the latent period, the more resistant the animal.

Statistical analysis.—We evaluated tumor incidence (frequency) by the chi-square method, tumor size and latent period by Student's *t*-test, and survival time by ANOVA. F-ratios were determined and where warranted, the data were further examined by the Newman-Keuls test to establish the allowable comparisons and the *P*-values for these comparisons.

Experimental design.—Experiment 1 was conducted in the spring of 1979, and its purpose was to study the effect of β-carotene on tumor incidence. For this reason, we used an inoculum size that did not produce tumors in all animals; thus we could detect if a treatment increased or decreased tumor incidence. Earlier we found that the TD_{80} for C3H/HeJ mice was approximately 10^4 cells (*6, 7*) and that some treatments could alter the tumor incidence when inoculated with TD_{80} for controls (*8*). Groups of 10 C3H/HeJ female mice each were fed one of the diets. Group I received the basal or control ration (Teklad). Group II mice received the vitamin A-supplemented diet, and group III mice received the β-carotene-supplemented diet. On the 4th day all mice were inoculated sc with 10^4 C3HBA tumor cells in the nipple line above the right inguinal lymph node.

Experiment 2 was conducted in the spring of 1978. Three groups of 10 C3H/HeJ female mice were established and maintained on the basal chow for 1 week. The mice were then inoculated with 2×10^5 C3HBA tumor cells as described for experiment 1. We used this inoculum ($2\times TD_{100}$) to ensure 100% tumor incidence (*8*); in this way we could study the influence of β-carotene on tumor latent period. Directly after inoculation, mice were fed one of the three Teklad-derived diets as described above.

Experiments 3 and 4 were started in November and December 1980, respectively. In experiment 3, 3 groups of 10 CBA/J male mice maintained on the Purina basal chow were inoculated in the outer aspect of the thigh with 2×10^5 C3HBA tumor cells. When the tumor sizes reached mean diameters of 6.2 mm 13 days later, 1 group of mice was continued on the basal chow, a second group was switched to the vitamin A-supplemented diet, and the third group was switched to the β-carotene-supplemented diet. Groups of mice without tumors were established in experiment 3; because they received the same amounts of vitamin A and β-carotene as did those with tumors, observations could be made on the toxicity of vitamin A and β-carotene over a long time period (*9*).

Experiment 5 was performed in the spring of 1981. Its purpose was to examine the possible effect of a single level of AA supplementation on C3HBA tumor growth and to uncover a possible AA–carotene interaction. Four groups of 10 female C3H/He mice, maintained on Purina Laboratory Chow, were inoculated with 2×10^5 C3HBA tumor cells. When tumor size reached 7.5 mm, the mice were treated with experimental diets as follows: 1 group was continued on the control ration, a second group received the control ration supplemented with β-carotene (90 mg/kg diet), a third group received the control ration supplemented with AA, (5 g/kg diet), and a fourth group received both β-carotene and AA supplements in the amounts described.

RESULTS

Growth and possible vitamin A toxicity.—In experiment 3, mice without tumors have been maintained on vitamin A- and β-carotene supplemented chow for 13 months. During the experimental period, the mice were weighed several times. All groups gained 14 g and the average weight at 13 months was 35±1.3 g. After the animals had been on the diets for 9 months, they were all subjected to diagnostic X-ray to determine if pathologic bone fractures were present.

TABLE 1.—*Effect of supplemental vitamin A and β-carotene on tumor incidence, latent period, and survival time in C3H/HeJ female mice inoculated with 1×10^4 C3HBA tumor cells (Expt 1)*

Group	Diet supplement	Tumor incidence[a]	Latent period, days[b]	Tumor size, mm[c]		Survival time, days[b,c]
				Day 32	Day 46	
I	None	6/10	21.7±3.2	5.0±0.4	13.5±0.5	70.2±4.0
II	Vitamin A 150 IU/g	1/10	28.0	1.0	4.0	120.0
III	β-Carotene 90 mg/kg	2/10	26.5±3.5	1.3±0.2	4.5±0.3	112.5±5.5
		Statistical analysis, *P*-values[d]				
I vs. II		<0.02	NA	NA	NA	NA
I vs. III		<0.05	NS	<0.001	<0.001	<0.006
II vs. III		NS	NA	NA	NA	NA

[a] No. of mice with tumor/no. of mice inoculated. Data were analyzed by the chi-square method.

[b] Values are means ± SE. Latent period and tumor size were analyzed by Student's *t*-test; survival time was analyzed by the ANOVA.

[c] Of the tumor-bearing animals.

[d] NS = not significant ($P>0.05$); NA = not allowable comparison. Mean is absent.

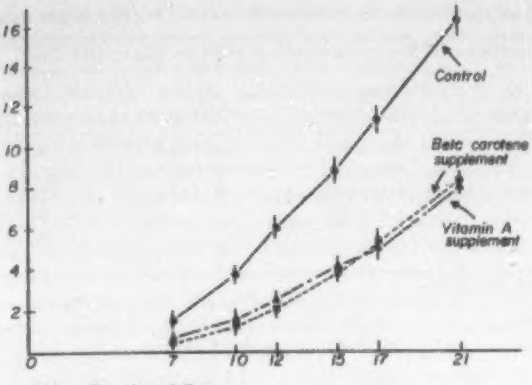

TEXT-FIGURE 1.—Female C3H/HeJ mice were inoculated with 2×10^5 syngeneic C3HBA cells. Feeding of supplemented diets was started several hours after inoculation.

We found no fractures and did not observe difficulty or pain in walking in any animal. Exfoliative or other dermatitis or dermatosis were not noted. Other signs of possible vitamin A toxicity have not, as yet, been explored.

Tumor incidence.—In experiment 1, the only experiment in which we began supplemental β-carotene feeding before tumor inoculation, each supplement decreased tumor incidence in mice inoculated with 1×10^4 tumor cells. There was no statistically significant difference between the effects of vitamin A ($P<0.02$) and β-carotene ($P<0.05$; table 1). All mice in experiments 2–5 developed tumors; thus neither vitamin A nor β-carotene influenced tumor incidence when 2×10^5 tumor cells were inoculated (expt 2).

Latent period.—The latent period for mice inoculated with 1×10^4 tumor cells was 21.7±3.2 days (expt 1), and 6.1±0.4 days for those receiving 2×10^5 cells (expt 2), $P<0.001$. The effect of vitamin A on the latent period for mice receiving 1×10^4 tumor cells could not be determined due to the diminished tumor incidence. Although β-carotene increased the latent period in the same experiment, the differences were not statistically significant. β-Carotene and vitamin A each increased the latent period significantly when the inoculum size was 2×10^5 cells (8.8±0.6 days for β-carotene, 8.9±0.5 for vitamin A vs. 6.1±0.4 for controls; $P<0.001$ for each treatment).

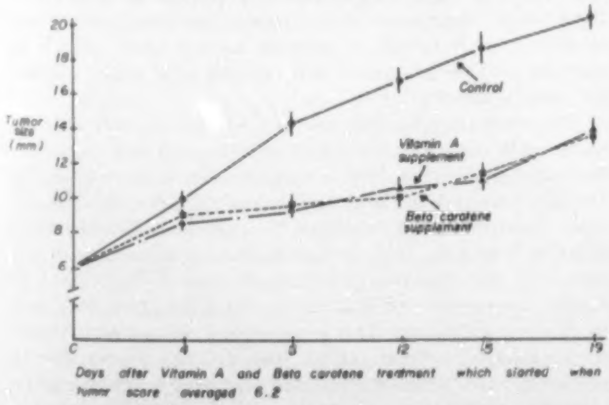

TEXT-FIGURE 2.—Male CBA/J mice were inoculated with 2×10^5 C3HBA tumor cells. Treatments were begun when tumor diameters were 6.2± 0.3 mm (mean ± SE; range=5.5–7.0 mm).

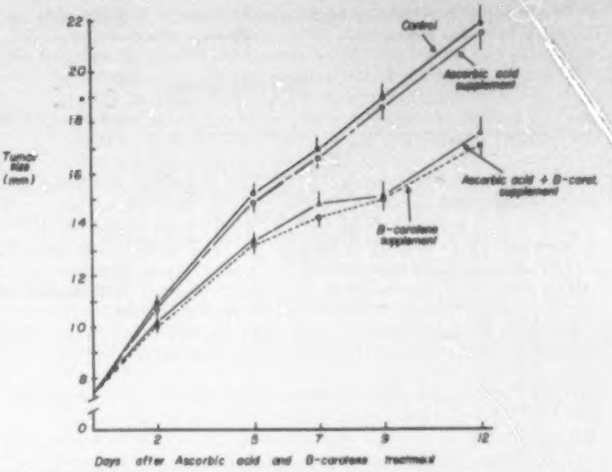

TEXT-FIGURE 3.—Female C3H/He mice were inoculated with 2×10^5 C3HBA tumor cells. Treatments were started when tumor diameters were 7.5±0.2 mm (mean ± SE; range=7.0–8.0 mm).

Tumor growth.—Supplemental β-carotene and vitamin A each slowed tumor growth in all experiments, but neither treatment caused tumor regression. Supplemental ascorbic acid by itself did not influence tumor growth rate, and it did not change the effect of β-carotene supplement. (*See* text-figs. 1–3.)

Survival time.—In all cases, supplemental β-carotene and vitamin A increased survival time significantly (tables 1, 2). This was true for experiments in which the vitamin A supplements were started after tumors were already present (expts 3 and 4) as well as for those in which vitamin A was fed before inoculation (expt 1) or beginning immediately after inoculation (expt 2). Supplemental β-carotene increased survival times to the same degree as did supplemental vitamin A. AA did not increase survival times of control (basal diet) or β-carotene-supplemented tumor-bearing mice.

DISCUSSION

In the present study, C3HBA (The Jackson Laboratory) tumor growth patterns and animal survival times were similar to those in syngeneic C3H/HeJ mice, closely related C3H/He mice, and allogeneic CBA/J mice. The patterns are similar to those we observed earlier in C3H/HeJ mice (*5, 8*). In each experiment supplemental vitamin A or β-carotene showed antitumor activity as measured by increased survival times. In each experiment vitamin A supplementation decreased tumor growth and prolonged survival to a degree previously reported for mice with C3HBA tumors (*10, 11*). The effects of supplemental β-carotene on tumor growth inhibition and increase in survival time were similar to those due to vitamin A.[7] Supplemental AA by

---

[7] The tumor preventive and therapeutic actions of β-carotene in mice inoculated with C3HBA cells were earlier described by us [NIH grant application (E. S.) entitled, "Anti-tumor actions of carotenoids," CA-16818-01A2, 1976].

TABLE 2.—*Effect of supplemental Vitamin A, β-carotene and AA on survival time in mice inoculated with C3HBA tumor cells*

Group	Diet supplement[a]	Survival time in various strains of male or female mice, days[b]			
		Expt 2 C3H/HeJ, ♀	Expt 3 CBA/J, ♂	Expt 4 CBA/J, ♂	Expt 5 C3H/He, ♀
I	None	34.9±1.1	40.0±2.8	41.1±2.5	36.3±1.3
II	Vitamin A, 150 IU/g diet	58.0±3.2	60.3±2.5	60.0±3.0	
III	β-Carotene 90 mg/kg diet	55.6±3.0	59.5±3.0	60.2±2.6	58.5±3.5
IV	AA, 5 g/kg diet				38.1±1.6
V	β-Carotene + AA, as in groups III and IV				56.7±1.5
	Statistical analysis, P-values[c]				
I vs. II		<0.001	<0.001	<0.001	—
I vs. III		<0.001	<0.001	<0.001	<0.001
I vs. IV		—	—	—	NS
II vs. III		NS	NS	NS	—
III vs. IV		—	—	—	<0.001
I vs. V		—	—	—	<0.001
IV vs. V		—	—	—	<0.001

[a] In experiment 2, vitamin A and β-carotene supplements were started immediately after tumor inoculation; in experiment 3, when tumor score averaged 6.2±0.3 mm; in experiment 4, when tumor score averaged 5.7±0.2 mm; and in experiment 5, vitamin A, β-carotene, and AA supplements were begun when tumor score averaged 7.5±0.2.

[b] Values are means ± SE; survival time was analyzed by the ANOVA.

[c] —=comparison could not be made.

itself did not influence tumor growth or animal survival, and it did not modify the antitumor action of supplemental β-carotene.

The basis of the anti-C3HBA tumor action of supplemental vitamin A has not been established. We have suggested that vitamin A influences host responses that limit tumor growth; at the dose we have used, vitamin A is not cytotoxic. We showed that this level of supplemental vitamin A stimulates immune responses in mice. The responses include *a*) lymphopoiesis (*12, 13*), thymopoiesis (*14, 15*), enhancement of allograft skin rejection (*16, 17*), and enhancement of antiviral host reactions directed against M-MuSV (*3*) or pox virus (*18*). It is a significant finding that supplemental vitamin A can stimulate these immune-related phenomena in animals that show depressed immune function due to tumor disease (*16*), chemical toxicity, or physical injury (*19*). Although differences in the effects of supplemental vitamin A and β-carotene on C3HBA tumor growth are not evident in our experiments, the data do not permit us to determine if the actions of β-carotene reported in this paper require that it be converted to vitamin A; the experiments were not designed to adduce this specific point. Supplemental β-carotene was as active as supplemental vitamin A in inhibiting tumor growth, which suggests either that 1) β-carotene need not be converted to vitamin A for this activity or that 2) the mouse is able to convert a sufficient portion of the β-carotene supplement to obtain a vitamin A-like antitumor response. This phenomenon has been discussed elsewhere (*19, 20*). Similarly, we have discussed the significance of the longer time required for dietary β-carotene to become liver vitamin A for tumor prevention and therapy (*19*).

In previous studies we used some graded doses of vitamin A (*21*) and found that a 150,000-IU/kg diet gives reproducible results and, in the time intervals we use, no discernible toxicity. Earlier in this discussion, we suggested that the antitumor action of vitamin A is not dependent on cytotoxicity against either the tumor or the host; i.e., vitamin A was not present under conditions that caused a decrease in tumor size or weight loss of the host. Vitamin A, in doses that cause lysosomal labilization, may be used under conditions (>350,000 IU/kg diet) that cause tumor regression; however, in our experience, these doses also cause weight loss and toxicity.

We considered the possibility that the C3HBA tumor-preventive action of β-carotene and vitamin A observed in experiments 1 and 2 is related to the effects of these compounds or that of their metabolites on maintenance of epithelial differentiation. If this were so, *all-trans*-retinoic acid (which promotes epithelial differentiation) would inhibit C3HBA tumorigenesis as it does in 7,12-dimethylbenz[*a*]anthracene tumorigenesis (*22*). However, we found that levels of retinoic acid that do not influence weight changes (10 mg/kg diet) do not alter C3HBA tumor incidence at the TD_{50}; larger amounts of retinoic acid cause both weight depression and increased tumor frequency and growth rate. Vitamin A protects against this toxicity of retinoic acid, which shows that retinoic acid toxicity is not vitamin A toxicity.

The results suggest that there are at least two mechanisms involved in the antitumor action of vitamin A and, therefore, in that of β-carotene. One of these mechanisms involves the role of vitamin A in the promotion of epithelial differentiation. This role can be fulfilled by chemicals lacking other vitamin A activity, such as reproduction or sense perception However, the other role of vitamin A (and of β-carotene) in tumor prevention and therapy involves lymphopoiesis and immune mechanisms. This requirement, in our experience, is not fulfilled by compounds that are not convertible to retinol in vivo. Although retinoic acid may stimulate an in vitro killer cell activity against tumor cells (*23*), the relevance of this action to the inhibition of tumor growth in vivo is highly questionable.

We examined the influence of supplemental AA in this system because of the current interest in a possible antitumor action of AA in C3H mice (*24*) and because we have considered a possible role for AA in the metabolism of *β*-carotene. AA was postulated by us (*20*) to be a cofactor for the dioxygenase enzyme that converts *β*-carotene to vitamin A (*25*). If this theory is correct, under some conditions dietary AA could promote the conversion of *β*-carotene to vitamin A. If the antitumor action of *β*-carotene were dependent on its conversion to vitamin A, dietary AA might contribute to the antitumor action of *β*-carotene. In the present experiments the inactivity of AA does not exclude the possibility that under certain conditions it has a tumor chemotherapeutic action, particularly in animals that require AA, such as guinea pigs or in mice that were fed an inhibitor of AA biosynthesis, e.g., lycorine.

REFERENCES

(*1*) Rettura G, Schittek A, Hardy M, Levenson SM, Demetriou A, Seifter E. *Brief communication:* Anti-tumor action of vitamin A in mice inoculated with adenocarcinoma cells. J Natl Cancer Inst 1975; 54:1489–1491.

(*2*) Seifter E, Rettura G, Stratford F, Goodwin P, Padawer J, Levenson SM. Supplemental vitamin A (A) and *β*-carotene (B): Suppression of C3HBA tumor growth following local X-irradiation. The 182nd national meeting of the American Chemical Society, Division of Medicinal Chemistry, New York, Aug 23–28, 1981. Abstract #93.

(*3*) Seifter E, Zisblatt M, Levine N, Rettura G. Inhibitory action of vitamin A on a murine sarcoma. Life Sci 1973; 13:945–951.

(*4*) Rettura G, Wolfe ES, Seifter E. Inhibition of BW10232 breast cancer growth by supplemental vitamin A. Fed Proc 1980; 39:1117.

(*5*) Seifter E, Rettura G, Stratford F, et al. Vitamin A inhibits some aspects of systemic disease due to local X-radiation. JPEN 1981; 5:288–294.

(*6*) Rettura G, Sarkar D, Padawer J, Levenson SM, Seifter E. Inhibition of tumor growth by metyrapone and deoxycorticosterone. Surg Forum 1976; 27:152–154.

(*7*) Seifter E, Rettura G, Levenson SM. Decreased resistance of C3H/HeHa mice to C3HBA tumor transplants: Increased resistance due to supplemental vitamin A. JNCI 1981; 67:467–472.

(*8*) Seifter E, Critselis A, Levenson SM, Rettura G. Effect of metyrapone and aminoglutethimide on the murine sarcoma (MuSV-M) and breast adenocarcinoma (C3HBA). J Surg Oncol 1979; 12:281–288.

(*9*) Seifter E, Rettura G, Stratford F, Goodwin P, Levenson SM. Supplemental *β*-carotene and vitamin A improve the anti-tumor response to radiation and chemotherapy. International Symposium on Carotenoids, July 26–31, 1981, Liverpool, England. Abstract.

(*10*) Rettura G, Barbul A, Levenson SM, Seifter E. Tumor excision and vitamin A supplementation increase survival of mice with C3H breast adenocarcinoma. Surg Forum 1978; 29:170–172.

(*11*) Lan S, Rettura G, Levenson SM, Richardson D, Seifter E. Paraneoplastic neutrophilia: Response to local tumor excision and vitamin A. Surg Forum 1980; 31:420–421.

(*12*) Barbul A, Thysen B, Rettura G, Levenson SM, Seifter E. White cell involvement in the inflammatory wound healing and immune actions of vitamin A. JPEN 1978; 2:129–140.

(*13*) Seifter E, Barbul A, Levenson SM, Rettura G. Lymphopoietic action of vitamin A in tumor bearing mice. Fed Proc 1978; 37:335.

(*14*) Seifter E, Rettura G, Seifter J, Davidson H, Levenson SM. Thymotropic action of vitamin A. Fed Proc 1973; 32:947.

(*15*) Seifter E, Rettura G. Vitamin A in animal tumor therapy: Adrenolytic, thymotropic and lymphopoietic actions. Cancer Cytology 1977; 17:22.

(*16*) Rettura G, Levenson SM, Schittek A, Seifter E. Vitamin A action on oncogenesis and graft rejection. Surg Forum 1975; 26:301–303.

(*17*) Seifter E, Hardy M, Levenson SM, Rettura G. Enhanced graft rejection due to vitamin A. The 5th International Congress of The Transplantation Society, Jerusalem, Israel, Aug 25–30, 1974. Abstract.

(*18*) Seifter E, Rettura G, Padawer J, Demetriou AA, Levenson S. Antipyretic and antiviral action of vitamin A in Moloney sarcoma virus- and poxvirus-inoculated mice. J Natl Cancer Inst 1976; 57:355–359.

(*19*) Seifter E, Rettura G, Levenson SM. Carotenoids and cell-mediated immune responses. In: Charalambous G, Inglett GE eds. Quality of food and beverages. Academic Press, New York, 1981:335–347.

(*20*) Seifter E. Ascorbic acid-beta carotene interactions: Hypothesis. The 181st national meeting of the American Chemical Society, Division of Biological Chemistry, Minneapolis, Minn. Aug 30–Sept 3, 1981.

(*21*) Seifter E, Padawer J, Dattner A, Levenson SM, Rettura G. Vitamin A alters adrenal and thymus responses in stressed mice. The 172nd national meeting of the American Chemical Society, Division of Agricultural and Food Chemistry, San Francisco, Calif. Aug 25–Sept 3, 1976.

(*22*) Bollag W, Matter A. From vitamin A to retinoids in experimental and clinical oncology: Achievements, failures, and outlook. In: DeLuca L, Shapiro SS, eds. Modulation of cellular interactions by vitamin A and derivatives (retinoids). The New York Academy of Sciences, New York, 1981:9–23.

(*23*) Lotan R. Effect of vitamin A and its analogs (retinoids) on normal and neoplastic cells. Biochim Biophys Acta 1980; 605:33–91.

(*24*) Sun M. At long last, Linus Pauling lands NCI grant. Science 1981; 212:1126–1127.

(*25*) Olson JA, Hayaishi O. The enzymatic cleavage of beta-carotene into vitamin A by soluble enzymes of rat liver and intestine. Proc Natl Acad Sci USA 1965; 54:1364–1370.

blank page

Flow Cytometric Analysis of R3327 Rat Prostate Adenocarcinoma Grown In Vivo and In Vitro[1,2,3]

Alice J. Claflin,[4] **Alan Pollack,**[4,5] **Theodore Malinin,**[4] **Norman L. Block,**[5,6] *and* **George L. Irvin**[4,5,7]

ABSTRACT—The Dunning R3327 transplantable prostate adenocarcinoma in the Copenhagen rat is an acceptable model for the human disease. The G-subline (a rapidly growing carcinoma) and the H-subline (a slow-growing, well-differentiated adenocarcinoma) represent the extremes of differentiation and growth rate of this tumor. Both sublines were found to have one population that was diploid and a second aneuploid population that was hyperdiploid in DNA content. The percentage of hyperdiploid cells was significantly higher in R3327-G tumors than in R3327-H tumors. The tumor cell population ratios were stable in vivo, but the in vitro culture conditions supported only cells with diploid DNA content following four to five subcultures. These predominantly diploid cultured cells, when injected into intact male rats, resulted in tumors that had both diploid and aneuploid cells.—JNCI 1982; 69:79–87.

The utilization of animal models of human disease often permits a more precise investigation than is possible with human subjects. The Dunning R3327 transplantable prostate adenocarcinoma is an acceptable model for this disease, with the same diversity as that of the disease in humans in relation to growth rate, cellular variation, differentiation, and response to a variety of therapeutic modalities (*1–4*). The tumor subline designated R3327-G is a rapidly growing, poorly differentiated, androgen-dependent carcinoma. The R3327-H tumor subline grows slowly and is well differentiated and androgen-dependent.

We have previously shown that the response of the poorly differentiated R3327-G subline to endocrine manipulation is reflected in population shifts as identified by FCM (*5–7*). The ratio of the number of hyperdiploid cells to the total number of cells (diploid + hyperdiploid) was used successfully to predict response to therapy. The proportion of hyperdiploid cells was chosen because in R3327-G tumors there appeared to be two proliferating cell types, of which one population was aneuploid (3.2C in G_0+G_1 phase). The possibility that two distinct cell populations with potentially different rates of proliferation coexist in a transplantable tumor prompted the following investigation.

In this communication we established that both R3327-G and R3327-H tumors contained two proliferating cell populations. Each subline consisted of one cell population with normal rat DNA content per cell (diploid) and 42 chromosomes, whereas the other was near-tetraploid and aneuploid in DNA content (hyperdiploid in G_0+G_1 phase). Thus the ratio of hyperdiploid to the total cell population (percent hyperdiploid) by FCM reflects the proportion of aneuploid cells in the tumors. The percentage of hyperdiploid cells was found to be significantly higher in R3327-G tumors than in R3327-H tumors. To investigate the mechanisms of in vivo coexistence and stability of two proliferating tumor subpopulations (diploid and aneuploid), we used cell culture techniques. We observed that aneuploid cell proliferation was limited in vitro. The following report is a systematic investigation of these in vitro changes by FCM.

MATERIALS AND METHODS

Cell culture.—Solid tumors (R3327-G and R3327-H), grown in male COP × F344 rats, were enzymatically dispersed to single cells as previously described (*2*). The tissue was minced and placed in trypsinization flasks with enzyme solution consisting of 0.25% trypsin, 0.02% EDTA, and 1,300 U collagenase/ml in PBS; the mixture was stirred at room temperature and the supernatant decanted at 20-minute intervals. Enzyme activity was reduced by the addition of cold CMRL-1415 medium (GIBCO, Grand Island, N.Y.) containing 10% calf serum. The cells were washed once, resuspended, and counted, and viability was determined by trypan blue exclusion. Approximately 10^6 dispersed tumor cells were seeded into 75-cm^2 plastic tissue culture flasks. Medium consisted of CMRL-1415 containing 2.0 mg $NaHCO_3$/ml, 100 U penicillin/ml, 100 µg streptomycin/ml, and 10% (vol/vol) newborn bovine serum. The flasks were gassed with 10% CO_2 in air to adjust the pH, caps were tightened, and the flasks were placed in a 37°C incubator. The medium was changed 1 day later and thereafter twice a week. The cells were subcultured at confluence (5–7 days) by treatment with 0.25% trypsin and 0.02% EDTA in PBS. The detached cells were washed and counted, and the flasks were reseeded with approximately 10^5 cells. The cultured

---

ABBREVIATIONS USED: CMRL=Connaught Medical Research Laboratories (Toronto, Canada); FCM=flow cytometric DNA histogram analysis (analyses); PBS=phosphate-buffered saline.

---

[1] Received August 20, 1981; accepted February 5, 1982.

[2] Supported by Public Health Service National Prostatic Cancer Project R26CA-21696-03 of the National Cancer Institute; by Federal grant #4321-001 from the Veterans Administration; by the Weeks Endowment Fund, Department of Urology, University of Miami School of Medicine; and by the Surgical Scholarship Fund of the Department of Surgery, University of Miami School of Medicine.

[3] Animals were maintained under the guidelines set forth in the "Guide for the Care and Use of Laboratory Animals" by the Institute of Laboratory Animal Resources, National Research Council.

[4] Department of Surgery, University of Miami School of Medicine, P.O. Box 016960, Miami, Fla. 33101.

[5] Veterans Administration Medical Center, Miami, Fla. 33125.

[6] Department of Urology, University of Miami School of Medicine.

[7] We thank Mercedes Fuentes, Richard M. Lipton, Anthony Risso, Sheila Long, and Teresa Garcia-Pons for their excellent technical assistance. We are also grateful to Marcelino Obaya for the illustrations and to Coulter Electronics Inc. (Hialeah, Fla.) for their support.

tumor cells were harvested by enzyme treatment and washed, and viability was determined. Cultured cells were injected sc with 10^7 viable cells per injection site.

Preparation of cells for karyotype determination.—The trypsin-dispersed tumor cells at their first subculture were seeded into 75-cm^2 plastic tissue culture flasks at a concentration of 1.5×10^5/ml (3×10^6/flask). After 24 hours in culture, 0.5 ml of 0.5 μg/ml vinblastine sulfate (Velban; Eli Lilly & Co., Indianapolis, Ind.) was added to each flask. The cells were incubated overnight in the presence of vinblastine sulfate and harvested by trypsinization. The cells were washed and suspended slowly in 5 ml of hypotonic solution (1 part fetal bovine serum:6.5 parts distilled water). The cells were incubated at 37°C for 17 minutes, and four to five drops of fixative (1 part glacial acetic acid:3 parts methanol) were added. The cells were washed once in freshly prepared fixative, and the slides were prepared. The cells were stained with Gurr Giemsa (Searle Diagnostics, High Wycombe, Bucks, England). Ten cells from the G-tumor and 12 cells from the H-tumor were analyzed.

FCM.—Solid tumor tissue or aliquots of 10^6 cells from each subculture were monitored by FCM for changes in ploidy. Small pieces of solid tumor tissue were frozen in teasing buffer [0.1 *M* Trizma Base, 5 ml/liter 37% HCl, and 0.08 *M* NaCl (pH 7.4)] as described previously (*5–8*). The tissue was thawed, teased in 0.5 ml of teasing buffer, and filtered through 60-μm nylon mesh. The suspension was diluted in 3.5 ml of staining solution (0.01 *M* Trizma Base, 700 U RNase 1-A/liter, 0.1% Nonidet P40, 10 m*M* NaCl, and 7.5×10^{-5} *M* propidium iodide). The concentrations of fluorescent nuclei were quantitated with the use of a hemacytometer in a fluorescence microscope. The nuclei were further diluted to a concentration of $1–2\times10^5$/ml and stored overnight at 4°C before they were run on the flow cytometer (TPS-1; Coulter Electronics Inc.). Since propidium iodide fluorescence is proportional to double-stranded nucleic acid (*9*) and measurements were made on isolated nuclei in the presence of RNase, the resulting fluorescence was proportional to DNA content. All DNA histograms were obtained with the use of a TPS-1 flow cytometer (Coulter Electronics Inc.). Those DNA histograms that were analyzed were smoothed, and the 2C peak was translocated to channel 25 (*10*). We obtained the percentage of hyperdiploid cells by summing the number of particles between 20 and 95 and multiplying the sum by 100 (*5, 7, 8*).

Two types of standards were used in the FCM. Rat spleen was prepared in the same manner as the tumor cells for use as an external 2C standard. At the beginning of each series of samples run on the cytometer, the spleen standard was positioned on channel 25. Periodically, between tumor samples, the rat spleen standard was analyzed to ensure that no fluctuation had occurred. Also, mixing experiments were performed, whereby the rat spleen standard was mixed with the tumor sample to further confirm the position of the diploid cells. In some of the samples, an internal fluorescent microsphere standard was included (1/8 brights; Coulter Electronics Inc.). These fluorescent microspheres were included to monitor changes in the coefficient of variation that might occur as a consequence of instrumentation (e.g., partial clogs) or staining problems.

RESULTS

Histology

Histologic examination of the tumor resulting from R3327-H cultured cells demonstrated a well-differentiated adenocarcinoma consisting of irregularly arranged glandular structures composed of multilayered uniformly appearing epithelial cells (fig. 1). Histologic examination of the tumor resulting from R3327-G cultured cells demonstrated a tumor composed of densely packed primitive cells in disarray and numerous blood vessels throughout (fig. 2). Histologically, the tumors resulting from cultured cells were not different from the tumor of origin.

FCM of R3327-H and R3327-G Tumors In Vivo

FCM of R3327-H and R3327-G tumors showed that both contained major hyperdiploid (greater than 2C) peaks characteristic of aneuploid G_0+G_1 cells (text-fig. 1). The hyperdiploid peak was at 3.2C for R3327-G tumors and 2.8C for R3327-H tumors. Along with this difference in peak position, there were more hyperdiploid cells in poorly differentiated R3327-G tumors than in well-differentiated R3327-

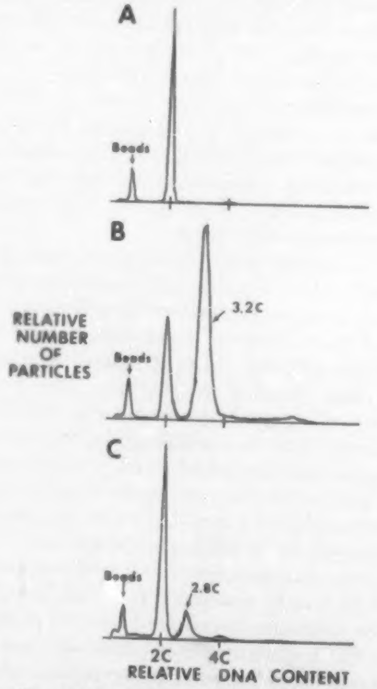

TEXT-FIGURE 1.—Representative flow cytometric DNA histograms of normal rat spleen cells (A), R3327-G rat prostate adenocarcinoma cells (B), and R3327-H cells (C). *Ordinate* represents relative number of particles, and the *abscissa* represents relative fluorescence intensity. Since the fluorochrome used was propidium iodide, fluorescence intensity is proportional to relative DNA content. The smaller peaks *to the left* (marked *beads*) are from 1/8 bright fluorescent microspheres (Coulter Electronics Inc.) that were added as an internal standard. The labels 2C and 4C mark the positions where diploid and tetraploid cells would be located, respectively. The R3327-G tumor (B) was harvested at day 50, and the R3327-H tumor (C) was harvested at day 100.

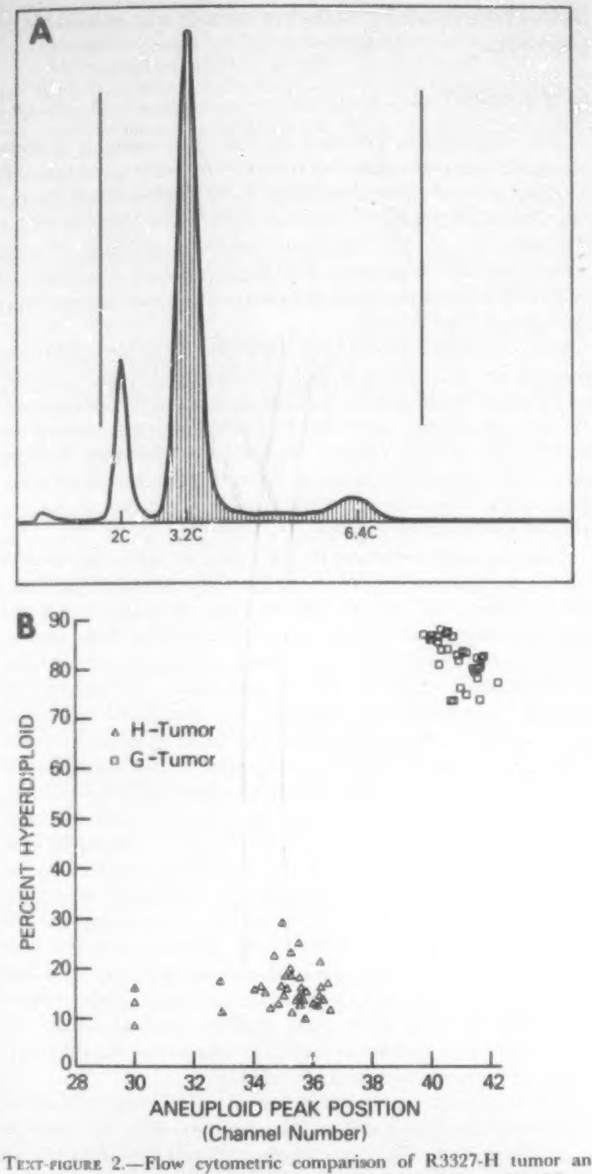

TEXT-FIGURE 2.—Flow cytometric comparison of R3327-H tumor and R3327-G tumor grown in intact male rats for 3–6 mo and 1–2.5 mo, respectively. Multiple pieces from 10 R3327-H tumors and 25 R3327-G tumors were analyzed. Each histogram was smoothed, the diploid peak translocated to channel 25 (*2*), the percentage of hyperdiploid cells calculated, and the aneuploid peak position determined. Panel A illustrates the areas used for the percent hyperdiploid calculation [the number of cells in the *shaded area* was divided by the number of cells between the *vertical lines* (*5, 7*)]. The results are displayed in panel B. In those histograms in which the computer could not find an aneuploid peak, the aneuploid peak position was said to be located at channel 30. R3327-G tumors had an average of 81.6%±4.7 (1 SD) hyperdiploid cells, and R3327-H tumors had an average of 16.4%±4.3 ($P<0.001$).

H tumors. These differences are shown quantitatively in text-figure 2. The two tumor sublines were found to be significantly different from each other ($P<0.001$) both in terms of the proportion of hyperdiploid cells and the position of the aneuploid G_0+G_1 peak. R3327-G tumors had an average of 81.6% hyperdiploid cells as compared to 16.4% for R3327-H tumors. We have shown previously that in R3327-G tumors the proportion of hyperdiploid cells remains relatively constant throughout the life of the tumor (*8*). Multiple biopsies of both tumor sublines showed that the R3327-G tumor has less variability than the R3327-H. When R3327-H tumors were left in vivo for 3–4 months, they frequently became multilobed, consisting of higher proportions of aneuploid cells in some sections as opposed to others. In some sections, detectable numbers of aneuploid R3327-H cells were lacking altogether.

FCM of R3327-G and R3327-H Tumor Cells In Vitro

The proliferation of enzyme-dispersed R3327-G and R3327-H tumor cells was further studied in cell culture by FCM. Text-figure 3B shows that when R3327-G cells were first subcultured (following 5 days of cell culture), the aneuploid population predominated. Although there were more aneuploid cells present at the first subculture, the proportion of proliferating aneuploid cells could not be determined by FCM alone. In fact, there were very few cells in aneuploid S-phase (approximately 3.4C to 6.2C). In subsequent passages the proportion of diploid cells increased such that by the fourth to fifth subculture (text-fig. 3E) no aneuploid cells were detectable by FCM. This decrease in the proportion of aneuploid cells to undetectable levels occurred in the absence of any change in ploidy. The aneuploid G_0+G_1 was located at approximately 3.2C, even when the proportion of aneuploid was less than 25% (text-fig. 3D). Chromosome analysis of vinblastine sulfate-blocked R3327-G cells in passages 4–5 in cell culture confirmed the

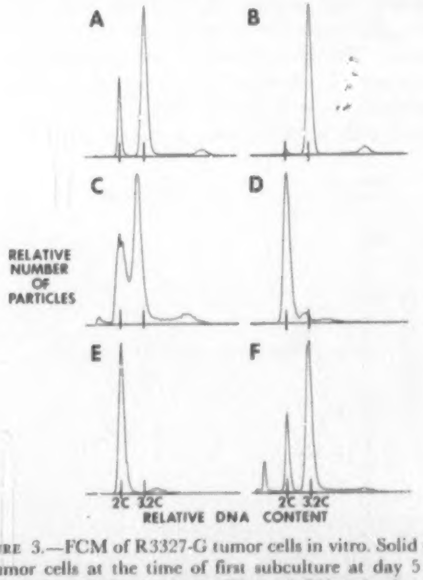

TEXT-FIGURE 3.—FCM of R3327-G tumor cells in vitro. Solid tumor tissue (A). Tumor cells at the time of first subculture at day 5 (B), second subculture (C), third subculture (D), and fifth subculture (E). Solid tissue from tumor that resulted from injected culture cells at the fifth subculture (F). *Small peak to the left of the 2C position in panel F* is from 1/8 bright fluorescent microspheres (Coulter Electronics Inc.) that were used as an internal standard.

FCM in that no aneuploid cells were found. The average chromosome number of these cells was always close to the normal somatic cell average of 42. The karyotype of these predominantly diploid cultured cells was similar to that of the diploid cultured cells at the first subculture.

The addition of 1–5 µg testosterone (Sigma Chemical Co., St. Louis, Mo.) in the culture media had no significant effect on the loss of the aneuploid population in vitro. The sc injection of these predominantly diploid cells into male rats gave rise to tumors that were palpable in the same amount of time as tumor cells that had not been cultured in vitro. Also, the tumors resulting from predominantly diploid cultured cells contained a large proportion of aneuploid cells, typical of tumors originating from an in vivo transfer (text-fig. 3F). These data suggest that *a*) diploid cells may give rise to aneuploid cells or *b*) aneuploid cells were present in vitro in small, undetectable numbers. In either case, the proportion of aneuploid cells returned to its usually high level (80–90%) and stabilized. This stability in the ratio of diploid to aneuploid tumor cells in vivo has been demonstrated previously (*8*).

Enzyme-dispersed R3327-H cells behaved like R3327-G cells in vitro. The aneuploid population in this case was lost more rapidly (one to two subcultures) and returned when predominantly diploid cells from the fourth to the fifth passage in vitro were implanted sc in intact male rats.

Chromosome Distribution

The diploid chromosome number of the normal rat is 42 with 20 autosome pairs, which consist of 7 pairs of metacentric, 9 pairs of telocentric, and 4 pairs of subtelocentric. The diploid and aneuploid cells of R3327-G tumors in metaphase at the time of the first subculture are shown in figures 3 and 4, respectively; the average diploid cell had 41.8 chromosomes per cell, while the average aneuploid cell had 77.9 chromosomes. The average R3327-H tumor diploid cell had 42.4 chromosomes, whereas the average aneuploid cell had 82.2 chromosomes (text-fig. 4). The proportions of diploid to aneuploid cells in text-figure 4 should not be compared, since a higher number of diploid spreads was acceptable for counting.

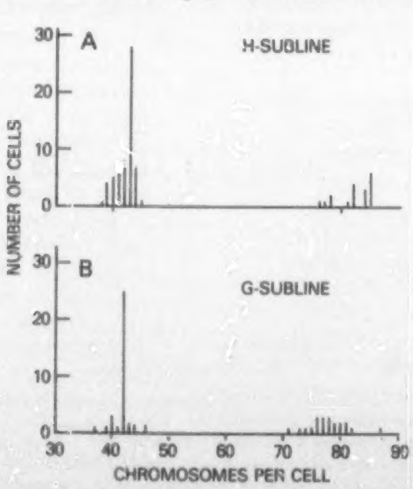

TEXT-FIGURE 4.—Distribution of the number of chromosomes per cell in R3327-G and R3327-H tumors.

DISCUSSION

The relationship between altered chromosomes and the change of normal cells to cancer cells remains an enigma. In human prostate carcinoma it has been observed that increasing anaplasia parallels the increasing occurrence of hyperdiploid cells (*11*, *12*). Our tumor model parallels the human disease in that anaplastic R3327-G has 80% hyperdiploid cells. Conversely, the well-differentiated H-subline has many fewer hyperdiploid cells.

We have shown that under the in vitro culture conditions selected for the growth of the diploid populations in the G- and H-sublines of the R-3327 rat prostate adenocarcinoma, the aneuploid cells appeared to proliferate only during the first 5 days of cell culture. Subsequent passages in vitro eventually resulted in a loss of detectable numbers of aneuploid cells. Thus the aneuploid cells appeared to have a limited proliferative capacity in vitro.

This disparity between in vivo and in vitro cell growth has been reported by others (*13*, *14*). Cells with increased DNA content do not appear to arise de novo under the condition described, and the apparent stability of the diploid cell in vitro reported here is striking. Implantation of these predominantly diploid cells sc into male rats resulted in tumors containing both diploid and aneuploid cells. The tumor growth rate and the ratio of diploid to aneuploid cells were the same as those for tumors from in vivo transplanted tumor cells. The selection of diploid tumor cells in vitro was, therefore, completely reversed by implantation in vivo. These data suggest that some factor(s) were missing in vitro which were *a*) necessary for the extended proliferation of aneuploid cells or *b*) necessary for the transition of diploid cells into aneuploid cells. In the former case, aneuploid cell proliferation would be reduced to undetectable levels in vitro. In the latter case, the proliferative capacity (number of cell divisions) of the aneuploid population is assumed to be limited in vivo or in vitro and the rate at which the transition from diploid to aneuploid occurred would determine the ratio of diploid to aneuploid.

It is doubtful that testosterone is solely responsible for sustaining aneuploid cell proliferation in vivo, since testosterone had little effect on aneuploid cell proliferation in vitro. We have recently reported that although a reduction in serum androgen levels affected an increase in the ratio of diploid to aneuploid cells, the proportion of aneuploid cells was reduced but not eliminated (*5*, *8*). Some other environmental factor(s) appear necessary to sustain aneuploid proliferation in vitro. In light of the results reported here, the constancy in the ratio of diploid to aneuploid tumor cells in vivo probably depends on several environmental conditions. Should these conditions be identified and characterized, our ability to limit aneuploid cell proliferation might be greatly enhanced.

REFERENCES

(*1*) DUNNING WF. Prostate cancer in the rat. Natl Cancer Inst Monogr 1963; 12:341–369.

(2) Claflin AJ, McKinney EC, Fletcher MA. Dunning R3327 prostate adenocarcinoma in the Fischer-Copenhagen F_1 rat: A useful model for immunologic studies. Oncology 1977; 34:105–109.

(3) Block NL, Camuzzi F, Stover B, Claflin AJ, Troner M, Politano VA. Further experience with chemotherapy in the Dunning prostatic adenocarcinoma. Trans Am Assoc Genitourin Surg 1979; 70:57–59.

(4) Smolev JK, Heston WD, Scott WW, Coffey DS. Characterization of the Dunning R3327 H rat prostatic adenocarcinoma: An appropriate model for prostatic cancer. Cancer Chemother Rep 1977; 61:273–287.

(5) Pollack A, Bagwell CB, Block NL, Irvin GL, Claflin AJ, Stover B. Flow cytometric analysis of the response of the R3327 G rat prostatic adenocarcinoma to endocrine manipulation. J Surg Oncol. In press.

(6) Bagwell CB, Block NL, Irvin GL. Flow cytometric monitoring of prostatic carcinoma. Surg Forum 1979; 30:556–557.

(7) Collins JM, Bagwell CB, Block NL, Cliflin AJ, Pollack A, Stover B. Flow cytometric monitoring of R3327 rat prostate carcinomas. Invest Urol 1981; 19:8–13.

(8) Pollack A, Irvin GL, Block NL, Lipton RM, Stover BJ, Claflin AJ. Hormone sensitivity of the R3327 G rat prostate adenocarcinoma. Growth rate, flow cytometry and hormone receptors. Cancer Res. In press.

(9) Lepecq JB, Paoletti C. A fluorescent complex between ethidium bromide and nucleic acids. Physical-chemical characterizations. J Mol Biol 1967; 27:87–106.

(10) Bagwell CB, Hudson JL, Irvin GL. Nonparametric flow cytometry analysis. J Histochem Cytochem 1979; 27:293–296.

(11) Bichel P, Frederiksen P, Kjear TB, Thommesen P, Vinvelov LL. Flow microfluorometry and transrectal fine needle biopsy in the classification of human prostatic carcinoma. Cancer 1977; 40:1206–1211.

(12) Ronstrom L, Tribukait B, Esposti PL. DNA pattern and cytological findings in the fine-needle aspirates of untreated prostatic tumors. A flow cytometric study. Prostate 1981; 2:79–88.

(13) Krishan A, Raychaudhuri R, Flowers A. Karyotype studies on human leukemic lymphoblasts in vitro and as serial transplants in neonatal Syrian hamsters. J Natl Cancer Inst 1969; 43:1203–1214.

(14) Kawamoto K, Herz F, Wolley RC, Hirano A, Koss LG. Flow cytometric analysis of the DNA content in cultured human brain tumor cells. Virchows Arch [Cell Pathol] 1980; 35:11–17.

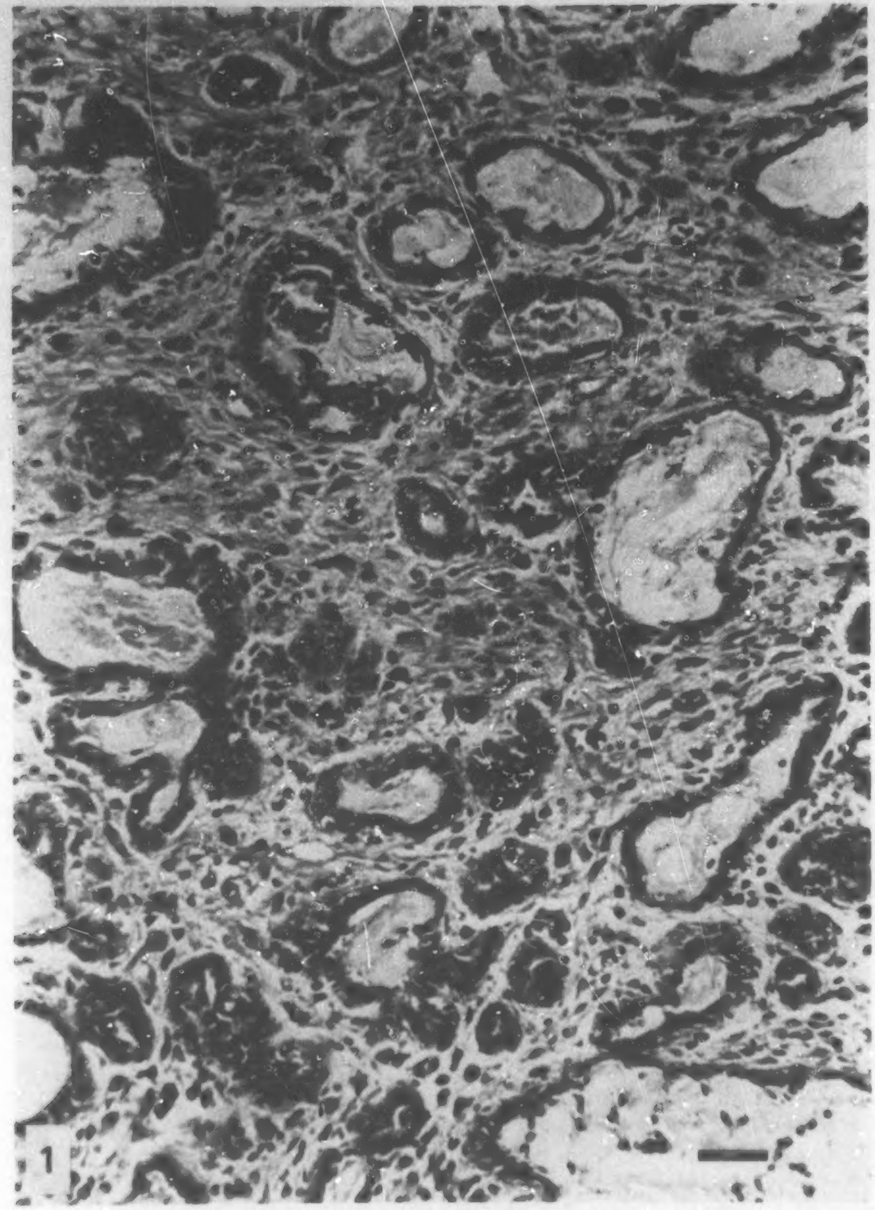

FIGURE 1.—Histology of the well-differentiated R3327-H subline consisting of irregularly arranged glandular structures composed of multilayered conglomerates of uniformly appearing epithelial cells. Hematoxylin and eosin. *Bar*=50 µm. × 200.

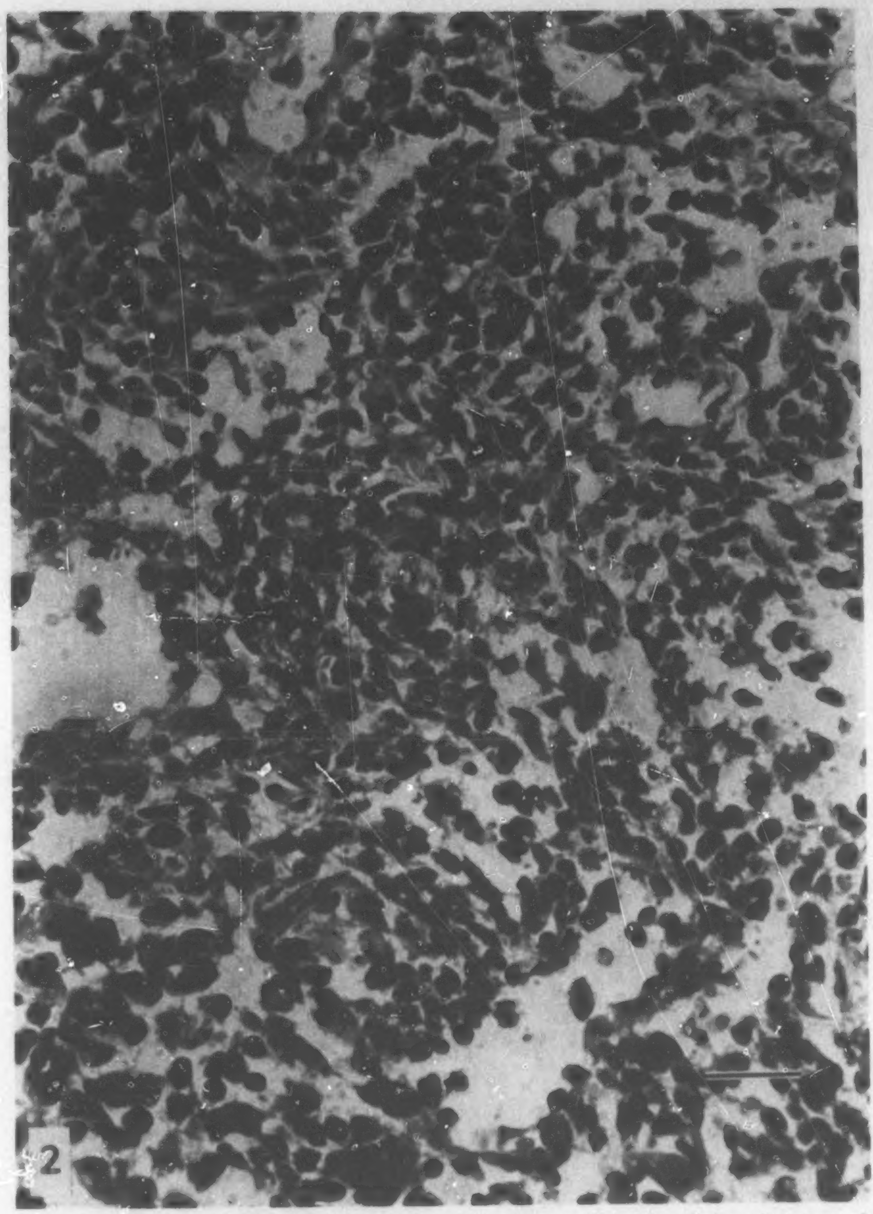

FIGURE 2.—Histology of the poorly differentiated R3327-G subline consisting of densely packed primitive cells in various stages of disarray, with numerous blood vessels throughout the tumor. Hematoxylin and eosin. *Bar*=50 µm. × 350.

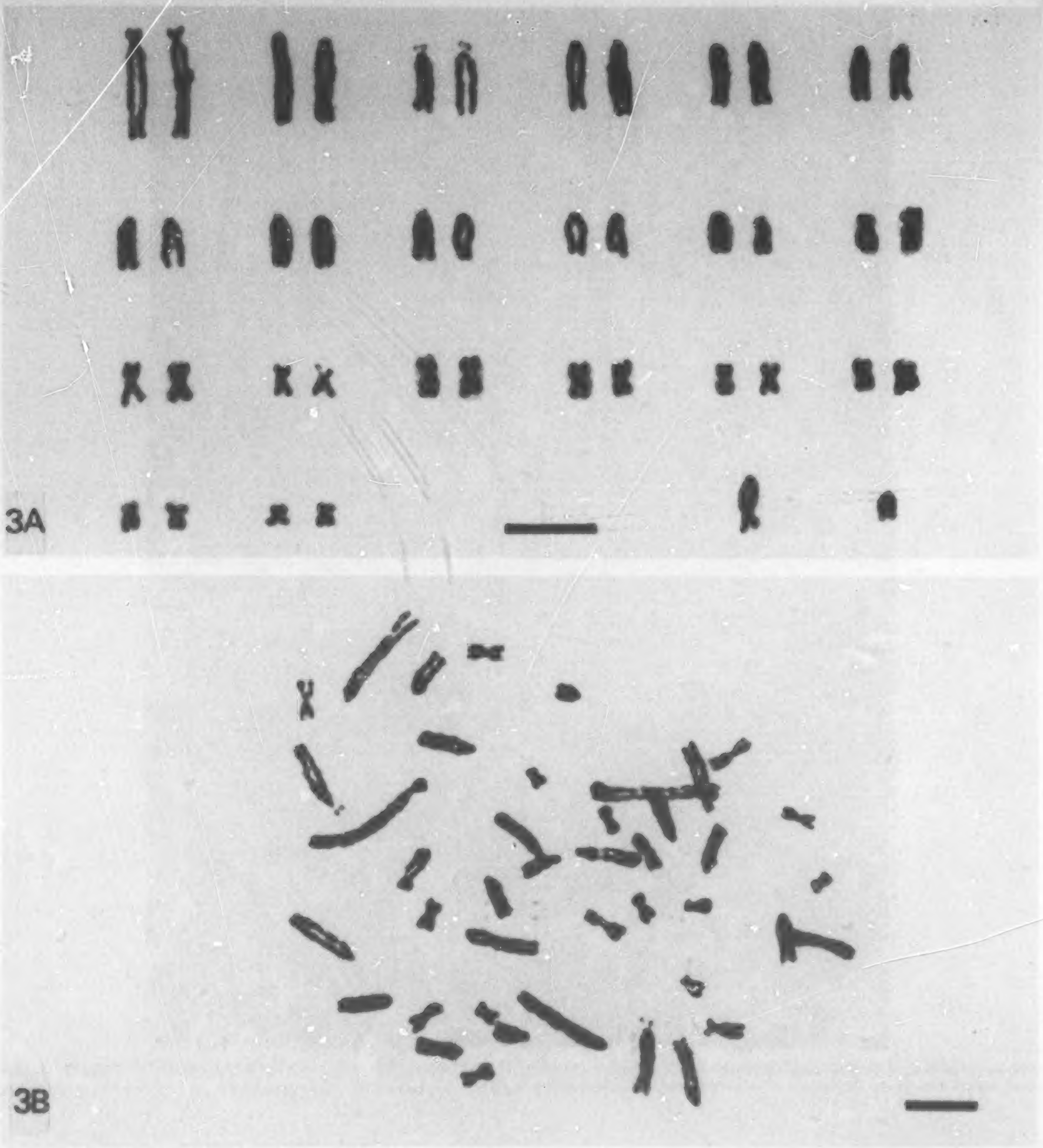

FIGURE 3.—Karyotype (A) and metaphase (B) of R3327-G diploid tumor cell with 42 chromosomes. Cells were treated with vinblastine sulfate at the first subculture. *Bars*=10 µm. × 1,500 (A); × 1,200 (B).

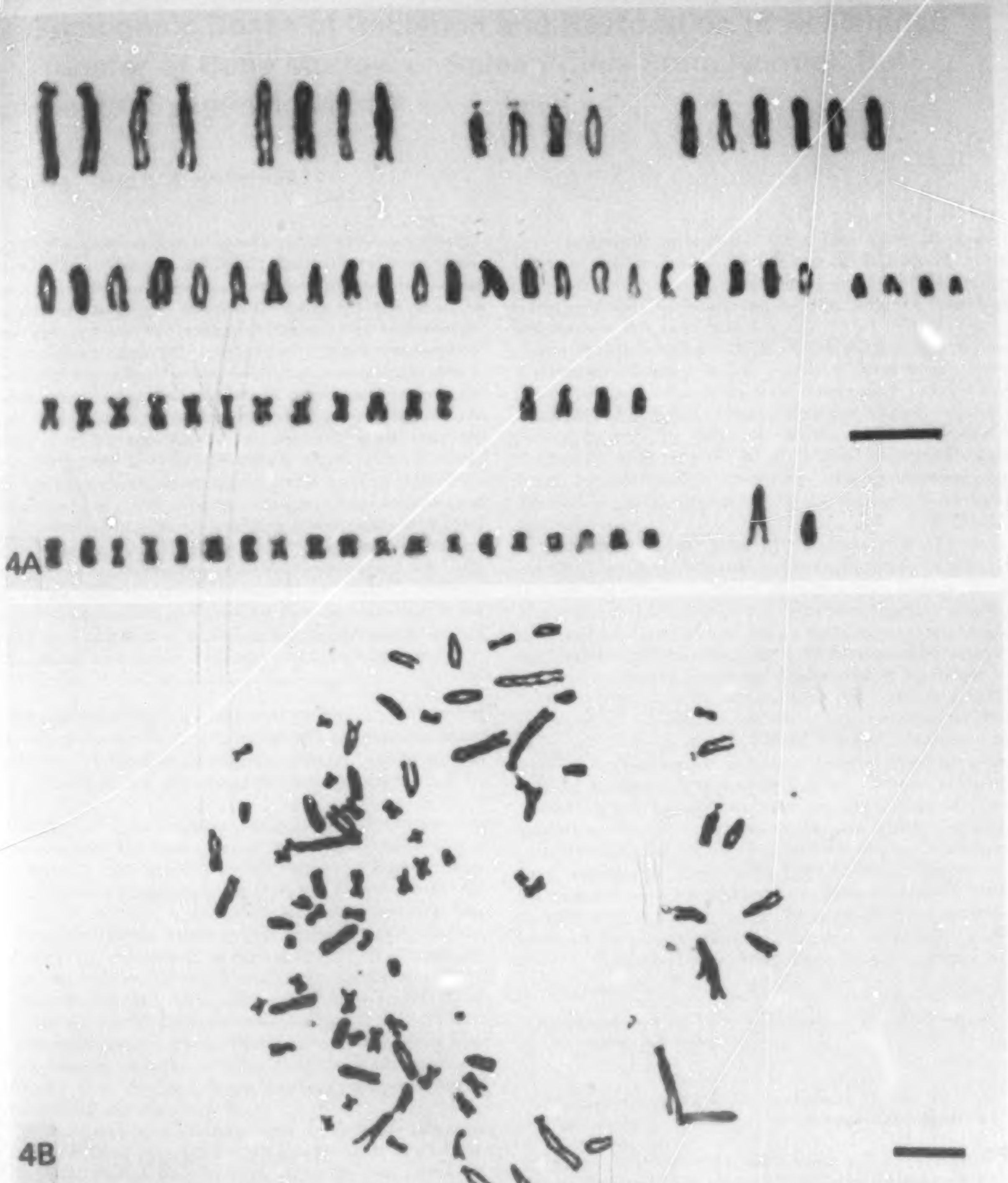

FIGURE 4.—Karyotype (A) and metaphase (B) of R3327-G hyperdiploid cells with 81 chromosomes. *Bars*=10 µm. × 1,500 (A); × 1,200 (B).

best copy available

blank page

Depression of Natural Antitumor Resistance of C57BL/6 Mice by Leukemogenic Doses of Radiation and Restoration of Resistance by Transfer of Bone Marrow or Spleen Cells From Normal, But Not Beige, Syngeneic Mice[1,2]

E. Gorelik[3,4] *and* **R. B. Herberman**[3,5]

ABSTRACT—Small fractionated doses of radiation (4 weekly doses of 179 rad) induced leukemia in 93% of C57BL/6J mice. These leukemogenic doses of radiation were associated with suppression of natural killer (NK) cell activity, as assessed in vitro by cytotoxic activity of spleen cells or in vivo by the ability of irradiated mice to eliminate iv inoculated radiolabeled YAC-1 lymphoma cells. This suppressive effect of irradiation was profound and prolonged, being detectable for at least 7 weeks after the last dose of radiation. NK reactivity of irradiated C57BL/6 +/+ or C57BL/6 beige mice could be reconstituted by iv transfer of 10×10^6 bone marrow cells or 50×10^6 spleen cells from normal C57BL/6 mice. In contrast, transfer of bone marrow or spleen cells from beige donors did not change the NK reactivity of irradiated C57BL/6 +/+ or C57BL/6 *bg/bg* recipients. It was also shown that the irradiation protocol did not eliminate potentially reactive NK cells, because following interferon incubation (10^3 U/ml), the NK activity of spleen cells of irradiated mice was substantially increased. This study supports the hypothesis of an important role for NK cells in radiation-induced leukemogenesis and forms the basis for exploration of the needed, more direct data on the effects of reconstitution of NK activity on subsequent development of tumors.—JNCI 1982; 69:89–93.

The concept of natural antitumor resistance predicts that NK cells and other natural effector cells play an important role in the elimination of malignant cells and can be considered as the first line of defense in immune surveillance (*1*, *2*).

Despite the attractiveness of this hypothesis, actual documentation of the participation of natural cell-mediated immunity in the prevention of primary spontaneous or induced carcinogenesis has been difficult. Experimental support for this concept would come from data showing that carcinogenic factors suppress NK reactivity and, further, that selective restoration of this reactivity in carcinogen-treated animals would interfere with carcinogenesis.

There already are a few pieces of evidence in this direction. Certain carcinogenic factors (irradiation, 7,12-dimethylbenz[*a*]anthracene, and urethan), in addition to their ability to suppress specific humoral and/or T-cell-mediated immunity, have also been shown to strongly suppress natural cell-mediated immunity (*3–5*).

The investigations on the suppressive effects of irradiation of NK cells have been performed mainly with single, relatively high (lethal or sublethal) doses of radiation. NK activity has usually been found to be relatively radioresistant, with little or no effect immediately or at 1 day after treatment (*3*, *6*). However, by 2 weeks after sublethal irradiation, NK activity of spleen cells dramatically declined (*3*). Transfer of normal bone marrow cells not only may protect mice from the lethal effects of irradiation but also may reconstitute their NK activity. The degree of reconstitution of NK reactivity has been found to depend on the genotype of the bone marrow donors, with high NK activity transferred only by bone marrow cells obtained from high NK-reactive strains of mice (*7*).

Bone marrow cells of C57BL/6J beige mice, which have a selective deficiency in NK reactivity, have been able to reconstitute several immunologic functions in lethally irradiated mice but failed to reconstitute the NK activity in the recipients (*8*). The doses of radiation and schedules of irradiation used in most of the above investigations are lethal. It is still unclear whether a carcinogenic schedule of irradiation can be suppressive for the natural cell-mediated immunity.

Small fractionated doses of radiation (160–170 rad, 4 weekly doses) have been shown to be particularly effective in inducing a high incidence of thymic lymphomas (*9*, *10*). It was found that transfer of normal bone marrow or spleen cells into mice treated with such a leukemogenic schedule of irradiation could strongly inhibit the development of tumors (*9*, *10*), but the mechanism of this protection is unclear.

In the present study, we analyzed the depression of NK reactivity of C57BL/6 mice by a leukemogenic schedule (179 rad, 4 weekly doses) of irradiation and examined the ability of transplanted syngeneic bone marrow or spleen cells to reconstitute their NK activity. This experimental model was particularly attractive because it allowed a comparison of the effects of transferred bone marrow or spleen cells from normal C57BL/6 mice with those of transferred bone marrow or spleen cells from C57BL/6 beige mice. Reconstitution of NK activity by cells from normal C57BL/6 mice and not from beige mice would provide strong evidence for a direct radiation-induced impairment in NK cells or their stem cells rather than for the presence of a

---

ABBREVIATIONS USED: CRA=^{51}Cr release assay; E:T=effector-to-target cell; IFN=interferon; NK=natural killer.

---

[1] Received August 21, 1981; accepted February 9, 1982.

[2] Animals were maintained under the guidelines set forth by the National Cancer Institute.

[3] Laboratory of Immunodiagnosis, Division of Cancer Biology and Diagnosis, National Cancer Institute (NCI), National Institutes of Health, Public Health Service, U.S. Department of Health and Human Services, Bethesda, Md. 20205.

[4] *Present address:* Surgery Branch, Division of Cancer Treatment, NCI.

[5] *Address reprint requests to* Dr. Herberman at his *present address:* NCI-Frederick Cancer Research Facility, Building 560, Room 31-93, Frederick, Md. 21701.

suppressive environment that inhibits the expression of NK cells. Furthermore, such findings should indicate the usefulness of this model for assessment of the role of NK cells in prevention of radiation-induced leukemogenesis.

MATERIALS AND METHODS

Mice.—C57BL/6J +/+ and C57BL/6J *bg/bg* mice were obtained from The Jackson Laboratory, Bar Harbor, Maine, at 3.5 weeks of age.

Tumor cells.—YAC-1, a tissue culture cell line of a Moloney virus-induced lymphoma of A/Sn origin, was used as target cells. This culture cell line was maintained in RPMI-1640 medium supplemented with 10% fetal bovine serum, 2 m*M* glutamine, 25 m*M* HEPES,[6] 50 μg gentamicin, and 100 μg penicillin and streptomycin (hereafter referred to as "complete medium").

Irradiation.—Whole-body irradiation was performed with the use of a cesium-137 source of irradiation. Gammacell 40, manufactured by Atomic Energy of Canada Limited, Ottawa, Canada, was used as the irradiation unit. The irradiation was started when the mice were 28±3 days old. Whole-body radiation at a dose of 179 rad (138 rad/min) was applied four times at weekly intervals.

Bone marrow or spleen cell reconstitution.—One or 2 days after the last dose of radiation, the mice were given iv 10×10^6 bone marrow cells or 50×10^6 spleen cells from nonirradiated 2- to 3-month-old C57BL/6 +/+ or C57BL/6 beige mouse donors.

CRA.—At different times after the last dose of radiation, 3–4 mice from every experimental group were killed, and spleen cell suspensions were prepared (*5*). YAC-1 cells, at 1×10^7 in 1 ml of RPMI-1640 medium, were incubated for 1 hour at 37°C with 200 μCi of $Na^{51}CrO_4$ (sp act, 1 mCi/mmol; Radiochemical Centre, Amersham, Buckinghamshire, England).

In some experiments tumor cells were labeled with ^{111}InOx according to the method of Wiltrout et al. (*11*). The relatively low level of spontaneous release of radioactivity from the ^{111}InOx-labeled tumor cells permitted the use of these cells in long-term cytotoxicity assays. YAC-1 cells, 10^7/ml, were incubated with 10 μCi ^{111}InOx for 10 minutes at room temperature in complete medium. After three washes, tumor cells were resuspended at 1×10^5/ml. Cytotoxic activity of the spleen cells was analyzed in a microcytotoxicity assay.

^{51}Cr-labeled tumor cells (5×10^3) were incubated with various concentrations of effector cells (ranging from 200:1 to 23:1 E:T ratios) in quadruplicate in microtiter plates (Linbro Scientific Inc., Hamden, Conn.) for 4 hours at 37°C. ^{111}InOx-labeled cells (5×10^3) were incubated with spleen cells for 16 hours. The supernatants were collected with the use of a Skatron Titertek rapid-harvesting system (Flow Laboratories, Inc., Rockville, Md.). The percent cytotoxicity was calculated (*5*). The differences between the means were consistently found to be significant ($P<0.05$) when $\Delta m_1 - m_2$ was more than 2 SD (or 4 SE) of m_1 or m_2.

IFN boosting of NK reactivity of spleen cells of the recipients.—Spleen cells (10^7) were obtained from mice at 4 weeks after the last dose of radiation and were incubated for 16 hours at 37°C with murine IFN (10^3 U/ml) in complete medium. Partially purified IFN (4.4×10^7 U/mg protein) was obtained from the late Dr. K. Paucker, the Medical College of Pennsylvania, Philadelphia, Pa. After incubation, cells were washed twice and tested in a 4-hour CRA against YAC-1 target cells.

In vivo cytotoxicity assay.—In vivo natural antitumor resistance was assessed by a modification of the method previously described (*12*). We found that the kinetics of clearance from the lungs of [^{125}I]deoxyuridine- and ^{51}Cr-labeled YAC-1 cells was identical, and in the present study ^{51}Cr-labeled YAC-1 cells (1×10^6/0.5 ml) were inoculated iv into the tail veins of mice at various times after the last dose of radiation. The level of radioactivity remaining in the lungs at 3 hours after tumor cell inoculation was measured in a gamma scintillation counter.

RESULTS

Irradiation with 179 rad weekly four times induced thymic lymphomas in 93% of irradiated C57BL/6 mice. The results presented in table 1 indicated that this irradiation schedule substantially depressed the NK activity of spleen cells. Even 4 weeks following the last dose of radiation, the cytotoxic activity of spleen cells was still depressed. After iv inoculation of 10×10^6 bone marrow cells of C57BL/6 +/+ mice into irradiated mice, the NK activity of spleen cells was significantly increased, although it did not reach the levels observed in nonirradiated C57BL/6 mice (table 1). Transfer of bone marrow cells from beige mice had little, if any, effect on the NK activity of spleen cells against YAC-1 cells. This evaluation of the effect of irradiation on NK activity of spleen cells had some limitations, since this activity is age-dependent. Spleen cells of mice develop cytotoxic activity at 3–4 weeks of age, their activity reaches a peak at 6–8 weeks, and then it declines to low levels (*1*). In our experiments, mice were irradiated between 4 and 8 weeks of age, and when NK activity was to be assessed 2–4 weeks later, the mice were already 10–12 weeks old. This probably explains the relatively low cytotoxicity by spleen cells of untreated C57BL/6 mice, which is slightly increased in the 16-hour cytotoxicity assay. Nevertheless, in all experiments performed, the pattern shown in table 1 was reproducible (e.g., *see* data in subsequent tables). One week following transfer of bone marrow cells from C57BL/6 +/+ mice, no reconstitution of splenic NK activity was seen (data not shown). Only after 2 weeks did the NK activity of these mice significantly increase.

To assess more precisely in vivo the NK reactivity of irradiated mice, we analyzed their ability to eliminate iv inoculated radiolabeled YAC-1 cells from the lungs. Elimination of radiolabeled YAC-1 cells from the lungs was significantly depressed in irradiated mice, with almost three times more cells remaining at 3 hours than in the lungs of nonirradiated control mice (table 1). After transfer of bone marrow cells from C57BL/6 +/+ mice, the ability to eliminate tumor cells from the lungs was considerably higher than it was in irradiated mice and was similar to that in

---

[6] 4-(2-Hydroxyethyl)-1-piperazine ethanesulfonic acid.

Table 1.—*Effect of irradiation on NK activity and on in vivo natural antitumor resistance of C57BL/6 mice and attempts to reconstitute these activities by transfer of bone marrow cells from normal or beige C57BL/6 mice*

Treatment[a]	Cytotoxicity at E:T ratio (±SE), %			cpm remaining in lungs (±SE)[b]	Radioactivity remaining in lungs, %
	100:1	33:1	11:1		
None	14.9 (0.6)	8.1 (0.8)	4.2 (0.2)	5,725 (406)	5
Irradiated, 179 rad four times	2.9 (0.3)	0.3 (0.3)	−0.2 (0.3)	15,544 (1,632)	13.7
Irradiated+BM +/+	9.4 (0.7)	4.7 (0.3)	2.0 (0.5)	7,389 (487)	6.5
Irradiated+BM *bg/bg*	5.8 (0.3)	2.1 (0.4)	0.3 (0.2)	14,042 (1,324)	12.4

[a] Mice were irradiated (179 rad) weekly for 4 wk. One day following the last dose (at 7 wk of age), mice were inoculated iv with 10×10^6 of bone marrow (BM) cells from normal C57BL/6 or beige mice. Four weeks later (at 11 wk of age) the cytotoxic activity of their spleen cells was tested in a 16-hr assay against ^{111}InOx-labeled YAC-1 cells, and clearance of radiolabeled tumor cells from the lungs was also evaluated.

[b] 0.5×10^6 ^{51}Cr-labeled YAC-1 cells were inoculated iv, and the level of radioactivity remaining in the lungs was determined 3 hr later. The number of radiolabeled YAC-1 cells in the lungs at 10 min following inoculation was the same in all groups of mice tested.

normal control C57BL/6 mice (table 1). In contrast, bone marrow cells from beige donors failed to restore the antitumor resistance of irradiated C57BL/6 mice. In the next series of experiments, beige mice also were irradiated and transplanted with bone marrow cells (table 2). In comparison with normal C57BL/6 mice, nonirradiated beige mice had a lower ability to destroy YAC-1 cells in vitro or in vivo. However, as previously reported (*13*), beige mice were not completely deficient in natural cytototoxic function, since after irradiation (179 rad four times) their ability to eliminate tumor cells after iv inoculation was further diminished (table 2). Also, by comparison of the natural antitumor resistance of irradiated C57BL/6 +/+ and C57BL/6 *bg/bg* mice, it appears that the schedule of irradiation did not suppress completely the antitumor activity in C57BL/6 +/+ mice, because their reactivity was still significantly greater than that of irradiated C57BL/6 beige mice (table 2).

Transfer of bone marrow cells of C57BL/6 +/+ mice into irradiated beige mice reconstituted the cytotoxic reactivity of these mice to levels above those of nonirradiated beige mice and close to, but not identical with, those in nonirradiated C57BL/6 +/+ mice. In contrast, transfer of bone marrow cells from beige donors did not significantly change the NK reactivity of irradiated C57BL/6 +/+ or C57BL/6 *bg/bg* recipients.

The weight of the thymus in irradiated mice was lower than that in nonirradiated mice (table 2). In irradiated and reconstituted mice the weight of the thymus was even higher than that in nonirradiated C57BL/6 +/+ or C57BL/6 *bg/bg* mice. Bone marrow of normal C57BL/6 +/+ and C57BL/6 *bg/bg* mice was equally efficient in the reconstitution of thymus weight in irradiated mice (table 2).

Transfer of spleen cells (50×10^6) gave results quite similar to those produced by bone marrow cells. Spleen cells from C57BL/6 +/+ mice, but not from C57BL/6 *bg/bg* mice, were efficient in the reconstitution of natural antitumor resistance of irradiated C57BL/6 +/+ or C57BL/6 *bg/bg* mice (table 3).

Thus our data indicate that small fractionated doses of radiation, a schedule that has been repeatedly shown to be strongly leukemogenic for C57BL/6 mice, substantially inhibit the natural cytotoxic reactivity of these mice. Even at 7 weeks following irradiation, the natural antitumor resistance of irradiated C57BL/6 +/+ or beige mice did not return to the levels of nonirradiated mice (table 3).

Although fractionated doses of radiation (179 rad four times) inhibited spontaneous NK reactivity, the treated mice still had IFN-responsive pre-NK cells. After 16 hours of incubation of their spleen cells with IFN (10^3 U/ml), NK activity dramatically increased (table 4). However, the levels of reactivity of spleen cells from irradiated mice did not reach those of IFN-treated spleen cells from nonirradiated

Table 2.—*Natural cell-mediated immunity of irradiated C57BL/6 +/+ and C57BL/6 beige mice inoculated with bone marrow cells*

Mice	Treatment[a]		Weight, mg of thymus (±SE)	In vitro cytotoxic activity of spleen cells at E:T ratio of 100:1 (±SE)[b]	In vivo elimination of radiolabeled YAC cells[c]	
	Irradiation, 179 rad four times	BM cell transplantation, 10^7			cpm remaining in lungs (±SE)	Radioactivity remaining in lungs, %
C57BL/6	−	—	65 (2)	8.4 (0.6)	9,291 (1,415)	5.4
C57BL/6	+	—	50 (5)	1.3 (0.5)	30,265 (3,197)	17.7
C57BL/6	+	Normal	114 (4)	4.6 (0.3)	8,537 (1,490)	5.0
C57BL/6	+	Beige	109 (4)	2.4 (0.5)	23,967 (2,679)	14.0
Beige	−	—	77 (3)	2.4 (0.9)	28,765 (3,847)	16.8
Beige	+	—	55 (5)	1.6 (1.0)	55,029 (5,811)	32.1
Beige	+	Normal	120 (4)	5.1 (0.9)	14,602 (961)	8.5
Beige	+	Beige	113 (5)	2.6 (0.5)	45,207 (7,249)	26.3

[a] +=irradiation; −=no irradiation. BM=bone marrow. —=no BM cells given.

[b] Mice were irradiated (179 rad four times). Two days following the last dose of radiation, 10×10^6 BM cells were inoculated iv. At 17 days following irradiation, the cytotoxic activity of their spleen cells was tested in a 4-hr CRA.

[c] 1×10^6 ^{51}Cr-labeled YAC-1 cells were inoculated iv, and 3 hr later the level of remaining radioactivity in the lungs was measured.

Table 3.—*Effect of spleen cells from C57BL/6 normal or beige mice on natural antitumor resistance of irradiated mice*

Mice	Treatment[a]		5 wk following spleen cell transplantation		7 wk following spleen cell transplantation	
	Irradiation, 179 rad four times[b]	Spleen transplantation[b]	cpm remaining in lungs (±SE)	Recovery, %	cpm remaining in lungs (±SE)	Recovery, %
C57BL/6	−	—	17,036 (2,084)	6.9	7,825 (1,262)	5.6
C57BL/6	+	—	31,914 (3,659)	13.0	33,239 (2,855)	23.6
C57BL/6	+	Normal	18,089 (1,927)	7.4	14,763 (605)	10.5
C57BL/6	+	*bg/bg*	39,549 (4,063)	16.1	35,137 (3,445)	24.9
Beige	−	—	31,563 (2,084)	12.8	29,290 (1,650)	20.8
Beige	+	—	53,853 (4,355)	21.9	60,548 (4,970)	42.9
Beige	+	Normal	20,939 (2,356)	8.5	19,028 (923)	13.5
Beige	+	*bg/bg*	43,317 (1,465)	17.6	Not tested	—

[a] Mice were irradiated (179 rad four times). Two days following irradiation, 50×10^5 spleen cells from C57BL/6 +/+ or C57BL/6 *bg/bg* mice were inoculated iv into irradiated recipients. Then 5 and 7 wk later, their ability to eliminate ^{51}Cr-labeled YAC-1 cells was analyzed. The level of radioactivity remaining in the lungs 3 hr following tumor cell inoculation was determined.

[b] +=irradiation; −=no irradiation. —=no transplantation.

Table 4.—*IFN boosting of NK activity of spleen cells of irradiated C57BL/6 mice*

Treatment[a]	Cytotoxicity (±SD) at E:T ratio of 100:1, %	
	Spleen cells preincubated without IFN	Spleen cells preincubated for 16 hr with IFN, 10^3 U/ml
None	8.3 (1.0)	62.6 (3.6)
Irradiated, 179 rad four times	2.1 (1.3)	41.0 (2.3)
Irradiated + BM +/+	6.2 (0.9)	60.3 (2.5)
Irradiated + BM *bg/bg*	1.5 (0.6)	64.2 (3.9)

[a] *See* footnote *a*, table 1. Spleen cells were incubated overnight (16 hr) with IFN. Cytotoxic activity of spleen cells was analyzed against YAC-1 cells in a 4-hr CRA.

or reconstituted mice. Transfer of 10×10^6 bone marrow cells from beige C57BL/6 mice into irradiated mice was unable to restore the spontaneous NK activity of spleen cells, but this procedure did efficiently reconstitute IFN-augmentable activity (table 4).

DISCUSSION

The first investigations of the effect of irradiation on the NK cell activity indicated that NK cell function is relatively radioresistant (*3, 6*). However, strong and prolonged suppression of NK activity of spleen cells was observed 2 weeks after irradiation (*3*). This decrease of NK reactivity was paralleled by the appearance of suppressor cells (*3*).

In the present study we analyzed the influence of small fractionated doses of radiation, a schedule that is strongly leukemogenic in C57BL/6 mice, on the NK reactivity of irradiated mice. Our data indicated that this schedule of irradiation (179 rad four times) very efficiently suppressed NK activity. This suppressive effect was profound and persisted for at least 7 weeks after the last dose of radiation. Such investigations on the duration of the suppressive effect of irradiation (or other factors) on the in vitro NK activity of spleen cells are complicated by the age dependence of NK activity. NK activity of spleen cells of mice older than 10 weeks gradually decreases and might come to the level observed in the treated mice. Parkinson et al. (*14*) reported depressed NK activity of spleen cells of mice treated with small split doses of radiation. However, the differences between irradiated and control mice tended to be small due to the problems discussed above of age-dependent decline of NK activity. We have found that the ability of mice to eliminate iv inoculated YAC-1 lymphoma cells is less age-dependent. At least at 12–14 weeks of age, when the spleen cells of normal C57BL/6 mice had low levels of NK activity, the mice were as efficient in the elimination of tumor cells from the lungs as were younger mice. Therefore, the analysis of the clearance of iv inoculated tumor cells may be a more useful method for assessment of the natural antitumor resistance of mice undergoing various treatments over a period of several weeks. NK reactivity of irradiated mice can be reconstituted. It was previously shown that NK activity could be restored by administration of normal C57BL/6 bone marrow cells to lethally irradiated mice (*8*). In contrast, bone marrow cells of beige mice failed to restore NK reactivity of lethally irradiated mice, although such treatment did restore other immunologic functions in these mice (*8*). Similarly, in our experiments bone marrow or spleen cells of normal C57BL/6 mice were able to reconstitute NK reactivity of C57BL/6 +/+ or C57BL/6 *bg/bg* mice irradiated with fractionated doses of sublethal radiation (179 rad four times), and bone marrow or spleen cells from beige donors were inefficient in the restoration of NK cell function. Also, transfer of bone marrow or spleen cells from C57BL/6 +/+ mice into fractionally irradiated beige mice resulted in a substantial increase in NK reactivity. These data support the hypothesis that the low levels of NK activity of beige mice are due to an intrinsic defect in the NK cells (*8*). In addition, the ability of bone marrow or spleen cells from normal C57BL/6 mice to reconstitute the NK activity of sublethally irradiated mice is consistent with the hypothesis that this treatment protocol does not induce an inhibitory or suppressive environment, but rather that the irradiation induces some deficit in pre-NK cells and/or their stem cells. Alternatively, the finding that spleen cells from irradiated mice can display quite substantial levels of NK activity after IFN treatment suggests that the radiation may induce a deficit in positive in vivo regulation of NK activity rather than in the NK cells themselves.

The split doses of radiation (179 rad four times) that we have shown to be strongly suppressive for NK cell activity of C57BL/6 mice have also been demonstrated to be strongly leukemogenic, with 93% of irradiated C57BL/6 mice developing thymomas by 6 months after irradiation. Transplantation of bone marrow or spleen cells into such irradiated mice by a protocol very similar to that shown here to reconstitute NK activity has been shown to inhibit the irradiation-induced leukemogenesis (*9, 10*). Thus these data are consistent with the hypothesis that NK cells play an important role in antileukemia defense. It will be of interest to examine the effects on natural antitumor resistance of the same schedule of irradiation in older C57BL/6 mice or in mice of other strains, which are relatively resistant to the leukemogenic effects of such treatments. Further experiments are needed also to define more precisely the mechanism of radiation-induced depression of NK activity and particularly to assess more directly the role of NK cells in resistance to radiation-induced leukemogenesis. Studies are now in progress to determine the incidence of radiation-induced lymphoma in beige mice and to determine the ability of bone marrow or spleen cells from beige mice to restore resistance to radiation-induced leukemogenesis.

REFERENCES

(*1*) Herberman R, Holden H. Natural cell-mediated immunity. Adv Cancer Res 1978; 27:305–337.

(*2*) Kiessling R, Wigzell H. An analysis of the murine NK cells as to structure, function and biological relevance. Immunol Rev 1979; 44:165–208.

(*3*) Hochman PS, Cudkowicz G, Dausset J. Decline of natural killer cell activity in sublethally irradiated mice. JNCI 1978; 61:265–268.

(*4*) Ehrlich R, Efrati M, Bar-Eyal A, et al. Natural cellular reactivities mediated by splenocytes from mice bearing three types of primary tumor. Int J Cancer 1980; 26:315–323.

(*5*) Gorelik E, Heberman RB. Inhibition of the activity of mouse natural killer cells by urethan. JNCI 1981; 66:543–548.

(*6*) Kiessling R, Hochman R, Haller O, et al. Evidence for a similar or common mechanism for natural killer cell activity and resistance to hemopoietic grafts. Eur J Immunol 1977; 7:655–663.

(*7*) Haller O, Orn A, Gidlund M, Wigzell H. In vivo activity of murine NK cells. In: Herberman RB, ed. Natural cell-mediated immunity against tumors. New York: Academic Press, 1980:1219–1270.

(*8*) Roder J. The beige mutation in the mouse. I. A stem cell predetermined impairment in natural killer cell function. J Immunol 1979; 123:2168–2173.

(*9*) Kaplan H. Leukemia and lymphoma in experimental and domestic animals. Ser Haematol 1974; 7:2–163.

(*10*) Haran-Ghera N. Pathogenesis of murine leukemia. In: Klein G, ed. Viral oncology. New York: Raven Press, 1980:161–185.

(*11*) Wiltrout RH, Frost P, Cummings GD. Isotope-release cytotoxicity assay with the use of indium-111: Advantage over chromium-51 in long-term assays. JNCI 1978; 61:183–188.

(*12*) Ricchardi C, Santoni A, Barlozzari T, et al. In vivo natural reactivity of mice against tumor cells. Int J Cancer 1980; 25:475–486.

(*13*) Brunda M, Holden H, Herberman R. Augmentation of natural killer cell activity of beige mice by interferon and interferon inducers. In: Herberman RB, ed. Natural cell-mediated immunity against tumors. New York: Academic Press, 1980:411–416.

(*14*) Parkinson D, Brightman R, Waksal S. Altered natural killer cell biology in C57BL/6 mice after leukemogenic split-dose irradiation. J Immunol 1981; 126:1460–1463.

blank page

Spontaneous Occurrence of Atypical Hyperplasia and Adenocarcinoma of the Uterus in Androgen-Sterilized SD Rats[1, 2]

Shinichi Morikawa,[3] Souei Sekiya,[3] Masabumi Naitoh,[3] Hiroshi Iwasawa,[3] Bin Takeda,[3] and Hiroyoshi Takamizawa[3]

ABSTRACT—In SD female rats sterilized by a single injection of testosterone propionate at 2 days after birth, the spontaneous occurrence of atypical hyperplasia and adenocarcinoma of the uterus was observed for a fairly long period (>2 yr). Two atypical hyperplasias and 2 adenocarcinomas were detected in 25 androgen-sterilized rats (ASR) after 500 days of age; in contrast, in 111 normal control rats no abnormal uterine proliferation was detected during a 750-day observation period. These results indicate that a persistence of both hormone imbalances and dysfunctional uteri in ASR induces abnormal uterine proliferation at a late age.—JNCI 1982; 69:95–101.

Anovulatory sterility is considered one of the major high-risk factors of endometrial hyperplasia and adenocarcinoma in humans (*1*). Although hormone imbalance characteristic of anovulatory sterility appears to be the cause of endometrial carcinogenesis (*2*), direct evidence for this explanation has not yet been obtained.

The rate of spontaneously occurring endometrial hyperplasia and adenocarcinoma is extremely low in both mice and rats as compared to the rate in old rabbits, in which such abnormal uterine proliferations are of relatively high incidence (*3, 4*). The highly varied patterns of endometrial hormone conditioning seen among these species seem to support this finding (*5*). In Sprague-Dawley rats, uterine tumors were detected in only 25 (0.9%) of 2,723 female rats at 600–800 days of age (*6–10*). Neither was atypical hyperplasia or adenocarcinoma of the uterus noted in these reports. We therefore set up an animal model of anovulatory sterility in Sprague-Dawley rats, and for the fairly long period of more than 2 years, we compared the spontaneous occurrence of uterine tumors in ASR with that in NR.

MATERIALS AND METHODS

Pregnant SD rats were purchased from a commercial breeder (Clea Japan, Inc., Tokyo). More than 200 newborn rats were used. They were housed in plastic cages in an air-conditioned (25±2°C), artificially illuminated room and were separated from their mothers after 3 weeks of age. Weaned rats were given commercial rations (Oriental M; Oriental Yeast Co., Ltd., Tokyo, Japan) and tap water ad libitum.

A single sc injection of 1.25 mg T propionate (Teikoku Hormone Manufacturing Co., Ltd., Kanagawa, Japan)/0.05 ml of sesame oil was given by the method of Barraclough (*11*) to each of 100 2-day-old female rats. Fertility of the ASR and an equal number of NR was checked at 70 days by the mating of 1 male:3 females for 30 days. Vaginal smears by the Papanicolaou staining method were examined daily for 2 weeks before autopsy.

After blood was collected from the portal veins of lightly ether-anesthetized rats, serial autopsies were performed on 70- to 750-day-old ASR and NR. Wet weights of the uteri, ovaries, adrenal glands, and pituitary glands were determined immediately after excision. These organs were then fixed in 10% neutral Formalin, sectioned serially, stained with hematoxylin and eosin, and examined by optical microscopy.

Plasma was obtained by centrifugation of the blood at 3,000 rpm for 15 minutes and was stored at −20°C until it was assayed. The plasma values of gonad steroids such as E_1, E_2, P, and T were estimated with CEA-IRE-SORIN radioimmunoassay kits (Japan Radioisotope Association, Tokyo). Effect of ovariectomy and E_2 on the uterus weight and peroxidase induction was examined in 70-day-old NR and ASR. Both NR and ASR were ovariectomized at 50 days of age and given a single injection of 40 µg E_2 (Sigma Chemical Co.)/kg body weight on the 18th day after ovariectomy. The animals were killed 48 hours after E_2 administration, and the uterus weights and peroxidase activities were measured, as described below. The cytosol E_2 receptor of the uterus was assayed according to the dextran-coated charcoal assay method of McGuire and DeLaGarza (*12*), as described previously (*13*). As described in a previous report (*14*), uterine peroxidase activity was assayed by the method of Himmelhoch et al. (*15*) with guaiacol as substrate. Protein was measured by the method of Lowry et al. (*16*).

RESULTS

Hormone Imbalance in ASR

In the ASR, vaginal opening was observed in only 63% of the animals, even after 300 days of age, whereas it was observed in all NR at about 45 days of age. The infertility rate of the ASR was 98%, and all ASR showed both a lack of sexual cyclicity and a persistence of estrus, as determined by vaginal smear after 70 days of age.

As shown in table 1, the body weights of the ASR were significantly greater than the body weights of the NR, and

---

ABBREVIATIONS USED: ASR=androgen-sterilized rats; E_1=estrone; E_2=17β-estradiol; H & E=hematoxylin and eosin; NR=normal control rats; P=progesterone; T=testosterone.

---

[1] Received September 24, 1981; accepted February 5, 1982.

[2] Supported by Grant-in-Aid 56-11 for Cancer Research from the Ministry of Health and Welfare of Japan.

[3] Department of Obstetrics and Gynecology, Chiba University School of Medicine, 1-8-1 Inohana, Chiba 280, Japan.

TABLE 1.—*Mean body and organ weights ± SE of NR and ASR with age*

Treatment group	Age, days	No. of rats	Body weight, g	Organ weight, mg			
				Uterus	Ovary	Adrenal glands	Pituitary gland
NR	100	9	267±12	641±60	78±3	99±4	25±2
ASR	100	11	267±5	473±20^{a}	92±10	113±9	25±3
NR	300	10	311±8	806±38	140±10	93±4	28±1
ASR	300	11	393±17^{b}	520±45^{b}	91±6^{b}	98±4	25±2
NR	550	11	332±19	845±66	179±19	167±18	28±4
ASR	550	22	406±10^{b}	611±40^{c}	114±14^{d}	120±6	32±3

[a] *P*<0.02.
[b] *P*<0.001 as compared to the values of NR.
[c] *P*<0.01 as compared to the values of NR.
[d] *P*<0.05 as compared to the values of NR.

obesity became prominent in the ASR with aging. In contrast to the body weights, although the organ weights of the uterus and ovary of the ASR increased with age, the significance of the increase was less than the significance of the increase in body weights.

As shown in text-figure 1, the response of uterus weight to ovariectomy in ASR was less as compared to the response in NR, and exogenous E_2 administration to ovariectomized ASR as young as 70 days old failed to exert any tropic action on the uterus weight. A similar phenomenon was also evident for uterine peroxidase induction by E_2 administration. However, no significant difference in the mean cytosol E_2 receptor content of the uteri of 5 rats was observed when ASR (138 fmol E_2/mg protein) were compared to NR (128 fmol E_2/mg protein).

As shown in text-figure 2, the plasma P values for ASR at both 300 and 750 days of age were significantly lower than the values for NR. This finding seems related to the absence of corpora lutea in the ovaries of the ASR. However, the values for the other gonad steroids E_1, E_2, and T were not significantly different between ASR and NR. Therefore, the plasma (E_1 + E_2):P ratio was increased in the ASR.

Spontaneous Occurrence of Atypical Hyperplasia and Adenocarcinoma of the Uterus in ASR

As shown in table 2, abnormal uterine proliferation was not detected in any of the 111 NR during a 750-day observation period. In contrast, 2 atypical hyperplasias were detected in 500-day-old (fig. 1) and 570-day-old ASR, respectively, and 2 adenocarcinomas of the uterus were detected in 25 ASR after 500 days of age. Both uterine carcinomas were characterized by cytologic atypia, such as enlarged nuclei and prominent nucleoli, as well as by histologic atypia, such as back-to-back arrangement of glands and mesenchymal destruction. One of the uterine adenocarcinomas was detected at 500 days of age and was histologically diagnosed as an adenocarcinoma composed of both differentiated (fig. 2) and poorly differentiated (fig. 3) types. The other uterine adenocarcinoma was detected at 730 days of age and was composed of an undifferentiated type of adenocarcinoma (fig. 4), a differentiated type of squamous cell carcinoma (fig. 5), and a squamous type of metaplasia. Metastasis was not found in either of these carcinomas.

Other tumors of nonuterine origin, such as mammary,

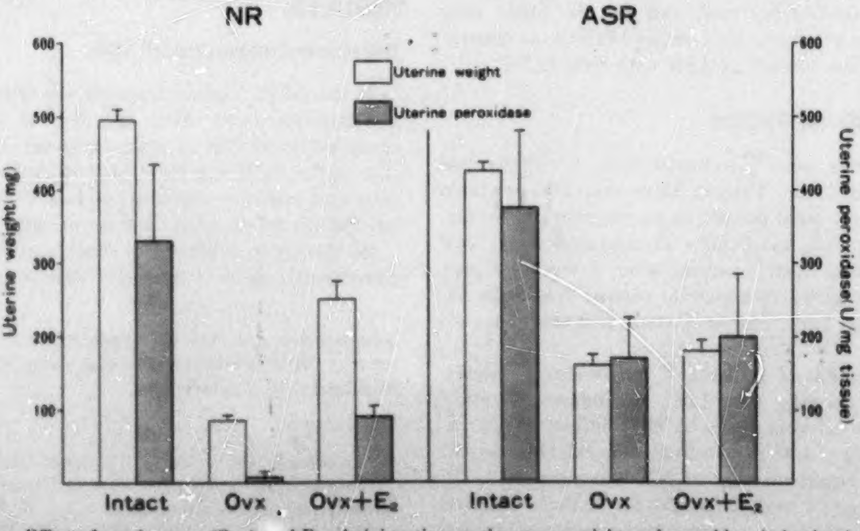

TEXT-FIGURE 1.—Effect of ovariectomy (Ovx) and E_2 administration on the uterus weight and peroxidase induction in 70-day-old NR and ASR. *Bars* represent means ± SE for 5 rats.

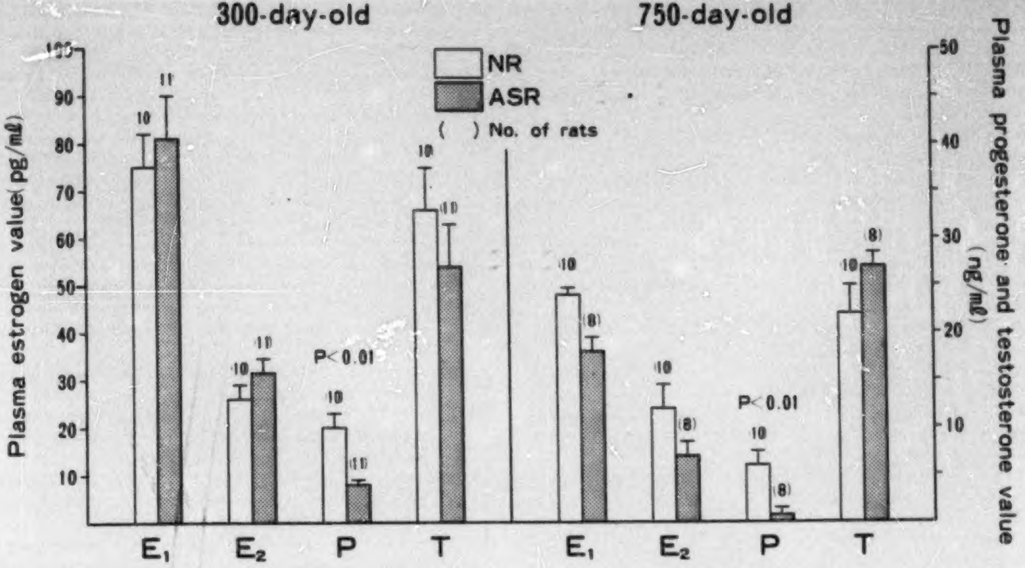

TEXT-FIGURE 2.—Plasma gonad steroid levels in 300- and 750-day-old NR and ASR.

adrenal, or pituitary tumors, were detected in 11 (33%) of 33 NR and in 4 (16%) of 25 ASR after 500 days of age. These results suggest that the spontaneous occurrence of endocrine-related tumors except those of the uterus was suppressed in ASR as compared to NR. Whereas squamous-type metaplasia of the uterine epithelium was detected in 25 (36%) of 70 ASR during a 750-day observation period and it increased with aging, no squamous metaplasia was observed in any of the 111 NR.

TABLE 2.—*Spontaneously occurring atypical hyperplasia and adenocarcinoma of the uterus in NR and ASR*

Treatment group	Age, days	No. of rats	Uterine tumors: Atypical hyperplasia	Uterine tumors: Adenocarcinoma	Other tumors
NR	70–499	78	0	0	0
NR	500–750	33	0	0	11[a]
ASR	70–499	45	0	0	0
ASR	500–750	25	2	2	4[b]

[a] Of the 11 tumors, 6 were of the mammary gland, 3 were of the adrenal gland, and 2 were of the pituitary gland.

[b] Of the 4 tumors, 2 were of the mammary gland and 2 were of the pituitary gland.

DISCUSSION

The effects of neonatal androgenization on the proliferation of rat uterine epithelium have been described by several investigators (*11, 17–19*). Tall columnar luminal epithelium, its squamous-type metaplasia, and pyometra (data not shown) are characteristic in ASR during a relatively short observation period of within 1 year. Such morphologic changes of the uterine epithelium in ASR are considered to be due to a continuous estrogen effect unopposed by P, inasmuch as the changes are similar to those produced by the administration of high doses of estrogens for prolonged periods (*17, 20, 21*). However, atypical hyperplasia and adenocarcinoma of the uterus so far have not been induced in rats by only excess estrogenic stimulation (*22, 23*), whereas their induction has been reported in rabbits (*24, 25*).

Spontaneously occurring uterine adenocarcinoma in hormonally imbalanced (persistent estrus) rats, i.e., without the use of any carcinogens including estrogens, has been reported only by Pfeiffer (*26*) who detected a uterine adenocarcinoma in an aged, 816-day-old female rat in which testes had been implanted at birth. However, hormone imbalance was not fully elucidated in his report.

The present study also provides direct evidence that atypical hyperplasia and adenocarcinoma of the uterus can occur spontaneously with fairly high incidences in aged ASR as compared to similarly aged NR. The cause of such abnormal uterine proliferations in ASR is not precisely known, but it is possibly a result of the complex hormone imbalances in ASR, such as lack of sexual cyclicity (persistent estrus) (*11, 27, 28*), decreased responsibility of the uterus particularly to exogenous estrogen (*27, 29–31*), and an increased endogenous E_2:P ratio (*29*), as observed in the present experiments. Among these causes, the E_2:P ratio seems to be important, because E_2:P in ASR with adenocarcinoma was about twice that in ASR without adenocarcinoma.

Such hormone imbalance of ASR occurring as early as 70 days of age precedes the occurrence of abnormal uterine proliferations, which are usually detected after 500 days of age. Thus the uterine carcinogenesis in ASR appears to require a fairly long time from the onset of both hormone imbalance and a dysfunctional uterus. Although a continuous estrogenic stimulation unopposed by P is needed in endometrial carcinogenesis, the present results obtained with androgenized rats suggest that a dysfunctional uterus of long duration is fundamental to endometrial carcinogenesis.

REFERENCES

(*1*) Lucas WE. Causal relationships between endocrine-metabolic variables in patients with endometrial carcinoma. Obstet Gynecol Surv 1974; 29:207-528.

(*2*) Gusberg SB. Hormone-dependence of endometrial cancer. Obstet Gynecol 1967; 30:287-293.

(*3*) Baba N, Von Haam E. Experimental carcinoma of the endometrium. Adenocarcinoma in rabbits and squamous cell carcinoma in rats and mice. Prog Exp Tumor Res 1967; 9:192-260.

(*4*) Cotchin E. Spontaneous uterine cancer in animals. Br J Cancer 1964; 18:209-227.

(*5*) Hertz R. Hormonal relationships of the endometrium in animals. Cancer Res 1965; 25:1188-1191.

(*6*) Davis RK, Stevenson GT, Busch KA. Tumor incidence in normal Sprague-Dawley female rats. Cancer Res 1956; 16:194-197.

(*7*) Mac Kenzie WF, Garner FM. Comparison of neoplasms in six sources of rats. J Natl Cancer Inst 1973; 50:1243-1257.

(*8*) Tannenbaum A, Vesselinovitch SD, Maltoni C, Mitchell DS. Multipotential carcinogenicity of urethan in the Sprague-Dawley rat. Cancer Res 1962; 22:1362-1371.

(*9*) Thompson SW, Huseby RA, Fox MA, Davis CL, Hunt RD. Spontaneous tumors in the Sprague-Dawley rat. J Natl Cancer Inst 1961; 27:1037-1057.

(*10*) Tsubura Y. Spontaneously occurring tumors in experimental animals. Gan Kagakuryoho 1981; 8:479-489 (in Japanese).

(*11*) Barraclough CA. Production of anovulatory, sterile rats by single injections of testosterone propionate. Endocrinology 1961; 68:62-67.

(*12*) McGuire WL, DeLaGarza M. Improved sensitivity in the measurement of estrogen receptor in human breast cancer. J Clin Endocrinol Metab 1973; 37:986-989.

(*13*) Morikawa S, Sekiya S, Takamizawa H. Studies on specific markers of hormone-dependence in endometrial carcinoma: Estradiol receptors and uterine peroxidase. Acta Obstet Gynaecol Jpn (Jpn Ed) 1981; 33:339-343 (in Japanese).

(*14*) Morikawa S, Kikuchi Y, Sekiya S, Takamizawa H. Study on uterine peroxidase as a specific marker of estrogen-dependence in rats. Acta Obstet Gynaecol Jpn (Jpn Ed) 1981; 33:499-505 (in Japanese).

(*15*) Himmelhoch SR, Evans WH, Mage MG, Peterson EA. Purification of myeloperoxidases from the bone marrow of the guinea pig. Biochemistry 1969; 8:914-921.

(*16*) Lowry OH, Rosebrough NJ, Farr AL, Randall RJ. Protein measurement with the Folin phenol reagent. J Biol Chem 1955; 193:265-275.

(*17*) Hayashi S. Hyperplasia and metaplasia of the uterine epithelium following estrone injection in ovariectomized adult rats given neonatal injections of sex steroids. Endocrinol Jpn 1968; 15:229-234.

(*18*) Lobl RT, Maenza RM. Androgenization: Alterations in uterine growth and morphology. Biol Reprod 1975; 13:255-268.

(*19*) Reiter RJ. Stratified squamous metaplasia of the uterine epithelium in early androgen-treated rats and its inhibition by light deprivation. Anat Rec 1969; 164:479-488.

(*20*) Kato T, Yakushiji M, Arima A, Hara I. Experimental studies on the morphologic changes of the endometrium following estrogen and progesterone administration. Kurume Med J 1974; 21:23-33.

(*21*) Takewaki K. Persistent changes in uterus and vagina in rats given injections of estrogen for the first thirty postnatal days. Proc Jpn Acad 1964; 40:42-47.

(*22*) McEuen, CS. Occurrence of cancer in rats treated with oestrone. Am J Cancer 1938; 34:184-195

(*23*) Noble RL, Hochachka BC, King D. Spontaneous and estrogen-produced tumors in Nb rats and their behavior after transplantation. Cancer Res 1975; 35:766-780.

(*24*) Griffiths CT, Tomic M, Craig JM, Kistner RW. Effect of progestins, estrogens and castration on induced endometrial carcinoma in the rabbit. Surg Forum 1963; 14:399-401.

(*25*) Meissner WA, Sommers S, Sherman G. Endometrial hyperplasia, endometrial carcinoma, and endometriosis produced experimentally by estrogen. Cancer 1957; 10:500-509.

(*26*) Pfeiffer CA. Adenocarcinoma in the uterus of an endocrine imbalance female rat. Cancer Res 1949; 9:347-349.

(*27*) Harris GW, Levin S. Sexual differentiation of the brain and its experimental control. J Physiol 1965; 181:379-400.

(*28*) Labhsetwar AP. Ovarian sensitivity to ovulatory stimuli in the androgen-induced persistent-oestrous rats. Acta Endocrinol (Copenh) 1971; 66:266-272.

(*29*) Barraclough CA, Fajer AB. Progestin secretion by gonadotropin-induced corpora lutea in ovaries of androgen-sterilized rats. Proc Soc Exp Biol Med 1968; 128:781-785.

(*30*) Van Rees GP, Gans E. Effect of gonadectomy and estrogen on pituitary LH-content and organ weights in the androgen-sensitized rat. Acta Endocrinol 1966; 52:471-477.

(*31*) Wrenn TR, Wood JR, Bitman J. Oestrogen responses of rats neonatally sterilized with steroids. J Endocrinol 1969; 45:415-420.

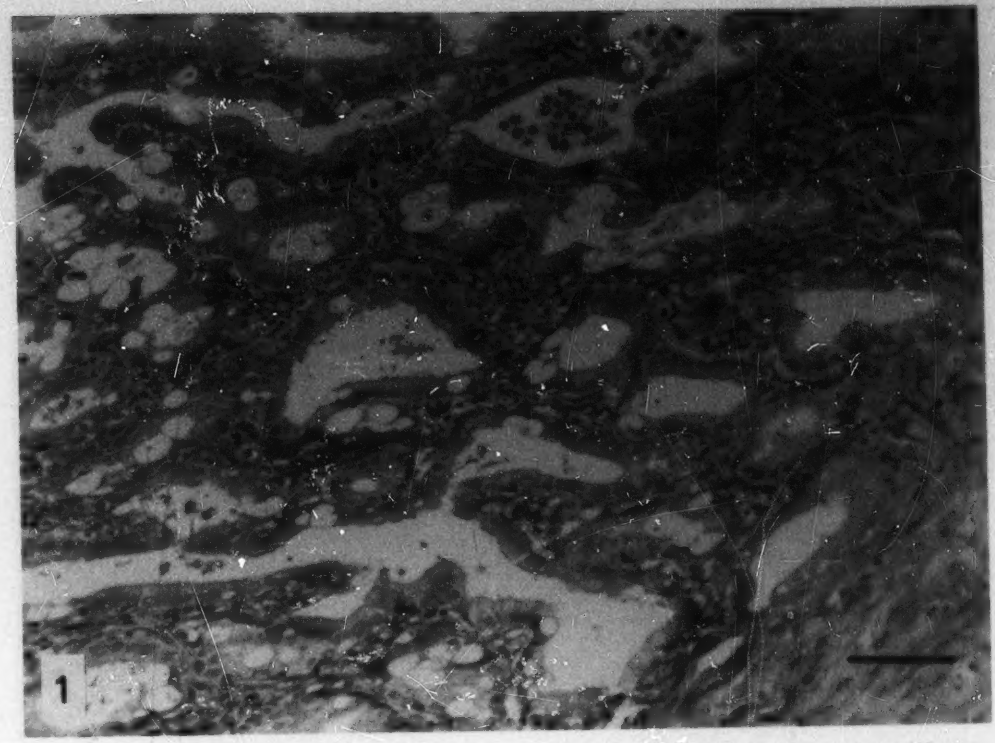

FIGURE 1.—Atypical hyperplasia of the uterus detected at 500 days in an ASR. H & E. *Bar*=50 µm. × 100

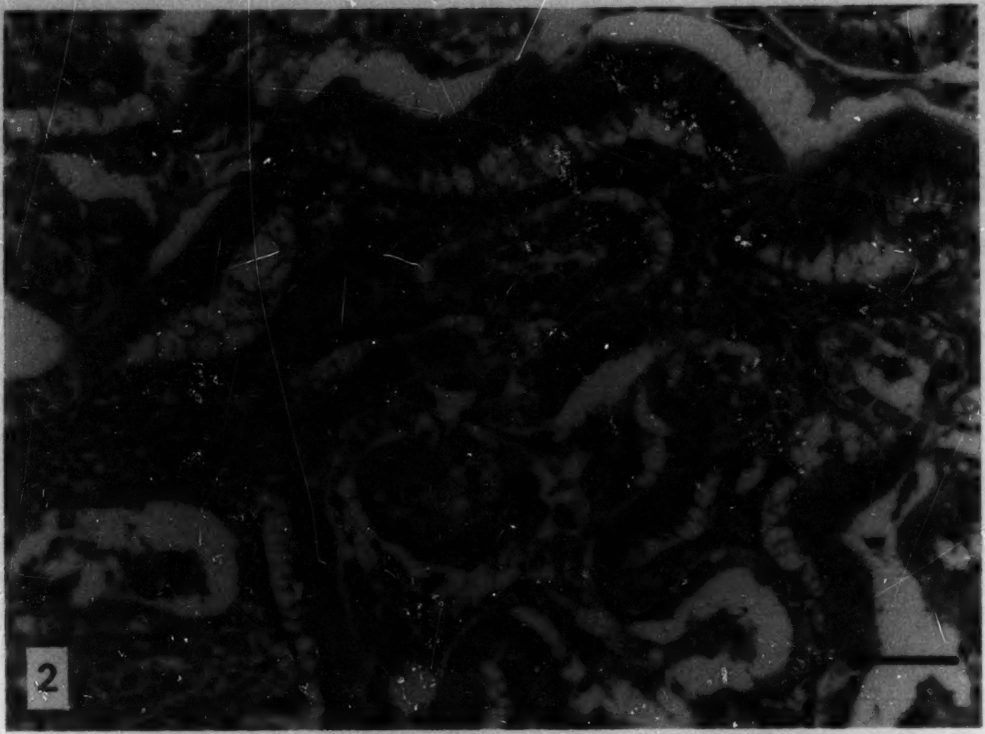

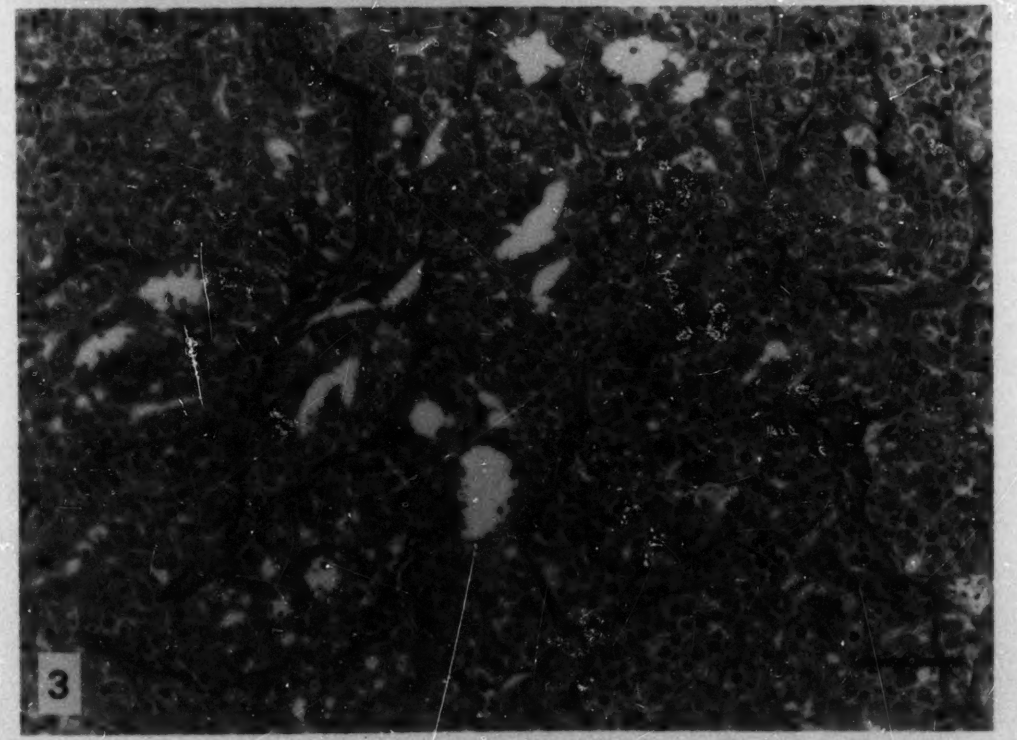

FIGURE 2.—Differentiated-type adenocarcinoma of the uterus detected at 500 days in an ASR. H & E. *Bar*=50 µm. × 100
FIGURE 3.—Poorly differentiated type of adenocarcinoma detected in the same uterus as that in fig. 2. H & E. *Bar*=50 µm. × 100

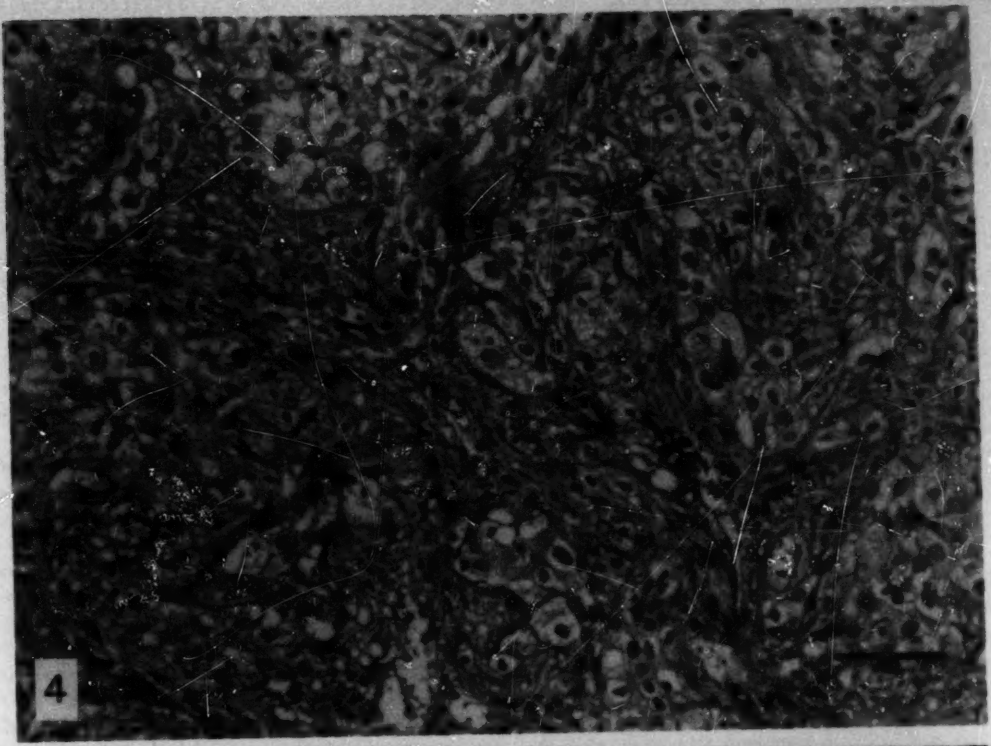

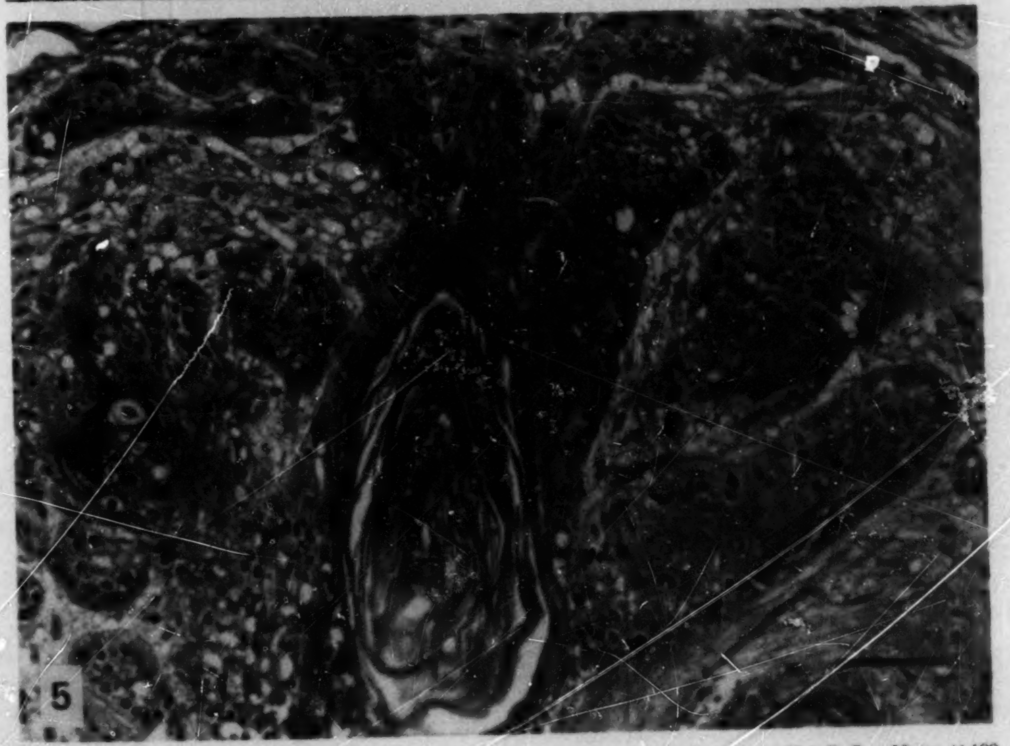

FIGURE 4.—Adenocarcinoma of the uterus detected at 730 days in an ASR. Undifferentiated type, H & E. *Bar*=50 µm. × 100

FIGURE 5.—Well-differentiated squamous cell carcinoma detected in the same uterus as that in fig. 4. H & E. *Bar*=50 µm. × 100

blank page

Combined Inhibitors of Carcinogenesis: Effect on Azoxymethane-Induced Intestinal Cancer in Rats[1,2,3]

Norman D. Nigro,[4] Arthur W. Bull,[4] Paulette S. Wilson,[4] Barbara K. Soullier,[4] *and* Majid A. Alousi[5,6]

ABSTRACT—Outbred male Sprague-Dawley CD rats were fed a complete semisynthetic diet and were given supplemental low doses (2 ppm) of selenium as H_2SeO_3 in their drinking water or 50 mg 13-*cis*-retinoic acid (13-*cis*-RA) and 2 g β-sitosterol/kg diet either singly, in combinations of two, or in combinations of all three. Intestinal tumors were induced with eight weekly sc injections of 8 mg azoxymethane (AOM)/kg body weight, and inhibition of tumor formation was determined by tumor counts after 26 weeks. Noncarcinogen controls for each dietary group received eight injections of sterile water. Tumor inhibition was statistically significant in 2 groups of animals: Dietary control animals had a tumor frequency of 5.07 tumors/rat, rats receiving selenium- plus 13-*cis*-RA supplementation had a tumor frequency of 3.77, and those being given the combination of all three inhibitors had 2.75 tumors/rat. Analysis of fecal steroids from 3 AOM groups (dietary controls, the β-sitosterol plus 13-*cis*-RA-supplemented group, and the group receiving all three additives) after 4 months of supplementation showed that the addition of β-sitosterol to the diet had no effect on acidic or neutral steroids, regardless of the observed difference in tumor frequency. These results suggest that subpharmacologic doses of inhibitors, particularly those that inhibit the process by different mechanisms, while ineffective alone, may provide significant inhibition of tumorigenesis when used in combination.—JNCI 1982; 69:103–107.

There is considerable evidence from epidemiologic and laboratory studies indicating that the etiology of cancer of the large intestine in humans is due to predominantly dietary factors. The dietary elements most suspect are a combination of excessive amounts of animal fat and relatively little fiber (*1*). Studies suggest that alterations of fat and fiber in the diet needed to reduce cancer incidence would have to be substantial. In fact, such profound dietary changes are not likely to be acceptable to the population in general (*2*).

However, prevention may be accomplished by other dietary measures. For example, cancer could be prevented best by eliminating or by effectively modifying the metabolism of the carcinogen. The difficulty with this approach is that the carcinogen responsible for intestinal cancer in humans is unknown, and it is extremely difficult to identify (*3*). In addition, known modifiers of initiation are few, and the time in which they act is short. However, we have more information about the inhibition of promotion. As a consequence, the use of inhibitors of the promotional phase appears to offer the best opportunity for reducing the high incidence of cancer of the large intestine (*4*).

Several chemicals have been shown to inhibit cancer formation in various organs in animals. These include selenium, the retinoids, and the plant steroids. Selenium has been shown by Jacobs (*5*) and Soullier et al. (*6*) to be an effective inhibitor of colon cancer in rats. The retinoids, especially 13-*cis*-RA, have been shown to inhibit cancer formation in the bladder, skin, breast, and lung (*7*). There is only limited evidence that 13-*cis*-RA inhibits intestinal cancer formation (*8*). Raicht et al. (*9*) have shown that β-sitosterol has some inhibitory effect on intestinal carcinogenesis in animals.

While the mode of action of these inhibitors is unknown, they appear to affect the process differently. There is precedent for suspecting that when small amounts of several inhibitors are used together they may enhance the total inhibitory effect significantly. The object of this experiment is to investigate that possibility.

MATERIALS AND METHODS

AOM was obtained from Ash-Stevens, Inc., Detroit, Mich., and was prepared as an aqueous solution for injection. Dextrose was purchased from a bakery supply house. Beef fat was donated by the Belmont Packing Co., Detroit, Mich., and was rendered in the laboratory. The 13-*cis*-RA was a gift from W. E. Scott, Hoffmann-La Roche Inc., Nutley, N.J. The β-sitosterol (95%) was donated by E. R. Diller, Eli Lilly & Co., Indianapolis, Ind. Other dietary components were obtained from Bioserve, Inc., Frenchtown, N.J. The same lot of each dietary component was used throughout the experiment. Selenium as H_2SeO_3 (99%) was purchased from the Ventron Corp., Alfa Products Division, Danvers, Mass.; it was prepared as a 1-g/liter stock solution, neutralized with NaOH, and added to double-distilled deionized water to a final concentration of 2 mg H_2SeO_3/liter. All other chemicals were obtained from sources previously described (*10*).

Outbred male Sprague-Dawley CD rats that weighed 100–125 g (6 wk old) were purchased from Charles River Breeding Laboratories, Wilmington, Mass. Animals were caged individually, diets and water were given ad libitum, body weights and water consumptions were recorded weekly, and food consumptions were determined every 4

ABBREVIATIONS USED: AOM=azoxymethane; 13-*cis*-RA=13-*cis*-retinoic acid.

---

[1] Received October 6, 1981; accepted February 12, 1982.

[2] Supported by the Matilda R. Wilson Fund.

[3] Animals were maintained under the guidelines of the Division of Laboratory Animal Resources, Wayne State University.

[4] Department of Surgery, Wayne State University School of Medicine, 540 East Canfield Ave., Detroit, Mich. 48201.

[5] Department of Pathology, Wayne State University School of Medicine.

[6] We acknowledge the excellent technical assistance of Mr. Marc Duchene and Ms. MaryAnne Buckley. We also thank Ms. Marie Stranad for skillful secretarial assistance.

TABLE 1.—*Basic diet: Composition*

Component	Weight, %	Total calories, %
Protein[a]	20.000	20.97
DL-Methionine	0.200	
Salt mix[b]	3.600	
Vitamin mix[c]	2.000	
Beef fat	5.000	11.80
Dextrose	45.155	47.31
Corn starch	19.000	19.92
Cellulose	5.000	
Placebo beadlets[d]	0.045	

[a] Vitamin-free casein (#11319; Bioserve, Inc.).

[b] Bernhart-Tomarelli salt mix, modified (#1468; Bioserve, Inc.) containing 735.0 g calcium phosphate, 81.0 g dipotassium phosphate, 68 g potassium sulfate, 30.6 g sodium chloride, 21.0 g calcium carbonate, 21.4 g disodium phosphate, 25.0 g magnesium oxide, 11.64 g ferric citrate, 810 mg zinc carbonate, 4.212 g manganese carbonate, 333 mg cupric carbonate, 7.2 mg potassium iodide, and 907.8 mg citric acid/kg salt mix.

[c] Vitamin mix (#1468; Bioserve, Inc.) containing 0.8 g vitamin A plamitate (250,000 U/g), 0.20 g vitamin D_2 (500,000 U/g), 15.4 g α-tocopherol (250 U/g), 100 g choline bitartrate, 0.05 g menadione, 4.5 g niacin, 0.5 g riboflavin, 0.7 g pyridoxine HCl, 0.1875 g thiamin HCl, 1.2 g calcium pantothenate, 0.03 g biotin, 0.2 g folic acid, 1.25 g vitamin B_{12}, and 874.9825 g sucrose/kg mixture.

[d] Stabilized gelatin beadlets.

weeks. Feces were collected over a 72-hour period during the 16th week of the experiment, their weights were recorded, and samples were frozen for subsequent neutral and acid steroid analysis. At least 15 animals in each dietary group were used for fecal collections, and samples from 2 animals were pooled.

The animals were divided into groups according to carcinogen administration and dietary supplementation. There were 8 groups of 30 rats given the carcinogen AOM (8 mg/kg body wt for 8 wk) and 8 groups (noncarcinogen controls) of 15 rats given injections of sterile water. The basic diet as defined in table 1 was supplemented with the inhibitors listed in table 2. Each supplement was given singly or in combination of two or of all three inhibitors as follows: Selenium was given in the drinking water at 2 ppm H_2SeO_3 (1.22 ppm Se^{4+}) in double-distilled deionized water, 13-*cis*-RA was added to the food (50 mg/kg diet) in stabilized gelatin beadlets (11% 13-*cis*-RA), and β-sitosterol was added to the food at 2 g/kg diet at the expense of cellulose. The dietary control groups were given the basic diet plus placebo gelatin beadlets.

After 26 weeks all animals were killed, necropsies were performed, and all tissues were examined grossly for tumors. The number, size, and location of intestinal tumors were recorded. Tumor distributions in the small intestine as well as the proximal and distal halves of the large intestine were also tabulated. Livers from 6 animals, and 15–20 representative intestinal tumors were removed from each group. These specimens were fixed in 10% Formalin, embedded in paraffin, and stained with hematoxylin and eosin.

Bile acids and neutral steroids were extracted from fecal samples of groups A, D, and H (table 2) according to the method of Cohen et al. (*11*). Thin-layer chromatography of bile acid samples was not necessary (*12*). Major bile acids that were detected and quantitated were lithocholic, hyodeoxycholic, deoxycholic, chenodeoxycholic, 12-ketolithocholic, and cholic acids. All data were analyzed with Student's *t*-test (*13*).

RESULTS

Body Weight and Food and Water Consumption

Weight curves for animals in the various groups are presented in text-figure 1. The administration of AOM to rats resulted in significantly ($P<0.05$) reduced body weights compared to those of noncarcinogen controls on the same diet for all groups except D, F, and G. There were no other significant differences in body weights among the various dietary groups. No differences were observed in either food

TABLE 2.—*Tumor incidence and frequency*

Group	Supplement[a]			No. of rats	Incidence, %		Frequency[b]				
							Average No. of tumors/rat				Total No. of tumors/rat
							Small bowel		Large bowel		
	13-*cis*-RA	β-Sitosterol	Selenium		Small bowel	Large bowel	Prox	Dist	Prox	Dist	
A	−	−	−	30	90	90	1.80	0	0.87	2.40	5.07
B	+	−	−	30	83.3	90	1.47	0	0.53	2.13	4.13
C	−	+	−	28	96.4	92.9	2.54[c]	0.07	1.04	2.29	5.93
D	+	+	−	29	65.5	100	1.34	0	0.90	2.55	4.79
E	−	−	+	29	93.1	93.1	1.86	0	1.03	1.83	4.72
F	+	−	+	31	77.4	74.1	1.58	0	0.39[d]	1.81	3.77[d]
G	−	+	+	29	89.7	93.1	2.14	0	0.79	2.28	5.21
H	+	+	+	28	60.7	78.6	0.93[c]	0	0.43[d]	1.39[f]	2.75[g]

[a] + = supplemented; − = not supplemented.

[b] Prox = proximal; Dist = distal.

[c] $P<0.025$ compared to control group A.

[d] $P<0.05$ compared to control group A.

[e] $P<0.0025$ compared to control group A.

[f] $P<0.01$ compared to control group A.

[g] $P<0.0005$ compared to control group A.

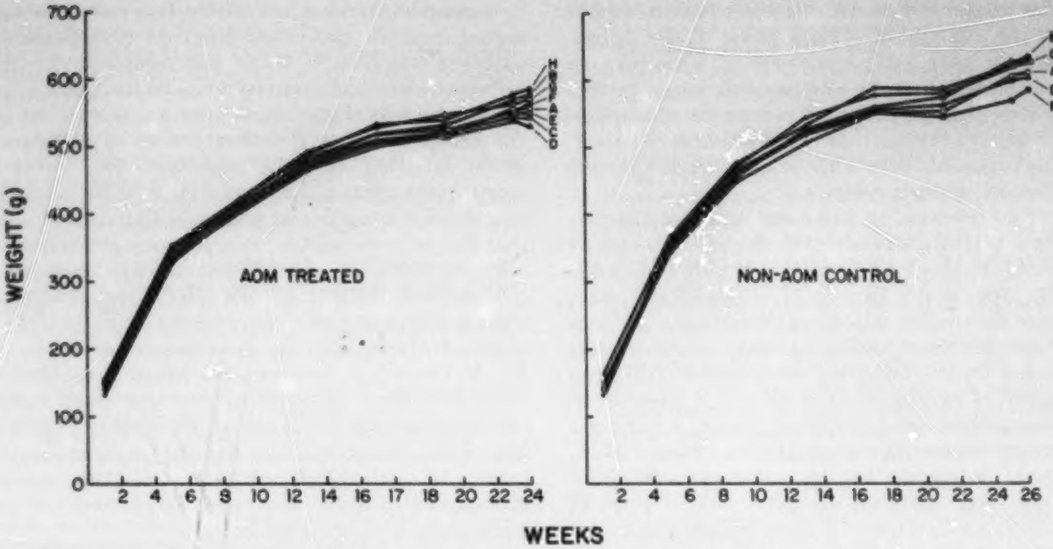

TEXT-FIGURE 1.—Average body weights of animals as a function of time. *See* table 2 for identification of treatment groups.

or water consumption throughout the study. The average daily intake of the different inhibitors was 38.8 μg Se^{4+}/rat, 1.31 mg 13-*cis*-RA/rat, and 49.8 mg β-sitosterol/rat.

Tumor Frequency and Distribution

Tumor frequency and incidence in rats treated with AOM are shown in table 2. Most animals receiving the carcinogen developed intestinal tumors, and the incidence varied from 90 to 100%. When compared to the dietary controls (group A), the total number of intestinal tumors per rat was significantly reduced when 13-*cis*-RA and selenium were administered in combination (group F, $P<0.05$). The reduction was even greater when all three inhibitors were given together (group H, $P<0.0005$). The degree of inhibition varied only slightly in the different segments of the intestinal tract. Group F rats had fewer tumors in the proximal half of the large intestine as compared to the number of tumors in rats in control group A. Group H had a reduction in tumors throughout the intestinal tract. However, when β-sitosterol was given alone (group C), the average number of tumors in the small intestine was significantly increased as compared to the number of tumors in the control group A ($P<0.025$).

TABLE 3.—*Fecal neutral steroids and bile acids*[a]

Group	Neutral steroids			Total bile acids[b]
	Coprostane	Cholesterol	β-Sitosterol	
A[c]	2.0±1.5	2.2±1.4	0.2±0.7	2.9±1.1
D[d]	2.0±1.7	3.5±2.1	14.6±7.9[e]	2.7±0.7
H[f]	1.9±1.4	2.7±1.7	10.4±5.3[e]	2.4±0.1

[a] Results are expressed as mg/g feces ± SD. Only trace levels of coprostanone were detected in all groups.

[b] Total bile acids = Σ cholic + chenodeoxycholic + deoxycholic + hyodeoxycholic + lithocholic + 12-ketolithocholic acids.

[c] Controls.

[d] β-Sitosterol plus 13-*cis*-RA supplemented.

[e] $P<0.01$ when compared to control group A.

[f] All three inhibitors combined.

One hundred fifty-five tumors, which varied in size from 2 mm to 2.2 cm, were examined histologically. All but 1 were malignant. However, 62% were early lesions, i.e., cancers limited to the intestinal wall, whereas the remaining 38% penetrated the wall and involved the surrounding fat. There were no significant differences between the various groups in the degree of anaplasia, the depth of invasion, or the size of the lesions.

Metastatic disease occurred in some animals in all groups. The most common form was intraperitoneal metastases, which occurred most frequently (50%) in group C. In control group A, only 3.3% had this complication, whereas the incidence in other groups was as much as 17% (groups D and G). Liver metastases occurred most often (17%) in rats in group G: All other groups had less than 7% liver involvement, except for group H which had none. Only two lung metastases were found: one in group C and one in group H. Because two or three ear tumors were found in each group, the inhibitors had no effect on this lesion.

Fecal Bile Acids and Neutral Steroids

In the 4th month of treatment, no significant differences were observed in fecal coprosterol, cholesterol, or bile acid concentrations in AOM-treated rats as a result of being fed the control diet (group A) or receiving the supplements β-sitosterol plus 13-*cis*-RA (group D) or the three inhibitors combined (group H). β-Sitosterol was significantly increased in both groups D and H ($P<0.01$). These data are presented in table 3.

DISCUSSION

Intestinal carcinogenesis is a long, complex process with multiple steps required for the development of clinical cancer (*14*). This complexity poses enormous problems for the discovery of the mechanism of each phase of the process. For example, we have little knowledge of what initiates intestinal cancer in humans or of how initiation or promotion occurs. However, the multistep process has one important advantage: It provides many opportunities for intervention. This is possible even without a full understanding of the mechanism of carcinogenesis.

Because of its reversibility and long duration, the promotional phase of carcinogenesis offers the best opportunity for interrupting the process, thereby preventing cancer formation (*15*). Most of our knowledge of promotion comes from studies of the murine skin cancer model, but evidence exists (*16*) that the same conditions apply to cancer promotion in other organs including the intestine. Although the mechanism of promotion is unknown, a number of compounds have been shown to inhibit this phase in several forms of cancer. Some appear to have a general effect, whereas others are specific for one tissue or organ (*17*). Unfortunately, most inhibitors are fairly toxic if given in large amounts over a long time. One possible solution to this problem is the use of very small amounts of two or three compounds which together might be inhibitory without being toxic. In the present study, the use of low doses of the individual inhibitors or any combination of them was not overtly toxic.

Epidemiologists have data that suggest that selenium may have cancer-preventive properties (*18*). Animal studies show that selenium inhibits cancer in several tissues including rat intestine (*5*). Soullier et al. (*6*) found selenium to be inhibitory in our laboratory even when the animals were given a potent carcinogen and a 30% fat diet, a combination that produces a strong cancer challenge. Selenium given at 4–5 ppm is not toxic to rats in 6-month experiments. However, we believe this dose is too high for consideration in any human application. Consequently, we used a much smaller dose (1.2 ppm) in this combination study. Selenium alone at this level had no inhibitory effect.

The rationale for the use of retinoids in chemoprevention is straightforward. Epithelial tissues are known to require retinoids for development and maintenance of cellular differentiation. Since carcinogenesis is a disease characterized by lack of cell differentiation, it seems reasonable to expect that retinoids might influence the process of carcinogenesis (*7*). We selected 13-*cis*-RA for this study because of its reported inhibitory effect in several cancer systems. We also hoped to provide information to resolve the conflicting reports of its ability to inhibit experimental colon cancer in rats (*8, 19*). As with selenium, we chose a lower dose of retinoid (50 mg/kg diet) than that which had been used by other investigators and thereby attempted to minimize the potential toxicity resulting from long-term use. The retinoid alone, at this level, had no inhibitory effect. Still the combination of 13-*cis*-RA and selenium, when given as a supplement to an adequate diet, inhibited the frequency of intestinal cancer induced by AOM. In another study a combination of selenium and retinyl acetate was shown to have an additive inhibitory effect on breast cancer in rats (*20*).

The plant steroid β-sitosterol is one of the major steroids in vegetables. When given orally, it is only minimally absorbed from the gastrointestinal tract (*21*). Because the β-sitosterol may alter fecal bile acid composition, it may also influence intestinal tumorigenesis. In the present study we analyzed the fecal steroids in 3 groups: the dietary controls, the group receiving β-sitosterol plus 13-*cis*-RA, and the group receiving all three inhibitors. The intent was to compare the effect of β-sitosterol on fecal steroids in animals that showed no reduction in tumors to the effect in animals that showed a reduced tumor frequency. β-Sitosterol had no effect on acidic or neutral fecal steroids, regardless of the difference in tumor frequency. The animal model provides some evidence that this plant steroid inhibits the formation of intestinal adenoma, the initial lesion in the cancer process (*9*). In this study, however, we found no evidence of an inhibitory effect when β-sitosterol was given alone or in combination with either one of the other two chemicals. In fact, when β-sitosterol was the only supplement, the frequency of small bowel tumors as well as the incidence of peritoneal metastases increased. At present we have no explanation for these observations.

In considering the inhibitory effect of selenium, 13-*cis*-RA, and β-sitosterol on carcinogenesis when administered singly, in combinations of two, and in combinations of all three, we found that the only combination of two that had any effect was that of selenium and 13-*cis*-RA. The reduction in the average number of tumors was marginally significant. However, when all three compounds were given as a supplement to an adequate diet, the inhibitory effect on the frequency of intestinal cancers was highly significant. In those groups with reduced tumor frequency, the tumors that did develop, while fewer, were approximately the same size, had the same degree of penetration, and were similarly anaplastic as tumors that developed in animals from the groups in which tumor frequency was not reduced. This suggests to us the possibility that the inhibitory effect may be an all-or-none phenomenon that occurs during a crucial transition from an initiated cell to a frankly tumorous cell, specifically, during promotion. While these experiments do not rigorously demonstrate inhibition of promotional processes as opposed to suppression of tumor growth, the fact that all tumors were approximately the same size and had the same degree of anaplasia, even in animals from groups with reduced tumor frequency, suggests that inhibition of promotional processes is the operational phenomenon.

The result of this study adds support to the concept that the use of small amounts of several agents that inhibit cancer by different mechanisms currently offers the best opportunity for development of a chemopreventive program in humans. No doubt other dietary changes would be a necessary part of the program; however, the use of effective inhibitors may permit relatively modest dietary changes that will be acceptable. Our results are encouraging, but it is apparent that more work is needed to identify the best group of inhibitors and to optimize their combined effects in a chemoprevention program.

REFERENCES

(*1*) Weisburger JH, Reddy BS, Wynder EL. Colon cancer: Its epidemiology and experimental production. Cancer 1977; 40:2414–2420.

(*2*) Walker AR. Colon cancer and diet, with special reference to intakes of fat and fiber. Am J Clin Nutr 1976; 29:1417-1426.

(*3*) Wilkins TD, Lederman M, Van Tassell RL, Kingston DG, Henion J. Characterization of a mutagenic bacterial product in human feces. Am J Clin Nutr 1980; 33:2513-2520.

(*4*) Nigro ND. Fat, fiber, and other modifiers of intestinal carcinogenesis: A strategy for prevention. In: Bruce RW, Correa P, Lipkin M, Tannenbaum SR, Wilkins TD, eds. Banbury report 7. New York: Cold Spring Harbor Laboratory, 1981:83-93.

(*5*) Jacobs MM. Inhibitory effects of selenium on 1,2-dimethylhydrazine and methylazoxymethanol colon carcinogenesis. Cancer 1977; 40:2557-2564.

(*6*) Soullier BK, Wilson PS, Nigro ND. Effect of selenium on azoxymethane-induced intestinal cancer in rats fed high fat diet. Cancer Lett 1981; 12:343-348.

(*7*) Sporn MB. Vitamin A and its analogs (retinoids) in cancer prevention. In: Winick M, ed. Nutrition and cancer. New York: Wiley, 1977:119-130.

(*8*) Newberne PM, Suphakarn V. Preventive role of vitamin A in colon carcinogenesis in rats. Cancer 1977; 40:2553-2556.

(*9*) Raicht RF, Cohen BI, Fazzini EP, Sarwal AN, Takahashi M. Protective effect of plant sterols against chemically induced colon tumors in rats. Cancer Res 1980; 40:403-405.

(*10*) Nigro ND, Campbell RL, Singh DV, Lin YN. Effect of diet high in beef fat on the composition of fecal bile acids during intestinal carcinogenesis in the rat. J Natl Cancer Inst 1976; 57:883-888.

(*11*) Cohen BI, Raicht RF, Salen G, Mosbach EH. An improved method for the isolation, quantitation and identification of bile acids in rat feces. Anal Biochem 1975; 64:567-577.

(*12*) Miettinen TA. Effects of neomycin alone and in combination with cholestyramine on serum cholesterol and fecal steroids in hypercholesterolemic subjects. J Clin Invest 1979; 64:1485-1493.

(*13*) Beyer W. Handbook of tables for probability and statistics. 2d ed. Cleveland: CRC Press, 1968:283.

(*14*) Reddy BS, Weisburger JH, Wynder EL. Colon cancer: Bile salts as tumor promoters. In: Slaga TJ, Sivak A, Boutwell RK, eds. Carcinogenesis: A comprehensive survey. Vol 2. New York: Raven Press, 1978:453-464.

(*15*) Boutwell RK. Some biological aspects of skin carcinogenesis. Prog Exp Tumor Res 1964; 4:207-250.

(*16*) Bull AW, Soullier BK, Wilson PS, Hayden MT, Nigro ND. Promotion of azoxymethane-induced intestinal cancer by high-fat diet in rats. Cancer Res 1979; 39:4956-4959.

(*17*) Wattenberg LW. Inhibitors of chemical carcinogenesis. Adv Cancer Res 1978; 26:197-226.

(*18*) Shamberger RJ, Willis CE. Selenium distribution and human cancer. CRC Crit Rev Clin Chem 1971; 2:211-221.

(*19*) Ward JM, Sporn MB, Wenk ML, Smith JM, Feeser D, Dean RJ. Dose response to intrarectal administration of *N*-methyl-*N*-nitrosourea and histopathologic evaluation of the effect of two retinoids on colon lesions induced in rats. J Natl Cancer Inst 1978; 60:1489-1493.

(*20*) Thompson HJ, Meeker LD, Becci PJ. Effect of combined selenium and retinyl acetate treatment on mammary carcinogenesis. Cancer Res 1981; 41:1413-1416.

(*21*) Sugano M, Morioka H, Ikeda I. A comparison of hypocholesterolemic activity of β-sitosterol and β-sitostanol in rats. J Nutr 1977; 107:2011-2019.

blank page

Generation of Long-Term T-Lymphoid Cell Lines With Specific Cytotoxic Reactivity for a Syngeneic Murine Lymphoma[1,2]

Timothy J. Eberlein, *M.D.*,[3,4] **Maury Rosenstein**, *Ph.D.*,[3] **Paul J. Spiess**, *M.S.*,[3] *and* **Steven A. Rosenberg**, *M.D., Ph.D.*[3]

ABSTRACT—The long-term in vitro growth in T-cell growth factor (TCGF) of murine cytotoxic T-lymphoid cells directed against syngeneic tumor antigens was investigated. C57BL/6 mice were immunized to syngeneic FBL-3 lymphoma by two ip injections of irradiated FBL-3 lymphoma cells. Splenocytes from these animals were injected into mice with disseminated lethal FBL-3 tumor. The injection of cyclophosphamide (Cy) plus immunized lymphocytes significantly improved survival with cure of 53% of 38 animals. In comparison, treatment with Cy alone resulted in 0 of 31 cured and treatment with Cy plus unimmunized cells resulted in 0 of 40 cured ($P<0.0005$). These in vivo immunized lymphocytes were reexposed to FBL-3 tumor in vitro for 5 days in lectin-free TCGF (LF-TCGF). Although in vivo and in vitro sensitized lymphocytes exhibited no cytotoxicity toward fresh FBL-3 tumor cells in an 18-hour ^{51}Cr release assay, expansion of appropriately sensitized cells in LF-TCGF resulted in significant lysis of fresh FBL-3 tumor cells. This significant lysis was specific and lysed syngeneic FBL-3 but not syngeneic MCA-103 fresh tumor targets. This maximal specific cytotoxicity was maintained for 2.5 months. A screening assay was developed that permitted rapid identification and isolation of low-frequency cytotoxic clones with reactivity specific for FBL-3 tumor. Several of these cloned cells were grown for almost 3 months with maintenance of high degrees of specific lysis (as much as 4,500 lytic U/10^6 cells). These cytotoxic lines and clones will be of value for the study of tumor-host immunologic interactions and perhaps for use in adoptive immunotherapy.—JNCI 1982; 69:109–116.

The use of passive immunotherapy for the treatment of malignant neoplasms has been the subject of numerous studies (*1*). This approach to therapy is dependent on obtaining lymphocytes or serum capable of eliminating tumor in vivo. In vitro assays of lymphocyte sensitization to tumor-related antigens on syngeneic tumor cells provided a useful guide to the generation of lymphoid cells of potential value in adoptive transfer (*2–21*), although exact correlation between in vitro and in vivo effects was not always observed.

The in vitro generation of lymphoid cells cytotoxic for syngeneic tumor cells proved to be difficult, and in most systems only weak cytotoxic responses were seen (*22, 23*). Attempts to enhance the in vitro generation of cytotoxic effector cells emphasized the importance of macrophage presentation of tumor antigen (*4, 6, 10, 24, 25*), the use of peritoneal exudate cells (*13, 26–28*), effector cells from in vivo immunized animals (*7–10, 12–15, 17, 27, 29*) or tumor-bearing animals (*12, 30–32*), removal of suppressor cells by mechanical means (*33, 34*) or by pretreatment of the host (*33, 35, 36*), isolation of lymphoid cell-infiltrating tumors (*37–41*), chemical modification or pretreatment the effector cell (*27, 33, 34, 42, 43*) or stimulator cell (*33, 43, 44*), or enhancement of the generation of cytotoxic cells with the use of soluble factors obtained from lymphoid cells (*21, 32, 45–47*).

It has been previously shown that LF-TCGF can cause the proliferation of previously activated cytotoxic T-lymphocytes (*48, 49*) and can actively enhance the cytotoxicity of T-cells sensitized in its presence (*50, 51*). Although we have been unable to consistently generate cytotoxic lymphoid cells against the syngeneic FBL-3 murine lymphoma in C57BL/6 mice by conventional techniques, the in vitro expansion of in vitro sensitized cells in LF-TCGF has enabled us to develop lymphoid cell lines with a high degree of specific cytotoxicity for this syngeneic lymphoma. The cloning of these cytotoxic cells with the use of limiting-dilution techniques has enabled us to generate cloned cell lines with specific cytotoxicity for fresh tumor at effector-to-target ratios of 0.01–1 in short-term in vitro cytotoxicity assays, with maintenance of this reactivity after growth for several months in vitro.

These techniques for the generation and cloning of cytotoxic lymphoid cells directed against syngeneic tumor may be applicable to the generation of cytotoxic cells directed against other murine and human tumors for studies of host responses to tumor antigens and perhaps for the adoptive immunotherapy of tumors.

MATERIALS AND METHODS

Animals.—Adult C57BL/6 female mice were obtained from The Jackson Laboratory, Bar Harbor, Maine.

Tumors.—FBL-3 is a Friend virus-induced syngeneic lymphoma–leukemia that is transplanted in its ascitic form. This tumor was supplied to us by Dr. C. C. Ting, National Cancer Institute. This tumor shares tumor-specific and/or viral antigens that cross-react with other tumors induced by Friend, Moloney, and Rauscher viruses (*52*).

MCA-103 is a sarcoma in C57BL/6 mice that was induced in our laboratory by the injection of 0.1 ml of 1% 3-methylcholanthrene in sesame oil into the hindlimb as previously

---

ABBREVIATIONS USED: CM=complete medium; Con A=concanavalin A; Cy=cyclophosphamide; FCS=fetal calf serum; HBSS=Hanks' balanced salt solution; IVS=in vitro sensitization(s); LF-TCGF=lectin-free T-cell growth factor; LU=lytic unit(s); TCGF=T-cell growth factor.

---

[1] Received October 20, 1981; accepted February 17, 1982.

[2] Animals were maintained under the guidelines set forth by the National Institutes of Health Policy on Humane Care and Use of Animals and by the Animal Welfare Act in facilities accredited by the American Association of Laboratory Animal Care.

[3] Surgery Branch, Division of Cancer Treatment, National Cancer Institute, National Institutes of Health, Public Health Service, U.S. Department of Health and Human Services, Bethesda, Md. 20205.

[4] *Address reprint requests to* Dr. Eberlein, Building 10, Room 10N116, National Institutes of Health, Bethesda, Md. 20205.

described (*53*). It was maintained by serial im passage and was used in these experiments in transplant generations 4–7.

In vivo immunization.—Adult C57BL/6 female mice were given two weekly ip injections of 2×10^7 FBL-3 tumor cells irradiated with 10,000 R. After 6 weeks, spleen cells were harvested and used for in vivo or in vitro experiments.

Spleen cell suspension.—Spleens were removed aseptically, pooled, teased apart with two sterile forceps, and then passed through a single layer of 100-mesh nylon in HBSS. The cells were centrifuged at $500\times g$ for 5 minutes, and the cell pellet was resuspended in buffered ammonium chloride solution for 1 minute at room temperature to lyse the red blood cells. The cells were washed three times and resuspended in CM. CM was composed of RPMI-1640 medium (Grand Island Biological Co., Grand Island, N.Y.) supplemented with 0.03% fresh glutamine (NIH Media Unit, National Institutes of Health), 1 μM sodium pyruvate (M.A. Bioproducts, Walkersville, Md.), 0.1 mM nonessential amino acids (M.A. Bioproducts), 5×10^{-5} M 2-mercaptoethanol, 100 U penicillin/ml, 100 µg streptomycin/ml, and 10% heat-inactivated FCS (Grand Island Biological Co.).

In vivo assay of in vivo immunized cells.—An adoptive chemoimmunotherapy model developed by Fass, Fefer, and coworkers (*54–56*) was used. Female 12-week-old C57BL/6 mice were given ip inoculations of 10^7 live FBL-3 tumor cells on day 0. By day 5, tumor cells could be found in the blood and lymph nodes and would have killed the animals if they were not treated. On day 5, mice were treated with 180 mg Cy/kg body weight, alone or in combination with ip administration of normal C57BL/6 lymphocytes or in vivo sensitized lymphocytes. Survival of mice was checked daily.

Production of LF-TCGF.—Optimal conditions for the production of LF-TCGF have been previously described (*51*). Single cell suspensions were prepared from spleens of exbreeder DBA/2 or BALB/c mice. A splenocyte preparation (50 ml) at a concentration of 4×10^7 cells/ml was incubated in 50-ml tubes (#2070; Falcon Plastics, Los Angeles, Calif.) with 10 µg Con A/ml (Miles Chemical Co., Elkhart, Ind.) at 37°C, in a 5% CO_2 atmosphere for 2 hours. The cells were then washed three times with HBSS, the pellet was resuspended in 50 ml CM without Con A, and 2 ml of the washed cell suspension was placed into individual wells of 24-well Costar plates (#3524; Cambridge, Mass.) and cultured for an additional 24 hours. Supernatants from these cultures were harvested, centrifuged, and passed through 0.45 filters (Millipore Corp., Bedford, Mass.). LF-TCGF supernatants prepared in this manner were more than 95% Con A-free as determined by absence of mitogenic activity on fresh lymphocytes and by measurement of removal of radiolabeled Con A.

IVS.—Stimulator cells were irradiated in a gamma irradiator with 10,000 R (FBL-3) or 2,000 R (normal C57BL/6 lymphocytes). Viable responder cells (6×10^7) and irradiated stimulator cells (1×10^6) were added to upright flasks (#3013; Costar) in a 20-ml total volume of CM (for generation of clones—*see* below) or 10 ml CM and 10 ml LF-TCGF (for generation of the whole population for expansion). Cells were harvested for expansion or in vitro tests on day 5. Yield of viable cells was approximately 25–31% of the initial concentration of responder cells.

Secondary IVS were performed by addition of 6×10^6 viable cells recovered from primary IVS on day 10 and 3×10^5 fresh irradiated tumor cells (or normal lymphocytes) to 24-well flat-bottomed plates (Costar) in 2 ml fresh CM. Tertiary IVS were performed in the same fashion on day 20 with the use of fresh CM and stimulators in exactly the same culture conditions as for secondary IVS.

Expansion of IVS lymphoid cells.—Cells were harvested from LF-TCGF flasks, centrifuged, and resuspended in fresh CM. Cell viability was assessed by trypan blue dye exclusion. These sensitized cells were adjusted to a concentration of 10^5 viable cells/ml in CM and then diluted in an equal volume of LF-TCGF (final concentration of 5×10^4 viable cells/ml). Of this final cell suspension 100 ml was placed in 750-ml tissue culture flasks (#3028; Falcon) lying flat, or 2 ml was placed in flat-bottomed tissue culture plates (#3524; Costar). The cells expanded sevenfold to tenfold in 6 days.

Cloning of IVS lymphoid T-cells.—Clones were generated with the use of a limiting-dilution technique in 96-well plates (#3596; Costar) from cells from primary, secondary, or tertiary IVS. Varying numbers of viable cells were plated per well (*57*).

^{51}Cr release cytotoxicity assays.—An 18-hour ^{51}Cr release assay was used under conditions previously described (*58*). Varying ratios of effector cells were plated in 96-well round-bottom plates (Linbro Titertek; Flow Laboratories, McLean, Va.) Viable fresh tumor targets (10^7) were labeled with 200 µCi of ^{51}Cr for 45 minutes at 37°C and in 5% CO_2. These targets were then washed three times, resuspended in RPMI-1640 medium and 10% heat-inactivated FCS, and plated at 10^4 viable cells/well. The plates were then centrifuged at $800\times g$ for 5 minutes and kept at 37°C and in a 5% CO_2 atmosphere for 18 hours. The plates were then centrifuged at $2{,}000\times g$ for 10 minutes and the supernatants harvested with the use of the Titertek Collecting System (Flow Laboratories).

Fresh FBL-3 tumor was harvested for each assay, washed, and labeled. One MCA-103 tumor was minced with fine scissors, trypsinized for 7 minutes, passed through a double layer of 100-mesh nylon, then washed three times, and freshly labeled. Spontaneous release was not greater than 50% in any experiment.

Screening assay to assess cytotoxicity of clones.—Clones were screened for cytotoxicity with the use of a replica-plating technique. Of the contents of each well of a 96-well plate (#3596; Costar), 0.1 ml was replica transferred to a fresh 96-well plate. Then 0.1 ml of the target suspension containing 10^4 ^{51}Cr-labeled targets (labeled as above) was added to each well. The second replica plate was centrifuged, incubated for 18 hours, recentrifuged, and harvested as above. The original plate had fresh LF-TCGF added (1:1 concentration of LF-TCGF and CM) and was available for further study and continuous growth. Clones that appeared "interesting" and required further growth were then transferred to the 2-ml flat-bottomed plates (Costar) in a 1:1 concentration of LF-TCGF and CM and expanded.

RESULTS

In vivo immunization against FBL-3 tumor.—Mice were immunized in vivo by two weekly ip injections of irradiated tumor cells. In multiple experiments, lymphocytes from these animals did not exhibit in vitro cytotoxicity in an 18-hour ^{51}Cr release assay (data not shown). These cells, however, were immune when tested by an adoptive transfer in vivo assay. A representative experiment is seen in text-figure 1. When compared to the transfer of spleen cells from normal mice, adoptive transfer of in vivo immunized lymphocytes conferred significant survival benefit. In all experiments combined, 53% of mice receiving Cy with in vivo immunized lymphocytes were cured (20/38) compared to 0 of 40 mice cured when mice were treated with Cy and normal lymphocytes or Cy alone (0/31 cured; $P<0.0005$ by paired log rank analysis).

In vitro cytotoxicity before and after expansion in LF-TCGF.—In an attempt to generate cells that exhibit cytotoxicity in vitro, in vivo sensitized lymphocytes were resensitized to irradiated FBL-3 cells in vitro for 5 days in the presence of LF-TCGF. Simultaneously, normal C57BL/6 lymphocytes were cocultured with normal C57BL/6 lymphocytes under identical conditions. Text-figure 2 shows a representative experiment. Both groups exhibited insignificant lysis of a fresh FBL-3 tumor in an 18-hour ^{51}Cr release cytotoxicity assay in six of eight experiments (text-fig. 2A). In the other two experiments low levels of lysis of fresh FBL-3 tumor were demonstrated only by the in vivo immunized lymphocytes resensitized to FBL-3 tumor and only at the effector-to-target ratio of 100:1 (data not shown). In eight of eight experiments, however, when these same IVS cells were expanded in LF-TCGF, there was a dramatic increase in cytotoxicity versus that seen with the fresh FBL-3 tumor only by the immunized cells (text-fig. 2B). Nonimmune cells cocultured with normal lymphocyte stimulators and then expanded in LF-TCGF showed low levels of lysis of fresh FBL-3 that did not change when they were expanded in LF-TCGF. When immune cells resensitized to FBL-3 tumor in vitro were expanded in LF-TCGF, lysis of fresh FBL-3 increased markedly (60% lysis at effector-to-target ratio of 1:1).

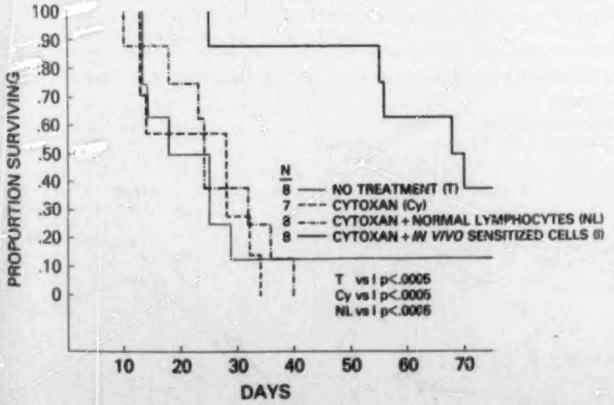

TEXT-FIGURE 1.—Survival of mice with disseminated FBL-3 lymphoma treated with in vivo immunized lymphocytes. When compared to treatment with Cy alone or Cy plus lymphocytes, treatment with Cy plus immune lymphocytes conferred significant survival benefit. All mice surviving at 75 days survived for >6 mo without tumor.

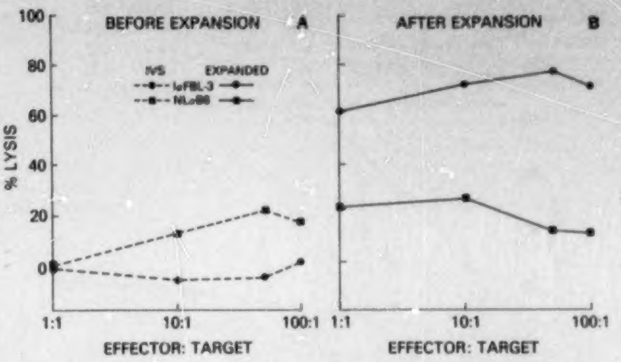

TEXT-FIGURE 2.—Cytotoxicity of IVS cells before and after expansion in LF-TCGF. A) No cytotoxicity after IVS; B) After expansion in LF-TCGF, only immune cells sensitized in vitro to FBL-3 tumor show significant cytotoxicity.

After expansion in LF-TCGF, only the combination of immune lymphocytes resensitized in vitro to irradiated FBL-3 tumor and then expanded in LF-TCGF showed this maximal lysis of fresh FBL-3 tumor (text-fig. 3). While the other three combinations of IVS (normal lymphocyte resensitized to FBL-3 tumor, immune lymphocyte cocultured with normal C57BL/6 lymphocytes, or normal nonimmune lymphocytes cocultured with normal lymphocyte stimulators) expanded in LF-TCGF showed some cytotoxicity of FBL-3, none had the same degree of lysis as immune lymphocytes cocultured with FBL-3 tumor. At an effector-to-target ratio of 1:1, maximal cytotoxicity was seen in the immune lymphocyte resensitized to FBL-3 tumor and then expanded in LF-TCGF. In subsequent experiments it was

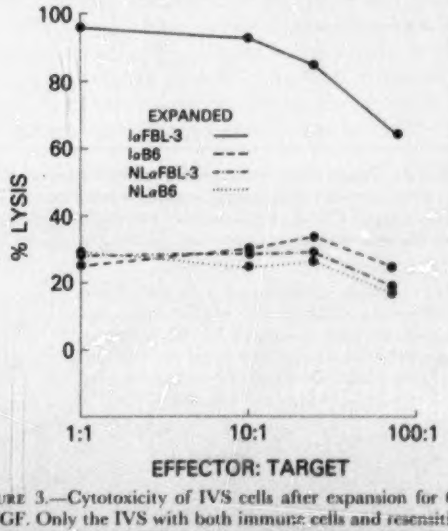

TEXT-FIGURE 3.—Cytotoxicity of IVS cells after expansion for 6 days in LF-TCGF. Only the IVS with both immune cells and resensitization to FBL-3 tumor in vitro (I$_{\alpha}$FBL-3) shows maximal cytotoxicity. Normal cell IVS to either FBL-3 (NL$_{\alpha}$FBL-3) or C57BL/6 (NL$_{\alpha}$B6) or immune cell IVS to C57BL/6 lymphocytes (I$_{\alpha}$B6) resulted in significantly less cytotoxicity.

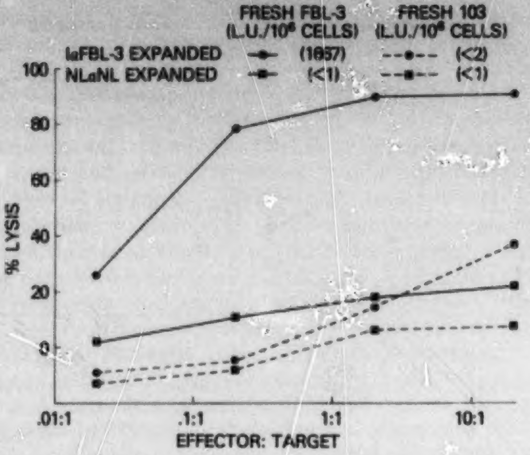

TEXT-FIGURE 4.—Specificity of lysis in a ^{51}Cr release assay. Whole populations of immune lymphocytes resensitized in vitro to FBL-3 tumor and then expanded in LF-TCGF exhibited significant cytotoxicity to fresh FBL-3 tumor but not to fresh syngeneic MCA-103 tumor.

necessary to reduce the effector-to-target ratio to 0.01:1 to reduce this lysis to near base-line levels.

Specificity of tumor lysis.—Immune lymphocytes resensitized in vitro to irradiated FBL-3 tumor and then expanded in LF-TCGF were tested for lysis of the FBL-3 tumor and a non-cross-reactive syngeneic MCA-103 tumor in the same assay. Lysis of fresh FBL-3 tumor but not MCA-103 tumor was seen in six of six experiments (text-fig. 4). Table 1 shows a representative experiment in which the immune cells cocultured with FBL-3 tumor and then placed in LF-TCGF had an 8,000-fold expansion and maintained their specific, high levels of cytotoxicity.

For a test of the relative ability of fresh FBL-3 and fresh MCA-103 targets to lyse, DBA/2 lymphocytes were sensitized in vitro to irradiated C57BL/6 lymphocytes in LF-TCGF. Text-figure 5 shows the in vitro lysis of FBL-3, MCA-103, and C57BL/6–Con A blasts at 4 hours and 18 hours when these allosensitized effectors were used. At both times the C57BL/6–Con A blast target demonstrated the most lysis. At 4 hours the relative abilities of fresh FBL-3 and fresh MCA-103 to lyse were equal (text-fig. 5A). At 18 hours these two targets again showed little difference in relative abilities to lyse (text-fig. 5B).

Screening assay for clones.—In all experiments described here, 10^3 cells per well were plated. There were 60 wells with growth of 288 wells plated from the immune sensitization and 121 wells with growth of 288 wells plated from the normal sensitization. On the basis of the Poisson distribution, the chance that growth in a single well arose from a single cell from the immune sensitization was 90% and the chance that growth was from a single cell from the normal sensitization was 75%.

With the use of the screening assay described in "Materials and Methods," we screened all clones from each

TABLE 1.—*Expansion of immune cells with maintenance of specific high-level cytotoxicity after coculture with FBL-3 tumor cells and subsequent placement in LF-TCGF*[a]

Day of expansion	I$_a$FBL-3[b]				NL$_a$NL[c]			
	No. of cells/ well × 10^5	Overall expansion	LU/10^6 cells		No. of cells/ well × 10^5	Overall expansion	LU/10^6 cells	
			Versus FBL-3	Versus MCA-103			Versus FBL-3	Versus MCA-103
0	1.0	—			1.0	—		
7	8.3	8.3	714	ND	5.4	5.4	<1	ND
11	4.4	36.3			4.5	24.3		
15	5.4	197.7			3.5	85		
18	—	—	3,226	<2	—	—	17.4	<2
20	5.2	1,029.7			5.2	442		
28[d]	8.2	8,443.5	1,724	<2	7.5	3,317	<1	<1

[a] At the time of each observation cells were split back to 10^5 cells/well with fresh CM and LF-TCGF. —=not observed. ND=not done.

[b] I$_a$FBL-3=in vivo immunized lymphocytes resensitized to FBL-3 tumor in vitro.

[c] NL$_a$NL=Normal C57BL/6 splenocytes resensitized to normal C57 irradiated stimulators in vitro.

[d] On day 26, cells were split to one-half concentration and fed with fresh CM and LF-TCGF.

TEXT-FIGURE 5.—Relative ability of fresh FBL-3 and MCA-103 tumors to lyse. An IVS of DBA/2 lymphocytes stimulated with irradiated C57BL/6 splenocytes was used. There is no difference in the inability to lyse of fresh FBL-3 tumor when compared to fresh MCA-103 tumor, at either 4 or 18 hr. B6=C57BL/6.

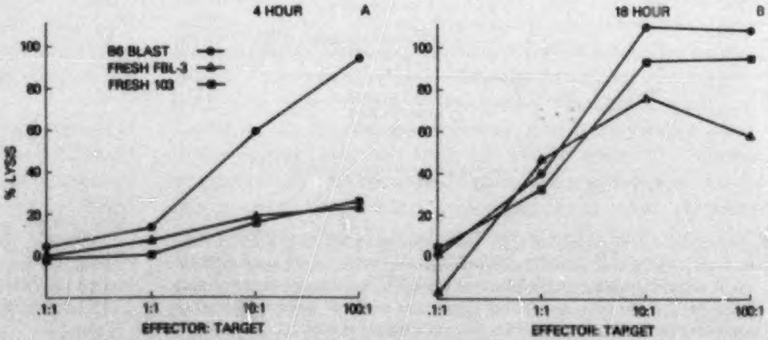

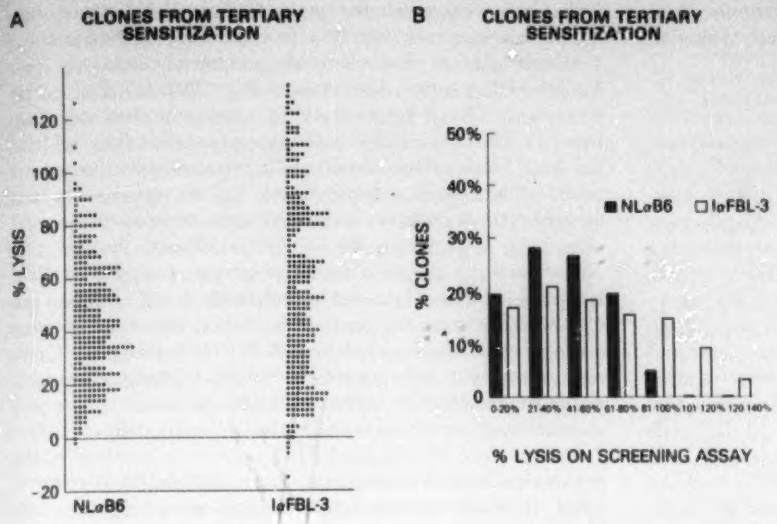

TEXT-FIGURE 6.—Results of a rapid screening assay for cloned lymphoid cells with the use of FBL-3 target cells. A) Results of one assay in which *each dot* represents an individual clone. B) The same data as a percentage of the total number of clones.

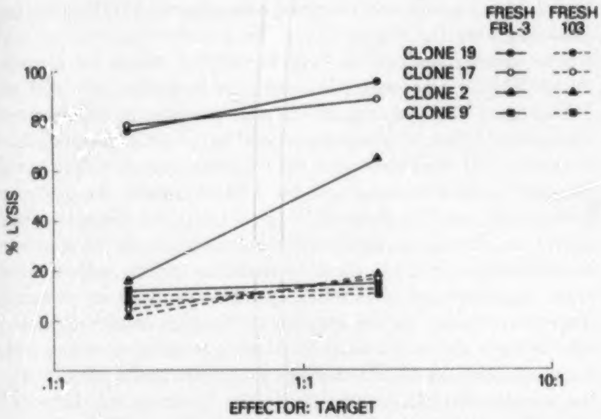

TEXT-FIGURE 7.—Cytotoxicity of several clones at known effector-to-target ratios after 1 mo in LF-TCGF. Clones 19, 17, and 2 were specifically lytic for fresh FBL-3 tumor cells and not for fresh MCA-103 tumor cells. Clone 9' (from an IVS of normal lymphocytes resensitized to normal lymphocytes) is not lytic for either target.

IVS at a single time. Text-figure 6A shows the results of screening clones from the tertiary IVS. Each dot represents one clone. The highest proportion of lytic clones resulted from the in vitro sensitization of the immune lymphocytes with FBL-3 tumor. The distribution of lytic clones is shown in text-figure 6B. Approximately 15% of the total number of clones from the immune cells cocultured with FBL-3 tumor in vitro had cytotoxicity more than 100% in our screening assay, whereas none of the control lymphocytes produced clones with this degree of lysis.

Specificity of clones in an 18-hour ^{51}Cr release assay.—From these screens three cytotoxic clones and one noncytotoxic clone were selected for further study. Text-figure 7 shows that clones 2, 17, and 19 (cytotoxic clones) but not clone 9' (the noncytotoxic clone) were specifically cytotoxic for the fresh FBL-3 tumor but not for the MCA-103 tumor at 1 month. This specific, high degree of cytotoxicity was maintained for 2.5 months. Text-figure 8 shows two assays testing these same four clones against both fresh syngeneic tumor targets. Again, the cytotoxic clones 2, 17, and 19 had extremely high specific cytotoxicity (up to 4,545 LU/10^6/

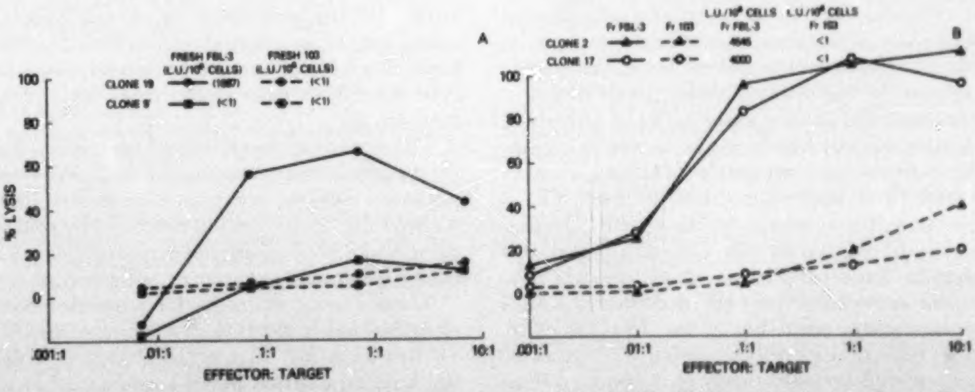

TEXT-FIGURE 8.—Clones from text-figure 7 tested after 2.5 mo of continuous growth in LF-TCGF. A) Clone 19 is shown to be specifically lytic for fresh FBL-3 cells. Clone 9' does not lyse either fresh FBL-3 or fresh MCA-103 tumor cells. B) Clones 2 and 17 are both highly lytic for fresh FBL-3 cells.

cells) compared to less than 1 LU for the noncytotoxic clone 9′. At no time did any of these clones lyse the fresh syngeneic MCA-103 target.

DISCUSSION

Many workers attempted to utilize in vitro sensitization techniques for the generation of cytotoxic lymphoid cells against tumors or tumor antigen (*2–21*). Macrophage presentation of tumor (*4, 6, 10, 24, 25*) and removal of suppressor cells (*33–36*) have been found to be effective in generating cytotoxicity against tumors. Chemically modifying or pretreating the effector population has enhanced cytotoxicity (*27, 33, 34, 42, 43*), and modifying the stimulator population (*33, 43, 44*) similarly has increased cytotoxicity in selected tumor systems. Cytotoxicity has been generated against tumor antigens with the use of peritoneal exudate cells (*13, 26–28*), cells from tumor-bearing animals (*12, 30–32*), cells from in vivo immunized animals (*7–10, 12–15, 17, 27, 29*), and lymphocytes infiltrating the tumor itself (*37–41*).

Helper factors produced by lymphoid cells have also been used to successfully enhance the in vitro generation of cytotoxicity against syngeneic tumors. Kilburn et al. (*45*) described the isolation of a helper factor that enhanced the generation of cytotoxic cells to P815 syngeneic tumor. Similarly, Reyser et al. (*46*) described a supernatant product of a secondary allogeneic mixed lymphocyte culture that, when added to a primary mixed leukocyte–tumor cell culture, increased lytic activity against the syngeneic tumor target. In addition, these authors found the same effect when supernatants from Con A-stimulated spleen cells were added to primary mixed leukocyte–tumor cell cultures.

Since the description by Gillis and Smith (*59*) of long-term culture of tumor-specific cytotoxic T-cells, much work has gone into attempts to grow and maintain cytotoxic T-cells and clones with the use of TCGF. We have previously noted (*51*) a marked enhancement of the generation and expansion of cytotoxic cells attributable to LF-TCGF in allogeneic in vitro sensitizations. Baker et al. (*60*) showed that long-term growth of clones generated from IVS cultures was possible with the use of TCGF with maintenance of specific cytotoxicity. More recently, TCGF has been used during in vitro sensitization of spleen cells from mice bearing the P815 syngeneic mastocytoma to generate high levels of cytotoxicity against the syngeneic tumor target (*32*). Cheever et al. (*47*) also used TCGF to expand cells from an in vitro sensitization of in vivo immunized lymphocytes resensitized to irradiated tumor. They achieved specific cytotoxicity against the cultured syngeneic tumor target.

In the studies reported in this paper we have attempted to generate lymphoid cells highly cytotoxic for the transplantable FBL-3 lymphoma, syngeneic in C57BL/6 mice. Fresh splenocytes from mice immunized to fresh FBL-3 tumor exhibited no in vitro cytotoxicity toward FBL-3 either before or after cocultivation with FBL-3 in vitro. Our results thus differed from those of Cheever et al. (*61–63*) who reported that immune splenocytes were cytotoxic for FBL-3 after in vitro incubation with this tumor. Cheever et al. utilized cultured tumor target cells, however, whereas in all of our experiments we have used tumor cells obtained fresh from the ascites of tumor-bearing mice. Culture of the FBL-3 tumor in xenogeneic serum, as performed by others, may lead to alterations in the lytic susceptibility of these cells.

We did, however, consistently generate cells highly lytic for the FBL-3 tumor by cocultivating cells from immunized mice with FBL-3 tumor cells in vitro and then exposing them to LF-TCGF. This technique generated cells exhibiting high levels of lysis in all eight experiments. The generation of lytic cells required both an in vivo immunized lymphocyte population and a reexposure to the tumor in vitro prior to growth in LF-TCGF (text-figs. 2, 3). Lymphocytes from nonimmune mice cocultivated with FBL-3 or lymphocytes from immune mice cocultivated with normal C57BL/6 splenocytes resulted in much less lysis of fresh FBL-3 tumor when grown in LF-TCGF (text-fig. 3). Cytotoxic lymphoid cells generated by this technique were capable of progressive exponential proliferation for up to 3 months with maintenance of cytotoxicity (text-fig. 4).

Lymphoid cells lytic for FBL-3 were not capable of lysing a non-cross-reactive syngeneic tumor, MCA-103 (text-fig. 4, table 1). Both tumors exhibited approximately the same lysis, however, when they were used as targets for DBA/2 lymphocytes sensitized in vitro to irradiated C57BL/6 lymphocytes (text-fig. 5).

The generation of cells lytic for FBL-3 tumor by growth in LF-TCGF is consistent with the hypothesized role of TCGF as a "second signal" in the generation of immune responses. Spleens obtained 6 weeks after immunization with the FBL-3 tumor probably contain small numbers of memory cells with receptors for FBL-3 tumor. Reexposure of these cells to FBL-3 tumor in vitro results in the activation of this small subpopulation of T-cells, although the number of activated cells is too small to cause consistent lysis (two of eight experiments) of FBL-3 in vitro. Growth of this cell suspension in LF-TCGF appears to result in selective expansion of the activated cells and not of the resting lymphocytes. Expansion could be accomplished in the absence of activating antigen in culture, similar to the findings of others (*50, 64, 65*), probably mediated by the binding of this lymphokine to activated T-cells (*66*). This hypothesis accounts for the requirements of both an in vivo immunized starting cell and a reexposure to the specific tumor cell in vitro prior to expansion in LF-TCGF.

The presence of only a small number of highly reactive cells following in vitro sensitization was also seen in our studies of the generation of cloned lymphoid lines after reexposure of immunized cells to FBL-3 in vitro (text-fig. 6). Only about 5% of immune lymphoid clones are more highly lytic for FBL-3 than clones from nonimmunized cultures (text-fig. 6).

The cytotoxic expanded cultures were totally dependent on the continued presence of TCGF. We have been able to maintain cultures in exponential growth for over 3 months without the "crisis" period described by others (*47, 67*). Cell growth and maintenance of cytotoxicity were not dependent on the continued presence of antigen (tumor cells).

The screening technique for cytotoxic clones that we have described has enabled us to select rare, highly cytotoxic cells for further study. The initial testing of cells directly from the limiting dilution plates is conducted at unknown effector-to-target ratios and results in an inherent advantage to rapidly growing cells. This technique might miss slowly growing, highly cytotoxic clones that are represented by very few cells. Suitable clones can then be selected and grown in LF-TCGF with maintenance of antitumor cytotoxic specificity for over 2.5 months (text-figs. 7, 8). On the basis of probabilities of cell distribution according to the Poisson distribution, the clones we have described have an 80% chance of having arisen from a single cell. These "clones" have now been "recloned" to increase the probability of derivation from a single effector cell.

When compared to the use of bulk T-cell cultures, the use of a cytolytic T-cell clone for studies of the cellular immune response to tumors offers several advantages. Presumably, all cells derived from cytolytic clones are themselves lytic. Moreover, the cloning of cytolytic cells provides the opportunity to remove suppressor or other modulator cells that might abrogate the effect of cytolytic T-cells on target tumor cells.

A potential problem exists in the selection of cells to be used in adoptive immunotherapy on the basis of in vitro reactivity in ^{51}Cr release cytotoxicity assays. In vivo effect may not correlate with the results of in vitro assays and in fact the primary effector cell in vivo may be a cell type other than a cytotoxic cell (i.e., helper cell). Indeed, this could explain why in vivo immunized cells (text-fig. 1) are effective in eradicating a tumor in vivo but demonstrate no cytotoxicity in vitro. This hypothesis is supported by the findings of Fernandez-Cruz et al. (*68*), who showed that the subset of T-cells most effective in in vivo tumor eradication was the least cytotoxic in an in vitro ^{51}Cr release assay. In experiments to be presented elsewhere, we have shown that adoptive transfer of lytic cells expanded in TCGF is effective in curing mice with disseminated FBL-3 lymphoma.

The methods described in this paper have been very effective in generating and maintaining cytotoxic effector cells directed against the syngeneic FBL-3 lymphoma. Further study of cytotoxic clones will be useful in the elucidation of tumor–effector cell interactions both in vitro and in vivo.

REFERENCES

(*1*) Rosenberg SA, Terry WD. Passive immunotherapy of cancer in animals and man. Adv Cancer Res 1977; 25:323–387.

(*2*) Treves AJ, Cohen IR, Feldman M. *Brief communication:* Immunotherapy of lethal metastases by lymphocytes sensitized against tumor cells in vitro. J Natl Cancer Inst 1975; 54:777–780.

(*3*) Bernstein ID, Wright PW, Cohen E. Generation of cytotoxic lymphocytes in vitro. Response of immune rat spleen cells to a syngeneic gross-virus induced lymphoma in mixed lymphocyte-tumor culture. J Immunol 1976; 116:1367–1372.

(*4*) Treves AJ, Feldman M, Kaplan HS. *Brief communication:* Macrophage mediated in vitro sensitization of T lymphocytes. I. Detection of murine leukemia virus-associated antigens. J Natl Cancer Inst 1977; 58:1527–1529.

(*5*) Kedar E, Schwartzbach M, Raanan Z, Hefetz S. In vitro induction of cell-mediated immunity to murine leukemia cells. II. Cytotoxic activity in vitro and tumor-neutralizing capacity of anti-leukemia cytotoxic lymphocytes generated in macrocultures. J Immunol Methods 1977; 16:39–58.

(*6*) Treves AJ, Schechter B, Cohen IR, Feldman M. Sensitization of T-lymphocytes in vitro by syngeneic macrophages fed with tumor antigens. J Immunol 1976; 116:1059–1064.

(*7*) Plata F, Cerottini JC, Brunner KT. Primary and secondary in vitro generation of cytolytic T-lymphocytes in the murine sarcoma virus system. Eur J Immunol 1975; 5:227–233.

(*8*) Glaser M, Herberman RB, Kirchner H, Djeu JY. Study of the cellular immune response to Gross-induced lymphoma by the mixed lymphocyte-tumor interaction. Cancer Res 1974; 34:2165–2171.

(*9*) Rollinghoff M. Secondary cytotoxic tumor immune response induced in vitro. J Immunol 1974; 112:1718–1725.

(*10*) De Landazuri MO, Herberman RB. In vitro activation of cellular immune response to Gross virus-induced lymphoma. J Exp Med 1972; 136:969–983.

(*11*) Wagner H, Rollinghoff M. In vitro induction of tumor specific immunity. I. Parameters of activation and cytotoxic reactivity of mouse lymphoid cells immunized in vitro against syngeneic and allogeneic plasma cell tumors. J Exp Med 1973; 138:1–15.

(*12*) Ting CC, Bonnard GD. Cell mediated immunity to Friend virus-induced leukemia. IV. In vitro generation and secondary cell mediated cytotoxic responses. J Immunol 1976; 116:1419–1425.

(*13*) Ting CC, Kirchner H, Rodriques D, Park JY, Herberman RB. Cell mediated immunity to Friend virus-induced leukemia. III. Characteristics of secondary cell-mediated cytotoxic response. J Immunol 1976; 116:244–252.

(*14*) Bernstein ID. Passive transfer of systemic tumor immunity with cells generated in vitro by a secondary immune response to a syngeneic rat Gross virus-induced lymphoma. J Immunol 1977; 118:122–128.

(*15*) Plata F, Jongeneel CV. Characterization of effector lymphocytes associated with immunity to murine sarcoma virus (MSV)-induced tumors. II. Repeated stimulation and proliferation in vitro of specific cytolytic T lymphocytes. J Immunol 1977; 119:623–629.

(*16*) Bartlett PF, Fenderson BA, Edidin M. Inhibition of tumor growth mediated by lymphocytes sensitized in vitro to a syngeneic murine teratocarcinoma 402AX. J Immunol 1978; 120:1211–1217.

(*17*) Kall MA, Hellström I, Hellström KE. In vitro generation of primary and secondary cytotoxic cell-mediated immune responses to chemically induced mouse sarcomas. Int J Cancer 1976; 18:488–497.

(*18*) Burton RC, Warner NL. In vitro induction of tumor specific immunity. IV. Specific adoptive immunotherapy with cytotoxic T cells induced in vitro to plasmacytoma antigens. Cancer Immunol Immunother 1977; 2:91–99.

(*19*) Kedar E, Schwartzbach M, Hefetz S, Raanan Z. In vitro induction of cell-mediated immunity to murine leukemia cells. V. Adoptive immunotherapy of leukemia in mice with lymphocytes sensitized in vitro to leukemia cells. Cancer Immunol Immunother 1978; 4:151–159.

(*20*) Röllinghoff M, Wagner H. *Brief communication:* In vivo protection against murine plasma cell tumor growth by in vitro activated syngeneic lymphocytes. J Natl Cancer Inst 1973; 51:1317–1318.

(*21*) Small M, Trainin N. Inhibition of syngeneic fibrosarcoma growth by lymphocytes sensitized on tumor cell monolayers in the presence of the thymic humoral factor. Int J Cancer 1975; 15:962–972.

(*22*) Hellström KE, Hellström I. Lymphocyte mediated cytotoxicity and blocking serum activity to tumor antigens. Adv Immunol 1974; 18:209–277.

(*23*) Lundak RL, Raidt DJ. Cellular immune response against [illegible] cells. I. In vitro immunization of allogeneic and syngeneic mouse spleen cell suspensions against DBA mastocytoma cells. Cell Immunol 1973; 9:60–66.

(*24*) Erb P, Feldman M. The role of macrophages in the generation of T-helper cells. III. Influence of macrophage derived factors in helper cell induction. J Immunol 1975; 5:759–766.

(*25*) Unanue ER. The regulatory role of macrophages in antigen stimulation. Adv Immunol 1972; 15:95–165.

(*26*) Chauvenet PH, McArthur CP, Smith RT. Demonstration in vitro of cytotoxic T cells with apparent specificity toward tumor-specific transplantation antigens on chemically induced tumors. J Immunol 1979; 123:2575–2581.

(*27*) Vasudevan DM, Brunner KT, Cerottini JC. Detection of cytotoxic T lymphocytes in the EL4 mouse leukemia system: Increased activity of immune spleen and peritoneal cells following preincubation and cell fractionation procedures. Int J Cancer 1974; 14:301–313.

(*28*) Hellström I, Hellström KE. Specific sensitization of lymphocytes to tumor antigens by co-cultivation with peritoneal cells exposed to such antigens. Int J Cancer 1976; 17:748–754.

(*29*) Glaser M, Bonnard GD, Herberman RB. In vitro generation of secondary [illegible]-mediated cytotoxic response against a syngeneic

Gross virus-induced lymphoma in rats. J Immunol 1976; 116:430-436.

(*30*) Takei F, Levy JG, Kiburn DG. In vitro induction of cytotoxicity against syngeneic mastocytoma and its suppression by spleen and thymus cells from tumor bearing mice. J Immunol 1976; 116:288-293.

(*31*) Schechter B, Treves AJ, Feldman M. Specific cytotoxicity in vitro in lymphocytes sensitized in culture against tumor cells. J Natl Cancer Inst 1976; 56:975-979.

(*32*) Mills GB, Paetkau V. Generation of cytotoxic lymphocytes to syngeneic tumor by using co-stimulator (interleukin 2). J Immunol 1980; 125:1897-1903.

(*33*) Kedar E, Lapu T, Schwartzbach M, Avraham Y. In vitro induction of cell mediated immunity to murine leukemia cells. VII. Methods for augmenting the induction and expression of cytotoxic response in vitro to syngeneic tumors. J Immunol Methods 1979; 26:157-171.

(*34*) Treves AJ, Feldman M, Kaplan H. In vitro sensitization of human lymphocytes against histiocytic lymphoma cell lines: I. Primary sensitization of lymphocyte subpopulations. J Immunol 1977; 119:955-960.

(*35*) Nachtigal D, Zanbar I, Feldman M. The role of specific suppressor T-cells in immune response. Transpl Rev 1975; 26:87-105.

(*36*) Röllinghoff M, Starzinski-Powitz A, Pfizenmaier K, Wagner H. Cyclophosphamide-sensitive T-lymphocytes suppress the in vivo generation of antigen-specific cytotoxic T-lymphocytes. J Exp Med 1977; 145:455-459.

(*37*) Gillespie GY, Hansen CB, Hoskins RG, Russell SW. Inflammatory cells in solid murine neoplasms. IV. Cytolytic T-lymphocytes isolated from regressing or progressing sarcomas. J Immunol 1977; 119:564-570.

(*38*) Klein E, Becker S, Svedmyr E, Jondal M, Vanky F. Tumor infiltrating lymphocytes. Ann NY Acad Sci 1976; 276:207-216.

(*39*) Haskill JS, Yamamura Y, Radov L. Host responses within solid tumors: Non-thymus derived specific cytotoxic cells within a murine mammary adenocarcinoma. Int J Cancer 1975; 16:798-809.

(*40*) Delustro F, Haskill JS. In situ cytotoxic T-cells in a methylcholanthrene-induced tumor. J Immunol 1978; 121:1007-1009.

(*41*) Yron I, Wood TA Jr, Spiess PJ, Rosenberg SA. In vitro growth of murine T-cells. V. The isolation and growth of lymphoid cells infiltrating syngeneic solid tumors. J Immunol 1980; 125:238-245.

(*42*) Ferguson R, Anderson SM, Schmidtke JR, Simmons RL. Effect of *Vibrio cholerae* neuraminidase on the generation of cell-mediated cytotoxicity in vitro. J Immunol 1976; 117:2150-2157.

(*43*) Kedar E, De Landazuri MO, Fahey JL. Enzymatic enhancement of cell mediated cytotoxicity and antibody-dependent cell cytotoxicity. J Immunol 1974; 112:26-36.

(*44*) Kedar E, Lupu T. In vitro induction of cell mediated immunity to murine leukemia cells. IV. Amplification of the generation of cytotoxic lymphocytes by enzymatically and chemically modified stimulator leukemic cells. J Immunol Methods 1978; 21:35-50.

(*45*) Kilburn DG, Talbot FO, Teh HS, Levy JG. A specific helper factor which enhances the cytotoxic response to a syngeneic tumour. Nature 1979; 277:474-476.

(*46*) Reyser J, Cerottini J, Brunner KT. Cell-mediated immunity to antigens associated with murine sarcoma virus-induced tumors: Augmentation of cytolytic T-lymphocyte activity by successive specific and non-specific stimulation in vitro. Eur J Immunol 1979; 9:179-184.

(*47*) Cheever MA, Greenberg PD, Fefer A. Specific adoptive therapy of established leukemia with syngeneic lymphocytes sequentially immunized in vivo and in vitro and non-specifically expanded by culture with interleukin 2. J Immunol 1981; 126:1318-1322.

(*48*) Smith KA, Baker PE, Gillis S, Ruscetti FW. Functional and molecular characteristics of T-cell growth factor. Mol Immunol 1980; 17:579-589.

(*49*) Rosenberg SA, Schwarz S, Spiess PJ, Brown JM. In vitro growth of murine T-cells. III. Method for separation of T-cell growth factor (TCGF) from concanavalin A and biological activity of the resulting TCGF. J Immunol Methods 1980; 33:337-350.

(*50*) Baker PE, Gillis S, Fern MM, Smith KA. The effect of T-cell growth factor on the generation of cytotoxic T-cells. J Immunol 1978; 121:2168-2173.

(*51*) Spiess PJ, Rosenberg SA. A simplified method for the production of murine T-cell growth factor free of lectin. J Immunol Methods 1981; 42:213-222.

(*52*) Glynn JP, McCoy JL, Fefer A. Cross-resistance to the transplantation of syngeneic Friend, Moloney and Rauscher virus-induced tumors. Cancer Res 1968; 28:434-439.

(*53*) Parker GA, Rosenberg SA. Serologic identification of multiple tumor-associated antigens on murine sarcomas. J Natl Cancer Inst 1977; 58:1303-1309.

(*54*) Fass L, Fefer A. Studies of adoptive chemoimmunotherapy of a Friend virus-induced lymphoma. Cancer Res 1972; 32:997-1001.

(*55*) ———. Factors related to therapeutic efficacy on adoptive chemoimmunotherapy of a Friend virus-induced lymphoma. Cancer Res 1972; 32:2427-2431.

(*56*) Fefer A, Einstein AB Jr, Cheever MA, Berenson JR. Models for syngeneic adoptive chemoimmunotherapy of murine leukemias. Ann NY Acad Sci 1976; 276:573-583.

(*57*) Rosenberg SA, Spiess PJ, Schwarz S. In vitro growth of murine T cells. IV. Use of T cell growth factor (TCGF) to clone lymphoid cells. Cell Immunol 1980; 54:293-306.

(*58*) Rosenberg SA, Schwarz S, Spiess PJ. In vitro growth of murine T cells. II. Growth of in vitro sensitized cells cytotoxic for alloantigens. J Immunol 1978; 121:1951-1955.

(*59*) Gillis S, Smith KA. Long term culture of tumour specific cytotoxic T cells. Nature 1977; 268:154-156.

(*60*) Baker PE, Gillis S, Smith KA. Monoclonal cytolytic T-cell lines. J Exp Med 1979; 149:273-279.

(*61*) Cheever MA, Kempf RA, Fefer A. Tumor neutralization immunotherapy and chemoimmunotherapy of a Friend leukemia with cells secondarily sensitized in vitro. J Immunol 1977; 119:714-718.

(*62*) Cheever MA, Greenberg PD, Fefer A. Specificity of adoptive chemoimmunotherapy of established syngeneic tumors. J Immunol 1980; 125:711-714.

(*63*) ———. Tumor neutralization, immunotherapy and chemoimmunotherapy of a Friend leukemia with cells secondarily sensitized in vitro. II. Comparison of cells cultured with and without tumor to noncultured immune cells. J Immunol 1978; 121:2220-2227.

(*64*) Ruscetti FW, Morgan DA, Gallo RC. Functional and morphologic characterization of human T-cells continuously grown in vitro. J Immunol 1977; 119:131-138.

(*65*) Gillis S, Fern MM, Ou W, Smith KA. T cell growth factor: Parameters of production and a quantitative microassay for activity. J Immunol 1978; 120:2027-2032.

(*66*) Smith KA, Gillis S, Baker PE, McKenzie D, Russetti FW. T cell growth factor mediated T-cell proliferation. Ann NY Acad Sci 1979; 332:423-432.

(*67*) Watson J. Continuous proliferation of murine antigen specific helper T-lymphocytes in culture. J Exp Med 1979; 150:1510-1519.

(*68*) Fernandez-Cruz E, Woda BA, Feldman M. Elimination of syngeneic sarcomas in rats by a subset of T-lymphocytes. J Exp Med 1980; 152:823-841.

Pathogenesis of Lesions Induced in Rat Lung by Chronic Tobacco Smoke Inhalation[1,2,3]

Carol A. Heckman, *Ph.D.*,[4] *and* **Walden E. Dalbey**, *Ph.D.*[4,5]

ABSTRACT—Lesions were induced in the lungs of specific-pathogen-free F344 rats by chronic tobacco smoke exposure. Animals exposed to 7 cigarettes/day were killed after 1, 1.5, or 2 years of exposure. Parallel lifetime exposures induced pulmonary tumors in 9% of the animals. In serially killed animals, four types of lesions were found: 1) perivascular or peribronchiolar accumulation of lymphoreticular cells, 2) fibrotic and cellular enlargement of peribronchiolar septa, 3) type II cell hyperplasia with septal fibrosis, and 4) air-space enlargement (emphysema). However, emphysema occurred only in animals exposed to a higher (10 cigarettes) dose of tobacco smoke. Ultrastructural studies showed all of the focal lesions to be infiltrated by cells typical of the inflammatory response. The type II hyperplastic and peribronchiolar alveolar lesions involved larger portions of the parenchyma in fibrotic changes but differed in structure, location, and frequency. The incidence of the peribronchiolar alveolar lesions was temporally related to tumor incidence.—JNCI 1982; 69:117–129.

Numerous previous reports have described the effects of tobacco smoke exposure on lung structure. In studies by Roe's group (*1, 2*), the major lesions induced in the rat lung by lifetime exposure were columnar, cuboidal, and squamous metaplasias of the alveolar epithelium. All three types of lesions were significantly more frequent in smoke-exposed than in control animals (*1*) and could be induced by intratracheal instillation of smoke condensate (*2*). However, neoplasms could be induced only by intratracheal instillation of the polycyclic aromatic hydrocarbon-containing fraction of smoke condensate (*2*). No statistically significant increase in pulmonary neoplasm incidence was found in animals exposed to smoke by inhalation, presumably because the animals died prematurely from chronic respiratory disease (*1*).

Short-term studies conducted independently by Walker et al. (*3*) on rats exposed to tobacco smoke for 6 weeks showed characteristic lesions at the level of the respiratory bronchiole, including peribronchiolar and perivascular infiltration by lymphocytes, focal pneumonitis, and alveolar cuboidal or columnar metaplasia. The metaplastic changes, along with increases in macrophage size and number, were thought to be dose-dependent. The other lesions were considered early manifestations of chronic pulmonary infection (*3*). Morphologic changes have also been induced in the lungs of beagle dogs by 2–5 years of tobacco smoke exposure (*4*). Marked fibrosis and emphysema were found, as were type II cell hyperplasia and squamous metaplasia of the alveolar epithelium. At the epithelial–mesenchymal interface, projections of the epithelial cells into the stroma and thickening and reduplication of the basal lamina (*5*) were also seen.

Despite the substantial number of experiments with chronic tobacco smoke inhalation, only two laboratories have reported significant induction of pulmonary tumors in exposed rodents. One report showed a twofold higher incidence of adenocarcinomas in smoke-exposed mice than in control mice. The gas phase of the smoke was found to induce an even higher tumor incidence than the whole smoke (*6*). More recently, a lifetime exposure of rats to tobacco smoke produced a 9% incidence of respiratory tract tumors, including adenomas, adenocarcinomas, and squamous cell carcinomas (*7*). In this experiment, animals exposed in parallel with those for the lifetime study were killed at earlier intervals for assessment of morphologic lesions induced by smoke inhalation. The present report characterizes those lesions. Many of the alterations appeared to be similar to those described above. However, 1 lesion was found that had not been found in previous experiments, i.e., fibrotic thickening of alveolar septa in peribronchiolar locations.

MATERIALS AND METHODS

Exposure conditions.—SPF female F344 rats were exposed to tobacco smoke in the Maddox/ORNL smoking machine as previously described (*7*). Beginning at 12–14 weeks of age, the animals were gradually exposed to increasing dosages of tobacco smoke from standard 85-mm, nonfiltered experimental cigarettes (National Cancer Institute code 16). Two final dose levels were used, 7 or 10 cigarettes/day, and the animals were killed at time intervals from 1 to 2 years after exposure began. The exact number of animals killed at various times in each dose group is shown in table 1. Since mortality was high in the 10-cigarette-per-day group, all the remaining animals in this group were killed at 1.5 years. Both untreated and sham-exposed groups were killed in parallel with the exposed animals. Additional data were

ABBREVIATION USED: SPF=specific-pathogen-free.

---

[1] Received July 27, 1981; revised January 9, 1982; accepted February 9, 1982.

[2] Supported by the Environmental Protection Agency under interagency agreement 81-D-X0533; by the National Cancer Institute under interagency agreement 40-484-74; and by the Office of Health and Environmental Research, U.S. Department of Energy, under contract W-7405-eng-26 with the Union Carbide Corporation.

[3] Animals were maintained under the guidelines set forth by the Biology Division, Oak Ridge National Laboratory.

[4] Biology Division, Oak Ridge National Laboratory, P.O. Box Y, Oak Ridge, Tenn. 37830.

[5] We are grateful to Dr. Paul Nettesheim, National Institute of Environmental Health Sciences, Durham, N.C.: to Dr. Michael Fry and Dr. Robert Ullrich, Oak Ridge National Laboratory, Oak Ridge, Tenn., for support and critical comments on the manuscript; and to Dr. Donald Swartzendruber, Oak Ridge Associated Universities, Oak Ridge, Tenn., for the use of his electron microscope facility. We thank Mr C. D. Farmer for technical assistance.

TABLE 1.—*Number of animals used for morphogenesis studies*

Duration of smoke exposure, yr	No. of animals			
	Treatment group: Untreated	Sham treated	7 cigarettes/day	10 cigarettes/day
1.0	10	10	10	8
1.5	9	9	9	14
2.0	10	12	11	0
2.5	2	4	6	0

obtained from animals in the lifetime study; these rats were killed after exposure for 2.5 years and maintenance for an additional 7 months without exposure. One animal from each treatment group was tested for infective organisms. Blood samples were tested by Microbiological Associates, Bethesda, Md., for the presence of serum antibodies to several viruses: PVM (pneumonia virus of mice), Reo-3 (reovirus type 3), GDVII (Theiler's mouse encephalomyelitis GDVII), k (newborn mouse pneumonitis, k-virus), polyomavirus, MVM (minute virus of mice), MHV (mouse hepatitis virus), Sendai virus, and RCV (rat corona virus). Cultures prepared from the postcaval lung lobe were tested for mycoplasma (*8*). All test results were negative.

Tissue preparation.—Before they were killed, the animals were anesthetized with 30 mg pentobarbital/kg body weight. For tissue fixation the trachea was cannalized; the airways and lungs were removed and fixed with buffered formaldehyde under 20 cm of pressure for 24–48 hours. The lung lobes were cut along the bronchus, except for the left lobe, which was cut in cross section just anterior to the entry of the bronchus. The tissues were embedded in paraffin. Sections from the right lobes were used to determine the number of fibrotic lesions in the lungs of smoke-exposed animals. All of the sections were examined, and the cumulative number of lesions, normalized to the number of animals killed, was used as an estimate of the frequency of each type of lesion. Sections from the left lobes, stained with hematoxylin and eosin, were used for morphometric analysis. For each sample, 10 fields were selected at random and viewed at 100× magnification through a Weibel ocular. Fields comprised of more than one-third conducting airways or vasculature were excluded. The mean linear intercept was determined, and point counts (420 points/lobe) were made to obtain the volume percent of alveolar versus nonalveolar air space and respiratory versus nonrespiratory tissue. Alveoli were defined as enclosed circles or as open semicircles with a radius greater than half the distance across the opening. Additional sections of the left lobes were stained with Snook's silver stain for reticulum, aldehyde fuchsin, and Lushbaugh's stain.

Each time rats were killed, tissues were also processed for electron microscopy by airway perfusion of a 2% glutaraldehyde solution containing 4.6% Tyrode's solution and 0.05 *M* collidine buffer (pH 7.3). The tissues were fixed for 2 hours under 15-cm pressure and retained in collidine buffer until further processing. After exposure to 2% osmium tetroxide in 0.1 *M* cacodylate for 3 hours, selected blocks of tissue were dehydrated in acetone and embedded in a standard epoxy mixture (*9*). Sections 2 μm in thickness were cut on the Sorvall JB-4 microtome and stained with 0.05% toluidine blue in 2.5% sodium carbonate. Selected areas of the blocks were thin sectioned on the Sorvall MT-2 ultramicrotome, mounted on Formvar-coated grids, and stained with uranyl acetate and lead citrate (*10*). Thin sections were examined with the Siemens 101 or Hitachi HU-11B electron microscope. For each pathologic change studied, at least four examples were examined ultrastructurally.

RESULTS

Some changes in the lung parenchyma following smoke exposure were readily apparent on a gross level. Lungs from animals exposed to 7 cigarettes/day for 1 year had dark foci about 1 mm in diameter scattered over their surfaces. With longer exposures or with exposure to 10 cigarettes/day, there were increasing numbers of larger white nodules about 1–4 mm in diameter. Four types of lesions could be distinguished microscopically in the pulmonary parenchyma: 1) perivascular or peribronchiolar accumulation of lymphoreticular cells, 2) fibrotic and cellular enlargement of peribronchiolar septa, 3) type II cell hyperplasia with septal fibrosis, and 4) air-space enlargement (emphysema). The first type of lesion was most common in the lungs of animals exposed to 7 cigarettes/day for 2 years. The last lesion type was seen only in animals exposed to 10 cigarettes/day.

Perivascular or Peribronchiolar Cell Accumulation

Perivascular lesions occurred frequently in the lung parenchyma after 2 years of smoke exposure, averaging 3 lesions/section of approximately 0.5 cm^2. The frequency after a 2-year exposure was approximately double that after a 1-year exposure. The lesions were characteristically associated with venules and arterioles in the parenchyma. They were most common in branches of the pulmonary vein located at or below the level of the terminal bronchiole (figs. 1A, 1B) and were also found in bronchial veins, but they were never seen in the adventitia of major arteries. Perivascular accumulations of cells were also found rarely in unexposed rats and consisted of large lymphocytes and macrophages (fig. 1C). The lesions of smoke-exposed lung tissues contained predominantly particulate-laden macrophages (figs. 1A, 1B). An ultrastructural analysis of several lesions associated with venules showed that lymphocytes, plasma cells, and, occasionally, fibroblasts were closely apposed to macrophages in the adventitia (fig. 2). While macrophages and lymphocytes were usually seen adjacent to the basal lamina of the epithelium, the cell mass was separated from the epithelium by a basement membrane in some lesions. In addition to the adventitial lesions, a separate lesion was sometimes found around major veins, consisting of lymphocytes within the lumen of lymphatic vessels. The lymphatic endothelium in these lesions frequently contained smoke particulates (figs. 3A, 3B). However, lesions with characteristics intermediate between those of the lymphatic and adventitial lesions were not found, so a common etiology seemed unlikely.

Lesions similar to the other adventitial perivascular lesions were also found near the bronchiolar–alveolar junction, most frequently between the bronchiole and the bronchial vein and extending only part of the way around the bronchiole. Therefore, most of these lesions were also perivascular in location.

Fibrotic and Cellular Enlargement of Peribronchiolar Septa

Septal enlargement was characteristic in peribronchiolar locations, but it was also found in type II hyperplasias. The enlarged septa in both lesions had similar ultrastructural features. Generally, both histologic types of lesions were larger than perivascular lesions and could be discerned readily in paraffin-embedded lung tissue. Neither type of lesion was found in the lungs of control animals, and the frequency of both types increased with the number of cigarettes smoked and the cumulative time of smoke exposure (table 2). The type II hyperplastic lesions always constituted more than 90% of the total number of large lesions. However, the total number of peribronchiolar lesions increased markedly in the later stages of exposure at a dose of 7 cigarettes/day. In animals exposed at the higher dose rate of 10 cigarettes/day for 1.5 years, the peribronchiolar lesions constituted only 2% of the large lesions, even though the cumulative dose of tobacco smoke was comparable to that delivered in the 2-year exposure at the lower dose rate. The peribronchiolar lesions constituted 7% of the large lesions under the latter conditions. In paraffin-embedded sections treated with Lushbaugh's stain for collagen, the amount of collagen seen in lesions showing septal enlargement appeared to increase in relation to the dose of tobacco smoke. No obvious increases in reticular fibers (Snook's silver stain) or elastic fibers (aldehyde fuchsin) were observed.

Although the two types of lesions exhibiting septal enlargement differed in location, frequency, and the type of lining epithelium present, the septal constituents were similar when examined ultrastructurally. Peribronchiolar lesions were characterized by an attenuated epithelium (fig. 4A) and by distortion of the normal semicircular profile of the alveoli (fig. 4B). In extreme cases, the septa were fused into a single mass. About half of the enlargement lesions in peribronchiolar locations also showed alveolar bronchiolization (fig. 4C), and a new columnar epithelium frequently appeared to extend into the alveolar duct (fig. 4A). Although septal thickening may also have occurred in loci separate from larger lesions, this was evidently rare; a few areas where enlargement was seen in isolation from neighboring lesions were found by serial sectioning to be adjacent to lesions. Type II hyperplastic lesions were observed most frequently at the pleura (figs. 5A–5C) but were also in the lung parenchyma adjacent to the distal airways (fig. 1B). In animals exposed to a dose of 7 cigarettes/day for 1 or 2 years, about 60% of the lesions were located on the pleura. When pleural lesions embedded in epoxy resins were serially sectioned, nearly all of them were found to be adjacent to sites where one or more alveolar ducts terminated on the pleura; about half were also distal to or surrounding perivascular lesions (fig. 5B). Fibrosis was obvious at the light microscopic level in the alveolar septa of all type II cell lesions.

The septal enlargements studied by electron microscopy contained numerous cells of the lymphoreticular system, i.e., plasma cells, lymphocytes, polymorphonuclear leukocytes, macrophages, and mast cells. Fibroblasts were also seen in all of the lesions and frequently appeared hypertrophic relative to those in unaffected septa (fig. 6). There were also extensive bundles of collagen fibers within the interstitium. Capillaries within the septa had swollen or hypertrophic endothelial cells that frequently occluded the lumen. In other areas the basal lamina showed extensive thickening, infolding, or reduplication (fig. 6).

The largest peribronchiolar lesions exhibited an aberrant morphology in which lengths of the basal lamina were completely surrounded by lymphoreticular cells, indicating areas of probable fusion of adjacent septa. Although the cellular constituents were similar to those in smaller lesions, they included fragments of cells embedded in an amorphous extracellular material resembling fibrin (fig. 7). These were thought to be derived from capillaries that were no longer patent. In densely fibrotic and cellular areas, there were relatively few capillaries of normal appearance. Both the squamous and type II epithelial cells in these areas sometimes contained an osmiophilic cytoplasm with an elaborate endoplasmic reticulum. Both epithelial cells and fibroblasts in these areas frequently contained osmiophilic granules resembling lipid droplets (fig. 7).

TABLE 2.—*Number and percent incidence of large lesions observed in lung after chronic tobacco smoke exposure*[a]

Duration of smoke exposure, yr	No. of large lesions and percent incidence			
	7 cigarettes/day		10 cigarettes/day	
	Peribronchiolar[b] (%)	Type II[b] (%)	Peribronchiolar[b] (%)	Type II[b] (%)
1.0	0.3±0.1 (33)[c]	9.1±2.6 (89)[d,e]	0.1±0.1 (14)	11.6±3.0 (86)[f]
1.5	0.7±0.4 (43)[g]	17.4±3.4 (86)[e,h]	0.5±0.2 (42)	25.5±2.5 (100)[f]
2.0	1.9±0.4 (90)[c,g]	25.3±4.5 (100)[d,h]	—	—

[a] *P*-values for the peribronchiolar comparisons were derived by a conditional exact test. Corresponding values for the type II lesion comparisons were derived by *t*-tests.

[b] Values are means ± SEM.

[c] $P \le 0.02$.

[d] $P \le 0.001$.

[e] $P \le 0.05$.

[f] $P \le 0.01$.

[g] $P \le 0.06$.

[h] $P \le 0.07$.

Type II Cell Hyperplasia

The cellular and extracellular constituents involved in enlargement of the interstitium in type II hyperplastic lesions were similar to those described in the preceding section. All of the type II lesions studied showed some degeneration of basal lamina structure; in areas where marked degeneration occurred, the type I epithelium was separated from the underlying connective tissue (fig. 8). Degenerative changes were frequently, though not always, found in areas where luminal macrophages were in close contact with the type I epithelium. The presence of phagocytes (i.e., macrophages and polymorphonuclear leukocytes) in the interstitium had little relationship to the position of basal lamina degeneration. The lining epithelium in hyperplastic lesions consisted of cells with an undifferentiated appearance, which could be flattened, distorted in shape, or hypertrophic. Some of the cells showed long microvilli on their luminal surfaces. In addition, most lesions contained cuboidal, type III cells, with an extensive endoplasmic reticulum rather than the lamellar bodies typical of type II cells (fig. 9). Other type III cells had a dense cytoplasm, abundant profiles of endoplasmic reticulum, and osmiophilic inclusions (fig. 10). Lymphocytes were frequently found as cellular constituents of the epithelium. Binucleate cells and evidence of stratification in the epithelium were seen in about half of the lesions. A few lesions also contained large cells with an exceptionally clear cytoplasm (fig. 8).

Air-Space Enlargement

In addition to the focal lesions described above, we detected a general tendency for enlargement of the air space in animals exposed to a high dose of tobacco smoke for 1 year or more. This trend was indicated by an increase in the apparent nonalveolar air space. Although a similar trend was seen in the surviving animals of the low-dose group, it fell short of statistical significance. Exposure of animals to 7 cigarettes/day for up to 2.5 years did not significantly influence the mean linear intercept (table 3). However, exposure to 10 cigarettes/day had a more pronounced effect on lung architecture: The mean linear intercept was increased significantly above control levels at both 1 and 1.5 years of exposure (table 3).

DISCUSSION

We obtained the present results on tobacco smoke inhalation in parallel with a lifetime study that demonstrated the induction of several types of lung tumors by tobacco smoke (*7*). The animals were maintained under SPF conditions; thus the histopathologic interpretation of pulmonary lesions was not complicated by chronic lung disease, and survival was not compromised by infection. In the lifetime experiment, the observation of tobacco smoke-induced tumors clearly was dependent on the long-term survival of the experimental animals. The mean survival time (± SD) was 2.3±0.6 years for rats exposed to 7 cigarettes/day, 2.4±0.4 years for untreated controls, and 2.6±0.4 years for sham-exposed controls. The survival curves for these 3 groups were not significantly different. The earliest of the 5 adenomas found among the treated animals appeared at 2.0 years, and the average age at death of the animals with these tumors was 2.6 years. For the 5 other lung and nasal tumors, which were adenocarcinomas and a squamous cell carincoma, the average age at death was 3.1 years. Only 1 alveologenic carcinoma was observed in the control animals over their life-span. The final incidences of respiratory tract tumors were 9 and 1% in the experimental and control groups, respectively.

The present studies have shown that the most common type of focal lesions to develop in the lungs of tobacco smoke-exposed animals consisted of accumulated lymphocytes and macrophages in the vascular adventitia. Similar accumulations were also found in the lamina propria of terminal bronchioles, where some of them were continuous with lesions surrounding the bronchial veins or branches of the pulmonary veins. While all of the focal lesions were found to include cellular infiltrates typical of the inflam-

TABLE 3.—*Morphometric analysis of lungs after exposure to cigarette smoke*[a]

		Percent of volume			
Duration of exposure	Mean linear intercept, μm	Air space		Tissue	
		Alveolar	Nonalveolar	Respiratory	Nonrespiratory
12 mo					
Age controls	74.8±3.7	50.6±2.8	26.8±3.5	21.0±4.7	1.6±0.6
10 cigarettes/day	82.6±7.0[b]	46.6±1.8[b]	32.1±4.4[b]	19.7±3.1	1.6±0.6
18 mo					
Age controls	70.0±5.2	49.8±1.6	25.9±3.7	22.9±4.2	1.5±0.9
10 cigarettes/day	86.8±4.6[b]	42.4±1.8[b]	36.1±2.6[b]	19.9±2.5	1.5±0.7
24 mo					
Age controls	71.5±3.6	45.8±3.9	31.4±3.7	21.3±3.2	1.4±0.9
7 cigarettes/day	67.6±3.8	43.8±2.7	30.9±3.1	23.7±2.9	1.5±0.6
30 mo[c]					
Age controls	67.8±1.9	43.7±2.8	33.5±3.2	20.7±4.0	2.0±1.2
7 cigarettes/day	69.7±9.2	34.0±2.5	39.9±6.5	24.4±7.0	0.6±0.4

[a] Values are means ± SD.
[b] Significantly different from untreated controls ($P<0.05$).
[c] Animals were exposed for 30 mo, followed by 7 mo without treatment.

matory response, the cell types found in the vascular adventitia were typically restricted to lymphocytes and macrophages. Similar accumulations of lymphoreticular cells in perivascular locations have been noted in the normal course of aging in the rat (*11*) and in cases of multiple sclerosis in humans (*12*).

Although perivascular lesions were often contained within some of the more extensive lesions, it is not clear whether they played an essential role in the pathogenesis of the larger lesions. The larger lesions could have been induced by infiltration of lymphoreticular cells into the surrounding parenchyma or could have been initiated independently. Since these locations were probably subjected to tobacco smoke exposure under similar local conditions, inflammatory responses could have resulted from the same, presumably chemotactic, biochemical intermediaries in both cases. However, the larger lesions showed the full spectrum of inflammatory cells, including polymorphonuclear leukocytes and mast cells. Another feature common to the more extensive lesions was degradation of the basal lamina, particularly under the type I or squamous epithelial cells. We considered this alteration a possible contributing factor in fibrogenesis and/or epithelial hyperplasia. The proximity of phagocytes, particularly macrophages, to these sites suggested that enzymes released from the cells during phagocytosis may affect the structure of the lamina. The presence of lymphocytes, monocytes, and macrophages in the interstitium has also been reported in human diffuse interstitial lung diseases (*13*).

Lesions of comparable structure to the type II hyperplastic and peribronchiolar fibrotic lesions have been induced in many previous studies of lung pathology, but authors have tended to classify the cuboidal and columnar metaplastic lesions together. The exceptions that particularly note "bronchiolization" of the peribronchiolar alveoli have been reports on mice and hamsters infected with influenza virus (*14*), mice exposed to synthetic smog or calcium chromate dust (*15*), and hamsters treated with chemical carcinogens (*16*). In experiments on rats treated with various agents, particularly intratracheal instillation of tobacco smoke condensate (*2*) or of casein and carbon particulates (*17*), or a single exposure to benzo[*a*]pyrene followed by lifetime tobacco smoke inhalation (*1*), bronchiolization appeared to have occurred but to have been classified with other types of metaplasia. Our studies, based on the improved structural detail obtained by the examination of tissues embedded in epoxy resins, suggest that the bronchiolar lesions differ in several respects from the more common cuboidal metaplasias, which were identified here as type II hyperplasias. Since only about half of the peribronchiolar lesions showed epithelial metaplasia, our studies are also the first performed on rodents to suggest that fibrotic and cellular enlargement of the peribronchiolar septa precedes the replacement of the squamous, type I epithelium with a columnar epithelium. However, prominent areas of peribronchiolar fibrosis without columnar metaplasia have also been noted in the lungs of human smokers and of nonsmokers exposed to lung irritants (*18*).

In the present studies, hyperplasia of the type II epithelium appeared concurrently with changes in the interstitium. Alveolar bronchiolization was rather infrequent and appeared to occur well after inflammatory and fibrotic changes in the interstitium. In addition, the two types of larger lesions differed in other respects: Their locations were typically dissimilar, the type II lesions being mainly at the pleura. More importantly, the frequency of the lesions was related to the duration of tobacco smoke exposure. Increasing the time of exposure at the lower dose of tobacco smoke from 1 to 2 years led to approximately a tripling in the frequency of type II hyperplasias but to a sixfold increase in the frequency of peribronchiolar lesions. While exposure to 10 cigarettes/day for 1.5 years induced as many type II hyperplasias as the 2-year exposure to 7 cigarettes/day, it induced far fewer peribronchiolar lesions. Thus the peribronchiolar lesions were dependent on the duration of exposure and/or on the age of the exposed animals.

In summary, the rat inhalation model offers a prototype of human syndromes induced by tobacco smoke exposure. However, the exposure level required for induction of emphysematous changes also leads to high mortality. The ultrastructure of the lesions appears to implicate the inflammatory response in their pathogenesis. The least common lesion seen, fibrosis of the peribronchiolar alveoli, is temporally related to tumor incidence and can be considered a precursor lesion.

REFERENCES

(*1*) Davis BR, Whitehead JK, Gill ME, Lee PN, Butterworth AD, Roe FJ. Response of rat lung to inhaled tobacco smoke with or without prior exposure to 3,4-benzpyrene (BP) given by intratracheal instillation. Br J Cancer 1975; 31:469–484.

(*2*) ———. Response of rat lung to tobacco smoke condensate or fractions derived from it administered repeatedly by intratracheal instillation. Br J Cancer 1975; 31:453–461.

(*3*) Walker D, Wilton LV, Binns R. Inhalation toxicity studies on cigarette smoke. VI. 6-week comparative experiments using modified flue-cured cigarettes: Histopathology of the lung. Toxicology 1978; 10:229–240.

(*4*) Frasca JM, Auerbach O, Parks VR, Jamieson JD. Electron microscopic observations on pulmonary fibrosis and emphysema in smoking dogs. Exp Mol Pathol 1971; 15:108–125.

(*5*) ———. Alveolar cell hyperplasia in the lungs of smoking dogs. Exp Mol Pathol 1974; 21:300–312.

(*6*) Leuchtenberger C, Leuchtenberger R. Effects of chronic inhalation of whole fresh cigarette smoke and of its gas phase on pulmonary tumorigenesis in Snell's mice. In: Nettesheim P, Hanna MG Jr, Deatherage JW Jr, eds. Morphology of experimental respiratory carcinogenesis. Vol 21. Oak Ridge, Tenn. USAEC Div Tech Inform, 1970:329–346.

(*7*) Dalbey WE, Nettesheim P, Griesemer R, Caton JE, Guerin MR. Chronic inhalation of cigarette smoke by F344 rats. JNCI 1980; 64:383–390.

(*8*) Forrester FT. The laboratory diagnosis of *Mycoplasma* infection. Atlanta: U.S. Department of Health, Education and Welfare, Center for Disease Control, 1975.

(*9*) Coulter HD. Rapid and improved methods for embedding tissues in Epon 812 and Araldite 502. J Ultrastruct Res 1967; 20:346–355.

(*10*) Reynolds ES. The use of lead citrate at high pH as an electron-opaque stain in electron microscopy. J Cell Biol 1963; 17:208–212.

(*11*) Burek JD. Pathology of aging rats. West Palm Beach, Fla.: CRC Press, 1978:94–97.

(*12*) Prineas JW. Multiple sclerosis: Presence of lymphatic capillaries and lymphoid tissue in the brain and spinal cord. Science 1979; 203:1123–1125.

(*13*) Davis GS, Brody AR, Craighead JE. Analysis of airspace and interstitial mononuclear cell populations in human diffuse interstitial lung disease. Am Rev Respir Dis 1978; 118:7–15.

(*14*) Baskerville A, Thomas G, Wood M, Harris WJ. Histology and ultrastructure of metaplasia of alveolar epithelium following infection of mice and hamsters with influenza virus. Br J Exp Pathol 1974; 55:130–137.

(*15*) Nettesheim P, Szakal AK. Morphogenesis of alveolar bronchiolization. Lab Invest 1972; 26:210–219.

(*16*) Stenback F. Morphology of experimentally induced respiratory tumors in Syrian golden hamster. Acta Otolaryngol [Suppl] 1977; 347:1–59.

(*17*) Davis BR, Whitehead JK, Gill ME, Lee PN, Butterworth AD, Roe FJ. Response of rat lung to 3,4-benzyprene administered by intratracheal instillation in infusine with or without carbon black. Br J Cancer 1975; 31:443–452.

(*18*) Niewoehner DE, Kleinerman J, Rice DB. Pathological changes in the peripheral airways of young cigarette smokers. N Engl J Med 1974; 291:755–758.

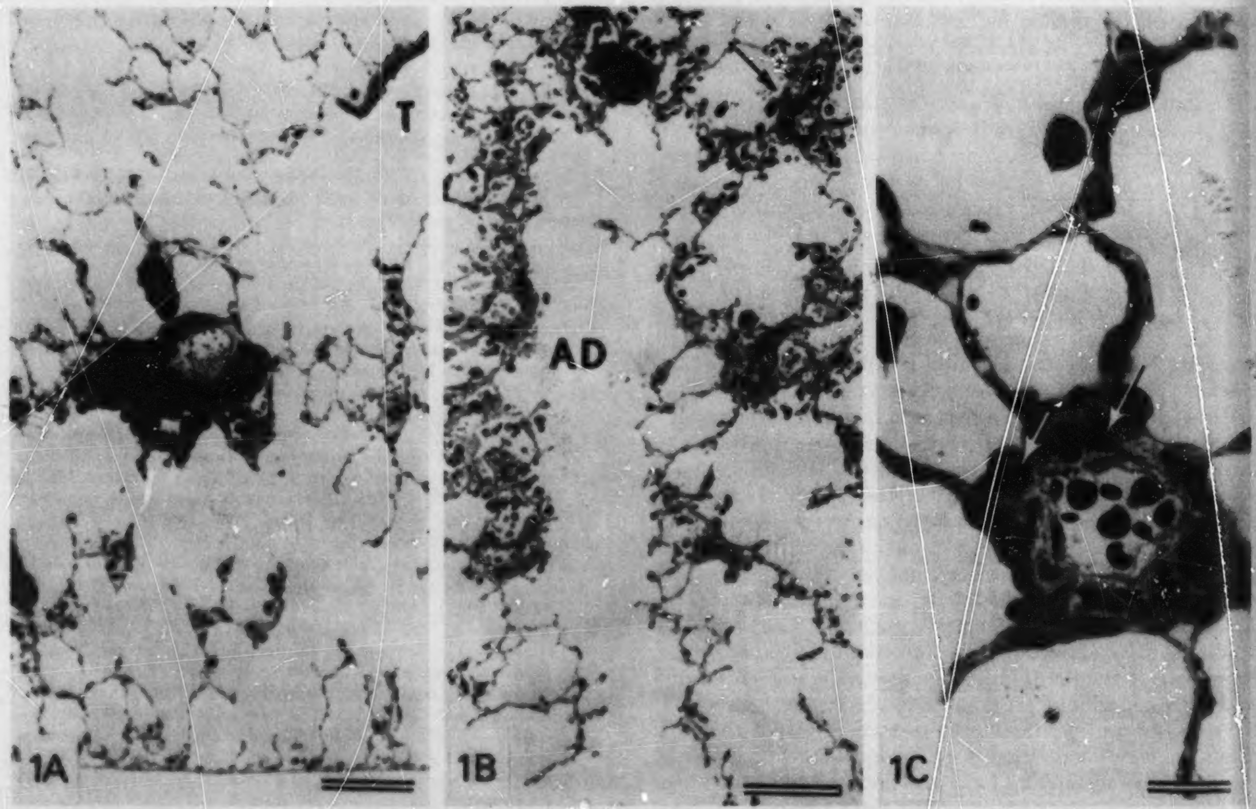

Figure 1.—Perivascular lesions. 1A) Particulate-laden macrophages forming a perivascular "cuff" in the parenchyma below the terminal bronchiole (T). Animal was exposed to 10 cigarettes/day for 1.5 yr. *Bar* = 200 μm. 1B) Perivascular lesion (*arrow*) associated with a small venule near the alveolar duc (AD). Animal was exposed to 7 cigarettes/day for 2 yr. *Bar* = 200 μm. × 70. 1C) Perivascular cuff of lymphocytes (*arrows*), untreated control animal at 1.5 yr. Toluidine blue. *Bar* = 20 μm. × 570

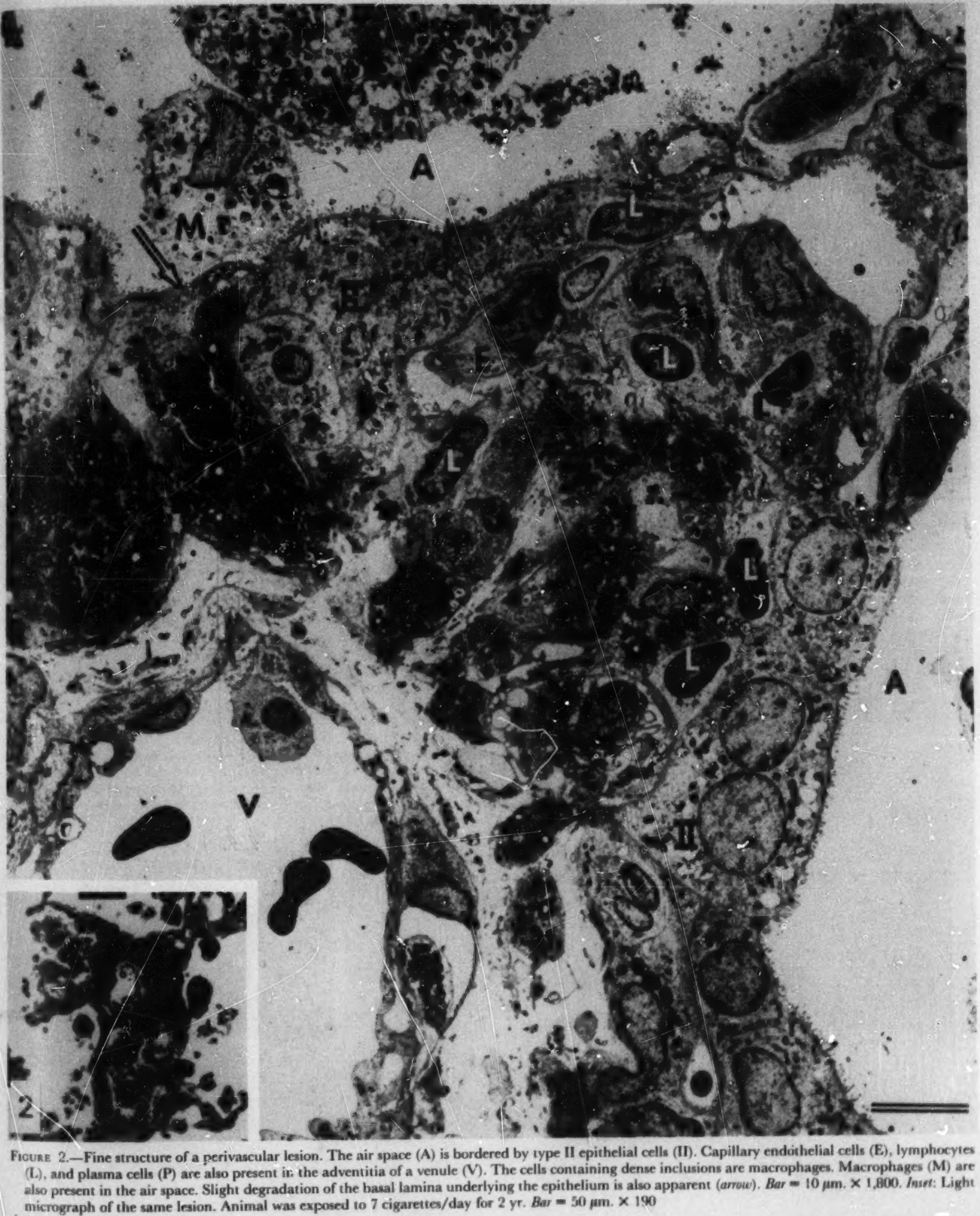

FIGURE 2.—Fine structure of a perivascular lesion. The air space (A) is bordered by type II epithelial cells (II). Capillary endothelial cells (E), lymphocytes (L), and plasma cells (P) are also present in the adventitia of a venule (V). The cells containing dense inclusions are macrophages. Macrophages (M) are also present in the air space. Slight degradation of the basal lamina underlying the epithelium is also apparent (*arrow*). *Bar* = 10 μm. × 1,800. *Inset*: Light micrograph of the same lesion. Animal was exposed to 7 cigarettes/day for 2 yr. *Bar* = 50 μm. × 190

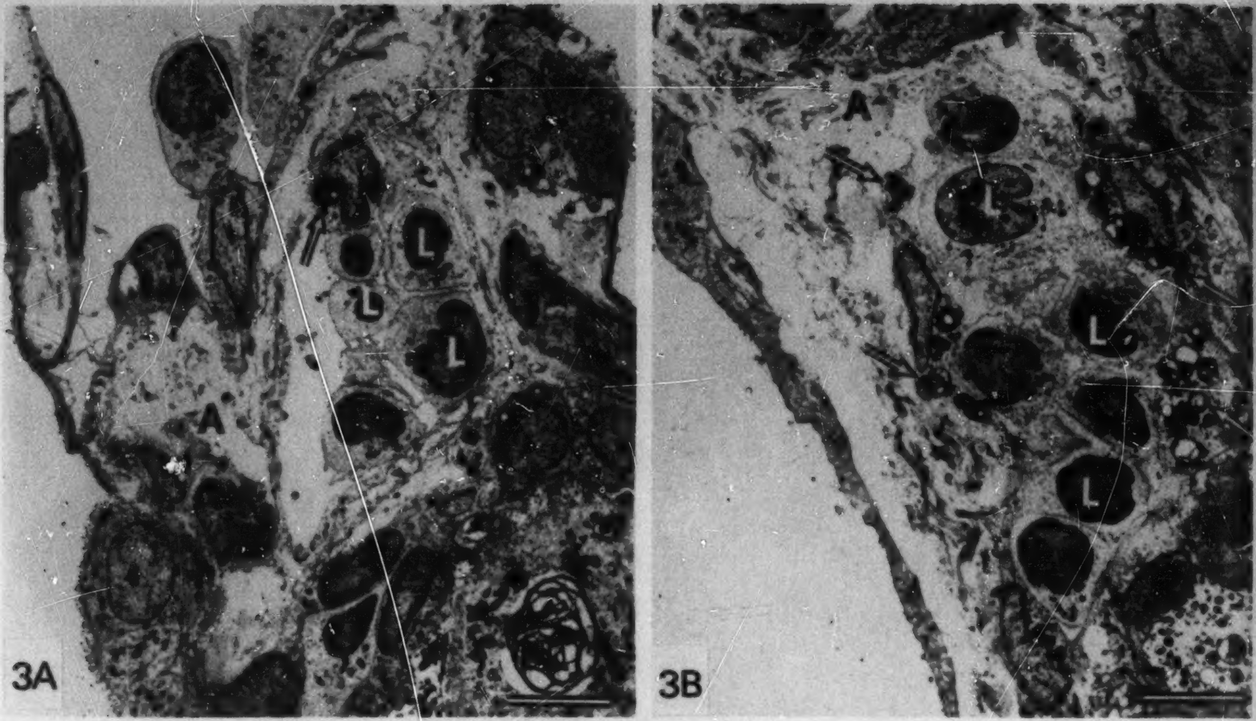

Figure 3.—Lymphocyte accumulation within lymphatic vessels located in vascular adventitia (A). A) Vessel containing lymphocytes (L) also has smoke particulates in lymphatic endothelium (*arrow*). *Bar* = 10 µm. B) Vessel occluded by large lymphocytes (L). *Note* that several of the lymphatic endothelial cells contain aggregated smoke particulates (*arrows*). Animal was exposed to 7 cigarettes/day for 2 yr. *Bar* = 10 µm. × 1,500

Figure 4.—Peribronchiolar septal lesions. 4A) Minimal fibrotic and cellular enlargement of septa, with an atypical airway epithelium in the distal part of terminal bronchiole (*arrows*). *Bar* = 100 µm. × 110. 4B) More extensive lesion showing peribronchiolar lymphoreticular cell accumulations (*arrows*) and distortion and fusion of alveolar septa adjacent to terminal bronchiole. *Bar* = 100 µm. × 50. 4C) Lesion showing a mucociliary bronchiolar epithelium on free surfaces of enlarged septa (*arrows*). Animals were exposed to 7 cigarettes/day for 2 yr. *Bar* = 100 µm. × 170

Figure 5.—Small pleural type II hyperplastic lesion. 5A) Type II hyperplasia distal to terminal bronchiole. *Bar* = 500 µm. × 25. 5B) Pulmonary vein with lymphoreticular cell accumulations (*arrows*) apical to type II hyperplastic lesion. *Bar* = 500 µm. × 25. 5C) High-magnification view of the epithelium, showing type II cells (*arrows*). Animal was exposed to 7 cigarettes/day for 2 yr. Toluidine blue. *Bar* = 10 µm. × 860

Figure 6.—Minimal septal enlargement at the periphery of a peribronchiolar fibrotic lesion. Plasma cells (P), lymphocytes (L), and hypertrophic fibroblasts (F) are present in interstitium. Collagenous thickenings (C) are also found at irregular intervals within alveolar septa. Thickening (*arrows*) and reduplication (*double arrows*) of basal lamina underlying the epithelium were also found. Most capillaries contained a hypertrophied endothelium (E), which frequently occluded the lumen completely. A few hypertrophic type II cells (II) were present. *Bar* = 10 µm. × 1,600. *Inset*: Higher magnification view of occluded capillary at top of micrograph (E) with an adjacent plasma cell (P). Capillary lumen is marked by *arrowheads*. *Note* extensive infolding of basal lamina (*double arrows*). Animal was exposed to 7 cigarettes/day for 2 yr. *Bar* = 3 µm. × 3,400

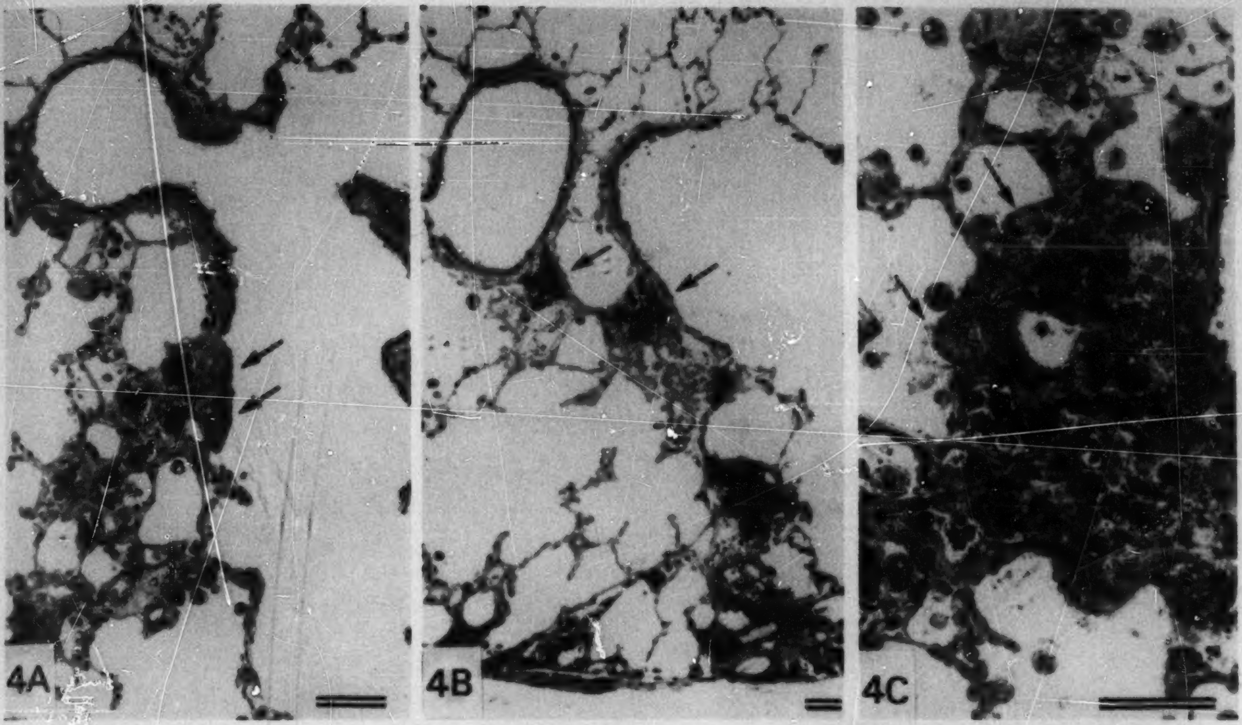
4A
4B
4C

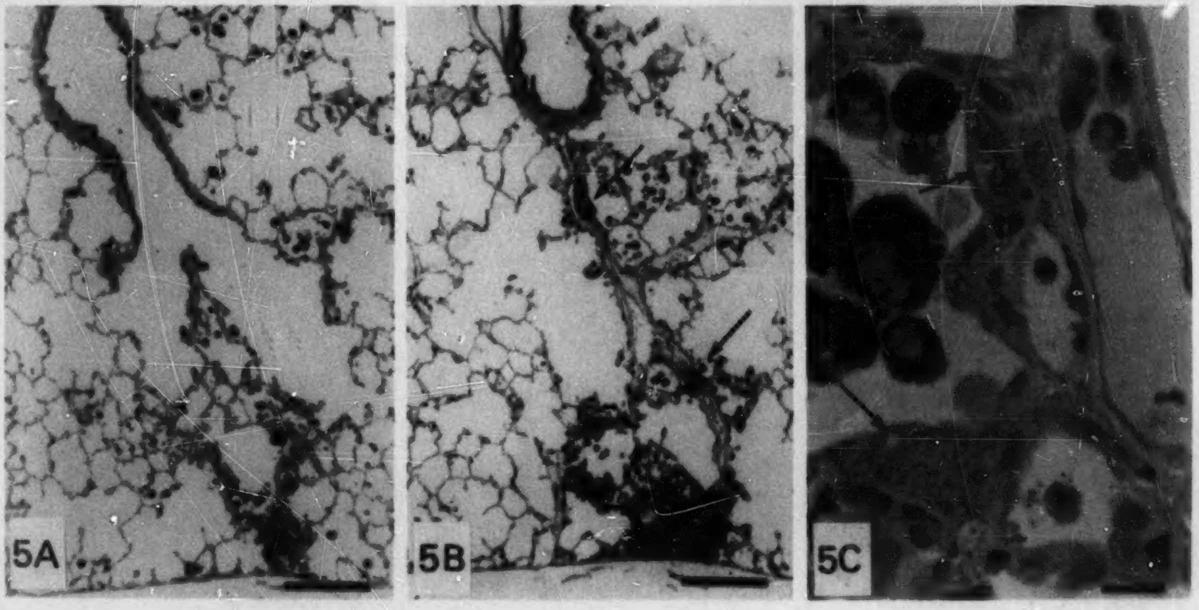
5A
5B
5C

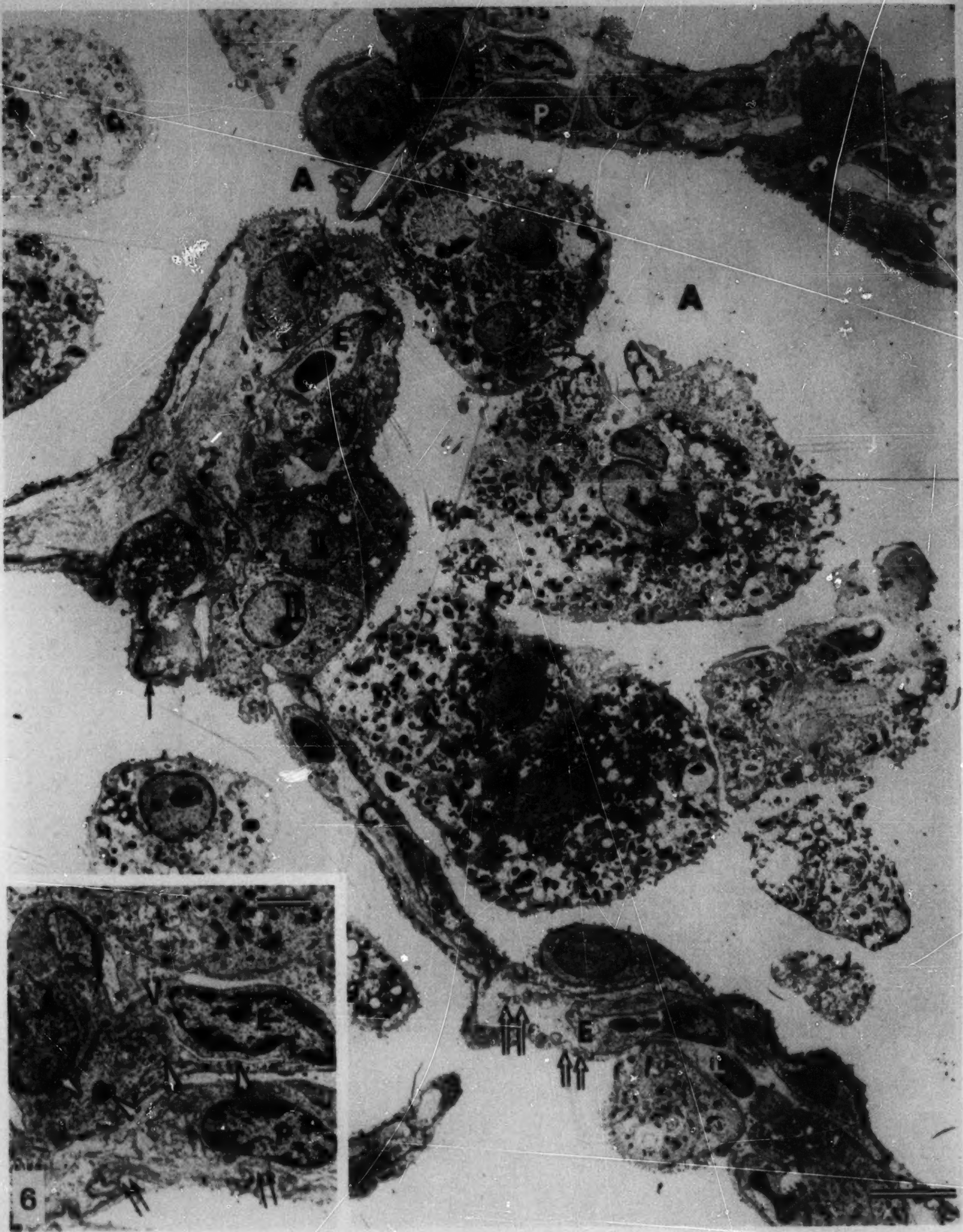
P
A
C
C
A
E
C
L
L
E
L
V
E
P

6

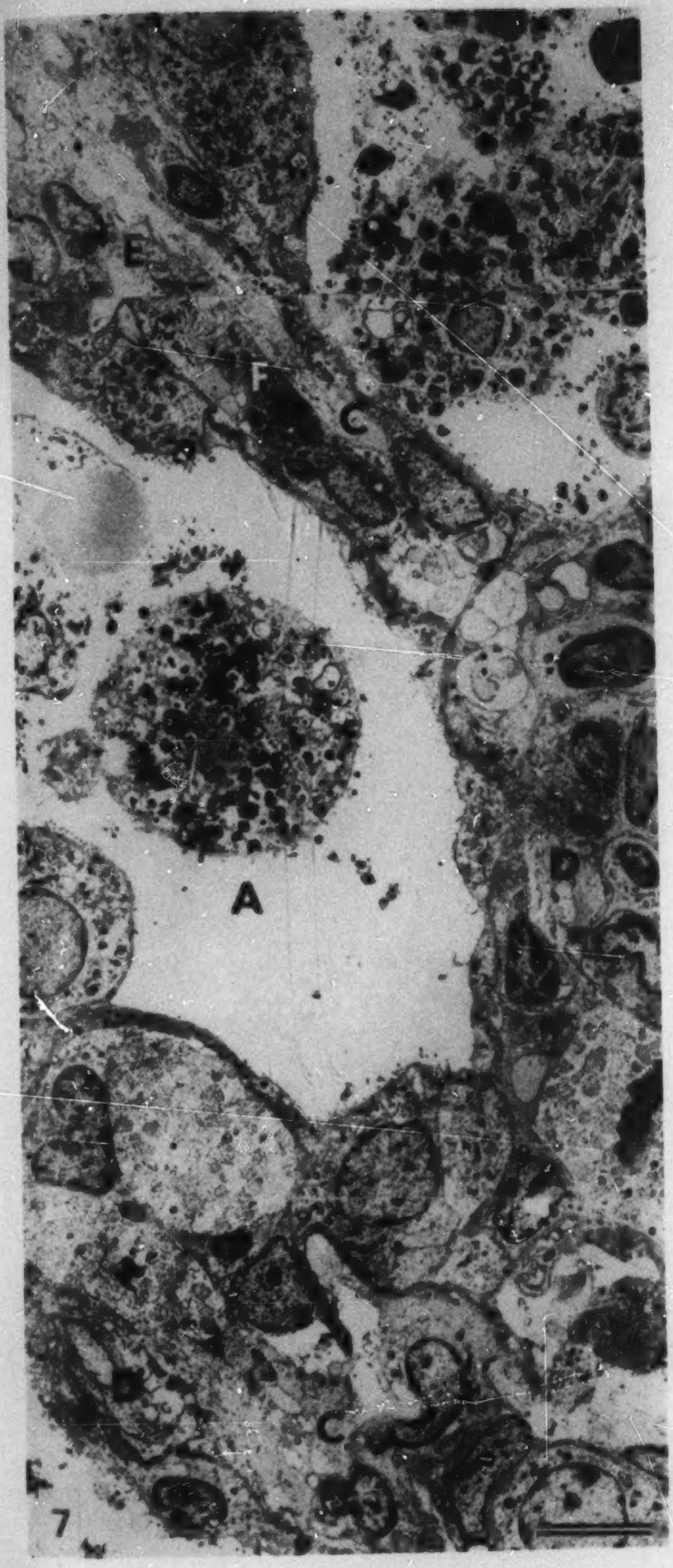

FIGURE 7.—Portion of a peribronchiolar fibrotic lesion that contains fibrotic septa showing collagenous thickenings (C), a fibroblast containing osmiophilic granules (F), and capillaries in which the endothelium appears to be degenerating (D). Animal was exposed to 7 cigarettes/day for 2 yr. *Bar* = 10 µm. × 1,700

FIGURE 8.—Portion of a type II hyperplastic lesion showing cuboidal epithelial cells with exceptionally clear cytoplasm and secretory inclusions (Se) and collagenous areas in the interstitium (C). Most of the cells comprising the cuboidal population are type II cells (II). Degradation of the basal lamina was extensive, leading to detachment of type I epithelial cells from the septum in some areas (*arrows*). Animal was exposed to 7 cigarettes/day for 2 yr. *Bar* = 10 µm. × 1,600

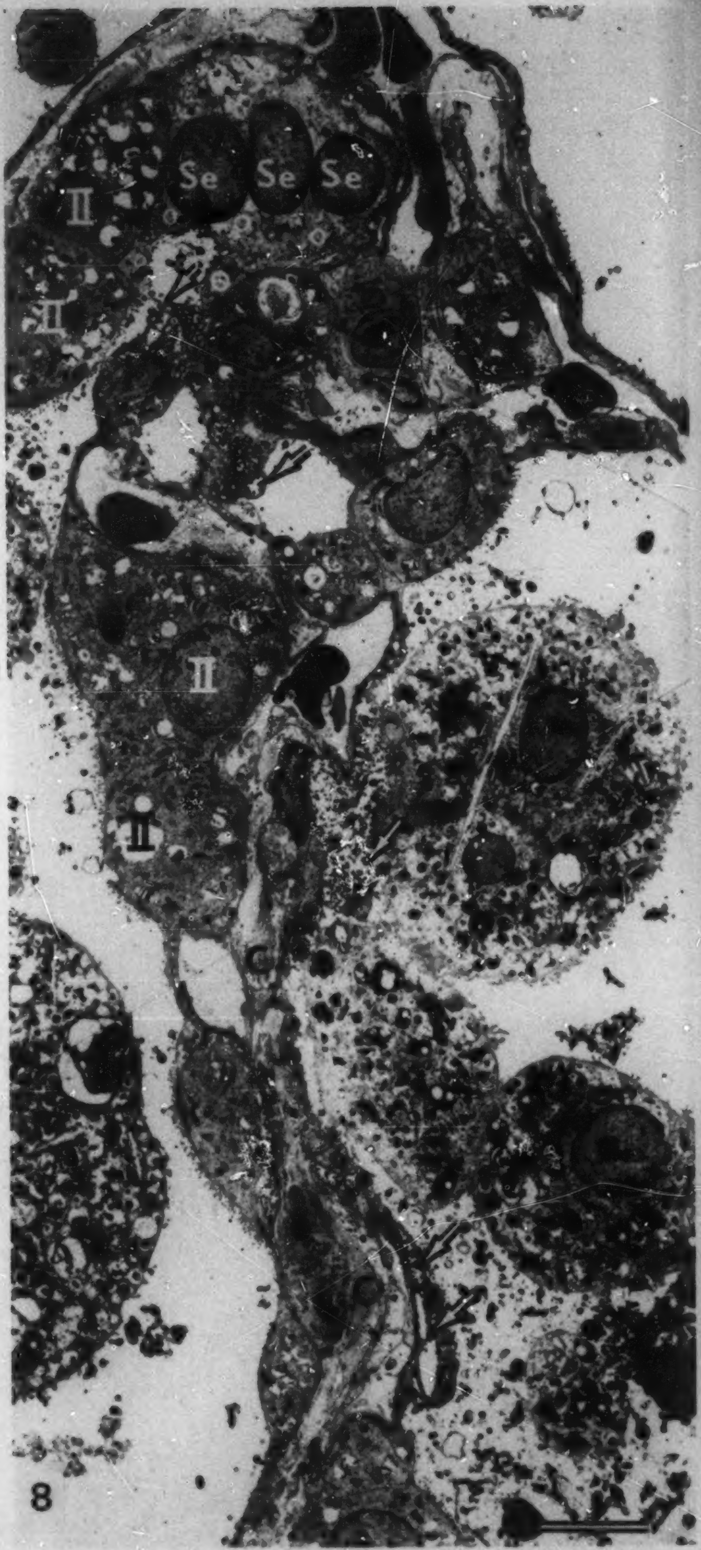

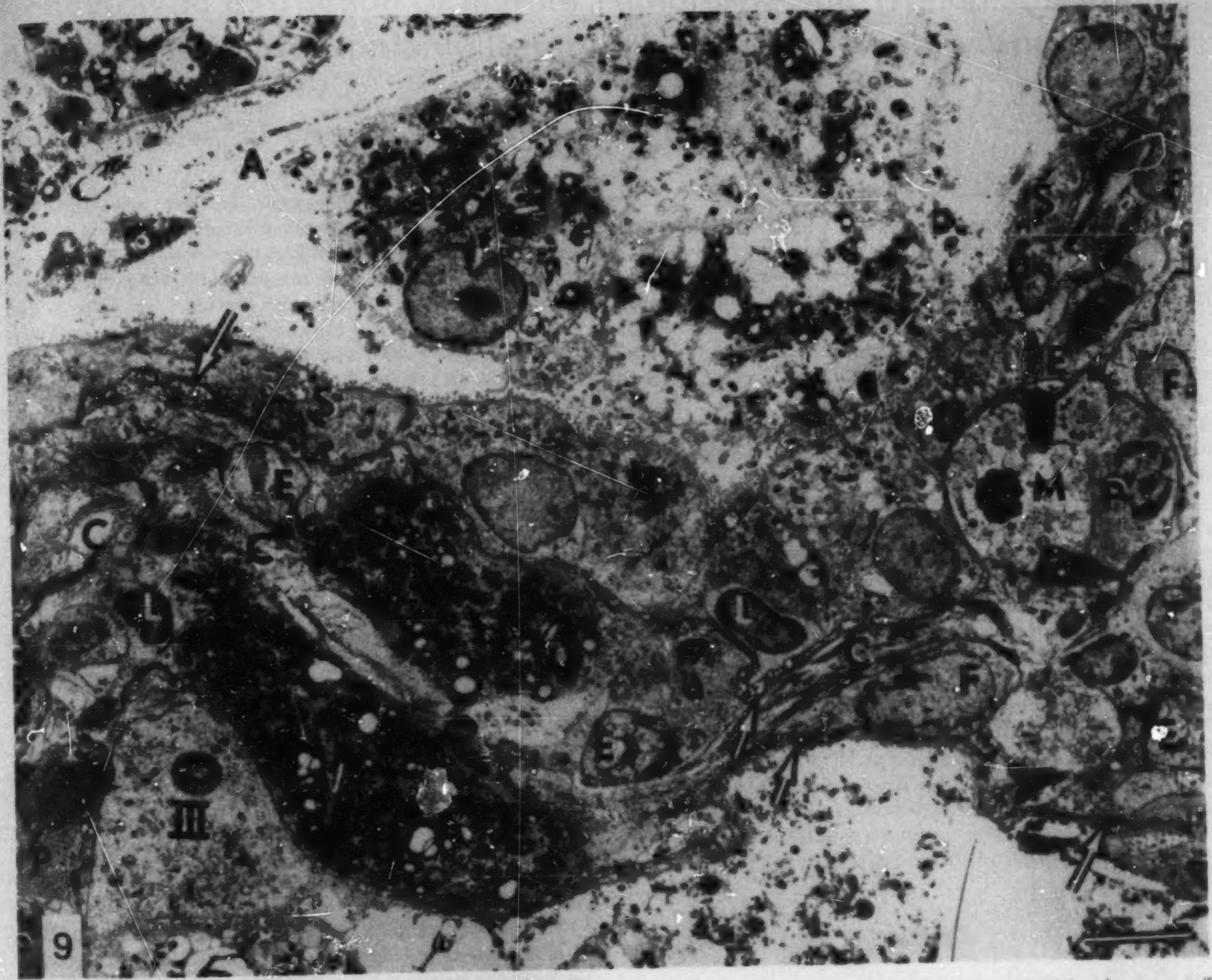

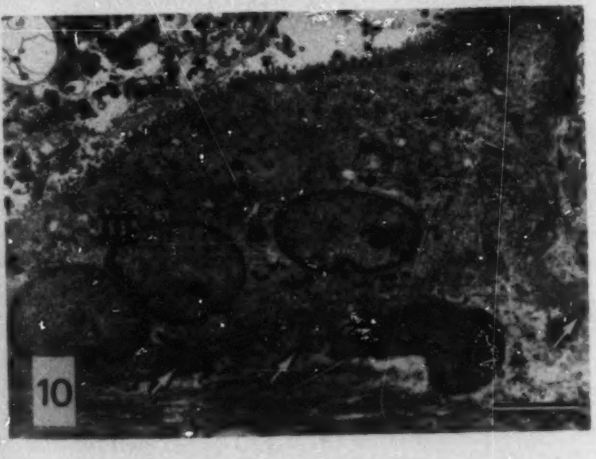

FIGURE 9.—Type II hyperplastic lesion showing cuboidal and squamous (S) epithelial cells. A columnar cell with extensive endoplasmic reticulum represented a third type of epithelial cell (III). Basal lamina underlying the epithelium is degraded in several areas (*arrows*). Lymphocytes (L) are present in both epithelium and interstitium. Interstitium also contains plasma cells (P), mast cells (M), macrophages with ingested particulate matter, and extensive areas filled with collagen fibers (C). Hypertrophic fibroblasts (F), were present. Nearly all capillary endothelial cells (E) were hypertrophied and occluded the capillary lumen. Profiles of linearly oriented acellular structures adjoined macrophages in the air space (A). Animal was exposed to 10 cigarettes/day for 1.5 yr. *Bar* = 10 μm. × 1,800

FIGURE 10.—Portion of a type II hyperplastic lesion containing cuboidal cells (III) that showed numerous profiles of endoplasmic reticulum and densely osmiophilic granules in the cytoplasm. Basal lamina also was reduplicated (*arrows*). Animal was exposed to 7 cigarettes/day for 2 yr. *Bar* = 5 μm. × 2,300

blank page

Noncytolytic Extraction of Murine Tumor-Specific Transplantation Antigens With the Nonionic Detergent Octyl-β-D-glucopyranoside[1,2,3]

Stephen J. LeGrue,[4,5,6] **Catherine M. Macek,**[5] *and* **Barry D. Kahan**[5,7]

ABSTRACT—The nonionic detergent octyl-β-D-glucopyranoside (C_8Glu) was used to extract immunogenic tumor-specific transplantation antigen (TSTA) from intact cells and purified plasma membranes of the 3-methylcholanthrene-induced fibrosarcoma MCA-F. Pretreatment of syngeneic C3H/HeJ mice with 100 μg of C_8Glu extracts induced specific immunoprotection such that mice resisted the outgrowth of MCA-F but not the antigenically distinct tumors MCA-D or MCA-2A. Incubation of intact cells with 7 m*M* (0.2%) C_8Glu for 30 minutes at 23°C was judged to be noncytolytic because extracted cells excluded trypan blue. Preparative isoelectric focusing partially purified the MCA-F-specific antigen from crude C_8Glu extracts into the pH 6.5–6.8 region of the gradient. Electrofocusing yielded 60% of the applied antigen activity and a fourfold to fivefold increase in specific activity. In addition, immunoprotective activity was obtained in 2% C_8Glu extracts of MCA-F plasma membranes, confirming the membrane localization of the MCA-F TSTA. Three properties of C_8Glu rendered it an attractive agent for the preparation of cell surface proteins: a nonionic character, large critical micellar concentration, and its capacity to extract antigens without complete membrane solubilization or cell disruption.—JNCI 1982; 69:131–136.

Carcinogen-induced murine neoplasms frequently express cell surface neoantigens that may serve as the focus of a host-tumor immune response (*1–4*). Vaccines containing whole-irradiated tumor cells (*5*, *6*), subcellular fractions (*4*, *7*, *8*), or crude cellular extracts (*3*, *7*, *9–11*) are capable of inducing tumor-specific host immunity, such that mice can reject or resist the outgrowth of the same, but not other, syngeneic tumors. Intact 3-methylcholanthrene-induced fibrosarcoma (MCA-F) cells of C3H/HeJ mice release substantial TSTA activity during brief incubation in solutions containing 2.5% 1-butanol (*12*). The observation that butanol extraction was not cytotoxic led to an investigation of other agents that might release TSTA activity without attendant cytolysis. One such agent is the nonionic detergent C_8Glu.

Nonionic and weakly ionic detergents have been used to solubilize neoantigens from both virus- and carcinogen-induced tumors (*4*, *10*, *11*, *13*, *14*). However, the ionic characteristics of compounds such as sodium dodecyl sulfate, sodium cholate, and sodium deoxycholate limit their use in protocols that employ pIEF (*6*, *12*, *15*). In addition, the low CMC and large micellar dimensions of detergents such as Nonidet P40 and Triton X-100 (*16*) contribute to the difficulty in removal of these detergents from the isolated proteins. Mixed detergent–protein micelles restrict resolution in pIEF and the accurate assessment of molecular size by gel filtration.

These problems may be avoided by the use of the detergent C_8Glu, a molecule consisting of an eight-carbon alkyl chain attached to carbon atom 1 of D-glucose by an O-linked β-glycosidic bond. C_8Glu is completely nonionic and freely dialyzable to concentrations below the 25-m*M* CMC (*17*, *18*). Since excess detergent can be removed from the extracted proteins, detergent-induced artifacts are minimized. Recently, C_8Glu has been used to solubilize the low-density lipoprotein receptor from human fibroblast membranes (*19*), the Ca^{2+} ATPase from sarcoplasmic reticulum (*20*), opsin from bovine retinal disks (*21*), a phosphoethanolamine transferase system from rat liver microsomes (*22*), and several enzyme activities from the membrane of *Streptococcus faecalis* (*18*). These workers report that C_8Glu concentrations ranging from 10 to 50 m*M* solubilize 25–100% of the protein from purified membranes. Maximum enzyme activity was usually observed in a narrow concentration range that was characteristic for each enzyme system.

C_8Glu extracted immunogenic TSTA activity from intact MCA-F cells. C_8Glu, like butanol, was not cytolytic at low concentrations. C_8Glu extracts of MCA-F cells possessed TSTA activity that was capable of inducing host resistance to challenge with viable MCA-F cells but not with the antigenically distinct MCA-D or MCA-2A tumors. Immunogenic activity was also observed in C_8Glu extracts of purified plasma membranes. The immunoprotective activity in C_8Glu extracts of MCA-F was partially purified by pIEF: Immunization with 23 μg of the pH 6.5–6.8 fraction significantly reduced subsequent homotypic tumor outgrowth. These results demonstrated that C_8Glu released substantial TSTA activity without cytolysis and that this detergent did not interfere with purification of the antigen by isoelectric focusing.

MATERIALS AND METHODS

Animals and tumors.—Fibrosarcomas MCA-F, MCA-D, and MCA-2A, induced with 3-methylcholanthrene (*9*, *23*),

---

ABBREVIATIONS USED: C_8Glu=octyl-β-D-glucopyranoside; CMC=critical micellar concentration; MTD=minimum tumorigenic dose; PBS=phosphate-buffered saline; pIEF=preparative isoelectric focusing; *r*=correlation coefficient; TSTA=tumor-specific transplantation antigen(s).

---

[1] Received October 27, 1981; accepted February 17, 1982.

[2] Supported by grant IM-62-G from the American Cancer Society and Public Health Service grant CA-29814 from the National Cancer Institute.

[3] Animals were maintained under guidelines set forth in the "Guide for the Care and Use of Laboratory Animals" by the Institute of Laboratory Animal Resources, National Research Council.

[4] Department of Biochemistry and Molecular Biology, The University of Texas Health Science Center, Houston, Tex. 77030.

[5] Department of Surgery, The University of Texas Health Science Center. *Address reprint requests to* Dr. LeGrue *at this address.*

[6] Recipient of National Research Service Award (postdoctoral fellowship) CA-06326 from the National Cancer Institute.

[7] We thank Ms. Elizabeth Costa for her expert technical assistance and Dr. N. Pellis for his helpful discussions and editorial assistance.

were maintained by serial sc transplantation in syngeneic C3H/HeJ female mice (The Jackson Laboratory, Bar Harbor, Maine). Tumors used for these studies were in transplant generations 4–7.

TSTA activity in crude extracts and plasma membranes was assessed according to the immunoprotection assay described in (*9*, *12*). Various doses of membrane or C_8Glu extract protein in Dulbecco's PBS (pH 7.4) were injected sc into groups of 10 syngeneic mice each. Hosts were challenged sc in the contralateral flank 10 days later with either 10^4 MCA-F, 10^4 MCA-2A, or 10^5 MCA-D cells (100 times the MTD). The mean tumor diameter of each group was calculated from individual tumor sizes, obtained as the average of two perpendicular measurements of tumor diameter with the use of a metric dial caliper. Significant differences in mean tumor diameters of control and antigen-treated groups were determined with the unpaired Student's *t*-test.

Specific activities of extracts and plasma membranes were determined with the immunoprotection assay. Specific activity was defined as the number of TSTA units per milligram of protein, where one TSTA unit is the milligram amount of protein necessary to reduce tumor growth by 33%.

Extraction of intact cells.—A single cell suspension of MCA-F was prepared by trypsin digestion of minced tumor tissue, as described in (*9*, *12*). The cells were washed twice and resuspended in Dulbecco's PBS (pH 7.4) containing the indicated concentrations of C_8Glu detergent (Calbiochem-Behring Corp., La Jolla, Calif.). Extraction in 7 m*M* C_8Glu for 30 minutes at 23°C maximized both the protein yield and viability of MCA-F cells. Following detergent extraction, cells were sedimented at 500×*g* for 10 minutes and washed three times prior to assessment of viability by trypan blue exclusion. The extract was dialyzed overnight against 100 vol of PBS, concentrated by dialysis against 50% sucrose in PBS, and redialyzed against PBS to remove the sucrose. After ultracentrifugation at 160,000×*g* (max) for 1 hour, the protein concentration of the supernatant fraction was determined with the use of the method of Bradford [(*24*); BioRad protein assay; Bio-Rad Laboratories, Richmond, Calif.] with ovalbumin as standard.

pIEF.—We achieved partial purification of the tumor antigen activity present in crude C_8Glu extracts by using pIEF (*6*, *12*, *15*). Crude C_8Glu extracts containing 40 mg protein in 1% glycine and 2% carrier ampholyte (pH 3.5–10) (LKB Instruments, Inc., Rockville, Md.) were electrofocused for 16 hours at 8 W, constant power, in a flatbed of Ultrodex (LKB Instruments, Inc.). After the gradient was sectioned into 31 fractions, the proteins were eluted into 10 ml of 0.3 *M* NaCl. The pH and protein concentration of each fraction were determined prior to assessment of immunoprotective activity.

Extraction of plasma membranes.—Partially purified plasma membranes were prepared from MCA-F cells by a modification of the method described by Brunette and Till (*25*). All procedures were performed on ice or at 4°C. Tumors were harvested from 10–30 hosts and minced over a fine-wire screen. The minced tissue was washed thrice in PBS, resuspended in a lysis buffer of PBS containing 1 m*M* $CaCl_2$, 1 m*M* $MgCl_2$, and 2 m*M* phenylmethylsulfonyl fluoride. Cells were lysed with 40–50 strokes of a Potter-Elvehjem homogenizer fitted with a motor-driven Teflon pestle. The homogenates were centrifuged for 10 minutes at 1,000×*g* (max), and the supernatant fractions were stored in ice. The pellets were rehomogenized in lysis buffer and recentrifuged. The low-speed supernatants containing microsomal components were centrifuged at 40,000×*g* for 20 minutes. The resulting pellets were resuspended in a two-phase polymer suspension (*26*, *27*) and centrifuged in a swinging-bucket rotor for 10 minutes with a force of 20,000×*g* at the interface. The pellets were discarded, and the polymer phases and interfacial material were remixed and recentrifuged. The membrane pellicles were removed from the polymer interfaces by aspiration into silanized Pasteur pipettes, pooled, and washed in at least 10 vol of PBS before storage at −70°C.

Plasma membranes were extracted with C_8Glu by addition of 20 mg of membrane protein (0.5 ml) to 4.5 ml of 2.2% of C_8Glu in PBS. Following a 30-minute incubation at 23°C, the material was ultracentrifuged for 30 minutes at 104,000×*g* (max) in an Airfuge (Beckman Instruments, Inc., Palo Alto, Calif.) fitted with a batch rotor. The supernatant fraction was dialyzed overnight against 100 vol of PBS to remove C_8Glu and the ultracentrifugation was repeated to remove insoluble material.

RESULTS

Noncytotoxic Extraction With C_8Glu

Incubation of intact sarcoma cells in solutions containing low concentrations of C_8Glu released cell surface proteins without significantly affecting the ability of the extracted cells to exclude the supravital dye trypan blue. Both the protein yield and resistance of the cells to detergent-induced lysis were temperature-dependent (text-fig. 1). Extraction of 10^7 MCA-F cells suspended in 1 ml PBS containing less than 7.5 m*M* C_8Glu for 30 minutes at room temperature was not cytotoxic. When the extraction was performed at 4°C, cells survived C_8Glu concentrations up to 15 m*M*. The maximum protein yield obtained without loss of cellular viability was slightly greater at the lower temperature. However, at equivalent detergent concentrations, more surface protein was recovered with incubations at room temperature. The standard extraction condition for intact cells of 7 m*M* (0.2%) C_8Glu at 23°C for 30 minutes yielded 3–20 μg protein/10^6 cells, an amount equivalent to that obtained with 2.5% 1-butanol at 23°C for 5 minutes (*12*). Text-figure 1 also demonstrates that the rate of protein release into the supernatant fraction increased markedly when cellular viability fell below 50%. Incubation of cells at room temperature in 20 m*M* C_8Glu (text-fig. 1B) released 43 μg protein per 10^6 cells, which is about 10% of the total cellular protein (0.55 mg/10^6 cells) (*12*), while 10 m*M* C_8Glu extracts contained 5 μg, or 1% of the total cellular protein. These results indicate that the greater protein yield associated with extraction at high detergent concentration reflects the release of cytoplasmic proteins following C_8Glu-induced membrane lysis.

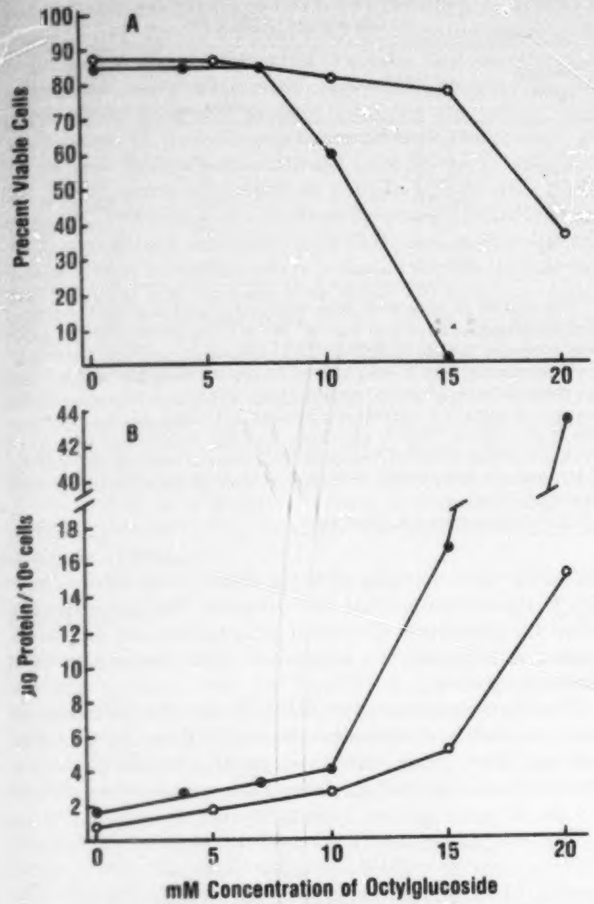

TEXT-FIGURE 1.—Effect of increasing C_8Glu concentration on cellular viability and protein yield. Intact MCA-F fibrosarcoma cells were incubated at 4°C (○) or 23°C (●) for 30 min in solutions containing C_8Glu. Viability was assessed by enumeration of cells excluding 0.01% trypan blue (A). Protein yield was determined following dialysis to remove excess detergent and ultracentrifugation (B).

Release of TSTA Activity From Intact Cells

Animals pretreated with 100 μg of a 7-m*M* C_8Glu extract prepared from intact MCA-F cells displayed a 45% reduction in the outgrowth of MCA-F tumor, when compared to the outgrowth in control mice (table 1). The specific activity of this extract (10 U/mg) is lower than that observed for butanol extracts (10–40 U/mg), but it is fivefold to tenfold greater than the specific activity of 3-*M* KCl extracts of MCA-F (*9*, *12*). To demonstrate that the tumor antigen activity released from cells by using 7 m*M* C_8Glu is specific for the tumor of origin, we immunized mice with 30 or 100 μg of crude C_8Glu extract from MCA-F cells and challenged them 10 days later with 100 times the MTD of MCA-F or 1 of 2 syngeneic but non-cross-reactive tumors, MCA-D or MCA-2A (table 2). Only animals pretreated with the homotypic extract displayed significant reduction in tumor outgrowth, when compared to control mice receiving PBS alone. Thus an immunogenic MCA-F-specific tumor antigen was among the polypeptides released from the surface of intact cells during incubation with low concentrations of C_8Glu.

TABLE 1.—*Immunoprotective activity of C_8Glu extracts prepared from intact MCA-F cells*[a]

Antigen	Dose, μg	Mean tumor diameter ± SE	Level of significance[b]
PBS	0	10.8±0.9	
C_8Glu extract	10	10.1±0.9	NS
	30	8.5±1.5	NS
	100	6.2±1.4	<0.02

[a] Extracts prepared by treatment of intact MCA-F cells with 7 m*M* C_8Glu were inoculated into groups of 10 syngeneic C3H mice each, which were challenged sc 10 days later with 10^4 MCA-F cells. Mean tumor diameters (mm) were determined 21 days post challenge.

[b] Determined by the two-tailed Student's *t*-test. NS=not significant.

Extraction of Plasma Membranes

The noncytolytic release of TSTA activity from MCA-F cells by C_8Glu suggested that TSTA was associated with the exterior surface of the plasma membrane. Localization of the antigen in the plasmalemma was confirmed by the potent immunoprotective activity of the partially purified membrane fraction from MCA-F cells. Pretreatment with 30 or 100 μg of membrane-associated protein reduced tumor outgrowth by 48 and 77%, respectively (text-fig. 2). Extraction of 20 mg of MCA-F membrane protein in 5 ml of 2% C_8Glu (30 min, 23°C) released 1.5 mg (7.5%) of protein into the high-speed supernatant fraction. Pretreatment of hosts with 10 or 100 μg of the 2% C_8Glu extract significantly reduced ($P<0.05$) the mean MCA-F tumor diameter measured 21 days post challenge (text-fig. 2). The degree of tumor growth reduction induced with C_8Glu membrane extracts was significantly less than that observed with 100 μg of intact membrane protein as the immunogen ($P<0.05$). However, there was no significant difference between groups immunized with C_8Glu extracts and those receiving 30 μg of membrane protein.

TABLE 2.—*Specificity of TSTA activity noncytolytically extracted from MCA-F cells with the use of C_8Glu*[a]

Challenge tumor	Dose of MCA-F extract, μg	Mean tumor diameter±SE, mm
MCA-F	0	16.2±0.7
MCA-F	30	14.2±1.2
MCA-F	100	10.6±1.0[b]
MCA-2A	0	16.3±1.5
MCA-2A	30	16.6±2.6
MCA-2A	100	14.7±1.8
MCA-D	0	15.4±1.4
MCA-D	30	14.2±1.0
MCA-D	100	14.8±0.8

[a] Groups of C3H mice were immunized with the indicated doses of crude 7 m*M* C_8Glu extract prepared from intact MCA-F cells. Ten days later, mice were challenged sc with 10^4 MCA-F, 10^4 MCA-2A, or 10^5 MCA-D (100 times the MTD).

[b] Level of significance, $P<0.001$.

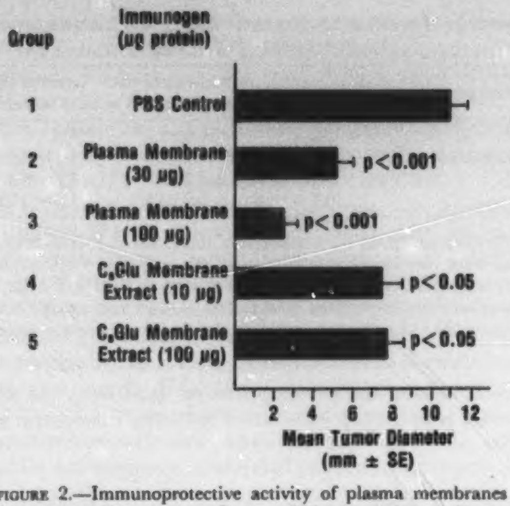

TEXT-FIGURE 2.—Immunoprotective activity of plasma membranes and C_8Glu extracts of membranes. Groups of 10 mice each were immunized with the indicated amounts of plasma membranes or 2% C_8Glu extract prepared from MCA-F plasma membranes. The mean MCA-F tumor diameters (mm ± SE) of control and experimental groups were determined 21 days post challenge. Statistically significant differences between antigen-treated mice and controls are shown. The significance of mean diameters between groups were as follows: group 2 vs. group 3, $P<0.05$; group 3 vs. group 4 or 5, $P<0.05$; all other comparisons were not significant.

Partial Purification of TSTA Activity by pIEF

The migration properties of MCA-F TSTA activity during electrofocusing are characteristic for the extraction technique used to obtain the antigen. Extracts prepared with 3 *M* KCl yielded immunoprotective activity at the pH 5.6–6.0 region of the gradient, while those prepared with 1-butanol electrofocused in the pH 6.4–6.5 region (*6*, *12*, *15*, *28*). The protein distribution and pH gradient obtained following electrofocusing of 40 mg crude C_8Glu extract (text-fig. 3) demonstrated that the detergent did not adversely affect the generation of a linear pH gradient nor did C_8Glu appear to influence the migration of the proteins to their isoelectric points.

The fractions obtained by pIEF of MCA-F C_8Glu extracts were assessed for immunoprotective TSTA activity. A significant reduction in tumor outgrowth ($P<0.005$), relative to that in control mice receiving PBS, was observed only in

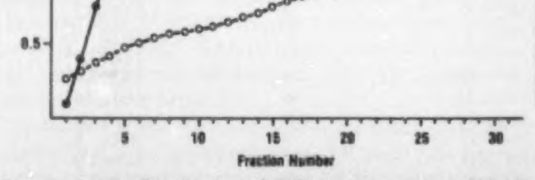

TEXT-FIGURE 3.—Distribution of C_8Glu extract protein following pIEF. Forty milligrams of a whole cell extract, prepared with the use of 7 m*M* C_8Glu, was electrofocused in a flatbed of Ultrodex containing 2% carrier ampholytes. After elution of the focused materials into 0.3 *M* NaCl, the pH and protein concentration of each fraction were determined. Fractions were pooled as indicated (A to I) for use in the immunoprotection assay (cf. table 3).

TABLE 3.—*Immunoprotective activity of pIEF fractions from a C_8Glu extract of MCA-F*[a]

Fraction pool	pH range	Immunizing dose, µg[b]	Mean tumor diameter ±SE, mm
	PBS-treated control	0	14.3±0.9
C	5.4–5.5	22	15.3±0.8
D	5.6–5.7	22	12.6±0.8
E	5.8–6.0	23	14.6±1.1
F	6.1–6.4	28	13.9±0.5
G	6.5–6.8	23	8.3±1.6[c]
H	6.9–7.1	25	15.7±0.4

[a] Groups of 10 mice each were immunized with the pIEF fractions and challenged 10 days later with 10^4 MCA-F; the mean tumor diameter was compared to that of PBS-treated controls 21 days post challenge.

[b] Immunizing dose was estimated to approximate the optimal dose for crude extract, with the formula $(mg_f)/(SA \times mg_t)$, where mg_f is the amount of protein in a particular fraction, *SA* is the specific activity of the crude extract (TSTA unit/mg), and mg_t is the total amount of protein recovered from all fractions. This formula assumes that activity is not preferentially lost or retained and that all the activity is present in a single fraction.

[c] Level of significance, $P<0.005$.

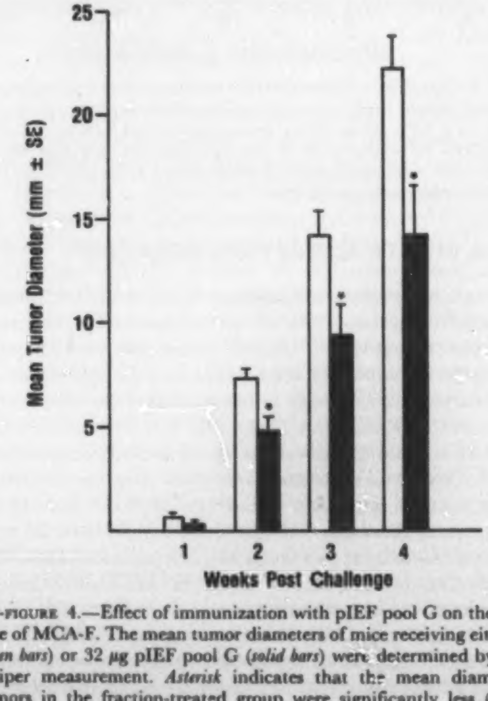

TEXT-FIGURE 4.—Effect of immunization with pIEF pool G on the growth rate of MCA-F. The mean tumor diameters of mice receiving either PBS (*open bars*) or 32 µg pIEF pool G (*solid bars*) were determined by weekly caliper measurement. *Asterisk* indicates that the mean diameters of tumors in the fraction-treated group were significantly less ($P<0.02$) than those in saline-treated controls.

mice pretreated with 23 μg of the pH 6.5–6.8 portion of the gradient (text-fig. 3, fraction pool G). Immunization with equivalent doses of other pIEF fractions had no effect on subsequent tumor outgrowth (table 3). The reduction in mean tumor diameter in mice receiving the pH 6.5–6.8 fraction was statistically significant ($P<0.02$ or greater) at 14, 21, and 28 days post challenge (text-fig. 4). In addition, the rate of tumor outgrowth in antigen-treated mice (0.67 mm/day, $r=0.999$) was significantly slower ($P<0.01$) than the rate of growth in control mice (1.01 mm/day, $r=0.999$). This degree of tumor growth retardation was comparable to that following pretreatment with either 100 μg of the crude, unfractionated C_8Glu extract or 30–100 μg of the crude butanol extract. Thus electrofocusing produced a fourfold to fivefold increase in specific antigen activity, relative to that in the crude C_8Glu preparation, with greater than 95% recovery of applied protein. The pH 6.5–6.8 fraction (pool G) contained 6.6% of the starting crude extract protein and 60% of the applied antigenic activity, calculated on the basis of the ability of a given milligram amount of crude or partially purified C_8Glu extract to effect a 33% reduction in mean tumor diameter.

DISCUSSION

Treatment of either intact cells or plasma membrane-enriched fractions from the 3-methylcholanthrene-induced fibrosarcoma MCA-F with solutions containing C_8Glu released significant immunoprotective TSTA activity. C_8Glu, a member of the alkylglucoside detergents described by Baron and Thompson (*18*), consists of an eight-carbon alkyl group attached to carbon atom 1 of D-glucose via an *O*-linked *β*-glycosidic bond. Thus C_8Glu is completely nonionic except under the most extreme alkaline conditions. The relatively high 25 m*M* CMC reported for C_8Glu (*17*) allows complete removal of excess detergent by simple dialysis (*18*). This is in sharp contrast to the properties of other detergents commonly used for the solubilization of membrane proteins, which have CMC's in the range of 0.1–1.0 m*M* (*16*). Detergents with low CMC's are intransigent to removal by dialysis or gel filtration (*18, 29*) because the monomer concentration is small compared to the total detergent concentration.

The ability of C_8Glu to liberate TSTA activity from the surface of intact cells without reducing cellular viability is similar to the noncytolytic butanol extraction procedure reported previously (*12*). However, extraction with C_8Glu differs from 1-butanol extraction in that 1) the cells may be incubated in low concentrations of C_8Glu for long periods of time at either 4°C or 23°C without loss of viability, 2) the protein yield and cellular viability are less dependent on pH and ionic strength in C_8Glu extraction, and 3) the specific activities of crude C_8Glu extracts are lower than those of crude 1-butanol extracts. The observation that both C_8Glu and 1-butanol release tumor antigen activity without attendant cytolysis suggests that the antigens are more weakly associated with the plasma membrane than are integral proteins such as histocompatibility antigens, which frequently require complete membrane solubilization to effect their release (*16, 30*).

The relatively mild conditions required to release TSTA activity from intact cells, together with the potent immunoprotective activity of plasma membranes, suggested that tumor antigen might also be obtained by treatment of purified tumor cell membranes with C_8Glu. Extraction of intact MCA-F cells with 10 m*M* C_8Glu released 5–10 μg protein/10^6 cells, an amount equivalent to that obtained (4–6 μg) by extraction of membranes prepared from 10^6 cells with the same concentration of detergent. Thus low concentrations of C_8Glu release proteins from both sources with equal efficacy. Complete solubilization of the isolated membranes was achieved by overnight incubation in 2% (68 m*M*) C_8Glu (data not shown), but only 60% of the protein remained in solution following dialysis and ultracentrifugation. Although the 2% detergent extract displayed significant immunoprotective activity, its specific activity was less than that of the intact plasma membranes. Thus pretreatment with 10 or 100 μg of extracted membrane protein reduced mean tumor size by 33%, while immunization with 100 μg of partially purified membranes effected a 77% reduction in tumor outgrowth. The greater ability of membranes, relative to membrane extracts, to elicit immunoprotective activity may be due to 1) the enhanced immunogenicity of particulate over soluble antigens (*4, 7*), 2) loss of TSTA during the processing of the crude extract, or 3) the masking or denaturation of immunogenic sites on the solubilized antigen resulting from the binding of detergent molecules (*20, 22*). Determination of an optimal C_8Glu concentration for the extraction of these antigens may reduce the disparity between the specific activities of the in situ and the extracted TSTA.

The biologically active TSTA moiety extracted from intact MCA-F cells with C_8Glu was partially purified by pIEF at the pH 6.5–6.8 region of the gradient. The apparent isoelectric pH of the C_8Glu-extracted antigen is slightly more basic than that reported for antigen released with the use of 1-butanol (*12*), and it is one full pH unit higher than the isoelectric pH of the 3-*M* KCl-extracted moiety (*6, 15*). The significantly greater isoelectric pH of the tumor antigens extracted by noncytolytic techniques, compared to TSTA released after exposure to 3 *M* KCl, may reflect differences in extraction mechanisms. The slightly different migration of 1-butanol- and C_8Glu-extracted antigens in pIEF might result from minor differences in the conformations of the antigens following extraction due to the association of residual extractant. However, if C_8Glu remains bound to the extracted antigen, it does not appear to affect the focusing of antigen into a discrete region of the pIEF gradient; 60% of the applied activity was recovered in 7% of the applied protein, resulting in a fourfold to fivefold increase in specific tumor antigen activity. Conversely, when extracts prepared with the nonionic detergent Nonidet P40 were electrofocused, the presence of mixed protein–detergent micelles resulted in a smearing of protein across the entire pH gradient, with no detectable TSTA activity in any fraction (data not shown).

Heretofore, the preparation of soluble tumor antigens suitable for immunoprotection assays and for biochemical characterization has relied on treatment of whole cells or subcellular fractions with detergents or hypertonic salt solutions. These techniques have yielded materials that are active but which often contain numerous extraneous components, complicating isolation and characterization of the extracted antigens. Noncytolytic extraction techniques, such as 1-butanol and C_8Glu extraction, yield biologically active membrane proteins unencumbered by cytoplasmic components or intransigent residual detergents. Thus noncytolytic extraction may facilitate analysis of certain plasma membrane antigens by providing preparations containing only membrane-associated molecules in a form amenable to fractionation by classical biochemical techniques.

REFERENCES

(*1*) Prehn RT, Main JM. Immunity to methylcholanthrene-induced tumors. J Natl Cancer Inst 1957; 18:769–778.

(*2*) Price MR, Baldwin RW. Preparation of aminoazo dye-induced rat hepatoma membrane fractions retaining tumour specific antigen. Br J Cancer 1974; 30:382–393.

(*3*) Pellis NR, Kahan BD. Specific tumor immunity induced with soluble materials: Restricted range of antigen dose and of challenge tumor load for immunoprotection. J Immunol 1975; 115:1717–1722.

(*4*) Natori T, Law LW, Appella E. Biologic and biochemical properties of detergent-solubilized tumor-specific transplantation antigen from a simian virus 40-induced neoplasm: *Brief communication*. J Natl Cancer Inst 1977; 59:1331–1333.

(*5*) Revesz L. Detection of antigenic differences in isologous host–tumor systems by pretreatment with heavily irradiated tumor cells. Cancer Res 1960; 20:443–437.

(*6*) Pellis NR, Yamagishi H, Macek CM, Kahan BD. Specificity and biological activity of extracted murine tumor specific transplantation antigens. Int J Cancer 1980; 26:443–449.

(*7*) Minami A, Mizushima Y, Takeichi N, Hosokawa M, Kobayashi H. Dissociation of anti-tumor immune responses in rats immunized with solubilized tumor-associated antigens from a methylcholanthrene-induced fibrosarcoma. Int J Cancer 1979; 23:358–365.

(*8*) DuBois GC, Appella E, Law LW, DeLeo AB, Old LJ. Immunogenic properties of soluble cytosol fractions of Meth A sarcoma cells. Cancer Res 1980; 40:4204–4208.

(*9*) Pellis NR, Kahan BD. Methods to demonstrate the immunogenicity of soluble tumor specific transplantation antigens. I. The immunoprophylaxis assay. In: Busch H, ed. Methods in cancer research. Vol 13. New York: Academic Press, 1976:291–330.

(*10*) Natori T, Law LW, Appella E. Immunochemical evidence of a tumor-specific surface antigen obtained by detergent solubilization of the membranes of a chemically induced sarcoma, Meth-A. Cancer Res 1978; 38:359–364.

(*11*) Prat M, Tarone G, Comoglio PM. Antigenic and immunogenic properties of membrane proteins solubilized by sodium desoxycholate, papain digestion or high ionic strength. Immunochemistry 1975; 12:9–17.

(*12*) LeGrue SJ, Kahan BD, Pellis NR. Extraction of a murine tumor-specific transplantation antigen with 1-butanol. I. Partial purification by isoelectric focusing. JNCI 1980; 65:191–196.

(*13*) Appella E, Law LW, Henriksen O. Biological and biochemical properties of soluble tumor-specific transplantation antigen of a simian virus-40 induced neoplasm. Cancer Res 1976; 36:3539–3544.

(*14*) Rogers MJ, Law, Pierotti MA, Parmiani G. Separation of the tumor associated transplantation antigen (TATA) from the alien H-2^k antigens expressed on a methylcholanthrene-induced tumor. Int J Cancer 1980; 25:105–109.

(*15*) Yamagishi H, Pellis NR, Kahan BD. Tumor-protective and -facilitating antigens from 3 *M* KCl solubilized tumor extracts. J Surg Res 1979; 26:392–399.

(*16*) Helenius A, Simons K. Solubilization of membranes by detergents. Biochim Biophys Acta 1975; 415:29–79.

(*17*) Shinoda K, Yamaguchi T, Hori R. The surface tension and the critical micelle concentration in aqueous solution of β-D-alkyl glucosides and their mixtures. Bull Chem Soc Japan 1961; 34:237–241.

(*18*) Baron C, Thompson TE. Solubilization of bacterial membrane proteins using alkyl glucosides and dioctanoyl phosphatidylcholine. Biochim Biophys Acta 1975; 382:276–285.

(*19*) Schneider WJ, Basu SK, McPhaul MJ, Goldstein JL, Brown MS. Solubilization of a low density lipoprotein receptor. Proc Natl Acad Sci USA 1979; 76:5577–5581.

(*20*) Banerjee R, Epstein M, Kandrach M, Zimniak P, Racker E. A new method of preparing Ca^{2+} ATPase from sarcoplasmic reticulum: Extraction with octylglucoside. Membr Biochem 1979; 2:283–296.

(*21*) Stubbs GW, Litman BJ. Effect of alterations in the amphipathic microenvironment on the conformational stability of bovine opsin. I. Mechanism of solubilization of disk membranes of the nonionic detergent octylglucoside. Am Chem Soc 1978; 17:215–219.

(*22*) Radominska-Pyrek A, Pilarska M, Zimniak P. Solubilization of microsomal phosphoethanolamine transferase by octylglucoside. Biochem Biophys Res Commun 1978; 85:1074–1081.

(*23*) Pellis NR, Tom BH, Kahan BD. Tumor-specific and allospecific immunogenicity of soluble extracts from chemically induced murine sarcomas. J Immunol 1974; 113:708–711.

(*24*) Bradford MM. A rapid and sensitive method for the quantitation of microgram quantities of protein utilizing the principle of protein-dye binding. Anal Biochem 1976; 72:248–254.

(*25*) Brunette DM, Till JE. A rapid method for the isolation of L-cell surface membranes using an aqueous two-phase polymer system. J Membr Biol 1971; 5:215–223.

(*26*) Stone KR, Smith RE, Joklik WK. Changes in membrane polypeptides that occur when chick embryo fibroblasts and NRK cells are transformed with avian sarcoma viruses. Virology 1974; 58:86–100.

(*27*) Kahan BD, Rutzky L, Berlin B, et al. Cell surface alterations on colon adenocarcinoma cells. Cancer Res 1976; 36:3526–3534.

(*28*) Macek CM, Kahan BD, Pellis NR. Delayed hypersensitivity to crude and partially purified murine tumor specific transplantation antigens and alloantigens utilizing the footpad swelling assay. J Immunol 1980; 125:1639–1643.

(*29*) Allen TM, Romans AY, Kercret H, Segrest JP. Detergent removal during membrane reconstitution. Biochim Biophys Acta 1980; 601:328–342.

(*30*) LeGrue SJ, Allison JP, Macek CM, Pellis NR, Kahan BD. Immunobiological properties of 1-butanol-extracted cell surface antigens. Cancer Res 1981; 41:3956–3960.

Use of Young Nude Mice for Selection of Subpopulations of Cells With Increased Metastatic Potential From Nonsyngeneic Neoplasms [1,2,3,4]

Vincent A. Pollack [5,6] *and* **Isaiah J. Fidler** [5,7]

ABSTRACT—The purpose of these studies was to investigate whether young (3-wk-old) nude mice, which lack functional T-lymphocytes and demonstrate low natural killer cell activity, could serve as in vivo models for the selection of metastatic subpopulations of cells from heterogeneous allogeneic melanomas. Three-week-old BALB/cAnN or N:NIH(S) nude mice received iv injections of single cells harvested from either the B16 or K-1735 melanoma. Individual pulmonary metastases were harvested 4 weeks later and implanted sc into nude mice to expand the population. Cells from each of these metastases colonized in the lungs of 3-week-old nude mice and 6-week-old normal syngeneic mice with significantly higher efficiency than did cells from the parent tumors. It was concluded that, in addition to being a useful in vivo model for ascertaining the metastatic potential of neoplasms, the healthy young nude mouse could be used for selecting and maintaining tumor cell variants of high metastatic potential from heterogeneous allogeneic tumors.—JNCI 1982; 69:137–141.

Cancer metastasis represents a complex series of tumor cell–host interactions that result in proliferation of tumor cells at organs distant from the primary neoplasm. Throughout this process, tumor cells are exposed to various host antitumor defenses, and the rules of "survival of the fittest" apply. As a result, metastasis is currently viewed as a process selective for preexistent metastatic cells that probably constitute a minor subpopulation of the primary tumor (*1–7*).

Recent evidence indicates that developing primary neoplasms may be comprised of subpopulations of cells with widely disparate phenotypes, a few subsets of which may confer selective survival advantages (*7, 8*). These include antigenic and immunogenic properties, growth rates, karyotypes, and cell surface receptors, among others (*2, 7, 8, 9–12*). Furthermore, malignant neoplasms are populated by cells of unequal invasive and metastatic capabilities (*13–15*). The heterogeneity of tumors with respect to response to cytotoxic drugs has profound implications for the way in which potential agents are selected for the treatment of metastases. Both human and animal tumors may contain subpopulations of cells with different sensitivity to cytotoxic agents (*7, 10, 12, 16–19*). Moreover, differences in response to drug treatment have been reported between primary neoplasms and their metastases (*16, 19*) and even among the metastases themselves (*19*). Taken together, these factors pose major problems to oncologists whose primary goal in cancer treatment is to eradicate metastases. Since the clinically important subpopulations of highly metastatic and/or chemotherapy-resistant tumor cells may represent minor subsets of the primary tumor, the sampling of primary tumors becomes problematic and such samples may not be representative of cells populating distant micrometastases (*7*).

Several methods have been described to isolate subpopulations of cells with increased metastatic potential from a heterogeneous malignant neoplasm. Perhaps the most widely used procedure is the one we initially described for the B16 melanoma. This procedure involves the isolation and propagation of variant lines from metastatic foci (*1*). In such diverse murine tumor systems as melanoma, fibrosarcoma, 3-methylcholanthrene-induced sarcoma, Lewis lung carcinoma, lymphoma, and lymphosarcoma, variants with different metastatic potential have been selected (*7, 9*). Essential to the success of such a procedure is the availability of normal syngeneic recipients for both the selection and the testing of the metastatic cells. Clearly, this is not a feature of autochthonous human tumors. The demonstration that 3-week-old nude mice, in which the NK cell system is not yet activated (*20, 21*), can be used for quantitation of the metastatic potential of neoplasms (*20, 22*) has encouraged us to use the athymic mouse for the selection of metastatic subpopulations from the allogeneic heterogeneous B16 melanoma and K-1735 melanoma parent tumor populations.

MATERIALS AND METHODS

Animals.—Five- to 6-week-old male B6C3F$_1$ mice (C57BL/6 × C3H/HeN mammary tumor virus negative) and 3-week-old male athymic (*nu/nu*) nude mice of N:NIH(S) and BALB/cAnN backgrounds were used. All mice were specific pathogen-free and were obtained from the Animal Production Area of the NCI–Frederick Cancer Research Facility.

Tumors.—The origin and maintenance of the spontaneous murine B16 melanoma, syngeneic to C57BL/6 mice, have

---

ABBREVIATIONS USED: HBSS=Hanks' balanced salt solution; NK=natural killer.

---

[1] Received December 2, 1981; accepted February 22, 1982.

[2] Supported by Public Health Service contract N01CO-75380 from the Office of the Director, National Cancer Institute, to Litton Bionetics Inc.

[3] The contents of this publication do not necessarily reflect the views or policies of the U.S. Department of Health and Human Services, nor does mention of trade names, commercial products, or organizations imply endorsement by the U.S. Government.

[4] Animals were maintained under the guidelines set forth by the National Institutes of Health Policy on Humane Care and Use of Animals and by the Animal Welfare Act in facilities accredited by the American Association for Accreditation of Laboratory Animal Care.

[5] Cancer Metastasis and Treatment Laboratory, NCI-Frederick Cancer Research Facility, P.O. Box B, Frederick, Md. 21701.

[6] *Present address:* Cancer Metastasis Research Group, Immunology and Infectious Diseases Department, Pfizer Central Research, Groton, Conn. 06340.

[7] *Address reprint requests to* Dr. Fidler.

been described previously (*1–3*). The melanoma's invasive and metastatic properties have been attributed to minor subpopulations of metastatic cells that preexist within the parent tumor (*13*). The induction and properties of the K-1735 melanoma, syngeneic to C3H/HeN mice, have been previously described (*23*). The in vitro production and characterization of many cloned cell lines, as well as the metastatic potentials of each, were also recently reported (*5, 14*). All tumor lines were maintained in vitro in complete Eagle's minimal essential medium that contained 5% fetal bovine serum and that was supplemented with glutamine, nonessential amino acids, and vitamins. Cultures were maintained at 37°C in a humidified atmosphere containing 5% CO_2. The tumor lines were free of mycoplasma and the following murine viruses: reovirus type 3, pneumonia virus of mice, K-virus, Theiler's virus, Sendai virus, ectromelia virus, and lactate dehydrogenase virus.

For in vivo studies, we harvested the tumor cells from cultures in their exponential growth phase by overlaying the cells with a thin layer of 0.25% trypsin–0.02% EDTA for 1 minute. The cells were washed and resuspended in HBSS. Tumor cell viability was assessed by trypan blue exclusion, and only single cell suspensions of greater than 95% viability were used in the study (*3*). For in vivo experiments involving sc passaged tumors (1–2 cm), single cell suspensions were prepared by enzymatic dissociation with the use of HBSS containing 0.14% collagenase type I, 0.03% DNase, and 50 µg gentamicin/ml). Enzymes were purchased from Sigma Chemical Co., St. Louis, Mo.

Selection of metastatic tumor cell variants in syngeneic mice.—In the first set of experiments, we isolated metastatic variants from the B16 melanoma and the K-1735 melanoma by recovering spontaneous lung metastases produced from a subcutaneous parent tumor implanted into the hind footpad of mice (*3*). Individual spontaneous metastases (designated as SMet-1, SMet-2, and so on) were removed aseptically and transplanted by trocar into syngeneic mice to expand their population before their metastatic potential was tested in both syngeneic and allogeneic nude mice.

Selection of metastatic tumor cell variants in allogeneic nude mice.—BALB/cAnN nude mice, 3 weeks old, received iv injections of 5×10^4 viable cells of either the B16 melanoma or the K-1735 melanoma. About 3–4 weeks later, the mice were killed, and solitary metastases harvested from different mice were transplanted by trocar implantation into the subcutis of nude mice (1 metastasis/mouse). The metastases were designated as NuMet-1, NuMet-2 and so on. After sc growth, both parent tumors (B16 and K-1735) and the various metastases were tested for their metastatic potential in both syngeneic mice and allogeneic nude mice. In all experiments, we took great care to prevent cross-contamination of tumor samples.

Testing of the metastatic potential of cells from the parent tumor and from their spontaneous metastases.—Parent tumors and individual metastases (selected either in syngeneic mice or in young nude mice) were transplanted sc into mice to expand their populations. Suspensions of single viable tumor cells were prepared from the individual subcutaneous tumor mass by a modification of the enzymatic dissociation technique described by Peters et al. (*24*). Individual subcutaneous tumors (1–2 cm) were aseptically excised, cut into 1-mm pieces, and rinsed several times with HBSS. The fragments were placed into a sterile vial containing a small magnetic stirring bar and two-thirds capacity (≈10 ml) of sterile dissociation medium (0.14% collagenase type I, 0.03% DNase, and 50 µg gentamicin/ml of HBSS). Vials were taped to the platform of a magnetic stirring device and gently agitated (without frothing) for 15–25 minutes at room temperature. All suspensions were filtered through a sterile silkscreen and centrifuged, and the cells were resuspended in HBSS. Cell viability was determined by the trypan blue dye exclusion test. After enumeration, the suspension was diluted to the [illegible] cell concentration.

We tested the metastatic potential of tumor lines by monitoring the induction of experimental pulmonary metastases as previously described (*3–5, 13*). Portions of cell suspensions (0.2 ml) were injected into the lateral tail vein of unanesthetized syngeneic $B6C3F_1$ mice or 3-week-old nude mice after disinfection of the site with 70% ethanol. After 21 days, the mice were killed and their lungs were placed in Bouin's fluid; peripheral lung colonies were counted with the use of a dissecting microscope. Results are expressed as the median and range of lung tumor counts. Differences between the groups were analyzed with the Mann-Whitney *U*-test (*13*).

RESULTS

In the first set of experiments, we examined whether tumor cells populating spontaneous metastases produced from a parent tumor growing in syngeneic mice had greater metastatic potential than cells populating the parent tumor. Moreover, we also confirmed our earlier data (*20, 21, 25*) that young (3-wk-old) nude mice are suitable for studies designed to distinguish cells with low or high metastatic potential. The data for the B16 system are summarized in table 1 and for the K-1735 system in table 2. Essentially, the data demonstrate that in both syngeneic mice and allogeneic nude mice, cells from spontaneous metastases

TABLE 1.—*Metastatic potential of cells from the parent B16 melanoma and spontaneous metastases (isolated in syngeneic mice) determined by measurement of experimental pulmonary metastasis in syngeneic ($B6C3F_1$) or allogeneic [N:NIH(S)] nude mice*

Source of cells	Median No. (range) of pulmonary tumor colonies[a]	
	Syngeneic mice, 6 wk old[b]	Allogeneic nude mice, 3 wk old[c]
$B16–F_1$ (parent)	39 (18–90)	2 (0–7)
B16 SMet-1	>400 (all >300)	>400 (all >400)
B16 SMet-2	236 (202–424)	198 (121–>300)
B16 SMet-3	198 (112–335)	126 (45–251)
B16 SMet-4	>300 (263–>300)	230 (103–400)
B16 SMet-5	197 (135–284)	254 (25–342)

[a] The median No. of tumor colonies differed significantly from that produced by cells of the parent tumor, $P<0.001$.

[b] Groups of 10 mice received iv inoculations of 25,000 viable cells/mouse in 0.2 ml of HBSS. Mice were killed 3 wk later, and their lung tumor colonies were counted under a dissecting microscope.

[c] Groups of 10 mice received iv inoculations of 12,500 viable cells/mouse and were killed 4 wk later.

produced significantly more experimental lung tumor nodules than cells isolated from the unselected parent population (*P*<0.005). It is important to note that, for the studies in nude mice, we used fewer tumor cells in the inoculum than we used for studies in syngeneic animals because of the increased sensitivity of young nude mice to the formation of experimental metastases (*21*). Nonetheless, cells of the metastatic variants were capable of greater lung colonization than cells from the unselected parent tumors. Despite the lower cell content of the inoculum, the metastatic variants SMet-2 and SMet-4 of the B16 melanoma produced extensive extrapulmonary (intrapleural) metastases. Variants SMet-1 and SMet-5 were particularly virulent, resulting in early deaths because of extensive pulmonary and extrapulmonary metastases. Collectively, these data confirm that young nude mice can be used to distinguish cells of low and high metastatic potential (*21*).

In the second set of experiments, we attempted to determine whether the iv injection of tumor cells into nude mice is selective for metastatic variants of allogeneic (B16 and K-1735) melanomas. Groups of 10 nude mice each received iv injections of serial twofold dilutions of either B16—F_1 parent melanoma cells or K-1735 parent melanoma cells. Four weeks later, solitary lung tumor colonies were harvested from the peripheral lung tissue of mice with well-isolated nodules (10–20 nodules/lung). Each nodule was transplanted by trocar into a single young nude mouse. In this manner, seven B16 isolates (designated B16 NuMet-1 to NuMet-7) were tested for their metastatic potential as compared to that of the unselected parent population (table 3). For these experiments mice received iv injections of 10^4 viable cells. Tested in nude mice, cells from 6 of 7 metastases were significantly more metastatic than cells of the parent B16 tumor (*P*<0.001). This enhanced metastatic potential of the cells was expressed not only in young nude mice: Similar data were obtained when the metastatic potential of parent B16 and metastases (isolated in nude mice) was tested in syngeneic mice. Cells from 5 of 7 metastases were significantly more metastatic than cells isolated from the parent tumor (*P*<0.001).

TABLE 2.—*Metastatic potential of cells from parent K-1735 melanoma and spontaneous metastases (isolated in syngeneic mice) determined by measurement of experimental pulmonary metastasis in syngeneic (C3H/HeN) or allogeneic [N:NIH(S)] nude mice*

Source of cells	Median No. (range) of pulmonary tumor colonies[a]	
	Syngeneic mice, 6 wk old[b]	Allogeneic nude mice, 3 wk old[c]
K-1735 (parent)	43 (6–165)	69 (21–331)
K-1735 SMet-1	360 (11–410)	205 (61–251)
K-1735 SMet-2	148 (9–365)	127 (44–223)
K-1735 SMet-3	101 (6–490)	154 (46–221)
K-1735 SMet-4	262 (44–>400)	215 (28–332)

[a] The median No. of tumor colonies differed significantly from that produced by cells of the parent tumor, *P*<0.01.

[b] Groups of 10 mice received iv inoculations of 50,000 viable cells in 0.2 ml HBSS. Mice were killed 4 wk later, and their lung tumor colonies were counted under a dissecting microscope.

[c] Groups of 10 mice received iv inoculations of 15,000 viable cells and were killed 4 wk later.

TABLE 3.—*Metastatic potential of parent B16—F_1 melanoma and putatively metastatic variants isolated in allogeneic (BALB/cAnN) nude mice determined by measurement of experimental pulmonary metastasis in allogeneic nude or syngeneic mice*

Source of cells	Median No. (range) of pulmonary tumor colonies	
	Allogeneic nude mice, 3 wk old[a]	Syngeneic mice, 6 wk old[a]
B16–F_1 (parent)	0.5 (0–7)	1.0 (0–11)
B16 NuMet-1	9.5 (1–39)[b]	8.0 (1–16)[b]
B16 NuMet-2	1.5 (0–16)	1.5 (0–8)
B16 NuMet-3	40.0 (3–101)[c]	27.0 (7–40)[c]
B16 NuMet-4	87.0 (37–298)[c]	68.0 (2–98)[c]
B16 NuMet-5	25.0 (4–56)[c]	11.0 (3–23)[c]
B16 NuMet-6	15.5 (0–67)[c]	2.5 (1–6)
B16 NuMet-7	31.0 (4–115)[c]	10.0 (4–28)[c]

[a] Groups of 10 mice received iv inoculations of 10,000 viable cells. Mice were killed 3 wk later, and their lung tumor colonies counted under a dissecting microscope.

[b] The median No. of lung tumor colonies differed significantly from that produced by cells of the parent tumor, *P*<0.01.

[c] The median No. of lung tumor colonies differed significantly from that produced by cells of the parent tumor, *P*<0.001.

TABLE 4.—*Metastatic potential of parent K-1735 melanoma and putatively metastatic variants isolated in allogeneic (BALB/cAnN) nude mice determined by measurement of experimental pulmonary metastasis in allogeneic nude or syngeneic mice*

Source of cells	Median No. (range) of pulmonary tumor colonies	
	Allogeneic nude mice, 3 wk old[a]	Syngeneic mice, 6 wk old[b]
K-1735 (parent)	19 (3–56)[c]	44 (10–148)[c]
K-1735 NuMet-1	>500 (all >500)	>500 (all >500)
K-1735 NuMet-2	406 (184–>500)	>500 (all >500)
K-1735 NuMet-3	>500 (all >500)	>500 (all >500)
K-1735 NuMet-4	124 (57–186)	200 (134–245)
K-1735 NuMet-5	>500 (all >500)	>500 (all >500)
K-1735 NuMet-6	>500 (all >500)	>500 (all >500)
K-1735 NuMet-7	385 (170–>500)	>500 (all >500)
K-1735 NuMet-8	378 (261–>500)	>500 (all >500)
K-1735 NuMet-9	>500 (all >500)	>500 (all >500)

[a] Groups of 10 mice received iv inoculations of 25,000 viable cells. Mice were killed 4 wk later, and their lung tumor colonies counted with a dissecting microscope.

[b] Groups of 10 mice received iv inoculations of 50,000 viable cells.

[c] The median No. of lung tumor colonies differed significantly from all other groups, *P*<0.001.

In a similar manner, putatively metastatic variants of the K-1735 melanoma were selected in the nude mouse and later tested for their metastatic potential in both adult syngeneic mice and 3-week-old BALB/cAnN nude mice (table 4). Cells of the parent K-1735 tumor produced a median of 19 lung tumor colonies (range, 3–56) in nude mice and a median of 44 lung tumor colonies (range, 17–148) in syngeneic mice. In contrast, the lines selected in the nude mice were uniformly highly metastatic and produced hundreds of peripheral lung tumor nodules. In each case, results of tests in the syngeneic mice paralleled those in nude mice. The results also indicate that sc growth did not affect the metastatic potential of either the parent or the metastatic variants. In subsequent experiments (data not shown), we have found that even several successive sc transplantations do not influence the metastatic potential of selected or unselected tumor populations.

DISCUSSION

Recent data from our laboratory have demonstrated that specific pathogen-free, 3-week-old nude mice, which lack functional T-lymphocytes (*26*) and which demonstrate low NK cell activity, could serve as in vivo models to ascertain the metastatic potential of allogeneic and xenogeneic tumors (*20, 21, 25*). Our present data confirm these observations and show, in addition, that young nude mice can be used to select from within a heterogeneous allogeneic tumor those subpopulations of cells that possess increased metastatic potential, in both nude mice and their original syngeneic hosts.

For the present studies, we used the B16 melanoma (*13*) and K-1735 melanoma (*14*) previously shown to be heterogeneous with regard to various biologic properties that include invasion and metastasis. Cells isolated from parent tumors or their spontaneous metastases were introduced into the circulation of either syngeneic mice or allogeneic nude mice. In both hosts, cells isolated from spontaneous metastases that had developed in the autochthonous (syngeneic) host produced significantly more experimental metastases ($P<0.005$) than cells isolated from the parent tumors. These data, therefore, demonstrate that the outcome of experimental metastasis in the young nude mice paralleled the pattern observed when parent and/or metastatic cells were injected iv into syngeneic $B6C3F_1$ recipients (tables 1, 2). The metastatic potential of tumor cells was ascertained by determining the production of "experimental" metastases after the introduction of cells into the circulation. This procedure eliminates the need for initial detachment of cells from the primary neoplasm and invasion into blood vessels. However, all the subsequent steps in the metastatic process must occur for the iv injected cells to establish a metastasis. Elimination of the initial steps in the process introduces the risk that noninvasive tumor cells might form metasases when injected iv but be unable to metastasize from a tumor growing sc or im. This question has been addressed by Kripke et al. (*15*) who studied the metastatic behavior of 21 clones of the UV-2237 fibrosarcoma syngeneic to the C3H mouse by using three different assays: 1) formation of experimental metastases after iv injection, 2) formation of experimental metastases after sc implantation, and 3) survival time of animals after receiving iv injections. When the clones were ranked in order of increasing metastatic behavior, a strong correlation was found among all three tests for 20 of 21 clones. Thus the production of experimental metastases is a valid assay for determining the potential of cells for spontaneous metastasis. Similar data have also been reported for the B16 melanoma system (*27*) and the K-1735 melanoma system (*14*).

The existence in heterogeneous neoplasms of minor but specialized subpopulations of cells that can give rise to metastases has profound implications for testing agents designed to treat disseminated disease (*7, 10, 11*). Differences in the response of primary and metastatic lesions (*2, 10, 16, 17*) or of various metastases (*19*) to therapeutic agents are well documented in clinical practice. Procedures that use unselected heterogeneous tumors to select effective agents for treatment of metastases may be unable to identify a beneficial response against the minor but fatal subpopulation of metastatic cells that exists in the neoplasm (*7*). Future assays to identify potential agents for treatment of metastases should ideally utilize tumor cell populations with defined metastatic capabilities (*9*).

Our studies demonstrate that young nude mice can be used for selection of populations of tumor cells with increased metastatic potential as tested in their original hosts (tables 3, 4). The ability of the athymic mouse to discriminate metastatic from nonmetastatic cells functions across major histocompatibility barriers, demonstrated by the fact that the N:NIH(S) and BALB/cAnN nude mice were allogeneic to the C57BL/6 and C3H/HeN mice from which the tumors were derived. We stress that the use of specific pathogen-free nude mice is mandatory to the success of the procedures we outlined. Nude mice infected with murine hepatitis virus or other pathogenic microorganisms exhibit increased activity of their NK system (*28*) and are resistant to the production of metastases (*20, 21*) or even growth of tumor allografts and/or xenografts at a subcutaneous site (*29–31*).

Taken together, our results suggest that the athymic nude mouse may be used for selection, isolation, and maintenance of tumor cell variants of high metastatic potential. They further suggest that since nude mice accept tissue grafts from a variety of sources (*32, 33*), they could be used for the identification and selection of metastatic cell variants across a greater (i.e., xenogeneic) histocompatibility barrier.

REFERENCES

(*1*) Fidler IJ. Selection of successive tumour lines for metastasis. Nature 1973; 242:148–149.

(*2*) ———. Tumor heterogeneity and the biology of cancer invasion and metastasis. Cancer Res 1978; 38:2651–2660.

(*3*) ———. General considerations for studies of experimental cancer metastasis. In: Bush H, ed. Methods in cancer research. New York: Academic Press, 1978:399–499.

(*4*) Fidler IJ, Gersten DM, Hart IR. The biology of cancer invasion and metastasis. Adv Cancer Res 1978; 28:149–250.

(*5*) Fidler IJ, Gruys E, Cifone MA, Barnes Z, Bucana C. Demonstration of multiple phenotypic diversity in a murine melanoma of recent origin. JNCI 1981; 67:947–956.

(*6*) Hart IR, Fidler IJ. Cancer invasion and metastasis. Quart Rev Biol 1980; 55:121–142.

(*7*) Poste G, Fidler IJ. The pathogenesis of cancer metastasis. Nature 1980; 283:139–146.

(*8*) Nowell PC. Clonal evolution of tumor cell populations. Science 1976; 194:23–28.

(*9*) Hart IR, Fidler IJ. The implications of tumor heterogeneity for studies on the biology and therapy of cancer metastasis. Biochim Biophys Acta 1981; 651:37–50.

(*10*) Heppner GH. The challenge of tumor heterogeneity. In: Bulbrook RD, Taylor DJ, eds. Commentaries on research in breast disease. New York: Liss, 1979:177–191.

(*11*) Kerbel RS. Implications of immunological heterogeneity of tumours. Nature 1979; 280:358–360.

(*12*) Trope, C. Different sensitivity to cytostatic drugs of primary tumor and metastasis of the Lewis carcinoma. Neoplasma 1975; 22:171–180.

(*13*) Fidler IJ, Kripke ML. Metastasis results from preexisting variant cells within a malignant tumor. Science 1977; 197:893–895.

(*14*) ———. Metastatic heterogeneity of cells from the K-1735 melanoma. In: Grundmann E, ed. Metastatic tumor growth. Stuttgart: Fischer-Verlag, 1980:71–81.

(*15*) Kripke ML, Gruys E, Fidler IJ. Metastatic heterogeneity of cells from an ultraviolet light-induced murine fibrosarcoma of recent origin. Cancer Res 1978; 38:2962–2967.

(*16*) Law LW. Origin of the resistance of leukaemic cells to folic acid antagonists. Nature 1952; 169:628–629.

(*17*) Fugmann RA, Anderson JC, Stolfi RL, Martin DS. Comparison of adjuvant chemotherapeutic activity against primary and metastatic spontaneous murine tumors. Cancer Res 1977; 39:496–500.

(*18*) Schabel RM Jr. Concepts for systemic treatment of micrometastases. Cancer 1975; 35:15–24.

(*19*) Tsuruo T, Fidler IJ. Differences in drug sensitivity among tumor cells from parental tumors, selected variants, and spontaneous metastases. Cancer Res 1981; 41:3058–3064.

(*20*) Hanna N. Expression of metastatic potential of tumor cells in young nude mice is correlated with low levels of natural killer cell-mediated cytotoxicity. Int J Cancer 1980; 26:675–680.

(*21*) Hanna N, Fidler IJ. Expression of metastatic potential of allogeneic and xenogeneic neoplasms in young nude mice. Cancer Res 1981; 41:438–444.

(*22*) Talmadge JE, Meyers KM, Prieur DJ, Starkey JR. Role of NK cells in tumour growth and metastasis in beige mice. Nature 1980; 284:622–624.

(*23*) Kripke ML. Speculations on the role of ultraviolet radiation in the development of malignant melanoma. JNCI 1979; 63:541–548.

(*24*) Peters LC, Brandhorst JS, Hanna MG Jr. Preparation of immunotherapeutic autologous tumor cell vaccines from solid tumors. Cancer Res 1979; 39:1353–1360.

(*25*) Hanna N, Fidler IJ. Role of natural killer cells in the destruction of circulating tumor emboli. JNCI 1980; 65:801–809.

(*26*) Riccardi C, Puccetti P, Santoni A, Herberman RB. Rapid in vivo assay of mouse natural killer cell activity. JNCI 1979; 63:1041–1045.

(*27*) Wang BS, McLoughlin GA, Richie JP, Mannick JA. Correlation of the production of plasminogen activator with tumor metastasis in B16 melanoma cell lines. Cancer Res 1980; 40:288–292.

(*28*) Clark EA, Russell PH, Egghart M, Horton MA. Characteristics and genetic control of NK-cell-mediated cytotoxicity activated by natural acquired infection in the mouse. Int J Cancer 1979; 24:688–699.

(*29*) Kameya T, Shimosato Y, Tumuraya M, Ohsawa N, Normura T. Human gastric choriocarcinoma serially transplanted in nude mice. J Natl Cancer Inst 1976; 56:325–332.

(*30*) Kyriazis, AP, Dipersio L, Michael JG, Pesce AJ. Influence of the mouse hepatitis virus (MHV) infection on the growth of human tumors in the athymic mouse. Int J Cancer 1979; 23:402–409.

(*31*) Reid LM, Holland J, Jones C, Wolf B, Sato G. Some of the variables affecting the success of transplantation of human tumors into the athymic nude mouse. In: Houchens DP, Ovejera AA, eds. Proceedings of the symposium on the use of athymic (nude) mice in cancer research. New York: Fischer-Verlag, 1978:107–121.

(32) Fogh J, Fogh JM, Orfeo T. One hundred and twenty-seven cultured human tumor cell lines producing tumors in nude mice. J Natl Cancer Inst 1977; 59:221–225.

(33) Fogh J, Giovanella BC, eds. The nude mouse in experimental and clinical research. New York: Academic Press, 1978.

blank page

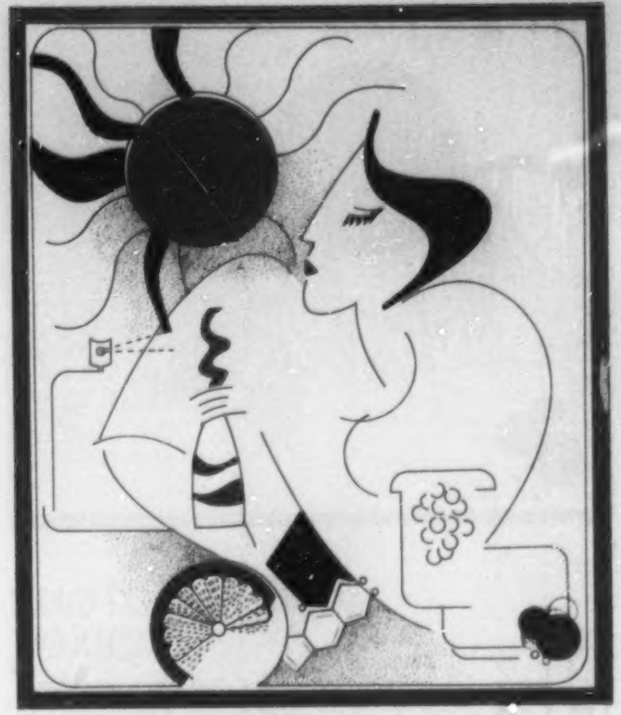

PHOTOCHEMICAL TOXICITY
Toxic, Allergic, and Carcinogenic Aspects with Emphasis on Predicting Effects in Humans

Proceedings of the seventh
in the series of Food and Drug
Administration Science Symposia

U.S. Department of Health
and Human Services
Public Health Service
Food and Drug Administration

blank page

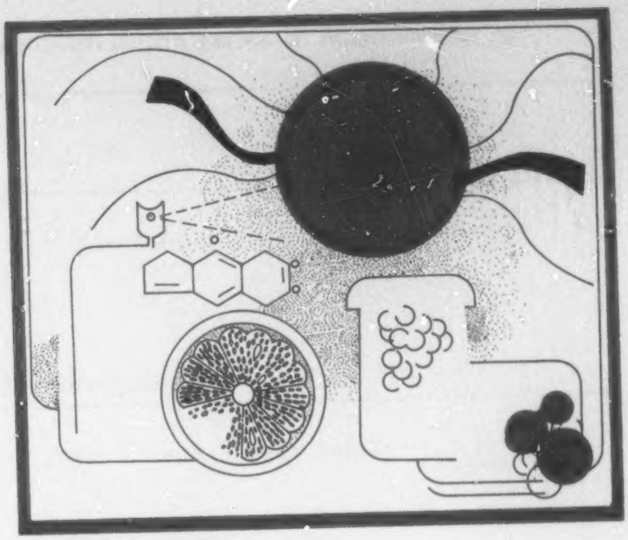

PHOTOCHEMICAL TOXICITY
Toxic, Allergic, and Carcinogenic Aspects with Emphasis on Predicting Effects in Humans

Proceedings of the seventh
in the series of Food and Drug
Administration Science Symposia

Held at the Uniformed Services
University of the Health Sciences
Bethesda, Maryland
March 16–17, 1981

Edited By:
F. Alan Andersen
Andrija Kornhauser
Constantine Zervos

Symposium Coordinator
and Technical Editor
Janet E. Cunningham

A limited number of reprints of this symposium are available from the Office of Health Affairs (Science), Food and Drug Administration, Public Health Service, Department of Health and Human Services, 5600 Fishers Lane (HFY-31), Rockville, Md. 20857.

Table of Contents

Photochemical Toxicity—Proceedings of the seventh in the series of Food and Drug Administration Science Symposia

Introduction

151	Photochemical toxicity: Toxic, allergic, and carcinogenic aspects with emphasis on predicting effects in humans—an introduction	*F. Alan Andersen*

Basic Chemistry, Physics, and Biology Relating to Photosensitization

155	Optical radiation measurements: Instrumentation and sources of error	*Robert J. Landry, F. Alan Andersen*
163	Molecular aspects of drug photosensitivity with special emphasis on psoralen photosensitization reaction	*Madhu A. Pathak*
171	Immunosuppressive effects of ultraviolet (280–320 nm) radiation and psoralen plus ultraviolet (320–400 nm) radiation in mice	*Margaret L. Kripke*

Cellular Assay Systems

177	Cell damage by near ultraviolet radiation: Role of DNA–protein cross-links	*A. Eisenstark, S. Kovacs, J. Terry*
183	Tumor virus induction and host cell capacity inactivation: Possible in vitro tests for photosensitizing chemicals	*L. E. Bockstahler, T. P. Coohill, C. D. Lytle, S. P. Moore, J. M. Cantwell, B. J. Schmidt*
189	Comparative photobiology of psoralens	*M. J. Ashwood-Smith, A. T. Natarajan, G. A. Poulton*
199	Genotoxic effects of sunlight-activated waste water in cultured mammalian cells	*Gary F. Strniste, David J. Chen, Richard T. Okinaka*
205	Interaction of oxygen and oxy-radicals with carotenoids	*Norman I. Krinsky, Susan M. Deneke*
211	A method to quantify the potency of photosensitizers that modify cell membranes	*John P. Pooler, Dennis P. Valenzeno*

Experimental Animal Systems

219	In vitro assay of the effects of psoralens plus ultraviolet radiation on human lymphoid cells	*Kenneth H. Kraemer*

229 Modification of photocarcinogenesis by chemical agents *Frederick Urbach, P. Donald Forbes, Ronald E. Davies*

237 Current status of predictive animal models for drug photoallergy and their correlation with drug photoallergy in humans *Leonard C. Harber, Robert B. Armstrong, Hideyuki Ichikawa*

245 Toxic effect of ultraviolet light on melanocytes: Use of animal models in pigment research *George Szabo, Frederick B. Blog, Andrija Kornhauser*

Animal Photochemical Toxicity Effects

253 Toxicologic aspects of photosensitization in livestock *A. Earl Johnson*

259 Chemical and biochemical aspects of photosensitization in livestock and poultry *G. Wayne Ivie*

Human Photochemical Toxicity Effects

265 Chemical phototoxicity in humans *John H. Epstein*

269 Human models for identification of photosensitizing chemicals *Albert M. Kligman, Kays H. Kaidbey*

274 Therapeutic in vivo photochemistry: Photochemical toxicity studies in humans *John A. Parrish*

279 Photosensitization by porphyrins and prevention of photosensitization by carotenoids *Micheline M. Mathews-Roth*

287 Ocular phototoxicity and psoralen plus ultraviolet radiation (320–400 nm) therapy: An experimental and clinical evaluation *Sidney Lerman*

Summary and Conclusions

305 Concluding remarks *Constantine Zervos*

307 Registrants

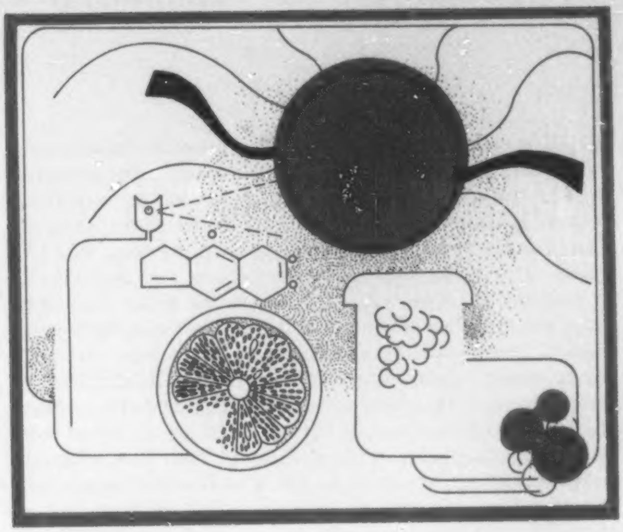

INTRODUCTION

Speaker: F. Alan Andersen
Food and Drug Administration

blank page

Photochemical Toxicity: Toxic, Allergic, and Carcinogenic Aspects With Emphasis on Predicting Effects in Humans—an Introduction[1]

F. Alan Andersen, *Ph.D.*[2]

In April 1975, the then Associate Commissioner for Science in the FDA, Dr. Lloyd Tepper, in a memorandum to all FDA Bureau Directors, included the following:

> It has been something of a surprise to note that light is implicated, to a greater or lesser degree, in the activities of each Bureau: cosmetics and photosensitization in the Bureau of Foods, chemophototherapy and photodermatitis in the Bureau of Drugs, phototherapy and various light products for the Bureau of Radiological Health and the Bureau of Medical Devices, microbiological control for the Bureau of Biologics, and laser analytical procedures used in the Bureau of Veterinary Medicine.

The interest is even broader now as a result of efforts to communicate the nature of the problem as it affects each Agency component. With this symposium, that communication is expanded to include affected industry and the medical, scientific, and consumer communities.

In a way, we are all coming in late. At the turn of the century, it was demonstrated that an acridine dye could act synergistically with light to produce oxygen-dependent killing of paramecia (*1*). In the 80 years that have passed, significant progress has been made in understanding the molecular basis for that early finding. Such basic research, however, has infrequently touched upon the implications for humans of sensitivity induced by a light-activated chemical. Moreover, this research has generated more questions.

For example, on the one hand, is light the great uncontrolled variable responsible for ambiguous chemical toxicity data, which FDA often faces in approval decisions? Could light, incident on individuals exposed to a chemical, on the other hand, be responsible for toxic reactions not uncovered in clinical or preclinical trials? Recent work suggests that the answer to both questions is yes (*2*).

Let us explore briefly just what is included in this area about which we are going to spend 2 days discussing. Chemical photosensitivity is a general term commonly used to describe abnormal or adverse light-induced chemical reactions in humans. Classically, this includes toxic and allergic responses to light plus chemicals. For purposes of this discussion, though, the general term is going to be expanded into three categories: chemical phototoxicity, chemical photoallergy, and (we are going to add) chemical photocarcinogenicity.

Chemical phototoxicity in humans is similar to many primary responses to irritants. Commonly, the skin response might mimic sunburn. Chemical photoallergy may be best described as getting a case of hives. Chemical photocarcinogenicity was suspected as early as 1937 for light-exposed mice subjected to sc injections of eosin or hematoporphyrin (*3*). More recently, an increased risk of nonmelanoma skin cancer has been found for patients treated with derivatives of the drug psoralen and UVA radiation (UV radiation between 320 and 380 nm) for severe psoriasis (*4*).

These responses in humans are serious consequences of simultaneous exposure to light and chemicals. It is important to emphasize that the responses might not be limited to body surfaces since circulating blood is also exposed to light. Because people are frequently exposed to light and because chemicals can be injected, ingested, or rubbed on, instances of simultaneous exposure are beyond calculation. Many chemicals cause photosensitivity, for example, because of their interaction with UV radiation. UV radiation can come from the sun or from a number of man-made sources, including high-intensity mercury vapor lamps, xenon lamps, medical phototherapy lamps, sunlamps, and even fluorescent lamps (*5, 6*). Because light sources can vary so in their intensity and their spectral quality, an important part of this symposium will be to introduce you to the topic of what is emitted from lights and how to measure it. We do not want you going back to your laboratories and checking out your lights with a light meter designed for your camera.

The number of chemical agents will also affect the magnitude of concern. A list, published in 1963, of photosensitizing chemicals contains at least 43 chemical agents, ranging from a buckwheat derivative to coal tars to various medications (*7*). A similar list, published in 1974 by essentially the same authors, had grown to 68 items, including dyes, essential oils, and additional medications (*8*). When we note that certain of these dyes are used in procedures such as retinal angiography (*9*) and that the earlier list already contained at least one agent used as an optical brightener in laundry detergent (*7*), the concern is further magnified.

Natural photosensitizers (endogenous biochemical species that interact with light) have also been described (*3*), and we will hear more about these during the symposium.

As a final piece of information relating to the magnitude of the problem from the chemical side, let me just note that one compilation includes 400 compounds that could act as sensitizers by interacting with molecular oxygen (*10*). This question of interaction is not limited to two dissimilar agents such as light and chemicals. A recent National Research Council report (*11*) noted that people normally are exposed to combinations of chemicals rather than to a single chemical, and, stating the obvious perhaps, it went on to note that "basic information on the effects of mixtures and

---

ABBREVIATION USED: FDA=Food and Drug Administration.

---

[1] Presented at the Seventh Food and Drug Administration Science Symposium ("Photochemical Toxicity: Toxic, Allergic, and Carcinogenic Aspects With Emphasis on Predicting Effects in Humans") held at the Uniformed Services University of the Health Sciences, Bethesda, Md., March 16–17, 1981.

[2] Bureau of Radiological Health, Food and Drug Administration, Public Health Service, U.S. Department of Health and Human Services, 8757 Georgia Ave. (HFK-300), Silver Spring, Md. 20910.

human body's reaction to them is lacking." It recommended further research on this difficult and complex problem and observed that, until a data base is available, the only practical approach is to test the specific mixtures of compounds for which information is needed.

To some extent, we face the same problem. Our information comes from both clinical and preclinical tests used for determining the potential of a given chemical to be a photosensitizer. Clinically, a photo-patch test is often used. Preclinical testing, however, can be done with the use of either animals or in vitro test systems. Currently, the guinea pig is used in most animal tests. As in the clinical studies, erythema is often the end point, and testing can be complete in a couple of weeks. In yet another system, the hairless mouse has been used to test for tumorigenesis by use of a procedure that can require 100 weeks to perform. In vitro tests include DNA cross-linking and induction of oncogenic virus. The assay for DNA cross-linking has also been used to detect chemical photosensitization in hairless mouse skin (*12*). Mammalian erythrocyte hemolysis is the classic assay for membrane chemical photosensitization, although, recently, effects on excitable cell membranes have shown themselves to be another quantifiable assay (*13*).

We will hear more about recent advances in all of these areas as the symposium progresses. In fact, that is what it is all about. As regulators, the FDA will have to decide how current test systems should be incorporated in the testing protocols for drugs and food additives. As part of the affected group, be it manufacturer, practitioner, scientist, or consumer, you need to participate. Such decisions will also influence the kind of test data the Agency will require to demonstrate that a cosmetic ingredient is harmful under normal conditions of use. So this symposium covers all areas of FDA, from foods to drugs to cosmetics, and includes radiation as a modifier in each of them.

In all of this future action, the evaluation of light-induced chemical carcinogenesis remains elusive. Current animal tests may take too long to serve as a screening tool. A test such as in vitro DNA cross-linking may not be sufficiently predictive of chemical photocarcinogenesis to be of use. We need a test system that can be used as a screen to determine whether a chemical should be tested in animal systems or not, and we need such a system soon.

REFERENCES

(*1*) Raab O. Über die Wirkung fluorescierender Stoffe auf Infusorien. Z Biol 1900; 39:524–546.

(*2*) Valenzeno DP, Pooler JP. Phototoxicity. The neglected factor. JAMA 1979; 242:453–454.

(*3*) Spikes JD. Photosensitization. In: Smith KC, ed. The science of photobiology. New York and London: Plenum, 1977:87–112.

(*4*) Stern RS, Thibodeau LA, Kleinerman RA, et al. Risk of cutaneous carcinoma in patients treated with oral methoxsalen photochemotherapy for psoriasis. N Engl J Med 1979; 300:809–813.

(*5*) Parrish JA, Anderson RR, Urbach F, Pitts D. UV-A: Biological effects of ultraviolet radiation with emphasis on human responses to longwave ultraviolet. New York and London: Plenum, 1978:7–35.

(*6*) Coakley JM. Activities in the control of noncoherent radiation. In: Hazzard DG, ed. Symposium on biological effects and measurement of light sources. Rockville, Md.: Food and Drug Administration, 1976:91–105 [DHEW publication No. (FDA)77-8002].

(*7*) Fitzpatrick TB, Pathak MA, Magnus IA, Curwen WL. Abnormal reactions of man to light. Annu Rev Med 1963; 14:195–214.

(*8*) Fitzpatrick TB, Pathak MA, Harber LC, Seiji M, Kukita A. An introduction to the problems of normal and abnormal responses of man's skin to solar radiation. In: Fitzpatrick TB, Pathak MA, Harber LC, Seiji M, Kukita A, eds. Sunlight and man: Normal and abnormal photobiologic responses. Tokyo: Univ Tokyo Press, 1974:3–14.

(*9*) Hochheimer BF, D'Anna SA. Angiography with new dyes. Exp Eye Res 1978; 27:i–116.

(*10*) Santamaria L, Prino G. List of the photodynamic substances. In: Gallo U, Santamaria L, eds. Vol 3, Part I. New York: Elsevier, 1972:xi–xxxv.

(*11*) National Research Council. Risk assessment/safety evaluation of food chemicals. Subcommittee of Food Toxicology, Committee on Food Protection, Food and Nutrition Board. Washington, D.C.: National Academy Press, 1980.

(*12*) Ley RD, Grube DD, Fry RJ. Photosensitizing effects of 8-methoxypsoralen on the skin of hairless mice. I. Formation of interstrand cross-links in epidermal DNA. Photochem Photobiol 1977; 25:265–268.

(*13*) Pooler JP, Valenzeno DP. Physiochemical determinants of the sensitizing effectiveness for photooxidation of nerve membranes by fluorescein derivatives. Photochem Photobiol 1979; 30:491–498.

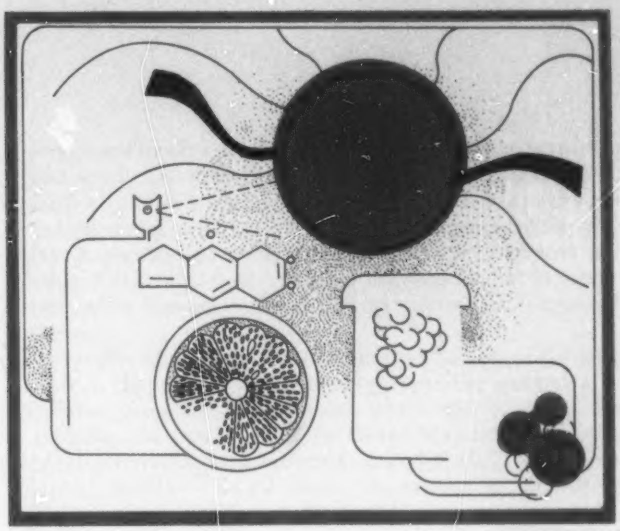

BASIC CHEMISTRY, PHYSICS, AND BIOLOGY RELATING TO PHOTOSENSITIZATION

Moderator: Andrija Kornhauser
Food and Drug Administration

blank page

Optical Radiation Measurements: Instrumentation and Sources of Error[1,2]

Robert J. Landry[3] *and* **F. Alan Andersen**[4]

ABSTRACT—Accurate measurement of optical radiation is required when sources of this radiation are used in biological research. The most difficult measurements of broadband noncoherent optical radiations usually must be performed by a highly trained specialist using sophisticated, complex, and expensive instruments. Presentation of the results of such measurement requires correct use of quantities and units with which many biological researchers are unfamiliar. The measurement process, physical quantities and units, measurement systems and instruments, and sources of error and uncertainties associated with optical radiation measurements are reviewed.—JNCI 1982; 69:155–161.

Accurate measurements of optical radiation are required for the proper description of radiation sources used in biological research. Measurements are also required for the design of products for various applications such as PUVA therapy devices for the treatment of psoriasis, photocopiers, and photopolymerization processes. Here, knowledge of the efficacy of the optical radiation is of paramount importance. The evaluation of potential hazards from optical radiation that may be associated with the various products such as welding arcs and high-intensity discharge lamps also requires accurate measurements. Unfortunately, accurate measurement of broadband noncoherent optical radiation is not trivial. It is best performed by a highly trained specialist and it requires the use of sophisticated, complex, and expensive instrumentation.

The measurement process is further complicated by the fact that the optical radiation quantity to be determined depends on the particular application. For example, the optical radiation quantity to be determined for accurate evaluation of the potential hazards to the retina of the eye is different from that quantity required for evaluation of the potential hazards to the skin and cornea of the eye. In addition, the presentation of the results of measurement processes requires correct use of quantities and units with which many biological researchers are unfamiliar.

This paper will outline important considerations in optical radiation measurements. The first section covers radiometric quantities and units, measurement systems, and instrumentation. Sources of error and uncertainties associated with optical radiation measurements are discussed in the second section.

RADIOMETRIC QUANTITIES AND UNITS, MEASUREMENT SYSTEMS, AND INSTRUMENTATION

Quantities and Units

The essential radiometric quantities and units of interest for the applications referred to in the introduction are listed and defined in table 1. For almost 10 years, work has progressed toward development of an approach to quantities and units that would be applicable to all radiation (*1–4*). Such a unified system requires compromise, of course, and certain quantities in table 1 could be presented differently (*4*). Regardless of the exact nature of the quantities and units, it is critical that nomenclature such as that in table 1 be used to express the results of optical radiation measurements.

Another aspect of nomenclature that warrants brief comment is the naming of various regions of the spectrum. To different people, the names can mean various things. For example, the separation of the visible from the UV portion of the electromagnetic spectrum is at 380×10^{-9} m for some and at 400×10^{-9} m for others; the lower limit of "UVA" may be at 315×10^{-9} m or 320×10^{-9} m, depending on who is using that jargon term; and the separation between "UVC" and "UVB" may be at 280×10^{-9} m or 290×10^{-9} m, again depending on who uses the terms. Therefore, if names must be used, precise definition of their meaning is necessary (*6*). As will be seen, the presentation of spectral radiometric data is a way to avoid any confusion on this issue.

Measurement Systems and Instruments

The quantities listed in table 1 are measured with an instrument called a radiometer, and they include the radiant power (Φ) or energy (Q), which have units of watts (W) and joules (J), respectively. Irradiance (E) is the radiant power incident upon a surface per unit area of the surface and has units of $W\cdot m^{-2}$, whereas radiance (L) is a quality of the source and is the radiant power emitted from a source per unit area of the source and into a unit solid angle. Radiance has units of $W\cdot sr^{-1}\cdot m^{-2}$. The energy equivalents of irradi-

---

ABBREVIATIONS USED: BRH=Bureau of Radiological Health; PM=photomultiplier; PUVA=psoralen plus UVA radiation.

---

[1] Presented at the Seventh Food and Drug Administration Science Symposium ("Photochemical Toxicity: Toxic, Allergic, and Carcinogenic Aspects With Emphasis on Predicting Effects in Humans") held at the Uniformed Services University of the Health Sciences, Bethesda, Md., March 16–17, 1981.

[2] The mention of commercial products, their sources, or their use in connection with material reported herein is not to be construed as either an actual or implied endorsement of such products by the Food and Drug Administration or the Department of Health and Human Services.

[3] Bureau of Radiological Health, Food and Drug Administration, Public Health Service, U.S. Department of Health and Human Services, 5600 Fishers Lane (HFX-220), Rockville, Md. 20857.

[4] Bureau of Radiological Health, Food and Drug Administration, 8757 Georgia Ave. (HFK-300), Silver Spring, Md. 20910.

TABLE 1.—*Selected radiometric quantities, symbols, defining equations, and units*[a]

Quantity[b]	Symbol	Defining equation	Units (abbreviations)
Radiant energy	Q		Joule (J)
Radiant power	Φ		Watt (W)
Irradiance	E	$E=d\Phi/dA$	Watt per square meter ($W \cdot m^{-2}$)
Radiant exposure	H	$H=dQ/dA$	Joule per square meter ($J \cdot m^{-2}$)
Radiance	L	$L=d^2\Phi/d\Omega dA \cos \theta$	Watt per steradian per square meter ($W \cdot sr^{-1} \cdot m^{-2}$)
Integrated radiance	tL	$tL=d^2Q/d\Omega dA \cos \theta$	Joule per steradian per square meter ($J \cdot sr^{-1} \cdot m^{-2}$)

[a] For a more complete listing of quantities and units, *see* (*5*).

[b] Quantities may be restricted to a narrow wavelength band (first derivative with respect to wavelength) by adding the word "spectral" and indicating the wavelength. The corresponding symbols are changed by adding the subscript λ.

ance (E) and radiance (L) are radiant exposure (H) and integrated radiance (tL), respectively.

The major components of a radiometer include input optics, a detector, signal processing components (usually electronics), and the readout. The input optics are used to define the field of view and sometimes the wavelength response of the instrument. The input optics, therefore, are components that the light passes through or reflects from before it reaches the detector. Included here are components such as transmission filters, windows, lenses, mirrors, and the like. The detector can be a silicon or vacuum photodiode, a lead sulfide or pyroelectric detector, a calorimeter, or a PM tube.

For measurement of the spectral quantities, dispersive optics such as a prism or diffraction grating monochromator or band-pass filters are located before the detector in the system described in the preceding paragraph. In this case, "dispersive" means to break up the radiation into its separate components as a function of wavelength. In addition, a hollow sphere, whose inside surface has a diffusely reflecting white finish and is referred to as an "integrating sphere," is commonly used in the input optics of a system which is used to measure the spectral quantities. Such a sphere provides the instrument with a uniform (cosine) angular response. A similar angular response can also be obtained with the use of a reflecting diffuser plate with a white finish. A more directional response can be obtained with the use of a transmissive plate of glass or quartz (fused silica) whose surface(s) has been ground or etched so that the incident optical radiation is diffused. Such diffusers are also sometimes used with radiometers to measure the radiometric quantities. Alignment of the optical system with respect to the source to be measured is usually much less critical with a system that uses a diffuser as opposed to a system that does not.

A functional block diagram of a spectroradiometer system used by the BRH to measure continuous wave or nonpulsed sources is shown in text-figure 1. Input optics for this system include selectable barium sulfate-coated integrating spheres with diameters of 3.81 cm (1.5 inches), 7.62 cm (3 inches), and 15.24 cm (6 inches) for the measurement of spectral irradiance or direct field-of-view optics for the measurement of spectral radiance. The input optics also include a filter wheel that allows placement of various short wavelength "cutoff" filters directly in front of the monochromator for spectral order-sorting purposes. The short wavelength cutoff filters eliminate radiation at wavelengths that would otherwise be simultaneously transmitted through grating monochromators when the desired radiation is at longer wavelengths—a characteristic of grating monochromators. The double-grating monochromator utilizes two sets of gratings to cover the wavelength range from 200×10^{-9} m through $2{,}500 \times 10^{-9}$ m, and it can be operated with various selectable bandwidths ranging from 1 to 20×10^{-9} m.

One set of gratings covers the wavelength range from 200 to 800×10^{-9} m, while the second set covers the wavelength range from 800 to $2{,}500 \times 10^{-9}$ m. The monochromator utilizes a precision stepping motor system to vary the wavelength being measured and to absolutely determine the monochromator's wavelength setting. A PM tube is used as a detector for measurements over the wavelength range from 200 to 800×10^{-9} m, whereas a lead sulfide detector is used for measurements in the IR region over the wavelength range of 800–$2{,}500 \times 10^{-9}$ m. Further, both detectors are thermoelectrically cooled to −20°C to improve the signal-to-noise characteristics. The electronic signal from the detector, which is proportional to the light incident upon it, is amplified, converted to a digital signal, and displayed on the system control console in relative units of microamperes. A MIDAS electronic interface system acts as an intermediary and translates control signals (messages) from the system minicomputer (a NOVA 3D) to the spectroradiometer and converts data from the spectroradiometer into a computer-acceptable format. The minicomputer controls overall system functions, as well as analysis of the data, through the use of specialized software. The sensitivities for various wavelengths for this spectroradiometer system are listed in table 2 in both SI units ($W \cdot m^{-3}$) and more familiar conventional units ($W \cdot cm^{-2} \cdot nm^{-1}$). The dynamic range for this system is six decades. Another similar but field portable spectroradiometer system that uses a microprocessor and desk top calculator for data reduction and processing is described elsewhere (*7*). Instruments similar to those described in this paper are available commercially from several vendors.

For accurate characterization of a source, it is sometimes necessary to measure the temporal characteristics of the optical radiation emitted. The major components of a sys-

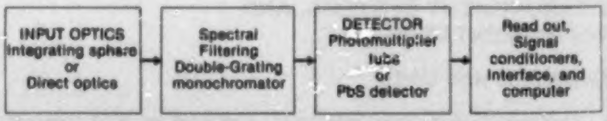

TEXT-FIGURE 1.—Block diagram of Optronic Laboratories' Model 747 laboratory scanning spectroradiometer system used to measure continuous wave or nonpulsed sources of optical radiation.

TABLE 2.—*BRH spectroradiometer system sensitivity with a 10-to-1 signal-to-noise ratio*

Wavelength range, 10^{-9} m	Sensitivity	
	$W \cdot m^{-3}$	$W \cdot cm^{-2} \cdot nm^{-1}$
200–250	10^5	10^{-8}
250–800	10^4	10^{-9}
800–2,500	10^7	10^{-6}
2,000–2,500	10^8	10^{-5}

tem to determine the temporal characteristics of pulsed or repetitively pulsed sources of optical radiation include input optics and a detector such as a photodiode or PM tube, with the addition of an oscilloscope as the signal readout. Care must be taken in the choice of the detector for this system to assure that its temporal response is much more rapid than any temporal characteristic of the radiation to be characterized. In addition, the bandwidth of the oscilloscope must be large enough so that it does not distort the shape of the pulse to be characterized.

There are several ways of displaying spectra data (*8*). Two are shown in text-figure 2, in which spectral irradiance data for a common fluorescent lamp at a distance of 2 m are plotted on both a logarithmic and linear scale as a function of wavelength over the range 250–700×10^{-9} m. From text-figure 2, it can be seen that an estimate of the spectral irradiance for wavelengths less than about 350×10^{-9} m can be obtained from the logarithmic plot, but not from the linear plot where the values are close to zero. Thus, in this case, the logarithmic plot is more useful. However, it is reasonable to use a linear plot when the spectral irradiance values are of the same order of magnitude over the wavelength range of interest.

Calibrations

Instruments for the measurement of power, energy, irradiance, or radiant exposure are usually calibrated with the use of electrically calibrated standard calorimeters (*9*) (e.g., calorimeters having a response that does not vary as a function of wavelength over a broad wavelength range). Spectroradiometers for the measurement of the spectral quantities are usually calibrated with the use of spectral standard lamps (*10*). Available standard lamps usually used for this purpose are listed in table 3. Since these standard lamps are calibrated at specific wavelengths over the wavelength range indictated, an interpolation procedure must be used to obtain values at intermediate wavelengths (*11*). Normally, the standard lamps are used to calibrate the instrument at the wavelengths of interest. The calibration factors obtained are then used to determine the values for the unknown source to be measured.

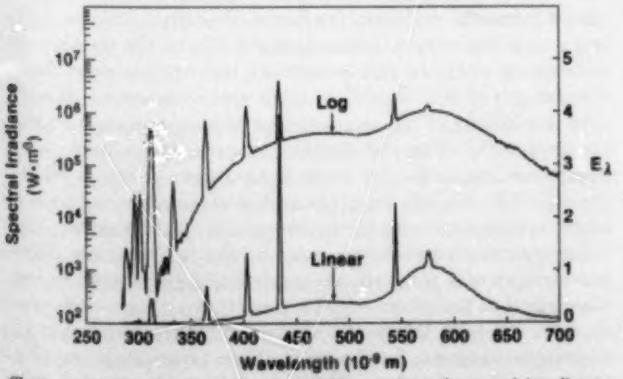

TEXT-FIGURE 2.—Semilogarithmic and linear plots of spectral irradiance for common fluorescent lamp at a distance of 2 m.

TABLE 3.—*Wavelength range and uncertainties associated with selected national spectral standard lamps*

Standard	Quantity	Wavelength range,[a] ×10^{-9} m	Uncertainty, ×10^{-9} m (%)	
Tungsten ribbon lamp	Spectral radiance	225–2,400	225	(2)
			1,000	(0.7)
			2,400	(0.6)
Quartz-halogen	Spectral irradiance	250–1,600	250	(2.6)
			555–1,100	(1.2)
Deuterium lamp	Spectral irradiance	200–350	200–350	(6)

[a] Standards of the National Bureau of Standards.

MEASUREMENT ERROR

Ultimately, the total uncertainty that may be associated with optical radiation measurement data should be specified. To accomplish this task, one must take into account the uncertainties that may be associated with the sources of error for each of the major components of the measurement system, including those associated with hardware components (input and dispersive optics, detector and electronics, and readout). Also, the operator and the instrument calibration can give rise to significant and large errors in the measurement data. The operator can be a source of error for both the calibration of the instrument and the subsequent measurements by not selecting proper components or by using poor operator techniques as discussed more fully elsewhere (*12*). With regard to calibration, it was noted in the preceding section that some uncertainty is associated with the calibration standards used. Some uncertainty is also associated with the transfer of the calibration to the instrument. These two sources of error must be accounted for so that a meaningful estimate of the uncertainty involved in the measurement data can be obtained.

The following is a list of selected sources of error in optical radiation measurements:

Alignment of optical components
Contamination of optical components
Degradation of optical components
Stray light (ambient)
Electronic noise
Meter response time
Nonlinearity of response
Accuracy of standards
General operator techniques
Stability of source
Temperature-dependent response
Lack of "out-of-band" rejection

While not a comprehensive listing, this list includes many of the important and common sources of error. More comprehensive discussions of sources of error in optical radiation measurements can be found elsewhere (*10, 12*).

Alignment of Optical Components

Alignment of optical components can become a very significant source of error, for example, when an instrument or measurement system is used that has a very narrow field of view or acceptance angle (e.g., 10^{-5} sr). For instance, in the measurement of radiance or spectral radiance, the slight misalignment of a lens used to image a small area of a relatively small source (e.g., an incandescent light bulb or a tungsten filament) onto the entrance aperture of the detector or monochromator can result in a significant error in the determination of the radiance of the source. In such a situation, the operator must use considerable care in aligning the lens or considerable error will result. The extent of the error can be estimated by repeated alignments and measurements.

Contamination and Degradation of Optical Components

Contamination of optical components is a very obvious source of error, but it is sometimes ignored. Dust, dirt, cigarette smoke, and fingertip grease on optical components such as lenses, mirrors, filters, and the like give rise to scattering and absorption of optical radiation and, therefore, to error. While the errors usually associated with contamination of optical components may be small, they should not be ignored. With regard to degradation of optical components, some components simply degrade with time. For example, it is well known that some thin-film interference filters degrade with time and the reflection and transmission characteristics of the filter change concomitantly (*12*). Errors associated with both contamination and degradation of optical components can be discovered by periodic checks on the calibration of the instrument. Degraded components should, of course, be either cleaned or replaced.

Ambient Stray Light

Ambient stray light can become a significant source of error when the order of magnitude of the radiation to be measured is the same as that of the ambient radiation. In such a situation, the operator must exercise care to take the ambient lighting or radiation levels into account either by eliminating them (e.g., turning off the room lights) or by measuring them and subtracting their contribution from the total reading.

Electronic Noise

Electronic noise, like ambient stray light, can become a significant source of error when the intensity of the signal of the radiation to be measured is of the same order of magnitude as that of the electronic noise of the measurement system itself (sometimes referred to as "darkage"). For weak signals, the darkage can give rise to a large uncertainty in the measurement data.

Meter Response Time

Meter response time or the rate at which the meter responds to the onset of radiation can be a source of error if the reading is taken before the instrument has had sufficient time to arrive at its true, final value. In this regard, it is important for the operator to account for the specific time constants for the instrument being used so that any uncertainty that may be associated with this source of error is minimized.

Nonlinearity of Response

Nonlinearity of response can become a significant source of error when the intensity of the radiation to be measured is very much larger or smaller than the intensity of the radiation associated with the calibration standard. In such cases, the accuracy of the reading obtained is dependent on the linearity of response of the measurement system. In some cases, the uncertainty may be fairly significant. Therefore, it should not be ignored for any measurement.

Accuracy of Standards and General Operator Technique

The uncertainties that may be associated with the calibration standards and general operator technique have been discussed in earlier sections of this paper and elsewhere (*8, 10, 12*).

Stability of Source

The instability associated with the source to be measured is unquestionably a source of uncertainty in measurement data. Further, the degree of the uncertainty is directly proportional to fluctuations of the radiation emissions from the source (i.e., the greater the instability, the larger the uncertainty).

Temperature-Dependent Response

The temperature-dependent response of some detectors can give rise to significant errors when measurements are made at an ambient temperature different from that prevailing when the instrument was calibrated. The temperature-dependent response for some detectors can be very large, as is illustrated in text-figure 3. There, the response of a biplanar vacuum photodiode at the helium–neon laser wavelength of 632.8×10^{-9} m is plotted in percent (normalized to 100% at 22°C) as a function of temperature over the range 4–50°C. For the detector tested, the temperature-dependent response near room temperature is about +0.3% per °C (*13*). Not all detectors and instruments have such a large temperature-dependent response. For example, the temperature-dependent response at the helium–neon laser wavelength of a p-i-n silicon photodiode instrument tested was found to be about −0.14% per °C near room temperature (22°C) (*13*). While the magnitude of the temperature-dependent response for the p-i-n silicon photodiode tested is not as large as that for the biplanar photodiode tested, it is still significant and should not be ignored if accurate mea-

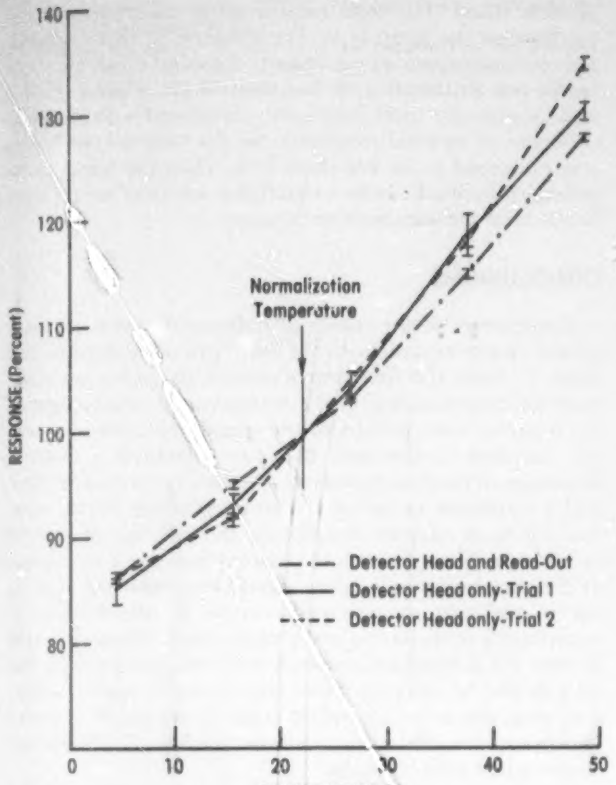

TEXT-FIGURE 3.—Temperature-dependent response of an S-5 surface response biplanar vacuum photodiode detector head and instrument to 632.8×10^{-9} m laser radiation.

surements are to be made. Finally, it should be noted that even calorimeters have a small but measurable temperature-dependent response (*13*). The temperature-dependent response of detectors and instruments is discussed more fully elsewhere (*13*).

Out-of-Band Leakage

While there is measurement error associated with all of the aforementioned items, the final item, lack of out-of-band rejection or out-of-band leakage, is a major and common source of error that can give rise to very large uncertainties or error in measurement data. In fact, if care is not taken, an error here can lead to spurious results. Basically, out-of-band rejection refers to the ability of monochromators or filters to transmit radiation only in the selected band pass. The extent of the error associated with out-of-band leakage depends on the following three factors: 1) the spectral irradiance characteristics of the source to be measured, 2) the out-of-band rejection characteristics of the monochromator (slit function) or filter being used, and 3) the spectral response characteristics of the detector being used.

As an example, if these factors have the characteristics similar to those sketched in text-figure 4, then out-of-band leakage will give rise to large errors and uncertainty. In text-figure 4, the spectral irradiance of the source to be measured and the relative monochromator throughput (when the monochromator is set to transmit radiation in a small band centered at wavelength λ_1) are plotted on logarithmic scales, whereas the spectral response of the detector (R_λ) to be used is plotted on a linear scale. From text-figure 4, it can be seen that the intensity of the emissions in the out-of-band radiation over a broad wavelength range is much greater than the intensity of the within-band radiation centered at wavelength λ_1. Text-figure 4 also shows that when the monochromator is set to transmit radiation within the small band centered at wavelength λ_1, it also simultaneously transmits a small percentage of the out-of-band radiation. In this particular example, the intensity of the out-of-band radiation transmitted through the monochromator to the detector would be of the same order of magnitude as the intensity of the within-band radiation centered at wavelength λ_1. Also, in this instructive example, since the detector to be used is much more responsive (*see* linear plot R_λ in text-fig. 4) to the out-of-band radiation than it is to the within-band radiation centered at wavelength λ_1, the reading obtained from the detector will be due primarily to the out-of-band leakage radiation and not to the within-band radiation to be measured.

The combination of error-prone elements just described can occur when a measurement system utilizing a single-grating monochromator and a detector more sensitive to visible than to UV radiation is calibrated with a 1,000-W quartz–halogen lamp in the UV range. In one such situation of which the authors are aware, about 80% of the reading obtained was due to out-of-band leakage radiation. In that situation, a 1,000-W quartz–halogen lamp was being used to calibrate a single-grating spectroradiometer system at 250×10^{-9} m with a 10×10^{-9} m bandwidth. In another situation, an error in measurements as large as 10,000% due to out-of-band leakage with a filter radiometer has been reported (*10*).

It is possible to obtain an estimate of the error that may be associated with out-of-band leakage through the use of a

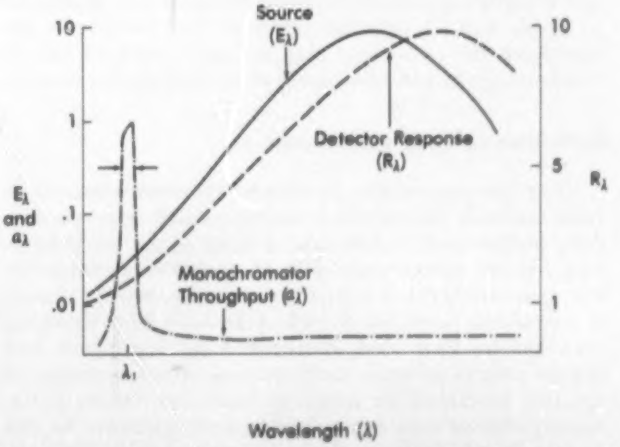

TEXT-FIGURE 4.—"Out-of-band" rejection. Semilogarithmic sketches of spectral irradiance (E_λ) of source to be measured and monochromator throughput (a_λ) and linear sketch of spectral detector response (R_λ).

TABLE 4.—*Measurement uncertainties (quartz-halogen lamps)*

Source of error	Uncertainty, %
Nonlinearity of response	2
Polarization of radiation	2.5
System instability	2
Lamp instability	0.5
Distance measurement	0.2
Wavelength scale inaccuracies	0.5
Uncertainties in working standard	5
Total	12.7

simple cutoff filter which, in the example described in the paragraph above, would absorb almost all of the within-band radiation to be measured centered at wavelength λ_1. Measurements are made with and without the cutoff filter in the optical path. The reading without the filter in the optical path is due to both the within-band radiation to be measured and the out-of-band radiation, whereas the reading with the cutoff filter in the optical path is due to the out-of-band leakage radiation only. Thus, in this example, the reading obtained with the cutoff filter in the optical path, after correction for reflection losses from the surfaces of the filter, is a direct estimate of the out-of-band leakage. When out-of-band leakage has been identified as a significant source of error, several techniques can and should be used to minimize the extent of the error as described in the following paragraph.

Usually, out-of-band leakage can be a significant source of error with a single-grating spectroradiometer system. Therefore, an obvious solution is to use a high-quality double-grating monochromator with high out-of-band rejection characteristics instead of a single-grating monochromator (*8*). Another approach is to use a band-pass filter in the optical path of the input optics which has a relatively strong absorption for the out-of-band radiation but a relatively high transmittance for the within-band radiation to be measured. Finally, a detector that is much more sensitive to the within-band radiation than it is to the out-of-band radiation can be used. Such a detector for the measurement of UV radiation is referred to as a "solar blind" detector, and it is relatively sensitive to UV radiation but insensitive to visible and IR radiation. If these three techniques are combined, the errors that may be associated with out-of-band leakage can be minimized, if not entirely eliminated.

Estimates of Total Uncertainty

Once the uncertainty for each of the known sources of error has been determined, it is then possible to prepare an error budget and to obtain an estimate of the total uncertainty in the measurement data. A typical error budget for one spectroradiometer system for the measurement of spectral irradiance is shown in table 4. In table 4 are listed the uncertainties that were determined for significant and known sources of error in the process of measurement of spectral irradiance for quartz-halogen-type lamps. Other sources of error were determined to be insignificant for this system. In this example, the total uncertainty in the measurement process is conservatively estimated to be the linear sum of the uncertainties associated with each of the sources of error listed. The total measurement uncertainty is dependent on the lamp type. For instance, in this example, the total measurement uncertainty for quartz-halogen-type lamps was estimated to be less than 12.7%, while with this same system, the total uncertainty associated with the measurement of spectral irradiance for fluorescent-type lamps was estimated to be less than 26%. Thus the lamp to be measured by itself can be a significant source of uncertainty in the total measurement uncertainty.

CONCLUSIONS

Presentation of the results of radiometric measurements should clearly be done with the use of correct quantities and units. To reach this final step of presenting results, one must have an understanding of the measurement process and of the inherent uncertainties of the specific instruments used. All too often radiometric data are presented without a discussion of measurement errors, including an error budget and a statement of the estimated uncertainty in the data. On the basis of past experience, the validity of optical radiation measurement data reported without a discussion of the uncertainty in the data should be questioned. This is not to say that measurements made in photobiological experiments must have a small uncertainty. However, even if there is a substantial uncertainty in the data (>30%), the data should be reported. Since large errors in optical radiation measurements can and do occur, a discussion of errors and an estimate of the uncertainty in the data should always be presented with the data.

REFERENCES

(*1*) JAGGER J. Dosimetry in photobiology. Photobiology 1974; 20:201.

(*2*) RUPERT CS. Dosimetric concepts in photobiology. Photochem Photobiol 1974; 20:203–212.

(*3*) ———. Uniform terminology for radiation. Photochem Photobiol 1978; 28:1.

(*4*) RUPERT CS, LATARJET R. Toward a nomenclature and dosimetric scheme applicable to all radiation. Photochem Photobiol 1978; 28:3–5.

(*5*) NICODEMUS FE. Self-study manual on optical radiation measurements: Part I—concepts, chapt 4. Gaithersburg, Md.: National Bureau of Standards, 1978 [National Bureau of Standards (USA) tech note 910-2].

(*6*) JAGGER J. The realm of the ultraviolet. Photochem Photobiol 1973; 18:353–354.

(*7*) KNIGHT WB, LANDRY RJ, BOSTROM RG. Recent BRH non-coherent optical radiation measurement instrumentation. In: Symposium on biological effects and measurement of light sources, June 9–10, 1980. Rockville, Md.: Food and Drug Administration, 1981 [HHS publication No. (FDA)81-8156].

(*8*) SLINEY DH, WOLBARSHT ML. Safety with lasers and other optical sources. New York: Plenum, 1980.

(*9*) JAMES RH. Optical radiation detectors and measurement devices. In: James RH, ed. National conference on measurements of laser emissions for regulatory purposes. Rockville, Md.: Food and Drug Administration, 1976:26–39 [DHEW publication No. (FDA)76-8037].

(*10*) KOSTKOWSKI HJ. Uncertainties in the measurement of incoherent radiation. In: Hazzard DG, ed. Symposium on biological effects and measurements of light sources, March 25–26, 1976. Rockville, Md.: Food and Drug Administration, 1977:197–216 [DHEW publication No. (FDA)77-8002].

(*11*) SAUNDERS RD, SHUMAKER JB. Optical radiation measurements: The NBS scale of spectral irradiance. Gaithersburg, Md.: National

Bureau of Standards, 1977:13 [National Bureau of Standards (USA) tech note 594-13].

(*12*) LANDRY RJ. Sources of error in optical measurement systems. In: James RH, ed. National conference on measurements of laser emissions for regulatory purposes. Rockville, Md.: Food and Drug Administration, 1976:40–58 [DHEW publication No. (FDA)76-8037].

(*13*) LANDRY RJ, PETERSON RW. Temperature dependent response of optical radiation measurement instrumentation. Applied Optics 1977; 16:2968–2971.

blank page

Molecular Aspects of Drug Photosensitivity With Special Emphasis on Psoralen Photosensitization Reaction[1,2]

Madhu A. Pathak[3]

ABSTRACT—Photosensitization reactions involve phototoxic reactions and photoallergic reactions, which are less common. Common drugs and chemicals that photosensitize humans are listed. Phototoxic reactions include the following: 1) direct photosensitization (type I reactions), in which the reactions of the triplet-state sensitizer are directly attributable to a component other than oxygen (e.g., DNA, proteins, and cell membranes), and 2) indirect photosensitization (type II reactions), in which the triplet state of a sensitizer reacts first with molecular oxygen, producing an "active oxygen" intermediate that subsequently reacts with the biologic system. The active oxygen intermediates are singlet oxygen ($^1O_2$), superoxide radical anions ($O_2^{\cdot-}$), and hydroxy radicals. Psoralen-induced skin photosensitization appears to involve both type I and type II reactions. The formation of monofunctional and bifunctional psoralen–DNA photoadducts (a type I reaction) is probably responsible for cell damage, cell death, mutation, and even skin carcinogenesis. The erythema response appears to be the result of a type II reaction.—JNCI 1982; 69:163–170.

In photobiology, it is well recognized that photons of certain wavelengths can be damaging to the cells. Absorption of photons, either directly or through energy transfer processes, by cellular constituents such as DNA, RNA, proteins, or lipoproteins can result in injury or damage to the cell nuclei, cell organelles, and cell membranes and can result in alterations of cellular proteins, in inactivation of enzymes, in mutagenesis, and even in carcinogenesis. The term "photosensitivity" has been interpreted in various ways and has often confused those who are unfamiliar with photon-induced cellular and molecular alterations in biological systems in general and cutaneous tissue in particular.

In simple terms, photosensitization may be defined as any observable change in a reaction system containing the biologic material *A* and the photosensitizer *S*, a change which occurs only as a result of irradiation of the mixture of *A* plus *S*. When such a biologic system is irradiated, the light-absorbing component *S* of a reaction system causes another component of the biologic system *A* to react to the absorbed radiation and to produce detectable biological changes. In this system, *S* may or may not be consumed in the reaction, but *S* most often significantly lowers the energy required to produce similar changes that radiation alone may be capable of evoking at significantly high radiation doses. In this presentation, a photosensitizing agent can be defined as a compound whose chemical configuration endows it with the ability to absorb UV radiation or visible radiation and to undergo a light-dependent photochemical reaction resulting in the generation of highly reactive, relatively metastable (long-lived) intermediate states (e.g., triplet state, free radical state, and ions) that cause chemical and functional modification in other molecules of biologic systems (*1*, *2*).

In fair-skinned individuals, sensitivity to sunlight is a common clinical problem. The interface between humans and their environment is the skin, and the physical (light) and chemical agents acting directly on human skin are important etiologic or precipitating factors in photosensitivity disorders. Most often, toxic chemicals when applied locally are irritants to the skin, but in photosensitivity reactions, chemicals and drugs by themselves may not act as contact irritants and are generally innocuous to skin in the absence of light exposure. However, under certain circumstances when the skin is challenged with the proper concentration of certain agents (e.g., 8-MOP) and the appropriate wavelengths of radiation (e.g., 320–400 nm), light-induced undesirable skin reactions could be enhanced by the presence of photosensitizing agents (e.g., erythema, edema, vesiculation, and other skin eruptions). "Cutaneous photosensitivity" is a general term used to refer to the abnormal reactions of human skin to the stimulus of light (*3*). Drug photosensitivity reactions or chemical photosensitivity reactions may be defined clinically as adverse skin responses resulting from the combination of exposure to certain therapeutic or chemical agents and to UV or visible radiation. Adverse cutaneous reactions can occur in individuals who either have ingested certain drugs or have been in contact with certain chemicals (tables 1, 2). These reactions may include an acute, exaggerated sunburn response followed by pigmentation or such abnormal responses as eczematous and urticarial reactions, vesicles, bullae, and papules. There may be desquamation and hyperpigmentation or hypopigmentation. These adverse photosensitivity reactions are classified into two broad categories: 1) phototoxic reactions and 2) photoallergic reactions.

PHOTOTOXIC AND PHOTOALLERGIC REACTIONS

Phototoxic reactions (*3–8*) are those damaging reactions of cutaneous cells that are exaggerated by the dual effect of a chemical agent plus UV or visible radiation in which there is no evidence of the participation of the immune system. These reactions most often can be reproduced in almost

---

ABBREVIATIONS USED: C_4=cyclobutane; 8-MOP=8-methoxypsoralen; Ps_0=ground state of psoralen; ^1Ps=singlet excited state of psoralen; ^3Ps=triplet excited state of psoralen; TMP=4,5′,8-trimethylpsoralen.

---

[1] Presented at the Seventh Food and Drug Administration Science Symposium ("Photochemical Toxicity: Toxic, Allergic, and Carcinogenic Aspects With Emphasis on Predicting Effects in Humans") held at the Uniformed Services University of the Health Sciences, Bethesda, Md., March 16–17, 1981.

[2] Supported by Public Health Service grant 2-R01CA-05003-23 from the National Cancer Institute.

[3] Department of Dermatology, Harvard Medical School, Massachusetts General Hospital, Boston, Mass. 02114.

TABLE 1.—*Contact photosensitizers: Chemicals that induce photosensitivity reactions in humans*[a]

Name[b]	Use	Reported clinical observations
Halogenated salicylanilides; 3,3′,4′,5-tetrachlorosalicylanilide; 3,4′,5- and 3,3′,5-trichlorosalicylanilide; 3,4′,5- and 3,3′,5-tribromosalicylanilide; 3,5- and 4,5′-dibromosalicylanilide	Deodorant, bacteriostatic agents in soaps	Phototoxic and eczematous photoallergic reactions, burning, itching, cross-photosensitivity reactions
Hexachlorophene	Antimicrobial, antiseptic	Phototoxic reactions
Bithionol or bis(2-hydroxy-3,5-dichlorophenyl) sulfide	Antimicrobial, antiseptic	Photoallergic reactions
Fentichlor (2,2′-dihydroxy-5,5′-dichlorodiphenylsulfide); multifungin (bromochlorosalicylanilide); Jadit (4-chloro-2-hydroxybenzoic acid *N*-*n*-butylamide)	Antifungal	Phototoxic and photoallergic reactions
5-Fluorouracil	Antineoplastic	Acceleration of inflammatory process
PABA and esters of PABA	Suncreen	Photoallergic reactions
4,4′-Bis(3-phenylureido)-2,2′-stilbenedisulfonic acid or blankophor	Fluorescent brightening agent for cellulose, nylon, or wool fibers	Phototoxic and photoallergic reactions
Cadmium sulfide	In tattoos	Erythema
Furocoumarins: psoralen, 8-MOP, 5-methoxypsoralen, TMP	In vitiligo for increased pigment formation and sun tolerance	Marked erythema, vesicles, bullae, hyperpigmentation
Essential oils: oil of bergamot, oil of lime, oil of cedar, oil of lavender, oil of citron, oil of sandalwood	Cosmetics and beauty aids	Phototoxic reactions and postinflammatory hyperpigmentation
Plants: *Umbelliferae*, *Rutaceae*	Used in perfumes or flavorings or as spices	Phytophotodermatitis, hyperpigmentation, vesicles, bullae
6-Methylcoumarin	Used in cosmetics	Photoallergic reactions
Musk ambrette	Used in cosmetics	Photoallergic reactions
Dyes: fluorescein, rose bengal, eosin, erythrocine, trypaflavin, orange red, paraphenylenediamine, methylene blue, toluidine blue, trypan blue, anthraquinone	Cosmetics and dye industry	Erythema, edema, vesicles, pigmentation, phototoxic reaction
Coal tar and coal tar derivatives containing anthracene, phenanthrene, naphthalene, thiophene, and many phenolic agents; pitch; acridine	In therapy for psoriasis and chronic eczema; in hair shampoos	Smarting, exaggerated sunburn, urticarial wheals, tar melanosis

[a] This table has been adapted and reproduced from Fitzpatrick TB, Pathak MA, Harber LC, Seiji M, Kukita K. An introduction to the problem of normal and abnormal responses of man's skin to solar radiation. In: Fitzpatrick TB, Pathak MA, Harber LC, Seiji M, Kukita A, eds. Sunlight and man: Normal and abnormal photobiologic responses. Tokyo: University of Tokyo Press, 1974:3–14, with permission.

[b] PABA=*p*-aminobenzoic acid.

every individual if an appropriate concentration of the agent is either applied topically or given orally and enough light energy of the appropriate wavelengths is delivered to elicit the reactions. Light plus the offending agent leads to an exaggerated sunburn reaction with or without painful edema, vesicles, and subsequent hyperpigmentation. The reaction usually is confined to the site of exposure and can occur within 5–18 hours after exposure to the sun and is maximum between 36 and 72 hours post exposure. Subsequent hyperpigmentation and desquamation can also occur. The severity depends on the route of entry of the chemical. Substances such as psoralens, pitch, tar, anthracene, and synthetic dyes, which when applied topically can readily reach the viable cells of the skin, may give early symptoms (e.g., burning, smarting, and itching sensations). Bullae or small vesicles may develop if the concentration of the implicated agent or if the exposure dose of UV or visible radiation is high.

Certain phototoxic reactions require the presence of molecular oxygen (e.g., hematoporphyrin or several xanthine dyes such as eosin and rose bengal). In such reactions, the triplet state of the photosensitizer reacts first with molecular oxygen, producing an active oxygen intermediate that subsequently reacts with a biologic substrate (*9*, *10*). The reactive oxygen intermediates are singlet oxygen ($^1O_2$), the superoxide anions (O_2^-), and hydroxy radicals. This oxygen-dependent reaction is referred to as a photodynamic reaction or type II reaction. However, many phototoxic reactions can occur in the absence of oxygen (e.g., psoralen and chlorpromazine photosensitization), and these oxygen-independent reactions are often referred to as drug or chemical photosensitization reactions (type I reactions). Although the term "photosensitization" (*11*, *12*) was originally proposed to indicate oxygen-independent biological sensitization reactions induced by psoralens, its current usage has now been expanded to include several other therapeutic agents and other chemicals used in cosmetics, food preservatives, hair dyes, fragrances, industrial products and by-products, and agricultural items (*3–8*). In a type I reaction, the so-called direct reaction, the triplet state of the sensitizer reacts directly with the key component of the biologic substrate, either through the hydrogen or the electron transfer process (*10*). In most of the drug or chemical photosensitization reactions, wavelengths that evoke abnormal reactions are usually but not always in the UV spectrum, which encompasses the 290–400 nm region. Most reactions have been reported to require UVA radiation (320–400 nm); however, certain phototoxic reactions can be initiated by UVB radiation (290–320 nm) as well as by visible radiation (400–700 nm).

Photoallergy to drugs is an acquired, altered capacity of the skin to respond to light in the presence of a light-absorbing chemical and involves the immune system (*3–8*). The absorbed light energy may promote a photochemical reaction between the drug that absorbs the radiation and the skin proteins. The drug may act to form a haptenic group, and it may either photoreact directly with skin proteins to form a "photoantigen" or first become photo-

TABLE 2.—*Systemic photosensitizers: Chemicals that induce photosensitivity reactions in humans*[a]

Name	Uses	Clinical observations	Action spectrum, nm
Sulfonamides: sulfanilamide, sulfathiazole, sulfapyridine, sulfamethazine, sulfaguanidine, sulfisoxazole, monochlorphenamide	Chemotherapy, antibacterial agents	Phototoxic and photoallergic reactions	290–320
Sulfonylurea: carbutamide, tolbutamide (Orinase), chlorpropamide (Diabinese)	Hypoglycemic or antidiabetic drugs	Phototoxic reactions	290–360
Chlorthiazides:			
6-Chloro-7-sulfamyl-3,4-dihydro-1,2,4-thiodiazine 1,1-dioxide (HydroDiuril)	Diuretics, antihypertensive	Papular and edematous eruption, plaques	290–320
Quinethazone (Diuril)	Antihypertensive	Phototoxic and photoallergic reactions	320–400
Phenothiazines: chlorpromazine (Thorazine), promethazine (Phenergan), mepazine, Stelazine, trimeprazine, Compazine, promazine (Sparine)	Tranquilizer, nematode infestation agent, urinary antiseptic, antihistamine	Exaggerated sunburn, maculopapular and urticarial eruptions, gray-blue hyperpigmentation	290–400
Antibiotics:			
Demethylchlortetracycline (Declomycin), chlortetracycline, oxytetracycline, doxycycline	Broad-spectrum antibiotic	Exaggerated sunburn, phototoxic reaction	320–400
Griseofulvin	Antimycotic	Exaggerated sunburn, phototoxic and photoallergic reactions	320–400
Nalidixic acid (NegGram)	Antibacterial	Erythema, bullae	320–400
Furocoumarins: TMP (trioxsalen), 8-MOP (methoxsalen), psoralen	In photochemotherapy of psoriasis and vitiligo; for sun tolerance and increased pigment formation	Erythema, bullae, hyperpigmentation	320–400
Estrogens and progesterones:			
Mestranol and norethynodrel, diethylstilbesterol	Oral contraceptives	Melasma, phototoxic reactions	?290–320
Chlordiazepoxide (Librium)	Tranquilizer, psychotropic	Eczematous eruption	290–360
Triacetyldiphenolisatin	Laxative	Eczematous photoallergic reaction	290–320
Cyclamates, calcium cyclamate, sodium cyclohexylsulfamate	Artificial sweeteners	Phototoxic and photoallergic reactions	290–360

[a] This table has been adapted and reproduced from Fitzpatrick TB, Pathak MA, Harber LC, Seiji M, Kukita K. An introduction to the problem of normal and abnormal responses of man's skin to solar radiation. In: Fitzpatrick TB, Pathak MA, Harber LC, Seiji M, Kukita A, eds. Sunlight and man: Normal and abnormal photobiologic responses. Tokyo: University of Tokyo Press, 1974:3–14, with permission.

chemically altered by the absorbed energy. This photochemically altered haptenic group then reacts with the proteins to form an antigen. The photoantigen is then processed by macrophages and is presumed to come in contact with T-lymphocytes to manifest any ordinary type of delayed hypersensitivity immunologic response. The complete photoantigen is recognized on subsequent exposure to sensitized T-lymphocytes in the form of eczematous or papulovesicular eruptions in a patient. As in allergic eczematous contact dermatitis, cross-reactivity with structurally related chemicals or drugs may be seen in drug-induced photoallergy.

Although photoallergic contact dermatitis has been shown to involve immunologic mechanisms by such techniques as patch testing, histopathologic criteria, the use of passive transfer, lymphocyte stimulation test, and macrophage inhibition (*8–13*), it may be difficult to distinguish clinically between a chronic phototoxic reaction and a photoallergic reaction. The clinical manifestations in drug-induced photoallergic reactions may range from acute urticarial lesions to eczematous or papular lesions appearing within 24 hours or later. The eruptions may extend beyond the exposure sites. In recurrent cases, flare-ups of the distant, previously uninvolved sites may also occur. The effective radiation is generally in the UVA region (320–400 nm), although some reactions may be triggered by UVB (280–320 nm) radiation also. Generally, less concentration of the drug and less energy of UV radiation are required in photoallergic reactions than are necessary for the production of phototoxic reactions (*8*, *13*). The various topical agents and systemic therapeutic drugs involved in phototoxic and photoallergic reactions in humans are listed in tables 1 and 2.

PHOTOREACTIVITY OF PSORALENS AND ISOPSORALENS

Furocoumarins (*14–23*) are heterocyclic, aromatic compounds derived from the condensation of a furan ring with a coumarin ring. Although this condensation may occur in several ways, in nature, however, only two forms of furan and coumarin fusion are generally seen: 1) a linear tricyclic structure resembling psoralen and 2) a nonlinear angular structure called angelicin (or isopsoralen) (text-fig. 1).

Linear psoralens (e.g., 8-MOP and TMP) and nonlinear psoralens (e.g., angelicin or isopsoralen and other methylated isopsoralens) when dissolved in ethanol or water exhibit a well-defined UV absorption spectrum with several characteristic peaks; the first peak is in the region of 300–335 nm, and the second is in the region below 330 nm (210–220 nm, 245–265 nm). The absorption band at 300–330 nm is attributable to $\pi \rightarrow \pi^*$ transition. When the photoreactive psoralens (e.g., 8-MOP and TMP) absorb radiation of 300–330 nm, the molecules are photoexcited to a short-lived (10^{-8} sec) ^{1}Ps. From this singlet excited state, certain potent photosensitizing molecules (e.g., 8-MOP and TMP) undergo

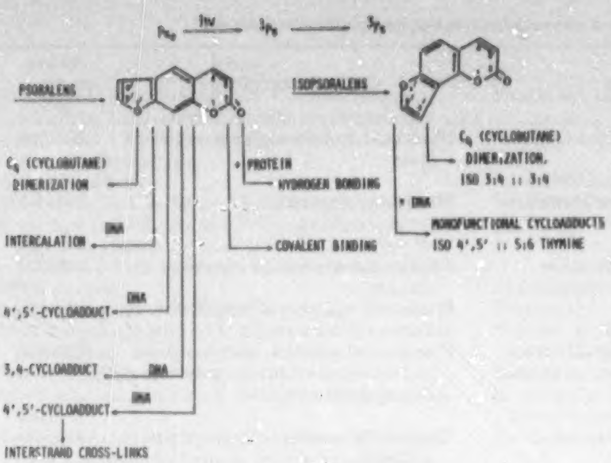
$Ps_0 \xrightarrow{h\nu} {}^1Ps \longrightarrow {}^3Ps$
PSORALENS
ISOPSORALENS
C4 (CYCLOBUTANE) DIMERIZATION
+ PROTEIN
HYDROGEN BONDING
C4 (CYCLOBUTANE) DIMERIZATION. ISO 3:4 :: 3:4
+ DNA
MONOFUNCTIONAL CYCLOADDUCTS ISO 4',5' :: 5:6 THYMINE
DNA
INTERCALATION
COVALENT BINDING
DNA
4',5'-CYCLOADDUCT
3,4-CYCLOADDUCT
DNA
DNA
4',5'-CYCLOADDUCT
INTERSTRAND CROSS-LINKS

TEXT-FIGURE 1.—Psoralen and isopsoralen photoreactions.

an intersystem crossing and are converted into the much longer-lived (10^{-3} sec) ^{3}Ps (text-fig. 2).

From the short-lived ^{1}Ps (10^{-8} sec) and the long-lived ^{3}Ps (10^{-3} sec), three events tend to occur: 1) a radiative decay, 2) a nonradiative transfer of energy (type I reaction), and 3) singlet oxygen production (type II reaction). In the radiative decay, the absorbed energy is dissipated either in the form of fluorescence (^{1}Ps to Ps_0) or in the form of phosphorescence (^{3}Ps to Ps_0) with the emission of light. This emitted energy may activate other molecules, but it may be wasted and not utilized in photochemical reactions. In the nonradiative transfer of energy from ^{3}Ps to biologic substrates, the triplet-state psoralen leads to certain specific chemical reactions which include *a*) dimerization of psoralens in which two psoralen molecules tend to react with each other and form both fluorescent and nonfluorescent dimers, *b*) C_4 addition to pyrimidines involving photochemical reaction with pyrimidine bases of nucleic acids, or *c*) photoreaction with amino acids of proteins. In the dimerization of psoralens, the formation of nonfluorescent dimers appears to dominate this reaction and involves C_4 dimers in which the 3:4 double bond of each psoralen molecule conjugates to form C_4 cycloadducts (text-fig. 1). The fluorescent dimers involving the 4′:5′ double bond are formed but usually in a lesser amount. The nonradiative reaction involves the formation of singlet oxygen by the transfer of energy from the photoexcited psoralen to any oxygen molecule, which leads to the formation of singlet oxygen.

The formation of photodimers from various furocoumarins has been reported by several workers (*18–21*). The characteristic absorption band in the range of 300–340 nm of monomeric psoralens disappears when photodimerization involving the 3:4 double bond occurs. The resultant dimerized product is devoid of the absorption band at 300–340 nm, and the product is nonfluorescent. The photodimers are nonphotosensitizing. They do not induce erythema and do not conjugate with DNA; however, they tend to be adsorbed and bind with epidermal proteins. The nature of this binding is, however, not covalent (*15*).

The photoreaction of psoralens with pyrimidines is one of the most important photochemical reactions which is not only of interest to photobiologists but is also of interest to dermatologists and geneticists. This reaction is responsible for elucidating the mutagenicity, carcinogenicity, and therapeutic effectiveness of psoralens in such diseases as psoriasis. The major photoreactions are schematically presented in text-figures 1 and 2 (*1–3*).

When linear psoralens are allowed to photoreact with pyrimidine bases (e.g., thymine, cytosine, or uracil) in the UVA region (320–365 nm) at room temperature in an aqueous solution, a decrease of the UV absorption band in

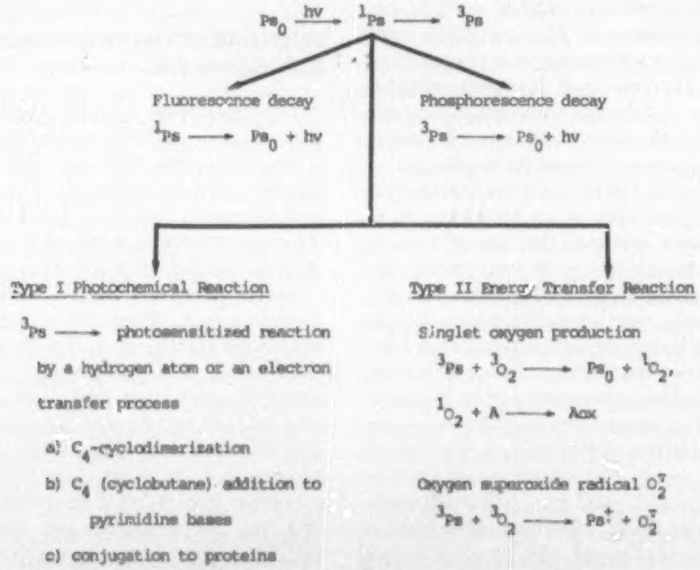
$Ps_0 \xrightarrow{h\nu} {}^1Ps \longrightarrow {}^3Ps$
Fluorescence decay
$^1Ps \longrightarrow Ps_0 + h\nu$
Phosphorescence decay
$^3Ps \longrightarrow Ps_0 + h\nu$
Type I Photochemical Reaction
$^3Ps \longrightarrow$ photosensitized reaction by a hydrogen atom or an electron transfer process
a) C_4-cyclodimerization
b) C_4 (cyclobutane) addition to pyrimidine bases
c) conjugation to proteins
Type II Energy Transfer Reaction
Singlet oxygen production
$^3Ps + {}^3O_2 \longrightarrow Ps_0 + {}^1O_2,$
$^1O_2 + A \longrightarrow Aox$
Oxygen superoxide radical $O_2^{\overline{\cdot}}$
$^3Ps + {}^3O_2 \longrightarrow Ps^{\dot{+}} + O_2^{\overline{\cdot}}$

TEXT-FIGURE 2.—Photoexcited states of psoralens and their photochemical reactions.

the region of 300–330 nm is seen, and a C_4 cycloaddition reaction product between the 3:4 double bond of psoralen and 5:6 double bond of pyrimidine occurs (*15, 22, 23*), which is nonfluorescent. In contrast, if the corresponding nucleosides or nucleotides of thymine or cytosine are allowed to react with psoralen in a frozen aqueous state in which the molecules are immobilized in an ice matrix, the formation of two types of new photoproducts can be demonstrated: 1) a fluorescent C_4 adduct and 2) a nonfluorescent C_4 adduct. The psoralen molecule has two reactive double bonds: the 4′:5′ double bond of the furan rings and the 3:4 double bond of the pyrone ring (*15, 16*). The psoralen can photoreact either at its 4′:5′ double bond or at its 3:4 double bond. When 4′:5′ double bond of psoralen photoreacts with 5:6 double bond of thymine, the resulting adduct is a fluorescent product; whereas if psoralen photoreacts at its 3:4 double bond with 5:6 double bond of thymine, the adduct is nonfluorescent. The 3:4- and 4′:5′-cycloadducts have different properties and UV absorption spectra (*24*). These two photochemical reactions are extremely important in understanding the reactivity of psoralens with DNA. The 3,4-cycloadduct usually does not further photoreact, whereas the 4′,5′-cycloadduct can be further photoexcited and give a second cycloaddition product with another pyrimidine base belonging to the opposite strand of DNA and can thus give rise to an interstrand cross-linkage, an event often very damaging to the cell (*15, 16*).

The photoreactions of linear and angular psoralens with DNA are schematically shown in text-figure 1. The first step involves the formation of a molecular complex between a furocoumarin and DNA; it occurs in the dark and involves the weak, hydrophobic van der Walls forces and hydrogen bonding (*24, 25*). The extent of this complex formation determines the rate of photoreaction and the number of psoralen molecules that form monofunctional and bifunctional adducts. Irradiation of this intercalated furocoumarin DNA complex gives rise to monofunctional and bifunctional (interstrand cross-linkage) adducts. Linear psoralens, like 8-MOP, TMP, and 5-methoxypsoralen, exhibit all three types of adducts with DNA; the angular isopsoralens (angelicin) have a remarkably low photobinding ability to DNA. Methyl-substituted psoralens (e.g., 4-methylpsoralen, 4,5′-dimethylpsoralen, and TMP) exhibit a greater ability to photobind with DNA than do nonmethylated psoralen molecules. Likewise, methyl-substituted isopsoralens (e.g., 5-methylisopsoralen and 4,5′-dimethylisopsoralen) also show a greater ability to bind with DNA than does the nonmethylated angelicin (*16, 24, 26–31*).

The interaction of furocoumarins (e.g., psoralen, 8-MOP, and TMP) and proteins (e.g., plasma proteins, albumin, globulin, and skin keratin) is not as strong as the photoreaction of psoralens with DNA or RNA. This weak interaction of furocoumarins with protein involves the 1) noncovalent conjugation in which the furocoumarins are bound by the weak forces of hydrogen bonding, 2) covalent photobinding of furocoumarins to certain amino acids in a protein molecule [this photoconjugation is not a major reaction (*15, 32*), and 3) photo-oxidation of certain amino acids. It appears that psoralens can photo-oxidize certain amino acids (e.g., histidine, cystine, and methionine). Preliminary evidence obtained in our laboratory suggests that the tryptophan of albumin also can be photo-oxidized by 8-MOP. It should be realized, however, that the interaction of psoralens with proteins is not a major photochemical reaction.

PSORALENS AND SINGLET OXYGEN PRODUCTION (TYPE II REACTIONS)

As stated earlier, certain phototoxic reactions require the presence of molecular oxygen (e.g., hematoporphyrin and several dyes). These oxygen-dependent reactions are referred to as photodynamic reactions (*9, 10*). The mechanism by which many photodynamic agents exert their photo-oxidizing action on biological substrates or other organic substrates involves the transfer of the photoexcitation energy to oxygen molecules present in the biologic milieu, i.e., the living cells. The normal oxygen molecule usually exists in the triplet state. The transfer of excitation energy of the photosensitizer *S* to the oxygen in its triplet state ($^3O_2$) results in the formation of a very reactive singlet oxygen ($^1O_2$) molecule, which causes the oxidation of the biological substrate. This may also lead to the formation of superoxide anions and hydroxy radicals. Interactions of these reactive species with biological substrates lead to the photo-oxidation of important cellular constituents essential for the viability and reproducibility of cells. This indirect reaction, often referred to as a type II reaction and involving a reactive species other than the light-absorbing molecule, can induce photosensitized damage to DNA, proteins, cell membranes, mitochondria, and other cellular components. The schematics of this reaction, in consecutive order, are as follows: $S_0 \xrightarrow{h\nu} {}^1S$, ${}^1S+{}^3O_2 \rightarrow S_0+{}^1O_2$, and ${}^1O_2$+biologic substrate→ photo-oxidation products.

These oxygen-dependent photodynamic reactions often cause vasodilation and are manifest as severe erythema, edema, and even bullae or vesiculation. It should be noted that the arterioles, venules, and capillaries which often become damaged in photosensitization reactions of the skin contain high concentrations of molecular oxygen. Formation of $^1O_2$ is thus a most likely event responsible for endothelial cell damage and subsequent vasodilation. The drug-induced or chemical photodynamic reactions involve photo-oxidative damage to DNA (e.g., oxidation of guanine), RNA, lysosomes (e.g., membrane damage, lipid oxidation, and liberation of hydrolytic enzymes), cell membranes (e.g., oxidation of lipids and formation of peroxides), and amino acids (oxidation) in proteins, including induction of cross-linkages in proteins.

Although it has long been recognized and carefully documented (*12, 15, 16*) that biological photosensitization involving psoralens was independent of oxygen and little or no photo-oxidation was involved when psoralens reacted in the presence of oxygen or other oxidizable substrates, recent evidence suggests that photoactivated psoralens can concomitantly induce type II reactions in vitro and in vivo (*33*). As early as 1961, Pathak et al. (*33*) demonstrated that photosensitizing psoralens in the presence of water or ethanol and oxygen exhibited a low-temperature phosphorescence and produced UV-induced free radicals. Cannistraro and Van de Vorst (*34*) also presented electron-spin resonance and optical absorption evidence for free radical involvement in the photosensitization action of furocoumarins and for their singlet oxygen production. Recently, Poppe and Grossweiner (*35*) demonstrated that 8-MOP and other psoralen derivatives in aqueous solution acted as photodynamic sensitizers and were able to produce biologic sensitization via the singlet oxygen mechanism by means of a type II or indirect photosensitization reaction that involved energy transfer from the excited triplet state of the psoralen derivative to oxygen. Studies by these investigators revealed that 8-MOP in the presence of UVA radiation and molecular oxygen generated $^1O_2$ by a triplet energy transfer reaction and that $^1O_2$ could inactivate lysozyme; if the irradiation was done in the absence of oxygen, no such inactivation occurred. Furthermore, they showed that the inactivation of lysozyme was much more evident when the psoralens were reacted in a deuterated water solution in the presence of oxygen, but the inactivation of lysozyme was strongly quenched when the reaction was done in the presence of a double-stranded polydeoxyribonucleotide, with which furocoumarins form intercalated complexes.

Veronese et al. (*32*) confirmed the inactivation of lysozyme by irradiation at 365 nm in the presence of 8-MOP and commented that this singlet oxygen effect of 8-MOP was very small when the effects were compared for the inactivation of several other enzymes in analogous reaction systems involving other well-known photodynamically active dyes such as rose bengal and methylene blue, which are known to produce singlet oxygen. Comparative studies involving the photo-oxidation of 17 amino acids revealed that limited oxidation (5–10%) of cystine, methionine, and histidine but no oxidation of tryptophan or tyrosine had occurred when 8-MOP was used as a photosensitizer. Singh and Vadsaz (*36*) also found that $^1O_2$ was the major reactive species produced in the inactivation of *Escherichia coli* ribosomes induced by the photosensitizing action of 8-MOP and TMP.

The formation of singlet molecular oxygen ($^1O_2$) by an energy transfer mechanism from the excited 8-MOP molecule (type II reaction) was also reported by DeMol et al. (*37*). This was done in three ways: 1) In the reaction of irradiated 8-MOP with $^1O_2$ acceptor 2-methyl-2-pentene, the characteristic oxidation products 2-methyl-3-pentene-2-ol and 2-methyl-1-pentene-3-ol could be identified; 2) the rate of 8-MOP-sensitized photo-oxidation with dopa (3,4-dihydroxyphenylalanine) mediated by $^1O_2$ was larger in D_2O than the rate was in water; and 3) the β-values for the reaction of $^1O_2$ with dopa in the presence of 8-MOP were in accord with the $^1O_2$-mediated photodecomposition reaction.

Even though the formation of singlet oxygen and superoxide anions with furocoumarins plus UVA in the presence of oxygen may be small, the effects may be extremely important in the explanation of the vascular damage that these photoreactive linear furocoumarins produce in the form of visible erythema and vesiculation reactions. These reactions appear to be analogous to those of porphyrins which produce endothelial cell damage and subsequent erythema. Interestingly, isopsoralens (e.g., angelicin and 5-methylangelicin) do not induce $^1O_2$ formation nor do they evoke cutaneous photosensitization in the form of the erythema reaction (*38*).

MONOFUNCTIONAL AND BIFUNCTIONAL ADDUCTS OF PSORALEN WITH DNA

The formation of psoralen–DNA photoadducts (monofunctional and bifunctional or interstrand cross-linkages) represents a type I reaction. The induction of monofunctional and bifunctional C_4 or C_4 adducts of psoralen with DNA signifies cell damage. Essentially, the role of monofunctional and bifunctional adducts appears to inhibit cell growth, induce lethality of cells, and inhibit DNA synthesis. These events subsequently can give rise to error-prone repair and mutagenicity. The extent of inhibition of DNA synthesis, inhibition of the template activity, and mutagenicity appear to be related more to the capacity of a given compound to form monoadducts rather than to the capacity to form interstrand cross-linkages. The degree of lethality can be correlated with the extent of the formation of bifunctional adducts (interstrand cross-linkages).

The question concerning the precise role of monofunctional and bifunctional adducts of psoralen with DNA in the induction of erythema reaction is difficult to assess. The studies reported by Musajo et al. (*16*), Rodighiero et al. (*28*), and Dall'Acqua et al. (*29*) and our own studies (*38–41*) indicated that skin photosensitizing activity can be correlated with the capacity to induce cross-linkages and not with the total photobinding of the furocoumarin to DNA.

On the basis of the observed correlation between skin photosensitization (erythema reaction) and the ability to form cross-linkages, it has been generally assumed that only cross-linking furocoumarins are able to induce skin photosensitization, and those furocoumarins that did not form interstrand cross-linkages were incapable of inducing the erythema reaction of the skin. For example, methyl-substituted isopsoralens (e.g., 5-methylangelicin, 4,5′-dimethylangelicin, and 3-carbethoxypsoralen) conjugate quite well with DNA, both in vitro and in vivo (*40, 41*), but they do not exhibit skin photosensitization reactions. These compounds form only monofunctional adducts and due to structural limitations, group substitutions, and steric hindrances do not form any cross-linkages. This observation supports the thesis that psoralen–DNA cross-linkages are in some way responsible for skin photosensitization and erythema reaction.

In my opinion, the photoconjugation of psoralen to DNA has very little to do with the induction of erythema, a reaction indicative of skin photosensitization. The event leading to the formation of psoralen–DNA adducts represents cellular damage, which in most instances leads to cell death but not to vasodilation. If cross-linking events were essential for the induction of an erythema reaction, then UVB (290–320 nm) radiation should be nonerythemogenic because it does not form any cross-linkages. The sunburn-producing UVB spectrum forms either thymine dimers or mixed dimers of other pyrimidine bases, and yet it is highly erythemogenic. Isopsoralens (e.g., angelicin and 5-methylangelicin), however, form single-strand adducts with pyrimidine bases but do not induce the erythema reaction. This damage to DNA is very similar to the damage caused by UVB radiation, an indication that the monofunctional adduct-forming event and the cross-linking event are not contributing to the induction of the erythema reaction.

The erythema reaction appears to be related to the ability of psoralen molecules to form singlet oxygen or superoxide anions. Nearly all photosensitizing molecules that evoke cutaneous photosensitization reaction (e.g., erythema and edema) are able to form the reactive oxygen species that subsequently reacts with biologic target molecules. For example, linear psoralens (e.g., 8-MOP, TMP, and psoralen) when irradiated in an oxygen-saturated system do show the formation of singlet oxygen. Nonlinear psoralens (e.g., angelicin, 5-methylangelicin, and linear psoralens such as 3-carbethoxypsoralen, 8-hydroxypsoralen, 5,8-dihydroxypsoralen, and 4′,5′-dihydroxypsoralen) forming only monofunctional adducts do not reveal any evidence for the formation of singlet oxygen (*38*). Furthermore, certain porphyrins (e.g., hematoporphyrin, uroporphyrins of types I and II, coproporphyrins of types I and II, and protoporphyrin) when exposed to radiation of 400–440 nm in the presence of O_2 can photosensitize the skin, induce an erythema reaction, and also form reactive singlet oxygen. The formation of $^1O_2$ can be demonstrated in D_2O and in quenching experiments in which $^1O_2$ quenchers such as histidine or dopa are also used (*41*, *42*). Thus psoralen-induced photosensitization reactions now appear to involve both type I and type II reactions, and both reactions can occur simultaneously in a biologic system such as the skin.

SUMMARY

Photosensitization may be defined as a process in which the combined action of a chemical or a drug and an appropriate wavelength of UV or visible radiation absorbed by the chemical or the drug leads to damaging effects in a biologic system, effects usually not observed in the absence of either modality. Absorption of radiant energy by the photosensitizer results in the generation of photoexcited states. Both the singlet excited state and the metastable (long-lived) triplet excited state of the photosensitizer can initiate chemical reactions with those components of the biologic system in close proximity to the photosensitizer. Drug-induced photosensitization reactions involve phototoxic reactions which are more frequent and photoallergic reactions which are less common. Common drugs and chemicals that cause phototoxic and photoallergic reactions in humans are listed in tables 1 and 2. Phototoxic reactions may be of two types: 1) Direct mechanisms, termed "type I reactions," are those in which the reactions of the triplet-state sensitizer are directly attributable to the key component of the biologic substrate other than oxygen (e.g., DNA, proteins, and cell membranes). 2) Indirect mechanisms, termed "type II reactions," include those reactions in which the triplet state of a sensitizer reacts first with molecular oxygen, producing an "active oxygen" intermediate that subsequently reacts with the biologic system. The active oxygen intermediates are singlet oxygen ($^1O_2$), superoxide radical anions (O_2^-), and hydroxy radicals. Interaction of these reactive oxygen species with biological substrates results in the photo-oxidation of molecules. Drug-induced photoallergic reactions appear to involve photoimmunologic mechanisms in which the drug or chemical acts as a haptenic group, and the absorption of the appropriate radiation wavelengths by the haptenic group of the drug causes photoconjugation with a carrier protein, resulting in the formation of a photoantigen. The biochemical avidity of the chemical or drug toward cellular constituents determines the site of reaction (whether in the nucleus or cytoplasm or with the proteins, cell membrane components, etc.). The psoralen-induced photosensitization reaction now appears to involve both type I and type II reactions. Until recently, it has been stated that oxygen is not required in biological photosensitization by furocoumarins (psoralens) and that the direct mechanism (type I) in which triplet-state psoralen reacts directly with the biologic substrate (e.g., DNA) was responsible for cutaneous photosensitization reactions. Recent evidence, however, suggests that the indirect mechanism involving the energy transfer and formation of an activated oxygen species [e.g., singlet oxygen ($^1O_2$), superoxide radical anions (O_2^-), and hydroxy radicals] also is responsible for manifesting the cutaneous photosensitization reaction. The formation of psoralen–DNA photoadducts (monofunctional and bifunctional or interstrand cross-linkages) represents a type I reaction, and these photoproducts are probably responsible for cell damage, cell death, mutation, and even for such phenomena as skin carcinogenesis. The psoralen-induced photosensitization reaction as manifested by erythema appears related to the formation of reactive singlet oxygen and superoxide anions, and it involves the energy transfer mechanism or type II reaction.

REFERENCES

(*1*) Pathak MA. Photosensitivity to drugs. In: Brodie BR, Gillette JR, eds. Drugs and enzymes. Proceedings of the second international pharmacological meeting, Prague, Czechoslovakia, Aug. 20–23, 1963. Oxford: Pergamon Press, 1965:419–440.

(*2*) Pathak MA. Mechanism of psoralen photosensitization and in vivo biological action spectrum of 8-methoxypsoralen. J Invest Dermatol 1961; 37:397–406.

(*3*) Pathak MA, Fitzpatrick TB, Parrish JA. Photosensitivity and other reactions to light, chapt 55. In: Isselbacher KJ, Adams RD, Braunwald E, Petersdorf RG, Wilson JD, eds. Harrison's principles of internal medicine. 9th ed. New York: McGraw-Hill, 1979:255–262.

(*4*) Harber LC, Baer RL. Pathogenic mechanisms of drug-induced photosensitivity. J Invest Dermatol 1972; 58:227–242.

(*5*) Pathak MA, Epstein JH. Normal and abnormal reactions of man to light. In: Fitzpatrick TB, Arndt KA, Clark WH Jr, Eisen AZ, Van Scott EJ, Vaughan JH, eds. Dermatology in general medicine. 1st ed. New York: McGraw-Hill, 1971:977–1036.

(*6*) Epstein JH. Adverse cutaneous reactions to the sun. In: Malkinson FD, Pearson RW, eds. Year book of dermatology. Chicago: Year Book Med Publ, 1971:5–43.

(*7*) Epstein JH. Phototoxicity and photoallergy: Clinical syndromes. In: Pathak MA, Harber LC, Seiji M, Kukita A, eds. Sunlight and man: Normal and abnormal photobiologic responses. Tokyo: Univ Tokyo Press, 1974:459–477.

(*8*) Harber LC, Baer RL, Bickers DR. Techniques of evaluation of phototoxicity and photoallergy in biologic systems, including man, with particular emphasis on immunologic aspects. In: Pathak MA, Harber LC, Seiji M. Kukita A, eds. Sunlight and man: Normal and abnormal photobiologic responses. Tokyo: Univ Tokyo Press, 1974:515–528.

(*9*) Blum HF. Photodynamic action and diseases caused by light. New York: Reinhold, 1941.

(*10*) Spikes JD. Photosensitization. In: Smith KC, ed. The science of photobiology. New York: Plenum, 1977:87–112.

(*11*) Fowlks WL. The mechanism of photodynamic effect. J Invest Dermatol 1959; 32:233–247.

(*12*) Oginsky EL, Green GS, Griffith G, Fowlks WL. Lethal photosensitization of bacteria with 8-methoxypsoralen to long wavelength ultraviolet radiation. J Bacteriol 1959; 78:821–833.

(*13*) Harber LC. Current status of mammalian and human models for predicting drug photosensitivity. J Invest Dermatol 1981; 77:65–70.

(*14*) Pathak MA, Daniels F, Fitzpatrick TB. The presently known distribution of furocoumarins (psoralens) in plants. J Invest Dermatol 1962; 39:225–239.

(*15*) Pathak MA, Krämer DM, Fitzpatrick TB. Photobiology and photochemistry of furocoumarins (psoralens). In: Pathak MA, Harber LC, Seiji M, Kukita A, eds. Sunlight and man: Normal and abnormal photobiologic responses. Tokyo: Univ Tokyo Press, 1974:335–368.

(*16*) Musajo L, Rodighiero G, Caporale G, et al. Photoreactions between skin-photosensitizing furocoumarins and nucleic acids. In: Pathak MA, Harber LC, Seiji M, Kupita A, eds. Sunlight and man: Normal and abnormal photobiologic responses. Tokyo: Univ Tokyo Press, 1974:369–387.

(*17*) Bensasson RV, Land EJ, Salet C. Triplet excited states of furocoumarins: Reaction with nucleic acid bases and amino acids. Photochem Photobiol 1978; 27:273–280.

(*18*) Wessely F, Kotlan J. Uber die Photodimerisierung von Furocumarinen und das Sphondylin. Monatsch Chem 1955; 86:430–436.

(*19*) Rodighiero G, Cappellina V. Richerche sulla fotodimerizzazione di alcune furocoumarine. Gazz Chim Ital 1961; 91:103–114.

(*20*) Rodighiero G, Dall'Acqua F, Chimenti G. Fotodimerizzazione della cumarina e di alcune furocumarine in matrice di ghiaccio. Ann Chim 1968; 58:551–561.

(*21*) Marciani S, Dall'Acqua F, Rodighiero P, Caporale G, Rodighiero G. Ricerche sulla foto-C_4-ciclo-dimerizzazione di alcuni metilpsoraleni. Gazz Chim Ital 1970; 110:435–451.

(*22*) Krauch CH, Krämer DM, Wacker A. Zum Wirkungsmechanismus photodynamischer Furocumarine Photoreaktion von Psoralen-(4-^{14}C) mit DNA, RNS, Homopolynucleotiden und Nucleosiden. Photochem Photobiol 1967; 6:341–354.

(*23*) Musajo L, Bordin F, Bevilacqua R. Photoreactions at 3655 Å linking the 3,4 double bond of furocoumarins with pyrimidine bases. Photochem Photobiol 1967; 6:927–931.

(*24*) Musajo L, Rodighiero G. Mode of photosensitizing action of furocoumarins. In: Giese AC, ed. Photophysiology. Vol VII. New York and London: Academic Press, 1972:115–147.

(*25*) Dall'Acqua F, Terbojevich M, Marciani S, Vedaldi D, Recher M. Investigation on the dark interaction between furocoumarins and DNA. Chem Biol Interact 1978; 21:103–115.

(*26*) Bordin F, Carlassare F, Baccichetti F, et al. 4,5'-Dimethyl-angelicin: A new DNA-photobinding monofunctional agent. Photochem Photobiol 1979; 29:1063–1070.

(*27*) Bordin F, Carlassare F, Baccichetti F, Guitto A, Rodighiero P. 5-Methyl-angelicin: A new highly photosensitizing furocoumarin. Experientia 1979; 35:1567–1568.

(*28*) Rodighiero G, Musajo L, Dall'Acqua F, Marciani S, Caporale G, Ciavatta L. Mechanism of skin-photosensitization by furocoumarins. Photoreactivity of various furocoumarins with native DNA and with ribosomal DNA. Biochim Biophys Acta 1970; 217:40–49.

(*29*) Dall'Acqua F, Marciani S, Ciavatta L, Rodighiero G. Formation of inter-strand cross-linkings in the photoreactions between furocoumarins and DNA. Z. Naturforsch 1971; 26:561–569.

(*30*) Cech T, Pathak MA, Biswas RK. An electron microscopic study of the photochemical cross-linking of DNA in guinea pig epidermis by psoralen derivatives. Biochim Biophys Acta 1979; 562:342–360.

(*31*) Johnston BH, Johnson MA, Moore CB, Hearst JE. Psoralen–DNA photoreaction: Controlled production of mono- and diadducts with nanosecond ultraviolet laser pulses. Science 1977; 197:906–908.

(*32*) Veronese FM, Schiavon O, Bevilacqua R, Rodighiero G. Drug-protein interaction: 8-Methoxypsoralen as a photosensitizer of enzymes and amino acids. Z Naturforsch 1979; 34:392–396.

(*33*) Pathak MA, Allen BT, Fellman JH, Ingram DJ. Photosensitization and the effect of ultraviolet radiation on the production of unpaired electrons in the presence of furocoumarins (psoralens). Biochim Biophys Acta 1961; 54:506–515.

(*34*) Cannistraro S, Van de Vorst A. ESR and optical absorption evidence for free radical involvement in the photosensitizing action of furocoumarin derivatives and for their singlet oxygen production. Biochim Biophys Acta 1977; 476:166–172.

(*35*) Poppe W, Grossweiner LI. Photodynamic sensitization by 8-methoxypsoralen via the singlet oxygen mechanism. Photochem Photobiol 1975; 22:217–219.

(*36*) Singh H, Vadasz JA. Singlet oxygen: A major reactive species in the furocoumarin photosensitized inactivation of *E. coli* ribosomes. Photochem Photobiol 1978; 28:539–545.

(*37*) Demol NJ, Beijersbergen van Henegouwen GM. Formation of singlet molecular oxygen by 8-methoxypsoralen. Photochem Photobiol 1979; 30:331–335.

(*38*) Cannistraro S, Pathak MA, Fitzpatrick TB. Photosensitized induction of singlet oxygen by furocoumarins (psoralens) and porphyrins. In: Book of abstracts, sixth annual meeting, American Society for Photobiology, Burlington, Vt., June 11–15, 1978. Bethesda, Md.: The American Society for Photobiology, 1978:65.

(*39*) Pathak MA, Rosario R, Parrish JA, Fitzpatrick TB. Role of psoralen–DNA monoadducts and cross-links in photochemotherapy of psoriasis. In: Book of abstracts, seventh annual meeting, American Society for Photobiology, Asilomar Conference Grounds, Pacific Grove, Calif., June 24–28, 1979. Bethesda, Md.: The American Society for Photobiology, 1979:97.

(*40*) Pathak MA, Biswas RK. Skin photosensitization and DNA cross-linking ability of photochemotherapeutic agent. J Invest Dermatol 1977; 68:abstract No. 236.

(*41*) Pathak MA, Fitzpatrick TB. Certain biological and therapeutic properties of linear and angular furocoumarins (psoralens and isopsoralens). In: Book of abstracts, ninth annual meeting, American Society for Photobiology, Williamsburg, Va., June 14–19, 1981. Bethesda, Md.: The American Society for Photobiology, 1981:109.

(*42*) West JD, Breitbart RE, Pathak MA. Photosensitization of DNA by uro-, copro-, and protoporphyrin. In: Book of abstracts, eighth international congress of photobiology, Strasbourg, France, July 20-25, 1980. London: Plenum, 1980:205.

Immunosuppressive Effects of Ultraviolet (280–320 nm) Radiation and Psoralen Plus Ultraviolet (320–400 nm) Radiation in Mice[1,2,3]

Margaret L. Kripke[4,5]

ABSTRACT—Contact hypersensitivity (CHS), a cell-mediated immunologic reaction, can be induced in mice by application of a contact-sensitizing chemical to the shaved skin. Exposing the animals to UV radiation from FS40 sunlamps inhibits this immune response. This inhibition is systemic, since the sensitizer need not be applied to the irradiated site of the animal. The mechanism whereby UV radiation prevents CHS appears to involve the production of suppressor T-lymphocytes. Recent evidence suggests that UV exposure of mice alters the way in which certain antigens are processed, and this altered processing or presentation of antigen results in the activation of the suppressor cell pathway, rather than leading to immunization. Treatment of mice with a photosensitizer, psoralen, plus UV (320–400 nm) radiation also suppresses CHS systemically, but whether the cellular mechanisms are the same as those underlying the suppression from the shorter UV wavelengths remains to be determined. The possible role of these immunosuppressive events in photocarcinogenesis is discussed.—JNCI 1982; 69:171–173.

Studies reviewed here concern the effects of UV radiation on the response of the host to certain chemicals that are applied topically. These particular chemicals all have the property of inducing CHS (allergic contact dermatitis), which is a specific type of immunologic response mediated by T-lymphocytes. Furthermore, the interaction between these chemicals and UV radiation is an indirect one. In contrast to chemical photosensitization, in which the radiation acts directly on the chemical agent to produce its biologic effect, the phenomenon that we are dealing with involves an effect of UV radiation on the host. This effect on the host alters the way in which the host subsequently responds to the chemical agent. In addition to being an interesting biological phenomenon, perhaps with some practical applicability, it is quite likely that this UV radiation-induced alteration has important consequences for carcinogenesis in skin.

CONTACT HYPERSENSITIVITY

To understand the effects of UV radiation on the host, one should know something about the mechanisms involved in the CHS reaction. CHS is an immune reaction of the delayed hypersensitivity type, the prototype of which is the tuberculin reaction. This state of immunity is transferable with T-lymphocytes, not with antibody; thus it is generally referred to as a cell-mediated immune response. Although many important details concerning how this reaction occurs are unknown, the sequence of events can be envisaged in the following simplified manner.

After gaining entry to the body, a foreign substance (antigen) becomes associated with a cell of macrophage lineage. Whether this association involves phagocytosis and alteration of the antigen by the macrophage ("antigen processing") is not clear. The antigen, in association with a specific cell surface marker on the macrophage (Ia molecule), is then "presented" to a T-lymphocyte that reacts specifically with that antigen. This interaction between the T-lymphocyte and the antigen plus Ia molecule activates the lymphocyte to undergo division and differentiation. This amplification process (or sensitization) results in the formation of a new population of T-lymphocytes that is long-lived and is capable of reacting again with the same antigen. A subsequent encounter with this same antigen triggers the effector or efferent portion of the immune response, which involves the production by the lymphocytes of soluble mediators, including vasoactive agents and proliferative and chemotactic substances, that act on other cells of the reticuloendothelial system. This second amplification process requires several hours to occur and usually reaches a maximum only after 24–48 hours. The infiltration of these cells, mainly blood monocytes and lymphocytes, into the site of antigen deposition in the skin accounts for the induration that characterizes this reaction.

CHS is a special form of delayed hypersensitivity in which the antigen (or contact allergen) is a reactive molecule that binds to cells and proteins in the skin following topical application. Thus the antigen is actually a chemically modified component of the host. A second distinctive feature of

---

ABBREVIATIONS USED: CHS=contact hypersensitivity; DNCB=2-chloro-1,3-dinitrobenzene; DNFB=1-fluoro-2,4-dinitrobenzene; PUVA=psoralen plus UV radiation (320–400 nm); TNCB=2-chloro-1,3,5-trinitrobenzene; UVA=UV, 320–400 nm; UVB=UV, 280–320 nm.

---

[1] Presented at the Seventh Food and Drug Administration Science Symposium ("Photochemical Toxicity; Toxic, Allergic, and Carcinogenic Aspects With Emphasis on Predicting Effects in Humans") held at the Uniformed Services University of the Health Sciences, Bethesda, Md., March 16–17, 1981.

[2] Supported by Public Health Service contract N01CO-75380 from the Office of the Director, National Cancer Institute, with Litton Bionetics, Inc. The contents of this publication do not necessarily reflect the views or policies of the U.S. Department of Health and Human Services, nor does mention of trade names, commercial products, or organizations imply endorsement by the U.S. Government.

[3] Animals were maintained under the guidelines set forth by the National Institutes of Health Policy on Humane Care and Use of Animals and by the Animal Welfare Act in facilities accredited by the American Association for Accreditation of Laboratory Animal Care.

[4] Cancer Biology Program, NCI-Frederick Cancer Research Facility, P.O. Box B, Frederick, Md. 21701.

[5] Dr. Frances Noonan, Dr. Edward De Fabo, Dr. J. M. Jessup, and Dr. Michael Fisher from this laboratory, Dr. Mark I. Greene and Dr. B. Benacerraf from the Department of Pathology, Harvard Medical School, and Dr. W. L. Morison and Dr. J. A. Parrish from the Dermatology Department, Harvard Medical School, have all contributed to the experimental data on which these comments are based and/or to the conceptual framework of this investigation.

the CHS reaction is that the processing and presentation of the antigen are probably performed by special cells distributed in network fashion throughout the epidermis. These cells, called Langerhans' cells, belong to the macrophage lineage and possess the Ia surface molecules essential for sensitization of lymphocytes (*1, 2*).

Effect of UV Radiation on CHS in the Mouse

In the mouse, CHS can be induced by the application of a contact allergen or a sensitizer, such as TNCB or oxazolone, to the shaved abdominal skin. After 5–7 days, the CHS reaction is elicited in the sensitized animal by application of a dilute solution of the sensitizing agent to both surfaces of the ears or by the intradermal injection of the agent into the rear footpads. The thickness of the ears or feet is measured with a spring-loaded micrometer before the challenge dose of the allergen is applied, and the thickness is measured again 24 hours later. The amount of specific swelling (i.e., ear swelling in sensitized mice minus ear swelling in unsensitized control mice) reflects the degree of edema and cellular infiltrate and hence the magnitude of the immune reaction.

Several years ago, we performed a series of experiments designed to assess the immunologic capabilities of mice exposed repeatedly to UV radiation for the induction of skin cancer. We found that, although many immune responses proceeded normally in these animals, exposure of the mice to UV radiation from unfiltered FS40 sunlamps inhibited a delayed hypersensitivity reaction to DNCB that was injected sc (*3*). More recently, we have shown that a single exposure of the shaved dorsum of BALB/c mice to UV radiation will prevent the subsequent induction of CHS to DNFB or TNCB (*4*). This UV radiation-mediated suppression is systemic, since in our protocol neither the site of sensitization (abdomen) nor the site of elicitation (ears) is directly exposed to UV radiation.

Several conclusions can be drawn from studies of the characteristics of the suppression of CHS by UV radiation: 1) The amount of suppression is directly related to the dose of UV radiation, 2) the amount of suppression is independent of dose fractionation and dose rate over a broad range of conditions, and 3) a minimum of 2–3 days must elapse between the time of UV radiation exposure and application of the contact sensitizer to allow for the manifestation of suppression (*4, 5*). The cellular basis for this immune suppression has been analyzed in some detail. Lymphoid cell transfer studies by Jessup et al. (*6*) demonstrated that UV irradiation of mice did not alter the responsiveness of their lymphocytes to the sensitizing antigen (DNCB). When lymphoid cells were removed from UV-irradiated mice and used to repopulate lethally X-irradiated recipients, the recipients responded normally to DNCB. This result demonstrated that the impaired response in UV-irradiated mice was not due to altered responsiveness or recognition by lymphocytes but must have been due to an impairment at the level of antigen processing, before lymphocytes were involved in the response, or at the effector portion of the immune reaction that occurs locally at the challenge site. So that these possibilities could be distinguished, lymphocytes from mice immune to DNCB were injected into UV-irradiated animals, and these recipients were tested for their ability to exhibit a CHS response following footpad challenge with DNCB. Since UV-irradiated mice responded as well as unirradiated mice, it was concluded that the afferent portion of the immune response had been affected by UV radiation, probably by altering antigen uptake, processing, or presentation by macrophages or Langerhans' cells.

Direct tests of the antigen-presenting capabilities of macrophages from UV-irradiated mice have been done by Greene and co-workers (*7*). In these studies, the antigen was chemically coupled to glass-adherent spleen cells (predominantly macrophages) from normal or donor mice exposed to UV radiation. These cells were then injected sc into normal or UV-irradiated recipients, and the recipients were tested for CHS. With this approach, it was found that antigen-coupled cells from normal donors could induce CHS in both normal and UV-irradiated recipients. Thus introduction of the antigen bound to a normal antigen-presenting cell bypassed the UV radiation-induced suppression of CHS. This observation strongly suggests that the impairment of CHS by UV radiation is mediated by an alteration in the antigen-presenting cell population in UV-irradiated mice. A second finding from this study was that attempts to immunize UV-irradiated mice with antigen-coupled cells from UV-irradiated donors not only failed to induce CHS but also resulted in the appearance of suppressor cells in the spleens of the recipients. These suppressor cells, shown to be T-lymphocytes, are capable of inhibiting the development of CHS to the coupled antigen when the cells are transferred to a normal recipient.

These results suggest that the failure of UV-irradiated mice to be sensitized after being skin painted with TNCB also might be associated with the production of suppressor T-lymphocytes. Recent experiments have demonstrated that this is indeed the case: UV-irradiated mice painted with TNCB or DNFB fail to develop a CHS reaction to the sensitizing agent but instead develop antigen-specific suppressor T-lymphocytes in their spleens. The induction of these suppressor cells requires both UV radiation exposure and the subsequent application of a contact-sensitizing agent (*5*).

Effects of Various UV Radiation Wavelengths in Suppression of CHS

To determine how UV radiation initiates these changes in immunologic function, we are evaluating the action spectrum for the suppression of CHS. Our preliminary data indicate that the wavelengths most effective in producing suppression are in the region of 260–270 nm. Furthermore, the shape of the action spectrum is consistent with the possibility that DNA may be the photoreceptor, although there are other compounds in skin that have similar absorption spectra (*5*). Because PUVA also damages DNA in skin (although the molecular lesions differ from those induced by UVB radiation) and because PUVA has been shown to be immunosuppressive in other species (*8*), we were interested in determining whether or not PUVA treatment of mice was capable of suppressing CHS systemically. The data presented in table 1 indicate that ip administration of methoxsalen, followed by exposure to radiation from Mylar-

TABLE 1.—*Effects of a single UVB radiation or PUVA treatment on the induction of CHS in C3H mice*

Expt. No.	Contact sensitizer[a]	Treatment[b]	Net ear swelling, cm×10^{-3}	Suppression, %
1	DNFB	Psoralen	9.7	0
		UVA radiation	11.1	0
		PUVA	3.0	62
		UVB radiation	2.0	74
		None	7.8	—
2	DNFB	PUVA	3.3	64
		UVB radiation	3.6	61
		None	9.2	—
	TNCB	PUVA	5.3	55
		UVB radiation	4.3	64
		None	11.8	—

[a] Mice were painted on the shaved abdomen with 100 µl of 5% TNCB or 30 µl of 0.5% DNFB in acetone 5 days after UV radiation treatment. The ear swelling reaction was elicited 6 days later by painting each ear surface with 5 µl of 1% TNCB or 0.2% DNFB, and the amount of swelling was measured 24 hr after application of the challenge dose.

[b] UVB radiation=$2.1\times10^4\ \mathrm{J\cdot m^{-2}}$; UVA radiation=$5.4\times10^4\ \mathrm{J\cdot m^{-2}}$; psoralen=0.4 mg methoxsalen administered ip (Kripke ML, Morison WL, Parrish JA: Unpublished data).

filtered Sylvania PUVA bulbs, can indeed reduce the development of CHS in mice. However, it has not yet been determined whether this immunosuppression is mediated by the same cellular pathway as that evoked following UVB radiation exposure, i.e., an alteration in antigen presentation, leading to the induction of T-suppressor cells. Furthermore, there is no firm evidence that the immunosuppression caused by either UVB radiation or PUVA is related to their effects on DNA. Thus the relationship between the immunosuppressive effects of UVB radiation and PUVA remains to be established.

CONCLUSIONS

Regardless of the molecular mechanisms involved, the studies reviewed here demonstrate that in vivo exposure of mice to UV radiation renders them systemically anergic to a subsequent application of a contact-sensitizing agent. Furthermore, this anergy does not represent merely the absence of a response; it also involves the induction of antigen-specific T-suppressor cells. Thus UV radiation exposure of mice changes their immunologic reactivity to contact-sensitizing antigens from a state of positive responsiveness to one of suppression.

It is not yet certain whether this immunosuppressive phenomenon is restricted to contact-sensitizing chemicals applied topically or whether the immune response to some other agents might be altered as well. Previous work has demonstrated that immune responses to histocompatibility antigens and to at least some particulate antigens are unaffected by UV irradiation of the test animal (*3, 9*). However, suppressor cells that inhibit the rejection of highly antigenic UV radiation-induced skin cancers can be found in UV-irradiated mice (*10–12*). Quite possibly, the UV radiation-induced alteration in the presentation of certain antigens is responsible for the induction of these suppressor cells that interfere with tumor immunity. Because these suppressor cells appear to be of considerable importance in the determination of the pathogenesis of UV radiation-induced skin cancers (Fisher MS, Kripke ML: Unpublished data), our current efforts are directed toward testing this hypothesis.

REFERENCES

(*1*) Stingl, G, Tamaki K, Katz SI. Origin and function of epidermal Langerhans cells. Immunol Rev 1980; 53:149–174.

(*2*) Steinman RM. Dendritic cells. Transplantation 1981; 31:151–155.

(*3*) Kripke ML, Lofgreen JS, Beard J, Jessup JM, Fisher MS. In vivo immune responses of mice during carcinogenesis by ultraviolet irradiation. J Natl Cancer Inst 1977; 59:1227-1230.

(*4*) Noonan FP, Kripke ML, Pedersen GM, Greene MI. Suppression of contact hypersensitivity in mice by ultraviolet radiation is associated with defective antigen presentation. Immunology 1981; 43:527–533.

(*5*) Noonan FP, De Fabo EC, Kripke ML. Suppression of contact hypersensitivity by ultraviolet radiation: An experimental model. Semin Hematol 1981; 4:293–304.

(*6*) Jessup JM, Hanna N, Palaszynski E, Kripke ML. Mechanisms of depressed reactivity to dinitrochlorobenzene and ultraviolet-induced tumors during ultraviolet carcinogenesis in BALB/c mice. Cell Immunol 1978; 38:105–115.

(*7*) Greene MI, Sy MS, Kripke ML, Benacerraf B. Impairment of antigen-presenting cell function by ultraviolet radiation. Proc Natl Acad Sci USA 1979; 76:6592-6595.

(*8*) Morison WL, Parrish JA, Woehler ME, Bloch KJ. The influence of ultraviolet radiation on allergic contact dermatitis in the guinea pig. II. Psoralen/UVA radiation. Br J Dermatol 1981; 104:165–168.

(*9*) Spellman CW, Woodward JG, Daynes RA. Modification of immunologic potential by ultraviolet radiation. I. Immune status of short-term UV-irradiated mice. Transplantation 1977; 24:112-119.

(*10*) Fisher MS, Kripke ML. Systemic alteration induced in mice by ultraviolet light irradiation and its relationship to ultraviolet carcinogenesis. Proc Natl Acad Sci USA 1977; 74:1688-1692.

(*11*) Spellman CW, Daynes RA. Modification of immunologic potential by ultraviolet radiation. II. Generation of suppressor cells in short-term UV-irradiated mice. Transplantation 1977; 24:120-126.

(*12*) Fisher MS, Kripke ML. Further studies on the tumor-specific suppressor cells induced by ultraviolet radiation. J Immunol 1978; 121:1139-1144.

blank page

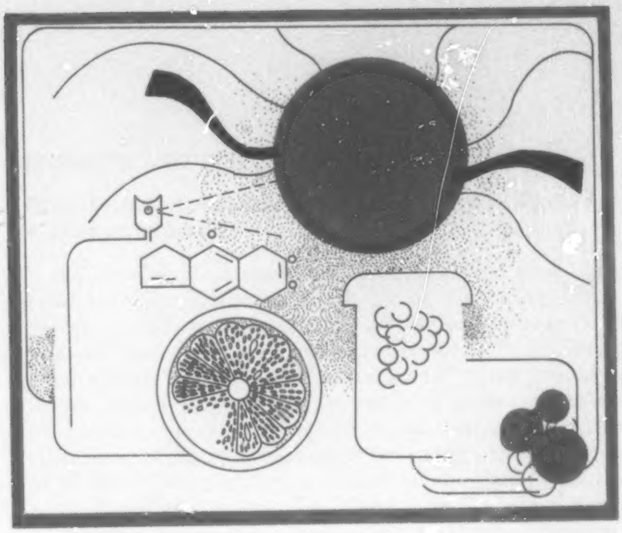

CELLULAR ASSAY SYSTEMS

Moderator: Sanford Miller
Food and Drug Administration

blank page

Cell Damage by Near Ultraviolet Radiation: Role of DNA–Protein Cross-links[1,2]

A. Eisenstark,[3] S. Kovacs,[3] *and* J. Terry[3]

ABSTRACT—Near UV radiation and hydrogen peroxide were found to act synergistically to damage bacteriophage (which contains only DNA and protein) and mammalian cells. DNA–protein cross-links are being considered as the critical molecular alteration that leads to biological damage.—JNCI 1982; 69:177–181.

Forty years ago, Stadler and Uber (*1*) discovered that the action spectrum for mutation in maize could be superimposed on the adsorption spectrum for DNA. However, when compared to the DNA adsorption spectrum, action spectra for inactivation of bacteria (*2*) or phage (*3*) have large deviations in the 300- to 400-nm region (NUV). This observation indicates that DNA is not the sole chromophore for biological damage by NUV radiation. In addition to action spectrum data, considerable evidence shows that the biological effects of NUV radiation are strikingly different from those of FUV radiation (200–300 nm) (*4–7*). As one of many illustrations of NUV and FUV differences, the bacterium *Micrococcus radiodurans* when compared to *Escherichia coli* is notoriously *less* sensitive to FUV radiation but is *more* sensitive than *E. coli* to NUV radiation [(*8*); Caimi P, Eisenstark A: Unpublished observations]. From these and numerous other observations, we conclude that the chromophore for FUV radiation, but not necessarily for NUV, is DNA.

In our research program, we are systematically examining the various biological effects of NUV radiation to identify specific chromophores, targets, molecular alterations, and repair mechanisms (both constitutive and induced). These effects are being tested in different environments (e.g., oxygen, nitrogen, or sensitizing agent).

During our studies, we discovered that tryptophan photoproducts (*9, 10*), especially H_2O_2 (*3, 7, 11, 12*), can act as sensitizers to NUV radiation; this report focuses on this synergistic effect of H_2O_2 and NUV radiation. We have irradiated bacterial cells, bacteriophage, mammalian cells, polypeptides, and amino acids in these studies.

We have been faced with a paradox that has confronted other investigators of NUV radiation; neither DNA nor protein has an absorption peak above 300 nm. Yet many biological effects are seen above the 300-nm wavelength. Even purified transforming DNA (*13*) and purified phage (*3*) can be inactivated by monochromatic NUV radiation above 300 nm.

MATERIALS AND METHODS

This report is derived from several distinct sets of experiments. Reference sources of materials and methods are: *a*) DNA–protein cross-links in phage T7 (*12*) and *b*) cross-links in L929 fibroblasts and B16 melanoma cells (*14*).

RESULTS AND DISCUSSION

DNA–Protein Cross-links via H_2O_2 Plus NUV Radiation Action on Phage T7

We have demonstrated that NUV radiation plus H_2O_2 synergistically inactivates phage T7 by producing DNA–protein cross-links, thus preventing injection of phage DNA into the host (*12*). Also, H_2O_2 enhances NUV radiation lethality and SS DNA breaks in bacteria (*7*), thus providing simple model systems for the study of these synergistic interactions. While action spectrum analysis indicates that synergism for phage is maximal at 340 nm (*4*), the frequency of SS DNA break induction cannot be correlated with the peak of cell killing (*12*); i.e., there is no apparent direct relationship between SS breaks and cell death. Therefore, we searched for other mechanisms of biological damage by H_2O_2 plus NUV radiation and found that the number of DNA–protein cross-links did correlate with the number of inactivated phage (*12*).

To identify cross-links, we appropriately treated double-labeled T7 phages (^3H-labeled DNA and ^{14}C-labeled protein) and sedimented them through CsCl block or step gradients (*12*). Alkaline sucrose gradients demonstrated that, while the overall pattern of protein separation was relatively unchanged, the DNA experienced a slight shift with H_2O_2 treatment and a considerable shift with NUV radiation plus H_2O_2 treatment. The fractions showing maximal ^3H radioactivity were pooled, dialyzed, and layered on CsCl step gradients. After centrifugation, fractions were collected and counted.

The peak of ^{14}C radioactivity (protein) cosedimenting with ^3H radioactivity (DNA) demonstrated a substantial increase in the cosedimentation complex only when phages were treated with both NUV radiation and H_2O_2. These results are most easily explained by DNA–protein cross-linkage induced by NUV radiation plus H_2O_2 treatment of phage T7. This argument is strengthened by the small, but reproducible, decrease in buoyant density of the DNA with NUV radiation plus H_2O_2 treatment (1.687 g/cm^3) versus

ABBREVIATIONS USED: FUV=far UV; NUV=near UV; PBS=phosphate-buffered saline; SS=single-strand; *trans*-Pt=*trans*-diaminedichloride platinum (II).

---

[1] Presented at the Seventh Food and Drug Administration Science Symposium ("Photochemical Toxicity: Toxic, Allergic, and Carcinogenic Aspects With Emphasis on Predicting Effects in Humans") held at the Uniformed Services University of the Health Sciences, Bethesda, Md., March 16–17, 1981.

[2] Supported by Public Health Service grant 2R01FD-00658 from the Food and Drug Administration.

[3] Division of Biological Sciences, University of Missouri, Columbia, Mo. 65211.

that with the control (1.704 g/cm^3), NUV radiation (1.702 g/cm^3), or H_2O_2 (1.701 g/cm^3) treatments. When NUV radiation plus H_2O_2-treated DNA fractions were pooled, dialyzed, digested with DNase I, and subjected to a second round of CsCl centrifugation, the liberated ^{14}C counts banded at about 1.3 g/cm^3, a position characteristic of protein.

This particular NUV radiation plus H_2O_2 treatment resulted in a surviving fraction of 5.9×10^{-5}, which corresponds to 9.7 lethal hits per phage. (One lethal hit is the dose that yields 37% survival.) Under these conditions, 1.48% of phage protein was cross-linked to DNA or 0.153% per lethal hit. Because the total molecular weight of the protein per phage T7 is 2.4×10^7, the contribution of the molecule (38,000 daltons) of the major head protein is 38,000 (2.4×10^7) or 0.158%.

The close agreement of these two values (0.153% vs. 0.158% theoretical cross-linked protein/lethal hit) suggests that one molecule of phage coat protein (gene 10) could cross-link with DNA per lethal event. Since this protein represents over 60% of the total protein in phage T7, it would be present in sufficient quantities for the juxtaposition necessary for cross-linkage to occur between DNA and protein, particularly since cross-linkage probably has no preferred location with respect to the T7 genome. That the cross-linkage is covalent was suggested by the fact that phages were lysed by either phenol or sodium dodecyl sulfate at high pH, which would have disrupted noncovalent bonds.

STUDIES WITH MAMMALIAN CELLS

In an effort to extrapolate the studies of DNA-protein cross-linking caused by NUV radiation and H_2O_2 to mammalian systems, we conducted experiments on established mouse cell lines, L929 fibroblasts and B16 melanoma cells. We used the DNA alkaline elution technique of Kohn (*14*) and Fornace and Kohn (*15*) for detection of DNA-protein cross-links. Alkaline elutions were run with internal reference cells (L1210 mouse leukemia) to facilitate cross-comparisons between treatments. The percentage of DNA retained on the filter when the L1210 DNA retention was 10% was termed "relative retention." Prior to elution but after treatment, the L929 and B16 cells received 440 rad of X-ray to introduce SS breaks and promote DNA elution by tetrapropylammonium hydroxide-EDTA eluting solution (*15*). The L1210 reference cells received 220 rad of X-ray.

L929 cells were apparently uninfluenced by black-light-bulb NUV radiation in doses between 2×10^5 J·m^{-2} and 6×10^5 J·m^{-2}. A slight replication delay was seen with 8×10^5 J·m^{-2} NUV radiation, but there was no long-term influence on cell cycle time. Irradiations were done with the cells immersed in PBS to obviate irradiated medium artifacts (*16*). A NUV radiation dose of 6×10^5 J·m^{-2} produced detectable DNA-protein cross-links as shown by the high filter retention of the NUV-radiation-treated cellular DNA over that of the control DNA (text-fig. 1). For these experiments, the control cells were incubated in PBS for 4.5 hours, which corresponded to the time that the irradiated cells were in PBS during the NUV radiation exposure. The filter retention was shown to be caused by DNA-protein cross-links (as opposed to DNA-DNA cross-links) because the retention was sensitive to proteinase K digestion (text-fig. 1); whereas the NUV radiation and control curves are quite separate without proteinase K treatment, the curves are nearly coincident after proteinase K treatment. The NUV-radiation-induced DNA-protein cross-links were effectively repaired within 24 hours after treatment as shown by the return of the relative retention to control levels after a 24 hour post-treatment incubation in complete medium (text-fig. 2).

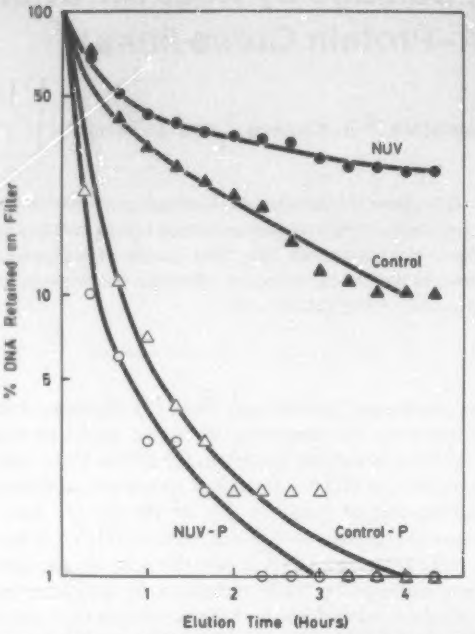

TEXT-FIGURE 1.—Fraction of L929 DNA retained on polyvinyl chloride filters vs. elution time with tetra-propylammonium hydroxide. NUV radiation=6×10^5 J·m^{-2} (black light bulb). *Solid symbols* were elutions run without proteinase K treatment. *Open symbols* and (−P) *designation* were elutions run with proteinase K treatment prior to elution.

To compare NUV-radiation-induced DNA-protein cross-links to chemically induced DNA-protein cross-links, we treated L929 cells with *trans*-Pt, a putative DNA-protein cross-linking agent (*17*). L929 cells were exposed to *trans*-Pt for 1 hour in medium without serum; control cells were incubated for 1 hour in medium without serum and without added *trans*-Pt. Either a 200-μM or a 400-μM concentration of *trans*-Pt caused about a 50% loss of cells within 24 hours of treatment. However, 200 μM of *trans*-Pt-treated cells restored replication capacity by either 4 or 7 days after treatment, whereas 400 μM of *trans*-Pt-treated cells showed no replication capacity by 4 days and only slight replication capacity by 7 days after treatment. DNA alkaline elution data showed that a 400-μM *trans*-Pt treatment produced DNA relative retention that was only slightly higher than that produced by 6×10^5 J·m^{-2} NUV radiation (table 1). The DNA-protein nature of this retention was shown by the considerable loss of retention following proteinase K treatment. However, a 200-μM *trans*-Pt treatment produced DNA relative retention that was essentially the same as that of the controls (table 1).

The NUV radiation effects on B16 survival and replication are contradictory. We have shown and reported an inhibition of replication with a NUV radiation dose as low as 4×10^5 J·m^{-2}; however, at other times the replication data were essentially identical to those obtained with L929, i.e., no extended effects for NUV radiation. The variation in NUV radiation sensitivity seems to be most readily attributable to the variation in pigmentation in these melanoma cells that occurs with extended periods of time in culture (the less pigmented cells being more NUV radiation-sensitive); this aspect is being pursued. The B16 alkaline elution data presented were obtained from cultures that had little pigmentation and therefore exhibited the greatest sensitivity to NUV radiation. NUV radiation (6×10^5 J·m^{-2}) induced DNA–protein cross-links in B16 cells, which as was observed in L929 cells were repaired within 24 hours after treatment (text-fig. 3). Proteinase K treatments confirmed the DNA–protein nature of this NUV radiation-induced DNA retention (data not shown). Thus B16 and L929 cells both exhibit similar DNA–protein damage and repair in response to NUV radiation.

Since NUV radiation plus H_2O_2 treatment has been shown to produce DNA–protein cross-linking in viruses (*12*), we were curious as to whether H_2O_2 might potentiate NUV radiation-induced DNA–protein cross-linking. Both L929 and B16 cells were extremely sensitive to H_2O_2 alone, with B16 showing slightly greater sensitivity. Coincident exposure to NUV radiation (6×10^5 J·m^{-2}) and H_2O_2 (1.5×10^{-4} *M*) did not significantly reduce cell survival. However, NUV radiation plus H_2O_2 did alter the DNA retention by alkaline elution (text-fig. 4). As before, NUV radiation alone showed retention greater than that of the control attributable to DNA–protein cross-links. H_2O_2 treatment alone showed less relative retention than controls; this result was anticipated since H_2O_2 is known to introduce SS breaks in DNA (*18–20*) and the alkaline elution of DNA is known to be accelerated by SS DNA breaks (*21*). The slightly lower retention by H_2O_2-treated B16 as compared to H_2O_2-treated L929 cells may indicate that the greater sensitivity of B16 to H_2O_2 is due to an increase in the number of SS breaks. Following the same reasoning, the even lower retention of NUV radiation plus H_2O_2-treated L929 DNA and B16 DNA may indicate that coincident NUV radiation treatment enhances SS breaking by H_2O_2 rather than increases DNA–protein cross-links.

TABLE 1.—*Relative retention of L929 DNA*[a]

Proteinase K treatment[b]	Untreated controls, %		Treated cells, %		
	NUV radiation[c,d]	*trans*-Pt[e]	NUV radiation[c,d]	*trans*-Pt[e]	
				200 µM	400 µM
Without	17	15	28	18	13
With	5.5	6.5	10	6.5	13.5

[a] Percentage of DNA retained on filter when L1210 DNA retention was 10%.

[b] Incubation for 30 min in 0.5 mg proteinase K/ml while cells are on filter, after lysis, and prior to elution.

[c] Dose=6×10^5 J·m^{-2}.

[d] Incubation for 4.5 hr in PBS.

[e] Incubation for 1 hr in RPMI-1640 without serum.

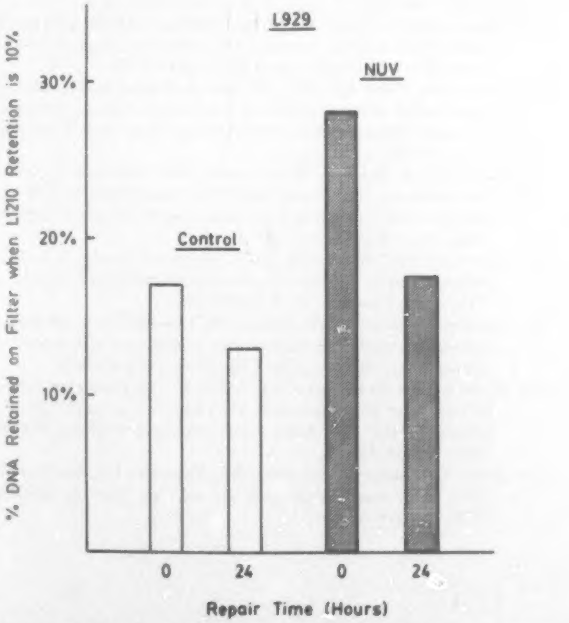

TEXT-FIGURE 2.—Repair of NUV radiation-induced DNA protein cross-links in L929 fibroblasts. Percent of L929 DNA retained on filter when L1210 DNA retention is 10% (relative retention) vs. repair time. 0 time=termination of experiment at the end of treatment. 24 hr=replacement of PBS with complete medium and incubation for 24 hr before termination. NUV radiation=6×10^5 J·m^{-2}.

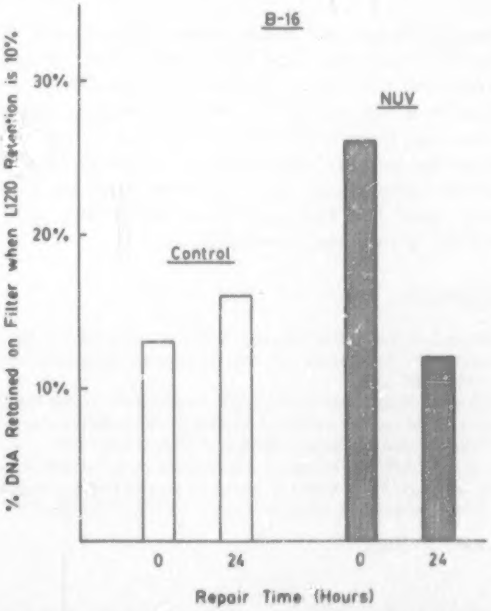

TEXT-FIGURE 3.—NUV radiation-induced DNA–protein cross-links and their repair in B16 melanoma cells. Percent of B16 DNA retained on filter when L1210 DNA retention is 10% (relative retention) vs. repair time. 0 time=termination of experiment at the end of treatment. 24 hr=replacement of PBS with complete medium and incubation for 24 hr before termination. NUV radiation=6×10^5 J·m^{-2}.

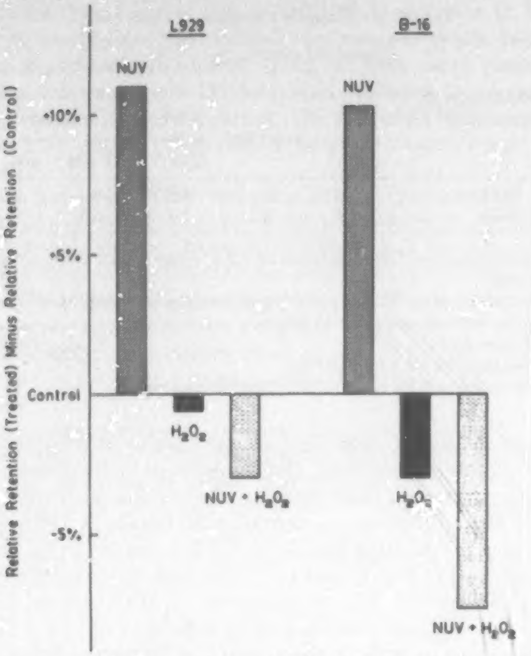

Text-figure 4.—Relative retention of DNA from NUV radiation, H_2O_2, and NUV radiation + H_2O_2-treated L929 fibroblasts and B16 melanoma cells. Relative retention (percent DNA retained on filter when L1210 DNA retention is 10%) of treated minus relative retention of control gives the percent of DNA retained above or below control. NUV radiation=6×10^5 $J\cdot m^{-2}$. $H_2O_2=1.5\times10^{-4}$ *M*. All incubations were for 4.5 hr in PBS.

Obviously, phage and mammalian cells respond differently to NUV radiation and H_2O_2 treatments. Whereas a NUV radiation plus H_2O_2 treatment creates DNA–protein cross-links in T7 phage while a NUV radiation treatment alone does not, the reverse seems to be true in mammalian cells. Since the protein "environment" of the DNA in these two systems varies widely, it is not surprising that a strong oxidizing agent like H_2O_2 should differentially alter the potential NUV radiation chromophores.

REFERENCES

(*1*) Stadler LD, Uber FM. Genetic effects of ultraviolet radiation in maize. IV. Comparison of monochromatic radiations. Genetics 1942; 27:84–118.

(*2*) Mackay D, Eisenstark A, Webb RB, Brown MS. Action spectra for lethality in recombinationless strains of *Salmonella typhimurium* and *Escherichia coli*. Photochem Photobiol 1976; 24:337–344.

(*3*) Ananthaswamy HN, Hartman PS, Eisenstark A. Synergistic lethality of phage T7 by near-UV radiation and hydrogen peroxide: An action spectrum. Photochem Photobiol 1979; 29:53–56.

(*4*) Eisenstark A. Mutagenic and lethal effects of visible and near-ultraviolet light on bacterial cells. Adv Genet 1971; 16:167–198.

(*5*) Ferron WL, Eisenstark A, Mackay D. Distinction between far- and near-ultraviolet light killing of recombinationless (*recA*) *Salmonella typhimurium*. Biochim Biophys Acta 1972; 277:651–658.

(*6*) Eisenstark A. Tryptophan photoproduct as a genetic probe: Effects on bacteria. Proceedings of the Stadler Symposium, April 17–18, 1973. Vol 5. Columbia, Mo.: Univ of Missouri Agricultural Experiment Station, 1973:49–60.

(*7*) Ananthaswamy HN, Eisenstark A. Near-UV-induced breaks in phage DNA: Sensitization by hydrogen peroxide (a tryptophan photoproduct). Photochem Photobiol 1976; 24:439–442.

(*8*) Webb RB. Lethal and mutagenic of near-ultraviolet radiation. In: Smith KC, ed. Photochemical and photobiological reviews. Vol 2. New York: Plenum, 1977:169–261.

(*9*) Yoakum G, Eisenstark A. Toxicity of L-tryptophan photoproduct on recombinationless (*rec*) mutants of *Salmonella typhimurium*. J Bacteriol 1972; 112:653–655.

(*10*) Yoakum G, Eisenstark A, Webb RB. Near-UV photoproduct(s) of L-tryptophan: An inhibitor of medium-dependent repair of X-ray-induced single-strand breaks in DNA which also inhibits replication-gap closure in *Escherichia coli* DNA. In: Hanawalt PC, Setlow RB, eds. Molecular mechanisms for repair of DNA. Part B. New York: Plenum, 1975:453–458.

(*11*) McCormick JP, Fischer JR, Pachlatko JP, Eisenstark A. Characterization of a cell-lethal product from the photooxidation of tryptophan: Hydrogen peroxide. Science 1967; 191:468–469.

(*12*) Hartman PS, Eisenstark A, Pauw PG. Inactivation of phage T7 by near-ultraviolet radiation plus hydrogen peroxide: DNA–protein crosslinks prevent DNA injection. Proc Natl Acad Sci USA 1979; 76:3228–3232.

(*13*) Cabrera-Juarez E, Swenson PA. Action spectrum for the oxygen-independent inactivation of *Haemophilus influenzae* transforming DNA with near ultra-violet light. Photochem Photobiol 1975; 21:193–196.

(*14*) Kohn KW. DNA as a target in cancer chemotherapy: Measurement of macromolecular DNA damage produced in mammalian cells by anti-cancer drugs and carcinogens. Methods Cancer Res 1979; 16:291–345.

(*15*) Fornace AJ, Jr, Kohn KW. DNA protein crosslinking by ultraviolet radiation in normal human and xeroderma pigmentosum fibroblasts. Biochim Biophys Acta 1976; 435:95–103.

(*16*) Stoien JD, Wang RJ. Effect of near-ultraviolet and visible light on mammalian cells in culture. II. Formation of toxic photoproducts in tissue culture medium by blacklight. Proc Natl Acad Sci USA 1974; 71:3961–3965.

(*17*) Zwelling LA, Bradley MO, Sharkey NA, Anderson T, Kohn KW. Mutagenicity, cytotoxicity and DNA crosslinking to V79 Chinese hamster cells treated with *cis-* and *trans*-Pt(II) diaminedichloride. Mutat Res 1979; 67:271–280.

(*18*) Hoffmann ME, Meneghini R. DNA strand breaks in mammalian cells exposed to light in the presence of riboflavin and tryptophan. Photochem Photobiol 1979; 29:299–303.

(*19*) Parshad R, Sanford KK, Jones GM, Tarone RE. Fluorescent light-induced chromosome damage and its prevention in mouse cells in culture. Proc Natl Acad Sci USA 1978; 75:1830–1833.

(*20*) Wang RJ, Ananthaswamy HN, Nixon BT, Hartman PS, Eisenstark A. Induction of single-strand DNA breaks in human cells by H_2O_2 formed in near-UV (black light)-irradiated medium. Radiat Res 1980; 82:269–276.

(*21*) Kohn KW, Erickson LC, Ewig RA, Friedman CA. Fractionation of DNA from mammalian cells by alkaline elution. Biochemistry 1976; 15:4629–4637.

DISCUSSION

N. Krinsky: I wonder if you would care to comment on the apparent presence of the DNA–protein cross-linking?

A. Eisenstark: We know that some cross-linking will persist in untreated cells. We check this by using still another mouse cell line (L1210) labeled with tritiated thymidine for 2 days. These control cells are always added to irradiated cells labeled with ^{14}C; thus we always do our experiments with two separate cell lines mixed together and we count the double labels. This provides an internal standard. Since the tritiated thymidine is always 5–10%, we choose a specific amount of ^{3}H label to compare with the ^{14}C. Our laboratory, as well as most other laboratories that use this elution technique, has chosen 10% as an internal standard; i.e., when 10% of the tritium remains on the filter, this is the figure that is compared with the ^{14}C-treated cells.

blank page

Tumor Virus Induction and Host Cell Capacity Inactivation: Possible In Vitro Tests for Photosensitizing Chemicals[1,2,3]

L. E. Bockstahler,[4] T. P. Coohill,[5] C. D. Lytle,[4] S. P. Moore,[5] J. M. Cantwell,[4] *and* B. J. Schmidt[4,6]

ABSTRACT—The responses of two in vitro mammalian virus-host cell systems to the photosensitizing chemicals proflavine sulfate and 8-methoxypsoralen (8-MOP) in the presence of light are described. Infectious simian virus 40 (SV40) could be induced from SV40-transformed hamster cells by treatment with proflavine plus visible light or 8-MOP plus near UV radiation. The same photosensitizing treatments inactivated the capacity of monkey cells to support the growth of herpes simplex virus. SV40 induction and inactivation of host cell capacity for herpesvirus growth might be useful as screening systems for testing the photosensitizing potential of chemicals. Advantages and disadvantages associated with each system are discussed.—JNCI 1982; 69:183–187.

Photosensitizing chemicals are unique in that exposures to both light and chemical are required for the production of photosensitized reactions. The most common chemically photosensitized reaction that occurs in humans is phototoxicity (*1–4*). The skin and eyes are the organs usually affected. Other reactions that can be induced by photosensitizing chemicals plus light include photoallergy (*1–4*) and photocarcinogenesis (*5*); however, the incidences of these reactions appear to be relatively small. UV or visible light from the sun or artificial light sources can elicit photosensitized reactions. Symptoms associated with chemically photosensitized reactions in humans and other clinical aspects are described elsewhere in these proceedings (*6–9*).

There are numerous known photosensitizing chemicals (*10*), and there is a need for the assessment of the photosensitizing potential of the hundreds of new chemicals placed on the market each year. Information useful for this assessment and for making effective risk–benefit decisions includes results from in vitro biological tests, animal studies, human clinical trials, and epidemiological investigations.

In vitro bacterial and mammalian cell systems for toxicity testing are valuable in that they can be used for large-scale prescreening. They yield relatively quick results and are generally less expensive than animal or human studies. Although numerous in vitro systems are available for chemical carcinogen testing, there has been little involvement in the development and utilization of such systems for the identification of potential photosensitizing chemicals. Examples of short-term tests that have been used for photochemical toxicity testing include the induction of bacterial and mammalian cell lethality, mutagenesis, and DNA-chromosome damage (*3, 11*).

In vitro tumor virus induction (*12, 13*) and inactivation of host cell capacity for virus growth (*14, 15*) are two mammalian virus-host cell systems that have been used extensively to investigate the phototoxic effects of UV radiation. The purpose of this report is to describe the responses of these systems to photosensitizing chemicals plus light. Two well-known chemical-light combinations, proflavine sulfate plus visible light and 8-MOP plus NUV radiation, were selected for photosensitization. The particular induction and capacity systems used were induction of SV40 from SV40-transformed hamster cells and inactivation of the capacity of monkey cells to serve as host cells for growth of herpes simplex virus. The results described suggest that these two systems might be useful as screens for potential photosensitizing chemicals.

TUMOR VIRUS INDUCTION

Several in vitro systems are available for investigating tumor virus induction by DNA-damaging agents (*12*). One of these is the SV40-transformed Syrian hamster kidney cell (clone E) system established by Kaplan et al. (*16*). In this inducible line the entire DNA genome of SV40 is integrated into the host cell DNA. Infectious SV40 can be induced by treatment of the cells with physical or chemical DNA-damaging agents such as UV radiation or mitomycin C (*13, 16*).

Induction of SV40 by photodynamic treatment of SV40-transformed cells with proflavine and visible light is shown in text-figure 1. The clone E line of SV40-transformed hamster cells (*16*) was used. Monolayers of clone E cells were treated with different concentrations of proflavine sulfate, irradiated with broadband radiation from fluorescent lamps (Sylvania "Daylight" fluorescent lamps, 26.7 W · m^{-2}) filtered with plate glass, and incubated (3 days) for virus expression. In addition to visible light, a relatively

ABBREVIATIONS USED: 8-MOP=8-methoxypsoralen; NUV=near UV; PFU=plaque-forming units; SV40=simian virus 40.

---

[1] Presented at the Seventh Food and Drug Administration Science Symposium ("Photochemical Toxicity: Toxic, Allergic, and Carcinogenic Aspects With Emphasis on Predicting Effects in Humans") held at the Uniformed Services University of the Health Sciences, Bethesda, Md., March 16–17, 1981.

[2] Part of the research was supported by contract No. 232-78-6018 from the Food and Drug Administration.

[3] The mention of commercial products, their sources, or their use in connection with material reported herein is not to be construed as either an actual or implied endorsement of such products by the Food and Drug Administration or the Department of Health and Human Services.

[4] Bureau of Radiological Health, Food and Drug Administration, Public Health Service, U.S. Department of Health and Human Services, 5600 Fishers Lane (HFX-120), Rockville, Md. 20857.

[5] Department of Biology, Western Kentucky University, Bowling Green, Ky. 42101.

[6] We thank L. D. Hester and L. C. James for help with the capacity studies, O. Ellingson for spectral irradiance measurements, J. C. Kaplan and P. H. Black for gifts of cell stock, and colleagues of the Bureau of Radiological Health for critical review of the manuscript.

small amount of NUV radiation was present; the plate glass effectively removed wavelengths of UV radiation below 320 nm. The amount of SV40 induced in each sample was determined by the measurement of the SV40 infectivity of cell extracts in permissive CV-1 monkey kidney cells. Further experimental details are given in (*17, 18*).

The maximum levels of SV40 induced for pretreatment with different proflavine concentrations (text-fig. 1) were similar in amount and represented about a thousandfold increase in virus production above the spontaneous background levels observed with untreated cells. As the concentration of proflavine was increased, less light exposure was needed to reach maximum virus induction. No virus induction above background levels was observed by treatment of the cells with either proflavine or light alone.

Induction of SV40 from clone E cells by treatment with 8-MOP plus NUV radiation is shown in text-figure 2. Monolayers of cells were treated with 0.1 m*M* 8-MOP, irradiated with 334 nm monochromatic NUV radiation, and incubated (4 days) for virus expression. The SV40 infectivity of cell extracts was determined by plaque assay in permissive CV-1 monkey kidney cells. Description of the irradiation system and further experimental details are given in (*15, 19*). NUV radiation plus 8-MOP gave a maximum induction level of approximately 5×10^3 above the spontaneous background level. Cell treatment with either NUV radiation alone or 8-MOP alone (text-fig. 2) did not induce virus above background levels. Experiments have also been conducted at additional wavelengths in the region 260–365 nm (*19*). 8-MOP was an effective photosensitizer for induction of SV40 at wavelengths tested between 302 and 365 nm. Wavelengths below 302 nm showed no consistently different response to 8-MOP plus UV radiation than to UV radiation alone.

The maximum levels of SV40 induced by either of the chemical photosensitization treatments described above were in excess of those observed with 254 nm UV radiation or γ-radiation of cells when the same induction system was utilized (*16, 19*).

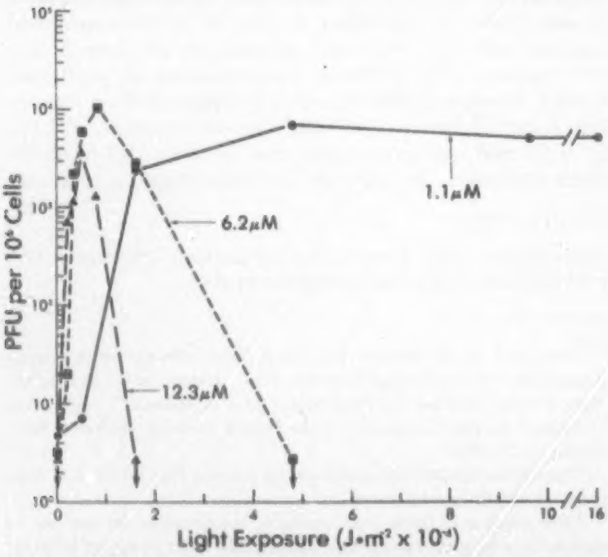

TEXT-FIGURE 1.—Induction of infectious SV40 from SV40-transformed hamster cells after treatment with proflavine plus visible light. Cultures of cells were pretreated with three different concentrations of proflavine sulfate, exposed to visible light, and incubated for virus expression. Induced virus was harvested and assayed for infectivity on permissive monkey cells. The induced virus yield is expressed as the average number of PFU per 10^6 cells. *Each point* represents the average of nine determinations (three separate experiments, in each of which cell extracts from three replicate samples were assayed once). Values lying below 3 PFU are lower than the detection limit of the assay and are indicated by points with *attached arrows*. Data from text-fig. 1B of (*17*) and text-fig. 1 of (*18*) are included.

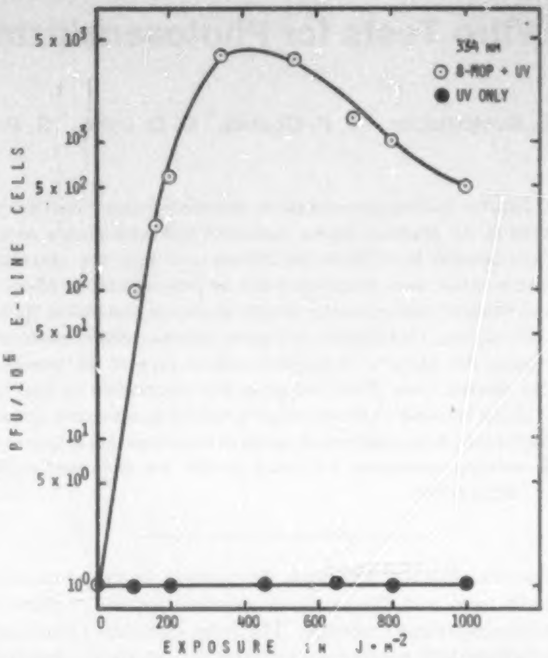

TEXT-FIGURE 2.—Induction of infectious SV40 from SV40-transformed hamster cells after treatment with 8-MOP plus NUV radiation. Same as text-fig. 1, except that cultures were either treated with 8-MOP (0.1 m*M*) and exposed to 334 nm UV radiation or treated with UV radiation alone. The data represent a typical experiment from (*19*).

INACTIVATION OF CAPACITY

The ability of a host cell to support virus growth is known as capacity. Inactivation of this cellular function can result from treatment of the cell with DNA-damaging agents. Herpes simplex virus, a DNA-containing human pathogenic virus, is particularly useful for mammalian cell capacity studies because it propagates in a wide variety of mammalian, including human, cells and has a relatively rapid growth cycle. Inactivation of host cell capacity for herpesvirus growth by UV irradiation (*14, 15*) and by chemical carcinogen treatment (*20*) has been investigated. In this section effects on capacity for herpesvirus growth by chemical photosensitization of host cells are described.

Inactivation of the capacity of CV-1 monkey kidney cells to support herpes simplex virus plaque formation by photodynamic treatment of the cells with proflavine and visible light is shown in text-figure 3. Confluent monolayers of CV-

1 cells were incubated with different concentrations of proflavine sulfate, exposed to broadband radiation from fluorescent lamps (Sylvania "White" fluorescent lamps, 17 W·m^{-2}) filtered with plate glass to remove UV radiation, and infected with herpes simplex virus (type 1). Virus growth was measured by plaque formation (2 days). Further experimental details are given in (*21*). The capacity curves in text-figure 3 are similar in shape to those obtained when the cells are UV irradiated (*15*). Inactivation of capacity was dependent on both light exposure time and dye concentration. A reciprocal relationship between these two variables was suggested from the data. That is, when the dye concentration was doubled, the radiation exposure needed to give a comparable effect was halved. Proflavine concentrations of 15 μM and higher in the dark resulted in cellular toxicity, as indicated by lowered plaque formation relative to the plaque formation in the untreated control. Light alone had no effect on plaque formation.

Use of the same capacity system to examine effects of 8-MOP plus NUV radiation is shown in text-figure 4. Confluent monolayers of CV-1 cells were incubated with 8-MOP at a concentration that had no effect on unirradiated monolayers (0.1 m*M*). The 8-MOP-treated monolayers and untreated controls were then treated with three different wavelengths of monochromatic NUV radiation and infected with herpesvirus. Virus growth was measured by plaque formation. Description of the radiation source and further experimental details are given in (*15, 22*). The results demonstrate inactivation of cell capacity for herpesvirus growth by treatment with NUV radiation plus 8-MOP. The exposures required to lower capacity in the presence of 8-MOP were about the same for UV radiation of wavelengths 320 and 327 nm. Little photosensitization due to 8-MOP occurred in the presence of 365 nm of UV radiation. For the wavelengths selected, no effect of UV radiation alone on cell capacity was observed. Further data obtained with this system have verified a wavelength dependence for 8-MOP-sensitized inactivation of capacity by UV radiation in the regions of 320–370 nm (*22*). The shorter wavelengths in this range were more effective than the longer ones. Little difference was observed between the responses of 8-MOP plus UV radiation and UV radiation alone at wavelengths 232–297 nm.

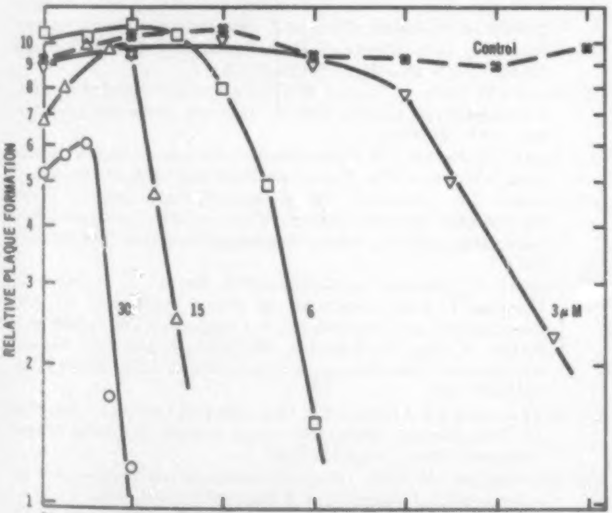

TEXT-FIGURE 3.—Inactivation by proflavine plus visible light of the capacity of monkey cells to support the growth of herpes simplex virus. The light intensity was 17 W·m^{-2}. Concentrations of proflavine were 0 μM (X), 3 μM (▽), 6 μM (□), 15 μM (△), and 30 μM (○). Virus infection immediately followed photodynamic treatment. Virus growth was measured by plaque formation. The data represent a typical experiment from (*21*).

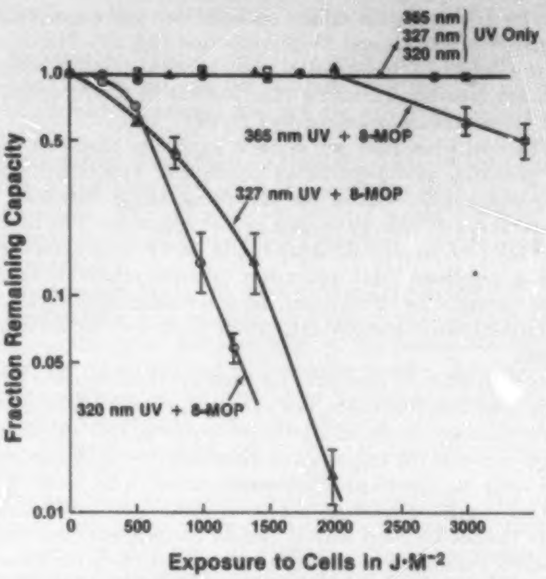

TEXT-FIGURE 4.—Inactivation by 8-MOP plus NUV radiation of the capacity of monkey cells to support the growth of herpes simplex virus. Cultures of cells were either treated with 8-MOP (0.1 m*M*) and exposed to UV radiation (*open symbols*) or treated with UV radiation alone (*closed symbols*). Wavelengths of UV radiation (in nanometers) are indicated. Virus infection immediately followed UV radiation exposure. Virus growth was measured by plaque formation. *Each curve* represents an average of three or more experiments. The data are from text-fig. 3 of (*22*).

DISCUSSION

The studies reviewed demonstrate the treatment with proflavine plus visible light or 8-MOP plus NUV radiation can inactivate the capacity of monkey cells to support the growth of herpesvirus and can induce SV40 from SV40-transformed hamster cells. Although the mechanisms of tumor induction and host cell capacity inactivation by chemical photosensitization are unknown, DNA damage is likely to be involved. It is known that both of the treatments described can damage DNA (*23, 24*). In general, DNA-damaging agents are efficient inducers of tumor viruses and inactivators of capacity.[7] UV radiation action spectrum studies have shown that DNA is an important target mole-

---

[7] An exception is X-ray treatment, which has relatively little effect on the capacity of monkey cells for herpesvirus growth (*25*).

best copy available

cule for UV radiation effects on both host cell capacity for herpesvirus growth and SV40 induction (*15*, *26*). However, other effects of UV radiation and chemical photosensitization are possible including inactivation of RNA, protein, and other cellular constituents (*23*, *24*).

The two virus–host cell systems might be useful as tests for potential photosensitizing chemicals. Treatment with microgram quantities of the photosensitizing chemicals in the presence of light gave measurable responses. The reproducibility of results obtainable should be satisfactory for testing purposes. Each procedure permits relatively large-scale testing. One of the tests, capacity inactivation, can be performed with human cells from a variety of different tissues.

As with most in vitro tests for toxicity, these systems have associated disadvantages. For example, virology laboratory experience and facilities would be required. Critical differences between the responses of virus-infected cells and normal cells to chemical photosensitization may exist. For several technical reasons, the virus induction system presently cannot be used with a variety of different host cells. Limited validation of the tests has been made with known photosensitizing and nonphotosensitizing chemicals. It is not known whether the systems would respond to treatments that cause primarily cell membrane damage.

The results described indicate that for screening purposes it would be important to use several different concentrations of chemical, light exposure times, and wavelengths of light. Knowledge of the light absorption spectrum for each chemical would be useful in helping select the appropriate wavelength band of light for irradiation. Use of broadband radiation is recommended so that the absorption bands of different chemicals would be included. The action spectra for clinical drug-induced photosensitivities are usually similar to the absorption spectra for phototoxic reactions and incude higher wavelengths than the absorption spectra for photoallergic reactions (*3*). Most known chemical-induced phototoxic and photoallergic reactions have action spectra in the UV radiation region of the spectrum between 320 and 380 nm (*3*). Little is known about action spectra for chemical photocarcinogenesis.

REFERENCES

(*1*) Jarratt M. Drug photosensitization. Int J Dermatol 1976; 15:317–325.

(*2*) Baer RI, Harber LC. Photosensitivity induced by drugs. JAMA 1965; 192:147–148.

(*3*) Parrish JA, Anderson RR, Urbach F, Pitts D. UV-A: Biological effects of ultraviolet radiation with emphasis on human responses to longwave ultraviolet. New York: Plenum, 1978:141–155.

(*4*) Epstein JH. Phototoxicity and photoallergy: Clinical syndromes. In: Fitzpatrick TB, Pathak MA, Harber LC, Seiji M, Kukita A, eds. Sunlight and man: Normal and abnormal photobiologic responses. Tokyo: Univ Tokyo Press, 1974:459–477.

(*5*) Stern RS, Thibodeau LA, Kleinerman RA, Parrish JA, Fitzpatrick TB. Risk of cutaneous carcinoma in patients treated with oral methoxsalen photochemotherapy for psoriasis. N Engl J Med 1979; 300:809–813.

(*6*) Epstein JH. Photochemical toxicity in humans. JNCI 1982; 69:265–268.

(*7*) Kligman A, Kaidbey KH. Human models for identification of photosensitizing chemicals. JNCI 1982; 69:269–272.

(*8*) Mathews-Roth MM. Photosensitization by porphyrins and prevention of photosensitization by carotenoids. JNCI 1982; 69:279–285.

(*9*) Lerman S. Ocular phototoxicity and psoralen plus UV radiation (320–400 nm) therapy: An experimental and clinical evaluation. JNCI 1982; 69:287–302.

(*10*) Fitzpatrick TB, Pathak MA, Harber LC, Seiji M, Kukita A. An introduction to the problem of normal and abnormal responses of man's skin to solar radiation. In: Fitzpatrick TB, Pathak MA, Harber LC, Seiji M, Kukita A, eds. Sunlight and man: Normal and abnormal photobiologic responses. Tokyo: Univ Tokyo Press, 1974:3–14.

(*11*) Ashwood-Smith MJ, Poulton GA, Barker M, Mildenberger M. 5-Methoxypsoralen, an ingredient in several suntan preparations, has lethal, mutagenic and clastogenic properties. Nature 1980; 285:407–409.

(*12*) Bockstahler LE, Hellman KB. Induction of oncogenic viruses by light. Photochem Photobiol 1979; 30:743–748.

(*13*) Zamansky GB, Little JB, Black PH, Kaplan JC. Inhibition of postreplication repair and the enhancement of induction of SV40 virus from transformed hamster kidney cells. Mutat Res 1978; 51:109–119.

(*14*) Lytle CD. Radiation-enhanced virus reactivation in mammalian cells. Natl Cancer Inst Monogr 1978; 50:145–149.

(*15*) Coohill TP, Moore SP, Drake S. The wavelength dependence of ultraviolet inactivation of host capacity in a mammalian cell–virus system. Photochem Photobiol 1977; 26:387–391.

(*16*) Kaplan JC, Wilbert SM, Collins JJ, Rakusanova T, Zamansky GB, Black PH. Isolation of simian virus 40-transformed inbred hamster cell lines heterogeneous for virus induction by chemicals or radiation. Virology 1975; 68:200–214.

(*17*) Bockstahler LE, Cantwell JM. Photodynamic induction of an oncogenic virus in vitro. Biophys J 1979; 25:209–213.

(*18*) Bockstahler LE. Induction and enhanced reactivation of mammalian viruses by light. Prog Nucleic Acid Res Mol Biol 1981; 26:303–313.

(*19*) Moore SP, Coohill TP. The effect of 8-methoxypsoralen on the activation of latent tumor viruses from mammalian cells. In: Symposium on biological effects and measurement of light sources. Rockville, Md.: Bureau of Radiological Health, 1981:216–225 [DHHS publication No. (FDA)81-8156].

(*20*) Lytle CD, Coppey J, Taylor WD. Enhanced survival of ultraviolet-irradiated herpes simplex virus in carcinogen-pretreated cells. Nature 1978; 272:60–62.

(*21*) Lytle CD, Hester LD. Photodynamic treatment of herpes simplex virus infection in vitro. Photochem Photobiol 1976; 24:443–448.

(*22*) Coohill TP, James LC. The wavelength dependence of 8-methoxypsoralen photosensitization of host capacity inactivation in a mammalian cell–virus system. Photochem Photobiol 1979; 30:243–246.

(*23*) Mizuno N, Tsuneishi S, Matsuhashi S, Kimura S, Fujimura Y, Ushijima T. Some aspects on the action mechanism of 8-methoxypsoralen photosensitization. In: Fitzpatrick TB, Pathak MA, Harber LC, Seiji M, Kukita A, eds. Sunlight and man: Normal and abnormal photobiologic responses. Tokyo: Univ Tokyo Press, 1974:389–409.

(*24*) Bockstahler LE, Coohill TP, Hellman KB, Lytle CD, Roberts JR. Photodynamic therapy for herpes simplex: A critical review. Pharmacol Ther 1979; 4:473–499.

(*25*) Bockstahler LE, Lytle CD. X-ray enhanced reactivation of ultraviolet-irradiated human virus. J Virol 1971; 8:601–602.

(*26*) Coohill TP, Moore SP, Knauer DJ, Fry D, Eichenbrenner TJ, Bockstahler LE. The wavelength dependence of ultraviolet radiation activation of latent tumor viruses from mammalian cells. In: Symposium on biological effects and measurement of light sources. Rockville, Md.: Bureau of Radiological Health, 1981:208–215 [DHHS publication No. (FDA)81-8156].

DISCUSSION

Anonymous: Have you looked at other psoralens as inducing agents, for example, in particular, 5-methoxypsoralen (5-MOP)?

L. E. Bockstahler: No, we have not been in the business of examining photosensitizing chemicals very long. We are interested in the different psoralens like 5-MOP. One would expect that 5-MOP would induce SV40. I know that Dr. M. J. Ashwood-Smith has shown that 5-MOP is active in a variety of in vitro test systems, so I would expect that it should give a positive response with our systems.

We are also interested in using some of the furocoumarins that do not make cross-links between the DNA strands, such as angelicin. We need to make sure that nonphotosensitizing chemicals do not give positive responses with our test systems.

E. Riklis: One basic question is that you are taking a target, which is actually viral DNA, and you are inserting this into a cell which has been treated; the viral DNA itself is not pretreated?

Bockstahler: Are you talking about the inactivation of capacity system?

Anonymous: Right.

Bockstahler: That is right. The virus is not treated.

Anonymous: So you are actually treating just the cell with the photosensitizer and not the entire virus-host cell system?

Bockstahler: Yes, When we treat the cells, we believe that DNA is the primary target; however, we have not really shown that. The response we observe might be due, for example, to a membrane effect. We have not really tested this possibility.

Anonymous: Have you tried treating the virus?

Bockstahler: Yes, in separate experiments we have tried treating the virus. For example, in the proflavine experiment, Dr. Lytle carried out separate studies showing that you can inactivate the virus alone by treating with proflavine plus visible light and then infecting.

F. Urbach: Do you get repair of this photodynamic damage to the virus?

Bockstahler: We really have not shown that. We need normal cells and a cell line in which we know that there is no repair of that type of damage—that is, a xeroderma pigmentosum-type-cell—and we do not have that yet.

blank page

Comparative Photobiology of Psoralens[1]

M. J. Ashwood-Smith,[2] **A. T. Natarajan,**[3] *and* **G. A. Poulton**[4]

ABSTRACT—The comparative photobiological effects of several furocoumarins [i.e., angelicin, psoralen, 8-methoxypsoralen (8-MOP), and 5-methoxypsoralen (5-MOP)] have been evaluated in a number of biological systems. The photosensitized induced lethality and genetic damage have been assessed in bacterial, animal, and human cells, and the rank order of effectiveness established psoralen as the most active compound followed by 8-MOP, 5-MOP, and angelicin. 5-MOP and 8-MOP are, however, essentially equally active in the production of chromosome damage in human cells in vitro.—JNCI 1982; 69:189–197.

The basic photobiology of furocoumarins has been the subject of two excellent and recent reviews by Song and Tapley (*1*) and by Parsons (*2*). That 8-MOP is a skin carcinogen in mice (*3*) has now been substantiated by a number of workers (*4*). The possibility that 8-MOP is a skin photocarcinogen in humans has been suggested by Stern et al. (*5*) after a careful analysis of the incidence of skin cancer in patients following PUVA therapy for psoriasis. The suggestion that PUVA therapy might prove to be carcinogenic was made by Ashwood-Smith and Grant (*6*) as a result of experimental studies of psoralens with Chinese hamster cells (*7*). Concerns about the safety of 5-MOP (bergaptene), an active ingredient of several suntan preparations, was expressed by Ashwood-Smith (*8*), and preliminary results concerning the photobiology of 5-MOP were published in 1980 (*4*).

The structure of 5-MOP as well as the structures of psoralen, angelicin, and 8-MOP is shown in text-figure 1. Recent work by Zajdela and Bisagni (*9*) at the Radium Institute in Paris, France, has clearly demonstrated that 5-MOP is almost as potent a skin photocarcinogen in mice as is 8-MOP. This paper presents the results of recent studies on the comparative photobiology of a number of furocoumarins including 5-MOP. The studies presented are joint work conducted in Canada and The Netherlands.

METHODS

Details of irradiation, furocoumarin chemistry, methodology, cell culture, and cytogenetics have been previously presented (*4*, *10*).

RESULTS AND DISCUSSION

The relative lethal photosensitizing activities toward bacteria of a series of furocoumarins examined at 40 μg/ml are illustrated in text-figure 2, and the mutation induction (try^- to try^+ for *Escherichia coli* WP2) is shown in text-figure 3. The rank order from the most active furocoumarin to the least was psoralen > 8-MOP > 5-MOP > angelicin for both lethal and mutagenic activities. For dark-induced frame shift mutation (*E. coli* $lac^- \rightarrow lac^+$), however, the rank order was psoralen > angelicin > 8-MOP > 5-MOP.

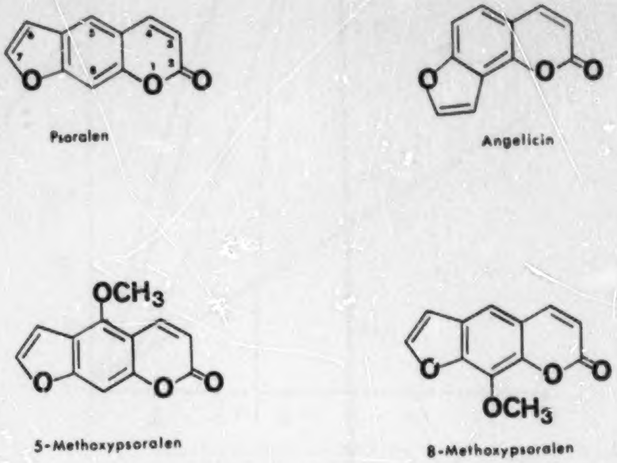

TEXT-FIGURE 1. —Chemical structures of furocoumarins.

The photosensitized killing of CHO cells in tissue culture is illustrated in text-figure 4. These results were obtained with the use of the standard Puck-type colony survival assays. Neither the UV irradiation nor the furocoumarins per se had any effect on cell survival. Again, at 40 μg/ml, the rank order was psoralen > 8-MOP > 5-MOP > angelicin. The induction of SCE in CHO cells is illustrated in text-figure 5. The responses to 5-MOP and 8-MOP were very similar and were typical. Angelicin (monoadduct formation only) was quite different, which is clearly apparent when SCE were plotted as a function of cell survival (text-fig. 6). Events other than observable damage to chromosomes were related to cellular death from angelicin photosensitization.

The responses of CHO cells to SCE are shown in table 1 in which the data are analyzed by the "unit dose concept"

ABBREVIATIONS USED: AT=ataxia telangiectasia; CHO=Chinese hamster ovary; 5-MOP=5-methoxypsoralen; 8-MOP=8-methoxypsoralen; NUV=near ultraviolet; PUVA=psoralen plus UV radiation (320–400 nm); SCE=sister chromatid exchange(s); UVA=UV, 320–400 nm; XP=xeroderma pigmentosum.

---

[1] Presented at the Seventh Food and Drug Administration Science Symposium ("Photochemical Toxicity: Toxic, Allergic, and Carcinogenic Aspects With Emphasis on Predicting Effects in Humans") held at the Uniformed Services University of the Health Sciences, Bethesda, Md., March 16–17, 1981.

[2] Environmental Toxicology Research Group, Department of Biology, University of Victoria, P.O. Box 1700, British Columbia V8W 2Y2, Canada.

[3] Department of Radiation Genetics and Chemical Mutagenesis, State University of Leiden, Leiden, The Netherlands.

[4] Department of Chemistry, University of Victoria.

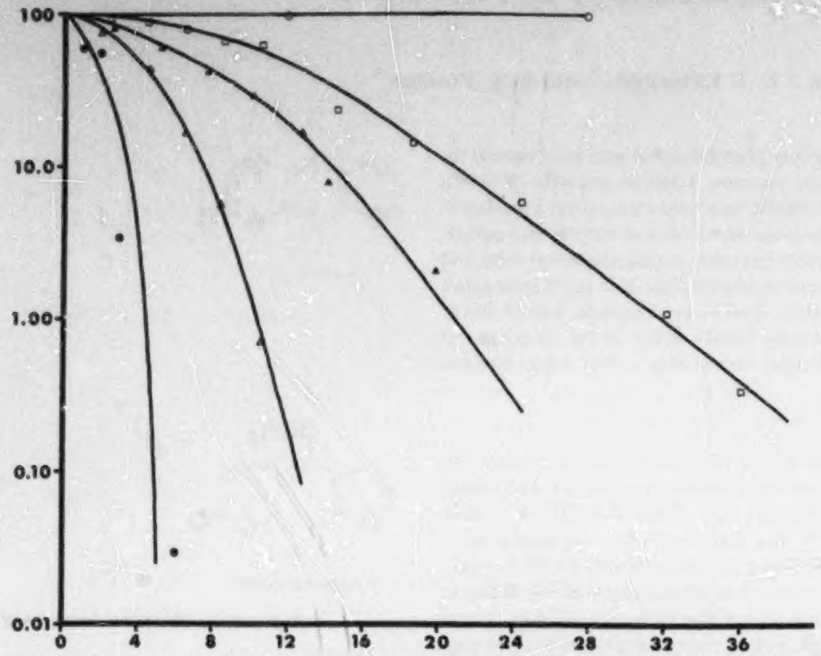

TEXT-FIGURE 2.—Lethal photosensitization of *E. coli* with various furocoumarins (40 µg/ml each). ●=psoralen; △=8-MOP; ▲=5-MOP; □=angelicin; ○=ethanol control. *E. coli* WP2 (*try*$^-$) was grown in nutrient broth at 22°C, and when bacteria were at a density of $\approx 5\times10^8$ cells/ml (logarithmic growth stage), they were filtered and resuspended in 0.07 *M* phosphate buffer at pH 7.2 before being irradiated for 5 min after addition of the furocoumarins. NUV radiation (320–380 nm) was produced by two parallel GEC black lamps (F20T12.BLB) emitting 13.4 $J\cdot m^{-2}$ as measured by chemical actinometry. Cells were plated on nutrient agar and colonies counted after 24 hr of incubation at 37°C. *Ordinate*: survival (%). *Abscissa*: NUV fluence (10^{-2} $J\cdot m^{-2}$).

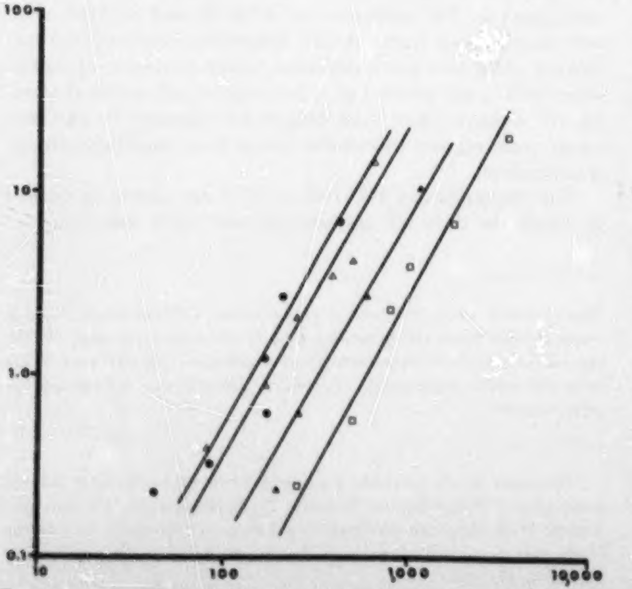

TEXT-FIGURE 3.—Mutagenesis in *E. coli* induced by furocoumarins (40 µg/ml) and NUV light. ●=psoralen; △=8-MOP; ▲=5-MOP; □=angelicin. *E. coli* WP2 (*try*$^-$) was grown as described in text-fig. 2 legend. Cell preparation and irradiation conditions were identical. Mutant (*try*$^+$) cells were detected on plates containing minimal agar 48 hr after incubation. *Ordinate*: log mutants per 10^8 viable cells. *Abscissa*: NUV fluence (log $J\cdot m^{-2}$).

of Burger and Simons (*11*) which is expressed as [observed SCE per cell/concentration of psoralen (µg/ml)×$J\cdot m^{-2}$]=*K*, the constant for any given psoralen. 5-MOP and 8-MOP gave values of 1.7×10^{-3} and 2.9×10^{-3}, respectively, while angelicin gave a lower yield of SCE at 5.8×10^{-4}.

The responses of human diploid fibroblasts (foreskin), AT cells, and XP cells to furocoumarins are shown in table 2. With normal cells 5-MOP resulted in 4.5×10^{-3} SCE/unit dose; the value of 8-MOP was 3.7×10^{-3}, and that for angelicin was 8.0×10^{-4}. These values are in surprisingly good agreement with the values obtained with CHO cells. They do, however, indicate that human cells are, in general, more sensitive to furocoumarins than are CHO cells and that 5-MOP and 8-MOP yield essentially the same number of SCE. The responses of AT and XP cells to the formation of SCE are illustrated in text-figure 7 and table 3. The increased sensitivity of AT and XP cells to angelicin is most interesting. Work is presently being done to see if AT heterozygotes are sensitive to angelicin inasmuch as it has been demonstrated that the individuals with AT are more prone to cancer than normal individuals (*12*). Chromosome breaks and exchanges in normal, AT, and XP cells were produced by 5-MOP, 8-MOP, and angelicin (table 3). All three furocoumarins produced considerably more aberrations in AT and XP cells than in normal human cells.

The formation of SCE in human peripheral blood lymphocytes has been reviewed by Burger and Simons (*11*) and is illustrated in table 4.

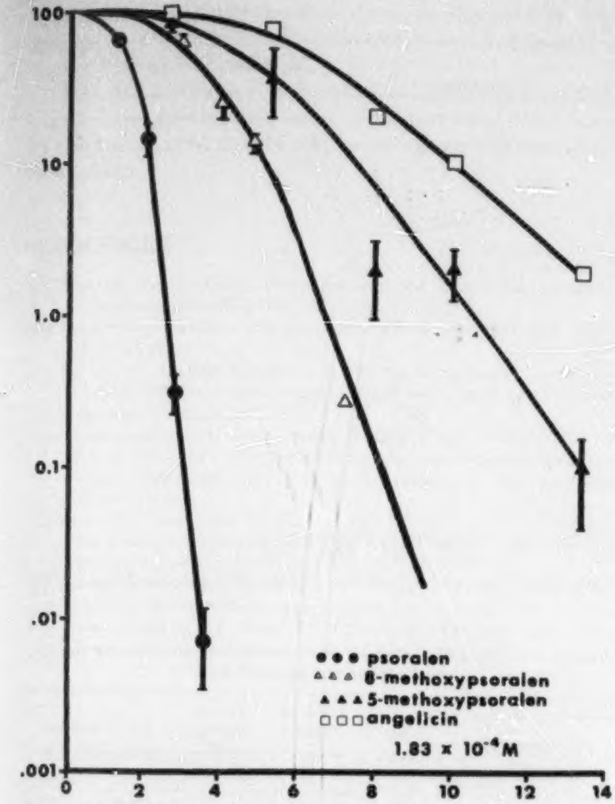

TEXT-FIGURE 4.—Lethal photosensitization of CHO cells by furocoumarins. *Ordinate*: percent cell survival (log). *Abscissa*: UVA fluence (J·m^{-2}×10^{-2}). Compounds were used at a final concentration of 40 μg/ml. Results are means ± SD.

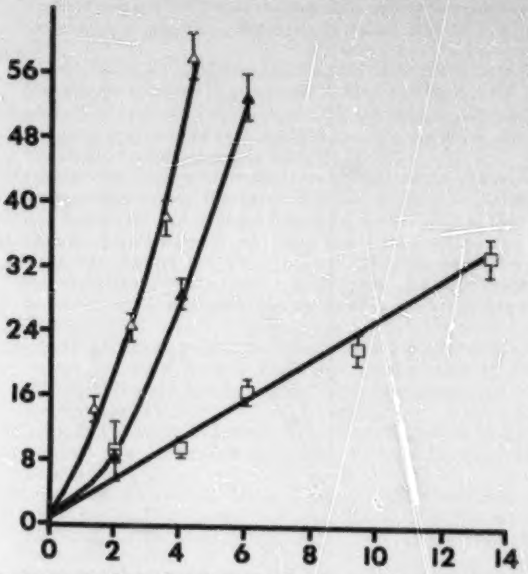

TEXT-FIGURE 5.—Induction of SCE in CHO cells by UVA radiation and furocoumarins. △=8-MOP; ▲=5-MOP; □=angelicin. *Ordinate*: average number of SCE per cell. *Abscissa*: NUV fluence (J·m^{-2}×10^{-2}). Compounds were used at a final concentration of 40 μg/ml. Results are means ± SE.

TABLE 1.—*Induction of SCE in CHO cells by furocoumarins and UVA radiation*

Furocoumarin[a]	UVA radiation, J·m^{-2}	No. of SCE/cell	No. of SCE/unit dose	Average No. of SCE/unit dose
Angelicin	201	7.23	8.9×10^{-4}	5.8×10^{-4}
	402	9.83	6.1×10^{-4}	
	603	16.53	6.8×10^{-4}	
	938	29.93	5.8×10^{-4}	
	1,346	33.73	1.6×10^{-4}	
5-MOP	201	8.50	1.0×10^{-3}	1.7×10^{-3}
	402	28.77	1.8×10^{-3}	
	603	53.26	2.2×10^{-3}	
8-MOP	134	14.6	2.7×10^{-3}	2.9×10^{-3}
	241	24.6	2.5×10^{-3}	
	348	38.5	2.8×10^{-3}	
	429	58.7	3.4×10^{-3}	

[a] All furocoumarins were used at a concentration of 40 μg/ml.

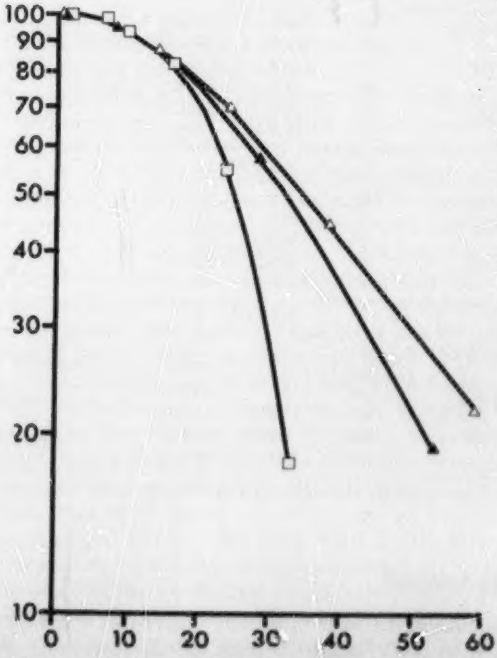

TEXT-FIGURE 6.—Survival of CHO cells as a function of the number of induced SCE per cell following photosensitization with furocoumarins. *Ordinate*: percent cell survival (log). *Abscissa*: SCE per cell. △=8-MOP; ▲=5-MOP; □=angelicin. Compounds were used at a final concentration of 40 μg/ml.

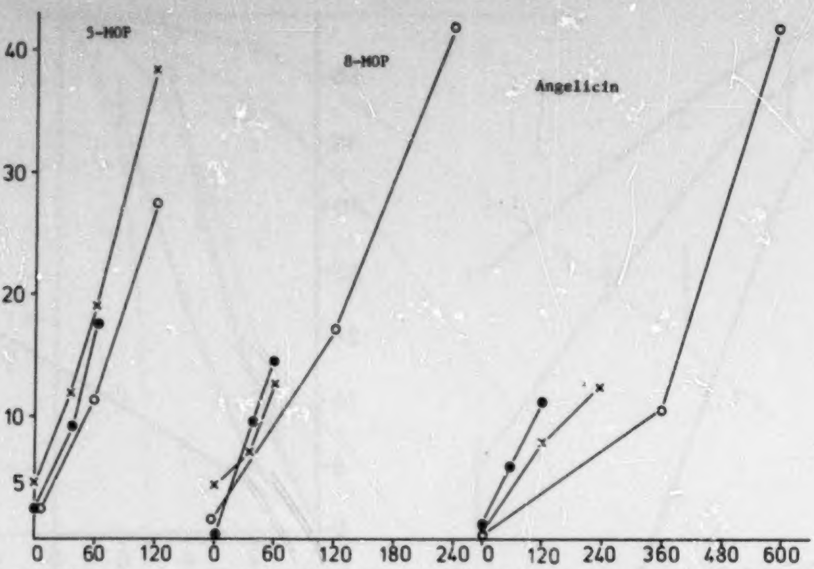

TEXT-FIGURE 7.—Induction of SCE in normal human diploid foreskin cell line (VH), AT cell line, and XP cell line. *Ordinate*: SCE per cell. *Abscissa*: UVA exposure in J·m^{-2}. ○=VH; ×=AT cells; ●=XP cells.

TABLE 2.—*Induction of SCE in human cells by furocoumarins and UVA radiation*

Furocoumarin[a]	UVA radiation, J·m^{-2}	No. of SCE/cell	No. of SCE/unit dose	Average No. of SCE/unit dose
		Human diploid fibroblasts		
Angelicin	360	10.2	7.0×10^{-4}	8.0×10^{-4}
	600	22.1	9.0×10^{-4}	
5-MOP	60	10.4	4.1×10^{-3}	4.5×10^{-3}
	120	24.4	5.0×10^{-3}	
8-MOP	120	15.7	3.3×10^{-3}	3.7×10^{-3}
	240	40.3	4.2×10^{-3}	
		AT cells		
Angelicin	120	8.0	1.7×10^{-3}	1.7×10^{-3}
5-MOP	36	8.2	5.6×10^{-3}	4.8×10^{-3}
	60	10.4	4.1×10^{-3}	
8-MOP	36	2.8	2.1×10^{-3}	3.1×10^{-3}
	60	8.9	4.1×10^{-3}	
		XP cells		
Angelicin	60	6.3	2.6×10^{-3}	2.3×10^{-3}
	120	9.6	2.1×10^{-3}	
5-MOP	36	7.1	4.9×10^{-3}	5.3×10^{-3}
	60	13.7	5.8×10^{-3}	
8-MOP	36	9.3	8.4×10^{-3}	6.2×10^{-3}
	60	14.4	6.0×10^{-3}	

[a] All furocoumarins were used at a concentration of 40 μg/ml.

CONCLUSIONS

Furocoumarins such as 8-MOP and 5-MOP when combined with NUV radiation have lethal, mutagenic, clastogenic, and carcinogenic effects. The unit dose concept of Burger and Simons (*11*) clearly indicates that setting an upper limit of furocoumarin concentration is meaningless inasmuch as a low concentration of furocoumarin and a

TABLE 3.—*Calculated number of chromosomal aberrations (breaks and exchanges) per unit dose*[a]

Furocoumarin	Cell type[b]	UVA radiation dose, J·m^{-2}	No. of aberrations/100 cells	No. of aberrations/unit dose
Angelicin	VH	240	2	0.021×10^{-4}
	AT	240	21	0.21×10^{-4}
	XP	240	28	0.29×10^{-4}
	VH	600	29	0.12×10^{-4}
	AT	600	80	0.33×10^{-4}
	XP	600	124	0.52×10^{-4}
5-MOP	VH	60	3	0.13×10^{-4}
	AT	60	7	0.31×10^{-4}
	XP	60	26	1.12×10^{-4}
	VH	120	35	0.72×10^{-4}
	AT	120	63	1.34×10^{-4}
	XP	120	103	2.12×10^{-4}
8-MOP	VH	120	26	0.52×10^{-4}
	AT	120	134	2.83×10^{-4}
	XP	120	70	1.53×10^{-4}
	VH	240	126	1.33×10^{-4}
	AT	240	256	2.72×10^{-4}
	XP	240	261	2.73×10^{-4}

[a] Numbers were calculated per μg furocoumarin/ml per J·m^{-2} based on data obtained at different NUV doses. Spontaneous and furocoumarin-induced aberrations have been deleted from these calculations.

[b] VH = human foreskin cells.

TABLE 4.—*Induction of SCE in human lymphocytes by 8-MOP and UVA radiation*

Investigator	Concentration, μg/ml	UVA radiation, J·m^{-2}	No. of SCE/unit dose
Carter et al. (*13*)	0.158	7,500	6.9×10^{-3}
	0.158	22,500	6.9×10^{-3}
Waksvik et al. (*14*)	25.0	471	6.5×10^{-4}
	50.0	314	3.0×10^{-4}
Gaynor et al. (*15*)	0.02	9,000	3.1×10^{-2}
	0.10	9,000	1.2×10^{-2}

large dose of light will result in the same degree of genetic damage as a higher concentration of furocoumarin and a smaller dose of UV radiation.

These compounds are very potent monoadduct and DNA cross-linking agents that, when combined with light, have an effect similar to that of alkylating agents and should be so classified.

REFERENCES

(*1*) Song PS, Tapley KJ Jr. Photochemistry and photobiology of psoralens. Photochem Photobiol 1979; 29:1177–1197.

(*2*) Parsons BJ. Psoralen photochemistry. Photochem Photobiol 1980; 32:813–821.

(*3*) Griffin AC, Hakim RE, Knox J. The wavelength effect upon erythemal and carcinogenic response in psoralen treated mice. J Invest Dermatol 1958; 31:289–295.

(*4*) Ashwood-Smith MJ, Poulton GA, Barker M, Mildenberger M. 5-Methoxypsoralen, an ingredient in several suntan preparations, has lethal, mutagenic and clastogenic properties. Nature 1980; 285:407–409.

(*5*) Stern RS, Thibodeau LA, Kleinerman RA, et al. Risk of cutaneous carcinoma in patients treated with oral methoxsalen photochemotherapy for psoriasis. N Engl J Med 1979; 300:809–813.

(*6*) Ashwood-Smith MJ, Grant EL. Chromosome damage produced by psoralen and ultraviolet light. Br Med J 1976; 1:342–343.

(*7*) Ashwood-Smith MJ, Grant EL, Heddle JA, Friedman GB. Chromosome damage in Chinese hamster cells sensitized to near-ultraviolet light by psoralen and angelicin. Mutat Res 1977; 43:377–385.

(*8*) Ashwood-Smith MJ. Possible cancer hazard associated with 5-methoxypsoralen in suntan preparations. Br Med J 1979; 2:1144.

(*9*) Zajdela F, Bisagni E. 5-Methoxypsoralen, the melanogenic additive in suntan preparations is tumorigenic in mice exposed to 365 nm UV radiation. Carcinogenesis 1981; 2:121–127.

(*10*) Natarajan AT, Verdegaal-Immerzeel EA, Meijer M, Zoetelief J, Ashwood-Smith MJ. Cytogenic response of ataxia telangiectasia cells to physical and chemical mutagens. In: Bridges BA, Harnden DG, eds. Ataxia telangiectasia. New York: Wiley. In press.

(*11*) Burger PM, Simons JW. Mutagenicity of 8-methoxypsoralen and long-wave ultraviolet irradiation in diploid human skin fibroblasts. An improved risk estimate in photochemotherapy. Mutat Res 1979; 63:371–380.

(*12*) Swift M. Malignant neoplasms in heterozygous carriers of genes for certain autosomal recessive syndromes. In: Mulvihill JJ, Miller RW, Fraumeni JF Jr, eds. Genetics of human cancer. New York: Raven, 1977:209–215.

(*13*) Carter DM, Wolff K, Schnedl W. 8-Methoxypsoralen and UVA promote sister chromatid exchanges. J Invest Dermatol 1976; 67:548–551.

(*14*) Waksvik H, Brogger A, Stene J. Psoralen/UVA treatment and chromosomes. I. Aberration and sister chromatid exchange in human lymphocytes in vitro and synergism with caffeine. Hum Genet 1977; 38:195–207.

(*15*) Gaynor AL, Carter DM. Greater promotion in sister chromatid exchanges by trimethylpsoralen than by 8-methoxypsoralen in the presence of UV light. J Invest Dermatol 1978; 71:257–259.

DISCUSSION

R. Goldemberg: I wish to ask a very simple question. A cosmetic preparation or sunscreen must contain enough 5-MOP to darken the skin. Is the amount necessary for the effect dangerous, for manufacturers of cosmetics and sunscreens are not interested in putting less 5-MOP than is necessary to create this effect? In other words, is there a safe level of 5-MOP in sunscreens and cosmetics?

M. J. Ashwood-Smith: I suppose I shouldn't be answering this question. But I can tell you that one of the legitimate industry objections is that the conditions of human dermal exposure and cellular exposure in vitro are different. 5-MOP or 8-MOP is being added as an alcoholic or acetone—in this case an alcoholic—solution to a cell culture. The reaction of the skin cell can be different when exposed to 5-MOP or 8-MOP in oil in the presence of many other compounds and chemical filtering agents, and the in vitro reaction may not be true in vivo.

I have quantitative information (now being prepared for presentation) that application of one of the suntan preparations to a monolayer of CHO cells followed by exposure to UV light leads to extensive cell death within 2 days. A few remaining cells have a large proportion of chromosome aberrations.

K. Kraemer: I am intrigued by your comments about the response of AT and XP cells to angelicin. Recently, M. C. Paterson and P. J. Smith have shown that cell lines are heterogeneous in their sensitivity to 4-nitroquinoline oxide, although the AT cell lines seem to be equally sensitive to X-rays. Also, use of other agents shows sensitivity differences among different AT cell lines, and it is well known that different XP patients have different degrees of defects. Have you tested more than one XP cell line?

Ashwood-Smith: At the moment, this is being done in Holland.

E. DeFabo: I understand that 5-MOP is a derivative of bergamot oil. Is it a light-induced derivative?

Ashwood-Smith: No, it is a constituent.

DeFabo: It is a constituent of the oil?

Ashwood-Smith: 5-MOP comprises about 0.3% of unpurified bergamot oil. The unpurified oil is commercially available and its 5-MOP content varies. Bergamot oil contained other psoralens. In fact, we have added different concentrations of different psoralens to see if there is interference, which is a possibility. At the moment, the data do not show that there is interference; i.e., there is no synergism, just straight additivity. But the data are scanty at this stage.

L. Freeman: Speaking for those of us interested in the power of in vitro and animal models to predict human responses, I am concerned with the magnitude of the jump you are making and I want to see if I am justified. Certainly, angelicin showed signs of problematic biological activity including, in one case at least, increased lethality. The presumption, I believe, is that it is not a photocarcinogen because it forms a monoadduct. Do you know if that presumption has been tested? If, as I believe, it is not a photocarcinogen, doesn't that raise some doubts about the adequacy of the translation between systems?

Ashwood-Smith: To the best of my knowledge, I am not sure about the assumption that a monoadduct-forming compound is not likely to be dangerous. Angelicin forms monoadducts and not cross-links. There are suggestions that in simple systems cross-links kill and monoadducts give rise to mutations. Therefore, my feeling is that angelicin might turn out to be a photocarcinogen as well if it were properly tested. But it has not been tested.

I can only rest my case on the results of our studies. We showed that angelicin and psoralen caused a lot of chromosome damage. As a result, Elizabeth Grant and I wrote a letter to the *British Medical Journal* suggesting that whatever its benefits, the phototherapy of psoriasis might lead to cancers.

We now all believe that this suggestion is probably valid. We are not certain if psoralens are direct carcinogens, promoters, or affectors of the immune system, or if they exert all three effects. So, I think the extrapolation we made from similar experiments in 1976, which seemed to be only too true, gives some credence to today's extrapolation as well. But I do make the point that, if pigment forms, it may well protect against future skin cancer production. I worry about what happens before the pigment forms and, as you know, that is a subject about which we do not have all the information.

F. Urbach: Have you done the same battery of studies with photodynamic agents, i.e., with anthracene, the dyes, or porphyrin? Do similar things happen with visible light?

Ashwood-Smith: We might have done such a study occasionally, but not deliberately, when we had hemoglobin in the serum.

R. Sayre: Everyone keeps saying how protective pigment really is. It really is not. This morning, a slide was presented that showed that short wavelengths were attenuated in the stratum corneum, longer wavelengths in the epidermis, and only UVA radiation and visible radiation penetrate the dermis.

Let me assure you that you will find some radiation of any wavelength you want to look for passing through the entire epidermis and dermis if you use radiation-detecting equipment that is sensitive enough. The concept that light is stopped by a few cell layers or at a certain skin depth must be wrong; also, the concept that a tan protects us must not be very good when we consider that a fairly dark-skinned person can suffer sunburns when exposed only to four to six times the energy that produces a sunburn in a light-skinned person. The fact that 5-MOP produces a skin pigment does not mean that light will not get through the skin to produce whatever adverse effect we are interested in.

The Food and Drug Administration (FDA) should perhaps be aware that enough adverse evidence is now available to indicate that psoralens should not be purchasable over the counter. Certainly, there is room for them in the bag of medical tricks because they have some very useful properties. But to smear them on people's bodies year in and year out is something else.

Ashwood-Smith: It is often said that CHO cells have a sensitivity that differs from that of human cells. That may be true, and the difference might be a threefold or fourfold one in some instances. I do not know if you noticed, but both in the SCE studies and in the chromosome aberration breakage and deletion studies, furocoumarins, dose for dose and joule for joule, are about three times as effective on human cells as they are in hamster cells. It is my judgment as a photobiologist that in the presence of light, the furocoumarins are, in fact, alkylating agents, and they should be classified as such by the FDA.

C. Zervos: The FDA cannot legally proscribe the use of any material in cosmetic preparations without proof that the material will cause harm. This situation is unlike the case of drugs and food additives in which the law requires premarketing proof of safety.

J. Epstein: Isn't the case about the same with saccharin?

Zervos: Absolutely not. In the case of saccharin, the law requires that the substance be shown to be safe to be marketable; in the case of cosmetic ingredients, there is no such requirement. The burden of proving harm or the potential for harm rests with the Government. In the case of food additives and drugs, the burden of proof of safety rests with the manufacturers.

Epstein: Are we talking about a sunscreen?

Zervos: Yes.

Epstein: Isn't that a medication?

Zervos: Not necessarily.

Epstein: Before we go one step further, I will restate the question I have: How much energy is required to produce a reasonable amount of pigment in a very light-skinned individual using suntanning material containing the usual level of psoralen? A response to this question, which I think is contained in a claim of the protection given the user, is a statement of efficacy. I can't imagine then that the preparation is not a medicine.

Zervos: Someone else from the FDA might wish to comment. I might be wrong, but I do think that the preparation could be a cosmetic.

M. Pathak: Sunscreens are not cosmetics. They alter the function of living cells. Accordingly, the FDA has classified them as topical drugs. Further, although I have been enjoying this discussion about what is safe and what is not and about whether 5-MOP or angelicin—a monofunctional adduct former—is carcinogenic or not, I must suggest that we recognize that any compound which intercalates with DNA as well as forms monoadducts or diadducts—it makes no difference—will be a carcinogen.

Finally, this is 1981. We need not design elegant experiments to get what the FDA requires. A lot of indirect evidence supports what Dr. Ashwood-Smith has been telling us. We have to make and pronounce a judgment. Remember, we are here talking about sick people (patients) as opposed to healthy people at risk. For patients, the physician is intelligent enough to determine what risks and what benefits are appropriate. But if the healthy public is in danger of being exposed to harmful substances such as the furocoumarins, the scientific community, the medical community, as well as the FDA must determine the guidelines of proven safety and whether this or that product should be approved. Thus there really is no question of across-the-board approval or disapproval.

H. Eiermann: I would like to clarify Dr. Zervos' statement. The classification of a product as a cosmetic or a drug depends on the statements made in regard to the product's use and the declarations on the label. More important yet are perceptions of the consumer.

If a product contains a sunscreen and the claim is made, truly or falsely, that it is a suntanning preparation which promotes a healthy tan, the product will be classified as a cosmetic. If the very same product is promoted as a suntanning preparation that screens out UV light and helps prevent sunburning, it would be classified as a drug, most likely an over-the-counter drug, depending on the sunscreen being used.

In the case of 5-MOP, if a statement is made that a product that contains 5-MOP accelerates tanning—which means that it affects the functions of the human body—that product may—and I have to emphasize "may"—be classified as a drug. To my knowledge, no firm decision has yet been made by the FDA; the matter is still under consideration.

If the 5-MOP-containing product is put to, or promoted for, a new use, a new purpose, e.g., to accelerate the tanning process, under the law it could be classified as a new drug, even though 5-MOP has been in use in fragrances for a long time. Under such circumstances, the manufacturer would have to submit to the FDA data and demonstrate safety and effectiveness before the product could be marketed. However, as of now, no firm decision has been made.

Urbach: Having been in many FDA meetings on psoralen and UVA radiation, I am uncertain whether anyone knows just how to classify psoralens. I wish instead to make two additional points.

First, Robert Sayre's statement that pigment doesn't protect the skin is misleading. A recent study by Kaidbey and Kligman showed that pieces of black skin used as a sunscreen provide a skin protection factor (SPF) of about 15, which is almost total protection. Please recall that on Mauna Loa, which is six degrees north of the Equator and 14,000 feet high, the largest insult we have ever measured was 21 minimal erythema doses. So, with 15 SPF protection, even an albino will not get much erythema.

Second and perhaps more important, 7 or 8 years ago when the PUVA business first started, I predicted we were going to find more skin cancers, but my prediction was made for a different reason than most. I wouldn't be at all surprised if we find UVA radiation- and psoralen-induced skin cancer in about another 7 or 8 years, i.e., after 10–15 years from the start of the PUVA therapy. What we are getting now is probably a promotion effect.

Also, not many patients will have been treated for 15 years. Patients get tired of it. It is too expensive, it doesn't work well, and patients have flare-ups; so 6 or 7 years from now, there will not be very many people at full risk, even in the large number of treatment installations.

Much more important than all that I have just said is what I will tell you tomorrow, i.e., that photocarcinogenesis, whether it is induced or augmented by UVB radiation, is described by a dose-response curve. As Harold Blum told me in 1951, if everybody lived long enough, everybody would get skin cancer; i.e., enough of a dose administered enough times presents a real risk provided that the exposed subjects do not die of old age.

The issue with the psoralens is exactly the same. They too produce dose-dependent effects. The question is one of how much. I have no reason to doubt that 5-MOP may be a little less effective in any one of the in vitro tests compared to 8-MOP, and the same may be true even in a usual photocarcinogenesis test.

The question, of course, is how all this information will be used. The really important questions are the following: How much exposure are people going to get, and how much damage are they going to sustain as a consequence? This is basically the point.

I recall I once asked why better instructions were not put in sunscreen packages, e.g., why they did not include instructions telling people to put the sunscreen on in the morning before going out and to use it every day. I was told that the average person who buys sunscreen buys one or two tubes at the beginning of the summer and then buys no more. So the use of sunscreens can't be overwhelming, even though a lot of tubes get sold. People do not really use these things very well.

With a tan you don't need to use anything. A long time ago in an early psoralen conference, we were able to tan people with 20 mg of psoralen/day in the desert. These people acquired a striking protecton against UVB radiation, and the tan lasted more than 6 months.

Pathak: One year.

Urbach: One year of tan with two or three doses of UV light and one or two oral doses of 20 mg of psoralen. If it produces persistent pigmentation that protects—an aspect which needs to be studied because a psoralen-induced tan is different from a UVA radiation-induced tan—it would not be surprising to find that this treatment is a low-risk exposure for the average person but probably not a low-risk exposure for the Celt who is so fair-skinned that he or she hasn't got any melanocytes or pigment anyhow.

The Government can only protect most of the people most of the time, or as the late Dr. Michael Halberstam said: "The Government can protect the innocent, but only God can protect a damned fool from being a damned fool." My point is that although I am in favor of regulating dangerous things, I do not think it should be done in the absence of some information. The information on this particular matter is not in yet. I am not saying it is good or bad, because I do not know. But things should not be condemned out of hand. There is a big difference between giving somebody 60 mg of 8-MOP three times a week along with 20 or even 10 J of UVA radiation year in and year out for years and using a sunscreen, assuming that it produces a tan which lasts a long time and which may or may not provide protection. I think there is a need to consider the dose-response curve of the sunscreen. It is not wise, after all, to dismiss things out of hand. Further, one might ask about that perfume that is full of bergamot oil. The more expensive the perfume is, the more bergamot oil it contains.

S. Zimmerman: I think it is necessary to amplify the notion that the Government tries to protect the people. Some of you have heard the Commissioner talk about the saccharin issue and why saccharin use was not banned after it was found to be a carcinogen. He indicated to a large audience that the decision was not purely scientific. The FDA elucidated the public health risks of saccharin consumption as best as could be done and attempted to take the action called for by the law, i.e., ban its use. It has been stymied there. The FDA can propose to ban the use of saccharin, but in the final analysis, it is the people in Congress and the political pressure groups that can abrogate the power to decide. If they say there are benefits that outweigh the risks, that is the way it is.

For a suntan lotion to be a drug, it must be claimed that it treats some kind of a disease or diseased state; i.e., there must be a claim of a therapeutic effect. Now I can't really see a therapeutic effect in putting a suntan lotion on the skin and getting a tan. There might be other situations in which a disease state could be helped by application of suntan lotion.

F. A. Andersen: Regardless of whether 5-MOP is added to a new drug, to an over-the-counter drug, or to a cosmetic, this basic question needs an answer: What are the risks of human exposure to this chemical? Today's scientific discussion yields, I think, two answers. The first is that there is a potential carcinogenic risk to people who apply this stuff to their skin; the second is that the risks have not been proved yet. I'd like anyone else who has some specific data or specific experience in this area to say yea or nay concerning this particular issue. It is, after all, the substance's actual potential for human carcinogenesis that will determine the ultimate fate of the substance, regardless of its classification.

Zervos: I think I have heard a half-answer to Dr. Andersen's question. There is a clear recognition of a possible carcinogenic danger from using this substance. That is the half-answer. However, there is also this matter of a dose-response function to be considered before discussing other aspects of 5-MOP. There is a need to consider the human cancer risks assumed by those exposed to the substance in suntan lotions.

L. Freeman: I would like to present a bit of additional evidence to that point, evidence that really is not yet finished and is not mine; so I will be very tentative about it.

Let me first return to the issue of classification. I think Mr. Eiermann indicated clearly that, for reasons I do not know if anybody can fully interpret, the problem of the classification of sun products has turned out to be a complex one. The same product can have two different labels and be a cosmetic or a drug accordingly. That is the way it is.

I have a personal bias that there ought to be another kind of a classification for substances which do something but do not treat a disease or a disease condition. There are no provisions for a class of regulated substances different from what we now call cosmetics that do not change the body function substantively and what we now call drugs which do. I wish there were one, and I think we would be better off if cosmetics were regulated that way.

However, the specific issue of the risk has been dealt with and is being dealt with by many people. Dr. Ashwood-Smith attempted to look at his model systems and at the formulations and used a product that contained some sunscreens. I do not know which product he used, but in the hairless mouse, an animal system very similar to that used by Professor Urbach and others, the incidences of tumors, as far as I know, were about the same in animals without protection—i.e., exposed to UV light only—and in animals exposed to sunscreens as well. Further, it is my impression from the work of Dr. Ian Magnus that tumors in exposed animals may be less malignant. However, to even elicit this kind of effect requires studies that have not been properly done.

I believe it is clear from the literature that sunscreens do, in fact, provide some protection against photocarcinogens. If, in fact, psoralens (which are quite ubiquitous) and specifically 5-MOP in sunscreens do not enhance photocarcinogenicity at low dose levels, if there is some enhancement of tanning, and if tanning has some benefit—whether cosmetic or the protection against carcinogenesis—I think we would be very rash to decide that psoralens and specifically 5-MOP are bad given the state of our knowledge.

Finally, if it is decided to call 5-MOP a drug, the following terrible paradox would ensue. Anyone eating a couple of tablespoons of parsley would be getting more 5-MOP than he or she could ever smear on by using sunscreens.

Zervos: The FDA faces such paradoxes day in and day out.

Freeman: The nitrite story is one example showing that, drawn far enough, some of the concepts of regulation are a bit ridiculous. The FDA has now taken the position that it will not forbid the use of nitrite in meat because it does prevent botulism.

Zervos: It is wrong to assume that in its deliberations the FDA does not recognize that, at some time or another, what the law dictates might be at odds with physical reality. Lead is a substance exemplifying the point, nitrite is a similar substance, and caffeine is a similar substance. I can go down a large list.

We are doing a disservice both to the FDA and most importantly to the public if against all indications to the contrary we repeat that the FDA does not recognize these paradoxes. But the law specifies that the Agency has to do certain things, and the Agency tries to abide by the law, to protect the public health to the extent the law provides for, and not to appear silly. The situation is difficult.

Epstein: I think that prevention is a very important aspect of disease control and certainly all here would agree that damage by sunlight will produce disease. Therefore, if it is advertised that some agent will protect the user from sunlight damage, then I would think the agent is a medication by definition.

Eiermann: I wish to make two points to set the record straight and hopefully to clarify a misconception. Classification is a decision that sets the record straight, whether a product is legally a drug or a cosmetic. The classification is strictly a legal matter, and it has implications as to how a product will be handled or regulated by the FDA.

The other point I wish to make is that the FDA does not make the laws. Earlier, the talk was about another product category, one intermediate between drugs and cosmetics. This category actually exists in the minds of the people in the cosmetics industry. They call the products in this category "treatment products." But to establish a category with legal standing would take an act of Congress. The FDA only interprets the law to the best of the ability of the people in the Agency, and classification is nothing else but an interpretation of the law made by Congress. If the law is not interpreted correctly, which is certainly possible, the FDA is taken to court, where it has been known to lose on occasion.

A. Kornhauser: I wish to summarize something regarding 5-MOP and 8-MOP. As far as we know today, both 5-MOP and 8-MOP have more or less similar topical effects. Taken orally, 5-MOP and 8-MOP show very different effects, both in animal models and in people. This had to be taken into account in a risk assessment of sunscreens. Cosmetics are not usually taken orally, but in the context of assessing the relative risks I would ask if there are differences in the potencies of pigmentation induced by 5-MOP and 8-MOP?

Pathak: Both 5-MOP and 8-MOP are melanogenic; i.e., they increase the melanocyte population by a factor of two or three or even five within 72–96 hours. Also, they increase the production of melanosomes and for Caucasians the size of the melanosomes as well. It is not known whether these are the results of somatic mutations or just a follicular contribution. In the hair follicles, the pigment is always large. Thus the changing sizes could represent the follicular hair melanosomes coming up the outer skin layers and contributing to the increased size of melanosome. Beyond that, it has been observed that 5-MOP causes a selective mitosis in melanocytes.

It is still to be determined whether we observed a selective mitosis or we were lucky to get a figure of mitotic melanocytes. But we feel that 5-MOP and 8-MOP have a selective effect on melanocytes, and some studies will have to be done to test this hypothesis.

Zervos: The statement was made, and I think correctly so, that looking at the structures of 5-MOP or 8-MOP one will conclude that each will be a carcinogen in an ultimate test in real animals. Subsequently, the statement was also made that the risk of carcinogenesis in exposed people will depend on the extent of human exposure as well as on the inherent carcinogenicity of the substances.

If today we must regulate these substances according to the degree of risk based on the extent of exposure necessary to obtain a desired effect, how do we go about comparing the relative risks of the different substances or estimating the absolute risks from each of these substances? These are the questions that the FDA must answer now and for some time to come. They are the questions posed by Congress, by the regulated industry, and by the people asked to use the various products. I wish to probe for some answers to these questions.

Urbach: I do not have answers, but I certainly do know that we have a lot of problems in getting an answer for you because of the difficulty of the questions. But let me give you an example with psoralen, although you could use any other agent.

The problem is that in any kind of interaction of a chemical, light, and a living system, any one of these elements can be modified. The chemical can be modified by the light; a lot of photochemistry can happen yielding breakdown products. Concerning the psoralens, i.e., 8-MOP, 5-MOP, or angelicin, whichever one you might select, it will also be a question of the degree of topical or oral exposure and a question of the dose of the administered radiation. Most important, however, a major question will arise with respect to the spectrum of radiation. Completely different effects will be observed with different spectra. The action spectrum for the psoralens does not really peak at 365 nm. It is pretty much a plateau up to 335 nm. At 365 nm, it is dropped by 1 log unit or by one order of magnitude.

Clearly, the results of photocarcinogenesis studies depend on the light source used and on the genetic strains of the test animals. The problem then is a very difficult one for a regulatory agency, and the answers are not easy. Unfortunately, chemical toxicology is not easy.

Again, the problem with light is that three components are present, and each interacts with the others. The immune system can change the host, the light frequently changes the chemical (I am going to spend most of my time tomorrow presenting evidence and data for this phenomenon), and the spectrum of light interacts with all. One can define effects for very specific conditions. The trouble is that when one is dealing with the skin and the sun, the light spectrum of importance absolutely refuses to stand still from one moment to another from one place to another. This is why we do not use the sun as an experimental tool very often. We cannot tell what it is doing.

So, this is a very difficult problem for which I have no immediate answer. Also, I can see that the problem is going to be a lot more complicated than we think.

Ashwood-Smith: I would like to end on a positive note, which has already been partially discussed. A recently improved technique for looking for guanine-resistant peripheral lymphocytes can be applied to individuals badly sunburned and treated with products A, B, and C or no products at all. We could look, for instance, at a population of students who want to get both a good tan and a good grade. We may be able to get an idea as to whether there is a risk in humans. Between 1 and 4% of the peripheral leukocytes are irradiated, so one way or the other mutations in these lymphocytes might be the first direct evidence of the adverse effects of these various psoralen products. Also, these studies may yield information on the mutation rates in normal individuals exposed to the sun under normal circumstances and when exposed to product X, Y, or Z as well.

blank page

Genotoxic Effects of Sunlight-Activated Waste Water in Cultured Mammalian Cells[1,2]

Gary F. Strniste,[3] David J. Chen,[3] *and* Richard T. Okinaka[3,4]

ABSTRACT—Cultured Chinese hamster ovary cells were incubated with dilutions of an oil shale retort process water and exposed to natural sunlight. An enhancement of sevenfold to ninefold was seen in photoinduced cytotoxicity (by a colony-forming assay) and mutagenicity [at the hypoxanthine phosphoribosyltransferase (*HPRT*) locus] for cells pretreated with the process water compared to effects seen in cells exposed to sunlight only. Significant photoinduced cytotoxicity was also observed in cultured human skin fibroblasts when exposed to the process water before being exposed to near UV (NUV) radiation. The mutation frequencies (determined for the *HPRT* locus) induced by the process water and NUV radiation were as great as those frequencies seen for far UV light alone. Increases in genotoxicity were observed in excision repair-deficient xeroderma pigmentosum skin fibroblasts when compared to the responses seen in normal cells. Risks to health resulting from the phototransformation of these oil shale retort process waste waters are unassessed at this time.—JNCI 1982; 69:199–203.

As natural petroleum reserves are consumed, it becomes more apparent that the United States will have to supplement its liquid energy supplies with synthetic fuels to meet projected energy demands. Of great promise are the organic reserves locked in vast oil shale deposits located primarily in the western United States. Estimates of hundreds of billions of barrels of economically recoverable crude oil have been made from surveys of oil shale deposits located in Colorado, Utah, and Wyoming (*1*). However, the processes involved in the mining, retorting, upgrading, and refining of oil shale will be accompanied by potential environmental and health-related risks.

One major problem associated with the development of an oil shale industry in this semiarid region will be the utilization of vast quantities of water and the production of process waters, a by-product of retorting which may amount to as much as two barrels of water for every barrel of crude oil produced. Due to its initimate contact with the oil during retorting, process waters, after separation in holding tanks, contain substantial amounts of aqueous-soluble organic materials. These dissolved components most likely contribute to the genotoxic properties of these waters when assessed in the Ames *Salmonella* bioassay (*2*).

For several years, our laboratory has been investigating the process of photoactivation by UV radiation of certain classes of promutagenic-procarcinogenic compounds in an attempt to relate DNA structural damage induced in vitro to the genotoxic effects witnessed in cultured mammalian cell assays (*3–6*). As an extension of this work, we have applied this "photoactivation process" to assess the genotoxic potential existing in by-products of shale oil (*2, 7–10*). This report will consider a particular retort process water and its cytotoxicity and mutagenicity in cultured rodent cells or human skin fibroblasts after activation by UV radiation.

MATERIALS AND METHODS

Test materials.—We have assessed the genotoxic potential of process waters obtained from three retort processes (above ground, modified in situ, and truly in situ) which utilized oil shale from deposits located in the Green River formation in the western United States. Although all waters exhibited photoinduced genotoxic properties (*2, 8, 9*), this report will concern only the most active water, which was obtained from a holding tank for shale oil produced by an above-ground retort. This process water was filtered through Whatman #42 paper and a Millipore 0.2-μm Swinnex unit before use.

Cell cultures.—CHO cells (line AA8-4) were obtained from Dr. L. Thompson (Lawrence Livermore National Laboratory, Livermore, Calif.). This cell line, heterozygous at the adenine phosphoribosyltransferase locus (*11*), was cultured under conditions described elsewhere (*9*). Text-figure 1 outlines the basic scheme for determining the cytotoxic and mutagenic events witnessed in CHO cells. The genetic marker examined in this report is the X-linked, recessive hypoxanthine phosphoribosyltransferase *HPRT* locus. This mutation assay system has been described elsewhere (*9, 12, 13*). Selection for HPRT$^-$ mutants is accomplished by growth of treated cell populations in medium containing 10 *μM* of the toxic base analog 6-TG, after maximal expression period of 8 days' incubation post treatment (*9, 14*). Plating efficiencies of untreated CHO cells are 90–100%.

Cultured human skin fibroblasts were purchased from the American Type Culture Collection (Rockville, Md.). NF (CRL 1295) and XP cells (CRL 1223 or XP12BE) were grown in DMEM containing 20% (vol/vol) FCS (*5*). A similar experimental protocol as diagramed in text-figure 1 for CHO cells was used for the determination of photoin-

---

ABBREVIATIONS USED: CHO=Chinese hamster ovary; D_{37}=exposure time required to reduce cell survival to 37%; DMEM=Dulbecco's modified Eagle's medium; EOP=efficiency of plating; FCS=fetal calf serum; FUV=far UV; HPRT=hypoxanthine phosphoribosyltransferase; HPRT$^-$=HRPT negative; NF=normal skin fibroblast(s); NUV=near UV; 6-TG=6-thioguanine; 6-TG^R=6-TG resistant; XP=xeroderma pigmentosum.

---

[1] Presented at the Seventh Food and Drug Administration Science Symposium ("Photochemical Toxicity: Toxic, Allergic, and Carcinogenic Aspects With Emphasis on Predicting Effects in Humans") held at the Uniformed Services University of the Health Sciences, Bethesda, Md., March 16–17, 1981.

[2] Supported by the U.S. Department of Energy.

[3] Genetics Group, Life Sciences Division, Los Alamos National Laboratory, Los Alamos, N. Mex. 87545.

[4] We gratefully acknowledge the technical assistance of Ms. J. Nickols, Ms. E. Wilmoth, and Mr. E. Martinez.

duced genotoxicity in human cells, with the following modifications: 1) For toxicity measurements, between 100 and 1,000 cells were plated, and for mutagenicity measurements, 3–6 plates at 10^5 cells/plate were used for each dose tested; 2) the cell attachment period was 20–22 hours; 3) for toxicity measurements, treated plates were incubated a total of 8–11 days with an intermittent feeding on the 5th day; 4) maximal expression of $HPRT^-$ mutants was obtained in 6–8 days (a minimum of four cell divisions); and 5) for selection of $HPRT^-$ mutants, cells were plated at 25 × 10^3/dish (35–40 dishes/dose) in DMEM with 10% FCS plus 30 μM 6-TG and incubated for 14 days with an intermittent feeding with selection medium on the 7th day. Corresponding EOP determinations were performed at each dose tested. The EOP for untreated NF was 30–40% and for XP cells, 15–25%.

Irradiation.—The source of FUV radiation (primarily 254 nm) was a single 15-W germicidal lamp (G15T8; General Electric Co., Denver, Colo.). The fluence of incident light was 0.5 $J \cdot m^{-2} \cdot sec^{-1}$. The source of NUV radiation (300–400 nm) was a pair of parallel 15-W black lights (F15T8 BLB; General Electric Co.). The incident fluence averaged 6.5 $J \cdot m^{-2} \cdot sec^{-1}$. Calibration of these sources is described elsewhere (*5, 9*). For experiments in which natural sunlight was used as the source of radiation, plates containing attached cells were exposed for various times on the rooftop of the Health Research Laboratory in Los Alamos, N. Mex. (lat. 35°53′11″ N., long. 106°18′58″ W. at an elevation of 7,450 ft above sea level). Sunlight experiments reported here were performed from 12:30 p.m. to 1:30 p.m. during December 1980 and January 1981; the total measured fluence (200- to 2,500-nm wavelength) was 850–950 $J \cdot m^{-2} \cdot sec^{-1}$.

RESULTS AND DISCUSSION

Pretreatment of CHO cells with oil shale retort process waters and subsequent exposure to NUV radiation has resulted in both cytotoxic and mutagenic responses (*2, 8–10*). Mutation frequencies induced at the *HPRT* locus were as great as 50% of those witnessed for the potent skin carcinogen FUV radiation (*9, 10*) at equivalent surviving fractions of cells. However, the magnitude of this genotoxic response was dependent on the process water used; in situ retort process waters were less photoactive than was a corresponding above-ground retort process water. These observations suggested that natural sunlight, which has an NUV component, may have a similar effect.

To test this hypothesis, we exposed CHO cells pretreated with above-ground retort process water (1:270 dilution for 1 hr in the dark) for various times to natural sunlight. The survival data (in terms of colony-forming ability) are shown in text-figure 2. The D_{37} was approximately 50 seconds, whereas untreated CHO cells were inactivated to 37% surviving fraction only after approximately 6 minutes' exposure to sunlight. This represented a sevenfold increase in the photosensitivity of CHO cells pretreated with retort process water as compared to the photosensitivity of untreated cells.

The estimated total solar irradiance (200–2,500 nm) in Los Alamos during December 1980 and January 1981 averaged approximately 900 $J \cdot m^{-2} \cdot sec^{-1}$. Approximately 3% of the solar spectrum is in the NUV range (300- to 400-nm wavelength). Therefore, the fluence of sunlight necessary to reduce survival to 37% for process water-treated CHO cells is 4.5×10^4 $J \cdot m^{-2}$, of which approximately 1,400 $J \cdot m^{-2}$ is NUV. This NUV dose is the same as that obtained in experiments in which NUV radiation was generated by black lights (*9*), indicating the role of this component of the solar spectrum in the photoactivation process.

In text-figure 3, the numbers of $HPRT^-$ mutants (cells resistant to 6-TG) induced by exposure of CHO cells to process water plus sunlight or to sunlight only are plotted versus the percent surviving fraction of cells. At the D_{37} for cell survival, there was a ninefold increase in the number of photoinduced mutants in CHO cells pretreated with process water as compared to untreated cells after subtraction of the natural background mutation frequency (averaged approximately 1/10^5 cells). As noted for photoinduced cytotoxicity, the frequencies of photoinduced mutations in process water-

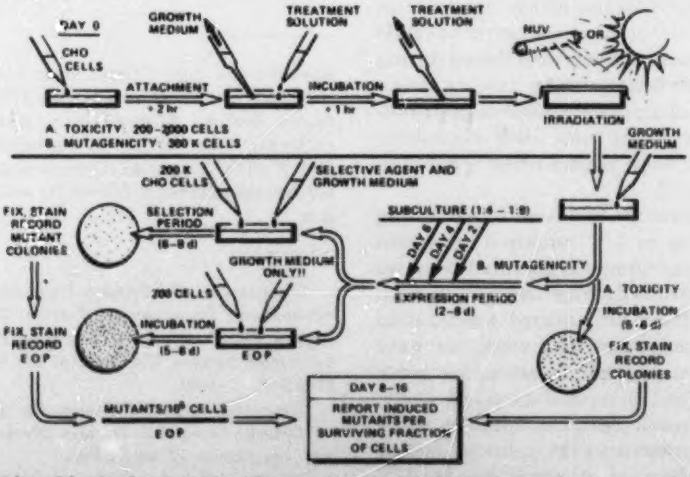
DAY 0
CHO CELLS
GROWTH MEDIUM
TREATMENT SOLUTION
TREATMENT SOLUTION
NUV
OR
ATTACHMENT
~2 hr
INCUBATION
~1 hr
IRRADIATION
A. TOXICITY: 200–2000 CELLS
B. MUTAGENICITY: 300 K CELLS
GROWTH MEDIUM
200 K CHO CELLS
SELECTIVE AGENT AND GROWTH MEDIUM
FIX, STAIN RECORD MUTANT COLONIES
SELECTION PERIOD (6–8 d)
SUBCULTURE (1:4 – 1:8)
DAY 6
DAY 4
DAY 2
B. MUTAGENICITY
GROWTH MEDIUM ONLY!!
200 CELLS
EXPRESSION PERIOD (2–8 d)
A. TOXICITY
INCUBATION (5–8 d)
FIX, STAIN RECORD EOP
INCUBATION (5–8 d)
EOP
FIX, STAIN RECORD COLONIES
DAY 8–16
REPORT INDUCED MUTANTS PER SURVIVING FRACTION OF CELLS
MUTANTS/10⁶ CELLS
EOP

TEXT-FIGURE 1.—Protocol used for the determination of genotoxic potential of light-activated mixtures in the CHO–HPRT mutation system. The selective agent used was 6-TG at 10 μM. *See* "Materials and Methods" for details.

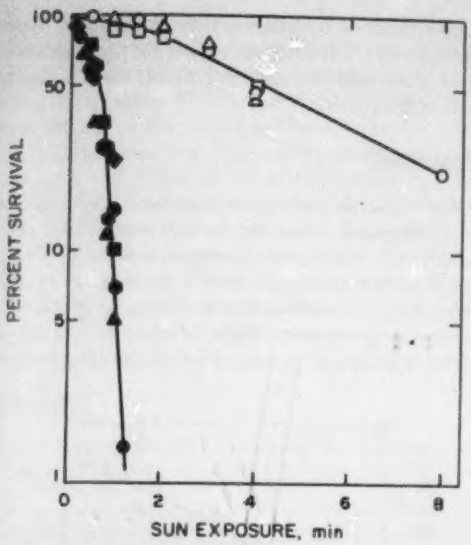

TEXT-FIGURE 2.—Loss of colony-forming ability of CHO cells exposed to oil shale retort process water plus natural sunlight (*closed symbols*) or to natural sunlight only (*open symbols*). Different symbols represent results from independently done experiments.

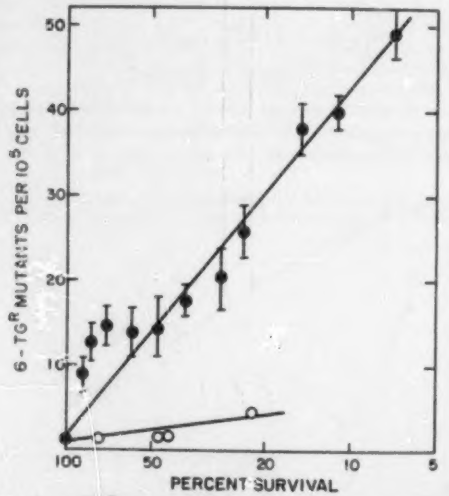

TEXT-FIGURE 3.—6-TG^R mutants (HPRT$^-$) induced per surviving fraction of CHO cells after exposure to oil shale retort process water plus natural sunlight (●) or to sunlight only (○). *Error bars*=±1 SD.

treated CHO cells were the same for equivalent fluences of sunlight or black light NUV radiation.

The potential environmental and health-related risks resulting from concomitant exposure to shale oil byproducts (including process waters) and natural or artificial light are unknown. However, a primary target in human exposure will be the skin. We designed the following experiments incorporating cultured human skin fibroblasts as targets to assess better photoinduced genotoxic properties (toward humans) of shale oil retort process waters. As in the CHO cell studies discussed above, only one process water obtained from an above-ground retort facility was used. For comparative purposes, analogous cytotoxic and mutagenic studies were performed with FUV radiation.

In text-figure 4, the survival (colony-forming ability) of NF is shown for NF pretreated with process water and subsequently NUV irradiated or exposed to FUV radiation only. Because of the extreme cytotoxic properties of this water toward cultured fibroblasts, a dilution of 1:700 was necessary to ensure that no cytotoxicity was induced by the process water only (1-hr exposure in the dark). At this dilution, a fluence of NUV of 1,700 J·m^{-2} was necessary to reduce NF survival to 37% that of the control, untreated cultures. Treatment of NF with process water only (1 hr in the dark) or with NUV radiation only (fluences up to 3,000 J·m^{-2}) resulted in no cytotoxicity or mutagenicity.

In text-figure 5, HPRT$^-$ mutants induced in NF by FUV radiation or process water plus NUV radiation are plotted versus radiation fluence. In these experiments, the average background mutation rate (0.3/10^5 cells) was subtracted from each data point. The establishment of conditions maximizing the response of this human cell–HPRT mutation assay has been determined with embryonic human skin fibroblasts (*7, 15*), and those protocols were used in the experiments reported here.

The data in text-figures 4 and 5 are replotted in text-figure 6 to show HPRT$^-$ mutants induced as a function of surviving fraction of cells. These data indicated that the frequency of induction of mutants (per surviving fraction of cells) at the *HPRT* locus was the same after treatment with either FUV radiation or process water plus NUV radiation. At 37% surviving fraction of cells, the number of mutants induced by above-ground retort process water and NUV radiation in NF was about 60% that observed in CHO cells, and the number of FUV radiation-induced mutants in NF was only about 20% that observed for CHO cells exposed to FUV radiation (*9*). These differences in mutation frequen-

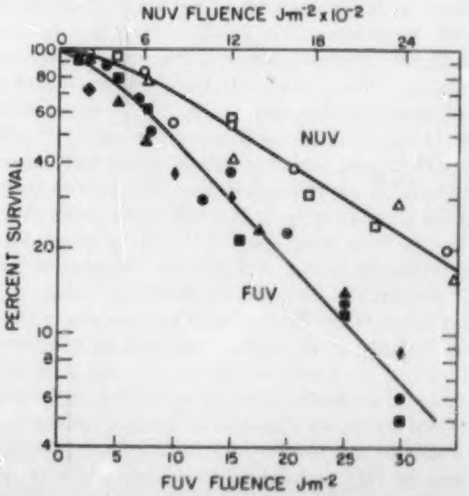

TEXT-FIGURE 4.—Loss of colony-forming ability of cultured NF exposed to oil shale retort process water plus NUV radiation (*open symbols*) or to FUV radiation only (*closed symbols*). Different symbols represent results from independently done experiments.

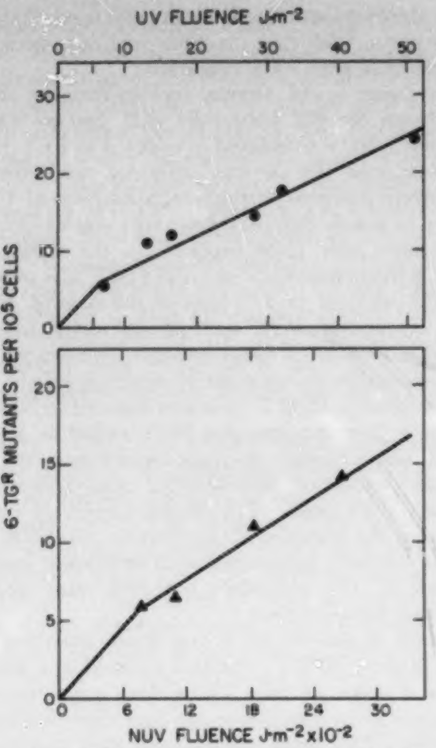

TEXT-FIGURE 5.—6-TG^R mutants (HPRT$^-$) induced in cultured NF exposed to FUV radiation (*upper curve*) or oil shale retort process water plus NUV radiation (*lower curve*).

cies observed can be accounted for, at least in part, by differences in repair capabilities in rodent versus human cells (*16, 17*).

In recent studies, we have examined the cytotoxic effects induced in repair-deficient human skin fibroblasts by process water and NUV radiation. XP cells obtained from a patient of complementation group A were used in this study. These cells are extremely sensitive because of deficiencies in their excision repair capacity to FUV radiation and certain classes of chemical compounds (*18, 19*). In text-figure 7 the survival (colony-forming ability) of NF and XP cells pretreated with process water (1:700 dilution) and subsequent exposure to NUV radiation is shown. The inset in text-figure 7 shows the survival of these two cell types exposed to FUV radiation. In both examples, XP cells showed an acute cytotoxic response as compared to the response of NF (five-fold and sixteenfold increases in sensitivity when the comparison is made of the D_{37} values of process water plus NUV radiation treatment or FUV radiation treatment alone, respectively). This result suggests that the magnitude of genotoxicity of photoactivated process water in human cells is influenced by repair capabilities existing in the cell. The decrease in the magnitude of sensitivity seen for XP cells (compared to NF) treated with process water plus NUV radiation versus FUV radiation only could possibly result from a contribution to cell toxicity by non-DNA damage (e.g., membrane damage). We have observed a similar reduction in sensitivity in XP cells (compared to NF) for cytotoxicity induced by photoactivated polycyclic aromatic hydrocarbons (*5*). The role of repair in the modulation of mutagenic potential induced in human cells is the subject of current investigation.

CONCLUSIONS

We reached the following conclusions: 1) Natural sunlight induces a genotoxic response in cultured CHO cells pretreated with oil shale retort process water. 2) The NUV component of the solar spectrum is the apparent radiation responsible for photoactivation. 3) Cultured NF are acutely sensitive to the genotoxic effects of photoactivated process water. The mutagenic potential of photoactivated process

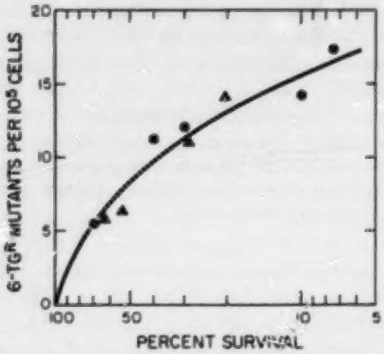

TEXT-FIGURE 6.—6-TG^R mutants (HPRT$^-$) induced per surviving fraction of NF after exposure to FUV radiation (▲) or oil shale retort process water plus NUV radiation (●).

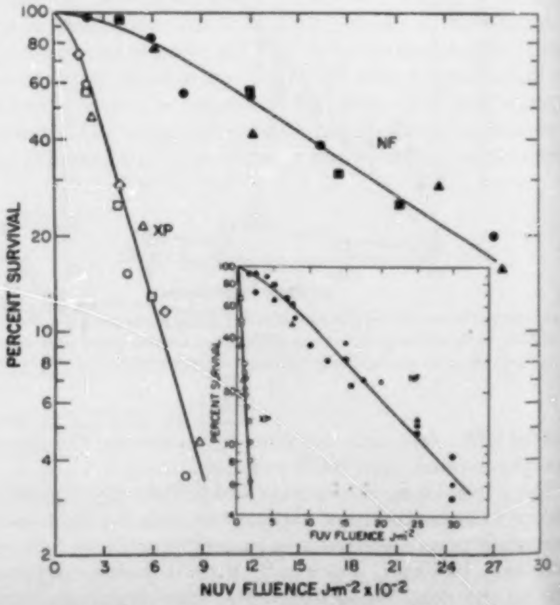

TEXT-FIGURE 7.—Loss of colony-forming ability in NF and in XP skin fibroblasts after exposure to oil shale retort process water plus NUV radiation. *Inset* represents loss of colony-forming ability in NF and XP cells after FUV radiation exposure. Different symbols represent results from independently done experiments.

water in human cells is the same as that witnessed for an equivalent killing dose of the potent skin carcinogen FUV radiation. 4) DNA repair processes are involved in modulating genotoxic effects of this photoinduced process. 5) The exact magnitude of the potential health-related and environmental risks resulting from photoactivation of retort process waters and other oil shale byproducts is unassessed at this time. Our demonstration that a significant rate of mutation occurs in cultured human cells exposed to high dilutions of process waters and fluences of NUV radiation comparable to those encountered during nominal exposure to sunlight suggests that such assessment is a prerequisite to the developement of our oil shale resources in a manner that will minimize health-related risks.

REFERENCES

(*1*) Yen TF, Chilingarian GV. Introduction to oil shales. In: Yen TF, Chilingarian GV, eds. Oil shale. Amsterdam and New York: Elsevier, 1976:1–12.

(*2*) Holland LM, Stafford CG, compilers. The Los Alamos integrated oil shale health and environmental program: A status report. Los Alamos, N. Mex.: Los Alamos National Laboratory, 1981:54–65 (Los Alamos National Laboratory Report LA-8565-SR).

(*3*) Hoard DE, Ratliff RL, Bingham JM, Strniste GF. Reactions induced in vitro between model DNA and benzo(*a*)pyrene by near ultraviolet light. Chem Biol Interact 1981; 33:179–194.

(*4*) Strniste GF, Brake RJ. Photoactivity of near ultraviolet light-irradiated benzo(*a*)pyrene. Fed Proc 1980; 39:2011.

(*5*) Strniste GF, Brake RJ. Cytotoxicity in human skin fibroblasts induced by photoactivated polycyclic aromatic hydrocarbons. In: Cooke M, Dennis AJ, eds. Polynuclear aromatic hydrocarbons: Chemical analysis and biological fate. Columbus, Ohio: Battelle Press, 1981:109–118.

(*6*) Strniste GF, Martinez AM, Martinez E, Brake RJ. Photo-induced reactions of benzo(*a*)pyrene with deoxyribonucleic acid in vitro. Cancer Res 1980; 40:245–252.

(*7*) Chen DJ, Okinaka RT, Barnhart BJ. Quantitation of mutations induced by metabolically activated mutagens in normal human fibroblasts. Environ Mutagen 1980; 2:294.

(*8*) Strniste GF, Brake RJ. Toxicity and mutagenicity of shale oil retort product waters photoactivated with near ultraviolet light. Environ Mutagen 1980; 2:268.

(*9*) Strniste GF, Chen DJ. Cytotoxic and mutagenic properties of shale oil byproducts. I. Activation of retort process waters with near ultraviolet light. Environ Mutagen 1981; 3:221–231.

(*10*) Strniste GF, Okinaka RT, Chen DJ. Photoactivation of shale oil byproducts. Environ Mutagen 1981; 3:308.

(*11*) Thompson LH, Fong S, Brookman K. Validation of conditions for efficient detection of HPRT and APRT mutations in suspension-cultured Chinese hamster ovary cells. Mutat Res 1980; 74:21–36.

(*12*) O'Neill JP, Brimer PA, Machanoff R, Hirsch GP, Hsie AW. A quantitative assay of mutation induction at the hypoxanthine-guanine phosphoribosyl transferase locus in Chinese hamster ovary cells (CHO/HGPRT system): Development and definition of the system. Mutat Res 1977; 45:91–101.

(*13*) O'Neill JP, Couch DB, Machanoff R, San Sebastian JR, Brimer PA, Hsie AW. A quantitative assay of mutation induction at the hypoxanthine–guanine phosphoribosyl transferase locus in Chinese hamster ovary cells (CHO/HGPRT system): Utilization with a variety of mutagenic agents. Mutat Res 1977; 45:103–109.

(*14*) Chen DJ, Strniste GF. Cytotoxic and mutagenic properties of shale oil byproducts. II Comparison of mutagenic effects at five genetic markers induced by retort process water plus near ultraviolet light in CHO cells. Environ Mutagen 1982. In press.

(*15*) Chen DJ, Okinaka RT, Strniste GF, Barnhart BJ. Induction of 6-thioguanine resistant mutations by rat liver homogenate (S9)-activated promutagens in human embryonic skin fibroblasts. Mutat Res 1982; 101:87–98.

(*16*) Painter RB, Cleaver JE. Repair replication, unscheduled DNA synthesis and the repair of mammalian DNA. Radiat Res 1969; 37:451–466.

(*17*) Trosko JE, Kasschau MR. Study of pyrimidine dimers in mammalian cells surviving low doses of ultraviolet radiation. Photochem Photobiol 1967; 6:215–219.

(*18*) Robbins JH, Kraemer KH, Lutzner MA, Festaff BW, Coon HG. Xeroderma pigmentosum: An inherited disease with sun sensitivity, multiple cutaneous neoplasms and abnormal DNA repair. Ann Intern Med 1974; 80:221–248.

(*19*) Setlow RB. Repair deficient human disorders and cancer. Nature 1978; 271:713–717.

blank page

Interaction of Oxygen and Oxy-radicals With Carotenoids[1]

Norman I. Krinsky[2] *and* **Susan M. Deneke**[3]

ABSTRACT—Dye-sensitized photo-oxidations of liposomes are inhibited by the presence of carotenoids in the membrane. Some carotenoid bleaching occurs during the reaction. It was shown that carotenoids are capable of inhibiting free-radical-induced lipid peroxidation in liposomes as well as singlet oxygen-induced lipid peroxidation. There is little direct effect of lipid peroxides on carotenoid bleaching during the photo-oxidative reactions. The carotenoid bleaching observed during the dye-photosensitized oxidations of the liposomes appears to be due to interactions between the carotenoid pigments and either radical intermediates from type I reactions or direct chemical reaction with singlet oxygen in a type II reaction. It was concluded that carotenoid pigments function as protective agents by quenching triplet sensitizers, singlet oxygen, and radical intermediates.—JNCI 1982; 69:205–210.

Carotenoid pigments are very widely distributed in nature. They are obligatory components of photosynthetic systems and are also present in many nonphotosynthetic organisms, particularly those that are normally exposed to light in their environment. The basis for carotenoid function in photosynthetic organisms was known to be related to their ability to capture radiant energy and transfer it to the photosynthetic pigments, either chlorophyll in green plants and algae or bacteriocholorphyll in photosynthetic bacteria (*1*), but an adequate explanation for their presence in nonphotosynthetic bacteria was not made available until the observations of Sistrom et al. (*2*) in 1956. These authors concluded that the carotenoid pigments were serving a specific function in protecting the purple sulfur bacterium *Rhodopseudomonas spheroides* from the effects of light, oxygen, and a photosensitizing dye. The harmful effects caused by light, oxygen, and a photosensitizing dye constitute the photodynamic effect, as defined by Blum (*3*). Following the observations of Sistrom et al. (*2*), there were a number of studies that correlated carotenoid presence with protection against photodynamic effects. These studies were done both in photosynthetic (*4, 5*) and in nonphotosynthetic organisms (*6, 7*). Mutant strains of various carotenoid-containing nonphotosynthetic organisms that lacked the ability to synthesize colored carotenoids were found to be sensitive to light in the presence of oxygen and either an exogenous photosensitizer (*6*) or even to endogenous pigments (*7*).

A specific proposal for explaining the mechanism of action of carotenoid pigments in conferring protection against photosensitized oxidation was formulated in 1968 by Foote and Denny (*8*) who demonstrated that carotenoid pigments had the capability of physically quenching singlet oxygen ($^1O_2$) generated during photosensitized reactions. The colored carotenoids are so effective in this process that there have been many conclusions presented in the literature that any protection observed in the presence of carotenoid pigments must be attributed to the presence of $^1O_2$ in the biological system under investigation. The material dealing with carotenoid-$^1O_2$ interactions has been reviewed earlier (*9*), and it is clear that other protective functions can be attributed to carotenoid pigments.

To investigate these processes, we have used the liposome model (*10*) and have demonstrated that carotenoid pigments protect against both photosensitized oxidations (*11*) as well as $^1O_2$ generated by a radio-frequency discharge apparatus (*12*). The liposome model has also been used by a number of investigators (*13–18*) to demonstrate sensitivity to photosensitized oxidations as well as protection by a variety of other compounds, such as vitamin E and cysteamine (*14*).

However, the question still remains whether carotenoid pigments can protect against oxygen-centered radicals or other radical species that can be generated either chemically, photochemically, or radiolytically. In this report, we present evidence that carotenoid pigments not only protect against $^1O_2$ generated during photosensitized oxidations, but also protect against other radical species that have the capacity for oxidizing the unsaturated fatty acids present in membranes and in liposomes.

MATERIALS AND METHODS

Liposomes were prepared by the method of Kinsky et al. (*10*), which utilized egg PC, DCP, and, in some preparations, cholesterol. These liposomes contained trapped glucose. Carotenoids were incorporated into the liposome membranes by inclusion of the desired carotenoid in the original lipid mixture as described previously (*11, 12*). In some preparations synthetic DL-α-phosphatidylcholine, dipalmitoyl (Sigma Chemical Co., St. Louis, Mo.) was used instead of egg PC. When synthetic PC was used all operations were at 50°C rather than at room temperature.

The procedure for toluidine blue O-sensitized photo-oxidations of liposomes has been described (*11*). The suspensions of liposomes containing the dye were illuminated with a Sylvania Sun Gun halogen source ($4.5\times10^3\ J\cdot m^{-2}\cdot sec^{-1}$) through a Rohm and Haas amber filter #2422 which removed all wavelengths below 530 nm.

UV radiation was used to initiate liposome oxidations. Samples maintained at 15°C in 10-ml beakers were illuminated from above with five General Electric germicidal

---

ABBREVIATIONS USED: BHT=butylated hydroxytoluene; DCP=dicetyl phosphate; MDA=malondialdehyde; PC=phosphatidylcholine.

---

[1] Presented at the Seventh Food and Drug Administration Science Symposium ("Photochemical Toxicity: Toxic, Allergic, and Carcinogenic Aspects With Emphasis on Predicting Effects in Humans") held at the Uniformed Services University of the Health Sciences, Bethesda, Md., March 16–17, 1981.

[2] Department of Biochemistry and Pharmacology, Tufts University School of Medicine, 136 Harrison Ave., Boston, Mass. 02111.

[3] Department of Medicine, New England Medical Center Hospital, Boston, Mass. 02111.

bulbs at a distance of 5 inches. The maximum wavelength of UV emission was 254 nm (in the UVC region which extends from 200 to 280 nm) and the intensity was 4.0×10^3 $J\cdot m^{-2}\cdot sec^{-1}$.

For ferrous ion-induced oxidations, the liposomes were incubated in 0.15 *M* choline chloride at 40°C as described by Leibowitz and Johnson (*19*) with 1 m*M* $FeCl_2$. Controls were incubated in air at 40°C without the added $FeCl_2$.

The extent of liposome peroxidation was determined by the thiobarbituric acid assay for MDA, a lipid peroxide breakdown product (*11*, *20*), as well as by the ferrous thiocyanate assay (*21*). Lysis of the liposomes was measured enzymatically by the release of the trapped glucose or by the loss in turbidity of the suspension as measured by the absorbance decrease at 700 nm (*11*).

Carotenoid concentrations were measured by extraction of the liposome suspensions with 1 volume of ethanol and 2 volumes of hexane and by measurement of the absorbance of the hexane layer in a Cary model 14 spectrophotometer. Dye concentrations were measured directly in the liposome suspensions.

Crystalline potassium tetraperoxochromate (K_3CrO_8) was obtained according to the procedure of Riesenfeld et al. (*22*).

RESULTS

As we have demonstrated earlier, carotenoid pigments such as β-carotene or canthaxanthin (4,4′-diketo-β-carotene) will prevent the loss of membrane integrity when liposomes are irradiated in air-saturated solutions of photosensitizing dyes such as toluidine blue (*11*, *12*). As shown in text-figure 1, carotenoid pigments are protective agents in this photosensitized system. Other workers have also demonstrated a protection against liposome lysis in irradiated systems by radical quenchers such as vitamin E or cysteamine (*14*).

To help identify the reactive species in this photosensitized system, we investigated the effect of K_3CrO_8 on the liposome preparation. This compound had been used by Hodgson and Fridovich (*23*) to generate $^1O_2$ as well as other oxy-radical species. It has also been used by Wörner et al. (*24*) in studying oxidant attack on platelets. As can be seen in text-figure 2, K_3CrO_8 produces a rapid appearance of lipid peroxides which results in liposome lysis. When liposomes prepared with β-carotene were exposed to K_3CrO_8, the rate of lipid peroxidation was markedly decreased. Control experiments in which potassium chromate (K_2CrO_4) was used showed no effect of this salt on lipid peroxidation and no effect of the added β-carotene. However, the K_3CrO_8 system does not generate solely $^1O_2$ but also apparently results in the formation of the superoxide radical and the hydroxyl radical (*24*). However, it is clear that carotenoids can protect against the product(s) of K_3CrO_8 decomposition.

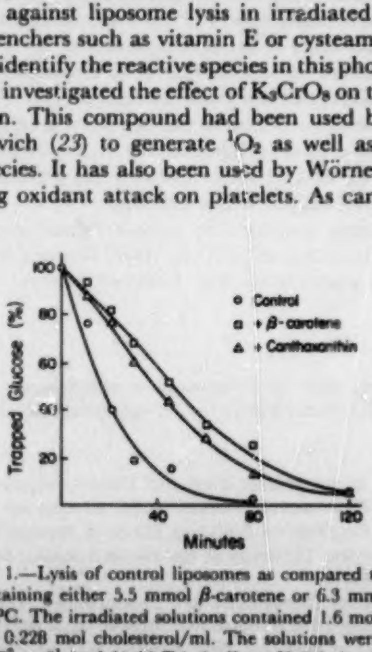

TEXT-FIGURE 1.—Lysis of control liposomes as compared to that of liposomes containing either 5.5 mmol β-carotene or 6.3 mmol canthaxanthin/mol PC. The irradiated solutions contained 1.6 mol PC, 0.45 mol DCP, and 0.228 mol cholesterol/ml. The solutions were irradiated at 0.45 $J\cdot cm^{-2}\cdot sec^{-1}$ in 0.01-*M* Tris buffer, pH 8.0, in the presence of 3×10^{-6} *M* toluidine blue at 10°C (*11*).

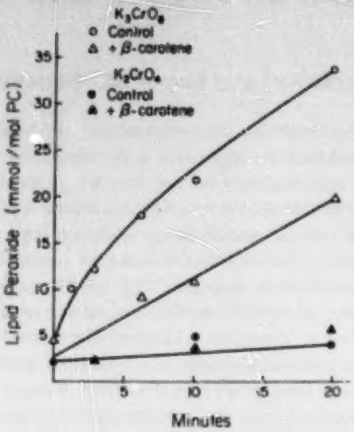

TEXT-FIGURE 2.—Liposomes were prepared as described in text-fig. 1. Either 40 mg of K_3CrO_8 or 40 mg of K_2CrO_4 was added with continuous agitation to 7.5 ml of liposome suspension at 40°C. Aliquots were analyzed for lipid peroxide formation by the ferrous thiocyanate assay (*21*).

UV light has long been known as being capable of initiating lipid peroxidation and starting the chain of radical reactions that leads to the loss of conjugated double bonds among unsaturated fatty acids (*25*). We tested the effect of UV light in our liposomes, prepared with either canthaxanthin or no pigment. The liposomes were exposed to UVC radiation at 254 nm from five germicidal lamps. As can be seen in text-figure 3, the presence of canthaxanthin resulted in a marginal delay in the onset of liposome lysis, as measured by the release of trapped glucose. The effect of the carotenoid pigment on MDA formation was much more pronounced, causing a 1-hour lag period in the appearance of MDA. In addition to measuring liposome lysis and MDA production, we also extracted the total pigment and measured the amount of canthaxanthin present in liposomes. As seen in text-figure 3, canthaxanthin disappeared rapidly with a half-life of approximately 1 hour. The appearance of MDA coincides with the disappearance of the canthaxanthin in the liposomes. Furthermore, lysis, as measured by release of trapped glucose, also seems to coincide with the plateau level of MDA formed in this system.

To assess if the bleaching of carotenoid in the UVC-irradiated liposome system was due solely to lipid peroxide formation, we prepared liposomes with either egg PC or synthetic dipalmitoyl PC, the synthetic compound containing only saturated fatty acids. The results of an experiment in which liposomes containing β-carotene and either unsaturated or saturated fatty acids were exposed to visible light in the presence of toluidine blue appear in text-figure 4. As can be seen, the production of MDA increased rapidly in the egg PC liposomes after a 10-minute lag period. In contrast, no MDA was observed in the liposomes made from dipalmitoyl PC. Of greater interest is the observation that β-carotene was bleached in both liposome systems at the same rate, indicating that the appearance of lipid peroxide was not required for the induction of bleaching of carotenoid pigments and that this bleaching can occur either through the direct interaction of β-carotene with the triplet sensitizer or by the chemical quenching of $^1O_2$ (*26*).

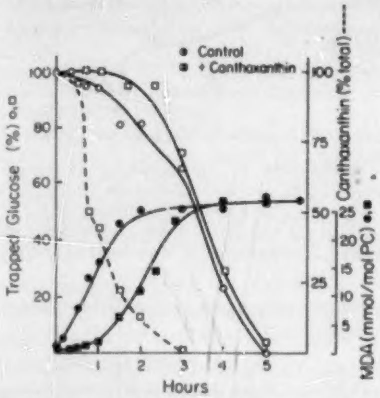

TEXT-FIGURE 3.—The effects of canthaxanthin on UV-induced lipid damage. Egg PC liposomes prepared with or without canthaxanthin were irradiated with germicidal UV lights (254 nm) at 0.4 J·cm^{-2}·sec^{-1} (*35*).

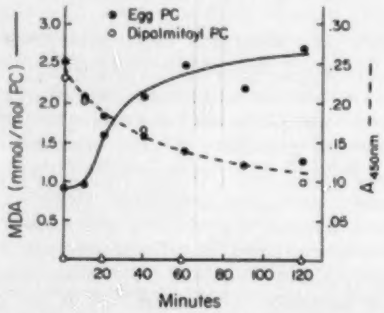

TEXT-FIGURE 4.—Photosensitized bleaching of β-carotene and formation of MDA in egg PC and in dipalmitoyl PC liposomes. Liposomes were irradiated with white light (>530 nm) at 0.45 J·cm^{-2}·sec^{-1} at pH 8 in the presence of 8×10^{-5} *M* toluidine blue.

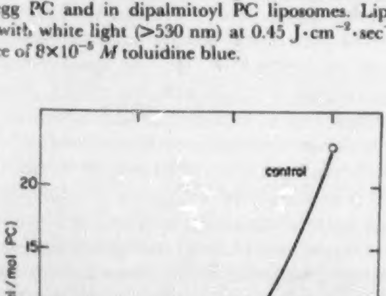

TEXT-FIGURE 5.—Fe^{2+}-generated radical oxidation of liposomes. Egg PC liposomes containing β-carotene, canthaxanthin, or no pigment were incubated with 0.1 *M* $FeCl_2$ for varying times, as indicated (*27*).

An additional means of generating radicals involves treating the unsaturated fatty acids with ferrous salts. As shown in text-figure 5, $FeCl_2$ was added to egg PC liposomes containing no carotenoid, β-carotene, or canthaxanthin. Under these circumstances, the incubation of the liposomes with $FeCl_2$ resulted in the appearance of MDA in the carotenoid-free preparation, whereas the liposomes containing carotenoid pigments were protected against radical-induced MDA formation.

DISCUSSION AND SUMMARY

The results of the experiments described here demonstrate clearly that carotenoid pigments are capable of inhibiting membrane lipid oxidations induced by mechanisms other than those involving $^1O_2$. As seen in text-figure 2, carotenoids protect liposomes from the radical species generated during the decomposition of K_3CrO_8. However, these results are still somewhat ambiguous inasmuch as the degradation of this tetraperoxyochromate can give rise not only to $^1O_2$ but also to the superoxide radical and the hydroxyl radical.

The primary products of UV radiation of unsaturated lipids are radicals produced by the expulsion of a hydrogen atom (*25*). These radicals, by reacting with oxygen to form peroxyradicals, can then initiate a chain reaction leading to extensive lipid peroxidation (*28*) and destruction of liposomes (*13, 15, 29*). As seen in text-figure 3, the progress of lipid peroxidation initated by UVC irradiation was significantly delayed in the presence of canthaxanthin. There is some small probability that canthaxanthin may be filtering some of the UVC radiation used for the initiation of lipid peroxidation. However, the absorbance of the carotenoid at this wavelength is very weak in comparison to the absorbance of the unsaturated lipids, and the carotenoid was maintained at a molar ratio of 0.01 of the phospholipid. A relationship was observed between the delay in the appearance of MDA and the destruction of the carotenoid pigment. In the control liposome preparation, MDA production proceeded without a lag period. In contrast, there was a 1-hour lag period in MDA production in the canthaxanthin liposomes, which coincided with the time necessary to bleach 50–60% of the carotenoid pigment. This observation indicates that the carotenoid strongly inhibited the process of lipid peroxidation. The carotenoid pigment was, however, much less effective with respect to maintaining the integrity of the liposome in the UVC-irradiated preparation in comparison to the visible light–photosensitizer preparation (text-fig. 1).

Another effective means for propagating lipid peroxidation consists of treating unsaturated lipids with the ferrous ion, either alone (*19*) or chelated with EDTA (*30*) or ascorbate (*31–33*). Dobretsov et al. (*31*) have suggested that the ferrous ion can accelerate lipid peroxidation reactions by propagating radical chain reactions in the presence of lipid peroxides, as demonstrated by $Fe^{2+} + ROOH \rightarrow Fe^{3+} + RO\cdot + OH^-$ and $Fe^{3+} + ROOH \rightarrow Fe^{2+} + ROO\cdot + H^+$.

In both reactions, the addition of the iron salts generates either alkoxy radicals or peroxyradicals, which continue the process of initiating lipid peroxidation. Also, as seen in text-figure 5, the addition of either β-carotene or canthaxanthin markedly delays the appearance of MDA from liposomes made with polyunsaturated fatty acids and treated with the ferrous ion. Antioxidants such as BHT (*19*, *30*) and vitamin E (*32–34*) display a similar inhibition of ferrous ion-induced lipid peroxidation.

Several likely mechanisms come to mind with respect to the ability of carotenoid pigments to inhibit these free-radical reactions. In one mechanism, the pigments could serve as free-radical quenchers, such as occurs when antioxidants such as vitamin E or BHT are added to a lipid-peroxidizing system. Another possibility is that the carotenoid pigments act as competitive substrates for radical-induced oxidations and therefore delay the onset or propagation of lipid peroxidation until such time as the pigments are consumed in the peroxidative reactions.

In text-figure 4, we demonstrate the effect of fatty acids on the rate of carotenoid bleaching in a photosensitized system in which toluidine blue was the photosensitizer. In this experiment, liposomes were prepared either with normal polyunsaturated fatty acids present in egg PC or with the saturated compound dipalmitoyl PC. As seen in text-figure 4, there was no MDA formation in the liposomes prepared with the saturated fatty acids, whereas there was extensive MDA formation in the liposomes made with unsaturated fatty acids. However, the rate of carotenoid bleaching was the same in both preparations. This observation strongly indicates that factors other than lipid peroxide can have a major impact on the bleaching of carotenoids.

From the work of Foote (*26*), approximately 0.1% of the carotenoid pigments interacting with the $^1O_2$ are known to undergo a chemical reaction resulting in destruction of the pigment. In addition, there is evidence (*35*, *36*) that carotenoid pigments can react with the triplet states of excited sensitizers, although it is not at all clear whether this reaction might lead to the bleaching of the carotenoid pigment. There is no question now that the formation of peroxyradicals can have a major impact on carotenoid bleaching, as demonstrated by the work of Packer et al. (*37*).

Packer et al. generated peroxyradicals by pulse radiolysis of CCl_4 in aerobic solutions, which leads to almost instantaneous bleaching of β-carotene. Also, by reaction with peroxyradicals, carotenoid pigments can inhibit the propagation of lipid peroxidation reactions. Such a mechanism may well explain the observations of Kellogg and Fridovich (*38*) who reported that β-carotene inhibited lipid peroxidation induced by xanthine oxidase and acetaldehyde.

We have therefore demonstrated that carotenoid pigments are capable of inhibiting lipid peroxidations induced by factors that lead to radical-mediated reactions other than those initiated by $^1O_2$. There have been other suggestions in the literature that would indicate that carotenoid pigments have a broader effectiveness than that of quenching $^1O_2$. For example, Yamane and Lamola (*39*) suggested that the inhibition of cholesterol-5α-hydroperoxide-induced erythrocyte lysis by β-carotene was due to a radical-quenching reaction on the part of the carotenoid. In addition, Mathews-Roth et al. (*40*) noted that the protective action of a series of carotenoid pigments in a biological system does not necessarily parallel the $^1O_2$-quenching ability of these pigments and suggested that the discrepancy might be due to carotenoids interfering with radical reactions initiated in vivo.

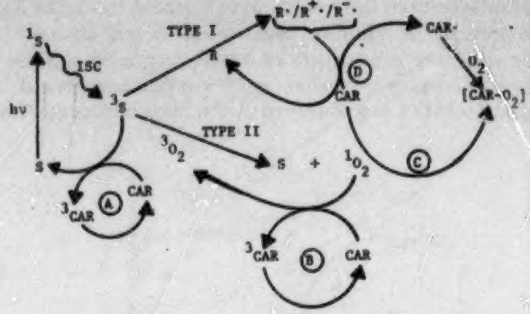

TEXT-FIGURE 6.—Mechanisms of carotenoid protection. Carotenoids (CAR) can quench triplet sensitizers Ⓐ, quench $^1O_2$ Ⓑ, chemically react with $^1O_2$ Ⓒ, or react with radical intermediates Ⓓ. "C" and "D" presumably result in the bleaching of the carotenoid pigment. ISC = intersystem crossing; S = sensitizer; R = an oxidizable substrate.

Clearly, these data show that carotenoids can effectively inhibit lipid oxidation initiated by mechanisms not involving $^1O_2$. The various mechanisms as depicted in text-figure 6 are indicated by *a*) carotenoid quenching of triplet sensitizers, *b*) carotenoid quenching of $^1O_2$, *c*) carotenoid reaction with $^1O_2$, and *d*) carotenoid reaction with radical species.

It is therefore clear that carotenoid pigments are very effective agents in terms of protecting cells against a variety of processes that can lead to cellular damage by several different and distinct mechanisms (*41*). Although the ability of carotenoid pigments to quench $^1O_2$ is an important function with respect to photosensitized oxidations or other reactions which might generate $^1O_2$, the observation of protection in the presence of carotenoids cannot necessarily be interpreted as being due to $^1O_2$ involvement in the process. The radical mechanisms described above would have to be ruled out before one could conclude that the mechanism under investigation indeed involved $^1O_2$. Furthermore, this broad spectrum of protective action exhibited by carotenoid pigments may be related to observations that in the case of some chemically induced mutations (*42*) or UVB-induced mutations (*42–44*), carotenoid pigments have exhibited protective effects. These observations have led to a proposal that carotenoid pigments might function as antitumor agents (*45*). Future experiments should help clarify this hypothesis.

REFERENCES

(*1*) KRINSKY NI. The protective function of carotenoid pigments. In: Giese AC, ed. Photophysiology. Vol 3. New York: Academic Press, 1968:123–195.

(*2*) SISTROM WR, GRIFFITHS M, STANIER RY. The biology of a photosynthetic bacterium which lacks colored carotenoids. J Cell Comp Physiol 1956; 48:473–515.

(*3*) Blum HF. Photodynamic action and diseases caused by light. New York: Reinhold (reprinted 1964, New York: Hafner Press), 1941.

(*4*) Anderson IC, Robertson DS. Role of carotenoids in protecting chlorophyll from photodestruction. Plant Physiol 1960; 35:531–534.

(*5*) Claes H. Analyse der biochemischen synthesekette für carotenoide mit hilfe von Chlorella-mutanten. Z Naturforsch 1954; 9B:461–470.

(*6*) Kunisawa R, Stanier RY. Studies on the role of carotenoid pigments in a chemoheterotrophic bacterium, *Corynebacterium poinsettiae*. Arch Mikrobiol 1958; 31:146–156.

(*7*) Mathews MM, Sistrom WR. Function of carotenoid pigments in non-photosynthetic bacteria. Nature 1959; 184:1892–1893.

(*8*) Foote CS, Denny RW. Chemistry of singlet oxygen. VII. Quenching by beta-carotene. J Am Chem Soc 1968; 90:6233–6235.

(*9*) Krinsky NI. Biological functions of singlet oxygen. In: Wasserman HH, Murray RW, eds. Singlet oxygen. New York: Academic Press, 1979:597–641.

(*10*) Kinsky SC, Haxby J, Kinsky CB, Demel RA, Van Deenen LL. Effect of cholesterol incorporation on the sensitivity of liposomes to the polyene antibiotic, filipin. Biochim Biophys Acta 1968; 152:174–185.

(*11*) Anderson SM, Krinsky NI. Protective action of carotenoid pigments against photodynamic damage to liposomes. Photochem Photobiol 1973; 18:403–408.

(*12*) Anderson SM, Krinsky NI, Stone MJ, Clagett DC. Effect of singlet oxygen quenchers on oxidative damage to liposomes initiated by photosensitization or by radiofrequency discharge. Photochem Photobiol 1974; 20:65–70.

(*13*) Roshchupkin DI, Pelenitsyn AB, Potapenkio AY, Talitsky VV, Vladimirov YuA. Study of the effects of ultraviolet light on biomembranes. IV. The effect of oxygen on UV-induced hemolysis and lipid photoperoxidation in rat erythrocytes and liposomes. Photochem Photobiol 1975; 21:63–69.

(*14*) Copeland ES, Alving CR, Grenan MM. Light-induced leakage of spin label marker from liposomes in the presence of phototoxic phenothiazines. Photochem Photobiol 1976; 24:41–48.

(*15*) Mandal TK, Ghose S, Sur P, Chatterjee SN. Effect of ultra-violet radiation on the liposomal membrane. Int J Radiat Biol 1978; 33:75–79.

(*16*) Suwa K, Kimura T, Schaap AP. Reaction of singlet oxygen with cholesterol in liposomal membranes. Effect of membrane fluidity on the photooxidation of cholesterol. Photochem Photobiol 1978; 28:469–473.

(*17*) Seligman ML, Mitamura J, Shera N, Demopoulos HB. Corticosteroid (methylprednisolone) modulation of photoperoxidation by ultraviolet light in liposomes. Photochem Photobiol 1979; 29:549–558.

(*18*) Muller-Runkel R, Blais J, Grossweiner LI. Photodynamic damage to egg lecithin liposomes. Photochem Photobiol 1981; 33:683–687.

(*19*) Leibowitz M, Johnson MC. Relation of lipid peroxidation to loss of cations trapped in liposomes. J Lipid Res 1971; 12:662–670.

(*20*) Placer ZA, Cushman L, Johnson BC. Estimation of product of lipid peroxidation (malonyl dialdehyde) in biochemical systems. Anal Biochem 1966; 16:359–364.

(*21*) Robey RF, Weise HK. Determination of peroxides in synthetic rubber. Anal Chem 1945; 17:425–426.

(*22*) Reisenfeld EH, Wohlers HE, Kutsch WA. Höhere oxydationsproducte des chroms. Chem Ber 1905; 38:1885–1898.

(*23*) Hodgson EK, Fridovich I. The production of superoxide radical during the decomposition of potassium peroxochromate (V). Biochemistry 1974; 13:3811–3815.

(*24*) Wörner P, Patscheke H, Paschen W. Response of platelets exposed to potassium tetraperoxochromate, an extracellular source of singlet oxygen, hydroxyl radicals, superoxide anions and hydrogen peroxide. Hoppe Seylers Z Physiol Chem 1979; 360:559–570.

(*25*) Livingston R. Photochemical autoxidation. In: Lundberg WO, ed. Autoxidation and antioxidants. Vol 1. New York: Interscience, 1961:249–298.

(*26*) Foote CS. Photosensitized oxidation and singlet oxygen: Consequences in biological systems. In: Pryor WA, ed. Free radicals in biology. Vol 2. New York: Academic Press, 1976:85–113.

(*27*) Krinsky NI. Carotenoid pigments: Multiple mechanisms for coping with the stress of photosensitized oxidation. In: Shilo M, ed. Strategies of microbial life in extreme environments. Berlin: Dahlem Konferenzen, 1979:163–177.

(*28*) Pryor WA. The formation of free radicals and the consequences of their reactions in vivo. Photochem Photobiol 1978; 28:787–801.

(*29*) Seligman ML, Demopoulos HB. Spin-probe analysis of membrane perturbations produced by chemical and physical agents. Ann NY Acad Sci 1973; 222:640–667.

(*30*) Svingen BA, Buege JA, O'Neal FO, Aust SD. The mechanism of NADPH-dependent lipid peroxidation. J Biol Chem 1979; 254:5892–5899

(*31*) Dobretsov GE, Borschevskaya TA, Petrov VA, Vladimirov YuA. The increase of phospholipid bilayer rigidity after lipid peroxidation. FEBS Lett 1977; 84:125–128.

(*32*) Arkhipenko IuV, Dobrina SK, Kagan VE, et al. Stabilizing action of vitamin E on biological membranes in the peroxide oxidation of lipids. Biokhimiia 1977; 42:1525–1531 (in Russian, English abstract).

(*33*) Gutteridge JM. The membrane effects of vitamin E, cholesterol and their acetates on peroxidative susceptibility. Res Commun Chem Pathol Pharmacol 1978; 22:563–572.

(*34*) Tappel AL. Vitamin E and free radical peroxidation of lipids. Ann NY Acad Sci 1972; 203:12–28.

(*35*) Fujimori E, Livingston R. Interactions of chlorophyll in its triplet state with oxygen, carotene, etc. Nature 1957; 180:1036–1038.

(*36*) Krinsky NI. Carotenoid protection against oxidation. Pure Appl Chem 1979; 51:649–660.

(*37*) Packer JE, Mahood JS, Mora-Arellano VO, Slater TF, Willson RL, Wolfenden BS. Free radicals and singlet oxygen scavengers: Reaction of a peroxy-radical with beta-carotene, diphenylfuran and 1,4-diazobicyclo-(2,2,2)-octane. Biochem Biophys Res Commun 1981; 98:901–906.

(*38*) Kellogg EW III, Fridovich I. Superoxide, hydrogen peroxide, and singlet oxygen in lipid peroxidation by a xanthine oxidase system. J Biol Chem 1975; 250:8812–8817.

(*39*) Yamane T, Lamola AA. Red blood cell lysis induced by a product of singlet oxygen and cholesterol. Abstracts of the first annual meeting of the American Society for Photobiology, Sarasota, Fla., June 10–14, 1973. Bethesda, Md.: American Society for Photobiology, 1973:66.

(*40*) Mathews-Roth MM, Wilson T, Fujimori E, Krinsky NI. Carotenoid chromophore length and protection against photosensitization. Photochem Photobiol 1974; 19:217–222.

(*41*) Krinsky NI. Photobiology of carotenoid protection. In: Regan JD, Parrish JA, eds. Photomedicine. New York: Plenum, 1982:397–403.

(*42*) Mathews-Roth MM. Anti-tumor activity of beta-carotene, canthaxanthin and phytoene. Oncology 1982; 39:33–37.

(*43*) Epstein JH. Effects of beta-carotene on ultraviolet induced cancer formation in the hairless mouse skin. Photochem Photobiol 1977; 25:211–213.

(*44*) Gruener N, Lockwood MP. Photodynamic mutagenicity in mammalian cells. Biochem Biophys Res Commun 1979; 90:460–465.

(*45*) Peto R, Doll R, Buckley JD, Sporn MB. Can dietary beta-carotene materially reduce human cancer rates? Nature 1981; 290:201–208.

DISCUSSION

L. De Luca: What is the specificity for the carotenoids? In any of these systems, do you get the same effects with retinoids?

N. Krinsky: The specificity with respect to singlet oxygen quenching is very much dependent on the polyene chain length, and there have been very good studies, both in vivo and in vitro, that have demonstrated that you need a minimum of nine conjugated double bonds for the carotenoid to act as an effective singlet oxygen quencher. The effectiveness is related to the triplet energy level of the carotenoid, with respect to the energy difference between singlet excited oxygen and ground-state oxygen.

With respect to triplet sensitization, that is also a function of the chain length of the carotenoid, but it also involves the triplet energy level of the sensitizer. For example, if chlorophyll is used as a sensitizer, one finds that one can use carotenoid pigments with only seven conjugated double bonds as protective agents because the energy level of triplet chlorophyll is lower than that of the energy difference between singlet oxygen and ground-state oxygen.

With respect to radical quenching, that is not at all as clear. One would expect that compounds such as the retinoids could also be readily oxidized by radical species. Under those circumstances, one would expect that retinol or any of the retinoids would also be effective quenchers of radical reactions, although it is not clear at all what might be happening to their radical products themselves.

W. Benson: Could you discuss water-soluble vitamin C as a radical scavenger in this case? It is not a fat-soluble carotenoid.

Krinsky: There is no question that vitamin C is a very effective radical quencher. In fact, if one does experiments in which one has used high-energy radiation to excite biological systems, the major radical species that can be observed after the irradiation turns out to be the radical of vitamin C. So the vitamin C may, in fact, be acting as a sink or a trap for collecting a variety of radicals that are formed within the body and, of course, that would only relate, therefore, to the more water-soluble radicals or those that the vitamin C could, in fact, come into contact with.

Vitamin E, also an effective radical quencher, would be localized, however, within lipophilic areas such as biological membranes and presumably would then be serving as a radical quencher or trap within that particular system.

P. Sundaresan: From the point of view of clinical application, would you suggest that β-carotene can be used as a sunscreen?

Krinsky: I will defer that question to the final speaker of the symposium, or do you want it answered now? I do not know very much about sunscreens, but Dr. Mathews-Roth does.

M. Mathews-Roth: As a sunscreen, Dr. M. A. Pathak, Dr. T. B. Fitzpatrick, Dr. E. H. Kass, and I looked at β-carotene, and although you get a statistically significant increase in the minimum erythema dose (MED), it is not clinically worth it. So I would have to say that β-carotene does not work as a sunscreen.

β-Carotene will be a protective agent against the photosensitization associated with porphyria, and that is what most of my talk tomorrow is going to be about. But we cannot recommend it as a sunscreen. Some people are using it as an artificial tanning agent, as was Man-Tan, but that is strictly for cosmetic purposes.

What we did find is that people who took β-carotene tanned a little easier, rather than being burned. But the MED was not significantly increased enough, again, to make it worthwhile. So the answer to your question is really no, you cannot recommend β-carotene as a sunscreen.

A Method To Quantify the Potency of Photosensitizers That Modify Cell Membranes[1]

John P. Pooler[2] *and* **Dennis P. Valenzeno**[3]

ABSTRACT—The numerical assessment of sensitizing potency of different species of photosensitizer molecules has historically been impracticable because of the difficulty of measuring all of the factors that must be taken into account. This paper describes a new method for quantifying relative sensitizer potency that obviates most of the past difficulties. The physical data needed to assess photosensitizing potency are the absorption spectrum of a sample of medium containing sensitizer, the illumination spectrum impinging on the preparation, the duration of illumination, and the amount of light-induced modification. The measurement of these quantities is relatively straightforward, but it is easy to overlook a number of artifacts that can distort the values for potency. Avoiding error requires careful attention to the optical properties of the system, particularly in the light path through the medium containing sensitizer.—JNCI 1982; 69:211–215.

Despite more than eight decades of research involving photosensitization of cells, little has been done to quantify the potency of different sensitizers. Review articles and book chapters on photosensitization generally list a handful of compounds as being good sensitizers (e.g., hematoporphyrin, eosin Y, acridine orange, and methylene blue) (*1*, *2*), but quantification is absent. A few reports have given some preliminary estimates of potency for fluorescein sensitizers (*3*, *4*) or porphyrins (*5*), while recent work by us has provided a thorough quantitative comparison of fluorescein sensitizers for photosensitization of nerve cell membranes (*6*) and erythrocytes (*7*). The purpose of this article is to explain the logic behind a general method for the quantification of sensitizer potency. While these ideas are centered on photosensitization of surface membrane function, much of the logic is applicable to modification of any cellular function.

A DILEMMA: HOW TO MEASURE ABSORPTION BY THE MOLECULES ACTUALLY DOING THE SENSITIZING

Reaction 1 outlines the process of membrane photosensitization.

$$\text{Normal membrane function} + \text{photosensitizer} + \text{light} \rightarrow \text{modified membrane function} \qquad [1]$$

In principle any measurable function could be involved in this process (e.g., membrane fluidity, receptor binding capacity, and solute transport rate). The main point is that the function must be quantifiable. Without quantification of the modification, then obviously quantification of sensitizer potency is not possible. Even with reliable quantitation of modification in hand, it is still not easy to derive sensitizer potency because modification also depends on the fluence. And not only is the total energy of light important but also its spectral makeup. The overlap between the illumination spectrum of the light and the absorption spectrum of the sensitizer is as important as total energy. Sensitizer concentration also plays a role. Higher concentrations absorb more photons and lead to greater modification. Just how this factor can be separated from the other factors involved may not be obvious. To sort these things out, one can begin with the photochemical concept of quantum yield (Φ) as given by equation 2. Quantum yield is a measure of potency for a homogeneous mixture of sensitizer and substrate in a reaction vessel.

$$\Phi = \frac{\text{Number of molecules reacted}}{\text{Number of photons absorbed}} \qquad [2]$$

The central concept here is that the amount of light-generated reaction is scaled to the number of photons absorbed. Therefore, any variation in illumination intensity, duration, spectral makeup, sensitizer absorption, and concentration is automatically taken into account. For the modification of cell membranes, unfortunately, one rarely knows which molecules have reacted or how to count them, and a direct assessment of quantum yield is impossible. One can define a potency as given by equation 3.

$$\text{Potency} = \frac{\text{Amount of membrane modification}}{\text{Number of photons absorbed}} \qquad [3]$$

This definition is analogous to that of quantum yield and involves the same essential concept, i.e., scaling modification to the photons absorbed. Even this definition is insufficient to define potency in a practical sense because not all individual sensitizer molecules in a heterogeneous cell membrane system will be equally effective in producing modification. This point is illustrated in text-figure 1. The sensitizer molecules are divided into three classes. Class I is within the membrane, removed from the aqueous environment; class II is adsorbed or bound to the external surface of the membrane; and class III is free in the aqueous environment at various distances from the membrane. A priori, one would expect molecules in class I to have the best chance of photosensitizing modification, whereas those far from the membrane in class III would have no chance. Molecules in class II and nearby ones in class III might have an intermediate chance. If one considers the dimensions of cell membranes, the vast majority of the absorption will occur

---

ABBREVIATION USED: OD=optical density (densities).

---

[1] Presented at the Seventh Food and Drug Administration Science Symposium ("Photochemical Toxicity: Toxic, Allergic, and Carcinogenic Aspects With Emphasis on Predicting Effects in Humans") held at the Uniformed Services University of the Health Sciences, Bethesda, Md., March 16-17, 1981.

[2] Department of Physiology, Emory University, Atlanta, Ga. 30322.

[3] Department of Physiology, University of Kansas, Kansas City, Kans. 66103.

in class III molecules, i.e., those which are not effective in producing modification. Thus in terms of scaling modification to absorption, it appears that one would scale to absorption having nothing to do with the modification. It might therefore seem logical to correct for absorption in the environment and only include absorption by classes I and II, but this method also involves difficulties. Effective sensitization can occur at sensitizer concentrations in the nanomolar range where OD becomes vanishingly small. At higher concentrations, the contribution of molecules at or near the membrane to total measurable absorption is still negligible. Even if the values could be obtained, one does not know the relative contributions to the modification by sensitizer molecules in classes I, II, and nearby regions of III. Thus a dilemma is created. How can one scale modification to absorption by the sensitizer molecules which actually do the sensitizing?

To solve this dilemma we must make the following two assumptions which obviate the need to assess directly absorption by only those molecules doing the sensitizing: 1) The concentration of effective sensitizer molecules is proportional to the concentration in the external medium, and 2) the absorption spectrum of effective sensitizer molecules has the same wavelength dependence as the absorption spectrum of the external medium. Together, these assumptions lead to a third assumption: The number of photons absorbed by effective sensitizer molecules is proportional to the number of photons absorbed in a thin layer of medium. By making this assumption, one can now define potency as modification scaled to absorption in a thin layer of medium. Conceptually, this is like finding the true quantum yield and multiplying it by factors that alter the capture of photons by effective sensitizer molecules relative to those in the bath. As an example, consider two sensitizers with equal concentrations and absorption spectra in the external medium but different concentrations in the effective region. The photon capture in the external medium will be the same for both sensitizers but different in the effective region. The sensitizer with the higher concentration in the effective region will capture more photons there and lead to greater modification. The sensitizer's potency, measured as modification scaled to absorption in the medium, will therefore be higher. In this definition of potency, it makes no difference whether increases in modification are due to more efficient transfer of captured photon energy to a reaction or simply to a greater capture of photons in the effective region—either way this manifests itself as an increase in modification. One utility of this definition is that it permits a simple measurement of medium absorption in a cuvette. Further consideration of the meaning and validity of the assumptions involved is provided later.

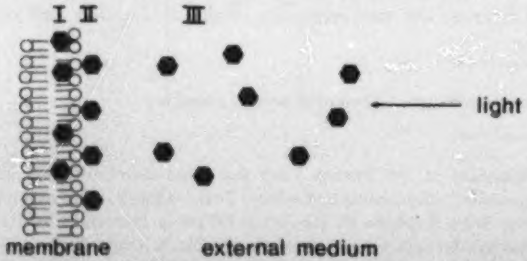

TEXT-FIGURE 1.—Location of sensitizer molecules with respect to the membrane. Sensitizer molecules (*solid symbols*) are classified as being within the membrane (class I), adsorbed or bound to the external surface (class II), or free in the external medium (class III).

CALCULATION OF ABSORBED PHOTONS

The energy capture per unit area in an absorbing medium is related to the OD by equation 4, where I and I_o are the transmitted and incident intensities, respectively.

$$I_o - I = I_o(1 - 10^{-\mathrm{OD}}) \qquad [4]$$

One can convert the energy capture to total photon capture by multiplying by illumination time (T), dividing by the energy per photon (hc/λ), and integrating across all wavelengths (equation 5).

$$\text{Absorbed photons} = T\int I_o(1 - 10^{-\mathrm{OD}})\,\frac{\lambda}{hc}\,d\lambda \qquad [5]$$

For low OD, which will always obtain for very short path lengths, the term in parentheses may be simplified according to equation 6.

$$1 - 10^{-\mathrm{OD}} \simeq 2.3\ \mathrm{OD} \qquad [6]$$

Combining equations 5 and 6 and replacing all constant terms by a single constant yield equation 7.

$$\text{Absorbed photons} = \text{constant}\ T\int I_o \mathrm{OD}\lambda d\lambda \qquad [7]$$

The OD at any particular concentration of the sensitizer C can be related to the OD at a standard concentration by equation 8.

$$\mathrm{OD} = \frac{C}{C^s}\,\mathrm{OD}^s, \qquad [8]$$

where the superscripts refer to the standard condition. Combining equations 7 and 8 gives equation 9.

$$\text{Absorbed photons} = \text{constant}\ T\,\frac{C}{C^s}\int I_o \mathrm{OD}^s\lambda d\lambda \qquad [9]$$

Equation 9 is a useful expression, for it permits calculation of absorbed photons under a standard condition and then a simple scaling of that result to any particular concentration and illumination time.

Integration of equation 9 is illustrated schematically in text-figure 2. The top three parts of the text-figure show the variation of each of the terms in the integral with wavelength. Wavelength, of course, is linear with itself. The illumination intensity represents a broadband source with a maximum at long wavelengths. The OD is the absorption spectrum of the sensitizer at a standard concentration. The sensitizer shown here absorbs maximally at short wavelengths. The bottom part of the text-figure shows the product of the three factors, which drops to zero at the long wavelength end because the sensitizer no longer absorbs at long wavelengths and drops to zero at the short wavelength end because the source intensity drops to zero there. The shaded area under this curve is the value of the integral. As one would expect, this value varies with intensity of the source, absorption efficiency of the sensitizer, and the degree

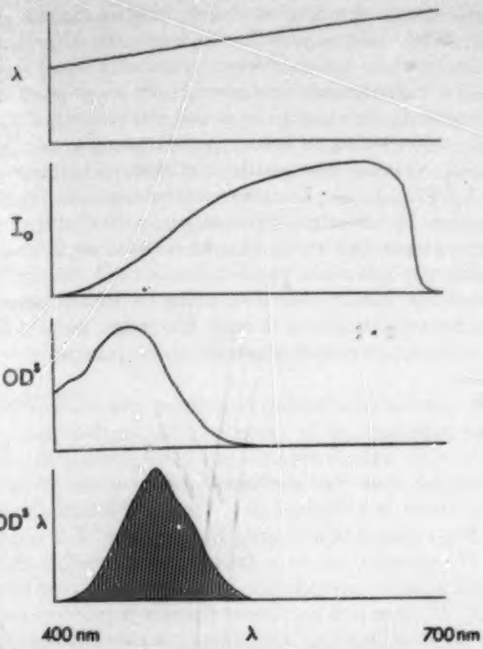

TEXT-FIGURE 2.—Wavelength-dependent terms that are integrated to calculate the number of absorbed photons. *Upper three panels* show the wavelength (λ), illumination spectrum (I_0), and the absorption spectrum of the external medium at a standard concentration (OD^s) plotted as a function of wavelength in the visible region. *Bottom panel* shows their product. The area under the product curve (*shaded region*) is the integral of equation 9.

of overlap between the two spectra. Multiplying this area by the other terms in equation 9 then yields the total absorption.

CALCULATION OF RELATIVE POTENCY

The previous section described the process of calculating the number of absorbed photons in an absorbing medium. This logic can be directly applied to the case of a thin layer of medium outside a cell membrane. Call the thickness of this thin layer δ. If the absorption properties of the medium are measured in a typical 1-cm path length cuvette, then the actual absorption will be δ times that value, since OD varies directly with path length. Let D = absorbed photons in a layer of medium δ thick, A = value of the integral in equation 9, M = amount of modification occurring in time T, and P = sensitizer potency.

$$D = \delta \text{ constant } T\frac{C}{C^s}A \qquad [10]$$

$$P = \frac{M}{D} \qquad [11]$$

Equation 11 is now the expression for sensitizer potency which scales modification to the number of absorbed photons in a thin layer of external medium. Although a numerical value for P (potency) may be obtained from this expression, it actually has no meaning without reference to the P-value for another sensitizer, since the units of M and the choice of δ are quite arbitrary. If, however, P for one sensitizer is compared to that for another, then a *relative* potency is obtained—the goal of this whole procedure. Consider now two sensitizers, 1 and 2, for which P-values have been obtained.

$$\frac{P_2}{P_1} = \frac{M_2D_1}{M_1D_2} \qquad [12]$$

$$\frac{P_2}{P_1} = \frac{M_2T_1(C_1/C_1^s)A_1}{M_1T_2(C_2/C_2^s)A_2} \qquad [13]$$

Equation 13 now expresses the potency of sensitizer 2 relative to that of sensitizer 1. Note that δ and the constants from equation 10 are canceled; therefore, one need not even bother with their values. Once the integral of equation 9 has been evaluated at standard concentrations, then the actual assessment of relative sensitizer potency involves measurement of the amounts of modification, the times of illumination, and the concentrations.

PHYSICAL TECHNIQUES

The assessment of modification is specific for the particular system involved and depends on the function and cell type being photosensitized. Therefore it will not be discussed here. The absorption spectrum of sensitizer is easily measured in a conventional spectrophotometer. The illumination spectrum can be obtained in several ways. One way is to use published spectra of the source employed, modified by any filter characteristics used in the system. Another method is to measure with a spectroradiometer the illumination spectrum impinging on the cell. With fairly broadband sources such as incandescent lamps, either method works reasonably well. One caveat to note here is the problem of screening. The illumination spectrum for this calculation is the spectrum actually reaching the cell membrane, not the spectrum on the outside of a thick layer of concentrated sensitizer. A container of colored sensitizer solution may appear perfectly

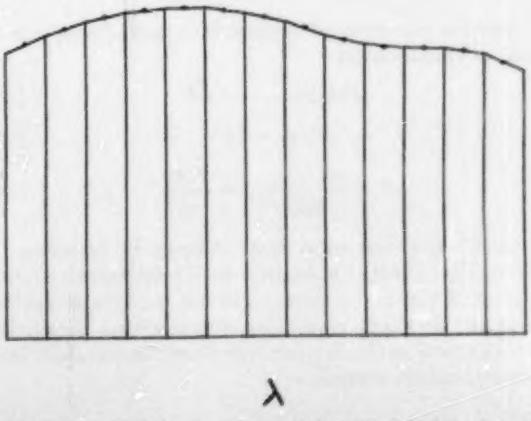

TEXT-FIGURE 3.—Division of wavelength-dependent function into small wavelength bands. A portion of the whole curve is shown over a limited region of wavelength. The midpoint within each band is multiplied by the midpoints of the other wavelength-dependent functions at corresponding wavelengths to obtain the points that form the product curve.

transparent, yet it can absorb the vast majority of light at the wavelengths of peak absorption efficiency. For typical sensitizers with a peak molar extinction coefficient of 10^5 and a 1-cm solution thickness, the majority of the light at the absorption maximum will be screened at all concentrations above 3 μM.

Evaluation of the integral of equation 9 is performed numerically. For each of the three terms within the integral, the total wavelength region of interest is divided into small bandwidth sections, as shown in text-figure 3. For each section the midpoints of the relations for each term (I_o, OD, λ) are multiplied together. Plotting these points against wavelength gives the product curve (bottom of text-fig. 2). The products are now summed, and the sum is multiplied by the bandwidth of the wavelength sections, which yields the area (integral of the product curve). While some sort of a digitizer-computer arrangement is very useful to aid in the computation, the process can be done with graph paper and a calculator.

POTENCY BASED ON RATE OF MODIFICATION

For the case of those modifications that proceed as an exponential decline in a function, it is an experimental convenience to base potency on rates of modification.

$$M = F_o(1 - e^{-k_1 t}) \qquad [14]$$

$$D = k_2 t \qquad [15]$$

Equations 14 and 15 express the amount of modification and absorbed photons during a time t. The k's are rate constants for the processes, and F_o is the value of the modified function before modification begins. For times short enough that M is small relative to F_o, the following approximation holds:

$$M \simeq F_o k_1 t \qquad [16]$$

This allows potency to be defined by equation 17.

$$P = \frac{M}{D} = \frac{F_o k_1 t}{k_2 t} = \frac{F_o k_1}{k_2} \qquad [17]$$

Now consider the rates of modification and absorption at the start of illumination.

$$(dM/dt)_{t=0} = F_o k_1 \qquad [18]$$

$$dD/dt = k_2 \qquad [19]$$

$$P = \frac{(dM/dt)_{t=0}}{dD/dt} = \frac{F_o k_1}{k_2} \qquad [20]$$

Equation 20 gives the same result as given by equation 17, indicating that scaling the initial rate of modification to rate of absorption yields the same value for potency as scaling the amounts. In many experimental conditions, measuring the rate of modification is more convenient or accurate than measuring a single amount.

COMMENT

The method described here was devised to cope with the apparently hopeless task of assessing sensitizer potency when the information required to define a true quantum yield is absent. While one would like to know the true quantum yield in order to have a better chance of identifying the molecular mechanisms underlying the modification, in a practical sense the concept of potency is more useful. When assessing the relative phototoxicity of a group of compounds, one wants to know how much modification will occur for a given light condition. The physicochemical factors affecting differences in sensitizer permeation and absorption efficiency in the actual region of sensitization are as important as is the true quantum yield in controlling the amount of modification. Ideally, one would like to express potency on a concentration basis, as is done for drugs, but there is no way to bypass the light absorption component of the calculation.

The assumptions underlying these calculations require further comment. It is assumed that modification varies directly with light intensity, sensitizer concentration, and illumination time. For the modification of nerve cell membranes, there is evidence that these conditions hold over fairly large ranges of intensity (*8*) and time.[4] For concentrations of sensitizer up to a range where possible shielding becomes a factor, modification is linear with concentration also (*9*). If there is a nonlinear fluence dependence, as was found for modification of erythrocyte membranes (*10, 11*), then defining a single potency parameter may not be possible. In such a situation, relative potency has to be defined at equivalent fluence for all sensitizers considered, or a new expression for potency must be defined that takes into account the specific fluence dependence.

The second-stated assumption says that the absorption spectra of effective and bath-located molecules have the same wavelength dependence. There is evidence that this assumption is somewhat in error since action spectra for modification of nerve membranes were found to be shifted to longer wavelengths by about 17 nm relative to absorption spectra of the bathing media (*9*). If the illumination spectrum is relatively flat in the region of maximum sensitizer absorption, the resulting error in calculated absorption will be insignificant. If, however, a source is employed with sharp peaks near the absorption maximum, then serious errors in calculated absorption can occur.[5]

Another complication that can confuse the results is a time dependence for distribution of sensitizer. If the arrival of sensitizer molecules at effective sites follows with a delay after the sensitizer is placed in the medium, then measured potency obviously will develop with a delay. For modification of nerve membranes, such a delay is not only significant but also variable from one sensitizer to the next (*6*). Ideally, a preillumination exposure time should be employed allowing a quasi-equilibrium distribution of sensitizer to be reached, or failing this, a standard preillumination time should be chosen for all sensitizers.

In the survey of the history of sensitized cell photomodification, there have been three barriers to the quantification of potency. The first barrier is the dependence of modification on a large number of variables and the difficulty of sorting them out experimentally, or even being aware of them. Overcoming this barrier involves thought about the optics of the system from emission to absorption and the performance of careful control experiments to eliminate unsuspected reasons for variations in potency. The second barrier is a difficulty in quantifying modification. Quantifying modification is a matter of bringing quantitative methods to the field of cell biology. The third barrier has been the subject of this paper—a definition of potency. We hope that these ideas will help future investigators define potency in a meaningful and quantitative way.

---

[4] Unpublished work by us shows that cutting the intensity and increasing the illumination duration by factors of 10 give equivalent modification.

[5] Equivalently, employing a monochrometer or using narrow band-pass filters can cause the same error. Source spectrum in this case means the spectrum actually reaching the effective sensitizer molecules.

REFERENCES

(*1*) Spikes JD. Photosensitization. In: Smith KC, ed. The science of photobiology. New York: Plenum, 1977:87-112.

(*2*) Smith KC, Hanawalt PC. Molecular photobiology. New York: Academic Press, 1969.

(*3*) Blum HF. Photosensitization of living systems. Cold Spring Harbor Symp Quant Biol 1935; 3:318-327.

(*4*) Kondo M, Kasai M. Photodynamic inactivation of sarcoplasmic reticulum vesicle membranes by xanthene dyes. Photochem Photobiol 1974; 19:35-41.

(*5*) Kessel D. Effects of photoactivated porphyrins at the cell surface of leukemia L1210 cells. Biochemistry 1977; 16:3443-3449.

(*6*) Pooler JP, Valenzeno DP. Physicochemical determinants of the sensitizing effectiveness for photooxidation of nerve membranes by fluorescein derivatives. Photochem Photobiol 1979; 30:491-498.

(*7*) Valenzeno DP, Pooler JP. Cell membrane photomodification: Relative effectiveness of halogenated fluoresceins for photohemolysis. Photochem Photobiol 1982; 35:343-350.

(*8*) Pooler JP. Photodynamic alteration of sodium currents in lobster axons. J Gen Physiol 1972; 60:367-387.

(*9*) Pooler JP, Valenzeno DP. Kinetic factors governing sensitized photooxidation of excitable cell membranes. Photochem Photobiol 1978; 28:219-226.

(*10*) Cook JS, Blum HF. Dose relationships and oxygen dependence in ultraviolet and photodynamic hemolysis. J Cell Comp Physiol 1959; 53:41-60.

(*11*) Valenzeno DP, Pooler JP. The concentration and fluence dependence of delayed photohemolysis. Photochem Photobiol 1982; 35:427-429.

DISCUSSION

J. Epstein: Which sensitizers have you rated?

J. P. Pooler: All of our work, as far as actually rating one with respect to the other, has been done with sensitizers of the fluorescein series. We have now done 10 different fluorescein sensitizers.

Anonymous: Are they rated?

Pooler: Yes, they can all be rated. Fluorescein is at the bottom, and rose bengal is at the top. The ratio of their potency is about 30,000 to 1—a huge range.

blank page

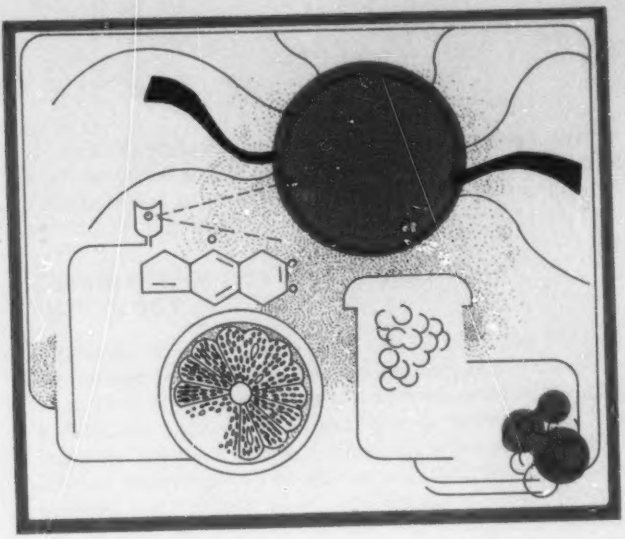

EXPERIMENTAL ANIMAL SYSTEMS

Moderator: F. Alan Andersen
Food and Drug Administration

blank page

In Vitro Assay of the Effects of Psoralens Plus Ultraviolet Radiation on Human Lymphoid Cells[1]

Kenneth H. Kraemer, *M.D.*[2,3]

ABSTRACT—An in vitro assay system that mimics some of the features of in vivo oral methoxsalen photochemotherapy (PUVA) in relation to human lymphoid cells was developed. In this assay, suspension cultures of human lymphoid cells were subjected to therapeutic concentrations of 8-MOP and to a UVA radiation spectrum modified to approximate the dermal exposure. The assay permitted correlation and quantitation of multiple 8-MOP plus UVA-induced biological and physical alterations in the same assay system. Thus were demonstrated inhibition of DNA synthesis, reduction of cell survival, production of DNA cross-links, and loss of mixed leukocyte reactivity induced by combinations of 8-MOP and UVA in or near the presumed therapeutic range. This assay may be useful for predicting lymphoid cellular toxicity of other photoactive agents as well as for examining the molecular effects of these agents.—JNCI 1982; 69:219–227.

A new type of clinical therapy, photochemotherapy, explicitly combining photoactive drugs with UV radiation is presently being investigated as a treatment of human diseases. PUVA therapy, the combination of oral 8-MOP plus long-wavelength UVA radiation with wavelengths between 320 and 400 nm, has been found effective in attaining clinical remissions in psoriasis and in the cutaneous lymphoma mycosis fungoides (*1–4*).

In oral 8-MOP photochemotherapy the skin is thought to be the primary treatment target, but circulating lymphoid cells are exposed and may also be affected. Inasmuch as the 8-MOP is taken orally, the drug is present in the blood, and there is a substantial circulation of blood through the dermis. In disease states this circulation may be increased, and leukocytes may leave the skin in considerable numbers and accumulate in the dermis. Short-wavelength UV radiation is absorbed by the epidermis, but long-wavelength UV radiation may penetrate the dermis and thus potentially interact with the psoralen-bathed lymphoid cells.

Oral PUVA treatment has been reported to induce immunologic abnormalities. These abnormalities include diminished cutaneous sensitization with dinitrochlorobenzene (*5*), decreased leukocyte dThd incorporation (*6, 7*), diminished leukocyte responsiveness to PHA (*7, 8*) or to $HgCl_2$ (*9*), decreased concentrations of circulating E-rosette-forming T-lymphocytes (*10–12*), and decreased neutrophil concentration (*13*). Increased frequencies of circulating thioguanine-resistant (possibly mutated) lymphocytes have been found in patients (*14*). In vitro UVA radiation exposure of human leukocytes either pretreated with 8-MOP (*7, 15–21*) or obtained from patients who had received oral 8-MOP (*22, 23*) resulted in decreased cell turnover, decreased dThd incorporation, diminished PHA responsiveness, and reduced mixed leukocyte culture reactivity.

In the in vitro assay system to be described (*17, 18*), we have reproduced some of the features of in vivo PUVA therapy. The assay system permits quantitation and simultaneous correlation of multiple biological and physical effects of photochemotherapy on human lymphoid cells. It may be useful in defining the direct actions of drug and radiation and in predicting possible effects in humans receiving such therapy.

CUTANEOUS OPTICS AND CIRCULATORY PHYSIOLOGY

Human skin serves as a filter of UV radiation (*24–26*). The shorter the radiation wavelength, the greater the filtration. This relationship is readily demonstrated if you hold a flashlight against your hand in a darkened room. The flashlight produces visible radiation of approximately 400–700-nm wavelength. The shorter wavelength radiation is blocked, but red light, with a wavelength of about 700 nm, can be seen passing through the entire thickness of skin. This phenomenon is utilized in medicine by pediatricians who transilluminate the crania of infants to diagnose nervous system abnormalities and by otolaryngologists who look for evidence of sinus inflammation.

The stratum corneum is the primary barrier to short-wavelength UV radiation and transmits less than 20% of the radiation below 300 nm (*24*). The entire epidermis, however, transmits about 45% of incident radiation in the UVA region (from 320 to 400 nm) (*24–26*). This UVA radiation may exert direct photobiological effects on dermal structures including blood within capillaries and lymphoid cells (*25*).

Blood flow through the skin has been measured to be about 500 ml/minute (*27*). Since the total blood volume is approximately 5,500 ml, the equivalent of the entire total blood volume circulates through the skin every 11 minutes in an individual at rest. One can formulate a crude estimate of the average dose of UVA radiation that a circulating

---

ABBREVIATIONS USED: dThd=thymidine; [^{3}H]dThd=tritiated dThd; GC=gas chromatography; GLC=gas–liquid chromatography; HPLC=high-pressure liquid chromatography; 8-MOP=8-methoxypsoralen; PHA=phytohemagglutinin; PUVA=psoralen (8-MOP) plus UV radiation (320–400 nm); SCE=sister chromatid exchanges; TLC=thin-layer chromatography.

---

[1] Presented at the Seventh Food and Drug Administration Science Symposium ("Photochemical Toxicity: Toxic, Allergic, and Carcinogenic Aspects With Emphasis on Predicting Effects in Humans") held at the Uniformed Services University of the Health Sciences, Bethesda, Md., March 16–17, 1981.

[2] Laboratory of Molecular Carcinogenesis, Division of Cancer Cause and Prevention, National Cancer Institute, National Institutes of Health, Public Health Service, U.S. Department of Health and Human Services, Bethesda, Md. 20205.

[3] *Address reprint requests to* Dr. Kraemer at Building 37, Room 3E24, National Institutes of Health, Bethesda, Md. 20205.

leukocyte would receive (D_L) from skin surface UVA radiation exposure (D_s) by considering the fraction of radiation transmitted by the epidermis (A_e), the treatment time (T), the rate of cutaneous blood flow (R), the number of circuits (n) a cell would make during the treatment time, the volume of blood in the body (V_b), and the volume of blood in the dermis (V_d).

Let p represent the fraction of the surface dose received by a leukocyte. Then

$$D_L = pD_s. \qquad [1]$$

Now

$$D_s = F_s \times T, \qquad [2]$$

where F_s is the fluence at the skin surface.

If F_d is the fluence in the dermis and t_L is the time a leukocyte spends in the dermis per circuit, then

$$D_L = F_d \times t_L \times n. \qquad [3]$$

Now

$$R = V_d/t_L = V_b/t_b, \qquad [4]$$

where t_b is the time for the total blood volume to pass through the dermis. This formula may be rearranged to

$$t_L/t_b = V_d/V_b. \qquad [4a]$$

But

$$n = T/t_b. \qquad [5]$$

Also,

$$F_d = A_e \times F_s. \qquad [6]$$

Thus $p = D_L/D_s = (F_d \times t_L \times n)/(F_s \times T) = (A_e \times F_s \times t_L \times T/t_b)/(F_s \times T) = A_e \times t_L/t_b$. Hence

$$p = A_e \times V_d/V_b. \qquad [7]$$

Equation 7 indicates that the fraction of the surface dose received by a circulating leukocyte is equal to the fraction of radiation transmitted by the epidermis times the ratio of the dermal blood volume to the total body blood volume. The epidermis transmits about 45% of the UVA radiation (A_e) (*24–26*), and the total blood volume (V_b) is about 5,500 ml (*6, 17, 27*). From these considerations, it is apparent that the crucial unmeasured component in determining the extent of UVA radiation exposure to leukocytes is the cutaneous blood volume. The flow rate is of secondary importance inasmuch as increases in flow rate resulting in less exposure per circuit are compensated for by more circuits during the period of exposure. I have been unable to find reliable estimates of human cutaneous blood volume. Data have been published for rodents and range from 20 to 70 µl blood/g of skin (*17*). If one assumes a human cutaneous blood volume of 100–500 ml (representing 50–250 µl/g skin), then circulating leukocytes would receive approximately $p = (0.45 \times 100\text{–}500 \text{ ml})/5{,}500 \text{ ml} = 0.8\text{–}4\%$ of the skin surface dose. Thus with a typical human skin surface exposure of 10,000 $\text{J}\cdot\text{m}^{-2}$ during photochemotherapy from a source delivering 100 $\text{J}\cdot\text{m}^{-2}\cdot\text{sec}^{-1}$, each lymphocyte would be estimated to receive 800–4,000 $\text{J}\cdot\text{m}^{-2}$ UVA radiation.

SERUM PSORALEN CONCENTRATIONS

Several methods have been described for the measurement of serum 8-MOP concentrations (table 1). The methods include TLC (*28–32*), GC (*35–39*), GLC (*34, 40, 41*), HPLC (*41–46*), and a bacterial bioassay (*47*). The standard dose of 8-MOP in PUVA therapy is about 0.6 mg/kg. Peak levels of 8-MOP have generally been found 2 hours after drug ingestion; however, variation is considerable among patients. Detectable peak levels have been reported to vary widely among patients; the range is from a low of 0.002 µg/ml to a high of 4 µg/ml. Some of this variation may be due to variations in drug composition or absorption (*37, 45*). However, even a single laboratory reports hundredfold differences in peak values among patients. Most laboratories found peak values between 0.1 and 1.0 µg/ml. Since 8-MOP is metabolized by hepatic enzymes, some of the reported values may include circulating metabolites. The possible effects of these metabolites have not been thoroughly investigated.

IN VITRO ASSAY SYSTEM

Human lymphoid cells were chosen for use in the in vitro assay (*17–21*). Primary cultures containing large numbers of lymphocytes were obtained by leukophoresis of normal donors and were further purified by flotation in lymphocyte separation medium. Lymphocytes could be maintained in short-term culture in RPMI-1640 medium supplemented with 17% fetal calf serum. This procedure resulted in a mild blastogenic response to the calf serum. These cells were used for short-term assessment of DNA synthesis. Smaller numbers of fresh leukocytes obtained by differential centrifugation of heparinized blood were used for the examination of immune reactivity.

For long-term cultures, Epstein-Barr virus-transformed lymphoblastoid cells were utilized from normal donors. These cells grow indefinitely in suspension in the culture medium. Their use permitted assessment of long-term cellular effects such as survival after treatment. We grew large numbers of the lymphoblastoid cells rapidly to facilitate measures of physical parameters such as DNA cross-linking.

The cells were exposed to radiation from the same type of lamp as that used for PUVA therapy. Our measurements of the spectrum of this lamp (*17, 18*) are shown in text-figure 1. Spectral irradiance on a $\log_{10}$ scale was plotted versus the wavelength. The peak energy of the unfiltered lamp was at 355–365 nm, and 98% of the measured UV radiation output was in the UVA region between 320 and 400 nm. Approximately 2% of the radiation from the unfiltered lamp was between 280 and 320 nm in the UVB region. This UVB radiation is known to be more active biologically than UVA radiation is, but UVB radiation is filtered out by the epidermis (*24–26*). Thus we used 6-mm-thick plate glass to filter out the UVB radiation. Text-figure 1 also shows the measured output through the plate glass filter. There was virtually no emission below 320 nm. Also shown in text-figure 1 is a calculation of the predicted spectral irradiance with the use of pigmented or unpigmented human epidermis as a filter to mimic the filtering effect of the epidermis on

TABLE 1.—*8-MOP therapeutic blood levels*

Assay method	No. of patients	8-MOP dose	Peak value		Reference
			Range, µg/ml	Time,[a] hr	
TLC	9	0.6–0.7 mg/kg	0.15–4.58	2–6	(*28*)
TLC	37	0.6–0.7 mg/kg	0.01–0.93	ND	(*29*)
TLC	7	40–50 mg	0.0–0.29	2–3	(*30*)
TLC	1	30 mg	3.0	2	(*31*)
TLC plus GC	5	50 mg	1.0–1.5	1–1.5	(*32*)
Radioactive 8-MOP	1	40 mg	1.2	2	(*33*)
Radioactive 8-MOP	1	20 mg	0.9	0.6	(*34*)
GC	5	Not stated	0.02–0.70	1–2	(*35*)
GC	5	0.6 mg/kg	0.250–0.700	0.5–2	(*36*)
GC	5	0.6 mg/kg	0.064–0.284	1.0–2.5	(*37*)
GC	1	40 mg	0.40	2	(*38*)
GC	21	0.6–0.8 mg/kg	0.046–0.289	1–4	(*39*)
GLC	31	Not stated	0.02–0.74	2–4	(*40*)
GLC	4	50 mg	0.40–1.5	1–1.5	(*34*)
GLC	10	0.6 mg/kg	0.065–0.191	ND	(*41*)
HPLC	3	0.56 mg/kg	0.09–0.15	1–2	(*42*)
HPLC	31	0.4–0.6 mg/kg	0.002–0.167	2–4	(*43*)
HPLC	8	0.5–0.6 mg/kg	0.158–0.550	0.5–1.5	(*44*)
HPLC	22	0.5–0.7 mg/kg	0.0–0.268	2–4	(*45*)
HPLC	8	0.6 mg/kg	0.04–0.22	ND	(*46*)
HPLC	42	0.6 mg/kg	0.02–0.70	ND	(*41*)
Bioassay (*Staphylococcus aureus*)	5	0.6 mg/kg	0.10–0.20	1.5–4	(*47*)

[a] ND=not determined (value listed was measured 2 hr after ingestion).

radiation impinging upon lymphocytes in the dermis. The plate glass partially mimics this filtering effect.

Cells were irradiated at 37°C from beneath the flasks (fig. 1). We suspended the cells in a UVA radiation-transmitting salt solution to minimize possible UV interactions with medium components and thereby to measure direct photochemical effects. The cells were kept in suspension and were exposed to different portions of the field during the time of irradiation by the plate glass being shaken at approximately 40 rpm.

8-MOP was added to the cells before the UVA radiation exposure. All manipulations were performed with gold fluorescent lamp illumination.

MEASUREMENTS OF DNA SYNTHESIS AFTER 8-MOP PLUS UVA TREATMENT

DNA synthesis was determined in a filter assay by the measurement of [^{3}H]dThd incorporation by the lymphoid cells during the first 2 hours after treatment (text-fig. 2). A dose-dependent decrease in DNA synthesis was apparent in primary lymphocyte cultures after exposure to UVA radiation in the absence of 8-MOP. Pretreatment with 8-MOP before UVA radiation exposure resulted in an additional decrease in DNA synthesis.

We had previously studied DNA synthesis in leukocytes of psoriasis patients receiving PUVA (*6*) by measuring [^{3}H]dThd incorporation in unstimulated leukocytes obtained immediately before and after UVA radiation treatment (text-fig. 3). The extent of the decrease in leukocyte DNA synthesis observed in vitro after 8-MOP plus UVA (text-fig. 2) was similar to that found in leukocytes of patients during PUVA treatment (≤60% inhibition in [^{3}H]dThd incorporation) (text-fig. 3). This finding is consistent with the thesis that the decreased DNA synthesis observed in vivo is a direct effect of the 8-MOP plus UVA treatment. Further, the crude assumptions made in predicting leukocyte UVA radiation exposure (*see* above) yield approximately congruent results: Thus 1,000–15,000 J·m^{-2} UVA radiation exposure after 8-MOP sensitization in vitro resulted in 40–60% inhibition of DNA synthesis (text-fig. 2); these values are similar to those observed following skin exposure of 50,000–300,000 J·m^{-2} in vivo (text-fig. 3).

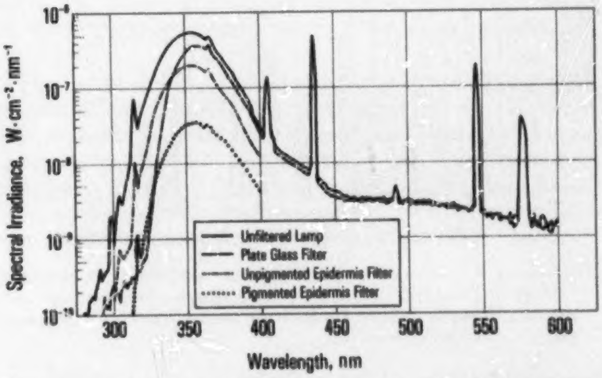

TEXT-FIGURE 1.—Filtering of PUVA fluorescent lamp radiation by plate glass or by human epidermis. The spectral irradiance of a Sylvania FR40T12 PUVA lamp operated at 115 V was measured at a distance of 2 m with and without a 6-mm plate glass filter. Predicted spectral irradiance with unpigmented or pigmented epidermis as a filter is also shown [reproduced from (*18*)].

DNA synthesis was similarly inhibited in the lymphoblastoid cells after UVA radiation exposure and was further decreased by pretreatment with 8-MOP (text-fig. 4). Within the range of doses studied, a tenfold increase in 8-MOP concentration resulted in an increase of approximately 20% in the extent of inhibition of [^{3}H]dThd incorporation, while

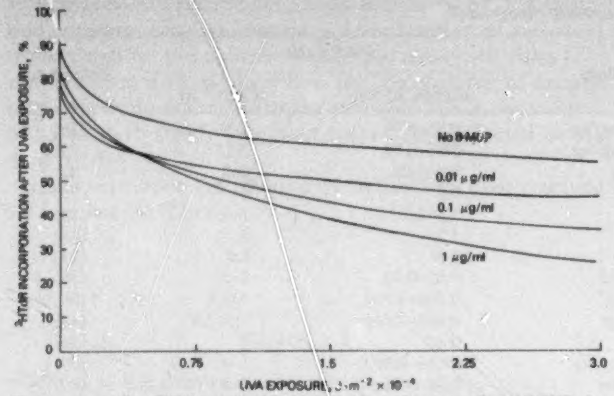

Text-figure 2.—DNA synthesis in human lymphocytes after 8-MOP plus UVA in vitro. Relative effect of in vitro exposure to UVA radiation and UVA plus 8-MOP (1.0, 0.1, and 0.01 μg 8-MOP/ml) on [^{3}H]dThd (^{3}HTdR) incorporation in lymphocytes from normal donors [modified from (*17, 18*)].

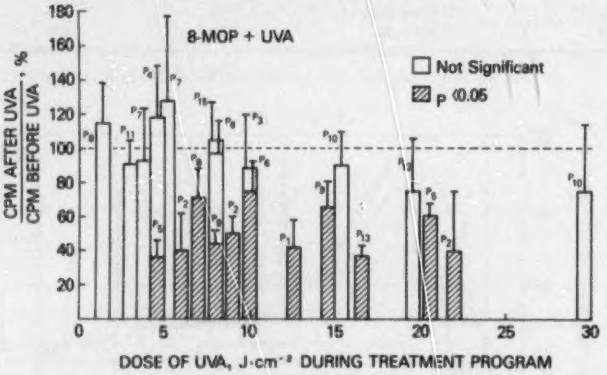

Text-figure 3.—Effect of in vivo PUVA on leukocyte DNA synthesis. Change in [^{3}H]dThd incorporation in leukocytes from patients with psoriasis in relation to UVA radiation exposure during PUVA treatment program [reproduced from (*6*)].

a tenfold increase in UVA radiation exposure resulted in an approximately 30% increase in the extent of inhibition of [^{3}H]dThd incorporation.

EFFECT OF 8-MOP PLUS UVA TREATMENT ON LYMPHOID CELL SURVIVAL

Cell proliferation ability could be evaluated in the lymphoblastoid cells after 8-MOP plus UVA treatment. Proliferation was measured by two methods: by daily hemacytometer counts of trypan blue dye-excluding cells and by growth of small numbers of cells in microtiter wells (*19*). Untreated cells grew exponentially in culture (text-fig. 5). This growth rate was not altered by treatment with either 1 μg 8-MOP/ml alone or 15,000 J·m^{-2} UVA radiation alone. Treatment with 8-MOP followed by UVA resulted in a dose-dependent decrease in cell proliferation. Thus pretreatment with 1 μg 8-MOP/ml followed by 15,000 J·m^{-2} UVA radiation resulted in no detectable viable cells after 1 week in culture.

Dose-dependent decreased cell survival was also evident when the microtiter well cloning method was used (text-fig. 6). UVA radiation exposure of 7,500 J·m^{-2} after pretreatment with 1.0, 0.1, or 0.01 μg 8-MOP/ml resulted in survivals of 0.03, 6, and 80%, respectively. Neither 8-MOP treatment alone nor UVA radiation exposure alone significantly reduced cell survival.

The in vitro assay permits correlation of decreased DNA synthesis immediately after 8-MOP plus UVA treatment with the subsequent cell survival (text-fig. 7). Survival was not altered by treatment which resulted in 60–70% of control [^{3}H]dThd incorporation remaining. However, treatment-induced reduction in [^{3}H]dThd incorporation to 50% of that of the control was associated with approximately 0.5% sur-

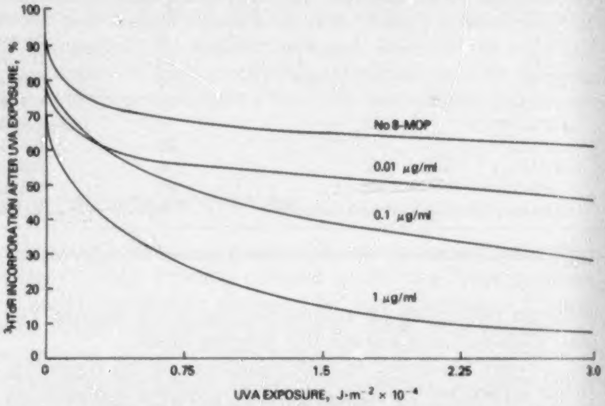

Text-figure 4.—DNA synthesis in a human lymphoblastoid cell line after 8-MOP plus UVA treatment in vitro. Relative effect of in vitro exposure to UVA radiation and UVA plus 8-MOP (1.0, 0.1, and 0.01 μg 8-MOP/ml) on [^{3}H]dThd (^{3}HTdR) incorporation in lymphoblastoid cell line E-1 [modified from (*17, 18*)].

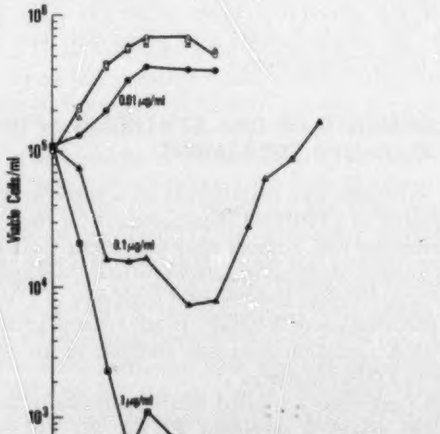

Text-figure 5.—Lymphoblastoid cell viability after 8-MOP plus UVA treatment in vitro. E-1 cells were treated with 0, 0.01, 0.1, and 1.0 μg 8-MOP/ml and were then exposed to 15,000 J·m^{-2} UVA radiation. Control cells received no treatment or received 0.1 μg 8-MOP/ml alone. Cell viability was determined by daily hemacytometer counts of cells that excluded trypan blue [reproduced from (*20*)].

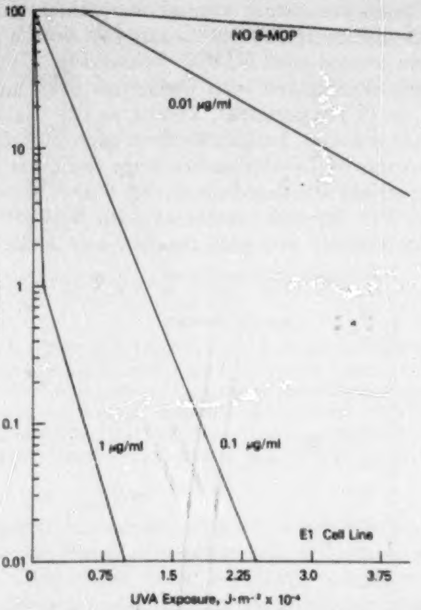

TEXT-FIGURE 6.—Survival of human lymphoblastoid cells after 8-MOP plus UVA treatment in vitro. Log-phase cells were treated with 0, 0.01, 0.1, or 1.0 μg 8-MOP/ml and were exposed to UVA radiation. Survival was measured by extrapolation from growth curves and by growth in microtiter wells [modified from (*18*)].

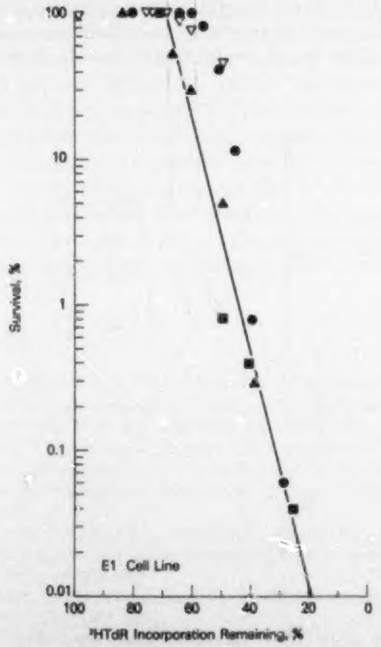

TEXT-FIGURE 7.—Relation of lymphoblastoid cell survival to DNA synthesis inhibition after 8-MOP plus UVA treatment. Mean survival after treatment with 0.01 (●), 0.1 (▲), 1.0 (■), or 0 (▽) μg 8-MOP/ml plus UVA was calculated from text-fig. 8 and was compared to the mean determinations of [^{3}H]dThd (^{3}HTdR) incorporation remaining (text-fig. 4). The coefficient of correlation between the log of the surviving fraction and the percent [^{3}H]dThd incorporation was 0.91 [reproduced from (*18*)].

vival. Similar survival was observed at similarly inhibited [^{3}H]dThd incorporation with different combinations of 8-MOP plus UVA. Some psoriasis patients receiving PUVA therapy had 50% reduction in leukocyte DNA synthesis immediately after treatment (text-fig. 3). This in vitro assay predicts that the proliferative ability of these cells would be impaired.

INDUCTION OF DNA CROSS-LINKS BY 8-MOP PLUS UVA

DNA cross-link induction in vitro was measured by a very sensitive technique known as alkaline elution (text-fig. 8) (*18, 20, 48, 49*). Cells in which DNA was labeled with radioactive dThd were irradiated with 300 rad X-ray so that the DNA would be broken into small fragments. The cells were layered on polyvinyl chloride filters with large (2-μm) pores and were then lysed. The DNA was slowly eluted with an alkaline solution at pH 12.1. The fragmented DNA was eluted through the filter relatively rapidly. DNA fragments that are cross-linked are retarded in their passage through the filter and are eluted more slowly.

This difference in elution rates may be used to measure DNA cross-links. Text-figure 9 shows that treatment of cells with 8-MOP plus UVA retards the elution of fragmented DNA. The extent of cross-link formation is related to both the 8-MOP concentration and the UVA exposure (text-fig. 10).

The extent of DNA cross-linking may be correlated with the inhibition of [^{3}H]dThd incorporation (text-fig. 11) measured immediately after PUVA treatment. When DNA synthesis was less than 50% that of the control, a dose-dependent increase in 8-MOP–DNA cross-linking was detected. Similarly, a linear relationship between cell survival and induction of DNA cross-links was detected (text-fig. 12). This

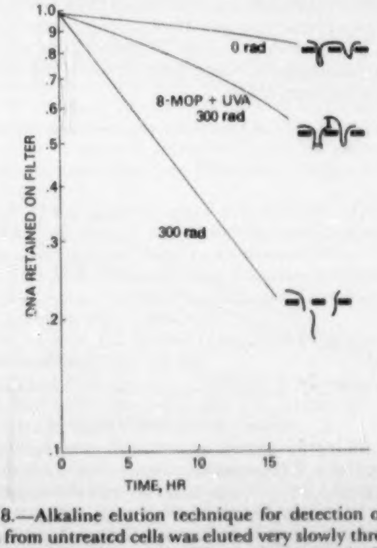

TEXT-FIGURE 8.—Alkaline elution technique for detection of DNA cross-links. DNA from untreated cells was eluted very slowly through the filter (*top curve*). Exposure to 300 rad X-radiation fragments the DNA resulting in more rapid elution (*bottom curve*). DNA cross-linked before 300 rad X-radiation has an intermediate elution rate (*middle curve*). (Diagram courtesy L. Cohen.)

suggests that the cytotoxic effects of photoactivated 8-MOP in human lymphoid cells may depend on DNA interstrand cross-links.

IMMUNOLOGIC EFFECTS OF 8-MOP PLUS UVA TREATMENT IN VITRO

The in vitro assay described was used to measure the effect of 8-MOP plus UVA on immune reactivity (*21*). The mixed leukocyte culture reaction was chosen as an assay of immune histocompatibility. Leukocytes from a normal donor were treated with 8-MOP followed by UVA exposure and were then mixed with leukocytes from an allogeneic donor. In this experiment, known as the two-way mixed leukocyte reaction, leukocytes from each individual stimulate division of T-lymphocytes from the other individual. DNA synthesis was determined after 6 days in culture (text-fig. 13). We see that treatment with 8-MOP plus UVA could completely abrogate the two-way mixed leukocyte

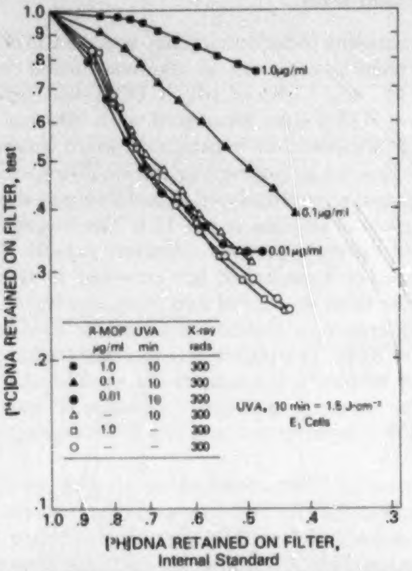

TEXT-FIGURE 9.—Measurement of 8-MOP–DNA cross-links by alkaline elution. [^{14}C]dThd-labeled human lymphoblastoid cells were treated as indicated, exposed to 300 rad X-radiation, and then mixed with [^{3}H]-dThd-labeled untreated mouse L1210 leukemia cells (internal standard) that had received 150 rad X-radiation. The cells were lysed on the membrane filter, and alkaline elution of the DNA was performed for 16 hr. The fraction of the ^{14}C-labeled DNA retained on the filter was plotted as a function of the retention of the ^{3}H-labeled DNA internal standard. Under these conditions, increased DNA retention indicates DNA cross-linking [modified from (*20*)].

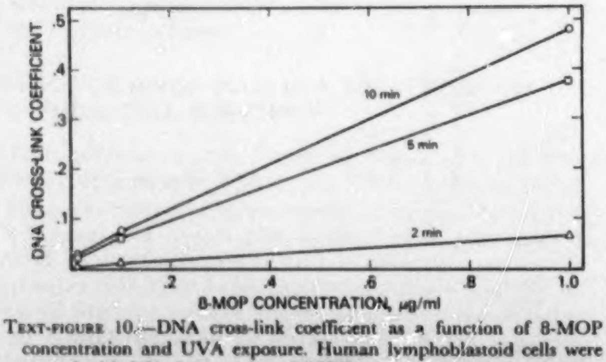

TEXT-FIGURE 10.—DNA cross-link coefficient as a function of 8-MOP concentration and UVA exposure. Human lymphoblastoid cells were treated with 0.01, 0.1, or 1.0 µg 8-MOP/ml and were then exposed to 15,000 J·m^{-2} (10 min), 7,500 J·m^{-2} (5 min), or 3,000 J·m^{-2} (2 min) UVA radiation. DNA cross-linking was measured by alkaline elution as indicated in text-fig. 9, and the DNA cross-link coefficient was calculated for each combination of 8-MOP and UVA. The DNA cross-link coefficient increased linearly with increasing 8-MOP concentration at each UVA radiation exposure level [modified from (*20*)].

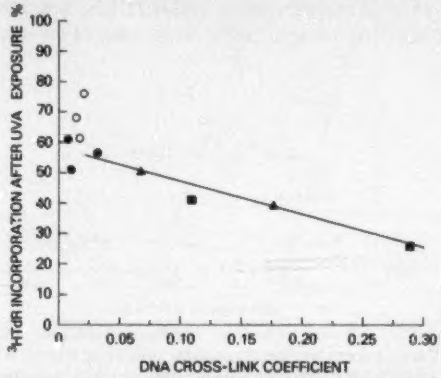

TEXT-FIGURE 11.—Relationship of DNA synthesis inhibition after 8-MOP plus UVA treatment to DNA 8-MOP cross-link induction. Human lymphoblastoid cells were incubated with 0 (○), 0.01 (●), 0.1 (▲), or 1.0 (■) µg 8-MOP/ml and were exposed to UVA radiation. [^{3}H]dThd (^{3}HTdR) incorporation was determined from the curves in text-fig. 3 for each combination of 8-MOP and UVA. The DNA cross-link coefficient was determined by use of the data in text-fig. 10 [reproduced from (*20*)].

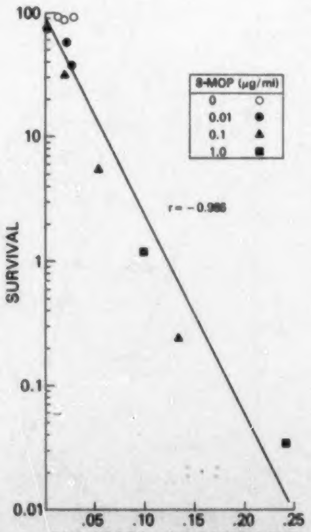

TEXT-FIGURE 12.—Relationship of DNA cross-link coefficient to cell survival after treatment with 8-MOP plus UVA. Survival data of E-1 cells after treatment with 8-MOP plus UVA were obtained from text-fig. 6 and DNA cross-link coefficient data were obtained from text-fig. 10. r =coefficient of correlation. Note that combinations of 8-MOP plus UVA yielding similar percent survivals also had similar DNA cross-link coefficients [modified from (*20*)].

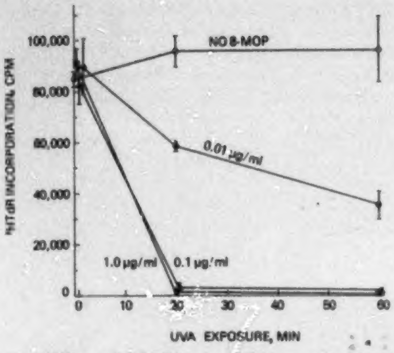

TEXT-FIGURE 13.—Effect of 8-MOP plus UVA on mixed leukocyte reaction. Leukocytes from a normal donor were treated with 0, 0.01, 0.1, or 1.0 µg 8-MOP/ml followed by UVA radiation and were then mixed with untreated leukocytes from an allogeneic normal donor. DNA synthesis was determined as [^{3}H]dThd (^{3}HTdR) after 6 days' incubation. (Kraemer K, Levis W, Cason J: Unpublished data.) [For further details, *see* (21).]

reaction. Similar experiments with one-way mixed leukocyte reactions demonstrated dose-dependent reductions in both stimulating ability and mixed leukocyte culture reaction-induced proliferation of peripheral blood leukocytes in vitro.

OTHER IN VITRO STUDIES

This assay has also been used to measure the frequency of 8-MOP plus UVA-induced SCE in vitro (*18*). We found at most a twofold increase in SCE.Higher doses of UVA radiation resulted in markedly increased cytotoxicity. These findings are in accord with the observations of Burger and Simons (*50*) on the failure to detect increased SCE in leukocytes of patients receiving PUVA therapy.

Psoriasis patients pretreated with oral retinoids have been reported to respond more rapidly to PUVA therapy (*51*). Accordingly, we decided to examine the effects of retinoids by use of the in vitro assay. Pretreatment of lymphoblastoid cells with 13-*cis*-retinoic acid for 15 minutes before 8-MOP plus UVA exposure did not significantly alter DNA synthesis or cell survival (*18*).

REFERENCES

(*1*) Parrish JA, Fitzpatrick TB, Tanenbaum L, Pathak MA. Photochemotherapy of psoriasis with oral methoxsalen and longwave ultraviolet light. N Engl J Med 1974; 291:1207-1222.

(*2*) Melski JW, Tanenbaum L, Parrish JA, Fitzpatrick TB, Bleich HL. Oral methoxsalen photochemotherapy for the treatment of psoriasis: A cooperative clinical trial. J Invest Dermatol 1977; 68:328-335.

(*3*) Gilchrest BA, Parrish JA, Tanenbaum L, Haynes HA, Fitzpatrick TB. Oral methoxsalen photochemotherapy of mycosis fungoides. Cancer 1976; 38:683-689.

(*4*) Roenigk HH. Photochemotherapy for mycosis fungoides. Arch Dermatol 1977; 113:1047-1051.

(*5*) Strauss GH, Bridges BA, Greaves M, Hall-Smith P, Price M, Vella-Briffa D. Inhibition of delayed hypersensitivity reaction in skin (DNCB test) by 8-methoxypsoralen photochemotherapy. Lancet 1980; 2:556-559.

(*6*) Kraemer KH, Weinstein GD. Decreased thymidine incorporation in circulating leukocytes after treatment of psoriasis with psoralen and long-wave ultraviolet light. J Invest Dermatol 1977; 69:211-214.

(*7*) Friedman PS, Rogers S. Photochemotherapy of psoriasis: DNA damage in blood lymphocytes. J Invest Dermatol 1980; 74:440-443.

(*8*) Morison WL, Parrish JA, Bloch KJ. Transient impairment of peripheral blood lymphocyte function during PUVA therapy. Clin Res 1978; 26:574A.

(*9*) Lischka G, Bohnert E, Bachtold G, Jung EG. Effects of 8-methoxypsoralen and UV-A on human lymphocytes. Arch Dermatol Res 1977; 259:293-298.

(*10*) Ortonne JP, Claudy AL, Alario A, Thivolet J. Decreased circulating E rosette forming cells in psoralen UV-A treated patients. Arch Dermatol Res 1977; 258:305-306.

(*11*) Cormane RH, Hamerlinck F, Simon M, Siddiqui AH. Photoimmunology in psoriasis. J Invest Dermatol 1977; 68:253.

(*12*) Haftek M, Glinski W, Jablonska S, Obalek S. T lymphocyte E rosette function during photochemotherapy (PUVA) of psoriasis. J Invest Dermatol 1979; 72:214-218.

(*13*) Dahl KB, Nyfors A, Brodthagen H. Decrease in neutrophils observed in vivo in psoriatics after PUVA therapy. Arch Dermatol Res 1978; 262:131-134.

(*14*) Strauss GH, Albertini RJ, Krusinski PA, Baughman RD. 6-Thioguanine resistant peripheral blood lymphocytes in humans following psoralen, long-wave ultraviolet light (PUVA) therapy. J Invest Dermatol 1979; 73:211-216.

(*15*) Wulf HC, Wettermark G. Toxic effects of 8-methoxypsoralen on lymphocyte division. Arch Dermatol Res 1977; 260:87-92.

(*16*) Kruger JP, Christophers E, Schlaak M. Dose-effects of 8-methoxypsoralen and UV-A in cultured human lymphocytes. Br J Dermatol 1978; 98:141-144.

(*17*) Kraemer KH, Waters HL, Ellingson OL, Tarone RE. Psoralen plus ultraviolet radiation-induced inhibition of DNA synthesis and viability in human lymphoid cells in vitro. Photochem Photobiol 1979; 30:263-270.

(*18*) Kraemer KH, Waters HL, Cohen LF, et al. Effects of 8-methoxypsoralen and ultraviolet radiation on human lymphoid cells in vitro. J Invest Dermatol 1981; 76:80-87.

(*19*) Kraemer KH, Waters HL, Buchanan JK. Survival of human lymphoblastoid cells after DNA damage measured by growth in microtiter wells. Mutat Res 1980; 72:285-294.

(*20*) Cohen LF, Kraemer KH, Waters HL, Kohn KW, Glaubiger DL. DNA crosslinking and cell survival in human lymphoid cells treated with 8-methoxypsoralen and long wavelength ultraviolet radiation. Mutat Res 1981; 80:347-356.

(*21*) Kraemer KH, Levis WR, Cason JC, Tarone RE. Inhibition of mixed leukocyte culture reaction by 8-methoxypsoralen and long wavelength ultraviolet radiation. J Invest Dermatol 1981; 77:235-239.

(*22*) Scherer R, Kern B, Braun-Falco O. UV-A induced inhibition of proliferation of PHA-stimulated lymphocytes from humans treated with 8-methoxypsoralen. Br J Dermatol 1977; 97:519-528.

(*23*) Edelson R, Jacobs D, Brin M, Kochevar I. Lymphocyte sensitivity to 8-methoxypsoralen and ultraviolet A. Clin Res 1977; 25:281A.

(*24*) Everett MA, Yeargers E, Sayre R, Olson RL. Penetration of the epidermis by ultraviolet rays. Photochem Photobiol 1966; 5:553-542.

(*25*) Parrish JA, Anderson RR, Urbach F, Pitts D. UV-A: Biological effects of ultraviolet radiation with emphasis on human responses to longwave ultraviolet. New York: Plenum, 1978.

(*26*) Kaidbey KH, Agin PP, Sayre RM, Kligman AM. Photoprotection by melanin—a comparison of black and Caucasian skin. J Am Acad Dermatol 1979; 1:249-260.

(*27*) Wade OL, Bishop JM. Cardiac output and regional blood flow. Oxford: Blackwell, 1962:92-93.

(*28*) Steiner I, Prey T, Gschnait F, Washuttl J, Greiter F. Serum level profiles of 8-methoxypsoralen after oral administration. Arch Dermatol Res 1977; 259:299-301.

(*29*) ———. Serum levels of 8-methoxypsoralen 2 hours after oral administration. Acta Derm Venereol (Stockh) 1978; 58:185-188.

(*30*) Herfst MJ, Koot-Gronsveld EA, de Wolff FA. Serum levels of 8-methoxypsoralen in psoriasis patients using a new fluorodensitometric method. Arch Dermatol Res 1978; 262:1-6.

(*31*) Chakrabarti SG, Gooray DA, Kenney JA Jr. Determination of 8-methoxypsoralen in plasma by scanning fluorometry after thin layer chromatography. Clin Chem 1978; 24:1155-1157.

(32) Gazith J, Schaefer H. 8-Methoxypsoralen: Its isolation and gas chromatographic determination from aqueous solutions and serum. Biochem Med 1977; 18:102–109.

(33) Busch U, Schmid J, Koss FW, Zipp H, Zimmer A. Pharmacokinetics and metabolite pattern of 8-methoxypsoralen in man following oral administration as compared to the pharmacokinetics in rat and dog. Arch Dermatol Res 1978; 262:255–265.

(34) Gazith J, Schalla W, Schaefer H. 8-Methoxypsoralen–gas chromatographic determinations and serum kinetics. Arch Dermatol Res 1978; 263:215–222.

(35) Ehrsson H, Eksborg S, Wallin I, Kallberg N, Swanbeck G. Determination of 8-methoxypsoralen in plasma by electron capture gas chromatography. J Chromatog 1977; 140:157–164.

(36) Swanbeck G, Ehrsson H, Ehrnebo M, Wallin I, Jonsson L. Serum concentration and phototoxic effect of methoxsalen in patients with psoriasis. Clin Pharmacol Ther 1979; 25:478–480.

(37) Ehrsson H, Nilsson S-O, Ehrnebo M, Wallin I, Wennersten G. Effect of food on kinetics of 8-methoxypsoralen. Clin Pharmacol Ther 1979; 25:167–171.

(38) Schmid J, Koss FW. Rapid sensitive gas chromatographic analysis of 8-methoxypsoralen in human plasma. J Chromatogr 1978; 146: 498–502.

(39) Wagner G, Hofman C, Busch U, Schmid J, Plewig G. 8-MOP plasma levels in PUVA problem cases with psoriasis. Br J Dermatol 1979; 101:285–292.

(40) Wilkinson DI, Farber EM. Gas-liquid chromatographic determination of 8-methoxypsoralen in serum. In: Farber EM, Cox AJ, Jacobs PH, Nall ML, eds. Psoriasis. Proceedings of the second international symposium, Stanford, Calif., 1976. New York: Yorke Medical Books, 1977:480–482.

(41) Hensby CP. The qualitative and quantitative analysis of 8-methoxypsoralen by HPLC-UV and GLC-MS. Clin Exp Dermatol 1978; 3:355–366.

(42) Puglisi CV, Arthur J, de Silva JA, Meyer JC. Determination of 8-methoxypsoralen, a photoactive compound, in blood by high pressure liquid chromatography. Anal Lett 1977; 10:39–50.

(43) Thune P, Volden G. Photochemotherapy of psoriasis with relevance to 8-methoxypsoralen plasma level and low intensity irradiation. Acta Derm Venereol (Stockh) 1977; 57:351–355.

(44) Thune P. Plasma levels of 8-methoxypsoralen and phototoxicity studies during PUVA treatment of psoriasis with meladinin tablets. Acta Derm Venereol (Stockh) 1978; 58:149–151.

(45) Ljunggren B, Carter DM, Albert J, Reid T. Plasma levels of 8-methoxypsoralen determined by high-pressure liquid chromatography in psoriatic patients ingesting drug from two manufacturers. J Invest Dermatol 1980; 74:59–62.

(46) Ljunggren B, Bjellerup M, Carter DM. Dose-response relations in phototoxicity due to 8-methoxypsoralen and UV-A in man. J Invest Dermatol 1981; 76:73–75.

(47) Glew WB, Roberts BS, Malinin GI, Nigra TP. Quantitative determination by bioassay of photoactive 8-methoxypsoralen in serum. J Invest Dermatol 1980; 75:230–234.

(48) Ewig RA, Kohn KW. DNA protein cross-linking and DNA interstrand cross-linking. Cancer Res 1978; 38:3197–3203.

(49) Kohn KW, Ewig RA, Erickson LC, Zwelling LA. Measurement of strand breaks and cross-links in DNA by alkaline elution, chapt 29. In: Friedberg E, Hanawalt P, eds. DNA repair: A laboratory manual of research procedures. New York: Marcel Dekker, 1981:379–401.

(50) Burger PM, Simons JW. Mutagenicity of 8-methoxypsoralen and long-wave ultraviolet irradiation in diploid human skin fibroblasts: An improved risk estimate in photochemotherapy. Mutat Res 1979; 63:371–380.

(51) Fritsch PO, Honigsmann H, Jaschke E, Wolff K. Augmentation of oral methoxsalen photochemotherapy with an oral retinoic acid derivative. J Invest Dermatol 1978; 70:178–182.

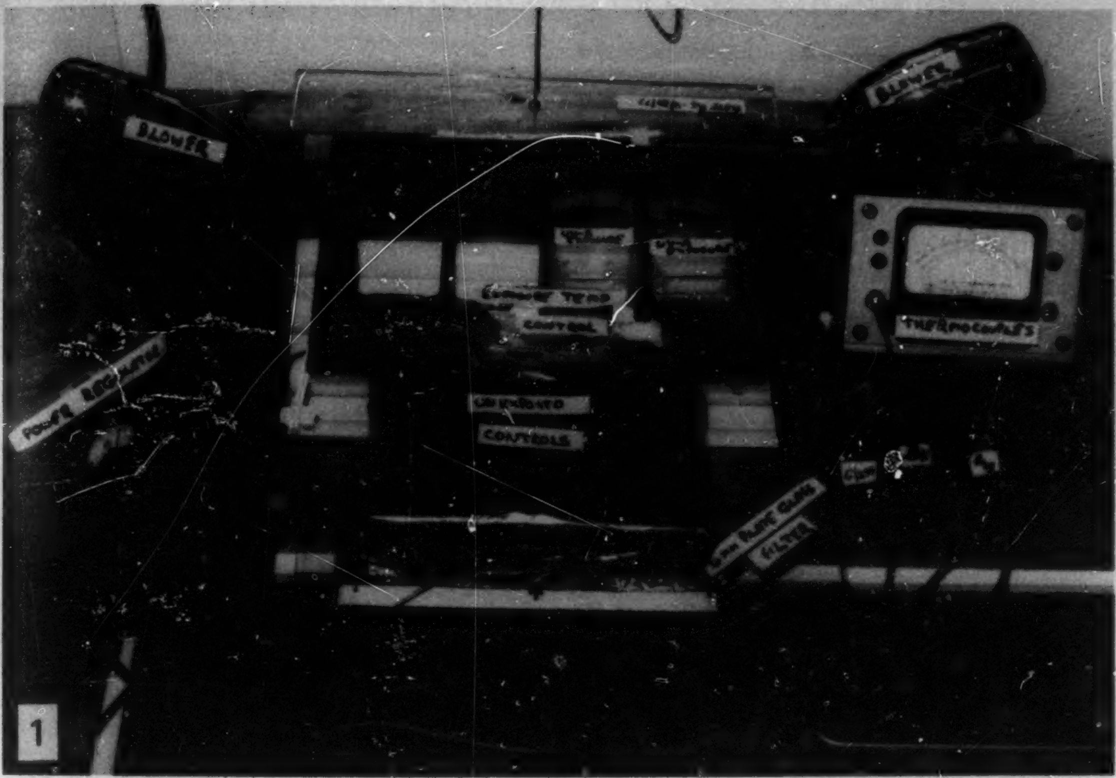
BLOWER
BLOWER
CONTROL
UNIRRADIATED
CONTROLS
POWER REGULATOR
THERMOCOUPLES
FILTER
1

FIGURE 1.—In vitro assay system apparatus. Lymphoid cells in suspension culture are placed in tissue culture flasks elevated above the surface of the plate glass filter over the center of four parallel fluorescent lamps. One edge of the plate glass rests on a mechanical shaker and the other is suspended by a wire passing through a hole in the glass. Control unirradiated cultures were placed in an opaque box on the shaker. Voltage supply to the lamps was regulated. Temperature was monitored via thermoprobes in flasks at the level of the treated cultures and in the opaque box. Temperature was regulated by use of hot or cool air blowers.

blank page

Modification of Photocarcinogenesis by Chemical Agents[1]

Frederick Urbach, *M.D.*,[2] **P. Donald Forbes**, *Ph.D.*,[2] *and* **Ronald E. Davies**, *Ph.D.*[2,3]

ABSTRACT—The evidence is long standing and compelling that chemical agents can modify the carcinogenic effects of light. Various types of chemical-light interaction are discussed, and events in chemical photocarcinogenesis, chemically enhanced photocarcinogenesis, and promotion of photocarcinogenesis are described. Specific examples of each type of process are given, and the importance of interaction of various wavelengths of UV radiation for these processes is stressed.—JNCI 1982; 69:229–235.

This paper is the result of more than a quarter of a century of research on photocarcinogenesis. It is widely accepted that UV radiation is the environmental agent most closely associated with the common forms of skin cancer, i.e., basal and squamous cell carcinomas. There is compelling evidence, based on both geographic and anatomic distribution of tumors, which suggests a causal association modified by genetic and occupational factors (*1*). Furthermore, animal studies have shown that UV radiation is sufficient for the production of squamous cell cancer of the skin (*2, 3*). This type of cancer is the single category of human cancer whose cause is most closely related to UV radiation (*1*).

The evidence is long-standing and compelling that chemical agents can modify the carcinogenic effect of light (*4–12*). As a matter of fact, the first experimental demonstration that one can induce skin cancer in animals with UV radiation was Findlay's in 1928 (*13*). His primary interest was in chemical carcinogenesis. He treated animals with coal tar, irradiated them with mercury arcs, and produced more tumors than if he had used tar alone. Being a good scientist, he ran a control experiment with UV radiation alone; this treatment also induced skin cancer, though not as much was induced as when the combined treatments were used. So this observation that chemical agents can modify the carcinogenic effect of light is clearly not new.

Although UV radiation may be the single most important etiologic agent in human skin cancer (≈400,000 new cases of nonmelanoma skin cancer/yr occur in the United States), nevertheless, the importance or the degree to which chemicals modify the effect of UV radiation on human skin is really not known.

TERMINOLOGY

Before giving a summary of our work, we need to define certain terms that will be used. These definitions may not be the same as everyone else's definitions, but at least our meaning will be clear.

The first concept to be defined is that of "carcinogenesis." As far as we are concerned, carcinogenesis refers to a response by a multicellular biologic system to a physical, chemical, or biologic stimulus; the agent capable of eliciting this response is called a carcinogen. The type of agent is usually specified, e.g., a "chemical" carcinogen or a "physical" carcinogen. The resulting process is similarly qualified, e.g., chemical carcinogenesis or physical carcinogenesis.

The term "photochemical carcinogenesis," as we use it, refers to the production of tumors in response to a combination of light and chemical. This use implies that the response is uniquely associated with a *combination*, and thus both elements must be present simultaneously if we are going to talk about photochemical carcinogenesis. Conceptually, the process is independent of the individual carcinogenicity of either the light or the chemical. In practice, these independent activities cause very serious problems in the identification and interpretation of the results.

Two other terms widely used are "initiation" and "promotion." These are complementary terms that describe certain interactive processes. An *initiator* is a carcinogen which, under the conditions of a particular experiment, may be an inadequate stimulus for the production of overt tumors but which, under varying conditions of dose, application frequency, or route of administration, is expected to produce tumors.

In contrast, a *promoter* is considered to be incapable of eliciting tumors under any conditions. However, after the action of an initiator, a promoter stimulates the appearance and growth of presumptive tumors; this phenomenon is generally explained in terms of two or more stages in the carcinogenic process.

There is obviously ambiguity because of the difficulty of defining a compound as being totally noncarcinogenic and therefore qualified to be a promoter. It is also conceivable that a compound can have such low carcinogenic activity that it can be detected only by its capacity for promotion.

Also important is the concept of "*cocarcinogenesis*," which has changed in the last 2 years. For a long time, cocarcinogenesis was used interchangeably with promotion, but it is not any more. Our use of the term will mean *the specific combined activity of two effective carcinogens*, although one or both may be used at a level too low to produce carcinogenesis by itself. It is possible that there is no fundamental difference between cocarcinogenesis and promotion, and lots of better people than we have argued this point to death.

ABBREVIATIONS USED: ALS=antilymphocyte serum; BP=benzo[*a*]pyrene; DMBA=7,12-dimethylbenz[*a*]anthracene; FS=fluorescent sun; MCA=3-methylcholanthrene; 8-MOP=8-methoxypsoralen; RA=retinoic acid.

---

[1] Presented at the Seventh Food and Drug Administration Science Symposium ("Photochemical Toxicity: Toxic, Allergic, and Carcinogenic Aspects With Emphasis on Predicting Effects in Humans") held at the Uniformed Services University of the Health Sciences, Bethesda, Md., March 16–17, 1981.

[2] The Center for Photobiology, Skin and Cancer Hospital, Temple University School of Medicine, Philadelphia, Pa. 19140.

[3] We acknowledge the work on light sources and measurements done by Mr. Daniel Berger and the genetic engineering of animal strains done by Dr. Stanley Mann, both in our laboratory.

Finally, we will use the term "*chemically enhanced photocarcinogenesis.*" You will notice a difference between the terms photochemical carcinogenesis and chemically enhanced photocarcinogenesis. In photochemical carcinogenesis, the chemical and the light must be present at the same time. In chemically enhanced photocarcinogenesis, the photochemical process serves as a promoter, and the carcinogenic light is the initiator.

The difference between chemically enhanced photocarcinogenesis and chemical promotion, as, for instance, with croton oil, lies in the fact that the former involves a photochemical process and the latter does not. One can obviously get cocarcinogenesis of this kind as well. The distinction between these various possibilities can impose methodologic problems. Such a distinction may be of very limited significance from a regulatory point of view, but these concepts are important because, under real conditions, one effective carcinogen (some form of radiation) is normally inevitably present. Sunshine, for example, always has some carcinogenic component, although it may be at ineffective levels; thus promotion or cocarcinogenesis may be of great importance.

PHOTOCARCINOGENESIS

In addition to the problems with chemical carcinogens, some very real problems in photocarcinogenesis have to do with only the physical aspect. The data from one particular photocarcinogenesis experiment are shown in text-figure 1. All animals are a strain of hairless mice irradiated with a solar simulator that contained carcinogenic UV radiation; absolutely no chemical was present, and the daily UV radiation dose was given for 5, 50, or 500 minutes/day. The total amount of radiation per day, per month, and per week is the same. The only difference is the rate of administration. Yield refers to the number of tumors per animal, and prevalence, the percentage affected. One can easily see that if the radiation exposure is protracted, many more tumors develop, and tumors develop much sooner.

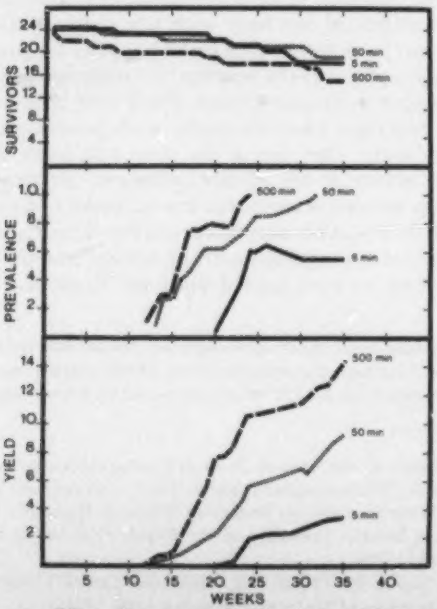

TEXT-FIGURE 1.—Effect of protracted UV irradiation. SK/h-1 mice were given the same daily doses of UV radiation for 5, 50, or 500 min. *Note* differences in proportion of mice with tumors (prevalence) and average number of tumors per survivor (yield).

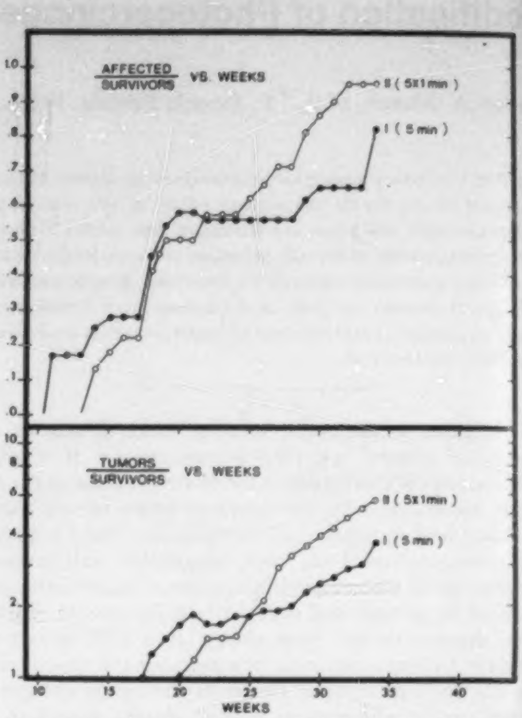

TEXT-FIGURE 2.—Effect of daily UV radiation dose when given in one 5-min period or in five 1-min periods 1 hr apart.

The question of course was, does this have to do with just the radiation intensity? We gave the dose for 5 minutes or in five 1-minute doses 1 hour apart so that the same time had elapsed. As seen in text-figure 2, there is very little difference between the two dose regimens as far as tumor development is concerned. We conclude that different dose rates are very important in photocarcinogenesis, and dose rates become another confounding factor to combine with such things as the animals' genetic makeup.

In table 1, classification or postulation of the reasonable possibilities for interactions of light and chemicals has been attempted. Some of these interactions we know exist. Others are just suggested. Two types of radiation, either noncarcinogenic or cancer producing, can occur, as can the same two types of chemicals.

An example of interactions that we know of is noncarcinogenic light and a noncarcinogenic chemical (anthracene), which will result in phototoxicity without photocarcinogenesis (*6*). But it is also possible to use noncarcinogenic light (UVA radiation, 320–380 nm) and 8-MOP (a noncarcinogenic chemical) to get photochemical carcinogenesis (*6*).

In the interaction categories, we have emphasized the distinction between *photochemical carcinogenesis*, for which we really have only one good example (interaction of noncarcinogenic light and the noncarcinogenic chemical 8-MOP)

TABLE 1.—*Interaction among light, chemicals, and biologic targets*[a]

Light	Chemical	
	Noncarcinogenic	Carcinogenic
Noncarcinogenic	*Phototoxicity* *Photochemical carcinogenesis* Photochemistry Optical filtration	*Photochemistry* *Phototoxicity* Promotion Host effects Optical filtration
Carcinogenic	*Optical filtration* *Promotion* *Photochemical cocarcinogenesis* *Host effects* Chemically enhanced photocarcinogenesis Phototoxicity Photochemistry	*Photochemistry* *Cocarcinogenesis* *Optical filtration* Chemically enhanced photocarcinogenesis Phototoxicity

[a] *Underlined categories* include known examples, and the remainder are not demonstrated or are of uncertain significance. Reproduced from (8).

and in which initiation of carcinogenesis occurs via photoexcitation, and *chemically enhanced carcinogenesis*, in which the chemical modifies the way in which the biologic targets respond to light. In the other interactions, the chemical can be altered, as with DMBA (*14*).

Until recently, few studies have been designed to distinguish between these various types of interactions. Unambiguous interpretations are generally impossible in studies in which polychromatic light sources and phototoxic or photolabile carcinogens were used intercurrently, unless the studies were specifically designed to look for this. That is a problem with a lot of the older studies. All kinds of interactions likely took place, but unless the study was specifically designed to examine these interactions, interpretation will be difficult. An example of this problem is DMBA, a highly carcinogenic compound, that when irradiated undergoes photo-oxygenation and rearrangements (*14*) with either a loss or a marked reduction of carcinogenicity.

As an aside, this whole series of experiments started because it was noted in some straight carcinogenesis experiments that animals kept on the top of a tier of racks in the animal colony developed much less skin cancer than those animals kept five racks below, i.e., on the bottom. The difference was purely proximity to ordinary, plain room-illuminating fluorescent lamps. A whole series of studies then ensued which showed that under appropriate circumstances a lot of the carcinogen, either MCA or DMBA, on the animal is destroyed before the carcinogen ever has an effect on the skin.

The alkyl-substituted polynuclear aromatic hydrocarbons such as DMBA and MCA are readily degraded by the kind of polychromatic light from the solar simulators that we use in our experiments. In contrast, BP is relatively light-stable. BP is relatively degradable in the presence of free carboxylic acid, however. In the presence of saturated fatty acids, a peculiar kind of photoacyloxylation develops. Text-figure 3 shows some of these results.

With unsaturated fatty acids the acylation is suppressed, but BP is consumed. Interestingly, these compounds of BP are extremely potent primary irritants although they do not seem to be carcinogenic. And since human skin, unlike animal skin, is covered with a film of fat containing free fatty acids, these reactions of BP with fatty acids may be of considerable significance not only from the point of view of irritancy but also perhaps even more from the point of view that BP is consumed. BP is the main carcinogen that everybody incriminates when they talk about shale oil or tar or whatever because BP is relatively photostable and therefore easily found in nature. Photoacyloxylation may very well be an important reaction, which incidentally takes place in the presence of light.

COCARCINOGENESIS

Cocarcinogenesis is another aspect of the problem. Nitrogen mustard, when painted on the skin of mice, is a carcinogen. We have been interested in nitrogen mustard because, as you know, it is used topically in the treatment of mycosis fungoides, and we have actually seen some keratoses and a few cancers in these treated patients. Text-figure 4 shows the results in hairless mice painted with nitrogen mustard.

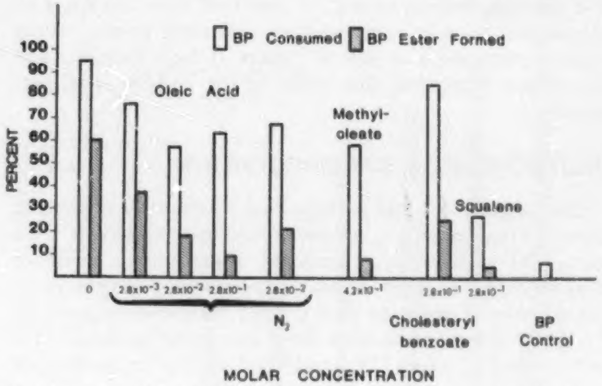

TEXT-FIGURE 3.—Effect of unsaturated compounds on photoacyloxylation. Reaction of BP with *n*-caproic acid.

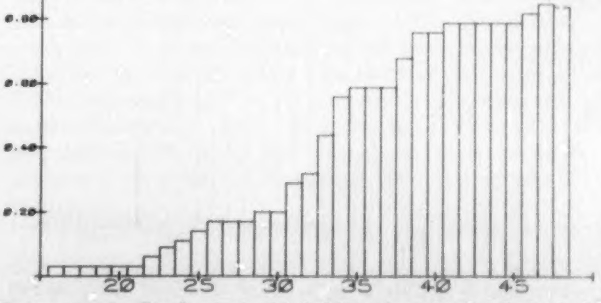

TEXT-FIGURE 4.—Results obtained in hairless mice painted daily for 5 wk with 20 μl of 0.02% nitrogen mustard in methanol (4 mg/mouse/day). *Ordinate values*=affected/survivors; *abscissa values*=wk.

You can see the number of tumors per survivor—you get a pretty good yield at the end of 50 weeks or so. Nitrogen mustard is, indeed, a complete carcinogen.

An interesting result is what happens when one irradiates nitrogen mustard-treated mice. Here one has a carcinogen, and in this case one is using a black light fluorescent lamp, unfiltered so it contains some UVB radiation (280–320 nm), but it primarily contains UVA radiation (320–380 nm). Text-figure 5 shows rather strikingly the huge potentiation of light plus nitrogen mustard, whereas, if one uses red light, which is totally inactive, one sees the background tumor incidence of the nitrogen mustard alone.

So in this case, there is cocarcinogenesis with two known carcinogens: The amount of UVB radiation is way below the threshold which is required to produce cancer in this period of time in these animals treated concurrently with nitrogen mustard. And incidentally, the nitrogen mustard is not phototoxic in the standard phototoxicity test. Even though dose-response data are insufficient at this time to permit precise comparison, it appears that the effect of the two carcinogens involved is additive; thus this seems to be a noninteractive form of cocarcinogenesis.

Since both nitrogen mustard and UV radiation are effective skin-pigmenting agents, we repeated these studies with pigmented hairless mice, and we produced lovely, strong hyperpigmentation as well as tumors in these animals. The interesting thing was that none of the tumors were pigmented.

PHOTOCHEMICAL CARCINOGENESIS

Let me go on to what perhaps may be the most important aspect of this paper, i.e., photochemical carcinogenesis. Two groups of workers have provided unambiguous evidence that 8-MOP can mediate photochemical carcinogenesis in the absence of radiation that is itself photocarcinogenic (*6*, *9*). Both groups of workers have irradiated animals with very carefully filtered UVA radiation sources; in the control experiment that ran concurrently, no animal developed any tumor when the UVA radiation source was used alone (*6*, *9*). The evidence is not clear at this moment for photochemical carcinogenesis with any compound we have tested or found in the literature, except for 8-MOP and some closely related psoralens.

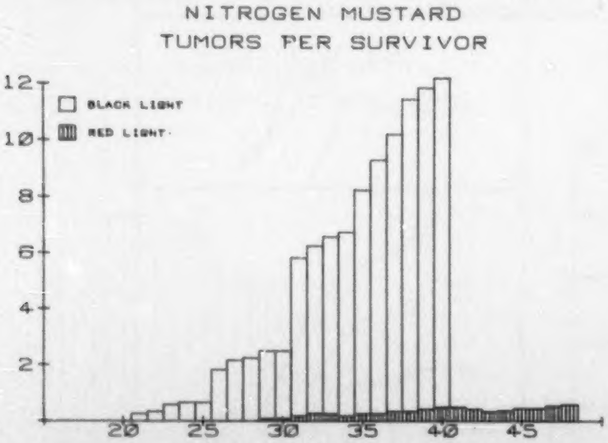

TEXT-FIGURE 5.—Potentiation effect of light plus nitrogen mustard. Mice were treated as specified in legend to text-fig. 4 and were irradiated continuously with either UVA (black-light lamps) or red fluorescent lamps. *Note* minimal effect with red light. *Ordinate values*=No. of tumors per survivor; *abscissa values*=wk.

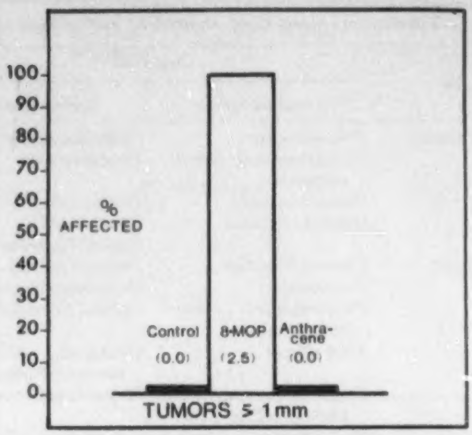

TEXT-FIGURE 6.—Results at 57 wk of exposure to chemical and UVA radiation. Hairless mice irradiated with UVA (black-light lamps F40T12BL which contain 1.5% UVB radiation) had been treated with 0.01% 8-MOP or 0.1% anthracene. *Note* marked enhancement of photocarcinogenesis with UVA radiation and 8-MOP but lack of effect with UVA radiation and anthracene.

Another compound in which we were interested because it is an extremely good topical phototoxic agent was anthracene. In text-figure 6 are the results of exposure to the chemical and UVA radiation. At the end of 57 weeks, 90% of the animals treated topically with 8-MOP had tumors, with an average number of 2.5 tumors/animal, and although the anthracene was phototoxic, no tumors developed.

This is seen in a different form in text-figure 7. In this case, the light source was a solar simulator, which contains UVB radiation and a lot of UVA radiation in roughly the same proportion as found in sunlight. The radiation exposure itself is carcinogenic. As can be seen for the vehicle control at the end of 36 weeks, 90% of the animals receiving it have tumors, and the animals have an average of about 12 tumors/survivor. With the 8-MOP, however, the onset of tumors is at 16 weeks instead of at 24 or so weeks. At 24 weeks, 100% of the animals have tumors, and the average number of tumors per survivor is 28. At 57 weeks, with topical 8-MOP and UVA radiation *without* UVB radiation, 100% of animals had tumors, with an average tumor number of 2.5. The presence of UVB radiation markedly enhances the photocarcinogenic effect of 8-MOP. Anthracene had no effect.

We looked at a number of photodynamic compounds, compounds that require oxygen to sensitize, that are apparently primarily membrane-effective, although in tissue culture they can affect DNA. In the intact animal, we hypothesize that the effect on the membrane is such that phototoxicity develops, and not much compound gets into the cell to affect DNA. Certainly, anthracene does not enhance photocarcinogenesis; neither does protoporphyrin, as based on the studies of Klaus Wolff (personal communication).

One other compound that we have looked at is amyl *o*-dimethylaminobenzoate. While amyl *p*-dimethylaminobenzoate is a good sunscreen, we find that amyl *o*-dimethylaminobenzoate is a very good phototoxic agent. We have used amyl *o*-dimethylaminobenzoate in this same kind of experiment, and we produced no photochemical carcinogenicity. All these compounds were tested so that the animals treated were kept in a mild state of chronic phototoxicity—not badly damaged, but sort of light pink.

PROMOTION

It has been shown that one can give mice small amounts of UV radiation (UVB) in an induction–promotion experiment, and when one paints the mice with croton oil, the mice develop tumors (*2, 7*). *All-trans*-RA acts similarly in an intercurrent experiment. One irradiates animals with a solar simulator, set so that roughly 15% of the animals will at 45 weeks have tumors 1 mm or more in diameter. And if one paints the animals with *all-trans*-RA just after the irradiation (because one certainly does not want to irradiate RA, for it is photolabile) 7 days/week, there is apparently an interaction: Photocarcinogenesis is enhanced (text-fig. 8).

This was an intercurrent experiment. Both treatment and radiation were done each day. Neither is *all-trans*-RA carcinogenic per se in lifetime painted animals nor is it phototoxic in skin. So the question now was, is this a promotion effect?

In text-figure 9, we show results from having treated the animals for 6 weeks with UVB radiation. This is not long enough for production of tumors by UVB radiation itself. A week after we stopped irradiating the animals, we painted them for the next 20 weeks with either 0.1% croton oil or 0.001% *all-trans*-RA. This is an initiation–promotion experiment which shows that 0.1% croton oil is a weak promoter and that the RA in this case was as good if not better as a promoter, when the same criterion was used, as was 0.1% croton oil.

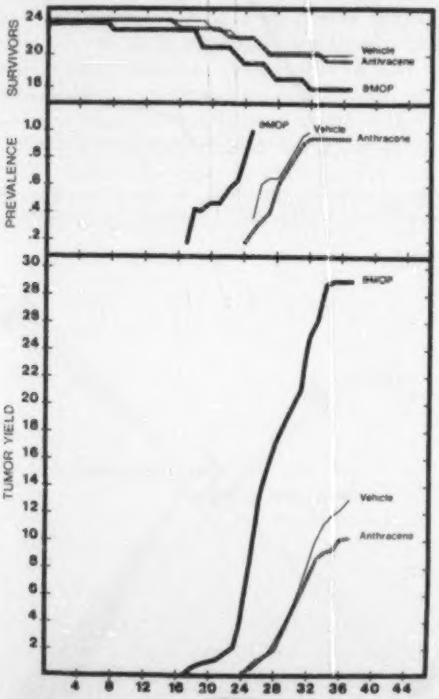

TEXT-FIGURE 7.—Effect of pretreatment with 8-MOP, anthracene, or the vehicle methyl alcohol on survival, the proportion of mice with tumors at any time (prevalence), and the average number of tumors per survivor (tumor yield) in groups of albino SK/h-1 mice irradiated chronically with a xenon arc simulator [from (*6*)].

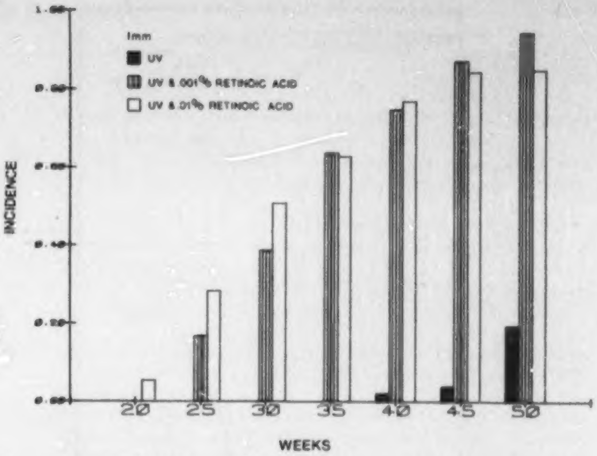

TEXT-FIGURE 8.—Incidence of skin tumors 1 mm in diameter in hairless mice irradiated 7 days/wk with a solar simulator, with a subsequent topical application of 20 μl of either 0.001% or 0.01% *all-trans*-RA acid in methanol. *Note* marked enhancement of photocarcinogenesis by posttreatment with RA [after (*10*)].

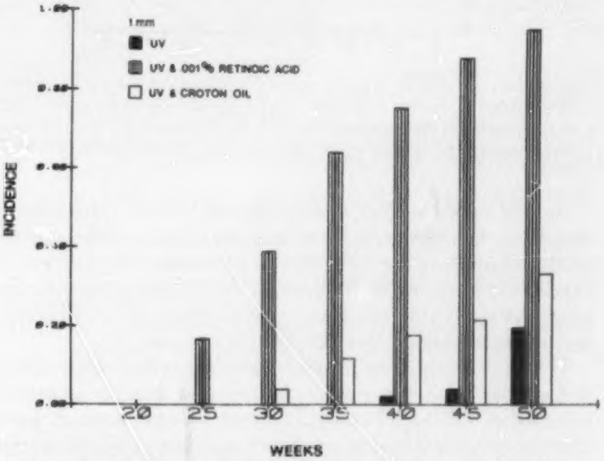

TEXT-FIGURE 9.—Results of an initiation–promotion experiment. Mice were irradiated as specified in legend to text-fig. 9 after they had been painted with either 0.001% *all-trans*-RA or 0.1% croton oil in methanol. *Note* promoting effect of croton oil as well as that of *all-trans*-RA.

Having done several experiments that seemed to show that *all-trans*-RA was a promoter of UV carcinogenesis, we did an experiment in which we used benz[*a*]anthracene as an initiator before we used RA, and nothing happened. However, when DMBA was used for initiation, *all-trans*-RA significantly promoted chemical carcinogenesis.

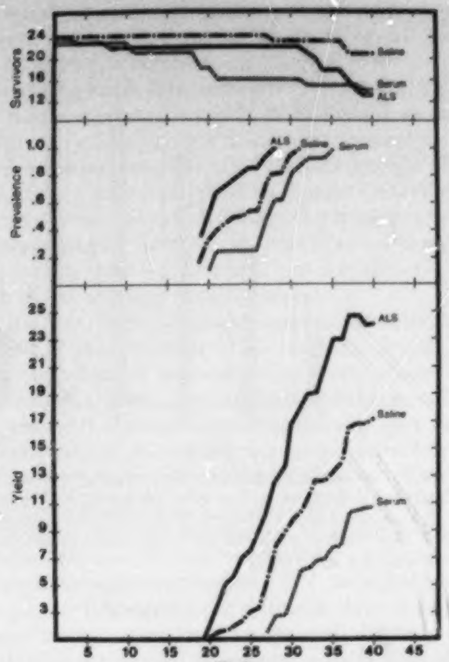

TEXT-FIGURE 10.—Effect of suppression of lymphocytic activity on photocarcinogenesis. Hairless mice were irradiated with a solar simulator after inoculation with rabbit anti-mouse ALS, saline, or normal rabbit serum. *Note* enhancement of photocarcinogenesis by immunosuppression with ALS.

As you might expect, this result was totally unexpected. Retinoids have been used as anticarcinogens; when given orally, vitamin A has been shown to reduce the number of chemically induced papillomas (*4*). So this result was totally unexpected. We do not know why it occurred. All we can say is that *all-trans*-RA is effective as a promoter.

We have inoculated animals (hairless mice) with rabbit anti-mouse ALS for a week before and during standard irradiation. We had 2 control groups: In one, animals were inoculated with saline; in the other, animals were inoculated with normal rabbit serum. Text-figure 10 shows that photocarcinogenesis was significantly increased when lymphocytic activity (presumably T-cell activity) was suppressed.

SUMMARY

For interpretation of results when dealing with the interaction of chemicals and light in carcinogenesis, we must consider three aspects simultaneously—light source, chemical, and host. We must first consider the *light source*, and that of course has to do not only with obvious things such as spectrum, with which all of you are familiar, but as I showed you at the very beginning, also with such things as dose rate and frequency and fractionation.

As an example of potential pitfalls, the following work is summarized. We initiated a very simple experiment in which we irradiated 1 group of animals with an FS lamp, which emits nearly pure UVB radiation, and we irradiated another group of animals with a solar simulator, which contains, by our measurements, the same amount (although not the same spectrum) of UVB radiation and also includes a lot of UVA radiation. When the solar simulator was used, the result was a huge increase of skin cancer over that produced by the fluorescent lamps. And that, of course, conclusively proved to us that UVA radiation indeed enhanced photocarcinogenesis, as Willis et al. (*15*) reported for skin erythema (text-fig. 11).

After we discovered the protraction effect described earlier, on review we realized that with the FS lamp the duration of exposure was 2 minutes, and with the solar simulator, the duration was 2 hours. So we began to wonder about our experiment. Repeating the previously described experiment with an FS lamp and solar simulator placed side by side and with the mice located so that the UVB radiation dose rate was similar from both light sources (text-fig. 12), we found that UVA radiation had no effect on UVB radiation photocarcinogenesis. What we had encountered was the "protraction effect."

The next problem, of course, is the interaction of light

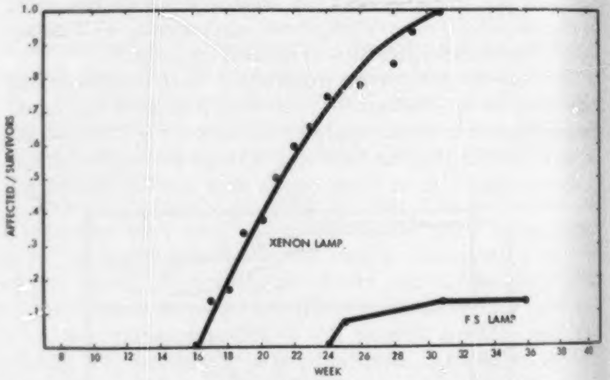

TEXT-FIGURE 11.—Tumor prevalence vs. wk of exposure. Xenon lamp contains primarily UVB and UVC (200–280 nm) radiation [from (*1*)].

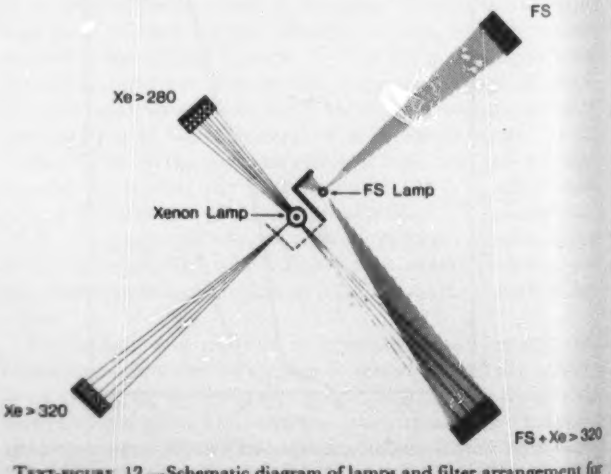

TEXT-FIGURE 12.—Schematic diagram of lamps and filter arrangement for comparing the effect of UVB radiation with that of UVB plus UVA radiation on photocarcinogenesis [from (*3*)]. Wavelengths are specified in nm.

and chemicals, and one of the things that is of great importance is the fact that UV radiation and visible radiation contain potent photons that are perfectly capable of doing photochemistry, and usually do so. Therefore, you can get photoproducts that may be more carcinogenic, less carcinogenic, more toxic, and certainly different. And depending on when you do what, you can affect the outcome of the experiment.

The next obvious problems are effects such as interactions with cocarcinogens and promoters like nitrogen mustard and RA. There may be any number of such compounds around, so the problem is complicated.

Finally, there is the problem of host modification. In addition to immunologic modification, a study is being done with 10 hairless mouse strains that are genetically different. Just doing straight photocarcinogenesis with the same light source and with the same filters—everything being the same—there is a huge difference in the susceptibility of different mouse strains to photocarcinogenesis, which is just genetically determined.

Different strains of animals have different genetic constitutions, and these differences do not seem to be related to the animals' immune systems. So you better be careful whose mice you use—not because one strain or stock is better than the other, but because each reacts differently and you will get different answers with psoralens, as Fry et al. (*9*) showed.

We are to the point of knowing some of the pitfalls and wanting to do experiments that are meaningful. These experiments will have to be done with very carefully calibrated light sources, with appropriate animals, and in an appropriate fashion. We can now begin to sort out and deliberately develop experiments for definition of specific problems. For instance, we really need to define this business as to whether UVA radiation plus UVB radiation and 8-MOP is really more carcinogenically effective than UVA radiation alone, and over what limits. The preliminary experiments strongly suggest a difference.

REFERENCES

(*1*) Urbach F, Epstein JH, Forbes PD. Ultraviolet carcinogenesis: Experimental, global, and genetic aspects. In: Fitzpatrick TB, Pathak MA, Harber LC, Seiji M, Kukita A, eds. Sunlight and man: Normal and abnormal photobiologic responses. Tokyo: Univ Tokyo Press, 1974:259–283.

(*2*) Pound AW. Induced cell proliferation and the initiation of skin tumor formation in mice with ultraviolet light. Pathology 1970; 2:269–273.

(*3*) Forbes PD, Davies RE, Urbach F. Experimental ultraviolet carcinogenesis: Wavelength interactions and time–dose relationships. Natl Cancer Inst Monogr 1978; 50:31–38.

(*4*) Davies RE. Effect of vitamin A on 7,12-dimethylbenz(α)anthracene-induced papillomas in rhino mouse skin. Cancer Res 1967; 27:237–241.

(*5*) Epstein JH, Roth HL. Experimental ultraviolet light carcinogenesis: A study of croton oil promoting effects. J Invest Dermatol 1968; 50:387–389.

(*6*) Forbes PD, Davies RE, Urbach F. Phototoxicity and photocarcinogenesis: Comparative effects of anthracene and 8-methoxypsoralen in the skin of mice. Food Cosmet Toxicol 1976; 14:303–306.

(*7*) Epstein JH. Chemicals and photocarcinogenesis. Australas J Dermatol 1977; 18:57–61.

(*8*) Davies RE. Interaction of light and chemicals in carcinogenesis. Natl Cancer Inst Monogr 1978; 50:45–50.

(*9*) Fry RJ, Ley RD, Grube DD. Photosensitized reactions and carcinogenesis. Natl Cancer Inst Monogr 1978; 50:39–43.

(*10*) Forbes PD, Urbach F, Davies RE. Enhancement of experimental photocarcinogenesis by topical retinoic acid. Cancer Lett 1979; 7:85–90.

(*11*) Forbes PD, Blum HF, Davies RE. Photocarcinogenesis in hairless mice: Dose-response and the influence of dose delivery. Photochem Photobiol 1981; 34:361–366.

(*12*) Logani MK, Austin WA, Davies RE. Light-induced interactions of benzo(*a*)pyrene with carboxylic acids. Photochem Photobiol 1981; 33:143–148.

(*13*) Findlay GM. Ultraviolet light and skin cancer. Lancet 1928; 2:1070–1073.

(*14*) Logani MK, Austin WA, Davies RE. A novel photo-rearrangement of 7,12-dimethylbenz(*a*)anthracene 7,12-epoxide into 6b,11b-dihydro-6b,11b-dimethyl-benzfuro(3,2-b)naphto(1,2-d)furan. Tetrahedron Lett 1978; 6:511–514.

(*15*) Willis I, Kligman A, Epstein J. Effects of long ultraviolet rays on human skin: Photoprotective or photoaugmentative? J Invest Dermatol 1973; 59:416–420.

blank page

Current Status of Predictive Animal Models for Drug Photoallergy and Their Correlation With Drug Photoallergy in Humans[1,2]

Leonard C. Harber, *M.D.*,[3] **Robert B. Armstrong**, *M.D.*,[3] *and* **Hideyuki Ichikawa**[4]

ABSTRACT—The number of adverse responses considered to be drug photosensitivity reactions account for only an exceedingly small percentage of the total undesirable effects from environmental chemicals. However, the rising incidence of and severe disability resulting from drug photosensitivity, especially when the photosensitivity is of the persistent light reactor type, indicate that increased photobiologic research and development efforts are required. Predictive tests are an obvious approach to minimize or eliminate those chemicals showing a risk-benefit ratio that is undesirable to society in general or to an unknowing individual in particular. Animal models with predictive value for determining the risk of photoallergic contact dermatitis in humans have undergone considerable modification during the past decade. This study reports an improved experimental guinea pig model for inducing photoallergic contact dermatitis to musk ambrette. In contrast to previously described models that used Freund's adjuvant, this model does not require nuchal stripping with cellophane tape. Control studies for primary irritancy, phototoxicity, allergic contact dermatitis, and "angry back" syndrome were included in the experimental design. Only photoallergic contact dermatitis was observed. Although the technique used to demonstrate this phenomenon is conducive to standardization, additional studies are required to ascertain whether or not other chemicals known to be photoallergic in humans can also be demonstrated with this animal model.—JNCI 1982; 69:237–244

The public in general and the scientific community in particular recognize that the introduction of innumerable new chemicals into our environment has been associated with both benefits and risks. Although these agents have been designed to aid the public, some have clearly entailed hazards of varying degree, as exemplified by hepatotoxic effects of vinyl chloride (*1*) and the oncogenic effects of diethylstilbestrol on vaginal tissue (*2*).

A subset of adverse reactions to environmental chemicals is photosensitivity reactions involving the skin. The term "drug photosensitivity" has been used to describe adverse reactions associated with patients exposed to sunlight after they have received particular medications. Although originally used in this limited clinically therapeutic sense, the term has been expanded in recent years to include reactions to chemicals used in cosmetics (*3*), food preservatives (*4*), household cleaners (*5*), fragrances (*6*), agricultural materials (*7*), and industrial by-products (*8*).

While the incidence of drug photosensitivity reactions has been quite low, it appears to be increasing. There is evidence in the literature of tens of thousands of persons affected with drug photosensitivity reactions during recent decades. In addition, there is a particular type of photosensitivity known as a persistent light reaction (*9*) that can be totally disabling. The increasing incidence and severity of this type of photosensitivity problem have served to illustrate the need for further photobiologic research efforts. It would be particularly desirable to have an animal model that could predict the potential of chemicals or drugs for producing the full range of adverse photosensitivity reactions.

Several models have been described and modifications continue to be developed. This paper is restricted solely to the subjects of development and evaluation of animal models for the induction of photoallergic contact dermatitis and for the assessment of their correlation with clinical events and photosensitivity tests in humans.

GENERAL REVIEW

A number of chemicals have been reported to cause photocontact dermatitis. These reactions are mediated by two broad mechanisms of action, phototoxic and photoallergic pathways. Their salient features are noted in table 1 and text-figure 1.

The mechanism involved in photoallergic contact dermatitis is immunologic and of the delayed hypersensitivity type. The role of light is restricted to photochemically altering the hapten or facilitating its combination with carrier protein (*10*). Following formation of this complete "photoantigen," it is believed that this unit is further processed by macrophages and comes in contact with T-lymphocytes in a manner similar to that of antigens associated with an ordinary delayed hypersensitivity immunologic response (*11*). The complete photoantigen is recognized as foreign on subsequent environmental exposure when sensitized T-lymphocytes are now present. An immunologic response is then initiated which results in erythema in laboratory animals and a papulovesicular, eczematous response in humans (*12*). This hypothesis has been supported by both in vitro and in vivo studies. The following are representative examples:

In Vitro Studies

The photoadducts of TCSA and Jadit (buclosamide) in combination with protein, when assayed with models such

---

ABBREVIATIONS USED: TCSA=3,3′,4′,5-tetrachlorosalicylanilide; UVA=UV, 320–400 nm; UVB=UV, 280–320 nm.

---

[1] Presented at the Seventh Food and Drug Administration Science Symposium ("Photochemical Toxicity: Toxic, Allergic, and Carcinogenic Aspects With Emphasis on Predicting Effects in Humans") held at the Uniformed Services University of the Health Sciences, Bethesda, Md., March 16–17, 1981.

[2] Supported in part by Public Health Service (PHS) grant ES-01041-08 from the National Institute of Environmental Health Sciences, by PHS grant RR-00645 from the Division of Research Resources (National Institutes of Health), and by the Shiseido Co., Ltd., Tokyo, Japan.

[3] Department of Dermatology, College of Physicians and Surgeons, Columbia University, 630 West 168th St., New York, N.Y. 10032.

[4] Laboratory of Dermatology and Toxicology, Shiseido Laboratories, Yokohama, Japan.

TABLE 1.—*Mechanisms of drug-induced photosensitivity: Comparison of phototoxic and photoallergic reactions in test models*

Mechanism	Reaction	
	Phototoxic	Photoallergic
Incidence	Usually relatively high (theoretically 100%)	Usually lower
Reaction possible on first exposure	Yes	No
Incubation period necessary after first exposure	No	Yes
Persistent light reaction possible	No	Yes
Cross-reactions to structurally related agents	No	Frequent
Passive transfer	No	Possible
Lymphocyte stimulation test	No	Possible
Macrophage migration inhibition test	No	Possible

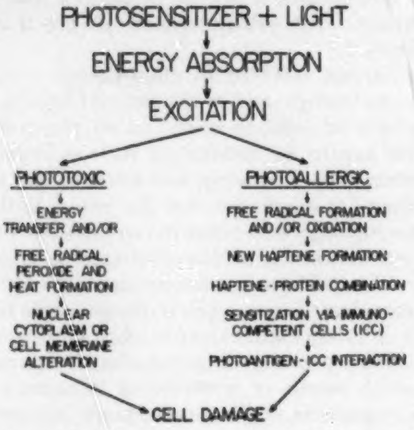
PHOTOSENSITIZER + LIGHT
ENERGY ABSORPTION
EXCITATION
PHOTOTOXIC
ENERGY TRANSFER AND/OR
FREE RADICAL, PEROXIDE AND HEAT FORMATION
NUCLEAR CYTOPLASM OR CELL MEMBRANE ALTERATION
PHOTOALLERGIC
FREE RADICAL FORMATION AND/OR OXIDATION
NEW HAPTENE FORMATION
HAPTENE-PROTEIN COMBINATION
SENSITIZATION VIA IMMUNO-COMPETENT CELLS (ICC)
PHOTOANTIGEN-ICC INTERACTION
CELL DAMAGE

TEXT-FIGURE 1.—Mechanism of phototoxic and photoallergic reactions.

as the macrophage inhibition and lymphocyte stimulation tests, have demonstrated positive results (*13*, *14*).

In Vivo Studies

Passive transfer of photosensitivity to TCSA with the use of peritoneal mononuclear cells from photosensitized guinea pigs has been demonstrated (*15*, *16*). The most comprehensive data in laboratory animals concerning induction of photoallergy to halogenated salicylanilides and its derivatives were those of Morikawa et al. (*17*). Recent studies by M. Takagawa and Y. Myochi (University of Kyoto, Kyoto, Japan) indicate the feasibility of using inbred strains of mice (BALB/c, DBA/2, C3H, and C57BL) for the induction of photoallergic contact dermatitis to TCSA, tribromsalan, and bithionol.

The first induction of experimental photoallergic contact dermatitis in guinea pigs was reported by Schwarz and Schwarz-Speck (*18*) in 1957. Their demonstration used sulfanilamide as a test model. Following this, Vinson and Borselli (*19*) induced contact photoallergic reactions with TCSA. Their technique has been considerably modified but basically confirmed by several other groups (*20–22*). More recently, contact photoallergies to musk ambrette (*22*, *23*) and 6-methylcoumarin (*24*, *25*) have been induced.

The guinea pig is presently the only experimental animal used to demonstrate photosensitivity of the delayed hypersensitivity type in all of the reported photoimmunologic animal studies. Hartley strain albino guinea pigs (375–425 g) are routinely used. Females appear to be preferable because there is likely to be less scratching of phototest sites.

Table 2 lists the techniques of inducing contact photoallergy in guinea pig models. In all the reported models, after induction and a suitable incubation period, elicitation is accomplished by topical application. These techniques are remarkably similar to those reported for inducing reactions in humans (*26*).

Clinical reports of photosensitivity in humans include reports on chlorpromazine (*27*), bithionol (*28*), Jadit (*29*), and promethazine (*30*). Table 3 presents a comprehensive list of agents reported to induce photoallergic contact dermatitis in humans.

Because of the risk and hazards of injury of test subjects by photosensitization (*31*), the following data in laboratory animals are stressed, indicating our preference for the use of a predictive animal-screening test model for photoallergic contact dermatitis before tests are initiated in humans.

Induction Techniques in Guinea Pigs

The typical induction procedure consists of the topical application of a relatively high concentration (10–100 times more than the lowest eliciting concentration) of the photosensitizer followed by UV irradiation. The entire induction procedure involves solely the nuchal region and is repeated five times during a 7- to 10-day period (table 2). Elicitation of photoallergic contact dermatitis is restricted to the depilated surface of the back.

Induction with UVB irradiation.—This model, introduced by Vinson and Borselli (*19*), has undergone numerous modifications and is an excellent one for inducing photosensitivity to halogenated salicylanilides. It uses both UVA and UVB radiations during the induction phase. As mentioned, although it has undergone extensive modification, this widely established model has been duplicated in several laboratories (*20–22*). However, it is ineffective in inducing photoallergy to 6-methylcoumarin and musk ambrette. A possible hazard involves corneal burns from UVB radiation expo-

TABLE 2.—*Techniques used to increase index of photoallergic contact dermatitis in guinea pigs*

Nuchal technique[a]	Example of photosensitizer
UVB radiation	Halogenated salicylanilides
Sodium lauryl sulfate	Halogenated salicylanilides
Skin "stripping" with cellophane tape	Musk ambrette
Stripping plus intradermal injection of Freund's adjuvant	Musk ambrette 6-Methylcoumarin
Intradermal injection of Freund's adjuvant without stripping	Musk ambrette

[a] These procedures precede irradiation of topically applied chemical with UVA radiation.

TABLE 3.—*Agents reported to induce photoallergic contact dermatitis in humans*

Agent[a]	Suggested concentration,%, for photopatch test
TCSA	0.1
3′,5′-Dibromosalicylanilide	1
4′,5′-Dibromosalicylanilide	1
Bithionol	1
Jadit	1
3,4′,5-Tribromosalicylanilide	1
Promethazine	1
Chlorpromazine	1
Dowicide 32	1
6-Methylcoumarin	5
Musk ambrette	5
Sulfonilamide	1
p-Aminobenzoic acid	1
2-Ethoxyethyl *p*-methoxycinnamate	1
Isoamyl dimethylaminobenzoate	5

[a] Petrolatum was used as a vehicle.

sure; therefore, the investigator's eyes must be protected with goggles.

Induction with sodium lauryl sulfate.—This model, introduced by Horio (*32*), offers promise and should be further evaluated. The induction procedure consists of the topical application of a 20% aqueous solution of sodium lauryl sulfate to the nuchal area. One hour later the photosensitizer is applied to the same site and immediately thereafter the site is exposed to UVA radiation. The procedure is repeated five to ten times during a 10-day period. The technique appears simple and effective. It is reported to produce a high index of photosensitization to halogenated salicylanilides and bithionol. Unfortunately, there are only limited reports of usage by photobiologists.

Induction with skin stripping with cellophane tape.—The induction phase consists of the repeated application of cellophane Scotch tape to the nuchal site until glistening is noted. The photosensitizer is then applied to this area, after which the site receives UVA radiation. The procedure is repeated three to five times during a 7-day period on the nuchal area. The rationale of stripping is presumed to involve increased percutaneous absorption of the photosensitizer, but the effectiveness of the model may also be related to the inflammatory response. This induction procedure appears analogous to the maximization test in humans and was successful for induction of musk ambrette photosensitivity in guinea pigs (*22*). However, in our studies, it was ineffective in inducing photoallergy to 6-methylcoumarin. A disadvantage of the technique is that a thick crust often forms on the nuchal induction site and impedes absorption.

Induction with Freund's complete adjuvant and cellophane stripping.—Freund's complete adjuvant, injected intradermally, has been demonstrated to increase the incidence of photosensitization to musk ambrette and 6-methylcoumarin in the guinea pig (*23*). This technique involves injecting Freund's adjuvant into four sites at the periphery of the depilated nuchal area, stripping with cellophane tape, applying the test substance, and exposing the region to UVA radiation. During the entire photosensitizing procedure, the adjuvant is injected only once, but the remainder of the induction steps are performed a total of five times (fig. 1). After 2 weeks, photosensitivity is assessed after depilation of the back for the first time, application of the test material to the back, and exposure of the back to UVA radiation (fig. 2). These experiments pose the disadvantage of variations in the manner by which and the extent to which cellophane tape stripping are accomplished and they make it difficult for other investigators to reproduce accurately and uniformly, in a controlled manner, the stripping procedures. Accordingly, the following studies were designed to test whether or not stripping was necessary for induction of photoallergic contact photosensitivity to musk ambrette.

MATERIALS AND METHODS

Experimental animals.—Twenty-three Hartley strain female albino guinea pigs weighing 375–450 g were tested. Musk ambrette (2-methoxy-3,5-dinitro-4-methylbutylbenzene) was used as a test agent. The purity of musk ambrette was assayed by high-pressure liquid chromatography and thin-layer chromatography.

Light sources.—Black light fluorescent tubes (General Electric Co.) emitting radiation in the 320- to 400-nm range were employed. The fluence rate measured at 12.5 cm through 3 mm of window glass was 2.85 $mW \cdot cm^{-2}$. All black light irradiation (10.2 $J \cdot cm^{-2}$) is nonerythrogenic in the absence of the photosensitizer.

Induction of photosensitivity in nonstripped nuchal skin.—The nuchal area (2.5×2.5 cm) of 11 guinea pigs was shaved and depilated with Nair, and 0.1 ml of a 10% solution of musk ambrette in acetone was applied. Before this procedure, 0.1 ml Freund's adjuvant (fig. 1) had been injected into four nuchal sites. Five treatments were given during a period of 10–11 days. Each treatment was followed by irradiation with black light fluorescent tubes as previously described.

Induction of photosensitivity in stripped nuchal skin (control).—The nuchal area of 12 guinea pigs was shaved, depilated with Nair, and stripped with cellophane tape for three or four of the five treatments. Freund's adjuvant was injected into four sectors. Musk ambrette (0.1 ml of a 10% solution in acetone) was applied within 15 minutes after stripping. The animals were irradiated with the same doses of light as were used for the nonstripped animals. The sensitization treatment of both the cellophane tape-stripped and nonstripped groups was performed five times during a period of 10–11 days.

Tests for elicitation of contact photosensitivity to musk ambrette.—The guinea pigs were challenged 17–22 days after the last nuchal sensitization exposure. The shaven and depilated lumbar area which had received no previous exposure to musk ambrette or light was demarcated into six sites (2.5×3.5 cm) with masking tape. The animals previously exposed to 10% musk ambrette in their nuchal region were challenged with 10, 1, and 0.1% concentrations of musk ambrette in ethanol on their dorsal lumbar skin (fig. 2). Each concentration (0.1 ml) was applied to symmetrical sites on the left and right sides of the animal. The right side was shielded with light-opaque material. A nonerythrogenic dose (10.2 $J \cdot cm^{-2}$) from black light fluorescent tubes was administered 30 minutes after application of the challenge solutions.

TABLE 4.—*Induction of photoallergic contact dermatitis to musk ambrette with the use of Freund's complete adjuvant, with and without cellophane tape stripping*

Procedure	Concentration of musk ambrette, %	No. of irradiated animals reacting/total No. of animals irradiated[a]			No. of unirradiated animals reacting/total No. of unirradiated animals
		1+	2+	Total No. of irradiated animals reacting/total No. of animals irradiated	
Nonstripping	0.1	4/11	0/11	4/11	0/11
	1.0	5/11	1/11	6/11	0/11
	10	5/11	1/11	6/11	0/11
Stripping	0.1	4/12	2/12	6/12	0/12
	1.0	6/12	4/12	10/12	0/12
	10	6/12	4/12	10/12	0/12

[a] Grading of reaction: 1+=mild erythema without edema; 2+=moderate to strong erythema without edema.

TABLE 5.—*Control studies for photoallergic contact dermatitis to musk ambrette*

Mechanisms evaluated	Chemical[a]	No. of animals	Result
Phototoxicity	100% musk ambrette	20	No primary irritant or phototoxic reaction noted on first exposure
Allergic vs. photoallergic contact dermatitis related to humans	$NiSO_4$	12	Contact allergy but no photocontact allergy induced with Freund's adjuvant
Allergic reactivity unrelated to humans	$CuSO_4$	12	No induction of allergic or photoallergic contact dermatitis
Nonspecific reactivity, angry back syndrome	TCSA, $CuSO_4$, and musk ambrette	12	No reaction to $CuSO_4$ and musk ambrette in animals photosensitized to TCSA and challenged with TCSA, $CuSO_4$, and musk ambrette

Evaluation of test results.—Erythema on the test sites was evaluated at 24 hours after irradiation with the use of a scoring system ranging from 0 to 3. A score of 1 or higher was considered a positive response.

RESULTS AND CONTROLS

Contact photoallergy to musk ambrette.—As noted in table 4, photosensitization to musk ambrette was induced with both the stripping and nonstripping procedures (fig. 3). The incidence of photosensitization and magnitude of response were greater in the stripped group.

Controls of photoallergy (*table 5*).—So that false-positive photosensitivity responses of a nonspecific nature could be ruled out, attempts were made to photosensitize guinea pigs to nickel sulfate, a known ordinary contact allergen in humans which has induced no cases of photoallergy in humans to date, and to cupric sulfate, a nonallergic agent in humans. Allergic contact but not photoallergic contact dermatitis was induced to nickel sulfate by use of Freund's adjuvant technique (Ichikawa H: Personal communication). Neither allergic nor photoallergic dermatitis was induced with cupric sulfate.

Controls for nonspecific reactivity ("angry back" syndrome).—Animals photosensitized to TCSA were challenged with TCSA and cupric sulfate. Reactions were noted only at TCSA-treated sites.

Control studies of phototoxicity: Phototoxicity to musk ambrette, anthracene, and 8-methoxypsoralen.—As previously described, 20 guinea pigs with no previous nuchal sensitization to musk ambrette were challenged with 50, 20, 10, 5, 3, and 1% concentrations of musk ambrette in acetone (*32*). With the use of radiation identical to that which elicited photoallergy, none of this group showed any visible reaction.

CONCLUSION

This modified experimental model for inducing photoallergic contact dermatitis in guinea pigs demonstrates the successful induction of photoallergic contact dermatitis to musk ambrette. In contrast to previously described models using Freund's adjuvant, this model did not require stripping with cellophane Scotch tape. Additional studies are needed to further demonstrate the correlation of the results seen with this model with events found in humans.

REFERENCES

(*1*) ROBBOY SJ, KAUFMAN RH, PRAT J, et al. Pathologic findings in young women enrolled in the National Cooperative Diethylstilbestrol Adenosis (DESAD) Project. Obstet Gynecol 1979; 53:309-317.

(*2*) PITOT HC, GOLDSWORTHY T, CAMPBELL HA, POLAND A. Quantitative evaluation of the promotion by 2,3,7,8-tetrachlorodibenzo-*p*-dioxin of the hepatocarcinogenesis from diethylnitrosamine. Cancer Res 1980; 40:3616–3620.

(*3*) FISHER AA. Contact dermatitis. In: Contact dermatitis. Philadelphia: Lea & Febiger, 1973:197–214.

(*4*) HARBER LC, LEVINE GM. Photosensitivity dermatitis from household products. General Practitioner 1969; 39:95–100.

(*5*) HARBER LC, HARRIS H, LEIDER M, BAER RL. Berloque (Berlock) dermatitis. Arch Dermatol 1964; 90:572–576.

(*6*) HARBER LC, BAER RL. Pathogenic mechanisms of drug-induced photosensitivity. J Invest Dermatol 1972; 58:327–342.

(*7*) EMMETT EA. Phototoxicity from exogenous agents. Photochem Photobiol 1979; 30:429–436.

(*8*) HJORTH N, MOELLER H. Phototoxic textile dermatitis ("bikini dermatitis"). Arch Dermatol 1976; 112:1645–1447.

(*9*) JILLSON OF, BAUGHMAN RD. Contact photodermatitis from bithionol.

Arch Dermatol 1963; 88:409–418.

(*10*) Herman PS, Sams WM Jr. Requirement for carrier protein in salicylanilide sensitivity: The migration-inhibition test in contact photoallergy. J Lab Clin Med 1971; 77:572–579.

(*11*) Harber LC, Baer RL, Bickers DR. Techniques of evaluation of phototoxicity and photoallergy in biologic systems, including man, with particular emphasis on immunologic aspects. In: Fitzpatrick TB, Pathak MA, Harber LC, Seiji M, Kukita A, eds. Sunlight and man: Normal and abnormal photobiologic responses. Tokyo: Univ Tokyo Press, 1974:515–528.

(*12*) Harber LC, Kochevar IE, Shalita AR. Mechanisms of photosensitization to drugs in man. In: Parrish J, ed. Photomedicine. New York: Plenum, 1980:143–144.

(*13*) Herman PS, Sams WM Jr. Immunologic investigation. In: Soap photodermatitis. Springfield, Ill.: Thomas, 1972:87–89.

(*14*) Jung EG, Hornke J, Hajdu P. Photoallergic durch 4-Chlor-2-Hydroxy-Benzoesauer-*N*-Butylamid. Arch Klin Exp Dermatol 1968; 233:287–295.

(*15*) Harber LC, Targovnik SE, Baer RL. Contact photosensitivity to halogenated salicylanilides: In man and guinea pigs. Arch Dermatol 1967; 96:646–656.

(*16*) Harber LC, Baer RL. Mechanisms of drug photosensitivity reactions. Toxicol Appl Pharmacol 1969; 3:58–67.

(*17*) Morikawa F, Nakayama Y, Fukuda M, et al. Techniques for evaluation of phototoxicity and photoallergy in laboratory animals and man. In: Fitzpatrick TB, Pathak MA, Harber LC, Seiji M, Kukita A, eds. Sunlight and man: Normal and abnormal photobiologic responses. Tokyo: Univ Tokyo Press, 1974:529–557.

(*18*) Schwarz K, Schwarz-Speck M. Experimentelle Untersuchungen zur Frage der Photoallergic der Sulfonamide. Dermatologica 1957; 114:232–243.

(*19*) Vinson LJ, Borselli VF. A guinea pig assay of the photosensitizing potential of topical germicides. J Soc Chem 1966; 17:123–130.

(*20*) Griffith J, Carter RD. Patterns of photoreactivity and cross reactivity in persons sensitive to TCSA. Toxicol Appl Pharmacol 1968; 12:304–309.

(*21*) Herman PS, Sams WM Jr. Requirement for carrier protein in salicylanilide sensitivity: The migration inhibition test in contact photoallergy. J Lab Clin Med 1971; 77:572–579.

(*22*) Kochevar IE, Zalar GL, Einbinder J, Harber LC. Assay of contact photosensitivity to musk ambrette in guinea pigs. J Invest Dermatol 1979; 73:144–146.

(*23*) Ichikawa H, Armstrong RB, Harber LC. Photoallergic contact dermatitis in guinea pigs: Improved induction technique using Freund's complete adjuvant. J Invest Dermatol 1981; 76:498–501.

(*24*) Giovinazzo VJ, Harber LC, Armstrong RB. Photoallergic contact dermatitis to musk ambrette, clinical report of two patients with persistent light reactor patterns. J Am Acad Dermatol 1980; 3:384–393.

(*25*) Harber LC. Current status of mammalian and human models for predicting drug photosensitivity. Soc Invest Dermatol. In press.

(*26*) Willis I, Kligman AM. The mechanism of photoallergic contact dermatitis. J Invest Dermatol 1968; 51:378–384.

(*27*) Epstein JH, Brunsting LA. Topical application of chlorpromazine; its effect on the erythema response to ultraviolet light. J Invest Dermatol 1958; 30:91–94.

(*28*) Jillson OF, Baughman RD. Contact photodermatitis from bithionol. Arch Dermatol 1963; 88:409–418.

(*29*) Burry JM, Hunter GA. Photocontact dermatitis from Jadit. Br J Dermatol 1970; 82:224–229.

(*30*) Sidi E, Hincky M, Gervais A. Allergic sensitization and photosensitization to phenergan cream. J Invest Dermatol 1955; 24:345–352.

(*31*) Willis I, Kligman AM. The mechanism of the persistent light reactor. J Invest Dermatol 1968; 51:385–394.

(*32*) Horio T. The induction of photocontact sensitivity in guinea pigs without UVB radiation. J Invest Dermatol 1976; 67:591–593.

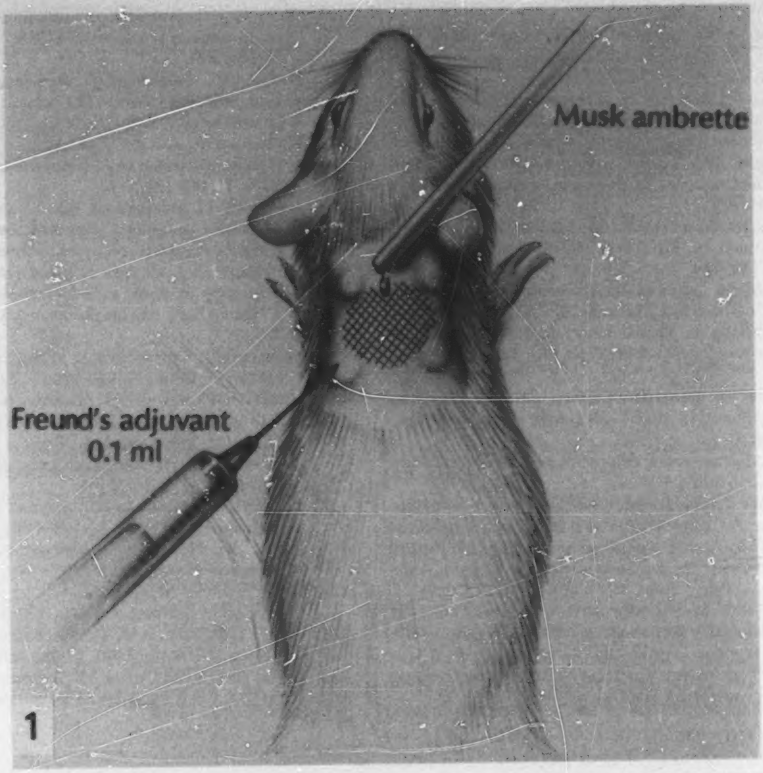
Musk ambrette
Freund's adjuvant 0.1 ml
1

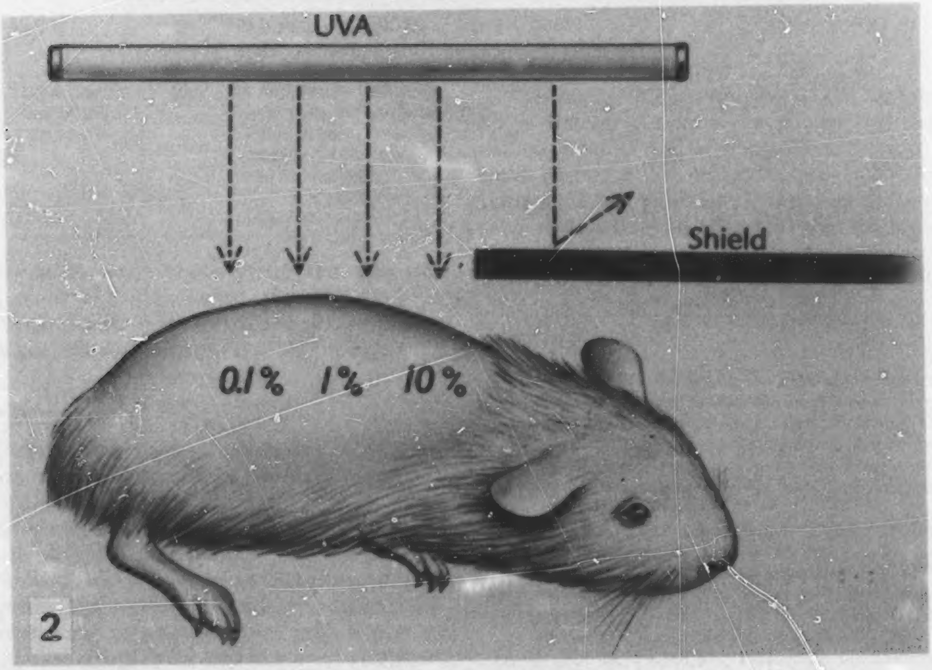
UVA
Shield
0.1% 1% 10%
2

FIGURE 1.—Induction of photosensitivity in the nuchal area with the use of Freund's adjuvant.
FIGURE 2.—Elicitation of photoallergic contact dermatitis to musk ambrette.

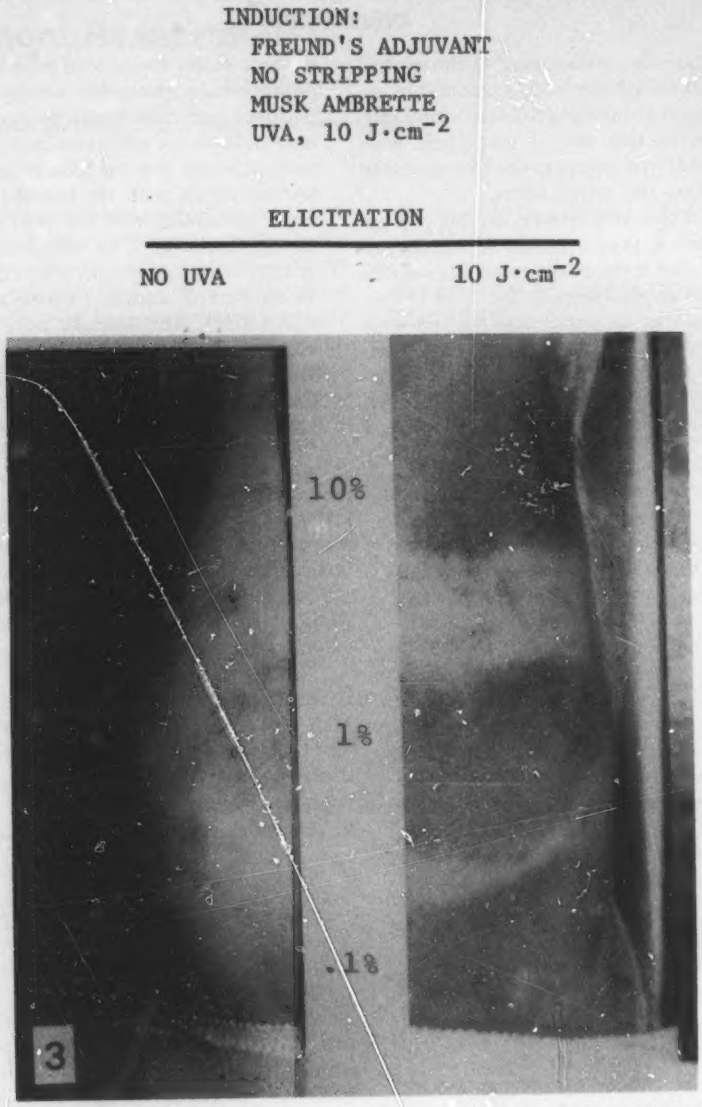
INDUCTION:
FREUND'S ADJUVANT
NO STRIPPING
MUSK AMBRETTE
UVA, 10 J·cm^{-2}
ELICITATION
NO UVA
10 J·cm^{-2}
10%
1%
.1%
3

FIGURE 3.—Erythema elicited 24 hr after exposure to 10, 1.0, and 0.1% musk ambrette and UVA radiation. Similar sites that were unirradiated showed no erythema.

DISCUSSION

J. Middleton: I have a question with regard to the control animals used in your studies. I have had considerable experience with the Magnusson guinea pig maximization test, which we use in Europe. In this test, if you inject with adjuvant, you can show that you increase the susceptibility not only to sensitization, but also to irritation.

My question is, in the studies you showed us, did you use adjuvant-pretreated animals as your controls? If not, do you think there is a possibility that some of the reactions may be photoirritation rather than photoallergy?

L. C. Harber: Our findings in patch test studies with humans regarding the "angry back" syndrome or "nonspecific" positive patch tests are in accord with those described by Dr. Mitchell. In terms of guinea pigs, however, we have not observed this phenomenon. Unfortunately, I have no direct experience with the Magnusson test, but our photobiology group has assessed in guinea pigs the angry back syndrome in regard to two photosensitizing fragrance materials, musk ambrette and 6-methylcoumarin. Specifically, relevant control studies concerning induction of photosensitization with the use of the Freund's adjuvant technique presented here involved an innocuous agent, cupric sulfate ($CuSO_4$). This compound has no known primary irritant or allergic properties in humans and thus was chosen for our control studies. Two weeks after attempted induction with $CuSO_4$, the animals were challenged simultaneously with 10% $CuSO_4$, 10% musk ambrette, and 10% 6-methylcoumarin. Each animal was assessed in the presence and absence of UVA light; 6 test sites were evaluated in each of 6 guinea pigs. No reactions were seen at any of the 36 sites.

Toxic Effect of Ultraviolet Light on Melanocytes: Use of Animal Models in Pigment Research[1,2]

George Szabo,[3] Frederick B. Blog,[4] *and* Andrija Kornhauser[5]

ABSTRACT—Quantitative histologic investigations on the effect of UV radiation on mammalian melanocytes have shown similarities in the response to carcinogenic chemicals, UV radiation, and 8-methoxypsoralen combined with UV radiation. With all three regimens the melanocyte number increased in mice, whereas long-wavelength UV radiation alone did not change the numerical distribution of these cells. Although it is too early to say that similarity in response of these agents indicates identity in harmful effects of these agents, great care should be exercised in the application of psoralens to human skin in a combined treatment with UV radiation.—JNCI 1982; 69:245-250.

A large body of evidence suggests a correlation between exposure to sunlight and the incidence of neoplasms of the skin (*1*). While the biological role of melanin is considered that of protection against harmful effects of UV radiation, the melanocytes (cells responsible for melanin production) are also known to undergo neoplastic changes possibly under the influence of sunlight.

In this article models used in the study of melanogenesis will be discussed followed by a presentation of our data regarding cytologic effects of exposure of mammalian melanocytes to UV radiation (UVA and UVB)[6] with or without treatment of the skin with a known chemical carcinogen (DMBA) or a photosensitizer widely used in treatment of psoriasis (8-MOP).

BIOLOGICAL MODELS IN PIGMENT RESEARCH

We believe that the melanocyte system of the mammalian epidermis is an excellent model for the study of melanogenesis and phototoxicity (*2-4*). This cell type produces a well-definable enzyme (tyrosinase) and a cell organelle (the melanosome). Inside this melanosome, tyrosinase becomes active and melanization takes place utilizing the substrate tyrosine. Finally, the melanosomes are transferred into keratinocytes by a unique cell-to-cell interaction (cytocrine activity). Ultrastructurally, the melanocytes are typical exocrine cells containing rough endoplasmic reticulum, Golgi zone, and melanosomes in various stages of formation (*4*).

These melanocytes are located in the basal layer of the epidermis, and in a dopa-treated epidermal preparation they can be counted easily. In the human epidermis there are about 1,000 melanocytes/mm^2 of skin surface in areas below the neck and about 2,000 in the head region (*5-9*). Although this distribution seemingly follows the extent of exposure to sun, there are some exceptions to this rule, inasmuch as 1,600 melanocytes can be found in some portions of the oral and nasal mucosae, about the same number can be seen in the epidermis of the sole and palm, and about 2,000 melanocytes can be found in the epidermis of the skin of the genital regions (*6*). There is no difference in the melanocyte number when one compares region by region the skin of the different color variants of the same species (*8-11*).

EFFECT OF UV RADIATION ON MAMMALIAN MELANOCYTES

It is well known that, as a first effect of exposure to sun, immediate pigment darkening of the skin can be observed within a few minutes, followed by new melanin formation 2-3 days after the initial exposure (*1*). Several separate steps are involved in this new melanin formation such as the synthesis of the enzyme tyrosinase, the formation of the melanin granule (the melanosome), the activation of tyrosinase within this melanosome, the polymerization of tyrosine into melanin, and the transfer of the melanized melanosome into the keratinocytes of the epidermis.

Solar radiation enhances the tyrosinase activity of melanocytes. This effect is well demonstrated in histologic preparations in which the melanocyte numbers of tyrosine-treated and dopa-treated portions of the same biopsy specimen are compared [*see* table 1 and (*6*)]. In the areas exposed to sun the number of melanocytes reacting with tyrosine is high and close to the number demonstrated with dopa, whereas in nonexposed areas either the tyrosinase reaction is entirely negative or only a very few melanocytes are positive. One should be aware of the fact, however, that tyrosine is also a suitable substrate to demonstrate melano-

---

ABBREVIATIONS USED: DMBA=7,12-dimethylbenz[*a*]anthracene; 8-MOP=8-methoxypsoralen; PUVA=psoralen plus UV radiation (320-400 nm).

---

[1] Presented at the Seventh Food and Drug Administration Science Symposium ("Photochemical Toxicity: Toxic, Allergic, and Carcinogenic Aspects With Emphasis on Predicting Effects in Humans") held at the Uniformed Services University of the Health Sciences, Bethesda, Md., March 16-17, 1981.

[2] Supported by research funds provided by the Department of Dermatology, Erasmus University, Rotterdam, The Netherlands, through Squibb B. V. Pharmaceutical Industry, Ryswyk, The Netherlands, and by Public Health Service grant AM-20669 from the National Institute of Arthritis, Diabetes, and Digestive and Kidney Diseases.

[3] Laboratory of Electron Microscopy, Harvard School of Dental Medicine, 188 Longwood Ave., Boston, Mass. 02115.

[4] Department of Dermatology, Erasmus University, Rotterdam, The Netherlands.

[5] Division of Toxicology, U.S. Food and Drug Administration, Public Health Service, U.S. Department of Health and Human Services, Washington, D.C. 20204.

[6] The UV spectrum can be divided into three regions: UVA (320-400 nm), noninflammatory and somewhat melanogenic; UVB (280-320 nm), inflammatory and melanogenic; and the germicidal UVC (shorter than 280 nm). UVC is absorbed in the stratospheric ozone layer and thus does not reach the earth's surface.

TABLE 1.—*Comparison of the regional frequency distribution of tyrosine-positive and dopa-positive cells*[a]

Area	No. of tyrosine-positive cells[b]	No. of dopa-positive cells[b]
Two areas from the same patients		
Temple	1,730±65	2,400±30
Thigh	0	790±50
Skin of the head		
Cheek	2,170±180	2,730±290
Cheek	1,600±120	1,980±120
Nose	1,990±110	1,890±110
Forehead	2,580±90	3,070±110
Behind ear	2,570±60	2,490±90
Behind ear	3,300±100	3,480±90
Rest of the body integument		
Frontal neck	0	2,050±130
Chest	0	700±30
Upper arm	0	690±20
Upper arm	0	1,660±100
Forearm	0	1,230±90
Thigh	0	1,580±150
Thigh	0	2,050±80
Thigh	0	710±50
Nasal mucosa	1,830±50	1,650±80
Buccal mucosa	0	1,395±30
Male genital region		
Scrotal sac	1,800±40	1,700±50
Foreskin, outer	920±30	1,290±70
Foreskin, inner	0	1,660±100
Foreskin, outer	1,560±60	2,700±110
Foreskin, inner	0	2,700±110

[a] Data are from (*6*).
[b] Per mm² ± SEM.

cytes in the skin areas of sex organs unexposed to solar radiation, which indicates that sex hormones can stimulate melanogenesis in specially receptive areas of the skin (table 1).

The tyrosinase activity of melanocytes is elevated after UV radiation; in addition, after multiple exposures the mitotic activity of melanocytes increases (*12*), resulting in an increase in melanocyte number which gradually returns to the preexposure level after the cessation of exposure (*10, 13*). Consequently, when one compares the numbers of dopa-positive melanocytes between habitually exposed and unexposed areas of the same individuals, one finds that the number is about twice as much on the exposed area than on the neighboring shielded regions (*14*).

It is not a prerequisite, however, that the melanocyte number increases following UV radiation, because if the skin is exposed to a single dose of UV radiation, pigmentation may increase without an increase in melanocyte number (*15*). In the following we shall turn our attention to experimental work on mice whose tail skins were exposed to UVA and UVB radiation (*16, 17*).

The tail skin of the mouse is very similar to human skin: Mouse skin is relatively hairless and contains functioning melanocytes in the basal layer; the epidermis is not as thin as in the general body skin of this species. The dorsal tail skin consists of a bricklike arrangement of pigmented blocks of skin surrounded and separated by nonpigmented areas (*11*). There are about 600 dopa-positive melanocytes per mm^2 in the pigmented areas, and none in between.

To answer the question whether UV light elicits toxicity similar to that of carcinogens or photosensitizers, we extended this study of the effect of UV radiation on skin by treating the skin with a known carcinogen, DMBA, and in separate experiments by treating the skin with the widely used photosensitizer 8-MOP combined with UVA radiation (PUVA).

We found that, in a sense, the mouse tail acts as a photometer (tables 2, 3); i.e., it "distinguished" between UVB and UVA radiation. The melanocyte number did not change after prolonged UVA radiation, whereas it doubled after UVB radiation. When psoralen and UVA radiation treatments were combined (PUVA), the numerical density of melanocytes became almost three times as high as that in normal or UVA radiation-treated animals. DMBA alone or DMBA combined with UVB radiation also resulted in an increase in melanocyte number. The morphologic changes were also revealing: After PUVA, DMBA plus UVB radiation, and UVB radiation treatment alone, melanocytes became large and irregular in shape, and the dendrites of melanocytes were shortened and clumped together. The outer root sheaths of hair follicles became laden with melanocytes in PUVA- and DMBA-treated animals. Most interestingly, the originally dopa-positive melanocyte-free interbrick areas of the tail skin became covered by melanocytes in the DMBA, UVB radiation, and PUVA series. UVA radiation alone or acetone (the vehicle for 8-MOP) did not produce these results. In our experiments, which were terminated after a 8-week application of DMBA with UVB radiation, no tumor formation was observed (tables 2, 3; figs. 1–5).

On the electron microscopic level, all these treatments resulted in an increase in melanosome formation. In some instances these melanosomes were sequestered into secondary lysosomes within the melanocytes instead of being trans-

TABLE 2.—*Changes in melanocyte number of mouse tail epidermis after treatment with PUVA and UVA radiation*[a]

Treatment	Treatment duration	Mean No. of melanocytes/mm² ± SEM, SD[b]
Control C57BL mouse	NA[c]	630±20, 70
PUVA	1 day	585±20, 65
UVA radiation	1 day	640±15, 50
PUVA	3 days	615±30, 85
UVA radiation	3 days	615±25, 80
PUVA	1 wk	705±20, 65
UVA radiation	1 wk	620±30, 100
PUVA	2 wk	1,285±35, 120
UVA radiation	2 wk	670±30, 90
PUVA	4 wk	1,760±40, 130
UVA radiation	4 wk	695±20, 70
PUVA	6 wk	1,760±35, 110
UVA radiation	6 wk	767±25, 80
PUVA	8 wk	1,670±30, 95
UVA radiation	8 wk	690±25, 75
Acetone	8 wk	655±25, 90
Acetone + UVA radiation	8 wk	650±30, 85

[a] Data are from (*16*).
[b] Mean number of melanocytes refers to mm² of surface of tail skin of 2 mice/experiment. Figures are rounded off to the nearest five.
[c] Not applicable.

TABLE 3.—*Changes in melanocyte number of mouse tail epidermis after treatment with DMBA and UVB radiation*[a]

Treatment	Treatment duration	Mean No. of melanocytes/mm^2 ± SEM, SD[b]
Control C57BL mouse	NA[c]	630±20, 70
DMBA	1 day	640±20, 80
DMBA + UVB radiation	1 day	655±25, 90
DMBA	3 days	755±20, 80
DMBA + UVB radiation	3 days	730±20, 70
DMBA	1 wk	1,410±25, 95
DMBA + UVB radiation	1 wk	1,370±30, 90
DMBA	4 wk	1,510±30, 90
DMBA + UVB radiation	4 wk	1,480±30, 95
DMBA	10 wk	[d]
DMBA + UVB radiation	10 wk	[d]
UVB radiation	10 wk	1,235±30, 85
Acetone	10 wk	655±25, 90

[a] Data are from Blog and Szabo (*17*).

[b] Mean number of melanocytes refers to mm^2 of surface of tail skin of 2 mice/experiment. Figures are rounded off to the nearest five.

[c] Not applicable.

[d] Due to high background pigmentation, counts were not possible.

ferred into keratinocytes. The melanosome structures, however, remained normal.

The covalent addition of psoralens as well as of some carcinogens to DNA is believed to be responsible for the inhibition of DNA synthesis in proliferating cells. Even now, nearly nothing is known about the mechanism of psoralen-induced melanogenesis. A few years ago we reported on the possible involvement of singlet oxygen in enzymatic and nonenzymatic melanin synthesis (*18*). It is known that psoralens under PUVA conditions can generate singlet oxygen (*19*). The relationship of this phenomenon to PUVA-induced melanogenesis, however, still needs to be established. Recently, we further extended our in vivo experiments by studying human melanocytes in cell cultures. These in vitro experiments (*20*) suggest that while UVB radiation is melanogenic, it can also be lethal. Pure cultures of human epidermal melanocytes were exposed to UVB radiation and were allowed to incorporate tritiated dopa (1.0 mCi/ml) from the growth medium for 48 hours. The single-exposure doses of UVB radiation were 0.1, 0.5, 10, and 50 $\mathrm{mJ \cdot cm^{-2}}$. The number of surviving melanocytes 48 hours after exposure was observed to decrease with increasing doses of UVB radiation. However, the incorporation of radiolabeled precursor (dopa) into melanocytes was found to increase at higher energy exposures. The highest dose tested, 50 $\mathrm{J \cdot cm^{-2}}$, resulted in a tenfold increase of dopa incorporation over control values. These results seem to be consistent with our previous findings, with the use of a retinal pigment cell culture system, that mitosis and melanogenesis are reciprocal cellular events. Possibly, UV radiation-induced melanogenesis is a specific instance of differentiation due to suppression of DNA synthesis (*21*).

DISCUSSION

This study has demonstrated that widely different factors when applied to melanocytes produce similar morphologic and functional results. In animals treated with UVB radiation, DMBA (with or without additional UVB radiation), and PUVA, the number of melanocytes and melanin production increased. UVB radiation and DMBA are known to be carcinogenic and seem to affect the melanocyte system in a very similar fashion. UVA radiation, which is not regarded as a carcinogen, did not increase the melanocyte number nor did it enhance melanogenesis to a noticeable degree. PUVA, however, produced results similar to those obtained with UVB radiation or DMBA treatment. One must also take into consideration the fact that UVA radiation delivers much less energy to the skin than UVB radiation. The difference in cellular response may be perhaps due not only to radiation spectrum but also to differences in the energy received by the skin.

The in vivo experiments reported here were done for only a short period and no tumor formation was observed. One should expand this investigation by studying the long-term effect of UVB radiation and DMBA and comparing their effect with that of PUVA. Furthermore, the effect of psoralen alone should also be studied.

In future experiments, one should also consider the observation made by Rosdahl (*22*) in regard to the possible systemic factors influencing melanogenesis in the entire melanocytic system following UV irradiation of a small area of the skin. Rosdahl observed that after exposure to UVB radiation, melanocytes increased in numbers both in a shielded area of the skin and in areas directly exposed to UVB radiation. This epoch-making observation indicates the existence of factor(s) controlling the mitotic cycle of melanocytes. It would be very important to know whether carcinogens or psoralens under PUVA conditions also exert their effect on remote areas of the integument by the same means.

In conclusion, from these studies a somewhat disturbing similarity emerges between the effects of UVB radiation and treatment by PUVA or by DMBA on mitotic division, melanogenic function, and morphology of melanocytes. The in vitro experiments indicate that UVB radiation can enhance melanogenesis and can be toxic at the same time. Great care should be exercised by physicians and by the general public, therefore, in regard to exposure to sun and the use of photosensitizers for cosmetic purposes.

REFERENCES

(*1*) JIMBOW K, PATHAK MA, SZABO G, FITZPATRICK TB. Ultrastructural changes in human melanocytes after ultraviolet radiation. In: Fitzpatrick TB, Pathak MA, Harber LC, Seiji M, Kukita A, eds. Sunlight and man: Normal and abnormal photobiologic responses. Tokyo: Univ Tokyo Press, 1974:195–215.

(*2*) FITZPATRICK TB, SZABO G. The melanocyte: Cytology and cytochemistry. J Invest Dermatol 1959; 32:197–209.

(*3*) KLAUS SN, ed. Biologic basis of pigmentation. Proceedings of the tenth international pigment cell conference, Cambridge, Mass., 1977. Part I. Basel: Karger, 1979:XVI–358.

(*4*) SZABO G. The biology of the pigment cell, chapt 3. In: Bittar E, Bittar N, eds. The biological basis of medicine. Vol VI. London and New York: Academic Press, 1969:59–91.

(*5*) ———. The number of melanocytes in human epidermis. Br Med J 1954; 1:1016–1017.

(*6*) ———. Tyrosinase in the epidermal melanocytes of white human skin: The histochemical demonstration and the numerical relationship of tyrosine-positive and dopa-positive cells. AMA Arch Dermatol 1957; 76:324–329.

(*7*) Staricco RJ, Pinkus H. Quantitative and qualitative data on the pigment cells of adult human epidermis. J Invest Dermatol 1957; 28:33–45.

(*8*) Billingham RE, Medawar PB. A study of the branched cells of the mammalian epidermis with special reference to the fate of their division products. Philos Trans R Soc Lond 1953; B237:151–171.

(*9*) Szabo G. Quantitative histological investigations on the melanocyte system of the human epidermis. In: Gordon M, ed. Pigment cell biology. New York: Academic Press, 1959:99–125.

(*10*) Gerald AB. Melanocyte number and function in man: Effects of ultraviolet irradiation in individuals of different races. Doctoral dissertation. Cambridge, Mass.: Harvard University, 1968.

(*11*) Gerson DE, Szabo G. The effects of single gene substitution on the mammalian melanocyte system—a qualitative and quantitative histological study in the C57BL and DBL mice. Am J Phys Antropol 1969; 31:363–382.

(*12*) Rosdahl IK Szabo G. Mitotic activity of epidermal melanocytes in UV-irradiated mouse skin. J Invest Dermatol 1978; 70:143–148.

(*13*) Szabo G. Photobiology of melanogenesis: Cytological aspects with special reference to differences in racial coloration. In: Montagna W, ed. Advances in biology of skin. VIII. The pigmentary system. New York: Pergamon Press, 1967:379–396.

(*14*) Gilchrest BA, Blog FB, Szabo G. Effects of aging and chronic sun exposure on melanocytes in human skin. J Invest Dermatol 1979; 73:141–143.

(*15*) Pathak MA, Sinesi SJ, Szabo G. The effect of a single dose of ultraviolet radiation on epidermal melanocytes. J Invest Dermatol 1965; 45:520–528.

(*16*) Blog FB, Szabo G. The effects of psoralen and UVA (PUVA) on epidermal melanocytes of the tail in C57BL mice. J Invest Dermatol 1979; 73:533–537.

(*17*) ———. The effects of UVB and 7,12-dimethylbenz(*a*)anthracene (DMBA) on epidermal melanocytes of the tail in C57BL mice. J Invest Dermatol 1979; 73:538–544.

(*18*) Kornhauser A, Garcia RI, Szabo G. Inhibition of the tyrosinase-DOPA reaction in epidermal melanocytes by sodium azide, phenylthiourea (PTU) and 1,4-diazabicyclo(2.2.2)octane (DABCO). Clin Res 1979; 27:530.

(*19*) Pope W, Grossweiner LI. Photodynamic sensitization by 8-methoxypsoralen via the singlet oxygen mechanism. Photochem Photobiol 1974; 2:217–219.

(*20*) Wilkins LM, Connell LB, Szabo G. Effect of ultraviolet light (UVB) on human melanocytes in vitro. J Cell Biol 1981; 91:31a.

(*21*) Garcia RI, Fuentes MA, Kornhauser A, Szabo G. Comparison of the effect of cyclic AMP and embryo extract on DNA and melanin synthesis in chick embryo retinal pigment cells in vitro. J Cell Biol 1975; 67:129a.

(*22*) Rosdahl IK. Local and systemic effects on the epidermal melanocyte population in UV-irradiated mouse skin. J Invest Dermatol 1979; 74:306–309.

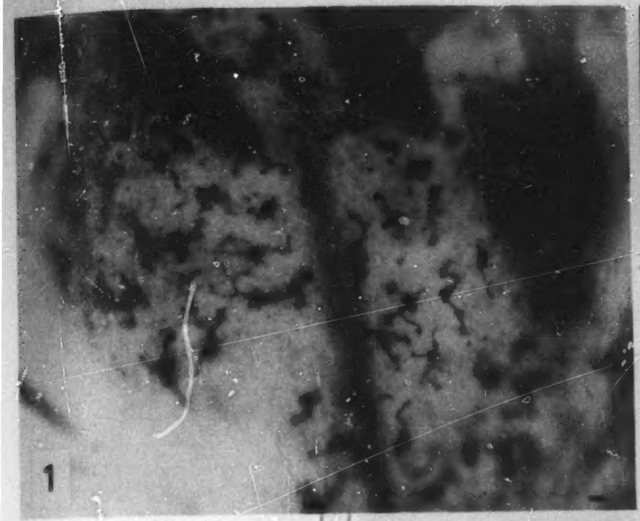

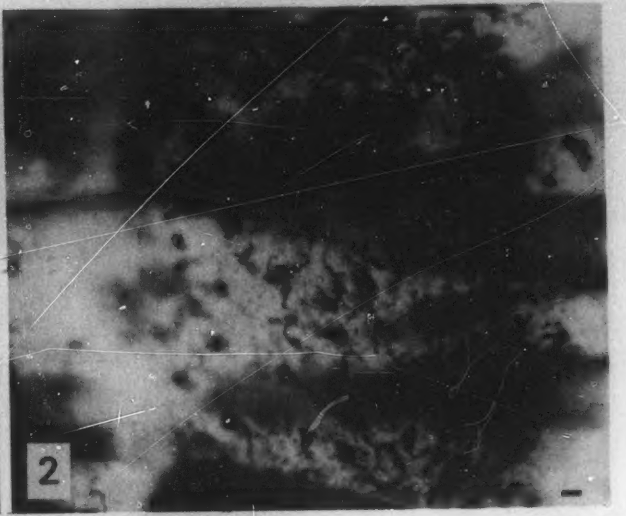

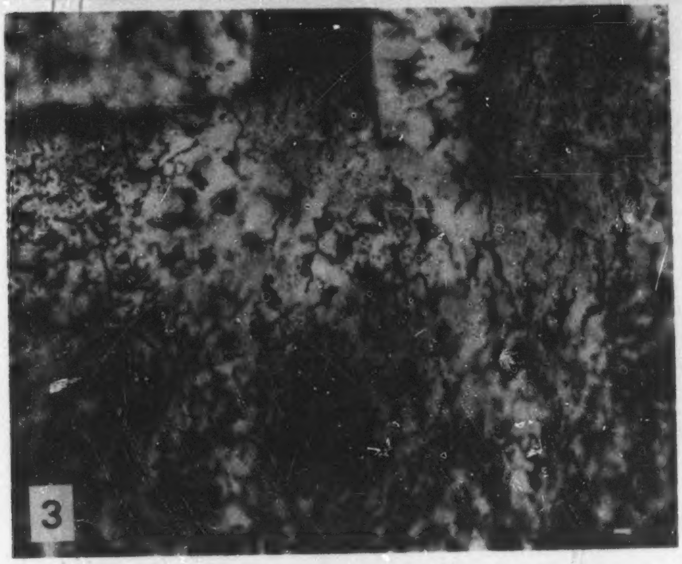

FIGURES 1–5.—Taken at the same magnification from dopa-treated epidermal sheets of mice. Selected from publications of Blog and Szabo (*16, 17*) with permission of the *Journal of Investigative Dermatology*. × 200

FIGURE 1.—Normal melanocytes in the mouse tail within one bricklike arrangement of pigmented epithelium. *Bar*=10 μm.

FIGURE 2.—Melanocytes after 10 wk of UVB radiation; the number of melanocytes has doubled. *Bar*=10 μm.

FIGURE 3.—Melanocytes after 4 wk of treatment with DMBA and UVB radiation; melanocytes are present not only in the originally pigmented bricklike area, but also in between. They have short, stubby dendrites, and they are also found on the junction of the outer root sheath of the hair follicles with the epidermis. *Bar*=10 μm.

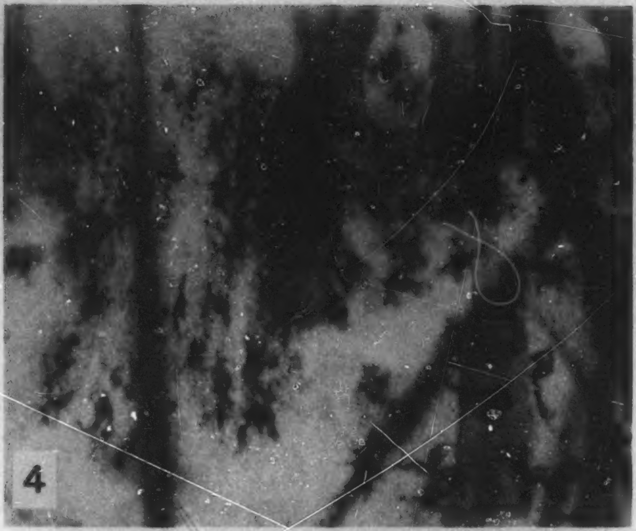

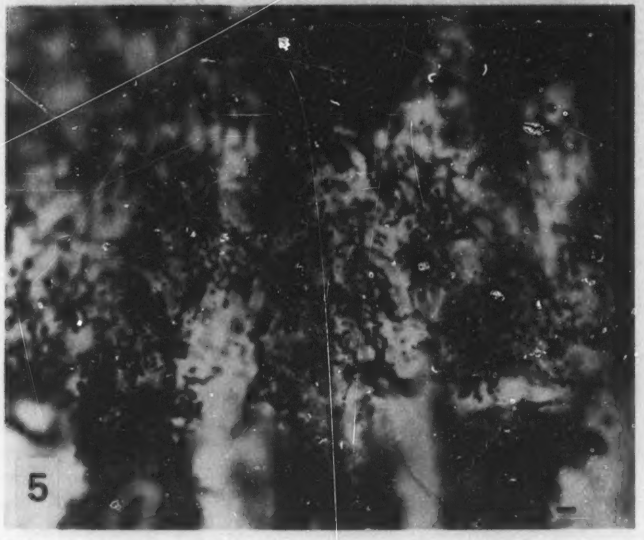

FIGURE 4.—Epidermis after 8 wk of UVA radiation treatment. Original bricklike pattern of melanocyte distribution, in contrast to that seen in figs. 2 and 3, is still present. *Bar*=10 μm.

FIGURE 5.—Melanocytes after 2 wk of PUVA treatment. Melanocytes are rounded with short, stubby dendrites and are located also on the outer root sheath of the hair follicles. They are somewhat similar to those shown in fig. 3 (DMBA plus UVB radiation treatment). *Bar*=10 μm.

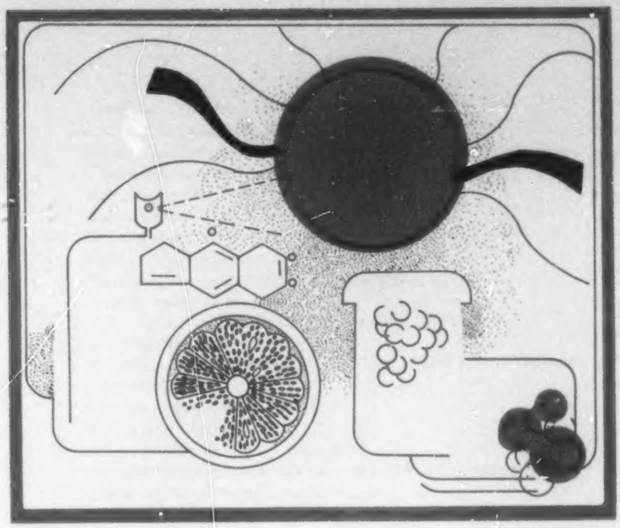

ANIMAL PHOTOCHEMICAL TOXICITY EFFECTS

Moderator: Irvin Asher
Food and Drug Administration

blank page

Toxicologic Aspects of Photosensitization in Livestock[1]

A. Earl Johnson[2]

ABSTRACT—Two types of plant-caused photosensitizations are recognized in livestock: 1) primary, wherein the phototoxic agent in the plant is ingested and reaches the skin chemically unchanged; and 2) secondary, wherein the phototoxic agent is the porphyrin phylloerythrin produced by chlorophyll degradation in ruminant stomachs. Phylloerythrin is normally excreted in bile but is allowed to reach the skin when hepatic damage interferes with the phylloerythrin-excreting mechanism. Primary photosensitizing plant toxins are few, whereas secondary photosensitizations can be caused by damage to the liver by a variety of plant and other toxins. Plants causing each type of photosensitization are discussed and clinical manifestations of the disease in livestock are summarized. *Tetradymia* species are one of the most economically important causes of phototoxicity in livestock. The etiology of this phototoxic syndrome in sheep and the importance of sagebrush species as preconditioning agents for phototoxicity are discussed.—JNCI 1982; 69:253–258.

Photosensitization in livestock, though little publicized and often neglected by researchers, is a significant problem to livestock producers. It occurs in most classes of livestock in all areas of the United States and throughout the world. Just as humans are exposed to an ever-increasing number of toxic chemicals, livestock in their varied environments are at hazard with a multitude of insecticides, herbicides, fertilizers, and other chemicals that may contaminate their feed and water. These agents, however, often photosensitize only a few animals and generally give rise to single exposure or nonrecurrent situations wherein the overall economic impact to an individual livestockman or to a localized group of livestockmen is minimal. Thus these outbreaks have not justified extensive investigations, and often the etiologic relationships have not been fully understood.

Poisonous plants, however, have caused phototoxic reactions in livestock for many decades, and photosensitization in livestock is generally considered a poisonous plant problem. Thus most research has concentrated on the more economically important plant-induced photosensitizations. This presentation focuses on some of these plant phototoxicities to 1) describe the importance of photosensitization problems in livestock, 2) review phototoxic manifestations in livestock, and 3) report on some of the interesting etiologic aspects of one of the most serious photosensitization problems in sheep in the West.

CLASSIFICATION OF PLANT-INDUCED PHOTOTOXICITIES

The following is a classification of some of the common plants that cause photosensitization in livestock:

- Primary photosensitizers:
  - *Hypericum perforatum* (St.-John's-wort, Klamath weed)—contains hypericin, a naphthodianthrone derivative
  - *Fagopyrum sagittatum* (buckwheat)—contains fagopyrin, a naphthodianthrone derivative
  - *Cymopterus watsoni* (spring parsley)—contains furocoumarins
  - *Ammi majus* (bishop's-weed)—contains furocoumarins
- Secondary or hepatogenous photosensitizers:
  - *Tetradymia glabrata*—spineless horsebrush
  - *Tetradymia canescens*—gray horsebrush
  - *Agave lecheguilla*—lechuguilla
  - *Nolina texana*—sacahuiste
  - *Tribulus terrestris*—puncture vine
  - *Lantana* spp.—lantana
  - *Panicum* spp.—panic grasses (kleingrass)
  - *Brassica napus*—cultivated rape
  - *Senecio* spp.—contain toxic pyrrolizidine alkaloids
- Other photosensitizers:
  - Common feeds: *Avena* (oats), *Medicago* (alfalfa), and *Trifolium* (clovers)
  - *Sorghum vulgare* (sudan grass)
  - Blue-green algae
  - Fungi (moldy Bermuda grass, etc.)
  - *Polygonum* spp. (smartweeds)—closely related to buckwheat
  - *Euphorbia maculata* (milk purslane)
  - *Kochia scoparia* (summer cyprus)
  - *Bassia hyssopifolia*
  - *Vicia* spp. (vetches)

In *primary photosensitization* the phototoxic or photosensitizing agent is a component of the feed. As the ingested feed moves through the animal's digestive system, the agent withstands metabolism and excretion and is absorbed unchanged to reach the general circulation and thus the skin where it can react with light (*1*).

Of the primary photosensitizing plants just listed, St.-John's-wort (*Hypericum perforatum*) is best known (*2*). It occurs in the Pacific Coast States and throughout the Southern United States and may affect any class of livestock that eats it. St.-John's-wort contains hypericin, a naphthodianthrone derivative, as the phototoxic agent (*3*).

Bishop's-weed (*Ammi majus*) and spring parsley (*Cymopterus watsoni*) contain furocoumarins (*4, 5*). Bishop's-weed causes photosensitization in poultry (*6*). Spring parsley grows in areas of the Southwestern United States and causes sporadic problems in sheep. Spring parsely gives rise to a somewhat unique problem in that the udders of sheep that are nursing lambs become photosensitized. The udders are hyperemic, sore, and too painful for the sheep to allow their lambs to nurse (*7*). Large numbers of lambs on some range lands may thus die of starvation and dehydration.

Animals affected by primary photosensitizing plants can usually be saved if the cause of the problem is recognized and the animals are removed from the source of the phototoxic agent, penned in the shade, and treated with ointments and antibiotics to hasten healing and prevent secondary infection.

---

[1] Presented at the Seventh Food and Drug Administration Science Symposium ("Photochemical Toxicity: Toxic, Allergic, and Carcinogenic Aspects With Emphasis on Predicting Effects in Humans") held at the Uniformed Services University of the Health Sciences, Bethesda, Md., March 16–17, 1981.

[2] Poisonous Plant Research Laboratory, Agricultural Research Service, U.S. Department of Agriculture, 1150 East 1400 North, Logan, Utah 84321.

In *secondary or hepatogenous photosensitization*, the phototoxic agent is phylloerythrin, a degradation product of chlorophyll (*8*). Phylloerythrin is produced in the stomach of ruminants by rumen microflora (*9*) and absorbed there into the bloodstream. In normal animals, phylloerythrin is eliminated in the bile and has no opportunity to be troublesome. Livers or biliary systems damaged in such a way that the phylloerythrin cannot be eliminated allow phylloerythrin to reach the skin where it reacts with light of appropriate wavelength as do other phototoxic agents. Any toxic plant or agent that causes interference with phylloerythrin excretion by the liver may cause secondary hepatogenous photosensitization if the animal is ingesting chlorophyll. Since chlorophyll is almost always present in the livestock diet, the true etiologic agent of such photosensitization is the hepatotoxic agent.

Secondary or hepatogenous photosensitizing plants cause most of the economically important losses in livestock because more than a phototoxic reaction is involved. Before photosensitization can occur, the damage to the phylloerythrin-excreting mechanism of the liver that must take place may be the result of subtle biochemical changes at the hepatocyte or membrane level or may involve more obvious intrahepatic biliary stasis. Ligation of the common bile duct (*10*) or cyst formation blocking this duct has shown that extrahepatic cholestasis also can generate hepatogenous photosensitization in ruminants on chlorophyll-rich diets. Furthermore, plants that cause cholestasis or blockage of phylloerythrin excretion often produce attendant and more serious hepatic damage and, indeed, some animals die from hepatotoxicity before photosensitization can develop. Thus secondary photosensitization often is less damaging than are the primary hepatic changes that give rise to it.

The *Tetradymia* species are perhaps the most economically important hepatogenous photosensitizing plants that I list and will be discussed in detail later. Lechuguilla and Sacahuiste are desert-type plants of southwestern United States and cause sporadic problems as do other plants in this group (*11, 12*). Kleingrass causes photosensitization in lambs (*13*) but is not toxic to adult sheep and cattle. Several aspects of this condition are presently being studied, and it may develop that the etiology of this disease is not as straightforward as might be expected. *Senecio* species are not usually listed as photosensitizing plants, but this is due to the critical nature of the hepatotoxicity that develops before photosensitization is seen.

A third type of photosensitization, *congenital porphyria*, is sometimes seen in cattle, swine, and cats. It results from a genetic metabolic defect in the synthesis of the heme pigment ferroprotoporphyrin. Free protoporphyrin, uroporphyrin, and coproporphyrin accumulate in serum and tissue of these animals, which leads to photosensitization (*14*).

CLINICAL MANIFESTATIONS

Signs of photosensitization in livestock are similar regardless of the causative agent. Signs, of course, may vary in degree, depending on the amount of reactive pigment present in the skin at a given time, the amount of activating light of appropriate wavelength (or the degree of exposure to that light), and the degree and type of attendant hepatic damage, if hepatogenous photosensitization is being considered.

Animals with photosensitization first exhibit a restlessness and discomfort due to itching of affected skin parts. The affected skin areas are those least protected by dense wool, hair, or pigmentation. In sheep the lips, eyelids, and the head in general are most affected. Occasionally, the external genitalia may be affected if the tail has been docked too closely. The udder of both sheep and cattle may be photosensitized, and in cattle and horses any white or light-colored skin may be affected. The itching parts are scratched in any way the animal can manage—against fences, trees, rocks, or other animals. The animal may appear depressed. Erythema may or may not develop followed by edema of varying degrees. Edema of the head is particularly common in sheep. Ears and lips are first affected. Ears droop as they become swollen and heavy. The sheep has no control of its ears, which may hang pendulously. Swelling then occurs around the eyes and under the chin and the entire head may be much enlarged (fig. 1). The lay term given photosensitization in sheep involving edema of the head is "bighead" or "swellhead." Tissue disruption may follow with external serum leakage that gives rise to scab formation and secondary infection. In addition, in some sheep photosensitizations, the coronet of the hoof (*15*) and the base of the horns may become red.

Recovery may leave seriously affected sheep with barren patches of skin where wool will not grow. Some animals may be left blind because of scar tissue formation that covers the eyes (fig. 2). Lips may be similarly scarred, resulting in the sheep's inability to graze properly. Cattle and horses may lose patches of skin that slough in large, hard, leather-like plaques, while adjacent black or darkly pigmented skin may be unaffected (fig. 3).

Livestock, though they often seek shade when phototoxicities are developing, cannot always find shade, or they may be fenced from it. Thus the period of exposure to sunlight may be long, resulting in much more severe photosensitizations than are commonly encountered in humans.

ETIOLOGIC STUDIES INVOLVING *TETRADYMIA GLABRATA*

Hepatogenous photosensitization as we have defined it is simple and straightforward and should be easily produced experimentally. This, however, is not the case in some plant-induced hepatogenous photosensitizations. Investigators working with *Tribulus*-induced (*16*), kleingrass-induced (Williams MC: Personal communication), and *Tetradymia*-induced (*17*) phototoxicities have found it difficult to induce phototoxic reactions experimentally in livestock, which indicates that other as yet unknown factors are important in the etiology of these syndromes. I have worked sporadically for many years with *Tetradymia* photosensitization in sheep and have found it to be a most interesting and frustrating problem. *Tetradymia glabrata* and *Tetradymia canescens* have been known to be toxic to sheep since 1922 (*18*) and to induce photosensitization in sheep since the 1930's (*19*), but attendant conditions important in the development of the toxic and phototoxic syndrome were not known. Outbreaks were sporadic and unpredictable and often economically devastating to livestockmen. Hundreds of sheep would be lost or affected in an individual herd at a single exposure. No further problems would be encountered for a few years and then another devastating outbreak would occur. The remainder of this presentation will acquaint you with this problem, perhaps give you an appreciation of some of the practical and economic aspects of livestock photosensitization as it happens in the field situation, and relate how we brought to light at least one etiologic agent important in this syndrome.

As background, you should have an appreciation of the land area and the management practices involved. Seventy percent of the land of Utah and adjacent Nevada is federally or state owned, so many sheepmen must graze their sheep on this land under a fee system. In summer sheep are grazed on National forest land in the Wasatch Mountains, a range of mountains that extends north and south through the center of Utah. In winter the sheep are grazed in semidesert areas south and west of the Great Salt Lake and into Nevada on land under the jurisdiction of the Bureau of Land Management. This desert land is lower and essentially free of snow in winter and consists of sparsely vegetated valleys interspersed at intervals of 5–20 miles with small mountain ranges. The land is essentially sagebrush range but contains enough desert-type plants to maintain sheep in winter and spring, if good management practices are employed.

A major problem is that these summer and winter ranges are 150–200 miles apart, and the sheep must therefore traverse this distance twice each year. Many sheepmen now truck their sheep, whereas others do not. Thus about 40,000–50,000 sheep are trailed twice each year 5 miles/day for a period of about 30–40 days each way. Much of this trail is in an extremely remote area—no stores, houses, ranches, or even paved roads for 50- to 100-mile stretches. When problems arise, the livestockmen must have the equipment, knowledge, and ingenuity to resolve them unaided.

Individual size of these trailing herds varies from a few hundred to 2,000 sheep. The possibilities for problems in herds of this size are unlimited as herders try to confine the sheep to a prescribed trail about a mile wide. Much of the trail follows the old Pony Express trail, and occasionally the trail narrows to one-fourth of a mile wide. Such is the case at Simpson Springs, a major Pony Express station and site of a small settlement of years ago. Through long years of use in this confined area around the spring, most of the vegetation has been replaced by *Tetradymia glabrata.* Inasmuch as most sheep must pass this spot, over the years literally thousands of sheep have died or become debilitated at this location from *Tetradymia*-related photosensitization and the attendant hepatic problems.

In the 1930's researchers found that the photosensitization and deaths were due to sheep ingesting *Tetradymia* (*19*). The sporadic poisonings were not fully understood, however, and these early investigators could cause only an occasional photosensitization in sheep by experimentally feeding the plant. These researchers did note that *Tetradymia glabrata* is one of the first desert plants to green in the spring, that it is active only 2–3 months, and that the new green buds that last only a short time are most readily eaten by sheep. They also noted that the most serious outbreaks of *Tetradymia* toxicity and photosensitization frequently followed spring rains or snowstorms and determined that sheep ate *Tetradymia* more freely at those times.

Thus as I became associated with the problem several years ago, much information from field outbreaks was available, but definitive information from experimental feedings was limited. My first efforts were to confirm that which was already reported and to establish toxicity levels by experimentally feeding sheep raised at our laboratory (*17*). These goals required several years because of the logistics of the problem and the fact that green *Tetradymia* is available for such a short time each year. At the expense of 40–50 sheep, we were able to determine the lethal dose under varying conditions; we monitored blood and histopathologic changes and became familiar with clinical symptoms, but we could not produce photosensitization. After we were assured that light conditions at the laboratory were the same as those at the desert area and after we unsuccessfully fed every conceivable combination of *Tetradymia* doses, animals were taken from our laboratory to the desert area for experimentation. Similar feeding efforts to produce photosensitization there were also unsuccessful.

The next effort was to take sheep from a desert herd and experimentally feed them *Tetradymia.* Of these sheep, 70% developed some degree of photosensitization; however, a similar experimental feeding the following year to confirm results was unsuccessful. The only controllable difference in the 2 years' experiments was that the sheep were taken from the herds at different locations on the range—locations that had different types of plant forage. Just prior to our getting them, sheep on one part of the range had been eating black sagebrush (*Artemisia nova*); sheep on the other range area had not been eating black sagebrush.

After experimental feedings to confirm this suspected sagebrush–*Tetradymia* relationship, we now know that black sagebrush, a good winter forage for sheep, preconditions sheep for the toxic action of the *Tetradymia.* Sheep that have not been eating black sagebrush for a few days can tolerate at least three times as much *Tetradymia* in their diet as those that have been eating black sagebrush just prior to their eating *Tetradymia.*

This small bit of information that took so much work to ferret out has the potential of saving hundreds of sheep annually. It is not the complete answer to the sporadic occurrence of *Tetradymia* toxicosis in sheep, for we cannot always produce a higher percentage of photosensitization in sheep preconditioned with black sagebrush (*20*). However, we are hopeful that further investigations into the relationship of toxic compounds in black sagebrush and *Tetradymia* may give us a better understanding of the etiology of this photosensitization and possibly other hepatogenous photosensitizations in livestock.

REFERENCES

(*1*) CLARE NT. Photosensitization in diseases of dometic animals. Review series No. 3 of the Commonwealth Bureau of Animal Health. Farnham Royal, Bucks, England: Commonwealth Agricultural Bureaux, 1952:11–17.

(2) Blum HF. Photodynamic action and diseases caused by light. American Chemical Society Monograph Series, No. 85. New York: Reinhold Publ Corp, 1941:134.

(3) Kingsbury JM. Poisonous plants of the United States and Canada. Englewood Cliffs, N.J.: Prentice-Hall, 1964:171–175.

(4) Williams MC. Xanthotoxin and bergapten in spring parsley. Weed Sci 1970; 18:479–480.

(5) Pathak MA, Daniels F Jr, Fitzpatrick TB. The presently known distribution of furocoumarins (psoralens) in plants. J Invest Dermatol 1962; 39:225–239.

(6) Egyed MN, Shlosberg A, Eilat A, Malkinson M. Acute and chronic manifestations of *Ammi majus*-induced photosensitisations in ducks. Vet Rec 1975; 97:193–199.

(7) Binns W, James LF, Brooksby W. *Cymopterus watsoni*: A photosensitizing plant for sheep. Vet Med/Small Anim Clinician 1964; 59:375–379.

(8) Rimington C, Quin JI. Studies on the photosensitisation of animals in South Africa. VII. The nature of the photosensitising agent in geeldikkop. Onderstepoort J Vet Sci Anim Ind 1934; 3:137–157.

(9) Quin JI, Rimington C, Roets GC. Studies on photosensitisation in animals in South Africa. VIII. The biological formation of phylloerythrin in the digestive tracts of various domesticated animals. Onderstepoort J Vet Sci Anim Ind 1935; 4:463–478.

(10) Quin JI. Studies on the photosensitization of animals in South Africa. VI. The effect of surgical obstruction of the normal bile flow. Onderstepoort J Vet Sci Anim Ind 1933; 1:505–526.

(11) Mathews FP. Lechugilla (*Agave lechegilla*) poisoning in sheep and goats. J Am Vet Med Assoc 1938; 93:168–175.

(12) ——. Poisoning in sheep and goats by sacahuiste (*Nolina texana*) buds and blossoms. Tex Agr Exp Station Bull 585, 1940.

(13) Dollahite JW, Younger RL, Jones LP. Photosensitization in lambs grazing kleingrass. J Am Vet Med Assoc 1977; 171:1264–1265.

(14) Rimington C. Some cases of congenital porphyrinuria in cattle. Chemical studies upon living animals and post-mortem material. Onderstepoort J Vet Sci Anim Ind 1936; 7:567–609.

(15) Quin JI, Rimington C. Geeldikkop. A critical review of the problem as it affects farming in the Karoo together with recommendations in the light of newer knowledge. J S Afr Vet Med Assoc 1935; 6:16–24.

(16) Blum HF. Photodynamic action and diseases caused by light. American Chemical Society Monograph Series, No. 85. New York: Reinhold Publ Corp, 1941:146.

(17) Johnson AE. Experimental photosensitization and toxicity in sheep produced by *Tetradymia glabrata*. Can J Comp Med 1974; 38:406–410.

(18) Fleming CE, Miller MR, Vawter LR. The spring rabbit brush (*Tetradymia glabrata*). A range plant poisonous to sheep. Univ Nevada Agr Exp Sta Bull No. 104, 1922:1–29.

(19) Clawson AB, Huffman WT. Bighead in sheep caused by plant poisoning. Natl Woolgrower 1937; 27:13–16.

(20) Johnson AE. *Tetradymia* toxicity—a new look at an old problem. In: Keeler R, Van Kampen K, James L, eds. Effects of poisonous plants on livestock. New York: Academic Press, 1978:209–216.

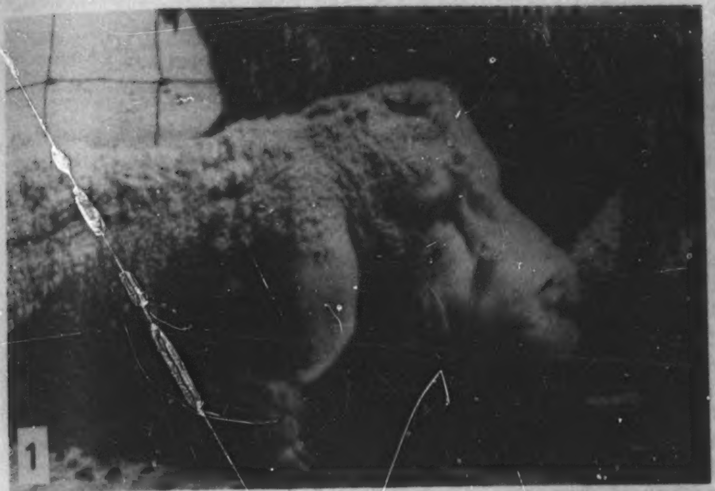

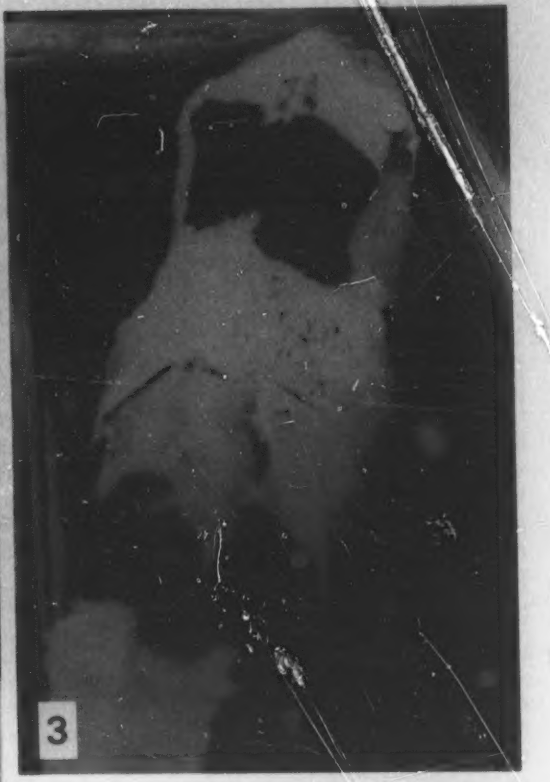

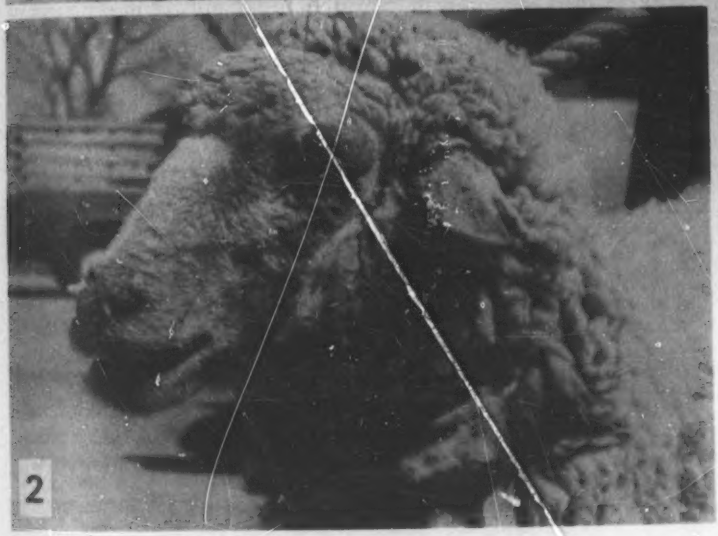

FIGURE 1.—Photosensitized sheep with full edema of the head. *Note* pendulous ears and edema of the lips, eyes, and throat.
FIGURE 2.—Sheep that has survived severe photosensitization. *Note* severe scarring of the lips, nose, and eyes. The sheep is also blind.
FIGURE 3.—Severely photosensitized Holstein cow. *Note* the large plaques of white skin that are sloughing, the unaffected darkly pigmented skin, and the general emaciation of the cow.

DISCUSSION

I. M. Asher: Could you speculate on the purpose of these photosensitizing agents to the plants themselves? Is it an evolutionary designed defense, or is it intrinsic to the plant unrelated to the photosensitizing effect of the agent?

A. E. Johnson: Are you speaking about the hepatogenous type of photosensitization?

Asher: Yes, what do the chemical agents do for the plants that contain them, and is what they do related to their ability to harm the animals that feed on such plants?

Johnson: As I said at the onset, hepatogenous photosensitization is a simple porphyrin type of photosensitization in that the phototoxic agent phylloerythrin is a breakdown product of chlorophyll. All sheep ingest chlorophyll, and the phylloerythrin that is produced from it is normally excreted in the bile. All you have to do, then, is to damage the liver in some way so that phylloerythrin is not excreted, and the very small amounts of phylloerythrin that reach the skin will cause this photosensitization. In fact, you can block phylloerythrin excretion by ligating the common bile duct and cause photosensitization this way when the animal is receiving chlorophyll in its diet.

Since this phototoxic reaction is secondary or incidental to the liver damage causing biliary stasis, it is not likely to relate to the plant's ability to harm those animals that feed upon it. In fact, most toxic agents in plants have not been shown to function in metabolic pathways in the plant. But even though their function is unknown, it is my belief that there is insufficient evidence to say that these toxins developed evolutionally in plants to harm animals that graze on them.

M. Pathak: I enjoyed this presentation very much and learned some things. The early work in this area was done by Professor C. Rimington of England, if you know about this, on the syndrome called geeldikkop.

But what interested me about the sagebrush story is that in desert areas around sagebrush, nothing seems to grow except sagebrush. It is not that other seeds are not able to germinate, but sagebrush produces very potent coumarin, as well as furocoumarin.

And if you extract the sagebrush, they do contain very highly fluorescent, phototoxic agents, some of which even induce reactions that have properties of a photoallergic type of reaction.

There is a plant called *Thamnosma montana* in the desert area; it has a furocoumarin that comes out in the root, preventing anything else from germinating. And that is the same thing with the sagebrush, I speculate. The fascinating thing is that the sagebrush has a photosensitizing agent which can actually cause a phototoxic reaction.

Johnson: Yes, I was very interested in those comments, and we have tried to cause photosensitization by feeding the sagebrush alone; however, we have been unsuccessful. We have not really delved into it, because there are many potential toxic agents in sagebrush, in addition to essential oils and sesquiterpene lactones.

K. Kraemer: You mentioned that the animals became sensitized by ingesting these plants. Do the levels of any of these sensitizers in the tissues in the milk or in the meat of the animals reach such concentrations that they would be dangerous to humans if they were to be ingested?

Johnson: Not that we are aware of. We cannot answer that question because we actually have not checked it out. But I would suspect not.

N. Salman: Is there any practical way to deal with the problem, to cover the sensitive parts of the sheep? I know that to study the plants and determine what type of photosensitizers they have is good, but is there meanwhile, any practical way, a quick way, to deal with the problem by maybe covering the sensitive parts of the sheep, for example, the head or any other vulnerable parts of the body, to overcome this serious and urgent problem?

Johnson: This, of course, if one of the problems of working with large numbers of animals. As I mentioned, we are talking about 2,000 sheep in some of these herds, and it is utterly impossible to cover that number. We have talked about protective compounds, carotenoids, tocopherol, and others, and there are some possibilities here that we need to investigate further; but even getting protective compounds into these sheep, under the conditions in which they are managed, is an extremely difficult thing to do.

Chemical and Biochemical Aspects of Photosensitization in Livestock and Poultry[1]

G. Wayne Ivie[2]

ABSTRACT—Certain synthetic and naturally occurring chemicals, particularly those found in some range plants, may interact with livestock and poultry in the presence of activating light to produce photosensitization. Such photosensitization may have serious implications for livestock producers as a result of causing reduced performance of and even death of affected animals. The mechanisms producing photosensitization in livestock and poultry are discussed in context with the chemical nature of major livestock photosensitizers. The possibility that photosensitizing agents for livestock may have toxicologic significance in humans consuming photoactive residues in meat or animal by-products is considered.—JNCI 1982; 69:259–262.

Livestock and poultry producers face many obstacles in their attempts to produce economically and profitably meat, edible animal by-products, and animal fibers. In addition to wide and often unpredictable fluctuations in production costs and market stability, animal disease and toxicity problems may be encountered that are often unanticipated but which may be devastating. Although many animal diseases may be dealt with quickly and effectively, either by prophylaxis or by prompt diagnosis and drug therapy, problems involving toxicants are generally more difficult to manage. This difficulty of management arises because causal agents in animal toxicoses are often difficult to define and effective treatment procedures are often lacking.

A wide variety of substances may interact with livestock and poultry, with toxicologic consequences. Among such substances are pesticides, animal drugs, and industrial chemicals. Certain natural products to which animals are exposed in the diet, particularly toxic range plants, are of special significance. While the nature of the toxic responses elicited by any one or combination of these toxic agents may vary greatly, depending on the mechanisms of action involved, this report will deal with only those agents known to elicit light-dependent toxicities in livestock and poultry.

MANIFESTATIONS OF PHOTOSENSITIZATION

Livestock.—From the perspective of the producer or veterinary diagnostician, livestock photosensitization can be defined as an abnormal blistering and peeling of skin due to increased sensitivity to sunlight. Although such a definition is overly simplistic and does not take into account all biochemical and physiologic ramifications of the syndrome, from a practical standpoint it is a workable and generally accurate description of photosensitization as normally observed in such animals as cattle, sheep, and horses. The lesions of photosensitization appear almost exclusively on light-skinned portions of animals not sufficiently protected from sunlight by the animal's coat or by anatomic location (eyelids, nose and muzzle, anus and vulva, udder and teats, and the coronary band of hooves and horns). Early acute reactions are, predictably, erythema and edema followed by blistering, scabbing, and peeling of the skin. In severely photosensitized animals, scarring, deformation (particularly of the ears), and blindness may be permanent effects (*1–3*).

Poultry.—In birds, photosensitization affects unfeathered or undowned portions of the body including the beak, ocular area, comb, wattles, and feet. Edema, blistering, and scabbing may be succeeded by blindness, sloughing of the comb and wattles, and deformation of the beak and feet. Deformities are particularly severe and often permanent in young birds photosensitized during active growth stages (*3–6*).

GENERAL MECHANISMS PRODUCING PHOTOSENSITIZATION

It is generally considered that livestock photosensitization can be classified into one of three categories depending upon the origin of the ultimate photosensitizing agent (*1, 2*). Some classifications include a fourth, "miscellaneous," category (*7*). In *primary* photosensitization, the photoactive chemical(s) arise from some source external to the animal, such as from a foodstuff. Once in the animal, these chemicals or their phototoxic metabolites reach the peripheral circulation where they absorb incident sunlight and transfer the absorbed energy to cellular components in such a manner that cellular damage results. *Hepatogenous* photosensitization occurs when exogenous chemicals or their metabolites, though not inherently phototoxic, cause hepatic damage that results in retention of photoactive bile pigments. Such pigments reach abnormally high concentrations in the peripheral circulation and, in the presence of sunlight, result in phototoxicity. *Congenital* photosensitizations in livestock are genetic disorders of porphyrin metabolism that result in unusually high concentrations of photoactive porphyrins or porphyrin precursors in the peripheral circulation. *Miscellaneous* syndromes of photosensitization represent those instances in which the etiology is unknown. Such photosensitizations are not hepatogenous because liver damage is not associated with the syndrome; they are not congenital because photosensitization is associated with some external source (such as a photosensitizing plant). Thus, of necessity, most if not all miscellaneous photosensitizers of an undefined type are probably primary photosensitizers in which the chemical nature of the photosensitizing agent is not known.

---

[1] Presented at the Seventh Food and Drug Administration Science Symposium ("Photochemical Toxicity: Toxic, Allergic, and Carcinogenic Aspects With Emphasis on Predicting Effects in Humans") held at the Uniformed Services University of the Health Sciences, Bethesda, Md., March 16–17, 1981.

[2] Veterinary Toxicology and Entomology Research Laboratory, Agricultural Research Service, U.S. Department of Agriculture, College Station, Tex. 77841.

Primary Photosensitization

Relatively few agents have been shown to cause primary photosensitization in livestock and poultry. A schematic representation of how such agents interact with animals to elicit phototoxic responses is shown in text-figure 1. Structures of some primary photosensitizing chemicals are shown in text-figure 2. Hypericin, fagopyrin, and protofagopyrin are highly conjugated naphthodianthrone derivatives that are responsible for the photosensitizing action of *Hypericum* spp. and *Fagopyrum* spp. in cattle and sheep (*8, 9*). Psoralens (linear furocoumarins) are well-known potent photosensitizers when activated by near UV light, and they occur in a large number of plant species from several families. Psoralens have been shown to account for the photosensitizing actions of *Ammi majus* and *Cymopterus* spp. in both livestock and poultry (*10–13*). The synthetic drug phenothiazine, used as an anthelmintic in several livestock species, can result in photosensitization under certain circumstances. It is thought that an oxidative metabolite, phenothiazine sulfoxide, may be the major photosensitizing agent in phenothiazine phototoxicity (*1, 2*).

Hepatogenous Photosensitization

Most agents known to elicit photosensitization in ruminants appear to be of the hepatogenous type. The progression of the syndrome is presented schematically in text-figure 3. In typical cases, foodstuffs such as range plants or moldy forage grasses that contain hepatotoxic chemicals or their precursors are consumed by the animals, and the toxin(s) are absorbed and transported to the liver. Hepatotoxicity ensues, which may be manifested as severe damage to liver cells and/or occlusion of the bile ducts. Ultimately, normal biliary excretion mechanisms are circumvented and photoactive bile pigments accumulate in the blood at abnormally high levels.

The chlorophyll derivative phylloerythrin is apparently the major ultimate photosensitizer in hepatogenous photosensitization in ruminants (*1, 2, 9*), although other photoactive bile pigments may possibly be involved. Phylloerythrin is a normal metabolite of the anaerobic fermentation of chlorophyll in the rumen (text-fig. 4). Phylloerythrin is a potent photosensitizer, but because it is normally eliminated rapidly through the bile, it usually has no significant effects on the animal. In liver-damaged animals, however, phylloerythrin is not eliminated normally; it accumulates in the blood, and its occurrence in the peripheral circulation at levels as low as 0.1 μg/ml, in the presence of sunlight, is sufficient to induce photosensitization (*14*).

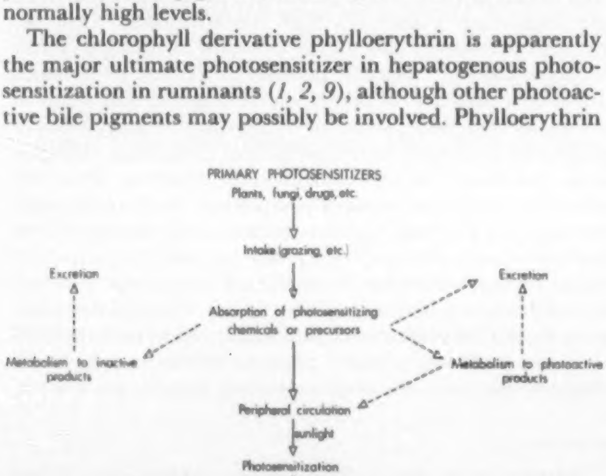
PRIMARY PHOTOSENSITIZERS
Plants, fungi, drugs, etc.
Intake (grazing, etc.)
Excretion
Absorption of photosensitizing chemicals or precursors
Excretion
Metabolism to inactive products
Metabolism to photoactive products
Peripheral circulation
sunlight
Photosensitization
Recovery
Death

TEXT-FIGURE 1.—Schematic representation of the interactions of primary photosensitizers with livestock and poultry. *Solid lines*=usual pathways; *broken lines*=pathways of lesser significance or that are more difficult to define experimentally.

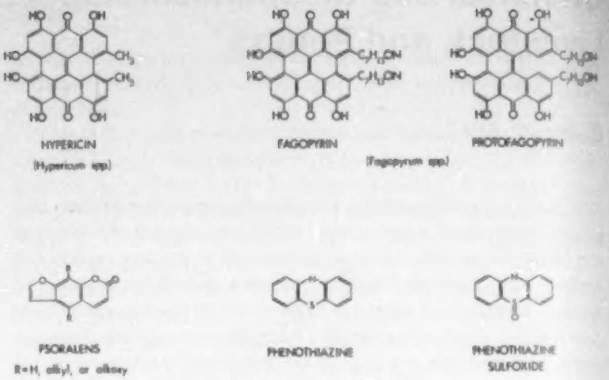

TEXT-FIGURE 2.—Structures of certain chemicals known to act as primary photosensitizers in livestock and/or poultry.

A number of agents are known to induce hepatogenous photosensitization in ruminants, on the basis of liver damage associated with photosensitivity, but the exact nature of the hepatotoxic chemicals is known in few cases. Two sources of such hepatotoxic chemicals are *Lantana* spp., which contain the hepatotoxins lantadene A and other closely related chemicals (*15*), and the fungus *Pithomyces chartarum*, a saprophyte of some forage plants, which contains the hepatotoxin sporidesmin (*16*) (text-fig. 5). It should be reemphasized that chemicals such as the lantadenes and sporidesmins are *hepatotoxic* and not inherently photoactive.

Hepatogenous photosensitization in ruminants has been associated almost exclusively with the consumption of certain forage plants, but it seems probable that in some cases metabolites of fungi or other micro-organisms associated with these plants may be the actual hepatotoxic agents involved. The occurrence of hepatogenous photosensitization in livestock is often sporadic, unpredictable, and difficult to reproduce experimentally. Further, hepatogenous photosensitivity is sometimes associated with very palatable and important forage plants including alfalfa and Bermuda grass (*8, 16*). These observations strongly suggest that in such cases the hepatotoxins associated with photosensitivity may not be normal constituents of the plant species themselves.

Congenital Photosensitization

Photosensitization associated with inherited disorders of porphyrin metabolism in livestock is known but is of little economic or practical significance in livestock production. Congenital protoporphyria occurs in cattle and swine, and the syndrome as observed in cattle may have importance as a human model of the disease (*17, 18*). In congenital pro-

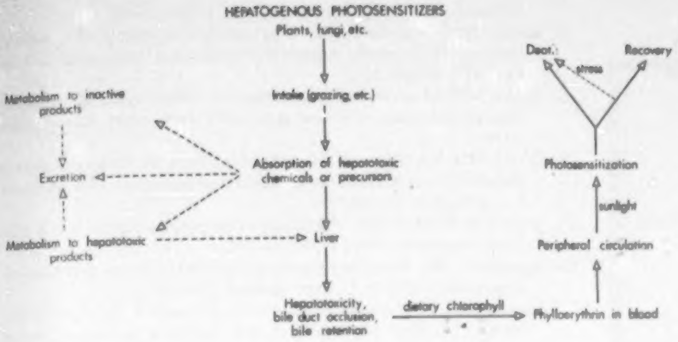
HEPATOGENOUS PHOTOSENSITIZERS
Plants, fungi, etc.
Intake (grazing, etc.)
Absorption of hepatotoxic chemicals or precursors
Liver
Hepatotoxicity, bile duct occlusion, bile retention
Metabolism to inactive products
Excretion
Metabolism to hepatotoxic products
dietary chlorophyll
Phylloerythrin in blood
Peripheral circulation
sunlight
Photosensitization
Death
stress
Recovery

Text-figure 3.—Schematic representation of the interactions of hepatogenous photosensitizers with livestock. *Solid lines*=usual pathways; *broken lines*=pathways of lesser significance or that are more difficult to define experimentally.

toporphyria, phototoxicity is caused by elevated levels of photoactive protoporphyrin in blood, which result from genetic deficiencies in heme biosynthesis (text-fig. 6).

Poultry disorders known as "turkey blindness syndrome" and "light-induced avian glaucoma" may occur when birds are reared under *continuous* artificial light (*19–21*). The mechanisms involved in producing these disorders are apparently not clearly understood, but it seems doubtful that such disorders should be classified as congenital photosensitizations in the context considered here.

ECONOMIC CONSIDERATIONS

It is probably safe to say that photosensitization, when considered in the context of other livestock diseases and toxicities, is not a major economic problem in livestock production. Photosensitization tends to occur sporadically and infrequently and may affect only a limited number of animals within a given herd. Also, photosensitization does not *usually* result in mortality, thus rapid action on the part of the producer to remove affected animals from the source of the photosensitizing agent or to provide protection from sunlight often results in the animals' rapid and complete recovery. This is not to imply, however, that livestock photosensitization is of no significant economic importance, for such is clearly not the case. Photosensitized animals, particularly those affected by hepatogenous photosensitizers, can in fact be killed by the disease or by complications arising from it, and surviving animals may be permanently affected (with blindness, scarring, deformation) such that their market value is destroyed or greatly reduced. In addition, weight gains may be affected, milk production may be reduced, animals photosensitized on the udder and teats may refuse to nurse their young, and the stresses associated with photosensitization may result in abortions. Thus, in some instances, livestock photosensitization can and does have significant economic impact. The relatively widespread occurrence of "facial eczema" in New Zealand among diary cattle grazing forage that contains *P. chartarum* is an example of a livestock photosensitization syndrome that has considerable local economic impact (*16*).

In contrast to the economic effects attributable to photosensitization in livestock, essentially *no* economic effects result from poultry phototoxicities because photosensitization in poultry is rare except under experimental conditions. I am aware of only one circumstance in which domestic poultry have suffered severe nonexperimental photosensitization, and that was in Israel among pasture-raised ducks and geese that grazed the psoralen-containing weed *A. majus* (*22*). The rarity of photosensitization in poultry is understandable in view of production practices in which dietary regimens are usually carefully regulated and because much of the poultry production worldwide is done indoors under relatively low-intensity artificial light. However, photosensitization of domestic poultry reared under less intensive practices, particularly among free ranging-birds, probably occurs periodically because of the widespread occurrence of photosensitizing agents in nature and because of the generally omnivorous dietary habits of many avian species.

RESEARCH NEEDS

Photosensitization is at present not a major economic problem in livestock production, except in localized situations, but it seems appropriate to continue to develop research data that will allow a more complete understanding of these disorders in livestock and poultry. Further studies aimed at defining the chemistry of livestock photosensitizing agents and their biochemical modes of action could lead to the development of more accurate procedures for predicting photosensitization and possibly even effective antidotes or prophylaxes. Because the expressions of photochemical toxicities in food animals and humans are often identical or very similar, studies in livestock reasonably may be expected to generate data applicable to a more complete understanding of certain photochemical disorders in humans.

Photoactive agents that interact with food animals are often extremely active biologically, certainly as photosensitizers but perhaps also through mechanisms not dependent on light. Therefore, it may be that some photosensitizing

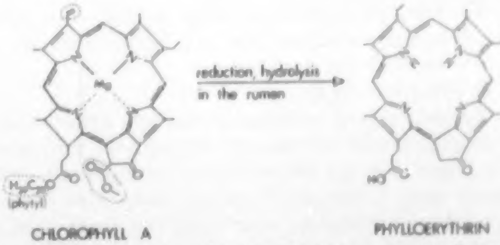

Text-figure 4.—Formation of phylloerythrin by anaerobic fermentation of chlorophyll a in the rumen.

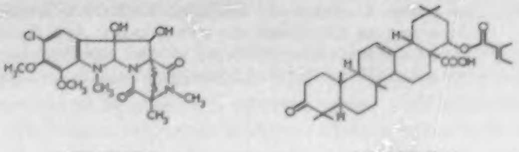

SPORIDESMIN (*Pithomyces chartarum*)

LANTADENE A (*Lantana camara*)

TEXT-FIGURE 5.—Structures of the hepatogenous photosensitizing chemicals sporidesmin and lantadene A.

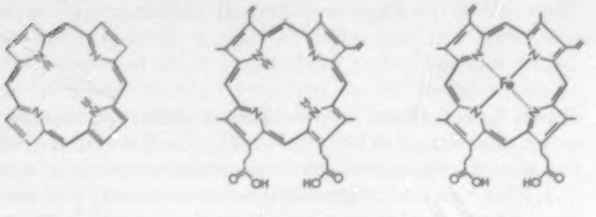

PORPHINE PROTOPORPHYRIN HEME

TEXT-FIGURE 6.—Structures of porphyrins. In congenital protoporphyria, genetic disorders in heme biosynthesis result in the accumulation of photoactive protoporphyrin in the peripheral circulation.

chemicals have direct toxicologic significance for humans, *if* these chemicals or their metabolites are retained by edible tissues or are secreted into milk or eggs. Such possibilities have thus far not been evaluated by suitable research approaches, although appropriate residue and metabolism studies with selected photosensitizers in food animals would provide data of considerable value toward an assessment of the toxicologic significance of these chemicals to humans.

REFERENCES

(*1*) CLARE NT. Photosensitization in diseases of domestic animals. Review series No. 3 of the Commonwealth Bureau of Animal Health. Farnham Royal, Bucks, England: Commonwealth Agricultural Bureaux, 1952.

(*2*) ———. Photosensitization in animals. Adv Vet Sci 1955; 2:182–211.

(*3*) IVIE GW. Toxicological significance of plant furocoumarins. In: Keeler R, Van Kampen K, James L, eds. Effects of poisonous plants on livestock. New York: Academic Press, 1978:475–485.

(*4*) EGYED MN, WILLIAMS MC. Photosensitizing effects of *Cymopterus watsonii* and *Cymopterus longipes* in chickens and turkey poults. Avian Dis 1977; 21:566–575.

(*5*) EGYED MN, MALKINSON M, SHLOSBERG A. Observation on the experimental poisoning of young geese with *Ammi majus*. Avian Pathol 1974; 3:79–87.

(*6*) EGYED MN, SHLOSBERG A, EILAT A, MALKINSON M. Acute and chronic manifestations of *Ammi majus* induced photosensitization in ducks. Vet Rec 1975; 97:193–199.

(*7*) JUBB KV, KENNEDY PC. Pathology of domestic animals. Vol 2. New York: Academic Press, 1970:590–594.

(*8*) KINGSBURY JM. Poisonous plants of the United States and Canada. Englewood Cliffs, N.J.: Prentice-Hall, 1964:52–57.

(*9*) PATHAK MA. Phytophotodermatitis. In: Fitzpatrick TB, Pathak MA, Harber LC, Seiji M, Kukita A, eds. Sunlight and man. Normal and abnormal photobiologic responses. Tokyo: Univ Tokyo Press, 1974:495–513.

(*10*) IVIE GW. Linear furocoumarins (psoralens) from the seed of Texas *Ammi majus* L. (Bishop's Weed). J Agric Food Chem 1978; 26:1394–1402.

(*11*) WILLIAMS MC. Xanthotoxin and bergapten in spring parsley. Weed Sci 1970; 18:479–480.

(*12*) STERMITZ FR, THOMAS RD, WILLIAMS MC. Furocoumarins of *Cymopterus watsonii*. Phytochemistry 1975; 14:1681.

(*13*) YOST GS, STERMITZ FR, WILLIAMS MC. Toxic furocoumarins of *Cymopterus longipes*. Phytochemistry 1977; 16:1097.

(*14*) FORD EJ, GOPINATH C. The excretion of phylloerythrin and bilirubin by calves and sheep. Res Vet Sci 1976; 21:12–18.

(*15*) SEAWRIGHT AA, HRDLICKA J. The oral toxicity for sheep of triterpene acids isolated from *Lantana camara*. Aust Vet J 1977; 53:230–235.

(*16*) RICHARD JL. Mycotoxin photosensitivity. J Am Vet Med Assoc 1973; 163:1298–1299.

(*17*) RUTH GR, SCHWARTZ S, STEPHENSON B. Bovine protoporphyria: The first nonhuman model of this hereditary photosensitizing disease. Science 1977; 198:199–201.

(*18*) BRENNER DA, BLOOMER JR. Comparison of human and bovine protoporphyria. Yale J Biol Med 1979; 52:449–454.

(*19*) ASHTON WL, PATTISON M, BARNETT KC. Light-induced eye abnormalities in turkeys and the turkey blindness syndrome. Res Vet Sci 1973; 14:42–46.

(*20*) LAUBER JK, SHUTZE JV, MCGINNIS J. Effects of exposure to continuous light on the eye of the growing chick. Proc Soc Exp Biol Med 1961; 106:871–872.

(*21*) KINNEAR A, LAUBER JK. Biochemical studies of the chicken vitreous in light-induced avian glaucoma. Comp Biochem Physiol [B] 1978; 61:107–110.

(*22*) EILAT A, MALKINSON M, SHLOSBERG A, EGYED MN. A field outbreak of photosensitization in goslings caused by the ingestion of *Ammi majus*. Refu Vet 1974; 31:83–86.

DISCUSSION

Anonymous: I was requesting from the speaker knowledge of the exposure situation whereby livestock meet the phenothiazine molecule.

G. W. Ivie: Phenothiazine is an anthelmintic used to control intestinal parasites. Earl, is it given orally, by injection, or whatever? Do you know?

A. E. Johnson: Orally.

N. Towers: I want to make a comment about what Dr. M. Pathak said after the last talk. In *Artemisia*, the photosensitizing chemicals are polyacetylinic compounds and not furocoumarins. I thought I should make that statement, because the Compositae, which are the largest group of flowering plants, have this very large group of photosensitizers in them. These compounds have a totally different mechanism in terms of photosensitization in that they act on cell membranes rather than on the nucleic acids.

T. Nigra: This is a comment, perhaps about evolution, but nature seems to have provided for protection automatically, at least in terms of psoralens, when they are eaten. Herbivores are extremely difficult to photosensitize if you try to feed them drugs by mouth, whereas omnivores are much easier to sensitize, and the carnivores are easier yet.

I think it is very interesting that there seems to be some natural protective mechanism. If you look at serum levels of psoralen when you give the drug by mouth, the amount needed by mouth to produce phototoxic-inducing serum levels in the herbivores is markedly higher than the amount needed in the carnivores.

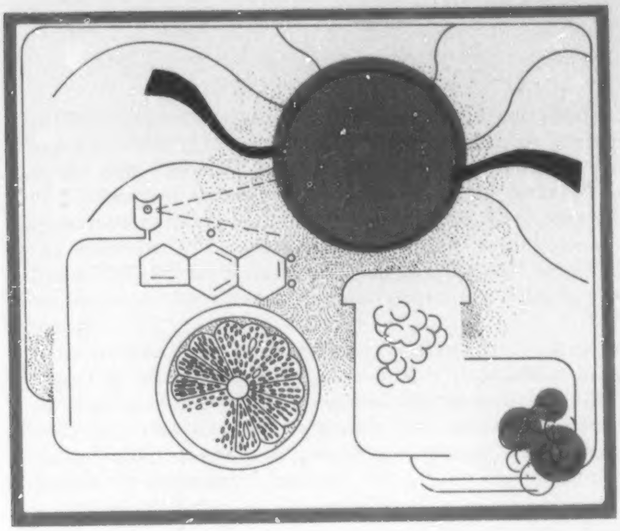

HUMAN PHOTOCHEMICAL TOXICITY EFFECTS

Moderator: Thomas Nigra
Washington Hospital Center

blank page

Chemical Phototoxicity in Humans[1,2]

John H. Epstein, *M.D.*[3,4]

ABSTRACT—Phototoxic reactions may be induced by endogenous or exogenous chemicals. Endogenous photosensitizers made by the body include porphyrin molecules which are responsible for the photocutaneous syndromes noted in the porphyrias. Exogenous photosensitizers may arrive on the skin through topical applications or may be distributed through the vasculature. Topical photosensitizers are found in cosmetics, medications, plants, and industrial and air pollutant emissions. Systemic photosensitizers consist primarily of therapeutic agents. Acute and chronic phototoxic reactions may occur. The acute response is generally characterized by erythema and edema followed by hyperpigmentation and desquamation. The end point of chronic damage may be cutaneous cancer formation. The mechanisms of these changes may well relate to nucleic acid injury, protein and membrane damage, and alterations in other nuclear and cytoplasmic molecular structures. However, translation of experimental information into human responses remains to be clarified. A great deal of investigation is still needed in developing assays for detecting phototoxic chemicals and for defining mechanisms involved in phototoxic events in human skin.—JNCI 1982; 69:265-268.

Injurious cutaneous photoreactions have become commonplace in the general population due *notably* to the sunbathing mania that pervades our society, but also due to the large quantities of photosensitizing chemicals being thrust into our environment from industrial, cosmetic, and pharmaceutical sources. The present report is concerned primarily with the last of these two conditions, i.e., the phototoxic effects of these chemicals on our collective skins.

LAWS AND DEFINITIONS

But before we examine the problems of photochemical toxicity in human skin, perhaps a brief discussion of certain basic concepts might be in order. Let us start with the basic law of photobiology. This law states that nonionizing radiation must be absorbed to produce a photochemical and thus the resultant photobiological reaction. This law then stipulates that the photosensitizer, chromophore, radiation absorber, or whatever term one wishes to use must be present at the time of radiation for a reaction to occur.

The action spectrum of a photochemical reaction and the resultant photobiological reaction consists of the wavelengths absorbed by a molecule which leads to a specific response. The action spectrum usually, but not always, simulates the absorption spectrum of a molecule. However, it must always be included in the absorption spectrum, since this radiation must be absorbed to produce a reaction.

"Photosensitivity" is the broad term used to connote adverse reactions to this radiation (*1*). Two types of reactions may occur: phototoxic or photoallergic. The phototoxic response can be divided into 2 subgroups: photodynamic and nonphotodynamic. Simplistically, the differentiation relates to the need of oxygen in the photodynamic process, though the process is much more complex (*2*).

Phototoxicity is common. It will occur in everybody if enough of the chromophore or photosensitizers are present in the skin. Clinically, the responses usually are comprised of a delayed erythema with or without edema, followed by hyperpigmentation and desquamation. Thus they resemble the ordinary UVB radiation (between 280 or 290 nm and 315 or 320 nm) sunburn response. In fact, the ordinary UVB sunburn is by far the most common phototoxic reaction that we see.

In contrast, photoallergy is uncommon (*3-5*). It is an acquired, altered reactivity, presumably dependent on an antigen-antibody or cell-mediated hypersensitivity. Clinically, it is characterized by unusual reactions. These reactions include immediate urticarial responses and delayed papular to eczematous lesions.

Almost all of the well-documented photobiological events that occur in the skin are induced by UVB radiation. Such radiation can inhibit DNA, RNA, and protein synthesis and mitosis formation, labilize lysosomal membranes, stimulate formation or release of vasoactive substances such as prostaglandins and kinins, induce a delayed erythema and new pigment formation, cause cancer, and produce vitamin D precursors in the epidermis. For practical purposes, this radiation does not pass through window glass. Thus a good sturdy piece of window glass will eliminate all of these cutaneous responses.

UVA radiation (315 or 320-400 nm) produces a few minor photobiological events such as immediate pigment darkening, due to photo-oxidation of melanin which is already present in the skin, and a transient immediate erythema response. However, UVA radiation is important to us for two reasons. UVA radiation markedly accentuates the injury produced by the UVB radiation and is responsible for the vast majority of exogenously photosensitized reactions that occur in the skin.

It is with this last issue (i.e., chemical phototoxicity) that this paper is concerned. Furthermore, this report is directed toward such a reaction in human skin. The initial consideration relates to the source and route of administration of these photosensitizing chemicals. The origin of these chemicals may be endogenous or exogenous.

---

[1] Presented at the Seventh Food and Drug Administration Science Symposium ("Photochemical Toxicity: Toxic, Allergic, and Carcinogenic Aspects With Emphasis on Predicting Effects in Humans") held at the Uniformed Services University of the Health Sciences, Bethesda, Md., March 16-17, 1981.

[2] Supported in part by Public Health Service grant CA-15605 from the National Cancer Institute.

[3] Department of Dermatology, University of California, San Francisco, Calif. 94102.

[4] *Address reprint requests to* Dr. Epstein at 450 Sutter St. #1306, San Francisco, Calif. 94108.

ENDOGENOUS PHOTOSENSITIZERS

Only one type of photosensitizing chemical is made in the body (*6, 7*). That is, or more properly, these are the porphyrin molecules which are responsible for the clinical manifestations of the porphyrias listed below:

The porphyrias

- I. Erythropoietic
  - A. Congenital erythropoietic porphyria
  - B. Erythropoietic coproporphyria
- II. Erythrohepatic: Erythropoietic protoporphyria
- III. Hepatic
  - A. Acute intermittent porphyria
  - B. Porphyria cutanea tarda
  - C. Variegate porphyria
  - D. Hereditary coproporphyria
  - E. Acquired porphyria

As noted, abnormal amounts of porphyrins may be made in the hematopoietic system as occurs in the congenital erythropoietic porphyria of the Günther variety and erythropoietic coproporphyria, or they may be made in hematopoietic tissue and at times possibly the liver as well, as appears to occur in erythropoietic protoporphyria which may be a misnomer (*8*). Perhaps a more appropriate name would be erythrohepatic protoporphyria. The abnormal amounts of porphyrins may be made in the liver alone as occurs in acute intermittent porphyria, porphyria cutanea tarda, variegate porphyria, hereditary coproporphyria, and the truly acquired porphyrias.

All of these porphyrias have photocutaneous syndromes associated with them except one, i.e., acute intermittent porphyria. The reason for this is that all of these porphyrias except acute intermittent porphyria are characterized by the overproduction of photoactive, preformed porphyrins. In acute intermittent porphyria the porphyrin precursors δ-aminolevulenic acid and porphobilinogen are produced in excess. These reactions range from the marked photodestruction noted in congenital erythropoietic porphyria to the fragility, blistering, denudation, superficial scarring, crusting, and milium formation noted in porphyria cutanea tarda.

In all of these instances, the nature of the process is phototoxic. The action spectrum appears to peak around 400 nm, which is the peak absorption spectrum of the naturally occurring porphyrins in the human body, i.e., uroporphyrin, coproporphyrin, and protoporphyrin. This is a prime example of a photodynamic process that appears to involve the production of peroxides (*7*). These peroxides in turn labilize membranes, presumably lysosomal membranes, in the upper dermal blood vessel endothelium, which in turn results in the release of hydrolytic enzymes (*9–11*). The resultant responses appear to be responsible for the clinical pictures noted in these diseases. Recent evidence indicates that photoactivation of these porphyrins can result in activation of the classical pathway of the complement system with generation of chemotactic factors through C5 (*12, 13*). This process may well contribute to the photodamage that occurs in these diseases.

EXOGENOUS PHOTOSENSITIZERS

Exogenous chemical photosensitizers may arrive on the skin topically or systemically through the vascular system.

The topical exogenous photosensitizers may be placed in the following categories:

- I. Cosmetics: Perfumes, creams, soaps, etc.
- II. Medications
  - A. Advertent: Psoralens, tars
  - B. Inadvertent: Phenothiazines, sulfonamides, halogenated salicylanilides (and related compounds), sunscreens, etc.
- III. Plants: Gas plant, lime rinds, celery, carrots, etc.

Topical exogenous photosensitizers may be applied to the skin in the form of cosmetics, perfumes, moisturizing creams, soaps, and the like. Certain medications are applied to the skin, some of which are intended to produce photoreactions, e.g., the psoralen compounds and, occasionally, tar.

Other medications arrive on the skin without the intent to photosensitize. These include phenothiazines, sulfonamides, antibacterial agents such as the halogenated salicylanilides and related compounds, and sunscreens.

A number of plants contain photosensitizing chemicals, primarily psoralen compounds, which can and do induce photosensitive reactions. These plants include carrots, celery (especially celery infected with pink rot disease), gas plant, lime rinds, and the like. The primary photosensitizers in these plants are psoralen compounds, though other photosensitizers are found in other plants (*14*).

Industrial emissions constitute another source of topical photoactive chemicals. These agents are primarily polycyclic hydrocarbons that can act as photosensitizers or additive carcinogens (*2, 15*). In addition, potential promoters of photocarcinogenesis may be found in industrial emissions (*15*).

The commonly used systemic photosensitizers may be placed in the following categories:

- I. Antibacterial sulfonamides
- II. Thiazide diuretic medications
- III. Sulfonylurea antidiabetic medications
- IV. Phenothiazines
- V. Antibiotics: Especially demeclocycline

Photosensitizing chemicals that reach the skin through the vasculature are generally medications. The numbers of systemic photosensitizers are immense. They include potent photosensitizers such as the psoralen compounds that are usually employed to produce photoreactions to weak photosensitizers such as the antihistamine Benadryl. Included in our list of commonly used systemic photosensitizers are antibacterial sulfonamides and their relatives the thiazide diuretics and the sulfonylurea antidiabetic drugs. The phenothiazines, especially chlorpromazine and certain antibiotics, are also included in this group. More complete lists of potential topical and systemic photosensitizers are available (*16–18*).

CLINICAL REACTIONS

Acute phototoxic responses are by far the most common reactions to these agents. These responses are usually characterized by a delayed erythema and edema followed by hyperpigmentation and desquamation or peeling. If the chemical is applied to the skin, the epidermis may be severely damaged such as seen in topical psoralen photosensitization. In contrast, if the agent reaches the skin through the vasculature, the primary site of injury may be in the dermis with little or no visible epidermal change. In both instances the inflammatory cellular response is very slight in the dermis in human skin (*17*). This is similar to the lack of cellular infiltration noted in human cutaneous acute UVB sunburn reactions.

Certain exogenous chemicals such as tetracycline hydrochloride, nalidixic acid, and the sulfones can produce low-grade phototoxic injuries that are expressed as blistering, fragility, denudation, scarring, and milium formation (*19, 20*). These changes are identical (clinically and microscopically) with those found in a number of the porphyrias (*9*).

Photosensitization by certain exogenous chemicals in humans is primarily or exclusively photoallergic. These chemicals include the halogenated salicylanilides, musk ambrette, and 6-methylcoumarin (*21–24*).

Chronic actinic damage and skin cancer formation are induced primarily by the UVB rays from the sun. In general, this process in humans has not been associated with exogenous chemicals.

However, such a relationship with certain forms of photochemotherapy has recently been established. In a large series of psoriatic patients treated with psoralens and UVA radiation, Stern et al. (*25*) noted a definite increase in cutaneous cancer formation. This increase was even more clinically significant because the cancers were found primarily on parts of the body usually not chronically exposed to the sun (*25*). More recently, these authors reported an increased skin cancer incidence in psoriatic patients who had received very extensive treatments with coal tar and UVB radiation (the Goeckerman regimen) (*26*). This may represent an additive carcinogenic effect between the tar and UVB radiation energy, since the action spectrum for coal tar photosensitization is in the UVA radiation range.

Thus patients with psoriasis may be at increased risk of developing skin cancer because of certain treatment modalities in wide use at the present time. However, a greater portion of the population may be at risk, i.e., individuals exposed to industrial contaminants and a great deal of radiation from the sun such as oil field workers and the like (*17*). Also air pollutants, many of which are photosensitizers, might cause chronic phototoxicity. But perhaps more importantly, these last two sources may relate to photocarcinogenesis as additive carcinogens and/or promoters. Experimentally, the carcinogenic effects of the polycyclic hydrocarbon 7,12-dimethylbenz[*a*]anthracene have been shown to be additive with the cancer-producing properties of UV radiation (*27*). In addition, certain essentially noncarcinogenic agents will promote UV carcinogenesis in experimental animals (*17, 28–30*). Possibly, industrial contaminants and air pollutants that contain both carcinogens and promoters accelerate cutaneous cancer formation in human skin similar to the acceleration of cutaneous cancer formation noted experimentally.

MECHANISMS OF CHEMICAL PHOTOTOXICITY

Although chemically induced phototoxic reactions have been described, specific evidence of how these reactions occur in human skin is not available in most instances.

Photodynamic processes appear to be responsible for reactions to certain dyes, to polycyclic hydrocarbons, and as noted previously and perhaps most commonly to porphyrin molecules in the porphyrias (*6, 7*). In this last instance, the photodynamic reactions may lead to peroxide formation which in turn may labilize lysosomal membranes and thus release hydrolytic enzymes that would lead to further cellular damage (*7*). The available evidence indicates that this initial photoinjury occurs primarily in the upper dermal blood vessel endothelial cells (*9–11*). As noted, porphyrin photosensitization in serum can lead to activation of the classical complement pathway and generate chemotactic activity derived from C5 (*12, 13*). This may also add to the cutaneous changes noted in the porphyrias.

As pointed out in previous papers in this symposium, certain psoralen compounds intercalate into the DNA helix. On photoactivation with UVA radiation, monofunctional and bifunctional adducts may be formed in the DNA (*31, 32*), which may lead to inhibition of DNA synthesis, cell damage, and cell death. Photoreactions with proteins containing aromatic amino acids can also occur (*32*).

Photoinduced DNA cross-links have been reported with coal tar extracts and anthracene (*33*). Also, lysosomal labilization has been accomplished with anthracene as well as with porphyrins (*34*). How this injury translates into the erythema, edema, and eventual dense hyperpigmentation that we see morphologically remains to be determined.

The production of a toxic photoproduct can cause membrane damage and result morphologically in an erythematous cutaneous response. Recent evidence indicates photoreactions at least in part can be due to this type of mechanism (*35–37*). In general, much more information is needed to clarify the mechanisms leading to the changes that occur in and during chemically induced phototoxic cutaneous responses.

ASSAYS FOR PHOTOTOXIC CHEMICALS IN HUMANS

Agents capable of producing phototoxic effects have been identified by use of a variety of in vitro and in vivo systems. However, the ultimate issue concerns the effect these molecules have on human tissue in vivo (*38*). In general, the following four techniques have been utilized: systemic administration, topical application with occlusion, topical application after the stratum corneum is stripped off, and intradermal injection of the molecules. Each of these techniques has disadvantages, among which are lack of distribution to the skin of the active photosensitizing molecule, metabolism of the chemical to a nonphotosensitizing structure, lack of metabolism to an active photosensitizing structure, lack of penetration to the appropriate target tissue, lack of irradiation with the appropriate wavelengths, and lack of irradiation at the appropriate time. Thus any human assay may well miss the target.

REFERENCES

(*1*) Epstein JH. Phototoxicity and photoallergy: Clinical syndromes. In: Fitzpatrick TB, Pathak MA, Harber LC, Seiji M, Kukita A, eds. Sunlight and man: Normal and abnormal photobiologic responses.

Tokyo: Univ Tokyo Press, 1974:459–477.

(*2*) Blum HF. Photodynamic action and diseases caused by light. American Chemical Society Monograph Series, No. 85. New York: Reinhold Publ Corp, 1941.

(*3*) Epstein JH. Photoallergy. Arch Dermatol 1972; 106:741–748.

(*4*) Morrison WL, Parrish JA, Epstein JH. Photoimmunology. Arch Dermatol 1979; 115:350–354.

(*5*) Kochevar IE. Photoallergic responses to chemicals. Photochem Photobiol 1979; 30:437–442.

(*6*) Meyer VA, Schmid R. The porphyrias. In: Stanbury JB, Wyngaarden JB, Fredrickson DS, eds. The metabolic basis of inherited diseases. 4th ed. New York: McGraw-Hill, 1978:1166–1220.

(*7*) Harber LC, Bickers DR. The porphyrias: Basic science aspects, clinical diagnosis and management. In: Malkinson FD, Pearson RW, eds. Year book of dermatology. Chicago: Year Book Med Publ, 1975:9–47.

(*8*) Poh-Fitzpatrick MB, Lamola AA, Lamon JM. Hepatic protoporphyrin production in human protoporphyria. J Invest Dermatol 1979; 72:208.

(*9*) Epstein JH, Tuffanelli DL, Epstein WL. Cutaneous changes in the porphyrias: A microscopic study. Arch Dermatol 1973; 107:689–698.

(*10*) Schnait FG, Wolff K, Konrad K. Erythropoietic protoporphyria—submicroscopic events during the acute photosensitivity flare. Br J Dermatol 1975; 92:545–557.

(*11*) Honigsmann H, Schnait FG, Konrad K, Stingl G, Wolff K. Mouse model for protoporphyria. III. Experimental production of chronic erythropoietic protoporphyria-like skin lesions. J Invest Dermatol 1976; 66:188–195.

(*12*) Gigli I, Schothorst AA, Soter NA. Erythropoietic protoporphyria: Photoactivation of the complement system. J Clin Invest 1980; 66:517–522.

(*13*) Lim HW, Perez HD, Poh-Fitzpatrick MB, Goldstein IM, Gigli I. Generation of chemotactic activity in serum from patients with erythropoietic photoporphyria and porphyria cutanea tarda. N Engl J Med 1981; 304:212–216.

(*14*) Pathak MA. Phytophotodermatitis. In: Fitzpatrick TB, Pathak MA, Harber LC, Seiji M, Kukita A, eds. Sunlight and man: Normal and abnormal photobiologic responses. Tokyo: Univ Tokyo Press, 1974:495–513.

(*15*) Epstein JH. Chemicals and photocarcinogenesis. Aust J Dermatol 1977; 18:57–61.

(*16*) Kirshbaum BA, Beerman H. Photosensitization due to drugs: A review of some of the recent literature. Am J Med Sci 1964; 248:445–468.

(*17*) Epstein JH. Adverse cutaneous reactions to the sun. In: Malkinson FD, Pearson RW, eds. Year book of dermatology. Chicago: Year Book Med Publ, 1971:5–43.

(*18*) Parrish JA, Pathak MA. Photomedicine. In: Fitzpatrick TB, Eisen AZ, Wolff K, Freedberg IM, Austen KF, eds. Dermatology in general medicine. 2d ed. New York: McGraw-Hill, 1979:942–994.

(*19*) Ramsay CA, Obreshkova E. Photosensitivity from nalidixic acid. Br J Dermatol 1974; 91:523–528.

(*20*) Epstein JH, Tuffanelli DL, Seibert JS, Epstein WL. Porphyria-like cutaneous changes induced by tetracycline hydrochloride photosensitization. Arch Dermatol 1976; 112:661–666.

(*21*) Herman PS, Sams WM Jr. Soap photodermatitis. Springfield, Ill.: Thomas, 1972.

(*22*) Raugi GJ, Storrs FJ, Larson WG. Photoallergic contact dermatitis to men's perfumes. Contact Dermatitis 1979; 5:251–260.

(*23*) Giovinazzo VJ, Ichikawa H, Kochevar IE, Armstrong RB, Harber LC. Photoallergic contact dermatitis to musk ambrette. J Am Acad Dermatol 1980; 3:384–393.

(*24*) Kaidbey KH, Kligman AM. Contact photoallergy to 6-methylcoumarin in proprietary sunscreens. Arch Dermatol 1978; 114:1709–1710.

(*25*) Stern RS, Thibodeau LA, Kleinerman RA, Parrish JA, Fitzpatrick TB. Risk of cutaneous carcinoma in patients treated with oral methoxsalen photochemotherapy for psoriasis. N Engl J Med 1979; 300:809–813.

(*26*) Stern RB, Ziebler S, Parrish JA. Skin carcinoma in patients with psoriasis treated with topical tar and artificial ultraviolet radiation. Lancet 1980; 1:732–735.

(*27*) Epstein JH. Comparison of the carcinogenic and cocarcinogenic effects of ultraviolet light on hairless mice. J Natl Cancer Inst 1965; 34:741–745.

(*28*) Epstein JH, Roth HL. Experimental ultraviolet light carcinogenesis: A study of croton oil promoting effects. J Invest Dermatol 1968; 50:387–389.

(*29*) Fry RJ, Ley RD, Grube DD. Photosensitized reactions and carcinogenesis. Natl Cancer Inst Monogr 1978; 50:39–43.

(*30*) Forbes PD, Urbach F, Davies RE. Enhancement of experimental photocarcinogenesis by topical retinoic acid. Cancer Lett 1979; 7:85–90.

(*31*) Song PS, Tapley KJ Jr. Photochemistry and photobiology of psoralens. Photochem Photobiol 1979; 29:1177–1197.

(*32*) Parsons BJ. Psoralen photochemistry. Photochem Photobiol 1980; 32:813–821.

(*33*) Pathak MA, Krämer DM, Fitzpatrick TB. Photobiology and photochemistry of furocoumarins (psoralens). In: Fitzpatrick TB, Pathak MA, Harber IC, Seiji M, Kukita A, eds. Sunlight and man: Normal and abnormal photobiologic responses. Tokyo: Univ Tokyo Press, 1974:335–368.

(*34*) Allison AC, Magnus IA, Young MR. Role of lysosomes and of cell membranes in photosensitization. Nature 1966; 209:874–878.

(*35*) Johnson BE. Cellular mechanisms of chlorpromazine photosensitivity. Proc R Soc Med 1974; 67:871–873.

(*36*) Ljunggren B. Phenothiazine phototoxicity: Toxic chlorpromazine photoproducts. J Invest Dermatol 1977; 69:383–386.

(*37*) Kochevar IE, Lamola AA. Chlorpromazine and protriptyline phototoxicity: Photosensitized oxygen independent red cell hemolysis. Photochem Photobiol 1979; 29:791–796.

(*38*) Emmett EA. Phototoxicity from exogenous agents. Photochem Photobiol 1979; 38:429–436.

Human Models for Identification of Photosensitizing Chemicals[1]

Albert M. Kligman, *M.D., Ph.D.,*[2] *and* **Kays H. Kaidbey,** *M.D.*[2]

ABSTRACT—The human is an appropriate and sensitive animal for identifying photosensitizing drugs administered either topically or systemically. Topically effective phototoxic agents are quite easily revealed when they are applied to normal or scarified skin which is subsequently exposed to 2×10^5 J·m^{-2} of near UV light (UVA, 320–400 nm). Systemically effective photoxic drugs can be identified by exposing intradermally injected sites to either solar-simulating or UVA radiation. Drugs that cause photocontact allergy can usually be recognized by irradiating pretreated sites six times over a 3-week period with a solar simulator and then challenging the sites with UVA. Existing models, the human model especially, should make it possible to recognize important photosensitizing drugs before they are marketed. JNCI 1982; 69:269–272.

It has long been known that, in the presence of light, certain chemicals can damage or kill many different kinds of cells such as bacteria, fungi, protozoa, and red blood cells, fibroblasts, and epidermal keratinocytes. That drugs can mediate abnormal reactions to sunlight in humans is relatively recent knowledge. The flood of new drugs introduced since midcentury has brought with it the painful awareness that very different kinds of molecules can induce abnormal light reactions through a number of mechanisms. We now know that photosensitizing chemicals abound in the environment, showing up in such diverse products as cosmetics, fragrances, soaps, household items, dyes (in bathing suits), sunscreens, topical medicaments, and drugs given orally or parenterally.

The inventory of chemically identified photosensitizers is large, numbering in the hundreds, and is diverse. Though most are aromatic compounds and very few are inorganic substances such as cadmium, their structures may be dissimilar. Except for congeners of well-known photosensitizers, the capacity of a new agent to provoke abnormal light reactions is impossible to predict by inspection of its molecular structure.

If in vitro models could be used to appraise photosensitizing potential, it would be ideal. In vitro techniques are quick, simple, and inexpensive, such as the one devised by Daniels (*1*) in which zones of inhibition develop around drug-impregnated paper disks placed on petri dish cultures of *Candida albicans* which have been irradiated. Regrettably, the killing of yeast cultures by light is relatively insensitive; some well-known photosensitizers are not detected by this screening technique. Other in vitro models in which cultured human lymphocytes or fibroblasts are used are not yet practical.

The crucial test for any model is whether it consistently identifies known photosensitizers. Too often, the test has high sensitivity for one class of chemicals, e.g., tetracyclines, but fails completely with sulfonamides. Potent photosensitizers such as the psoralens are quite easily recognized. (The Egyptians pioneered the field centuries ago.) Mild photosensitizers are often difficult to detect. Although we automatically think of photosensitizers as harmful, psoralens and coal tar have proved very beneficial in the photochemotherapy of psoriasis. Clearly, there are positive and negative medical implications, but here our main concern is adverse effects.

Animals should be used to an advantage in the detection of photosensitizers. Albino murine species should be ideal because they lack native photoprotection. Numerous attempts, most notably by Morikawa et al. (*2*), have been made to develop animal models. These workers compared photosensitizers in various species. Their experience typifies the problem. Some known photosensitizers were confirmed, but tetracyclines and sulfonamides were not. False-negative results for important photosensitizers are found in many animal models. This is true for the guinea pig ear model of Stott et al. (*3*) and for the hairless mouse model of Gloxhuber (*4*) and of others who used oral, ip, and topical applications.

Part of the difficulty is the uniqueness of human skin, which really has no true animal counterpart. For example, the vasculature of the murine species is sparse compared to the rich venular plexuses of the human. Accordingly, the inflammatory display, in which vessels are crucial, is greatly diminished in animals. This restriction lessens the likelihood of recognizing weak photosensitizers.

Very few photosensitizing drugs have been identified before their widespread clinical use. Only recently have appropriate tests been developed to meet the need for revealing photosensitizing potential before a drug is marketed. Unfortunately, inquiry into the possibility of photosensitization is still not routine in the development of systemic drugs.

PERSPECTIVES

The term "photosensitization" applies to chemicals that cause unusual reactions to sunlight. Two forms of photosensitization will be discussed here: phototoxicity and photoallergy. Theoretically, phototoxic responses can be elicited in all persons given enough drug and enough light, though susceptibility varies a great deal among individuals and races. Phototoxic chemicals give rise to a varied repertoire of skin lesions, ranging from wheals to acute dermatitis to bullae. Some damage cell membranes, others damage organelles, and still others interact with DNA. This diversity of expressions tells us not to depend on rigid routines such

---

ABBREVIATIONS USED: id=intradermally; MED=minimum erythema dose(s).

---

[1] Presented at the Seventh Food and Drug Administration Science Symposium ("Photochemical Toxicity: Toxic, Allergic, and Carcinogenic Aspects With Emphasis on Predicting Effects in Humans") held at the Uniformed Services University of the Health Sciences, Bethesda, Md., March 16–17, 1981.

[2] Duhring Laboratories, Department of Dermatology, University of Pennsylvania School of Medicine, Medical Education Building, 36th and Hamilton Walk, Philadelphia, Pa. 19104.

as single readings at some convenient interval such as 1 day, a traditional favorite. For example, if readings are made at 24 hours, one may miss wheals that develop shortly after irradiation but that fade in an hour or two. Likewise, phototoxic reactions to furocoumarins generally do not peak until 72 hours.

By contrast, photoallergic reactions do not show a diversity of clinical expressions and are set apart by being immunologically mediated. They are T-cell-dependent, delayed hypersensitivity responses akin to allergic contact dermatitis.

Phototoxic drugs outnumber photoallergic ones by a large margin. Most of the photoallergic drugs belong to a single class of compounds, i.e., the halogenated phenols. Their harmful effects are apparent after topical applications and are, therefore, examples of photocontact allergy. Bona fide instances of orally administered photoallergic drugs are quite rare and are not without diagnostic ambiguities. Chlorothiazide is probably the only unequivocal example and sulfonamides may perhaps sometimes qualify. Even a potent photocontact allergen like chlorpromazine very rarely causes photoallergic reactions when taken orally. Still, as clinicians, physicians must be forever watchful for the unexpected if diagnostic disasters are to be avoided.

Very few drugs are both phototoxic *and* photoallergic. 3,3′,4′,5-Tetrachlorsalicylanilide, an antibacterial that caused a famous epidemic of photocontact allergy, is the best example. It was initially thought that phototoxicity was a prerequisite for a chemical to be photoallergic. This was a mistaken idea, for the two are usually dissociated and have no common denominator. Each quality must be separately tested.

There are many examples of phototoxic chemicals that are capable of causing skin disease both when topically applied and when systemically administered. Phototoxic agents that are topically applied are the commonest, but orally administered ones are also important. Topical and oral agents are tested in different ways. The best known orally sensitizing phototoxic drugs are the tetracyclines and the phenothiazines. It is worth emphasizing that these drugs continue to be widely used, mainly because they are valuable therapeutic agents whose photoreactivity is well known to all. These orally administered drugs are not necessarily disqualified because they are phototoxic. This contrasts with topically sensitizing photoallergens whose uses are much less important. Besides there is a special urgency to identifying photocontact allergens, for once sensitized, the victim may be reactive to light for years after the last exposure. The plight of the persistent light reactor is a compelling reason why all new topical substances should be routinely examined for their capacity to induce photoallergy.

Once identified, topical phototoxic chemicals are best avoided. This precaution becomes especially important when a sunscreen ingredient turns out to be phototoxic. This actually happened in the case of the amyldimethylester of *p*-aminobenzoic acid, otherwise an effective absorber of UV radiation (*5*).

With the use of human skin tests, it is unlikely that significant phototoxic chemicals and drugs will not be detected by the laboratory screening procedures. We emphasize the value of the human model because human skin is plentiful, only a small test area is required, and the reactions are transient and easily borne. Furthermore, the findings are likely to be the most relevant.

LIGHT SOURCE

The professional tester must have an apparatus that emits a continuous spectrum of UV radiation covering the UVB (290–320 nm) and the UVA (320–400 nm) ranges and extending into the visible region. The xenon arc is the most versatile and most suitable of the available light sources. It produces high-intensity radiation which with appropriate filters can yield a spectrum resembling sunlight. Xenon solar simulators are now commercially available at reasonable cost. The action spectrum for the great majority of photosensitizing drugs, phototoxic and photoallergic, lies in the UVA region. With the Schott WG 345 filter, all xenon rays below 320 nm can be excluded; thus sunburning radiation is abolished and only UVA radiation and visible light remain. Visible light is important for certain photodynamic dyes such as the xanthene and anthraquinone dyes, which are activated by rays beyond 400 nm. IR radiation must be attenuated to avoid nonspecific or painful heating effects.

Though not common, certain orally effective phototoxic drugs are activated by UVB radiation, e.g., chlorothiazide. The solar simulator is quite suitable for such agents because concomitant exposure to UVA radiation is of no consequence and need not be filtered out. If desired, inexpensive radiometers are available for determining exposure levels. Alternatively, the amount of radiation may be expressed as the MED, that exposure just producing a uniform erythema in 24 hours.

IDENTIFICATION OF TOPICALLY EFFECTIVE PHOTOTOXIC CHEMICALS

Topical phototoxic chemicals can be evaluated by a relatively simple and straightforward procedure described previously from this laboratory (*6*). Nonirritating concentrations of the chemicals are applied to 2×2-cm areas of skin at a topical dose of 5 $\mu l/cm^2$. Soluble substances can be dissolved in ethanol or water at 1–2%, whereas insoluble material can be suspended at 5% in an oil and water cream such as hydrophilic ointment U.S.P. The skin site is covered by a nonabsorbing cotton cloth and an impermeable adhesive tape (blenderm) for 6 hours and is then exposed to xenon radiation with the sunburning rays filtered out. An appropriate light dose is 2×10^5 $J \cdot m^{-2}$, which is generally less than that which will produce erythema on untanned white skin, with the exception of individuals who burn very easily. The threshold photoactivating dose may be and usually is very much lower, i.e., often $2\text{-}3 \times 10^4$ $J \cdot m^{-2}$. Controls include a drug-treated unirradiated site and a vehicle-treated irradiated site.

The development of immediate abnormal reactions such as burning and stinging, erythema, wheal, and flare, which may occur during or within 5–10 minutes of exposure, is diagnostic of phototoxicity. Crude coal tar is the classic example. The burning is perceived first, and it may be nearly intolerable. Generally, the erythema and flare fade in an hour or so; 24 hours later, the exposure site shows a sunburn-type erythematous reaction. Most topically active phototoxic chemicals show only delayed sunburn-type reactions, generally beginning in about 8 hours and peaking at 24. These sunburn-type responses are certainly not sunburns in the strict sense. Histologically, they are quite different, lacking the telltale sunburn cells. The appearance of erythema can also be delayed for 48–72 hours after exposure, as when the furocoumarins are used. Blisters are the ultimate expression of psoralen phototoxicity.

A negative reaction does not enable one to conclude that the substance lacks phototoxic properties. One further test is necessary to account for those chemicals that bind strongly to the horny layer and thus do not penetrate the viable tissue where the photosensitivity reaction takes place. Xanthene dyes such as eosin and rose bengal are typical of this class. When eosin was widely used in lipsticks, severe lip dermatitis was common; yet eosin on normal skin is quite harmless in the presence of light. The necessary modification for eliciting the adverse reaction is to apply the dye to skin lightly scarified with a fine, 30-gauge needle. With the barrier breached, wheals can be provoked immediately, and erythema is delayed until 24–48 hours later. Once photosensitization has been demonstrated, more precise determinations can be secured; i.e., the threshold dose for provoking a given response such as a wheal and flare or a delayed "sunburn" can be examined. If desired, one can narrow down the activating wavelengths by using band-pass filters or better still monochromatic radiation. The UVA region is quite broad, and for particular chemicals certain portions within this range are more effective than others. Sometimes only a relatively narrow band comprises the action spectrum, as with the porphyrins (406 nm). As a rule, the absorption spectrum and the action spectrum of topically effective photosensitizers correspond rather well. The following agents produce demonstrable phototoxicity when they are applied topically to humans:

Essential oils, e.g., oil of bergamot, rue oil, lemon oil, lime oil
Synthetic fragrances, e.g., dimethylanthranilate, 7-methoxycoumarin
Sunscreens, e.g., amyldimethylaminobenzoate
Furocoumarins, e.g., 5-methoxypsoralen, trimethylpsoralen, 8-methoxypsoralen
Coal tar and coal tar products
Polycyclic hydrocarbons, e.g., anthracene, fluoranthene
Phenothiazines, e.g., chlorpromazine
Anthraquinone dyes, e.g., disperse blue
Xanthene dyes, e.g., eosin, rose bengal; activity demonstrable only in scarified skin
Thiazine dyes, e.g., methylene blue; activity demonstrable only in scarified skin

SYSTEMICALLY EFFECTIVE PHOTOTOXIC DRUGS

Therapeutic agents designed for oral and parenteral use can be screened for photosensitizing potential by injections id into untanned lower back skin (*7*). The procedure is simple and highly reliable. So far all known phototoxic drugs can be readily identified. Pretest injections of 0.1–0.3% of the drug in normal saline are made id, and thereby a nonirritating dose is found. Ideally, the drug should be solubilized, but this is often not necessary. With drugs like nalidixic acid and benoxaprofen, the injection of sonicated suspensions gives negative results. Usually, if an appropriate pH is chosen, solubilization can be obtained; the material can then be nearly neutralized. Either 0.05 or 0.1 ml of the material is injected id, and within 5–10 minutes the back skin is exposed to UV light.

Since systemic drugs can be activated by a wide range of wavelengths, exposures to solar-simulating radiation should be done first. This requires individual determination of the MED, after which injected sites receive 0.5 and 1.0 MED. Controls consist of saline-injected irradiated sites and drug-injected unirradiated sites.

Systemically effective phototoxic drugs can provoke immediate-type reactions similar to those of topically effective phototoxic chemicals. Subjective sensations such as burning, stinging, and pruritus developing during irradiation are an important clue. Most often, the drug-injected site will show an intensified, infiltrated erythema with variable edema at 24–48 hours. Threshold doses for a selected concentration can then be determined along with appropriate dose-response measurements. Discomfort is minimal because of the small size of the test area.

The results of intradermal testing should not be too narrowly interpreted. Substances may be found to yield phototoxic reactions at very low concentrations, and yet these same drugs taken orally only rarely cause photosensitivity. This is typical of the tetracyclines, of which only demeclocycline is a clinical photosensitizer of importance. Actually, after oral administration only small concentrations are present in the skin, and by the time the drug perfuses the skin, it may have been transformed into its nonphotosensitizing metabolites. Thus a positive intradermal result means only that the drug has the potential to photosensitize. Whether this potential is likely to be realized can be checked in volunteers who ingest the drug at double doses. Because the action spectrum is already known, the drug should be given for at least 3 days before the exposure, which will allow the level of drug in the skin to accumulate. Administration of 0.5 and 1.0 MED of either UVB or UVA radiation must be individually determined beforehand. Observations should be made shortly after exposure as well as at 24–28 hours. Determinants for activity of common phototoxic drugs are given in table 1.

TABLE 1.—*Phototoxicity from id-injected drugs in humans*

Substance	Injected dose, μg	Activating waveband
Sulfanilamide	500	UVB
Sulfapyridine	500	UVB
Vinblastine	0.2	UVB
Nalidixic acid	150	UVA
Griseofulvin	200	UVA
Chlorothiazide	250	UVB and UVA
Demeclocycline	200	UVA
Tetracycline base	200	UVA
Furosemide	500	UVA
Quinidine	250	UVA
Prochlorperazine	250	UVA
Chlorpromazine	100	UVA
Benoxaprofen	500	UVA

Intradermal testing furnishes an additional benefit in that it helps rule out drugs which have been declared photosensitizers in clinical reports but which in fact are not. A surprising number of drugs have been labeled photosensitizers and show up regularly in published lists; yet the evidence is often flimsy at best and is frequently unconvincing. One can, of course, become sunburned while taking any drug. We believe the following drugs are some examples of falsely identified phototoxic agents: estrogens, saccharin, chlordiazepoxide, and tolbutamide. Photosensitivity reactions attributed to oral antidiabetic agents by clinicians are therefore probably examples of photoallergy.

PHOTOCONTACT ALLERGENS

The photomaximization test is simply a modification of the maximization test for detecting ordinary contact sensitizers. The difference is that solar-simulating radiation is added during induction (*8*). In fact, photocontact allergy is similar in every respect to contact allergy except that UV radiation is required for both induction and elicitation. The procedure entails occlusive applications of drug at 5% in hydrophilic ointment U.S.P. with subsequent exposure to three MED of solar-simulating radiation. Six such exposures are given to the same site after the drug is freshly applied each time. At 10–14 days after the last induction exposure, the drug is applied at 1% to a fresh site for 24 hours which is then irradiated with 4×10^4 $J\cdot m^{-2}$ of filtered UVA radiation. The development of a vesicular or an infiltrated, spreading erythematous reaction in the irradiated site but not in the control, unirradiated drug-treated site signifies the development of photoallergic contact dermatitis.

This method has been successfully used to demonstrate the photosensitizing capacity of a group of halogenated salicylanilides, notably those that have produced outbreaks of photosensitivity in the past, as well as of other chemicals such as coumarin derivatives (table 2). Experience with this technique in humans is still limited. However, some substances which have occasionally produced photoallergic contact sensitization in humans are not recognized in the photomaximization assay. These presumably false-negative trials include 3,4′,5-tribromosalicylanilide uncontaminated by dibrominated derivatives that are potent photoallergens and the fragrance musk ambrette. Recently, using improved methods of induction in the guinea pig, Jordan (*9*) and Ichikawa et al. (*10*) have succeeded in inducing photocontact sensitization to musk ambrette as well as to 6-methylcoumarin; however, Mauer et al. (*11*) found 6-methylcoumarin to be inactive in the guinea pig. The improved techniques including the use of Freund's complete adjuvant and scarification of the skin appear to greatly enhance the sensitivity of the guinea pig model for the detection of photoallergic contact sensitizers. Species differences in sensitivity, however, may exist, and more information is needed in this regard.

TABLE 2.—*Photoallergic contact sensitization by the photomaximization test*

Substance	No. of photosensitized subjects, n=25	Substance	No. of photosensitized subjects, n=25
3,3′,4′,5-Tetrachlorosalicylanilide	8	Coumarin	0
3,4′,5-Tribromosalicylanilide (pure)	0	6-Methylcoumarin	15
3,4′,5-Tribromosalicylanilide (impure)	2	7-Methoxycoumarin	11
4,5-Dibromosalicylanilide	3	Hexahydrocoumarin	0
3,5-Dibromosalicylanilide	10	Isoeugenol	0
5-Monobromosalicylanilide	0	Musk ambrette	0
Bithionol	3	Chlorpromazine	6
3,4,4′-Trichlorocarbanilide	0	5-Fluorouracil	0
Hexachlorophene	0	Benzoyl peroxide	0
		p-Aminobenzoic acid	0
		Sodium Omadine	6
		Zinc Omadine	0

SUMMARY

Our present view is that the photomaximization test is sensitive enough to detect all potent photocontact allergens. Those such as musk ambrette which rarely sensitize humans or do so under special conditions, as in shaving, may escape detection. It may be that the guinea pig is the animal of choice for photocontact allergy.

On the basis of studies with coumarin and its derivatives in humans, it appears that photoallergenic activity may be greatly influenced by small changes in the structure of the molecule. Furthermore, although coumarin itself possesses little or no photosensitizing potential, it can elicit photosensitization reactions in subjects sensitized to more potent derivatives.

REFERENCES

(*1*) DANIELS F. A simple microbiological method for demonstrating phototoxic compounds. J Invest Dermatol 1965; 44:259–263.

(*2*) MORIKAWA F, NAKAYAMA Y, FUKUDA M, et al. Techniques for evaluation of phototoxicity and photoallergy in laboratory animals and man. In: Fitzpatrick TB, Pathak MA, Harber LC, Seiji M, Kukita A, eds. Sunlight and man: Normal and abnormal photobiologic responses. Tokyo: Univ Tokyo Press 1974:529–557.

(*3*) STOTT CW, STASSE J, BONOMO R, CAMPBELL AH. Evaluation of the phototoxic potential of topically applied agents using long-wave ultraviolet light. J Invest Dermatol 1970; 55:335–338.

(*4*) GLOXHUBER C. Prufung von Kosmetik-grundstoffen auf fototoxische Wirkung. J Soc Cosmet Chem 1970; 21:825–833.

(*5*) KAIDBEY KH, KLIGMAN AM. Phototoxicity to a sunscreen ingredient. Arch Dermatol 1978; 114:547–549.

(*6*) ———. Identification of topical photosensitizing agents in humans. J Invest Dermatol 1978; 70:149–151.

(*7*) ———. Identification of systemic phototoxic drugs by human intradermal assay. J Invest Dermatol 1978; 70:272–274.

(*8*) ———. Photomaximization test for identifying photoallergic contact sensitizers. Contact Dermatitis 1980; 6:161–169.

(*9*) JORDAN WP. The guinea pig as a model for predicting photoallergic contact dermatitis. Contact Dermatitis 1982; 8:109–116.

(*10*) ICHIKAWA H, ARMSTRONG RB, HARBER LC. Photoallergic contact dermatitis in guinea pigs: Improved induction technique using Freund's complete adjuvant. J Invest Dermatol 1981; 76:498–501.

(*11*) MAURER TH, WEIRICH EG, HESS R. Evaluation of the photocontact allergenic potential of 6-methylcoumarin in the guinea pig. Contact Dermatitis 1980; 6:275–278.

Therapeutic In Vivo Photochemistry: Photochemical Toxicity Studies in Humans[1,2]

John A. Parrish, *M.D.*[3]

ABSTRACT—Information obtained by studies of phototherapy and photochemotherapy is reviewed and some of the advantages and disadvantages of using in vivo photochemistry to treat disease are examined. Selective in vivo photochemistry is used to treat a variety of diseases. Study of the dosimetric aspects of these treatments and quantitative analysis of acute risks are instructive to individuals interested in photochemical toxicity in humans. Results from prospective short-term and long-term clinical trials are especially instructive because the model used is the intact living human. These studies provide important data about toxic, allergic, and carcinogenic aspects of photochemical toxicity, which could not be obtained in routine animal toxicity experiments. Work done to develop, explain, or improve these treatments also provides insight into molecular mechanisms of photon-induced cell injury and the sequelae of that injury.—JNCI 1982; 69:273–278.

Selective in vivo photochemical toxicity is used to treat a variety of diseases. Dosimetric aspects of these treatments, quantitative analysis of acute risks, and prospective studies of long-term effects are instructive to individuals interested in photochemical toxicity in humans. Clinical trials of various forms of phototherapy and photochemotherapy provide the largest animal phototoxicity studies, and the model used is the intact living human. These studies obtain important data about toxic, allergic, and carcinogenic aspects of photochemical toxicity, which could not be obtained in toxicity experiments. The basic science studies used to develop, explain, or improve these treatments provide insight into molecular mechanisms of photon-induced cell injury and the sequelae of that injury. This manuscript reviews some of the information obtained by studies of phototherapy and photochemotherapy and also examines some of the advantages and disadvantages of using in vivo photochemistry to treat disease.

Phototoxicity is a general term often used simply to describe cell injury or tissue alterations induced by nonionizing electromagnetic radiation with or without photosensitizing chemicals. Phototoxicity is toxicity induced by photons. The radiation most often considered is within the UV and visible ranges. This radiation has appropriate quantum energy to cause electronic excitation and subsequent alterations in cell chemistry which can be specific and can lead to major alteration in cell function or viability. Photon-induced cell injury can be by mechanisms other than photochemistry because absorbed energy affects vibrational or rotational modes recorded as heating of tissues. However, use of the term "*photochemical* toxicity" usually not only implies that the mechanism of photon-induced toxicity is via photochemistry but also means that an exogenous chromophore has been supplied to initiate or augment the reaction. The singular term "phototoxicity" has also been used with more specific meaning, but unfortunately the specific meaning varies. Some authors use the term only when identified chemical photosensitizers are involved; others use it only when no known photosensitizer is present.

In the context of describing in vivo chemical photosensitization, the term is also used to separate nonimmunologic (phototoxic) responses from those effects involving immune mechanisms (photoallergic). Phototoxicity is also used to describe acute or chronic, morphologic or histologic alterations of skin by UV or visible radiation with or without the addition of chemical photosensitizers. Therefore, when one uses the term "phototoxicity," it is best to define the term clearly, avoid using it, or use it only in a general way to mean cell injury or toxicity induced by photons.

OPTICAL AND DOSIMETRIC PROPERTIES OF SKIN AND BLOOD

All photobiologic responses of skin are influenced by the optical properties of the skin. These properties determine the dosimetry of optical radiation within the tissue. Radiation transmitted into skin and cutaneous blood vessels has an internal dosimetric depth profile because penetration of UV and visible radiation into soft tissue is very wavelength-dependent.

The first optical interaction occurs at the surface of the stratum corneum, where some fraction of the incident radiation is scattered backward (reflected), since the refractive index of stratum corneum ($n_D \cong 1.55$) (*1*) is much different from that of air (1.00). Because it is well described by Fresnel's laws of reflection, this fraction is called regular reflectance, and it typically accounts for 5–7% of nearly perpendicularly incident radiation. The regular reflectance component is nearly constant for all optical wavelengths and is the same for normal black and normal white skin (*2*). Of the radiation that enters the skin, part is scattered back to the environment, part is absorbed in various layers, and part is transmitted inward to successive layers of cells until the energy of the incident beam has been dissipated (text-fig. 1). Remitted (returning back from the surface) radiation

---

ABBREVIATIONS USED: NIR=near IR; PUVA=psoralen plus UVA radiation (320–400 nm).

---

[1] Presented at the Seventh Food and Drug Administration Science Symposium ("Photochemical Toxicity: Allergic, and Carcinogenic Aspects With Emphasis on Predicting Effects in Humans") held at the Uniformed Services University of the Health Sciences, Bethesda, Md., March 16–17, 1981.

[2] Supported by Public Health Service grant AM-25395-02 from the National Institute of Arthritis, Metabolism, and Digestive Diseases and by funds from The Wellman Laboratories.

[3] Department of Dermatology, Harvard Medical School, Massachusetts General Hospital, Boston, Mass. 02114.

includes the regular reflectance from the surface plus that radiation which enters the skin and is subsequently backscattered outward. In the UVA (320–400 nm), visible, and NIR regions, most of the remittance of Caucasian skin is radiation which has traversed the epidermis, been backscattered by the dermis, and returned again through epidermis.

In the epidermis, aromatic amino acids both free and in protein, urocanic acid, nucleic acids, and melanin are the major absorbing chromophores. Transmission of Caucasian stratum corneum (text-fig. 2) closely resembles a solution of protein containing the aromatic amino acids tryptophan and tyrosine and having a minimum transmittance near 275 nm due to absorption by these and other aromatic chromophores (text-fig. 3). Nucleic acids, with an absorption maximum near 260 nm, and numerous small aromatic molecules, especially urocanic acid with an absorption maximum at 277 nm at pH 7.4, also contribute to the broad 275-nm absorption band seen in the epidermis and stratum corneum. Melanin content and distribution also play a major role in determining epidermal transmission. Across the UVA, visible, and NIR spectral regions, melanin is by far the most important epidermal chromophore, showing a smoothly declining absorption toward longer wavelengths out to 1,200 nm, a result of its highly conjugated, amorphic polymeric chromophoric backbone (text-fig. 3).

Optical scattering within the dermis largely determines the average path length and depth of penetration of radiation at various wavelengths. Dermal scattering is an inverse function of wavelength. The approximately 50% of UVA radiation which penetrates fair Caucasian epidermis is largely attenuated within the first 50 μm of the papillary dermis. However, a longer wavelength radiation such as 500 nm (green) may penetrate several hundred microns, and red and NIR radiation may penetrate several millimeters or more, or the entire thickness of the dermis. Another result of dermal scattering is that shorter wavelengths are remitted from the relatively more superficial layers of dermis, and these remitted rays experience, in general, a shorter average dermal path length than do longer wavelengths (table 1).

When the skin is irradiated in the UV and visible ranges, the blood and important components of the immune system are also being exposed. If one considers only metabolic need, the skin is highly overperfused. The mean blood flow to the skin is 20–30 times greater than the flow rate necessary for metabolic demands of the skin cells, and the maximum flow may be more than 100 times the minimum flow. This great variation of flow occurs largely because the cutaneous vascular system participates in the regulation of body temperature. The design of the cutaneous vascular system for temperature control is such that an unusually large portion of the blood is available near the surface of the body for exposure to nonionizing electromagnetic radiation.

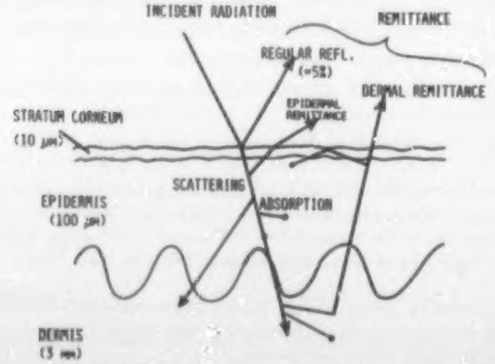

TEXT-FIGURE 1.—Schematic diagram of optical pathways in skin. REFL.=reflectance.

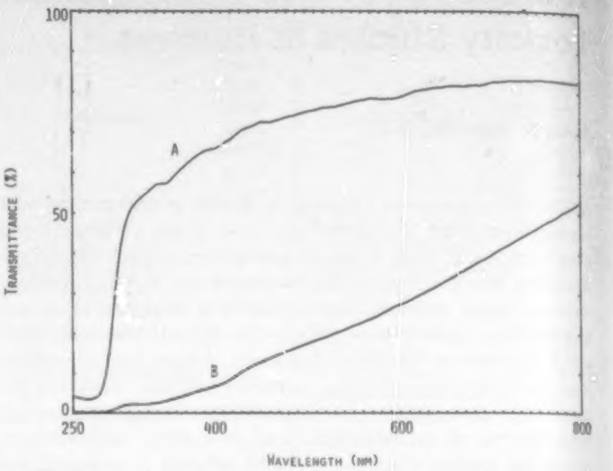

TEXT-FIGURE 2.—Human epidermis: transmittance from 250 to 800 nm. Surgical specimen was separated from dermis by being soaked in 60°C water for 30 sec and was mounted on integrating sphere in special container which allowed continuous wetting of basement membrane. A=fair Caucasian epidermis; B=black epidermis.

Skin blood flow has been measured by a variety of techniques. A nude subject at rest has an average cutaneous blood flow rate of 200–400 ml/m^2 body surface/minute (*3, 4*). This can be greatly increased, and flow rates up to 2,000 ml/m^2/minute have been reported (*5*). Flow varies from site to site, being greatest in digits and the face, especially the perioral areas. When cutaneous blood flow is accelerated, the skin blood content usually also increases, but these two parameters do not always run precisely parallel to one another.

Cutaneous blood flow accounts for about 10% of basal cardiac output; as much as 10% of the blood may be in the skin during any time period. This amount can be increased significantly by exercise or by inducing a heat load on the skin or host. At rest, an equivalent of the entire blood volume may pass through the skin two or more times during the time required for one minimal erythema dose (≈20 min) of sunlight. Much of this blood is exposed to UVA, visible, and NIR radiation.

The immune system is well represented in the skin with Langerhans' cells in the epidermis, mast cells and lymphocytes in the dermis, and other elements percolating through the lymphatics and capillaries of the dermis. All these components of the immune system are therefore exposed to environmental and therapeutic nonionizing radiation, and evidence is increasing that alterations of immune function

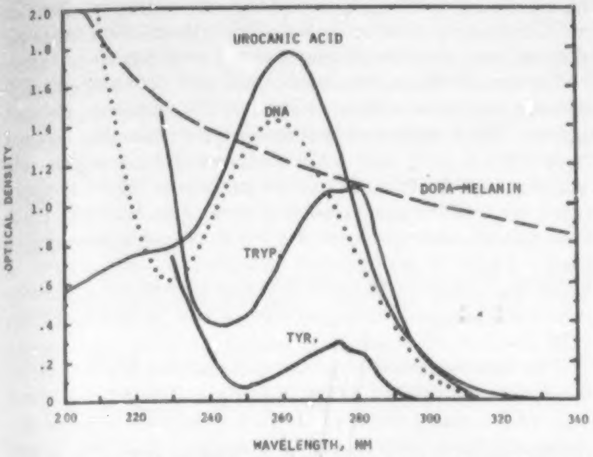

Text-figure 3.—UV absorption spectra of the major epidermal chromophores at the following concentrations: 1.5 mg dopa-melanin/100 ml H_2O; 10^{-4} *M* urocanic acid/H_2O; 10 mg calf thumus DNA/100 ml H_2O (pH 4.5); 2×10^{-4} *M* tryptophan (TRYP.) (pH 7); and 2×10^{-4} *M* tyrosine (TYR.) (pH 7).

occur as a result of such exposure. Exposure of mice or guinea pigs to UV radiation results in a suppression of delayed hypersensitivity responses to contact allergens (*6, 7*) and injected hapten-protein conjugates (*8*). In rabbits, the rejection of full-thickness skin grafts is delayed by treatment with PUVA (*9*). The rejection of antigenic UVB radiation (280–320 nm)-induced skin tumors in mice is prevented by exposures to UV radiation; the mechanism appears to involve the generation of specific suppressor lymphocytes (*10*). In normal human volunteers, single exposures to erythemogenic doses of UVB radiation or PUVA produce an alteration in the distribution and function of subpopulations of circulating lymphocytes (*11, 12*).

PHOTOTHERAPY AND PHOTOCHEMOTHERAPY: IN VIVO THERAPEUTIC PHOTOCHEMISTRY

Phototoxicity is a likely mechanism for several forms of phototherapy and photochemotherapy. The use of photons as therapeutic agents has the advantage of selectivity of site (exposed skin) and depth of effect (wavelength-dependent dosimetric depth profile). Photochemical effects can also be quite selective, affecting specific chromophores within tissue or cells but not affecting adjacent molecules. In complex tissues, the possibilities for significant selective effects far exceed those available in which biochemical reactions are conventionally thermally accelerated. Nevertheless, the disadvantages of phototherapy and photochemotherapy involve unwanted acute and chronic phototoxic side effects. Definition and quantification of these unwarranted effects give massive information about photochemical toxicity in human tissues.

With some qualitative and quantitative differences, the cellular alterations and cascade of events known to occur in normal skin that has been UV irradiated most likely also occur in diseased skin that has been similarly treated. The differences in response may lead to improvement of diseased skin without irreversible or unacceptable damage to normal skin. For example, UV irradiation may decrease abnormal hyperproliferation or may interfere with function or viability of abnormal cells intricately involved in expression of skin disease. In some cases of skin diseases, abnormal cells associated with the diseases may be more sensitive to radiation than are normal cells. Paradoxically, certain photodermatoses can be improved by controlled exposures to UV or visible radiation. Phototherapy and photochemotherapy of photodermatoses may induce melanogenesis or injure cells involved in the pathogenesis of the photosensitivity. In polymorphic light eruption for instance, it is likely that both of these mechanisms are involved (*13*). Radiation may be cytotoxic to lymphocytes necessary to support the disease process, and UV radiation-induced delayed melanogenesis and thickening of the epidermis provide photoprotection. Lymphocytotoxicity may also operate in successful PUVA therapy of mycosis fungoides (*14*), lichen planus (*15*), or vitiligo (*16*).

Phototoxicity is probably also the therapeutic basis of the treatment of psoriasis with UV radiation. The exact therapeutic mechanism is unknown. It is assumed that photons must reach the proliferative compartment, and DNA is thought to be an important therapeutic target because psoriasis is a hyperproliferative disease. UV radiation temporarily decreases DNA synthesis in normal skin, and other agents known to be effective in psoriasis, including tar, affect DNA. Other potential mechanisms include preferential lethal effects on abnormal cells, inhibition of cell recruitment, gene effects, effects on dermal blood vessels, inhibition or killing of leukocytes, or photoimmunologic effects. Repeated exposures at phototoxic doses are required.

The mechanism of action of some forms of phototherapy appears to be direct photochemical alteration of extracellular chemicals present in skin and blood. Generalized pruritus, a common symptom of chronic renal failure, has been reported to be diminished by six to eight exposures of erythemogenic doses of UVB radiation (*17*). In patients with uremic pruritus, phototherapy of one side of the body results in generalized improvement, and the beneficial effect is not limited to only the exposed side. This observation suggests that the therapeutic effects may result from photoinactivation of a pruritus-producing circulating substance present in uremia (*18*).

Direct in situ intracutaneous extracellular photochemistry also seems the most likely mechanism in phototherapy of hyperbilirubinemia. In this disorder an insoluble form of bilirubin accumulates in tissues and may cause discoloration

Table 1.—*Penetration of radiation in fair Caucasian skin*[a]

Wavelength, nm	Depth, µm
350	60
400	90
450	150
500	230
600	550
700	750
800	1,200

[a] Approximate depth of penetration is one-third (37%) of the incident energy density.

(jaundice) of skin and permanent damage to the central nervous system. Photoisomerization of unconjugated bilirubin results in a more water-soluble form which can apparently pass directly into the bile (*19*). This photoisomerization and subsequent water solubility of bilirubin lead to reduced tissue levels of bilirubin and may prevent brain injury.

Photochemotherapy is the use of a chemical plus subsequent nonionizing electromagnetic radiation to achieve a therapeutic benefit. An exogenous chromophore or photosensitizer is added in an attempt to influence the site and nature of the photochemistry and subsequent photobiologic effects. Usually, in the doses used, the chemical alone or the radiation alone has no significant biologic effect. The chemical component of photochemotherapy may be given topically or parenterally, but it must reach viable cells which absorb subsequent radiation. Four major therapeutic regimens claim to use this form of in vivo photochemistry: 1) The Goeckerman regimen was conceived to be augmented phototherapy, i.e., topically photosensitized with crude coal tar, but this treatment as used today appears to be mainly UVB radiation phototherapy. The topical vehicle used to apply the tar alters the optical properties of the surface of the psoriatic tissue and thereby increases its transmission of UV radiation. It is unlikely that chemical photosensitization by tar plays a major role in the Goeckerman treatment as commonly used (*20*). 2) "Dye-light" treatment of recurrent herpes simplex with neutral red or proflavine and subsequent UVA or visible light radiation has not proved to be an effective therapy (*21*). 3) Another example of photochemotherapy is hematoporphyrin-visible light therapy of human cancer (*22*). This therapy, also called photoradiation therapy, has been successfully used to selectively destroy a certain cancer metastatic to skin. The future applications of this treatment are not certain at present. 4) PUVA therapy was discovered thousands of years ago and remains the best example of successful photochemotherapy.

For PUVA therapy and UV radiation phototherapy, in which phototoxicity is the most likely central therapeutic mechanism, the lists of potential long-term side effects are similar. However, there are major differences between these two methods of using photons to injure or alter cells. These differences are instructive to individuals considering chemical phototoxicity of human tissue. The depth profiles and average depth of in vivo photochemistry are different for PUVA therapy and UVB radiation phototherapy. Psoralen-DNA photoproducts and psoralen-UVA radiation-induced cross-links are quite different from UVB radiation-induced changes in DNA. They most likely have different effects on cells and are repaired differently. The most stable, easily isolated, and most studied photoproduct of DNA irradiation by UVB is the pyrimidine dimer. Other photoproducts also occur, but cross-links are very rare. PUVA therapy may be more lethal to certain cells or may be more effective as a mutagen because the resultant monofunctional or bifunctional photoadducts may be repaired by pathways different from the major DNA repair pathways that have evolved to restore the more usual DNA photoproducts. Monofunctional psoralen-DNA photoadducts may lead to a frameshift type of mutation. However, cross-linking may be less mutagenic than frameshifts in absolute terms because cross-linking is a more lethal event. A smaller surviving fraction may in effect display fewer mutations.

The non-DNA mechanisms of cell phototoxicity also differ, but less is known about in vivo UV radiation-induced protein, RNA, or membrane lesions. For example, whereas both PUVA (*23*) and UVB (*24*) are known to decrease viability and function of human peripheral blood lymphocytes, the relative mechanisms of their phototoxicities are at least qualitatively different. For UVB, trypan blue exclusion (most likely a membrane function) is diminished at lower doses than required to diminish phytohemagglutinin-induced blastogenic response. The reverse is true for PUVA (*24*).

The inflammatory response induced by PUVA differs from that induced by UVB. Prostaglandins are associated with the initial portion of the UVB-induced delayed erythema. Indirect evidence to date suggests that this prostaglandin involvement does not seem to be true for PUVA (*25*). Generalized symptomatic UVB-induced erythema is accompanied by a polymorphonuclear leukocytosis, which is not seen with PUVA (*26*). Delayed erythema after sufficient UVB radiation exposure begins after a latent period of a few hours and peaks at 12–24 hours. After PUVA, erythema usually does not begin for 24 hours and peaks at 48–96 hours. The erythema dose-response curve is more steep with PUVA than with UVB. Histologic studies show that in normal skin PUVA has more effect on blood vessels and that epidermal alterations last much longer (*27*).

The importance of these differences is not known. Both agents are known photocarcinogens, and both are expected to add to cumulative actinic insult of skin. Both are lymphocytotoxic with potential long-term effects. The greater depth effect and affected tissue volume of in vivo photochemistry may explain why several studies have found PUVA therapy to be more rapidly effective than UVB radiation phototherapy in some patients with psoriasis and why topical lubricants enhance the therapeutic effect of PUVA therapy less than they enhance the effect of UVB radiation phototherapy. However, PUVA therapy may be more likely to cause irreversible actinic changes because of its greater percentage of dermal effects. The viability and function of lymphocytes or other cells in the dermis may be more easily affected by PUVA therapy, and thus therapeutic or nontherapeutic effects may be increased. The best example of a qualitatively different risk associated with the two treatments is the primary eye hazard. Unintentional overexposure to UVB radiation causes an acutely symptomatic photokeratitis, which is usually reversible (*28*). The major risk to the unprotected eye of the patient receiving PUVA therapy is the development of cataract (*29*), a permanent decrease in visual acuity whose onset and maturity may be delayed for years to decades.

THE FUTURE OF THERAPEUTIC IN VIVO PHOTOCHEMISTRY

Advances in optics technology and the science of photobiology make it possible to think beyond therapy that depends on direct photochemical alteration of metabolites or on direct phototoxic insult to cells. Another generation of photomedical therapy will include in vivo photoactivation of medicines, photon-dependent drug delivery, and creative manipulation of host and exposure source to maximize therapeutic index (*30*). Clinical trials of these treatments will provide much additional information about photochemical toxicity in humans.

REFERENCES

(*1*) Scheuplein RJ. Survey of some fundamental aspects of the absorption and reflection of light by tissue. J Soc Cosmet Chem 1964; 15:111–122.

(*2*) Anderson RR, Hu J, Parrish JA. Optical radiation transfer in the human skin and applications in in vivo remittance spectroscopy. In: Proceedings of the symposium on bioengineering and the skin, Cardiff, Wales, July 19–21, 1979. London: MTP Press, 1982. In press.

(*3*) Hertzman AB. Vasomotor regulation of cutaneous circulation. Physiol Rev 1959; 39:280–306.

(*4*) Tsuchida Y. Rate of skin blood flow in various regions of the body. Plast Reconstr Surg 1979; 64:505–508.

(*5*) Hardy JD, Soderstrom GF. Heat loss from the nude body and peripheral blood flow at temperatures of 22°C to 35°C. J Nutr 1938; 16:493.

(*6*) Jessup JM, Hanna H, Palaszynski E, Kripke ML. Mechanisms of depressed reactivity to dinitrochlorobenzene and ultraviolet-induced tumors during ultraviolet carcinogenesis in BALB/c mice. Cell Immunol 1978; 38:105–115.

(*7*) Morison WL, Parrish JA, Woehler ME, Bloch KJ. The influence of ultraviolet radiation on allergic contact dermatitis in the guinea pig. I. UVB radiation. Br J Dermatol 1981; 104:161–164.

(*8*) Morison WL, Parrish JA, Woehler ME, Krugler JI, Bloch KJ. The influence of PUVA and UVB radiation on delayed hypersensitivity in the guinea pig. J Invest Dermatol 1981; 76:484–488.

(*9*) Morison WL, Parrish JA, Woehler ME, Bloch KJ. The influence of PUVA and UVB radiation on skin-graft survival in rabbits. J Invest Dermatol 1980; 75:331–333.

(*10*) Fisher MS, Kripke ML. Further studies on the tumor specific suppressor cells induced by ultraviolet radiation. J Immunol 1978; 121:1139–1144.

(*11*) Morison WL, Parrish JA, Bloch KJ, Krugler JI. In vivo effect of UV-B on lymphocyte function. Br J Dermatol 1979; 101:513–520.

(*12*) ———. In vivo effects of PUVA on lymphocyte function. Br J Dermatol 1981; 104:405–413.

(*13*) Parrish JA, Le Vine MJ, Morison WL, Gonzalez E, Fitzpatrick TB. Comparison of PUVA and beta-carotene in the treatment of polymorphous light eruption. Br J Dermatol 1979; 100:187–192.

(*14*) Gilchrest BA, Parrish JA, Tanenbaum L, Haynes HA, Fitzpatrick TB. Oral methoxsalen photochemotherapy of mycosis fungoides. Cancer 1976; 38:683–689.

(*15*) Ortonne JP, Thivolet J, Sannwald C. Oral photochemotherapy in the treatment of lichen planus (LP). Br J Dermatol 1978; 99:77–88.

(*16*) Parrish JA, Fitzpatrick TB, Shea C, Pathak MA. Photochemotherapy of vitiligo: Use of orally administered psoralens and a high-intensity long-wave ultraviolet light system. Arch Dermatol 1976; 112:1531–1534.

(*17*) Gilchrest BA, Rowe JW, Brown RS, Steinman TI. Relief of uremic pruritis with ultraviolet phototherapy. N Engl J Med 1977; 297:136–138.

(*18*) Gilchrest BA, Rowe JW, Brown RS, Steinman TI, Arndt KA. Ultraviolet phototherapy of uremic pruritis. Ann Intern Med 1979; 91:17–21.

(*19*) McDonagh AF, Lightner DA, Wooldridge A. Geometric isomerization of bilirubin-IX(*a*)dimethyl ester. Chem Commun (J Chem Soc Sect D) 1979; 3:110–112.

(*20*) Parrish JA. Photomedicine. In: Regan JD, Parrish JA, eds. The science of photomedicine. New York: Plenum, 1982. In press.

(*21*) Myers MG, Oxman MN, Clark JE, Arndt KA. Failure of neutral-red photodynamic inactivation in recurrent herpes simplex virus infections. N Engl J Med 1975; 293:945–949.

(*22*) Dougherty TJ, Kaufman J, Goldfar A, Weishaupt KR, Boyle DG, Mittelman A. Photoradiation therapy for the treatment of malignant tumors. Cancer Res 1978; 38:2628–2635.

(*23*) Morison WL, Parrish JA, McAuliffe DJ, Bloch KJ. Sensitivity of mononuclear cells to PUVA: Effect on subsequent stimulation with nitrogens and on exclusion of trypan blue dye. Clin Exp Dermatol 1981; 6:273–277.

(*24*) Morison WL, Parrish JA, Anderson RR, Bloch KJ. Sensitivity of mononuclear cells to UV radiation. Photochem Photobiol 1979; 29:1045–1047.

(*25*) Morison WL, Paul BS, Parrish JA. The effects of indomethacin on long-wave ultraviolet-induced delayed erythema. J Invest Dermatol 1977; 68:130–133.

(*26*) Morison WL, Parrish JA, Bloch KJ, Krugler JI. In vivo effects of PUVA on lymphocyte function. Br J Dermatol 1981; 104:405–413.

(*27*) Rosario R, Mark GJ, Parrish JA, Mihm MC. Histological changes produced in skin by equally erythemogenic doses of UV-A, UV-B, UV-C and UV-A with psoralens. Br J Dermatol 1979; 101:299–308.

(*28*) Lerman S. Radiant energy and the eye. New York: Macmillan, 1980:321.

(*29*) Parrish JA. Photoimmunologic, carcinogenic and ocular effects of in vivo psoralen photochemistry in humans. In: Pathak MA, ed. Proceedings of NATO advanced study institute's program on molecular basis of dermatological diseases. New York: Plenum, 1982. In press.

(*30*) Parrish JA. New concepts in therapeutic photomedicine: Photochemistry, optical targeting in the therapeutic window. J Invest Dermatol 1981; 77:305–310.

DISCUSSION

K. Kraemer: That was a very nice review of the current status of photomedicine. I would like to clarify one point: On theoretical grounds, if you were to manipulate the various factors and want to increase the radiant exposure to circulating cells in the skin, what you really need to do is to increase the volume of blood that is in the skin at a given time. If you just increase the flow rate, all that will mean is that the cells go through the skin faster. So at first approximation, it would mean that you would actually have less exposure to the circulating cells. Again, I request, if anyone knows of measurements of cutaneous blood volume in humans, this would be a very important factor to take into consideration. Then, if we manipulate skin blood volume, we can directly see what changes are induced.

J. A. Parrish: That is a very good point. There does not necessarily have to be a one-to-one correlation between increased flow and increased volume. I think, however, that anything that makes the skin subsequently red most likely has increased blood volume as well as increased flow, because your eye is telling you that there is more blood present there. By the time the photons scatter back to your eye, the blood has, of course, not travelled far. The photons travel much faster (186,000 mile/sec) than the blood flowing through the skin. So I think that the fact that you see the skin is red means that more than likely there is more blood present.

Also, there are a variety of ways to change the permeability of vessels, which may be more important than changing flow or content, because then you can release more substance into the tissue and subsequently photoactivate it. In summary, you are correct that we cannot assume that increased blood flow has a one-to-one correlation with increased blood content at any one time, because that may not necessarily be the same. There is inadequate information about this topic.

Photosensitization by Porphyrins and Prevention of Photosensitization by Carotenoids[1]

Micheline M. Mathews-Roth[2,3]

ABSTRACT—Photosensitization by porphyrins and the use of carotenoid pigments as protective agents against photosensitization are examined. The use of carotenoids in the treatment of erythropoietic protoporphyria as well as other diseases of photosensitivity is reviewed. Possible mechanisms for the protective action of carotenoids are mentioned.—JNCI 1982; 69:279–285.

Photosensitization can occur not only from the ingestion or the topical application of a photosensitizing compound, but in some diseases it can occur from the endogenous formation of a photosensitizer. Examples of powerful endogenous photosensitizers in human disease are the various porphyrin compounds produced as a result of the metabolic defects in the photosensitive porphyrias (table 1). In these diseases, the presence of the abnormal porphyrins in the blood and skin results in the production of photosensitivity reactions, such as itching, redness, swelling, and formation of various lesions in skin exposed to light.

A "porphyric state" leading to photosensitization as well as other skin changes can be induced in otherwise healthy individuals by the ingestion of certain chemicals. An example of this was the accidental ingestion of the fungicide hexachlorobenzene by several thousand individuals in Turkey, where the chemical was used as a herbicide on the wheat crop. This compound caused a porphyria cutanea tarda-like syndrome. Most of the people afflicted continued to excrete abnormally high levels of porphyrins and experience photosensitivity for several years after hexachlorobenzene ingestion. Some of the characteristic skin changes of porphyria cutanea tarda, such as hypertrichosis and hyperpigmentation, persisted for many years longer. Additional examples of photosensitive porphyria-inducing chemicals in man and experimental animals, and more detailed descriptions of the various porphyrias, were reviewed by Meyer and Schmid (*1*).

Recently, the use of iv-administered hematoporphyrin and light exposure to delineate or treat human cancers has been introduced. This treatment renders the patients who received the hematoporphyrin extremely photosensitive for several months; casual exposure of unprotected skin to the sun results in the development of severe erythema, edema, and/or papule formation (*2*). This mode of therapy is still experimental, but if it proves successful, rigorous safeguards for protecting patients against photosensitization obviously will have to be developed.

What are the available means for protection against photosensitization by porphyrins? In the case of drug-induced porphyric states, avoidance of the drug is obvious. Also obvious is the instruction for patients to avoid unnecessary sun exposure and, when patients must go out, to shield the skin with appropriate clothing. The sunscreens that are effective against sunburn are ineffective in the case of the porphyrias. Opaque sunscreens, such as those made with titanium dioxide or zinc oxide provide some protection, but in most cases, patients find them cosmetically unacceptable.

A possible approach to the treatment of diseases with sensitivity to visible light such as the porphyrias was suggested from work on photosensitization and photoprotection in bacteria and plants. Sistrom et al. (*3*) found that the carotenoid pigments of the photosynthetic bacterium *Rhodopseudomonas spheroides* could protect these bacteria against lethal photosensitization by their own chlorophyll. These workers found that when a mutant of this organism, which could not synthesize colored carotenoids, was grown in the presence of light and air, growth stopped, chlorophyll was destroyed, and the cells were killed. However, the wild type, with its carotenoid pigments, was not injured by growth in light and air.

These workers further demonstrated that the bacteriochlorophyll was responsible for the lethal photo-oxidation of the blue-green mutant and that both oxygen and light were necessary for the destructive reaction. The carotenoid pigments of the organism were functioning as protective agents against this killing, and the bacteriochlorophyll was the photosensitizer responsible for the lethal photosensitization.

Many nonphotosynthetic bacteria also have carotenoid pigments. These organisms do not contain large amounts of potential photosensitizers as do the photosynthetic bacteria with their ample supply of chlorophyll. Nonphotosynthetic bacteria do contain small amounts of compounds such as porphyrins and flavins that can cause photosensitization. Sistrom and I (*4*) studied the wild-type and a colorless mutant of the nonphotosynthetic bacterium *Sarcina lutea* and found that in this organism also, the carotenoids of the wild-type were protective against lethal photosensitization. The pigments protected the organism against photosensitization by photosensitizers added to the medium, as well as against sensitizers naturally present within the cell. The ability of carotenoid pigments to protect against lethal photosensiti-

---

ABBREVIATIONS USED: EPP=erythropoietic protoporphyria; PMLE=polymorphous light eruption.

---

[1] Presented at the Seventh Food and Drug Administration Science Symposium ("Photochemical Toxicity: Toxic, Allergic, and Carcinogenic Aspects With Emphasis on Predicting Effects in Humans") held at the Uniformed Services University of the Health Sciences, Bethesda, Md., March 16–17, 1981.

[2] Channing Laboratory, Department of Medicine, Harvard Medical School, and Brigham and Women's Hospital, Boston, Mass. 02115.

[3] *Address reprint requests to* Dr. Mathews-Roth *at* Channing Laboratory, 180 Longwood Ave., Boston, Mass. 02115.

TABLE 1.—*Photosensitive porphyrias*

Disease	Biochemical lesion
Congenital porphyria (Günther's disease)	Functional imbalance between uroporphyrinogen I synthetase and uroporphyrinogen III cosynthetase. Elevated levels of uroporphyrin I and coproporphyrin I in erythrocytes, plasma, stool, and urine.
Erythropoietic protoporphyria	Partial deficiency of ferrochelatase. Elevated levels of protoporphyrin and often coproporphyrin in erythrocytes, plasma, and stool. Urine levels normal.
Porphyria cutanea tarda	Partial deficiency of uroporphyrinogen decarboxylase. Uroporphyrin and coproporphyrin in urine, occasionally in stool. Erythrocyte levels normal.
Variegate porphyria	Enzymatic lesion not definitely established. Elevated levels of protoporphyrin and coproporphyrin in feces, often also in urine. Erythrocyte levels normal.
Hereditary coproporphyria	Partial deficiency of coproporphyrinogen oxidase. Elevated levels of coproporphyrin in feces and to a lesser degree in urine. Erythrocyte levels normal.

zation has now been demonstrated in many other bacteria, both photosynthetic and nonphotosynthetic and also in green plants (*5*).

Lethal photosensitization can be induced also in mammals by the administration of hematoporphyrin and exposure to strong light (*6*). Because of the striking protective action of carotenoids in bacteria and in plants, it seemed possible that carotenoids might prevent this lethal effect also. To test this possibility, mice were given 1 mg of hematoporphyrin ip before exposure to strong visible light. Half of the animals had received 3 mg of β-carotene ip 18–24 hours before receiving the injection of hematoporphyrin and being exposed to light. Significantly more animals that received the β-carotene survived the treatment with hematoporphyrin and light than did those mice that had not received the β-carotene (table 2). Controls showed that the vehicle in which the β-carotene was suspended, a mixture of Tween-80 and saline, offered no protection against photosensitization and that control animals given either β-carotene or hematoporphyrin survived well if kept in the dark. Thus β-carotene was effective in preventing the lethal photosensitization of mice induced by the injection of hematoporphyrin and exposure to visible light (*7*).

From the results of the studies in bacteria and in animals, it now seemed feasible, because of the lack of toxicity of carotenoids in man, to administer β-carotene to patients with photosensitivity. The disease chosen for study was EPP. Patients with this abnormality of porphyrin metabolism complain of itching, burning, redness, and swelling of the skin exposed to the sun (*1*). Erythrocyte, plasma, and stool protoporphyrin levels are increased, but urine porphyrin levels are within normal limits (table 1). Typical lesions may be induced by exposure of the patients' skin to sunlight or to strong artificial light (e.g., xenon arc filtered to transmit light from 380 to 600 nm) under controlled conditions in the laboratory.

Could carotenoid pigments, which can protect against the photosensitization induced by the porphyrin group of chlorophyll, also protect against the photosensitization induced by the porphyrin group of protoporphyrin? In collaboration with Dr. Edward H. Kass, Dr. Madhu Pathak, and Dr. Thomas B. Fitzpatrick, Harvard Medical School and Massachusetts General Hospital, and Dr. Leonard C. Harber, Columbia College of Physicians and Surgeons, we treated with β-carotene (15–90 mg/day) 3 patients with EPP, each of whom had elevated erythrocyte, plasma, and stool protoporphyrin levels. All 3 patients, a 10-year-old girl, her 39-year-old father, and an unrelated 35-year-old man, showed marked improvement in their ability to tolerate exposure to sunlight, as well as an increased ability to tolerate exposure to a xenon arc lamp (phototesting) after they had taken β-carotene for 4–6 weeks. Protection continued as long as β-carotene was taken; when the medication was stopped, photosensitivity returned (*8, 9*).

TABLE 2.—*Protective effect of β-carotene on photosensitization of mice by hematoporphyrin and visible light*[a]

Treatment	Light exposure	No. of animals	No. of dead animals	No. of animals alive
Hematoporphyrin[b]	Yes	27	21	6
Hematoporphyrin and carotene[b, c]	Yes	27	9	18
Hematoporphyrin and Tween 80–saline[b]	Yes	8	7	1
Hematoporphyrin[b]	No	8	0	8
Carotene[c]	No	8	0	8

[a] Data taken from (*7*).

[b] Animals received 1 mg ip before exposure to light.

[c] Carotene was suspended in Tween 80–saline. Animals received 3 mg β-carotene ip 18–24 hr before exposure to light.

Since publication of the report on these 3 patients in 1970, we have treated 130 additional patients with β-carotene in collaboration with their personal physicians (*10, 11*). From our experience with this larger number of patients, we found that we often had to use higher doses of β-carotene beadlets (up to 180 mg/day) than we used with the first 3 patients; the dosage must be individualized for each patient (*10, 11*). Of the 133 patients treated with these individualized dosages, 22 reported little or no improvement and the remaining 111 reported significant improvement in their ability to tolerate sunlight without developing symptoms of photosensitivity (table 3). Over 75% of the patients report a fourfold or more increase in tolerance to sunlight. The majority now engage in outdoor activities from which they excluded themselves before β-carotene treatment started. Most of the children can now play outside in daylight. Some patients still get reactions when they expose themselves for a long time to the sun. Others can spend all day outdoors with no trouble, and some only an hour or two before developing symptoms. In general, the treated patients report that they can tolerate sunlight better now than before treatment.

In addition to the patients' subjective reactions of improved tolerance to sunlight, we used phototesting with

TABLE 3.—*Effect of β-carotene on tolerance to sunlight of patients with erythropoietic protoporphyria*[a]

No. of patients	Percent of total	Protection index[b]
10	16	1[c]
12		2[c]
27	84	3–5
39		6–10
15		11–15
6		16–20
24		>21
Total 133	100	

[a] Data taken from (*10, 11*).

[b] Protection index is defined as the number of minutes of summer sunlight tolerated with the development of symptoms after therapy divided by the number of minutes of summer sunlight tolerated without the development of symptoms before therapy. An index of less than 3 represents no improvement.

[c] Patients showed little or no improvement despite blood carotene levels of at least 400 μg/dl following intake of highest dose appropriate for their ages.

xenon arc light before and during β-carotene therapy as an objective method of evaluating the effect of this treatment (*10, 12*). Tolerance to this light increased in those patients who reported benefit from carotene therapy. No increased tolerance was found in those patients reporting no improvement (table 4).

In the 6-year period of the study (1969–75), no toxic side effects (other than occasional transient loose stools) from the ingestion of these high doses of β-carotene (the equivalent of up to 4 pounds of carrots a day) were found. The carotenodermia which usually develops has not bothered most of the patients. Although we found in another study that β-carotene had no effect in preventing sunburn (*13*), it appears to have a small effect in increasing tanning as opposed to burning. Many of our patients reported that for the first time in their lives they were able to develop a tan.

Treatment with β-carotene has had no effect on the abnormalities of porphyrin metabolism that characterize EPP. All of the 133 patients had elevated erythrocyte, plasma, and stool porphyrins when they entered the study, and their porphyrins have remained elevated in spite of β-carotene treatment.

In 22 reports of the successful use of β-carotene for the treatment of photosensitivity in EPP, over 75% of the patients treated reported a significant improvement in their ability to tolerate light exposure, and no side effects from the use of β-carotene were observed (*14–35*). One study reporting little or no improvement has also appeared (*36*); however, these workers used a much lower dosage of β-carotene than that recommended by us (*10, 11*). Later, some of the patients from the unsuccessfully treated group were given higher doses of β-carotene by another investigator (*35*), and the patients noted some increased tolerance to sun while taking the higher doses. These results emphasize the importance, as we have mentioned (*10, 11*), of individualizing the dose to each patient and increasing the dose until the patient reports some improvement.

The problem of individualizing treatment is also important in the conduct of a controlled trial and makes double-blind designs almost impossible. At a minimum, such trials should use a dose of β-carotene large enough to produce amelioration of symptoms in most patients (a minimum period of 3 months' treatment at doses giving blood levels ≥800 μg/dl; for adults at least 180 mg/day should be given).

From our results and those of other workers it can be concluded that β-carotene administered in sufficiently high doses can be an effective therapy for ameliorating photosensitivity in most patients with EPP. However, it must be pointed out that there are limits to the protective ability of carotenoids. As can be seen from our data, some patients receive little or no benefit from carotene treatment. In general, these are patients who have very high levels of red cell and/or plasma porphyrins. Carotenoid administration seems also to offer a slight degree of protection in patients given iv hematoporphyrin for cancer investigation, but this protection is not sufficient to allow unrestricted activity (*2*). Thus it is important to realize that even when carotene doses are increased to the highest achievable levels, significant protection may not occur in the presence of extremely high levels of porphyrins.

Since β-carotene administration seemed effective in protecting against photosensitization in EPP, it seemed logical to see if it could prevent photosensitization in other photosensitivity diseases. There have been seven reports (*26, 37–42*) on the use of carotenoids in the treatment of congenital porphyria (Günther's disease). Five report some decrease in the number of new lesions produced, in some cases the patient is allowed fairly normal exposure to light. Seip et al.

TABLE 4.—*Tolerance to xenon arc light*[a]

Patient	Development time for minimal erythema, min	
	Before therapy[b]	During therapy[c]
1	13.33	36.67
2	20.00	40.00
3	.75	5.64
4	18.33	25.71
5	8.00	16.67
7	5.20	12.00
8	6.00	9.33
9	23.33	38.30
10	8.33	31.67
11	3.67	31.67
12	5.00	14.00
13	10.00	41.67
14	6.25	13.75
15	6.25	13.33
16	10.00	15.56
34	3.75	8.75
35	6.67	20.00
37	4.00	15.00
38	12.50	25.00
39	2.00	10.00
42	5.00	15.00

[a] Data taken from (*12*). $P<0.001$ from paired *t*-test on data in table.

[b] Average for each patient of all phototests before therapy started, when patient first entered study, as well as tests done before therapy started in subsequent years of the study, when patient had not taken β-carotene during winter (serum carotene level <250 μg/dl) in all years patient was in study.

[c] Average for each patient of all phototests in which blood β-carotene level exceeded 400 μg/dl in all years patient was in study.

(*37*) report phototesting 1 patient with the use of a xenon arc light. Before treatment the patient reacted with marked erythema after 10 minutes' exposure to this light, and during treatment he developed only mild erythema after 40 minutes of exposure. These authors stressed, as we do, the importance of maintaining high levels of carotene in the blood. Here, as in EPP, carotenoids do not correct the biochemical defect, so it is important that whatever hematologic treatment the patient is receiving must be continued during carotenoid therapy. Carotene treatment will not heal old scars—hence the best cosmetic effects will occur if therapy is started when patients are very young.

Several groups of workers have reported the use of carotenoids (usually a mixture of β-carotene and canthaxanthin) in the treatment of PMLE with varying degrees of success (*33, 43–47*). Jansen (*43*) treated 66 patients, 51 of whom responded favorably. Wennersten and Swanbeck (*44*) treated 8 patients, all of whom showed improvements in the minimal erythema dose tested with an appropriately filtered xenon arc lamp. Thune (*45*) treated 17 patients, only 5 of whom showed a more than threefold increase in tolerance to sunlight. On phototesting, he found "a significant increase in MED [the minimum erythema dose] for unfiltered light (xenon arc) at the 5% level of probability." Some of the patients also needed a sunscreen to achieve maximal therapeutic effect. Haeger-Aronsen et al. (*33*) found improvement in 15 of 18 patients with PMLE. Parrish et al. (*46*) found complete remission in only 6 of 19 patients and got much better results using psoralen plus UV radiation treatment. In our collaborative study (*11*), only 9 out of 27 patients reported improvement with carotene treatment with most also needing the concurrent application of a sunscreen, though sunscreen alone was not beneficial.

Fusaro and Johnson (*47*) reported success in treating the hereditary form of PMLE found in American Indians with high doses of β-carotene. They treated 5 patients and stated that each patient was able to perform normal activities outdoors without avoiding the sun and without showing symptoms of photosensitivity and reappearance of skin lesions.

Although some workers have shown objective evidence by phototest of improved light tolerance in PMLE with carotene treatment, it is obvious from these various reports that carotenoids are not as effective in the treatment of PMLE as they are in the treatment of EPP. It would seem sensible to use carotenoids in the therapy of PMLE only when the usual modes of therapy are ineffective, impractical, or contraindicated.

Carotenoids have been found by other workers as well as by our group to be ineffective in the treatment of actinic reticuloid (*11, 48*), porphyria cutanea tarda (*11, 49, 50*), solar urticaria (*11, 26, 48*), and hydroa aestivale (*11*). Two groups of workers (*33, 51*) have found a beneficial effect of carotenoid treatment in lupus erythematosus, but another group had success in only 1 of 26 patients (*52*). Bickers et al. (*53*) suggest that β-carotene may be effective in ameliorating the photosensitivity in hydroa vaccineforme, and Husquinet et al. (*54*) have reported some success in a patient with porphyria variegata who developed no lesions for 2 years while taking β-carotene, in spite of elevated stool and urine porphyrins. Eales (*30*) reported also some success in treating this disease. Pietzcker (*55*) reports successfully using carotenoids to ameliorate the appearance of certain patients with vitilligo.

Since few patients with these various diseases have been treated with carotenoids, we still do not know the extent of the pigment's effectiveness in these conditions; clearly more work needs to be done. However, since the above-described studies have also reported no significant toxicity from carotenoid ingestion, it is probably sensible to give a trial of β-carotene (or β-carotene and canthaxanthin, as is used in Europe) to patients with any kind of photosensitivity disease, who have not responded to other forms of therapy. In EPP, carotenoids seem to be the treatment of choice.

How carotenoids might be exercising their protective function is being actively investigated at this time. Studies to date suggest that the high levels of protoporphyrin present in the erythocytes, plasma, or extracellular fluid of the skin can be stimulated to an excited (triplet) state by visible light, which can penetrate skin to the level of the dermal capillaries (*56*). The excited protoporphyrin may either destroy cell components directly or may react with molecular oxygen to form singlet oxygen, a moiety that can be highly damaging to cellular components. Direct cell damage, or damage to cells or cellular organelles such as lysosomes, with release of chemical mediators that in turn damage other cells or organelles, would then cause the manifestations of itching, burning, erythema, and edema experienced by the patient with EPP.

β-carotene can quench singlet oxygen and inhibit free radical formation in vitro (*57, 58*) as you have heard in Dr. Krinsky's presentation at this meeting (*59*), and the ability of bacterial carotenoids to confer protection is correlated with the ability of the carotenoids to quench singlet oxygen in vitro (*60*). However, some degree of free radical inhibition by carotenoids is a possible alternative mechanism of action. Mechanisms of carotenoid protection in EPP have not yet been studied in an animal model. Further work should elucidate the definitive mode of action of the carotenoids' protective effect in animal models and eventually in patients with EPP.

In nonporphyric photosensitivity diseases, the chromophore responsible for the abnormal reactions is not known and is in all likelihood different from that in EPP: The mechanisms responsible for the induction of abnormal responses may not have the same molecular basis. Thus it is not surprising to see that for some diseases carotenoids may not be as an effective a photoprotector as they are in EPP. Here also, much work must be done on the mechanisms of photosensitization in these diseases.

The results of studies done by us and other workers show that carotenoid therapy—when given in high enough dose—is usually effective in ameliorating the photosensitivity in EPP, and it may be of some value in certain patients with other forms of photosensitivity.

REFERENCES

(*1*) Meyer UA, Schmid R. The porphyrias. In: Stanbury JB, Wyngaarden JD, Fredrickson DS, eds. The metabolic basis of inherited disease. New York: McGraw-Hill, 1978:1166–1220.

(2) Zalar GL, Poh-Fitzpatrick MB, Krohn DL, Jacobs R, Harber LC. Induction of drug photosensitization in man after parenteral exposure to hematoporphyrin. Arch Dermatol 1977; 113:1392–1397.
(3) Sistrom WR, Griffith M, Stanier RY. Biology of a photosynthetic bacterium which lacks colored carotenoids. J Gen Physiol 1956; 48:473–515.
(4) Mathews MM, Sistrom WR. The function of the carotenoid pigments of *Sarcina lutea*. Arch Mikrobiol 1960; 35:139–146.
(5) Krinsky NI. The protective function of carotenoid pigments. In: Giese AC, ed. Photophysiology. Vol 3. New York: Academic Press, 1968:123–195.
(6) Lipson RL, Blades EJ. The photodynamic properties of a particular hematoporphyrin derivative. Arch Dermatol 1960; 82:508–516.
(7) Mathews MM. Protective effect of beta-carotene against lethal photosensitization by hematoporphyrin. Nature 1964; 203:1092.
(8) Mathews-Roth MM, Pathak MA, Fitzpatrick TB, Harber LC, Kass EH. Beta-carotene as a photoprotective agent in erythropoietic protoporphyria. Trans Assoc Am Physicians 1970; 83:176–184.
(9) Mathews-Roth MM, Pathak MA, Fitzpatrick TB, Harber LC, Kass EH. Beta-carotene as a photoprotective agent in erythropoietic protoporphyria. N Engl J Med 1970; 282:1231–1234.
(10) Mathews-Roth MM, Pathak MA, Fitzpatrick TB, Harber LC, Kass EH. Beta-carotene as an oral photoprotective agent in erythropoietic protoporphyria. JAMA 1974; 228:1004–1008.
(11) Mathews-Roth MM, Pathak MA, Fitzpatrick TB, Harber LC, Kass EH. Beta-carotene therapy for erythropoietic protoporphyria and other photosensitivity diseases. Arch Dermatol 1977; 113:1229–1232.
(12) Mathews-Roth MM, Kass EH, Fitzpatrick TB, Pathak MA, Harber LC. Phototesting as an objective measure of improvement in erythropoietic protoporphyria. Arch Dermatol 1979; 115:1381–1382.
(13) Mathews-Roth MM, Pathak MA, Parrish JA, et al. A clinical trial of the effects of oral beta-carotene on the responses of human skin to solar radiation. J Invest Dermatol 1972; 59:349–353.
(14) Baart de la Faille H, Suurmond D, Went LN, Van Steveninck J, Schorthorst AA. Beta-carotene as a treatment for photo-hypersensitivity due to erythropoietic protoporphyria. Dermatologica 1972; 145:389–394.
(15) Lewis MB. Effect of beta-carotene on serum vitamin A levels in erythropoietic protoporphyria. Aust J Dermatol 1972; 13:75–78.
(16) Chapel TA, Stewart RH, Webster SB. Erythropoietic protoporphyria: Report of a case successfully treated with beta-carotene. Arch Dermatol 1972; 105:572–573.
(17) Anderson CR. Erythropoietic protoporphyria. Arch Dermatol 1972; 106:412–413.
(18) Würzer I. Protoporphyrinamische lichdermatose bei vitium cordis Z Haut Geschlechtskr 1972; 47:1006–1007.
(19) Hopsu-Havu VK, Terho PE, Hollmen T. Erythropoietic protoporphyria. The first case in Finland. Ann Clin Res 1973; 5:111–185.
(20) Moynahan EJ, Leppard B. Erythropoietic protoporphyria. Proc R Soc Med 1973; 66:1085–1086.
(21) Gschnait F, Wolff K. Die erythropoetische Protoporphyrie. Hautarzt 1974; 25:72–80.
(22) Grupper GH, Girard G, Davatchy C. Protoporphyrie erythropoetique familiale. Protection par beta-carotene. Bull Soc Fr Dermatol Syphiligr 1975; 82:249–250.
(23) Beckert E, Metz J. Zur Beta-Karotin Behandlung der erythropoetischen Protoporphyrie. Hautarzt 1974; 25:195–196.
(24) Marsden RA, Dawber RP. Erythropoietic protoporphyria with onycholysis. Proc R Soc Med 1977; 70:572–574.
(25) Zaynoun ST, Hunter JA, Darby FJ, Zakembski P, Johnson BE, Frain-Bell W. The treatment of erythropoietic porphyria-experience with beta-carotene. Br J Dermatol 1977; 97:663–668.
(26) Goerz G, Ippen H. Carotinoid-Behandlung von Lichtdermatosen. Dtsch Med Wochenschr 1977; 102:1051–1055.
(27) Nonaka S, Hirowatari T, Honda T, et al. Erythropoietic protoporphyria. Jpn J Dermatol 1977; 87:7–32.
(28) Barth J. Protoporphyrinämische Lichtdermatose, papulös-urticarielle Form. Dermatol Monatsschr 1978; 160:601.
(29) Weston WL. EPP masquerading as angioedema. J Allergy Clin Immunol 1978; 61:408.
(30) Eales L. The effects of canthaxanthin on the photocutaneous manifestations of porphyria. S Afr Med J 1978; 54:1050–1052.
(31) Rossi E, Curnow DH, Schenberg H. The detection of porphyria in photosensitive patients. Pathology 1978; 10:17–26.
(32) Niebauer G, Mischer P, Formanek I. Light-sensitive dermatoses in children. Mod Probl Paediatr 1978; 20:86–101.
(33) Haeger-Aronsen B, Krook G, Abdulla M. Oral carotenoids for photohypersensitivity in patients with erythropoietic protoporphyria, polymorphous light eruptions and lupus erythematodes discoides. Int J Dermatol 1979; 18:73–82.
(34) Thomsen K, Schmidt H, Fischer A. Beta-carotene in erythropoietic protoporphyria: 5 years' experience. Dermatologica 1979; 159:82–86.
(35) Shafrir A. Comments on a case of erythropoietic protoporphyria with onycholysis. Proc R Soc Med 1977; 70:574.
(36) Corbett MF, Herxheimer A, Magnus IA, Ramsay CA, Kobza-Black A. The long-term treatment with beta-carotene in erythropoietic protoporphyria—a controlled trial. Br J Dermatol 1977; 97:655–662.
(37) Seip M, Thune PO, Eriksen L. Treatment of photosensitivity in congenital erythropoietic porphyria with beta-carotene. Acta DermVenereol 1974; 54:239–240.
(38) Sneddon IB. Congenital porphyria. Proc R Soc Med 1974; 67:593–594.
(39) Jung EC. Porphyria erythropoetica congenita Günther. Arztliche Führung Dtsch Med Wochenschr 1977; 102:279–280.
(40) Mathews-Roth MM, Haining RG, Kinney TR. Congenital erythropoietic porphyria. Am J Dis Child 1977; 131:366.
(41) Stretcher GS. Beta-carotene in congenital porphyria. Arch Dermatol 1978; 114:1242–1243.
(42) Storck H, Kaufmann J. Kongenitale erythropoetische Porphyrie, Morbus Günther. Dermatologica 1978; 157: 323–333.
(43) Jansen CT. Beta-carotene treatment of polymorphous light eruption. Dermatologica 1974; 149:363–373.
(44) Wennersten G, Swanbeck G. Treatment of light-sensitivity with carotenoids. Acta DermVenereol 1974; 54:491.
(45) Thune P. Chronic polymorphic light eruption. Particular wavebands and the effects of carotene therapy. Acta DermVenereol 1976; 56:127–133.
(46) Parrish JA, Levine MJ, Morison WL, Gonzalez E, Fitzpatrick TB. Comparison of PUVA and beta-carotene in the treatment of polymorphous light eruption. Br J Dermatol 1979; 100:187–192.
(47) Fusaro RM, Johnson JA. Hereditary polymorphic light eruption in American Indians. JAMA 1980; 244:1456–1459.
(48) Kobza A, Ramsay CA, Magnus IA. Oral beta-carotene therapy in actinic reticuloid and solar articaria. Br J Dermatol 1973; 88:157–166.
(49) Ippen H. Allgemeinsymptome der späten Hant Porphyria (porphyria cutanea tarda) alshinweise für deren Behandlung. Dtsch Med Wochenschr 1961; 86:127–133.
(50) Ippen H, Goerz G, Botsch C. Photoprotection in porphyrias and the role of phlebotomy. In. Fitzpatrick TB, Pathak MA, Harber LC, Seiji M, Kukita A, eds. Sunlight and man: Normal and abnormal photobiologic responses. Tokyo: Univ Tokyo Press, 1974:655–658.
(51) Newbold CH. Beta-carotene in the treatment of discoid lupus erythematosus. Br J Dermatol 1976; 95:100–101.
(52) Durois EL, Patterson C. Ineffectiveness of beta-carotene in lupus erythematosus. JAMA 1976; 236:138–139.
(53) Bickers DR, Demar LK, De Leo V, Poh-Fitzpatrick MB, Aronberg JM, Harber LC. Hydroa vaccineforme. Arch Dermatol 1978; 114:1193–1196.
(54) Husquinet H, Noirfalise A, Parent MT. Porphyria variegata. J Genet Hum 1978; 26:367–383.
(55) Pietzcker F, Kuner-Beck V. Pigmentausgleich dursch beta-Karotin oral. Hautarzt 1979; 30:308–311.
(56) De Leo VA, Poh-Fitzpatrick M, Mathews-Roth MM, Harber LC. Erythropoietic protoporphyria—10 years' experience. Am J Med 1976; 60:8–22.
(57) Fujimori E, Tavla M. Light-induced electron transfer between chlorophyll and hydroquinone and the effect of oxygen and beta-carotene. Photochem Photobiol 1966; 5:877–887.
(58) Foote CS, Denny RW. Chemistry of singlet oxygen. VII. Quenching by beta-carotene. J Am Chem Soc 1968; 98:6233–6235.
(59) Krinsky NI, Deneke SM. Interaction of oxygen and oxy-radicals with

best copy available

carotenoids. JNCI 1982; 69:205–210.

(60) Mathews-Roth MM, Wilson T, Fujimori E, Krinsky NI. Carotenoid chromophore length and protection against photosensitization. Photochem Photobiol 1974; 19:217–222.

DISCUSSION

P. Sundaresan: I was wondering about the variation you were getting with the different patients. Was the carotene administered orally in these patients?

M. Mathews-Roth: Yes, β-carotene was administered orally. Humans are "yellow fat" animals, and if we take β-carotene by mouth, we accumulate high levels in the skin and in the blood. Yes, it is true there is physiologic variation from people to people as to blood levels. Also, in some of our patients, compliance might not have been as good. We really could not totally push them to take six pills a day all the time. Some people just refused to take six pills a day, and we just took their blood, determined the β-carotene level, and took their word for their reaction. Some of that variation is probably due to the fact that some of the people were not taking enough pills to attain drug levels as high as they should have been.

Sundaresan: Probably the variation is also due to poor absorption of carotene. Because carotene is very poorly absorbed, as you know, I was wondering if there is any way of improving the patients' absorption. You might then be able to give the carotene at a lower dose.

Mathews-Roth: It is very true that crystalline β-carotene is extremely hard to absorb. What we have been using are the Hoffman-LaRoche β-carotene beadlets, which the FDA had approved for use as a food color. This is a water-miscible beadlet, and I think it is about the best way to get carotenoids into anyone. We did a well-controlled study on carotene intake in the sunburn study that I referred to (*13*). This was done with Dr. Fitzpatrick's collaborative investigators at the Arizona State Prison, and the men in the study were taking their pills judiciously. They indeed developed high levels fairly soon, in 4–6 weeks. That time is fairly standard for that dose of carotene. When they took their pills, these people did develop the kinds of levels that theoretically we thought they should.

I think that the β-carotene preparation we have is probably about the best we can get, and unless Hoffman La-Roche comes out with a better water-miscible formulation, I think we are doing pretty well with the one we have.

If I can also add my request to the FDA for what drugs they should investigate, it would be that hematoporphyrin derivative. For one thing, it concerns me that investigators are giving this material that they are preparing in their own labs intravenously to patients and that these patients remain photosensitive for weeks. If this therapy ever does get a bit more use, and admittedly people are trying to use it topically, the FDA should be attempting to monitor its use.

Another thing that you might be interested in (and I think the FDA is aware of it) is that people are marketing in Europe canthaxanthin as the European answer to Man-Tan. Instead of having to smear something on you to look tanned and attractive, you can take a pill. Indeed, the patients in Europe who are taking, for porphyria, the mixture of β-carotene and canthaxanthin do like the cosmetic appearance much better than our patients in the United States who are just taking the β-carotene.

So far, no toxicity has occurred. However, we do not know as much about canthaxanthin as we do about β-carotene. It would seem to me that the oral use of canthaxanthin should be classified as a drug, be it for a cosmetic purpose or not, because of the fact that its users are taking it by mouth and they are taking it in the same range of dose that people with porphyria are taking it. It would seem to me that some studies comparable to those that we did to get the new drug approval for β-carotene (Solatene) should be done by these people who want to market canthaxanthin for a tanning effect. It works: There is no doubt about the efficacy. People who take it look great. In fact, I do not know if Dr. M. Pathak remembers, but when we first started out and did a β-carotene UV study, some of our residents wanted to stay on it (β-carotene) because they looked so good.

N. Krinsky: I wonder if you could just comment on the level of vitamin A in the serum of the people on the high β-carotene regimen, and also if you have any idea what happens to vitamin A storage in the liver?

Mathews-Roth: One of the things that you always read in pharmacology books is that if you administer vitamin A as a β-carotene, you do not get high levels of vitamin A. The body shuts off the vitamin A converting mechanism, and indeed we found this to be true. Our patients never exceeded the normal range of blood vitamin A. Now, this vitamin A determination was admittedly not done by liquid chromatographic methods but done by the standard clinical lab test for vitamin A. This has been reported routinely in the literature from old studies done from β-carotene administration. It has been confirmed as far as I can tell in all of the studies on protoporphyria. None of these studies reported high levels of vitamin A, and it was confirmed also in our prisoner study. The subjects' vitamin A levels stayed within the normal range.

We had the opportunity to look at livers of 2 patients who were receiving β-carotene, one of whom was a protoporphyria patient who had a gallbladder attack. Her gallbladder was removed, and her surgeon provided us with a small amount of her liver. The other one was a child with a genetic disease who was being given β-carotene at the request of her father to improve the skin appearance. She died of a totally unrelated cause. We were able to get some liver from her, and both of these livers did contain a normal level of vitamin A. There are several reports in the literature of people who were caratonemic and also had normal liver vitamin A levels. Also, liver β-carotene was not particularly increased. I think this was also shown by Hoffman LaRoche years back in some animal studies that they had done, and again, the administration of carotene does not lead to abnormally high stores in the liver of either carotene or vitamin A, which is why it is such a great compound to use for this kind of work.

M. Pathak: The textbook of biochemistry that you and I studied had to be changed because the enzyme system just does not convert under in vivo conditions one molecule of β-carotene to two molecules of vitamin A. I think there are a couple of good papers published from the Massachusetts Institute of Technology showing that the enzyme actually gets inhibited by high levels of vitamin A.

Mathews-Roth: Right, and thereby keeping the vitamin A levels at normal ranges. Yes, anyway, theoretically, β-carotene should cleave to two molecules, and I think in vitro it does it, but in vivo it does not. So β-carotene is a nice safe preparation to use.

blank page

Ocular Phototoxicity and Psoralen Plus Ultraviolet Radiation (320–400 nm) Therapy: An Experimental and Clinical Evaluation[1,2,3]

Sidney Lerman, *M.D.*[4,5]

ABSTRACT—The increase in fluorescent chromophores within the human ocular lens is age related, leading to an increasingly yellow core (nucleus) that presumably results from UV radiation exposure. In approximately 10% of our population this process progresses more rapidly, resulting in the formation of the brown (nuclear) cataract. Some lenticular discoloration may be beneficial, since it enables the mature lens to filter UV and short-wavelength visible radiation, thus protecting the retina from potential photodamage. Aphakic primate retinas can be irreversibly damaged by exposure to approximately 5 $mW \cdot cm^{-2}$ long-wavelength UV (>325 nm) radiation. Photosensitized damage to the lens and retina with psoralen plus UV radiation (320–400 mm) (PUVA) has been demonstrated in experimental animals, and cataracts have recently been reported in patients given PUVA therapy. A new method to screen patients for lens damage is by enhanced fluorescence measurements. This method, UV slit-lamp densitography, permits detection of lenticular photodamage at a molecular level, years before visible opacities become manifest by conventional slit-lamp examination. This procedure has also demonstrated a significantly lower level of lens fluorescence (hence decreased filtering capacity) in patients with retinal degenerative diseases, suggesting UV photodamage as a factor in the progression and perhaps pathogenesis of these conditions.—JNCI 1982; 69:287–302.

Aside from the skin, the eye is the only organ or tissue in the body that is particularly sensitive to the nonionizing wavelengths of radiation normally present in our environment (wavelengths >280 nm). We are constantly exposed to UV radiation (solar and man-made) throughout life; approximately 8% (110 $W \cdot m^{-2}$) of solar radiation above the atmosphere is estimated to be UV. At sea level the amount of UV radiation declines to 20–50 $W \cdot m^{-2}$, depending on geographic location and season. Aside from solar radiation, man-made UV radiation may also play a role in ocular phototoxicity, albeit a relatively minor one under normal circumstances. The spectral output of commonly used fluorescent lamps is relatively low at these wavelengths and should not pose a problem except in special circumstances, e.g., in patients who are being treated with photosensitizing drugs. However, exposure to photoflood lamps or the black light lamps frequently used in various laboratories might present a potential hazard because their output can approach approximately 5–10% of the average levels of solar radiation in our atmosphere. Furthermore, a much more significant hazard exists in certain industries that utilize UV radiation in catalytic polymerization processes.

UV radiation-induced changes in human and animal ocular tissues can be attributed to two mechanisms: a direct or intrinsic process in which the radiation is absorbed by specific naturally occurring chromophores within these tissues (e.g., the nucleic acids or aromatic amino acid residues) and an indirect or photosensitized process in which the radiation is initially absorbed by a photosensitizing drug or other extraneous compound (text-fig. 1).

DIRECT UV RADIATION EFFECTS

Corneal photodamage from UV radiation has been appreciated and recorded for a long time, a typical example being snow blindness experienced by polar explorers. This type of photokeratitis is due to the relatively high levels of UV radiation that can be reflected by snow compared with less than 5% of UV radiation that is reflected from earth or grass. Aside from the well-known polar and industrial photokeratitis, UV radiation has also been implicated in a variety of conjunctival and corneal lesions. These lesions include pingueculae and pterygiums, exposure keratosis (which involves epithelial changes related to actinic radiation and is analogous to actinic keratosis of the skin), nodular band-shaped keratopathy, experimentally induced tumors in animals, and the relatively rare dysplasia and intraepithelial carcinoma. Certain corneal diseases can also be triggered by exposure to UV radiation, e.g., herpes simplex keratitis and recurrent erosions of the cornea. Experimental UV photokeratitis is generally associated with an action spectrum in which the major peak is at 280 nm and the minor one is approximately 260 nm (*1*, *2*).

The normal human cornea and aqueous humor transmit nearly all UV radiation longer than 300 nm; however, there is a small but progressive decline in the percent of UV radiation transmitted as the cornea ages, which may be due to an accumulation of UV radiation-induced fluorescent chromophores in the aging cornea (*2*). Thus the human ocular lens is constantly exposed to ambient UV radiation (300–400 nm) throughout life. One consequence of cumulative photochemical damage is an increasing absorption of UV radiation and visible light due to the presence of

---

ABBREVIATIONS USED: 3-AT=aminotriazole; ESR=electron spin resonance; 8-MOP=8-methoxypsoralen; PAS=photoacoustic spectroscopy; PUVA=psoralen plus UV radiation (320–400 nm); Trp=tryptophan.

---

[1] Presented at the Seventh Food and Drug Administration Science Symposium ("Photochemical Toxicity: Toxic, Allergic, and Carcinogenic Aspects With Emphasis on Predicting Effects in Humans") held at the Uniformed Services University of the Health Sciences, Bethesda, Md., March 16–17, 1981.

[2] Supported by Public Health Service (PHS) grant EY-01575 from the National Eye Institute, by PHS grant AG-01309 from the National Institute on Aging, and by a grant from Precision-Cosmet, Inc., Minnetonka, Minn.

[3] Research procedures were in accord with the ethical standards of the Human Investigations Committee of Emory University, and animals were maintained under the guidelines of Emory University.

[4] Emory University and Georgia Institute of Technology, Atlanta, Ga. 30322.

[5] *Address reprint requests to* Dr. Lerman at Laboratory for Ophthalmic Research, Emory University School of Medicine, 1708 Haygood Dr., N.E., Atlanta, Ga. 30322.

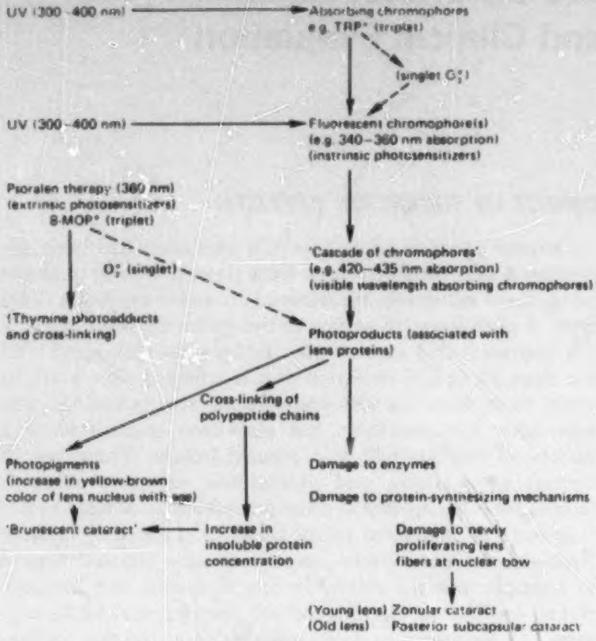
UV (300–400 nm)
Absorbing chromophores
e.g. TRP* (triplet)
(singlet O_2^*)
UV (300–400 nm)
Fluorescent chromophore(s)
(e.g. 340–360 nm absorption)
(instrinsic photosensitizers)
Psoralen therapy (360 nm)
(extrinsic photosensitizers)
8-MOP* (triplet)
O_2^* (singlet)
'Cascade of chromophores'
(e.g. 420–435 nm absorption)
(visible wavelength absorbing chromophores)
(Thymine photoadducts
and cross-linking)
Photoproducts (associated with
lens proteins)
Cross-linking of
polypeptide chains
Photopigments
(increase in yellow-brown
color of lens nucleus with age)
Damage to enzymes
Damage to protein-synthesizing mechanisms
'Brunescent cataract'
Increase in
insoluble protein
concentration
Damage to newly
proliferating lens
fibers at nuclear bow
(Young lens) Zonular cataract
(Old lens) Posterior subcapsular cataract

TEXT-FIGURE 1.—UV radiation effects on the ocular lens with particular emphasis on lens protein photoreaction.

intrinsic and photochemically generated lens chromophores (*1–20*).

We have demonstrated that UV radiation can markedly affect the intact lens by direct absorption, both in vivo and in vitro. In vitro UV radiation-induced changes in human lenses include increased fluorescence intensities at 440 and 520 nm and increased pigmentation (*13–16*). Similar fluorescence enhancement can be observed in UV-irradiated rat lenses both in vitro and in vivo (*16*). Our studies indicate that these photochemical changes are similar to the increasing fluorescence seen in normally aging human lenses (*13, 15*). The cumulative effects of chronic exposure to ambient UV radiation appear to include the generation of a series of fluorescent chromophores (absorbing at increasingly longer wavelengths), an increasingly yellow lens nucleus, and a progressive increase in the level of insoluble lens proteins. The increase in the level of insoluble lens protein may also be related to the cross-linking of previously soluble polypeptides by some of the fluorescent pigments (*6, 9, 11, 15*) as well as to the formation of disulfide bonds (*15, 20, 21*).

Our UV radiation and visible light transmission studies on normal human lenses ranging in age from 6 months to 82 years have shown that more than 75% of the UV radiation (300–400 nm) is transmitted by lenses less than 10 years of age, whereas transmission of the same radiation by lenses more than 25 years of age drops markedly to 20% or less (*13, 15, 20*) (text-fig. 2). These data are consistent with the relative lack of UV radiation-absorbing chromophores in the young lens and the increasing concentration of such chromophores as the lens ages. Accompanying the measured increase in these chromophores and decrease in light transmission is an increase in the yellowness of the lens nucleus as it ages (fig. 1). These pigments are mainly confined to the nucleus and may be a factor in the development of nuclear sclerosis. The extreme example of such an aging process is the brown or black nuclear cataract (fig. 1J).

PAS performed on normal aging lenses and brown nuclear cataracts reveals an absorption band at 340–360 nm which increases in intensity as the lens ages and is particularly pronounced in brown cataracts (*22*). The intensity of this PAS-absorbing region is directly correlated with the degree of coloration of the lens nucleus. These data provide further evidence that UV radiation-absorbing pigments accumulate in the aging lens and brown nuclear cataract and are associated with the changes in light transmission and fluorescence in such lenses.

In comparing the action spectrum for production of fluorescent material in lenses (*23*) with that for photochemical destruction of Trp in aqueous solution (*24*), we suggested that Trp residues in lens proteins could be the initial light-absorbing and photochemically active species in UV radiation-induced lens damage. ESR studies point to an initial free radical mechanism for this photochemical lens damage (*25*). Further evidence regarding this mechanism derives from our studies with D-penicillamine. This free radical scavenger greatly reduces the free radical signal in UV-irradiated lenses and prevents the photochemical generation of fluorescent chromophores (*15, 25*). Lens tissue has built-in mechanisms for combating free radical damage. One of these mechanisms utilizes glutathione (which is present in very high concentration, particularly in the cortex) as a free radical scavenger. If this protective mechanism were suppressed, the damage due to UV radiation exposure would be significantly increased.

Our in vitro studies with whole lens incubates (mouse, rat, and human) have demonstrated that the production of fluorescent chromophores can be markedly accelerated if the lenses were incubated in the presence of 3-AT during UV irradiation (*16*). Because 3-AT is a catalase inhibitor, more glutathione is consumed in such lenses, resulting in the depletion of this important lens free radical scavenger and thereby increasing the sensitivity of the lenses to UV radiation. The high concentration of glutathione in the cortex

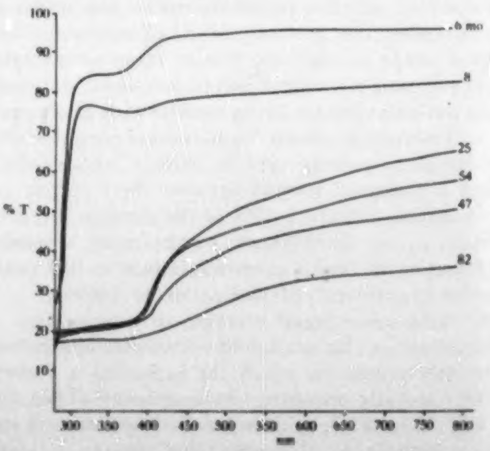

TEXT-FIGURE 2.—Percent transmission (% T) of UV radiation and visible light of normal human lenses 6 mo to 82 yr of age.

would prevent (or abort) a free radical-induced photochemical generation of these fluorescent chromophores while the lens nucleus, which has a much lower level of glutathione, does not have such an effective protective mechanism and would, therefore, accumulate these photochemically generated pigments (*13, 15, 16*). This enables the cortex to remain clear while the aging nucleus becomes progressively more yellow to brown. In addition to UV radiation-induced free radicals, singlet oxygen is also involved in direct UV radiation photodamage as well as in the photodynamic action of 8-MOP on lens proteins (*26, 27*).

Thus it is now generally accepted that chronic exposure to UV radiation (300–400 nm) over an individual's lifetime leads to the generation and increased accumulation of various fluorescent chromophores in the lens; these fluorescent chromophores are, to some extent, responsible for the increased yellowing of the lens nucleus as it ages. [In about 10% of our population this process progresses more rapidly, resulting in the development of the brown (nuclear) cataract.] This type of discoloration, in moderation, is actually beneficial because it enables our lens to become a very effective filter for UV and short-wavelength visible radiation (by our second to third decade), thus protecting our retina from cumulative photochemical damage which could occur during our lifetime. Laboratory studies have shown that such radiation can cause irreversible retinal photodamage (*28*). Interestingly, nature has provided us with the ability to develop a lenticular UV radiation filter to protect our retina from continuous radiation exposure which could be harmful, particularly in the older individual whose retinal metabolism and repair processes are no longer as effective as they are in the younger individual. We are now beginning to see confirmation of our hypothesis that long-wavelength UV radiation may play a role in certain retinal diseases (e.g., cystoid macular edema) which tend to occur in older patients after their cataractous lenses are removed.

Aside from the effects of chronic exposure to ambient UV radiation, acute exposure to higher radiation levels can produce cortical opacities in human, rat, and rabbit lenses in vitro and in vivo (*29–32*). Thus more intense UV radiation (≥300 nm) can induce lens changes involving the cortex, whereas chronic exposure mainly affects the lens nucleus. These effects appear to be dose and time related (*31, 32*). Our UV radiation exposure experiments have demonstrated that cortical opacities can be induced in young rat lenses (in vitro) by exposure doses (at 300 nm) greater than 26 J, concentrated within a relatively short time period (*32*). We have previously demonstrated that rat lenses will develop an increasing level of 440-nm fluorescence and become yellow at irradiance levels of 0.4 mW·cm^{-2} within 6 hours (*16*). However, when the irradiance is increased by a factor of four or more, cortical opacities develop within 4–6 hours, and these anterior cortical opacities appear to prevent any marked increase in lens fluorescence (*32*). It is postulated that this more intense UV radiation is capable of inducing severe photochemical damage to important enzyme systems (e.g., catalase and glutathione dehydrogenase). Chronic exposure of these enzymes to lower levels of irradiance could be overcome by the lenticular reparative mechanism enabling the photochemically induced fluorescence changes within the structural lens proteins (e.g., 440- and 520-nm fluorescence) to proceed and become manifest. There is also the possibility that more intense UV radiation may affect the protein–water order within the lens, resulting in the formation of "water lakes" associated with protein aggregates. The formation of water lakes would give rise to localized areas of marked changes in refractive index in the injured site and result in light scattering and opacification. Recent studies on rabbit lenses exposed to 337 nm of laser radiation demonstrate marked changes in their water component (*33*). These wavelengths have sufficient photon energies (~1–1.5 eV) to disrupt the protein–water order in the lens and give rise to sudden changes in refractive index resulting in localized opacities.

PHOTOSENSITIZED UV RADIATION EFFECTS

In addition to the demonstrated direct photochemical action of UV radiation on the ocular lens, photobiologic damage is possible by means of photosensitized reactions due to the accumulation of certain drugs within this organ. After the 13-mm stage of development, the ocular lens is completely encapsulated and never sheds its cells throughout life. Therefore, after 8-MOP therapy, photobound 8-MOP could be retained and accumulate with repeated therapy. We have demonstrated the presence of 8-MOP in human lenses 12 hours after the patient had ingested a single therapeutic dose of this drug (*26, 34*) (text-fig. 3). "Free" 8-MOP can also be detected within 2 hours in rat and dogfish lenses after one ip injection, and we have shown that it diffuses out of these lenses within 24 hours if the animals are kept in the dark (*35–37*).

In the presence of photic stimuli [ambient room light as well as direct UV (320–380 nm) radiation], lenticular fluorescence and phosphorescence are enhanced (*36*). Our spectroscopic studies have shown that photoaddition products (at 360 nm exposure) can be generated with lens proteins as well as with Trp (in vitro) in the presence of 8-MOP and oxygen (*26, 38*). Such a reaction in vivo would result in the

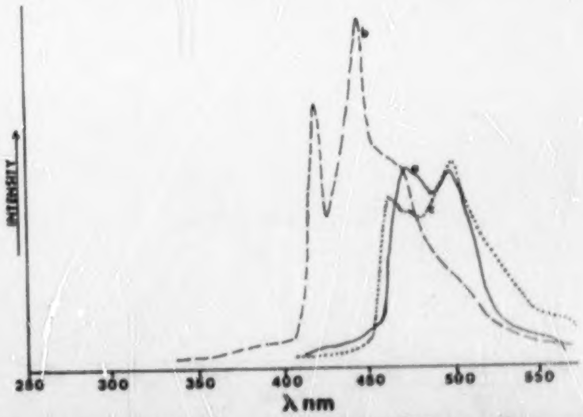

TEXT-FIGURE 3.—Phosphorescence spectra (at 77°K) at various wavelengths (λ) of a 27-yr-old lens (derived from an enucleated eye 12 hr after the patient was given 0.75 mg 8-MOP/kg). a) 8-MOP phosphorescence (——) in lens (equivalent to 10^{-7}-*M* concentration); b) Trp phosphorescence (-----); c) 8-MOP solution in ethylene glycol (•••••).

permanent retention of the photoproduct within the ocular lens. One such photoproduct has recently been demonstrated in lenses derived from rats given 8-MOP (1 mg ip) and exposed to UVA (320–390 nm) radiation (*39*) (text-figs. 4, 5).

The photosensitizing action of the psoralen compounds has been correlated with the generation of cyclobutane photoaddition products with thymine in DNA molecules (*40*). A similar mechanism has been proposed for 8-MOP-photosensitized lens damage (*41*). The effect of such binding would be an enhanced potentiation of the photosensitizing action of the psoralens; i.e., the 4′,5′-cyclobutane photoadduct between 8-MOP and thymine could act as a new photosensitizer (absorbing at 365 nm), resulting in the formation of interchain cross-links in DNA (*42*). 8-MOP may also exert a photodynamic action involving singlet oxygen in the lens and forming photoproducts with aromatic amino acids, particularly Trp residues. Nuclear magnetic resonance analyses of the photoreaction between 8-MOP and Trp demonstrate the loss of hydrogen at the 3,4,4′ and 5′ positions of 8-MOP and at the indole C_2 position of Trp, with concomitant changes in the aliphatic regions of the spectra (*38*). Since the positions involved in this reaction are the same as those reported in cyclobutane photoadduct formation with thymine, the reaction between 8-MOP and Trp could involve a cyclobutane type of photoproduct.

We have also demonstrated that 8-MOP is capable of entering the corneal epithelium, the ciliary processes, the ocular lens, and the retina (of young rat and dogfish eyes) within 2 hours after a single ip dose of 1 mg labeled 8-MOP (*43*). When the animals are maintained in the dark, no 8-MOP can be demonstrated by spectroscopic methods, by autoradiography, or by scintillation counts after 24 hours. However, when the animals are exposed to relatively low levels of 365 nm of UV radiation, a photoreaction (or photoreactions) occurs which results in the binding of 8-MOP within these tissues (text-fig. 6; figs. 2, 3). In the cornea, bound 8-MOP accumulates mainly in the epithelium, but because of its excellent reparative mechanisms, the bound 8-MOP disappears within 3 or 4 days in spite of continuous UV radiation exposure. Therefore, 8-MOP therapy should not prove to be a significant hazard to the cornea. However, since the 8-MOP in the retina is capable of being stimulated by 365 nm of radiation (the lenses in these young animals are not effective filters for this wavelength), 8-MOP photoproducts quickly develop in the inner nuclear layer. It would thus appear that photobound 8-MOP can accumulate in the retina as well as the ocular lens in animals whose lens is not an effective UVA radiation filter. Repeated injections of 8-MOP to such animals could result in an increasing accumulation of photoproducts in these two ocular tissues. Such photoproducts could then act as new photosensitizing agents within these tissues, thereby enhancing photochemical damage caused by UV radiation. The preceding data demonstrate that 8-MOP therapy could pose a potential hazard not only to the ocular lens but also to the retina in young people whose lenses are not effective UV radiation absorbers and/or in aphakic and pseudophakic individuals, particularly if they are exposed to repeated PUVA therapy.

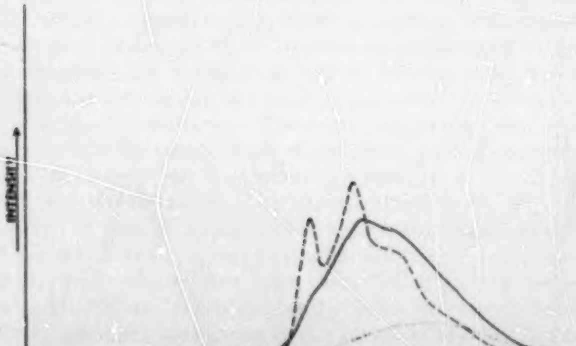

TEXT-FIGURE 4.—Phosphorescence spectra at various wavelengths (λ) of a rat lens treated with 8-MOP and UVA radiation. New phosphorescence (325-nm excitation) is now apparent (——) as well as is a relatively structureless 360-nm excitation phosphorescence (·····) which represents intrinsic chromophore phosphorescence in such lenses. Trp phosphorescence (– – –) is also shown.

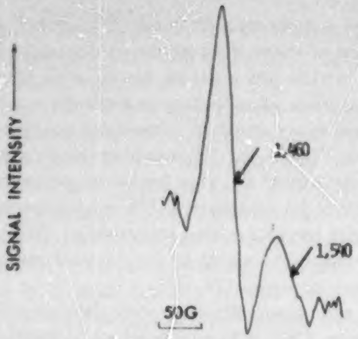

TEXT-FIGURE 5.—ESR spectra of same lens as shown in text-fig. 4. Aside from the Trp triplet [at 1,460 gauss (G)], a new triplet at 1,540 G is now present (υ = 9.10 GHz). These two triplets correspond to the triplets noted by phosphorescence spectroscopy for Trp (290-nm excitation) and the new 325-nm excited photoproduct as shown in text-fig. 4. Their respective lifetimes are 6.8 sec (Trp) and 2.4 sec for the photoproduct.

Because laboratory studies have demonstrated enhanced fluorescence in the ocular lens to be associated with aging and PUVA therapy and because presumptive PUVA cataracts have recently been reported (*44*), we have developed a method to monitor lens fluorescence in vivo (*45*). A new slit-lamp densitographic apparatus constructed on the Scheimpflug principle, capable of accurately and reproducibly recording visible changes in lens density as the lens ages, was recently introduced (*46–48*). We have modified this apparatus to utilize UV radiation at wavelengths of 300–400 nm, to excite the UV radiation-absorbing chromophores in the lens, and to reproducibly photograph the ensuing fluorescence. Because the regions of lens fluorescence (440 and 520 nm) require wavelengths of 340–360 nm and 400–420 nm, respectively, for excitation, we can utilize UV radiation to measure and quantitate the age-related fluorescence levels in the normal lens in vivo and correlate them with our in vitro data reported in previous communications (*13–15*) (text-fig. 7). We can also detect abnormal fluores-

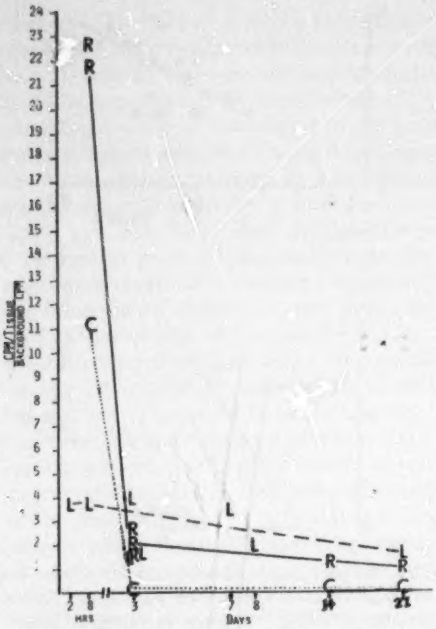

TEXT-FIGURE 6.—Total radioactivity expressed as a ratio of cpm per tissue divided by background cpm in retina (R) (——), cornea (C) (·····), and lens (L) (-----) derived from rat and dogfish eyes following one injection of ^{3}H- or ^{13}C-labeled 8-MOP and exposed to UVA radiation for varying times. This ratio was used because the experiments were performed in two different scintillation counters (Marine Biological Laboratory and Emory University).

cence levels or emission wavelengths in patients exposed to levels of UV radiation that exceed ambient levels and/or to photosensitizing agents.

UV SLIT-LAMP DENSITOGRAPHY

We have modified a Topcon (Topcon USA) visible radiation slit-lamp densitography apparatus to obtain in vivo lens fluorescence data. Specially coated quartz filters (which transmit only UV radiation ~290–410 nm) are placed in front of the 200-W xenon lamp light source. Since the regions of lens fluorescence that we are currently evaluating require wavelengths of 340–360 and 400–420 nm for excitation, these filters permit us to utilize UV and short-wavelength visible radiation to measure and quantitate the age-related fluorescence levels in the normal lens in vivo and to correlate these data with the in vitro data previously reported. We have refined our present in vivo studies by adding new filters so that we can obtain fluorescence measurements in vivo at 20-nm bandwidths (e.g., 340–360, etc.). The 200-W xenon light source in the camera has sufficient spectral output in the 320- to 420-nm region so that we are able to utilize these filters and obtain levels of irradiance at the lens (in vivo) sufficient to excite its chromophores and obtain reproducible fluorescence data which can be analyzed by microdensitography. We used the conventional slit lamp to examine all patients with mydriasis (7- to 8-mm pupillary diameter) and then photographed them with our apparatus first with visible radiation and then with UV radiation. The camera position for all photographs is at 0° and 180°. The resulting negative strips are analyzed by microdensitography, and the data are plotted as densitograms. Three specific regions can be selected from the UV radiation densitograms, and two of these have been correlated with the 440- and 520-nm emission peaks obtained from our in vitro studies with fluorescence spectroscopy on whole normal lenses. We are thus able to obtain fluorescence emission data which can be attributed to and quantified for

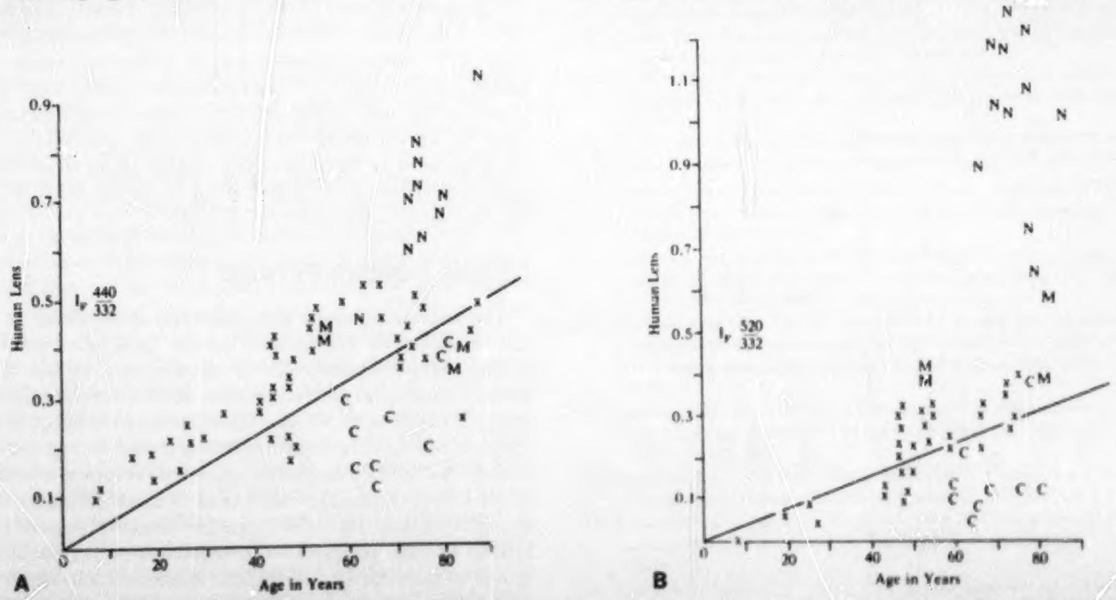

TEXT-FIGURE 7.—Increase in A) 440-nm and B) 520-nm fluorescence emission levels in the normal aging human lens (x) expressed as I_F 440/332 and I_F 520/332, respectively. Each ratio represents the measured fluorescence intensity divided by the intrinsic Trp fluorescence emission at 332 nm in the lens. Similar measurements show marked elevations of the 440- and 520-nm fluorescence levels in nuclear cataracts (N), slight elevations in mixed nuclear plus cortical cataracts (M), and below normal levels in anterior cortical cataracts (C).

specific emission peaks so that in vivo data can be compared with in vitro whole-lens fluorescence spectroscopy.

Representative in vivo UV and visible radiation slit-lamp photographs obtained from normal individuals at 26, 37, 44, and 71 years of age and corresponding densitograms from these photographs are shown in figure 4 and text-figure 8. Detailed analyses of such densitograms on a series of normal eyes ranging in age from 17 to 85 years demonstrate an age-related increase in three peaks. Two of these peaks were determined to correspond to the 440- and 520-nm fluorescence peaks derived from our in vitro whole-lens fluorescence spectroscopy data, and a close correlation can be observed (text-figs. 7, 9). We are currently attempting to define and correlate the third in vivo densitography region with more detailed analyses of the simulated in vivo UV radiation densitograms (on whole donor eyes) and subsequent fluorescence spectroscopy on the cornea and lens. Aside from the age-related increase in lens fluorescence determined by these in vivo studies, we have also noted a posterior shift of the fluorescent peaks with increasing age. Our data also demonstrate a small but significant increase in corneal fluorescence with age, which correlates with our previous in vitro observations (*2*, *20*). Thus UV radiation slit-lamp densitography should provide an objective and reproducible method for monitoring at least one parameter of lens aging.

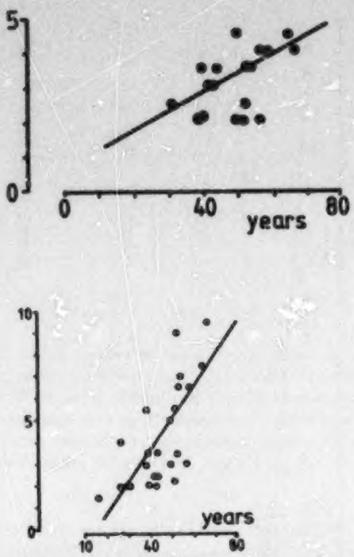

TEXT-FIGURE 9.—Increase in the two densitographic regions ● and ○ that correspond, respectively, to 440-nm (text-fig. 7A) and 520-nm (text-fig. 7B) fluorescence emission levels obtained in vitro. *Ordinate values* are arbitrary units.

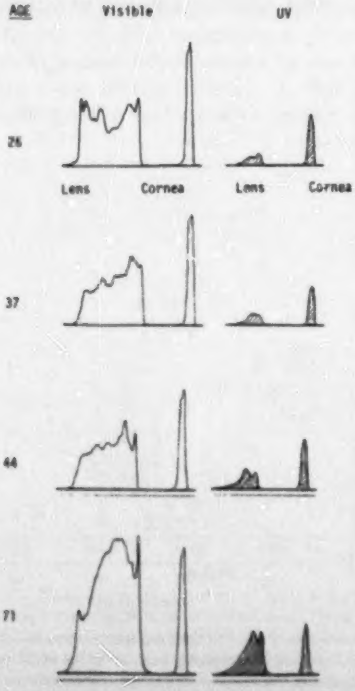

TEXT-FIGURE 8.—Densitograms corresponding to eyes shown in fig. 3.

Preliminary studies of patients accidently exposed to levels of UV radiation that exceed ambient levels and/or to photosensitizing agents such as the psoralens demonstate an enhancement of lenticular fluorescence (figs. 5, 6). This demonstration could provide us with a useful diagnostic and prognostic tool in such patients as well as provide a relatively simple screening procedure. Inasmuch as enhanced lens fluorescence appears to occur months to years before lens opacities become manifest by conventional slit-lamp examination, measures could be instituted which at least retard or prevent UV radiation-induced (direct or photosensitized) lens opacities. One simple approach (which we are now utilizing for patients on PUVA therapy) consists of advising those individuals who have abnormal fluorescence levels to wear UV radiation-absorbing or reflecting lenses. These lenses permit over 90% transmission of visible light and can therefore be worn with comfort indoors as well as outdoors. This is of particular importance for patients receiving PUVA therapy because even indoor fluorescent lighting contains sufficient UV radiation to cause 8-MOP photobinding within the lens (*20*, *32*, *34*).

FUTURE CONSIDERATIONS

The increasing use of phototherapy in medicine as well as the fact that we are located in the "sun belt" provides us with a unique opportunity to develop a program whereby we will be able to screen patients and determine which ones are risk candidates for the development of direct and photosensitized UV radiation photodamage to certain ocular tissues. Aside from detecting abnormal levels or wavelengths of lens fluorescence in the living eye, we can also test our hypothesis that the UV radiation-filtering capacity of the lens in certain patients with degenerative retinal disease is less than normal; i.e., the ocular lens in such individuals has not developed enough photochemically induced chromophores for it to absorb all the UV radiation. By the time 90% of the population reaches its fourth to fifth decade, the lens has become a very effective filter for UV and shortwave visible radiation (320–450 nm), thereby protecting the aging (and metabolically less efficient) retina from potential damage. These wavelengths can cause retinal photodamage as demonstrated by experiments in primate eyes (*28*), and we can now determine whether this occurs in the human. We have begun a program whereby we are examining all patients with retinal disease (referred by our retina service). These patients are evaluated by UV radiation slit-lamp densitography and also have their retinas independently evaluated by fundus photography and fluorescein angiography. Preliminary results demonstrate a significantly lower level of lens fluorescence in patients with degenerative retinal disease (compared with corresponding values for their age group), indicating that their lenses are less effective in filtering out the 320- to 450-nm wavelengths of radiation. A larger clinical study is required to prove that the inability to completely remove these wavelengths may play a significant role in the development and/or acceleration of certain forms of degenerative retinal disease in the older population. In view of the increasing use of plastic intraocular lenses, which transmit much more UV radiation than do glass lenses (i.e., they effectively transmit wavelengths shorter than 320 nm), questions have been raised regarding potential UV and shortwave visible (320–450 nm) radiation damage to such patients. For example, Dr. J. Tennant (personal communications) has indicated that protecting such patients with UV radiation-absorbing glasses significantly reduces the incidence of postoperative cystoid macular edema. Thus the demonstration that UV radiation can play a role in the pathogenesis of retinal degeneration in certain "phakic" individuals would indirectly corroborate the possible relationship between retinal disease and 320- to 450-nm radiation in phakic as well as aphakic individuals. We believe that our clinical UV radiation slit-lamp densitography study can provide hard data to answer this question.

In view of the confusion and controversial claims regarding the efficacy of commercially available sunglasses in protecting the eye from UV radiation photodamage, we have recently analyzed a large series of such lenses to determine their transmission characteristics. Their ability to transmit UV and visible radiation (280–750 nm) was measured in a recording spectrophotometer. Photon flux measurements were also performed (with a Hewlett-Packard calibrated flux meter) with the lenses exposed to a 200-W mercury light source filtered to transmit only 280- to 390-nm radiation. These studies (*49*) demonstrated a wide variation in the UV radiation transmission characteristics of the sunglasses evaluated, ranging from 1.5 to 40% with similar transmission values noted when the sunglasses were tested for more discrete wavelengths, i.e., 340–380 nm. Only the Spectra-Shield and UV 400 lenses were more than 99% effective in filtering the UV radiation. It should also be noted that visible radiation is significantly decreased in certain darkly tinted sunglasses, whereas these sunglasses still transmit some long-wavelength UV radiation. In patients with blue, gray, or hazel eyes who wear such sunglasses, a 50% or more decrease in visible radiation can result in pupillary enlargement of 0.25–0.5 mm, thereby increasing the UV radiation incident on the intraocular tissues.

REFERENCES

(*1*) Kurzel RB, Wolbarsht ML, Yamanashi BS. UV radiation effects on the human eye. In: Smith KC, ed. Photochemistry and photobiology review. Vol 2. New York: Pergamon Press, 1977:133–167.

(*2*) Lerman S. Susceptibility of ocular tissues to radiant energy, chapt 2; biologic and chemical effects of ultraviolet radiation, chapt 3. In: Radiant energy and the eye. New York: Macmillan, 1980:29–186.

(*3*) Lerman S, Tann TT, Louis D, Hollander M. Anomalous absorptivity of lens proteins due to a fluorogen. Ophthalmic Res 1970; 1:338–343.

(*4*) Zigman S. Eye lens color: Formation and function. Science 1971; 171:807–809.

(*5*) Lerman S. Lens proteins and fluorescence. Isr J Med Sci 1972; 8:1583–1589.

(*6*) Pirie A. Effect of sunlight on proteins of the lens. In: Bellows J, ed. Contemporary ophthalmology. Baltimore: Williams & Wilkins, 1972:484–501.

(*7*) Satoh K, Bando M, Nakajima A. Fluorescence in human lens. Exp Eye Res 1973; 16:167–172.

(*8*) Augusteyn RC. Human lens albuminoid. Jpn J Ophthalmol 1974; 18:127–134.

(*9*) Dilley KJ, Pirie A. Changes to the proteins of the human lens nucleus in cataract. Exp Eye Res 1974; 19:59–72.

(*10*) Augusteyn RC. Distribution of fluorescence in the human cataractous lens. Ophthalmic Res 1975; 7:217–224.

(*11*) Spector A, Roy O, Stauffer J. Isolation and characterization of an age-dependent polypeptide from human lens with non-tryptophan fluorescence. Exp Eye Res 1975; 21:9–24.

(*12*) Bando M, Nakajima A, Satoh K. Coloration of human lens protein. Exp Eye Res 1975; 20:489–492.

(*13*) Lerman S. Lens fluorescence in aging and cataract formation. Doc Ophthalmol Proc Series 1976; 8:241–260.

(*14*) Lerman S, Borkman RF. Spectroscopic evaluation and classification of the normal, aging and cataractous lens. Ophthalmic Res 1976; 8:335–353.

(*15*) ——— Photochemistry and lens aging. In: von Hahn HP, ed. Interdisciplinary topics in gerontology: Gerontological aspects of eye research. Vol 13. Basel: Karger, 1978:154–182.

(*16*) Lerman S, Kuck JF, Borkman R, Saker E. Induction, acceleration and prevention (in vitro) of an aging parameter in the ocular lens. Ophthalmic Res 1976; 8:213–226.

(*17*) Zigman S, Datiler M, Torozynshi E. Sunlight and human cataract. Invest Ophthalmol Vis Sci 1979; 18:462–467.

(*18*) Castineiras SG, Dillon J, Spector A. Effects of reduction on absorption and fluorescence of human lens proteins. Exp Eye Res 1979; 29:573–575.

(*19*) Yu NT, Kuck JF, Askren CC. Red fluorescence in older and brunescent human lenses. Invest Ophthalmol Vis Sci 1979; 18:1278–1280.

(*20*) Lerman S. Lens transparency and aging. In: Regnault F, Hockwin O, Courtour Y, eds. Aging of the lens. Amsterdam: Elsevier/North-Holland, 1980:263–279.

(*21*) Garner MH, Spector A. Selective oxidation of cysteine and methionine in normal and senile cataractous lenses. Proc Natl Acad Sci USA 1980; 77:1274–1277.

(*22*) Lerman S, Yamanashi B, Palmer RA, Roark JC, Borkman RF. Photoacoustic, fluorescence and light transmission spectra of normal aging and cataractous lenses. Ophthalmic Res 1978; 10:168–176.

(*23*) Borkman RF, Dalrymple A, Lerman S. Ultraviolet action spectrum for fluorogen production in the ocular lens. Photochem Photobiol 1977; 26:129–132.

(*24*) Borkman RF. Ultraviolet action spectrum for tryptophan destruction in aqueous solution. Photochem Photobiol 1977; 26:163–166.

(*25*) Borkman RF, Lerman S. Evidence for a free radical mechanism in aging and UV irradiated ocular lenses. Exp Eye Res 1977; 26:303–309.

(*26*) Lerman S, Megaw J, Willis I. The photoreaction of 8-MOP with tryptophan and lens proteins. Photochem Photobiol 1980; 31:235–242.

(*27*) Goosey JD, Zigler JS Jr, Kinoshita JH. Cross-linking of lens crystallins in a photodynamic system: A process mediated by singlet oxygen. Science 1980; 208:1278–1280.

(28) Ham WT, Muller HA, Buffalo JJ. Retinal effects of blue light exposure. Ocular effects of ion-ionizing radiation. Society for Photo-Optical Instrumentation Engineering, 1980; 229:46–50.

(29) Zigman S, Vaughn T. Near UV light effects on the lenses and retinas of mice. Invest Ophthalmol Vis Sci 1974; 13:462–465.

(30) Pitts DG, Hacker PD, Parr WH. Ocular ultraviolet effects from 295 nm to 400 nm in the rabbit eye. Washington, D.C.: U.S. Govt Print Off, 1977 [DHEW publication No. (NIOSH)77–175].

(31) Lerman S. Human UV radiation cataracts. Ophthalmic Res 1980; 12:303–314.

(32) Lerman S, Gardner K, Megaw J, Borkman RF. The prevention of direct and photosensitized UV radiation damage to the ocular lens. Ophthalmic Res, 1981; 13:284–292.

(33) Thomas DM, Schepler KL. Raman spectra of normal and ultraviolet-induced cataractous rabbit lens. Invest Ophthalmol Vis Sci 1980; 19:904–912.

(34) Lerman S, Megaw J, Willis I. Potential ocular complications of PUVA therapy and their prevention. J Invest Dermatol 1980; 74:197–199.

(35) Lerman S, Borkman RF. A method for detecting 8-methoxypsoralen in the ocular lens. Science 1977; 197:1287–1288.

(36) Lerman S, Jocoy M, Borkman RF. Photosensitization of the lens by 8-methoxypsoralen. Invest Ophthalmol Vis Sci 1977; 16:1065–1068.

(37) Lerman S, Megaw J, Takei Y. The photosensitizing action of psoralens in dogfish ocular tissues. Biol Bull 1979; 157:379.

(38) Megaw J, Lee J, Lerman S. NMR analyses of tryptophan-8-methoxypsoralen photoreaction products. Photochem Photobiol 1980; 32:265–269.

(39) Koch HR, Beitzen R, Dremer F, Lerman S. Effect of 8-methoxypsoralen and long UV on the rat lens. Invest Ophthalmol Vis Sci 1979; suppl 18:218.

(40) Song PS, Tapley KJ Jr. Photochemistry and photobiology of psoralens. Photochem Photobiol 1979; 29:1177–1197.

(41) Jose JG, Yielding KL. Photosensitive cataractogens, chlorpromazine and methoxypsoralen, cause DNA repair synthesis in lens epithelial cells. Invest Ophthalmol Vis Sci 1978; 17:687–691.

(42) Dall'Acqua S, Marciani M, Zamobon F, Rodighiero G. Kinetic analysis of the reaction (365 nm) between psoralen and DNA. Photochem Photobiol 1979; 24:489.

(43) Lerman S, Megaw J, Gardner K, Takei Y, Willis I. Localization of 8-methoxypsoralen in ocular tissues. Ophthalmic Res 1981; 13:106–116.

(44) Crylin MN, Pedvis-Leftick A, Sugar J. Cataract formation in association with ultraviolet photosensitivity. Ann Ophthalmol 1980; 12:786.

(45) Lerman S, Hockwin O, Dragomirescu V. In vivo lens fluorescence photography. Ophthalmic Res 1981; 13:224–228.

(46) Dragomirescu V, Hockwin O, Koch HR. Photo-cell device for slit-beam adjustment to the optical axis of the eye in Scheimpflug photography. Ophthalmic Res 1980; 12:78–86.

(47) Dragomirescu V, Hockwin O, Koch HR, Sasaki K. Development of a new equipment for rotating slit image photography according to Scheimpflug's principle. In: von Hahn HP, ed. Interdisciplinary topics in gerontology: Gerontological aspects of eye research. Vol 13. Basel: Karger, 1978: 118–130.

(48) Hockwin O, Sasaki K, Dragomirescu V. Lens transparency. In: Srivastava S, ed. Red blood cells and lens metabolism. Amsterdam: Elsevier/North-Holland, 1980; 9:435–441.

(49) Lerman S. The role of commercial sunglasses in protecting the eye from UV radiation damage. Proceedings of the ninth annual meeting of the American Society for Photobiology, Williamsburg, Va., June 14–19, 1981. New York: Pergamon Press, 1981:180.

DISCUSSION

D. Valenzeno: Given the fact that light above 400 nm can get through to the retina, what do we know about retinal sensitization by sensitizers that absorb in the visible range?

S. Lerman: Do you mean the porphyrins?

Valenzeno: Yes.

Lerman: I do not know of any reported problems. Actually, as I have noted, most of our lenses act as very good short-wavelength visible filters, as well as UV radiation filters; and we really do not need any of that radiation below 500 nm for central visual activity. Thus a good deal of that radiation is filtered out as well, protecting the retina from the photosensitizers, which are activated at or below those wavelengths.

T. Nigra: I would like to ask about the posterior subcapsular cataract that is induced by steroids versus the cataract you showed in that patient who you said had a PUVA-induced cataract, and did that patient by any chance have steroids?

Lerman: No, he did not, and actually that was not a posterior subcapsular cataract. As I tried to point out, to look at a lens and say what caused the cataract is, in my opinion, rather questionable because a lot of lens changes can look alike and be caused by a variety of different insults (drugs, radiation, endocrine, and metabolic problems). However, if a person is on long-term steroids and has posterior subcapsular changes which have a certain pattern, it is at present acceptable to classify the cataract as a steroid cataract, assuming you have ruled out other cataractogenic factors.

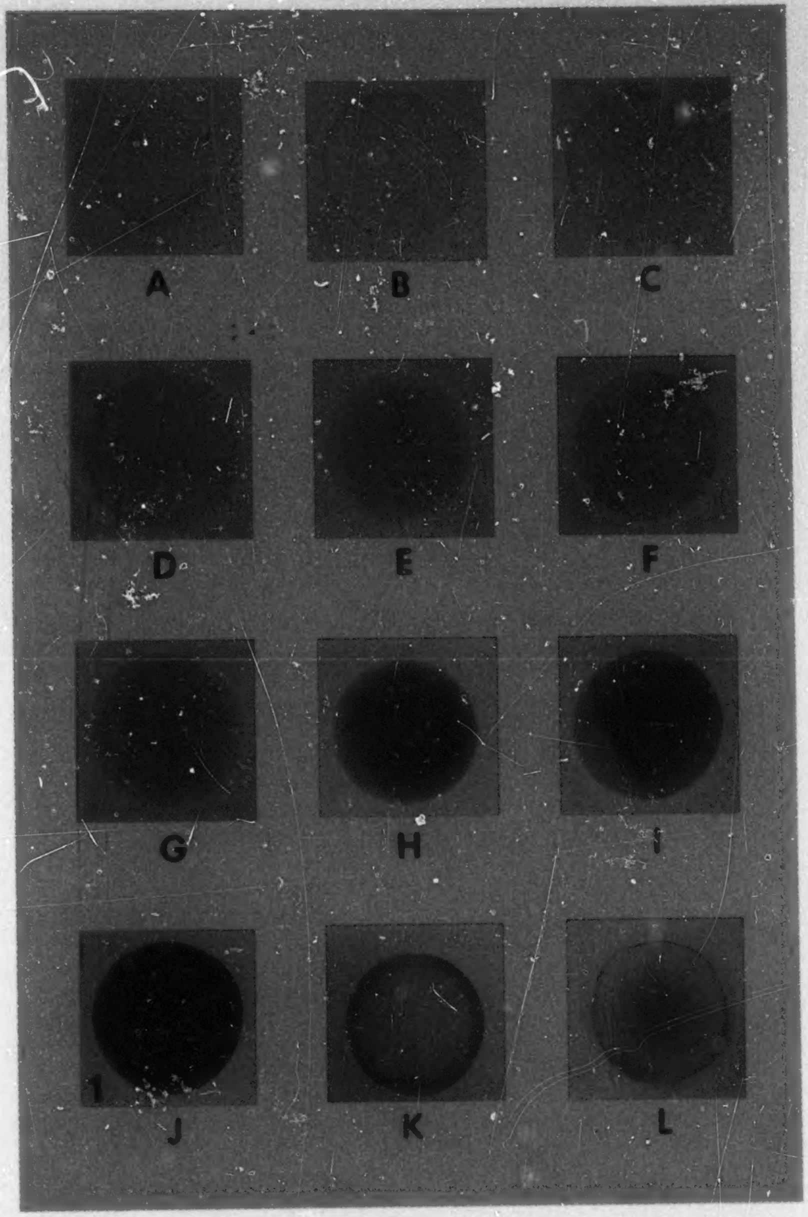

FIGURE 1.—Increasingly yellow to yellow-brown in the normal aging human lens nucleus. A) 6 mo, B) 8 yr, C) 12 yr, D) 25 yr, E) 47 yr, F) 60 yr, G) 70 yr, H) 82 yr, I) 91 yr, J) nuclear cataract (70 yr), K) cortical cataract (68 yr), and L) mixed nuclear and cortical cataract (74 yr).

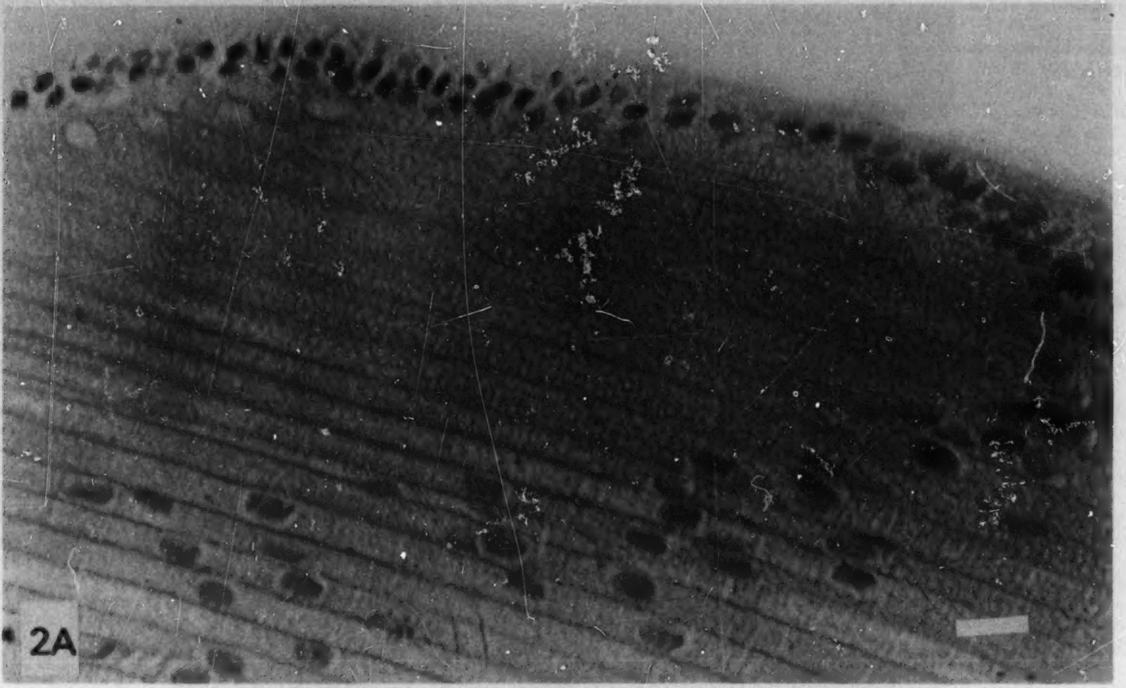

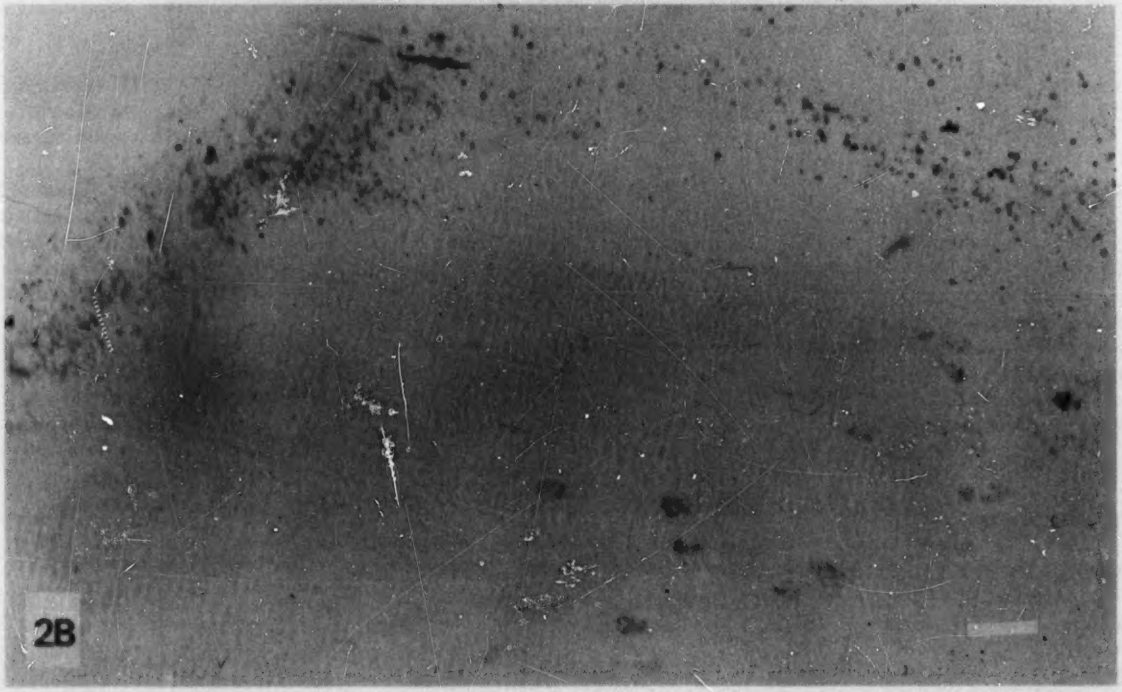

FIGURE 2A.—Hematoxylin-and-eosin-stained section of 8-MOP-treated rat lens (after 3 wk UVA radiation exposure) showing germinative zone. *Bar*=10 µm. × 750

FIGURE 2B.—Autoradiograph of corresponding region showing significant number of grains in epithelium and cortical fibers. *Bar*=10 µm. × 750

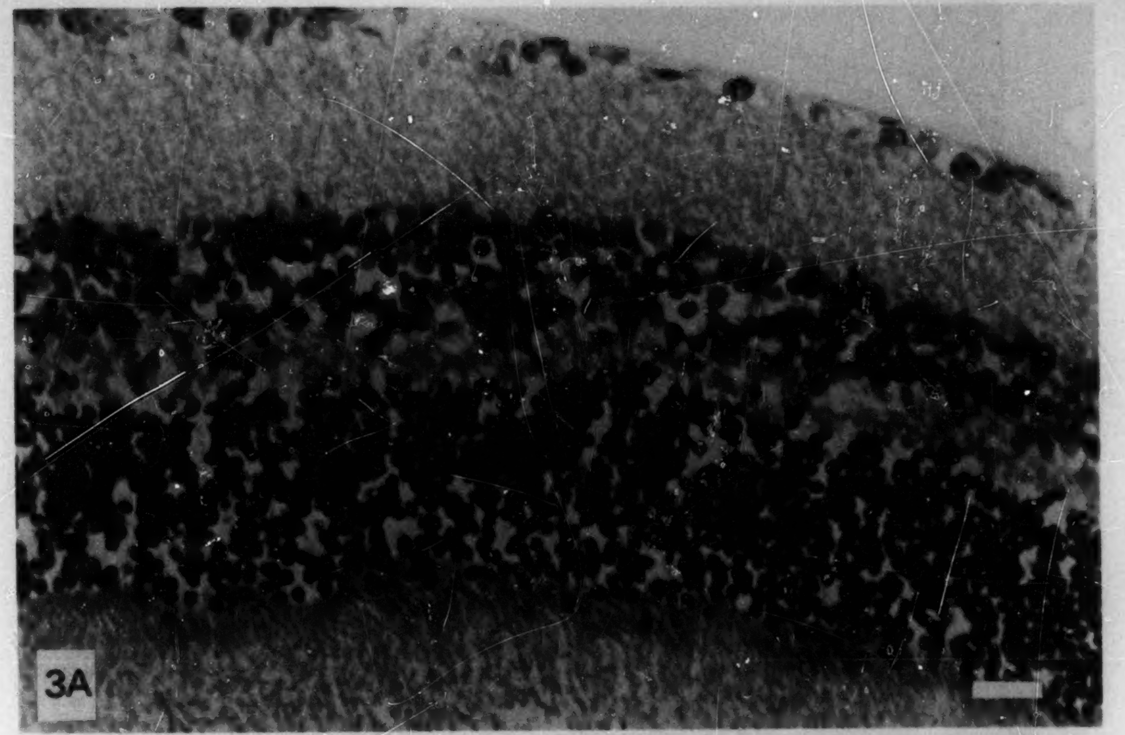

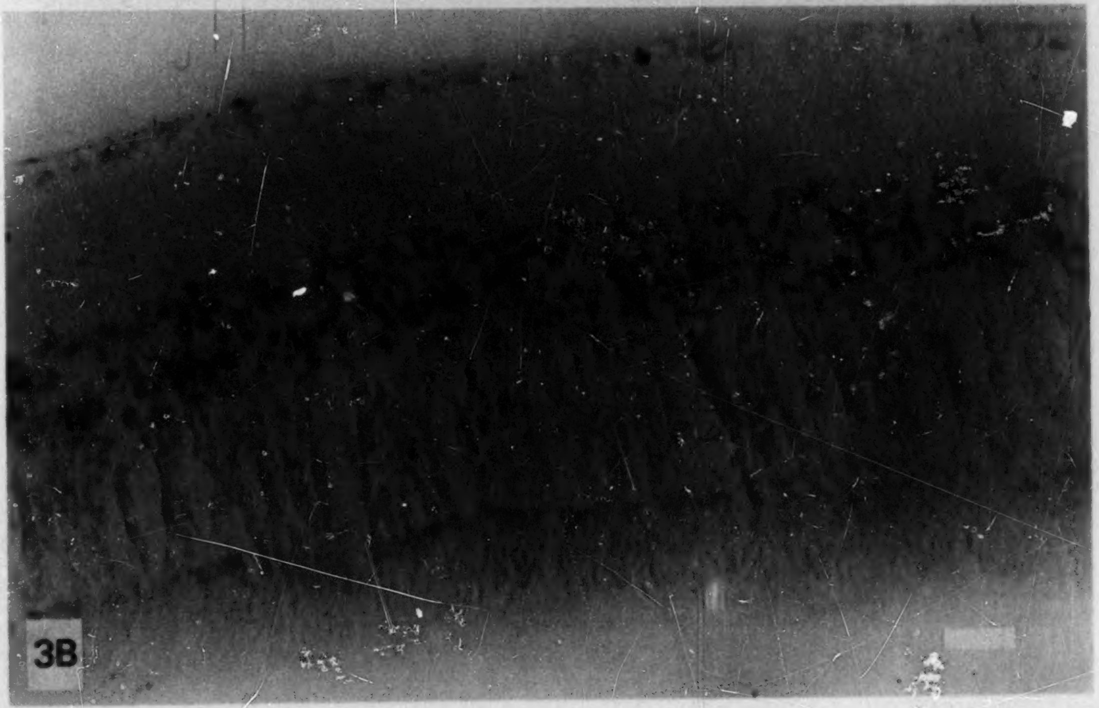

FIGURE 3A.—Hematoxylin-and-eosin-stained section of 8-MOP-treated rat retina (after 3 wk UVA radiation exposure). *Bar*=10 μm. × 750

FIGURE 3B.—Autoradiograph of corresponding region showing significant number of grains in nuclear layer. *Bar*=10 μm. × 750

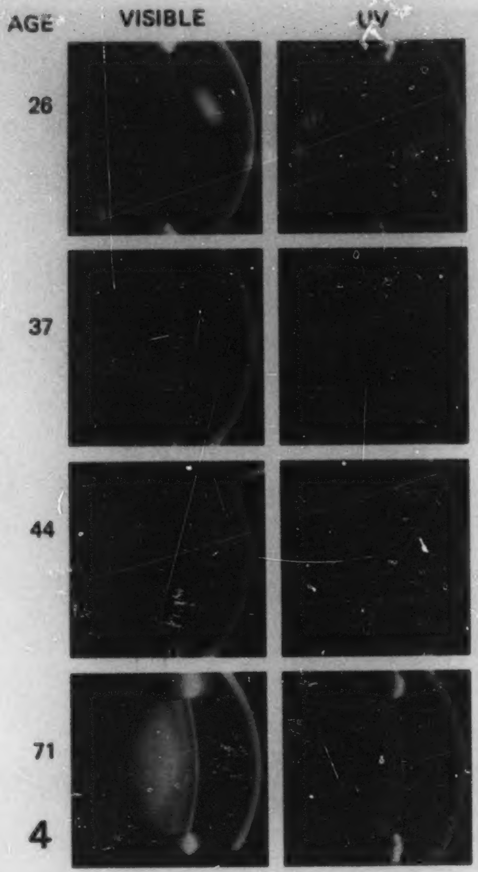
AGE
VISIBLE
UV
26
37
44
71
4

FIGURE 4.—Representative visible and UV radiation slit-lamp photographs of normal eyes at 26, 37, 44, and 71 yr of age (*left*) and corresponding densitograms (*right*).

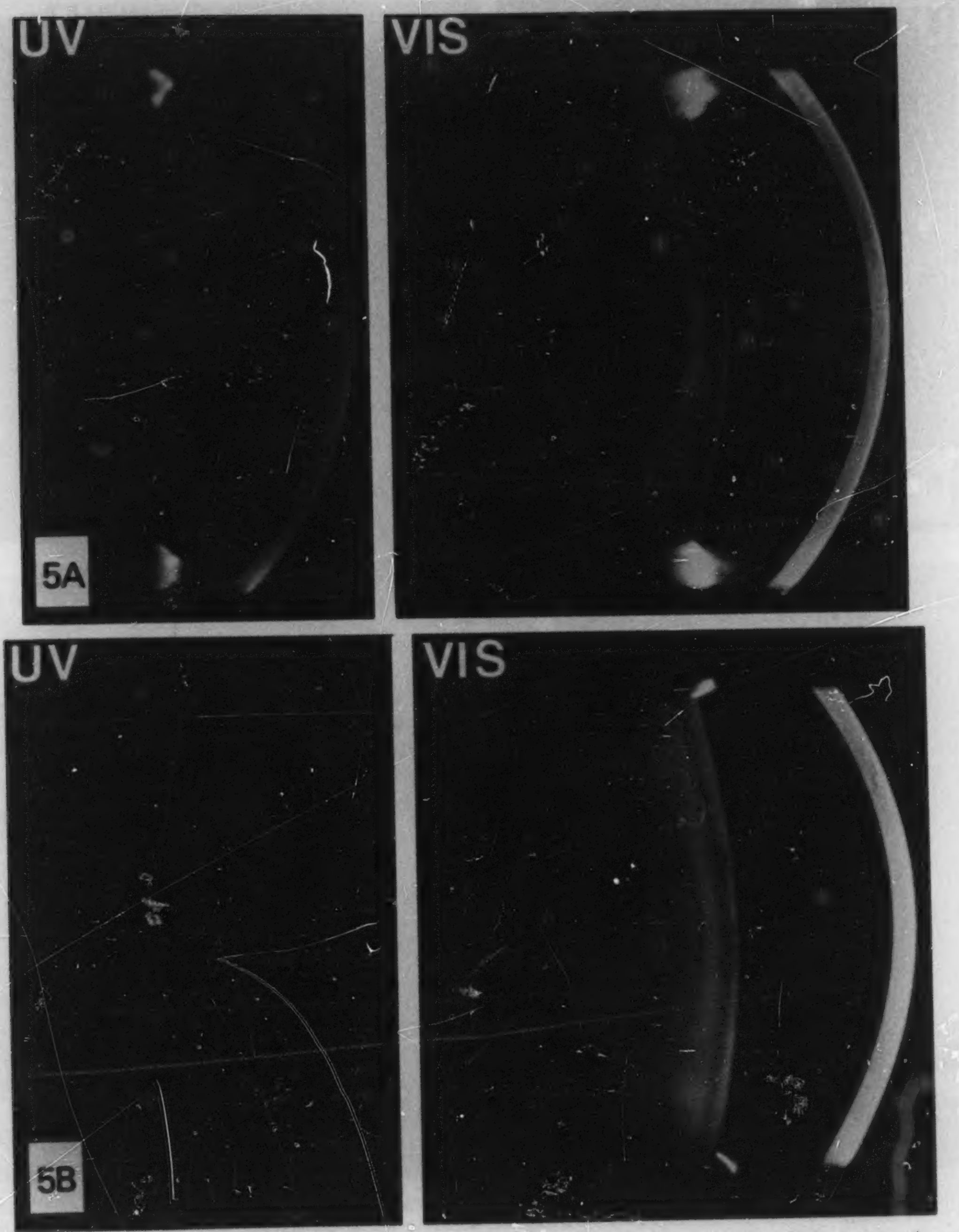

FIGURE 5.—UV and visible (VIS) radiation slit-lamp photographs of 40-yr-old patient with history of excessive UV radiation exposure (occupational). *Note* marked enhancement of lenticular fluorescence (A) compared with normal fluorescence level in a 41-yr-old individual (B). The fluorescence levels in fig. 5A are comparable to the values seen in lenses from the seventh decade as shown in photographs of the right (fig. 5C) and left (fig. 5D) eyes of a 76-yr-old normal patient.

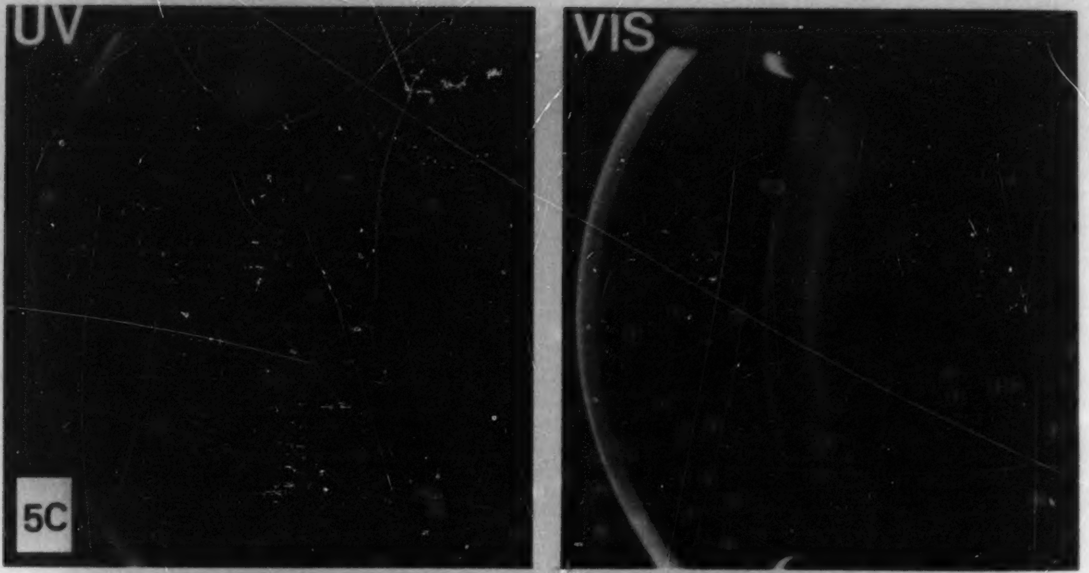

5C

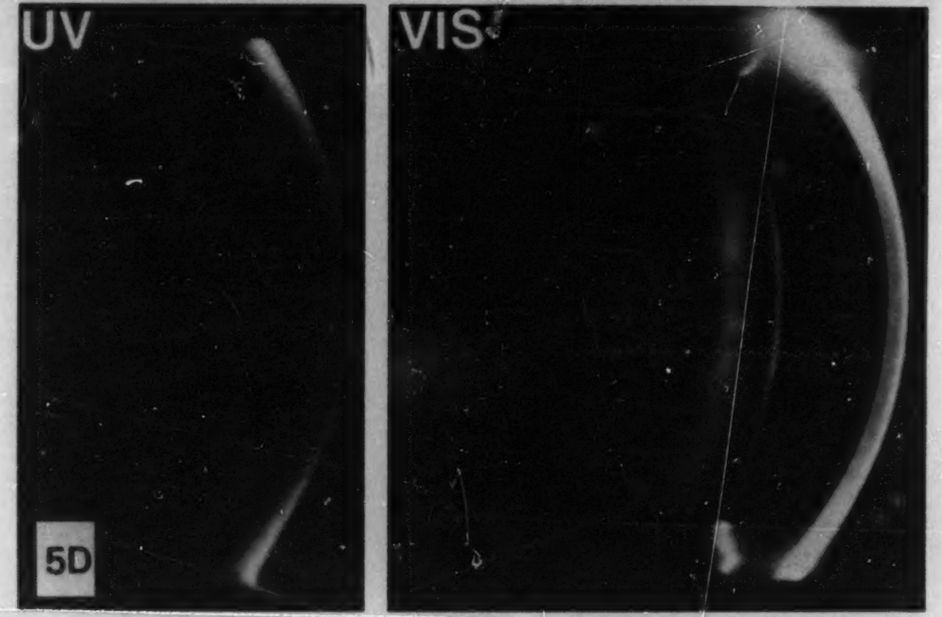

5D

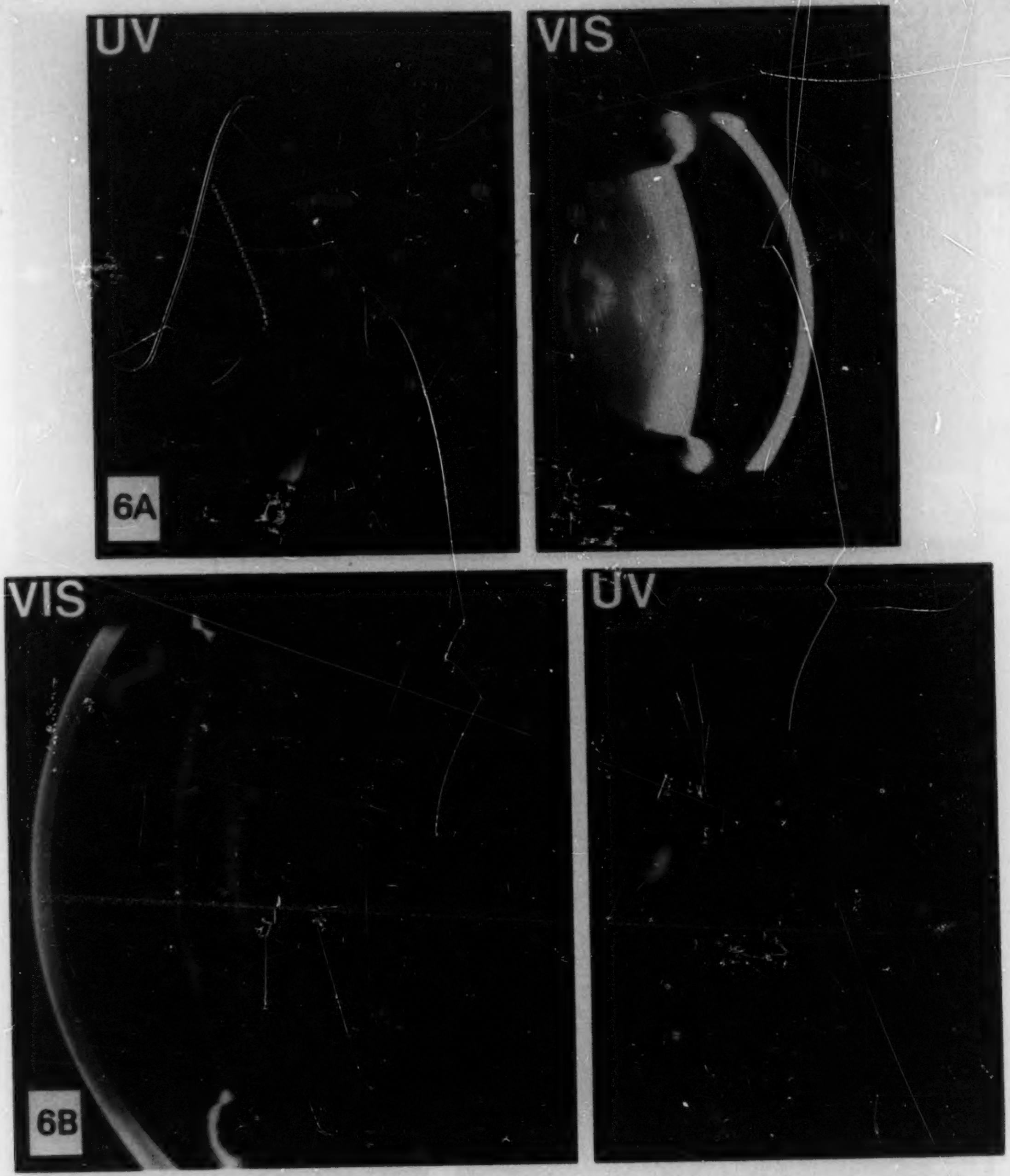

FIGURES 6A, 6B.—UV and visible (VIS) radiation slit-lamp photographs of 59-yr-old patient on PUVA therapy for 4 yr (not protected by special lenses during the first 2 yr of therapy). *Note* abnormal fluorescence (A) compared with fluorescence in a 58-yr-old normal individual (B).

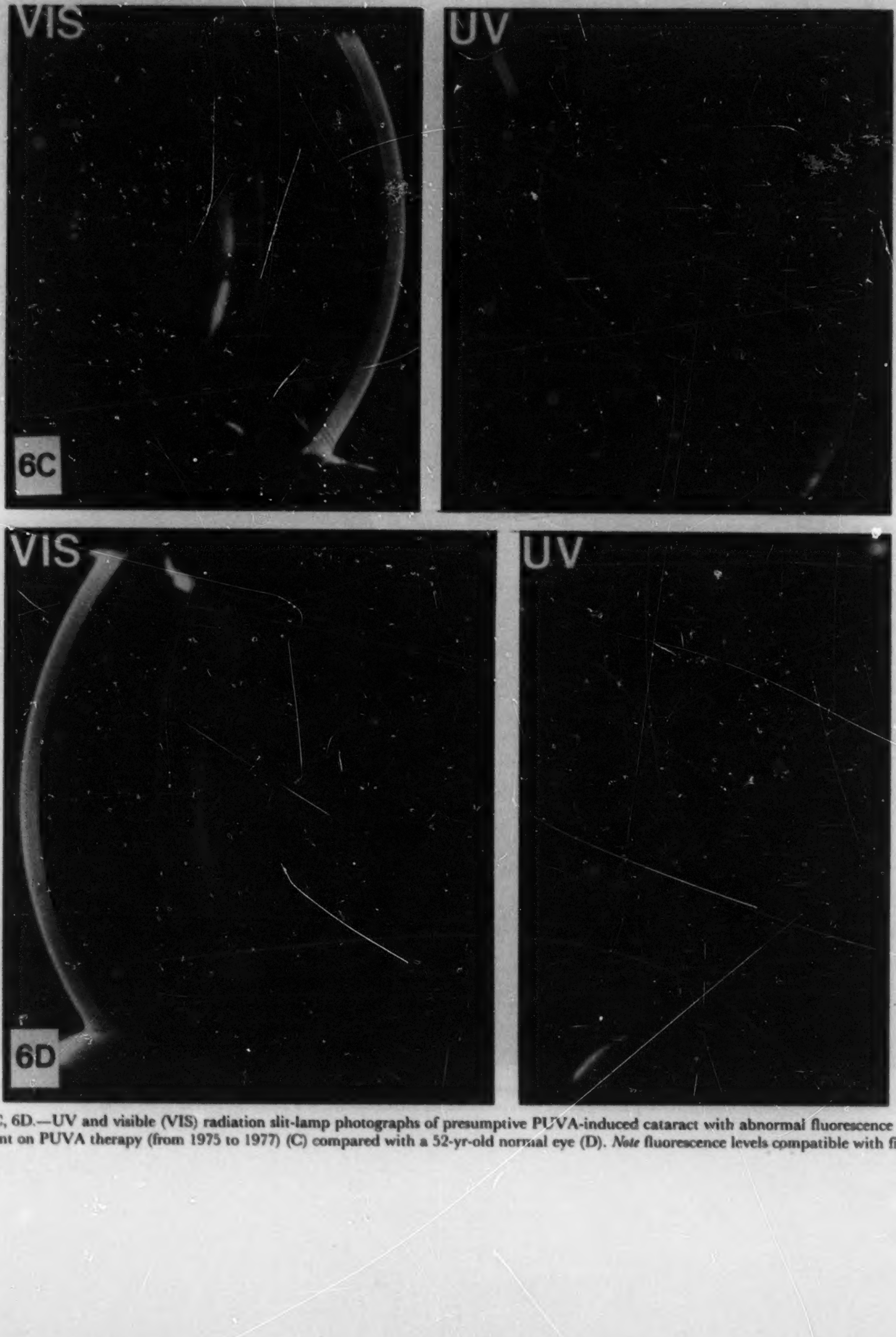

FIGURES 6C, 6D.—UV and visible (VIS) radiation slit-lamp photographs of presumptive PUVA-induced cataract with abnormal fluorescence in a 52-yr-old patient on PUVA therapy (from 1975 to 1977) (C) compared with a 52-yr-old normal eye (D). *Note* fluorescence levels compatible with fifth decade values.

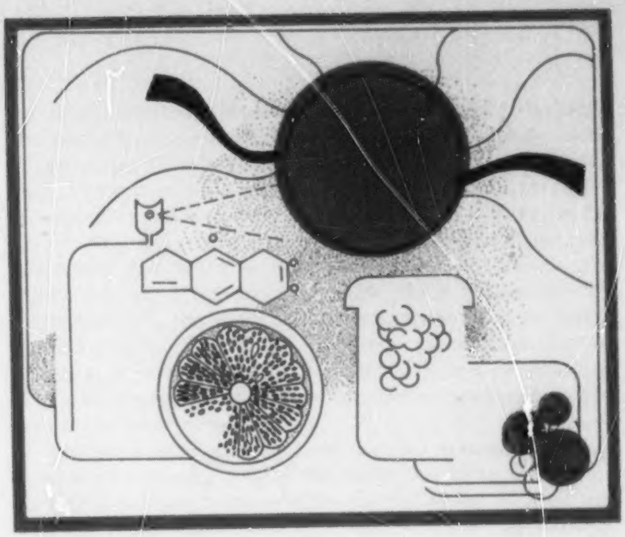

SUMMARY AND CONCLUSIONS

Speaker: Constantine Zervos
Food and Drug Administration

blank page

Concluding Remarks[1]

Constantine Zervos[2]

We have come to the end of this symposium on photochemical toxicity, and I would like to take a few minutes to thank a lot of people and to briefly summarize our accomplishments over the last 2 days.

Let me begin by thanking the speakers who provided us with excellent presentations describing the frontiers of the field of photochemical toxicity. I also thank the symposium participants, the audience, who have also been excellent. Mrs. Janet Cunningham deserves a special thanks for her handling of the administrative aspects of this symposium and so do Dr. F. Alan Andersen and Dr. Andrija Kornhauser for their handling of the scientific aspects. Last but not least I thank the people at the Uniformed Services University of the Health Sciences for providing us with the excellent facilities to hold our program.

Let me now proceed with a short summary of the symposium. To begin, let me tell you how this symposium was born. Sometime last year, Dr. Andersen approached me and my colleagues at the FDA Office of Health Affairs (Science) and expressed concern about the fact that light is an important but often neglected variable in carcinogenesis bioassay experiments.

At the same time, my colleagues and I in the Office of Health Affairs (Science) were hearing that in cancer bioassays the position of the animal cage relative to the sources of illumination was an important determinant of the outcome of the study. Dr. Andersen and we at the FDA Office of Health Affairs (Science) agreed that agency scientists should be made aware of the effects of light on the outcome of carcinogenesis bioassays. Subsequently, Dr. Kornhauser visited my office with a request for help to fund a research proposal to study the toxic interactions of light and chemicals. Having no money to offer in support of Dr. Kornhauser's research, I offered instead to support this symposium, and Dr. Andersen and Dr. Kornhauser were enthusiastic at the opportunity. Thus the dedicated efforts of Dr. Andersen and Dr. Kornhauser converted an idea to reality.

Now, what did we learn yesterday and today? First, we learned that in experiments with whole animal systems and with systems of lower levels of aggregation, e.g., cells and macromolecules, we usually think we are dealing with the classic two-body system. Since yesterday, we have come to know better; we have come to know that we deal with a three-body system. But classical physics and quantum mechanics say that three-body systems present much more complex problems compared to the problems presented by the two-body system. The three-body system provides for greater variability in the experimental results that one can obtain and for a greater number of parameters that one needs to control.

The three-body system of concern here consists of the part of a living organism or the living organism itself, the chemical, and light. Further, we usually look at light as a single agent, which is not providing for the greater complexity of light. Light is many agents, as many agents as the distinct bands of wavelength that one wishes to consider. Also there are many living organisms and many distinct subdivisions of organisms as well. Finally, there are many, many chemicals. These chemicals may be drugs, industrial chemicals, natural chemicals, and chemicals produced by living organisms; they may be endogenous or exogenous to people. Yesterday and today we have heard that the effects produced by the interactions of these three bodies can be beneficial and, therefore, the system can be used for beneficial purposes. The effects of these interactions can be synergistic; they can be immediate; they can be delayed; they can be degenerative. They have many properties, some useful and some dreadful.

Yesterday and today we have learned that we can study interactions among two of the three bodies in the system and that we can then consider the influence of the third body as a perturbation of this, the two-body, interaction. We have heard of studies done at the molecular level, the subcellular level, the cellular level with mammalian cells or with microorganisms, or at the whole animal level. The purpose of this experimentation is to study the adverse effects that animals can suffer as a consequence of simultaneous or sequential exposure to light and chemicals.

The questions that arise in connection with a symposium such as this are: Where to next? What do the FDA and the other regulatory agencies need next? Outlines for some of the answers were formulated at the evening discussion session. We can work at a number of levels of living-system organizations. But matters that come before agencies such as the FDA involve decisions concerning limiting or permitting exposures of living systems to chemicals and light exposures that are either simultaneous or sequential. For the purpose of answering the regulatory questions, we are usually unable to integrate all the information obtained from studies at different levels of living-system organizations because of concerns over extrapolation.

So, even though we have a lot of good work being done in the field of photochemical toxicity, which parallels the more complex aspects of the work done in the field of chemical toxicity, we do not appear to link what scientific research can offer and what is needed to make practical regulatory decisions that have consequences in terms of economics, creature comforts, and the quality of life of individuals or groups of people.

ABBREVIATION USED: FDA=Food and Drug Administration.

---

[1] Presented at the Seventh Food and Drug Administration Science Symposium ("Photochemical Toxicity: Toxic, Allergic, and Carcinogenic Aspects With Emphasis on Predicting Effects in Humans") held at the Uniformed Services University of the Health Sciences, Bethesda, Md., March 16–17, 1981.

[2] Office of Health Affairs (Science), Food and Drug Administration, Public Health Service, U.S. Department of Health and Human Services, 5600 Fishers Lane (HFY-31), Rockville, Md. 20857.

I will close, then, with a plea that applies both to researchers interested in photochemical toxicity as well as to those interested in chemical toxicity itself. Please remember in your research that knowing for the sake of knowledge or collecting information for the sake of knowledge is, of course, a very noble undertaking; however, look also into the practical aspects of the information that you collect and try to see whether you can pose questions and obtain answers that make possible the necessary everyday decisions of the FDA and other regulatory agencies.

REGISTRANTS

Lucile Adamson
Occupational Safety and Health Administration
519 Underwood St., N.W.
Washington, D.C. 20012

Frank Akin
Plough, Inc.
P.O. Box 377
Memphis, Tenn. 38151

Robert M. Albrecht
Food and Drug Administration
5600 Fishers Lane (HFX-130)
Rockville, Md. 20857

Alvito P. Alvares
Department of Pharmacology
Uniformed Services University of the Health Sciences
4301 Jones Bridge Rd.
Bethesda, Md. 20014

H. N. Ananthaswamy
Cancer Biology Program
NCI-Frederick Cancer Research Facility
Frederick, Md. 21701

F. Alan Andersen
Food and Drug Administration
5600 Fishers Lane (HFX-140)
Rockville, Md. 20857

N. G. Andersen
Towson State University
Towson, Md. 21214

Richard Angerhofer
Toxicology Division, Edgewood Area
U.S. Army Environmental Hygiene Agency
Aberdeen Proving Ground, Md. 21010

Bernard Armbrecht
Food and Drug Administration
5600 Fishers Lane (HFV-112)
Rockville, Md. 20857

Donald Aronson
Food and Drug Administration
5600 Fishers Lane (HFD-313)
Rockville, Md. 20857

Irvin M. Asher
AID/SCI, Room 5758
New State
Department of State
Washington, D.C. 20520

M. J. Ashwood-Smith
Environmental Toxicology Research Group
Department of Biology
University of Victoria
P.O. Box 1700
Victoria, British Columbia V8W 2Y2, Canada

Arthur Auer
Food and Drug Administration
5600 Fishers Lane (HFD-310)
Rockville, Md. 20857

Murl Bailey
Food and Drug Administration
5600 Fishers Lane (HFV-222)
Rockville, Md. 20857

Tibor Balazs
Food and Drug Administration
200 C St., S.W. (HFD-414)
Washington, D.C. 20204

Donald Barnes
Office of Pesticide and Toxic Substances
Environmental Protection Agency
401 M St., S.W. (TS-788)
Washington, D.C. 20460

Estela Barry
Food and Drug Administration
5600 Fishers Lane (HFD-510)
Rockville, Md. 20857

Karam V. Batra
Food and Drug Administration
8757 Georgia Ave. (HFK-450)
Silver Spring, Md. 20910

Lois Ann Beaver
Food and Drug Administration
5600 Fishers Lane (HFY-31)
Rockville, Md. 20857

Janusz Z. Beer
Food and Drug Administration
5600 Fishers Lane (HFX-120)
Rockville, Md. 20857

Michael Behrman
Health Research Group
2000 P St., N.W.
Suite 708
Washington, D.C. 20036

Sandra Bell
Food and Drug Administration
200 C St., S.W. (HFF-436)
Washington, D.C. 20204

Saul A. Bell
Chesebrough-Pond's Inc.
Trumbull Industrial Park
Trumbull, Conn. 06611

Walter Benson
Food and Drug Administration
200 C St., S.W. (HFD-420)
Washington, D.C. 20204

Garfield Biddle
Food and Drug Administration
200 C St., S.W. (HFF-159)
Washington, D.C. 20204

Ronald Biskup
Food and Drug Administration
200 C St., S.W. (HFF-158)
Washington, D.C. 20204

Marvin Bleiberg
Food and Drug Administration
200 C St., S.W. (HFF-156)
Washington, D.C. 20204

Larry Bockstahler
Food and Drug Administration
5600 Fishers Lane (HFX-120)
Rockville, Md. 20857

Michael Bolger
Food and Drug Administration
200 C St., S.W. (HFF-159)
Washington, D.C. 20204

Charles Bonfield
Regulatory Associates, Inc.
1834 Woodgate Lane
McLean, Va. 22101

Allen Brands
National Institute for Occupational Safety and Health
5600 Fishers Lane
Rockville, Md. 20857

Kathy Briscoe
Food and Drug Administration
5600 Fishers Lane (HFY-31)
Rockville, Md. 20857

Robert Bronaugh
Food and Drug Administration
200 C St., S.W. (HFF-164)
Washington, D.C. 20204

Elise Brown
U.S. Department of Agriculture
6811 Nesbitt Place
McLean, Va. 22101

Natalie Brown
Food and Drug Administration
5600 Fishers Lane (HFX-120)
Rockville, Md. 20857

Mary Bruch
Food and Drug Administration
5600 Fishers Lane (HFD-140)
Rockville, Md. 20857

Mary Bruenik
Food, Drug, and Cosmetic Reports, Inc.
One National Press Building
Washington, D.C. 20045

Jerry Brunton
The Animal Health Institute
1717 K St., N.W.
Suite 1009
Washington, D.C. 20036

Michael Byrne
3034 South Buchanan St.
Arlington, Va. 22206

Lorri Cameron
Division of Occupational Medicine
The Johns Hopkins School of Hygiene and Public Health
615 North Wolfe St.
Baltimore, Md. 21218

Karen Campbell
Food and Drug Administration
5600 Fishers Lane (HFV-222)
Rockville, Md. 20857

Janet Cantwell
Food and Drug Administration
5600 Fishers Lane (HFX-120)
Rockville, Md. 20857

Andy Chen
Mitre Corporation
1820 Dolley Madison Blvd.
McLean, Va. 22102

M. A. Chirigos
Litton Bionetics, Inc.
Kensington, Md. 20795

Pei-Lu Chiu
Department of Pharmacology
Uniformed Services University of the Health Sciences
4301 Jones Bridge Rd.
Bethesda, Md. 20014

Choong Chung
Food and Drug Administration
200 C St., S.W. (HFF-164)
Washington, D.C. 20204

George Clarke
Food and Drug Administration
5600 Fishers Lane (HFD-312)
Rockville, Md. 20857

John Clayton
Plough, Inc.
P.O. Box 377
Memphis, Tenn. 38151

Marvin Cohen
Enviro Control, Inc.
11300 Rockville Pike
Rockville, Md. 20852

David Conine
Hilltop Research Inc.
P.O. Box 42501
Cincinnati, Ohio 45242

Laurel Conley
Johnson & Johnson Baby Products Co.
Grandview Rd.
Skillman, N.J. 08558

Robert Coon
Food and Drug Administration
200 C St., S.W. (HFF-9)
Washington, D.C. 20204

Edmund Copeland
Grants Division
National Institutes of Health
Bethesda, Md. 20205

George Cosmides
National Library of Medicine
National Institutes of Health
Bethesda, Md. 20205

Boris Cumpelik
Vandyke and Company, Inc.
William St.
Belleville, N.J. 07109

Janet Cunningham
Food and Drug Administration
5600 Fishers Lane (HFY-31)
Rockville, Md. 20857

W. Howard Cyr
Food and Drug Administration
5600 Fishers Lane (HFX-120)
Rockville, Md. 20857

Robert Dailey
Food and Drug Administration
200 C St., S.W. (HFF-169)
Washington, D.C. 20204

Susan Davis
Food and Drug Administration
8757 Georgia Ave. (HFK-420)
Silver Spring, Md. 20910

John Davitt
Food and Drug Administration
5600 Fishers Lane (HFD-140)
Rockville, Md. 20857

E. DeFabo
NCI-Frederick Cancer Research Facility
Building 539
Frederick, Md. 21701

Luigi DeLuca
National Cancer Institute
National Institutes of Health
Bethesda, Md. 20205

Rosalie Donnelly
Food and Drug Administration
200 C St., S.W. (HFF-166)
Washington, D.C. 20204

Robert Doyle
Food and Drug Administration
200 C St., S.W. (HFF-403)
Washington, D.C. 20204

June Dunnick
National Toxicology Program
National Institutes of Health
P.O. Box 12233
Research Triangle Park, N.C. 27709

Elizabeth Earley
Food and Drug Administration
8800 Rockville Pike (HFB-500)
Bethesda, Md. 20205

Heinz Eiermann
Food and Drug Administration
200 C St., S.W. (HFF-440)
Washington, D.C. 20204

Abraham Eisenstark
Division of Biological Sciences
University of Missouri
Tucker Hall UMC
Columbia, Mo. 65211

Robert Elder
Cosmetic, Toiletry and Fragrance Association, Inc.
1110 Vermont Ave.
Suite 810
Washington, D.C. 20005

Sydney Ellis
Food and Drug Administration
200 C St., S.W. (HFD-410)
Washington, D.C. 20204

Kurt Enslein
Health Designs, Inc.
183 Main St., E.
Suite 1428
Rochester, N.Y. 14604

Robert Eppley
Food and Drug Administration
200 C St., S.W. (HFF-454)
Washington, D.C. 20204

John Epstein
450 Sutter St., #1306
San Francisco, Calif. 94108

C. Evans
Food and Drug Administration
5600 Fishers Lane (HFD-140)
Rockville, Md. 20857

Elizabeth Facchine
Food and Drug Administration
5600 Fishers Lane (HFX-25)
Rockville, Md. 20857

Homer Fairchild
Department of Agriculture
Federal Center Building
APHIS, PPO Room 642-A
Hyattsville, Md. 20782

Theodore Farber
Food and Drug Administration
200 C St., S.W. (HFF-154)
Washington, D.C. 20204

Richard Felten
Food and Drug Administration
5600 Fishers Lane (HFX-120)
Rockville, Md. 20857

Michael Fisher
NCI-Frederick Cancer Research Facility
Frederick, Md. 21701

W. Gary Flamm
Food and Drug Administration
5600 Fishers Lane (HFY-3)
Rockville, Md. 20857

Edgar Flint
CIBA-GEIGY Corporation
Ardsley, N.Y. 10502

Paul Forlot
Laboratoires Goupil
30 Avenue de President Wilson
F94230 Cachan, France

Mark Fow
Food and Drug Administration
5600 Fishers Lane (HFD-240)
Rockville, Md. 20857

Vasilios Frankos
Food and Drug Administration
5600 Fishers Lane (HFY-31)
Rockville, Md. 20857

Charles Frazier
Food and Drug Administration
200 C St., S.W. (HFF-158)
Washington, D.C. 20204

Leon Freeman
Pharmaquest Corporation
101 Casa Buena Dr.
Corte Madera, Calif. 94925

Leonard Friedman
Food and Drug Administration
200 C St., S.W. (HFF-169)
Washington, D.C. 20204

Kearby Fugate
Food and Drug Administration
8757 Georgia Ave. (HFK-440)
Silver Spring, Md. 20910

Seishiro Fujii
Shiseido Co., Ltd.
100 Tokeneke Rd.
Darien, Conn. 06820

Karl Gabriel
BioResearch, Inc.
P.O. Box 8598
Philadelphia, Pa. 19101

Raymond Gantt
National Cancer Institute
National Institutes of Health
Bethesda, Md. 20205

Albert Giles, Jr.
Food and Drug Administration
200 C St., S.W. (HFF-164)
Washington, D.C. 20204

Hyman Gittes
Consulting Toxicologist
4254 Briars Rd.
Olney, Md. 20832

Vera Glocklin
Food and Drug Administration
5600 Fishers Lane (HFD-102)
Rockville, Md. 20857

Marcia Goldberg
Health Research Group
2000 P St., N.W.
Suite 708
Washington, D.C. 20036

Robert Goldemberg
Raduma Laboratories, Inc.
P.O. Box 1083
South Hackensack, N.J. 07606

Evelyn Gordon
Food and Drug Administration
5600 Fishers Lane (HFX-4)
Rockville, Md. 20857

Nat Gordon
Midwest Research Institute
1750 K St., N.W.
Suite 250
Washington, D.C. 20006

Cheryl Graham
Food and Drug Administration
5600 Fishers Lane (HFD-210)
Rockville, Md. 20857

Arthur Gregory
Health Sciences Directorate
Consumer Product Safety Commission
Washington, D.C. 20207

F. Grundschober
International Fragrance Association
8 rue Charles-Humbert
1205 Geneva, Switzerland

Joseph Gubernick
Estee Lauder Inc.
210 Marcus Blvd.
Hauppauge, N.Y. 11787

Karen Hamernik
Department of Pharmacology
Uniformed Services University of the Health Sciences
4301 Jones Bridge Rd.
Bethesda, Md. 20014

James Hamilton
Food and Drug Administration
5600 Fishers Lane (HFD-310)
Rockville, Md. 20857

Leonard Harber
Department of Dermatology
College of Physicians and Surgeons
Columbia University
630 West 168th St.
New York, N.Y. 10032

Lester Hardy
Gillette Company
1413 Research Blvd.
Rockville, Md. 20850

B. Harris
Food and Drug Administration
200 C St., S.W. (HFF-154)
Washington, D.C. 20204

Lynne Harrison
FDRL
60 Evergreen Place
East Orange, N.J. 07018

David Hattan
Food and Drug Administration
200 C St., S.W. (HFF-156)
Washington, D.C. 20204

Annabel Hecht
Food and Drug Administration
5600 Fishers Lane (HFI-20)
Rockville, Md. 20857

Kiki Hellman
Food and Drug Administration
5600 Fishers Lane (HFX-120)
Rockville, Md. 20857

Sara Henry
Food and Drug Administration
200 C St., S.W. (HFF-159)
Washington, D.C. 20204

Paul Hepp
Food and Drug Administration
5600 Fishers Lane (HFD-522)
Rockville, Md. 20857

William Herman
Food and Drug Administration
5600 Fishers Lane (HFX-200)
Rockville, Md. 20857

James Herrera
The Wella Corporation
524 Grand Ave.
Englewood, N.J. 07631

Gloria Hicks
Food and Drug Administration
5600 Fishers Lane (HFV-136)
Rockville, Md. 20857

Shirley Hicks
Gillette Medical Evaluation Laboratories
1413 Research Blvd.
Rockville, Md. 20850

Richard Hill
Office of Pesticide and Toxic Substances
Environmental Protection Agency
401 M St., S.W. (TS-788)
Washington, D.C. 20460

Paul Hillery
Food and Drug Administration
5600 Fishers Lane (HFD-150)
Rockville, Md. 20857

Vicki Hitchins
Food and Drug Administration
5600 Fishers Lane (HFX-120)
Rockville, Md. 20857

Richard Hollingsworth
Food and Drug Administration
200 C St., S.W. (HFF-158)
Washington, D.C. 20204

George Holmes
Department of Microbiology
College of Medicine
Howard University
520 W St., N.W.
Washington, D.C. 20059

Steve Horwitz
Department of Dermatology
Mt. Sinai Medical Center
4300 Jalton Rd.
Miami Beach, Fla. 33140

Albert Houk
Food and Drug Administration
5600 Fishers Lane (HFD-102)
Rockville, Md. 20857

Kirk Huber
Lever Brothers Company
45 River Rd.
Edgewater, N.J. 07020

Phillis Huene
Food and Drug Administration
5600 Fishers Lane (HFD-140)
Rockville, Md. 20857

D. Hughes
The Procter and Gamble Company
5299 Spring Grove Ave.
Cincinnati, Ohio 45217

Shang W. Hwang
Food and Drug Administration
8757 Georgia Ave. (HFK-450)
Silver Spring, Md. 20910

G. Wayne Ivie
Veterinary Toxicology and Entomology Research Laboratory
Agricultural Research
Science and Education Administration
U.S. Department of Agriculture
College Station, Tex. 77841

Benjamin Jackson
Food and Drug Administration
200 C St., S.W. (HFF-158)
Washington, D.C. 20204

Edward Jackson
Noxell Corporation
P.O. Box 1799
Baltimore, Md. 21203

Elizabeth Jacobson
Food and Drug Administration
5600 Fishers Lane (HFX-120)
Rockville, Md. 20857

George James
Food and Drug Administration
5600 Fishers Lane (HFD-140)
Rockville, Md. 20857

George Jan
Food and Drug Administration
5600 Fishers Lane (HFX-430)
Rockville, Md. 20857

Herman Jass
315 Tall Oak Lane
Somerville, N.J. 08876

Jack Jawitz
4614 Harvard Rd.
College Park, Md. 20740

Phillip Johns
Food and Drug Administration
200 C St., S.W. (HFF-156)
Washington, D.C. 20204

A. Earl Johnson
Poisonous Plant Research Laboratory
Science and Education Administration
U.S. Department of Agriculture
1150 East 1400 North
Logan, Utah 84321

Garland T. Johnson
Enviro Control, Inc.
11300 Rockville Pike
Rockville, Md. 20852

Jean M. Johnson
Food and Drug Administration
5600 Fishers Lane (HFD-110)
Rockville, Md. 20857

William Jordan, Jr.
Department of Dermatology
Medical College of Virginia
Box 296—MCV
Richmond, Va. 23298

Hildegard Jorgensen
Washington Hospital Center
110 Irving St., N.W.
Washington, D.C. 20010

A. Joshi
Food and Drug Administration
200 C St., S.W. (HFF-454)
Washington, D.C. 20204

S. A. Joshi
Food and Drug Administration
5600 Fishers Lane (HFD-140)
Rockville, Md. 20857

Attila Kadar
Food and Drug Administration
5600 Fishers Lane (HFO-620)
Rockville, Md. 20857

David Kalins
Food and Drug Administration
5600 Fishers Lane (HFX-430)
Rockville, Md. 20857

Vincent Karusaites
Food and Drug Administration
5600 Fishers Lane (HFD-530)
Rockville, Md. 20857

Michael Kennedy
Food and Drug Administration
5600 Fishers Lane (HFD-514)
Rockville, Md. 20857

Jagjitsingh Khalsa
Food and Drug Administration
200 C St., S.W. (HFF-156)
Washington, D.C. 20204

Mushtaq Khan
Food and Drug Administration
200 C St., S.W. (HFF-154)
Washington, D.C. 20204

Albert Kligman
Department of Dermatology
Dhuring Laboratory
University of Pennsylvania School of Medicine
244 Medical Education Building
36th and Hamilton Walk—GM
Philadelphia, Pa. 19104

Denise Knott
Food and Drug Administration
5600 Fishers Lane (HFX-120)
Rockville, Md. 20857

B. M. Kong
Colgate Palmolive Company
909 River Rd.
Piscataway, N.J. 08854

Charma Konnor
Food and Drug Administration
5600 Fishers Lane (HFD-512)
Rockville, Md. 20857

Andrija Kornhauser
Food and Drug Administration
200 C St., S.W. (HFF-164)
Washington, D.C. 20204

Katalin Korossy
11227 Woodson Ave.
Kensington, Md. 20795

Kenneth Kraemer
National Cancer Institute
National Institutes of Health
Bethesda, Md. 20205

Kenneth Krell
Food and Drug Administration
5600 Fishers Lane (HFX-120)
Rockville, Md. 20857

Norman Krinsky
Department of Biochemistry and Pharmacology
Tufts University School of Medicine
136 Harrison Ave.
Boston, Mass. 02111

Margaret Kripke
NCI-Frederick Cancer Research Facility
P.O. Box B
Frederick, Md. 21701

Lark Lambert
Food and Drug Administration
200 C St., S.W. (HFF-164)
Washington, D.C. 20204

Angelo Lamola
Bell Telephone Laboratories
Murray Hill, N.J. 07974

Robert Landry
Food and Drug Administration
5600 Fishers Lane (HFX-220)
Rockville, Md. 20857

Sidney Lerman
Laboratory for Ophthalmic Research
Emory University School of Medicine
1708 Haygood Dr., N.E.
Atlanta, Ga. 30322

Jerome Levine
Food and Drug Administration
5600 Fishers Lane (HFX-140)
Rockville, Md. 20857

Allen Lewis
Food and Drug Administration
5600 Fishers Lane (HFD-180)
Rockville, Md. 20857

Chiu Lin
Food and Drug Administration
200 C St., S.W. (HFF-156)
Washington, D.C. 20204

Scott Lindemann
Food and Drug Administration
5600 Fishers Lane (HFX-120)
Rockville, Md. 20857

S. Lomvardias
Beverly Hospital
Beverly, Mass. 01915

Ed Losiewicz
Food and Drug Administration
5600 Fishers Lane (HFO-610)
Rockville, Md. 20857

Maria Lugo
Food and Drug Administration
5600 Fishers Lane (HFX-120)
Rockville, Md. 20857

Jasper Lynch
Food and Drug Administration
5600 Fishers Lane (HFX-120)
Rockville, Md. 20857

C. D. Lytle
Food and Drug Administration
5600 Fishers Lane (HFX-120)
Rockville, Md. 20857

Joseph Macko
Toxicology Division, Edgewood Area
U.S. Army Environmental Hygiene Agency
Aberdeen Proving Ground, Md. 21010

Louise Magruder
Food and Drug Administration
5600 Fishers Lane (HFF-265)
Rockville, Md. 20857

Howard Maibach
Department of Dermatology
University of California
School of Medicine
San Francisco, Calif. 94143

Keisuke Makino
National Cancer Institute
National Institutes of Health
Bethesda, Md. 20205

Zenona Mally
1712 Eye St., N.W.
#604
Washington, D.C. 20006

Milton Manowitz
Givaudan Corporation
125 Delawanna Ave.
Clifton, N.J. 07014

Randall Margolis
George Washington University
1827 Kalorama Rd.
Washington, D.C. 20009

Luch Markarian
Gillette Medical Evaluation Laboratories
1413 Research Blvd.
Rockville, Md. 20850

Edgar Martin
Food and Drug Administration
5600 Fishers Lane (HFD-140)
Rockville, Md. 20857

Frank Marzulli
Food and Drug Administration
200 C St., S.W. (HFF-160)
Washington, D.C. 20204

Micheline Mathews-Roth
Channing Laboratory
Department of Medicine
Harvard Medical School and Brigham and Women's Hospital
180 Longwood Ave.
Boston, Mass. 02115

Vernon Mayer, Jr.
Food and Drug Administration
200 C St., S.W. (HFF-166)
Washington, D.C. 20204

John McCurdy
Food and Drug Administration
5600 Fishers Lane (HFV-222)
Rockville, Md. 20857

James McDermott
The Procter and Gamble Company
5299 Spring Grove Ave.
Cincinnati, Ohio 45217

John McDowell
Food and Drug Administration
5600 Fishers Lane (HFV-222)
Rockville, Md. 20857

G. N. McEwen, Jr.
Cosmetic, Toiletry and Fragrance Association, Inc.
1110 Vermont Ave.
Suite 800
Washington, D.C. 20005

Darrel McKenzie
Medical Service Corp
U.S. Navy
National Naval Medical Center
Bethesda, Md. 20014

James McNerney
Cosmetic, Toiletry and Fragrance Association, Inc.
1110 Vermont Ave., N.W.
Washington, D.C. 20005

Robert McQuate
The Armour Research Center
15101 N. Scotsdale Rd.
Scotsdale, Ariz. 85260

Meryl Melnicoff
BioResearch Inc.
Philadelphia, Pa. 19104

John Middleton
Proprietary Perfumes Ltd.
50 Williams Dr.
Ramsey, N.J. 07446

David B. Miller
Naval Medical Research Institute
Bethesda, Md. 20014

David J. Miller
1200 15th St., N.W.
#504
Washington, D.C. 20004

Dee Miller
Food, Drug, and Cosmetic Reports, Inc.
One National Press Building
Washington, D.C. 20045

Eugene Miller
Food and Drug Administration
200 C St., S.W. (HFF-169)
Washington, D.C. 20204

Sanford Miller
Food and Drug Administration
200 C St., S.W. (HFF-1)
Washington, D.C. 20204

Loren Mills
Food and Drug Administration
5600 Fishers Lane (HFX-140)
Rockville, Md. 20857

Frances W. S. Min
Food and Drug Administration
200 C St., S.W. (HFD-140)
Rockville, Md. 20857

Krishna Misra
Food and Drug Administration
200 C St., S.W. (HFF-156)
Washington, D.C. 20204

Stephen Montgomery
Food and Drug Administration
200 C St., S.W. (HFF-158)
Washington, D.C. 20204

Warwick Morison
NCI-Frederick Cancer Research Facility
P.O. Box B
Frederick, Md. 21701

W. Morris
Revlon Research Center
945 Zerega Ave.
Bronx, N.Y. 10473

Alan N. Moshell
National Institute for Occupational Safety and Health
5600 Fishers Lane
Rockville, Md. 20857

Magdi Mossoba
National Cancer Institute
National Institutes of Health
Bethesda, Md. 20205

Richard Nicklas
Food and Drug Administration
5600 Fishers Lane (HFD-160)
Rockville, Md. 20857

Thomas Nigra
Department of Dermatology
The Washington Hospital Center
110 Irving St., N.W.
Room 2B-33
Washington, D.C. 20010

Philip Noguchi
Food and Drug Administration
8000 Rockville Pike (HFB-400)
Bethesda, Md. 20014

Frances Noonan
NCI-Frederick Cancer Research Facility
Frederick, Md. 20034

Winston Nottingham
National Science Foundation
1800 G St., N.W.
Washington, D.C. 20550

Leszek Ochota
Food and Drug Administration
5600 Fishers Lane (HFD-150)
Rockville, Md. 20857

Mamoru Ohashi
Food and Drug Administration
200 C St., S.W. (HFD-420)
Washington, D.C. 20204

Chester Opalsky
Environmental Protection Agency
401 M St., S.W. (TS-796)
Washington, D.C. 20460

Donald Opdyke
Research Institute for Fragrance Materials, Inc.
375 Sylvan Ave.
Englewood Cliffs, N.J. 07632

John O'Rangers
Food and Drug Administration
5600 Fishers Lane (HFO-620)
Rockville, Md. 20857

S. W. Page
Food and Drug Administration
200 C St., S.W. (HFF-454)
Washington, D.C. 20204

Kaniambaka Pani
Food and Drug Administration
5600 Fishers Lane (HFD-140)
Rockville, Md. 20857

Douglas Park
Food and Drug Administration
5600 Fishers Lane (HFY-31)
Rockville, Md. 20857

John Parrish
Harvard Medical School
Massachusetts General Hospital
Boston, Mass. 02114

M. E. Paterson
Proprietary Perfumes Limited
50 Williams Dr.
Ramsey, N.J. 07446

Madhu Pathak
Department of Dermatology
Harvard Medical School
Massachusetts General Hospital
Warren 5, Room 566
Boston, Mass. 02114

Jeffrey Perrman
Food and Drug Administration
5600 Fishers Lane (HFX-130)
Rockville, Md. 20857

Stephen Pijar
Food and Drug Administration
5600 Fishers Lane (HFX-70)
Rockville, Md. 20857

Wolfgang Pilz
Haarmann & Reimer GmbH
Postfach 139
3450 Holzminden
Federal Republic of Germany

Sal Pinella
Food and Drug Administration
5600 Fishers Lane (HFO-610)
Rockville, Md. 20857

Albert Pohland
Food and Drug Administration
200 C St., S.W. (HFF-452)
Washington, D.C. 20204

John Pooler
Department of Physiology
Emory University
Atlanta, Ga. 30322

William Powell
Food and Drug Administration
5600 Fishers Lane (HFD-140)
Rockville, Md. 20857

Ronald Rafft
Bristol Myers Products
1350 Liberty Ave.
Hillside, N.J. 07207

Gopa Rakhit
Food and Drug Administration
5600 Fishers Lane (HFD-410)
Rockville, Md. 20857

V. Rao
University of Mississippi
Medical Center
2500 North State St.
Jackson, Miss. 39216

Guruva Reddy
Food and Drug Administration
5600 Fishers Lane (HFV-125)
Rockville, Md. 20857

Peter Reisz
National Cancer Institute
National Institutes of Health
Bethesda, Md. 20205

Anthony Ridolfo
Lilly Laboratories for Clinical Research
Eli Lilly & Company
Wishard Memorial Hospital
Indianapolis, Ind. 46202

Emanuel Riklis
Armed Forces Radiobiology Research Institute
National Naval Medical Center
Bethesda, Md. 20014

Jane Robens
Agricultural Research
Science and Education Administration
U.S. Department of Agriculture
Beltsville, Md. 20705

Earl Robinson
Food and Drug Administration
5600 Fishers Lane (HFX-430)
Rockville, Md. 20857

Janice Rogers
Gillette Medical Evaluation Laboratories
1413 Research Blvd.
Rockville, Md. 20850

Joyce Rollings
Food and Drug Administration
5600 Fishers Lane (HFX-76)
Rockville, Md. 20857

Walter Rosen
National Academy of Science
2101 Constitution Ave. (WG-1007)
Washington, D.C. 20418

Ionel Rosenthal
National Cancer Institute
National Institutes of Health
Bethesda, Md. 20205

Barbara Rude
Food and Drug Administration
5600 Fishers Lane (HFI-22)
Rockville, Md. 20857

Naser Salman
Food and Drug Administration
8757 Georgia Ave. (HFK-410)
Silver Spring, Md. 20910

Carol Salzberg
Enviro Control, Inc.
11300 Rockville Pike
Rockville, Md. 20852

Deborah Salzberg
9834 Marcliff Court
Vienna, Va. 22180

John Sanders
Food and Drug Administration
5600 Fishers Lane (HFD-140)
Rockville, Md. 20857

Leonard Saslaw
Food and Drug Administration
200 C St., S.W. (HFF-154)
Washington, D.C. 20204

Neil Sass
Food and Drug Administration
200 C St., S.W. (HFF-158)
Washington, D.C. 20204

Robert Sayre
Plough, Inc.
P.O. Box 377
Memphis, Tenn. 38151

A. F. Scafidi
Food and Drug Administration
5600 Fishers Lane (HFD-140)
Rockville, Md. 20857

Ronald Scarpinato
National Cancer Institute
National Institutes of Health
Bethesda, Md. 20205

Jurgen Scheide
Haarmann & Reimer Corporation
111 Highway 22
P.O. Box 175
Springfield, N.J. 07081

Robert Scheuplein
Food and Drug Administration
200 C St., S.W. (HFF-350)
Washington, D.C. 20204

Roger Schneider
Food and Drug Administration
5600 Fishers Lane (HFX-200)
Rockville, Md. 20857

John Scigliano
Food and Drug Administration
5600 Fishers Lane (HFD-120)
Rockville, Md. 20857

Marvin Seife
Food and Drug Administration
5600 Fishers Lane (HFD-530)
Rockville, Md. 20857

Edward Seis
Norda, Inc.
140 Route 10
East Hanover, N.J. 07936

Charles Selander
Food and Drug Administration
8757 Georgia Ave. (HFK-128)
Silver Spring, Md. 20910

Mukund Shah
JRB Associates
8400 Westpark Dr.
McLean, Va. 22102

Barclay Shepard
Veterans Administration
810 Vermont Ave., N.W.
Washington, D.C. 20420

Samuel Shibko
Food and Drug Administration
200 C St., S.W. (HFF-152)
Washington, D.C. 20204

Bernard Shleien
Food and Drug Administration
5600 Fishers Lane (HFX-4)
Rockville, Md. 20857

Moris Shore
Food and Drug Administration
5600 Fishers Lane (HFX-100)
Rockville, Md. 20857

Charlotte Silverman
Food and Drug Administration
5600 Fishers Lane (HFX-101)
Rockville, Md. 20857

Patrick Siu
Food and Drug Administration
200 C St., S.W. (HFF-156)
Washington, D.C. 20204

Wallace Snipes
Pennsylvania State University
618 Mueller Laboratory
University Park, Pa. 16802

James Sphon
Food and Drug Administration
200 C St., S.W. (HFF-459)
Washington, D.C. 20204

Stephen Springer
Vick Divisions Research and Development
56 Harrison St.
New Rochelle, N.Y. 10801

Joseph Stanfield
Westwood Pharmaceuticals
468 Dewitt St.
Buffalo, N.Y. 14213

Joycelyn Stewart
Food and Drug Administration
200 C St., S.W. (HFF-154)
Washington, D.C. 20204

Jan Stofberg
PFW, Division of Hercules
33 Sprague Ave.
Middleton, N.Y. 10940

Fred Stone
Firmenich, Inc.
P.O. Box 5880
Princeton, N.J. 08540

John Strange
Franklin Research Center
1320 Fenwick Lane
Silver Spring, Md. 20910

Amparo Strickland
Food and Drug Administration
5600 Fishers Lane (HFX-120)
Rockville, Md. 20857

Gary Strniste
Genetics Group
Los Alamos National Laboratory
Los Alamos, N. Mex. 87545

Fred Stults
International Flavor and Fragrances
1515 Highway 36
Union Beach, N.J. 07735

Joseph Sun
Food and Drug Administration
5600 Fishers Lane (HFD-413)
Rockville, Md. 20857

P. Sundaresan
Food and Drug Administration
200 C St., S.W. (HFF-154)
Washington, D.C. 20204

Allan Susten
National Institute of Occupational Safety and Health
4676 Columbia Parkway
Cincinnati, Ohio 45226

C. Swentzel
Food and Drug Administration
200 C St., S.W. (HFF-154)
Washington, D.C. 20204

Stephen Sykes
Food and Drug Administration
5600 Fishers Lane (HFX-120)
Rockville, Md. 20857

George Szabo
Laboratory of Electron Microscopy
Harvard School of Dental Medicine
188 Longwood Ave.
Boston, Mass. 02115

Jean Taylor
Food and Drug Administration
200 C St., S.W. (HFF-158)
Washington, D.C. 20204

Richard Teske
Food and Drug Administration
200 C St., S.W. (HFV-500)
Washington, D.C. 20204

Paul Thau
Cosmair, Inc.
285 Terminal Ave.
Clark, N.J. 07066

Paul Tobin
1719 35th Street, N.W.
Apartment 1
Washington, D.C. 20007

Michael Topper
Toxicology Division, Edgewood Area
U.S. Army Environmental Hygiene Agency
Aberdeen Proving Ground, Md. 21010

Neil Towers
Botany Department
University of British Columbia
Vancouver, British Columbia, Canada

Eugiene Triantas
Food and Drug Administration
5600 Fishers Lane (HFD-110)
Rockville, Md. 20857

Chet Trybus
801 Quince Orchard Blvd. #32
Gaithersburg, Md. 20760

Miin-Rong Tsai
Food and Drug Administration
8757 Georgia Ave. (HFK-470)
Silver Spring, Md. 20910

Paul Turkeltaub
Food and Drug Administration
8000 Rockville Pike (HFB-500)
Bethesda, Md. 20014

Frederick Urbach
The Center for Photobiology
Skin and Cancer Hospital
Temple University School of Medicine
3322 North Broad St.
Philadelphia, Pa. 19140

L. Valcovic
Food and Drug Administration
200 C St., S.W. (HFF-154)
Washington, D.C. 20204

Dennis Valenzeno
Department of Physiology
University of Kansas Medical Center
39th and Rainbow Blvd.
Kansas City, Kans. 66103

Marcia Van Gemert
Food and Drug Administration
200 C St., S.W. (HFF-156)
Washington, D.C. 20204

Adele Vessey
Food and Drug Administration
200 C St., S.W. (HFF-265)
Washington, D.C. 20204

Carl Vest
Battelle
2030 M St., N.W.
Washington, D.C. 20036

Michael Wade
Food and Drug Administration
200 C St., S.W. (HFF-159)
Washington, D.C. 20204

Stephen Wagner
Pennsylvania State University
617 Mueller Laboratory
University Park, Pa. 16802

Wayne Wamer
Food and Drug Administration
200 C St., S.W. (HFF-164)
Washington, D.C. 20204

Andrea Wargo
Food and Drug Administration
8757 Georgia Ave. (HFK-420)
Silver Spring, Md. 20910

James Weaver
The Procter and Gamble Company
Sharon Woods Technical Center
11520 Reed Hartman Highway
Cincinnati, Ohio 45241

Robert Webb
Division of Biological and Medical Research (D202)
Argonne National Laboratory
Argonne, Ill. 60439

Henri Weems
Department of Pharmacology
Uniformed Services University of the Health Sciences
4301 Jones Bridge Rd.
Bethesda, Md. 20014

Stephanie Weisbroth
BioSafe Systems, Inc.
1804 Plaza Ave.
New Hyde Park, N.Y. 11040

Gerald Weiss
Food and Drug Administration
5600 Fishers Lane (HFD-110)
Rockville, Md. 20857

Alfred Weissler
5510 Uppingham St.
Chevy Chase, Md. 20015

John Wenninger
Food and Drug Administration
200 C St., S.W. (HFF-441)
Washington, D.C. 20204

Dorothy Wheeler
Food and Drug Administration
5600 Fishers Lane (HFD-14)
Rockville, Md. 20857

Clarence Wilson
Food and Drug Administration
8757 Georgia Ave. (HFK-128)
Silver Spring, Md. 20910

John Winkert
12301 Mikia Lane
Bowie, Md. 20715

Herbert Wiser
Environmental Protection Agency
401 M St., S.W. (RD-676)
Washington, D.C. 20460

Thomas Withrow
Food and Drug Administration
5600 Fishers Lane (HFX-120)
Rockville, Md. 20857

Garnett Wood
Food and Drug Administration
200 C St., S.W. (HFF-454)
Washington, D.C. 20204

William Workman
5221 42d St., N.W.
Washington, D.C. 20015

Ronald Wulf
Carter-Wallace, Inc.
Half Acre Rd.
Cranbury, N.J. 08512

Arthur Wykes
Toxicology Information Program
National Library of Medicine
National Institutes of Health
Bethesda, Md. 20205

George Yang
Food and Drug Administration
200 C St., S.W. (HFF-454)
Washington, D.C. 20204

Shen Yang
Department of Pharmacology
Uniformed Services University of the Health Sciences
4301 Jones Bridge Rd.
Bethesda, Md. 20014

Terrye Zaremba
Food and Drug Administration
5600 Fishers Lane (HFX-120)
Rockville, Md. 20857

Howard Zell
Food and Drug Administration
5600 Fishers Lane (HFD-140)
Rockville, Md. 20857

Constantine Zervos
Food and Drug Administration
5600 Fishers Lane (HFY-31)
Rockville, Md. 20857

John Ziegler
National Cancer Institute
National Institutes of Health
Bethesda, Md. 20205

Stuart Zimmerman
Food and Drug Administration
5600 Fishers Lane (HFD-110)
Rockville, Md. 20857

Correction

June 1981, vol 66, No. 6

In "The Causes of Cancer: Quantitative Estimates of Avoidable Risks of Cancer in the United States Today," by Richard Doll and Richard Peto, add the following after table 6 on page 1203: *Note*: Occupational exposure to phenoxyacid and/or chlorphenol herbicides (or their impurities) is a reasonably well-established cause of soft tissue sarcomas and perhaps lymphomas.

In the same article, page 1233, column 2, the following changes should be noted: 1) Delete "mammary" from line 10. 2) ¶In lines 16–19, replace text between comma and period by "but 32 nonfatal spontaneous tumors arose among the 40 continuously fed mice, whereas only 4 arose among the 40 intermittently fed mice."

Announcements

The Journal *will publish notices of major meetings dealing with cancer. Submission of notices 6 months in advance is requested to permit timely publication.*

Second International Congress on Hormones and Cancer

Monte Carlo will be the site of this conference, sponsored by the International Association for Hormones and Cancer, to be held on September 18–23, 1983. The scientific program will include invited lectures and a limited number of free communications.

Information on speakers, the scientific program and committee, and satellite meetings may be obtained by writing to Dr. S. Iacobelli, Scientific Secretary, Laboratorio di Endocrinologia Molecolare, Università Cattolica del S.Cuore, L.go Gemelli, 8-00168 Rome, Italy (telephone: (06) 33054496 Telex 611330 unicatro).

Workshop Conference on Diet and Cancer

"Diet and Cancer, From Basic Research to Policy Implications" will be the subject of this conference to be held at Cornell University, Ithaca, New York, on August 16–18, 1982. Research, risk assessment, regulation, and public policy issues on the carcinogenic effects of nutrients will be addressed.

For further information please contact Mr. T. Colin Campbell, Division of Nutritional Sciences, Cornell University, MVR N-206, Ithaca, New York 14853.

Annual Symposium on Diagnostic Imaging

The Radiation Medicine Section of Brown University and the Department of Diagnostic Radiology of Rhode Island Hospital will cosponsor this symposium to be held at the Sheraton-Islander Inn, Newport, Rhode Island, on August 16–19, 1982. The symposium will emphasize use, techniques, comparisons, and trends among the diagnostic imaging modalities. Discussions will focus on the GI tract, renal system, retroperitoneum and pelvis, and head and spine.

Informal workshops will provide faculty-registrant interchange on nuclear cardiology, venography and pulmonary angiography, chest biopsy and chest CT, abdominal nuclear imaging and CT, noninvasive carotid imaging, CT of the head and spine, and ultrasound of the newborn head.

Approved accreditation is for 20 hours, Category I, AMA Physician's Recognition Award. For additional information please contact Educational Resources Associates, Inc., P.O. Box 369, Brookline, Massachusetts 02146 (telephone: 617-738-8859/8861).

Fourth International Symposium on Nasopharyngeal Carcinoma

The University of Malaya will sponsor this symposium to be held at the University of Malaya, Kuala Lumpur, Malaysia on September 27–29, 1982. The theme of the program will be the application of field and laboratory studies to the control of nasopharyngeal carcinoma.

For additional information please contact the Secretariat, NPC International Symposium, Department of ENT, Faculty of Medicine, University of Malaya, Kuala Lumpur 22-11, Malaysia.

Fifth Annual Bristol-Myers Symposium on Cancer Research

The Bristol-Myers Company will sponsor this symposium entitled "Chromosomes and Cancer: From Molecules to Man" to be held at the University of Chicago, Chicago, Illinois, on October 18–19, 1982. The symposium will focus on the consistent chromosome abnormalities that occur in human tumors and will explore the use of new techniques that can elucidate the role of chromosome abnormalities in malignant transformation.

Information regarding registration, for which there is no fee, may be obtained from Dr. Janet D. Rowley or Dr. John E. Ultmann, the University of Chicago Cancer Research Center, Box 444, 950 E. 59th Street, Chicago, Illinois 60637.

Twenty-Sixth Annual Clinical Conference

The University of Texas M. D. Anderson Hospital and Tumor Institute will sponsor this conference entitled "Current Controversies in Breast Cancer" to be held in Houston, Texas, at the Shamrock Hilton Hotel on

November 3–5, 1982. The conference will discuss the current status of therapeutic and diagnostic controversies surrounding breast cancer, and will focus on issues of limited mastectomy and irradiation; pathologic prognostic factors; breast cancer screening; long-term results on adjuvant chemotherapy; the value of biological markers; strategies for complete remission of metastatic disease; and second- and third-line therapies for advanced disease.

For additional information please contact Mr. Stephen C. Stuyck, Director, Public Information and Education, M. D. Anderson Hospital and Tumor Institute, Houston, Texas 77030 (telephone: 713-792-3030).

European Organization for Research on Treatment of Cancer Symposium

"Paraneoplasia: Basic Concepts and Clinical Aspects" will be the subject of this symposium to be held in Brussels, Belgium, on November 5–6, 1982. Invited speakers will lecture on endocrine paraneoplasia, neurological paraneoplasia, coagulopathies, and non-hormonal tumor markers. In addition, free communications of 10 minutes each are accepted. An abstract must be sent before September 30, 1982, to Dr. M. Staquet, Director, EORTC Data Center, rue Héger-Bordet 1, 1000 Brussels, Belgium.

Seating is limited and preregistration is recommended. For further information and registration contact Dr. M. Staquet at the above-mentioned address (telephone: [2] 538.57.90—telex: 22773).

Thirtieth Annual Scientific Meeting of the American Society of Cytology

Chicago, Illinois, will be the site of this meeting to be held at the Hyatt Regency Hotel, on November 8–13, 1982. The general outline of the scientific program will include a seminar for cytotechnology program faculties, cytology workshops, scientific papers and discussions, and a diagnostic cytology seminar.

The Continuing Education Program of the American Society of Cytology has been granted full approval by the Council on Medical Education of the American Medical Association. Physicians may earn credit hours for Category I, Physician's Recognition Award of the American Medical Association.

For additional information please contact Dr. Warren R. Lang, Secretary-Treasurer, 130 South 9th Street, Suite 810, Philadelphia, Pennsylvania 19107.

Sixteenth Midyear Topical Symposium of the Health Physics Society

The Rio Grande Chapter of the Health Physics Society will sponsor this meeting to be held at the Albuquerque Convention Center, Albuquerque, New Mexico, on January 10–14, 1983. "Epidemiology Applied to Health Physics" will be the subject of this meeting and invited speakers will participate in sessions dealing with: the relation of epidemiologic studies to radiation protection standards, epidemiological and statistical methods applied to research on health effects and radiation exposure, and risk estimation and its application to other areas.

Individuals who are interested should submit an abstract not exceeding 200 words by July 30, 1982 to Dr. Gregg S. Wilkinson, Chairman, Technical Program Committee, Epidemiology Group, Health Division, MS-404, Los Alamos National Laboratory, P.O. Box 1663, Los Alamos, New Mexico 87545.

Requests for information and registration materials should be sent to Mr. A. Wendell Holmes, 3800 Camino Don Diego N.E., Albuquerque, New Mexico 87111.

Urological Cancer Symposium

The USC Comprehensive Cancer Center, USC Division of Urology, USC Division of Postgraduate Medicine, and the Los Angeles Urological Society will sponsor this symposium to be held at the USC Health Science Campus, Los Angeles, California on January 14–15, 1983. The target audience includes urologists, medical oncologists, surgical oncologists, radiation oncologists, and general practitioners.

Interested persons should contact Ms. Katie Eisenberg, Regional Activities Program, 1721 Griffin Avenue, Los Angeles, California 90031 (telephone: 213-224-7416).

☆ U.S. GOVERNMENT PRINTING OFFICE: 1982-361-145/56

JNCI (NIH Publication No. 82-13)

69/2

JNCI

Journal of the National Cancer Institute

August 1982
Volume 69
Number 2

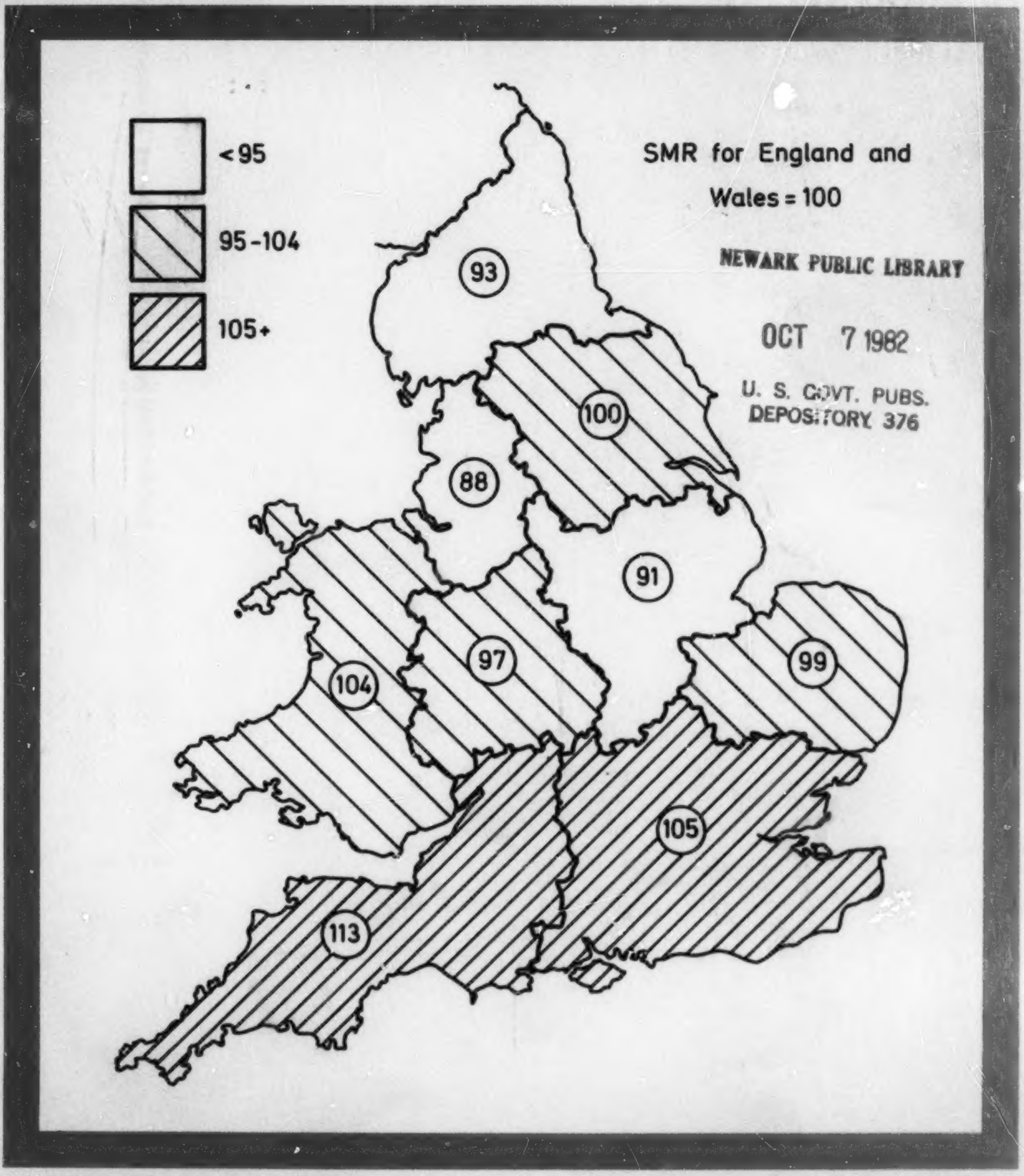

<95
95-104
105+
SMR for England and Wales = 100
93
100
88
91
104
97
99
105
113

NEWARK PUBLIC LIBRARY
OCT 7 1982
U. S. GOVT. PUBS.
DEPOSITORY 376

U.S. DEPARTMENT OF HEALTH AND HUMAN SERVICES Public Health Service National Institutes of Health

HE 20.3161:

The map on this month's cover depicts the mortality ratios for multiple myeloma in different regions of England and Wales (*see* paper by Velez et al. on pages 387–392).

JNCI

Journal of the National Cancer Institute

August 1982
Volume 69
Number 2

THE JOURNAL of the National Cancer Institute solicits manuscripts on original observations in laboratory and clinical research from all scientists. A manuscript is considered for publication with the understanding that it has not been published previously and is submitted exclusively to the Journal. Opinions expressed by the authors are not necessarily those of the publisher or its editors.

THE JOURNAL is published monthly (two volumes a year). The Secretary of Health and Human Services has determined that the publication of this periodical is necessary in the transaction of the public business required by law of this Department.

A MONOGRAPH SERIES covering proceedings of scientific meetings pertaining to cancer is also published. These books may be purchased from the Superintendent of Documents. Series subscriptions are not available and monographs are not included in a subscription to the Journal.

THE JOURNAL is for sale by the Superintendent of Documents, U.S. Government Printing Office, Washington, D.C. 20402. Price per copy, $7.00. Subscription price for two volumes per year in the United States, $70.00; foreign, $87.50. Payment is required in advance, and check or money order should be made payable to the Superintendent of Documents.

All inquiries regarding purchase of subscriptions or depository library distribution, including inquiries about missing issues and change of address, should be addressed to the Government Printing Office. The Government Printing Office requires payment in advance on all orders. Inquiries regarding missing issues or change of address for official subscriptions should be addressed to the Editorial Office, Room 850, Westwood Building, 5333 Westbard Avenue, Bethesda, Md. 20816.

VINCENT T. DEVITA, JR., *Director, National Cancer Institute*

BOARD OF EDITORS

PETER GREENWALD, *Editor in Chief*
ELIZABETH K. WEISBURGER, *Assistant Editor in Chief*
STUART A. AARONSON, *Associate Editor*
CHARLES H. EVANS, *Associate Editor*
MARY A. FINK, *Associate Editor*
JANET W. HARTLEY, *Associate Editor*
DONALD HENSON, *Associate Editor*
RONALD B. HERBERMAN, *Associate Editor*
GEORGE S. JOHNSON, *Associate Editor*
KURT W. KOHN, *Associate Editor*
ARTHUR S. LEVINE, *Associate Editor*
JOHN J. MULVIHILL, *Associate Editor*
ALAN S. RABSON, *Associate Editor*
RICHARD M. SIMON, *Associate Editor*

EDITORIAL STAFF

EDWIN A. HAUGH, *Managing Editor*
PAMELA T. ALLEN, *Assistant Managing Editor*
FLORENCE I. GREGORIC, *Monograph Editor*
Editors: DOROTHY D. KATZ, MERCEDES B. LA CHARITY, I. AGNES REVESZ, JOAN O'BRIEN RODRIGUEZ, CONSTANCE R. STONESTREET, and ANNA B. WITTIG

JNCI (NIH Publication No. 82-13)

U.S. DEPARTMENT OF HEALTH AND HUMAN SERVICES   Public Health Service   National Institutes of Health

Instructions to Authors

Text: Send one original and two copies. **Text-figures** (graphs, charts, and line drawings): Send one original and two copies. **Figures** (photomicrographs and photographs): Send three original glossy prints, unmounted. **Tables:** Send tabular material in typewritten form; do not submit tables as glossy prints to be photographed. The entire manuscript including footnotes, legends, and references must be typed double spaced. Single-spaced portions of a manuscript will be returned to the author for retyping. The mailing address is: Journal of the National Cancer Institute, Westwood Building, Room 850, 5333 Westbard Avenue, Bethesda, Maryland 20816.

Manuscripts should be accompanied by a covering letter from the author responsible for correspondence about the manuscript. The covering letter should contain a statement that the manuscript has been seen and approved by all authors and that all persons listed as authors have made significant (not merely administrative, technical, or supervisory) contributions to the content of the paper. The letter should also state that the manuscript or substantial portions thereof have not been previously published nor are they under consideration for publication in another journal.

Data too extensive for inclusion in a manuscript, but which may be of interest to other investigators, may be deposited with the National Auxiliary Publications Service (NAPS), c/o Microfiche Publications, P.O. Box 3513, Grand Central Station, New York, New York 10017. Authors using the NAPS facilities should indicate in a footnote how their additional data may be obtained.

Approximately one-half of all manuscripts submitted to the Journal are accepted for publication. Publication of manuscripts is contingent on transfer of copyright to the Journal. Forms for this purpose will be sent to authors when a manuscript has been approved for publication. All material published in the Journal is in the public domain; therefore, permission to reproduce any portions is not necessary. As a matter of courtesy, communication should be made to the author(s) concerned.

TITLE: Be brief (no more than 14 words, if possible), but for indexing purposes include all key words. The annual subject index is prepared directly from the titles. Titles that form complete sentences are not acceptable. Do not use abbreviations or chemical formulas in titles.

BYLINE: Supply the complete first name, middle initial, and last name of each author. Avoid use of nicknames. Academic degree is optional; however, if a degree is provided for one author, it should be provided for all authors on a manuscript. Include the name of the institution, address, and zip code for each author. Indicate address for reprint requests in a footnote on the byline.

ACKNOWLEDGMENTS: Financial aid in support of research should be recognized in a footnote. Aid in technical fields, animal care, photography, stenography, and other areas may be mentioned in a separate footnote. Indicate the title (Dr., Mr., Mrs., Miss, Ms.) and affiliation of each person acknowledged.

ABSTRACT: Provide an abstract, 150 words or less, on a separate page. The abstract should describe only *results* of the work being reported. Speculation, historical background, or reference to published works will be deleted from abstracts. Any inbred strains, noninbred stocks, cell lines, or other living materials used in the work should be noted in the abstract.

TEXT: Avoid the use of laboratory jargon and abbreviations not in common usage. When possible, refrain from the use of abbreviations that form words (exceptions are PAGE, ALL). Whenever possible, write mathematical equations and chemical formulas on a single line; submit complicated chemical structures as artwork. Avoid repetition of data in the text when it is presented in tables or text-figures.

Use the following style sources: Webster's *Third New International Dictionary* and Dorland's *Illustrated Medical Dictionary* (25th ed) for spelling; *Council of Biology Editors Style Manual* (4th ed) for scientific abbreviations and symbols: *Government Printing Office Style Manual* for other abbreviations and symbols, punctuation, and hyphenation; *Biochemical Nomenclature and Related Documents* (IUB, 1978) for abbreviations of chemical substances; *Enzyme Nomenclature*, recommendations (1978) of the IUB for recommended names of enzymes and information on nomenclature of isozymes; *The Merck Index* (9th ed) for chemical compounds; "Standard Nomenclature for Inbred Strains of Mice: Seventh Listing" by Joan Staats (Cancer Res 1980;40: 2083-2128) for inbred mouse strains; "Standardized Nomenclature for Inbred Strains of Rats: Fourth Listing" by Joan Staats and Michael Festing (Transplantation 1973;16:221-245) for designations of inbred rat strains; *Animals for Research* (9th ed) prepared by the Institute of Laboratory Animal Resources, National Academy of Sciences, for designations of laboratory animal stocks and strains.

TABLES: Submit tabular material typed double spaced on a separate page. Computer print-outs of tables are acceptable only if they are double spaced and with satisfactory title, column headings, legends and other textual material. Provide headings for all columns of a table and indicate units of measurement where applicable.

TEXT-FIGURES: Refer to graphs, charts, and line drawings as text-figures. Make the abbreviations on text-figures identical to the abbreviations used in the text and legends. Symbols and lettering should be large enough to be legible if reduced. Glossy prints or original drawings in black ink are acceptable; orient vertically instead of horizontally.

FIGURES: Refer to photomicrographs and photographs as figures. Figures and their legends should fit a 7.5- by 9-inch dimension. Calculate that nine typewritten lines of legend will require 1 inch of vertical space. Type figure legends on a separate sheet and identify in the legend any lettering used on the figure. Trim photographs to show only important areas. Do not number face of photographs; use the back or overlay to indicate the top and number of each. Printed indicators may be included on photographs; do not use hand-drawn indicators. *Insert internal scale markers on all photomicrographs.* Color photographs must be grouped as a single plate. For color reproduction, submit both color transparencies and high-quality black and white reproductions. The need for color must be documented before it will be considered.

REFERENCES: Use any recent issue of the Journal as a style guide for reference lists. Number references in order of citation in both text and reference list. For periodicals, provide author(s), title of paper, journal, year, volume, and first and last page numbers. For books, give the author(s), title, name(s) of editor(s), location and name of publisher, year, pertinent chapter or section title, and page numbers. Follow *Index Merdicus* for punctuation and abbreviations. Citations of papers in preparation or submitted for publication, unpublished observations, and personal communications should be noted parenthetically in the text. Do *not* include them in the reference list. The accuracy of all references is the responsibility of the authors and not of the editorial staff.

LETTERS TO THE EDITOR should pertain to recent articles in the Journal and should not contain new data unless relevant to the discussion of a particular paper. The authors addressed will be invited to reply to comments before correspondence is published. Letters will be edited by the Staff, subject to contributor approval.

FURTHER DETAILS on the preparation of manuscripts are set forth in the document "Uniform Requirements for Manuscripts Submitted to Biomedical Journals" prepared by the International Steering Committee of medical editors (*see* Am Rev Respir Dis 1979;119:3-10/Ann Intern Med 1979;90:95-99/Br Med J 1979;1:532-535/ or Lancet 1979;1:428-430).

UNITED STATES GOVERNMENT PRINTING OFFICE, WASHINGTON, D.C.: 1982

Table of Contents

Vol. 69, No. 2——August 1982

Letters to the Editor

319	*Trans* fatty acids in tumor development	*J. Edward Hunter*
320	Reply	*Atif B. Awad*

Investigations on Man

323	Multiple myeloma among atomic bomb survivors in Hiroshima and Nagasaki, 1950–76: Relationship to radiation dose absorbed by marrow	*Michito Ichimaru, Toranosuke Ishimaru, Motoko Mikami, Masako Matsunaga*
329	Possible association of radioprotective and chemoprotective aminophosphorothioate drug activity with polyamine oxidase susceptibility	*Joseph M. Gaugas*
333	Search for evidence of feline leukemia virus infection in humans with leukemias, lymphomas, or soft tissue sarcomas	*Peter P. Sordillo, R. Pincow Markovich, William D. Hardy, Jr.*
339	Interferon and prostaglandins: Effects on human natural and lectin-induced cytotoxicity	*Nicholas P. Lang, John R. Ortaldo, Guy D. Bonnard, Ronald B. Herberman*
345	Indirect macrophage migration inhibition response to 3-*M* KCl extract of gastric carcinoma	*Tsuyoshi Akiyoshi, Fumio Koba, Michihiro Kawaguchi, Soichiro Miyazaki, Hideo Tsuji*
349	Ten- to fourteen-year effect of screening on breast cancer mortality	*Sam Shapiro, Wanda Venet, Philip Strax, Louis Venet, Ruth Roeser*
357	Antigenic heterogeneity of human colorectal cancer cell lines analyzed by a panel of monoclonal antibodies. I. Heterogeneous expression of Ia-like and HLA-like antigenic determinants	*Grant D. MacLean, Jutta Seehafer, Andrew R. E. Shaw, Mark W. Kieran, B. Michael Longenecker*
365	Changes in skin cancer morbidity between 1971–72 and 1977–78	*Thomas R. Fears, Joseph Scotto*
371	Isolation and partial characterization of surface components of cell line MDA-MB-231 derived from a human metastatic breast carcinoma	*Evelyne Walker-Nasir, John F. Codington, Marianne R. Jahnke, Thomas C. Fuller, Roger W. Jeanloz*
381	α_1-Protease inhibitor production by human adenocarcinomas xenotransplanted into nude mice	*Dorothy Lee, Dan Shochat, David V. Gold*

387 Increasing trends of multiple myeloma mortality in England and Wales; 1950–79: Are the changes real? *Ramon Velez, Valerie Beral, Jack Cuzick*

393 Changes in clonal expression during the course of acute leukemia: Possible subsets in childhood leukemia *Hie-Won L. Hann, Peter C. Nowell, Penelope Koch, Jun Minowada, John E. Leitmeyer, Charles S. August*

401 Coproduction of carcinoembryonic antigen and nonspecific cross-reacting antigen by a continuous cell line from a human pancreatic tumor *Masahide Kuroki, Sadanori Ichiki, Motomu Kuroki, Yuji Matsuoka*

409 Repair of chromosome damage induced by X-irradiation during G_2 phase in a line of normal human fibroblasts and its malignant derivative *Ram Parshad, Raymond Gantt, Katherine K. Sanford, Gary M. Jones, Robert E. Tarone*

Investigations on Nonhuman Systems

415 Role of anchorage in the expression of tumorigenicity of untransformed mouse cell lines *Robert S. Wells, Evelyn W. Campbell, Douglas E. Swartzendruber, Lawrence M. Holland, Paul M. Kraemer*

425 Chromosome changes associated with the progression of cell lines from preneoplastic to tumorigenic phenotype during transformation of mouse salivary gland epithelium in vitro *John K. Cowell, Caroline B. Wigley*

435 Effect of type C viral expression and cellular karyotype on human B-lymphoblast tumorigenicity in nude mice *Anton F. Steuer, Robert C. Ting, Phillip D. Markham, Zaki Salahuddin, Robert C. Gallo*

443 Hormone dependence of 7,12-dimethylbenz[*a*]-anthracene-induced mammary tumor growth: Correlation with prostaglandin E_2 content *M. Katherine Foecking, William E. Kibbey, Hussein Abou-Issa, Richard H. Matthews, John P. Minton*

447 Comparison of ovariectomy and retinyl acetate on the growth of established 7,12-dimethylbenz[*a*]anthracene-induced mammary tumors in the rat *Philippe Gandilhon, Réjean Melancon, Jean Djiane, Paul A. Kelly*

453 Growth and differentiation of hyperplastic outgrowths derived from mouse mammary epithelial cells transformed in organ culture *Nivedita Ganguly, Ranjan Ganguly, Nozer M. Mehta, Mihir R. Banerjee*

465 Effect of immunomodulation on the fate of tumor cells in the central nervous system and systemic organs of mice. Distribution of $[^{125}I]$5-iodo-2′-deoxyuridine-labeled KHT tumor cells after left intracardial injection *Frances K. Conley*

475 Role of prostaglandin E_1 and copper in angiogenesis *Marina Ziche, John Jones, Pietro M. Gullino*

483 Angiogenesis and neoplastic progression in vitro *Marina Ziche, Pietro M. Gullino*

489 Immunization against transplantable leukemia impaired in copper-deficient mice — *Omelan A. Lukasewycz, Joseph R. Prohaska*

495 Effects of different fractions of *Corynebacterium parvum* on the cytotoxic T-cell response to alloantigens in mice — *Alan Lichtenstein, Richard Tuttle, John Cantrell, Jacob Zighelboim*

503 Chemical cocarcinogenesis with the use of a subclone derived from Balb/3T3 cells with catechol as cocarcinogen — *Mahalakshmi Atchison, Ching-shan Chu, Takeo Kakunaga, Benjamin L. Van Duuren*

509 Immunotherapy of a murine leukemia virus-infected, chemically induced murine sarcoma with antiviral antibodies — *Edward C. Ward, J. Dirk Iglehart, Kent J. Weinhold, Dani P. Bolognesi*

517 Proliferation of ductal outgrowths by carcinogen-induced rat mammary tumors in gland-free mammary fat pads — *Evelyn M. Rivera, Srinivasan Vijayaraghavan*

527 Individually distinct tumor-specific cell surface antigen identified by monoclonal antibody on a Rous sarcoma virus-induced mouse tumor — *Noboru Kuzumaki, Hidetaka Minakawa, Takashige Miyazaki, Soichi Haraguchi, Tetsumichi Matsuo, Takato O. Yoshida*

531 Neoplastic transformation of Syrian hamster cells by putative epoxide metabolites of commercially utilized chloroalkenes — *Joseph A. DiPaolo, Jay Doniger*

535 Derivation of transplantable 7,12-dimethylbenz[*a*]anthracene-induced chicken fibrosarcoma lines: Differences in metastasizing properties and organ specificity — *J. E. Galton, B. Xue, G. M. Hochwald, G. J. Thorbecke*

Meeting Highlights

543 Cytogenetics and somatic cell genetics of malignancy workshop — *Warren W. Nichols, Alfred G. Knudson, Louis Siminovitch*

544 Brief summary of the third joint meeting of the United States–Japan Cooperative Cancer Research Program on cell interactions and cancer — *Ira Pastan, Yoji Ikawa*

Corrections

547 May 1982, vol 68, No. 5, page 878: "Comparison of In Vitro and In Vivo Effects of Thymidine on L1210 Leukemia in Mice" NCI Monograph No. 58, page 47: "Carcinogenic and Mutagenic N-Substituted Aryl Compounds" — *Daniel S. Zaharko, Lori M. Ramonas*

Announcements

547 Temporomandibular Joint——Pain and Dysfunction Course

547 Second Annual International Symposium on the Clinical Applications of Cardiopulmonary Imaging
547 Fifteenth Annual Malignant Disease Symposium
547 Pediatric Radiology Course
547 New Monographs Available
548 Public Health Controversies—Food Safety Laws: Delaney and Other Dilemmas

Letters to the Editor

Trans Fatty Acids in Tumor Development

SIR: The Institute of Shortening and Edible Oils, Inc., submits the following comments about the recent paper by Awad[1].

1) Concerning experimental diets, comparison of the feeding of a triglyceride (olive oil) to the feeding of a free fatty acid (elaidic acid) is not a correctly controlled experiment. A properly controlled experiment would have been comparison of the feeding of olive oil with the feeding of elaidic acid in triglyceride form or the feeding of controls with a corresponding amount of free oleic acid. Furthermore, the experimental fats had substantial differences in fatty acid composition and therefore are not directly comparable. The reported levels of 16:0 in the olive oil and elaidic acid diets were 13.3 and 2.9%, respectively; total monoene levels, 60.0 and 7.8%, respectively; and 18:2 levels, 23.3 and 8.5%, respectively (table 1). Considering these large differences in non-*trans* acids between the two diets, the author cannot conclude that the reduced survival times of mice fed the elaidic acid diet were due to elaidic acid exclusively. It would be equally valid to conclude that the high levels of 18:2 (or 16:0) were *protective* of the animals fed the olive oil diet.

In addition, the feeding of free fatty acid of m.p. 44.5–45.5°C should be of concern because the higher melting fats usually are poorly digested. This fact alone is suggestive of a possible cause for the growth suppression (≈8% in 4 wk, table 2), even though the *trans*-fed mice ate about 17% more than did the olive oil group.

2) Some of the reported fatty acid composition data in table 1 are of questionable accuracy. For example, considering that corn oil comprised ⅔ of the total dietary lipid, the level of 18:2 in the elaidic acid diet should have been about 16.4%, yet the reported value was only 8.5%. Similarly, the expected level of 18:0 in the elaidic acid diet should have been about 0.5%, yet 2.6% was reported. These discrepancies suggest erroneous fatty acid analyses of the dietary fats.

If the actual level of 18:2 in the total fat of the elaidic acid diet were 8.5% as reported, then the level of 18:2 in this diet would have been about 0.6%, which would barely satisfy the essential fatty acid (EFA) requirement of the animals.[2] The animals fed this diet may have been borderline EFA-deficient, despite Dr. Awad's claims to the contrary. Thus the "host survival" data may reflect poor adaptation to the diet high in free fatty acid (as elaidic) and low in EFA.

3) The validity of the experiments involving thymidine uptake by the Ehrlich ascites tumor cells (table 3) may be questioned because there were no measurements of cell survival during the incubation period. Furthermore, the author did not report any cytological examination of these cells to determine if they were uniformly tumor cells or whether they also contained leukocytes which may be common in ascites tumor cells. Differences in proportions of tumor and nontumor cells in these ascites preparations might account for differences in thymidine uptake.

4) There is no correspondence between the in vitro thymidine uptake studies (table 3) and the weights of solid tumors 14 days after tumor inoculation (table 6). If *trans* acids were really stimulating tumor promotion as suggested by Dr. Awad (table 3), then the solid tumors in these animals should have been larger than those in the animals fed the olive oil diet. However, the data in table 6 indicate that "elaidic acid feeding did not significantly increase the weight of the solid tumor" after 14 days. No reason is offered for this apparent inconsistency. Borderline EFA deficiency may be an explanation since it has been shown that tumor cells also have minimum EFA requirements.[3]

The method used for measurement of tumor weight (difference in weight between tumor-bearing leg and opposite leg) may not be accurate since the presence of the tumor may lead to disuse atrophy of the tumor-bearing leg and perhaps hypertrophy of the noninvolved leg. Additionally, if the tumors are large, they may impair circulation or cause edema, so that weight differences may be misleading.

5) The Ehrlich ascites tumor is *not* a normal tumor for the mouse, in contrast to a tumor that might develop in response to treatment of the animal with a carcinogen. Thus Dr. Awad's study is somewhat artificial since it evaluates how mice fed particular diets handle one type of foreign tumor. Other tumor systems should have been evaluated for assessment of the general applicability of these results.

6) Among erroneous or misleading statements in this paper are the following:

a) *Trans* fatty acids are *not* "unnatural substances" as referred to by the author. They occur naturally in ruminant fats and thus have been in the diets of humans for centuries. Reliable estimates of *trans* acid intake by Americans, however, have not been published in spite of Dr. Awad's citation of Enig and co-workers'[4] reported intake range of 3.3–7% calories. The lower end of this range is supported by the recent work of Ohlrogge et al.,[5] which showed a close correlation between levels of isomeric fatty acids in the diet and in various human tissues and a range of 2.0–5.8% *trans* fatty acids in human adipose tissue. The 7% calorie figure is not supported by valid data and is probably too high.

b) Dr. Awad cited the recent report of Enig et al.[4] as indicating "possible negative health ramifications of the widespread ingestion of dietary *trans* acids" and "a possible linkage between the consumption of *trans* fatty acids and the incidence of cancer in the United States." However, Dr. Awad overlooked the fact that the work of Enig et al. was severely criticized in letters by Applewhite,[6] Bailar,[7] and Meyer.[8] Both the report by Enig et al. and the one by Dr. Awad failed to consider published studies in which high levels of *trans* fatty acids were fed to animals for long periods of time without any overall adverse effects.[9-12]

c) Dr. Awad's claim that ". . . the level of *trans* fatty acids used in these studies is lower than that present in some hydrogenated products . . ." is also incorrect. The *level* of elaidic acid *in the dietary fat* was 78%, and this is the crux of the argument. Had the author studied a diet truly parallel-ing the human diet, he should have reduced this value to less than 10% of the total fat. There are no commercial products containing 78% elaidic acid. The study of this pure compound as a free fatty acid adds confusion and does little to clarify a complex issue.

d) Dr. Awad's suggestion that "more studies . . . are needed . . . (to determine) . . . the safety of these unnatural (*trans* fatty acids)" ignores the many animal metabolic studies without any evidence of deleterious effects of *trans* fatty acids. The safety of hydrogenated fats and *trans*-monoenes for human use has been scrutinized repeatedly [cf. Applewhite[13]]. The closing quotation in Applewhite's article[13] best sums up the subject: "Trans, *trans*- 18:2 excepted, and with adequate linoleate intake, there is no strong evidence that they (*trans*-monoenes) are more harmful than any other fatty acid class."

J. Edward Hunter, *Ph.D.*
Biological Subcommittee
Institute of Shortening and Edible Oils, Inc.
1750 New York Avenue, N. W.
Washington, D.C. 20006

---

[1] Awad AB. *Trans* fatty acids in tumor development and the host survival. JNCI 1981; 67:189-192.

[2] National Research Council. In: Nutrient requirements of laboratory animals. 3d ed. Washington, D.C.: National Academy of Sciences, 1978:44.

[3] Carroll KK, Hopkins GJ. Dietary polyunsaturated fat versus saturated fat in relation to mammary carcinogenesis. Lipids 1979; 14:155-158.

[4] Enig, G. Munn RJ, Keeney M. Dietary fat and cancer trends—a critique. Fed Proc 1978; 37:2215-2220.

[5] Ohlrogge JB, Emken EA, Gulley, RM. Human tissue lipids: Occurrence of fatty acid isomers from dietary hydrogenated oils. J Lipid Res 1981; 22:955-960.

[6] Applewhite TH. Statistical "correlations" relating *trans*-fats to cancer: A commentary. Fed Proc 1979; 38:2435.

[7] Bailar JC III. Dietary fat and cancer trends—a further critique. Fed Proc 1979; 38:2435-2436.

[8] Meyer WH. Further comments. Fed Proc 1979; 38:2436-2437.

[9] Alfin-Slater R, Aftergood L. Nutritional role of hydrogenated fats (in rats). In: Emken EA, Dutton HJ, eds. Geometrical and positional fatty acid isomers. Champaign, Ill.: Am Oil Chem Soc, 1979:53-72.

[10] Mattson FH. An investigation of the essential fatty acid activity of some of the geometrical isomers of unsaturated fatty acids. J Nutr 1960; 71:366-370.

[11] Alfin-Slater RB, Wells AF, Aftergood L, Deuel HJ. Nutritive value and safety of hydrogenated vegetable fats as evaluated by long-term feeding experiments with rats. J Nutr 1957; 63:241-261.

[12] Aaes-Jorgensen E, Funch JP, Dam JH. The role of fat in the diet of rats. 8. Influence on growth of shortening products, emulsifiers and polymerised linseed oil. Br J Nutr 1956; 10:317-324.

[13] Applewhite TH. Nutritional effects of hydrogenated soya oil. J Am Oil Chem Soc 1981; 58:260-269.

Sir: *This is a reply to Dr. Hunter's critique on my paper published in the July 1981 issue of JNCI.*

1) The author is aware that oleic acid would be more appropriat as a control to elaidic acid than olive oil. However, our previous work[1] *demonstrated that the commercial oleic acid (United States Biochemical Corp., Cleveland, Ohio) contains about 2.9% elaidic acid. The ideal control then would be a pure oleic acid, which is very costly for feeding, and thus our choice was limited to the oil (olive oil) from which most of the commercial oleic acid is obtained.*

It is well known to the experimental scientist that it is difficult, if not impossible, to exactly duplicate the concentrations of all other fatty acids in the experimental diet to resemble those of the control unless pure fatty acids are used. The work of Carroll and Hopkins[2] *argues against the possibility that high levels of 18:2 in the olive oil diet is protective against cancer. Their studies demonstrated that 20% sunflower oil diet induced more tumors in rats as compared with the number of tumors induced in rats fed 3% sunflower oil diet. Feeding the two experimental diets, as stated in the paper (table 2), revealed no significant effect for elaidic acid on body weight gain; we also stated that the increase in food consumption in animals fed elaidic acid as compared with the controls (olive oil diet) cannot be tested for significance since the individual observations of food consumption were not recorded.*

2) The data presented for the fatty acid composition of the experimental diets were obtained by actual gas-liquid chromatography analysis after mixing the diets and were not derived by calculation from published chemical analysis for the fats used. Regarding reference 2 in Dr. Hunter's critique for the EFA requirements for mice, I would like to mention that Dr. Hunter unfortunately misread the statement in that reference. It was stated that "In the absence of specific studies in the mouse, the concentration of 0.3% linoleic acid, as recommended for the rat has been adopted." Thus our diets that contained double the recommended level should be more than sufficient, and the animals were not borderline EFA-deficient. *This was supported by the nonsignificant difference in growth rate between animals fed an elaidic acid or an olive oil diet.*

3) We tested the viability of tumor cells from animals fed elaidic acid diet or olive oil diet on several occasions, and it was found to be similar and ranged between 92 and 94%. This viability was not affected by incubation for 1 hour. Similar work by King and Spector[3] *using in vitro incubation of Ehrlich ascites tumor cells under similar conditions demonstrated that this tumor can survive up to 4 hours without a decrease in its viability. The tumor cells were washed three times in saline after the blood cells were lysed by brief exposure to water. We checked for the presence of erythrocytes and leukocytes, and we could not detect any by light microscopy. This information was supplied to one of the reviewers of the* JNCI *during the reviewing process of the paper.*

4) Measuring the size of the solid tumor by weighing its mass or by measuring its size would not be as accurate as biochemical indices to give ideas on the tumor growth and development. This could be the reason for not seeing differences in solid tumor mass by feeding the experimental diets.

5) It is well known that Ehrlich ascites tumor cell line has been originated in mice several decades ago by the use of chemical carcinogens. As Dr. Hunter stated in this regard, the issue of trans *fatty acids in the diet and how they affect normal and abnormal processes in the body is complex. For that reason we have decided to study* trans *fatty acids by using only one fatty acid at a time. In this particular study, we used the predominant* trans *fatty acid in hydrogenated vegetable oils, i.e., elaidic acid.*

6) a) There is a difference in the position of the double bond between the trans *fatty acids produced by rumen bacteria and those produced by industrial hydrogenation of vegetable oil* ($18{:}1^{\Delta 11}$ *vs.* $18{:}1^{\Delta 9}$)*. This difference results in differences in fatty acid metabolism by the mammalian system.*[4] *For that reason, elaidic acid is considered* *to be unnatural. Studies by Ohlrogge et al.*[5] *reported differences in the concentrations of* trans *fatty acids in human tissues, and the values of 2–5.8% were reported for* adipose tissues. *There were no data in Ohlrogge and co-workers' paper for the* trans *fatty acid content of the human diet. These tissues were obtained at autopsy, and the dietary records for the deceased persons were not available.*

b) We are not aware of any other studies that have been done to examine trans *fatty acid's effect on tumor development, and it was not appropriate to discuss cancer with other diseases as Dr. Hunter suggested.*

c) For testing a hypothesis, especially with a rapidly growing tumor (14 days in the ascites form), one has to increase the level of the tested substance to greater than that present in the human diet. The increase was modest—11 versus 7% of dietary calories in human diet.

d) I believe that my paper contains useful information and further investigation in this area is warranted.

In conclusion, I can see that Dr. Hunter, as a representative for the Institute of Shortening and Edible Oils, Inc., is disturbed by the results of our studies since they could affect the marketing of their products. However, issues such as those related to diet and health of the American public should be subject to extensive independent investigation.

Atif B. Awad, *Ph.D.*
Department of Biochemistry
Kirksville College of Osteopathic Medicine
Kirksville, Missouri 63501

---

[1] Awad AB. The effect of elaidic acid incorporation upon the lipid composition of Ehrlich ascites tumor cells and the host's liver. Lipids 1978; 13:850–859.

[2] Carroll KK, Hopkins GJ. Dietary polyunsaturated fat versus saturated fat in relation to mammary carcinogenesis. Lipids 1979; 14:155–158.

[3] King ME, Spector AA. Effect of specific fatty acyl enrichments on membrane physical properties detected with spin label probe. J Biol Chem 1978; 253:6493–6501.

[4] Lawson LD, Kummerow FA. β-Oxidation of the coenzyme A esters of vaccenic, elaidic and petroselaidic acids by rat heart mitochondria. Lipids 1979; 14:501–503.

[5] Ohlrogge JB, Emken EA, Gulley RM. Human tissue lipids: Occurrence of fatty acid isomers from dietary hydrogenated oils. J Lipid Res 1981; 22:955–960.

blank page

Multiple Myeloma Among Atomic Bomb Survivors in Hiroshima and Nagasaki, 1950–76: Relationship to Radiation Dose Absorbed by Marrow[1,2]

Michito Ichimaru, *M.D.*,[3] **Toranosuke Ishimaru**, *M.D., M.P.H.*,[4,5] **Motoko Mikami**, *M.D.*,[6] *and* **Masako Matsunaga**, *M.D.*[6,7,8]

ABSTRACT—The relationship between atomic bomb exposure and the incidence of multiple myeloma has been examined in a fixed cohort of atomic bomb survivors and controls in the life-span study sample for Hiroshima and Nagasaki. From October 1950 to December 1976, 29 cases of multiple myeloma were confirmed in this sample. Our analysis shows that the standardized relative risk (RR) adjusted for city, sex, and age at the time of bombings (ATB) increased with marrow-absorbed radiation dose. The increased RR does not appear to differ between cities or sexes and is demonstrable only for those survivors whose age ATB was between 20 and 59 years. The estimated risk in these individuals is approximately 0.48 cases/million person-years/rad for bone marrow total dose. This excess risk did not become apparent in individuals receiving 50 rad or more in marrow total dose until 20 years or more after exposure.—JNCI 1982; 69:323–328.

Although leukemia has long been known to be a late effect of atomic bomb exposure (*1*, *2*), the incidence of multiple myeloma previously has not been found to be significantly elevated among atomic bomb survivors. On the basis of the autopsy material obtained by the ABCC in 1948–62, Anderson and Ishida (*3*) reported that the incidence of multiple myeloma among atomic bomb survivors in Hiroshima was slightly increased in the group exposed within 1,400 m of the detonation, as compared to the incidence in those individuals exposed beyond that distance; however, in the group within 1,400 m, there was only 1 multiple myeloma case. Up to September 1964, Ichimaru et al. (*4*, *5*) found 8 cases of multiple myeloma among the Nagasaki atomic bomb survivors, but they observed no unusual clinical features of the disease in these instances. These investigators did not examine the relationship of distance to risk of multiple myeloma. Yamamoto and Wakabayashi (*6*) reported an absence of evidence of radiation-induced bone tumors, including multiple myeloma in atomic bomb survivors in Hiroshima and Nagasaki during 1950–65. Nishiyama et al. (*7*) also made a study of malignant lymphoma and multiple myeloma in the same fixed cohort of atomic bomb survivors, but they could not demonstrate a significant excess risk of multiple myeloma in the heavily exposed. Thus for 20 years after the atomic bombings, no persuasive evidence of an excess of multiple myeloma among the survivors was found.

Inasmuch as 10 years have elapsed since Yamamoto and Wakabayashi (*6*) and Nishiyama and his colleagues (*7*) reported their findings, we thought it timely to examine again the effect of radiation on the risk of multiple myeloma, based on further follow-up of the cohort of atomic bomb survivors. Moreover, in 1980 an improved dosimetry, based on a new epicenter in Nagasaki proposed by Kerr and Solomon (*8*), became available for survivors belonging to the RERF fixed cohort. As a result of the formulas developed by Kerr (*9*) for bone marrow-absorbed dose per kerma dose conversion factors, bone marrow-absorbed dose is also now available for each atomic bomb survivor in this fixed cohort. These atomic doses may be changed, however, as the result of an ongoing review of atomic bomb dosimetry. Our risk estimates, although probably not the major conclusions presented in this paper, may require revision when that review has been completed.

On the basis of bone marrow-absorbed radiation dose, an analysis is presented herein of the multiple myeloma incidence among atomic bomb survivors and controls in the fixed cohort of the ongoing LSS (*10*) of the RERF in a 26-year period from October 1950 to December 1976.

MATERIALS AND METHODS

Subjects.—The death of 109,000 atomic bomb survivors and their controls in Hiroshima and Nagasaki has been under scrutiny since October 1, 1950, first at ABCC and later at RERF. In connection with this mortality surveil-

---

ABBREVIATIONS USED: ABCC=Atomic Bomb Casualty Commission; ATB=at time of bombings; LSS=life-span study; NIC=not in the city; P-Y=person-years; RERF=Radiation Effects Research Foundation; RR=relative risk.

---

[1] Received August 9, 1979; revised October 23, 1981; accepted February 14, 1982.

[2] Supported by the Radiation Effects Research Foundation (formerly the Atomic Bomb Casualty Commission), a cooperative Japan–United States research organization; and by a cancer research grant from the Japanese Ministry of Education.

[3] Department of Hematology, Atomic Bomb Disease Institute, Nagasaki University School of Medicine, Nagasaki 852, Japan.

[4] Department of Epidemiology and Statistics, Radiation Effects Research Foundation (RERF), 5-2 Hijiyama Park, Hiroshima 730, Japan; and Department of Epidemiology, Tokyo University School of Health Science, Tokyo 113, Japan.

[5] *Address reprint requests to* Dr. T. Ishimaru at RERF.

[6] Department of Medicine, RERF.

[7] Department of Internal Medicine, Atomic Bomb Disease Institute, Nagasaki University School of Medicine.

[8] We express our sincere appreciation to Dr. William J. Schull, former Chief of the Department of Epidemiology and Statistics, RERF, for his advice and encouragement. We are also grateful to the many physicians at the university and community hospitals in Hiroshima and Nagasaki and to the staffs of the tumor registries in those cities for their continued support of the Leukemia Registry at RERF. We thank Mrs. Nobuko Shimba for her assistance in the statistical analysis of the data and Mr. K. Joji, Chief of the Translation Section, RERF, for his editorial assistance.

TABLE 1.—*Distribution of atomic bomb survivors and controls (by city and marrow total dose) in the LSS sample, October 1950-December 1976, Hiroshima and Nagasaki*

Marrow total dose exposure, rad	Hiroshima				Nagasaki			
	Average dose, rad		Subjects		Average dose, rad		Subjects	
	Gamma	Neutron	No.	Percent	Gamma	Neutron	No.	Percent
≥150	193.0	32.7	726	1.0	227.1	2.3	743	3.1
100–149	105.8	15.9	557	0.8	119.8	1.0	707	2.9
50–99	61.0	8.3	1,511	2.1	72.7	0.5	1,165	4.8
10–49	19.7	2.3	6,921	9.4	23.7	0.0	3,135	12.9
1–9	2.8	0.4	17,163	23.4	3.1	0.0	8,143	33.6
Control[a]	0.0	0.0	46,435[b]	63.3	0.0	0.0	10,338	42.7
Total			72,313	100.0			24,231	100.0

[a] 0 rad and NIC ATB.

[b] Subjects in the NIC ATB group in Hiroshima were selected in 1950, 1951, and 1953.

lance from 1961 to 1975, an intensive autopsy procurement program (*11*) existed, which was directed toward the original LSS sample (*12*) and excluded the extended part of the sample. Because the efficiency with which case findings of multiple myeloma were reported seems to differ between the original LSS sample and the extended portion, the present analysis is confined to the original LSS sample which totaled approximately 100,000 subjects.

Dosimetry.—In 1980 the RERF Department of Epidemiology and Statistics, using a new epicenter in Nagasaki and a standardized rounding procedure, recalculated the estimated atomic bomb radiation dose received by each survivor in this sample. The improved dosimetry system is called the "T65D revised system" or T65DR. If the total kerma for a survivor were calculated to be 600 rad or more and to avoid distortions arising from probable erroneous estimates (*13*), the investigators arbitrarily set the gamma dose for that survivor in Hiroshima at 439 rad and the neutron dose at 161 rad, whereas in Nagasaki the gamma dose was set at 587 rad and the neutron dose was set at 13 rad. Hiroshima had 165 such cases and Nagasaki had 138. There were 1,706 survivors for whom the estimated dose could not be calculated either because the information regarding their exposure was incomplete or the shielding configuration was unusually complex. Those survivors whose doses are unknown were excluded from the present analysis.

Individual bone marrow doses were calculated by means of Kerr's proposed formulas (*9*) for bone marrow dose per kerma dose conversion factors for Japanese atomic bomb survivors: $(D\gamma/K\gamma) = 0.56$, $(Dn/Kn) = 0.28$, and $(Dn, \gamma/Kn) = 0.067$, where $K\gamma$ = gamma kerma dose, Kn = neutron kerma dose, $D\gamma$ = marrow gamma dose converted by kerma gamma dose, Dn = marrow neutron dose converted by kerma neutron dose, and Dn, γ = marrow gamma dose converted by kerma neutron dose.

A degree of uncertainty still exists about the quality and quantity of radiation released by these two atomic bombs. Some recent estimates (*14, 15*) suggest that the total kerma was somewhat higher in Hiroshima and somewhat lower in Nagasaki than the present T65DR dosimetry system and that the present estimate of neutrons is grossly erroneous. If warranted by future dose assessments, the RR reported in this paper will be reanalyzed and subsequently reported.

Ascertainment.—The koseki system on which the mortality surveillance is based ensures virtually complete identification of deaths and causes of death in this fixed sample. All deaths ascribed to multiple myeloma among those individuals were screened. Pathologic studies intensively conducted under the ABCC-RERF autopsy procurement program since 1961 (*11*) provide supportive observations. Furthermore, almost complete screening of possible multiple myeloma from various medical sources was made through the Leukemia and Related Disorders Detection Program at

TABLE 2.—*Annual incidence of multiple myeloma (by marrow total dose) in the LSS sample, October 1950-December 1976, Hiroshima and Nagasaki*

Specification	Controls	T65DR marrow total dose, rad		Totals
		1–49	≥50	
Average dose, rad	0	8.6	125.3	—
P·Y	1,273,647	803,080	123,851	2,200,578
Observed No.	14	10	5	29
Expected No.[a]	16.0	11.2	1.8	29.0
Crude incidence rate, 10^5	1.10	1.25	4.04	1.32
Standardized incidence[b] rate, 10^5	1.29	1.47	4.67	—
Standardized RR[c]	1.0	1.0	3.2	—
Statistical test of significance for linearity[d]: $\chi^2_{[1]}=7.43$, $P<0.01$				

[a] Adjusted for city, sex, and age.

[b] LSS subjects standardized according to sex and age ATB (0–19, 20–39, 40–59, and ≥60 yr).

[c] Calculation was made by Miettinen's procedure (*18*).

[d] Extension of the Mantel-Haenzel procedure (*17*).

TABLE 3.—*Specific annual incidence of multiple myeloma (by marrow total dose, sex, city, and age ATB) in the LSS sample, October 1950–December 1976, Hiroshima and Nagasaki*

Specification	Controls	Marrow total dose, rad		Totals
		1–49	≥50	
		Male		
P-Y	517,563	322,571	53,255	893,389
No. of cases	4	3	3	10
Rate, 10^5	0.77	0.93	5.63	1.12
Crude RR	1.0	1.2	6.4	—
		Female		
P-Y	756,083	480,509	70,597	1,307,189
No. of cases	10	7	2	19
Rate, 10^5	1.32	1.46	2.83	1.45
Crude RR	1.0	1.1	2.1	—
		Hiroshima		
P-Y	1,032,403	543,374	62,575	1,638,352
No. of cases	11	6	2	19
Rate, 10^5	1.07	1.10	3.20	1.16
Crude RR	1.0	1.0	3.0	—
		Nagasaki		
P-Y	241,243	259,706	61,276	562,225
No. of cases	3	4	3	10
Rate, 10^5	1.24	1.54	4.90	1.78
Crude RR	1.0	1.2	4.0	—
		Age ATB: 0–19		
P-Y	577,303	373,998	59,606	1,010,907
No. of cases	1	0	0	1
Rate, 10^5	0.17	0.0	0.0	0.10
Crude RR	1.0	—	—	—
		Age ATB: 20–39		
P-Y	391,526	228,147	37,527	657,200
No. of cases	3	2	2	7
Rate, 10^5	0.77	0.88	5.33	1.07
Crude RR	1.0	1.1	6.9	—
		Age ATB: 40–59		
P-Y	272,033	178,330	24,817	475,180
No. of cases	9	8	3	20
Rate, 10^5	3.31	4.49	12.09	4.21
Crude RR	1.0	1.4	3.7	—
		Age ATB: ≥60		
P-Y	32,785	22,605	1,902	57,292
No. of cases	1	0	0	1
Rate, 10^5	3.05	0.0	0.0	1.75
Crude RR	1.0	—	—	—

ABCC and later at RERF in Hiroshima and Nagasaki (*16*). With the aid of a standardized registration procedure, hematologists recorded all pertinent information available at the community hospitals and clinics to confirm a diagnosis of multiple myeloma. In the present analysis 3 hematologists (M. I., M. O. M., and M. A. M.) reviewed these records for possible multiple myeloma cases. Microscopic evidence of myeloma cells, laboratory tests of immunoglobulins, X-ray findings of bone, and autopsy findings were all used to establish the diagnosis. The final judgment was made by the senior hematologist (M. I.). Through the foregoing screening procedure, 35 cases of possible multiple myeloma were identified in the original LSS sample from October 1950 to December 1976. On the basis of available medical data, the diagnosis of multiple myeloma was accepted in 29 instances: 22 individuals who were exposed to the atomic bomb and 7 individuals who were NIC ATB.

Table 1 shows the distribution of atomic bomb survivors and controls in the LSS sample by city and marrow total dose. The sample consists of 97,544 persons—73,313 in Hiroshima and 24,231 in Nagasaki. Hiroshima NIC subjects were selected in 1950, 1951, and 1953; hence the observation periods differ from those for individuals who had been exposed to the atomic bomb. Hiroshima survivors, at least until recently, have been assumed to have received mixed gamma and neutron exposure at all dose levels, whereas Nagasaki survivors received largely gamma exposures except at the higher dose levels, but even in Nagasaki the neutron exposure was small when contrasted with that in Hiroshima.

RESULTS

Annual Incidence Rate of Multiple Myeloma in LSS Sample by Marrow Total Dose

Table 2 shows the crude and standardized annual incidence rates adjusted for city, sex, and age ATB for 3 dose

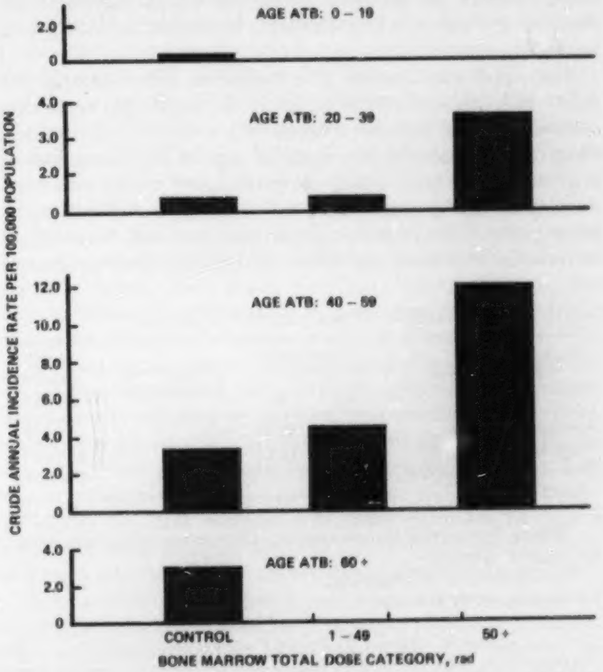

TEXT-FIGURE 1.—Crude annual incidence rate of multiple myeloma (by age ATB and total marrow dose) for atomic bomb survivors and controls in the LSS sample, Oct. 1950–Dec. 1976, Hiroshima and Nagasaki.

TABLE 4.—*Age at onset of multiple myeloma in the LSS sample, October 1950–December 1976, Hiroshima and Nagasaki*

Age, yr	No. of cases	Percent
<60	7	24.1
60–69	14	48.3
≥70	8	27.6
Total	29	100.0

classes. The RR significantly increases with marrow total dose after adjustment for city, sex, and age ATB ($P<0.01$), as judged by an extension of the Mantel-Haenszel procedure (*17*). The standardized RR is approximately 3 among those individuals who received 50 rad or more in marrow doses, as compared to the RR for controls. The RR was calculated by Miettinen's procedure (*18*).

Table 3 gives the specific annual incidence rate by sex, city, and age ATB for 3 dose classes. The RR tends to increase with dose for both sexes in both cities in the 20- to 59-year age ATB group. When the data were examined by dividing them into 12 categories (3 dose groups and 4 age ATB groups), the number of cases in each category was small. However, a dose effect is not evident among those individuals whose age ATB was less than 20 years or 60 or more years, although the risk tends to increase in the control group with age. Text-figure 1 shows the age ATB-specific annual incidence rate by dose for the 4 age ATB groups, and apparently the dose effect does differ.

The distribution of age at onset of the 29 confirmed cases in the present study is shown in table 4. Clearly, multiple myeloma occurs frequently after 60 years of age, and thus the failure to see an effect in the under-20-year group may merely reflect the fact that these individuals have not yet reached the age at which multiple myeloma is more prone to develop.

The apparent absence of a radiation effect among the oldest individuals (≥60 yr of age ATB) is thought to be due to other reasons. Because a dose effect is evident only among those individuals 20-59 years of age ATB, a regression analysis based on a linear dose-response model was conducted for this group to estimate the risk of multiple myeloma per million population per year per rad. Tables 5-7 summarize the linear regression analysis for dose response of multiple myeloma among atomic bomb survivors and controls whose age ATB was between 20 and 59 years in the LSS sample. Tables 5 and 6 present summaries of the results of fitting two linear dose-response models to these data. Model I (table 5) assumes a linear dependence on marrow total dose, and model II (table 6) assumes a linear dependence on γ-rays and neutrons, separately. The analysis revealed that model I fits the data well (small chi-square and large-tail probability), and the regression coefficient is suggestively significant ($0.05<P<0.10$). The estimated risk is approximately 0.48 cases (SE, 0.29)/million P-Y/rad for bone marrow total dose. When a dose-response model was tested that assumes a linear dependence for both γ-rays and neutrons (table 6), the model again fit the data well. However, the regression coefficients for both γ-rays and neutrons were not significantly different from zero nor even suggestively so.

TABLE 5.—*Model I:* $P_{ij}\times10^{-6}=\alpha_i+\beta_1 D_{ij}$[a]

Specification	Constant[b]		Regression coefficient $\hat{\beta}_1$	Goodness-of-fit test
	$\hat{\alpha}_H$	$\hat{\alpha}_N$		
Average	15.80	30.57	0.48	$\chi^2=1.20$
Standard error	4.52	12.43	0.29	df[c] = 5
Test of significance for coefficient			$\chi^2_{[1]}=2.84$, $0.05<P<0.10$	$P>0.10$

[a] Where P=probability, α=constant, D=marrow total dose, i=city, and j=dose category.

[b] H=Hiroshima, N=Nagasaki.

[c] df=degrees of freedom.

TABLE 6.—*Model II:* $P_{ij}\times10^{-6}=\alpha_i+\beta_1 D\gamma_{ij}+\beta_2 Dn_{ij}$[a]

Specification	Constant[b]		Regression coefficient		Goodness-of-fit test
	$\hat{\alpha}_H$	$\hat{\alpha}_N$	$\hat{\beta}_1$	$\hat{\beta}_2$	
Average	15.94	29.53	0.59	−0.73	$\chi^2=1.19$
Standard error	4.57	12.75	0.51	4.33	df[c] = 4
Test of significance for coefficient			$\chi^2_{[1]}=1.33$, $P>0.10$	$\chi^2_{[1]}=0.03$, $P>0.10$	$P>0.10$

[a] Where P=probability, α=constant, $D\gamma$=marrow gamma dose, Dn=marrow neutron dose, i=city, and j=dose category.

[b] H=Hiroshima, N=Nagasaki.

[c] df=degrees of freedom.

TABLE 7.—*Basic table for regression analysis for dose response of multiple myeloma among atomic bomb survivors and controls (aged 20-59 yr ATB) in the LSS sample, October 1950-1976, Hiroshima and Nagasaki*

Marrow total dose exposure, rad	Average dose, rad		Total dose, rad	P-Y	No. of cases	Rate, 10^6
	Gamma	Neutron				
Hiroshima						
Survivors						
≥100	154	24	178	15,920	2	125.6
50-99	62	8	70	19,698	0	0.0
1-49	8	1	9	295,417	6	20.3
Controls	0	0	0	556,240	9	16.2
Total				887,275	15	16.9
Nagasaki						
Survivors						
≥100	178	2	180	14,741	2	135.7
50-99	72	0	72	11,984	1	83.4
1-49	9	0	9	111,059	4	36.0
Controls	0	0	0	107,318	3	28.0
Total				245,102	10	40.8

Cumulative Hazard Rates of Multiple Myeloma By Three Marrow Dose Groups

We used a simple graphical method called "hazard plotting" (*19, 20*) to compare the cumulative risk of multiple myeloma in 3 dose groups in relation to years after exposure. Text-figure 2 shows the cumulative hazard rates for individuals aged 20-59 ATB in 3 marrow dose groups (≥50, 1-49, and <1 rad) from October 1950 to December 1976. An increased risk in the high-dose group (≥50 rad) does not become apparent until 20 years after exposure.

Clinical Features of Multiple Myeloma

Although the available records on the clinical course of multiple myeloma cases have limited value and the observed number of individuals in the high-dose group is small, the clinical and autopsy findings and immunoglobulin properties are not unique for the high-dose survivors when compared to those for the control group. The type of immuno-

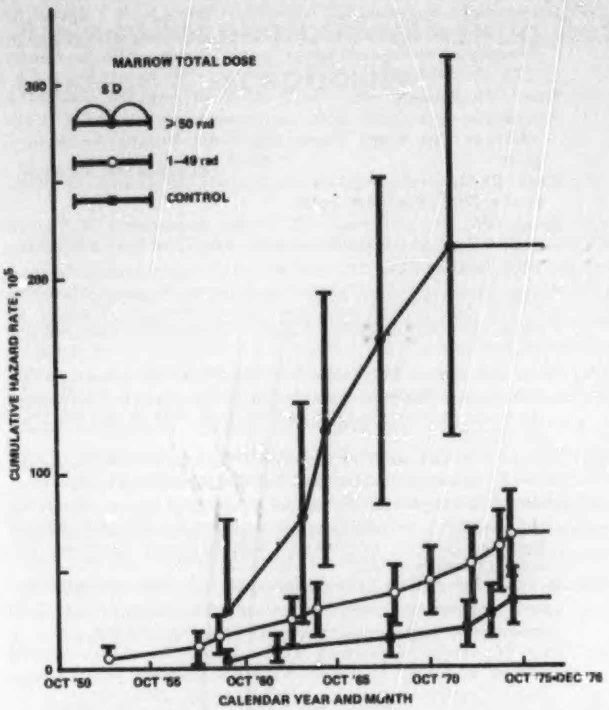

TEXT-FIGURE 2.—Cumulative hazard rates for atomic bomb survivors and controls (aged 20–59 yr ATB) in the LSS sample, Oct. 1950–Dec. 1976, Hiroshima and Nagasaki. The controls, selected in Oct. 1950, were individuals who had received <1 rad radiation or were NIC ATB.

globulin seen in myeloma was recorded for 4 of 17 patients (24%) in whom onset of the disease occurred before 1971 and for 5 of 12 patients (42%) in whom onset occurred in 1971 or later, which suggests that the techniques for the diagnosis of multiple myeloma have improved in recent years. A clinical diagnosis of multiple myeloma could not be confirmed by autopsy in 2 of 6 possible cases.

DISCUSSION

Only a few studies exist on the relationship of death from multiple myeloma to occupational long-term, continuous low-dose, ionizing radiation exposure. Lewis (*21*) noted that the observed mortality from multiple myeloma among American radiologists was significantly higher than expected. In 1977, Mancuso et al. (*22*) reported an excess mortality due to bone marrow cancers, including myelomas and myeloid leukemias, among Hanford workers who received radiation exposure during the manufacture of radioactive substances. Subsequently, Gilbert and Marks (*23*) and Hutchinson et al. (*24*) reanalyzed these data. Both analyses indicated a significant relationship of radiation exposure to cancer of the pancreas and multiple myeloma among Hanford workers who received significant radiation exposure, but no evidence of a dose effect was seen for cancers of other sites including those more typically associated with radiation exposure, such as myeloid leukemia and lung cancer. In 1977, independently of the Hanford studies, we initiated the present study based on the Leukemia Registry at RERF because of our interest in examining whether an induction of multiple myeloma among atomic bomb survivors could be demonstrated 20 years after exposure to the bomb. Earlier studies on the incidence of multiple myeloma among atomic bomb survivors had failed to demonstrate a significantly increased risk with dose (*3, 6, 7*).

The present analysis was conducted on a fixed cohort of survivors and controls 5–31 years after exposure; thus data on the entire life-spans of the subjects in this cohort were not examined. Evaluation of the latent period was complicated by the fact that the number of cases is not large enough to permit examination of the development pattern of radiation-induced multiple myeloma in relation to age ATB. By the end of 1976, attrition due to death was about 28% for the entire cohort: Death had occurred in approximately 98% of the individuals aged 60 years or more ATB, in 60% of those aged 40–59 years ATB, in 15% of those aged 20–39 years ATB, and in 5% of those aged less than 20 years ATB. Thus further investigation of this cohort will not result in the detection of any new cases among individuals aged 60 years or more ATB in the high-radiation-dose category.

Our analysis suggests that the latent period of radiation-induced multiple myeloma is longer the younger the age ATB, except for those survivors whose age ATB was 60 years or more. The pattern of development of radiation-induced leukemia among atomic bomb survivors suggests an earlier development of leukemia in the younger age ATB groups and later development of the disease in older age ATB groups (*2, 25*). Thus the pattern of development (latent period and effect of age ATB) of radiation-related multiple myeloma appears to differ from that of leukemia.

A relationship of multiple myeloma mortality to radiation exposure in the fixed cohort of atomic bomb survivors was not reported until 1974 (*26*); however, Kato and Schull (*27*) recently noted, from death certificate information for the period between 1950 and 1978, an excess risk of multiple myeloma mortality in atomic bomb survivors.

Although the present analysis failed to produce a significance dose-response function for the incidence of multiple myeloma in relation to gamma and neutron doses separately, the risk of multiple myeloma among survivors whose age ATB was 20–59 years is estimated to be about 0.48 cases/million P-Y/rad for marrow dose under a linear dependence on total marrow dose. Risk estimates for excess mortality from multiple myeloma in Hanford workers have not been reported due to the small number of cases (*22–24*).

Excess multiple myeloma mortality has been reported among employees in nuclear processing plants at Hanford. The original report by Mancuso et al. (*22*) showed an increased mortality from bone marrow cancers, including myeloid leukemia and multiple myeloma, and from pancreas cancer and lung cancer. Gilbert and Marks (*23*) and Hutchinson et al. (*24*) subsequently reanalyzed the data on these workers and reported that the excess proportional deaths from cancer of the pancreas and multiple myeloma occurred in employees who received significant radiation from occupational exposure, but these investigators failed to demonstrate the effect of radiation on those cancers that are more commonly associated with radiation exposure, such as myeloid leukemia and lung cancer. Thus the results of Mancuso et al. now seem to be discounted.

Cuzick (*28*) recently reviewed multiple myeloma mortality in several cohort studies of persons exposed to radiation. He reported that an excess in incidence of myeloma was found in most cohorts but that the incidence was negligible in groups irradiated for uterine neoplasms. Most of the radiation-related cases of multiple myeloma occurred 15–25 years after exposure.

Although the incidence of multiple myeloma was significantly elevated among heavily exposed persons in our study, the observed number of cases in the high-radiation-dose group was small, and the clinical findings, immunoglobulin properties, and autopsy findings were not unique when compared to the data for the control group. The cases we studied were identified by retrospective review of available records accumulated over the 3 postwar decades. Unfortunately, these records are not uniformly detailed insofar as the clinical course of the disease is concerned, and an immunoelectrophoretic examination was not done routinely. The older cases, in contrast to the more recent ones, do not have records of immunological laboratory tests. However, despite improvements over the years in techniques for the diagnosis of multiple myeloma, it is unlikely that the newer immunological laboratory tests for the diagnosis of multiple myeloma create a bias in case detection by dose.

Myelomatous cells are considered to be of B-cell lineage, as are malignant neoplasms of the lymphatic system. They differ, however, from the malignant lymphoma cells which proliferate in lymphatic tissues, primarily in the lymph nodes. Spontaneous myeloma is a disease frequently found in advanced age groups, and possibly an immunoinsufficiency due to aging contributes to the development of this disease together with the late effect of atomic bomb exposure. The mechanism for development of radiation-induced myeloma apparently is different from that for radiation leukemogenesis. According to reports of follow-up studies on patients who received radiotherapy for ankylosing spondylitis and tinea capitas, bone tumors can be induced by radiation exposure (*29–31*). In those studies, multiple myeloma was not classified as a bone tumor. We also consider multiple myeloma to be different from malignant neoplasms of the bone, although an earlier report by Yamamoto and Wakabayashi (*6*) showed a negative effect of radiation for the induction of bone tumors including multiple myeloma.

(*1*) Ishimaru T, Hoshino T, Ichimaru M, et al. Leukemia in atomic bomb survivors, Hiroshima and Nagasaki, 1 October 1950–30 September 1966. Radiat Res 1971; 45:216–233.

(*2*) Ichimaru M, Ishimaru T, Belsky JL. Incidence of leukemia in atomic bomb survivors belonging to a fixed cohort in Hiroshima and Nagasaki, 1950–71. Radiation dose, years after exposure, age at exposure, and type of leukemia. J Radiat Res 1978; 19:262–282.

(*3*) Anderson RE, Ishida K. Malignant lymphoma in the survivors of the atomic bomb in Hiroshima. Ann Intern Med 1964; 61:853–862.

(*4*) Ichimaru M, Yasuhi S, Ootsuru S. Twelve cases of multiple myeloma in Nagasaki (7 cases from atomic bomb survivors). Nagasaki Igakkai Zasshi–Nagasaki Med J 1963; 38:109–113.

(*5*) Ichimaru M, Yasuhi S, Danno H, et al. Additional two cases of multiple myeloma in atomic bomb survivors. Nagasaki Igakkai Zasshi–Nagasaki Med J 1965; 40:608–611.

(*6*) Yamamoto T, Wakabayashi T. Bone tumors among the atomic bomb survivors of Hiroshima and Nagasaki. Acta Pathol Jpn 1969; 19:201–212.

(*7*) Nishiyama H, Anderson RE, Ishimaru T, Ishida K, It Y, Okabe N. The incidence of malignant lymphoma and multiple myeloma in Hiroshima and Nagasaki atomic bomb survivors, 1945–65. Cancer 1973; 32:1301–1309.

(*8*) Kerr GD, Solomon DL. The epicenter of Nagasaki weapon: A reanalysis of available data with recommended values. ORNT-TM-5139. Oak Ridge, Tenn.: Oak Ridge National Laboratory, 1976.

(*9*) Kerr GD. Organ dose estimates for Japanese atomic bomb survivors. Health Phys 1979; 37:487–508.

(*10*) Beebe GW, Kato H, Land CE. Studies of mortality of A-bomb survivors. 4. Mortality and radiation dose, 1950–1966. Radiat Res 1971; 48:613–649.

(*11*) Atomic Bomb Casualty Commission–Japanese National Institute of Health. ABCC–JNIH pathology studies, Hiroshima-Nagasaki, research plan. Atomic Bomb Casualty Commission technical report, 1962:12–62.

(*12*) Beebe GW, Ishida M, Jablon S. JNIH–ABCC life-span study, Hiroshima and Nagasaki. report 1: Description of study. Mortality in the medical subsample, October 1950–June 1958. Radiat Res 1962; 16:253–280.

(*13*) Jablon, S. Atomic bomb radiation dose estimation at ABCC. Atomic Bomb Casualty Commission technical report, 1971:23–71.

(*14*) Loewe WE, Mendelson E. Revised estimates of dose at Hiroshima and Nagasaki, and possible consequences for radiation-induced leukemia. D-80-14. Livermore, Calif.: Lawrence Livermore National Laboratory, 1980.

(*15*) Marshall E. New A-bomb studies alter radiation estimates. The basis of 15 years of radiation research may be in error; radiation toxicity may be understated. Science 1981; 212:900–903.

(*16*) Finch SC, Hrubec Z, Nefzger MD, et al. Detection of leukemia and related disorders, Hiroshima-Nagasaki, research plan. Atomic Bomb Casualty Commission technical report, 1965:5–65.

(*17*) Mantel N. Chi-square tests with one degree of freedom: Extensions of the Mantel-Haenszel procedure. Am Stat Assoc J 1963; 58:690–700.

(*18*) Miettinen OS. Standardization of risk ratios. Am J Epidemiol 1972; 96:383–388.

(*19*) Nelson W. Theory and applications of hazard plotting for censored failure data. Technometrics 1972; 14:945–965.

(*20*) Aalen O. Non-parametric inference in connection with multiple decrement models. Scand J Statist 1976; 3:15–27.

(*21*) Lewis EB. Leukemia, multiple myeloma and aplastic anemia in American radiologists. Science 1963; 42:1492–1494.

(*22*) Mancuso TF, Stewart A, Kneale G. Radiation exposure of Hanford workers dying from cancer and other causes. Health Phys 1977; 33:369–385.

(*23*) Gilbert ES, Marks S. An analysis of the mortality of workers in a nuclear facility. Radiat Res 1979; 79:122–148.

(*24*) Hutchinson GB, MacMahon B, Jablon S, Land CE. Review of report by Mancuso, Stewart and Kneale of radiation exposure of Hanford workers. Health Phys 1979; 37:207–220.

(*25*) Ichimaru M, Ishimaru T, Mikami M, Yamada Y, Ohkita T. Incidence of leukemia in atomic bomb survivors and controls in a fixed cohort, Hiroshima and Nagasaki, October 1950–December 1978. Radiation Effects Research Foundation technical report, 1981:13–81.

(*26*) Beebe GW, Kato H, Land CE. Studies of the mortality of A-bomb survivors. 6. Mortality and radiation dose, 1950–1974. Radiat Res 1978; 75:138–201.

(*27*) Kato H, Schull WJ. Life-span study, report 9, part 1: Cancer mortality among atomic bomb survivors, 1950–1978. Radiation Effects Research Foundation technical report, 1980:12–80.

(*28*) Cuzick J. Radiation-induced myelomatosis. N Engl J Med 1981; 304:204–210.

(*29*) Court Brown WM, Doll R. Mortality from cancer and other causes after radiotherapy for ankylosing spondylitis. Br Med J 1965; 2:1327–1332.

(*30*) Modan B, Baidatz D, Mart H, et al. Radiation-induced head and neck tumours. Lancet 1974; 1:277–279.

(*31*) Shore RE, Albert RE, Pasternack BS. Follow-up study of patients treated by X-ray epilation for tinea capitis. Arch Environ Health 1976; 31:21–28.

Possible Association of Radioprotective and Chemoprotective Aminophosphorothioate Drug Activity With Polyamine Oxidase Susceptibility[1,2]

Joseph M. Gaugas[3,4,5]

ABSTRACT—The aminophosphorothioate drug *S*-2-(3-aminopropylamino)ethylphosphorothioate (WR-2721) is both radioprotective and chemoprotective, with potential clinical use in cancer therapies. These distinct properties may be associated with its catabolism by polyamine oxidase (EC 1.4.3.4), which is found in varying amounts in different body tissues. Unfortunately, the metabolite is probably a cytotoxic aldehyde, but it should be detoxified in vivo following adduction with tissue sulfhydryls. Whether conversion and adduction benefit or hinder pharmacologic activity is not known, inasmuch as aldehydes may reduce oxygen-dependent free radicals generated by irradiation of tissues. *S*-2-(3-aminopropylamino)propylphosphorothioate was similarly a substrate for polyamine oxidase, and the product was cytotoxic. Other aminophosphorothioates [*S*-2-(4-aminobutaneamino)ethylphosphorothioate, *S*-2-(5-aminopentylamino)ethylphosphorothioate, and *S*-2-(4-aminobutaneamino)propylphosphorothioate] were poor substrates and less radioprotective.—JNCI 1982; 69:329–332.

Radiation injury of normal tissues contiguous to solid tumor is a major problem in radiotherapy. Injury imposes a limitation on the size of tumor suitable for radical radiotherapy, restricts dosage, and a course of radiotherapy is rarely repeated should regrowth of the tumor occur [(*1*) and references therein].

For decades it has been well known that both biogenic and synthetic sulfhydryls, such as L-cysteine, β-mercaptoethylamine, and 2-aminoethylisothiourea, afford significant protection of animals against lethal-dose radiation. Administration of the aminophosphorothioate drug *S*-2-(3-aminopropylamino)ethylphosphorothioate (WR-2721) reduced the radiosensitivity of many body tissues and evoked a 2.6-fold increase in the whole-body dose of radiation lethal for 50% of mice by day 30 ($LD_{50/30}$) (*2*).

Undoubtedly, need exists in the cancer clinic for drugs that preferentially protect normal rather than neoplastic tissue against radiation injury. The aminophosphorothioate drugs (particularly WR-2721) have been extensively studied in animals and fulfill such criteria (*2–8*), because WR-2721 does not penetrate as quickly into many types of tumor as it does into normal tissues (except the central nervous system) (*4–6*). More recently, WR-2721 was also shown to preferentially protect normal rather than neoplastic tissue against the side effects of alkylating agents (*7*), with implications for its use as an adjunct in cancer chemotherapy (*8–10*).

We noticed that the aminophosphorothioate drugs of the WR series listed in table 1 possess the substrate requirement (*11*) for PAO. PAO is found mostly in the pancreas, liver, spleen, and kidney (*12*) as the PAO–flavin form (*11*) and in ruminant sera as the PAO–pyridoxal form (*13*). PAO converts biogenic polyamines, spermidine, and spermine to labile aminoaldehydes which are extremely cytotoxic [(*14*) and references therein]. WR-2721 was similarly converted, possibly to a cytotoxic thiolaminoaldehyde [i.e., aldehyde of *N*-(2-mercaptoethyl)-1,3-diaminopropane (WR-1065)] (*15*). In this preliminary investigation any association between PAO susceptibility and radioprotective ability was noted for certain aminophosphorothioate drugs in the WR series. In addition, the in vitro cytotoxicity of the drugs was evaluated.

MATERIALS AND METHODS

Cell culture bioassay.—Cells (Bri8 human B-lymphocytes) were seeded at low density in 1.0-cm³ cultures (in triplicate) of RMPI-1640 medium, supplemented with L-glutamine and antibiotics (Flow Laboratories Limited), 10% FCS (Sera-Labs Ltd.), which is known to have such endogenous PAO activity, and catalase (Sigma London Chemical Co., Ltd.), as fully described elsewhere (*14, 15*). After 4 days' incubation of the cultures at 37°C in an atmosphere of 5.0% CO_2 in air, the cells, which had a doubling time of about 21 hours, were dispersed with isotonic EDTA buffer and counted in an automatic Coulter Counter. PAO activity could be completely ablated by addition of 3-hydroxybenzyloxyamine (10 μ*M*) with no effect on cell proliferation (*14, 15*). Aminophosphorothioates were solubilized just before their addition to the cultures on day 0 to minimize any autodephosphorylation (*16*). Sterile precautions were taken throughout the procedures. The ability of the aminophosphorothioates to inhibit cell proliferation in the presence of FCS, FCS with added purified PAO (Miles Laboratories, Ltd.), and FCS when its PAO activity had been ablated was measured, and the results were compared (table 1).

PAO substrate assay.—The PAO susceptibility of substrates (spermidine and aminophosphorothioates) was assayed by a colorimetric method (*17*), as well as by the foregoing bioassay.

ABBREVIATIONS USED: FCS=fetal calf serum; PAO=polyamine oxidase.

---

[1] Received May 12, 1981; revised February 15, 1982; accepted March 8, 1982.

[2] Supported by the Cancer Research Campaign of the United Kingdom.

[3] Gray Laboratory, Cancer Research Campaign, Mount Vernon Hospital, Northwood, Middlesex HA6 2RN, England.

[4] *Address reprint requests to* Dr. Gaugas at his *present address*: Int'l Immunotechnology Corp., 4904 West Cypress St., Tampa, Fla. 33607.

[5] I thank Colonel D. D. Davidson, Walter Reed Research Institute, Washington, D.C., for a gift of aminophosphorothioate drugs and Dr. J. W. Purdie, Defence Research Establishment, Ottawa, Canada, for a gift of *N*-(2-mercaptoethyl)-1,3-diaminopropane.

TABLE 1.—*Aminophosphorothioates: Oxidation by PAO, susceptibility to PAO,[a] and radioprotection rating[b]*

Compound	Formula	In vitro cytotoxicity,[c] μM, in the presence of:			Susceptibility to PAO[g]	Radioprotection rating[b,h] for:				
		10% FCS[d]	Inactivated PAO[e]	Added PAO[f]		HTD_{50}	HTD_{25}	$HTD_{12.5}$	$HTD_{6.25}$	Controls
Spermidine	$NH_2(CH_2)_3NH(CH_2)_4NH_2$	36	2,000	10	100					
Aminophosphorothioates										
WR-2[illegible]1	$NH_2(CH_2)_3NH(CH_2)_2SPO_3H$	300	3,750	150	8.5	+	+	+	+	0
WR-1065	$NH_2(CH_2)_3NH(CH_2)_2SH$	150	260	80	8.5	+	+	+	0	0
WR-44923	$NH_2(CH_2)_3NH(CH_2)_3SPO_3H$	330	1,200	120	10.5	+	+	+	±	0
WR-2822	$NH_2(CH_2)_4NH(CH_2)_2SPO_3H$	376	240[i]	NT	<1.0	+	+	0	0	0
WR-2823[j]	$NH_2(CH_2)_5NH(CH_2)_2SPO_3H$	3,600	3,800	NT	<1.0	+(T)	+	+	0	0
WR-80855	$NH_2(CH_2)_4NH(CH_2)_3SPO_3H$	1,100	820[i]	1,600[d]	<1.0	0	0	0	0	0

[a] Data obtained by author.

[b] Data obtained from Walter Reed Research Institute, Washington, D.C. (*6*).

[c] Inhibitory dose causing 50% reduction in cell proliferation.

[d] FCS has endogenous PAO activity equivalent to 4.0 $\mu g \cdot cm^{-3}$ of the purified PAO (29.2 $U \cdot g^{-1}$, where 1.0 U converted 1.0 $\mu mol \cdot min^{-1}$ benzylamine at pH 7.2).

[e] Inactivated in FCS by addition of 3-hydroxybenzyloxyamine (10 μ*M*).

[f] 10 $\mu g \cdot cm^{-3}$ PAO. NT = not tested.

[g] Determined by colorimetric assay (also by rough bioassay guide obtained by comparison of results in columns 3, 4, and 5).

[h] HTD = highest tolerated dose at which test mice survived. HTD_{50}, indicates 50% survival; HTD_{25}, 20–49% survival; $HTD_{12.5}$, 20% survival; $HTD_{6.25}$, <20% survival. Forty mice at each HTD level were exposed to 8.0 Gy whole-body radiation. ± = few survivors, (T) = some deaths due to interaction of drug and radiation.

[i] Some detoxification due to PAO activity of the FCS.

[j] *S*-2-(5-aminopentylamino)ethylphosphorothioate.

RESULTS

The antiproliferative or cytotoxic effects of WR-2721, WR-1065, and *S*-2-(3-aminopropylamino)propylphosphorothioate (WR-44923) on cultured cells are shown in text-figure 1 and table 1; the effects of other aminophosphorothioates are summarized in table 1. Cytotoxicity of WR-2721, WR-1065, and WR-44923, but not of the other compounds, was substantially increased when the drugs were oxidized by PAO. In contrast, *S*-2-(4-aminobutaneamino)ethylphosphorothioate (WR-2822) and *S*-2-(4-aminobutaneamino)propylphosphorothioate (WR-80855) were poor substrates for PAO, and they also afforded significantly less radioprotection (table 1) (*6*). The degree of cytotoxicity of the polyamine-like drugs in the WR series varied considerably when the PAO (in FCS nutrient) was completely inhibited by 3-hydroxybenzyloxyamine. More importantly, there apparently is an association between the radioprotective potency and PAO susceptibility of the drugs, as measured by the antiproliferative effect of the drugs when oxidized and when the radioprotective ratings of the drugs are considered (table 1).

The cytotoxicity of the oxidized aminophosphorothioate drugs generally could be prevented by addition to cultures of 2 m*M* of the sulfhydryls L-cysteine, reduced glutathione, and DL-homocysteine, as had been reported previously for WR-2721 (*14*). Note that dephosphorylation of WR-2721 in solution at neutral pH was completed within 2 hours, as determined by pH change (*14, 16*). Therefore, the relative loss in WR-2721 toxicity beyond approximately 600 μ*M* probably was due to adduction of the thiolaminoaldehyde product with the dephosphorylated (i.e., free sulfhydryl) product. This finding of autodephosphorylation agrees with recently published data (*16*).

As determined by colorimetric assay, the relative PAO substrate activity of WR-2721 and WR-44923 was 10.5% relative to spermidine as 100%; the activity of the remaining drugs in the WR-series (table 1) was not detectable.

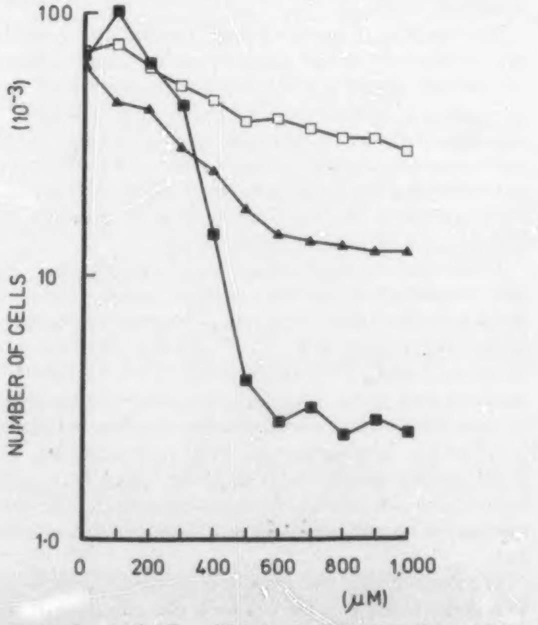

TEXT-FIGURE 1.—Arrest of cell proliferation by WR-2721 (▲) and WR-44923 (■) and its partial prevention by PAO inactivation by added 3-hydroxybenzyloxyamine (□). Similarly, partial prevention of WR-2721 cytotoxicity was obtained by PAO inactivation [*see* (*15*)]. Results are expressed as mean cell counts (triplicate cultures) after 4-days' growth; coefficient of variation, <10% of mean.

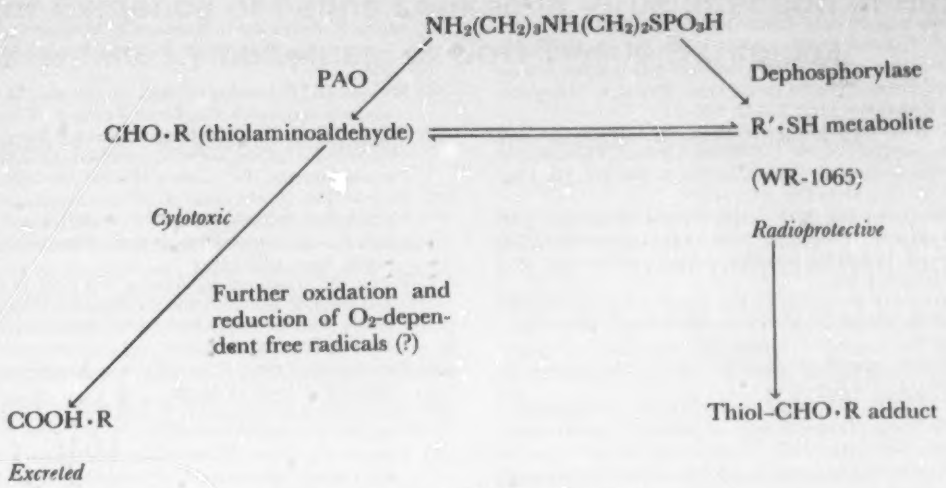

TEXT-FIGURE 2.—Catabolism of WT-2721.

DISCUSSION

The radioprotective ability of aminophosphorothioates probably is due to slow in vitro dephosphorylation of the R·SPO_3H moiety to R·SH (i.e., WR-1065) (*15*, *16*), which can scavenge the tissue-damaging free radicals generated by radiation (*2–8*). Substitution of the R·SPO_3H moiety with either R·SH or R·SSO_3H afforded less radioprotection of mice (*6*).

Adduction of oxidized aminophosphorothioates (thiolaminoaldehydes) with nonprotein sulfhydryls (e.g., L-cysteine), which abound in body tissues, probably causes an in vivo detoxification. The radioprotective efficacy of the adduct has yet to be ascertained.

Presumably, the catabolism of WR-2721, for example, proceeds as in text-figure 2, with a stable end product (R·COOH) excreted into the urine. Since PAO distribution in tissues varies considerably, with low levels in lungs and muscle (*12*), the extent of the catabolism of WR-2721 and WR-44923 by both PAO and dephosphorylase could influence their radioprotective activity for different tissues. Combined administration of a PAO inhibitor drug (pyridoxal and/or flavin cofactor inactivators) with WR-2721 or WR-44923 might spare the radioprotective capability of these WR drugs while decreasing their toxicity. This expediency may benefit tumor radiotherapy and tumor chemotherapy with alkylating agents.

Since aminoaldehydes are potent reducing agents (*14*), they may reduce tissue-damaging, oxygen-dependent free radicals generated by tissue irradiation. This possibility is currently under investigation, and preliminary data show that the aldehyde of WR-2721 is a much more powerful reducing agent than the aldehyde of oxidized spermidine (Gaugas JM, Dewey DL, Stratford MR, Minchington AI: Unpublished data). Therefore, if both the CHO and SH moiety of a WR-2721 metabolite are radioprotective to some degree, then the kinetics of metabolite production and lability could account for differences observed in the radioprotective ability of WR-2721 and closely related compounds (e.g., those listed in table 1), which may or may not be more susceptible to PAO. The chain length of aldehydes determines whether they exist in a free (RCHO) or hydrated ($RCH(OH)_2$) state (*18*). It is not known which of the two states would function better in vivo as reducing agent for certain free radicals.

Phase I clinical trials for WR-2721 in the United States have progressed to the stage where the results are being reported to the National Cancer Institute in preparation for a Phase II radiotherapy trial of WR-2721 in which dosage levels known to be safe will be used (*9*, *19*, *20*). Those doses would not give the full degree of radioprotection, however, that would be obtainable with the higher doses already proved satisfactory in laboratory animals (*2*, *9*, *19*, *20*).

So far I am able to conclude from my work with aminophosphorothioate drugs [*see also* (*15*)] that their deamination by PAO may somehow facilitate their radioprotective efficacy. If so, it should be possible to design protective drugs that would be more susceptible than WR-2721 or WR-44923 to PAO activity and that would be better prospects for clinical use. If not, it should be possible to modify the structure of WR-2721 or WR-44923 to make them insusceptible to PAO and, as a consequence, less toxic. Then those of us working in this field could decide whether or not the in vivo PAO catabolism of aminophosphorothioates increases their pharmacologic efficacy and whether further development of drugs is necessary.

REFERENCES

(*1*) FOWLER JR. Nuclear particles in cancer treatment. Bristol, England: Hilger, 1980:1–21.

(*2*) YUHAS JM. Biological factors affecting the radioprotective effectiveness of *S*-2-(3-aminopropylamino)ethylphosphorothioic acid WR-2721: $LD_{50/30}$ doses. Radiat Res 1970; 44:621–628.

(*3*) UTLEY JF, PHILLIPS TL, KANE LJ. Protection of normal tissues by WR-2721 during fractionated irradiation. Int J Radiat Oncol Biol Phys 1976; 1:695–703.

(*4*) KOLLMAN G, YUHAS JM, LEONE S, SHAPIRO B. Mechanism of differential radiation protection of normal tissue versus tumor by WR-

2721 in tumor-bearing mice. Radiat Res 1973; 55:603.

(*5*) Washburn LC, Carlton JE, Hayes RL, Yuhas JM. Distribution of WR-2721 in normal and malignant tissues of mice and rats bearing solid tumors: Dependence on tumor type, drug dose and species differences. Radiat Res 1974; 59:475–483.

(*6*) Sweeney TR. A survey of compounds from the antiradiation drug development program of the U.S. Army Medical Research and Developmental Command. Publication No. 0-303-138. Washington, D.C.: U.S. Govt Print Off, 1979:1–771.

(*7*) Yuhas JM, Spellman JM, Jordan SW, Pardini MC, Afzal SM, Culo F. Treatment of tumours with the combination of WR-2721 and cisplatinum (II) dichlorodiamine or cyclophosphamide. Br J Cancer 1980; 42:574–585.

(*8*) Yuhas JM, Spellman JM, Culo F. The role of WR-2721 in radiotherapy and/or chemotherapy. Cancer Clin Trials 1980; 3:211–216.

(*9*) Yuhas JM. A more general role for WR-2721 in cancer therapy. Br J Cancer 1980; 41:832–834.

(*10*) Spooner D. WR-2721 (aminopropylamino ethyl phosphorothioate): A radio and chemoprotective drug of potential clinical value. Cancer Topics 1981; 3:50.

(*11*) Tabor CW, Tabor H, Bachrach U. Identification of the aminoaldehydes produced by the oxidation of spermine and spermidine with purified plasma amine oxidase. J Biol Chem 1964; 239:2194–2203.

(*12*) Seiler N, Bolkenius B, Knodgen B, Mamont P. Polyamine oxidase in rat tissues (BBA 69012). Biochim Biophys Acta 1980; 615:329–336.

(*13*) Morgan DL. Polyamine oxidases. In: Gaugas JM, ed. Polyamines in biomedical research. Chichester, England: Wiley, 1980:285–302.

(*14*) Gaugas JM, Dewey DL. Oxygen-dependent free radicals in spermine oxidation cytostasis and chemiluminescence and the role of superoxide dismutase. Br J Cancer 1980; 41:946–955.

(*15*) Gaugas JM. Mechanisms of *S*-2-(3-aminopropylamino)ethylphosphorothioic acid cytotoxicity. In: Caldarera CM, Zappia V, Bachrach U, eds. Polyamines in normal and neoplastic cells. New York: Raven Press, 1981:441–450.

(*16*) Purdie JW. Dephosphorylation of WR-2721 to WR-1065 in vitro and effect of WR-1065 and misonidazole in combination in irradiated cells. In: Brady LW, ed. Radiation sensitizers. New York: Masson, 1981:330–333.

(*17*) Bachrach U, Reches B. Enzymic assay for spermine and spermidine. Anal Chem 1966; 17:38–48.

(*18*) Schauenstein E, Esterbauer H, Zollner H. Aldehydes in biological systems. London: Pion, 1980:4.

(*19*) Phillips TL. Rationale for initial clinical trials and future development of radioprotectors. In: Brady LW, ed. Radiation sensitizers. New York: Masson, 1981:321–328.

(*20*) Kligerman MM, Shaw MT, Slavik M, Yuhas JM. Phase I clinical studies with WR-2721. Cancer Clin Trials 1980; 3:217–221.

Search for Evidence of Feline Leukemia Virus Infection in Humans With Leukemias, Lymphomas, or Soft Tissue Sarcomas[1,2,3]

Peter P. Sordillo, *M.D.,*[4] **R. Pincow Markovich,** *B.S.,*[4] *and* **William D. Hardy, Jr.,** *V.M.D.*[4]

ABSTRACT—Two-hundred and thirty-nine patients, including 66 with soft tissue sarcomas and 173 with hematologic cancers, were investigated for evidence of infection with feline leukemia virus (FeLV). Included in this group were 2 patients with acute lymphocytic leukemia who had lived in the same household with leukemic cats. None of the patients demonstrated measurable levels of neutralizing antibody to FeLV or had detectable FeLV antigens in peripheral blood normal leukocytes or leukemic cells. In a smaller number of patients, there was no evidence of antibody to FOCMA or of FOCMA on tumor cells in the bone marrow.—JNCI 1982; 69:333–337.

In 1969, natural field isolates of FeLV were found to be able to infect and replicate in human cell cultures (*1*). This observation and the finding, in 1973, that FeLV is spread contagiously among cats via the saliva brought concern that FeLV might be able to infect and cause disease in humans (*2–6*). FeLV is oncogenic in a species other than the cat. When inoculated into newborn puppies, FeLV can induce virus-positive lymphosarcomas (*7*). Since FeLV can infect and replicate in human lymphoid cells in culture, it is possible that FeLV induces lymphoid tumors in humans (*8*, *9*). Experimental challenge of humans with FeLV can, of course, never be done; thus the possible oncogenicity of FeLV in humans can only be determined by long-term observation of individuals living with infected cats or by examination of human patients with tumors for evidence of FeLV.

Several oncoviruses (RNA tumor viruses) have been transmitted naturally from one species to another. FeLV originated in ancestral rats and spread to the ancestor of the pet cat; the gibbon ape leukemia virus originated in Asian mice and spread to Asian gibbon apes; and the bovine leukemia virus originated from an unknown and possibly extinct species and spread to cattle (*10*, *11*). In each of the recipient species, the viruses are spread contagiously and induce neoplastic disease. Due to these observations and concerns and because FeLV is probably the only known tumor virus of any animal to which humans are frequently and intimately exposed, epidemiologic and seroepidemiologic studies have been done to determine if FeLV is associated with disease in humans (*12*, *13*).

Sarcoma viruses of birds, mice, rats, cats, and subhuman primates are derived by replication competent leukemia viruses of each species recombining with a host cellular gene (*14*). The resulting replication-defective sarcoma virus is highly oncogenic in the host species and often in other species as well. The FeSV, which are derived by recombination of FeLV with cat cellular *onc* genes, induce virus-producer sarcomas in young pet cats (*15*, *16*). In addition, FeSV can induce, by experimental inoculation, virus-nonproducer tumors in dogs, cattle, sheep, and primates [for review, *see* (*16*)]. However, although cells transformed by FeSV in nonfeline species often do not produce infectious FeLV or FeSV, they do possess FeLV structural antigens, proteins of 15,000 12,000, and 27,000 daltons (p15, p12, p27) (*17*).

Thus we undertook a study using the IFA test for FeLV antigens and serologic tests to determine if humans with hematologic tumors or with sarcomas have antibody to FeLV antigens or to the FOCMA, an FeLV- and FeSV-induced tumor-specific antigen (*18–22*). A total of 239 patients (192 adults and 47 children) with various types of cancer and seen at Sloan-Kettering Institute for Cancer Research between May 1, 1978 and December 31, 1980 were tested for neutralizing antibody to FeLV. Of these patients, 191 were also tested for FeLV antigens and 20 for antibody to FOCMA. In addition, tumor cells from the bone marrows of 20 of these patients were tested for FOCMA.

MATERIALS AND METHODS

IFA test for FeLV antigens (*18*).—Blood smears from each patient were fixed for 8 minutes in absolute methanol, and 0.05 ml rabbit anti-FeLV group-specific serum was placed in a small well made with a marker pencil on each slide. The smears were incubated at 37°C for 1 hour and then washed twice for 5 minutes in PBS. We then placed 0.05 ml goat anti-rabbit IgG–FITC conjugate (Miles Laboratory, Elkhart, Ind.) (1:80) in each well. After incubation at 37°C for 1 hour, the smears were washed. Then they were counterstained with Evans' blue for 2 minutes, washed twice in PBS, and dried. Control, FeLV-infected cat blood smears were tested along with all human blood smears. The slides were examined under a Zeiss UV microscope.

Absorption test for FOCMA (*21*).—We mixed 0.2 ml bone marrow cells ($\approx 3\times10^8$ cells/ml) with 0.2 ml cat serum containing FOCMA antibody at its 50% end point dilution

---

Abbreviations used: FeLV=feline leukemia virus; FeSV=feline sarcoma virus(s); FITC=fluorescein isothiocyanate; FLF=feline lung fibroblasts; FOCMA=feline oncovirus-associated cell membrane antigen; IFA=immunofluorescent antibody; LTR=long terminal repeats; PBS=phosphate-buffered saline; SN=serum neutralizing.

---

[1] Received July 7, 1981; revised February 15, 1982; accepted March 15, 1982.

[2] Supported by Public Health Service grants CA-16599 and CA-19072 from the National Cancer Institute.

[3] Research procedures were in accord with the ethical standards of the Memorial Sloan-Kettering Cancer Center and the Helsinki Declaration of 1975.

[4] Sloan-Kettering Institute for Cancer Research, 1275 York Ave., New York, N.Y. 10021.

(1:64). For comparison, 0.2 ml serum without cells was handled exactly as the samples being absorbed. All were incubated on ice for 1 hour and at room temperature for 1 hour. Following incubations, all samples were centrifuged for 20 minutes at 2,000 rpm. Supernatants (sera) were aliquoted equally into three portions and stored at −70°C. A direct test for expression of FOCMA was done as described in the test for FOCMA antibody, but we used the absorbed serum. Lack of absorption of the FOCMA antibody indicated a lack of FOCMA expression in the human cells tested.

Test for SN antibody to FeLV.—The FLF cells (FLF-3) in 0.05 ml culture medium (2.5×10^5 cells/ml) were placed on multispot fluorescent slides (Hendley Co., Essex, England) and allowed to attach to the wells by incubation of the slides for 24 hours at 37°C. Serum from each patient was heat inactivated at 56°C for 30 minutes. Dilutions of 1:2 and 1:10 of the sera were mixed with 40 infectious units of FeLV serotypes A and B. For the infection control, a mixture of equal volumes of media and 40 infectious units FeLV was used. The neutralization control consisted of 1:30 dilution of cat serum containing a titer greater than 1:30 of SN antibody mixed with 40 infectious units FeLV and media. The test sera and FeLV mixtures and controls were incubated for 1 hour at 37°C in CO_2. The medium was then removed from the wells of the seeded slides, leaving FLF monolayers attached to the wells. One drop (0.05 ml) of each test serum-virus mixture was placed in its appropriate well and incubated for 1 hour at 37°C to allow for FeLV attachment to the susceptible FLF cells. The serum-virus mixtures were then replaced with fresh medium and incubated for 3 days at 37°C. After incubation, the slides were washed and fixed for 8 minutes in absolute methanol. The IFA test for FeLV as previously described was then done on the cells. The presence of any fluorescent-positive cells indicated that SN antibody to FeLV was not detectable at the dilution of serum tested.

Test for FOCMA antibody (*20, 21*).—FeLV-positive feline lymphosarcoma cells (FL-74) were washed three times in medium 199 and centrifuged for 5 minutes at 400 rpm and for 5 minutes at 800 rpm (*23*). From each patient 0.05 ml serum at dilutions of 1:4, 1:16, and 1:32 was mixed in 15-ml tubes with 0.05 ml cells (15×10^6 cells/ml). A mixture of 0.05 ml cells and 0.05 media was used as a conjugate control. As a positive FOCMA antibody control, a cat serum containing a titer of 1:64 or greater of FOCMA antibody was used at the same dilutions as the human serum being tested. The FL-74 cells were incubated on ice for 30 minutes and then washed twice in medium. Following the second wash, the medium was removed from the pelleted cells, and the tubes were inverted and rimmed with cotton swabs to ensure complete removal of all wash medium. Rabbit anti-cat IgG FITC conjugate was diluted to 1:20 in medium 199 and 0.05 ml was placed onto each FL-74 cell pellet. The cells were suspended in the conjugate and incubated for 30 minutes on ice.

NFL-74 cells were washed twice in medium 199, and each pellet was resuspended with one drop of 50% glycerol in PBS and placed on a slide. We read the test within 2 hours using a Zeiss fluorescent microscope.

TABLE 1.—*Test for FeLV antigens in human cells*

Malignant disease	Total No. of patients tested	No. of patients tested for:		No. of patients positive for FeLV antigens
		Normal leukocytes in peripheral blood	Tumor cells in peripheral blood	
Acute lymphocytic leukemia	43	43	35	0
Acute nonlymphocytic leukemia	38	38	31	0
Chronic leukemias	21	21	21	0
Lymphomas	40	40	22	0
Soft tissue sarcomas	49	49	0	0
Total	191	191	109	0

RESULTS

Antigen Studies

FeLV Antigens

A total of 191 patients were tested for FeLV antigens in their normal peripheral blood leukocytes or in tumor cells present in the peripheral blood (table 1). Of these, 49 patients had soft tissue sarcomas and 142 patients had hematologic cancers. All patients were negative for FeLV antigens in the cytoplasm of their peripheral blood normal leukocytes or of tumor cells in their peripheral blood. Two of the patients tested developed acute lymphocytic leukemia after having lived with cats who had died of FeLV-positive lymphosarcoma. In both patients, FeLV antigens were not found either in the leukemia cells at diagnosis or later in the normal peripheral blood leukocytes when the cancer was in remission.

FOCMA Absorption Tests

None of the 20 patients tested with hematologic tumors had FOCMA expressed on the cell membranes of tumor cells from their bone marrows (table 2).

Antibody Studies

SN Antibody to FeLV

We tested 239 patients for SN antibody against FeLV subgroups A and B. None of the 66 patients with soft tissue sarcomas and none of the 173 patients with hematologic cancers had SN antibody to FeLV at a titer of 1:2 or above (table 3).

TABLE 2.—*FOCMA absorption test on human cells*

Malignant disease	Total No. of patients tested	No. of patients with FOCMA-positive cells
Acute lymphocytic leukemia	6	0
Acute nonlymphocytic leukemia	10	0
Chronic leukemias	0	0
Lymphomas	4	0
Soft tissue sarcomas	0	0
Total	20	0

TABLE 3.—*Serologic tests of human cancer patients for SN antibody to FeLV and FOCMA antibody*

Malignant disease	SN antibody test against FeLV		FOCMA antibody test	
	No. of patients tested	No. of patients positive for SN antibody to FeLV	No. of patients tested	No. of patients positive for FOCMA antibody
Acute lymphocytic leukemia	49	0	6	0
Acute nonlymphocytic leukemia	46	0	7	0
Chronic leukemias	28	0	0	0
Lymphomas	50	0	4	0
Soft tissue sarcomas	66	0	3	0
Total	239	0	20	0

FOCMA Antibody

None of the 20 patients with hematologic cancers had antibody to FOCMA at a titer of 1:2 or above on FL-74 target cells (table 3).

Patients Exposed to FeLV-Positive Cats With Lymphosarcoma

Two patients with acute lymphocytic leukemia had lived with FeLV-positive cats with lymphosarcoma. Both patients were negative for SN antibody to FeLV and FOCMA antibody at the time of their diagnosis. In addition, both patients were still negative for these antibodies while in remission 12 months after diagnosis. We judge these findings significant considering that each patient developed the same type of neoplasia as did their FeLV-positive cats.

DISCUSSION

For the past 10 years, both epidemiologic and seroepidemiologic (immunologic) studies have been done to determine if humans exposed to cats or FeLV had an increased risk of developing cancer.

Several epidemiologic studies of veterinarians or of children and adults exposed to cats have been done with conflicting results. Veterinarians have a high occupational exposure to FeLV. Five mortality studies of a total of 23,249 U.S. veterinarians have been reported. In two of these studies of 876 veterinarians, no increase in the occurrence of any type of cancer was noted in veterinarians compared to the occurrence in the general public (*24, 25*). In another study, skin melanomas were found in excess among veterinarians (*26*). However, two recent studies of many veterinarians have revealed a significant increase in the occurrence of lymphoid tumors. The first study reported an 80% increase in the mortality due to lymphoma among 19,000 veterinarians who died over the age of 45 years (*27*). The second study also showed a significant excess occurrence of leukemia and Hodgkin's disease among 1,551 male veterinarians in clinical practice (*28*). The authors of (*27, 28*) were unable to prove a cause for the excess number of these tumors among veterinarians, although FeLV certainly must be considered.

Two retrospective studies of the exposure to cats of 328 children with leukemia have been done. A twofold increase in exposure to cats was found in houses in London where children developed lymphoid cancers compared to those where children developed other forms of cancer (*29*). Similarly, in a study performed in the United States of 300 children with leukemia and 831 control children, the relative risk among leukemic children exposed to "sick" cats was more than double that of the control children (*30*). In contrast, in retrospective studies of more than 1,965 adults exposed to cats, no increase in occurrence of cancer was found in individuals exposed to cats with lymphosarcoma or to healthy cats (*31–33*).

Seroepidemiologic or immunologic tests are more definitive methods of determining if FeLV can infect humans. These tests consist of immunologic procedures to determine if FeLV antigens exist in humans exposed to cats or if antibodies to FeLV or to FOCMA are produced by people exposed to infected cats. Eight studies to determine if antibody to FeLV occurred in a total of 4,069 people have been done and have yielded conflicting results. Four of the studies found antibody to FeLV antigens in 224 of 2,089 people (10.7%) (*34–37*). In four other studies, no antibody to FeLV was found in 1,538 healthy people, in 631 people with cancer, in 209 people with nonneoplastic diseases, or in 662 healthy veterinarians (*19, 38–40*).

There have been only four studies that attempted to detect FeLV antigens in people. In one study, FeLV antigens were found in immune complexes in the glomeruli of 2 people with acute myelogenous leukemia (*41*). In another study, FeLV-related antigens were detected on the leukemia cell surface of 43 (81%) of 53 patients with myeloid leukemias and of 35 (97%) of 36 patients with lymphoid leukemia or lymphoma, but not on normal lymphocytes from 12 healthy people (*42*). No FeLV antigens were found in 439 people, of whom 4 had been bitten by FeLV-infected cats, 52 were veterinarians, 200 had lymphoid tumors, and 59 had carcinomas or sarcomas (*19*). Similarly, no soluble FeLV antigens were found in the sera of any of 1,324 people, 490 of whom had hematologic cancers (*40*).

Because 4 groups of investigators using various immunologic tests found antibody to FeLV (*34–37*), we attempted to confirm these observations on a larger series of human patients with soft tissue sarcomas or hematologic cancers. We chose to determine if FeLV was present in patients by the use of an indirect IFA test. A positive IFA test for FeLV in cats correlates with the ability to isolate FeLV from the plasma in 97.5% of cats studied (*18, 43*). In addition, we used the FOCMA test on human cells to determine if FeLV or FeSV was involved in the induction of transformation of these cells, inasmuch as these viruses induce FOCMA in cat cells, which they transform (*20–22*). Most cats that are exposed to FeLV and then reject the virus and become immune produce both SN antibody to FeLV and FOCMA antibody (*19*). Therefore, as an indication of a history of FeLV or FeSV exposure, we chose to test human sera for these antibodies. Our study represents the most complete immunologic analysis of FeLV exposure in humans inasmuch as some of our patients had tests for FOCMA expression on the membranes of their tumor cells as well as tests for FeLV and for FeLV and FOCMA antibodies. This study is also significant because we were able to test 66 patients with soft tissue sarcoma, which is a relatively rare tumor in humans (comprising <1% of human malignant tumors) but is a type of tumor (multicentric fibrosarcoma) induced by the FeSV in pet cats.

In 191 human patients with various forms of cancer, we found no evidence of the presence of active FeLV replication in any of the patients. Nor did we find any evidence of *past* FeLV infection, as judged by the absence of FeLV SN antibody, in 239 human patients. Even the 2 patients with acute lymphocytic leukemia, who had lived in close contact in the same household with their FeLV-infected leukemic pet cats, were repeatedly negative for FeLV antigens and for SN antibody to FeLV. In addition, none of the 20 patients tested were positive for FOCMA antibody. We have not found any evidence of active FeLV infection or a history of past FeLV infection in any of the patients that we tested.

We must be cautious in the interpretation of these negative data, however, because 30% of the pet cats who developed lymphosarcoma as a result of known past exposure to the virus have neither FeLV antigens nor FeLV SN or FOCMA antibodies (*43–45*). However, we did not find FOCMA expression on the tumor cells from the bone marrows of 20 of these patients. This is the most reassuring evidence that FeLV or FeSV was not involved in the etiology of these tumors because FOCMA is expressed on the cell surface of all FeLV and FeSV-induced tumors of cats, as well as on experimentally induced tumors of other species (*21–23*).

Although we did not find evidence supporting a role for FeLV or FeSV as causative factors in human tumors, more studies are needed. Molecular biologic studies of the DNA of human tumors should be done for detection of either complete copies or fragments of FeLV or FeSV sequences (*46*). The etiology of FeLV-negative lymphosarcomas of pet cats may be the insertion of FeLV noncoding sequences called "long terminal repeats" (LTR), which may promote downstream expression of a cat oncogene (*47–48*). Similarly, a fragment of the FeLV genome (LTR) may integrate into human cells and induce transformation without expression of that sequence. Until definitive molecular biologic studies have been done, we recommend that FeLV-infected cats should not be kept as pets.

REFERENCES

(*1*) Jarrett O, Laird HM, Hay D. Growth of feline leukaemia virus in human cells. Nature 1969; 224:1208–1209.

(*2*) Hardy WD Jr, Old LJ, Hess PW, Essex M, Cotter S. Horizontal transmission of feline leukaemia virus. Nature 1973; 244:266–269.

(*3*) Jarrett W, Jarrett O, Mackey L, Laird H, Hardy W Jr, Essex M. Horizontal transmission of leukemia virus and leukemia in the cat. J Natl Cancer Inst 1973; 51:833–841.

(*4*) Hardy WD Jr, Geering G, Old LJ, DeHarven E, Brodey RS, McDonough S. Feline leukemia virus: Occurrence of viral antigen in the tissues of cats with lymhosarcoma and other diseases. Science 1969: 166:1019-1021.

(*5*) Gardner MB, Rongey RW, Johnson EY, DeJournett R, Huebner RJ. C-type tumor virus particles in salivary tissue of domestic cats. J Natl Cancer Inst 1971; 47:561–568.

(*6*) Francis DP, Essex M, Hardy WD Jr. Excretion of feline leukaemia virus by naturally infected pet cats. Nature 1977; 269:252–254.

(*7*) Richard CG, Post JE, De Norouha F, Barr LM. Interspecies infection by feline leukemia virus: Serial cell-free transmission in dogs of malignant lymphoma induced by feline leukemia virus. In: Dutcher RM, Chieco-Bianchi L, eds. Unifying concepts of leukemia. Basel: Karger, 1973:102–112.

(*8*) Essex M, Klein G, Deinhardt F, et al. Induction of the feline oncornavirus-associated cell membrane antigen in human cells. Nature [New Biol] 1972; 238:187–189.

(*9*) Azocar J, Essex M. Susceptibility of human cell lines to feline leukemia virus and feline sarcoma virus. JNCI 1979; 63:1179–1184.

(*10*) Benveniste RE, Sherr CJ, Todaro GJ. Evolution of type C viral genes: Origin of feline leukemia virus. Science 1975; 190:886–888.

(*11*) Todaro GJ. Interspecies transmission of mammalian retroviruses. In: Klein G, ed. Viral oncology. New York: Raven Press, 1980:291–309.

(*12*) Hardy WD Jr, McClelland AJ, Hess PW, MacEwen EG. Feline leukemia virus and public health awareness. J Am Vet Med Assoc 1974; 165:1020-1021.

(*13*) Levy SB. Cat leukemia: A threat to man? N Engl J Med 1974; 290:513–514.

(*14*) Shih Ty, Scolnick EM. Molecular biology of mammalian sarcoma viruses. In: Klein G, ed. Viral oncology. New York: Raven Press, 1980:135–160.

(*15*) Frankel AE, Gilbert JH, Porzig KJ, Scolnick EM, Aaronson SA. Nature and distribution of feline sarcoma virus nucleotide sequences. J Virol 1979; 30:821–827.

(*16*) Hardy WD Jr. The biology and virology of the feline sarcoma viruses. In: Hardy WD Jr, Essex M, McCelland AJ, eds. Feline leukemia virus. Amsterdam: Elsevier/North-Holland, 1980:79–118.

(*17*) Sherr CJ, Sen A, Todaro GJ, Sliski A, Essex M. Pseudotypes of feline sarcoma virus contain an 85,000-dalton protein with feline oncornavirus-associated cell membrane antigen (FOCMA) activity. Proc Natl Acad Sci USA 1978; 75:1505–1509.

(*18*) Hardy WD Jr, Hirshaut Y, Hess P. Detection of the feline leukemia virus and other mammalian oncornaviruses by immunofluorescence. Bibl Haematol 1973; 39:778–799.

(*19*) Hardy WD Jr, Hess PW, MacEwen EG, et al. Biology of feline leukemia virus in the natural environment. Cancer Res 1976; 36:582–583.

(*20*) Essex M, Klein G, Snyder SP, Harrold JB. Feline sarcoma virus-induced tumours: Correlation between humoral antibody and tumour regression. Nature 1971; 233:195–196.

(*21*) Hardy WD Jr, Zuckerman EE, MacEwen EG, Hayes AA, Essex M. A feline leukaemia virus- and sarcoma virus-induced tumour-specific antigen. Nature 1977; 270:249–251.

(*22*) Essex M, Cotter SM, Stephenson JR, Aaronson SA, Hardy WD Jr. Leukemia, lymphoma and fibrosarcoma of cats as models for similar diseases of man. In: Hiatt HH, Watson JN, Winsten JA, eds. Origins of human cancer. Cold Spring Harbor, N.Y.: Cold Spring Harbor Laboratory, 1977:1197–1214.

(*23*) Theilen GH, Kawakami TG, Rush JD, Munn RJ. Replication of cat leukaemia virus in cell suspension cultures. Nature 1969; 222:589–590.

(*24*) Potts RP, Edlavitch S, Payne G. Mortality of Missouri veterinarians. J Am Vet Med Assoc 1966; 149:499–504.

(*25*) Schnurrenberger PR, Martin RJ, Walker JF. Mortality of Illinois veterinarians. J Am Vet Med Assoc 1977; 170:1071–1075.

(*26*) Fasal E, Jackson EV, Klauber MR. Mortality in California veterinarians. J Chron Dis 1966; 19:293–306.

(*27*) Gutenson N, Essex M, Francis DP, Hardy WD Jr. Risk to humans from exposure to feline leukemia virus: Epidemiological considerations. In: Viruses in naturally occurring cancers. Cold Spring Harbor Conferences on Cell Proliferation. Vol 7. New York: Cold Spring Harbor Laboratory, 1980:699–706.

(*28*) Blair A, Hayes HM. Cancer and other causes of death among U.S. veterinarians, 1966–1977. Int J Cancer 1980; 25:181–185.

(*29*) Penrose M. Cat leukaemia. Br Med J 1970; 1:755.

(*30*) Bross ID, Gibson R. Cats and childhood leukemia. J Med 1970; 1:180–187.

(*31*) Schneider R. The natural history of malignant lymphoma and sarcoma in cats and their associations with cancer in man and dog. J Am Vet Med Assoc 1970; 157:1753–1758.

(*32*) ———. Human cancer in households containing cats with malignant lymphoma. Int J Cancer 1972; 10:338–344.

(*33*) Hanes B, Gardner MB, Loosli CG, et al. Pet association with selected human cancers: A household questionnaire survey. J Natl Cancer Inst 1970; 45:1155–1162.

(*34*) Fink MA, Sibal LR, Plata EJ. Serologic detection of feline leukemia virus antigens or antibodies. J Am Vet Med Assoc 1971; 158:1070–1075.

(*35*) Olsen RG, Mathes LE, Yohn DS. Complement-fixation-inhibition as a test for antibodies in cats and humans to C-type RNA tumor virus antigen. Bibl Haematol 1975; 40:419–429.

(*36*) Caldwell GG, Baumgartener L, Carter C, et al. Seroepidemiologic testing in man for evidence of antibodies to feline leukemia virus and bovine leukemia virus. Bibl Haematol 1976; 43:238–241.

(*37*) Jacquemin PC, Saxinger C, Gallo RC. Surface antibodies of human myelogenous leukaemia leukocytes reactive with specific type-C viral reverse transcriptases. Nature 1978; 276:230–236.

(*38*) Schneider R, Riggs JL. A serologic survey of veterinarians for antibody to feline leukemia. J Am Vet Med Assoc, 1973; 162:217–219.

(*39*) Sarma PS, Sharar A, Walters V, Gardner M. A survey of cats and humans for prevalence of feline leukemia-sarcoma virus neutralizing serum antibodies. Proc Soc Exp Biol Med 1974; 145:560–564.

(*40*) Krakower JM, Aaronson SA. Seroepidemiologic assessment of feline leukaemia virus infection risk for man. Nature 1978; 273:463–464.

(*41*) Sutherland JC, Mardiney MR Jr. Immune complex disease in the kidneys of lymphoma-leukemia patients: The presence of an oncornavirus-related antigen. J Natl Cancer Inst 1973; 50:633–644.

(*42*) Metzgar RS, Mohanakumar T, Bolognesi DP. Antigenic relationships between murine, feline and primate RNA tumor viruses and membrane antigens of human leukemic cells. Bibl Haematol 1976; 43:549–554.

(*43*) Hardy WD Jr, McClelland AJ, Zuckerman EE, et al. Development of virus non-producer lymphosarcomas in pet cats exposed to FeLV. Nature 1980; 288:90–92

(*44*) Francis DP, Essex M, Cotter SM, Gutensohn N, Jakowski R, Hardy WD Jr. Epidemiologic association between virus-negative feline leukemia and the horizontally transmitted feline leukemia virus. Cancer Lett 1981; 12:37–42.

(*45*) Sliski AH, Essex M, Meyer C, Todaro GJ. Feline oncornavirus-associated cell membrane antigen (FOCMA): Expression on feline sarcoma virus-transformed nonproducer mink cells. Science 1977; 196:1336–1339.

(*46*) Gallo RC, Saxinger WC, Gallagher RE, Gillespie DH, Aulekh GS, Wong-Staal F. Some ideas on the origin of leukemia in man and recent evidence of the presence of type-C viral related information. In: Hiatt HH, Watson JD, Winsten JA, eds. Origins of human cancer. New York: Cold Spring Harbor Laboratory, 1977:1253–1258.

(*47*) Blair DG, Oskarsson M, Wood TG, McClements WL, Fischinger PJ, Vandewoude GG. Activation of the transforming potential of a normal cell sequence: A molecular model for oncogenesis. Science 1981; 212:941–943.

(*48*) Hayward WS, Neel BG, Astrin SM. Activation of a cellular *onc* gene by promoter insertion in ALV-induced lymphoid leukosis. Nature 1981; 290:475–480.

blank page

Interferon and Prostaglandins: Effects on Human Natural and Lectin-Induced Cytotoxicity[1]

Nicholas P. Lang,[2,3] **John R. Ortaldo,**[2,4] **Guy D. Bonnard,**[2] *and* **Ronald B. Herberman**[2]

ABSTRACT—Effects of interferons (IFN) and E-series prostaglandins (PGE) were evaluated on subpopulations of human peripheral blood mononuclear lymphocytes (PBL) that mediate natural killer (NK) activity, antibody-dependent cell-mediated cytotoxicity (ADCC), or lectin-induced cellular cytotoxicity (LICC). When PBL were separated into subpopulations depending on the presence or absence of receptors for sheep erythrocytes (E^+ or E^-, respectively) or for the Fcγ receptor ($Fc\gamma R^+$ or $Fc\gamma R^-$, respectively), LICC was mainly associated with the $E^+Fc\gamma R^-$ cells and to a considerably lesser extent with $E^+Fc\gamma R^+$ cells. In contrast, NK activity and ADCC were associated with the E^+ and E^- subpopulations that had FcγR. IFN treatment had stronger effects on the $Fc\gamma R^+$ subpopulations. Boosting of LICC occurred maximally in the $E^+Fc\gamma R^+$ subpopulation, and the activity of the $E^+Fc\gamma R^-$ cells increased only modestly. IFN had a greater augmenting effect on the NK activity and ADCC of $E^+Fc\gamma R^+$ cells than on $E^-Fc\gamma R^+$ cells. PGE strongly inhibited all three types of cell-mediated cytotoxicity and was effective on IFN-boosted cells as well as on untreated cells.—JNCI 1982; 69:339–343.

Recent data from this laboratory (*1, 2*) and from other laboratories have indicated that IFN is an important mediator of activation or boosting of human and rodent NK and ADCC cells. Additional evidence that IFN can boost cytotoxic reactivity of human and rodent monocytes (*3–5*) indicates that IFN is involved in the positive regulation of a variety of cytotoxic effector cells. Although addition of IFN to human mixed lymphocyte cultures resulted in the development of higher levels of cytotoxicity, short-term IFN treatment did not boost the activity of the CTL after they were generated (*6*).

The apparently divergent effects of IFN on NK cells and CTL raised the possibility that only certain types of cytotoxic effector cells or subpopulations of lymphoid cells are responsive to augmentation by IFN. In vitro generated human CTL are found exclusively in subpopulations of T-cells forming rosettes with E and lacking detectable FcγR (i.e., $E^+Fc\gamma R^-$ cells), whereas NK activity and ADCC have been associated only with $Fc\gamma R^+$ cells, both E^+ and E^-. The cells mediating cytotoxicity in the presence of the lectin PHA have been found to have similar surface characteristics as in vitro generated CTL (*7, 8*). In the present study, we have examined the effects of IFN on NK activity, ADCC, and LICC of various subpopulations of PBL.

It has also been of interest to determine the factors involved in negative regulation of cell-mediated cytotoxicity and other immune functions. PGE appear to play an important role, possibly exerting their effect by stimulating adenyl cyclase and thereby causing an intracellular increase in cAMP (*9*). PGE has been shown to suppress blastogenesis, to inhibit leukocyte inhibitory factor production (*10*), to increase granulocyte migration (*11*), to boost IFN-induced suppression of antibody production (*12*), and to suppress ADCC (*5*) and NK activity in rodents (*13*). CTL activity (*14, 15*) and activated macrophage cytolysis in rodents (*16*) are also suppressed by PGE. PGE also could suppress IFN production by mitogen-stimulated human PBL (*17*). As with IFN, there are indications for some selectivity of the effects of PGE on various lymphoid cell subpopulations. PGE did not affect the activity of resting macrophages (*16*). Furthermore, others (*18*) have shown that PGE could inhibit the lymphoproliferative responses of one subpopulation of T-cells but actually augment the reactivity of another subpopulation.

It was therefore of interest to determine the effects of PGE on various human effector cell activities and subpopulations and to determine whether cells activated by IFN were as sensitive to inhibition as were unstimulated cells.

MATERIALS AND METHODS

Culture medium.—RPMI-1640 tissue culture medium (Biofluids Inc., Rockville, Md.), buffered with 10 m*M* HEPES[5] (M.A. Bioproducts, Walkersville, Md.), was used for all cell cultures and cytotoxicity assays. The medium was supplemented with 1 m*M* glutamine (National Institutes of Health Media Unit), 55 μg gentamicin reagent solution/ml (Schering Corp., Kenilworth, N.J.), and 10% FBS (Grand Island Biological Co., Grand Island, N.Y.). FBS was routinely heat inactivated and filtered through a 0.22-μm micropore filter before use in tissue culture medium.

IFN treatment.—PBL ($1\text{-}5\times10^6$/ml) were incubated in RPMI-1640 medium containing 10% FBS at 37°C for specified times, with or without IFN (1,000 U/ml) (HEM Re-

---

ABBREVIATIONS USED: ADCC=antibody-dependent cell-mediated cytotoxicity; cAMP=cyclic AMP; db-cAMP=N^6,$O^{2'}$-dibutyryl cAMP; cGMP=cyclic GMP; db-cGMP=N^6,$O^{2'}$-dibutyryl cGMP; CRA=^{51}Cr release assay; CTL=cytotoxic T-lymphocyte(s); E=erythrocyte(s); EA=E-antibody; E:T=effector-to-target cell; FBS=fetal bovine serum; FcγR=Fcγ receptor; IFN=interferon; K=killer; LICC=lectin-induced cellular cytotoxicity; LU=lytic unit(s); NK=natural killer; PBL=peripheral blood mononuclear lymphocytes; PG=prostaglandin(s); PGE=E-series PG; PHA=phytohemagglutinin.

---

[1] Received July 8, 1981; revised February 26, 1982; accepted April 2, 1982.

[2] Laboratory of Immunodiagnosis, Division of Cancer Biology and Diagnosis, National Cancer Institute, National Institutes of Health, Public Health Service, U.S. Department of Health and Human Services, Bethesda, Md. 20205.

[3] Department of Surgery, University of Arkansas Medical Sciences, 4301 West Markham, Little Rock, Ark. 72205.

[4] *Address reprint requests to* Dr. Ortaldo at his *present address*: NCI-Frederick Cancer Research Facility, Building 560, Room 31-16(23), Frederick, Md. 21701.

[5] 4(-2-Hydroxyethyl)-1-piperazine ethanesulfonic acid.

search Inc., Rockville, Md.). This IFN is type β, induced in human fibroblasts by polyinosinic-polycytidylic acid, and purified by hydrophobic affinity chromatography to approximately 3×10^7 U/mg. Unless specified, lymphocytes were washed with complete medium before treatment or testing.

Effector cells.—Mononuclear cells were isolated from heparinized peripheral blood of healthy normal volunteers by centrifugation on Ficoll–Hypaque. Whole blood was diluted 1:1 (vol/vol) with phosphate-buffered 0.83% NaCl solution and then overlaid on a Ficoll–Hypaque solution (lymphocyte-separating medium; Litton Bionetics Inc., Kensington, Md.). The blood was centrifuged at $450\times g$ for 30 minutes as previously described (*19*) or at $900\times g$ for 8 minutes. Cells were recovered from the interface, washed twice with Hanks' balanced salt solution without serum, and adjusted to appropriate concentrations for use.

Cell separation techniques—Spontaneous sheep rosette PBL were mixed with sheep E, rosettes were allowed to form spontaneously at 4°C, and E^+ and E^- cells were separated by centrifugation on Ficoll–Hypaque. The red blood cells in the pellet containing E^+ cells were lysed by addition of 3 ml of distilled H_2O to the pellet followed in 15 seconds by 25 ml of FBS for prevention of lymphocyte damage. This population contained greater than 98% E^+ cells, as measured by the 4°C sheep E-rosette assay. The E^- fraction contained 2–3% E^+ contaminating cells by the same assay.

FcγR separation.—The E^+ and E^- fractions were then further separated into $Fc\gamma R^+$ and $Fc\gamma R^-$ cells by two methods. The first method (*19*) involved separation by $Fc\gamma R^+$ depletion on an antigen–antibody monolayer. We removed the $Fc\gamma R^+$ cells (which adhered to the monolayer) by rinsing the monolayer with 0.01% EDTA in phosphate-buffered 0.83% NaCl solution and by scraping cells with a rubber policeman. Before being tested, the subpopulations of cells were incubated overnight at 37°C in 5% CO_2. Recovery after the procedure ranged from 60 to 85% with more than 90% viability at the time of testing.

The second method involved separation with the use of bovine E and IgG anti-bovine EA (Cappel Laboratories, Inc., Thurd Ridge Farm, Cochranville, Pa.). The procedure was a slight modification of the technique reported by Shaw et al. (*20*). EA^+ and EA^- cells were incubated with bovine E coated with IgG (EA–IgG) at 4°C for 1 hour. The cells were then separated on a Ficoll–Hypaque gradient. The pelleted cells were termed "$Fc\gamma R^+$," and the interface cells were termed "$Fc\gamma R^-$." Adherent E were lysed with H_2O as described above. The lymphocytes were then cultured overnight at 37°C in 5% CO_2 as above before they were tested. The purity of each fraction was evaluated with the use of E-rosettes and EA rosettes. The $E^+Fc\gamma R^+$ fraction contained 3% $Fc\gamma R^-$ cells, and the $E^+Fc\gamma R^-$ fraction had less than 1% $Fc\gamma R^+$ cells. The $E^-Fc\gamma R^+$ fraction had an average of 10% $Fc\gamma R^-$ contamination, whereas the $E^-Fc\gamma R^-$ fraction had an average of 7% $Fc\gamma R^+$ cells.

Culture conditions.—A total of 5–10^7 lymphocytes in 1–2 ml of complete medium was added to 17×100-mm plastic tubes (#2057; Falcon Plastics, Oxnard, Calif.) and incubated overnight at 37°C in a 5% CO_2 atmosphere. At the end of the culture, the lymphocytes were washed, adjusted to the desired concentrations, and tested for cytotoxicity.

Target cells.—The human myeloid cell line K562 (*21*) was used as a target cell for the detection of natural cytotoxicity as previously described (*19*).

Chang liver cells (*22*) were used as target cells in the LICC and ADCC assays. The Chang cells used in the ADCC assay were sensitized with a 1/50,000 dilution of rabbit anti-Chang antisera (*19*). DNase (Sigma Chemical Co., St. Louis, Mo.) at a final concentration of 0.1 μg/ml was added to Chang cells during ^{51}Cr labeling for prevention of clumping.

CRA.—The CRA for NK activity (and ADCC and LICC where indicated) was slightly modified from that which we described earlier (*19*). Target cells ($\approx2\times10^6$ in 0.5 ml medium containing 10% FBS) were labeled by incubation with 0.15 ml (200 μCi) of ^{51}Cr as sodium chromate (New England Nuclear Corp., Boston, Mass.) for 45 minutes at 37°C, washed twice in 50 ml of medium, and resuspended at 1×10^5 cells/ml. The 5×10^3 ^{51}Cr-labeled cells in 0.05 ml were added to 0.05 ml of varying concentrations of effector lymphocytes, ranging from 100:1 to 1:1 E:T ratios in medium in 0.2-ml wells of a 96-well Linbro plate (catalogue #76-311-05; Flow Laboratories, Inc., Rockville, Md.). The plates were incubated for 4 hours at 37°C in a 5% CO_2 humidified incubator. The supernatants were harvested by means of a Titertek harvester (Flow Laboratories), and their ^{51}Cr content was measured in a Biogamma II counter (Beckman Instruments, Fullerton, Calif.). All test combinations were performed in triplicate. Both an autologous control and a medium control were included in all assays and consisted of unlabeled target cells or medium alone, respectively, added in place of (and at the same concentration as) effector lymphocytes. These controls provided the measurement of base-line release of ^{51}Cr from target cells under the conditions of both high cell densities (as was encountered at high E:T ratios) or in medium alone, which usually ranged from 5 to 12% of the total label incorporated.

The percentage of specific ^{51}Cr release was calculated as $(A-B)/T\times100$, where A=mean cpm of test samples; B=mean cpm of autologous control; and T=mean cpm of the total amount of ^{51}Cr incorporated into the target cells at the time of labeling; background cpm of the gamma counter were first subtracted from each of these parameters (*19*). This calculation, which does not subtract spontaneous release from the denominator, gives somewhat lower percentages of cytotoxicity than those reported by other investigators, as has been discussed by Herberman et al. (*23*).

LICC.—This assay was performed by addition of PHA (H-16; Burroughs Wellcome Co., Research Triangle Park, N.C.) as the lectin, at specified final concentrations, to the 4-hour CRA. ^{51}Cr-labeled Chang cells were used as the target at 5×10^3 cells/well as in the CRA and ADCC assay.

Calculation of LU.—As previously described (*19*), we obtained dose-response curves by plotting the percentages of specific ^{51}Cr release obtained at each of several E:T ratios. An LU was then defined as that number of effector cells, extrapolated from the dose-response curve, required to achieve 30% specific target cell lysis. To more easily compare the lytic capacity of different cell populations which may have differed in cell yield or recovery, we frequently expressed the data as LU/10^7 effector cells.

Treatment with PG or cyclic nucleotides.—PGA_1, PGA_2, PGB_1, PGB_2, PGE_1, PGE_2, $PGF_{1\alpha}$, $PGF_{2\alpha}$, and cyclic nucleotides (db-cAMP and db-cGMP) (Sigma Chemical Co.) were dissolved in 95% ethanol as stock solutions and stored at −70°C. The reagents used in experiments were then prepared as 1/100 to 1/10,000 (vol/vol) dilutions of stock solutions with the use of RPMI-1640. Controls with the use of 1/100 dilutions of 95% ethanol showed no change from medium controls. Concentrations of each reagent are indicated in the tables.

RESULTS

Pretreatment of PBL with IFN resulted in substantial augmentation of LICC as well as NK activity and ADCC. To look for possible heterogeneous effects on subpopulations of cells, we made separations according to the presence or absence of receptors for E and of FcγR.

Table 1 shows the results of four experiments with subpopulations of PBL when tested for LICC and NK activity, with or without IFN augmentation. No significant activity (5% cytotoxicity at 50/1) was seen against Chang targets in the 4-hour CRA; however, addition of PHA efficiently elicited LICC. As previously reported (*8*), most LICC was associated with the $E^+FC\gamma R^-$ fraction, and LICC was significantly increased by IFN. The $E^+Fc\gamma R^+$ cells had very low LICC, but LICC was markedly increased after IFN treatment. Significant NK activity and boosting were seen only with $Fc\gamma R^+$ populations. Whereas higher spontaneous activity was seen in the $E^-Fc\gamma R^+$ cells, IFN caused relatively more augmentation of activity of the $E^+Fc\gamma R^+$ cells. The large boost in LICC seen with the $E^+Fc\gamma R^+$ cells was not due to NK activity, since IFN-treated effectors gave only a mean of 7 LU (data not shown) on Chang cells in the absence of PHA, compared to the 112 LU with lectin addition. Recovery of lytic activity (*see* footnote, table 1) demonstrated that manipulation on populations did not account for these results.

Table 2 shows the effects of PG addition to NK and K-cell assays. PGE and $PGF_{2\alpha}$ were the only consistent inhibitors of cytotoxic activity. Preincubation of effectors for 30 minutes and then removal of PG had no significant effect on NK or K-cell activity, demonstrating the rapid reversibility of these agents. As can be seen, PGE_1 and PGE_2 significantly depressed NK and K-cell activities and also LICC. The $PGF_{2\alpha}$ depression shown in table 2 was not consistent in repeat experiments, and $PGF_{1\alpha}$ had minimal inhibitory effects and often enhanced cytolysis. PGA_1, PGA_2, PGB_1, and PGB_2 had no effects on the results (data not shown). Since PG are known to result in changes in cyclic nucleotides, db-cAMP and db-cGMP were also tested. As expected, cAMP (only when present during the assay) and not cGMP inhibited NK and K-cell killing and also LICC.

TABLE 1.—*Effect of IFN on lymphoid subpopulations mediating NK activity and LICC*

Subpopulation	IFN	Cytotoxicity, LU/10^7 cells[a]			
		LICC		NK activity	
		Mean	Range	Mean	Range
$E^+Fc\gamma R^+$	−	2.95	1.4–4	54.6	3.4–117
	+	112	28–224	252	43–662
$E+Fc\gamma R^-$	−	20.3	3.8–38	0	—
	+	83.7	32–135	2	0–6
$E^-Fc\gamma R^+$	−	0.17	0–0.5	110	3–309
	+	4.2	0–11.2	235	9.6–486
$E^-Fc\gamma R^-$	−	0	—	0	—
	+	6.5	0.9–12	4.2	0.1–8.4

[a] For LICC, mean unseparated PBL activity prior to separation was 30.8 LU without IFN (75% recovery) and 267 LU with IFN (77% recovery); for NK activity, it was 181 LU without IFN (91% recovery) and 404 LU with IFN (122% recovery).

TABLE 2.—*Effect of PG and cyclic nucleotides when present in assay for 4 hours*

Agent added to assay (concentration, *M*)	Cytotoxicity activity, LU/10^7 cells		
	NK	LICC[a]	ADCC
Medium	225	87	46.7
PGE_1 (10^{-5})	29.8	12	3.0
PGE_2 (10^{-6})	20.0	7	14.7
$PGF_{1\alpha}$ (10^{-5})	171	NT	79.3
$PGF_{2\alpha}$ (10^{-5})	87.4	NT	15.1
cAMP (10^{-3})	12.0	5	7.0
cGMP (10^{-3})	194	91	72.6

[a] NT=not tested.

TABLE 3.—*Effects of cAMP on spontaneous and IFN-boosted NK activity*[a]

Treatment	Concentration, *M*	Cytotoxic activity			
		Without IFN		With IFN	
		LU/10^7 cells	Percent control	LU/10^7 cells	Percent control
Medium	—	147	—	226	—
cAMP	10^{-3}	7	5	75	33
cAMP	10^{-5}	107	72	144	77
cAMP	10^{-7}	209	142	219	97
cAMP	10^{-9}	219	148	244	107

[a] Results with cGMP (doses of 10^{-3}–10^{-9} *M*) showed no significant depression of NK activity, and data are not shown.

Since IFN and PGE had opposite effects on NK activity and since PG seemed to act through changes in cyclic nucleotides, it was of interest to determine how cAMP would affect IFN-augmented NK cells. As shown in table 3, a similar dose-dependent inhibition of both spontaneous and IFN-augmented NK activity was seen with cAMP. However, in contrast to spontaneous activity, the activity of boosted cells could never be completely inhibited, which suggests some resistance to negative regulation by the IFN-activated cells.

DISCUSSION

IFN has been shown here to have quantitatively different effects on various subpopulations of PBL. These observations are compatible with the previous observations that IFN did not augment the cytotoxicity by CTL against allogeneic blasts (*6*). It remains possible that long-term exposure of cells to IFN in mixed lymphocyte reaction might render them less sensitive or insensitive to augmentation. However, the $E^+Fc\gamma R^-$ cells involved in LICC show the same cell surface marker characteristics as CTL (*24*) and were augmented significantly by IFN (with short exposure), but not to the marked extent seen with $E^+Fc\gamma R^+$ cells. The $E^+Fc\gamma R^+$ cells accounted for most (60–80%) of the IFN-induced augmentation in NK and LICC reactivities. $E^-Fc\gamma R^+$ or $E^-Fc\gamma R^-$ cells appeared to lack the ability to mediate LICC, even after treatment with IFN.

Our results show that IFN is capable of augmenting both NK activity and LICC. The differential effect of IFN on E^+ and E^- populations could be explained by either a decrease in the number of cells present in the E population that are sensitive to IFN stimulation or a decrease in the sensitivity of all cells in the population to stimulation by IFN. This is consistent with the point previously made (*7*) that LICC effector cells and NK cells are differently distributed between E^+ and E^- cells, and it indicates that only cells with the inherent ability to moderate a particular effector function can be activated to do so by IFN.

Another interesting finding in this study is the tendency of $Fc\gamma R^+$ cell populations to be more susceptible to boosting by IFN. This feature was observed with the subpopulations involved in LICC and NK functions in addition to monocyte and polymorphonuclear leukocytes. This finding is particularly interesting because there is little evidence that the FcγR is directly involved in LICC or NK activity. The FcγR may simply make a cell population that is particularly receptive to boosting by IFN.

The data concerning the effects of PG on ADCC support work previously reported (*25*). In addition to confirming this study, we have also shown that PG could affect the cytolytic function of human NK cells and of LICC. Previous reports suggested that PGE has its effect on lymphocytes by stimulating adenyl cyclase to produce an increase in intracellular cAMP (*26*). Our data show similar effects by these two agents and would support these conclusions. These two agents appear to be capable of inhibiting a wide array of cytolytic activities. These cytolytic activities may have a final common pathway that is being blocked by PGE_1 and db-cAMP.

Although data available at this time suggest that IFN and PGE have opposite effects on cytolysis, there is no evidence that these compounds have any influence at the same step in the cytolytic pathway. PGE was capable of depressing cytolytic function of IFN-boosted human PBL, but to get the same degree of suppression required increased levels of PGE (data not shown). The suppression by PGE was not absolute following stimulation by IFN; the PGE treatment caused suppression of cytotoxic activity to levels below those of unstimulated PBL but not to the levels of depression seen in PBL treated with PGE alone. The temporal sequences required for the IFN and PGE effects were different. IFN pretreatment, even for a very short time (5 min), still produced a sustained effect on cytotoxicity, which suggests that IFN acts as a trigger for the production of relatively long-lived products. PGE, however, seems to produce its inhibitory effects through a much more evanescent product. A recent report has indicated that more prolonged pretreatment of human PBL with PGE may lead to stimulation of NK activity (*27*), which points out the possible complex and pleiotropic effects of PG.

It is very important to understand both the positive and negative regulatory facts on cytolytic effector cells. Increased knowledge in the area might lead to rational protocols for in vivo manipulation of the levels of cytolytic effector activities. Immune adjuvants may act largely via their ability to induce IFN and thereby activate or augment the activity of cytolytic cells. Conversely, elimination or reduction of PGE production might overcome inhibition of cytotoxic activity. In vivo data in mice from our laboratory and from other laboratories (*28*) have demonstrated decreased tumor growth in indomethacin-treated mice, which supports this hypothesis.

REFERENCES

(*1*) Perussia B, Santoli D, Trinchieri G. Interferon modulation of natural killer cell activity. In: Regulatory functions of interferons. Ann NY Acad Sci 1980; 350:55–62.

(*2*) Herberman RB, Ortaldo JR, Djeu JY, et al. Role of interferon in regulation of cytotoxicity by natural killer cells and macrophages. In: Regulatory functions of interferons. Ann NY Acad Sci 1980; 350:63–71.

(*3*) Lindahl P, Leary P, Gresser I. Enhancement by interferon of the specific cytotoxicity of sensitized lymphocytes. Proc Natl Acad Sci USA 1972; 69:721–725.

(*4*) Jett JR, Mantovani A, Jerrells TR, et al. Interferon enhancement of spontaneous human monocyte cytolysis. Proc Am Assoc Cancer Res 1980; 21:236.

(*5*) Wisloff F, Christoffersen T. Role of cyclic nucleotides in human lymphocyte-mediated antibody dependent cytotoxicity. Int Arch Allergy Appl Immunol 1977; 53:42–49.

(*6*) Zarling J, Sosmon J, Borden E, et al. Enhancement of allogencically induced cytotoxic lymphocyte response by purified human fibroblast interferon. Proc Am Assoc Cancer Res 1978; 19:108.

(*7*) Pichler WJ, Lum LG, Broder S. Fc-receptors on human T lymphocytes. I. Transition of T gamma to T mu cells. J Immunol 1978; 121:1540–1549.

(*8*) De Landazuri MO, Silva A, Alvarez J, et al. Evidence that natural cytotoxicity and antibody-dependent cellular cytotoxicity are mediated in humans by the same effector cell populations. J Immunol 1979; 123:252–258.

(*9*) Novogrodsky A, Rubin AL, Stenzel KH. Selective suppression by adherent cells, prostaglandin, and cyclic AMP analogues of blastogenesis induced by different mitogens. J Immunol 1979; 122:1–7.

(*10*) Lomnitzer R, Rubson AR, Kornhof HJ. The effects of cyclic AMP on leucocyte inhibitory factor (LIF) production and on the inhibition of leucocyte migration. Clin Exp Immunol 1976; 24:42–48.

(*11*) Van Epps DE, Wiik A, Garcia ML, et al. Enhancement of human neutrophil migration by prostaglandins E_2. Cell Immunol 1978; 37:142–150.

(*12*) Johnson HM, Baron S. Evaluation of effects of interferon and interferon inducers on immune response. In: Pestka S, ed. Pharmacology and therapeutics. Part A. Chemotherapy toxicology and metabolic inhibitors. Vol 1. Oxford: Pergamon Press, 1977:349–367.

(*13*) Brunda MJ, Herberman RB, Holden HT. Inhibition of murine natural killer cell activity by prostaglandins. J Immunol 1980; 124:2682–2687.

(*14*) Henry CS, Lichtenstein LM. The role of cyclic AMP in the cytolytic activity of lymphocytes. J Immunol 1972; 108:1526–1534.

(*15*) Henny CS, Bourne HR, Lichtenstein LR. The role of cyclic 3′,5′-adenosine monophosphate in the specific cytolytic activity of lymphocytes. J Immunol 1971; 107:610–621.

(*16*) Schultz RM, Pavlidis NA, Stylos WA, et al. Regulation of macrophage tumoricidal function: A role for prostaglandins of the E series. Science 1978; 202:320–321.

(*17*) Epstein LB, Bourne HR. Interferon production in mitogen stimulated lymphocytes: Cyclic AMP mediated inhibition by cholera toxin. In: Oppenheim JJ, Rosenstreich DL, eds. Mitogens in immunobiology. New York: Academic Press, 1976:433–462.

(*18*) Picker LJ, Raff HV, Goldyne ME, et al. Metabolic heterogeneity among human monocytes and its modulation by PGE_2. J Immunol 1980; 124:2557–2562.

(*19*) Kay HD, Bonnard GD, Herberman RB. Evaluation of the role of IgG antibodies in human natural cell-mediated cytotoxicity against the myeloid cell line K562. J Immunol 1979; 122:675–685.

(*20*) Shaw S, Pichler WJ, Nelson DL. Fc receptors on human T-lymphocytes. J Immunol 1979; 122:599–604.

(*21*) Lozzio CB, Lozzio BB. Human chronic myelogenous leukemia cell-line with positive Philadelphia chromosome (21406). Blood 1975; 45:321–333.

(*22*) Chang RS-M. Continuous subcultivation of epithelial-like cells from normal human tissues. Proc Soc Exp Biol Med 1954; 87:440–443.

(*23*) Herberman RB, Oldham RK, Connor RJ. Statistical analysis of baseline controls in cytotoxicity assays. In: Bloom RB, David JR, eds. In vitro methods in cell-mediated and tumor immunity. New York: Academic Press, 1976:481–488.

(*24*) Bonnard GD, West WH. Cell-mediated cytotoxicity in humans. A critical review of experimental models and clinically oriented studies. In: Herberman RB, McIntire KR, eds. Immunodiagnosis of cancer. Part 2. New York: Marcel-Dekker, 1979:1032–1105.

(*25*) Droller MJ, Schneider MU, Perlman P. A possible role of prostaglandins in the inhibition of natural and antibody-development cell-mediated cytotoxicity against tumor cells. Cell Immunol 1978; 39:165–177.

(*26*) Butcher RW, Baird CE. Effects of prostaglandins on adenosine 3′,5′-monophosphate levels in fat and other tissues. J Biol Chem 1968; 243:1713–1721.

(*27*) Kendall RA, Targan S. The dual effect of prostaglandin and ethanol on the natural killer cytolytic process effector activation and natural killer cell target cell conjugate lytic inhibition. J Immunol 1980; 125:2770–2777.

(*28*) Brunda MJ, Herberman RB, Holden HT. Inhibition of murine natural killer cell activity by prostaglandins. J Immunol 1980; 124:2682–2687.

blank page

Indirect Macrophage Migration Inhibition Response to 3-*M* KCl Extract of Gastric Carcinoma[1]

Tsuyoshi Akiyoshi,[2] Fumio Koba,[2] Michihiro Kawaguchi,[2] Soichiro Miyazaki,[2] *and* Hideo Tsuji[2]

ABSTRACT—With the use of indirect macrophage migration inhibition (MMI) test, the MMI response to 3-*M* KCl extract from gastric carcinoma or adjacent normal tissue was studied in patients with gastric carcinoma, in patients with other types of carcinoma, and in normal controls. The migration index (MI) of less than 75, which was 2 SD below the mean MI of normal controls, was considered positive. Twelve (23%) of 52 patients with gastric carcinoma showed positive response to autologous tumor extract, whereas only 2 (6%) of 35 patients responded to autologous normal tissue extract ($P<0.03$). Positive response to allogeneic gastric carcinoma extract occurred in 4 (9%) of 47 patients with gastric carcinoma and in none of 25 patients with other types of carcinoma. None of 39 patients with gastric carcinoma and 19 patients with nongastric carcinoma responded to allogeneic normal tissue extract. These results appeared to show a lower degree of sensitivity but a relatively higher degree of specificity in the indirect MMI test, as compared to those in the direct leukocyte migration inhibition test, for detection of the cell-mediated immune response to tumor-associated antigens in patients with gastric carcinoma.—JNCI 1982; 69:345-347.

The MMI test has proved to be a sensitive in vitro method for detection of cellular immune response to purified antigens in experimental animals and has been modified for use in clinical studies, whereas the LMI test has been monitored. The direct LMI assay is now widely accepted as a means of examining cell-mediated immunity against human neoplasms, and it has revealed discrimination in reactivity between healthy donors and patients with various malignant tumors (*1-9*). As for gastric carcinoma, however, few results have been reported (*10*).

Conversely, the indirect MMI test (*11*) has been scarcely utilized for detection of cell-mediated immunity in patients with malignant tumors (*12-14*), although it has been used as an in vitro method in the detection of cellular immune response to purified antigens in humans. The indirect MMI technique as well as the indirect LMI test (*15, 16*) could decrease the possibility of false-positive migration inhibition reactions that might occur in the direct LMI test as a result of toxicity of antigen preparation on leukocytes.

Using the indirect MMI test in the present study, we examined the cell-mediated immune response to autologous 3-*M* KCl extract of tumor or adjacent normal tissue in patients with gastric carcinoma. These responses were compared with those produced by patients with gastric carcinoma to allogeneic extract, by patients with other types of carcinoma, and by normal control subjects.

MATERIALS AND METHODS

Patients.—Heparinized whole blood was obtained from 86 patients with gastric carcinoma and from 31 patients with the other types of carcinoma. Patients were tested before the operation or in the postoperative period (7-21 days) prior to chemotherapy, radiotherapy, and/or immunotherapy. Blood specimens were also obtained from 42 normal controls.

Extracts.—Extracts of tumor (3 *M* KCl) and adjacent normal tissue were prepared by modifications of the method described by Meltzer et al. (*17*). Tissue samples were dissected from surgical specimens under sterile condition and minced finely with a scalpel. Minced tissue was suspended in cold 3-*M* KCl solution at pH 7.3 and incubated at 4°C for 16-24 hours. The mixture was then centrifuged at 40,000×g for 60 minutes at 4°C. The supernatant was desalted twice against 200-volume distilled water for 1 hour. The desalted supernatant was centrifuged at 40,000×g for 15 minutes and dialyzed against 200-volume phosphate-buffered saline for 1 hour. The dialyzed extract was sterilized by Millipore membrane filtration, and protein concentration was determined by Lowry's method (*18*). Samples of each extract were stored at −80°C.

Indirect MMI assay.—The method described by Rocklin and David (*11*) was used with minor modifications. Mononuclear cells from heparinized peripheral blood, prepared by Ficoll-Conray separation, were suspended in medium 199 supplemented with 100 U penicillin/ml and 100 µg streptomycin/ml to a concentration of 3×10^6 cells/ml for culture. A concentration of 250 µg 3-*M*-KCl extract/ml was added to the cells, and mononuclear cell cultures were then incubated at 37°C in a humidified 5% CO_2 atmosphere for 3 days. The cell-free supernatants were carefully removed each day and, medium with and without the original extracts was replaced to maintain the original volume. The collected supernatants were dialyzed in cold against 0.9% NaCl, redialyzed against distilled water, and concentrated by lyophilization. The lyophilized supernatants were resuspended in medium 199 containing 10% guinea pig serum and 5% fetal calf serum at one-third of the original volume, sterilized by Millipore membrane filtration, and adjusted to pH 7.4 with CO_2 in air. Controls consisted of the cell-free supernatant from similar mononuclear cell culture incubated without extract; the extract was added after the total collection.

To measure the macrophage migration inhibitory factor activity in these supernatants, we utilized modifications of

---

ABBREVIATIONS USED: LMI=leukocyte migration inhibition; MI=migration index (indices); MMI=macrophage migration inhibition.

---

[1] Received July 30, 1981; revised December 27, 1981; accepted February 17, 1982

[2] Department of Surgery, Research Institute of Balneotherapeutics, Kyushu University, Beppu 874 Japan.

the capillary migration technique of Rocklin and David (*11*). Capillary tubes were filled with the cell suspension of peritoneal exudate cells from normal guinea pig and centrifuged. The tubes were cut, and the portion containing the cells was placed in Mackaness-type chambers, two capillaries per chamber. The chambers were filled with the media to be assayed and incubated at 37°C for 24 hours. Then the area of migration of cells from capillary tubes was projected and measured by planimetry, and percentage migration (MI) was calculated from the following formula: Migration index = (average area of test supernatant/average area of control supernatant) × 100. The average area was calculated with at least six capillary tubes.

RESULTS

A total of 307 indirect MMI tests were performed on 86 patients with gastric carcinoma, 31 patients with nongastric carcinoma, and 42 normal controls. All individuals were tested with 3-*M* KCl extracts derived from gastric carcinoma or adjacent normal tissue. The results obtained from normal control subjects were shown in text-figure 1. The mean MI were 103.1±13.0 with tumor extract and 100.9±13.9 with normal tissue extracts, respectively. Therefore, the limit for a positive assay was set at 75, which was 2 SD below the mean (102.1±13.4) of normal controls tested with both tumor and normal tissue extract.

For evaluation of the accuracy of the indirect MMI assay, we divided the cells from the same patient and tested duplicate specimens simultaneously and separately for the MMI response to autologous tumor extract. As shown in table 1 MI values rarely differed more than 20, and frequently the difference was less than 10.

Table 1.—*Accuracy of the indirect MMI assay in gastric cancer patients with autologous tumor extract*

Patient No.	MI	
	Expt 1	Expt 2
1	113	108
2	59	70
3	74	83
4	106	104
5	70	74
6	93	99
7	102	103
8	112	104
9	89	105
10	94	104
11	92	105
12	79	60
13	102	80
14	75	74
15	94	110

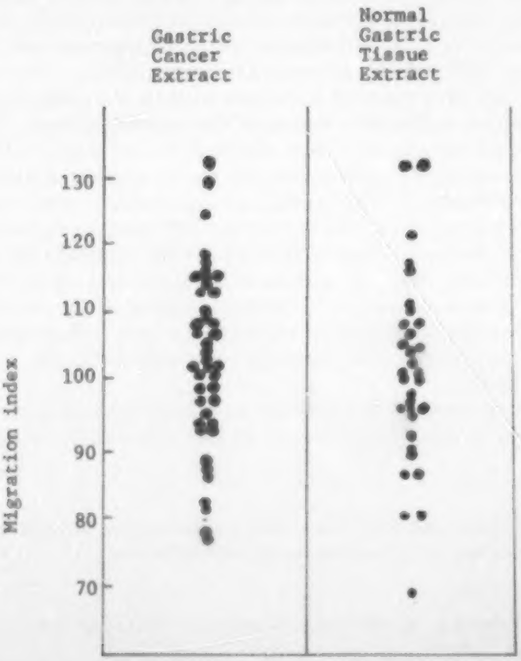

Text-figure 1.—Indirect MMI responses of normal controls to 3-*M* KCl extract of gastric carcinoma and adjacent normal tissue.

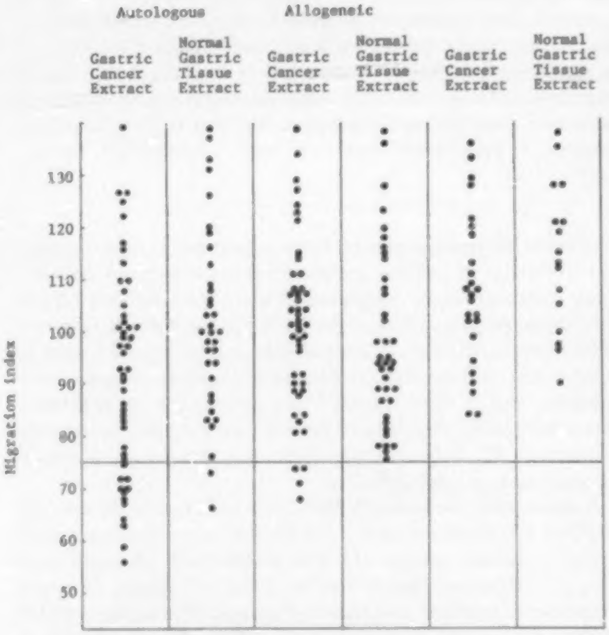

Text-figure 2.—Indirect MMI responses of patients with gastric carcinoma and other types of carcinoma to 3-*M* KCl extract of gastric carcinoma and adjacent normal tissue

As shown in text-figure 2, a positive MMI response to autologous tumor extract was found in 12 (23%) of 52 patients with gastric carcinoma. In contrast, only 2 (6%) of 35 patients with gastric carcinoma showed positive response against autologous normal tissue extract. The difference was statistically significant ($P<0.03$; Fisher's exact probability test). The MMI response to extract derived from allogeneic gastric tissue was measured in 47 patients with tumor extract and in 39 patients with normal tissue extract. Four (9%) of 47 patients responded to extract of allogeneic gastric cancer tissue, whereas none of 39 patients responded to the extract of allogeneic adjacent normal tissue. None of the patients with other types of carcinoma responded to the extract of gastric carcinoma (25 tested) or adjacent normal tissue (19 tested).

DISCUSSION

In this study we have measured the indirect MMI response of gastric carcinoma patients to 3-*M* KCl extract derived from gastric carcinoma or adjacent normal tissue. We have additionally evaluated the MMI response in patients with nongastric carcinomas to 3-*M* KCl extract of normal and cancerous gastric tissue.

Our response rate to autologous tumor extract was 23%, and it was significantly different from that to autologous normal tissue extract. However, the rate was relatively lower than that reported by other investigators which was obtained with the use of the direct LMI test in patients with various carcinomas (*2, 7, 9*). It may be partially related to the timing of the tests relative to surgery because our tests were performed in the postoperative period (7–21 days), which is a time of immune suppression as reported by several authors (*19, 20*).

The results of this study similarly showed low frequency of positive response in patients with gastric carcinoma to allogeneic tumor extract compared to the LMI response to various carcinomas reported by other investigators (*1–6, 8–10*), although none of 39 patients showed positive response to allogeneic normal tissue extract. With the use of the direct LMI test, Zöller et al. (*10*) found that 39 (91%) of 43 patients with gastric carcinoma, compared to 5% of patients with nonmalignant diseases and 3% of normal controls, responded to a panel of allogeneic 3-*M* KCl tumor extracts, whereas patients with nongastric carcinoma were sensitized in 36% (49/135) of the cases.

In the present study we utilized the indirect MMI test in which inhibition was not due to toxicity of tumor extract as it might be seen in the direct LMI test (*21*). In this system, involvement of histocompatibility antigens was unlikely because none of these patients with carcinoma showed positive response to allogeneic normal tissue extract. Furthermore, the present results showed the lack of reactivity in patients with gastric carcinoma to allogeneic normal gastric tissue extract. Thus the indirect MMI reactivity might be largely directed against tumor-associated antigens of gastric carcinoma. Our lower response rates to autologous or allogeneic tumor extract appeared to be related to the reasons described above.

Of 81 autologous tests 5 were associated with an MI greater than 129, which might suggest enhancement of migration (*22*). This enhancement also occurred in those in the presence of allogeneic tissue extract (8 of 130 tests). The significance of this phenomenon remains to be determined.

The results of the present study suggested that the indirect MMI test appeared to have a lower degree of sensitivity but a relatively higher degree of specificity, as compared to the direct LMI test, for detection of cell-mediated immune response to tumor-associated antigens in patients with gastric carcinoma. To determine the significance of the test in comparison with direct or indirect LMI assay, further studies with this test in patients with other types of carcinoma are presently under way.

REFERENCES

(*1*) McCoy JL, Jerome LF, Dean JH, et al. Inhibition of leukocyte migration by tumor-associated antigens in soluble extracts of human malignant melanoma. J Natl Cancer Inst 1975; 55:19–23.

(*2*) Cochran AJ, Grant RM, Spilg WG, et al. Sensitization to tumor associated antigens in human breast carcinoma. Int J Cancer 1974; 14:19–25.

(*3*) McCoy JL, Jerome LF, Dean JH, et al. Inhibition of leukocyte migration by tumor-associated antigens in soluble extracts of human breast carcinoma. J Natl Cancer Inst 1974; 53:11–17.

(*4*) Lavergne JA, Lamm DL, Radwin HW, Harrington JT. Leukocyte migration inhibition in vitro in bladder carcinoma. Cancer Res 1979; 39:1985–1988.

(*5*) Boddie AW, Holmes, EC, Roth JA, Morton DJ. Inhibition of human leukocyte migration in agarose by KCl extracts of carcinomas of the lung. Int J Cancer 1975; 15:823–829.

(*6*) McCoy JL, Jerome LF, Cannon GB, Neese JL, Herberman RB. Reactivity of lung cancer patients in leukocyte migration inhibition assay to 3-*M* potassium chloride extracts of fresh tumor and tissue-cultured cells derived from lung cancer. J Natl Cancer Inst 1977; 59:1413–1418.

(*7*) Elias EG, Elias LL, Didolker MS, Hebel JR. Cellular immunity in patients with colorectal adenocarcinoma measured by autologous leukocyte migration inhibition. Cancer 1977; 40:687–692.

(*8*) Faiferman I, Gleicher N, Cohen CJ, Koffler D. Leukocyte migration in ovarian carcinoma: Comparison of inhibitory activity of tumor extracts. J Natl Cancer Inst 1977; 59:1593–1597.

(*9*) Fukuda M, Wanebo HJ, Tsuei L, Sarker NH. Leukocyte migration response to various antigen preparation of autologous and homologous breast cancer in patients with primary breast cancer. JNCI 1979; 63:1161–1169.

(*10*) Zöller M, Matzku S, Schulz U. Leukocyte migration studies in gastric cancer detection: An approach toward improved specificity and sensitivity. J Natl Cancer Inst 1977; 58:897–904.

(*11*) Rocklin RE, David JR. Method for the production of MIF by human blood lymphocytes. In: Bloom BR, Glade PR, eds. In vitro methods in cell-mediated immunity. New York and London: Academic Press, 1971:281–288.

(*12*) Hilberg RW, Balcerzak SP, Lobuglio AF. A migration inhibition factor assay for tumor immunity in man. Cell Immunol 1973; 7:152–158.

(*13*) Akiyoshi T, Hata A, Tsuji H. In vitro cellular responses to autologous tumor extract detected by inhibition of macrophage migration. Gan 1975; 66:167–174.

(*14*) Rocklin RE, Gagel R, Feldman Z, Tashjian AH. Cellular immune responses in familial medullary thyroid carcinoma. N Engl J Med 1977; 296:835–838.

(*15*) Suslov I, McCoy JL, Herberman RB. Indirect leukocyte migration inhibition reactions to a 3-*M* KCl extract of lung adenocarcinoma by lung cancer patients. JNCI 1981; 66:233–237.

(*16*) Suslov IM, McCoy JL, Cannon GB, Herberman KB. High incidence of migration inhibition reactivity to lung tumor-associated antigen by normal donors in close contact with lung cancer patients or materials. JNCI 1980; 65:709–713.

(*17*) Meltzer MS, Leonard EJ, Rapp HJ, Borsos T. Tumor-specific antigen solubilized by hypertonic potassium chloride. J Natl Cancer Inst 1971; 47:703–709.

(*18*) Lowry OH, Rosebrough NJ, Farr AL, Randall RJ. Protein measurement with the Folin phenol reagent. J Biol Chem 1951; 193:265–275.

(*19*) Black MM, Leis HP Jr. Cellular responses to autologous breast cancer tissue. Correlation with stage and lymphoreticuloendothelial reactive. Cancer 1971; 28:263–273.

(*20*) Cochran AL, Spilg WG, Machie RM, Thomas CE. Postoperative depression of tumour-directed cell-mediated immunity in patients with malignant disease. Br Med J 1972; 14:47–70.

(*21*) Wolberg WH. Inhibition of migration of human autologous and allogeneic leukocytes by extracts of patients' cancers. Cancer Res 1971; 31:798–802.

(*22*) Weisbart RH, Blustone R, Goldberg LS, Pearson CM. Migration enhancement factor: A new lymphokine. Proc Natl Acad Sci USA 1974; 71:875–879.

blank page

Ten- to Fourteen-Year Effect of Screening on Breast Cancer Mortality[1,2]

Sam Shapiro, *B.S.*,[3] **Wanda Venet**, *B.S., R.N.*,[4] **Philip Strax**, *M.D.*,[5]
Louis Venet, *M.D.*,[6] *and* **Ruth Roeser**, *M.A.*[4,7]

ABSTRACT—Results from the randomized trial conducted by the Health Insurance Plan (HIP) to determine the efficacy of breast cancer screening with mammography and palpation are reported for longer periods than previously available. By the end of 10 years after entry, the study group's mortality due to breast cancer was about 30% below the control group's. Arithmetic gains due to screening were maintained through year 14; relative gains declined. With increases in the period of follow-up, cumulative survival rates among cases detected by mammography alone (palpation negative during screening), decreased more rapidly than rates among other subgroups, but survival rates for mammography cases remained relatively high. Study women aged 40–49 years at entry began to show lower breast cancer mortality than those in the control group as duration of follow-up increased. Reservations are advanced about the acceptance of this finding as evidence of the efficacy of screening under age 50 under the conditions of the HIP study. The reservations are based on the observation that the decrease of mortality among the study group aged 45–49 at entry is concentrated entirely among cases diagnosed after they reached 50 years of age.—JNCI 1982; 69:349–355.

The favorable impact of periodic screening with mammography and clinical examination of the breast on mortality from breast cancer shown by the HIP Study has been extensively reported for the short-term period of 5 years after the start of screening and for several subsequent years (*1*). Stimulated by these results, a number of issues have attracted attention that affect the spread of large-scale screening programs, e.g., the independent contribution of mammography (*2*), the age groups that benefit from screening, the radiogenic effect of mammography, and the risk-benefit effects of screening at various intervals (*3–5*). At the same time, it has been well recognized that the efficacy of screening will not be adequately comprehended until we know the long-term effects on mortality.

Short- to intermediate-term reduction in mortality is close to one-third, but the absence of information on the natural history of breast cancer detected through screening leaves uncertain whether this reduction represents a cure or a postponement in mortality from breast cancer. Evidence on this issue would have great significance not only for screening but also for the more general understanding of the biology of breast cancer. At this point, the data on breast cancer detected in clinical practice show that even among cases diagnosed at a localized stage, there continues to be excess mortality for long periods after diagnosis (*6*).

The discussion that follows represents a start in addressing the question of long-term effects related to screening through an extension of previously reported observations into a 12- to 14-year period of follow-up.

METHODS

Population source and observation methods.—To test the efficacy of periodic screening with mammography and clinical examination, we selected two systematic random samples, each consisting of about 31,000 women aged 40–64 years, from members of HIP, a comprehensive, prepaid group practice. Study women were offered screening examinations; the 65% who appeared for an initial examination were offered three additional examinations at annual intervals unless earlier follow-up or biopsy was indicated. All but a small proportion (12%) had at least one additional annual examination. Screening consisted of a clinical examination, usually by a surgeon; mammography, in which two views were taken of the breast (cephalocaudad and lateral); and an interview to obtain relevant demographic information and a health history. Independence between the two examining modalities was strictly maintained. Initial screenings began in December 1963 and continued through June 1966; annual rescreenings ended in June 1970. Control women continued to receive their usual medical care. The extent to which women in the study and control groups had general physical examinations (including breast examinations) or engaged in breast self-examination after the completion of the screening project is not known. At HIP, mammography was utilized extensively for differential diagnostic purposes but not as part of a program for early detection among asymptomatic women.

Follow-up procedures.—All observations relate to women in the study and to control groups with no breast cancer diagnosed prior to their entry into the study. Follow-up procedures for identification of breast cancers and deaths due to breast cancer or other causes have been applied equally to the study and control groups. These include periodic communication with women (or their next of kin) on the breast cancer registries established in the study, searches of hospital insurance and death records, and surveys

---

ABBREVIATIONS USED: CFR=case fatality rate(s); CSR=case survival rate(s); HIP=Health Insurance Plan of Greater New York.

---

[1] Received August 21, 1981; accepted February 26, 1982.

[2] Supported in part by Public Health Service (PHS) contract N01CP-43278 from the Division of Cancer Cause and Prevention, National Cancer Institute; and by PHS contract NIH-69-88 to The Health Insurance Plan of Greater New York from the National Cancer Institute.

[3] Health Services Research and Development Center, The Johns Hopkins University School of Hygiene and Public Health, 624 North Broadway, Baltimore, Md. 21205.

[4] The Health Insurance Plan of Greater New York, 220 West 58th St., New York, N.Y. 10019.

[5] New York Medical College, Valhalla, N.Y. 10595.

[6] Department of Surgery, Beth Israel Medical Center, 10 Nathan D. Perlman Place, New York, N.Y. 10003.

[7] We thank Dr. George B. Hutchison of the Department of Epidemiology, Harvard University School of Public Health for his valuable suggestions on reviewing the draft of this paper.

5 and 10 years after entry of all 62,000 women whose status was not already known through other sources. Other tracing methods are being applied for residual groups, and a new survey 15–17 years after entry is under way. Results thus far indicate that nearly all cases of breast cancer that occurred during the first 10 years after entry are now known; however, this may not be so for later years. Accordingly, mortality due to breast cancer, the primary measure for determining efficacy of screening, is restricted to cases detected in the 10-year interval. The end point for detection of breast cancer deaths among these cases is 14 years from entry; all study and control group women were observed for this period of time, and survival status of all cases on the breast cancer register has been ascertained.

Also presented are case survival rates among women with breast cancer histologically confirmed during the first 5 years after entry. The secondary position given to these rates in the determination of efficacy of screening results from *a*) the lead time in detection gained by the cases detected through screening and from *b*) the tendency of screening to select individuals with longer mean duration of preclinical disease. (In these instances each subsequent stage of disease may be more indolent, giving rise to a bias termed "length-biased sampling" (*7–9*), the effect of which diminishes as new cases are accrued.)

Life-table methods have been applied with the use of 6-month intervals after diagnosis. All breast cancer cases had a minimum of 9.5 years of exposure by December 31, 1980, the cut-off date for this report. The maximum period for which survival rates are given is 12 years[a] after which the numbers of cases withdrawn due to incomplete exposure become relatively large. Recalculation of survival rates between 9.5 and 12 years with the use of 1-month intervals shows that the resulting cumulative survival rates differ from the rates based on 6-month calculations by less than 1%.

Comparability of study and control groups.—High levels of comparability between the study and control groups have been demonstrated for a wide range of demographic and other characteristics (*10*) and for general mortality other than breast cancer (table 1). There are, however, large differences in general mortality between the study women who participated in the screening program and those who refused. The differential appears to be decreasing as the interval from entry increases, but the margin is still large (28%)—6–10 years from entry. This evidence of bias in the self-selection for screening has emphasized the importance of comparisons based on the total study group (screenees and refusers combined).

RESULTS

Breast Cancer Detection

Case detection information has been described elsewhere in detail (*1*); only a few of the results will be given here. By the end of 5 years from entry, which covers about 1.5 years after the last screening cycle, the gap between the breast cancer rates of the total study and control groups had become small (2.03 and 1.94/1,000 person-yr, respectively). Women who refused screening had a low rate of breast cancer (1.58/1,000) as compared with the rate among controls, indicating that women with a higher risk for breast cancer tended to self-select themselves for screening. Clinical and mammography examinations both contributed cases not detected by the other; the relative contribution of mammography (in the absence of clinical findings) was less among women under 50 years of age at diagnosis than among those 50 and over (14.4 vs. 37.6%). The proportion with no histologic evidence of axillary nodal involvement was higher among study cases than in the control group (56.4 vs. 46.3%). Breast cancers detected through screening had an especially high proportion with no nodal involvement (70.5%).

TABLE 1.—*Mortality from all causes excluding breast cancer: 10-year follow-up after entry*[a]

Population	Mortality at following intervals from entry:		
	10 yr	1–5 yr	6–10 yr
Total study	65.5	54.9	76.7
Screened	54.9	42.3	68.1
Refused screening	87.2	80.4	94.3
Control	64.8	56.5	73.4

[a] Rates per 10,000 person-yr.

Mortality Differentials

The primary measure in the determination of the efficacy of screening is the differential between study women (those screened one time or more plus those who refuse screening) and control women in the number or rate of deaths with breast cancer as the underlying cause. Included are *a*) deaths due to breast cancer among women with histologically confirmed breast cancer and *b*) deaths among women with breast cancer as the underlying cause of death but with no histologic confirmation prior to death. Category *b*) consists of deaths among women for whom clinical or autopsy evidence indicated that breast cancer was the underlying cause of death. There were 9 and 16 such cases in the study and control groups, respectively, during the first 10 years after entry.

Follow-up periods of 5, 7, 10, and 14 years from date of entry are included to indicate changes in relationships as observations progress from short to intermediate to long intervals of follow-up.

Text-figure 1 displays two trend series. The curves representing cumulative breast cancer mortality from entry date among women with breast cancer diagnosed in the first 5 years have previously served as the basis for conclusions about the impact of periodic screening. Five years has been of interest because it includes an average of 3.5 years of screening and 1.5 years post screening—an interval that extends only moderately beyond the point when women would have been due for an additional examination if the program had continued. The gap between the curves for the

---

[a] In the total study group, there were 176 women alive at the start of follow-up interval 9.5–10 yr; over the next 1.5 yr 12 women had incomplete exposure; at the start of interval 11–11.5 yr, there were 146 women alive, 29 of whom had incomplete exposure by the end of yr 12. Corresponding figures for the control group are similar.

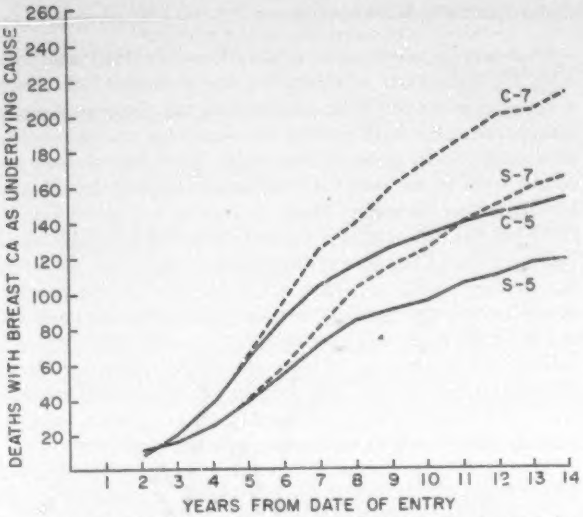

TEXT-FIGURE 1.—Cumulative breast cancer deaths by time interval from date of entry. S-5 and C-5 refer to breast cancer deaths within 5 yr of entry; S-7 and C-7 refer to corresponding situation for cancers diagnosed within 7 yr of entry. S=total study; C=controls.

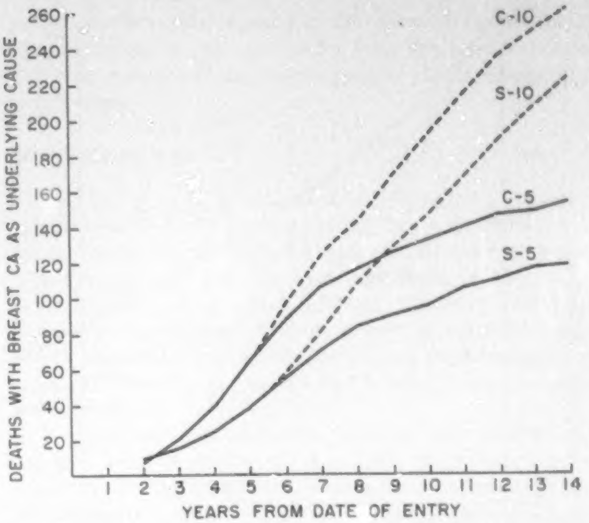

TEXT-FIGURE 2.—Cumulative breast cancer deaths by time interval from date of entry. S-5 and C-5 refer to breast cancer deaths among cancers diagnosed within 5 yr of entry. S-10 and C-10 refer to corresponding situation for cancers diagnosed within 10 yr of entry. S=total study; C=controls.

study and control groups widens numerically until year 6 or 7 from entry and then remains fairly constant through year 14 (table 2).

Addition of breast cancer deaths to cases diagnosed through year 7 results in increased numerical differentials between study and control groups; no further increases occur with the inclusion of mortality among cases diagnosed in years 8–10 (text-fig. 2). From this, it would appear that mortality due to breast cancer among cases detected starting 3–3.5 years after screening ended became very similar for study and control groups of women.

TABLE 2.—*Cumulative numbers of deaths due to breast cancer by selected time intervals from date of entry*

Interval to breast cancer diagnosis, yr	No. of breast cancers[a]	No. of deaths with breast cancer as underlying cause through following yr after entry:			
		5	7	10	14
Within 5					
Study	306	39	71	95	118
Control	300	63	106	133	153
Difference, %		(38.1)[b]	(33.0)[c]	(28.6)[b]	(22.9)[b]
Within 7					
Study	425	39	81	123	165
Control	443	63	124	174	212
Difference, %		(38.1)[b]	(34.7)[c]	(29.3)[c]	(22.2)[b]
Within 10					
Study	600	39	81	146	218
Control	604	63	124	192	262
Difference, %		(38.1)[b]	(34.7)[c]	(24.0)[b]	(16.8)[b]

[a] No. indicate breast cancers histologically confirmed within a specified interval after entry plus deaths among women with breast cancer as the underlying cause but with no histologically confirmed diagnosis prior to death.

[b] $0.01 < P < 0.05$. Conditional 2-tailed test of the ratio between 2 Poisson parameters (study:control No. of deaths due to breast cancer) applied.

[c] $P < 0.01$. Statistical test same as explained under footnote *b*.

Thus far, the discussion has been concerned with numerical differences. For purposes of estimating the influence of screening on reduction in the breast cancer mortality rate of a population, relative differences are important. Table 2 shows that the percent decrease becomes smaller with increases in duration from entry. This follows from the constancy in arithmetic differences just presented. Addition of breast cancers diagnosed through year 10 also reduces the differential between study and control groups in breast cancer mortality. The attenuation reflects the effect on breast cancer mortality in a population that participated in screening, because the cases are added long after screening ends. The magnitude of the attenuation is appreciable as suggested by the "observed" percentages in text-figure 3.

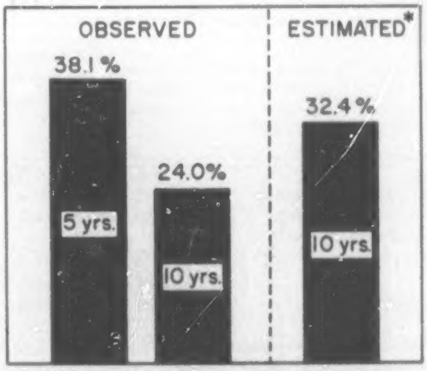

*Estimated under assumption screening program renewed in years 6-10 after entry.

TEXT-FIGURE 3.—Difference between total study and control group deaths due to breast cancer 5 and 10 yr after entry.

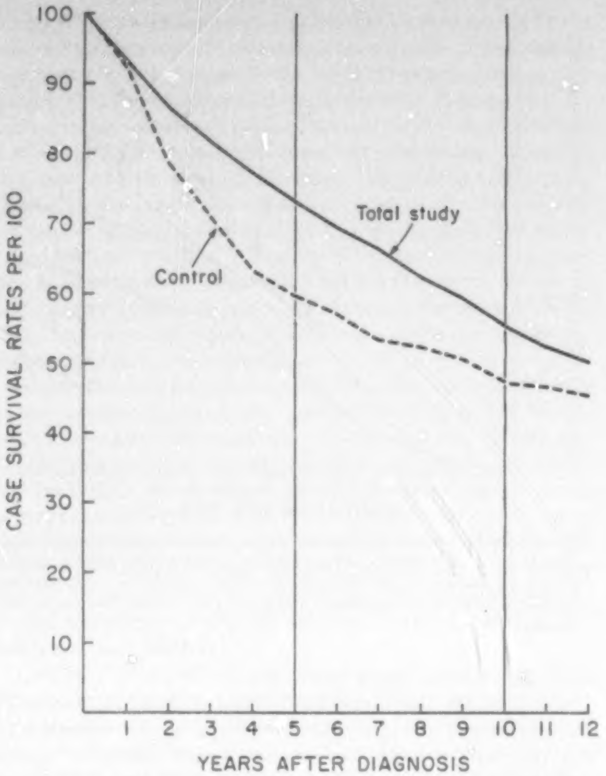

TEXT-FIGURE 4.—CSR by interval from diagnosis in total study breast cancer patients and in controls.

Under the assumption that a new cycle of screening in years 6–10 among the women aged 45–64 years resulted in the same reduction in mortality as that found in years 1–5, the margin between study and control groups is 32.4%. This is to be compared with a differential of 24.0% under the condition of no continuation in screening as in the HIP study. Nevertheless, there is some decrease between the 5-year effect of screening and the effect over a 10-year period.

TABLE 3.—*Cumulative CSR (per 100) among confirmed breast cancer cases*[a]

Population	No. of cases	CSR through following yr after diagnosis:[b] 5	10	12
Total study	303	73.9	54.8	50.4 (2.9)
Detected through screening	132	87.1	64.4	59.7 (4.3)
Screened but not detected through screening	93	62.4	46.2	44.7 (5.2)
Refused screening	78	65.4	48.7	41.9 (5.6)
Control	294	59.5	46.3	43.1 (2.9)
Total study, adjusted[c]	303	71.3	53.8	48.9 (2.9)

[a] Included are cases histologically confirmed within 5 yr of entry.

[b] *Numbers in parentheses* are standard errors due to sampling variability.

[c] Lead time of 1 yr is included for cases detected through screening. The adjusted CSR through yr *n* is derived as a weighted average of the rates for screened cases (yr *n*+1), screened but not detected through screening (yr *n*), and refused screening (yr *n*).

Case Survival Differentials

Past presentations on mortality from the HIP study parallel the discussions of mortality due to breast cancer with a consideration of CFR, adjusted to take into account an estimated 1-year lead time in the detection of cases through screening (*8*). In general, the results have been highly consistent with those from the analysis of the population-based breast cancer mortality data. A reason for turning to the CFR has been that this is the only possible approach to the examination of the course of mortality related to the screening process itself, i.e., how CFR vary with the mode of detection (mammography or clinical examination) and with the round of screening examinations (initial examination vs. subsequent screenings). There are major restrictions in the interpretation of such CFR because of the uncertainty about how lead time or length-biased sampling, previously discussed, varies with the subgroup of cases detected.

The data to be discussed from this point represent a shift from CFR to CSR. All of the considerations related to CFR are applicable to CSR. The shift to CSR is useful because it places the experience in the study within the context of the usual analysis of breast cancer experience as exemplified by publications from the Cancer Surveillance, Epidemiology, and End Results (SEER) Program (*6*).

Text-figure 4 and table 3 show that screening has had a profound effect on the contour of the trend in cumulative CSR among breast cancer cases diagnosed in the total study

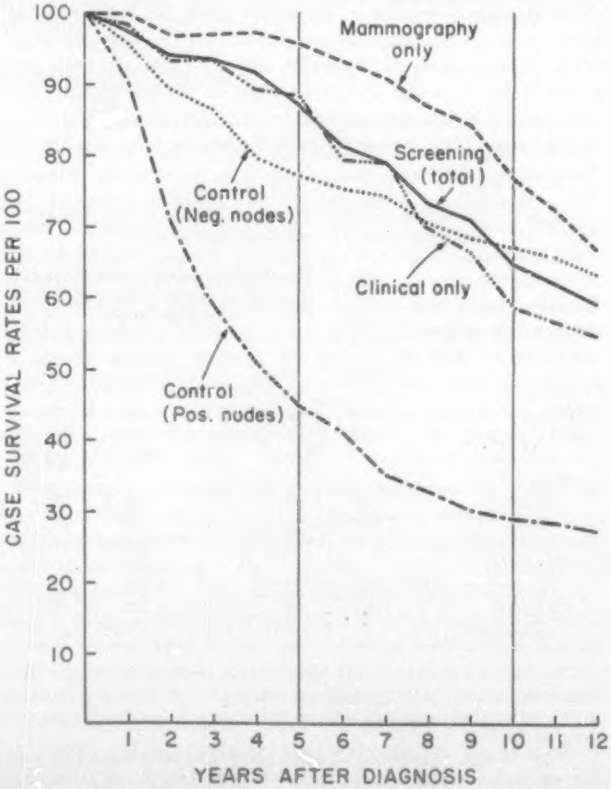

TEXT-FIGURE 5.—CSR by interval from diagnosis of breast cancers detected in screening and control cases.

TABLE 4.—*CSR (per 100) among breast cancer cases detected on screening by modality and control cases*[a]

Breast cancer category of cases	No. of cases	CSR through following yr after diagnosis:[b]		
		5	10	12
Detected through screening[c]				
Total	132	87.1	64.4	59.7 (4.3)
Mammography only	44	95.5	77.3	67.8 (7.1)
Clinical only	59	88.1	59.3	55.9 (6.5)
Mammography and clinical	29	72.4	55.2	55.2 (9.2)
Control				
Negative nodes[d]	136.	77.2	66.9	62.5 (4.2)
Positive nodes[d]	123	44.7	29.3	27.4 (4.0)

[a] Included are cases histologically confirmed within 5 yr of entry.

[b] *Numbers in parentheses* are standard errors due to sampling variability.

[c] Initial evidence for biopsy recommendation made independently by the two modalities.

[d] Classification based on histologic evidence of axillary nodal involvement. Not shown are 35 cases with unknown nodal involvement.

group within 5 years after entry. The corresponding control cases have a marked convex curve similar to what is seen in general population series based on relative CSR. In contrast, the total study group barely begins to flatten out at year 10, and, in fact, a linear regression equation fits the time series quite well.

Clearly, within this time period there has been a fundamental alteration in the survival experience among breast cancer cases in the study group. The large bulge between the two trend lines is in the interval 4–8 years post diagnosis. At all subsequent points on the survival curve for the study group, the rate in the control group is 3–4 years earlier, which is well beyond the effect of introducing a 1-year average lead time for cases detected through screening, and provides a basis for estimation of person-years of life gained by the study group. Relative survival rates are currently being developed that take into account age distributions of breast cancer cases detected in the HIP study and age-specific general mortality in the study and control groups. Preliminary results indicate that the relationships discussed in this paper are not materially affected when based on relative survival rates.

Text-figure 5 and table 4 give further evidence of the complex changes that occur in cumulative CSR in a screening program. The solid line represents rates among all cases detected through sceening and is slightly concave. Data plotted for subgroups of these cases are based on small numbers and are subject to large sampling variability. Nevertheless, it would appear that the trend in CSR for cases detected on mammography only is decidedly concave. For "clinical only" cases, the trend is slightly concave. In contrast, the control cases with negative nodes show a modest convex trend in CSR, and by 12 years post diagnosis the cumulative CSR in this group is higher than that in the clinical only cases (≈3/4 of which were diagnosed with negative nodes). Finally, the difference between cumulative CSR for mammography only and clinical only cases appears to peak in year 10 after diagnosis. Some reductions may then occur. Only additional years of observation will determine whether this represents the start of closure or just chance variation. As expected, a wide gap persists between the rates for control cases with positive nodes and all of the other rates.

Mortality by Age

The last issue to be discussed in this paper concerns the much debated question whether the lowered mortality from breast cancer among study women is related to age at entry. Table 5 indicates that the direction of the difference is in favor of the study group at all ages. However, the firmest statements have been related to age group 50–59 years, which showed a statistically significant difference through year 10 ($P<0.05$); in year 14 the difference was not significant ($P>0.10$).

A major issue that has arisen concerns the situation in the age group 40–49 years at entry (*11, 12*) when there has been an increasing differential in breast cancer mortality in favor of the study group. At no time has the difference been statistically significant. In addition, the reason for our conclusion that the study has not demonstrated a benefit at ages under 50 is the observation that for this age group the smaller number of breast cancer deaths in the study group is almost entirely attributable to fewer deaths among cases diagnosed after women advanced to ages 50–54 years.

The rationale for examination of data by age at diagnosis in addition to age at entry is that a repetitive screening program that begins at young ages would eventually show benefits as women advanced beyond age 50, according to the HIP study. The relevant group of women were 45–49 years of age at entry; increasing proportions of these women passed their 50th birthday in successive rounds of screening.

As noted in table 6, the observed difference in numbers of deaths due to breast cancer between study and control groups 45–49 years old at entry (28 vs. 35, respectively, in 14 yr of follow-up) is attributable to the situation among cases diagnosed when the women were 50–54 years of age. The question that might be raised is whether this finding reflects relatively large numbers in the study group of breast cancer cases diagnosed under age 50 and small numbers at 50–54 years of age. However, ratios between deaths and cancer cases classified by age at diagnosis show no difference

TABLE 5.—*Breast cancer deaths by age at entry 5 and 14 years from entry*[a]

Age at entry, yr	No. of deaths through following yr after entry			
	5		14	
	Study	Control	Study	Control
Total	39	63	118	153
40–49	19	20	46	61
40–44	9	11	18	26
45–49	10	9	28	35
50–59	15	33	53	68
50–54	8	23	29	36
55–59	7	10	24	32
≥60	5	10	19	24

[a] Included are deaths with breast cancer as an underlying cause among breast cancers diagnosed during the first 5 yr after entry.

TABLE 6.—*Breast cancer deaths and cases with age at entry, at 40–49 years, by age at diagnosis, 14 years from entry*[a]

Age at diagnosis, yr	Deaths due to breast cancer		Breast cancer cases	
	Study	Control	Study	Control
		Age at entry 40–44 yr		
40–49	18	26	49	46
40–44	7	11	17	15
45–49	11	15	32	31
		Age at entry 45–49 yr		
45–54	28	35	68	68
45–49	18	12	40	30
50–54	10	23	28	38

[a] Included are deaths with breast cancer as an underlying cause among breast cancers diagnosed during the first 5 yr after entry.

between study and control groups at ages 45–49 (0.45 vs. 0.40), but they show a major difference at ages 50–54 (0.36 vs. 0.61).

Women 40–44 years old at entry remained under 50 in the interval 5 years after entry. If the deaths are aggregated by age at diagnosis, there is no difference between the study and control groups at 45–49 years (11+18, study group vs. 15+12, control group). The numbers at 40–44 years, age at diagnosis, are too small for meaningful assessment.

DISCUSSION

Follow-up in the HIP randomized trial for determination of efficacy of periodic screening for breast cancer with mammography and palpation of the breast has started to produce information beyond the short to intermediate periods after the start of screening. Results continue to be promising for a role for screening in secondary prevention of breast cancer mortality, although some changes are taking place in the magnitude of differentials that indicate effects.

It seems clear that repetitive screening has led to about a 30% reduction in breast cancer mortality over a 10-year period. The impact of screening on mortality was felt rapidly, and the margin between study and control groups of women in mortality due to breast cancer reached a peak in the first 6–7 years after screening started. The arithmetic gains made by year 7 have been maintained through year 14; relative gains have declined to about 20%. Information from follow-up now under way will determine the nature of changes in differentials over the long run, thereby providing a basis for deriving estimates of person-years of life saved through screening.

Cumulative CSR have been exceptionally favorable among women with breast cancer detected through screening after allowance is made for an estimated 1-year lead time. This accounts for the entire difference between the total study group (screenees and refusers combined) and the control group in their CSR through year 12 after diagnosis of breast cancer. Nevertheless, as the interval from diagnosis increases, trends in CSR differ among various subgroups, the net effect of which is to reduce the differential between the study and control groups' rates. In the early years, cases detected on screening had relatively high CSR even when compared with the rates for control cases diagnosed with negative nodes. But with follow-up approaching 10 years, the advantage is eliminated.

CSR among "mammography only" cases were extraordinarily high the first 5 years after diagnosis and then started to decrease fairly rapidly. One possible explanation is that the mammography only cases were markedly affected by the lead time and length-biased sampling factors. Accordingly, the experience thus far indicates that caution needs to be exercised in drawing conclusions about the advantage for long-term prognosis attributable to screening with mammography from rates over a short period. Differentials in breast cancer mortality by age at entry may also be entering a new phase. From the early years of the study, screening's impact on mortality has appeared at ages 50–59; at entry ages 40–49, study–control differences show up later (although not statistically significant at any time). A complicating factor is the age at diagnosis, which, when introduced in the case of the age group 45–49, strongly suggests that whatever gain may have occurred is attributable to cases diagnosed after the women passed their 50th birthday. At this point, the prudent conclusion is that for ages under 50 years, the HIP study does not provide evidence that screening has had an effect on mortality. Small numbers may be a factor as well as the level of effectiveness of case detection under screening conditions in the 1960's.

All of the preceding observations are derived from an experiment in which mammography was in an earlier stage of development than it is now, and that screening ended after the offering of an initial examination and three additional screening examinations at annual intervals to women in the study group. Despite these limitations, there have been gains in the saving of lives from breast cancer or postponement of death among women with breast cancer. While it is important to assess the longer run impact of screening, the gains have extended over a sufficiently long period of time (12–14 yr) to be significant.

The questions that remain have been well defined (*13*). A high-priority question is whether repetitive screening with physical examination tied to instruction in breast self-examination achieves most of the effects found in screening that also utilizes mammography. Reduced costs for screening and elimination of radiation exposure, although very low under controlled conditions, are the issues at stake. At the same time, improvement in early case detection among women under age 50 and among older women through modern mammography has been demonstrated (*13*). This fact raises the possibility that under present conditions, screening would have a beneficial effect under age 50. Resolution of the issues of relative value of palpation alone versus palpation and mammography and the efficacy of screening under age 50 has such great consequences for the spread of breast cancer screening to merit new investments in appropriately designed randomized trials. Fortunately, a move in this direction has already been taken by the National Cancer Institute of Canada (*14*).

REFERENCES

(*1*) SHAPIRO S. Evidence on screening for breast cancer from a randomized trial. Cancer 1977; 39 (suppl 6):2772–2782.

(*2*) Bailar JC III. Mammography—a contrary view. Ann Intern Med 1976; 84:770–784.

(*3*) Schwartz M. Analysis of the benefits of serial screening to detect early breast cancer. Cancer 1978; 41:1550–1564.

(*4*) Eddy DM. A theory of screening. In: Screening for cancer: Theory, analysis and design. Englewood Cliffs, N.J.: Prentice-Hall, 1980.

(*5*) Chiacchierini RP, Lundin FE, Scheidt PC. A risk/benefit analysis of life table modeling of an annual breast cancer screening program which includes X-ray mammography. In: Niebergs H, ed. Proceedings of the third international symposium on detection and prevention of cancer, New York City, April 26–May 1, 1976. New York: Marcel Dekker, 1980.

(*6*) Axtell L, Asire JA, Meyers MH. Cancer patient survival. Report No. 5. Washington, D.C.: U.S. Govt Print Off, 1976 [DHEW publication No. (NIH) 77-992].

(*7*) Zelen M. Theory of early detection of breast cancer in the general population. Heuson JC, Mattheiem WH, Rosencweig M, ed. Breast cancer: Trends in research and treatment. New York: Raven Press 1976:287–300.

(*8*) Shapiro S, Goldberg J, Hutchison G. Lead time in breast cancer detection and implication of periodicity of screening. Am J Epidemiol 1974; 100:357–366.

(*9*) Prorok PC. The theory of periodic screening. I. Lead time and proportion detected. Adv Appl Prob 1976; 8:127–143.

(*10*) Fink R, Shapiro S, Lewison J. The reluctant participant in a breast cancer screening program, 1968. Public Health Rep 83:479–490.

(*11*) Dubin N. Benefits of screening for breast cancer: Application of a probabilistic model to a breast cancer detection project. J Chron Dis 1979; 32:145–151.

(*12*) Prorok PC, Hankey BF, Bundy BN. Concepts and problems in the evaluation of screening programs. J Chron Dis 1981; 34:159–171.

(*13*) Beahrs OH, Shapiro S, Smart C, et al. Report of the working group; to review the National Cancer Institute-American Cancer Society breast cancer detection demonstration projects. I. General issues related to breast cancer screening. JNCI 1979; 62:655–662.

(*14*) Miller AB, Howe GR, Wall C. The national study of breast cancer screening. Clin Invest Med. In press.

blank page

Antigenic Heterogeneity of Human Colorectal Cancer Cell Lines Analyzed by a Panel of Monoclonal Antibodies. I. Heterogeneous Expression of Ia-Like and HLA-Like Antigenic Determinants[1,2]

Grant D. MacLean,[3,4] Jutta Seehafer,[4] Andrew R. E. Shaw,[4] Mark W. Kieran,[3] *and* B. Michael Longenecker[3,5,6,7]

ABSTRACT—The pattern of reactivity of 10 monoclonal antibodies (MCA) developed against human lymphoid leukemia cells and tested with human T-cells, B-cells, as well as T-lymphoma and B-lymphoma cell lines suggested that six of them detect Ia-like determinants, three detect HLA-like determinants, and the remaining one detects a non-Ia B-cell antigen. With the use of three binding assays, the six MCA that appeared to detect Ia-like determinants reacted strongly with the human colorectal cancer cell (CCC) line LoVo, and none of the three MCA that reacted with HLA-like determinants reacted with this cell line. Immunoprecipitation and polyacrylamide gel electrophoresis analysis confirmed the apparent specificities of the MCA for Ia-like and HLA molecules, demonstrated the presence of Ia-like molecules in LoVo, and failed to detect HLA in these cells. The cellular enzyme-linked immunosorbent assay was used for the testing of our anti-Ia and anti-HLA MCA with 15 other CCC lines. Marked heterogeneity was found in the expression of different Ia-like and HLA determinants defined by different or overlapping subsets of MCA, which suggested that these determinants might be present on different molecules or that different conformations of the same molecules exist in various CCC lines. Analysis of the surface phenotype of subclones of LoVo cells revealed the presence of stable variant cell subpopulations, which lost reactivity with four out of six of the anti-Ia-like MCA but retained at least one Ia-like molecule recognized by two of our MCA. All of the subclones maintained the HLA-negative phenotype. The possible immunologic and diagnostic consequences of the presence or absence of Ia-like or HLA markers on nonlymphoid tumor cells are discussed.—JNCI 1982; 69:357–364.

In recent years it has become apparent that despite their monoclonal origin many experimental tumors are comprised of subpopulations of cells of varying phenotypes (*1*). This heterogeneity of tumors has been demonstrated with respect to several traits including susceptibility to cytotoxic drugs (*2*), immunogenicity (*3*), and antigenicity (*4*). Tumors also consist of subpopulations of cells with widely differing metastatic properties. Clonal variation in metastatic potential was first demonstrated by Fidler and Kripke (*5*) using the B-16 melanoma mouse model. These workers demonstrated the existence of tumor cell population clones that differed widely in their abilities to form lung metastases, showing that the potential to form lung metastases was inherent in certain clones within the unselected tumor cell population. We have recently demonstrated clonal variation in the ability of lymphoma clones to form liver-specific metastases (*6*). Furthermore, with use of an MCA, we identified an antigenic determinant whose expression correlates with the metastatic capacity of a given clonal variant, which suggests that this molecule might have a functional role in the interaction of blood-borne, metastasizing tumor cells with a specific target organ (*6, 7*).

Little work has been done with the antigenic heterogeneity of human tumors, chiefly because of the lack of suitable probes for the detection of antigenic variants of human tumors. The unexpected expression of Ia-like antigens on human melanomas as well as various other nonlymphoid human cancers has recently been reported (*8–16*). Because the presence or absence of Ia-like and HLA antigens on solid tumors might have a profound influence on the biology of tumors and on the interaction of the tumor with the host's immune system (*17, 18*), we began an analysis of the antigenic heterogeneity of solid human tumors with a panel of 10 MCA that appear to detect HLA and Ia-like determinants. In preliminary experiments we found that one human CCC line appeared to possess the interesting and unexpected phenotype Ia^+, HLA^-. Thus we wished to extend our studies to include 15 other human CCC lines as well as individual subclones of one line to attempt the detection of tumor heterogeneity in the expression of Ia-like and HLA-like antigens. For these studies we used Leibovitz's SW series of well-characterized human colorectal tumors (*19*).

MATERIALS AND METHODS

1) *MCA nomenclature.*—All MCA were produced in our laboratories. Most have a code name that includes "H" denoting human cells were used for immunization. The negative control MCA D228b was produced against a *Neis-*

ABBREVIATIONS USED: CCC=colorectal cancer cell(s); CEA=carcinoembryonic antigen; ELISA=enzyme-linked immunosorbent assay; IF=immunofluorescence; MCA=monoclonal antibody (antibodies); PAGE=polyacrylamide gel electrophoresis; RIA=radioimmunoassay; SDS=sodium dodecyl sulfate.

---

[1] Received August 20, 1981; accepted February 26, 1982.

[2] This research is funded by an Alberta Heritage Savings Trust Fund grant and in part by the National Cancer Institute of Canada and the Medical Research Council of Canada.

[3] Department of Immunology, University of Alberta, Edmonton, Alberta, Canada T6G 2H7.

[4] Department of Medicine, Cross Cancer Institute, 11560 University Ave., Edmonton, Alberta, Canada T6G 1Z2.

[5] *Address reprint requests to* Dr. Longenecker.

[6] Dr. Longenecker is a Research Associate of the National Cancer Institute of Canada.

[7] We thank the many laboratory technologists who have assisted in this work, particularly Mr. L. Hartel, Mrs. M. Hájek, Mrs. M. J. Meeker, Mrs. T. Tan, and Mrs. B. Widtmen. We also thank our clinical and research colleagues who are part of this expanding project.

seria meningitidis serotype (*20*). The nonreacting hybridoma 8H2A1 was used for production of control ascites.

2) *Immunizations.*—The H series MCA were produced after immunization of mice as follows: 7H—CLL blood leukocytes (>95% lymphocytes); 8H—cells from the Raji line (derived from Burkitt's lymphoma); 9H—CML blood leukocytes; 10H—ALL bone marrow leukocytes; 41H—spleen lymphoid cells from a patient with hairy cell leukemia (>65% "hairy cells"); and 50H—cells from the malignant melanoma cell line MEL-T-1.

3) *Fusions.*—The fusion technique is modified from that of Köhler and Milstein (*21*) and has been previously described (*22*).

4) *Cells used for specificity testing.*—*a*) Lymphocytes from peripheral blood samples from random normal human donors were separated first with Ficoll-Hypaque and then into "T"- and "B"-subsets after incubation with nylon wool. (The B-cell subfraction, comprising 50–70% cells reacting with a fluorescent goat antihuman immunoglobulin heterologous antiserum, also includes monocytes.)

b) The cell lines Raji and MEL-T-1 have been passaged in our laboratories for many years. The Daudi lines (Burkitt's lymphoma derived) were provided by Dr. P. J. M. Mannoni, Blood Transfusion Services, Edmonton, Canada. CCRF-SB (B-cell type) and MOLT-4 (T-cell type), 2 acute lymphocytic leukemia-derived cell lines, were provided by Dr. J. Menezes, Hospital Sainte-Justine, Montreal, Canada.

c) LoVo, a CEA-producing human CCC line (*23, 24*) was supplied recently by Dr. Benjamin Drewinko, M. D. Anderson Hospital and Tumor Institute, Houston, Tex. The SW series of human CCC lines (*19*) were recently provided by Dr. W. B. McCombs and Dr. O. D. Holton, Scott and White Clinic, Temple, Tex. The other human CCC line, WiDR, was recently purchased from the American Type Culture Collection, Rockville, Md.

5) *Specificity testing.*—*a, b*) Testing of lymphocytes and lymphoid cell lines was by both complement-mediated cytotoxicity (at 37°C with Cedarlane Low-Tox rabbit complement; Cedarlane Laboratories, Hornby, Canada) and indirect immunofluorescence [at 4°C with fluorescein-labeled $F(ab')_2$ (Cappel Laboratories, Cochranville, Pa.) goat-anti-mouse immunoglobulin, and azide to prevent capping]. This testing was used to avoid missing any potentially important positive reactions. *c*) The CCC lines were tested initially by ELISA with the β-D-galactosidase system (Bethesda Research Laboratories, Inc., Gaithersburg, Md.). The cells were trypsinized (trypsin-EDTA), added at 10^5 cells per well to Nunc 96-well flat-bottom tissue culture plates (A/S Nunc, Copenhagen, Denmark), and allowed to grow over 24 hours into a confluent adherent layer. The cells were then fixed in 0.1% glutaraldehyde in 0.1 *M* $NaHCO_3$ and incubated with 10% fetal calf serum in phosphate-buffered saline (pH 7.4) for blocking of nonspecific MCA binding. The fixed, blocked tumor cells were then assayed by the ELISA method with use of β-D-galactosidase recording the optical denisty in each well with a Titertek Multiskan. Controls for nonspecific binding of MCA included myeloma proteins from all known IgG subclasses, IgM and IgA. No nonspecific binding was detected. Testing was repeated on at least 3 different days for each CCC line with consistency of results.

The LoVo line was tested by indirect immunofluorescence. A cell suspension was prepared with trypsin-EDTA plus RPMI-1640 medium (1:1) and tested as in 4*b* above.

d) Selected MCA were also intrinsically labeled with [^{35}S]methionine (*25*) for analysis by RIA of selected cell lines.

6) *MCA dilution.*—The 41H and 50H MCA were tested as neat culture supernatant with medium as negative control. The other MCA were derived from the ascites of pristane-primed mice given injections ip of the hybridomas with use of 8H2A1 as negative control ascites. These ascites-derived MCA were used at a dilution of 1:500 because our titration studies (unpublished observations) showed 1:500 to be on the plateau of the dose-response curve, well clear of the prozone often observed at high concentration, with most MCA reactive to a dilution of $1{:}10^6$.

7) *Immunoprecipitation of radiolabeled antigens.*—Cells from the Raji line and the LoVo line were intrinsically labeled with [^{3}H]leucine [2×10^6 cells pulsed with 100 µCi of [^{3}H]-leucine-55 mCi/mmol (New England Nuclear Corp., Boston, Mass.) for 5 hr]. Labeled proteins were extracted from washed cells with 0.5% sodium deoxycholate and 0.5% Nonidet P-40 in 20 m*M* Tris-HCl phosphate buffer (pH 8.0) in the presence of protease inhibitors phenol methylsulfonyl fluoride (1 m*M*) and chloromethyl L-(2-phenyl-1-*p*-toluenesulfonamido)ethyl ketone (0.5 m*M*). Lysates were sonicated and clarified by centrifugation (15,000 rotational centrifugal force) before addition of MCA-containing ascites at concentrations of 1:100–1:1,000. Antibody-bound antigens were precipitated with *Staphylococcus aureaus* protein-A bound to Sepharose CL4B (Pharmacia Fine Chemicals, Piscataway, N. J.). Precipitated complexes were solubilized in 1% SDS, 5% 2-mercaptoethanol, and separated in a 12.5% polyacrylamide slab gel in 1 m*M* 3-mercaptoproprionate according to the method of Laemmli (*26*). Gels were calibrated with fluorescein-tagged marker proteins visualized by fluorography (*27*). (The marker proteins were provided by Dr. Robert Duke, Hahnemann Medical College, Philadelphia, Pa.).

RESULTS

Characterization of MCA.—The MCA we used to detect Ia-like and HLA antigens (on the colorectal tumor cells) were characterized in two ways. First, their reactivity to a panel of T-lymphocytes, B-lymphocytes, and lymphomas was evaluated by immunofluorescence and complement-mediated cytotoxicity assays. Second, proteins precipitated by some of the antibodies were characterized in terms of molecular weight by SDS-PAGE (*see* below). Table 1 illustrates the specificity of 10 MCA tested against T-lymphocytes, non-T-cells (B-lymphocytes and monocytes), and three lymphoma cell lines—Raji, Daudi, and MOLT-4. Raji is a line of B-cell origin and expresses Ia-like and HLA, A-, B-, and C-antigens. Daudi is also B-cell derived and expresses Ia-like antigens, but not membrane-bound HLA (*28, 30*). MOLT-4, a T-cell leukemia, expresses HLA, but it does not express Ia antigens. Antibodies 7H.3, 8H.6, 8H.7, 8H.18, 41H.20, and 41H.30 react with B-lymphocytes and B-lymphoma

TABLE 1.—*Specificity of MCA used in these studies*

MCA	Cell lines				
	B-cells[a]	T-cells[a]	Daudi[b]	Raji[b]	MOLT-4[b]
7H.3	11/11	0/10	81±6	87±9	1±0
8H.6	11/11	0/10	84±4	76±13	2±1
8H.7	8/11	0/10	53±1	63±7	0±0
8H.18	8/11	0/10	NT	NT	NT
41H.16	11/11	0/10	2±2	75±10	0±1
41H.20	5/7	0/7	NT	NT	NT
41H.30	10/11	0/10	NT	NT	NT
9H.1	11/11	10/10	−2±3	89±8	35±10
10H.7	11/11	10/10	1±0	77±8	50±2
41H.5	11/11	10/10	NT	NT	NT

[a] No. of positive/No. of donors tested. All positive MCA listed here are both cytotoxicity- and immunofluorescence-positive and showed excellent concordance of results.

[b] Values are mean percentages of cytotoxicity±SD after correction for background cell death. NT=not tested.

TABLE 2.—*MCA reactivity with LoVo cells demonstrated with the use of three assays*

MCA	Assay		
	ELISA[a]	IF[b,c]	RIA[c,d]
7H.3	0.92±0.21	40,50	8,500±700
8H.6	0.43±0.09	30,35	8,300±940
8H.7	0.41±0.07	25,35	9,400±830
8H.18	0.48±0.06	25,30	6,000±570
41H.16	0.07±0.01	0,1	50±10
41H.20	0.81±0.10	30,35	10,600±770
41H.30	0.54±0.02	40,40	6,300±520
9H.1	0.01±0.00	0,0	40±10
10H.7	0.06±0.01	0,2	60±20
41H.5	0.03±0.01	0,0	NT
50H.19[e]	0.99±0.20	NT	NT
D228b[f]	0.06±0.03	NT	NT

[a] Mean optical density per ELISA well ± SD.

[b] Percent fluorescing cells; duplicate wells were each read by different persons.

[c] NT=not tested.

[d] Mean cpm ^{35}S per cell pellet ± SD.

[e] Positive control, reacts with all human solid tumors tested.

[f] Negative control, reacts with a single *N. meningiditis* serotype (*19*).

lines, but they do not react with T-cells. Consequently, they may recognize Ia-like antigens. Antibody 41H.16 reacts with all B-cells, but it does not react with Daudi which expresses Ia antigens; hence it may recognize a non-Ia B-cell marker. Its immunoprecipitation product is uncharacterized.

Antibodies 9H.1, 10H.7, and 41H.5 recognize T- and B-lymphocytes from all individuals and failed to react with surface HLA-negative Daudi cells, which suggests that these MCA might recognize HLA, A-, B-, and C-antigens.

Reactivity of MCA with the human colorectal carcinoma cell line LoVo.—Table 2 illustrates the reactivity of the MCA panel with LoVo with the use of three cellular binding assays: ELISA, indirect immunofluorescence, and RIA. The last two assays were done with trypsinized cells, and the ELISA was done with nontrypsinized, gluteraldehyde-fixed cells. Despite the differing types of treatments of the cells, the three assays showed excellent concordance, also demonstrating that the cellular ELISA assay can be used reliably for detection of cell surface antigens on adherent cell lines. The six MCA that reacted with the Ia-bearing B-cells but not T-cells reacted strongly with LoVo cells. In contrast, none of the three HLA-like MCA reacting with B-cells, T-cells, Raji, and MOLT-4 but not Daudi reacted with LoVo cells.

Immunoprecipitation of Ia-like, but not HLA-like, molecules from LoVo cells.—These results suggest that LoVo cells might bear surface Ia-like but not HLA-like determinants. Figure 1 demonstrates that three of our anti-B-cell MCA precipitate a bimolecular complex (heavy-chain mol wt = 34,000 and light-chain mol wt = 30,500) from LoVo cells. Consequently, they appear to recognize Ia-like antigens. The other three anti-B-cell MCA that react with LoVo (8H.7, 8H.18, 41H.20) were not good immunoprecipitating antibodies, although longer exposure time of the autoradiograms clearly showed two faint bands in the Ia region (data not shown). Figure 2 shows that three putative anti-HLA MCA (9H.1, 10H.7, and 41H.5) indeed precipitate a two-chain complex of molecular weights 44,000 and 12,500 from Raji cells. Consequently, they appear to recognize HLA, A-, B-, and C-antigens. However, the two anti-HLA MCA that were tested with LoVo (9H.1 and 41H.5) do not immunoprecipitate anything detectable from these cells.

Reactivity of the MCA panel with 16 human CCC lines.—We used the cellular ELISA assay for testing the MCA panel against human CCC lines. The MCA D228b, which reacts against a serotype-specific antigen of *N. meningiditis*, was used as a negative control, whereas 50H.19, which reacts with all human solid tumors we have tested, served as a positive control. In addition, we have tested myeloma proteins of all known isotypes and IgG subclasses and did not detect significant binding to CCC (data not shown). Marked heterogeneity in the expression of Ia-like and HLA markers detected by our MCA panel was noted (table 3). Two additional CCC lines were found to react with the same six anti-Ia-like MCA that reacted with LoVo. Unlike LoVo, these two CCC lines reacted strongly with all three anti-HLA MCA. Two of the CCC lines, SW-48 and SW-707, reacted only with the positive control MCA and did not react detectably with any of the anti-HLA or anti-Ia-like MCA. These are the only two lines classified in Leibovitz's group 1 (*19*). The two CCC lines from Leibovitz's group 2 (SW-480 and SW-620), which were derived from tumors at different sites from the same patient, reacted identically with all three anti-HLA MCA and none of the anti-Ia or other anti-B-cell MCA. Heterogeneity in the expression of different Ia-like and HLA determinants detected by our MCA among the CCC lines was also found. For example, WiDR expressed the determinants detected by anti-HLA MCA 9H.1 but not the HLA determinants detected by 10H.7 or 41H.5. SW-1116 and SW-1398, both Ia-like-negative, reacted with 9H.1 and 41H.5 but not with 10H.7. Two of the CCC lines, SW-948 and SW-1463, reacted with only one of the anti-Ia-like MCA, 7H.3, again suggesting heterogeneity in the expression of Ia-like determinants among the cell lines. None of the CCC lines reacted with MCA 41H.16, another B-cell marker possibly unrelated to Ia.

Binding of ^{35}S-labeled anti-Ia-like and anti-HLA MCA to selected CCC lines.—To confirm the results obtained by ELISA, we used another more quantitative assay, the cellular RIA, to

TABLE 3.—*ELISA reactivity of MCA with human CCC lines*[a]

MCA	Cell line															
	LoVo	WiDr	SW-48	SW-707	SW-480	SW-620	SW-403	SW-742	SW-837	SW-948	SW-1116	SW-1222	SW-1345	SW-1398	SW-1417	SW-1463
7H.3[b]	6	—	—	—	—	—	—	—	6	2	—	—	—	—	6	6
8H.6[b]	6	—	—	—	—	—	—	—	2	—	—	—	—	—	2	—
8H.7[b]	6	—	—	—	—	—	—	—	2	—	—	—	—	—	2	—
8H.18[b]	6	—	—	—	—	—	—	—	3	—	—	—	—	—	6	—
41H.16[c]	—	—	—	—	—	—	—	—	—	—	—	—	—	—	—	—
41H.20[b]	6	—	—	—	—	—	—	—	5	—	—	—	—	—	6	—
41H.30[b]	6	—	—	—	—	—	—	—	3	—	—	—	—	—	3	—
9H.1[d]	—	6	—	—	6	6	6	6	6	6	6	6	6	6	6	6
10H;7[d]	—	—	—	—	5	6	3	6	2	5	—	5	3	—	6	6
41H.5[d]	—	—	—	—	6	5	6	6	6	6	6	2	5	6	2	6
50H.19[e]	6	6	6	6	6	6	6	6	6	6	6	6	6	6	6	6
D228b[f]	—	—	—	—	—	—	—	—	—	—	—	—	—	—	—	—
Leibovitz's group			1	1	2	2	3	3	3	3	3					

[a] All lines were tested three times giving identical patterns of reactivity. In each test each MCA was tested in duplicate. Only results significantly above the background mean ($P<0.05$) are recorded as positive. —=negative reaction. Positive results are expressed as the number of standard deviations above the background mean, a value of 6 being >6 SD above the background mean.

[b] Detect Ia-like specificities.

[c] Detect a non-Ia B-cell marker.

[d] Detect HLA-like specificities.

[e] Positive control.

[f] Negative control.

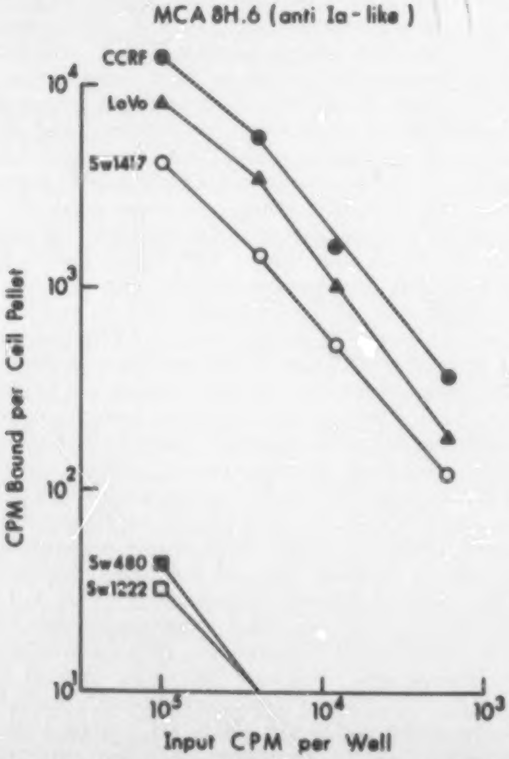

TEXT-FIGURE 1.—Cellular RIA with the use of ^{35}S-labeled MCA 8H.6, which detects an Ia-like antigen. CCRF-SB cells, a human B-leukemia cell line, was used as a positive control for binding. Two CCC lines (LoVo and SW-1417) showed a dose-dependent binding of the antibody, and two other CCC lines (SW-480 and SW-1222) did not show significant binding ($P>0.05$ at the highest antibody concentration compared to background). 5×10^4 CCC cells and 10^5 B-leukemia cells per well were used.

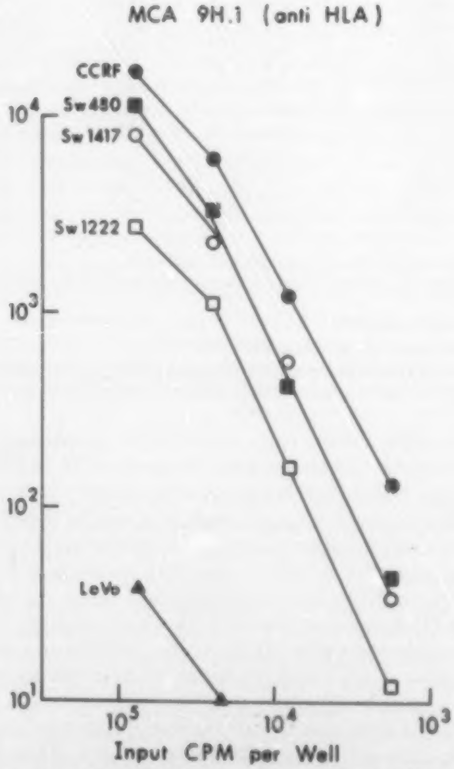

TEXT-FIGURE 2.—Cellular RIA with the use of ^{35}S-labeled 9H.1, which detects an HLA-like antigen. The only cell line that did not show significant binding was the human CCC line LoVo.

measure the reactive binding of ^{35}S-labeled 8H.6 (anti-Ia-like) and 9H.1 (anti-HLA) MCA to selected CCC lines. As a positive control for binding, we used the B-leukemia cell

TABLE 4.—*Reactivity by ELISA and IF of MCA with 12 LoVo subclones*

MCA	ELISA subclones[a]		IF subclones		
	1–3, 5, 7–12	4, 6	1	4	6
7H.3[b]	6	6	40	40	35
8H.6[b]	6	—	40	0	1
8H.7[b]	6	—	25	0	0
8H.18[b]	6	—	30	0	0
41H.16[c]	—	—	0	1	1
41H.20[b]	6	6	30	25	30
41H.30[b]	6	—	45	0	1
9H.1[d]	—	—	0	0	0
10H.7[d]	—	—	0	0	0
41H.5[d]	—	—	0	0	0
50H.19[e]	6	6	100	100	100
D228b[f]	—	—	0	0	0

[a] —=negative reaction.

[b] Detect Ia-like specificities.

[c] Detect a non-Ia B-cell marker.

[d] Detect HLA-like specificities.

[e] Positive control.

[f] Negative control.

line CCRF-SB. Text-figure 1 demonstrates that 8H.6 binds to CCRF-SB LoVo, and SW-1417 but not significantly to SW-480 or SW-1222, and text-figure 2 shows that 9H.1 binds to all cell lines tested except LoVo, confirming the ELISA results.

HLA and Ia-like phenotype of LoVo subclones.—We established 12 limiting dilution subclones of LoVo to determine whether significant antigenic heterogeneity exists within the LoVo line. Like the parental line, all 12 subclones lacked all three HLA markers. Two out of 12 of the subclones failed to express Ia-like markers detected by MCA 8H.6, 8H.7, 8H.18, and 41H.30, but they continued to express strongly 7H.3 and 41H.20 (table 4). Immunofluorescence tests on subclones 4 and 6 confirmed the ELISA results and showed, as in the parental line (*see* table 2), that approximately 25–40% of the cells stained after treatment with 7H.3 or 41H.20.

DISCUSSION

It has become generally accepted that at least one explanation for tumor progression is the production in the tumor of variant clones of cells that vary in their malignant phenotypes (*31, 33*). Those clones with a survival advantage will become dominant in a tumor but will, in turn, give rise to more variant clones. Conditions in vivo may result in the emergence of more aggressive and/or less antigenic variant sublines from the parent population. This hypothesis is supported by the data of several workers (*34–37*), who noted marked heterogeneity among tumor subclones. The results presented here demonstrate marked heterogeneity in the expression of Ia-like and HLA-like molecules on different human CCC lines as well as on subclones of one CCC line. One of our most interesting observations was the heterogeneity in the expression of different Ia-like and HLA determinants showing not only that some of our MCA detect different determinants but also suggesting that these determinants might be present on different molecules or that different conformations of the same molecules exist in various CCC lines. Our sequential immunoprecipitation data (unpublished observations) suggest that our anti-Ia-like MCA detect at least two and possibly three different Ia-like molecules on human lymphoblastoid cell lines. The data obtained from the LoVo subclones also suggest the existence of at least two Ia-like molecules on human CCC lines. The results of several recent studies in which MCA were used have suggested that the human Ia-like molecular pool is composed of several subsets of molecules (*38–44*). More work will be required to determine whether tissue polymorphism in the expression of different Ia-like molecules occurs and whether different Ia-like molecules have different functions or different effects on the immune system when present on tumor cell membranes.

Ia-like determinants have been unexpectedly detected most frequently on malignant melanoma cells (*8–12*) but also on several other types of nonlymphoid tumors (*10–15*). To the best of our knowledge this communication represents the first description of Ia-like antigens on human colorectal cancer cells, although others have reported negative findings based on testing only a few tumors (*10*). Five out of the 16 CCC lines reproducibly expressed at least one Ia-like marker. The reason for the variable expression of Ia-like antigens on certain solid tumors is not understood and could be due to abnormal expression of genes in cancer cells. Conversely, the presence of these molecules may be related to cell differentiation because Ia-like antigens may be restricted to particular stages of differentiation within certain cell lineages (*16*). Nevertheless, Ia-like antigens may serve as important tumor markers for immunodiagnostic purposes. The expression of these markers could relate to certain clinical parameters, such as extent of disease, ease and duration of remission induction, and perhaps survival. Indeed, it is known that Ia-like antigens control the specificity of several immunologic reactions and have been shown to affect the immunogenicity of certain tumor-specific antigens (*17, 18*).

The immunofluorescence tests presented in table 2 showed that although most of the LoVo cells do not react with anti-Ia-like MCA, distinct subpopulation(s) of cells, comprising 25–50% of the total population, react strongly with MCA. We considered two mechanisms to explain the intratumor Ia-like antigen heterogeneity: 1) the existence of stable variants of Ia-positive cells in the cell line or 2) cell cycle regulation of Ia antigen expression. Two out of 12 of the subclones we generated lost reactivity to four of the anti-Ia-like MCA, but all retained at least one Ia-like molecule recognized by two of our MCA. We retested these subclones four times and found that the two variant subclones were highly stable. These data suggest that stable phenotypic variants exist within the LoVo tumor. Further biochemical studies will be required to determine whether or not the variant subclones synthesize the Ia-like molecules, which are undetectable at the cell surface. If we assume that similar Ia variants are found in fresh tumor tissue, it is possible that immunoselection of such variants could occur. It is of interest in this regard that Ia-like antigens on nonlymphoid human tumor cells can serve as efficient targets for antibody-dependent cellular cytotoxicity (*14*). The LoVo subclones were retested with use of the immunofluorescence test. Like the parental tumor, the percentage of Ia-positive cells remained in the 20–50% range, which suggested that cell cycle-related events are also responsible for the Ia antigen heterogeneity. This type of Ia antigen heterogeneity has recently been described for the cell cycle-related Ia expression on a murine B-lymphoma cell line (*45*).

Recent reports demonstrate the presence of Ia-like molecules on human endothelial cell surfaces, which can function in antigen presentation and lymphocyte triggering (*46, 47*). Inasmuch as lymphocytes must cross endothelial barriers to enter extravascular tissues during immune reactions and tumor cells must cross the same barriers to metastasize, Ia-like molecules might represent important recognition structures for organ-specific homing of both lymphocytes and tumor cells, especially in view of the recent reports suggesting the existence of multiple Ia-like molecules (*38–44*). The demonstration of tissue polymorphism in the expression of different Ia-like molecules might lend credence to this hypothesis.

Three indirect binding assays described in this paper failed to detect the HLA-like molecules detected by all three of our MCA on the surfaces of three of the human CCC lines. The apparent lack of detectable HLA was examined in detail with the LoVo CCC line. The immunoprecipitation experiments also failed to detect these molecules in the parental LoVo line. Twelve subclones of LoVo were found to remain HLA-negative, which suggested that if HLA-positive variant clones exist they must be present at relatively low frequency. Nevertheless, these cells may have contained HLA antigens but at a level undetectable by all the methods used. Using our MCA, we have found that the only other cell line that has the same phenotype is the Daudi Burkitt's lymphoma cell line. This cell line is known not to express cell surface HLA because it cannot synthesize β_2 microglobulin (*28–30*). Recently, Woda and co-workers (*48*) described 3 malignant lymphomas of the diffuse histiocytic type in which most of the tumor cells express monoclonal surface immunoglobulin and HLA-DR antigens but do not express HLA, A, B, C, or $\beta_2\mu$. Because it is possible that at least some of our anti-HLA MCA react against $\beta_2\mu$, we cannot rule out the possibility that heavy chain is also synthesized by these CCC lines.

LoVo was derived from a lymph node metastasis of a colorectal cancer patient. It maintains the characteristic morphologic and physiologic properties of a colorectal cancer, including the formation of acinar structures and the production of CEA [(*23, 24, 49*) and our unpublished results] and has been used as an important model for chemotherapy of colorectal cancer (*50*). The two CCC lines of Leibovitz's SW series, which were negative for all three HLA markers, were the only group 1 CCC lines included in our study. According to Leibovitz et al. (*19*), group 1 cell lines have a modal chromosome number of about 47 and synthesize small-to-moderate amounts of CEA. The WiDR cell line was found to lack two HLA markers, and the SW-1116 and SW-1398 lines lacked only one marker. This phenomenon might reflect tissue polymorphism in the expression of different HLA markers or molecules or indicate that HLA molecules exist in different configurations. The reduction of type I MHC molecules on tumor cells may have important biologic implications, e.g., for the associative recognition of tumor antigens by T-cells and hence for immunosurveillance (*18*). The apparent loss of HLA could have been due to immunoselection of HLA loss variants.

Further studies are in progress to determine whether clones of HLA-loss variants exist in fresh human tumors. It is of interest in this regard that a high proportion of non-transfused cancer patients may possess relatively high titers of cytotoxic anti-HLA and possibly anti-Ia antibodies in their sera (*51*).

REFERENCES

(*1*) Fidler IJ and Hart IR. The origin of metastatic heterogeneity in tumors. Eur J Cancer 1981; 17:487–494.

(*2*) Heppner GH, Dexter DL, DeNucci T, Miller FR, Calabresi P. Heterogeneity in drug sensitivity among tumor cell subpopulations of a single mammary tumor. Cancer Res 1978; 38:3758–3763.

(*3*) Kerbel RS. Implications of immunological heterogeneity of tumours. Nature 1979; 280:358–359.

(*4*) Prehn RT. Analysis of antigenic heterogeneity within individual 3-methylcholanthrene-induced mouse sarcomas. J Natl Cancer Inst 1970; 45:1039–1045.

(*5*) Fidler IJ, Kripke ML. Metastasis results from preexisting variant cells within a malignant tumor. Science 1977; 197:893–895.

(*6*) Shearman PJ, Longenecker BM. Clonal variation and functional correlation of organ-specific metastasis and an organ-specific metastasis-associated antigen. Int J Cancer 1981; 27:387–395.

(*7*) Shearman PJ, Gallatin WM, Longenecker BM. Detection of a cell-surface antigen correlated with organ-specific metastasis. Nature 1980; 286:267–269.

(*8*) Winchester RJ, Wang CY, Gibofsky A, Kunkel HG, Lloyd KO, Old LJ. Expression of Ia-like antigens on cultured human malignant melanoma cell lines. Proc Natl Acad Sci USA 1978; 75:6235–6239.

(*9*) Wilson BS, Indiveri F, Pellegrino MA, Ferrone S. DR (Ia-like) antigens on human melanoma cells, serological detection and immunochemical characterization. J Exp Med 1979; 149:658–668.

(*10*) Howe AJ, Seeger RC, Molinaro GA, Ferrone S. Analysis of human tumor cells for Ia-like antigens with monoclonal antibodies. JNCI 1981; 66:827–829.

(*11*) Lloyd KO, Ng J, Dippold WG. Analysis of the biosynthesis of HLA-DR glycoproteins in human malignant melanoma cell lines. J Immunol 1981; 126:2408–2413.

(*12*) Lloyd KO, Travassos LR, Takahashi RT, Old LJ. Cell surface glycoproteins of human tumor cell lines: Unusual characteristics of malignant melanoma. JNCI 1979; 63:623–634.

(*13*) Carrel S, Gross N, Heumann D, Mach JP. Expression of "Ia-like" antigens on cells from endometrial carcinoma cell line, END-1. Transplantation 1979; 27:431–433.

(*14*) Ng A, Pellegrino MA, Imai K, Ferrone S. HLA-A, B antigens, Ia-like antigens, and tumor-associated antigens on prostate carcinoma cell lines: Serologic and immunochemical analysis with monoclonal antibodies. J Immunol 1981; 127:443–447.

(*15*) Pellegino MA, Natal PG, Ng AK, et al. Unorthodox expression of Ia-like antigens on human tumor cells of non-lymphoid origin: Immunological properties, structural profile and clinical relevance. In: Nakamura RM, ed. Recent progress in diagnostic laboratory immunology. New York: Masson. In press.

(*16*) Winchester RJ. Aspects of surface membrane differentiation during maturation of human hematopoietic and tumor cells: The Ia system. In: Moscon AA, Monroy A, eds. Current trends in developmental biology. New York: Academic Press, 1980:115–125.

(*17*) Forni G, Shevach EM, Green I. Mutant lines of guinea pig L2C leukemia. I. Deletion of Ia alloantigens is associated with a loss in immunogenicity of tumor-associated transplantation antigens. J Exp Med 1976; 143:1067–1081.

(*18*) Festenstein H, Schmidt W. Variation in MHC antigenic profiles of tumour cells and its biological effects. Immunol Rev 1981; 60:85–127.

(19) Leibovitz A, Stinson JC, McCombs WB III, McCoy CE, Mazur KC, Mabry ND. Classification of human colorectal adenocarcinoma cell lines. Cancer Res 1976; 36:4562–4569.

(20) Mackie EB, Mosmann TR, Bryan LE, Longenecker BM. A strong, specific response of mice to serotype-specific antigenic determinants of *Neisseria meningitidis* analyzed with mouse monoclonal antibodies. J Immunol 1981; 127:387–388.

(21) Köhler G, Milstein C. Continuous cultures of fused cells secreting antibody of predefined specificity. Nature 1975; 256:495–497.

(22) Longenecker BM, Mosmann TR, Shiozawa C. A strong, preferential response of mice to polymorphic antigenic determinants of the chicken MHC, analyzed with mouse hybridoma (monoclonal) antibodies. Immunogenetics 1979; 9:137–147.

(23) Drewinko B, Romsdahl MM, Yang LY, Ahearn MJ, Trujillo JM Establishment of a human carcinoembryonic antigen-producing colon adenocarcinoma cell line. Cancer Res 1976; 36:467–475.

(24) Drewinko B, Yang LY, Barlogie B, et al. Further biologic characteristics of a human carcinoembryonic antigen-producing colon carcinoma cell line. JNCI 1978; 61:75–83.

(25) Mosmann TR, Gravel Y, Williamson AR, Baumal R. Modification and fate of J chain in myeloma cells in the presence or absence of polymeric immunoglobulin secretion. Eur J Immunol 1978; 8:94–99.

(26) Laemmli UK. Cleavage of structural proteins during the assembly of the head of bacteriophage T4. Nature 1970; 227:680–685.

(27) Bonner WH, Laskey RA. A film detection method for tritium-labeled proteins and nucleic acids in polyacrylamide gels. Eur J Biochem 1974; 46:83–88.

(28) Ploegh HL, Cannon LE, Strominger JL. Cell-free translation of the mRNAs for the heavy and light chains of HLA-A and HLA-B antigens. Proc Natl Acad Sci USA 1979; 76:2273–2276.

(29) Parham P, Barnstable CJ, Bodmer WF. Use of monoclonal antibody (W6/32) in structural studies on HLA-A, -B, -C antigens. J Immunol 1979; 123:342–348.

(30) Krangel MS, Orr JT, Strominger JL. Assembly and maturation of HLA-A and HLA-B antigens in vivo. Cell 1979; 18:979–984.

(31) Nowell PC. The clonal evolution of tumor cell populations. Science 1976; 194:23–28.

(32) Fidler IJ, Gersten DM, Hart IR. The biology of cancer invasion and metastasis. Adv Cancer Res 1978; 28:149–250.

(33) Poste G, Fidler IJ. The pathogenesis of cancer metastasis. Nature 1980; 283:139–146.

(34) Fidler IJ. Tumor heterogeneity and the biology of cancer invasion and metastasis. Cancer Res 1978; 38:2651–2660.

(35) Dexter KL, Kowalski HM, Blazer BA, Fligiel Z, Vogel R, Heppner GH. Heterogeneity of tumor cells from a single mouse mammary tumor. Cancer Res 1978; 38:3174–3179.

(36) Kripke ML, Gruys E, Fidler IJ. Metastatic heterogeneity of cells from an ultraviolet light-induced murine fibrosarcoma of recent origin. Cancer Res 1978, 38:2962–2967.

(37) Suzuki N, Withers HL, Koehler MW. Heterogeneity and variability of artificial lung colony forming ability among clones from mouse fibrosarcoma. Cancer Res 1978; 38:3349–3351.

(38) Lampson LA, Levy R. Two populations of Ia-like molecules on human B-cell line. J Immunol 1980; 125:293–299.

(39) Accolla RS, Tosi R, Tanigaki N, Carmagnola AL, Gross N, Carrel S. Human Ia isotypes. Eighth Int Histol Work Newslett 1980; 1980:46.

(40) Carrel S, Tosi R, Gross N, Tanigaki N, Carmagnola AL, Accolla RS. Subsets of human Ia-like molecules defined by monoclonal antibodies. Mol Immunol 1981; 18:403–410.

(41) Assolla RS, Gross N, Carrel S, Corte G. Distinct forms of both α and β subunits are present in the human Ia molecular pool. Proc Natl Sci USA 1981; 78:4549–4552.

(42) Tanigaki N, Tosi R, Centis D, Ferrara GB, Pressman D. Further characterisation of two "DR supratypic" specificities. Additional evidence that they reside on molecules different from those carrying HLA-DR locus specificities. Hum Immunol 1981; 3:93–108.

(43) Nadler LM, Stashenko P, Hardy R, Pesando JM, Yanis EJ, Schlossman SF. Monoclonal antibodies defining serologically distinct HLA-D/DR related Ia-like antigens in man. Hum Immunol 1981; 1:77–90.

(44) Pesando JM, Nadler LM, Lazarus H, et al. Human cell lines express multiple populations of Ia-like molecules. Hum Immunol 1981; 3:67–76.

(45) Lanier LL, Warner NL. Cell cycle related heterogeneity of Ia antigen expression on a murine B lymphoma cell line: Analysis by flow cytometry. J Immunol 1981; 126:626–631.

(46) Hirschberg H. Presentation of viral antigens by human vascular endothelial cells in vitro. Hum Immunol 1981; 2:235–246.

(47) Burger DR, Ford D, Vetto RM, et al. Endothelial cell presentation of antigen to human T-cells. Hum Immunol 1981; 3:209–230.

(48) Woda BA, Racklin B, Rappaport H. Altered expression of histocompatibility antigens on 'B' large cell lymphomas. Blood 1981; 57:802–804.

(49) Stragand JJ, Bergerat J-P, White RA, Hokanson J, Drewinko B. Biological and cell kinetic properties of a human colonic adenocarcinoma (LoVo) grown in athymic mice. Cancer Res 1980; 40:2846–2852.

(50) Drewinko B, Corry P, Bergerat J-P, Barlogie B. Cisplatin, current status and new developments. In: Prestayko AW, Brooke ST, Carter SK, eds. The lethal activity of platinum compounds in combination with pyrimidine derivatives. New York: Academic Press, 1980:37–55.

(51) Laurentaci G, Favoino B. Cytotoxic antibodies in cancer patients: Possibilities of correlation with HLA antigens. Boll Ist Sieroter Milan 1981; 60:52–57.

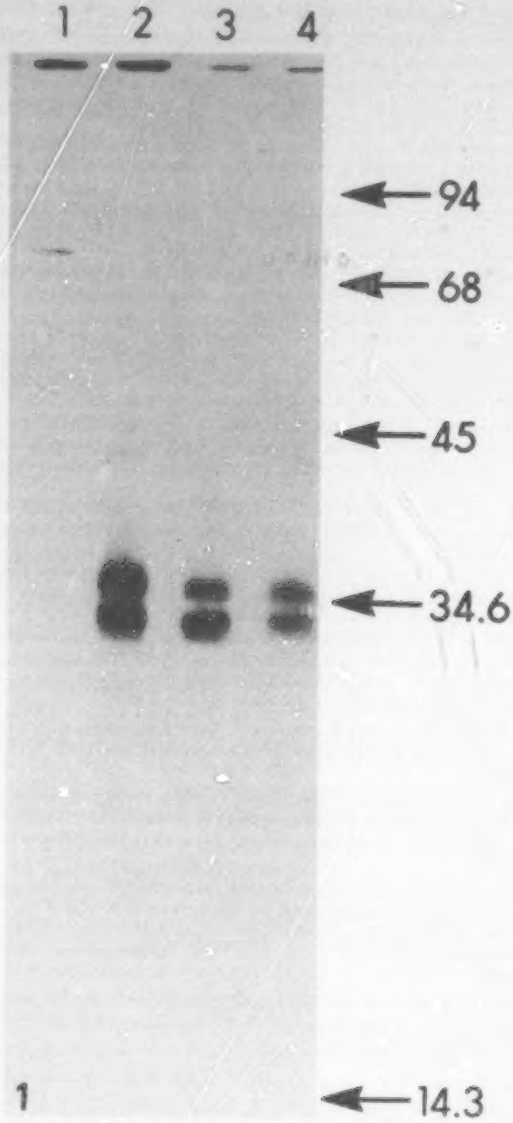

1

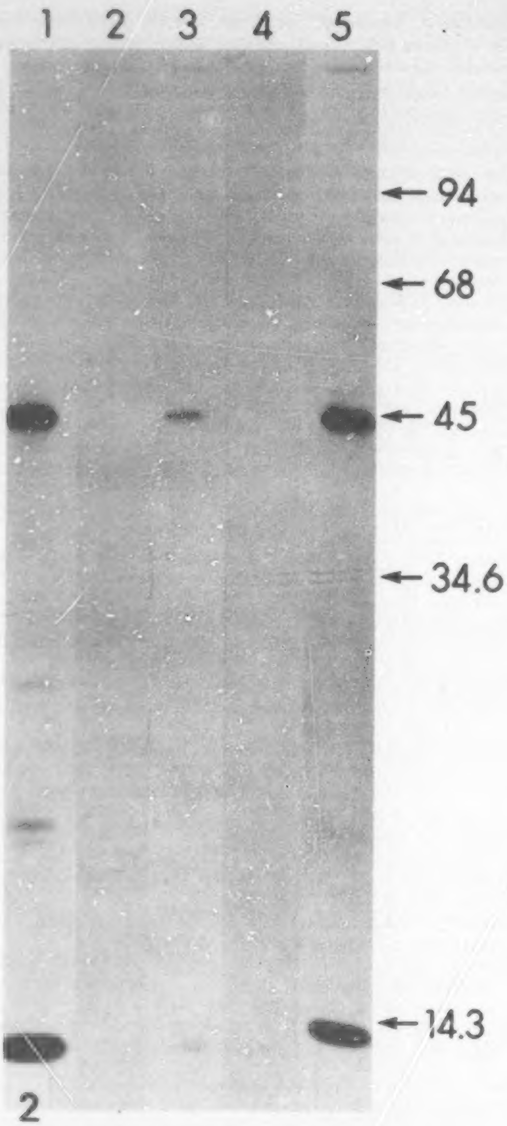

2

FIGURE 1.—SDS-PAGE analysis of proteins immunoprecipitated from lysates of LoVo cells with the following MCA: lane 1, 8H.2A1, negative control; lane 2, 8H.6; lane 3, 7H.3; lane 4, 41H.30. Molecular weight standards were FITC-labeled lysozyme (mol wt 14,300), carboxypeptidase A (mol wt 34,600), ovalbumin (mol wt 45,000), bovine serum albumin (mol wt 68,000), and phosphorylase (mol wt 94,000).

FIGURE 2.—SDS-PAGE analysis of proteins immunoprecipitated from lysates of LoVo or Raji cells. Lanes 1, 3, and 5: Raji; 9H.1, 10H.7, and 41H.5, respectively. Lanes 2 and 4: LoVo; 9H.1 and 41H.5, respectively.

Changes in Skin Cancer Morbidity Between 1971–72 and 1977–78[1]

Thomas R. Fears[2,3] *and* **Joseph Scotto**[2,4]

ABSTRACT—Skin cancer incidence rates for two geographic areas of the United States were analyzed for detection of significant changes in risk over a 6-year period (1971–72 to 1977–78). Changes in rates were examined by cell type, anatomic site, sex, and age. In general risk has increased, but the size of the increase varied by cell type, sex, and anatomic site. Statistically significant increases were limited to tumors of the basal type. The risk of basal cell skin cancer appears to have increased about 18% or almost 3% per year. Increases did not depend on age group. Among males the increases were most notable for sites other than face, head, and neck, whereas among females the increases were not associated with site.—JNCI 1982; 69:365–370.

In 1971–72 age-adjusted nonmelanoma skin cancer incidence rates ranged from 151 to 379 per 100,000 in four geographic areas of the Third National Cancer Survey (*1*). These incidence rates were far higher than the rate for any other single cancer site and substantially higher than any previously reported skin cancer incidence rates for the United States. In one location, Minneapolis–St. Paul, incidence apparently doubled in just 5 years (*2*). Unfortunately, the meaning of the increase was not clear. The average annual risk of developing the disease could have increased, but the change in incidence rates could have been due to varied or improved case ascertainment methodologies. To provide more data on skin cancer, the National Cancer Institute conducted a skin cancer survey during 1977–78 at several locations in the United States. Two of these locations, Minneapolis–St. Paul and San Francisco–Oakland, were also part of the 1971–72 study and were included in the new survey to provide the data needed to determine if the risk of developing skin cancer is changing. This report contains a summary of the data currently available from these two locations and an analysis of the observed changes in skin cancer incidence rates over the 6-year period by age, sex, anatomic site, and cell type.

MATERIALS AND METHODS

The data used in this report are from two special skin cancer surveys. The first study, covering a 6-month survey period, September 1971 through February 1972, was conducted as a part of the Third National Cancer Survey (*1*). Four locations participated. The second study was reported only recently (*3*) and covered a full 1-year period from June 1977 through May 1978. Eight locations participated. The two studies used the same protocol for the identification and recording of all nonrecurring nonmelanoma skin cancer (i.e., squamous cell or basal cell carcinomas). In addition to obtaining data from outpatient hospital files, special efforts were made to contact the offices of dermatologists, pathologists, radiotherapists, surgeons, and other physicians who see or treat skin cancer patients. Although clinically diagnosed cases were accepted, over 95% of the reported tumors were microscopically confirmed. Uniform reporting and monitoring procedures (both manual and by computer) were maintained at all study locations. The procedures and forms used are detailed elsewhere (*4*). We know of no substantive changes in registry methodology, methods of treatment, or medical care patterns in these locations, which would differentially affect the observed incidence. Two locations, Minneapolis–St. Paul and San Francisco–Oakland, are common to the two surveys. Only for these two locations can we obtain direct estimates of changes in incidence, which may have occurred between 1971–72 and 1977–78. Because the reporting of skin cancer is usually highest during the summer months, the difference in survey periods between the two studies must be considered. To adjust for any differences in reporting by month of diagnosis, we based the analysis on the incidence of newly diagnosed cases that occurred during the 6-month period common to both surveys, i.e., September through February. Because skin cancer is rare among nonwhites, analysis is limited to Caucasians only. The incidence rates given in this report are 6-month incidence rates among whites, which refer only to the September-through-February period in each survey.

The 1971–72 survey used population data from the 1970 census. For the 1977–78 survey, intercensal population estimates were required. Total population estimates for 1977 were provided by the Federal–State Cooperative Program for Population Estimates for each study location. Detailed estimates according to age, race, sex, and location were then obtained with data from the U.S. Bureau of Census to incorporate changes in birth, death, and migration patterns.

We assume throughout that for a particular age and sex stratum the distribution of the number of cases can be approximated by a Poisson distribution with a mean and variance equal to the expected number of cases. Such an approximation is quite good for large populations with a moderate average probability of developing the disease. We take the mean of these Poisson variables to be proportional to the population size and an exponential function of cell type, anatomic site, survey year, area, and age effects.

Let P_1 and P_2 represent the probability of developing skin cancer of a particular cell type at a given anatomic site during the first and second surveys, respectively. Then the

---

ABBREVIATIONS USED: FHN=face, head, and neck; SMSA=standard metropolitan statistical area.

---

[1] Received August 24, 1981; revised February 16, 1982; accepted March 2, 1982.

[2] Biometry Branch, Field Studies and Statistics, Division of Cancer Cause and Prevention, National Cancer Institute, National Institutes of Health, Public Health Service, U.S. Department of Health and Human Services, Bethesda, Md. 20205.

[3] *Address reprint requests to* Dr. Fears at the Landow Building, Room 1007, 7910 Woodmont Ave., Bethesda, Md. 20205.

[4] We thank Mrs. Alroy Smith who implemented the methodology.

TABLE 1.—*Age-specific incidence rates per 100,000 and number of basal cell skin cancer patients by anatomic site, age, sex, geographic area, and survey year*

Age, yr	Incidence rates and No. of patients: Basal cell skin cancer															
	Males								Females							
	Minneapolis-St. Paul				San Francisco-Oakland				Minneapolis-St. Paul				San Francisco-Oakland			
	1971-72		1977-78		1971-72		1977-78		1971-72		1977-78		1971-72		1977-78	
	No. of patients	Rate	No. of patients	Rate	No. of patients	Rate	No. of patients	Rate	No. of patients	Rate	No. of patients	Rate	No. of patients	Rate	No. of patients	Rate
	All sites combined															
25-34	11	9.0	14	8.9	35	19.0	37	15.6	14	11.4	16	10.4	25	13.9	52	23.3
35-44	48	50.3	35	35.7	97	63.6	83	55.2	30	31.2	44	44.6	62	41.2	84	57.3
45-54	80	91.9	121	138.5	237	148.0	273	182.3	62	67.4	100	111.9	180	106.7	207	132.5
55-64	124	199.1	177	259.1	334	278.4	460	360.7	92	127.5	123	160.7	235	176.3	266	190.5
65-74	136	363.7	167	419.9	299	442.0	383	518.7	118	215.6	155	264.6	172	185.6	239	234.3
75-84	128	673.3	132	693.0	159	518.1	201	632.7	113	351.0	130	348.3	174	329.7	181	305.4
	FHN only															
25-34	10	8.2	9	5.7	27	14.6	26	11.0	13	10.6	14	9.1	17	9.5	39	17.5
35-44	41	42.9	25	25.5	66	43.3	54	35.9	29	30.1	38	38.5	47	31.2	67	45.7
45-54	69	79.2	91	104.1	190	118.7	206	137.5	51	55.4	81	90.6	143	84.8	148	94.7
55-64	111	178.3	139	203.4	269	224.2	320	250.9	84	116.4	107	139.8	196	147.0	219	156.9
65-74	115	307.6	134	336.9	248	366.6	282	381.9	103	188.2	137	233.9	133	143.5	202	198.0
75-84	117	615.4	112	588.0	134	436.6	172	541.4	99	307.5	111	297.4	148	280.4	159	268.3
	At least one site other than FHN															
25-34	1	0.8	5	3.2	8	4.3	11	4.6	1	0.8	2	1.3	8	4.5	13	5.8
35-44	7	7.3	10	10.2	31	20.3	29	19.3	1	1.0	6	6.1	15	10.0	17	11.6
45-54	11	12.6	30	34.3	47	29.4	67	44.7	11	11.9	19	21.3	37	21.9	59	37.8
55-64	13	20.9	38	55.6	65	54.2	140	109.8	8	11.1	16	20.9	39	29.3	47	33.7
65-74	21	56.2	33	83.0	51	75.4	101	136.8	15	27.4	18	30.7	39	42.1	37	36.3
75-84	11	57.9	20	105.0	25	81.5	29	91.3	14	43.5	19	50.9	26	49.3	22	37.1

survey ratio, denoted by R, is simply P_1 divided by P_2, and $(R-1)\times 100\%$ is the relative change in the probability of developing the disease. Our analysis of the data from these surveys consisted of detailed testing and estimation of the relative change in incidences for a given sex, cell type, anatomic site, and age stratum. We assumed that the relative changes in incidence were the same for all age groups at both locations. We tested the appropriateness of the assumption by calculating the conditional maximum likelihood estimate of the common relative changes for each set of incidences and used that estimate to obtain goodness-of-fit chi-squares. We also considered the data for each individual geographic area. We took relative changes to be the same for all age groups but different for each location. In this case the assumption was further tested against the alternative that the relative change varied according to age by use of weighted regression on logarithms of relative changes. If the assumption appeared appropriate, using a normal deviate test we tested the hypothesis $H_0{:}R=1$ against the alternative $H_1{:}R\neq 1$.

The methods used here are based on the conditional distribution of test statistics in which the conditioning is on the sufficient statistics of nuisance parameters. These methods are quite accurate even when expected values are small. A detailed mathematical presentation of the methods is outside the scope of this report. The interested reader is, however, referred to Gart (*5*),[5] in which there is a careful mathematical derivation of the methods.

RESULTS

The Data

For San Francisco-Oakland and for Minneapolis-St. Paul, the number of patients and the 6-month incidence rates were tabulated for males and for females. Six age groups were used: 25-34, 35-44, 45-54, 55-64, 65-74, and 75-84. Rates and counts were tabulated for patients with basal cell carcinomas only and for patients with at least 1 squamous cell carcinoma. Since squamous cell carcinoma is not as common as basal cell carcinoma, the few cases with simultaneously diagnosed skin cancers of both cell types were included in the squamous cell counts only. The tabulations were made for 2 general groups of anatomic sites: The sites most frequently exposed to sunlight by both sexes FHN and the sites other than FHN that are less frequently exposed, such as upper extremities, trunk, and lower extremities. Cases with multiple cancer sites were included in the count for sites other than FHN if at least one of the sites was not FHN, whereas cases with multiple cancer sites of the FHN only were included in FHN only. Table 1 presents the tabulations for basal cell cancers, and table 2 provides a summary for squamous cell cancers. Table 3 summarizes the statistical analysis of the data. In text-figure 1 we plot the relative changes and their standard errors for each sex, cell type, area, and site group. A horizontal line at zero in these figures represents no change in the incidence rate.

---

[5] The computer program and documentation are available upon request to Mrs. A. Smith, Mathematical Statistics and Applied Mathematics Section, Biometry Branch, National Cancer Institute.

Basal Cell Skin Cancer Among Males

After adjusting for geographic area, the assumption of constant relative increase over age groups fit the data for basal cell incidence rates among males. Basal cell skin cancer incidence rates among males have increased during 1971–72 to 1977–78. The increase is estimated to have been 18% over the 6 age strata. This increase was significant ($P<0.001$). The relative changes were not, however, consistent by site group. Basal incidence rates adjusted for age and area increased only 8% for FHN ($P=0.043$), quite different from a 69% increase found in sites other than FHN ($P<0.001$).

Changes in incidence rates for the individual FHN sites were inconsistent between geographic areas. For at least one geographic area, decreases occurred in the rates of scalp or forehead, eyelid, ear, and neck or supraclavicular tumors. Nevertheless, the rates for FHN sites when adjusted for area increased for each individual site except eyelid, but not one of these changes was significant. Changes in incidence rates for individual sites other than FHN indicated an increase at both geographic areas and all sites. There was a 91% adjusted increase in male basal incidence rates for upper extremities and a 54% increase in the incidence rates for lower extremities. Increases were notable for skin tumors on the trunk. However, the magnitude of the relative change at this site seemed to depend on age or geographic area. The incidence rates for San Francisco-Oakland increased 75–100% in the age groups 55–64, 65–74, and 75–84, whereas decreases were observed in younger age groups. The increases in San Francisco-Oakland are consistent with the increase observed in Minneapolis-St. Paul.

Basal Cell Skin Cancer Among Females

Basal cell skin cancer incidence rates among females increased during 1971–72 to 1977–78. For all sites combined there was an estimated increase of 18.5% ($P<0.001$). In contrast to the patterns observed among men, changes for women apparently do not depend on anatomic site. Area-adjusted incidence rates increased by 18% ($P<0.001$) for the more exposed FHN sites and by 23% ($P<0.026$) for sites other than FHN.

In regard to the individual sites of the FHN, increases were observed for tumors of the scalp or forehead, nose, cheek, chin, or jaw, neck, and lip. The increases in female

TABLE 2.—*Age-specific incidence rates per 100,000 and number of squamous cell skin cancer patients by anatomic site, age, sex, geographic area, and survey year*

Age, yr	Incidence rates and No. of patients: Squamous cell skin cancer															
	Males								Females							
	Minneapolis–St. Paul				San Francisco–Oakland				Minneapolis–St. Paul				San Francisco–Oakland			
	1971–72		1977–78		1971–72		1977–78		1971–72		1977–78		1971–72		1977–78	
	No. of patients	Rate	No. of patients	Rate	No. of patients	Rate	No. of patients	Rate	No. of patients	Rate	No. of patients	Rate	No. of patients	Rate	No. of patients	Rate
	All sites combined															
25–34	0	0.0	0	0.0	0	0.0	4	1.7	2	1.6	0	0.0	1	0.6	2	0.9
35–44	2	2.1	4	4.1	10	6.6	9	6.0	0	0.0	4	4.1	4	2.7	5	3.4
45–54	15	17.2	15	17.2	38	23.7	41	27.4	9	9.8	6	6.7	17	10.1	21	13.4
55–64	26	41.8	24	35.1	76	63.3	85	66.7	10	13.9	8	10.5	20	15.0	35	25.1
65–74	29	77.6	42	105.6	92	136.0	110	149.0	12	21.9	18	30.7	31	33.4	41	40.2
75–84	37	194.6	34	178.5	70	228.1	66	207.7	20	62.1	21	56.3	35	66.3	38	64.1
	FHN only															
25–34	0	0.0	0	0.0	0	0.0	3	1.3	0	0.0	0	0.0	0	0.0	1	0.4
35–44	2	2.1	2	2.0	9	5.9	6	4.0	0	0.0	3	3.0	0	0.0	2	1.4
45–54	11	12.6	12	13.7	32	20.0	31	20.7	5	5.4	3	3.4	9	5.3	12	7.7
55–64	24	38.5	17	24.9	56	46.7	65	51.0	2	2.8	6	7.8	14	10.5	15	10.7
65–74	19	50.8	34	85.5	69	102.0	77	104.3	11	20.1	11	18.8	19	20.5	25	24.5
75–84	25	131.5	27	141.7	56	182.5	54	170.0	9	28.0	11	29.5	22	41.7	21	35.4
	At least one site other than FHN															
25–34	0	0.0	0	0.0	0	0.0	1	0.4	2	1.6	0	0.0	1	0.6	1	0.4
35–44	0	0.0	2	2.0	1	0.7	3	2.0	0	0.0	1	1.0	4	2.7	3	2.0
45–54	4	4.6	3	3.4	6	3.7	10	6.7	4	4.3	3	3.4	8	4.7	9	5.8
55–64	2	3.2	7	10.2	20	16.7	20	15.7	8	11.1	2	2.6	6	4.5	20	14.3
65–74	10	26.7	8	20.1	23	34.0	33	44.7	1	1.8	7	11.9	12	12.9	16	15.7
75–84	12	63.1	7	36.7	14	45.6	12	37.8	11	34.2	10	26.8	13	24.6	17	28.7

TABLE 3.—*Relative change in skin cancer incidence rates by cell type, anatomic site, sex, and geographic location, 1971–72 to 1977–78*

Anatomic site	Relative change in incidence, %					
	Males			Females		
	Minneapolis	San Francisco	Adjusted for area	Minneapolis	San Francisco	Adjusted for area
			Basal cell cancer			
All sites combined	16.8[a]	19.0[a]	18.3[a]	23.4[a]	15.9[a]	18.5[a]
FHN sites	*5.1*	*9.1*[b]	*7.8*[c]	*19.8*[a]	*16.2*[a]	*17.5*[a]
Scalp or forehead	−4.6	6.1	2.4	9.5	23.0	16.7
Eyelid	−22.7	−5.2	−11.6	−9.4	−32.1[c]	−24.9[b]
Ear	42.5	−1.1	8.5	26.0	−34.9	−23.5
Nose	5.2	19.5[b]	14.7	12.2	26.9[c]	22.1[c,d]
Cheek, chin, or jaw	16.3	1.6	6.6	8.1	14.9	12.2
Neck-supraclavicular	−28.0	43.3[c]	14.2	81.3[b]	6.2	23.5
Lip	11.6	1.8	5.0	192.4[a]	58.0[c]	96.9[a]
Sites other than FHN	*102.0*[a]	*59.7*[a]	*68.9*[a]	*49.9*[c]	*14.7*	*23.0*[c]
Trunk	129.7[a]	41.5[a,d,e]	63.4[a,d]	46.9	−8.0	6.7
Upper extremities	31.8	106.4[a]	90.8[a]	137.0	13.4[c]	27.7
Lower extremities	136.0	42.1	53.8	17.6	64.1[b]	53.4[b]
			Squamous cell cancer			
All sites combined	4.8	5.2	5.0	−1.1	23.7	15.5
FHN sites	*8.9*	*1.7*	*3.6*	*16.5*	*11.3*	*12.9*
Scalp or forehead	43.6	15.2	21.4	171.7	−48.4	−0.4
Eyelid	−76.5	−50.3	−63.7	42.2	−64.5	−43.2
Ear	2.3	27.7	20.9	−6.6	183.6	88.3
Nose	11.0	−4.1	−0.9	−7.2	16.2	9.3
Cheek, chin, or jaw	41.0	−12.1	0.8	19.5	7.2	10.5
Neck-supraclavicular	53.2	33.5	38.5	169.4	82.3	104.1[d]
Lip	−17.4	−23.7	−21.6	−53.1	317.9[c]	104.9
Sites other than FHN	*−7.1*	*17.2*	*9.9*	*−19.3*	*41.7*[b]	*18.8*
Trunk	466.9	70.6[d]	110.5[b]	−4.5	−19.4	−16.4
Upper extremities	−35.5	9.0[c]	−6.3	116.8	78.1[b]	89.0[c]
Lower extremities		−25.6				

[a] $P<0.01$.
[b] $P<0.10$.
[c] $P<0.05$.
[d] Lack of fit significant at $P<0.05$.
[e] Regression significant at $P<0.05$.

incidence rates were substantially larger than the increases for males at the same anatomic sites. By far the largest increase, 97%, occurred in the incidence rates for lip. This difference cannot be explained by changes in morphology coding (i.e., eighth to ninth revision of the International Classification of Diseases for Oncology) because anatomic site charts were utilized for identification of the exact tumor locations on the body. There were decreases in the rates for skin cancer of the ear in San Francisco–Oakland and of the eyelid in both locations. There were increases in the incidence rates for skin cancer of sites other than FHN, but they were less dramatic than those observed for males. Increases of 28, 53, and 40% were found for upper extremities, lower extremities, and multiple sites, respectively.

Squamous Cell Skin Cancer

Squamous cell skin cancer incidence rates are relatively small. They are based on few cases, and under the Poisson assumption they are quite variable. Small nonsignificant increases in rates for males were obtained. The rates for all sites combined increased 5%, the rates for FHN sites increased 4%, and the rates for sites other than FHN increased 10%. The increases in squamous cell skin cancer among rates for females are larger than those observed for males, 13% for FHN sites and 19% for sites other than FHN. The increases among females are consistent in size with those observed for basal cell skin cancer rates, but because of the higher variability of the rates for squamous cell tumors, these increases, like those for males, are not significant.

DISCUSSION

Recent changes in skin cancer incidence show that there have been increases in the incidence of the superficial, nonspreading tumors of the basal cell type. Changes in the incidence of squamous cell type are not definitive. There have been increases in general, but the changes seem to vary by sex and anatomic site. Certainly, more data are needed. The apparent difference between cell types is not easily explained. Perhaps the latent period for squamous cell carcinoma is different from that for basal cell carcinoma.

Among males increases in the basal cell incidence rates appear to be site-dependent with areas of the body not routinely exposed to sunlight showing the largest increases.

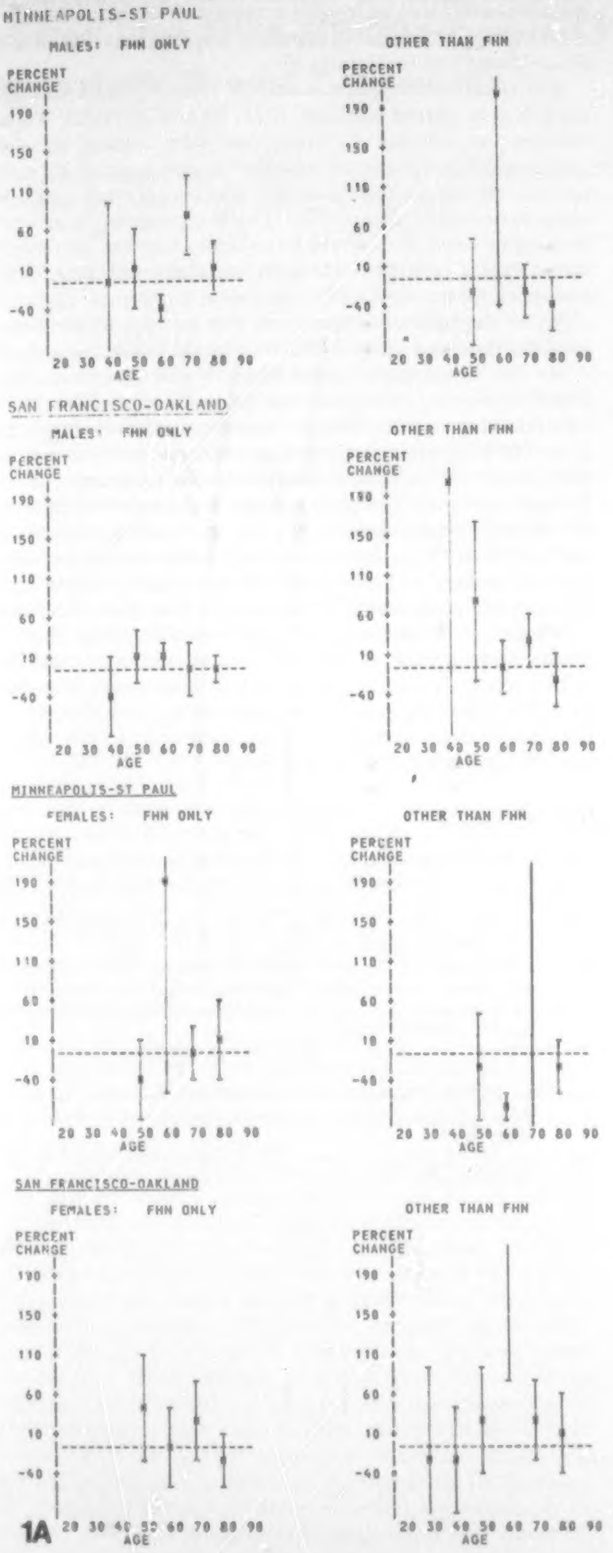

1A

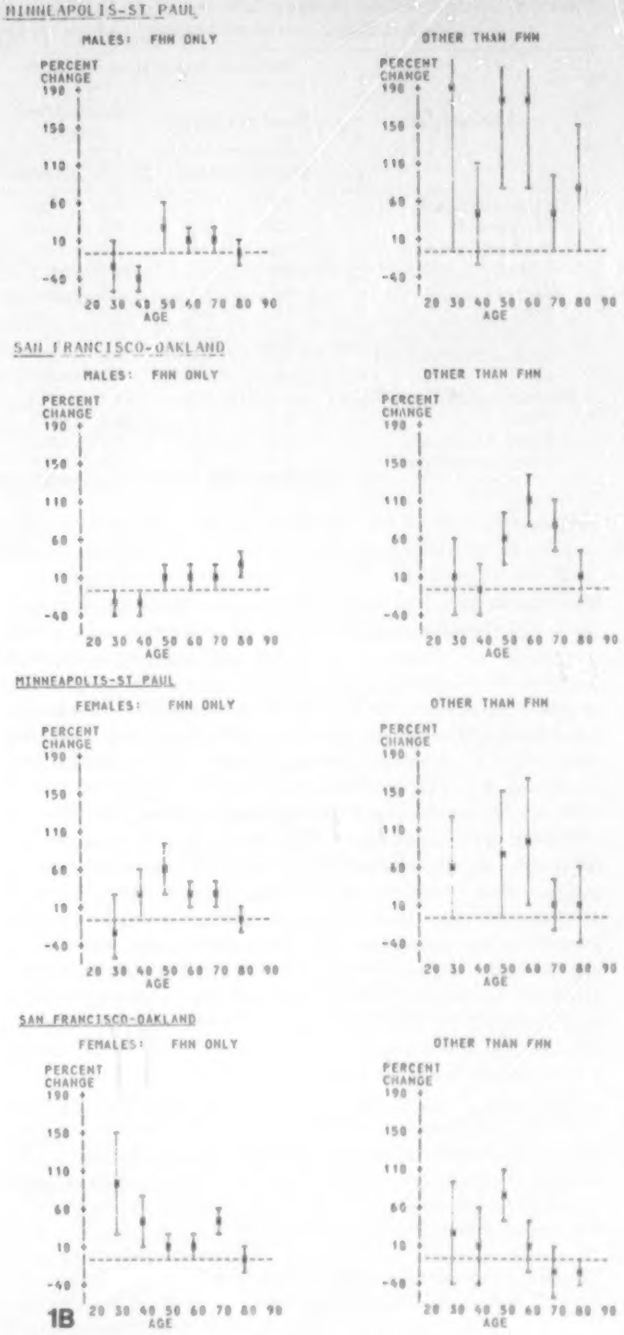

1B

TEXT-FIGURE 1.—Relative change in age-specific skin cancer incidence with standard error by cell type, sex, anatomic sites, and geographic area, 1971–72 to 1977–78. Let r_1 be the incidence rate of skin cancer in 1971–72 and r_2 be the incidence rate of skin cancer in 1977–78. Then $\mathrm{Var}(R)=\mathrm{Var}(r_2/r_1)$ is estimated by $[\mathrm{Var}(r_2)+R^2\mathrm{Var}(r_1)]/r^2_1$. A) Squamous cell carcinoma. B) Basal cell carcinoma.

TABLE 4.—*Annual relative change in skin cancer incidence rates by sex, cell type, and anatomic site*

Anatomic site	Relative change in incidence, %			
	Basal cell cancer		Squamous cell cancer	
	Males	Females	Males	Females
All sites combined	2.8^{a}	2.9^{a}	0.8	2.4
FHN subsites	1.3^{b}	2.7^{a}	0.6	2.0
Scalp or forehead	0.4	2.6	3.3	−0.1
Eyelid	−2.0	−4.7	−15.5	−9.0
Ear	1.4	−4.4	3.2	11.1
Nose	2.3	3.4^{b}	−0.2	1.5
Cheek, chin, or jaw	1.1	1.9	0.1	1.7
Neck-supraclavicular	2.2	3.6	5.6	12.6
Lip	0.8	12.0^{a}	−4.0	12.7
Subsites other than FHN	9.1^{a}	3.5^{a}	1.6	2.9
Trunk	8.5^{a}	1.1	13.2	−2.9
Upper extremities	11.4^{a}	4.2	−1.1	11.2^{b}
Lower extremities	7.4	7.4	1.9	1.9

^{a} $P<0.01$.
^{b} $P<0.05$.

The small change in basal cell incidence rates among males for FHN therefore suggests to us that males increased the frequency or duration of their sunlight exposure only slightly. The large increase at the usually unexposed sites suggests, however, that the nature of exposure at these sites has changed. Perhaps men are wearing shorts and removing their shirts more often. Among females the incidence rates increased, but the increases were not so clearly associated with site. Rates for the frequently exposed sites of the FHN indicated large increases as did the incidence rates for less frequently exposed parts of the body. This general increase suggests that frequency and/or duration as well as manner of exposure may have changed among females. Perhaps women are spending more time outdoors today than in the past and wearing less protective clothing. The large increases observed for basal cell carcinoma of the lip among women may coincide with the practice in recent years of wearing less lipstick. Decreases in the rates for tumors of the eyelid are consistent with the practice of wearing sunglasses.

We found little or no evidence to support the hypothesis that relative changes in basal cell or squamous cell skin cancer depended on age for any site group, site, or sex. This finding is important since it implies that changes in nonmelanoma skin cancer incidence rates shift but do not distort the observed relationship between age and logarithmically transformed incidence rates (*6*).

The relative changes in incidence rates reported here are for a 6-year period between 1971–72 and 1977–78. These increases should not be compared with annual relative changes that are reported for other tumor types (e.g., melanoma). If we assume that the relative increase was the same in each year, then $(R^{1/6}-1)\times 100$ represents the annual relative increase that would have been observed. In table 4 we provide this estimate of the annual change in skin cancer incidence rates by sex, cell type, and site group.

There are problems that make the interpretation of the results of our study difficult: 1) We have used as our unit of study the populations of two SMSA's and concerned ourselves with population incidence rates. Care must be taken when making inference about the risks to individuals within these SMSA's, since the population hazard need not reflect changes in the individual hazard. 2) No measurements of the sizes of populations in these areas are currently available. Therefore, we must assume that our estimates of population size for 1977–78 do not contain any systematic errors over ages. If, in fact, such systematic errors are present, changes in incidence rates would be observed when there had been no change in the average probability of disease. 3) Finally, other factors of etiologic significance have not been included in this report. Since the probability of skin cancer is known to differ markedly among subpopulations, any change in the relative sizes of subpopulations could dramatically affect the average probability of the disease.

REFERENCES

(*1*) Scotto J, Kopf A, Urbach F. Nonmelanoma skin cancer among Caucasians in four areas of the United States. Cancer 1974; 34:1333–1338.

(*2*) Lynch FW, Seidman H, Hammond EC. Incidence of cutaneous cancer in Minnesota. Cancer 1970; 25:83–91.

(*3*) Scotto J, Fears TR, Lisiecki E, et al. Incidence of nonmelanoma skin cancer in the United States, 1977–78. Preliminary report. Washington, D.C.: U.S. Govt Print Office, 1980 [DHEW publication No. (NIH)80-2154].

(*4*) Scotto J, Fears TR. Skin cancer epidemiology: Research needs. Natl Cancer Inst Monogr 1978; 50:169–177.

(*5*) Gart JJ. The analysis of ratios and cross-product ratios of Poisson variates with application to incidence rates. Commun Stat Theor Methods 1978; A7:917–937.

(*6*) Cook PJ, Doll R, Fellingham SA. A mathematical model for the age distribution of cancer in man. Int J Cancer 1969; 4:93–112.

Isolation and Partial Characterization of Surface Components of Cell Line MDA-MB-231 Derived From a Human Metastatic Breast Carcinoma[1,2,3]

Evelyne Walker-Nasir,[4] John F. Codington,[4] Marianne R. Jahnke,[4,5] Thomas C. Fuller,[6] *and* Roger W. Jeanloz[4,7,8]

ABSTRACT—Neuraminidase (*Vibrio cholerae*) treatment of human metastatic mammary carcinoma MDA-MB-231 cells grown in culture released 0.60–0.63 mg of *N*-acetylneuraminic acid from 10^9 cells. Incubation of intact cells with a modified trypsin and fractionation by gel filtration gave mainly *O*-glycopeptides. The presence of *O*-glycosyl-linked chains having one or two carbohydrate residues was confirmed by treatment of the glycopeptide fractions with galactose oxidase, followed by reduction with alkaline sodium borotritide and fractionation. The major glycopeptide fraction, which consisted of 53% carbohydrate and 47% protein, and a minor glycopeptide fraction each inhibited hemagglutination by peanut lectin. These results suggest the presence of *O*-β-D-galactopyranosyl-(1→3)-*O*-(2-acetamido-2-deoxy-α-D-galactopyranosyl)-(1→3)-L-serine (threonine) residues. The absorptive capacities for anti-HLA-A2 and anti-HLA-B8 antisera were slightly greater for intact than for lyophilized cells, which suggested that masking of these major histocompatibility antigens did not occur in intact cells.—JNCI 1982; 69:371–380.

Attempts by many laboratories during the past decade to correlate metastatic properties with the presence of macromolecular structures at the cell surface have not been conclusive. Some investigators, for example, have reported a correlation between metastatic potential and low concentrations of cell surface glycoproteins in mammary tumor cells (*1*), whereas others (*2–4*) have observed the presence of high concentrations of high-molecular-weight, endogenous *O*-glycoproteins in metastatic mammary carcinoma cells grown in vivo. However, metastatic potential may be achieved by more than one mechanism (*4*), and cell surface features involved directly in this process may vary with cell type, host, and environmental circumstances. The need for more intensive work in this area involving physicochemical and immunologic determinations on various metastatic tumor cell types is clearly indicated.

The availability of the well-characterized, metastatic cell line, derived from a human breast tumor, MDA-MB-231 (*5, 6*), which was reported to grow rapidly in culture (*6, 7*), offered the opportunity to study the chemical, immunochemical, and immunologic characteristics of the surface components of this cell and the possible role of these components in metastasis. Of particular interest was investigation of the possible presence of cell surface *O*-glycoproteins having high concentrations of carbohydrate chains. Investigators have reported the presence of large endogenous *O*-glycoproteins in high concentration at the surfaces of both mouse (*4, 8*) and rat (*9*) mammary carcinoma ascites cells with high metastatic potential. Furthermore, the presence of Thomsen-Friedenreich antigenic activity, presumably resulting from *O*-β-D-galactopyranosyl-(1→3)-*O*-2-acetamido-2-deoxy-α-D-galactopyranosyl residues linked to serine or threonine in the polypeptide backbone, has recently been observed in human mammary carcinoma tissue but not in normal breast tissue (*10, 11*). In our investigation of macromolecular structures at the surface of the MDA-MB-231 cell, particular attention was given to the possible presence of glycoproteins containing the Thomsen-Friedenreich antigen-like structure.

MATERIALS AND METHODS

Cells.—Cell line MDA-MB-231, established from the pleural effusion of a patient with metastasized mammary carcinoma (*5*), was obtained in the frozen state at the 75th passage from EG&G Mason Research Institute, Rockville, Md., at the suggestion of Dr. P. Gullino, National Cancer Institute, Bethesda, Md.

Cell culture and harvest.—Cells were grown in monolayer culture in Dulbecco's modified Eagle's minimum essential medium with L-glutamine (Grand Island Biological Co., Grand Island, N.Y.) and supplemented with 10% fetal bovine serum (M.A. Bioproducts, Walkersville, Md.), 100 U penicillin/ml, and 100 μg streptomycin/ml. Cells in 100-mm-diameter plastic tissue culture dishes (Falcon Plastics, Oxnard, Calif.) were incubated in humidified 5% CO_2–95%

ABBREVIATIONS USED: GLC=gas-liquid chromatography; MS=mass spectrometry; *m/z*=mass divided by charge; NHS=normal human serum; PAGE=polyacrylamide gel electrophoresis; SDS=sodium dodecyl sulfate; TPCK=chloromethyl L-(2-phenyl-1-*p*-toluenesulfonamido)ethyl ketone; T_R=retention time(s).

---

[1] Received October 7, 1981; revised February 24, 1982; accepted March 15, 1982.

[2] Supported by Public Health Service grant CA-19763-2 from the National Cancer Institute.

[3] Publication No. 891 of the Robert W. Lovett Memorial Group for the Study of Diseases Causing Deformities, Harvard Medical School and Massachusetts General Hospital.

[4] Laboratory for Carbohydrate Research, Departments of Biological Chemistry and Medicine, Massachusetts General Hospital and Harvard Medical School, Boston, Mass. 02114.

[5] *Present address*: Department of Microbiology, State University of New York, Stony Brook, N.Y. 11794.

[6] Blood Transfusion Service and Transplantation Unit, Department of Surgery, Massachusetts General Hospital and Harvard Medical School.

[7] *Address reprint requests to* Dr. Jeanloz.

[8] We thank Dr. Vernon N. Reinhold, Laboratory of Human Reproduction and Reproductive Biology, Harvard Medical School, for the gas chromatography-mass spectroscopy analyses. We also thank Mr. Keyes B. Linsley, Dr. Hasi R. Das, and Mrs. Cyla Silber from this laboratory for gas-liquid, polyacrylamide gel, and chemical analyses, respectively.

best copy available

air at 37°C. Cells free of mycoplasma[9] were used between their 11th and 20th passages. From monolayer culture, the cells were adapted to growth in suspension culture in spinner flasks at 37°C in the same medium as described above. Inocula of 5×10^5 cells/ml were used. After 4 days the cells ($\approx2\times10^6$ cells/ml) were harvested, washed, and counted with a hemacytometer, and their viability was determined by trypan blue exclusion (*12*). For this investigation, 1.2×10^9 cells (in six separate runs) were utilized.

Enzymes.—Neuraminidase (EC 3.2.1.18 from *Vibrio cholerae*, protease-free, 500 U/ml; Behring Diagnostics, Somerville, N.J.) was obtained in 1-ml vials. TPCK-treated trypsin (TPCK-trypsin, EC 3.4.21.4; Sigma Chemical Co., St. Louis, Mo.) was purified as described in (*13*). α-Amylase (EC 3.2.1.1, from porcine pancreas) was obtained from Sigma Chemical Co.; galactose oxidase (EC 1.1.3.9), glucose oxidase (EC 1.1.3.4, from *Aspergillus niger*), and peroxidase (from horse-radish) were obtained from Worthington Biochemical Corp., Freehold, N.J.

Physicochemical analyses.—The dry weight of cells was estimated as previously described (*13*). Cell surface sialic acid was determined by the thiobarbituric acid method (*14*) after incubation for 80 minutes with neuraminidase (150 U/ml in phosphate-buffered saline solution) at 37°C, with crystalline *N*-acetylneuraminic acid (Sigma Chemical Co.) as standard. The total amount of sialic acid in the washed cells was estimated as the sum of neuraminidase-liberated sialic acid plus the sialic acid detected (*14*) after treatment of the residual, neuraminidase-treated cells with 50 m*M* sulfuric acid for 1 hour at 80°C, neutralization of the cooled solution with barium carbonate, filtration, and passage of the solution through a column of Dowex 50W-X16 (H^+) ion-exchange resin (Bio-Rad Laboratories, Richmond, Calif.). The amount and composition of sialic acid were also determined by GLC (*15*). Protein was determined by the method of Lowry et al. (*16*) with bovine serum albumin (Sigma Chemical Co.) as standard. Hexoses were determined by the phenol-sulfuric acid procedure (*17*) with D-galactose as standard. Uronic acid was determined by GLC and by the procedure of Blumenkrantz and Asboe-Hansen (*18*) with D-glucuronic acid as standard and identified by GLC–MS (*see* below). Sulfate was estimated by the rhodizonate dye assay (*19*), after hydrolysis of the sample with 2 *M* HCl for 14 hours at 100°C, and by evaporation of the solvent under a stream of nitrogen.

GLC.—The carbohydrate composition of the lyophilized samples was determined after methanolysis, acetylation, *O*-deacetylation, and per-*O*-(trimethylsilyl)ation as previously described (*20*). The T_R are given relative to hexa-*O*-trimethylsilyl-*myo*-inositol. Amino acid analyses were performed by the method of Zumwalt et al. (*21*) on the same samples after hydrolysis with 6 *M* HCl for 24 hours at 110°C.

GLC–MS.—Fraction F100-III, eluted from a Biogel P-200 column (100–200 mesh; Bio-Rad Laboratories), was methanolized (≈35 hr at 85°C). The product was acetylated, *O*-deacetylated, reduced with sodium borodeuteride as previously described (*22*), and analyzed by GLC–MS with an instrument equipped with a computer. Methyl 2,3,4,6-tetra-*O*-trimethylsilyl-α-D-glucopyranoside and 1,6-anhydro-2,3,4-tri-*O*-trimethylsilyl-α-L-idopyranose were used as reference standards in MS. The intensities of the following diagnostic ions, compared with those of the corresponding deuterated fragments, observed after treatment of fraction F100-III, as just described, were *m/z* 231, 133, 117, 103, and 89 and 305, 133, 129, 117, 103, and 89, respectively.

Column chromatography.—Fractionations were performed at 4°C on columns of Biogel P-4 (200–400 mesh), Biogel P-100 (100–200 mesh), and Sepharose 6B (Pharmacia Fine Chemicals, Piscataway, N.J.) with 50 m*M* pyridine acetate (pH 5.3) as eluent. The void volume of the gel-filtration columns was determined with blue dextran 2000 (Pharmacia Fine Chemicals).

Gel electrophoresis.—PAGE (10%) with SDS (0.1%) was performed according to the method of Laemmli (*23*) in Tris-HCl buffer (pH 8.0) with bovine serum albumin and α_1-acid glycoprotein as standards. The bands were stained with 0.1% Coomassie brilliant blue in 45% methanol and 7.5% acetic acid.

Proteolysis of viable cells.—Batches of $2\text{–}5\times10^8$ viable cells were incubated at 4°C in Dulbecco's phosphate-buffered saline (pH 7.0) with a modified trypsin (18 μg/ml), as previously described (*24*). The supernatants were lyophilized, and bound sialic acid [after treatment with neuraminidase (*25*)], protein (*16*), and total hexose (*17*) were determined.

Purification and fractionation of cell surface components.—A solution of lyophilized trypsinates in pyridine acetate (50 m*M*, pH 5.3) was applied to a column (2.2×84 cm) of Biogel P-4. Fractions (6.0 ml) were eluted with the same buffer and monitored for protein (*16*) and total hexose (*17*). The major carbohydrate- and protein-containing fractions from the first peak (F4-I, 6.5 mg) (text-fig. 1) were combined and passed through a column (2.7×91 cm) of Biogel P-100 (text-fig. 2). Fractions (6.0 ml) were examined for protein (*16*) and total hexose (*17*). Material eluted just after the void volume (F100-II, 1.0 mg) was fractionated on a column (0.8×45 cm) of Sepharose 6B. Fractions (0.5 ml) were analyzed for protein content by absorbance at 278 nm and, on this basis, were divided into five fractions

Adsorption of Vicia graminea *lectin by intact cells.*—As previously described (*26, 27*), the amount of lectin adsorbed was calculated from the amount remaining in solution (following incubation with intact cells), a value determined by the capacity of the unadsorbed lectin to agglutinate human erythrocytes of N-blood group specificity.

Adsorption–inhibition assays.—The inhibitory activity of glycopeptide fractions for the agglutination of neuraminidase-treated, human type O erythrocytes by *Arachis hypogaea* (peanut) lectin (Sigma Chemical Co.) was determined according to a modified procedure of Osawa et al. (*28*). After incubation of 25 μl of the lectin (amount previously found to agglutinate 50% of the erythrocytes) and 25 μl of each glycopeptide fraction at appropriate twofold dilutions for 3 minutes, 50 μl of sialic acid-free erythrocytes (7×10^8 cells/ml) was added. The concentration of lectin that completely inhibited the agglutination of the erythrocytes within 60 minutes was recorded.

---

[9] Mycoplasma contamination was tested by the Bacteriology Department, Massachusetts General Hospital, on batches of cells grown in antibiotic-free medium.

Alloantiserum adsorptions.—Expression of the HLA histocompatibility alloantigens at the surface of the tumor cells was determined by the adsorption-inhibition lymphocytotoxic assay. The following alloantisera were used: MGH No. 29 with HLA-A2 antibody specificity, CW-2, anti-HLA-B8, GLO-2, anti-HLA-A1, and NHS. Antiserum (50 μl at the optimal dilution) was incubated with viable or lyophilized cells at three concentrations (1×10^5, 1×10^6, and 1×10^7 cells). Comparison was made of suspension- and monolayer-grown viable and lyophilized cells, respectively. After 60 minutes with intermittent mixing at room temperature, the adsorbed antiserum was separated from the cells by centrifugation (5 min, 15,000×*g*) and kept frozen at −30°C until back-titration was performed. Both adsorbed and unadsorbed sera were assayed for residual cytotoxic antibody with the National Institutes of Health cytotoxicity technique (*29*) and the more sensitive Amos modification of this method, which incorporates a wash step following the incubation of target cells with the antiserum (*30*). All sera were tested undiluted and diluted 1:2 with fresh rabbit serum (Pel-Freez Biologicals, Inc., Rogers, Ark.) as a source of complement. Two unrelated individuals, who possessed the antigens reported (*31*) to be expressed on the cell line (HLA-A2 and HLA-B8), donated target lymphocytes for back-titration of the antisera as described above. In addition, for specificity control, a nonadsorbable HLA antiserum (GLO-2, anti-HLA-A1) and NHS were also incorporated; the unrelated individuals also expressed HLA-A1 for this purpose.

Labeling of terminal D*-galactose and 2-acetamido-2-deoxy-*D*-galactose residues with tritium: Cleavage of carbohydrate chains and fractionation in a gel-filtration column.*—Incubation of 100–200 μg of each sample with 5 U of galactose oxidase (150 U/mg) in phosphate-buffered saline solution (pH 7.0) was performed for 30 minutes at 37°C. Approximately 500 μCi of sodium borotritide (246 Ci/mol) was added. After 1–2 hours at 22°C, 700 μg of sodium borohydride (Ventron Corp., Alfa Products Division, Danvers, Mass.) was added, and the solution was kept for an additional 45 minutes. The mixture was acidified with acetic acid and kept for 2 hours before the addition of sodium hydroxide to a 0.1-*M* concentration and of sodium borohydride to a 1.0-*M* concentration. The mixture was incubated for 72 hours at 37°C and then acidified with acetic acid. After evaporation to dryness in vacuo, the residue was dissolved in anhydrous methanol, and the solution was evaporated to dryness. The residue was dried by several additions and evaporations of methanol in vacuo.

Each residue dissolved in 0.1 *M* pyridine acetate (pH 5.3) was applied to and eluted at 4°C from a column (1.5×127 cm) of Biogel P-2 (200–400 mesh) with 0.1 *M* pyridine acetate (pH 5.3). The radioactivity of aliquots of fractions (2.5 ml) was counted in a Packard scintillation counter. The column had been previously calibrated with a sample of 2-acetamido-2-deoxy-D-galactitol, prepared by reduction of 2-acetamido-2-deoxy-D-galactose (Pfanstiehl Laboratories, Inc., Waukegan, Ill.) with excess sodium borohydride at neutral pH, with a sample of the reduced disaccharide 2-acetamido-2-deoxy-3-*O*-β-D-galactopyranosyl-D-galactitol obtained from epiglycanin, as previously described (*32*), and with a sample of α_1-acid glycoprotein.

RESULTS

Release of Glycoprotein Material From the Cell Surface

The amounts of sialic acid, neutral carbohydrate, and protein material removed by the action of enzymes from viable MDA-MB-231 cells grown under monolayer and suspension culture conditions were similar for both growth conditions, although the trypsinates of suspension-grown cells appeared to contain slightly more glycoprotein material (table 1). The cells possess a large surface area, and the diameter of the cells grown under each set of conditions was found to be similar (≈15 μm). The amount of cell surface sialic acid liberated by neuraminidase represents about 70–75% of the total sialic acid of the cells (*24*), because approximately 25–30% more sialic acid was detected after mild acid hydrolysis of the viable, neuraminidase-treated cells. No free sialic acid was detected before neuraminidase treatment, and the only sialic acid detected at the surface of MDA-MB-231 cells was *N*-acetylneuraminic acid; no *O*-acylated derivatives were observed, because identical sialic acid values were obtained for untreated samples and for samples briefly pretreated with sodium hydroxide and neutralized with hydrochloric acid prior to incubation with neuraminidase (*15*). No neutral carbohydrate was detected in material released from the cell surfaces in the control incubations without added proteolytic enzyme; some protein, however, was liberated (5–9% of the amount released by trypsin).

Fractionation of Cell Surface Fragments Removed by Proteolysis

Chromatography on a column of Biogel P-4 of the material released by TPCK-trypsin from viable, suspension-

TABLE 1.—*Glycoprotein material removed from the surfaces of viable MDA-MB-231 cells*

Components	Released by:	Cells grown in vitro			
		Monolayer		Suspension	
		$\mu g/10^9$ cells[a]	Percent[b]	$\mu g/10^9$ cells[a]	Percent[b]
Sialic acid[c]	Neuraminidase[d]	633	0.25	598	0.23
	Proteolysis,[e] followed by neuraminidase[d]	203	0.08	356	0.14
Neutral carbohydrate[f]	Proteolysis[e]	2,969	1.2	3,250	1.3
Protein[g]	Proteolysis[e]	22,410	8.8	25,150	9.8

[a] Mean value of duplicate determinations performed on two to three cell batches.

[b] Calculated on the basis of the dry weight, which was determined on the lyophilized cells: 254±15 mg/10^9 monolayer-grown cells, 256±20 mg/10^9 suspension-grown cells.

[c] Determined by the thiobarbituric acid method of Warren (*14*).

[d] *V. cholerae* neuraminidase, 150 U/ml, 80 min at 37°C.

[e] According to (*13*).

[f] Determined by the phenol–sulfuric acid method (*17*).

[g] Determined by the method of Lowry et al. (*16*).

grown MDA-MB-231 cells gave, at the void volume, a major peak (F4-I; text-fig. 1) (≈6–7 mg/10^9 cells), which represents about 21–25% of the total surface glycoprotein material (28.5 mg) recovered from the Biogel P-4 column. (For carbohydrate and amino acid composition, *see* table 2.) Other fractions eluted later from the Biogel P-4 column represented minor components of glycopeptide nature and were not further studied. Fractionation of F4-I on a column of Biogel P-100 gave three major peaks (F100-I, F100-II, and F100-III; text-fig. 2) at fractions 25, 47, and 66, respectively. (For carbohydrate and amino acid compositions, *see* table 3.) All three F100-fractions contained uronic acid and sulfate.

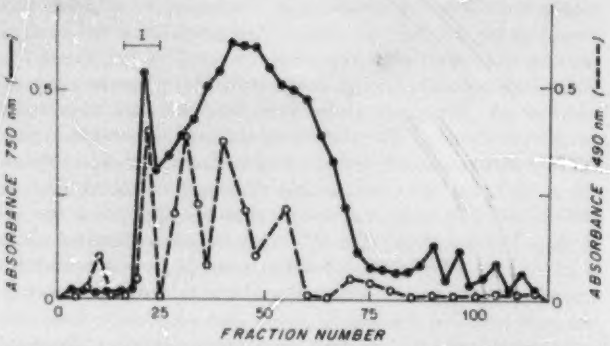

TEXT-FIGURE 1.—Fractionation on a column of Biogel P-4 of the cell surface material released by TPCK-trypsin. Eluent: 50 m*M* pyridine acetate (pH 5.3). Protein (——) and total hexose (-----) in column fractions were plotted against the effluent volume.

TABLE 2.—*Composition of Biogel P-4 fraction F4-I*

Carbohydrates[a]	Molar ratio[b]
Mannose	1.7
Galactose	3.7
Glucose	17.0
N-Acetylgalactosamine	+ND
N-Acetylglucosamine	3.3
N-Acetylneuraminic acid	1.0
Uronic acid and derivatives[c]	1.3
Sulfate[d]	+
Total carbohydrates[a]	16[e]
Amino acids[a]	**Residues per 1,000 residues**
Alanine	94
Valine	70
Glycine	100
Isoleucine	43
Leucine	84
Proline	71
Threonine	63
Serine	63
Phenylalanine	33
Aspartic acid	141
Glutamic acid	173
Lysine	70

[a] Determined by GLC.

[b] Molar ratio relative to the amount of *N*-acetylneuraminic acid taken as a unit. +=present; ND=not detected.

[c] Determined colorimetrically (*18*) and by GLC.

[d] Qualitatively determined by the rhodizonic acid method (*19*).

[e] Percent relative to weight of fraction.

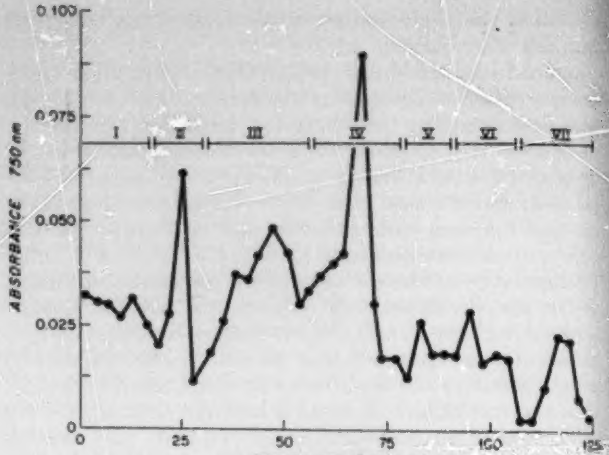

TEXT-FIGURE 2.—Chromatography on a column of Biogel P-100 of fraction F4-I. Eluent: 50 m*M* pyridine acetate (pH 5.3). Protein (——) in column fractions was plotted against the effluent volume.

TABLE 3.—*Composition of Biogel fractions F100*

Components	Fraction F100		
	I	II	III
Carbohydrates[a]	**Molar ratio[b]**		
Mannose	7.6	2.4	3.1
Galactose	4.8	4.8	4.1
Glucose	59.2	11.1	3.2
N-Acetylgalactosamine	1.0	1.0	1.0
N-Acetylglucosamine	2.1	2.3	3.3
N-Acetylneuraminic acid	0.6	1.8	3.1
Uronic acid and derivatives[c]	37.5	2.4	1.7
Sulfate[d]	62	+NQ	15
Total carbohydrates[a]	30[e]	65[e]	15[e]
Amino acids[a]	**Residues per 1,000 residues**		
Alanine	61	93	120
Valine	66	80	75
Glycine	87	88	81
Isoleucine	41	54	45
Leucine	60	76	67
Proline	59	63	75
Threonine	74	93	94
Serine	114	87	79
Phenylalanine	68	40	24
Aspartic acid	164	114	116
Glutamic acid	205	161	182
Lysine	+NQ	52	42

[a] Determined by GLC.

[b] Molar ratio relative to ratio of *N*-acetylgalactosamine. +=present; NQ=quantitative determination not performed.

[c] Determined colorimetrically (*18*) and by GLC.

[d] Determined by the rhodizonic acid method (*19*).

[e] Percent relative to weight of fraction.

Fraction F100-II (1.3–1.4 mg, corresponding to ≈ 5% of the original cell surface glycoprotein material) was further fractionated on a column of Sepharose 6B. Four major fractions (F6B-I, F6B-II, F6B-III, and F6B-V) were eluted at 6, 18, 21, and 45 ml, respectively. (For carbohydrate and amino acid compositions, *see* table 4.) Fraction F6B-I was partly excluded from the column and contained a high

TABLE 4.—*Composition of Sepharose 6B fractions F6B*

Components	Fraction F6B			
	I	II	III	V
Carbohydrates[a]	Molar ratio[b]			
Xylose	1.1		1.1	1.2
Mannose	2.4	2.6	1.8	1.8
Galactose	7.8	8.0	2.8	1.1
Glucose	41.2	1.6	5.0	3.2
N-Acetylgalactosamine	2.0	2.0	2.0	ND
N-Acetylglucosamine	4.1	4.3	1.1	23.2
N-Acetylneuraminic acid	3.1	4.1	0.9	ND
Uronic acid and derivatives[c]	2.0		2.0	23.9
Sulfate[d]	14.7		7.0	+NQ
Total carbohydrates[a]	52[e]	53[e]	15[e]	26[e]
Amino acids[a]	Residues per 1,000 residues			
Alanine	77	83	70	82
Valine	44	67	108	112
Glycine	92	37	99	75
Isoleucine	41	42	29	42
Leucine	75	75	51	74
Proline	60	16	50	ND
Threonine	85	145	124	47
Serine	110	168	140	131
Phenylalanine	40	40	30	49
Aspartic acid	114	137	94	135
Glutamic acid	158	153	136	163
Lysine	105	38	68	90

[a] Determined by GLC.

[b] Molar ratio relative to ratio of *N*-acetylgalactosamine=2.0; for F6B-V, relative to ratio of mannose=1.8. +=present; NQ=quantitative determination not performed; ND=not detected.

[c] Determined colorimetrically (*18*) and by GLC.[f]

[d] Determined by the rhodizonic acid method (*19*).

[e] Percent relative to weight of fraction.

proportion of glucose, i.e., over 60% of the total carbohydrate. Fractions F6B-I, F6B-III, and F6B-V contained sulfate and uronic acid (table 4), the proportion of uronic acid being the highest and that of sulfate being the lowest in fraction F6B-V. The presence of glycogen in F100-I and F6B-I was suggested by the characteristic mahogany color observed under the microscope after addition of Lugol's iodine reagent; it was further indicated by treatment of both fractions with α-amylase, followed by the determination of the D-glucose liberated with glucose oxidase, according to the method of Dahlqvist (*33*). Control samples of both fractions were treated under identical conditions but without the addition of α-amylase; no free D-glucose was detected in the samples.

D-Glucose was identified in all material obtained from the cell surface, although the relative amounts of this sugar differed widely in the various samples. D-Glucose is not a constitutent of most glycoproteins, although it has been found as an integral part of a few glycoproteins (*34–36*) and of glycopeptides isolated from the membranes of rat liver mitochondria (*37*). However, in the high-molecular-weight fractions from both the Biogel P-100 and Sepharose 6B columns, the large quantities of glucose observed seem to arise from a glucose polymer, possibly glycogen, which might have accumulated on the cell membrane as a result of the growth conditions of the cells and the high glucose content of the medium used (*38*). However, a high-molecular-weight glucose polymer that appears to be a metabolically stable form of glycogen or limit-dextrin has recently been found in rat brain glycopeptide preparations (*39*). Removal of the glucose polymer before fractionation was not possible.

The proportions of uronic acid in the various column fractions (tables 2–4) correspond to the sum of the values obtained by the colorimetric method (*18*) (found to be more sensitive for free uronic acid than the determination by GLC) and the values obtained by GLC of uronic acid derivatives, possibly in the forms of an iduronolactone (T_R 0.83; Walker-Nasir E, Reinhold VN, Jeanloz RW: Unpublished results) and uronic acid-containing oligosaccharides. These oligosaccharides, which did not react in the colorimetric procedure (*18*), were present in small amounts in many column fractions because of the unusual resistance of the D-glucuronic acid glycosidic linkages to acid-catalyzed hydrolysis. By subjection of the materials to two cycles of methanolysis (*see* "Materials and Methods"), the release of free uronic acid was increased, but arabinose (T_R 0.56) arising from decarboxylation of glucuronic acid was also formed in a large amount; a peak at T_R 1.27 (unidentified 2-amino-2-deoxyhexose) was also observed. Under the methanolysis conditions used in the present study, only a trace amount of arabinose was observed on the chromatograms of all the fractions described, except for F6B-II. In fraction F6B-V, a uronic acid disaccharide represented the major component; peaks corresponding to uronic acid-containing oligosaccharides were also observed on the chromatogram. These components might have arisen from hyaluronic acid, which appears to represent the preponderant glycosaminoglycan in this fraction (*see* table 4) and which is rather resistant to methanolysis (*40*).

The uronic acids present in fraction F6B-I, as well as in F100-III, were identified as described in "Materials and Methods." A net increase in the size of the glucose peak on GLC (T_R 0.90), observed after reduction with sodium borodeuteride, and deuterium incorporation into that particular hexose (*m/z* 233, 135, 119, 105, and 91) established the presence of glucuronic acid as the major uronic acid in the original, surface-associated glycosaminoglycans. Deuterium was also incorporated into another hexose, which was observed as a minor peak in the chromatogram after reduction; this sugar was tentatively identified (GLC–MS) as idose (T_R 0.95; *m/z* 233, 135, 119, 105, and 91), indicating the presence of iduronic acid (arising from the iduronolactone derivative, T_R 0.83) as the second uronic acid at the surface of the MDA-MB-231 cell. Additional evidence for the presence of iduronic acid was obtained by the identification (GLC–MS) of a small proportion of 1,6-anhydro-[^{2}H]idose (T_R 0.80; *m/z* 307, 135, 131, 119, 105, and 91). No other deuterated carbohydrate component was found. Peaks probably corresponding to arabinose, xylose, gluco-4,5-enepyranosyluronic acid, an unidentified hexosamine, and reduced *N*-acetylneuraminic acid derivatives were also observed on the chromatogram.

Fraction F6B-II consisted of glycopeptides only and showed the highest values for total carbohydrates and amino acids, as well as the highest proportions of both serine and threonine; the values for aspartic acid and glutamic acid were also high. The yield of this purified glycopeptide fraction from the crude, high-molecular-weight glycopeptide fraction (F100-II) was about 10–15%, and it accounted for about 0.75% of the total cell surface glycoprotein material released by mild proteolysis. Fraction F6B-V contained neutral sugars, *N*-acetylglucosamine, and uronic acid; no sialic acid, *N*-acetylgalactosamine, or proline was detected, and only a minor amount of threonine was observed (GLC). On SDS–PAGE, fraction F6B-V did not enter the gel and gave a single, narrow band at the origin, which was stained with Coomassie blue. The molecular weight of this fraction may be estimated superior to 100,000.

V. graminea Lectin Adsorption Experiments

In experiments performed with intact, suspension-grown, washed tumor cells from two passage numbers, no adsorption was observed, suggesting that these cells do not have exposed *V. graminea* receptors on their surface.

Determination of Inhibitory Activity Against Hemagglutination by *A. hypogaea* (Peanut) Lectin

Fraction F6B-II completely inhibited the agglutination of neuraminidase-treated erythrocytes with peanut lectin at a concentration of 2.5 µg/ml, whereas fraction F6B-III completely inhibited the agglutination at 20 µg/ml. Fractions F6B-I and F6B-V showed no inhibitory activity. These data suggest that both fractions F6B-II and F6B-III contain receptors for peanut lectin, fraction F6B-II possessing a much stronger inhibitory activity than fraction F6B-III.

Antiserum Adsorptions

In these experiments (*see* table 5), no reactivity was observed with NHS (negative control) antiserum, indicating that the adsorption procedure used released no lymphocytotoxins. Experiments with GLO-2 alloantiserum (having HLA-A1 specificity) clearly showed that the adsorption procedure did not remove antibody in a nonspecific way. (HLA-A1 is not expressed on the cell surface of the adsorbing cell line.)

All the cells tested, suspension- and monolayer-grown, viable as well as lyophilized, consistently adsorbed a large amount of HLA-A2 antiserum, even at the lowest concentration of cells, i.e., 10^5 cells. The data also indicate that slightly more HLA-A2 antigen is present on the viable than on the lyophilized cells. The results of the experiment performed with the HLA-B8 antiserum are less clear, but nevertheless they seem to indicate that HLA-B8 is weakly expressed on the cells tested, possibly in a slightly higher concentration or site density on the viable than on the lyophilized cells.

Identification of *O*-Glycosyl-Linked Carbohydrate Chains

Carbohydrate chains containing tritium-labeled terminal galactose and 2-acetamido-2-deoxygalactose residues were tentatively identified by comparison of their effluent volumes with those of labeled authentic monosaccharides and disaccharides. No detectable amounts of chains longer than two residues appeared to be released from fraction F6B-II or F6B-V, as shown in text-figure 3. Fraction F6B-III gave peaks that corresponded to those of both authentic samples, 2-acetamido-2-deoxy-3-*O*-*β*-D-galactopyranosyl-D-galactitol and 2-acetamido-2-deoxy-D-galactitol. Two additional peaks appeared, however, in the region where the reduced disaccharide was expected. The identity of the two (possibly three) reduced oligosaccharides has not been established. No additional peak appeared after treatment of fraction F6B-III with *V. cholerae* neuraminidase (*15*) prior to labeling and cleavage from the macromolecule. Indeed, a shoulder present in the elution profile of the untreated material disappeared after treatment with the enzyme. Fraction F6B-III as well as fractions F6B-II and F6B-V exhibited a prominent peak that corresponded to that of 2-acetamido-2-deoxy-D-galactitol. Fraction F6B-V appeared to possess a small amount of labeled disaccharide material, but this peak

TABLE 5.—*Adsorption*[a] *of lymphocytotoxic HLA alloantibody by intact and lyophilized suspension- and monolayer-grown MDA-MB-231 cells*

HLA antiserum (specificity)	Adsorbing cell concentration	Percent cytotoxicity in cell state[b]							
		S		SL		M		ML	
		LD A	LD B	LD A	LD B	LD A	LD B	LD A	LD B
MGH No. 29 (HLA-A2)	0	100	100						
	10^5	20	10	20	10	20	10	100	100
	10^6	20	20	20	20	10	20	10	10
	10^7	20	10	10	10	10	10	10	10
CW-2/2 (HLA-B8)	0	100	100						
	10^5	40	40	100	60	100	60	60	60
	10^6	60	20	60	40	60	20	60	60
	10^7	40	40	60		60	20	60	60
GLO-2 (HLA-A1)	0	100	100						
	10^5	40	60	60	60	40	60	60	60
	10^6	60	60	100	60	100	60	60	100
	10^7	40	60	100	100	40	40	100	100

[a] *See* "Materials and Methods" for details.

[b] MDA-MB-231 cell state: S=suspension, viable; SL=suspension, lyophilized; M=monolayer, viable; ML=monolayer, lyophilized. LD=lymphocyte donor: A=HLA-A1, 2; B8, w21; C−. B=HLA-A1, 2; B8, 17; C−.

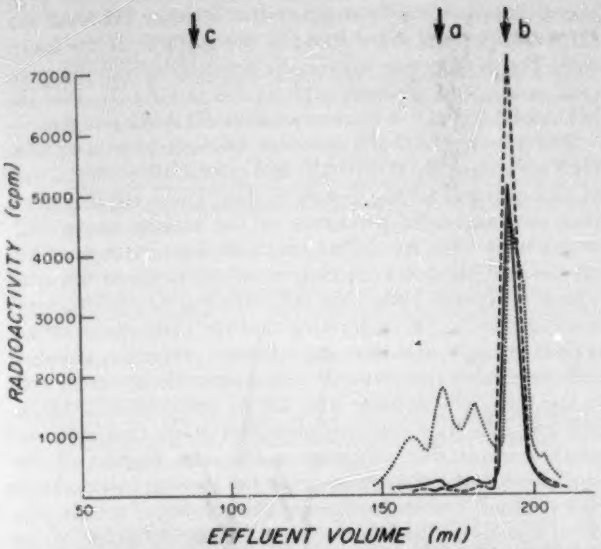

TEXT-FIGURE 3.—Fractionation on a column of Biogel P-2 of tritium-labeled, reduced oligosaccharides cleaved from glycopeptides by alkaline borohydride reduction. Eluent: 0.1 *M* pyridine acetate (pH 5.3). Tritium (cpm) in products derived from F6B-II (-----), F6B-III (····), and F6B-V (——) was plotted against the effluent volume. Authentic standards were a) 2-acetamido-2-deoxy-3-*O*-β-D-galactopyranosyl-D-galactitol, b) 2-acetamido-2-deoxy-D-galactitol, and c) α_1-acid glycoprotein.

was missing in the elution profile of fraction F6B-II, which indicated the release of a chain of only one residue.

DISCUSSION

In an attempt to relate the metastatic properties of the human mammary ductal carcinoma MDA-MB-231 cell line to the concentration and type of carbohydrate-containing macromolecules at the cell surface, we discovered several types of structures previously found to be associated with cancer in general and metastasis in particular on the surfaces of these cells. The presence of an unusually high concentration of sialic acid (1.2×10^9 residues/cell) would result in a large net negative charge on these cells (*41*). It has been suggested that the charge from sialic acid at the cell surface may be responsible for allotransplantability in mouse ascites cells (*42*). Furthermore, sialic acid has been shown to prevent tumor rejection by masking antigen sites on the cell surface (*43*).

These investigations confirmed the findings of other workers (*44*) that high concentrations of glycosaminoglycans are present at the surfaces of these cells grown in culture. Indeed, uronic acids and sulfate groups, resulting from the cleavage of cell-associated glycosaminoglycuronans by mild proteolysis, were identified in the major column fractions (with the exception of fraction F6B-II), in addition to glycopeptide components (tables 3, 4). The presence of heparan sulfate at the surface of the MDA-MB-231 cell has been described (*44*). The high content of sulfate and the high molar ratio (almost 2:1) of sulfate to uronic acid in fraction F100-I (*see* table 3) are possibly due to a disulfated disaccharide structure in this material. The possible presence of sulfated glycoprotein fragments in fractions F100-I and F100-III must also be considered. In any case, the unusually high sulfate content in some of these fractions probably reflects a complex array of sulfated glycoproteins and glycosaminoglycans at the MDA-MB-231 cell surface. Although the role(s) of such substances as heparan sulfate at the cell surface of tumor cells is not understood (*45*), shielding of cell surface receptors has been suggested (*46*). A role for hyaluronic acid in masking cell surface antigens in a variety of mouse fibrosarcoma and carcinoma cells has recently been suggested (*47*).

The presence of glycoproteins containing *O*-glycosyl-linked carbohydrate chains at the surfaces of MDA-MB-231 cells was first suggested by the carbohydrate and amino acid compositions of isolated glycopeptide fractions (table 4). The proportion of *N*-acetylgalactosamine in fractions F6B-II and F6B-III is higher than that reported for other types of cell surface glycopeptides (*48, 49*). The presence of *N*-acetylgalactosamine as well as galactose in fractions F6B-I, F6B-II, and F6B-III indicates the occurrence of *O*-glycosyl-linked chains at the surfaces of these cells. The proportion of serine and threonine is likewise high, especially in fraction F6B-II, which was obtained from the crude, high-molecular-weight material in 10–15% yield, and thus appears to represent the major glycopeptide fraction of these cells. In this fraction these two residues represent 31% of the amino acids, and the carbohydrate content represents 53% of the weight of the material. In addition to sialic acid, *N*-acetylgalactosamine, and galactose, this fraction contained *N*-acetylglucosamine, mannose, and glucose; the proportion of aspartic acid was also high. These data suggest the presence of both *N*- and *O*-glycosyl-linked oligosaccharides in the glycoprotein molecules. The hemagglutination inhibition studies indicate that in fraction F6B-II *O*-glycopeptides are preponderant or that they are exposed (*50*). Fractions F6B-I, F6B-III, and F6B-V probably contain mixtures of both *N*- and *O*-linked carbohydrate chains as well as glycosaminoglycans. These components have been found at the surface of Ehrlich ascites carcinoma (*41, 51*), hepatoma ascites (*49, 50, 52*), and melanoma cells (*53*). The major glycoprotein fraction from the plasma membranes of AH-66 rat hepatoma cells was reported (*52*) to contain both *O*- and *N*-glycopeptides having related chemical composition, in analogy with our findings.

Consistent with the presence of short *O*-glycosyl-linked chains was the capacity of both fractions F6B-II and F6B-III to inhibit the agglutination of neuraminidase-treated human erythrocytes by peanut lectin. It has been suggested that the receptor for this lectin in macromolecules is the serine- or threonine-linked disaccharide β-D-Gal*p*-(1→3)-D-GalNAc (*54*). This structure is similar to that proposed for the Thomsen-Friedenreich antigen, which is reported to be the carbohydrate precursor of both M- and N-blood group substances (*55*). It has been reported (*56, 57*) that this structure is associated with human malignant, but not benign, mammary tumors, and its detection by a tuberculin-like skin test has been used as a diagnostic test for human breast cancer (*58*). However, recent observations (*59, 60*) point to a more complex interpretation, and possibly the antigenic specificity of the disaccharide is strongly affected by the amino acid sequence adjacent to the site of chain attachment.

The presence of *O*-glycosyl chains in isolated glycopeptide fractions (table 4) was confirmed by the use of labeling techniques (text-fig. 3). The terminal galactose residues of the intact glycopeptides were labeled with tritium by galactose-oxidase treatment, followed by reduction of the 6-aldehyde group with sodium borotritide (*61*). Cleavage of the *O*-glycosyl chains under reductive conditions was followed by gel-filtration fractionation (text-fig. 3). Only fraction F6B-III, which demonstrated weak hemagglutination-inhibitory activity, showed a major peak corresponding to that of a standard sample of the reduced disaccharide. A second peak, corresponding to that of authentic *N*-acetylgalactosaminitol, was also obtained from this fraction. Surprisingly, fraction F6B-II, which had the highest inhibitory activity in the peanut-lectin experiment, gave only this peak. Fraction F6B-V, which demonstrated no inhibitory activity, showed a major monosaccharide and a minor disaccharide peak. These seemingly contradictory results may be explained either by failure of the alkaline borohydride reduction to release the disaccharide or by failure of investigators to recognize that the *N*-acetylhexosamine itself may serve as a receptor for the lectin in macromolecules (*62*).

It is somewhat surprising that *O*-glycoproteins should represent important cell surface components of the MDA-MB-231 cell line after a prolonged period in culture (95 passages), since it has been shown (*42*) that the environment in which a cell line grows is essential for the biosynthesis of some surface components. Thus the large, endogenous glycoprotein epiglycanin of the TA3-Ha mammary carcinoma cell of the strain A mouse is hardly detectable after several weeks in suspension culture (*63*), whereas it represents the major surface component when the cell is grown in the ascites form. A similar observation has been made in the case of the 13762 rat mammary adenocarcinoma (*64*). Attempts have been made to grow the MDA-MB-231 cells in the ascites form in the nude (*nu/nu*) mouse (Walker-Nasir E, Codington JF, Jeanloz RW: Manuscript in preparation) to observe the formation of the surface glycoproteins under these conditions; it was found, however, that this cell line, like most human carcinoma cell lines reported (*65*), does not grow as an ascites tumor. In spite of the in vitro suspension culture conditions used in the present study, glycopeptides with *O*-glycosyl carbohydrate chains were isolated from the surfaces of these cells; it seems possible that these glycopeptides represent major surface components in the original carcinoma from human metastatic cells.

The HLA antigens of the MDA-MB-231 cell line were reported (*31*) as HLA-A2, HLA-B8, and HLA-W14. Previous observations, made in this laboratory, had demonstrated that the adsorptive capacity of the non-strain-specific, murine TA3-Ha cells for anti-H-2^a antibody was increased manyfold by disruption of the cell surface by lyophilization. This effect is probably due to unmasking of H-2^a antigens at the cell surface (*66*). It was of interest, therefore, to test this hypothesis in human tumor cells by the use of antisera specific for the reported HLA-A and HLA-B determinants of the aforementioned line. The observation that the adsorptive capacity in intact and lyophilized cells did not differ significantly suggests that neither HLA-A2 nor HLA-B8 antigens are masked at the surfaces of the intact cells. The data further suggest the possibility, from the quasi total removal of antibody with as few as 10^5 cells, that the MDA-MB-231 cell is homozygous for HLA-A2 antigens.

The presence of *O*-glycoproteins has been associated with both allotransplantability (*67*) and metastatic potential (*64*) in experimental tumors grown in vivo. The possibility exists that the metastatic properties of the human tumor cells might have been lost in culture, and the results described here would then not necessarily relate to those obtained with the original cancer cells. According to data from several investigators (*1, 68*) suggesting that the property of metastasis is intrinsic and that the inherent properties of tumor cells determine the metastatic character of the tumor cells in the host, it is possible that the in vitro cultured MDA-MB-231 cells have retained their metastatic character and would exhibit this property in vivo. In support of this hypothesis is the observation that the in vitro cultured cells had retained the characteristics (morphology, growth pattern, karyotype, and histocompatibility antigens) of the original tumor cells isolated from the pleural effusion (*5*).

An ideal situation would, of course, involve a comparison of primary and metastatic tumors of the same cell types. The difficulties inherent in such a study with human material are, however, obvious. Large quantities of cells from an established and stable line, derived from the original metastatic cells, would be required, and no reliable method for the determination of the metastatic character of the established line is available.

Although it seems possible that the presence of *O*-glycoproteins is associated with the metastatic character of the MDA-MB-231 tumor cells, several other factors, including those discussed in this report (i.e., high sialic acid and glycosaminoglycan concentrations), may play a role in this phenomenon. The complex process of metastasis may be accompanied by other events that might vary with each type of cell or tumor and with the environmental circumstances of the cell itself.

REFERENCES

(*1*) Kim U, Baumler A, Carruthers C, Bielat K. Immunological escape mechanism in spontaneously metastasizing mammary tumors. Proc Natl Acad Sci USA 1975; 72:1012-1016.

(*2*) Codington JF. Masking of cell-surface antigens by ectoglycoproteins. In: Walborg EF Jr, ed. Glycoproteins and glycolipids in disease processes. Washington, D.C.: Am Chem Soc, symposium series No. 80, 1978:277-294.

(*3*) Carraway K, Huggins JW, Sherblom AP, et al. Membrane glycoproteins of rat mammary gland and its metastasizing and nonmetastasizing tumors. In: Walborg EF Jr, ed. Glycoproteins and glycolipids in disease processes. Washington, D.C.: Am Chem Soc, symposium series No. 80, 1978:432-445.

(*4*) Cooper A, Morgello S, Miller D, Brown M. Role of surface glycoproteins in tumor growth. In: Day SB, Myers WP, Stansly P, Garattini S, Lewis MG, eds. Cancer invasion and metastasis: Biological mechanisms and therapy. New York: Raven Press, 1977:49-64.

(*5*) Cailleau R, Young R, Olivé M, Reeves WJ Jr. Breast tumor cell lines from pleural effusions. J Natl Cancer Inst 1974; 53:661-674.

(*6*) Cailleau RM. Old and new problems in human tumor cell cultivation. In: Fogh J, ed. Human tumor cells in vitro. New York: Plenum Press, 1975:79-114.

(7) Beall PT, Asch BB, Hazlewood CF. NMR relaxation times of water in human cancer cell lines: Correlation with cytoskeletal structures. J Cell Biol 1977; 75:274a.

(8) Codington JF. Masking of cell surface antigens on cancer cells. In: Cellular membranes and tumor cell behavior. Baltimore: Williams & Wilkins, 1975:395-419.

(9) Sherblom AP, Buck RL, Carraway KL. Purification of the major sialoglycoproteins of 13762 MAT-B1 and MAT-C1 rat ascites mammary adenocarcinoma cells by density gradient centrifugation in cesium chloride and guanidine hydrochloride. J Biol Chem 1980; 255:783-790.

(10) Springer GF, Desai PR, Murthy MS, Scanlon EF. Human carcinoma-associated precursors of the blood group MN antigens. In: Walborg EF Jr, ed. Glycoproteins and glycolipids in disease processes. Washington, D.C.: Am Chem Soc, symposium series No. 80, 1978:311-325.

(11) Springer GF, Desai PR, Murthy MS, Yang HJ, Scanlon EF. Precursors of the blood group MN antigens as human carcinoma-associated antigens. Transfusion 1979; 19:233-249.

(12) Phillips HJ. Dye exclusion test for cell viability. In: Kruse PE Jr, Patterson MK, eds. Tissue culture. Methods and applications. New York: Academic Press, 1973;406-408.

(13) Codington JF, Sanford BH, Jeanloz RW. Glycoprotein coat of the TA3 cell. Isolation and partial characterization of a sialic acid-containing glycoprotein fraction. Biochemistry 1972; 11:2559-2564.

(14) Warren L. The thiobarbituric acid assay of sialic acids. J Biol Chem 1959; 234:1971-1975.

(15) Codington JF, Linsley KB, Silber C. Removal of sialic aids from glycoproteins by chemical methods and determination of sialic acids. Methods Carbohydr Chem 1976; 7:226-232.

(16) Lowry OH, Rosebrough NJ, Farr AL, Randall RJ. Protein measurement with the Folin phenol reagent. J Biol Chem 1951; 193:265-275.

(17) Dubois MF, Gilles KA, Hamilton JK, Rebers PA, Smith F. Colorimetric method for determination of sugars. Anal Chem 1956; 28:350-356.

(18) Blumenkrantz N, Asboe-Hansen G. New method for quantitative determination of uronic acids. Anal Biochem 1973; 54:484-489.

(19) Waheed A, Van Etten RL. A spectrophotometric determination of sulfate ion and its application in studies of substrate purity and of aryl sulfatase A kinetics. Anal Biochem 1978; 89:550-560.

(20) Reinhold VN. Gas-liquid chromatographic analysis of constituent carbohydrates in glycoproteins. Methods Enzymol 1972; 25:244-249.

(21) Zumwalt RW, Kuo K, Gehrke CW. A nanogram and picogram method for amino acid analysis by gas-liquid chromatography. J Chromatogr 1971; 57:193-208.

(22) Nash TE, Nasir-ud-Din, Jeanloz RW. Further purification and characterization of a circulating antigen in schistosomiasis. J Immunol 1977; 119:1627-1633.

(23) Laemmli UK. Cleavage of structural proteins during the assembly of the head of bacteriophage T4. Nature 1970; 227:680-685.

(24) Codington JF, Sanford BH, Jeanloz RW. Glycoprotein coat of the TA$_3$ cell. I. Removal of carbohydrate and protein material from viable cells. J Natl Cancer Inst 1970; 45:637-647.

(25) Codington JF, Linsley KB, Jeanloz RW, Irimura T, Osawa T. Immunochemical and chemical investigations of the structure of glycoprotein fragments obtained from epiglycanin, a glycoprotein at the surface of the TA3-Ha cancer cell. Carbohydr Res 1975; 40:171-182.

(26) Cooper AG, Codington JF, Miller DK, Brown MC. Loss of strain specificity of the TA3-St subline: Evidence for the role of epiglycanin in mouse allogeneic tumor growth. JNCI 1979; 63:163-169.

(27) Cooper AG, Codington JF, Brown MC. In vivo release of glycoprotein I from the Ha subline of TA3 murine tumor into ascites fluid and serum. Proc Natl Acad Sci USA 1974; 71:1224-1228.

(28) Osawa T, Terao T, Kawaguchi T, Fukuda M, Toyoshima S, Irimura T. Some problems in the application of phytohemagglutinins to the structural studies of complex carbohydrates. Colloq Int Cent Nat Rech Sci 1974; 221:765-776.

(29) Ray JG, Hare DB, Pedersen PD, Mullally DI. NIAID manual of tissue typing techniques. Washington, D.C.: Govt Print Off, 1976:22 [DHEW publication No. (NIH)76-545].

(30) Amos DB. In: Ray JG, Hare DB, Pedersen PD, Mullally DI, eds. NIAID manual of tissue typing techniques. Washington, D.C.: Govt Print Off, 1976:25 [DHEW publication No. (NIH)76-543].

(31) EG&G Mason Research Institute. MDA-MB-231 cell line summary sheet. Rockville, Md.: EG&G Mason Research Inst, 1976.

(32) Van Den Eijnden DH, Evans NA, Codington JF, Reinhold VN, Silber C, Jeanloz RW. Chemical structure of epiglycanin, the major glycoprotein of the TA3-Ha ascites cell. J Biol Chem 1979; 254:12,153-12,159.

(33) Dahlqvist A. Assay of intestinal disaccharidases. Anal Biochem 1968; 22:99-107.

(34) Radhakrishnamurthy B, Fishkin AF, Berenson GS. A glucose-containing glycopeptide from bovine aorta glycoprotein. Biochim Biophys Acta 1965; 101:127-129.

(35) Wagh PV, Roberts BI. Purification and characterization of a glycoprotein from the intimal region of porcine aorta. Biochemistry 1972; 11:4222-4227.

(36) Cynkin MA, Knowlton M. Studies on the carbohydrate components of ferritin. In: Brown EB, ed. Proteins of iron metabolism. New York: Grune, 1977:115-120.

(37) Itoh N, Kawasaki T, Yamashina I. Isolation and characterization of glycopeptides from rat liver mitochondria. J Biochem (Tokyo) 1974; 76:459-466.

(38) Racker E, Wu R, Alpers JB. Carbohydrate metabolism in ascites tumor and HeLa cells. In: Edsall JT, ed. Amino acids, proteins and cancer biochemistry. New York: Academic Press, 1960:175-189.

(39) Margolis RK, Margolis RU. Structure and distribution of glycoproteins and glycosaminoglycans. In: Margolis RU, Margolis RK, eds. Complex carbohydrates of nervous tissue. New York: Plenum Press, 1979:45-73.

(40) Jeanloz RW, Jeanloz DA. The degradation of hyaluronic acid by methanolysis. Biochemistry 1964; 3:121-123.

(41) Langley OK, Ambrose EJ. The linkage of sialic acid in the Ehrlich ascites-carcinoma cell surface membrane. Biochem J 1967; 102:367-372.

(42) Jeanloz RW, Codington JF. The biological role of sialic acid at the surface of the cell. In: Rosenberg A, Schengrund C-L. Biological roles of sialic acid. New York: Plenum Press, 1976:201-238.

(43) Codington JF. The masking of cancer cell surface antigens. In: Waters H, ed. The handbook of cancer immunology. Vol 8. Tumor antigens: Structure and function. New York and London: Garland, 1981:171-203.

(44) Chandrasekaran EV, Davidson EA. Glycosaminoglycans of normal and malignant cultured human mammary cells. Cancer Res 1979; 39:870-880.

(45) Lindahl U, Höök M. Glycosaminoglycans and their binding to biological macromolecules. Annu Rev Biochem 1978; 47:385-417.

(46) Kraemer PM, Smith DA. High molecular-weight heparan sulfate from the cell surface. Biochem Biophys Res Commun 1974; 56:423-430.

(47) McBride WH, Bard JB. Hyaluronidase-sensitive halos around adherent cells. Their role in blocking lymphocyte-mediated cytolysis. J Exp Med 1979; 149:507-515.

(48) Shen L, Ginsburg V. Release of sugars from HeLa cells by trypsin. In: Manson LA, ed. Biological properties of the mammalian surface membrane. Philadelphia: Wistar Inst, monograph No. 8, 1968:67-71.

(49) Walborg EF, Lantz RS, Wray VP. Isolation and chemical characterization of a cell-surface sialoglycopeptide fraction from Novikoff ascites cells. Cancer Res 1969; 29:2034-2038.

(50) Funakoshi I, Nakada H, Yamashina I. The isolation and characterization of glycopeptides from plasma membranes of an ascites hepatoma, AH 66. J Biochem (Tokyo) 1974; 76:319-333.

(51) Molnar J, Teegarden DW, Winzler RJ. The biosynthesis of glycoproteins. VI. Production of extracellular radioactive macromolecules by Ehrlich ascites carcinoma cells during incubation with glucosamine-^{14}C. Cancer Res 1965; 25:1860-1866.

(52) Nakajo S, Nakaya K, Nakamura Y. Isolation and partial characterization of the major glycoprotein from the plasma membranes of AH-66 hepatoma cells. Biochim Biophys Acta 1979; 579:88-94.

(53) Bhavanandan VP, Umemoto J, Banks JR, Davidson EA. Isolation and partial characterization of sialoglycopeptides produced by a murine melanoma. Biochemistry 1977; 16:4426-4437.

(*54*) Goldstein IJ, Hayes CE. The lectins: Carbohydrate-binding proteins of plants and animals. Adv Carbohydr Chem Biochem 1978; 35:127–340.

(*55*) Vaith P, Uhlenbruck G. The Thomsen agglutination phenomenon: A discovery revisited 50 years later. Z Immunitaetsforsch Immunobiol [Suppl] 1978; 154:1–14.

(*56*) Springer GF, Desai PR, Banatwala I. Blood group MN specific substances and precursors in normal and malignant human breast tissues. Naturwissenschaften 1974; 61:457.

(*57*) Springer GF, Desai PR, Murthy MS, Tegtmeyer H, Scanlon EF. Human carcinoma-associated precursor antigens in the blood group MN system and the host's immune response to them. Prog Allergy 1979; 26:42–96.

(*58*) Springer GF, Desai PR, Yang HJ, Murthy MS. Carcinoma-associated blood group MN precursor antigens against which all humans possess antibodies. Clin Immunol Immunopathol 1977; 7:426–441.

(*59*) Newman RA, Klein PJ, Uhlenbruck G, Citoler P, Karduck D. The presence and significance of the Thomsen-Friedenreich antigen in breast cancer. I. Serological studies. J Cancer Res Clin Oncol 1979; 93:181–188.

(*60*) Klein PJ, Newman RA, Müller P, et al. The presence and significance of the Thomsen-Friedenreich antigen in mammary gland. II. Its topochemistry in normal, hyperplastic and carcinoma tissue of the breast. J Cancer Res Clin Oncol 1979; 93:205–214.

(*61*) Gahmberg CG, Hakomori S. External labeling of cell surface galactose and galactosamine in glycolipid and glycoprotein of human erythrocytes. J Biol Chem 1973; 248:4311–4317.

(*62*) Uhlenbruck G, Pardoe GI, Bird GW. Studies on lectins with a broad agglutination spectrum. II. Studies on the nature of the T-antigen and the specific receptors for the lectin of *Arachis hypogea* (ground-nut). Z Immunitaetsforsch 1969; 138:423–433.

(*63*) Miller DK, Cooper AG, Brown MC, Jeanloz RW. *Brief communication*: Reversible loss in suspension culture of a major cell-surface glycoprotein of the TA3-Ha mouse tumor. J Natl Cancer Inst 1975; 55:1249–1252.

(*64*) Howard SC, Sherblom AP, Chesnut RW, Carothers-Carraway CA, Carraway KL. Changes on expression of a major sialoglycoprotein associated with ascites forms of a mammary adenocarcinoma. Biochim Biophys Acta 1980; 631:79–89.

(*65*) Ueyama Y, Morita K, Yokoyama M, et al. Establishment and maintenance of human malignant tumors serially transplanted to nude mice. In: Nomura T, Ohsawa N, Tamaoki N, Fujiwara K, eds. Proceedings of the second international workshop on nude mice. Stuttgart and New York: Fischer-Verlag, 1977:365–374.

(*66*) Sanford BH, Codington JF, Jeanloz RW, Palmer PD. Transplantability and antigenicity of two sublines of the TA3 tumor. J Immunol 1973; 110:1233–1237.

(*67*) Codington JF, Sanford BH, Jeanloz RW. Cell-surface glycoproteins of two sublines of the TA3 tumor. J Natl Cancer Inst 1973; 51:585–591.

(*68*) Fidler IJ, Gerstein DM, Hart IR. The biology of cancer invasion and metastasis. Adv Cancer Res 1978; 28:149–250.

α_1-Proteinase Inhibitor Production by Human Adenocarcinomas Xenotransplanted Into Nude Mice[1,2,3]

Dorothy Lee,[4,5] **Dan Shochat,**[6] *and* **David V. Gold**[6]

ABSTRACT—Human colon adenocarcinomas xenotransplanted into BALB/c nude mice were examined for the ectopic synthesis of α_1-proteinase inhibitor(s) (α_1Pi). Tumor extracts were prepared by homogenization followed by molecular sieve chromatography on Sepharose 4B. Fractions with immunoreactive α_1Pi were concentrated and adsorbed onto a concanavalin A-Sepharose 4B affinity column, then eluted, concentrated, and analyzed. All 4 colon tumors examined produced α_1Pi with full antigenic identity to normal human plasma α_1Pi. Electrophoretic mobilities of 3 of the tumor-derived α_1Pi were different from the electrophoretic mobility of the normal human plasma α_1Pi. Activities of the inhibitors were determined by the reaction of each tumor extract with pancreatic elastase (PE) followed by immunoelectrophoresis of the reaction mixture against both anti-human α_1Pi and anti-PE antisera. Two of the tumor-derived α_1Pi examined were active in inhibiting PE. —JNCI 1982; 69:381–385.

The suggestion has been made that tumor cell proteinases may facilitate invasion of host tissues by the malignant tumor (*1*). In support of this suggestion are the many observations of increased levels of proteinases capable of digesting connective tissue matrix components within the tumor environment. High concentrations of plasminogen activators were shown to be produced by a number of different transformed cell lines (*2–4*). Increased cathepsin-B activity in malignant tumors as compared to the activity in benign tumors has been correlated with increased metastatic potential (*5, 6*). Liotta et al. (*7*) described the production of a specific basement membrane type IV collagenase by a metastatic tumor.

As a consequence of these studies, interest has arisen in regard to the distribution of Pi in tumors. Maintenance of a balance between proteinases and Pi within the tumor cell microenvironment may be critical in tumor growth regulation. The major serum Pi (α_1Pi) has been found associated with tumors. Yoshimura et al. (*8*) reported the synthesis of α_1Pi by yolk sac, hepatoblastoma, renal cell, and colon carcinomas xenotransplanted into nude mice. Later, Akatsuka et al. (*9*) confirmed these findings by immuno-electron microscopic localization of the α_1Pi in the endoplasmic reticulum and Golgi apparatus. In the present study we have isolated α_1Pi produced by human colon carcinomas xenotransplanted into nude mice and examined their antiproteinase activities and immunochemical properties.

MATERIALS AND METHODS

Tumors.—Human colon carcinomas xenotransplanted into nude mice were supplied by Dr. D. Dexter (Roger Williams General Hospital, Providence, R.I.). The tumors were transferred in nude BALB/c mice for at least 15, but not more than 30 generations. Tumors were transferred when they approximated 1×1×1.5 cm in size. The tumors were carefully excised, cleaned of obvious connective tissues, and minced into 1- to 2-mm cubes. A 25% suspension was prepared with Hanks' balanced salt solution, and 0.5 ml of this suspension was injected sc into the backs of the mice. Generation time for each of the tumors was about 3–4 weeks. DLD-1 was a poorly to moderately differentiated adenocarcinoma. Clone A and clone D were derived from DLD-1 by the soft agar method. Clone A was aneuploid, whereas clone D was diploid. DLD-2 was a moderately differentiated adenocarcinoma. The in vitro characteristics of the cell lines were described in (*10*).

Partial purification of α_1Pi from the tumors.—The tumors (2 g) were washed with cold deionized water, minced into 1- to 2-mm cubes, and then homogenized with 0.1 M NH_4HCO_3 containing 0.5 M NaCl (5 ml/g wet weight of tissue) in a homogenizing chamber (Omnimixer; Ivan Sorvall Inc., Norwalk, Conn.) at high speed for 2 minutes while on ice. The homogenate was centrifuged at 48,000×*g* for 30 minutes, the supernatant was collected, and 10-ml aliquots were chromatographed on a Sepharose 4B column (2.5×100 cm), equilibrated, and eluted with the same buffer. The column was previously calibrated with normal human serum to determine the elution volume of α_1Pi. The fractions within the α_1Pi region were pooled and concentrated by ultrafiltration (PM10 membranes; Amicon Corp., Lexington, Mass.) to about twice the size of the starting volume. This material was dialyzed against 1 liter of deionized water and then two changes of 2 liters of 0.1 M sodium acetate buffer (pH 6.0) containing 0.15 M NaCl and 0.001 M each of $CaCl_2$, $MgCl_2$, and $MnCl_2$. The dialyzed material was applied to a Sepharose-Con A (Pharmacia, Piscataway, N.J.) column 2.5×10 cm, equilibrated, and eluted with the same buffer. The attached fraction was desorbed with 0.2 M α-methylglucoside prepared in the buffer. The partially purified α_1Pi was dialyzed against several changes of 0.5 M NH_4HCO_3 and

---

ABBREVIATIONS USED: α_1Pi=α1-proteinase inhibitor(s); Con A=concanavalin A; PE=pancreatic elastase; Pi=proteinase inhibitor(s).

---

[1] Received October 15, 1981; revised February 5, 1982; accepted March 17, 1982.

[2] Supported by Public Health Service (PHS) grants GM-14262 and GM-24481-05 from the National Institute of General Medical Sciences, PHS grant R26CA-29489 from the National Cancer Institute (NCI), and PHS contract 1CB-84259-31 from the Division of Cancer Biology and Diagnosis, NCI.

[3] Animals were maintained under the guidelines set forth by the University of Kentucky.

[4] Department of Pathology, Health Sciences Center, State University of New York at Stony Brook, Stony Brook, N.Y. 11794.

[5] *Present address:* Department of Dermatology, New York University Medical Center, Rm. 831, 455 First Ave., New York, N.Y. 10016.

[6] Division of Experimental Pathology, Department of Pathology, University of Kentucky Medical Center, Lexington, Ky. 40536.

lyophilized. The lyophilized preparation was redissolved with a minimum amount of buffer (100–200 μl) and was used for further study.

Analytic procedures.—Immunodiffusion, immunoelectrophoresis, and rocket immunoelectrophoresis were performed according to the methods of Ouchterlony (*11*), Grabar and Williams (*12*), and Laurell (*13*), respectively. Normal human serum was employed as a standard. Purified mouse α_1Pi was from Dr. S. K. Chan (University of Kentucky, Lexington). Rabbit anti-α_1Pi was obtained from Dako through Accurate Chemical and Scientific Corp., Hicksville, N.Y. The activity of the isolated α_1Pi preparations was demonstrated by their ability to inhibit PE. To 50 μl of the α_1Pi preparation we added 2 μl of a stock solution of porcine PE, 5 μg/μl in 0.07 *M* barbital buffer (pH 8.6; Elastin Products, St. Louis, Mo.), at room temperature for 20 minutes with constant stirring. Samples (10 μl) of the reaction mixture were subjected to immunoelectrophoresis with the simultaneous use of rabbit anti-α_1Pi (Dako) and rabbit anti-porcine PE (provided by Dr. H. Carp and Dr. A. Janoff, State University of New York at Stony Brook). Immunoelectrophoresis was conducted in 0.016 *M* sodium barbital and 0.014 *M* sodium acetate buffer (pH 8.8), with 3 V/cm of agarose gel for 90 minutes at room temperature.

RESULTS

Extracts (1 g tissue/5 ml buffer) of xenotransplanted human colon carcinomas were examined by immunodiffusion for the presence of α_1Pi. A weak precipitin line was noted for the DLD-2 extract, whereas no precipitin lines were observed for the other tumors. The possibility existed that the concentration of α_1Pi in these other tumors was below the detection limit of the method employed. When we attempted to examine a more concentrated sample however, we found that these tumor extracts could not simply be concentrated due to the presence of relatively large quantities of mucin, which formed highly viscous solutions upon concentration. To avoid this difficulty, we performed a semipurification of the α_1Pi by molecular sieve chromatography on a calibrated column to obtain an α_1Pi-containing fraction and a subsequent lectin affinity chromatography on a Con A–Sepharose 4B column. All the α_1Pi antigen-reactive material, as determined by immunodiffusion, was adsorbed to the Con A–lectin column. The desorbed material, after lyophilization and reconstitution, served as our sample for further analyses. The yields of semipurified α_1Pi (quantitated by rocket immunoelectrophoresis with the use of normal human serum as a standard) were 34.5, 70.5, and 49.5 μg/g tissue for DLD-1, DLD-2, and clone D, respectively. The material obtained from clone A was insufficient for this analysis.

Immunodiffusion performed with rabbit anti-human α_1Pi antiserum demonstrated that human plasma and xenotransplanted human colon carcinomas contained immunologically identical α_1Pi (fig. 1). Moreover, when absorbed with tumor-derived α_1Pi preparations, the antiserum lost all its reactivity against the plasma α_1Pi. A mouse plasma fraction that had been prepared in an identical manner did not react with the antiserum in immunodiffusion. In addition, purified mouse α_1Pi (0.5–5 mg/ml) did not react with the antiserum in immunodiffusion. By immunoelectrophoresis we confirmed that the DLD-1-derived α_1Pi had an electrophoretic mobility identical to that of the human plasma α_1Pi, whereas the mobilities of the α_1Pi isolated from DLD-2, clone A, and clone D were slower than the mobility of the plasma inhibitor (fig. 2).

We examined the biologic activities of three of the isolated tumor-derived α_1Pi preparations by testing the abilities of these preparations to form complexes with porcine PE. The α_1Pi concentrations in the preparations used in the experiment were determined by rocket immunoelectrophoresis and were found to be 9.4, 4.6, 6.6, and 17.4 μg/μl for DLD-1, DLD-2, clone D, and the diluted human plasma, respectively. When free, active α_1Pi was allowed to react with porcine PE, an enzyme inhibitor complex was formed that was reactive with both anti-α_1Pi antiserum and anti-PE antiserum. This complex had an electrophoretic mobility intermediate between that of the cathodal PE and anodal α_1Pi (fig. 3). The α_1Pi isolated from DLD-1 and DLD-2 were biologically active, whereas the α_1Pi from clone D was inactive.

DISCUSSION

Several lines of evidence suggest that proteases may play an important role in the tumor–host relationship. Consequently, maintenance of a proper balance between proteases and Pi may be essential in the regulation of tumor growth. Indeed, many synthetic and natural antiproteinases have the ability to retard tumor growth. Active site-alkylating agents such as the chloromethyl ketones *N*-tosyl-L-lysyl chloromethyl ketone and *N*-tosyl-L-phenylalanyl chloromethyl ketone reduced the growth of several transformed mouse and hamster cell lines (*14–16*). These inhibitors as well as the competitive inhibitor tosyl-L-arginyl methyl ester inhibited tumorigenesis in mouse skin (*17, 18*). Leupeptin, antipain, chymostatin, elastatinal, pepstatin, and bestatin have been found in many cases to inhibit the early stages of transformation (*18–21*). Natural antiproteinases such as soybean trypsin inhibitor, beef pancreas trypsin inhibitor, ovomucoid, and Trasylol (aprotinin) have been shown to inhibit the growth of a variety of transformed cell lines (*14, 15, 22*).

Colon epithelium in its normal state is not considered to be a plasma protein-producing organ. Our results, however, show that some colon carcinomas produce a protein which is antigenically identical with plasma α_1Pi of the tumor donor's species (and in some cases is an active Pi). The tumor xenografts that we studied did not secrete sufficient protein to enable its detection in the sera of their hosts, but the inhibitor could be demonstrated in extracts of the tumors.

The observed slower electrophoretic mobility of three of the tumor-derived α_1Pi may indicate the existence of either structural differences between the plasma and the tumor α_1Pi or different Pi phenotypes. Since more than 90% of the general population produce α_1Pi of the Pi MM phenotype (*23*), it would be a rare coincidence to have such a large population of variant Pi phenotypes in such a small sample. It would appear that the first explanation for the variant electrophoretic mobilities of the tumor-derived α_1Pi is more tenable.

Activity of α_1Pi was clearly established in 2 of these tumors, DLD-1 and DLD-2. The inactivity of α_1Pi from clone D may have resulted from prior interaction with proteinases liberated by clone D tumor cells, although the normal electrophoretic mobility of the clone D inhibitor would not be consistent with degraded or complexed α_1Pi. Alternatively, α_1Pi from clone D may have been more susceptible to denaturation during processing. Since human α_1Pi can be inactivated by cell-generated oxygen-free radicals (*24, 25*), clone D cells may be metabolically more active in this regard than DLD-1 or DLD-2 tumor cells. Of course, clone D tumor cells may simply synthesize an inactive form of α_1Pi.

The physiologic significance of antiproteinase production by tumor cells is unknown. Local concentrations of active Pi may be important in modulating tumor proteinases and in this manner affect neoplastic spread. Conversely, because these same antiproteinases also inhibit enzymes released from host leukocytes (some of which participate in immune cytolysis of tumor cells), the production of these antiproteinases may compromise a vital, host defense mechanism. Clearly, further exploration of the regulatory effect of tumor cell products on tumor growth is warranted.

REFERENCES

(*1*) Nicolson GL. Cancer metastasis. Sci Am 1979; 79:50-60.

(*2*) Unkeless J, Tobia A, Ossowski L, Quigley J, Rifkin D, Reich E. An enzymatic function associated with transformation of fibroblasts by oncogenic viruses. I. Chick embryo fibroblast cultures transformed by avian RNA tumor viruses. J Exp Med 1973; 137:85–111.

(*3*) Ossowski L, Unkeless J, Tobia A, Quigley J, Rifkin D, Reich E. An enzymatic function associated with transformation of fibroblasts by oncogenic viruses. II. Mammalian fibroblast cultures transformed by DNA and RNA tumor viruses. J Exp Med 1973; 137:112–126.

(*4*) Unkeless J, Dano K, Kellerman GM, Reich E. Fibrinolysis associated with oncogenic transformation. Partial purification and characterization of the cell factor, a plasminogen activator. J Biol Chem 1974; 249:4295–4305.

(*5*) Poole AR, Tiltman KJ, Recklies AD, Stoker TA. Differences in secretion of the proteinase cathespin B at the edges of human breast cancer and fibroadenoma. Nature 1978; 273:454–547.

(*6*) Sloane BF, Dunn JR, Honn KV. Lysosomal cathepsin B: Correlation with metastatic potential. Science 1981; 212:1151–1153.

(*7*) Liotta LA, Abe S, Robey PG, Martin GR. Preferential digestion of basement membrane collagen by an enzyme derived from a metastatic murine tumor. Proc Natl Acad Sci USA 1979; 76:2268–2271.

(*8*) Yoshimura S, Tamaoki N, Ueyama Y, Hata J. Plasma protein production by human tumor xenotransplanted in nude mice. Cancer Res 1978; 38:3474–3478.

(*9*) Akatsuka A, Yoshimura S, Hata J, Tamaoki N, Ueyama Y. Intracellular localization of human plasma proteins revealed by peroxidase-antibody method in human tumors transplanted in nude mice. J Electron Microsc (Tokyo) 1979; 28:93–99.

(*10*) Dexter DL, Barbosa JA, Calabresi P. *N,N*-Dimethylformamide-induced alteration of cell culture characteristics and loss of tumorigenicity in cultured human colon carcinoma cells. Cancer Res 1979; 39:1020–1025.

(*11*) Ouchterlony O. Diffusion-in-gel methods for immunological analysis. Prog Allergy 1958; 5:1–78.

(*12*) Grabar P, Williams CA. Methods permettant l'étude conjugée des propriétés électrophorétiques et immunochimique d'un mélange de protéines. Application au serum sanguin. Biochim Biophys Acta 1953; 10:193–194.

(*13*) Laurell CB. A screening test for α_1-antitrypsin deficiency. Scand J Clin Lab Invest 1972; 29:247–248.

(*14*) Schnebli HP, Burger MM. Selective inhibition of growth of transformed cells by proteinase inhibitors. Proc Natl Acad Sci USA 1972; 69:3825–3827.

(*15*) Goetz IE, Weinstein C, Roberts E. Effects of proteinase inhibitors on growth of hamster tumor cells in culture. Cancer Res 1972; 32:2469–2474.

(*16*) Weber MJ. Inhibition of protease activity in cultures of Rous sarcoma virus-transformed cells: Effect on the transformed phenotype. Cell 1975; 5:253–261.

(*17*) Troll W, Klassen A, Janoff A. Tumorigenesis in mouse skin: Inhibition by synthetic inhibitors of proteases. Science 1970; 169:1211–1213.

(*18*) Rossman TG, Troll W. Protease inhibitors in carcinogenesis: Possible sites of action. In: Slaga TJ, ed. Carcinogenesis. Vol 5. New York: Raven Press, 1980:127–143.

(*19*) McIlhinney A, Hagan BL. Effects of inhibitors of proteolytic enzymes on the growth of normal and polyoma transformed BHK cells. Biochem Biophys Res Commun 1974; 60:348–354.

(*20*) Umezawa H. Protease inhibitors produced by microorganisms. Acta Biol Med Ger 1977; 36:1899–1915.

(*21*) Hozumai M, Osawa M, Sugimura T, Tukeuchi T, Umezawa H. Inhibition of tumorigenesis in mouse skin by leupeptin, a protease inhibitor from actinomyces. Cancer Res 1972; 32:1725–1728.

(*22*) Troll W, Weisner R, Belman S, Shellaburger CJ. Inhibition of carcinogenesis by feeding diets containing soybeans. Proc Am Assoc Cancer Res 1979; 20:265.

(*23*) Fagerhol MR. Genetics of the Pi system. In: Mittman C, ed. Pulmonary emphysema and proteolysis New York: Academic Press, 1972:123–131.

(*24*) Carp H, Janoff A. Potential mediators of inflammation J Clin Invest 1980; 66:987–995.

(*25*) Matheson NR, Wong PS, Travis J. Enzymatic inactivation of human alpha-1-proteinase inhibitor by neutrophil myeloperoxidase. Biochem Biophys Res Commun 1979; 88:402–409.

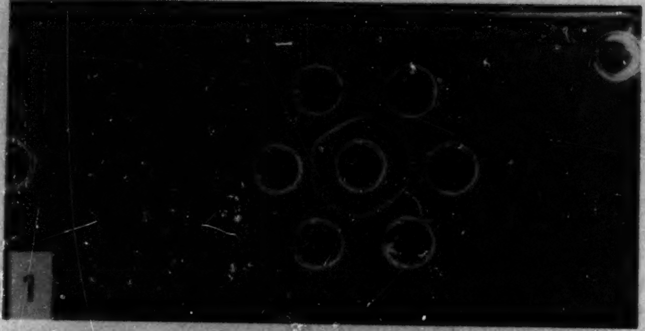

1

FIGURE 1.—Immunodiffusion plate demonstrates immunologic identity between tumor-derived and human plasma α_1Pi. *Center well* contains rabbit anti-human α_1Pi. *Outer wells* contain tumor extracts from clone D (CLD), clone A (CLA), DLD-1, DLD-2, and normal human serum (HS), prepared the same way as were the tumor extracts.

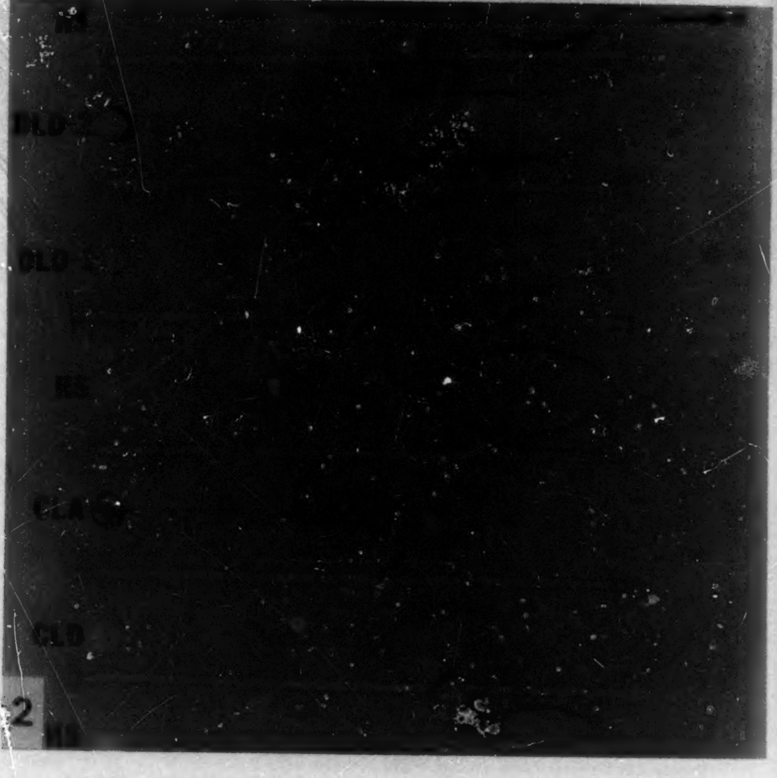

2

FIGURE 2.—Immunoelectrophoresis of partially purified α_1Pi preparations. All antibody *troughs* contain rabbit anti-human α_1Pi. HS=normal human serum; tumor preparations DLD-2, DLD-1, clone A (CLA), and clone D (CLD) are *in the wells*. *Arrows* indicate precipitation arcs.

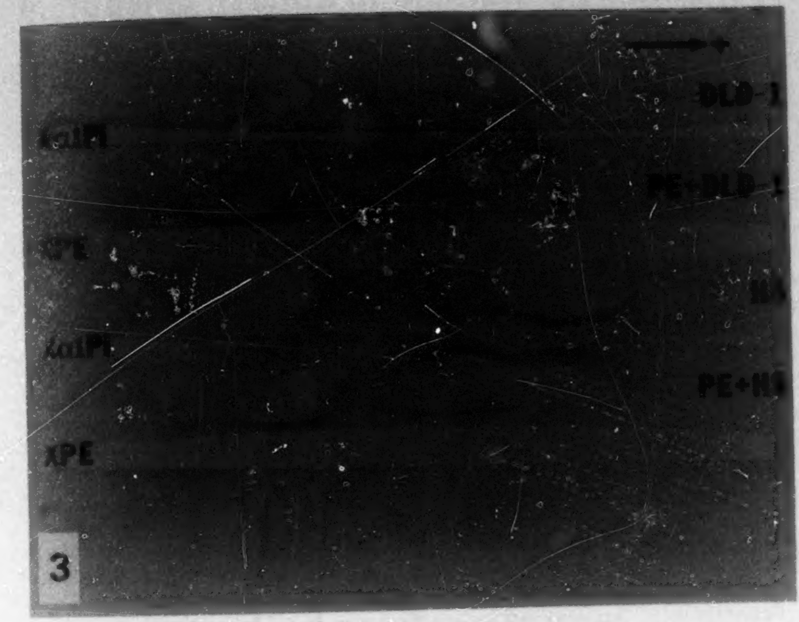
+
Xα_1Pi
DLD-1
PE+DLD-1
XPE
HS
Xα_1Pi
PE+HS
XPE
3

FIGURE 3.—Analysis of antipr
1 partially purified α_1Pi.
plus 2 µl of PE (10 µg/2 µl)
20 min at room temperature
mixture was applied to a w
was allowed to undergo el
for 1 hr at room temperatu
placed in each of the wel
serum (HS)] and 7.5 µg (
anti-α_1Pi-rabbit anti-α_1Pi
PE as indicated.

blank page

Increasing Trends of Multiple Myeloma Mortality in England and Wales; 1950–79: Are the Changes Real?[1,2,3]

Ramon **Velez**, *M.D., M.Sc.*,[4,5,6] **Valerie Beral**, *M.R.C.P.*,[7] *and* **Jack Cuzick**, *Ph.D.*[8,9]

ABSTRACT—National statistics for England and Wales for the period of 1950–79 were examined to study the secular trends in multiple myeloma mortality and to evaluate the extent to which these changes may be due to biases associated with improvements in medical care. Age-adjusted mortality has increased more than fivefold during this 30-year period. Contrary to the impression obtained from clinical series, a slightly greater increase in age-adjusted mortality has occurred in males. Examination of age- and sex-specific mortality trends showed that the greatest apparent increase in myeloma mortality occurred in individuals over 70 years of age. The data are consistent with either a cohort effect, indicating a true increase in mortality, or an age-dependent diagnostic effect in which a greater percentage of deaths among the elderly are now being certified as myeloma. Analyses of mortality data by social class and region point toward improved case ascertainment being responsible for at least part of the apparent increase in reported mortality. The increase in reported mortality in the younger age groups may reflect a true increase in the incidence of this disease. This increase, however, would account for only a proportion of the total increase, even when extrapolated to the older age groups.—JNCI 1982; 69:387–392.

The apparent increase in incidence and mortality from multiple myeloma has become the subject of increasing interest. In the United States the reported increase in incidence of myeloma has been proportionally greater than that for any other site of cancer (*1–3*). However, a recent study of the population of Olmsted County, Minnesota, which has been under careful medical surveillance by the Mayo Clinic for several decades, has failed to show any increase in the incidence of the disease (*4*). The purpose of this study was to determine whether a similar trend in myeloma mortality has occurred in England and Wales and to assess the extent to which these changes may be due to change in diagnostic factors. Our analyses are based largely on routinely collected, published, and unpublished vital statistics for England and Wales. Comparisons have also been made with data from a cancer registry in Texas, where secular trends are tabulated for 3 ethnic groups (*5*).

MATERIALS AND METHODS

Mortality data were obtained from the Registrar General's Statistical Review for England and Wales (*6*) for the period of 1950–73 and from the OPCS Mortality Statistics (*7*) for the period of 1974–79. Unpublished mortality data by region for England and Wales were also obtained from OPCS.

Multiple myeloma has been separately classified under the ICD rubric 203 since the sixth revision of the ICD in 1948. There have been no changes in this classification in subsequent revisions.

The denominators for rate calculations for England and Wales are based on census year populations and intercensal estimates published by the Registrar General and OPCS. Age- and sex-adjusted myeloma mortality rates for England and Wales were calculated by the direct method with the use of the World Health Organization's European population standard. The data on standardized mortality ratios by social class were obtained from the Registrar General's decennial supplements (*8–10*). The regression lines of logarithm of incidence versus calendar year fitted to the Texas Cancer Registry data have been determined by the least-squares method. The analyses of age, cohort, and calendar year effects by a log-linear model was done by the same method as that used by Holman et al. (*11*).

RESULTS

Review of vital statistics.—In 1979 there were 1,602 deaths attributed to multiple myeloma (ICD 203) in England and Wales (*7*). This statistic represents approximately 1% of all cancer deaths and 18% of deaths from cancers of the lymphatic and hematopoietic system. Although these numbers by themselves are not particularly striking, the proportional increase in mortality from myeloma since 1950 is noteworthy. Since the case fatality rate for multiple myeloma is high, changes in mortality should reflect changes in incidence rates over time.

ABBREVIATIONS USED: df=degree(s) of freedom; ICD=International Classification of Diseases; OPCS=Office of Population Censuses and Surveys (England); SMR=standardized mortality ratio(s).

---

[1] Received October 27, 1981; accepted February 26, 1982.

[2] Supported in part by the Milbank Memorial Fund and the Imperial Cancer Research Fund.

[3] This work was initiated by Dr. Velez while in the Department of Medical Statistics and Epidemiology, London School of Hygiene and Tropical Medicine, and in the Department of Community Medicine, St. Thomas' Hospital Medical School, London, England.

[4] Department of Medicine, Duke University Medical Center, Durham, N.C. 27710.

[5] *Address reprint requests to* Dr. Velez, HSR & D and Clinical Epidemiology Unit, Durham Veterans Administration Medical Center, 508 Fulton St., Durham, N.C. 27705.

[6] Recipient of a Milbank Memorial Fund fellowship in clinical epidemiology.

[7] Department of Medical Statistics and Epidemiology, London School of Hygiene and Tropical Medicine, Keppel St., London WC1E 7HT.

[8] Cancer Epidemiology and Clinical Trials Unit, University of Oxford, 9 Keble Rd., Oxford, OX1 3QG, England.

[9] We thank Sir Richard Doll (Oxford University), Professor Geoffrey Rose and Mr. Peter Smith (London School of Hygiene and Tropical Medicine) for their advice and encouragement. We also thank Miss Naomi Klein for editorial assistance, Miss Carol Hermon and Mrs. Irene Stratton for computing assistance, and Mrs. Celia A. Murphy for preparation of the manuscript.

TEXT-FIGURE 1.—Death rates for multiple myeloma in England and Wales, 1950–79. Age-adjusted to the European standard population.

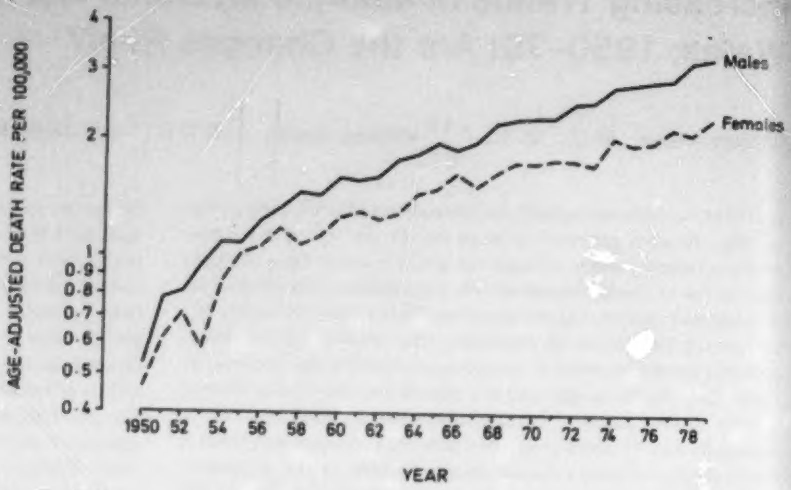

The age-adjusted mortality trends for both sexes from 1950 to 1979 are shown in text-figure 1. The proportionate increase during this 30-year period was 515% for males and 398% for females.

The sex ratio of age-adjusted mortality rates shows an excess of males which, remarkably, has increased in recent times. In 1950 the male:female ratio was 1.15, whereas it was 1.26 in 1960, 1.31 in 1970, and 1.42 in 1979.

Text-figure 2 illustrates the changes in age- and sex-specific multiple myeloma mortality rates for the 5-year periods 1953–57, 1963–67, and 1973–77. Although some increase has occurred in all age groups, most of the increase in myeloma mortality has been concentrated in the older age groups. Consequently, the shape of the age-mortality curve has changed over time: In 1953–57 peak mortality was at ages 65–69 in males and 70–74 in females, but in 1973–77 the mortality rates continued to increase with advancing age for both sexes.

Social class.—Text-figure 3 summarizes SMR by social class for occupied males and females for the periods of 1949–53, 1959–63, and 1970–72. During 1949–53 a high SMR was found among social class I males and females, while other groups were similar and no clear trend was seen across social classes II through V. The same pattern was apparent during 1959–63, but the excess SMR was smaller in social class I. By the last 5-year period excess SMR had almost disappeared, and the rates among different social classes became similar.

It is useful to compare these observations with the change for leukemia which occurred at an earlier time. Table 1 compares mortalities for all types of leukemias and for all cancers for occupied males by social class for the periods of 1930–32, 1949–53, 1959–63, and 1970–72. The general pattern for leukemias is similar to that for myeloma, although a clear trend is not seen for high SMR among the higher social classes (I and II) and low SMR in the lower social classes (IV and V). These differences were most marked for the period 1930–32 and again have diminished over time. In contrast, the pattern for mortality from all cancer by social class shows a gradient in the opposite direction, with excess mortality among classes IV and V and lesser mortality among the other social classes. For all cancers, the trend with social class has become more marked in recent times—a reflection, for the most part, of the greater reduction in

TEXT-FIGURE 2.—Age and sex-specific death rates for multiple myeloma over 5-yr periods during the last 3 decades in England and Wales.

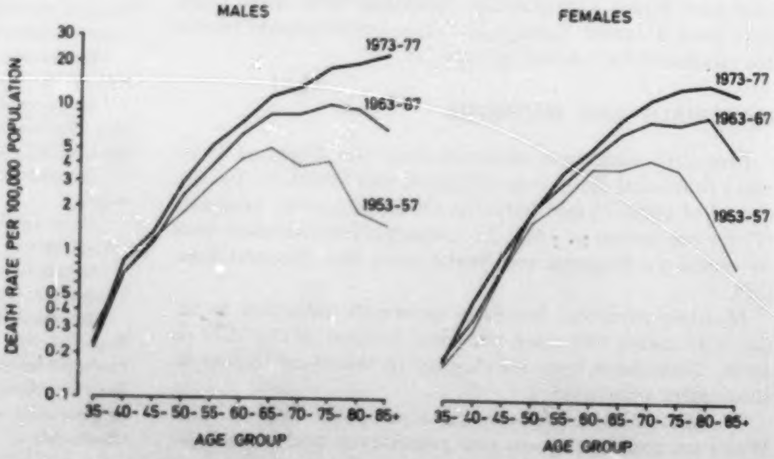

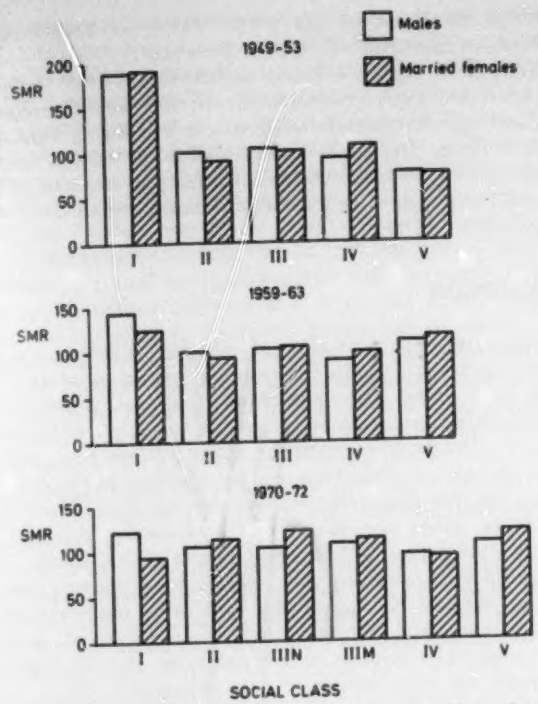

TEXT-FIGURE 3.—Standardized mortality ratios for multiple myeloma by social class in England and Wales.

smoking which has led to less lung cancer among social classes I and II.

Geographic variations.—Text-figure 4 shows the SMR for multiple myeloma for the standard regions of England and Wales (1976–78). There was some variation in SMR by region with the highest mortality in the Southwest (SMR=113) and Southeast (SMR=105) and the lowest mortality in the Northwest (SMR=88) and East Midlands (SMR=91).

Cohort analysis.—Text-figure 5 portrays mortality by birth cohort. This is plotted on a log-log scale so that a power law age-incidence curve appears as a straight line. This simple type of age-incidence curve is suggested by general principles (*12*) and provides a good fit for cancer at a number of sites (*13*). The fit to the present data is also quite good. The shifting of the curves to the left with more recent cohorts is what one would expect if successive cohorts were experiencing a greater mortality from this disease. The increases are largest between the earlier cohorts but continue until the 1905 birth cohort when the curves appear to have almost stabilized. A more mathematical analysis (*11*) can be based on a model that includes terms to account for both cohort effects and calendar year effects (that could arise from an age-independent change in diagnostic or certification practices). Such a model attributes the bulk of the increase to a cohort effect. A model that corrects for age and birth cohort fits the data extremely well (χ^2 for error =42.07 on 30 df), and no further improvement is obtained if calender year terms are included (χ^2 for error =38.65 on 27 df). A model that includes only age and calendar year terms does not fit so well (χ^2 for error =561.8 on 40 df), and a much better fit is obtained when the cohort terms are included (χ^2 for error =38.65 on 27 df). However, the calendar year variables do not accommodate an age-dependent improvement in diagnosis and certification (which could masquerade as a cohort effect), and this likely possibility must be considered in the assessment of the validity of this model. This model assumes that the logarithm of the expected mortality rates in each 5-year calendar period and 5-year age group is a linear combination of indicator func-

TABLE 1.—*Standardized mortality ratios by social class: occupied males in England and Wales during four 5-year periods*[a]

Period, yr	Social class[b]					
	I	II	IIIN	IIIM	IV	V
			Leukemias			
1930–32	153	125	96		94	85
1949–53	107	98	104		93	89
1959–63	106	100	103		97	108
1970–72	113	100	107	101	104	95
			All cancers			
1930–32	83	92	99		102	115
1949–53	94	86	104		95	113
1959–63	73	80	104		102	139
1970–72	75	80	92	113	116	131

[a] Source: Occupational Mortality Tables (*8, 9*).
[b] N = nonmanual occupations; M = manual occupations.

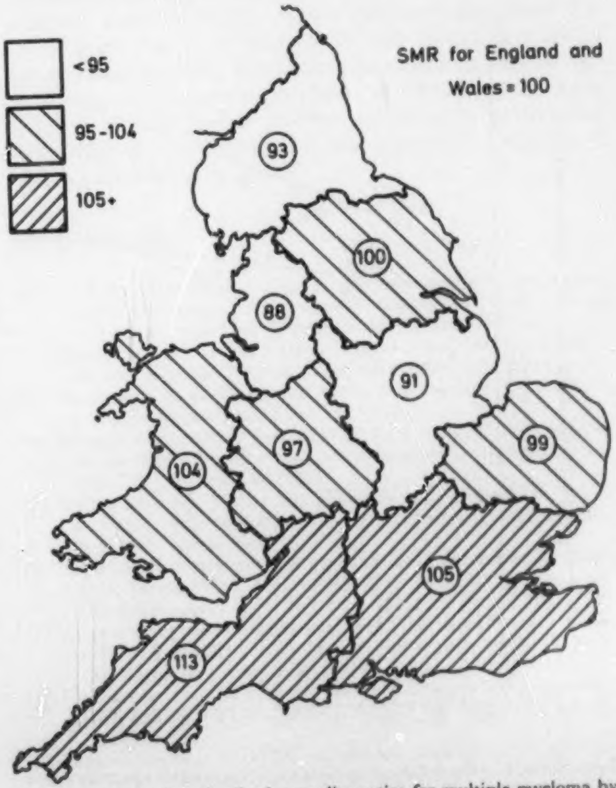

TEXT-FIGURE 4.—Standardized mortality ratios for multiple myeloma by region in England and Wales. Males and females aged ≥25 yr, 1976–78.

tions for 5-year age groups, 5-year birth cohorts, and 5-year calendar periods, and that the variations from the expected rates are independent Poisson random variables. A more detailed discussion of this model based on data from a number of countries will appear elsewhere.

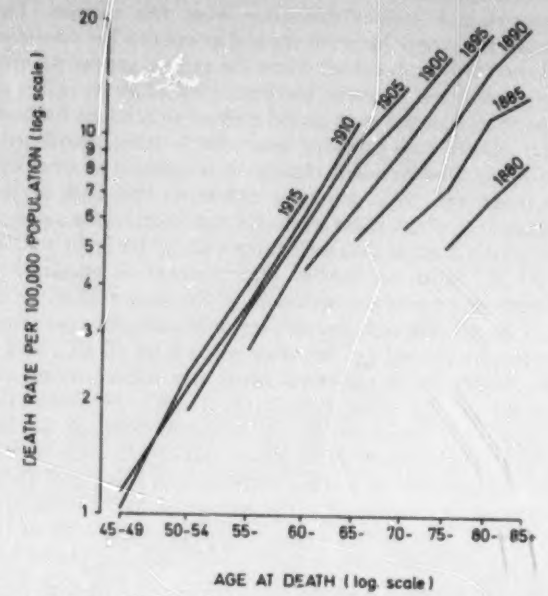

TEXT-FIGURE 5.—Mortality from multiple myeloma in England and Wales in different cohorts born in 5-yr periods between 1880 and 1915.

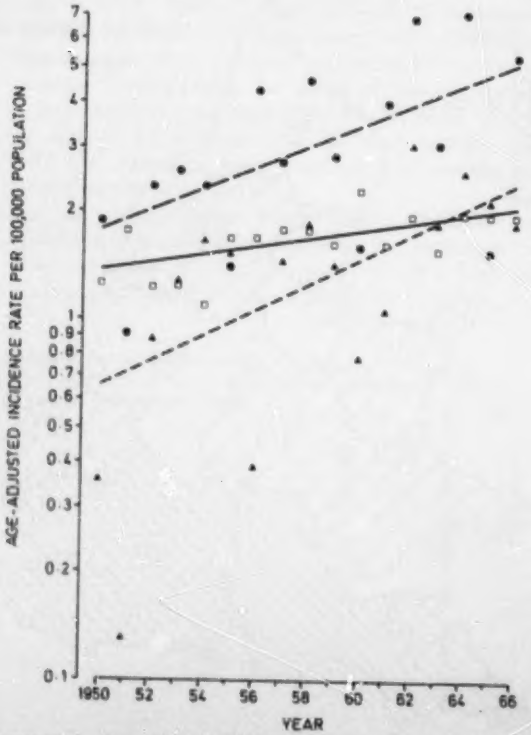

TEXT-FIGURE 6.—Age-adjusted multiple myeloma incidence rates by ethnic group in Texas, 1950–1966. 1960 U.S. population used as standard. □——□, whites; ●– – –●, non-whites; ▲-----▲, Spanish surnamed.

Texas cancer registry.—Shown in text-figure 6 are the age-adjusted multiple myeloma incidence rates for white, Spanish, and nonwhite populations living in a defined geographic area in Texas. The slopes of the rise of the regression lines of logarithm of incidence versus calendar year are steeper for Spanish and nonwhite populations compared to the white population.

DISCUSSION

The clinical presentation of multiple myeloma varies widely, with initial symptoms ranging from vague migratory bone pain, back pain, pathologic fractures, pneumonia, neurologic symptoms, and/or anemia to acute renal failure (*14, 15*). Diagnosis requires the aid of various tests, which have changed in their type and availability in the last 50 years. The first diagnostic test was the examination of urine for Bence Jones protein (*16*). Unfortunately, this test is positive in less than 50% of proven cases of this disease (*17, 18*). Thus other ancillary tests, such as bone marrow examination, skeletal X-rays, serum, and urine electrophoresis must be employed when this diagnosis is suspected. Before these procedures became widely available, the diagnosis of myeloma was often confirmed only at autopsy (*19*).

The gradual introduction of these diagnostic tests has spanned nearly 4 decades. Although bone marow examinations were first performed in 1929 (*20*), it was not until 1938 that the value of this procedure was recognized in the diagnosis of myeloma (*21*). It remained an infrequently used procedure, however, until the late 1940's, when a greater understanding of the cell types in normal marrow made the identification of abnormalities easier (*22*). Needle biopsies, that could be taken easily under local anesthetic, as opposed to the more difficult and painful trephine cuts used previously, became available in the 1950's and early 1960's and also led to the wider use of bone marrow investigation (*23, 24*). Similarly, serum electrophoresis was first described as being of diagnostic value in myeloma in 1938 (*25*). However, the method was laborious and remained a research tool until the 1950's (*26–28*), when, with the development of paper and cellulose acetate electrophoresis, this procedure became more widely available. We inquired at 10 London teaching hospitals to establish the time when serum electrophoresis became available. The responses gave the average year when this occurred as 1956, with a range from 1950 to 1962.

A diagnosis of multiple myeloma is highly dependent on the use of medical facilities and laboratory tests. The effects of these factors must be taken into consideration when one interprets mortality statistics (*29*). The sharpest increase in reported mortality rates occurred between 1950 and 1960 (text-fig. 1). This increase coincides with the period of the most rapid advances in the laboratory diagnosis of this disease.

The age-adjusted male-to-female mortality ratio reveals a slight excess of males in the 1950's that has increased in the next 2 decades. This finding is in striking contrast to the impression gained from clinical series in which a larger male preponderance was seen in the early part of this century (*19*) and is less apparent now. In 1961 Martin (*30*) reported the male-to-female ratio of cases of myeloma seen in London teaching hospitals as 3:2. More recently, Waldenstrom (*31*) has pointed out that in his recent experience the sex ratio has shifted toward a preponderance of females. The early large male excess is possibly partly an artifact due to a bias that used to exist (particularly before the introduction of the National Health Service) in favor of hospital referral of males rather than females for the investigation of obscure diseases (*32*), and its disappearance may be partly due to changes in referral patterns and in the sex distribution of the aged population. A greater percentage of females are now alive in the age groups in which myeloma incidence is highest, and the early case series were based on numbers and not rates. For example, in 1979 64% of the population of England and Wales above age 70 were female, whereas in 1950 only 59% were female. This bias can be removed by studying age-adjusted rates instead of cases for the two sexes (text-fig. 1), where the size of the normal population is accounted for.

Kyle et al. (*33*) examined the death certification of 31 patients in whom myeloma had been diagnosed at the Mayo Clinic in Olmsted County, Minnesota, during the period of 1945–64. He found that myeloma had been recorded as the underlying cause of death in 23 cases (74%). By contrast, in studying the recorded cause of deaths in a sample of incident cases from the Third National Cancer Survey, 1970–71, Percy et al. (*34*) found that 96% of the 699 incident cases of myeloma were certified as dying of this disease. This suggests that an increased awareness by clinicians of multiple myeloma, associated with changes in diagnostic habit and death certification, may contribute to the apparent increase in mortality trends.

MacMahon (*35*) has previously commented on the greater reported mortality from myeloma in social class I in the period 1949–53. A trend in the same direction has also been seen for the leukemias. The proportionate increase in mortality from leukemias earlier this century has been exceeded only by greater increases in lung cancer and coronary heart disease mortality (*36*). Although radiation exposure has been implicated as a causative factor in both leukemia (*37*) and myeloma (*38*), the increase in leukemia has been attributed primarily, although not exclusively (*37*), to improvements in diagnosis and better access to medical care (*36*), which may well be true also for myeloma.

Further support for the hypothesis that underascertainment is related to social class and access to medical care is provided by an examination of the data from a cancer registry in Texas (*5*), where cancer incidence in white, Spanish, and non-white populations has been analyzed. Both the Spanish and the non-white group represent socioeconomically disadvantaged populations. Over time both of these groups have benefited from greater access to medical care, and the increase in incidence of myeloma has been more pronounced in these 2 ethnic groups (text-fig. 6).

Studies of leukemia incidence have indicated that there is a consistent selective underascertainment among the elderly (*39–41*). Meadors (*40*) has suggested that this is the result of attributing leukemia deaths in the elderly to diseases of old age and infections. If correct diagnosis is a factor in myeloma mortality rates, as laboratory investigations increase, the greatest increases in registered mortality would be among the elderly where underdiagnosis is most prevalent. It is apparent from text-figure 2 that while myeloma mortality rates have increased in all age groups, the change is far greater in the older age groups.

Regional mortality data for England and Wales also support the view that access to medical care may be important in the diagnosis of myeloma. Mortality from all causes and all cancers is highest in regions in the North and lowest in the Southeast (*42*), but the reverse is true for myeloma (text-fig. 4). This observation is consonant with the disproportionately greater availability of medical facilities in the South (*43*).

In conclusion, it appears that technical improvements in the diagnosis of myeloma, as well as greater access to medical care especially among the elderly, have contributed to the increased recognition, and hence to the reported mortality, from this disease. Similar arguments were put forward to explain the reported increase in lung cancer earlier this century (*44, 45*), yet the increase in lung cancer was real. In the case of lung cancer, the increases were first noted in males, suggesting a specific etiologic agent much of which was later identified as cigarette smoking (*46*). For myeloma, the increase occurred in both sexes and has been only slightly greater in males, suggesting that any major new putative factor must have been introduced across broad sections of the population. The extremely good fit of the data to a model with only cohort effects also suggested that the increase may be at least partly real. Although much of the apparent increase in incidence of myeloma may be due to changes in diagnostic practice and referral, myeloma is certainly not as rare as it once was thought to be. Our knowledge of the etiology of this disease is meager and requires further investigation.

REFERENCES

(*1*) Blattner WA. Epidemiology of multiple myeloma and related plasma cell disorders: An analytic review. In: Potter M, ed. Progress in myeloma. New York: Elsevier/North-Holland, 1980:1–65.

(*2*) Devesa SS, Silverman DT. Cancer incidence and mortality trends in the United States: 1935–74. J Natl Cancer Inst 1978; 60:545–571.

(*3*) Fraumeni JF Jr. Environmental and genetic determinants of cancer. J Environ Pathol Toxicol 1977; 1:19–30.

(*4*) Linos A, Kyle RA, O'Fallon WM, Kurland LT. Incidence and secular trend of multiple myeloma in Olmsted County, Minnesota: 1965–77. JNCI 1981; 66:17–20.

(*5*) MacDonald EJ, Heinze EB. Epidemiology of cancer in Texas: Incidence analyzed by type, ethnic group, and geographic location. New York: Raven Press, 1978.

(*6*) Registrar General. Statistical review of England and Wales 1950–1973. London: Her Majesty's Stat Off, 1952–1975. [Separate annual publications].

(*7*) Office of Population Censuses and Surveys. Mortality statistics: Cause 1974–79 (series DH2 No. 1). London: Her Majesty's Stat Off, 1977–1981. [Separate annual publications].

(*8*) Registrar General. Decennial supplement. England and Wales 1931, Occupational mortality tables. London: Her Majesty's Stat Off, 1938.

(*9*) Registrar General. Decennial supplement. England and Wales 1951 and 1961. Occupational mortality tables. London: Her Majesty's Stat Off, 1957 and 1971.

(10) Office of Population Censuses and Surveys. Decennial supplement. England and Wales 1970–72 (series DS No. 1). Microfiche. London: Her Majesty's Stat Off, 1978.

(11) Holman CD, James IR, Gatey PH, Armstrong BK. An analysis of trends in mortality from malignant melanoma of the skin in Australia. Int J Cancer 1980; 26:703–709.

(12) Armitage P, Doll R. Stochastic models for carcinogenesis. In: Neyman J, ed. Proceedings of the Fourth Berkeley symposium on mathematical statistics and probability. Berkeley: Univ Calif Press, 1961:19–38.

(13) Doll R. The age distribution of cancer: Implications for models of carcinogenesis. J R Statist Soc 1971; A, 134:133–166.

(14) Schwartz SO, Cataldo M. Some clinical caprices of multiple myeloma: 15 case reports from a study of 75 cases. Ann Intern Med 1953; 39:1267–80.

(15) Doll DC, Weiss RB. Unusual presentation of multiple myeloma. Postgrad Med 1977; 61:116–121.

(16) Jones HB. On a new substance occurring in the urine of a patient with mollities ossium. Philos Trans R Soc London [Biol] 1948; 138:55–62.

(17) Adams WS, Alling EL, Lawrence JS. Multiple myeloma: Its clinical and laboratory diagnosis with emphasis on electrophoretic abnormalities. Am J Med 1949; 6:141–161.

(18) Hobbs JR. Immunoglobulins in clinical chemistry. Adv Clin Chem 1971; 14:219–317.

(19) Geschickter CF, Copeland MM. Multiple myeloma. Arch Surg 1928; 16:807–863.

(20) Snapper I, Turner LB, Moscovitz HL. Multiple myeloma. New York: Grune, 1953.

(21) Rosenthal N, Vogel P. Value of the sternal puncture in the diagnosis of multiple myeloma. J Mt Sinai Hosp 1938; 4:1001–1019.

(22) Vaughan SL, Brockmyre F. Normal bone marrow as obtained by sternal puncture. Blood 1947; 1:54–59.

(23) Brody JI, Finch SC. Bone marrow needle biopsy. Am J Med Sci 1959; 238:140–145.

(24) Ellis LD, Jensen WN, Westerman MP. Needle biopsy of bone and marrow. Arch Intern Med 1964; 114:213–221.

(25) Longsworth LG, Shedlovsky T, MacInnes DA. Electrophoretic patterns of normal and pathological human blood serum and plasma. J Exp Med 1938; 70:399–413.

(26) Waldenstrom J. Abnormal proteins in multiple myeloma. In: Advances in internal medicine. Vol 5. Chicago: Year Book Med Publ, 1952:398–440.

(27) Rundles RW, Cooper GR, Willett RW. Multiple myeloma. IV. Abnormal serum components and Bence Jones protein. J. Clin Invest 1951; 30:1125–1142.

(28) Reiner M, Stern KG. Application of electrophoretic studies on the distribution in the serum of multiple myeloma patients. Acta Hematol 1953; 9:19–29.

(29) Newton PA. Multiple myeloma: Uncommon or uncommonly diagnosed. Postgrad Med 1977, 61:107–110.

(30) Martin NH. The incidence of myelomatosis. Lancet 1961; 1:237–239.

(31) Waldenstrom J. Diagnosis and treatment of multiple myeloma. New York: Grune, 1970:3.

(32) ———. Malignancy of the hematopoietic system and ageing. In: Engel A, Larrson T, eds. Thule international symposium No. 2. Cancer and ageing, 1967. Stockholm: Nordiska Bokhandelns Forlag. 1968:155–165.

(33) Kyle RA, Nobrega FT, Kurland LT. Multiple myeloma in Olmsted County, Minnesota, 1945–1969. Blood 1969; 33:739–745.

(34) Percy C, Stanek E, Gloeckler L. Accuracy of cancer death certificates and its effects on cancer mortality statistics. Am J Public Health 1981; 71:242–250.

(35) MacMahon B. Epidemiology of Hodgkin's disease. Cancer Res 1966: 26:1189–1200.

(36) Office of Health Economics. Leukemia: Towards control. London: Office of Health Economics, 1980:1–47.

(37) Court Brown WM, Doll R. Leukaemia in childhood and young adult life: Trends in mortality in relation to etiology. Br Med J 1961; 2:981–988.

(38) Cuzick J. Radiation-induced myelomatosis. N Engl J Med 1981; 304:204–210.

(39) McPhedran P, Health CW Jr, Garcia JS. Racial variation in leukemia: Incidence among the elderly. J Natl Cancer Inst 1970; 45:25–28.

(40) Meadors GF. Epidemiology of leukemia. Public Health Rep 1956; 71:103–108.

(41) Hewitt D. Geographical pathology of leukemia in England and Wales. Acta Un Int Cancr 1960; 16:1643–1647.

(42) Office of Population Censuses and Surveys. Area mortality decennial supplement. England and Wales 1969–1973 (series DS No. 1). London: Her Majesty's Stat Off, 1981.

(43) West PA. The nation's health and the NHS. King's fund project paper No. RC14. London: King's Fund Centre, 1980:32–34.

(44) Gillian A. Trends of mortality attributed to carcinoma of the lung: Possible effects of faulty certification of deaths to other respiratory diseases. Cancer 1949; 3:311–320.

(45) Heady JA, Kennaway EL. The increase in deaths attributed to cancer of the lung. Br J Cancer 1949; 3:311–320.

(46) Doll R, Hill AB. A study of the aetiology of carcinoma of the lung. Br Med J 1952; 2:1271–1286.

Changes in Clonal Expression During the Course of Acute Leukemia: Possible Subsets in Childhood Leukemia[1,2]

Hie-Won L. Hann, *M.D.*,[3,4,5,6] **Peter C. Nowell**, *M.D.*,[7] **Penelope Koch**, *M.D.*,[4,5] **Jun Minowada**, *M.D.*,[8] **John E. Leitmeyer**, *B.A.*,[3] *and* **Charles S. August**, *M.D.*[4,5,9]

ABSTRACT—We studied cell surface markers and chromosomes in the leukemia cells of a boy with the initial diagnosis of acute lymphocytic leukemia during 18 months from diagnosis to demise. During this time he received induction therapy, underwent bone marrow transplantation, and relapsed. The leukemia cells expressed three membrane phenotypes during different stages of disease: T-cell at diagnosis; T-cell, E-cell, and monocyte during the induction period; T-cell in the first relapse after bone marrow transplantation; and T-cell and B-cell during the terminal stage. Some cells expressed markers of two cell types, indicating a common origin of these cells. Cytogenetic studies during post-transplantation relapse showed abnormal marker chromosomes that indicated two major sublines. However, there was enough sharing of other aberrant chromosomes to suggest that these two populations presented sublines within the same neoplastic clone. We suggest that these leukemia cells were derived from a pluripotential cell prior to differentiation into cells of the lymphoid and monocytic series. This particular case may represent a subset of acute leukemia and may account for the resistance to conventional therapy.—JNCI 1982; 69:393–399.

The ALL of childhood is considered to have its origin in the lineage of lymphoid cells. Alternatively, in CML cytogenetic and enzyme evidence (*1–7*) indicates origin from a pluripotent marrow stem cell.

Recently, a case of biclonal lymphoblastic and myeloblastic leukemia (*8*) was described, although the possibility that these two cell lines might have originated from a single clone was not completely excluded.

We have made a similar observation in a child who was considered to have ALL at diagnosis. During the course of leukemia, however, the malignant cells underwent a series of changes demonstrated by morphology, histochemistry, immunological surface markers, and cytogenetic studies. Moreover, evidence suggested that the cells were derived from a single malignant clone. The response of the patient to antileukemia chemotherapy was extremely poor, and the disease recurred after bone marrow transplantation.

CASE SUMMARY

A 6-year-old white boy was hospitalized in March 1978 because of pallor, lethargy, and swelling of the eyes, hands, and abdomen. Spleen and liver were palpable 12 and 3 cm below their respective costal margins. The WBC count was 319,000/mm^3 with 92% blasts. A bone marrow aspirate revealed 96% undifferentiated lymphoblastoid cells. They were most similar to lymphoblastic leukemia L_2 by French-American-British criteria (*9*). Both PAS and Sudan black stains were negative. Chest X-ray was normal. The diagnosis of ALL was made. The patient was treated with vincristine, prednisone, and L-asparaginase with only a temporary reduction in the number of peripheral blast cells. When the WBC count rose to 141,000/mm^3 with 88% blasts on the 16th day of therapy (April 78), a repeat bone marrow aspirate revealed 76% primitive cells, which appeared more like monoblasts than lymphoblasts. These cells reacted minimally with PAS stain and not with Sudan black. They stained positively for nonspecific esterase and did not react with naphthol AS-D chloroacetate esterase stain. The diagnosis was therefore changed to acute undifferentiated leukemia. Chemotherapy was continued with the addition of daunomycin and β-cytosine arabinoside, and a bone marrow remission was obtained.

Because of concern about the patient's long-term prognosis and because he had a younger brother with identical HLA-A, HLA-B, and HLA-D, the decision was made to undertake bone marrow transplantation while he was in complete remission. After informed consent was obtained (*10*), the patient was prepared with 2 doses of 60 mg

---

ABBREVIATIONS USED: ALL=acute lymphocytic leukemia; cIg=cytoplasmic immunoglobulins; CML=chronic myelocytic leukemia; E=erythrocyte; EA=E-antibody; EAC=EA-complement; PAS=periodic acid-Schiff; sIg=surface immunoglobulin; SRBC=sheep red blood cell(s); T-LCL=T-lymphoid cell line; WBC=white blood cell.

---

[1] Received October 28, 1981; accepted February 26, 1982.

[2] Supported by Public Health Service (PHS) grants RR-00240 and RR-05539 from the General Clinical Research Centers Program, Division of Research Resources, National Institutes of Health; by Public Health Service grants CA-06551, CA-06927, CA-14413, and CA-14489 from the National Cancer Institute; by The Philadelphia Eagles Fly for Leukemia Fund; and by an appropriation from the Commonwealth of Pennsylvania.

[3] The Institute for Cancer Research, The Fox Chase Cancer Center, Philadelphia, Pa. 19111.

[4] The Children's Cancer Research Center and the Bone Marrow Transplant Unit, The Children's Hospital of Philadelphia, Philadelphia, Pa. 19104.

[5] Department of Pediatrics, University of Pennsylvania, Philadelphia, Pa. 19104.

[6] *Address reprint requests to* Dr. Hann at The Institute for Cancer Research, The Fox Chase Cancer Center, 7701 Burholme Ave., Philadelphia, Pa. 19111.

[7] Department of Pathology, University of Pennsylvania.

[8] Roswell Park Memorial Institute, Buffalo, N.Y. 14263.

[9] The authors thank Dr. W. Elkins, The Children's Hospital of Philadelphia, for providing stored leukemia cells of the patient for us to reexamine and confirm our initial observation; Ms. Janet Finan for her technical assistance on the chromosome study; Dr. H. W. Lischner, St. Christopher's Hospital for Children, and Dr. R. S. Hann, Hahnemann Medical College and Hospital, Philadelphia, for their invaluable technical and scientific advice; Dr. W. T. London, The Institute for Cancer Research, Philadelphia, and Dr. G. D'Angio, The Children's Hospital of Philadelphia, for their review and helpful criticism of this paper; and Ms. M. Walsh for her excellent typing of the manuscript.

cyclophosphamide/kg body weight/day, followed by a single 800-rad dose of total-body irradiation. The bone marrow transplant was performed on January 15, 1979, when the patient received 6.5×10^8 nucleated marrow cells/kg body weight. Thereafter, he received methotrexate at regular intervals for prevention of graft versus host disease (*11*). Extensive red cell typing had been done on both donor and recipient before transplantation. A repeat red cell antigen profile done in March 1979 revealed the patient to have c-antigen of the Rh group, the one informative antigen that distinguished the donor from the recipient. This finding indicated that the regenerated bone marrow was of donor origin. He fared well until the 56th post-transplant day when papilledema of the left optic disc was noted. Bone marrow examination did not show leukemia blasts at this time. X-ray therapy (600 rad) was delivered to the left eye. On the 112th day after the graft, his WBC count rose to 175,000/mm^3 with 82% blasts. Bone marrow examination confirmed the relapse. The cells were slightly positive for PAS and negative for Sudan black. Although palliative treatment with vincristine, prednisone, 6-mercaptopurine, and methotrexate was given for the next 4 months, leukemia cells appeared in the spinal fluid, and lymphoblasts persisted at low levels in the peripheral blood. Two months later (Sept. 79), the WBC count rose to 138,000/mm^3, of which 88% were blasts. The boy died of leukemia shortly thereafter, 8 months after the bone marrow graft.

MATERIALS AND METHODS

Studies were performed on bone marrow and/or peripheral blood which were obtained at diagnosis, during relapses, and in remission.

Cell marker studies.—Lymphoid cells including leukemia cells were separated on a Ficoll-metrizoate gradient (*12, 13*) and used in the following assays: T-cell markers: 1) E-rosettes (E$^+$). The spontaneous rosette formation technique of Jondal et al. (*14*) was used with a minor modification as described previously (*15*). When leukemia cells were tested on two occasions during the relapse after bone marrow transplantation, E-rosettes were assayed after incubation of leukemia cells with SRBC at 4, 25, and 37°C for 1 hour or longer. After leukemia cells were mixed with SRBC and incubated at 37°C in 5% CO_2 for 10 minutes, this cell suspension was divided into four aliquots and treated in the following manner. Three aliquots were first centrifuged at $200\times g$ for 5 minutes and incubated at 4, 25, and 37°C. The fourth aliquot was not centrifuged but sedimented by gravity at 25°C. Incubation time of these aliquots was 1 hour or longer.

2) Indirect membrane immunofluorescence with the use of anti-T-cell serum. Rabbit antiserum specific to T-cell antigen (T-LCL) (*16*) was prepared and characterized according to methods previously reported. Using this antiserum as a primary reagent and fluorescein-conjugated goat anti-rabbit globulin serum as the secondary reagent, we performed indirect membrane immunofluorescence for detection of membrane antigen. The T-LCL antigen is expressed on normal T-lymphocytes, thymocytes, and T-cell leukemia-lymphoma cells (*17*).

B-cell markers: 1) Direct immunofluorescence for sIg. The method of Grey et al. (*18*) was used. Fluorescein-conjugated goat anti-human immunoglobulins (polyvalent and monovalent for γ, α, μ, δ, ϵ, κ, and λ (Meloy Laboratories Inc., Springfield, Va.) and fluorescein-conjugated $F(ab')_2$ fragments of anti-human IgG, IgM, and IgA (Cappel Laboratories, Inc., Cochranville, Pa.) were used as the reagents.

2) Detection of Fc receptor. *a*) Heat-aggregated human IgG. Fc receptors were detected by fluorescein-conjugated heat-aggregated IgG prepared by the method described by Dickler and Kunkel (*19*). *b*) EA rosettes. Rosette formation with bovine EA complex (*20*) was used.

3) Detection of complement receptor by EAC rosettes. Rosette formation with bovine EAC complex (*21*) was used.

Detection of Ia-like B-cell-associated (gp28,30) antigens.—Rabbit antiserum specific to Ia-like gp28,30 antigen (Ia-like) was prepared and characterized by the method described by Schlossman et al. (*22*). Indirect membrane immunofluorescence was used for detection of this antigen. This Ia-like antigen is expressed on normal peripheral B-lymphocytes, B-cell leukemia-lymphoma cells, cells from non-T-cell, non-B-cell leukemia (common ALL), and most acute myelocytic leukemia and CML in blast crisis (*17*).

cIg.—Cells were tested for cIg by means of the method described previously (*23*).

Latex phagocytosis.—Leukemia cells were incubated with a latex particle suspension (1:100, size 0.81 μm) (Difco Laboratories, Detroit, Mich.) as described by Schmidt and Douglas (*24*) with a minor modification.

Combined test for T-cell, B-cell, and monocytic markers in the same cells.—Tests for the three markers (E-rosettes, sIg, and phagocytosis) were done sequentially on the same cells. Cells were first incubated with latex particles, washed, and incubated with fluorescein-conjugated antisera to human immunoglobulins, washed, and finally incubated with SRBC for detection of rosette-forming cells. Individual cells were then examined alternately under phase contrast and fluorescein illumination by UV light for detection of latex particle and both T-marker and B-marker presence on the same cells.

Common form of ALL antigen.—Rabbit antiserum specific to the common form of ALL antigen (common ALL) was prepared and characterized by the method described by Greaves et al. (*25*).

Cytogenetics.—Chromosome studies were done on bone marrow processed by a direct preparative technique and on peripheral blood cultured for 24 hours without mitogen (*26*). Slides were prepared by the air-drying technique and G banded. This quality of the preparations did not permit complete characterization of the abnormal karyotypes, but aberrant "marker" chromosomes were sufficiently distinctive to be recognized readily in different metaphases.

RESULTS

Cell Membrane Phenotypes

Membrane phenotypes were studied at diagnosis, on the 16th day of induction therapy when leukemia cells reappeared, and on two occasions (April 79, Sept. 79) during a 6-month-long relapse after bone marrow transplantation.

Results are shown in table 1. At diagnosis 27% of leukemia cells were E^+, and no cells were positive for sIg. On the 16th day of induction, leukemia cells appeared more monoblastic than lymphoblastic. Fifty percent of these cells were E^+ and 80% were positive for sIg (tested with polyvalent antiserum). When tested with monospecific antisera, 100% of cells were positive for λ-light chain only. Also, 50% of these cells phagocytized latex particles (fig. 1). When the procedures were combined (*see* "Materials and Methods"), six populations of leukemia cells were observed: 1) E^+ cells, 21%; 2) E^+ cells with positive phagocytosis, 15% (fig. 1); 3) sIg^+ cells, 16%; 4) sIg^+ with phagocytosis, 33%; 5) cells with phagocytosis only, 7%; and 6) cells with no markers, 8%. With the combined procedures, sIg^+ cells were 49% (16 + 33%) compared with 80% by a single test (table 1), probably because combined tests were done on cells stored at 4°C for 2 days, and the three steps of analysis tended to lower the percentage of positive cells.

Shortly after the post-transplant relapse (April 79), there were 48% E^+ cells and no cells with sIg or positive EA rosettes. Less than 1% of the cells were positive for T-LCL antigen. All were positive for Ia-like gp28,30 antigen, and 30% were positive for common ALL antigen. No cells were positive for cIg or phagocytized latex particles.

During the terminal stage (Sept. 79), E^+ cells ranged from 29 to 44%. T-LCL antigen-positive cells were 0.8%. Twenty-five to 30% of the cells were positive for sIg of lambda light chain. Some cells were weakly positive for μ-heavy chain. There were 10–15% of cells with Fc receptors demonstrated by EA rosettes and heat-aggregated IgG. EAC rosette-positive cells ranged from 2.3 to 15%. No cells phagocytized latex particles. All cells were negative for cIg. When the

TABLE 1.—*Membrane phenotype and cytogenetic data*[a]

Study	Pre-BM transplantation[b]		Post BM transplantation[b]		
	Diagnosis, 3/78, BM, 96%	During induction, 4/78, BM, 76%	First relapse, 4/79, BM, 82%		Terminal stage, 9/79, blood,[c] 88%
I) Cell marker, %[d]					
T-cell					
E-rosette, E^+	27	50	48[e]		29–44[e]
T-LCL	ND	ND	<1		0.8
B-cell					
sIg					
Polyvalent	0	80	0		23
μ, F(ab′)₂	ND	0	ND		30
γ, F(ab′)₂	ND	0	ND		0
α, F(ab′)₂	ND	0	ND		0
δ	ND	0	ND		0
ε	ND	0	ND		0
κ	ND	0	ND		0
λ	ND	100	ND		25–30
Fc receptor					
EA rosette	ND	ND	0		10
Heat-aggregated IgG	ND	ND	ND		15
Complement receptor by EAC rosettes	ND	ND	1		2.3–15
Ia-like gp28,30 antigen	ND	ND	100		90
cIg	ND	ND	0		0
Latex phagocytosis	ND	50	0		0
Combined tests	ND	T[f] 21 T+latex 15 Latex 7 B+latex 33 B[g] 16 No marker 8	ND		T 19 T+B 8 B 28 No marker 45
Common ALL antigen	ND	ND	30		ND
			Blood	BM	Blood
II) Cytogenetic study	ND	ND			
Normal, No. of cells			7	9	0
Abnormal					
Subline 1 (M 1)			5	14	24
Subline 2 (M 2, M 3)			9	0	9

[a] BM=bone marrow; ND=not done.

[b] After dates below, specimen and percent blasts are given.

[c] 138,000/mm³.

[d] Normal control values of cell markers in our laboratories arte E^+, 55–80%; sIg, 10–30% (IgM, 10.3%; IgG, 8%; IgA, 5%; IgD, 2%; IgE, <1%; κ, 8.6%; λ, 6.2%), T-LCL, 65–85%; Ia, 15–25%; EAC, 8–16%.

[e] Done at 4, 25, and 37°C.

[f] T-cell percentage by E-rosettes.

[g] B-cell percentage by sIg.

procedures were combined, four populations of cells were observed: 1) E^+ cells, 19%; 2) E^+ and sIg^+ cells, 8%; 3) sIg^+ cells, 28%; 4) cells with no markers, 45%.

Cytogenetic Studies

Chromosome studies were done twice during the relapse after transplantation (April 79, Sept. 79) (table 1).

During the first relapse, material for study was obtained from blood (cultured for 24 hr without mitogen) and marrow. Twenty-one cells were counted from the blood: 7 were normal, and the remaining 14 metaphases had 46 chromosomes but showed multiple abnormalities. These included at least eight different aberrant marker chromosomes. The three most conspicuous markers indicated two major sublines: five metaphases contained marker 1, and nine metaphases contained markers 2 and 3. Marker 1 (M 1) was a large B-type chromosome, apparently a $5q^+$ (fig. 2A). Markers 2 and 3 (M 2, M 3) were large D-type chromosomes, with different banding patterns, whose origins could not be determined (fig. 2B). Every abnormal metaphase contained either M 1 or M 2 and M 3, and there was enough sharing of other aberrant chromosomes to indicate that these two populations presented sublines within the same neoplastic clone. Among the shared markers was an apparent $17p^-$ and a smaller abnormal chromosome with a similar banding pattern (figs. 2A, 2B).

In the bone marrow, 23 cells were counted: 9 were normal, and 14 metaphases were from the M 1 subline. No cells of the M 2, M 3 line were observed in the marrow.

In the terminal stage, 33 metaphases were obtained from blood cultures grown for 24 hours without mitogen. All were abnormal: 24 of the M 1 line, and 9 of the M 2, M 3 line. Some of the cells in the M 1 line now had 47 chromosomes, suggesting continuing evolution.

DISCUSSION

In this patient, different membrane phenotypes on the neoplastic cells were detected during the course of disease. If E-rosette formation at 4, 20, and 37°C are considered to represent T-cells, and E-rosettes at 37°C (*27*) and at 25°C by sedimentation are lymphoblasts with T-cell characteristics, then after transplantation more than 25% of this patient's leukemia cells retained T-cell markers throughout relapse. T-cell antigen (T-LCL) tested only in post-transplant relapse was not detected. Expression of T-antigen has been shown to precede that of SRBC receptor (E-rosette formation) during T-lymphocyte development (*28-32*). Some forms of lymphoblastic leukemia appear to represent cells arrested in a stage of development characterized by the expression of T-antigens but not SRBC receptors (*29*). Conversely, leukemia cells with a reversed expression of these markers have not been reported. Since T-cell antigen was not tested before the transplantation, we do not have an explanation for our finding of the reversed expression. During the first relapse after the graft, cells were negative for sIg and EA rosettes, and less than 1% were positive for EAC rosettes, indicating absence of the commonly recognized B-cell markers. However, Ia antigens were positive. In the terminal stage, Ia antigens were detected again and so were the other B-cell markers (sIg, Fc receptors, and EAC rosettes). Ia antigens on both occasions could have represented early lymphoid cell lines or stem cells common to lymphoid and granulocytic cell lines rather than B-cells. Another possibility is that the other B-cell markers except Ia antigen were selectively lost during the first relapse.

The monocyte marker used was the phagocytosis of latex particles by neoplastic cells and was detected only on one occasion when the cells morphologically also appeared more monoblastic than lymphoblastic. Fifty percent of cells showed phagocytosis, and one-third of these were also sIg^+, the remaining two-thirds were E^+ (fig. 1), and only a few were without either E^+ or sIg^+ markers (table 1). There was no cell with all three markers. We do not know whether the three-step procedures with multiple washing and handling of cells caused the loss of one or two markers or whether there was indeed no such cell. Nonetheless, this observation suggested that the neoplastic cells probably originated from a cell line that could express both lymphoid and monocytic characteristics.

Taking these observations together, the patient showed three types of surface markers throughout his course of leukemia: T-cell at diagnosis, T-, B-, and monocytic markers during the initial induction therapy, T-cell in the first relapse following the bone marrow transplantation, and T- and B-cells in the terminal stage. Occasionally, there were cells with double markers, which suggested that they were derived from a single common cell line.

Further evidence for this hypothesis is provided by the cytogenetic studies that were done during the post-transplantation relapse period. Two major abnormal sublines were detected in the cells studied. Both populations had multiple rearrangements, presumably from the large doses of radiation and chemotherapy preceding transplantation, but there was enough sharing of abnormal marker chromosomes between the sublines to indicate that they were from a common origin, with different proportions in the blood and bone marrow at different stages.

It is difficult to compare the chromosome data with the membrane marker studies done at various times, because there are only two time points in common. However, it may be significant that bone marrow cells from the first relapse post transplantation showed T-cell characteristics and that cytogenetically only one of two major abnormal sublines (subline 1) was found in the marrow at that time. When blood was studied in the terminal stage just prior to death, however, there was a mixture of cells with T- and B-cell characteristics, and the chromosome data indicated the presence in the blood of both major sublines. It is tempting to speculate that the cells identified cytogenetically as subline 1 had T-cell characteristics and that subline 2 had B-cell properties.

The results of this study support the view that as clonal evolution occurs during the clinical and biological progression of a malignant disease, more than one subpopulation may develop and coexist within the neoplasm. Such subpopulations were distinguishable in our patient by morphology, membrane phenotype, and genotype. A possible pattern for the clonal expression of leukemia cells in this case is illustrated in table 2.

This phenomenon has been reported in some patients

TABLE 2.—*Proposed clonal expression of leukemia cells*

Specification	Diagnosis, marrow	Induction, marrow	First relapse, marrow	Terminal stage, blood
Apparent cell types	T-cell	T-cell, B-cell monocyte	T-cell	T-cell, B-cell
Surface markers	E$^+$, sIg$^-$	E$^+$, sIg$^+$, phagocytosis$^+$	E$^+$, sIg$^-$, phagocytosis$^-$	E$^+$, sIg$^+$, phagocytosis$^-$
Chromosomes	Not done	Not done	Subline 1	Sublines 1, 2

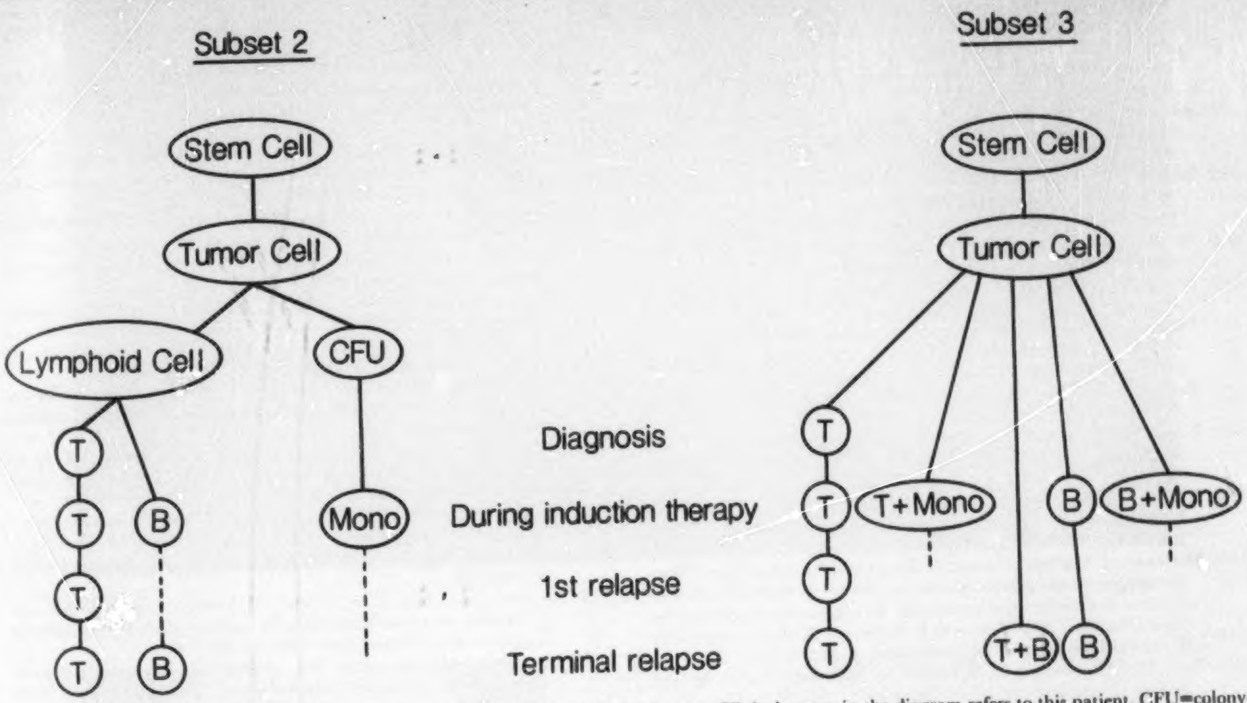

TEXT-FIGURE 1.—Proposed subsets of acute leukemia. Subset 1 is described in the text. Clinical course in the diagram refers to this patient. CFU=colony-forming unit.

with CML and in rare patients with ALL (*33–36*). Recently, we have observed 2 more patients with ALL who changed membrane phenotypes from diagnosis to relapse. Apparently, drug-resistant subclones within a leukemia cell clone appear and sometimes dominate in the patient's bone marrow tissue and peripheral blood after the initially dominant drug-sensitive subclones of blast cells disappear. The clinical course of this particular patient was marked by poor responses to a variety of chemotherapy regimens. A successful bone marrow transplant was performed, but leukemia recurred. Since the donor was the same sex as the patient, we cannot determine whether or not the recurrent leukemia was the same as the original one, but surface markers suggest that it was the original leukemia that recurred. It has been shown that more than 95% of the observed post-transplantation relapses have been in host-type cells, presumably the original leukemia clone (*37*).

These results lead us to propose the hypothesis that there are subsets in childhood leukemia: 1) Acute leukemia originating from a lymphoid cell lineage and expressed as a single end cell of a lymphoid line, such as T-cell, B-cell, or null cell; 2) Acute leukemia originating from a stem cell and expressed as a mixture of different end cells that carry one marker in each cell, such as T-cells, B-cells, or monocytes (text-fig. 1); and 3) acute leukemia originating from a stem cell but having mixed characteristics of T-cells, B-cells, or monocytes in the same cells (text-fig. 1).

This case would belong to the last hypothetical subset (subset 3 in text-fig. 1). At diagnosis and during the first relapse after bone marrow transplantation, only T-cell characteristics were expressed, whereas during the induction period and the terminal stage, there were cells with mixed markers in the same cells. The clinical evolution of our patient indicates that if he was, in fact, an example of one of the two postulated subgroups, management by ordinary or even extraordinary means will prove to be very difficult.

REFERENCES

(*1*) BOGGS DR. Hematopoietic stem cell theory in relation to possible lymphoblastic conversion of chronic myeloid leukemia (editorial). Blood 1974; 44:449–453.

(*2*) NOWELL PC, HUNGERFORD DA. Chromosome studies on normal and leukemic human leukocytes. J Natl Cancer Inst 1960; 25:85–109.

(*3*) ROWLEY JD. A new consistent chromosomal abnormality in chronic myelogenous leukaemia identified by quinacrine fluorescence and Giemsa staining. Nature 1973; 243:290–293.

(*4*) FIALKOW PJ, LISKER R, DETTER J, GIBLETT ER, ZAVALA C. 6-Phosphogluconate dehydrogenase: Hemizygous manifestation in a patient with leukemia. Science 1969; 163:194–195.

(5) Fialkow PJ, Lisker R, Giblett ER, Zavala C, Cobo A, Detter J. Genetic markers in chronic myelocytic leukemia: Evidence opposing autosomal inactivation and favouring 6-PGD-Rh linkage. Ann Hum Genet 1972; 35:321–326.

(6) Fialkow PJ. The origin and development of human tumors studied with cell markers. N Engl J Med 1974; 291:26–35.

(7) ———. Clonal origin and stem cell evolution of human tumors. In: Mulvihill JJ, Miller RW, Fraumeni JF Jr., eds. Genetics of human cancer. New York: Raven Press, 1977:439–453.

(8) Andreeff M, Gee T, Mertelsmann R, et al. Biclonal lymphoblastic and myeloblastic acute leukemia. Proc Am Assoc Cancer Res 1980; 21:54.

(9) Bennett JM, Catovsky D, Daniel MT, et al. Proposals for the classification of the acute leukaemias. Br J Haematol 1976; 33:451–458.

(10) Serota FT, August CS, O'Shea AT, Woodward WT, Koch PA. Role of a child advocate in the selection of donors for pediatric bone marrow transplantation. J Pediatr 1981; 98:847–850.

(11) Storb R, Thomas ED, Buckner CD, et al. Allogeneic marrow grafting for treatment of aplastic anemia. Blood 1974; 43:157–180.

(12) Böyum A. Separation of leukocytes from blood and bone marrow. Scand J Clin Lab Invest 1968; 21 (suppl 97):57–76.

(13) Thorsby E, Bratlie A. A rapid method for preparation of pure lymphocyte suspensions. In: Terasaki PI, ed. Histocompatibility testing. Copenhagen:Munksgaard, 1970:655–656.

(14) Jondal M, Holm G, Wigzell H. Surface markers on human T and B lymphocytes. J Exp Med 1972; 136:207–215.

(15) Hann HL, London WT, Evans AE. Lymphoblasts with T-cell markers in five girls with acute lymphocytic leukemia. Cancer 1977; 39:2001–2003.

(16) Tsubota T, Minowada J, Pressman D. Reaction of T-lymphoid and B-lymphoid cell lines with rabbit antisera against these lines. J Natl Cancer Inst 1977; 59:399–404.

(17) Minowada J. Markers of human leukemia-lymphoma cell lines reflect hematopoietic cell differentiation. In: Serrou B, Rosenfeld C, eds. Human lymphocyte differentiation: Its application to cancer. Institute National de la Santé et de la Recherche Médicale symposium 8. Amsterdam: Elsevier/North-Holland, 1978:337–344.

(18) Grey HM, Rabellino E, Pirofsky B. Immunoglobulins on the surface of lymphocytes. J Clin Invest 1971; 50:2368–2375.

(19) Dickler HB, Kunkel HG. Interaction of aggregated γ-globulin with B lymphocytes. J Exp Med 1972; 136:191–196.

(20) Frøland SS, Michaelsen TE, Wisløff F, Natvig JB. Specificity of receptors for IgG on human lymphocyte-like cells. Scand J Immunol 1974; 3:509–517.

(21) Han T, Minowada J, Subramanian S, Sinks LF. Human thymus cells: Excellent responders but poor stimulators in "one-way" mixed lymphocyte reaction. Immunology 1976; 30:361–366.

(22) Schlossman SF, Chess L, Humphreys RE, Strominger JL. Distribution of Ia-like molecules on the surface of normal and leukemic human cells. Proc Natl Acad Sci USA 1976; 73:1288–1292.

(23) Hurwitz R, Hozier J, LeBien T, et al. Characterization of a leukemic cell line of the pre-B phenotype. Int J Cancer 1979; 23:174–180.

(24) Schmidt ME, Douglas SD. Disappearance and recovery of human monocyte IgG receptor activity after phagocytosis. J Immunol 1972; 109:914–917.

(25) Greaves MF, Brown G, Rapson NT, Lister TA. Antisera to acute lymphoblastic leukemia cells. Clin Immunol Immunopathol 1975; 4:67–84.

(26) Nowell PC, Glick J, Bucolo A, Finan J, Creech R. Cytogenetic studies of bone marrow in breast cancer patients after adjuvant chemotherapy. Cancer 1981; 48:667–673.

(27) Borella L, Sen L. E receptors on blasts from untreated acute lymphocytic leukemia (ALL): Comparison of temperature dependence of E rosettes formed by normal and leukemic lymphoid cells. J Immunol 1975; 114:187–190.

(28) Balch CM, Dougherty PA, Dagg MK, Diethelm AG, Lawton AR. Detection of human T cells using anti-monkey thymocyte antisera: Tissue distribution and evidence for antigenic heterogeneity. Clin Immunol Immunopathol 1977; 8:448–460.

(29) Greaves MF, Janossy G, Roberts M, et al. Membrane phenotyping: Diagnosis, monitoring and classification of acute "lymphoid" leukaemias. In: Thierfelder S, Rodt H, Thiel E, eds. Hematology and blood transfusion. New York:Springer-Verlag, 1977:61–75.

(30) Aiuti F, Schirrmacher V, Ammirati P, Fiorilli M. Effect of thymus factor on human precursor T lymphocytes. Clin Exp Immunol 1975; 20:499–503.

(31) Incefy GS, L'Esperance P, Good RA. In vitro differentiation of human marrow cells into T lymphocytes by thymic extracts using the rosette technique. Clin Exp Immunol 1975; 19:475–483.

(32) Touraine JL, Incefy GS, Touraine F, Rho YM, Good RA. Differentiation of human bone marrow cells into T-lymphocytes by in vitro incubation with thymic extracts. Clin Exp Immunol 1974; 17:151–158.

(33) Grouchy J de, Nava C de, Cantu J-M, Bilski-Pasquier G, Bousser J. Models for clonal evolutions: A study of chronic myelogenous leukemia. Am J Hum Genet 1966; 18:485–503.

(34) Goldstone AH, McVerry BA, Janossy G, Walker H. Clonal identification in acute lymphoblastic leukemia. Blood 1979; 53:892–898.

(35) Borella L, Casper JT, Lauer SJ. Shifts in expression of cell membrane phenotypes in childhood lymphoid malignancies at relapse. Blood 1979; 54:64–71.

(36) Andersson LC, Wegelius R, Borgström GH, Gahmberg CG. Change in cellular phenotype from lymphoid to erythroid in a case of ALL. Scand J Haematol 1980; 24:115–121.

(37) Thomas ED. Marrow transplantation for leukemia. J Clin Immunol 1981; 1:137–140.

Figure 1.—a) Leukemia cell that has formed a rosette with SRBC without phagocytosis of latex particles. b) Two leukemia cells that have phagocytized latex particles but have not formed rosettes with SRBC. c) A leukemia cell that has formed a rosette with SRBC and phagocytized latex particles. *Bar*=5 µm.

Figure 2.—A) Metaphase with large abnormal chromosome (M 1), probably a $5q^+$, which characterized one major leukemia subline (subline 1). *Small arrow* indicates an abnormal marker chromosome, which was also identified in subline 2. B) Metaphase with two large D-type chromosomes (M 2, M 3), which characterized the second major leukemia subline (subline 2). *Small arrow* indicates the same small marker as in fig. 2A.

1

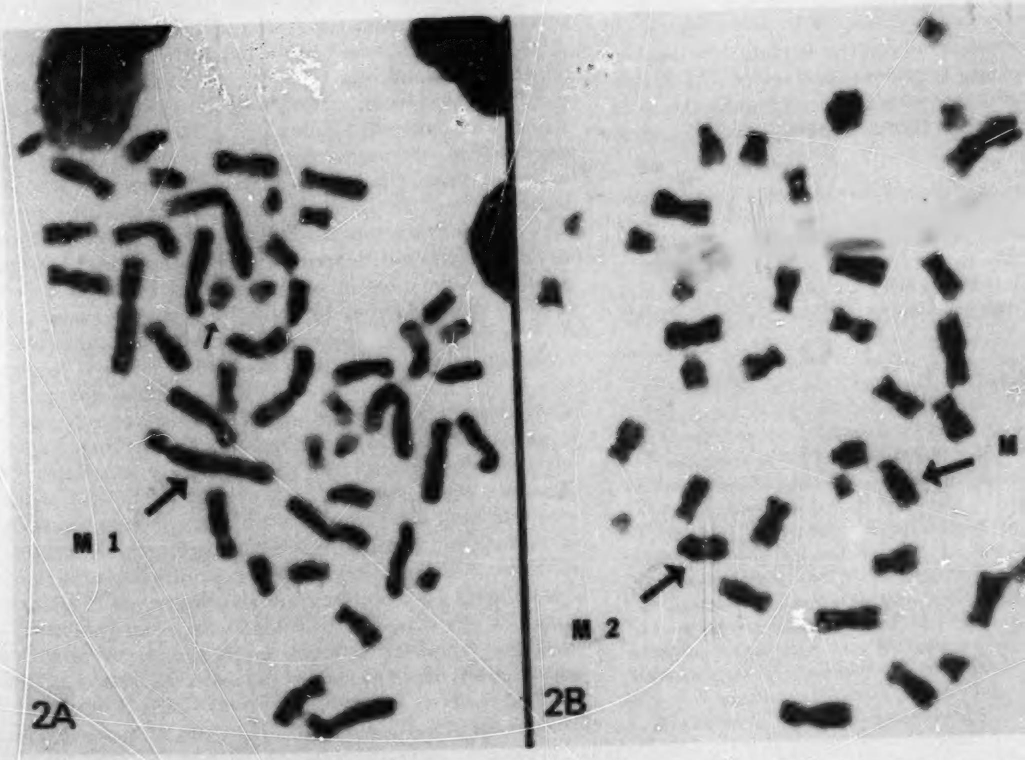
M 1
2A
M 2
2B
M

blank page

Coproduction of Carcinoembryonic Antigen and Nonspecific Cross-Reacting Antigen by a Continuous Cell Line From a Human Pancreatic Tumor[1,2]

Masahide Kuroki,[3] Sadanori Ichiki,[3] Motomu Kuroki,[3] *and* Yuji Matsuoka[3,4,5]

ABSTRACT—A simultaneous production of nonspecific cross-reacting antigen (NCA) and carcinoembryonic antigen (CEA) by the same individual cells of an established human pancreatic cell line (QGP-1) was demonstrated by the immunoperoxidase method. Kinetics of cell proliferation and production of CEA and NCA were analyzed, and active synthesis of both antigens was found to be accompanied with the active proliferation of cultured cells. Both antigens in culture medium were purified by immunoadsorption and gel filtration. Immunochemical studies confirmed that CEA and NCA produced by the QGP-1 cells had properties identical to those of authentic CEA derived from metastatic colorectal carcinoma and to those of NCA from normal lungs, respectively.—JNCI 1982; 69:401–408.

Although the cancer specificity of CEA is, at present, rather controversial, its clinical usefulness is being widely accepted, especially in monitoring the response to therapy in cancer patients with elevated serum levels of CEA (*1, 2*). From the basic oncologic point of view, CEA is one of the most interesting glycoprotein antigens because the ontogenic and oncologic molecular differentiation process may be traced by the comparative structural analyses of CEA and related antigens in fetal tissues and in normal adult tissues or secretions (*3–5*). In this context, a number of CEA-related antigens in normal tissues have become significant (*6–9*). Among them, NCA (*10*), which is also known as normal glycoprotein [NGP (*11*)], glycoprotein related to CEA [CEX (*12*) and CCEA-2 (*13*)], and colon carcinoma antigen-III [CCA-III (*14*)], seems to be very important because this antigen is frequently detected in malignant tissues as well as normal tissues and has been reported to have a partial identity with CEA chemically and antigenically (*10, 15*). The NCA has been detected in normal blood granulocytes and macrophages of mesodermal origin (*16, 17*), but a controversy exists as to whether the epithelial cells of entodermal origin produced NCA or not, though some data suggested that the entodermal epithelial cells also produced NCA as well as CEA (*18*).

Thus the established CEA-producing cell lines seem to be of great significance for investigation of the mechanism of CEA expression by cancer cells and for understanding the biologic role of CEA (*19–25*). Although there are some suggestions that several CEA-producing cell lines also produced the NCA molecules (*26–28*), whether the same individual cells simultaneously produce both the CEA and NCA molecules or not remains to be determined. We investigated, as described herein, an established cell line from a human pancreatic tumor and found that this cell line coproduced the CEA and NCA molecules in the same cells, each having the immunochemical properties identical to those of CEA from colon tumors and of NCA from normal lungs.

MATERIALS AND METHODS

Cell Culture.—The human pancreatic cancer cell line QGP-1 was initially developed by Dr. Kaku at Kyushu Cancer Center, Fukuoka. It was originally established from a tumor mass surgically obtained from a 61-year-old Japanese male who had a circulating plasma CEA level of 1,369 ng/ml (measured by the CEA-Roche kit). By histologic examination, the cells were determined to be of islet cell origin. The characteristics of QGP-1 cells, such as morphology, biologic features, and CEA synthesis, have been outlined elsewhere (*29*). We received this cell line in 1979. The cells were maintained as monolayer cultures in RPMI-1640 medium supplemented with 5% fetal bovine serum (GIBCO, Grand Island, N.Y.), 5% newborn calf serum (GIBCO), 10^5 U penicillin/ml, and 100 µg streptomycin/ml. Confluent cell monolayers were passaged by treatment with trypsin-EDTA solution (0.25% trypsin and 0.075% EDTA in 0.1 *M* phosphate-buffered saline). All cultures were gassed with 5% CO_2 in air and incubated at 37°C.

Reference CEA and NCA preparations.—Reference CEA was prepared from metastatic liver tumors from colorectal cancer by use of a purification procedure described earlier (*30, 31*). NCA was purified from pooled normal human lungs by combination of an affinity chromatography on immunoadsorbent and gel filtration as described in (*9*). The CEA and NCA preparations contained practically pure antigens as demonstrated by immunoelectrophoresis and by sodium dodecyl sulfate–polyacrylamide gel electrophoresis (*9*).

ABBREVIATIONS USED: CEA=carcinoembryonic antigen; Go-a-CEA=goat anti-CEA antiserum; NCA=nonspecific cross-reacting antigen; Go-a-NCA=goat anti-NCA antiserum; Q-CEA=CEA produced by QGP-1 cells; Q-NCA=NCA produced by QGP-1 cells; R-a-CEA=rabbit anti-CEA antiserum; R-a-NCA=rabbit anti-NCA antiserum; R-a-Q-CEA=rabbit anti-Q-CEA antiserum; R-a-Q-NCA=rabbit anti-Q-NCA antiserum.

---

[1] Received November 17, 1981; accepted March 2, 1982.

[2] Supported in part by Grant-in-Aid for Cancer Research from the Ministry of Education, Science and Culture, Japan.

[3] Department of Biochemistry, School of Medicine, Fukuoka University, 34 Nanakuma, Nishi-ku, Fukuoka 814-01, Japan.

[4] *Address reprint requests to* Dr. Matsuoka.

[5] We thank Dr. M. Kaku, Kyushu Cancer Center, Fukuoka, Japan, for supplying the QGP-1 cell line; Dr. M. Kikuchi, School of Medicine, Fukuoka University, Dr. A. Horie, School of Medicine, University of Occupational and Environmental Health, Kitakyushu, Japan, and Dr. Y. Katsuta, Kyushu Cancer Center, for their kind supply of cancerous and noncancerous materials; Miss M. Kichimoto and Miss R. Iida, School of Medicine, Fukuoka University, for expert technical assistance; Dr. Y. Yagi, Nippon Roche Research Center, for reviewing the manuscript; and Miss N. Kawakami for typing the manuscript.

Antisera.—Two anti-CEA preparations were used in this study. Go-a-CEA and R-a-CEA against a preparation of CEA from tumor tissue were prepared as described previously (*31*). Go-a-CEA was specifically purified by adsorption to CEA–Sepharose 4B (*see below*) and by elution with 0.175 *M* glycine–HCl buffer (pH 2.8). The purified antibody preparation was used without further absorption or after complete absorption with NCA. An IgG-rich fraction of R-a-CEA obtained by salting out with 40% saturation of $(NH_4)_2SO_4$ was completely absorbed with NCA–Sepharose 4B and was used for the immunoperoxidase staining.

Go-a-NCA and R-a-NCA against lung NCA were obtained as described previously (*32*). Go-a-NCA was specifically purified by adsorption to and elution from NCA–Sepharose 4B. The purified antibody preparation was used after complete absorption with CEA. An IgG-rich fraction of R-a-NCA was completely absorbed with CEA–Sepharose 4B and used for the immunoperoxidase staining.

An antiserum against the CEA produced by QGP-1 cells (Q-CEA) (*see below*) was prepared in a rabbit that was immunized twice at five weekly intervals, each time with 200 μg of partially purified Q-CEA in complete Freund's adjuvant (Difco Laboratories, Detroit, Mich.). This antiserum was designated R-a-Q-CEA. An antiserum against the NCA produced by QGP-1 cells (Q-NCA) (*see below*) was raised as mentioned above, each time with 100 μg of partially purified Q-NCA and designated R-a-Q-NCA. R-a-Q-CEA and R-a-Q-NCA were used after absorption with fetal bovine serum and newborn calf serum.

We prepared a goat anti-rabbit IgG antiserum by immunizing with rabbit IgG purified by salting out with 40% $(NH_4)_2SO_4$ and by performing ion-exchange chromatography on DEAE–cellulose. A rabbit antiperoxidase antiserum was obtained by immunization with purified horse-radish peroxidase (type IV; Sigma Chemical Co., St. Louis, Mo.).

Antigen and antibody adsorbents.—Purified CEA and NCA were coupled with CNBr-activated Sepharose 4B (10 mg/g dry gel; Pharmacia Fine Chemicals AB, Uppsala, Sweden) according to the manufacturer's instructions.

Go-a-CEA specifically purified by CEA–Sepharose 4B was conjugated to CNBr-activated Sepharose 4B (10 mg/g dry gel) and used for specific purification of the antigens in QGP-1 culture media.

Immunoperoxidase staining.—We applied an unlabeled antibody enzyme method (*33*) to identify the CEA- or NCA-producing cells. Packed cells obtained from confluent culture were fixed in 10% buffered Formalin (pH 7.4) and embedded in paraffin by the usual techniques. Paraffin sections (2 μm) were treated with xylene and graded ethanol solution and finally with 0.05 *M* Tris–saline (pH 7.6). Serial sections were used to determine whether CEA and NCA are produced by the same cells or not.

Staining procedures were as follows: 1) We incubated the sections in 0.3% hydrogen peroxide in methanol to block endogenous peroxidase. 2) We added goat serum diluted twentyfold to the sections for 30 minutes to reduce nonspecific background staining. 3) We applied R-a-CEA absorbed with NCA, R-a-NCA absorbed with CEA, or control serum (each diluted 1:100) to the sections for 30 minutes. 4) We included goat anti-rabbit IgG (diluted 1:50) to the sections for 30 minutes. 5) We applied horse-radish peroxidase-rabbit antiperoxidase complex, which was synthesized according to the instruction of Sternberger et al. (*33*), to the sections for 30 minutes. 6) We effected 3,3′-diaminobenzidine (0.05%) reaction in the presence of 0.05% hydrogen peroxide for 5 minutes. All incubation steps were performed at 37°C, and washings after incubation were performed with Tris buffer. In these experiments, we always used in parallel for the control serum the normal rabbit serum, R-a-CEA absorbed with CEA, or R-a-NCA absorbed with NCA. The sections were finally counterstained with hematoxylin for 10 minutes, dehydrated in graded ethanol solutions and xylene, and mounted in Permount (Fisher Scientific Co., Fair Lawn, N.J.)

Gel filtrations.—Gel filtrations were performed with 0.05 *M* sodium phosphate buffer (pH 5.2).

Radioimmunoassay.—We estimated CEA in spent culture medium and in Sephadex G-200 column fractions by using previously described sandwich-type solid-phase methods (*32*). In this system NCA showed a negligible reactivity (10,000 ng of NCA corresponded to 3 ng of CEA). NCA was also determined by a similar method with the use of Go-a-NCA absorbed with CEA. In this system, 10,000 ng CEA gave a reaction equivalent to only 0.5 ng NCA. Fresh culture medium gave no reaction by these two assay systems.

Immunoelectrophoresis and immunodiffusion tests.—Immunoelectrophoresis and microscale immunodiffusion tests were performed in 1.2% agarose layer as described in (*31*).

RESULTS

Immunohistochemical Studies

The QGP-1 cells harvested by treatment with trypsin–EDTA solution are morphologically heterogenous and can be roughly categorized into two types: small cells and large cells (fig. 1). The large cells were not the cells spread after death since most of large cells were found to exclude trypan blue dye as did the small ones. Interrelation between these two types of cells is unclear at present. When the serial sections of packed QGP-1 cells were examined by the immunoperoxidase method, the cytoplasm of almost all the cells was stained diffusely or granularly both with specific R-a-CEA and with specific R-a-NCA (figs. 1A, 1B), though the staining of the large cells was generally rather faint. Obviously, the same individual cell was stained with both antibody reagents. This clearly indicated that both CEA and NCA were present in the cytoplasm of the same cells. No positive staining of the nuclei was observed by examination of the sections just before counterstaining with hematoxylin. None of the QGP-1 cells were stained with any of the control sera: normal rabbit serum, R-a-CEA absorbed with CEA, or R-a-NCA absorbed with NCA, confirming the immunologic specificity of the staining.

Growth Rate and Kinetics of CEA and NCA Production

To determine the growth rate and the output of Q-CEA and Q-NCA, 1.4×10^5 cells were seeded into each of 30 petri dishes (35 mm in diameter) containing 2 ml of nutrient medium. At intervals of 2 or 3 days, all the cells and spent culture medium of three dishes were individually harvested for the ensuing 14 days, and the average cell number per dish and viability at a given culture period were counted by trypan blue dye exclusion test with the use of a hemacytometer. The concentrations of CEA and NCA in spent culture medium of each dish were separately estimated by radioimmunoassay, and the average antigen concentrations in medium at a given culture period were calculated. No fresh medium was added to the cultures during the course of the experiment.

As can be seen in text-figure 1, after 1-day lag phase, the QGP-1 cells started to proliferate with the doubling time of about 3.5 days and reached confluence at day 12 of culture. Both CEA and NCA also started to accumulate in the medium after 1-day lag phase and kept increasing up to culture day 12 when the cells stopped proliferating (text-fig. 1). The concentrations of both CEA and NCA in medium accumulated by day 7 of culture were 37.7 and 15.7 ng/ml, respectively.

Isolation of CEA and NCA From Spent Culture Medium of QGP-1 Cells

We tried to isolate CEA and NCA from spent culture medium by immunoadsorption and gel filtration. The perchloric acid extraction technique for precipitation of the protein, a technique frequently employed for the purification of CEA or CEA-related antigens, was not used in this study in order to minimize the loss of antigens. About 7.5 liters of spent medium of the QGP-1 cell line was collected, filtered through a 1.2-μm Millipore filter, and concentrated about fortyfold by pervaporation. The antigens in the concentrated medium (≈180 ml) were drawn into and eluted from the Go-a-CEA (not absorbed with NCA) adsorbent containing about 10 mg of purified antibody. The eluate was concentrated and applied to a Sephadex G-200 column. The elution profile is shown in text-figure 2. The major peak of optical density at 280 nm was due primarily to calf serum proteins contaminating the eluate. In fraction II, we detected the antigen reactive with specific anti-CEA antibody. The NCA activity was detected in fraction V. The concentrated fraction II was chromatographed on another Sephadex G-200 column. The antigen with CEA activity was eluted from the column as a single peak and designated Q-CEA. The antigen with NCA activity in fraction V was further chromatographed on a Sephadex G-200 column and eluted in a single peak and designated Q-NCA. The elution position of Q-CEA or Q-NCA on the Sephadex G-200 column was identical with that of reference CEA or NCA, respectively (text-fig. 2).

Immunochemical Studies of the Purified Q-CEA and Q-NCA Preparations

As can be seen in figure 2A, the precipitate line of Q-CEA with R-a-CEA coalesced completely with that of CEA from

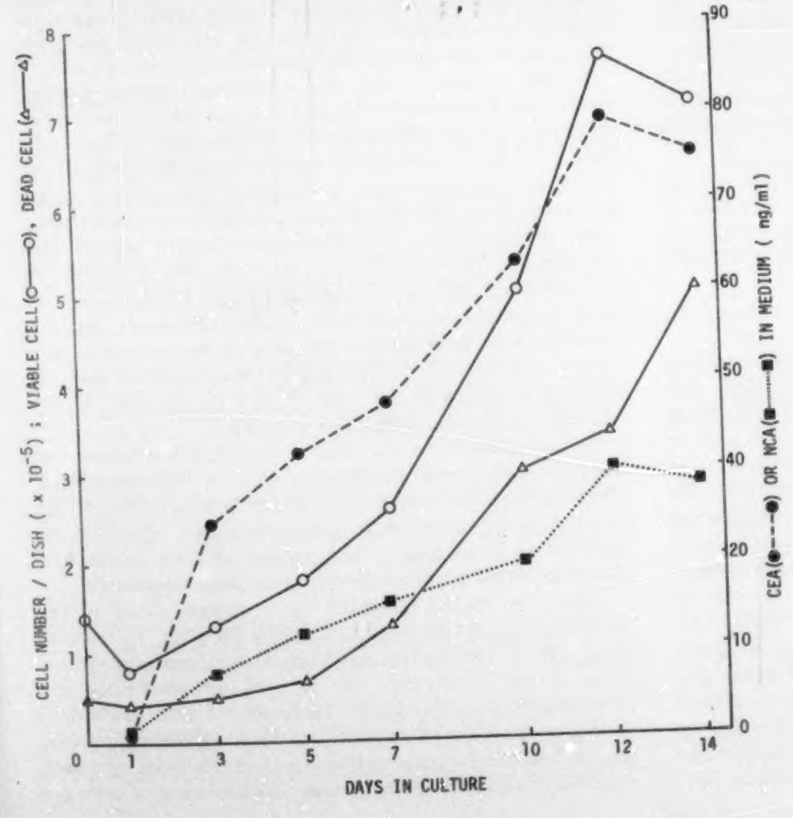

TEXT-FIGURE 1.—Growth rate of the QGP-1 cells at passage 12 after recovery from liquid nitrogen storage and kinetics of CEA and NCA production by these cells. QGP-1 cells, 1.4×10^5, were seeded into 35-mm petri dishes with 2 ml medium, and then at indicated times the cell number and viability were estimated by a hemacytometer, and the CEA or NCA activity in supernatants of the dishes was determined by radioimmunoassay (*see text*).

TEXT-FIGURE 2.—Sephadex G-200 chromatography of the eluate from an anti-CEA adsorbent. Sample (1.2 ml) was applied to the column (1.7×100.0 cm). The effluent was collected in 1.5-ml portions and combined as indicated. Elution positions of colon carcinoma CEA and lung NCA are shown in references. O.D.=optical density.

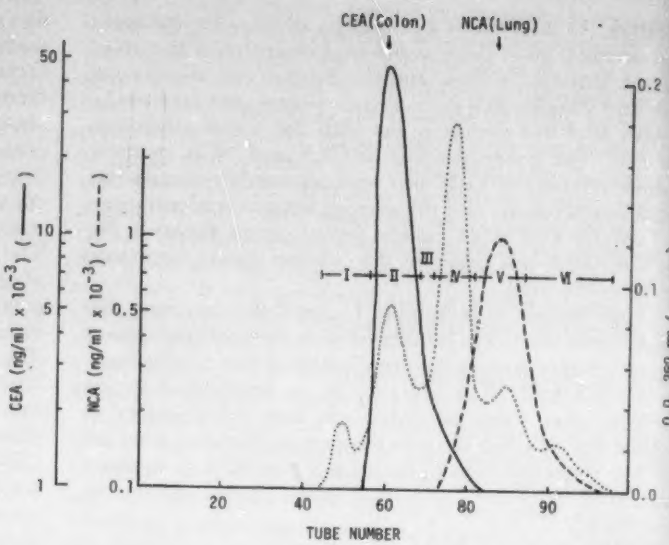

tumor tissues. The precipitate line of Q-NCA fused partially with that of CEA and, in turn, the line of NCA fused partially with Q-CEA. The lines of NCA and Q-NCA with R-a-CEA coalesced completely with each other (fig. 2B). When tested with R-a-NCA absorbed with CEA, the line of Q-NCA also coalesced with that of NCA (fig. 2C). Furthermore, the immunologic reactivities of R-a-Q-CEA and R-a-Q-NCA were demonstrated to be the same as those of R-a-CEA and R-a-NCA, respectively (figs. 3A, 3B). These results indicated that antigenically Q-CEA was indistinguishable from CEA from tumor tissues, that Q-NCA was antigenically identical with NCA from lung, and that Q-NCA had a distinctive determinant (NCA distinctive determinant) in addition to the NCA common determinant as well as did authentic NCA (*9, 10, 12*).

The immunoelectrophoretic patterns of Q-CEA and Q-NCA are shown in figure 4 in comparison with those of CEA and NCA. No difference in mobility was observed between Q-CEA and CEA and between Q-NCA and NCA.

DISCUSSION

NCA was first identified in perchloric extracts of normal lung or spleen (*10, 11*) as a glycoprotein antigen that partially shares antigenic determinants with CEA; NCA then was also found in normal colon mucosa (*18*) and in normal sera (*34*). NCA has also been frequently seen in association with CEA in the tumor tissues (*12, 18*). In addition, NCA was found to be a normal constituent of blood granulocytes and macrophages (*16, 17*), which leads to the suggestion that the presence of NCA in the tumor tissues is a result of infiltration of granulocytes due to inflammatory process in the tissues. However, several histologic examinations of the tissue samples revealed no correlation between the degree of granulocyte infiltration and concentration of NCA in the corresponding tissue extracts (*35*). The question has occurred, therefore, of whether or not NCA is also produced by the tumor cells themselves. In 1975, by using the immunofluorescence technique, von Kleist et al. (*27*) revealed that NCA was synthesized by a CEA-producing colon tumor cell line (HT-29). This finding was followed by a report (*28*) demonstrating the presence of NCA on the cells from this HT-29 cell line by means of the antibody-dependent, cell-mediated cytotoxicity assay. In addition, Heumann et al. (*36*) demonstrated that a colon carcinoma cell line produced NCA even after passage in nude mice. However, it has not been determined whether or not CEA and NCA are produced by the same cells, and no immunochemical characterization has been made about the NCA synthesized by the CEA-producing tumor cell line.

In the present study, the immunoperoxidase method clearly demonstrated that both CEA and NCA were synthesized by the same individual cells of pancreatic tumor origin (figs. 1A, 1B). A preliminary experiment with the use of the double-staining procedure by the respective antisera conjugated with two different fluorochromes (tetramethylrhodamine isothiocyanate and fluorescein isothiocyanate) also detected the CEA and NCA on the same cells of QGP-1 cell line (data not shown). To our knowledge, NCA has not yet been described on pancreatic tumor cell lines. NCA is frequently elevated also in the sera of patients with pancreatic tumor (*12, 34*) and can be demonstrated easily in fetal pancreatic extracts (*37*). Hence its presence on the cultured pancreatic cells is not illogical.

Immunoperoxidase staining of the QGP-1 cells revealed the intracytoplasmic localization of both CEA and NCA. These findings are strong evidence favoring the idea of CEA or NCA being synthesized in the cytoplasm. Granular deposits may be related to the storage of CEA or NCA in distended ergastoplasmic cisternae of Golgi apparatus.

From the results obtained by a kinetic study of cell proliferation and antigen production (text-fig. 1), it seems clear that: 1) During the lag phase no antigens were synthesized, 2) the production rate of both antigens CEA and NCA was most active in the early period after seeding, 3) the active synthesis of antigens was observed during a period in which the cells also proliferate actively, 4) after cells have reached confluence neither active proliferation of cells nor active production of the antigens was observed and, therefore, 5) accumulation of the antigens in culture medium does not seem to be due to passive release of antigens from the dead or dying cells.

The production rate of CEA by QGP-1 cells is comparable to that reported for other CEA-producing cell lines such as HT-29 cells (*19*) and HRT-18 or HCT-8 cells (*20*). The rate of NCA production by QGP-1 cells was about the same as that of CEA production, on the molecular basis; but this may be variable depending on the nature of cell line established.

Immunochemical analyses indicate that Q-CEA and Q-NCA have antigenic and physicochemical properties identical to those of authentic colon carcinoma CEA and lung NCA, respectively. Q-NCA seems not to be simply a fragment of the CEA (Q-CEA) molecule since Q-NCA possessed a unique determinant identical to that of lung NCA, and there are enough immunologic and chemical differences proving that NCA and CEA are distinct molecules (*6*, *15*). Shively et al. (*7*) have suggested that CEA and NCA were products of sister (or daughter) genes derived from a single primordial gene by replication and evolutionary divergence inasmuch as the similarity between the NH_2 terminal sequences of CEA and NCA was demonstrated (*15*). The fact that the Q-NCA having immunochemical properties similar to those of lung NCA was coproduced by the very CEA-producing cells suggests that these sister genes are simultaneously active in some tumor cells.

Further characterization of the QGP-1 cell line and chemical analyses of Q-CEA and Q-NCA produced by this line may help us to understand in what way CEA is related to the normal tissue component NCA.

REFERENCES

(*1*) Gold P, Shuster J. Historical development and potential uses of tumor antigens as markers of human tumor growth. Cancer Res 1981; 40:2973–2976.

(*2*) National Institutes of Health Consensus Development Conference Statement. Carcinoembryonic antigen: Its role as a marker in the management of cancer. Cancer Res 1981; 41:2017–2018.

(*3*) Rule AH, Kirch ME. Gene activation of molecules with carcinoembryonic antigen determinants in fetal development and in adenocarcinoma of the colon. Cancer Res 1976; 36:3503–3509.

(*4*) Shively JE, Todd CW. The assay and structure of carcinoembryonic antigens. In: Waters H, ed. The handbook of cancer immunology. Vol 8. New York: Carland STPM Press, 1981:321–338.

(*5*) Matsuoka Y, Kuroki M, Koga Y, Kuriyama H, Mori T, Kosaki G. Immunochemical differences among carcinoembryonic antigen in tumor tissues and related antigens in meconium and adult feces. Cancer Res. In press.

(*6*) Burtin P. The carcinoembryonic antigen of the digestive system (CEA) and the antigens cross-reacting with it. Ann Immunol (Paris) 1978; 129:185–198.

(*7*) Shively JE, Glassman JN, Engvall E, Todd CW. Amino acid sequence of CEA and CEA related antigens. In: Lehmann F-G, ed. Carcinoembryonic proteins. Amsterdam: Elsevier/North-Holland, 1979; 1:9–15.

(*8*) von Kleist S. Antigens crossreacting with CEA. Evaluation of their interrelationship and clinical role. Vol 1. In: Lehmann F-G, ed. Carcinoembryonic proteins. Amsterdam: Elsevier/North-Holland, 1979:35–39.

(*9*) Kuroki M, Koga Y, Matusoka Y. Purification and characterization of carcinoembryonic antigen-related antigens in normal adult feces. Cancer Res 1981; 41:713–720.

(*10*) von Kleist S, Chavanel G, Burtin P. Identification of an antigen from normal human tissue that crossreacts with the carcinoembryonic antigen. Proc Natl Acad Sci USA 1972; 69:2492–2494.

(*11*) Mach J-P, Pusztaszeri G. Carcinoembryonic antigen (CEA): Demonstration of a partial identity between CEA and a normal glycoprotein. Immunochemistry 1972; 9:1031–1034.

(*12*) Darcy DA, Turberville C, James R. Immunological study of carcinoembryonic antigen (CEA) and a related glycoprotein. Br J Cancer 1973; 28:147–160.

(*13*) Turberville C, Darcy DA, Laurence DJ, Johns EW, Neville AM. Studies on carcinoembryonic antigen (CEA) and a related glycoprotein, CCEA-2. Preparation and chemical characterization. Immunochemistry 1973; 10:841–843.

(*14*) Newman ES, Petras SE, Georgiadis A, Hansen HJ. Interrelationship of carcinoembryonic antigen and colon carcinoma antigen-III. Cancer Res 1974; 34:2125–2130.

(*15*) Engvall E, Shively JE, Wrann M. Isolation and characterization of the normal crossreacting antigen: Homology of its NH_2-terminal amino acid sequence with that of carcinoembryonic antigen. Proc Natl Acad Sci USA 1978; 75:1670–1674.

(*16*) Bordes M, Knobel S, Martin F. Carcinoembryonic antigen (CEA) and related antigens in blood cells and hematopoietic tissues. Eur J Cancer 1975; 11:783–786.

(*17*) Burtin P, Quan PC, Sabine MC. Nonspecific cross reacting antigen as a marker for human polymorphs, macrophages and monocytes. Nature 1975; 255:714–716.

(*18*) Burtin P, von Kleist S, Sabine MC, King M. Immunohistological localization of carcinoembryonic antigen and nonspecific cross-reacting antigen in gastrointestinal normal and tumoral tissues. Cancer Res 1973; 33:3299–3305.

(*19*) Egan ML, Todd CW. *Brief communication:* Carcinoembryonic antigen: Synthesis by a continuous line of adenocarcinoma cells. J Natl Cancer Inst 1972; 49:887–889.

(*20*) Tompkins WA, Watrach AM, Schmale JD, Schultz RM, Harris JA. Cultural and antigenic properties of newly established cell strains derived from adenocarcinomas of the human colon and rectum. J Natl Cancer Inst 1974; 52:1101–1110.

(*21*) Carrel S, Sordat B, Merenda C. Establishment of a cell line (Co-115) from a human colon carcinoma transplanted into nude mice. Cancer Res 1976; 36:3978–3984.

(*22*) Leibovitz A, Stinson JC, McCombs WB III, McCoy CE, Mazur KC, Mabry ND. Classification of human colorectal adenocarcinoma cell lines. Cancer Res 1976; 36:4562–4569.

(*23*) Ellison ML, Lamb D, Rivett J, Neville AM. Quantitative aspects of carcinoembryonic antigen output by a human lung carcinoma cell line. J Natl Cancer Inst 1977; 59:309–312.

(*24*) Drewinko B, Yang L-Y, Barlogie B, et al. Further biologic characteristics of a human carcinoembryonic antigen-producing colon carcinoma cell line. JNCI 1978; 61:75–83.

(*25*) Rosenthal KL, Tompkins WA, Rawls WE. Factors affecting the expression of carcinoembryonic antigen at the surface of cultured human colon carcinoma cells. Cancer Res 1980; 40:4744–4750.

(*26*) Breborowicz J, Easty GC, Birbeck M, Robertson D, Nery R, Neville AM. The monolayer and organ culture of human colorectal carcinomata and the associated "normal" colonic mucosa and their production of carcinoembryonic antigens. Br J Cancer 1975; 31:559–569.

(*27*) von Kleist S, Chany E, Burtin P, King M, Fogh J. Immunohistology of the antigenic pattern of a continuous cell line from a human colon tumor. J Natl Cancer Inst 1975; 55:555–560.

(*28*) Hammarström S, Troye M, Wahlund G, Svenberg T, Perlmann P. K cell mediated lysis of cultured colon carcinoma and urinary bladder carcinoma cells induced by monospecific antisera against carcinoembryonic antigen (CEA) and two CEA-related normal glycoproteins. Int J Cancer 1977; 19:756–766.

(*29*) Kaku M, Nishiyama T, Yagawa K, Abe M. Establishment of a carcinoembryonic antigen-producing cell line from human pancreatic carcinoma. Gan 1980; 71:596–601.

(*30*) Matsuoka Y, Tsuru E, Sawada H. Preparation and evaluation antisera directed against cancer specific moiety of antigenic determinants on carcinoembryonic antigen. Immunochemistry 1975; 12:779–782.

(*31*) Matsuoka Y, Koga Y, Maruta H, Yoshino M, Tsuru E. Proteolytic release of antigenic fragments corresponding to normal fecal antigen and non-specific cross-reacting antigen from carcinoembryonic antigen. Int J Cancer 1978; 21:604–610.

(*32*) Kuroki M, Shinoda T, Takayasu T, Koga Y, Matsuoka Y. Immunological characterization and structural studies of normal fecal antigen-1 related to carcinoembryonic antigen. Mol Immunol 1982; 19:399–406.

(*33*) Sternberger LA, Hardy PH Jr, Cuculis JJ, Meyer HG. The unlabeled antibody enzyme method of immunohistochemistry. Preparation and properties of soluble antigen–antibody complex (horseradish peroxidase–antihorseradish peroxidase) and its use in identification of spirochetes. J Histochem Cytochem 1970; 18:315–333.

(*34*) von Kleist S, Troupel S, King M, Burtin P. A clinical comparison between nonspecific cross-reacting antigen and CEA in patients' sera. Br J Cancer 1977; 35:875–880.

(*35*) Nielsen CS, Wandall JH. Nonspecific crossreacting antigen (NCA) in human mammary carcinoma extracts. Scand J Immunol 1978; 8 (suppl 8):479–484.

(*36*) Heumann D, Candardjis P, Carrel S, Mach J-P. Identification of the normal glycoprotein (NGP) crossreacting with CEA as a differentiation antigen of myeloid cells and macrophages. In: Lehmann F-G, ed. Carcinoembryonic proteins. Vol 2. Amsterdam: Elsevier/North-Holland, 1979:3–14.

(*37*) Gadler H, Gremme K, Wahren B. Distribution of tumor-associated antigen CEA and cross-reacting NCA in fetal organs. Int J Cancer 1980; 25:91–94.

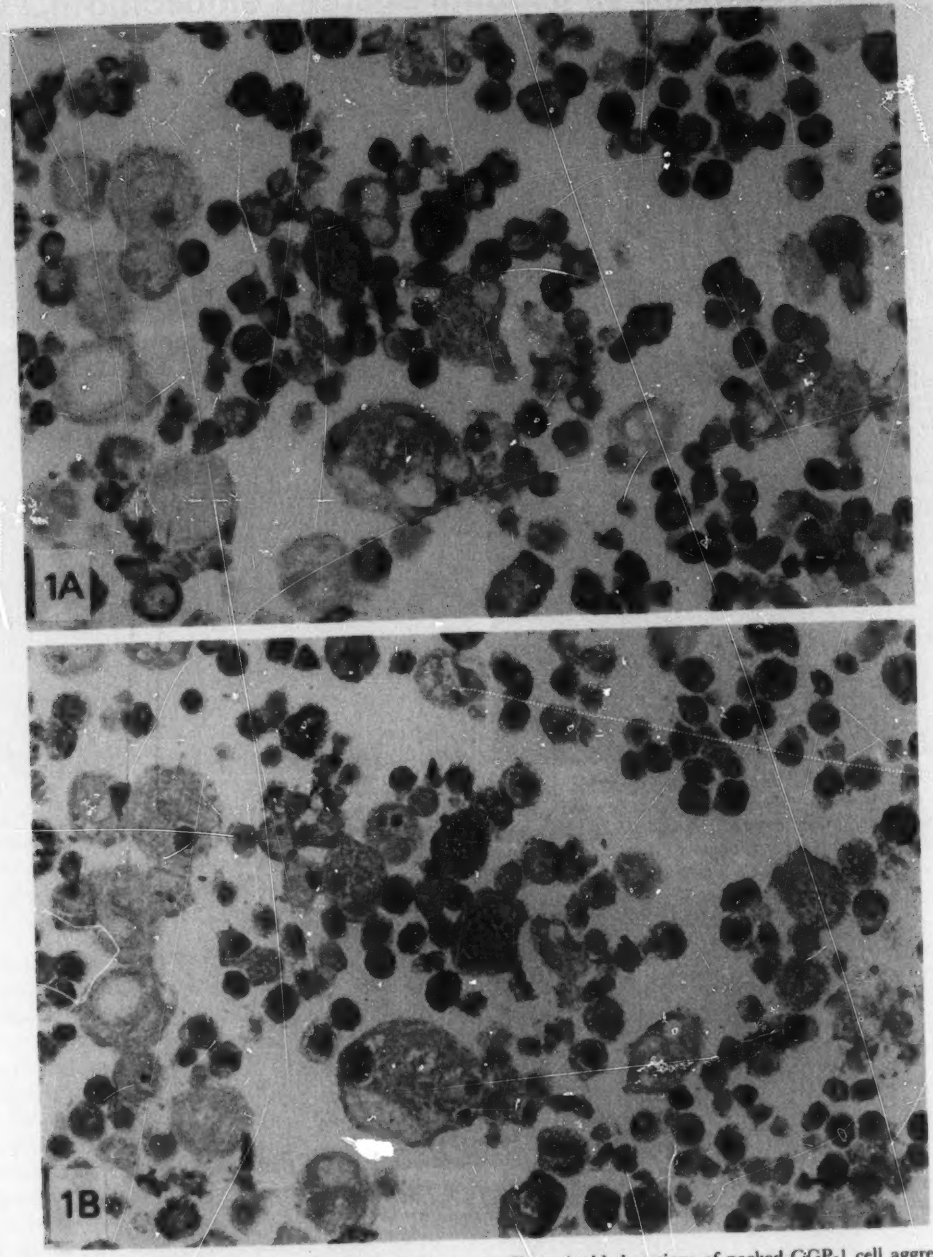

FIGURE 1.—Immunoperoxidase staining of the Formalin-fixed, paraffin-embedded sections of packed QGP-1 cell aggregates. Two serial sections were stained by rabbit anti-CEA antiserum absorbed with NCA (A) and rabbit anti-NCA antiserum absorbed with CEA (B). Nuclei were finally counterstained with hematoxylin. *Bar*=20 µm. × 200

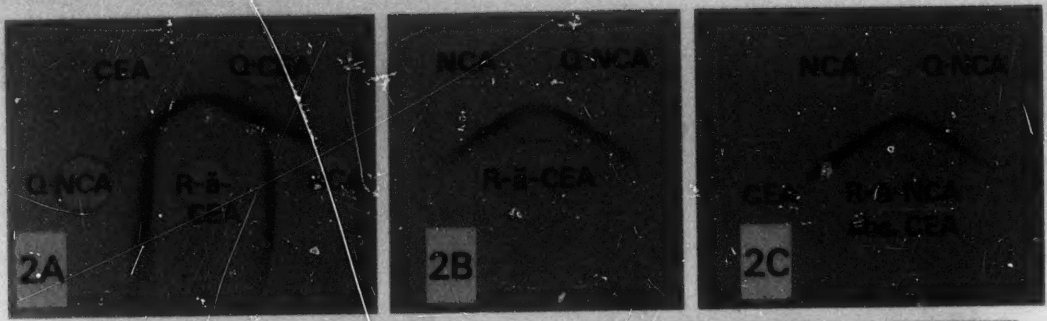
CEA
Q·CEA
Q·NCA
R-ā-CEA
NCA
2A
NCA
Q·NCA
R-ā-CEA
2B
NCA
Q·NCA
CEA
R-ā-NCA abs. CEA
2C

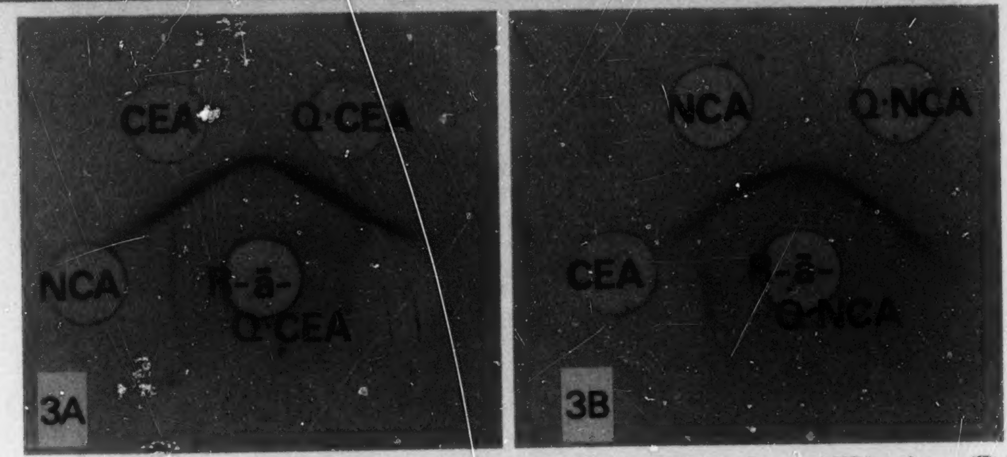
CEA
Q·CEA
NCA
R-ā-Q·CEA
3A
NCA
Q·NCA
CEA
R-ā-Q·NCA
3B

FIGURE 2—Immunodiffusion analyses of the isolated antigen preparations with anti-CEA (A, B) or anti-NCA antiserum (C). CEA, reference CEA (colon carcinoma); NCA, reference NCA (lung); Q·CEA, CEA isolated from QGP-1 culture media; Q·NCA, NCA isolated from QGP-1 culture media; R-ā-CEA, a rabbit antireference CEA antiserum; R-ā-NCA abs. CEA, a rabbit antireference NCA antiserum absorbed with reference CEA.

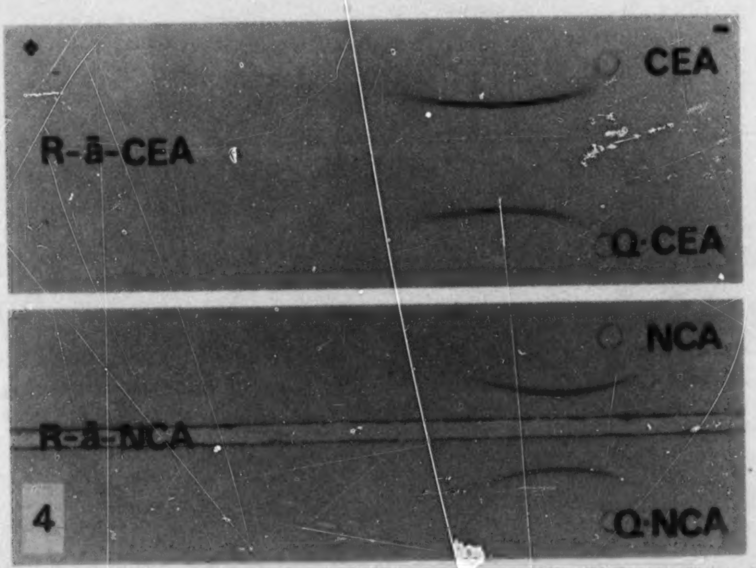
+
−
CEA
R-ā-CEA
Q·CEA
NCA
R-ā-NCA
4
Q·NCA

FIGURE 3.—Immunologic reactivities of anti-Q·CEA (A) and anti-Q·NCA antisera (B) with the purified antigens: R-ā-Q·CEA, a rabbit anti-Q·CEA antiserum; R-ā-Q·NCA, a rabbit anti-Q·NCA antiserum. For descriptions of CEA, Q·CEA, NCA, and Q·NCA, *see* legend for fig. 2.

FIGURE 4—Immunoelectrophoresis of the isolated antigens. R-ā-CEA, a rabbit antireference CEA antiserum; R-ā-NCA, a rabbit antireference NCA antiserum. For descriptions of CEA, Q·CEA, NCA, and Q·NCA, *see* legend for fig. 2.

Repair of Chromosome Damage Induced by X-Irradiation During G_2 Phase in a Line of Normal Human Fibroblasts and Its Malignant Derivative[1]

Ram Parshad,[2] Raymond Gantt,[3] Katherine K. Sanford,[3,4] Gary M. Jones,[3] *and* Robert E. Tarone[5]

ABSTRACT—A line of normal human skin fibroblasts (KD) differed from its malignant derivative (HUT-14) in the extent of cytogenetic damage induced by X-irradiation during G_2 phase. Malignant cells had significantly more chromatid breaks and gaps after exposure to 25, 50, or 100 rad. On the assumption that each chromatid contains a single continuous DNA double helix, chromatid breaks would represent unrepaired DNA double-strand breaks; the gaps may represent single-strand breaks. Results from alkaline elution of cellular DNA immediately after irradiation showed that the normal and malignant cells in asynchronous population were equally sensitive to DNA single-strand breakage by X-irradiation. Caffeine or β-cytosine arabinoside (ara-C), inhibitors of DNA repair, when added directly following G_2 phase exposure, significantly increased the incidence of radiation-induced chromatid damage in the normal cells. In contrast, similar treatment of the malignant cells had little influence. Ara-C differed from caffeine in its effects; whereas both agents increased the frequency of chromatid breaks and gaps, only ara-C increased the frequency of gaps to the level observed in the irradiated malignant cells. Addition of catalase, which destroys H_2O_2, or mannitol, a scavenger of the derivative free hydroxyl radical (·OH), to the cultures of malignant cells before, during, and following irradiation significantly reduced the chromatid damage; and catalase prevented formation of chromatid gaps. The DNA damage induced by X-ray during G_2 phase in the normal KD cells was apparently repaired by a caffeine- and ara-C-sensitive mechanism(s) that was deficient or absent in their malignant derivatives.—JNCI 1982; 69:409–414.

Cytogenetic findings in recent years implicate chromosome DNA damage and deficient repair in the process of malignant neoplastic transformation. Cells from individuals predisposed to a high risk of cancer, such as those with xeroderma pigmentosum, ataxia telangiectasia, Fanconi's anemia, or Bloom's syndrome, show abnormally increased chromosome breakage on exposure to various DNA-damaging agents and/or are prone to spontaneous chromosome breaks in culture (*1*). Furthermore, such individuals may show an impaired capacity to repair DNA damage. In addition, both mouse and human cells transformed to malignant cells in culture show an increased incidence of chromatid breaks after exposure to fluorescent light, as compared with their normal counterparts (*2*, *3*). This increased incidence results from an impaired capacity to repair DNA strand breaks [(*4*); Parshad R, Sanford KK, Jones GM, Tarone RE: Submitted for publication]. The extent of DNA repair is also influenced by the phase of the cell cycle at the time of exposure to the damaging agent. For example, both normal and malignant human cells showed comparable chromatid damage when exposed to light prior to S-phase, but only the malignant cells showed unrepaired chromatid breaks when exposed during the late S-G_2 period. These results imply a difference between normal and malignant cells in their capacity to repair light-induced damage, particularly when inflicted during late S-G_2. Because this light-induced damage is mediated through the intracellular generation of H_2O_2 and its derivative free hydroxyl radical (·OH) (*5*, *6*), both of which are produced during X-irradiation (*7*), we compared in the present study the incidence of chromatid breaks following X-irradiation during G_2 phase in a line of normal human fibroblasts (KD) and its malignant derivative (HUT-14). By examining metaphase cells 1–1.5 hour after irradiation, we could be assured that the cells were in G_2 at the time of X-irradiation. In one set of experiments, catalase, which decomposes H_2O_2, and mannitol, an ·OH scavenger, were added to the cultures before, during, and after X-irradiation for evaluation of the extent of chromatid damage attributable to these two agents.

An increased incidence of chromatid breaks could result from an enhanced susceptibility to DNA damage or from an impaired capacity to repair such damage. Therefore, we also evaluated in asynchronous populations the relative susceptibility of the cells to DNA breakage by X-ray and the influence of inhibitors of DNA repair such as caffeine (*8*) and ara-C (*9*) on radiation-induced chromatid breaks.

MATERIALS AND METHODS

Cell culture, irradiation, and cytogenetic procedures.—A line of human skin fibroblasts (KD) and its malignant derivative (HUT-14) transformed in culture by 4-nitroquinoline 1-oxide were provided by Dr. T. Kakunaga, National Cancer Institute (*10*). Because the KD line is diploid and nontumorigenic, it is referred to as "normal" in this paper. Stock cultures were grown in Dulbecco's modified Eagle's minimum essential medium supplemented with 10% fetal bovine serum (Flow Laboratories, Inc., McLean, Va.) as described in (*3*). For chromosome studies, 0.5–1.0×10^5 cells in 2 ml medium were inoculated into Leighton tubes each containing a 9×50-mm cover slip (#1 thickness; Bellco Glass, Inc., Vineland, N.J.). After 48 hours of incubation at 37°C, cultures were irradiated by means of two Philips RT250

ABBREVIATION USED: ara-C=β-cytosine arabinoside.

---

[1] Received December 16, 1981; accepted April 2, 1982.

[2] Department of Pathology, Howard University College of Medicine, Washington, D.C. 20059.

[3] Laboratory of Cellular and Molecular Biology, Division of Cancer Cause and Prevention (DCCP), National Cancer Institute (NCI), National Institutes of Health, Public Health Service, U.S. Department of Health and Human Services, Bethesda, Md. 20205.

[4] *Address reprint requests to* Dr. Sanford, Building 37, Room 2D02, NCI, National Institutes of Health, Bethesda, Md. 20205.

[5] Biometry Branch, DCCP, NCI.

opposing therapeutic 250-kV potential X-ray tubes operated at 235 kV, 15 mA, with 0.25-mm Cu and 0.55-mm Al filters (half-value layer, 0.9 mm Cu) and at a dose rate of 126 R/minute at 54-cm target distance. After irradiation, culture fluid was renewed within approximately 10–30 minutes, and 0.1 μg Colcemid/ml (GIBCO, Grand Island, N.Y.) was added for 1 hour either immediately or after 1- or 2-hour incubation, as indicated in the text. Caffeine, ara-C, catalase (Sigma Chemical Co., St. Louis, Mo.), and mannitol (Calbiochem-Behring Corp., La Jolla, Calif.) were added to the culture medium as described later. For chromosome analysis, the experimental and control cells were processed in situ on cover slips by techniques described (*11*). Chromosome analyses were made on randomized, coded preparations; four cultures were used for each variable. Only complete, well-spread metaphase cells were analyzed. The statistical analyses were based on both the number of chromatid breaks or gaps per cell and the percentage of cells showing these abnormalities. Abnormalities scored as breaks showed distinct dislocation and misalignment of the chromatid fragment, whereas gaps were achromatic lesions showing no dislocation.

In one experiment, normal and malignant cells were cocultivated by inoculation of 3×10^4 KD cells and 2×10^4 HUT-14 cells per Leighton tube; 48 hours later cultures were irradiated and processed as described above. The KD and HUT-14 metaphase cells were identified on the basis of chromosome numbers since KD cells are predominantly diploid (46 chromosomes) in contrast to subdiploid chromosome 43–45 in HUT-14.

In the experiment on the influence of 50 μg caffeine/ml on mitotic delay induced by X-irradiation, four cultures per variable were scanned for total number of metaphase cells. Mitotic inhibition was determined for postirradiation periods of 1.5 and 2 hours, during which time cells were exposed to caffeine. Cells were arrested in metaphase by Colcemid treatment for 1 hour before fixation. In the nonirradiated controls, 198 and 816 metaphase cells were enumerated in KD and HUT-14, respectively.

Technique for determination of irradiation-induced DNA strand breakage.—Cellular DNA size indicative of strand breakage was determined by the alkaline elution method of Kohn (*12*) with minor variations. In Kohn's method (with or without minor variation), the elution rate is dependent on the DNA strand length. (The higher the molecular weight, the slower the elution rate.) Cells of the two lines were prelabeled, one with [2-^{14}C]thymidine (15 nCi/ml) and the other with [*methyl*-^{3}H]thymidine (30 nCi/ml); cells were cocultivated in a T-25 flask (7.5×10^4 malignant and 1.5×10^5 normal cells). After 24 hours, the cells were chilled to 0°C, X-irradiated, and mechanically removed in 3 ml fresh medium. The cells were then placed on a polyvinyl chloride membrane (2-μm pore, BSWP02500; Millipore, Corp., Bedford, Mass.) and lysed with 20 m*M* EDTA (pH 10.2) containing 0.2% Sarkosyl (wt/vol) and 2 *M* NaCl. The DNA was fragmented with a burst of air from a syringe fitted to the filter holder (*13*) and eluted at a flow rate of 0.04 ml/minute with 20 m*M* EDTA (free-acid form) titrated to pH 12.2 with tetra-propylammonium hydroxide. Fractions were collected every 90 minutes for 18–20 hours, and the radioactivity remaining on the filter and in the filter holder was determined. The cells and DNA were shielded from light or exposed only to light through gold filters during culture, filtration, and elution.

RESULTS

X-ray-Induced Chromatid Damage in Normal and Malignant Human Cells

In the first posttreatment metaphase after X-irradiation of cells in G_2 phase, only two types of chromosome aberrations, chromatid breaks and gaps, were observed. In the normal cell population, cells entered metaphase only during the 1st hour after irradiation, whereas in the malignant cell population some cells were still entering metaphase even 3 hours after treatment. Thus the malignant cells, in contrast to the normal cells, did not show the distinct radiation-induced G_2 block or mitotic delay.

The malignant cells (HUT-14) had significantly more

TABLE 1.—*Chromatid damage in a line of normal skin fibroblasts (KD) and its malignant derivative (HUT-14) after X-irradiation in G_2 phase*

X-ray dose, rad	Hr post treatment		Normal			Malignant		
	Before Colcemid	With Colcemid	No. of cells studied[a]	Average No. per cell[b]		No. of cells studied	Average No. per cell[c]	
				Chromatid breaks	Chromatid gaps		Chromatid breaks	Chromatid gaps
25	0	1	132	0.045	0	121	0.298[d]	0.033
	1	1	—			46	0.478	0
	2	1	—			38	0.526	0
50	0	1	95	0.032	0.032	92	0.478[d]	0.043
	0	1	105	0.038	0.010	34	0.618[d]	0.088
100	0	1	200	0.065	0.010	126	1.294[d,e]	0.103[d]
	1	1	—			86	3.698	0.337
	2	1	—			22	2.318	0.318
None			200	0.010	0	200	0.055	0

[a] Number does not indicate total metaphase cells per variable (*see* Materials and Methods). No metaphase cell observed, —.

[b] Normal cells were predominantly diploid (46 chromosomes).

[c] Malignant cells were predominantly subdiploid (43–45 chromosomes).

[d] $P<10^{-4}$ and $P=0.003$ in comparisons of malignant vs. normal for chromatid breaks and gaps, respectively.

[e] $P<10^{-4}$ for increase in chromatid breaks with increasing radiation dose.

chromatid breaks than did their normal counterparts (KD) after exposure to 25, 50, or 100 rad ($P<10^{-4}$) and a slightly higher spontaneous chromatid breakage as seen in the unirradiated controls (table 1). They also showed a significant increase in chromatid breaks with increasing radiation dose ($P<10^{-4}$), whereas in the normal KD cells the increase was significant only with 100 rad ($P=0.05$). In addition, the malignant cells compared to the normal cells had increased frequencies of chromatid gaps following 25, 50, or 100 rad, although the increase was significant only at 100-rad exposure ($P=0.003$). These differential responses of normal and malignant cells to X-irradiation were further confirmed in a cocultivation experiment.

In certain experiments, the incubation period after irradiation was increased to allow additional time for repair of DNA damage (table 1). Periods of 1, 2, or 3 hours after 25 rad did not significantly alter the frequency of chromatid breaks or gaps in the malignant cells. However, after 100 rad chromatid breaks and gaps increased significantly at 2 hours of posttreatment as compared to 1 hour ($P<10^{-4}$ and $P=0.007$, respectively). No increase was observed during the 3d hour. As noted earlier, normal cells did not enter metaphase between 1 and 2 hours after treatment.

X-ray-Induced DNA Fragmentation and Repair in Normal and Malignant Cells

The initial susceptibility of normal as compared with malignant cells to X-ray-induced strand breaks was evaluated by determination of the relative molecular weights of DNA in the two cell populations immediately after irradiation. The elution rates of the DNA were essentially the same for both cell lines at each X-ray dose tested (text-fig. 1). These results indicated that irradiation caused an equivalent number of DNA strand breaks and that the two populations were similar in their susceptibility to irradiation as measured by DNA single-strand breaks.

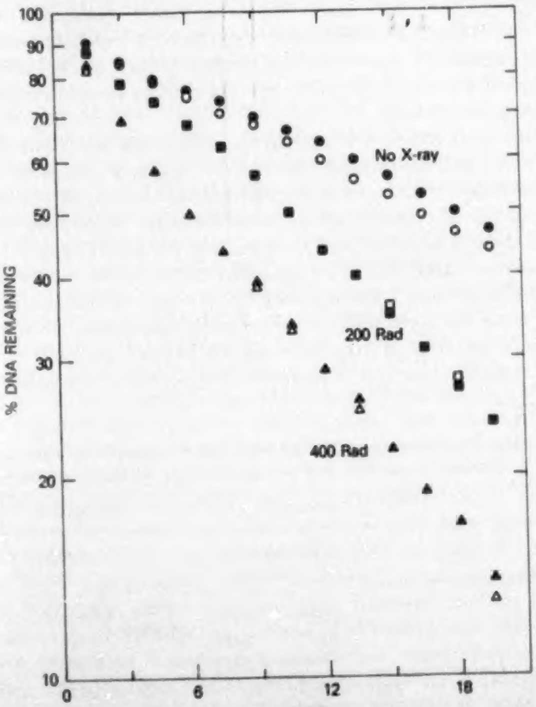

TEXT-FIGURE 1.—Effect of X-ray irradiation on the alkaline elution rates of DNA from normal and malignant cells. *Open symbols* represent malignant cells; *closed symbols* represent normal cells. ○, ●, no X-ray; □, ■, 200 rad; △, ▲, 400 rad.

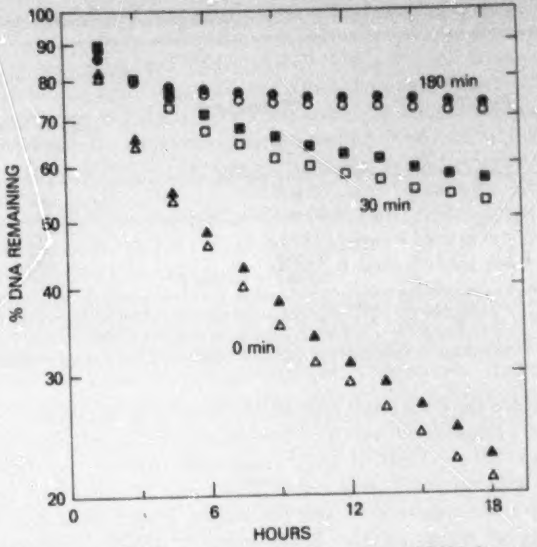

TEXT-FIGURE 2.—Effect of time on the elution rates of DNA from malignant and normal cells after induction of DNA strand breaks by 400 rad of X-ray. *Open symbols* represent malignant cells; *closed symbols* represent normal cells. △, ▲, zero time; □, ■, 30 min after irradiation; ○, ●, 3 hr after irradiation.

Relative rates of DNA repair in cells of the two lines were compared; cells were prelabeled, cocultivated, and exposed to 400 rad; DNA elution rates were determined at three time points (text-fig. 2). At zero time, the DNA eluted

TABLE 2.—*Influence of catalase and mannitol on X-ray-induced chromatid damage of malignant cells (HUT-14) during G_2 phase*

Treatment[a]	No. of cells studied	Average No. per cell		
		Chromatid breaks	Chromatid gaps	Chromatid exchanges
None	200	0.030	0	0
50 rad	150	0.533	0.120	0.007
50 rad + 1 μg catalase/ml	200	0.460	0.145	0
50 rad + 5 μg catalase/ml	186	0.339	0.097	0
50 rad + 10 μg catalase/ml	189	0.153[b]	0[b]	0
50 rad + 5 m*M* mannitol	200	0.365	0.100	0
50 rad + 10 m*M* mannitol	190	0.158[c]	0.058[c]	0
50 rad + 20 m*M* mannitol	197	0.173	0.066	0

[a] Culture medium was renewed ≈20 min after radiation. Colcemid was added at the time of medium renewal. Mannitol or catalase was added 1 hr before X-ray and during Colcemid treatment.

[b] $P=10^{-4}$ and $P<10^{-4}$ for dose-related decrease in chromatid breaks and gaps, respectively.

[c] $P=0.003$ and $P=0.03$ for dose-related decrease in chromatid breaks and gaps, respectively, with no additional decrease after 10 m*M*.

TABLE 3.—*Influence of 50 µg caffeine/ml on chromatid damage in normal and malignant human cells after X-irradiation in G_2 phase*

Expt No.	Treatment	Normal: No. of cells examined	Normal: Average No. per cell: Chromatid breaks	Normal: Average No. per cell: Chromatid gaps	Malignant: No. of cells examined	Malignant: Average No. of cell: Chromatid breaks	Malignant: Average No. of cell: Chromatid gaps
1	50 rad	200	0.020	0.010	200	0.385	0.170
	50 rad + caffeine	200	0.105[a]	0.065	200	0.420[b]	0.170
2[c]	None	149	0.007	0	117	0.034	0
	50 rad	200	0.015	0.005	159	0.484	0.145
	50 rad + caffeine	137	0.073[a]	0.073	115	0.512[b]	0.163

[a] P=0.005 and P=0.030 in comparisons with irradiated control cells in expt 1 and 2, respectively.

[b] P=0.014 and P=0.002 in comparisons with irradiated control cells in expt 1 and 2, respectively.

[c] Control and experimental cultures chilled on ice during irradiation and until medium renewal.

rapidly for both lines and after 30 minutes the elution rate was substantially slower; these results indicated that more than half the DNA strand breaks were repaired. By 3 hours the elution rates were essentially those of untreated cells. From the results with this technique, it appeared that the rates of repair of the X-ray-induced DNA single-strand breaks were similar.

Influence of Catalase and Mannitol on X-irradiation-Induced Chromatid Damage

Addition of catalase to the cultures of malignant cells before, during, and after irradiation produced a dose-related decrease in the frequency of chromatid breaks ($P=10^{-4}$) and chromatid gaps ($P<10^{-4}$) (table 2). At the highest dose of catalase, the frequency of breaks was still significantly greater than that in nonirradiated cells ($P=2\times10^{-4}$), whereas the frequency of gaps was identical to that in the nonirradiated controls.

Addition of mannitol before, during, and after irradiation was also associated with a dose-related decrease in the frequency of both chromatid breaks (P=0.003) and chromatid gaps (P=0.03) with no additional decrease after 10 m*M*. The frequencies of both breaks and gaps even at the highest dose of mannitol were significantly greater than those in the nonirradiated cells ($P<10^{-4}$ and P=0.002, respectively).

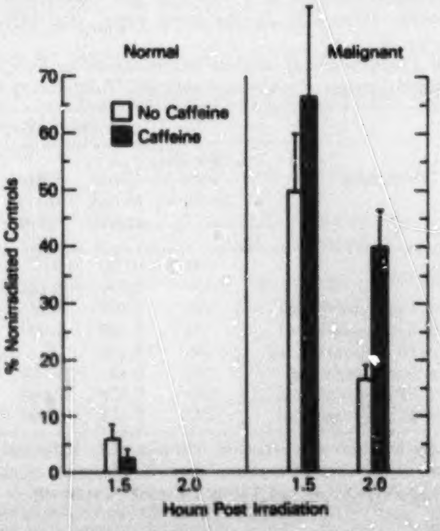

TEXT-FIGURE 3.—Influence of caffeine (50 µg/ml) and postirradiation time (hr) on number of metaphase cells following X-irradiation (50 rad) in normal and malignant human cells. *Bar* indicates 1 SE.

Influence of Inhibitors of DNA Repair on Chromatid Damage From X-irradiation in G_2

Caffeine had little influence on malignant cells with respect to chromatid breaks or gaps when added directly following irradiation and during Colcemid treatment. In contrast, similar treatment of normal cells with caffeine in two experiments significantly increased both chromatid breaks (P=0.005 and P=0.030) and chromatid gaps (P=0.014 and P=0.002) as compared with irradiated control cells (table 3). However, the levels attained in the caffeine-treated normal cells were less than those in the irradiated malignant cells.

Because caffeine is known to reduce the duration of X-ray-induced G_2 phase delay (14–17), the increase in irradiation-induced damage in the normal cells after caffeine treatment could result from a "breakthrough" of the G_2 block, allowing a shorter period available for DNA repair (*17*). However, addition of 50 µg caffeine/ml to the normal cells did not initiate a breakthrough since such addition did not increase the number of cells entering metaphase during the 2 hours after treatment (text-fig. 3). In contrast, caffeine did increase the number of metaphase cells in the malignant cell population.

TABLE 4.—*Influence of 10^{-5} M ara-C on X-ray-induced chromatid damage in normal and malignant cells during G_2 phase*

Treatment	Normal: No. of cells studied	Normal: Average No. per cell: Chromatid breaks	Normal: Average No. per cell: Chromatid gaps	Malignant: No. of cells studied	Malignant: Average No. per cell: Chromatid breaks	Malignant: Average No. per cell: Chromatid gaps
None	200	0.010	0	113	0.027	0.027
Ara-C	200	0.015	0	129	0.031	0
50 rad	200	0.010	0.010	150	0.573	0.140
50 rad + ara-C	185	0.065[a]	0.124[a]	115	0.548	0.122

[a] P=0.009 and $P=10^{-4}$ in comparison with untreated irradiated controls for chromatid breaks and gaps, respectively.

Like caffeine, ara-C significantly increased the frequency of X-ray-induced chromatid breaks and gaps in the normal cells (P=0.009 and P=10^{-4}, respectively) (table 4). The frequency of chromatid gaps was particularly enhanced by ara-C to a level comparable to that in the X-irradiated malignant cells. In the malignant cells, however, ara-C had no influence on the X-ray-induced chromatid breaks or gaps.

DISCUSSION

An extensive literature (*18–20*) details the cytogenetic effects of ionizing irradiation on mammalian cells in culture. The present study is unique in the comparison of the chromatid damage in normal cells and their malignant derivatives following X-irradiation exclusively in the G_2 phase of the cell cycle or within 1–1.5 hours of metaphase. X-irradiation is known to induce several types of lesions in DNA, including single- and double-strand breaks, crosslinks, and endonuclease-sensitive sites, presumably representing base damage. On the assumption that each chromatid contains a single, continuous DNA double helix, chromatid breaks seen in the first metaphase following G_2 irradiation must represent unrepaired double-strand DNA breaks. These double-strand breaks could arise directly or indirectly as the result of repair processes (*4, 9, 19–22*). Achromatic lesions or gaps especially prevalent in cells irradiated in early prophase or late G_2 (*23*) may represent single-strand breaks (*20, 24, 25*). In the present study, the chromatid gaps induced in the malignant cells by X-irradiation during G_2 were completely prevented by addition of catalase before, during, and after irradiation. In the normal cells, the low incidence of gaps induced by X-irradiation during G_2 was significantly enhanced by addition of ara-C following irradiation. Ara-C has also been shown to increase the incidence of chromatid deletions in normal human lymphocytes X-irradiated during G_2 (*9*). It was suggested that ara-C molecules incorporated into the repair–replicating DNA distort the helix, prevent the polymerase from functioning, and inhibit repair of base damage (*9, 22*). In studies on the excision repair of UV-induced base damage in normal human fibroblasts, ara-C seemed to inhibit the rejoining of breaks formed by the endonuclease, probably through inhibition of polymerase activity (*26*). In accordance with these observations and interpretations, the chromatid gaps observed in the present study may result from incomplete excision repair of base damage produced by X-irradiation during G_2.

Although the malignant cells as compared with their normal counterparts have a slightly higher spontaneous chromatid breakage as seen in unirradiated control cells, they show significantly more chromatid breaks and gaps after X-irradiation during G_2. These findings confirm and extend our previous observations that malignant cells of either mouse or human origin develop more chromatid breaks than do their normal counterparts when exposed to fluorescent light during late S–G_2 [(*4*); Parshad R, Sanford KK, Jones GM, Tarone RE: Submitted for publication].

The increased incidence of chromatid damage in the malignant cells as compared with their normal counterparts
could result from greater initial DNA dam
tion, from a decreased radiation-induced m
lowing less time for DNA repair (*16, 1*
impaired capacity to repair the DNA dam
from alkaline elution of DNA immediately
show that the malignant and normal ce
sensitive to DNA single-strand breakage by
From our results (table 1, text-fig. 3), the C
induced by X-irradiation in both cell lines
lesser extent in HUT-14) occurs somewhere
2 hours before metaphase. Therefore, those c
metaphase during the 1st hour after X-irra
late G_2 and would not have been subject to t
since they would have passed the "transitio
the time of irradiation. Furthermore, if chr
in the malignant cells results from inadequa
repair, a decreasing yield of chromatid da
expected in cells sampled at increasing po
tervals. Such was not the case, and the in
chromatid breaks and gaps was significant
and 3 hours post-irradiation.

Our results from use of inhibitors of DNA
and ara-C, suggest that the increased chrom
the malignant cells results from an impa
repair radiation-induced DNA damage inf
Exposure of cells to caffeine directly follo
significantly increased the X-ray-induced
age in the normal cells but had little i
malignant cells. Because caffeine is also kno
mitotic delay produced by irradiation, th
matid damage in the normal cells could
resulting from the shorter time available fo
However, at the concentration used, caffei
ence the mitotic delay in the normal cells
reduce this delay in the malignant cells. A
in inhibiting DNA repair, other than da
pair, has not been established in eukaryot
genetic observations support the concept
hibits repair of DNA damage inflicted by
or by fluorescent light during late S–G_2 [(*4*
R, Sanford KK, Jones GM, Tarone R
publication]. Like caffeine, ara-C added d
of normal cells following irradiation durin
increased X-ray-induced chromatid brea
had no influence on the malignant cells.

No difference in the rate or extent of
induced DNA strand breaks could be det
line elution technique. However, the alka
nique measures repair of single-strand br
cytogenetic procedure measures unrepai
breaks after at least 1-hour incubation of
the repair of most single-strand breaks
doses of 400 rad (text-fig. 2). Some of the u
strand breaks may result from incomplet
cision repair of base damage. Further, th
technique was applied to asynchronous
whereas the cytogenetic analyses were lim
at the time of irradiation. Finally, the
alkaline elution technique is insufficient
of unrepaired DNA double-strand br

breaks/cell) observed by these cytogenetic procedures (*30*).

The present results indicate that the DNA damage induced by X-ray during G_2 in the normal KD cells is almost completely repaired by a mechanism(s) sensitive to caffeine and ara-C, whereas the malignant derivatives are deficient in this repair mechanism(s).

REFERENCES

(*1*) German J. Genes which increase chromosomal instability in somatic cells and predispose to cancer. Prog Med Genet 1972; 8:61–101.

(*2*) Parshad R, Sanford KK, Tarone RE, Jones GM, Baeck AE. Increased susceptibility of mouse cells to fluorescent light-induced chromosome damage after long-term culture and malignant transformation. Cancer Res 1979; 39:929–933.

(*3*) Parshad R, Gantt R, Sanford KK, Jones GM, Camalier RF. Light-induced chromatid damage in human skin fibroblasts in culture in relation to their neoplastic potential. Int J Cancer 1981; 28:335–340.

(*4*) Parshad R, Sanford KK, Jones GM, Tarone RE, Hoffman HA, Grier AH. Susceptibility to fluorescent light-induced chromatid breaks associated with DNA repair deficiency and malignant transformation in culture. Cancer Res 1980; 40:4415–4419.

(*5*) Parshad R, Sanford KK, Jones GM, Tarone RE. Fluorescent light-induced chromosome damage and its prevention in mouse cells in culture. Proc Natl Acad Sci USA 1978; 75:1830–1833.

(*6*) Parshad R, Taylor WG, Sanford KK, Camalier RF, Gantt R, Tarone RE. Fluorescent light-induced chromosome damage in human IMR-90 fibroblasts: Role of hydrogen peroxide and related free radicals. Mutat Res 1980; 73:115–124.

(*7*) Johns HE, Cunningham JR. The physics of radiology. Springfield, Ill: Thomas, 1969:680–686.

(*8*) Kihlman BA. Caffeine and chromosomes. Amsterdam: Elsevier/North Holland, 1977.

(*9*) Preston RJ. DNA repair and chromosome aberrations: The effect of cytosine arabinoside on the frequency of chromosome aberrations induced by radiation and chemicals. Teratogenesis, Carcinogen, and Mutagen 1980; 1:147–159.

(*10*) Kakunaga T. Neoplastic transformation of human diploid fibroblast cells by chemical carcinogens. Proc Natl Acad Sci USA 1978; 75:1334–1338.

(*11*) Gantt R, Parshad R, Ewig RA, et al. Fluorescent light-induced DNA crosslinkage and chromatid breaks in mouse cells in culture. Proc Natl Acad Sci USA 1978; 75:3809–3812.

(*12*) Kohn KW. DNA as a target in cancer chemotherapy: Measurement of macromolecular DNA damage produced in mammalian cells by anti-cancer agents and carcinogens. Methods Cancer Res 1979; 16:291–345.

(*13*) Gantt R, Jones GM, Stephens EV, Baeck AE, Sanford KK. Visible light-induced DNA crosslinks in cultured mouse and human cells. Biochim Biophys Acta 1979; 565:231–240.

(*14*) Walters RA, Gurley LR, Tobey RA. Effects of caffeine on radiation-induced phenomena associated with cell-cycle traverse of mammalian cells. Biophys J 1974; 14:99–118.

(*15*) Tolmach LJ, Busse PM. The action of caffeine on x-irradiated HeLa cells. IV. Progression delays and enhanced cell killing at high caffeine concentrations. Radiat Res 1980; 82:374–392.

(*16*) Zampetti-Bosseler F, Scott D. Cell death, chromosome damage and mitotic delay in normal human, ataxia telangiectasia and retinoblastoma fibroblasts after x-irradiation. Int J Radiat Biol 1981; 39:547–558.

(*17*) Painter RB, Young BR. Radiosensitivity in ataxia telangiectasia: A new explanation. Proc Natl Acad Sci USA 1980; 77:7315–7317.

(*18*) Evans HJ. Chromosome aberrations induced by ionizing radiations. Int Rev Cytol 1962; 13:221–321.

(*19*) Evans HJ. Molecular mechanisms in the induction of chromosome aberrations. In: Scott D, Bridges BA, Sobels FH, eds. Progress in genetic toxicology. Amsterdam: Elsevier/North Holland, 1977:57–74.

(*20*) Bender MA, Griggs HG, Bedford JS. Mechanisms of chromosomal aberration production. III. Chemicals and ionizing radiation. Mutat Res 1974; 23:197–212.

(*21*) Taylor AM. Unrepaired DNA strand breaks in irradiated ataxia telangiectasia suggested from cytogenetic observations. Mutat Res 1978; 50:407–418.

(*22*) Preston RJ. The effect of cytosine arabinoside on the frequency of x-ray-induced chromosome aberrations in normal human leukocytes. Mutat Res 1980; 69:71–79.

(*23*) Savage JR. Classification and relationships of induced chromosomal structural changes. J Med Genet 1975; 13:103–122.

(*24*) Taylor JH, Haut WF, Tung J. Effects of fluorodeoxyuridine on DNA replication, chromosome breakage, and reunion. Proc Natl Acad Sci USA 1962; 48:190–198.

(*25*) Natarajan AT, Obe G, van Zeeland AA, Palitti F, Meijers M, Verdegaal-Immerzeel EA. Molecular mechanisms involved in the production of chromosomal aberrations. II. Utilization of neurospora endonuclease for the study of aberration production by x-rays in G_1 and G_2 studies of cell cycle. Mutat Res 1980; 69:293–305.

(*26*) Erixon K, Ahnström G. Single-strand breaks in DNA during repair of UV-induced damage in normal human and xeroderma pigmentosum cells as determined by alkaline DNA unwinding and hydroxylapatite chromatography. Effects of hydroxyurea, 5 fluorodeoxyuridine and 1-β-D-arabinofuranosylcytosine on the kinetics of repair. Mutat Res 1979; 59:257–271.

(*27*) Hodge FA, Nachtwey DS. X-ray-induced delay of cell division in synchronized Tetrahymena pyriformis. Radiat Res 1972; 52:603–617.

(*28*) Natarajan AT, Obe G, Dulout FN. The effect of caffeine post-treatment on X-ray-induced chromosomal aberrations in human blood lymphocytes in vitro. Hum Genet 1980; 54:183–189.

(*29*) Saugabaeva K, Eidus LK, Ganassi EE. Modifying of radiation damages of chromosomes of Chinese hamster fibroblasts in a cell culture. Radiobiologiia 1978; 18:511–514.

(*30*) Kohn KW, Erickson LC, Ewig RA, Friedman CA. Fractionation of DNA from mammalian cells by alkaline elution. Biochemistry 1976; 15:4629–4637.

Role of Anchorage in the Expression of Tumorigenicity of Untransformed Mouse Cell Lines[1,2,3]

Robert S. Wells,[4] **Evelyn W. Campbell,**[5] **Douglas E. Swartzendruber,**[6] **Lawrence M. Holland,**[5] *and* **Paul M. Kraemer**[5,7,8]

ABSTRACT—Cultured mouse cells were tested for tumorigenicity in nude mice with both a conventional assay (injection of cell suspensions) and a new test involving implantation of cells grown on gelatin sponges. Sublines of Balb/3T3 cells, obtained from different sources, varied in their tumorigenic potential with either assay. One subline (A) formed distinctive precancerous nodules only in the sponge assay; these nodules often became progressive after a latent period of 3–4 months. However, suspensions of cells of this subline also caused tumors after a similar latent period, but no nodular phase preceded tumor formation. Another subline of Balb/3T3 (M) has failed to form tumors in either assay. The Balb/3T3 sublines did not differ in in vitro properties, such as low saturation density, failure to grow in methylcellulose, and monolayer morphology. A second experimental approach involved tests on nude BALB/c mouse-embryo fibroblasts at various passage levels. The cells were passaged from primary culture, through crisis, to heteroploid, established cell lines. Tumorigenicity was demonstrable earlier in the sponge assay, at which time in vitro parameters putatively associated with malignant behavior were unchanged. Possible relationships with the in vivo phenomenon of solid-surface sarcomagenesis are discussed.—JNCI 1982; 69:415–423.

Tumorigenicity studies in nude mice have been used to investigate the biological significance of in vitro cell transformation (*1–16*). Questions have arisen, however, concerning the methods commonly used to test cells for tumorigenic potential. For instance, Boone and Jacobs (*7*) and Boone (*17*) have shown that two commonly used untransformed mouse cell lines (Balb/3T3 and C3H/10T½) were tumorigenic if the cells were anchored to substrate (plastic platelets or glass beads) at the time of implantation. Using the same plastic platelet method, Boone et al. (*18*) also showed that freshly explanted adult connective tissue cells were tumorigenic after subculture in vitro. By contrast, the same type of cells was not tumorigenic when a conventional assay was used (injection of at least 10^6 cells in suspension).

The present report describes initial results with a tumorigenicity assay system that, like Boone's, provides anchorage for the cells. The system is based on the subcutaneous implantation into nude mice of Gelfoam sponge disks containing 10^4–10^5 growing cells. The system has a number of practical advantages and can be applied to the specific goal of investigating the role of anchorage in the expression of tumorigenic potential of untransformed cultured mouse cells. The role of anchorage is of interest because Boone's results suggest that anchorage to certain nonbiologic substrates (plastic and glass) exerts a tumor-promoting or tumor-initiating effect on mouse cells. Since routine tissue culture employs anchorage to these same substrates, a clearer understanding of the matter would influence the interpretation of studies of in vitro transformation by viruses, chemicals, or radiation. Clearly, spontaneous transformation of rodent cells in culture (*8*) is already a complicating feature of these systems.

MATERIALS AND METHODS

Cells.—Subline A of Balb/3T3 cells was obtained from the American Type Culture Collection, Rockville, Md.; subline C of Balb/3T3 cells was from Dr. Lloyd Culp (Case Western Reserve University, Cleveland, Ohio); subline M of Balb/3T3 cells was from Dr. Gerd Maul (Wistar Institute, Philadelphia, Pa.). Each subline was initially grown to a population of about 10^7 cells and frozen in equal parts of 20% glycerol–saline and medium. For routine use, an aliquot of 10^6 cells was thawed and recultured. Except for certain specific experiments, Balb/3T3 cells were split 1:20 to 1:100 once or twice weekly as needed to minimize cell-to-cell contact (as judged with an inverted microscope).

The nude BALB/c mouse fibroblasts were initiated as a cell strain in our laboratory. Embryos at day 16 of gestation, which were the product of a (*nu/nu*) × (*nu/nu*) homozygous mating, were removed aseptically, minced, and digested with 0.25% trypsin (Difco Laboratories, Detroit, Mich.) in Puck's saline A (*9*) for 45 minutes at 20°C in a stirring apparatus. The trypsinized preparation was spun at 500×*g* for 10 minutes, and the cells were resuspended in medium and distributed to three T150 flasks. As cultures reached confluence, they were split at a 1:2 ratio every 3–4 days into T75 flasks until culture crisis occurred at passage 8. From passages 8 through 12, growth slowed and 7–10 days were required to reach confluence. After crisis, split

---

ABBREVIATIONS USED: FCS=fetal calf serum; H & E=hematoxylin and eosin; TPA=12-*O*-tetradecanoylphorbol 13-acetate; WNME=whole nude mouse-embryo fibroblasts in tissue culture.

---

[1] Received September 28, 1979; revised January 7, 1982; accepted March 18, 1982.

[2] Supported by U.S. Department of Energy contract W-7405-ENG. 36.

[3] Animals were maintained under the guidelines set forth by the Los Alamos National Laboratory and in the "Guide for the Care and Use of Laboratory Animals" by the Institute of Laboratory Animal Resources, National Research Council.

[4] Department of Pathology, University of Colorado Medical Center, Denver, Colo. 80220.

[5] Experimental Pathology Group, Los Alamos National Laboratory, University of California, Los Alamos, N. Mex. 87545.

[6] Department of Developmental Therapeutics, M. D. Anderson Hospital and Tumor Institute, Texas Medical Center, Houston, Tex. 77030.

[7] *Address reprint requests to* Dr. Kraemer, Group LS-4, MS 888, Los Alamos National Laboratory, Los Alamos, N. Mex. 87545.

[8] We thank Ms. Mary R. Brooks for expert care of the nude mouse colony and Ms. Julie Wilson for help with experiments.

ratios of 1:5 to 1:10 were used. Every fifth passage about 10^7 cells were frozen in 10% glycerol–medium, and preparations were made for chromosome studies. For experiments, samples of the various passages were used within two passages of thawing. SVT2 cells, a simian virus 40-transformed line of Balb/3T3, were obtained from Dr. Lloyd Culp. Human diploid fibroblasts (CRL 1295, passages 12–20) were provided by Dr. Gary Strniste (Los Alamos National Laboratory).

Culture conditions.—Monolayer cell cultures were grown in T75 or T150 flasks (Falcon Plastics, Los Angeles, Calif.) in Dulbecco's modified Eagle's minimum essential medium (GIBCO, Grand Island, N.Y.) with 10% FCS. However, human diploid fibroblasts recieved medium containing 20% serum. The cells were grown in 5% CO_2 at 37°C and passaged with 0.25% trypsin in Puck's saline A. For some experiments, cultures were maintained in medium with 0.1 mg TPA/ml obtained from Dr. Peter Borchert (University of Minnesota, Minneapolis, Minn.) and 0.005% acetone (Matheson, Coleman, & Bell, East Rutherford, N.J.); control cultures with 0.005% acetone were used.

For sponge cultures, 10^6–10^7 cells obtained from monolayer culture by trypsinization were resuspended in 5-ml sterile plastic tubes (Falcon Plastics). The tubes were kept in the same incubator as that used for monolayer culture. Gelfoam (The Upjohn Co., Kalamazoo, Mich.) sponges (≈200 mm^3 in vol) were prepared from individually wrapped, presterilized, 20×60×7-mm slabs by means of a sterilized office paper punch. The sponges were hydrated in media and spun at 300 rpm for 20 minutes for removal of air. The number of cells per sponge was determined by incubation of individual sponges in 10 ml of the 0.25% trypsin solution containing 0.04 mg collagenase/ml (Worthington Biochemical Corp., Freehold, N.J.) for 10–15 minutes. Cells were then enumerated with a Coulter counter with the use of blank sponges as controls. For studies of cell growth fewer cells were seeded initially (10^5 for 20 sponges), and the media were changed twice weekly. Sample sponges were removed daily and counted. For routine sponge tumorigenicity tests, cultures were used within 1–3 days, at which time the samples were counted and fixed in 10% Formalin for histologic examination.

Tumorigenicity tests.—We performed sponge assays by decanting sponge cultures into 10-mm petri dishes (Falcon Plastics) and using forceps to implant individual sponges in the subcutaneous space (or other site) of mice; for some experiments, intraperitoneal implantation was done in the same manner; in either case, a 5-mm incision was made in mice that had been given intraperitoneal anesthesia with 60 mg pentobarbital/kg body weight. The incision was closed with a 9-mm Autoclip (Clay Adams, Inc., Parsippany, N.J.), which was removed 10 days later. Some implants were later removed from animals by similar surgical techniques. Such sampled implants were fixed in 10% buffered Formalin for histologic examination or minced and recultured in monolayer. Some implants were digested with stirring, with the use of the trypsin–collagenase mixture mentioned above, and the recovered cells were then processed for determination of DNA content (*see* below).

Suspension cell assays for tumorigenicity were done with the use of 10^6 trypsinized single cells suspended in 0.2 ml of media injected sc.

Transformation assays.—We determined saturation density by seeding 60-mm petri dishes with 5×10^4 cells; media were changed, and trypsinized cells were counted every other day for 10 days. Growth of cells suspended in Methocel was tested by the method of Risser and Pollack (*10*). Cells determined to be at least 99% free of microscopic cell clumps were suspended in Methocel at concentrations of 10^5, 10^4, 10^3, and 10^2 cells/plate with three replicates at each concentration. We determined that colonies with at least 25 cells could be directly visualized. Such colonies were scored and the number was confirmed with the use of an inverted microscope. Plating efficiency was calculated for plates with the appropriate cell concentration as the average number of colonies per plate divided by the number of cells plated. If no colonies formed with the highest number (10^5), then these plates were evaluated for more limited growth. We scanned at least 10^3 cells at random looking for microscopic colonies. Plating efficiencies of 0%, therefore, mean that fewer than 1 of 3×10^5 cells formed macrocolonies (>25 cells) and that no more than 1% of cells grew in a more limited fashion. SVT2 cells with a high colony-forming efficiency in Methocel were used as positive controls in all assays.

Chromosome studies.—Confluent monolayers of WNME were split every fifth passage to provide a 24-hour culture in exponential growth for chromosome preparation. They were blocked with Colcemid (0.06 µg/ml) for 2 hours, harvested by trypsinization, and pelleted by slow centrifugation. The pellet was resuspended in 1 ml medium that was made hypotonic by addition of 0.07 *N* KCl for 7 minutes. The cells were again gently pelleted and fixed by repeated dispersions (at least three times) in freshly prepared 3:1 methanol–acetic acid for 10-minute intervals. The final pellet was resuspended in fixative, spread on cold, wet slides, and air dried. The slides were stained with 10% Giemsa (G. P. Gurr, Ltd., London, England) at a pH of 6.8 for 10 minutes.

Photomicrographs were made of 30 metaphases on each slide, and the chromosomes per metaphase were counted.

DNA content determinations.—Single cell suspensions were spun at 1,500 rpm for 10 minutes, resuspended in 70% ethanol, and stored at 4°C for at least 24 hours. The cells were then removed from the ethanol and resuspended in mithramycin (Pfizer Inc., Groton, Conn.), 100 mg/ml in 0.15 *M* NaCl with 15 m*M* $MgCl_2$ at a final concentration of 10^5 cells/ml (*11*). DNA content distributions were determined with the use of the Los Alamos flow cytometer, which has been described in detail elsewhere (*12*).

Animals.—The nude mice in our colony originated from five breeding pairs (*nu/nu* males × *nu*/+ females) of BALB/c mice obtained from ARS/Sprague-Dawley Division, The Mongul Corporation, Madison, Wis., in January 1978. Since that time all experimental mice have been produced from similar life-mated pairs. For some studies homozygous (*nu/nu* × *nu/nu*) matings were employed. A single room was used for animal housing and all in vivo manipulations. The ventilation system was High-Efficiency Particle Arrestance filtered and provided a slight positive pressure in relationship to adjacent rooms. Entry was re-

TABLE 1.—*Tumorigenicity of Balb/3T3 strains with various assays*

Strain	Assay	No. of tumors/No. of mice	Inoculum, $\times 10^{-4}$ cells	Latent period,[a] mode/range in mo
A	Sponge	24/32	2–4	4/3–8
	Sponge	0/5[b]	4	>9
	Suspension	7/8	20–200	4/3–8
C	Sponge	2/3	1	4, 5
M	Sponge	0/19	2–54	>9
	Sponge	0/10[b]	2	>9
	Suspension	0/15	100	>9
SVT2	Sponge	3/3	3	4/1–4
Blank	Sponge	0/13	0	>8

[a] Calculation of mode and range was done only on animals with tumors. When no tumors were obtained, the period of observation is given preceded by >.

[b] In this experiment syngeneic, immunocompetent (*nu*/+) mice were used.

stricted to personnel directly associated with the experiments, and individuals were required to pass through an air lock-change room where they put on sterile gowns, shoe covers, masks, and gloves. Autoclaved cages, bedding, food, and water were changed twice weekly, and the mice were checked weekly for tumors. Routine serologic tests for a standard array of murine viruses have all been negative. Pathogenic bacteria have not been detected by frequent culture of utensils or excreta. Fewer than 20 nonexperimental deaths out of over 1,000 deaths have occurred since the colony started. For some studies, heterozygous (*nu*/+) mice produced in the colony were used as immunocompetent controls.

RESULTS

Tumorigenicity of Balb/3T3 Sublines

Of the three Balb/3T3 sublines studied, sublines A and C were tumorigenic in nude mice after a latent period of 3–4 months, but subline M did not produce tumors in several trials (table 1). When immunocompetent (*nu*/+) syngeneic mice were used as hosts, no tumor formation was demonstrated with subline A.

The differences in tumorigenicity between sublines A and M were not accompanied by differences in in vitro characteristics. Both sublines A and M failed to grow in Methocel, and both had low saturation densities in monolayer culture and on sponges (table 2). Cultures allowed to reach confluence did not show morphologic alterations in monolayer pattern.

TABLE 2.—*Saturation densities of cells in monolayer and sponge culture*

Cell type	Monolayer: Cells/cm$^2\times 10^{-4}$	Sponge: Cells/sponge$\times 10^{-4}$
Balb/3T3 strain A	2	4
Balb/3T3 strain M	2	2
WNME, passage 20	15	16
WNME, passage 65	13	17

Phases in Tumor Formation by Balb/3T3 Subline A

In the initial testing of subline A by the sponge method, three phases of tumor formation were noted.

Phase I (wk 1–8): The subline A implants were not grossly or histologically distinguishable from the subline M implants or from blank sponges (without cells) except that subline A implants persisted and enlarged slightly.

Phase II (wk 8–14): Nodules formed at each implant site. The nodules persisted at about 7 mm in mean diameter. By this time the implants of subline M and the blank sponges could not be detected either by external inspection or by dissection. During a similar time period, mice tested with suspensions of subline A cells (some of these mice would eventually develop tumors) showed no externally discernible lesions.

Phase III (later than 14 wk): Some of the nodules resorbed spontaneously, whereas others became rapidly progressive tumors at various times after 14 weeks. Also in the same time period, the mice tested with suspensions of subline A cells began to show rapidly progressive tumors without a preceding nodular phase. The fibrosarcomas produced by both assays were moderately well differentiated with occasional hypocellular, myxoid areas.

A more detailed study of subline A tumor formation was made with the use of 18 nude mice, 8 of which were implanted with two sponges each. One of the two sponges was removed from 1 or 2 of the mice at 2-week intervals and examined for histology or for DNA content (either in a direct manner or after reculture in monolayer). Table 3 shows that three phases occurred as before.

The histology of this series of implants is illustrated in figure 1. Vascularization and proliferation of subline A cells within the sponge were seen at 2 weeks. Between 4 and 8 weeks, the sponge was replaced by an encapsulated, myxoid proliferation of cells, including rare signet-ring cells resembling lipoblasts. Subline M implants also showed the myxoid proliferation during the period before their involution. These hypocellular nodules were similar to the myxoid areas in the tumors. Implants removed after 10 weeks tended to show hypercellularity in their capsules, a pattern consistent with that of a fibrosarcoma. Histologic sections of blank sponges removed at 2-week intervals during phase I showed minimal inflammatory response and progressive organization by granulation tissue (fig. 2). The granulation tissue included ingrowing blood vessels and collagen deposition.

TABLE 3.—*Fate of Balb/3T3 sponge implants by time*

Phases	Subline[a]		Blank sponge[a,b]
	A	M[b]	
Phase I: Nodules before 8 wk	16/18	19/19	13/13
Phase II: Nodules at wk 8–14	16/18	0/19	0/13
Phase III:			
Progressive tumors after 14 wk	11/18	0/19	0/13
Spontaneous resolution after 14 wk	4/18	19/19	13/13
Persistent nodule after 14 wk	3/18	0/19	0/13

[a] Results are expressed as No. of animals with nodules/total No. of animals examined.

[b] The results obtained with subline M and blank sponge are taken from table 1 for comparison with the results of the subline A study.

TABLE 4.—*DNA content of cells recovered from strain A implants versus parent strain in culture*

Time after implant	Recovery method	G_1 DNA content[a]
6 wk	Explant culture	1.79
8 wk	Nodule digestion	1.33
10 wk	Explant culture	1.96
10 wk	Explant culture	1.92
Parent strain	Routine culture	1.61

[a] This content is the DNA content of cells which are in the G_1 portion of the cycle relative to that of normal diploid controls. It is measured as the ratio of G_1 fluorescent intensity (modal channel number of the G_1 peak) of mithramycin-stained test cells over that of diploid control cells. The G_1-to-G_2 modal channel ratio was 2.08:2.17 for all diploid controls. Sample peaks showed coefficients of variation ≤4% and represented at least 10^4 cells.

Analysis of the DNA content of cells recovered from the subline A implants showed amounts distinct from those of the parent subline in cell culture (table 4). Of the four samples from the implants, the one obtained directly by digestion of the nodule and recovery of the cells was different from the other three as well as from the parent subline. This result indicated in vivo cell selection during phase I of tumor formation (as well as possibly during reculture of the implant). A minor peak of diploid cells of host stromal origin was also present in each suspension. Such peaks provided internal control for the G_1 phase ratio determinations.

Tumorigenicity of WNME

WNME at passage 35 formed tumors in the sponge assay as early as 3 months after implantation, but with the suspension test only one of the mice developed a tumor at 7 months (table 5). Earlier passages tested were nontumorigenic, whereas later ones were rapidly tumorigenic by both methods. Exposure of cells to TPA for 2 or 3 weeks before implantation did not materially change the results. Samples for histologic study of sponge implants from passages 35 and 50 were taken at 8 weeks. The passage 35 implants (barely large enough to sample at this time) showed foci of spindle cells within and surrounding the remnants of sponge matrix. The passage 50 implants were much more cellular and sufficiently atypical to be called sarcomatous. Implants of earlier passages (5 and 20) were too small to be visualized reliably by 8 weeks.

TABLE 5.—*Tumorigenicity of WNME at various passages*

Passage No.	Assay	No. of tumors/No. of mice	Inoculum, ×10^{-4} cells	Latent period,[a] mode/range in mo
5	Sponge	0/17	6–28	>9
20	Sponge	0/18	16–32	>9
	Suspension	0/9	160–320	>9
	Sponge TPA	0/7	52	>9
35	Sponge	3/9	15	3, 5
	Suspension	1/7	310	7
	Sponge TPA	7/8	62	4/3–5
50	Sponge	14/16	10–58	3/2–4
	Suspension	5/8	230	5/3–7
	Sponge TPA	6/7	56	3/2–5
65	Sponge	8/8	10	2/1–2
	Suspension	5/17	100	2/1–4

[a] Each entry is the result of a separate experiment. Calculation of mode and range includes only mice with tumors. If <3 tumors were obtained, the actual data are presented. When no tumors were obtained, the period of observation is given preceded by >.

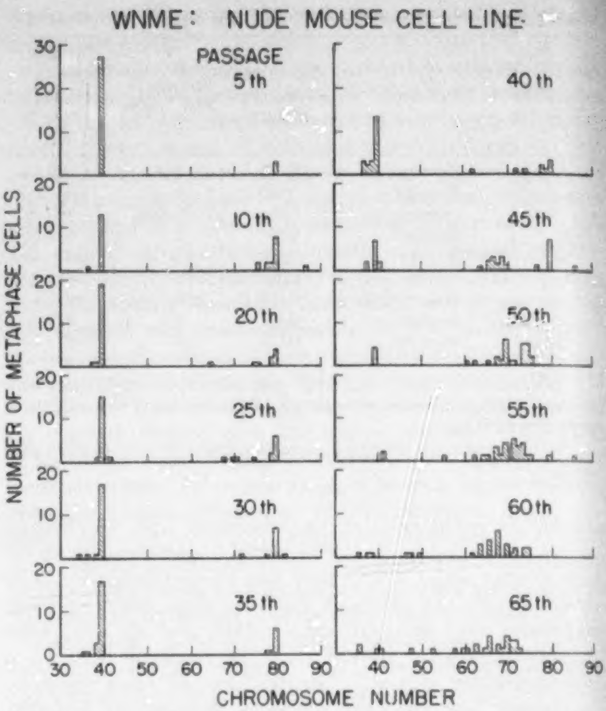

TEXT-FIGURE 1.—Histogram of the number of chromosomes per cell in various passages of WNME. Thirty metaphases were counted for each passage.

Comparison of in vitro characteristics (chromosome number, saturation density, and growth in Methocel) of post-

TABLE 6.—*Saturation density (cells/cm²×10^{-5})*[a]

Cells (passage No.)	No. TPA		TPA		Methocel: Plating efficiency[b]	
	10% FCS	1% FCS	10% FCS	10% FCS	No TPA	TPA
WNME, primary	10.3[c]	ND	ND	ND	ND	ND
WNME (5)	ND	ND	ND	ND	0	0
WNME (20)	1.6	0.2	2.9	0.6	0	0
WNME (35)[d]	3.2	0.5	5.0	0.9	0	0
WNME (50)[e]	2.7	0.5	4.8	0.9	0	0.0005
WNME (60)[e]	1.3	0.4	2.3	0.8	0	0
Balb/3T3 (subline M)	0.2	<0.1	0.3	<0.1	0	0
SVT2	2.0	1.2	2.7	1.4	35	81

[a] Cells were plated at 0.05×10^5 cells/cm² with and without 0.1 mg/ml TPA. ND = not done.

[b] Zero means <1 colony in 10^5 cells. The TPA concentration was 0.1 g/ml.

[c] This value was calculated from cultures in T150 flasks with twice weekly refeeding for 1–2 wk.

[d] The cells formed tumors in the sponge assay only (as per table 5).

[e] The cells formed tumors in both assays (as per table 5).

crisis passages before and after passage 35 showed that the only obvious change was in karyotype. Fully tumorigenic passage 50 cells were blatantly heteroploid, but both passages 20 and 35 showed minor aneuploid subpopulations as did all crisis and post-crisis passages (text-fig. 1).

Saturation density did not change significantly and had not changed from the value calculated for primary cultures of WNME; growth in Methocel was not demonstrable (table 6).

These passage levels were also tested for in vitro response to TPA. TPA increased saturation density in all passages and allowed a very low frequency of growth in Methocel at passage 50 (table 6). Likewise, it produced morphological changes in all cases (fig. 3).

DISCUSSION

Collagenous sponges have been shown to be suitable growth substrates for a wide variety of cells (*13-16*). The use of collagenous sponges for studies of tumorigenicity was also encouraged by the ability of collagen to stimulate angiogenesis in vivo (*19*). Sponges implanted sc in nude mice are externally visible and can be recovered from the animals and the cells can then be recultured. The specific use of the system reportd here was to investigate the expression of the spontaneously acquired tumorigenicity that is characteristic of rodent cells when they are carried in routine culture for extended periods. In particular, we wished to examine further the possibility suggested by the studies of Boone and co-workers (*17,18*) that such culture conditions (which imply attachment to glass or plastic) followed by implantation while still attached to plastic plates combine to initiate and/or promote spontaneous malignant change. In the studies of Boone et al., this kind of effect was seen for both untransformed, permanent cell lines and for early-passage adult mouse connective tissue cells. One question that we asked was whether the highly fenestrated surface of our gelatin sponges could replace the plastic plates in the second stage of Boone's system. This question was asked both for sublines of the untransformed Balb/3T3 cell line and for WNME at varying levels of passage.

For the Balb/3T3 sublines the answer was that anchorage to fenestrated gelatin did not replace the effect of plastic plates. Balb/3T3 subline M was not tumorigenic on gelatin. Nor did variations in the site of inoculation (ip), with the use of Sephadex beads (Superbeads TM, Microcarriers; Flow Laboratories) as the substrate, or coinjection with 10^7 human diploid fibroblasts [by the method of Sager and Kovac (*20*)] suffice to allow subline M to form tumors (Kraemer PM, Wells RS: Unpublished data). Balb/3T3 subline A did not require the gelatin substrate to form tumors, but it did require the environment of the nude mouse since it was not tumorigenic in immunocompetent (nu^+) syngeneic hosts (comparable to the normal BALB/c hosts used by Boone). Further, the slow tumor formation of subline A in nude mice did not appear to be simple selection of a single preexisting variant or subclone. First, the subline A sponge tumors went through a distinctive myxoid nodule stage before either forming progressive tumor or resolving. Second, 4 of 4 such nodules whose cells were analyzed for DNA content had unique values (i.e., were from separate stem lines or clones).

One possible explanation for these data is that the Balb/3T3 sublines are initiated cells that require further promotion. Such promotion might be provided by plastic plates (in the case of subline M) via a mechanism analogous to in vivo solid-surface sarcomagenesis as proposed by Boone et al. (*18*). In contrast, the highly fenestrated gelatin surface does not meet the geometric requirement in order to promote foreign-body sarcomas (*21*). Also, subline A cells might be beyond the need for this promotion step but still not fully tumorigenic in immunocompetent, syngeneic hosts.

An alternative explanation is that some untransformed cell lines do not form tumors in immunocompetent hosts because they have neoantigens. In that case the plastic plates might exert their effect by an immunosuppressive effect; this effect could be generalized or localized, such as the effect suggested for UV light-induced skin carcinogenesis in which altered antigen processing in the skin has been incriminated (*22*). It would be interesting to know if Boone's Balb/3T3 and C3H/10T½ cells are tumorigenic in nude mice.

For the WNME our data show that anchorage to gelatin sponges enhanced the expression of tumorigenicity of early post-crisis cell populations. These results are consistent with the data of Boone et al. (*18*) for adult mouse connective tissue cells, in that carrying cells on plastic surfaces yielded premalignant, but anchorage-dependent lineages. However, our results and the results of Boone et al. differ markedly. The effect of Boone et al. was demonstrable for cells after 1 passage in culture, while our effect required over 20 passages. This inconsistency may reflect any one of several differences between adult connective tissue lineages and cultures initiated with whole mouse fetuses. More definitive experiments are now in progress, i.e., studies of lineages initiated and cultured exclusively on gelatin sponges.

The results with both study systems confirm those of other reports (*2, 6, 23-25*) which indicate weaknesses in the predictive usefulness of in vitro parameters of cancer. In the case of our study of permanent cell line evolution, these parameters did not herald the onset of tumorigenicity, and even passage levels that were frankly heteroploid and tumorigenic by conventional assay were not transformed according to these in vitro parameters.

Similarly, the differences between Balb/3T3 sublines were not paralleled by differences in in vitro behavior. Nor did vascularization or initial cell proliferation on the sponges in vivo predict tumor formation. One advantage of the sponge assay is that such in vivo factors can be evaluated up to 2 months after the cells are implanted. The rapidly tumorigenic, 50th and 60th passage nude mouse embryo cells that evolved in culture were not transformed as defined by our in vitro assays (except for being frankly heteroploid as were the other untransformed permanent cell lines). In particular, they were not anchorage-independent (anchorage-independent cells were not detected in samples many times as large as a tumorigenic dose), indicating that anchorage independence is not the only mechanism by which WNME became independent of the sponges for progressive tumor formation.

In this study "promotability" with TPA was not found, and in vitro responses to TPA did not prove to be markers of tumorigenic potential. Since all sponge implants were vascularized, this also does not appear to be the limiting step for expression of the tumorigenic phenotype as suggested by Folkman (*26*). Indeed, angiogenesis may be a very early attribute of initiated cells as suggested by Brem et al. (*27*). In summary, the spontaneous acquisition of tumorigenicity during serial cultivation of mouse cells was not predicted by commonly used in vitro indicators. This conclusion is also suggested in the work of Reid et al. (*28*).

REFERENCES

(*1*) Freedman VH, Shin S. Cellular tumorigenicity in nude mice: Correlation with cell growth in semi-solid medium. Cell 1974; 3:355–359.

(*2*) Stiles CD, Desmond W, Chuman LM, Sato G, Saier MH Jr. Relationship of cell growth behavior in vitro to tumorigenicity in athymic mice. Cancer Res 1976; 36:3300–3305.

(*3*) Shin S, Freedmann VH, Risser R, Pollack R. Tumorigenicity of virus-transformed cells in nude mice is correlated specifically with anchorage independent growth in vitro. Proc Natl Acad Sci USA 1975; 72:4435–4439.

(*4*) Stiles CD, Desmond W, Sato G, Saier MH Jr. Failure of human cells transformed by simian virus 40 to form tumors in athymic mice. Proc Natl Acad Sci USA 1975; 72:4971–4975.

(*5*) Koprowski H, Croce C. Tumorigenicity of simian virus 40-transformed human cells and mousel-human hybrids in nude mice. Proc Natl Acad Sci USA 1977; 74:1142–1146.

(*6*) Gallimore PH, McDougall JK, Chen LB. In vitro traits of adenovirus-transformed cell lines and their relevance to tumorigenicity in nude mice. Cell 1977; 10:669–678.

(*7*) Boone CW, Jacobs JB. Sarcomas routinely produced from putatively nontumorigenic Balb/3T3 and C3H/10T½ cells by subcutaneous inoculation attached to plastic platelets. J Supramol Struct 1976, 5:131–137.

(*8*) Sanford KK. "Spontaneous" neoplastic transformation of cells in vitro: Some facts and theories. Natl Cancer Inst Monogr 1967; 26:387–418.

(*9*) Coriell LL. Amniocentesis. In: Kruse PF Jr, Patterson MK Jr, eds. Tissue culture, methods and applications. New York and London: Academic Press, 1973:63.

(*10*) Risser R, Pollack R. A nonselective analysis of SV40 transformation of mouse 3T3 cells. Virology 1974; 59:477–489.

(*11*) Crissman HA, Tobey RA. Cell cycle analysis in 20 minutes. Science 1974; 21:1297–1298.

(*12*) Holm DM, Cram LS. An improved flow microfluorometer for rapid measurements of cell fluorescence. Exp Cell Res 1973; 80:105–110.

(*13*) Pontén J, MacIntyre EH. Long term culture of normal and neoplastic human glia. Acta Pathol Microbiol Scand 1968; 74:465–486.

(*14*) Leighton J, Mark R, Justh A. Patterns of three-dimensional growth in vitro in collagen-coated cellulose sponge: Carcinomas and embryonic tissues. Cancer Res 1968; 28:286–296.

(*15*) Rubinstein LG, Herman MM, Foley VL. In vitro characteristics of human glioblastomas maintained in organ culture systems. Am J Pathol 1973; 71:61–76.

(*16*) Douglas WH, Moorman GW, Teel RW. The formation of histotypic structures from monodisperse fetal rat lung cells cultured on a three-dimensional substrate. In Vitro 1976; 12:373–381.

(*17*) Boone CW. Malignant hemangioendotheliomas produced by subcutaneous inoculation of Balb/c 3T3 cells attached to glass beads. Science 1975; 188:68–70.

(*18*) Boone CW, Takeichi N, Eaton SD, Paranjpe M. "Spontaneous" neoplastic transformation in vitro: A form of foreign body (smooth surface) tumorigenesis. Science 1979; 204:177–179.

(*19*) Shubik P, Feldman R, Garcia H, Warren BA. Vascularization induced in the cheek pouch of the Syrian hamster by tumor and nontumor substances. J Natl Cancer Inst 1976; 57:769–774.

(*20*) Sager R, Kovac PE. Genetic analysis of tumorigenesis: Expression of tumor-forming ability in hamster hybrid cell lines. Somatic Cell Genet 1978; 4:375–392.

(*21*) Fergusen DJ. Cellular attachment to implanted foreign bodies in relation to tumorigenesis. Cancer Res 1977; 37:4367–4371.

(*22*) Kripke MC. Immunology of UV induced skin cancer. Photochem Photobiol 1980; 32:837–839.

(*23*) Stanbridge EJ, Wilkinson J. Analysis of malignancy in human cells: Malignant and transformed phenotypes are under separate genetic control. Proc Natl Acad Sci USA 1978; 75:1466–1469.

(*24*) Freeman VH, Shin S. Isolation of human diploid cell variants with enhanced colony-forming efficiency in semisolid medium after a single-step chemical mutagenesis: *Brief communication.* J Natl Cancer Inst 1977; 58:1873–1875.

(*25*) Defendi V, Lehman J, Kraemer P. "Morphologically normal" hamster cells with malignant properties. Virology 1963; 19:592–598.

(*26*) Folkman J. Tumor angiogenesis, chapt 13. In: Becker FF, ed. Cancer. A comprehensive treatise. Vol 3. New York and London: Plenum Press, 1975:355–388.

(*27*) Brem SS, Gullino PM, Medina D. Angiogenesis: A marker for neoplastic transformation of mammary papillary hyperplasia. Science 1977; 195:880–882.

(*28*) Reid LM, Stiles CD, Saier MH Jr, Rindler MJ. Growth of nontumorigenic cells in Millipore diffusion chambers implanted in mice and implications for in vivo growth regulation. Cancer Res 1979; 39:1467–1473.

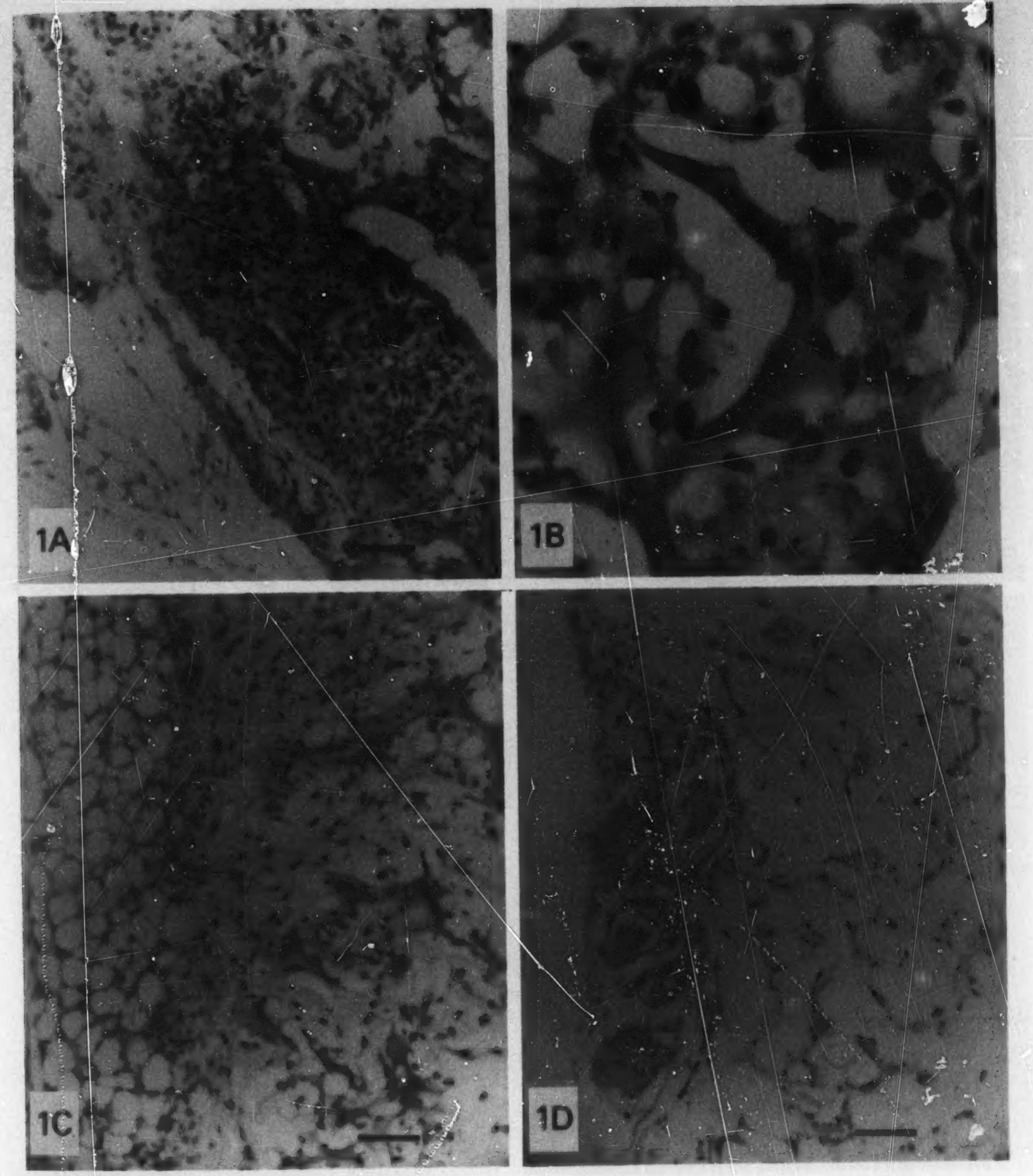

FIGURE 1.—Histologic evolution of Balb/3T3 subline A sponge implants during the first 8 wk (phase I). H & E. A: Sponge implant after 2 wk illustrating cell proliferation within sponge matrix. *Bar*=100 µm. × 100. B: Higher power view at 2 wk shows capillaries intermingled with subline A cells. *Bar*=25 µm. × 400. C: Implant (4 wk old) shows myxoid change of the subline A tissue within the sponge. Adjacent host adipose tissue is seen at *left*. *Bar*=100 µm. × 100. D: Nodules (6 and 8 wk old) were myxoid with total replacement of the sponge. Compressed peripheral nerve is present at *edge of nodule*. *Bar*=100 µm. × 100

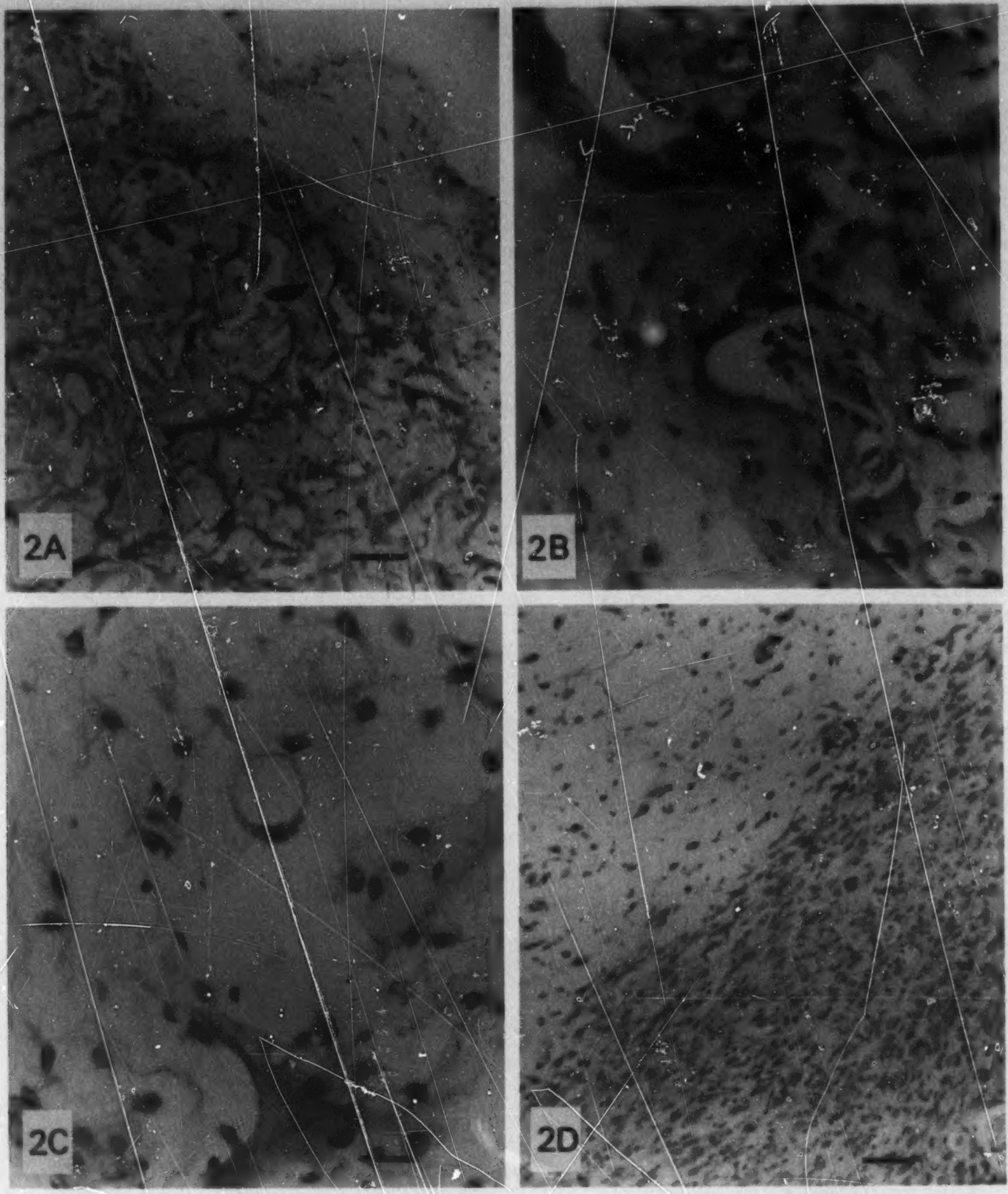

FIGURE 2.—A: Blank sponge implant at 4 wk shows dense collagen and fibroblasts scattered within the sponge matrix. Adjacent host stroma contains little inflammation. H & E. *Bar*=100 μm. × 100. B: Higher power view of same blank sponge implant as in fig. 2A shows no atypia of nuclei. *Bar*=40 μm. × 250. C: Higher power view of subline A implant at 4 wk shows a signet-ring cell in myxoid tissue with atypical cells. H & E. *Bar*=35 μm. × 400. D: Some subline A fibrosarcomas have myxoid areas. H & E. *Bar*=100 μm. × 100

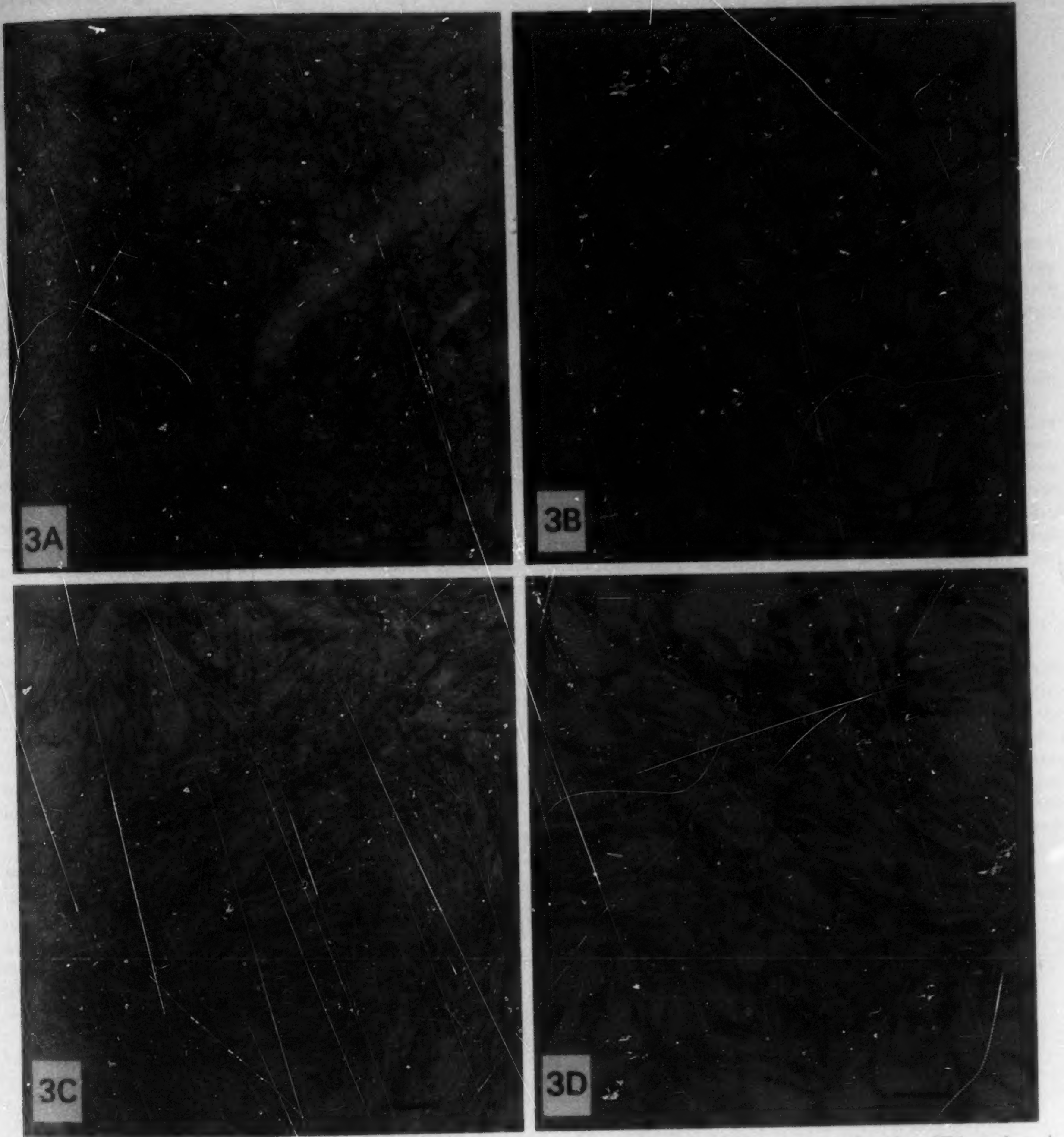

FIGURE 3.—Pseudotransformation was produced in passage 35 WNME by 0.1 g TPA/ml in figs. 3A and 3B. Passage 35 cells without TPA are shown in figs. 3C and 3D. TPA induced pseudotransformation in passages 20 and 50 as well. May-Grünwald-Giemsa. A: *Bar*=100 µm; × 100. B: *Bar*=40 µm; × 250. C: *Bar*=100 µm; × 100. D: *Bar*=40 µm; × 250

blank page

Chromosome Changes Associated With the Progression of Cell Lines From Preneoplastic to Tumorigenic Phenotype During Transformation of Mouse Salivary Gland Epithelium In Vitro[1]

John K. Cowell[2,3] *and* **Caroline B. Wigley**[2,4,5]

ABSTRACT—Two mouse salivary gland epithelial cell lines, CSG 211 and CSG 205/2B1, isolated during carcinogen-induced neoplastic transformation in vitro, were analyzed cytogenetically before and after they acquired the ability to produce carcinomas in syngeneic animals. With the use of Giemsa banding techniques, chromosome changes were identified that were associated with the transition from a preneoplastic to a fully transformed (tumorigenic) phenotype during serial passage in vitro. Results were compared with those from a third cell line of similar origin, CSG 225, which was tumorigenic at the earliest passage tested. These cell lines were found to be subtetraploid, which confirms previous data, and the tumorigenic lines showed consistent losses of copies of chromosomes 1, 4, 7, 9, and 14. Compared with their preneoplastic counterparts, the loss of no single chromosome seems to be sufficient to generate the tumorigenic phenotype, but the loss of a combination of some or all of these chromosomes appears to be important in the phenotypic transition. In CSG 211 the loss of chromosome 7 is probably more important in this respect than loss of the other chromosomes listed. The karyotype of this cell line undergoes major structural rearrangement, which suggests that loss of specific regions of chromosomes 1 and 9 is also important.—JNCI 1982; 69:425–433.

The majority of tumor cells from humans and experimental animals show substantial numerical and structural chromosome aberrations (*1*, *2*), but it is not always possible to determine whether the observed changes are related causally to the expression of the malignant phenotype or are a later consequence. In a few cases where analysis has been possible, chromosome aberrations have been shown to be associated with the progression from premalignant (preinvasive) to malignant (invasive) cells (*3–5*). The progression of myelocytic leukemia, often considered a preleukemia stage (*2*), to the acute blast crisis of the disease is frequently associated with the appearance of new chromosome aberrations (*2*, *6*).

Most human cancers are epithelial in origin, but the study of these cells in vivo is complicated by many factors (*7*). As yet, there is no in vitro transformation system for human epithelium, but recently it became possible to follow closely the development of neoplasia in vitro in epithelial tissue from experimental animals (*8*). In one particular system, chemically induced transformation in vitro of mouse salivary gland epithelium can be followed through a series of defined stages, resulting in the eventual production of fully transformed epithelial cell lines (*9–11*).

During in vitro transformation of mouse salivary gland epithelium, an increase occurred in the proportion of tetraploid cells in the preneoplastic foci (*12*). Accurate quantitation [*see* (*13*)] showed that in the later stages of transformation the DNA content of individual cells decreased, suggesting that chromosomes were being eliminated from these tetraploid cells, a process which eventually gives rise to subtetraploid cell lines (*12*). In the same study evidence was presented which suggested that similar events involving the same cell type occur during in vivo carcinogenesis.

A detailed analysis of eight well-established, tumor-producing cell lines showed that a nonrandom loss of certain chromosomes occurred (*14*). Although chromosomes 1, 4, 7, 9, and 14 were invariably lost, the time of their loss, whether before or after onset of tumorigenicity, could not be determined. In this study we have attempted to identify those chromosomes whose loss is specifically associated with the acquisition of tumorigenicity by preneoplastic cell lines. We hope to dissociate such specific changes from changes that occur randomly without selective advantage or that are involved in adaptation to growth in tissue culture.

MATERIALS AND METHODS

Cell lines.—Three cell lines, CSG 205/2B1, CSG 211, and CSG 225, were derived from mouse submandibular salivary gland ductal epithelium (*11*) transformed in vitro with the use of the hydrocarbon carcinogen BP. Foci of altered preneoplastic cells were isolated from BP-treated primary cultures. Most of the resulting cell lines could be subcultured for many passages before becoming tumorigenic in syngeneic animals. For a fuller account of the derivation and characterization of preneoplastic and fully transformed (tumorigenic) salivary epithelial cell lines, *see* (*10*).

The epithelial tumor cell line CMT 148 was derived from explant cultures of a tumor from CSG 205/2B1 cells.

All cell lines were maintained in Dulbecco's modified Eagle's minimum essential medium supplemented with 10%

Abbreviation used: BP=benzo[*a*]pyrene.

---

[1] Received July 28, 1981; revised January 25, 1982; accepted February 26, 1982.

[2] Imperial Cancer Research Fund, Lincoln's Inn Fields, London, WC2 3PX, England.

[3] *Present address*: Department of Human Genetics and Development, College of Physicians and Surgeons, Columbia University, 701 West 168th St., New York, N.Y. 10032.

[4] *Address reprint requests to* Dr. Wigley.

[5] We thank Dr. L. M. Franks, Imperial Cancer Research Fund (ICRF), and Dr. C. J. Marshall, Institute of Cancer Research, London, England, for their critical reading of the manuscript. We also thank Mrs. T. Barnes, Miss J. Southgate, and Mr. A. Carbonell, all of ICRF, for their technical assistance.

newborn calf serum and 1% kanamycin sulfate. Cells were harvested with the use of EDTA-pronase (*10*) and were passaged with a 1:10 split ratio.

Chromosome analysis.—Chromosome preparations and subsequent trypsin-Giemsa banding analyses were usually performed as described previously (*15*). However, the presence of keratinizing cells in CSG 211, which seemed to prevent penetration of vinblastine and inhibited chromosome spreading, necessitated that the procedure be modified slightly for this cell line. The cells were harvested and treated with vinblastine in suspension; this procedure was followed by longer than usual hypotonic treatment (at least 20 min).

For each cell line, 20 well-banded metaphases were analyzed. From these analyses, modal karyotypes were constructed representing consistent features of the cell line. [For further discussion, *see* (*14*)]. All karyotypes were based on the previously presented normal karyotype (*15*) from mouse embryo fibroblasts. The nomenclature used throughout is that of Nesbitt and Francke (*16*).

Tumorigenicity assays.—Cell lines, at the earliest possible passage after their isolation, were tested for tumorigenicity by sc injections of 2-5×10^6 cells into syngeneic hosts. Subsequently, the cell lines were tested at appropriate regular intervals. These numbers of cells were chosen for routine testing of tumorigenicity after it had been shown that the most malignant salivary epithelial cell lines available in our laboratory [e.g., CSG 120/7 (*9*)] failed to produce tumors consistently from inocula of less than 10^6 cells and that there was no advantage with respect to tumor incidence or growth rate in injecting more than 5×10^6 cells (Wigley CB: Unpublished data).

RESULTS

Three cell lines were isolated from preneoplastic foci before the occurrence of change in growth pattern and before evidence of morphology characteristic of tumorigenic cells (*10*). Two cell lines, CSG 211 and CSG 205/2B1, were nontumorigenic at early passages and, therefore, have a preneoplastic stage (table 1), but CSG 225 was tumorigenic from the outset. Both of the preneoplastic cell lines eventually gave rise to tumorigenic cell lines after varying lengths of time in culture. In an attempt to detect specific chromosome changes associated with the onset of tumorigenicity, we undertook a detailed G-band chromosome analysis of the preneoplastic and tumorigenic cell lines.

CSG 211 Cells

Preneoplastic.—A representative karyotype with modal number 67 from passage 11 is shown in figure 1. The main feature of this karyotype is the absence of copies of individual chromosomes that presumably were lost from progenitor tetraploid cells (*12*). Details of these losses are summarized in table 2. There was only one structural chromosome rearrangement which involved the translocation of a small chromosome region onto the distal end of 4q (fig. 1), with the breakpoint in band 4C3. The difficulty in identifying the origin of the translocated region was due to the fact that the translocation is not a reciprocal one; i.e., no other chromosome in the karyotype shows a deletion. We must assume, therefore, that after the rearrangement event the chromosome from which the translocated segment arose was lost. If this is the case, then the most likely source of the extra chromosome material is chromosome 13.

TABLE 1.—*Summary of cell line tumorigenicity as related to passage level of inoculated cells*

Cell line	Passage level	No. of tumors/No. of mice
CSG 211	5–18	0/11
	23–37	7/7
CSG 205/2B1	6–12	0/5
	14	2/4
	16–26	11/13

TABLE 2.—*Chromosome losses in preneoplastic and tumorigenic salivary gland epithelial cell lines*

Cell line (passage level)	Modal chromosome No.	Chromosome losses[a]	Rearrangements
CSG 211			
Preneoplastic (11)	67	1, 2, 3, 4, 9, 13, 14, 15, 16, 17 (2), 18, Y	T(?;4)
Tumorigenic (33)	59	1 (2), 2, 3, 4 (2), 7, 8, 9 (2), 10, 11, 12 (2), 13, 14 (3), 15 (2), 16 (2), 17 (2), Y (2)	T(1;5), T(9;10), T(14;?), T(4;?), M5
CSG 205/2B1			
Preneoplastic (13)	71	1, 2, 4, 7, 8, 9 (2), 12 (2), 13, 14 (2), 15 (2), 17	T(8;12), T(6;?), M3, M4, M5, del 4
Tumorigenic (26)	69	1, 2 (2), 3, 4, 6, 7, 8, 9, 12, 14 (2), 15, 17, Y	T(8;12), T(6;?), M3, del 4, del 14
CMT 148[b]	71	1, 2, 3, 4, 6, 7, 8, 9, 12 (2), 14, 17, Y	T(8;12), M2, M3, del 4, del 6, del 14

[a] One chromosome copy from each group was missing from a tetraploid cell unless otherwise specified *in parentheses*.

[b] Derived from explant cultures of CSG 205/2B1 cells at passage 16.

Tumorigenic.—The mean chromosome number of passage 33 cells is 59, eight fewer than that of the preneoplastic cells. The karyotype of the tumorigenic cells is shown in figure 2. During evolution of this cell line, several structural rearrangements have arisen (fig. 3). A description and tentative identification of these rearrangements follows: M1—T(1;15)(1D;15D2); M2—T(9;10)(9D;10D2); M3—deletion of the distal region of the marker chromosome in CSG 211/11 (fig. 1), which was replaced by a small unidentified chromosome region, with the breakpoint in band 4C3; M4—translocation of chromosome 14, possibly with a centromeric breakpoint to the proximal region of an unidentified chromosome; and M5—rearrangement could not be identified.

Changes in karyotype—A study of the modal chromosome numbers alone shows that there was a loss of eight chromosomes during the transition from preneoplastic to tumorigenic cell line. However, as shown in table 3, when the chromosome markers were analyzed in more detail, only copies of chromosomes 7, 11, 12, 14, and 16, in addition to the Y-chromosome, were completely missing, and there was a gain of one copy of chromosome 18. Often regions of other chromosomes were lost as a result of chromosome rearrangement (table 3). In CSG 211/11 the marker chromosome, tentatively identified as the translocation of 13D→ter to 4C3, was no longer present in the same form but appeared to have undergone further rearrangement.

CSG 205/2B1 Cells

Preneoplastic.—Up to passage 12, no cell implant had produced tumors within the 18-month observation period (table 1). Passage 14 cells showed a 50% tumor incidence after a long latency period, suggesting that selection of variant tumorigenic cells from a heterogeneous population had taken place in vivo. The earliest passage level at which good G-banded preparations were obtained was passage 13 where the majority of cells could be considered to be nontumorigenic (preneoplastic). The karyotype of passage 13 cells is shown in figure 4 and has a modal number of 71. Losses of individual chromosomes are summarized in table 2. At least five and sometimes six copies of chromosome 5 were present in all cells at this passage. Unlike the preneoplastic CSG 211 cells, several structural rearrangements occurred in the early passage of CSG 205/2B1 cells. These are shown in figure 3. A consistent feature of the cell line was the terminal deletion of chromosome 4, with the breakpoint at band 4C7. Other consistent chromosome changes were: M1—a complex translocation apparently involving deletion of chromosome 8 distal to band 8D1, with the possible duplication of band 8D1 and the translocation of most of chromosome 12 distal to band 12B onto the duplicated region; and M2—translocation of a large chromosome region to the distal tip of chromosome 6, with the breakpoint in 6F1. This translocated region does not resemble that of any other chromosome, and possibly the relocated region originated from several chromosomes.

Chromosome markers M3, M4, and M5 were small chromosomes that arose from the proximal region of unidentified chromosomes. Similar fragments were also characteristic of many other salivary gland cell lines (*14*), but relevance to the phenotype of these cells was difficult to assess because of their variable presence in individual cells of any particular cell line.

At passage level 13, two Y-chromosomes were present in the majority of cells.

Tumorigenic.—Passage 24 cells produced carcinomas after 4–6 weeks (table 1), as compared to longer times at earlier passage levels. Karyotype analysis at passage 26
as representative of the fully tumorigenic cell
The modal chromosome number is 69. A detai
some analysis revealed that major karyotypic re
occurred, the details of which are summarize
Five copies of chromosome 5, the terminal dele
mosome 4, and the two large marker chromoso
M2 were also retained in the tumorigenic cells
small chromosome markers were lost in the tun
line. The only new structural aberration in th
formed cells involved the terminal deletion of
14 distal to band 14E2.

Although the Y-chromosome is included in t
in figure 5, it was missing in half of the cells a

Changes in karyotype.—The reduction in chron
ber by two during the transition of the CSG
from a preneoplastic to a tumorigenic cell lin
retically be accounted for by the loss of th
chromosome markers. Closer analysis reveal
explanation was too simple, inasmuch as consi
mosome reorganization had occurred (table 3)
emphasizes the caution that must be exercis
draws conclusions from chromosome counts a

Terminal deletion of chromosome 14 repre
new chromosome aberration associated with th
cells, but losses of chromosomes 2, 3, and
chromosome also occurred. The tumorigeni
copies of chromosomes 9, 12, and 13, when c
the preneoplastic cells, presumably as a res
junction. Cowell in (*14*) suggested that in th
cell lines certain chromosomes carry mutatio
excess may be responsible for the expression of
phenotype. These imbalances may be achiev
of one or both of the "normal" homologues. S
chromosome 9 have been found in all of th
salivary gland cell lines, often with two copi
205/2B1 cells at passage 13 have already lost t
homologues, then nondisjunction of one of
chromosomes, while increasing the number
represents a chromosome imbalance.

At regular intervals during in vitro passag
205/2B1 and CSG 211, cells were tested for
(table 1). Although cell implants from CS
negative for many passages, the findings for
were not so clearly definable. Cell implan
passage 16 of CSG 205/2B1 produced tumor
many months in vivo, and the latent per
longer than that for cells of later passages.
therefore, to determine whether the cells i
were derived as a result of the selection in viv
population of cells preexisting in vitro or wh
ulation arose de novo after inoculation in viv
tumors was cultured, and cell line CMT 148
to distinguish between the two possibilities.

TABLE 3.—*Chromosome changes associated with progression of CSG 211 and CSG 205/2B1 from preneoplastic to tumorigenic cell lines*

Cell line	Whole chromosome changes[a]	Deleted chromosome regions[b]
CSG 211	−7, −8, −11, −12 (2), −14, −16, +18, −Y, +M5	1 cen→1D 15D2→ter, 10D2→ter, 9cen→9D
CSG 205/2B1	−2, −3, −6, +9, +12, +13, +15, −Y, −M3, −M5	14F2→ter

[a] One chromosome copy from each group was missing from a tetraploid cell unless otherwise specified *in parentheses*.

[b] Breakpoint terminology is according to Nesbitt and Francke (*16*).

CMT 148 Cells

The karyotype of cells from passage 8 o
given in figure 6. The cells have a moda
number of 71. Losses of individual chromos

in table 2, and a comparison of the karyotype of the CMT 148 cell line (derived from passage 16 of CSG 205/2B1 cells) with the karyotypes of preneoplastic and tumorigenic CSG 205/2B1 cells is summarized in table 4.

Certain chromosome abnormalities common to both the preneoplastic and tumorigenic cell lines, such as the terminal deletion of chromosome 4 and the excess of chromosome 5, are also present in CMT 148. With the exception of the variable presence of the small marker fragments, the CMT 148 tumor cell line only resembled the preneoplastic cell line in two respects (table 4), and the overall karyotype resembled the tumorigenic cell line at passage 26. The only new structural aberration was the deletion of the terminal region of chromosome 6 distal to band 6E. Chromosome gains had occurred in normal copies of chromosomes 14 and 15. CMT 148 now has four copies of chromosome 15, presumably as a result of nondisjunction.

CSG 225 Cells

This cell line was isolated from primary culture in the same way as were lines CSG 211 and CSG 205/2B1, but even at passage 9 it consistently produced invasive carcinomas (*10*). Clones from an early passage of CSG 225 cells were also tumorigenic (Wigley CB: Unpublished data) and had, therefore, no detectable preneoplastic stage. A description of this cell line was included for comparison with lines CSG 211 and CSG 205/2B1. Detailed chromosome analysis of cells from passage 9 showed that the majority were in the suboctaploid range, with only a minor subpopulation of cells in the subtetraploid range. Therefore, these higher ploidy cells apparently have a selective advantage in culture and presumably arose as a result of endoreduplication of the subtetraploid cells. A similar situation was described in another salivary gland cell line, CAE 553 (*14*). A modal karyotype could not be constructed from the very limited number of subtetraploid cells available, but a sample karyotype of a single CSG 225 cell (fig. 7) shows that there were many chromosome losses. The average chromosome number was in the range 62–65, and chromosomes 1, 4, 7, 9, and 14 and the Y-chromosome were missing. These losses were consistent with findings for the tumorigenic cell lines described in this paper and previously (*14*). Another consistent feature was the excess of chromosome 5; chromosome 19 was also in excess.

DISCUSSION

The loss of certain chromosomes from tetraploid cells has been implicated in the transformation of mouse salivary gland epithelium (*14*). All three tumorigenic cell lines described in this paper were also subtetraploid and, within a background of random loss, chromosomes 1, 4, 7, 9, and 14 were missing consistently, confirming previous results (*14*). In the experiments reported in this paper it was possible to analyze the chromosomes of preneoplastic cells, follow them through the transformation process, and compare their karyotypes with those of the tumorigenic derivatives. No single chromosome change apparently was associated with this transition. In cell line CSG 211, complete copies of chromosomes 7 and 14 were lost during the transition from a preneoplastic to a tumorigenic phenotype, with most of one copy each of chromosomes 1 and 9 also lost. Thus of the nonrandom changes noted previously in the fully transformed cell lines, apparently only chromosome 4 was not involved (*see* later). In CSG 205 cells a small region of chromosome 14 was lost during the transition—the only change common to both cell lines. In line CSG 225, no preneoplastic phase could be identified, but chromosomes 1, 4, 7, 9, and 14 were also underrepresented in the tumorigenic cells.

TABLE 4.—*Comparison of CMT 148 karyotype with karyotypes of preneoplastic and tumorigenic CSG 205/2B1 cell lines*

CSG 205/2B1 cell lines	CMT 148 chromosome aberrations	
	In common with CSG 205/2B1*	Different from CSG 205/2B1
Preneoplastic (P)	−2, −12 (2), M3, M5	—
Tumorigenic (T)	−3, −6, −9, +13, −Y, del 14	—
Both P and T	−1, −4, +5, −7, −8, −17, del 4, M1	del 6, +14, +15

*One chromosome copy from each group was missing from a tetraploid cell unless otherwise specified *in parentheses*.

The two cell lines CSG 211 and CSG 205/2B1 behaved differently during their progression from preneoplastic to tumorigenic cell lines. The differences in behavior also were reflected in their karyotypic changes. CSG 211 was in continuous culture for more than 5 months, from the initial karyotyping at passage 11 to passage 23 when the cells were consistently tumorigenic. During this time the cells were tested at regular intervals, and within the 18-month period of animal observation no tumor arose from CSG 211 cells before passage 23, four passages earlier than stated in the preliminary data presented previously (*10*). During this time in vitro, the cells had undergone major karyotypic changes. In comparison, cell line CSG 205/2B1 was first karyotyped at passage 13 and was initially considered to be tumorigenic at passage 22 (*10*). Since these observations, a proportion of tumorigenicity tests have proved positive at earlier passages but only after a long latent period in vivo. This finding indicates that whereas CSG 211 may have undergone the relevant structural chromosome reorganization fairly late in its culture history, the tumorigenic subpopulation of CSG 205/2B1 appears to have evolved relatively early, although selection for this subpopulation in vitro occurred gradually over a longer period. Analysis of CMT 148, the cell line derived from the tumor that arose from passage 16 of CSG 205/2B1 cells, reveals karyotypic features of both the preneoplastic and tumorigenic cell lines, but features of the tumorigenic line predominate. This observation suggests that these cells were selected in vivo, just as they were selected in vitro, from a heterogeneous parent population. Of possible relevance is the deletion of part of chromosome 14. The importance of the loss of this chromosome has been implicated in all other cell lines. [*See* above and (*14*).]

CSG 211 perhaps offers better insight into the changes involved in the transition of preneoplastic cells to tumorigenic cells, inasmuch as the transition seems to be relatively abrupt in this cell line. Perhaps of most interest is the finding that chromosomes 1, 7, 9, and 14 are involved, particularly chromosome 7. The preneoplastic cells have four copies of chromosome 7, whereas one copy of chromosome 7 is missing in the tumorigenic cells. An additional chromosome 14 is lost, leaving only two, a common feature of the other tumorigenic cell lines (*14*), particularly those transformed in vivo. The other chromosomes, 9 and 1, were involved in rearrangements resulting in the loss of parts of these chromosomes. That these karyotype changes are simply an adaptation to in vitro growth is unlikely inasmuch as CSG 211 cells had grown rapidly from the first passage, with no marked increase in growth rate associated with the acquisition of tumorigenicity.

Unlike any of the tumorigenic cell lines reported in this paper or previously (*14*), CSG 211 cells at passage 33 contained many structural chromosome rearrangements in addition to the small marker chromosomes so often seen. Possibly simple loss of whole chromosomes in this cell line is insufficient to generate the malignant phenotype. Analysis of the markers has shown that as a result of nonreciprocal chromosome rearrangements, certain parts of chromosomes were lost, notably from chromosomes 1 and 9. These observations may indicate that these regions carry important information that controls expression of the malignant phenotype. Why should rearrangement, rather than whole chromosome losses, occur in this cell line? One possibility is that these cell lines carry recessive mutations so that loss of the whole homologous chromosome would be lethal. However, loss of certain regions may be required to create a genetic imbalance and allow expression of the malignant phenotype (*17*). As a result of rearrangement, these regions could be lost or their expression suppressed while the lethal mutations remain balanced. This may also account for the long preneoplastic period inasmuch as appearance of these rearrangements is likely to be a rare event. From the analysis of the two cell lines, particularly of CSG 211, a combination of chromosomes or chromosome regions apparently must be lost to allow expression of the malignant phenotype.

In both CSG 211 and CSG 205/2B1, chromosome 4 was shown to be structurally abnormal. In CSG 205/2B1 a terminal deletion of chromosome 4 occurred, and in CSG 211 two rearrangements resulted that involved the same terminal region although the nature of the rearrangement changed during the transition from preneoplastic to tumorigenic cells. In addition to the structural rearrangement, one copy of chromosome 4 was missing, which was also one of the consistent features of tumorigenic salivary gland cell lines (*14*). In these cell lines the same terminal region of chromosome 4 was also involved in structural rearrangements, suggesting that the region was a nonrandom site for chromosome rearrangement. These findings are not restricted to salivary gland cell lines, and the terminal region of chromosome 4 also was reported to be involved in structural rearrangements in mouse bladder epithelial cell lines (*15*). The invariable loss of at least one copy of chromosome 4 in salivary gland cell lines might suggest some correlation with the expression of tumorigenicity in these cells, but the correlation could not be demonstrated conclusively in these studies. Whether structural rearrangement of the terminal region of chromosome 4 is important in the expression of the malignant phenotype is also uncertain. Somatic cell hybridization studies strongly implicated chromosome 4 in the expression of the malignant phenotype in the mouse (*18*). Recently, Lin and Ruddle (*19*) demonstrated that murine chromosome 4 is the probable site of a gene (or genes) for DNA repair synthesis that has been implicated in the development of cancer (*20*). Whether the enzymes involved in DNA repair are located in the terminal region of chromosome 4 is not known.

REFERENCES

(*1*) Mitelman F. Cytogenetics of experimental neoplasms and non-random chromosome correlations in man. Clin Haematol 1980; 9:195–219.

(*2*) Sandberg AA. The chromosomes in human cancer and leukaemia. Amsterdam and New York: Elsevier, 1980.

(*3*) Granberg I. Chromosomes in preinvasive, microinvasive and invasive cervical carcinomas. Hereditas 1971; 68:165–218.

(*4*) Mitelman F, Mark J, Nilsson PG, Dencker H, Norrvd C. Chromosome banding pattern in human colonic polyps. Hereditas 1974; 78:63–68.

(*5*) Sandberg AA. Chromosome markers and progression in bladder cancer. Cancer Res 1977; 37:2950–2956.

(*6*) Trujillo JM, Ahearn MJ, Cork A. General implications of chromosome alterations in human leukaemia. Hum Pathol 1974; 5:675–686.

(*7*) Harnden DG, Taylor AMR. Chromosomes and neoplasia. Hum Genet 1979; 9:1–70.

(*8*) Franks LM, Wigley CB. Neoplastic transformation in differentiated epithelial cell systems in vitro. New York and London: Academic Press, 1979.

(*9*) Knowles MA, Franks LM. Stages in neoplastic transformation of adult epithelial cells by 7,12-dimethylbenz(*a*)anthracene in vitro. Cancer Res 1977; 37:3917–3924.

(*10*) Wigley CB. Transformation in vitro of adult mouse salivary gland epithelium: A system for studies on mechanisms of initiation and promotion. In: Franks LM, Wigley CB, eds. Neoplastic transformation in differentiated epithelial cell systems in vitro. New York and London: Academic Press, 1979:3–34.

(*11*) Wigley CB, Franks LM. Salivary epithelial cells in primary culture: Characterization of their growth and functional properties. J Cell Sci 1976; 20:149–165.

(*12*) Cowell JK, Wigley CB. Changes in DNA content during in vitro transformation of mouse salivary gland epithelium. JNCI 1980; 64:1443–1449.

(*13*) Cowell JK, Franks LM. A rapid method for accurate DNA measurements in single cells in situ using a simple microfluorimeter and Hoechst 33258 as a quantitative fluorochrome. J Histochem Cytochem 1980; 28:206–210.

(*14*) Cowell JK. Chromosome abnormalities associated with salivary gland epithelial cell lines transformed in vitro and in vivo with evidence of a role for genetic imbalance in transformation. Cancer Res 1981; 41:1508–1517.

(*15*) ———. Consistent chromosome abnormalities associated with mouse bladder epithelial cell lines transformed in vitro. JNCI 1980; 65:955–961.

(*16*) Nesbitt MN, Francke U. A system of nomenclature for band patterns of mouse chromosomes. Chromosoma 1973; 41:145–158.

(*17*) Cowell JK. Chromosome changes associated with epithelial cell transformation with special reference to in vitro systems. In: Franks LM, Wigley CB, eds. Neoplastic transformation in differentiated epithelial cell systems in vitro. New York and London: Academic Press, 1979:259–286.

(*18*) Jonasson N, Povey S, Harris H. The analysis of malignancy by cell fusion. VII. Cytogenetic analysis of hybrids between malignant and diploid cells and tumours derived from them. J Cell Sci 1977; 24:217–254.

(*19*) Lin PF, Ruddle FH. Murine DNA repair gene located on chromosome 4. Nature 1981; 289:191–194.

(*20*) Setlow RB. Repair deficient human disorders and cancer. Nature 1978; 271:713–717.

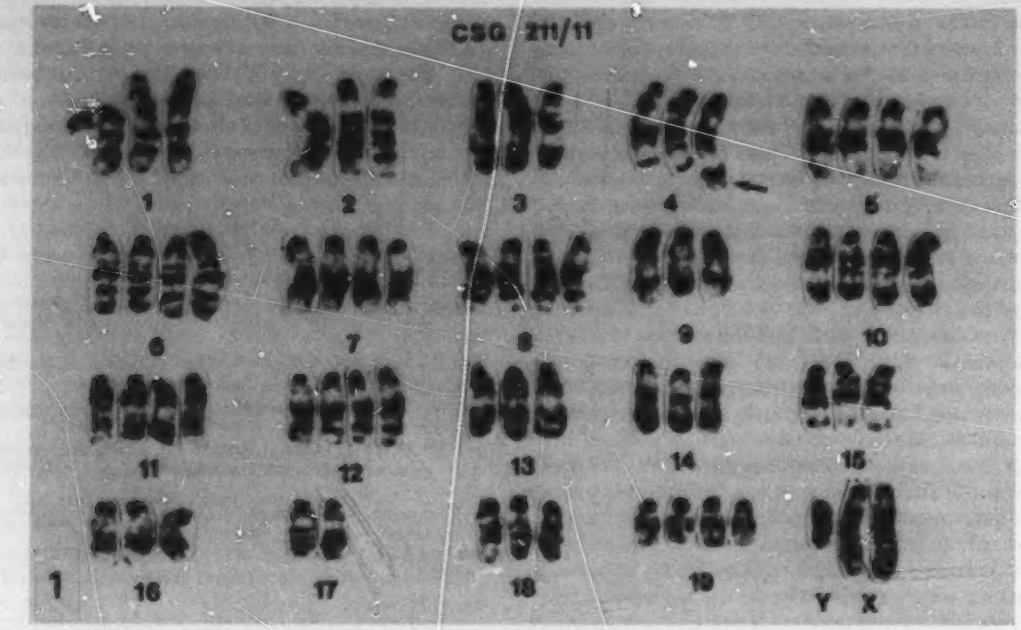
CSG 211/11
1
2
3
4
5
6
7
8
9
10
11
12
13
14
15
16
17
18
19
Y X
1

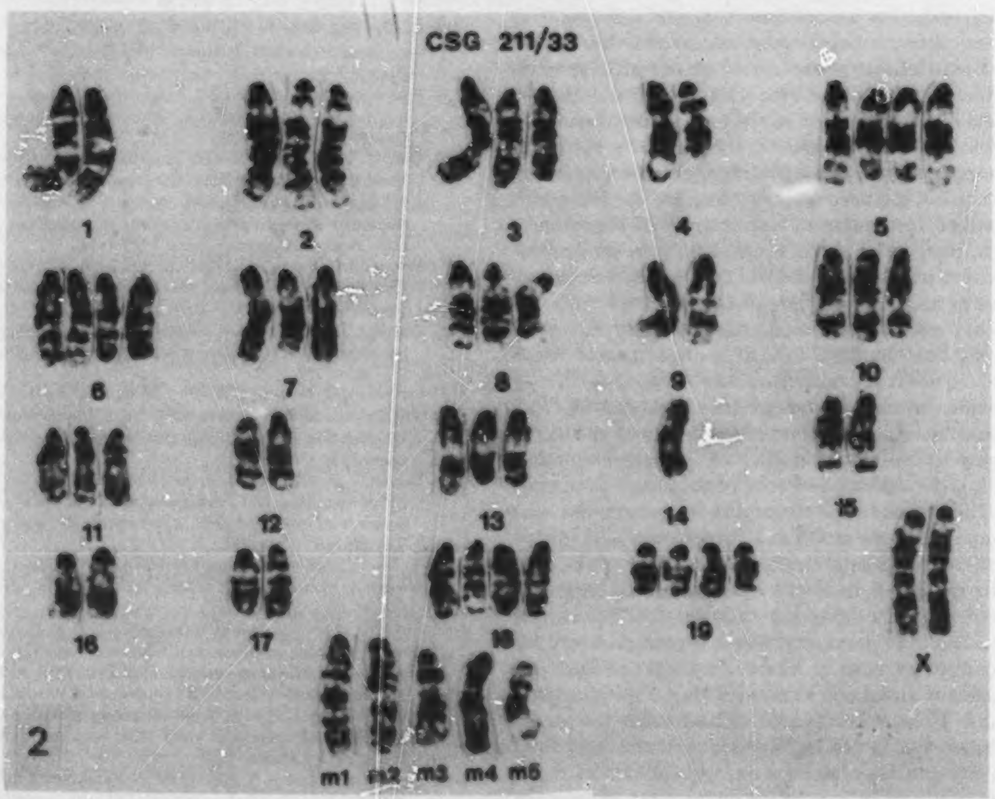
CSG 211/33
1
2
3
4
5
6
7
8
9
10
11
12
13
14
15
16
17
18
19
X
m1 m2 m3 m4 m5
2

FIGURE 1.—Giemsa-banded karyotype of in vitro transformed salivary gland epithelial cell line CSG 211 (preneoplastic cells at passage 11). *Arrow* indicates the only structural rearrangement.

FIGURE 2.—Giemsa-banded karyotype of in vitro transformed mouse salivary gland cell line CSG 211 (tumorigenic cells at passage 33).

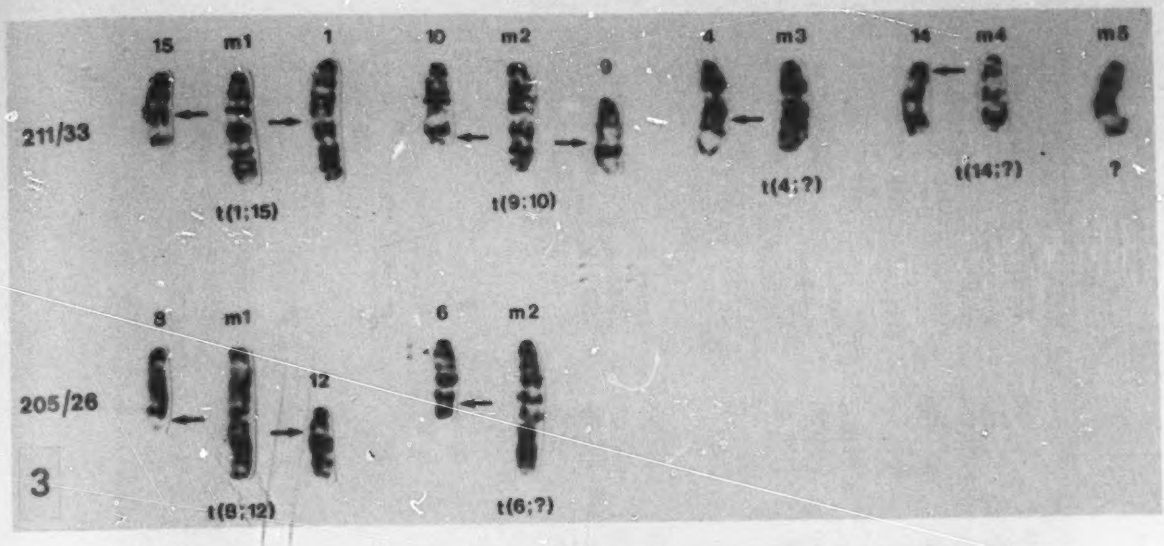
211/33
15
m1
1
10
m2
9
4
m3
14
m4
m5
t(1;15)
t(9;10)
t(4;?)
t(14;?)
?
205/26
8
m1
12
6
m2
t(8;12)
t(6;?)
3

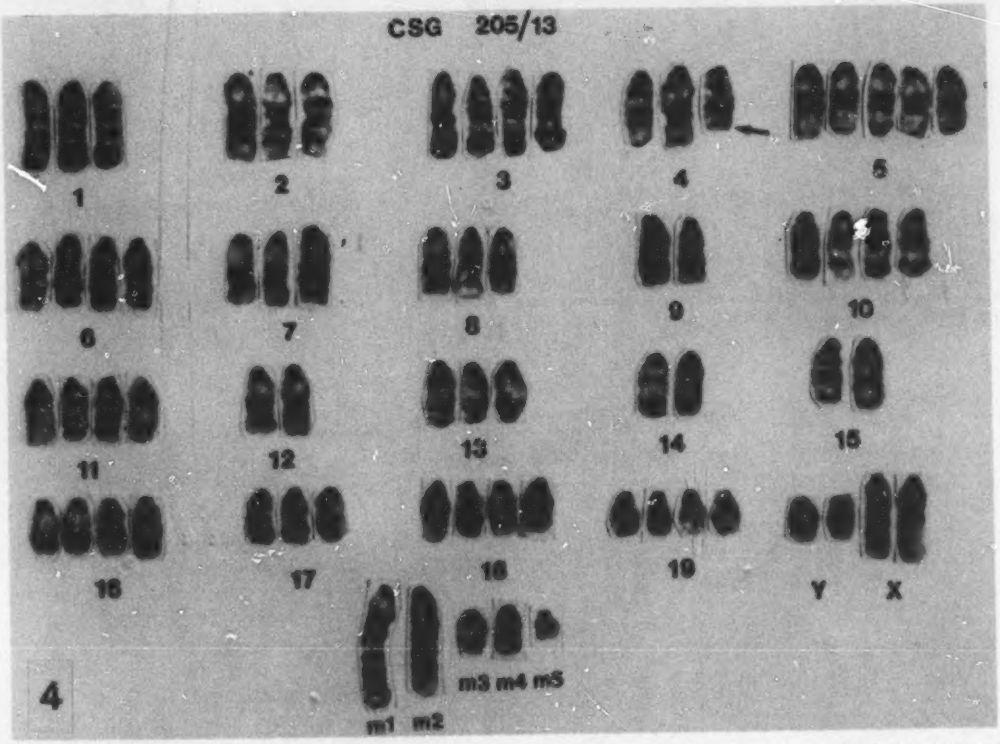
CSG 205/13
1
2
3
4
5
6
7
8
9
10
11
12
13
14
15
16
17
18
19
Y
X
m1
m2
m3
m4
m5
4

Figure 3.—Tentative identification of major structural rearrangements in chromosomes of tumorigenic cells from CSG 211 (*top*) and CSG 205/2B1 (*bottom*). *Arrows* indicate suggested breakpoints in normal homologues from which markers were derived.

Figure 4.—Giemsa-banded karyotype of in vitro transformed salivary gland epithelial cell line CSG 205/2B1 (preneoplastic cells at passage 13). *Arrow* indicates terminal deletion of chromosome 4.

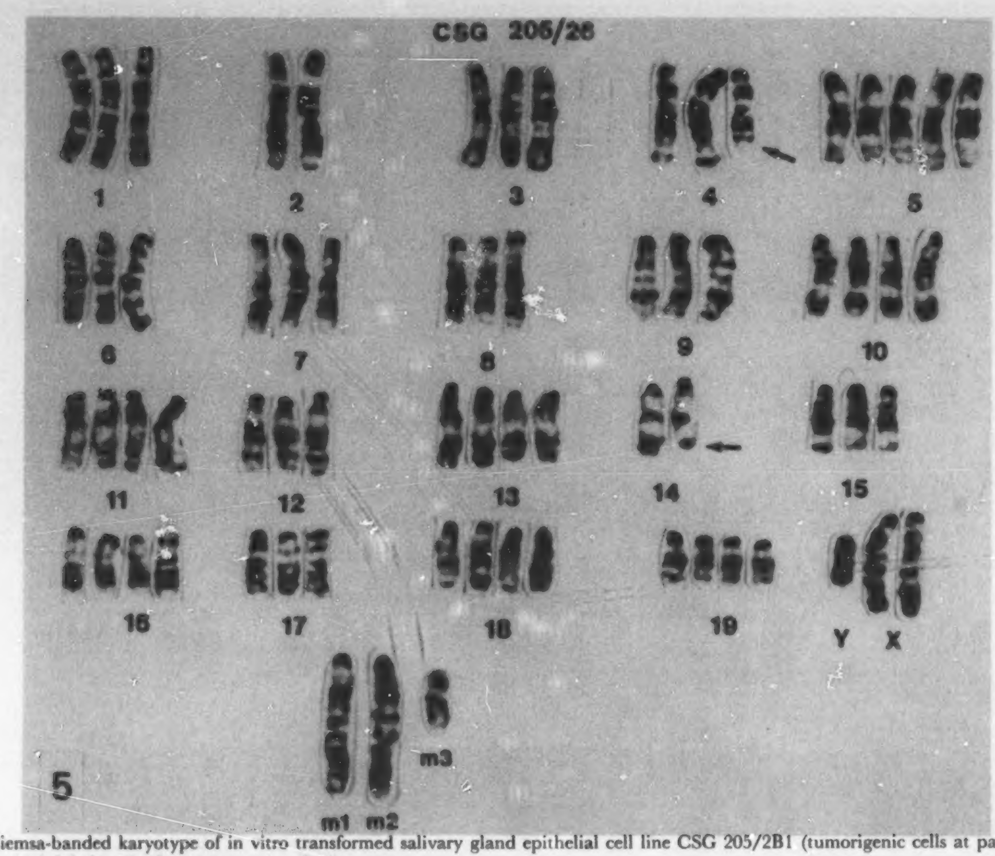
CSG 205/26
1
2
3
4
5
6
7
8
9
10
11
12
13
14
15
16
17
18
19
Y X
m1 m2
m3
5

FIGURE 5.—Giemsa-banded karyotype of in vitro transformed salivary gland epithelial cell line CSG 205/2B1 (tumorigenic cells at passage 26). *Arrows* indicate terminal deletions in chromosomes 4 and 14.

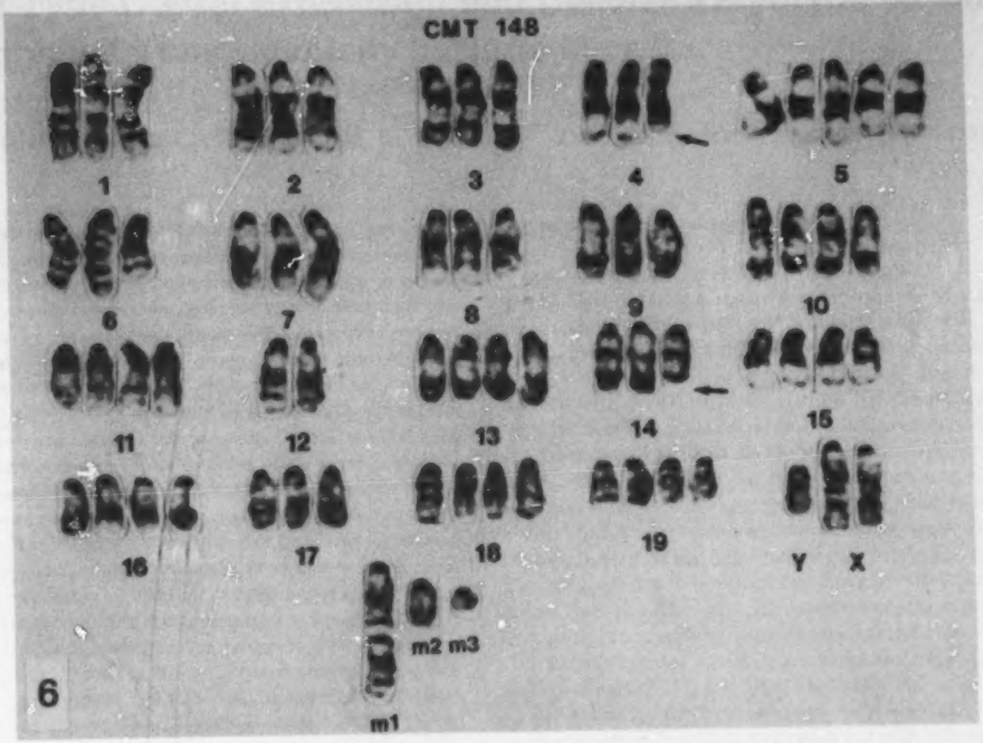
CMT 148
1
2
3
4
5
6
7
8
9
10
11
12
13
14
15
16
17
18
19
Y
X
m1
m2
m3
6

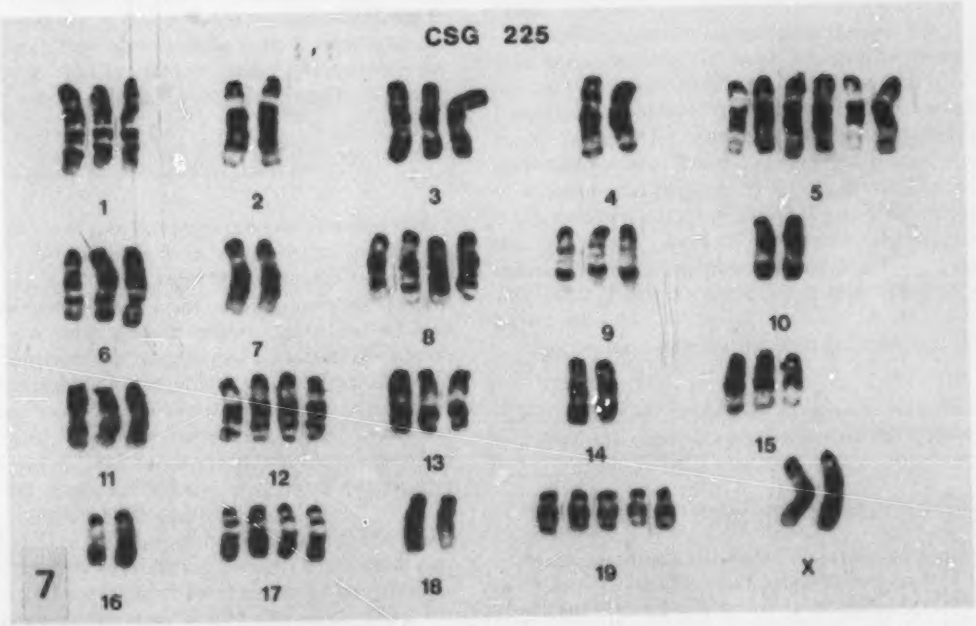
CSG 225
1
2
3
4
5
6
7
8
9
10
11
12
13
14
15
16
17
18
19
X
7

FIGURE 6.—Giemsa-banded karyotype of salivary gland cell line CMT 148 (passage 8) derived from a tumor of CSG 205/2B1 (passage 16).

FIGURE 7.—Giemsa-banded karyotype of in vitro transformed salivary gland epithelial cell line CSG 225 (passage 8).

blank page

Effect of Type C Viral Expression and Cellular Karyotype on Human B-Lymphoblast Tumorigenicity in Nude Mice[1, 2]

Anton F. Steuer,[3] Robert C. Ting,[3] Phillip D. Markham,[4] Zaki Salahuddin,[4] *and* Robert C. Gallo[5]

ABSTRACT—Cultured human hematopoietic cells from several normal and leukemic sources, including those cells initiated after exposure to primate type C retroviruses were tested for their capacity to induce tumors in young athymic BALB/c (*nu/nu*) mice after sc inoculation. An attempt was made to correlate these results with virus expression and chromosome patterns. Progressively growing tumor formation was observed in 5 of 18 normal diploid B-lymphoblast lines from normal peripheral blood and in one of three diploid B-lymphoblast lines from leukemic donors established after infection with primate type C viruses (gibbon ape leukemia virus or simian sarcoma virus). In contrast, none of eight spontaneously transformed B-lymphoblast lines with normal diploid karyotypes formed progressively growing tumors, although one formed a tumor that remained the same size (0.5 cm) for several months. Progressive tumor formation occurred in four of seven previously established cell lines of different cell types that had abnormal karyotypes. Of the normal diploid B-lymphoblast cultures exposed to type C viruses, 12 were tested for the presence of viral RNA and structural proteins (p12, p30, gp70), and this information was correlated with tumorigenicity. Four of the six cultures expressing viral RNA or proteins were tumorigenic, whereas only one of six cultures that did not express virus information was positive. The results of this study suggest that expression of type C viral RNA and proteins by human B-lymphoblasts increases their tumorigenicity in nude mice. It is also apparent that caution must be used in attempts to correlate cell tumorigenicity and chromosome abnormalities in nude mice.—JNCI 1982; 69:435–441.

The athymic nude mouse has been used for the assessment of tumorigenicity by cell lines from a number of species (*1*–*4*). Nilsson et al. (*5*) have reported that EBV-carrying human lymphoblastoid cell lines with a normal diploid karyotype did not form tumors when inoculated sc into nude mice. In contrast, the majority of lymphoblastoid cell lines with an aneuploid karyotype gave rise to malignant tumors. A recent study by Giovanella et al. (*6*) indicated that EBV-carrying human lymphoblastoid cell lines that exhibited a normal diploid karyotype could form tumors in nude mice under immunologically privileged conditions, such as after intracerebral inoculation.

We report here on 36 human hematopoietic cell lines, many of them recently established, which underwent karyologic analysis and were tested for their ability to produce subcutaneous growths in young adult nude mice. Some (6/20) human lymphoblast lines initiated with certain primate type C viruses produced subcutaneous tumors in nude mice despite their maintenance of a normal diploid karyotype. A characterization of these cells for expression of type C viral RNA and proteins demonstrated a correlation between tumorigenicity and virus expression. Several other human leukocyte lines with abnormal karyotypes did not always give rise to tumors.

MATERIALS AND METHODS

Human hematopoietic cells.—New B-lymphoblast lines established after infection with primate type C viruses: Human lymphoblast lines were established after type C virus infection of peripheral blood leukocytes or bone marrow obtained from EBV-seropositive normal human donors and adult donors with AML or from normal EBV-negative umbilical cord blood. The establishment and characterization of these lymphoblast cell lines have been described previously by Markham et al. (*7*). A bat lung fibroblast line (CCL88) was infected and used for the production of the type C retroviruses GALV or SSV, which in turn were used for the establishment of the cell lines of this study (*7*). In summary, the cell lines are B-lymphoblast lines by several criteria; e.g., all contain the EBV genome, positive erythrocyte–antibody–complement rosetting, and surface-bound immunoglobulin. These cells express variable amounts and types of viral RNA and proteins (*8*, *9*), but they generally fail to produce virus. Some cell lines were established spontaneously or with special growth conditions but without the use of exogenous virus.

Miscellaneous hematopoietic cell lines: The following human hematopoietic cell lines, which have been cultured for several years, were also used in this study: *1*) K-562, derived from the pleural fluid of a patient with chronic ML in blast crisis; *2*) NALM-1, derived from the peripheral blood of a leukemic patient; *3*) DHL-2, derived from the pleural fluid of a lymphoma patient; *4*) KG-1, derived from the peripheral blood of a patient with AML; *5*) U-43195, derived from the peripheral blood of a normal subject; and *6*) 8226, derived from the peripheral blood of a patient with multiple myeloma. Table 1 contains the references on these established cell lines.

Prior to their inoculation into animals, cell lines less than

---

ABBREVIATIONS USED: AML=acute myelogenous leukemia; EBV=Epstein-Barr virus; GALV=gibbon ape leukemia virus; SSV=simian sarcoma virus.

---

[1] Received June 25, 1981; revised February 15, 1982; accepted March 8, 1982.

[2] Animals were maintained under the guidelines set forth by the National Institutes of Health Policy on Humane Care and Use of Animals and by the Animal Welfare Act in facilities accredited by the American Association of Laboratory Animal Care.

[3] Department of Cell Biology, Biotech Research Laboratories, Inc., 3 Taft Ct., Rockville, Md. 20850.

[4] Department of Cell Biology, Litton Bionetics, Inc., Kensington, Md. 20852.

[5] Laboratory of Tumor Cell Biology, Division of Cancer Treatment, National Cancer Institute, National Institutes of Health, Public Health Service, U.S. Department of Health and Human Services, Bethesda, Md. 20205.

TABLE 1.—*Tumorigenicity in mice by established human leukocyte cell lines with abnormal karyotypes*

Cell designation	Diagnosis	Type of cell in culture	Reference No.	Tumorigenicity[a]	Karyotype
LB$_V$-16A3	Normal (type-C virus-initiated)	B-lymphoblast	(*7*)	1/3	1.5% pseudodiploid
K-562	Chronic myelogenous leukemia in blast crisis	Undiffrentiated myeloid–erythroid	(*10*)	3/3	Aneuploid
NALM-1	Leukemia	Pre-T lymphoblast		0/3	Aneuploid
DHL-2	Lymphoma	Histiocyte	(*11*)	0/2	Aneuploid
KG-1	AML	Myeloblast	(*12*)	3/3	Aneuploid
U-43915	Normal	B-lymphoblast	(*13*)	0/3	Aneuploid
8226	Multiple myeloma	Plasma cell	(*14*)	3/3	Aneuploid

[a] Tumorigenicity=No. of nude mice with tumors/No. of mice inoculated. All cell lines were inoculated sc at a cell concentration of 10^7/nude mouse.

6 months old were maintained in vitro as suspension cultures in RPMI-1640 medium supplemented with either 10 or 20% fetal bovine serum. All leukocyte lines were tested for the presence of mycoplasma at regular intervals by standard procedures (*15*, *16*). Only mycoplasma-free cultures were utilized for tumorigenicity experiments.

Karyotype analysis.—Karyotype analysis was performed on leukocyte lines with the use of standard procedures and trypsin–Giemsa banding techniques (*17*, *18*).

Tumorigenicity studies in nude mice.—Lymphoblast and other cell lines were tested for their ability to induce tumors in 6- to 15-week-old athymic BALB/c (*nu/nu*) mice (ARS/Sprague-Dawley, Division, The Mogul Corp., Madison, Wis.). After sc inoculation of 10^7 viable cells into the neck region, the mice were observed for the formation of tumors on a regular basis for a minimum of 6 weeks before an experiment would be considered negative for tumor growth. Tumors were removed and processed for histologic examination by fixation, thin sectioning, and hematoxylin–eosin staining. Results were considered positive for tumorigenicity when the cells formed a mass of at least 0.5 cm in diameter and also exhibited a progressive increase in size. A growth smaller than 0.5 cm was considered a nodule.

Detection of type C viral RNA and structural proteins.—Viral RNA was detected by molecular hybridization procedures, and viral p12, p30, and gp70 were detected by competition radioimmunoassay as described by Markham et al. (*8*).

RESULTS

The tumorigenicity and karyotype results for the 36 leukocyte cell lines are presented in tables 1–3. These cell lines consisted of 29 of the newly established B-lymphoblast lines, 21 were established after infection with a retrovirus, and eight were spontaneously established cell lines (*7–9*). Of these cell lines 23 were from normal donors and six were from patients with AML. In addition, seven previously established cell lines of various lineage were tested.

One of the three normal diploid B-lymphoblast lines from leukemic donors established after retrovirus infection formed a progressively growing tumor. Also, five of the 18 normal diploid B-lymphoblast lines from normal peripheral blood formed growing tumors. An example of a normal diploid karyotype of cells that produced progressive tumors is shown in figure 1. In contrast, the eight spontaneously transformed B-lymphoblast lines with normal diploid karyotypes did not form tumors. However, one of these lines formed a small, 0.5-cm tumor which persisted for several months without any further growth. Four of the seven previously established cell lines (LB$_V$-16A3, K562, KG-1, and 8226) exhibiting abnormal karyotypes formed progressive tumors.

TABLE 2.—*Tumorigenicity in nude mice of normal diploid human B-lymphoblast cultures*[a]

Cell source	Treatment	Subcutaneous tumors[b]		
		None	Regressive	Invasive
Peripheral blood (adult and cord blood)	Type C virus-initiated	6	7	5
	Spontaneous	4	0	1[c]
Adult leukemic peripheral blood	Type C virus-initiated	1	1	1
	Spontaneous	1	2	0

[a] B-lymphoblast cultures were initiated from normal or leukemic donors either after exposure to type-C retroviruses, GALV (*30*), or SSV (*31*), or spontaneously. Chromosomes were analyzed as described in "Materials and Methods."

[b] Mice were inoculated sc with 10^7 viable cells. All tests were performed in triplicates. None=no visible or palpable cell growth; regressive=small nodules (<0.5 cm in diameter) appeared but gradually regressed; invasive tumor=tumor reaching size >0.5 cm in diameter in at least 1/3 inoculated mice.

[c] Persisting tumor only.

Of the normal diploid B-lymphoblast lines established with type C viruses, such as GALV or SSV, 12 were tested for the presence of viral RNA and the structural proteins p12, p30, and gp70. Those results and correlations with tumorigenicity are presented in table 3. Of the six lines positive for viral RNA or proteins, four were tumorigenic. In contrast, only one of the six lines negative for virus expression was tumorigenic.

Examination of sections of the tumor formed by one of the karyotypically normal diploid lines showed a population of lymphoblasts that appeared homogeneous (fig. 2). No metastases of these lymphomatous tumors were observed. Tumors were removed, a cell suspension was obtained, and the cells were grown again in culture. Karyologic analysis involving trypsin–Giemsa banding techniques of cultured cells derived from the tumors again showed normal diploid

TABLE 3.—*Tumorigenicity in nude mice and expression of type C virus-related nucleic acids or proteins by normal diploid human B-lymphoblast cultures*

Cell line[a]	Virus expression[b]	No. of mice with tumors/No. of mice inoculated[c]
$\mathrm{LB_V}$-4A	Positive for low-level virus production	1/3
$\mathrm{LB_V}$-12A	Positive for viral RNA, no proteins detected	3/3
$\mathrm{LB_V}$-16A1	Positive for RNA and proteins	2/3 NR
$\mathrm{LB_V}$-17A	Positive for RNA and proteins	1/3
$\mathrm{LB_V}$-20A	Positive for RNA and proteins	1/3
$\mathrm{LB_V}$-20B	Positive for RNA and proteins	0/3
$\mathrm{LB_V}$-13A	Negative	2/3 NR
$\mathrm{LB_V}$-13B	Negative	1/3 NR
$\mathrm{LB_V}$-14C	Negative	1/3
CB-51 AF	Negative	0/3
CB-51 BE	Negative	0/3
CB-456	Negative	0/3

[a] B-lymphoblast cultures initiated as described in "Materials and Methods" and in (*7*).

[b] Cells were tested for the presence of viral RNA by molecular hybridization and for viral structural proteins p12, p30, gp70 by radioimmunoassays.

[c] NR=nodule regressed.

karyotypes and normal banding patterns (fig. 3). Ten of the normal diploid cell lines that formed nodules that regressed also exhibited normal diploid karyotypes.

The aneuploid cell lines (table 1) either formed progressive tumors or no tumors at all. Fresh leukocyte specimens from leukemic or normal donors did not form tumors (data not shown). These specimens included peripheral blood lymphocytes and other mononuclear cells treated with protein A or with pokeweed mitogen.

DISCUSSION

Previous studies by Nilsson et al. (*5*) have shown that normal diploid human lymphoid cell lines do not form subcutaneous tumors in nude mice. In agreement with this finding, in the present study the majority of normal diploid cell lines did not give rise to progressive tumors either. However, a significant number of our normal diploid B-lymphoblast lines formed lymphomatous masses. This is not necessarily in conflict with the finding of Nilsson and coworkers because in our study the five normal diploid cell lines that induced tumors were established after infection with primate type C oncogenic retroviruses, whereas the cells tested by Nilsson et al. were spontaneously established lines. The results suggest a correlation between tumorigenicity and the presence of type C viral information or expression in human B-lymphoblasts. One possibility that may explain these results is that the presence of retrovirus or of retrovirus proteins could cause further immunosuppression in nude mice. Several studies (*19–21*) have suggested that immunosuppression may follow retrovirus infection in a number of animals, and a more recent study has shown that a virion polypeptide from feline leukemia virus has immunosuppressive properties (*23*). A report by Giovanelli et al. (*6*) indicated that normal diploid human lymphoid cells, which fail to grow subcutaneously, formed tumors in immunologically privileged sites such as the brain; Watanabe et al. (*24*) reported that normal diploid lymphoblastoid cells gave rise to subcutaneous tumors in splenectomized nude mice that had received whole-body irradiation. The nude mouse has not been the only host system used for tumor formation by normal diploid cells. For example, Miyoshi et al. (*25*) demonstrated that antilymphocyte-treated newborn hamsters supported tumor formation of normal human leukocytes derived from peripheral blood of adults or from cord blood. Twelve lymphoblastoid cell lines established from these lymphoid tumors also exhibited a normal diploid karyotype. It is therefore clear that tumor masses can form in test animals in the absence of any detectable chromosome abnormality.

We do not know the mechanisms (immunologic and/or nonimmunologic) that favor or prevent tumor growth in the subcutaneous environment of the nude mouse and that contribute to the substantial variation in results from animal to animal. Factors such as origin of lymphoid cells, patient diagnosis, sex and age of the mouse, and cell concentration of the inoculum do not seem to account for these results alone. Immunologic factors may play an important role in lymphoid cell fate in the subcutaneous space of the nude mouse. The nude mouse does exhibit some immunologic function, such as immunoglobulin production (*26*) and natural killer cell activity (*27*). Nonimmunologic factors could also determine the fate of inoculated lymphoid cells. For example, factors in the subcutaneous microenvironment, such as nutrient availability and lymphoid cell interactions with host cells, could vary from mouse to mouse, which could explain the inconsistency in tumor "takes." Which, if any, of these mechanisms actually plays a role in inhibition of tumor formation or progression is not known.

The crucial question to be asked with regard to tumor formation by diploid cells in nude mice, is whether or not tumor growth, in either the brain or in subcutaneous space represents a true malignant neoplasm. Two useful criteria in the definition of cancerous growth are transplantability and metastasis. In other studies we observed that the human promyelocytic leukemia cell line HL-60 (*28*) could not be serially transplanted beyond one animal passage despite the clear leukemic nature of these cells (*29*). Moreover, metastases were not observed in any of the nude mice inoculated with aneuploid or diploid human leukemia leukocytes. It is clear then that a cell may be neoplastic and not be able to grow in nude mice and not exhibit features characteristic of neoplastic cells. Therefore, the use of nude mice for tumorigenicity testing must be viewed with caution.

REFERENCES

(*1*) FREEDMAN VH, SHIN S. Cellular tumorigenicity in nude mice: Correlation with cell growth in semi-solid medium. Cell 1974; 3:355–356.

(*2*) STILES CD, DESMOND W, CHUMAN L, SATO G, SAIER MH. Growth control of heterologous tissue culture cells in the congenitally athymic nude mouse. Cancer Res 1976; 36:1353–1360.

(*3*) FREEDMAN VH, SHIN S. FOGH J, GIOVANELLA B, eds. The nude mouse in experimental and clinical research. New York: Academic Press, 1978:353.

(*4*) SHIN S. Use of nude mice for tumorigenicity testing and mass propagation. Methods Enzymol 1979; 58:370–379.

(*5*) Nilsson K, Giovanella BC, Stehlin JS, Klein G. Tumorigenicity of human hematopoietic cell lines in athymic nude mice. Int J Cancer 1977; 19:337–344.

(*6*) Giovanella B, Nilsson K, Zech L, Yim O, Klein G, Stehlin JS. Growth of diploid, Epstein-Barr virus carrying human lymphoblastoid cell lines heterotransplanted into nude mice under immunologically privileged conditions. Int J Cancer. In press.

(*7*) Markham PD, Ruscetti F, Salahuddin SZ, Gallagher RE, Gallo RC. Enhanced induction of growth of B-lymphoblasts from fresh human blood by primate type-C retroviruses (gibbon ape leukemia virus and simian sarcoma virus). Int J Cancer 1979; 23:148–156.

(*8*) Markham PD, Ruscetti F, Kalyanaraman VS, et al. Restricted expression of retrovirus nucleic acid and protein in primate type-C virus initiated human B-lymphoblast cultures. Cancer Res 1981; 41:2738–2744.

(*9*) Ceccherini-Nelli L, Dalla-Favera R, Markham PD, et al. Restricted expression of integrated primate type-C virus proviral DNA in non-productively infected human B-lymphoblasts. Virology. In press.

(*10*) Lozzio CB, Lozzio BB. Human chronic myelogeneous leukemia cell line with positive Philadelphia chromosome. Blood 1975; 45:321–334.

(*11*) Kaplan HS, Goodenow R, Epstein A, Gartner S, Decleve A, Rosenthal P. Isolation of a Type-C RNA virus from an established human histiocytic lymphoma cell line. Proc Natl Acad Sci USA 1977; 74:2564–2568.

(*12*) Koeffler HP, Golde DW. Acute myelogenous leukemia: A human cell line responsive to colony-stimulating activity. Science 1978; 200:1153–1154.

(*13*) Bechet JM, Fialkow P, Nilsson K, Klein G. Immunoglobulin synthesis and glucose-6-phosphate dehydrogenase as cell markers in human lymphoblastoid cell lines. Exp Cell Res 1974; 89:275–282.

(*14*) Matsuoka Y, Moore GE, Yagi Y, Pressman D. Production of free light chains immunoglobulin by a hematopoietic cell line derived from a patient with multiple myeloma. Proc Soc Exp Biol Med 1967; 125:1246–1250.

(*15*) Hayflick L. Screening tissue cultures for mycoplasma infection. In: Kruse PF, Patterson MD, eds. Tissue culture methods and applications. New York: Academic Press, 1973:772–728.

(*16*) Chen TR. In situ detection of mycoplasma contamination in cell cultures by fluorescent Hoechst 33258 stain. Exp Cell Res 1977; 104:255–262.

(*17*) Seabright M. A rapid banding technique for human chromosomes. Lancet 1971; 2:971–972.

(*18*) Wang HC, Fedoroff S. Banding in human chromosomes treated with trypsin. Nature 1972; 235:52–53.

(*19*) Dent PB. Immunodepression by oncogenic viruses. Prog Med Virol 1972; 14:1–35.

(*20*) Wood GW. Suppression of Moloney sarcoma virus immunity following sensitization with attenuated virus. Cancer Res 1976; 36:4552–4557.

(*21*) Olsen RG, Hoover EA, Schaller JP, Mathes LE, Wolff LH. Abrogation of resistance to feline oncornavirus disease by immunization with killed feline leukemia virus. Cancer Res 1977; 37:2082–2085.

(*22*) Schaller JP, Hoover EA, Olsen RG. Active and passive immunization of cats with inactivated feline oncornaviruses. J Natl Cancer Inst 1977; 59:1441–1450.

(*23*) Mathes LE, Olsen RG, Hebebrand LC, et al. Immunosuppressive properties of a virion polypeptide, a 15,000-dalton protein, from feline leukemia virus. Cancer Res 1979; 39:950–955.

(*24*) Watanabe S, Shimosato Y, Kuroki M, Sato Y, Nakajima T. Transplantability of human lymphoid cell line, lymphoma, and leukemia in splenectomized and/or irradiated nude mice. Cancer Res 1980; 40:2588–2595.

(*25*) Miyoshi I, Kubonsiki I, Uchida H, et al. Production of lymphoid tumors in hamsters by direct implantation of normal human peripheral and umbilical cord leukocytes. Int J Cancer 1976; 18:67–75.

(*26*) Brogren CH, Warren HS, Nielsen E, Rygaard J. Quantitative immunoelectrophoretic analysis of serum proteins and immunoglobulins in the serum and produced by spleen cell cultures of individual nude mice. In: Nomura T, Ohsawa N, Tamoaki N, Fujiwara K, eds. Proceedings of the second international workshop in nude mice, Tokyo, 1976:157–165.

(*27*) Sprent J. Migration and lifespan of circulating B lymphocytes of nude (*nu/nu*) mice. In: Rygaard J, Povlsen CO, eds. Proceedings of the first workshop on nude mice, Aarhus, Denmark, 1973. Stuttgart: Fischer, 1973:11–12.

(*28*) Collins SJ, Gallo RC, Gallagher RE. Continuous growth and differentiation of human myeloid leukaemic cells in suspension culture. Nature 1977; 270:347–349.

(*29*) Gallagher R, Collins S, Trujillo K, McCredie M. Characterization of the continuous differentiating myeloid cell lines (HL-60) from a patient with acute promyelocytic leukemia. Blood 1979; 54:713–733.

(*30*) Gallo RC, Gallagher RE, Wong-Staal F, et al. Isolation and tissue distribution of type-C virus and viral components from a gibbon ape (*Hylobates lar*) with lymphocyte leukemia. Virology 1978; 84:359–373.

(*31*) Wolfe LG, Deinhardt F, Theilen GH, Rabin H, Kawakami T, Bustad LK. Induction of tumors in marmoset monkeys by simian sarcoma virus type-1 (*Lagothrix*): A preliminary report. J Natl Cancer Inst 1971; 47:1115–1120.

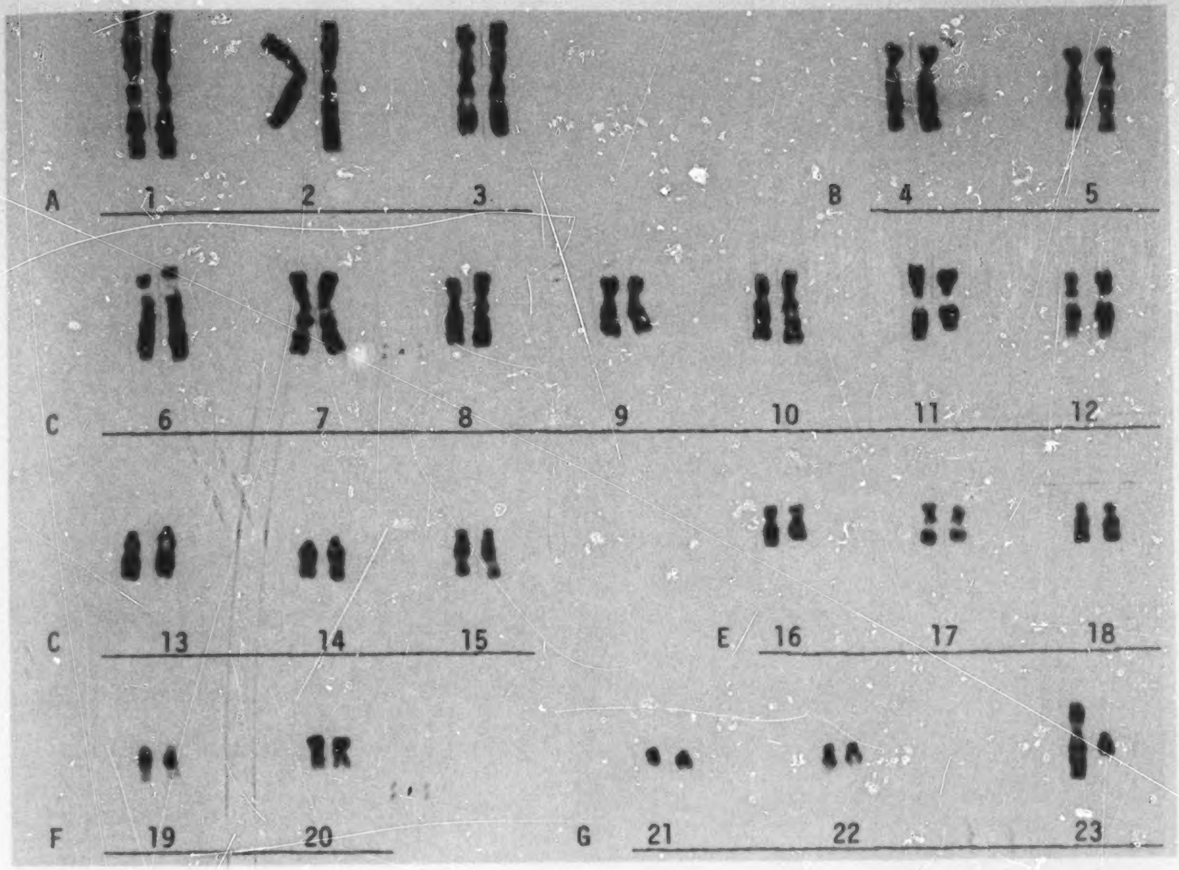
A
1
2
3
B
4
5
C
6
7
8
9
10
11
12
C
13
14
15
E
16
17
18
F
19
20
G
21
22
23

1

Figure 1.—Typical karyotype of a normal diploid human lymphoid cell line (LBv-12a).

2

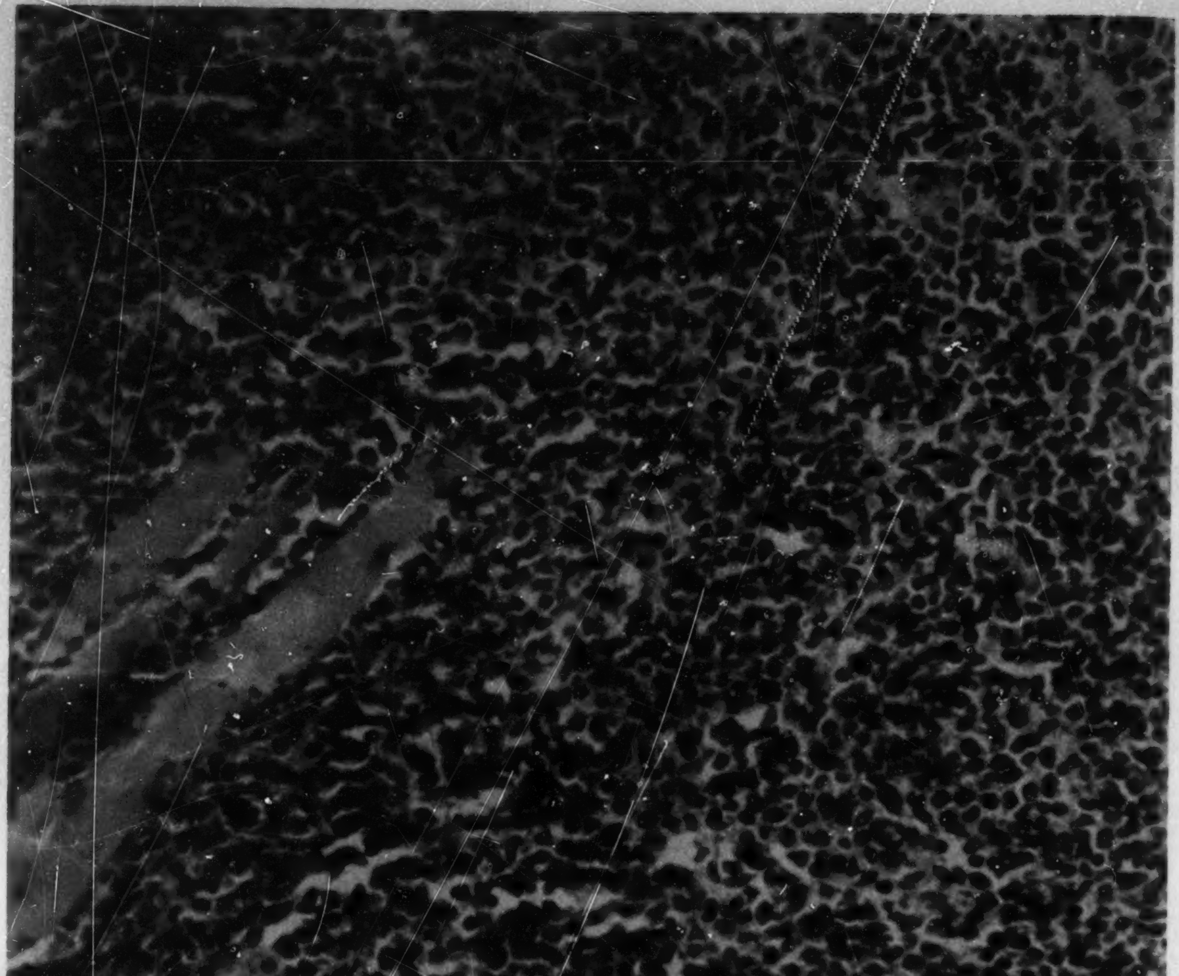

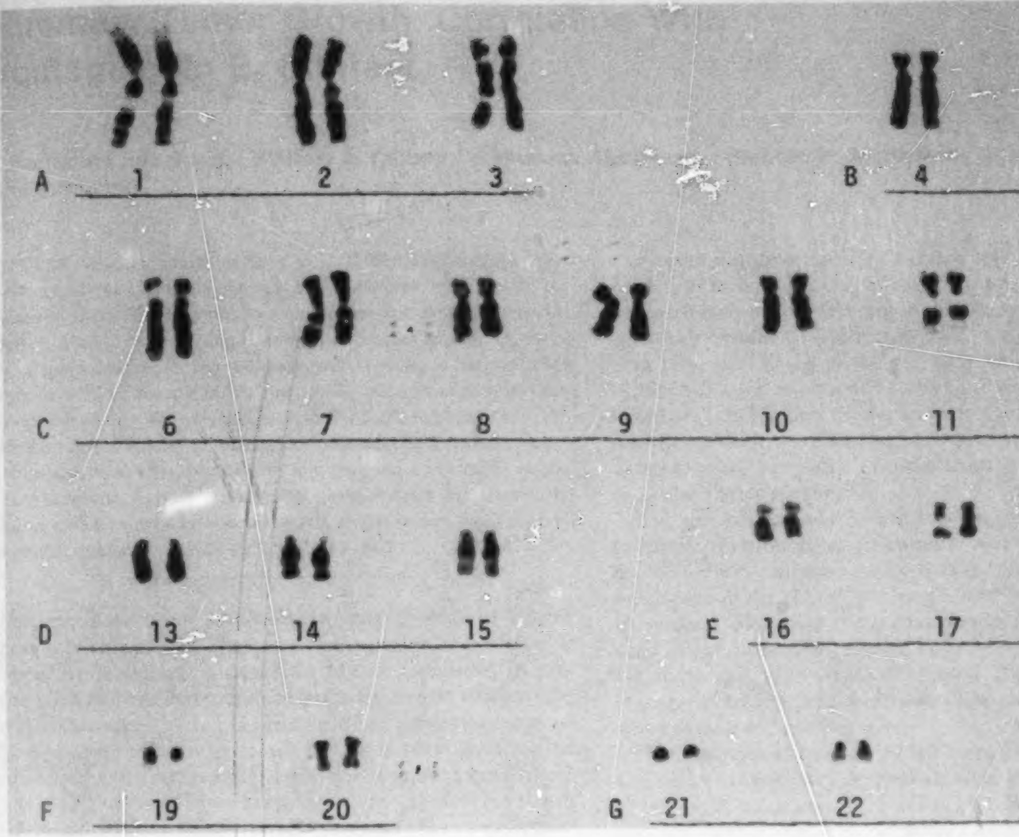
A
1
2
3
B
4
C
6
7
8
9
10
11
D
13
14
15
E
16
17
F
19
20
G
21
22

3

FIGURE 3.—Karyotype of a normal diploid human lymphoid cell line (LB$_{V}$-12A) reestablished from a nude mous

FIGURE 2.—Histopathologic section of a lymphoid tumor induced in a nude mouse by the inoculation of a human lymphoblast c
eosin. × 512

blank page

Hormone Dependence of 7,12-Dimethylbenz[*a*]anthracene-Induced Mammary Tumor Growth: Correlation With Prostaglandin E_2 Content[1,2,3]

M. Katherine Foecking,[4] William E. Kibbey,[5,6] Hussein Abou-Issa,[5] Richard H. Matthews,[4] *and* John P. Minton[5,7]

ABSTRACT—Prostaglandin content in 7,12-dimethylbenz[*a*]anthracene-induced rat mammary tumors was correlated with growth responses to alterations in endogenous estrogen and prolactin. Prostaglandin E_2 (PGE_2) content varied inversely with tumor latency. Ovariectomy of tumor-bearing Sprague-Dawley rats resulted in regression of tumors in 90% of the castrated rats. PGE_2 content in tumors from ovariectomized rats was elevated twofold ($P<0.05$) compared to PGE_2 content in tumors from intact controls. Haloperidol treatment promoted tumor growth even after ovariectomy and returned tumor PGE_2 values to control levels. Tumors grouped by growth status irrespective of hormone status showed an inverse relationship between PGE_2 content and growth response.—JNCI 1982; 69:443–446.

PG stimulate bone resorption in the process of breast cancer metastasis (*1*). The pain due to bone metastases is relieved by levodopa, a prolactin release inhibitor, in patients with hormone-dependent primary breast cancer (*2*). These facts suggest that PG production in mammary cancer may be hormonally modulated. PG have been reported to mediate some prolactin actions in normal murine mammary tissue (*3–5*), and PG have been shown to vary in this tissue with the fluctuation of ovarian hormones in the estrus cycle (*6*).

The role of PG in the control of tumor cell growth has been investigated in vivo and in vitro, and the reports showed conflicting results. Exogenously applied and endogenously produced PGE have been reported to inhibit the growth of several different cell lines in vitro (*7–9*), and $PGF_{2\alpha}$ inhibited tumor growth in vivo (*10*). In contrast, inhibition of PG synthesis by indomethacin has been reported to inhibit tumor growth and cell proliferation in vivo (*11–13*), and $PGF_{2\alpha}$ promoted the initiation of proliferation in mouse fibroblasts in vitro (*14*).

The purpose of this study is to investigate the possibility that PG play some role in hormone-dependent mammary cancer by correlation of in vivo hormone manipulation effects to tumor growth and changes in PG levels that accompany it.

MATERIALS AND METHODS

Mammary tumors were induced by injection of a 1-ml emulsion containing 5 mg of DMBA (provided by Dr. Paul Schurr, The Upjohn Co., Kalamazoo, Mich.) into the tail veins of 50–55-day-old female Sprague-Dawley Cox:(SD) outbred rats (*15, 16*). The rats were maintained on standard laboratory chow and water ad libitum. Sprague-Dawley rats with DMBA-induced mammary tumors were also obtained from commercial sources (Hazleton Laboratories, Vienna, Va.). Hormone manipulations were begun on rats bearing 1 or more visible mammary tumors >1.0×1.0 cm in size. A depletion in endogenous estrogen was accomplished by bilateral ovariectomy. Serum prolactin levels were elevated with haloperidol (*17*) injected daily for 4 consecutive days at a dose of 120 µg in 0.2 ml olive oil (*18*). Control rats received 0.2-ml injections of olive oil alone. The rats were killed on the 5th day by decapitation and the tumors were rapidly excised and frozen in liquid nitrogen (−196°C). Tumors were similarly excised from ovariectomized rats 5–11 days after surgery.

The growth response of the tumors to the various in vivo hormone manipulation treatments was measured with the use of vernier calipers. A regressing tumor was defined as one in which the sum of the length and width was decreased by at least 20% from the measurement taken at the beginning of the treatment period. A growing tumor was one in which length plus width increased 20% or more. If the change in length plus width was less than 20%, the tumor was considered stable in size.

The individual tumors, which were excised and frozen at the end of the treatment period, were pulverized, homogenized in 9 volumes of 50 m*M* Tris-HCl-44 m*M* EDTA solution (pH 7.5) at 4°C, with the use of a Potter-Elvehjem type tissue grinder with a Teflon pestle, and then acidified with 1 *M* citric acid. PG were extracted into cold redistilled ethyl acetate (MC&B Manufacturing Chemists, Cincinnati, Ohio) and subjected to purification by silicic acid column chromatography as described earlier (*19*). The fraction containing all the PGE was then used to determine PGE_2 by radioimmunoassay, according to Caldwell et al. (*20*). Antibody to PGE_2 was provided by Dr. Thomas Ferris, Department of Medicine, Ohio State University, Columbus, Ohio.

ABBREVIATIONS USED: cAMP=cyclic AMP; DMBA=7,12-dimethylbenz[*a*]anthracene; PG=prostaglandin(s); PGE_2=prostaglandin E_2.

---

[1] Received August 3, 1981; revised February 22, 1982; accepted March 15, 1982.

[2] Supported by Public Health Service grant CA-22892-02 from the National Cancer Institute.

[3] Animals were maintained under the guidelines set forth in the "Guide for the Care and Use of Laboratory Animals" by the Institute of Laboratory Animal Resources, National Research Council.

[4] Department of Physiological Chemistry, Ohio State University, 333 West 10th Ave., Columbus, Ohio 43210.

[5] Department of Surgery, Ohio State University Hospitals, 410 West 10th Ave., Columbus, Ohio 43210.

[6] *Present address:* Fairbanks Clinic, 1867 Airport Rd., Fairbanks, Alaska 99701.

[7] American Cancer Society Professor of Clinical Oncology.

PGE_2 was donated by Dr. John Pike, The Upjohn Company. [5,6,8,11,12,14,15-^3H(N)]PGE_2 was purchased from the New England Nuclear Corp., Boston, Mass.

RESULTS

Administration of DMBA to Sprague-Dawley rats resulted in the appearance of mammary tumors from 2.5 to 11 months after exposure to the carcinogen. PG production was seen to vary with tumor latency, which is the time between DMBA administration and the appearance of the tumor. The PGE_2 content of the tumors is inversely related to tumor latency (r=0.94; table 1). Therefore, to eliminate complicating variables, we made experimental comparisons in tumors of matched latency in age-matched rats.

The response of mammary tumor PGE_2 content to hormone manipulations is shown in table 2. PGE_2 content was elevated approximately twofold in tumors from ovariectomized rats compared to PGE_2 content in tumors from intact rats ($P<0.05$). Ovariectomy results in a decrease in serum prolactin subsequent to depletion of estrogen since it is known that estrogen stimulates prolactin release (*18*). Tumors from rats treated with haloperidol showed similar PGE_2 levels to those in tumors from non-hormone-manipulated control rats. To determine if the effect of ovariectomy on PGE_2 levels was due primarily to the decrease in estrogen or the subsequent decrease in prolactin, we ovariectomized the rats and then treated them with haloperidol, so that serum prolactin levels would be maintained in the absence of estrogen. PGE_2 levels in tumors from these rats were not different from the levels in tumors from non-hormone-manipulated controls.

The modifications resulting from the various treatments resulted in alterations in the growth response of the DMBA-induced mammary tumors. Ovariectomy resulted in regression of tumors in 90% of the castrated rats. When the rats were treated with haloperidol after ovariectomy, tumor growth was maintained. Tumor growth was also maintained in haloperidol-treated intact rats.

TABLE 1.—*Effect of tumor latency on PGE_2 content in DMBA-induced mammary tumors*

Average tumor latency, days	No. of tumors	ng PGE_2/g tissue, mean ± SE
80	12	117±19
97	10	76±16
183	7	67±35
289	8	14±4

TABLE 2.—*PGE_2 content and growth response in DMBA-induced tumors from hormonally manipulated rats*

Treatment	No. of rats	ng PGE_2/g tissue, mean ± SE	P-value, compared to OVX	Change in tumor size,[a] %, mean ± SE
Intact	10	65±15	<0.05	118±8.6
Ovariectomy	8	120±28		79±6.2
Haloperidol	11	75±23	<0.1	116±9
Ovariectomy + haloperidol	4	64±32	<0.1	110±9

[a] Tumor size at beginning of treatment=100%.

TABLE 3.—*PGE_2 levels in growing, static, and regressing tumors*[a]

Tumor status	ng PGE_2/g tissue, mean ± SE
Growing	39±15
Static	84±26
Regressing	161±42

[a] P-values: Growing vs. regressing—$P<0.006$; static vs. regressing—$P<0.1$.

The changes in tumor PGE_2 levels corresponded with their growth response to these treatments. In actively growing or stable tumors in intact rats, PGE_2 levels were 65±15 ng/g tissue. In intact rats treated with haloperidol, continued growth was accompanied by PGE_2 levels similar to those in tumors from intact rats not treated with haloperidol. The doubling of PGE_2 levels upon ovariectomy was accompanied by regression of the tumors. However, haloperidol treatment of ovariectomized rats resulted in continued growth of the tumor along with PGE_2 levels, which were very similar to those of the growing tumors from the intact non-hormone-manipulated rats. Whereas most of the tumors from the intact rats were found to be actively growing at the time of PG determination, in some tumors the growth rate had reached a plateau. To correlate tumor PGE_2 levels with the growth rate further, we classified tumors as growing, stable, or regressing (as described in "Materials and Methods"), without regard to hormone treatment. An inverse relationship between tumor growth and tumor PGE_2 content was observed (table 3). PGE_2 tissue content was highest in regressing tumors, intermediate in stable tumors, and lowest in growing tumors.

DISCUSSION

Our results show that PG content in DMBA-induced mammary tumors is inversely related to tumor latency. The loss of the ability of tumors from older rats to produce PG may be due to the age and hormonal status of the animals and/or the morphologic or the hormone characteristics of the tumors that appear at different times after DMBA administration. Investigators have shown that tumors that appear sooner after induction by DMBA show a greater degree of hormone responsiveness than tumors with longer latent periods (*18*). However, the differences in PG levels between young and old tumors do not appear to be due to the characteristic of hormone dependence or independence. We have found that PGE_2 is produced at approximately equal rates by hormone-dependent and hormone-independent human and rat mammary tumors (Kibbey WE, Foecking MK: Unpublished observations). Furthermore, Rolland et al. (*12*) reported that steroid-receptor-negative human mammary tumors produce more PG than do steroid-receptor-positive tumors. Older rats with longer latent periods, however, demonstrate a high rate of spontaneous regression, and their tumors are often morphologically classified as benign adenomas (*18*). Therefore, the decline in PG production in older tumors may be a function of the morphologic characteristics of the tumors. The interpretation of comparisons between benign tumors and adenocarcinomas is problematic due to the differences in the degree of differentiation of the two types of tumors. Rolland reported that tumors with a lower degree of differentiation synthesize more PG than those with a higher degree of differentiation (*21*). The observation that PG content is lower in benign tumors than in adenocarcinomas but is elevated in regressing adenocarcinomas is not necessarily a contradiction, because the process that takes place during regression in in vivo tumors is not identical to the redifferentiation observed in cells in culture. Therefore, an awareness of the variation of morphology, hormone responsiveness, and PG production with age and tumor latency is necessary for proper experimental design when hormone effects on PG production are studied in the DMBA-induced mammary tumors in rats.

The increase of PGE_2 levels in the tumors from ovariectomized rats compared to PGE_2 levels in tumors from intact, nonovariectomized rats suggests that hormones that are depleted by ovariectomy are involved in the regulation of PG synthesis in cancerous mammary tissue. This postulate is consistent with the work of Knazek et al. (*6*), who showed that PGE_2 synthesis in normal murine mammary tissue varies with the stage of the estrus cycle, which suggests that PG production by mammary tissue is sensitive to fluctuations in ovarian hormones. The effect of hormonal changes in PGE_2 levels corresponds with the growth response to the alterations in hormone levels. The increase in tumor PGE_2 levels after ovariectomy of the tumor-bearing rats is accompanied by regression of these tumors. Tumor growth is observed in intact rats. When prolactin levels are elevated in intact rats by haloperidol treatment, the continued growth is accompanied by PGE_2 levels similar to the levels in tumors from the intact controls. When prolactin levels are maintained in ovariectomized rats, the tumor growth is also maintained, and the observed PGE_2 levels are not different from levels in tumors from nonmanipulated intact controls. Thus prolactin overcomes the effect of ovariectomy on tumor growth response and PGE_2 levels. These results are consistent with the work of Meites et al. (*18, 22*), who showed that the increase of serum prolactin by haloperidol promotes tumor growth even in the absence of the ovaries, which implies that prolactin may be more important than estrogen in the hormonal control of DMBA-induced mammary tumors. Pearson and co-workers (*23, 24*) also reported that prolactin is the major growth stimulant in DMBA-induced tumors and that estrogen enhances tumor growth through the stimulation of prolactin release. In contrast, our results are inconsistent with the report of Sinha et al. (*25*), who found that the stimulation of mammary tumor growth by prolactin is dependent on the presence of ovarian hormones, primarily of estrogen.

The causal connection between hormone manipulations and changes in PGE_2 levels has not been established. Prolactin effects may be mediated by PG in normal mammary tissue (*2-5*). On the basis of our results, the relationship between prolactin and PG in cancerous mammary tissue appears to be an inverse relationship in which prolactin suppresses PG synthesis. Future investigations will determine whether greater increases in serum prolactin would result in a depression of PGE_2 levels or whether the PGE_2 level observed in growing tumors is a basal level for that tissue. Work is in progress in our laboratory to further characterize the relationship between alterations in serum prolactin, separately and in combination with alterations in ovarian hormones, and the effects on PG production.

The inverse relationship between PGE_2 content and tumor growth rates (table 3) indicates that PG may be functionally involved in the regulation of tumor growth. Our results showed that regressing tumors exhibit a high PGE_2 content, whereas actively growing tumors exhibit low PGE_2 levels and static tumors exhibit intermediate PGE_2 levels. These results are consistent with those of previous reports, which showed that inhibition of tumor growth is influenced by PG (*9, 10, 26*). PG have been shown to stimulate adenylate cyclase activity in many cells including mammary cells (*27, 28*) and thus increase their intracellular cAMP content. cAMP has been reported to be involved in mammary tumor regression (*29-31*). Recent studies have also shown that growing DMBA-induced mammary tumors have lower cAMP levels and adenylate cyclase activities than regressing tumors, whereas static tumors have intermediate values (*31*). In view of these studies it is possible that the action of PG on tumor growth behavior is expressed via regulation of cAMP production. Further studies are in progress in our laboratory to correlate PGE_2 and cAMP levels in growing, static, and regressing mammary tumors.

REFERENCES

(*1*) Powles TJ, Clark SA, Easty GC, Neville AM. The inhibition by aspirin and indomethacin of osteolytic tumour deposits and hypercalcaemia in rats with Walker tumour, and its possible application to human breast cancer. Br J Cancer 1973; 28:316-321.

(*2*) Minton JP. The repsonse of breast cancer patients with bone pain to L-dopa. Cancer 1974; 33:358-363.

(*3*) Rilemma JA. Possible role of prostaglandin F_2 in mediating effect of prolactin on RNA synthesis in mammary gland explants of mice. Nature 1975; 253:466-467.

(*4*) ———. Effects of arachidonic acid on RNA metabolism in mammary gland explants of mice. Prostaglandins 1975; 10:307-312.

(*5*) ———. Efffects of prostaglandins on RNA and casein synthesis in mammary gland explants of mice. Endocrinology 1976; 99:490-495.

(*6*) Knazek RA, Watson KC, Lim MF, Cannizzaro AM, Christy RJ., Liu SC. Prostaglandin synthesis by murine mammary gland is modified by the state of the estrus cycle. Prostaglandins 1980; 19:891-897.

(*7*) Thomas DR, Philpott GW, Jaffe BM. The relationship between concentration of prostaglandin E and rates of cell replication. Exp Cell Res 1974; 84:40-46.

(*8*) Karmali RA, Horrobin DF, Menezes J, Patel P. The relationship between concentrations of prostaglandin A_1, E_1, E_2 and F_2 alpha and rates of cell proliferation. Pharmacol Res Commun 1979; 11:69-75.

(*9*) Claesson HE, Lindgren JA, Hammarström S. Endogenous prostaglandin E_2 production inhibits proliferation of polyoma virus-transformed 3T3 cells: Correlation with cellular levels of cyclic AMP. Adv Prostaglandin Thromboxane Res 1980; 6:541-545.

(*10*) Jubiz W, Frailey J, Smith JB. Inhibitory effect of prostaglandin $F_{2\alpha}$ on the growth of a hormone-dependent mammary tumor. Cancer Res 1979; 39:998-1000.

(*11*) Humes JL, Cupo JJ, Strausser HR. Effects of indomethacin on Maloney sarcoma virus-induced tumors. Prostaglandins 1974; 6:463-473.

(*12*) Lynch NR, Salomon JC. Tumor growth inhibition and potentiation of immunotherapy by indomethacin in mice. JNCI 1979; 62:117-121.

(*13*) Fürstenberger G, Marks F. Indomethacin inhibition of cell proliferation induced by the phorbal ester TPA is reversed by prostaglandin E_2 in mouse epidermis in vivo. Biochem Biophys Res Commun 1978; 84:1103–1111.

(*14*) DeAsua LJ, Clingan D, Rudland PS. Initiation of cell proliferation in cultured mouse fibroblasts by prostaglandin $F_{2\alpha}$. Proc Natl Acad Sci USA 1975; 72:2724–2728.

(*15*) Huggins CB. Experimental leukemia and mammary cancer. Chicago and London: Univ Chicago Press. 1979:81.

(*16*) Schurr PE. Composition and preparation of experimental intravenous fat emulsions. Cancer Res 1969; 29:258–260.

(*17*) Dickerman S, Clark J, Dickerman E, Meites J. Effects of haloperidol on serum and pituitary prolactin and on hypothalamic PIF in rats. Neuroendocrinology 1972; 9:332–340.

(*18*) Bradley CJ, Kledzik GS, Meites J. Prolactin and estrogen dependency of rat mammary cancers at early and late stages of development. Cancer Res 1976; 36:319–324.

(*19*) Kibbey WE, Bronn DG, Minton JP. Chromatographic patterns of prostaglandins using different lots of silicic acid. Prostaglandins 1977; 13:1023–1032.

(*20*) Caldwell BV, Speroff L, Brock WA, et al. Development and application of a radioimmunoassay for F prostaglandins. In: Southern EM, ed. The prostaglandins: Clinical applications in human reproduction. Mount Kisco, N.Y.: Futura, 1972:257.

(*21*) Rolland PH, Martin PM, Jacquemier J, Rolland AM, Toga M. Prostaglandin in human breast cancer: Evidence suggesting that an elevated prostaglandin production is a marker of high metastatic potential for neoplastic cells. JNCI 1980; 64:1061–1070.

(*22*) Quadri SK, Kledzik GS, Meites J. Enhanced regression of DMBA-induced mammary cancers in rats by combination of ergocornine with ovariectomy or high doses of estrogen. Cancer Res 1974; 34:499–501.

(*23*) Manni A, Trujillo JE, Pearson OH. Predominant role of prolactin in stimulating the growth of 7,12-dimethylbenz(*a*)anthracene-induced rat mammary tumor. Cancer Res 1977; 37:1216–1219.

(*24*) Arafah BM, Manni A, Pearson OH. Effect of hypophysectomy and hormone replacement on hormone receptor levels and the growth of 7,12-dimethylbenz(*a*)anthracene-induced mammary tumors in the rat. Endocrinology 1980; 107:1364–1369.

(*25*) Sinha D, Cooper D, Dao TL. The nature of estrogen and prolactin effect on mammary tumorigenesis. Cancer Res 1973; 33:411–414.

(*26*) Santoro MG, Philpott GW, Jaffe BM. Inhibition of tumour growth in vivo and in vitro by prostaglandin E. Nature 1976; 263:777–779.

(*27*) Bar HP. Epinephrine and prostaglandin-sensitive adenyl cyclase in mammary gland. Biochim Biophys Acta 1973; 321:397–406.

(*28*) Schorr I, Russell A. Properties of adenylate cyclase of murine mammary carcinoma. Biochim Biophys Acta 1974; 364:174–180.

(*29*) Cho-Chung YS, Newcomer SF. Adenylate cyclase, cyclic adenosine 3′:5′-monophosphate phosphodiesterase, and regression of Walker 256 mammary carcinoma. Cancer Res 1977; 37:4493–4499.

(*30*) Cho-Chung YS. In vivo inhibition of tumor growth by cyclic adenosine 3′,5′-monophosphate derivatives. Cancer Res 1974; 34:3492–3496.

(*31*) Ip C, Dao TL. Regulation of cyclic adenosine 3′,5′-monophosphate in relation to growth of dimethylbenz(*a*)anthracene-induced mammary tumors in rats. Cancer Lett 1980; 8:227–233.

Comparison of Ovariectomy and Retinyl Acetate on the Growth of Established 7,12-Dimethylbenz[*a*]anthracene-Induced Mammary Tumors in the Rat[1,2,3]

Philippe Gandilhon,[4,5] Réjean Melancon,[4] Jean Djiane,[6] *and* Paul A. Kelly[4]

ABSTRACT—Prolonged exposure to retinyl acetate (RA) in the diet inhibits the development of 7,12-dimethylbenz[*a*]anthracene (DMBA)-induced mammary cancers in rats. The effectiveness of RA was examined when given 6 months after the administration of DMBA. Noninbred female Sprague-Dawley rats with DMBA-induced mammary tumors were divided into 3 groups and treated for 4 weeks as follows: Group 1 served as controls, group 2 was ovariectomized, and group 3 received 328 mg RA/kg diet. Ovariectomy (OVX) markedly reduced both the number and size of the tumors. RA administration failed to induce any significant regression in tumor number but significantly retarded tumor growth when compared to tumor growth in group 1 controls. The levels of estradiol, progestin, and prolactin (PRL) receptors were significantly reduced after OVX, whereas only the levels of PRL receptors declined significantly after RA administration. Circulating progesterone concentrations were not affected in the RA-treated group but the plasma PRL level was significantly increased. The present studies show that if treatment with RA is delayed until 6 months after carcinogen administration, the protective effect of RA can still be observed although its effectiveness is less dramatic than when it is administered earlier.—JNCI 1982; 69:447–451.

Retinoids are known to be involvd in the induction or enhancement of cellular differentiation, and the use of retinoids in the prophylaxis of cancer may therefore represent a physiologic approach to arrest the process of carcinogenesis (*1*). Retinoids have been shown to be highly effective in preventing mammary cancer induced in the rat by DMBA (*2–4*) or MNU (*5–7*). In addition, it has been reported that dietary vitamin A acetate (RA) supplements can inhibit the late phase (growth and development of palpable tumors from transformed cells) of DMBA-induced (*3*) and benzo[*a*-]pyrene-induced (*8*) mammary carcinogenesis since RA administration can be initiated 1 week after carcinogen administration or can be delayed beyond 1 week with no alteration in the chemoprotective effects of RA. These observations suggest some role of the retinoids in controlling growth of transformed cells. The aim of the present study is to determine the ability of RA to inhibit mammary tumor growth when retinoid treatment is delayed in rats bearing established DMBA-induced tumors. In addition, the effect of an endocrine therapy (OVX) is compared with the effect of RA treatment on established tumor growth and hormone receptor levels.

MATERIALS AND METHODS

Animals and treatments.—Noninbred female Sprague-Dawley rats (Canadian Breeding Farms, St. Constant, Quebec) were given a single intragastric dose of 10 mg DMBA in 0.5 ml sesame oil at 50–55 days of age. All animals were housed 2 per cage in a room controlled for light cycle (lights on between 5 a.m. and 7 p.m.) and were allowed free access to drinking water and Purina Rat Chow.

Tumors began to appear about 1 month after DMBA administration. Six months after DMBA administration, 60 rats bearing DMBA-induced mammary tumors were selected and divided into 3 groups of 20 animals each. Each group was adjusted to a similar tumor number (70–72 tumors/group) and to a similar tumor area (145–150 cm^2/group). The first group served as control, the second group underwent OVX and the third group received RA. To treat animals with retinoid, we blended RA into the stock diet in the form of stable gelatinized beadlets at a concentration of 328 mg RA/kg diet, which corresponded to a daily intake of approximately 5 mg. Control rats were fed gelatinized beadlets without RA. All rats were palpated once a week for mammary tumors, and the number of tumors per rat was recorded. The two largest perpendicular diameters of each tumor were measured with calipers, and the product of these diameters was used as an estimate of tumor size. This value was expressed as the average tumor area (cm^2) per tumor. Tumor development was followed up to 5 weeks. The body weight of each animal was recorded at the beginning and at the end of the 4-week observation period. All animals were decapitated between 9 and 11 a.m. on the last day of the 4-week period. Trunk blood was collected in heparinized beakers. After separation by centrifugation, plasma was stored at −20°C until hormones were assayed. The tumors were removed immediately after the animals were decapitated. They were frozen and stored at −80°C until receptor studies were performed. Some tumor fractions were fixed in Bouin's fluid for histologic diagnosis.

ABBREVIATIONS USED: BSA=bovine serum albumin; DCC=dextran-coated charcoal; DMBA=7,12-dimethylbenz[*a*]anthracene; hGH=human growth hormone; MNU=methyl-*N*-nitrosourea; oPRL=ovine prolactin; OVX=ovariectomy; PRL=prolactin; R2848=11β-methoxyethinyl-17β-estradiol (Moxestrol); R5020=17,21-dimethyl-19-nor-pregna-4,9-diene-3,20 dione (Promegestone); RA=retinyl acetate; RIA=radioimmunoassay.

---

[1] Received August 13, 1981; revised March 3, 1982; accepted March 15, 1982.

[2] Supported by a grant from the Medical Research Council of Canada and the National Cancer Institute of Canada.

[3] Animals were maintained under the guidelines set forth by Laval University.

[4] Department of Molecular Endocrinology, Le Centre Hospitalier de l'Université Laval, Quebec G1V 4G2, Canada.

[5] Exchange student from the Laboratoire de Biochimie Cellulaire, UER de Sciences, 86000 Poitiers, France.

[6] Laboratoire de Physiologie de la Lactation, Institut National de Recherche Agronomique, CNRZ, 78350, Jouy-en-Josas, France.

Hormone solutions.—$[^3H]$R2858 (87 Ci/mmol) and $[^3H]$-R5020 (87 Ci/mmol) were obtained from New England Nuclear Corp., Boston, Mass., and the corresponding unlabeled steroids were synthesized at the Roussel Research Center, Romainville, France. Dexamethasone was purchased from Sigma Chemical Co., St. Louis, Mo. Stock solutions of the unlabeled steroids were kept at 2–4°C at a concentration of 4 m*M* in ethanol. The desired steroid solutions were prepared by serial dilution with buffer B [10 m*M* Tris-HCl (pH 7.4), 1.5 m*M* EDTA, and 10 m*M* thioglycerol]. The final concentration of ethanol in the assays never exceeded 0.2%, a concentration that does not affect steroid binding.

We obtained hGH (lot #HS-2160E; 1.71 U/mg), oPRL (lot #NIH-P-S13; 30 U/mg), and materials for the RIA of rat PRL from the National Pituitary Agency, National Institutes of Health, Bethesda, MD.

Preparation of cytosol and membrane fractions.—After thawing, tumors or tumor fractions were weighed and homogenized in 6 volumes (wt/vol) of buffer A [25 m*M* Tris-HCl (pH 7.4), 1.5 m*M* EDTA, 10 m*M* thioglycerol, and 10% glycerol) with the use of a Polytron PT-10 homogenizer at a setting of 5 for 2 or 3 periods of 10 seconds with an interval of 10 seconds for cooling. The homogenate was then centrifuged at 1,500×*g* for 15 minutes, and the resulting supernatant centrifuged at 105,000×*g* for 90 minutes to obtain the cytosol (supernatant fraction). All steroid-binding assays were performed with freshly prepared cytosol fractions. The 105,000×*g* pellet was resuspended in 25 m*M* Tris-HCl (pH 7.4) and 10 m*M* MgCl$_2$ with a Teflon and glass homogenizer and stored at −20°C until PRL-binding assays. Protein concentrations were measured with BSA as standard (*9*).

Estrogen and progesterone receptor levels.—$[^3H]$R2858 binding and $[^3H]$R5020 binding were measured with the use of the protamine sulfate and DCC assays, respectively (*10*). In the standard assay, 0.2-ml aliquots of the cytosol were incubated with 0.1 ml of 5 n*M* $[^3H]$R2858 or 8 n*M* $[^3H]$R5020 in the presence or absence of a 100-*M* excess of the unlabeled steroid for 5 hours at 25°C or for 16–20 hours at 0–4°C. Time-course studies have been performed, and the times utilized represent equilibrium or steady-state conditions. An excess of dexamethasone was always added to the $[^3H]$R5020 solution to saturate all glucocorticoid receptors. For the $[^3H]$R5020-binding assay, unbound steroids were removed by incubation for 10 minutes at 0–4°C with 0.3 ml of 0.5% Norit-A–0.05% Dextran T-70 (DCC) in buffer B and centrifugation at 2,000×*g* for 10 minutes at the same temperature. Then 0.3-ml aliquots of supernatant were removed. After addition of 8 ml of Aquasol, the radioactivity was measured in a Beckman liquid scintillation spectrometer at a 40% counting efficiency. For the $[^3H]$R2858-binding assay, 0.3 ml of a 2% protamine sulfate solution in buffer B was added and the tubes incubated for 10 minutes. The resulting precipitate was filtered and washed in buffer B, and the filters were counted. The extent of specific binding was obtained by subtraction of nonspecific radioactivity from total bound radioactivity.

Dissociation of endogenously bound PRL.—Since a large portion of PRL still remained bound to the receptors at the end of the membrane fraction preparation, it was necessary to remove endogenously bound PRL to measure total PRL receptor levels (*11*). We added 0.5 ml of 3 *M* MgCl$_2$ to 1.5 mg of DMBA-induced mammary tumor membrane protein in 12×75-mm glass tubes. The tubes were mixed on a vortex and after 3 minutes, 3.5 ml of the assay buffer [25 m*M* Tris-HCl (pH 7.4), 10 m*M* MgCl$_2$, and 0.1% BSA] was added to each tube. The tubes were centrifuged at 2,300×*g* for 15 minutes, and the resulting supernatant was aspirated. The pellets were resuspended in 0.5 ml of the assay buffer and binding studies were performed.

PRL receptor levels.—It was shown previously that ^{125}I-labeled hGH binds with the same affinity and specificity as ^{125}I-labeled oPRL to membrane fractions prepared from PRL-responsive tissues. We used ^{125}I-labeled hGH for PRL binding since labeled samples of this hormone have proved more stable than labeled PRL. A modification of the method of Hunter and Greenwood (*12*), in which 500 ng chloramine-T and 5 μg hGH were incubated for 3 minutes at 23°C, was employed to iodinate hGH (*11*). The iodinated hormone was purified on a column of Sephadex G-75 (0.9×100 cm), and the tubes of radioactivity comprising the protein peak were diluted in assay buffer and could be stored for as long as 3 weeks at 4°C. Specific activities, as calculated by isotope recovery, ranged between 75 and 95 μCi/μg. The integrity of the iodinated hGH was verified after each iodination with the use of a laboratory standard receptor preparation. At

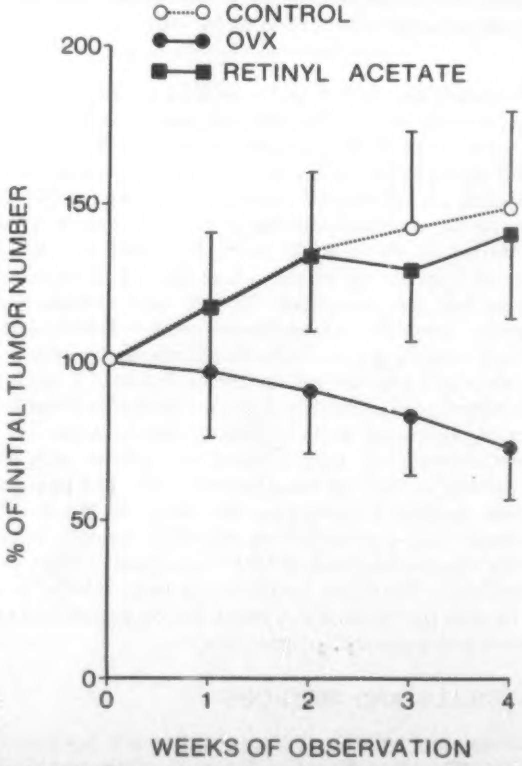

TEXT-FIGURE 1.—Tumor numbers throughout a 4-wk period of observation. Tumor numbers are presented as percent of the initial (time 0) values for each group: control, 3.32±0.46; OVX, 3.58±0.54; and RA, 3.55±0.41. *Vertical bars* show SEM.

the concentration of the mammary gland receptor used (300 μg), at least 40% of the iodinated hGH was specifically bound before the tracer was considered acceptable.

DMBA-induced mammary tumor membranes (300 μg) were incubated with approximately 100,000 cpm ^{125}I-labeled hGH both in the presence and absence of an excess (1 μg) of unlabeled oPRL. Specific binding was calculated as the difference between the cpm bound in the absence and presence of excess unlabeled hormone and was expressed as a percentage of the total radioactivity added to the tube.

Measurement of plasma PRL and progesterone and calculations.—Plasma PRL was measured by a double-antibody RIA with the use of rat hormones and rabbit antisera. Plasma progesterone concentrations were determined by specific double-antibody RIA. Plasma was extracted with benzene. Assays were performed with the use of antibodies developed against progesterone-12-(*O*-carboxymethyl)-oxime. ^{125}I-labeled progesterone-12-(*O*-carboxymethyl)-oxime tyrosine methyl ester was used as labeled tracer (*13*). RIA data were analyzed with the use of a program based on model II of Rodbard and Lewald (*14*). Receptor assays were calculated with the use of a program developed in this laboratory. Calculations were performed with Hewlett-Packard 9845T desk-top calculator. Statistical significance was determined by Student's *t*-test, Duncan-Kramer multiple range test (*15*), or the χ^2 test. All data presented are means plus or minus standard errors of the means. Each assay was performed with at least duplicate determinations.

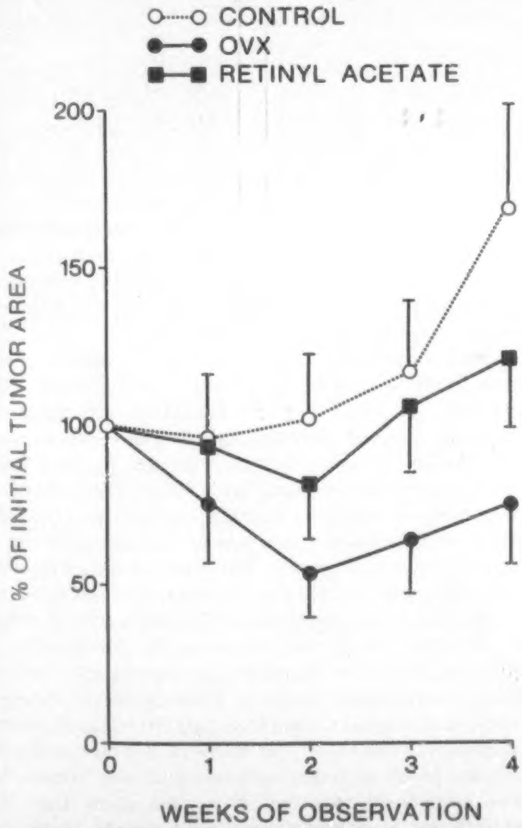

TEXT-FIGURE 2.—Tumor area throughout a 4-wk period of observation. Tumor areas are presented as percent of initial (time 0) values for each group: control, 1.91±0.28 cm^2; OVX, 1.99±0.28 cm^2; and RA, 2.12±0.27 cm^2. *Vertical bars* show SEM.

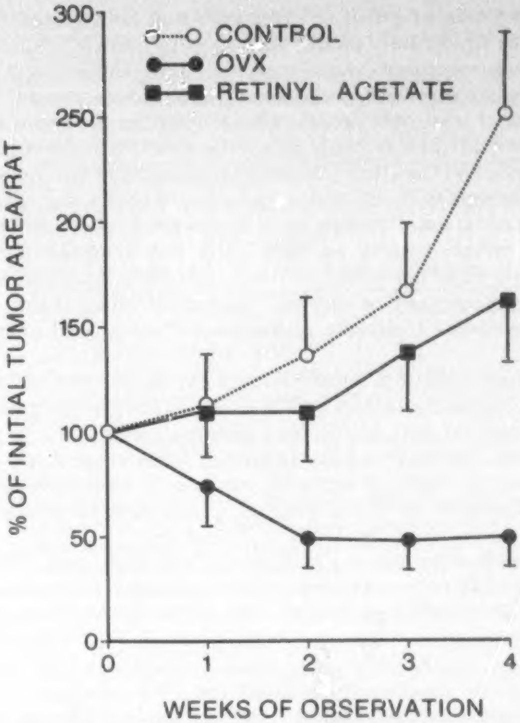

TEXT-FIGURE 3.—Total tumor area per rat throughout a 4-wk period of observation. Tumor area per rat is presented as a percent of initial (time 0) values for each group: control, 6.34±0.94 cm^2/rat; OVX, 7.12±0.99 cm^2/rat; and RA, 7.51±0.95 cm^2/rat. *Vertical bars* show SEM.

RESULTS

The response in tumor number to OVX and RA treatment is shown in text-figure 1. The number of tumors at time 0 was 63 (control), 68 (OVX), and 71 (RA treatment). OVX significantly reduced tumor number (27%; $P<0.01$) compared to the number of tumors in the control group which increased steadily and reached 149±29% of the initial tumor number at the end of the experiment. RA administration failed to induce any significant regression in tumor number, although there was a slight regressing effect during the last 2 weeks of the treatment.

The average tumor size (text-fig. 2) increased only slightly during the first 3 weeks in control animals, but it increased sharply (to 168%) at the 4th week of observation (from 1.91±0.28 cm^2 to 3.2±0.3 cm^2). During the first 2 weeks of treatment, OVX induced a maximum regression (to 53%) in tumor size which was 1.99±0.28 cm^2 at time 0, whereas the effect of RA was less pronounced (only a 19% decrease). During the last 2 weeks of the observation, tumors began to grow again in both the RA-treated and OVX-treated groups; however, at the end of the treatment period, tumors were smaller (1.5±0.2 cm^2) in OVX-treated animals than in the RA-treated group (2.5±0.2 cm^2) and both groups had tumors significantly smaller than those of controls ($P<0.05$). When tumor numbers and tumor size are combined and the results are expressed as the average tumor area per rat, the effects of treatment become clearer (text-fig. 3). There was a steady increase of initial tumor size to 251% in the control animals and the effect was most pronounced in the 3rd and 4th weeks. OVX induced a regression in tumor size, which was maximum at 2 weeks (to 51% of control values; $P<0.01$) after which growth was stabilized. RA retarded tumor growth when compared to tumor growth in controls, and the area increased to only 162% of control values at the end of the 4-week treatment period ($P<0.05$ compared to control).

Table 1 shows a subdivision of the tumor growth into those regressing tumors (<50% of initial size), static tumors (between 50 and 110%), and growing tumors (>10% increase). Two-thirds of the tumors in OVX-treated rats regressed ($P<0.001$; χ^2 analysis), whereas the ratio of regressing tumors in the RA-treated group was three times higher than that in controls ($P<0.03$; χ^2 analysis).

Specific binding of [^{3}H]R2858, [^{3}H]R5020, and ^{125}I-labeled hGH to tumors from treated animals is summarized in table 2. OVX significantly reduced the levels of estradiol and progesterone receptors ($P<0.01$), whereas RA treatment did not significantly affect steroid receptor levels. Both treatments significantly reduced the PRL receptor levels ($P<0.01$): OVX resulted in a 79% decline in PRL receptor levels ($P<0.01$), whereas the RA diet resulted in a slight but equally significant (21%) decline of PRL binding. If only regressing tumors are considered for PRL receptor levels, there was no significant difference in the RA-treated group compared to the control group (7.0±0.6 and 7.7±1.3%, respectively; data not shown).

Plasma progesterone and PRL levels at the time of death are shown in table 3. RA significantly increased circulating PRL concentrations ($P<0.01$) but did not affect plasma progesterone levels.

No significant differences were observed in body weights between controls and either of the treated groups, which suggests an absence of toxic effect of RA. All tumors examined histologically were adenocarcinomas.

TABLE 1.—*Response to treatments expressed as percent of regressing, static, or growing tumors*

Group	Total No. of tumors	Total tumor growth, %		
		Regressing[a]	Static[b]	Growing[c]
Control	98	5.10	5.10	89.80
Ovx	79	64.56	16.45	18.98
RA	102	14.71	10.78	74.51

[a] Defined as <50% of initial size.

[b] Defined as between 50% and 110% of initial size.

[c] Defined as >110% of initial size.

TABLE 2.—*Effects of treatments on specific binding of [^{3}H]R2858, [^{3}H]R5020, and ^{125}I-labeled hGH to DMBA-induced tumors*

Group	No. of tumors	Protein, fmol/mg ± SEM		Specific binding/300 μg protein, % ± SEM: ^{125}I-labeled hGH
		[^{3}H]R2858	[^{3}H]R5020	
Control	59	62.0±5.8	68.7±10.4	11.7±0.7
OVX	28	15.6±6.4[a]	11.0±3.4[a]	2.5±0.6[a]
RA	57	73.3±7.6	86.4±19.2	9.2±0.6[a]

[a] $P<0.01$, when compared to control.

TABLE 3.—*Plasma progesterone and PRL concentrations at the time of death*

Group	No. of animals	ng/ml ± SEM	
		Progesterone	PRL
Control	19	4.91±1.23	14.09±2.94
OVX	19	0.34±0.05[a]	6.39±0.91[a]
RA	20	5.36±1.22	39.29±9.14[a]

[a] $P<0.01$, when compared to control.

DISCUSSION

RA feeding has previously been reported to suppress the development of carcinogen-induced cancers in rats (*3–5, 7*). However, this approach had been extensively used only in the prevention of experimental mammary tumorigenesis. The specific role of RA in the regression of established DMBA-induced mammary tumors or a possible influence of this retinoid on hormonal factors regulating tumor growth has not previously been reported.

DMBA-induced rat mammary carcinogenesis was significantly inhibited by the chronic administration of a dietary supplement of RA beginning 1 week after carcinogen administration (*3*). In the present study, we have shown that if treatment with RA was delayed for 6 months after carcinogen administration and then a dose of retinoid sufficient to assure an intake of 5 mg per day was given, there was a lack of any substantial protective effect on tumor induction. As expected, OVX remained effective in inhibiting mammary carcinogenesis, although its effectiveness was less dramatic than that in animals with younger tumors.

Very little information is available on the ability of RA to reduce DMBA-induced mammary tumor growth. McCormick et al. (*3*) found that 12% of DMBA-induced mammary tumors regressed spontaneously in Lewis rats as compared to 29% in the retinoid-treated groups. In the present study in Sprague-Dawley rats, only 5% of the tumors regressed in controls versus 15% in RA-treated rats ($P<0.03$). Moreover, we have shown that a short dietary exposure to retinoid reduced tumor growth. The effect on tumor number was most noticeable in the first 2 weeks, and the effect on tumor area was more apparent in the last weeks of observation. However, when one compares the effectiveness of RA to that of OVX, the endocrine therapy clearly remains superior to the retinoid treatment. Although several reports have noted that vaginal smears from rats fed retinoid showed normal estrous cycles (*3, 4*), the effect of RA on circulating progesterone levels and steroid binding in the tumors has not been previously reported. Our data show that RA feeding did not alter circulating progesterone levels nor steroid binding to DMBA-induced mammary tumors, which suggests that the ability of RA to limit tumor growth in the rat is not mediated by an alteration of ovarian function, or tumor responsiveness to estrogen or progesterone.

Welsch et al. (*7*) reported a synergistic effect of chronic PRL suppression and retinoid treatment in the propylaxis of MNU-induced mammary tumorigenesis in female Sprague-Dawley rats. In the present study, an elevated level of circulating PRL in the RA-treated group could explain the failure of this treatment to reduce tumor number. There was a slight decline in PRL receptor levels in the RA-treated group in which a limited effect on tumor growth was observed, which suggests a possible direct effect of the retinoid on tumor membranes. Specific retinoic acid-binding proteins have been reported in the cytosols of mammary gland as well as in carcinogen-induced mammary tumors, and an increased relationship between steroid receptors and retinoid receptors in mammary tumors has been noted (*16*). This fact, coupled with the failure of RA to alter the ovarian function in rats, is in agreement with an hypothesis of direct cellular effects. Moreover, Lotan and Nicolson (*17*) have shown that the growth of a considerable number of both transformed cells and tumor cells (which form rat DMBA mammary adenocarcinoma cells lines) could be inhibited in vitro by retinoids, which suggests that the antitumor activity of retinoids observed in vivo is at least partly due to direct inhibition of cell proliferation. The reduced RA effect in the present report might be due to a diminished cellular sensitivity to retinoids in tumors from animals 6 months after DMBA administration.

The present study demonstrates that RA when administered to animals in advanced stages of the disease remains effective in inhibiting established tumor growth, but the effectiveness of RA is reduced compared to the effectiveness of RA administered at earlier periods of tumor development.

REFERENCES

(*1*) Sporn MB, Newton DL. Chemoprevention of cancer with retinoids. Fed Proc 1979; 38:2528–2534.

(*2*) Grubbs CJ, Moon RC, Sporn MB, Newton DL. Inhibition of mammary cancer by retinyl methyl ether. Cancer Res 1977; 37:599–602.

(*3*) McCormick DL, Burns FJ, Albert RE. Inhibition of rat mammary carcinogenesis by short dietary exposure to retinyl acetate. Cancer Res 1980; 40:1140–1143.

(*4*) Moon RC, Grubbs CJ, Sporn MB. Inhibition of 7,12-dimethylbenz(*a*)anthracene-induced mammary carcinogenesis by retinyl acetate. Cancer Res 1976; 36:2626–2630.

(*5*) Moon RC, Grubbs CJ, Sporn MB, Goodman DG. Retinyl acetate inhibits mammary carcinogenesis induced by *N*-methyl-*N*-nitrosourea. Nature 1977; 267:620–621.

(*6*) Moon RC, Thompson HJ, Becci PJ, et al. *N*-(4-Hydroxyphenyl) retinamide, a new retinoid for prevention of breast cancer in the rat. Cancer Res 1979; 39:1339–1346.

(*7*) Welsch CW, Brown CK, Goodrich-Smith M, Chiusano J, Moon RC. Synergistic effect of chronic prolactin suppression and retinoid treatment in the prophylaxis of *N*-methyl-*N*-nitrosomethylurea-induced mammary tumorigenesis in female Sprague-Dawley rats. Cancer Res 1980; 40:3095–3098.

(*8*) McCormick DL, Burns FJ, Albert RE. Inhibition of benzo[*a*]pyrene-induced mammary carcinogenesis by retinyl acetate. JNCI 1981; 66:559–564.

(*9*) Lowry OH, Rosebrough NJ, Farr AL, Randall RJ. Protein measurement with the Folin phenol reagent. J Biol Chem 1951; 193:265–275.

(*10*) Turcot-Lemay L, Kelly PA. Characterization of estradiol, progesterone and prolactin receptors in nitrosomethylurea-induced mammary tumors and effect of anti-estrogen treatment on the development and growth of these tumors. Cancer Res 1980; 40:3232–3240.

(*11*) Kelly PA, Leblanc G, Djiane J. Estimation of total prolactin-binding sites after in vitro desaturation. Endocrinology 1979; 104:1631–1638.

(*12*) Hunter WM, Greenwood FC. Preparation of iodine-131 labeled human growth hormone of high specific activity. Nature 1962; 194:495.

(*13*) Belanger A, Caron S, Picard V. Simultaneous radioimmunoassay of progestin, androgen and estrogen in adult rat testes. J Steroid Biochem 1980; 13:185–190.

(*14*) Rodbard D, Lewald JE. Computer analysis of radio-ligand assays and radioimmunoassay data. In: Diczfalusy E, ed. Second Karolinska symposium on research in reproductive endocrinology. Copenhagen: Bogtrykkeriet Forum, 1970:79–103.

(*15*) Kramer CY. Extension of multiple-range tests to group means with unequal numbers of replications. Biometrics 1956; 12:307–310.

(*16*) Moon RC, Mehta RG. Retinoid Inhibition of mammary carcinogenesis: receptors. Cancer Treat Rep 1979; 63:1177.

(*17*) Lotan R, Nicolson GL. Inhibitory effects of retinoic acid or retinyl acetate on the growth of untransformed, transformed, and tumor cells in vitro. J Natl Cancer Inst 1977; 59:1717–1722.

blank page

Growth and Differentiation of Hyperplastic Outgrowths Derived From Mouse Mammary Epithelial Cells Transformed in Organ Culture[1,2,3]

Nivedita Ganguly,[4,5] **Ranjan Ganguly,**[4,5] **Nozer M. Mehta,**[4] *and* **Mihir R. Banerjee**[4,6,7]

ABSTRACT—Potentially neoplastic outgrowths of BALB/c mouse mammary hyperplasia(s) (MH) derived from 7,12-dimethylbenz[a]anthracene-transformed epithelial cells in organ culture were characterized for responses to the hormones normally required for morphogenesis and functional differentiation of the mammary tissue. In a new culture model of the gland-free mammary fat pad, DNA synthesis in the MH outgrowths increased to a single peak during 6 days of incubation in a serum-free medium containing insulin, prolactin, aldosterone, and cortisol. The rise in DNA synthesis was accompanied by increased cell number and lobuloalveolar morphogenesis filling 50–70% of the fat pad; the rate of growth was variable among the MH outgrowth lines. Certain MH tissue showed some growth response in medium with aldosterone, cortisol, or estrogen, and progesterone in the presence of insulin. The hormone mixture insulin-prolactin was conducive to maximal growth, which suggested an altered sensitivity of the MH outgrowths to the mammogenic steroid hormones. Functional differentiation in the MH outgrowths was assessed in vivo by determination of the casein messenger RNA (mRNAcsn) levels measured by a specific complementary DNA probe. In MH-1 and MH-5 outgrowth lines, mRNAcsn was measurable in lactating hosts. In MH-9 outgrowth essentially the same concentration of mRNAcsn was present both in virgin and lactating hosts. Although mRNAcsn was present in MH outgrowths in lactating hosts, the concentration of the mRNA was only 0.056–0.88% of that present in the lactating host's own mammary gland. Virtually no mRNAcsn was measurable in the mammary tumors, regardless of the endocrine environment of the host animal. The results indicate a transformation-associated altered pattern of mammary cell-specific gene expression.—JNCI 1982; 69:453–463.

Recent studies have established that the murine mammary parenchyma in an isolated whole organ in vitro can mimic the stages of mammogenesis, functional differentiation, and alveolar regression (involution) in a chemically defined medium supplemented with hormones (*1–3*). With the use of this unique culture model of the whole mammary organ, it has been demonstrated (*4–6*) that the carcinogenic hydrocarbon DMBA can induce neoplastic transformation of the epithelial cells in the gland in vitro and that the process is associated with appearance of a type of dysplasia referred to as "NLAL." The NLAL are sustained in a hormone-deficient medium, which suggests that the alveolar epithelium in these lesions exhibits a state of transformation with respect to its hormonal requirement. DMBA apparently is metabolized by the mammary cells in organ culture, because incubation of the glands in medium with the hydrocarbon results in covalent binding of the carcinogen with cellular DNA (*6*). Therefore, the molecular interactions of DMBA with mammary gland in vitro is characteristic of similar interactions associated with the transforming action of DMBA in other cell types (*7, 8*). Subsequent studies have shown that a variety of oncogenic chemicals, direct-acting as well as those requiring metabolic activation, also induced NLAL in the mammary organ under similar culture conditions (*9, 10*). The incidence of NLAL, induced by a low concentration of procarcinogen, is preventable by a retinoid, a vitamin A analogue (*11*), which has been found to inhibit mammary tumorigenesis in rats (*12, 13*).

Studies in our laboratory have indicated that the transformed mammary epithelial cells (including those in NLAL) in the mammary organ in culture include potentially neoplastic cells (*14*). After transplantation into gland-free mammary fat pads of syngeneic female mice, the transformed cells initially produce hyperplastic lobulo-alveolar outgrowths in virgin hosts. Subsequently, mammary tumors appear in these MH outgrowths. Serial transplantation studies further showed that the pattern of sequential appearance of MH outgrowths and mammary tumors is analogous to that of the preneoplastic HAN (*15*). Thus the mammary epithelial cells transformed in vitro by DMBA mimic the multistage genesis of murine mammary neoplasia in vivo (*16–19*). This accomplishment of neoplastic transformation of the mammary epithelial cells in an isolated whole organ in culture presents a unique in vitro model for assessment of responses of the epithelial cells to various exogenous agents, including potential carcinogenic and chemopreventive chemicals. This model then prompts a detailed analysis of the characteristics of the cells transformed in vitro. This report presents the results of the studies on responses of different MH outgrowth lines to the regulatory hormones needed for morphogenetic and functional differentiation of the normal mammary glands of the mouse.

ABBREVIATIONS USED: cDNAcsn=complementary DNA to 15S mouse casein messenger RNA; DMBA=7,12-dimethylbenz[*a*]anthracene; HAN=hyperplastic alveolar nodule(s); $[^3H]$dThd=tritiated thymidine; MH=mammary hyperplasia (hyperplastic); mRNAcsn=casein messenger RNA; NLAL=nodule-like alveolar lesions; R_0t=moles of ribonucleotides·sec·L^{-1}; $R_0t_{1/2}$=R_0t needed to reach 50% hybridization; TCA=trichloroacetic acid.

---

[1] Received August 31, 1981; revised February 9, 1982; accepted March 8, 1982.

[2] Supported by Public Health Service grants CA-25304 and CA-11058 from the National Cancer Institute.

[3] Animals were maintained under the guidelines set forth by the University of Nebraska.

[4] Tumor Biology Laboratory, School of Life Sciences, University of Nebraska, 201 Lyman Hall, Lincoln, Nebr. 68588.

[5] *Present address:* Department of Molecular Biology and Biochemistry, School of Biological Sciences, University of California, Irvine, Calif. 92717.

[6] *Address reprint requests* to Dr. Banerjee.

[7] We thank Ms. Linda R. Crump, Ms. Susette Mittag, and Mr. Anand P. Iyer for technical assistance and Mr. Arvilla Kirchhoff for editorial assistance.

MATERIALS AND METHODS

Animals.—BALB/cAnN mice obtained from the National Cancer Institute were used.

MH outgrowth lines.—The four MH outgrowth lines used in the present studies were derived from the mammary epithelial cells transformed by DMBA in an in vitro carcinogenesis model of the whole mammary organ (*15*). The MH outgrowth lines were maintained by serial transplantation with the use of the standard procedure (*20*) into gland-free inguinal (fourth) mammary fat pads of syngeneic virgin hosts. The origin and biologic characteristics, including the tumorigenic potential of the MH outgrowth lines, have been recently described (*15*) and are summarized in table 1.

Proliferation of MH outgrowth lines.—The rate of cell proliferation in the MH outgrowth lines was measured during growth of the implant in the gland-free mammary fat pad in vivo and in vitro. In vivo cell proliferation: Small pieces of the MH tissues were transplanted with the use of the standard procedure (*20*) into the gland-free inguinal (fourth) mammary fat pads of 3-week-old syngeneic mice. At different times the entire inguinal mammary fat pad was isolated and stained with alum carmine, and the total area of the fat pad occupied by the outgrowth tissue was determined microscopically (*21*).

In vitro cell proliferation: Previously, we have observed that HAN tissue implanted into the gland-free mammary fat pad is capable of spatial proliferation in vitro filling the fat pad in a chemically defined medium that contained appropriate hormones (*22*). This gland-free mammary fat pad organ culture procedure was used to measure the growth characteristics of the MH lines and their responses to the growth-promoting hormones in a controlled in vitro environment. In these studies pieces of MH outgrowth tissue were first transplanted into the gland-free mammary fat pads (fourth) of the 3-week-old female syngeneic mice. According to the standard procedure (*22, 23*) the whole fat pad, which carried the MH tissue, was excised on a Dacron raft 3 weeks later and incubated in Waymouth's medium in the presence of a 95% O$_2$–5% CO$_2$ atmosphere. The rate of DNA synthesis, increase in cell numbers, and percent area of the fat pad filled by the MH tissue during a 6-day incubation in medium with combinations of insulin, prolactin, aldosterone, cortisol, estrogen, and progesterone were determined for measurement of growth. Procedures used for determination of each of these parameters are described in legends of appropriate text-figures.

TABLE 1.—*Characteristics of DMBA-induced MH lines*[a]

MH lines	Morphology	Animals with tumors, %	Latent period of tumor incidence, wk	Mammary tumor type
MH-1	Lobulo-alveolar	30–35	20	Lobular
MH-3	Lobulo-alveolar	20–25	20	Lobular
MH-5	Mixed lobulo-alveolar ductal	45–50	25–30	Lobular
MH-9	Lobulo-alveolar	80–85	10–15	Lobular

[a] For further detail, *see* (*14*) and (*15*).

Expression of functional differentiation.—Accumulation of mRNAcsn in different MH outgrowth lines and their tumors in vivo was used as a measure of functional differentiation. MH tissues were transplanted into the gland-free inguinal (fourth) mammary fat pads of 3-week-old BALB/cAnN female mice, and 10–12 weeks later the gland-free fat pads carrying the outgrowth tissue were collected from the virgin hosts. To measure the responses of the MH outgrowths and their tumors to the lactogenic hormone stimulation, we mated 9-week-old virgin host animals carrying the different outgrowth lines with BALB/c males (6 wks after transplantation). After the normal period of gestation, the fat pads carrying the MH tissues were collected from post-partum mice on the fifth day of lactation. In some cases tumors appeared in MH outgrowths carried in lactating hosts, and these tumors were also collected for measurement of functional differentiation. Until the animals were killed, the lactating mice were allowed to nurse their pups.

Nucleic acid hybridization: Total RNA from the MH, HAN-D8, and the mammary tumors was isolated by the phenol–chloroform method (*24*). Purification of 15S mRNAcsn and synthesis of a [^{3}H]-labeled cDNAcsn to the mRNAcsn were done as previously described (*25–27*). Concentration of the mRNAcsn in the total RNA of different mammary tissues was determined by RNA excess hybridization to the cDNAcsn probe (*25–27*). Test RNA's were incubated with [^{3}H]cDNAcsn probe (500 cpm; 4×10^6 cpm/µg) at 68°C for various times in a buffer containing 0.6 *M* NaCl, 10 m*M* HEPES[8] (pH 7.0), and 2 m*M* Na$_2$EDTA. At the end of the incubation the reaction mixtures were adjusted to 0.1 *M* sodium acetate (pH 4.5), 0.2 *M* NaCl, and 1.2 m*M* ZnCl$_2$. S$_1$-nuclease was added at 1,000 U/ml, and the reaction mixtures were incubated at 37°C for 2 hours. S$_1$-nuclease-resistant cDNA–RNA hybrids were precipitated on filters (Millipore Corp., Bedford, Mass.), and radioactivity was determined by liquid scintillation spectrometry. S$_1$-nuclease-resistant radioactivity in the reactions without any RNA was considered as background and was subtracted from all values. The mRNAcsn concentration in test RNA was determined as follows: $Rot_{1/2}$ of pure mRNAcsn: $Rot_{1/2}$ of test RNA×100.

RESULTS

Proliferation of MH Outgrowth Cell Lines in Gland-Free Mammary Fat Pads In Vitro

The whole gland-free mammary fat pad culture model was used to measure the growth rate of the MH lines in an in vitro controlled environment. MH outgrowth lines were derived from the mammary cells transformed by DMBA, apparently during lobulo-alveolar growth of the gland in the culture medium containing the hormones insulin, prolactin, aldosterone, and cortisol. Accordingly, the growth rate of the MH outgrowth lines in vitro was also measured in the presence of the same hormone mixture in the culture medium.

---

[8] 4-(2-Hydroxyethyl)-1-piperazine ethanesulfonic acid.

DNA Synthesis in MH Outgrowth Lines In Vitro

Incorporation of [^{3}H]dThd into the MH tissue was used as a measure of DNA synthesis, and the data are shown in text-figure 1. The general pattern of the kinetics of DNA synthesis in the different MH outgrowth lines was essentially similar during the 6-day incubation period. In each MH outgrowth line, incorporation of [^{3}H]dThd increased steadily to a peak on the fourth day and then declined sharply. The rise of DNA synthesis in MH-1 was rather slow (1.4-fold) during the initial 2 days, although it rose threefold reaching a peak on the fourth day. The increase of DNA synthesis in MH-3 was 2.9-fold at the peak period after 4 days of incubation. In MH-5 DNA synthesis increased at a near linear rate showing a 4.18-fold rise between 0 and 4 days. In MH-9 a 2.3-fold rise occurred between 0 and 2 days, and on the fourth day the total increase reached 2.8-fold. In addition to the variability of the rate of DNA synthesis, the initial zero time values were also variable for the different MH outgrowth lines.

Epithelial Cell Number

The measure of DNA synthesis is likely to provide an average value of the total cell population in the MH tissues. Therefore, a measure of epithelial cell number in the MH outgrowth lines was also obtained after collagenase dissociation of the outgrowth tissues at different times in culture.

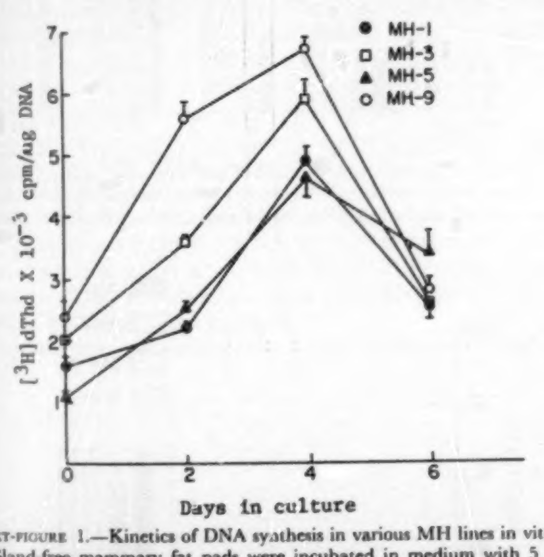

TEXT-FIGURE 1.—Kinetics of DNA synthesis in various MH lines in vitro. Gland-free mammary fat pads were incubated in medium with 5 μg insulin/ml, 5 μg prolactin/ml, 1 μg aldosterone/ml, and 5 μg cortisol/ml as described in "Materials and Methods." During the last 1 hr of culture, the fat pads were incubated in medium containing 5 Ci/ml [^{3}H]dThd (20 Ci/mmol; New England Nuclear Corp., Boston, Mass.). At the end of the labeling period, the fat pads were removed, rinsed with cold 0.9% NaCl and blot-dried. For each time point, 15 fat pads containing MH tissue were pooled and defatted with two extractions, each with ethanol:ether (1:1) and ether. The fat pads were then homogenized in cold 5% TCA, and the acid-precipitable material was recovered. After three washes with 5% cold TCA, DNA content and radioactivity were determined in the acid-precipitable material by diphenylamine assay (*20*) and liquid scintillation spectrometry. *Each time point* is a mean of three experiments. *Vertical lines* = positive side of standard deviation.

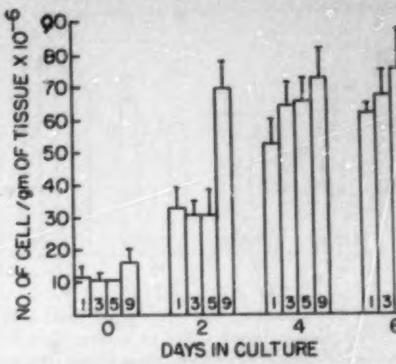

TEXT-FIGURE 2.—Determination of cell number in MH t
bation in hormonal medium as described in text-fig.
interval 20–30 fat pads containing MH tissue were pool
incubated with vigorous agitation in Waymouth's mec
0.1% collagenase, 0.1% hyaluronidase, and 0.04% DNas
min. At the end of the incubation, the reaction mixt
through cheese cloth and then centrifuged at 700×*g* fo
the pellet were suspended in Waymouth's medium a
hemacytometer. Mammary cells isolated by this proced
viable epithelial cells (*14*, *15*). *Each bar* is the mean of th
Vertical lines = positive side of standard deviation.

Data in text-figure 2 show that between 0 a
incubation the number of epithelial cells in
MH outgrowths increased sixfold to eightfol
cell number remained essentially similar a
MH-3, and MH-5 tissues on different days du
6-day incubation, in MH-9 the increase in cel
markedly greater than others between 0 a
culture. Subsequently, however, the overall ra
(between 2 and 6 days) in MH-9 was lower t
three MH outgrowths.

Spatial Proliferation of MH Cells in the Fa

Text-figure 3 shows the data on spatial gro
ured by percentage of the fat pad filled by t
tissues at different times in vitro. It is clear th
6-day culture period each of the MH outgrov
spatially filling 50–70% of the mammary fat pa
the rate of spatial growth followed a similar p

Figure 1 illustrates the morphology of the M
the gland-free mammary fat pad in vitro. The
lobulo-alveolar structures at different times
filled nearly 70% of the fat pad in the chem
medium, supplemented with insulin, prolacti
and cortisol. Figure 2 illustrates the spatial g
of the MH-5 mixed outgrowth (lobulo-alveol
at different times during in vitro incubation i
of the same hormone mixture. The character
ogy of this mixed outgrowth tissue was ma
during the in vitro spatial proliferation of
ductal component of the outgrowth failed to
mammogenic action of the hormone mixture i
(*5*).

Proliferation of the MH outgrowth lines v
ured in vivo (text-fig. 4). All four MH outgro
found to grow filling nearly 100% of the fat

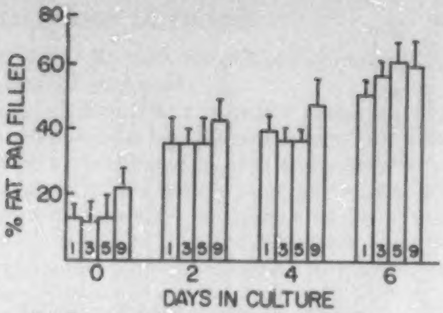

TEXT-FIGURE 3.—Percent area of fat pad filled by different MH tissues at various times of incubation in vitro. Fat pads containing MH tissues were incubated in the hormone medium as described in text-fig. 1. At each time point fat pads were removed, fixed, and stained with alum carmine. With use of dissecting microscope, the total area of each fat pad and the area occupied by MH tissue were measured (*22*). *Each bar* is mean value of 3–5 fat pads. *No. within bars* indicate different MH tissues. *Vertical lines*=positive side of standard deviation.

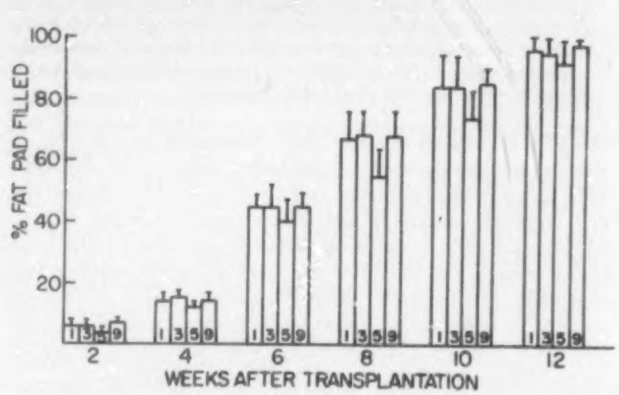

TEXT-FIGURE 4.—Percent area of fat pads filled by different MH tissues during their spatial growth in vivo. Other details are as in text-fig. 3. *Bar*=mean value of four fat pads. *Vertical lines*=positive side of standard deviation.

12-week period after transplantation. The growth rate also showed a similar pattern, although MH-5 appeared to be slightly slower. Figure 3 illustrates the morphology of a lobulo-alveolar MH outgrowth line at different times of its spatial growth in the gland-free mammary fat pad in vivo.

Response of the MH Outgrowth Cell Lines to the Growth-Promoting Action of Hormones

Hormonal influence on growth of the MH outgrowth lines was assessed in vitro by the measurement of the percentage of fat pad filled by the outgrowth tissues after a 6-day incubation period. Responses to different combinations of the hormones insulin, prolactin, aldosterone, cortisol, estrogen, and progesterone were measured. Essentially no growth was observed in the MH tissues after 6 days of incubation in medium without any hormone compared to 0 day (text-fig. 5). Addition of insulin to the medium also failed to promote any noticeable increase in growth in MH-1, MH-3, and MH-9 tissues. However, compared to the medium without any hormone, a 1.8-fold increase in growth was observed in MH-5 tissue in medium with insulin alone. Addition of aldosterone and cortisol to insulin-containing medium failed to increase growth in MH-1, MH-3, and MH-9 tissues. However, MH-5 tissue showed a 2.5-fold increase in growth in medium with insulin and the adrenal steroid hormones. A three- to fourfold increase in growth in all four MH tissues was observed in medium with insulin and prolactin compared to the medium without hormone. Although addition of aldosterone and cortisol to the insulin-prolactin hormone mixture stimulated a noticeably increased growth of MH-1, the growth rate of MH-3, MH-5, and MH-9 remained essentially unaltered in the presence of insulin, prolactin, and adrenal steroid hormones.

Text-figure 6 shows the data on responses of the MH outgrowth lines to the growth stimulatory action of the ovarian steroid hormones in the presence of insulin or insulin plus prolactin. In medium with insulin, estrogen, and progesterone, a twofold increase in growth was evident in MH-1, MH-3, and MH-5; in MH-9 the increase was only 1.3-fold. However, addition of prolactin to medium with insulin, estrogen, and progesterone promoted a marked increase in

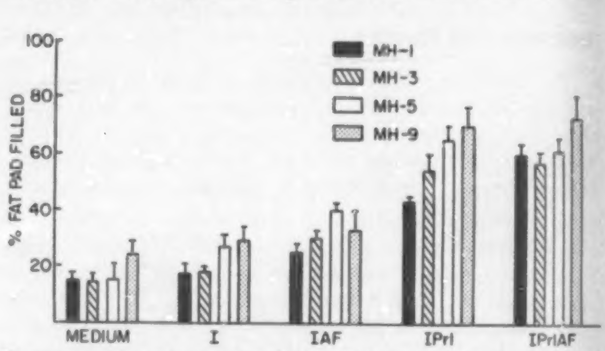

TEXT-FIGURE 5.—Area of fat pad (%) filled by the MH tissues in the presence of different combinations of the hormones insulin, prolactin, cortisol, and aldosterone during a 6-day incubation period. Other details are as in text-fig. 1. I=insulin; Prl=prolactin; F=cortisol; A=aldosterone.

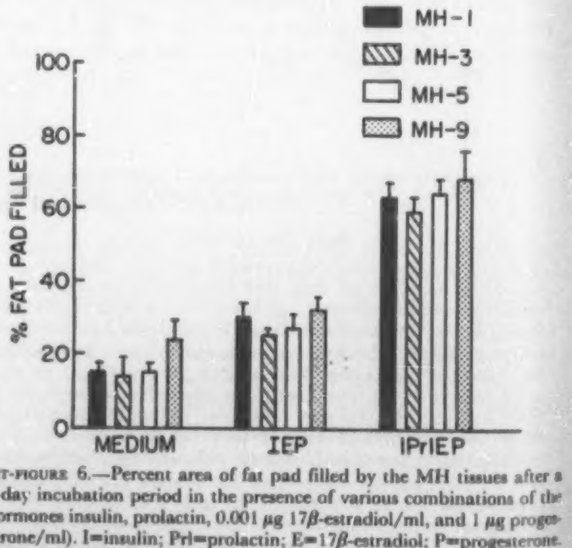

TEXT-FIGURE 6.—Percent area of fat pad filled by the MH tissues after a 6-day incubation period in the presence of various combinations of the hormones insulin, prolactin, 0.001 μg 17β-estradiol/ml, and 1 μg progesterone/ml). I=insulin; Prl=prolactin; E=17β-estradiol; P=progesterone. Other details and concentrations of hormones are as in text-fig. 1.

growth in all the MH outgrowth lines, which suggests that the growth potential of the MH tissues is dependent principally on the pituitary polypeptide hormone.

Expression of Functional Differentiation

Functional differentiation was assessed by quantitative measurement of the cellular concentration of mRNAcsn in the MH-1, MH-5, and MH-9 outgrowth lines in vivo. Text-figure 7A shows that in virgin hosts MH-1 and MH-5 tissues failed to accumulate a measurable level of mRNAcsn. However, mRNAcsn was measurable in the same two MH-outgrowth lines carried in lactating hosts, and the $R_0t_{1/2}$ values were 74.13 and 234.4 mol·sec·L^{-1} for MH-1 and MH-5, respectively. Quantitative estimates based on these data showed that concentrations of mRNAcsn in total RNA were 0.0044% in MH-1 and 0.0014% in MH-5.

RNA samples obtained from MH-9 outgrowth tissue carried in virgin hosts hybridized to the cDNAcsn probe to completion with a $R_0t_{1/2}$ of 14.8 mol·sec·L^{-1} giving a 0.022% mRNAcsn concentration in the total RNA of the tissue (text-fig. 7B). A 100% level of hybridization was also shown by RNA samples from MH-9 cells carried in lactating hosts, and concentration of mRNAcsn sequences in the total RNA was 0.017%. Mammary tumors derived from MH-9 tissue failed to show a measurable level of mRNAcsn in virgin or lactating hosts (text-fig. 7B).

For the purpose of comparison, the HAN-D8 line was included in the present studies. The HAN-D8 is one of the D-series HAN lines which were derived from mammary glands of an old virgin BALB/c mouse chronically hyperstimulated with a pituitary isograft in the renal capsule (*19*). Molecular hybridization data demonstrate that HAN-D8 tissue carried in virgin hosts failed to accumulate a measurable level of mRNAcsn sequences (text-fig. 8). However, RNA from HAN-D8 cells carried in lactating hosts reached a near 100% hybridization with a $R_0t_{1/2}$ of 56.2 mol·sec·L^{-1}, reflecting a 0.006% mRNAcsn level in the total RNA. Mammary tumors obtained from HAN-D8 (text-fig. 8) line failed to show a measurable level of mRNAcsn in virgin hosts as well as in lactating hosts.

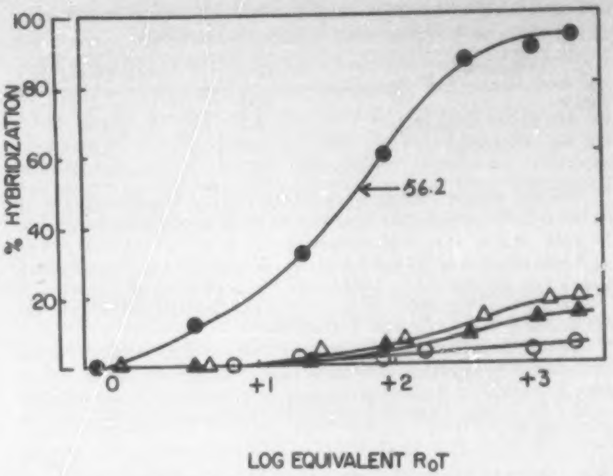

TEXT-FIGURE 8.—Hybridization kinetics of the cDNAcsn probe to total RNA from HAN-D8 tissue and its tumors. ○, HAN in virgin host; ●, HAN in lactating host; △, tumor in virgin host; ▲, tumor in lactating host. *Arrow* indicates $R_0t_{1/2}$ value. Tumors in virgin hosts appeared 15 wk after transplantation. For tumors in lactating hosts *see* "Materials and Methods."

To determine the level of expression of the casein gene in the MH and HAN-D8 tissues in virgin and/or lactating hosts, we compared the concentration of mRNAcsn in these preneoplastic tissues to that observed in the normal mammary glands. Accordingly, mRNAcsn concentrations in the normal mammary glands (second thoracic glands) of the host animals were determined by the molecular hybridization assays, and the data are shown in table 2. Whereas no mRNAcsn was detectable in the normal mammary glands of virgin hosts even at R_0t values of 1,000 mol·sec·L^{-1}, levels of mRNAcsn in normal glands of pregnant and lactating mice were 0.09 and 2.5% of the total RNA mass, respectively. These results are in agreement with earlier findings in the mammary glands of BALB/c mice (*29*). Since the MH outgrowth lines were derived from the mammary glands incubated for 6 days in medium with insulin, prolactin, aldosterone, and cortisol, mRNAcsn levels in the glands incubated in medium containing the same hormones were also determined. Consistent with our earlier finding (*30*),

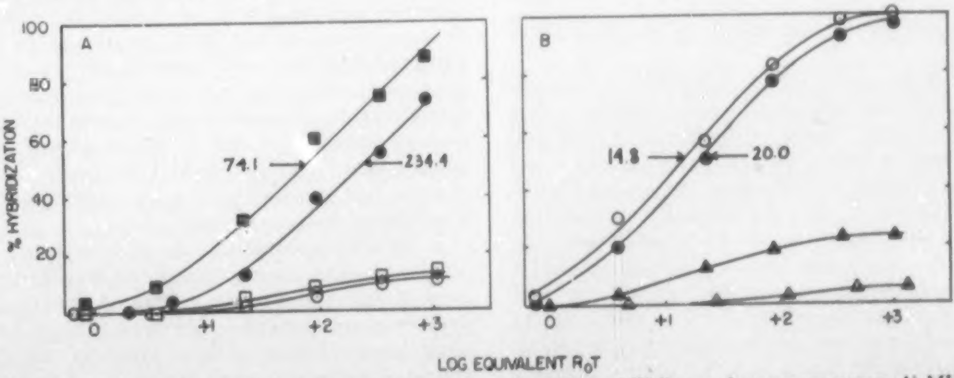

TEXT-FIGURE 7.—Hybridization kinetics of cDNAcsn probe to total RNA from the different MH lines and mammary tumors. A) MH-1; □, virgin host; ■, lactating host; MH-5: ⊙, virgin host; ●, lactating host; B) MH-9: ⊙, virgin host; ●, lactating host; △, MH-9 tumor in virgin host; ▲, MH-9 tumor in lactating host. *Arrows* indicate the $R_0t_{1/2}$ values. Tumors in the MH-9 tissue carried in virgin hosts appeared 15–20 wk after transplantation. For tumors in lactating hosts, *see* "Materials and Methods."

TABLE 2.—*Concentration of mRNAcsn in the normal mammary glands from mice in different conditions*

Condition[a]	$R_0t_{1/2}$	mRNAcsn,[b] %
Virgin	NM	—
14–15th day of pregnancy	3.7	0.09
5th day of lactation	0.13	2.5
In vitro[c]	17.4	0.019

[a] Normal second thoracic glands were used of virgin, pregnant, or lactating hosts carrying MH tissue in the gland-free inguinal mammary fat pads.

[b] Concentration of the mRNAcsn in the total RNA of the mammary glands was determined by cDNA-RNA hybridization as described in "Materials and Methods." $R_0t_{1/2}$ of the purified 15S mRNAcsn was 0.0033 mol·sec·L^{-1}. NM=not measurable.

[c] Second thoracic mammary glands of 3-wk-old BALB/cAnN female mice primed daily with 1 μg estrogen and 1 mg progesterone for 9 days were incubated in medium with insulin, prolactin, aldosterone, and cortisol for 6 days. Concentrations of the hormones were the same as in text-fig. 1.

TABLE 3.—*Levels of mRNAcsn in total RNA from preneoplastic MH outgrowths compared to mRNAcsn levels in normal mammary glands*

Tissue	Host mice	mRNAcsn,[a] %	Normal gland mRNAcsn levels, % of	
			Lactating mice[b]	In vitro[c]
MH-1	Virgin	NM	—	—
	Lactating	0.0044	0.18	23.1
MH-5	Virgin	NM	—	—
	Lactating	0.0014	0.056	7.3
MH-9	Virgin	0.022	0.88	115.7
	Lactating	0.017	0.68	89.5
HAN-D8	Virgin	NM	—	—
	Lactating	0.006	0.24	31.5

[a] Concentrations of the mRNAcsn were derived from the $R_0t_{1/2}$ values shown in text-figs. 7 and 8. NM=not measurable.

[b] Normal lactating mammary glands are the second thoracic mammary glands of MH- or HAN-D8-carrying lactating hosts. For mRNAcsn levels in these glands, *see* table 2.

[c] Normal mammary glands in vitro were the second thoracic mammary glands incubated in hormone medium as described in footnote *c*, table 2.

mRNAcsn in these glands was 0.019% of the total RNA (table 2).

On the basis of the above results, mRNAcsn concentrations in MH and HAN tissues were analyzed relative to that in the normal mammary glands of the lactating mice and the mammary gland in vitro (table 3). Although MH-1 and MH-5 tissues accumulate mRNAcsn in the lactating hosts, a quantitative analysis of the data (table 3) revealed that concentration of the mRNA in the MH tissues was only 0.056–0.88% of the hosts' own lactating glands. In MH-1 tissue mRNAcsn concentration in virgin hosts was not measurable, and in the lactating animal the level was 0.18% of that in the normal mammary glands of the respective hosts. The concentrations of mRNAcsn in MH-9 carried in virgin and lactating hosts were 0.88 and 0.68% of that present in the normal glands of the lactating hosts. Compared to that of the normal lactating mammary gland, the level of mRNAcsn in the HAN-D8 tissue was also very low (table 3).

The levels of mRNAcsn in MH-1, MH-5, and HAN-D8 tissues were also lower than the mRNAcsn levels found in the mammary glands after 6 days of incubation in insulin, prolactin, aldosterone, and cortisol. However, the mRNAcsn level in MH-9 tissue in virgin as well as in lactating hosts was as high as that in mammary glands in vitro (table 3).

DISCUSSION

In the present study growth potential of the MH outgrowths was measured during their spatial proliferation filling the gland-free mammary fat pads in a chemically defined medium. The ability of the preneoplastic MH outgrowths to faithfully mimic the characteristic morphogenesis in the culture medium provides a unique in vitro model for measurement of their proliferative potential in a controlled environment.

In a medium containing the hormones insulin, prolactin, aldosterone, and cortisol, the MH outgrowths showed a single wave of DNA synthesis rising to a peak on the 4th day and then declining to their respective near-basal level on the 6th day. A similar single wave of DNA synthesis was also found to be associated with a preneoplastic HAN (D1) outgrowth line during its proliferation in the gland-free mammary fat pad in vitro under similar culture conditions (*22*). Thus the kinetics of DNA synthesis in the MH and HAN outgrowths appear to exhibit a similar pattern during morphogenesis in vitro, even though the etiology and the mode of origin of the two populations of transformed cells are different. In contrast, in the normal mammary gland DNA synthesis rises in two waves during 6 days of lobulo-alveolar morphogenesis in vitro in a medium containing the same hormone mixture (*5*). This suggests an alteration of the kinetic pattern of DNA synthesis in the MH and HAN outgrowths during their lobulo-alveolar morphogenesis in vitro. The increase in DNA synthesis in the MH tissues was accompanied by a rise in epithelial cell number, lobulo-alveolar morphogenesis, and spatial growth filling the fat pad in vitro. This finding suggests that although the kinetics of DNA synthesis in the MH outgrowths has been altered, the MH outgrowth tissues maintain the sequential processes normally associated with lobulo-alveolar morphogenesis of the parenchyma within the constraints of the mammary fat pad. Although the overall growth pattern of the four MH outgrowths examined was essentially similar, each outgrowth line maintained its own characteristic rate of growth increase during the 6-day culture period. The variable growth rate of the different MH outgrowths, however, failed to show any correlation with the tumorigenic potential of the different outgrowth lines.

In MH-5 outgrowth the ductal component of the tissue was maintained during its proliferation filling the fat pad, even though the medium contained insulin, prolactin, aldosterone, and cortisol—a hormone mixture known to stimulate lobulo-alveolar differentiation of the ductal parenchyma of the normal gland in vitro (*5*). This finding suggests that the ductal epithelium in the MH-5 outgrowth line is also in a state of transformation at least with respect to its hormone sensitivity.

Endogenous hormonal milieu in virgin mice is not likely to provide the endocrine environment conducive for lobulo-alveolar morphogenesis of the mammary parenchyma, yet the MH outgrowths fill the gland-free mammary fat pads with lobulo-alveolar structures in virgin hosts. This characteristic suggests an escape of the epithelial cells in the MH outgrowths from the normal endocrine regulation on lobulo-alveolar differentiation. A similar escape from normal hormone regulation is also associated with the HAN tissues (*19*). Thus the MH outgrowths are analogous to HAN with respect to the requirement of the growth-promoting hormones in vivo. With regard to hormone sensitivity of the MH outgrowth in vitro, the medium containing prolactin and insulin is capable of promoting maximal development of lobulo-alveolar structures in MH outgrowth tissues filling the fat pad. Addition of the steroid hormones, aldosterone plus cortisol or estrogen plus progesterone, to the medium generally failed to produce any additive effect on the growth of the MH tissues in the presence of prolactin and insulin in the medium; MH-5 outgrowth showed some responses to the steroid hormones. In contrast, presence of the adrenal and/or the ovarian steroid hormones is essential for stimulation of lobulo-alveolar morphogenesis in the normal glands in vitro (*5, 31*). Thus the ability of MH outgrowths to fill the fat pads with lobulo-alveolar outgrowths in the presence of insulin and prolactin strongly indicates an altered sensitivity of the MH tissues to the mammary growth regulatory steroid hormones. This escape of the MH outgrowths from the growth regulatory actions of the adrenal and the ovarian steroid hormones also corresponds to similar altered sensitivity of the HAN tissues to the steroid hormones. HAN outgrowths have been reported to be maintained in adrenoovariectomized hosts treated with prolactin (*32*). Thus the potentially tumorigenic MH tissues from mammary cells transformed in vitro exhibit an altered hormone requirement for their growth potential essentially similar to that of HAN, induced by the mammary tumor virus or carcinogenic chemical (*19*).

Expression of functional differentiation as measured by accumulation of mRNAcsn in MH-1, MH-5, and HAN-D8 outgrowth lines showed an expected pattern of endocrine response. Accumulation of mRNAcsn in these tissues remained suppressed in the endocrine environment of the virgin hosts, and in the lactating hosts mRNAcsn was measurable in the same outgrowth lines, which suggests that the epithelial cells in these MH outgrowths have retained their sensitivity to the lactogenic hormones. Expression of the casein gene in MH-9 outgrowth, however, was measurable, presumably in the absence of the lactogenic hormone stimulation in the virgin hosts. This measurable expression indicates that the casein gene(s) in MH-9 outgrowth has escaped from the modulatory action of the lactogenic hormones prolactin and glucocorticoid. This abnormality was possibly acquired by the mammary cells during the transformation process, initiated apparently, in consequence to interactions between the electrophilic reactants of DMBA and the mammary cell DNA (*7, 8*). Expression of the casein gene in the mammary gland in vitro is dependent on hormone induction (*30*). The mechanisms associated with expression of the casein gene in MH-9 outgrowth in the inadequate endocrine environment of the virgin hosts are intriguing, and future studies are likely to provide some interesting information. Accumulation of mRNAcsn in MH-9 outgrowth, exposed to the lactogenic hormone environment of the nursing mother, may be considered an usual response of the tissue, except that the concentration of the mRNA sequences remains essentially similar to that observed in the same tissue in the virgin host. This then raises the possibility that the cells accumulating the mRNAcsn in virgin and lactating hosts represent the same population.

Another point of interest about the characteristic of casein gene expression observed in the MH outgrowths and HAN-D8 lines concerns concentration of the mRNAcsn accumulated in these tissues. Although mRNAcsn was measurable in these preneoplastic tissues when exposed to the lactogenic endocrine environment of the post-partum animals, concentrations of the mRNAcsn sequences in the different preneoplastic tissues represent only 0.056–0.88% of that observed in the normal lactating mammary glands of the host animals. This reduced level of casein gene expression in the MH and HAN outgrowths may not reflect hormone responses of a micropopulation of normal mammary cells present in the preneoplastic tissue, because normal mammary cells have a finite life expectancy of 9–11 serial transplant generations (*33*). MH outgrowths have been carried in our laboratory through 20–25 transplant generations, and likewise HAN-D8 has been maintained since 1969. Thus the reason for the reduced level of expression of the casein gene in the MH and HAN tissues remains unclear at this time. However, the reduced level of mRNAcsn accumulation in the MH outgrowths may reflect expression of the casein gene in micropopulation of transformed cells which have retained their ability to respond to the modulatory action of the lactogenic hormones. Partial inactivation and/or loss of the specific hormone receptors may also cause a reduced sensitivity of the cells to the lactogenic hormones. A loss of certain steroid hormone receptors in some HAN lines has been reported (*34*). Studies in our laboratory have also shown a depletion of glucocorticoid receptor in the MH outgrowths (Majumder P, Banerjee MR: Unpublished observation).

Mammary tumors obtained from the MH and HAN-D8 outgrowths in general failed to show a detectable level of mRNAcsn, regardless of the endocrine status of the host. This finding indicates a virtual absence of casein gene expression in the neoplastic mammary tissue of the mouse. Thus it appears that during the multistep transformation process the mammary cells progressively lose their ability to respond to the hormones regulating expression of functional differentiation. A similar trend of reduced functional activity also has been reported to be associated with liver carcinogenesis in rats. In normal liver albumin mRNA constitutes 10% of the total poly(A) RNA, but its concentration is reduced significantly in Morris hepatomas (*35*).

Rat mammary tumor cell line R3230AC as well as DMBA-induced rat mammary tumors are mostly nonresponsive to prolactin and/or estrogen stimulation of mRNAcsn accumulation (*36, 37*). Consistent with the present results, several hormone- or DMBA-induced HAN lines of BALB/c mice have been reported to be only moderately responsive to exogenous hormone stimulation (prolactin and dexamethasone), and mammary tumors derived from these preneoplastic tissues in general are nonresponsive (*38*).

In conclusion, results of the present studies provide further evidence that altered responses of the MH outgrowths to the hormones that regulate growth and functional differentiation of the mammary cells are similar to those of the HAN tissues found in mouse mammary glands. Thus the preneoplastic MH outgrowths derived from mouse mammary cells transformed in organ culture are analogous to the HAN tissues derived from transformed cells in mouse mammary gland in vivo.

REFERENCES

(*1*) Banerjee MR. Responses of mammary cells to hormones. Int Rev Cytol 1976; 46:1-97.

(*2*) Ichinose RR, Nandi S. Influence of hormones on lobuloalveolar differentiation of mouse mammary gland in vitro. J Endocrinol 1966; 35:331-340.

(*3*) Wood BG, Washburn LL, Mukherjee AS, Banerjee MR. Hormonal regulation of lobuloalveolar growth, functional differentiation and regression of whole mammary gland in organ culture. J Endocrinol 1975; 65:1-6.

(*4*) Banerjee MR, Wood BG, Washburn LL. *Brief communication:* Chemical carcinogen-induced alveolar nodules in organ culture of mouse mammary gland. J Natl Cancer Inst 1974; 53:1387-1393.

(*5*) Lin FK, Banerjee MR, Crump LR. Cell Cycle-related hormone carcinogen interaction during chemical carcinogen induction of nodule-like mammary lesions in organ culture. Cancer Res 1976; 36:1607-1614.

(*6*) Kundu AB, Telang NT, Banerjee MR. The binding of 7,12-dimethylbenz[*a*]anthracene to BALB/c mouse mammary cell DNA in organ culture. JNCI 1978; 61:465-469.

(*7*) Miller EC, Miller JA. Mechanism of chemical carcinogenesis, nature of proximate carcinogens and interactions with macromolecules. Pharmacol Rev 1966; 18:805-838.

(*8*) Heidelberger C. Chemical carcinogenesis. Ann Rev Biochem 1975; 44:79-121.

(*9*) Tonelli QJ, Custer RP, Sorof S. Transformation of cultured mouse mammary glands by aromatic amines and amides and their derivatives. Cancer Res 1979; 39:1784-1792.

(*10*) Dickens MS, Sorof S. Retinoid prevents transformation of cultured mammary glands but not by nonactivated procarcinogens. Nature 1980; 285:581-584.

(*11*) Dickens MS, Custer RP, Sorof S. Retinoid prevents mammary gland transformation by carcinogenic hydrocarbon in whole organ culture. Proc Natl Acad Sci USA 1979; 76:5891-5895.

(*12*) Moon RC, Grubbs CJ, Sporn MB. Inhibition of 7,12-dimethylbenz[a] anthracene-induced mammary carcinogenesis by retinyl acetate. Cancer Res 1977; 36:2626-2630.

(*13*) Sporn MB, Newton DL. Chemoprevention of cancers with retinoids. Fed Proc 1979; 38:2528-2534.

(*14*) Telang NT, Banerjee MR, Iyer AP, Kundu AB. Neoplastic transformation of epithelial cells in whole mammary gland in vitro. Proc Natl Acad Sci USA 1979; 76:5886-5890.

(*15*) Iyer AP, Banerjee MR. Sequential expression of preneoplastic and neoplastic characteristics of mouse mammary epithelial cells transformed in organ culture. JNCI 1981; 66:893-905.

(*16*) DeOme KB. The mammary tumor system in mice. A brief review. In: Burdette J, ed. Viruses inducing cancer. Salt Lake City: Univ of Utah Press. 1966:127-137.

(*17*) Blair PB, DeOme KB, Nandi S. The preneoplastic state in mouse mammary carcinogenesis. In: Brennan M, ed. Biological interactions in normal and neoplastic cells: Boston: Little, Brown & Co. 1962;371-389.

(*18*) Medina D. Preneoplastic lesions in murine mammary cancer. Methods Cancer Res 1973; 7:3-53.

(*19*) ———. Preneoplasia in breast cancer. In: Mcguire WL, ed. Breast cancer. New York: Plenum. 1978:2:47-102.

(*20*) DeOme KB, Faulkin LT Jr, Bern HA, Blair PB. Development of mammary tumors from hyperplastic alveolar nodule transplanted into gland-free mammary fat pad of female C3H mice. Cancer Res 1959; 19:515-520.

(*21*) Adamson RD, Banerjee MR, Medina D. Susceptibility of mammary-tumor-virus-free BALB/c mouse mammary nodule outgrowth cells in DNA synthesis to 3-methylcholanthrene tumorigenesis. J Natl Cancer Inst 1971; 46:899-907.

(*22*) Mehta RG, Washburn LL, Young PN, Banerjee MR, Bern HA. *Brief communication:* Proliferation of preneoplastic mammary nodule outgrowth in mammary fat pads of BALB/c mice in organ culture. J Natl Cancer Inst 1974; 52:1013-1017.

(*23*) Banerjee MR, Wood BH, Lin FK, Crump LR. Organ culture of the whole mammary gland of the mouse. In: Sanford KK, ed. Tissue culture association manual. Vol 2. Gaithersburg, Md.: Tissue Culture Association, Inc., 1976:457-462.

(*24*) Palmiter RD. Magnesium precipitation of ribonucleoprotein complexes. Expedient technique for isolation of undegraded polysomes and messenger ribonucleicacid. Biochemistry 1974; 13:3606-3615.

(*25*) Ganguly R, Mehta NM, Ganguly N, Banerjee MR. Glucocorticoid modulation of casein gene transcription in mouse mammary gland. Proc Natl Acad Sci USA 1979; 76:6466-6470.

(*26*) Banerjee MR, Ganguly N, Mehta NM, Iyer AP, Ganguly R. Functional differentiation and neoplastic transformation in an isolated whole mammary organ in vitro. In: McGrath C, Brennan M, Rich M, eds. Cell biology of breast cancer. New York: Academic Press. 1980:485-516.

(*27*) Mehta NM, Ganguly N, Ganguly R, Banerjee MR. Hormonal modulation of the casein gene expression in a mammogenesis-lactogenesis two-step culture model of whole mammary gland of the mouse. J Biol Chem 1980; 255:4430-4434.

(*28*) Burton K. A study of the conditions and mechanisms of the diphenylamine reaction for the corometric estimation of deoxyribonucleic acid. Biochem J 1956; 62:315-326.

(*29*) Pauley RJ, Rosen JM, Socher SH. Mammary tumor virus and casein gene transcription during mammary development. Nature 1978; 275:455-457.

(*30*) Ganguly N, Ganguly R, Mehta NM, Crump LR, Banerjee MR. Simultaneous occurrence of pregnancy-like lobuloalveolar morphogenesis and casein gene expression in a culture of the whole mammary gland. In Vitro 1981; 17:55-60.

(*31*) Mehta RG, Banerjee MR. Action of growth promoting hormones on macromolecular biosynthesis during lobuloalveolar development of the entire mammary gland in organ culture. Acta Endocrinol 1975; 80:501-516.

(*32*) Yanai R, Nagasawa H. Enhancement by pituitary isograft of mammary hyperplastic nodules in adreno-ovariectomized mice. J Natl Cancer Inst 1971; 46:1251-1255.

(*33*) Daniel CW, DeOme KB, Young LJ, Blair PB, Faulkin LF Jr. The in vivo life span of normal and preneoplastic mouse mammary glands: A serial transplantation study. Proc Natl Acad Sci USA 1968; 61:53-60.

(*34*) Medina D, Iramian CA, Clark JH. Hormone dependence and estrogen receptor in the D-series of mammary nodule outgrowth lines and tumors. Cancer Res 1975; 35:2355-2360.

(*35*) Tse TP, Morris HP, Taylor JM. Molecular basis of reduced albumin synthesis in Morris hepatoma 7777. Biochemistry 1978; 17:3121-3128.

(*36*) Nadacci NJ, McGuire WL. Casein and α-lactalbumin mRNA in experimental breast cancer. Cancer Res 1977; 37:1186-1190.

(*37*) Rosen JM, Socher SH. Detection of casein messenger RNA in hormone dependent mammary cancer by molecular hybridisation. Nature 1977; 269:83-86.

(*38*) Pauley RJ, Socher SH. Hormonal influence on the expression of casein messenger RNA during mouse mammary tumorigenesis. Cancer Res 1980; 40:362-367.

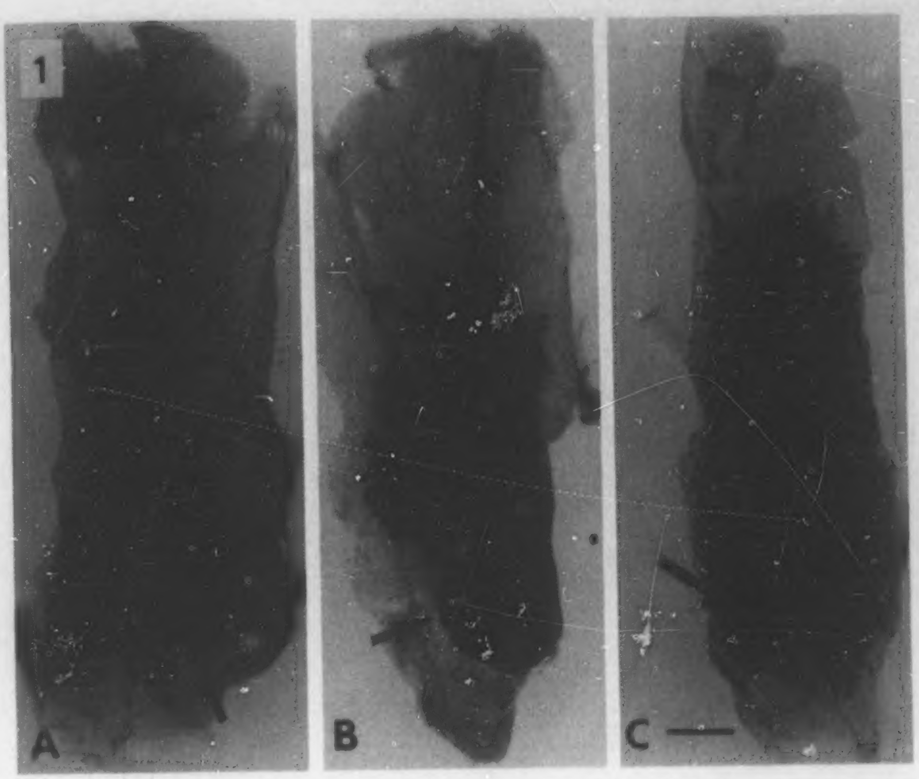

FIGURE 1.—Spatial growth of the lobulo-alveolar MH-9 tissue filling the gland-free mammary fat pad at different times during incubation in vitro. A) at zero time; B) at 4 days; C) at 6 days. *Arrows* point to lymph nodes. *Bar*=1 mm. × 10

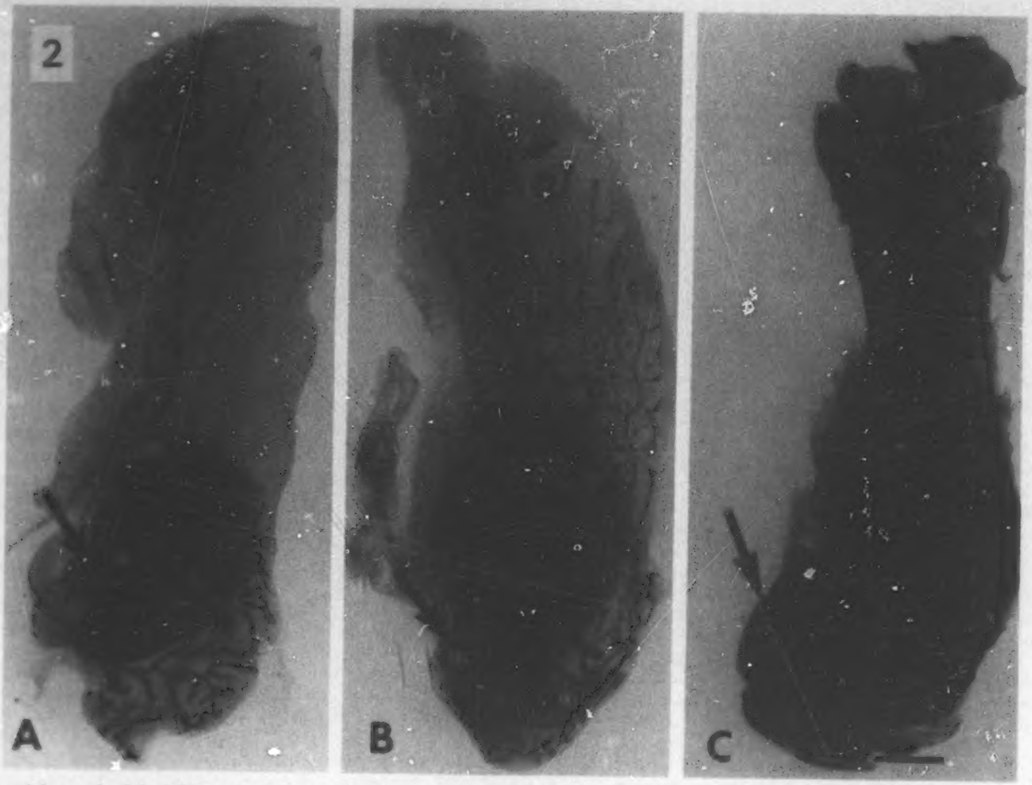

FIGURE 2.—Spatial growth of the MH-5 mixed (ductal-lobulo-alveolar) outgrowth tissue filling the gland-free fat pad at different times during incubation in vitro. A) at zero time; B) at 4 days; C) at 6 days. *Arrows* point to lymph nodes. *Bar*=1 mm. × 10

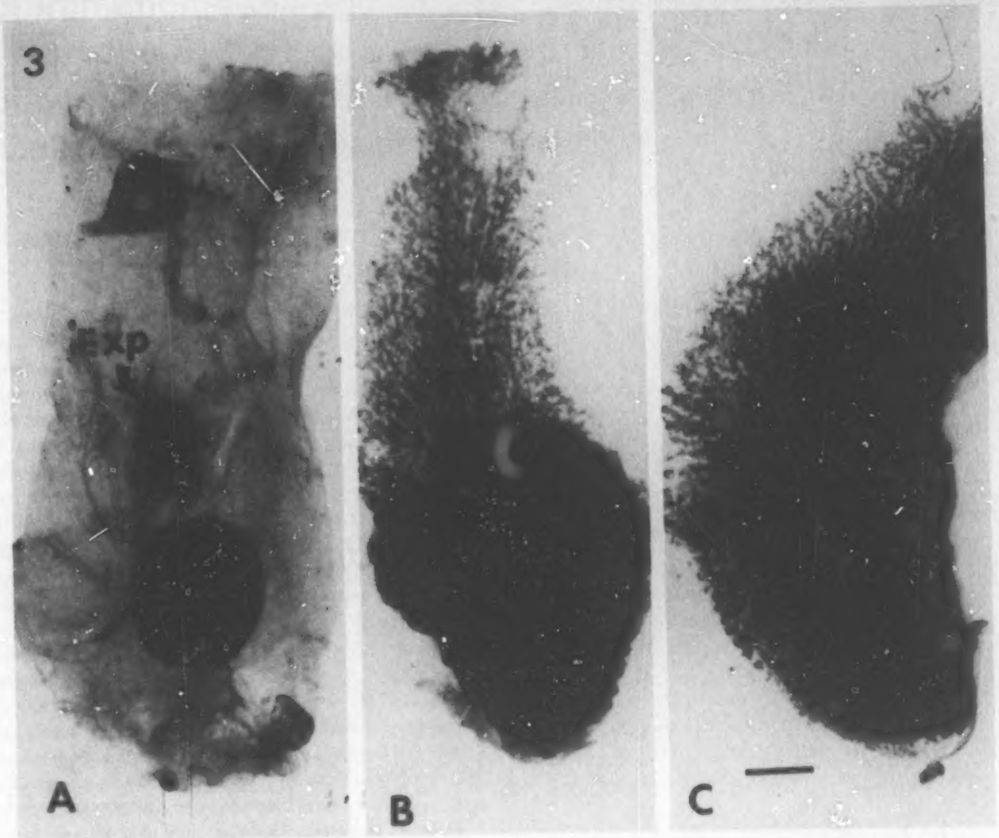

FIGURE 3.—Spatial proliferation of the lobulo-alveolar MH filling the gland-free mammary fat pad at different times in vivo. A) at zero time; B) at 6 wk; C) at 10 wk. *Arrows* point to lymph nodes. Exp=explant. *Bar*=1 mm. × 10

blank page

Effect of Immunomodulation on the Fate of Tumor Cells in the Central Nervous System and Systemic Organs of Mice. Distribution of [^{125}I]5-Iodo-2′-deoxyuridine-Labeled KHT Tumor Cells After Left Intracardial Injection[1,2]

Frances K. Conley[3,4,5]

ABSTRACT—The effect of systemic immunomodulation on tumor cell arrest and retention in the central nervous system was studied by following radioactively labeled tumor cells. KHT mouse sarcoma tumor cells were labeled in vitro with [^{125}I]IdUrd, and 1×10^5 tumor cells were injected into the left side of the hearts of syngeneic C3H mice. Experimental groups consisted of untreated normal mice, mice pretreated iv with *Corynebacterium parvum*, and mice chronically infected with *Toxoplasma gondii*; in this model both groups of immunomodulated mice are protected from developing systemic metastatic tumor, but only *Toxoplasma*-infected mice have protection against metastatic brain tumor. At time intervals from 1 to 96 hours, groups of mice from each experimental group were killed, and the brain and other organs were monitored for radioactivity to determine the number of viable tumor cells that had been present at the time of death. Normal mice demonstrated significant retention of tumor cells in the brain and kidneys plus adrenals at 96 hours. By contrast, in both groups of immunomodulated mice tumor cells were rapidly eliminated from systemic organs, but tumor cells were significantly retained in the central nervous system even at 96 hours after tumor cell injections. The results indicated that generalized immunomodulation had more effect in elimination of tumor cells from systemic organs than from the brain and that the elimination of tumor cells from the brain in *Toxoplasma*-infected mice was a delayed phenomenon.—JNCI 1982; 69:465–473.

The ultimate control of cancer will depend on the development of therapeutic mechanisms that will successfully stop the metastatic spread of cancer cells. In attempts to define the biologic behavior of the arrest and trapping of tumor cells that have been released into the circulation, many investigators have followed the fate of radioactively labeled, iv injected tumor cells. [^{125}I]IdUrd has become the radioactive label of choice for these studies because it is incorporated into the DNA of viable, proliferating cells and is rapidly eliminated upon cell death with negligible reutilization (*1–3*). Following iv injection of cells, the lung is the initial recipient organ of the tumor cell bolus and thus is the organ studied most extensively. Several immunologic and mechanical factors, such as immune status of the host (*4–6*), immunogenicity and viability of the tumor cells injected (*7–10*), deformability of tumor cells (*11–13*), anticoagulation status of the host (*7*), or thromboplastic activity of the tumor (*14*), can influence the arrest and retention pattern of tumor cells in the lung. Tumor cell traffic to other organs following passage through the pulmonary vasculature has also been explored (*15, 16*).

Because in human oncology the brain is a frequent site of symptomatic metastatic disease, we have been interested in defining arrest and retention patterns of tumor cells in the CNS. In humans most tumor emboli reach the brain from an arterial source (*17*), and we have developed a metastatic brain tumor model in mice in which the tumor cells are injected into the left side of the heart and thus are initially distributed to the brain by arteries (*18*). Tumor also develops in the kidneys, adrenals, and ovaries. Using this model in prior work, we explored the ability of two agents that cause systemic immunomodulation to affect the ultimate development of metastatic brain tumor, and we were able to document that the treatment with *Corynebacterium parvum* eliminated systemic tumor but had no effect whatever on brain tumor metastasis, whereas chronic infection with *Toxoplasma gondii* was able to eliminate both systemic and CNS tumor (*19*). In the present study we have followed the fate of [^{125}I]IdUrd-labeled tumor cells following ic injections in normal mice, *C. parvum*-treated mice, and *Toxoplasma*-infected mice to define the effect of immunomodulation on the arrest and retention pattern of tumor cells in the brain and to compare this pattern of tumor cell traffic in the CNS with that in systemic organs.

MATERIALS AND METHODS

Mice.—C3H/HeN/MTV-negative syngeneic female mice were obtained from Simonsen Laboratories, Gilroy, Calif., and were 2–4 months old at the beginning of the experiments. For each experiment all mice were age matched. Starting 3–4 days before injection of labeled tumor cells, the drinking water was supplemented with 0.1% sodium iodide

---

ABBREVIATIONS USED: CNS=central nervous system; FAA=formaldehyde-ethyl alcohol-glacial acetic acid; H & E=hematoxylin and eosin; ic=intracardial(ly); [^{125}I]IdUrd=[^{125}I]5-iodo-2′-deoxyuridine; NK=natural killer.

---

[1] Received September 3, 1981; revised January 6, 1982; accepted March 17, 1982.

[2] Supported by the Veteran's Administration.

[3] Division of Neurosurgery, Department of Surgery, Stanford University School of Medicine, Stanford University Medical Center, Stanford, Calif. 94305; and Neurosurgery Section, Veterans Administration Medical Center, Palo Alto, Calif. 94304.

[4] *Address reprint requests to* Dr. Conley *at* Division of Neurosurgery, Department of Surgery, Stanford University School of Medicine, Stanford University Medical Center, 300 Pasteur Dr., Stanford Calif. 94305.

[5] I acknowledge Ms. Kay Ann Jenkins and Mrs. Bonnie Bell for superb technical help, Mrs. Ruth Uhrhammer for typing the manuscript, and Dr. Jon Kosek and the Medical Media Service of the Veterans Administration Medical Center, Palo Alto, for the photomicrographs and graphs.

for prevention of radioactive iodine accumulation by the thyroid gland.

Infection with T. gondii.—To establish a chronic infection with *Toxoplasma,* we gave mice inoculations ip of 1×10^5 of the C56 strain of *T. gondii* in the tachyzoite state and treated them with sulfadiazine for 3 weeks as previously described (*20*). Mice received tumor cell injections 3–8 weeks after termination of sulfadiazine therapy.

Treatment with C. parvum.—A suspension of killed *C. parvum* (lot #CA771/B; 7 mg/ml dry wt) was obtained from Burroughs-Wellcome Ltd., Beckenham, England. *C. parvum* was administered iv 3 days before tumor cell inoculations at a concentration of 700 μg/mouse in a total volume of 0.2 ml of normal saline. Prior work from our laboratory had determined that this dose and schedule of *C. parvum* administration protected mice from developing systemic metastatic tumor but that it did not provide protection against metastatic tumor to the brain (*19*).

Tumor.—Cell lines of the KHT mouse sarcoma, a tumor that arose spontaneously in a C3H mouse, were grown in Eagle's minimum essential medium (Grand Island Biological Co., Grand Island, N.Y.) and supplemented with 15% fetal calf serum, l-glutamine, sodium bicarbonate, and kanamycin (1 g/100 ml). Cell cultures were incubated at 37°C in a humidified atmosphere containing 5% CO_2. All studies were done with cell populations in the exponential growth phase.

Preparation of cells for study of cell arrest and dissemination in vivo.—KHT cells were labeled with [^{125}I]IdUrd (Amersham Corp., Arlington Heights, Ill.) at a labeling dose of either 0.05 or 0.02 μCi/ml of medium for 48 hours. After incubation the cells were harvested and washed three times for removal of nonbound isotope. Cells were resuspended in Hanks' balanced salt solution with kanamycin (1 g/100 ml), checked for viability by exclusion of trypan blue (90–95% viable), and diluted to yield an inoculum dose of 1×10^5 viable cells per 0.2 ml of cell suspension. To determine the percentage of cell labeling, we made cytocentrifuge preparations from a 1:10 dilution of the inoculum dose and autoradiographed them. Representative inoculum doses were monitored in a well-type scintillation counter (Searle gamma counter, model #1185; G. D. Searle & Co., Des Plaines, Ill. 60018). Triplicate samples were collected both before and after animal injections, and these aliquots of 1×10^5 cells yielded similar counts in each individual experiment.

Inoculation and evaluation of labeled tumor cells.—Mice received 0.2 ml of labeled tumor cells by iv injection into a lateral tail vein (normal mice only) or by direct left ic injection (normal and *Toxoplasma*-infected and *C. parvum*-treated mice.) At time periods from 1 to 96 hours after injection, 5 mice from each experimental group were rapidly exsanguinated; blood, brain, lungs, spleen, and kidneys plus adrenals (in all experiments both kidneys and both adrenals from each mouse were removed and counted together) were collected from each animal. In some experiments the liver was also included. Solid organs were placed in individual vials containing FAA fixative (10 ml of 37–40% formaldehyde, 90 ml of 80% ethyl alcohol, 5 ml of glacial acetic acid). The fixative was changed every 24 hours for 3 days for removal of the acid-soluble fraction of ^{125}I (*21, 22*) released from the DNA of dead tumor cells (*23*). We had previously determined that the FAA fixative was as effective as 70% ethyl alcohol in eluting the acid-soluble fraction and that it was much superior to 70% ethyl alcohol for tissue preservation for subsequent histologic examination and autoradiography. Blood and solid organs were monitored in a well-type scintillation counter, and the number of viable tumor cells present in each organ was determined from the radioactivity counts. The number of tumor cells in each organ was expressed as a percentage of the total injected dose. Experiments in which tumor cells were injected ic were repeated six times, but not all time intervals were sampled in every experiment. Because the organ counts changed in the same direction at the same time intervals in all experiments, the results were pooled. Statistical evaluations for significance were done by Student's *t*-test.

Evaluation of distribution and arrest of heat-killed tumor cells.—Labeled tumor cells were killed by being heated to 70°C for 10 minutes, and 1×10^5 cells in 0.2 ml media plus antibiotic were injected ic into normal mice. For each time period (1, 2, 4, 24, and 48 hr) 5 mice were rapidly exsanguinated, and blood and organs were collected and processed as above.

Preparation of material for histologic examination.—After counting the total radioactivity of each individual organ, we processed the organs for light microscopy. We cut representative paraffin-embedded tissue sections at 5 μm, autoradiographed them using NTB 2 emulsion (Eastman Kodak Co., Rochester, N.Y.) at an exposure time of 3 weeks, and stained them with H & E.

RESULTS

Cell Labeling and Evaluation of Metastatic Potential

In preliminary experiments we used three concentrations of [^{125}I]IdUrd for labeling tumor cells in vitro. Almost 100% of KHT cells incubated for 24 hours with 0.5 μCi [^{125}I]-IdUrd/ml medium were heavily labeled. Tumor cells labeled with 0.05 μCi [^{125}I]IdUrd/ml or 0.02 μCi [^{125}I]IdUrd/ml for 24 hours demonstrated 70–75% labeling; if the incubation time was extended to 48 hours at these concentrations, the percentage labeling improved to 90–95% and the amount of label per cell was increased.

We assessed metastatic capability by giving normal mice ic injections of either 1×10^5 labeled tumor cells or 1×10^5 nonlabeled tumor cells and by following the animals to time of death. All mice were autopsied and the gross numbers of parenchymal brain tumor metastases visible on the surface of the brain were counted with a dissecting microscope. [A proportionality exists between the dose of tumor cells injected ic and the number of visible metastatic tumor deposits that can be counted on the surface of the brain at the time of death (Conley FK: Unpublished data).] When a concentration of 0.5 μCi [^{125}I]IdUrd/ml was used as a labeling dose, mice receiving injections of labeled cells died an average of 4 days later than did mice receiving the same dose of unlabeled tumor cells and had fewer tumor nodules in the brain, indicating that this concentration of radioactive label was toxic to the tumor cells. Mice receiving KHT cells labeled with [^{125}I]IdUrd at concentrations of 0.05 or 0.02

μCi/ml and an incubation time of 48 hours died at the same time as did mice receiving nonlabeled cells; the average and median counts of brain tumor metastases were identical between the 2 groups. At the lowest concentration of [^{125}I]-IdUrd, 0.02 μCi/ml, the counts per cell ranged from 0.16 to 0.36 in individual experiments, providing sufficient radioactivity to follow cells adequately after injection; this labeling concentration was used in all subsequent experiments.

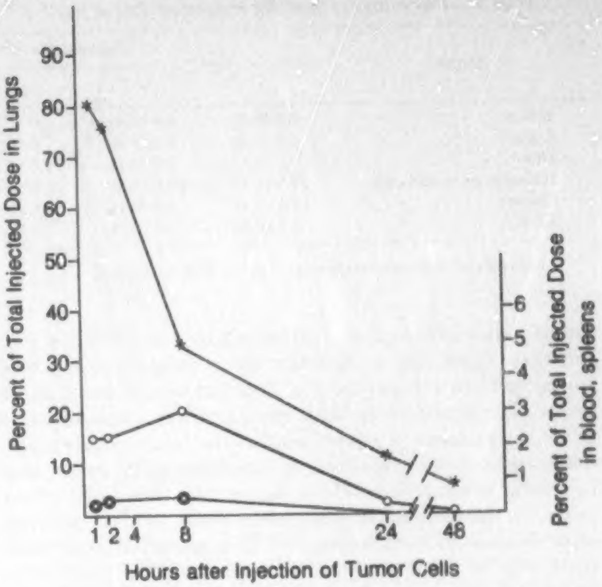

TEXT-FIGURE 1.—Percent of [^{125}I]IdUrd-labeled KHT tumor cells in lungs, blood, and spleen after iv injection of 1×10^{5} tumor cells. lungs, *; blood, ○; spleen, *white star within black circle.*

Fate and Distribution of KHT Tumor Cells Following Injection in Normal Mice

Following iv injection of KHT sarcoma, the lung is the only organ to consistently develop tumor nodules, and at the dose of 1×10^{5} cells the tumor in the lungs is confluent at the time of death. The organ distribution of labeled KHT cells from a single experiment in normal mice is shown in table 1 and text-figure 1. At 1 hour 81% of the total injected dose was in the lungs. By 8 hours this figure had dropped to 33%; at 48 hours 6.3% of the original inoculum of tumor cells still resided in the lungs. Very small numbers of tumor cells were detectable in the spleens and kidneys plus adrenals for the first 8 hours, and none were detectable by 24 hours after tumor cell injections. Tumor cells were not detectable in the brain at any time interval. From 1 to 8 hours after injections, radioactivity counts in the blood rose from 2.3 to 3.1%, but radioactivity was absent from the blood at 48 hours.

Dissemination and Arrest of Labeled Tumor Cells Following Left ic Injection in Normal Mice

A marked discrepancy of radioactivity counts between lungs and brain in individual animals made it easy for us to determine when the tumor cell bolus had not been injected into the left side of the heart. Any animal that had received a "missed injection" was eliminated from all tabulation of results. Table 2 and text-figures 2–5 give composite results from multiple experiments of the distribution of labeled tumor cells in various organs at time intervals following left ic injection. Unlike the distribution of tumor cells following iv injection, appreciable numbers of arterially disseminated cells reached the brain and kidneys plus adrenals, and in normal mice a constant number of tumor cells tended to remain in these organs over the first 8 hours. By 96 hours 1% of the total injected dose was still detectable in the brain, and 2% of the total injected dose was still present in the kidneys plus adrenals. Radioactivity counts in the blood and spleen were stable over the first 8 hours, but both fell to 0.1% by 48 hours post injection. The number of tumor cells arresting in the lungs increased over the first 4 hours, then gradually declined so that by 96 hours only 0.2% of the total injected dose remained. At no time interval did greater numbers of tumor cells exist in the lungs than in the brain.

Dissemination and Arrest of Labeled Tumor Cells Following Left ic Injection in Immunomodulated Mice

The dissemination of labeled tumor cells in various organs in *Toxoplasma*-infected mice and *C. parvum*-treated mice are presented in tables 3 and 4 and text-figures 2–5, all of which represent composite data from multiple experiments. When compared to normal mice, both groups of immunomodulated mice demonstrated a different pattern of arrest of tumor cells between systemic organs and the brain. In *C. parvum*-treated mice 10% of the total injected dose of tumor cells was present in the brain at 1 hour. This percentage dropped over the next hour to 6.5% but then remained relatively constant for the first 8 hours after ic injection. Similarly, in the *Toxoplasma*-infected mice, there was a drop in the num-

TABLE 1.—*Percentage of total iv injected dose of 1×10^{5} [^{125}I]IdUrd-labeled KHT tumor cells remaining in organs of normal mice*[a]

Organ	Percentage of dose (SE) remaining after tumor cell injections at hr:				
	1	2	8	24	48
Brain	—	—	—	—	—
Lungs	80.8 (7.5)	76.8 (5.7)	32.8 (2.8)	10.6 (2.6)	6.3 (0.7)
Blood	2.3 (0.2)	2.3 (0.2)	3.1 (0.5)	0.3 (0.1)	—
Kidneys plus adrenals	0.1 (0.01)	0.2 (0.03)	0.1 (0.01)	—	—
Spleen	0.3 (0.04)	0.4 (0.02)	0.5 (0.04)	—	—

[a] —=levels of radioactivity undetectable.

TABLE 2.—*Percentage of total left ic injected dose of 1×10⁵ [^{125}I]IdUrd-labeled KHT tumor cells remaining in organs of normal mice*[a]

Organ	Percentage of dose (SE) remaining after tumor cell injections at hr:							
	1	2	4	8	24	48	72	96
Brain	8.2 (0.9)	8.8 (0.6)	8.0 (1.3)	9.1 (0.6)	3.2 (0.3)	1.4 (0.2)	1.4 (0.2)	1.0 (0.2)
Lungs	4.9 (0.9)	5.2 (0.9)	7.0 (1.7)	3.9 (0.6)	1.7 (0.6)	0.4 (0.2)	0.3 (0.2)	0.2 (0.03)
Blood	1.5 (0.1)	1.6 (0.1)	1.6 (0.2)	1.7 (0.2)	0.4 (0.1)	0.1 (0.02)	—	—
Kidneys plus adrenals	10.1 (1.4)	10.6 (1.6)	11.8 (3.4)	9.9 (1.0)	6.4 (0.7)	3.1 (0.7)	3.4 (0.9)	1.9 (0.6)
Spleen	0.5 (0.1)	0.4 (0.1)	0.5 (0.1)	0.6 (0.1)	0.3 (0.1)	0.1 (0.02)	0.1 (0.02)	—
Livers	1.7 (0.6)	1.4 (0.1)	1.0 (0.1)	1.6 (0.2)	ND	ND	ND	ND

[a] —=levels of radioactivity undetectable. ND=not done.

ber of tumor cells in the brain from 1 to 2 hours (8.3–4.1%), but then there was a tendency for a constant number of tumor cells to remain for the first 8 hours. From 8 to 48 hours after injections in both groups of immunomodulated mice, the number of tumor cells in the brain progressively declined but then stabilized, so that even at 96 hours after injections detectable levels of tumor cells remained in the brain. In the systemic organs, by contrast, at time intervals after 1 hour in both groups of immunomodulated mice, there was a rapid progressive decline in the number of tumor cells present in the lungs and kidneys plus adrenals; by 48 hours after tumor cell injections, cells were undetectable in these organs. We noted a small progressive increase in radioactivity counts in the blood over the first 8 hours and then a rapid decline to undetectable levels by 48 hours. When compared to normal mice, immunomodulated mice had increased numbers of tumor cells lodged in the spleens; but no significant peak of splenic uptake of tumor cells was seen in either group at any time period, and by 48 hours the number of tumor cells in the spleen was the same in normal and immunomodulated mice.

Dissemination and Arrest of Labeled Heat-Killed Tumor Cells After ic Injection in Normal Mice

The results of this single experiment are shown in table 5. When dead tumor cells were injected intra-arterially, these cells were eliminated extremely rapidly from systemic organs over the first 2 hours. Not as many dead tumor cells initially lodged in the brain as did live tumor cells, and a progressive gradual decline in cell numbers was seen over the first 4 hours; negligible numbers of tumor cells remained in the brain by 24 hours. The only organ to maintain detectable radioactivity counts at 24 hours was the spleen, but no peak of splenic sequestration was encountered at the time intervals sampled.

Histologic Examination and Autoradiography

Labeled tumor cells were readily visualized in brain, lungs, and kidney plus adrenals. By light microscopy it was often impossible to determine with certainty the intravascular or extravascular location of a given labeled tumor cell.

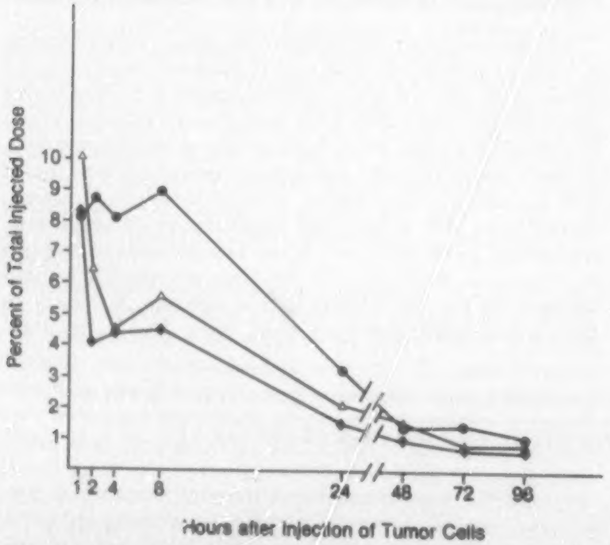

TEXT-FIGURE 2.—Percent of [^{125}I]IdUrd-labeled KHT tumor cells in the brains of normal mice, *Toxoplasma*-infected mice, and *C. parvum*-treated mice following left ic injection of 1×10⁵ tumor cells. Normal, ●; *Toxoplasma* infected, ◆; *C. parvum* treated, △.

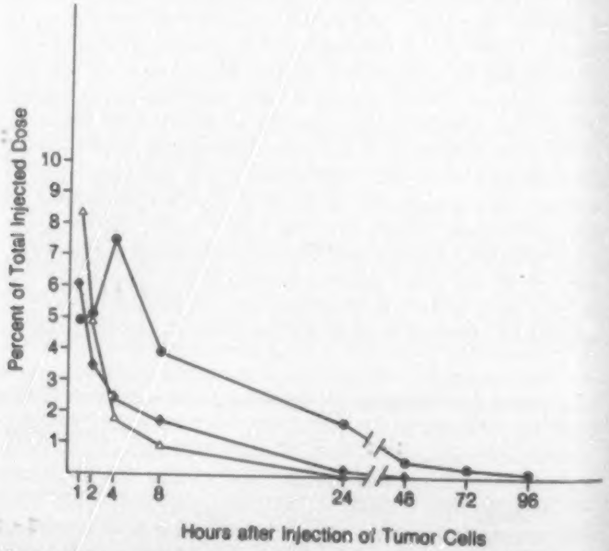

TEXT-FIGURE 3.—Percent of [^{125}I]IdUrd-labeled KHT tumor cells in the lungs of normal mice, *Toxoplasma*-infected mice, and *C. parvum*-treated mice after left ic injection of 1×10⁵ tumor cells. Normal, ●; *Toxoplasma* infected, ◆; *C. parvum* treated, △.

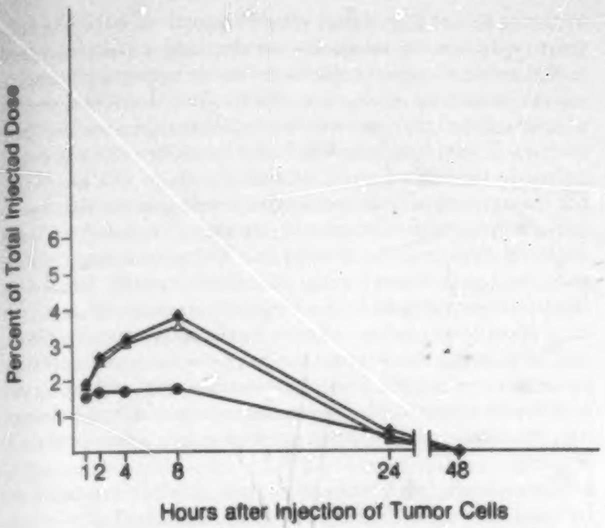

TEXT-FIGURE 4.—Percent of [^{125}I]IdUrd-labeled KHT tumor cells in the blood of normal mice, *Toxoplasma*-infected mice, and *C. parvum*-treated mice after left ic injection of 1×10^5 tumor cells. Normal, ●; *Toxoplasma* infected, ◆; *C. parvum* treated, △.

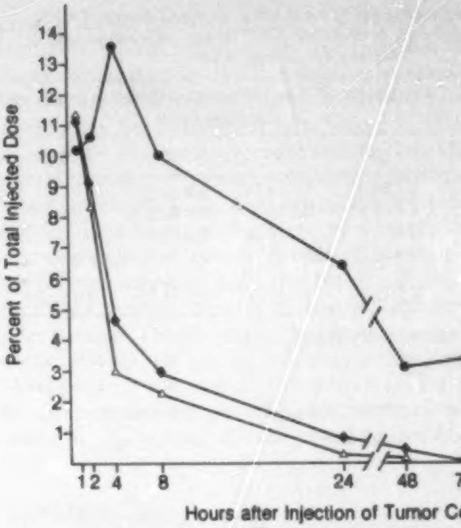

TEXT-FIGURE 5.—Percent of [^{125}I]IdUrd-labeled KHT t kidneys plus adrenals of normal mice, *Toxoplasma*-infe *parvum*-treated mice after left ic injection of 1×10^5 tur ●; *Toxoplasma* infected, ◆; *C. parvum* treated, △.

In the brain, tumor cells were randomly distributed and initially appeared to be trapped in capillaries (fig. 1), but even at 96 hours after tumor cell injections the occasional labeled cell was found still in what appeared to be an intravascular location. Forty-eight hours after injections, however, more labeled tumor cells appeare chymal than intracapillary. Tumor cells in normal or *C. parvum*-treated mice elicited no chymal reaction (fig. 2). By contrast, tum brains of *Toxoplasma*-infected mice very frequ

TABLE 3.—*Percentage of total left ic injected dose of 1×10^5 [^{125}I]IdUrd-labeled KHT tumor cells remaining i organs of* Toxoplasma-*infected mice*[a]

Organ	Percentage of dose (SE) remaining after tumor cell injections at hr:						
	1	2	4	8	24	48	72
Brain	8.3 (1.1)	4.1 (0.6)[b]	4.5 (0.8)[b]	4.6 (0.6)[b]	1.6 (0.4)[b]	1.1 (0.3)	0.8 (0.2)
Lungs	6.1 (1.3)	3.5 (0.6)	2.5 (0.6)[b]	1.7 (0.5)[b]	0.2 (0.1)[b]	0.1 (0.02)[b]	—
Blood	1.9 (0.2)	2.2 (0.2)[b]	3.0 (0.6)	3.7 (0.3)[b]	0.5 (0.2)	0.1 (0.02)	—
Kidneys plus adrenels	11.1 (1.9)	9.1 (2.1)	4.7 (1.0)[b]	3.0 (0.5)[b]	0.8 (0.4)[b]	0.4 (0.1)[b]	0.1 (0.04)[b]
Spleen		1.0 (0.2)[b]	1.2 (0.3)[b]	1.6 (0.2)[b]	1.3 (0.2)[b]	0.4 (0.04)	0.1 (0.01)
Liver	3.1 (0.2)	1.7 (0.4)	1.7 (0.2)	1.8 (0.1)	ND	ND	ND

[a] —=levels of radioactivity undetectable. ND=not done.

[b] *P*-value is ≤0.05 when *Toxoplasma*-infected mice are compared to normal mice; no significant differences were found w infected mice were compared to *C-parvum*-treated mice.

TABLE 4.—*Percentage of total left ic injected dose of 1×10^5 [^{125}I]IdUrd-labeled KHT tumor cells remaining organs of* C. parvum-*treated mice*[a]

Organ	Percentage of dose (SE) remaining after tumor cell injection at hr:						
	1	2	4	8	24	48	72
Brain	10.2 (1.2)	6.5 (1.0)	4.6 (0.7)[b]	5.7 (0.9)[b]	2.1 (0.5)	1.6 (0.2)	0.8 (0.2)
Lungs	8.5 (1.0)[b]	4.9 (1.2)	1.8 (0.4)[b]	0.9 (0.2)[b]	0.1 (0.03)	—	—
Blood	1.9 (0.3)	2.5 (0.7)	3.0 (0.5)[b]	3.5 (0.1)[b]	0.3 (0.1)	0.1 (0.03)	—
Kidneys plus adrenals	11.4 (1.4)	8.8 (1.3)	3.0 (0.7)[b]	2.4 (0.6)[b]	0.3 (0.1)[b]	0.3 (0.1)[b]	—
Spleen	1.5 (0.3)[b]	1.5 (0.3)[b]	1.3 (0.2)[b]	1.3 (0.2)[b]	0.5 (0.1)	0.2 (0.05)	0.3 (0.1)
Livers	4.5 (1.2)	2.8 (0.3)[b]	1.7 (0.3)	1.1 (0.1)	ND	ND	ND

[a] —=levels of radioactivity undetectable. ND=not done.

[b] *P*-value is ≤0.05 when *C. parvum*-treated mice are compared to normal mice; no significant differences were found when mice were compared to *Toxoplasma*-infected mice.

best cop

TABLE 5.—*Percentage of total left ic injected dose of 1×10^5 $[^{125}I]$IdUrd-labeled, heat-killed KHT tumor cells remaining in organs of normal mice*[a]

Organ	Percentage of dose (SE) remaining after tumor cell injection at hr:			
	1	2	4	24
Brain	4.7 (0.9)	1.1 (0.1)	0.3 (0.1)	—
Lungs	4.6 (0.8)	0.5 (0.2)	0.1 (0.01)	—
Blood	2.8[b]	4.8 (0.4)	3.3 (0.3)	—
Kidneys plus adrenals	6.0 (0.2)	0.6 (0.1)	0.1 (0.01)	—
Spleen	0.7 (0.2)	0.6 (0.1)	0.5 (0.1)	0.3 (0.02)

[a] —=levels of radioactivity undetectable.

[b] SE not available.

always, resided in close proximity to collections of small mononuclear cells (figs. 3, 4).

DISCUSSION

This study demonstrated that with the KHT tumor a considerable number of tumor cells reach the brain but only after arterial dissemination and that systemic immunomodulation had a much greater influence on the arrest and retention of tumor cells in systemic organs than in the brain. Following ic injections a tumor nodule develops at the injection site in the heart and uniformly tumor deposits are present in the brain, kidneys plus adrenals, and ovaries. The occasional mouse will also develop 1 or 2 tumor nodules in the lungs. The number of tumor cells arrested and retained in the organs of normal mice in this study would predict this pattern of ultimate tumor growth. The brain and kidneys plus adrenals were the organs that collected the largest percentage of labeled tumor cells, and in normal mice at both of these sites there was significant retention of viable tumor cells at 96 hours following the tumor cell injections. Whereas some tumor cells initially did arrest in the lungs, a subsequent steady decline was seen in the number of viable cells such that by 96 hours only 0.2% of the total injected dose remained; the lung is not a primary target organ of KHT tumor growth after ic injection of tumor cell suspensions as it is after iv injections.

Previous work by our laboratory (*9*) had documented that both *C. parvum*-treated mice and mice chronically infected with *Toxoplasma* had excellent protection against the development of systemic KHT tumor following ic injection of tumor cells. The pattern of tumor cell arrest in the lungs and the kidneys plus adrenals was very different in both groups of immunomodulated mice when compared to that in normal mice. With immunomodulation there was a rapid loss of viable tumor cells from these systemic organ sites over the first 4 hours after injections, followed by a progressive but less rapid loss such that tumor cells were undetectable in the lungs at 48 hours and not detectable in the kidneys plus adrenals at 72 hours. KHT tumor rarely develops in these organs in *C. parvum*-treated mice or *Toxoplasma*-infected mice. We can only speculate as to mechanisms responsible for the observed decrease in tumor cell numbers and ultimate tumor growth in our immunologically modified animals. In a study involving immunologic manipulation, Fidler et al. (*4*) found that after iv injections of tumor cells mice with specific immunity to the tumor had increased initial arrest of tumor cells in the lungs whereas thymectomized, irradiated adult mice did not but that both groups of mice resisted the ultimate development of metastatic lung nodules. They (*4*) concluded that immunomodulation could influence the initial arrest of tumor cells in the lungs but not the amount of final metastatic tumor growth. Similar to our results where nonspecific immune mechanisms were explored, Glaves (*24*) reported that, compared to untreated mice, mice pretreated with endotoxin rapidly cleared iv injected tumor cells from the lungs, demonstrated a concomitant short-term increase of tumor cells trapped by the liver, and developed fewer ultimate lung tumor nodules. Close comparison of results from these studies and ours, however, is difficult because of differences in experimental design; e.g., the mice used by Glaves, treated or not, were all tumor-bearing.

Recent work by other investigators (*25–33*) suggested an important role for the NK cell in the elimination of circulating metastatic tumor cells; the curves we obtained of tumor cell arrest and retention following ic injection are consistent with intracirculatory NK cell activity in our immunomodulated mice. *C. parvum* treatment produces increased numbers of NK cells (*29*), and recently Hauser et al. (*34*) demonstrated that both acute and chronic *Toxoplasma* infection in mice is associated with increased NK cell activity; so both groups of our immunomodulated mice should have had more NK cells than our normal, control mice, many of which were old enough at the time of experiments to have lost much of their natural NK cell activity, which probably peaks at 5–10 weeks of age in the mouse (*33*). Electron microscopy has demonstrated that KHT tumor cells, having escaped intracirculatory destruction, can be within the lung parenchyma by 6 hours after iv injection (*7*). Beyond 8 hours in our study, the curves of viable tumor cell loss in normal mice following ic tumor cell injection and in both groups of immunomodulated mice were roughly parallel, indicating perhaps that continued destruction of tumor cells trapped in the organs themselves did not differ between normal and immunomodulated mice. Thus the fact that immunomodulated mice develop very little systemic tumor may be on the basis of early elimination of sheer numbers of tumor cells after their injection into the circulation (i.e., by NK cells) rather than on the basis of nonspecific immunologic mechanisms acting within the parenchyma of a target organ. A similar explanation of results was used by Brown and Parker (*7*) who studied the effect of immunomodulation on iv injected radiolabeled KHT tumor cells in the lungs and by Bishop and Donald (*35*) working with 2 other murine tumor lines; their explanations would agree also with the conclusions of Fidler et al. (*4*). Also, possibly the slow loss of viable tumor cells from systemic organs represents delayed, nonimmunologically mediated death of cells damaged by circulation through the pulmonary vasculature, as suggested by Weiss (*15*).

In light of the above possibilities, the effect of immunomodulation on the arrest and trapping of tumor cells in the brain holds interest for investigators. Similar to observations in the systemic organs is the observation of an immediate decline in the number of viable tumor cells in the brains of both groups of immunomodulated mice over the first 2 hours after ic tumor cell injections, with the number of tumor cells remaining fairly constant for the next 6 hours (8 hr after injections). In the normal mice an immediate rapid loss of cells was not observed, and the number of tumor cells in the brain remained at a constant level approximately twice that of the immunomodulated mice for the first 8 hours. Subsequently, in all 3 groups of mice a steady, gradual decline occurred in the number of viable cells until 48 hours after injection, when the number of tumor cells remaining again became constant at approximately the same number of cells in the brains of both normal and immunomodulated mice. A decline in the number of viable cells to undetectable levels in the brains of immunomodulated mice did not occur as had been observed in the systemic organs, and the brain was the only organ to sequester and hold a constant number of viable tumor cells regardless of the immunologic status of the animal. (Killed tumor cells were eliminated from the brain very rapidly.) This dichotomy suggests that in systemic organs nonspecific immune mechanisms, possibly via the activated macrophage (*36-41*), are present and can inactivate or kill tumor cells in the parenchyma of a particular organ but that the brain does not develop similar antineoplastic ability as a result of systemic immunomodulation at least for the first 96 hours following tumor cell injections.

However, it is known that *Toxoplasma*-infected mice resist the development and growth of both directly implanted and metastatic tumor to the brain, whereas *C. parvum*-treated mice do not (*19, 42, 43*). Only minute quantities of *C. parvum* reach the brain when it is given iv (*44, 45*), and the brains of our *C. parvum*-treated mice showed no histologic changes. In our previous work we had documented a remarkable increase in a base-line inflammatory cell reaction in the brains of *Toxoplasma*-infected mice following ic injection of KHT tumor cells and had postulated that this inflammatory response was responsible for elimination of metastatic tumor. The base-line inflammatory response is present in the brain as a direct result of *Toxoplasma* organisms invading the brain parenchyma and leaving a long-standing antigenic stimulus (*46*). Our autoradiographic, histologic studies demonstrated that labeled tumor cells in the brains of *Toxoplasma*-infected mice were surrounded by small mononuclear cells much more frequently than were labeled tumor cells in the brains of normal mice or *C. parvum*-treated mice. Whether these observations by light microscopy have significance remains speculative, but our results indicate that measurable tumor cell destruction in the brain induced by *Toxoplasma* infection probably did not occur within the first 96 hours after tumor cell injections. Unfortunately, the technique of following labeled intra-arterially injected tumor cells was not sufficiently sensitive to allow us accurately to follow tumor cell elimination for time periods beyond 96 hours, so we do not yet know the time course of tumor cell stasis or lysis in the brain of a *Toxoplasma*-infected mouse. Our study does suggest, however, that in the brain, and possibly in other organs, little hope exists that nonspecific immunologic activity that is induced after a tumor has disseminated will be effective against metastatic tumor growth unless mechanisms are developed that will directly stimulate a parenchymal immune response in a particular organ. A population of NK cells may be essential for reduction of the viable tumor burden detaching and entering the circulation, but there must be subsequent local specific and nonspecific immunologic mechanisms that act to eliminate a small number of viable tumor cells remaining in an organ. The brain apparently does not develop parenchymal nonspecific immunologic reactivity as a result of systemic immunomodulation, unless, as with *Toxoplasma* infection, the stimulating agent actually reaches the brain. The observed increased number of patients who develop brain metastases after successful treatment of the primary tumor and systemic metastatic disease (*17, 47, 48*) may be the result not only of chemotherapeutic agents failing to reach the brain but also of a present lack of a therapeutic mechanism which would result in production of local immunologic reactivity in the CNS.

REFERENCES

(*1*) Commerford SL. Biological stability of 5-iodo-2′-deoxyuridine labelled with iodine-125 after its incorporation into the deoxyribonucleic acid of the mouse. Nature 1965; 206:949-950.

(*2*) Hofer KG, Prensky W, Hughes WL. Death and metastatic distribution of tumor cells in mice monitored with ^{125}I-iododeoxyuridine. J Natl Cancer Inst 1969; 43:763-773.

(*3*) Hofer KG, Swartzendruber DC. ^{67}Ga-citrate and ^{125}I-iododeoxyuridine as markers for in vivo evaluation of tumor cell metastasis and death. J Natl Cancer Inst 1973; 50:1039-1045.

(*4*) Fidler IJ, Gersten DM, Riggs CW. Relationship of host immune status to tumor cell arrest, distribution, and survival in experimental metastasis. Cancer 1977; 40:46-55.

(*5*) Glaves D, Weiss L. Metastasis and the reticuloendothelial system. II. Effect of triamcinolone acetonide on organ retention of malignant cells in endotoxin-treated mice. Int J Cancer 1981; 27:475-479.

(*6*) Weiss L, Glaves D, Waite DA. The influence of host immunity on the arrest of circulating cancer cells and its modification by neuraminidase. Int J Cancer 1974; 13:850-862.

(*7*) Brown JM, Parker ET. Host treatments affecting artificial pulmonary metastases: Interpretation of loss of radioactively labelled cells from the lung. Br J Cancer 1979; 40:677-688.

(*8*) Fidler IJ. The relationship of embolic homogeneity, number, size and viability to the incidence of experimental metastasis. Eur J Cancer 1973; 9:223-227.

(*9*) Fidler IJ, Gersten DM, Kripke ML. Influence of immune status on the metastasis of three murine fibrosarcomas of different immunogenicities. Cancer Res 1979; 39:3816-3821.

(*10*) Fidler IJ, Kripke ML. Tumor cell antigenicity, host immunity, and cancer metastasis. Cancer Immunol Immunother 1980; 7:201-205.

(*11*) Kawaguchi T, Nakamura K. Relationship between transcerebral passage of tumor cells and brain metastasis. Gan 1977; 68:65-71.

(*12*) Sato H, Khato J, Sato T, Suzuki M. Deformability and filterability of tumor cells through "nuclepore" filter, with reference to viability and metastatic spread. Gan Monogr 1977; 20:3-13.

(*13*) Zeidman I. The fate of circulating tumor cells. I. Passage of cells through capillaries. Cancer Res 1961; 21:38-39.

(*14*) Naito S, Kinjo M, Tanaka K. Fate of intravenously injected cultured human cancer cells in the lungs of congenitally athymic nude mice. Acta Pathol Jpn 1980; 30:541-547.

(*15*) Weiss L. Cancer cell traffic from the lungs to the liver: An example of metastatic inefficiency. Int J Cancer 1980; 25:385-392.

(*16*) Zeidman I, Buss JM. Transpulmonary passage of tumor cell emboli. Cancer Res 1952; 12:731-733.

(*17*) Posner JB. Brain metastases: A clinician's view. In: Weiss L, Gilbert HA, Posner JB, eds. Brain metastasis. Boston: Hall, 1980:2-29.

(*18*) Conley FK. Development of a metastatic brain tumor model in mice. Cancer Res 1979; 39:1001-1007.

(*19*) ———. Effect of *Corynebacterium parvum* and chronic *Toxoplasma* infection on metastatic brain tumors in mice. JNCI 1979; 63:1237–1244.

(*20*) Ruskin J, McIntosh J, Remington JS. Studies on the mechanisms of resistance to phylogenetically diverse intracellular organisms. J Immunol 1969; 103:252–259.

(*21*) Bryant BJ, Cole LJ. Evidence for pluropotentiality of marrow stem cells: Modification of tissue distribution of in vivo ^{125}I-Udr labeled transplanted marrow. In: Toffey JM, ed. The lymphocyte in immunology and haemopoiesis. London: Arnold, 1967:170–182.

(*22*) Hughes WL, Commerford SL, Gitlin D, et al. Deoxyribonucleic acid metabolism in vivo. I. Cell proliferation and death as measured by incorporation and elimination of iododeoxyuridine. Fed Proc 1964; 23:640–648.

(*23*) Hofer KG. Radiation effects on death and migration of tumor cells in mice. Radiat Res 1970; 43:663–667.

(*24*) Glaves D. Metastasis: Reticuloendothelial system and organ retention of disseminated malignant cells. Int J Cancer 1980; 26:115–122.

(*25*) Hanna N. Expression of metastatic potential of tumor cells in young nude mice is correlated with low levels of natural killer cell-mediated cytotoxicity. Int J Cancer 1980; 26:675–680.

(*26*) Hanna N, Fidler IJ. Role of natural killer cells in the destruction of circulating tumor emboli. JNCI 1980; 65:801–809.

(*27*) Henney CS, Tracey D, Durdik JM, Klimpel G. Natural killer cells. In vitro and in vivo. Am J Pathol 1978; 93:459–467.

(*28*) Herberman RB, Holden HT. Guest editorial. Natural killer cells as antitumor effector cells. JNCI 1979; 62:441–445.

(*29*) Riccardi C, Puccetti P, Santoni A, Herberman RB. Rapid in vivo assay of mouse natural killer cell activity. JNCI 1979; 63:1041–1045.

(*30*) Riccardi C, Barlozzari T, Santoni A, Herberman RB, Cesarini C. Transfer to cyclophosphamide-treated mice of natural killer (NK) cells and in vivo natural reactivity against tumors. J Immunol 1981; 126:1284–1289.

(*31*) Riesenfeld I, Örn A, Gidlund M, Axberg I, Alm GV, Wigzell H. Positive correlation between in vitro NK activity and in vivo resistance towards AKR lymphoma cells. Int J Cancer 1980; 25:399–403.

(*32*) Talmadge JE, Meyers KM, Prieur DJ, Starkey JR. Role of NK cells in tumour growth and metastasis in *beige* mice. Nature 1980; 284:622–624.

(*33*) ———. Role of natural killer cells in tumor growth and metastasis: C57BL/6 normal and beige mice. JNCI 1980; 65:929–935.

(*34*) Hauser WE, Sharma SD, Remington JS. Natural killer cells induced by acute and chronic Toxoplasma infection. Cell Immunol. In press.

(*35*) Bishop CJ, Donald KJ. Non-immunological cell death of intravenously injected murine tumour cells. Br J Exp Pathol 1979; 60:29–37.

(*36*) Droller MJ, Remington JS. A role for the macrophage in in vivo and in vitro resistance to murine bladder tumor cell growth. Cancer Res 1975; 35:49–53.

(*37*) Evans R, Cox H, Alexander P. Immunologically specific activation of macrophages armed with the specific macrophage arming factor (SMAF). Proc Soc Exp Biol Med 1973; 143:256–259.

(*38*) Hibbs JB, Lambert LH, Remington JS. Possible role of macrophage mediated nonspecific cytotoxicity in tumour resistance. Nature 1972; 235:48–50.

(*39*) ———. Control of carcinogenesis: A possible role for the activated macrophage. Science 1972; 177:998–1000.

(*40*) Mantovani A, Tagliabue A, Vecchi A, Spreafico F. Effect of *Corynebacterium parvum* on cellular and humoral antitumoral immune effector mechanisms. Eur J Cancer 1976; 12:113–123.

(*41*) Morahan PS, Kaplan AM. Macrophage activation and anti-tumor activity of biologic and synthetic agents. Int J Cancer 1976; 17:82–89.

(*42*) Conley FK, Remington JS. Nonspecific inhibition of tumor growth in the central nervous system: Observations of intracerebral ependymoblastoma in mice with chronic *Toxoplasma* infection. J Natl Cancer Inst 1977; 59:963–973.

(*43*) ———. Effect of *Corynebacterium parvum* on tumor growth in the central nervous system of mice. JNCI 1978; 61:827–832.

(*44*) Dimitrov NV, Greenberg CS, Denny T. Organ distribution of *Corynebacterium parvum* labeled with iodine-125. J Natl Cancer Inst 1977; 58:287–294.

(*45*) Sadler TE, Cramp WA, Castro JE. Radiolabelling of *Corynebacterium parvum* and its distribution in mice. Br J Cancer 1977; 35:357–368.

(*46*) Conley FK, Jenkins KA. Immunohistological study of the anatomic relationship of Toxoplasma antigens to the inflammatory response in the brains of mice chronically infected with *Toxoplasma gondii*. Infect Immun 1981; 31:1184–1192.

(*47*) Gerovich FG, Luna MA, Gottlieb JA. Increased incidence of cerebral metastases in sarcoma patients with prolonged survival from chemotherapy: Report of cases of leiomyosarcoma and chondrosarcoma. Cancer 1975; 36:1843–1851.

(*48*) Grooms GA, Eilber FR, Morton DL. Failure of adjuvant immunotherapy to prevent central nervous system metastases in malignant melanoma patients. J Surg Oncol 1977; 9:147–153.

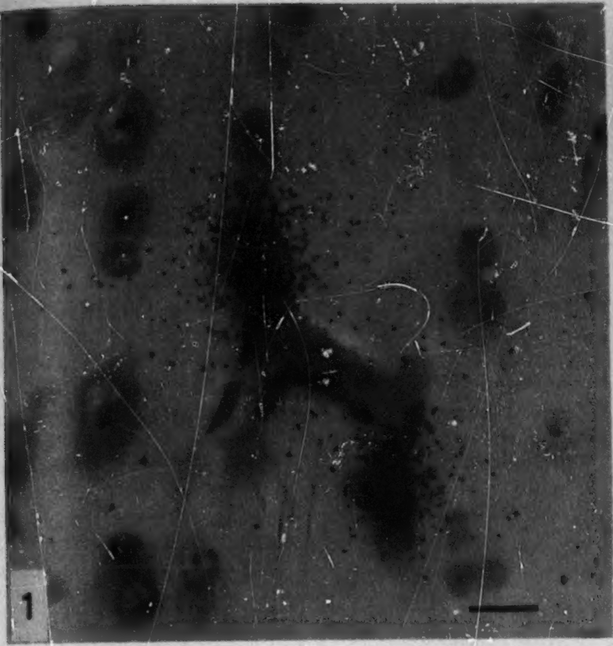

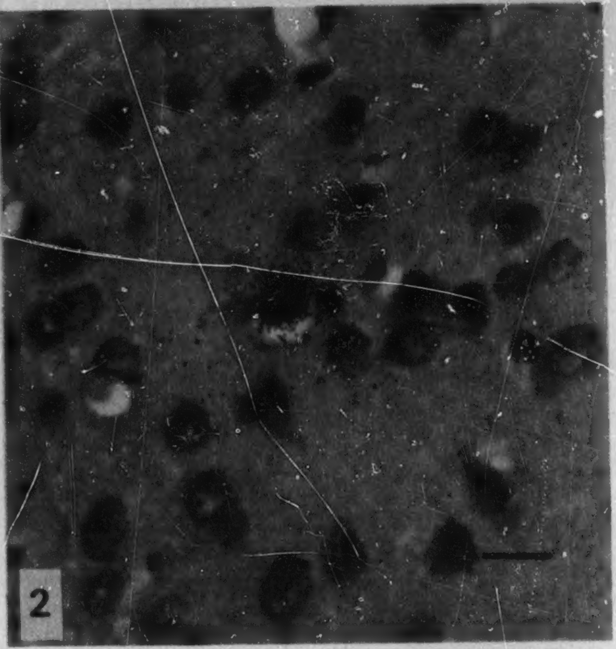

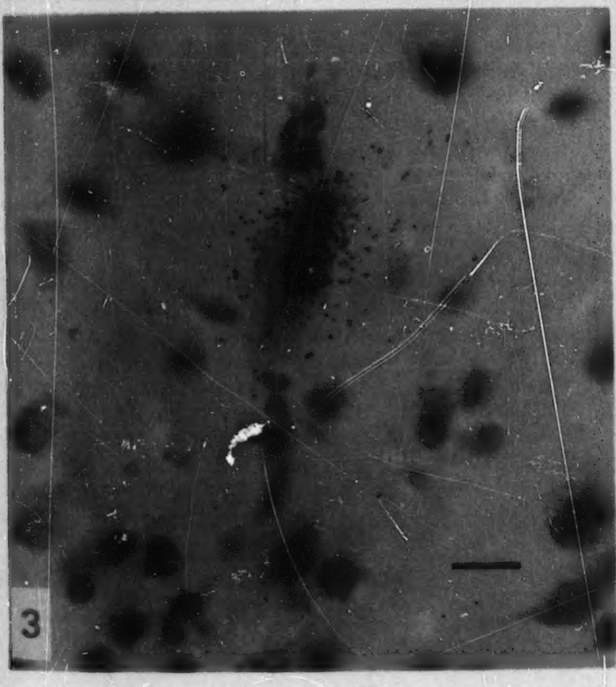

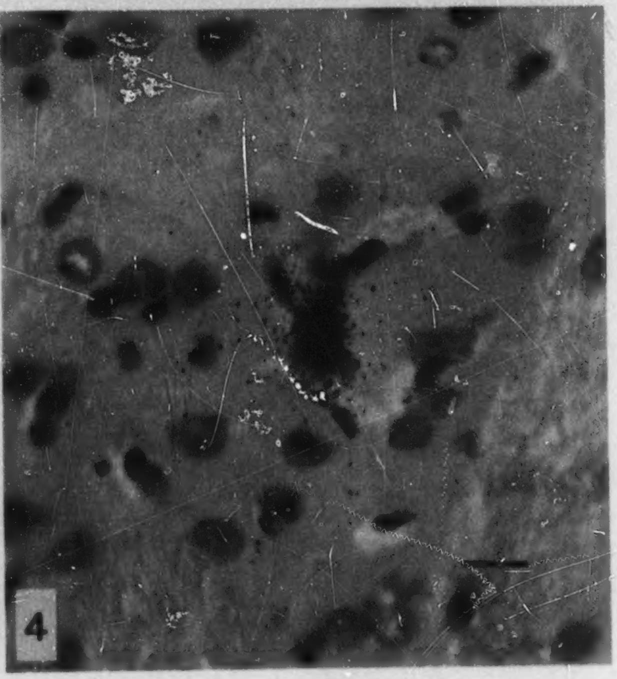

FIGURE 1.—KHT tumor cells labeled with $[^{125}\text{I}]$IdUrd trapped in a capillary in the brain of a normal mouse 8 hr after left ic injection of tumor cells. H & E. *Bar*=13 μm. FIGURE 2.—KHT tumor cell labeled with $[^{125}\text{I}]$IdUrd in the brain of a normal mouse 48 hr after left ic injection of tumor cells. H & E. *Bar*=14 μm. FIGURE 3.—KHT tumor cell labeled with $[^{125}\text{I}]$IdUrd in the brain of a *Toxoplasma*-infected mouse 24 hr after left ic injection of tumor cells. The cell probably still is in a capillary, but there are many surrounding small mononuclear cells. H & E. *Bar*=15 μm. FIGURE 4.—KHT tumor cell labeled with $[^{125}\text{I}]$IdUrd in the brain of a *Toxoplasma*-infected mouse 48 hr after left ic injection of tumor cells; *cf.* fig. 2; both tumor cells were lodged in the same region of the brain, but the tumor cell in the brain of the *Toxoplasma*-infected mouse is surrounded by many small mononuclear cells. H & E. *Bar*=13 μm.

blank page

Role of Prostaglandin E_1 and Copper in Angiogenesis[1,2]

Marina Ziche,[3,4] John Jones,[5] *and* Pietro M. Gullino[3,6,7]

ABSTRACT—The interstitial fluid of MTW9A and Walker carcinomas and their ethanol extract induced strong angiogenic response in the rabbit (New Zealand White) corneal test. The fluid collected in vivo was rich in E-type prostaglandins, and prostaglandin E_1 (PGE_1) in particular was strongly angiogenic at the lowest dose as compared with the angiogenic responses of prostaglandins E_2, I_2, and $F_{2\alpha}$. Neoplastic fibroblasts also induced a strong angiogenic response, but in indomethacin-treated rabbits neovascularization failed to occur. Copper was concentrated in the cornea during PGE_1-induced neovascularization, and copper-deficient rabbits were unable to mount an angiogenic response in the corneal test. Ceruloplasmin, the copper carrier of plasma, was found to be angiogenic at high doses. In indomethacin-treated rabbits, however, ceruloplasmin at the same high doses failed to induce angiogenesis. The experiments are interpreted to indicate that angiogenesis is the end result of a sequence of events, two of which are PGE_1 production and copper mobilization in the tissue where neovascularization occurs.—JNCI 1982; 69:475–482.

New formation of vessels is an event common to a variety of physiologic and pathologic processes. Tumor growth in particular depends on new formation of a large number of vessels, and experiments have been performed which indicate that the lack of angiogenesis prevents or arrests tumor growth (*1–3*). Recent evidence suggests also that acquisition of angiogenic capacity by tissues normally deprived of this capacity may indicate a high risk of neoplastic transformation (*4–6*).

The morphogenesis of a capillary involves a sequence of events usually described as mobilization of the endothelium in a controlled direction, cellular proliferation, canalization of a solid bud, and production of a periendothelial stroma. The conditions necessary to trigger this sequence of events are poorly understood. As a contribution to the understanding of the mechanism of angiogenesis, experiments have been conducted with the use of the rabbit corneal test. The results reported here indicate that production of PGE_1 and increased concentration of copper in the cornea to be invaded by capillaries are two events that occur during the angiogenesis process.

MATERIALS AND METHODS

Rabbits.—Male or female New Zealand White rabbits, 2–3 kg in body weight, were utilized for the angiogenesis test. The animals were kept in an air-filtered room with a 12-hour dark-light cycle. The normal diet was Purina Rabbit Chow 5321 (Ralston Purina Co., St. Louis, Mo.) and tap water ad libitum. The copper-deficient diet was #901409 (Nutritional Biochemicals Corp., Cleveland, Ohio) and deionized water.

Rabbits fed the copper-deficient diet reduced their total food consumption about 25%, and the weight gain at the end of 1 month averaged 35% less than that for rabbits receiving a normal diet. This diet did not severely impair the animals' health; upon return to a normal diet, the rabbits regained weight promptly and in about 3 weeks their weight matched the weight of rabbits on a normal diet. After the animals were on the deficient diet for 4 weeks, the copper content of their sera was usually reduced to 50% of the initial values. In about 20% of the rabbits, however, the serum copper level never decreased below 70–80% of the initial values, and these animals were not used in the experiments. The copper concentration in serum was utilized so that we could ascertain that copper deficiency was established and could select rabbits with comparable depression of serum copper concentration to ensure uniformity of response. To enhance the removal of available copper 6 days before and during the experiment, we gave each deficient rabbit three 20-mg doses orally of D-penicillamine (#4875; Sigma Chemical Co., St. Louis, Mo.) in deionized water at about 9 a.m., noon, and 4 p.m.

Surgical procedures were performed under sodium Nembutal anesthesia (30 mg/kg, #8612; Abbott Laboratories, North Chicago, Ill). In addition, after the eye was proptosed, a few drops of 0.5% tetracaine hydrochloride were placed on the cornea. After surgery, the observation of the implant with the slit-lamp stereomicroscope did not require anesthesia.

Rabbits undergoing indomethacin treatment were kept on a normal diet and received orally three 25-mg capsules of Indocin (#3316; Wholesale Drug Co., Landover, Md.) each day at about 9 a.m., noon, and 4 p.m. Treatment was started 6 days before corneal implant and continued during the entire observation period. In addition, after the corneal implant was completed, a drop of Vaseline containing about 20 mg of indomethacin was placed on the eye bulb three times a day for enhancement of the anti-PGE_1 effect.

Rats.—MTW9A carcinomas (*7*) transplanted subcutaneously in WF female rats, 2–3 months old, were utilized for the TIF sampling. The technique has been previously de-

---

ABBREVIATIONS USED: DMEM=Dulbecco's modified Eagle's minimum essential medium; FBS=fetal bovine serum; PBS=phosphate-buffered saline; PGE_1=prostaglandin E_1; PGI_2=prostaglandin I_2; TIF=tumor interstitial fluid.

---

[1] Received October 6, 1981; accepted March 17, 1982.

[2] Animals were maintained under the guidelines set forth by the National Institutes of Health.

[3] Laboratory of Pathophysiology, Division of Cancer Biology and Diagnosis, National Cancer Institute, National Institutes of Health, Public Health Service, U.S. Department of Health and Human Services, Bethesda, Md. 20205.

[4] *Present address:* Via Circondaria 37, 50127 Florence, Italy.

[5] Division of Chemical Technology, Food and Drug Administration, Washington, D.C. 20204.

[6] *Address reprint requests to* Dr. Gullino at Building 10, Room 5B36, National Institutes of Health, Bethesda, Md. 20205.

[7] We gratefully acknowledge the technical help of Mrs. Jane Earhardt.

scribed in detail (*8*). A chamber about 13 mm in diameter, with walls constituted by Millipore filters (0.45-μm pore size) and bearing a PE50 catheter (Clay, Adams Inc., Parsippany, N.J.), was inserted in a pouch of the subcutaneous tissue of the interscapular region. About 200 mg of tumor slurry was injected into the subcutaneous pouch around the Millipore chamber. Within 5–6 days a 3- to 4-g tumor had incorporated the chamber. The neoplastic cells grew against the Millipore filter but did not penetrate the chamber's cavity, whereas the fluid surrounding the neoplastic cells did penetrate and was sampled via the catheter. The fluid volume was about 150 μl for each chamber, and the color was like that of serum. As the tumor grew larger, the fluid became hemorrhagic and was not utilized.

Walker carcinoma (*9*) transplanted subcutaneously in noninbred Sprague-Dawley females, 2–3 months old, was also used in several determinations of TIF angiogenic capacity. No appreciable difference was found between the two fluids.

Cell cultures.—Fibroblasts from the subcutaneous tissue of BALB/c male mice 6 weeks old were utilized for induction of angiogenesis. The cells were removed from the donor by injection of 3 ml of a 0.5% bacterial collagenase (#4196, code CLS; Worthington Biochemical Corp., Freehold, N.J.) and 0.5% trypsin solution in PBS (GIBCO, Grand Island, N.Y.) into the subcutaneous tissue of the dorsum. After 45 minutes, 5 ml of DMEM plus 10% FBS (#12-332-45; Flow Laboratories, McLean, Va.) was injected into the same area for neutralization of the enzymatic activity.

The fluid of the subcutaneous pouch was gently sucked and extruded three times and then was centrifuged at 2,000 rpm for 5 minutes. The pellet of cells was resuspended in complete DMEM and transferred to T75 flasks. The cultures reached confluence in 3 days and were passaged every 4 days. For the experiments the cells were utilized at confluence.

Angiogenesis test.—The angiogenic capacity of samples was evaluated by the rabbit cornea test, as previously described (*10*). One pocket about 2×3 mm was surgically prepared in the cornea of a rabbit. Special care was taken to have the bottom of this pocket at 2 mm from the limbus and to avoid any rupture of the pocket's walls. The material to be tested was introduced into the pocket either in the form of a pellet or as a cell suspension. The pellet assured slow release of the angiogenic stimuli, an essential condition for angiogenesis to occur (*11*). The pellet consisted of an ethylene–vinyl acetate copolymer (Elvax 40; du Pont de Nemours, Wilmington, Del.) prepared from a casting solution of 10% Elvax in methylene chloride. Under sterile conditions the test material was carefully incorporated by the polymer; then the methylene chloride was evaporated, and the repolymerized Elvax was cut into 1×1×0.5-mm pellets. Before use the pellets were kept under vacuum at 4°C overnight.

The cells were removed from the culture flask with 0.1% trypsin in PBS, washed twice in complete DMEM plus 10% FBS, and concentrated. A dose of 2×10^5 cells was used for each corneal implant. If the tension of the cornea was not reduced, a substantial number of cells were extruded from the pocket. To ensure retention, we aspirated about 50 μl of fluid with a 30-gauge needle from the anterior chamber of the eye before corneal implantation. The Elvax pellet, on the contrary, was easily retained within the corneal pocket when a slight pressure was applied after insertion.

The implants were examined daily with a slit-lamp Zeiss stereomicroscope. A slight corneal opacity was visible around the pocket after surgery, but it disappeared during the 2d day. For the angiogenesis-positive pellets, budding capillaries started to appear at day 4; by day 7 a dense network of newly formed vessels surrounded the pellet. For angiogenesis-positive cells, the budding capillaries appeared at the end of day 5 or at the beginning of day 6; by day 10 the implant was fully colonized by vessels. As a routine we considered as negative the implants unable to stimulate angiogenesis by day 7 for the pellets and by day 10 for the cells. Occasionally, a few capillaries could bud from the limbal vessels but were unable to reach the pellets. These implants were scored as negative.

Serial histologic sections were performed on corneas for each experiment so that we could exclude the possibility that the procedure induced an inflammatory process (fig. 3). To an expert examiner any inflammatory reaction is rapidly revealed by a change in the transparency of the cornea.

Removal of corneas for copper determination.—Special care was required for the evaluation of copper content in the corneas. The initial incision for performing the corneal pocket was done with a glass knife, and all instruments used were coated with a film of fluorocarbon (National Institutes of Health instrument shop) so that contamination would be avoided. The instruments were kept in a 30% HNO_3 solution and were washed exhaustively in sterile deionized water before use. The implant was observed twice daily. As soon as the capillary buds appeared on the limbal vessel, the cornea was removed. The rabbit was anesthetized, the eye was proptosed, and the cornea was frozen by the spraying of a solution of dichlorodifluoromethane (Criokwik 15145-266, VWR Scientific Div., UNIVAR, Baltimore, Md.). With a glass knife we then quickly removed the cornea by cutting about 0.5 mm above the limbus and carefully avoiding the vessels. The frozen corneas were stored in Dry Ice in plastic vials, previously washed with HNO_3 and deionized sterile water. Twenty corneas were utilized for each copper determination. To avoid contamination by blood, we removed all corneas before any vessels had migrated into the stroma. The frozen sample was transferred to a 70-ml Teflon pressure decomposition vessel (Uniseal; Columbia Organic Chemicals Co., Inc., Columbia, S.C.), treated with 1.0 ml high-purity concentration nitric acid, sealed with a Teflon cap inside a steel jacket, and heated for 16 hours at 125°C. We transferred the digested sample solution to a Teflon bottle with 5 ml deionized water to obtain a solution with a total volume of approximately 6.5 ml. We measured volumes with calibrated polypropylene pipettes.

Copper content of these sample solutions was determined by inductively coupled argon plasma-emission spectroscopy (model 975; Jarrell-Ash Div., Fisher Scientific Co., Waltham, Mass.). Copper emission was measured at 324.7 nm against copper standards prepared in 10% (vol/vol) nitric acid. Triplicate analyses were performed on each sample solution.

RESULTS

Angiogenesis by TIF

Walker carcinoma was implanted with the Millipore chamber in 30 rats. After 5-6 days when the tumors were 4-5 g and had incorporated the chambers, TIF was sampled. The fluid was removed under sterile conditions and collected in a single vial kept at +1°C during sampling. The composition of TIF, the conditions of the tissue surrounding the Millipore chamber, and the reasons supporting the belief that TIF represents the fluid bathing the neoplastic cells in vivo have been discussed in previous publications reported in (*8*). In this experiment the objective was to establish whether TIF was angiogenic or not.

The pooled fluid was subdivided in five samples of 1 ml each. Each sample was lyophilized, and the residue of each was incorporated into an Elvax pellet in the appropriate dose. The experiment was repeated with the use of the ethanol extract of TIF treated similarly.

TIF from MTW9A carcinomas was utilized in a similar set of experiments. The results indicate that both the fluid surrounding the neoplastic cells in vivo and the ethanol extract of this fluid are able to induce corneal neovascularization (fig. 1). Table 1 reports the relationship between dose of TIF and frequency of angiogenic response.

Angiogenesis by PGE$_1$

The content of E-type prostaglandins was measured in the interstitial fluid of MTW9A carcinomas by chloroform extraction, purification on silica gel, and specific prostaglandin radioimmunoassay (*12*). The fluid was sampled during the 5th day of tumor growth and was compared with the subcutaneous fluid of non-tumor-bearing animals matched for age and weight. The subcutaneous interstitial fluid was also removed 5 days after the implant of the Millipore chamber without tumor. In five of six determinations, the prostaglandin E content of the TIF was higher than that in normal subcutaneous fluid (table 2).

The angiogenic capacity of several prostaglandins was then tested. Known amounts of prostaglandins were added to a solution of Elvax in methylene chloride, and the pellets containing the appropriate dose were implanted in the cornea (table 3). In the positive implants, newly formed capillaries had penetrated the cornea by day 4, and a dense network was evident around the pellet by day 6 (fig. 2). If the pellet was removed, the capillaries started to regress within a few days.

TABLE 1.—*Angiogenic activity of TIF and its ethanol extract sampled from Walker carcinomas*[a]

Dose, mg/pellet[b]	TIF, positive/total	EtOH·supernatant, positive/total
0.1	2/6	4/6
0.2	2/4	6/6
0.4	—	5/5
0.5	4/6	4/4
1.0	4/5	—

[a] Similar data were obtained with TIF from MTW9A carcinomas.
[b] 1.0 ml of TIF corresponds to ≃34 mg of dry material.

TABLE 2.—*Prostaglandin E content of MTW9A TIF*[a]

Sample	Tumor	Subcutaneous tissue
1	1,376±121	592±119
2	998±76	959±64
3	1,073±57	321±15
4	1,148±84	147±6
5	669±40	304±21
6	995±57	110±5

[a] Values are means ± SD for three determinations in pg/ml. Prostaglandin E content of TIF was measured on samples removed from the tumor via a Millipore chamber (*7*) and compared with that of samples removed with an identical procedure from the subcutaneous tissue of rats on the same diet, matched for age and weight but without tumor. The determinations were done by Mrs. S. C. Liu in the laboratory of Dr. R. A. Knazek (*10*).

TABLE 3.—*Angiogenic activity of prostaglandins*

Prostaglandin	Doses and angiogenic activity, positive/total[a]					
	0.1 µg	0.25 µg	0.5 µg	1.0 µg	5.0 µg	10.0 µg
E$_1$	5/8	6/9	11/11	11/11	7/8	8/8
E$_2$	1/8	1/9	4/10	3/10	—	6/8
I$_2$	—	—	—	0/5	0/5	0/5
F$_{2\alpha}$	—	—	0/3	0/3	0/3	4/4

[a] Appropriate dose was incorporated into an Elvax pellet, and angiogenesis was scored at day 6. — = not done.

PGE$_1$ was able to induce the highest frequency of angiogenesis at the lowest dose when compared with angiogenesis induction by prostaglandins E$_2$, I$_2$, and F$_{2\alpha}$ (table 3). For both prostaglandins E$_1$ and E$_2$, a mobilization of inflammatory type of cells was not detected in serial histologic sections when the dose per pellet was equal to or less than 1 µg, and the cornea was examined at the end of day 3 after implantation. It is important to establish whether or not an infiltration of inflammatory type of cells is present before vessel invasion (fig. 3). After day 3 when the cornea is colonized by capillaries, one can find leukocytes in the surrounding stroma (*13*); but it is impossible at this time to determine whether they had migrated before the vessels colonized the cornea or whether they had merely escaped from the budding capillaries during vasculogenesis.

With the assumption that PGE$_1$ production was necessary for neovascularization to occur, we used indomethacin-treated rabbits in the angiogenesis test to ascertain whether a block of prostaglandin production impaired neovascularization (*14*).

Angiogenesis was produced by BALB/c fibroblasts, 2×10^5 cells for each corneal pocket. In an experiment to be reported in the following paper (*15*), it had been observed that normal fibroblasts of BALB/c skin cultivated in vitro lack angiogenic capacity for the first three to four passages. By passage 5 angiogenesis was induced by about 50% of implants, and by passage 8 almost all implants were angiogenic. After passage 15 the fibroblasts were able not only to induce angiogenesis but also to produce a sarcoma upon transplantation in the BALB/c donor.

Rabbits receiving indomethacin and untreated controls were implanted with fibroblasts of the first transfer generation unable to induce angiogenesis, fibroblasts of the 10th and 14th transfer generations, able to induce angiogenesis but not yet neoplastic, and fibroblasts of the 22d transfer generation, both angiogenic and oncogenic. As expected, the fibroblasts of the first passage were not angiogenic in both treated and untreated rabbits. However, passages 10, 14, and 22, strongly angiogenic in untreated rabbits, were unable to induce angiogenesis in the rabbits treated with indomethacin (table 4). The inability of passage 10, 14, and 22 fibroblasts to induce corneal neovascularization appeared to be due to lack of prostaglandin production, which is blocked by indomethacin.

Copper Content of Corneal Tissue During Angiogenesis

McAuslan and Reilly (*16*) reported that copper ions stimulated the mobility of bovine aortic endothelium in vitro. Since new formation of capillaries requires mobilization of endothelium, we determined whether an increment of copper ion concentration was detectable in the rabbit corneas before the capillaries had invaded the tissue. In one experiment 20 rabbits received in the right cornea an Elvax pellet containing 1 μg PGE_1 and in the left cornea a similar pellet containing 1 μg PGI_2. At this dose PGE_1 is angiogenic; PGI_2 is not and served as the control. At the end of day 3 post implantation, the animals were anesthetized and the corneas were removed. By day 3 the vessels of the limbal plexus facing the PGE_1 pellet started to bud but had not yet penetrated the cornea; thus contamination by blood carried by newly formed vessels was avoided. In a separate group of 10 rabbits the corneas were also removed without any previous treatment. Copper content was determined in the 3 groups, and corneas bearing the PGE_1 pellet were found to contain the largest amount of copper (table 5).

In a second experiment 20 rabbits received an Elvax pellet containing 1 μg PGE_1 in the left eye and an identical pellet in the right eye containing 1 μg PGE_2, poorly angiogenic at this dose. Each of another group of 20 rabbits was implanted with a pellet containing 1 μg PGI_2 in one cornea, whereas the contralateral cornea was left untreated. Also, in this experiment the copper concentration was elevated only in the PGE_1-treated corneas (table 5).

The concentrations of Ca, Fe, Mg, P, Zn, and K were not significantly changed in the samples utilized for copper determination.

Assuming that enhanced copper concentration in the corneas about to be invaded by capillaries was an indispensable event during angiogenesis, we used rabbits fed a copper-deficient diet to evaluate the angiogenic response induced by PGE_1 and BALB/c fibroblasts. Before being tested, the rabbits were fed the copper-deficient diet until the serum level of copper was about 50% lower than normal. Under these conditions the frequency of angiogenesis produced either by PGE_1 or by BALB/c fibroblasts was drastically reduced (table 6). Deficient rabbits showed a regular angiogenic response to PGE_1 challenge after they were returned to a normal diet for 3 weeks. The data suggest that the lack of copper impaired the angiogenic response.

TABLE 4.—*Block of angiogenesis by indomethacin*

Cell passage, 2×10^5 cells[a]	Indomethacin treatment,[b] positive/total	Controls, positive/total
1	0/7	0/5
10	0/7	13/15
14	0/10	14/17
22	0/8	8/8

[a] BALB/c fibroblasts from the subcutaneous tissue; 2×10^5 cells were in each implant.

[b] 25 mg/dose, three times a day for 6 days before and 8 days after grafting. Local treatment with indomethacin was also applied after grafting (see "Materials and Methods").

TABLE 5.—*Copper content of corneal tissue during angiogenesis*[a]

Expt No.	PGE_1	PGE_2	PGI_2	Untreated
1	80.7±0.4	—	60.0±4.8	58.6±1.0
2	68.5±2.3	55.5±5.4	51.4±1.8	48.1±3.9

[a] Values are means ± SD in μg/100 g. In experiment 1, PGE_1 (1.0 μg/pellet) and PGI_2 (1.0 μg/pellet) were implanted in the left and right corneas, respectively, of the same rabbit. A separate group of untreated rabbits served as the control. In experiment 2, PGE_1 (1.0 μg/pellet) and PGE_2 (1.0 μg/pellet) were implanted in the right and left corneas, respectively, of the same rabbit. In a second group of rabbits, PGI_2 (1.0 μg/pellet) was implanted in the right cornea, and the left cornea was left untreated. There were 20 corneas for each determination. $P = <0.005$ as compared to untreated.

TABLE 6.—*Angiogenesis in copper-deficient rabbits*

	Copper-deficient diet		Controls	
Angiogenic stimuli	Copper in serum,[a] μg/dl	Angiogenesis, positive/total	Copper in serum,[a] μg/dl	Angiogenesis, positive/total
0.5 μg PGE_1/pellet	54.4±8.0	1/11	99.3±8.3	9/12
1.0 μg PGE_1/pellet	54.4±8.0	1/11	99.3±8.3	11/12
BALB/c—fibroblast, 2×10^5	48.5±5.7	1/6	84.7±5.0	11/13
1.0 μg PGE_1/pellet	58.0±10	1/12	101.3±7.5	10/12[b]

[a] Rabbits were left on a copper-deficient diet until serum concentration of copper was about one-half the normal values (≈4 wk). Frequency of angiogenic response was drastically reduced in copper-deficient rabbits. Determination was done by Biometrics Medical Laboratory, Kensington, Md., using atomic absorption spectrophotometry.

[b] *Note* that the last group was constituted by rabbits kept on a copper-deficient diet for 4 wk and returned to a normal diet for 3 wk. Angiogenesis response was tested in the left cornea while the animals were on a copper-deficient diet and in the right cornea of the same animals after 3 wk on a normal diet.

Relationship Between PGE_1 Production and Copper Concentration During Angiogenesis

The results reported in the previous sections suggested that both PGE_1 and copper play a role in angiogenesis. Assuming that a cascade of events is necessary for angiogenesis to occur, we investigated whether PGE_1 production preceded or followed copper concentration in the cornea. To this end we assumed that an enhancement of copper content in the cornea could induce angiogenesis, and ceruloplasmin (human ceruloplasmin type III; Sigma Chemical Co., St. Louis, Mo.), the copper carrier protein of serum, was selected as an angiogenesis "factor." At a dose of 100 μg/Elvax pellet, ceruloplasmin induced angiogenesis in about 70% of corneal implants (12 positive implants/18). However, when the rabbits were treated with indomethacin, the ceruloplasmin-containing pellets were unable to induce angiogenesis (0 positive/15 implants). This observation suggests that the increment of copper concentration per se is not sufficient to induce angiogenesis and that prostaglandin production probably precedes copper mobilization.

DISCUSSION

The experiments showed that the fluid surrounding the neoplastic cells in vivo had the capacity to induce corneal neovascularization when incorporated as lyophilized material into a slow-release polymer. The angiogenic capacity was manifested by the complete fluid as well as the ethanol extract of TIF. Culture media of several types of cells, neoplastic or not, have been previously shown to possess the capacity to induce neovascularization or to stimulate growth of the endothelium (*17-21*). Our experiments established that in vivo angiogenic factor(s) are also released in the fluid surrounding the cells. This observation suggests that the often visible halo of "hyperemia" and vascular proliferation observed around nodules of tumors growing in the mesenterium or other surfaces may be due to TIF, which oozes at the periphery of the node and stimulates vessel proliferation in the surrounding tissue.

The presence of angiogenic stimuli in the fluid surrounding a tumor is also important for diagnosis of neoplasia. For instance, Tapper et al. (*22*) described angiogenic activity in ocular fluid in contact with retinoblastomas, and Chodak et al. (*23*) described angiogenic activity in the urine of patients with carcinomas of transitional epithelium.

Prostaglandin E content of TIF was higher than that of the interstitial fluid from the normal subcutaneous area where the tumor was implanted. Consequently, we tested the angiogenic capacity of several prostaglandins and observed that PGE_1 was the most effective inducer of neovasculogenesis.

We assumed that the release rate of each prostaglandin from the pellet was similar on the basis that the pellet preparation was identical for all of them. Since removal of the pellet was followed by regression of the newly formed capillaries, persistence of the prostaglandin gradient seems necessary not only for the onset of neovascularization but also for the maintenance of the capillary network. We also assumed that the prostaglandin dose found in each pellet could maintain this gradient during the 5-6 days necessary for the test to be completed. Under our experimental conditions, however, a difference in prostaglandin lability may alter the dose-response profile observed.

A PGE_1 dose of 1 μg/pellet or less was unable to stimulate any appreciable inflammatory response, but it induced a strong neovascularization. Inflammatory type cells have been shown to be highly angiogenic (*24-26*); however, the experiments with low doses of PGE_1 indicated that angiogenesis could be obtained without inducing an inflammatory response as evaluated on serial sections of the corneal implants (fig. 3). The interpretation that PGE_1 plays the role of a mediator in angiogenesis (*13, 27*) was sustained by the experiment in which corneal neovascularization was induced by fibroblasts. Cultured skin fibroblasts were not angiogenic for the first three passages, but from passage 4 onward they became angiogenic (*15*). Neovascularization of the cornea was induced by the fibroblasts without mobilization of inflammatory cells, and in rabbits treated with indomethacin angiogenesis failed to develop; these findings suggest that prostaglandin production was the missing link in the process. An effective block of angiogenesis could be obtained only when the indomethacin treatment followed the procedure described in "Materials and Methods."

The work of McAuslan and Reilly (*16*) on copper ions and mobility of endothelium suggested to us the possibility that copper was involved in the corneal penetration by capillaries. We found that in PGE_1-treated corneas copper accumulation occurred before the capillaries penetrated the cornea. Indeed, rabbits on a copper-deficient diet implanted with PGE_1 or fibroblasts were unable to mount an angiogenic response, provided that copper in serum was lowered to about one-half the normal level or less. Both findings, coupled with the observation that the angiogenic response returned to normal when copper-deficient rabbits were returned to the standard diet, suggest that mobilization of copper ions is involved in neovascularization.

On this assumption we tested the angiogenic capacity of ceruloplasmin, the copper carrier of serum. We found that ceruloplasmin was able to induce neovascularization of the cornea but at a relatively high dose, probably because only a fraction of the molecule carries the active site (*28*). Indeed, ceruloplasmin deprived of copper lacked angiogenic capacity (Raju KS, Alessandri G, Ziche M, Gullino PM: Unpublished data). The angiogenic capacity of ceruloplasmin was utilized so we could evaluate whether PGE_1 production and copper accumulation were interdependent. We found that ceruloplasmin lost the angiogenic capacity in rabbits treated with indomethacin. This finding suggests that prostaglandin production probably precedes copper concentration.

The biologic significance of these two events during neovascularization is not clear. Cu^{2+} added to homogenates of sheep vesicular tissue has been shown to stimulate conversion of arachidonic acid into prostaglandins (*29, 30*). In a preliminary experiment we were unable to find substantial changes in arachidonic acid content of corneas during fibroblast-induced angiogenesis.

Growing tumors have been found to produce prostaglandins of the E-series not only in our models but also in other natural and induced tumors (*31*). In sarcomas induced by Moloney virus, prostaglandin production was sufficiently high to cause bone deformities (*32*). Moreover, several examples have been reported of reduction of tumor growth by suppression of prostaglandin synthesis (*14, 31, 33, 34*). Investigators observed that growing tumors have substantially increased ceruloplasmin levels in blood (*35, 36*), and for Walker carcinoma a direct correlation has been found between increment of copper concentration in plasma and [^{3}H]thymidine uptake (*37*). Endothelium from umbilical and mesenteric arteries and veins produces in vitro prostaglandins of the F- and E-series. Synthesis is decreased by aspirin-like agents, but it is enhanced by vasoactive substances (*38, 39*), and bradykinin in particular appears to selectively increase prostaglandin-like agents in arteries and prostaglandin-like substances in veins (*40*).

All these observations suggest that the interdependence between PGE$_1$ production and copper mobilization during angiogenesis is a plausible event. One must be aware, however, that mammalian cells seem to disgorge prostaglandins at the slightest provocation. It seems, therefore, unlikely that the simple release of a prostaglandin can by itself initiate and direct a specific response of cell populations able to complete a morphogenetic event, such as the formation of a capillary network. Yet from the knowledge accumulated since Folkman promulgated the notion that angiogenesis and tumor growth are interdependent (*1, 41*), one has the impression that neovascularization results from a cascade of events that presumably follow a pattern. The data reported here indicate that PGE$_1$ and copper are part of this cascade.

REFERENCES

(*1*) Folkman J, Cotran R. Relation of vascular proliferation to tumor growth. Int Rev Exp Pathol 1976; 16:207–224.

(*2*) Langer R, Conn H, Vacanti J, Haudenschild C, Folkman J. Control of tumor growth in animals by infusion of an angiogenesis inhibitor. Proc Natl Acad Sci USA 1980; 77:4331–4335.

(*3*). Brem S, Brem H, Folkman J, Finkelstein D, Patz A. Biological tumor dormancy by prevention of neovascularization in the vitreous. Cancer Res 1976; 36:2807–2812.

(*4*) Gimbrone MA, Gullino PM. Angiogenic capacity of preneoplastic lesions of the murine mammary gland as a marker of neoplastic transformation. Cancer Res 1976; 36:2611–2620.

(*5*) Brem SS, Jensen HM, Gullino PM. Angiogenesis as a marker of preneoplastic lesions of the human breast. Cancer 1978; 41:239–244.

(*6*) Maiorana A, Gullino PM. Acquisition of angiogenic capacity and neoplastic transformation in the rat mammary gland. Cancer Res 1978; 38:4409–4414.

(*7*) Kim V, Furth J. Relation of mammotropes to mammary tumors. IV. Development of highly hormone dependent mammary tumors. Proc Soc Exp Biol Med 1960; 105:490–492.

(*8*) Gullino PM. Techniques for the study of physiopathology. Methods Cancer Res 1970; 5:45–91.

(*9*) Stewart HL, Snell KC, Dunham LJ, Schlyen SM. Walker carcinosarcoma 256. Rat. In: Transplantable and transmissible tumors of animals. Washington, D.C.: Armed Forces Institute of Pathology, 1959:261–271 (Atlas of tumor pathology, sect. XII, fasc. 40).

(*10*) Gimbrone MA Jr, Cotran RS, Leapman SB, Folkman J. Tumor growth and neovascularization: An experimental model using the rabbit cornea. J Natl Cancer Inst 1974; 52:413–427.

(*11*) Langer R, Folkman J. Polymers for the sustained release of proteins and other macromolecules. Nature 1976; 263:797–800.

(*12*) Knazek RA, Watson KC, Lim MF, Cannizzaro AM, Christy RJ, Liu SC. Prostaglandin synthesis by murine mammary gland is modified by the state of the estrus cycle. Prostaglandins 1980; 19:891–897.

(*13*) Ben Ezra D. Neovasculogenic ability of prostaglandins, growth factors, and synthetic chemo attractants. Am J Ophthalmol 1978; 86:455–461.

(*14*) Lynch NR, Castes M, Astoin M. Mechanism of inhibition of tumour growth by aspirin and indomethacin. Br J Cancer 1978; 38:503–512.

(*15*) Ziche M, Gullino PM. Angiogenesis and neoplastic progression in vitro. JNCI 1982; 69:483–487.

(*16*) McAuslan BR, Reilly W. Endothelial cell phagokinesis in response to specific metal ions. Exp Cell Res 1980; 130:147–157.

(*17*) Klagsbrun M, Knighton D, Folkman J. Tumor angiogenesis activity in cells grown in tissue culture. Cancer Res 1976; 36:110–113.

(*18*) Kelly PJ, Suddith RL, Hutchison HT, Werrbach K, Haber B. Endothelial growth factor present in tissue culture of CNS tumors. J Neurosurg 1976; 44:342–346.

(*19*) Birdwell CR, Gospodarowicz D, Nicolson GL. Factors from 3T3 cells stimulate proliferation of cultured vascular endothelial cells. Nature 1977; 268:528–531.

(*20*) Pliskin ME, Ginsberg SM, Carp N. Induction of neovascularization by mitogen-activated spleen-cells and their supernatants. Transplantation 1980; 29:255–258.

(*21*). Castellot JJ, Karnovsky MJ, Spiegelman BM. Potent stimulation of vascular endothelial cell growth by differentiated 3T3 adipocytes. Proc Natl Acad Sci USA 1980; 77:6007–6011.

(*22*) Tapper D, Langer R, Bellows R, Folkman J. Angiogenesis capacity as a diagnostic marker for human eye tumors. Surgery 1979; 86:36–40.

(*23*) Chodak GW, Scheiner CJ, Zetter BR. Urine from patients with transitional cell carcinoma stimulates endothelial cell migration. N Engl J Med 1981; 305:869–874.

(*24*) Auerbach R, Sidky YA. Nature of the stimulus leading to lymphocyte-induced angiogenesis. J Immunol 1979; 123:751–754.

(*25*) Jakobisiak M, Kaminska G, Kaminski M, Majewski S. Angiogenic activity of cells isolated from the infiltration of the skin allograft in mice. Bull Acad Pol Sci [Biol] 1979; 26:823–826.

(*26*) Polverini PJ, Cotran RS, Gimbrone J, Unanue ER. Activated macrophages induce vascular proliferation. Nature 1977; 269:804–806.

(*27*) Ben Ezra D. Neovasculogenesis—triggering factors and possible mechanisms. Surg Ophthalmol 1979; 24:167–176.

(*28*) McAuslan BR. A new theory of neovascularization based on identification of an angiogenic factor and its effect on cultured endothelial cells. In: Jumenez de Asua L, Shields R, Levi-Montalcini R, Iacobelli S, eds. Control mechanisms in animal cells. New York: Raven Press, 1980:285–292.

(*29*) Lee RE, Lands WE. Cofactors in the biosynthesis of prostaglandins $F_{1\alpha}$ and $F_{2\alpha}$. Biochim Biophys Acta 1972; 260:203–211.

(*30*) Maddox IS. The role of copper in prostaglandin synthesis. Biochim Biophys Acta 1973; 306:74–81.

(*31*) Hial V, Horakova Z, Shaff RE, Beaven MA. Alteration of tumor growth by aspirin and indomethacin: Studies with two transplantable tumors in mouse. Eur J Pharmacol 1976; 37:367–376.

(*32*) Strausser HR, Humes JL. Prostaglandin synthesis inhibition: Effect on bone changes and sarcoma tumor induction in BALB/c mice. Int J Cancer 1975; 15:724–730.

(*33*) Goodwin JS, Husby G, Williams RC Jr. Prostaglandin E and cancer growth. Cancer Immunol Immunother 1980; 8:3–7.

(*34*) Leaper DJ, French BT, Bennett A. Breast cancer and prostaglandins: A new approach to treatment. Br J Surg 1979; 66:683–685.

(*35*) Ungar-Waron H, Gluckman A, Spira E, Waron M, Trainin Z. Ceruloplasmin as a marker of neoplastic activity in rabbits bearing the VX-2 carcinoma. Cancer Res 1978; 38:1298–1299.

(*36*) Linder MC, Bryant RR, Lim S, Scott LE, Moor JE. Ceruloplasmin elevation and synthesis in rats with transplantable tumors. Enzyme 1979; 24:85–95.

(*37*) Volm W, Wayss K, Wesch H, Zimmerer J. Korrelation zwischen der Kupfer und Caeruloplasminkonzentration im Plasma und dem ^{3}H-Thymidin-Einbau des Walker Karzinosarkoms. Arch Geschwulstforsch 1972; 40:248–258.

(*38*) Joyner WL, Strand JC. Differential release of prostaglandin E-like and F-like substances by endothelial cells cultured from human umbilical arteries and veins. Microvasc Res 1978; 16:119–131.

(*39*) Dumonde DC, Jose PJ, Page DA, Williams TJ. Production of prostaglandins by porcine endothelial cells in culture. Br J Pharmacol 1977; 61:504–505.

(*40*) Terragno DA, Crowshaw K, Terragno NA, McGiff JC. Prostaglandin synthesis by bovine mesenteric arteries and veins. Circ Res 1975; 36, 37 (suppl I):176–180.

(*41*) Folkman J. Tumor angiogenesis: Role in regulation of tumor growth. In: Hay EO, King TJ, Papaconstantinou J, eds. Macromolecular regulating growth and development. New York: Academic Press, 1974:43–52.

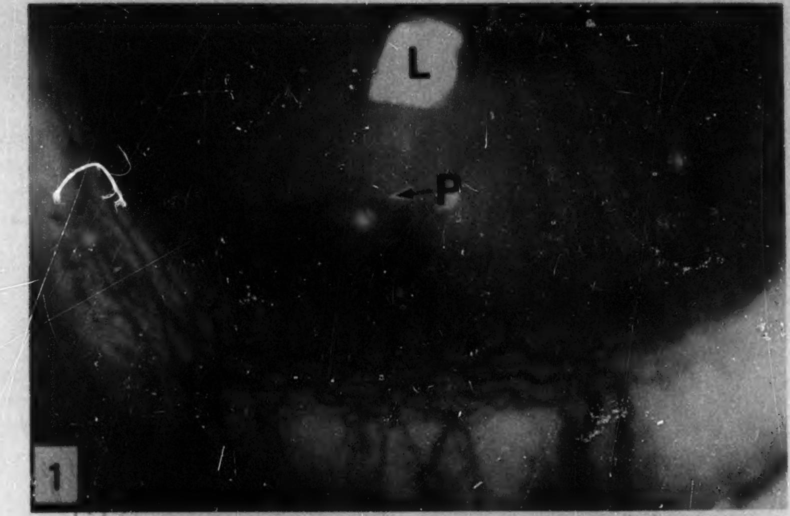

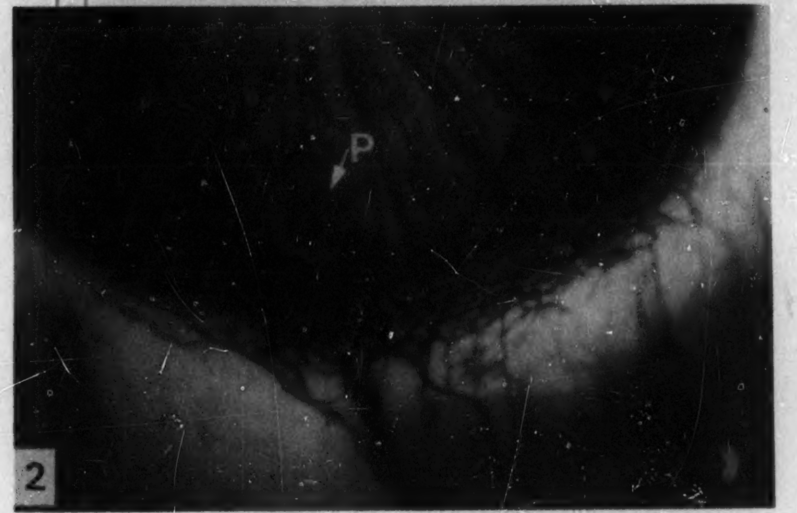

FIGURE 1.—Elvax pellet (P) containing the lyophilized ethanol extract of TIF (409 μl TIF). Photograph was taken in the unanesthetized rabbit 5 days after implantation. *Note* new formation of capillaries penetrating the cornea from the limbus and surrounding the pellet. L = reflection of lamp filament. Zeiss stereomicroscope. × 10

FIGURE 2.—Elvax pellet (P) containing 1.0 μg PGE_1 implanted in the cornea 5 days earlier. Newly formed vessels coming from the limbus and sharply localized around the pellet had penetrated the cornea. By focusing, one can reveal a much denser network than that visible in one plane. *Note* vessels of the iris, visible through the transparent cornea, in a spoke-like distribution, and out of focus for their deeper localization. Photograph was taken with a Zeiss stereomicroscope in an unanesthetized rabbit. × 10

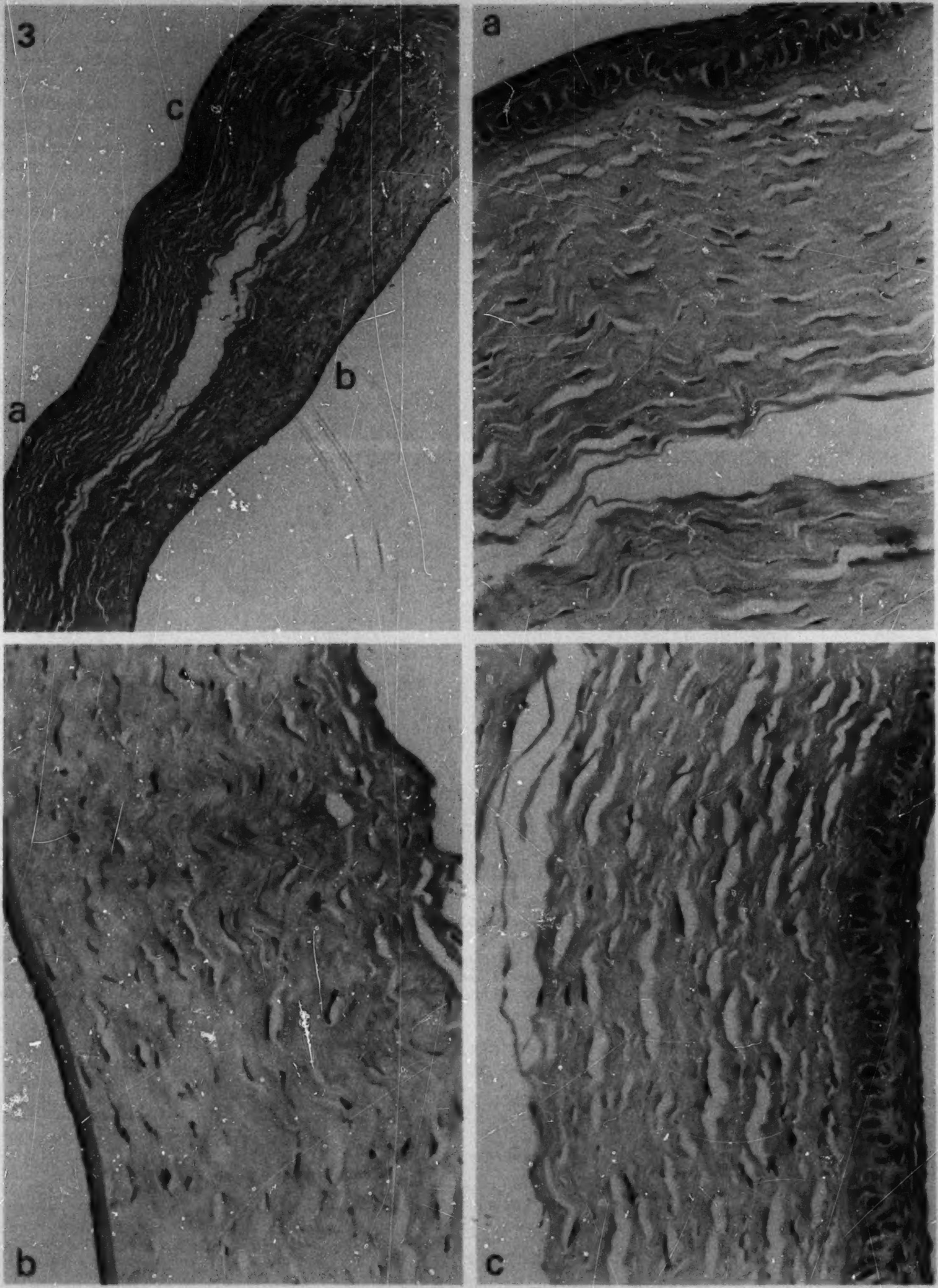

FIGURE 3.—*Upper left:* cross section of a cornea bearing an Elvax pellet with 1.0 μg PGE_1. H & E. × 68. The cornea was removed about 80 hr after the implant. *Note* absence of an inflammatory infiltrate at the time capillary buds from limbal vessels start to penetrate the cornea. a, b, and c are areas of the same cornea at × 330. (The Elvax pellet was removed after fixation for facilitation of serial sectioning.)

Angiogenesis and Neoplastic Progression In Vitro[1,2]

Marina Ziche[3,4] *and* **Pietro M. Gullino**[3,5,6]

ABSTRACT—In vivo cell populations at high risk of neoplastic transformation have been shown to acquire the ability to induce new formation of vessels. The present experiments tested whether the same change occurred during neoplastic transformation in vitro. In four cell populations (human HBL 100 mammary epithelium, BALB/c fibroblasts, C57BL-MG epithelium, and Syrian golden hamster embryo cells), angiogenic capacity appeared during their cultivation in vitro and was evident long before a neoplastic transformation could be recognized. The data were interpreted to support the hypothesis that acquisition of angiogenic capacity by a cell population normally devoid of this capacity indicates an increased risk of neoplastic transformation.—JNCI 1982; 69:483–487.

Previous work performed in our laboratory showed that in vivo the hyperplastic epithelium of the human mammary gland acquired the ability to induce neovascularization in about 30% of specimens tested at random (*1*). No other known characteristics distinguished the angiogenesis-positive specimens from the remaining 70% lacking angiogenic capacity. Because a high percentage of human primary mammary carcinomas are angiogenic but normal, adult mammary tissue is not (*1-3*), we hypothesized that the capacity to induce neovascularization is a property acquired by cell populations progressing toward neoplastic transformation.

The validity of this hypothesis was tested under two experimental conditions in which the risk of neoplastic transformation was predictable. The first concerned hyperplastic outgrowths of mouse mammary gland. These outgrowths are often transplantable in the inguinal fat pad free of mammary parenchyma. Medina (*4*) developed two lines, D_1 and D_2, morphologically identical but different in the frequency of neoplastic transformation (<10% in the D_1 line and >40% in the D_2 line). We observed that long before any neoplastic transformation was demonstrable, the D_2 line, at higher risk of neoplastic transformation, induced angiogenesis at a frequency twice as high as that of the D_1 line at lower risk (*5*).

In another experiment we took advantage of the observation of Brand (*6*) and Brand et al. (*7*) on oncogenesis by plastics. In the subcutaneous tissue of CBA mice, large (25×15×0.2 mm) plastic cover slips produced sarcomas in a higher number and at an earlier date than did smaller (15×7×0.2 mm) cover slips. We observed that within a few weeks after implantation in the same mouse, the cells attached to the large cover slip induced angiogenesis at a frequency severalfold higher than cells attached to the small cover slip. This was observed long before any tumor was present or was expected to occur (*8*).

The experiments reported here were performed to establish *a*) whether cells undergoing neoplastic transformation in vitro acquired angiogenic capacity in the process and *b*) whether onset of the angiogenic capacity occurred before oncogenesis, defined as the ability to produce a tumor upon transplantation. The major objective was to corroborate the hypothesis generated by the experiments with hyperplastic outgrowths (*1-3*) and plastic cover slips (*8*), namely, that a cell population, normally lacking angiogenic capacity, is at higher risk of becoming neoplastic when it has acquired angiogenic capacity. Moreover, if the angiogenic capacity is acquired before oncogenesis is demonstrable, it may reveal a preneoplastic condition and have prognostic value.

MATERIALS AND METHODS

Human line.—The HBL 100 line of human mammary epithelium was utilized for the angiogenesis test at passages 6, 23, and 130. This line was developed from the milk of a 27-year-old Caucasian obtained at day 3 after delivery (Gaffney EV: Personal communication). The primary culture of the milk-cell pellet was initiated in McCoy's 5-A medium supplemented with 10% FBS and was characterized by a number of mitoses higher than usual. At passage 5 enough cells were available for characterization. Metaphases contained human chromosomes in numbers ranging from 58 to 72. In later passages the range was 58–67, and the mode was 63. HeLa marker chromosomes were absent. The cells in culture were able to produce a small amount of lactose but not α-lactalbumin. They possessed human type B glucose-6-phosphate dehydrogenase activity.

At passage 12, HBL 100 grew rapidly in soft agar (0.3%) supplemented with 10% FBS. Inocula of 10^7 cells in 0.4 ml McCoy's 5-A medium from passages 9–20 failed to produce tumors in Swiss athymic mice receiving the implants ip or iv or in the cleared fat pad and observed for 14 months. Carcinomas consistently appeared when passage 103 or later passages were inoculated (10^7 cells) in the mammary fat pad. After passage 35, HBL 100 produced tumors occasionally when inoculated intracerebrally in untreated Swiss

---

ABBREVIATIONS USED: DMEM=Dulbecco's modified Eagle's minimum essential medium; FBS=fetal bovine serum; HMEM=Hanks' modified Eagle's minimum essential medium; MuMTV=murine mammary tumor virus.

---

[1] Received December 14, 1981; accepted April 2, 1982.

[2] Animals were maintained under the guidelines set forth by the National Institutes of Health.

[3] Laboratory of Pathophysiology, Division of Cancer Biology and Diagnosis, National Cancer Institute, National Institutes of Health, Public Health Service, U.S. Department of Health and Human Services, Bethesda, Md. 20205

[4] *Present address:* Via Circondaria 37, 50127 Florence, Italy.

[5] *Address reprint requests to* Dr. Gullino, Building 10, Room 5B36, National Institutes of Health, Bethesda, Md. 20205.

[6] We are particularly grateful to Dr. D. K. Howard, International Minerals and Chemicals Corp., Terre Haute, Ind., and Dr. P. E. Kirby, EG & G Mason Research Institute, Rockville, Md., for the gift of the cell populations tested; and to Dr. H. Pettigrew, National Cancer Institute, for statistical evaluation of the data.

athymic nude mice or sc in nude mice heavily treated with antilymphocyte serum (*9*).

The milk donor was followed for 6 years with clinical and mammographic evaluations at regular intervals, but the presence of a breast carcinoma was never revealed.

Murine lines.—Fibroblasts were harvested from the subcutaneous tissue of BALB/c male mice that were 6 weeks old and had been raised on standard Zeigler diet (Zeigler Bros., Gardners, Pa.). About 3 ml of a phosphate-buffered saline solution containing 0.5% bacteria collagenase (Worthington Biochemical Corp., Freehold, N.J.) and 0.5% trypsin (GIBCO, Grand Island, N.Y.) was injected sc into the dorsal region. The solution was left for 45 minutes, and then 5 ml of DMEM was injected into the same area. Slowly, the culture medium was sucked in and out of the syringe several times to "wash out" the pouch produced by the initial injection of lytic enzymes. The fluid collected from 3 mice was pooled and centrifuged at about 2,000×*g*, and the pellet containing the fibroblasts was washed and resuspended in DMEM supplemented with 10% fetal calf serum and seeded in T75 plastic flasks (Falcon Plastics, Oxnard, Calif.). The fibroblasts reached confluence in 3 days and were passaged every 4–5 days. For the determination of angiogenic capacity the cultures were tested at day 4.

The C57BL-MG line was obtained from Dr. D. K. Howard (*10, 11*) and was originally developed by Vaidya et al. (*12*) from the mammary gland of a 23-week-old C57BL/6 female. The cells had epithelial morphology and were cultivated in HMEM containing 10 µg insulin/ml and 10% FBS. From passage 31 of the parent line, Howard et al. isolated several clones by end-point dilution. Three of these clones indicated as 2, 18, and 22 were readily susceptible to MuMTV infection (*10, 11*) and were utilized for tests of the effect of MuMTV infection on angiogenesis.

The infected cells were unable to produce a tumor when they were injected sc into the mammary fat pad of athymic nude or syngeneic mice. The MuMTV-infected clones become tumorigenic only when treated with appropriate doses of 7,12-dimethylbenz[α]anthracene (*11*). Clones 2, 18, and 22, MuMTV infected and uninfected, as well as the uninfected parent line and clones 1 and 3 were tested for angiogenic capacity at several passages.

Hamster embryo line.—From 72-day-old Syrian golden hamster embryos, Dr. Kirby developed a line that was cultivated in complete DMEM for 16 passages (*13*). At this time the cell population was cloned by end-point dilution, and clone 220D6 was selected because it had the least "abnormal" morphology. Two sublines, designated A and B, were separated from clone 220D6 and subcultured twice weekly with a 1:40 split ratio. Dr. Kirby compared the two lines for serum dependency, plating efficiency, ability to grow in 0.32% agar, and tumor formation by 10^6 cells inoculated sc into 4-day-old Syrian golden hamsters. The objective was evaluation of the appearance of new properties in cell populations derived from the same clone and undergoing simultaneous neoplastic transformation in vitro. We utilized both clones at several passages, preserved frozen, to compare the angiogenic capacity with their ability to grow in agar and to be tumorigenic upon transplantation.

Angiogenesis test.—Angiogenesis was evaluated by the rabbit cornea test as previously described (*14*). A 2×3-mm pocket was prepared in the cornea of an adult New Zealand White rabbit, male or female. The bottom of the pocket must be 1.5–2.0 mm from the limbus. A 30-gauge needle was inserted into the anterior chamber of the eye, and about 50 µl of fluid was removed to partially collapse the cornea. Then 1–2×10^5 cells in 5–10 µl medium were injected into the corneal pocket, and a slight pressure was exerted so the open border of the pocket would collapse. Reduction of corneal tension is indispensable to ensure retention of a sufficient number of cells to start a colony. About 5 days after implantation, a whitish area was visible around the pocket examined with a slit-lamp stereomicroscope. In positive tests sprouts of capillaries started to penetrate the cornea from the limbus by days 5–6, and by day 10 a bunch of newly formed capillaries was clearly visible (figs. 1A, 1B). Implants unable to induce neovascularization by day 10 were scored as negative. For each experiment a few corneas were removed for histologic examination. Occasionally, a few capillaries could bud from the limbal vessels but were unable to colonize the implant. They were scored as negative. Surgical procedures were performed under Nembutal anesthesia (30 mg/kg). Daily evaluation of the angiogenic response with the slit-lamp stereomicroscope did not require anesthesia. Strict asepsis is indispensable at every step of the procedure. After cells were grafted, each rabbit was given an injection im of 20 mg triamincinolone acetonide/kg body weight; this chemical is a synthetic corticosteroid with a marked anti-inflammatory action that minimizes the possible interference of an inflammatory reaction.

RESULTS

Mammary human line.—The angiogenic capacity of HBL 100 was evaluated for three passages and compared with the tumorigenicity as tested in the Swiss athymic nude mice. Table 1 shows that passage 6, which consistently failed to produce tumors upon transplantation or to grow in soft agar, was already angiogenic. Passage 23 elicited an angiogenic response but no tumors, and passage 130 consistently produced rapidly growing tumors and was consistently angiogenic. HBL 100 represents one example of a human line of mammary epithelium in which angiogenic capacity was present long before a neoplastic transformation could be demonstrated in the original donor or after transplantation in athymic nudes. In the past it had been demonstrated that normal adult human mammary tissue is not angiogenic (*1*).

Fibroblasts of BALB/c mice.—The objective of these exper-

TABLE 1.—*Angiogenesis and tumorigenicity of HBL 100 cells at different passages*

HBL 100 passage	Angiogenesis, 1.5×10^5 cells, positive/total[a]	Tumorigenicity in Swiss adult athymic mice[b]
6	4/6	0
23	8/13	0
103	—	14/20
120	7/7	19/20

[a] The medium without cells was not angiogenic.

[b] Each of 20 mice received 10^7 cells injected ip or sc.

iments was comparison of the angiogenic capacity of subcutaneous fibroblasts maintained in culture from passage 1 onward, until a sarcoma could be induced upon transplantation into the syngeneic host. In three experiments we found that angiogenic capacity was absent for the first two to three passages, it was detected at passages 3–4, and it was present in almost every implant by passages 7–10 (table 2). Sarcomas developed only after passage 15, never at passage 10 or earlier. In this experimental system, as for the human mammary line HBL 100, angiogenesis appeared long before any neoplastic transformation was detectable.

C57BL/6 mammary epithelium.—The objective of these experiments was to ascertain whether mouse mammary epithelium acquired angiogenic capacity in culture and whether infection with a MuMTV influenced the angiogenic response. The parent line at the time of cloning was at the 31st passage and already showed angiogenic capacity. Since normal adult mammary mouse epithelium is not angiogenic (*2, 5*), the capacity to induce neovascularization was acquired during the cultivation in vitro, although the exact time of appearance could not be ascertained. The four clones tested had about the same angiogenic capacity as that of the parent line. The MuMTV infection of three clones did not induce any striking modification of the angiogenesis pattern (table 3). A small increase of angiogenic activity after MuMTV infection was observed in all three experiments, but the difference was so slight that an extensive analysis was considered unwarranted. Transplantation of these cells never produced a tumor.

The experiment with subcutaneous fibroblasts (table 2) showed that the angiogenic response increased in frequency as the number of passages in cultures increased, and by the time the cells produced a tumor, practically all implants were angiogenic. We could not detect the same behavior in the C57BL mammary epithelium. For instance, the angiogenic activity of clone 2 at passage 16 was not substantially different from that of clone 2 at passage 24; the same can be said for clone 18 at passage 16 versus passage 28 (table 3). This question was more carefully analyzed with hamster embryo cells.

Table 2.—*Angiogenesis induced by BALB/c fibroblasts*[a]

Expt No.	Positive/total at passage							
	1	2	3	4	5	6	7	10
I	0/4	0/6	0/8	4/8	5/8	5/7	10/10	20/20
II	0/6	0/9	0/8	4/6	3/7	—	6/7	16/16
III	0/10	0/7	1/6	1/8	3/8	6/10	—	24/28

[a] The formation of a sarcoma after transplantation of 10^7 cells in the subcutaneous tissue of the interscapular region appeared after passage 15 for line I, after passage 20 for line II, and after passage 21 for line III. Capacity to induce angiogenesis in all three lines already appeared at the third to fourth passage.

Table 3.—*Angiogenesis induced by C57BL-MG epithelium*

Cell population	Passage in culture	MuMTV infection	Angiogenic response, positive/total
Parent line	34	0	3/10
Clone 1	11	0	5/10
Clone 2	24	0	4/9
Clone 3	23	0	3/9
Clone 18	16	0	2/9
Clone 2	16	0	3/16
	15	+	7/10
Clone 18	28	0	0/16
	28	+	4/16
Clone 22	10	0	0/6
	10	+	2/6

Table 4.—*Angiogenesis induced by hamster embryo cells*

Clone	Passage	Angiogenic response, positive/total	Growth in 0.3% agar	Tumor formation, %[a]
220D6A	3	4/7	No	0
	9	3/8	No	0
	15	3/6	No	0
	18	—	Yes	20
	49	4/6	Yes	50
220D6B	5	0/6	No	0
	10	2/8	No	0
	16	2/6	No	0
	19	—	Yes	20
	50	3/6	Yes	100

[a] Each 4-day-old hamster was inoculated sc with 10^6 cells; 10 animals were in each group (*13*).

Hamster embryo cells.—Two cell populations from the same clone were cultured under identical conditions, and their angiogenic capacity was compared at subsequent passages with the ability to grow in 0.3% agar and to form tumors. Angiogenesis appeared in both cell populations before the capacity to grow in agar or to produce tumors was established (table 4). The number of implants showing an angiogenic response did not change appreciably as the number of passages in culture progressed. In these cells, as for the mammary epithelium of C57BL/6 mice, not every implant was angiogenic when the neoplastic transformation was established.

DISCUSSION

Since the observation that a neoplastic cell population could form a tumor only when new formation of vessels was elicited from the host (*15, 16*), angiogenesis was studied by oncologists mainly with the objective of finding the factor(s) involved in the process (*17–19*). The majority of adult tissues where tumors originate are not angiogenic, but the neoplastic tissues are; therefore, the capacity to elicit new formation of vessels is acquired during neoplastic transformation. Cultivation in vitro represents a special condition for mammalian cell populations known to favor neoplastic transformation in a large number of cases. In four cell populations cultivated in vitro, we observed that angiogenic capacity appeared long before the neoplastic transformation was demonstrable by transplantation in vivo. Consequently, the appearance of angiogenesis in a tissue normally devoid of it should indicate that a step toward neoplastic transformation has occurred. The presence of an angiogenic response before the neoplastic transformation could be demonstrated was unequivocal in the four experimental models utilized here. The early appearance of angiogenic capacity during neoplastic transformation is therefore a property expressed under in vitro conditions as it was previously observed in vivo (*1, 3, 5, 8*).

The question as to whether MuMTV infection of mammary epithelium is a determinant factor in eliciting angiogenic capacity could not be answered in a satisfactory manner. The C57BL/6 parent line went through 31 culture passages before cloned cell populations capable of being infected by MuMTV were obtained. The in vitro cultivation was sufficiently long to induce an already high frequency of angiogenic response in the uninfected clones. The MuMTV infection failed to enhance the angiogenic response of the clones to a sufficiently high frequency to convincingly indicate that MuMTV played a decisive role in inducing angiogenic capacity of infected cells.

The interdependence, if any, between angiogenesis and oncogenesis is still difficult to envisage. In vivo we have observed that tumors were highly angiogenic; however, a fraction of tumor fragments was consistently unable to induce angiogenesis (*1, 2, 3, 8*). Cultured neoplastic cells were also highly angiogenic; however, several implants also were unable to elicit neovascularization. Thus angiogenesis does not appear to be an obligatory property of every neoplastic cell in a tumor. Heterogeneity of the tumor cell population is a well-known event and may be responsible for this finding.

Since angiogenic capacity appears early during oncogenesis, one would expect a gradual increment in the number of angiogenesis-positive implants as the time of neoplastic transformation approaches. This phenomenon, however, was observed only for the subcutaneous fibroblasts (table 2) and not for human and mouse mammary epithelia or for hamster embryo cells in culture. Similarly, the above correlation was not observed in vivo for hyperplastic outgrowths of murine mammary glands (*2*) or for cells around plastic cover slips producing sarcomas (*8*). An interdependence between angiogenesis and oncogenesis is not demonstrable at this time; however, it is clear that angiogenic activity appears consistently in a variety of cell populations before neoplastic transformation is evident, either in vitro or in vivo.

The possibility of using angiogenesis as a marker of a cell population at high risk of neoplastic transformation or of a cell population already tumorigenic is presently hampered by our limited knowledge of the sequence of events necessary for angiogenesis to occur. However, two observations of clinical importance are already available. Because neoplastic cells in vivo release the angiogenic factor(s) into the surrounding fluid, the presence of a tumor can be revealed by the angiogenic capacity of fluids bathing the tumor: Tapper et al. (*20*) reported this observation for retinoblastomas, and Chodak et al. (*21*) reported it for bladder carcinomas.

REFERENCES

(*1*) Brem SS, Jensen HM, Gullino PM. Angiogenesis as a marker of preneoplastic lesions of the human breast. Cancer 1978; 41:239–244.

(*2*) Gimbrone MA Jr, Gullino PM. Neovascularization induced by intraocular xenografts of normal, preneoplastic, and neoplastic mouse mammary tissues. J Natl Cancer Inst 1976; 56:305–318.

(*3*) Maiorana A, Gullino PM. Acquisition of angiogenic capacity and neoplastic transformation in the rat mammary gland. Cancer Res 1978; 38:4409–4414.

(*4*) Medina D. Preneoplastic lesions in mouse mammary tumorigenesis. Methods Cancer Res 1973; 7:3–53.

(*5*) Gimbrone MA Jr, Gullino PM. Angiogenic capacity of preneoplastic lesions of the murine mammary gland as a marker of neoplastic transformation. Cancer Res 1976; 36:2611–2620.

(*6*) Brand KG. Foreign body induced sarcomas. In: Becker FF, ed. Cancer: A comprehensive treatise. Vol 1. New York: Plenum Press, 1975:485–511.

(*7*) Brand KG, Bouen LC, Brand I. Carcinogenesis from polymer implants: New aspects from chromosomal and transplantation studies during premalignancy. J Natl Cancer Inst 1967; 39:663–679.

(*8*) Ziche M, Gullino PM. Angiogenesis and prediction of sarcoma formation by plastic. Cancer Res 1981; 41:5060–5063.

(*9*) Giovanella BC, Gaffney EV, Yim SO, Stehlin JS. Increase of the malignant potential of human line HBL 100 with long term passage in vitro. In Vitro 1980; 16:211.

(*10*) Howard DK, Hand PH, Schlom J. In vitro infection of mammary and nonmammary cells by mammary tumor viruses. In: McGrath CM, Brennen M, Rich MA, eds. Cell biology of breast cancer. New York: Academic Press, 1980:451–466.

(*11*) Howard DK, Fisher PB, Schlom J. Transformation of cloned mammary epithelial cells following combined treatment with mouse mammary tumor virus and dimethylbenz(α)anthracene. In: Rich M, Formanski P, eds. Biological carcinogenesis. New York: Marcel Dekker. In press.

(*12*) Vaidya AB, Lasfargues EY, Sheffield JB, Coutinho WG. Murine mammary tumor virus (MuMTV) infection of an epithelial cell line established from C57BL/6 mouse mammary glands. Virology 1978; 90:12–22.

(*13*) Kirby PE. Stages of tumorigenicity in spontaneously transformed hamster cells in culture. Ph.D. thesis. Washington, D.C.: Catholic University of America, 1978.

(*14*) Gullino PM. Angiogenesis factor(s). In: Baserga RO, ed. Tissue growth factors. Handbook of experimental pharmacology. Vol 57. New York: Springer-Verlag, 1981:427–449.

(*15*) Greene HS. Heterologous transplantation of mammalian tumors. I. The transfer of rabbit tumors to alien species. J Exp Med 1941; 73:461–474.

(*16*) ———. Heterologous transplantation of mammalian tumors. II. The transfer of human tumors to alien species. J Exp Med 1941; 73:475–486.

(*17*) Tuan D, Smith S, Folkman J, Merler E. Isolation of nonhistone proteins of rat Walker carcinoma 256. Their association with tumor angiogenesis. Biochemistry 1973; 12:3159–3165.

(*18*) Weiss JB, Brown RA, Kumar S, Phillips P. An angiogenic factor isolated from tumours: A potent low-molecular weight compound. Br J Cancer 1979; 40:493–496.

(*19*) Fenselau A, Mello RJ. Growth stimulation of cultured endothelial cells by tumor cell homogenates. Cancer Res 1976; 36:3269–3273.

(*20*) Tapper D, Langer R, Bellows RA, Folkman J. Angiogenesis capacity as a diagnostic marker for human eye tumors. Surgery 1979; 86:36–40.

(*21*) Chodak GW, Scheiner CJ, Zetter BR. Urine from patients with transitional cell carcinoma stimulates migration of capillary endothelial cell. N Engl J Med 1981; 305:869–874.

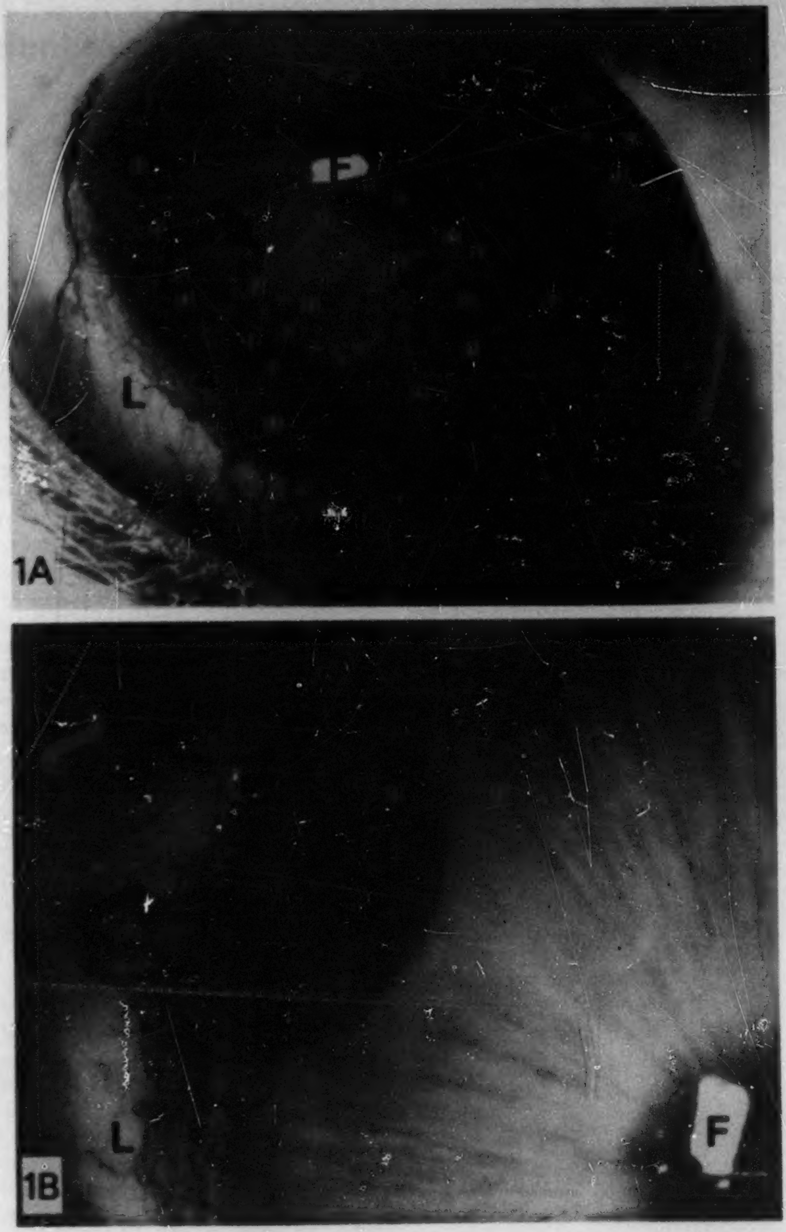

FIGURE 1A.—Proptosed rabbit eye. *Arrows* point toward a whitish area in the cornea where 2×10^5 HBL 100 cells had been implanted 6 days earlier. *Note* the brush of capillaries invading the cornea and moving from the limbus (L) toward the area occupied by the cells. F=filament of the stereomicroscope lamp. In vivo photograph. × 5. FIGURE 1B.—Same as in fig. 1A but at day 8. In vivo photograph. × 10.

blank page

Immunization Against Transplantable Leukemia Impaired in Copper-Deficient Mice[1,2,3]

Omelan A. Lukasewycz[4] *and* **Joseph R. Prohaska**[5,6]

ABSTRACT—Inbred C58 mice, kept on a copper-deficient (−Cu) diet from birth, were tested for their ability to be immunized to, and subsequently challenged with, line I_b syngeneic transplantable malignant lymphocytes (I_b cells). −Cu mice had significantly lowered hematocrits and serum ceruloplasmin (EC 1.16.3.1) values in contrast to those of the copper-supplemented (+Cu) controls. All male +Cu mice (17/17) survived the immunization regimen (consisting of $\approx 10^3$ viable and 10^7 inactivated I_b cells) and the challenge dose (10^6 viable I_b cells). Male −Cu mice had a survival rate of only 15% (4/27) after the immunization process and an overall survival rate of 11% (3/27). Female +Cu mice had survival rates of 86% (19/22) after immunization and of 74% (14/19) after the challenge dose, compared to 54% (15/28) and 47% (7/15) survival rates, respectively, for the female −Cu mice. Overall, the +Cu mice had a 79% (31/39) survival of both immunization and challenge compared to an 18% (10/55) survival for the −Cu mice. These results indicate that the initiation and maintenance of cell-mediated immunity to leukemia cells are severely impaired in −Cu animals.—JNCI 1982; 69:489–493.

We have utilized a mouse model, the C58 mouse-line I_b syngeneic leukemia system, to evaluate and characterize the lymphoid subpopulations operative in leukemia immunity (*1-5*). Immunity in this model is predominately cellular in nature (*3, 6*) and is mediated by a lymphocyte cell population that appears to consist of Thy 1.2^+, surface immunoglobulin-negative, Ly 4.2^- T-cells (*3, 4*) that possess the Ia determinants (*5*).

Appropriate nutrition is crucial to the well-being of any organism. Malnutrition has been shown to have a profound influence on both the humoral and cell-mediated immune responses (*7*). Martinez et al. (*8*) have shown that starvation, even for 48 hours, will severely suppress cellular immunity in the C58-I_b system. Investigators in our laboratory have recently shown that an impaired humoral immune response is observed in mice with severe as well as marginal −Cu and that the magnitude of this impairment is highly correlated with the degree of functional −Cu (*9*). We thus wished to explore the effect of −Cu on the cellular arm of the immune system, and we describe here the effect of −Cu on the cell-mediated immunity to syngeneic malignant lymphocytes.

MATERIALS AND METHODS

Mice.—Inbred C58 mice, originally from Dr. William H. Murphy Jr., Department of Microbiology, University of Michigan Medical School, Ann Arbor, Mich., have been maintained at the animal facilities of the School of Medicine, University of Minnesota, Duluth, Minn., since 1975.

Pregnant dams were housed in polyethylene cages with stainless steel covers and wood shavings (American Excelsior Co.) for bedding. Offspring were transferred at 3 weeks of age to stainless steel cages with wire mesh floors. Mice were used in I_b immunization experiments at 5–9 weeks of age.

Diet.—On the day of parturition, C58 dams were switched from a nonpurified diet (Purina Mouse Chow; Ralston Purina Co., St. Louis, Mo.) containing 12 mg Cu/kg to a purified mouse diet, formulated to omit Cu from the salt mix (modified AIN-76; Teklad Inc., Madison, Wis.) and containing no more than 0.6 mg Cu/kg. This diet has previously been used to establish −Cu in mice (*10*). Approximately half of the dams were given supplemental Cu (20 μg$CuSO_4$/ml) in the drinking water, whereas the remaining dams were given deionized water to drink. Pups were maintained on the diet of their respective dams until the experiments began. +Cu and −Cu animals were matched for age, sex, and weight for each experiment.

Hematocrit.—Hematocrit determinations were done by retro-orbital bleeding of etherized mice into heparinized microhematocrit capillary tubes (Scientific Products).

Ceruloplasmin levels.—Plasma from individual microhematocrit tubes was assayed for ceruloplasmin (EC 1.16.3.1) activity, with *o*-dianisidine as substrate as described by Prohaska (*10*). Ceruloplasmin, a cuproenzyme, was routinely used to monitor Cu status of the mice (*9*).

Line I_b cells.—The origin of I_b syngeneic malignant lymphocytes was described by Lin et al. (*6*). Fresh suspensions of I_b cells were prepared by aseptic removal of spleens from C58 mice moribund with transplanted leukemia frozen stock (passage 79); spleens were then injected with HBSS, sectioned with scalpels, and a single cell suspension prepared.

ABBREVIATIONS USED: −Cu=copper-deficient (deficiency); +Cu=copper-supplemented; HBSS=Hank's balanced salt solution; LD_{50}=median lethal dose.

---

[1] Received October 7, 1981; accepted March 8, 1982.

[2] Supported in part by Public Health Service grant HD-15491 from the National Institute of Child Health and Human Development, by a University of Minnesota Graduate School research grant, and by the American Cancer Society Institutional grants IN-13-S-46 and IN-13-T-23.

[3] Animals were maintained under the guidelines set forth by the University of Minnesota and in the "Guide for the Care and Use of Laboratory Animals" by the Institute of Laboratory Animal Resources, National Research Council.

[4] Department of Medical Microbiology and Immunology, School of Medicine, University of Minnesota, Duluth, Minn. 55812.

[5] Department of Biochemistry, School of Medicine, University of Minnesota.

[6] We appreciate the technical assistance and expertise of Susan B. Meyer in all aspects of this work.

Gross particles were discarded and cells were washed two more times in HBSS (250×*g* for 5 min each). Total and viable cell counts by trypan blue exclusion (*11*) were performed at this time.

I_b cells treated with Formalin.—Cells were prepared by dilution of I_b cells in HBSS to a concentration of 2×10^7 cells/ml and then diluted 1:2 with a 1:250 dilution of a Formalin solution (37.4% analytical grade formaldehyde solution diluted 1:10 in HBSS). Cells were incubated with the Formalin solution (final dilution 1:500) at 4°C for 18 hours and then used for immunization of mice.

This Formalin treatment results in a preparation that still harbors approximately 1×10^2 viable cells from the initial 1×10^7 I_b cell load; i.e., Formalin inactivates 99.999% of all the cells (*6*). This preparation is highly immunogenic and will protect normal mice against a subsequent challenge of at least 1×10^7 viable I_b cells ($LD_{50}>1\times10^7$ viable I_b cells); mice immunized with preparations that harbor no viable cells die at lower challenge doses ($LD_{50}=1\times10^{5.9}$ viable I_b cells) (*1*). Nonimmunized mice will succumb to challenge of a single viable I_b cell (*6*). There is a linear relationship between time of death and the $\log_{10}$ dose of viable I_b cells administered (*1*).

Immunization and challenge of mice.—Mice received a single 1.0-ml ip injection of cells treated with Formalin as an immunization regimen. Immunocompromised mice will succumb to the viable I_b cells that remain in the "Formalinized" cell preparation (*2*). Mice were observed for 21 days for determination of leukemia deaths due to the immunizing preparation. All deaths recorded in these experiments were consistent with the time course and gross pathology of I_b leukemia. A challenge dose was administered 3 weeks after immunization; it consisted of a 1.0-ml ip injection containing 1×10^6 viable I_b cells. These animals were then followed for an additional 15 days to ascertain leukemia deaths. Dose-response experiments were conducted in unimmunized mice, both in controls and in −Cu animals, by the injection of viable I_b cells into mice of each group at each of three doses—10^3, 10^5, and 10^7 cells. Leukemia deaths were monitored twice daily.

Statistics.—Hematocrit and ceruloplasmin means were compared with the use of the *F*-variance ratio and two-tailed Student's *t*-test. Survival data were treated by chi-square analysis. Linear regression analyses were performed on the dose-response data.

RESULTS

The effect of dietary −Cu was manifest quite rapidly in both hematocrits (text-fig. 1) and ceruloplasmin levels (text-fig. 2). Hematocrit levels of −Cu mice were below those of +Cu mice as early as 1 week after weaning (wk 4). The hematocrits in −Cu mice tended to decrease further during weeks 5–7. The decreased hematocrits appeared much more pronounced in the −Cu male population compared to those in females.

Ceruloplasmin values, determined on the same group of mice, also show a decrease by week 4. During the subsequent weeks ceruloplasmin levels began to increase, especially among −Cu females, and possibly approached +Cu values by week 10. We have found that the hematocrit and ceruloplasmin values varied in individual −Cu mice, even though they were treated identically from birth. Animals were selected for further study based on the time course of their Cu depletion.

The effect of −Cu on immunization to I_b cells and subsequent challenge was studied in −Cu mice and compared to that in +Cu mice (table 1). Male +Cu mice responded exactly as did Cu-adequate (chow-fed) mice studied previously (*1*), i.e., a 100% survival of the immunization and challenge regimens. Male −Cu mice, however, showed only a 15% survival of immunization and an overall survival rate of only 11%. All deaths recorded in these experiments were

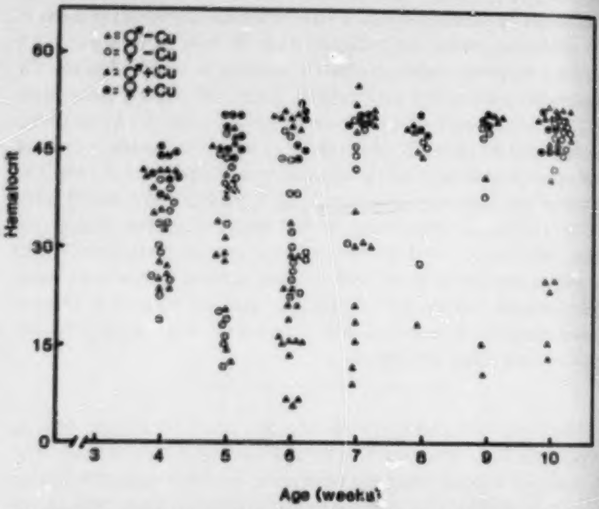

TEXT-FIGURE 1.—Hematocrit determination of C58 mice. A pool of mice, separate from those used for the immunization-challenge experiments, were bled retro-orbitally on a weekly basis after weaning. *Points* represent means of triplicate determinations in individual animals. △, −Cu males; ▲, +Cu males; ○, −Cu females; ●, +Cu females.

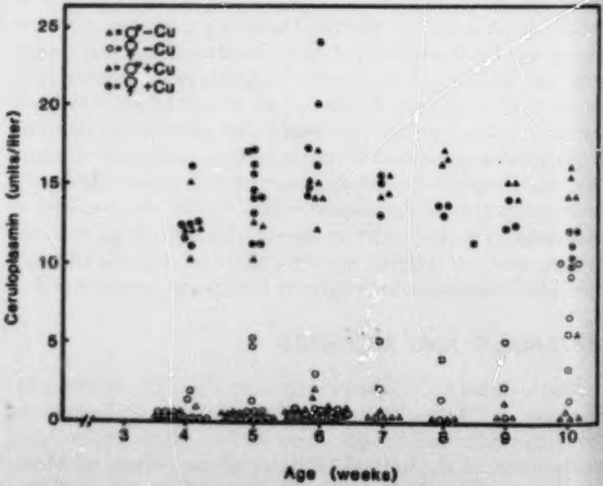

TEXT-FIGURE 2.—Ceruloplasmin activity in plasma of C58 mice. Plasma was obtained from the same mice as were used for hematocrit determinations (text-fig. 1). *Points* represent activities of individual animals.

TABLE 1.—*Effect of −Cu on immunization to lymphocytic leukemia*[a]

Group	Preimmunization[b]			Postimmunization[c]			Survivors/total No. immunized and challenged (%)
	Hematocrit, mean ± SD (No. of mice)	Ceruloplasmin, U/liter, mean ± SD (No. of mice)	Survivors/total No. immunized (%)[d]	Hematocrit, mean ± SD (No. of mice)	Ceruloplasmin, U/liter, mean ± SD (No. of mice)	Survivors/total No. challenged (%)[e]	
+Cu ♂	52.8±4.0 (6)	16.6±2.4 (6)	17/17 (100)	51.0±0.5 (3)	19.4±5.6 (3)	17/17 (100)	17/17 (100)
−Cu ♂	12.4±5.3 (8)[f]	0.4±0.6 (8)[f]	4/27 (15)[g]	45.3±3.9 (4)	10.8±4.3 (4)	3/4 (75)	3/27 (11)[g]
+Cu ♀	47.8±1.4 (6)	18.0±3.0 (6)	19/22 (86)	48.2±2.4 (6)	20.1±3.7 (6)	14/19 (74)	14/22 (64)
−Cu ♀	26.6±3.2 (5)[f]	0.0±0.0 (5)[f]	15/28 (54)[h]	43.6±7.2 (7)	7.2±7.0 (7)[f]	7/15 (47)	7/28 (25)[h]
Total +Cu	—	—	36/39 (92)	—	—	31/36 (86)	31/39 (79)
Total −Cu	—	—	19/55 (35)[g]	—	—	10/19 (53)[h]	10/55 (18)[g]

[a] Table is a composite of three replicate experiments with male and female mice.

[b] Preimmunization determinations performed 24 hr before immunization regimen was started.

[c] Postimmunization determinations performed 15–20 days after immunization and therefore included only survivors of the regimen.

[d] Immunization regimen consisted of ip injection of 1.0 ml Formalinized cells containing ≈10^7 inactivated and 10^3 viable I_b cells. Survivors were scored over a 15-day period.

[e] Challenge dose contained 1×10^6 viable I_b cells in a 1.0-ml ip bolus. Survivors counted at a 15-day end point.

[f] Means are significantly different from controls (+Cu) $P<0.001$, by Student's *t*-test.

[g] Significantly different from controls (+Cu), $P<0.01$, by chi-square test.

[h] Significantly different from controls (+Cu), $P<0.05$, by chi-square test.

consistent with the time course and gross pathology of I_b leukemia. Female +Cu mice also exhibited a high survival immunization (86%) as compared to that of female −Cu mice (54%). More than half of the −Cu females that survived immunization failed to survive the challenge of 10^6 viable I_b cells. Only 7 of 28 (25%) of the −Cu females survived immunization and challenge as opposed to 64% survival (14/22) of +Cu females. The totals indicate that the +Cu mice fared very well in contrast to the −Cu mice in immunization (92 vs. 35%) and challenge (86 vs. 53%) survival rates. The overall picture is even more striking: 31 of 39 (79%) +Cu mice survived both immunization and challenge compared to 10 of 55 (18%) −Cu mice.

We observed that survivors of immunization, both +Cu and −Cu animals, had near normal hematocrits and higher ceruloplasmin values than those seen prior to immunization (table 1). This increase was not due to induction of ceruloplasmin from the Cu contained in the Formalinized I_b preparation. Replicate samples of the immunization preparation were analyzed by atomic absorption spectroscopy after wet ashing in HNO_3. The immunization bolus contained 0.045 μg Cu, an amount equal to only 5% of that which a mouse would absorb in 1 day from the low Cu diet. Therefore, a different mechanism seemed plausible.

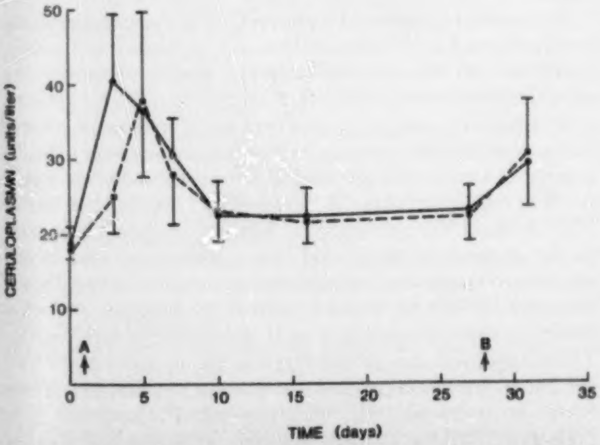

TEXT-FIGURE 3.—Plasma ceruloplasmin activity of normal, chow-fed C58 mice after inoculation of Formalinized I_b cells (●) or the Formalin vehicle alone (■). Values are the means ± SD of 12 animals (6 males and 6 females). Both groups A) were given injections on day 1 of their respective treatments, and B) all mice were challenged on day 28 with 10^6 viable I_b cells. All unimmunized animals died within 6 days after administration of the challenge dose (by day 33).

The capacity of the I_b immunization preparation and its Formalin vehicle to induce serum ceruloplasmin was determined in chow-fed animals (text-fig. 3). After immunization with I_b cells, C58 mice demonstrated a rapid 221% rise in ceruloplasmin activity ($P<0.01$), which subsequently fell but remained elevated (126%) even 26 days after injection ($P<0.01$) (text-fig. 3). The Formalin-injected mice also showed a rapid rise in ceruloplasmin activity; however, 2 days after injection the Formalin-treated mice had lower ceruloplasmin activities than those given injections of I_b cells ($P<0.01$). This difference was eliminated by day 5, and as with I_b-immunization, the Formalin treatment also caused a prolonged 125% elevation of ceruloplasmin activity (text-fig. 3). Challenge with I_b cells further increased plasma ceruloplasmin activity ($P<0.01$) in both immunized and Formalin-treated animals (text-fig. 3). All unimmunized animals (i.e., those given only the Formalin vehicle) were dead of leukemia within 6 days after administration of the challenge dose. The increases from prechallenge levels were equivalent in I_b-treated (129%) and Formalin-treated mice (138%). Males and females gave equivalent responses to the injection regimens.

Nutritional factors may modify the sequence of events leading to death by malignant lymphocytes. Accordingly, a study was conducted to determine the time course of death from the I_b leukemia in −Cu mice compared to that in +Cu controls (table 2). There were no significant differences in the time of death at any of the three doses employed. Furthermore, linear regression and slope analysis demonstrated that both groups responded similarly.

TABLE 2.—*Effect of −Cu on survival times of nonimmunized mice to line I_b malignant lymphocytes*[a]

Dose of viable I_b cells	Time of death, mean days ± SD (No. of mice)	
	+Cu	−Cu
10^3	9.8±1.6 (8)	10.0±0.8 (11)
10^5	6.9±0.5 (9)	7.4±0.6 (11)
10^7	4.6±0.9 (10)	4.7±0.7 (12)

[a] Each mouse received a single ip injection of the appropriate dose; survival and death due to leukemia were evaluated twice daily. All mice died of leukemia. Mean comparisons were made by Student's *t*-test, and no significant differences were observed.

DISCUSSION

−Cu in animals is known to lead to alterations in several biologic systems—hematologic, cardiovascular, central nervous, and skeletal. The immune system should now be added to this list. The severity of the alterations depends, to a large extent, on the degree of deficiency and the sensitivity of the system to Cu depletion. The immune system must be very sensitive to Cu depletion because profound effects on both humoral (*9*) and cell-mediated immunity (table 1) are observed in −Cu mice that display only modest changes in the other biologic systems sensitive to Cu deprivation.

Unlike dietary −Cu in other species, mice show variable responses to treatment as determined by hematocrit values (text-fig. 1) and plasma ceruloplasmin activities (text-fig. 2). This variable response of mice to the −Cu diet has been noted previously (*9*) and most probably reflects the individual animal's unique growth requirement. Contributing to this variability is the amount of Cu transferred during lactation and the efficiency in metabolizing the small amount of Cu that remains in the purified diet.

Despite individual variability, the results indicate that dietary −Cu severely impairs the ability of C58 mice to be immunized to line I_b syngeneic malignant lymphocytes (table 1), a known T-cell response (*3, 4*). Thus −Cu mice appear to have not only an impaired humoral response to sheep red blood cells (*9*) but also a definite decline in cell-mediated immunity as well. It is as yet too early to speculate which of the immunologic triad, B-cells, T-cells, or macrophages, is most affected by −Cu. Preliminary results in our laboratory indicate that the mitogen reactivity of both T- and B-cells is diminished in −Cu mice. Indeed, it appears that reactivity of T-cells from −Cu mice spleens is impaired in proportion to the plasma ceruloplasmin concentrations (Lukasewycz OA, Prohaska JR: Unpublished results). In vitro generation of cytotoxic T-cells is reduced in acute −Cu (Cu-depleted media), and this effect is most likely due to an impairment of T-cell helper function (*12*). If these findings can be extended in vivo, the loss of T-helper cell function could explain the loss of both humoral and cellular immune function seen in −Cu mice.

The exact mechanism by which immunocompetent cells and/or their subsets might be affected by Cu deprivation is unknown. One intriguing possibility is that the cytocidal function of immunocompetent cells is lowered due to −Cu. Boyne and Arthur (*13*) have shown that Cu-deprived cattle have neutrophils with decreased microbicidal activity. Whether this observation can be extended to a tumor system is yet to be determined.

−Cu leads to myriad physiologic changes, which are thought to be due to decreases in the Cu-dependent enzymes, such as ceruloplasmin, cytochrome oxidase, dopamine *β*-hydroxylase, lysyl oxidase, superoxide dismutase, and tyrosinase (*14*). Ceruloplasmin itself exhibits a multitude of properties (*15–17*), which include the mobilization of iron into the serum (ferroxidase), serum antioxidant activity (iron and superoxide radical scavenger), an acute-phase reactant, and Cu transport. It has recently been shown in in vitro studies with human peripheral lymphocytes that ceruloplasmin (*18*), especially in the presence of thiols (*19*), can significantly modify T-cell function. Thus the ceruloplasmin deficit seen in −Cu mice might affect the immune system directly, although the role of other cuproenzymes cannot be excluded. For example, Leuthauser et al. (*20*) have recently shown that a Cu chelate with superoxide dismutase activity has antitumor properties. Thus −Cu mice, with low superoxide dismutase activity, may be more likely to succumb to lymphocytic leukemia than those with normal enzyme levels.

The increase in ceruloplasmin evident in the C58-I_b system (text-fig. 3) is similar to the increase seen in human chronic lymphocytic leukemia (*21*) and in Hodgkin's disease (*18*). Both +Cu and −Cu mice exhibit elevated ceruloplasmin activity after I_b immunization (table 1). The rise in ceruloplasmin does not require the presence of I_b cells because Formalin-treated mice also exhibit long-term hyperceruloplasminemia (text-fig. 3). This response in −Cu mice is analogous to that seen in −Cu rats stimulated by carrageenan (*22*). The increase in ceruloplasmin is believed to be the result of its synthesis by liver due to the action of lymphocyte-activating factor released by stimulated macrophages (*23*). What the precise role of rising ceruloplasmin concentrations might be in response to tumors or as an acute-phase reactant to inflammation is yet to be determined.

Starvation experiments with the C58-I_b system performed by Martinez et al. (*8*) showed that a 2-day starvation period, bracketing the time of immunization, greatly suppresses the cellular immune response to I_b cells. Starvation also affected established immunity: Immunized mice that were starved had a significantly lower survival rate to a challenge regimen compared to that of mice that were not starved with regard to −Cu (table 1). There is, however, a considerable difference between the two systems. Starvation causes decreases in the number of peripheral blood leukocytes and in the number of nucleated splenocytes, as well as a significant reduction in spleen, thymus, and body weights (*8*). −Cu results in splenomegaly and near normal body weights (*9*). There appears to be no difference in the number of peripheral blood lymphocytes, and the number of nucleated splenocytes is increased over +Cu controls (Lukasewycz OA, Prohaska JR: Unpublished results). Adoptive cell transfer experiments showed that the immunocompetence of individual spleen immunocytes was not reduced by starvation (*8*). We are currently in the process of determining whether this is true for −Cu mouse splenocytes. This is probably not the case because of the preliminary results with in vitro mitogen assays, which indicate that the reactivity of T-cells of −Cu mice to concanavalin A is substantially below that of their +Cu counterparts.

The suppression of immunity seen here with Cu depletion also appears to be distinct from that seen with other trace element deficiencies. Zinc-deficient animals also have both an impaired humoral (*24*, *25*) and a cell-mediated (*26*) immune response, which appear to be dependent on T-helper cell function (*24*, *27*). Zinc deficiency affects cell-mediated immunity as measured by depressed T-killer cell activity against EL-4 tumors and leads to a low natural killer cell activity but essentially a normal antibody-dependent cell-mediated cytotoxicity response (*26*). However, zinc-deficient mice are characterized by an atrophic spleen and thymus, a situation that does not occur in −Cu (*9*). Furthermore, zinc metabolism is unaltered by −Cu (*28*). Lastly, many transplantable tumors show restricted growth in animals maintained on a zinc-deficient diet (*29–32*). Although the growth of those tumors has not yet been evaluated in −Cu mice, the growth of I_b cells does not appear to be slowed.

Perturbations in iron metabolism in the −Cu mice may explain both the decrease in antibody production (*9*) and the impairment of cell-mediated immunity (table 1), since iron deficiency itself can alter both humoral and cell-mediated immunity (*7*). We do not believe that iron deficiency is a major factor in the immunologic impairment seen in −Cu mice. Mice with minimal anemia and normal liver iron levels still show an impaired antibody response to sheep red blood cells (*9*). Also, a nonanemic state does not predict survival, especially in the I_b challenge of −Cu mice (table 1).

The biochemical and immunologic mechanisms in which Cu is required for a competent immune system are not known. The data herein establish that an adequate dietary level of Cu is necessary for an effective cell-mediated immune response to tumor cells.

REFERENCES

(*1*) Lukasewycz OA, Martinez D, Murphy WH. Immune mechanisms in leukemia: Evaluation of immunocompetent cell populations. J Immunol 1975; 114:1491–1496.

(*2*) Martinez D, Lukasewycz OA, Murphy WH. Immune mechanisms in leukemia: Suppression of cellular immunity by drugs and X-irradiation. J Immunol 1975; 115:724–729.

(*3*) Lukasewycz OA, Duffey PS, Murphy WH. Immune mechanisms in leukemia: Protective capacity of the major lymphoid cell compartments. J Immunol 1976; 116:976–981.

(*4*) Duffey PS, Lukasewycz OA, Olson DS, Murphy WH. Differential protective effects of immune lymphoid cells against transplanted line I_b leukemia and immune polioencephalomyelitis. J Immunol 1978; 121:2316–2321.

(*5*) Lukasewycz OA, Frelinger JA. Immune mechanisms in leukemia: Role of the Ia antigens. J Exp Med 1977; 145:1077–1081.

(*6*) Lin JS, Huber N, Murphy WH. Immunization of C58 mice to line I_b leukemia. Cancer Res 1969; 29:2157–2162.

(*7*) Gross RL, Newberne PM. Role of nutrition in immunologic function. Physiol Rev 1980; 60:188–302.

(*8*) Martinez D, Cox S, Lukasewycz OA, Murphy WH. Immune mechanisms in leukemia: Suppression of cellular immunity by starvation. J Natl Cancer Inst 1975; 55:935–939.

(*9*) Prohaska JR, Lukasewycz OA. Copper deficiency suppresses the immune response of mice. Science 1981; 213:559–561.

(*10*) Prohaska JR. Comparison between dietary and genetic copper deficiency in mice: Copper-dependent anemia. Nutr Res 1981; 1:159–167.

(*11*) Tennant JR. Evaluation of the trypan blue technique for determination of cell viability. Transplantation 1964; 2:685–694.

(*12*) Flynn A, Yen BR. Mineral deficiency effects on the generation of cytotoxic T-cells and T-helper cell factors in vitro. J Nutr 1981; 111:907–913.

(*13*) Boyne R, Arthur JR. Effects of selenium and copper deficiency on neutrophil function in cattle. J Comp Pathol 1981; 91:271–276.

(*14*) Underwood EJ. Trace elements in human and animal nutrition. 4th ed. New York: Academic Press, 1977.

(*15*) Frieden E, Hsieh HS. Ceruloplasmin: The essential copper transport protein with essential oxidase activity. Adv Enzymol 1976; 44:187–236.

(*16*) Frieden E. Ceruloplasmin: the serum copper transport protein with oxidase activity. In: Nriagu JO, ed. Copper in the environment. Part II. New York: Wiley. 1979:241–284.

(*17*) ———. Caeruloplasmin: A multi-functional metalloprotein of vertebrate plasma. Biological roles of copper. Excerpta Medica 1980:93–124.

(*18*) Larsen B, Heron I, Thorling EB. Elevated serum Cu in Hodgkin's disease and inhibitory effects of ceruloplasmin on lymphocyte response in vitro. Eur J Cancer 1980; 16:415–421.

(*19*) Lipsky PE. Modulation of T lymphocyte function by copper and thiols. Agents Actions 1981; 8:85–102.

(*20*) Leuthauser SW, Oberley LW, Oberley TD, Sorenson JR, Ramakrishna K. Antitumor effect of a copper coordination compound with superoxide dismutase-like activity. JNCI 1981; 66:1077–1081.

(*21*) Green JA, Pocklington T, Dawson AA, Foster M. Electron spin resonance studies on caeruloplasmin and iron transferrin in patients with chronic lymphocytic leukaemia. Br J Cancer 1980; 41:356–359.

(*22*) Milanino R, Passarella E, Velo GP. Copper and the inflammatory process. Adv Inflamm Res 1979; 1:281–291.

(*23*) Pekarek RS, Powanda MC, Wannemacher, RW Jr. The effect of leukocytic endogenous mediator (LEM) on serum copper and ceruloplasmin concentrations in the rat. Proc Soc Exp Biol Med 1972; 141:1029–1031.

(*24*) Fraker PJ, Haas SM, Luecke RW. Effect of zinc deficiency on the immune response of the young adult A/J mouse. J Nutr 1977; 107:1889–1895.

(*25*) Frost P, Chen JC, Rabbani I, Smith J, Prasad AS. The effect of zinc deficiency on the immune response in zinc metabolism. In: Brewer GJ, Prasad AS, eds. Zinc metabolism: Current aspects in health and disease. New York: Liss, 1977:211–236.

(*26*) Fernandes G, Nair M, Onoe K, Tanaka T, Floyd R, Good RA. Impairment of cell-mediated immunity functions by dietary zinc deficiency in mice. Proc Natl Acad Sci USA 1979; 76:457–461.

(*27*) Beach RS, Gershwin ME, Makishima RK, Hurley LS. Impaired immunologic ontogeny in post-natal zinc deprivation. J Nutr 1980; 11:805–815.

(*28*) Alfaro B, Heaton FW. Relationships between copper, zinc and iron in the plasma, soft tissues and skeleton of the rat during Cu deficiency. Br J Nutr 1973; 29:73–84.

(*29*) DeWys W, Pories WJ, Richter MC, Strain WH. Inhibition of Walker 256 carcinosarcoma growth by dietary zinc deficiency. Proc Soc Exp Biol Med 1970; 13:17–22.

(*30*) DeWys W, Pories W. Inhibition of a spectrum of animal tumors by dietary zinc deficiency. J Natl Cancer Inst 1972; 48:375–381.

(*31*) Barr DH, Harris JW. Growth of the P388 leukemia as an ascites tumor in zinc deficient mice. Proc Soc Exp Biol Med 1973; 144:284–287.

(*32*) Fenton MR, Burke JP, Tursi FD, Arena FP. Effect of a zinc-deficient diet on the growth of an IgM-secreting plasmacytoma (TEPC-183). JNCI 1980; 65:1271–1272.

blank page

Effects of Different Fractions of *Corynebacterium parvum* on the Cytotoxic T-Cell Response to Alloantigens in Mice[1,2,3]

Alan Lichtenstein,[4] **Richard Tuttle,**[5] **John Cantrell,**[6] *and* **Jacob Zighelboim**[7,8]

ABSTRACT—The effects of several biochemically derived fractions of *Corynebacterium parvum* and chemically treated intact organisms on the generation of cytotoxic T-lymphocytes (CTL) were assessed in a tumor allograft model with the use of C57BL/6 and DBA/2 mice. The acid-modified, active and inactive fragmented preparations and pyridine extract and residue were all capable of inhibiting primary spleen cell allocytotoxicity. Only the active fragmented, pyridine residue and unfractionated preparations caused splenomegaly and prevented the secondary in vitro generation of CTL. Periodate treatment, acid modification, and pyridine extraction abrogated the ability of *C. parvum* to activate suppressor macrophages. Although incapable of activating suppressor macrophages, the phenol and pyridine extracts significantly enhanced suppressor T-cell activity. The effect of whole *C. parvum* organisms on T-cell-mediated cytotoxicity is thus extremely complex and due to the direct activation or inhibition of various cell types that interact with each other.—JNCI 1982; 69:495–501.

The BRM *Corynebacterium parvum* potentiates many aspects of the immune system. It augments antibody responses (*1*), increases clearance function of the reticuloendothelial system (*2*), and activates cytotoxic macrophages (*3*). Paradoxically, it can also cause immunosuppression, inhibiting graft-versus-host reactivity (*4*), delayed cutaneous hypersensitivity (*5*), proliferative responses to mitogens and alloantigens (*6, 7*), and cytotoxic responses to tumor-associated viral antigens and alloantigens (*8, 9*). The paradox extends to the more recently described cytotoxicity mediated by natural killer cells, which has been reported to be amplified (*10*) as well as suppressed (*11*) by injections of *C. parvum*.

These diverse contrasting effects might be explained by an indiscriminant activation of macrophages by the drug and the subsequent interaction between these cells and other varied cell types of the immune system. Enhancement of cytotoxic or accessory macrophages as well as suppressor macrophage function could account for simultaneous positive and negative effects on the host.

An alternative explanation is that the *C. parvum* organism contains multiple determinants that independently activate different subsets of lymphoid cells with different functions. We have explored this hypothesis by examining the effects of several biochemically derived fractions of *C. parvum* and chemically treated intact organisms on the generation of T-CMC in a tumor allograft model. The depression of primary spleen cell cytotoxicity, inhibition of secondary in vitro generated CMC, and activation of suppressor cells appear to be due to separate components of the organism. In addition, several fractions were identified that activate suppressor T-cells independently of suppressor macrophage activation, whereas others activated suppressor T-cells and macrophages simultaneously.

MATERIALS AND METHODS

Animals.—Male C57BL/6 mice (The Jackson Laboratory, Bar Harbor Maine) were obtained at 6 weeks of age. They rested at least 1 week before the initiation of an experiment.

Immunization.—The P815 mastocytoma was maintained in ascites form by weekly ip passage in female DBA/2 mice (The Jackson Laboratory), the strain of origin. C57BL/6 mice were immunized on day 0 by an sc injection of 2×10^7 P815 cells. Seven days later, one group of mice received injections iv in the lateral tail vein with 0.2 ml of phosphate-buffered saline containing 500 µg of *C. parvum* (strain CN 6143; Burroughs-Wellcome Co., Research Triangle Park, N.C.) or one of its fractions. All mice were killed on day 14 for assay of spleen cell cytotoxic activity, for in vitro restimulation of splenocytes, and for the ability to suppress primary or secondary in vitro generation of CTL.

In vitro stimulations.—Spleens were removed aseptically from naive or alloimmunized mice (14 days post alloimmunization with 2×10^7 P815 sc), and a single cell suspension was prepared by filtration of the organ through a stainless-steel mesh. Spleen cells (5×10^6) were cultured with 5×10^6 mitomycin C-treated P815 in 2.5 ml of Eagle's minimum essential medium (M.A. Bioproducts, Walkersville, Md.) supplemented with 10% fetal calf serum, L-glutamine, antibiotics, and 5×10^{-5} *M* 2-mercaptoethanol. The cultures were maintained at 37°C for 5 days in a humidified CO_2 incubator, after which the cells remaining in culture were harvested and tested for cytotoxic activity. To test for suppressor cell activity, we added 5×10^6 spleen cells from *C. parvum*- or fraction-treated alloimmunized mice to 5×10^6

ABBREVIATIONS USED: ATS=antithymocyte serum; BRM=biologic response modifier(s); C=complement; CMC=cell-mediated cytotoxicity; CTL=cytotoxic T-lymphocyte(s); E:T=effector-to-target cell ratio(s); T-CMC=T-cell CMC.

---

[1] Received October 20, 1981; accepted March 24, 1982.

[2] Supported by a grant from the California Institute for Cancer Research and by an American Cancer Society–University of California at Los Angeles (UCLA) institutional grant.

[3] Animals were maintained under the guidelines set forth by the UCLA Medical School and by the Wadsworth Veterans Administration Hospital.

[4] Department of Medicine, Wadsworth Veterans Administration Medical Center, Los Angeles, Calif. 90073.

[5] Tumor Biology Section, Molecular Biology Department, Burroughs-Wellcome Co., Research Triangle Park, N.C. 27709.

[6] Ribi Immuno Research Inc., Hamilton, Mont. 59840.

[7] Departments of Medicine and Microbiology and Immunology, University of California at Los Angeles School of Medicine, Los Angeles, Calif. 90024.

[8] We thank Melané Ali for expert technical assistance.

spleen cells from alloimmunized control (secondary stimulation) or naive control (primary stimulation) animals prior to the initiation of culture. Addition of spleen cells from naive or alloimmunized mice had no significant effect on the specific cytotoxic activity of stimulated cells. As we have previously reported (*12*), addition of spleen cells from naive mice given iv injections of 700 µg *C. parvum* up to 7 days prior to assay has no effect on in vitro CTL generation, although spleen cells from naive mice given injections of 1,400 µg are significantly suppressive to CTL generation.

Test for CMC.—Spleen cells taken directly from mice or harvested from 5-day cultures were tested for cytotoxic activity against ^{51}Cr-labeled P815 by the method of Brunner et al. (*13*). Cytotoxicity was measured at several E:T with the use of an incubation period of 4 hours. Results are expressed as percent specific release calculated as follows: Percent specific release = [(percent release experimental group − percent minimum release)/percent maximum release] × 100. Maximum release was determined by addition of concentrated HCl to a final dilution of 1 *M* and was generally between 80 and 90% of total incorporated counts. Minimum release was a medium control and ranged from 7 to 15% of total incorporated counts. One lytic unit was defined as the number of effector cells required to yield 25% specific release in primary cultures and primary in vivo spleen cytotoxicity and 50% specific release in secondary cultures.

Fractionation of C. parvum.—The fractions investigated in this study are listed in table 1 with their composition if known.

Phenol-water extraction.—Killed *C. parvum* was extracted with hot phenol-water (1:1) by the standard Westphal method as previously described (*14*). Material extracted in the phenol phase was designated the "phenol extract" (fraction A). The pelleted residue material was resuspended and centrifuged at 30×*g* for 10 minutes, and the supernatant was obtained and designated the "light residue" (fraction B). We have previously reported on some of the effects of the phenol extract and light residue on T-CMC (*15*).

Disruption.—The active fragmented fraction C was supplied by Dr. V. Riveros-Moreno, Burroughs-Wellcome Ltd., Beckenham, England. The fraction was prepared by disruption in an X-press in the presence of 20 m*M* dithiothreitol as previously described (*16*). The preparation was lyophilized and stored. Some of its properties have been previously reported (*17*).

TABLE 1.—*Composition of* C. parvum *fractions*[a]

Fraction	Percent of recovered material	Percent of fraction by weight		
		Protein	Fatty acid	Total sugar
Whole cells	—	29.2	36.2	11.8
A: Phenol extract	9	40.5	39.6	2.3
B: Light residue	88	26.6	31.2	10.5
C: Active fragmented	NT	NT	NT	NT
D: Inactive fragmented	NT	2.5	NT	14.5
E: Pyridine extract	9	12.1	47.2	12.4
F: Pyridine residue	91	21.4	33.6	12.2
G: Periodate modified	NT	NT	NT	NT
H: HCl modified	NT	NT	NT	NT

[a] NT=not tested.

The inactive fragmented preparation (fraction D) was also a gift of Dr. V. Riveros-Moreno and prepared as described by Riveros-Moreno et al. in (*18*). Whole bacteria were broken in a Novotny cell disruptor. After the cells were resuspended in 0.1 *M* Tris buffer (pH 7.6), Ballotini beads (#12) were added, and the mixture was prepared at 10,000 rpm for 1.5 minutes on ice and NaCl in a homogenizer. The homogenate was filtered and the glass beads were washed. The material was centrifuged at 1,000×*g* for 20 minutes at 4°C, and the resulting supernatant was treated sequentially with 2% sodium dodecyl sulfate, trypsin, DNase, and RNase as previously described (*18*). Some of the properties of this preparation have been previously reported (*18*).

Pyridine extraction.—Ninety grams (wet weight) of washed *C. parvum* whole-cell paste was added to 200 ml of neat pyridine, reagent grade (J. T. Baker Chemical Co., Phillipsburg, N.J.). The extraction mixture was stirred for 18 hours at 37°C. Supernatant fraction obtained after centrifugation of the mixture at 17,000×*g* for 1 hour at 4°C was designated the "pyridine extract" (fraction E). Pelleted materials were extracted two times more in the original volume of pyridine. After filtration, the pyridine soluble extracts were pooled and the solvent was removed by evaporation at 50°C in a Buchi Rotavapor (Brinkmann Instruments, Inc., Westbury, N.Y.). The dried pyridine extract was dialyzed against distilled water, freeze dried, and lyophilized. The insoluble residue (fraction F) was washed three times with sterile, distilled water. After centrifugation at 17,000×*g* for 1 hour at 4°C, the residue was suspended in distilled water, dialyzed for 7 days, and then lyophilized.

Periodate and HCl modifications.—Periodate and HCl modifications of whole organisms were performed as previously described (*19*). Organisms suspended in phosphate-buffered saline were mixed with sodium metaperiodate (pH 5.0) and held in the dark for 30 seconds. The final molarity of periodate was 250 m*M*. The action of the oxidant was stopped by addition of 20% glucose solution. This preparation (fraction G) and its effect on spleen weight have been previously reported (*19*). Lyophilized organisms were suspended in 0.1 *N* HCl in a stoppered tube and held in a temperature-controlled water bath for 10 minutes. This preparation (fraction H) and its effect on spleen weight have been previously reported (*19*).

Fractionation of suppressor cells.—Phagocytic cells were removed by incubation of spleen cells with carbonyl iron (GAF Corp., New York, N.Y.) for 30 minutes at 37°C followed by separation over a magnet. Recovery was between 40 and 60% of starting cell numbers. This treatment reduced the percentage of nonspecific esterase-positive cells in spleens from *C. parvum*-treated mice from 20 to 25% to less than 1%.

T-cells were removed by incubation of 10^7 cells/ml in a 1:45 dilution of absorbed rabbit anti-mouse thymocyte serum (M.A. Bioproducts) for 30 minutes at 4°C. The cells were centrifuged and incubated at the same concentration in a 1:15 dilution of agarose-absorbed guinea pig C (M.A. Bioproducts) for 30 minutes at 37°C. This concentration killed 100% of thymocytes, less than 10% of bone marrow cells, and 40–50% of spleen cells. The treatment also abrogated the proliferative response to the T-cell mitogen phytohemagglutinin. The cells were washed and resuspended at the desired concentration of viable cells.

Statistics.—The *t*-test was utilized to determine *P*-values between experimental and control groups.

RESULTS

Effect of iv injection of C. parvum *fractions on generation of primary T-CMC in spleen.*—Administration of iv *C. parvum* to alloimmunized mice depresses the subsequent generation of alloreactive splenic CTL (*20*). We investigated whether several biochemically derived fractions of active organisms or chemically treated intact organisms can also mediate this inhibition of CMC. Mice were alloimmunized and given injections of 500 μg of various *C. parvum* fractions on day 7. (Immunized mice not given injections served as the control group.) Fourteen days after alloimmunization (day +14), mice were killed and spleen cells assayed for cytotoxicity to allogeneic tumor cells. Table 2 demonstrates that unfractionated *C. parvum*, as well as the active fragmented fraction, markedly depresses the generation of cytotoxic splenocytes. In addition, the HCl-modified preparation, pyridine extract, and pyridine residue were all capable of depressing primary splenic CMC. The periodate-modified fraction had a minimal effect on cytotoxicity. A somewhat surprising finding was that the inactive fragmented fraction caused significant depression of splenic CMC.

Induction of splenomegaly by C. parvum *fractions.*—Table 3 demonstrates that the depressive effects of the various fractions on spleen CMC were not simply due to induction of splenomegaly and dilution of CTL by influx of irrelevant cells. Spleen cell indices were measured in alloimmunized mice at the time of assay 7 days after fractions were injected (500 μg). Only the unfractionated organism, the active fragmented preparation, and the pyridine residue clearly induced splenomegaly.

Effect of C. parvum *fractions on secondary in vitro generation of CMC.*—Administration of *C. parvum* to alloimmunized mice prevents the subsequent generation of secondary CTL following rechallenge in vivo and in vitro (*9, 21*). Table 4 shows the effects of the different fractions on the generation of secondary CTL in vitro. Alloimmunized mice were either not given injections (control group) or given injections of 500 μg of various fractions 7 days after alloimmunization. On day +14, mice were killed and spleen cells were restimulated for 5 days in vitro with allogeneic tumor cells. As shown, only unfractionated *C. parvum*, the active fragmented preparation, and the pyridine residue were effective in inhibiting the subsequent generation of secondary CTL in vitro.

TABLE 2.—*Effect of* C. parvum *fractions on generation of primary splenic allocytotoxicity*[a]

Agent injected	Percent specific release at E:T		
	100:1	20:1	4:1
Control	27±5	13±3	5±1
Whole *C. parvum*	2±.4[b]	1±.2[b]	1±.3[b]
Fraction C: Active fragmented	3±1[b]	2±.6[b]	1±.5[b]
Fraction D: Inactive fragmented	7±1[b]	5±.4[b]	1±.4[b]
Fraction H: HCl modified	10±3[b]	6±1.1[b]	2±.6[b]
Fraction G: Periodate modified	19±6	8±4	3.5±1
Fraction E: Pyridine extract	15±5[b]	6±2[b]	2±.5[b]
Fraction F: Pyridine residue	5±2[b]	3±1[b]	1±.2[b]

[a] Primary spleen cytotoxicity was assayed in a ^{51}Cr release assay against chromated P815 cells 14 days after alloimmunization and 7 days after injection of whole or fractionated *C. parvum* organisms (500 μg). Results are mean percentages of specific lysis ± SD of three experiments (2–3 mice/each group/each individual expt). Lysis was determined at three E:T.

[b] Significantly different from control, $P<0.05$.

TABLE 3.—*Effects of* C. parvum *fractions on splenic cellularity*[a]

Agent injected	Spleen cell index
Whole *C. parvum*	2.54±0.29
Fraction C: Active fragmented	2.18±0.21
Fraction D: Inactive fragmented	1.13±0.09
Fraction H: HCl modified	1.11±0.11
Fraction G: Periodate modified	1.34±0.14
Fraction E: Pyridine extract	1.30±0.13
Fraction F: Pyridine residue	2.10±0.24

[a] Splenic cellularity was determined 14 days after alloimmunization and 7 days after injection of whole or unfractionated *C. parvum* organisms (500 μg). Spleen cell index was calculated by the following formula: (Cellularity/spleen of whole or fraction treated mice)/(cellularity/spleen of control mice). Results are means ± SD of four experiments (2–3 mice/group/expt).

TABLE 4.—*Effect of* C. parvum *fractions on generation of secondary in vitro CMC*[a]

Agent injected	Percent specific release at E:T		
	25:1	5:1	1:1
Control	83±4	70±6	41±3
Whole *C. parvum*	10±2[b]	2±1[b]	1±.4[b]
Fraction C: Active fragmented	19±3[b]	6±1[b]	3±1[b]
Fraction D: Inactive fragmented	—	59±3	35±6
Fraction H: HCl modified	78±2	73±8	33±4
Fraction G: Periodate modified	79±1	76±6	34±7
Fraction E: Pyridine extract	83±3	67±4	28±1
Fraction F: Pyridine residue	56±3[b]	15±3[b]	3±1[b]

[a] Alloimmune control or alloimmunized mice that received iv injections of whole or fractionated *C. parvum* were killed 14 days after immunization (2×10^7 P815 cells), and spleen cells were restimulated with P815 for 5 days after which secondary CTL generation was assayed against chromated P815 targets. Results are mean percentages of specific lysis ± SD of three experiments (2–3 mice/each group/each expt). Lysis was determined at three E:T.

[b] Significantly different from control, $P<0.05$.

Activation of suppressor cells.—We have previously reported that *C. parvum* activates suppressor macrophages and T-cells (*12*). The former markedly curtail primary and secondary in vitro generation of CTL, whereas the latter are only effective in preventing primary in vitro CMC. Text-figure 1 demonstrates the ability of spleen cells from fraction-treated alloimmune mice to suppress the generation of secondary CTL in vitro. The active fragmented preparation is as effective as the whole organism in this regard. In contrast, periodate modification, HCl modification, and pyridine extraction alter the organism so that it no longer activates suppressor macrophages.

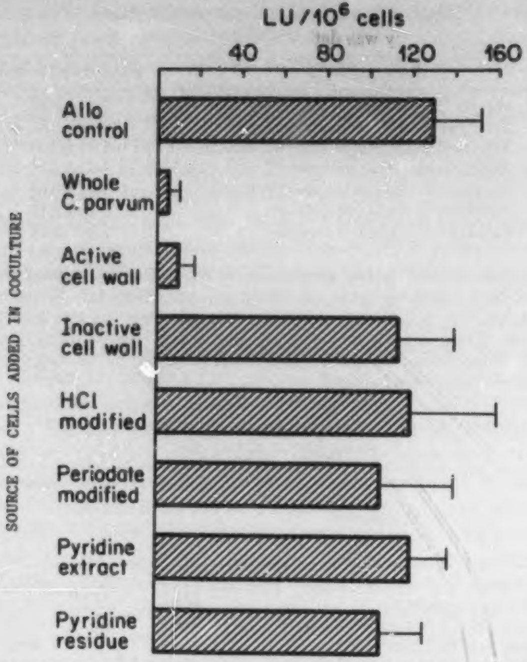

TEXT-FIGURE 1.—Activation of suppressor cells that curtail in vitro generation of secondary CTL by various *C. parvum* fractions. Suppressor spleen cells were obtained 7 days after injection of whole or fractionated *C. parvum* (14 days after alloimmunization) and added to spleen cells from alloimmune control (Allo control) mice (14 days after alloimmunization). These cocultures were restimulated with mitomycin C-treated P815 for 5 days, and the generation of secondary CTL was assessed against P815 targets. Addition of equivalent numbers of spleen cells from alloimmune control mice to secondary cultures resulted in cytotoxicity identical to that generated in secondary cultures alone, and this control is not shown. Results are lytic units (LU)/10^6 cells generated in culture, mean ± SD of four experiments. Active cell wall=active fragmented fraction C; inactive cell wall=inactive fragmented fraction D.

TABLE 5.—*Activation of either suppressor macrophages or T-cells by* C. parvum *fractions*[a]

Suppressor cell source	Fractionation	Lytic units/ 10^6 cells generated in culture
Naive control	—	5±1.3
Whole *C. parvum* injected	—	1.7±0.3[b]
Whole *C. parvum* injected	Iron and magnet	1.8±0.4[b]
Whole *C. parvum* injected	ATS and C	1.6±0.2[b]
Whole *C. parvum* injected	Iron and magnet-ATS and C	4.7±1
Light residue injected	—	1.8±0.1[b]
Light residue injected	Iron and magnet	1.7±0.2[b]
Light residue injected	ATS and C	1.6±0.2[b]
Light residue injected	Iron and magnet-ATS and C	4.5±1.1

[a] Putative suppressor spleen cells from whole *C. parvum*- or light residue-treated alloimmunized mice were added to primary sensitizations or first fractionated to remove phagocytic or theta-bearing cells before addition to primary cultures. After 5 days of culture, cytotoxicity to chromated P815 targets (the stimulating cells) was assessed. Results are mean lytic units/10^6 cells in culture ± SD of three experiments.

[b] Significantly different from control, $P<0.05$.

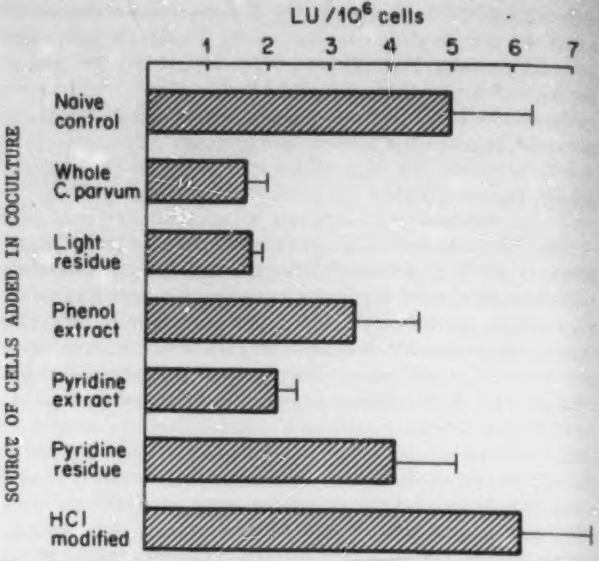

TEXT-FIGURE 2.—Activation of suppressor cells that curtail in vitro generation of primary CTL by various *C. parvum* fractions. Suppressor spleen cells were obtained 7 days after injection of whole or fractionated *C. parvum* (14 days after alloimmunization) and added to spleen cells from naive mice. These cocultures were stimulated with mitomycin C-treated P815 for 5 days, and the generation of primary CTL was assessed against P815 targets. Suppressor cells were treated with mitomycin C before addition to culture for prevention of their clonal expansion when encountering P815, the alloantigen to which they had been primed. Addition of mitomycin C-treated alloimmune control splenocytes to primary cultures resulted in cytotoxicity identical to that generated in primary cultures alone, and this control is not shown. Results are lytic units (LU)/10^6 cells generated in culture, mean ± SD of four experiments.

TABLE 6.—*Activation of either suppressor macrophages or T-cells by* C. parvum *fractions*[a]

Suppressor cell source	Fractionation	Lytic units/10^6 cells generated in culture
Naive control	—	5.4±1.7
Phenol extract	—	3.4±1.1[b]
Phenol extract	Iron and magnet	2±0.2[b]
Phenol extract	ATS and C	4.6±1.2
Pyridine extract	—	2.2±0.2[b]
Pyridine extract	Iron and magnet	1.8±0.3[b]
Pyridine extract	ATS and C	4.9±1

[a] Putative suppressor spleen cells from phenol- or pyridine extract-treated alloimmunized mice were added to primary sensitizations or first fractionated to remove phagocytic or theta-bearing cells before addition to primary cultures. After 5 days of culture, cytotoxicity to chromated P815 targets (the stimulating cells) was assessed. Results are mean lytic units/10^6 cells in culture ± SD of three experiments.

[b] Significantly different from control, $P<0.05$.

The fractions were also assayed for their ability to activate suppressor cells that prevent primary in vitro CMC. Text-figure 2 demonstrates that unfractionated *C. parvum*, light residue (obtained after phenol–water extraction), and the pyridine extract significantly activate suppressor cells that prevent the generation of primary CMC. The phenol extract modestly activates suppressor cells, whereas HCl-modified and pyridine residue fractions are without effect.

Prior to the addition of putative suppressor cells to primary cultures, suppressor cells were depleted of T-cells by treatment with ATS and C or of macrophages by incubation with iron fillings and exposure to a magnet. Although depletion of T-cells and macrophages independently had no effect on suppression mediated by spleen cells from mice treated with whole *C. parvum* or light residue, suppression was abrogated when the spleens were depleted of T-cells and macrophages by sequential use of both fractionation procedures (table 5). We have interpreted these results to indicate the simultaneous activation of suppressor T-cells and macrophages. In contrast, suppression of primary CMC mediated by spleen cells from mice given injections of phenol and pyridine extracts is completely abrogated by treatment with ATS and C, indicating the sole activation of suppressor T-cells (table 6).

DISCUSSION

The results of the current study confirm and extend our previous observations utilizing different fractions of *C. parvum* (*15*) in regard to several points. First, the inhibition of T-CMC by *C. parvum* appears to be due to the effects of several biochemical moieties of the organism that function independently to modulate various aspects of T-CMC. Acid modification and pyridine extraction yield preparations that have lost the ability to inhibit secondary CMC but effectively curtail primary spleen cytotoxicity, indicating the distinctness of the structures that induce these effects. These results also indicate that, under certain conditions, the generation of primary allocytotoxic T-lymphocytes can be completely dissociated from the expression of secondary CMC.

Second, while the pyridine residue administered in vivo to immunized mice markedly inhibited in vitro secondary CMC generation, it did not generate cells that suppressed secondary stimulation in coculture experiments. Thus *C. parvum* appears to inhibit secondary CMC by at least two mechanisms: the activation of suppressor cells and a second effect that is possibly exerted on the priming process. Alternatively, this second mechanism may simply be a dilution of secondary CTL precursors by a marked influx of irrelevant cells into the spleen, because only the fractions capable of inducing splenomegaly could inhibit the restimulation in vitro.

The action of the various distinct *C. parvum* determinants may be exerted on different cell types of the immune system to account for the diversity of effects. One possible hypothesis is that each determinant activates a specific macrophage subpopulation with a predetermined function. The report by Lee and Berry (*22*) on the physical separation of accessory and suppressor–cytotoxic macrophages activated by *C. parvum* is consistent with this concept. Furthermore, Scott and Warner (*23*) described the activation of macrophages cytostatic for tumor cells by low doses of *C. parvum* without the accompanying activation of macrophages suppressive for T-cell responses, which suggests that the threshold dose for activation of different macrophage subsets may vary. Our results also support the activation of different subsets of macrophages by *C. parvum*. Although the pyridine extract has been reported to activate cytotoxic macrophages (*24*), we found it incapable of activating suppressor macrophages. In a similar fashion, the periodate-treated residue fraction obtained from phenol–water extraction has been reported to activate peritoneal cytotoxic macrophages (*14*), although it (*15*) and the periodate-modified whole-cell preparation used in the current study could not activate suppressor macrophages.

Although *C. parvum* is best known for its macrophage-activating properties, some of its multiple effects may also be due to stimulation of other cell types by other determinants. In this regard, the induction of suppressor T-cells by the phenol extract and the pyridine extract suggests that some components of the *C. parvum* organism can directly activate subsets of T-cells. We had previously noted an inhibition of C-dependent cytotoxic antibody titers caused by administration of the phenol extract to alloimmunized mice, whereas other fractions derived from phenol–water extraction had no effect on the antibody response (*15*). It is tempting to relate this inhibition of alloantibody response to the induction of suppressor T-cells by the phenol extract.

The effects of *C. parvum* fractionation on the ability of the agent to modulate CMC provide some insight into the nature of the determinants responsible for this phenomenon. The active fragmented preparation was comparable to unfractionated *C. parvum* in its inhibition of primary and secondary CMC and activation of suppressor cells, suggesting that at least some of the relevant inhibitory determinants are located in the cell wall structure. In contrast, the inactive fragmented preparation was incapable of inhibiting secondary CMC or activating suppressor cells. Like most other cell wall preparations, the inactive fragmented fraction does not induce splenomegaly (*18*), whereas the active fragmented preparation is an unusual one in that it does induce splenomegaly (*17*). The active one is prepared by fracturing the organism in the presence of the reducing agent dithiothreitol, which may have allowed preservation of the ability to modulate CMC as well as to induce splenomegaly.

In contrast, administration of the inactive fragmented fraction significantly inhibited the generation of primary spleen cytotoxicity. Apparently, the requirements for inhibiting this cytotoxic function are less restricted because most of the fractions tested significantly inhibited the development of primary CMC. In preliminary experiments, a related organism that did not induce splenomegaly (*Corynebacterium granulosum*, CN5888; Burroughs-Wellcome Co.) was capable of inhibiting the generation of primary CMC. This phenomenon raises the question of whether this inhibition is a biologic activity that is unique to the "active" (reticuloendothelial system-stimulating) strains of *Propionibacterium*. Alternatively, these "inactive" preparations may be inactive only insofar as induction of splenomegaly is concerned. In fact, inactive *C. granulosum* is capable of producing chemotactic factors for macrophages (*25*) and can significantly reduce the incidence of tumor nodules in the lung (*26*) although less effectively than does unfractionated *C. parvum*. Although splenomegaly has historically been used as an indicator of biologic activity, these and other data suggest that the activity of a preparation must be defined by the assay used. To further investigate this question, we are devising experiments to assess whether inhibition of primary CMC can be mediated by injection of unrelated organisms or inert particles.

Periodate treatment and HCl treatment of whole organisms abrogate the ability of the adjuvant to inhibit the development of secondary CMC and to activate suppressor macrophages. Although these preparations have not yet been assayed biochemically, both these procedures are reported to markedly liberate galactose residues (*14*, *27*), which suggests that these carbohydrates are important in inducing these effects on the immune system. Since the HCl-modified fraction effectively inhibits primary spleen cytotoxicity, galactose residues are probably not critical in that immunosuppressive action. Neither are galactose residues important in inducing splenomegaly, since *Propionibacterium* species type II can induce splenomegaly and does not contain galactose (*28*). Assaying type II species for their ability to inhibit secondary CMC and to activate suppressor cells will assist in supporting or refuting the hypothesis that galactose residues are prerequisites for these effects.

A dose of 500 µg/mouse was selected for this study because previous experiments indicated that the effects of whole *C. parvum* on T-CMC were lost when a dose of less than 70 µg was used (*29*), and we have seen significant mortality (50–75% of mice) when doses greater than 1,000 µg are administered iv. Comparing fractions at a standard dose (500 µg/mouse) allowed for the detection of significant biologic effects of certain fractions that are present in minimal quantities in unfractionated organisms (i.e., phenol- and pyridine-extractable fractions). However, since extensive dose-response curves for all the fractions have not been completed, it is unclear whether the above active fractions contribute to the overall effects following administration of whole *C. parvum*. Since these active fractions consist of approximately only 10% of recovered material (table 1), injection of 500 µg of purified material is a great enrichment compared to equivalent doses of unfractionated *C. parvum*.

Several laboratories are now actively producing and assessing fractions of *C. parvum* organisms. Simpler preparations with more selective effects on immune and antitumor responses theoretically provide better BRM for use in immunotherapy of cancer. Brunda et al. (*30*) have shown that the inhibitory and stimulating effects of *C. parvum* on natural killer cytotoxicity reside on separate components of the organism. We have also identified fractions that appear to be enriched for the determinants enhancing natural killer cytotoxicity and others that lack these determinants (*31*). A prime candidate for antitumor therapy would be the pyridine extract, which has antitumor activity in animal models (*24*), stimulates natural killer cytotoxicity (*31*) in rats following ip injection, and has no effect on secondary CMC and is not capable of activating suppressor cells.

A secondary important use for these fractions is as probes for the study of the cellular interactions of normal immune responses. A good example of this is our own model for enhancing suppressor cell activity. While this model allows for interesting comparisons between the effects of suppressor T-cells and macrophages induced within the same animal by the same conditions, it is cumbersome when one is attempting to isolate and to study only one suppressor cell type. The availability of fractions (phenol and pyridine extract) that can selectively activate suppressor T-cells is an important tool for the continued study of these cells within this system.

REFERENCES

(*1*) Howard JG, Christie GH, Scott MT. Biological effects of *Corynebacterium parvum*. IV. Adjuvant and inhibitory activities on B lymphocytes. Cell Immunol 1973; 7:290–296.

(*2*) Adlam C, Scott MT. Lympho-reticular stimulatory properties of *Corynebacterium parvum* and related bacteria. J Med Microbiol 1972; 6:261–274.

(*3*) Olivotto M, Bomford R. In vitro inhibition of tumor cell growth and DNA synthesis by peritoneal and lung macrophages from mice injected with *Corynebacterium parvum*. Int J Cancer 1974; 13:478–488.

(*4*) Howard JG, Biozzi G, Stiffel C, et al. An analysis of the inhibitory effect of *Corynebacterium parvum* on graft-versus-host disease. Transplantation 1962; 5:1510–1515.

(*5*) Scott MT. Depression of delayed-type hypersensitivity by *Corynebacterium parvum*: Mandatory role of the spleen. Cell Immunol 1974; 13:251–263.

(*6*) ———. Biological effects of the adjuvant *Corynebacterium parvum*. I. Inhibition of PHA, mixed lymphocyte, and graft-versus-host reactivity. Cell Immunol 1972; 5:459–468.

(*7*) ———. Biological effects of the adjuvant *Corynebacterium parvum*. II. Evidence for macrophage–T cell interactions. Cell Immunol 1972; 5:469–476.

(*8*) Kirchner H, Glaser M, Herberman RB. Suppression of cell mediated tumour immunity by *Corynebacterium parvum*. Nature 1975; 257:396–398.

(*9*) Berd DA, Mitchell MS. Immunological enhancement of leukemia L1210 by *Corynebacterium parvum* in allogeneic mice. Cancer Res 1976; 36:4119–4124.

(*10*) Oehler JR, Lindsay LR, Nunn ME, et al. Natural cell-mediated cytotoxicity in rats. II. In vivo augmentation of NK-cell activity. Int J Cancer 1978; 21:210–218.

(*11*) Flexman JP, Shellam GR. Factors affecting stimulation of natural cytotoxicity to a rat lymphoma by *Corynebacterium parvum*. Br J Cancer 1980; 42:41–51.

(*12*) Lichtenstein A, Murahata RI, Sugasawara R, et al. Suppressor T cells and suppressor macrophages induced by *Corynebacterium parvum*. Cell Immunol 1981; 58:257–268.

(*13*) Brunner KT, Engers HD, Cerotinni J-C. The ^{51}Cr release assay as used for the quantitative measurement of cell-mediated cytolysis in vitro. In: Bloom BR, David JR, eds. In vitro methods in cell-mediated immunity. New York: Academic Press, 1976:423–428.

(*14*) Cantrell JL, Wheat RW. Antitumor activity and lymphoreticular stimulation properties of fractions isolated from *Corynebacterium parvum*. Cancer Res 1979; 39:3554–3563.

(*15*) Murahata RI, Cantrell J, Lichtenstein A, et al. Dissociation of biological activities of *Corynebacterium parvum* by chemical fractionation. Int J Immunopharmacol 1980; 2:47–53.

(*16*) Riveros-Moreno V, Niblock A. Chemical properties of the principle in *C. parvum* that produces splenomegaly in mice. Immunology 1979; 36:495–501.

(*17*) ———. Analysis of the effect of periodate oxidation and phenol extraction on the antitumor properties of *C. parvum*. Cancer Immunol Immunother 1980; 8:265–272.

(*18*) Riveros-Moreno V, Bomford R, Scott MT. Antitumor activity of purified cell walls from *Corynebacterium parvum*. J Natl Cancer Inst 1978; 60:653–658.

(*19*) Cummins CS, Stimpson SA, Tuttle TL, et al. Observations on the nature of the determinants in anaerobic coryneforms which produce splenomegaly. J Reticuloendothel Soc 1981; 29:1–13.

(*20*) Murahata RI, Zighelboim J. Inhibition of cell mediated cytotoxicity to tumor alloantigens by systemic administration of *Corynebacterium parvum*. Cancer Immunol Immunother 1979; 6:101–106.

(*21*) ———. Inhibition of memory cell-mediated cytotoxic response by systemic administration of *Corynebacterium parvum*. Cell Immunol 1981; 58:289-297.

(*22*) Lee K-C, Berry D. Functional heterogeneity in macrophages activated by *Corynebacterium parvum*: Characterization of subpopulations with different activities in promoting immune responses and suppressing tumor cell growth. J Immunol 1977; 118:1530-1540.

(23) Scott MT, Warner SL. The accumulated effects of repeated systemic or local injections of low doses of *Corynebacterium parvum* in mice. Cancer Res 1976; 36:1335-1338.

(24) Cantrell JL. Antitumor activity of a soluble component isolated from *C. parvum*. Proc Am Assoc Cancer Res 1980; 21:225.

(25) Wilkinson PC, O'Neill GJ, Wapshaw KG. Role of anaerobic coryneforms in specific and non-specific immunological reactions. II. Production of a chemotactic factor specific for macrophages. Immunology 1973; 24:997-1006.

(26) Adlam C, Reid DE. Comparative studies on the cell wall composition of some anaerobic coryneforms of varying lymphoreticular stimulatory activity. International symposium on biological preparations in the treatment of cancer. Dev Biol Stand 1978; 38:115-120.

(27) Johnson JL, Cummins CS. Cell wall composition and deoxyribonucleic acid similarities among the anaerobic coryneforms, classical propionibacteria and strains of *Arachnia propionica*. J Bacteriol 1972; 109:1047-1054.

(28) Cummins CS, Linn DM. Reticulostimulating properties of killed vaccines of anaerobic coryneforms and other organisms. J Natl Cancer Inst 1977; 59:1697-1708.

(29) Lichtenstein A, Murahata R, Zighelboim J. Inhibition of cell-mediated cytotoxicity by *Corynebacterium parvum*. Cancer Immunol Immunother 1980; 8:39-44.

(30) Brunda MJ, Holden HT, Tuttle R. Modulation of natural killer cell activity by anaerobic Corynebacteria. Proc Am Assoc Cancer Res 1980; 21:209.

(31) Bick AB, Lichtenstein A, Sugasawara R, et al. Activation of natural killer cells by *Corynebacterium parvum* fractions. Proc Am Assoc Cancer Res 1981; 22:275.

blank page

Chemical Cocarcinogenesis With the Use of a Subclone Derived From Balb/3T3 Cells With Catechol as Cocarcinogen[1,2]

Mahalakshmi Atchison,[3] Ching-shan Chu,[4] Takeo Kakunaga,[5] *and* Benjamin L. Van Duuren[3,6]

ABSTRACT—This study was performed for the detection of cocarcinogens by transformation in vitro with the use of a subclone of a Balb/3T3 cell line. Dose response, cytotoxicity, and transformation studies were done with the use of an indirect-acting carcinogen, benzo[*a*]pyrene (B[*a*]P), a direct-acting alkylating carcinogen, β-propiolactone (BPL), and the mouse skin cocarcinogen catechol. The rate of transformation was notably higher in groups treated with B[*a*]P and catechol or BPL and catechol than in groups treated with either B[*a*]P or BPL. Catechol alone did not induce any transformation. All the cells isolated from the transformed foci showed characteristics of malignantly transformed cells, such as anchorage-independent growth. Thus chemical cocarcinogenesis was accomplished in vitro similar to that accomplished in in vivo studies reported earlier on mouse skin.—JNCI 1982; 69:503–508.

A series of compounds shows the effect of enhancing significantly the incidence of benign and malignant tumors induced by B[*a*]P on mouse skin when the carcinogen B[*a*]P and cocarcinogen are applied simultaneously and repeatedly (*1–4*). These compounds are not carcinogenic, and most of them are not tumor-promoting agents in the classical two-stage carcinogenesis experiment, i.e., initiation–promotion on mouse skin (*4*). They are referred to as cocarcinogens. There is, therefore, a clear-cut operational difference in the two types of experiments. Not all cocarcinogens are tumor promoters and *vice versa*. These definitions are those of Berenblum (*1*), and they have also been used in our earlier work (*4*). Cocarcinogens for mouse skin belong to various classes of chemicals including polyphenols, aromatic hydrocarbons, long-chain aliphatic hydrocarbons, and others, and hence they probably act by different mechanisms (*4, 5*).

To extend the possibilities for studies on the mechanism of action of cocarcinogens, we undertook the present study to develop a cell culture system for cocarcinogenesis.

The cells selected for the present work are the A31-1-1 subclone isolated from clone A31-1 of Balb/3T3 cells (*6*). These early-passage cells, 50 generations, exhibit a high degree of contact inhibition, homogeneous cell morphology, and a low incidence of spontaneous transformation. Malignant transformation has been observed with the use of these cells treated with several carcinogens, e.g., 4-nitroquinoline-*N*-oxide (*7*).

Catechol, a potent mouse skin cocarcinogen (*4*), occurs in plants (*8, 9*), is manufactured and used in diverse industries (*9*), and is the major phenolic component in cigarette smoke condensate (*10*). In a recent study catechol was shown to be the major cocarcinogen in a subfraction of cigarette smoke condensate on the basis of mouse skin bioassays with the use of B[*a*]P as carcinogen (*11*). It is not carcinogenic by skin application in mice (*4*) and is not a promoter in two-stage carcinogenesis on mouse skin (*4*). It was used in the present work with two carcinogens in separate in vitro cocarcinogenesis experiments: B[*a*]P, an indirect-acting carcinogen, and BPL, a direct-acting alkylating carcinogen.

MATERIALS AND METHODS

Cells.—A subclone, A31-1-1, derived from Balb/3T3 cells and described earlier (*6, 7, 12–14*), was used for all the experiments. For all the experiments, cells were cultured in 60-mm plastic petri dishes (Falcon Plastics, Oxnard, Calif.). Stock cultures were maintained in plastic tissue culture flasks (75 cm^2; Falcon Plastics). The complete medium used in all experiments and in stock cultures was EMEM (GIBCO, Grand Island, N. Y.) containing 100 U penicillin, 100 μg streptomycin, and 0.25 μg amphotericin B/ml (GIBCO) and supplemented with 10% FCS from Biofluids Inc., Rockville, Md. All washing procedures were done in HBSS (GIBCO) containing 400 U penicillin, 400 μg streptomycin, and 1.0 μg amphotericin B/ml. The cultures were incubated in a humidified incubator at 37°C in an atmosphere of 5% CO$_2$ in air. The media were changed two or three times a week. Passage of cultures was performed with the use of 0.25% trypsin (GIBCO).

Chemicals.—B[*a*]P, BPL, and catechol were purified and characterized as described before (*4, 15*). Solutions of the test compounds B[*a*]P and catechol were prepared in amber containers. The compounds were dissolved in acetone and diluted with complete medium at 37°C for preparation of appropriate stock solutions. The compounds were further diluted in complete medium so that the required dose would be obtained in a final concentration of 0.1% acetone. Control

---

ABBREVIATIONS USED: B[*a*]P=benzo[*a*]pyrene; B[*e*]P=benzo[*e*]pyrene; BPL=β-propiolactone; CE=cloning efficiency; CE$_{50}$=median CE; EMEM=Eagle's minimum essential medium; FCS=fetal calf serum; HBSS=Hanks' balanced salt solution; RCE=relative CE.

---

[1] Received October 27, 1981; accepted March 25, 1982.

[2] Supported in part by Public Health Service (PHS) grant ES-00260 from the National Institute of Environmental Health Sciences and by PHS grant CA-13343 from the National Cancer Institute.

[3] Laboratory of Organic Chemistry and Carcinogenesis, Institute of Environmental Medicine, New York University Medical Center, 550 First Ave., New York, N.Y. 10016.

[4] Visiting Scientist from Beijing Medical College, Beijing, Peoples Republic of China.

[5] Laboratory of Molecular Carcinogenesis, Division of Cell Genetics, National Cancer Institute, National Institutes of Health, Public Health Service, U.S. Department of Health and Human Services, Bethesda, Md. 20205.

[6] We are indebted to Mr. Michael Atchison for statistical calculations and interpretation and to Dr. Milton Adesnik for making cell culture hood and other facilities available for this work. Both men are from the Department of Cell Biology, New York University Medical Center.

cultures received only 0.1% acetone, which was nontoxic at this concentration. Stock solutions of BPL were freshly prepared, 1.14 mg/ml of culture medium, and the experimental solutions were then prepared immediately before use by serial dilution of the stock solution with the culture medium to give the final desired concentrations. All the experimental solutions of the compounds were freshly prepared, and the carcinogen plus cocarcinogen solutions in medium were then made up in one solution so that they were applied simultaneously to cultures.

Cytotoxicity, cloning efficiency, and transformation.—Cells obtained from freshly confluent stock flasks were seeded at 5×10^2 cells/60-mm petri dish for cytotoxicity assays and at 1×10^3 cells/60-mm petri dish for transformation assays 24 hours before chemical treatment. Each experiment was divided into 8 groups, 10 dishes per group. B[*a*]P was used at 0.02, 0.01, and 0.005 µg/ml; catechol was used at 2.0, 1.0, and 0.5 µg/ml; there were six experiments in which B[*a*]P and catechol were used in combination as given under "Results." In addition, B[*a*]P and catechol each were examined alone at all the above doses in the control experiments. Other controls were the medium control and an acetone control. Similar protocols were used for cotransformation studies with the use of simultaneous exposure of BPL and catechol. The concentrations of BPL were 4, 2, 1, and 0.5 µg/ml, and the concentration of catechol was 1 µg/ml with 10 dishes per group. In a reverse experiment the concentrations of catechol were 2.0, 1.0, and 0.5 µg/ml, respectively, and the concentration of BPL was 1.0 µg/ml. Cells were exposed to carcinogen and cocarcinogen as described above for 72 hours in 6 ml of medium per dish. Thereafter, they were washed twice with HBSS and maintained in the culture medium alone. Medium was changed twice weekly. At the end of the experiment, the dishes were washed twice with HBSS, fixed with methanol, and stained with Giemsa at 8 days for CE studies and at 23–26 days for transformation assays. The CE is defined as the number of colonies formed as a percentage of the number of cells seeded. The RCE is expressed as the number of colonies in the treated cultures as a percentage of those in the untreated cultures and acetone controls. Morphologic transformation was defined as an increase in cell density accompanied by numerous cells growing on the surface of the cell sheet forming foci with a loss of polar orientation of the cells on the background monolayer as shown in figure 1 (*12–14*). This was used as the criterion of the transformed phenotype. Such transformed areas were collected by the ring-isolation technique (*16*) for growth in soft agar and subsequently in culture.

Growth in soft agar.—The procedure used was described earlier (*17*). The cell suspension was mixed with agar (Difco Laboratories, Detroit, Mich.) at 44°C and diluted with agar to a final concentration of about 1×10^5 cells/dish in 0.3% agar. This suspension of cells in agar was layered over 5 ml of 0.5% agar base layer prepared in double-strength synthetic medium supplemented with 20% FCS in 60-mm dishes. The dishes were incubated in an atmosphere of 5% CO_2 in air. A total of 51 dishes, three dishes per group, were seeded with cells in agar. The dishes were held for 40 days to score for colonies larger than 1 mm. Such colonies were isolated from each group of dishes and were grown in 75-cm^2 flasks to raise the stock cells of transformed line and were stored in liquid nitrogen for future use and characterization.

RESULTS

To determine the dosage of the three test chemicals to be used in the transformation assays, we first obtained CE$_{50}$ values (*18*). The CE$_{50}$ values for B[*a*]P, BPL, and catechol (in µg/ml of medium) were 0.015, 3.60, and 1.0, respectively. The nontoxic doses were 0.005, 1.0, and 0.5 µg/ml of medium for the three chemicals, respectively. The highest doses used were 0.02, 4.0, and 2.0 µg/ml for B[*a*]P, BPL, and catechol, respectively. Concentrations slightly above the maximum values given above rapidly resulted in complete cell lethality. The doses used in the transformation assays were based on the CE$_{50}$ values. The CE of the 0.1% acetone control was 42.53%, and this concentration of acetone gave the same CE as control cultures without acetone.

The detailed results of the transformation experiments with the use of B[*a*]P and catechol are given in table 1. The number of cells plated for the transformation experiments was 10^3/dish; this cell number was optimal for all of our transformation experiments with the use of this early-passage subclone. Cells treated with catechol alone did not produce any transformed foci. B[*a*]P alone at 0.02, 0.01, and 0.005 µg/ml induced the same average number of transformed foci per dish, i.e., 0.5. Simultaneous treatment of cells with the above concentrations of B[*a*]P plus 1 µg catechol/ml for each dose of B[*a*]P gave 4.4-, 2.6-, and 5.2-

TABLE 1.—*CE and transformation frequencies of A31-1-1 cells treated with B[a]P and catechol*[a]

B[*a*]P concentration, µg/ml	Catechol concentration, µg/ml	RCE, %	No. of foci per dish[b]	Transformation frequencies per 10^3 surviving cells	*P*[c]
0	0	100	0	0	—
0.005	0	65.1	0.5±0.31	1.8	—
0.01	0	53.1	0.5±0.15	2.2	—
0.02	0	38.9	0.5±0.41	3.0	—
0	0.5	86.2	0	0	—
0	1.0	50.1	0	0	—
0	2.0	27.0	0	0	—
0.005	1.0	43.3	2.6±2.87	14.4	<0.05
0.01	1.0	37.6	1.3±0.80	8.1	<0.025
0.02	1.0	31.8	2.2±1.47	16.3	<0.025
0.01	0.5	43.4	0.5±0.27	2.7	—
0.01	1.0	37.6	1.2±0.25	7.5	<0.025
0.01	2.0	9.7	2.3±0.59	55.8	<0.05

[a] 5×10^2 cells/60-mm dish for RCE; 1×10^3 cells for transformation assays. Dishes for RCE were fixed and stained 8 days after plating; dishes for transformation were fixed and stained 21 days after plating.

[b] Average number ± SD from 10 plates.

[c] Statistically compared with the group of B[*a*]P-alone treatment on the basis of number of foci per dish with the use of a two-sample *t*-test. When transformation frequencies were used for calculation, statistical significance was larger. —=statistical calculation not significant or not needed.

TABLE 2.—*CE and transformation frequency of A31-1-1 cells treated with BPL and catechol*[a]

BPL concentration, μg/ml	Catechol concentration, μg/ml	RCE, %	No. of foci per dish[b]	Transformation frequencies per 10^3 surviving cells	P[c]
0	0	100	0	0	—
0.5	0	69.3	ND	ND	—
1.0	0	58.9	0.4±0.23	1.6	—
2.0	0	41.4	0.8±0.22	4.3	—
4.0	0	27.0	2.8±0.26	24.4	—
0	0.5	86.2	0	0	—
0	1.0	50.1	0	0	—
0	2.0	27.0	0	0	—
0.5	1.0	40.4	ND	ND	—
1.0	1.0	30.4	2.0±0.54	15.5	<0.025
2.0	1.0	27.8	4.5±0.95	38.1	<0.025
4.0	1.0	23.7	3.5±0.51	34.7	<0.1

[a] 5×10^2 cells/60-mm dish for RCE; 1×10^3 cells for transformation assays. Dishes for RCE were fixed and stained 8 days after plating; dishes for transformation were fixed and stained 21 days after plating.

[b] Average number ± SD from 10 plates. ND=not determined.

[c] Statistically compared with the group of BPL-alone treatment on the basis of number of foci per dish with the use of a two-sample *t*-test. When transformation frequencies were used for calculation, statistical significance was larger. —=statistical calculation not significant or not needed.

fold increases, respectively, compared to the increases seen with B[*a*]P alone. The transformation frequency was highest at the lowest dose of B[*a*]P with 1 μg catechol/ml.

Treatment of cells with various concentrations of catechol, 2, 1, and 0.5 μg/ml, with 0.01 μg B[*a*]P/ml gave 4.6-, 2.4-, and 1.0-fold increases in B[*a*]P transformation, respectively, compared to the increases seen in cultures treated with B[*a*]P alone. The rate of transformation was linear up to 2 μg catechol/ml added. All experiments with B[*a*]P at the above three doses (0.02, 0.01, and 0.005 μg/ml) in combination with catechol at 1.0 or 2.0 μg/ml resulted in increased transformation levels over those seen with B[*a*]P alone at $P<0.05$ with the use of a two-sample *t*-test. When catechol was used at 0.5 μg/ml with B[*a*]P at 0.01 μg/ml, no increase in transformation was seen.

The data on the transformation frequency of BPL alone and BPL together with catechol are summarized in table 2. Cells treated with BPL alone at 4, 2, and 1.0 μg/ml gave 2.8, 0.75, and 0.4 foci/dish, respectively; i.e., there was a linear increase in transformation frequency with increased BPL concentration. When the same BPL concentrations were used simultaneously with 1 μg catechol/ml, the transformation frequency increased by 1.25, 6.0, and 5.0 times when compared to that of cultures treated with BPL alone. The frequency of transformation was highest at 2 μg BPL/ml together with 1 μg catechol/ml added and the transformation frequency decreased slightly at 4 μg BPL/ml with 1 μg catechol/ml. This decrease may be due to the combined toxic effects of the compounds on cells.

When cells were isolated from individual transformed foci, all produced populations of typical transformed cells in culture and demonstrated a loss of contact inhibition and oriented growth. They subsequently gave rise to colonies of anchorage-independent cells (fig. 2), whereas the control cultures did not. Dense, multilayer areas of untransformed cells isolated from treated or control cultures also failed to produce colonies in soft agar. A transformed line was isolated from the colonies that developed in soft agar from transformed foci treated with B[*a*]P (0.005 μg/ml) and catechol (1 μg/ml) 23 days after cell seeding. This cell line (TCL3a) is shown in figure 3.

DISCUSSION

Cocarcinogenesis in vivo has been established in various laboratories (*1–5*). Many of these studies have focused on mouse skin experiments (*1*, *2*, *4*). Because of the range of chemical structural types that exhibit cocarcinogenicity, it appears unlikely that all these compounds affect the target organ in the same way. This is supported by a recently reported study of the effects of five chemicals that enhance mixed-function oxidase activity in vivo (*19*). When tested in an in vitro mouse embryo fibroblast system, C3H10T½/CL8, with B[*a*]P as carcinogen, four of the five agents enhanced B[*a*]P-induced transformation; the exception was Aroclor 1254, a well-known inducer of mixed-function oxygenases in mouse liver (*20*). These findings suggest, as the authors point out (*19*), that certain metabolic pathways and the pharmacokinetics that are operative in vivo do not necessarily occur in vitro. Another recent report describing the effect of B[*e*]P on B[*a*]P metabolites showed that the relative proportions of B[*a*]P metabolites formed in hamster embryo cells are altered in the presence of B[*e*]P (*21*). A third in vitro cocarcinogenesis report concerns the effect of B[*e*]P on B[*a*]P carcinogenesis in respiratory tract mucosa in organ culture (*22*). B[*e*]P, a mouse skin cocarcinogen, was not cocarcinogenic for respiratory tract carcinoma induction in organ culture but did enhance tracheal and peritracheal sarcomas twofold to threefold in the same experiments.

With these complications in mind, it is still highly desirable to perform cocarcinogenesis studies in vitro. The in vitro system provides the obvious advantage of one cell type, for which some of the biochemical and biological characteristics have been described before.

Because catechol did not show tumor-promoting activity on mouse skin (*4*), it was not tested in the present in vitro system for tumor-promoting activity.

The results presented in this report clearly demonstrate the cocarcinogenic activity of catechol on B[*a*]P- as well as BPL-induced transformation in vitro. This system is potentially useful for the study of mechanisms of action of mouse skin cocarcinogens in vitro. It may also develop to be an in vitro screen for other potential cocarcinogenic agents, once a larger number of mouse skin cocarcinogens have been successfully tested in vitro as cocarcinogens.

In an earlier report we have enumerated several possible modes of action of cocarcinogens (*5*). The present findings suggest that the effect of catechol may involve an interference with repair of DNA damaged by the direct-acting carcinogen BPL in which alteration in metabolic pathways is not involved; the latter effect can occur with B[*a*]P as carcinogen.

REFERENCES

(*1*) Berenblum I. The mechanism of carcinogenesis. A study of the significance of cocarcinogenic action and related phenomena. Cancer Res 1941; 1:807–814.

(*2*) Bingham E, Falk HL. Environmental carcinogens. The modifying effect of cocarcinogens on the threshold response. Arch Environ Health 1969; 19:779–783.

(*3*) Van Duuren BL, Katz C, Goldschmidt BM. *Brief communication*: Cocarcinogenic agents in tobacco carcinogenesis. J Natl Cancer Inst 1973; 51:703–705.

(*4*) Van Duuren BL, Goldschmidt BM. Cocarcinogenic and tumor-promoting agents in tobacco carcinogenesis. J Natl Cancer Inst 1976; 56:1237–1242.

(*5*) Van Duuren BL, Melchionne S. Cofactors in environmental health and disease: Cocarcinogens and tumor promoters, chapt 17. In: McKinney JD, ed. Environmental health chemistry. The chemistry of environmental agents as potential human hazards. Ann Arbor, Mich.: Ann Arbor Sci Publ, 1980:337–364.

(*6*) Kakunaga T, Crow JD. Cell variants showing differential susceptibility to ultraviolet light-induced transformation. Science 1980; 209:505–507.

(*7*) Kakunaga T. Factors affecting polycyclic hydrocarbon-induced cell transformation. In: Gelboin HV, Ts'o PO, eds. Polycyclic hydrocarbons and cancer. Vol 2. New York: Academic Press, 1978:293–304.

(*8*) Rodd EH, ed. Chemistry of carbon compounds. Vol 3A. Amsterdam: Elsevier, 1956:480.

(*9*) International Agency for Research on Cancer. Some fumigants, the herbicides 2,4-D and 2,4,5-T, chlorinated dibenzodioxins and miscellaneous industrial chemicals. IARC Monogr Eval Carcinog Risk Chem Man 1977; 15:165.

(*10*) Waltz P, Häusermann M, Krull A. Methoden der quantitativen Bestimmung des Brenzcatechins im Cigarettenrauch. Beitr Tabakforsch 1965; 3:263–277.

(*11*) Hecht SS, Carmella S, Mori H, Hoffmann D. A study of tobacco carcinogenesis. XX. Role of catechol as a major cocarcinogen in the weakly acidic fraction of smoke condensate. JNCI 1981; 66:163–169.

(*12*) Kakunaga T. A quantitative system for assay of malignant transformation by chemical carcinogens using a clone derived from Balb/3T3. Int J Cancer 1973; 12:463–473.

(*13*) ———. Requirement for cell replication in the fixation and expression of the transformed state in mouse cells treated with 4-nitroquinoline-1-oxide. Int J Cancer 1974; 13:736–742.

(*14*) ———. The role of cell division in the malignant transformation of mouse cells treated with 3-methylcholanthrene. Cancer Res 1975; 35:1637–1642.

(*15*) Van Duuren BL, Goldschmidt BM. Carcinogenicity of epoxides, lactones, and peroxy compounds. III. Biological activity and chemical reactivity. J Med Chem 1966; 9:77–79.

(*16*) Puck TT, Marcus PI, Cieciura SJ. Clonal growth of mammalian cells in vitro. Growth characteristics of colonies from single HeLa cells with and without "feeder" layer. J Exp Med 1956; 103:273–284.

(*17*) Macpherson I, Montagnier L. Agar suspension culture for the selective assay of cells transformed by polyoma virus. Virology 1964; 23:291–294.

(*18*) Miller LC, Tainter ML. Estimation of ED_{50} and its error by means of logarithmic probit graph paper. Proc Soc Exp Biol Med 1944; 57:261–264.

(*19*) Nesnow S, Leavitt S, Garland H, et al. Identification of cocarcinogens and their potential mechanisms of action using C3H/10T½/CL8 mouse embryo fibroblasts. Cancer Res 1981; 41:3071–3076.

(*20*) Hutton JJ, Meier J, Hackney C. Comparison of the in vitro mutagenicity and metabolism of dimethylnitrosamine and benzo(*a*)pyrene in tissues of inbred mice treated with phenobarbital, 3-methylcholanthrene or polychlorinated biphenyls. Mutat Res 1979; 66:75–94.

(*21*) Baird WM, Diamond L. Effects of the carcinogen benzo(*e*)pyrene on metabolism of the carcinogen benzo(*a*)pyrene in hamster embryo cell cultures. Proc Am Assoc Cancer Res 1981; 22:96.

(*22*) Topping DC, Martin DH, Nettesheim P. Determination of cocarcinogenic activity of benzo(*e*)pyrene for respiratory tract mucosa. Cancer Lett 1981; 11:315–321.

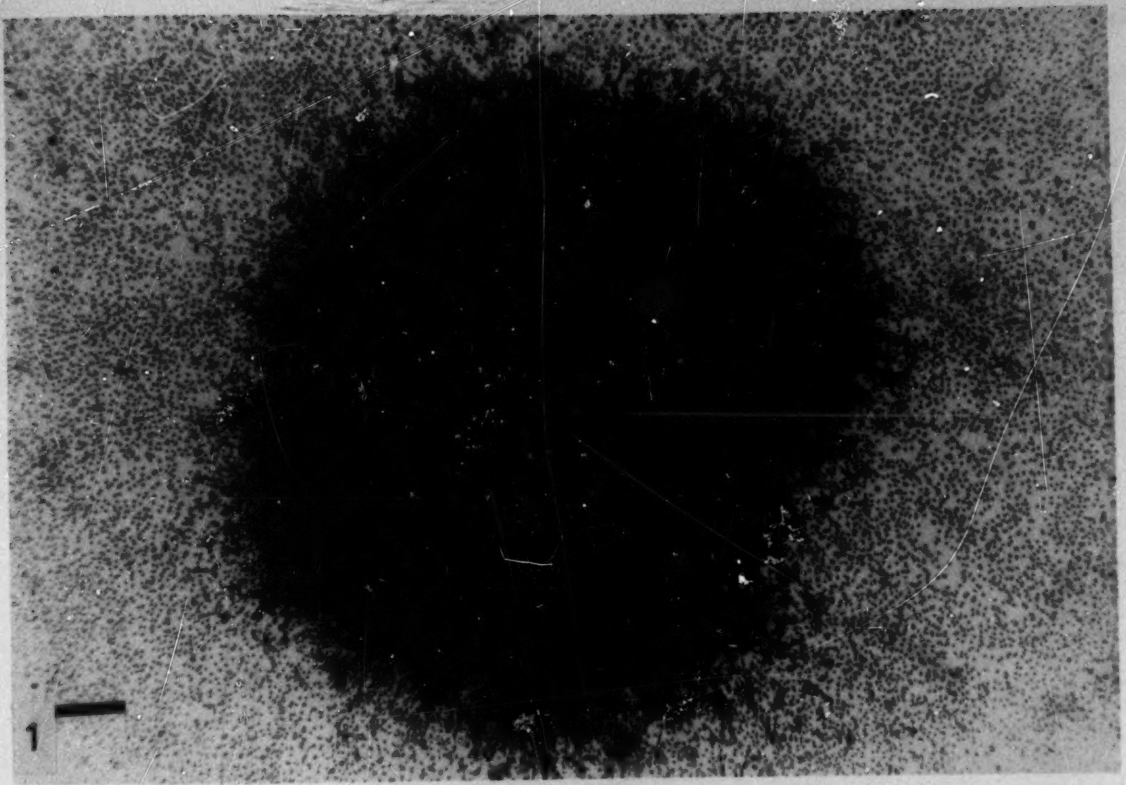

FIGURE 1.—A transformed focus of Balb/3T3 subclone (C1-1-1) against the normal monolayer background of cells. *Bar*=500 µm. × 20

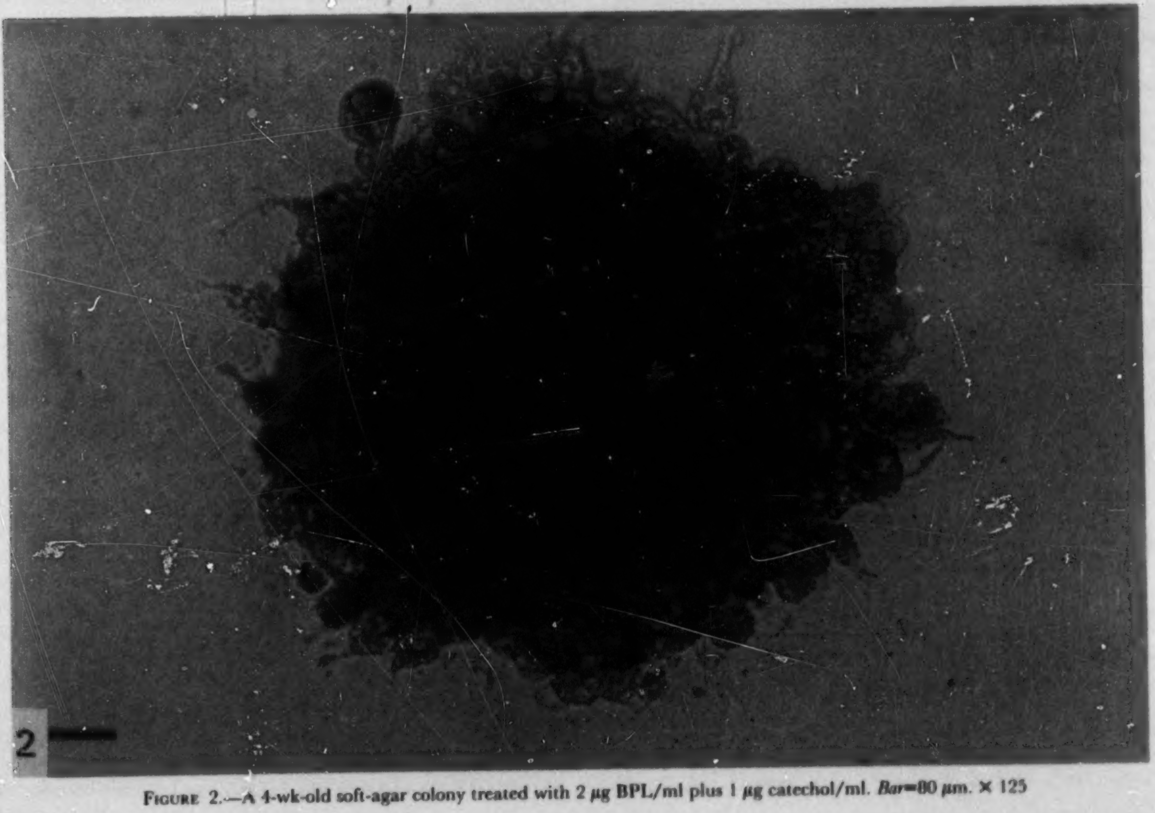

FIGURE 2.—A 4-wk-old soft-agar colony treated with 2 µg BPL/ml plus 1 µg catechol/ml. *Bar*=80 µm. × 125

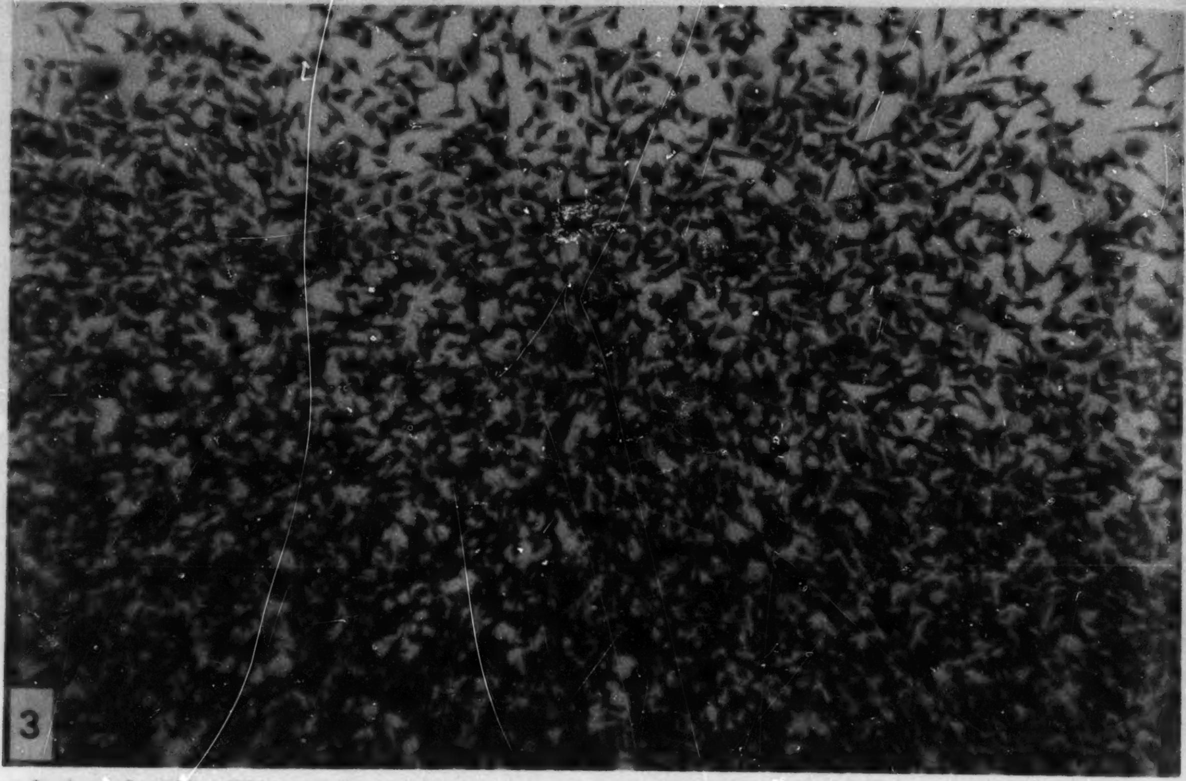

FIGURE 3.—A transformed line (TCL3a) in a low magnification treated with B[*a*]P (0.005 µg/ml) and catechol (1 µg/ml) to show the central peripheral edge of actively growing cells in living culture. *Bar*=227 µm. × 44

Immunotherapy of a Murine Leukemia Virus-Infected, Chemically Induced Murine Sarcoma With Antiviral Antibodies [1,2,3]

Edward C. Ward, [4,5,6] **J. Dirk Iglehart,** [7] **Kent J. Weinhold,** [7] *and* **Dani P. Bolognesi** [7,8,9]

ABSTRACT—Many murine tumor models associated with murine leukemia virus(es) (MuLV) have been successfully treated by passive administration of antiviral antibodies. There is a large body of virus-negative tumors, however, which are lowly antigenic and thus refractory to such approaches. Therefore, an investigation was done for determination of whether such tumors could be rendered susceptible to passive serum therapy by introduction of MuLV antigens onto the tumor cell surface. For this purpose a 3-methylcholanthrene-induced fibrosarcoma from inbred C57BL/6J mice was chosen. Following infection of the tumor in vitro with Friend murine leukemia virus (F-MuLV), the tumor was found to be susceptible to treatment with a high-titered heterologous anti-F-MuLV gp71 antiserum. The specificity of the treatment was determined by conduction of the therapy on the uninfected parental tumor, in which case there was no effect. In addition, therapy could be initiated at time points when demonstrable tumors were present and successfully treated animals were resistant to rechallenge with the infected tumor. Thus conversion of a lowly antigenic virus-negative tumor to an MuLV-positive antigenic tumor rendered such growths susceptible to immunologic management.—JNCI 1982; 69:509–515.

Many murine tumor models are directly induced by or intimately associated with type C retroviruses. Such tumor cells usually express virus structural components on the cell surface, predominantly the virus envelope antigens gp71 and p15(E) (*1*). This has led to the development of immunotherapeutic regimens against MuLV-induced or -associated neoplasia, which utilize these antigens as specific targets for immunotherapeutic protocols. In this regard, both xenogeneic and syngeneic antisera against viral antigens have been shown to influence tumor growth in vivo in both the murine and feline type C retrovirus tumor systems (*2–5*). In contrast to tumors expressing retroviral antigens, virus-negative tumors, including many spontaneous or chemically induced neoplasms, are in general weakly antigenic, often producing an immune response difficult to measure (*6*). Although transplantation resistance may be elicited by immunization against such neoplasms (*7–12*), the antigens responsible for this phenomenon have proved difficult to isolate and identify (*13–16*). Moreover, each tumor, even when induced by the same chemical, has been shown to display unique transplantation antigens (*8, 9, 11, 17, 18*). Therefore, even if a therapeutic modality could be developed for such cancers by the use of these antigens, its applicability would be restricted to a single tumor.

An approach toward the successful immunologic management of such tumors could be derived from manipulations that would increase their antigenicity. To test this, we have chosen a chemically induced tumor arising in an inbred mouse strain and infected the tumor cells in vitro with a nonpathogenic MuLV. Subsequently, immunologic control of tumor growth was attempted by passive administration of antibodies directed against the major surface glycoprotein of the infecting virus. Our results, based on suppression of tumor growth, demonstrate that the superimposed viral antigen functions as an effective immunologic target in vivo.

MATERIALS AND METHODS

Mice.—All experiments were done with inbred C57BL/6J (B6) female mice used at 10–14 weeks of age (The Jackson Laboratory, Bar Harbor, Maine).

Virus.—F-MuLV was from a cell line derived from STU mouse embryo fibroblasts (Eveline) infected with F-MuLV (*19*). This cell line produces only the helper component of the Friend virus complex.

Cell lines.—A fibrosarcoma of B6 origin was induced in vivo with MCA and maintained in vitro. This line is designated MCA-FS and was provided by Dr. D. Adams (Department of Pathology, Duke University Medical Center, Durham, N.C.). An additional cell line was derived from this MCA-induced parental cell line in our laboratory by infection with F-MuLV and was designated MCA-FS-F-MuLV. Sarcoma-positive, leukemia-negative cells (Fg10) were obtained from Dr. P. J. Fischinger (National Cancer Institute, National Institutes of Health, Bethesda, Md.) and were used for determination of the ecotropic virus content of the cell lines. All 3 cell lines were grown as monolayers in

---

ABBREVIATIONS USED: cRIA=competition radioimmunoassay; FI=fluorescence index; IF=immunofluorescence; LD_{50}=median lethal dose; MCA=3-methylcholanthrene; MCA-FS=MCA-induced fibrosarcoma syngeneic to C57BL/6 mice; MuLV=murine leukemia virus; F-MuLV=Friend MuLV; MCA-FS-F-MuLV=MCA-FS (tumor) superinfected with F-MuLV; R-MuLV=Rauscher MuLV; NGS=normal goat serum; PBS=phosphate-buffered saline.

---

[1] Received November 5, 1981; accepted March 15, 1982.

[2] Supported by Public Health Service (PHS) contract N01CP-33308 from the Division of Cancer Cause and Prevention, National Cancer Institute (NCI); by PHS grant 5-P01CA-25863 from the NCI; and by PHS training grants 5-T32CA-09111 (to E. C. W.), 5-T32CA-09058 (to J. D. I.), and 2-T32CA-09058 (to K. J. W.) from the NCI.

[3] Animals were maintained under the guidelines of the National Research Council.

[4] Department of Microbiology and Immunology, Duke University Medical Center, Durham, N.C. 27710.

[5] These studies are in partial fulfillment of the requirements for the Ph.D. degree in the Department of Microbiology and Immunology, Duke University Medical Center.

[6] *Address reprint requests to* Dr. Ward at the Department of Surgery, P.O. Box 2926, Duke University Medical Center, Durham, N.C. 27710.

[7] Department of Surgery, Duke University Medical Center.

[8] Recipient of faculty research award FRA-141 from the American Cancer Society.

[9] The authors thank Dr. J. J. Collins and Dr. T. J. Matthews, Department of Surgery, Duke University Medical Center, for their helpful discussions. We also thank Ms. Donna Wilson for assembly of this manuscript.

plastic T-flasks. Cell lines MCA-FS and MCA-FS-F-MuLV were grown in modified Eagle's minimum essential medium with 10% newborn calf serum, whereas the Fg10 cells were maintained in modified McCoy's 5-A medium containing 10% fetal calf serum (Grand Island Biological Co., Grand Island, N.Y.).

Infectious virus assay.—Ecotropic MuLV were titrated on Fg10 cells as previously described (*20*). Tissue culture supernatants were filtered (0.45 μm) prior to testing.

Sera.—Hyperimmune goat serum against purified F-MuLV gp71 was provided by Dr. Werner Schäfer (Max-Planck Institut Virusforschung, Tübingen, Federal Republic of Germany), and the corresponding IgG was prepared as described in (*2*). The IgG preparation appeared homogeneous on gels and was reconstituted to 15 mg protein/ml. The radioimmunoassay titer was determined as previously described (*21*) and was comparable to that of whole goat anti-gp71 sera. NGS was obtained from Dr. H.-J. Thiel (Bundesforschungsanstalt für Viruskrankheiten der Tiere, Tübingen, Federal Republic of Germany), and the IgG was extracted from it in a manner similar to that reported in (*2*). Rabbit antisera against R-MuLV gp71 and MuLV p30 were prepared as previously described (*19*). Rabbit anti-F-MuLV gp71 antiserum was provided by Dr. D. Bigner, Duke University Medical Center. Fluorescein-conjugated goat anti-rabbit IgG serum was obtained from Meloy Laboratories Inc., Springfield, Va.

IF.—IF with the rabbit anti-F-MuLV gp71 antiserum was performed as in (*22*). Monolayer cells were lightly trypsinized and washed three times with PBS; 1×10^6 cells were placed into dilution tubes. Each tube was incubated with 100 μl of either normal rabbit serum or rabbit anti-F-MuLV gp71 serum for 1 hour at 37°C. The cells were then washed three times with PBS and incubated with 100 μl of a mixture of fluorescein-conjugated goat anti-rabbit IgG (1:10 final dilution) and rhodamine counterstain (1:40 final dilution). After incubation for an additional 30 minutes at 37°C on a shaker platform, the cells were washed three times in PBS and dispersed in a drop of buffered glycerol. They were then mounted on glass slides, stored at 4°C, and examined within 24 hours for staining under UV illumination (Carl Zeiss, Oberkochen, Federal Republic of Germany). The results were expressed as an FI, where FI = (percent negative control cells − percent negative test cells)/percent negative control cells. An FI of greater than or equal to 0.20 is taken to reflect significant staining.

cRIA.—The methodology used in cRIA with the rabbit anti-R-MuLV gp71 and p30 has been described (*23*). We prepared cell extracts by washing cell monolayers with PBS and treating with disruption buffer [20 m*M* Tris-HCl and 100 m*M* NaCl (pH 7.6) with 1 m*M* EDTA and 1% Triton X-100]. The extracts were then sonicated and clarified by centrifugation first at 1,500 rpm (10 min) and then at 10,000 rpm (5 min). Protein content was determined by the method of Lowry et al. (*24*).

Inoculation of tumor cells.—Tumor cells for in vivo transplantation were prepared by light trypsinization with 0.05% trypsin and 0.1% EDTA in calcium-magnesium-free PBS, washed with PBS, and then enumerated. Cells were then inoculated sc in the dorsal region of the animal.

TABLE 1.—*Characteristics of tumor cell lines*

Cell line	Plaque-forming units/ml[a]	F-MuLV proteins, ng/mg protein[b]		LD_{50}[c]
		p30	gp71	
MCA-FS	≤10	≤80	≤25	5×10^5
MCA-FS-F-MuLV	3×10^5	1,900	436	1.8×10^6

[a] Amount of infectious virus per 1 ml 24-hr tissue culture supernatants as determined in the Fg10 assay.

[b] Determined by cRIA. *See* "Materials and Methods."

[c] Determined by the method of Reed and Muench (*25*).

RESULTS

Characteristics of Tumor Cell Lines

To determine the amount of virus being produced by the cells, we tested culture fluids for the presence of viable virus in the Fg10 assay. Table 1 shows that the MCA-FS-F-MuLV cell line synthesized infectious virus, whereas the parental MCA-FS cell line was virus-negative.

The cell lines were also examined for viral antigen content in a cRIA. As can be seen in table 1, the infected cell line exhibited elevated levels of the internal virus structural protein p30 as compared to the uninfected parental line. Additionally, the assay for F-MuLV gp71 detected the envelope glycoprotein only in the MCA-FS-F-MuLV cells (table 1).

Because we intended to do passive immunotherapy studies using antiviral antibodies, we wanted to ensure that the appropriate virion antigen was prominently expressed at the cell surface. We therefore performed membrane IF analyses with the rabbit anti-F-MuLV gp71 antibodies. Text-figure 1 shows that the MCA-FS-F-MuLV cell line exhibits a significantly higher FI with the rabbit anti-F-MuLV gp71 serum than that of the parental cell line. The positive fluorescence with the MCA-FS cell line presumably reflects reactivity of group-specific antibodies in this serum with endogenous gp71 known to be expressed on some MCA-induced tumors (*26*).

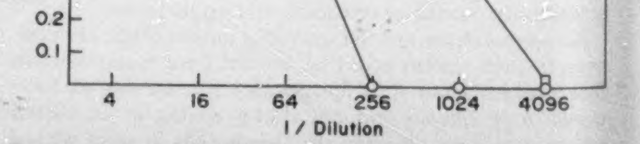

TEXT-FIGURE 1.—Immunofluorescent analysis of the MCA-induced cell lines with the rabbit anti-F-MuLV gp71 serum as described in "Materials and Methods." Parental non-virus-expressing MCA-FS cell line (○—○) was compared to MCA-FS-F-MuLV cell line (□—□).

Tumorigenicity

To determine the cell dose to use for tumor induction, we determined the tumorigenicity of each cell line by sc inoculation of graded numbers of tumor cells on the dorsum of the mouse. The infection of the parental cell line with F-MuLV, as compared to the uninfected parental cell line, was found to cause approximately a threefold increase in the number of cells needed to kill 50% of the animals (table 1). Thus, as predicted, infection with F-MuLV enhances antigenicity, although not to an extent that completely suppresses tumor growth. We therefore investigated the possibility that complete suppression of tumor growth could be achieved by administration of antiviral antibody. A challenge dose of three times the LD$_{50}$ was used in all subsequent studies. This correlated to approximately 3×10^6 cells of MCA-FS-F-MuLV and 1×10^6 cells of MCA-FS per mouse.

Passive Serum Therapy of MCA-Induced Tumors

On the basis of our success using the hyperimmune goat anti-gp71 antisera in other tumor systems (*2–4*), we tested its therapeutic potential on mice inoculated with the MCA-FS-F-MuLV tumor cells. The basic serum therapy protocol consisted of ip inoculation of 0.5 ml whole serum or its equivalent, mixed with an equal volume of PBS, every other day. The therapy was initiated the day following tumor inoculation and continued for a course of six treatments, except where noted. Text-figure 2 is a composite of the results from four experiments on more than 25 mice per group. The goat anti-gp71 serum afforded a highly significant degree of protection (4% with tumors) when compared to the untreated controls (60% with tumors) and those mice treated with NGS (80% with tumors). To ascertain that the effect seen with the hyperimmune serum was specific for the infected cells, we subjected mice inoculated with the MCA-FS parental cell line to the identical treatment protocol. Text-figure 3 demonstrates that treatment with the goat anti-gp71 serum had no effect on either the latency or lethality of the MCA-FS.

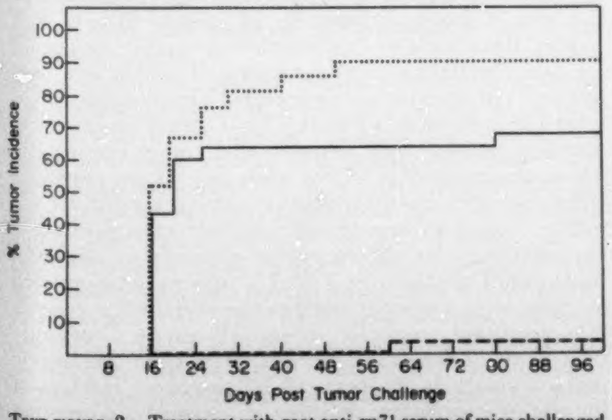

TEXT-FIGURE 2.—Treatment with goat anti-gp71 serum of mice challenged with MCA-FS-F-MuLV. No treatment (——), NGS treatment (···), or goat anti-gp71 treatment (– – –) were performed as described in "Materials and Methods."

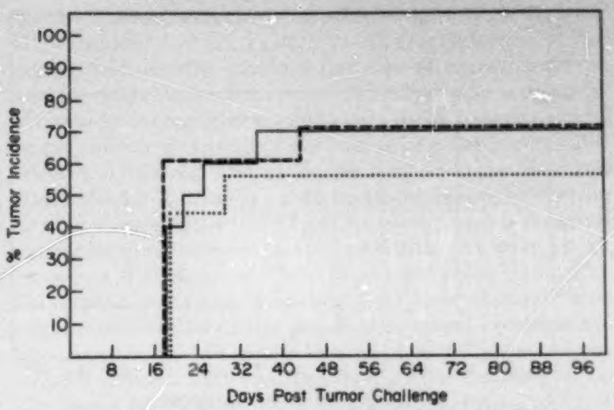

TEXT-FIGURE 3.—Treatment of MCA-FS tumor-bearing mice with goat anti-gp71 serum. Tumors were treated as in fig. 2. No treatment (——), NGS treatment (···), goat anti-gp71 treatment (– – –).

To investigate whether the protective effect of the immune serum truly reflected an antibody activity, we tested IgG preparations from both normal and hyperimmune goat anti-gp71 sera for their protective capability. Text-figure 4 is a composite of three experiments in which all of the animals treated with IgG equivalent to 0.5 ml of goat anti-gp71 serum per inoculum showed results of complete protection against outgrowth of tumor compared to a 70% tumor incidence in mice treated with normal goat IgG. These mice have been observed for longer than 1 year, and none of the protected animals have demonstrated any sign of tumor recurrence. Therefore, the protective activity resides in the IgG fraction of the hyperimmune serum.

In an effort to determine the effectiveness of the treatment in relation to tumor mass, therapy with purified IgG was initiated at varying time points after tumor inoculation. The results shown in text-figure 5 demonstrate that therapy may be initiated as late as 3 days post inoculation without the efficacy of the treatment regimen being decreased. Furthermore, serum treatment has an appreciable effect on the

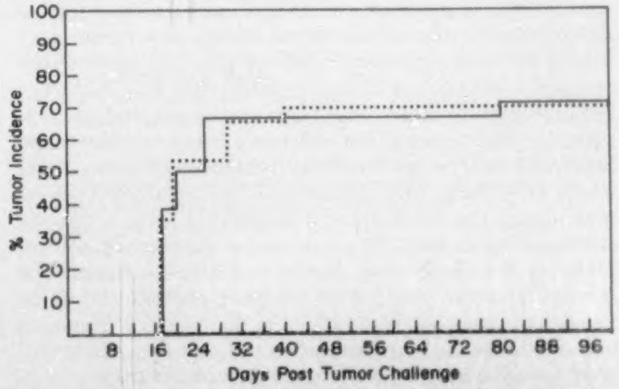

TEXT-FIGURE 4.—Treatment of MCA-FS-F-MuLV with purified IgG. Mice challenged with MCA-FS-F-MuLV were treated with 500 µl whole-serum equivalents of normal goat IgG (···) or goat anti-gp71 IgG (– – –) or left untreated (——). Treatment was as described in fig. 2 legend.

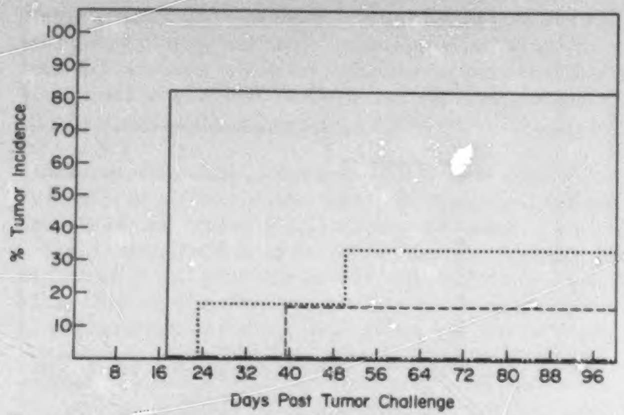

TEXT-FIGURE 5.—Treatment of MCA-FS-F-MuLV-bearing mice with 500-μl equivalents of goat anti-gp71 IgG starting on days 1 (— —), 3 (·· ··), 5 (– – –), or 7 (···) and nontreatment (——) following tumor challenge. Therapy was continued for six courses of treatment from the time it was initiated.

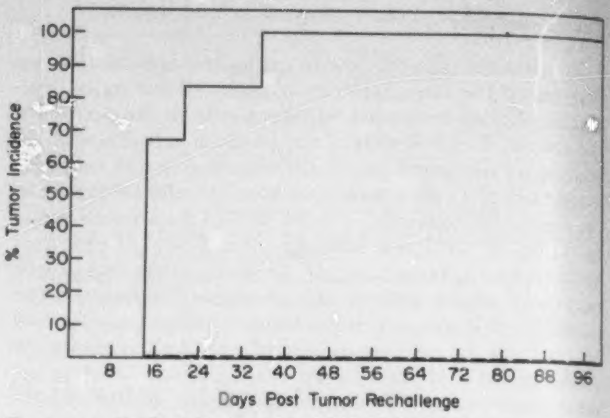

TEXT-FIGURE 6.—Rechallenge with MCA-FS-F-MuLV of successfully treated MCA-FS-F-MuLV-inoculated mice. For details, *see* text. Age matched controls (——); rechallenged mice (– – –).

tumor outgrowth even when begun as late as 7 days post inoculation.

Histologic Examination of Treated and Untreated Tumors

We next wished to determine whether the positive effect observed was directed against a definable tumor mass. Thus we performed autopsies on animals at various times following administration of the standard dose of tumor cells to ascertain the earliest time at which a demonstrable tumor was present. Animals autopsied as early as 2 days post challenge were found to bear histologically identified cancerous nodules (fig. 1A) with a well-defined capsule surrounding the tumor. By day 5 there was some necrosis at the center of the tumor, although the cells at the periphery appeared viable (fig. 1B). Several tumor cells were multinucleated and highly vacuolar, and in general the tumor appeared anaplastic with a wide heterogeneity in the size of both the cells and the nuclei. Additionally, there was little or no inflammatory reaction within the tumor sheath. In contrast to the appearance of a day-5 tumor in an untreated mouse, examination of the tumor nodule in a mouse after having received two inoculations of goat anti-gp71 serum revealed a large degree of tumor necrosis (fig. 1C). A marked inflammatory exudate, with large monocytes and plasmacytes was also present. The difference between treated and untreated tumors was even more pronounced by day 10, at which time there were virtually no viable tumor cells remaining in the serum-treated mouse (fig. 1E), while the untreated tumor (fig. 1D) progressed to the point that it was invading the underlying muscle and adipose tissue. The therapy protocol resulted in complete elimination of the tumor and was not an induction of tumor stasis inasmuch as treated animals, when autopsied 100 days after treatment, were found to have no histologic evidence of tumor.

Rechallenge of Treated Mice

Previous studies with virus-induced and associated cancers indicated that one important effect of successful immunotherapy was the development of a host immune response against the viral antigens (*4, 27, 28*). The biologic significance of such a response could be demonstrated since rechallenge of the animals with virus resulted in resistance to infection (*28, 29*). To determine whether the current serum therapy protocol conferred any long-term immunity to tumor rechallenge in successfully treated mice, we rechallenged such animals with the standard dose of MCA-FS-F-MuLV cells (3×10^6) 200 days following cessation of the initial treatment protocol. As can be seen in text-figure 6, successful treatment led to functional immunologic memory, inasmuch as all of the treated animals remained tumor-free, whereas untreated age-matched controls developed lethal tumors.

DISCUSSION

As an approach toward the immunotherapeutic management of non-virus-associated, weakly antigenic tumors, a transplantable MCA-induced sarcoma was infected with a type C retrovirus (F-MuLV), followed by treatment with antiviral antibodies. The resulting data support the contention that if strong antigens can be introduced onto such tumors, these antigens can function as specific targets for the immune elimination of the growth. The optimum therapy protocol currently entails repeated large doses of a high-titered xenogeneic anti-F-MuLV gp71 serum (or the corresponding purified IgG) initiated after tumor inoculation. The main conclusions of this study are: 1) the beneficial effect seen with the treatment protocol is specific for the infected tumor as the parental non-virus-infected tumor is not influenced by the treatment protocol; 2) successful treatment of the MCA-FS-F-MuLV tumor can be initiated at times when well-established tumor nodules are present; 3) a significant proportion of animals can be successfully treated up to 7 days post tumor challenge; 4) the therapeutic protocol results in an increased inflammatory reaction at the site of inoculation, resulting in necrosis and eventual elimination of the tumor; and 5) successfully treated mice are resistant to rechallenge with the infected tumor as late as 6 months after the initial treatment.

Two concerns regarding the general applicability of this protocol pertain to potential harmful effects to the host of the virus as well as the introduction of such large quantities of foreign antibody. The virus used in these studies contains only the helper component of the Friend erythroleukemia virus stock and has no detectable oncogenic potential in the mouse strain utilized in these studies (*30*) presumably reflecting attenuation by prolonged passage in tissue culture. Likewise, animals inoculated systemically with this agent demonstrated no other adverse side effects inducible by infection with the helper F-MuLV (*30*). In addition, animals into which relatively large doses of F-MuLV (10^7 F-MuLV) were introduced did not exhibit a significant pattern of generalized infection (*31*), a consideration of importance in relation to the subsequent therapy with antiviral antibodies that could have an adverse effect on normal tissues expressing viral antigens.

The possible immunosuppressive effect of large amounts of anti-gp71 antibodies against T- and B-cells that express endogenous gp71 demonstrated by Wecker et al. (*32*) has been addressed in a similar therapy system by Schwarz et al. (*33*). They found that the treatment of AKR leukemia with comparable amounts of goat anti-gp71 IgG did not result in suppression of a T-cell-dependent humoral response. Although an adverse reaction (i.e., serum sickness and/or anaphylaxis) to the large amounts of foreign protein being administered in the treatment protocol is a possibility, no evidence of such a phenomenon has been seen in the current model.

The mechanism by which the antiviral antibodies affords protection to the tumor-bearing host, as well as the involvement of the host in the rejection process, has yet to be elucidated. However, the histologic examination of tumors shortly after the initiation of serum therapy revealed an increased inflammatory reaction when compared to untreated controls, suggesting that the rejection process is possibly mediated by a host effector cell. Preliminary results have indicated that serum-protected mice mount a humoral response to gp71 that does not arise until approximately 2 months after the treatment protocol. This finding is similar to the results seen by Schäfer et al. (*2*) in the STU F-MuLV system. Experiments are currently under way to delineate if this or other host responses are involved in the serum protection process.

The ability of successfully treated mice to resist a second tumor challenge with MCA-FS-F-MuLV cells as late as 6 months after serum therapy indicates that treated mice mount an immune response. In addition, preliminary studies show that treated mice also resist tumor outgrowth of parental MCA-FS cells. Confirmation of these results would suggest that virus infection of the MCA-FS cells has enhanced the immunogenicity of a cellular antigen responsible for tumor rejection in a manner similar to that described by Al-Ghazzouli et al. (*34*). Whether this increased immunogenic potential of the MCA-induced tumor antigens is necessary for effective therapy remains to be determined.

The results of this current paper form the basis for development of model systems for immunotherapy of weakly antigenic tumors. However, for such models to have practical value, the targeting of the tumor would have to be accomplished in situ. As we have previously reported (*30*), systemic administration of F-MuLV into mice bearing MCA-induced tumors resulted in efficient infection of the tumor. Additionally, minimal infection of normal host tissues was found in such animals (*31*). If therapy were to be initiated following in vivo infection, a prime concern would be the time at which all of the tumor cells are successfully infected. However, studies under way indicate that the tumor burden at this time may be too large for the current therapy to be effective. We hope to overcome this problem by establishing better therapy modalities as well as by increasing the efficiency of the in vivo infection process. In this regard, we have recently found that therapy with antiviral antibodies in the presence of rabbit complement has a greater benefit in the treatment of a Harvey virus-induced sarcoma than has the treatment with serum alone (Weinhold K: Manuscript in preparation). Presumably, if the parameters of the in vivo infection and therapy can be established for the system involved in MCA-induced tumors, then such findings could be extended to other systems involving naturally occurring tumors.

REFERENCES

(*1*) Schäfer W, Bolognesi DP. Mammalian C-type oncornaviruses: Relationship between viral structural and cell surface antigens and their possible significance in immunological defense mechanisms. In: Rapp F, Hanna MG, eds. Contemporary topics in immunobiology. New York: Plenum Press, 1977:127–167.

(*2*) Schäfer W, Schwarz H, Thiel H-J, Wecker E, Bolognesi DP. Properties of mouse leukemia viruses. XIII. Serum therapy of virus-induced murine leukemias. Virology 1976; 75:401–418.

(*3*) de Noronha F, Schäfer W, Baggs R, Bolognesi DP. Prevention of oncornavirus-induced sarcomas in cats by treatment with antiviral antibodies. Nature 1977; 267:54–56.

(*4*) Schwarz H, Fischinger PJ, Ihle JN, et al. Properties of mouse leukemia viruses. XVI. Suppression of spontaneous fatal leukemias in AKR mice by treatment with broadly reacting antibody against the viral glycoprotein gp71. Virology 1979; 93:159–174.

(*5*) Haagensen DE Jr, Roloson G, Collins JJ, Wells SA Jr, Bolognesi DP, Hansen HJ. Immunologic control of the ascites form of murine adenocarcinoma 755. I. Protection with syngeneic immune serum or lymphoid cells. J. Natl Cancer Inst 1978; 60:131–139.

(*6*) Klein G, Klein E. Rejectability of virus-induced tumors and nonrejectability of spontaneous tumors: A lesson in contrasts. Transplant Proc 1977; 9:1095–1104.

(*7*) Foley EJ. Antigenic properties of methylcholanthrene-induced tumors in mice of the strain of origin. Cancer Res 1953; 13:835–837.

(*8*) Prehn RI, Main JM. Immunity to methylcholanthrene-induced sarcomas. J Natl Cancer Inst 1957; 18:769–778.

(*9*) Wahl DV, Chapman WH, Hellström I, Hellström KE. Transplantation immunity to individually unique antigens of chemically induced bladder tumors in mice. Int J Cancer 1974; 14:114–121.

(*10*) Klein G, Sjogren O, Klein E, Hellström KE. Demonstration of resistance against methylcholanthrene-induced sarcomas in the primary autochthonous host. Cancer Res 1960; 20:1561–1572.

(*11*) Old LJ, Boyse EA, Clarke DA, Cresswell EA. Antigenic properties of chemically induced tumors. Ann NY Acad Sci 1962; 101:80–106.

(*12*) Pellis NR, Tom BH, Kahan BD. Tumor-specific and allospecific immunogenicity of soluble extracts from chemically-induced murine sarcomas. J Immunol 1974; 113:708–711.

(*13*) DeLeo AB, Shiku H, Takahashi MJ, Old LJ. Cell surface antigens of chemically induced sarcomas of the mouse. J Exp Med 1977; 146:720–734.

(*14*) Natori T, Law LW, Appella E. Biological and bicohemical properties of Nonidet p40-solubilized and partially purified tumor-specific antigens of the transplantation type from plasma membranes of a methylcholanthrene-induced sarcoma. Cancer Res 1977; 37:3406–3413.

(*15*) ———. Immunochemical evidence of a tumor-specific surface antigen obtained by detergent solubilization of the membranes of a chemically induced sarcoma, Meth A. Cancer Res 1978; 38:359–364.

(*16*) Pellis NR, Shulan DJ, Kahan BD. Specific tumor immunity induced with soluble materials: Purification of antigens inducing tumor resistance. Biochem Biophys Res Commun 1976; 71:1251–1256.

(*17*) Basombrio MA. Search for common antigenicities among twenty-five sarcomas induced by methylcholanthrene. Cancer Res 1970; 30:2458–2462.

(*18*) Forbes JT, Nakao Y, Smith RT. Evidence for immunologic specificity and shared antigenicity in lymphocyte responses to soluble tumor antigens: Tumor-specific immunity to chemically induced tumors. J Exp Med 1975; 141:1181–1200.

(*19*) Seifert E, Claviez M, Frank H, Hunsmann G, Schwarz H, Schäfer W. Properties of mouse leukemia viruses. XII. Production of substantial amounts of Friend leukemia virus by a suspension tissue culture line (Eveline suspension cells). Z Naturforsch [C] 1975; 30:698–700.

(*20*) Bassin RH, Tuttle N, Fischinger PJ. Rapid cell culture assay technique for murine leukaemia viruses. Nature 1971; 229:564–566.

(*21*) Strand M, August JT. Structural proteins of oncogenic RNA viruses: Interspecies II, a new interspecies antigen. J Biol Chem. 1973; 248:5627–5633.

(*22*) Collins JJ, Montelaro RC, Denny TP, Ishizaki R, Langlois AJ, Bolognesi DP. Normal chicken cells (chf$^-$) express a surface antigen which cross-reacts with determinants of the major envelope glycoprotein (gp85) of avian myeloblastosis virus. Virology 1978; 86:205–216.

(*23*) Bolognesi DP, Collins JJ, Leis JP, Moennig V, Schäfer W, Atkinson PH. Role of carbohydrate in determining the immunochemical properties of the major glycoprotein (gp71) of Friend murine leukemia virus. J Virol 1975; 16:1453–1463.

(*24*) Lowry OH, Rosebrough NJ, Farr AL. Protein measurement with the Folin phenol reagent. J Biol Chem 1951; 193:265–275.

(*25*) Reed LJ, Muench H. A simple method of estimating fifty-percent endpoints. Am J Hygiene 1938; 27:493–497.

(*26*) Grant JP, Bioner DB, Fischinger PJ, Bolognesi DP. Expression of murine leukemia virus structural antigens on the surface of chemically induced murine sarcomas. Proc Natl Acad Sci USA 1974; 71:5037–5041.

(*27*) Collins JJ, Sanfilippo F, Tsong-Chou L, Ishizaki R, Metzgar RS. Immunotherapy of murine leukemia. I. Protection against Friend leukemia virus-induced disease by passive serum therapy. Int J Cancer 1978; 21:51–61.

(*28*) de Noronha F, Schäfer W, Essex M, Bolognesi DP. Influence of antisera to oncornavirus glycoprotein (gp71) on infection of cats with feline leukemia virus. Virology 1978; 85:617–621.

(*29*) Genovesi G, Livnat D, Collins JJ. Immunotherapy of murine leukemia. VI. Development of immunological memory in mice protected against Friend leukemia virus-induced disease by passive serum therapy. Leuk Res. In press.

(*30*) Iglehart JD, Ward EC, Thiel K, Huper G, Geier SS, Bolognesi DP. In vivo antigenic modification of tumor cells. I. Introduction of murine leukemia virus antigens on non-virus-producing murine sarcomas. JNCI 1981; 67:107–115.

(*31*) Iglehart JD, Ward EC, Huper G, Thiel K, Bolognesi DP. In vivo antigenic modification of tumor cells. II. Distribution of virus in sarcoma-bearing animals. JNCI 1981; 67:117–122.

(*32*) Wecker E, Schimpl A, Hünig T. Expression of MuLV gp71-like antigen in normal mouse spleen cells induced by antigenic stimulation. Nature 1977; 269:598–600.

(*33*) Schwarz H, Ihle JN, Wecker E, et al. Properties of mouse leukemia viruses. XVII. Factors required for successful treatment of spontaneous AKR leukemia by antibodies against gp71. Virology 1981; 111:568–578.

(*34*) Al-Ghazzouli IK, Donahoe RM, Huang K-Y, Sass B, Peters RL, Kelloff GJ. Immunity to virus-free syngeneic tumor cell transplantation in the BALB/c mouse after immunization with homologous tumor cells infected with type C virus. J Immunol 1976; 117:2239–2248.

FIGURE 1.—Hematoxylin and eosin cross sections of MCA-FS-F-MuLV tumors, treated and untreated. A) Tumor 2 days following challenge. *Bar*=160 μm. × 48. B) Tumor 5 days following challenge, untreated. *Bar*=40 μm. × 190. C) Tumor 5 days following challenge, having received two shots of immune serum. *Bar*=40 μm. × 190. D) Tumor 10 days following challenge, untreated. *Bar*=40 μm. × 190. E) Tumor 10 days following challenge, having received five shots of immune serum. *Bar*=40 μm. × 190

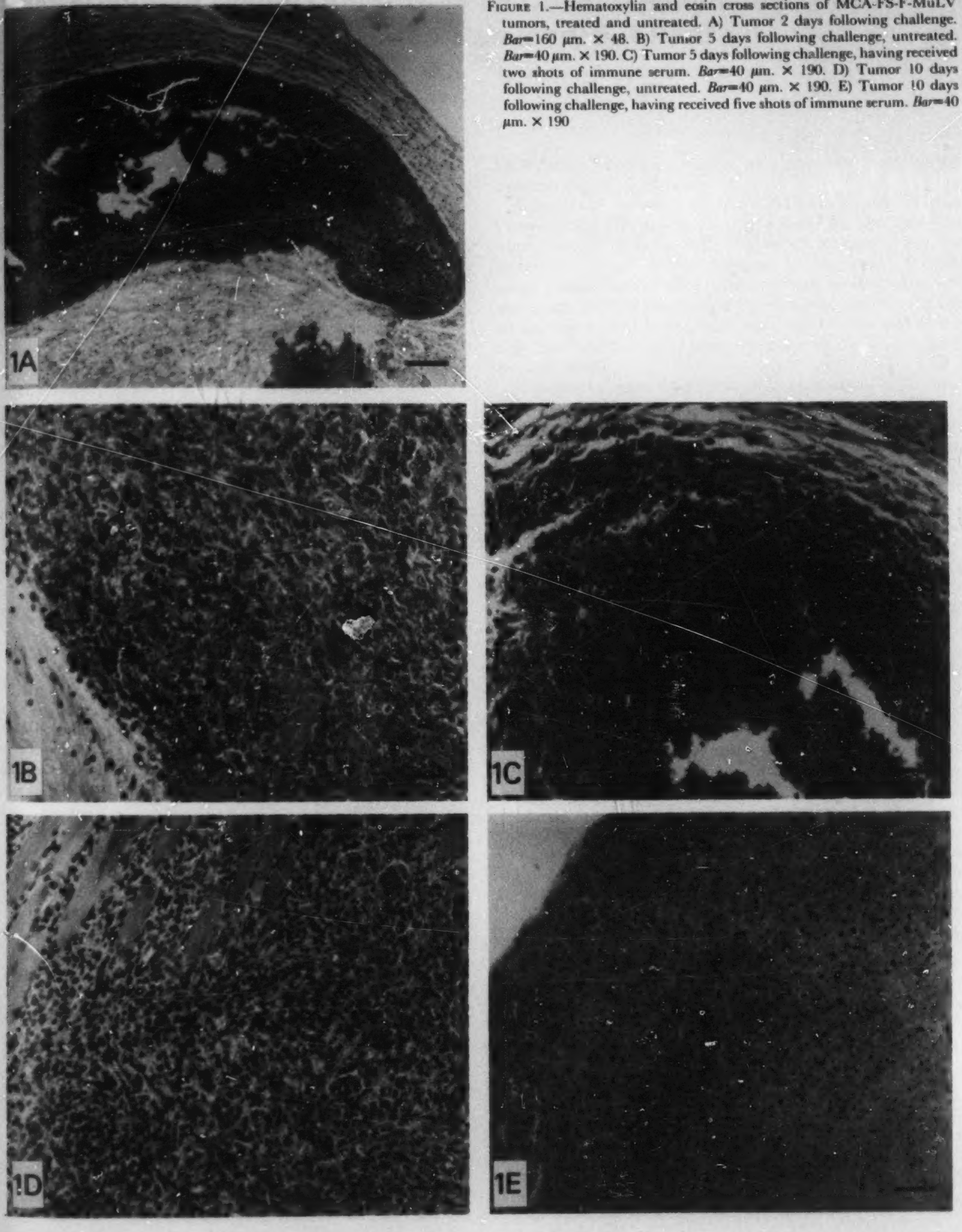

blank page

Proliferation of Ductal Outgrowths by Carcinogen-Induced Rat Mammary Tumors in Gland-Free Mammary Fat Pads[1,2,3]

Evelyn M. Rivera[4] *and* **Srinivasan Vijayaraghavan**[4,5]

ABSTRACT—The purpose of this study was to evaluate the gland-free mammary fat pad as a preferential site for transplantation of 7,12-dimethylbenz[a]anthracene (DMBA)-induced rat mammary tumors, since previous studies indicated their frequent failure to grow when transplanted in ectopic sites. Accordingly, samples from 14 primary mammary tumors (9 randomly selected and 5 ovarian-independent) were transplanted into the inguinal pairs of gland-free mammary fat pads of syngeneic female Lewis rats (9–12 wk of age). Although the percentage of takes was high (88%), the growth and morphogenetic capabilities of the transplants were strikingly different. Whereas transplants of ovarian-independent tumors consistently developed palpable carcinomas, transplants of all but 1 of the tumors selected at random (most of which were presumably ovarian-dependent) gave rise mainly to apparently normal ductal and hyperplastic outgrowths. The growth behavior of the transplants could not be correlated with the presence or absence in the tumors of mononuclear cells of the immune system. Unless the mammary fat pad selected against the growth of tumor cells, it seemed that the main alternative to tumor formation by the transplants was the proliferation of nontumorous outgrowths. These results draw attention to differences in the phenotypic stability of primary mammary tumors induced by DMBA and open up for further study the question of whether these differences reflect their cellular heterogeneity or their potential to undergo differentiation.—JNCI 1982; 69:517–525.

Mammary tumors induced in rats by the administration of DMBA frequently fail to grow when transplanted into subcutaneous and intramuscular sites (*1–4*). Even after autotransplantation, 33% of the mammary tumor transplants remain dormant in subcutaneous sites (*4*). Although the tumors have been serially transplanted in ectopic sites, the drawback is that they lose within a few generations the morphologic and hormone-dependent properties that characterized the primary tumors from which they originated (*2, 3, 5–7*). In the course of evaluating the mammary fat pad as a preferred site for transplantation, we noted that transplants of randomly selected DMBA-induced mammary tumors only infrequently grew to palpability but proliferated instead a variety of nontumorous outgrowths. In contrast, transplants of ovarian-independent mammary tumors consistently grew to palpability without forming outgrowths. These unexpected findings, which provide a new perspective on the growth potential of mammary tumors, are the subject of this paper.

MATERIALS AND METHODS

Rats.—Two sublines of Lewis strain rats were used in this study. They have been maintained separately and inbred by brother-sister matings in our laboratory since 1976. The original breeding pairs were obtained from the National Institutes of Health, Bethesda, Md. (strain LEW/SsN) and from Simonsen's Laboratories, Gilroy, Calif. (strain LEW/Sim). Mammary tumors were not cross-transplanted between the two sublines.

Induction of mammary tumors.—DMBA (20 mg; Sigma Chemical Co., St. Louis, Mo.) in sesame oil was administered to virgin females, beginning at 45–50 days of age, by gastric intubation in two feedings (10 mg each) 1 week apart. About 50% of the treated animals developed mammary tumors by 7 weeks, and by 16 weeks after treatment all animals had at least 1 mammary tumor. The age of the rats from which tumors were taken for study ranged from 16 to 22 weeks.

Preparation of mammary fat pads for transplantation.—The major pair of inguinal mammary fat pads of female rats was used as the site of transplantation. In rats, these fat pads contain the fourth and fifth pairs of mammary anlagen, which were removed surgically by cautery from 20- to 22-day-old females by a modification of the method of DeOme et al. (*8*). In our modification, the fat pad lymph nodes were removed, and the anesthetic used was ether rather than pentabarbital sodium. After surgery, wound clips were applied to the skin incisions, and the animals were held until transplantation.

Transplantation of mammary tumors.—Nine randomly selected primary tumors (≈1.0–1.5 cm in diameter), each from a different rat, were excised under sterile conditions. Portions of each tumor, excluding the capsule, were cut with the aid of a stereomicroscope into the approximately 1-mm cubes (to exclude pieces consisting only of connective tissue) and placed on saline-saturated filter paper in a petri dish. Tumor samples were transplanted singly into the gland-free mammary fat pads of syngeneic virgin hosts 9–12 weeks of age. In experiments A, B, and C (table 1), in which 2 tumors were used per experiment, samples from 1 tumor were transplanted into the right fat pad of each host, and samples of the second tumor were transplanted into the contralateral fat pad. Corresponding samples of the tumors were fixed in Carnoy's solution and processed for histologic examination.

Ovarian-independent tumors were also studied when it was recognized that tumors selected at random generally

---

ABBREVIATIONS USED: DH=ductal hyperplasia(s); TDH=terminal ductal hyperplasia(s).

---

[1] Received November 25, 1981; accepted February 26, 1982.

[2] Supported by Public Health Service grant CA-17862 from the National Cancer Institute.

[3] Animals were maintained under the guidelines set forth by Michigan State University.

[4] Department of Zoology, Michigan State University, East Lansing, Mich. 48824.

[5] We thank Ms. Mary Taylor and Ms. Martha Hunt for their expert technical assistance.

failed to grow to palpability. In these cases, rats bearing primary mammary tumors were bilaterally ovariectomized, and samples from 5 tumors that continued to grow after ovariectomy (≈1.0–1.5 cm in diameter) were transplanted into gland-free mammary fat pads as described above.

Evaluation of growth and morphogenetic capabilities of the tumors.—Within 1 week after transplantation, mammary fat pads were palpated for tumors twice weekly. Tumor latency was determined to be the number of days elapsing between transplantation and initial palpability of the tumor. Tumors were allowed to grow until they were at least 1.0–1.5 cm in diameter before termination. At this time, samples of tumors (if present) were removed for histologic examination, and the remaining fat pads were removed intact, spread on filter papers, and fixed on the papers in buffered 15% Formalin; the papers were removed after fixation, and the fat pads were processed for wholemount examination as described previously (*9*).

In cases in which no palpable growths occurred, the animals were usually held for 1 year before termination, and the mammary fat pads were processed as described above for whole-gland examination. Each fat pad was evaluated according to the growth patterns found, which are listed in tables 1 and 2. Representative portions of the outgrowths were removed and processed for histologic examination. Photographs were taken of some of the wholemounts and of the portions removed for histologic examination.

RESULTS

Transplantation of randomly selected mammary tumors.—The primary tumors that provided the transplants were mammary adenocarcinomas (figs. 1, 2) with histologic variations (*10*) within and among different tumors. In 4 of the 9 primary tumors, the intraepithelial stroma was infiltrated with mononuclear cells, mostly lymphocytes (fig. 2). Those tumors showing this infiltration were one of the two sources used in experiment A and the sources of experiments D, E, and F (table 1). However, there was no correlation between growth fates of the tumors and the presence of lymphocytes.

The overall results are summarized in tables 1 and 2. The major finding was that although nearly 90% (87/100) of the transplants did take in mammary fat pads, most transplants (70%, 61/87) gave rise to outgrowths that were predominantly ductal or ductal-alveolar in morphology (figs. 3–6, 10, 12, 18, 21). DH and/or alveolar hyperplasias were also present in many of the outgrowths (figs. 3, 6, 12, 13, 18, 19), but only a few outgrowths contained tumors (figs. 7, 8, 21, 22). Transplants developing palpable tumors generally did not proliferate outgrowths (24%, 21/87), and 17 of the 21 transplants of this type were from a single tumor source (*see* below). Of the transplants, 7% formed localized atypical ducts (figs. 14–16).

Variations among the primary tumor sources.—As noted above, all but 1 of the 9 randomly selected tumors produced outgrowth in mammary fat pads. The exception was the tumor source in experiment D (tables 1, 2), from which all samples gave rise to palpable carcinomas. In general, transplants that proliferated outgrowths rarely developed palpable tumors (table 1). Only two tumor sources gave rise to regressing tumors (experiment B, table 1).

Variations among transplants from individual tumors.—In experiment A (table 1), the same tumor was the source of both a palpable adenocarcinoma and a nonpalpable adenoacanthoma. In experiments E and F (table 1), transplants from both tumor sources generated outgrowths, palpable and nonpalpable tumors, and localized takes, but the tumor source in experiment F gave rise to a broader spectrum of outgrowths than did the source in experiment E (table 2).

Histologic examination of the mammary outgrowths.—The epithelial portions of the outgrowths that were ductal, ductal-alveolar, and hyperplastic-alveolar in subgross appearance were shown by histologic examination to consist of normal-appearing, cuboidal cells with scant cytoplasm (figs. 15, 23). There were variations in the same outgrowth in the size and shape of the cells (cf. figs. 15, 17, 20) and in the thickness of the connective tissue stroma (cf. figs. 15, 17). DH occurred at terminal portions of ducts (TDH) (fig. 9) and in proximal portions (figs. 18, 19). Hyperplasias also varied in size, number, and shape (cf. figs. 9, 19) and in the amount of associated connective tissue (cf. figs. 9, 13). Other atypias included atrophic ducts and structures with variable histol-

TABLE 1.—*Growth potential of mammary tumors transplanted into gland-free mammary fat pads*

Specification	Growth potential in expt						Total
	A	B	C	D	E	F	
No. of tumor sources	2	2	2	1	1	1	9
No. of takes/No. of samples transplanted	14/16	15/18	8/8	17/18	16/20	17/20	87/100
No. of transplants that developed tumors that were:							
Palpable[a]	1	2	1	17	2[b]	1[b]	24
Palpable, then regressed		6[c]					6
Nonpalpable	1[d]	1	2		4	2	10
No. of transplants that developed:							
Tumors only	1[d]			17	3		21
Tumors and outgrowths	1	8	3[e]		2	3	17
Outgrowths only	10	7	5		8	13	43
Localized takes, ductal	2				3	1	6

[a] All palpable tumors were adenocarcinomas.

[b] Small tumors noted only at termination.

[c] Of the 6 tumors, 1 was a fibroadenoma; the remainder were adenocarcinomas.

[d] This tumor was an adenoacanthoma, the only one found in the study.

[e] Of the 3 tumors, 2 were fibroadenomas.

TABLE 2.—*Morphology of outgrowths of mammary tumor transplants in gland-free mammary fat pads*

Morphologic pattern[a]	No. of outgrowths showing morphology indicated in expt						Total showing morphology indicated
	A	B	C	D	E	F	
Ductal, nonhyperplastic	4	2	3		3	2	14
Ductal + TDH	3	4	4		7		18
Ductal + non-TDH	1	1				2	4
Ductal + non-TDH + TDH	1					1	2
Ductal–alveolar	1	6	1			6	14
Ductal–alveolar + TDH		1				3	4
Ductal–alveolar + hyperplastic alveolar	1	1				1	3
Hyperplastic alveolar + TDH						1	1
No. of outgrowths/expt	11	15	8	0	10	16	

[a] A portion of most of the outgrowths was ductal or ductal–alveolar in morphology, regardless of whether other growths (tumors or hyperplasias) were also present.

ogy (figs. 13, 19, 22) that appeared as microscopic densities in wholemounts (figs. 12, 18, 21).

Tumor latencies.—The latencies for palpability (excluding tumors that regressed after initial palpability) ranged from 9 to 119 days ($\bar{x}$, 32 days). If we consider separately the case in which all transplants from a single source gave rise to palpable tumors without outgrowths (experiment D, table 1), the latencies were 9–51 days ($\bar{x}$, 19 days). In contrast, the latencies of the remaining tumors ranged from 28 to 119 days ($\bar{x}$, 61 days). Latencies of the tumors that regressed after initial palpability were 25–78 days ($\bar{x}$, 41 days).

Transplantation of ovarian-independent tumors.—These tumors were remarkably consistent in developing palpable tumors without also forming outgrowths. Five ovarian-independent tumors were the sources of 32 transplants in the fat pads of 16 hosts, of which 88% took (28/32) and grew to palpability. Only 2 of the 28 transplants produced outgrowths as well as tumors, and these outgrowths were ductal–alveolar in morphology and derived from the same tumor. Latencies for palpability were 9–53 days ($\bar{x}$, 28 days). The tumors and their transplanted derivatives were adenocarcinomas (fig. 25). Only one of the five sources was infiltrated with lymphocytes, but all transplants from that source developed tumors without outgrowths.

DISCUSSION

It is now well documented that transplants of normal and hyperplastic mammary tissue proliferate better in gland-free mammary fat pads of syngeneic hosts than in ectopic sites (*8, 11, 12*). It was therefore expected that transplants of DMBA-induced mammary tumors, which frequently failed to grow in ectopic sites (*1–4*), would develop palpable carcinomas in mammary fat pads, their normal site of development. However, as the present study shows, this was not always the case.

Despite the high percentage of takes, there was a striking difference in the growth and morphogenetic capabilities of the tumors. Most of the transplants of *randomly selected* tumors proliferated mainly ductal and ductal–alveolar outgrowths, with and without hyperplastic components, but only rarely did they develop palpable tumors. In contrast, transplants of *ovarian-independent* tumors consistently gave rise to palpable tumors but rarely to outgrowths. This last finding and the fact that most mammary tumors induced in rats by DMBA are ovarian-dependent (*6, 13–16*) suggest that most of those selected at random were ovarian-dependent. This characteristic is consistent with the finding that transplants of only 1 of 9 randomly selected tumors gave rise to tumors without outgrowths (as did the ovarian-independent tumors), and transplants from only two sources displayed spontaneous regression (see table 2).

The major questions raised by this study concern the differential growth behavior of the tumors, i.e., why the ovarian-dependent majority formed nontumorous outgrowths, whereas the ovarian-independent minority were more likely to "breed true" and give rise only to palpable carcinomas.

We considered the possibility that the nontumorous outgrowths were a reflection of the heterogeneous cell composition of the tumors and therefore the result of proliferation of preexisting normal and hyperplastic cells. Although cellular heterogeneity may account in part for the diversity in outgrowth morphology as well as in the proliferative potential of randomly selected tumors, what was remarkable was the infrequency with which transplants of these tumors gave rise to palpable carcinomas. Thus if preexisting cell variants were the major source of the outgrowths, this would imply that selection occurred in the mammary fat pads against the growth of tumor cells. This possibility is difficult to reconcile with the fact that the tumors did originate and grow in the fat pads in the first place. Furthermore, assuming that the tumors were heterogeneous (i.e., each differing in content of normal, hyperplastic, and tumor cells), then some of the transplants from all of the tumor sources should have developed palpable tumors. However, this activity did not occur with most tumors selected at random.

Differences in the hormonal environment and microenvironment of the transplant recipients (9- to 12-wk-old virgins) and transplant donors (16- to 22-wk-old DMBA-treated virgins) may exert some selection in the transplants. Experiments are planned to pursue this possibility. One study in progress indicates that pretreatment of the recipients with DMBA does not enhance the formation of palpable growths from transplants of randomly selected tumors.

The possibility that immune rejection could account for the growth failure of the tumors was also considered, since these tumors have been found to express tumor antigens (*2, 17*). Although tumor immunogenicity was not studied, histologic studies revealed no correlation between the presence of mononuclear cells in the tumor sources and their subsequent behavior on transplantation. Portions of some outgrowths did contain lymphocytes (see fig. 16), but most did not. Perhaps the strongest argument against immune rejection playing a significant role in tumor growth failure was the invariability with which ovarian-independent tumors grew to palpability. Moreover, even with well-defined rejection antigens, tumors are still able to grow progressively (*18*).

Whatever the ultimate explanation, the remarkable finding was that tumor transplants that failed to breed true appeared to have other growth options: generally, to proliferate normal-appearing and hyperplastic outgrowths or, more infrequently, to proliferate mixed tumor–ductal outgrowths or to form localized ducts (limited proliferative potential). If our assumption that the mammary fat pad does not select against tumor cells is correct, then an alternative explanation for the development of outgrowths is that it reflects the potential of the tumors to undergo differentiation. Transplantation into gland-free mammary fat pads must in some way have triggered the expression of this potential. This indicates that the neoplastic phenotype is not a fixed property of most DMBA-induced mammary tumors but is subject to modulation. Conversely, the general failure of ovarian-independent tumors to form outgrowths implies a more stable phenotype in autonomous than in dependent tumors. As occurs in normal differentiation, the number of avenues open to a cell becomes decreased as it becomes committed to a particular phenotype. A similar commitment may hold for ovarian-independent tumor cells.

That most DMBA-induced mammary tumors are ovarian-dependent (*6, 13–16*) and at least some are spontaneous regressors (*15, 19*) may be viewed as evidence for their phenotypic lability and sensitivity to environmental shifts. Indeed, the phenotypes of other tumors can be altered and even normalized by shifts in their microenvironment (*20–24*), and it is possible that the gland-free mammary fat pad represents an environmental shift for mammary tumor cells. Pregnancy-dependent mammary tumors in mice also appear to be phenotypically labile, since during serial transplantation they alternate between ductal and tumorous phases of growth, depending on the hormonal environment (*25*). We plan also to determine whether similar alternation occurs in carcinogen-induced mammary tumors, and to this end we are attempting to develop a serially transplantable ductal tissue line derived from a tumor (fig. 26).

Although cloning studies of the tumors are clearly needed to specify the cellular origin of the mammary outgrowths, the absence of specific markers for mammary tumor cells (except for their tumorigenicity in vivo) poses problems. For example, anchorage independence in agarose cultures, a widely used criterion for tumorigenicity, is not always linked to mammary tumorigenicity in vivo (*26*). Furthermore, both anchorage-dependent and anchorage-independent cell lines from mouse mammary tumors have been shown to be tumorigenic in vivo (*27*), indicating that the tumor cells themselves are heterogeneous.

Nevertheless, the recent work of Dulbecco et al. (*28, 29*) and Rudland et al. (*30, 31*) is of special relevance to the present study. These researchers have developed cell clones derived from DMBA-induced rat mammary tumors, which give rise in vitro to normal-appearing mammary cells. One clonal line, Rama-25, may be a stem cell line since it gives rise to the main differentiated cell types of the mammary gland (*31*). Furthermore, depending on the composition of the medium (*29*) or of the substrate (*32*), the clones form structures that may be analogous to normal mammary ducts, ductal end buds, and hyperplasias. Thus our results may be in the in vivo counterpart for these studies in cell culture.

In a broader context, there is considerable evidence for tumor cell heterogeneity (*33–35*) and increasing evidence for the differentiative potential of tumor cells (*36–39*). Thus while it is possible that the growth characteristics reported here may be peculiar to certain types of mammary tumors, they open up for further exploration the question of their heterogeneous cell composition and/or potential to undergo differentiation.

REFERENCES

(*1*) Takizawa S, Ito A, Kawamura Y, Nakano M. Growth characteristics of chemically induced rat mammary tumors in autochthonous and secondary hosts. Gan 1973; 64:465–474.

(*2*) Piessens WF, Churchill WH. Transplantable mammary tumors in Wistar/Furth rats: Development, antigenicity, and effect of hormone manipulations. J Natl Cancer Inst 1977; 59:911–917.

(*3*) Horn H, Erlichman I, Geier A, Levij IS. Changes in morphology and hormone dependency following transplantation of rat 9,10-dimethyl-1,2-benzathracene-induced mammary adenocarcinoma. Eur J Cancer 1976; 12:189–194.

(*4*) Lee C, Shih A, Oyasu R. Multiple autotransplantation of rat mammary tumors induced by 7,12-dimethylbenz[*a*]anthracene: *Brief communication*. J Natl Cancer Inst 1978; 60:473–476.

(*5*) Sander S, Jakobsen A, Sander J. Transplantable breast tumours in rats. Acta Pathol Microbiol Scand [A] 1973; 81:91–94.

(*6*) DeSombre ER, Kledzik G, Marshall S, Meites J. Estrogen and prolactin receptor concentrations in rat mammary tumors and response to endocrine ablation. Cancer Res 1976; 36:354–358.

(*7*) Hilf R, Johnson MM, Breuer C, Freeman JJ, Borman A. Comparative biochemistry of three transplantable mammary tumors as influenced by steroid therapy. J Natl Cancer Inst 1963; 31:541–555.

(*8*) DeOme KB, Faulkin LJ Jr, Bern HA, Blair PB. Development of mammary tumors from hyperplastic alveolar nodules transplanted into gland-free mammary fat pads of female C3H mice. Cancer Res 1959; 19:515–520.

(*9*) Rivera EM, Hill SD, Taylor M. Organ culture passage enhances oncogenicity of carcinogen-induced hyperplastic mammary nodules. In Vitro 1981; 17:159–166.

(*10*) Young S, Hallowes RC. Tumors of the mammary gland. In: Turosov VS, ed. Pathology of tumors in laboratory animals. Vol 1. IARC Sci Publ 1973; 5:31–73.

(*11*) Medina D. Preneoplastic lesions in mouse mammary tumorigenesis. Methods Cancer Res 1973; 7:3–53.

(*12*) Hoshino K. Mammary transplantation and its histogenesis in mice. In: Yokoyama A, Mizuno H, Nagasawa H, eds. Physiology of mammary glands. Baltimore: Univ Park Press, 1980:163–228.

(*13*) Dao TL. Studies on mechanism of carcinogenesis in the mammary gland. Prog Exp Tumor Res 1969; 11:235–261.

(*14*) Huggins C, Briziarelli G, Sutton H. Rapid induction of mammary carcinoma in the rat and the influence of hormones on the tumors. J Exp Med 1959; 109:25–41.

(*15*) Haslam SZ. Age as a modifying factor of 7,12-dimethylbenz-(*a*)anthracene-induced mammary carcinogenesis in the Lewis rat. Int J Cancer 1979; 23:374–379.

(*16*) Rivera EM, Vijayaraghavan S. Rat mammary tumors from carcinogen-induced nodules and their responsiveness to ovariectomy. Eur J Cancer Clin Oncol 1982; 18:53–58.

(*17*) Silinskas KC, Fang W, Mukkus TK. Demonstration of tumor-associated transplantation antigen in rat mammary tumors induced by 7,12-dimethylbenz(*a*)anthracene. Oncology 1974; 29:273–282.

(*18*) Baldwin RW, Price MR. Immunobiology of rat mammary neoplasia. Ann NY Acad Sci 1976; 276:3–10.

(*19*) Young S, Cowan DM, Sutherland LE. The histology of induced mammary tumors in rats. J Pathol Bacteriol 1963; 85:331–340.

(*20*) Kleinsmith LJ, Pierce GB. Multipotentiality of single embryonal carcinoma cells. Cancer Res 1964; 24:1544–1551.

(*21*) Fibach E, Hayashi M, Sachs L. Control of normal differentiation of myeloid leukemic cells to macrophages and granulocytes. Proc Natl Acad Sci USA 1973; 70:343–346.

(*22*) Illmensee K, Mintz B. Totipotency and normal differentiation of single teratocarcinoma cells cloned by injection into blastocysts. Proc Natl Acad Sci USA 1976; 73:549–553.

(*23*) Schirrmacher V. Shifts in tumor cell phenotypes induced by signals from the microenvironment. Immunobiology 1980; 157:89–98.

(*24*) Brouty-Boye D, Gresser I. Reversibility of the transformed and neoplastic phenotype. I. Progressive reversion of the phenotype of X-ray-transformed C3H/10½ cells under prolonged treatment with interferon. Int J Cancer 1981; 28:165–173.

(*25*) Aidells BD, Daniel CW. Hormone-dependent mammary tumors in strain GR/A mice. I. Alteration between ductal and tumorous phases of growth during serial transplanation. J Natl Cancer Inst 1974; 52:1855–1863.

(*26*) Butel J, Dudley JP, Medina D. Comparison of the growth properties in vitro and transplantability of continuous mouse mammary tumor cell lines and clonal derivatives. Cancer Res 1977; 37:1892–1900.

(*27*) Danielson KG, Anderson LW, Hosick HL. Selection and characterization in culture of mammary tumor cells with distinctive growth properties in vivo. Cancer Res 1980; 40:1812–1819.

(*28*) Dulbecco R, Bologna M, Unger M. Differentiation of a rat mammary cell line in vitro. Proc Natl Acad Sci USA 1979; 76:1256–1280.

(*29*) Dulbecco R, Okada S. Differentiation and morphogenesis of mammary cells in vitro. Proc R Soc Lond [Biol] 1980; 208:399–408.

(*30*) Rudland PS, Bennett DC, Warburton MJ. Isolation and characterisation of epithelial stem-cell lines from the rat mammary gland. Br J Cancer 1980; 41:666–668.

(*31*) Rudland PS, Ormerod EJ, Paterson FC. Stem cells in rat mammary development and cancer: A review. J R Soc Med 1980; 73:437–442.

(*32*) Bennett DC. Morphogenesis of branching tubules in cultures of cloned mammary epithelial cells. Nature 1980; 285:657–659.

(*33*) Fidler IJ. Tumor heterogeneity and the biology of cancer invasion and metastasis. Cancer Res 1978; 38:2651–2660.

(*34*) Dexter DL, Kowalski HM, Blazar BA, Fligiel Z, Vogel R, Heppner GH. Heterogeneity of tumor cells from a single mouse mammary tumor. Cancer Res 1978; 38:3174–3181.

(*35*) Schmitt M, Daynes RA. Heterogeneity of tumorigenicity phenotype in murine tumors. J Exp Med 1981; 153:1344–1359.

(*36*) Braun AC. On the origin of the cancer cell. Am Sci 1970; 58:307–320.

(*37*) Pierce GB. Neoplasms, differentiations, and mutations. Am J Pathol 1974; 77:103–118.

(*38*) Saunders GF, ed. Cell differentiation and neoplasia. New York: Raven Press, 1978.

(*39*) Mintz B, Fleischman RA. Teratocarcinomas and other neoplasms as developmental defects in gene expression. Adv Cancer Res 1981; 34:211–278.

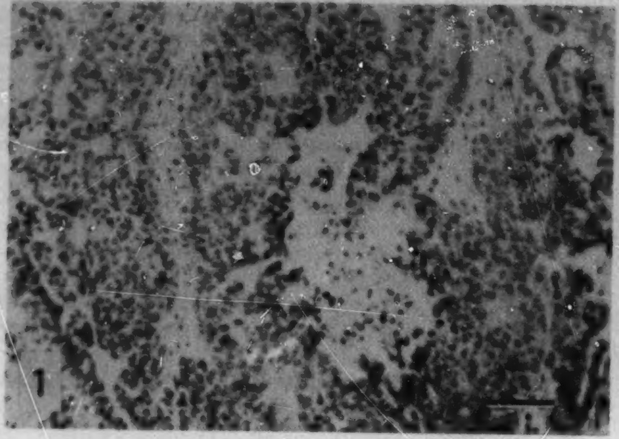

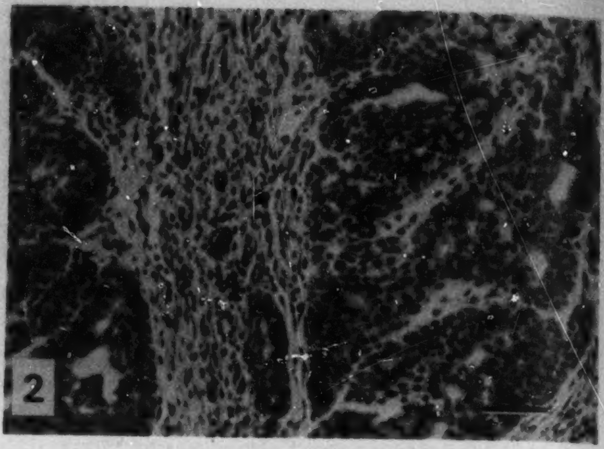

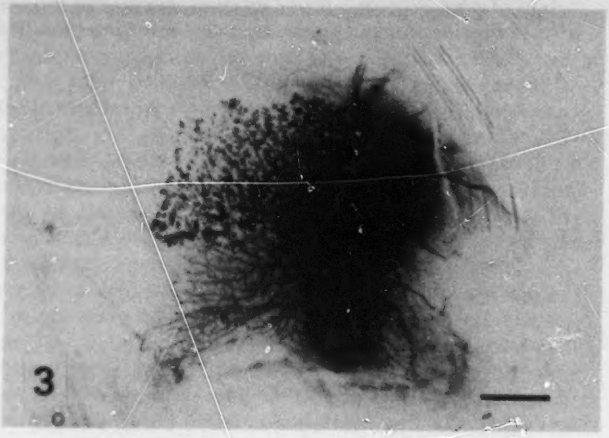

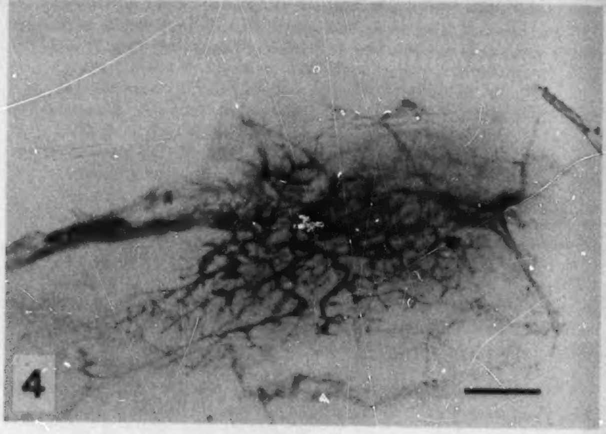

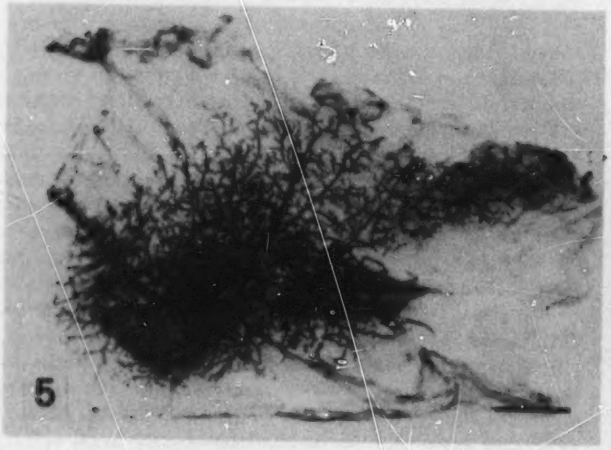

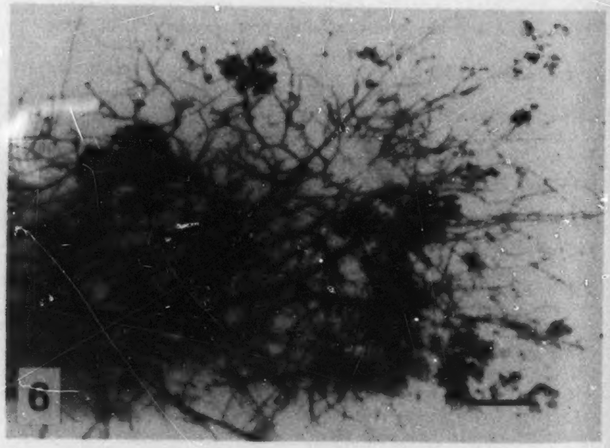

Figures 1–26.—Wholemounts were stained with hematoxylin, and tissue sections were stained with hematoxylin and eosin.

Figure 1.—Histologic section of mammary tumor source of experiment B, showing adenocarcinoma cells and minimal stroma. *Bar*=50 µm. × 190

Figure 2.—Histologic section of mammary tumor source of experiment D, showing lymphocytic infiltration of intraepithelial stroma. *Bar*=50 µm. × 190

Figure 3.—Wholemount showing hyperplastic alveolar (*upper portion*) and ductal (*lower portion*) areas of mammary outgrowth. *Bar*=5 mm. × 1.9

Figure 4.—Wholemount showing atypical ductal outgrowth. *Bar*=5 mm. × 2.2

Figure 5.—Wholemount showing ductal–alveolar outgrowth and non-TDH (*lower right*). *Bar*=5 mm. × 2.2

Figure 6.—Wholemount showing ductal outgrowth with several hyperplastic alveolar clusters. *Bar*=2.5 mm. × 3.8

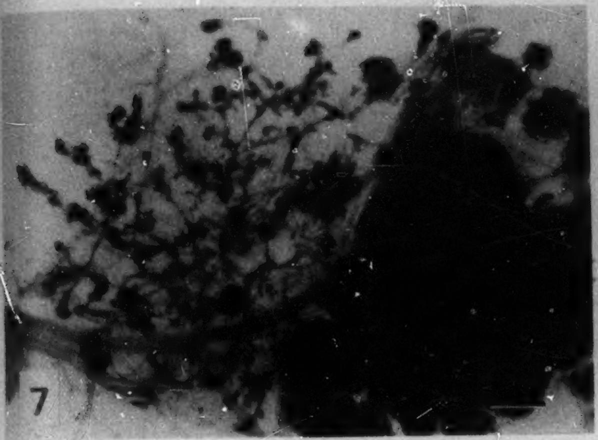

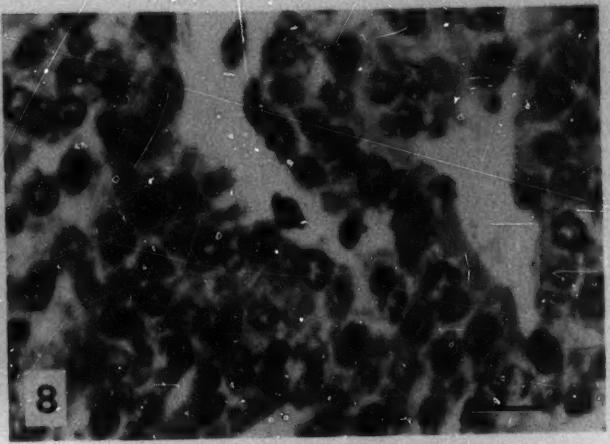

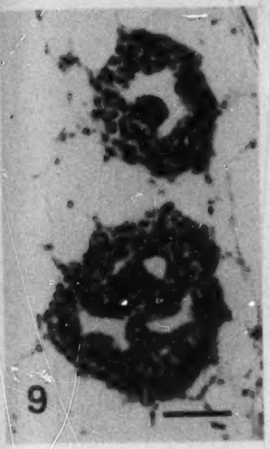

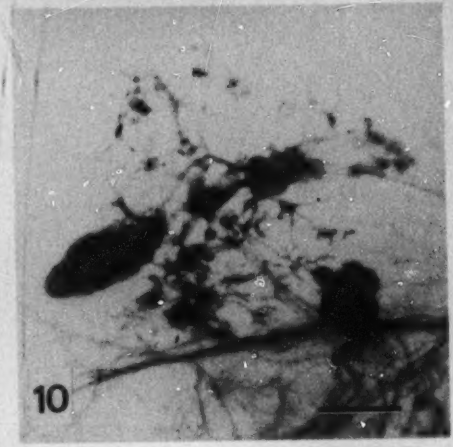

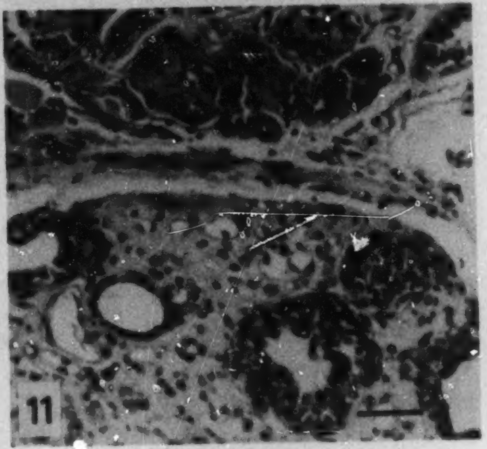

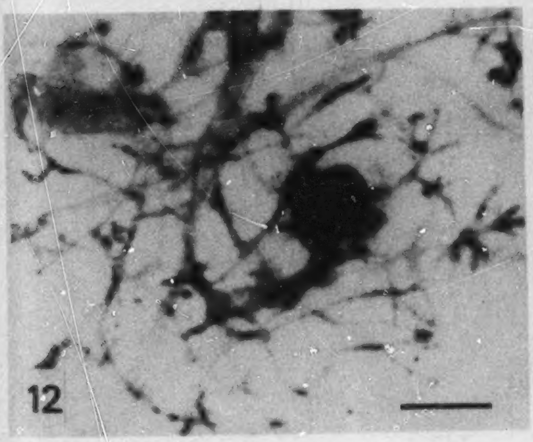

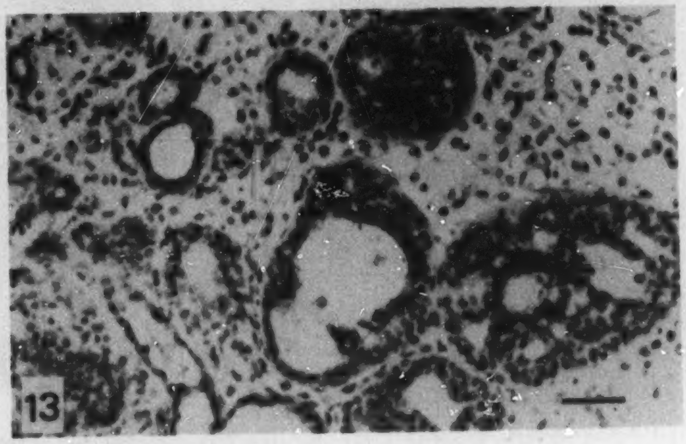

FIGURE 7.—Wholemount showing palpable tumor (density at *right*) and TDH (*left half* of photo). *Bar*=1 mm. × 8

FIGURE 8.—Histologic section of tumor in fig. 7, showing typical carcinoma cells. *Bar*=13.2 µm. × 760

FIGURE 9.—Histologic section of a TDH in fig. 7. *Bar*=50 µm. × 190

FIGURE 10.—Wholemount showing several small densities in ductal outgrowth. *Bar*=2 mm. × 6

FIGURE 11.—Histologic section of density at *extreme left* in fig. 10, showing fibroadenoma (*upper portion*) and DH embedded in fibrous stroma (*lower right*). *Bar*=50 µm. × 190

FIGURE 12.—Wholemount showing small density in ductal outgrowth. *Bar*=1 mm. × 13

FIGURE 13.—Histologic section of density in fig. 12, showing several DH. *Bar*=50 µm. × 190

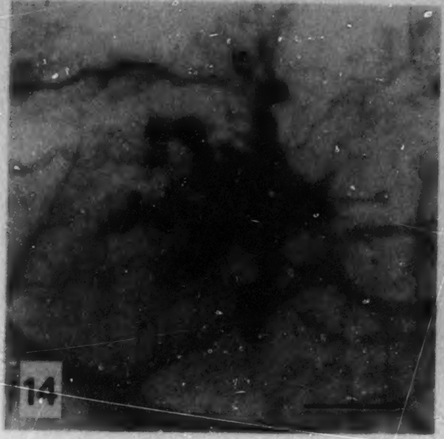

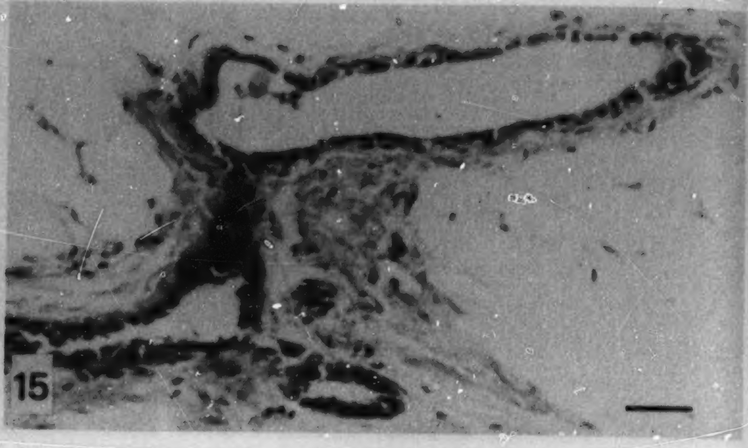

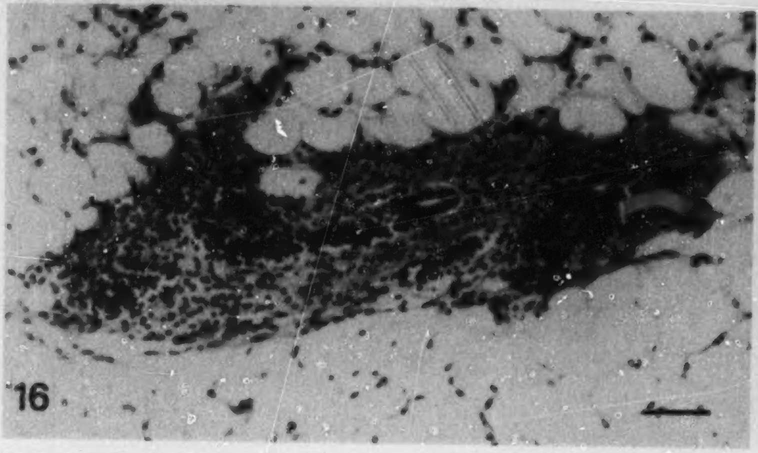

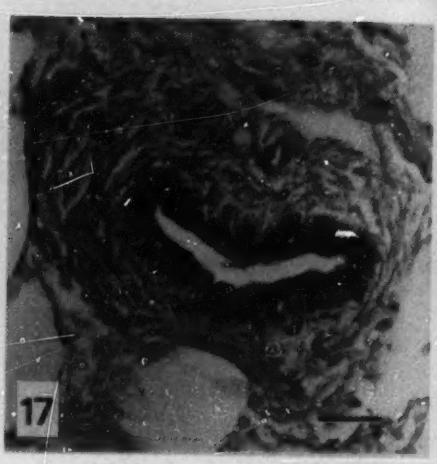

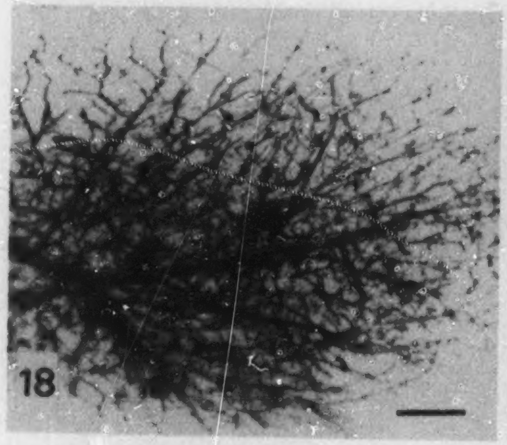

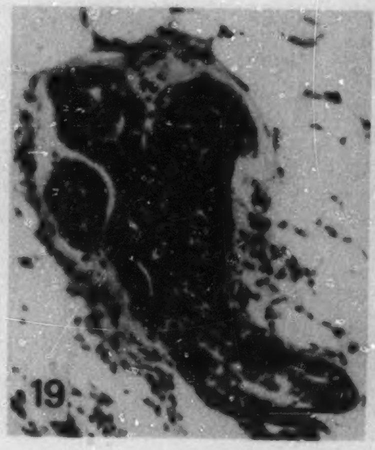

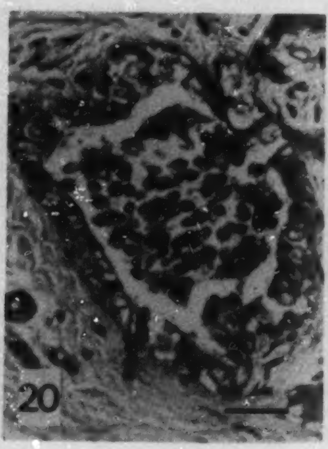

Figure 14.—Wholemount showing appearance of localized ducts. *Bar*=1 mm. × 13

Figure 15.—Histologic section of a portion of fig. 14, showing normal-appearing ducts. *Bar*=50 µm. × 190

Figure 16.—Histologic section of another portion of fig. 14, showing fibrous stroma of ducts infiltrated with lymphocytes. *Bar*=50 µm. × 190

Figure 17.—Histologic section of portion of ductal outgrowth with dense fibrous stroma and normal-appearing ductal epithelium. *Bar*=25 µm. × 380

Figure 18.—Wholemount showing ductal outgrowth with non-TDH (two dense areas near center). *Bar*=2.5 mm. × 3.8

Figure 19.—Histologic section of DH in fig. 18, showing atypical structure. *Bar*=25 µm. × 380

Figure 20.—Histologic section of portion of ductal outgrowth showing fibrosis. *Note* two types of epithelial cells: small, darkly stained and large cells with clear cytoplasm and nuclei. *Bar*=25 µm. × 380

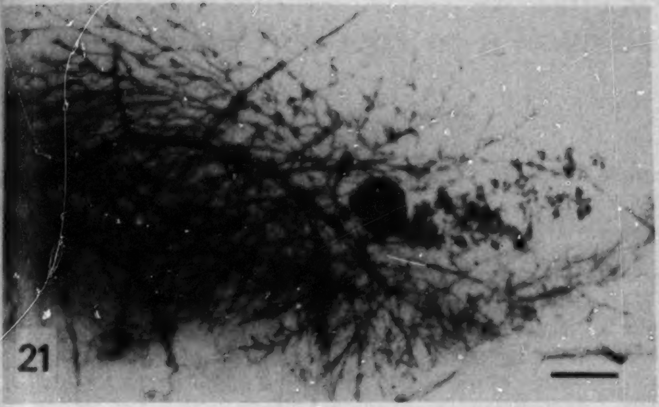

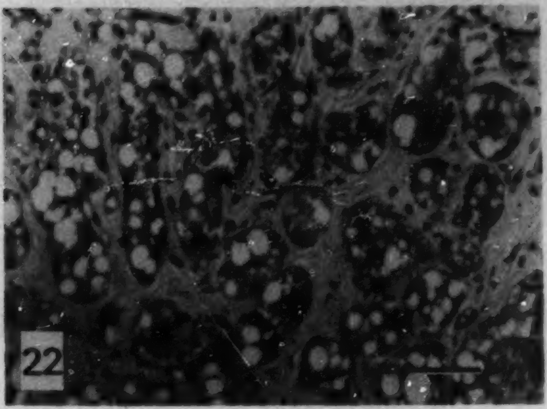

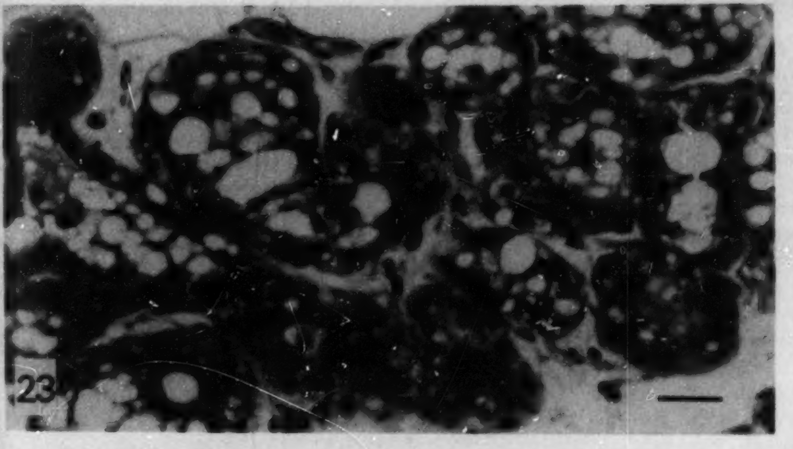

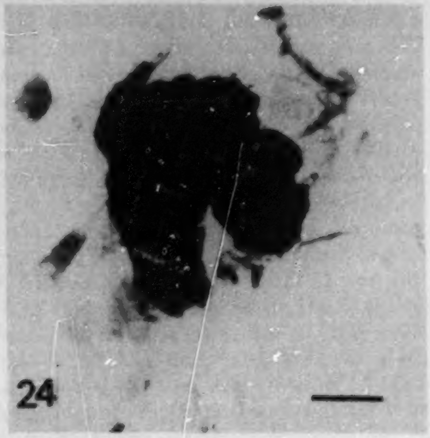

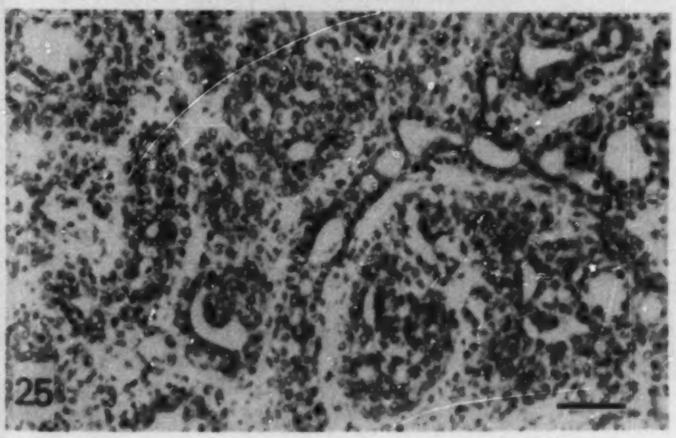

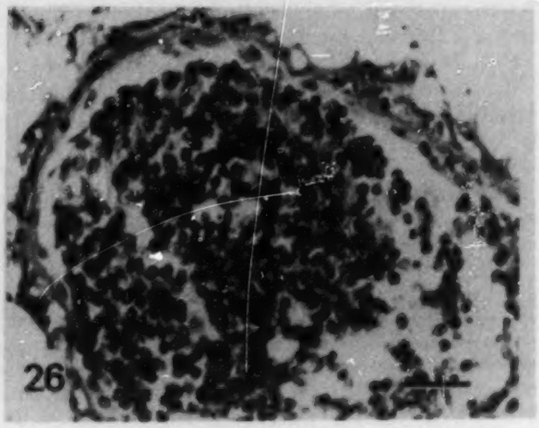

FIGURE 21.—Wholemount showing ductal outgrowth with small density (*right* of center) and hyperplastic alveolar cluster (*right* of density). *Bar*=2.5 mm. × 3.8

FIGURE 22.—Histologic section of density in fig. 21, a secretory fibroadenoma. *Bar*=50 µm. × 190

FIGURE 23.—Histologic section of hyperplastic alveoli in fig. 21, showing typical secretory alveoli. *Bar*=25 µm. × 380

FIGURE 24.—Wholemount showing gross appearance of a transplanted ovarian-independent tumor. *Note* absence of outgrowth from tumor. *Bar*=5 mm. × 2

FIGURE 25.—Histologic section of tumor in fig. 24. *Bar*=50 mm. × 190

FIGURE 26.—Histologic section of hyperplastic ductal outgrowth derived from a mammary tumor and serially transplanted for 5 generations in gland-free mammary fat pads. Hyperplastic appearance is maintained as seen in this photograph at the fifth generation. *Note* occlusion of lumen by ductal cells. *Bar*=25 µm. × 380

blank page

Individually Distinct Tumor-Specific Cell Surface Antigen Identified by Monoclonal Antibody on a Rous Sarcoma Virus-Induced Mouse Tumor[1,2]

Noboru Kuzumaki,[3,4] **Hidetaka Minakawa,**[3] **Takashige Miyazaki,**[3] **Soichi Haraguchi,**[3] **Tetsumichi Matsuo,**[3] *and* **Takato O. Yoshida**[3,5]

ABSTRACT—Hybrid cell lines were prepared by the fusion of BALB/c myeloma P3U-1 cells with the lymphocytes of BALB/c mice that were immunized with syngeneic Rous sarcoma virus (RSV)-induced tumor CSA1M cells. Three clones of the hybrid progeny (3.4B2, 3.4C6, and 3.5C11) produced cytotoxic IgM antibodies against CSA1M cells. One of the clones, 3.5C11, was chosen for analysis of the detailed specificity. Both direct cytotoxicity assays and absorption tests revealed that monoclonal antibody from 3.5C11 was positive only with CSA1M cells and that it failed to react with other tumors, including 20 RSV-induced mouse tumors, and normal cells. The 3.5C11 monoclonal antibody alone, with or without exogenous complement, was suppressive in the therapy of ip injected CSA1M tumor in syngeneic hosts, and significant prolongation in survival was seen in the treated mice. These results clearly showed presence of an individually distinct tumor-specific cell surface antigen on an RSV-induced mouse tumor.—JNCI 1982; 69:527–530.

Chemical carcinogen-induced tumors carry surface antigens that are generally unique to each tumor and do not cross-react with other tumors in vivo, even when these are induced by the same carcinogen in the same strain of mice and have the same morphology (*1*). Conversely, all tumors induced by an oncogenic virus, even those induced by that virus in different species of rodents, share cross-reacting tumor-associated antigens. In addition to common antigens, however, individual specificities of non-virus-associated antigens have been demonstrated in murine mammary tumor virus-induced tumors (*2, 3*), SJL mouse reticulum cell sarcomas (*4*), SV40-induced tumors (*5*), AKR mouse leukemias (*6*), and feline leukemias (*7*).

In the ASV system, ASV-induced avian and mammalian tumors express a common TSSA (*8*). Recent progress in the production of monoclonal antibody in vitro (*9*) has prompted many investigators to use this technique to investigate cell surface antigens on tumor cells in experimental animal (*10–13*) and human (*14–17*) systems.

We have used this approach and obtained a syngeneic monoclonal mouse antibody that identifies a new individually distinct TSSA of an RSV-induced tumor.

MATERIALS AND METHODS

Mice.—Mice BALB/cCrl mice were obtained from Shizuoka Argicultural Cooperative Association for Laboratory Animals, Hamamatsu, Japan. Homozygosity of the inbred mice was identified by genetic monitoring with use of biochemical markers of Id-1, Dip-1, Car-2, Mup-1, Gpd-1, Pgm-1, Ldr-1, Gpi-1, Hbb, Es-1, Es-2, Es-11, Prt-2, Mod-1, Trf, Es-3, and Ce-2.

Cells.—The cell lines used in this work are the following: The SR-RSV-induced mouse tumors CSA1M, CSA7M, CSA8M, CSA9F, CSA10F, CBr2F, C3SA1F, B6SA3F, BDSA3F, B10Br2F, D2SA1M, B10ABr2M, and B10ABr1F. C, C3, BD, and D2 stand for mouse strains BALB/c, C3H, BDF_1, and B10D2. SA and Br stand for sarcoma and brain tumor, 1–10 for the serial number of the tumor, and M and F for male or female. These tumors were established in our laboratory (*18*). S1018.B10, S908.D2, S623.BR, S826.BA, S1229.4R, S325.5R, S319.BS, and S208.9R are also SR-RSV-induced tumors and were provided by Dr. S. Fujimoto (Kochi University School of Medicine, Kochi, Japan). Three MCA-induced tumors (MCSA4M, MCSA2F, and CMC-11; obtained from Dr. T. Takahashi, Aichi Cancer Center, Nagoya, Japan), 3 murine leukemias (RL♂1, Kaplan-1, and P815; also from Dr. T. Takahashi), and a wild mouse embryo cell line (SC-1; obtained from Dr. A. Ishimoto, Virus Research Institute, Kyoto University, Kyoto, Japan) were also used. A Fischer rat fibroblast line 3Y1 and SR-RSV-transformed 3Y1 line were provided by Dr. S. Kawai (Research Institute of Medical Science, Tokyo University, Tokyo, Japan), and B77ASV-transformed 3Y1 was a gift from Dr. H. Mitsui (Tokyo Metropolitan Institute of Medical Science, Tokyo, Japan). Eight human cell lines were also used: Namalva, Raji, and RPMI 8226 (from Dr. G. Klein, Karolinska Institute, Stockholm, Sweden), CCRF-CEM (from Dr. M. Katagiri, Asahikawa University School of Medicine, Asahikawa, Japan), K562 (from Dr. Y. Koide, Hamamatsu University School of Medicine, Hamamatsu, Japan), SK-MEL-28 (from Dr. T. Takahashi), SCH (established by Dr. S. Ooboshi, Niigata University School of Medicine, Niigata, Japan), and A204 (from Dr. M. Hatano, Cancer Research Institute, Kanazawa University, Kanazawa, Japan). All cell lines were maintained in DMEM or RPMI-1640 medium supplemented by 5–10% newborn or

---

ABBREVIATIONS USED: ASV=avian sarcoma virus; CDC=complement-dependent cytotoxicity; CI=cytotoxicity index; DMEM=Dulbecco's modified Eagle's minimum essential medium; FCS=fetal calf serum; MCA=3-methylcholanthrene; RSV=Rous sarcoma virus; SR-RSV=Schmidt-Ruppin strain of RSV; SV40=simian virus 40; TSSA=tumor-specific cell surface antigen.

---

[1] Received November 27, 1981; accepted March 17, 1982.

[2] Supported in part by a Grant-in-Aid for Cancer Research from the Ministry of Education, Science and Culture, Japan.

[3] The Department of Microbiology and Immunology, Hamamatsu University School of Medicine 3600, Handa-cho, Hamamatsu 431-31, Japan.

[4] *Present address*: Laboratory of Genetics, Cancer Institute, Hokkaido University School of Medicine, Sapporo 060, Japan.

[5] We thank Mr. T. Ito for his skilled technical assistance.

FCS and antibiotics. 8-Azaguanine-resistant BALB/c myeloma cells, P3U-1, were provided by Dr. T. Watanabe (Saga University School of Medicine, Saga, Japan). This line originated from Dr. M. D. Scharff (*19*). P3U-1 cells were grown in RPMI-1640 medium supplemented with 10% FCS and L-glutamine (300 mg/liter). Embryo cells from 14-day gestation BALB/c and NZB/Ta1 embryos (from Dr. T. Shirai, Kyoto University School of Medicine, Kyoto, Japan) and normal spleen cells from BALB/c, C57BL/6, C57BL/10, B10.D2, BALB.B, CBA, B10.BR, B10.A, B10.A(3R), B10.A(5R), BTK/Osb (from Dr. Kawamata, Microbiological Disease Institute, Osaka University, Osaka, Japan), NZB/Ta1, and NZW/Ta1 (from Dr. T. Shirai) were also used.

Production of hybridomas.—Male BALB/c mice, 6 weeks old, were immunized by 2–4 weekly ip inoculations of both 5–100×10^3 viable and 1×10^7 mitomycin C-treated CSA1M cells and were killed 4 days after the last injection. The fusion of immune splenocytes with mouse myeloma P3U-1 cells was performed by the addition of a mixture of 30% polyethylene glycol 1500 (Katayama Chemical Co. Ltd., Nagoya, Japan) and 10% dimethyl sulfoxide in RPMI-1640 medium. Fused cells were seeded in wells of tissue culture plates (Falcon #3040). Hybrids were selected according to establish techniques in a medium containing hypoxanthine–aminopterine–thymidine (*20*). Supernatants were screened for cytotoxicity against cultured CSA1M cells and other target cells with the use of microcytotoxicity assays. Established hybridoma cultures were cloned by limiting dilutions. Hybridomas were expanded by growth in tissue culture and were also grown in the peritoneal cavity of BALB/c mice.

Immunoglobulin isotypes were determined by the Ouchterlony technique with the use of goat anti-mouse IgG_1, IgG_2, and IgM (obtained from Meloy Laboratories, Inc., Springfield, Va.) and rabbit anti-mouse IgG_3 (Miles Laboratory, Inc., Elkhart, Ind.).

CDC assays.—A microassay was used; 2 µl of serial dilutions of culture supernatants or of ascitic fluid were injected under paraffin oil into wells of a Terasaki Microtest plate (Falcon #3034). To each well 1,000 target cells in 1 µl were added, and the plates were incubated for 20 minutes at 37°C. Subsequently, 1 µl rabbit complement was added. Plates were further incubated for 45 minutes. Thereafter, 0.5 µl trypan blue was added to each well, and the results were read microscopically. CI was calculated as follows: $CI=1-t/c$, where t=the percentage of unstained cells in the test sample and c=the percentage of unstained cells in the control sample. A CI exceeding 0.20 was regarded as positive.

Absorption test.—An equal volume of culture supernatant containing hybridoma antibodies, diluted one or two wells below the CI of 0.50 to the CSA1M cells, as well as the washed packed cells (5×10^6) to be tested were incubated for 30 minutes at 37°C and then for 30 minutes at 4°C. Thereafter, the mixtures were centrifuged. After centrifugation, the residual cytotoxicity of the supernatants was measured at 1:1 and 1:2 dilutions against the CSA1M cells by CDC assays. Percent absorption (Ab) was calculated as follows: Percent $Ab=(1-a/u)\times 100$, where a=CI by absorbed culture supernatant and u=CI by unabsorbed culture supernatant. A percent Ab less than 20% was regarded as negative.

Immunotherapy.—Fifty-seven male BALB/c mice (6 wk old) were each inoculated ip with 5×10^5 syngeneic CSA1M cells (a dose 1 log >100% lethal dose). The mice were then separated into 5 groups for treatment, which was initiated 2 hours after tumor inoculation and continued for 4 days. All injections were made ip. Mice in 1 test group were each given an injection of 900 µl ascitic fluid containing monoclonal antibody (20 mg) to CSA1M cells with a titer of 7×10^{-5} in CDC assays. Mice in 2d group were each given an injection of 100 µl suckling rabbit serum, which did not show any cytotoxicity for CSA1M cells in vitro. Mice in a 3d group each received an injection of 900 µl ascitic fluid containing antibody and 100 µl suckling rabbit serum. Two additional groups were used as controls; one 900 µl P3U-1 ascitic fluid, whereas the other was untreated. They were kept for an observation period of 90 days.

RESULTS

Two out of 17 fusions produced hybridomas, some of whose supernatants showed activity against CSA1M cells. In the first experiment, 2 hybridomas were reactive not only with CSA1M cells but also with other RSV-induced mouse tumors, CSA9F or B6SA3F, but neither reacted with the MCA-induced mouse tumor MCSA4M or the BALB/c leukemia RL♂1. After repeated testing, these hybridomas showed gradually decreasing reactivity with the CSA1M cells. The other hybridomas 3.4B, 3.4C, and 3.5C reacted exclusively with CSA1M cells and remained strongly and consistently positive against CSA1M cells. These hybridomas were cloned by the limiting dilution method, and clones that were found to produce a high titer of antibody reactive with the CSA1M cells were isolated. A supernatant of 3.5C11 and ascitic fluid or serum from 3.5C11-bearing BALB/c mice showed very strong cytotoxicity against CSA1M cells with titers of 1:5,120, 1:409,600, and 1:409,600, respectively (table 1). Two other clones, 3.4B2 and 3.4C6, had similar titers. Determination of immunoglobulin class showed that all the antibodies secreted by 3.4B2, 3.4C6, and 3.5C11 were IgM.

One of the clones selected, 3.5C11, has been extensively tested for specificity against various target cells (table 2). Using culture supernatant from 3.5C11, we saw no cytotoxicity with 20 other RSV-induced tumors from 12 different

TABLE 1.—*Titer and immunoglobulin class of cytotoxic antibodies produced by cloned hybridomas in culture supernatant, ascitic fluid, and serum against CSA1M cells*

Hybridomas	Cytotoxicity titer[a] with:			Immunoglobulin class
	Culture supernatant	Ascitic fluid	Serum[b]	
3.4B2	2,560	204,800	NT	IgM
3.4C6	5,120	819,200	NT	IgM
3.5C11	5,120	409,600	409,600	IgM

[a] Reciprocal of serum dilution producing >0.20 of CI. Mean value of five times experiments.

[b] NT = not tested.

TABLE 2.—*Specificity of cytotoxic antibody produced by a cloned hybridoma 3.5C11 in culture supernatant against various target cells*

Target cells	Direct sensitivity[a]	Absorption of cytotoxicity against CSA1M, %[b]
CAS1M	5,120	100
20 other mouse RSV tumors	—	—
3 mouse MC tumors	—	—
4 mouse leukemias	—	—
Embryo cells from 3 mouse strains	—	—
Normal splenocytes from 13 strains	—	—
2 rat ASV tumors	—	—
1 rat fibroblast line	—	—
8 human tumor cell lines	—	—

[a] Cytotoxicity titer. — = no positive reaction at a 1:10 dilution.

[b] — = <20%.

TABLE 3.—*Suppressive effect of tumor-specific monoclonal antibody with or without complement on an RSV-induced mouse tumor (CSA1M) in syngeneic hosts*

Treatment[a]	Incidence of lethal growth (%)	Mean survival days (range)	Students' *t*-test[b]
3.5C11 ascitic fluid	10/10 (100)	33.0 (24–49)	<0.001
Rabbit serum	10/10 (100)	22.4 (22–23)	NS
3.5C11 ascitic fluid plus rabbit serum	15/15 (100)	37.2 (24–73)	<0.01
P3U-1 ascitic fluid	10/10 (100)	23.0 (21–26)	NS
None	10/10 (100)	21.8 (21–23)	

[a] Mice were inoculated ip with 5×10^5 CSA1M cells. Treatment was initiated 2 hr later and continued for 4 days. All injections were ip.

[b] NS = not significant.

mouse strains, a rat fibroblast cell line transformed by SR-RSV or B77ASV, MCA-induced mouse tumors, 3 murine leukemias, P3U-1 cells, or 8 human tumor cell lines. The hybridoma antibody was also tested against normal cells; a wild mouse embryo fibroblast line, SC-1, BALB/c, and NZB embryo cells at 14-day gestation, normal mouse splenocytes from BALB/c, NZB, B10.D2, C57BL/6, C57BL/10, BALB.B, BTK, CBA, B10.BR, NZW, B10.A, B10.A(3R), and B10.A(5R), and a noninfected rat fibroblast line, 3Y1. All tests were negative at all serial dilutions of the hybridoma culture supernatant from 1:10 out. Even ascitic fluid from 3.5C11-bearing mice was noncytotoxic to target cells other than those of CSA1M (data not shown). Absorption tests showed that the antibody secreted by hybridoma 3.5C11 completely lost its cytotoxicity for CSA1M cells when preabsorbed with CSA1M cells. Other tumors and normal cells did not absorb the cytotoxicity of the hybridoma antibody for CSA1M cells (table 2).

For its therapeutic activity in vivo against a transplant of CSA1M cells, as shown in table 3, CSA1M cells inoculated into peritoneal cavity grew progressively in the treated and untreated mice. The median survival time for mice treated with rabbit serum or P3U-1 ascitic fluid alone and untreated mice was from 21 to 23 days. In contrast, mice treated with the 3.5C11 ascitic fluid alone or with the ascitic fluid and rabbit serum as exogenous complement showed prolonged survival, with a median of 33 and 37 days, respectively.

DISCUSSION

It was previously demonstrated that SR-RSV-induced mouse tumors had common TSSA and transplantation antigens (*8*). Using transplantation resistance, Bubeník et al. (*21*) suggested that in addition to a group-specific antigen shared by tumors induced with different variants of RSV, SR-RSV, Prague-RSV, and Bryan-RSV, there were specific antigens for individual tumors. We know of no report concerning the presence of individually distinct antigens on different tumors induced by the same type of RSV.

We have demonstrated an individually distinct antigen at the cell surface of an SR-RSV-induced mouse tumor by serologic technique using monoclonal antibodies from hybridomas. The antigen is not shared by any of a wide range of tissues tested, including other mouse or rat tumors induced by SR-RSV or B77ASV, chemically or physically induced mouse tumors, murine leukemias, various human tumor cell lines, mouse and rat embryo cells, and normal spleen cells from various strains of mice.

This strongly suggests the previously canvassed possibility (*3*) that individually distinct antigens on virus-induced tumors are overshadowed in conventional transplantation tests and serologic studies with the use of immune serum by cross-reactive antigens. The presence of the individually distinct antigen on an SR-RSV-induced mouse tumor indicates that it was at least partly coded by a cellular gene, as in tumors induced by chemical carcinogens. The integration or interaction of the viral genome with the cellular genome, if it occurs, would most often occur in a defined and confined site providing the basis for common antigens. A slight shift of the integration or interaction site may occasionally occur, leading to the expression of individual antigens that coexist with the common antigen.

It has been shown by serologic, histogenetic, and biochemical approaches that murine tumors of different etiologic origins may express alien H-2 and non-H-2 histocompatibility antigens (*22, 23*). That the individually distinct antigen on our RSV mouse tumor is such an alien histocompatibility antigen is unlikely since several anti-H-2 sera showed no alien H-2 antigens at the cell surface of CSA1M cells that expressed the individually distinct antigen (Mizuno M: Unpublished observation), and the unique antigen was not expressed on other normal and tumor cells from a range of mouse strains including congenic and recombinant mice.

All vertebrate normal cells possess one or a few genes (*c-src*) homologous with the ASV *src* gene (*24*). Such sequences are expressed, at a low frequency, as a 60,000-dalton phosphoprotein, $\text{pp}60^{c\text{-}src}$ (*25–28*). Hanafusa et al. (*29*) and Vigne et al. (*30*) have shown that viruses with partial deletion of the *src* gene can recover a fully functional *src* gene during passage through a chicken. Partial analysis of the sequence of the *src* gene of the recovered viruses suggests that much of it is derived from the cellular *src* gene (*31*). Parsons et al. (*32*) showed that injection of RSV-transformed cells into syngeneic mice resulted in an antiserum specific for the ASV gene product $\text{pp}60^{src}$. Analysis of the cross-reactivity of these antisera demonstrated at least three to four antigenic determinants on $pp60^{src}$ including one cross-reactive with normal cell *src* protein. Whether the monoclonal antibody from our hybridoma recognizes an antigen associated with the cellular *src* gene remains to be analyzed.

One of the important questions to be answered is whether the serologically defined antigens correspond to transplantation antigens. In this report, using monoclonal antibody, we have demonstrated that antibody against an individually distinct TSSA is responsible for the tumor growth inhibition. These results suggest that the unique TSSA on an RSV-induced mouse tumor can function as a transplantation antigen.

REFERENCES

(*1*) Klein G. Tumor antigens. Annu Rev Microbiol 1966; 20:223–252.
(*2*) Vaage J. Nonvirus-associated antigens in virus-induced mouse mammary tumors. Cancer Res 1968; 28:2477–2483.
(*3*) Kuzumaki N, Klein G. Serologically defined, unique surface antigen on a mouse mammary adenocarcinoma. 1979; 62:619–622.
(*4*) Carswell EA, Wanebo HJ, Old LJ, Boyse EA. Immunogenic properties of reticulum cell sarcomas of SJL/J mice. J Natl Cancer Inst 1970; 44:1281–1288.
(*5*) Collins JJ, Black PH. Analysis of surface antigens on simian virus 40-transformed cells. I. Unique antigenicity of simian virus 40-transformed outbred hamster kidney cell lines. J Natl Cancer Inst 1973; 51:95–114.
(*6*) Okazaki E, Aoki T, De Kozlowski SJ. AKR leukemia-specific surface antigens acquired by malignant transformation: Their common and individual specificities. Int J Cancer 1976; 17:640–646.
(*7*) Grant CK, Michalek MT. Feline leukemia-unique and cross-reacting antigens on individual virus-producing tumors identified by complement-dependent antibody. Int J Cancer 1981; 28:209–217.
(*8*) Kurth R, Bauer H. Avian tumor viruses: A model for studying tumor associated cell surface alterations. Biochim Biophys Acta 1975; 417:1–23.
(*9*) Köhler G, Milstein C. Continuous cultures of fused cells secreting antibodies of predefined specificity. Nature 1975; 256:495–497.
(*10*) Goodfellow PN, Lennson JR, Williams VE, McDevitt HO. Monoclonal antibodies reacting with murine teratocarcinoma cells. Proc Natl Acad Sci USA 1979; 76:377–380.
(*11*) Simrell CR, Klein RA. Antibody responses of tumor-bearing mice to their own tumors captured and perpetuated as hybridomas. J Immunol 1979; 123:2386–2394.
(*12*) Tax A, Manson LA, Kennet RH. Production of monoclonal antibodies against MTV and mammary tumors by lymphocyte hybridomas. Fed Proc 1979; 38:1422.
(*13*) Gunn B, Embleton MJ, Middle JG, Baldwin RW. Monoclonal antibody against a naturally occurring rat mammary carcinoma. Int J Cancer 1980; 26:325–330.
(*14*) Herlyn M, Steplewski Z, Herlyn D, Koprowski H. Colorectal carcinoma-specific antigen: Detection by means of monoclonal antibodies. Proc Natl Acad Sci USA 1979; 76:1438–1442.
(*15*) Yeh M-Y, Hellström I, Brown JP, Warner GA, Hansen JA, Hellström KE. Cell surface antigens of human melanoma identified by monoclonal antibody. Proc Natl Acad Sci USA 1979; 76:2927–2931.
(*16*) Kennet RH, Gilbert F. Myeloma producing antibodies against a human neuroblastoma antigen present on fetal brain. Science 1979; 203:1120–1121.
(*17*) Dippold WG, Lloyd KO, Li LT, Ikeda H, Oettgen HF, Old LJ. Cell surface antigens of human malignant melanoma: Definition of six antigenic systems with mouse monoclonal antibodies. Proc Natl Acad Sci USA 1980; 77:6114–6118.
(*18*) Yoshida TO, Haraguchi S, Miyamoto H, Matsuo T. Recognition of RSV induced tumor cells in syngeneic mice and semisyngeneic reciprocal hybrid mice. Gan Monogr Cancer Res 1979; 23:201–212.
(*19*) Yelton DE, Diamond BA, Kwan S-P, Scharff MD. Fusion of mouse myeloma and spleen cells. Curr Top Microbiol Immunol 1978; 81:1–7.
(*20*) Littlefield WJ. Selection of hybrids from matings of fibroblasts in vitro and their presumed recombinants. Science 1964; 145:709–710.
(*21*) Bubeník J, Koldovský P, Svoboda J, Klement V, Dvořák R. Induction of tumours in mice with three variants of Rous sarcoma virus and studies on the immunobiology of these tumours. Folia Biol (Praha) 1967; 13:29–39.
(*22*) Parmiani G, Carbone G, Invernizzi G, et al. Alien histocompatibility antigens on tumor cells. Immunogenetics 1979; 9:1–24.
(*23*) Parmiani G, Colombo M, Balliari D. Expression of alien minor histocompatibility antigens distinct from tumor-specific transplantation antigen on a murine fibrosarcoma. Int J Cancer 1980; 26:461–465.
(*24*) Spector D, Varmus HE, Bishop JM. Nucleotide sequences related to transforming gene of avian sarcoma virus are present in DNA of uninfected vertebrates. Proc Natl Acad Sci USA 1978; 75:4102–4106.
(*25*) Collet MS, Brugge JS, Erikson RL. Characterization of a normal avian cell protein related to the avian sarcoma transforming gene product. Cell 1978; 15:1363–1370.
(*26*) Oppermann H, Levinson AD, Varmus HE, Levintow L, Bishop JM. Uninfected vertebrate cells contain a protein that is closely related to the product of the avian sarcoma virus transforming gene (*src*). Proc Natl Acad Sci USA 1979; 76:1804–1808.
(*27*) Karess RE, Hayward WS, Hanafusa H. Cellular information in the genome of recovered avian sarcoma virus directs the synthesis of transforming protein. Proc Natl Acad Sci USA 1979; 76:3154–3158.
(*28*) Rohrschneider LR, Eisenman RN, Leitch CR. Identification of a Rous sarcoma virus transformation-related protein in normal avian and mammalian cells. Proc Natl Acad Sci USA 1979; 76:4479–4483.
(*29*) Hanafusa H, Halpern CC, Buchhagen DL, Kawai S. Recovery of avian sarcoma virus from tumors induced by transformation-defective mutants. J Exp Med 1977; 146:1735–1747.
(*30*) Vigne R, Breitman ML, Moscovici C, Vogt PK. Restriction of fibroblast-transforming ability in *src* deletion mutants of avian sarcoma virus during animal passage. Virology 1979; 93:413–426.
(*31*) Wang L-H, Halpern CC, Nadel M, Hanafusa H. Recombination between viral and cellular sequences generates transforming sarcoma virus. Proc Natl Acad Sci USA 1978; 75:5812–5816.
(*32*) Parsons SJ, Riley SC, Mullen EE, et al. Immune response to the *src* gene product in mice bearing tumors induced by injection of avian sarcoma virus-transformed mouse cells. Virology 1979; 32:40–46.

Neoplastic Transformation of Syrian Hamster Cells by Putative Epoxide Metabolites of Commercially Utilized Chloroalkenes[1,2]

Joseph A. DiPaolo[3,4] *and* **Jay Doniger**[3,5]

ABSTRACT—The transforming ability of six epoxides of structurally related chloroalkenes was determined with a quantitative Syrian hamster embryo cell model. The epoxides used were *cis*-1-chloropropene oxide (*c*-CPO), *trans*-1-chloropropene oxide (*t*-CPO), *cis*-1,3-dichloropropene oxide, *trans*-1,3-dichloropropene oxide, trichloroethylene oxide (TCEO), and tetrachloroethylene oxide (PCEO). All six epoxides induced morphologic transformation of Syrian hamster embryo cells and caused cell lethality as reflected in the reduced cloning efficiency; in all instances, transformation was observed with less than 25% toxicity. The potency of the various epoxides was influenced by the difference in stability of the compounds. The results with *c*-CPO, *t*-CPO, TCEO, and PCEO were consistent with a linear dose response. The transformation results reflect the carcinogenicity of the parental chloroalkenes tested thus far. Furthermore, if the epoxides are metabolic intermediates of the chloropropene parent chloropropenes, the epoxides are probably proximate carcinogens.—JNCI 1982; 69:531–534.

The observation of angiosarcomas and portal cirrhosis of the liver in workers exposed to vinyl chloride monomer was followed by a series of experiments in animals to reproduce the disease (*1*, *2*). More recent investigations have demonstrated that the mutagenic effect of vinyl chloride occurred after metabolic activation in yeast and bacteria (*3–6*). In addition, malignant transformation of embryonic Syrian hamster cells occurred only after pregnant hamsters were exposed to the compound at fairly high concentrations of 20% (vol/vol) in air and not by direct treatment of the cells (*7*). Therefore, the preponderance of the results indicates that vinyl chloride gives rise to metabolites responsible for mediating the various deleterious effects. The highly reactive chloroethylene oxide is considered the most plausible of these metabolites and, as discussed by Van Duuren (*8*), is probably responsible for the carcinogenic action of vinyl chloride. Evidence for this assumption is based on experiments in which 3,4-dichlorobenzenethiol served as a trapping agent for the reactive metabolites formed in vitro from vinyl chloride in the presence of a liver microsomal system (*9*). Epoxide derivatives from chlorinated olefins including the one from vinyl chloride are direct-acting mutagens in both bacteria and yeast (*6*, *10*, *11*). The mutagenicity was correlated with the reactivity of the postulated epoxide intermediates of six chlorinated olefins of economic importance (*10*).

In the present work, the transformation of Syrian hamster cells by this series of six epoxides from chloro-olefins was determined and the transforming ability of these epoxides was compared to their mutagenicity so that we could obtain a measure of their relative activities. The results of this study provide insight into the potential carcinogenicity of the parental chloroalkenes. The epoxides *c*-CPO, *t*-CPO, *c*-DCPO, *t*-DCPO, TCEO, and PCEO (text-fig. 1) were synthesized and characterized by Kline et al. (*12*). The comparative study on the transformation as a function of exposure dose suggests that *c*-DCPO and *t*-DCPO are the most effective compounds.

MATERIALS AND METHODS

Chemicals.—The *c*-CPO, *t*-CPO, *c*-DCPO, and *t*-DCPO were obtained by *m*-chloroperbenzoic acid oxidation of the two parental chloroalkenes; PCEO was the reaction solvent. The *c*-DCPO and *t*-DCPO were similarly prepared from the corresponding alkenes except that the reactions utilized methylene chloride as solvent. The TCEO and PCEO were synthesized by auto-oxygenation of the TCEO and PCEO, and the chloride by-products formed were removed by extraction with 0.5 *N* sodium hydroxide. All compounds were provided pure as determined by nuclear magnetic resonance analysis (*12*) and were stored at −70°C.

Cell cultures.—Hamster cells were derived from Syrian hamster embryos at 12–13 days of gestation as described (*13*). We obtained primary cultures from trypsinized embryos by seeding 10^7 cells/100-mm dish. We prepared secondary cultures 2–3 days later by seeding 5×10^6 cells/10 ml in complete medium in 100-mm dishes. Mass cultures were grown in modified Dulbecco's minimum essential medium supplemented with 10% fetal bovine serum (*14*) in incubators in an 11% CO_2 atmosphere.

Hamster embryo cell transformation assay.—Three hundred cells from the secondary cultures were plated in complete medium with 20% serum in 60-mm plastic dishes along with 6×10^4 cells that had been irradiated as confluent monolayer cultures. The feeder cells were irradiated with a total of 4,400 rad in air at a distance of 22 cm. After 2-day incuba-

ABBREVIATIONS USED: *c*-CPO=*cis*-1-chloropropene oxide; *t*-CPO=*trans*-1-chloropropene oxide; *c*-DCPO=*cis*-1,3-dichloropropene oxide; *t*-DCPO=*trans*-1,3-dichloropropene oxide; PBS=phosphate-buffered saline; PCEO=tetrachloroethylene oxide; TCEO=trichloroethylene oxide.

---

[1] Received February 3, 1982; accepted April 7, 1982.

[2] Animals were maintained under the guidelines set forth by the National Institutes of Health Policy on Humane Care and Use of Animals.

[3] Laboratory of Biology, Division of Cancer Cause and Prevention, National Cancer Institute, National Institutes of Health, Public Health Service, U.S. Department of Health and Human Services, Bethesda, Md. 20205.

[4] *Address reprint requests to* Dr. DiPaolo, Building 37, Room 2A19, National Institutes of Health, Bethesda, Md. 20205.

[5] We thank Dr. Benjamin L. Van Duuren and Dr. Stanley A. Kline, both of the Laboratory of Organic Chemistry and Carcinogenesis, Institute of Environmental Medicine, New York University Medical Center, New York, N.Y., for providing the epoxides used. We also thank Mr. Anthony J. DeMarinis, Laboratory of Biology, National Cancer Institute, for technical assistance.

TEXT-FIGURE 1.—Structures and stability of chloroalkene oxides. Half-life values are in minutes and were measured at pH 7.4 and 37°C as determined by Kline et al. (*12*).

Compound	Structure	Half-Life(min)
cis-1-Chloropropene oxide (*c*-CPO)	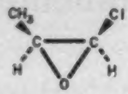	11
trans-1-Chloropropene oxide (*t*-CPO)	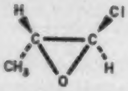	4.3
cis-1,3-Dichloropropene oxide (*c*-DCPO)	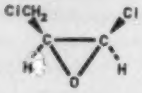	290
trans-1,3-Dichloropropene oxide (*t*-DCPO)	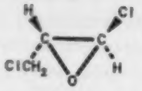	300
Trichloroethylene oxide (TCEO)	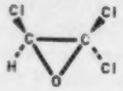	1.3
Tetrachloroethylene oxide (PCEO)	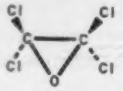	12

tions, the medium was removed, the cells were washed with PBS, and the appropriate dilution of the test chemicals was added to the cells in 4 ml PBS. The PBS was removed after incubation at 37°C for 30 minutes, the cells were washed, and fresh complete medium was added. After 5 more days of incubation, the cells were washed with PBS, fixed, and stained with Giemsa. Colonies (minimum 2-mm in diameter) were counted to determine cloning efficiency and examined for morphologic transformation. Morphologic transformation is defined as an altered colony morphology consisting of crisscrossing and piled-up cells not observed in controls (*15*). The transformation frequency is calculated relative to surviving colonies and to the initial number of cells plated. A total of 12 dishes were used at each concentration.

RESULTS AND DISCUSSION

The advantage of using the quantitative hamster embryo culture model to study carcinogenesis is that the effect of physical and chemical agents can be observed at the target cell level without the complications of host-modifying factors. Whereas the morphology of colonies formed by nontreated hamster embryo cells consisted of oriented cell arrangements, colonies classified as transformed by the chloroalkene oxides were similar to those induced by carcinogens such as benzo[*a*]pyrene. The relevance of morphologic transformation to neoplasia is that greater than 90% of transformed hamster cell colonies result in transformed cell lines that produce tumors when injected into nude mice or newborn hamsters (*16*).

All six chloroalkene epoxides induced morphologic transformation and cytotoxicity in hamster embryo cultures (table 1, text-fig. 2). The transformation results obtained with different concentrations of *c*-CPO, *t*-CPO, TCEO, and PCEO were consistent with the linear dose response. On a molar basis the most effective compounds were *c*-DCPO and *t*-DCPO, which induced transformation in the range of 0.01 m*M*; the least effective compounds were TCEO and PCEO, which required more than 1.0 m*M* (text-fig. 2). Although in all cases the cells were exposed to chemical for 30 minutes, the effective reaction time probably varied because of the instability of some compounds. This is especially true for TCEO and *t*-CPO, which have half-lives of less than 5 minutes. With *c*-DCPO and *t*-CPO the decrease in the transformation frequency at the higher concentrations is a reflection of the increased toxicity; in all cases, however, transformation was observed even when toxicity was less than 25% (table 1). Consideration of transformation on the basis of the number of cells seeded (absolute number) confirms the inductive nature of transformation by the chloroalkene oxides (table 1).

In general, the more stable the compound, the lower the concentration required; *c*-DCPO and *t*-DCPO, which are at least 25–30 times as stable as the other compounds, induced transformation at a hundredfold or lower concentrations. Therefore, in this assay, some relationship between chemical stability and biological potency exists. However, the *trans*-isomer compared to the *cis*-isomer induced twofold more transformation (absolute number) at the same concentration with similar toxicity (table 1) even though the half-lives of the *trans*-isomer and the *cis*-isomer were essentially identical (text-fig. 1). Moreover, tenfold more PCEO was required to induce transformation than was required with *c*-CPO even though the half-lives of PCEO and *c*-CPO are the same, which suggests that the bulky chlorine atoms on PCEO limit its ability to interact with DNA. Therefore, half-life alone does not correlate with carcinogenic potency.

The effects of these same chloroalkene oxides in bacterial systems have recently been reported (*10*). The mutagenicity of all six epoxides in *Salmonella typhimurium* TA 1535 and in *Escherichia coli* WP-2 UV light-sensitive gene A and their effects in *E. coli* (DNA polymerase A$^-$/DNA polymerase B$^+$) were determined in the absence of metabolic activation and compared to the transformation results (table 2). All six compounds induced cytotoxicity in *E. coli* and *S. typhimurium*; again, *c*-DCPO and *t*-DCPO were the most potent. PCEO was effective in only the *Salmonella* system, whereas TCEO induced no mutations in either system. Therefore, except for TECO, there is a reasonable quantitative agreement between the bacterial tests and the in vitro hamster transformation assay in terms of biological effectiveness of these chloralkene epoxides. Possibly, the highly unstable TCEO might have been inactivated before it reached most of the cells in the mutagenesis assays because treatment was performed on a concentrated number of cells suspended in culture medium; in the hamster embryo cell assay, the cells were treated in the presence of PBS.

TABLE 1.—*Transformation and survival of Syrian hamster embryo cells treated with diverse chloroalkene oxides*[a]

Compound	Dose, m*M*	Percent survival	Total transformed colonies	Average transformations/cells seeded, ×10^3
Acetone		100 (29)[b]	0	
c-CPO	0.11	110	4	1.1
	0.27	94	5	1.4
	0.55	90	6	1.7
	1.1	50	12	3.3
t-CPO	0.22	96	0	—
	0.55	78	2	0.56
	1.1	54	6	1.7
	2.2	12	1	0.26
c-DCPO	0.005	92	1	0.26
	0.01	93	3	0.83
	0.02	81	1	0.26
t-DCPO	0.01	89	8	2.2
	0.025	85	8	2.2
	0.05	44	4	1.1
TCEO	1.1	91	1	0.26
	2.5	86	1	0.26
	5.0	73	4	1.1
PCEO	0.87	98	0	—
	4.3	96	3	0.83
	8.7	100	2	0.56
	17.1	70	5	1.4

[a] Plastic dishes (60 mm) were seeded with 300 cells from a secondary culture with irradiated hamster cells (6×10^4) for a feeder, grown for 2 days, and incubated with the test chemical in PBS in the absence of growth medium for 30 min at 37°C. Cells were washed, fed again, and incubated for 7 days after which colonies were stained, counted for survival data, and scored for morphologic transformation. Twelve dishes were used for each treatment.

[b] *Number in parenthesis* is the absolute cloning efficiency of solvent-treated cultures.

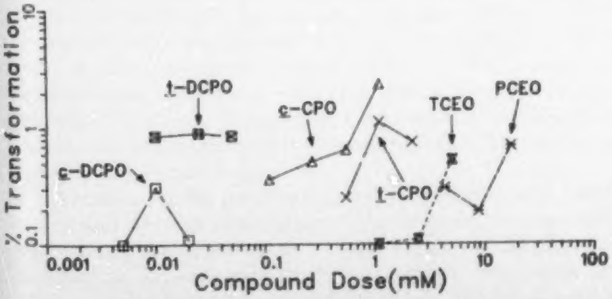

TEXT-FIGURE 2.—Frequency of transformed colonies relative to survival and chemical concentration. The transformation frequency is total number of transformed colonies observed relative to the total number of colonies counted.

TABLE 2.—*Comparison of biological activities of diverse chloroalkene oxides*

Compound	Mutagenicity[a,b]		Genotoxicity:[a] *E. coli* pol A/pol A^{+}[b]	Transformation of hamster embryo cells[b]
	S. typhimurium TA 1535	*E. coli* WP-2		
c-CPO	++	+	+	++
t-CPO	+	+	+	++
c-DCPO	+++	+++	++++	++++
t-DCPO	+++	++	++++	++++
TCEO	−	−	++	+
PCEO	+	−	+	+

[a] *See* (*10*).

[b] Each plus represents one order of magnitude less compound (μg/ml) needed to produce a similar biological response. Maximum amount used is represented by a single plus. Minus indicates no effect at any concentration.

If these labile (text-fig. 1) putative proximate carcinogens are actual metabolites that survive detoxification, then the results provide an explanation for the carcinogenicity of the parental chloralkenes. In fact, a mixture of *cis*-isomers and *trans*-isomers of *c*-CPO, as well as *c*-DCPO, TCEO, and PCEO induced carcinomas of the forestomach, or subcutaneous sarcomas, or hepatocellular carcinomas in mice (*17*, *18*). Although *c*-CPO, *t*-CPO, and *t*-DCPO have not been tested, our in vitro results indicate that they are also potential carcinogens.

REFERENCES

(*1*) VIOLA PL, BIGOTTI I, CAPUTO A. Oncogenic response of rat skin, lungs and bones to vinyl chloride. Cancer Res 1971; 31:516–522.

(*2*) MALTONI C, LEFEMINE G. Carcinogenicity bioassays of vinyl chloride. I. Research plan and early results. Environ Res 1974; 7:387–405.

(*3*) LOPRIENO N, BARALE R, BARONCELLI S, et al. Evaluation of the genetic effects induced by vinyl chloride monomer (VCM) under mammalian metabolic activation: In vitro and in vivo studies. Mutat Res 1976; 40:85–96.

(*4*) RANNUG U, JOHANSSON A, RAMEL C, WACHTMEISTER CA. The mutagenicity of vinyl chloride after metabolic activation. Ambio 1974; 3:194–197.

(*5*) BARTSCH H, MALAVEILLE C, MONTESANO R. Human, rat and mouse liver-mediated mutagenicity of vinyl chloride in *S. typhimurium* strains. Int J Cancer 1975; 15:429–437.

(*6*) MALAVEILLE C, BARTSCH H, BARBIN A, CAMUS AM, MONTESANO R. Mutagenicity of vinyl chloride, chloroethylene oxide and chloroacetaldehyde. Biochem Biophys Res Commun 1975; 63:363–370.

(*7*) DIPAOLO JA. Modulation of induced quantitative mammalian cell transformation. In: Kolber A, Wong T, eds. In vitro toxicity testing: Current and future possibilities. Amsterdam: Elsevier/North-Holland. In press.

(*8*) VAN DUUREN BL. On the possible mechanism of carcinogenic action of vinyl chloride. Ann NY Acad Sci 1975; 246:258–267.

(*9*) GÖTHE R, CALLEMAN CJ, EHRENBERG L, WACHTMEISTER CA. Trapping with 3,4-dichlorobenzenethiol of reactive intermediates formed in vitro from the carcinogen vinyl chloride. Ambio 1974; 3:234–236.

(*10*) KLINE SA, MCCOY EC, ROSENKRANZ HS, VAN DUUREN BL. Mutagenicity of chloroalkene epoxides in bacterial systems. Mutat Res 1982; 101:115–125.

(*11*) Loprieno N, Barale R, Baroncelli S, et al. Induction of gene mutations and gene conversions by vinyl chloride metabolites in yeast. Cancer Res 1977; 56:253–257.

(*12*) Kline SA, Solomon JJ, Van Duuren BL. Synthesis and reactions of chloroalkene epoxides. J Org Chem 1978; 43:3596–3600.

(*13*) DiPaolo JA, Donovan P, Nelson R. Quantitative studies of in vitro transformation by chemical carcinogens. J Natl Cancer Inst 1969; 42:867–876.

(*14*) Evans CH, DiPaolo JA. Equivalency of endothelial cell growth supplement to irradiated feeder cells in carcinogen-induced morphologic transformation of Syrian hamster embryo cells. JNCI 1982; 68:127–132.

(*15*) DiPaolo JA, Donovan PJ, Popescu NC. Kinetics of Syrian hamster cells during X-irradiation enhancement of transformation in vitro by chemical carcinogen. Radiat Res 1976; 66:310–325.

(*16*) DiPaolo JA, Nelson RL, Donovan PJ. Morphological, oncogenic, and karyological characteristics of Syrian hamster embryo cells transformed in vitro by carcinogenic polycyclic hydrocarbons. Cancer Res 1971; 31:1118–1127.

(*17*) Van Duuren BL, Goldschmidt BM, Loewengart G, et al. Carcinogenicity of halogenated olefinic and aliphatic hydrocarbons in mice. JNCI 1979; 63:1433–1439.

(*18*) Weisburger EK. Carcinogenicity studies on halogenated hydrocarbons. Environ Health Perspect 1977; 21:7–16.

Derivation of Transplantable 7,12-Dimethylbenz[*a*]anthracene-Induced Chicken Fibrosarcoma Lines: Differences in Metastasizing Properties and Organ Specificity[1,2,3]

J. E. Galton,[4,5] B. Xue,[4] G. M. Hochwald,[6] *and* G. J. Thorbecke[4,7]

ABSTRACT—Several transplantable 7,12-dimethylbenz[a]anthracene-induced SC chicken fibrosarcoma (CHCT-NYU) lines were studied for their ability to grow in internal organs after iv injection (artificial metastases) into 1- to 3-week-old chickens. Some tumor lines were recently derived, whereas others were studied after many serial subcutaneous transplantations. Striking similarities as well as differences were found between tumor lines' ability to grow in various organs. Artificial metastases were seen primarily in the stomach, pancreas, lungs, heart, and muscle, and occasionally also in the kidneys and in the liver. Agammaglobulinemic recipients showed more extensive organ involvement than normal recipients of the same age. Whole-body γ-irradiation also enhanced the incidence of artificial metastases, particularly in lungs. Antibody from the serum of a primary tumor-bearing host reduced the growth of the corresponding tumor in many organs. The metastatic pattern of line CHCT-NYU4 was a relatively stable property, since there was little difference in the internal localization of these tumor cells studied before and after 15 serial subcutaneous transplants. However, intravenous transplantation of tumor cells from line CHCT-NYU4 taken from the liver, lungs, and pancreas of a single recipient established sublines with changes in organ specificity. After a few such serial transplants of liver-derived tumor, a line was derived that grew virtually in the liver alone. A subline with preference for growth in lungs was also obtained, but its ability to grow in the pancreas persisted. A pancreas-derived tumor line also grew in the liver and lungs. Subcutaneous transplants of tissue fragments of the lung-derived tumor line caused the appearance of spontaneous metastases in lungs. The incidence of spontaneous metastases with the lung-derived line was much greater than that with the liver-derived line or with the original CHCT-NYU4 line.—JNCI 1982; 69:535–541.

In a previous study (*1*) with transplantable DMBA-induced fibrosarcomas, we showed that after iv injection into immature, histocompatible chickens, these tumors grew in a variety of internal organs. While we observed a similar organ distribution pattern with three tumor lines, we saw a higher propensity for growth in muscle with one line and a higher frequency of growth in lungs with another. The organ distribution of growth after injection of 2×10^7 CHCT-NYU4 cells (originally named SCFSIV) into 3-week-old unirradiated recipients was pancreas>stomach>heart>kidneys>lungs (*1*). Nonspecific stimulation of the immune system with *Corynebacterium parvum* inhibited fibrosarcoma growth in internal organs.

In studies on the metastatic ability of murine B16 melanoma and Abelson virus-induced lymphoma (*2–5*), repeated retrieval of metastases from a single organ, combined with periods of in vitro growth, led to variant lines with an enhanced tendency to metastasize to the organ of origin. Thus tumor lines were derived that preferentially grew in liver, brain, adrenals, ovaries, or lungs. The tendency of a transplantable Marek's lymphoma line to grow in the liver of SC chickens could also be enhanced by similar in vivo–in vitro procedures (*6*). In all these examples 5–10 repeated transplants and in vitro growth periods were needed before significant differences in metastatic properties were observed.

To test the generality of this phenomenon with respect to tumor cell type, we have attempted to derive organ-specific sublines from CHCT-NYU4 by serial intravenous transplants of tumor cell suspensions made from a tumor dissected from a single organ. The wide variety of organs in which these chicken fibrosarcomas can grow makes them an excellent tool for such a study. The present report shows that tumor lines with preference for growth in specific organs can readily be obtained in some cases within two serial transplants, without an intervening in vitro growth period. In addition, a subline is described with increased ability to metastasize spontaneously. The influence of some immunologic parameters on the sites of fibrosarcoma growth after iv tumor cell injection is also examined.

MATERIALS AND METHODS

Animals.—SC chickens, homozygous at the major histocompatibility B-locus (B2/B2), were used throughout the experiments. Chicken eggs were obtained from Hyline Poultry Farms (Dallas Center, Iowa). In some experiments, chickens received 300 rad of γ-irradiation from a ^{137}Cs source delivering 550 rad/minute (Isomedix, Parsippany, N.J.). BX was performed as previously described (*7*).

Tumor cells.—The fibrosarcomas CHCT-NYU1, CHCT-NYU2, and CHCT-NYU4 were derived from DMBA-induced (Eastman Kodak) primary tumors. These tumors grow only in SC chickens and were originally called "SCFS1,

---

ABBREVIATIONS USED: BX=chemical bursectomy (bursectomized); DMBA=7,12-dimethylbenz[*a*]anthracene; DPBS=Dulbecco's phosphate-buffered saline; GI=growth index (indices); TB=tumor burden.

---

[1] Received December 10, 1981; accepted March 9, 1982.

[2] Supported by Public Health Service grant CA-16247 from the National Cancer Institute.

[3] Animals were maintained under the guidelines set forth in the "Guide for the Care and Use of Laboratory Animals" by the Institute of Laboratory Animal Resources, National Research Council.

[4] Department of Pathology, School of Medicine, New York University Medical Center, 550 First Ave., New York, N.Y. 10016.

[5] *Present address*: Department of Surgery, University of California at Los Angeles, Los Angeles, Calif. 90024.

[6] Department of Neurology and Department of Physiology and Biophysics, School of Medicine, New York University Medical Center.

[7] *Address reprint requests to* Dr. Thorbecke.

SCFS2, and SCFS4," but they have been renamed according to a new nomenclature (*8*). CHCT-NYU1, the oldest tumor studied here, was shown to be rejected not only by B-locus-incompatible FP (B15/B21) chickens, but also, similarly to SC chickens, by RPRL lines 63 and 72 both B2/B2 (donated by the U.S. Department of Agriculture Regional Poultry Research Laboratory, East Lansing, Mich.). At the time of these experiments, CHCT-NYU1 (of female origin) was in its 60th monthly transfer in vivo, and CHCT-NYU2 and CHCT-NYU4 (of male origin) were in the 40th and 20th–40th transfers, respectively. The 2 other tumors, CHCT-NYU8984 and CHCT-NYU9136, more recently derived from DMBA-induced primary tumors, were in their 5th–10th transfer in vivo.

The tumor was dissociated into cell suspensions by incubation for 15 minutes at 37°C in a combination of 0.5% trypsin (1:250 hog pancreas; ICN Pharmaceuticals, Inc., Cleveland, Ohio) and 0.25% collagenase (Worthington Biochemical Corp., Freehold, N.J.) in 0.165 *M* DPBS (pH 7.2; Associated Biomedic Systems, Inc., Buffalo, N.Y.) containing 2% normal chicken serum (Flow Laboratories, Inc., Rockville, Md.). The resulting cell suspensions, 95% viable, were filtered through gauze and washed three times in DPBS. Only large typical tumor cells were included in the cell count. Contaminating smaller cells rarely exceeded 5%.

Antiserum.—Antiserum to CHCT-NYU8984 was obtained from the primary tumor-bearing chicken 8984, which received an injection of 8 mg DMBA 5 months previously. The 1:10 diluted serum was tested for the presence of antibody with the use of a triple-layer immunofluorescence technique (*9, 10*) and stained 40% of CHCT-NYU8984 tumor cells (Galton JE, Thorbecke GJ: Manuscript in preparation).

Treatment of tumor cells with antibody.—One milliliter of 2×10^7 CHCT-NYU8984 tumor cells was incubated on ice for 45 minutes with 1 ml of the antiserum. Without washing, 10^6 tumor cells were injected into 3-week-old γ-irradiated (300 R) chickens. The chickens were killed 14 days after receiving the tumor cell injection.

Experimental metastases.—In most experiments 3-week-old chickens received iv injections of $5\text{–}10\times10^5$ tumor cells in the wing web, and tumor growth in various organs was observed macroscopically 2–3 weeks later. The results were expressed as tumor incidence and TB or as GI to give both a semiquantitative and qualitative assessment of tumor growth. The presence of tumor in small nodules was verified microscopically after Formalin fixation and staining with hematoxylin and eosin. TB of each organ was estimated on a 1+ to 5+ scale: 1+=single to 3 small nodules, depending on the organ involved. For organs such as lungs, liver, and pancreas, complete infiltration or more than 15 nodules=5+; for stomach and kidneys, 10 nodules=5+; for heart and skeletal muscles of the leg, 5 nodules=5+. Tumor GI was calculated as the product of tumor incidence and the average TB for each organ. "Organ-specific" tumor lines were derived and maintained by serial intravenous passage of tumor cells taken from liver, pancreas, or lungs.

RESULTS

Experimental Metastasis Patterns of the CHCT-NYU4 Tumor

To minimize immunologic influences, we determined the pattern of experimental metastases of the CHCT-NYU4 tumor in 1-week-old chickens after iv injection of varying doses of tumor cells (table 1). The organ involvement was much greater than that found previously in 3-week-old recipients, but there was a similar distribution pattern, with 100% incidence of metastases in pancreas and stomach at a tumor dose of 2×10^5. A dose as low as 2×10^3 tumor cells still caused a significant involvement of stomach and lungs. The lowest dose injected, 2×10^2, did not result in any macroscopically detectable tumor growth within the 2-week observation period.

The pattern of organ distribution of tumor growth after iv injection of 10^6 or 10^7 CHCT-NYU4 cells was similar in unirradiated and γ-irradiated 3-week-old chickens (cf. text-fig. 1 and table 2). We observed much more tumor growth in internal organs with immunosuppressed (irradiated) chickens, and for this reason we used 3-week-old irradiated recipients in subsequent experiments.

Tumor Growth After iv Injection of Tumor Cells From Two Different Primary Tumors

The pattern of organ distribution of tumor growth after iv injection of CHCT-NYU4 tumor cells of the transplantable line was compared to that of 2 recently derived transplantable DMBA-induced fibrosarcomas. Tumor cells from CHCT-NYU8984 and CHCT-NYU9136 were injected into 3-week-old, γ-irradiated chickens, and internal tumor growth was determined (table 3). More than 70% of the recipients had tumor growth in the stomach, pancreas, lungs, and heart 3 weeks after the injection of CHCT-

TABLE 1.—*Tumor incidence and TB in internal organs after iv injection of varying numbers of CHCT-NYU4 cells*[a]

No. of tumor cells injected	No. of chickens	Tumor incidence, %, and (TB)[b] in:						
		Stomach	Pancreas	Liver	Lungs	Kidneys	Heart	Muscle
2×10^5	4	100 (3.5)	100 (3.3)[c]	25 (1.0)[c]	75 (1.5)[c]	0	0	0
2×10^4	9	78 (3.2)	67 (1.1)	0	44 (0.8)	0	0	0
2×10^3	19	53 (1.1)	5 (0.1)	0	53 (1.2)	0	0	0
2×10^2	20	0	0	0	0	0	0	0

[a] Recipients were 1 wk old at time of tumor cell injection and were killed 2 wk later.

[b] Tumor incidence is expressed as percentage of animals with tumor in an organ; No. and size of nodules per organ (TB) are averaged for all animals in the group. TB was estimated for each organ on a 1–5+ scale: 1+=single nodule; 5+=complete infiltration of organ with multiple nodules (*see* "Materials and Methods").

[c] The tumor-bearing organs in 1 of these recipients were used for the derivation of organ-specific transplant lines.

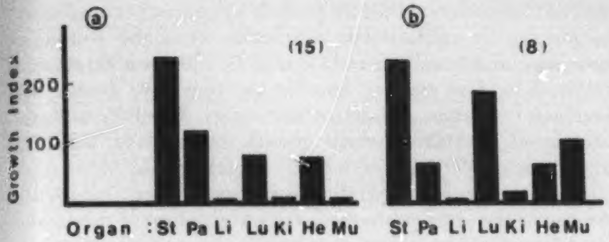

TEXT-FIGURE 1.—Tumor growth after iv injection of 10^6 tumor cells from the original CHCT-NYU4 line transplanted locally throughout period of subline derivation: a) at start of study and b) after ≈15 intervening serial local transplants. GI represents the average TB for recipients multiplied by the percentage of recipients with growth in that organ. Animals were 3 wk old and γ-irradiated (300 rad). No. of animals in group is given *in parentheses*.

NYU8984 cells. In contrast with the CHCT-NYU4 tumor cells, however, there was a much higher incidence of tumor involvement in the muscle, kidneys, and liver. Transplants of tumor cells obtained from the heart of recipients from the first serial transfer resulted in slightly increased tumor growth in heart and muscle (GI 139 and 65, respectively) and in decreased growth in other organs (table 3).

It proved difficult to establish experimental metastases from the CHCT-NYU9136 tumor. Injection of as many as 2×10^7 cells into 3-week-old irradiated chickens did not result in tumor growth (data not shown). The results shown in table 3 are those from an experiment in which 1-week-old chickens were killed 2 months after iv injection of 5×10^6 tumor cells. Chickens killed before this time showed no macroscopic tumor growth. There was preferential growth in the stomach (63%) and lungs (50%), and 25% of the recipients showed tumor growth in the pancreas and kidneys. There was no growth in the heart, muscle, or liver.

Effect of BX on Tumor Growth of CHCT-NYU4 Cells

To explore the influence of host immune responsiveness, we analyzed the effect of recipient BX on tumor growth. Unirradiated 3-week-old normal and BX chickens were given injections of 10^5–10^7 CHCT-NYU4 cells, and tumor growth was determined 15 days later (table 2). When as many as 10^7 cells were injected into normal chickens, tumor growth was found in the stomach, pancreas, and lungs. When the number of cells injected was 10^5, tumor growth was limited to the stomach. In contrast, BX chickens were much more susceptible to the induction of experimental metastases. At the highest cell dose injected, tumor growth was apparent in most organs of all recipients, and with as few as 10^5 cells, there was still tumor growth in the stomach, pancreas, lungs, and kidneys. We did not observe tumor growth in the liver in either normal or BX chickens.

Thus it appeared that BX resulted in an increase in the incidence of experimental metastases. It was not clear, however, whether this was due to the general poor health of BX animals or, in fact, to a lack of specific antibody production. To test the role of antibody in the control of experimental metastases more directly, we studied the effect of passively administered antiserum to CHCT-NYU8984 on tumor growth (text-fig. 2). CHCT-NYU8984 cells were incubated with the antiserum and injected at a dose that would give, in the absence of antiserum, a high incidence of experimental metastases. Tumor growth was apparent in all organs

TABLE 2.—*Effect of BX of host on tumor incidence and TB in internal organs after iv injection of CHCT-NYU4*[a]

No. of tumor cells injected	Pretreatment	No. of chickens	Tumor incidence, %, and (TB)[b] in:						
			Stomach	Pancreas	Liver	Lungs	Kidneys	Heart	Muscle
10^7	None	4	100 (2.8)	50 (1.5)	0	50 (0.5)	0	0	0
10^7	BX	4	100 (3.5)	100 (2.5)	0	100 (1.3)	25 (0.3)	100 (2.0)	100 (1.3)
10^6	None	4	75 (0.8)	0	0	25 (0.3)	0	0	0
10^6	BX	6	100 (3.2)	100 (1.8)	0	67 (0.8)	0	100 (1.3)	33 (0.8)
10^5	None	4	100 (1.0)	0	0	0	0	0	0
10^5	BX	6	100 (1.7)	67 (0.7)	0	50 (0.5)	0	17 (0.2)	0

[a] Unirradiated 3-wk-old recipients.

[b] Tumor incidence was examined 15 days after tumor cell injection and is expressed as percentage of animals with tumor in an organ; No. and size of nodules per organ (TB) are averaged for all animals in the group. TB was estimated for each organ on a 1–5+ scale: 1+=simple nodule; 5+=complete infiltration of organ with multiple nodules (*see* "Materials and Methods").

TABLE 3.—*Patterns of organ distribution of tumor growth after iv injection of tumor cells from 2 different primary tumors*[a]

Primary tumor source: Chicken	No. of serial iv transplants	No. of tumor cells injected	No. of chickens	Tumor incidence, %, and (TB)[b] in:						
				Stomach	Pancreas	Liver	Lungs	Kidneys	Heart	Muscle
8984	1	$2–5\times10^6$	14	93 (2.5)	79 (1.4)	21 (0.3)	71 (1.6)	43 (0.6)	71 (1.6)	50 (0.6)
	2+3[c]	5×10^5	13	62 (2.3)	69 (1.6)	0	31 (0.8)	23 (0.6)	77 (1.8)	54 (1.2)
9136	1	5×10^6	8	63 (0.8)	25 (0.5)	0	50 (1.6)	25 (0.8)	0	0

[a] Primary tumors were taken from 2 carcinogen-injected chickens. Recipients of tumor 8984 showed growth in internal organs 3 wk after transfer, but recipients of 9136 showed no tumor growth until 2 mo after transfer. Recipients were 3-wk-old, γ-irradiated (8984) or 1-wk-old chickens (9136).

[b] Tumor incidence is expressed as percentage of animals with tumor in an organ; No. and size of nodules per organ (TB) were averaged for all animals in the group. TB was estimated for each organ on a 1–5+ scale: 1+=single nodule; 5+=complete infiltration of organ with multiple nodules (*see* "Materials and Methods").

[c] Heart tumor from primary transplant recipient used as donor cells.

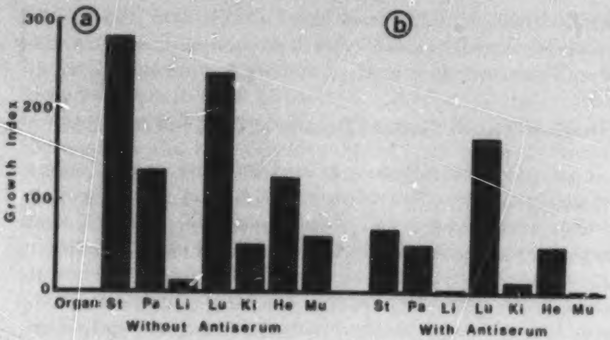

TEXT-FIGURE 2.—Growth of 10^6 iv injected cells from tumor CHCT-NYU8984 after preincubation with a) normal chicken serum, or b) antibody-containing serum from primary host chicken 8984. ≈1 ml of serum was injected together with the tumor cells into 3-wk-old γ-irradiated (300 rad). Recipients, and the tumor growth was determined 2 wk later. No. of recipients was 9 from group a) and 3 from group b).

observed after iv injection of untreated CHCT-NYU8984 cells. Although the number of animals given injections of antiserum-treated CHCT-NYU8984 cells was small, there was a decrease in the tumor incidence and TB in most organs. The absence of growth in the muscle was striking, particularly in view of the previous experiments (table 3) in which animals that received as few as 5×10^5 untreated CHCT-NYU8984 cells also showed a more than 50% tumor incidence in this organ.

In an additional experiment (data not shown), iv injection of antibody to CHCT-NYU4 with corresponding tumor cells also resulted in a decrease in tumor growth in the muscle (GI=4 vs. 105), but there was little effect on the growth in other organs.

Development of Organ-Specific Tumor Lines

Text-figure 1A shows the extent of tumor growth, expressed as GI, of 10^6 "parent" CHCT-NYU4 cells after injection into 3-week-old irradiated chickens. There was a similar distribution of tumor growth compared to that found previously in unirradiated recipients. Thus the stomach, pancreas, and heart showed GI of 250, 120, and 70, respectively. The low dose of irradiation, however, caused an increase in tumor growth in the lungs (GI=80), and an occasional bird also showed growth in the liver, kidneys, and muscle. After approximately 15 additional serial subcutaneous transplants, tumor growth was reexamined with the use of the same protocol at the termination of this study (text-fig. 1B). The organ distribution was not significantly different from that observed at the start of the study, although the extent of organ involvement had increased for lungs (GI=180) and muscle (GI=100) and decreased for pancreas and heart (GI=60). Again, there was an occasional chicken that exhibited growth in the liver and kidneys. Thus the ability of the parent line to localize and/or to grow in internal organs was a relatively stable property.

Although CHCT-NYU4 cells rarely showed tumor growth in the liver, one of the recipient chickens (table 1) showed tumor growth in liver, lungs, and pancreas. It was from this chicken that we attempted to develop tumor lines with organ specificity by repeated serial intravenous transfers of tumor cells taken from these organ sites. After as few as two to three serial intravenous transplants of liver-derived tumor, a different growth pattern was obtained, and by the fourth to fifth transplant of this subline 87% of recipients had extensive growth in the liver (GI=180), whereas the incidence of both pancreas and lung involvement was only 17% (GI=40) (text-fig. 3). After nine transplants, the liver line formed multiple nodules in the livers of virtually all of the recipients. In many chickens, livers were almost replaced by tumors within 2 weeks after injection of the tumor cells, whereas there was only sporadic growth in other organs.

This liver specificity was maintained over many transplantations. Even when the liver-specific tumor was transplanted from wing web to wing web several times before it was again injected iv, it maintained its specificity for growth in liver. In this experiment, 10^4 liver-line tumor cells, injected iv into 2-week-old γ-irradiated recipients, grew in

TEXT-FIGURE 3.—Tumor growth of the three sublines derived from CHCT-NYU4 by serial intravenous transplantation of 10^6 tumor cells taken each time from lungs, liver, or pancreas. The numbers of serial intravenous transplants are given at the *bottom*. GI is represented as in text-fig. 1. All recipients were 3 wk old and γ-irradiated (300 rad). No. of recipients is given *in parentheses*.

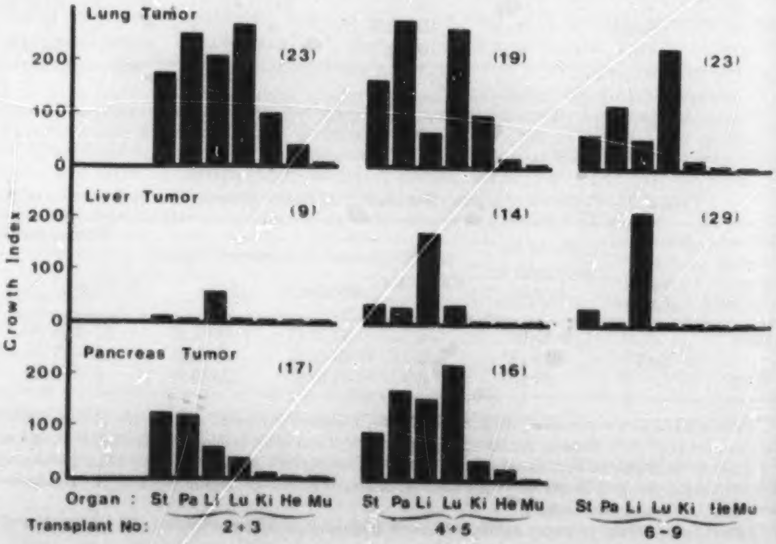

TABLE 4.—*Metastatic potential and organ specificity of transplantable CHCT-NYU tumor lines*[a]

Tumor line	Method and site of inoculation	Total No. of recipients	Percent of recipients with tumors in:				
			Stomach	Pancreas	Lungs	Liver	Heart
CHCT-NYU1	10^6 cells in both wings	45	0	0	0	0	0
CHCT-NYU2	10^6 cells in both wings	65	6.1	4.6	3.1	0	1.5
CHCT-NYU4	10^6 cells in both wings	70	10.0	7.1	1.4	0	0
CHCT-NYU4 "liver"	Fragments in wings	28	0	0	0	7.1	0
CHCT-NYU4 "lung"	Fragments in wings	40	0	7.5	47.5	2.5	0

[a] Chickens were 1 wk old and were γ-irradiated prior to receiving tumor fragment injection or 2 wk after injection of tumor cells in the wings.

67% of the receipients' livers (GI=89) within 3 weeks. Among the other organs only the lung showed a small amount of tumor growth (GI=7; incidence 22%). In an additional study, iv injection of 10^9 killed *Corynebacterium parvum* organisms, just prior to injection of the liver subline, prevented all tumor growth in 9 of 10 animals (data not shown). In the remaining animal, only a single liver nodule was found compared to massive TB in the livers of control animals (GI=160).

Five serial intravenous transplants of lung-derived tumor cells resulted in 95–100% involvement of both lungs and pancreas (GI=200), with much less growth in liver. After the ninth passage, the lung-derived tumor cells grew in 100% of the recipients' lungs, and to a much lesser extent in the stomach, pancreas, heart, and liver (text-fig. 3). After further transplantation (data not shown) the lungs remained the primary target for this tumor line, and the incidence of concomitant growth in the pancreas did not change.

Serial transplantation of pancreas-derived tumor did not result in similar organ specificity: GI of the pancreas, as well as of the lungs and liver increased, but that of the stomach decreased (text-fig. 3). After five passages, transplantation of this subline was discontinued.

Metastatic Potential and Organ Specificity of Transplantable CHCT-NYU Cell Lines

An attempt was also made to determine whether the transplantable organ-specific CHCT lines could metastasize spontaneously. One-week-old chickens were inoculated with CHCT-NYU1, CHCT-NYU2, and CHCT-NYU4 tumor cells in both wing webs, irradiated on day 14, and dissected 2 weeks later (table 4). There was no tumor growth in any organ of the 45 chickens given injections of CHCT-NYU1 cells, although previous studies had shown extensive growth of this tumor in internal organs after iv injection of tumor cells (*1*). After injection of CHCT-NYU2 and CHCT-NYU4 tumor cells in the wing webs, a small number of chickens did exhibit metastases, primarily in the stomach and pancreas, and occasionally in the lungs and heart. The possibility, however, that a small number of tumor cells was inadvertently injected intravascularly could not be excluded. This could explain the formation of these "spontaneous" metastases, because as few as 2,000 iv injected CHCT-NYU4 cells resulted in tumor growth in the stomach, pancreas, and lungs of 1-week-old chickens (table 1).

To minimize direct cell entry into the blood, we inoculated small washed fragments, rather than cell suspensions, of organ-specific tumors into both wing webs of 1- to 2-week-old γ-irradiated chickens (table 4). Almost 50% of the 40 chickens given injections of lung subline tumor fragments showed tumor growth in the lungs. Occasionally, a few tumor nodules were also found in the pancreas (8%) and liver (3%). After wing web inoculation of the liver subline tumor fragments, metastases were confined to the liver, but these occurred in only 8% of recipients. Tumor invariably grew progressively in the wing webs of both liver- and lung-line recipients.

The metastatic potential of these lung- and liver-specific sublines was further tested by ip injection of tumor cells into 2-week-old chickens (not included in tables). Four weeks later, 78% of the 9 birds given injections of liver subline tumor cells showed extensive growth in the liver (GI=250). There was no evidence of growth in any other organ. The lung subline exhibited some growth in the liver, but much less than the liver line, and metastasized to lung in 1 of the 4 recipients.

DISCUSSION

The patterns of artificial metastatic growth of the five randomly selected lines of DMBA-induced fibrosarcomas, studied previously (*1*) and in the present report, show some striking similarities as well as differences. The stomach and pancreas are common localization sites for all five tumor lines, and three of these lines also show heart and skeletal muscle as major sites. Lung localization was very much enhanced by irradiation of recipients similarly to many mammalian tumor systems (*11*). Immunologic incompetence of recipients resulting from BX (agammaglobulinemia) also greatly increased tumor growth in lungs and in some cases in heart and muscle. This observation suggests an antibody role in the limitation of tumor growth in internal organs, which is in agreement with the finding that passively acquired antibodies obtained from the primary host abolish the growth of line CHCT-NYU8984 in the muscle. Of the five tumor lines studied, only one (CHCT-NYU2) exhibited preferential growth in the liver (*1*), and another (CHCT-NYU8984) grew well in the kidneys.

It seems likely that patterns of metastases are influenced by the nature of the tumor cells. Only a few studies on transplantable tumors in chickens are available for comparison (*6, 12*). These studies concern Marek's disease T-cell lymphoma, and the patterns of lymphoma localization include the ovaries, the kidneys, and the liver. They are thus different from those of fibrosarcomas reported in the present study. Comparison of lymphomas derived from cells that normally migrate, with fibrosarcomas may not be appropriate. Studies of human soft tissue sarcomas show preferential metastatic sites, primarily the lung (*13*).

Organ-specific sublines were obtained rapidly from tumor line CHCT-NYU4 in the present study. Further experiments are needed to determine whether adaptation to an organ during growth in that organ is involved in this phenomenon, or whether there is a preexisting heterogeneity with respect to organ preference in CHCT-NYU4 at the time of intravenous transplantation. Studies by Fidler and Kripke (*14*) on B16 melanoma in mice showed heterogeneity of the tumor itself to be a major factor in causing variation in metastatic behavior. Chow and Greenberg (*15*) showed that heterogeneity of a lymphoma clone was generated within a short time in the syngeneic host. In addition, Nicolson and Custead's recent finding (*16*)—that forcing a tumor to grow in the lungs does not improve its ability to produce experimental metastases on the same site—also refutes the idea of organ adaptation. The chicken lymphoma system studied by Shearman and Longenecker (*17*), in which liver metastases could be prevented by preincubation of tumor cells with a monoclonal antibody without an effect on metastases in other sites, strongly supports the concept of organ-specific receptors.

In the present studies with chicken fibrosarcoma, a liver-specific tumor line was readily derived. The ability to grow in pancreas was never completely dissociated from growth in the lungs. Selection for growth in lungs resulted in a variant that grew best in lungs, but it still metastasized to the pancreas. Metastases to heart and skeletal muscle also appeared to be linked, but no attempt was made to separate tumor sublines metastasizing to these sites. Localization of metastases in muscle is rare in most mammalian systems studied thus far. This finding is attributed to the fact that embolic tumor cells are trapped in arterioles and do not reach the capillary beds in the muscle, thyroid gland, and spleen (*18*).

Hypotheses such as "favorable environment of the soil" (*19*), which causes preferential tumor growth in a given organ, and existence of cell surface receptors, which (*12, 20*) cause selective retention of tumor cells in organ sites, have been put forth as explanations for organ specificity of metastasis (*21*). Some preliminary experiments have been performed to analyze which possibility might be applicable to the present results. No evidence for organ-specific receptors on the tumor cells could be found, since attachment of tumor cells from the liver and lung sublines to sections of various organs (*22*) was not different from controls. Moreover, when cells of the liver-adapted line labeled with ^{125}I-labeled uridine deoxyriboside were injected iv, a much higher percentage of the labeled cells was seen in the lungs than in the liver during the first 24 hours, even though the tumor rarely grew in the lungs.

There are many factors that influence the ability of tumors to metastasize spontaneously (*21, 23*). In our studies, the lung-adapted line had definite metastatic properties. Lung metastases also arose when tumor pieces, rather than cell suspensions, were used for injection in the wing web to minimize accidental iv injection of viable tumor cells. The incidence of spontaneous metastases of the liver-specific sublines was much lower. Since the liver line grows very well in liver after iv or ip injection, these findings show that a major factor that determines the difference between the metastatic abilities of the liver and lung localizing lines may reside in their relative capacity to get into the circulation. However, if only a few cells gain access to the circulation, the first organ encountered will be the lung. Therefore, the metastatic capacity of cells able to grow in the lungs will be detected more readily than that of cells, which according to the "soil hypothesis," prefer to grow in the liver. Further studies are needed to analyze some of the possible characteristics associated with these metastatic properties (*24–33*).

The present results show that relatively stable transplantable lines with a high degree of organ preference can be rapidly derived from the DMBA-induced chicken fibrosarcomas. They suggest that this tumor model provides an excellent tool for further study of this phenomenon.

REFERENCES

(*1*) PALLADINO MA, GALTON JE, HOCHWALD GM, THORBECKE GJ. Immunity to carcinogen-induced transplantable fibrosarcomas in B2/B2 chickens. IV. Effect of whole-body gamma radiation on localization and growth of intravenously injected tumor cells. J Natl Cancer Inst 1979; 63:737–743.

(*2*) FIDLER IJ. Selection of successive tumor lines for metastasis. Nature [New Biol] 1973; 242:148–149.

(*3*) FIDLER IJ, NICOLSON GL. *Brief communication:* Organ selectivity for implantation survival and growth of B16 melanoma variant tumor lines. J Natl Cancer Inst 1976; 57:1199–1202.

(*4*) HART IR, FIDLER IJ. Role of organ selectivity in the determination of metastatic patterns of B16 melanoma. Cancer Res 1980; 40:2281–2287.

(*5*) BRUNSON KW, NICOLSON GL. Selection and biologic properties of malignant variants of a murine lymphosarcoma. JNCI 1978; 61:1499–1502.

(*6*) SHEARMAN PJ, LONGENECKER BM. Selection for virulence and organ-specific metastasis of herpes virus-transformed lymphoma cells. Int J Cancer 1980; 25:363–369.

(*7*) LERMAN SP, WEIDANZ WP. Antibody deficiency syndromes resulting from cyclophosphamide treatment of bursectomized chickens. Bacteriol Proc 1969; 69:91.

(*8*) WITTER RI. A proposed method for designating avian cell lines and transplantable tumors. Avian Pathol 1979; 8:487–498.

(*9*) GALTON J, IVANY J. An immunofluorescent technique for the detection of lymphocyte alloantigens. J Immunol Methods 1977; 17:57–61.

(*10*) GALTON J, PALLADINO MA, THORBECKE GJ. Immunity to carcinogen-induced transplantable fibrosarcoma in B2/B2 chickens. V. Relationship to tumor cell-specific delayed hypersensitivity and serum antibody. Cell Immunol. In press.

(*11*) FIDLER IJ, ZEIDMAN I. Enhancement of experimental metastasis. J Exp Med 1972; 3:172–177.

(*12*) SHEARMAN PJ, GALLATIN WM, LONGENECKER BM. Detection of a cell-surface antigen correlated with organ-specific metastasis. Nature 1980; 286:267–269.

(*13*) GILBERT HA, KAGAN AR. Metastases incidence, detection and evaluation without histologic confirmation. In: Weiss L, ed. Fundamental aspects of metastasis, Amsterdam: Elsevier/North-Holland, 1976:385–405.

(*14*) FIDLER IJ, KRIPKE ML. Metastasis results from pre-existing variant cells within a malignant tumor. Science 1977; 197:893–895.

(*15*) CHOW DA, GREENBERG AH. The generation of tumor heterogeneity in vivo. Int J Cancer 1980; 25:261–265.

(*16*) NICOLSON GL, CUSTEAD SE. Tumor metastasis is not due to adaptation of cells to a new organ environment. Science 1982; 215:176–178.

(*17*) SHEARMAN PJ, LONGENECKER BM. Clonal variation and functional correlation of organ-specific metastasis and an organ-specific metastasis-associated antigen. Int J Cancer 1981; 27:387–395.

(*18*) COMAN DR, DELONG RP, MCCUTCHEON M. Studies on the mechanisms of metastasis. The distribution of tumors in various organs in relation to the distribution of arterial emboli. Cancer Res 1951; 11:648–651.

(19) Paget S. The distribution of secondary growth in cancer of the breast. Lancet 1889; 1:571–573.

(20) Nicolson GL, Winkelhaake JL. Organ specificity of blood-borne tumour metastasis determined by cell adhesion? Nature 1975; 255:230–232.

(21) Fidler IJ, Gersten DM, Hart IR. The biology of cancer invasion and metastasis. Adv Cancer Res 1978; 28:150–250.

(22) Woodruff JJ, Rasmussen RA. In vitro adherence of lymphocytes to unfixed and fixed high endothelial cells of lymph nodes. J Immunol 1979; 123:2369–2372.

(23) Poste G, Fidler IJ. The pathogenesis of cancer metastasis. Nature 1980; 283:139–146.

(24) Sato H, Suzuki M. Deformability and viability of tumor cells by transcapillary passage, with reference to organ affinity of metastasis in cancer. In: Weiss L, ed. Fundamental aspects of metastasis. Amsterdam: Elsevier/North Holland, 1976:311–317.

(25) Bosman HB, Bieber GF, Brown AE. Biochemical parameters correlated with tumour cell implantation. Nature 1973; 246:487–489.

(26) Strauch L. The role of collagenases in tumor invasion. In: Tarin D, ed. Tissue interactions in carcinogenesis. London: Academic Press, 1972:399–407.

(27) Winkelhake JL, Nicolson GL. Determination of adhesive properties of variant metastatic melanoma cells to BALB/3T3 cells and their virus-transformed derivatives by a monolayer attachment assay. J Natl Cancer Inst 1976; 56:285–291.

(28) Pearlstein E, Salk PL, Yogeeswaran G, Karpatkin S. Correlation between spontaneous metastatic potential, platelet-aggregating activity of cell surface extracts, and cell surface sialylation in 10 metastatic-variant derivatives of a rat renal sarcoma cell line. Proc Natl Acad Sci USA 1980; 77:4336–4339.

(29) Hagmar B, Ryd W. Tumor cell locomotion: A factor in metastasis formation? Influence of cytochalasin B on a tumor dissemination pattern. Int J Cancer 1977; 19:576–580.

(30) Leighton J. Invasive growth and metastasis in tissue culture systems. Methods Cancer Res 1968; 4:86–104.

(31) Fitzpatrick FA, Stringfellow DA. Prostaglandin D_2 formation by malignant melanoma cells correlates inversely with cellular metastatic potential. Proc Natl Acad Sci USA 1979; 76:1765–1769.

(32) Kim U. Factors influencing metastasis of breast cancer. Breast Cancer 1979; 3:1–49.

(33) Kerbel RS, Twiddy RR, Robertson DM. Induction of a tumor with greatly increased metastatic growth potential by injection of cells from a low-metastatic H-2 heterozygous tumor cell line into an H-2 incompatible parental strain. Int J Cancer 1978; 22:583–594.

blank page

Meeting Highlights

Cytogenetics and Somatic Cell Genetics of Malignancy Workshop

This workshop on November 9–10, 1981 was sponsored by the Division of Cancer Cause and Prevention of the National Cancer Institute, National Institutes of Health, Public Health Service, U.S. Department of Health and Human Services, Bethesda, Md. The stated objectives were 1) to explore genetic areas that have potential interdisciplinary overlap with other areas of cancer research; 2) to bring together individuals in different disciplines, with the hope of stimulating and initiating collaborations; 3) to explore environmental and genetic interactions in the multifactorial origins of cancer; and 4) to identify areas to be examined for fundamental changes in carcinogenesis mechanisms and areas in which gaps in knowledge exist, for the purpose of making recommendations for future research.

In the three sessions of the 1.5-day workshop program, the interactions of the disciplines of cytogenetics, somatic cell genetics, molecular genetics, DNA repair, epidemiology, virology, chemical transformation, immunology, and molecular biology were discussed in relation to the mechanisms of carcinogenesis.

In the first session, the chairman Dr. Alfred G. Knudson indicated that genetic change related to cancer could be in the cancer genes or the accessory genes. The cancer genes may be dominant in cells and behave like oncogenes or recessive genes that behave like the retinoblastoma or polyposis genes. Accessory genes can influence the rate at which changes occur in these cancer genes. Dr. Janet Rowley analyzed the cytogenetic findings in human leukemias and lymphomas, noting particularly that in Burkitt's lymphoma and chronic myelocytic leukemia more than one kind of chromosome translocation is characteristic, but that a common segment is found. Thus the Burkitt's aberration can be an apparently reciprocal translocation between chromosome 8 and any of chromosomes 14, 2, or 22. Segments of chromosomes 14, 2, and 22 code, respectively, for heavy, κ- and λ-chains of the immunoglobulins. Dr. Peter Nowell discussed chromosome abnormalities in leukemia and noted that stimulation of B-cells by terephthalate permits analysis of chromosome changes in chronic lymphocytic leukemia.

The rare but interesting cases of prezygotic chromosome lesions that predispose to cancer were discussed by Dr. Uta Francke. In retinoblastoma, band 13q14.3 is critical. In Wilms' tumor associated with aniridia, band 11p34 is deleted. This deletion was found in 18 individuals with aniridia, although some did not have Wilms' tumor. Dr. Louise Strong presented data on a family in which multiple offspring with retinoblastoma had the characteristic chromosome deletion. The parents of the affected individuals were carriers of a translocation that involves the same segment of chromosome 13. All four of the possible segregants of the translocation were found. Such a pedigree shows an irregular pattern of inheritance, with a 25% ration of affected children among the offspring carriers. This pedigree may be a paradigm for previously reported instances of so-called "premutation."

Dr. Mary Clare King discussed the linkage of a breast cancer gene with the gene for glutamate–pyruvate transaminase. Syndromes that characteristically show chromosome fragility were reviewed by Dr. James German. In xeroderma pigmentosum (XP) chromosome instability is seen after UV irradiation. In Werner's syndrome, chromosome mutations are observed, although breakage rates are not increased. In ataxia telangiectasia and Fanconi's syndrome, breakage and translocations are characteristic. In Bloom's syndrome, breakage and homologous chromosome exchange are prominent. Heterozygotes for ataxia telangiectasia have been shown by Dr. Michael Swift to be at increased risk for cancer. Inasmuch as such heterozygotes represent between 0.5 and 1.0% of the population, they could be making an important contribution to the incidence of cancer.

Dr. John Little discussed the in vitro repair to damaged DNA as a function of the interval of time after administration of a breaking agent to a confluent culture. A rapid component is concerned with repair of thymidine dimers and of chromosome aberrations, whereas a slow component is associated with DNA cross-links and sister chromatid exchanges. Dr. Malcolm Paterson noted that in the neurologic forms of XP, but not in the nonneurologic forms, nonphotoreactable sites are affected.

The second session of the workshop was chaired by Dr. Louis Siminovitch. In introductory remarks, he described some work in his laboratory by Dr. Irene Andrulis, who has been working with the gene system that controls asparagine synthetase. This gene was transferred into CHO cells by means of DNA. One of the transformed isolates contained highly elevated levels of the enzyme and a homogeneously staining region (HSR). The isolate, therefore, probably represents an example of gene duplication. Similar high levels of asparagine synthetase were achieved by the growing of wild type cells in increasing concentrations of albiizzin.

Dr. Warren Nichols described some of the consequences of transformation of human diploid cells with wild type and mutant simian virus 40 (SV40). Most of such cells undergo senescence similar to that of uninfected cells. Some mutants showed positive transformation when assayed in monolayer but were negative when tested in soft agar, indicating that the agar was more exigent and that possibly multiple events were involved. It also appears that SV40-transformed human diploid cells show increased sister chromatid exchanges (SCE) and chromosome anomalies at the same time as the T-antigen production increased. Dr. N. C. Popescu reported a correlation between SCE and morphologic transformation in Syrian hamster cells after treatment with benzo[*a*]anthracene, *N*-methyl-*N*′-nitro-*N*-nitrosoguanidine, methyl methanesulfonate, and *N*-hydroxy-*N*-2-fluorenylacetamide. After X-irradiation, however, SCE was increased without morphologic transformation.

Dr. Susan Astrin described studies she made in collaboration with Dr. W. S. Hayward on the activation of cellular genes by means of promoter sequences. In earlier studies they had demonstrated such activation for the *myc* gene in tumors in an avian system. Inasmuch as humans also carry the *myc* gene, Dr. Astrin and Dr. Hayward explored its possible activation in human acute lymphocytic leukemia (ALL), chronic lymphocytic leukemia (CLL), and Hodgkin's disease. By blot hybridization analysis with the use of a *myc* DNA probe, elevated levels of the *myc* gene RNA were found in some of the CLL, ALL, and Hodgkin's disease patients. Dr. E. Skolnik presented some examples of cellular gene activation by promoters. He also described examples in which the cellular *onc* gene had been amplified.

Dr. R. Weinberg reported on his recent studies on transformation, in which he used DNA from a variety of murine and human tumors. Examination of the restriction enzyme sensitivity of various tumor-derived DNA's indicated that the same gene may be activated in each tissue type. Dr. Weinberg has also been cloning some of these genes and examining their sequence interrelationships. Two different bladder carcinomas seem to have activated the same gene sequence. In the case of a colon carcinoma, the gene was found to be present in normal cells, supporting the concept of activation of sequences during carcinogenesis.

Dr. B. D. Crawford is involved in studies that examine the multistep nature of carcinogenesis as indicated by the successive appearance of new cancer phenotypes. Dr. P. Lalley, by analysis of XP human–murine cell hybrids, has been attempting to map the genes involved in UV radiation repair. The present data support the concept that chromosomes 3 and 8 are involved.

In the third session, chaired by Warren W. Nichols, Dr. Michael Potter discussed the differential susceptibility of various mouse strains to plasmacytoma induction by injections of pristane. BALB/cAn mice are quite susceptible to this procedure, whereas most other mouse strains are resistant. Susceptibility and resistance genes differ within strains. BALB/c pristane-induced plasmacytomas all showed translocations involving chromosome 15 and either chromosome 6 or 12. Chromosome 6 and 12 breakpoints are associated with regions that code for Igκ and Igλ complex loci, respectively, with the breakpoint on chromosome 15 the same in both translocations. Dr. June Biedler commented on the high frequency of trisomic chromosome 15 observed in mouse leukemias.

Dr. Robert Schimke discussed the loss of cellular restraint by increased synthesis of specific cellular proteins. One of the mechanisms of the increased protein production is gene amplification, which has been associated with the acquisition of drug resistance, reversion of auxotrophy, and in embryonic development. Cytogenetically, HSR's and double minute chromosomes (DM) have been associated with the phenomenon, and amplified genes have been mapped to these areas. Dr. June Biedler and Dr. Gloria Balaban reported on the occurrence of HSR's and DM in clinical and experimental tumor material.

Dr. T. Mohandas discussed gene regulation by methylation of DNA. The modification of DNA that methylation produces has been proposed as a mechanism of X-chromosome inactivation. Use of 5-azacytidine results in hypomethylation of DNA. The addition of this chemical to a mouse–human hybrid cell that contained the inactive X-chromosome as the only human chromosome resulted in the reactivation of human hypoxanthine phosphoribosyltransferase (HPRT) at a frequency of 1 in 700 cells in comparison to a frequency of 1×10^{-6} in untreated cells. DNA isolated from cells with a reactivated chromosome X was competent in a transformation assay with an HPRT line, demonstrating that the changes were at the DNA level. Dr. O. J. Miller described studies with rat hepatoma cells containing a large HSR associated with ribosomal gene amplification. Staining of nucleolar organizing region demonstrated that only a few of these genes are active, and antibodies against methylcytosine reacted with the amplified genes.

Following session 3, a general and very active discussion period was held concerning the greatest opportunities for progress. There was unanimity regarding the importance of interactions and communications between disciplines. Means of communication that were discussed included meetings similar to the one just completed, Gordon conferences, newsletters, and listings of accessible biologic materials, such as the listing of available recombinant DNA probes that Dr. Francke and Dr. Skolnick are in the process of compiling. Making available materials that are standardized but usually not readily obtainable can stimulate research.

Communication and interactions are the keys to interdisciplinary collaboration, as illustrated by at least four proposed collaborative efforts that resulted from the current meeting. Interdisciplinary training programs and task force approaches were also suggested. The need for initial support in new areas and in interdisciplinary areas and the development of lists of available biologic supplies, as mentioned above, were considered to be especially important in assuring progress. In more than 25 letters and phone calls after the conclusion of the workshop, other important areas were suggested—too many to be recounted here.

WARREN W. NICHOLS, *M.D., Ph.D.*
Department of Cytogenetics
Institute for Medical Research
Camden, New Jersey 08103
ALFRED G. KNUDSON, *M.D., Ph.D.*
The Institute for Cancer Research
Philadelphia, Pennsylvania 19111
LOUIS SIMINOVITCH, *Ph.D.*
Department of Medical Genetics
University of Toronto
Toronto, Canada

Brief Summary of the Third Joint Meeting of the United States–Japan Cooperative Cancer Research Program on Cell Interactions and Cancer

The third joint meeting of the Cellular and Molecular Biology Sub-area of the United States–Japan Cooperative Cancer Research Program was held in Kyoto from November 5–7, 1981, on the subject of cell interactions and cancer.

The 17 participants, 5 from the United States and 12 from Japan, were of various backgrounds related to cell interaction and/or cancer. The presentations covered a diverse series of topics ranging from cell-to-cell adhesion in the cellular slime molds to studies of the pathology of human cancer. In spite of this wide diversity of topics, the discussions were lively, reflecting the commonality of interests of the participants and the common tools of their research effort.

In the first two sessions cell adhesion was discussed in relation to morphogenesis and differentiation. A number of cellular systems were discussed in which the cell surface changes in a systematic way during development. Included in these discussions was extensive work on the cellular slime mold (Ikuo Takeuchi, Samuel Barondes) as well as studies of cell lineage and the maintenance of the cell proportions in differentiation mutants of hydra (Tsutomu Sugiyama). Cell adhesion also influences the growth in differentiation of cells, as has been demonstrated in fibroblasts (3T3 cells and Schwann cells) under culture conditions (Luis Glaser). In these and other simple systems, analysis of factors involved in cell–cell interaction appears promising. Although several cell-adhesion molecules have been identified in several systems, it was recognized that we are far from understanding the molecular events regulating cell behavior and the precise way in which cell surface molecules participate in these events. This is true not only for the complex phenomena discussed at the meeting but also for the interaction of more defined cell molecules, such as hormones, with the cell surface. Before any generalizations can be made, each of these systems will have to be examined in greater detail and at a more detailed molecular level than has been achieved so far.

The neuronal connection, a phenomenon in which cell recognition is potentially involved, was discussed in particular in relation to retino-tectal projection by Hajime Fujisawa. Dr. Fujisawa followed the developmental pathway of retinal fibers that had been labeled with horse-radish peroxidase and succeeded in showing for the first time that the pathway by which these axons reached their target cells in the tectum involves a great deal of trial and error in search rather than a totally directed transit to the cells. These elegant experiments served to rule out a number of currently popular models by which the retino-tectal connections are made and strongly suggest that trial and error is at least in this instance a major mechanism for reaching a correct target. The precise molecular mechanism by which the growth count of an axon differentiates among surface molecules to reach a preferred adhesion site is one of the more exciting puzzles in the cell-adhesion field.

Strong evidence was given that cell surface receptors do play decisive roles for cell interaction and hence for normal development. Specific lymphocyte homing in the lymphoid organ of the frog was demonstrated (Shin Tochinai), and such homing of migratory cells was shown to be regulated in mice by the binding of lymphocytes to high endothelial venule and organ-specific surface cells via genetically restricted receptors (Irving Weissman).

The third and fourth sessions dealt with phenomena more directly related to cancer. The differentiation of tissue mast cells and growth of leukemia cells in vitro were reported to depend on microenvironment (Yukihiko Kitamura, Hiroshi Hiai). Since collagen and fibronectin are of primary importance as extracellular microenvironments in situ and decrease after malignant transformation, studies on the structure and regulation of these molecules are of interest. Binding sites for collagen, heparin, and other macromolecules have been precisely mapped on fibronectin molecules (Kenneth Yamada). The structure of a type I collagen gene was analyzed and shown to have a unique regulatory region containing three large, inverted repeats; it was suggested that hypothetical regulatory proteins that interact with this region may be modified in transformed cells (Ira Pastan).

In the discussion of adhesion of transformed cells, alteration of adhesion properties of in situ cancer cells was demonstrated as well as in vitro cell lines (Hideo Hayashi, Masatoshi Take-ichi, Hideko Urushihara). Malignant types of gastric carcinoma constituted of dissociative cells were examined with the use of electron microscopy and [^{3}H]-thymidine autoradiography. [^{3}H]thymidine-labeled growing cells were shown to be abnormally distributed in cancerous areas because of decreased adhesiveness and peculiar motility (Setsuya Fujita).

The meeting was a mixed demonstration of clear molecular study and of complicated phenomena in higher organisms. This impression no doubt summarizes the present status of the study of cancer at the cellular level.

Our overall evaluation of this meeting was that it was an excellent exchange of science by professionals with varying approaches. There were ample opportunities both during the formal presentations of papers and in relaxation times for broad-ranging discussions among the participants, and these appeared to be utilized fully. It was a productive 3-day period for all involved.

The public symposium that followed at the close of the "formal" meetings attracted an audience of 100, some from as far away as Nagoya and Tokyo. The audience was made up of professionals and interested students. This symposium was entitled simply "Cell Interaction," and four speakers from the United States presented their views and work during the 3-hour session. This type of sharing of knowledge is perhaps too rare among the generations, and the fact that it was so well attended would appear to testify to the fact that more such presentations would be welcomed.

IRA PASTAN, *M.D.*
National Cancer Institute
Building 37, Room 4B27
Bethesda, Maryland 20205

YOJI IKAWA, *M.D.*
Department of Viral Oncology
Cancer Institute
Kami-Ikebukuro,
Toshima-ku, 170 Tokyo, Japan

blank page

Corrections

May 1982, vol 68, No. 5

In "Comparison of In Vitro and In Vivo Effects of Thymidine on L1210 Leukemia in Mice," by Daniel S. Zaharko and Lori M. Ramonas, page 878, the last sentence in the legend to text-figure 5 should read: N/N_0=No. of cells at time=*t*/No. of cells at time=0 (*not* N/NO=No. of cells in drug-treated tubes/No. of cells in control tubes).

NCI Monograph No. 58

In "Carcinogenic and Mutagenic N-Substituted Aryl Compounds," NCI Monograph No. 58, page 47, the sentences beginning in the second line of the right column should read:

> Smaller molecular weight arylamines have lower overall carcinogenic and oncogenic effects than do larger molecules. When the amino group is alpha to an anelated ring position in a polycyclic arylamine, such as 1-NA or 2-BPA, current views are that such chemicals are not carcinogenic because they cannot undergo the required biochemical N-hydroxylation reaction to a sufficient extent.

Announcements

The Journal *will publish notices of major meetings dealing with cancer. Submission of notices 6 months in advance is requested to permit timely publication.*

Temporomandibular Joint—Pain and Dysfunction Course

The University of Rochester Medical Center School of Medicine and Dentistry and Strong Memorial Hospital will sponsor this course to be held at the Plaza Hotel, New York City, on September 24-26, 1982. This course is designed for persons involved with diagnosis, assessment, and treatment of temporomandibular joint (TMJ) disease. Course offerings will include clinical evaluation and arthrographic and differential diagnosis of the disease, use of contrast media and plain film techniques, and both surgical and nonsurgical methods of managing TMJ pain and dysfunction. Coverage will also extend to pathophysiology of mandibular dysfunction, myofacial pain dysfunction syndrome, and degenerative joint disease.

Accreditation approved AMA Category I credit for 16 hours; approved by the ADA Continuing Education Registry for 16 hours. For additional information please contact Educational Resources Associates, Inc., P. O. Box 369, Brookline, Massachusetts 02146 (telephone: 617-738-8859).

Second Annual International Symposium on the Clinical Applications of Cardiopulmonary Imaging

This 4-day cardiopulmonary course, to be held at the Hyatt Lake Tahoe, Lake Tahoe, Nevada, on September 29-October 2, 1982, is designed for all practitioners who desire a comprehensive "patient-oriented" learning experience in the newest cardiopulmonary imaging techniques. The course will update and refine assessments of the different imaging techniques and their application to diagnosis and management of patients with cardiopulmonary diseases.

AMA Category I accreditation has been approved for 24 hours. Additional information on tuition and registration is available from Educational Resources Associates, Inc., P. O. Box 369, Brookline, Massachusetts 02146 (telephone: 617-738-8859/8861).

Fifteenth Annual Malignant Disease Symposium

"Cancer and Nutrition—An Oncology Update" will be the subject of this symposium to be held at Chapel Hill, North Carolina, on October 22-23, 1982. Mounting evidence from current epidemiological and clinical research studies points to an association of nutritional excesses or deficiencies with certain cancers. This symposium has been organized to bring the most up-to-date information about these developments to practicing physicians, house staff, nurses, and health professionals involved with cancer patients.

For additional information please contact Dr. William D. Heizer, Cancer Research Center, Box 30, MacNider Building, The University of North Carolina School of Medicine, Chapel Hill, North Carolina 27514.

Pediatric Radiology Course

Cambridge, Massachusetts, will be the site of this course to be held at the Hyatt Regency Hotel on November 1-3, 1982. This 3-day course, sponsored by the Department of Radiology of the Children's Hospital Medical Center and Harvard Medical School, will review the diagnostic and therapeutic imaging techniques employed in pediatric radiology, with emphasis on the application of these techniques to diagnostic problems in children.

Accreditation has been approved for 22 hours AMA Category I. For additional information please contact Educational Resources Associates, Inc., P. O. Box 369, Brookline, Massachusetts 02146 (telephone: 617-738-8859).

New Monographs Available

No. 58: Carcinogenic and Mutagenic N-Substituted Aryl Compounds
  GPO Stock No.: 017-042-00155-2, $12.00 in the United States, Canada, and Mexico; $15.00 elsewhere
No. 59: Cancer Mortality in the United States: 1950-1977
  GPO Stock No.: 017-042-00161-7, $18.00 in the United States, Canada, and Mexico; $22.50 elsewhere

Copies are for sale **only** by the Superintendent of Documents, U.S. Government Printing Office, Washington, D.C. 20402. When ordering, please be sure to make the check or money order payable to the Superintendent of Documents and include the title and stock number of the volume desired. Payment is required in advance.

Public Health Controversies—Food Safety Laws: Delaney and Other Dilemmas

The first in a series of national conferences on public health issues, sponsored by Boston University School of Public Health, will be held at the Capital Hilton in Washington, D. C., on September 23–24, 1982. The conference will be attended by the principal interests from the food industry, consumer groups, academia, the legal profession, and government. The program will focus on the latest efforts to frame workable food safety regulations; the projected legal implications of the passage of less stringent legislation, including questions of liability; the current and projected state of the art in food testing; and the public health and ethical issues raised by changing the current law.

For further information please contact Ms. Elizabeth M. Ollen, Conference Coordinator, Boston University School of Public Health, 80 East Concord Street, Boston, Massachusetts 02118 (telephone: 617-247-6201 or 617-247-6016).

U.S. GOVERNMENT PRINTING OFFICE: 1982-311-216/57

JNCI (NIH Publication No. 82-13)

69/3

NEWARK PUBLIC LIBRARY

OCT 25

U. S. GOVT. PUB.
DEPOSITORY 376

JNCI
Journal of the National Cancer Institute
September 1982
Volume 69
Number 3

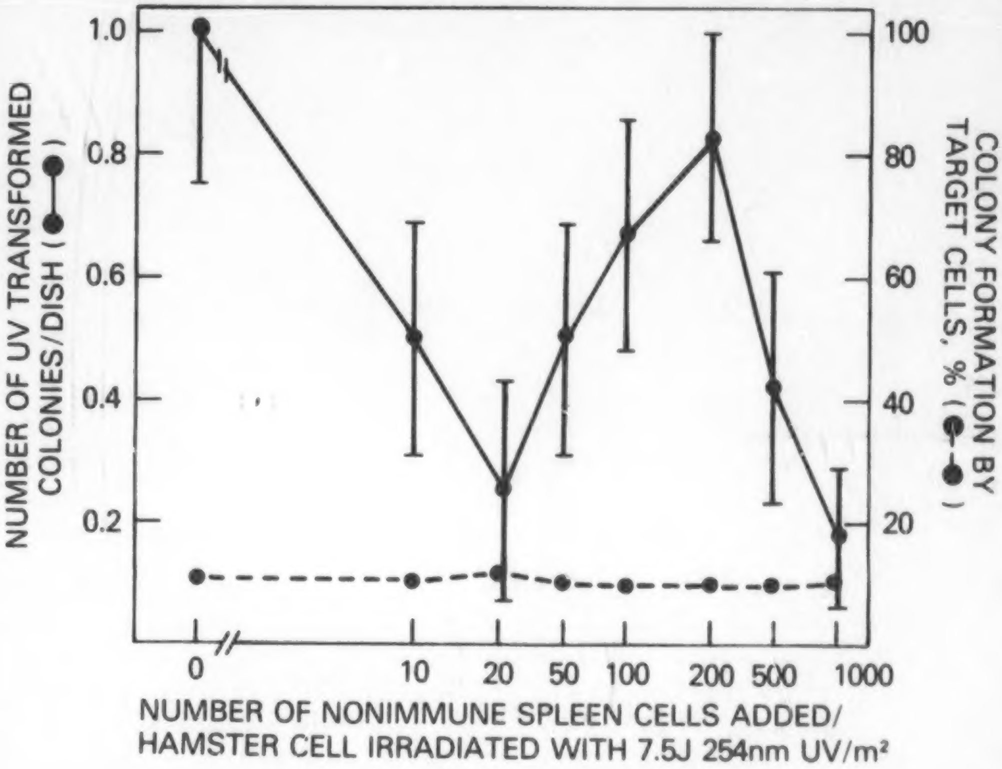

U.S. DEPARTMENT OF HEALTH AND HUMAN SERVICES   Public Health Service   National Institutes of Health

HE 20.3161:

The cover illustrates biphasic inhibition of UV radiation-induced morphologic transformation of hamster fibroblasts by normal (naturally immune) spleen lymphocytes. Modulation of carcinogenesis at this early stage can result from immunoregulation of the immunologic hormone and anticarcinogenic lymphokine lymphotoxin. This study by Evans et al. (*see* paper on pages 737–740) dissects mechanisms of natural immunity that affect carcinogenesis.

JNCI

Journal of the National
Cancer Institute

September 1982
Volume 69
Number 3

THE JOURNAL of the National Cancer Institute solicits manuscripts on original observations in laboratory and clinical research from all scientists. A manuscript is considered for publication with the understanding that it has not been published previously and is submitted exclusively to the Journal. Opinions expressed by the authors are not necessarily those of the publisher or its editors.

THE JOURNAL is published monthly (two volumes a year). The Secretary of Health and Human Services has determined that the publication of this periodical is necessary in the transaction of the public business required by law of this Department.

A MONOGRAPH SERIES covering proceedings of scientific meetings pertaining to cancer is also published. These books may be purchased from the Superintendent of Documents. Series subscriptions are not available and monographs are not included in a subscription to the Journal.

THE JOURNAL is for sale by the Superintendent of Documents, U.S. Government Printing Office, Washington, D.C. 20402. Price per copy, $7.00. Subscription price for two volumes per year in the United States, $70.00; foreign, $87.50. Payment is required in advance, and check or money order should be made payable to the Superintendent of Documents.

All inquiries regarding purchase of subscriptions or depository library distribution, including inquiries about missing issues and change of address, should be addressed to the Government Printing Office. The Government Printing Office requires payment in advance on all orders. Inquiries regarding missing issues or change of address for official subscriptions should be addressed to the Editorial Office, Room 850, Westwood Building, 5333 Westbard Avenue, Bethesda, Md. 20816.

VINCENT T. DEVITA, JR., *Director, National Cancer Institute*

BOARD OF EDITORS

PETER GREENWALD, *Editor in Chief*
ELIZABETH K. WEISBURGER, *Assistant Editor in Chief*
STUART A. AARONSON, *Associate Editor*
CHARLES H. EVANS, *Associate Editor*
MARY A. FINK, *Associate Editor*
JANET W. HARTLEY, *Associate Editor*
DONALD HENSON, *Associate Editor*
RONALD B. HERBERMAN, *Associate Editor*
GEORGE S. JOHNSON, *Associate Editor*
KURT W. KOHN, *Associate Editor*
ARTHUR S. LEVINE, *Associate Editor*
JOHN J. MULVIHILL, *Associate Editor*
ALAN S. RABSON, *Associate Editor*
RICHARD M. SIMON, *Associate Editor*

EDITORIAL STAFF

EDWIN A. HAUGH, *Managing Editor*
PAMELA T. ALLEN, *Assistant Managing Editor*
FLORENCE I. GREGORIC, *Monograph Editor*
Editors: DOROTHY D. KATZ, MERCEDES B. LA CHARITY,
I. AGNES REVESZ, JOAN O'BRIEN RODRIGUEZ,
CONSTANCE R. STONESTREET, and ANNA B. WITTIG

JNCI (NIH Publication No. 82-13)

U.S. DEPARTMENT OF HEALTH AND HUMAN SERVICES Public Health Service National Institutes of Health

Instructions to Authors

Text: Send one original and two copies. **Text-figures** (graphs, charts, and line drawings): Send one original and two copies. **Figures** (photomicrographs and photographs): Send three original glossy prints, unmounted. **Tables:** Send tabular material in typewritten form; do not submit tables as glossy prints to be photographed. The entire manuscript including footnotes, legends, and references must be typed double spaced. Single-spaced portions of a manuscript will be returned to the author for retyping. The mailing address is: Journal of the National Cancer Institute, Westwood Building, Room 850, 5333 Westbard Avenue, Bethesda, Maryland 20816.

Manuscripts should be accompanied by a covering letter from the author responsible for correspondence about the manuscript. The covering letter should contain a statement that the manuscript has been seen and approved by all authors and that all persons listed as authors have made significant (not merely administrative, technical, or supervisory) contributions to the content of the paper. The letter should also state that the manuscript or substantial portions thereof have not been previously published nor are they under consideration for publication in another journal.

Data too extensive for inclusion in a manuscript, but which may be of interest to other investigators, may be deposited with the National Auxiliary Publications Service (NAPS), c/o Microfiche Publications, P.O. Box 3513, Grand Central Station, New York, New York 10017. Authors using the NAPS facilities should indicate in a footnote how their additional data may be obtained.

Approximately one-half of all manuscripts submitted to the Journal are accepted for publication. Publication of manuscripts is contingent on transfer of copyright to the Journal. Forms for this purpose will be sent to authors when a manuscript has been approved for publication. All material published in the Journal is in the public domain; therefore, permission to reproduce any portions is not necessary. As a matter of courtesy, communication should be made to the author(s) concerned.

TITLE: Be brief (no more than 14 words, if possible), but for indexing purposes include all key words. The annual subject index is prepared directly from the titles. Titles that form complete sentences are not acceptable. Do not use abbreviations or chemical formulas in titles.

BYLINE: Supply the complete first name, middle initial, and last name of each author. Avoid use of nicknames. Academic degree is optional; however, if a degree is provided for one author, it should be provided for all authors on a manuscript. Include the name of the institution, address, and zip code for each author. Indicate address for reprint requests in a footnote on the byline.

ACKNOWLEDGMENTS: Financial aid in support of research should be recognized in a footnote. Aid in technical fields, animal care, photography, stenography, and other areas may be mentioned in a separate footnote. Indicate the title (Dr., Mr., Mrs., Miss, Ms.) and affiliation of each person acknowledged.

ABSTRACT: Provide an abstract, 150 words or less, on a separate page. The abstract should describe only *results* of the work being reported. Speculation, historical background, or reference to published works will be deleted from abstracts. Any inbred strains, noninbred stocks, cell lines, or other living materials used in the work should be noted in the abstract.

TEXT: Avoid the use of laboratory jargon and abbreviations not in common usage. When possible, refrain from the use of abbreviations that form words (exceptions are PAGE, ALL). Whenever possible, write mathematical equations and chemical formulas on a single line; submit complicated chemical structures as artwork. Avoid repetition of data in the text when it is presented in tables or text-figures.

Use the following style sources: Webster's *Third New International Dictionary* and Dorland's *Illustrated Medical Dictionary* (25th ed) for spelling; *Council of Biology Editors Style Manual* (4th ed) for scientific abbreviations and symbols; *Government Printing Office Style Manual* for other abbreviations and symbols, punctuation, and hyphenation; *Biochemical Nomenclature and Related Documents* (IUB, 1978) for abbreviations of chemical substances; *Enzyme Nomenclature*, recommendations (1978) of the IUB for recommended names of enzymes and information on nomenclature of isozymes; *The Merck Index* (9th ed) for chemical compounds; "Standard Nomenclature for Inbred Strains of Mice: Seventh Listing" by Joan Staats (Cancer Res 1980;40: 2083-2128) for inbred mouse strains; "Standardized Nomenclature for Inbred Strains of Rats: Fourth Listing" by Joan Staats and Michael Festing (Transplantation 1973;16:221-245) for designations of inbred rat strains; *Animals for Research* (9th ed) prepared by the Institute of Laboratory Animal Resources, National Academy of Sciences, for designations of laboratory animal stocks and strains.

TABLES: Submit tabular material typed double spaced on a separate page. Computer print-outs of tables are acceptable only if they are double spaced and with satisfactory title, column headings, legends, and other textual material. Provide headings for all columns of a table and indicate units of measurement where applicable.

TEXT-FIGURES: Refer to graphs, charts, and line drawings as text-figures. Make the abbreviations on text-figures identical to the abbreviations used in the text and legends. Symbols and lettering should be large enough to be legible if reduced. Glossy prints or original drawings in black ink are acceptable; orient vertically instead of horizontally.

FIGURES: Refer to photomicrographs and photographs as figures. Figures and their legends should fit a 7.5- by 9-inch dimension. Calculate that nine typewritten lines of legend will require 1 inch of vertical space. Type figure legends on a separate sheet and identify in the legend any lettering used on the figure. Trim photographs to show only important areas. Do not number face of photographs; use the back or overlay to indicate the top and number of each. Printed indicators may be included on photographs; do not use hand-drawn indicators. *Insert internal scale markers on all photomicrographs.* Color photographs must be grouped as a single plate. For color reproduction, submit both color transparencies and high-quality black and white reproductions. The need for color must be documented before it will be considered.

REFERENCES: Use any recent issue of the Journal as a style guide for reference lists. Number references in order of citation in both text and reference list. For periodicals, provide author(s), title of paper, journal, year, volume, and first and last page numbers. For books, give the author(s), title, name(s) of editor(s), location and name of publisher, year, pertinent chapter or section title, and page numbers. Follow *Index Medicus* for punctuation and abbreviations. Citations of papers in preparation or submitted for publication, unpublished observations, and personal communications should be noted parenthetically in the text. Do *not* include them in the reference list. The accuracy of all references is the responsibility of the authors and not of the editorial staff.

LETTERS TO THE EDITOR should pertain to recent articles in the Journal and should not contain new data unless relevant to the discussion of a particular paper. The authors addressed will be invited to reply to comments before correspondence is published. Letters will be edited by the Staff, subject to contributor approval.

FURTHER DETAILS on the preparation of manuscripts are set forth in the document "Uniform Requirements for Manuscripts Submitted to Biomedical Journals" prepared by the International Steering Committee of medical editors (*see* Am Rev Respir Dis 1979;119:3-10/Ann Intern Med 1979;90:95-99/Br Med J 1979;1:532-535/ or Lancet 1979;1:428-430).

UNITED STATES GOVERNMENT PRINTING OFFICE, WASHINGTON, D.C.: 1982

Table of Contents

Vol. 69, No. 3——September 1982

Letters to the Editor

549 Morbidity versus mortality — *Johannes Clemmesen, Arne Nielsen*

550 Reply — *Richard Doll, Richard Peto*

Investigations on Man

551 Immunity to tumor-associated antigens in vasectomized men — *Deborah J. Anderson, Nancy J. Alexander, David L. Fulgham, Arthur A. Vandenbark, Denis R. Burger*

557 Unscheduled DNA synthesis in human oral mucosa treated with chemical carcinogens in short-term organ culture — *Fumio Ide, Takatoshi Ishikawa, Minoru Takagi, Shinichiro Umemura, Shozo Takayama*

565 Distribution of hepatitis B surface and core antigens in human liver cell carcinoma and surrounding nontumorous liver — *Setsuo Hirohashi, Yukio Shimosato, Yoshinori Ino, Kiyozo Kishi*

569 Elevated dTTPase activities in sera of patients with advanced cancer — *Nicolaus Dahlmann*

573 Breath methane excretion in patients with unresected colorectal cancer — *David A. Karlin, R. D. Jones, John R. Stroehlein, Anthony J. Mastromarino, Gregory D. Potter*

577 *N*-Methyl-*N*-nitrosourea and saccharin: Effects on epithelium of normal human urinary bladder in vitro — *Shadia El-Gerzawi, Barry M. Heatfield, Benjamin F. Trump*

585 Persistence of transforming and nontransforming Epstein-Barr virus in high passages of P3HR-1 cell lines — *Paul Gerber, Dharam Ablashi, Ian Magrath, Gary Armstrong, Philip Andersen, Luba Trach*

Investigations on Nonhuman Systems

591 A deletion in chromosome 1 in cells of a transplantable granulocytic leukemia (GL 13) in guinea pigs — *Dorothy E. Moore, Warren H. Evans, Michael G. Mage*

595 Establishment and immunologic characterization of 3-methylcholanthrene-induced sarcoma cell lines metastasizing widely in mice and exhibiting distinct and selective propensities for the mode of metastasis — *Yuso Kodama, Toshio Seyama, Kenji Kamiya, Kenjiro Yokoro*

607 Modulation of cell-mediated alloimmunity by BCG. I. Antagonism and potentiation of immunosuppression caused by cytarabine — *Richard I. Murahata, Malcolm S. Mitchell*

613	Modulation of cell-mediated alloimmunity by BCG. II. Induction of specific, nonadherent, non-T-killer cells by BCG and alloantigen	*Richard I. Murahata, Malcolm S. Mitchell*
619	Alloantigenic phenotype of radiation-induced thymomas in the mouse	*P. Mark Hogarth, Margaret M. Henning, Ian F. C. McKenzie*
627	Formation of symbiotic complex by microenvironment-dependent mouse leukemias and thymic epithelial reticular cells	*Yoshimi Nishi, Kazuhiro Yoshikawa, Hiroshi Hiai, Kunihiro Notake, Hayase Shisa, Yasuaki Nishizuka*
639	A high-tumor-incidence subline of the D1 mouse mammary hyperplastic outgrowth line: Effect of carcinogens	*Rhoda L. Ashley, Robert D. Cardiff, Terry S. Pratt, Leslie J. Faulkin*
647	Antitumor immunity induced by hybrid murine tumor cells: Requirements for optimal immunization	*Craig S. McCune, Robert W. O'Donnell, Paul K. Horan, Hollis S. Budd, Janice L. Spennacchio, Christy Chuang, Edgar C. Henshaw*
653	Inhibitory effect of interferon on the growth of spontaneous mammary tumors in mice	*Erik De Clercq, Zhen-Xi Zhang, Kris Huygen, Roger Leyten*
659	Influence of cause-of-death assignment on time-to-tumor analyses in animal carcinogenesis studies	*Ralph L. Kodell, John H. Farmer, David W. Gaylor, Alexander M. Cameron*
665	Murine lymph node natural killer cells: Regulatory mechanisms of activation or suppression	*Goro Hisano, Nabil Hanna*
673	Androgen control of cytosol progesterone receptor levels in the MT-W9B transplantable mammary tumor in the rat	*Margot M. Ip, Richard J. Milholland, Untae Kim, Fred Rosen*
683	In vitro measurement of resistance to phalloidin and γ-glutamyltransferase of carcinogen-induced preneoplastic hepatocytes of rats	*Norimasa Sawada, Kazunori Furukawa, Hideyuki Tsukada*
687	Chicken resistance to dimethylnitrosamine acute effects on the liver: A comparative study with other species	*H. M. Godoy, M. I. Díaz Gómez, A. Marzi, E. C. de Ferreyra, O. M. de Fenos, J. A. Castro*
693	Effects of sublethal irradiation on changes in crypts of the mouse colon during treatment with 1,2-dimethylhydrazine	*Thomas C. Richards, David E. Tacha*
699	Tumor-induced neovascularization in the mouse eye	*V. R. Muthukkaruppan, L. Kubai, R. Auerbach*
709	In vitro infection of lymphocytes with Marek's disease virus	*Bruce W. Calnek, Karel A. Schat, William R. Shek, Chen-Lo H. Chen*
715	Surface antigens on Marek's disease lymphoblastoid tumor cell lines	*Karel A. Schat, Chen-Lo H. Chen, William R. Shek, Bruce W. Calnek*
721	Some effects of the tumor promoter 12-*O*-tetradecanoylphorbol 13-acetate on cell interactions in vitro	*David E. Maslow, Eric G. Mayhew, Charles E. Wenner*

725 Mouse skin tumor-initiating activity of 5-, 7-, and 12-methyl- and fluorine-substituted benz[*a*]anthracenes *Alexander W. Wood, Wayne Levin, Richard L. Chang, Allan H. Conney, Thomas J. Slaga, Robert F. O'Malley, Melvin S. Newman, Donald R. Buhler, Donald M. Jerina*

729 Free amino acid pools of rodent mammary tumors *Martin J. Pine, Untae Kim, Clement Ip*

737 Immunomodulation of the lymphoresponsive phases of carcinogenesis: Mechanisms of natural immunity *Charles H. Evans, Joseph A. DiPaolo, Jeffrey A. Heinbaugh, Anthony J. DeMarinis*

741 Lymphotoxin prevention of diethylnitrosamine carcinogenesis in vivo *Janet H. Ransom, Charles H. Evans, Joseph A. DiPaolo*

Announcements

745 Advances in Pediatric Oncology Seminar

745 Thirty-Sixth Annual Symposium on Fundamental Cancer Research

745 Twenty-Fourth Postgraduate Institute for Pathologists in Clinical Cytopathology

745 Accredited Visiting Faculty Program on Colorectal Cancer

Letters to the Editor

Morbidity Versus Mortality

SIR: Our experience from Danish cancer registration since 1942 fails to support the opinions of Doll and Peto stated in their report to the U.S. Congress[1] in which they prefer mortality data, because trends in incidence data "are difficult to interpret because of the difficulty of allowing for the effects of more complete registration and of more screening."

In the beginning of their paper, the authors accept morbidity data from everywhere taken at face value for ages between 35 and 64 for subtraction of low rates from high rates to determine the amount of avoidable cancer. Nevertheless, in the end they find mortality data more reliable, doubting observations by the cancer registries with the longest records, those of Connecticut and upstate New York.

Doll and Peto further argue from an assumed bias caused by difficulty in delimitation of populations at risk and by changes in definitions and in the interest of physicians reporting—supposed to affect morbidity data more than mortality rates.

Some evidence to the contrary is the following: For the years up to 1950 we found age curves for upstate New York and Copenhagen closely similar for Hodgkin's disease, leukemia, and multiple myeloma,[2] and the similarity extends to a special study in leukemia morbidity in Brooklyn[2] and Hodgkin's disease around 1970. Is it credible that a bias in the estimate of the population at risk for upstate New York would result in rates similar to those for Copenhagen where the bias does not exist?

A bias from increasing inclusion of cases previously grouped as papilloma is suggested by Doll and Peto for urinary bladder tumors, although for once they accept for this site the increasing morbidity rates as more reliable than the decreasing mortality rates for the United States. However, morbidity rates for Denmark, where papillomas have always been included, show an increase in morbidity rates of the same pattern as that seen in Connecticut, and not too different from that of upstate New York.[3-6]

The influence on morbidity rates from screening has been analyzed for breast cancer on Danish data[2] without explaining the steady increase in morbidity, whereas screening for cervical carcinoma in situ appears to have turned an increase in invasive carcinoma into a decrease, both in Copenhagen and Connecticut.[3]

In contrast, U.S. mortality data compared with hospital data for the same persons have recently shown deficits up to 43.8% as reported for rectal cancer.[7]

While there is every reason to avoid exaggeration of the obvious gradual increase of many nontobacco cancers,[8] it is still more important not to disregard this trend or the valuable contributions to cancer registration from Connecticut and upstate New York.

JOHANNES CLEMMESEN
Stockholmsgade 43
ARNE NIELSEN
Institute of Human Genetics
Tagensvej 14
Copenhagen, Denmark

SIR: Drs. Clemmesen and Nielsen appear to have misunderstood our main purpose, because most of their criticisms are not relevant to it. In our review of the causes of cancer in the United States,[1] we needed to examine the trends in U.S. cancer onset rates, and for this purpose two chief types of data (mortality and morbidity) were available, neither of which is wholly reliable.

Mortality data are in error when the underlying cause of death is miscertified, which it quite often is. Trends in the accuracy with which causes of death are certified can therefore produce artifactual trends in recorded mortality, either for cancer as a whole or for particular types of cancer.

Morbidity data derive from cancer registries that seek to record all cases of cancer that occur among the residents of a defined geographic area, such as the State of Connecticut or upstate New York. These may be in error not only when the cancer is misdiagnosed but also when a cancer that has been diagnosed is not reported. The likelihood that a life-threatening cancer will never be diagnosed is small, but the prevalence of asymptomatic, undiagnosed lumps in an old person that would be described as "cancer" and registered if they were biopsied and examined histologically can be large. For example, in a special study of the prostate glands of 70-year-old men dying of unrelated diseases, 25% were found to have cancer,[2] although the cumulative incidence of prostate cancer that is diagnosed clinically by the age of 70 is only 3%. In other words, about 90% of prostate cancer in 70-year-old men is at present undiagnosed, so any change in the intensity with which healthy, unhealthy, or dead old men are examined might produce an appreciable artifactual trend in recorded morbidity, perhaps of the order of several percent in the last decade.

Furthermore, 30 years ago about 20% of the people certified as dying of cancer in the State of Connecticut did so without generating either any medical record of cancer that was forwarded to the registry or even any such record that, knowing the patient to have died of

---

[1] Doll R, Peto R. The causes of cancer: Quantitative estimates of avoidable risks of cancer in the United States today. JNCI 1981; 66:1191-1308.

[2] Clemmesen J. Statistical studies in the aetiology of malignant neoplasms. 1. Review and results. Acta Pathol Microbiol Scand 1965 (suppl 174):271-276; 454-464.

[3] ———. Statistical studies in the aetiology of malignant neoplasms. 5. Trends and risks. Acta Pathol Microbiol Scand 1977 (suppl 261):30-37; 110-139.

[4] Eisenberger H. Cancer in Connecticut, 1953-62. Connecticut State Department of Health, 1966.

[5] Ferber B, Handy VH, Gerhardt PR, et al. Cancer in New York State exclusive of New York City, 1941-60. Bureau of Cancer Control, New York State Department of Health, 1962.

[6] Waterhouse J, Muir C, Correa P, et al, eds. Cancer incidence in five continents. Vol III. Lyon: IARC, 1976:196-199; 224-227.

[7] Percy C, Stanek E, Gloeckler L. Accuracy of cancer death certificates and its effect on cancer mortality statistics. Am J Public Health 1981; 71:242-250.

[8] A diagram (text-fig. 2) in the July 1981 issue of JNCI (vol. 67, p. 9) failed to show the latest Danish rates increasing for male lung and prostate cancers.

cancer, the registry could, subsequently trace. By the 1970's, the corresponding figure was only about 2%. To the extent to which this change was due to progressively more thorough coverage of medical records by the registry, a concomitant trend toward more complete registration of nonfatal cancers would be expected. This will produce artifactual increases in disease registration rates that may, for some types of cancer, amount in some periods to a few percent per decade.

When, in 1979–80, we began our report, we intended to estimate the trends in U.S. cancer onset rates chiefly by means of morbidity data, because the site of origin and type of a cancer are likely to be recorded more reliably by a cancer registry than on a death certificate; moreover, trends in registration rates should not be biased by trends in the effects of cancer therapy. When we came to examine the available data, however, we were reluctantly forced to the conclusion that, for the common types of cancer, the U.S. trends since 1950 would be estimated more reliably from the mortality data (among Americans <65 yr) than from the morbidity data. This was not a conclusion that we welcomed because it prevented us from examining the separate trends for certain subtypes of cancer that are not separated in the published mortality data. The evidence that forced us to this conclusion was therefore presented at some length (pp. 1270–1281) in "Appendix C" of our report. For some of the less common types of cancer, such as Hodgkin's disease, childhood leukemia, and various embryonal neoplasms, of course, improvement in therapy dominate the trends in mortality. However, for the common cancers, no such large improvements in curative treatment occurred during the third quarter of the century. Despite this, however, some quite marked divergences still exist between the trends in recorded mortality and those in recorded morbidity (see text and text-figs. C4, C5, and C6 in our paper), and we eventually concluded that these divergences must be due chiefly to artifacts in the U.S. morbidity trends rather than in the U.S. mortality trends.

Our general preference for mortality data, however, relates to the assessment of recent trends only in the United States. It does not imply that we believe that U.S. cancer mortality data for other epidemiologic purposes, or that trends in registry data in other countries are necessarily less reliable than mortality data, either for the assessment of trends or for the purpose of comparing the absolute cancer onset rates in different countries. (Indeed, in many parts of the world where mortality data are poor, cancer registry data may be far more reliable, which is why we used them in section 3 of our report.) None of the points made by Drs. Clemmesen and Nielsen bear directly on the limited question of the relative merits of U.S. mortality data and U.S. morbidity data for the assessment of U.S. trends, and certainly none outweigh the many considerations listed in "Appendix C" to our original report.

Turning to their detailed points that do have some bearing on this main issue, 1) we do not regard the trends in morbidity data as preferable for bladder neoplasms; 2) the trends in U.S. breast cancer morbidity data are far from steady; they are grossly irregular, with a 15% increase over one 3-year period (1971–4) being followed by a 5–10% decrease over the next 3 years; 3) we noted in our text the beneficial effects of screening on cervical cancer (and the generally decreasing proportion of women with a cervix); and 4) precisely because of the increasing tendency for rectal cancer to be misdiagnosed as colon cancer (which we recognized and discussed), we examined only the trends in death certification for the aggregate of rectum, colon, large intestine (part unspecified), small intestine, and intestine (part unspecified).

Subject to the various sources of uncertainty noted in our original report, we still do not accept that there is at present any good evidence for a generalized increase in U.S. cancer onset rates over and above what could plausibly be ascribed to tobacco. Thus, although we hesitate to disagree with Dr. Clemmesen, who directly or indirectly has taught us so much about the value and limitations of the data from cancer registries worldwide,[3,4] we cannot see that his arguments require us to modify our main conclusions. It is, however, a pleasure to end by acknowledging the important contribution that continues to be made both by his own and by the Connecticut and New York cancer registries.

RICHARD DOLL
RICHARD PETO
Clinical Trial Service Unit
Radcliffe Infirmary
University of Oxford
Oxford OX2 6HE, United Kingdom

---

[1] DOLL R, PETO R. The causes of cancer: Quantitative estimates of avoidable risks of cancer in the United States today. JNCI 1981; 66:1191–1308.

[2] BRESLOW N, CHAN CW, DOHM G, et al. Latent carcinoma of the prostate at autopsy in seven areas. Int J Cancer 1977; 20:680–688.

[3] DOLL R, PAYNE P, WATERHOUSE JA, eds. Cancer incidence in five continents. Vol 1. UICC technical report. Berlin: Springer-Verlag, 1966.

[4] DOLL R, MUIR CS, WATERHOUSE JA, eds. Cancer incidence in five continents. Vol 2. Geneva: IARC, WHO, 1970.

Immunity to Tumor-Associated Antigens in Vasectomized Men [1,2,3,4]

Deborah J. Anderson, [5,6] **Nancy J. Alexander,** [5,7] **David L. Fulgham,** [5] **Arthur A. Vandenbark,** [8] *and* **Denis R. Burger** [8,9]

ABSTRACT—Leukocytes from 49 vasectomized and 57 age-matched nonvasectomized men were tested in the leukocyte adherence inhibition (LAI) assay for reactivity to sperm and various 3-*M* KCl human tumor extracts. Forty-four percent of the vasectomized men and 15% of the control group were reactive to the sperm antigen preparation ($P \leq 0.03$). Similarly, a significantly higher percentage of vasectomized men responded to 3 of 5 tumor extracts tested: melanoma I (34.7 vs. 15.8%, $P \leq 0.04$), squamous cell carcinoma (48.8 vs. 26.0%, $P \leq 0.04$), and breast carcinoma (19.5 vs. 4%, $P \leq 0.04$). Thirty percent of vasectomized versus 4% of the control group responded to more than two tumor antigens ($P \leq 0.03$). The degree of LAI reactivity to each tumor extract was highly correlated with degree of antisperm LAI reactivity, and the degree of LAI responsiveness to one of the melanoma extracts was significantly correlated with antisperm antibody titer as measured by the sperm-immobilization assay. Furthermore, nonresponsive leukocytes from the control population converted to tumor antigen-responsive when incubated with sera from vasectomized LAI-positive men. Data from this study indicated that a large percentage of vasectomized men with sperm immunity were responsive to tumor-associated antigens in the LAI test and that antisperm antibodies or other serum factors played a role in this response. These results and the evidence that most tumor antigen-responsive cancer patients also have serum antibodies that reacted with sperm suggested that vasectomized men and cancer patients frequently responded to immunologically cross-reactive antigenic determinants present on both sperm and tumor cells.—JNCI 1982; 69:551–555.

Autoimmunity to spermatozoa often develops after vasectomy in experimental animals and men (*1*). Immunohistologic studies performed by us and others [for review, *see* (*1*)] have revealed that a variety of sperm antigens can elicit autoimmune responses and, furthermore, that considerable individual variation exists in the dynamics and specificity of vasectomy-induced antisperm responses (*1, 2*). Since spermatozoa appear to express antigens similar in structure to surface markers found on early embryos (*3*) and malignant tissues (*4*) and since such differentiation antigens have been demonstrated to elicit immune responses in adult syngeneic animals (*5*), we designed the present study to determine whether vasectomized men with antisperm immunity demonstrate cross-reacting immunity to tumor-associated antigens.

MATERIALS AND METHODS

The LAI assay used in this study has been described in detail elsewhere (*6*). Soluble antigens were extracted from various human tumors (2 melanomas from different individuals, a pool of 7 squamous cell carcinomas of the head and neck, a single breast ductule carcinoma, and a single neuroblastoma) or from normal human breast (control) tissue with 3 *M* KCl according to the method of Meltzer and associates (*7*). Additionally, antigens were obtained from thrice-washed human ejaculated sperm by 0.4 m*M* 1,4-dithiothreitol treatment (sonication, 3×20 sec). Heparinized blood was drawn from 49 vasectomized and 57 age-matched nonvasectomized (control) men between the ages of 28 and 59 years. Leukocytes obtained by dextran sedimentation were incubated with several concentrations of each antigen or with medium alone (incubated control), were subsequently transferred to wettable plastic tubes, and then incubated for an additional 2 hours at 37°C so that adherence could occur. Nonadherent cells were enumerated in a Coulter counter, and LAI values were calculated by the formula: Percent inhibition = {[nonadherent cells (test sample − incubated control sample)]/(total cells − nonadherent incubated control cells)} × 100.

Plasma samples were analyzed for antisperm antibodies by: *a*) the macroscopic SA test in gelatin, *b*) the complement-dependent SI assay; and *c*) indirect immunofluorescence on methanol-fixed, intact or 1,4-dithiothreitol-treated sperm (*8*).

Arming of control (nonreactive) leukocytes with sera from LAI-reactive vasectomized men was performed according to the method of Thompson et al. (*9*) to determine if serum factors (such as antisperm antibodies) were mediators of LAI reactivity in these studies.

Data were subjected to frequency analysis by contingency table testing for independence and were corrected for continuity (Yates' correction). For this statistical test, vasectomy

---

ABBREVIATIONS USED: ANOVA=analysis of variance; IF=immunofluorescence (immunofluorescent); K-S=Kolmogorov-Smirnov; LAI=leukocyte adherence inhibition; SA=sperm-agglutination (agglutinating); SI=sperm-immobilization (immobilizing); SSH=swollen sperm head.

---

[1] Received September 22, 1981; revised January 25, 1982; accepted April 16, 1982.

[2] Supported by Public Health Service (PHS) grant RR-00163 from the Division of Research Resources, National Institutes of Health; by PHS grant HD-42866 from the National Institute of Child Health and Human Developments; and by PHS interagency agreement N01CB-53954 from the Division of Cancer Biology and Diagnosis, National Cancer Institute.

[3] Publication No. 1211 from the Oregon Regional Primate Research Center.

[4] Research procedures were in accord with the ethical standards of the Human Subjects Committee, Oregon Regional Primate Research Center.

[5] Oregon Regional Primate Research Center, 505 N.W. 185th Ave., Beaverton, Oreg. 97006.

[6] *Present address:* Division of Immunogenetics, Sidney Farber Cancer Institute, Harvard Medical School, 44 Binney St., Boston, Mass. 02115.

[7] *Address reprint requests to* Dr. Alexander.

[8] Veterans Administration Hospital, 3700 S.W. U.S. Veterans Hospital Rd., Portland, Oreg. 97207.

[9] The authors acknowledge Ms. Barbara Mixon and Ms. Patsy Kimzey, Oregon Regional Primate Research Center, and Ms. Patti Finke, Ms. Sallie Olson, and Ms. Karen Williams, the Veterans Administration, for their assistance.

Table 1.—*Sperm immunity in Vx and age-matched C-men*[a]

Statistical assay		SA		SI		IF antibodies[b]								LAI to sperm extract[c]	
						IgG		IgM		IgA		SSH			
		C	Vx	C	Vx	C	Vx	C	Vx	C	Vx	C	Vx	C	Vx
n		56	47	55	49	56	49	56	48	35	27	42	41	27	34
χ^2 95%[d]	%+[e]	3.6	68	5.5	34.7	1.8	12.2	14.5	20.8	0	0	9.5	29.3	3.7	29.4
	P≤	0.001		0.001		NS		NS		NS		0.005		0.001	
χ^2 K-S[f]	%+[e]	3.6	68.1	30.9	69.4	16.1	38.8	28.6	41.7	2.9	3.7	9.5	29.3	14.8	44.1
	P≤	0.001		0.001		0.016		NS		NS		0.045		0.030	
ANOVA,[g] *P*≤		0.001		0.001		0.007		NS		NS		0.02		NS	

[a] Vx=vasectomized; C=control. NS=not significant.

[b] Sperm-specific antibodies as revealed by IF for immunoglobulins and antibodies to protamine.

[c] Optimal reactivity was obtained with a 1:400 dilution of sperm antigen.

[d] χ^2 95%=cut-off for chi-square: Titers ≥10 in the SA and IF assays and SI values (% motile sperm control/% motile sperm test) ≥5.0 were considered positive.

[e] %+=percent positive.

[f] χ^2 K-S, approach for determination of the point of maximum difference in the cumulative frequency distribution between the C-group and vasectomy group.

[g] ANOVA with the use of the Mann-Whitney *U* test.

group LAI values were considered positive for a certain antigen if they were greater than values obtained from 95% of the control population tested against the same antigen at the same concentration. (By this definition, ≈5% of the control population reacted to each antigen.) For this same analysis, we considered any titer (SA or IF) greater than or equal to 10 and SI values (percent sperm motile in control/percent motile in test) of greater than or equal to 5.0 to be positive. This analysis was termed the 95% cutoff method. A second method, the K-S two-sample test, was also used to determine the LAI cutoff value giving the maximum difference between percent responders in the control and vasectomy groups for each antigen tested (*10*). The data were also analyzed by Kendall's coefficient of rank correlation, a distribution-free statistical test, for correlation of degree of antisperm immunity (in humoral and LAI assays) to degree of antitumor reactivity and by two sample ANOVA with the Mann-Whitney *U* test (*11*).

RESULTS

Antisperm Immunity

When the 95% cutoff method was used to determine significant reactivity levels, 77.6% of the vasectomized men and only 17.5% of the controls had detectable antisperm immunity in at least one of the assays (*P*≤0.001). Of the vasectomized men, 68% had SA antibodies, 34.7% had SI antibodies, and by IF assay 12.2% had IgG and 20.8% had IgM antisperm antibodies. Antibodies to protamine, a sperm nuclear antigen, were found in 29.3% of the vasectomy group. Only 3.6 and 5.5% of the control group had detectable SA or SI antisperm antibody titers, respectively; 1.8% had IgG IF antibodies, 14.5% had IgM IF antibodies, and 9.5% had antiprotamine IF antibodies (SSH) (table 1).

When the K-S method was used for statistical evaluation, we found that 68.1% of the vasectomized men had SA antibodies, 69.4% had SI antibodies, 38.8% had IgG antibodies, 41.7% had IgM antibodies, and 29.3% had antiprotamine antibodies, compared to the controls with values of 30.9% for SI antibodies, 16.1% for IgG antibodies, 28.6% for IgM antibodies, and 9.5% for antiprotamine antibodies. By both statistical analyses the percentage of vasectomized men positive for SA, SI, and antiprotamine antisperm antibodies was significantly higher than that of the control group (table 1).

By the K-S method, 15 (44.1%) of 34 vasectomized men were significantly (*P*≤0.03) reactive to sperm antigen in the LAI test, and of these 15 men 14 (93.3%) had antisperm antibodies as detected by SA or SI tests. Only 4 (14.8%) of 27 nonvasectomized controls were LAI-reactive to sperm antigen (*P*≤0.03). Antisperm LAI reactivity significantly correlated with the presence of antisperm immobilizing antibodies (*P*≤0.05) but did not correlate with any other types of antisperm antibodies.

Analysis of variance (Mann-Whitney *U* test) generally confirmed the other statistical analyses. Vasectomized men had significantly more SA (*P*≤0.001), SI (*P*≤0.001), IgG (*P*≤0.007), and antiprotamine (*P*≤0.02) antibodies but did not have significantly more immunity to sperm as measured by LAI (table 1).

We also tested sera from cancer patients with known LAI reactivity (*6*) in the IF assay for IgG antisperm antibodies. From 32 of these cancer patients, 24 (75%) had antisperm antibodies (table 2). Compared to the sera of the control group, significantly more cancer patient sera exhibited antibodies (*P*≤0.005).

Table 2.—*Antisperm antibodies*[a] *in cancer patients with positive LAI reactivity to correponding tumor extract*

Group	No. tested	No. with antisperm antibodies (%)
Control (nonvasectomized men)[b]	14	3 (21)
Total cancer patients	32	24 (75)
Neuroblastoma	6	5 (83)
Squamous cell carcinoma	16	12 (75)
Melanoma	10	7 (70)

[a] Indirect IF with fluorescein isothiocyanate–goat antihuman IgG.

[b] Nonvasectomized men who responded in the LAI assay to at least one or more antigens.

Antitumor Immunity

By K-S evaluation, significantly more vasectomized men than control men responded to squamous cell carcinoma (48.8 vs. 26.0%, $P \leq 0.04$), breast carcinoma (19.5 vs. 4%, $P \leq 0.04$), and melanoma I extract (34.7 vs. 15.8%, $P \leq 0.04$). In contrast, reactivity of vasectomized men to the normal breast antigen (control) was not significantly different from that of the control group at any protein concentration in the range of those tested for the tumor extracts. Results of all statistical evaluations are shown in table 3.

Of the total study group, 90% responding to breast carcinoma antigen, 88.9% responding to melanoma II, 85.7% responding to neuroblastoma, 80.8% responding to melanoma I, and 72.5% responding to squamous cell carcinoma in the LAI assay had antisperm immunity detectable in LAI or antibody assays. The percent of men with antisperm immunity was 45.3%; thus the frequency of antisperm immunity in all the tumor antigen-positive groups was significantly higher than expected by chance. By Kendall's statistical test, antisperm LAI reactivity was highly correlated with reactivity to each of the tumor extracts ($P \leq 0.001$). Various types of antisperm antibody titers were also significantly correlated with LAI reactivity to certain of the tumor antigens (table 4).

Of those 54 individuals tested against all five antigens, 48% of the vasectomized men versus 33% of the controls responded to at least one of the five tumor antigens tested. Thirty-seven percent of the vasectomized men versus 15% of the control group responded to at least two different tumor antigens, and 30% of the vasectomized but only 4% of the control group responded to three or more tumor antigens ($P \leq 0.03$). Fifteen percent of the vasectomized and none of the control group responded to all five antigens. All of the vasectomized men and half of the control men that responded to at least one tumor antigen (82%) had detectable antisperm immunity in either the LAI or antibody assays; 100% of the men in both groups responding to three or more tumor antigens had detectable antisperm immunity (text-fig. 1).

Arming Study

We used sera from tumor antigen-responsive vasectomized men with antisperm antibodies and sera from control men with no demonstrable antisperm antibodies in an arming study to determine if serum factors confer LAI responsiveness to nonresponsive (control) leukocytes. The data are presented in table 5. Significant arming was obtained when squamous cell carcinoma extract was used as the test antigen ($P \leq 0.01$) and when the data for all antigens were pooled ($P \leq 0.005$).

TABLE 3.—*Reactivity to tumor extracts of C-group and Vx group*[a]

Statistical assay		Melanoma I		Melanoma II		Squamous cell carcinoma		Breast carcinoma		Neuroblastoma	
		C	Vx	C	Vx	C	Vx	C	Vx	C	Vx
n		57	49	34	35	50	41	50	41	52	41
χ^2 95%[b]	%+[c]	5.3	16.3	5.9	20.0	4.0	22.0	4.0	19.5	7.7	14.6
	$P \leq$	NS		NS		0.02		0.04		NS	
χ^2 K-S[d]	%+[c]	15.8	34.7	5.9	20.0	26.0	48.8	4.0	19.5	3.6	22.0
	$P \leq$	0.04		NS		0.04		0.04		NS	
ANOVA,[e]	$P \leq$	0.02		NS		NS		NS		NS	

[a] C=control; Vx=vasectomized. Antigen dilutions giving optimum LAI reactivity were: melanoma I, 1:320; melanoma II, 1:200; squamous cell carcinoma, 1:200; breast carcinoma, 1:40; neuroblastoma, 1:100. NS=not significant.

[b] χ^2 95%, cut-off for chi-square: Titers ≥10 in the SA and IF assays and SI values ≥5.0 were considered positive.

[c] %+=percent positive.

[d] χ^2 K-S, approach to determine the point of maximum difference in the cumulative frequency distribution between control and vasectomy groups.

[e] ANOVA with the use of the Mann-Whitney *U* test.

TABLE 4.—*Statistical correlations by Kendall's coefficient of rank order correlation test*

Group	LAI reactivity to extracts[a]					
	Sperm antigen	Melanoma I	Melanoma II	Squamous cell carcinoma	Breast carcinoma	Neuroblastoma
LAI response to sperm antigen		$P \leq 0.01$	$P \leq 0.01$	$P \leq 0.01$	$P \leq 0.01$	$P \leq 0.01$
Antisperm antibodies revealed by:						
SA	NS	NS	NS	NS	NS	NS
SI	$P \leq 0.05$	$P \leq 0.05$	NS	NS	NS	NS
IF for IgG	NS	NS	NS	NS	NS	NS
IF for IgM	NS	NS	NS	NS	$P \leq 0.01$	$P \leq 0.01$
IF for IgA	NS	NS	NS	NS	NS	NS
IF for SSH[b]	NS	NS	NS	NS	NS	NS

[a] NS=not significant.

[b] Protamine.

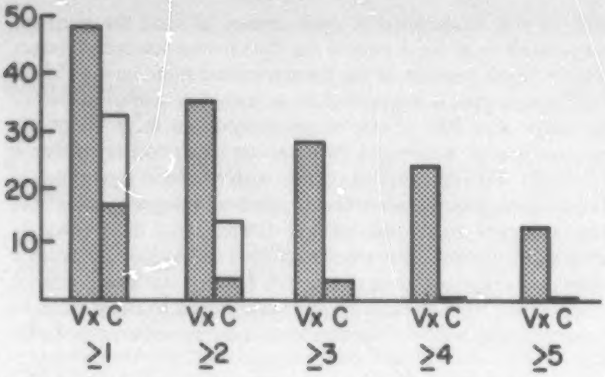

TEXT-FIGURE 1.—Percent of vasectomized (Vx) and control (C) men responding to tumor antigens in the LAI assay. Leukocytes were tested for reactivity against five different human tumor antigen preparations: melanoma I, melanoma II, squamous cell carcinoma, breast carcinoma, and neuroblastoma. *Ordinate* shows percent responders and *abscissa* represents Vx and C-groups that responded from one to all five tumor antigens. *Stippled bars*, antisperm immunity.

TABLE 5.—*Donor-specific serum transfer of LAI responses*

Antigen tested	n[a]	Donor		Recipient		Transfer P[b]
		Reaction	Percent LAI±SD	Reaction	Percent LAI±SD	
Squamous cell carcinoma	8	+	68±28	+	45±12	0.01
	3	+	41±10	–	18±3	
	1	–	0	+	33	
	9	–	9±8	–	19±8	
Neuroblastoma	1	+	28	+	24	NS
	5	+	53±26	–	2±4	
	2	–	0	+	30±5	
	14	–	1±1	–	10±6	
Melanoma	6	+	62±31	+	34±16	NS
	13	+	47±19	–	7±7	
	0	–	–	+	–	
	13	–	7±7	–	8±6	
Sperm	9	+	63±32	+	29±7	NS
	7	+	60±28	–	8±7	
	1	–	0	+	22	
	1	–	2	–	0	
All antigens	24	+	63±30	+	35±13	0.005
	28	+	51±22	–	8±7	
	4	–	0	+	29±5	
	37	–	5±7	–	11±8	

[a] No. of donor sera tested in arming study.

[b] χ^2 analysis for transfer of reactivity. NS=not significant.

DISCUSSION

The LAI assay, originally described by Halliday and Miller (*12*), has proved to be a sensitive in vitro method for detection of specific immunity to a variety of antigens in both experimental animals and man (*13*). Several clinical research groups currently use the LAI assay to monitor specific reactivity to tumor-associated antigens in cancer patients (*6*), and this assay has also been used to detect antisperm immunity in animals and man (*14*). At least two separate mechanisms appear to underlie the LAI response: *a*) adherence inhibition mediated by a soluble lymphokine-like factor (LAI factor) released by sensitized lymphocytes upon contact with specific antigen (*15*) and *b*) nonadherence of monocytes and possibly other leukocytes induced by the binding of antigen to cytophilic antibody on the cell surface (*9*). Our ability to arm nonresponder leukocytes with sera from tumor-responsive vasectomized men suggests that one mechanism in our model is cytophilic antibody-dependent. Absorption–elution studies with serum arming factors could provide an approach for characterization of the antigens involved in this response.

The various forms and large amount of data assimilated in this study made thorough statistical analysis crucial. We used a number of specialized statistical analyses: The K-S cutoff method, which is nonparametric, was perhaps the most appropriate and in general agreed with the more standard tests for comparison of two populations (χ^2 analysis with 95% cut-off, analysis of variance). These tests revealed that vasectomized men had significantly higher antisperm antibody titers than did the controls in most antibody assays and that significantly more vasectomized men responded to the melanoma I, squamous cell carcinoma, and breast carcinoma extracts. The Kendall's rank order test is a powerful statistical tool that enabled us to make the statement that degree of reactivity to the melanoma extract was positively correlated with antisperm antibody level (SI test).

Embryonic antigens are known to be reexpressed on some malignant tissues, and several of these have been biochemically characterized (*16, 17*). Sperm express differentiation antigens that are found on early embryos (although these have not been well characterized), and sperm antigens can also be found on malignant tissues (*18*). The biologic function of these cell surface structures is not known. Vasectomized men did not respond to the control antigen (normal breast tissue) used in this study, but a larger panel of both normal and malignant tissues should be used in future tests to show more conclusively a tumor association and identify the types of tumors expressing these antigens.

Our preliminary observation that many cancer patients have high titers of antisperm antibodies is interesting in the context of this report because it further reports the hypothesis that sperm and malignant cells express immunologically cross-reactive antigens that readily stimulate a host autoimmune response. Serologic studies including absorption of antisperm reactivity in cancer sera with various types of tumor tissue should reveal the distribution of these antigens.

There is accumulating evidence that immunity to tumor-associated oncofetal antigens can affect the subsequent development of tumors (*19, 20*). However, although LAI reactivity to tumor extracts appears to arise from exposure to specific tumor antigens (i.e., in cancer patients) (*6*), the expected inverse correlation between LAI reactivity and tumor incidence or tumor growth rate has yet to be established. Nonetheless, from the data presented here, a tempting speculation is that the development of neoplastic disease in some vasectomized men with antisperm immunity could be affected by a cross-reacting immune sensitivity to tumor-associated antigens.

REFERENCES

(*1*) ALEXANDER NJ, ANDERSON DJ. Vasectomy: Consequences of autoimmunity to sperm antigens. Fertil Steril 1979; 32:253–260.

(*2*) TUNG KS. Human sperm antigens and antisperm antibodies. I. Studies on vasectomy patients. Clin Exp Immunol 1975; 20:93–104.

(*3*) Menge AC, Fleming CH. Detection of sperm antigens on mouse ova and early embryos. Dev Biol 1978; 63:111–117.

(*4*) Fellous M, Gachelin G, Buc-Caron M, Dubois P, Jacob F. Similar location of an early embryonic antigen on mouse and human spermatozoa. Dev Biol 1974; 41:331–337.

(*5*) Coggin JH, Ambrose KR, Anderson NG. Fetal antigen capable of inducing transplantation immunity against SV40 hamster tumor cells. J Immunol 1970; 105:524–526.

(*6*) Burger DR, Vandenbark AA, Finke P, et al. Assessment of reactivity to tumor extracts by leukocyte adherence inhibition and dermal testing. J Natl Cancer Inst 1977; 59:317–323.

(*7*) Meltzer MS, Leonard EJ, Rapp HJ, Borsos T. Tumor-specific antigen solubilized by hypertonic potassium chloride. J Natl Cancer Inst 1971; 47:703–709.

(*8*) Rose NR, Hjort T, Rümke P, Harper MJ, Vyazov O. Techniques for detection of iso- and autoantibodies to human spermatozoa. Clin Exp Immunol 1976; 23:175–199.

(*9*) Thompson DM, Grosser N. Immunological mechanisms of tube leukocyte adherence inhibition. Cancer Res 1979; 39:576–581.

(*10*) Siegel S. Nonparametric statistics for the behavioral sciences. New York: McGraw-Hill, 1956.

(*11*) Sokal R, Rohlf FJ. Biometry: The principles and practice of statistics in biologic research. San Francisco: Freedman, 1969:776.

(*12*) Halliday WJ, Miller S. Leukocyte adherence inhibition: A simple test for cell-mediated tumour immunity and serum blocking factors. Int J Cancer 1972; 9:477–483.

(*13*) Burger DR. Leukocyte adherence inhibition. In: Herberman RB, McIntire KB, eds. Immunodiagnosis of cancer. New York: Marcel-Dekker, 1979:1124–1145.

(*14*) Dorsman BG, Tumboh-Oeri AG, Roberts TK. Detection of cell-mediated immunity to spermatozoa in mice and man by the leucocyte adherence-inhibition test. J Reprod Fertil 1978; 53:277–283.

(*15*) Powell A, Sloss AM, Smith RN, Murrell H. Antigenic specificity and cellular mechanisms in leukocyte adherence inhibition analysis of immunity to simple proteins and hapten-protein conjugates. Cancer Res 1979; 39:570–575.

(*16*) Evans DL, Parker DV, Frank MK. Biochemical and physical characterizations of tumor-associated fetal antigens. Cancer Res 1979; 39:2006–2015.

(*17*) Chandrasekaran K, McFarland VW, Simmons DT, Dziadek M, Gurney EG, Mora PT. Quantitation and characterization of a species-specific and embryo stage-dependent 55-kilodalton phosphoprotein also present in cells transformed by simian virus 40. Proc Natl Acad Sci USA 1981; 78:6953–6957.

(*18*) Goldberg EH, Tokuda S. Evidence for related antigens on sperm, tumor, and fetal cells in the mouse. Transplant Proc 1977; 9:1363–1365.

(*19*) Baldwin RW, Embleton, JJ, Price MR, Vose BM. Embryonic antigen expression on experimental rat tumors. Transplant Rev 1974; 20:77–99.

(*20*) Chism SE, Wallis S, Burton RC, Warner NL. Analysis of murine oncofetal antigens as tumor-associated transplantation antigens. J Immunol 1976; 117:1870–1877.

blank page

Unscheduled DNA Synthesis in Human Oral Mucosa Treated With Chemical Carcinogens in Short-Term Organ Culture[1,2]

Fumio Ide,[3,4] Takatoshi Ishikawa,[3,5] Minoru Takagi,[6] Shinichiro Umemura,[4] *and* Shozo Takayama[3,7]

ABSTRACT—Unscheduled DNA synthesis (UDS) was investigated by autoradiography in human oral mucosa treated with 10 representative chemical carcinogens. Small sections of gingiva in short-term organ culture were exposed for 2 hours to chemical carcinogens plus [*methyl*-^{3}H]thymidine. Significant numbers of silver grains, indicating UDS, were detected over the nuclei of both epithelial cells and fibroblasts. All ultimate or proximate carcinogens tested induced UDS. Of five procarcinogens tested, only benzo[*a*]pyrene (BP) did not induce UDS, but the more activated metabolite of BP, (±)-*trans*-7β-8α-dihydroxy-9α,10α-epoxy-7,8,9,10-tetrahydrobenzo[*a*]pyrene (BPDE I), was very effective in inducing UDS. Ultimate or proximate carcinogens induced higher levels of UDS than did procarcinogens. All the carcinogens that induced UDS showed clear dose-dependent effects. UDS levels were twofold to fivefold higher in the epithelial cells than in the fibroblasts, regardless of the type of carcinogen tested. Comparisons of the levels of UDS induced by 4-(hydroxyamino)quinoline 1-oxide, methyl methanesulfonate, or BPDE I did not reveal any significant differences. These findings indicate that human gingival epithelial UDS assay should be useful for short-term detection of environmental carcinogens that induce cancer in human oral mucosa.—JNCI 1982; 69:557–563.

Because most chemical carcinogens in their ultimate reactive form are electrophils that react with DNA, they may induce DNA repair (*1*). Thus measurement of DNA repair could be a reliable method for determination of their carcinogenic potential (*2, 3*). Inasmuch as DNA damage and repair synthesis in various human tissues obviously cannot be measured by in vivo administration of chemicals, as has been done in experimental animals, an in vitro model must be developed that can be applied to human tissue. Several studies have shown that UDS in cultured human cells is a suitable marker for use in in vitro bioassay of carcinogens (*4–11*).

The oral cavity probably is the region of the body exposed to the highest levels of naturally occurring and synthetic chemical carcinogens present in the food and atmosphere, but no attempts have been made to assay UDS induced by carcinogens in oral tissues. We previously showed that UDS was induced in short-term organ culture of the oral tissues of adult rats and hamster embryos after application of two carcinogens (*12*). The organ culture system is more similar to the in vivo state than are cell culture systems, and it may eventually prove valuable for identification of possible carcinogens and of critical target populations of cells within a tissue.

This paper presents our findings on the abilities of 10 representative chemical carcinogens to induce UDS in human gingiva, on the differences between DNA repair in epithelial cells and fibroblasts, and on the individual differences in UDS in explants from several patients.

MATERIALS AND METHODS

Chemicals.—The following chemicals were purchased from the sources indicated: MMS, BP, DENA, and DMN from Tokyo Kasei Co., Tokyo, Japan; MNU, 4HAQO, and 4NQO from Iwai Chemical Co., Tokyo; MNNG from Wako Pure Chemical Co., Tokyo; mitomycin C from Kyowa Hakko Kogyo Co., Ltd., Tokyo; and [*methyl*-^{3}H]dThd (sp act, 60 Ci/mmol) from New England Nuclear Corp., Boston, Mass. The purities of these chemicals were as specified by the manufacturers. The following chemicals were gifts: N-OH-2-FAA from Dr. K. Umezawa, University of Tokyo, Tokyo; BPDE I and BPE from IIT Research Institute, Chicago, Ill., under the auspices of Dr. D. Longfellow, the National Cancer Institute, Bethesda, Md.

Induction of UDS in human oral mucosa.—Human gingivae were obtained from 20 gingivectomized patients at the Department of Periodontology, Faculty of Dentistry, Tokyo Medical and Dental University. Healthy portions of tissue were cut from the specimens. These specimens were brought within 2 hours to our laboratory in L-15 (Grand Island Biological Co., Grand Island, N. Y.) containing streptomycin (500 μg/ml) and penicillin (500 IU/ml) at 4°C. An

---

ABBREVIATIONS USED: BP=benzo[*a*]pyrene; BPDE I=(±)-*trans*-7β-8α-dihydroxy-9α,10α-epoxy-7,8,9,10-tetrahydrobenzo[*a*]pyrene; BPE=(±)-4,5-dihydrobenzo[*a*]pyrene-4,5-epoxide; DENA=diethylnitrosamine; DMN=dimethylnitrosamine; DMSO=dimethyl sulfoxide; dThd=thymidine; [^{3}H]-dThd=tritiated dThd; H & E=hematoxylin and eosin; 4HAQO=4-(hydroxyamino)quinoline 1-oxide; L-15=Leibovitz's L-15 medium; MMS=methyl methanesulfonate; MNNG=*N*-methyl-*N'*-nitro-*N*-nitrosoguanidine; MNU=*N*-methyl-*N*-nitrosourea; N-OH-2-FAA=*N*-hydroxy-*N*-2-fluorenylacetamide; 4NQO=4-nitroquinoline 1-oxide; UDS=unscheduled DNA synthesis.

---

[1] Received January 30, 1981; revised March 26, 1982; accepted April 21, 1982.

[2] Supported by a Grant-in-Aid for cancer research from the Ministry of Education, Science and Culture, Japan; and by grants from the Society for the Promotion of Cancer Research, Japan; from the Japan Tobacco and Salt Public Corporation; and from the Princess Takamatsu Cancer Research Fund, Japan.

[3] Department of Experimental Pathology, Cancer Institute, 1-37-1 Kami-Ikebukuro, Toshima-ku, Tokyo 170, Japan.

[4] Department of Pathology, Nihon University School of Dentistry, 1-8 Surugadai Kanda, Chiyoda-ku, Tokyo 101, Japan.

[5] *Address reprint requests to* Dr. Ishikawa.

[6] Department of Oral Pathology, Faculty of Dentistry, Tokyo Medical and Dental University, 1-5-45, Yushima, Bunkyo-ku,Tokyo 113, Japan.

[7] We express our gratitude to the Cancer Research Program, Division of Cancer Cause and Prevention, National Cancer Institute, Bethesda, Md., for providing us with ultimate metabolites of benzo[*a*]pyrene. We also thank Mr. Y. Matsui and Ms. K. Kawana for their devoted assistance.

best copy available

outline of the procedure for organ culture was reported in (*12*); specific details were as follows:

All specimens were cut with a sharp razor into pieces of about 1 mm^3 under a dissecting microscope. Small pieces (5 or 6) were then incubated together for 2 hours at 37°C in an organ culture dish in 2 ml of L-15 containing [*methyl*-^{3}H]dThd (10 μCi/ml) and a carcinogen. Organ culture dishes were maintained in a chamber in an atmosphere of 50% N_2 and 50% O_2. Water-soluble carcinogens were dissolved directly in L-15 with stirring. Other carcinogens were dissolved in DMSO and then diluted with L-15 (highest final concentration of DMSO, 1%). All carcinogens were tested at three different doses. Carcinogen dose ranges were determined on the basis of previous reports (*6, 9, 12–14*). Each carcinogen was tested in tissue from a single patient, partly because of the scarcity of the material. Controls were included for all experiments; i.e., specimens were in either L-15 containing [*methyl*-^{3}H]dThd or in L-15 containing [*methyl*-^{3}H]dThd plus DMSO.

After incubation, the specimens were washed several times with cold L-15 and fixed with 10% neutral Formalin. All the specimens in a dish were embedded together in paraffin, with the same orientation relative to the surface of the epithelium as determined under a dissecting microscope. The usual histologic sections of 4- to 5-μm thickness were cut and then were treated with 3% perchloric acid for 45 minutes, with three changes of solution at 4°C for removal of the acid-soluble fraction. Sections were dip covered with NR-M_2 emulsion (Konishiroku Photo Co., Tokyo) and placed in the dark for 5 weeks at 4°C. Autoradiographs were developed, fixed, and then lightly stained with H & E.

Grain counting, under a 100× objective lens of a Nikon microscope, was done on 300–400 nuclei of randomly selected cells from the spinous layer of the epithelium of each explant (*12*). Counts were also made on subepithelial fibroblasts for comparison. Background numbers of grains were counted in the same way.

Estimation of the dThd pool.—The possibility of a difference between the dThd pools of epithelial cells and fibroblasts was studied by means of control autoradiographs. With autoradiographic procedures as described for the UDS study, but with a shorter exposure period (3 days), the numbers of silver grains on S-phase cells could readily be counted. Grains were counted on 50 epithelial cells and 50 fibroblasts. Because the numbers of S-phase cells were relatively few, grain counts were collectively made on tissues obtained from 5 individuals.

Comparisons of UDS.—Comparisons were made of UDS levels in tissues from 4 patients who had been simultaneously treated with the most effective UDS-inducing dose of 4HAQO or MMS. Similarly, tissues were examined from 3 other patients who had been exposed to BPDE I or BPE.

RESULTS

Induction of UDS in human oral mucosa.—Of the 10 carcinogens tested, 5 were ultimate or proximate carcinogens (MMS, MNU, MNNG, 4HAQO, and N-OH-2-FAA) and 5 were procarcinogens that require metabolic activation (BP, DENA, DMN, 4NQO, and mitomycin C). After treatment with each of the carcinogens (except BP), UDS could be clearly seen as silver grains on the nuclei of gingival epithelial cells and fibroblasts (figs. 1–3). The amount of UDS was greater near the edge than in the center of the specimens, probably because of the limited diffusion of [^{3}H]dThd and the carcinogen, as mentioned by Cleaver (*15*). However, the numbers of grains were constant in a zone of about 200 μm from the lateral edge of all explants. Thus we counted grains on the nuclei of randomly selected cells from the spinous layer within this zone, which contained approximately 1,000 cells. In the present study, UDS grains were clearly distinguished from grains of S-phase cells, inasmuch as S-phase cells were heavily labeled and were mainly located in the basal layer of the epithelium. Only background numbers of grains (0.2–0.4 grain/cell) were seen on the nuclei of control specimens (fig. 4). Mean values with standard deviations of the mean for the grain count on each explant are given in table 1.

All of the ultimate or proximate carcinogens tested induced UDS at various levels. Of the procarcinogens, DENA, DMN, 4NQO, and mitomycin C induced UDS, but BP did not.

As shown in table 1, the highest average grain number in carcinogen-treated groups was about 50 times that in the

TABLE 1.—*UDS in human oral mucosa after exposure to carcinogens*

Carcinogen	Dose, *M*[a]	Grains/cell[b]	
		Epithelial cell	Fibroblast
MMS	10^{-2}	10.1±1.0	4.5±0.7
	10^{-3}	6.8±0.8	4.6±0.7
	10^{-4}	2.1±0.2	1.9±0.3
MNNG	10^{-3}	7.0±0.5	3.0±0.2
	10^{-4}	3.6±0.6	1.8±0.4
	10^{-5}	1.3±0.3	0.7±0.3
MNU	10^{-2}	8.5±0.3	3.2±0.2
	10^{-3}	2.8±0.4	1.9±0.4
	10^{-4}	1.1±0.3	0.8±0.2
4HAQO	10^{-5}	10.2±0.7	5.1±0.3
	10^{-6}	6.7±0.4	4.5±0.5
	10^{-7}	2.0±0.3	2.1±0.6
N-OH-2-FAA	10^{-4}	6.3±0.5	2.0±0.2
	10^{-5}	3.0±0.3	1.2±0.1
	10^{-6}	1.1±0.1	0.7±0.1
DMN	10^{-2}	5.8±0.4	1.6±0.1
	10^{-3}	6.3±0.4	0.9±0.1
	10^{-4}	2.1±0.4	0.3±0.1
DENA	10^{-2}	4.4±0.7	1.8±0.4
	10^{-3}	6.0±0.5	1.2±0.1
	10^{-4}	2.0±0.3	0.8±0.2
4NQO	10^{-4}	6.7±0.4	3.2±0.6
	10^{-5}	7.1±0.3	3.7±0.7
	10^{-6}	1.7±0.2	2.0±0.3
Mitomycin C	0.2[c]	3.4±0.3	1.7±0.1
	0.02[c]	1.8±0.3	0.8±0.3
	0.002[c]	0.9±0.1	0.3±0.1
BP	10^{-5}	0.3±0.1	0.3±0.2
	10^{-6}	0.3±0.1	0.2±0.2
	10^{-7}	0.3±0.3	0.2±0.1
Controls	0	0.3±0.9	0.2±0.4
Controls (DMSO)[d]	0	0.4±0.6	0.4±0.5

[a] *M* unless otherwise indicated.

[b] Values are means ± SD for each explant from 1 patient.

[c] IU/ml.

[d] Final concentration, 1%.

TABLE 2.—*Comparison of grains on S-phase cells*

Cell	Grains/cell[a]
Epithelial	12.1±0.4
Fibroblast	11.7±0.9

[a] Values are means ± SD for 50 S-phase epithelial cells and 50 S-phase fibroblasts. S-phase grains were collectively counted on 50 epithelial cells and 50 fibroblasts from several tissues obtained from 5 individuals. Autoradiographs were exposed for a short time (3 days).

TABLE 3.—*Comparison of UDS in human oral mucosa from 4 patients*

Patient	Cell	Grains/cell[a]	
		4HAQO, 10^{-5} *M*	MMS, 10^{-2} *M*
A	Epithelial	8.9±0.4	9.4±0.6
	Fibroblast	3.8±0.9	3.6±0.8
B	Epithelial	9.0±0.9	9.6±0.6
	Fibroblast	3.4±0.8	2.6±0.7
C	Epithelial	8.4±0.4	11.0±0.7
	Fibroblast	3.1±0.8	3.2±0.9
D	Epithelial	10.0±0.8	10.6±0.6
	Fibroblast	3.6±0.9	3.1±0.8

[a] Values are means ± SD for each explant from 1 patient.

TABLE 4.—*USD in human oral mucosa exposed to BPDE I or BPE*

Patient	Cell	Grains/cell[a]	
		BPDE I, 10^{-5} *M*	BPE, 10^{-5} *M*
A	Epithelial	9.4±0.5	0.4±0.5
	Fibroblast	5.0±0.4	0.4±0.7
B	Epithelial	9.4±0.7	0.3±0.5
	Fibroblast	3.5±0.9	0.3±0.7
C	Epithelial	10.0±0.6	0.4±0.6
	Fibroblast	2.7±0.8	0.2±0.9

[a] Values are means ± SD for each explant from 1 patient.

control group. All of the carcinogens that induce UDS showed clear dose-dependent effects. Ultimate or proximate carcinogens induced higher levels of UDS than procarcinogens. UDS levels were twofold to fivefold higher in the epithelial cells than in the fibroblasts, regardless of the type of carcinogen tested.

Estimation of the dThd pool. The mean grain numbers formed on S-phase nuclei of both epithelial cells and fibroblasts are given in table 2. No marked differences were observed in the average number of grains on the S-phase nuclei of epithelial cells and fibroblasts.

Comparisons of UDS.—Comparisons of UDS in human oral mucosae from 4 patients are shown in table 3. The amounts of UDS induced by 4HAQO or MMS were not significantly different in these tissues. Similar results were obtained with BPDE I (fig. 5). However, the K-region epoxide BPE gave a negative result within 2 hours (table 4).

DISCUSSION

Apparently, most human cancers have an environmental etiology (*16, 17*). Thus it is important to detect environmental carcinogens to which humans are exposed and to remove these carcinogens from the environment. The best evidence for the carcinogenic potential of a chemical obviously is cancer induction in experimental animals, but tests on animals are expensive and time consuming. The feasibility of detection of carcinogenic chemicals by the induction of UDS being measured in various cultured cells has been explored (*3*). Many bioassay methods have been developed in which human fibroblasts are used (*6*), but these methods provide only limited information inasmuch as most human cancer of clinical significance appears to originate in epithelial cells rather than in fibroblasts (*8, 10, 18*). The ideal cells for use in development of a practical and reliable in vitro UDS assay are those from a readily accessible, differentiated epithelium—cells that are able to metabolize a large variety of procarcinogens and that have high activity in excision repair pathways (*8*).

Several studies on in vitro cultivation of human oral keratinocytes have been reported (*19–22*). However, so far as we know, no reports have appeared with regard to UDS assay of these cells. Recently, Lake et al. (*8*) demonstrated, by scintillation counting, the chemical induction of UDS in human foreskin epithelial cell cultures. These investigators mentioned that they first attempted to use autoradiography for detection of UDS in organotypic primary skin cultures, but because the epidermal keratinocytes are multilayered and are at various stages of differentiation, Lake and his colleagues observed significant variation in grain counts due to self absorption of [^{3}H]dThd. The results obtained in our studies indicate that autoradiography permits quantitative analysis of UDS in both epithelial cells and fibroblasts in architecturally and functionally intact human gingival tissue in organ culture.

As indicated under "Results," DENA and DMN induced UDS. These nitrosamines are present in the atmosphere of certain urban areas (*23*), in tobacco smoke (*24*), and in food (*25*), and may be formed in vivo by the reaction of secondary and tertiary amines with nitrites under acidic conditions (*26*). Although direct evidence is lacking, these findings suggest that these nitrosamines may induce cancer in human oral mucosa. However, BP, one of several important carcinogenic hydrocarbons found in the environment (*27*), did not induce UDS. The metabolism of BP by human skin epithelial cells has been studied in detail in organ culture (*28, 29*) and in cell culture (*30–32*). We believe that these observations indicate that BP may require a long time for metabolic activation and may not bind covalently to DNA within 2 hours, inasmuch as the more activated metabolite of BP, BPDE I, induced UDS in our present study.

Mitomycin C, which is widely used as a cancer chemotherapeutic agent, induced UDS in our system. This chemical was shown to induce interstrand cross-links in DNA, and these DNA-DNA cross-links may be repaired by both base and nucleotide excision repair pathways (*33*).

In the absence of direct information on biochemical measurement of DNA adducts, our autoradiographic method for studying DNA repair is speculative. Nevertheless, the results obtained in our studies provided evidence that epithelial cells are more proficient in DNA excision repair, as measured by UDS, than are fibroblasts, regardless of the type of carcinogen tested. The dThd pool, estimated from the intensities of S-phase cells, revealed little difference in epithelial cells and fibroblasts. Thus, we believe that the

UDS value would reflect DNA repair efficiency. Recently, Taichman and Setlow (*34*) reported that the extent of UV light-induced repair was similar in cultured human epidermal cells and dermal fibroblasts. Whether this difference reflects differences in experimental approach or in types of DNA damaging agents is not yet clear. Remember, however, that several studies have shown that the metabolism of carcinogenic hydrocarbons is higher in human skin epithelial cells than in fibroblasts (*8, 29, 30, 35*).

Much evidence exists for a prophylactic role of DNA excision repair in chemical carcinogenesis (*36, 37*). Other factors, such as the percentage of cells undergoing the cell cycle and the chance of exposure to carcinogens, may contribute to carcinogenesis (*38, 39*). The apparent lack of cell division in fibroblasts in vivo could render them less susceptible than dividing epithelial cells to the carcinogenic effects of chemicals, even if equal amounts of carcinogen are bound to the cell's DNA (*31*). These findings suggest that the role of excision repair in rapidly renewed epithelial cells is important in preventing carcinogenic initiation. Note that carcinogen-induced DNA damage, if not repaired before cell proliferation, is intimately related to the initiation-fixation process of carcinogenesis (*40, 41*).

The use of human tissues should be helpful in providing a link between studies on experimental animal and human cancers, for assessment of the validity of extrapolating carcinogenicity data on experimental animals to human beings.

REFERENCES

(*1*) Miller EC, Miller JA. The metabolism of chemical carcinogens to reactive electrophils and their possible mechanisms of action in carcinogenesis. In: Searle CE, ed. Chemical carcinogenesis. Washington, D.C.: Am Chem Soc, 1976:737–762.

(*2*) Bridges BA. Short term screening tests for carcinogens. Nature 1976; 261:195–200.

(*3*) Hollstein M, McCann J, Angelosanto FA, Nicholas WW. Short-term tests for carcinogens and mutagens. Mutat Res 1979; 65:160–163.

(*4*) Lieberman MW, Baney RN, Lee RE, Sell S, Farber E. Studies on DNA repair in human lymphocytes treated with proximate carcinogens and alkylating agents. Cancer Res 1971; 31:1297–1306.

(*5*) Trosko JE, Yager JD. A sensitive method to measure physical and chemical carcinogen-induced "unscheduled DNA synthesis" in rapidly dividing eukaryotic cells. Exp Cell Res 1974; 88:47–55.

(*6*) San RH, Stich HF. DNA repair synthesis of cultured human cells as a rapid bioassay for chemical carcinogens. Int J Cancer 1975; 16:284–291.

(*7*) Painter RB. Rapid test to detect agents that damage human DNA. Nature 1977; 265:650–651.

(*8*) Lake RS, Kropko ML, Pezzutti MR, Schoemaker RH, Igel HJ. Chemical induction of unscheduled DNA synthesis in human skin epithelial cell cultures. Cancer Res 1978; 38:2091–2098.

(*9*) Martin CN, McDermid AC, Garner RC. Testing of known carcinogens and noncarcinogens for their ability to induce unscheduled DNA synthesis in HeLa cells. Cancer Res 1978; 38:2621–2627.

(*10*) Freeman HJ, San RH. Use of unscheduled DNA synthesis in freshly isolated human intestinal mucosal cells for carcinogen detection. Cancer Res 1980; 40:3155–3157.

(*11*) Lake RS, Kropko ML, McLachlan S, Pezzutti MR, Schoemaker RH, Igel HJ. Chemical carcinogen induction of DNA-repair synthesis in human peripheral blood monocytes. Mutat Res 1980; 74:357–377.

(*12*) Ide F, Ishikawa T, Takayama S, Umemura S. Autoradiographic demonstration of unscheduled DNA synthesis in oral tissues treated with chemical carcinogens in short-term organ culture. J Oral Pathol 1981; 10:113–123.

(*13*) Ishikawa T, Takayama S, Ide F. Autoradiographic demonstration of DNA repair synthesis in rat tracheal epithelium treated with chemical carcinogens in vitro. Cancer Res 1980; 40:2898–2903.

(*14*) Ide F, Ishikawa T, Takayama S. Detection of chemical carcinogens by assay of unscheduled DNA synthesis in rat tracheal epithelium in short-term organ culture. J Cancer Res Clin Oncol 1981; 102:115–126.

(*15*) Cleaver JE. Methods for studying repair of DNA damage by physical and chemical carcinogens. Methods Cancer Res 1975; 11:123–165.

(*16*) Higginson J. The role of the pathologist in environmental medicine and public health. Am J Pathol 1977; 86:459–484.

(*17*) Higginson J, Muir CS. *Guest Editorial*: Environmental carcinogenesis: Misconceptions and limitations to cancer control. JNCI 1979; 63:1291–1298.

(*18*) Harris CC, Autrup H, Stoner GD, Trump BF. Carcinogenesis studies in human respiratory epithelium: An experimental model system. In: Harris CC, ed. Pathogenesis and therapy of lung cancer. New York: Marcel Dekker, 1978:559–607.

(*19*) Flaxman BA, Lutzner MA, Van Scott EJ. Cell maturation and tissue organization in epithelial outgrowth from skin and buccal mucosa in vitro. J Invest Dermatol 1967; 49:322–329.

(*20*) Mlinek A, Buchner A. In vitro cultivation of adult human gingiva. I. Primary epithelial outgrowth from gingival explants. J Periodont Res 1975; 10:73–78.

(*21*) Birkendal-Hansen H, Moe K, Dabelsteen E, Rheinholdt J. Propagation of a keratinizing human gingival epithelial cell line in vitro. J Dent Res 1978;57A.

(*22*) Taichman L, Reilly S, Garant PR. In-vitro cultivation of human oral keratinocytes. Arch Oral Biol 1979; 24:335–341.

(*23*) Fine DH, Rounbehler DP, Belcher NM, Epstein SS. N-Nitroso compounds: Detection in ambient air. Science 1976; 192:1328–1330.

(*24*) McCormick A, Nicholson MJ, Baylisma MA, Underwood JC. Nitrosamines in cigarette smoke condensate. Nature 1973; 244:237–238.

(*25*) Eisenbrand G, Spiegelhalder B, Janzowski C, Kann J, Preussmann R. Volatile and nonvolatile N-nitroso compounds in food and other environmental media. In: Walker EA, Griciute L, Castegnaro M, Lyle RE, Davis W, eds. Environmental aspects of N-nitroso compounds. Lyon: IARC, 1978:311–324.

(*26*) Tannenbaum SR. Endogeneous formation of nitrite and N-nitroso compounds. In: Miller EC, Miller JA, Hirono I, Sugimura T, Takayama S, eds. Naturally occurring carcinogens—mutagens and modulators of carcinogenesis. Proceedings of the 9th International Symposium of the Princess Takamatsu Cancer Research Fund, Tokyo, 1979. Baltimore: Univ Park Press, 1979:211–220.

(*27*) Committee on Biological Effects of Atmospheric Pollutants. Particulate polycyclic organic matter. Washington, D.C.: National Acad Sci, 1972:1–355.

(*28*) Levin W, Conney A, Alvares A, Merkatz I, Kappas A. Induction of benzo(*a*)pyrene hydroxylase in human skin. Science 1972; 176:419–420.

(*29*) Fox CH, Selkirk JK, Price FM, Croy RG, Sanford KK, Cottler-Fox M. Metabolism of benzo(*a*)pyrene by human epithelial cells in vitro. Cancer Res 1975; 35:3551–3557.

(*30*) Hurberman E, Sachs L. Metabolism of carcinogenic hydrocarbon benzo(*a*)pyrene in human fibroblast and epithelial cells. Int J Cancer 1973; 11:412–418.

(*31*) Parkinson EK, Newbold RF. Benzo(*a*)pyrene metabolism and DNA adduct formation in serially cultivated strains of human epidermal keratinocytes. Int J Cancer 1980; 26:289–299.

(*32*) Kuroki T, Nemoto N, Kitano Y. Metabolism of benzo(*a*)pyrene in human epidermal keratinocytes in culture. Carcinogenesis 1980; 1:559–565.

(*33*) Cleaver JE. DNA repair and its coupling to DNA replication in eukaryotic cells. Biochim Biophys Acta 1978; 516:489–516.

(*34*) Taichman LB, Setlow RB. Repair of ultraviolet light damage to the DNA of cultured human epidermal keratinocytes and fibroblasts. J Invest Dermatol 1979; 73:217–219.

(*35*) Freeman AE, Lake RS, Igel HJ, et al. Heteroploid conversion of human skin cells by methylcholanthrene. Proc Natl Acad Sci USA 1977; 74:2451–2455.

(36) Trosko JE, Chu EH. The role of DNA repair and somatic mutation in carcinogenesis. Adv Cancer Res 1975; 21:391–425.

(37) Hart RW, Hays S, Brash D, Daniel FB, Davis MT, Lewis NJ. In vitro assessment and mechanism of action of environmental pollutants. Ann NY Acad Sci 1977; 298:141–158.

(38) Bertman JS, Heidelberger C. Cell cycle dependency of oncogenic transformation induced by *N*-methyl-*N'*-nitro-*N*-nitrosoguanidine in culture. Cancer Res 1974; 34:526–537.

(39) Kakunaga T. Rerquirement for cell replication in the fixation and expression of the transformed state in mouse cells treated with 4-nitroquinoline 1-oxide. Int J Cancer 1974; 14:737–742.

(40) Ikenaga M, Kakunaga T. Excision of 4-nitroquinoline 1-oxide damage and transformation in mouse cells. Cancer Res 1977; 37:3672–3678.

(41) Ishikawa T, Takayama S, Kitagawa T. Correlation between time of partial hepatectomy after a single treatment with diethylnitrosamine and induction of adenosinetriphosphatase-deficient islands in rat liver. Cancer Res 1980; 40:4261–4264.

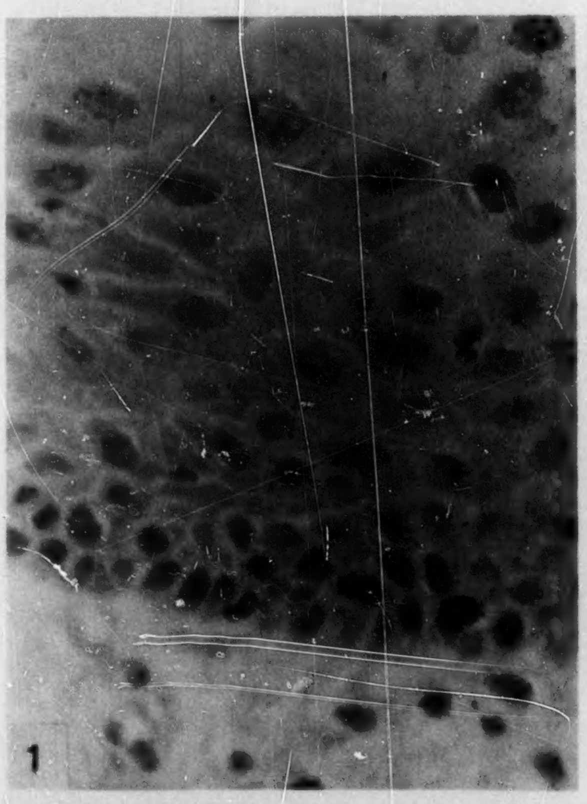

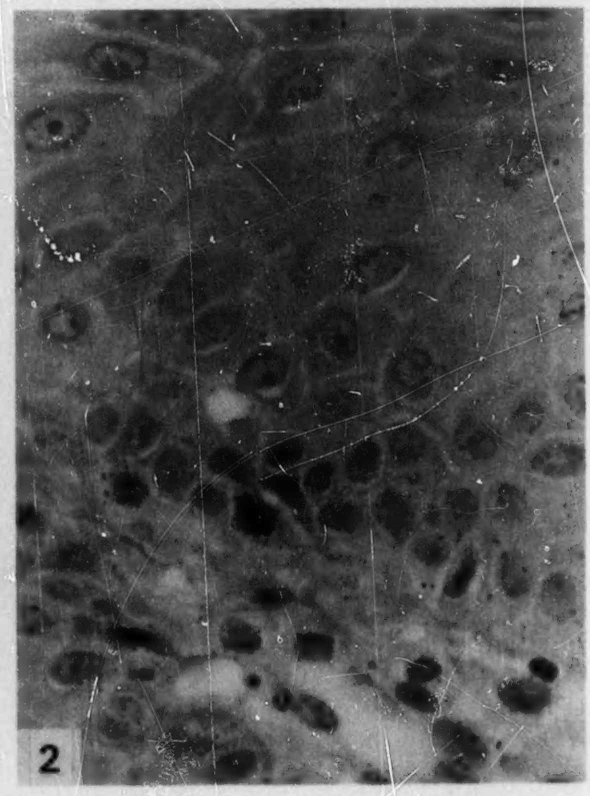

Figure 1.—Autoradiograph showing silver grains on the nuclei of gingival epithelial cells and fibroblasts, indicative of UDS after treatment with 10^{-5} *M* 4HAQO and [*methyl*-^{3}H]dThd (10 μCi/ml) for 2 hr. Lightly stained with H & E. × 1,000

Figure 2.—Autoradiograph of gingiva after treatment with 10^{-3} *M* DENA and [*methyl*-^{3}H]dThd for 2 hr. H & E. × 1,000

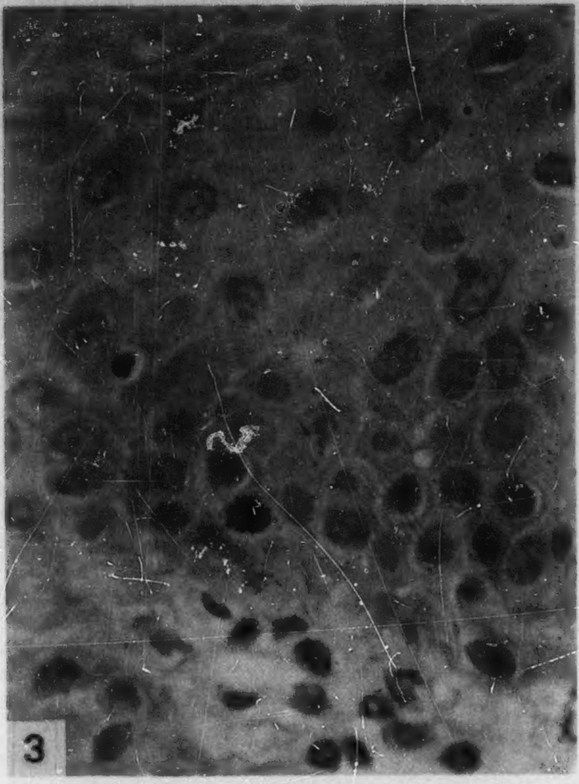

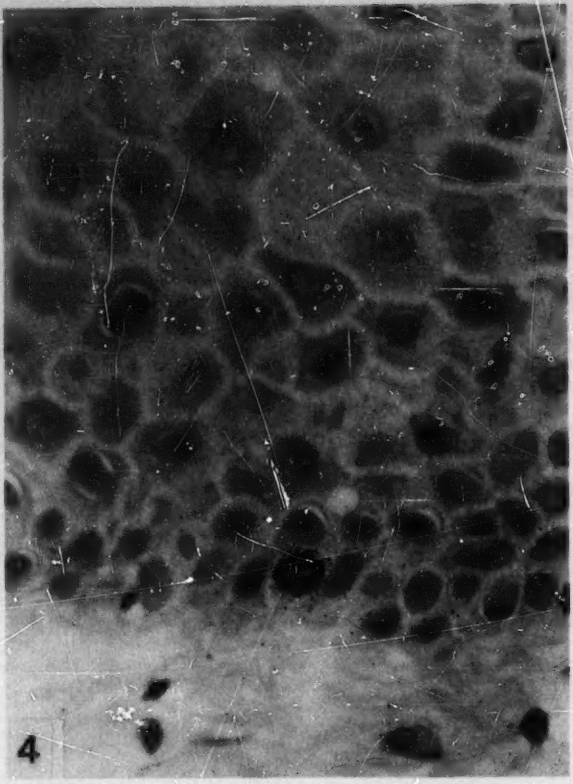

FIGURE 3.—Autoradiograph of gingiva exposed to 0.2 IU mitomycin C. H & E. × 1,000

FIGURE 4.—Control autoradiograph showing few background grains. The gingiva was treated with [*methyl*-^{3}H]dThd. Cells with heavily labeled nuclei seen in the basal layer of the epithelium were in the S-phase during incubation (*see also* figs. 1-3). H & E. × 1,000

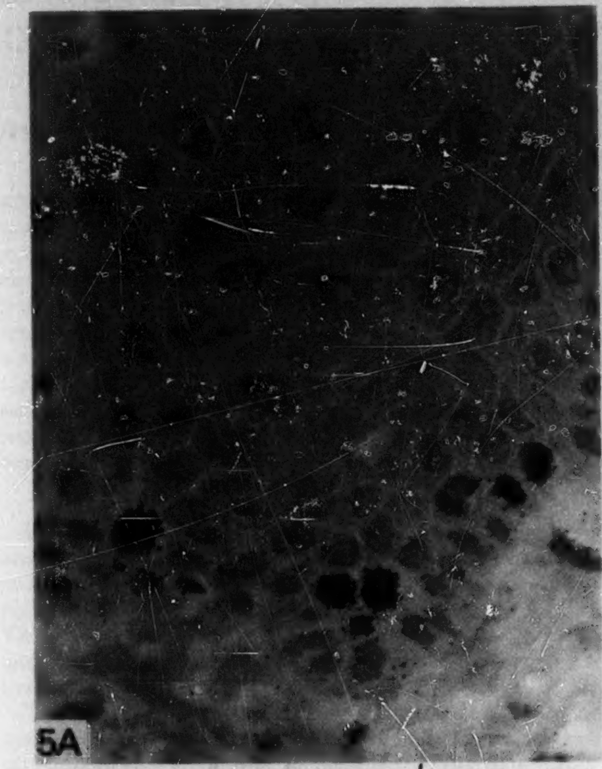

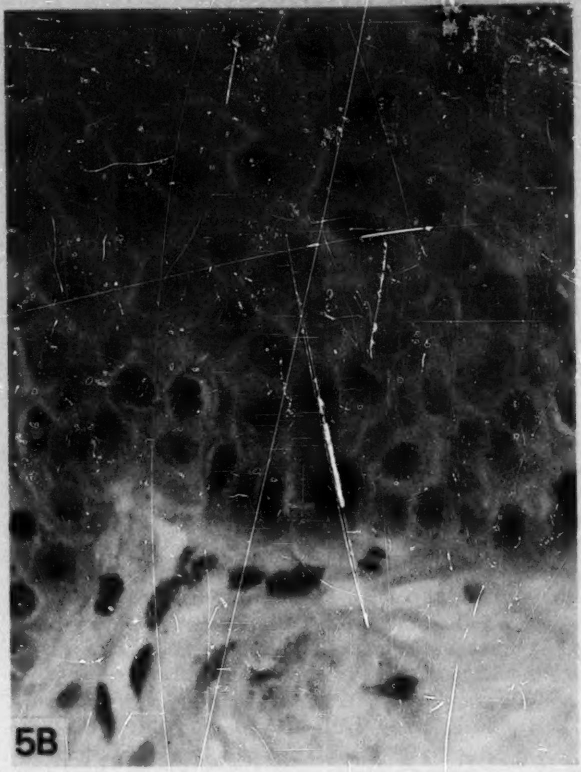

FIGURE 5.—Autoradiographic demonstration of UDS in gingiva from 3 patients (5A, 5B, 5C). Tissues were treated with 10^{-6} *M* BPDE I and [*methyl*-^{3}H]dThd for 2 hr. Spinous layer cells from 3 other patients showed similar numbers of grains on the nuclei. H & E. × 1,000

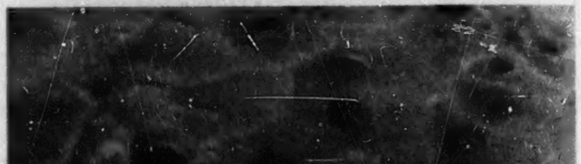

blank page

Distribution of Hepatitis B Surface and Core Antigens in Human Liver Cell Carcinoma and Surrounding Nontumorous Liver[1,2]

Setsuo Hirohashi,[3] Yukio Shimosato,[3] Yoshinori Ino,[3] *and* Kiyozo Kishi[3,4]

ABSTRACT—The distribution of hepatitis B surface antigen (HBsAg) and core antigen (HBcAg) in surgically removed liver cell carcinomas of 60 Japanese patients was studied by an immunohistochemical method. HBsAg was localized in the cytoplasm, and HBcAg was mainly in the nuclei of normal-appearing liver cells, dysplastic liver cells, and tumor cells. In some instances both HBsAg and HBcAg were contained in the tumor cells and liver cells. HBsAg was found in the nontumorous liver tissue of 30 patients (50%); nine of the HBsAg-containing nontumorous livers also contained HBcAg. HBsAg and/or HBcAg was detected in tumor cells in 7 (23%) of 30 cases with HBsAg-positive liver diseases.—JNCI 1982; 69:565–568.

It is well known that liver cell carcinoma and cirrhosis are frequently associated with each other; HBsAg frequently occurs in sera of patients with liver cell carcinoma and in populations whose incidence of liver cell carcinoma is high. These phenomena suggest that both infection with HBV and cirrhosis play important roles in the development of liver cell carcinomas.

The presence of HBsAg in cells of liver cell carcinomas has been demonstrated with the use of immunohistochemical methods (*1–7*), whereas the presence of HBcAg in tumor cells remains questionable (*1, 2, 4, 5*).

In Japan, the incidence of liver cell carcinoma is relatively high, and surgical treatment of this carcinoma has been successful in some cases. With the use of surgically resected livers and a sensitive immunohistochemical method, we studied the distribution of HBsAg and HBcAg in liver cell carcinomas and in surrounding nontumorous livers. We also studied the relationship between HBV infection and the histology of nontumorous regions of livers in which neoplastic transformation had developed. The intent of this study was to clarify whether not only HBsAg but also HBcAg could be produced by liver cell carcinomas and to evaluate the roles of HBV and cirrhosis in human liver cell carcinogenesis.

MATERIALS AND METHODS

Cases.—Sixty primary liver cell carcinomas of Japanese patients were studied. They had been surgically resected at the National Cancer Center Hospital during the last 10 years. Hepatoblastomas and pure bile duct carcinomas were excluded from this study. Serum HBsAg of patients was measured by the reversed passive hemagglutination test (AUSCELL; Abbott Laboratories, North Chicago, Ill.), and anti-HBsAg was measured by the passive hemagglutination test (PHA Test Eisai Kit; Eisai Co., Ltd., Tokyo, Japan).

Immunohistochemical staining of HBsAg and HBcAg.—The unlabeled antibody PAP method of Sternberger (*8*) was used to demonstrate HBsAg and HBcAg on Formalin-fixed, paraffin-embedded sections. One section each of tumor tissue and nontumorous liver was initially selected at random and studied for each case, and in cases in which either or both of two antigens were positive in nontumorous liver, 4 more sections of tumor tissue were examined. Each section was about 2×3 cm in size. We used anti-HBsAg rabbit serum (Medical and Biological Laboratories Ltd., Nagoya, Japan), anti-HBcAg rabbit serum (*9*), swine immunoglobulins to rabbit immunoglobulins (DAKO-Immunoglobulins Ltd., Copenhagen, Denmark), and PAP complex (DAKO Immunoglobulins). These antisera were diluted with 0.01 *M* phosphate buffer (pH 7.2) with 0.8% NaCl (PBS) containing 10% normal swine serum to block nonspecific binding. Sections were deparaffinized in xylene, cleared in ethanol, and then incubated for 30 minutes in methanol that contained 0.3% hydrogen peroxide to remove the endogenous peroxidase activity. After being washed in PBS, the rabbit antiserum to HBsAg or HBcAg (diluted 1:100) was applied and incubated for 30 minutes at room temperature and then washed and incubated with swine immunoglobulins to rabbit immunoglobulins (diluted 1:20). After being washed, the sections were incubated with PAP complex (diluted 1:50), washed again, and developed for 5–10 minutes in 0.05 *M* Tris buffer (pH 7.6), that contained 0.02% DAB and 0.005% hydrogen peroxide. Subsequently, the sections were counterstained with Mayer's hematoxylin.

The specificity of the immunohistochemical staining was confirmed by the following controls: 1) replacement of the primary antiserum by the normal rabbit serum and 2) absorption of the primary antisera with excess amount of purified HBsAg and HBcAg. HBsAg was purified by affinity

---

ABBREVIATIONS USED: anti-HBcAg=antibody to hepatitis B core antigen; anti-HBsAg=serum antibody to hepatitis B surface antigen; DAB=3,3′-diaminobenzidine tetrahydrochloride; HBcAg=hepatitis B core antigen; HBsAg=hepatitis B surface antigen; HBV=hepatitis B virus; PAP=peroxidase-antiperoxidase; PAP complex=soluble complex of horse-radish peroxidase-rabbit antiperoxidase; PBS=phosphate-buffered saline.

---

[1] Received June 25, 1981; revised March 4, 1982; accepted March 30, 1982.

[2] Supported in part by grant 577184 from the Ministry of Education, Science and Culture, Japan.

[3] Pathology Division, National Cancer Center Research Institute, 5-1-1 Tsukiji Chuoku, Tokyo, Japan.

[4] We are indebted to Dr. Shinobu Matsuda (Central Research Division, Takeda Chemical Industries, Osaka, Japan) for the gift of anti-HBcAg rabbit serum and to Dr. Masayasu Inoue (Kanagawa Prefecture Public Health Laboratory, Yokohama, Japan) for the gift of purified HBsAg and HBcAg. Surgical materials were provided by Dr. Hiroshi Hasegawa (National Cancer Center Hospital, Tokyo), photomicrographs were prepared by Mr. Etsuji Nishizaki (National Cancer Center, Tokyo), and the manuscript was reviewed by Mr. J. Patrick Barron (St. Marianna University School of Medicine, Kawasaki, Japan).

chromatography and HBcAg by zonal ultracentrifugation with metrizamide discontinuous gradient.

Double immunohistochemical staining.—To observe HBsAg and HBcAg simultaneously in the tissue, we studied all the sections with both antigens by the method described by Sternberger (*8*). The reactions were initially stained for HBcAg with the use of DAB as substrate. Then the antibodies bound were removed by elution in 0.1 *M* glycine-HCl buffer (pH 2.2) for 1 hour. After being washed in PBS, the sections were stained for HBsAg and developed for 20–30 minutes in Tris buffer that contained 0.02% 4-chloro-1-naphthol and 0.005% hydrogen peroxide at 37°C.

RESULTS

Cases and histology.—Of the 60 patients, 49 were male and 11 were female. The patients' ages ranged from 16 to 77 years with an average age of 52.1 years. The nontumorous livers were classified according to the recommendations by the World Health Organization (*10*) (table 1). Accumulation of dysplastic liver cells in nontumorous livers, named "liver cell dysplasia" by Anthony et al. (*11*), was found in 32 cases (53%), 22 of which showed the histologic characteristics of macronodular cirrhosis. Liver cell dysplasia was marked in 17 cases and was slight in 15 cases (table 2). The 60 tumors were histologically divided into 56 pure liver cell carcinomas and 4 combined liver cell and bile duct carcinomas, and the predominant area of the tumors was classified by the grading system of differentiation (table 3) introduced by Edmondson and Steiner (*12*).

Specificity of immunohistochemical staining.—Immunohistochemical staining of HBsAg and HBcAg resulted in brown reaction products with DAB and in pale-blue reaction products with 4-chloro-1-naphthol. Nonspecific background staining was virtually absent. Absorption of antisera against HBsAg and HBcAg by the respective antigens resulted in unstained sections. No reactions were obtained when the primary antisera were replaced by normal rabbit serum.

HBsAg and HBcAg in nontumorous livers.—Table 1 shows the results of immunohistochemical detection of HBsAg and HBcAg in relation to the histology of nontumorous livers, and table 4 compares the results obtained with serum HBsAg and anti-HBsAg.

The number of HBsAg-positive cells in nontumorous livers varied from case to case. HBsAg was localized diffusely in the cytoplasm or localized as cytoplasmic inclusion bodies (fig. 1).

TABLE 1.—*Hepatitis B antigens in nontumorous livers*

Histology of nontumorous liver	No. of cases (% of total)	HBsAg-positive and HBcAg-positive	HBsAg-positive and HBcAg-negative	HBsAg-negative and HBcAg-positive	HBsAg-negative and HBcAg-negative
Cirrhosis					
Macronodular	34 (56.7)	9	6	0	19
Micronodular	3 (5)	0	0	0	3
Chronic active hepatitis	5 (8.3)	0	5	0	0
Chronic persistent hepatitis	9 (15)	0	8	0	1
Almost normal[a]	9 (15)	0	2	0	7
Total (%)	60	9 (15)	21 (35)	0	30 (50)

[a] Schistosomiasis was present in 1 case.

TABLE 2.—*Liver cell dysplasia and hepatitis B antigens*

Hepatitis B antigens	Liver cell dysplasia,[a] No. of cases		
	Marked	Slight	Absent
HBsAg-positive and HBcAg-positive	8	1	0
HBsAg-positive and HBcAg-negative	7	8	6
HBsAg-negative and HBcAg-negative	2	6	22
Total	17	15	28

[a] Marked = frequent prominent lesions of liver cell dysplasia; slight = a few lesions of liver cell dysplasia per section.

TABLE 3.—*Hepatitis B antigens in tumors*

Tumor grade[a]	No. of cases	No. HBsAg-positive and HBcAg-positive	No. HBsAg-positive and HBcAg-negative	No. HBsAg-negative and HBcAg-positive
I	1	0	0	0
II	27	0	2	2
III	31	2	1	0
IV	1	0	0	0
Total	60	2	3	2

[a] According to Edmondson and Steiner (*12*).

TABLE 4.—*Serum HBsAg and anti-HBs in relation to HBsAg in nontumorous liver*

Liver antigens[a]	Serum antigens or antibodies, No./liver antigens, No. (%)	
	HBsAg-positive[b]	anti-HBsAg-positive[c]
HBsAg-positive	29/29 (100)	0/28 (0)
HBsAg-negative	0/30 (0)	11/29 (37.9)
Total	29/59 (49.2)	11/57 (19.1)

[a] Results of immunohistochemical determinations.

[b] Assayed by reversed passive hemagglutination test.

[c] Assayed by passive hemagglutination test.

HBcAg was localized mainly in the nuclei of liver cells (fig. 1), but occasionally small amounts were also localized in the cytoplasm of liver cells. HBcAg-positive cells were often distributed in clusters, and their number varied from case to case. HBsAg was detected in all cases in which HBcAg was detected (table 1), and HBsAg-positive cells were more frequent than HBcAg-positive cells in most cases. HBsAg and HBcAg usually occurred in different cells, but a few scattered cells were observed to contain both HBsAg and HBcAg (fig. 1).

Table 2 shows the incidence of liver cell dysplasia in relation to the presence of HBsAg and/or HBcAg in nontumorous livers. HBsAg was localized in some of the dysplastic liver cells (fig. 2), but HBcAg was seldom seen.

HBsAg and HBcAg in tumors.—HBsAg and/or HBcAg was detected in various numbers of tumor cells in 7 cases (table 3), although tumor cells were predominantly negative for both antigens. In 2 cases, in which both HBsAg and HBcAg were detected, HBsAg-positive tumor cells were more frequent than HBcAg-positive tumor cells; tumor cells that contained both HBsAg and HBcAg were present in only one case; even in that case such cells were rare (fig. 3). In tumor cells, HBsAg was localized in the cytoplasm only, whereas HBcAg was mainly localized in the nuclei (fig. 3).

DISCUSSION

In autopsy studies, cirrhosis is recognized in more than 80% of patients with liver cell carcinoma in Japan (*13*). However, cirrhosis was present in only 61.7% of the cases in the present study of surgically resected livers. This is probably due to the fact that the cases in this series were operable. Cases without cirrhosis showed histologic findings of chronic active hepatitis, chronic persistent hepatitis, or almost normal liver. It is now clear that fully developed cirrhosis is not a prerequisite for the development of liver cell carcinoma (*13, 14*). However, cirrhosis is suspected of being able to play an important role in carcinoma development. The histologic type of cirrhosis (the so-called "posthepatitic cirrhosis") associated with liver cell carcinoma is predominantly macronodular: In this cirrhosis liver cell regeneration is prominent. Conversely, micronodular cirrhosis, in which liver cell regeneration is not so prominent, is rarely associated with liver cell carcinoma. Since liver cell regeneration increases susceptibility to carcinogens in animal experiments (*15, 16*), macronodular cirrhosis might be expected to play a similar role in human liver cell carcinogenesis.

HBsAg and HBcAg were clearly demonstrated in Formalin-fixed, paraffin-embedded sections of surgically resected livers by Sternberger's PAP method, the specificity of which was confirmed by adequate controls. In addition, the high sensitivity of the method was shown by the fact that the results of HBsAg localization in nontumorous livers completely coincided with the results of serum HBsAg measured by reversed passive hemagglutination test.

We observed a close relationship between liver cell carcinoma and HBV infection. HBsAg was detected in 30 cases (50%), and anti-HBsAg was detected in 11 cases (18%); therefore 68% of our series were cases with active HBV infection or a history of HBV infection.

Tumor tissues containing HBsAg and/or HBcAg were observed in 7 cases. In addition, a few tumor cells simultaneously contained both HBsAg and HBcAg. The results suggest production of complete virus by tumor cells and the presence of complete virus genomes in tumor cells. Recently, a cultured human liver cell carcinoma (PLC/PRF/5) was shown by molecular hybridization technique to possess complete genomes of HBV as an integrated form in host DNA (*17-20*). These findings are consistent with those seen in several oncogenic viruses in animals and indicate that HBV probably plays a major role in liver cell carcinogenesis.

If the HBV genomes were integrated in host DNA, all the tumor cells would contain the virus genomes. However, one tumor was composed of cells that contained either HBsAg or HBcAg, or both HBsAg and HBcAg, or neither HBsAg nor HBcAg. From this finding, it is speculated that HBV genes coding for HBsAg and HBcAg would be expressed under different and independent regulation at least in tumor cells.

Anthony et al. (*11*) and Anthony (*21*) reported that liver cell dysplasia was a precancerous lesion and was related to HBV infection. We do not know if dysplastic liver cells progress to cancer or not, but a close relation between liver cell dysplasia and HBV infection was observed in this study. In addition, the presence of HBsAg in some dysplastic liver cells may suggest the presence of integrated HBV genomes in dysplastic liver cells.

Our review of 60 resected cases shows that both HBsAg and HBcAg can be produced by liver cell carcinomas, and it further suggests important roles played by HBV and cirrhosis in the development of liver cell carcinoma.

REFERENCES

(*1*) Nayak NC, Dhar A, Sachdeva R, et al. Association of human hepatocellular carcinoma and cirrhosis with hepatitis B virus surface and core antigens in the liver. Int J Cancer 1977; 20:643-654.

(*2*) Nazarewicz T, Krawczynski K, Slusarczyk J, Nowoslawski A. Cellular localization of hepatitis B virus antigens in patients with hepatocellular carcinoma coexisting with liver cirrhosis. J Infect Dis 1977; 135:298-302.

(*3*) Turbitt ML, Patrick RS, Goudie RB, Buchanan WM. Incidence in Southwest Scotland of hepatitis B surface antigen in the liver of patients with hepatocellular carcinoma. J Clin Pathol 1977; 30:1124-1128.

(*4*) Trevisan A, Realdi G, Losi C, Ninfo V, Rugge M, Rampinelli L. Hepatitis B virus antigens in primary hepatic carcinoma: Immunofluorescent techniques on fixed liver tissue. J Clin Pathol 1978; 31:1133-1139.

(*5*) Thung SN, Gerber MA, Sarno E, Popper H. Distribution of five antigens in hepatocellular carcinoma. Lab Invest 1979; 41:101-105.

(*6*) Ilardi CF, Ying YY, Ackerman LV, Elias JM. Hepatitis B surface antigen and hepatocellular carcinoma in the People's Republic of China. Cancer 1980; 46:1612-1616.

(*7*) Kew MC, Ray MB, Desmet VJ, Desmyter J. Hepatitis-B surface antigen in tumuor tissue and non-tumourous liver in black patients with hepatocellular carcinoma. Br J Cancer 1980; 41:399-406.

(*8*) Sternberger LA. The unlabeled antibody peroxidase-antiperoxidase (PAP) method. In: Immunocytochemistry. 2d ed. New York: Wiley, 1979:104-169.

(*9*) Onda H, Matsuda S, Oka Y. Hepatitis B core particles with endogenous DNA polymerase activity from chimpanzee liver. Intervirology 1978; 10:254-264.

(*10*) Anthony PP, Ishak KG, Nayak NC, Poulsen HE, Scheuer PJ, Sobin LH. The morphology of cirrhosis. Recommendations on definition, nomenclature, and classification by a working group sponsored by the World Health Organization. J Clin Pathol 1978; 31:395-414.

(*11*) Anthony PP, Vogel CL, Barker LF. Liver cell dysplasia: A premalignant condition. J Clin Pathol 1973; 26:217-223.

(*12*) Edmondson HA, Steiner PE. Primary carcinoma of the liver. A study of 100 cases among 48,900 necropsies. Cancer 1954; 7:462-503.

(*13*) Shikata T. Primary liver carcinoma and liver cirrhosis. In: Okuda K, Peters RL, eds. Hepatocellular carcinoma. New York: Wiley, 1976:53-71.

(*14*) Shikata T, Yamazaki S, Uzawa T. Hepatocellular carcinoma and chronic persistent hepatitis. Acta Pathol Jpn 1977; 27:297-304.

(*15*) Craddock VM. Liver carcinomas induced in rats by single administration of dimethylnitrosamine after partial hepatectomy. J Natl Cancer Inst 1971; 47:899-907.

(*16*) Hollander CF, Bentvelzen P. Enhancement of urethan induction of hepatomas in mice by prior partial hepatectomy. J Natl Cancer Inst 1968; 41:1303-1306.

(*17*) Marion PL, Salazar FH, Alexander JF, Robinson WS. State of hepatitis B viral DNA in a human hepatoma cell line. J Virol 1980; 33:795-806.

(*18*) Chakrabotory PR, Ruiz-Opazo N, Shouval D, Shafritz DA. Identification of integrated hepatitis B virus DNA and expression of viral RNA in an HBsAg-producing human hepatocellular carcinoma cell line. Nature 1980; 286:531–533.

(19) Brechot C, Pourcel C, Louise A, Rain B, Tiollais P. Presence of integrated hepatitis B virus DNA sequences in cellular DNA of human hepatocellular carcinoma. Nature 1980; 286:533–535.

(20) Edman JC, Gray P, Valenzuela P, Rall LB, Rutter WJ. Integration of hepatitis B virus sequences and their expression in a human hepatoma cell. Nature 1980; 286:535–538.

(21) Anthony PP. Precursor lesions for liver cancer in humans. Cancer Res 1976; 36:2579–2583.

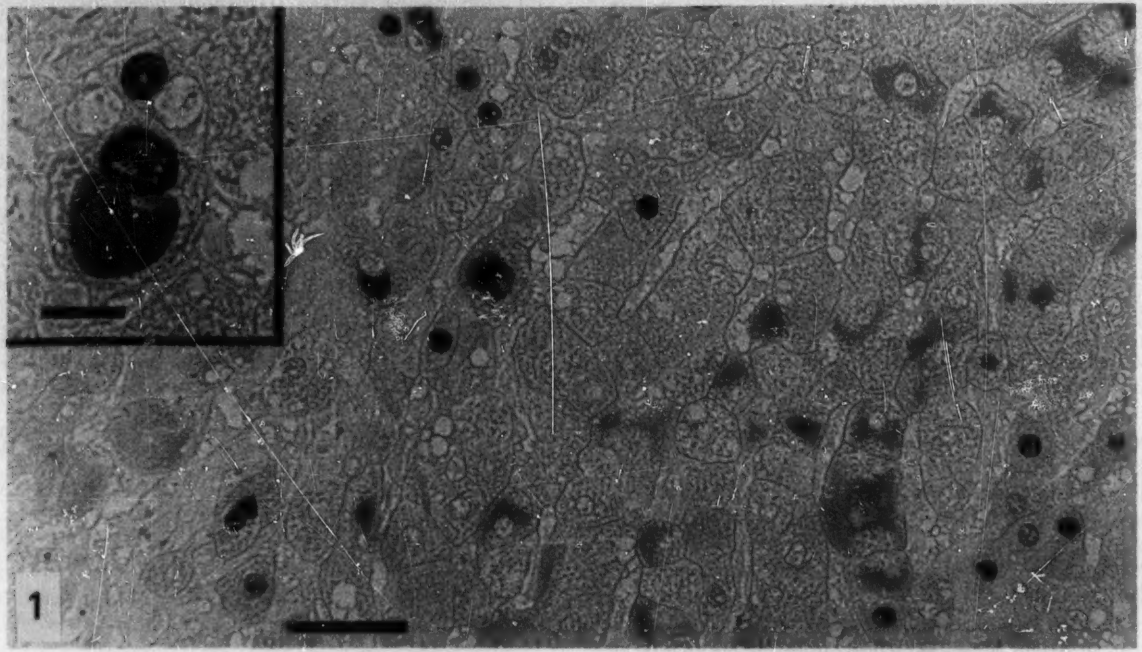

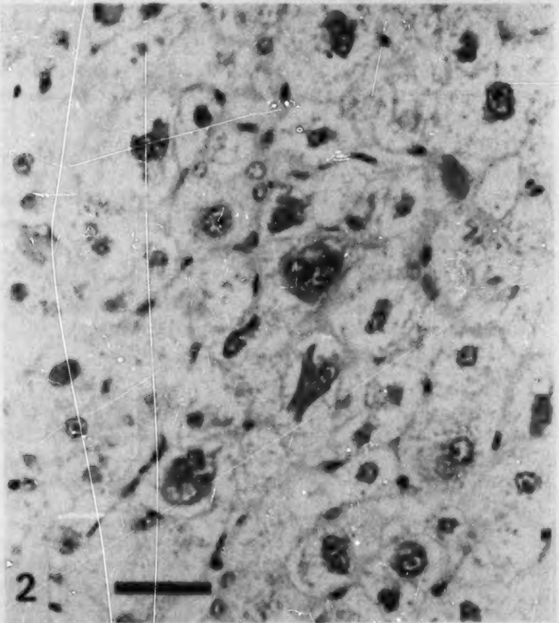

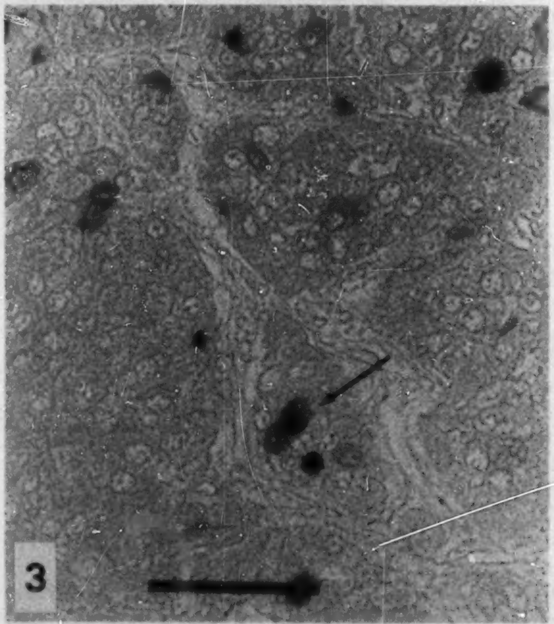

Figure 1.—Nontumorous liver. Double staining of HBsAg (originally pale-blue reaction product in the cytoplasm) and HBcAg (originally dark-brown reaction product in the nuclei) by Sternberger's PAP method (*8*). HBsAg and HBcAg were distributed independently. *Bar*=50 µm. × 350. *Inset:* A few cells contained both antigens. *Bar*=10 µm. × 1,200

Figure 2.—Dysplastic liver cells that show multinucleation and nuclear pleomorphism contain HBsAg. Staining of HBsAg by Sternberger's PAP method and counterstain with Mayer's hematoxylin. *Bar*=20 µm. × 700

Figure 3.—Liver cell carcinoma, grade III. Double staining of HBsAg and HBcAg by Sternberger's PAP method. HBsAg was localized in the cytoplasm and HBcAg in the nuclei of tumor cells. *Arrow* indicates a few tumor cells that contain both HBsAg and HBcAg. *Bar*=50 µm. × 500

Elevated dTTPase Activities in Sera of Patients With Advanced Cancer[1,2,3]

Nicolaus Dahlmann, *M.D.*[4,5]

ABSTRACT—dTTPase activities were determined in the sera of 108 healthy blood donors, 43 nonseriously ill patients, 66 seriously ill patients, 95 patients with untreated malignant diseases, 41 patients with breast carcinoma, and 53 umbilical cord blood samples. Values of 300 mU/liter or higher were taken as abnormal activity. Whereas the dTTPase activities of the nonseriously ill patients and the breast carcinoma patients were not significantly elevated, the dTTPase activities of 52% of the seriously ill patients and 82% of the patients with untreated malignant diseases were lying above the two standard deviation range.—JNCI 1982; 69:569–572.

Previously, we described a novel enzyme activity present in human serum (*1*). This enzyme, dTTPase, catalyzes the conversion of dTTP to dTDP. No measurable hydrolysis of nucleoside triphosphate to the diphosphate was observed with any of the other three standard deoxyribonucleoside triphosphates.

The unique characteristics of this enzyme suggest that it might be involved in the regulation of the rate of dTTP synthesis and thus may play an important role in the control of DNA synthesis (*2*). To date, positive correlations between growth rate of mammalian tumors and the levels of activity of key enzymes of pyrimidine synthesis in these tissues have been reported (*3*). The enzymes studied include dCMP deaminase (dCMP aminohydrolase, EC 3.5.4.12), thymidylate synthetase (N^{5},N^{10}-methylenetetrahydrofolate: 2′-deoxyuridylate *C*-methyltransferase, EC 2.1.1.45), and dTMP kinase (ATP deoxythymidinemonophosphate phosphotransferase, EC 2.7.4.9) (*4*). Therefore, the idea was to see if the dTTPase activity was elevated in sera of cancer patients. Indeed, preliminary studies revealed increased levels of dTTPase activity in 19 sera obtained from patients with various untreated cancers as compared to the levels of dTTPase activity in sera obtained from healthy blood donors (*5*).

In the present paper, serum dTTPase levels are compared in *a*) healthy blood donors, *b*) nonseriously ill patients, *c*) seriously ill patients, *d*) patients with untreated malignant diseases, *e*) breast cancer patients, and *f*) umbilical cord blood samples. The objectives of this investigation were to determine *a*) whether elevated levels of dTTPase activity in the serum may serve as a marker for diagnosis of tumors, *b*) whether there is a specificity for different tumors, and *c*) whether there is any indication that the dTTPase is involved in a neoplastic process.

MATERIALS AND METHODS

Substrates.—Tetrasodium dTTP was obtained from Boehringer-Mannheim, Mannheim, Federal Republic of Germany. The ammonium salt of [methyl-^{3}H]dTTP was purchased from The Radiochemical Centre, Amersham, England, and diluted with unlabeled nucleotide solution to a concentration of 7–8 μCi/nmol.

Other chemicals.—Disodium dTMP and trisodium dTDP were obtained from Boehringer-Mannheim. Dithiothreitol was purchased from Sigma Chemical Co., München, Federal Republic of Germany. Polygram CEL 300 PEI precoated sheets were supplied by Macherey-Nagel Co., Düren, Federal Republic of Germany. Other standard reagents, all of analytical grade, were purchased from E. Merck A.G., Darmstadt, Federal Republic of Germany.

dTTPase assay.—The assay was based on the conversion of [^{3}H]dTTP to [^{3}H]dTDP and was performed under optimized conditions for each component. Each assay mixture contained, in a final volume of 50 μl, 10 m*M* Tris-HCl (pH 7.8), 0.5 m*M* MnCl$_2$, 8 m*M* dithiothreitol, 6 μ*M* [^{3}H]dTTP (7–8 μCi/nmol), and 5 μl serum. Both the reaction mixture and the serum were pipetted with a Hamilton digital diluter (Hamilton Bonaduz A.G., Bonaduz, Switzerland). Incubation was at 30°C for 1 hour, and the reaction was terminated by the addition of 5 μl of 50% formic acid (vol/vol) containing unlabeled dTTP, dTDP, and dTMP, all at 5 m*M*.

The reaction mixtures were immediately centrifuged (2 min, 10,000×*g*), and 5-μl aliquots of 20 supernatants were simultaneously applied to the PEI cellulose sheets with the Desaga autospotter (DesagA GmbH., Heidelberg, Federal Republic of Germany). The chromatograms were developed at room temperature with 1 *M* acetic acid containing 0.85 *M* LiCl, were dried, and were examined with UV light. The dTTP, dTDP, and dTMP spots were cut out, and radioactivity in each spot was determined by liquid scintillation spectrometry.

The enzyme activity was calculated from the amount of the hydrolyzed product formed. One international unit represented the production of 1 μmol dTDP/minute. The reaction rates were linear with time and enzyme concentrations up to 350 mU/liter under the conditions used.

Serum samples.—Blood was collected from patients and allowed to clot in the absence of any additives. The serum was separated by centrifugation and was stored at −20°C until assayed. The enzyme activity was stable to three cycles of freezing and thawing.

---

[1] Received August 31, 1981; revised March 3, 1982; accepted April 2, 1982.

[2] Supported in part by the Tumorzentrum Hamburg, Hamburger Stiftung zur Förderung der Krebsbekämpfung, Hamburger Landesverband für Krebsbekämpfung und Krebsforschung eV., Holstein Fond für Krebsforschung.

[3] Research procedures were in accord with the ethical standards of the Universität Hamburg and the Helsinki Declaration of 1975.

[4] Physiologisch-Chemisches Institut, Abteilung Molekularbiologie, Grindelallee 117, D-2000 Hamburg 13, Federal Republic of Germany.

[5] I am grateful to Prof. Gebhard Koch for helpful discussions.

Sera of healthy blood donors were obtained from Dr. M. Moskophides, Chirurgische Universitätsklinik, Hamburg, Federal Republic of Germany, and from Professor Dr. K. Hoppe, Allgemeines Krankenhaus Eilbek, Hamburg. Various members of the staff of the Medizinische Universitätsklinik Hamburg provided patients' sera. Dr. F. Bode and Dr. G. Steinmann provided sera from both seriously and nonseriously ill patients, Professor Dr. R. Klapdor provided sera from patients with pancreatic and biliary tract carcinomas, and Dr. R. Pompecki provided sera from patients with gastrointestinal carcinomas. Sera from patients with laryngeal–pharyngeal carcinomas were obtained from Dr. R. Skoblo, Universitätsklinikum Steglitz, Berlin, Federal Republic of Germany, and sera from patients with hematologic tumors were obtained from Professor Dr. H. Stein, Pathologisches Institut der Universität, Kiel, Federal Republic of Germany. Professor G. Trams provided sera from breast carcinoma patients; the histologic examinations of the various samples were performed by Professor H. E. Stegner. Umbilical cord blood samples were obtained by Dr. H. Jagella, Krankenhaus Elim, Hamburg. All sera from the patients with untreated malignant diseases, as obtained from the persons mentioned above, suffered from carcinomas of stage 3.

RESULTS

Blood donors.—The dTTPase activity in the sera of the healthy blood donors (n=108) is demonstrated in text-figure 1. For normal blood donors the dTTPase level did not vary. Thus the data for the 67 males and 41 females were taken together, and a Gaussian distribution was seen. The average dTTPase value of 229 mU/liter and two standard deviations (SD=34 mU/liter) for the normal control are indicated on the scattergram. This cutoff limit was chosen so that about 95% of a healthy population had values below the limit.

Nonseriously ill patients.—Analysis of patients with diseases other than neoplasia showed a biphasic distribution in dTTPase activity. We divided the population into 2 groups, which we called nonseriously ill patients and seriously ill patients (characterized by severe destruction of tissues and serious inflammations) according to the diseases that are summarized in the tables for these 2 groups. Diseases of the nonseriously ill patients are listed in table 1. Although the numbers of the cases in the various disease categories were not high enough to be statistically significant for each disease, the reactions of the nonseriously ill patients were clearly similar to the reactions of the blood donors. The following values were obtained: $\bar{x}$=263 mU/liter and SD = 37 mU/liter. Only 16% were found to lie above the two standard deviations of the normal mean.

Seriously ill patients.—The diseases summarized for this group (table 2) all involved severe destruction of tissue. From a total of 66 patients, 52% had positive dTTPase values, which means that their dTTPase values lay in the pathologic range (>300 mU/liter). The number of patients with dTTPase values above the two standard deviations of the normal mean per the total number of patients with

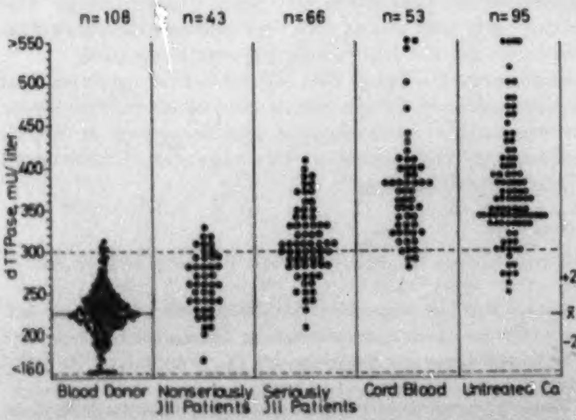

TEXT-FIGURE 1.—dTTPase activities expressed in mU/liter for healthy blood donors, nonseriously ill patients, seriously ill patients, umbilical cord blood samples, and patients with untreated malignant carcinoma (Ca).

TABLE 1.—*dTTPase activity: Nonseriously ill patients*

Disease	Patients			Enzyme activity, mU/liter		
	Total No.	No. positive[a]	Percent	Mean	SD	Range
Diabetes without organic complications	4	1	25	265	48	200–310
Heart disease	5	2	40	278	54	210–330
Polyposis of stomach or colon	4	2	50	295	19	270–310
Anemia	3	0	0	253	31	220–280
Pancytopenia	6	0	0	243	10	230–260
Hypertonia	6	1	17	247	59	170–320
Asthma–bronchitis	4	0	0	285	6	280–290
Liver: cirrhosis	3	0	0	250	27	220–270
All other diseases	8	1	13	263	23	240–310
Total	43	7	16	263	37	170–330

[a] Positives are all patients whose enzyme activity values are above the two standard deviation range of the normal mean (≥300 mU/liter).

TABLE 2.—*dTTPase activity: Seriously ill patients*

Disease	Patients			Enzyme activity, mU/liter		
	Total No.	No. positive[a]	Percent	Mean	SD	Range
Diabetes with organic complications	4	3	75	320	58	250–390
Cardiac infarction	9	6	67	319	26	280–360
Apoplexy	16	9	56	309	29	260–350
Inflammation	28	11	39	298	46	210–380
Renal insufficiency, terminal	6	4	67	345	70	250–410
Thrombosis	3	1	33	333	58	300–400
Total	66	34	52	311	45	210–410

[a] Positives are all patients whose enzyme activity values are above the two standard deviation range of the normal mean (≥300 mU/liter).

TABLE 3.—*dTTPase activity: Untreated malignant diseases*

Disease, stage 3	Patients			Enzyme activity, mU/liter		
	Total No.	No. positive[a]	Percent	Mean	SD	Range
Polycythemia vera	5	5	100	482	73	430–610
Chronic lymphatic leukemia	12	12	100	453	111	320–650
Malignant lymphoma	5	3	60	324	49	250–370
Carcinoma						
Stomach	6	4	67	418	94	300–500
Jejunum	5	4	80	340	46	270–390
Colon–sigmoid	14	12	86	344	37	290–440
Rectal	17	16	94	359	42	270–420
Pancreatic	14	11	79	350	58	260–480
Biliary tract	5	5	100	352	26	320–390
Ovarian	6	4	67	358	86	280–520
Laryngeal–pharyngeal	6	6	100	372	18	350–390
Total	95	82	86	375	76	250–650

[a] Positives are all patients whose enzyme activity values are above the two standard deviation range of the normal mean (≥300 mU/liter).

specific diseases studied were 3/4 for diabetes with organic complications, 6/9 for cardiac infarction, 11/28 for inflammations, 4/6 for terminal renal insufficiency, and 1/3 for thrombosis. These results show that the sera of some patients with serious diseases other than cancer may have elevated dTTPase activities and that such increases are not restricted to cancer.

Malignant diseases.—All patients of this group as given in table 3 had a progessive malignant disease (stage 3) and were untreated. The mean and standard deviation for these probands were $\bar{x}$=375 and SD=76 mU/liter. Of 95 patients, 86% lay above the two standard deviation range. Positive values of 100% or nearly 100% were seen for patients with polycythemia vera, chronic lymphatic leukemia, rectal carcinoma, and laryngeal–pharyngeal carcinoma. The other diseases and the number of patients with dTTPase activities in the pathologic range per the total number of patients with specific diseases studied were 3/5 for malignant lymphoma, 12/14 for colon–sigmoid carcinoma, 11/14 for pancreatic carcinoma, and 4/6 for ovarian carcinoma.

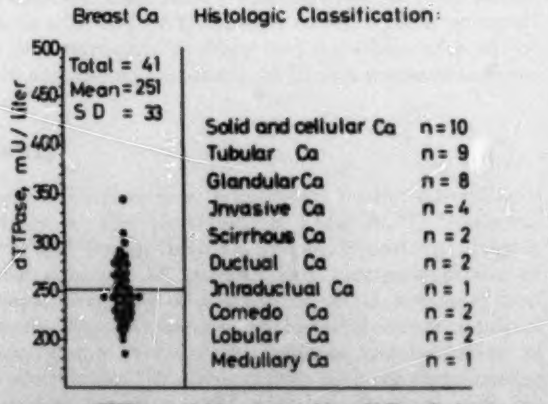

TEXT-FIGURE 2.—dTTPase activities expressed in mU/liter for breast carcinoma (Ca) of different histologic groups.

Patients with breast carcinoma.—In contrast to the sera from patients with other monitored malignant diseases, sera from breast carcinoma patients revealed an average dTTPase activity of 251 mU/liter (SD=33 mU/liter) with a distribution quite similar to the distribution of the blood donors. (text-fig. 2). Because of the relatively large group of 41 breast carcinomas analyzed and their different histologic classifications, it is quite probable that patients with breast carcinoma do not have an elevated dTTPase activity. The reason for this result is not known, and further investigations of the biochemical and clinical aspects of breast carcinoma must be done to clarify this observation.

Umbilical cord blood samples.—Values for sera from umbilical cord bloods are shown in text-figure 1. The distribution of the data resembled the distribution for untreated malignant diseases inasmuch as about 90% of the 53 values lay above the two standard deviation level. The dTTPase activity in cord blood ranged from 280 to greater than 550 mU/liter.

DISCUSSION

This report describes elevated serum dTTPase activities in association with some nonmalignant diseases and with various untreated malignant diseases. The nonmalignant diseases could be divided into 2 groups, inasmuch as the nonseriously ill patients had serum dTTPase activities like those of healthy blood donors. However, 52% of the seriously ill patients had serum dTTPase activities above the two standard deviation range of values found for sera from healthy blood donors. In terms of a potential tumor marker, these results are by no means satisfactory because of the apparent lack of specificity for malignant disease. One must also consider that elevated serum dTTPase activities are restricted to patients with specific disease entities that are characterized by severe destruction of tissue. Under circumstances of a differential diagnosis, the determination of dTTPase activity in human sera might be a useful tool for monitoring the presence of cancer, inasmuch as the true positive rate for untreated human malignant diseases is greater than 80%. The only exception known so far is breast carcinoma, and this finding is not well understood because we have insufficient knowledge regarding the function and origin of dTTPase activity in human sera.

The test system as described above is simple, inexpensive, and accurate; it is not time consuming and could be used as a mass screening test for cancer. Other diseases such as cardiac infarction or apoplexy that result in increased levels of dTTPase activity in the serum could be easily diagnosed.

Furthermore, we speculate that the dTTPase assay can be made more specific because about 25% of the sera from patients with untreated carcinomas have values above the two standard deviation range of 400 mU/liter of the seriously ill patients, indicating that in serum in general at least two enzymes are acting on the dTTP substrate, one enzyme being an unspecific degrading enzyme and the other being specific and involved in the proliferation process. This suggestion is supported by the fact that the samples of the umbilical cord blood used as a model for a proliferating tissue show a distribution of dTTPase activity that is absolutely similar to the pattern exhibited by sera from untreated carcinomas.

The elevation of the dTTPase activity in cord blood is interesting to note because in another paper a DNA-binding protein was described that was elevated in the sera of patients with various untreated malignant diseases but was not elevated in umbilical cord blood samples (*6*). Another hint for the existence of more than one enzyme acting on dTTP as a substrate was the attempted determination of the K_m (Michaelis constant) value from a reciprocal plot, which led to a downward-bent hyperbolic curve typical for the hydrolysis of one substrate by two enzymes (Dahlmann N: Unpublished observations). So the future task is to see if really two or more enzymes are hydrolyzing the dTTP and if there might be one which is specifically regulating the proliferation process as formerly discussed (*1*).

REFERENCES

(*1*) Dahlmann N, Müller D. Thymidine-5′-triphosphatase: A new human serum enzyme activity and its significance in malignant diseases. Hoppe Seylers Z Physiol Chem 1980; 361:1851–1854.

(*2*) Beltz RE. Comparison of the content of thymidylate synthetase, deoxycytidylate deaminase and deoxyribonucleoside kinases in normal and regenerating rat liver. Arch Biochem Biophys 1962; 99:304–312.

(*3*) Sneider TW, Potter VR, Morris HP. Enzymes of thymidine triphosphate synthesis in selected Morris hepatomas. Cancer Res 1969; 29:40–54.

(*4*) Cummins RR, Balinsky D. Activities of some enzymes of pyrimidine and DNA synthesis in a rat transplantable hepatoma and human primary hepatomas, in cell lines derived from these tissues, and in human fetal liver. Cancer Res 1980; 40:1235–1239.

(*5*) Dahlmann N. Elevated dTTPase activity as a new marker for clinical diagnosis of tumors. J Clin Chem Clin Biochem 1980; 18:683.

(*6*) Katsunuma [illegible], Tsuda M, Kusumi T, et al. Purification of a serum DNA binding protein (64DP) with a molecular weight of 64,000 and its diagnostic significance in malignant diseases. Biochem Biphys Res Commun 1980; 93:552–557.

Breath Methane Excretion in Patients With Unresected Colorectal Cancer[1,2]

David A. Karlin, *M.D.,*[3] **R. D. Jones,** *M.S.,*[3] **John R. Stroehlein,** *M.D.,*[3] **Anthony J. Mastromarino,** *Ph.D.,*[3] *and* **Gregory D. Potter,** *M.D.*[3]

ABSTRACT—The objective of our study was to verify or refute the observation that patients with unresected colorectal cancer are more likely to be breath methane excretors than the general population. Intracolonic heme had no effect on breath methane excretion of 11 normal volunteers given oral hemoglobin. Laxative–enema colonoscopy preparation had a profound effect on the subsequent measurement of breath methane. Three of 4 volunteer methane excretors became nonexcretors, and 2 remained nonexcretors for 21 days and 7 months, respectively. No significant difference was found in the frequency and the amount of breath methane excretion in 55 patients with unresected colorectal cancer and in 99 control subjects. However, 13 patients with unresected descending or sigmoid colon cancers were almost twice as likely to be breath methane excretors as 38 patients with colorectal cancer at other sites.—JNCI 1982; 69:573–576.

Large bowel cancer is a leading cause of morbidity and mortality in the United States (*1*). Because the etiology is unknown, current research concerns the detection of premalignant conditions, the screening of large populations by proctosigmoidoscopy, and tests for fecal occult blood (*2, 3*). To enhance the cost-effectiveness of screening, simpler or more effective tests are needed for screening large populations for selection of subgroups that are at increased risk for developing large bowel cancer.

Although it has been suggested that the colonic microflora plays a role in the etiology of colorectal cancer, significant differences in the flora composition have been difficult to demonstrate. However, significant differences in metabolic activities of the flora have been reported (*4–7*). Because breath methane excretion is an indirect measurement of the metabolism of the anaerobic colonic flora, the breath methane content in patients with carcinoma of the large bowel has been studied. In a prospective study, Haines et al. (*8*) found that 80% of 30 patients with unresected large bowel cancer excreted more than 1 ppm methane in their breath compared with 40% of 272 control subjects. Here we report results of a retrospective study and the effects of heme or laxative and enema treatment on breath methane concentrations.

METHODS

Subjects.—This study was approved by the Surveillance Committee at The University of Texas M. D. Anderson Hospital and Tumor Institute, and study participants gave informed consent. All patients had roentgenographic or endoscopic diagnosis of a colon or rectal neoplasm and subsequent biopsy or resection for histologic confirmation of adenocarcinoma. None of the patients had symptoms of bowel obstruction. Fifty-five patients with colorectal cancer were studied before surgical resection. Prestudy data included age, sex, race, anatomic location of large bowel cancer, history of previous intestinal surgery, colorectal polyps and use of antibacterial medication, chemotherapy, laxatives, enemas, and antibowel motility drugs during the preceding month. Ninety-nine control subjects were comprised of patients' spouses and normal volunteers.

Collection, storage, and transport of breath samples.—We collected duplicate end-expiratory breath samples from all subjects by using an apparatus consisting of a 2-liter rubber anesthesia bag connected to a one-way valve with an air sample tap and on-off valve and a female connector on the bag side of the one-way valve. The mouth side of the one-way valve was connected to a mouthpiece with a segment of flexible tubing. The first of three end-expiratory breath samples was discarded for reduction of dead-space error.

To validate our method for storage and transport of breath samples, we collected end-expiratory breath samples from 2 subjects known to be breath methane excretors. With use of a gas-tight syringe, 20 50-ml aliquots from each subject were transferred to 20-cm^3 plain Venoject nonsiliconized rubber-stoppered evacuated tubes. Ten tubes each of 5 and 43.5 ppm methane in nitrogen standard, ambient air, and nitrogen were stored under identical conditions at room temperature up to 4 weeks. Five-milliliter samples were withdrawn at base-line and weekly intervals from unknown, standard, ambient air, and nitrogen tubes for gas chromatographic analysis. Up to four samples could be withdrawn from each tube.

Effect of laxative–enema preparation.—Because most of the subjects with large bowel cancer had radiographic or endoscopic confirmation of their diagnosis prior to referral, it was necessary to determine the length of time for the recovery of breath methane excretion in known excretors following laxative–enema colonoscopy preparation. Daily end-expiratory breath methane concentrations were determined on 4 healthy volunteers (table 1). On day −2 a full liquid diet was consumed; on day −1 a clear liquid diet was consumed. On the evening of day −1, 300-ml magnesium citrate and four bisacodyl tablets were taken. On the morning of day 0, two to three tap water enemas were given until all liquid return was clear.

Effect of oral hemoglobin.—Eleven healthy volunteers (7 methane excretors and 4 nonmethane excretors) ingested 2.5 g bovine hemoglobin in chocolate syrup three times a day

---

[1] Received November 2, 1981; accepted March 23, 1982.

[2] Supported in part by Public Health Service (PHS) grant RR-5511-18-BR-47 from the Division of Research Resources, National Institutes of Health; and by PHS grant 1-R01CA-29056-01 from the National Cancer Institute.

[3] Department of Medicine, Gastroenterology Section, The University of Texas System Cancer Center, M. D. Anderson Hospital and Tumor Institute, Houston, Tex. 77030.

TABLE 1.—*Effect of laxative-enema preparation on breath methane*

Subject	Age, yr	Sex	Daily mean breath methane, ppm[a]							
			−2	−1	0	+1	+2	+3	+4	+5
1	27	♂	7.8	5.0	0.1	0.5	0.0	0.0	0.1	0.0
2	28	♀	2.0	6.4	0.7	0.2	0.4	0.0	0.2	0.1
3	33	♂	22.8	25.4	15.4	3.4	6.4	18.9	22.3	25.0
4	27	♀	1.2	1.4	0.7	0.3	0.3	4.1	4.3	5.4

[a] Laxative-enema colonoscopy preparation from day −2–0, the day colonoscopy would be performed; days +1–+5 postpreparation recovery.

for 5 days. During a subsequent period, 3 of the same volunteers (all 3 methane excretors) ingested 6.7 g bovine hemoglobin in gelatin capsules three times a day for 5 days. Starting 7 days before hemoglobin administration and finishing several days after the last day of oral hemoglobin, we determined end-expiratory breath methane concentrations. We determined the presence of occult blood in stool specimens using the Hemoccult slide test.

Breath sample analysis.—Breath samples were tapped from the Venoject tubes and analyzed for methane on a gas chromatograph. Methane was identified and quantified by comparison of retention time and peak areas with those of standards consisting of 5 and 43.5 ppm methane in nitrogen. A sample of ambient air was collected with each pair of breath samples, and the breath methane levels were calculated as the difference between the means of the methane levels in the paired breath samples and the mean methane level of the ambient air (*9, 11*). A breath methane excretor was defined as having greater than 1 ppm methane in an end-expiratory breath sample (*9–12*).

RESULTS

Collection, storage, and transport of breath samples.—Weekly analyses showed that samples and standards could be stored for 4 weeks at room temperature without detectable loss of methane. Analysis of variance for determination of the magnitude and significance of possible sampling error and week-to-week differences demonstrated that these effects were not significant.

Effect of laxative-enema preparation.—Laxative-enema preparation reduced breath methane by 75–90% (table 1). Two subjects returned to 100% or more of pretreatment levels after 3 and 5 days; however, 2 subjects had a prolonged absence of breath methane excretion. Subject 2 returned to pretreatment levels after 21 days, and subject 1 returned after 7 months.

Effect of oral hemoglobin.—During the pretreatment week prior to oral hemoglobin, the methane excretors and nonexcretors had average breath methane levels of 12.0 ppm ± 1.9 SEM and 0.6 ppm ± 0.2 SEM, respectively. During the oral administration of 2.5 g hemoglobin three times each day, methane excretors and nonexcretors had average breath methane levels of 11.7 ppm ± 1.5 SEM and 0.2 ppm ± 0.1 SEM, respectively. The stool Hemoccult slide test became positive in 8 of 9 subjects tested within 3–8 days after the start of oral hemoglobin.

During the pretreatment week and the first 2 days of oral administration of 6.7 g hemoglobin three times each day, the stool had no occult blood. On the 3rd day, stools of all 3 subjects had occult blood. For each of the 3 methane excretors there was a slight increase in the mean breath methane excretion during the 5–9 days that stools contained

TABLE 2.—*Incidence of breath methane in unresected colorectal cancer patients and controls*

Study population characteristics					Methane excretors		
Group and lesion location[a]	No.	Mean age, yr ± SEM	Percent male (No.)	Percent female (No.)	Percent CH_4+[b] (No.)	Mean methane, ppm ± SEM	Mean age, yr ± SEM
Control	99	45.7±1.6	45.5 (45)	55.5 (55)	46.5 (46)[c]	12.8±1.5	48.2±2.4
Cancer patients	55	61.5±1.7	60.0 (33)	40.0 (22)	41.8 (23)[d]	16.5±2.9	65.7±2.8
Proximal	16	66.9±2.4	50.0 (8)	50.0 (8)	37.5 (6)[e]	15.4±7.5	72.0±3.4
Distal	15	60.7±3.3	66.7 (10)	33.3 (5)	60.0 (9)[f]	14.2±5.5	63.2±4.6
Rectum	24	58.3±2.9	62.5 (15)	37.5 (9)	33.3 (8)[g]	21.2±3.9	63.9±5.4

[a] Proximal = cecum, ascending, and transverse. Distal = descending and sigmoid.

[b] CH_4+ = breath methane excretor. Chi-square analysis: *c* vs. *d*, *c* vs. *e*, *c* vs. *f*, and *c* vs. *g*, not significant. *f* vs. *e* plus *g*, $0.1>P>0.05$.

TABLE 3.—*Incidence of breath methane in unresected colorectal cancer patients off antibiotics for greater than 6 days and in controls*

Study population characteristics					Methane excretors		
Group and lesion location[a]	No.	Mean age, yr ± SEM	Percent male (No.)	Percent female (No.)	Percent CH_4+[b] (No.)	Mean methane, ppm ± SEM	Mean age, yr ± SEM
Control	94	45.8±1.6	45.7 (43)	54.3 (51)	47.9 (45)[c]	12.6±1.5	48.6±2.4
Cancer patients	51	61.9±1.8	58.8 (30)	41.2 (21)	45.1 (23)[d]	16.5±2.9	65.7±2.8
Proximal	16	66.9±2.4	50.0 (8)	50.0 (8)	37.5 (6)[e]	15.4±7.5	72.0±3.4
Distal	13	60.9±3.5	69.2 (9)	30.8 (4)	69.2 (9)[f]	14.2±5.5	63.2±4.6
Rectum	22	58.9±2.9	59.1 (13)	40.9 (9)	36.4 (8)[g]	21.2±3.9	63.9±5.4

[a] Proximal = cecum, ascending, and transverse. Distal = descending and sigmoid.

[b] CH_4+ = breath methane excretor. Chi-square analysis: *c* vs. *d*, *c* vs. *e*, *c* vs. *f*, and *c* vs. *g*, not significant. *f* vs. *e* plus *g*, $0.05>P>0.01$.

TABLE 4.—*Incidence of breath methane in unresected colorectal cancer patients off enemas, laxatives, and antibiotics for greater than 6 days and in controls*

	Study population characteristics				Methane excretors		
Group and lesion location[a]	No.	Mean age, yr ± SEM	Percent male (No.)	Percent female (No.)	Percent CH$_4$+[b] (No.)	Mean methane ppm ± SEM	Mean age, yr ± SEM
Control	93	45.8±1.7	46.2 (43)	53.8 (50)	47.3 (44)[c]	13.5±1.9	48.6±2.5
Cancer patients	35	63.7±2.3	68.6 (24)	31.4 (11)	54.3 (19)[d]	18.1±3.3	67.4±2.6
Proximal	13	69.6±2.3	53.8 (7)	46.2 (6)	46.2 (6)[e]	15.4±7.5	72.0±3.4
Distal	7	65.1±3.4	85.7 (6)	14.3 (1)	71.4 (5)[f]	18.5±9.0	67.6±3.3
Rectum	15	57.9±4.1	73.3 (11)	26.7 (4)	53.3 (8)[g]	21.2±3.9	63.9±5.4

[a] Proximal = cecum, ascending, and transverse. Distal = descending and sigmoid.

[b] CH$_4$+ = breath methane excretor. Chi-square analysis: *c* vs. *d*, *c* vs. *e*, *c* vs. *f*, and *c* vs, *g*, not significant. *f* vs. *e* plus *g*, not significant.

occult blood, but this increase was not statistically significant.

Patients with unresected colorectal cancer.—There was no significant difference in the frequency or the amount of breath methane excretion in patients with unresected colorectal cancer and control subjects (table 2). This finding remained true even if patients and controls on antibiotics or patients and controls on either laxatives or enemas or antibiotics within 6 days of the breath sample collection were excluded (tables 3, 4). Patients with large bowel cancer having unresected descending or sigmoid colon cancers were more likely to be breath methane excretors than patients with colorectal cancer at other sites ($0.1>P>0.05$) (table 2). Exclusion of patients and controls on antibiotics administered within 6 days of sample collected revealed that patients with descending or sigmoid colon cancers were almost twice as likely to be breath methane excretors as were patients with colorectal cancers in other locations ($0.05>P>0.01$) (table 3). The additional exclusion of patients and controls on either laxatives or enemas within 6 days of sample collection demonstrated the same trend, but this was not significant (table 4). Breath methane excretion was unrelated to age or sex (table 5).

TABLE 5.—*Incidence of breuth methane by age and sex in unresected colorectal cancer patients off enemas, laxatives, and antibiotics for greater than 6 days and in controls*

Age, yr	Controls		Cancer patients	
	No.	Percent CH$_4$+[a] (No.)[b]	No.	Percent CH$_4$+[a] (No.)[b]
20–29	22	36.4 (8)	1	0 (0)
30–39	16	43.8 (7)	—	— —
40–49	11	45.4 (5)	3	33.3 (1)
50–59	25	60 (15)	7	42.8 (3)
60–69	15	46.7 (7)	11	45.4 (5)
70–79	1	0 (0)	11	72.7 (8)
80–89	2	50 (1)	2	100 (2)
90–99	1	100 (1)	—	— —
Total	93	47.3 (44)	35	54.3 (19)
Female	50	44.0 (22)[c, d]	11	54.6 (6)[c, d]
Male	43	51.2 (22)[c, e]	24	54.2 (13)[c, e]

[a] CH$_4$+ = breath methane excretor.

[b] Chi-square analysis: CH$_4$+ vs. age (decade), not significant.

[c] Female vs. male, not significant.

[d] Female (control) vs. femle (cancer patient), not significant.

[e] Male (control) vs. male (cancer patient), not significant.

DISCUSSION

Our retrospective study failed to confirm the observation of Haines et al. (*8*) that patients with unresected colorectal cancer are twice as likely as control subjects to be breath methane excretors. In their study, endoscopic or roentgenographic diagnostic procedures were not performed prior to breath sample collection from out-patients who came in with symptoms suggestive of large bowel cancer (personal communication). The reduced number of cancer patients excreting breath methane in our study may be due to the use of laxatives and enemas by virtually all patients before breath collection. Many of the cancer patients who did not excrete breath methane might have been methane excretors prior to laxative-enema preparation. Although bowel cleansing has been shown to decrease intracolonic methane and breath methane excretion, the length of time required to regain methane excretion has not been studied (*11*). In our study of the effect of standard colonoscopy preparation on breath methane excretion, 2 of the 4 volunteer breath methane excretors became nonexcretors for over 6 days.

Substantial differences in the anatomic distribution of colorectal cancers in the two studies might also account for the differences in our results. We have demonstrated that patients with descending or sigmoid colon cancers are twice as likely to be breath methane excretors as patients with lesions in other parts of the large bowel. A lower percentage of patients with descending and sigmoid colon cancers than was present in the study of Haines et al. (*8*) might account for our inability to confirm their observation.

Heme has been shown to be an essential in vitro growth factor for some anaerobic microflora of the human colon (*13*). Therefore, oral hemoglobin was administered for testing of the hypothesis that degraded blood from an unresected large bowel cancer provides heme to the colonic microflora, thus stimulating colonic methane production and accounting for the difference observed between cancer patients and controls of Haines et al. (*8*). In spite of delivering adequate amounts of heme to the colon, as shown by positive Hemoccult testing, no effect on breath methane excretion could be demonstrated.

The nature of the relationship between breath methane excretion and colorectal cancer remains unclear. Two additional hypotheses might account for the differences between the observation of Haines et al. (*8*) and our observation. A partial large bowel obstruction might alter the ecology of the colonic microflora, favoring the growth of methane-producing bacteria. The predominance of left-sided large bowel cancers, which are more likely to partially obstruct, in the study of Haines et al. (personal communication) compared to our study supports this hypothesis. However, our subgroup with rectal cancer did not have a higher percentage of breath methane excretors than our subgroup with cancers in the cecum, ascending colon, and transverse colon. Furthermore, none of our patients had evidence of bowel obstruction.

The second hypothesis is that breath methane excretion is a marker of the metabolism of the colonic microflora of a subgroup at greater risk for developing large bowel cancer. Studies of patients with adenomatous polyps, members of colon cancer families, and large prospective studies of the general population will be necessary to prove this hypothesis. Should this be proved to be correct, breath methane excretion might be useful for screening for the selection of a subgroup that is at increased risk for developing large bowel cancer.

REFERENCES

(*1*) American Cancer Society. Cancer facts and figures 1981. New York: Am Cancer Soc, 1981.

(*2*) Winawer SJ, Andrews M, Flehinger B, Sherlock P, Schottenfeld D, Miller DG. Progress report on controlled trial of fecal occult blood testing for the detection of colorectal neoplasia. Cancer 1980; 45:2959–2964.

(*3*) Sherlock P, Lipkin M, Winawer SJ. The prevention of colon cancer Am J Med 1980; 68:917–931.

(*4*) Hill MJ, Drasar BS, Williams RE, et al. Fecal bile acids, clostridia and the etiology of cancer of the large bowel: A case-comparison study. Lancet 1975; 1:535–539.

(*5*) Mastromarino A, Reddy BS, Wynder EL. Metabolic epidemiology of colon cancer: Enzymic activity of fecal flora. Am J Clin Nutr 1976; 29:1455–1460.

(*6*) Reddy BS, Mastromarino A, Wynder EL. Diet and metabolism Large bowel cancer. Cancer 1977; 39:1815–1819.

(*7*) Reddy BS, Wynder EL. Metabolic epidemiology of colon cancer Fecal bile acids and neutral sterols in colon cancer patients and patients with adenomatous polyps. Cancer 1977; 39:2523–2539.

(*8*) Haines A, Metz G, Dilawari J, Blendis L, Wiggins H. Breath methane in patients with cancer of the large bowel. Lancet 1977; 2:481–483.

(*9*) Bond JH, Engel RR, Levitt MD. Factors influencing pulmonary methane excretion in man: An indirect method of studying the in situ metabolism of the methane-producing colonic bacteria. J Exp Med 1971; 133:572–588.

(*10*) Calloway DH. Respiratory hydrogen and methane as affected by consumption of gas-forming foods. Gastroenterology 1966; 51:383–389.

(*11*) Bond JH, Levitt MD. Factors affecting the concentration of combustible gases in the colon during colonoscopy. Gastroenterology 1975; 68:1445–1448.

(*12*) Levitt MD, Bond JH. Volume, composition and course of intestinal gas. Gastroenterology 1970; 59:921–929.

(*13*) Bryant MP. Nutritional features and ecology of predominant anaerobic bacteria of the intestinal tract. Am J Clin Nutr 1974; 27:1313–1319.

N-Methyl-*N*-nitrosourea and Saccharin: Effects on Epithelium of Normal Human Urinary Bladder In Vitro[1,2,3]

Shadia El-Gerzawi,[4,5] Barry M. Heatfield,[4] *and* Benjamin F. Trump[4,6,7,8]

ABSTRACT—The effects of *N*-methyl-*N*-nitrosourea (MNU) and saccharin on the histology of normal human bladder "urothelium" (i.e., the epithelium of the urinary bladder) were studied in long-term explant cultures. In MNU-treated cultures, a dose response was observed. Single doses of 1-100 μg MNU/ml induced atypical focal hyperplasia, which reverted to a single or a double cell layer as seen in controls. Exophytic, papillary-like hyperplastic structures were noted after a single dose of 10 or 100 μg MNU/ml. In contrast to single doses, multiple doses (given every 2 wk) of MNU at 5 or 10 μg/ml resulted in striking focal proliferation of dysplastic spindle cells in as little as 6 weeks (three doses of MNU). At 0.5% saccharin, urothelium on explant surfaces resembled that of controls, except in one instance in which mild focal hyperplasia persisted. In the presence of saccharin, hyperplasia induced by a single dose of MNU persisted. Following three multiple doses of MNU in the presence of saccharin, spindle cell hyperplasia was induced similar to that seen with multiple doses of MNU alone, although nuclei appeared more pleomorphic and hyperchromatic in the presence of saccharin.—JNCI 1982; 69:577-583.

The etiology, pathogenesis, and progression of bladder cancer are poorly understood, as reflected by the continuing high rates of deaths associated with this disease in the United States (*1*). Epidemiologic studies have linked bladder cancer and occupational exposure or other exposure to environmental chemical substances such as those encountered in the dye, rubber, leather, and printing industries and in cigarette smoke (*2*). The hypothesis that these and other naturally occurring or synthetic chemicals that contaminate food, drinking water, and the atmosphere may result in bladder cancer (*3-5*) is in keeping with the prevailing opinion that 80-90% of human cancers are caused by environmental agents including chemical carcinogens (*6*). Although an association between exposure to chemicals and development of bladder cancer in humans is supported by the results of experimental studies with animal models in which various chemical agents are used in vivo (*7*), direct evidence of such an association in humans is not yet available.

The understanding of the pathogenesis and progression of bladder cancer in humans is largely based on extrapolation from in vivo animal studies, which can provide a continuum of development stages. Certain features of the animal tumor have their counterparts in the human tumor, although early, preneoplastic changes are difficult to obtain and assess in the human tumor. Despite similarities between the neoplasm in human and animal models, extrapolation from one to the other is often difficult. This has led to attempts to develop models based on human tissues. However, use of human tissue presents some unique problems. First, because of the obvious risks to the individual, exposure of human bladder "urothelium" (i.e., the epithelium of the urinary bladder) to potentially toxic or carcinogenic substances under experimental conditions can only be undertaken in vitro. Second, bladder tissue obtained at the time of surgery for neoplastic or nonneoplastic disease, usually in older individuals, is not suitable for studies of the effects of carcinogens on human bladder urothelium in vitro, because of the possibility that focal preneoplastic changes are already present in the urothelium, even though the urothelium may otherwise appear histologically normal. The presence of such changes would, of course, invalidate conclusions on the induction of neoplastic transformation in vitro following exposure to carcinogens.

In the present report, we describe the results of in vitro studies on chemical carcinogenesis in which we used bladder urothelium obtained from young individuals at the time of immediate autopsy (*8*) following accidental death. This paper represents the first attempt to study the response of normal human bladder urothelium to chemical carcinogens in vitro and to evaluate the effects of saccharin directly on human urothelial cells.

MATERIALS AND METHODS

Tissues.—Normal human bladder was obtained at immediate autopsy (*8*) of 9 male and 3 female patients who ranged in age from 16 to 33 years and who had died of accidental causes. None of the patients had any history of neoplastic disease of the bladder. The entire bladder was removed within a few minutes following somatic death, opened, and immersed in chilled L-15 (*9*) medium.

Culture conditions.—In a laminar flow hood, the mucosa of the entire bladder was carefully trimmed from the bladder wall. It was then rinsed several times in L-15 medium and cut into 0.5×1-cm pieces. Areas showing evidence of hem-

ABBREVIATIONS USED: AB-PAS=Alcian blue at pH 2.5-periodic acid-Schiff; DMSO=dimethyl sulfoxide; H & E=hematoxylin and eosin; MNU=*N*-methyl-*N*-nitrosourea.

---

[1] Received November 10, 1981; accepted April 26, 1982.

[2] Contribution #1106 from the Cellular Pathobiology Laboratory, Department of Pathology, University of Maryland School of Medicine.

[3] Research procedures were in accord with the ethical standards of the Human Volunteers Research Committee, University of Maryland School of Medicine.

[4] Department of Pathology, University of Maryland School of Medicine, 10 South Pine St., Baltimore, Md. 21201.

[5] *Present address*: 1 Samir Sayed Ahmmed St., El Manial-Cairo, Egypt.

[6] *Address reprint requests to* Dr. Trump.

[7] American Cancer Society Professor of Clinical Oncology.

[8] We thank Mr. Robert Pendergrass and staff for histologic sections, Ms. Pat Miller for typing the manuscript, and Mr. Carl Larsson and staff for photographic prints.

orrhage, usually as a consequence of catheterization, were excluded. Explants of the mucosa were then placed with the urothelial surface uppermost in 60-mm plastic petri dishes (Falcon Plastics, Oxnard, Calif.). The medium used was CMRL-1066 (GIBCO, Grand Island, N.Y.) supplemented with 0.1 mg hydrocortisone hemisuccinate/ml (Sigma Chemical Co., St. Louis, Mo.), 1 μg bovine recrystallized insulin/ml (Schwarz/Mann Division, Becton, Dickinson & Co., Orangeburg, N.Y.), 200 U amphotericin B/ml, 2 m*M* L-glutamine, and 5% heat-inactivated fetal calf serum (GIBCO). The culture dishes were then placed in controlled atmosphere chambers (Bellco Glass, Inc., Vineland, N.J.) and gassed for about 5 minutes with 45% O_2, 50% N_2, and 5% CO_2. The chambers were placed on rocker platforms that rocked at 10 cycles/minute, and they were incubated at 36.5–37°C. The medium and atmosphere were changed twice each week.

For our experiments, as many as 70 explants could be prepared from a single bladder. However, the number of explants from a given case was insufficient for simultaneous use in all experimental protocols. Nevertheless, enough explants were always available to permit the use of untreated explants from the same case as controls in those experiments performed.

MNU.—Explants were cultured for several days to 1 week before carcinogen treatment to allow recovery and acclimation of tissues to culture conditions. MNU (Ash-Stevens, Inc., Detroit, Mich.) was purified and provided by the National Cancer Institute, Bethesda, Md. MNU was dissolved in DMSO (Fisher Scientific Co., Springfield, N.J.). Because MNU has a short half-life, it was freshly prepared and used within 15–30 minutes (*10*). MNU was added to the culture medium at final concentrations of 1, 5, 10, or 100 μg/ml. The final concentration of DMSO in experimental and control cultures was 1%. The culture medium was always changed the day after treatment.

Specific safety procedures for protection of laboratory personnel included use of disposable gloves, masks, and gowns during preparation and handling of MNU and treatment of cultures. The exhausted medium and remaining carcinogen-containing solutions were placed in double plastic bags and incinerated.

Saccharin—A concentrated solution of saccharin (*o*-sulfobenzimide, sodium salt; Sigma Chemical Co., St. Louis, Mo.) was prepared in culture medium. The pH was adjusted, and the solution was sterilized through a 0.2-μm Nalgene filter unit (Nalgene-Sybron Co., Rochester, N.Y.). The solution of saccharin was then mixed with the medium to a final concentration of 0.02%, or 0.5%; 10% or 20% saccharin was toxic. Saccharin was added to the cultures with each change of medium.

In dosing cultures with MNU and/or saccharin in the various experiments, we used the following protocols:

1) A single dose of MNU was added to the culture medium at concentrations of 1, 10, and 100 μg/ml. Explants were sampled at 2-week intervals for 8 weeks. 2) Multiple doses of MNU were administered by the addition of the carcinogen at 2-week intervals to the culture medium at concentrations of 5 or 10 μg/ml up to 12 weeks, with final sampling at 14 weeks, 2 weeks after the last dose of MNU. 3) Saccharin was added to the culture medium at concentrations of 0.2, 0.5, 10, or 20% for 8 weeks. 4) A single dose of MNU was added to the culture medium at a concentration of 10 μg/ml; then 3 weeks later 0.5% saccharin was added, with a final sampling after 7 weeks. 5) Multiple doses of MNU were administered by the addition of the carcinogen at 2-week intervals to the culture medium (containing 0.5% saccharin) at a concentration of 5 μg/ml, with final sampling at 8 weeks, 2 weeks after the last dose of MNU.

Fixation and sampling.—The tissues were fixed immediately before culture (time 0 culture) and at the time of first treatment with MNU. Cultured explants were then sampled at 2 week intervals up to 14 weeks. In each experiment, explants were sampled 2 weeks after the last dose of MNU. All tissues were fixed in 4% formaldehyde–1% glutaraldehyde in 200 mOs*M* phosphate buffer (*11*). For light microscopy, fixed tissues were embedded in paraffin, and serial, transverse sections were cut 5 μm in thickness and stained with H & E or the AB-PAS sequence for detection of mucosubstances.

RESULTS

The results in most experiments are based on examination of explants from at least 2 patients. During the period of culture, some explants were occasionally lost due to contamination. Despite losses, three to five explants were usually available for sampling from most cases at each interval. Variability in morphologic response was noted among treated explants of the same patient under identical experimental conditions as well as among the different patients studied. In part, this variability can be attributed to the focal nature of the response. In general, examples of the morphologic responses of treated groups illustrated below represent the maximum observed.

Time 0 cultures.—Histologic examination of human urothelium before culture (time 0 cultures) revealed approximately six to eight layers of cells arranged in an ascending pattern of differentiation, from small basal cells with slightly hyperchromatic nuclei adjacent to the basement membrane, to elongated intermediate cells, and finally, to large, mature superficial cells with pale cytoplasm and abundant vacuoles at the luminal surface (fig. 1). Intermediate and superficial urothelial cells contained periodic acid–Schiff-positive granules, some of which also were Alcian blue-positive. No areas of histologic abnormalities were observed.

Control explants.—At early periods of culture (2–3 days) in control explants in the presence or absence of DMSO, urothelial cells adjacent to cut surfaces began to flatten and migrate (fig. 2). The superficial cells sometimes could be seen at the surface of some explants at this interval, but they usually sloughed and were lost. By 2 weeks, there was gradual thinning of the urothelium; small intracellular vacuoles and rounded glandlike spaces of variable size and sometimes containing mucosubstances appeared (figs. 3, 4). Mitotic figures were rare. By 4–6 weeks (fig. 5), the urothelium consisted of only one or two layers of short, columnar or cuboidal cells with only occasional glandlike spaces. Mitotic figures were rare. By the 8th week and later (fig. 6), explants were covered by a single layer of cuboidal or flattened cells, with no evidence of mucus production or presence of glandlike spaces. During culture the stroma also showed a gradual decrease in viable cells, appearing necrotic by the end of the 8th week (*see* fig. 6).

Effects of a single dose of MNU at different concentrations.—In explants of normal human urothelium exposed to a single dose of MNU at concentrations of 1, 10, or 100 µg/ml, a dose-dependent response was noted. Two weeks after a single dose of MNU (1 µg/ml), the urothelium showed areas of microscopic, focal atypical hyperplasia with foci of cellular necrosis (fig. 7). The contour of the luminal surface was irregular, and cell orientation was disturbed with occasional hyperchromatic nuclei in some cells. Glandlike spaces were present and appeared to contain necrotic cell debris (*see* fig. 8) as well as mucosubstances (AB-PAS). At a dose of 10 µg/ml, the typical hyperplasia was characterized by the formation of microscopic papillary-like proliferations of atypical urothelial cells, which frequently projected from the upper surface of explants (fig. 8). The glandlike spaces seemed larger and more numerous compared to those of the controls (*see* fig. 3) or to those in explants treated with MNU at a concentration of 1 µg/ml (*see* fig. 7). These atypical changes were more marked in explants receiving a single dose of 100 µg MNU/ml (fig. 9). Although the degree of hyperplasia and extent of necrosis varied from explant to explant, the atypical changes with numerous, large glandlike spaces were the principal features characterizing the explants. These changes eventually reverted to the more typical single cell layer seen in untreated explants (*see* fig. 6) after about 6 weeks at concentrations of 1 µg/ml and after about 6-8 weeks at concentrations of 10 or 100 µg/ml.

Effects of multiple doses of MNU at different concentrations.—Because multiple doses of MNU at a concentration of 100 µg/ml resulted in severe toxic and necrotic changes in the explants, they were discontinued. In contrast to bladder explants exposed to single doses, bladder explants exposed to multiple doses of MNU at a concentration of either 5 or 10 µg/ml over 8-14 weeks showed marked hyperplasia that appeared focally on the surface of explants. These changes consisted of multiple layers of dysplastic, spindle-shaped cells (figs. 10, 11) sometimes arranged in whorl-like configurations. The cells varied in size and shape. They possessed large, elongated nuclei, particularly in cells near the surface, and had conspicuous nucleoli. Mitotic figures were common both in the deep and superficial layers (fig. 10). Glandlike spaces were absent.

These spindle-shaped cells differed morphologically from the hyperplastic cells seen in explants following a single dose of MNU (cf. figs. 7-9). Moreover, atypical spindle cell hyperplastic changes persisted, in contrast to the lack of persistence of hyperplastic changes in explants treated with a single dose of MNU.

Effects of saccharin.—In these experiments, continuous exposure of explants to saccharin alone at concentrations of 0.2 or 0.5% resulted in only mild, if any, urothelial changes different from changes seen in untreated controls. Differences between treated cultures and controls were mainly reflected by a possible increase in the number of small glandlike structures in treated cultures. However, in one sample after 8 weeks, focal hyperplasia was noted and resembled that seen at early time periods following a single dose of MNU (fig. 12).

Effects of MNU in single or multiple doses followed by saccharin.—In explants receiving only a single dose of 10 µg MNU/ml followed 3 weeks later by continuous exposure to 0.5% saccharin for 4 weeks (total of 7 wk), urothelial changes in the form of focal atypical hyperplasias with numerous glandlike spaces containing mucosubstances were noted (fig. 13); spindle cell hyperplasia was not seen. The persistence of these changes in the presence of saccharin was dramatic in these explants compared to lesions that reverted and resembled untreated controls 6-8 weeks after a single dose of 10 µg MNU/ml alone.

In contast to the histologic effects induced by saccharin following single doses of MNU, explants exposed to as few as three multiple doses of MNU at a concentration of 5 µg/ml in the presence of 0.5% saccharin showed marked focal, atypical hyperplasia of the spindle cell type by 6 weeks (figs. 14, 15). Mitotic figures were frequently observed. These hyperplastic changes were similar to those seen in explants receiving four or five doses of MNU at a concentration of 10 µg/ml in the absence of saccharin. However, nuclei appeared more pleomorphic and hyperchromatic (fig. 15). Focal hyperplasias induced by single doses of MNU were not seen in explants exposed to multiple doses of MNU in the presence or absence of saccharin.

DISCUSSION

Our previous studies characterized the surface features of untreated human bladder urothelium by scanning electron microscopy during long-term explant culture (*12*). In the present investigation, the histologic features of untreated human bladder urothelium during long-term explant culture are consistent with our earlier observations. Overall, these studies demonstrate an early loss of mature superficial cells and survival of intermediate and basal cell types, followed by a gradual reduction in the overall thickness of the urothelium. Residual urothelial cells are probably basal cells, which are the mitotic cell component of mammalian urothelium.

In sharp contrast to untreated explant cultures, in treated explant cultures the present study has clearly demonstrated a marked focal, hyperplastic response to single or multiple doses of MNU in vitro. Two distinctive patterns of response were observed in these experiments: 1) glandular and 2) spindle cell.

The glandular pattern, induced by a single dose of MNU, was characterized by a thickening of the urothelium, with loss of cell orientation. Importantly, the surface of these focal hyperplastic changes was irregular, frequently appearing papillary in profile. In animal models and in the human, the pattern of growth of transitional cell carcinoma of the bladder in approximately 90% of the cases is papillary (*4*). Presumably, the pathogenesis of this disease involves an initial focal increase in urothelial cells followed by protrusion of hyperplastic buds into the bladder lumen. Buds contain supporting fibrovascular tissue, which eventually forms the stalk of the papillary growth. Continued proliferation of urothelial cells into the bladder lumen gives rise to papillary tumors. Epithelium, similar to normal urothelium, covers papillary tumors; invasion of the bladder wall follows increases in cell atypia and in cell numbers. Hyperplastic changes noted here after a single dose of MNU resemble early neoplastic or preneoplastic alterations in mammalian urothelium, although in vitro an internal supporting stroma and vascular supply cannot, of course, develop.

In response to multiple doses of MNU, in the presence or absence of saccharin, the second pattern of response developed, which involved a striking proliferation of spindle-shaped cells. These spindle cells resemble those comprising papillary carcinoma of the bladder [*see* (*4*)]. We have not yet obtained morphologic evidence of a progression from focal hyperplastic changes in urothelial cells in response to a single dose of MNU to spindle cell lesions seen after multiple doses of MNU, with or without the addition of saccharin. The lack of such evidence at the present time could reflect a sampling error due to the focal distribution of the lesions. Further, it remains to be determined if spindle cell lesions represent carcinoma in situ or possess invasive properties. Study by electron microscopy will be needed to fully characterize these cells and to determine their reversibility or irreversibility and neoplastic potential.

The role of the artificial sweetener saccharin in the induction of neoplasms in the human remains controversial (*13*). However, in animal models some investigators have reported that administration of chemical carcinogens, such as MNU, in small, nonneoplastic doses results in neoplastic changes in bladder urothelium if this regimen is followed by administration of other compounds that may act as promoters or cocarcinogens. For example, Hicks et al. (*14*) reported that the incidence of bladder cancer in rats receiving a single initiating, but noncarcinogenic, dose of MNU followed by a diet containing saccharin was 58% compared to an incidence of only 2% when a similar dose of MNU was administered alone. Recently, Hooson et al. (*15*) observed an increase in proliferative lesions and a shorter latent period in development of lesions in rats following a carcinogenic dose of MNU. In recent lifetime feeding studies, saccharin alone produced mild urothelial hyperplasia in male and female rats and a low incidence of bladder tumors in male rats (*16*). Similarly, Cohen et al. (*17*) reported that a diet containing another carcinogen, *N*-[4-(5-nitro-2-furyl)-2-thiazolyl]formamide, induced bladder cancer in less than 20% of rats after 6 weeks, but if administration of this carcinogen was followed by a diet containing saccharin, nearly 90% of the animals developed tumors. More recently, Fukushima and Cohen (*18*) noted an increase in the rate of DNA synthesis, which paralleled mild focal hyperplasia in rats fed saccharin. By scanning electron microscopy, pleomorphic microvilli were seen, suggestive of more than a simple regenerative response. Saccharin administered simultaneously with or after *N*-butyl-*N*-(4-hydroxybutyl)-nitrosamine has also been shown to enhance the induction of hyperplastic responses in rats (*19*, *20*). Thus, possibly acting as a weak carcinogen or promoter, at least in animal models, saccharin appears to enhance the incidence of urothelial tumors. Our observations suggest prolongation of a hyperplastic urothelium by saccharin alone and are not inconsistent with the concept of sacchrin as a weak carcinogen or promoter. In combination with multiple doses of MNU, nuclei of focal, dysplastic spindle cell hyperplasias induced in the presence of saccharin appeared more pleomorphic and hyperchromatic compared to nuclei from explants treated with MNU alone. However, further studies are needed to assess the biologic significance of these alterations.

REFERENCES

(*1*) Cole P. Lower urinary tract, chapt 10. In: Schottenfeld D, ed. Cancer epidemiology and prevention. Springfield, Ill.: Thomas, 1975: 233-262.

(*2*) Clayson DB, Cooper EH. Cancer of the urinary tract. Adv Cancer Res 1970; 13:271–381.

(*3*) Armstrong B, Doll R. Environmental factors and cancer incidence and mortality in different countries, with special reference to dietary practices. Int J Cancer 1975; 15:617–631.

(*4*) Koss LG. Tumors of the urinary bladder. In: Firminger H, ed. Atlas of tumor pathology. Washington, D.C.: Armed Forces Inst Pathol, 1975, fascicle 11, series 2, p 31 (fig. 35).

(*5*) Wynder EL, Fori GB. Guest editorial: Contribution of the environment to cancer incidence: An epidemiologic exercise. J Natl Cancer Inst 1975; 58:825–832.

(*6*) Higginson J. The role of the pathologist in environmental medicine and public health. Am J Pathol 1977; 86:459–484.

(*7*) Bryan GT. The pathogenesis of experimental bladder cancer. Cancer Res 1977; 37:2813–2816.

(*8*) Trump BF, Valigorsky JM, Jones RT, Mergner WJ, Garcia JH, Cowley RA. The application of electron microscopy and cellular biochemistry to the autopsy. Observations on cellular changes in human shock. Hum Pathol 1975; 6:499–516.

(*9*) Leibovitz A. The growth and maintenance of tissue-cell cultures in free gas exchange with the atmosphere. Am J Hyg 1963; 78:173-183.

(*10*) Hicks RM, Chowaniec J. Experimental induction, histology, and ultrastructure of hyperplasia and neoplasia of the urinary bladder epithelium. Int Rev Exp Pathol 1978; 18:199–280.

(*11*) McDowell EM, Trump BF. Histologic fixatives suitable for diagnostic light and electron microscopy. Arch Pathol Lab Med 1976; 100:405–414.

(*12*) Heatfield BM, Sanefuji H, El-Gerzawi S, Urso B, Trump BF. Surface alterations in urothelium of normal human bladder during long-term explant culture. Scan Electron Microsc 1980; 3:61–69.

(*13*) Cranmer MF. Saccharin. Park Forrest, Ill.: Pathotox Publishers, 1980.

(*14*) Hicks RM, Wakefield JS, Chowaniec J. Evaluation of a new model to detect bladder carcinogens or co-carcinogens; results obtained with saccharin, cyclamate and cyclophosphamide. Chem Biol Interact 1975; 11:225–233.

(*15*) Hooson J, Hicks RM, Grasso P, Chowaniec J. Ortho-toluene sulphonamide and saccharin in the promotion of bladder cancer in the rat. Br J Cancer 1980; 42:129–147.

(*16*) Chowaniec J, Hicks RM. Response of the rat to saccharin with particular reference to the urinary bladder. Br J Cancer 1979; 39:355–375.

(*17*) Cohen SM, Arai M, Jacobs JB, Friedell GH. Promoting effect of DL-tryptophan and saccharin in urinary bladder carcinogenesis in the rat. Cancer Res 1979; 39:1207–1217.

(*18*) Fukushima S, Cohen SM. Saccharin-induced hyperplasia of the rat urinary bladder. Cancer Res 1980; 40:734–736.

(*19*) Nakanishi K, Hirose M, Ogiso T, Hasegawa R, Arai M, Ito N. Effects of sodium saccharin and caffeine on the urinary bladder of rats treated with *N*-butyl-*N*-(4-hydroxybutyl)nitrosamine. Gan 1980; 71:490–500.

(*20*) Nakanishi K, Hagiwara A, Shibata M, Imaida K, Tatematsu M, Ito N. Dose response of saccharin in induction of urinary bladder hyperplasias in Fischer 344 rats pretreated with *N*-butyl-*N*-(4-hydroxybutyl)nitrosamine. JNCI 1980; 65:1005–1010.

Figures 1-15.—*Bars*=50 μm.

Figure 1.—Urothelium of normal human bladder employed as starting material. Urothelial cells are arranged in an ascending series of maturational stages from undifferentiated basal cells (B), to immature intermediate cells (I), and finally to mature superficial cells (S) at the luminal surface. H & E. × 350

Figure 2.—Control urothelium, 2-wk culture. Edge of migrating sheet of urothelial cells, which eventually covers cut surfaces of the explant is shown. H & E. × 350

Figure 3.—Control urothelium, 2-wk culture. Gradual thinning of the urothelium, coupled with loss of superficial cells and appearance of rounded glandlike spaces, characterizes cultures at this time period. H & E. × 350

Figure 4.—Control urothelium 2-wk culture. Mucosubstances are present within glandlike spaces of the urothelium. AB-PAS. × 350

Figure 5.—Control urothelium, 6-wk culture. Urothelium consists of one or two layers of low columnar or cuboidal cells, enclosing occasional rounded, glandlike spaces. H & E. × 350

Figure 6.—Control urothelium, 11-wk culture. At this interval the urothelium typically consists of a single cell layer. Few cellular elements are seen within the adjacent stroma. H & E. × 350

Figure 7.—Urothelium, 2-wk culture, following a single dose of 1 μg MNU/ml. Urothelium shows atypical changes including irregularity in height and contour of the luminal surface. Some nuclei are hyperchromatic, and cells appear disoriented. Small glandlike spaces contain necrotic cell debris (*arrow*). H & E. × 350

Figure 8.—Urothelium, 2-wk culture, following a single dose of 10 μg MNU/ml. Focal, papillary proliferations of atypical urothelial cells are seen projecting from the explant surface. These papillary structures do not represent cleavage artifacts but are exophytic growths. Small glandlike spaces also are present. H & E. × 350

Figure 9.—Urothelium, 2-wk culture, following a single dose of 100 μg MNU/ml. Compared to control urothelia (figs. 2, 3), the urothelium shows marked atypical, focal hyperplastic changes. Cells lack orientation. Some nuclei are hyperchromatic. Small-to-large glandlike spaces are seen. H & E. × 350

Figure 10.—Marked, atypical hyperplasia at the explant surface, 2 wk following five doses of 10 μg MNU/ml at 2-wk intervals for 10 wk. Dysplastic, spindle-shaped cells possess elongated nuclei and occur in whorl-like patterns closely resembling patterns of spindle cell carcinoma. *Arrow* indicates one of several mitotic figures in this lesion. H & E. × 350

Figure 11.—Higher magnification of dysplastic, spindle-shaped cells with pleomorphic nuclei shown in fig. 10. H & E. × 700

Figure 12.—Urothelium after continuous exposure to 0.5% saccharin for 8 wk. Focal hyperplasia is similar to that seen following a single dose of MNU. H & E. × 350

Figure 13.—Urothelium after a single dose of 10 μg MNU/ml, followed at 3 wk by 0.5% saccharin for 4 wk. Compared to control urothelia (fig. 5), the urothelium is markedly hyperplastic with numerous small-to-large glandlike spaces enclosing eosinophilic material similar to that shown in fig. 9. H & E. × 350

Figure 14.—Marked hyperplasia is seen at the explant surface following three doses of 5 μg MNU/ml at 2-wk intervals for 6 wk in medium containing 0.5% saccharin. Dysplastic, spindle cells are arranged in whorl-like configurations similar to those seen in fig. 11; however, nuclei appear more pleomorphic and hyperchromatic. H & E. × 350

Figure 15.—Higher magnification of dysplastic, spindle-shaped cells with pleomorphic and hyperchromatic nuclei shown in fig. 14. H & E. × 700

1

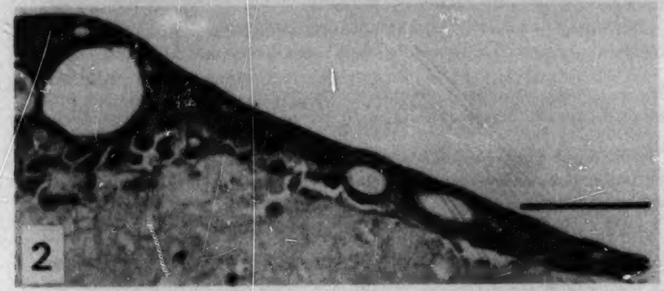
2

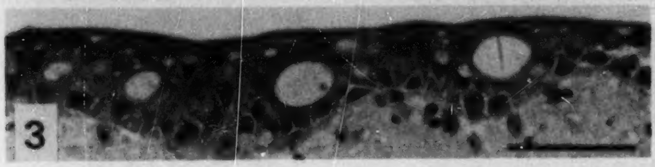
3

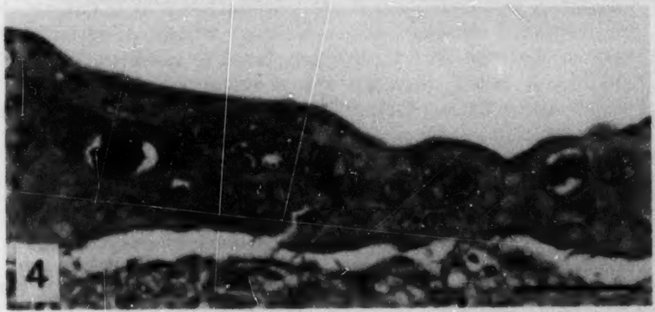
4

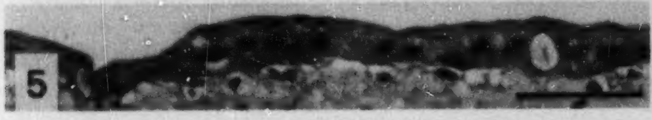
5

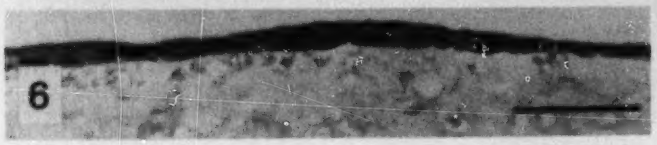
6

7

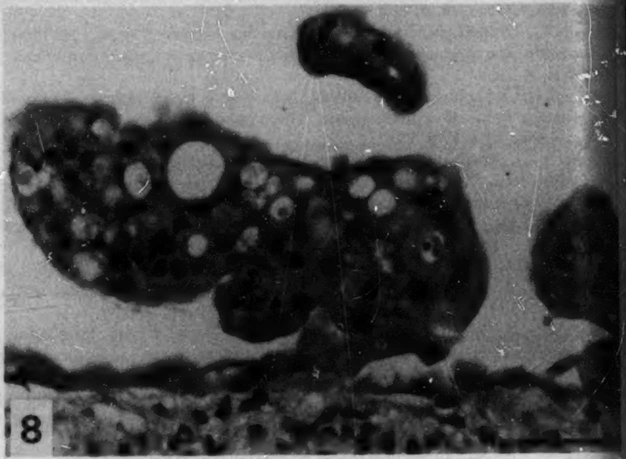
8

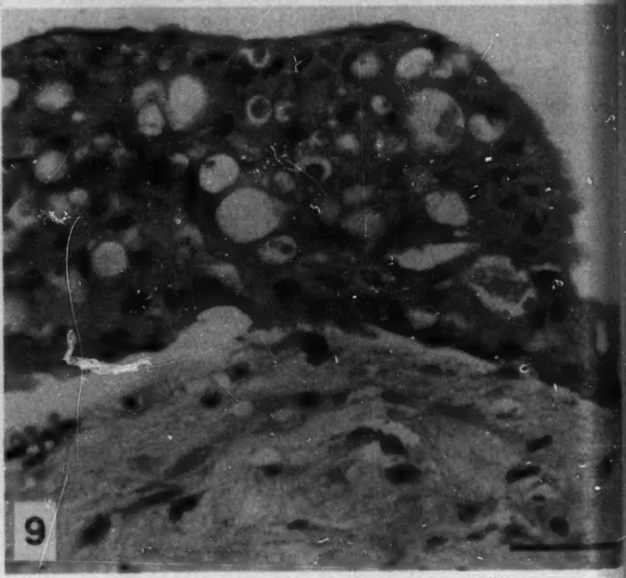
9

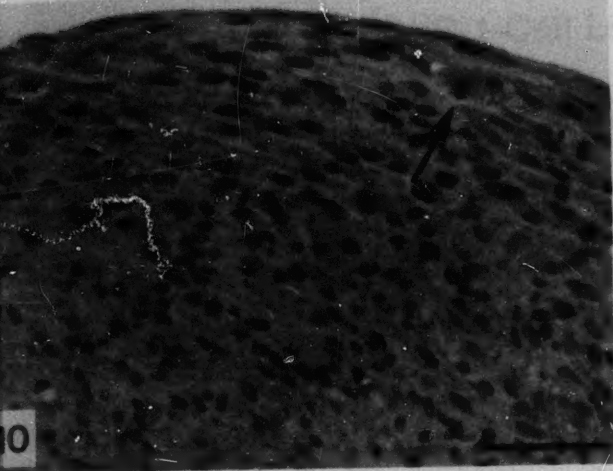
0

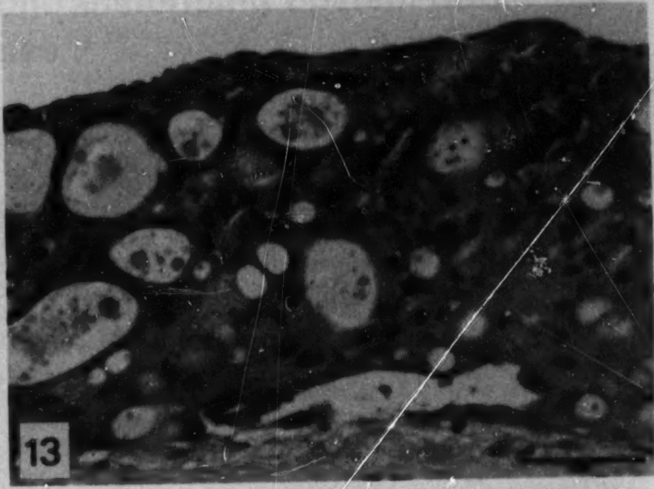
13

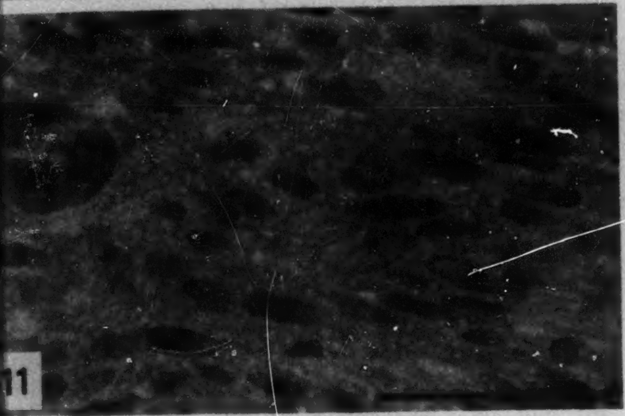
11

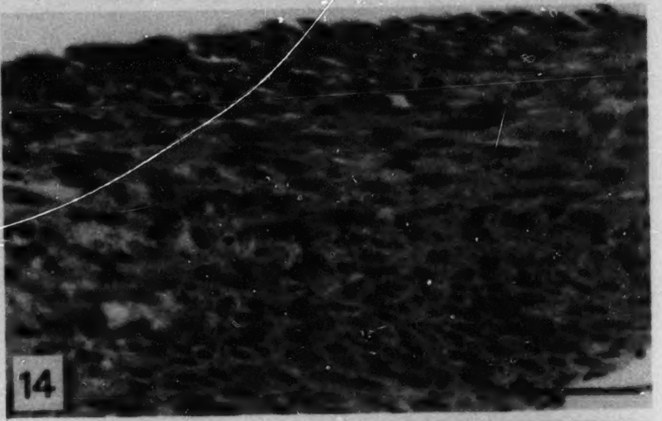
14

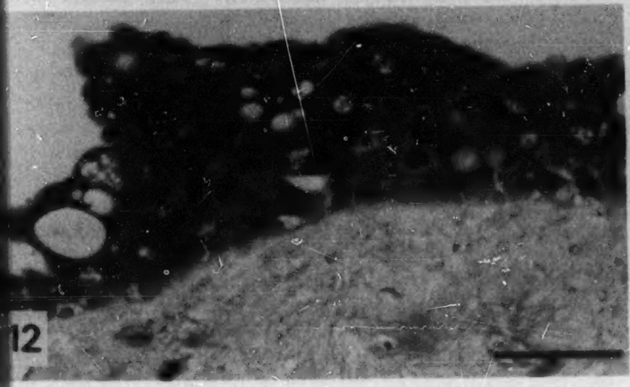
12

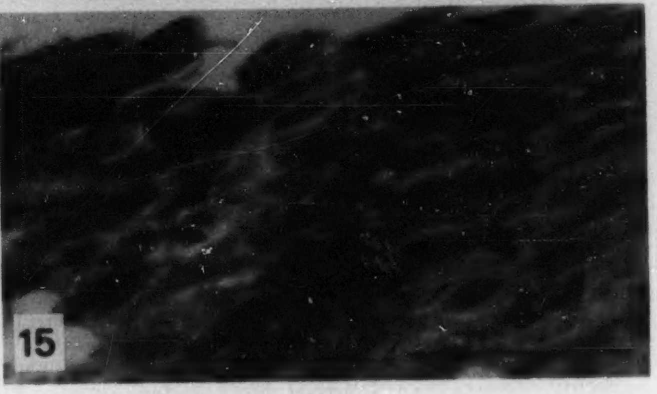
15

blank page

Persistence of Transforming and Nontransforming Epstein-Barr Virus in High Passages of P3HR-1 Cell Lines[1,2,3]

Paul Gerber,[4] Dharam Ablashi,[5,6] Ian Magrath,[7] Gary Armstrong,[5] Philip Andersen,[5] *and* Luba Trach[4,8,9]

ABSTRACT—At least three laboratories have reported that the P3HR-1 line, which had originally produced transforming Epstein-Barr virus (EBV), now produces only the nontransforming variant. Studies to determine whether these findings were universal or a consequence of specific cell lines or culture conditions were undertaken in P3HR-1 cultures of identical HLA types from five sources. All of the EBV preparations derived from cell lines cultured at 32, 34, and 35°C transformed cord blood lymphocytes, whereas virus propagated at 37°C did not usually transform. Furthermore, indirect immunofluorescence revealed that a monoclonal antibody directed against transforming EBV membrane glycoprotein bound to 10–12% of the P3HR-1 cells that had been continuously propagated at 34°C, but the antibody did not bind to the same cells cultured at 37°C. Although virus expression was completely repressed in transformed cord blood cells, transforming virus could be rescued by superinfection with nontransforming P3HR-1 EBV. Cells transformed with P3HR-1 virus induced poorly differentiated lymphomas in athymic nude mice after seven or eight passages. Whether all P3HR-1 cells have the potential to produce detectable quantities of transforming virus remains to be determined.—JNCI 1982; 69:585–590.

Currently, most investigators accept that there are two major classes or "strains" of EBV, which are characterized in terms of their ability to transform human cord blood lymphocytes and to induce the EBV EA in EBV DNA-containing but EBV-nonproducing cell lines, such as Raji. All known EBV, with one exception, fall into the "transforming" group; i.e., they will transform cord blood lymphocytes or lymphocytes from EBV-seronegative donors, but they will not induce EA in Raji cells (*1–3*). The exceptional virus is that produced by the P3HR-1 cell line (*4*), a clonal derivative of the Jijoye (P3J) line originally isolated by Pulvertaft (*5*) from a Nigerian patient with Burkitt's lymphoma (table 1). Menezes et al. (*3*) and Miller et al. (*1*) were unable to demonstrate transformation with P3HR-1 virus, but this virus will readily induce EA in Raji cells (*6*).

The differences in the biologic properties of the two virus classes should permit the identification of the DNA sequences and molecular events resulting in transformation as opposed to productive infection and may therefore provide insights into the molecular basis for the oncogenic potential of EBV (*7*). Such studies, however, require stable homogeneous preparations of virus particles and are ideally performed with cloned stocks of mutant viruses that can be compared with the parental strain. In this regard and in view of the recent reports that P3HR-1 virus does not transform, it is of considerable interest that the parental cell line of P3HR-1 (P3J) released only transforming virus (*8*). Moreover, early passages of P3HR-1 appear to have released transforming virus, since cell lines that were derived by infection of cord blood cells with EBV from early isolates of P3HR-1 have been reported (table 1) (*9, 10*). Quite possibly, the P3HR-1 virus has since undergone a mutation that resulted in the loss of its transforming potential (*1*). Aya and Osato (*11*), however, have recently shown that their P3HR-1 cell line releases viruses capable of inducing DNA synthesis and EBNA in cord blood cells (table 1), both of which are associated with and are possibly a prerequisite to transformation. Aya and Osato did not, however, report the induction of continuous cell lines with P3HR-1-derived virus. The question arises, therefore, as to whether high-passage P3HR-1 cells release a mixture of viruses with different biologic properties. If so, the composition of virus preparations may vary.

In view of these findings, we have studied the P3HR-1 viruses produced by cell lines maintained in different laboratories and have examined the effect of culture conditions on the properties of the released virus particles. Virus preparations obtained from cell lines continuously cultured in separate laboratories may have different properties in any given cell line. Further, since the conditions of culture differ in different laboratories, the properties of any given virus preparation may be in part dependent on these conditions.

ABBREVIATIONS USED: EA=early antigen; EBV=Epstein-Barr virus(es); EBNA=EBV nuclear antigen; EMEM=Eagle's minimum essential medium; FCS=fetal calf serum; MA=membrane antigen; VCA=viral capsid antigen.

---

[1] Received December 10, 1981; accepted April 7, 1982.

[2] Supported by Public Health Service contract N01CP-45617 from the National Cancer Institute.

[3] We followed the guidelines set forth in the "Guide for the Care and Use of Laboratory Animals" by the Institute of Laboratory Animal Resources, National Research Council.

[4] Bureau of Biologics, Food and Drug Administration, Bethesda, Md. 20205.

[5] Laboratory of Cellular and Molecular Biology, Division of Cancer Cause and Prevention, National Cancer Institute, National Institutes of Health, Public Health Service, U.S. Department of Health and Human Services, Bethesda, Md. 20205.

[6] *Address reprint requests to* Dr. Ablashi, Building 37, Room 1A07, National Institutes of Health, Bethesda, Md. 20205.

[7] Pediatric Oncology Branch, Division of Cancer Treatment, National Cancer Institute.

[8] We regret to inform readers of the untimely death of Dr. Paul Gerber. This is his last contribution to the field of Epstein-Barr virus research, an area in which he was a pioneer.

[9] We extend our thanks to Dr. Gerald Quinnan, Jr., Division of Virology, Bureau of Biologics, for making available Dr. Gerber's data, books, and laboratory materials to finish this work. We thank Dr. John S. Cole, National Cancer Institute, for providing nontransforming P3HR-1 EBV through the Resource and Logistics Program. We also thank Dr. Paul Terasaki, University of California at Los Angeles, for HLA typing of our cell lines.

Temperature may be particularly important in this regard since the amount of virus released by P3HR-1 cells is increased at low temperature. In addition, Sairenji and Hinuma (*12*) have demonstrated that the Jijoye line, the parental line of P3HR-1 (table 1), releases transforming virus at 33°C but not at 37°C. Virus release from the B95-8 cell line is not affected by the temperature of incubation (at least between 32 and 37°C).

MATERIALS AND METHODS

Cells.—The origins of P3HR-1 cells from which EBV preparations were obtained are given in table 2. The precise duration of continuous culture for each of the P3HR-1 lines is not known, but in all cases the lines had been subpassaged over several years.

Raji cells were used to assay for EA induction.

All cells were grown and maintained in RPMI-1640 medium with 10% heat-inactivated FCS, 100 U penicillin/ml, and 100 μg streptomycin/ml.

HLA.—P3HR-1 cells from different sources were typed for HLA antigens. Four of the P3HR-1 cell lines were HLA A3, B17, and BW35 [identical to that reported by Traul et al. (*10*)], and one cell line from Dr. Osato (#4 in table 2) expressed only A3. The human cord blood cell lines obtained by transformation with P3HR-1 EBV were also examined for HLA so that any contamination with P3HR-1 cells would be ruled out.

Virus preparation.—As shown in table 2, cells were routinely cultured at 37°C and then at either 32 or 35°C for virus preparation. One set of P3HR-1 cells, obtained from Dr. W. Henle, The Children's Hospital of Philadelphia, Philadelphia, Pa., was consistently carried at 34°C (5*b*, table 2).

The virus was prepared as follows: 1) P3HR-1 cells were cultured at a concentration of 5×10^5 cells/ml at 37°C and were allowed to age for 6 days at 37, 35, or 32°C. On the day of harvest, supernatants were clarified by low-speed centrifugation and then concentrated by ultrafiltration (Millipore pellicon casette system with a mol wt of 1–3 million) according to the procedure of Magrath et al. (*13*). The supernatant concentrates were then passed through a 0.45-μm nitrocellulose filter and centrifuged in an SW 27 rotor at 26°K for 1 hour. Pellets were resuspended in spent medium, sonicated for 10 seconds twice on ice, and passed again through a 0.45-μm Millipore filter. Final suspension was adjusted to a concentration factor up to 1,000. Then 1- to 3-ml aliquots of virus were stored at −70°C.

2) A monoclonal antibody was used for detection of a membrane glycoprotein associated with transforming virus for virus preparation from P3HR-1-reactive and nonreactive cells. Monoclonal antibody 2F5.6 (supplied by Dr. Gary Pearson, Mayo Clinic, Rochester, Minn.) was used for identification of cells producing transforming virus by an indirect membrane immunofluorescence technique. This antibody is directed against an antigenic determinant on the major membrane glycoprotein (320°K), which is common to transforming EBV (B95-8 and AG-876) but absent from the lytic P3HR-1 EBV (*14*). We routinely used this antibody to follow the P3HR-1 cultures to detect the MA-producing cells. This antibody failed to show MA-positive cells in P3HR-1 cells carried at 37°C, but it detected between 8 and 12% MA-positive cells in P3HR-1 cells carried at 34°C (fig. 1). Thus both 2F5.6 MA-reactive and nonreactive cells were used for virus preparation from source 5 (table 2).

P3HR-1 cells at a concentration of 1×10^6/ml from source 5 (table 2) were continuously carried at 37 and 34°C for 10 days without a change of medium. On the day of virus preparation, cells were rapidly frozen and thawed twice in a small volume of their own supernatant and then mixed with the rest of the supernatant. The supernatants were clarified at low speed, filtered through a 0.45-μm filter, and concentrated by ultracentrifugation at $70\times10^3\times g$ for 1.5 hours. The pellets were then resuspended in spent medium at a final concentration of 75-fold. The virus was stored in 1-ml vials in liquid nitrogen. The cell lines from each source were examined for VCA-producing cells. There was a greater fraction of VCA-producing cells at lower temperatures, but this number varied from one preparation to another, as previously shown by Magrath et al. (*13*) with P3HR-1, AG-876 and B95-8 EBV preparations.

TABLE 1.—*Human lymphoblastoid cell line from African Burkitt's lymphoma producing infectious (lytic-nontransforming) and transforming EBV (established by Pulvertaft, 1964)*

P3J (Jijoye)—transforming virus [Henle et al. (*8*), 1967; Sairenji and Hinuma (*12*), 1980]
↓
HR-1 clone [Hinuma and Grace (*4*), 1967]
↓
HR-1 virus
↓
Infectivity
↓

Transforming–nontransforming			Nontransforming		
↓	↓	↓	↓	↓	↓
Gerber et al. (*9*), 1969: Adult donor lymphocyte cell lines AV_1 and AV_2	Aya and Osato (*11*), 1974: Human cord mononuclear cells—presence of EBNA and DNA synthesis	Traul et al. (*10*), 1977: Superinfection of 6410 nonproducer cells; these cells produce EBV (transforming and nontransforming)	Miller et al. (*1*), 1974: P3HR-1 virus lacks transforming activity but has EA induction of Raji cells.	Menezes et al. (*3*), 1975: Biological differences between EBV strains	Klein et al. (*2*), 1978: The Jijoye line differs from the P3HR-1 line in that it is susceptible to infection with P3HR-1 virus.

Assay of EBV from P3HR-1 cells by induction of EA and transformation.—For assay of EA induction, 5×10^5 Raji or LDV/7 cells showing 85% or more viability were superinfected with tenfold dilutions of virus in 1.0-ml amounts. These cells were examined for EA at 48 and 72 hours post infection for calculation of EA-inducing units according to the procedure of Henle et al. (*15*).

Transforming EBV was assayed by measurement of the ability of the virus to transform human cord lymphocytes with or without treatment with Polybrene. Cord blood mononuclear cells were treated overnight with 2 μg Polybrene/ml, washed with RPMI-1640 medium, infected with 0.2 ml of virus (5×10^6 cells/ml) in a small plastic tube (12×75 mm), and incubated at 37°C. After 2 hours, the cells were washed, fed with medium, and incubated at 37°C. Half the volume of medium was changed weekly. Transformation was judged initially by morphologic changes and later by the presence of EBNA, immortalization, and EBV DNA. The transformed cells were examined for VCA and EA production. Titers were expressed as median transformation dose per milliliter (TD$_{50}$/ml) based on 50% transformation (*16*). Some transformed cord blood lymphocytes were also typed for HLA antigens (table 2).

Rescue of transforming virus from P3HR-1-transformed cord blood cells.—Transforming virus was rescued from transformed cord blood cells according to the method described by Yajima et al. (*17*) with slight modification. One specific P3HR-1 virus preparation (400× concentration) obtained from Pfizer and Co., Inc., Maywood, N.J., was found to possess 10^6/ml EA-inducing titer in Raji cells by serial dilutions. This P3HR-1 EBV lot also failed to induce transformation in cord blood lymphocytes over 8 weeks. This preparation thus only possessed lytic EBV and was used for rescue experiments.

The P3HR-1 virus-transformed cord blood lymphocytes were washed three times with phosphate-free EMEM containing 2% dialyzed FCS and adjusted to contain 1×10^6 cells/ml. Cells from 10 ml of this cell suspension were pelleted, and the supernatant was discarded. Pfizer P3HR-1 EBV with an EA-inducing titer in Raji cells of 10^6 was diluted 1:5 in EMEM containing 2% dialyzed FCS, and the cord blood cells were resuspended in 1 ml of virus suspension and absorbed for 2 hours. After absorption the cells were washed three times in EMEM and resuspended in 10 ml of phosphate-free EMEM containing 2% dialyzed FCS and incubated at 37°C for 72 hours. The cells were then frozen and thawed in their supernatant, clarified, filtered through a 0.45-μm Millipore filter, and concentrated to 100× as previously described.

Nucleic acid hybridization.—EBV DNA from P3HR-1 cells (supplied by Dr. Nonoyama, Showa University Research Institute, St. Petersburg, Fla., under National Cancer Institute contract) was used for hybridization with DNA from P3HR-1-transformed cells and P3HR-1 cells grown at 37°C (5*b*; table 2) according to the method of Fresen et al. (*7*). EBV genome-negative BJAB cell DNA was used as a negative control.

Induction of tumors in athymic nude mice.—Transformed cord blood cells (10^8) in their seventh or eighth passage were injected sc into each of ten 6-week-old noninbred N:NIH(S) *nu/nu* athymic nude mice (1, 2, and 5*b*; table 2). The mice had been treated with antithymocyte serum 1 week before and 2 weeks after inoculation according to the procedure of Ablashi et al. (*18*).

RESULTS AND DISCUSSION

Properties of P3HR-1 Virus Preparations

Table 2 shows the characteristics of EBV preparations from cells aged at 32, 35, and 34°C that contained EA-inducing and EA-transforming EBV. The virus preparations (75×) from P3HR-1 cells consistently carried at 34°C contained 10$^{2.5}$–10$^{4.5}$ transforming virus (6/10 attempts), but they failed to release any transforming virus at 37°C (5*b*; table 2). The virus preparations (100× or 200×) from cells aged at 32 and 35°C (1, 2, 3, 4, 5*a* and 6; table 2) always released low amounts of transforming virus (10$^{1.0}$–10$^{2.5}$), regardless of the source of the P3HR-1 cells, although preparations from cells cultured at 37°C were inconsistent in their transforming abilities. Transformation was never shown by preparations concentrated less than a hundredfold (3, 5*b*; table 2) or by a preparation obtained from Pfizer, although the Pfizer preparation was a potential inducer of EA (*see* "Materials and Methods").

Table 2 shows that cord blood cells transformed by various preparations of P3HR-1 virus had different HLA types from the P3HR-1 cell line itself, which rules out contamination of the cord blood cells with P3HR-1. The transformed cells contained EBNA and EBV DNA, but they did not express any EA or VCA.

Table 2 also shows that virus preparations from all sources were also able to induce EA, although to a variable extent. EBV preparations from 5*b* (75×) at 37 and 34°C consistently contained large amounts of EA-inducing virus (≥10$^{4.0}$).

Detection of Transforming Virus-Associated Antigens With a Monoclonal Antibody

Our data demonstrating the presence of transforming EBV in P3HR-1 are strongly supported by the reactivity of specific EBV monoclonal antibody. The antibody gave punctate as well as full-ring fluorescence in 10–12% of the P3HR-1 cells from 5*b*, table 2, maintained at 34°C (figs. 1A, B). It also reacted with approximately 5–7% AG-876 as well as B95-8 cells (both of which release transforming virus), but it failed to react with P3HR-1 cells continuously passaged at 37°C from 5*b* or with the P3HR-1 cell line obtained from Dr. Pearson (data not included). The antibody did not react with Raji and BJAB cells. The P3HR-1 cell line subpassaged at 34°C generally showed punctate staining of cells (fig. 1A) after 3–4 days, and as the cells were further aged, brilliant membrane fluorescence was observed (fig. 1B). Thus 2F5.6 monoclonal antibody (*14*) is a valuable reagent in distinguishing between lytic and transforming EBV as well as in monitoring the production of transforming virus.

Rescue of Transforming Virus From Cord Blood Cell Lines

A number of investigators have shown that transforming

TABLE 2.—*Recovery of nontransforming (lytic) and transforming EBV from P3HR-1 cells from different sources*[a]

Origin of P3HR-1 cells for virus preparations	EBV VCA-EA, %	Virus preparation: Aged at temperature, °C	Virus preparation: Description	Infectivity of virus preparation: EA induction on Raji cells and/or LDV/7 cells	Infectivity of virus preparation: Transformation of human cord cells[b] (amount of transforming virus recovered)	HLA type of transformed cells[c,d]	EBNA[d,e]	EBV-DNA
1) Cells were grown for several years in continuous culture, frozen in 1971, and revived in 1980 by P. Gerber.	15–18	32	Cells were grown at 37°C and aged at these temperatures.	+	+	A3, AW23, BW16, BW35[f]	+	+
		35		+	+		+	ND
					(1.0–2.5 logs)			
2) Cells were frozen in Jan. 1978 and revived in Oct. 1979 by Gerber.	12–15	32	Cells were grown at 37°C and aged at these temperatures.	+	+	A3, AW30, B7, BW44[f]	+	+
		35		+	+		+	ND
		37		+	+		ND	ND
					(1.0–2.5 logs)			
3) Cells were given to Gerber at end of March 1980 by D. V. Ablashi, who received these cells from R. Glaser in 1975 and froze them in Dec. 1975. Glaser had received these cells from M. Nonoyama.	15–20	32	As in 1	+	+	A3, AW30, B7, BW44	+	+
		35	As in 1	+	+		+	ND
		37	As in 2	+	+			
				+	−			
					(1.0–2.5 logs)			
4) Cells received by Gerber from T. Osato in Feb. 1975, were frozen the same year, and revived in May 1980.	12–15	32	As in 1	+	+	A3, AW23, BW16, BW35	+	+
		35	As in 1	+	+		+	ND
		37	As in 2	+	+		ND	ND
					(1.0–2.5 logs)			
5) Cells obtained from W. Henle in July–Aug. 1980 independently by *a*) Gerber and *b*) Ablashi.	18–22	32	As in 1	+	+	A1, A3, BW35[f]	+	+
		35		+	+		+	ND
		34	Cells were grown and aged at these temperatures.	+	+		ND	ND
		37		+	−			
					(2.5–4.5 logs)			
6) Cells obtained by Gerber from E. Kieff in Sept. 1980 were originally received from G. Klein.	12–15	32	As in 1	+	+	A3, AW23, BW16, BW35	+	+
		35	As in 1	+	+		+	ND
		37	As in 2	+	+		ND	ND
					(1.0–2.5 logs)			

[a] HLA of P3HR-1 cells from 1, 2, 3, 5, and 6 were A3, B17, and BW35; for 4 it was A3 only. +=contain virus or transformed human cord cell or detected EBNA or cell DNA hybridized with EBV-DNA. −=no transformation.

[b] Cord blood mononuclear cells were treated with 2 μg Polybrene/ml in Ablashi's laboratory but not in Gerber's laboratory. The amount of virus recovered from cells aged at 37°C was always less (≤1.0 log) in comparison to that recovered from cells aged at 32 and 35°C (≥1.0–≤2.5 logs).

[c] Cord blood mononuclear cells from same donor were used for transformation with virus preparations from 1, 4, and 6. A separate donor was used for 2 and 3, and a third for 5.

[d] EBNA test was performed usually on days 12, 14, and 18. Cells were also examined for VCA–EA.

[e] ND=not done.

[f] Cell lines inoculated into nude mice. Tumors usually appeared between 15 and 60 days, and on the average 50% of the mice had tumors with single or multiple nodules.

virus can be obtained from EBV DNA-containing, but nonvirus-producing cell lines, such as Raji, by superinfection with P3HR-1. The released transforming virus may be a recombinant between P3HR-1 and the resident viral genomes, although simple selection and amplification of P3HR-1-derived transforming particles have not been excluded.

We therefore attempted to superinfect nonproducer cell lines, which had themselves been obtained by transforming cord blood lymphocytes with P3HR-1 virus (1 and 5*b*; table 2). The filtered cell lysates from cells superinfected with nontransforming Pfizer P3HR-1 virus preparation were able to transform cord blood cells, but they were not able to induce EA in Raji cells. Thus the rescued EBV appears to be a homogeneous preparation of transforming virus particles. This strongly suggests that P3HR-1 cell lines release mixtures of virus particles with different biologic properties. Our rescued transforming P3HR-1 virus will be useful for molecular and biologic comparisons with virus derived from B95-8 and AG-876 cell lines and putative recombinants between these viruses and P3HR-1 (*7, 16, 19, 20*). In particular, it will be important to determine whether the rescued transforming virus from P3HR-1-transformed cord blood lines is identical to that rescued from P3HR-1-superinfected

Raji cells, since this determination should reveal whether or not the second virus is a recombinant or a selected subpopulation of P3HR-1 virus.

Propagation of Transformed Cell Lines in Nude Mice

Several P3HR-1 virus-transformed human cord blood lymphocyte lines inoculated into nude mice continued to proliferate as poorly differentiated lymphomas in 50% of the animals (table 2). These tumors contained human chromosomes. The tumors in most cases were composed of a single nodule, but multiple nodules were also observed. Cultured cells from these tumors contained EBNA but no EA or VCA (*18*).

Attempts are being made to transform marmoset and stump tail monkey peripheral lymphocytes with P3HR-1-transforming virus for establishment of a high-virus-producing cell line permitting further molecular and biologic comparisons between isolates.

Our data in 5*b* of table 2 are consistent with the findings of Sairenji and Hinuma (*12*) who reported high yields of transforming EBV at 33°C but not at 37°C from Jijoye (P3J) cells. However, unlike Jijoye cells, which do not yield EA-inducing virus, P3HR-1 cells produce EA-inducing virus at both 33 and 37°C. Furthermore, our recent findings with AG-876 cells maintained at 34°C show at least 2 logs more transforming virus than is obtained from cells cultured at 37°C. Therefore, the results of Sairenji and Hinuma (*12*) and our results with respect to transforming EBV suggest that growing and culturing appropriate lines at lower temperatures markedly enhance release of transforming EBV. In P3HR-1 cell lines that produce very low amounts of transforming virus, such virus may be detectable only when cells are cultured at lower temperature.

We have shown that P3HR-1 virus from cell lines propagated in several laboratories is capable of both transformation and EA induction in Raji cells. Whether individual virus particles possess both properties, whether there is a mixture of virus particles, as has been suggested by others, or whether individual nontransforming mutants can complement each other at high multiplicity and induce transformation is unknown. However, the possibility of complementation seems very unlikely in view of the fact that at least one P3HR-1 virus preparation, that obtained from Pfizer, is unable to transform at all, in spite of the fact that it contains large amounts of virus, as demonstrated by its potent ability to induce EA in Raji cells. If there are mixtures of transforming and nontransforming properties, as our rescue experiments suggest, it would be important to determine *a*) whether individual P3HR-1 cells produce one or both kinds of virus and *b*) the nature of the difference between these particles. Cloning of cells may provide the means to answer these questions.

REFERENCES

(*1*) Miller G, Robinson J, Heston L, Lipman M. Difference between laboratory strains of Epstein-Barr virus based on immortalization, abortive infection and interference. Proc Natl Acad Sci USA 1974; 71:4006-4010.

(*2*) Klein G, Yefenof E, Falk K, West A. Relationship between Epstein-Barr virus (EBV)—production and the loss of the EBV receptor/complement complex in a series of sublines derived from the same original Burkitt's lymphoma. Int J Cancer 1978; 21:552-560.

(*3*) Menezes J, Leibold W, Klein G. Biological differences between Epstein-Barr virus strains with regard to lymphocyte transforming ability, superinfection antigen induction. Exp Cell Res 1975; 92:478-484.

(*4*) Hinuma Y, Grace JT Jr. Cloning of immunoglobulin-producing human leukemic and lymphoma cells in long term cultures. Proc Soc Exp Biol Med 1967; 124:107-117.

(*5*) Pulvertaft RJ. Cytology of Burkitt's lymphoma (African lymphoma). Lancet 1964; 1:238-240.

(*6*) Gergely L, Klein G, Ernberg I. Appearance of Epstein-Barr virus associated antigens in infected Raji cells. Virology 1971; 45:10-21.

(*7*) Fresen KO, Merkt B, Bornkamm GW, Zur Hausen H. Heterogeneity of Epstein-Barr virus originating from P3HR-1 cells. I. Studies on EBNA induction. Int J Cancer 1977; 19:317-323.

(*8*) Henle W, Diehl V, Kohn G, Zur Hausen H, Henle G. Herpes-type virus and chromosome marker in normal leukocytes after growth with irradiated Burkitt's cells. Science 1967; 157:1064-1065.

(*9*) Gerber P, Whang-Peng J, Monroe JH. Transformation and chromosome changes induced by Epstein-Barr virus in normal human leukocyte culture. Proc Natl Acad Sci USA 1969; 63:740-747.

(*10*) Traul KA, Stephens R, Gerber P, Peterson WD. Productive Epstein-Barr viral infection of the human lymphoblastoid cell line 6410 with release of early antigen inducing and transforming virus. Int J Cancer 1977; 20:247-255.

(*11*) Aya T, Osato T. Early events in transformation of human cord leukocytes by Epstein-Barr virus: Induction of DNA synthesis, mitosis and virus associated nuclear antigen synthesis. Int J Cancer 1974; 14:341-347.

(*12*) Sairenji T, Hinuma Y. Re-evaluation of transforming strain of Epstein-Barr virus from the Burkitt's lymphoma cell line, Jijoye. Int J Cancer 1980; 26:337-342.

(*13*) Magrath IT, Pizzo PA, Novikovs L, Levine AS. Enhancement of Epstein-Barr virus replication in producer cell lines by combination of low temperature and corticosteroids. Virology 1979; 97:477-481.

(*14*) Qualtiere LF, Chase R, Vroman B, Pearson GR. Identification of Epstein-Barr virus strain differences with monoclonal antibody to membrane glycoprotein. Proc Natl Acad Sci USA 1982; 79:616-620.

(*15*) Henle W, Henle G, Zajac B, Pearson G, Wanbke R, Scriba M. Differential reactivity of human serums with early antigens induced by Epstein-Barr virus. Science 1970; 169:188-190.

(*16*) Miller G, Lipman M. Release of infectious Epstein-Barr virus by transformed marmoset leukocytes. Proc Natl Acad Sci USA 1973; 70:190-191.

(*17*) Yajima Y, Marczynska B, Nonoyama M. Transforming activity of Epstein-Barr virus obtained by superinfection of Raji cells. Proc Natl Acad Sci USA 1978; 75:2008-2010.

(*18*) Ablashi DV, Glaser R, Easton JM, Nonoyama M, Armstrong GR. Athymic nude mice: Induction of tumors containing Epstein-Barr virus using Burkitt's-related cell lines. Exp Hematol 1978; 6:365-374.

(*19*) Dambaugh T, Raab-Traub N, Heller, M, et al. Variation among isolates of Epstein-Barr virus. Ann NY Acad Sci 1980; 354:309-325.

(*20*) Pizzo PA, Magrath IT, Chattopadhyay SK, Biggar RJ, Gerber P. A new tumor-derived transforming strain of Epstein-Barr virus. Nature 1978; 272:629-631.

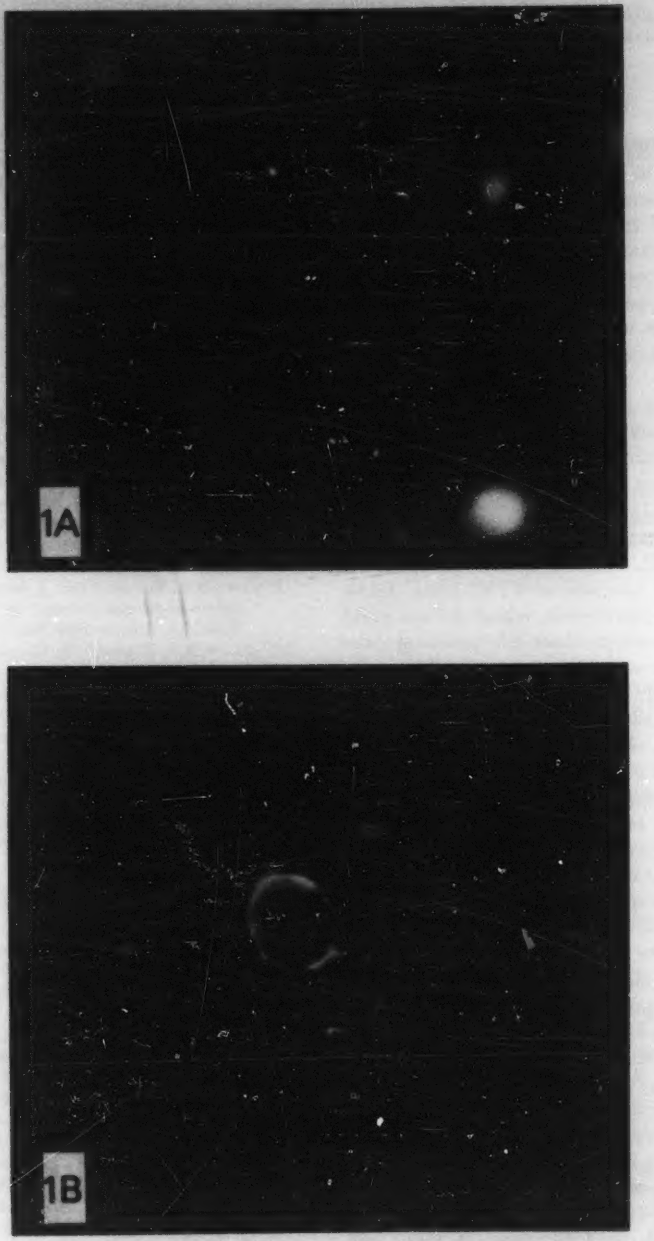

FIGURE 1.—Reactivity of monoclonal antibody (320°K) with P3HR-1 cells, producing transforming (A+B) or lytic (C) EBV. A) Cells propagated and maintained at 34°C, showing punctate immunofluorescence. × 752. B) Cells *continuously* propagated and aged at 34°C, showing partial and full-ring immunofluorescence. × 752.

A Deletion in Chromosome 1 in Cells of a Transplantable Granulocytic Leukemia (GL-13) in Guinea Pigs[1,2]

Dorothy E. Moore,[3,4] **Warren H. Evans,**[3] *and* **Michael G. Mage**[3,5]

ABSTRACT—Chromosomes were examined in leukocytes from a unique transplantable granulocytic leukemia (GL-13) of strain 13 guinea pigs. The GL-13 leukemia has many similarities to human chronic myelogenous leukemia (CML). It has remained predominantly diploid after 90 transplant generations and is characterized cytogenetically by a terminal deletion of the long arm of one of the #1 pair of chromosomes. No other chromosomal abnormality was observed. These findings lend further support to the conclusion that the GL-13 leukemia may be a useful model for the study of human CML.—JNCI 1982; 69:591–594.

In 1978, Evans et al. (*1*) described a transplantable granulocytic leukemia in a 13/N guinea pig that had been fed *N*-nitroso-*N*-butylurea. To our knowledge, this is the only existing granulocytic leukemia in guinea pigs. Some of the properties of this transplantable leukemia (now referred to as GL-13 leukemia) resemble those of human CML. The leukemic granulocytes in the blood and marrow of the guinea pig show the complete range of cell maturity, and the leukemia cells infiltrating the spleen, liver, and other body organs are exclusively granulocytes and their precursors. In addition, a pronounced anemia develops and the marrow becomes hypoplastic as the normal and leukemia cells in the marrow are replaced by fibroblast-like cells. These properties raised the possibility that the GL-13 leukemia might serve as a useful model for the study of human CML.

It is now well documented that most cases of human CML are accompanied by a characteristic chromosome abnormality in the leukocytes called the "Ph^1 chromosome" (*2*). Because no cytogenetic studies have been performed yet on the GL-13 leukemia cells, we have examined the chromosomes in these cells to determine whether the GL-13 leukemia model resembles human CML in its cytogenetic properties.

MATERIALS AND METHODS

Blood culture.—The GL-13 leukemia originated in a strain 13 female guinea pig and has been passaged for 90 transplant generations. The techniques for passaging the leukemia have been described previously (*1*). To differentiate leukemia cells from normal female cells, we used only inbred male leukemic guinea pigs for cytogenetic analysis. Blood cultures were initiated according to the method of Shevach et al. (*3*) when the leukocyte count had reached a concentration of greater than 50,000/mm^3 and death of the guinea pig was imminent. Duplicate 10-ml cultures were initiated at a concentration of 1×10^6 cells/ml and incubated for 24–48 hours at 37°C with 95% air–5% Co_2. More than 7 different blood cultures from 7 different transplant generations were set up over a 3-year period, and the chromosomes of at least 20 cells per culture were examined.

Blood cultures from normal female guinea pigs were set up as controls. Phytohemagglutinin (6 μg/10 ml) was added to stimulate cell division. These cultures were incubated for 48–72 hours.

Metaphase preparation.—Colcemid was added 0–1 hour before harvest to give a final concentration of 0.25 μg/ml. Metaphase preparations were made according to standard procedures. The slides were stored at room temperature for 1 week before Giemsa banding (*4*) and R-banding (*5*).

RESULTS

A karyotype of the normal diploid chromosomes of the strain 13/N guinea pig can be seen in figure 1. The chromosomes are arranged according to the diploid guinea pig karyotype described by Whang-Peng et al. (*6*). The location of the centromere and the size of the chromosome determine the position of the chromosome. Chromosomes 1–16 have a definite short arm and are arranged in decreasing size. Because of their size, the sex chromosomes are placed after chromosome 2. Chromosomes 17–31 are acrocentric and are also arranged according to decreasing total length.

A typical leukemic karyotype can be seen in figure 2A. One of the chromosomes in pair 1 has a deletion at the end of the long arm (1q−). The other chromosome 1 of this pair is normal. There is no obvious translocation of the deleted material to other chromosomes in this karyotype or in other karyotypes that were studied. This chromosome abnormality was present in all the cells of all 7 cell passages studied. The only difference consistently found between the normal and leukemic chromosomes was the deletion in one leukemic

---

ABBREVIATION USED: CML=chronic myelogenous leukemia.

---

[1] Received July 16, 1981; revised February 23, 1982; accepted March 15, 1982.

[2] Animals were maintained under the guidelines set forth by the National Institutes of Health Policy on Humane Care and Use of Animals.

[3] Laboratory of Biochemistry, Division of Cancer Biology and Diagnosis, National Cancer Institute, National Institutes of Health, Public Health Service, U.S. Department of Health and Human Services, Bethesda, Md. 20205.

[4] *Address reprint requests to* D. Moore, Building 37, Room 4C16, National Institutes of Health, Bethesda, Md. 20205.

[5] We thank Dr. Jacqueline Whang-Peng (National Cancer Institute), Dr. Beverly White (National Institute of Arthritis, Diabetes, and Digestive and Kidney Diseases), and Dr. Elizabeth Earley (Bureau of Biologics, Food and Drug Administration) for review of the manuscript and for helpful advice; Mrs. D. Susan Koch and Mr. John Graham (NCI-Frederick Cancer Research Facility, Frederick, Md.) for maintenance of the transplantable leukemia cells in vivo; and Mrs. Jean Regan and Ms. Gail Taff for excellent secretarial assistance.

chromosome 1. Since the 50th transplant generation, a blast crisis similar to that seen in human CML has been associated with the terminal phase of the GL-13 leukemia (Evans W and Miller D: Submitted for publication). Leukemia cells from the blast crisis stage as well as from preblast crisis stages had karyotypes the same as the karyotype seen in figure 2A. Figure 2B shows in more detail several leukemic chromosome 1 pairs. A small amount of the dark bottom band can be seen in the deleted chromosome 1. Therefore, the terminal unstained band plus a portion of the dark band is missing. Technical difficulties encountered in obtaining well-spread chromosomes and evenly stained preparations made identification of some chromosomes in some preparations tentative. In particular, one chromosome 11 was often difficult to identify. The significance of this is unclear. Slides stained by R-banding added no additional information.

The leukemia cells have an essentially diploid number of chromosomes. In a count of 87 well-spread leukemia cells, 74 contained the normal diploid number of 64 chromosomes, 2 had 128, 1 had 123, and the remaining 10 contained less than 64. Two of such hypodiploid cells contained a dense micronuclei-like body, which may have been a condensed chromosome. No cells with normal karyotypes were found in any leukemic blood culture.

Inasmuch as others have reported differences in the chromosome patterns of rat leukemic leukocytes transplanted by different routes of injection (*7*), we compared the chromosomes of GL-13 leukemic leukocytes transplanted intraperitoneally with those transplanted subcutaneously. We could detect no differences.

DISCUSSION

The results of our chromosome analyses of the GL-13 leukemic granulocytes show that the only consistent, detectable alteration in these cells is a terminal deletion in one of the long arms of a single chromosome. No obvious translocation of the deleted portion to another chromosome was detected.

The Ph^1 chromosome, present in about 85% of the cases of human CML (*8*), was identified as a deleted chromosome 22 (*9*) with a portion of the long arm translocated to the long arm of chromosome 9 (*10*) except in less than 10% of the cases in which the translocation was to chromosomes other than 9 (*11*). In less than 1% of the cases, no translocation of the portion was found (*11–13*). These findings appear to indicate that the deletion of chromosome 22 is the crucial event related to the development of CML rather than the site of translocation (*11*).

The GL-13 leukemia may be a useful model for the study of human CML because it has hematologic similarities to human CML as previously described (*1*) and is now found to have a consistent single chromosome deletion. At present it is not known whether this anomaly is typical of guinea pig myelogenous leukemia since no other cases are available to examine in this species. Possible homology of the deletion in GL-13 leukemia to that in human CML can be examined when, in the future, gene loci are mapped for the terminal ends of the long arm of guinea pig chromosome 1 and compared to genes already known to be present on the terminal end of the long arm of human chromosome 22.

Although various viruses are known to cause breaks in chromosomes of mammalian cells (*14*), the oncornavirus type A particles, which have been found in the GL-13 tumor, have not been implicated in either chromosome breakage or in the development of leukemia. In addition, using cell-free extracts of leukemia cells, we have been unable thus far to produce leukemia in strain 13/N guinea pigs (Evans WH, Smith GH, Hsu CK: Unpublished results).

The availability of the new techniques of gene mapping, such as somatic cell hybridization, chromosome and DNA transfer into cells, and plasmid-gene amplification, should make possible future investigation of the question as to whether any of the abnormalities of granulocyte proliferation and differentiation in GL-13 leukemia are linked to the chromosomal defect described in the present study.

REFERENCES

(*1*) Evans WH, Mage MG, Hsu CK, Himmelhoch SR, Smith GH. Transplantable granulocytic leukemia in strain 13 guinea pigs. Cancer Res 1978; 38:130–136.

(*2*) Nowell PC, Hungerford DA. A minute chromosome in human chronic granulocytic leukemia. Science 1960; 132:1497.

(*3*) Shevach EM, Rosenstreich DL, Green I. The distribution of histocompatibility antigens on T and B cells in the guinea pig. Transplantation 1973; 16:126.

(*4*) Seabright M. A rapid banding technique for human chromosomes. Lancet 1971; 2:971–972.

(*5*) Prantera G, Bonaccorsi S, Pimpinelli S. Simultaneous production of Q and R bands after staining with chromomycin A_3 or olivomycin. Science 1979; 204:79–80.

(*6*) Whang-Peng J, Lee EC, Forni G, Green I. Mutant lines of guinea pig L_2C leukemia. II. Comparative cytogenetic studies and banding analyses of normal and leukemic karyotypes. J Natl Cancer Inst 1976; 57:897–905.

(*7*) Ishidate M, Aoshima M, Sakurai Y. Population changes of a rat leukemia by different routes of transplantation. J Natl Cancer Inst 1974; 53:773–781.

(*8*) Whang-Peng J, Canellos GP, Carbone PP, Tijo JH. Clinical implications of cytogenetic variants in CML. Blood 1968; 32:755–766.

(*9*) Caspersson T, Gahrton G, Lindsten J, Zech L. Identification of the Philadelphia chromosome as a number 22 by quinacrine mustard fluorescence analysis. Exp Cell Res 1970; 63:238–240.

(*10*) Rowley JD. A new consistent chromosomal abnormality in chronic myelogenous leukaemia identified by quinacrine fluorescence and Giemsa staining. Nature 1973; 243:290–293.

(*11*) Sandberg AA. Chronic myelocytic leukemia. In: The chromosomes in human cancer and leukemia. New York and Amsterdam: Elsevier, 1980:134–261.

(*12*) ——— Chromosomes in Ph^1-positive chronic granulocytic leukaemia. In: First international workshop on chromosomes in leukaemia. Br J Haematol 1978; 39:305–309.

(*13*) Mitelman F, Levan G. Clustering of aberrations to specific chromosomes in human neoplasms. II. A survey of 287 neoplasms. Hereditas 1976; 82:167–174.

(*14*) Nichols WW. Viruses and chromosomes. In: Busch H, ed. The cell nucleus. Vol 2. New York: Academic Press, 1974:437–458.

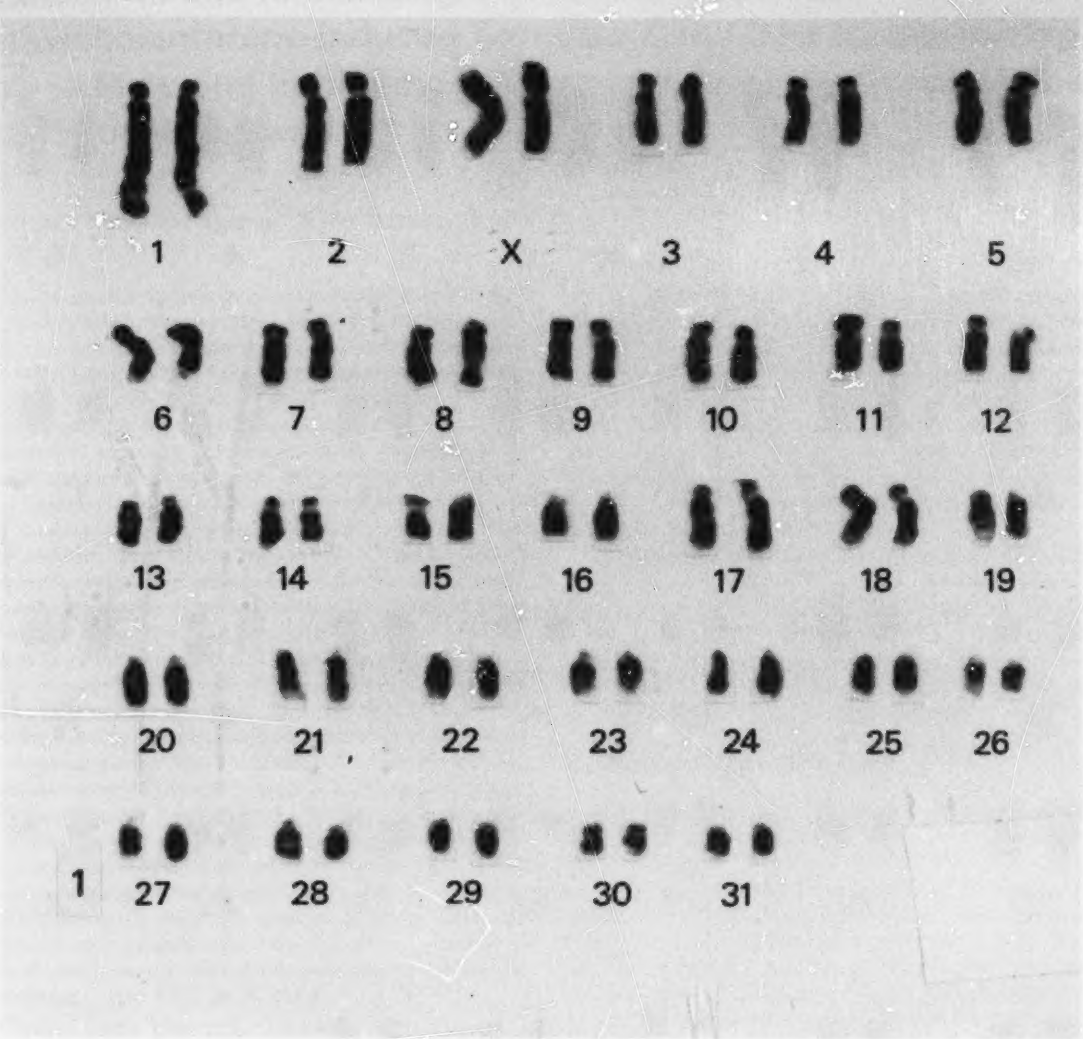
1
2
X
3
4
5
6
7
8
9
10
11
12
13
14
15
16
17
18
19
20
21
22
23
24
25
26
1
27
28
29
30
31

FIGURE 1.—Normal diploid karyotype of strain 13 guinea pig blood leukocyte chromosomes.

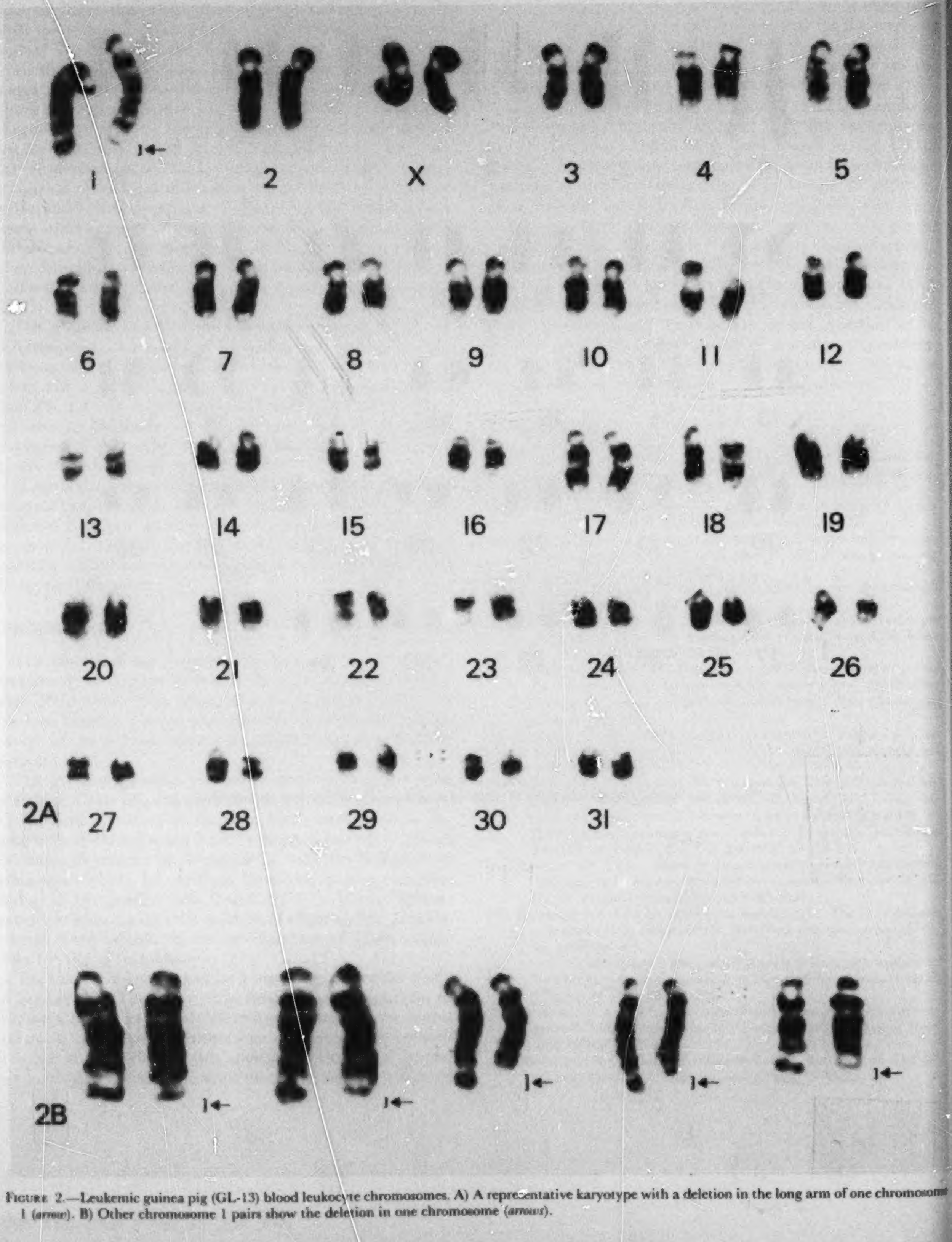
1
2
X
3
4
5
6
7
8
9
10
11
12
13
14
15
16
17
18
19
20
21
22
23
24
25
26
2A
27
28
29
30
31
2B

FIGURE 2.—Leukemic guinea pig (GL-13) blood leukocyte chromosomes. A) A representative karyotype with a deletion in the long arm of one chromosome 1 (*arrow*). B) Other chromosome 1 pairs show the deletion in one chromosome (*arrows*).

Establishment and Immunologic Characterization of 3-Methylcholanthrene-Induced Sarcoma Cell Lines Metastasizing Widely in Mice and Exhibiting Distinct and Selective Propensities for the Mode of Metastasis[1,2]

Yuso Kodama,[3] **Toshio Seyama,**[3] **Kenji Kamiya,**[3] *and* **Kenjiro Yokoro**[3,4]

ABSTRACT—Successive transplantations of metastatic secondary tumors of a 3-methylcholanthrene-induced sarcoma in (C57BL/Ka × C3H/He)F_1 male and female syngeneic mice resulted in the establishment of two unique tumor cell lines with enhanced metastatic potential. Moreover, each line showed distinct and selective propensities for the mode of metastasis. The 1101Pn tumor line, obtained by successive transplantations of metastatic pulmonary nodules, metastasized to many visceral organs via the bloodstream. Another tumor line, 1101Ln, selected by repeated transplantations of lymph node metastases, metastasized to almost all lymph nodes and to the lungs. When the metastatic pulmonary tumor of mice bearing 1101Ln was subcutaneously implanted on the backs of syngeneic mice, the tumor grew locally and eventually metastasized via the lymphatics, with systemic involvement of the lymph nodes. This finding is an indication that the intrinsic properties of tumor cells that form pulmonary metastases in 1101Ln tumor-bearing mice are distinct from those in 1101Pn tumor-bearing mice in terms of metastatic mode. The 1101Pn and 1101Ln tumor lines were nonimmunogenic or less immunogenic than the 505 tumor (the parental, nonselected tumor line). The growth and metastatic action of 505 tumors were enhanced by 400 R whole-body X-radiation, but no such effect was seen with 1101Pn tumors. Pretreatment of mice with OK-432, an immunopotentiator, retarded the growth and metastasis of 505 tumors but exerted little or no effect on 1101Pn tumors. The experimental results suggest that a tumor is composed of a heterogeneous cell population with respect to metastatic potential, metastatic mode, and tumor immunogenicity and that some intrinsic properties of the tumor cell have a primary role in the determination of the mode of cancer metastasis.—JNCI 1982; 69:595–605.

Cancer is characterized by uncontrolled growth and metastasis to distant organs. The development of metastasis involves four major sequential steps: 1) invasion of tumor cells into the surrounding tissues with penetration of blood and/or lymph vessels, 2) transport of tumor cells by blood or lymph flow, 3) arrest of the circulating tumor cells in small vascular beds of various organs or in lymph nodes, and 4) progressive growth of secondary tumors at extravascular sites. The detailed mechanism of metastasis formation is, however, largely obscure.

With regard to the mode of metastasis, tumor cells give rise to distant metastases through two routes: hematogenous and lymphogenous. Using ^{51}Cr-labeled tumor cells, Fisher and Fisher (*1, 2*) demonstrated direct communication between the blood and lymphatic circulations. They proposed that it was no longer practical to consider these routes as separate modes of neoplastic dissemination. Their conclusions, however, were drawn mainly from the anatomic point of view, and for the full understanding of metastatic action it is necessary to consider the biophysical properties of the tumor cell itself. Fidler, Nicolson, and co-workers (*3–6*), using both in vivo and in vitro selection systems, developed B16 melanoma variant lines that showed enhanced metastatic potential to the lungs. They suggested that tumor cell properties were instrumental in the outcome of metastasis.

We have established two separate tumor cell lines of MCA-induced sarcomas that metastasize in selective modes. The biologic behaviors of these tumor cell lines suggest that intrinsic properties of tumor cells are determining factors of the mode of the metastasis.

Tumor-specific antigens have been demonstrated in many experimental tumors and in some human tumors (*7–13*). Kim (*14*) showed that chemically induced rat mammary carcinomas with low immunogenicity have high metastatic potentials. We have studied the immunogenicity of established tumor cell lines and confirmed the results presented by Kim (*14*) in our murine sarcoma system.

MATERIALS AND METHODS

Animals.—Male and female 2- to 4-month-old (C57BL/Ka × C3H/He)F_1 mice, produced in our laboratory, were used throughout the study. C57BL/Ka mice, supplied by Professor H. S. Kaplan (Department of Radiology, Stanford University, Stanford, Calif.), have been maintained by brother × sister mating in our laboratory since 1964. C3H/He mice, obtained from Dr. K. Suzuki (Institute of Medical Science, Tokyo University, Tokyo, Japan), have been propagated in our laboratory since 1971. The mice were kept in metal wire cages, 6–7 mice per cage, in an air-conditioned room. They were given commercial pellets and tap water ad libitum.

Tumor.—MCA-induced fibrosarcoma was used throughout this study. A subcutaneous fibrosarcoma was induced

---

ABBREVIATIONS USED: H & E=hematoxylin and eosin; KE=Klinische Einheit [clinical unit(s)]; MCA=3-methylcholanthrene; TSTA=tumor-specific transplantation antigen.

---

[1] Received July 28, 1981; revised March 16, 1982; accepted April 9, 1982.

[2] Animals were maintained under the guidelines set forth in the "Guide for the Care and Use of Laboratory Animals" by the Institute of Laboratory Animal Resources, National Research Council.

[3] Department of Pathology, Research Institute for Nuclear Medicine and Biology, Hiroshima University, Kasumi 1-2-3, Minami-ku, Hiroshima, Japan.

[4] We thank Mr. T. Nishioka, Mr. K. Shitasue, Miss A. Kinomura, and Mrs. T. Matsuura for their excellent technical assistance.

on the back of a female (C57BL/Ka × C3H/He)F_1 mouse by the injection of 1.0 mg MCA dissolved in olive oil. It has been maintained by serial subcutaneous transplantation on the backs of syngeneic mice. When the fibrosarcoma reached the eighth transplant generation, metastasis developed in the lungs. This feature of metastasis to the lungs has been maintained ever since.

When several pieces of tumor (2–3 mm in diameter) weighing about 30 mg are subcutaneously implanted on the backs of mice, the tumor kills the host within 50 days. There have been no sex-related differences in the growth rate and metastatic behavior of the tumor.

Successive and selective transplantation of metastatic tumors.—For the study of the characteristics of the tumor cells that form the metastatic nodules, metastatic tumors in the lung were serially subcutaneously transplanted on the backs of syngeneic mice. The method of selective transplantation of metastatic nodules is shown in text-figure 1. After transplant generation 12, metastatic tumor nodules in the lungs were cut with scissors into small blocks, 2–3 mm in diameter, and subcutaneously implanted on the backs of syngeneic mice. The recipient mice were killed at the preterminal stage, their lungs with the metastatic nodules were removed, and small pieces of nodules were again implanted on other syngeneic mice. The procedure was then repeated. At the third selective transplant generation, metastasis formation was found in the left axillary lymph node, the regional node of the grafted site. Metastasis to the same node was formed from the third to the eighth selective transplant generations. After the sixth selective transplantation, the metastatic axillary node of a female mouse, BC 1101, was cut into small blocks and subcutaneously implanted on the backs of syngeneic mice. When the tumor metastasized to the regional lymph nodes of these mice, blocks of these nodes were in turn implanted into other syngeneic mice. The procedure was repeated in the same manner as that employed for pulmonary metastatic nodules.

By continuing these procedures, we obtained two distinct metastatic tumor cell lines, both originally derived from the metastatic pulmonary tumor-grafted mouse BC 1101. We designated the pulmonary nodule line as 1101Pn and the lymph node nodule line as 1101Ln. The parental, nonselected tumor cell line was named 505.

Preparation of single cell suspensions.—Single cell suspensions were obtained by trypsin digestion of tumor fragments. Tumor fragments were agitated three times for 15 minutes each on a magnetic stirrer in phosphate-buffered saline containing 0.2% trypsin at 37.0°C. Trypsinization was stopped by placement of the cell-containing flask in ice water. The tumor cell suspension was washed three times by centrifugation at 1,200 rpm for 15 minutes, and the cell pellets were resuspended in Eagle's minimum essential medium supplemented with 9% fetal calf serum. Cell concentration for injection was determined by use of a hemacytometer. The viability of the tumor cell preparation, tested by trypan blue exclusion, was usually over 95%.

Immunization with tumor cells.—Mice were immunized once with heavily irradiated tumor cells of each line. Tumor cells ($2.2–2.6 \times 10^6$), irradiated with 8,000–10,000 rad of either X-rays or ^{60}Co γ-rays, were injected sc into bilateral axillary and inguinal regions and ip into syngeneic mice.

Thymectomy.—When mice were 6–7 weeks old, thymectomies were performed through a midsternal incision. The mice were under Nembutal anesthesia. The incisions were closed with silk thread.

Whole-body X-irradiation.—Mice were given whole-body X-radiation with a Toshiba KXC-18 X-ray generator at 180 kVp, 25 mA, a half value layer of 1.08 mm Cu, a focus–target distance of 60 cm, and a dose rate of 50 rad/minute.

Pretreatment with OK-432.—A streptococcal preparation, manufactured by Chugai Pharmaceutical Co., Ltd., Tokyo, and designated OK-432, has been demonstrated to possess both direct cytocidal and indirect host-mediated immunopotentiating activities (*15–18*). The content of streptococci

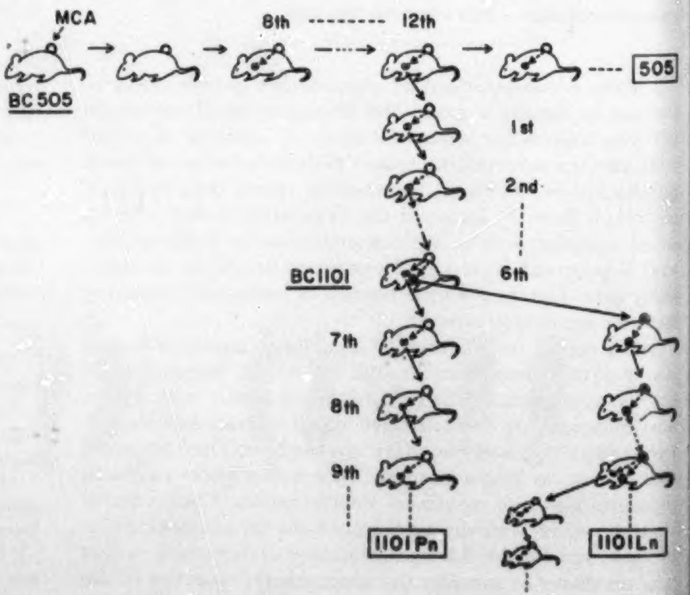

TEXT-FIGURE 1.—Schematic representation of the serial transplantation of metastatic tumors. Pulmonary nodules of 1101Ln-bearing mice at the ninth selective transplant generation were subcutaneously implanted on the backs of syngeneic mice. Successive transplantations of the pulmonary metastases of this line were performed in the same manner as that used for the 1101Pn line.

is expressed in KE; 1 KE corresponds to 0.1 mg dried streptococci. A fixed dose of the preparation, 0.5 KE of OK-432, dissolved in 0.2 ml physiologic saline was injected into the peritoneal cavities of syngeneic mice for 7 consecutive days (a total of 3.5 KE/mouse) before tumor implantation. Mice pretreated with OK-432 were grafted subcutaneously on the backs with tumor cells 1 day after the termination of the OK-432 treatment. In instances of iv injection of tumor cells, the injection was postponed for 5 days after OK-432 treatment to avoid the possible direct effect of OK-432 on circulating tumor cells.

Autopsy and histologic examination.—A complete autopsy was performed on every mouse. The entire body of the mouse was examined for metastases, and metastatic nodules on the surface of the lungs were counted independently by two persons with a dissecting microscope. Freshly removed organs were weighed routinely by a microbalance. For histologic examination organs were fixed in a 10% neutral Formalin solution, and paraffin-embedded tissues were cut into 5-μm-thick sections. The sections were stained with H & E. Serial sections were observed when necessary.

Analysis of results.—The results were statistically evaluated by Student's *t*-test.

RESULTS

Metastatic Spread of Cell Lines of the MCA-Induced Sarcoma

The metastatic spread of each tumor cell line is shown in tables 1 and 2. The metastatic spread of 1101Pn tended to increase as the number of transplant generations advanced (table 1). At the first and second transplant generations, the tumor metastasized only to the lungs. At the third generation, however, it metastasized to the kidneys, adrenal glands, spleen, and left axillary lymph node in addition to the lungs

TABLE 2.—*Metastatic spread of lymphatic nodule line of MCA-induced sarcoma, 1101Ln*

Transplant generation	Animal No.	Days after transplant	Organ with metastasis,[a] ○		
			Lungs	Kidneys	Lymph node, grade[b]
1	BC 1134	40	○		○ +
	BC 1136	40	○		○ +
2	BC 1152	37	○	○	○ ++
3	BC 1163	35	○	○	○ ++
4	BC 1185	35	○	○	○ +++
	BC 1189	41	○		○ ++
5	BC 1202	33	○		○ ++
	BC 1205	37	○		○ +++
6	BC 1216	34	○		○ ++++
	BC 1218	38	○		○ ++
7	BC 1224	35	○		○ ++
8	BC 1241	33	○		○ ++++
	BC 1243	35	○		○ ++++
9	BC 1259	31	○		○ +++
	BC 1262	36	○		○ ++
10	BC 1333	35	○		○ +++
	BC 1337	36	○		○ ++
11	BC 1370	28	○		○ ++++
	BC 1371	28	○		○ +++

[a] No metastases were observed in the adrenal glands, spleen, brain, and heart.

[b] += metastasis to the left axillary lymph node only; ++= metastasis to the left axillary and inguinal lymph nodes and occasionally to the mediastinal or retroperitoneal nodes; +++= metastasis to lymph node at the right side of the body plus ++; ++++= metastasis to almost all lymph nodes.

TABLE 1.—*Metastatic spread of the 1101Pn pulmonary nodule line of an MCA-induced sarcoma, 1101Pn*

Transplant generation	Animal No.	Days after transplant	Organ with metastasis, ○						
			Lungs	Kidneys	Adrenal glands	Spleen	Brain	Heart	Left axillary lymph node
1	BC 912	31	○						
2	BC 938	42	○						
	BC 942	44	○						
	BC 1022	49	○		○				
3	BC 1030	58	○	○	○	○			○
4	BC 1039	37	○	○	○	○			○
	BC 1096	92	○				○	○	
5	BC 1074	39	○	○	○				○
	BC 1093	47	○	○		○			○
6	BC 1101	36	○		○	○			○[a]
7	BC 1135	40	○	○	○	○			○
	BC 1137	40	○				○		
8	BC 1154	45	○	○	○	○	○		○
9	BC 1167	34	○						
	BC 1173	42	○						
10	BC 1197	43	○					○	
	BC 1200	49	○	○	○	○	○		
11	BC 1209	33	○	○					
	BC 1214	42	○	○	○	○	○	○	
	BC 1215	42	○	○	○	○		○	
12	BC 1232	42	○	○		○	○		
	BC 1234	46	○	○			○	○	

[a] Beginning with the left axillary lymph node of BC 1101, metastatic nodules in the left axillary nodes of tumor-bearing mice were repeatedly implanted subcutaneously on the backs of syngeneic mice. The procedure resulted in the selection of the tumor cell line 1101Ln (table 2).

(fig. 1). Metastasis to the regional lymph node, i.e., the left axillary lymph node, was seen from the third to the eighth transplant generations. In further generations, however, no metastatic involvement of lymph nodes was seen. Instead, in later generations hematogenous metastasis began to involve the brain and the heart more consistently (figs. 2–4).

The 1101Ln, the selective cell line derived from the metastatic tumor in the left axillary lymph node of the BC 1101 mouse (6th generation; table 1), showed a distinctly different pattern of metastasis from that of 1101Pn (table 2). The metastasis of 1101Ln that developed first only in the left axillary lymph node came to involve more and more nodes and finally involved all nodes except the mesenteric lymph node (fig. 5). Conversely, no metastatic foci were observed in organs other than the lungs, except for microscopic metastases in the kidneys of the second, third, and fourth transplant generations. It is of particular interest that the extent of pulmonary metastases decreased, whereas that of lymphatic metastases increased in later transplant generations. The findings in the lungs are well reflected in the changes in lung weights which decreased steadily with serial passage (table 3).

Biologic Properties of Tumor Cells Forming Pulmonary Nodules in 1101Ln-Bearing Mice

To clarify the characteristics of tumor cells that form pulmonary nodules in 1101Ln-bearing mice, we cut into small pieces pulmonary metastases of BC 1259 and BC 1262 mice (ninth transplant generation; table 2) and implanted them subcutaneously on the backs of syngeneic mice. When the animals appeared moribund 35–40 days later, they were killed and autopsied. We found that almost all lymph nodes were systemically involved with metastatic tumors, but there was no secondary growth in other organs except the lungs (first generation; table 4).

The tumor nodules that were formed in the lungs were again subjected to successive and selective transplantations in the same manner as in the selection of the 1101Pn tumor line, to test whether it was possible to obtain a tumor cell line that showed a different mode of metastasis. To express it in a different way, we wanted to see if the metastatic mode of 1101Ln cells may be converted into that of 1101Pn cells by repeated transplantation of pulmonary nodules of 1101Ln-bearing mice. The results revealed that the metastatic pattern remained unchanged; i.e., the tumor metastasized systemically to the lymph nodes and to the lungs and only occasionally to the kidneys (table 4).

TABLE 3.—*Lung weights of 1101Ln-bearing mice after successive transplantations of metastatic axillary lymph nodes*[a]

Transplant generation	Animal No.	Lung weight, mg
1	BC 1134	705
	BC 1136	573
2	BC 1152	453
3	BC 1163	429
4	BC 1185	472
	BC 1189	406
5	BC 1202	312
	BC 1205	322
6	BC 1216	246
	BC 1218	240
7	BC 1224	135
8	BC 1241	188
	BC 1243	273
9	BC 1259	199
	BC 1262	177
10	BC 1333	199
	BC 1337	189
11	BC 1370	168
	BC 1371	176

[a] Mean weight of normal lungs ± SE: 173.4±3.4 mg.

TABLE 4.—*Metastatic spread of the 1101Ln pulmonary metastatic tumor*

Transplant generation	Animal No.	Days after transplant	Organ with metastasis,[a] ○		
			Lung	Kidneys	Lymph node, grade[b]
1	BC 1334	35	○		○ ++
	BC 1335	39	○		○ +++
	BC 1342	40	○		○ ++
	BC 1343	40	○		○ ++++
2	BC 1421	35	○		○ +++
	BC 1422	35	○		○ ++++
3	BC 1496	38	○		○ ++++
	BC 1509	43	○		○ ++++
4	BC 1595	41	○	○	○ ++
	BC 1604	41	○		○ ++
5	BC 1651	41	○		○ ++++
	BC 1663	48	○		○ ++++
6	BC 1767	38	○		○ ++
	BC 1768	38	○	○	○ ++++
7	BC 1900	44	○		○ ++++
8	BC 1930	36	○		○ ++++
	BC 1931	36	○		○ ++
9	BC 2069	53	○		○ ++++
	BC 2070	53	○		○ ++

[a] No metastases were observed in the adrenal glands, spleen, brain, and heart.

[b] ++=metastasis to the left axillary and inguinal lymph nodes and occasionally to the mediastinal or retroperitoneal nodes; +++=metastasis to lymph node at the right side of the body plus ++; ++++=metastasis to almost all lymph nodes.

These results indicate that the intrinsic properties of tumor cells forming pulmonary metastases of 1101Ln-bearing mice are distinct from those of 1101Pn-bearing mice in terms of metastatic mode and that the properties are stationary in nature.

Immunogenicity of Tumor Lines

Syngeneic mice were given multiple sc and single ip injections of tumor cells of each line (505, 1101Pn, or 1101Ln), preirradiated with 8,000–10,000 rad of X-rays or ^{60}Co γ-rays. Then 7–14 days later, the immunized mice were challenged with an sc injection of live tumor cells of the respective line, and the growth of the implanted tumor was recorded. Untreated or mice treated with 400 R of whole-body X-radiation served as controls. Results are shown in table 5. When the implanted tumor cell doses were small (expts. 1, 2), there was no distinct difference in the growth of the implants in 505 and 1101Pn hosts; no tumor growth was observed in either 505 or 1101Pn hosts preimmunized with the respective tumor cells; the tumor grew only in a

TABLE 5.—*Evaluation of the immunogenicity of cell lines derived from the MCA-induced sarcoma*

Expt No.	No. of tumor cells challenged	Immune status of recipients	No. of mice with tumor/ No. challenged		
			505	1101Pn	1101Ln
1	1.5×10^5	Untreated control	0/5	1/5	—
		Immunized[a]	0/5	0/5	—
2	6.0×10^5	Untreated control	0/6	2/6	—
		Immunized[a]	0/6	0/6	—
3	1.3×10^6	X-irradiated[b]	8/9	8/8	9/10
		Untreated control	7/12	9/9	14/14
		Immunized[a]	1/12	8/8	15/15

[a] Immunized with heavily irradiated tumor cells.

[b] Mice were given 400 R of whole-body X-radiation a few hours before tumor challenge.

few nonimmunized 1101Pn hosts. However, in experiment 3, in which the recipients were challenged with a larger number of tumor cells, none of the mice preimmunized with either 1101Pn or 1101Ln rejected the implanted tumors. Alternatively, all but 1 of 12 mice preimmunized with 505 rejected the implants. These findings indicate a distinct difference in immunogenicity among these cell lines and show a clear inverse correlation between the immunogenicity and metastatic potential of the tumor cells, regardless of their metastatic mode.

Growth of Tumor Lines in Immunosuppressed Hosts

The growth patterns of the 505 and 1101Pn tumor lines were compared in mice treated with 400 R of whole-body X-radiation. Irradiated mice and nonirradiated controls were implanted subcutaneously with 1.24–1.27×10^6 tumor cells of each line; the implants were allowed to grow for 31–38 days. At autopsy, the grafted tumors were removed and weighed, and the formation of metastatic foci was carefully examined microscopically and macroscopically. The 505 line grew much faster in X-irradiated mice than in control mice, whereas 1101Pn grew equally well in both irradiated and control mice (table 6).

Metastatic Behavior of Tumor Lines in Immunosuppressed Hosts

The metastatic behavior of each tumor line was studied in thymectomized, X-irradiated mice. Recipient mice were thymectomized 7 days before they received 400 R of whole-body X-radiation. Twenty-two days after the irradiation, tumor cells of each line were injected into the tail vein. Recipients of the 505 and 1101Pn lines were killed 2 and 3 weeks after the cell injection, respectively. The shortened observation period for the 505 tumor line was due to the unexpected early deaths of the hosts. Lungs were removed and weighed, and the metastatic nodules on the surface were counted with the aid of a dissecting microscope. The other organs were also removed and examined for metastases. As shown in table 7, the formation of pulmonary metastatic nodules by 505 tumor cells was distinctly enhanced in the immunosuppressed hosts, whereas the formation of the nodules by 1101Pn was not affected by the immunologic status of the host. The lung of the immunosuppressed host, however, was slightly heavier than that of the intact host.

Effects of Pretreatment With OK-432 on Growth of Tumor Lines Subcutaneously Implanted on the Back

Subcutaneously implanted tumors were allowed to grow for 38–40 days in intact hosts or in hosts pretreated with OK-432 for 7 consecutive days so that we could observe the effect of the treatment on the tumor growth of each cell line. Table 8 shows that the growth of the 505 line tended to be inhibited by OK-432 treatment, whereas that of the 1101Pn line was not.

Effects of Pretreatment with OK-432 on Metastasis of Tumor Lines Injected Intravenously in Tail Vein

Tumor cells of each line were injected into the tail veins of intact mice or mice pretreated with OK-432. The mice were killed 21 days later, and the pattern of metastasis formation was examined. Results are shown in table 9. Again, pretreatment of OK-432 brought about an apparent decrease in both the number of pulmonary metastatic nodules and the weight of the lungs of 505 tumor-bearing hosts, whereas the effect was less marked in 1101Pn tumor-bearing hosts. The distinct response of the respective tumor-bearing hosts to OK-432 treatment may be interpreted in terms of the difference in immunogenicity of the tumor lines.

DISCUSSION

Successive transplantations of metastatic secondary tu-

TABLE 6.—*Effect of whole-body X-irradiation on the behavior of cell lines subcutaneously implanted on the backs of syngeneic mice and observed for 31–38 days*

Tumor cell line	Cell dose	Host treatment	Tumor weight gain, g[a]	Incidence of metastasis to:[b]			
				Lungs (No. of metastatic nodules)[a]	Kidneys	Brain	Mediastinal lymph node
505	1.27×10^6	None	1.24±0.30	2/7 (0.6±0.4)	—	—	—
		400 R of radiation	3.04±0.33[c]	4/8 (7.3±3.0)	—	—	1/8
1101Pn	1.24×10^6	None	2.69±0.49	9/9 (5.9±0.8)	1/9	1/9	—
		400 R of radiation	1.98±0.34	8/8 (19.7±4.7)	—	—	—

[a] Means ± SE.

[b] Results are numbers of mice with metastasis/total number of mice challenged.

[c] Significantly different from untreated controls ($P<0.01$).

TABLE 7.—*Effect of whole-body X-radiation on the behavior of cell lines injected iv into the tail veins of mice 22 days after X-irradiation*

Tumor cell line	Cell dose	Host treatment	Lungs			Incidence of metastasis to:[a]		
			Metastasis incidence[a]	No. of metastatic nodules[b]	Organ weight, mg[b]	Kidneys	Brain	Mediastinal lymph node
505	1.80×10^6	None	15/15	141.4±21.5	476.2±61.8	2/15	2/15	1/5
		Tx[c]+400 R of radiation	14/14	298.8±17.2[d]	739.7±49.5[e]	3/14	8/14	7/14
1101Pn	1.00×10^6	None	15/15	86.8±10.5	279.0±21.8	2/15	6/15	2/15
		Tx[c]+400 R of radiation	14/14	84.5±14.5	367.7±27.9	5/14	5/14	1/14

[a] Results are numbers of mice with metastasis/total number of mice challenged.
[b] Means ± SE.
[c] Tx=thymectomy was performed 7 days before X-irradiation.
[d] Significantly different from untreated controls ($P<0.001$).
[e] Significantly different from untreated controls ($P<0.01$).

TABLE 8.—*Effect of pretreatment with OK-432 on the behavior of cell lines subcutaneously implanted on the backs of syngeneic mice and observed for 38–40 days*

Tumor cell line	Cell dose	Host treatment[a]	Tumor weight gain, g[b]	Incidence of metastasis to:[c]		
				Lungs (No. of metastatic nodules[b])	Kidneys	Brain
505	1.85×10^6	None	3.93±0.53	8/15 (1.5±0.4)	—	—
		OK-432	2.60±0.31[d]	5/14 (0.7±0.3)	—	—
1101Pn	1.40×10^6	None	2.60±0.23	13/15 (6.7±2.0)	1/15	—
		OK-432	2.56±0.18	13/15 (6.0±1.4)	2/15	1/15

[a] Each mouse received ip injections of 0.5 KE OK-432 for 7 consecutive days. Tumor cells were implanted subcutaneously on the backs of mice 1 day after the last injection.
[b] Means ± SE.
[c] Results are numbers of mice with metastasis/total number of mice challenged.
[d] Not significant ($P>0.05$).

TABLE 9.—*Effect of pretreatment with OK-432 on the behavior of cell lines injected iv into the tail veins of mice*[a]

Tumor cell line	Cell dose	Host treatment[b]	Lungs			Incidence of metastasis to:[c]			
			Metastasis incidence[d]	No. of metastatic nodules[e]	Organ weight, mg[e]	Kidneys	Brain	Adrenal glands	Heart
505	2.37×10^6	None	12/12	160.4±15.6	529.8±90.1	2/11	1/11	—	1/11
		OK-432	12/13	83.9±12.6[c]	280.8±32.4[f]	1/13	2/13	2/11	—
1101Pn	1.35×10^6	None	10/10	223.1±10.6	619.9±53.8	7/10	7/10	—	1/10
		OK-432	11/11	206.5±33.1	443.9±71.2	5/11	6/11	—	1/11

[a] Mice were killed 3 wk after the tumor challenge.
[b] 0.5 KE OK-432/mouse/day was injected ip for 7 consecutive days. Tumor cells were given iv 5 days after the last injection.
[c] Significantly different from untreated controls ($P<0.001$).
[d] Results are numbers of mice with metastasis/total number of mice challenged.
[e] Means ± SE.
[f] Significantly different from untreated controls ($P<0.05$).

mors of MCA-induced sarcoma into syngeneic mice resulted in the establishment of unique cell lines with enhanced metastatic potential. Furthermore, each line exhibited distinct and selective propensities for the mode of metastasis. The 1101Pn tumor line, obtained by repeated transplantations of pulmonary metastases, widely metastasizes to the viscera via the bloodstream. Alternatively, the 1101Ln tumor line, derived from a metastatic nodule in the lymph node, spreads via lymphatic vessels involving almost all lymph nodes and the lungs (text-fig. 2). Both lines are the progeny of the tumor line 505 and have been obtained by repeated transplantations of each metastatic tumor originating in the lungs and in the left axillary lymph node of a single mouse (BC 1101). A study of the characteristics of tumor cells forming the pulmonary nodules of 1101Ln-bearing mice revealed that the implanted pulmonary tumors grew and eventually metastasized by the lymphogenous route, and their serial passage in syngeneic mice never resulted in alteration of the mode of metastasis. These results demonstrate that intrinsic properties of tumor cells of pulmonary nodules of 1101Ln-bearing mice are distinct from those of 1101Pn-bearing mice in terms of metastatic mode and that the properties are stable through successive in vivo transplantations.

Pressman and Simon (*19*) reported the existence of a direct anatomic connection between lymph nodes and venous channels. Fisher and Fisher (*1*) recovered iv injected ^{51}Cr-labeled tumor cells from the thoracic lymph shortly

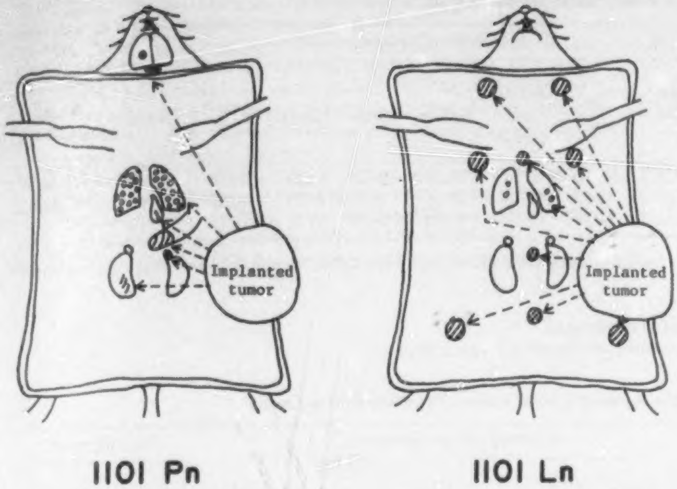

TEXT-FIGURE 2.—Schematic representation of the metastatic spread of each cell line. The 1101Pn line metastasizes to the brain, lungs, heart, spleen, adrenal glands, and kidneys. In contrast, 1101Ln metastasizes systemically to almost all lymph nodes, i.e., the cervical, axillary, brachial, inguinal, mediastinal, and retroperitoneal lymph nodes. The 1101Ln tumor also metastasizes to the lungs to a small degree.

after injection. These reports indicate a close relationship between two vascular systems from the anatomic point of view, but they do not directly lead to the conclusion that a tumor metastasizes randomly irrespective of the nature of the tumor cell.

Fidler (*3*) was able to select B16 melanoma variant lines with enhanced metastatic potential to the lungs by in vivo and in vitro selection systems. Brunson et al. (*20*) obtained a brain-specific melanoma line by a procedure similar to that of Fidler (*3*). Brunson et al. (*20*) suggested that intrinsic properties of the tumor cell are important for the outcome of metastasis, and our results are in strong agreement with this conclusion. However, the results of the present study are not in accord with those obtained by other authors in that they have established cell lines with a particular organ specificity by repeatedly transferring secondary tumors developing in the respective organs. For example, B16 melanoma variant lines with a specific metastatic preference for lungs (*3*), brain (*20*), and liver (*21*) were selected by repeated transplantations of each metastasis. In our tumor system, however, successive transplants of pulmonary metastases did not result in selection of a cell population with a preference for only lungs but rather with a specificity for metastatic mode. A trial to obtain a tumor line with a kidney preference by repeated transfers of secondary kidney tumors was unsuccessful. It also resulted in a tumor line that metastasized in the same fashion as that of the widely metastasizing 1101Pn and 1153Pn lines (data not shown).

The metastatic tumor nodules that developed in the left axillary lymph nodes during the selection of 1101Pn (table 1) were derived from pulmonary metastases. This suggests that pulmonary metastatic nodules were composed of two tumor cell populations which differ from one another in their metastatic mode, even though pulmonary metastases consist of cells arriving at the lungs through blood vessels. We concluded, therefore, that the repeated transplantations of pulmonary nodules might have resulted in the selective adoption of a cell population with a preference for blood vessels where it survives better, minimizing the cell population that prefers the lymphatic system (table 3). In that sense, the process of the establishment of each cell line might be a selective one. Fidler (*22*) and Suzuki et al. (*23*) reported that the tumors were heterogeneous and contained many clones with different metastatic potentials. Conceivably, our tumor cell lines might have preexisted in the original 505 tumor before they were selected.

We also obtained two other tumor lines, 1153Pn and 1153Ln, from the 505 tumor by the same selection procedure as that of 1101Pn and 1101Ln. The 1153Pn and 1153Ln lines show more vigorous metastatic action than the 1101Pn and 1101Ln lines (fig. 6). Table 10 shows the results of the experiment in which 30-mg blocks of each tumor were subcutaneously implanted on the backs of syngeneic mice. A marked difference could be observed between the metastatic patterns of 1153Pn and 1153Ln: 1153Pn involved many visceral organs at a high rate of metastatic spread, whereas 1153Ln involved the lymph nodes extensively, but never metastasized to organs that were preferred by 1153Pn.

We have observed that the 1153Pn tumor line metastasized to the regional lymph nodes as well as to other organs. Consequently, we investigated the properties of tumor cells that proliferated in the regional lymph node of 1153Pn-bearing mice. Blocks of the metastatic lymph node of 1153Pn tumor-bearing mice were implanted subcutaneously on the backs of syngeneic mice. Table 11 shows that the implanted tumors eventually metastasized in the same manner as 1153Pn. This indicates that the metastatic mode of the lymph node metastases of 1153Pn tumor-bearing mice is hematogenous. The facts that 1153Pn metastasizes to the lymph nodes and its metastases consist of cells that are hematogenous imply that 1153Pn contains cell clones that show no specific preference for the metastatic mode.

When we considered the facts that tumor cell properties were maintained unchanged in spite of successive in vivo transfers and that our tumor lines contained a large cell population rigid in the selection of the metastatic mode and a small population that showed no preference for the mode, we concluded that the intrinsic properties of the tumor cell play an important role in the choice of metastatic mode.

Studies on the immunogenicity of selected lines of the MCA-induced sarcoma revealed that the widely metastasizing 1101Pn and 1101Ln tumor lines were less immuno-

TABLE 10.—*Metastases of the selected tumor cell lines 1153Pn and 1153Ln*[a]

Tumor cell line	No. of mice	Tumor-bearing period, day	Weight of tumor on back, g[b]	Lungs			Incidence of metastasis to:[c]						Lymph node	
				Metastasis incidence[c]	No. of metastatic nodules[b]	Organ weight, mg[b]	Kidneys	Adrenal glands	Spleen	Brain	Heart	Lymph node	Grade[d]	Total weight, mg
1153Pn	18	35–46	5.01±0.40	18/18	80.7±9.4	365.8±15.2	18/18	8/18	9/18	10/18	0/18	15/18	+	215.0±61.7
1153Ln	13	33–36	10.83±1.03	13/13	13.3±2.0	276.4±27.2	0/13	0/13	0/13	0/13	0/13	13/13	++++	4,727.6±0.4
505	12	37–51	8.52±1.10	11/12	8.9±2.1	216.7±11.4	0/12	0/12	0/12	0/12	0/12	0/12		

[a] Tumor blocks (30 mg) were implanted subcutaneously on the backs of syngeneic mice that were killed and autopsied when they appeared moribund.

[b] Means ± SE.

[c] Results are numbers of mice with metastasis/total number of mice challenged.

[d] +=metastasis to the left axillary lymph node only; ++++=metastasis to almost all lymph nodes.

TABLE 11.—*Metastasis of tumors of the regional lymph nodes of 1153Pn-bearing mice*[a]

No. of mice	Tumor-bearing period, day	Lungs			Incidence of metastasis to:[b]						Lymph node	
		Metastasis incidence[b]	No. of metastatic nodules[c]	Organ weight, mg[c]	Kidneys	Adrenal glands	Spleen	Brain	Heart	Lymph node	Grade[d]	Total weight, mg[c]
8	30–43	8/8	106.5±13.3	408.3±41.3	8/8	5/8	1/8	5/8	0/8	7/8	+	306.3±62.4

[a] Small blocks of lymph node metastases of 1153Pn tumor-bearing mice were implanted subcutaneously on the backs of syngeneic mice that were killed and autopsied when they appeared moribund.

[b] Results are numbers of mice with metastasis/total number of mice challenged.

[c] Means ± SE.

[d] +=metastasis to the left axillary lymph node only.

genic or nonimmunogenic to the host, whereas 505, the parental tumor line that metastasized only to the lungs and only to a small extent, was distinctly immunogenic to the host. We concluded, therefore, that the metastatic potential and the immunogenicity of the tumor cell correlated well. Tumor 505 was rejected by specifically preimmunized hosts, whereas no such protection against the implanted tumor was observed with 1101Pn and 1101Ln. These findings indicate that 505 has distinct TSTA on the cell membrane, whereas no recognizable TSTA exists on the cell surfaces of 1101Pn and 1101Ln. The immunosuppressive state induced by whole-body X-irradiation facilitated the growth and metastasis of 505 but had little or no effect on 1101Pn. Pretreatment of the host with OK-432, an immunopotentiator, suppressed the local and metastatic growth of 505, but it had little or no effect on 1101Pn.

These results demonstrate that the immunogenicity of the tumor cell is one of the critical factors in determining the outcome of metastasis regardless of the metastatic mode; the lower the immunogenicity, the higher the metastatic potential of the tumor cell.

It is assumed that human tumors, which often widely metastasize in a manner similar to that of our tumor line 1101Pn or 1101Ln, might be weakly immunogenic or nonimmunogenic to the human hosts.

Our tumor cell lines are new in the sense that there is no previous record of such highly metastasizable MCA-induced sarcoma cell lines in spite of the intensive use of MCA-induced sarcomas for experiments in the past. We believe that our tumor lines are useful additions to the few spontaneously metastasizing tumor models currently in use in the study of the mechanism of cancer metastasis.

REFERENCES

(*1*) Fisher B, Fisher ER. The interrelationship of hematogenous and lymphatic tumor cell dissemination. Surg Gynecol Obstet 1966; 122:791–798.

(*2*) Fisher ER, Fisher B. Recent observations on concepts of metastasis. Arch Pathol 1967; 83:321–324.

(*3*) Fidler IJ. Selection of successive tumour lines for metastasis. Nature [New Biol] 1973; 242:148–149.

(*4*) ———. Biological behavior of malignant melanoma cells correlated to their survival in vivo. Cancer Res 1975; 35:218–224.

(*5*) Fidler IJ, Nicolson GL. *Brief communication*: Organ selectivity for implantation survival and growth of B16 melanoma variant tumor lines. J Natl Cancer Inst 1976; 57:1199–1202.

(*6*) Nicolson GL, Winkelhake JL, Nussey AC. An approach to studying the cellular properties associated with metastasis: Some in vitro properties of tumor variants selected in vivo for enhanced metastasis. In: Weiss L, ed. Fundamental aspects of metastasis. Amsterdam and Oxford: North-Holland, 1976:291–303.

(*7*) Foley EJ. Antigenic properties of methylcholanthrene-induced tumors in mice of the strain of origin. Cancer Res 1953; 13:835–837.

(*8*) Prehn RT, Main JM. Immunity to methylcholanthrene-induced sarcomas. J Natl Cancer Inst 1957; 18:769–778.

(*9*) Klein G, Sjögren HO, Klein E, Hellström KE. Demonstration of resistance against methylcholanthrene-induced sarcomas in the primary autochthonous host. Cancer Res 1960; 20:1561–1572.

(*10*) Old LJ, Boyse EA, Clarke DA, Carswell EA. Antigenic properties of chemically induced tumors. Ann NY Acad Sci 1962; 101:80–106.

(*11*) Bubeník J, Perlmann P, Helmstein K, Moberger G. Immune response to urinary bladder tumours in man. Int J Cancer 1970; 5:39–46.

(*12*) Baldwin RW, Embleton MJ, Jones JS. Cell-mediated and humoral immune reactions to human tumours. Int J Cancer 1973; 12:73–83.

(*13*) Braatz JA, McIntire KR, Princler GL, Kortright KH, Herberman RB. Purification and characterization of a human lung tumor associated antigen. JNCI 1978; 61:1035–1046.

(*14*) Kim U. Metastasizing mammary carcinomas in rats: Induction and study of their immunogenicity. Science 1970; 167:72–74.

(*15*) Okamoto H, Minami M. Shoin S. Experimental anticancer studies

XXXI. On the streptococcal preparation having potent anticancer activity. Jpn J Exp Med 1966; 36:175–186.

(16) Ono T, Kurata S, Wakabayashi K, Sugawara Y, Saito M, Ogawa H. Inhibitory effect of a streptococcal preparation (OK-432) on the nucleic acid synthesis in tumor cells in vitro. Gan 1973; 64:59–69.

(17) Suzuki S, Yamamoto A, Ogawa H. Inhibitory effect of a streptococcal preparation (OK-432) on induction of splenomegaly by Friend leukemia virus. Gan 1975; 66:455–456.

(18) Aoki T, Kvedar JP, Hollis VW Jr, Bushar GS. *Brief communication: Streptococcus pyogenes* preparation OK-432: Immunoprophylactic and immunotherapeutic effects on the incidence of spontaneous leukemia in AKR mice. J Natl Cancer Inst 1976; 56:687–690.

(19) Pressman JJ, Simon MB. Experimental evidence of direct communications between lymph nodes and veins. Surg Gynecol Obstet 1961; 113:537–541.

(20) Brunson KW, Beattie G, Nicolson GL. Selection and altered properties of brain-colonizing metastatic melanoma. Nature 1978; 272:543–545.

(21) Tao T, Matter A, Vogel K, Burger MM. Liver-colonizing melanoma cells selected from B-16 melanoma. Int J Cancer 1979; 23:854–857.

(22) Fidler IJ. Tumor heterogeneity and the biology of cancer invasion and metastasis. Cancer Res 1978; 38:2651–2660.

(23) Suzuki N, Withers HR, Koehler MW. Heterogeneity and variability of artificial lung colony-forming ability among clones from mouse fibrosarcoma. Cancer Res 1978; 38:3349–3351.

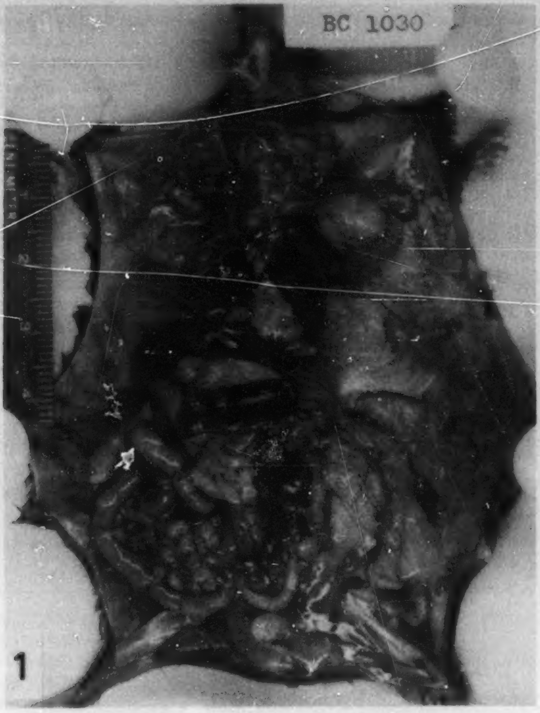

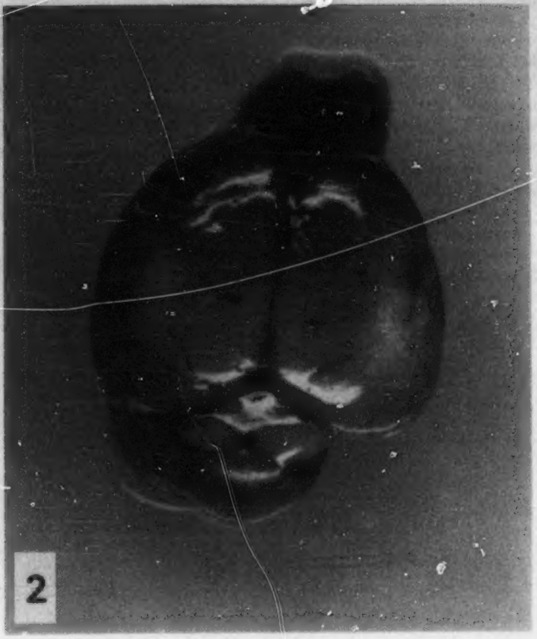

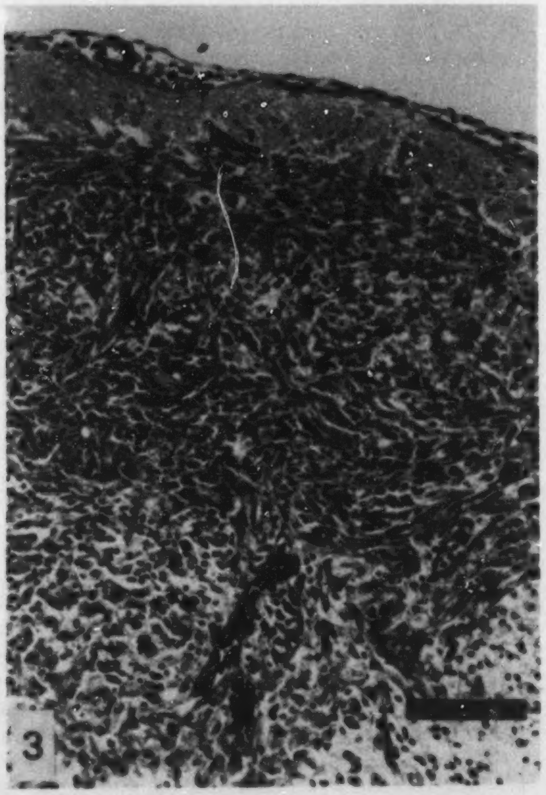

FIGURE 1.—Autopsy findings of a mouse (BC 1030) bearing the pulmonary nodule line at the third transplant generation. The tumor, subcutaneously implanted on the back, has metastasized to the lungs, spleen, adrenal glands, kidneys, and the left axillary lymph node. Tumor nodules developed in the mesenterium as a result of peritoneal carcinomatosis (table 1).

FIGURE 2.—Mouse brain with metastatic lesions. The 1101Pn tumor has developed metastatic foci in both hemispheres.

FIGURE 3.—Section of the left hemisphere of the brain shown in fig. 2. Tumor cells have proliferated around the blood vessels. H & E. *Bar*=0.1 mm. × 175.

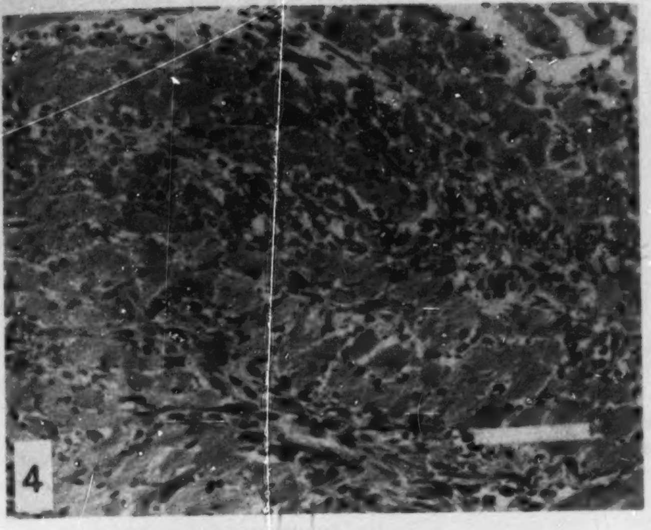

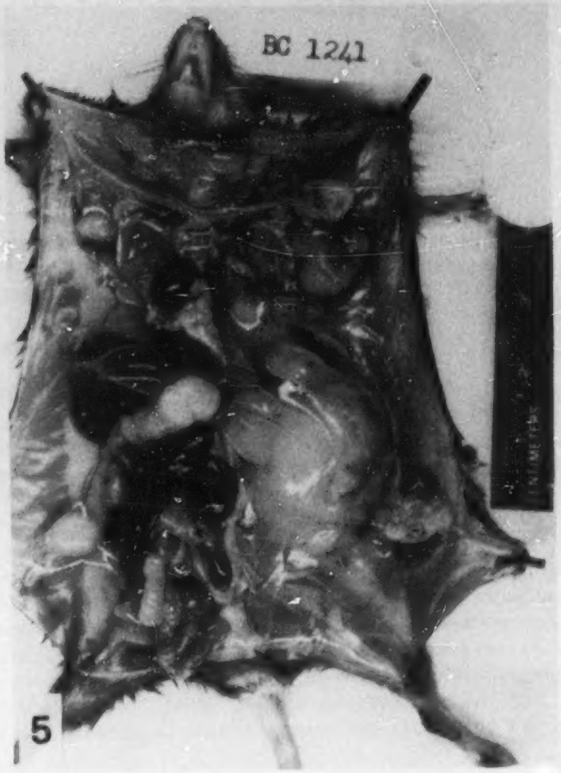

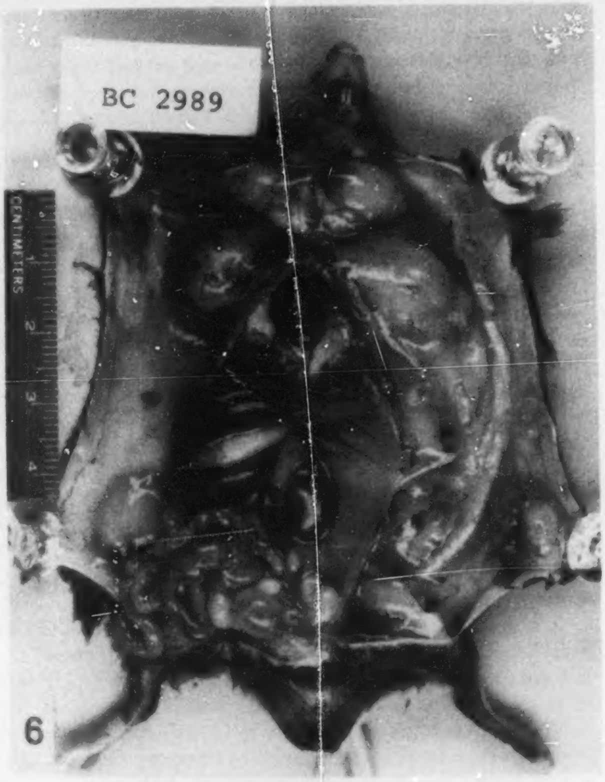

FIGURE 4.—Heart of a 1101Pn tumor-bearing mouse. Tumor cells propagated in the muscle plates. H. & E. *Bar*=0.1 mm. × 175.

FIGURE 5.—Mouse (BC 1241) bearing a 1101Ln tumor at the eighth selective transplant generation. Besides the lungs, the tumor has metastasized into the left cervical lymph node, into the bilateral axillary, inguinal, and lumbar lymph nodes (table 2).

FIGURE 6.—Mouse (BC 2989) bearing an 1153Ln tumor, another line selected from the 505 tumor and implanted subcutaneously on the back. The tumor has developed massive lymphogenous metastases, involving cervical, axillary, inguinal, lumbar, and renal lymph nodes.

blank page

Modulation of Cell-Mediated Alloimmunity by BCG. I. Antagonism and Potentiation of Immunosuppression Caused by Cytarabine[1,2,3]

Richard I. Murahata[4,5] *and* **Malcolm S. Mitchell**[6,7,8]

ABSTRACT—The ability of iv administered BCG to antagonize immunosuppression caused by injection of the antimetabolite cytarabine (β-cytosine arabinoside; ara-C) was investigated in C57BL/6 mice. Treatment with BCG 10 days before alloimmunization with killed L1210 tumor cells decreased spleen T-cell-mediated cytolysis against allogeneic P815Y tumor cells, as measured by a short-term ^{51}Cr release assay, and potentiated immunosuppression due to ara-C. In contrast, spleen cell-mediated immunity (CMI) that was assayed by a 48-hour microcytotoxicity assay (MCA) was augmented by systemic BCG administered before alloimmunization. Pretreatment with BCG resulted in a complete and long-lasting protection against the immunosuppressive effects of ara-C on this CMI as measured by the MCA. Treatment with BCG after cytoreductive therapy resulted in a significant, although transient, reversal of immunosuppression. Depending on the type of response and thus the type of effector cell measured, BCG acts as a moderate immunosuppressive agent or a strong immunopotentiator of CMI.—JNCI 1982; 69:607–612.

BCG has been used extensively as an immunologic adjuvant. Among its reported effects are accelerated skin graft rejection (*1–3*), increased antibody production (*4*, *5*), and an augmented resistance to tumors in man (*6*, *7*) and experimental animals (*8–12*). Perhaps the most well-studied tumor model is the transplantable hepatoma in the Sewall-Wright guinea pig (*10–12*), in which tumor cell–BCG vaccines or intralesional BCG caused the regression of a significant proportion of tumors and the development of systemic immunity in the animals whose tumors regressed. These results have not been consistently observed in mice or hamsters (*13–16*), and the cellular basis of the rejection is unclear. Probably, different cellular mechanisms are involved in the rejection of intralesionally injected tumors and in the expression of systemic immunity to the tumor. The inhibition of tumor growth by systemically administered BCG (*17*, *18*) may be a manifestation of yet another effect of BCG on the host's response to a tumor.

One of the more intriguing and potentially exploitable features of BCG is its ability to reverse or protect against the immunosuppressive effects of various agents, such as 3-methylcholanthrene (*5*) or cyclophosphamide (*19*, *20*). BCG also has been reported to increase the effectiveness of high-dose therapy with cyclophosphamide in an L1210 tumor model, presumably with antagonizing immunosuppression (*17*). BCG treatment can also reverse or protect against immune complex-induced suppression of macrophage receptors for cytophilic antibody (Rao VS, Mitchell MS: Data to be published). Yet, paradoxically, BCG can induce suppressor cells that inhibit the in vitro alloimmunization of cytotoxic T-cells (*21*, *22*)—which emphasizes the modulatory rather than strictly adjuvant properties of BCG.

Our study investigated the ability of systemically administered BCG to modulate the immune response to allogeneic tumor cells in the mouse, especially in conjunction with the administration of a cytoreductive agent, ara-C.

MATERIALS AND METHODS

Mice.—Female C57BL/6 mice (H-2^b) (from The Jackson Laboratory, Bar Harbor, Maine, or Charles River Breeding Laboratories, Inc., Wilmington, Mass.) were used for the preparation of all spleen cell suspensions. Animals were 8–10 weeks old at the beginning of the experiments. Adult male (C57BL/6 × DBA/2)F$_1$ (B6D2F$_1$) mice were used for the in vivo passage of the L1210 tumor line.

Cell lines.—The L1210 leukemia, which originated in a DBA/2 mouse (H-2^d), was maintained by weekly intraperitoneal passage in B6D2F$_1$ mice. The P815Y mastocytoma, also of DBA/2 origin, is a long-term tissue culture line that was maintained in FM supplemented with antibiotics and 10% horse serum (M.A. Bioproducts, Walkersville, Md.). The cells growing in suspension were passaged every 2 or 3 days.

Immunization.—BCG (Tice strain; National Institutes of Health, Bethesda, Md.) was obtained as lyophilized material packaged at $5\pm3\times10^8$ viable units/ampule. One container was reconstituted with 6 ml sterile saline, and mice were given iv injections of 0.2 ml (≈0.5 mg material or 2×10^7 viable units). Mice given other doses of BCG also received

---

Abbreviations used: ara-C=cytarabine (β-cytosine arabinoside); CMI=cell-mediated immunity; CRA=^{51}Cr release assay; E:T=effector-to-target cell ratio(s); FM=Fischer's medium; FM-S=FM+10% horse serum; K=killer; MCA=microcytotoxicity assay; NK=natural killer; R-ATS=rabbit anti-mouse thymocyte serum.

---

[1] Received August 31, 1981; revised March 1, 1982; accepted March 24, 1982.

[2] Supported by Public Health Service grant CA-13105 from the National Cancer Institute and by grant IM-50B from the American Cancer Society.

[3] Animals were maintained under the guidelines of the Yale University School of Medicine and of the National Research Council.

[4] Department of Pharmacology, Yale University School of Medicine, New Haven, Conn. 06510.

[5] *Present address*: Division of Dermatology, Department of Medicine, University of California at Los Angeles School of Medicine, Los Angeles, Calif. 90024.

[6] Departments of Medicine and Pharmacology, Yale University School of Medicine.

[7] Recipient of a Research Career Development Award from the National Cancer Institute.

[8] *Address reprint requests to* Dr. Mitchell at his *present address*: Director for Clinical Investigations, University of Southern California Comprehensive Cancer Center, 2025 Zonal Ave., Los Angeles, Calif. 90033.

a total volume of 0.2 ml. Control mice received an equal volume of saline.

C57BL/6 mice were immunized against DBA/2 alloantigens on day 0 by an ip injection of 20×10^6 L1210 cells, which had been killed by 2,800 rad X-radiation immediately before BCG injection. This radiation dose prevented growth of L1210 cells in the syngeneic strain, as judged by the survival of the host for more than 30 days after inoculation.

Cytoreductive therapy.—The ara-C (The Upjohn Company, Kalamazoo, Mich.) was diluted to 2 mg/ml in sterile saline, and mice were given ip injections of either 20 or 40 mg/kg/day on days 3–7 after antigen administration. Control mice received an equal volume of saline.

Labeling of target cells.—Target cells for the measurement of CMI by the CRA were labeled by incubation of 5×10^6 cells/ml in FM with 0.1 mCi ^{51}Cr (200–500 Ci/g; New England Nuclear Corp., Boston, Mass.) for 30–60 minutes at 37°C. The target cells were washed four times with FM before use.

CMI as measured by CRA.—The spleen was removed aseptically and gently disrupted by hand in a glass tissue grinder. Cells were washed three times and diluted in FM-S to the desired concentration of trypan blue-excluding cells. In the CRA [used as described in (*23*)], 10^5 target cells/ml, and generally 10^7 spleen cells/ml (E:T=100:1), were incubated for 6 hours at 37°C. Specific release was calculated according to the following equation: Percent specific release$=100\times(X-C)/T$, where X is cpm released in the presence of test splenocytes, C is the release in the presence of normal lymphocytes, and T is total incorporated counts. Maximum releasable counts were 80–90%, and C was generally less than 10–15%.

CMI as measured by the MCA.—The MCA procedure was similar to that of the CRA, except for the following: *a*) The incubation period was 48 hours at 37°C in an atmosphere of 5% CO_2 in air and b) the target cells remaining were counted in a hemacytometer by light microscopy. The results are expressed as percent specific inhibition of target cell growth, which was calculated according to the following equation: Percent specific inhibition$=[1-(T/N)]\times100$, where T is the number of target cells remaining in the presence of test lymphocytes and N is the number of target cells remaining in the presence of normal lymphocytes.

Assays were performed in duplicate on samples from individual spleens. Values for CMI are the means of 3–4 different experiments, in which duplicate determinations were made on 5–8 spleens. Results were analyzed by a two-tailed Student's *t*-test. Differences with a *P*-value less than 0.05 were considered to be statistically significant.

R-ATS treatment of spleen cells.—R-ATS (M.A. Bioproducts) was twice absorbed with liver homogenate from C57BL/6 mice (6 ml of a 1:3 dilution of R-ATS to 1 ml packed liver homogenate) for 30 minutes at room temperature. Spleen cells (20×10^6/ml) were added to an equal volume of R-ATS and incubated for 60 minutes at 0°C. The tubes were centrifuged, the supernatants were discarded, and the cells were resuspended to the same concentration in agarose-absorbed guinea pig complement. After incubation at 37°C for 60 minutes, the cells were centrifuged and resuspended in FM-S at the desired concentration of trypan blue-excluding cells. Treatment with R-ATS at a dilution of 1:40 killed approximately 50% of spleen cells, greater than 95% of thymocytes, and less than 10% of bone marrow cells; these cells were from several strains of mice. The response of R-ATS-treated spleen cells to concanavalin A was reduced by approximately 90%; the response to lipopolysaccharide was not decreased.

RESULTS

Preliminary experiments had established that the ip injection of 2×10^7 X-irradiated L1210 cells would elicit a submaximal immune response when the spleen cells were examined in the MCA 14 days later. This standard immunizing dose was used in all studies reported here.

Immune Response of Alloimmunized Mice

The kinetics of the development of CMI in the spleen as measured by the CRA are shown in text-figure 1. Activity was easily demonstrated by day 3. It peaked on day 6 and declined to low, but detectable, levels by day 14. Inhibition of tumor cell growth (a combination of cytotoxic and cyto-

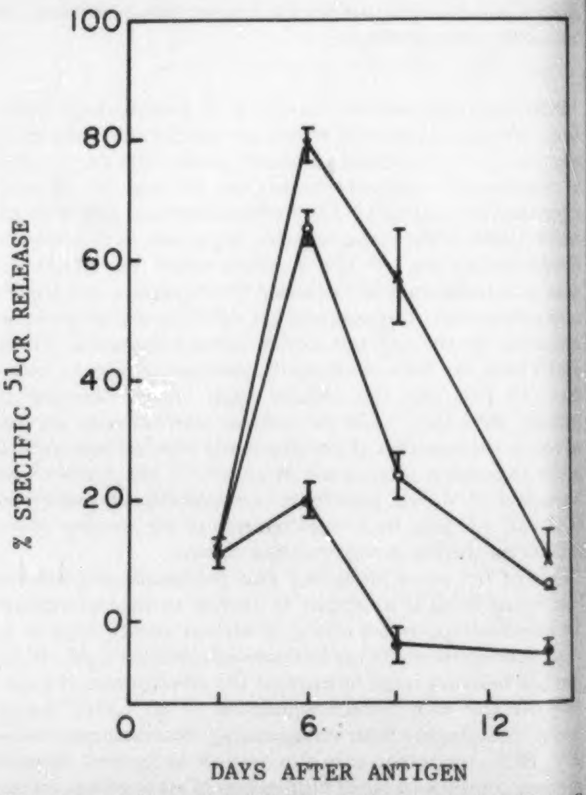

TEXT-FIGURE 1.—Suppression of CMI by ara-C as measured by CRA. All animals were given ip injections of 20×10^6 killed L1210 cells on day 0. Mice receiving ara-C were given ip injections of the indicated dose on days 3–7. ×——×, saline; ○——○, ara-C, 20 mg/kg/day; ●——●, ara-C, 40 mg/kg/day. All data points in this and subsequent figures represent the mean of duplicate determinations on 15–18 spleens per group. Bars indicate ±1 SEM.

static events) as measured by the 48-hour MCA was greater than 90% on day 6, was 48% on day 15, and was still significant (30%) on day 19. The contribution of immediately cytolytic T-cells was assessed by removal of θ-positive cells before the addition of spleen cells to the assay. This treatment reduced the activity of day-6 cells from 90 to 66%, but it had no effect on the activity of cells assayed on day 14. The time period from 14 to 16 days after antigen administration was chosen for all further experiments in which the MCA was used, because this was the earliest time after immunization when the contribution of the effector cells active in the CRA (primarily cytotoxic T-cells) would not mask the effect of other cell populations active in the MCA. θ-Positive cells were not routinely removed in other experiments.

Effect of Chemotherapy With ara-C

A 5-day course of ara-C, given ip on days 3-7 after antigen administration, resulted in a dose-dependent suppression of spleen cell activity in the CRA (text-fig. 1). The activity in the MCA 14 days after immunization was also subject to dose-dependent suppression (table 1).

Effects of Immunotherapy With BCG

Spleen cells from mice that had received 0.5 mg BCG iv 10 days before alloimmunization were less active in the CRA than those from alloimmune control animals (text-fig. 2). BCG pretreatment appeared to inhibit the generation of the primary cytotoxic response, the spleen cytotoxicity being significantly suppressed on both days 9 and 14. BCG pretreatment in combination with chemotherapy was more suppressive than was chemotherapy alone.

In contrast, BCG pretreatment resulted in a significant increase in spleen cell activity as measured by the MCA (text-fig. 3). BCG pretreatment completely abrogated the suppressive effect of subsequent chemotherapy with 20 mg ara-C/kg/day. The CMI of spleen cells obtained from mice that had received combination therapy was not significantly different from that seen with cells obtained from alloimmunized control mice. Pretreatment with BCG was partially protective against the suppressive effects of the higher dose of ara-C (text-fig. 4). Immunotherapy with BCG in combination with 40 mg ara-C/kg/day resulted in spleen cell immunity intermediate between that of alloimmune control mice and mice treated with chemotherapy alone. The protective effect of BCG was observed with doses from 0.25-1.0

Table 1.—*Suppressive effect of ara-C on spleen cell activity in the MCA*[a]

ara-C, mg/kg/day[b]	Percent inhibition of target cell growth[c]
—	47.7±7.9
20	19.1±4.3
40	1.5±5.2

[a] Mice were alloimmunized ip with 20×10^6 killed L1210 cells on day 0 and were killed for assay on day 14.

[b] Injected ip on days 3-7.

[c] Values are means ± SE.

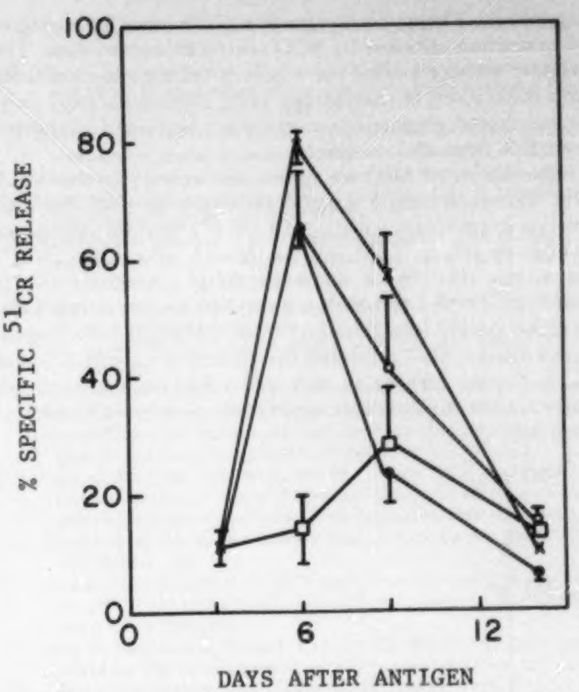

Text-figure 2.—Effect of BCG administration on CMI as measured by the CRA. Animals were immunized ip with 20×10^6 killed L1210 cells on day 0. Animals receiving ara-C were given ip injections of 20 mg/kg/day on days 3-7. Mice receiving BCG were given iv injections of 0.5 mg on day −10. ×——×, saline; ○——○, ara-C; ●——●, BCG; □——□, ara-C and BCG.

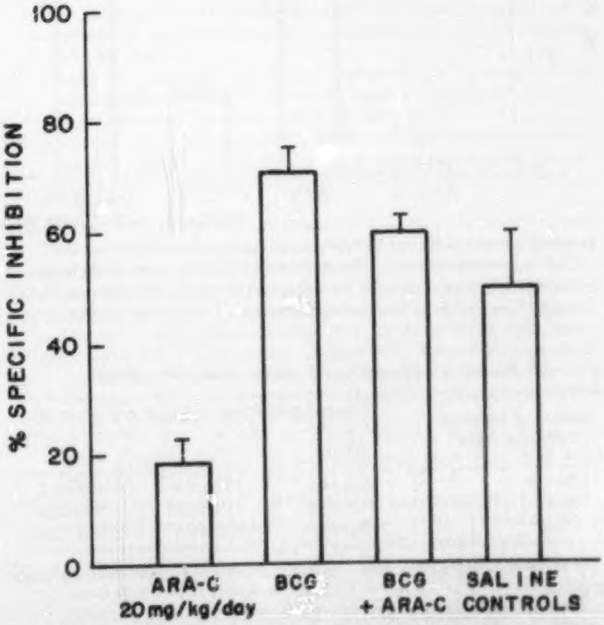

Text-figure 3.—Effect of BCG, in combination with low-dose ara-C, on CMI as measured by the MCA. Animals were treated as described in text-fig. 2. All animals were assayed 14 days after alloimmunization (24 days after BCG administration).

mg/mouse. There was no significant difference in the degree of protection afforded by BCG within this dose range. The relative activity among the 4 groups (alloimmune controls, and mice given chemotherapy only, immunotherapy only, or combined chemoimmunotherapy) remained consistent over E:T from 25:1 to 250:1.

The effects of BCG on spleen cell activity in the MCA was immunologically specific inasmuch as cells from all groups immunized with L1210 (*H-2*^{d}) had no significant inhibitory effect (11%) on the growth of a C3H (*H-2*^{k}) hepatoma (H-129) or an AKR (*H-2*^{k}) leukemia (SL-1) (table 2). These 2 tumors were sensitive targets in this assay because spleen cells obtained from C57BL/6 mice immunized against SL-1 inhibited the growth of both H-129 and SL-1. Spleen cells from mice given BCG alone were not active in the MCA at this time (24 days) after BCG administration.

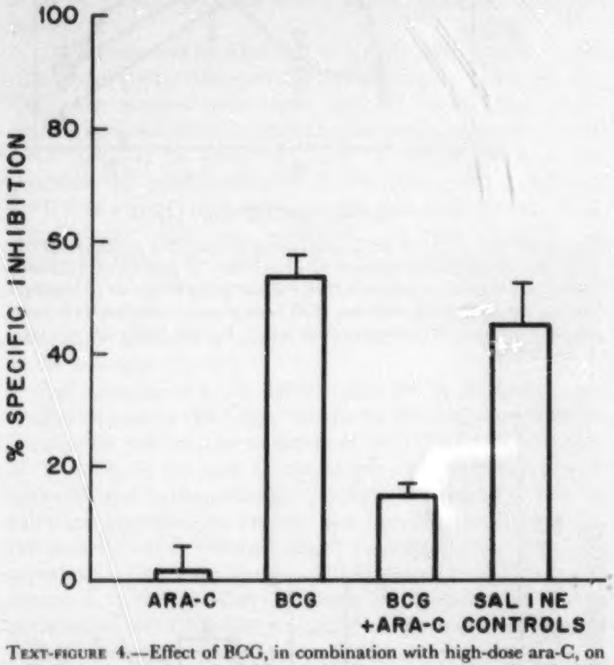

TEXT-FIGURE 4.—Effect of BCG, in combination with high-dose ara-C, on CMI as measured by the MCA. Animals were treated as described in text-fig. 2, except that mice receiving ara-C were given injections of 40 mg/kg/day. All mice were killed for assay 14 days after alloimmunization.

TABLE 2.—*Specificity of spleen cells in the MCA*[a]

Source of immune effector cells	Percent inhibition of target cell growth[b]		
	P815Y	SL-1	H-129
L1210[c]	32.4±4.1	−10.0±7.8	−13.2±8.5
BCG + L1210[d]	71.1±2.6	11.0±8.9	11.5±3.8
SL-1[e]	5.6±6.0	51.2±9.1	42.8±11.1

[a] Mice were killed for assay on day 14 (24 days after BCG administration).

[b] Values are means ± SE.

[c] Mice were alloimmunized ip with 20×10^6 killed L1210 cells.

[d] Mice received 0.5 mg BCG, iv, 10 days before alloimmunization with L1210 cells.

[e] Mice were alloimmunized ip with 20×10^6 killed SL-1 cells;

TABLE 3.—*Reversal of immunosuppression by BCG*[a]

BCG	ara-C	Percent inhibition of target cell growth at:[b, c]	
		Day 12	Day 19
−	−	36.5±4.1	44.8±3.1
−	+[d]	15.8±3.3	16.2±6.2
+[e]	−	64.8±1.8	35.3±4.4
+[e]	+[d]	33.1±5.9	19.0±4.6

[a] All mice received ip injections of 20×10^6 killed L1210 cells on day 0.

[b] Mice were killed on day 12 or day 19, and their spleen cell activity was measured by the MCA.

[c] Values are means ± SE.

[d] 20 mg ara-C/kg/day, was administered ip on days 3–7.

[e] BCG, 0.5 mg, was administered iv on day 10 and day 13 to the indicated groups.

Because BCG administration could protect against subsequent immunosuppression by ara-C, the ability of BCG to reverse the suppressed state was investigated (table 3). ara-C was given on days 3–7; BCG was given on days 10 and 13. The suppressive effect of ara-C was transiently, but significantly, reversed by BCG. On day 12, the activity of spleen cells from animals that had received combination therapy was equal to that of cells from alloimmunized control mice and significantly greater than that seen with cells from mice treated only with ara-C. The effect of BCG therapy in this protocol was no longer apparent on day 19.

DISCUSSION

The findings of this study indicate that systemically administered BCG augments the spleen cell-mediated immune response to alloantigens measured by the MCA. Furthermore, BCG administration before ara-C inoculation completely antagonized the immunosuppressive effects of the cytotoxic drug on the cells active in this assay. When the CRA was used to measure immunity (due mainly to T-cells), BCG decreased the response to alloantigens and potentiated immunosuppression by ara-C.

The mechanisms by which systemically administered BCG interacts with chemotherapy or other modes of cytoreductive therapy may be several. Mathé et al. (*17*) suggested that BCG acts by protecting against the myelosuppressive rather than the immunosuppressive effects of cyclophosphamide. Our study supports the thesis that treatment with an immunologic adjuvant, such as BCG, in conjunction with specific immunization can act by increasing the activity of specifically armed effector cells. These effector cells may be immature members of the macrophage–monocyte family and are the subject of a companion study (*24*). The augmentation of non-T-CMI demonstrated in the present study may be related to BCG's ability to elicit other non-T-effector cells, e.g., non-specific, nonadherent cytotoxic cells (*25*), NK cells (*26*), and K cells active in antibody-dependent, cell-mediated cytotoxicity, (*27*). The lack of activity of spleen cells activated by BCG in a 6-hour CRA and the alloantigen-specific killing observed in this investigation are both inconsistent with a major role for NK cells as effectors. The relationship of the nonspecific, adjuvant-induced effectors reported earlier (*25*) to the specific effector cells reported in the present study is not clear. Specificity is probably conferred by the alloimmunization procedure added to the administration of BCG. Alternatively, the nonspecific component may be short lived and, therefore, not detected 24 days after BCG injection. In any event, BCG pretreatment in this study substantially increased the immune response to the specific tumor allograft, a true adjuvanticity. We could not determine whether BCG increased the activity per cell or simply increased the number of cells that reacted in the spleen; both are plausible. A definitive answer awaits the development of a single cell assay applicable to long-term cytotoxicity—an assay similar to those that have been developed to assess short-term cytotoxicity (*28*, *29*).

The inability of BCG pretreatment to augment cytotoxic T-cell activity, and indeed the suppression of such activity as measured in the CRA, is consistent with observations from this and other laboratories. Systemic administration of BCG in mice elicits macrophage-like cells in the spleen that inhibit proliferation in response to T-cell mitogens (*22*, *25*). Similar cells, derived from "natural suppressor" cells present in normal bone marrow, suppress the generation of cytotoxic T-cells in vitro (*21*, *22*). This, too, may well be an antiproliferative effect. Systemic administration of *Corynebacterium parvum* can also inhibit the generation of cytotoxic T-cells in vivo (*30*) and results in the generation of spleen cells that can suppress the generation of primary and memory cytotoxic T-lymphocytes in vitro (*31*). Reinisch et al. (*32*) reported that immunization of mice with allogeneic tumor cells in complete Freund's adjuvant containing mycobacteria suppressed the generation of cytotoxic T-cells while having no effect on the generation of helper or memory T-cells.

Whether the non-T cytotoxic cells discussed above are in the same family of monocytes–macrophages as the suppressor cells generated concomitantly is under investigation. In any event BCG clearly stimulates a variety of responses such that its ultimate effect on the host can be considered to be the resultant of conflicting vectors.

The ability of BCG to increase one form of CMI to tumor alloantigens and to significantly protect against the immunosuppressive effects of the clinically effective cytotoxic agent ara-C illustrates one possible cellular mechanism underlying successful immunotherapy and chemoimmunotherapy. Preliminary studies in our laboratory indicate that $B6D2F_1$ mice cured of L1210 leukemia by chemoimmunotherapy with ara-C and BCG are resistant to high-dose rechallenge [ten times the 100%-effective lethal dose ($10{\times}LD_{100}$)], whereas mice cured by chemotherapy alone are not resistant. Further immunopharmacologic studies are required to define the cellular and molecular mechanisms by which agents such as BCG modulate host resistance.

REFERENCES

(*1*) Balner H, Old LJ, Clarke DA. Accelerated rejection of male skin isografts by female C57BL mice infected with Bacillus Calmette-Guérin (BCG). Proc Soc Exp Biol Med 1962; 109:58–62.

(*2*) Peters LC, Hanna MG Jr, Gutterman JV, Mavligit CM, Hersh EM. Modulations of the immune response of guinea pigs by repeated BCG scarification. Proc Soc Exp Biol Med 1974; 147:344–349.

(*3*) Vitale B, Allegretti N. Influence of Bacillus Calmette-Guérin infection on the intensity of homograft rejection in rats. Nature 1963; 199:507–509.

(*4*) Miller TE, Mackaness GB, Lagrange PH. Immunopotentiation with BCG. II. Modulation of the response to sheep red blood cells. J Natl Cancer Inst 1973; 51:1669–1676

(*5*) Stjernswärd J. Effect of Bacillus Calmette-Guérin and/or methylcholanthrene on the antibody-forming cells measured at the cellular level by a hemolytic plaque test. Cancer Res 1966; 26:1591–1594.

(*6*) Morton DL. Immunotherapy of human melanomas and sarcomas. Natl Cancer Inst Monogr 1972; 35:375–378.

(*7*) Nathanson L. Regression of intradermal malignant melanoma after intralesion injection of *Mycobacterium bovis* strain BCG. Cancer Chemother Rep 1972; 56:659–665.

(*8*) Biozzi G, Stiffel C, Halpern BN, Mouton D. Effet de l'inoculation du bacille du Calmette-Guérin sur le développement de la tumeur ascitique d'Ehrlich chez la souris. C R Soc Biol (Paris) 1959; 153:987–989.

(*9*) Halpern BN, Biozzi G, Stiffel C, Mouton D. Effet de la stimulation du système reticuloendothelial par l'inoculation du bacille du Calmette-Guérin sur le développement de l'épithelioma atypique T-de Guérin chez le rat. C R Soc Biol (Paris) 1959; 153:919–923.

(*10*) Zbar B, Bernstein ID, Bartlett BL, Hanna MG Jr, Rapp HJ. Immunotherapy of cancer: Regression of intradermal tumors and prevention of growth of lymph node matastases after intralesional injection of living *Mycobacterium bovis*. J Natl Cancer Inst 1972; 49:119–130.

(*11*) Zbar B, Bernstein ID, Rapp HJ. Suppression of tumor growth at the site of infection with living Bacillus Calmette-Guérin. J Natl Cancer Inst 1971; 46:831–839.

(*12*) Zbar B, Bernstein I, Tanaka T, Rapp HJ. Tumor immunity produced by the intradermal inoculation of living tumor cells and living *Mycobacterium bovis* (strain BCG). Science 1970; 170:1217–1218.

(*13*) Bartlett GL, Zbar B, Rapp HJ. Suppression of murine tumor growth by immune reaction of the Bacillus Calmette-Guérin strain of *Mycobacterium bovis*. J Natl Cancer Inst 1972; 48:245–257.

(*14*) Meltzer MS, Leonard EJ. Enhanced tumor growth in animals treated with complete Freund's adjuvant. J Natl Cancer Inst 1973; 50:209–218.

(*15*) Mathé G, Kamel M, Dezfulian M, Halle-Pannenko O, Bourut C. An experimental screening system for "systemic adjuvants of immunity" applicable in cancer immunotherapy. Cancer Res 1973; 33:1987–1997.

(*16*) Sparks FC, Breeding JH. Tumor regression and enhancement resulting from immunotherapy with Bacillus Calmette-Guérin and neuraminidase. Cancer Res 1974; 34:3262–3269.

(*17*) Mathé G, Halle-Pannenko O, Bourut C. Immune manipulation by BCG administered before or after cyclophosphamide for chemoimmunotherapy of L1210 leukemia. Eur J Cancer 1974; 10:661–666.

(*18*) Ungaro PC, Drake WP, Mardiney MR Jr. Repetitive administration of BCG in prevention and treatment of spontaneous leukemia of AKR mice. J Natl Cancer Inst 1973; 50:125–128.

(*19*) Houchens DP, Gaston MR, Kinney Y, Goldin A. Prevention of cyclophosphamide immunosuppression by Bacillus Calmette-Guérin. Cancer Chemother Rep (Part 1) 1974; 58:931–933.

(*20*) Houchens DP, Goldberg AI, Gaston MR, Kende M, Goldin A. Studies of the effects of Bacillus Calmette-Guérin on Moloney sarcoma virus-induced tumors in normal and immunosuppressed mice. Cancer Res 1973; 33:685–690.

(*21*) Bennett JA, Rao VS, Mitchell MS. Systemic Bacillus Calmette-Guérin (BCG) activates natural suppressor cells. Proc Natl Acad Sci USA 1978; 75:5142–5144.

(*22*) Klimpel GR, Henney CS. BCG-induced suppressor cell. I. Demonstration of a macrophage-like suppressor cell that inhibits cytotoxic T cell generation in vitro. J Immunol 1978; 120:563–569.

(*23*) Brunner KT, Manuel J, Cerottini JC, Chapuis B. Quantitative assay of the lytic action of immune lymphoid cells in vitro: Inhibition by isoantibody and drugs. Immunology 1968; 14:181–196.

(*24*) Murahata RI, Mitchell MS. Modulation of cell-mediated alloimmunity by BCG. II. Induction of specific, nonadherent, non-T-killer cells by BCG and alloantigen. JNCI 1982; 69:613–618.

(*25*) Mitchell MS, Kirkpatrick D, Mokyr MB, Gery I. On the mode of action of BCG. Nature [New Biol] 1973; 243:216–218.

(*26*) Wolfe SA, Tracey DE, Henney CS. Induction of "natural killer" cells by BCG. Nature 1976; 262:584–586.

(*27*) Pollack SB. Effect of BCG-SS on K cell activity in mice. Proc Am Assoc Cancer Res 1976; 17:89.

(*28*) Berke G, Gabison D, Feldman M. The frequency of effector cell populations containing cytotoxic T lymphocytes. Eur J Immunol 1975; 5:813–818.

(*29*) Grimm E, Bonavida B. Mechanism of cell-mediated cytotoxicity at the single cell level. I. Estimation of cytotoxic T lymphocyte frequency and relative lytic efficiency. J Immunol 1979; 123:2861–2869.

(*30*) Murahata RI, Zighelboim J. Inhibition of memory cell-mediated cytotoxic response by systemic administration of *Corynebacterium parvum*. Cell Immunol 1979; 42:289–297.

(*31*) ———. Inhibition of cell-mediated cytotoxicity to tumor alloantigens by systemic administration of *Corynebacterium parvum*. Cancer Immunol Immunother 1979; 6:101–106.

(*32*) Reinisch CL, Gleiner NA, Schlossman SL. Adjuvant regulation of T cell function. J Immunol 1976; 116:710–715.

Modulation of Cell-Mediated Alloimmunity by BCG. II. Induction of Specific, Nonadherent, Non-T-Killer Cells by BCG and Alloantigen[1,2,3]

Richard I. Murahata[4,5] *and* **Malcolm S. Mitchell**[6,7,8]

ABSTRACT—The cellular basis of the augmentation of cell-mediated immunity (CMI) by systemically administered BCG was investigated in C57BL/6 mice. BCG pretreatment potentiated the CMI to alloantigens as measured by a 48-hour microcytotoxicity assay (MCA) against P815Y tumor cells. The effector cell was not a T-cell, as demonstrated by its lack of sensitivity to antithymocyte serum and complement and its failure to kill in a short-term ^{51}Cr release assay. The effector cell also was not a classical macrophage, because it was not depleted by treatment with silica. CMI as measured by the MCA was consistently depleted by magnetic separation after incubation with carbonyl iron. The active cell(s) showed variable adherence properties. The augmentation of alloimmunity was alloantigen-specific. The specificity appeared to be due to the interaction between effector cells without inherent specificity and sensitized T-cells.—JNCI 1982; 69:613–618.

BCG is a powerful immunoadjuvant which, in appropriate doses and schedules, can potentiate both humoral (*1, 2*) and cellular (*3–5*) immune responses. It has been reported to antagonize immunosuppression due to a chemical carcinogen (*5*), cytotoxic chemotherapeutic agents (*6, 7*), and antigen-antibody complexes (*8*). Of particular interest has been its ability to augment resistance to tumors in humans (*9, 10*) and experimental animals (*11–15*). The cellular basis of many of these effects has not been clearly elucidated, although many mechanisms have been proposed including increased nonspecific trapping in the draining lymph nodes (*16*) and increased localization of specifically recruited lymphocytes (*17*).

The antitumor effects of BCG have been variously ascribed to a nonspecific activation of the reticuloendothelial system (*3, 18*), to nonspecific stimulation of lymphoid cell proliferation in lymph nodes and spleen (*1, 19*), and to a specific enhancement of the immune response (a true adjuvanticity) due to stimulation of helper-accessory cells, such as helper T-cells and macrophages (*20*). Systemic administration of BCG has been reported to result in the production of nonspecific cytotoxic cells such as macrophages (*21, 22*), K cells (*23*), and NK cells (*24*).

Spleen cell immunity, measured by the 48-hour MCA was augmented by systemic BCG in a murine allogeneic tumor model (*25*). Pretreatment with BCG resulted in complete and long-lasting protection against immunosuppression by cytarabine (β-cytosine arabinoside) in that model. The study reported here characterizes the cell types involved in a CMI-R evoked by alloantigens and BCG in mice. A cellular model for the ability of BCG to augment specific alloreactivity is proposed.

MATERIALS AND METHODS

Mice.—Female C57BL/6 mice (*H-2^b*) (The Jackson Laboratory, Bar Harbor, Maine, or Charles River Breeding Laboratories, Inc., Wilmington, Mass.) were used for the preparation of all spleen cell suspensions. Animals were 8–10 weeks old at the beginning of the experiments. Adult male (C57BL/6 × DBA/2)F$_1$ (B6D2F$_1$) mice were used for the in vivo passage of the L1210 tumor line.

Cell lines.—The L1210 leukemia, which originated in a DBA/2 mouse (*H-2^d*), was maintained by weekly intraperitoneal passage in B6D2F$_1$ mice. The P815Y mastocytoma, also of DBA/2 origin, is a long-term tissue culture line which was maintained in FM-S supplemented with antibiotics (M.A. Bioproducts, Walkersville, Md.). The cells growing in suspension were passaged every 2 or 3 days.

Immunization. BCG (Tice strain; National Institutes of Health, Bethesda, Md.) was obtained as lyophilized material packaged at 5±3 viable units/ampule. One container was reconstituted with 6 ml sterile saline, and mice were given iv injections of 0.2 ml (≈0.5 mg of material or 2×10^7 viable units). Mice given other doses of BCG also received a total volume of 0.2 ml. Control mice received an equal volume of sterile saline.

C57BL/6 mice were immunized against DBA/2 alloan-

ABBREVIATIONS USED: CMI=cell-mediated immunity; CMI-R=cell-mediated immune response; CRA=^{51}Cr release assay; FM-S=Fischer's medium + 10% horse serum; K=killer; MCA=microcytotoxicity assay; NK=natural killer; PEC=peritoneal exudate cells; R-ATS=rabbit anti-mouse thymocyte serum; SRBC=sheep red blood cells.

---

[1] Received August 31, 1981; revised March 1, 1982; accepted March 24, 1982.

[2] Supported by Public Health Service grant CA-13105 from the National Cancer Institute and by grant IM-50B from the American Cancer Society.

[3] Animals were maintained under the guidelines of the Yale University School of Medicine and of the National Research Council.

[4] Department of Pharmacology, Yale University School of Medicine, New Haven, Conn. 06510.

[5] *Present address*: Division of Dermatology, Department of Medicine, University of California at Los Angeles School of Medicine, Los Angeles, Calif. 90024.

[6] Departments of Medicine and Pharmacology, Yale University School of Medicine.

[7] Recipient of a Research Career Development Award from the National Cancer Institute.

[8] *Address reprint requests to* Dr. Mitchell at his *present address*: Director for Clinical Investigations, University of Southern California Comprehensive Cancer Center, 2025 Zonal Ave., Los Angeles, Calif. 90033.

tigens on day 0 by an ip injection of 20×10⁶ L1210 cells, which had been killed by 2,800 rad X-radiation immediately before injection. This radiation dose prevented growth of L1210 cells in the syngeneic strain, as judged by the observation of the host 30 days after inoculation.

CMI as measured by the MCA.—The spleen was removed aseptically and gently disrupted by hand in a glass tissue grinder. Cells were washed three times and diluted in FM-S to the desired concentration of trypan blue-excluding cells. Spleen cells were mixed with P815Y cells at effector-to-target cell ratios (E:T) from 5:1 to 250:1, and the mixtures were incubated for 48 hours at 37°C in an atmosphere of 5% CO_2 in air. At the end of the incubation, the remaining target cells were counted in a hemacytometer by light microscopy. The results are expressed as the percent specific inhibition of target cell growth, which was calculated according to the following equation: Percent specific inhibition $= [1 - (T/N)] \times 100$, where T is the number of target cells remaining in the presence of test lymphocytes and N is the number of target cells remaining in the presence of normal lymphocytes.

Assays were performed in duplicate on samples from individual spleens. Values shown are the means of three to four experiments in which duplicate determinations were made on 5–8 spleens. Results were analyzed by a two-tailed Student's t test. Differences with a P-value less than 0.05 were considered to be statistically significant.

Fractionation of effector cells.—R-ATS treatment of spleen cells: R-ATS (M.A. Bioproducts) was twice absorbed with liver homogenate from C57BL/6 mice (6 ml of a 1:3 dilution of R-ATS to 1 ml packed liver homogenate) for 30 minutes at room temperature. Spleen cells (20×10^6/ml) were added to an equal volume of R-ATS and incubated for 60 minutes at 0°C. The tubes were centrifuged, the supernatants were discarded, and the cells were resuspended to the same concentration in guinea pig complement. After incubation at 37°C for 60 minutes, the cells were centrifuged and resuspended in FM-S at the desired concentration of trypan blue-excluding cells. Treatment with R-ATS at a dilution of 1:40 killed approximately 50% of spleen cells, greater than 95% of thymocytes, and less then 10% of bone marrow cells; these cells were from several strains of mice. The response of R-ATS-treated spleen cells to concanavalin A was reduced by approximately 90%; the response to lipopolysaccharide was not decreased.

Treatment with carbonyl iron powder: Spleen cells (4×10^6/ml) in FM-S were incubated with 4 mg carbonyl iron powder/ml (AF-special; a gift of the General Aniline and Film Corp., New York, N.Y.) for 30 minutes at 37°C, with occasional agitation. At the end of the incubation, the tube was placed between the poles of two magnets, and the phagocytic cells and excess iron were allowed to settle for 1 minute. With the magnets in place, the contents of the tube were transferred to another tube, and the process was repeated. The depleted cell population was washed once, and the appropriate concentration in FM-S was adjusted. The overall recovery of viable cells ranged from 35 to 55%; of these, approximately 85% were susceptible to lysis by R-ATS and complement. Less than 0.5% were macrophages, as determined by the acridine orange staining method (*26*).

Removal of plastic adherent cells: On 15×100-mm plastic tissue culture dishes, 6 ml spleen cells (20×10^6/ml) in FM-S were incubated for 40 minutes at 37°C. The nonadherent cells were removed by gently pipetting the medium, and they were placed on a fresh dish. The adsorption procedure was repeated three times. In one experiment, the cells were fractionated by causing them to adhere to glass of surface area equivalent to the tissue culture dishes. Less than 1% of the nonadherent cells were macrophages, as determined by the acridine orange staining technique.

Fractionation by nylon wool columns: Nylon wool columns were prepared by the method of Trizio and Cudkowicz (*27*) as modified by Bennett et al. (*28*). Spleen cells (1-5×10^8) were added to the columns, which were sealed and incubated at 37°C for 45 minutes. Nonadherent cells were recovered by dropwise elution with 25 ml prewarmed medium. Adherent cells were recovered by placing the nylon wool in 40 ml of medium and by agitating them vigorously with forceps. The cells were washed and adjusted to the desired concentration in FM-S.

X-irradiation.—The spleen cells were irradiated immediately before being placed in the assay. Various doses were used, each given at a rate of 140 rad/min on a Stabilipan (250-kV source; Siemens Corp. Medical/Industrial Groups, Iselin, N. J.).

RESULTS

Systemic administration of BCG prior to alloimmunization resulted in a marked increase in CMI as measured by the MCA (table 1). This increase was observed only in animals that were also alloimmunized. BCG administration alone had no effect. Characterization of effector cells is given below.

R-ATS-Treated Cells

Although the spleen cells were only minimally active 14 days after alloimmunization when CMI was assayed by the CRA—a test in which T-cells are at least one major type of effector cell (*26*, *29*)—the T-cells possibly were acting in a role other than that of rapidly cytolytic cells. The results of depleting T-cells by treatment with R-ATS and complement are shown in table 2. This treatment did not reduce the activity of any group in the 48-hour MCA. The increased activity in the R-ATS-treated groups probably was due to an enrichment of the non-T-effector cell population and not

TABLE 1.—*Effect of BCG on spleen cell activity in the MCA*[a]

L1210 cells[b]	BCG[c]	Percent inhibition of target cell growth[d]
−	+	11.4±3.0
+	−	36.4±2.1
+	+	45.9±4.2

[a] Mice were killed on day 14, and their spleen cells were assayed for activity.

[b] + indicates mice received standard immunizing dose of L1210 cells on day 0.

[c] + indicates mice received 0.5 mg BCG, iv, on day −10.

[d] Values are means ± SEM.

to removal of a suppressor cell; however, removal of a suppressor cell as a possible cause of the increased activity cannot be ruled out.

Removal of Phagocytic or Adherent Cells

Peritoneal adherent cells (primarily macrophages) activated by BCG in the absence of specific antigen have been reported to be nonspecifically cytotoxic to transformed cell lines in vitro (*22, 30*). Macrophages are also active in several types of antibody-dependent cellular cytotoxicity reactions (*31*), and possibly they were the effector cells in our study. Macrophages were killed by the addition of 100 μg silica/ml (final concentration) (Santocel; Monsanto Co., St. Louis, Mo.) to the assay mixture (*32*). This procedure did not significantly decrease the activity of the spleen cells in the MCA (66±5% vs. 60±3%) while destroying approximately 95% of the adherent cells derived from a proteose–peptone starch-induced peritoneal exudate, as measured by their detachment from the substrate and by their being stained by trypan blue.

Inasmuch as the cytotoxic and cytostatic activities of activated macrophages have been ascribed to nonphagocytic mechanisms (*31, 33*), we thought it entirely possible that macrophages were involved but that they were acting in a nonphagocytic capacity, or that nonphagocytic or immature monocytes were involved. We, therefore, tested the effect of removal of adherent cells on the CMI mediated by spleen cells. There was no diminution of the growth inhibitory activity of the spleen cells after removal of cells adherent to plastic or glass (three serial adsorptions) (table 3). Both nylon wool-nonadherent cells and nylon wool-adherent cells had significant growth inhibitory activity (table 4). The reason for our inability to separate the effector function on the basis of adherence is not clear, although it is known that the nonadherent cells from BCG-treated spleens are qualitatively different from those obtained from the spleen of a normal mouse. Alternatively, activated suppressor macrophages that adhere tightly to the nylon wool (*34, 35*) can be removed by this procedure, which may result in increased cytotoxic activity of the nonadherent as well as the adherent fraction.

TABLE 2.—*Effect of R-ATS and complement on spleen cell activity in the MCA*[a]

BCG[b]	Percent inhibition of target cell growth[c]	
	Untreated cells	Cells treated with R-ATS + complement[d]
–	41.1±7.5	64.0±0.4
+	55.2±3.5	75.4±3.1

[a] Mice received standard immunizing dose of L1210 cells on day 0. On day 14 mice were killed, and their spleen cells were assayed for activity.

[b] + indicates mice received 0.5 mg BCG, iv, on day −10.

[c] Values are means ± SEM.

[d] Cells were treated immediately before initiation of assay.

TABLE 3.—*Effect of removal of plastic-adherent cells on spleen cell activity in the MCA*[a]

BCG[b]	Percent inhibition of target cell growth[c]	
	Unfractionated cells[d]	Nonadherent cells
–	47.7±4.5	51.8±3.0
+	75.5±2.8	79.0±2.0

[a] Mice received standard immunizing dose of L1210 cells on day 0. On day 14 mice were killed, and their spleen cells were assayed for activity.

[b] + indicates mice received 0.5 mg BCG, iv, on day −10.

[c] Values are means ± SEM.

[d] Plastic adherent cells were removed by three serial adsorptions to plastic tissue culture dishes.

TABLE 4.—*Immunological activity of fractions derived from passage through nylon wool*[a]

BCG[b]	Percent inhibition of target cell growth[c]		
	Unfractionated cells	Nonadherent cells	Adherent cells
–	24.9±7.5	36.5±3.8	55.6±1.9
+	29.6±7.1	43.4±4.3	62.8±1.3

[a] Mice received standard immunizing dose of L1210 cells on day 0. On day 14 mice were killed, and their spleen cells were assayed for activity in the MCA, before or after fractionation with a nylon wool column.

[b] + indicates mice received 0.5 mg BCG, iv, on day −10.

[c] Values are means ± SEM.

Diminution of CMI by Carbonyl Iron and Restoration by PEC

Treatment of the spleen cells with carbonyl iron and magnet reduced the number of macrophages to less than 0.5%, as determined by acridine orange staining and by phagocytosis of antibody-coated SRBC (*36*). Although this separation was most likely dependent upon adherence to, as well as phagocytosis of, the iron, for convenience the resultant fractions will be referred to as "phagocytic" and "nonphagocytic." Removal of phagocytic cells from the spleens of animals that had received BCG resulted in a significant reduction of activity (text-fig. 1). Immunity of the controls was not significantly affected by this procedure. PEC obtained from mice given ip injections of sterile proteose–peptone starch solution (2 ml of a 6% solution) significantly augmented the tumor-inhibitory activity of the nonphagocytic population (text-fig. 1). Heat-killed PEC were not able to restore the activity of immune spleen cells depleted of the phagocytic cells (table 5).

Addition of normal PEC to the unfractionated immune spleen cells led to an increased CMI activity (tables 6, 7). PEC did not inhibit tumor cell growth by themselves or when added to normal spleen cells. Inasmuch as sensitized T-cells can arm macrophages in vitro (*37*), the immune spleen cells were treated with R-ATS and complement before addition to the assay. This treatment abolished the ability of the spleen cells to cooperate with the nonimmune PEC (table 6). In the converse experiment, treatment of the PEC with R-ATS and complement did not influence the cooperation (table 7).

The spleen cells active in the MCA thus appeared to be monocyte-like cells found in sensitized mice but not in normal mice; there monocyte-like cells may have acquired

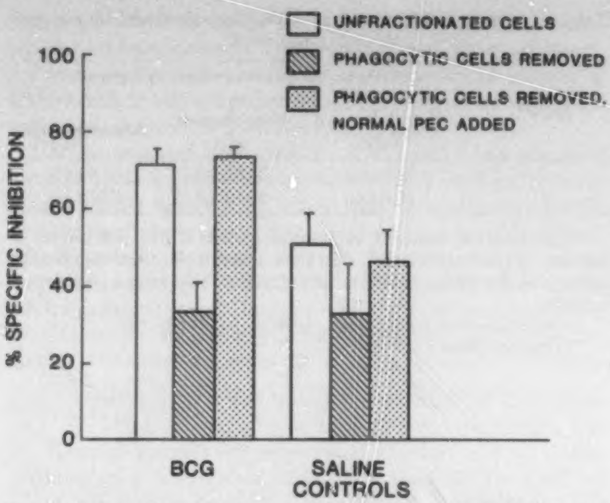

TEXT-FIGURE 1.—Decrease of growth inhibition measured by MCA after removal of spleen cells adhering to and/or ingesting carbonyl iron particles (phagocytic cells) and the restoration of activity by the addition of normal PEC, 5×10^5 cells/culture. All groups were given 20×10^6 irradiated cells and either BCG or saline, 14 days before MCA.

TABLE 5.—*Restoration of activity to nonphagocytic cells by normal PEC*[a]

BCG[b]	Percent inhibition of target cell growth[c]			
	Unfractionated cells	Nonphagocytic cells		
		Untreated	+ PEC[d]	+ killed PEC[e]
–	27.2±3.0	2.4±5.4	59.8±1.2	6.3±2.8
+	40.9±6.5	6.5±4.5	66.9±3.0	7.2±2.9

[a] Mice received standard immunizing dose of L1210 cells on day 0. On day 14 mice were killed, and their spleen cells were assayed for activity in the MCA, before or after fractionation by treatment with carbonyl iron and magnet.

[b] + indicates mice received 0.5 mg BCG, iv, on day −10.

[c] Values are means ± SEM.

[d] Normal PEC (5×10^5) were added to cultures.

[e] PEC were killed by heating to 56°C for 30 min before addition to cultures.

specificity from interaction with sensitized T-cells. Thus far our attempts to isolate a soluble cytotoxic or arming factor in this system have not been successful. Cytophilic antibody was not found in the serum nor was arming factor detectable in supernatants from spleen cell incubation mixtures. As effectors in an antibody-dependent, cell-mediated cytotoxicity assay, when antibody to SRBC was added, spleen cells from mice pretreated with BCG were not more active than those from controls. Attempts to remove any arming factors by treatment of spleen cells with trypsin were also unsuccessful. (For brevity, data from these experiments are not included.) These observations, combined with the abrogation of the ability of spleen cells to recruit specific peritoneal exudate cytotoxic cells after R-ATS treatment of the spleen, indicate that an antibody-dependent phenomenon is not involved and that the specificity is due to a direct interaction of immune T-cells and macrophages.

X-Irradiation of Effector Cells

Because macrophages are more radioresistant than lymphocytes, and activated macrophages even more so tha resting cells, the effect of radiation on the effectors elicite by BCG was tested. Spleen cells were exposed to X-radiatio immediately prior to the in vitro assay. A dose of 500 ra significantly reduced the CMI of control spleen cell whereas the activity of spleen cells from animals that ha received various doses of BCG and alloantigen was no affected. A 1,000-rad dose was similarly ineffective in inhibiting the CMI of BCG-treated alloimmune spleen cell

TABLE 6.—*Effect of R-ATS treatment of immune spleen cells on their ability to cooperate with normal PEC*[a]

BCG[b]	R-ATS	Percent inhibition of target cell growth[c]	
		Spleen cells	Spleen cells + PEC[d]
–	–	43.9±2.8	68.8±2.7
–	+	52.2±7.3	59.5±6.3
+	–	51.4±4.8	65.1±2.0
+	+	73.7±3.2	61.7±9.7

[a] Mice received standard immunizing dose of L1210 cells on day On day 14 mice were killed, and their spleen cells were assayed fo activity in MCA, before or after fractionation with R-ATS and complement.

[b] + indicates mice received 0.5 mg BCG, iv, on day −10.

[c] Values are means ± SEM.

[d] 5×10^5 normal PEC were added to cultures.

TABLE 7.—*Effect of R-ATS treatment of PEC on their ability to cooperate with immune spleen cells*[a]

BCG[b]	Percent inhibition of target cell growth[c]		
	Untreated spleen cells	Spleen cells + PEC[d]	Spleen cells + R-ATS-treated PEC[e]
–	51.9±2.5	87.7±0.4	82.5±0.7
+	68.3±2.2	87.6±0.4	85.5±1.5

[a] Mice received standard immunizing dose of L1210 cells on day On day 14 mice were killed for assay.

[b] + indicates mice received 0.5 mg BCG, iv, on day −10.

[c] Values are means ± SEM.

[d] Untreated PEC (5×10^5) were added to cultures immediately befo initiation of assay.

[e] Normal PEC (5×10^5) treated until R-ATS + complement we added to cultures immediately before initiation of assay.

TABLE 8.—*Radioresistance of effector cells in the MCA*[a, b]

BCG[c]	Percent inhibition of target cell growth after X-radiation[d]			
	0 rad	500 rad	1,000 rad	3,000 rad
–	22.6±3.7	12.2±4.4	13.5±3.0	9.7±4.4
+	32.2±3.0	36.3±4.0	28.9±3.3	18.0±2.8

[a] Mice received standard immunizing dose of L1210 cells on day On day 14 mice were killed for assay.

[b] Spleen cells received the indicated dose of X-radiation immediate before their addition to assay.

[c] + indicates mice received 0.5 mg BCG, iv, on day −10.

[d] Values are means ± SEM.

Not until high (3,000 rad) radiation doses were administered was the activity of the BCG-treated spleen cells reduced (table 8), again suggesting the involvement of a nonlymphocytic cell. Note, however, that activated and/or immune lymphocytes are also relatively radioresistant, and that the BCG may result in T-cell populations that are less susceptible to radiation damage.

DISCUSSION

The findings presented in this paper indicate that systemically administered BCG potentiates the spleen CMI-R to alloantigens in the mouse, as measured by the 48-hour MCA. BCG and alloantigens elicit immunologically specific cytotoxic effectors that are not T-cells but neither do they resemble classical mature macrophages. The data support the thesis that treatment with an immunologic adjuvant in conjunction with specific immunization can increase the production of specific, variably adherent, non-T-effector cells. The potentiation of specific non-T-CMI reported in this paper may be related to BCG's demonstrated ability to elicit other non-T-effectors, such as nonspecific, nonadherent spleen cytotoxic cells (*21*), NK cells (*24*), and spleen K cells (*23*). However, the lack of reactivity in the short-term CRA (*25*) and the specificity of killing we observed in this study are both inconsistent with a role for NK cells such as Wolfe and his co-workers have induced with BCG (*24*). In earlier work (*21*), BCG given alone to C57BL/6 mice caused the production of nonadherent effector cells in the spleen that inhibited P815Y mastocytoma cells in vitro. This nonspecific inhibitory activity, which also extended to *H-2*^{k} tumors, was found with the MCA, but not with the CRA, 10–14 days after administration of BCG (Kinder BK, Mitchell MS: Unpublished data). In the present study, the specificity demonstrated by the spleen cells most likely was due to the alloimmunization and the longer interval between BCG inoculation and the assay. It could not be determined whether the increased immunity was due to an increased number of effector cells or an increased activity per effector cell, but both are plausible explanations.

The inability in the MCA of ATS-treated spleen cells to cooperate in the restoration of activity by normal PEC suggests that T-cells are necessary for the development of augmented specific systemic immunity after administration of BCG and antigen. However, the non-T-effector cell in the spleen appears to be the limiting factor in the expression of that immunity. Treatment of unfractionated immune spleen cells with ATS and complement did not decrease their activity in the MCA, presumably because the effector cells had already interacted with T-cells in vivo. Only when effector cells were depleted did the importance of the interaction with T-cells become manifest.

A considerable literature implicates the macrophage as an effector in antitumor immunity (*38*). In our studies a number of methods known to deplete mature macrophages had no effect on the inhibitory activity of the spleen. Poisoning the spleen cells with silica did not decrease CMI, as measured by the MCA, nor did the removal of glass- or plastic-adherent cells. Yet a good deal of evidence suggests a cell of the monocyte–macrophage lineage. When nylon-adherent cells were examined, they, as well as the nonadherent cells, showed strong activity. The presence of reactive cells in both populations may reflect a variation in the adherence properties of the same class of effector cell rather than two distinct types of cell. Bennett and Mitchell (*39*) noted a number of immature macrophages with suppressive activity in BCG spleens, which had migrated from the bone marrow. Recent evidence (Hengst JC, Mitchell MS: Unpublished data) supports this observation, inasmuch as progenitors of red blood cells, granulocytes and macrophages were found in profusion 2–3 weeks after iv inoculation with BCG. Thus poorly adherent immature macrophages and adherent more-mature macrophages might both be implicated. The decrease in activity after treatment with carbonyl iron and magnet was probably due as much to the depletion of cells adhering to the iron as to removal of cells that ingested it. This would explain the discrepancy in results with silica which poisons truly phagocytic cells.

Radioresistance also favors a cell of the macrophage series. BCG led to a considerable increase in the radioresistance of spleen CMI (as compared to the resistance induced by antigen alone), which could be due either to a greater number of radioresistant cells or to greater activation of effector cells. That the increased radioresistance is due to greater activation of effector cells is consistent with the studies of Den Otter et al. (40), who, with a 24- to 40-hour MCA, found that the resistance to ionizing radiation could be correlated with the degree of activation of the cytotoxic macrophages. Armed macrophages activated in vitro by incubation with the antigen or with lipopolysaccharide also showed increased radioresistance over that of armed unactivated cells.

The role of cytophilic antibody in this system appears to be minimal, as demonstrated by the following observations: *a*) the lack of detectable lymphocyte-dependent antibody in the sera of mice or in the supernatant of incubation mixtures and *b*) the failure of BCG to potentiate K cell activity in the spleens of treated animals. More likely, the observed specificity is conferred on the ultimate effector cell through direct interaction with immune T-cells in a manner described by other investigators (*37, 41*).

The inability of BCG pretreatment to increase cytotoxic T-cell activity measurable by the CRA is consistent with recent results from this and other laboratories. Systemic BCG elicits cells in the spleen that can inhibit T-cell proliferation to mitogens (*21*; Murahata RI: Unpublished observations) and suppress the generation of cytotoxic T-cells in vitro (*34, 35*). Reinisch et al. (*42*) reported that immunization of mice with allogeneic tumor cells in complete Freund's adjuvant suppressed the generation of cytotoxic T-cells while having no effect on the generation of helper or memory T-cells. A similar phenomenon may be occurring in our study, if the T-cells that remain capable of cooperating with macrophages are helper cells.

REFERENCES

(*1*) Miller TE, Mackaness GB, Lagrange PH. Immunopotentiation with BCG. II. Modulation of the response to sheep red blood cells. J Natl Cancer Inst 1973, 51:1669–1676.

(*2*) Stjernswärd J. Effect of Bacillus Calmette-Guérin and/or methylcholanthrene on the antibody-forming cells measured at the cellular level by a hemolytic plaque test. Cancer Res 1966; 26:1591-1594.

(3) Balner H, Old LJ, Clarke DA. Accelerated rejection of male skin isografts by female C57BL mice infected with Bacillus Calmette-Guérin (BCG). Proc Soc Exp Biol Med 1962; 109:58-62.

(4) Peters LC, Hanna MG Jr, Gutterman JV, Mavligit CM, Hersh EM. Modulations of the immune response of guinea pigs by repeated BCG scarification. Proc Soc Exp Biol Med 1974; 147:344-349.

(5) Vitale B, Allegretti N. Influence of Bacillus Calmette-Guérin infection on the intensity of homograft rejection in rats. Nature 1963; 199:507-509.

(6) Mathé G, Halle-Pannenko O, Bourut C. Immune manipulation by BCG administered before or after cyclophosphamide for chemoimmunotherapy of L1210 leukemia. Eur J Cancer 1974; 10:661-666.

(7) Houchens DP, Gaston MR, Kinney Y, Goldin A. Prevention of cyclophosphamide immunosuppression by Bacillus Calmette-Guérin. Cancer Chemother Rep (Part 1) 1974; 58:931-933.

(8) Rao VS, Mitchell MS. BCG prevents suppression of macrophage mediated immunity induced by soluble immune complexes. Proc Am Assoc Cancer Res 1981; 22:247.

(9) Morton DL. Immunotherapy of human melanomas and sarcomas. Natl Cancer Inst Monogr 1972; 35:375-378.

(10) Nathanson L. Regression of intradermal malignant melanoma after intralesion injection of *Mycobacterium bovis* strain BCG. Cancer Chemother Rep 1972; 56:659-665.

(11) Biozzi G, Stiffel C, Halpern BN, Mouton D. Effet de l'inoculation du bacille du Calmette-Guérin sur le développement de la tumeur ascitique d'Ehrlich chez la souris. C R Soc Biol (Paris) 1959; 153:987-989.

(12) Halpern BN, Biozzi G, Stiffel C, Mouton D. Effet de la stimulation du système reticulendothelial par l'inoculation du bacille du Calmette-Guérin sur le développement de l'épithelioma atypique T-de Guérin chez le rat. C R Soc Biol (Paris) 1959; 153:919-923.

(13) Zbar B, Bernstein ID, Bartlett BL, Hanna MG Jr, Rapp HJ. Immunotherapy of cancer: Regression of intradermal tumors and prevention of growth of lymph node metastases after intralesional injection of living *Mycobacterium bovis*. J Natl Cancer Inst 1972; 49:119-130.

(14) Zbar B, Bernstein I, Tanaka T, Rapp HJ. Tumor immunity produced by the intradermal inoculation of living tumor cells and living *Mycobacterium bovis* (strain BCG). Science 1970; 170:1217-1218.

(15) Bartlett GL, Zbar B, Rapp HJ. Suppression of murine tumor growth by immune reaction of the Bacillus Calmette-Guérin strain of *Mycobacterium bovis*. J Natl Cancer Inst 1972; 48:245-257.

(16) Zatz MD. Effects of BCG on lymphocyte trapping. J Immunol 1976; 116:1587-1591.

(17) Emeson EE. Adjuvant-induced selective recruitment of specifically reactive lymphocytes: A probable mechanism of adjuvant action. J Immunol 1980; 124:2222-2230.

(18) Biozzi G, Stiffel C, Halpern BN, Mouton D. Etude de la fonction phagocytaire du S.R.E. au cours du développement de tumeurs malignes experimentales chez le rat et la souris. Ann Inst Pasteur 1958; 94:681-693.

(19) White RG, Coons AH, Connolly JM. Studies on antibody production. IV. The role of a wax D fraction of *Mycobacterium tuberculosis* in adjuvant emulsions on the production of antibody to egg albumin. J Exp Med 1955; 102:83-104.

(20) Mokyr MB, Mitchell MS. Activation of lymphoid cells by BCG in vitro. Cell Immunol 1975; 15:264-73.

(21) Mitchell MS, Kirkpatrick D, Mokyr MB, Gery I. On the mode of action of BCG. Nature [New Biol] 1973; 243:216-218.

(22) Cleveland RP, Meltzer MS, Zbar B. Tumor cytotoxicity in vitro by macrophages from mice infected with *Mycobacterium bovis* strain BCG. J Natl Cancer Inst 1974; 52:1887-1895.

(23) Pollack SB. Effect of BCG-SS on K cell activity in mice. Proc Am Assoc Cancer Res 1976; 17:89.

(24) Wolfe SA, Tracey DE, Henney CS. Induction of "natural killer" cells by BCG. Nature 1976; 262:584-586.

(25) Murahata RI, Mitchell MS. Modulation of cell-mediated alloimmunity by BCG. I. Antagonism and potentiation of immunosuppression caused by cytarabine. JNCI 1982; 69:607-612.

(26) Goldstein P, Blomgren H. Further evidence for the autonomy of T cells mediating specific in vitro cytotoxicity: Efficiency of very small amounts of highly purified T cells. Cell Immunol 1973; 9:127-141.

(27) Trizio D, Cudkowicz G. Separation of T and B lymphocytes by nylon wool columns: Evaluation of efficacy by functional assays in vivo. J Immunol 1974; 113:1093-1097.

(28) Bennett J, Ehrke C, Dave C, et al. Selective effects of methylglyoxyl-bis-(guanylhydrazone) on the development of antibody-forming cells in mice. Biochem Pharmacol 1977; 26:723-728.

(29) Herberman RB, Nunn ME, Lavrin DH, Asofsky R. Effect of antibody to θ antigen on cell-mediated immunity induced in syngeneic mice by murine sarcoma virus. J Natl Cancer Inst 1973; 51:1509-1512.

(30) Holtermann OA, Klein E, Casale GP. Selective cytotoxicity of peritoneal leucocytes for neoplastic cells. Cell Immunol 1973; 9:339-352.

(31) Temple A, Loewi G, Davies P, Howard A. Cytotoxicity of immune guinea-pig cells. II. The mechanisms of macrophage cytotoxicity. Immunology 1973; 24:655-669.

(32) Allison AC, Harington JS, Birbeck M. An examination of the effects of silica on macrophages. J Exp Med 1966; 124:141-154.

(33) Lohmann-Matthes ML, Schipper H, Fischer H. Macrophage-mediated cytotoxicity against allogeneic target cells in vitro. Eur J Immunol 1972; 2:45-49.

(34) Klimpel GR, Henney CS. BCG-induced suppressor cells. I. Demonstration of a macrophage-like suppressor cell that inhibits cytotoxic T cell generation in vitro. J Immunol 1978; 120:563-569.

(35) Bennett JA, Rao VS, Mitchell MS. Systemic Bacillus Calmette-Guérin (BCG) activates natural suppressor cells. Proc Natl Acad Sci USA 1978; 75:5142-5144.

(36) Hersey P. Macrophage effector function. An in vitro system of assessment. Transplant 1973; 15:282-290.

(37) Evans R, Grant CK, Cox H, Steele K, Alexander P. Thymus-derived lymphocytes produce an immunologically specific macrophage-arming factor. J Exp Med 1972; 136:1318-1322.

(38) Fink MA, ed. The macrophage in neoplasia. New York: Academic Press, 1976.

(39) Bennett JA, Mitchell MS. Induction of suppressor cells by intravenous administration of Bacillus Calmette-Guérin and its modulation by cyclophosphamide. Biochem Pharmacol 1979; 28:1947-1952.

(40) Den Otter W, Evans R, Alexander P. Differentiation of immunologically specific cytotoxic macrophages into two types on the basis of radiosensitivity. Transplantation 1974; 18:421-428.

(41) Gallily R, Eliahu H. Mechanism and specificity of macrophage-mediated cytotoxicity. Cell Immunol 1976; 25:245-255.

(42) Reinisch CL, Gleiner NA, Schlossman SL. Adjuvant regulation of T cell function. J Immunol 1976; 116:710-715.

Alloantigenic Phenotype of Radiation-Induced Thymomas in the Mouse[1,2,3]

P. Mark Hogarth,[4] Margaret M. Henning,[4] *and* Ian F. C. McKenzie[4]

ABSTRACT—The alloantigenic phenotype of 21 radiation-induced thymomas is described. Monoclonal antibodies and conventional antisera, absorbed to remove contaminating antibodies, were used to test the thymomas directly for the presence of H-2, Ia, Ly-1, Ly-2, Ly-4, Ly-5, Ly-6, Ly-9, Ly-15, Thy-1, TL, and Qa-2 antigens, and for surface immunoglobulin. The phenotypes obtained by direct tests were also confirmed by absorption studies. The tumors were all of T-cell origin (Thy-1$^+$Ig$^-$) and showed a restricted heterogeneity of their cell surface phenotype, concordant with the known alloantigenic phenotypes of functional T-cells. Thus the thymomas could be classified into 7 groups based on the differing expressions of Ia, Ly-1, Ly-2, Ly-4, and Ly-6 specificities; all tumors were H-2$^+$, Ly-5$^+$, Ly-9$^+$, and Ly-15$^+$. Thus a wide variety of phenotypically diverse tumors could be detected; if these represent the clonal expansion of different functional subsets, they could provide a valuable set of functional T-cells.—JNCI 1982; 69:619–626.

T-lymphocyte functions in the mouse are mediated by various populations of T-cells that can be identified by their expression of cell surface markers (*1*). T-helper cells, T-suppressor cells, and T-cytotoxic cells can be distinguished on the basis of their Ly-1, Ly-2, Ly-3, Ly-6, and Ia phenotype (*1–3*). Thus cell surface markers have been useful in categorizing different functional T-cell subsets. Based on this, various T-cell differentiation pathways have also been suggested (*4, 5*). However, these experiments involve the depletion of Ly$^+$ lymphocytes from whole lymphoid cell suspensions, which may result in the loss of several different Ly$^+$ populations. Several approaches may be used to overcome this problem and enable the analysis of a single T-cell function. These are, first of all, creating monoclonal T-cell lines by hybridization of functional T-cells with T-cell tumors, which is, in general, unsuccessful. The second possibility, the establishment of cloned normal T-cell lines under special conditions in vitro, has been successfully achieved, although with some difficulty (*6*). Finally, T-cell tumors that grow readily in vivo or in vitro and that possess the cell surface phenotype of a particular T-cell could be induced to function as a normal T-cell of that phenotype. This approach has been successful for the study of B-cell differentiation (*7, 8*). It is also well documented that T-cell tumors can mediate functions attributed to normal cells (*9, 10*). Recently, such T-cell-like function has been demonstrated for cells of the appropriate phenotype: Ly-1$^-$2$^+$ tumor cells could specifically mediate suppression of immune function (*11*). Thus studies of the cell surface phenotype of tumors may be of great value in providing functional T-cell tumor lines.

This paper describes the testing of 21 radiation-induced thymomas with monoclonal and conventional antisera; this testing recognized 13 different cell surface antigenic systems. The aim of this study was to answer several questions: 1) Do tumors represent a monoclonal expansion of a single cell arrested at a particular stage of differentiation? 2) Are the Ly alloantigenic phenotypes the result of random gene derepression, or do they reflect the phenotype of the originally transformed T-cell? 3) What is the role of antiviral antibodies in the results obtained, and can these be overcome by the use of absorption tests or by tests with MoAb?

MATERIALS AND METHODS

Mice.—Strains of mice used for the generation of thymomas are shown in table 1. The distribution of alloantigenic specificities among these strains is also shown.

Induction and maintenance of thymomas.—Thymic lymphomas were induced in C57BL/6 mice and in related strains and in CE/J mice by repeated X-irradiation as described (*12*). Four-week-old mice received 150 rad of X-irradiation per week for 4 weeks from a Philips Ortholux machine. Thymomas appeared in 7–9 months and were maintained by serial passage in syngeneic mice by subcutaneous implantation or by ip injection and subsequent harvest of ascitic fluid. The cells were also preserved frozen in liquid nitrogen. Some tumors were not transplantable after their primary appearance, and some did not withstand cryopreservation.

Antisera.—Conventional anti-H-2 antisera used in this study were obtained from the National Institutes of Health, Bethesda, Md., and are fully described in the "Catalog of Mouse Alloantisera." The antibodies used were anti-H-2.2 (D-2), H-2.33 (D-33), H-2.23 (D-23), and H-2.32 (D-32), which were absorbed with DBA/2 lymphoid cells to remove contaminating antibodies as described below. Anti-H-2.4 (D-4) and H-2.31 (D-31) were absorbed with AKR cells, and an anti-Ia^k made as A.TH anti-A.TL was absorbed with SJL cells. Conventional anti-Ly, Thy-1, and TL antisera were made in the donor recipient combinations shown in table 2 as described (*1*). MoAb used in this study are listed in table 3.

ABBREVIATIONS USED: FcR=Fc receptor; ITT=irradiation-induced thymus tumor; MoAb=monoclonal antibody (antibodies); MuLV=murine leukemia virus; SAMIg=sheep anti-mouse immunoglobulin; sIg=surface immunoglobulin.

---

[1] Received September 17, 1981; revised February 22, 1982; accepted March 24, 1982.

[2] Supported by funds from the National Health and Medical Research Council of Australia, and by Public Health Service grant CA-22080 from the National Cancer Institute.

[3] Animals were maintained under the guidelines set forth in the "Guide for the Care and Use of Laboratory Animals" by the Institute of Laboratory Animal Resources, National Research Council.

[4] Department of Pathology, University of Melbourne, Parkville, Victoria, 3052 Australia.

TABLE 1.—*Alloantigenic specificities of strains used for thymoma induction*

Strain	H-2 haplotype of origin			Alloantigenic specificities									
	H-2K	*I*	*H-2D*	Ly-1	Ly-2	Ly-4	Ly-5	Ly-6	Ly-9	Ly-15	Thy-1	TL	Qa-2
C57BL/6	*b*	*b*	*b*	2	2	2	1	2	2	2	2	—	+
B10.BR	*k*	*k*	*k*	2	2	2	1	2	2	2	2	1, 2, 3, 5	–
B10.A	*k*	*k/d*	*d*	2	2	2	1	2	2	2	2	1, 2, 3, 5	+
B10.A(5R)	*b*	*b/k/d*	*d*	2	2	2	1	2	2	2	2	1, 2, 3, 5	+
B10.T(6R)	*q*	*q*	*d*	2	2	2	1	2	2	2	2	1, 2, 3, 5	+
AQR	*q*	*k/d*	*d*	2	2	2	1	2	2	2	2	1, 2, 3, 5	+
B6.*Ly-1*^{a}/Cy	*b*	*b*	*b*	1	2	2	1	2	2	2	2	—	+
B6.PL(75NS)	*b*	*b*	*b*	2	1	2	1	2	2	2	2	—	+
B10.C(28NX)	*b*	*b*	*b*	2	2	1	1	2	2	2	2	—	+
CE/J	*k*	*k*	*k*	2	1	1	1	1	1	2	2	—	–

Absorption of antisera.—For removal of autoantibodies, antiviral antibodies, and other contaminating antibodies, all conventional antisera were absorbed. Thymus and spleen cells for absorption were obtained from 10 mice and were prepared as a single cell suspension; the cells were washed twice in medium and mixed with 0.5 ml of antiserum diluted in an equal volume of medium. The suspension was mixed and incubated for 15 minutes at room temperature, 15 minutes on ice, and then centrifuged at 500×*g* for 5 minutes. The absorbed serum was recovered, and cytotoxicity assay was performed to establish specific antibody activity.

Contaminating antibodies to known cell surface antigens were removed in the same way with the use of cells from mice with reciprocal specificity to that accorded to the antiserum (table 2). For removal of antiviral antibodies, antisera were also absorbed with lymphoid cells from aged DBA/2, NZB, or AKR mice known to express high levels of MuLV (*16, 17*) (table 2). No separate determination of antivirus titer was performed after absorption.

Serologic studies.—Direct tests: Thymoma cells were prepared as a single cell suspension and were typed directly with the use of the cytotoxicity test (*18*) with absorbed conventional antisera or SAMIg rosetting (*19*) with MoAb. We performed the tests in triplicate at one dilution of antibody (1/10–1/20) on several occasions.

Absorption studies: Absorption methods were also used to serotype tumors and were performed by the mixing of 5×10^7 tumor cells or lymphoid cells prepared as above with 100 µl antiserum at an appropriate dilution (2 tubes less than the highest dilution giving maximum lysis or rosettes). We incubated the cell–antibody mixture at room temperature for 15 minutes, then on ice for 15 minutes. The cells were removed by centrifugation at 500×*g* for 5 minutes, and the serum was then tested for residual activity on appropriate target cells. Antigen-positive and antigen-negative normal cell controls were included in the absorption as specificity controls. A positive result was obtained when absorption reduced the antibody titer by more than two tubes. Negative results showed a less than two-tube variation in titer.

Detection of FcR and sIg.—The FcR was detected with the use of sheep red blood cell–anti-sheep red blood cell complexes as described (*20*). The sIg was detected with the use of the SAMIg rosetting assay.

Nomenclature of thymomas.—The thymomas are referred to by the prefix ITT. The number after the prefix distinguishes the tumor from others that have arisen in the same strain.

RESULTS

The results of direct serologic typing of 21 radiation-induced thymomas, for 12 alloantigenic markers in C57BL/6 and related mice and CE/J mice are shown in tables 4–6. With the use of conventionally prepared antisera or MoAb, the thymomas were tested for the presence of the alloanti-

TABLE 2.—*Conventional anti-Ly, Thy-1, and TL antisera used in this study*

Specificity	Donor	Recipient	Possible contaminating antibodies	Strains used for absorptions	Remaining antibodies
Ly-1.1	B6.Ly-1^a	(C57BL/6 × LP.RIII)F$_1$	Ly-10.2	NZB	Ly-1.1
Ly-1.2	CE	C3H	Negligible	DBA/2	Ly-1.2
Ly-2.1	CE	C57BR/cd	Ly-4.1, Ly-6.1, Ly-9.1 Ly-10.1, Ly-12.2, Ly-13.2, Ly-16.2	NZB	Ly-2.1
Ly-2.2	B10.BR	(C3H × BDP)F$_1$	Ly-4.2	DBA/2, B6.*Ly-2*^{a}*Ly-3*^{a}	Ly-2.2
Ly-4.2	B10.D2	(BALB/c × SWR)F$_1$	Ly-9.2, Ly-15.2	DBA/2 B6-C(18NX)	Ly-4.2
Ly-6.1	C3H	(C3H.B6-*Ly-6*^{b} × C57BL/6)F$_1$	? Ly-8.1	DBA/2	Ly-6.1 ? Ly-8.1
Ly-6.2	CXBE	(CXBG × A)F$_1$	Ly-8.2, H9/25	NZB	Ly-6.2 Ly-8.2 H9/25
Thy-1.2	C57BL/6	(B6.PL-*Thy-1*^{a} × RF)F$_1$	Negligible	AKR	Thy-1.2
TL-1, 2, 3	B10.BR	(C3H × C57BL/6)F$_1$	Negligible	AKR	TL-1, 2, 3

gens H-2, Ia, Ly-1, Ly-2, Ly-4, Ly-5, Ly-6, Ly-9, Ly-15, Thy-1, TL, and Qa-2, and also for sIg. Thirteen tumors were available for only a single initial test because they were either rejected on initial transplantation into syngeneic mice or could not be recovered from preservation in liquid nitrogen. Eight thymomas have been repeatedly tested by direct methods with conventional antibodies and MoAb and these results have been confirmed by absorption studies. The thymomas have been classified into groups based on similarity of Ly-1, Ly-2, Ly-4, and Ia antigenic phenotype.

Initial typing of thymomas.—In initial tests of thymomas with use of conventional alloantisera, all thymomas were positive with all the antisera (group 1, table 5). This finding implied that the antisera were contaminated with antibodies to other cell surface alloantigens (table 2) and with antiviral antibodies (*21, 22*) or autoantibodies (*23*). Contaminating autoantibodies and antibodies to other cell surface antigens were removed by absorption of the antisera with thymus and spleen cells from mice bearing the appropriate antithetical specificity, and antiviral antibodies were removed by absorption with thymus and spleen cells from mice that showed a high expression of endogenous MuLV. Antisera were considered specific when they showed: 1) a positive reaction with cells from mice carrying the allele for the specificity detected by that antiserum but not on mice congenic for that locus; and 2) no reactivity with the rat cell line W/Fu-G, which expresses high levels of the endogenous MuLV and associated antigens. All thymomas were then typed directly with the absorbed antisera by cytotoxicity assay, and where possible, these results were confirmed with the use of MoAb and SAMIg rosetting. The direct test results were then verified by absorption tests (tables 4, 5), which also confirmed the occurrence of an antigen that may be present in quantities too small to be detected by direct methods.

General comments on the cell surface phenotype of the thymomas.—The conclusion that the radiation-induced tumors were of thymic origin is based on the evidence that: 1) all thymomas were Thy-1^+ sIg^-; 2) approximately half of the thymomas were TL^+—an antigen found only on T-cells; 3) all thymomas were Ly-6^- and Qa-2^-, which implied a lack of maturity since more than 90% of the peripheral T-cells are Ly-6^+, Qa-2^+, whereas thymus cells are Ly-6^-, Qa-2^-. The data presented below also show that with the exception of 1 thymoma, ITT(1)CE, which appears to be related to a pre-T-cell, all tumors expressed Ly-2, but surprisingly most thymomas were Ly-1^-; i.e., most were Ly-1^-2^+. This is an unusual phenotype, which has not been detected in normal thymocytes and which is difficult to detect among peripheral T-cells (*24, 25*).

Another significant observation was that no Ly-1^+2^- thymoma was detected. The reason for this is not clear and may mean that such cells are resistant to the dose of radiation given and do not form tumors or that they are extremely radiosensitive.

Alloantigenic phenotype of thymomas.—The alloantigenic phenotype for each group of thymomas is shown in tables 4 and 5. Although each tumor in the groups bears the same Ia and Ly phenotype, there is considerable heterogeneity in the

TABLE 3.—*MoAb used in this study*

Specificity[a]	Clone designation	Reference
Ly-1 (framework)	53-7.313	*13*
Ly-2 (framework)	53-6.72	*13*
Ly-2.1	49-31.1	*14*
Ly-5 (T200) (framework)	30-G-12	*13*
Ly-6.2	237-43	*14*
Ly-9.2 (Lgp 100)	20-1.5	*13*
Ly-15.2	8-6.4	*14*
Thy-1.2	23-64.10	*14*
Qa-2	141-15.8	*14*
Ia.20	93-20	*14*
Ia.17^c	N-22	*14*
Ia.17^p	10-2.16	*15*
Ia.2	11-5.2	*15*

[a] Ia.20 specificity is coded for by *I-A^b* genes only. Ia.17 specificity is coded for by genes in the *I-A* subregion of *H-2^k*, *H-2^f*, *H-2^r*, and *H-2^s*. Ia.2 specificity is coded for by *I-A^k* genes only.

TABLE 4.—*Alloantigenic phenotype of radiation-induced thymomas*

Group	Tumor	Assay[a]	Alloantigenic specificities[b]												
			H-2	Ia	Ly-1	Ly-2	Ly-4	Ly-5	Ly-6	Ly-9	Ly-15	Thy-1	TL	Qa-2	sIg[c]
1	ITT(1)B10.A	C	+	+	+	+	+	·	+	·	·	+	+	·	−
	ITT(3)B10.A	C	+	+	+	+	+	·	+	·	·	+	+	·	−
	ITT(1)B10.T.6R	C	+	+	+	+	+	·	+	·	·	+	+	·	−
	ITT(1)*B6-Ly-1^a*	C	+	+	+	+	+	·	+	·	·	+	+	·	−
2	ITT(1)B6	C	+	−	+	+	−	+	+	·	·	+	−	·	−
	ITT(2)B6	C	+	−	+	+	−	+	+	·	·	+	+	·	−
	ITT(1)28NX	C	+	−	+	+	−	+	+	·	·	+	−	·	−
3	ITT(2)B10.A	C	+	−	+	+	+	+	−	·	·	+	+	·	−
		MC	·	−	+	+	·	+	·	+	+	+	·	−	
		Abs	·	·	+	+	+	+	−	·	·	+	·	·	
	ITT(1)5R	C	+	−	−	+	+	+	−	+	+	+	+	·	−
		MC	·	−	+	+	·	+	−	·	·	+	·	−	

[a] Thymomas were tested by direct serologic methods with the use of cytotoxicity testing with C, absorbed conventional antisera; MC, SAMIg rosetting with monoclonal antibodies; or by Abs, absorption.

[b] Positive results in direct testing gave >70% lysis or rosette-forming cells, whereas negative results were background levels of <10%. Absorption results were positive when absorbed sera showed a >2 tube reduction in titer relative to negative control. · = not determined.

[c] sIg was detected by SAMIg rosetting.

TABLE 5.—*Alloantigenic phenotype of radiation-induced thymomas*

Group	Tumor	Assay[a]	Specificity detected[b]												
			H-2	Ia	Ly-1	Ly-2	Ly-4	Ly-5	Ly-6	Ly-9	Ly-15	Thy-1	TL	Qa-2	sIg[c]
4	ITT(2)AQR	C	+	−	−	+	−	·	−	·	·	−	−	·	−
	ITT(5)B10.A	C	+	−	−	+	−	·	−	·	·	+	+	·	−
	ITT(4)B10.A	C	+	−	−	+	−	·	−	·	·	+	+	·	−
	ITT(1)AQR	C	+	−	−	+	−	·	−	·	·	+	−	·	−
	ITT(3)AQR	C	+	−	−	+	−	·	−	·	·	+	+	·	−
	ITT(3)B10.BR	C	+	−	−	+	−	+	−	·	·	+	·	·	−
	ITT(1)75NS	C	+	−	−	+	−	+	−	·	·	+	−	·	−
		MC	+	−	−	+	−	+	−	+	+	+	·	−	
		Abs	·	−		+	−	+	−	·	·	+	·	·	
		W	·			+		+	·	·	·	+	·	·	
5	ITT(3)28NX	C	+	−	−	+	+	+	−	·	·	+	+	·	−
		MC	·	·	−	+	·	+	−	+	+	+	·	−	
		Abs	·	·	−	+	·	+	·	·	·	+	+	·	
	ITT(2)B10.BR	C	+	−	−	+	+	·	−	·	·	+	+	·	−
		MC	·	·	·	+	·	+	−	+	+	+	·	−	
		Abs	·	·	·	+	·	+	·	·	·	+	·	·	
	ITT(4)B10.BR	C	+	−	−	+	+	+	−	·	·	+	+	·	−
		MC	·	·	−	+	·	+	−	+	+	+	·	−	
		Abs	·	·	−	+	+	+	−	·	·	·	+	·	
6	ITT(4)B6	C	+	+	−	+	+	+	−	+	+	+	+	− (Fc^-R^+)	
		MC	+	−	−	+		+							
		Abs	·	+	−	+	+	+	·	·	·	+	+	·	
		W	·	+	·	+	+		·	·	·	+	+	·	
7	ITT(1)CE	C	+	−	−	[illegible]	−	+	−	·	·	+	−	·	−
		MC	+	−	−	−	·	+	−	·	+	+	·	·	
		Abs	·	·	−	−	−	+	·	·	·	+	·	·	

[a] Thymomas were tested by direct serologic methods with the use of cytotoxicity testing with C, absorbed conventional antisera; MC, SAMI rosetting with MoAb; or by Abs, absorption. W=direct cytotoxicity testing of ITT(1)75NS with conventional antisera absorbed as described in tex and additionally absorbed with the rat leukemia W/Fu infected with MuLV-Gross.

[b] Positive results in direct testing gave >70% lysis or rosette-forming cells, whereas negative results were background levels of <10%. Absorptio results were positive when absorbed sera showed a >2 tube reduction in titer relative to negative control. ·=not determined.

[c] sIg was detected by SAMIg rosetting.

TABLE 6.—*Summary of alloantigenic phenotype of thymomas*[a]

Group[b]	Specificity detected												
	H-2	Ia	Ly-1	Ly-2	Ly-4	Ly-5	Ly-6	Ly-9	Ly-15	Thy-1	TL	Qa-2	sIg
1	+	+	+	[illegible]	+	·	+	·	·	+	+	+	−
2	+	−	+	+	−	+	−	·	·	+	±	·	−
3	+	−	+	+	+	+	−	+	+	+	+	−	−
4	+	−	−	+	−	+	−	+	+	+	±	−	−
5	+	−	−	+	+	+	−	+	+	+	+	−	−
6	+	+	−	+	+	+	−	+	+	+	+	−	−
7	+	−	−	−	−	+	−	·	+	+	+	·	−

[a] +=possession of the antigen; −=absence of antigen; ·=not determined.

[b] Thymomas were grouped on the basis of similarity of phenotype. Group 1 thymomas were tested only once with unabsorbed conventiona antisera (*see* "Results"). They were rejected on subsequent transplantation and could not be retyped.

expression of TL within each group. Since the TL$^-$ phenotype can be converted during transformation to TL$^+$, it was considered that grouping the tumors on the basis of TL phenotype was unsatisfactory.

Group 1 (Ly-1$^+$2$^+$4$^+$Ia$^+$) thymomas.—These tumors arose independently at the same time and were the first to be typed by direct testing with the use of *unabsorbed* conventional antisera. All antisera gave strong positive reactions on all thymomas i.e., these cells appear H-2$^+$Ia$^+$Ly-1$^+$Ly-2$^+$Ly-4$^+$Ly-6$^+$Thy-1$^+$TL$^+$. It would appear that this phenotype is due to the presence of contaminating antibodies in the antisera. Thus the antisera were absorbed (as described in "Materials and Methods") to remove autoantibodies, antiviral antibodies, and antibodies recognizing other cell surface specificities. Following this absorption protocol, we did not observe this phenotype for any other tumor. It is therefore presumed that the positive reactions obtained with these tumors were due, in part, to contaminating antibodies. This assumption, however, cannot be formally demonstrated, because the group 1 thymomas were rejected after initial transplantation and could not be retyped with the absorbed antisera.

Group 2 (Ly-1$^+$2$^+$3$^-$Ia$^-$) thymomas.—These thymomas arose in the C57BL/6 and the *Ly-4* congenic strain

B10.C(28NX) which are both *H-2^b* (table 4). The thymomas were typed with the use of conventional antisera absorbed to remove contaminating antibodies. The 3 thymomas in this group possess the phenotype of the majority of thymocytes, i.e., Ly-1$^+$2$^+$4$^-$Ia$^-$, and all were Ly-5$^+$. Their possible relationship to normal thymocytes was further reinforced since they were Ly-6$^-$, as are 90% of thymocytes (*26*).

Group 3 (Ly-1$^+$2$^+$4$^+$Ia$^-$) thymomas.—Two thymomas, B10.A and B10.A(5R), in this group which arose in *H-2* recombinant mice had an almost identical phenotype as did the group 2 thymomas (table 4). However, unlike group 2, they were Ly-4$^+$ i.e., Ly-1$^+$2$^+$4$^+$Ia$^-$. The results obtained with the absorbed conventional antisera were confirmed by absorption studies and by direct tests with MoAb. MoAb tests also demonstrated that these cells are Ly-9$^+$, Ly-15$^+$, and Qa-2$^-$, as are all thymocytes. This phenotype is equivalent to that seen for a subpopulation of thymocytes or mature T-cells in the periphery which expresses Ly-4 (*27*). However, because these thymomas also lacked Ly-6, the phenotypes resembles that of the thymocyte.

There is one interesting discrepancy in the Ly-1 expression on ITT(1)5R cells. As shown by the rat MoAb test that detects a framework determinant on the Ly-1 molecule common to both Ly-1.1 and Ly-1.2 strains, the cells were clearly Ly-1$^+$. However, the conventional antiserum failed to detect the Ly-1.2 specificity. This finding may be due to one of several causes. The Ly-1.2 specificity may be present in low density, and it was not detected by cytotoxicity assay, but it was detected by SAMIg rosetting, which is a more sensitive technique (*19, 28*) that may detect low Ly-1 density with the rat MoAb. Alternatively, the allotypic Ly-1.2 specificity could be absent from the Ly-1 molecule of these cells, the backbone of which is present, as detected with the MoAb test.

Group 4 (Ly-1$^-$2$^+$4$^-$Ia$^-$) thymomas.—This group contains the largest number of tumors, 7 in all, and they have a more "differentiated" phenotype (Ia$^-$Ly-1$^-$2$^+$) than the group 2 or 3 thymomas (table 5). The tumors arose in the *H-2* recombinant strains AQR and B10.A, and the *H-2^k* congenic strain B10.BR, as well as in the *Ly-2* congenic strain B6.PL(75NS). These thymomas were Ly-4$^-$, and as a measure of their immaturity they were Ly-6$^-$, but all were Ly-5$^+$. TL was variably expressed among the tumors. The ITT(1)75NS tumor was tested with the MoAb test and by absorption, which confirmed the phenotype as Ia$^-$Ly-1$^-$Ly-2$^+$Ly-4$^-$Ly-5$^+$Ly-6$^-$Ly-9$^+$Ly-15$^+$Thy-1$^+$Qa-2$^-$. The Ly-9 antigen was detected by the mouse MoAb as was the Ly-15 antigen, but Qa-2 was absent (table 5). This phenotype Ia$^-$Ly-1$^-$2$^+$ has been observed for several functional T-cell populations in the mouse including suppressor T-cells (*2*), and cells involved in feedback inhibition (*29*). However, knowledge on the expression of the other Ly markers on these cells is somewhat limited.

Group 5 (Ly-1$^-$2$^+$4$^+$Ia$^-$) thymomas.—This group comprised 3 thymomas that arose in the *H-2^k* congenic strain B10.BR and in the *Ly-4* congenic strain B10.C(28NX) (table 5). These tumors had an identical phenotype to that of the group 3 thymomas except that they were all Ly-4$^+$; i.e., they were Ia$^-$Ly-1$^-$2$^+$4$^+$5$^+$6$^-$, which was confirmed by testing with MoAb and by absorption tests. These tumors expressed Ly-4, which may indicate that they were somewhat more mature than the group 4 thymomas. Ly-4 is present on only a small population of thymocytes (10%), but it is present on about 90% of the peripheral T-cells (*27*). The Ly-9 and Ly-15 antigens that are present on all thymocytes were also present on the group 5 tumors. Qa-2 is absent from most thymocytes and appeared to be absent from the thymomas as well. As mentioned for the group 3 thymomas, there are several T-cell functions mediated by Ly-1$^-$2$^+$Ia$^-$ cell types; however, the presence of Ly-4 on these functional T-cells has not been investigated.

Group 6 (Ly-1$^-$2$^+$4$^+$Ia$^+$) thymoma.—Although there was only 1 tumor in this group, ITT(4)B6, derived from a C57BL/6 mouse, it shows some very interesting features (table 5). The phenotype of H-2$^+$Ia$^+$-Ly-1$^-$2$^+$4$^+$5$^+$6$^-$9$^+$15$^+$Thy-1$^+$TL$^+$Qa-2$^-$FcR$^+$ was confirmed by three different assays and reflected the phenotype of a mature peripheral T-cell. The thymoma was unique among all those tested because it was Ia$^+$Ly-1$^-$2$^+$. The Ia antigen expressed was detected by conventional antisera and was clearly confirmed by absorption, but the Ia antigens expressed were not Ia.20$^-$ with the use of the MoAb test. As mentioned above, the Ly-1$^-$2$^+$ phenotype is found on several populations of functional T-cells in the periphery or is "inducible" from thymocytes (*30*). This, together with the Ly4$^+$6$^-$ phenotype of these cells, indicates a possible relationship with functional T-cells, possibly precursor cells, which may be Ly-6$^-$ (*1*). Another remarkable finding was that this thymoma was FcR$^+$, a quality of more mature T-cells rather than of the majority of thymocytes (*31*). Ly-9, Ly-15, and Thy-1 were present on all thymocytes and peripheral T-cells. The presence of TL antigens on the surfaces of ITT(4)B6 cells was detected with conventional antisera and confirmed by absorption. Because TL antigen is restricted in its distribution to thymocytes, the phenotype of the ITT(4)B6 thymoma is totally consistent with that of a mature thymocyte.

Group 7 (Ly-1$^-$2$^-$Ia$^-$) thymoma.—This thymoma was derived from CE mice (*H-2^k*), and the alloantigenic phenotype appears to be that of a very primitive T-cell (table 5). After repeated testing both by direct serologic assays with conventional and monoclonal antisera and by absorption, this tumor was not found to possess the Ly-1 or Ly-2 antigens. Furthermore, the cells did not have Ly-4, Ly-6, TL, or Ia antigens, but they possessed H-2, Ly-5, Ly-15, and Thy-1. Although Ly-5 was originally thought to be restricted to T-cells (*1*), it has now been shown to have a wider distribution including pre-T-cells (*32, 33*). The distribution of Ly-15 on immature lymphoid cells has not been investigated, but its presence on this tumor suggests that it may also be a marker of pre-T-cells.

Alloantigenic phenotype of BALENTL-5.—The BALENTL-5 tumor is a thymic lymphoma derived from a BALB/c mouse treated with 1-ethyl-1-nitrosourea (*34*). This tumor was included as a control because it has been typed independently for cell surface markers in another laboratory with the use of different Ly antisera (*34*). With the use of the same reagents that were used to type the other thymomas, the BALENTL-5 tumor was found to be H-2$^+$Ia$^-$Ly-1$^-$Ly-2$^+$Ly-5$^+$Thy-1$^+$, and these results are in agreement with those of

Mathieson et al. (*34*) that showed the tumor to be Ly-1^-2^+Thy-1^+TL$^+$.

Removal of antiviral antibodies.—It is unlikely that antiviral antibodies were responsible for the phenotyping results obtained with conventional antisera. This was evident when the MoAb confirmed the positive results obtained with conventional antisera and the tumor cells could specifically absorb positive antibody activity. For confirmation that antiviral antibodies make no contribution to the positive results, the conventional antisera were further absorbed with a MuLV-Gross-infected rat leukemia that expresses cell surface antigens associated with this widespread MuLV. The absorbed antisera were tested on ITT(1)75NS and ITT(4)B6 (table 5). No differences in positive reactivity were seen between sera absorbed with lymphoid cells and those absorbed additionally with the rat leukemia. Clearly, absorption of antisera with normal lymphoid cells as described removed contaminating antibodies that may otherwise have given rise to anomalous results. This point will be fully discussed later.

Stability of phenotype.—All the thymomas were tested upon initial removal from the mouse and, where available, were repeatedly tested over 3 years. In all cases, the phenotype was found to be unchanged during successive transplants or after recovery from being frozen in liquid nitrogen.

DISCUSSION

With the use of MoAb or conventional antisera that recognize 13 cell surface antigenic systems, the cell surface phenotypes of 21 radiation-induced thymomas were determined. Several conclusions can be drawn of the results presented above: 1) The thymomas are clearly of T-cell origin but heterogeneous with respect to alloantigen expression; 2) the alloantigenic phenotypes of all thymomas are in accord with the phenotypes of normal T-cells detected by direct serologic assays or by functional assays; 3) the phenotypes found suggest that the tumor cells represent a clonal expansion of a T-cell, arrested at a certain stage of differentiation.

The remarkable feature of these thymomas is that the majority of them have the phenotype of differentiated T-cells (Ly-1^-2^+) and not the phenotype of the majority of thymocytes which are Ly-1^+2^+. This could mean that either there is a subpopulation of these "differentiated" cells within the thymus that are selectively transformed by X-irradiation, or that a peripheral T-cell is transformed by X-irradiation and then returns to the thymic microenvironment to become an overt lymphoma. The first possibility seems most likely because all the thymomas were Ly-6^- and Qa-2^-, which marked them as immature T-cells as the vast majority of thymocytes [90% of the thymocytes are Ly-6^--Qa$^-$, whereas 99% of the peripheral T-cells are Ly-6^+ Qa-2^+ (*1*)]. Furthermore, approximately half of the thymomas expressed the TL antigen, which is present on thymocytes and detectable only with difficulty on peripheral T-cells. Alternatively, expression of the Ly-1 antigen may be readily disrupted by radiation or transformation. It is difficult to determine which possibility is correct; however, the possible radiosensitivity of Ly-1 antigen expression would have to be a selective phenomenon as Ly1^+2^+ thymomas arise.

Since these phenotypes have been described for normal T-cells, it is tempting to postulate that the thymomas represent a clonal expansion of a T-cell, transformed at a particular stage of differentiation. Thus it would appear that group 2 thymomas (table 4) were derived from the pool of the majority of thymocytes which are Ly-$1^+2^+4^-$Ia$^-$, whereas group 3 (table 4) thymomas represent a somewhat more differentiated thymocyte that had acquired the Ly-4 antigen i.e., Ly-$1^+2^+4^+$Ia$^-$. However, the majority of the thymomas exhibited more "differentiated" phenotypes in terms of Ly-1 and Ly-2 expression. Group 4 thymomas are Ly-$1^-2^+4^-$Ia$^-$, whereas group 5 thymomas (table 5) are apparently more mature on the basis of their acquisition of Ly-4, i.e., Ly-$1^-2^+4^+$Ia$^-$. These phenotypes occur with cytotoxic T-cells or suppressor T-cells (*1, 3*), or cells involved in immunoregulatory circuits (*29, 35*).

One final point of interest is that the Ly-4 antigen was clearly selectively expressed on different thymomas. This implies that, if these tumors have arisen from T-cells at different stages of development, then Ly-4, despite its predominant B-cell distribution, may be useful in the definition of different T-cell subsets. The group 6 thymoma ITT(4)B6 (table 5) is extremely interesting, because it had a different Ly phenotype and is unlike all other thymomas in that it had Ia antigens on the cell surface and expressed a FcR; i.e., the tumor is Ly-$1^-2^+4^+$Ia$^+$FcR$^+$. These Ia antigens are also expressed on B-cells, although the T-cell expression of B-cell Ia antigens has been documented (*36*). Finally, the 1 thymoma in group 7 ITT(1)CE (table 5) appears to have been derived from a primitive T-cell, since the tumor cells express Thy-1 but do not express the other T-cell alloantigens Ly-1 or Ly-2. However, it is not possible to determine what stage of early differentiation this thymoma represents. Notwithstanding, this phenotype has been described for the natural killer cell in the mouse (*37*).

As suggested above, the phenotype of the thymomas may be accounted for by clonal expansion of a known T-cell which retains its phenotype after transformation. However, several other explanations for the observed phenotypes are possible and are discussed below.

Derepression of Inactive Cellular Genes

This is a plausible explanation of the observed phenotypes and will be difficult to resolve. There have been reports on the acquisition of foreign H-2 antigens on certain virus-transformed cells (*38*), i.e., unexpected H-2 antigens from another haplotype. This implies that the new antigens are the result of an association with the virus or are the gene products of derepressed genes. However, indirect evidence suggests that this may not be the case for thymomas in our study. There were no unusual phenotypes; that is, the phenotypes observed are all found on normal T-cells. Furthermore, if the genes were randomly derepressed, then it would be expected that there would be a random expression of antigens. Since the presence or absence of 13 different antigens was investigated, it would be expected that there are 13^2 or 169 possible antigenic phenotypes; the study demonstrated only 6 antigenic phenotypes (table 6). It is possible, however, that derepression may be selective and only certain loci are affected. However, the strong correlation between the absence of markers from these tumors that are also not present on more than 90% of the thymocytes (sIg, Ly-6, Qa-2, Ia) indicates that these phenotypes do not arise randomly. In addition, markers known to be present on all thymocytes (Ly-5, Thy-1) are present as expected. Ly-2, which is also present on 90% of thymocytes, is also found on all the thymomas.

Perhaps the only way to resolve this issue would be the testing of the thymomas for functional T-cell activity of the attempt to induce such activity that would be expected of a T-cell with this phenotype. Indeed, such functional studies have been undertaken with BALB/c mouse T-lymphomas that show restricted Ly phenotype (*11*). In this study, Ly-1^-2^+ tumor cells could suppress certain mixed lymphocyte reactions or mitogen activation, as do Ly-1^-2^+ normal cells (*1-3*).

Effective Removal of Antiviral Antibodies

There are indeed many reports of the presence of a variety of antiviral antibodies or other antibodies which bind to cell surface antigens in conventional alloantisera (*1, 21, 22, 39*). These antibodies can and do lead to anomalous results, especially when tumors grown in vitro are tested (*39, 40*). It was clear that the unabsorbed antisera used in this study contained antibodies leading to anomalous results, such as in group 1, where all tumors reacted with all the antisera. However, after absorption, this ubiquity of reaction did not occur again. The absorptions were performed to achieve two aims: 1) the removal of antiviral and autoantibodies by absorption of antisera with thymus and spleen cells from mice whose tissues contained high levels of MuLV (NZB, AKR, DBA/2) (*16, 17*); and 2) the removal of antibodies reactive with other cell surface antigens by absorption with lymphoid cells from appropriately selected strains.

The alloantigenic phenotypes of the tumors obtained by direct testing with this absorbed antisera were real and did not include anomalous results due to antiviral or contaminating antibodies because: 1) Testing with MoAb preparations that contained no other antibody invariably agreed with the positive reactions obtained with the absorbed conventional antisera. 2) In all cases where antisera gave positive reactions, the tumor could specifically absorb antibody activity. There was no instance of a positive result with conventional antisera being negative by absorption. 3) Further absorption of the antisera with a rat leukemia, infected with MuLV-Gross (endogenous MuLV) did not change the reactivity of the antisera with the thymoma ITT(1)75NS or ITT(4)B6 (table 5). MuLV-Gross is closely related to MuLV-AKR which is wide-spread in mice (*41*), and the naturally occurring antiviral antibodies act predominantly against the major envelope glycoprotein gp70 of this virus and against cell surface antigens of infected cells associated with the virus (*41-44*). Thus if significant levels of antiviral antibodies still remained in the antisera after absorption with mouse lymphoid cells, these should have been removed by absorption with the infected rat leukemia. 4) Antiviral antibodies are highly reactive with in vitro cultured cell lines (*21, 40*), and while such reactivity is found with tumors grown in vivo, it is detectable only at high concentrations of antibody (<1/6) (*45, 46*), whereas for testing of the thymomas the antisera were used at 1/10 dilution. This finding may be due to the very rare occurrence of type C virus particles (MuLV) in in vivo grown tumors which increase in number when adapted to in vitro growth (*17*). 5) It is well documented that *radiation-induced* thymic lymphomas in C57BL/10 and related mice do not express readily detectable MuLV antigens (*41, 47, 48*). Furthermore, active viral RNA was also rarely found in radiation-induced thymomas (*41*). 6) It is conceivable that the presence of circulating antiviral antibodies in the mice leads to modulation of antigen or selection of cells that express low levels of MuLV antigens or none at all. Thus in this situation even if antiviral antibodies had not been completely removed by the procedures employed, it is unlikely that they would give rise to false-positive results.

Taken together, the evidence presented above strongly suggests that the absorption protocol for conventional antisera adequately removes contaminating antibodies and results in the production of specific, H-2, Ia, Ly, Thy-1, or TL antisera and that antiviral antibodies do not play a role in the positive reactions seen with these tumors.

The thymomas described may be of use in many areas. The selective expression of Ly antigens may provide cells for more specific immunization for Ly antibodies (conventional or monoclonal) than is possible with unfractionated spleen lymph node cells. Furthermore, if the thymomas represent transformed normal T-cells from a particular subpopulation, they may be useful as immunogens to define new antigens specific for that particular subpopulation. In addition, the possibility that these thymomas represent T-cells at a particular stage of differentiation could make them useful for the study of normal T-cell functions: killing, suppression, or factor elaboration. The production of suitable clones of normal T-cells is difficult but can be achieved. Attempts at the production of T-cell hybridomas have largely been unsuccessful. Thus the provision of readily transplantable, stable, and functional T-cell tumors would be of great benefit to cellular immunologists.

Finally, the advantages of the use of MoAb are clearly seen with the typing of tumors. Although with one exception there were no differences between typing with conventional or monoclonal antisera, the conventional sera were difficult to produce and contained other antibodies that gave rise to anomalous results. Conventional antisera therefore required extensive absorption that resulted in a concomitant loss of specific antibody activity. The use of the MoAb overcame these problems and greatly simplified serotyping of the thymomas.

REFERENCES

(*1*) McKenzie IF, Potter TA. Murine cell surface alloantigens. Adv Immunol 1979; 27:179-338.

(*2*) Jandinski J, Cantor H, Tadakuma D, Peary DL, Pearce CW. Separation of helper T cells from suppressor T cells expressing different Ly components. I. Polyclonal activation: Suppressor and helper activities are inherent properties of distinct T cell subclasses. J Exp Med 1976; 143:1382-1390.

(*3*) Al-Adra AR, Pilaski LM, McKenzie IF. Surface markers on the T cells that regulate cytotoxic T cell responses. I. The Ly phenotype of suppressor T cells changes as a function of time and is distinct from that of helper or cytotoxic T cells. Immunogenetics 1980; 10:521–533.

(*4*) Cantor H, Boyse EA. Lymphocytes as models for the study of mammalian cellular differentiation. Immunol Rev 1977; 33:105–124.

(*5*) Scollay R, Weismann IL. T cell maturation: Thymocyte and thymus migrant subpopulations defined with monoclonal antibodies to the antigens Lyt-1, Lyt-2 and ThB. J Immunol 1980; 124:2841–2844.

(*6*) Von Boehmer H, Haas W, Pohlit H, Hengartner H, Nabholz M. T cell clones: Their use in the study of specificity, induction and effector function of T cells. Springer Semin Immunopathol 1980; 3:23–37.

(*7*) Potter M. Immunoglobulin producing tumors and myeloma proteins of mice. Physiol Rev 1972; 52:631–719.

(*8*) Kim KJ, Kanellopolous-Langerin C, Merwin RM, Sachs DH, Asofsky R. Establishment and characterisation of BALB/c lymphoma lines with B cell properties. J Immunol 1979; 122:549–554.

(*9*) Proffitt MR, Hirsch MS, Geridian B, McKenzie IF, Black PH. Immunological mechanisms in the pathogenesis of virus induced murine leukemia. I. Autoreactivity. Int J Cancer 1975; 15:221–229.

(*10*) Roman JM, Golub ES. Leukemia in AKR mice. I. Effects of leukemic cells on antibody-forming potential of syngeneic and allogeneic normal cells. J Exp Med 1976; 143:482–496.

(*11*) Kim KJ, Weinbaum FI, Asofsky R. Functional characteristics of BALB/c T cell lines: Suppression in the mixed lymphocyte response and cell mediated lysis. J Immunol 1978; 121:2299–2304.

(*12*) Kaplan HS. The role of radiation on experimental leukemogenesis. Natl Cancer Inst Monogr 1964; 14:207–220.

(*13*) Ledbetter JA, Herzenberg LA. Xenogeneic monoclonal antibodies to mouse lymphoid differentiation antigens. Immunol Rev 1979; 47:63–90.

(*14*) Hogarth PM, McKenzie IF. Monoclonal antibodies to lymphocyte differentiation antigens. In: Hammerling G, Hammerling U, Kearney J, eds. Monoclonal antibodies and T cell hybridomas. New York: Elsevier, 1981. In press.

(*15*) Oi VT, Jones PP, Goding JW, Herzenberg LA, Herzenberg LA. Properties of monoclonal antibodies to mouse Ig allotypes, H-2, and Ia antigens. Curr Top Microbiol Immunol 1978; 81:115–120.

(*16*) Morse HC III, Chused TM, Boehm-Truitt M, Mathieson BJ, Sharrow SO, Hartley JW. XenCSA: Cell surface antigens related to the major glycoproteins (gp70) of xenotropic murine leukemia viruses. J Immunol 1979; 122:443–454.

(*17*) Kim KJ, Weinbaum FI, Mathieson BJ, McKeever PE, Asofsky R. Characteristics of BALB/c T cell lymphomas grown as continuous in vitro lines. J Immunol 1978; 121:339–344.

(*18*) McKenzie IF, Snell GD. A cell membrane alloantigen of murine B lymphocytes I. Population studies. J Immunol 1975; 114:848–855.

(*19*) Parish CR, McKenzie IF. A sensitive rosetting method for detecting subpopulations of lymphocytes which react with alloantisera. J Immunol Methods 1978; 20:173–183.

(*20*) Parish CR, Hayward JA. The lymphocyte surface. I. Relation between Fc receptors, C'3 receptors and surface immunoglobulin. [illegible]oc Roy Soc Lond [Biol] 1974; 187:47–63.

(*21*) [illegible]owinski RC, Klein P. Anomalous reaction of mouse alloantisera with cultured tumor cells. II. Cytotoxicity is caused by antibodies to leukemia viruses. J Immunol 1975; 115:1261–1268.

(*22*) Langdon WY, Shellam GR, Morgan GM, McKenzie IF. High titers of antibody to murine leukemia virus in lymphocyte (Ly) alloantisera. Immunogenetics 1980; 10:141–150.

(*23*) Boyse EA, Bressler E, Iritani CA, Lardis M. A cytotoxic γ M autoantibody in mouse alloantisera. Transplantation 1970; 9:339–341.

(*24*) Mathieson BJ, Sharrow SO, Campbell PS, Asofsky R. An Lyt-differentiated thymocyte subpopulation detected by flow microfluorometry. Nature 1979; 277:478–480.

(*25*) Ledbetter JA, Rouse RV, Micklem S, Herzenberg LA. T cell subsets defined by expression of Ly123 and Thy-1 antigens. Two parameter immunofluorescence and cytotoxicity analysis modifies current views. J Exp Med 1980; 152:280–295.

(*26*) Potter TA, McKenzie IF, Morgan GM, Cherry MC. Murine lymphocyte alloantigens. I. The *Ly-6* locus. J Immunol 1980; 125:541–545.

(*27*) Potter TA, McKenzie IF, Cherry MC. Murine lymphocyte alloantigens: The *Ly-4* locus. J Immunogenet 1981; 8:15–26.

(*28*) Sandrin MS, Potter TA, Morgan GM, McKenzie IF. Detection of mouse alloantibodies by rosetting with protein A coated sheep red blood cells. Transplantation 1978; 26:126–130.

(*29*) McDougal JS, Shen FW, Cort SP, Barot J. Feedback suppression: Phenotypes of T cell subsets involved in the Ly-1 T cell induced immunoregulatory circuit. J Immunol 1980; 125:1157–1160.

(*30*) Pilaski LM, Al-Adra AR, McKenzie IF. Surface markers on T cells that regulate cytotoxic cell responses. II. Distribution of Ly-6.1 and Ly-7.2. Selective expression of Ly-7.2 on helper T cell effectors. J Immunol 1980; 125:365–369.

(*31*) Stout RD, Herzenberg LA. The Fc receptor on thymus derived lymphocytes I. Detection of a subpopulation of murine T lymphocytes bearing the Fc receptor. J Exp Med 1975; 142:611–621.

(*32*) Sheid M, Triglia D. Further description of the Ly-5 system. Immunogenetics 1979; 9:423–433.

(*33*) Triglia D. Expression of Ly-5 on yolk sac and fetal liver cells of the mouse. Immunogenetics 1980; 11:303–306.

(*34*) Mathieson BJ, Campbell PS, Potter M, Asofsky R. Expression of Ly-1, Ly-2, Thy-1 and TL differentiation antigens on mouse T cell tumors. J Exp Med 1978; 147:1267–1279.

(*35*) Germain RN, Benaceraff B. Helper and suppressor T cell factors. Springer Semin Immunopathol 1980; 3:129–144.

(*36*) Michaelides M, McKenzie IF. Detection of Ia alloantigens on PHA-T blast cells. Transplantation 1981; 31:330–333.

(*37*) Cantor H, Kasai M, Shen FW, Leclerc JC, Glimcher L. Immunogenetic analysis of "natural killer" activity in the mouse. Immunol Rev 1979; 44:3–12.

(*38*) Garrido F, Schirrmacher V, Festenstein H. H-2-like specificities of foreign haplotypes appearing on a mouse sarcoma after *Vaccinia* virus infection. Nature 1976; 259:228–230.

(*39*) Wettstein PJ, Krammer P, Nowinski RC, David CS, Frelinger JA, Schreffer DC. A cautionary note regarding Ia and H-2 typing of murine lymphoid tumors. Immunogenetics 1976; 3:507–516.

(*40*) Klein P. Anomalous reactions of mouse alloantisera with cultured tumor cells. I. Demonstration of widespread occurrence using reference typing sera. J Immunol 1975; 115:1254–1260.

(*41*) Ihle JN, Joseph DR, Pazmino NH. Radiation leukemia in C57BL/6 mice. II. Lack of ecotropic virus expression in the majority of lymphomas. J Exp Med 1976; 144:1406–1423.

(*42*) Lee JC, Hanna MG, Ihle JN, Aaronson SA. Autogenous immunity to endogenous RNA tumor virus: Differential reactivities of immunoglobulins M and G to virus envelope antigens. J Virol 1974; 14:773–781.

(*43*) Ihle JN, Hanna MG, Robertson LE, Kenney FT. Autogenous immunity to endogenous RNA tumor virus. Identification of antibody reactivity to select viral antigens. J Exp Med 1974; 139:1568-1581.

(*44*) Stephenson JR, Peters RL, Hino S, et al. Natural immunity in mice to structural polypeptides of endogenous Type C RNA viruses. J Virol 1978; 19:890–898.

(*45*) Aoki T, Boyse EA, Old LJ. Occurrence of natural antibody to the G (Gross) leukemia antigen in mice. Cancer Res 1976; 26:1415-1419.

(*46*) Martin SE, Martin WJ. Anti-tumor antibodies in normal mouse sera. Int J Cancer 1975; 15:658–664.

(*47*) De Cleve A, Sato C, Lieberman M, Kaplan H. Selective thymic localisation of murine leukemia virus-related antigens in C57BL/Ka mice after innoculation with radiation leukemia virus. Proc Natl Acad Sci USA 1974; 71:3124–3128.

(*48*) Lieberman M, Kaplan HS, De Cleve A. Anomalous viral expression in radiogenic lymphomas of C57BL/Ka mice. In: Yuhas JM, Tennant RW, Regan JD, eds. Biology of radiation carcinogenesis. New York: Raven Press, 1976:237–244.

Formation of Symbiotic Complex by Microenvironment-Dependent Mouse Leukemias and Thymic Epithelial Reticular Cells [1,2]

Yoshimi Nishi, [3] **Kazuhiro Yoshikawa,** [4] **Hiroshi Hiai,** [5,6] **Kunihiro Notake,** [4] **Hayase Shisa,** [7] *and* **Yasuaki Nishizuka** [5,8]

ABSTRACT—Developing thymic leukemias of the mouse have been assumed to form symbiotic complexes with thymic microenvironments. This symbiosis is morphologically based on pseudoemperipolesis (PEMP). The mechanism of the association of microenvironment-dependent leukemia cells with thymic epithelial reticular cells (TER) was analyzed in vitro by scanning electron microscopy, microcinematography, and a quantitative assessment of PEMP. PEMP was a consequence of active locomotion of the leukemia cells, with TER passively accepting the leukemia cells' "crawling" under their cytoplasm. The integrity of the cytoskeletal system of both cells was essentially required for PEMP, since cytochalasins and colchicine were highly inhibitory to PEMP. The mechanism of action of these compounds was probably dual: inhibition of the locomotive movements of the leukemia cells. A similar inhibition of PEMP was also observed with the tumor promoter 12-*O*-tetradecanoylphorbol 13-acetate—JNCI 1982; 69: 627-637.

TER are the major cellular components of thymic microenvironments supporting differentiation and proliferation of thymocytes, which are progeny of migrating prethymocytes from the hematopoietic compartment. The function of TER is mediated at least in part by soluble factors elaborated by TER, and several biologically active substances have been identified (*1*). In contrast, the cell interaction involving close cell contact is also suggested to play a role in supporting differentiation and proliferation of thymocytes (*2*). Wekerle et al. (*3*) isolated the lymphoepithelial cell complexes from the normal murine thymus, in which lymphoid cells are localized in cytoplasmic caveolae of Ia determinant-bearing TER. From leukemic thymuses, we have shown that morphologically similar complexes of leukemic lymphocytes and TER can be isolated in vitro, and from such complexes the symbiotic cell lines are consistently obtained, in which leukemia cells depend on occasional contact with TER for their in vitro survival and growth (*4*). The leukemia cells in such cultures are frequently observed to be confined to a space between the cytoplasm of glass-adherent TER and the substrate. We have defined this form of cell interaction as PEMP (*4, 5*) to distinguish it from true "emperipolesis" (*6*) involving actual invasion of viable cells into other cells or cytophagocytosis. Although the biological significance of PEMP is still obscure, PEMP has been observed not only in symbiotic leukemias but also rather widely between various hematolymphoid cells and TER or other stromal cells [(*5*); Hiai H, Nakamura H, Kaneshima H, Nishi Y, Sato C, Nishizuka H: In preparation]. Conceivably, PEMP may represent a crucial form of cell interaction involved in the association of hematolymphoid cells with their microenvironments. Symbiotic complexes of mouse lymphoid leukemias may be a promising in vitro model for analysis of such a cell interaction.

In the present paper, the dynamic morphology of the formation of symbiotic complexes is studied by means of SEM and microcinematography. We gave particular attention to the mechanism of the leukemia cells' entry into and exit from the microenvironment formed by TER. We showed that the association of leukemia cells with TER was based on active locomotion of the leukemia cells, and the integrity of the cytoskeleton of both leukemia cells and TER was essentially required for PEMP.

MATERIALS AND METHODS

Tissue culture.—Symbiotic cell lines were established from spontaneous thymic leukemias in AKR/Ms mice as described previously (*4*). The leukemic thymus was mechanically disrupted between two sheets of a frosted glass slide, vigorously pipetted, and allowed to stand for a few minutes. After the free leukemia cells were removed, tissue fragments were explanted in a culture flask. After 1-2 weeks, leukemia cells started to grow and were associated with the outgrowth of the glass-adherent TER-like cells from the explants. In earlier stages of such cultures, leukemia cells depended on the adherent cells for their in vitro survival and growth and PEMP was consistently observed. In this paper, we used the AKRL-16 cell line except when otherwise noted because of its stable growth behavior and high efficiency in PEMP.

Abbreviations used: DMEM=Dulbecco's modified Eagle's minimum essential medium; DMSO=dimethyl sulfoxide; FCS=fetal calf serum; MEM=minimum essential medium; PBS=phosphate-buffered saline; PEMP=pseudoemperipolesis; %PEMP(≥1)=percentage of A17A cells holding one leukemia cell or more under their cytoplasm; %PEMP(≥5)=percentage of A17A cells holding five leukemia cells or more under their cytoplasm; SEM=scanning electron microscopy; TER=thymic epithelial reticular cell(s); TPA=12-*O*-tetradecanoylphorbol 13-acetate.

---

[1] Received September 24, 1981; revised March 24, 1982; accepted April 9, 1982.

[2] Supported in part by a Grant-in-Aid for Cancer Research from the Ministry of Education, Science and Culture, Japan.

[3] Laboratory of Service Section, Aichi Cancer Center Research Institute, Chikusa-ku, Nagoya 464, Japan.

[4] Department of Microbiology, Aichi Medical University, Nagakute, Aichi 480-11, Japan.

[5] Laboratory of Experimental Pathology, Aichi Cancer Center Research Institute.

[6] *Address reprint requests to* Dr. Hiai.

[7] Laboratory of Pathology, Saitama Cancer Center, Research Institute, Ina, Saitama 362, Japan.

[8] We thank Dr. M. Matsuyama for critical reading of the manuscript and Mrs. Y. Oguro and Mr. S. Nakamura for excellent technical assistance.

The medium was the high-glucose version of DMEM (GIBCO, Grand Island, N.Y.) with 10% unheated FCS. One liter of DMEM was also supplemented with 60 mg kanamycin sulfate, 110 mg sodium pyruvate, 860 mg MEM amino acids-vitamins (Nissui Seiyaku Co. Ltd., Tokyo, Japan), and 10 ml of a 100 times concentrated MEM nonessential amino acid solution (GIBCO). Cultures were kept in a CO_2 incubator with 6% CO_2 and 94% fully humidified air. Medium was changed twice a week.

Isolation of intrinsic adherent cells from symbiotic stock culture.—The method for the isolation of thymic nurse cells from normal thymus described by Wekerle et al. (*3*) was used with modifications. The symbiotic stock culture was washed with three changes of Ca^{2+}-free and Mg^{2+}-free Dulbecco's PBS and digested with 5 ml of 0.01 *M* EDTA-0.25% trypsin in Dulbecco's PBS for 10 minutes at 37°C. After two washes in serum-free DMEM, the digest in 1 ml was overlaid on 4 ml FCS in a 10-ml culture tube and kept standing at room temperature for 15 minutes. Subsequently, the top one-third layer containing mainly leukemia cells was aspirated off, and the bottom layer enriched with adherent cells was spun down. After two washes, the cells in 5 ml DMEM with 2% FCS were propagated in a TD-40 glass flask with a surface area of approximately 40 cm^2. Two hours later, nonadherent cells were removed by being repeatedly washed with Dulbecco's PBS, and the adherent cells were fed with DMEM plus 10% FCS and kept in culture. The entire procedure was repeated daily until all leukemia cells were removed. In this work, a colonial clone A17A isolated from symbiotic AKRL-17 leukemia was used throughout.

Assay of PEMP.—The degree of PEMP was measured as in (*5, 7*) with modification. A17A cells, 5×10^4 in 3 ml of medium, were plated in a 60-mm plastic petri dish. One day later the monolayer was washed twice with Dulbecco's PBS, and 3×10^6 washed leukemia cells in 4 ml of DMEM plus 1% FCS were overlaid. After 6 hours of incubation at 37°C, free leukemia cells were washed out by three changes of Dulbecco's PBS, and the monolayer was fixed with methanol and stained with Giemsa. The %PEMP($\geq$1) and %PEMP($\geq$5) were determined by the examination of approximately 1,000 A17A cells under a microscope. Although %PEMP($\geq$5) roughly paralleled %PEMP($\geq$1), %PEMP($\geq$5) was a more sensitive measure for the effects of the various inhibitors.

Chemicals.—Cytochalasin B and cytochalasin A (Aldrich Chemical Co., Milwaukee, Wis.) were dissolved at 1 mg/ml in DMSO, colchicine (Wako Pure Chemical Co., Osaka, Japan) was dissolved at 10 m*M* in culture medium, and TPA (Consolidated Midland Corp., Brewster, N.Y.) was dissolved at 100 μg/ml in absolute ethanol. All stock solutions were stored frozen at −20°C and diluted in culture medium immediately before use.

Evaluation of inhibitory effects on PEMP.—Leukemia cells, 3×10^6 in 4 ml of the medium containing a test chemical at an appropriate final concentration, were seeded on top of A17A cells. After 6 hours of incubation, the %PEMP($\geq$1) and %PEMP($\geq$5) were measured as above. Inhibition of the preformed PEMP was studied by incubation of the leukemia cells on top of the A17A cells for 6 hours without an inhibitor and subsequently by replacement of the medium with 4 ml fresh medium with or without the inhibitor. The %PEMP($\geq$1) and %PEMP($\geq$5) were determined 5, 10, 20, 30, 45, and 60 minutes after addition of the inhibitor. To determine the target of action of the chemicals, we preincubated either leukemia or adherent cells with the chemicals and we examined the capacity of PEMP as follows: Leukemia cells, 8×10^6, were incubated for 1 hour at 37°C in 5 ml of the medium with or without an inhibitor. Also similarly incubated were 5×10^4 A17A cells plated 1 day earlier in a 60-mm plastic petri dish. After the treatment adherent cells and leukemia cells were washed carefully by three changes of fresh medium, and PEMP was determined in combination with untreated cells. The viability of the cells was determined by the trypan blue dye exclusion test.

Microcinematography.—A Nikon inverted phase-contrast microscope with a built-in incubator maintained at 37°C was used as optical equipment. With the use of a Borex H16 camera with a Nikon CFMA cine-autotimer, photographs were taken on 16-mm Fujicolor RT500 cinefilm. Intervals of exposures (2, 4, 15, or 30 sec) were selected depending on the duration of observation.

Electron microscopy.—SEM was done as in (*4, 5*).

RESULTS

PEMP of Symbiotic Leukemia Cells

As shown previously (*4, 5*), in vitro survival and growth of leukemia cells of symbiotic cell lines in earlier passage generations required close association with glass-adherent stromal cells, and the complexes containing both types of cells formed a germinative layer. Localization of the leukemia cells under adherent cells, i.e., PEMP, was a prevalent morphologic feature in this layer (fig. 1). The degree of PEMP could be measured by the %PEMP($\geq$1) and the

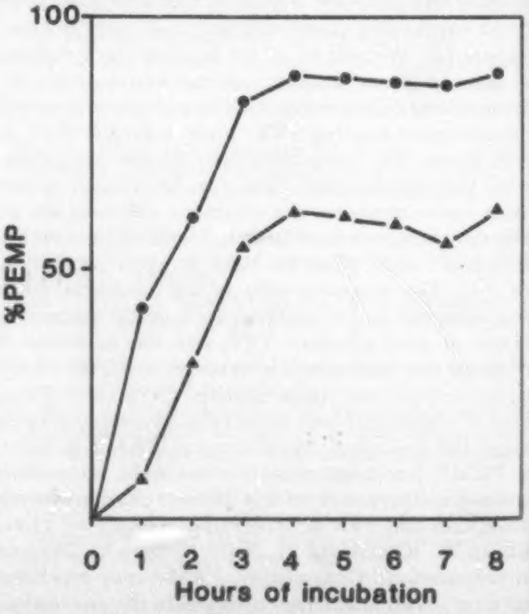

TEXT-FIGURE 1.—Kinetics of PEMP. AKRL-16 leukemia cells under A17A adherent cells. ●: %PEMP($\geq$1); ▲: %PEMP($\geq$5).

%PEMP(≥5). As a source of the adherent cells for PEMP assay, the cloned cell line A17A was used throughout. It was isolated from a symbiotic stock of AKRL-17 leukemia and had a TER-like morphology (fig. 2). Text-figure 1 depicts the time course of PEMP of AKRL-16 leukemia cells under A17A cells. Approximately 5-6 hours after the cells were plated, a plateau was attained and the average number of leukemia cells under an A17A cell was maximum (data not shown). Leukemia cells from all of eight different symbiotic cell lines were capable of PEMP with A17A cells but at varying degrees (table 1). Thereafter, a combination of AKRL-16 leukemia cells and A17A cells was used, since it gave highly consistent results in the PEMP assay.

Microcinematographic Observation

To determine whether PEMP occurred by active movement of the leukemia cells or by passive entrapment by the adherent cells, we observed the process of PEMP by time-lapse cinematography. After being plated on a sparse culture of A17A cells, leukemia cells exhibited active locomotion on the substrate or on A17A cells. The locomotion was nondirectional, and the association of leukemia cells with A17A cells appeared to occur by chance. Some leukemia cells anchored on the surface of A17A cells by their uropods and frequently twirled on one spot. Others "crawled" around the periphery of A17A cells, occasionally touching the periphery with pseudopods as if investigating the cell margin. In contrast, A17A cells were relatively stationary with the exception of slower ruffling of lamellipods.

Invasion of leukemia cells under A17A cells usually took place without any predictable changes in motility of both cells. In figures 3A-3E, three leukemia cells were seen to move in under an A17A cell. The leukemia cell in contact with the A17A cell at the cell margin (fig. 3A) rapidly protruded pseudopods and extruded them under the A17A cell (figs. 3B-3D). Figure 4 is an SEM picture showing a leukemia cell in the process of PEMP. The portion of the leukemia cell cytoplasm already under the A17A cell could be seen through the thin cytoplasmic membrane. The gateway of entry appeared to be narrow, since the leukemia cells moving in were considerably constricted at the site (figs. 3B, 3C). But once the leukemia cells were under the adherent cells, the motility of the leukemia cells looked as unrestricted as that seen when the leukemia cells were outside the A17A cells. During the entry of the leukemia cells under an A17A cell, the A17A cell remained almost unmoved. The time required for the entry varied (5-15 min on the average). Under adherent cells, leukemia cells twirled on the spot or "crawled" around. Occasionally, a group of cells became involved in a sudden rotatory movement. When an A17A cell with many leukemia cells in PEMP divided, the leukecemia cells were expelled as the dividing A17A cell rounded up. However, the leukemia cells were somehow bound to the A17A cell, since they were rapidly accommodated again under the daughter A17A cells after division. Leukemia cells stayed under an A17A cell for varying periods ranging from 15 minutes to over 6 hours, and the fate of each cell was apparently determined individually. Exit of the leukemia cells occurred as an almost exact reverse of their entry.

TABLE 1.—*PEMP of various symbiotic leukemia cells under A17A cells*

Cell line	%PEMP(≥1)[a]	%PEMP(≥5)[a]
AKRL-16	56.3±2.5	26.1±2.0
AKRL-17	48.6±3.2	25.8±1.1
AKRL-25	56.1±1.8	19.2±2.7
AKRL-26	46.3±0.6	17.2±1.9
AKRL-36	81.3±4.2	40.0±2.3
AKRL-38	62.1±1.8	23.3±0.8
AKRL-46	28.9±2.0	8.6±0.6
AKRL-47	27.9±1.7	7.2±1.1

[a] Results are means ± standard deviations. Assays were done in triplicate.

Effect of Cytochalasins

Cytochalasins (microfilament-disrupting agents) were found to be potent inhibitors of PEMP. In the presence of 2.5 µg or more cytochalasin B/ml, PEMP did not occur and the minimum effective concentration was 0.04 µg/ml (text-fig. 2A). The solvent DMSO was inhibitory to PEMP at 1%, but it did not affect PEMP below 0.5% (text-fig. 2A). The inhibitory effect of cytochalasin A was approximately five times as strong as that of cytochalasin B (data not shown).

To determine whether the leukemia cells or adherent cells were the target of cytochalasins, we treated the cells with either cytochalasin A or cytochalasin B for 1 hour, washed them extensively, and examined them for the capacity of PEMP by combining the treated and untreated cells. As shown in table 2, pretreatment of both cells with cytochalasin A abolished PEMP. The leukemia cells were more susceptible than were the A17A cells, since 50% specific inhibition in %PEMP(≥1) was observed in leukemia cells at 0.25 µg/ml, whereas in A17A cells it was observed at 2 µg/ml. Similar treatment with 2.5 µg cytochalasin B/ml was without effect inasmuch as its action was reversible (*8*). Microcinematography showed that addition of 2.5 µg cytochalasin/ml almost instantly inhibited the locomotion of leukemia cells, caused cessation of the crawling movement under the A17A cells, and caused rapid retraction of the cytoplasm of the A17A cell. Since cytochalasin B did not affect the adherence of A17A cells to the substrate, the retraction of the cytoplasmic sector between adherence sites produced a bizarre stellate morphology in A17A cells. When cytochalasin B was added to the A17A cells with many leukemia cells in PEMP, the leukemia cells were quickly liberated (text-fig. 2B)—a result of the rapid retraction of the covering A17A cell cytoplasm as revealed by microcinematography and SEM (figs. 5, 6). That the effects of cytochalasins on PEMP were due to sublethal cell damage is unlikely, since the viability of both cells after 6 hours of incubation with 2 µg cytochalasin A/ml or 2.5 µg cytochalasin B/ml remained over 85%, as judged by the trypan blue dye exclusion test. Therefore, the effects of cytochalasins on PEMP seemed to be dual: inhibition of the active locomotion of leukemia cells and contraction of the adherent cell cytoplasm.

Effect of Colchicine

Colchicine (a representative microtubule poison of the

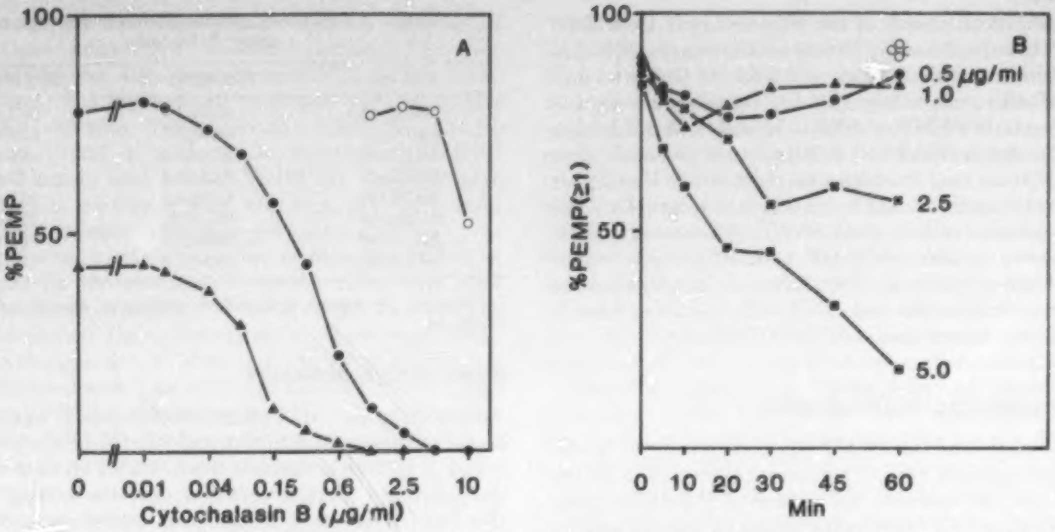

TEXT-FIGURE 2.—Effect of cytochalasin B on PEMP. A) Dose-effect relationship. ●: %PEMP(≥1) in the presence of cytochalasin B; ▲: %PEMP(≥5) in the presence of cytochalasin B. ○: %PEMP(≥1) of solvent control. As 1 mg cytochalasin B was dissolved in 1 ml DMSO, the solution of 10 μg cytochalasin B/ml, for example, contained 1% DMSO. B) Inhibition of PEMP by addition of cytochalasin B after 6 hr of incubation without the chemical. ●: 0.5 μg/ml; ▲: 1 μg/ml; ×: 2.5 μg/ml; ■: 5 μg/ml; ○: medium control.

TABLE 2.—*Effect of pretreatment of either A17A cells or leukemia cells with cytochalasins or colchicine*

Pretreatment drug	Pretreatment concentration for:		%PEMP(≥1)[a]	%PEMP(≥5)[a]
	Leukemia cells	A17A cells		
Cytochalasin A	0	0	54.2±2.3 (0)	25.1±2.2 (0)
	0.25 μg/ml	0	28.1±3.4 (48.4)	7.5±1.4 (70.1)
	0.5 μg/ml	0	3.1±0.2 (94.3)	0.3±0.1 (98.8)
	1 μg/ml	0	0.9±0.3 (98.3)	0.0±0.0 (100.0)
	2 μg/ml	0	0.0±0.0 (100.0)	0.0±0.0 (100.0)
	0	0.25 μg/ml	53.7±3.2 (0.9)	25.2±1.5 (−0.4)
	0	0.5 μg/ml	53.8±2.3 (0.7)	22.9±2.4 (8.8)
	0	1 μg/ml	47.2±2.8 (12.9)	6.2±1.9 (75.3)
	0	2 μg/ml	21.1±3.7 (61.1)	1.1±0.3 (95.6)
Cytochalasin B	0	0	53.3±2.5 (0)	24.3±1.2 (0)
	2.5 μg/ml	0	52.3±2.7 (1.9)	24.1±2.0 (0.8)
	0	2.5 μg/ml	54.7±3.3 (−2.6)	25.2±1.8 (−3.7)
Colchicine	0	0	53.4±3.1 (0)	24.1±2.1 (0)
	0.01 m*M*	0	43.3±3.1 (18.9)	13.2±1.1 (45.2)
	0.1 m*M*	0	32.3±1.5 (39.5)	8.4±2.0 (65.1)
	0	0.01 m*M*	48.1±3.3 (9.9)	19.7±2.3 (22.4)
	0	0.1 m*M*	46.3±4.2 (13.2)	16.0±1.1 (33.6)

[a] Results are means ± standard deviations. Assays were done in triplicate. *Numbers in parentheses* are percentages of specific inhibition of solvent control for each chemical. Percent specific inhibition=(% PEMP in solvent control−% PEMP in experimental/% PEMP in solvent control) ×100.

Vinca alkaloids) was also a strong inhibitor of PEMP. It suppressed PEMP at 10^{-4} m*M* or at higher concentrations (text-fig. 3A). Microcinematography showed that the locomotion of the leukemia cells was inhibited and the A17A cell cytoplasm was contracted immediately after addition of colchicine. Rapid release of the leukemia cells was observed from preformed PEMP complexes after addition of colchicine, depending on its concentration (text-fig. 3B). This rapid release was the result of the contraction of the covering A17A cell cytoplasm as shown by microcinematography as well as by SEM (Figs. 6C, 6D). When either leukemia cells or A17A cells were pretreated with colchicine for 1 hour and washed and their capacity for PEMP was examined, there was a moderate, but definitive, inhibition in PEMP by either treatment (table 2). The effect was more visible in %PEMP(≥5) than in %PEMP(≥1). The leukemia cells were more susceptible to this treatment than were A17A cells. Both leukemia cells and A17A cells remained over 85% viable after 6 hours of incubation in 10^{-1} m*M* colchicine.

Effect of TPA

Previously, we learned that tumor-promoting phorbol esters are inhibitory to PEMP (*7*). This finding was con-

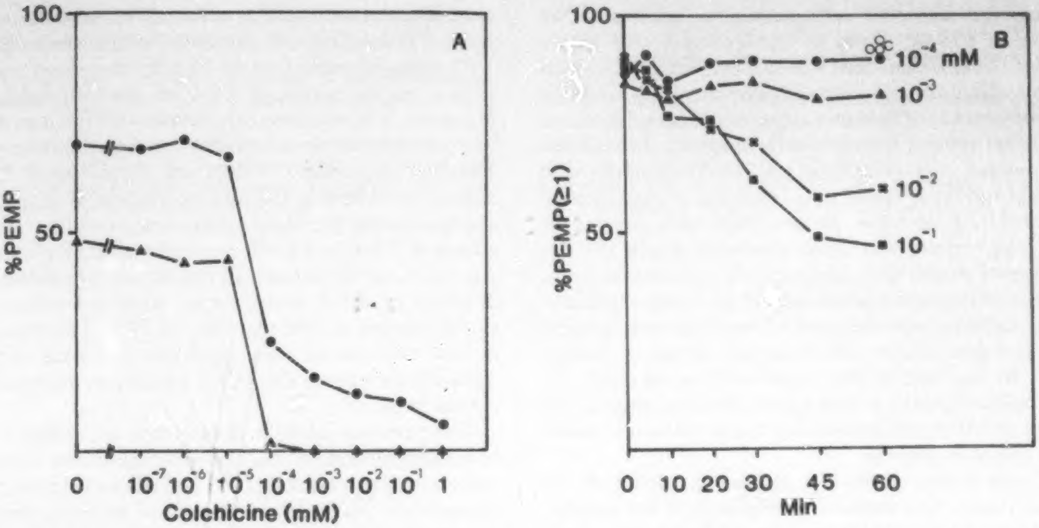

TEXT-FIGURE 3.—Effect of colchicine on PEMP. A) Dose-effect relationship. ●: %PEMP(≥1); ▲: %PEMP(≥5). B) Inhibition of PEMP by addition of colchicine after 6 hr of incubation without the chemical. ●: 10^{-4} m*M*; ▲: 10^{-6} m*M*; ×: 10^{-2} m*M*; ■: 10^{-1} m*M*; ○: medium control.

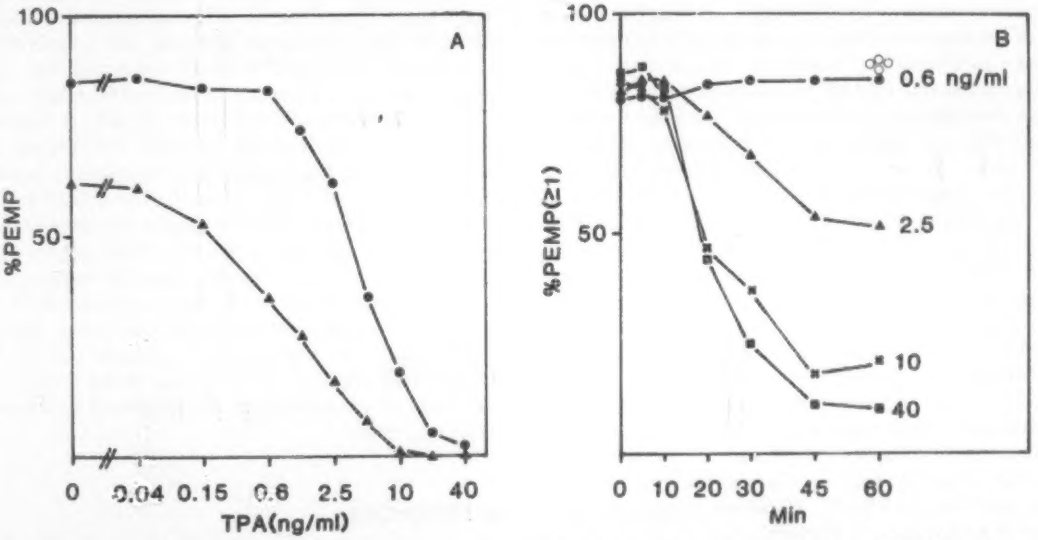

TEXT-FIGURE 4.—Effect of TPA on PEMP. A) Dose-effect relationship. ●: %PEMP(≥1); ▲: %PEMP(≥5). B) Inhibition of PEMP by addition of TPA after 6 hr of incubation without the chemical. ●: 0.6 ng/ml; ▲: 2.5 ng/ml; ×: 10 ng/ml; ■: 40 ng/ml; ○: medium control.

firmed when a combination of the AKRL-16 leukemia cells and A17A cells was studied (text-fig. 4A). Addition of TPA to preformed PEMP complexes released the leukemia cells in a dose-dependent way (text-fig. 4B). Unlike the immediate action of cytochalasins and colchicine (text-figs. 2B, 3B), there was an approximately 10-minute delay before any measurable effect of TPA on PEMP became manifest. Microcinematography and SEM revealed that the effects of TPA were also to inhibit locomotion of the leukemia cells and to contract the A17A cell cytoplasm. The release of leukemia cells from complexes was caused by retraction of the A17A cell cytoplasm (figs. 6E, 6F). TPA was not toxic to either leukemia cells or A17A cells by 6 hours of incubation at 40 ng/ml.

DISCUSSION

Observation of the dynamic morphology of symbiotic complex formation by murine leukemias revealed that association of leukemia cells with their microenvironments in the form of PEMP was a consequence of the leukemia cells' actively moving in under the adherent cells. Apparently, this movement occurred as nondirectional motility of leukemia cells rather than as adherent cell-directed chemotaxis.

In contrast, the adherent cells seemed to play a rather passive role in PEMP. Entry of the leukemia cells into a space under the adherent cells was usually observed to start from the margin of the adherent cell. The currently available method with the use of cultured symbiotic leukemias allows observation of the cell interaction in only two dimensions. In vivo, however, such complexes may well be composed of a three-dimensional network of interwoven thymic epithelium forming a basket-like packet filled with normal or leukemic lymphocytes and other elements. Clark (*9*) has proposed such a packet as a unit structure of normal thymus. Immigration of lymphoid precursors of extrinsic origin into the thymic rudiment was observed by microcinematography in a thymus organ culture of a 4-day-old larvae of *Xenopus laevis* (*10*). In contrast to the organ culture method, our symbiotic culture has the advantage of allowing more direct observation of cell-to-cell interaction. It also allows for quantitation of the phenomenon.

The present study revealed that the integrity of the cytoskeletal system was essentially required for the association of leukemia cells with their microenvironments. Both cytochalasins and colchicine strongly inhibited PEMP at concentrations without toxic injury to either leukemia cells or A17A cells. The action of both compounds was probably dual. The primary target of these compounds was the motile apparatus of the leukemia cells, inasmuch as the compounds paralyzed the locomotion of leukemia cells and thus prevented the occurrence of PEMP. However, these compounds caused rapid contraction of the A17A cell cytoplasm, so that the affected cells were unable to hold leukemia cells under them. The release of the leukemia cells immediately after addition of the chemicals to preformed complexes was a result of contraction of the A17A cells, as visualized in microcinematography and SEM. The effect of pretreatment of cells with these chemicals was less evident in the adherent cells than in the leukemia cells. The pretreated adherent cells could accept leukemia cells to a lesser or greater degree despite marked deformity and contraction of the cytoplasm. Such a difference in susceptibility to the pretreatment seemed partly due to the passive role of the adherent cells in complex formation. Inasmuch as the selective actions of cytochalasins on microfilaments (*11*) and colchicine on microtubules (*12*) have been well established, both cytoskeletal systems are involved in PEMP. However, details of their mechanisms of action remain unclear.

Previously, we reported that tumor-promoting phorbol esters stimulate in vitro growth of many microenvironment-dependent leukemias and at the same time inhibit PEMP (*7*). The present study confirmed and extended the findings with regard to the inhibition of PEMP. Microcinematography as well as SEM revealed that TPA inhibited the locomotion of leukemia cells and also caused contraction of adherent cells at nontoxic concentrations. We concluded previously (*7*) that the primary action of TPA was on the leukemia cells, since the pretreatment of the leukemia cells prevented PEMP but pretreatment of the adherent cells had a negligible effect. In light of the present study, however, the action of TPA seemed to be dual also. The action of TPA was apparently similar to the actions of cytochalasins and colchicine. TPA has been proved to disorganize the cytoskeletal system of the cells and to modulate their phenotype, mimicking the phenotype of transformed cells (*13*). TPA-induced inhibition of PEMP, therefore, may well be related to the action of TPA on the cytoskeletal system. However, it is not currently known if TPA acts directly on the cytoskeleton or on another motile apparatus or if TPA somehow secondarily affects the cytoskeleton. Unlike the almost immediate action of cytochalasin B or colchicine, an approximately 10-minute delay was noted by us before the effects of TPA on PEMP became visible. Rifkin et al. (*13*) reported that the action of TPA on the cytoskeleton requires synthesis of RNA and protein, since actinomycin D and cycloheximide abolish the effect of TPA. The observed delay in our experiment may represent the time required for intracellular events ultimately leading to modulation of the cytoskeleton.

Our previous study indicates that an indispensable step of leukemogenesis is that developing mouse thymic leukemias must form symbiotic complexes with thymic microenvironments (*4, 7*). Since growth of microenvironment-dependent leukemias requires close cell association with TER, any interference of the interaction may well cure or prevent the disease. The present study clearly showed that the integrity of the cytoskeleton was essential for the complex formation. Therefore, for this hypothetical approach to chemotherapy, chemicals affecting the cytoskeleton would be of choice. In a parallel study, we found that chemotherapeutic agents of *Vinca* alkaloids having a high affinity for microtubules strongly inhibited PEMP at concentrations without direct cytotoxicity (Hiai H, Fukushima M, Oguro Y, Nishizuka Y: Manuscript in preparation). Selective clinical indication of these agents for lymphoid malignancies might be explained at least in part by their action on the cell interaction proper to the lymphoid system rather than toxicity on growing cells. For further exploration of this possibility, the nature of the interaction between normal or neoplastic hematolymphoid cells and their microenvironments has to be elucidated. Symbiotic culture of mouse leukemias, therefore, will provide a useful in vitro model for the study of chemotherapy of lymphoid leukemias in this novel approach.

REFERENCES

(*1*) GOLDSTEIN G. Polypeptides regulating lymphocyte differentiation. In: Clarkson B, Marks PA, Till JE, eds. Differentiation of normal and neoplastic hematopoietic cells. Cold Spring Harbor conferences on cell proliferation. Vol. 5. Cold Spring Harbor, N.Y.: Cold Spring Harbor Laboratory, 1978:455–465.

(*2*) ZINKERNAGEL RM. Thymus and lymphohemopoietic cells: Their role in T cell maturation in selection of T cells' H-2-restriction-specificity and H-2-linked *Ir* gene control. Immunol Rev 1978; 42:224-270.

(*3*) WEKERLE H, KETELSEN U-P, ERNST M. Thymic nurse cells. Lymphoepithelial cell complexes in murine thymuses: Morphological and serological characterization. J Exp Med 1980; 151:925–944.

(*4*) HIAI H, NISHI Y, MIYAZAWA T, MATSUDAIRA Y, NISHIZUKA Y. Mouse lymphoid leukemias: Symbiotic complexes of neoplastic lymphocytes and their microenvironments. JNCI 1981; 66:713–722.

(*5*) HIAI H, SHISA H, NISHI Y, et al. Symbiotic culture of mouse leukemias: Regulation of cell interaction by a serum activity. Virchows Arch [Cell Pathol] 1980; 32:261–279.

(*6*) Humble JG, Jayne WH, Pulvertafts RJ. Biological interaction between lymphocytes and other cells. Br J Haematol 1956: 2:283-294.

(*7*) Hiai H, Nishizuka Y. Growth stimulation of microenvironment-dependent mouse leukemias by tumor-promoting phorbol esters. JNCI 1981; 67:1333-1340.

(*8*) Goodman GC, Miranda AF. Cellular contractility and the visible effects of cytochalasin. In: Tanenbaum SW, ed. Cytochalasins: Biochemical and cell biological aspects. Amsterdam, New York, and Oxford: North-Holland, 1978:277-429.

(*9*) Clark SL Jr. The thymus in mice of strain 129/J studied with the electron microscope. Am J Anat 1963; 112:1-33.

(*10*) Tochinai S. Direct observation of cell migration into *Xenopus* thymus rudiments through mesenchyme. Dev Comp Immunol 1980; 4:273-282.

(*11*) Spudich JA. On the effect of cytochalasin B on actin filaments. Cold Spring Harbor Symp Quant Biol 1973; 37:585-593.

(*12*) Dustin P. Microtubule poisons. In: Microtubules. Berlin and Heidelberg: Springer-Verlag, 1978:167-225.

(*13*) Rifkin DB, Crowe RM, Pollack. R. Tumor promoters induce changes in the chick embryo fibroblast cytoskeleton. Cell 1979; 18:361-368.

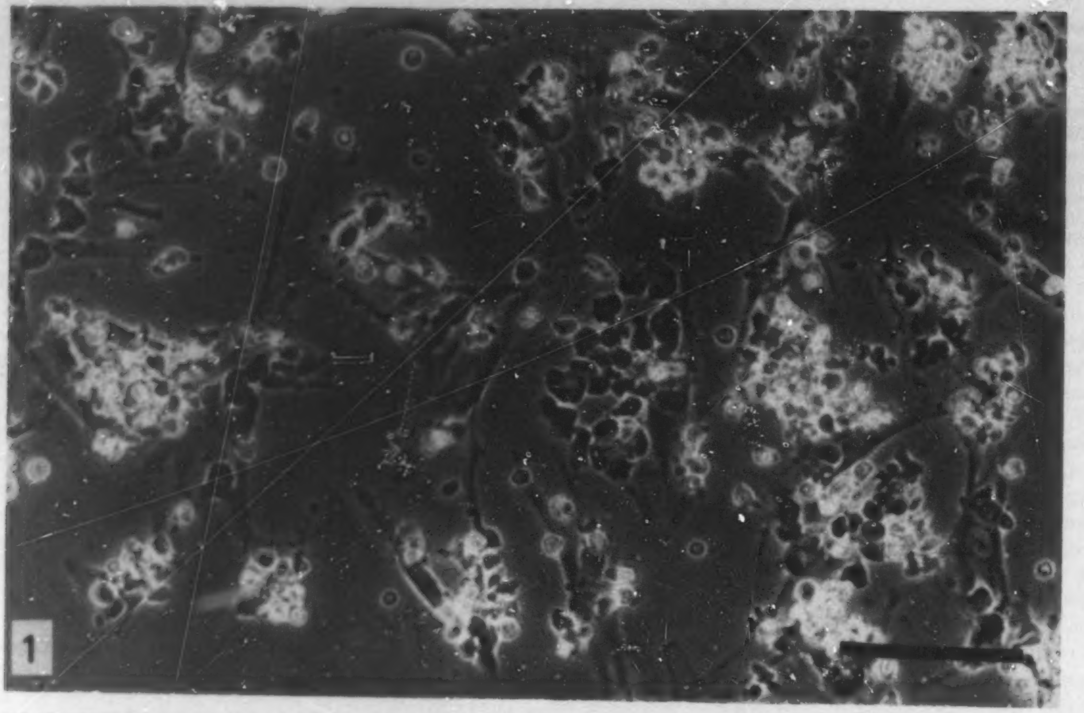

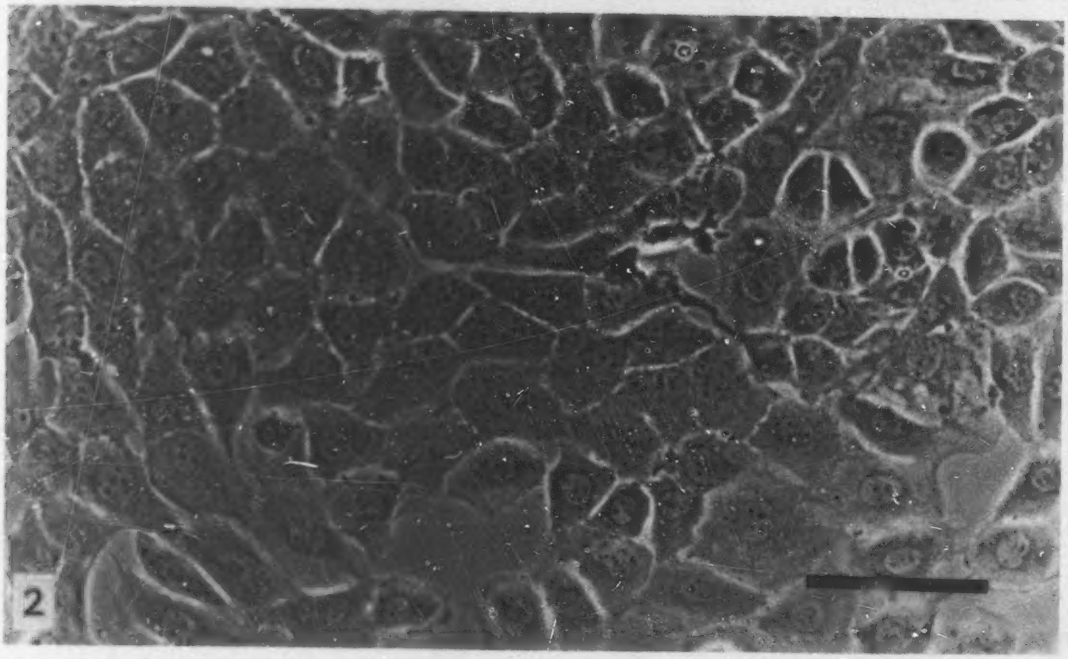

FIGURE 1.—Germinative layer of a representative symbiotic leukemia AKRL-16. *Note* many leukemia cells were in PEMP under adherent cells. Phase contrast. *Bar* = 100 µm. × 200

FIGURE 2.—Cloned adherent A17A cells, isolated from the symbiotic stock AKRL-17. Phase contrast. *Bar* = 100 µm. × 200

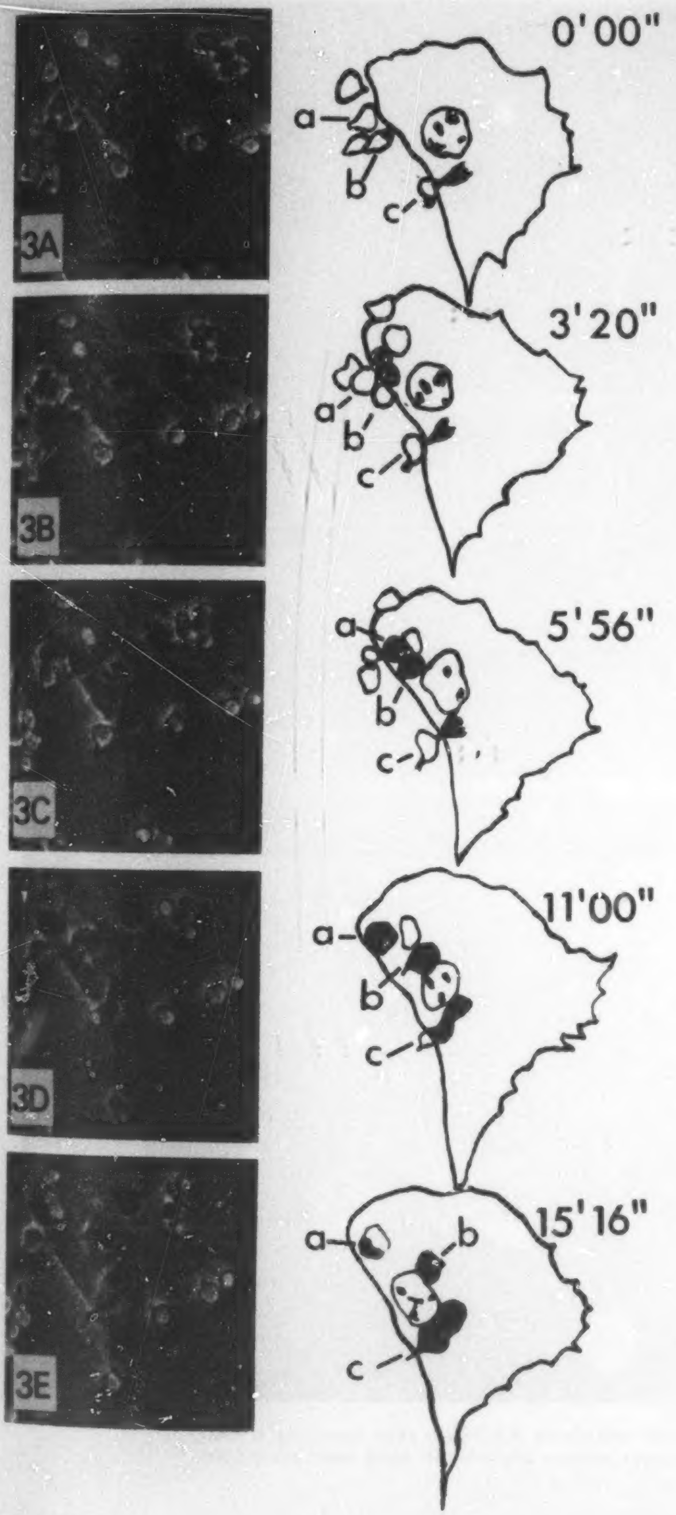

FIGURE 3.—Process of PEMP observed by microcinematography. Figs. 3A–3E were reproduced from cinefilms, and the drawings were added to help orientation. Figures on the *upper right corner* of each drawing represent time in minutes calculated from numbers of frames. *Frame A* was regarded as time 0. Phase contrast. *Bar*=50 µm. × 200. A: The leukemia cells (a) and (b) were in touch with the margin of the A17A cell. The cell (c) had already extruded its pseudopod under the A17A cell. B: All three leukemia cells were trying to push themselves under the adherent cell. C: The cell (b) was now under the A17A cell. D: Also the cell (a) was under the A17A cell. E: The cell (c) finally moved in under the A17A cell. The cell (b) had "run away" from the cell margin.

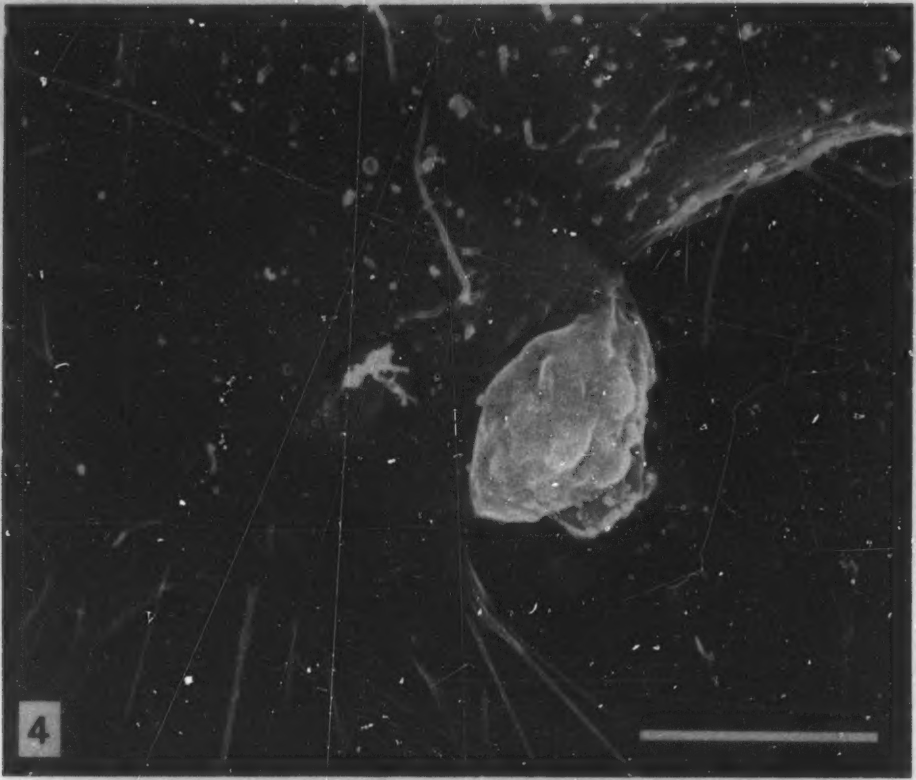

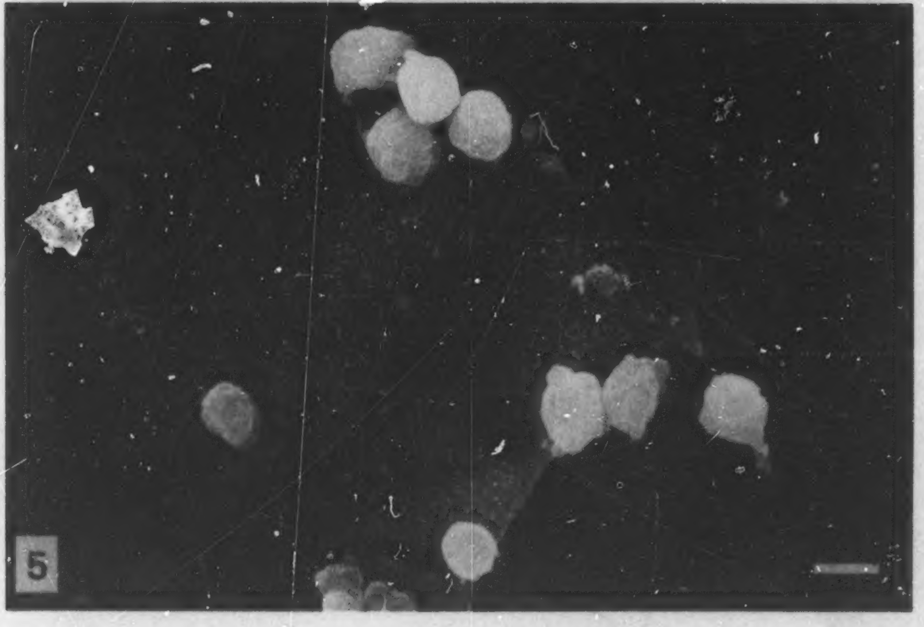

FIGURE 4.—Leukemia cell in the course of PEMP from margin of A17A cell. SEM. *Bar*= 5 μm. × 7,000
FIGURE 5.—Control culture of A17A cell with many leukemia cells in PEMP. SEM. *Bar*=5 μm. × 2,000

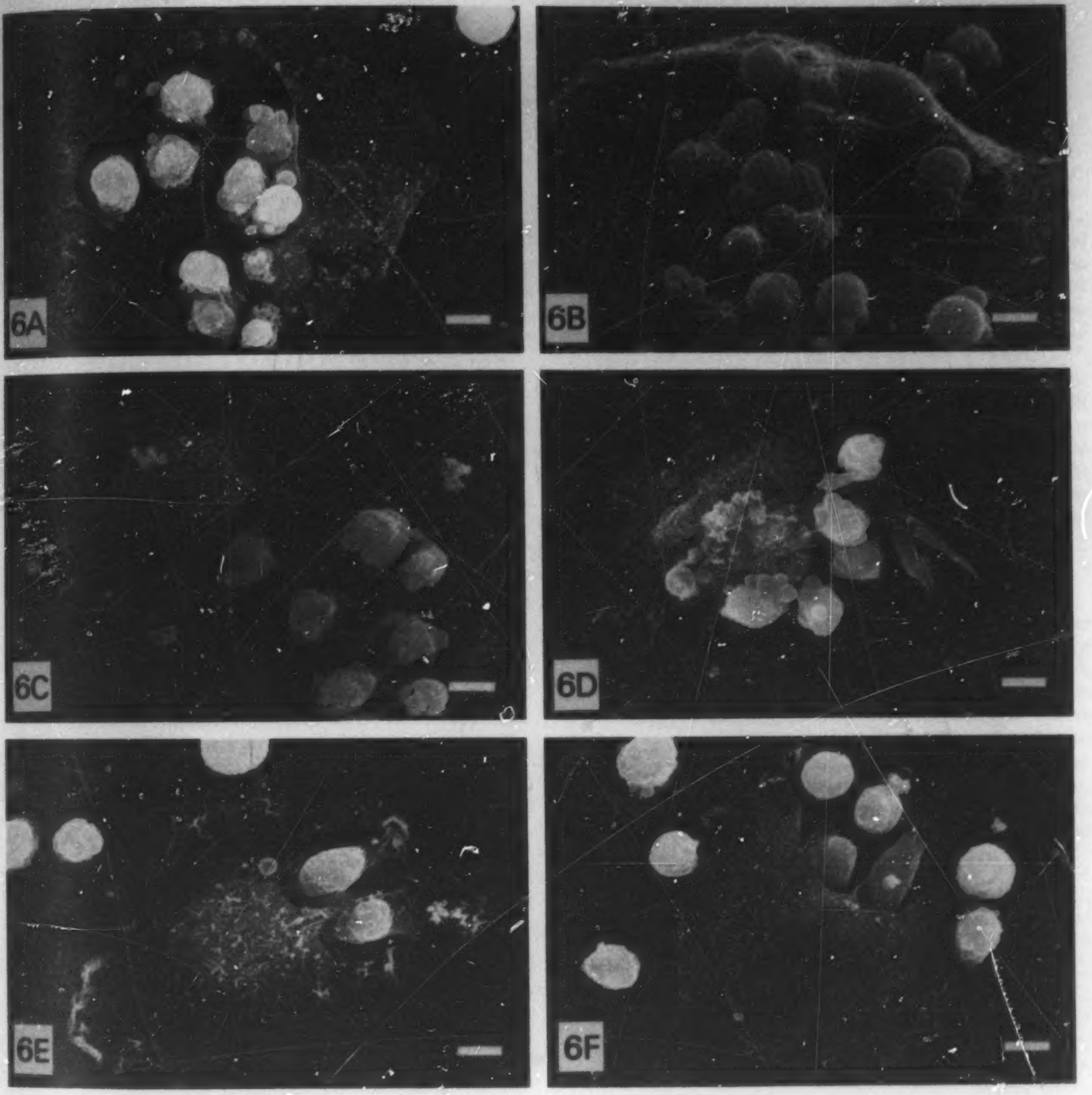

FIGURE 6.—Effect of various chemicals on PEMP observed by SEM. *Bar* = 5 μm. × 1,500. Ten (A) and 30 (B) min after addition of 2.5 μg cytochalasin B/ml. Ten (C) and 30 (D) min after addition of 10^{-2} m*M* colchicine. Ten (E) and 30 (F) min after addition of 10 ng TPA/ml.

blank page

A High-Tumor-Incidence Subline of the D1 Mouse Mammary Hyperplastic Outgrowth Line: Effect of Carcinogens[1,2,3]

Rhoda L. Ashley,[4,5] Robert D. Cardiff,[4,6] Terry S. Pratt,[4] *and* Leslie J. Faulkin[7,8]

ABSTRACT—Mammary tumorigenesis in some mouse strains is characterized by the appearance of a preneoplastic lesion, the hyperplastic alveolar nodule (HAN). The biology of the HAN has been characterized primarily through the study of stable outgrowth lines of serially transplanted HAN. One outgrowth line, DI, which was developed and carried in female BALB/c mice, has been described as a low-tumor-incidence line that does not express murine mammary tumor virus (MuMTV) and is susceptible to hormonal, chemical, and viral carcinogens. In this report, a high-tumor-incidence subline of DI, DI/UCD, is described. Although DI/UCD, like DI, is susceptible to the chemical carcinogen 7,12-dimethylbenz[a]anthracene, an increase in tumor incidence was not observed when DI/UCD outgrowth was exposed to hormones by means of pituitary isografts. Unlike DI, DI/UCD is refractory to the carcinogenic action of MuMTV. Both DI and the DI/UCD subline contained the endogenous MuMTV provirus but did not contain exogenous MuMTV provirus sequences. MuMTV antigen was not detected in DI/UCD outgrowths or tumors. RNA hybridizable to MuMTV complementary DNA was detected in some DI/UCD outgrowths and tumors but did not appear to correlate with tumorigenesis.—JNCI 1982; 69:639–645.

Mammary tumorigenesis in certain mouse strains is a multistage process characterized by an intermediate, biologically distinct, proliferative lesion or HAN (*1*). The cells of the HAN are at higher risk for tumor development than are those of the surrounding mammary parenchyma (*2, 3*). Therefore, HAN have been termed "preneoplastic" (*4*). Unlike normal lactating mammary epithelium, the HAN does not require lactogenic hormone stimulation for maintenance and is able to survive indefinite serial transplantation in the gland-free mammary fat pad of syngeneic hosts (*3, 5*). In vivo transplantation techniques have provided a means for studying the biology of premalignant neoplasia (*1, 6–8*). Stable outgrowth lines that have been developed from individual HAN are particularly useful for identification and analysis of factors that affect the emergence of tumors from preneoplastic lesions.

One of these lines, DI, was developed from a BALB/c HAN that arose after hormonal stimulation of the host (*9*). Outgrowths from early transplant generations of this line rarely developed tumors but were shown to be highly susceptible to the action of various carcinogens, as evidenced by increased tumor incidence and reduced latent periods for tumor development. Prolonged hormonal stimulation and chemical carcinogens, such as DMBA and the MuMTV, have been shown to increase tumor incidence in DI tissue (*9, 10*).

In our recent work with DI we used outgrowth tissue from the 40th to the 45th transplant generation. In these later generations, the DI differs from early transplant generations in its increased tumor incidence and in its lowered response to the tumorigenic effects of MuMTV infection. The tumor incidence of DI in the BALB/c host is greater than 70% at 9 months (*6*), as compared to the less than 30% incidence at 12 months reported by other investigators (*10, 11*). In contrast to previous studies with MuMTV, repeated studies in this laboratory demonstrated that the mean latent period for tumors from DI outgrowths in the BALB/cfC3H host is as much as 3 months longer than that observed in DI outgrowths in the BALB/c host (*6*). Because of these changes, we consider the later generations of DI in our laboratory as a distinct subline of DI and call it "DI/UCD."

This report of our continuing studies on DI/UCD describes the kinetics of tumorigenesis of DI/UCD outgrowth and the effects of MuMTV and other tumor-inducing agents on tumor incidence and latency. DI/UCD outgrowths and tumors from carcinogen-treated and untreated animals were also analyzed for MuMTV antigen and RNA to determine whether overt changes in the virology of DI were associated with the observed biologic changes.

MATERIALS AND METHODS

Transplantation.—Female BALB/c mice (3 wk old) were obtained from Simenson Laboratories, Gilroy, Calif. Mice were anesthetized, and the inguinal mammary fat pads were surgically exposed and cleared of all epithelial elements, as described in (*2*). Transplants of BALB/c DI outgrowth were made into the cleared fat pads. The DI outgrowth was originally obtained in transplant generation 40 from the Cancer Research Laboratory, University of California, Berkeley, Calif. Transplant recipients were held 5 per cage, as virgins, under controlled conditions of temperature and light. Water and food were provided ad libitum.

ABBREVIATIONS USED: cDNA=complementary DNA; df=degrees of freedom; DMBA=7,12-dimethylbenz[*a*]anthracene; HAN=hyperplastic alveolar nodule; IP=immunoperoxidase; MuMTV=murine mammary tumor virus; SDS=sodium dodecyl sulfate.

---

[1] Received October 20, 1981; accepted April 16, 1982.

[2] Supported by Public Health Service contract N01CP-61013 from the Virus Cancer Program, Division of Cancer Cause and Prevention, National Cancer Institute.

[3] Animals were maintained under the guidelines set forth by the University of California.

[4] Department of Pathology, School of Medicine, University of California, Davis, Calif. 95616.

[5] *Present address:* Department of Immunology and Microbiology, School of Medicine, University of Washington, Seattle, Wash. 98195.

[6] *Address reprint requests to* Dr. Cardiff.

[7] Department of Veterinary Anatomy, School of Veterinary Medicine, University of California, Davis.

[8] We are grateful to Mr. D. J. Mitchell and Ms. J. Walls (Department of Veterinary Anatomy, School of Veterinary Medicine) and to Ms. J. K. Lund and Dr. T. G. Fanning (Department of Pathology, School of Medicine) for their technical assistance.

By gastric intubation, 1 group of Dl recipients (Dl generation 42) received 0.5 mg DMBA (Sigma Chemical Co., St. Louis, Mo.) at 4 weeks and again at 6 weeks post transplantation. This experiment was repeated with recipients of Dl from generation 43. The dose of DMBA remained at 0.5 mg but was administered at 12 and 14 weeks post transplantation. Another group of transplant recipients (Dl generations 42 and 43) received two or three male pituitary isografts by subrenal capsule implantation at the time of transplantation of the Dl/UCD. Finally, a group of mice (recipients of Dl generation 43 or 44) were held as untreated controls.

Animals from all groups were checked weekly for tumor development in transplant sites and in host mammary glands. One tumor was detected in a host gland site in a DMBA-treated host and was identified as a sarcoma. No mammary tumors were observed in host tissues during the course of the study. Autopsies were performed on tumor bearers to confirm the presence of tumors in the transplant sites and to confirm growth of contralateral transplants. At the termination of each experiment, all animals were killed and autopsies were performed. Only those transplants that had filled at least 50% of the fat pad were considered in the incidence calculations. Hormonal stimulation was confirmed at autopsy in those animals that received pituitary isografts by the noting of secretion in the host mammary glands and transplants. All tumor bearers in these groups showed evidence of hormonal stimulation. The low number (<1%) of those mice that were not obviously stimulated did not develop tumors and were not considered in calculations of the incidence figures.

At 12 weeks post transplantation, 30–40 mice from each group were killed, and hyperplastic outgrowths, tumors, host mammary glands, livers, kidneys, and spleens were collected. Portions of these tissues were taken for IP staining, and the remaining tissue was held at −70°C. Those animals that were killed at 12 weeks post transplantation were not considered in compiling tumor incidence data.

Tumors were collected when they reached approximately 1–2 g. Host mammary glands, livers, kidneys, and spleens from tumor bearers were collected and frozen. Most animals at the time they were killed for large tumors had smaller tumors in the contralateral transplant. Portions of all tumors were fixed for PAP staining and the remaining tissue was held at −70°C.

IP staining.—To test for the presence of MuMTV antigen, we used a modification of the immunocytochemical methods of St. George et al. (*12*) and Vacquier and Cardiff (*13*), as described in detail in (*6*).

RNA extraction.—The RNA was extracted as previously described (*6, 8*). Frozen tissue was weighed and, while frozen, 2–5 g was minced before suspension in 10 vol/g TE buffer.[9] The slurry was homogenized and adjusted to 0.1 *M* NaCl and 0.5% SDS. Nucleic acids were extracted twice with phenol and once with phenol-chloroform-isoamyl alcohol (50:50:1). The aqueous phase was adjusted to 0.3 *M* NaCl, and 1 volume of cold absolute ethanol was added. After the DNA was spooled onto glass rods, a second volume of ethanol was added, and RNA was precipitated twice from ethanol at −20°C. The RNA was treated with DNase as described in (*6*), extracted with phenol, and stored at −70°C in TE buffer[9] (pH 7.4). MuMTV RNA was extracted from virions purified from tissue culture fluid as previously described (*6, 8, 14*).

[^{32}P]cDNA.—Labeled DNA complementary to MuMTV RNA was synthesized in a 100-μl reaction mixture containing 200 m*M* each of dTTP, dCTP, and dGTP; 50 m*M* Tris-HCl (pH 8.1); 75 m*M* KCl; 10 m*M* $MgCl_2$; 2 m*M* dithiothreitol; 25 μg actinomycin D/ml; 100 μCi α-[^{32}P]dATP (2,000–3,000 Ci/mmol; Amersham Corp., Arlington Heights, Ill.); 1.0 μg MuMTV RNA; 1.2 μg calf thymus DNA primers (*15*); and 100 U avian myeloblastosis virus RNA-dependent DNA polymerase provided by Dr. J. Beard (Life Sciences, Inc., St. Petersburg, Fla., through the Research Resources, Biological Carcinogenesis Branch, National Cancer Institute). After 30 minutes at 37°C, the reaction was stopped by the addition of EDTA, SDS, an NaOH to final concentrations of 0.05 *M*, 0.5%, and 0.3 *M*, respectively, and the mixture was incubated at 65°C for 3-4 hours to hydrolyze the RNA. The mixture was neutralized and then was passed over a Sephadex G-50 column. The excluded fractions were pooled, were precipitated in ethanol, and then were suspended in 10 m*M* Tris–HCl (pH 8.0) and 1 m*M* EDTA. The final cDNA had a specific activity of 2×10^4 cpm/pg (*8*). The probe was characterized as described below.

Characterization of the [^{32}P]cDNA probe.—Hybridization levels of the [^{32}P]cDNA in reactions containing MuLV RNA or yeast RNA were minimal (<5%), indicating specificity for MuMTV. The cDNA hybridized to template RNA to a 65% maximum and at a $C_rt_{1/2}$[10] of 6×10^{-2} mol×sec×liter^{-1} (*8*). To test the extent to which the probe represented the MuMTV genome, we used aliquots of the [^{32}P]cDNA in the Southern blot technique (*16*) to detect Pst I endonuclease fragments from DNA containing the MuMTV endogenous and exogenous proviruses. The fragment pattern reported by Cohen et al. (*17*) was consistently reproduced with this probe (*6, 14*). These results indicate that all of the 35S genome was represented in our probe. However, since the probe was not reannealed back to 35S RNA before use, some degree of over-representation of subgenome portions of the template RNA was possible. To directly test the extent of subgenome over-representation in the probe, we used the cDNA to protect ^{125}I-labeled MuMTV 35S RNA from RNase A degradation. The probe protected 85% of the RNA at a ratio of 10:1, indicating a low level of sequences present in excess of other sequences.

RNA:[^{32}P]cDNA liquid hybridization.—The annealing mixture contained 0.3 *M* NaCl, 25 m*M* Tris–HCl (pH 7.4), 2 m*M* EDTA, 30,000 cpm [^{32}P]cDNA, and 5–7 mg RNA/ml in a total volume of 150 μl (750–1,050 μg RNA) (*8*). Nucleic acids were boiled for 1 minute and quickly chilled on ice before addition of the remaining components of the reaction mixture. Hybridizations were conducted up to 96 hours at 68°C; C_rt[10] values were varied by time (*8*). Periodically, 10-

---

[9] 10 m*M* Tris (pH 9.2) and 1 m*M* EDTA.

[10] C_rt=product of concentration and time (mol×sec×l^{-1}); $C_rt_{1/2}$=50% of the product of RNA concentration and time.

μl aliquots of the reaction mixture were removed and placed into 1.1 ml ice-cold, freshly-made Sl buffer.[11] Two 0.5-ml aliquots from this mixture were then removed, and 12 μl Sl nuclease (5 μg; Miles Laboratories, Inc., Elkhart, Ind.) was added to 1 aliquot. All samples were then incubated for 2 hours at 50°C. Nucleic acids were precipitated with 2.0 ml cold 10% trichloroacetic acid in the presence of yeast RNA and were counted in phase combining system scintillation fluid.

RESULTS

Tumor Incidence in D1/UCD Outgrowth

Tumor incidence in postgeneration 40 D1 outgrowth (D1/UCD) was greater than 70% by 9 months post transplantation. When D1/UCD was exposed to MuMTV by transplantation into BALB/cfC3H animals, tumor incidence at 9 months was approximately 30%; after 12 months, 70% tumor incidence was attained in this group (*6*). Thus the major effect of MuMTV on D1/UCD outgrowth was to substantially prolong the mean latent period of tumorigenic development.

The effect of other tumor-inducing regimens, including treatment with DMBA and introduction of pituitary isografts, was examined in this study. The experiments were designed in such a way that periodic samples of the hyperplastic outgrowth were taken from each group for virologic analysis. Because of these experimental manipulations and accidental loss of animals, the number of fat pads at risk of tumor development diminished with time. Therefore, to provide an accurate description of tumor development in D1/UCD outgrowths, we have expressed the data in three forms: 1) Tumor incidence was calculated at a given time post transplantation as the number of tumors per total viable transplants (table 1); 2) cumulative tumor incidence was determined by amending the total number of tumors at weekly intervals over the entire recorded period (text-fig. 1); and 3) age-specific incidence data (*18*) were also generated from the number of tumors arising in a given month relative to updated values for transplants at risk due to prior tumor development, experimental manipulation, or animal death (table 2; text-fig. 2).

When DMBA was given 4–6 weeks post transplantation, 71% of the D1/UCD transplants developed tumors by 14 weeks post transplantation. In contrast, 2.5% of the D1/UCD in untreated animals had developed tumors at that time. The experiment was repeated to generate data on the kinetics of tumor development after DMBA treatment. We chose the same dose of DMBA (0.5 mg) and administered it 12 and 14 weeks post transplantation. A rapid increase in tumors was observed in this second DMBA trial as reflected in the cumulative tumor incidence curve (text-fig. 1). The overall tumor incidence in this second group was 85% (table 1) at 29 weeks when all of the transplants at risk had developed tumors (table 2). This incidence compared with the 45% tumor incidence in D1/UCD from untreated controls (table 1), a significant difference by the chi-square test (df=1; $P<0.001$]. In contrast to the DMBA-treated animals, a significant number of D1/UCD transplants in untreated animals had not developed tumors when the experiment was terminated at 39 weeks (table 2; text-fig. 2).

TABLE 1.—*Tumor incidence in D1/UCD transplants[a] with carcinogen treatment*

Treatment	D1 generation	No. of tumors/No. of transplants	Percent tumors	Mean latent period, wk	Termination, wk
None	43	2/80	2.5	—	14
DMBA[b]	42	103/145	71.0	—	14
None	43	36/80	45.0	22.0	29
DMBA[c]	43	29/34	85.3	23.8	29
None	43	43/80	56.3	24.5	34
Hormones[d]	42	38/87	43.7	23.0	34

[a] D1/UCD was transplanted bilaterally into cleared mammary fat pads of BALB/c females, and each transplant site was examined weekly to determine the total No. of palpable tumors at the time of termination. Total transplants were determined by autopsy; transplants that failed to fill 50% of the host fat pads were not recorded. Palpated tumors were confirmed by autopsy.

[b] DMBA was administered 4 and 6 wk post transplantation.

[c] DMBA was administered at 12 and 14 wk post transplantation.

[d] Hormones were supplied by pituitary isografts as described in "Materials and Methods."

D1/UCD transplants in pituitary-treated animals initially developed tumors at the same rate as did D1/UCD transplants in untreated animals (text-fig. 1). The tumor incidence of the D1/UCD in treated animals, however, began to drop after the 6th month (table 2; text-fig. 2), whereas the tumor incidence continued to rise in the untreated animals (table 2; text-fig. 2). This resulted in a distinct plateau in the cumulative tumor incidence of D1/UCD in treated animals (text-fig. 1). When the experiment with pituitary-treated animals was terminated at 34 weeks, the overall incidence was 45%, as compared to 53% in the control group at the same time. This difference was not significant by the chi-square test (df=1; $P=0.1$). Further, the mean latent periods of 23.5 and 24 weeks were the same.

These data can be compared with the tumor incidence observed with the D1/UCD transplants in BALB/cfC3H animals (*6*) (text-figs. 1, 2). With MuMTV exposure, the mean latent period was prolonged, and the age-adjusted kinetics of tumor development were slower than those of the other groups. This distinctive kinetics profile of the D1/UCD tumors arising in BALB/cfC3H animals is consistent with the earlier observation that the biology of the D1/UCD in the BALB/cfC3H system is different from previous descriptions of the D1 line (*19*). These data suggest that while DMBA treatment increases the rate of tumor development in D1/UCD, other treatments, including hormone stimulation and exposure to MuMTV, do not increase either the incidence of tumors or the rate of tumor development.

Analysis of D1/UCD Tissues for MuMTV Antigen by IP

The D1/UCD outgrowth and D1/UCD tumors contained only the endogenous MuMTV proviruses (*6*). To determine

---

[11] 30 mm sodium acetate (pH 4.5), 3 m*M* $ZnSO_4$, 30 m*M* NaCl, and 10 μg alkaline-denatured DNA/ml.

TABLE 2.—*Age-specific tumor incidence in D1/UCD outgrowth*[a] *exposed to carcinogens*

Treatment[b,c]	Months post transplantation:[b,c]									
	3	4	5	6	7	8	9	10	11	12
DMBA										
No. of sites at risk			34	32	24	5				
Tumors										
No.			2	8	17	5				
Percent			5.9	25.0	70.8	100.0				
Hormones										
No. of sites at risk	171	168	154	122	100	96	94			
Tumors										
No.	3	9	13	30	3	2	1			
Percent	1.8	5.4	8.4	16.4	2.0	2.1	1.1			
MuMTV										
No. of sites at risk			38	34	39	27	22	21	15	12
Tumors										
No.			4	3	2	4	0	5	3	4
Percent			10.5	8.8	6.7	14.8	—	23.8	20.0	33.3
None										
No. of sites at risk	130	126	120	105	83	56	41			
Tumors										
No.	4	4	13	21	25	10	4			
Percent	3.1	3.2	10.8	20.0	30.1	17.9	9.8			

[a] D1/UCD outgrowth was transplanted into BALB/c mice that were treated with DMBA, received isografts of pituitary glands, or were untreated. D1/UCD outgrowth was also transplanted into BALB/cfC3H hosts for exposure to MuMTV. D1/UCD from generation 42 was transplanted into virus-positive animals, D1/UCD from generations 42 and 43 was exposed to hormone stimulation, D1/UCD from generation 43 was exposed to DMBA, and D1/UCD from generations 43 and 44 were untreated.

[b] No. of sites at risk was determined for each 1-mo period post transplantation by subtraction of those transplants that were no longer at risk due to tumor development or animal death.

[c] No. of tumors includes those tumors that became palpable within each 1-mo period and that were later confirmed by autopsy.

whether viral expression was a feature of the D1/UCD subline, we analyzed outgrowths and tumors for the presence of MuMTV antigen. We analyzed numerous samples of outgrowth and tumor from hormonally stimulated or DMBA-treated hosts with similar tissues from untreated D1/UCD hosts. MuMTV antigen could not be demonstrated in these tissues. However, antigen could be detected in D1/UCD outgrowths and tumors in BALB/cfC3H hosts (*6*). While the effect of sampling error cannot be ruled out, the results of this study indicate that expression of virus structural antigen in D1/UCD outgrowth or tumors from BALB/c hosts is, at best, a rare occurrence and is not induced in detectable levels by either treatment.

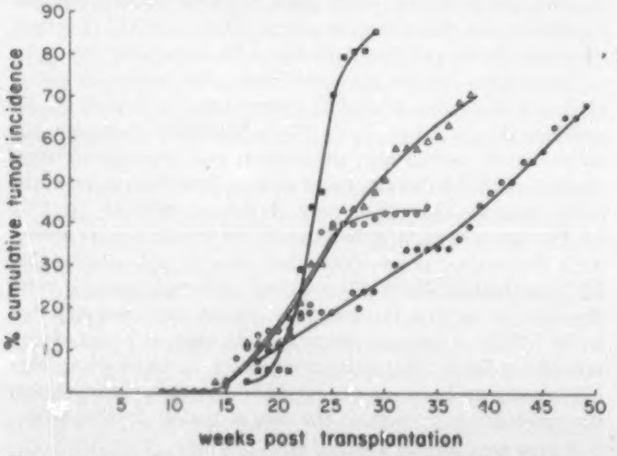

TEXT-FIGURE 1.—Cumulative tumor incidence in D1/UCD outgrowth. Total tumor incidence was calculated weekly from the initial transplants at risk. Both palpable tumors and transplants were confirmed by autopsy. D1/UCD tumors arose in DMBA-treated BALB/c hosts (■), hormone-stimulated BALB/c hosts (○), untreated BALB/c hosts (△); and MuMTV-infected BALB/cfC3H hosts (●).

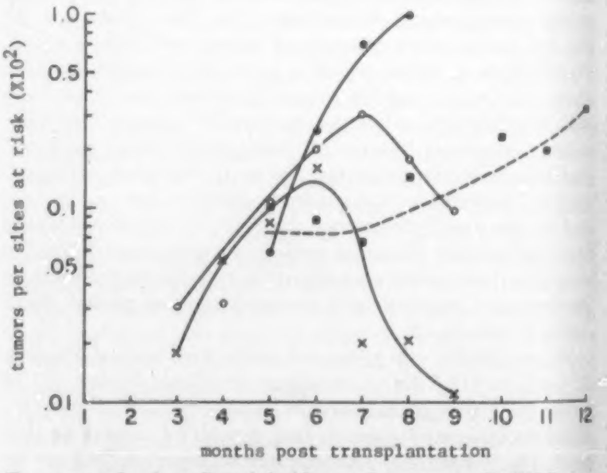

TEXT-FIGURE 2.—Age-adjusted incidence of tumors in D1/UCD outgrowth. Incidence of palpable tumors was calculated every 4 wk post treatment from the total number of tumors arising in D1/UCD transplants during the period and the total number of transplants at risk during the period. D1/UCD tumors arose in DMBA-treated BALB/c hosts (●), BALB/c recipients of pituitary isografts (×), untreated BALB/c hosts (○), and MuMTV-infected BALB/cfC3H hosts (■). Tabulated data are presented in table 2.

Analysis of D1/UCD Outgrowth RNA by Nucleic Acid Hybridization

D1/UCD tissues were also analyzed for MuMTV RNA. RNA from outgrowth obtained from hormone-stimulated animals had detectable levels of RNA that hybridized to our probe (text-fig. 3C). At high C_rt^{10} values, D1/UCD outgrowth RNA from DMBA-treated animals hybridized to a greater extent (14%) than did that from pooled livers and host glands from this group (text-fig. 3B). Although these data are suggestive of MuMTV RNA expression, the low maximum hybridization level precludes quantitative comparisons with other tissues. Little or no hybridizable RNA was detected in any of the nontumor tissues tested from the BALB/c controls (text-fig. 3A).

Analysis of D1/UCD Tumor RNA by Nucleic Acid Hybridization

RNA hybridizable to the MuMTV cDNA was detected in RNA from 2 of 8 D1/UCD tumors from untreated hosts (text-fig. 4). The RNA was tested from 6 randomly selected D1/UCD tumors occurring in the DMBA-treated hosts. In addition, 6 RNA preparations from D1/UCD tumors in the hormone group were tested. All 12 of these tumors contained RNA that hybridized to the MuMTV cDNA (text-fig. 4).

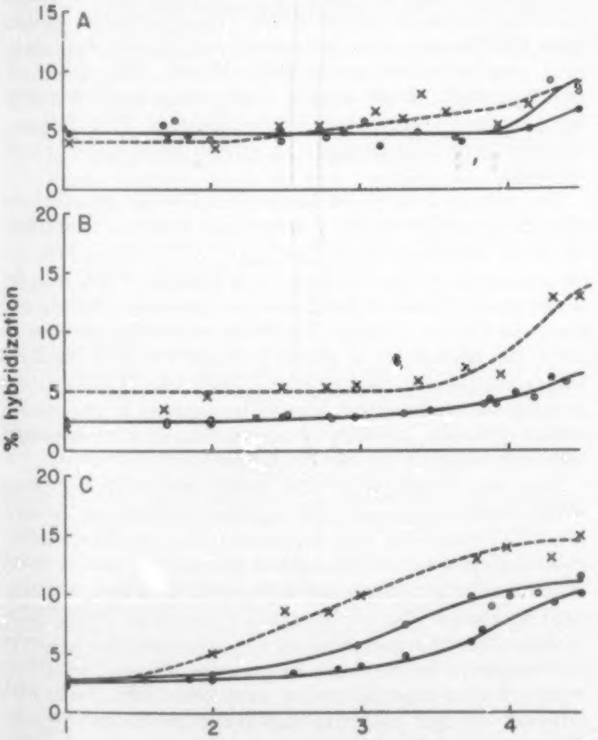

TEXT-FIGURE 3.—MuMTV RNA in D1/UCD outgrowth. D1/UCD outgrowths were pooled at 12 wk post transplantation or post treatment (DMBA-treated animals) from A) untreated BALB/c hosts, B) DMBA-treated BALB/c hosts, and C) BALB/c hosts with pituitary isografts. The RNA from the separate pools was hybridized to [^{32}P]cDNA as outlined in "Materials and Methods." D1/UCD outgrowths (×), host mammary gland (○), and liver (●) RNA preparations were tested from each group.

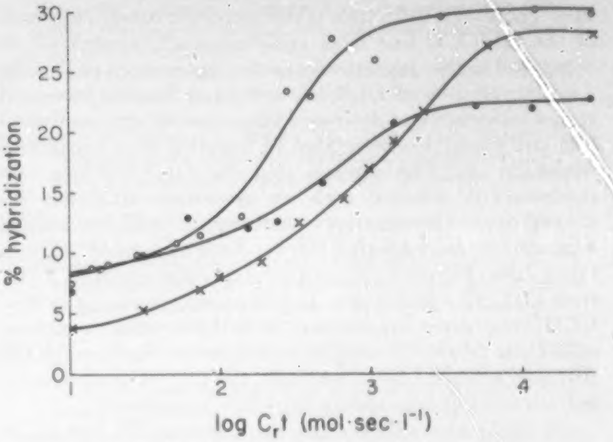

TEXT-FIGURE 4.—MuMTV RNA in D1/UCD tumors arising in untreated BALB/c hosts (●), DMBA-treated BALB/c hosts (○), or BALB/c hosts with pituitary isografts (×). RNA from individual tumors was hybridized to [^{32}P]cDNA as outlined in "Materials and Methods." Representative reactions from these tumors are presented.

The maximum extent of hybridization differed according to the treatment of the D1/UCD hosts. RNA samples from DMBA-treated hosts hybridized to a higher maximum value (30%) than those from the hormone-treated and control groups (text-fig. 4). The level of hybridization was too low to reach a conclusion based on a quantitative comparison.

DISCUSSION

The D1 subline has been widely used as a source of hyperplastic tissue of lower tumor incidence. We, like many investigators, began our studies with the assumption that D1 was a low-tumor-incidence outgrowth line. In the course of a long-term study of carcinogen effects on D1 outgrowth, we observed the increased tumor incidence reported here and elsewhere (*6*). Several investigators indicated to us that they had observed a comparable increase in the D1 tumor incidence (Medina D: Personal communication; Guzman, R: Personal communication).

All D1 lines may have become highly tumorigenic or maybe only the subline we obtained from the University of California, Berkeley, has a high tumor incidence. To facilitate comparison and maintain clarity in future reports, we have designated the outgrowth in our laboratory as "D1/UCD." As other laboratories publish their observations, the origin of the increased tumor incidence in D1/UCD may be resolved. In the meantime we report our observations on the increased, intrinsic, long-term tumor incidence in D1/UCD, and we further describe the effect of a chemical carcinogen and hormones on tumor incidence. We believe that in light of these data other investigators should carefully analyze their own D1 outgrowths before proceeding with experiments based on an assumption of low tumorigenicity.

The biologic characteristics of the D1/UCD subline differ in several respects from those of the parental D1 outgrowth line. The major difference is the increased tumor incidence of the D1/UCD line from generations 42 through 46, as compared to that reported for earlier generations of D1 (*10, 11*). Our analysis of D1/UCD indicated that the increased tumor incidence and decreased latent period were reproducible and could not be related to infection with exogenous MuMTV (*6*). The concern that the D1/UCD line was inadvertently infected with an exogenous virus was increased with the discovery that several BALB/c strains appeared in the restriction maps to have additional provirus DNA (*20*). However, numerous restriction maps of DNA from D1/UCD outgrowths and from tumors arising in D1/UCD outgrowths maintained in BALB/c mice contained only those MuMTV restriction fragments expected in the BALB/c genome (*6*). In addition, the D1/UCD outgrowth and tumors did not contain MuMTV antigens (*6*).

D1/UCD also differs from the parental D1 line in its relative lack of response to MuMTV as a tumor-inducing agent (*6*). In light of these pronounced differences, we examined the effect of other putative tumor-inducing agents on the new D1/UCD subline. The effects of chemical carcinogens and pituitary explants on the parental D1 line have been described (*1*). In D1, DMBA increased the tumor incidence from 4 to 67% and decreased the mean latent period from 404 to 207 days (*1*). Pituitary isografts had only marginal effects on tumor incidence, with an increase to 7% and a mean latent period of 371 days (*1*).

The DMBA treatment of hosts bearing D1/UCD resulted in accelerated tumor development. The effect of DMBA in terms of decreased mean latent period was clear with two different experimental designs: Treatment at 4 and 6 weeks resulted in rapid onset 8 weeks later, and treatment at 12 and 14 weeks resulted in an exponential rise in tumors 6–8 weeks later. Because of the differences in experimental design, direct comparisons between parental D1 and D1/UCD cannot be made. However, it is quite apparent that both are sensitive to chemical carcinogens.

The effects of pituitary isografts on the D1/UCD are difficult to interpret. The initial rise in tumor incidence was identical to that of the control curve, and the mean latent periods were similar. However, the appearance of new tumors suddenly slowed at 30 weeks. This phenomenon was reflected in both the cumulative tumor incidence and the age-specific incidence curves. We have no ready explanation for these observations, and inasmuch as the tumor incidence of the parental D1 was not analyzed in the same way, direct comparisons cannot be made. Clearly, tumor kinetics is a complex function that must be analyzed with the use of various parameters. Pituitary isografts resulted in a set of kinetics curves that differed from those generated by data from the control group.

As previously reported, transplantation of D1/UCD in BALB/cfC3H led to a prolonged latent period (*6*). The tumor kinetics curves for these transplants differ from those for the control group. The tumor kinetics for each experimental group were unique, and each differed from the kinetics predicted by the control group's curve. These studies helped delineate the biologic characteristics of the D1/UCD subline.

The second major issue explored in these studies was the possible association of detectable MuMTV antigen a
RNA with tumorigenesis in the D1/UCD system. The
outgrowth line originated in BALB/c (*9*). BALB/c mi
have endogenous MuMTV provirus DNA sequences (*2*
The MuMTV sequences appear to be highly repres
because MuMTV RNA is either very low or undetectab
in mammary glands or tumors (*22–26*). Virion expres
and antigen expression occasionally have been detected
spontaneous BALB/c tumors (*27–29*). These findings m
be explained by undetected exogenous infection (*20*). Ho
mone induction of BALB/c tumors has been reported to
associated with some increase in virus RNA levels (*3*
However, DMBA-induced BALB/c tumors have had lit
or no detectable MuMTV RNA (*31–33*).

Tissue such as D1 outgrowth has been used to determi
whether virus expression may occur in premalignant ne
plasia. Several investigations have suggested that MuMT
RNA levels are higher in tumors than in outgrowths (*3*
33, 34). We found no appreciable differences in the levels
virus RNA in BALB/cfC3H premalignant hyperplastic ou
growths and their tumors (*6*).

The analysis of D1/UCD RNA with MuMTV-speci
cDNA probe revealed little or no increase in MuMTV RN
in the outgrowths as compared to that in BALB/c liver
lactating mammary gland RNA. D1/UCD RNA sampl
from DMBA and hormone-treated outgrowths hybridiz
to a greater extent to MuMTV cDNA. The differenc
although slight, might suggest some expression of MuMT
RNA in the D1/UCD from treated animals. Viral antigen
however, were not detected in any of these tissues by
methods.

The tumors from treated and untreated outgrowths we
also analyzed for MuMTV RNA and antigens. Hybridiz
ble RNA was detected in 2 of 8 D1/UCD tumors from th
untreated group. In contrast, hybridizable RNA was d
tected in all of the D1/UCD tumors from the DMBA- an
hormone-treated animals. While these findings are provo
ative, the percentage of putative MuMTV RNA detecte
was extremely low. Because of this low level of hybridizatio
and the failure to detect MuMTV antigens in any tumo
virus expression probably is not correlated with increase
tumor incidence in the D1/UCD subline.

The data reported in this study extend our previo
observations concerning the biologic differences betwe
D1/UCD outgrowth and the parental D1 line. These diffe
ences may provide an example of phenotypic drift resulti
from selective pressure in serial passage. Although premali
nant outgrowth lines are generally quite stable biologicall
evidence has been presented for the heterogeneous nature
premalignant lesions and outgrowths (*8, 11, 35*). Wi
repeated serial transplantation, subpopulations of cells wi
different biologic potential may dominate outgrowth po
ulation. Whether genetic alteration accounts for the ph
notype changes seen in D1/UCD is uncertain. Studies usin
restriction endonuclease mapping suggest that the endog
nous MuMTV provirus has remained stable in D1 and D1
UCD (*6, 21, 22*). Alteration of other genetic loci, howeve
cannot be ruled out as the possible basis for the differ
between D1/UCD and D1.

The increased D1/UCD tumor incidence apparently not due to introduction and maintenance of virus expression, as neither D1/UCD outgrowth nor most of the tumors studied from untreated hosts contained detectable MuMTV RNA or MuMTV antigens. The relative increase in D1/UCD tumor incidence with DMBA treatment was accompanied by detection of RNA that hybridized to the MuMTV cDNA in all of the D1/UCD tissues (outgrowths and tumors) tested. However, hybridizable RNA was also detected in all D1/UCD tissues after hormone treatment without an increase in tumor incidence. Further, the levels of RNA detected were extremely low, thereby limiting comparisons and conclusions. Even with these technical limitations the presence of hybridizable RNA in carcinogen-treated tissues could not be correlated with tumorigenesis. These conclusions serve to confirm and extend the observation that full MuMTV expression is not necessary for the maintenance of the malignant phenotype in BALB/c mice (*32*).

REFERENCES

(*1*) Medina D. Preneoplastic lesions in mouse mammary tumorigenesis. Methods Cancer Res 1973; 7:3.

(*2*) DeOme KB, Faulkin LJ, Bern HA, Blair PB. Development of mammary tumors from hyperplastic alveolar nodules transplanted into the gland-free mammary fat pads of female C3H mice. Cancer Res 1959; 19:515–520.

(*3*) Medina D. Preneoplasia in breast cancer. In: McGuire WL, ed. Breast cancer. Vol 2. New York: Plenum Press, 1978:47–102.

(*4*) Cardiff RD, Wellings SR, Faulkin LJ. Biology of breast preneoplasia. Cancer 1977; 39:2734–2746.

(*5*) Daniels C, DeOme K, Young LJ, Blair PB, Faulkin LJ Jr. The in vivo life span of normal and preneoplastic mouse mammary glands: A serial transplantation study. Proc Natl Acad Sci USA 1968; 61:53–60.

(*6*) Ashley RL, Cardiff RD, Fanning TG. Reevaluation of the effect of mouse mammary tumor virus infection on the BALB/c mouse hyperplastic outgrowth. JNCI 1980; 65:977–986.

(*7*) Faulkin LJ Jr, DeOme KB. Regulation of growth and spacing of gland elements in the mammary fat pad of the C3H mouse. J Natl Cancer Inst 1960; 24:953–969.

(*8*) Ashley RL, Cardiff RD, Mitchell DJ, Faulkin LJ, Lund JK. Development and characterization of mouse hyperplastic mammary outgrowth lines from BALB/cfC3H hyperplastic alveolar nodules. Cancer Res 1980; 40:4232–4242.

(*9*) Medina D, DeOme KB. Influence of mammary tumor virus on the tumor-producing capabilities of nodule outgrowth free of mammary tumor virus. J Natl Cancer Inst 1968; 40:1303–1308.

(*10*) ———. Effects of various oncogenic agents on tumor-producing capabilities of series D BALB/c mammary nodule outgrowth lines. J Natl Cancer Inst 1970; 45:353–363.

(*11*) Medina D, Shepherd DF, Gropp T. Enhancement of the tumorigenicity of preneoplastic mammary nodule lines by enzymatic dissociation. J Natl Cancer Inst 1978; 60:1121–1126.

(*12*) St. George JA, Cardiff RD, Young LJ, Faulkin LJ. The immunocytochemical distribution of mouse mammary tumor virus antigens in BALB/cfC3H mammary epithelium. JNCI 1979; 63:813–818.

(*13*) Vacquier JP, Cardiff RD. In vitro infectivity assay for mouse mammary tumor virus. Proc Natl Acad Sci USA 1979; 76:4117–4121.

(*14*) Cardiff RD, Fanning TG, Morris DW, Ashley RL, Faulkin LJ. Restriction endonuclease studies of hyperplastic outgrowth lines from BALB/cfC3H mouse hyperplastic mammary nodules. Cancer Res 1981; 41:3024–3029.

(*15*) Taylor JM, Illmensee R, Summers J. Efficient transcription of RNA into DNA by avian sarcoma virus polymerase. Biochim Biophys Acta 1976; 442:324–330.

(*16*) Southern EM. Detection of specific sequences among DNA fragments separated by gel electrophoresis. J Mol Biol 1975; 98:503–517.

(*17*) Cohen JC, Shank PR, Morris VL, Cardiff RD, Varmus HE. Integration of the DNA of mouse mammary tumor virus in virus-infected normal and neoplastic tissue of the mouse. Cell 1979; 16:333–345.

(*18*) Prehn R. Rate-limiting step in the progression of mouse breast tumors. Int J Cancer 1977; 19:670–672.

(*19*) Medina D, DeOme KB. Response of hyperplastic outgrowth line D1 to mammary tumor virus, nodule-inducing virus, and prolonged hormonal stimulation acting singly and in combination. J Natl Cancer Inst 1969; 42:303–310.

(*20*) Morris VL, Vlasschaert JE, Beard CL, Milazzo MF, Bradbury WC. Mammary tumors from BALB/c mice with a reported high mammary tumor incidence have acquired new mammary tumor virus DNA sequences. Virology 1980; 100:101–109.

(*21*) Cohen JC, Majors JE, Varmus HE. Organization of mouse mammary tumor virus-specific DNA endogenous to BALB/c mice. J Virol 1979; 32:483–496.

(*22*) Long CA, Dumaswala UJ, Tancin SL, Vaidya AB. Organization and expression of endogenous murine mammary tumor virus genes in mice congenic at the H-2 complex. Virology 1980; 103:167–177.

(*23*) Varmus HE, Quintrell N, Medeiros E, Bishop JM, Nowinski RC, Sarkar NH. Transcription of mouse mammary tumor virus genes in tissues from high and low incidence mouse strains. J Mol Biol 1973; 79:663–679.

(*24*) Michalides R, Van Deemtes L, Nusse R, Röpcke G, Boot L. Involvement of mouse mammary tumor virus in spontaneous and hormone-induced mammary tumors in low mammary tumor mouse strains. J Virol 1978; 27:551–559.

(*25*) Michalides R, Vlahakis G, Schlom J. A biochemical approach to the study of the transmission of mouse mammary tumor viruses in mouse strains RIII and C3H. Int J Cancer 1976; 18:105–115.

(*26*) Schlom J, Colcher D, Drohan W, et al. Differences in mouse mammary tumor viruses. Relationship to early and late occurring mammary tumors. Cancer 1977; 39:2727–2733.

(*27*) Bentvelzen P. Endogenous mammary tumor viruses in mice. Cold Spring Harbor Symp Quant Biol 1975; 39:1145–1150.

(*28*) Hilgers J, Theuns GH, Van Nie R. Mammary tumor virus (MTV) antigens in normal and tumor-bearing mice. Int J Cancer 1973; 12:568–576.

(*29*) Moore DH, Sarkar NH, Holben JA, Sheffield JB. Idiopathic mammary tumors in BALB/c mice. Int J Cancer 1979; 23:713–717.

(*30*) McGrath CM, Marineau EJ, Vogels BA. Changes in MuMTV DNA and RNA levels in BALB/c mammary epithelium during malignant transformation by exogenous MuMTV and by hormones. Virology 1978; 87:339–353.

(*31*) Dusing-Swartz S, Medina D, Butel JS, Socher SH. Mouse mammary tumor virus genome expression in chemical carcinogen-induced mammary tumors in low and high tumor incidence mouse strains. Proc Natl Acad Sci USA 1979; 76:5360–5364.

(*32*) Dudley JP, Butel JS, Socher SH, Rosen JM. Detection of mouse mammary tumor virus RNA in BALB/c tumor cell lines of nonviral etiologies. J Virol 1978; 28:743–752.

(*33*) Pauley RJ, Medina D, Socher S. Murine mammary tumor virus expression during mammary tumorigenesis in BALB/c mice. J Virol 1979; 29:483–493.

(*34*) ———. Hormonal regulation of murine mammary tumor virus RNA expression during mammary tumorigenesis in BALB/c mice. J Virol 1979; 32:557–566.

(*35*) DeOme KB, Blair PB, Faulkin LJ Jr. Some characteristics of the preneoplastic hyperplastic alveolar nodules of the C3H/Crgl mice. Acta Unio Int Contra Cancrum 1961; 17:973–982.

blank page

Antitumor Immunity Induced by Hybrid Murine Tumor Cells: Requirements for Optimal Immunization[1,2,3]

Craig S. McCune,[4] Robert W. O'Donnell,[4] Paul K. Horan,[5] Hollis S. Budd,[4] Janice L. Spennacchio,[4] Christy Chuang,[6] *and* Edgar C. Henshaw[4,7]

ABSTRACT—Hybrid tumor cells have been evaluated for their ability to induce specific antitumor immunity in inbred female C3H/He mice challenged with the syngeneic BA tumor. Hybrid cells were produced by fusion of BA cells with a BALB/c renal adenocarcinoma, which is hypoxanthine phosphoribosyl transferase-deficient and grows well in culture. *Corynebacterium parvum* was evaluated as an adjuvant for BA and hybrid cells. The BA tumor was shown to be poorly immunogenic, and four weekly injections of BA cells alone or *C. parvum* alone did not confer significant immunity. When BA cells and *C. parvum* were mixed, survival time was prolonged and most mice remained tumor-free. Hybrid cell lines derived from the BA tumor were produced in culture in unlimited quantities and were successfully used as immunogens. The addition of *C. parvum* to hybrids gave a significant incremental increase in survival when compared to the survival resulting from immunization by hybrids without adjuvant. When hybrids without adjuvant were used, several weekly injections were required for effective immunization. Irradiated and unirradiated hybrids were compared, and it was found that irradiation did not diminish hybrid immunogenicity. The potential problems and advantages of this concept of therapy are discussed.—JNCI 1982; 69:647–652.

Highly specific immune responses directed at tumor cells have been successfully produced in animals by injection of a suspension of viable irradiated syngeneic tumor cells mixed with an adjuvant (*1–4*). This approach evolved from an earlier observation by Zbar and Tanaka (*5*) that BCG injected into tumor nodules produced both local and regional destruction of tumor cells. The immune responses produced by tumor cell-adjuvant preparations have frequently rendered the animals tumor-free, and long-term immunologic memory has been demonstrated by a later rechallenge (*4*).

Successful clinical trials have been conducted on the basis of the methodology of these animal tumor models. Autologous tumor cells were used, and *Corynebacterium parvum* and BCG were employed as adjuvants. Regressions were noted in patients with malignant melanoma (*6*) and renal carcinoma (*7*). A major limitation to the tumor cell-adjuvant concept of treatment became apparent during the clinical trials: The quantity of autologous tumor cells obtained by tissue dissociation was often very small.

An alternative method to induce specific antitumor immunity is to substitute HTC for the syngeneic-autologous tumor cells. This possibility was entertained early in the development of cell fusion technology by Watkins and Chen (*8*) who successfully used hybrids to immunize mice against the Ehrlich ascites tumor. Several investigators have confirmed the potential of HTC as immunogens in a variety of animal tumor models (*9–15*). HTC have several potential advantages: First, they can be grown in culture to produce unlimited quantities. This attribute is acquired by selecting as one parent a permanent cell line which grows readily in culture. Second, there is empirical evidence that HTC express the TAA required for initiating antitumor immunity. Therefore, the essential antigens are also available in unlimited quantity. Third, the HTC surface membranes express foreign transplantation antigens. Because of the presentation of TAA in close proximity to foreign transplantation antigens, advantages have been postulated for the recognition process (*9*, *13*). Fourth, several clones of HTC can be produced. Each clone represents a separate fusion with an individual tumor cell. This permits a new approach to the problem of tumor heterogeneity. Small subpopulations of antigenically distinct tumor cells can be represented on individual hybrid clones and amplified in culture.

In the experiments that we are now reporting, several potential requirements for optimal immunization with HTC have been evaluated: single versus repeated immunizations, irradiated versus unirradiated hybrids, injection with or without an adjuvant, and treatment with a single hybrid cell line versus a pool of three lines.

MATERIALS AND METHODS

Animals.—Inbred C3H/He female mice (Flow Laboratories Inc., Rockville, Md.) 6–10 weeks old were used.

Tumor lines.—The murine mammary adenocarcinoma C3H BA (M.A. Bioproducts, Walkersville, Md.) was origi-

---

Abbreviations used: AHB=animal hybrid; BSA=bovine serum albumin; DMEM=Dulbecco's modified Eagle's minimum essential medium; FBS=fetal bovine serum; HAT=hypoxanthine, aminopterin, and thymidine; HPRT=hypoxanthine phosphoribosyl transferase; HTC=hybrid tumor cell(s); id=intradermally; LPF=long-pass filter(s); M199=medium 199; PBS=phosphate-buffered saline; PEG=polyethylene glycol 6000; PMT=photomultiplier tube(s); RAG=renal adenocarcinoma; TAA=tumor-associated antigens.

---

[1] Received October 28, 1981; accepted March 30, 1982.

[2] Supported by Public Health Service (PHS) grants CA-27625 and CA-11198 from the National Cancer Institute, by PHS grant RR-05403 from the Division of Research Resources, by PHS grant GM-23088 from the National Institute of General Medical Sciences, and by a grant from the Elsa U. Pardee Foundation.

[3] Animals were maintained under the guidelines of the University of Rochester Vivarium.

[4] University of Rochester Cancer Center, 601 Elmwood Ave., Rochester, N.Y. 14642.

[5] Department of Pathology, University of Rochester Medical Center, Rochester, N.Y. 14642.

[6] Division of Biostatistics, University of Rochester Medical Center.

[7] We thank Mrs. Helen Ochej and Dr. Irene Evans for their assistance at the Animal Tumor Research Facility, Dr. Thomas Shows for the RAG cell line, and the Burroughs Wellcome Co. for the *Corynebacterium parvum*.

nally a spontaneous tumor which has been passaged in syngeneic mice for several years. The RAG line was derived from a BALB/cf/Cd renal adenocarcinoma (*16*). A mutant subline which lacks the enzyme HPRT was obtained from Dr. Thomas Shows, Roswell Park Memorial Institute, Buffalo, N.Y. This cell line is maintained in culture in DMEM and 10% FBS and dies when exposed to HAT selective medium.

Enzymes.—Collagenase type I (Worthington Biochemical Corp., Freehold, N.J.), hyaluronidase type I (Sigma Chemical Co., St. Louis, Mo.), pronase B-grade (Calbiochem-Behring Corp., La Jolla, Calif.), and DNase type I bovine pancreas (Worthington Biochemical Corp.) were used for disaggregation of the tumor.

Chemicals and media.—PEG (J. T. Baker Chemical Co., Philadelphia, Pa.), HAT (Sigma Chemical Co.), RPMI-1640 medium, DMEM, and FBS (GIBCO, Grand Island, N.Y.) were used in the procedures described below.

C. parvum.—This is a Formalin-killed preparation; 7 mg *C. parvum*/ml was provided by the Burroughs Welcome Co., Research Triangle Park, N.C.

Antisera.—Mouse H-2 alloantisera were obtained from the Serum Bank, National Institute of Allergy and Infectious Disease, Bethesda, Md. The H-2 antigens of the RAG line (BALb/c) were demonstrated with an anti-D^d serum (catalog Y1-8-03-29-04) and the C3H BA antigens with an anti-K^k serum (catalog Y1-9-03-15-03).

C3H BA tumor cell suspensions.—For cell fusion, immunotherapy, or tumor challenge, we prepared cell suspensions from tumors transplanted as tissue fragments 14–17 days previously. After excision the tissue was minced by scalpel blades and enzymatically disaggregated in three separate incubations at 37°C while being shaken in a water bath. The tumor mince was incubated in 10 ml of Earle's balanced salt solution (pH 7.8) for 15 minutes. The supernatant was discarded, and 10 ml of M199 containing collagenase (250 μg/ml), hyaluronidase (0.12%), and salt-poor BSA (4% made from Sigma Chemical Co. fraction V BSA by dialysis with distilled water) was added and incubated for 45 minutes. The supernatant was again discarded and 10 ml of a 1% pronase solution (in M199) was added for 45 minutes. After this final incubation, 1 ml of 0.04% DNase was added, followed immediately by the addition of 30 ml of M199. The supernatant cells were retained, filtered through glass wool, and washed. Testing of this fraction by trypan blue exclusion has consistently shown a cell viability of 85% or greater.

Cell fusion.—To develop the HTC lines, we fused BA cells with RAG cells by using 35% PEG as the "fusogen." The BA cells were freshly dissociated and the RAG cells were harvested with 0.125% trypsin and 0.05% EDTA. Both cell types were washed in serum-free RPMI-1640 medium for removal of enzymes and serum. When 5×10^6 of each cell type was placed in round-bottom tubes, the cells were centrifuged at 250×*g* for 5 minutes at room temperature. The supernatants were removed, and the cells were gently resuspended in 0.5 ml of PEG for 8 minutes. Then 5 ml of serum-free RPMI-1640 medium was added, and the tubes were centrifuged at 250×*g* for 5 minutes. The supernatant was removed, and the cells were resuspended in RPMI-1640 medium containing FBS and were plated in small tissu culture flasks (25 cm^2) at a final concentration of 1×10 cells/flask. Control flasks of each parent cell were als plated. After 24 hours, the medium was replaced with HAT-RPMI-1640-selective medium (1×10^{-4} *M* hypoxanthine 4×10^{-7} *M* aminopterin, and 1.6×10^{-5} *M* thymidine).

Flow cytometry of hybrid cells.—Flow cytometric analysis wa done with a Coulter EPICS-V flow cytometer and sorte (Coulter Electronics Inc., Hialeah, Fla.). The excitatio source was a 164-05 Spectra-Physics argon ion laser (Spectra-Physics Inc., Mountain View, Calif.) which was tune to 488 nm with an output of 500 mW. Fluorescein—ethidium bromide fluorescence was collected through the following filters for two-color analysis: The barrier filter was a 510-nm interference filter, and the red fluorescence wa separated from the green fluorencence with a 590-nm dichroic mirror. Glass LPF were placed in front of the re PMT (590 nm LPF) and the green PMT (515 nm LPF) to ensure that any scattered light escaping the interferenc filter through a manufacturing defect was not allowed to enter the PMT. We used the multiparameter data acquisition and display system of the EPICS-V to collect and display two-color fluorescence signals and light scatter signals. More detailed descriptions of the flow cytometric methodology are described elsewhere (*17, 18*).

Flow cytometric analysis of H-2.—Cells to be used for immunofluorescence analysis were dispersed with trypsin and EDTA and, after dispersion was complete, were placed in PBS containing 0.1% sodium azide (PBS azide). Then, 2×10^6 cells of each type to be analyzed were incubated in the appropriate dilution of mouse anti-H-2 K^k or anti-H-2 D^d. At the end of this 4°C, 30-minute incubation, cells were diluted in PBS azide and washed twice in the cold. After being washed, the cells were placed in the appropriate dilution of a fluorescein-conjugated goat $F(ab')_2$ IgG anti-mouse IgG (Cappel Laboratories, Cochranville, Pa.). Cells were incubated in the conjugate for 30 minutes at 4°C. After this incubation, cells were washed twice in PBS azide while on ice and were then made ready for flow cytometric analysis.

Indirect immunofluorescence analysis on flow cytometers requires that dead cells be distinguished from live cells. Two drops from a Pasteur pipette of a solution of 20 μg ethidium bromide/ml of PBS azide were placed into each tube containing 2×10^6 fluorescein-stained cells in 1 ml of PBS azide. With this procedure nuclei of all dead cells stained with ethidium bromide, whereas live cells did not permit the penetration of ethidium bromide (*19*). Immunofluorescence profiles of each sample were obtained when identical high-voltage and gain settings were used. Gate windows were established such that green fluorescence signals were acquired for only those cells that did not fluoresce with ethidium bromide and had a light scatter intensity equal to that of cells and not of debris.

Immunotherapy.—Immunizations were given weekly. Those cell suspensions being irradiated were exposed to a cesium source and received 10,000 rad. When *C. parvum* was included in the immunizing preparations, it was added at 35 μg/10^7 tumor cells. The desired number of tumor cells was made up to 0.1 ml in M199 and was administered id to the abdominal area.

Tumor challenge.—C3H BA cell suspensions that had not been irradiated were injected id over the chest wall.

Statistics.—The effectiveness of each immunogen was evaluated by the determination of the survival times of mice that had received a tumor challenge after being immunized. The differences in immunogenicity were most apparent in the later stages of an experiment when fewer mice remained alive. Therefore, we used the generalized Savage (Mantel-Cox) method to compare the survival curves.

RESULTS

Hybrid Cell Characteristics

At 14 days after cell fusion, several colonies were observed in each HAT-containing flask. Because BA cells do not grow in culture and HPRT-deficient RAG cells died in control flasks grown in selective medium, these colonies were presumed to be hybrids. Each flask which attained confluence was designated as a noncloned AHB line (lines 1–7) and passaged. Three lines, AHB 1, 4, and 5, were selected for immunizing experiments on the basis of the practical consideration that they grew rapidly in culture. To confirm their hybrid origin, we analyzed AHB 1, 4, and 5 cells for expression of parental H-2 antigens by flow cytometry. Text-figure 1 illustrates that BA cells (derived from mice with the $H\text{-}2^K$ haplotype) have an immunofluorescence profile positive for anti-K^k serum but not for anti-D^d serum and that RAG cells (derived from mice with the $H\text{-}2^D$, haplotype) react positively with anti-D^d serum but not with anti-K^k serum. Each of the three hybrid cell lines analyzed showed immunofluorescence profiles positive for both anti-K^k and anti-D^d sera. Table 1 further demonstrates the hybrid origin of the cell lines by quantifying in each population the percentage of cells having a fluorescence intensity above an arbitrary level.

Syngeneic Tumor Cells as Immunogens

Syngeneic BA tumor cells and *C. parvum* were injected separately or together for 4 weeks (text-fig. 2). The survival time of those mice receiving *C. parvum* was on the average shorter than that of the untreated control group ($P<0.01$). Injections of BA tumor cells only, for 4 weeks, did not significantly affect the survival time when compared to that of the control group ($P>0.24$), although 2 of 15 mice remained tumor-free. When *C. parvum* was added to the BA cells, a single injection was ineffective, but four weekly injections resulted in prolonged survival ($P<0.001$) and 10 of 15 mice remained tumor-free.

HTC as Immunogens

AHB tumor lines 1, 4, and 5 were pooled and given as weekly injections. Each injection contained 3.3×10^6 viable cells of each hybrid (total, 9.9×10^6) and 35 μg *C. parvum*/10^7 tumor cells. All hybrid cells were preserved in liquid nitrogen until used and were given unirradiated unless otherwise indicated. Their viability after being frozen and thawed was consistently greater than 80%. The injected hybrid cells

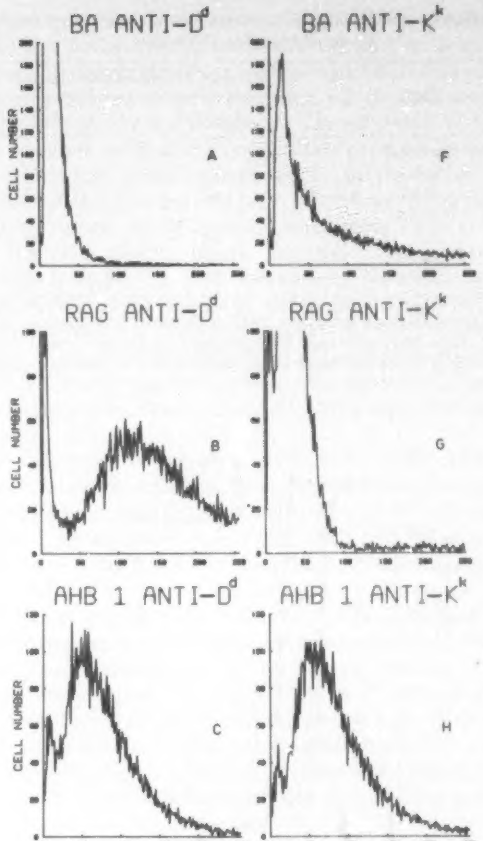

TEXT-FIGURE 1.—Fluorescence intensity of parent (BA, RAG) and hybrid (AHB 1, 4, and 5) cells as determined by flow cytometry. The anti-D^d antiserum identifies the H-2^d antigens of RAG cells. The anti-K^k antiserum identifies H-2^k antigens of BA cells. BA cells were freshly dissociated from tumor, whereas RAG and all hybrids were harvested from culture.

TABLE 1.—*H-2 antigens of parent and hybrid cells analyzed by fluorescent antibodies*

Cells	Percent of cells above channel 60[a]	
	Anti-D^d	Anti-K^k
Parental		
BA	4	47
RAG	82	15
Hybrids		
AHB 1	58	63
AHB 4	65	71
AHB 5	77	68

[a] Channel 60 is an arbitrary level of fluorescence intensity selected so that those cells with only background fluorescence could be distinguished from those that have absorbed anti-H-2 fluorescent antibodies.

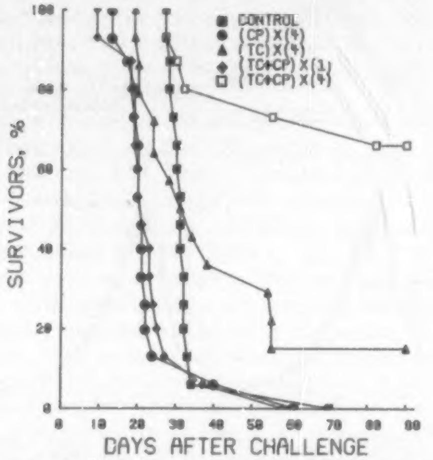

TEXT-FIGURE 2.—Comparison of survival of groups of mice receiving no treatment (CONTROL), 35 μg *C. parvum* id weekly for 4 wk [(CP)×(4)], 10^7 irradiated tumor cells id weekly for 4 wk [(TC)×(4)], and 10^7 irradiated tumor cells mixed with 35 μg *C. parvum* id weekly for 1 wk [(TC+CP)×(1)] and for 4 wk [(TC+CP)×(4)]. The weekly injections ended 7 days before the challenge with 2×10^6 live BA cells. Groups contained 14–15 mice.

formed small nodules which disappeared by 7 days. A challenge of 1.2×10^6 viable BA cells obtained from freshly dissociated tumor was given id over the chest wall 7 days after the last immunizing injection. All mice were challenged on the same day in a particular experiment.

An experiment in which the hybrid cells were given weekly for 1, 3, and 5 weeks is shown in text-figure 3. All control-group unimmunized animals died by day 45. A single injection of pooled hybrid cells resulted in 3 of 12 animals remaining tumor-free, but the difference in the survival time was not significant($P>0.16$). Three weekly injections prolonged the survival time ($P<0.009$), but only 2 of 11 remained tumor-free. Five weekly injections improved overall survival time ($P<0.007$), and 6 of 11 mice were tumor-free (all of these three comparisons were against the survival time in the control group). The difference between one and five injections did not attain significance at the 0.05 level.

Adjuvant and Radiation Effects

The role of *C. parvum* and a comparison of viable vers
irradiated hybrids were evaluated in the experiment show
in text-figure 4. All test groups of mice received weekl
injections for 5 weeks. When 35 μg of *C. parvum* was give
alone, no significant change in the survival time from tha
of the control group was observed. Pooled hybrid cells i
the absence of *C. parvum* were immunogenic compared wit
the control group ($P<0.005$), and 7 of 14 animals remaine
tumor-free; however, when *C. parvum* was added to th
hybrid cells, the improvement in the survival time was eve
greater ($P<0.02$ compared to the survival obtained when C
parvum was not added to the hybrids) and 14 of 15 mic
remained tumor-free. When the hybrid cells were irradiate
and given with *C. parvum*, the decrease in the survival tim

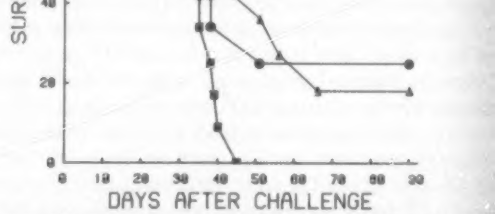

TEXT-FIGURE 3.—Comparison of survival of groups of mice receiving pooled unirradiated hybrids with 35 μg *C. parvum*/10^7 tumor cells. Groups wer immunized for 1, 3, or 5 wk (WEEKLY×1, 3, and 5); challenge wa with 1.2×10^6 live BA cells 7 days after the last immunization. Group contained 11–12 mice.

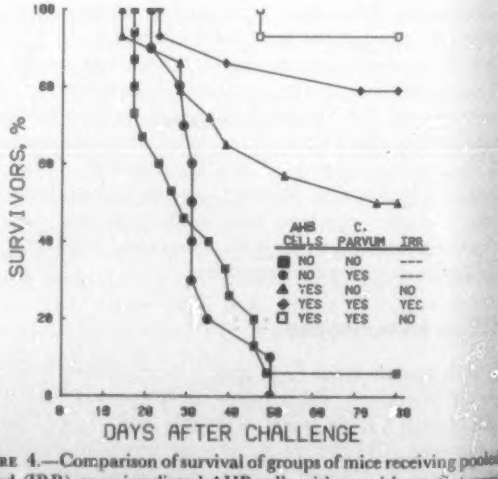

TEXT-FIGURE 4.—Comparison of survival of groups of mice receiving poole irradiated (IRR) or unirradiated AHB cells with or without C. Immunizations were given for 5 wk; challenge was with 1.2×10^6 live B cells. Groups contained 10–15 mice.

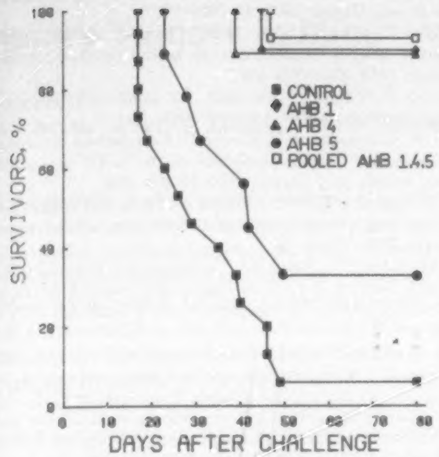

TEXT-FIGURE 5.—Comparison of survival of groups of mice receiving five weekly immunizations with single or pooled unirradiated hybrids (AHB 1, 4, and 5) with *C. parvum*. Challenge was with 1.2×10⁶ live BA cells. Groups contained 10–15 mice.

was not significant when compared to that when unirradiated hybrids were given with *C. parvum* ($P>0.28$).

Single Hybrid Lines Versus Pooled Hybrid Lines

The immunogenicity of individual hybrid lines was compared with the pool of three hybrids in the experiment shown in text-figure 5. This experiment was performed concurrently with the experiment presented in text-figure 3, and the control and pooled groups were common to both experiments. The immunizing cells for all groups were unirradiated, had *C. parvum* added, and were given as five weekly injections before the challenge. AHB lines 1 and 4 both produced an improvement in the survival time ($P<0.0001$), which is similar to that of the pool of three hybrids. In contrast AHB line 5 was weakly immunogenic, and the survival curve for this group did not differ significantly from that of the control group ($P>0.06$).

Multiple comparisons have been made with the data of each experiment. They might inflate the type I error in testing the equality of the survival curves beyond the 0.05 level. However, most of the *P*-values that we cited to establish differences are fairly low, which tends to justify our claims.

DISCUSSION

We have demonstrated in this study that the BA tumor cell line which will not grow in culture can be fused readily with the RAG cell line which does grow in culture to produce hybrid cell lines that can grow apparently indefinitely in culture and will produce large numbers of cells for immunization. The results also show that some cell lines so generated can serve very effectively as immunogens in protecting against the targeted parent tumor (BA). Thus in the animal model we can reach several of the goals that we hope to attain in human patients. In additon, we have examined several methodologic questions relevant to optimal immunization.

In the experiment shown in text-figure 2, we determined some of the background parameters relevant to antitumor immunity in this model. Four weekly injections of irradiated tumor cells did not protect the mice, which indicates that this tumor is poorly immunogenic. The adjuvant *C. parvum* which we used in these studies did not produce a survival advantage when given independently in the small doses desirable for an adjuvant role (*1, 4, 20*). However, adjuvant-facilitated tumor cell recognition does occur in this model when BA cells plus *C. parvum* are given for four weekly injections (text-fig. 2). This tumor was found to require several weekly immunizations, although a single injection has been adequate in other models (*4, 20*). When the question of single versus serial injections was looked at with hybrids as immunogens (text-fig. 3), significant survival effects were again seen only with three and five weekly injections.

The beneficial effect of an adjuvant when added to syngeneic tumors cells has been demonstrated in animal models of active specific immunotherapy (*1–4*). We wished to know if an adjuvant would also assist hybrids as immunogens. The hybrid cells in these experiments express histocompatibility antigens ($H\text{-}2^d$) foreign to the mouse strain (C3H/He) of origin of the BA tumor. The presumed TAA of the BA tumor would be expressed in association with the foreign $H\text{-}2^d$ antigens on the surface membrane of these hybrids. We surmised that the foreign $H\text{-}2^d$ might fulfill an adjuvant role and the addition of *C. parvum* to hybrids might be noncontributory. Indeed, we did find that HTC without adjuvant were effective immunogens; however, the addition of *C. parvum* improved survival significantly beyond that attained with hybrids alone (text-fig. 4).

Hybrid cells can be injected for immunizing purposes when fully viable as contrasted with killed or irradiated cells, which is the requirement for syngeneic cells. Parkman (*9*) and Kim et al. (*12*) found that injected viable hybrids never grow lethally in the syngeneic hosts of the target tumor but may be observed to grow briefly before an immune response develops. Our hypothesis was that immunization with viable hybrid cells might be superior to immunization with irradiated hybrids because the viable hybrid cells remain alive and proliferate in the host until their immunologic rejection. However, as seen in text-figure 4, irradiation did not significantly alter the immunogenic function of these hybrids. This retention of immunogenic function is supported in part by the observation that irradiated tumor cells do persist for several days at the injection site (*21*) and that they may function as immunogens for a time similar to the interval noted for unirradiated hybrids.

Therapeutic effectiveness has been noted to vary among hybrid lines derived from the same parent cells (*9, 12*). The hybrid lines AHB 1 and 4 were individually immunogenic at a level equal to that of a pool of all three lines, whereas AHB 5 was strikingly ineffective (text-fig. 5). A troublesome problem is that hybrid cells may lose critical surface antigens required for antitumor immunization. This may occur through elimination of chromosomes or through extinction of the expression of chromosomes although the chromosomes themselves are retained. Hybrid lines AHB 1 and 4 have been maintained in culture for more than 1 year and still retain the relevant tumor antigens. Whether AHB 5 lost immunogenicity with time or was never very protective cannot be determined from our experiments, inasmuch as AHB 5 was not used separately until after many passages in culture. However, these results demonstrate the retention of relevant antigens in two of three lines.

Hybrids may also be expected to vary in immunogenicity as a consequence of the postulated antigenic heterogeneity within the tumor parent (*22-24*). A hybrid line might antigenically represent a very uncommon subpopulation and be totally ineffective when used as a single immunogen, but hybrid lines might also be the means for totally representing an entire tumor if several hybrid lines are pooled. Hence pooled HTC provide a means of representing all populations within a tumor in adequate antigenic doses for the initiation of multideterminant antitumor immunity.

We have not directly compared the immunogenicity of individual hybrid lines versus parental BA cells in these experiments. Such comparisons are under way with a larger series of hybrid lines in experiments in which our particular interest is the evaluation of those parameters which may be predictive of greater immunogenicity.

REFERENCES

(*1*) Bartlett GL, Zbar B. Tumor-specific vaccine containing *Mycobacterium bovis* and tumor cells: Safety and efficacy. J Natl Cancer Inst 1972; 48:1709-1726.

(*2*) Hanna MG Jr, Brandhorst JS, Peters LC. Active specific immunotherapy of residual micrometastasis: An evaluation of sources, doses and ratios of BCG with tumor cells. Cancer Immunol Immunother 1979; 7:165-173.

(*3*) Minden P, McClatchy JK, Brunda MJ. Suppression and immunotherapy of the guinea pig line-10 hepatocarcinoma mediated by nonviable *Staphylococcus aureus*. JNCI 1978; 61:535-538.

(*4*) Scott MT. Potentiation of the tumor-specific immune response by *Corynebacterium parvum*. J Natl Cancer Inst 1975; 55:65-72.

(*5*) Zbar B, Tanaka T. Immunotherapy of cancer: Regression of tumors after intralesional injection of living *Mycobacterium bovis*. Science 1971; 172:271-273.

(*6*) Laucius JF, Bodurtha AJ, Mastrangelo MJ, Bellet RE. A phase II study of autologous irradiated tumor cells plus BCG in patients with metastatic malignant melanoma. Cancer 1977; 40:2091-2093.

(*7*) McCune CS, Schapira DV, Henshaw EC. Specific immunotherapy of advanced renal carcinoma: Evidence for the polyclonality of metastases. Cancer 1981; 47:1984-1987.

(*8*) Watkins JF, Chen L. Immunization of mice against Ehrlich ascites tumour using a hamster/Ehrlich ascites tumour hybrid cell line. Nature 1969; 223:1018-1022.

(*9*) Parkman R. Tumor hybrid cells: An immunotherapeutic agent. J Natl Cancer Inst 1974; 52:1541-1545.

(*10*) Favre R, Carcassonne Y, Meyer G. Comparison between different techniques of immunoprotection in the A-SW mouse/SEWA tumour system. Br J Cancer 1974; 29:300-304.

(*11*) Jami J, Rubio N, Ritz E. Cellular and humoral response to immunization with semi-allogeneic hybrid cells in the mouse. Eur J Cancer 1976; 12:13-18.

(*12*) Kim BS, Liang W, Cohen EP. Tumor-specific immunity induced by somatic hybrids. I. Lack of relationship between immunogenicity and tumorigenicity of selected hybrids. J Immunol 1979; 123:733-738.

(*13*) Klein G, Klein E. Induction of tumor cell rejection in the low responsive YAC-lymphoma strain A host combination by immunization with somatic cell hybrids. Eur J Cancer 1979; 15:551-557.

(*14*) Dei T, Tachibana T. Induced resistance in normal mice and growth enhancement in tumor-bearing mice by inoculation with syngeneic hybrid cells. JNCI 1980; 65:739-749.

(*15*) Baumal R, Marks A. Protective effect of an interspecies hybridoma on the tumorigenicity of mouse myeloma cells. Cancer Res 1981; 41:2598-2604.

(*16*) Felluga B, Claude A, Mrena E. Electron microscope observations on virus particles associated with a transplantable renal adenocarcinoma in BALB/cf/Cd mice. J Natl Cancer Inst 1969; 43:319-333.

(*17*) Horan PK, Wheeless LL. Quantitative single cell analysis and sorting. Science 1977; 198:149-157.

(*18*) Loken MR, Stout RD, Herzenberg LA. Lymphoid cell analysis and sorting. In: Melamed M, Mullaney P, Mendelsohn M, eds. Flow cytometry and sorting. New York: Wiley, 1979:505-528.

(*19*) Horan PK, Kappler JW. Automated fluorescent analysis for cytotoxicity assays. J Immunol Methods 1977; 18:309-316.

(*20*) Bomford R. Active specific immunotherapy of mouse methylcholanthrene induced tumours with *Corynebacterium parvum* and irradiated tumour cells. Br J Cancer 1975; 32:551-557.

(*21*) Hanna MG Jr, Bucanna CD. Active specific immunotherapy of residual micrometastasis: The acute and chronic inflammatory response in induction of tumor immunity by BCG-tumor cell immunization. J Reticuloendothel Soc 1979; 26:439-452.

(*22*) Olsson L, Ebbesen P. Natural polyclonality of spontaneous AKR leukemia and its consequences for so-called specific immunotherapy. JNCI 1979; 62:623-627.

(*23*) Sugarbaker EV, Cohen AM. Altered antigenicity in spontaneous pulmonary metastases from an antigenic murine sarcoma. Surgery 1972; 72:155-161.

(*24*) Fidler IJ, Kripke ML. Metastasis results from pre-existing variant cells within a malignant tumor. Science 1977; 197:893-895.

Inhibitory Effect of Interferon on the Growth of Spontaneous Mammary Tumors in Mice[1,2,3,4]

Erik De Clercq,[5] Zhen-Xi Zhang,[5,6] Kris Huygen,[7] *and* Roger Leyten[8,9]

ABSTRACT—Partially purified mouse interferon type I (Mu IFN-β), crude mouse interferon type II (Mu IFN-γ) serum, and the interferon inducer polyinosinic acid-polycytidylic acid (poly I:C) were evaluated for their effects on the growth of spontaneously occurring mammary carcinomas in BALB/c mice. As soon as their tumors had reached a palpable size (diameter: 3–5 mm), the mice received three ip injections of Mu IFN-β, Mu IFN-γ, or poly I:C per week for 6 weeks. A significant (fourfold to fivefold) reduction in tumor size was achieved with Mu IFN-β (at 10^6 U/mouse), Mu IFN-γ (at 10^3 U/mouse), and poly I:C (at 1 mg/mouse). A similar reduction in tumor size was noted when the mice were treated with cyclophosphamide (2.5 mg/mouse, three ip injections per wk for 6 wk). Treatment with Mu IFN-β combined with Mu IFN-γ resulted in a greater tumor growth-inhibitory effect than treatment with either Mu IFN-β or Mu IFN-γ alone. In addition to inhibiting the growth of primary tumors, interferon also reduced the incidence of lung metastases. However, complete tumor regression was not observed in any mouse while under interferon therapy.—JNCI 1982; 69:653–657.

IFN therapy has been attempted in a number of patients with osteosarcoma, myeloma, lymphoma, melanoma, breast cancer, lung cancer, or other neoplasms (*1*). Partial or complete remissions have been observed in only a small percentage of the patients, ranging from 0% of the patients with lung cancer or diffuse histiocytic lymphoma to approximately 30% of the patients with myeloma or breast cancer. Of a series of 17 patients with advanced breast cancer who were treated with human IFN-α, 6 patients achieved a partial remission, 1 patient showed a less than partial remission, and 10 patients did not respond; none of the patients acquired a complete remission (*2*).

Although IFN has been administered to a relatively large number of patients with breast cancer, there is little, if any, evidence that IFN may cause regression of spontaneous or carcinogen-induced mammary tumors in animal models. The only study pertaining to the effect of IFN treatment on mammary tumors in animals (mice) is that of Came and Moore (*3, 4*). These authors found that IFN treatment initiated early in life (at the age of 6 wk) could retard the appearance of spontaneous mammary carcinomas in RIII mice. However, they noted no such delay in tumor appearance if IFN treatment was started at 22 weeks of age, and they did not attempt to assess the potential antitumor effects of IFN in mice that had already developed mammary tumors.

We have now evaluated the effects of IFN and the IFN inducer poly I:C in mice that had developed a palpable mammary tumor at the time treatment was started. In addition to our evaluation of the effects of Mu IFN-β, we have determined the effects of Mu IFN-γ, since IFN-γ has, per unit of antivirus activity, a significantly greater anticellular activity than IFN-β or IFN-α (*5, 6*). Furthermore, Mu IFN-γ preparations have been shown to inhibit the growth of transplanted osteogenic sarcomas in mice at a dose a hundredfold less than that required for Mu IFN-β (*7*). In view of the apparent synergism in the antivirus activities of Mu IFN-β and Mu IFN-γ (*8*), which was recently extended to the antitumor effects of Mu IFN-β and Mu IFN-γ (*9*), we have also investigated the combined effects of Mu IFN-β and Mu IFN-γ on the growth of mammary tumors. This investigation was further prompted by our recent observations (*10*) that treatment with Mu IFN-β combined with Mu IFN-γ significantly increased the survival of mice inoculated with murine leukemia L1210 cells.

MATERIALS AND METHODS

Animals.—Female BALB/c mice were used throughout. Approximately 20% of these mice developed mammary carcinomas. The mice were bred in the Laboratory Animal Center (Proefdierencentrum) of the University of Leuven and were followed regularly for the development of mammary tumors. Treatment was started as soon as the tumor was palpable (at a diameter of 3–5 mm), which occurred in the mice at an average age of 189 days (range: 110–318 days).

Compounds.—Poly I:C was constituted from the individual homopolymers polyinosinic acid and polycytidylic acid, both purchased from P-L Biochemicals, Inc., Milwaukee, Wis. The sedimentation coefficients corrected to water at 20°C of polyinosinic acid and polycytidylic acid were 9.4 *s* and 10.0 *s*, respectively. Poly I:C was prepared at 1 mg/ml in Dulbecco's phosphate-buffered saline. Mu IFN-β was induced with Newcastle disease virus in mouse L-929 fibro-

---

ABBREVIATIONS USED: ADCC=antibody-dependent cell-mediated cytotoxicity; IFN=interferon; IFN-α=leukocyte IFN; IFN-β=fibroblast IFN; IFN-γ=immune IFN; Mu IFN-β=mouse IFN type I; Mu IFN-γ=mouse IFN type II; NK=natural killer; poly I:C=polyinosinic-polycytidylic acid; PPD=purified protein derivative.

---

[1] Received November 10, 1981; accepted April 16, 1982.

[2] Supported by grant No. 30048.75 from the Belgian Fonds voor Geneeskundig Wetenscheppelijk Onderzoek and grant No. 76/81-IV from the Belgian Geconcerteerde Onderzoeksacties.

[3] Presented in part at the Fifth International Congress of Virology, Strasbourg, France, held August 1–7, 1981.

[4] Animals were maintained under the guidelines set forth by our local Laboratory Animal Center (R. Leyten, Proefdierencentrum).

[5] Rega Institute for Medical Research, Katholieke Universiteit Leuven, Minderbroedersstraat 10, B-3000 Leuven, Belgium.

[6] *Present address*: Department of Virology, Institute of Antibiotics, Tientan, Beijing, People's Republic of China.

[7] Pasteur Institute, Stoomsleperstraat 28, B-1040 Brussels, Belgium.

[8] Proefdierencentrum, Katholieke Universiteit Leuven, de Croylaan 34, B-3030 Heverlee, Belgium.

[9] We gratefully acknowledge the excellent technical assistance of H. Baplu.

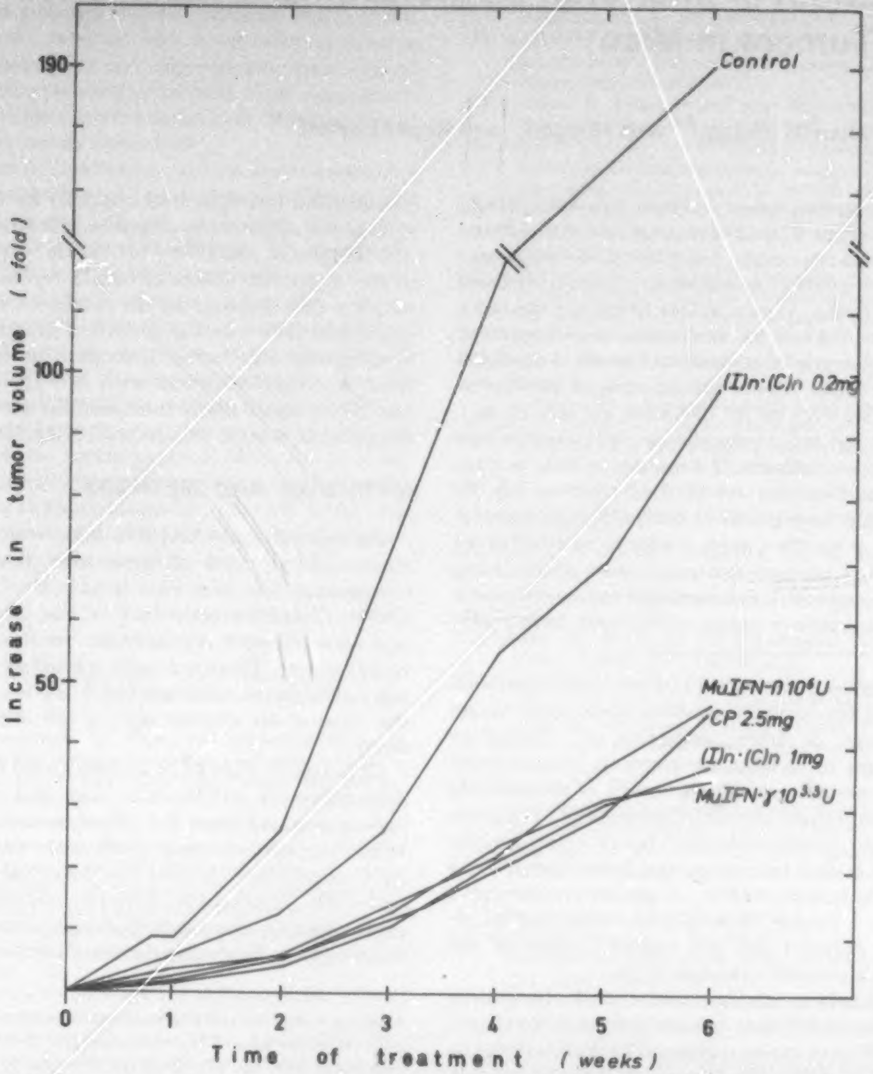

TEXT-FIGURE 1.—Inhibitory effects of poly I:C [(I)n·(C)n], Mu IFN-β, Mu IFN-γ, and cyclophosphamide (CP) on the growth of mammary tumors in BALB/c mice. Number of mice per group: 53 in the control (untreated) group, 21 in the group treated with 0.2 mg poly I:C/mouse, 21 in the group treated with 10^6 U Mu IFN-β, 22 in the group treated with 2.5 mg cyclophosphamide/mouse, 20 in the group treated with 1 mg poly I:C/mouse, and 32 in the group treated with $10^{3.3}$ U Mu IFN-γ/mouse.

blasts, as described previously (*11*). It was purified by $(NH_4)_2SO_4$ precipitation to a specific activity of 10^6 U protein/mg. Mu IFN-γ was obtained from the sera of Swiss mice that had been sensitized with BCG (immuno-BCG GL2, grown as a surface pellicle) (1 mg/mouse, iv), boosted 2 weeks later with PPD (1 mg/mouse, iv), and bled 5 hours after the PPD injection. The specific activity of the Mu IFN-γ preparation was 60 U/mg protein. BCG serum was derived from mice that had been given iv injections of BCG 2 weeks before they were bled and their sera sampled (IFN titer: <10 U/ml). PPD serum was derived from mice that had received iv injections of PPD 5 hours before they were bled and their sera sampled (IFN titer: <10 U/ml). Cyclophosphamide (Endoxan) was purchased from Cilag-Chemie, Herentals, Belgium.

Treatment.—Mice bearing palpable mammary tumors were allocated at random to the different treatment groups. Treatment consisted of three ip injections per week for 6 weeks. Poly I:C was administered at either 0.2 mg/mouse (8 mg/kg) or 1 mg/mouse (40 mg/kg). Mu IFN-β was given at 10^4, 10^5, or 10^6 U/mouse, Mu IFN-γ at 10^2, 10^3, or $10^{3.3}$ U/mouse, and cyclophosphamide at 2.5 mg/mouse (100 mg/kg). BCG serum and PPD serum were administered at 0.2 ml/mouse. The number of mice per group is indicated in the legends to the text-figures.

Tumor volume measurements.—The length and width of the mammary tumors were determined weekly with calipers, and tumor volume was calculated according to the formula

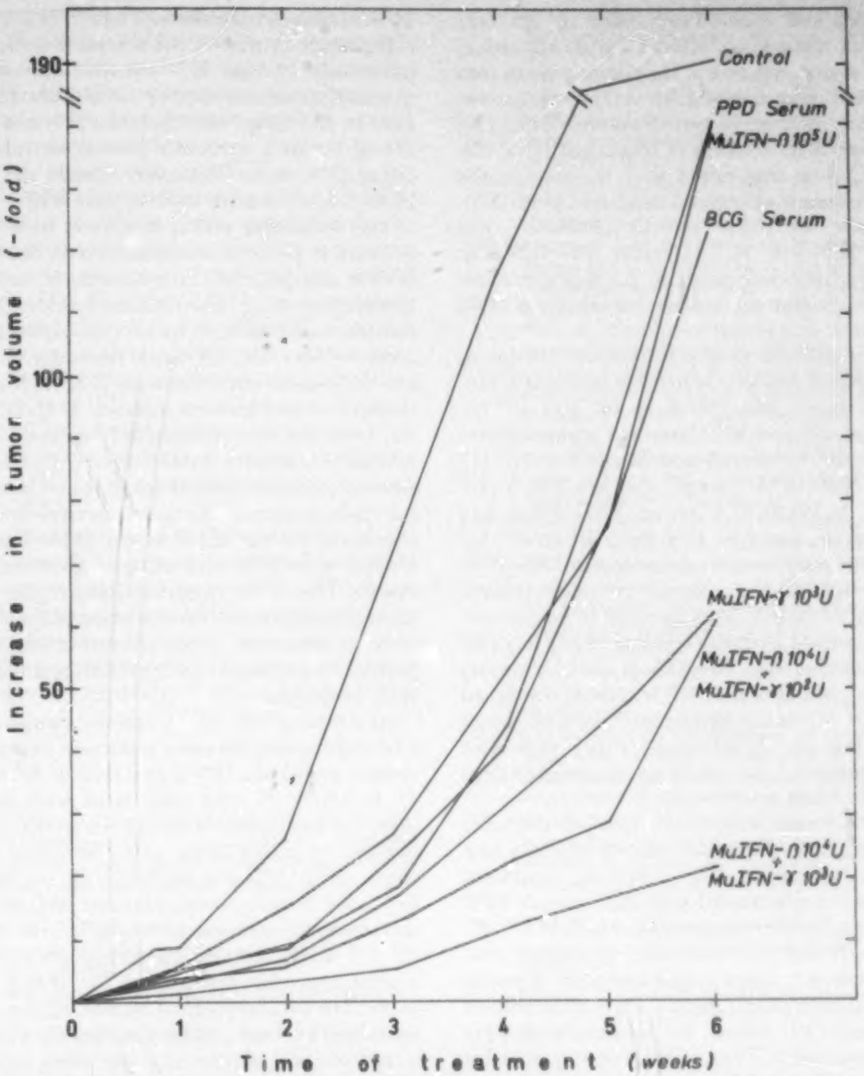

TEXT-FIGURE 2.—Inhibitory effects of BCG serum, PPD serum, Mu IFN-β, Mu IFN-γ, and combinations of Mu IFN-β and Mu IFN-γ on the growth of mammary tumors in BALB/c mice. Number of mice per group: 53 in the control (untreated) group, 20 in the group treated with PPD serum, 18 in the group treated with 10^5 U Mu IFN-β/mouse, 22 in the group treated with BCG serum, 16 in the group treated with 10^3 U Mu IFN-γ/mouse, 20 in the group treated with the combination of Mu IFN-β (10^4 U/mouse) and Mu IFN-γ (10^2 U/mouse), and 20 in the group treated with the combination of Mu IFN-β (10^4 U/mouse) and Mu IFN-γ (10^3 U/mouse).

$V = 4/3\ \pi L/2(W/2)^2$. The number of tumors arising in individual mice varied from 1 to 7; the frequency of mice developing 1, 2, 3, 4, 5, 6, or 7 tumors was 30, 25.5, 24.5, 9, 6.5, 3.5, and 1%, respectively. For those mice that developed more than 1 tumor, tumor volumes were measured separately. These tumor volumes were combined in the calculation of the total tumor volume per mouse, and the tumor volumes indicated in text-figures 1 and 2 refer to the average tumor volumes per mouse.

Statistical analysis.—Differences in tumor volume per mouse between the control (untreated) and treated groups at the end of the 6-week treatment period were assessed for statistical significance by Student's *t*-test.

Histologic examination.—Tumor specimens removed from control mice were identified as mammary carcinoma upon microscopic examination (courtesy of Dr. H. Sobis, Rega Institute for Medical Research). For those mice that were killed at the end of the 6-week treatment period, the lungs were examined macroscopically and microscopically for metastases.

RESULTS

In the first experiment we evaluated the tumor-inhibiting properties of the following treatment regimens: poly I:C at 0.2 and 1 mg/mouse, Mu IFN-β at 10^6 U/mouse, Mu IFN-

pages tightly bound

best copy available

γ at $10^{3.3}$ U/mouse, and cyclophosphamide at 2.5 mg/mouse. All treatment regimens effected a significant reduction in tumor growth as compared to the tumor growth seen in control (untreated) mice (text-fig. 1). At 0.2 mg/mouse, poly I:C reduced the increase in tumor volume from 190-fold to a hundredfold after 6 weeks of treatment ($P<0.05$). When the poly I:C dose was raised to 1 mg/mouse, the increase in tumor volume was reduced to 35-fold ($P<0.001$). A similar reduction in tumor growth ($P<0.001$) was achieved with Mu IFN-γ at $10^{3.3}$ U/mouse. Mu IFN-β at 10^6 U/mouse and cyclophosphamide at 2.5 mg/mouse reduced the increase in tumor volume to about 47-fold ($P<0.005$) (text-fig. 1).

In the second experiment various additional treatment regimens were compared for their antitumor potentials, viz., BCG serum, PPD serum, Mu IFN-β at 10^4 and 10^5 U/mouse, Mu IFN-γ at 10^2 and 10^3 U/mouse, and combinations of Mu IFN-β (10^4 U/mouse) and Mu IFN-γ (10^2 U/mouse) and Mu IFN-β (10^4 U/mouse) and Mu IFN-γ (10^3 U/mouse) (text-fig. 2). While BCG serum, PPD serum, Mu IFN-γ at 10^2 U/mouse, and Mu IFN-β at 10^4 or 10^5 U/mouse did not significantly inhibit tumor growth, Mu IFN-γ at 10^3 U/mouse reduced the increase in tumor volume from 190- to 63-fold ($P<0.05$). This increase in tumor volume was further decreased to only 22-fold if Mu IFN-γ (10^3 U/mouse) was combined with Mu IFN-β (10^4 U/mouse) ($P<0.005$). Similarly, Mu IFN-β at 10^4 U/mouse combined with Mu IFN-γ at 10^2 U/mouse significantly reduced tumor growth ($P<0.05$) (text-fig. 2), although either IFN dose regimen used separately did not confer an appreciable diminution of tumor size (data not shown).

At the end of the 6-week observation period, the mice were killed and their lungs examined macroscopically and microscopically for metastases. The following treatment groups were examined: mice treated with BCG serum, PPD serum, cyclophosphamide (2.5 mg/mouse), Mu IFN-γ ($10^{3.3}$ U/mouse), and Mu IFN-β (10^4 U/mouse) combined with Mu IFN-γ (10^2 U/mouse). Lung metastases were detected in 84% of the control (untreated) mice. Of the mice treated with BCG serum and PPD serum, the frequency showing lung metastases amounted to 77 and 75%, respectively; this is not significantly different from the frequency of mice showing lung metastases in the control group. However, the other treatment regimens brought about a significant reduction in the percentage of mice developing lung metastases; i.e., cyclophosphamide (2.5 mg/mouse) resulted in a 52% reduction ($P<0.05$), Mu IFN-γ ($10^{3.3}$ U/mouse) resulted in an 18% reduction ($P<0.001$), and Mu IFN-β (10^4 U/mouse) plus Mu IFN-γ (10^2 U/mouse) resulted in a 60% reduction ($P=0.05$).

DISCUSSION

The results of our study demonstrate that both IFN and poly I:C reduced, but did not completely suppress, the growth rate of mammary carcinomas in BALB/c mice; that the tumor-inhibiting effects of IFN and poly I:C were dose-dependent; that Mu IFN-γ, per antiviral unit, exerted a significantly greater antitumor effect that did Mu IFN-β; that the antitumor activity of low doses of Mu IFN-γ (10^3 U/mouse) and high doses of Mu IFN-β (10^6 U/mouse) was comparable to that of the standard anticancer drug cyclophosphamide; that IFN reduced not only the growth of primary mammary tumors but also the formation of metastases in the lungs; and that Mu IFN-γ combined with Mu IFN-β led to a markedly greater antitumor activity than either IFN alone. However, tumors did not regress completely in any mouse treated with IFN.

The antitumor effects described here for IFN and poly I:C extend previous investigations on the antitumor activity of IFN and poly I:C in a number of experimental murine models, including virus-induced tumors, chemically induced tumors, transplantable tumors, and spontaneous tumors [for a review, *see* (*12*)]. Of direct relevance to the present study are the results obtained with IFN in the prophylaxis and therapy of spontaneous tumors. If given prophylactically, i.e., from the day of birth, IFN delayed the appearance of lymphoid leukemia in AKR mice (*13*), but even if treatment was started after clinical diagnosis of lymphoma, IFN substantially increased the mean survival time (*14*). Yet tumor regression did not occur in any of the leukemic AKR mice treated with IFN, and all mice eventually died from the disease. Hence the results obtained with IFN in the treatment of spontaneous murine leukemia are quite comparable to those obtained in the present study, in that IFN only partially suppressed tumor growth and did not cure the host of its neoplasia.

At a dose of 10^3–$10^{3.3}$ U/mouse (text-figs. 1, 2), Mu IFN-γ brought about the same reduction in growth of mammary tumors as did Mu IFN-β at a dose of 10^6 U/mouse (text-fig. 1). In C57BL/6 mice inoculated with osteogenic sarcoma cells, a 7-day course of Mu IFN-γ at 600 U/mouse/day was as effective in inhibiting tumor development as was a 7-day course of Mu IFN-β at 60,000 U/mouse/day (*7*); in C3HeB/FeJ mice bearing transplantable MC-36 sarcomas, direct intratumoral injection of Mu IFN-γ at 300 U/mouse/day for 3–4 weeks reduced the tumor mass by 98%, whereas a similar treatment regimen for Mu IFN-β did not show any protective activity (*15*). The Mu IFN-γ preparations that were used in these previous studies (*7, 15*) as well as in ours were from sera of mice that had been sensitized with BCG, challenged 2–3 weeks later with PPD, and exsanguinated 3–5 hours after PPD injection. These sera contained not only IFN but also other lymphokines (e.g., migration inhibitory factor and interleukin 1), released concomitantly with IFN. These lymphokines may have contributed to the antitumor effects of the Mu IFN-γ preparations. Some lymphokines might themselves inhibit tumor growth, whereas others might modulate (either diminish or potentiate) the antitumor activity of Mu IFN-γ.

Several mechanisms could be envisaged to account for the inhibitory effects of Mu IFN-β and Mu IFN-γ on mammary tumor growth (*16*), i.e., *a*) inhibition of mammary tumor virus multiplication [which would be unlikely, according to the findings of Came and Moore (*3*)], *b*) direct antimitotic action on the tumor cells, *c*) increased expression of cell surface antigens, *d*) activation of the cytotoxicity of macrophages for tumor cells, and *e*) stimulation of the NK activity and ADCC of lymphocytes for tumor cells. The antitumor activity of IFN may be achieved by a cooperation of some of these effector mechanisms, i.e., *c* and *e*. As suggested by Yagi and Bekesi (*17*), exposure of the mammary tumor cells to IFN may induce alteration in the antigenic composition of the cells (*c*). This increased antigenicity may lead to a heightened host recognition and immune response against the growing tumor, which could, in turn, be further enhanced by contact of the host cells with IFN (*e*).

If one assumes that the antitumor activity of the Mu IFN-γ preparations reside in Mu IFN-γ per se, which remains to be proved, one could readily explain why the inhibitory effects of Mu IFN-γ on mammary tumor growth should exceed those of Mu IFN-*β*. Indeed, IFN-γ is a far more potent anticellular agent than IFN-*β* or IFN-*α* (*5, 6*) and is also far more active as an immunoregulatory agent than IFN-*β* or IFN-*α* (*18, 19*). This superiority may extend to various other properties of IFN, e.g., its enhancing effects on macrophage activity, cell surface antigen expression, NK activity, and ADCC. As has been demonstrated recently by Catalona et al. (*20*), IFN-γ is a potent stimulator of both NK activity and ADCC.

In keeping with the observations of Fleischmann et al. (*9*) and our own observations (*10*) in mice inoculated with P388 or L1210 cells, combined administration of Mu IFN-*β* and Mu IFN-γ effected a much greater inhibition of mammary tumor growth than did either IFN given alone (text-fig. 2). The reason(s) for this synergism remain unclear but may be related to differences in the mode of action of Mu IFN-*β* and Mu IFN-γ.

REFERENCES

(*1*) Sikora K. Does interferon cure cancer? Br Med J 1980; 281:855–858.

(*2*) Gutterman JU, Blumenschein GR, Alexanian R, et al. Leukocyte interferon-induced tumor regression in human metastatic breast cancer, multiple myeloma, and malignant lymphoma. Ann Intern Med 1980; 93:399–406.

(*3*) Came PE, Moore DH. Inhibition of spontaneous mammary carcinoma of mice by treatment with interferon and poly I:C. Proc Soc Exp Biol Med 1971; 137:304–305.

(*4*) ———. Effect of exogenous interferon treatment on mouse mammary tumors. J Natl Cancer Inst 1972; 48:1151–1154.

(*5*) Blalock JE, Georgiades JA, Langford MP, Johnson HM. Purified human immune interferon has more potent anticellular activity than fibroblast or leukocyte interferon. Cell Immunol 1980; 49:390–394.

(*6*) Zhang Z-X, De Clercq E, Heremans H, Verhaegen-Lewalle M, Content J. Antiviral and anticellular activities of human and murine type I and type II interferons in human cells monosomic, disomic and trisomic for chromosome-21. Proc Soc Exp Biol Med 1982; 170:103–111.

(*7*) Crane JL Jr, Glasgow LA, Kern ER, Youngner JS. Inhibition of murine osteogenic sarcomas by treatment with type I or type II interferon. JNCI 1978; 61:871–874.

(*8*) Fleischmann WR Jr, Georgiades JA, Osborne LC, Johnson HM. Potentiation of interferon activity by mixed preparations of fibroblast and immune interferon. Infect Immun 1979; 26:248–253.

(*9*) Fleischmann WR Jr, Kleyn KM, Baron S. Potentiation of antitumor effect of virus-induced interferon by mouse immune interferon preparations. JNCI 1980; 65:963–966.

(*10*) De Clercq E, Zhang Z-X, Huygen K. Synergism in the antitumor effects of type I and type II interferon in mice inoculated with leukemia L1210 cells. Cancer Lett. 1982; 15:223–228.

(*11*) Braude IA, De Clercq E. Purification of mouse interferon by sequential chromatography. J Chromatogr 1979; 172:207–219.

(*12*) Gresser I, Tovey MG. Antitumor effects of interferon. Biochim Biophys Acta 1978; 516:231–247.

(*13*) Gresser I, Coppey J, Bourali C. Interferon and murine leukemia. VI. Effect of interferon preparations on the lymphoid leukemia of AKR mice. J Natl Cancer Inst 1969; 43:1083–1089.

(*14*) Gresser I, Maury C, Tovey M. Interferon and murine leukemia. VII. Therapeutic effect of interferon preparations after diagnosis of lymphoma in AKR mice. Int J Cancer 1976; 17:647–651.

(*15*) Salvin SB, Youngner JS, Nishio J, Neta R. *Brief communication*: Tumor suppression by a lymphokine released into the circulation of mice with delayed hypersensitivity. J Natl Cancer Inst 1975; 55:1233–1236.

(*16*) De Clercq E. Effects of interferon on human tumor cell growth in nude mice. In: Fogh J, Giovanella B, eds. The nude mouse in experimental and clinical research. Vol II. New York: Academic Press, 1982:439–449.

(*17*) Yagi MJ, Bekesi JG. Interferon activity against murine mammary tumors. Proc Am Assoc Cancer Res 1981; abstract 1295.

(*18*) Sonnenfeld G, Mandel AD, Merigan TC. The immunosuppressive effect of type II mouse interferon preparations on antibody production. Cell Immunol 1977; 34:193–206.

(*19*) ———. Time and dosage dependence of immunoenhancement by murine type II interferon preparations. Cell Immunol 1978; 40:285–293.

(*20*) Catalona WJ, Ratliff TL, McCool RE. γ Interferon induced by *S. aureus* protein A augments natural killing and ADCC. Nature 1981; 291:77–79.

blank page

Influence of Cause-of-Death Assignment on Time-to-Tumor Analyses in Animal Carcinogenesis Studies[1,2]

Ralph L. Kodell,[3] John H. Farmer,[3,4] David W. Gaylor,[3] *and* Alexander M. Cameron[3,5]

ABSTRACT—The importance of cause-of-death determination in an animal carcinogenesis study with respect to estimation of time-to-tumor distributions of internally occurring (occult) tumors is discussed. A nontechnical description of time-to-tumor estimation is presented. The information obtained from time-to-tumor estimation when cause-of-death designation was used is illustrated for liver tumors in female mice of the inbred strain BALB/cStCrlfC3Hf/Nctr from the ED$_{01}$ study with *N*-2-fluorenylacetamide done at the National Center for Toxicological Research. A time-to-tumor analysis of reticulum cell sarcoma data from the same study has provided insight into some difficulties involved in routine case-by-case determination of cause of death. A more flexible system for assigning of cause of death to dead animals and cause of morbidity to moribund animals is described as a way to improve cause-of-death assignment.—JNCI 1982; 69:659–664.

Variation in reported latent periods among various neoplasms has been observed for both humans and experimental animals. This variation has led investigators of potential chemical carcinogens to recognize the importance of time to occurrence of spontaneous and induced tumors in animal bioassay studies in addition to the importance of simply the frequency of tumor occurrence. There has been no clear consensus due to several problems in the collection of data as to what constitutes a proper time-to-tumor analysis. The purpose of this paper is threefold: 1) to demonstrate that assignment of cause of death of each animal enhances most statistical analyses of time to tumor, 2) to show by example the extent to which the analysis is sensitive to the correct assignment and use of cause of death, and 3) to suggest a more flexible method of assigning cause of death which does not place unrealistic constraints on the examining pathologist.

In the context of this paper, the term *time to tumor* will mean the time from the beginning of an experiment until the time when a tumor is *first detectable* by the most appropriate observation method. For externally observable tumors, accurate measurement of time to grossly visible tumor is possible because constant surveillance can be maintained. For internally occurring (occult) tumors, because time to tumor as defined above means the time when a tumor is just large enough to be observed histologically, exact time to tumor cannot be measured inasmuch as histologic examination will not likely be conducted at the instant of first histologic detectability.

The three basic problems that have hampered statistical analyses of time-to-tumor data are inherent in the manner in which animal bioassay data are gathered. Animals that die (or are otherwise removed) without a particular tumor of interest during the course of an experiment constitute right-censored observations with respect to the time-to-tumor probability distribution, because it is only known that the animals might have developed a tumor sometime in the future. Animals that die (or are removed) for reasons other than an occult tumor of interest but that have already developed such a tumor (i.e., incidental tumor) constitute left-censored observations with respect to the time-to-tumor distribution, because it is only known that they developed a tumor sometime in the past. Finally, animals that die as a result of an occult tumor of interest (i.e., fatal tumor) constitute not only left-censored observations with respect to time to tumor but also the observed tumors arise from a biased sampling mechanism, namely, death from the tumor of interest.

Various parametric models for the analysis of time-to-tumor data have been proposed in the literature. For example, Albert and Altshuler (*1*) proposed a version of the lognormal probability distribution for time to tumor, as an extension of the work of Druckrey (*2*). Peto and Lee (*3*) discussed analyzing time-to-tumor data with the Weibull distribution, as earlier proposed by Pike (*4*). Hartley and Sielken (*5*) developed the general product model (which includes dose of carcinogen in addition to time to tumor) as an extension of earlier work by Armitage and Doll (*6*). Kodell and Nelson (*7*) proposed fitting independent Weibull distributions of time to onset of tumor and time to death after onset, with the assumption that the difference between fatal and incidental occurrence of tumors could be distinguished.

An early nonparametric approach was proposed by Hoel and Walburg (*8*) who first recognized that different animals provide different kinds of time-to-tumor information, dependent on the censoring involved. For externally observed or rapidly lethal tumors, they proposed estimation of the time-to-tumor distribution by the nonparametric survival estimator of Kaplan and Meier (*9*), because only right censoring is involved in those cases. For strictly nonlethal occult tumors, Hoel and Walburg (*8*) suggested nonparametric time-to-tumor estimation that uses the available time-to-tumor information in each of the right-censored and left-censored (but unbiased) observations. Peto (*10*) suggested testing methods for time-adjusted comparisons of tumor rates, which take into account the censoring-deter-

---

ABBREVIATIONS USED: ED$_{01}$=dose that produces a 1% tumor response; 2-FAA=*N*-2-fluorenylacetamide; RCS=reticulum cell sarcoma.

---

[1] Received November 17, 1981; accepted April 9, 1982.

[2] Animals were maintained under the guidelines of the National Center for Toxicological Research.

[3] National Center for Toxicological Research, Food and Drug Administration, Public Health Service, Department of Health & Human Services, Jefferson, Ark. 72079.

[4] *Present address*: Headquarters, Training and Doctrine Command, Combined Arms Testing Activity, Fort Hood, Tex. 76541.

[5] *Present address*: McNeil Pharmaceutical, Spring House, Pa. 19477.

mined time-to-tumor information provided by each animal. An enlargement of Peto's work has resulted in a comprehensive testing methodology for animal carcinogenesis bioassays proposed by the International Agency for Research on Cancer (*11*).

The nonparametric time-to-tumor estimation procedure illustrated in the present paper was developed by Kodell et al. (*12*) as an extension of the estimation procedures of Kaplan and Meier (*9*), Hoel and Walburg (*8*), and Kodell and Nelson (*7*), whereas many of the underlying concepts overlap those of the testing procedure of Peto (*10*) and Peto et al. (*11*). The estimation procedure is based on the assumptions that each animal in a carcinogenesis bioassay can be assigned an appropriate cause of death upon necropsy or subsequent histopathologic examination and that causes of death (or removal) other than the tumor of interest censor the time to onset of tumor or time to death after onset in a noninformative manner.

Let $S(t)$ represent the net probability of not developing the tumor of interest by time t, and let $P(t)$ represent the net probability of not dying from the tumor of interest by time t, both conditional on survival with respect to all other causes of death up to time t. The respective estimators $\hat{P}(t)$ and $\hat{S}(t)$ of $P(t)$ and $S(t)$ proposed by Kodell et al. (*12*) are the Kaplan-Meier survival estimator (*9*) and the product of the Kaplan-Meier survival estimator and "one minus" the Hoel-Walburg estimator of prevalence of a nonlethal disease (*8*). Under the condition that the prevalence $1-S(t)/P(t)$ of the tumor of interest is a monotone nondecreasing function of t, the estimator $\hat{P}(t)$ is a generalized maximum likelihood estimator of $P(t)$ and $\hat{S}(t)$ coincides with the generalized maximum likelihood estimator of $S(t)$ over certain time intervals. The related estimators of Dinse and Lagakos (*13*) and B. W. Turnbull and T. J. Mitchell [Nonparametric estimation of the distributions of time to onset and time to death for specific diseases in survival-sacrifice experiments. Presentation at the meeting of the Biometric Society (ENAR), March 16-18, 1981, in Richmond, Va.], which do not restrict the prevalence to be monotone, may also be used to estimate the distributions of time to tumor and time to death. These estimators also depend on the important condition that fatal and incidental observations of the tumor of interest can be distinguished through the assignment of a cause of death for each animal. It is this condition that makes the functions $S(t)$ and $P(t)$ identifiable (*see 14*), thus permitting estimation of the time-to-tumor distribution function $1-S(t)$.

When an analysis is restricted to a particular type of tumor, it is only necessary to determine whether the particular tumor type under consideration caused the death of an animal. If not, then the exact cause of death is not required. Admittedly, cause-of-death determination requires a subjective judgment on the part of pathologists, and such a requirement sometimes places unfair constraints on them. The intent of this paper is to demonstrate the desirability of assigning cause of death (mortality) or illness (morbidity) whenever possible, to present a real-data example of the effect of misclassification of cause of death, and to suggest a more flexible way of assigning cause of death that will be acceptable to pathologists and statisticians alike. A theoretical investigation of the effects of misclassification of cause of death has been presented by Lagakos (*14*) in a testing context.

DATA-BASED PERFORMANCE ASSESSMENT

Application of the time-to-tumor estimation procedure of Kodell et al. (*12*) to data obtained from a large-scale carcinogenesis bioassay (the so-called "ED_{01} Study") conducted at the National Center for Toxicological Research illustrates the importance of cause-of-death determination. The procedure is first applied to liver tumor data (hepatocellular adenomas and carcinomas) and is then applied to reticulum cell sarcoma data (including all types and organs).

Complete details of the design and execution of the ED_{01} study, as well as of several selected analyses, are provided in the proceedings of the symposium Innovations in Cancer Risk Assessment (ED_{01} Study) presented by the ED_{01} Working Group (*15*). The study involved continuously feeding 2-FAA, a known bladder and liver carcinogen in mice, to inbred female BALB/cStCrlfC3Hf/Nctr mice until their death or their removal when moribund or until their scheduled killing at times ranging from 9 months (273 days) to 33 months (1,001 days). Concentrations of 2-FAA in the feed were 0, 30, 35, 45, 60, 75, 100, and 150 ppm. The study was originally scheduled as six identical replicates, conducted in six identical rooms, which were loaded sequentially over 10 months in reverse numerical order of room numbers: 146, 145, 144, 143, 142, and 141. Because of low mortality in all rooms and a lower bladder tumor prevalence than expected at the 18-month scheduled killing in the first three replicates (rooms 146, 145, 144), all scheduled killings not yet completed in the last three replicates (rooms 143, 142, 141) were extended to 24 months (728 days) and were not conducted as originally planned (table 1).

In the analysis of liver tumors, only animals for which that organ was histologically examined were included, after all animals for which autolysis precluded a diagnosis of the cause of death had been excluded. Text-figures 1 and 2 display the time-to-tumor ($1-\hat{S}(t)$) and time-to-death ($1-\hat{P}(t)$) curves for the 150-ppm dose groups of rooms 144 and 143, respectively. Note that time to tumor and time to death were accelerated for animals in room 143 when compared to the same parameters for animals in room 144. This is representative of a general tendency in all of the last three replicates (rooms 143, 142, 141) for animals to respond earlier than they did in the first three replicates (rooms 146, 145, 144) [*see* (*16*)]. The estimated median time to liver tumor at 150 ppm in room 144 was 824 versus 728 days in room 143.

The time-to-tumor distribution curve $1-\hat{S}(t)$, which estimates the probability of occurrence of occult liver tumors at any prespecified time t, provides important information not available on time to onset of tumor without assignment of cause of death. Sometimes prevalence estimates obtained from scheduled killing data have been mistakenly used as estimates of the time-to-tumor distribution. In other instances cumulative proportions of animals observed with tumors at specific times, without regard to mode of death, have been incorrectly claimed as estimates of the time-to-

Table 1.—*Altered scheduled killings*[a]

Dose, ppm 2-FAA	Scheduled removal from study,[b] mo								
	33	24[c]	18	17	16	15	14	12	9
150	All	4, 5, 6	1, 2, 3	1, 2, 3	1, 2, 3, 4	1, 2, 3, 4	1, 2, 3, 4, 5	All	All
100	All	4, 5, 6	1, 2, 3	1, 2, 3	1, 2, 3, 4	1, 2, 3, 4	1, 2, 3, 4, 5	All	All
75	All	4, 5, 6	1, 2, 3	1, 2, 3	1, 2, 3, 4	1, 2, 3, 4	1, 2, 3, 4, 5	All	All
60	All	4, 5, 6	1, 2, 3	1, 2, 3	1, 2, 3, 4	1, 2, 3, 4	1, 2, 3, 4, 5	All	All
45	All	4, 5, 6	1, 2, 3	1, 2, 3	1, 2, 3, 4				
35	All	4, 5, 6	1, 2, 3	1, 2, 3					
30	All	4, 5, 6	1, 2, 3						
0	All	4, 5, 6	1, 2, 3	1, 2, 3	1, 2, 3, 4	1, 2, 3, 4	1, 2, 3, 4, 5	All	All

[a] The six replicates are shown by dose and month for the continuous feeding portion of the ED_{01} study. Before alteration of schedules, killings were to have been conducted in all replicates at all times indicated, except that no killings were scheduled originally at 24 mo.

[b] Where no replicates are noted as having been removed, no killings were done.

[c] Killings were conducted at 24 mo for replicates 4, 5, and 6.

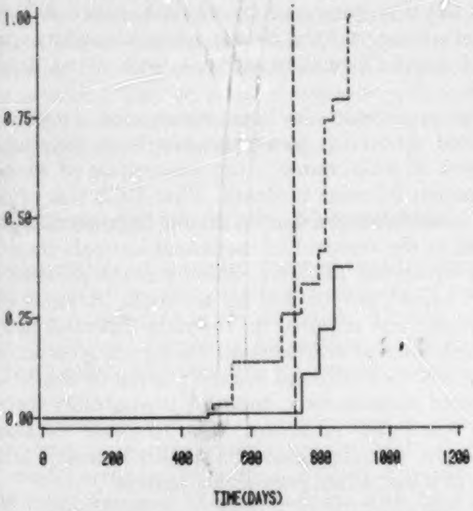

Text-figure 1.—Time-to-tumor and mortality curves with respect to liver tumors for female BALB/c mice fed 150 ppm 2-FAA (room 144). Dashed step function: $1-\hat{S}(t)$=estimated time-to-onset distribution; solid step function: $1-\hat{P}(t)$=estimated time-to-death distribution; *dashed, vertical line* at 728 days (24-mo killing).

tumor distribution. By properly accounting for mode of removal of an animal, the time-to-tumor curves represented in text-figures 1 and 2 actually estimate the underlying but unspecified time-to-tumor distribution functions. In addition to the direct use of time-to-tumor information, such as in refining risk extrapolation of carcinogenic compounds (*17*), one can use the time separation of $1-\hat{S}(t)$ and $1-\hat{P}(t)$ to arrive at a rough estimate of the time lapse between histologic observability of an internal tumor and the resultant death or morbidity of an animal. From text-figures 1 and 2, an estimate of approximately 5 months (150 days) is obtained for death from liver tumor after onset. Using a parametric procedure, Kodell et al. (*18*) obtained a similar estimate irrespective of dose group.

All animals except those in which autolysis precluded a diagnosis of the cause of death were used in the RCS analysis. Because the histopathologic criteria utilized in this study were those recommended by Dunn (*19*), the various types of lymphoma were excluded from this analysis. An additional study combining RCS with lesions classified as lymphomatous was also done, with the same basic results and conclusions as those reported below for RCS alone.

Text-figures 3 and 4 display time-to-tumor and time-to-death curves for the 150-ppm dose groups of rooms 144 and 143, respectively. The most striking feature of these plots is the large "jump" in the time-to-tumor curve for room 143, in contrast to the time-to-tumor curve for room 144. In fact, the time-to-tumor and time-to-death curves for room 144 stay very close together throughout the animals' lifetimes, whereas for room 143, after the large jump at approximately 728 days (time indicated by a dashed vertical line on all plots), the curves tend to stay apart, although they were nearly coincident until that time. The closeness of $1-\hat{S}(t)$ to $1-\hat{P}(t)$ evident for room 144 was characteristic of all dose groups housed in rooms 146, 145, and 144 (first three replicates). In contrast, the large jump phenomenon at 728

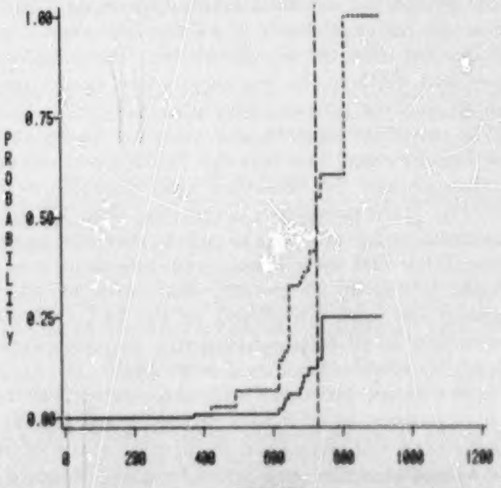

Text-figure 2.—Time-to-tumor and mortality curves with respect to liver tumors for female BALB/c mice fed 150 ppm 2-FAA (room 143). Dashed step function: $1-\hat{S}(t)$=estimated time-to-onset distribution; solid step function: $1-\hat{P}(t)$=estimated time-to-death distribution; *dashed, vertical line* at 728 days (24 mo killing).

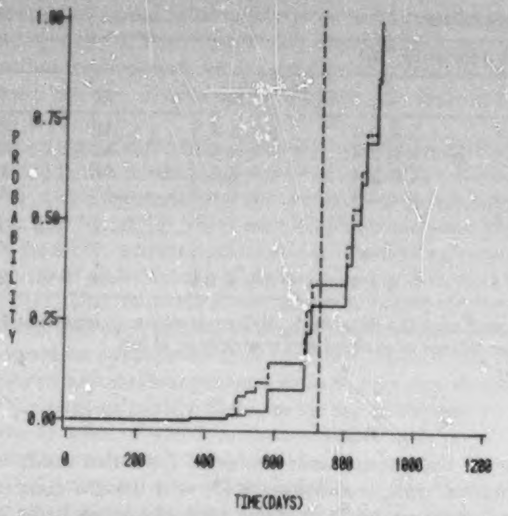

TEXT-FIGURE 3.—Time-to-tumor and mortality curves for RCS in female BALB/c mice fed 150 ppm 2-FAA (room 144). Dashed step function: $1-\hat{S}(t)$=estimated time-to-onset distribution; solid step function: $1-\hat{P}(t)$=estimated time-to-death distribution; *dashed, vertical line* at 728 days (24 mo killing).

days for $1-\hat{S}(t)$ characterized all dose groups of rooms 143, 142, and 141 (last three replicates).

The contradiction in time-to-tumor distributions between the first and last three replicates apparently resulted because throughout the experiment RCS was classified as cause of death more often than was appropriate. Because RCS is a malignant disease, there was a tendency for pathologists to assign it as the cause of death when it was present at necropsy in dead or moribund animals for which no other information was available on which to base the cause of death. Approximately 90% of the RCS which occurred in lifetime groups (i.e., uncontaminated by being killed) was listed as the cause of death. If RCS really were a rapidly lethal disease, then the prevalence, i.e., the proportion of animals with RCS in the live population, would never be very high, and the time-to-tumor and time-to-death curves would lie very close together, as is generally the situation for rooms 146, 145, and 144 (text-fig. 3). This premise can be seen theoretically by observing that prevalence equals $1-S(t)/P(t)$. If the prevalence is very low, then $S(t)$ and $P(t)$ must necessarily be very close to one another, and vice versa. Because in the first three rooms (144–146) there was not a scheduled killing at 24 months, the notion of low RCS prevalence was not contradicted. At the 18-month killing, the prevalence of RCS (a late-occurring disease) was indeed low (e.g., 7/130=5% in controls, room 144).

Whereas in the last three replicates (rooms 141–143) a similar impression of RCS as a rapidly lethal disease with low prevalence was given until 24 months, at the 24-month killing an unexpectedly large prevalence was observed (e.g., 42/103=41% in controls, room 143). Both before and after this time, practically every dead or moribund animal with RCS present was assigned RCS as the cause of death, even though a substantial number of animals without RCS were assigned other causes of death. Because the 24-month killing data reflects a high prevalence of RCS and because causes of death other than RCS were responsible for the death of animals *without* RCS, one would expect that these other causes were also responsible for deaths of some animals *with* RCS. Thus more animals with RCS than were reported to have died of other causes should have died of other causes before dying of RCS. This would have resulted in more incidental and fewer fatal classifications of RCS before and after 24 months, so that the prevalence estimate obtained from dead and moribund animals would then reflect the true high prevalence, if one assumes that the prevalence did not change at approximately 24 months. Thus the 24-month killing data contradicted the impression of the degree of lethality of RCS obtained from data from only dead and moribund animals. In addition, a surprisingly large number of animals killed at 24 months had several organs affected with RCS, which is also inconsistent with the picture of rapid lethality portrayed by virtually every RCS-bearing animal's dying from the disease, whereas a substantial number of non-RCS-bearing animals were dying from other causes.

Thus it appears that one assumption underlying the proposed estimation procedure has been violated in the situation of RCS, namely, the assumption of an accurate designation of cause of death. That RCS was apparently given heavier weight than it should have been is probably related to the removal of moribund animals from experiments by animal handlers, which was the practice so that tissues would not be lost to autolysis. A cause-of-death assignment was required by the data-collection system for all moribund and dead animals, thus forcing the pathologist to "project" a moribund animal's cause of death. If some moribund animals were removed prematurely, i.e., before death was really imminent, then in those situations the pathologist was improperly compelled to assign a cause of death to a live, albeit possibly ill, animal.

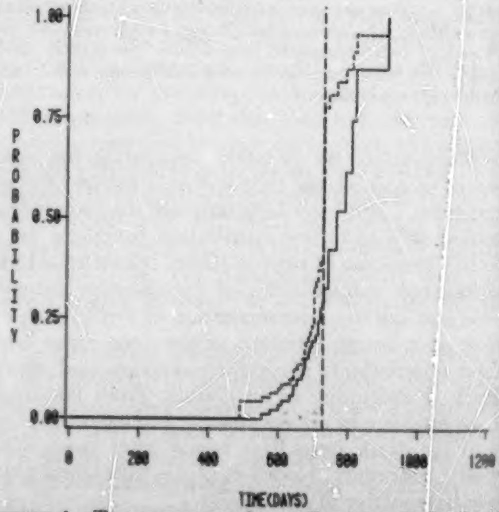

TEXT-FIGURE 4.—Time-to-tumor and mortality curves for RCS in female BALB/c mice fed 150 ppm 2-FAA (room 143). Dashed step function: $1-\hat{S}(t)$=estimated time-to-onset distribution; solid step function: $1-\hat{P}(t)$=estimated time-to-death distribution; *dashed, vertical line* at 728 days (24 mo killing).

No such discrepancy between early and late replicates with respect to time to liver tumor was noted (text-figs. 1, 2). The lack of a large jump at 24 months in room 143 at 150 ppm is representative of all dose groups in the last three rooms. This lack of a large jump indicates that the estimated prevalence at the 24-month killing was in line with what was expected on the basis of dead and moribund animal data up to that time. This suggests that cause of death determination was more accurate for liver tumor mortality than for RCS mortality, which is gratifying inasmuch as liver tumor was a dose-related end point of interest. The other principal dose-related end point of interest, bladder carcinoma, exhibited the same consistency in cause-of-death assignment as did liver tumor. Both the liver and bladder tumor data support the applicability of the recommended time-to-tumor estimation procedure. And although the cause-of-death assumption may have been violated in the case of RCS, nevertheless when the recommended procedure was used, it helped demonstrate that RCS is not as rapidly lethal as had been thought. The question remains as to what, if anything, can be done to improve assignment of cause of death in an animal bioassay for carcinogenesis. This question is addressed in the next section.

IMPROVING CAUSE OF DEATH ASSIGNMENT

The assumption of accurate cause-of-death assignment has been required for many statistical analyses of survival data that have appeared in the literature. Thus it is not a new concept in the foregoing estimation of ,the time-to-tumor distribution, although it is a necessary condition for accurate analysis.

Because scheduled sacrifice data were used for detection of a discrepancy in prevalence estimates of RCS in the present study, one experimental modification would be to schedule more frequent killings, perhaps with only a few animals being killed each time. This schedule would help keep the true prevalence in proper perspective, although it would not affect overdesignation of a particular cause of death.

With the removal of moribund animals in lieu of letting them die, a possible early-removal bias can be introduced. So that the examining pathologist would be allowed more flexibility, a moribund animal should be assigned a cause of *morbidity* rather than a cause of death. In this way the pathologist would not be forced to concur with the animal caretaker who removed the animal that death was imminent.

The pathology system should also incorporate a graded response into cause-of-death and cause-of-morbidity assignments. If the examining pathologist is able to identify a single entity as causing death or morbidity, he should then assign this as the *primary* cause. If more than 1 lesion is determined to be responsible for removal of an animal, then each lesion should be assigned as a *contributing* cause, and no primary cause should be recorded. Finally, lesions that are thought to have had a possible influence on an animal's death or morbidity may be listed as *equivocal* causes. If no condition classifiable as a primary, a contributing, or an equivocal cause of death is found in an animal, then that animal should be classified as having died from an unknown cause.

Distinguishing between primary and contributing causes of death will offer some flexibility to the statistician as well as to the pathologist in the classification of moribund animals with respect to fatal or incidental occurrence of tumors, in the interest of alleviating problems such as those encountered with RCS. For example, in analyzing a particular type of tumor, one might investigate the impact of classifying occurrences of that tumor as fatal only if they are primary causes of death (morbidity) as opposed to treating both primary and contributing causes as fatal.

The introduction of cause of morbidity for moribund animals will not be of direct help to the statistician, who must continue to treat cause of morbidity and cause of death identically in the performance of a time-to-tumor estimation. That is, the statistician must use both cause of death and cause of morbidity as "cause of removal" to distinguish between fatal and incidental tumors. In this sense, for example, a tumor classified as the primary cause of morbidity for a moribund animal would be treated as a fatal tumor in a statistical analysis of time to tumor.

A cause-of-death–cause-of-morbidity system which incorporates the above concepts is being developed at the National Center for Toxicological Research in the spirit of that recommended by the International Agency for Research on Cancer (*11*), although the system at the National Center for Toxicological Research is not identical with the recommendations of the International Agency for Research on Cancer. In the future it will be of interest to evaluate this new system with respect to RCS cause-of-death diagnosis to measure any improvement over the present system.

REFERENCES

(*1*) Albert RE, Altshuler B. Considerations relating to the formulation of limits for unavoidable population exposures to environmental carcinogens. In: Ballow JE, Busch RH, Mahlum DD, Sanders CL, eds. Radionuclide carcinogenesis. Springfield, Va.: Atomic Energy Commission (Symposium series, CONF-72050, NTIS), 1973:233-253.

(*2*) Druckrey H. Quantitative aspects in chemical carcinogenesis. In: Truhart L, ed. Potential carcinogenic hazards from drugs (evaluation of risk). New York: Springer-Verlag, 1967:60–78.

(*3*) Peto R, Lee P. Weibull distributions for continuous carcinogenesis experiments. Biometrics 1973; 29:457–470.

(*4*) Pike MC. A method of analysis of a certain class of experiments in carcinogenesis. Biometrics 1966; 22:142–161.

(*5*) Hartley HO, Sielken RL. Estimation of "safe doses" in carcinogenic experiments. Biometrics 1977; 33:1–30.

(*6*) Armitage P, Doll R. Stochastic models for carcinogenesis. In: Le Cam L, Neyman J, eds. Proceedings of the fourth Berkeley symposium on mathematical statistics and probability. Vol 4. Berkeley and Los Angeles: Univ California Press, 1961:19–38.

(*7*) Kodell RL, Nelson CJ. An illness–death model for the study of the carcinogenic process using survival/sacrifice data. Biometrics 1980; 36:267–277.

(*8*) Hoel DG, Walburg HE Jr. Statistical analysis of survival experiments. J Natl Cancer Inst 1972; 49:361–372.

(*9*) Kaplan EL, Meier P. Nonparametric estimation from incomplete observations. J Am Stat Assoc 1958; 53:457–481.

(*10*) Peto R. Editorial: Guidelines on the analysis of tumor rates and death rates in experimental animals. Br J Cancer 1974; 29:101-105.

(*11*) Peto R, Pike MC, Day NE, et al. Annex to: Long-term and short-term screening assays for carcinogens: A critical appraisal. Guidelines for simple, sensitive significant tests for carcinogenic effects in long-term animal experiments. Lyon, France: IARC, suppl 2:311–425.

(*12*) Kodell RL, Shaw GW, Johnson AM. Nonparametric joint estimators for disease resistance and survival functions in survival/sacrifice experiments. Biometrics 1982; 38:43–58.

(*13*) Dinse GE, Lagakos SW. Nonparametric estimation of the prevalence and survival functions from incomplete observations. Biometrics 1982. In press.

(*14*) Lagakos SW. An evaluation of some two-sample tests used to analyze animal carcinogenicity experiments. Utilitas Mathematica 1982. In press.

(*15*) Staffa J, Mehlman M, eds. Innovations in cancer risk assessment (ED_{01} study). J Environ Pathol Toxicol 1980; 3 (special issue): 1–250.

(*16*) Kodell RL, Farmer JH, Littlefield NA, Frith CH. Analysis of life-shortening effects in female BALB/c mice fed 2-acetylaminofluorene. J Environ Pathol Toxicol 1980; 3:69–87.

(*17*) Farmer JH, Kodell RL, Gaylor DW. Estimation and extrapolation of tumor probabilities from a mouse bioassay with survival/sacrifice components. Risk Analysis 1982. In press.

(*18*) Kodell RL, Farmer JH, Greenman DL, Frith CH. Estimation of distributions of time to appearance of tumor and time to death from tumor after appearance in mice fed 2-acetylaminofluorene. J Environ Pathol Toxicol 1980; 3:89–102.

(*19*) Dunn TB. Normal and pathologic anatomy of the reticular tissue in laboratory mice, with a classification and discussion of neoplasms. J Natl Cancer Inst 1954; 14:1281–1433.

Murine Lymph Node Natural Killer Cells: Regulatory Mechanisms of Activation or Suppression [1,2,3]

Goro Hisano [4,5] *and* Nabil Hanna [4,6]

ABSTRACT—The kinetics and organ distribution patterns of lymph node natural killer (NK) cell activation or suppression were found to vary according to the type, dose, and route of administration of *Corynebacterium parvum* or polyinosinic-polycytidylic acid (poly I·poly C). Activation of lymph node NK cells by local injections of *C. parvum* into the footpad or the peritoneum was restricted to the regional lymph nodes; contralateral and distant lymph nodes were not involved. This selectivity persisted even though splenic and peripheral blood NK cells were strongly activated by the same treatment. Conversely, poly I·poly C induced systemic activation of NK cells without selectively activating the regional lymph nodes. The decline of NK cell activity observed 2 weeks after *C. parvum* treatment was associated with a state of unresponsiveness to a second injection of NK cell stimulants. The expression of *C. parvum*-induced suppression could be systemic or restricted to the regional lymph nodes. Possible mechanisms for the anatomical compartmentalization of NK cell activation or suppression and the implications for the control of tumor growth and dissemination in vivo are discussed.—JNCI 1982; 69:665–671.

The possible role for NK cells in the in vivo resistance against transplantable lymphomas and nonlymphoma solid tumors has been suggested by several studies (*1–8*). For example, adult nude mice exhibit high NK cell activity and strong resistance against syngeneic, allogeneic, and xenogeneic lymphoma cells (*1, 2, 9*). Furthermore, B16 melanoma cells injected into beige mice, which are known to be deficient in NK cell activity, exhibit shorter induction time, faster growth rate, and higher incidence of experimental and spontaneous metastases (*7, 10*) than those injected into normal syngeneic mice. Several recent studies showed that NK cells play a major role in the destruction of circulating tumor cells (*8, 11*) and in the inhibition of hematogenous metastatic spread (*8*). However, they also showed that NK cells are less effective in destroying tumor cells that have extravasated into the lung parenchyma. Thus regulation of the activity of NK cells within the anatomical compartments to which they are confined is important in the control of tumor growth and dissemination. NK cells have a characteristic organ distribution. The activity of NK cells is highest in peripheral blood, followed in descending order by spleen, lymph nodes, and bone marrow (*12, 13*). The lymph nodes are common sites for spontaneous metastases from local primary tumors. Therefore, the induction and maintenance of high levels of NK cell activity in lymph nodes are biologically and perhaps clinically significant. The use of BRM that activate NK cells and macrophages in the prevention and therapy of lymph node metastases has been described previously (*14, 15*). However, depending on the type, dose, and route of administration of the BRM, augmentation or suppression of NK cell-mediated cytotoxicity may be obtained (*16–18*).

In this study, we investigated the kinetics, regulation, and mode of activation of NK cells in lymph nodes by local or systemic administration of the bacterial adjuvant *C. parvum* and the IFN inducer poly I·poly C. Also, we examined the effect of these BRM on the generation of local or systemic suppression, which may interfere with the reactivation and maintenance of high NK cell activity in lymph nodes.

MATERIALS AND METHODS

Animals.—Specific-pathogen-free (C3H/HeN mammary tumor virus-negative (C3H⁻) and athymic BALB/c nude mice were obtained from the Animal Production Area, NCI-Frederick Cancer Research Facility, Frederick, Md. Within a single experiment all mice were age and sex matched and were 3–6 weeks old at the beginning of most experiments.

Reagents.—*C. parvum* (7.0 mg/ml; Burroughs Wellcome Co., Research Triangle Park, N.C.) was diluted in PBS before injection. Poly I·poly C (Sigma Chemical Co., St. Louis, Mo.) was prepared in PBS (1.0 mg/ml) and stored at −70°C until use. Mouse fibroblast IFN (10^6 U/ml) was purchased from Calbiochem-Behring Corp., La Jolla, Calif. IFN levels in sera of mice treated with BRM were determined by virus-inhibition assay in vitro (Biofluids Inc., Rockville, Md.).

Tumors.—The YAC-1, a Moloney virus-induced lymphoma of A/Sn origin (*19*), was maintained in culture with CMEM (Flow Laboratories, Rockville, Md.). The cell line was tested and found to be free of mycoplasma.

In vitro assay for NK cell-mediated cytotoxicity.—Mice were killed by cervical dislocation, and their spleen and lymph

---

ABBREVIATIONS USED: BRM=biological response modifier(s); CMEM=Eagle's minimum essential medium supplemented with 5% fetal bovine serum, L-glutamine, nonessential amino acids, and vitamins; E:T=effector-to-target cell; IFN=interferon; ifp=intrafootpad; LU=lytic unit(s); NK=natural killer; PBS=phosphate-buffered saline; poly I·poly C=polyinosinic-polycytidylic acid.

---

[1] Received November 17, 1981; accepted April 7, 1982.

[2] Supported by Public Health Service contract N01CO-75380 from the Office of the Director, National Cancer Institute, with Litton Bionetics, Inc. The contents of this publication do not necessarily reflect the views or policies of the U.S. Department of Health and Human Services, nor does mention of trade names, commercial products, or organizations imply endorsement by the U.S. Government.

[3] Animals were maintained under the guidelines set forth by the National Institutes of Health Policy on Humane Care and Use of Animals and by the Animal Welfare Act in facilities accredited by the American Association for Accreditation of Laboratory Animal Care.

[4] Cancer Metastasis and Treatment Laboratory, NCI-Frederick Cancer Research Facility, P.O. Box B, Frederick, Md. 21701.

[5] Visiting scientist from the Third Department of Internal Medicine, School of Medicine, Tokushima University, Tokushima, Japan.

[6] *Address reprint requests to* Dr. Hanna at his *present address:* Smith Kline & French, 620 Allendale Rd., King of Prussia, Pa. 19406.

nodes (popliteal, inguinal, and mesenteric) were removed. We prepared single cell suspensions by mechanically disrupting the lymphoid organs and forcing them through a 60-mesh wire screen. We dispersed cell aggregates by gentle pipetting and then filtered the cell suspensions through a 200-mesh nylon screen. The red blood cells in the spleen cell preparations were removed by water lysis, and all lymphoid cells were washed and resuspended in CMEM. The final concentration was 5 × 10^6 cells/ml. For isolation of effector cells from peripheral blood, mice were anesthesized in ether, and blood was drawn by cardiac puncture with the use of 20 U heparin/ml as anticoagulant. The blood was diluted 1:3 in Ca^{2+}-free and Mg^{2+}-free Hanks' balanced salt solution that contained 10 U heparin/ml and layered on Ficoll–metrozoate gradient. After centrifugation at 1,000×*g* for 30 minutes, the cells at the interface were collected, washed, and resuspended in CMEM. Effector cells from 5 mice per group were pooled for the in vitro cytotoxicity assay.

The in vitro NK cell-mediated killing of YAC-1 lymphoma target cells was evaluated by the 4-hour ^{51}Cr release assay. YAC-1 cells (1×10^7/0.2 ml) obtained from cultures in exponential growth phase were incubated with 200 μCi of $Na^{51}CrO_4$ for 1 hour at 37°C. The labeled cells were washed thoroughly and adjusted to a final concentration of 10^5 cells/ml in CMEM. Portions (0.1 ml) of lymphoid effector cell suspension were added to 10^4 radiolabeled YAC-1 lymphoma target cells in U-shaped wells of microtiter plates to yield E:T ratios of 50:1, 25:1, 12:1, and 6:1. The plates were centrifuged at 60×*g* for 5 minutes and incubated for 4 hours at 37°C in a humidified incubator with 5% CO_2. The amount of ^{51}Cr released into the medium was measured, and percent killing was calculated by the formula: Percent cytotoxicity=$[(E-C)/T] \times 100$, where *E*=cpm released in the presence of effector cells, *C*=cpm released by target cells incubated alone in medium, and *T*=total cpm input per well. The experimental error for triplicate determinations (95% confidence interval) was less than 5% of the mean cytotoxicity, except for cytotoxicity values less than 15% for which it was ±3%.

In several experiments the suppressive effect of treatment with *C. parvum* on activation of NK cells was studied. Percent suppression was calculated according to the formula: Percent suppression = $1 - [(A - B)/(C - D)] \times 100$, where group A received one injection 14 days before testing and a second injection 3 days before testing, groups B and C received single injections at 14 or 3 days before testing, respectively, and group D served as untreated control. The responses were expressed in LU per 10^7 lymphoid effector cells, which were calculated from the linear parts of the cytotoxicity curves. In most cases the number of lymphoid cells that killed 10% (LU_{10}) or 20% (LU_{20}) of the labeled target cells constituted 1 LU. In instances in which NK cell-mediated cytotoxicity was very low (e.g., unstimulated lymph node cells), the least-squares linear fit was calculated and the lines were extrapolated.

Statistical analysis—Student's *t*-test was used.

RESULTS

Kinetics of Activation of Lymph Node NK Cells

Lymphoid cells from popliteal, inguinal, and mesenteric lymph nodes of normal or *C. parvum*-treated mice were tested for NK cell activity against YAC-1 lymphoma target cells in a 4-hour ^{51}Cr release assay.

In 22 separate experiments, the levels of NK cell activity

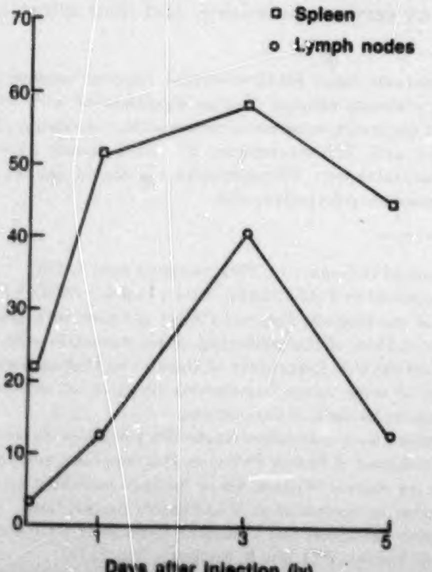

TEXT-FIGURE 1.—Kinetics of NK cell activation in spleen and popliteal lymph nodes after iv injection of *C. parvum* (160 μg/mouse) into 6-wk-old C3H$^-$ mice. Percent cytotoxicity was at an E:T ratio of 50:1.

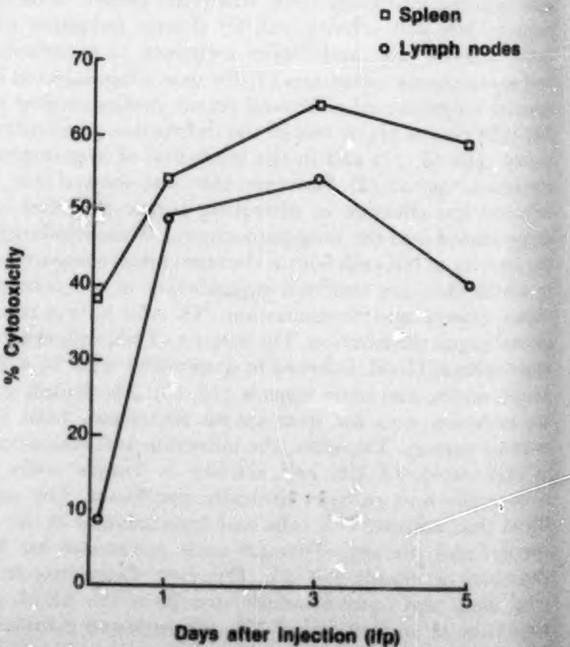

TEXT-FIGURE 2.—Kinetics of NK cell activation in spleen and lymph nodes after ifp injection of *C. parvum* (10 μg/mouse) into 6-wk-old C3H$^-$ mice. Percent cytotoxicity was at an E:T ratio of 50:1.

in lymph nodes of normal 4- to 12-week-old C3H⁻ mice averaged 5.2±3.0% cytotoxicity (range, 2.0–11.8%) at an E:T ratio of 50:1. In the same experiments, spleen cells exhibited higher levels of cytotoxic activity, with a mean of 29.4±8.0% (range, 20.1–52.7%). The activity of both splenic and popliteal lymph node NK cells could be boosted by systemic (iv) or local (ifp) injections of *C. parvum* (text-figs. 1, 2). Although the activity of spleen and lymph node NK cells reached a peak on day 3 after injection, the route of administration of *C. parvum* significantly affected the onset and decline of the natural cytotoxicity. Thus following iv injection of *C. parvum*, we observed only a slight activation of popliteal lymph node cells 24 hours after treatment, a peak response on day 3, and a sharp decline to pretreatment levels by day 5 (text-fig. 1). In contrast, ifp injection of *C. parvum* caused a marked activation of NK cells in regional (popliteal) lymph nodes 24 hours after treatment, and high levels of activity were maintained through day 5 after treatment (text-fig. 2). Two weeks after *C. parvum* injection, the NK cell activity in the spleen and popliteal lymph nodes was four times higher in mice given ifp injections than in those given iv injections or in normal controls. (*See* tables 3, 4.)

The optimal doses of *C. parvum* that activate NK cells in popliteal lymph nodes were found to be highly dependent on the route of administration (text-fig. 3). A marked activation of NK cells was observed 3 days after ifp injection of as little as 5 μg of *C. parvum*, and maximum activity was obtained with 20 μg of adjuvant. In contrast, for optimal activation of lymph node NK cells by the iv route, large doses of *C. parvum* (160–320 μg/mouse) were required.

The quantitative evaluation of NK cell activation and suppression can be affected by the adjuvant-induced alterations in the cellularity of the lymph nodes and spleen. For example, after iv injection of large doses (160 μg) of *C. parvum*, an increase in the number of cells in the popliteal lymph nodes was observed on day 3 (3.1 times that of untreated controls); this subsided to pretreatment levels by day 14 post injection. The same treatment, however, led to a marked splenomegaly, which was most pronounced 14 days after treatment (yield of 150×10⁶ cells as compared to 50×10⁶ cells/spleen in untreated mice). Conversely, the ifp injection of as little as 10 μg of *C. parvum* led to a marked increase in the number of cells in the regional popliteal lymph nodes by day 3 after injection (4–7 times that of untreated controls) and reached maximal levels by day 14 (6–10 times that of normal lymph nodes). The same treatment had only a modest effect on the cellularity of the spleen. The increase in the number of spleen cells was dose-dependent and ranged from 1.1 to 2.2 times that of untreated controls.

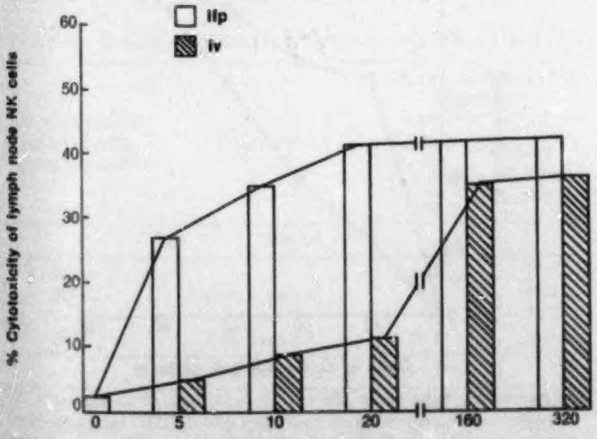

TEXT-FIGURE 3.—Effect of dose and route of administration of *C. parvum* on activation of lymph node NK cells. Cytotoxicity of popliteal lymph node cells was assessed 3 days after ifp or iv injections of *C. parvum* into 6-wk-old C3H⁻ mice. Percent killing was at an E:T ratio of 50:1.

Dependence of Organ Selectivity of NK Cell Activation on Route of *C. parvum* Administration

Using 3- to 4-week-old C3H⁻ mice with initially low NK cell activity, we next studied the anatomical compartmentalization of NK cell activation following iv, ip, or ifp injection of *C. parvum*. The data presented in table 1 show that ifp injection of 10 μg of *C. parvum* markedly activated NK cells in the regional popliteal lymph nodes, spleen, and peripheral blood. In contrast, no activation of NK cells in the contralateral popliteal lymph nodes or mesenteric lymph nodes and only a moderate stimulation in the regional inguinal lymph nodes could be detected. Doses up to 160 μg of *C. parvum* administered ifp also failed to activate NK cells in the contralateral popliteal lymph nodes, even though NK cells in the spleen and peripheral blood were highly activated (data not shown).

A different pattern of activation was observed after the ip injection of 10 μg of adjuvant. Whereas NK cells in the spleen and peripheral blood were highly activated on day 3 after adjuvant treatment, NK cells in the popliteal lymph

TABLE 1.—*Dependence of pattern of NK cell activation on route of* C. parvum *administration*

Source of lymphoid cells	NK cell-mediated cytotoxicity,[a] $LU_{20}/10^7$ lymphoid cells					
	Expt I			Expt II		
	Control	*C. parvum*, 10 μg/mouse		Control	*C. parvum*, iv	
		ifp	ip		10 μg/mouse	160 μg/mouse
Spleen	9.6	40.0	53.5	16.0	140.8	251.5
Lymph nodes						
Popliteal						
Regional	3.5	65.0	3.4[b]	3.8[b]	7.8[b]	80.0[b]
Contralateral	3.5	3.0				
Inguinal	3.4	8.3[c]	14.5[b]			
Mesenteric	4.8	5.0	12.7	5.1	15.6	16.0
Peripheral blood	8.4	41.9	55.8			

[a] NK cell-mediated killing was measured 3 days after *C. parvum* injection into 3- or 4-wk-old C3H⁻ mice. Each treatment group contained 5 mice.

[b] Lymph nodes from both sides were pooled.

[c] Regional lymph nodes only.

nodes were not activated, and NK cells in the inguinal and mesenteric lymph nodes were only moderately stimulated. These patterns of organ selectivity were found to be unchanged at days 5, 8, and 11 after ip or ifp injection of *C. parvum*. Although iv administration of *C. parvum* activated NK cells in the spleen and the mesenteric and popliteal lymph nodes, the activation of the NK cells in the popliteal lymph nodes required relatively high doses of the adjuvant (table 1, expt II). Moreover, under optimal stimulation conditions, the overall NK cell activity generated in mesenteric lymph nodes was consistently lower than that detected in popliteal lymph nodes. Thus both the route of injection and the dose of *C. parvum* affect the levels and the organ localization of activated NK cells.

Generalized Activation of Lymph Node NK Cells by Poly I•Poly C

Since IFN plays a significant role in the regulation of NK cell activity, the levels of IFN produced by different BRM may influence the activation of NK cells at different sites. Thus we investigated the pattern of NK cell activation after the injection of poly I·poly C, a potent IFN inducer and NK cell activator (*20*). The range of IFN levels in the blood 16 hours after injection of poly I·poly C or *C. parvum* was 500–1,580 and 5–20 IU/ml, respectively. The results (table 2) clearly demonstrate that organ selectivity or site restriction of NK cell activation did not occur after local poly I·poly C injection. Thus unlike *C. parvum*, ifp injection of poly I·poly C activated NK cells in the regional as well as the contralateral popliteal lymph nodes. Moreover, NK cell activity in popliteal lymph nodes was enhanced also when poly I·poly C was administered ip.

Suppression of NK Cell Activity in Spleen and Lymph Nodes

The iv injection of large doses of *C. parvum* induces severe and long-lasting suppression of spleen NK cell activity that occurs after the early and transient activation period (*16*). In the following experiments, we investigated whether the *C. parvum*-induced suppression of NK cell activation is confined to the spleen or is generated also in lymph nodes and whether the suppression is influenced by the dose and route of adjuvant administration. Groups of mice were given iv injections of 10–160 μg of *C. parvum*; 11 days later, they were given a second iv injection of 160 μg of the adjuvant; 3 days later, NK cell-mediated cytotoxicity in spleen and lymph nodes was monitored in vitro. The results (table 3) show that an initial treatment with 160 μg of *C. parvum* markedly suppressed the ability of a second injection of the same adjuvant to activate NK cells in the spleen and lymph nodes. Similarly, NK cells were not reactivated when poly I·poly C was injected into mice initially treated iv with large doses of *C. parvum* (table 3). Although the degree of suppression of NK cell activation was dependent on the dose of *C. parvum* used in the initial treatment, at lower doses the suppression was more pronounced in the spleen than in the lymph nodes (text-fig. 4).

TABLE 2.—*Lack of site restriction of NK cell activation by poly I·poly C*

Route of poly I·poly C treatment, 50 μg/mouse	NK cell-mediated cytotoxicity,[a] $LU_{20}/10^7$ lymphoid cells		
	Popliteal lymph nodes		Spleen
	Regional	Contralateral	
None (control)	2.5	2.5	28.6
ifp	28.6	24.2	139.3
ip	16.7	16.7	94.5

[a] NK cell-mediated killing was measured 1 day after poly I·poly C injection into 5-wk-old $C3H^-$ mice.

We then examined the systemic and/or local suppression of NK cell-mediated cytotoxicity induced by ifp injection of *C. parvum*. Mice were inoculated with 10 or 160 μg of *C. parvum* into one hind footpad. Eleven days later, the animals received a second iv injection of 160 μg of adjuvant. NK cell-mediated cytotoxicity in the spleen and regional and contralateral popliteal lymph nodes was assayed in vitro 3

TABLE 3.—C. parvum-*induced suppression of NK cell activation*

Treatment, iv[a]		NK cell-mediated cytotoxicity,[b] $LU_{20}/10^7$ lymphoid cells	
Day 0	Day 11	Lymph nodes	Spleen
—	—	3.6	18.6
—	*C. parvum*	72.7	187.8
—	Poly I·poly C	16.0	144.9
C. parvum	—	4.0	4.0
C. parvum	*C. parvum*	5.3 (98)	4.6 (100)
C. parvum	Poly I·poly C	6.3 (82)	17.0 (90)

[a] 6-wk-old $C3H^-$ mice were given iv injections of 160 μg *C. parvum* or 10 μg poly I·poly C.

[b] NK cell cytotoxicity was tested in vitro on day 14. *Numbers in parentheses* are percentages of inhibition of NK cell activation.

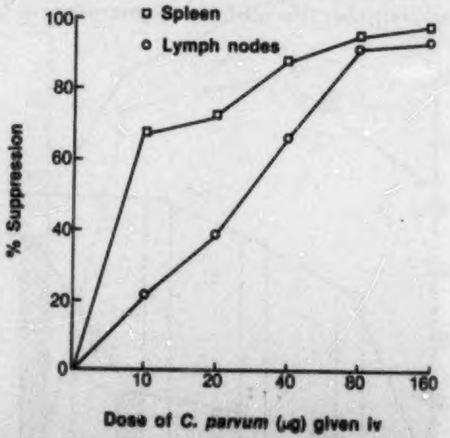

TEXT-FIGURE 4.—Suppressive effects of iv injections of *C. parvum* on the activation of NK cells in lymph nodes and spleen. $C3H^-$ mice were given iv injections of 10, 20, 40, 80, and 160 μg of *C. parvum*. Eleven days later, they received an iv challenge of 160 μg of *C. parvum*; 3 days later, NK cell-mediated cytotoxicity was assayed. Percent suppression was calculated as described in "Materials and Methods." The differences in percent suppression of spleen vs. lymph node NK cell activity observed with doses of 10 and 20 μg *C. parvum* were highly significant ($P<0.001$).

days after the iv challenge. The results (table 4) indicate that, unlike the generalized suppression observed following iv injection of *C. parvum*, NK cell suppression initiated by ifp injection of *C. parvum* was confined to the regional lymph nodes draining the site of inoculation. Thus ifp injection of 10-160 μg of *C. parvum* abrogated the response of NK cells in the regional popliteal lymph node, but not in the contralateral lymph node or spleen, to a second injection of *C. parvum* administered 11 days later. Local suppression of NK cell activity in the regional lymph nodes, but not in the spleen, also was detected when the second challenge with *C. parvum* was given into the same footpad rather than systemically (data not shown).

In Vitro Activation of Lymph Node NK Cells by Poly I•Poly C and IFN

We have demonstrated that activation and suppression of NK cells by local injections of *C. parvum* are compartmentalized and display restricted organ distribution patterns. To delineate further this phenomenon, we investigated whether lymph nodes from normal untreated mice contain cells that could be activated in vitro by IFN and IFN inducers. Under such in vitro conditions, the problems of in vivo recruitment and redistribution of activated cytotoxic cells are bypassed. Thus lymphoid cells pooled from popliteal, inguinal, axillary, and submandibular lymph nodes were incubated in vitro with either 0.5 μg poly I·poly C/ml for 24 hours or 500 U IFN/ml for 2 hours. The data shown in table 5 demonstrate that a brief incubation with IFN enhanced NK cell-mediated cytotoxicity in both spleen and lymph node cell preparations. Similarly, a 24-hour incubation with poly I·poly C activated lymph node NK cells, but only after the addition of 1-2% peritoneal adherent cells at the initiation of the incubation period (table 5). Quantitatively, the levels of NK cell-mediated cytotoxicity detected after in vivo or in vitro activation were uniformly higher in the spleen than in the lymph nodes.

TABLE 4.—*Localized suppression of NK cell activity in lymph nodes after ifp injection of* C. parvum

Treatment with *C. parvum*, dose/mouse		NK cell-mediated cytotoxicity,[a] LU_{20}/10^7 lymphoid cells		
		Popliteal lymph nodes		
Day 0, ifp	Day 11, iv	Regional[b]	Contralateral	Spleen
—	—	4.4	4.4	30.2
—	160	59.3	59.3	238.1
160	—	16.0	6.7	121.2
160	160	10.0 (100)	83.3	251.6
10	—	19.0	5.6	111.0
10	160	24.0 (91)	50.0	266.0

[a] NK cell cytotoxicity was tested in vitro on day 14.

[b] *Numbers in parentheses* are percentages of inhibition of NK cell activation.

TABLE 5.—*In vitro activation of NK cells by poly I·poly C and IFN*

No. of peritoneal adherent cells added per well[a]	Treatment[b]	NK cell-mediated cytotoxicity	
		Lymph nodes, LU_{10}/10^7 cells	Spleen, LU_{20}/10^7 cells
Expt I			
None	—	3.0	11.3
None	Poly I·poly C	3.5	48.9
2×10^5	—	6.7	15.5
2×10^5	Poly I·poly C	23.5	65.2
Expt II			
None	—	10.5	22.0
None	IFN	55.8	125.0

[a] Resident peritoneal cells were harvested from normal $C3H^-$ mice, and 2×10^5 adherent cells were added to the cultures as indicated.

[b] Lymph node or spleen cells (10^7 cells/well) obtained from 5-wk-old $C3H^-$ mice were incubated with 0.5 μg poly I·poly C/well or 500 U IFN/well for 24 and 2 hr, respectively.

DISCUSSION

Our findings demonstrate that activation or suppression of NK cells could be systemic or restricted to certain anatomical compartments, depending on the type, dose, and route of administration of the BRM. Also, the onset and/or duration of NK cell activation is affected primarily by the route of injection of the activating agent. Thus low doses of *C. parvum* injected into the footpad were highly effective in activating NK cells in the regional lymph nodes, spleen, and peripheral blood, but they failed to activate NK cells in mesenteric or contralateral popliteal lymph nodes. In contrast, when *C. parvum* was administered iv, large doses were required to activate lymph node NK cells, and the activity persisted for a much shorter time than activity induced by local ifp injection. At lower doses of *C. parvum*, NK cells were selectively activated in the spleen and peripheral blood, but not in popliteal lymph nodes. Similarly, ip injection of *C. parvum* activated NK cells in the spleen, peripheral blood, and mesenteric and inguinal lymph nodes but not in popliteal lymph nodes.

This result is in agreement with some (*21, 22*), but not all (*16*), recent reports that demonstrated successful activation of spleen NK cells after ip injection of bacterial adjuvants. Such discrepancies may be attributed to differences in the strain or age of the mice used. The anatomical compartmentalization of NK cell activation suggests that the evaluation of NK cell-mediated cytotoxicity at one site (spleen or peripheral blood) does not necessarily reflect activity at a different location (lymph nodes). Moreover, the absence of detectable NK cell activation in lymph nodes, despite the strong activation of peripheral blood NK cells, suggests that circulating activated NK cells do not migrate freely into normal, unstimulated lymph nodes. This is not surprising since recent studies have shown that activated NK cells differ from their naive counterparts in several characteristics (*23*). Thus activation of lymph node NK cells with *C. parvum* probably requires it to be delivered, perhaps within macrophages, to the site of activation where local production of small amounts of IFN is sufficient to activate NK cells in situ. This conclusion is substantiated by our observation of dose-dependent differences in NK cell activation in the popliteal lymph nodes induced by ifp or iv administration of *C. parvum* (text-fig. 3). Further evidence that the low blood levels of IFN induced by *C. parvum* treatment may be the limiting factor in attaining a generalized activation of NK cells is provided by the findings that local ifp injections of potent IFN inducers, such as poly I·poly C, activate NK cells in the regional as well as the contralateral lymph nodes. Thus when high blood levels of IFN were achieved, a more generalized activation of NK cells was observed without site restriction, such as restriction to the regional draining lymph nodes.

Recent evidence has indicated that stimulation of NK cell-mediated cytotoxicity by IFN involves the activation of precursors of NK cells and their maturation into highly cytotoxic effectors (*24, 25*). Therefore, in situ activation of NK cells in lymph nodes requires that such NK cell precursors be present at or recruited to the site of activation. Indeed, the natural cytotoxic activity of lymphoid cells from normal, unstimulated lymph nodes may be boosted in vitro by IFN or poly I·poly C. However, poly I·poly C-induced activation of lymph node NK cells in vitro required the addition of 1–2% normal peritoneal adherent cells. This finding agrees with that of previous studies showing that removal of macrophages inhibits the activation of NK cells by poly I·poly C but not by IFN (*26*). Although these experiments demonstrate that precursors of NK cells exist as a normal cellular constituent of unstimulated lymph nodes, they do not rule out that local injection of BRM such as *C. parvum* may recruit unactivated NK cells and/or their precursors together with accessory cells to the local draining lymph nodes. The hypercellularity observed in draining lymph nodes as early as 3 days after *C. parvum* injection suggests that local NK cell recruitment could be a significant component of the host response.

Recent studies have indicated that macrophages are required for stimulation of NK cell activity by BRM (*26–28*) and for the maintenance of normal levels of natural cytotoxicity in vivo (*26*). However, following activation with reticuloendothelial system stimulants, macrophages were found, although not invariably (*17*), to suppress the lytic activity of NK cells (*18*). Our findings indicate that the decline of NK cell activity that follows the early and transient activation by *C. parvum* is associated with a state of resistance to reactivation by the same or other unrelated NK cell stimulants. For example, an optimal challenge with *C. parvum* or poly I·poly C failed to boost NK cell activity in recipients treated 2 weeks earlier with an iv injection of *C. parvum*. Whereas low doses were sufficient to suppress selectively spleen NK cell reactivity, larger doses of *C. parvum* also induced suppression in lymph nodes. In contrast, local ifp injection of *C. parvum* inhibited the reactivation of NK cells in the draining lymph nodes without affecting the subsequent responsiveness of the spleen and the contralateral lymph nodes.

Although the suppressive mechanism may be mediated by suppressor cells, such as activated macrophages, it is clear that these cells do not migrate freely into all lymphoid organs. The possibility that site-specific utilization or depletion of NK cells and/or their precursors by the first adjuvant injection might be responsible for the inhibition of subsequent NK cell activation seems very remote, since nylon wool-purified lymph node cells obtained from "suppressed" *C. parvum*-treated mice could be activated in vitro with IFN (Hisano G: Unpublished observation). Dilution of NK cells by unrelated noncytotoxic cells recruited to the enlarged spleen or lymph nodes by *C. parvum* injection does not seem to contribute significantly to the observed suppression. For example, the number of lymphoid cells recovered from unresponsive popliteal lymph nodes 2 weeks after ifp injection of adjuvant was only 1.3 times higher than that found in lymph nodes at the peak of NK cell response (day 3). Also, large doses of *C. parvum* administered iv markedly suppressed the subsequent activation of lymph node NK cells without increasing the total number of cells per lymph node. However, it could not be ruled out that *C. parvum*-induced histologic alteration in lymph node structure may also contribute to the suppressed response.

In any event, the type and route of administration of NK cell stimulants are important for achievement and maintenance of high levels of NK cell activity at specific lymph nodes. Moreover, the possible generation of long-lasting local or systemic suppression of NK cells indicates that multiple injections of BRM are not necessarily effective in maintaining the high levels of NK cell activity required for the control of tumor cell growth and dissemination.

REFERENCES

(*1*) Warner NL, Woodruff MF, Burton RC. Inhibition of the growth of lymphoid tumours in syngeneic athymic (nude) mice. Int J Cancer 1977; 20:146–155.

(*2*) Minato N, Bloom BR, Jones C, Holland J, Reid LM. Mechanism of rejection of virus persistently infected tumor cells by athymic nude mice. J Exp Med 1979; 149:1117–1133.

(*3*) Hanna N. Expression of metastatic potential of tumour cells in young nude mice is correlated with low levels of natural killer cell-mediated cytotoxicity. Int J Cancer 1980; 26:675–680.

(*4*) Riesenfeld I, Orn A, Gidlund M, Axberg I, Alm GU, Wigzell H. Positive correlation between in vitro NK activity and in vivo resistance towards AKR lymphoma cells. Int J Cancer 1980; 25:399–403.

(*5*) Kasai M, Leclerc JC, McVay-Boudreau L, Shen FW, Cantor H. Direct evidence that natural killer cells in nonimmune spleen cell populations prevent tumor growth in vivo. J Exp Med 1979; 149:1260–1264.

(*6*) Gorelick E, Fogel M, Feldman M, Segal S. Differences in resistance of metastatic tumor cells and cells from local tumor growth to cytotoxicity of natural killer cells. JNCI 1979; 63:1397–1404.

(*7*) Talmadge JE, Meyers KM, Prieur DJ, Starkey JR. Role of NK cells in tumour growth and metastasis in beige mice. Nature 1980; 284:622.

(*8*) Hanna N, Fidler IJ. Role of natural killer cells in the destruction of circulating tumor emboli. JNCI 1980; 65:801–809.

(*9*) Campanile F, Crino L, Bonmassor E, Houchens E, Goldin A. Radioresistant inhibition of lymphoma growth in congenitally athymic (nude) mice. Cancer Res 1977; 37:394–398.

(*10*) Hanna N, Fidler IJ. Relationship between metastatic potential and resistance to natural killer cell-mediated cytotoxicity in three murine tumor systems. JNCI 1981; 66:1183–1190.

(*11*) Riccardi C, Puccetti P, Santoni A, Herberman RB. Rapid in vivo assay of mouse natural killer cell activity. JNCI 1979; 63:1041–1045.

(*12*) Herberman RB, Nunn ME, Lavrin DH. Natural cytotoxic reactivity of mouse lymphoid cells against syngeneic and allogeneic tumours. I. Distribution of reactivity and specificity. Int J Cancer 1975; 16:216–229.

(*13*) Kiessling R, Klein E, Wigzell H. Natural killer cells in the mouse

A. Cytotoxic cells with specificity for mouse Moloney leukemia cells. Specificity and distribution according to genotype. Eur J Immunol 1975; 5:112–117.

(14) Hanna MG Jr, Peters LC. Efficacy of intralesional BCG therapy in guinea pigs with disseminated tumor. Cancer 1975; 36:1298–1304.

(15) Zbar B, Bernstein ID, Bartlett GL, Hanna MG Jr, Rapp HJ. Immunotherapy of cancer: Regression of intradermal tumors and prevention of growth of lymph node metastases after intralesional injection of living *Mycobacterium bovis*. J Natl Cancer Inst 1972; 49:119–130.

(16) Ojo E, Haller O, Kimura A, Wigzell H. An analysis of conditions allowing *Corynebacterium parvum* to cause either augmentation or inhibition of natural killer cell activity against tumour cells in mice. Int J Cancer 1978; 21:444–452.

(17) Lotzova E. *C. parvum*-mediated suppression of the phenomenon of natural killing and its analysis. In: Herbermann RB, ed. Natural cell-mediated immunity against tumors. New York: Academic Press, 1980:735–752.

(18) Santoni A, Riccardi C, Barlozzari T, Herberman RB. Suppression of activity of mouse natural killer (NK) cells by activated macrophages from mice treated with pyran copolymer. Int J Cancer 1980; 26:837–843.

(19) Cikes M, Friberg S Jr, Klein G. Progressive loss of H-2 antigens with concomitant increase of cell-surface antigen(s) determined by Moloney leukemia virus in cultured murine lymphomas. J Natl Cancer Inst 1973: 50:347–362.

(20) Djeu JY, Heinbaugh JA, Holden HT, Herberman RB. Augmentation of mouse natural killer cell activity by interferon and interferon inducers. J Immunol 1979; 122:175–181.

(21) Herberman RB, Nunn ME, Holden HT, Staal S, Djeu JR. Augmentation of natural cytotoxic reactivity of mouse lymphoid cells against syngeneic and allogeneic target cells. Int J Cancer 1977; 19:555–564.

(22) Nasrallah AG, Gallagher MT, Priest EL, Trentin JJ. Comparative effects of different strains of *Corynebacterium parvum* on natural cell-mediated cytotoxicity. Cancer Res 1980; 40:4159–4164.

(23) Welsh RM Jr. Mouse natural killer cells: Induction specificity, and function. J Immunol 1978; 121:1631–1635.

(24) Minato N, Reid L, Cantor H, Lengyel P, Bloom B. Mode of regulation of natural killer cell activity by interferon. J Exp Med 1980; 152:124–137.

(25) Targan S, Dorey F. Interferon activation of "Pre-spontaneous killer" (Pre-SK) cells and alteration in kinetics of lysis of both "Pre-SK" and active SK cells. J Immunol 1980; 124:2157–2161.

(26) Djeu JY, Heinbaugh JA, Holden HT. Role of macrophages in the augmentation of mouse natural killer cell activity by poly I·C and interferon. J Immunol 1979; 122:182–188.

(27) Tracey DE. The requirement for macrophages in the augmentation of natural killer cell activity by BCG. J Immunol 1979; 123:840–845.

(28) Puccetti P, Santoni A, Riccardi C, Holden H, Herberman RB. Activation of mouse macrophages by pyran copolymer and role in augmentation of natural killer activity. Int J Cancer 1979; 24:819–830.

blank page

Androgen Control of Cytosol Progesterone Receptor Levels in the MT-W9B Transplantable Mammary Tumor in the Rat[1,2,3]

Margot M. Ip,[4] Richard J. Milholland,[4] Untae Kim,[5] *and* Fred Rosen[4,6]

ABSTRACT—The effect of androgen on the levels of the cytosol progesterone receptor was examined in the transplantable rat mammary tumor MT-W9B and in the normal uteri of inbred WF rats. Progesterone receptor levels were barely detectable in tumors grown in male WF rats but were increased after castration or administration of 17β-estradiol. Both effects were blocked by testosterone. In tumors grown in intact female rats, both testosterone and dihydrotestosterone decreased progesterone receptor levels in a dose-dependent manner, and testosterone completely blocked the estradiol-induced increase in progesterone receptor levels in tumors from ovariectomized rats. The inhibitory effect of testosterone in female rats was blocked by the antiandrogen flutamide, suggesting an androgen receptor-dependent mechanism. Neither dihydrotestosterone nor testosterone had any effect on basal levels of progesterone receptor in tumors from ovariectomized rats. In uterus, up to 5 mg dihydrotestosterone/kg did not affect progesterone receptor levels, and a dose of 5 mg/kg was also uterotropic. This fact plus the finding that testosterone only partially blocked the estradiol-induced increase in uterine progesterone receptor levels suggested stimulation of different cell types by testosterone and estradiol. This did not appear to be the case in the tumor, however. Androgen is suggested to act as a negative modulator of progesterone receptor levels, which might have clinical relevance in terms of hormone therapy of breast cancer.—JNCI 1982; 69:673–681.

Androgens were shown to be effective in the treatment of many cases of human breast cancer (*1*); however, the mechanism by which this occurs is still not understood. On the basis of studies in animal model systems, such as the DMBA-induced mammary tumor in rats, several possibilities have been proposed to account for androgen-induced tumor regression. Quadri et al. (*2*) found, for example, that although prolactin secretion was not decreased after the administration of androgens, the administration of prolactin concurrently with androgen could overcome the inhibitory effect. They suggested that androgen might be acting by blocking the peripheral ability of prolactin to promote mammary tumor growth. In agreement with this concept is the finding of Costlow et al. (*3*) that androgen-induced tumor regression was accompanied by a decrease in the level of prolactin receptors in the tumor, although this decrease was not thought to be sufficient to account for the regression. Also, androgen administration decreases estrogen receptor levels in regressing DMBA-induced mammary tumors (*4*), thereby possibly resulting in a decreased sensitivity to estrogen in this estrogen-dependent tumor.

In addition to inhibitory effects of androgen on tumor growth, stimulatory effects have also been observed (*5–7*), which instills concern in regard to patient treatment. Approximately 30% of human breast cancers contain the androgen receptor (*8*); so they are potentially sensitive to the stimulatory effects of androgens via an androgen receptor-dependent mechanism. Androgen receptors have also been demonstrated to be present in several rodent mammary tumors (9–11); at least one of these, the Shionogi mammary tumor, has been shown to be androgen dependent (*10*). Biphasic effects of androgens on the growth of the 7,12-dimethylbenz[*a*]anthracene-induced mammary tumor and the transplantable mammary tumor MT-W9A have also been demonstrated (*5, 12*). The stimulatory effect observed at very high doses may occur via an estrogen receptor-dependent mechanism, since at these concentrations androgens have been shown to cause nuclear translocation of the estrogen receptor in several systems including the 7,12-dimethylbenz[*a*]anthracene-induced mammary tumor (*13, 14*), the human breast cancer cell line MCF-7 (*7*), and the rat uterus (*15–19*). That this translocation is functional is evidenced by an increased synthesis of estrogen-dependent proteins, including the induced protein of uterus and the progesterone receptor (*7, 13, 16, 18, 20, 21*).

Our interest in this topic arose from preliminary observations that suggested that in contrast to the situation observed with estrogen-dependent tissues and tumors, both physiologic and pharmacologic doses of androgens appeared to decrease progesterone receptor levels in the estrogen-independent mammary tumor MT-W9B (*22*). This tumor is considered estrogen independent by virtue of its growth in both male and female syngeneic WF rats and by lack of effect on its growth rate by ovariectomy or hypophysectomy (*23*). Receptors for androgen (*9*), estrogen (*24*), progesterone (*24*), and dexamethasone (Ip MM, Milholland RJ, Rosen F: Unpublished observations) are present in the tumor and, despite the lack of effect of estrogen on growth, estrogen is involved in regulation of progesterone receptor levels (*24*). Tumor regression was not observed in response to pharmacologic doses of either androgen (*9*) or estrogen (*24*). Since estrogen regulation of progesterone receptor levels has been reported in many systems (normal tissues as well as tumors) (*25–30*), we thought it important to further clarify androgen effects on the progesterone receptor and in particular to examine androgen–estrogen interactions in this regard.

MATERIALS AND METHODS

Animals and tumors.—The MT-W9B mammary tumor (*23*)

---

[1] Received November 25, 1981; accepted April 7, 1982.

[2] Supported in part by American Cancer Society grant PDT-76E and by Public Health Service grants CA-22761 and CA-24538 from the National Cancer Institute.

[3] Guidelines for the care and use of laboratory animals are followed as set forth by the Roswell Park Memorial Institute.

[4] Department of Experimental Therapeutics, Grace Cancer Drug Center, Roswell Park Memorial Institute, New York State Department of Health, 666 Elm St., Buffalo, N.Y. 14263.

[5] Department of Pathology, Roswell Park Memorial Institute.

[6] We thank Ms. Wendy Shea, Mrs. Doris Robinson, and Mr. Tom Turnbull for excellent technical assistance.

was transplanted by trocar into 8- to 10-week-old inbred male (200–250 g) or female (140–160 g) WF rats (M.A. Bioproducts, Walkersville, Md.) and became palpable in about 3–3.5 weeks. All rats were maintained in temperature-controlled rooms with a 12-hour light–12-hour dark schedule and were fed ad libitum Teklad rat chow (Teklad Inc., Madison, Wis.) and water. Gonadectomies were performed under pentobarbital sodium anesthesia in our laboratory at various times after tumor transplant. The exact details for each experiment are given in the appropriate table, text-figure, or figure legend.

Reagents.—[1,2,6,7-^{3}H]progesterone (110 Ci/mmol) was purchased from Amersham/Searle Corp., Arlington Heights, Ill. All unlabeled steroids were obtained from Sigma Chemical Co., St. Louis, Mo. Flutamide was a gift of Dr. Arthur Watnick, Schering Corp., Bloomfield, N.J. Dextran-coated charcoal was prepared as described previously (*9*). The scintillation fluid 3a70 was a product of Research Products International Corp., Elk Grove Village, Ill.

Receptor assays.—Cytosol was prepared and stripped of endogenous steroids as described in (*9*). Binding of [^{3}H]-progesterone to tumor cytosol was measured by incubation of 75 µl charcoal-treated cytosol with 5 µl [^{3}H]progesterone (final assay concentration, 20 n*M*) or 5 µl [^{3}H]progesterone containing a hundredfold-molar excess of unlabeled progesterone for 2 hours at 4°C in conical Microtiter plates. We also added a thousandfold-molar excess of hydrocortisone to all incubations to correct for binding of progesterone to the hydrocortisone-binding globulin. At the end of the incubation, bound steroid was separated from free by the addition of 25 µl of a suspension of 5% charcoal–0.5% dextran directly to the Microtiter plate. This incubation mixture with charcoal–dextran was allowed to stand for 2 minutes and then was centrifuged at 850×*g* for 10 minutes, and 75 µl of the supernatant was counted. We made radioactivity measurements in 5 ml scintillation fluid by means of a Beckman LS-100C or LS-150 liquid scintillation counter. Counting efficiency for ^{3}H averaged 40–45%. Specific binding was defined as the difference between total binding and binding in the presence of a hundredfold-molar excess of unlabeled progesterone. Protein in the cytosol was determined according to the procedure of Lowry et al. (*31*).

Statistics—The significance of the difference between two means was evaluated on the basis of Student's *t*-test.

RESULTS

Progesterone receptor levels in tumors grown in male or female rats.—As can be seen in table 1, progesterone receptor levels were near the lower limit of detection in tumors grown in male rats; however, substantial quantities were present in tumors from female rats. Tumors grew well in both male and female rats but were slightly larger (*P*<0.02) in males at the time the rats were killed (table 1).

Estrogen and androgen interactions on progesterone receptor levels in tumors grown in male rats.—To help elucidate the hormonal regulation of progesterone receptor levels in tumors grown in male or female rats, we did an experiment to determine if the progesterone receptor could be induced by estrogen in tumors grown in male rats, and if so, if the effect could be blocked by the concurrent administration of androgen. Text-figure 1 shows that administration of estradiol benzoate at a dose of 25 µg/kg body weight caused a substantial increase in progesterone receptor levels in tumors from both intact and castrated rats. Castration in rats also caused an increase in tumor progesterone receptor levels—a fivefold increase, which was blocked by the administration of 5 mg testosterone propionate/kg (text-fig. 1). Testosterone propionate at the same dose also completely blocked the 17β-estradiol-stimulated enhancement of progesterone receptor levels (text-fig. 1). None of these treatments had any signif-

TABLE 1.—*Effect of sex on tumor progesterone receptor and tumor weight*[a]

Sex	Progesterone receptor, fmol/mg protein	Tumor wt, g
Male	16.7±7.1	4.44±0.51
Female	288±38[b]	2.37±0.53[c]

[a] MT-W9B tumor was transplanted into either male or female WF rats, and rats were killed 42 days later. Values are means ± SEM of 10 rats/group.

[b] Statistically different (*P*<0.01) compared to male.

[c] Statistically different (*P*<0.02) compared to male.

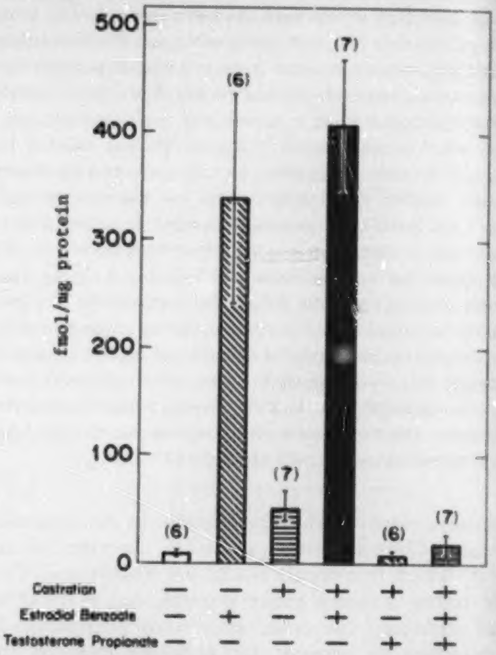

TEXT-FIGURE 1.—Effect of castration, estradiol benzoate, and testosterone propionate on progesterone receptor levels in the MT-W9B tumor grown in WF male rats. Rats were castrated or sham castrated 27 days after tumor transplant, and injections of estradiol benzoate (25 µg/kg), testosterone propionate (5 mg/kg), or the corn oil vehicle were initiated 28 days after transplant. Injections were given sc five times/wk. Rats were killed 24 hr after the last injection, 37 days after transplant (seven total injections). *Each bar* represents mean ± SEM. Number of rats/group is shown *in parentheses*. Statistical significance: intact vs. intact + estradiol benzoate, *P*<0.01; intact vs. castrated, *P*<0.01; castrated vs. castrated + estradiol benzoate, *P*<0.01; castrated vs. castrated + testosterone propionate, *P*<0.02; castrated + estradiol benzoate vs. castrated + estradiol benzoate + testosterone propionate, *P*<0.01. Treatment or lack thereof is indicated by *plus* or *minus signs*, respectively.

TABLE 2.—*Effect of castration, estradiol benzoate, and testosterone propionate on tumor and seminal vesicle weight*[a]

Rat group	Tumor wt, g	Seminal vesicle wt, g
Sham castrated	2.08±0.43	0.82±0.02
Sham castrated + estradiol benzoate	2.43±0.39	0.30±0.02
Castrated	1.36±0.36	0.20±0.01
Castrated + estradiol benzoate	1.89±0.16	0.29±0.03
Castrated + testosterone	2.21±0.15	1.65±0.21
Castrated + estradiol benzoate + testosterone	1.55±0.18	1.74±0.11

[a] These data are from the experiment described in the legend to text-fig. 1. Values are means ± SEM. Statistical significance of the data is as follows—none of the tumor wt are significantly different; for the seminal vesicles: intact vs. intact + estradiol benzoate, $P<0.01$; intact vs. castrated, $P<0.01$; castrated vs. castrated + estradiol benzoate, $P<0.02$; castrated vs. castrated + testosterone propionate, $P<0.01$; castrated + estradiol benzoate vs. castrated + estradiol benzoate + testosterone propionate, not significant.

icant effect on tumor growth (table 2), although a tendency was seen for the tumor to be smaller in untreated castrated rats than in intact controls. We have observed that a longer period of castration than that used in this experiment does significantly retard growth of this tumor in male rats (Ip MM, Milholland RJ: Unpublished observations). Seminal vesicle weights are also presented in table 2 as an index of the effectiveness of the hormonal manipulations.

Estrogen and androgen interactions on progesterone receptor levels in tumors grown in female rats.—The data from the male rats suggested that testosterone could be a physiologic negative modulator of progesterone receptor levels; we were interested to determine if testosterone would also exhibit an inhibitory influence in tumors grown in female rats. Text-figure 2 shows that this was the case. As previously described (*24*), progesterone receptor levels were decreased by ovariectomy and induced by the administration of 17β-estradiol to ovariectomized rats; however, this increase was blocked by concurrent administration of testosterone propionate. Testosterone propionate alone at 5 mg/kg had no significant effect on progesterone receptor levels in tumors from ovariectomized rats (text-fig. 2). None of the treatments had any effect on tumor growth (table 3); however, it is interesting that testosterone propionate (5 mg/kg) increased the weight of the uterus from these ovariectomized rats to the same extent as did 25 µg estradiol benzoate/kg. Also, the combination of estradiol and testosterone was more uterotropic than either hormone administered alone.

Estrogen and androgen interactions on progesterone receptor levels in uterus.—In the preceding experiment testosterone appeared to be acting as an antiestrogen in terms of its effect on progesterone receptor levels in the tumor and as an estrogen in terms of its effect on uterine growth. Thus we measured progesterone receptor levels in the uterus of the same animals (text-fig. 3). When the data were expressed as femtomoles per milligram protein (text-fig. 3A), ovariectomy showed no effect on progesterone receptor levels; however, 17β-estradiol administration to ovariectomized rats caused a significant stimulation. This was not blocked by concurrent administration of testosterone propionate, but the administration of testosterone propionate alone to ovariectomized rats significantly decreased uterine progesterone receptor levels ($P<0.02$). When the data were expressed as femtomoles per uterus (text-fig. 3B), ovariectomy significantly decreased the total progesterone receptor content of the uterus, whereas both 17β-estradiol and testosterone independently caused a significant increase (eightfold and twofold, respectively). Testosterone administration concurrently with 17β-estradiol only slightly blocked the stimula-

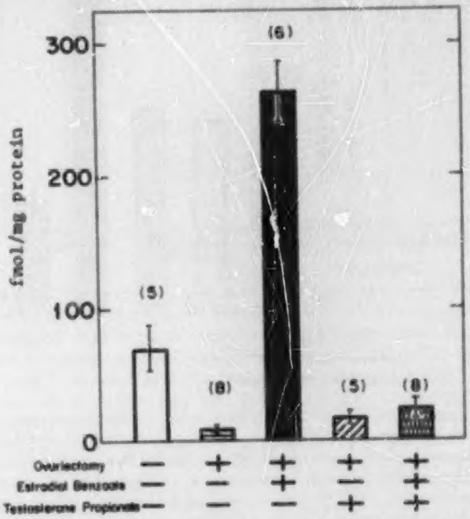

TEXT-FIGURE 2.—Effect of ovariectomy, estradiol benzoate, and testosterone propionate on progesterone receptor levels in the MT-W9B tumor grown in WF female rats. Rats were ovariectomized or sham ovariectomized 38 days after tumor transplant, and injections of estradiol benzoate (25 µg/kg), testosterone propionate (5 mg/kg), or the corn oil vehicle were initiated 39 days after transplant. Injections were given sc five times/wk. Rats were killed 24 hr after the last injection, 52 days after transplant (nine total injections). Statistical significance: intact vs. ovariectomized, $P<0.01$; ovariectomized vs. ovariectomized + estradiol benzoate, $P<0.01$; ovariectomized vs. ovariectomized + testosterone propionate, not significant; ovariectomized + estradiol benzoate vs. ovariectomized + estradiol benzoate + testosterone propionate, $P<0.01$. For meanings of *bar*, *numbers in parentheses*, and *minus and plus signs*, see legend for text-fig. 1.

TABLE 3.—*Effect of ovariectomy, estradiol benzoate, and testosterone propionate on tumor and uterus weight*[a]

Rat group	Tumor wt, g	Uterus wt, g
Sham ovariectomized	5.93±0.87	0.34±0.02
Ovariectomized	5.09±0.93	0.15±0.01
Ovariectomized + estradiol benzoate	5.72±0.49	0.40±0.01
Ovariectomized + testosterone propionate	4.64±0.77	0.38±0.02
Ovariectomized + estradiol benzoate + testosterone propionate	4.66±0.95	0.46±0.02

[a] These data are from the experiment described in the legend to text-fig. 2. Values are means ± SEM. Statistical significance of the data is as follows—none of the tumor wt are significantly different; for the uterus: sham ovariectomized vs. ovariectomized, $P<0.01$; ovariectomized vs. ovariectomized + estradiol benzoate, $P<0.01$; ovariectomized vs. ovariectomized + testosterone propionate, $P<0.01$; ovariectomized + estradiol benzoate vs. ovariectomized + estradiol benzoate + testosterone propionate, $P<0.05$; ovariectomized + testosterone propionate vs. ovariectomized + estradiol benzoate + testosterone propionate, $P<0.02$.

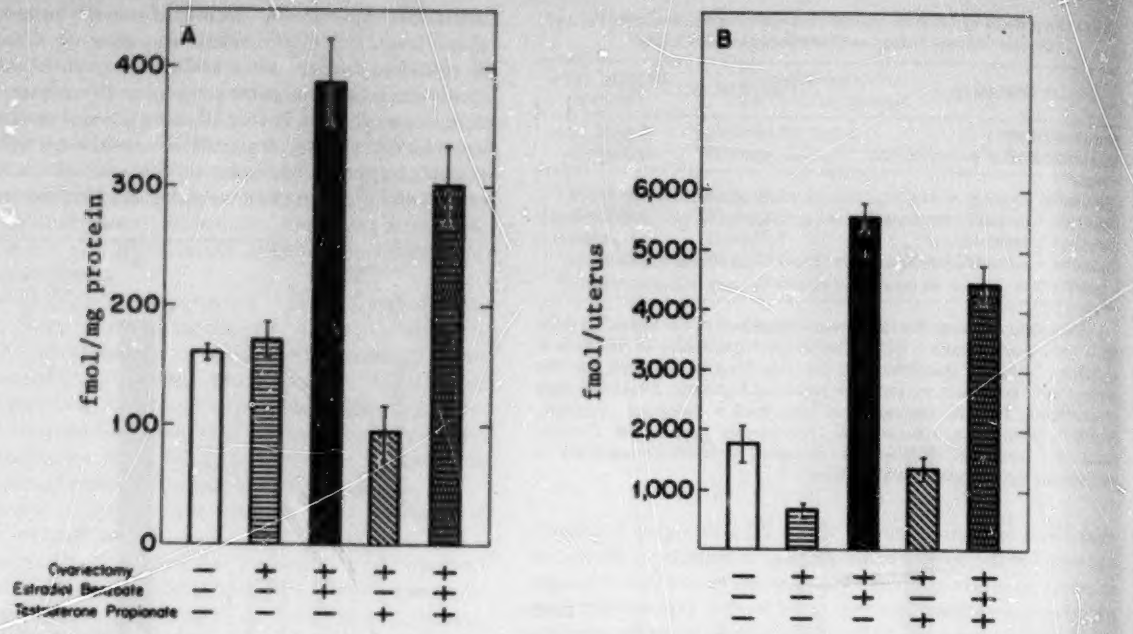

TEXT-FIGURE 3.—Effect of ovariectomy, estradiol benzoate, and testosterone propionate on progesterone receptor levels in uterus. Uteri are from the same animals described in the legend to text-fig. 2. Statistical significance: progesterone receptor as fmol/mg protein: intact vs. ovariectomized, not significant; ovariectomized vs. ovariectomized + estradiol benzoate, $P<0.01$; ovariectomized vs. ovariectomized + testosterone propionate, $P<0.02$; ovariectomized + 17β-estradiol vs. ovariectomized + 17β-estradiol + testosterone propionate, not significant. Progesterone receptor as fmol/uterus: intact vs. ovariectomized, $P<0.01$; ovariectomized vs. ovariectomized + estradiol benzoate, $P<0.01$; ovariectomized vs. ovariectomized + testosterone propionate, $P<0.01$; ovariectomized + estradiol benzoate vs. ovariectomized + 17β-estradiol + testosterone propionate, $P<0.05$. For meanings of *bar* and *plus and minus signs, see* legends to text-fig. 1.

tory effect of 17β-estradiol. The apparent discrepancy between the effects of testosterone alone on progesterone receptor levels when expressed as femtomoles per milligram protein and as femtomoles per uterus basis (decrease and increase, respectively) is due to the uterine weight being more than doubled as a result of this treatment (2.5-fold increase; table 3) and the uterine protein concentration being slightly increased (1.5-fold) after treatment.[7]

Effect of varying doses of dihydrotestosterone benzoate and testosterone propionate on progesterone receptor levels in the MT-W9B tumor and in uterus from intact rats.—In addition to examining the effect of testosterone in ovariectomized rats, we also tested the effect of testosterone in intact rats and compared the effect of dihydrotestosterone, the active metabolite of testosterone in many tissues, with that of testosterone. Text-figure 4 shows a comparison of the dose-response relationship between dihydrotestosterone benzoate and testosterone propionate on progesterone receptor levels in the tumor. Both dihydrotestosterone and testosterone were equally effective in reducing tumor progesterone receptor levels. The response appeared to be dose related, although only the dose of 5 mg/kg was statistically significant. In other experiments (text-fig. 5 and data not shown), 0.5 mg testosterone propionate/kg did cause a significant decrease in progesterone receptor levels in the tumor. Increase in the dose of testosterone propionate to 50 mg/kg did not have any further effect on progesterone receptor levels beyond that seen with 5 mg/kg (data not shown). Tumor weights were not significantly affected by dihydrotestosterone or testosterone in the experiment described in text-figure 4 or by doses of 0.05, 0.5, or 5.0 mg dihydrotestosterone benzoate/kg in ovariectomized rats (data not shown). In addition, dihydrotestosterone benzoate, at the same three doses noted in the legend to text-figure 4, had no effect on progesterone receptor levels in tumors from ovariectomized rats (data not shown).

In uterus, increasing doses of dihydrotestosterone benzoate had no effect on progesterone receptor levels when expressed on the basis of femtomoles per milligram protein (text-fig. 6A). On the basis of femtomoles per uterus, the highest dose resulted in an approximate 50% decrease in progesterone receptor levels, reflecting the similar decrease in uterine weight (text-fig. 6B). The same three doses of dihydrotestosterone benzoate had no effect on uterine weight in ovariectomized rats (data not shown). In contrast to dihydrotestosterone benzoate, testosterone propionate showed a dose-dependent decrease in progesterone receptor levels in uterus from intact rats when results were expressed as femtomoles per milligram protein. On the basis of femtomoles per uterus, progesterone receptor levels were decreased by both doses at 0.5 and 5 mg/kg; however, the decrease at dose 5 mg/kg was not as remarkable because this dose also doubled the size of the uterus (text-fig. 6B).

Effect of flutamide on progesterone receptor levels in tumor and uterus from control and testosterone-treated intact rats.—To test

---

[7] In none of the other experiments described in this paper did a change in protein concentration as a result of hormone manipulation affect the results presented.

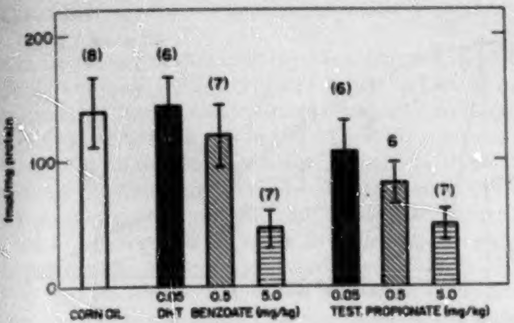

TEXT-FIGURE 4.—Effect of varying doses of dihydrotestosterone (DHT) benzoate and testosterone (TEST.) propionate on progesterone receptor levels in the MT-W9B tumor grown in WF female rats. Rats were given sc injections five times/wk, starting 32 days after transplant, with DHT benzoate (0.05, 0.5, or 5 mg/kg body wt), TEST. propionate (0.05, 0.5, or 5 mg/kg), or the corn oil vehicle. Rats were killed 24 hr after the last injection, 49 days after transplant (13 total injections). Statistical significance: control vs. DHT (0.05), not significant; control vs. DHT (0.5), not significant; control vs. DHT (5), $P<0.02$; control vs. TEST. propionate (0.05), not significant; control vs. TEST. propionate (0.5), not significant; control vs. TEST. propionate (5), $P<0.02$. For meanings of *bar* and *numbers in parentheses*, *see* legend for text-fig. 1.

whether the androgen effect was mediated through an androgen receptor mechanism, we performed an experiment to determine if the antiandrogen flutamide would block the response. Flutamide, at a dose of 20 mg/kg, completely blocked the inhibitory effect of 0.5 mg testosterone propionate/kg on progesterone receptor levels in the MT-W9B tumor (text-fig. 5). By itself, flutamide had no significant effect. Tumor weight was slightly, although not significantly, increased by testosterone propionate and decreased by flutamide (table 4). Tumors from rats receiving the combined regimen were significantly ($P<0.05$) smaller than those from the control animals.

In uterus from the same animals, neither testosterone nor flutamide had any significant effect on progesterone receptor levels; however, the combination resulted in a significant increase when expressed both as femtomoles per milligram protein and as femtomoles per uterus (text-fig. 7). None of these treatments had any effect on the weight of the uterus (table 4).

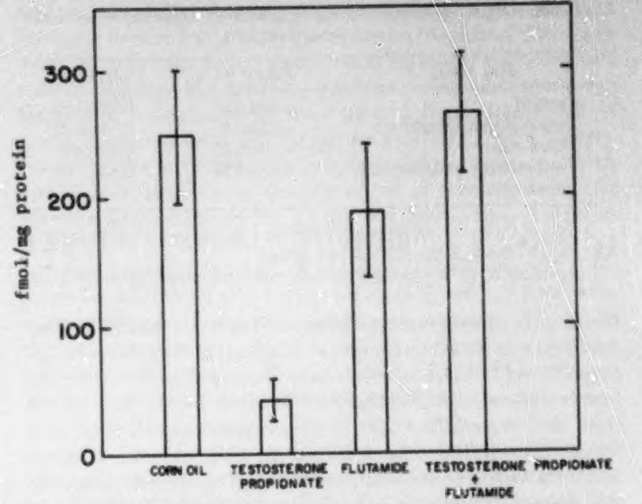

TEXT-FIGURE 5.—Effect of flutamide on the testosterone-induced decrease in cytosol progesterone receptor levels in the MT-W9B tumor grown in WF female rats. Rats were given sc injections five times/wk starting 25 days after transplant, with testosterone propionate (0.5 mg/kg), flutamide (20 mg/kg), the combination of testosterone propionate and flutamide, or the corn oil vehicle. Rats were killed 24 hr after the last injection, 37 days after transplant (eight total injections). *Each bar* represents mean ± SEM of 10 rats/group. Statistical significance: control vs. testosterone propionate, $P<0.01$; testosterone propionate vs. testosterone propionate + flutamide, $P<0.01$; control vs. flutamide, not significant; control vs. testosterone propionate + flutamide, not significant.

Competition of dihydrotestosterone and testosterone for binding of [^{3}H]progesterone to tumor and uterus.—Both testosterone and dihydrotestosterone competed for [^{3}H]progesterone binding to tumor; however, the affinity was much less than that of progesterone (text-fig. 8). Similar observations were made in the uterus (data not shown). Physiologically, this would result in interference of the action of progesterone only if

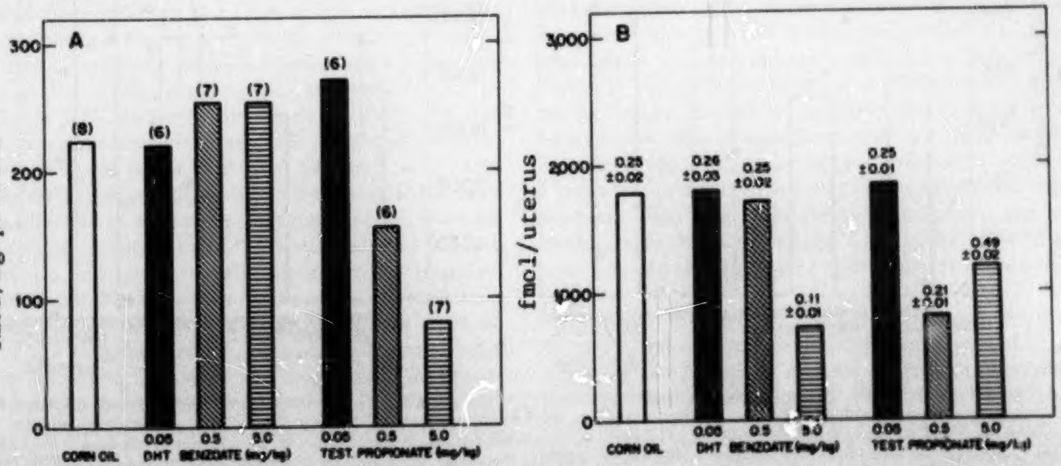

TEXT-FIGURE 6.—Effect of varying doses of dihydrotestosterone (DHT) benzoate and testosterone (TEST.) propionate on progesterone receptor levels in uterus. Uteri are from the same animals described in the legend to text-fig. 4. Assays were done on pooled uteri (3-10 uteri/group, depending on size of uterus). A) *Numbers in parentheses* represent No. of rats/group. B) *Numbers above bars* represent mean wt (g) of the uterus ± SEM.

TABLE 4.—*Effect of testosterone propionate and flutamide on tumor and uterus weight*[a]

Rat group	Tumor wt, g	Uterus wt, g
Control	3.52±0.63	0.36±0.02
Testosterone propionate	4.65±0.81	0.35±0.02
Flutamide	2.73±0.45	0.35±0.02
Testosterone propionate + flutamide	2.50±0.39[b]	0.35±0.01

[a] This is the same experiment described in the legend to text-fig. 5. Values are means ± SEM of 10 rats/group.

[b] Significantly different than testosterone propionate alone ($P<0.05$).

the level of androgen relative to progesterone was high. One could argue that our observed effect of testosterone on progesterone receptor levels was due to the fact that the testosterone was not sufficiently cleared by the rats at the time they were killed (24 hr after injection) and that, as a result, testosterone interfered in the progesterone receptor assay by virtue of its binding to the progesterone receptor. We do not think this is so, however, on the basis of two additional experiments. In the first of these, we found that tumor cytosol progesterone receptor levels returned to normal 16 hours after a single injection of 5 mg testosterone/kg. Whereas the decrease observed at earlier time periods could have been due to testosterone occupation of progesterone receptor sites, this testosterone occupation did not result in nuclear translocation of this receptor (data not shown). In the second experiment, we found that the effect of testosterone on progesterone receptor levels in the tumor was not manifested until after 4 days of therapy (5 mg testosterone/kg, daily, with the rats being killed 24 hr after the final injection). If testosterone was simply interfering in the progesterone receptor assay, the effect would have been observed after only a single injection (data not shown). Possibly, endogenous androgen partially interfered in the progesterone receptor assay in tumors from male rats; a portion of the increase in progesterone receptor levels after castration could be due to clearance of this endogenous androgen.

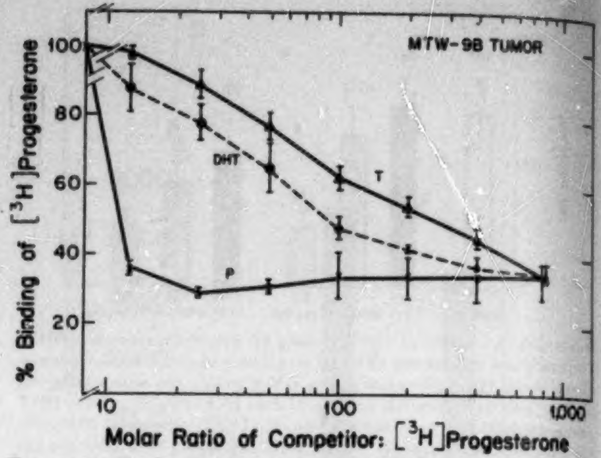

TEXT-FIGURE 8.—Competition of progesterone (P), dihydrotestosterone (DHT), and testosterone (T) for [^{3}H]P binding to MT-W9B mammary tumor cytosol. Cytosol was incubated in the presence of 11 n*M* [^{3}H]P plus varying concentrations of unlabeled steroid as described in "Materials and Methods." *Each bar* represents the mean ± SEM of three separate determinations and is plotted as specific binding. A thousand-fold-molar excess of hydrocortisone was present in all cases to correct for binding of P to the hydrocortisone-binding globulin.

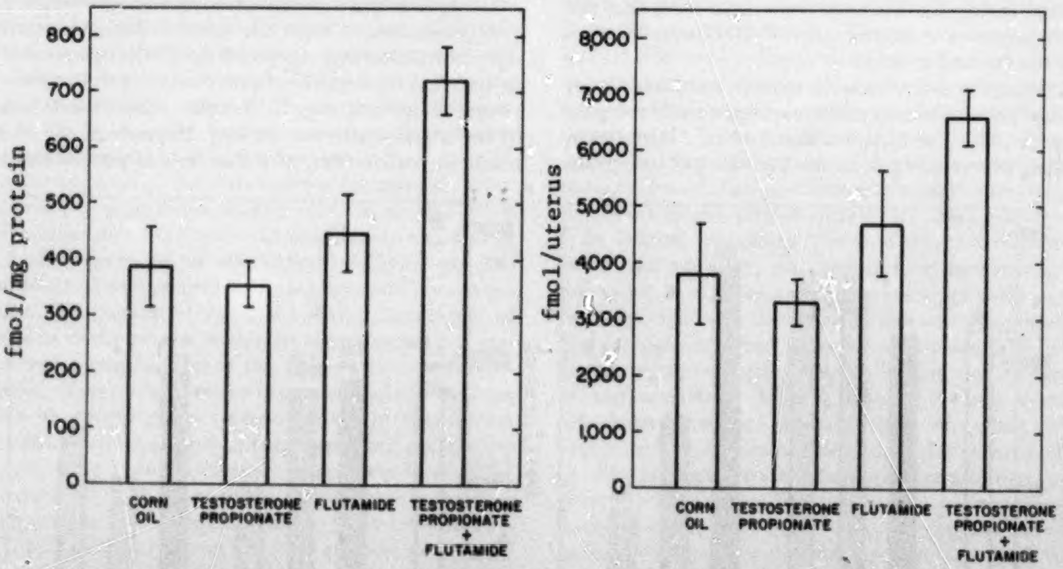

TEXT-FIGURE 7.—Effect of flutamide and testosterone on progesterone receptor levels in uterus. Uteri are from the same animals described in legend to text-fig. 5 and were assayed individually. *Each bar* represents mean ± SEM of 10 rats/group. Statistical significance: progesterone receptor as fmol/mg protein: control vs. testosterone propionate, not significant; control vs. flutamide, not significant; control vs. testosterone propionate + flutamide, $P<0.01$; testosterone propionate vs. testosterone propionate + flutamide, $P<0.01$; flutamide vs. testosterone propionate + flutamide, $P<0.01$. Progesterone receptor as fmol/uterus: control vs. testosterone propionate, not significant; control vs. flutamide, not significant; control vs. testosterone propionate + flutamide, $P<0.02$; testosterone propionate vs. testosterone propionate + flutamide, $P<0.01$; flutamide vs. testosterone propionate + flutamide, not significant.

DISCUSSION

Our results suggest that androgen is a negative modulator of the cytosol progesterone receptor in the MT-W9B mammary tumor. However, the inhibitory effects of androgen on progesterone receptor levels in the MT-W9B tumor and in the uterus as found in this study appear to differ from several reports: Zava and McGuire (*7*), for example, showed that high concentrations (10^{-6} *M*) of dihydrotestosterone resulted in a threefold increase in progesterone receptor levels in the human breast cancer cell line MCF-7, whereas 10^{-8} *M* had no effect. This result appeared to be due to translocation of the estrogen receptor by high, but not low, concentrations of dihydrotestosterone (*7*) and was accompanied by an increased incorporation of leucine and thymidine into protein and DNA, respectively, (*6*, *32*) and by a stimulation of cell growth (*7*). Garcia and Rochefort (*13*) also noted that a very high dose of dihydrotestosterone (50 mg/rat) increased progesterone receptor levels and [^{3}H]leucine incorporation in DMBA-induced mammary tumors and concluded also that this was the result of translocation of the estrogen receptor. Testosterone and dihydrotestosterone have also been shown to cause movement of the estrogen receptor into uterine nuclei. This was demonstrated both in vitro at concentrations greater than 10^{-7} *M* (*15*, *16*, *18*, *21*, *33*) and in vivo when the androgen in an oil vehicle was injected at a dose greater than 3 mg per rat (*17*, *20*). Accompanying this increase in nuclear estrogen receptor was an increased synthesis of induced protein (*18*, *20*, *21*) and an increased level of progesterone receptor (*19*). Lower doses in vivo (0.3 mg/rat) of dihydrotestosterone in oil (*19*) had no effect, either stimulatory or inhibitory, on progesterone receptor levels.

In our experiments we did not see an increase in progesterone receptor levels (expressed as fmol/mg protein) in uterus after the administration of high doses of 5 mg dihydrotestosterone/kg and 50 mg testosterone propionate/kg (data not shown). In fact, testosterone propionate at doses greater than 0.5 mg/kg caused a decrease. Our results with dihydrotestosterone are in agreement with those reported by Schmidt and Katzenellenbogen (*19*), if it is assumed that the doses we used, 5 mg/kg and lower, were too small to exert an effect on estrogen receptor translocation. That this might be the case is also suggested by the work of Garcia and Rochefort (*20*) and of Schmidt et al. (*18*). To our knowledge, no one has reported any effect of testosterone on progesterone receptor levels in uterus, although in in vitro experiments testosterone was shown to be less effective than dihydrotestosterone in stimulating synthesis of the induced protein (*18*, *21*). Schmidt et al. (*18*) showed that 0.5 mg testosterone (in oil) given to an immature rat (roughly comparable to our 5 mg/kg in a mature rat) did not cause translocation of the estrogen receptor and did not increase synthesis of the induced protein, although uterine weight was slightly increased. Our dose of 5 mg/kg causd a uterotrophic response in both intact and ovariectomized rats and decreased progesterone receptor concentrations (expressed as fmol/mg protein) in both groups of rats.

The lack of stimulation of progesterone receptor levels in the MT-W9B tumor by either dihydrotestosterone or testosterone could be explained on the basis of an insufficient dose to cause translocation of the estrogen receptor, although even 50 mg testosterone propionate/kg given to intact rats was inhibitory. We believe, however, that androgens are important modulators in their own right, independent of any estrogenic effects that might be exerted at high concentrations. The antiestrogenic properties of androgen are well established, and an inhibitory effect of androgen on the estrogen-induced increase in progesterone receptor levels, as reported here, has also been described, for example, in hamster kidney (*34*) and in the MCF-7 cell line (*35*, *36*). Such an inhibitory effect may be mediated by a decreased concentration (*4*) or a decreased replenishment (*37*, *38*) of the cytosol estrogen receptor or by competition for the nuclear binding site(s). The inhibitory effect of physiologic levels of androgen on progesterone receptor concentrations in tumors from castrated and intact male rats has not, however, been previously described, nor has the inhibitory effect of relatively low concentrations of dihydrotestosterone or testosterone in tumors from female rats. Whereas the androgen effect on progesterone receptor levels could still represent antagonism of physiologic levels of estrogen in both male and female rats, we theorize that the androgen is the controlling factor, an argument further strengthened by the data showing that androgen is acting via an androgen receptor-dependent mechanism. Furthermore, the antiestrogen tamoxifen, at doses that blocked the estrogen-induced progesterone receptor response in ovariectomized rats, has no effect on basal levels of progesterone receptor in this tumor (*39*), again suggesting that in the present experiments androgen is acting through an androgen receptor-dependent mechanism rather than as an antiestrogen.

The apparent inhibitory effect of androgen on progesterone receptor levels could, also, be the result of selection of cells with different biochemical properties—an explanation applicable as well to the uterus, since both 5 mg testosterone/kg and 17β-estradiol stimulated uterine growth in ovariectomized rats, whereas testosterone decreased and estrogen increased progesterone receptor levels. Thus testosterone and 17β-estradiol may be stimulating growth of different subpopulations of uterine cells [as has been demonstrated histologically (*40*)], and either the population stimulated by testosterone might have inherently lower levels of progesterone receptor or testosterone might exert an inhibitory control on progesterone receptor levels. The observation that testosterone was not able to block the estrogen-induced increase in progesterone receptor levels in ovariectomized rats to any significant extent is in agreement with the idea that different subpopulations are being induced, as is the fact that the combination of 17β-estradiol and testosterone indicates synergism in terms of uterine weight.

In the tumor, however, we believe that the results cannot be explained on the basis of differential stimulation of cell types for the following reasons: 1) In ovariectomized rats, androgen completely blocked the estrogen-induced increase in progesterone receptor levels. If it is assumed that estrogen and androgen each stimulate different cell types (as in uterus, for example), then different cell types should be present when both hormones are given, and we might expect to see what appears to be only a partial block, as was observed in the uteri from the same animals. A complete block as found in the tumor suggests that androgen is not acting as a selective inducer to a specific cell type but rather (in the presence of estrogen) as an antiestrogen. 2) Flutamide is an antiandrogen that is thought to act by an inhibition of androgen uptake and/or by inhibition of nuclear binding of androgens in the target tissues (*41*). If androgen were to select for growth of a specific cell type, then flutamide would be an unlikely blocker. Rather, the ability of flutamide to prevent the androgen-induced decrease in tumor progesterone receptor levels suggests that the androgen effect is a direct one.

The physiologic significance of the decrease in progesterone receptor levels in the MT-W9B mammary tumor as a result of androgen treatment remains to be established. However, Walters and Clark (*42*) demonstrated that the progesterone-induced decrease in progesterone receptor levels in uterus does result in a decreased ability to respond to progesterone. With the widespread use of progestogens, such as medroxyprogesterone acetate in the treatment of breast cancer (*43*), androgen modulation of progesterone receptor levels has clinical relevance; studies in this laboratory are continuing in an effort to more clearly understand the mechanisms involved.

REFERENCES

(*1*) American Medical Association Committee on Research. Androgens and estrogens in the treatment of disseminated mammary carcinoma. JAMA 1960; 172:1271-1283.

(*2*) Quadri SK, Kledzik GS, Meites J. Counteraction by prolactin of androgen-induced inhibition of mammary tumor growth in rats. J Natl Cancer Inst 1974; 52:875-878.

(*3*) Costlow ME, Buschow RA, McGuire WL. Prolactin receptors and androgen-induced regression of 7,12-dimethylbenz(*a*)anthracene-induced mammary carcinoma. Cancer Res 1976; 36:3324-3329.

(*4*) Zava DT, McGuire WL. Estrogen receptors in androgen-induced breast tumor regression. Cancer Res 1977; 37:1608-1610.

(*5*) Heise E, Gorlich M. Growth and therapy of mammary tumours induced by 7,12-dimethylbenzanthracene. Br J Cancer 1966; 20:539-545.

(*6*) Lippman ME, Bolan G, Huff K. Human breast cancer responsive to androgen in long term tissue culture. Nature 1975; 258:339-341.

(*7*) Zava DT, McGuire WL. Androgen action through estrogen receptor in a human breast cancer cell line. Endocrinology 1978; 103:624-631.

(*8*) Allegra JC, Lippman ME, Thompson EB, et al., Distribution, frequency and quantitative analysis of estrogen, progesterone, androgen, and glucocorticoid receptors in human breast cancer. Cancer Res 1979; 39:1447-1454.

(*9*) Ip MM, Milholland RJ, Kim U, Rosen F. Characterization of androgen receptors in 7,12-dimethylbenz(*a*)anthracene-induced and transplantable rat mammary tumors. Cancer Res 1978; 38:2879-2885.

(*10*) Bruchovsky N, Sutherland DJ, Meakin JW, Minesita T. Androgen receptors: Relationship to growth response and to intracellular androgen transport in nine variant lines of the Shionogi mouse carcinoma. Biochim Biophys Acta 1975; 381:61-71.

(*11*) Sluvser M, Evers SG, DeGoeij CC. Sex hormone receptors in mammary tumours of GR mice. Nature 1976; 263:386-389.

(*12*) Kim U. Pituitary function and hormonal therapy of experimental breast cancer. Cancer Res 1965; 25:1146-1161.

(*13*) Garcia M, Rochefort H. Androgen effects mediated by estrogen receptor in 7,12-dimethylbenz(*a*)anthracene-induced rat mammary tumors. Cancer Res 1978; 38:3922-3929.

(*14*) Nicholson RI, Davies P, Griffiths K. Interaction of androgens with oestradiol-17beta receptor proteins in DMBA-induced mammary tumours—a possible oncolytic mechanism. Eur J Cancer 1978; 14:439-445.

(*15*) Rochefort H, Lignon F, Capony F. Formation of estrogen nuclear receptor in uterus: Effect of androgens, estrone, and nafoxidine. Biochem Biophys Res Commun 1972; 47:662-670.

(*16*) Ruh TS, Wassilak SG, Ruh MF. Androgen-induced nuclear accumulation of the estrogen receptor. Steroids 1975; 25:257-273.

(*17*) Rochefort H, Garcia M. Androgen on the estrogen receptor. I. Binding and in vivo nuclear translocation. Steroids 1976; 28:549-560.

(*18*) Schmidt WN, Sadler MA, Katzenellenbogen BS. Androgen-uterine interaction: Nuclear translocation of the estrogen receptor and induction of the synthesis of the uterine-induced protein (IP) by high concentrations of androgens in vitro but not in vivo. Endocrinology 1976; 98:702-716.

(*19*) Schmidt WN, Katzenellenbogen BS. Androgen-uterine interactions: An assessment of androgen interaction with the testosterone- and estrogen-receptor systems and stimulation of uterine growth and progesterone-receptor synthesis. Mol Cell Endocrinol 1979; 15:91-108.

(*20*) Garcia M, Rochefort H. Androgens on the estrogen receptor. II. Correlation between nuclear translocation and uterine protein synthesis. Steroids 1977; 29:111-126.

(*21*) Ruh TS, Ruh MF. Androgen induction of a specific uterine protein. Endocrinology 1975; 97:1144-1150.

(*22*) Ip MM, Milholland RJ, Kim U, Rosen F. Effect of androgens on steroid hormone receptor in the MT-W9B transplantable rat mammary tumor. Proc Am Assoc Cancer Res 1979; 20:123.

(*23*) Kim U, Depowski M. Progression from hormone dependence to autonomy in mammary tumors as an in vivo manifestation of sequential clonal selection. Cancer Res 1975; 35:2068-2077.

(*24*) Ip M, Milholland RJ, Rosen F, Kim U. Mammary cancer: Selective action of the estrogen receptor complex. Science 1979; 203:361-363.

(*25*) Sherman MR, Corval PL, O'Malley BW. Progesterone-binding components of chick oviduct. I. Preliminary characterization of cytoplasmic components. J Biol Chem 1970; 245:6085-6096.

(*26*) Rao BR, Wiest WG. Estradiol-17β stimulation of progesterone binding in rabbit uterus. Fed Proc 1971; 30:1213.

(*27*) Toft DO, O'Malley BW. Target tissue receptors for progesterone: The influence of estrogen treatment. Endocrinology 1972; 90:1041-1045.

(*28*) Asselin J, Kelly PA, Caron MG, Labrie F. Control of hormone receptor levels and growth of 7,12-dimethylbenz(*a*)anthracene-induced mammary tumors by estrogens, progesterone and prolactin. Endocrinology 1977; 101:666-671.

(*29*) Tsai T-L, Katzenellenbogen BS. Antagonism of development and growth of 7,12-dimethylbenz(*a*)anthracene-induced rat mammary tumors by the antiestrogen U23, 469 and effects on estrogen and progesterone receptors. Cancer Res 1977; 37:1537-1543.

(*30*) Horwitz BK, McGuire WL. Estrogen control of progesterone receptor in human breast cancer. Correlation with nuclear processing of estrogen receptor. J Biol Chem 1978; 253:2223-2228.

(*31*) Lowry OH, Rosebrough NJ, Farr AL, Randall RJ. Protein measurement with the Folin phenol reagent. J Biol Chem 1951; 193:265-275.

(*32*) Lippman M, Bolan G, Huff K. The effects of androgens and antiandrogens on hormone-responsive human breast cancer in long-term tissue culture. Cancer Res 1976; 36:4610-4618.

(*33*) Rochefort H, Lignon F. Differences between the estradiol and testosterone receptors in rat uterus. Eur J Biochem 1974; 48:503-512.

(*34*) Li SA, Li JJ. Estrogen-induced progesterone receptor in the Syrian hamster kidney. I. Modulation by antiestrogens and androgens. Endocrinology 1978; 103:2119-2128.

(*35*) MacIndoe JH, Etre LA. Androgens inhibit estrogen action in MCF-7 human breast cancer cells. Life Sci 1980; 27:1643-1648.

(*36*) ———. An antiestrogenic action of androgens in human breast cancer cells. J Clin Endocrinol Metab 1981; 53:836-842.

(*37*) Hsueh AJ, Peck EJ, Clark JH. Control of uterine estrogen receptor levels by progesterone. Endocrinology 1976; 98:438-444.

(*38*) Bhakoo HS, Katzenellenbogen BS. Progesterone modulation of estrogen-stimulated biosynthetic events and estrogen receptor levels. Mol Cell Endocrinol 1977; 8:121-134.

(*39*) Ip MM, Milholland RJ, Rosen F, Kim U. Dichotomous effects of tamoxifen on a transplantable rat mammary tumor. Cancer Res 1981; 41:984-988.

(*40*) Datta JK, Roy S, Das RP. Effect of clomiphene on the ponderal, histological and biochemical changes induced by stilbestrol and testosterone in the uterus of rats. Steroids 1975; 25:163-168.

(*41*) Peets EA, Henson MF, Neri R. On the mechanism of the antiandrogenic action of flutamide, (α-α-α-trifluoro-2-methyl-4′-nitro-*m*-propionotoluidide) in the rat. Endocrinology 1974; 94:532-540.

(*42*) Walters MR, Clark JH. Estrogen and progesterone modulation of progesterone receptor content in the rat uterus. In: Beato M, ed. Steroid-induced uterine proteins. Amsterdam: Elsevier/North-Holland, 1980; 183-196.

(*43*) Ganzina F. High dose medroxyprogesterone acetate (MPA) treatment in advanced breast cancer. A review. Tumori 1979; 65:563-585.

blank page

In Vitro Measurement of Resistance to Phalloidin and γ-Glutamyltransferase of Carcinogen-Induced Preneoplastic Hepatocytes of Rats[1,2]

Norimasa Sawada,[3] Kazunori Furukawa,[3] *and* Hideyuki Tsukada[3,4]

ABSTRACT—Male inbred F344 rats weighing about 150 g were fed continuously a diet containing 0.02% *N*-2-fluorenylacetamide for 14–15 weeks. The presumptively preneoplastic hepatocytes were transferred to an in vitro system after dispersion by a collagenase-perfusion technique. Sensitivity to phalloidin in terms of formation of cytoplasmic blebs on the cell surface was less in the presumptively preneoplastic hepatocytes than in normal hepatocytes. Among the presumptively preneoplastic hepatocytes, the γ-glutamyltransferase (GGT)-positive cells were less sensitive to phalloidin than GGT-negative cells, indicating a greater contribution to the decrease in the sensitivity to phalloidin of the presumptively preneoplastic cells.—JNCI 1982; 69:683–686.

It has been well documented that acquisition of resistance of hepatocytes to acute cytotoxicity of hepatocarcinogens or hepatotoxins is a unique biologic property of the cells emerging during hepatocarcinogenesis (*1–8*).

Phalloidin is a specific hepatotoxin (*9*) that induces the formation of cytoplasmic blebs over the cell membranes in an in vitro experiment (*10*). Furthermore, the formation of the blebs was reported to decrease as the treatment of rats with a carcinogen was prolonged, resulting presumably from a decrease in the cellular uptake of the toxin (*6*). However, GGT is one of the most widely used markers for presumptive preneoplasia (*11–16*). Furthermore, it was possible that GGT-positive hepatocytes would acquire relative resistance to cytotoxic effects of 2-FAA (*17*).

In the present experiments, sensitivity to phalloidin of presumptively preneoplastic hepatocytes of rats induced by 2-FAA was quantitatively assessed in the in vitro system, and correlation between the sensitivity and GGT-positiveness of the cells was investigated cytochemically.

MATERIALS AND METHODS

Animals.—Male F344 rats weighing about 150 g were fed a commercial diet (NMF; Oriental Yeast Co., Tokyo, Japan) containing 0.02% 2-FAA for 14–15 weeks ad libitum. Prior to examinations, the animals were placed on the diet without 2-FAA for 5 days. Animals were maintained at 22±1°C and subjected to a standard 12-hour light–dark schedule (6 a.m.–6 p.m.).

Isolation of hepatocytes.—Hepatocytes were isolated by a collagenase perfusion technique as described previously in detail (*7, 18*). In the present experiments, the perfusion time of Ca^{2+}-free Hanks' balanced salt solution containing 130 U collagenase/ml (Sigma Chemical Co., St. Louis, Mo.) was 10 minutes, and the flow rate of the perfusion was 57 ml/minute. Presumptively preneoplastic hepatocytes were obtained from whole livers of rats administered 2-FAA. After viability of the cells was examined by the trypan blue exclusion test (viabilities in this experiments were 85–90%), the cell suspension was prepared at a concentration of 6×10^5 viable cells/ml in Williams' medium E (Flow Laboratories, Inc., Rockville, Md.) supplemented with 10% calf serum (GIBCO, Grand Island, N.Y.), 0.5 μg insulin/ml, 0.04 mg streptomycin/ml, and 40 IU penicillin-G/ml.

Treatment with phalloidin and GGT cytochemistry.—To 1 ml of the cell suspension containing 6×10^5 viable cells was added 1 ml of the medium containing various concentrations of phalloidin (Sigma Chemical Co.) but devoid of serum, and they were incubated for 20 minutes at 37°C with slow shaking (*19*). After incubation, the mixtures were immediately cooled to stop the phalloidin action (*20*). After added trypan blue solution, the cells that were viable and that had formed cytoplasmic blebs were counted in each examination. The phalloidin response was expressed as a percentage of the number of the cells that had formed the multiple blebs over the cell surface to the total number of the observed viable cells. Phalloidin-induced bleb formation was observed only in viable cells but not in nonviable cells as reported by Frimmer et al. (*21*). In GGT cytochemical examination, 1.5 ml of the cell suspension was inoculated into 35-mm plastic dishes in which cover glasses were placed. After 3-hour cultivation in a CO_2-incubator, the cells were washed three times with the culture medium and then incubated with 1.5 ml of the phalloidin-containing medium for 20 minutes at 37°C. After the incubation, more than 95% of the cells attached to the cover glasses were viable, even in the presence of 10 μg phalloidin/ml, when examined by trypan blue exclusion test. The cells on the cover glasses were fixed in ice-cold acetone for 15 minutes and stained for GGT activity according to the method of Rutenberg et al. (*22*).

RESULTS

As for the purity of the cell suspensions, obtained from both normal and the carcinogen-induced preneoplastic livers, more than 98% of the cells were identified as hepatocytes

---

ABBREVIATIONS USED: 2-FAA=*N*-2-fluorenylacetamide; GGT=γ-glutamyltransferase.

---

[1] Received November 27, 1981; accepted April 16, 1982.

[2] Supported in part by Grant-in-Aid for Scientific Research 448143 and by Grants-in-Aid for Cancer Research 501054 and 501569 from the Ministry of Education, Science and Culture, Japan.

[3] Department of Pathology, Cancer Research Institute, Sapporo Medical College, Minami-1, Nishi-17, Chuo-ku, Sapporo 060, Japan.

[4] We are indebted to Miss Y. Takahashi and Mrs. M. Kuwano for their skillful technical assistance.

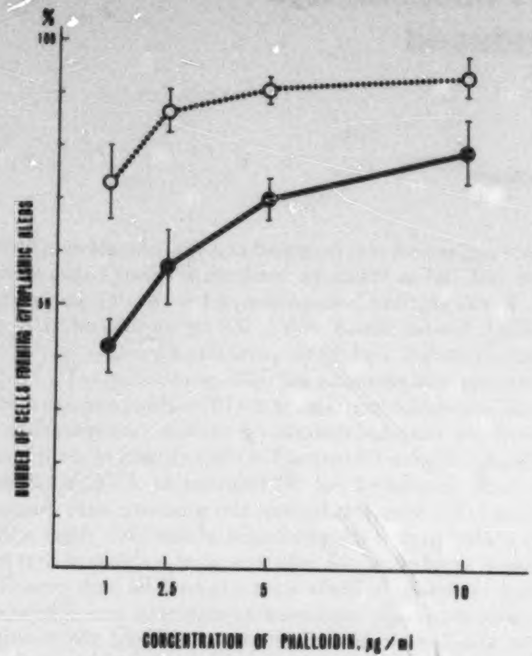

TEXT-FIGURE 1.—Sensitivity to phalloidin of normal and preneoplastic hepatocytes. ○=normal hepatocytes (n=6). ●=preneoplastic hepatocytes (n=6). Values are means ± SD.

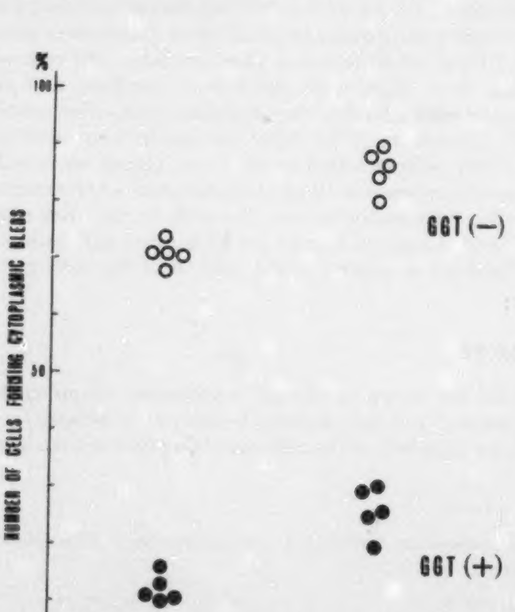

TEXT-FIGURE 2.—Sensitivity to phalloidin of GGT-positive and GGT-negative carcinogen-altered hepatocytes. ○=GGT-negative cells. ●=GGT-positive cells.

by the aid of alkaline 3,3′-diaminobenzidine staining for peroxisomes.

As shown in figures 1 and 2, we quantitatively assessed sensitivity to phalloidin of hepatocytes by counting the proportion of the cells that had formed multiple cytoplasmic blebs. Text-figure 1 shows that at every concentration of the toxin examined the cells obtained from the carcinogen-treated rats were more resistant to phalloidin than normal hepatocytes. The difference in the degree of the sensitivity between those two cell populations was more conspicuous as the concentration of phalloidin was lower.

The presumptively preneoplastic hepatocytes were divided into 2 groups according to GGT cytochemistry. One group was GGT-positive and the other was GGT-negative (figs. 3, 4). Of the presumptively preneoplastic hepatocytes, 30–40% were GGT-positive cells. The sensitivity of these groups of cells was examined. As shown in text-figure 2, at concentrations of 2.5 and 10 µg phalloidin/ml, the sensitivity of GGT-positive cells was about 10 and 25%, respectively. In contrast, the sensitivity of GGT-negative cells was about 70 and 85%, respectively. GGT-positive cells were more resistant to phalloidin than were GGT-negative cells, the former cell group making a greater contribution to the increase in the resistance of presumptively preneoplastic hepatocytes than the latter.

DISCUSSION

Resistance of presumptively preneoplastic hepatocytes to hepatocarcinogens or hepatotoxins is considered as one of characteristic features that the cells were rendered to survive and proliferate selectively during the carcinogenesis. In this context, resistance of presumptively preneoplastic rat hepatocytes to aflatoxin (*5, 6*), methotrexate (*8*), cycloheximide (*8*), adriamycin (*8*), and dimethylnitrosamine (*7*) was reported on in vitro experiments, which were favorable for a quantitative assessment of the degree of the resistance. Furthermore, our previous experiments (*7, 18*) on dimethylnitrosamine cytotoxicity showed that resistance of preneoplastic rat hepatocytes induced by 2-FAA was increased as the preneoplastic stages progressed.

Phalloidin is a polypeptide that acts specifically on hepatocytes resulting in vitro in the formation of cytoplasmic blebs. In contrast to the above-mentioned cytotoxic agents, phalloidin was reported to act on the cell membranes inducing the cell death in an environment containing an excess of Ca^{2+} ions (*23*). However, the cytoplasmic bleb formation test might be much more sensitive than the trypan blue exclusion test in assessing the sensitivity of the cells to phalloidin, since much smaller amounts of the toxin and a shorter period of the treatment were observed to be enough for the cytoplasmic bleb formation test.

During hepatocarcinogenesis, sensitivity of the cells to phalloidin was reported to be decreased progressively as the carcinogen-treatment period was prolonged, presumably due to an impairment in the transport system of the toxin across the cell membranes or to an alteration of the receptor for the toxin on the cell surface (*6*). These findings that the phalloidin response was decreased in carcinogen-altered hepatocytes might agree with those of the present results.

Expression of GGT activity of hepatocytes in carcinogenesis is considered to be a fetal phenotypic expression and may be due to an alteration of cell membrane (*24*). In the present study it was demonstrated that the increase in GGT activity was well correlated with the decrease in sensitivity to phalloidin. It is suggested that alterations of the cell membranes occur in a preneoplastic state in terms of expression of GGT activity, on the one hand, and decrease in phalloidin response, on the other hand.

REFERENCES

(*1*) Williams GM, Klaiber M, Parker SE, Farber E. Nature of early appearing, carcinogen-induced liver lesions resistant to iron accumulation. J Natl Cancer Inst 1976; 57:157-165.

(*2*) Farber E, Parker S, Gruenstein M. The resistance of putative premalignant liver cell populations, hyperplastic nodules, to the acute cytotoxic effects of some hepatocarcinogens. Cancer Res 1976; 36:3879-3887.

(*3*) Gans JH. Diethylnitrosamine-induced changes in mouse liver morphology and function. Proc Soc Exp Biol Med 1976; 53:116-120.

(*4*) Judah DJ, Legg RF, Neal GE. Development of resistance to cytotoxicity during aflatoxin carcinogenesis. Nature 1977; 265:343-345.

(*5*) Laishes BA, Roberts E, Farber E. In vitro measurement of carcinogen-resistant liver cells during hepatocarcinogenesis. Int J Cancer 1978; 21:186-193.

(*6*) Ziegler K, Petzinger E, Frimmer M. Decreased phalloidin response, phallotoxin uptake and bile acid transport in hepatocytes prepared from Wistar rats treated chronically with diethylnitrosamine. Naunyn Schmiedebergs Arch Pharmacol 1980; 310:245-247.

(*7*) Sawada N, Furukawa K, Gotoh M, Mochizuki Y, Tsukada H. Estimation of resistance to dimethylnitrosamine of normal hepatocytes, hyperplastic nodule cells and hepatoma cells of rats in primary culture. Gan 1981; 72:318-321.

(*8*) Carr BI, Laishes BA. Carcinogen-induced drug resistance in rat hepatocytes. Cancer Res 1981; 41:1715-1719.

(*9*) Wieland T, Faulstich H. Amatoxins, phallotoxins, phallolysin, and antamide: The biologically active components of poisonous Amanita mushroom. CRC Crit Revbiochem 1978; 5:185-260.

(*10*) Weiss E, Sterz I, Frimmer M. Electron microscopy of isolated rat hepatocytes before and after treatment with phalloidin. Beitr Pathol 1973; 150:345-356.

(*11*) Fiala S, Fiala ES. Activation by chemical carcinogens of γ-glutamyl transpeptidase in rat and mouse liver. J Natl Cancer Inst 1973; 51:151-158.

(*12*) Harada M, Okabe K, Shibata K, Masuda H, Miyata K, Enomoto M. Histochemical demonstration of increased activity of γ-glutamyl transpeptidase in rat liver during hepatocarcinogenesis. Acta Histochem Cytochem 1976; 9:168-179.

(*13*) Kalengayi MM, Ronchi G, Desmet VJ. Histochemistry of gamma-glutamyl transpeptidase in rat liver during aflatoxin B_1-induced carcinogenesis. J Natl Cancer Inst 1975; 55:579-588.

(*14*) Cameron R, Kellen J, Kolin A, Malkin A, Farber E. γ-Glutamyltranspeptidase in putative premalignant liver cell populations during hepatocarcinogenesis. Cancer Res 1978; 38:823-829.

(*15*) Laishes BA, Ogawa K, Roberts E, Farber E. Gamma-glutamyl transpeptidase: A positive marker for cultured rat liver cells derived from putative premalignant and malignant lesions. J Natl Cancer Inst 1978; 60:1009-1016.

(*16*) Jacobs JM, Pretlow TP, Fausto N, Pitts AM, Pretlow TG II. Separation of two populations of cells with gamma-glutamyl transpeptidase from carcinogen-treated rat liver. JNCI 1981; 66:967-973.

(*17*) Solt D, Farber E. New principle for analysis of chemical carcinogenesis. Nature 1976; 263:701-703.

(*18*) Sawada N, Furukawa K, Gotoh M, Mochizuki Y, Tsukada H. Primary culture of preneoplastic hepatocytes from rats treated with 2-acetylaminofluorene and clofibrate: Relationship between resistance to dimethylnitrosamine and responsiveness of peroxisomes. Gan 1982; 73:1-6.

(*19*) Frimmer M, Kroker R, Porstendörfer J. The mode of action of phalloidin: Demonstration of rapid deformation of isolated hepatocytes. Naunyn Schmiedebergs Arch Pharmacol 1974; 284:395-398.

(*20*) Frimmer M, Rufeger U. Temperature dependence of phalloidin response in isolated rat hepatocytes. Naunyn Schmiedebergs Arch Pharmacol 1977; 300:193-194.

(*21*) Frimmer M, Petzinger E, Rufeger U, Veil LB. Trypsin protection of hepatocytes against phalloidin. Naunyn Schmiedebergs Arch Pharmacol 1977; 300:163-171.

(*22*) Rutenberg AM, Kim H, Fischbein JW, Hanker JS, Wasserkurg HL, Seligman AM. Histochemical and ultrastructural demonstration of γ-glutamyl transpeptidase activity. J Histochem Cytochem 1969; 17:517-526.

(*23*) Kane AB, Young EE, Schanne FA, Farber JL. Calcium dependence of phalloidin-induced liver cell death. Proc Natl Acad Sci USA 1980; 77:1177-1180.

(*24*) Williams GM, Ohmori T, Katayama S, Rice JM. Alteration by phenobarbital of membrane-associated enzymes including gamma glutamyl transpeptidase in mouse liver neoplasms. Carcinogenesis 1980; 1:813-818.

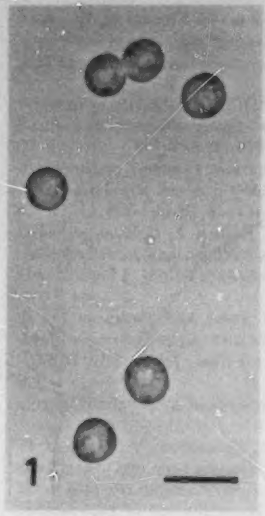

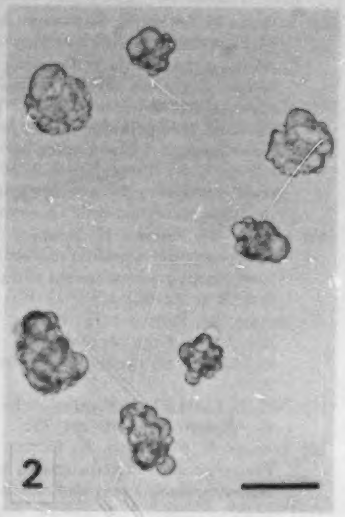

FIGURE 1.—Isolated normal hepatocytes without phalloidin treatment. *Bar*=40 µm. × 270

FIGURE 2.—Isolated normal hepatocytes treated with 10 µg phalloidin/ml for 20 min. *Bar*=40 µm. × 270

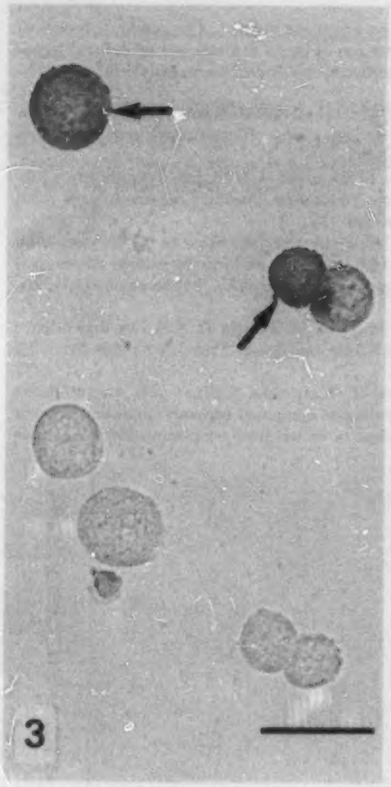

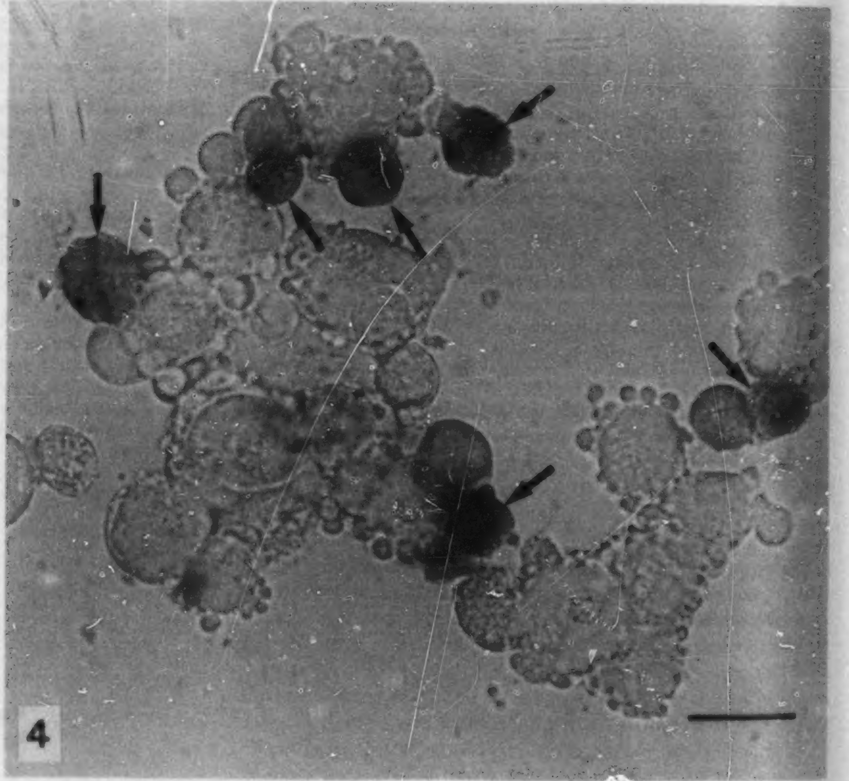

FIGURE 3.—Carcinogen-altered hepatocytes in 3-hr culture without phalloidin treatment. *Bar*=40 µm. × 405

FIGURE 4.—Carcinogen-altered hepatocytes in 3-hr culture treated with 10 µg phalloidin/ml for 20 min. *Bar*=40 µm. × 405. *Arrows* in figs. 3 and 4 indicate GGT-positive cells.

Chicken Resistance to Dimethylnitrosamine Acute Effects on the Liver: A Comparative Study With Other Species[1,2,3]

H. M. Godoy,[4] M. I. Díaz Gómez,[4] A. Marzi,[4] E. C. de Ferreyra,[4] O. M. de Fenos,[4] *and* J. A. Castro[4,5]

ABSTRACT—Dimethylnitrosamine (DMN)-induced liver damage, as measured by the increase in plasma isocitrate dehydrogenase as well as by histologic assessment of necrosis, was marked after DMN ip administration (70 mg/kg) in males of all noninbred species tested (BALB/c mouse, Sprague-Dawley rat, Syrian golden hamster, general purpose guinea pig) but not in the noninbred White Leghorn chicken. At 1 and 3 hours after DMN injection, liver DMN levels were not lower in the chicken as compared to levels in the other species. Furthermore, in all species except the chicken, significant decreases were found at 3 hours as compared to 1 hour after DMN administration. DMN metabolism to CO_2 and to formaldehyde, as well as covalent binding of DMN-reactive metabolites to either proteins or nucleic acid, was measured with the use of liver slices, microsomes, and/or 9,000×*g* supernatants. Results indicated that chicken liver had a very low capacity for metabolism and activation (29–3,166 times lower than comparable data in mice or hamsters).—JNCI 1982; 69:687–691.

Nitrosamines have been implicated as acute liver toxicants, mutagens, carcinogens, and teratogens (*1–3*). Biologic effects of nitrosamines are thought to be mediated through the formation of reactive metabolites that react with cellular macromolecules (*1, 2*). Numerous animal species, including mammals, birds, fish, and amphibia, are susceptible to the carcinogenic action of an N-nitrosamine (*1–4*). Relatively less information is available about species susceptibility to nitrosamines' acute effects on the liver (*1–4*). The chicken is remarkably resistant to acute liver effects produced by a hepatotoxin, such as carbon tetrachloride, that causes injury by metabolic activation (*5–8*). In this work, we studied whether chicken liver is also resistant to DMN acute toxic effects. In addition, we compared the susceptibility to DMN acute effects on the liver of the chicken with that of other species, such as the mouse, rat, hamster, and guinea pig. We also attempted to correlate the observed effects with the intensity of different parameters related to DMN metabolism and/or activation to reactive metabolites.

MATERIALS AND METHODS

Chemicals.—Gold label quality DMN was purchased from the Aldrich Chemical Co., Milwaukee, Wis., and [^{14}C]DMN (50.1 mCi/mmol, purity >99% by GLC) from New England Nuclear Corp., Boston, Mass. All other chemicals were of the best quality available.

Animals and treatment.—All the experiments were performed with animals of the following noninbred species fasted for 12–14 hours: male Sprague-Dawley rats, 250–350 g each; male BALB/c mice, 20–25 g; male general purpose guinea pigs, 280–300 g (purchased from Centro Panamericano de Zoonosis, Buenos Aires, Argentina); male Syrian golden hamsters (purchased from the Centro Panamericano de Zoonosis), 90–100 g; White Leghorn chickens (from Romanelli Laboratories, Buenos Aires), 1,500–1,900 g.

DMN was given ip in 0.9% NaCl solution at a dose of 70 mg/kg. Controls received 0.9% NaCl solution. In the toxicity studies, animals were killed 24 hours after DMN administration. Blood samples were taken with a heparinized syringe under light ether anesthesia from the inferior venae cava.

Tissue preparations for determination and measurements.—Liver slices were prepared with a Stadie Riggs hand microtome. The slices (≈200 mg) were equilibrated with O_2 in Warburg flasks containing 2.8 ml Krebs-Ringer buffer-glucose (2 mg/ml) (*9*). [^{14}C]DMN was added from the side arm, and $^{14}CO_2$ was trapped in NaOH (0.2 ml, 10% wt/vol). The NaOH was then removed from the well, the [^{14}C]carbonate was precipitated as barium carbonate, and the radioactivity was determined (*10*). Binding of ^{14}C from [^{14}C]DMN to nucleic acids in tissue slices was performed by isolation of nucleic acids according to the procedure described by Korn (*11*) followed by hydrolysis with 5% TCA at 90°C for 15 minutes. Radioactivity on an aliquot was counted with the use of a cocktail composed of 0.6% PPO in Triton X-100–toluene (1:4, vol/vol). The in vitro metabolism to formaldehyde and the activation of DMN to reactive metabolites by 9,000×*g* supernatants or microsomes were determined as described by McLean and Day (*12*), but [^{14}C]DMN (0.17 m*M*, 1.8 × 10^6 dpm/ml) was used instead of DMN. Samples were incubated in a Dubnoff shaker for 10 minutes at 37°C, and the reaction was stopped with an equal volume of 10% TCA. The irreversibly bound radioactivity was determined in the acid-insoluble precipitate as described (*13*). [^{14}C]formaldehyde produced from [^{14}C]DMN was measured in the TCA-soluble fraction as previously described (*14*).

NADPH-linked ICDH activity was measured according to the method of Sterkel et al. (*15*). One unit of activity was the amount of enzyme producing 1 mmol NADPH/ml plasma/hour at 25°C.

DMN levels in liver were determined as follows: Liver homogenates (30% wt/vol in water) were deproteinized with a mixture (20% wt/vol of zinc sulfate and saturated barium

---

ABBREVIATIONS USED: CB=covalent binding; DMN=dimethylnitrosamine; GLC=gas-liquid chromatography; ICDH=isocitrate dehydrogenase; PPO=2,5-diphenyloxazole; TCA=trichloroacetic acid.

---

[1] Received December 10, 1981; accepted April 2, 1982.

[2] Supported by Public Health Service grant AM-13195-12 from the National Institute of Arthritis, Metabolism and Digestive Diseases; and by the Consejo Nacional de Investigaciones Científicas y Técnicas (CONICET), Argentina.

[3] Animals were maintained under the guidelines set forth by Centro de Investigaciones Toxicológicas (CEITOX), Instituto de Investigaciones Científicas y Técnicas de las Fuerzas Armadas (CITEFA)-CONICET.

[4] CEITOX, CITEFA/CONICET, Zufriategui y Varela, 1603 Villa Martelli, Pcia. de Buenos Aires, Argentina.

[5] *Address reprint requests to* Dr. Castro.

hydroxide). After centrifugation, aliquots of supernatants were saturated with sodium chloride and extracted with an equal volume of methylene chloride. The methylene chloride extracts were dried with anhydrous sodium sulfate, and DMN concentrations were determined by GLC coupled to a thermal energy analyzer (Thermal Electron Corp., Waltham, Mass.). Separation was performed in 20 *M* Carbowax/0.5% KOH on Chromosorb W/HP 80–100 mesh. Column temperature was 175°C. The recovery of known amounts of DMN spiked in liver homogenates was 70–75%. Reported values were corrected for loss.

Histologic techniques.—After the liver was removed, small portions from the left and central lobes were immediately fixed in Bouin's solution, embedded in paraffin, and stained with hematoxylin and eosin. The specimens were coded to avoid bias and were evaluated histologically by at least two independent observers. To quantify the morphologic changes, we graded liver sections according to hydropic degeneration or necrosis by means of an arbitrary scale (+=light; ++=moderate; +++=marked; ++++=very intense).

Statistical method.—Results reported as representative for each experimental condition were the means of all the observations made. Five livers per group and five sections per liver were inspected. The significance of the difference between two mean values was assessed by Student's *t*-test (*16*).

RESULTS

DMN metabolism to CO_2 and CB of DMN metabolites to nucleic acids in experiments with liver slices from different animal species.—All the species tested were able to metabolize DMN to CO_2 and to give DMN-reactive metabolites, which to some extent bound covalently to nucleic acids (table 1). However, there are very large differences among the species in their ability to carry forward both processes. Metabolism of DMN was 25 times more intense in hamsters than in chickens. The intensity of the CB of ^{14}C from [^{14}C]DMN to the nucleic acids in liver slices from different animal species followed a similar pattern, but differences between the species were not so large as they were for metabolism of DMN to CO_2 (table 1).

TABLE 1.—*DMN metabolism to CO_2 and CB of DMN metabolites to nucleic acids in experiments with liver slices[a] from different animal species*

Species	10^{-2} μmol DMN transformed to CO_2/g liver, mean±SD[b]	10^{-3} μmol DMN bound to nucleic acids/g liver, mean±SD[b]
Mouse	5.2±0.81	1.3±0.04
Guinea pig	2.0±0.29	0.43±0.05
Hamster	22.9±1.61	2.02±0.46
Rat	4.7±0.95	1.53±0.6
Chicken	0.79±0.18	0.16±0.03

[a] Liver slices were equilibrated with O_2 in a Warburg flask containing Krebs-Ringer buffer-glucose. [^{14}C]DMN (0.1 m*M* final concentration, 1×10^6 dpm/ml) was added from the side arm, and $^{14}CO_2$ was taken up with NaOH at the center well, precipitated as barium carbonate, and counted, as detailed in "Materials and Methods." Liver slices were taken from 3 rats.

[b] Reported $^{14}CO_2$ production or CB values correspond to incubation periods of 120 min at 37°C.

TABLE 2.—*Formaldehyde formation from DMN and CB of ^{14}C from [^{14}C]DMN to proteins by microsomes or 9,000×g supernatants from liver of different animal species[a]*

Species	Microsomes	9,000×*g* supernatants
Formaldehyde formed, 10^{-6} μmol/g liver/10 min[b]		
Mouse	180,400±15,500	37,950±9,900
Guinea pig	55,560±17,510	45,500±11,500
Hamster	150,300±23,500	127,740±32,100
Rat	5,700±2,300	16,500±5,000
Chicken	492±339	197±338[d]
CB, μmol/g liver, $\times10^{-6}$[c]		
Mouse	3,886±935	3,235±863
Guinea pig	9,440±2,295	4,072±886
Hamster	29,760±4,200	12,950±3,590
Rat	183±60	1,164±650
Chicken	9.4±19.0[d]	18.4±29.0[d]

[a] Livers were blended with 0.15 *M* KCl in a Potter-Elvehjem homogenizer and centrifuged 20 min at 9,000×*g*. The supernatant was then centrifuged 60 min at 105,000×*g* to obtain microsome fraction.

[b] The final protein concentration in the incubation mixture was 2.5–3.8 mg/ml for microsomes and 8–10 mg/ml for 9,000×*g* supernatants. The incubation mixture contained [^{14}C]DMN (0.17 m*M*, 1.6×10^6 dpm/ml) and an NADPH-generating system. Samples were incubated for 10 min at 37°C. Results are the means of three determinations. For formaldehyde determinations in the incubation mixture, a known amount of carrier formaldehyde was added and precipitated with 5,5-dimethyl-1,3-cyclohexanedione. A weighed portion of formaldemethone formed was counted in a toluene–PPO mixture. *See* "Materials and Methods" for other details. Values are means ±SD.

[c] For CB studies, proteins were precipitated with TCA, delipidated, and dried with successive washings with the use of a mixture of ethanol plus ether plus chloroform (2:2:1), acetone, and ether; finally, they were dissolved in concentrated formic acid and counted with a Butyl Cellosolve–PPO mixture. *See* "Materials and Methods" for details. Values are means ± SD.

[d] Not significantly different from zero.

Formaldehyde formation from DMN by microsomes or 9,000×g supernatants from livers of different animal species.—Both microsomes and 9,000×*g* supernatants from the mouse, guinea pig, hamster, or rat were able to metabolize DMN to formaldehyde. The chicken, in contrast, exhibited DMN demethylase values either not significantly different from zero or extremely low (table 2). The ratio between DMN demethylase activity in microsomes to that in 9,000×*g* supernatant varies from one species to another. For example, for the mouse and chicken a higher activity was found in microsomes than that in 9,000×*g* supernatants, whereas the ratios were similar in the guinea pig or hamster; in the rat 9,000×*g* supernatants exhibited higher activity than did the microsomes (table 2).

*CB of ^{14}C from [^{14}C]DMN to protein in microsomes and 9,000×*g *supernatants from livers of different animal species.*—Both microsomes and 9,000×*g* supernatants from the livers of the different animal species except the chicken were able to activate DMN to reactive metabolites that bind covalently to proteins (table 2). For the chicken, values were not significantly different from zero. The extent of the CB in the hamster was higher than that in the other species in both microsomes and 9,000×*g* supernatants and was more than three times as intense as that in the guinea pig. CB in the guinea pig was of the same order of magnitude of that in the mouse, which in turn was far more intense than that

TABLE 3.—*DMN levels in livers from animals of different species 1 or 3 hours after administration*[a]

Species	DMN content, μg/g liver, at hr:	
	1	3
Mouse	26.9±6.4	4.6±2.6
Guinea pig	71.7±8.9	48.8±6.4
Hamster	43.2±22.6	13.5±2.0
Rat	58.1±5.8	50.1±8.2
Chicken	67.1±20.3	84.8±12.6

[a] Animals received an ip injection of 70 mg DMN/kg and were killed at 1 or 3 hr after injection. Their livers were homogenized, extracted with methylene choride, and analyzed by GLC coupled to a thermal energy analyzer. Each group had 8 animals. Values are means ± SD.

in the rat. In the hamster and guinea pig the intensity of the CB was higher with microsomal than with 9,000×*g* supernatant preparations. In the mouse, the intensity of the CB was similar in both fractions, whereas in the rat it was far more intense in 9,000×*g* supernatant preparations than in microsomes (table 2).

DMN levels in livers from different animal species 1 to 3 hours after administration.—Administration ip of 70 mg DMN/kg body weight to animals of different species led at 1 hour to liver DMN levels of the same order but of different magnitude (table 3). The differences were larger at 3 hours. Decreases in the liver DMN content at this time were more pronounced in the mouse than in the hamster, and these decreases in the hamster were larger than that observed either in the guinea pig or in the rat. DMN levels in the liver from a chicken at 3 hours did not decrease but rather increased slightly (table 3).

DMN-induced damage in livers of animals of different species.—Twenty-four hours after ip administration of a single dose of 70 mg DMN/kg, centrilobular necrosis of the liver was observed in all species except the chicken, as evidenced by determinations of ICDH in plasma (table 4). Hepatic necrosis also was assessed by histologic examination. The administration of DMN to mice produced a very intense (++++) centrolobular necrosis at 24 hours, associated with hemorrhage and edema. The liver cells of the periportal zones were enlarged, and in that area the normal architectural pattern was lost. Administration of DMN to guinea pigs and hamsters produced centrolobular necrosis at 24 hours (++ and +, respectively). The cells of the periportal zones also exhibited different degrees of necrosis. Administration of DMN to rats produced a centrolobular necrosis (++), little hemorrhage and edema were seen, and the liver cells of the periportal zones were well preserved. At this dose no necrosis was observed in chicken livers.

TABLE 4.—*Effect of DMN 24 hours after administration on ICDH in different animal species*[a]

Species	Treatment	ICDH, U±SD[b]	Degree of histologically observable necrosis[c]
Mouse	Control	160±100	—
	DMN	26,700±10,810[d]	++++
Guinea pig	Control	4,200±1,250	—
	DMN	91,000±3,300[d]	++
Hamster	Control	1,200±1,020	—
	DMN	10,710±6,840[e]	+
Rat	Control	200±60	—
	DMN	7,850±1,450[d]	++
Chicken	Control	675±200	—
	DMN	960±540	—

[a] Controls received 0.9% NaCl solution. Animals were killed 24 hr after DMN administration. Blood samples were taken and plasma was assessed for ICDH activity. Each group had 5 animals.

[b] One unit of enzyme is that required to form 1 nmol NADPH/ml plasma/hr at 25°C.

[c] For meanings of *plus signs, see* "Materials and Methods" (histologic techniques). *Dash* indicates no histologic observable necrosis.

[d] $P<0.001$.

[e] $P<0.01$.

DISCUSSION

Our histologic and enzymatic observations reported here show that chicken liver is resistant to DMN acute necrogenic effects. This behavior resembles the one previously reported for the other hepatotoxin acting on chicken liver, CCl_4 (*5–8*). In the case of CCl_4, this lack of necrogenic effect was attributed to a poor capacity of chicken liver to biotransform CCl_4 to trichloromethyl-free radicals or to the associated lack of production of lipid peroxidation (*7, 8*). Similar reasons might be in operation in the failure of chicken liver to respond to the DMN's acute effects. Chicken liver has far less ability to metabolize and/or activate DMN to reactive metabolites than do the livers of the other species tested. For example, metabolism of DMN to CO_2 in liver is about 29 times less intense in the chicken than in the hamster and 6, 7, and 4 times less than in the rat, mice, or guinea pig, respectively. These results on metabolism of DMN to CO_2 are in agreement with those previously reported by Montesano and Magee (*17*) for hamsters and rats. Again, the ability to activate DMN to reactive metabolites that bind covalently to nucleic acids in the liver is 13 times less intense in the chicken than in the hamster and 10, 8, and 3 times less than that in the rat, mouse, or guinea pig, respectively. Similarly, liver microsomal DMN demethylase in the chicken is 366 times less active than in the mouse and 305, 113, and 12 times less than that in the hamster, guinea pig, or rat, respectively. These results on microsomal DMN demethylase are in agreement with those previously reported by Lotlikar et al. (*18, 19*) for the rat, hamster, and guinea pig. A recent work also reported good correlation between rates of DMN demethylation and relative acute liver toxicities in species such as the monkey, cat, lizard, duck, rat, and guinea pig (*20*).

The covalent binding of DMN-reactive metabolites to liver microsomal proteins, however, is 3,166 times less intense in the chicken than in the hamster and 1,004, 413, and 19 times less than that in the guinea pig, mouse, or rat, respectively. A similar behavior was observed for DMN demethylase activity in liver 9,000×*g* supernatants. In this case, values for the chicken were 648 times less than for the hamster and 231, 193, and 84 times less than the value for the guinea pig, mouse, or rat, respectively. Finally, the CB value of each reactive DMN metabolite to liver 9,000×*g* supernatant protein in chickens is 704 times less than the value in hamsters and 221, 176, and 63 times less than that in guinea pigs or rats, respectively. Moreover, assuming that the time necessary for distribution of DMN through the body is negligible in relation to 3 hours and that the given dose is uniformly distributed among the different tissues, as seems to be the case (*1, 17, 21*), then we may consider that about 70 µg DMN/g liver would be approximately the zero time concentration in livers of the different species receiving ip a dose of 70 mg/kg. The amounts of DMN remaining in the livers after 3 hours revealed that 93.4% of the original amount of DMN was metabolized in mice; 80.7%, in hamster; 30.3%, in guinea pig; and 28.42%, in the rat. In the chicken no decreases were detected in the liver concentrations of DMN; rather a 21.14% increase was observed. This apparent increase probably derives from the comparison based on theoretical assumptions made for this analysis. Results show that the chicken, which is the species less susceptible to deleterious effects by DMN on the liver, is also the one less able to process DMN through different metabolic pathways. The preceding analysis might reasonably explain the large difference in the acute liver response of the chicken to DMN when compared to the responses of other species. However, it is not possible to explain with a similar analysis the different response of the liver to DMN acute effects in species other than the chicken.

An absolute lack of correlation was observed between the necrogenic response of DMN in the liver of the mouse, guinea pig, hamster, and rat and metabolism of DMN to CO_2 or DMN demethylase activity in $9{,}000\times g$ supernatants or the CB of DMN reactive metabolites to proteins either from microsomes or from $9{,}000\times g$ supernatants. Among different species, a partial degree of correlation was observed for necrosis in liver, for DMN demethylase activity in liver microsomes, and for DMN disappearance in 3 hours in livers. In regard to these last two parameters, however, there is an inversion in the correlation for hamsters in relation to that of guinea pigs, inasmuch as the latter are more susceptible to DMN necrogenic effect than the former, whereas the intensity of the above-cited parameters is greater in hamster livers than in guinea pig livers. This lack of correlation between several parameters and DMN-induced liver injury in different species is in contrast with our past findings about correlation between CB to $9{,}000\times g$ supernatant proteins and injury observed in rats (*22–24*). Factors other than DMN metabolism and/or activation might be relevant to inherent susceptibility of livers from different species to DMN necrogenic effects. For example, the cell response to injury as well as its intrinsic ability for repair could be different in the livers of different animal species, thus obscuring correlations with other parameters. Within a given species, e.g., the rat, we (*22–24*) previously reported that DMN acute effects on the liver correlated with extents of CB of DMN metabolites to $9{,}000\times g$ supernatant proteins, but in the present experiments this does not seem to be the case.

Much remains to be learned about the different factors involved in the liver response to injury by DMN and other nitrosamines. That knowledge would be relevant also to long-term carcinogenic effects of these chemicals, inasmuch as cell necrosis is believed to modulate to a great extent the course of the cancer induction by chemicals in organs such as the liver, which are quiescent with respect to cell proliferation (*25*). The mechanism of this effect appears to be an induction of compensatory liver cell proliferation (*26*). Whether chicken liver is susceptible to DMN carcinogenic effects would be of interest. Recent results by Schmähl et al. (*27*) indicated that another nitrosamine, diethylnitrosamine, causes liver cancer in chickens. However, diethylnitrosamine is a more potent carcinogen than is DMN (*1, 2, 4*); nonetheless, no species ever tested against carcinogenic nitrosamines proved to be unsusceptible (*28*).

REFERENCES

(*1*) MAGEE PN, BARNES JM. Carcinogenic nitroso compounds. Adv Cancer Res 1967; 10:163–246.

(*2*) MONTESANO R, BARTSCH H. Mutagenic and carcinogenic N-nitroso compounds: Possible environmental hazards. Mutat Res 1976; 32:179–228.

(*3*) SHANK R. Toxicology of N-nitroso compounds. Toxicol Appl Pharmacol 1975; 35:361–368.

(*4*) MAGEE PN, MONTESANO R, PREUSSMANN R. N-nitroso compounds and related carcinogenesis. Chemical carcinogens. Am Chem Soc Monogr 1967; 173:491–625.

(*5*) HALL M, SCHILLINGER J. Miscellaneous tests of carbon tetrachloride as an anthelmintic. J Agric Res 1923; 23:163–192.

(*6*) CAMERON C, KARUNARATNE W. Carbon tetrachloride cirrhosis in relation to liver regeneration. J Pathol Bacteriol 1936; 42:1–21.

(*7*) SLATER TF. Necrogenic action of carbon tetrachloride in the rat: A speculative mechanism based on activation. Nature 1965; 209:36–40.

(*8*) DÍAZ GÓMEZ MI, DE CASTRO CR, D'ACOSTA N, DE FENOS OM, DE FERREYRA EC, CASTRO JA. Species differences in carbon tetrachloride-induced hepatotoxicity: The role of CCl_4 activation and of lipid peroxidation. Toxicol Appl Pharmacol 1975; 34:102–114.

(*9*) UMBREIT WW, BURRIS RH, STAUFFER JF. Manometric techniques. Minneapolis: Burgess 1964:149.

(*10*) SWANN PF, MCLEAN AE. Cellular injury and carcinogenesis. The effect of a protein-free high carbohydrate diet on the metaoblism of dimethylnitrosamine in the rat. Biochem J 1971; 4:632–634.

(*11*) KORN ED. Purines and pyrimidines. Methods Enzymol 1957; 4:632–634.

(*12*) MCLEAN AE, DAY PA. The use of new methods to measure the effect of diet and inducers of microsomal enzyme system of cytochrome P-450 in liver homogenates and on metabolism of dimethylnitrosamine. Biochem Pharmacol 1974; 23:1173–1180.

(*13*) DÍAZ GÓMEZ MI, CASTRO JA, DE FERREYRA EC, D'ACOSTA N, DE CASTRO CR. Irreversible binding of $^{14}CCl_4$ to liver microsomal lipids and proteins from rats pretreated with compounds altering microsomals mixed-function oxygenase activity. Toxicol Appl Pharmacol 1973; 25:534–541.

(*14*) PAIK WK, KIM S. E-alkyl lysinase: New assay method, purification, and biological significance. Arch Biochem Biophys 1974; 165:369–378.

(*15*) STERKEL RL, SPENCER JA, WOLFSON SW, WILLIAMS-ASHMAN H. Serum isocitric dehydrogenase activity with particular reference to liver disease. J Lab Clin Med 1958; 52:176–184.

(*16*) BANCROFT H. Introducción a la bioestadística. Buenos Aires: Eudeba, 1960:205–211.

(*17*) MONTESANO R, MAGEE PN, eds. Comparative metabolism in vitro of nitrosamines in various animal species including man. IARC Sci Publ 1974; 10:39–55.

(*18*) LOTLIKAR PD, BALDY WJ, DWYER EN. Dimethylnitrosamine demethylation by reconstituted liver microsomal cytochrome P-450 enzyme system. Biochem J 1975; 152:705–708.

(*19*) LOTLIKAR PD, SOOK HONG Y, BALDY WJ. Effect of dimethylnitrosamine concentration on its demethylation by liver microsomes from control and 3-methylcholanthrene pretreated rats, hamsters and guinea pigs. Cancer Lett 1978; 4:355–361.

(*20*) MADUAGWA EN, BASSIN O. Comparative in vitro metabolism of dimethylnitrosamine in animals of six different species. J Environ Pathol Toxicol 1980; 4:229–235.

(*21*) Johansson-Brittebo EB, Tajäve H. The distribution of (^{14}C) dimethylnitrosamine in mice. Autoradiographic studies in mice with inhibited and non-inhibited dimethylnitrosamine metabolism and a comparison with the distribution of (^{14}C) formaldehyde. Toxicol Appl Pharmacol 1978; 45:565–575.

(*22*) Godoy HM, Díaz Gómez MI, Castro JA. Mechanism of dimethylnitrosamine metabolism and activation in rats. JNCI 1978; 61:1285–1289.

(*23*) Godoy HM, Díaz, Gómez MI, Castro JA. Relationship between dimethylnitrosamine metabolism or activation and its ability to induce liver necrosis in rats. JNCI 1980; 64:533–537.

(*24*) Díaz Gómez MI, Godoy HM, Castro JA. Further studies on dimethylnitrosamine metabolism, activation and its ability to cause liver injury. Arch Toxicol 1981; 47:159–168.

(*25*) Farber E. The genesis of cancer with chemicals. Arch Pathol Lab Med 1980; 104:499–502.

(*26*) Ying TS, Sarma DS, Farber E. Role of acute hepatic necrosis in the induction of early steps in liver carcinogenesis by dimethylnitrosamine. Cancer Res 1981; 41:2096–2102.

(*27*) Schmähl D, Habs M, Ivankovic S. Carcinogenesis of *N*-nitrosodiethylnitrosamine (DENA) in chickens and domestic cats. Int J Cancer 1978; 22:552–557.

(*28*) Bogovski P, Bogovski S. Animal species in which N-nitroso compounds induce cancer. Int J Cancer 1981; 27:471–474.

blank page

Effects of Sublethal Irradiation on Changes in Crypts of the Mouse Colon During Treatment With 1,2-Dimethylhydrazine[1,2,3]

Thomas C. Richards[4] *and* David E. Tacha[4]

ABSTRACT—The effects of low-dose X-irradiation on the progression of early neoplastic changes induced in the colon by 1,2-dimethylhydrazine (DMH) were assessed. Outbred female Swiss-Webster mice were treated with DMH only, DMH–irradiation, irradiation only, or 0.001 *M* EDTA. Animals were pulsed with [^{3}H]thymidine for 1 hour, and the distal colon was radioautographed. The number of labeled cells per crypt in animals treated with DMH–irradiation was greater (P<0.01) than the number in "DMH-only" animals, but a corresponding increase in the length of the crypts did not occur. After 16 weeks of treatment, the percentage of animals with focal atypia was similar in the DMH–irradiation group (87%), and the DMH-only group (100%), but there were more focal atypias per animal in the DMH-only group. After 20 weeks, 14% of the DMH–irradiation group had visible tumors compared to 63% of the DMH-only group. The results suggest that DMH increased the number of cells at risk for irradiation; thus the surge in proliferation subsequent to cell depletion was amplified. However, the development of precancerous lesions was not promoted.—JNCI 1982; 69:693–697.

Low-dose, whole-body irradiation is cytotoxic to populations of mitotic cells in the proliferative zone of crypts of the mouse colon. The extent of mucosal damage is dependent on the dose level and frequency of irradiation (*1*). The injured or dead cells were sloughed and the colon epithelium is renewed by a compensatory proliferative surge of the remaining stem cells (*2*). The lower regions of crypts in mice begin to show some cell loss 36 hours after high-dose irradiation, and by 60 hours the lower halves of the crypts are depleted. Foci of surviving clonogenic cells become visible in the lower crypt, and within 5 days the number of mitotically active cells will have increased dramatically (*3*).

These alterations in the growth characteristics of crypts may influence the development and progression of lesions induced in the mucosa by the carcinogen DMH. At least two possible events may occur: 1) An increase in proliferative activity may enhance carcinogenesis by the reduction of the latent period for the appearance of focal atypia, or 2) irradiation-induced sloughing of cells, already altered by DMH, may delay carcinogenesis because repopulation of crypts could occur from relatively unaffected stem cells. The purpose of this study was to determine whether the cytokinetics of crypts is different in groups given DMH–irradiation compared to those given DMH alone, and to determine whether the induction of neoplastic lesions by DMH is similar in the 2 groups.

MATERIALS AND METHODS

Animals and treatments.—Outbred, female Swiss-Webster mice, at least 60 days old and 20 g in body weight, were housed 5 animals per cage and given free access to food and water (standard rodent chow; Oregon State University, Corvallis, Oreg.). Nine groups of animals were treated for 1–20 weeks. Each group was divided into 4 subgroups (5 animals/subgroup) and treated with DMH alone, or DMH–irradiation, or irradiation alone, or 0.001 *M* EDTA. More animals were added to those groups that were treated for 16 and 20 weeks. DMH (American Scientific, Portland, Oreg.) was dissolved in 0.001 *M* EDTA and adjusted to pH 6.5 with $NaHCO_3$. Controls were given comparable volumes of 0.001 *M* EDTA. Those subgroups that received DMH or EDTA were given sc injections at a dose of 20 mg/kg body weight on Mondays each week. Subgroups that received irradiation were given 390 rad of whole-body irradiation on Fridays before the beginning of weeks 1, 3, and 6 of the experiment. The mice were irradiated before these weeks of the experiment so that irradiation effects on initial DMH-induced changes in the cells could be tested. All the animals of a group were killed on Thursdays, 3 days after the beginning of weeks 1, 2, 3, 4, 6, 8, 12, 16, or 20 of the experiment.

Irradiation was performed in a cesium-37 irradiator (Mark I, model 68; J.L. Shepherd and Assoc., Glendale, Calif.). Animals in groups of 5 were placed in a transparent plastic box with ample ventilation, rotated slowly on a turntable in the irradiation chamber, and exposed to 223 rad per minute for 1.75 minutes for a total dose of 390 rad. The lethal dose of radiation for mice is about 1,000 rad, so the 390-rad dose was low enough to initiate a proliferative response in the crypt cells without killing the animals (*4, 5*).

Tissue preparation.—Mice were given injections of 0.5 μCi [^{3}H]dThd/g body weight (20 Ci/mmol; New England Nuclear Corp., Boston, Mass.) 1 hour before they were killed. The entire descending colon of the mouse was quickly removed. A section of the distal colon at the pelvic rim 1.0–1.5 cm above the anus was dissected, washed in cold 0.9% NaCl, divided into two sections, each 3–5 mm in length, and fixed in 4% paraformaldehyde–1% glutaraldehyde solution for at least 24 hours. The two sections from each animal were embedded together in one block of glycol methacrylate and oriented so that transverse sections of the colon could be taken. The remainder of the colon was slit lengthwise, washed free of its contents, stained with 1% Alcian blue, and examined under a 2× dissecting micro-

ABBREVIATIONS USED: DMH=1,2-dimethylhydrazine; [^{3}H]dThd=tritiated thymidine.

---

[1] Received December 11, 1981; accepted April 16, 1982.

[2] Supported by Public Health Service grant CA-21480 from the National Large Bowel Cancer Project of the National Cancer Institute.

[3] Animals were maintained under the guidelines set forth by the Oregon Health Sciences University.

[4] Department of Anatomy, School of Medicine, Oregon Health Sciences University, Portland, Oreg. 97201.

scope. The number of grossly visible tumors was counted in this tissue.

Analysis of tissues.—Two types of microscopic analyses were completed on sections of each colon: 1) radioautographic analysis for identification of cells that incorporate [^{3}H]dThd, and 2) histologic analysis for the presence of focal atypia and other induced lesions. Several sections (2–3-μm thick) were cut on a Sorvall JB-4 microtome and mounted on slides, then 300–500 μm were trimmed from the block, and additional sections were cut. The slides of colon used for radioautography were hydrolyzed in 1 *N* HCl for 10 minutes, stained by the Feulgen method, and dried. These slides were then processed for radioautography with the use of standard procedures (*6*).

The rest of the slides were stained with hematoxylin, counterstained with methylene blue, and the number of abnormal crypts, focal atypias, microcarcinomas, and cysts per section were counted. Focal atypias were characterized by high mitotic activity, disrupted crypt architecture, and anaplastic or abnormal cell structure and size (*7*). When these changes were confined to a single crypt, it was defined as an abnormal crypt (*8*). Microcarcinomas were defined as tumors that were too small to be identified with a dissecting microscope. The presence of mucosal cysts, indicative of disrupted cell kinetics in the glands, were also noted. The intent of this study was to compare relative differences in the number of lesions observed between groups rather than an analysis of the total number of lesions induced per animal.

Thirty crypt columns per animal were scanned for the presence of [^{3}H]dThd-labeled cells. The number of labeled cells and their positions in the crypt column were recorded. Differences in cell proliferation among the 4 subgroups of animals after 2, 4, 8, and 16 weeks of treatment were chosen as representative times during the course of the experiment to analyze changes in the distribution of labeled cells. Further details concerning procedures used to analyze the radioautographs can be found elsewhere (*9*).

A one-way analysis of variance was used to test the differences in values among subgroups at any particular point during treatment. Differences in distribution of labeled cells after each time interval among the treatment groups were determined by a two-way analysis of variance (*10*).

RESULTS

Three consecutive whole-body irradiations, spaced 2 to 3 weeks apart, at sublethal doses of 390 rad per animal resulted in an increase in pyknotic nuclei along the lower halves of crypts as the target cells were killed by irradiation. Instead of the entire mucosa sloughing as occurs with larger doses of radiation, the damaged individual cells were extruded into the crypt lumen and lost from the epithelium.

Radioautographs of colon sections from animals treated with DMH, DMH–irradiation, irradiation only, or untreated were analyzed for the total number of cells and the number of labeled cells per crypt column. In the DMH-treated group we observed an initial, rapid increase in the number of labeled cells and in the total number of cells in the crypts followed by a more gradual enlargement of crypts as the mucosa became severely altered. In contrast, the number of labeled cells per crypt column increased significantly ($P<0.01$) after the 3d week of treatment in the DMH–irradiation group compared to the numbers in the other groups (text-figs. 1, 2). There was no additional acute response to irradiation during the 6th week of DMH treatment, although the expanded level of cell proliferation was sustained until the 12th treatment week in the DMH-irradiation group. A corresponding increase in the total number of cells per column did not accompany the increase in labeled cells. Animals that received only irradiation showed some increase in labeled cells per crypt above control levels; however, the proliferative response was not nearly of the magnitude of that observed in the DMH–irradiation group.

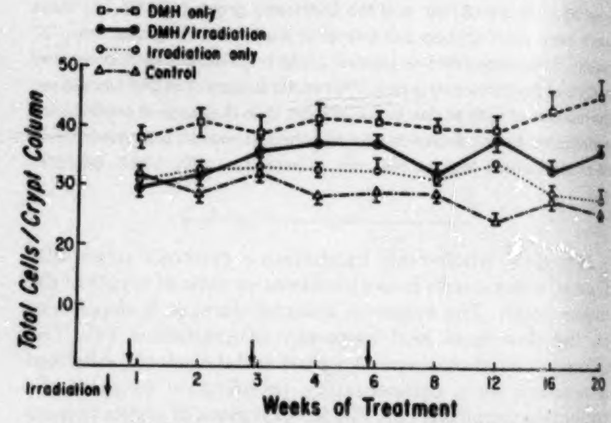

TEXT-FIGURE 1.—Comparison of the changes in the No. of cells/crypt over time in the treatment groups. *Each point* represents the mean value from 5 animals; *bracketed lines* represent the SE of the mean. *Arrows* along the *abscissa* indicate the times of irradiation. Irradiation appears not to affect the total No. of cells in mucosal glands of the mouse colon.

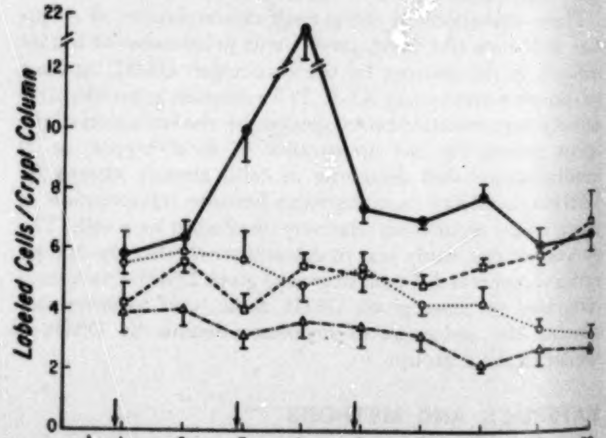

TEXT-FIGURE 2.—Comparison of the changes in the No. of labeled cells/crypt over time in the 4 treatment groups. Symbols are the same as in text-fig. 1. Irradiation dramatically increased the No. of labeled cells/crypt in animals that received DMH.

The distribution of labeled cells in crypts after DMH-irradiation treatment showed an increase of the labeling index of each segment and a marked shift of the labeled cells toward the surface. The proliferative zone expanded to include a larger proportion of the total crypt column (text-figs. 3-6). The largest change in the relative size of the proliferative zone occurred after 4 weeks of DMH treatment, when labeled cells appeared in all segments of the crypt column and on the surface epithelium. This pattern persisted after 8 and 16 weeks of DMH treatment, although the early effects of the irradiation became progressively less pronounced in these later groups.

In groups of animals that received irradiation only, we observed a similar but smaller cell proliferation response. Changes in number and distribution of proliferative cells in crypts were significantly different ($P<0.05$) from those of control animals 2 weeks after the first irradiation. However, at later treatments only the presence of a few labeled cells in crypt column segments close to the surface distinguished the animals that received irradiation alone from untreated controls.

Relative differences in the number of distinct lesions and the times of their appearance in the colonic mucosa of irradiated and nonirradiated animals treated with DMH are shown in table 1. The important difference between the groups was not the uniqueness of a particular lesion to a treatment, but that the overall level of mucosal transformation in nonirradiated animals was much greater than that in irradiated mice. The irradiated group had fewer tumors after 20 weeks of DMH treatment than the group that received DMH alone. Focal atypias were present in approximately the same proportion of animals in the 2 groups, but there were more focal atypias per animal in those that were not irradiated. In addition, microcarcinomas were present only in the nonirradiated group after 16 weeks of DMH treatment. Mice in the DMH-irradiation group developed about the same number of mucosal cysts compared to the number in nonirradiated animals that received DMH. The cysts usually formed in the base of the crypts, apparently as a consequence of disruption in the normal cell

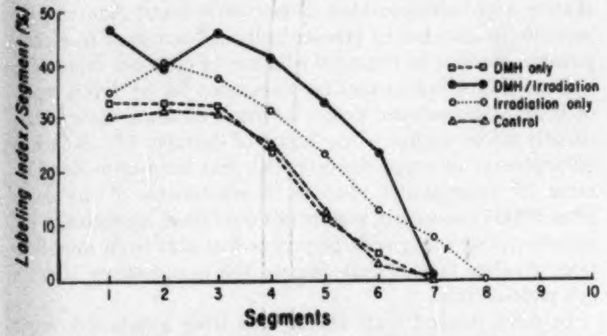

TEXT-FIGURE 3.—Comparison of the relative differences in distribution of labeled cells in mucosal glands 2 wk after the start of the experiment. *Each point* represents the mean percentage of labeled cells in 5 animals. The relative size of the proliferative zone increased groups that received DMH-irradiation. The overall mean No. of cells/crypt column/group of animals was divided into 10 equal segments. The percent labeled cells/segment was determined by the division of the No. of labeled cells/crypt segment by the total No. of cells/segment ×100.

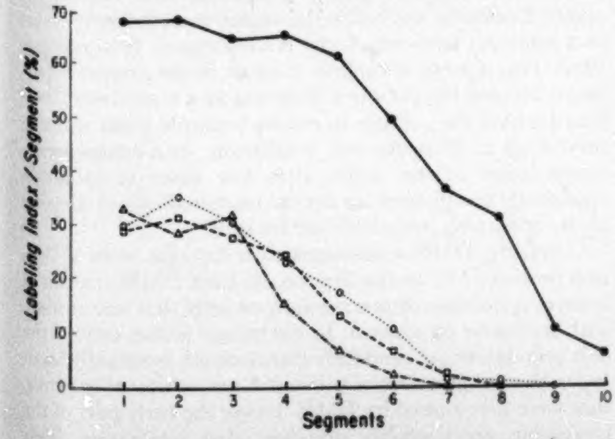

TEXT-FIGURE 4.—Comparison of the relative differences in distribution of labeled cells in mucosal glands 4 wk after the start of the experiment. Symbols are the same as in text-fig. 3. The proliferative zone of the crypts of the DMH-irradiation group has expanded greatly.

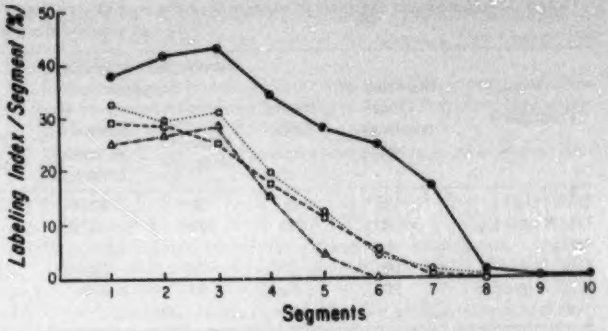

TEXT-FIGURE 5.—Comparison of the relative differences in distribution of labeled cells in mucosal glands 8 wk after the start of the experiment. Symbols are the same as in text-fig. 3. Even though the proliferative zone of the crypts of the DMH-irradiation group is smaller than it was at 4 wk, it is still relatively larger than that of other groups.

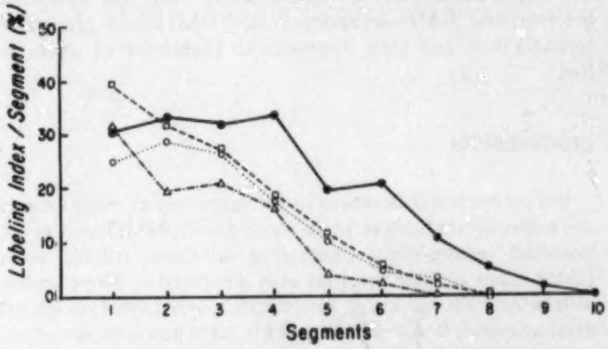

TEXT-FIGURE 6.—Comparison of the relative differences in distribution of labeled cells in mucosal glands 16 wk after the start of the experiment. Symbols are the same as in text-fig. 3. The proliferative zone of the DMH-irradiation group has reduced in size even further; however, labeled cells were still found in the upper segment of the crypts in animals of this group.

TABLE 1.—*Histologic analysis of segments of the mid-descending colon of mice treated with DMH for 16 or 20 weeks and irradiated with 39 rad per mouse before weeks 1, 3, and 6 of treatment*[a]

Treatment	Duration of DMH treatment, wk	No. of mice	Abnormal crypts/focal atypias		Microcarcinomas		Cysts		Visible tumors	
			Total No. observed	Mice with at least 1 lesion, %	Total No. observed	Mice with at least 1 lesion, %	Total No. observed	Mice with at least 1 lesion, %	Total No. observed	Mice with at least 1 lesion, %
DMH only	16	10	30	100	3	30	8	70	—	—
DMH-irradiation	16	8	16	87.5	—	—	17	62.5	—	—
DMH only	20	16	70	100	11	56.2	22	68.7	18	63
DMH-irradiation	20	14	32	100	4	28.2	19	57.1	3	14.2

[a] Abnormalities were recorded from representative step-serial sections. Two levels of the colon, separated by 300–500 μm, were analyzed. Type of lesions observed have been defined in the text.

organization in the upper regions of the glands. Finally, histologic differences in the mucosa were less apparent between the DMH-irradiation and DMH-only groups of animals that had been treated with DMH for 12 weeks or less.

DISCUSSION

We compared differences in the responses of crypt cells of the colon epithelium in mice treated with DMH and given low-dose, whole-body irradiation to those treated with DMH alone or that received only irradiation. The number of labeled cells per crypt in animals given DMH increased dramatically after irradiation. This surge has been shown to occur because the epithelium compensates for the induced loss of cells by increasing the proliferative activity in the remaining cells (*2*). The magnitude of compensation is a function of the level of cell depletion which, in turn, is related to the total dose and frequency of the irradiation (*1*). The radiation dose we used was sufficient to kill a proportion of the most susceptible target cells, the mitotic cells, but not large enough to kill many cells in other phases of the cell cycle more resistant to irradiation (*1*). In the irradiated tissue cellularity decreases as dead cells are removed, and repopulation begins only when damaged proliferative cells exhaust their limited division potential and undamaged stem cells begin to divide (*11*).

When groups given DMH for 3 weeks were irradiated, both the labeling index and the proliferation zone increased significantly to the extent that labeled cells were observed in the upper crypt segments and in the surface epithelium. In contrast, we observed a much lower response in animals that were irradiated but were not given DMH. These findings suggest that treatment with DMH accentuates the effect of irradiation by an increase of the number of target cells at risk to radiation and results in an amplification of the compensatory surge of the remaining proliferative cells. This amplification did not recur after the third irradiation, after 6 weeks of DMH treatment because DMH-induced changes in the cell population were reduced by the earlier sloughing of altered cells.

A surge in proliferation usually leads to an overshoot in the number of cells retained in the upper crypt and an enlargement of the overall size of the crypt (*12*). In the present model, [^{3}H]dThd-labeled cells were observed in high positions in the crypts after irradiation, because the proliferative zone had expanded. However, it is not clear why the increase in number of labeled cells did not lead to a comparable increase in the total number of cells per crypt. The increased labeling cannot be accounted for by DNA repair of irradiation-induced errors in the cells since these events usually occur within a few hours of damage (*3*). A lack of enlargement in crypt size suggests that long-term development of hyperplastic mucosa, characteristic of the colon after DMH treatment, results not only from increases in the number of dividing cells per crypt but also from modification of other factors that control the homeostasis of crypt cell populations.

In mice treated with DMH and then irradiated, fewer identifiable lesions of the colon developed than in DMH-treated unirradiated animals. Moreover, those lesions that were present required longer periods of time to develop. These observations indicate that irradiation in some way delays the transformation of the mucosa. Hamilton (*13*) has demonstrated that after a large single dose of radiation, the denuded crypts are regenerated from single clonogenic cells located in the upper region of the proliferative zone of the crypts. Evidently, any cell in this region can randomly revert to a stem cell from which the entire crypt is then repopulated. This pattern is unlikely to occur in the present experiment because the radiation dose was at a much lower level that enabled the animals to receive multiple doses and still survive up to 20 weeks post irradiation. As a consequence, repopulation of the crypts after low doses of radiation apparently results from an overall increased rate of division of the remaining mitotically active cells.

Currently, DMH carcinogenesis is thought to be a two-step process (*14*). In the first phase, each DMH treatment induces a number of pretransformed cells that accumulate with successive treatments. In the second phase, cells of the first population are randomly transformed, eventually leading to the development of tumors. A proportion of the cells, that were first altered by DMH during the early part of the treatment, are probably sloughed after irradiation. This results in an overall reduction in the relative transformation of the mucosa and ultimately decreases the number of tumors that develop in 20 weeks.

REFERENCES

(*1*) WITHERS HR. Cell renewal system concepts and the radiation response. Front Radiat Ther Oncol 1972; 6:93–107.

(*2*) HAGEMANN RF, LESHER S. Irradiation of the G.I. tract: Compensatory response of stomach, jejunum and colon. Br J Radiol 1971; 44:599–602.

(*3*) WITHERS HR, MASON KA. The kinetics of recovery in irradiated colonic mucosa of the mouse. Cancer 1974; 34:896–903.

(*4*) HAGEMANN RF, SIGDESTAD CP, LESHER S. Intestinal crypt survival and total and per crypt levels of proliferative cellularity following irradiation: Fractionated X-ray exposures. Radiat Res 1971; 47:149–158.

(*5*) HAMILTON E. Differences in survival of mouse colon after whole- or partial-body irradiation. Int J Radiat Biol 1977; 31:341–347.

(*6*) TACHA DE, RICHARDS TC. Comparison of glycol methacrylate and paraffin-embedded tissues for identification of tritium-labeled cells after emulsion radioautography. J Histotech 1981; 4:59–61.

(*7*) DESCHNER EE. Experimentally induced cancer of the colon. Cancer 1974; 34:824–828.

(*8*) CHANG WW. Histogenesis of symmetrical 1,2-dimethylhydrazine-induced neoplasms of the colon in the mouse. J Natl Cancer Inst 1978; 60:1405–1418.

(*9*) RICHARDS TC. Early changes in the dynamics of crypt cell populations in mouse colon following administration of 1,2-dimethylhydrazine. Cancer Res 1977; 37:1680–1685.

(*10*) STEEL RG, TORRIE JH. Principles and procedures of statistics. New York: McGraw-Hill, 1960:99–160.

(*11*) FABRIKANT JI. Radiation effects on rapidly and slowly proliferating cell renewal systems. Front Radiat Ther Oncol 1972; 6:57–78.

(*12*) HAMILTON E. Cell proliferation and ageing in mouse colon. I. Repopulation after repeated X-ray injury in young and old mice. Cell Tissue Kinet 1978; 11:423–431.

(*13*) ———. Diurnal variation in proliferative compartments and their relation to cryptogenic cells in the mouse colon. Cell Tissue Kinet 1979; 12:91–100.

(*14*) MASKENS AP. Confirmation of the two-step nature of chemical carcinogenesis in the rat colon adenocarcinoma model. Cancer Res 1981; 41:1240–1245.

blank page

Tumor-Induced Neovascularization in the Mouse Eye[1,2,3]

V. R. Muthukkaruppan,[4] **L. Kubai,**[5] *and* **R. Auerbach**[5,6,7]

ABSTRACT—Tumor fragments implanted in the mouse cornea induce a neovascular reaction characterized by the penetration of new blood vessels into the avascular cornea that ultimately reach the tumor to permit its further rapid growth. A method to achieve angiogenesis in the mouse cornea was studied, as well as the histologic and gross manifestations of the neovascular reaction and the effect of tumor cells or host irradiation on the observed angiogenic response. Sequential stages of tumor-induced neovascularization are described and documented for sarcoma 180- and C755 mammary adenocarcinoma-induced angiogenesis. A number of distinct processes of the angiogenesis response to tumors are discussed which suggest that several families of angiogenesis-inducing factors may mediate each of these processes. The importance of the development of a mouse model for the study of angiogenesis is stressed.—JNCI 1982; 69:699–708.

Neovascularization is now recognized as a major component of a variety of disease processes ranging from lymphadenopathies to the development and spread of cancer. Its role in inflammatory reactions, in graft maintenance and rejection, and in delayed hypersensitivity is beginning to be more fully appreciated. The generation of new blood vessels, angiogenesis, has been studied in a variety of test systems (*1-3*). Aside from making direct observations in situ of growing tumors, of inflammatory lesions, or of capillary regeneration after injury, the principal approach has been to transplant angiogenesis-inducing tissues ectopically into a dorsal air sac of the rat, into the cheek pouch of hamsters, as grafts on the CAM of chick embryos, or into the adult mammalian avascular cornea. Efforts to obtain in vitro correlates of angiogenesis reactions have recently begun to show some success as well (*4, 5*). Both mitogenesis and cell migration of endothelial cells have been used in these in vitro test systems, but it is not yet clear how reliable as indicators of in vivo responses these cell culture systems will be. Because most in vitro tests have used endothelial cells from large vessels and because the measured responses are of quite general biologic reactions, continued reference to in vivo tests of angiogenesis is essential for studies of neovascularization.

Our research group has, over the past several years, begun to develop both in vivo and in vitro tests of angiogenesis that will permit the examination, under genetically controlled conditions, of the cellular and subcellular factors leading to angiogenesis. For this reason, we have concentrated on the development of techniques for studies of angiogenesis systems involving the mouse, since this species has major advantages through the extensive range of genetically characterized tumors, reagents for delineation, fine dissection of cell types on the basis of differentiation antigens, and genetically homogenous inbred lines and mutants that represent a wide range of disease models. Among the test systems we have developed are the LIA assay system involving the introduction of angiogenesis-inducing lymphocytes intradermally into syngeneic or allogeneic irradiated adult host animals (*6, 7*); xenogeneic assays in which murine effector cells, tissues, or extracts are placed on the CAM of explanted chick embryos (*8*); in vitro assays of mitogenesis and cell migration of mouse capillary endothelial cells (Joseph J, Form D, Watt S, Auerbach R: Unpublished observations); and the murine intracorneal assay in which angiogenesis-inducing tissues or slow release pellets are placed into an intrastromal corneal pocket of adult mice (*9*).

Of all the test systems for neovascular reactions, the intracorneal response is the most definitive, inasmuch as new blood vessels must penetrate an avascular space to reach the angiogenesis-inducing stimulus. Moreover, in contrast to the in vitro tests, the intracorneal response permits the assessment of systemic host factors that influence the progress of neovascularization. To permit the mouse corneal angiogenesis reaction to be used effectively for the analysis of the neovascular process, we now present a detailed description of the sequence of gross and histologic events that occur after the implantation of tumors into the cornea.

MATERIALS AND METHODS

Mice.—BALB/cAu, C57BL/6Au, and ICR/HaAu strains of mice were obtained from our own inbred mouse colony. For several experiments we used the C57BL/6c2J albino mutant and (BALB/cAu × 129/J)F_1 and (ICR/HaAu × C57BL/6c2J)F_1 hybrids. (BALB/cJ × A/J)F_1 (CAF_1) mice were obtained from The Jackson Laboratory, Bar Harbor, Maine.

Tumors.—The C755 mammary adenocarcinoma work was initiated with tumors obtained from Dr. Kelly Clifton,

---

ABBREVIATIONS USED: CAM=chorioallantoic membrane; LIA=lymphocyte-induced angiogenesis; S180=sarcoma 180.

---

[1] Received December 11, 1981; accepted March 30, 1982.

[2] Supported by Public Health Service grants EY-3243 from the National Eye Institute and AI-14607 from the National Institute of Allergy and Infectious Diseases.

[3] Animals were maintained under the guidelines set forth in the "Guide for the Care and Use of Laboratory Animals" by the Institute of Laboratory Animal Resources, National Research Council.

[4] Department of Immunology, Madurai Kamaraj University, Madurai, India.

[5] Department of Zoology, University of Wisconsin, Madison, Wisc. 53706.

[6] *Address reprint requests to* Dr. Auerbach.

[7] The experimental work was performed at the University of Wisconsin. We appreciate the administrative and editorial assistance of Barbara Houser, M.S., the help with photography of Gilbert Burns, Donald Chandler, Hilary French, and Laura Vanderpooeg, the assistance of Wanda Auerbach, M.L.S., and Bich Van Nguyen with literature retrieval, and the excellent animal care provided for our research animals by Patricia Cofta, Philip Corona, John Gundlach, Robert Peterson, and William Peterson. We appreciate the scientific discussions with our colleagues David Form, Ph.D., Jeymohan Joseph, M.S., and Younan A. Sidky, Ph.D. We thank Jacqueline Grieves and Gwendolyn Holbrow for technical assistance.

University of Wisconsin-Madison, which were subsequently maintained by subcutaneous passage in C57BL/6 mice. Subsequently, tumor morphology became somewhat atypical, and a new stock of C755 tumor was obtained from the tumor bank of the National Institutes of Health (Bethesda, Md.) and was maintained in similar fashion. The S180 studies in the present paper were done with the use of a tumor line maintained in vitro in Dulbecco's modified Eagle's minimum essential medium with fetal calf serum. Additional experiments, not included in the present study but with similar results, involved fresh S180 tumors obtained from the National Institutes of Health tumor bank and maintained either in BALB/c or in ICR/Ha mice.

Grafting procedures.—The intracorneal grafting method was one modified from that described by Gimbrone et al. (*10*) and outlined briefly in our earlier report (*9*). Mice were anesthesized with tribromoethanol (1:1 in tertiary amyl alcohol diluted 1:50 in 10% ethanol and administered as 0.01 ml/g body wt; Avertin). This anesthetic proved to be particularly useful since it was gentle, it did not lead to pupil dilation, and it was tolerated over a fairly wide dose range. If animals recovered from anesthesia before surgery could be completed, additional anesthetic could be administered safely. The eye was irrigated with antibiotics (500 U penicillin and 500 μg streptomycin/ml phosphate-buffered saline). A transverse 1-mm incision was made in the cornea with the use of a #65 Beaver blade (Beaver Instruments, Waltham, Mass.). The cut penetrated about halfway through the cornea, deep enough to permit insertion of a spatula, but not so deep as to penetrate the anterior chamber of the eye. The pocket was prepared with a malleable iris spatula (V. Mueller Co., Chicago, Ill.) ground down extensively to yield a fine, thin edge. The pocket was extended to reach within about 0.8 mm of the limbus. Tissue fragments (0.5 mm^3) were then inserted into the pocket by means of the same spatula. Tumor cells from culture were implanted with a small-bore (0.1–0.2 mm in inside diameter), orally controlled micropipette. The entire surgical procedure was performed by lighting supplied either by a Luxo surgical lamp cooled by light passage through a long plastic extension tube or by fiber optic illumination with additional heat-absorbing filters placed between the light source and the fiber extension tube. We found lighting to be critical, and the importance of cooling the light source cannot be overemphasized, since corneal damage can result from excessive heat and may lead to spurious neovascular reactions.

Preparation of material for examination.—Histologic preparations were made from Formalin- or Bouin's-fixed material embedded in paraffin, sectioned at 7 μm, and generally stained with hematoxylin and eosin. Other fixatives and stains were used for specific experimental purposes.

India ink perfusions were accomplished by retrograde injection of filtered Pelikan-brand india ink after extensive perfusion with 0.9% saline to clear erythrocytes from the circulation. After the ocular vasculature became filled with india ink, the eyes were bathed in 10% Formalin buffered at pH 7 and further fixed in Formalin, followed by clearance in 50% glycerin.

Photographs were taken with standard illumination on mildly anesthesized animals or with a flash attachment on unanesthesized animals. The mouse was held at a sharp enough angle to obtain corneal vascular images similar to those obtained by use of a slit lamp.

Other angiogenesis assays.—Intradermal neovascular responses were done as described previously (*6*). Test cell suspensions were inoculated into sublethally irradiated adult mice, with the amount of the intradermal inoculum held constant at 0.1 ml. The animals were killed 3 days later, a skin flap was opened up, and the extra blood vessels visible around the inoculation site were enumerated to obtain a measure of the vascular reaction.

Angiogenesis on the chick CAM was performed on embryos grown in petri dish culture (*11*). Eggs were incubated for 3.5 days, the egg contents were placed in 100-mm petri dishes, and the uncovered dish was placed inside a larger (150 mm) petri dish (covered) for humidification and incubation. Five days later grafts were made onto the CAM by means of a small incision into which the tissue to be tested was placed. Care was taken to ensure that the incision was small enough that the graft would not slip through the membrane. Neovascularization was monitored daily for 4-5 days.

RESULTS

Vascular Response in Control Grafts

Normal mammary gland tissue from nonlactating adult female C57BL/6 mice was implanted into the corneal stroma of syngeneic recipients to serve as a reasonably normal counterpart for the C755 mammary tumor. Additional control grafts were made with the use of inguinal and mesenteric lymph node fragments from syngeneic mice (table 1).

For 2 days after a pocket is made in the cornea, limbal activity can be observed. This activity is transient and vasodilatory in nature and disappears within 2 days after trauma. The grafting of normal mammary gland or syngeneic lymph node fragments causes no additional reaction. Carbon perfusion of corneas bearing mammary gland or syngeneic lymph node implants prepared several days after

TABLE 1.—*Tumor-induced angiogenesis in the mouse cornea*

Host strain	Source of graft	Total no. of grafts	No. of grafts with:		
			No growth	Growth	Angiogenesis
C57BL/6J	C57BL/6 mammary gland	4	4	0	0
	C57BL/6 lymph node	3	3	0	0
	C755 mammary adenocarcinoma	10	4	6	6
C57BL/6c2J	C57BL/6 mammary gland	6	6	0	0
	C57BL/6 lymph node	6	6	0	0
	C755 mammary adenocarcinoma	18	4	14	14
BALB/c	S180	12	0	12	12

grafting revealed the normal pattern of limbal blood vessels (fig. 1). Opacity, corneal edema, or other signs of an inflammatory reaction were almost universally absent, being observed in fewer than 5% of the corneal grafts prepared in our laboratory. We routinely exclude those implants (corneal and experimental) that show a broad inflammatory reaction within the first 2 days; such reactions generally accompany infection.

Tumor-Induced Angiogenesis

To determine the extent and nature of angiogenesis induced by various tumors, we selected the C755 mammary adenocarcinoma and the S180 as primary tumor types. C755 grows only in C57BL/6 or F_1 hybrids derived from this strain of mice. Conversely, S180 grows rapidly in all the strains we tested, although we generally used mice that carried the histocompatibility genes ($H\text{-}2^d$) of the strain of tumor origin (BALB/c or F_1 animals which included BALB/c as one of the parents). The C755 tumor was originally transplanted into black mice, but subsequently we used congenic C57BL/6c2J albino mice to facilitate making in situ observations of the graft and the vascular response.

Of 28 C755 tumor grafts implanted into syngeneic animals, 20 induced angiogenesis, and in these cases tumor growth was consistently observed (table 1; fig. 2). S180 induced vascularization and developed as growing tumor masses in all 12 of the grafts made (table 1). In all instances, vessel outgrowth began in the limbal region most directly apposed to the edge of the corneal pocket, and the progress of vessel penetration into the cornea could be monitored by daily measurements with an ocular micrometer.

Sequence of Tumor-Induced Vascular Events

Several corneas bearing tumor implants were monitored critically by sequential photographs as well as by routine measurements. One representative series obtained with a C755 tumor graft is shown in text-figure 1. Whereas the

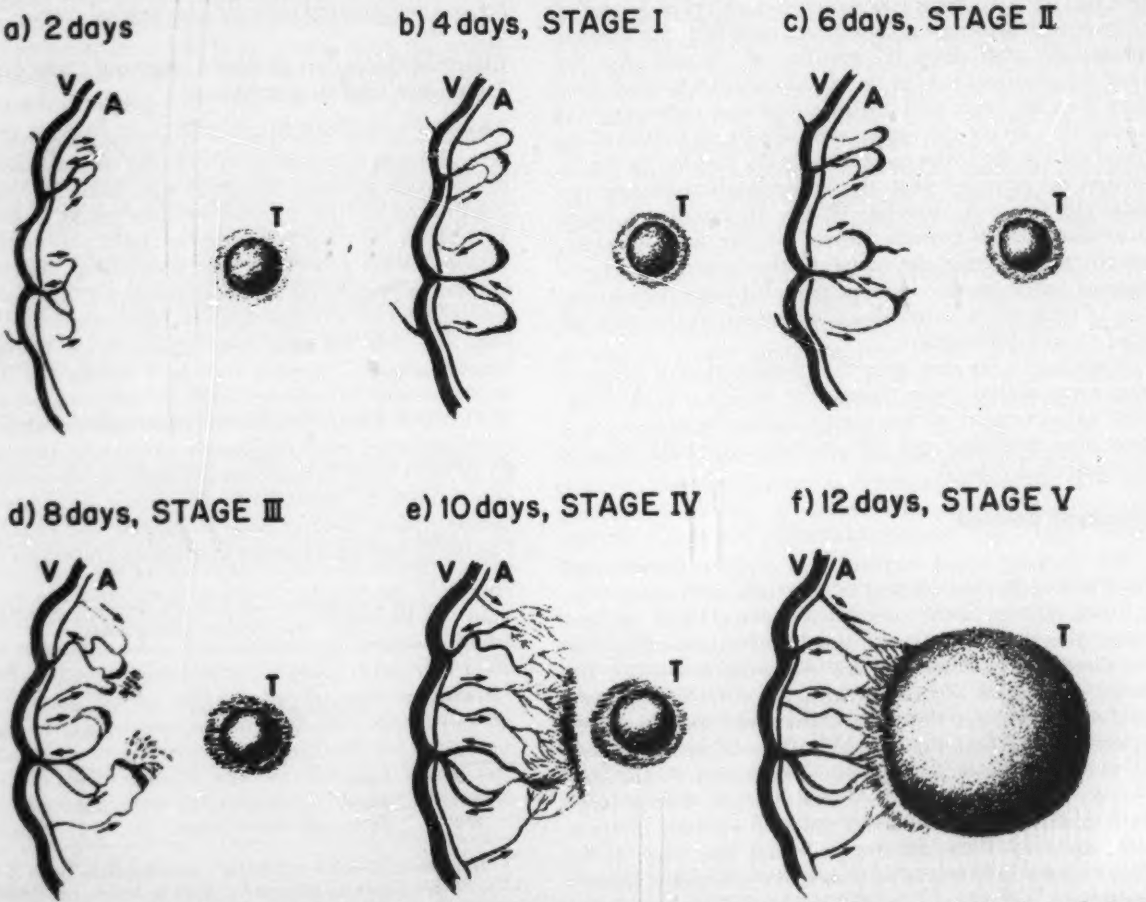

TEXT-FIGURE 1.—Sequence of vascular responses seen in the cornea of C57BL/6c2J mice after implantation of C755 mammary adenocarcinoma fragments. The drawings of the living cornea were made under a stereomicroscope at a) 2 days after grafting and b) 4 days after grafting, stage I. *Note* elongation of loops and thickening of microvessels at the apices c) 6 days after grafting, stage II. Blind-end single-channel sprouts form at the apices d) 8 days after grafting, stage III. More sprouts form, directed toward the graft, e) 10 days after grafting, stage IV. New channels form from the original sprouts; a brush border is seen at the advancing vascular front f) 14 days after grafting, stage V. Tumor is now vascularized, and three-dimensional growth has been initiated. Each of the stages has also been identified with carbon-perfused corneal preparations. For comparison with S180 grown in BALB/c mice, *see* table 3. V=vein; T=tumor; A=artery.

initial limbal activity in the control cornea subsided within 2 days, the tumor-bearing cornea exhibited elongation of the initial loops as much as 0.4 mm from the limbal vessels toward the tumor by day 4 (text-fig. 1a, 1b). We consider tumor-induced angiogenesis to be initiated after 2 days only and classify the response seen by day 4 as stage I, with the recognition that events in the first 48 hours may also be tumor-specific but may simply be masked from characterization by virtue of the general limbal response to preparation of the pocket.

In stage I, the apices of the vascular loops appeared thicker than the remaining parts of the microvasculature (text-fig. 1b). The vascular loops were intact, allowing normal blood flow from the arteriole to the venule of the limbus to continue. At this point, the tumor implant appeared to have spread slightly from the original pocket.

By day 6, single blind-end channels or sprouts developed from the apices of the loops toward the tumor implant, and blood flow was sluggish in these sprouts in contrast to the original loops where circulation remained normal (stage II; text-fig. 1c). This event was soon followed by the formation of more such sprouts that lengthened with their tips directed toward the graft (stage III; text-fig. 1d). Shortly after this time the proximal ends of the sprouts showed normal blood flow from the loops, and the distal tips were all arranged in a row, thus giving the appearance of a brush border of red blood cells in the living cornea (stage IV; text-fig. 1e; fig. 3). Within the next 2–4 days, the tumor implant became vascularized (stage V; text-fig. 1f; fig. 4), leading to rapid, three-dimensional growth, corneal bulging, and ultimately exophytic progress of the tumor. Carbon-perfused preparations of tumor-bearing corneas provided clear documentation of each of the stages described by sequential observations on individual grafts.

Vascular events seen after the implantation of S180 tumors were similar, even though the timing was different. S180 tumors could induce sprout formation as early as 3 days after grafting, and the implants generally became vascularized by day 8.

Histologic Studies

The growing tumor implant was initially found to be contained within the corneal stroma, and both epithelium and endothelium of the cornea were intact. Until the new vessels penetrated the tumor, growth remained effectively two dimensional. After the new microvessels reached the tumor, a number of blood vessels could be seen in and around the graft, and the center of the tumor mass appeared necrotic by the time the corneal surface became ruptured due to the exophytic development of the tumor. At the zone between the limbus and the tumor implant, several large blood vessels could be seen in the stroma, most of them being distributed toward the epithelial side (figs. 5, 6). Inflammatory infiltration of leukocytes was conspicuously absent.

Allogeneic Tumor-Induced Angiogenesis

The mouse cornea model was used to analyze the nature of tumor-induced vascular responses in allogeneic tumor–host combinations. C755 mammary tumor cells (C57BL/6, $H\text{-}2^b$ origin) were grafted into the corneas of BALB/c ($H\text{-}2^d$) animals. Of 14 tumor grafts, 13 induced angiogenesis and became vascularized by day 13. The kinetics of the angiogenic response from stages I to IV was similar to that seen in syngeneic grafts. A major difference in the response was seen first in the fact that the typical brush borders of stages IV and V did not develop. The vessels in the tumor implant consisted mainly of vascular loops of a nonleaky nature, and extravasation of red blood cells was not observed. Though vascularized, tumors did not continue to grow and by day 17 appeared necrotic. However, the original vascular loops persisted with intact blood flow for several more days, regressing only at about the 25th day after grafting of the tumor.

Histologic analysis revealed an accumulation of lymphocytes around the tumor and the blood vessels in the stroma and in the limbus region (fig. 7). At that time (day 10), the tumor cells appeared viable, and several large blood vessels could be seen in the stroma around the graft. Tumor cell destruction occurred over the next several days.

Effect of Depletion of Host Lymphoid Cells on Tumor-Induced Angiogenesis

Insofar as the experiments involving allogeneic tumors demonstrated that host lymphoid cells were associated with the rejection of tumor allografts seen following tumor vascularization in the cornea, we believed it important to analyze the role that lymphocytes might play in the initial vascularization process as well, apart from allogenetically induced responses. We therefore examined the effect of host lymphocytes on a tumor that was histocompatible with the host and that also had been described as being of low immunogenicity, growing well in a number of unrelated murine strains. We selected S180 (BALB/c origin) and used (BALB/c × 129/J)F_1 hosts for these experiments. Tumors were implanted into hosts shortly after a sublethal dose (550 R) of total-body X-rays was delivered to these mice. The results (table 2), indicate that the tumor grafts were vascularized equally well in both irradiated and control mice. The initial vascular response in irradiated hosts was different

TABLE 2.—*Effect of sublethal irradiation of host mice on tumor-induced angiogenesis*

Irradiation,[a] R	Additional treatment[b]	No. of grafts made[c]	No. of tumors becoming vascularized[d]
0	None	7	6
550	None	14	13
550	Spleen cell reconstitution	4	3

[a] Host mice, (BALB/c × 129/J)F_1, were irradiated with X-rays (250 kVp, 20 mA, 1 mm Al, 0.5 mm Cu) 0–24 hr before transplantation of tumors. Dose was measured in air with a Victoreen dosimeter.

[b] Spleen cell reconstitution was performed by the injection of 10^7 syngeneic spleen cells immediately before tumor transplantation.

[c] Grafts of S180 cells obtained from confluent cultures were placed within 1 mm of the limbus.

[d] Tumors became vascularized within 8 days of grafting and subsequently underwent exophytic growth.

TABLE 3.—*Angiogenesis induction by irradiated tumor cells*

Irradiation,[a] rad	No. of grafts	Loops on 2d day, mm	Loops on 3d day, mm	No. of grafts on:									No. of growing tumors at 10th day
				4th day at stage				6th day at stage				8th day at stage V	
				I	II	III	IV	I	II	III	IV		
0	7	0.35	0.52	1	1	4	1	0	0	3	4	7	7
2,000	3	0.35	0.35	0	2[b]	0	0	0	0	3	0	3[c]	0
4,000	5	0.45	0.45	0	1[b]	1	0	1[b]	1	1	1	2[c]	0

[a] Cultures of S180 were irradiated from a gamma (cesium) source before intracorneal grafting into BALB/c mice.

[b] Remaining grafts had not progressed beyond loop formation at this time.

[c] Although the tumors were vascularized, the number of sprouts were reduced and the typical brush border effect was not seen. The remaining grafts failed to become vascularized.

to the extent that a general increased vasodilation and limbal activity were seen in the first few days after irradiation. The localized vascular outgrowth and penetration toward the pocket containing the tumor graft were visibly greater in irradiated animals, but the timing was comparable. It is likely that the increased visibility of the neovasculature was due to vasodilation and altered blood flow characteristics rather than to any basic alteration in the angiogenesis reaction itself. At any rate, there was no indication of a diminished angiogenesis response in hosts irradiated sufficiently to lead to a 90–95% reduction in circulating leukocyte levels (data not shown).

To be certain that the neovascular response we observed was similar because of offsetting effects of irradiation on the endothelial cells and on leukocyte levels, we performed reconstitution experiments by reinjecting syngeneic spleen cells into irradiated hosts prior to implantation of tumor fragments (table 2). The addition of unirradiated leukocytes to the irradiated hosts did not alter the timing or extent of the neovascular reaction.

Angiogenesis Induced by Irradiated Tumor Cells

To analyze the nature and extent of neovascularization induced by heavily irradiated tumor cells, we exposed S180 tumors to either 2,000 or 4,000 rad γ-irradiation from a cesium source immediately before they were grafted. As shown in table 3, the extent of induced loop formation was similar for irradiated and unirradiated tumors. However, the effect of irradiation was readily apparent for the later stages of vascularization. The number of vascular sprouts was greatly reduced, especially in the group exposed to 4,000 rad. The brush border effect typically accompanied by extravasation of erythrocytes was uniformly absent (fig. 8). Even though the irradiated tumor implants could become vascularized, tumor growth was not observed, which suggests that the irradiation had effectively blocked tumor cell replication.

DISCUSSION

Our description of the events accompanying neovascularization of tumor grafts placed in the corneas of adult mice is basically similar to that provided for the angiogenesis response previously documented for the rabbit (*10*). In both systems an implant of angiogenesis-inducing tissue can evoke vascular outgrowth from the limbal vessels into the avascular cornea, and in both instances the growth of tumors becomes rapid and three dimensional only after the blood vessels have penetrated the grafted tumor.

The delineation of reasonably distinct phases in the angiogenesis response not only provides a convenient set of markers for the process of vessel formation in response to grafting but also reflects the rather separate events that accompany the reaction. Initial activity of the limbal region is transient for control tissues or simple surgical manipulation alone. However, in the presence of angiogenesis-inducing stimuli, elongation of capillary loops occurs over the control level. Such activity may be an essential first step that must take place as a prelude to the later events of vascular penetration and endothelial cell migration and proliferation.

Loop formation and capillary sprouting appear to be distinct entities, and differences in vascular permeability (Muthukkaruppan VR, Auerbach R: Unpublished observations) at points along the new vessels (loop region vs. brush border region) suggest yet a third separate manifestation of the response. The extravasation of red blood cells and of injected carbon particles at the brush border was found to be characteristic of tumor-induced angiogenesis; however, the tight junctions between endothelial cells appear to be normal, as revealed by electron microscopic analysis (Clark AW, Muthukkaruppan VR: Unpublished observations).

It seems quite likely that the induction of angiogenesis involves several, not necessarily related, effector mechanisms. Factors that stimulate vasodilation, cell migration, loop formation (which is itself possibly a manifestation of migration), endothelial cell proliferation (both proximal in the limbal region and distal at the brush border form of the new microvessels), and changes in vascular permeability may all play a significant part in leading to the extensive vascular reaction associated with tumor growth (*1, 10, 12*).

The dissociation of some of these factors has already been suggested by our earlier observation that LIA can elicit vascular loops but apparently fails to yield a brush-border-type advancing sprouting edge (*9, 13, 14*). It is interesting in this regard that irradiated tumors as well as tumors placed in immunologically inhospitable environments fail to lead to the formation of this active advancing edge of the new capillaries. In this connection, the published figures of Folkman and his associates (*15, 16*) suggest that in the presence of cartilage-derived angiogenesis inhibitor, vascular loops are formed but sprouts appear to be absent and that already existing sprouts disappear from the cornea soon after removal of an angiogenesis-inducing stimulus (tumor angiogenesis factor in ethyl vinylacetate copolymer) from the corneal pocket, whereas the residual capillary loops remain for extended periods (*17*).

Further support for several discrete mechanisms for action of mediators of neovascularization comes from the fact that the isolation of angiogenesis-inducing chemical factors appears to have led to several distinct classes of factors, some of low molecular weight (prostaglandin-type), some macromolecular (growth factor types such as fibroblast growth factor or epidermal growth factor), and some in the general group of vasoactive mediators (e.g., heparin). The question of angiogenesis-inducing factors has been discussed in detail in a recent review (*3*) which can be consulted for detailed documentation and literature citations.

The ability of irradiated tumors to elicit angiogenesis in our experiments confirms for the mouse system what we have previously reported for tumor grafts placed on the CAM or in rabbit eyes (*18*). Irradiation also fails to prevent the initial neovascular reactions seen after intradermal inoculation of angiogenesis-stimulating allogeneic lymphocytes (*6*) or tumor cell suspensions (data not shown). It may be significant, however, that the extraction of tumor angiogenesis factor from irradiated tumor cell cultures by Folkman and his associates (*18*) appears to yield an active nondialyzable factor that is larger than the factor obtained by Weiss and her colleagues (*19*), who, using unirradiated tumors, report isolation of a smaller, dialyzable material (*3*). Our own observations on prostaglandin-associated angiogenesis (*20, 21*) as well as on the effects of prostaglandin synthetase inhibitors such as indomethacin (Sidky YA, Form OM, Auerbach R: Unpublished observations) suggest that the prostaglandin-associated angiogenesis effect may include stimulation of endothelial cell proliferation.

Form and Auerbach (submitted for publication) have proposed that since the amount of prostaglandin E_2 necessary to induce angiogenesis on the CAM is as little as 0.2 ng/day in their experiments—an amount less than the amount known to be released by activated macrophages or by many tumors and less than the amount reported to be present in inflammatory exudates or synovial fluids—this mediator alone may be adequate for initiation of angiogenesis in a variety of known biologic systems. An additional role of vasoactive factors released from mast cells (*22*) may provide further stimulation. It would be most attractive if the two factors acted synergistically, one inducing proliferation and the other inducing migration of endothelial cells. The perhaps special ability of tumors to further enhance the angiogenesis response may reflect action of yet a third class of agents, able to cause dissolution or perturbation of the growing edge of the capillary loops, leading to the observed brush border morphology and extensive capillary sprouting. It is in this phase of angiogenesis that the larger, tumor-associated, perhaps enzymatically active angiogenesis factors may be of major importance.

The use of mouse assay systems for the analysis of the angiogenesis reaction is clearly of major advantage for numerous reasons. Even with the use of the intradermal test assay system we have already been able to address such questions as assessment of the role of various subsets of the *H-2* complex in LIA, the effect of host T-cell deficiency (*nu/nu* athymic animals) on neovascular reactions, and the efficacy of T-cell subsets (Lyt antigens) in inducing LIA (*7, 23*). The availability of mutants of strains high or deficient in natural cytotoxic activities, of lines susceptible to the induction of tumors, and of inbred lines capable of sustaining growth of so many well-characterized tumor cell lines and the broad range of reagents developed especially for murine systems (e.g., antibodies directed against differentiation antigens and tumor-specific antigens) make mouse models most attractive. The availability, therefore, of an in vivo test system for angiogenesis in the mouse that can clearly distinguish between neovascularization and other vascular events, permits continued in situ observations without anesthesia, can be performed on large numbers of animals, and can be done with predictability should facilitate study of induced vascular reactions.

REFERENCES

(*1*) Folkman J, Cotran R. Relation of vascular proliferation to tumor growth. Int Rev Exp Pathol 1976; 16:207–248.

(*2*) Haudenschild CC. Growth control of endothelial cells in atherogenesis and tumor angiogenesis. Adv Microcirc 1980; 9:226–251.

(*3*) Auerbach R. Angiogenesis-inducing factors: A review. Lymphokines 1981; 4:69–88.

(*4*) Fenselau A, Watt S, Mello RJ. Tumor angiogenic factor: Purification from the Walker 256 rat tumor. J Biol Chem 1981; 256:9605-9611.

(*5*) Folkman J, Haudenschild CC, Zetter BR. Long-term culture of capillary endothelial cells. Proc Natl Acad Sci USA 1979; 76:5217-5221.

(*6*) Sidky YA, Auerbach R. Lymphocyte-induced angiogenesis (LIA): A quantitative and sensitive assay of the graft-vs.-host reaction. J Exp Med 1975; 141:1084–1100.

(*7*) Auerbach R, Sidky YA. Nature of the stimulus leading to lymphocyte-induced angiogenesis. J Immunol 1979; 123:751–754.

(*8*) Auerbach R, Kubai L, Sidky YA. Angiogenesis induction by tumors, embryonic tissues and lymphocytes. Cancer Res 1976; 36:3435-3440.

(*9*) Muthukkaruppan VR, Auerbach R. Angiogenesis in the mouse cornea. Science 1979; 205:1416–1418.

(*10*) Gimbrone MA Jr, Cotran RA, Leapman SB, Folkman J. Tumor growth and neovascularization: An experimental model using the rabbit cornea. J Natl Cancer Inst 1974; 52:413–427.

(*11*) Auerbach R, Kubai L, Knighton D, Folkman J. A simple procedure for the long-term cultivation of chicken embryos. Dev Biol 1974; 41:391–394.

(*12*) Ausprunk DH, Folkman J. Migration and proliferation of endothelial cells in preformed and newly formed blood vessels during tumor angiogenesis. Microvasc Res 1977; 14:53–65.

(*13*) Epstein RJ, Hughes WE. Lymphocyte-induced corneal neovascularization: A morphological assessment. Invest Ophthalmol Vis Sci 1981; 21:87–94.

(*14*) Fromer CH, Klintworth GK. An evaluation of the role of leukocytes in the pathogenesis of experimentally induced corneal vascularization. III. Studies related to the vasoproliferative capability of polymorphonuclear leukocytes and lymphocytes. Am J Pathol 1976; 82:157–170.

(*15*) Brem H, Folkman J. Inhibition of tumor angiogenesis mediated by cartilage. J Exp Med 1975; 141:427–439.

(*16*) Langer R, Conn H, Vacanti J, Haudenschild C, Folkman J. Control of tumor growth in animals by infusion of angiogenesis inhibitor. Proc Natl Acad Sci USA 1980; 77:4331–4335.

(17) Ausprunk DH, Falterman K, Folkman J. The sequence of events in the regression of corneal capillaries. Lab Invest 1978; 38:284–294.

(18) Auerbach R, Arensman R, Kubai L, Folkman J. Tumor angiogenesis: Lack of inhibition by irradiation. Int J Cancer 1975; 15:241–245.

(19) Weiss JB, Brown RA, Kumar S, Phillips P. An angiogenic factor isolate from tumours: A potent low-molecular-weight compound. Br J Cancer 1979; 40:493–496.

(20) Form DM, Sidky YA, Kubai L, Auerbach R. PGE$_2$-induced angiogenesis. In: Prostaglandins and cancer: First international conference. New York: Liss, 1982:685–689.

(21) Ben Ezra D. Neovascuologenic ability of prostaglandins, growth factors and synthetic attractants. Am J Ophthalmol 1978; 86:455–461.

(22) Azizkhan RG, Azizkhan JC, Zetter BR, Folkman J. Mast cell heparin stimulates migration of capillary endothelial cells in vitro. J Exp Med 1980; 152:931–944.

(23) Roehm NW, Sidky YA, Auerbach R. Lyt phenotype analysis of the effector cells responsible for evoking lymphocyte-induced angiogenesis (LIA).Cell Immunol 1981; 63:272–278.

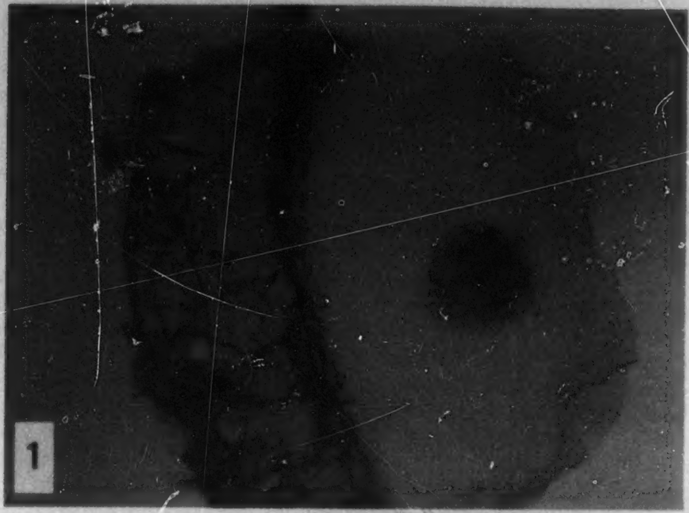

FIGURE 1.—Cornea of CAF$_1$ mouse with syngeneic lymph node graft 5 days after grafting. *Note* absence of vascular response. *Bar*=1 mm.

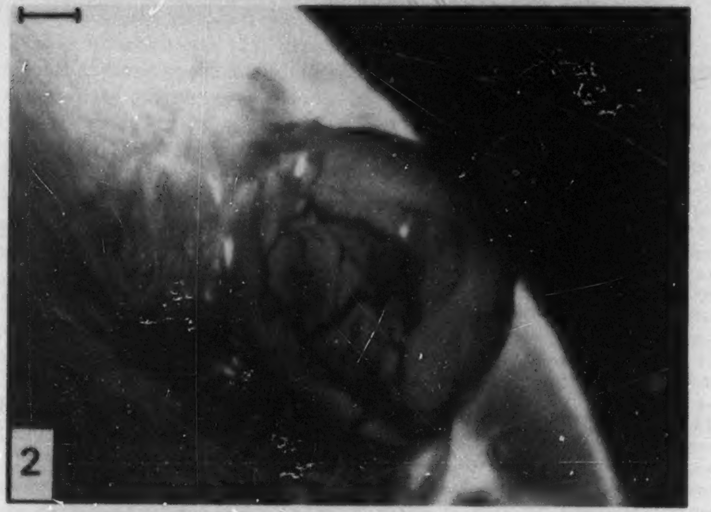

FIGURE 2.—Living cornea of C57BL/6c2J mouse bearing C755 mammary adenocarcinoma graft 12 days after grafting. *Bar*=1 mm.

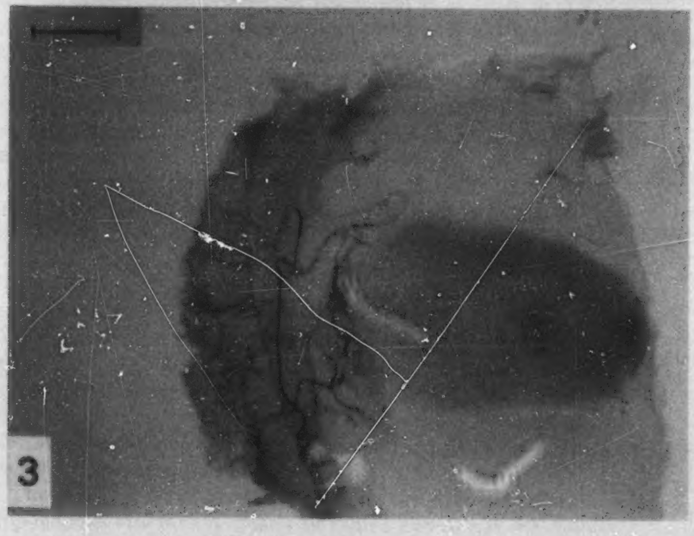

FIGURE 3.—C57BL/6c2J cornea with C755 mammary adenocarcinoma 9 days after grafting; carbon perfused, stage IV. *Bar*=1 mm.

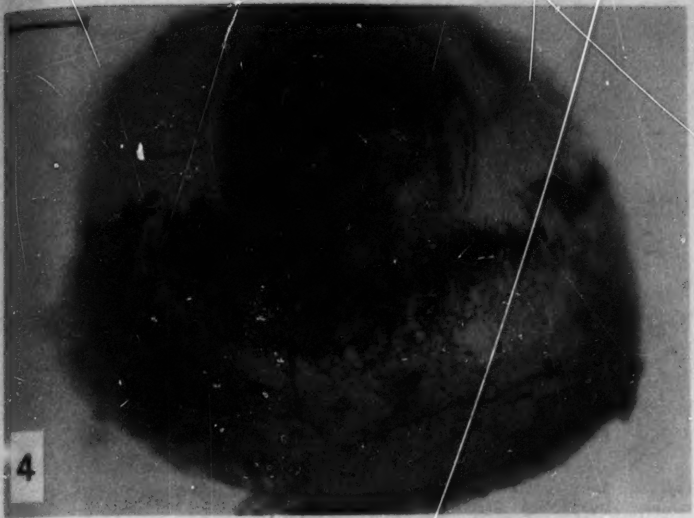

FIGURE 4.—C57BL/6c2J cornea with C755 mammary adenocarcinoma implant 14 days after grafting; stage V. Tumor is vascularized. *Bar*=1 mm.

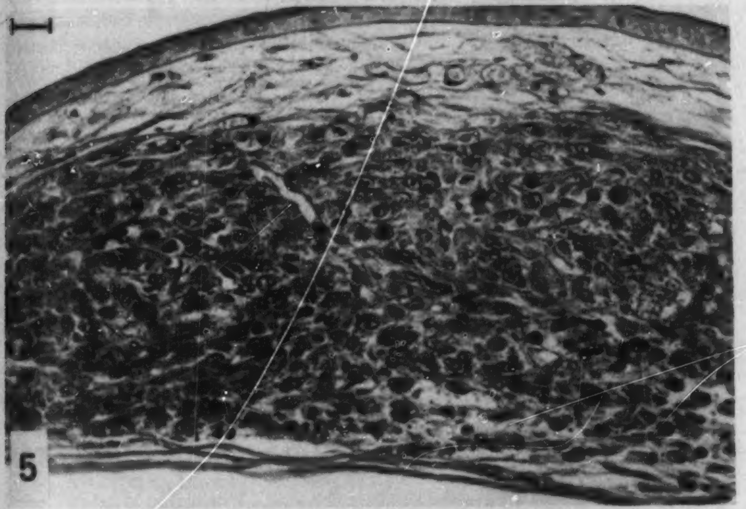

FIGURE 5.—Section of BALB/c cornea showing vascularized S180 tumor graft. *Note* several cross sections of microvessels in the stroma and in the tumor itself and the presence of numerous tumor cells undergoing cell division. *Bar*=0.5mm.

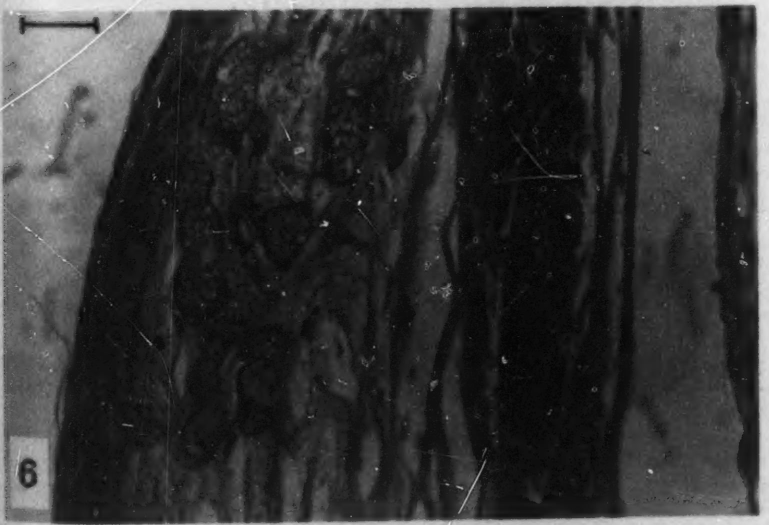

FIGURE 6.—Section of BALB/c mouse cornea bearing S180 tumor graft. Preparation shows blood vessels in the stroma, mainly distributed toward the epithelial surface. *Note* the absence of inflammatory infiltration of leukocytes. *Bar*=0.5 mm.

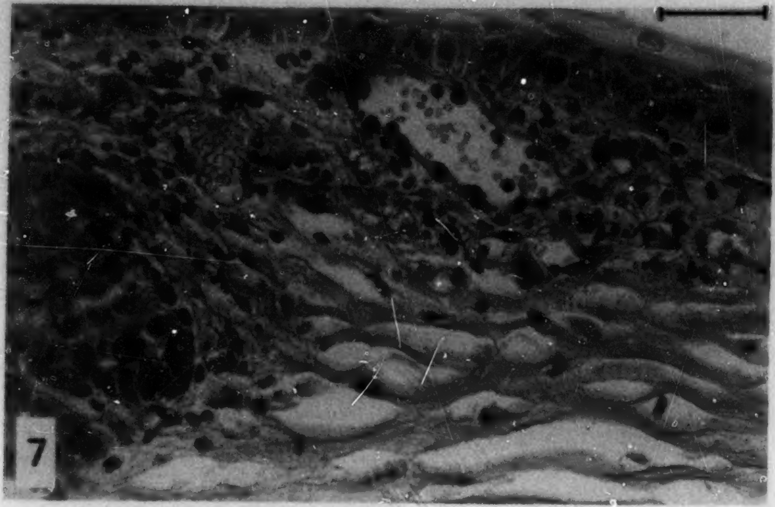

FIGURE 7.—BALB/c cornea bearing C755 mammary adenocarcinoma graft (histoincompatible), 10 days after grafting. *Note* extensive lymphocytic infiltration. *Bar*=0.5 mm.

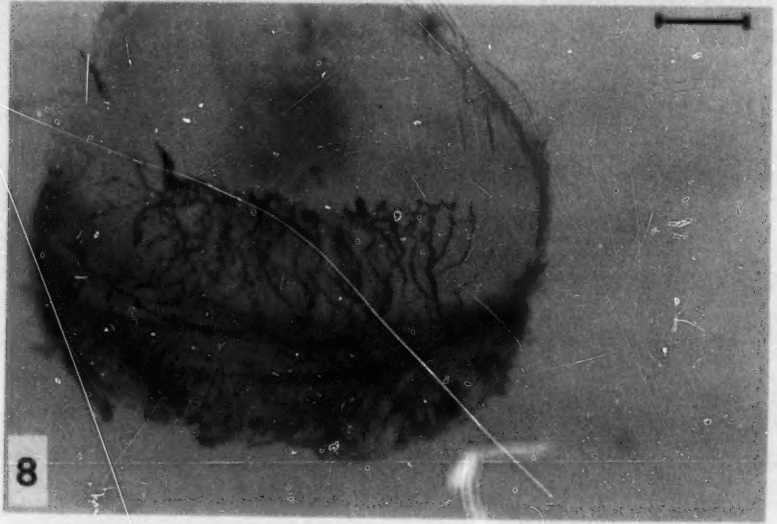

FIGURE 8.—Cornea of BALB/c mouse bearing S180 tumor graft, 8 days after grafting. Tumor cells were irradiated with 4,000 rad before implantation. Carbon perfusion shows vascularized graft, but absence of typical brush border. *Bar*=1 mm.

In Vitro Infection of Lymphocytes With Marek's Disease Virus[1,2,3]

Bruce W. Calnek,[4] Karel A. Schat,[4] William R. Shek,[4] *and* Chen-Lo H. Chen[5,6]

ABSTRACT—Suspension cultures of splenic lymphocytes, incubated at 41°C, became infected with Marek's disease virus (MDV) following exposure to *a*) other infected lymphocytes, *b*) infected chicken kidney monolayer cultures, or *c*) cell-free MDV. Both viral antigen expression and virus isolation could be demonstrated after more than 40 passages made by the addition of fresh spleen cells at 2- to 3-day intervals. Susceptibility of spleen cells from bursectomized chickens was markedly lower than that of cells from intact birds. Furthermore, when spleen cell suspensions were depleted of cells having characteristics of bursa-derived cells, e.g., those with surface IgM, Fc receptors, or ability to adhere to nylon wool, the susceptibility of the cell suspension was diminished. Enrichment of the suspension with cells having those features enhanced overall susceptibility. The target cells for virus infection in vitro also were shown to be nonphagocytic, to be of low or medium density, and to bear Ia-like antigen. In vitro susceptibility to infection of spleen cells did not correlate with the genetic susceptibility of the donor to Marek's disease.—JNCI 1982; 69:709–713.

MD, a naturally occurring lymphomatous disease of fowl, is caused by a cell-associated herpesvirus which may be isolated from latently infected lymphocytes by cocultivation with susceptible cell cultures such as CK monolayers (*1*). In vivo, the infection is biphasic, causing a cytolytic infection in lymphoid organs such as the spleen, thymus, and bursa of Fabricius during the 1st week, followed by a predominantly latent infection of lymphocytes thereafter. Lymphomas, which subsequently develop in a variable proportion of genetically susceptible chickens, are the result of neoplastic transformation of thymus-derived (T)-lymphocytes (*1*). Both T- and bursa-derived (B)-lymphocytes were reported to be involved in latent infections (*2*).

It was postulated that various subpopulations of lymphocytes were the targets of the different types of infection with MDV, i.e., cytolytic (productive-restrictive), latent, transforming (*1*). We (Shek WR, Calnek BW, Schat KA, Chen CH: Submitted for publication) have now obtained very substantial evidence that different subpopulations are involved. A very significant finding was that B-cells are the primary target of the early cytolytic infection, whereas the latent infection is largely associated with non-B-lymphocytes. These studies were conducted by the fractionation of cells infected in vivo.

In vivo infection patterns are probably influenced by a great many pathogenetic complexities in addition to the inherent susceptibility of various cell populations. In an effort to obviate that problem, we attempted to infect chicken lymphocytes in vitro where direct exposure of various cell types could be used to assess their susceptibility and response to MDV. This paper demonstrates that lymphocyte infection does occur following in vitro exposure to virus and that infection spreads among lymphocytes under culture conditions. Furthermore, we corroborate the conclusions of the in vivo studies by showing that B-cells are a major target of cytolytic infection in vitro.

MATERIALS AND METHODS

Viruses.—JM-10 and GA-5 clones of MDV have been described (*3*) and were used as cell-associated inocula consisting of infected CK cells from infected monolayer cultures or spleen cells from infected birds. Cell-free JM strain MDV was prepared as a skin extract (*4*) from chickens infected with uncloned virus.

Experimental birds.—Specific-pathogen-free chickens from departmental flocks of P-2, N-2, UCD-003, PDRC, and S-strain genetic lines were the sources of lymphocytes for in vitro infection studies. The P-2, N-2, and UCD-003 lines were, respectively, homozygous for the major histocompatibility alleles $B^{19}B^{19}$, $B^{21}B^{21}$, and $B^{17}B^{17}$ (*5, 6*); PDRC (*7*) and S-strain (*8*) birds are uncharacterized for these alleles. P-2 and S-strain chickens are genetically highly susceptible to MD, and the N-2 strain is highly resistant to MD; the susceptibility of UCD-003 and PDRC to MD is intermediate (*6*). Chickens that were donors of spleens, thymuses, or bursas of Fabricius were 2–4 weeks old.

For some experiments, PDRC or P-2 donors of spleen cells were EBx on the 17th day of incubation as described elsewhere (*9*). The efficacy of the treatment was assessed by examination of spleen cells for the presence of surface IgM in an indirect immunofluorescence test with mouse monoclonal anti-chicken IgM (μ-chain). This reagent is described elsewhere (Shek WR, Calnek BW, Schat KA, Chen CH: Submitted for publication). For some experiments, 3- to 4-week-old P-2 and N-2 birds, infected 5–13 days earlier with JM-10 or GA-5 virus, were donors of infected spleen cells. In one trial, spleen cells from two 5-week-old turkeys were compared with chicken spleen cells. These turkeys were

---

ABBREVIATIONS USED: CK=chicken kidney; EBx=embryonally bursectomized; MD=Marek's disease; MDV=MD virus; PFU=plaque-forming units; SRBC=sheep red blood cell(s); VIA=viral internal antigen.

---

[1] Received December 15, 1981; accepted April 21, 1982.

[2] Supported in part by Public Health Service research grant CA-06709-19 from the National Cancer Institute.

[3] Animals were maintained under the guidelines set forth by Cornell University.

[4] Department of Avian and Aquatic Animal Medicine, New York State College of Veterinary Medicine, Cornell University, Ithaca, N.Y. 14853.

[5] Departments of Pediatrics and Microbiology, University of Alabama in Birmingham, School of Medicine, Comprehensive Cancer Center Cellular Immunobiology Unit, University Station, Ala. 35294.

[6] We thank Mr. Raymond Harris for excellent technical assistance and Mrs. Gwen Troise for typing the manuscript.

hatched and raised in isolation and were known to be free of turkey herpesvirus (*10*) and MDV infections.

Preparation of cells for in vitro studies.—Spleens, bursas of Fabricius, and thymuses were collected aseptically and gently forced through an autoclavable 60-μm mesh (Tetko Inc., Elmsford, N.Y.). Cells were suspended in phosphate-buffered saline (pH 7.3) and centrifuged over Ficoll–Paque (Pharmacia, Inc., Piscataway, N.J.). Lymphocytes, collected from the interface, were washed once and resuspended in LM-Hahn medium (*11*) at a concentration of 2–3×10^6/ml.

For some studies spleen cells were fractionated into subpopulations by procedures described in detail elsewhere (Shek WR, Calnek BW, Schat KA, Chen CH: Submitted for publication). Leukocytes were isopyknically separated by flotation in continuous Percoll (Pharmacia Chemicals AB, Uppsala, Sweden) gradients. Adherent cells were depleted with nylon wool or carbonyl iron (Sigma Chemical Co., St. Louis, Mo.). Cells with Fc receptors were separated from those without Fc receptors by adherence to chicken IgG-coated SRBC monolayers. We separated B-cells from non-B-cells by mixing SRBC coated with *Staphylococcus* protein A (Pharmacia Chemicals AB) with spleen cell suspensions pretreated with mouse monoclonal IgG (Y2b) anti-chicken IgM. The B-cell rosettes that formed were separated from the nonrosetted cells by centrifugation over Ficoll–Paque. Cells bearing Ia-like antigen were eliminated by lysis with mouse monoclonal IgM (υK) anti-chicken Ia and guinea pig complement.

In vitro infection and culture conditions.—Lymphocytes to be exposed to MDV were suspended in LM-Hahn medium, counted in a hemacytometer, and adjusted to a concentration of 2–3×10^6 viable cells (on the basis of trypan blue dye exclusion)/ml. MDV exposure was effected by cocultivation with infected lymphocytes or infected CK monolayers or by the addition of cell-free virus to the lymphocyte suspension. Infected lymphocyte inocula consisted of *a*) primary cultures of spleen cells obtained from infected chickens prepared as above and incubated at 41°C for 48 hours or *b*) 48-hour spleen cell cultures representing up to the 43d serial passage. The ratio of infected to uninfected cells was from 1:1 to 1:7. For exposure to infected CK cells, lymphocyte suspensions were added to heavily infected (>50% cytopathic effect) CK monolayers at the rate of 5 ml/60-mm petri dish culture. The lymphocytes were washed off after incubation at 41°C for 24–48 hours. Cell-free virus, with a titer of about 3,000 PFU/ml, was added to lymphocyte suspensions at a ratio of 1:10 (vol/vol).

All lymphocyte cultures consisted of 2 ml per plastic tube (#2057; Falcon Plastics, Oxnard, Calif.). Caps were left loose, and incubation was at 41°C in a humidified atmosphere of 5% CO_2 in air.

Serial passages of MDV infection in spleen cells were performed by the addition of freshly prepared uninfected spleen cells to an infected culture at 2- to 3-day intervals. Generally, the ratio of fresh to infected cells was 3:1. With few exceptions, passages were done with cells from P-2 chickens.

Tests for infected cells in cultures.—Virus isolations were performed by inoculation of 0.5 ml of cultured lymphocyte suspensions onto primary CK monolayers in 35-mm plastic petri dishes. The number of PFU was determined 6 or 7 days later and recorded in terms of PFU/ml.

The number of cells per milliliter expressing VIA was determined as described elsewhere (*11*). The lymphocyte suspension was concentrated ten times by centrifugation and resuspension in phosphate-buffered saline, and 10-μl drop smears were air dried on glass slides. Acetone-fixed smears were stained with fluorescein isothiocyanate-conjugated MDV antibodies, and the number of positive cells was enumerated with epi-illumination with the use of a Leitz Dialux fluorescence microscope. VIA-positive cells were recorded as the number positive per milliliter.

Statistical analyses.—Data were compared with the use of Student's *t*-test (*12*).

RESULTS

General Characteristics of In Vitro Infection and Passage of Virus in Splenic Lymphocytes

Table 1 contains data from representative trials that illustrate the successful infection and passage of virus in suspension cultures of splenic lymphocytes. Infection could be initiated with cell-free virus as well as with cell-associated virus from cultured CK cells or spleen cells from infected birds. VIA expression rates exceeded virus isolation rates by a substantial margin (up to 3 $\log_{10}$) in most instances when parallel assays were done. This observation is similar to earlier observations on virus genome expression in vitro (*2, 11*). VIA was detected in both the nucleus and cytoplasm of cells stained in immunofluorescence tests.

The number of positive cells per milliliter increased sub-

TABLE 1.—*Serial passage of MDV in cultured spleen cells from P-2 chickens*[a]

Spleen cell culture passage No.	No. of cells positive, $\log_{10}$/ml for VIA or virus isolation (PFU)[b]			
	Trial 1: Inoculum = GA-5 spleen[c]	Trial 2: Inoculum = JM-10 spleen[c]	Trial 3: Inoculum = GA-5 CK culture[d]	Trial 4: Inoculum = cell-free JM
1	3.2	3.4 (1.9)	ND	0
2	1.8	2.7 (1.0)	ND	1.6 (1.7)
3	1.8	3.1 (0.1)	3.2	1.9
4	3.3 (1.4)	3.6 (1.4)	3.0	1.8
5	3.5	3.4 (2.9)	2.9	2.3
6	3.9	ND	3.9	3.6
7	3.9	ND	ND	ND
8	3.8 (1.3)	ND	ND	ND
35	ND	4.3 (2.1)	ND	4.2 (2.2)
43	3.7 (2.0)	ND	ND	ND

[a] Passages were made every 2–3 days by addition of freshly prepared spleen cells at a concentration of 2–3×10^6/ml. Ratio of fresh to infected culture cells was 1:1–3:1. Inocula incubated without addition of fresh spleen cells were all negative for VIA or infectivity by 3–4 passages. ND = not done.

[b] Smears to detect VIA by immunofluorescence or virus isolations to assay PFU were done at 48 hr after passage.

[c] Cells (2×10^6/ml) were cultured at 41°C for 2 days before use as inoculum.

[d] Passage 1 was done by the addition of spleen cells to infected monolayers; the spleen cells were washed off 48 hr later.

stantially between days 1 and 2 after inoculation, but not thereafter. Both VIA expression and virus isolation rates were higher with incubation at 41°C than at 37°C. As previously noted (*2*), the viability of cultured lymphocytes dropped rapidly, so that generally less than 10% of the lymphocytes were alive after 72 hours of incubation. Thus passages were more successful when done at 2-day intervals than at 3- or 4-day intervals. Removal of dead cells by centrifugation over Ficoll-Paque reduced the number of VIA-positive cells by 65–70%. Two trials were done to determine if cell-to-cell transfer of MDV required shared major histocompatibility antigens or if the rate of virus infection was influenced by the genetic constitution of the spleen cell donors. The results, summarized in table 2, show that there was no allogeneic restriction; levels of infection were as high or higher in histoincompatible cells as in histocompatible cells. Furthermore, it was clear that susceptibility of lymphocytes to in vitro infection from infected cultured spleen cells did not follow the pattern of genetic susceptibility to tumor development seen in the various chicken strains. In fact, cells from the most resistant donors (N-2) showed the highest (albeit not significant) level of in vitro infection, whereas the UCD-003 strain, in which donors are of intermediate susceptibility to MD, had the lowest ($P<0.005$). In other trials, continued serial passage of GA-5 or JM-10 virus in parallel in P-2 or N-2 spleen cell cultures resulted in essentially identical titers as determined by VIA expression and virus isolations.

Characterization of Target Cells

We conducted several experiments to identify the cell type(s) susceptible to in vitro infection with MDV. In the first experiment, spleen cells from P-2 chickens were fractionated by methods found to be useful in identifying types of infected cells in vivo (Shek WR, Calnek BW, Schat KA, Chen CH: Submitted for publication). Data recorded in table 3 characterized the susceptible cell population(s) as being of low or medium density, readily adherent to nylon wool, and refractory to removal attempts with carbonyl iron. Furthermore, the susceptible cells had Fc receptors and surface IgM.

TABLE 2.—*Effect of genetic strain on susceptibility of spleen cells to in vitro infection with MDV*

Spleen cells exposed in vitro[a]	VIA-positive cells/ml				
	Trial 1: Inocula = spleen cells 5 days post inoculation from individual GA-5-infected birds[b]				Trial 2: Inoculum = 35th passage JM-10 in P-2 spleen cells[c]
	P-2 #1	P-2 #2	N-2 #1	N-2 #2	
P-2	2,720	120	1,830	770	426±62*
N-2	2,450	260	920	290	659±170*
UCD-003	ND	ND	ND	ND	194±46†
S-strain	ND	ND	ND	ND	432±42*

[a] Suspensions of 2.5–3.0×10^6/ml uninfected spleen cells from various donors (pools for trial 1; 4 individual birds for trial 2) were mixed with infected spleen cell suspensions at a ratio of 1:1 (trial 1) or 10:1 (trial 2).

[b] Data from trial 1 (48 hr post in vitro exposure) were from single samples. ND = not done.

[c] Data from trial 2 (72 hr post in vitro exposure) show the means ± SE from 4 spleen samples/group. *Means followed by the same superscript symbol* were not significantly different ($P>0.05$, Student's *t*-test).

TABLE 3.—*Susceptibility of various fractions of spleen cell suspensions to in vitro infection with GA-5 MDV*[a]

Criterion for selection	Fraction	VIA-positive cells/ml at 48 hr after passage, means ± SEM[b]
Density	Whole spleen (control)	1,012±83*
	Low density (1.03–1.06 g/liter)	481±155†
	Medium density (1.06–1.07 g/liter)	1,378±170*
	High density (1.07–1.08 g/liter)	106±44‡
Fc receptors	Control	1,212±372*
	Fc receptor-positive	1,475±296*
	Fc receptor-negative	362±53†
Nylon wool adherence	Adherent	929±256*
	Nonadherent	295±109†
Rosetting with antisera	Control rosetted	15±10*
	Control nonrosetted	1,387±533†
	Anti-μ rosetted	615±245*
	Anti-μ nonrosetted	32±23†
Depletion by carbonyl iron	Depleted	1,030±258*
	Nondepleted	1,233±209*

[a] Inoculum = 48-hr culture of the 21st serial passage of GA-5 virus in P-2 spleen cell cultures. Four passages were made at 2-day intervals by the addition of 3 parts of freshly fractionated cells from uninfected P-2 spleens to 1 part of infected cultured cells.

[b] Means were based on 8 samples; there were 2 replicates for each passage (4 samples; 1 each passage for rosetted fractions). *Means followed by same superscript symbol* within groups were not significantly different ($P>0.05$, Student's *t*-test).

Three trials in the second experiment (table 4) showed that the target cells for MDV infection bore Ia-like antigens on their membranes since depletion of Ia-bearing cells by complement lysis with mouse monoclonal anti-Ia reduced the susceptibility of spleen cell suspensions in which MDV was serially passaged four times.

Two trials were conducted to determine the relative susceptibility of spleen cells from EBx versus intact donors (table 5). Within each trial the donors were from the same

TABLE 4.—*Effect of complement lysis with anti-Ia on the susceptibility of P-2 spleen cells to in vitro infection with MDV*

Trial[a]	Treatment of spleen cells for passage[b]	VIA-positive cells/ml at 48 hr after passage			
		Passage 1	Passage 2	Passage 3	Passage 4
1	C alone	2,180	460	100	480
	C + anti-Ia	570	270	30	0
2	C alone	220	60	200	1,360
	C + anti-Ia	110	140	20	30
3	C alone	3,060	1,880	2,880	2,560
	C + anti-Ia	1,630	270	80	120

[a] Inocula for trials 1 and 2 were individual MDV-infected spleen cell suspensions from GA-5-infected P-2 chickens; inoculum for trial 3 was 48-hr 4th passage of GA-5 virus-infected P-2 spleen cells.

[b] Uninfected, freshly prepared spleen cells were treated with complement (C) alone or C plus monoclonal anti-Ia and then were added to inoculum (passage 1) or to 48-hr cultures (passages 2–4) at a ratio of 1:1 (trials 1 and 2) or 3:1 (trial 3). All suspensions were at 3×10^6 cells/ml.

TABLE 5.—*Comparative susceptibility of lymphocytes from bursa of Fabricius, thymus, or spleen of intact or EBx chickens or turkeys to in vitro infection with MDV*

Trial	Lymphocyte source		No. of samples	Positive cells/ml 48 hr after inoculation with MDV-infected cultured spleen cells, means ± SEM[a]	
	Bird	Tissue		VIA	PFU
1	P-2	Spleen	4	9,065±690*	181±21*
	EBx P-2	Spleen	6	1,230±344†	83±9†
	Turkey	Spleen	2	320±100‡	0‡
2	(Inoculum control)		3	217±22*	
	PDRC	Spleen	3	1,003±152†	
	EBx PDRC	Spleen	3	217±52*	
3	(Inoculum control)		4	225±18*	
	P-2	Spleen	4	2,110±572†	
	P-2	Bursa	4	798±384*†	
	P-2	Thymus	4	683±243*†	

[a] Inocula were added to fresh lymphocytes at a ratio of 1:3. Infected cells were from 21st to 43d passages of JM-10 or GA-5 in P-2 cells. *Means followed by same superscript symbol* were not significantly different ($P>0.05$, Student's *t*-test).

hatch. In trial 1, turkey spleen cells were also compared to spleen cells from intact or EBx P-2 chickens. The number of VIA-positive cells in the turkey cell culture after 48 hours was approximately that expected from the inoculum cells alone (as in trials 2 and 3) and virus could not be isolated; thus the turkey cells were considered refractory to infection. In contrast, the spleen cells from EBx donors in that trial showed evidence of susceptibility when these cells were compared with the turkey spleen cells ($P<0.05$), but at a markedly reduced level when compared to the level found in the cells from intact donors ($P<0.05$). However, in trial 2, spleen cells from 3 EBx donors failed to evidence even a low level of susceptibility. The percentage of spleen cells of trial 1 birds that could be shown by immunofluorescence to have surface IgM was determined for the 4 intact and 6 EBx chickens. The respective means ± SE were 28.86±3.17 and 1.58±0.39 ($P<0.001$). Only 2 of the 6 EBx donor spleens had more than 1% positive cells (1.33 and 6.31), whereas all intact donor spleens had over 20% positive cells. The VIA and virus isolation rates from EBx donor spleen cell cultures did not appear to correlate with the percentage of IgM-bearing cells.

In the final trial (table 5, trial 3), lymphocytes from the spleens, thymuses, and bursas of Fabricius of 4 P-2 donor birds were compared. The number of VIA-positive cells in bursa or thymus cell cultures was in each case less than that in the spleen cell culture. Viability of bursa cells dropped much more rapidly than that of either spleen or thymus cells. Because of the short viability period of bursa cells in vitro, the data on the relative susceptibility to in vitro infection of these cells compared to spleen cells are not considered to be meaningful. Conversely, the viability of thymus cells in vitro was equivalent to that of spleen cells, and therefore the susceptibility of these cells to in vitro infection could be compared. The data comparing VIA expression by spleen and thymus cells in table 5 are from the first of three serial passages made on four samples. In all but 1 of the 12 assays, the ratios of VIA-positive spleen cells to VIA-positive thymus cells were greater than 1 (median, 4.2; range, 0.8–10.7; $P<0.01$, Wilcoxon signed rank test).

DISCUSSION

To our knowledge, this constitutes the first report of successful in vitro infection of lymphocytes with MDV. The evidence that lymphocytes were infected is very strong. 1) Both VIA expression and virus isolation could be demonstrated after more than 40 serial passages of virus in spleen cell suspensions which, because of preparative methods, should have contained few cells other than lymphocytes and macrophages. Macrophage depletion did not reduce the number of susceptible cells. 2) Immunofluorescence methods were used to localize viral antigen in cells that appeared to be lymphocytes on the basis of size and general morphology. 3) Techniques that specifically reduced the number of susceptible cells in a given suspension were those that were designed to eliminate certain subpopulations of lymphocytes.

To serially passage virus, we had to add fresh splenic lymphocyte suspensions at frequent intervals (ideally, every 1–2 days) since cells were not long lived. It was not necessary to match histocompatibility antigens between donor and recipient cells. However, because spleen cells from one genetic strain (UCD-003) appeared less susceptible ($P<0.05$) than those from others (P-2, N-2, S-strain), the question of genetic control over susceptibility to in vitro infection should remain open. Gallatin and Longenecker (*13*) have claimed a genetically controlled difference in prevalence of receptors for the antigenically related turkey herpesvirus on cells from chicken strains differing in susceptibility to MD. In any case, genetic differences important in determining the outcome of in vivo infection, as between resistant N-2 and susceptible P-2 chickens, were clearly not expressed in vitro. This was not surprising since the level of early cytolytic infection in lymphoid organs was shown (*14*) not to correlate with the tumor response, which is the usual criterion for assessing genetic resistance of chicken strains.

The experiments done in attempts to identify the target(s) of in vitro infection gave results mostly in agreement with those we obtained from in vivo infection studies (Shek WR, Calnek BW, Schat KA, Chen CH: Submitted for publication). As in the early phase of in vivo infection, the cells that were found infected after exposure in vitro were among the subpopulations characterized by 1) low or medium density, 2) nylon wool adherence, 3) Fc receptors, 4) surface IgM, and 5) surface Ia-like antigen. The data from our in vivo studies showing that targets of cytolytic infection display Fc receptors and Ia-like antigen could not distinguish between the possibility that these antigens were expressed as a result of herpesvirus infection (*15*) as opposed to the alternate possibility that the susceptible subpopulation was already expressing them. The in vitro experiments reported here prove that the alternate possibility is the true interpretation since removal of cells bearing either antigen significantly decreased the susceptibility of the cell suspension. It is known that B-cells express Ia antigen. However, the question as to whether non-B-lymphocytes express Ia prior to infection remains unresolved.

Carbonyl iron treatment did not remove cells susceptible to cytolytic infection in vitro. In contrast, this treatment caused significant depletion of lymphocytes that were cytolytically infected in vivo. This observation suggests that infection with MDV enhanced depletion of B-cells by carbonyl iron treatment.

The percentage of susceptible cells was higher in the spleen than in the thymus. This observation is not surprising since we (Shek WR, Calnek BW, Schat KA, Chen CH: Submitted for publication) found that VIA-positive cells in the thymus during the cytolytic period of in vivo infection were B-cells, and the proportion of B-cells in the spleen is considerably higher than that in the thymus. Along this line, Gallatin and Longenecker (*13*) found few receptors for turkey herpesvirus on thymus cells.

The bursa also appeared to have a lower number of target cells than the spleen, but caution in interpretation is indicated in that case. While the viability of cultured thymic cells dropped off at the same (or at a slower) rate as that of spleen cells, bursa cells died much more rapidly and this probably affected the assays for infected cells. The results of the trials in which the susceptibility of spleen cells from EBx and intact donors was compared demonstrated the importance of the bursa as a probable origin of target cells. Taken together, the data uniformly support the conclusion that B-cells are the major target for in vitro cytolytic infection. The only suggestion that non-B-cells might also serve as a target for cytolytic infection came from trial 1 (table 5) in which spleen cells from EBx donors had both VIA and virus isolation rates above those expected from inoculum cells alone. Although the percentage of IgM-bearing cells from EBx donors was very low, absolute freedom from B-cells was not established. Thus additional study of this point is warranted.

Little was learned about the target(s) for latent infection. It may be necessary to use DNA hybridization methods to address this very important aspect. The finding of Schat et al. (*16*) that EBx birds exposed to MDV lack cytolytic infections of lymphoid organs but do develop latent infections of splenic and peripheral blood lymphocytes suggests that additional efforts with in vitro infection of cells from EBx donors might be fruitful. Finally, it should be obvious that the methodology reported here might be successfully adapted for studies leading to in vitro transformation. The potential for the use of the in vitro system in the study of the factors that determine the outcome of the virus–lymphocyte encounter is great indeed.

REFERENCES

(*1*) Calnek BW. Marek's disease virus and lymphoma, chapt 5. In: Rapp F, ed. Oncogenic herpesviruses. Vol I. Boca Raton, Fla.: CRC Press, 1980:103–144

(*2*) Calnek BW, Shek WR, Schat KA. Latent infections with Marek's disease virus and turkey herpesvirus. JNCI 1981; 66:585–590.

(*3*) Calnek BW. Influence of age at exposure on the pathogenesis of Marek's disease. J Natl Cancer Inst 1973; 51:929–939.

(*4*) Calnek BW, Adldinger HK, Kahn DE. Feather follicle epithelium: A source of enveloped and infectious cell-free herpesvirus from Marek's disease. Avian Dis 1970; 14:219–233.

(*5*) Schat KA, Calnek BW. In vitro cytotoxicity of spleen lymphocytes against Marek's disease tumor cells: Induction by SB-1, an apparently nononcogenic Marek's disease virus. In: Biggs PM, ed. Resistance and immunity to Marek's disease. Luxembourg: EEC Publ, 1980:301–319.

(*6*) Schat KA, Calnek BW, Fabricant J, Abplanalp H. Influence of oncogenicity of Marek's disease virus on evaluation of genetic resistance. Poultry Sci 1981; 60:2559–2566.

(*7*) Calnek BW, Hitchner SB. Localization of viral antigen in chickens infected with Marek's disease herpesvirus. J Natl Cancer Inst 1969; 43:935–949.

(*8*) Hutt FB, Cole RK. The interaction of genetic and environmental influences affecting the incidence of avian leukosis. Science 1953; 117:695–697.

(*9*) Calnek BW, Fabricant J, Schat KA, Murthy KK. Rejection of a transplantable Marek's disease lymphoma in normal versus immunologically deficient chickens. J Natl Cancer Inst 1978; 60:623–631.

(*10*) Witter RL, Nazerian K, Purchase HG, Burgoyne GH. Isolation from turkeys of a cell-associated herpesvirus antigenically related to Marek's disease virus. Am J Vet Res 1970; 31:525–538.

(*11*) Calnek BW, Shek WR, Schat KA. Spontaneous and induced herpesvirus genome expression in Marek's disease tumor cell lines. Infect Immun 1981; 34:483–491.

(*12*) Snedecor GE, Cochran WG. Statistical methods. 6th ed. Ames, Iowa: Iowa State Univ Press, 1971:130–131.

(*13*) Gallatin WM, Longenecker BM. Expression of genetic resistance to an oncogenic herpesvirus at the target cell level. Nature 1979; 380:587–589.

(*14*) Fabricant J, Ianconescu M, Calnek BW. Comparative effects of host and viral factors on early pathogenesis of Marek's disease. Infect Immun 1977; 16:136–144.

(*15*) Dorvall G, Bourka AE, Menezcs J. Comparative studies on the expression of Fc receptor, Ia antigens and B_2 microglobulin following in vitro herpes simplex virus infection of human lymphoid cells. Clin Exp Immunol 1979; 37:477–485.

(*16*) Schat KA, Calnek BW, Fabricant J. Influence of the bursa of Fabricius on the pathogenesis of Marek's disease. Infect Immun 1981; 31:199–207.

blank page

Surface Antigens on Marek's Disease Lymphoblastoid Tumor Cell Lines[1,2,3]

Karel A. Schat,[4] Chen-Lo H. Chen,[5] William R. Shek,[4] *and* Bruce W. Calnek[4,6]

ABSTRACT—A total of 32 Marek's disease virus (MDV)-induced cell lines, 1 avian leukosis virus-induced cell line, and 1 reticuloendotheliosis virus (REV)-induced lymphoblastoid cell line were investigated for the presence of Fc receptors, surface IgM, and Ia-like antigen. Surface IgM and Fc receptors could not be demonstrated on any of the cell lines. Ia-like antigen was detected on all MDV-induced cell lines and on the 1 REV-induced cell line. Ia-like antigen was unrelated to other antigens reported to be present on Marek's disease tumor cells. It was also unimportant as a target antigen for MDV-related, allogeneic cell-mediated cytotoxicity. The densities of the cells of 5 MDV-induced cell lines were established on continuous Percoll gradients. Most cells had densities between 1.05 and 1.06 g/ml.—JNCI 1982; 69:715-720.

It is generally accepted that the thymus-derived lymphocyte (T-cell) is the target cell for transformation by MDV. Evidence for this is mainly that MD lymphoblastoid cell lines are positive for T-cell antigens, when these cells are tested with antisera prepared against thymocytes (*1-4*). Using lactoperoxidase-catalyzed iodination techniques, Ross et al. (*5*), however, were unable to demonstrate the major thymus-specific polypeptide. It was not clear if this inability reflected technical problems or a real absence of this polypeptide. A more definitive description of the subset(s) of lymphocytes transformed by MDV has to await better defined reagents.

Other antigens have been described on transformed cells. The major histocompatibility antigen defined by the *B*-locus and the minor histocompatibility C-antigen are present (*6, 7*). A number of antigens not present on nontransformed lymphocytes can be detected on the surface of tumor cells. Powell et al. (*1*) and later Witter et al. (*8*) described an MATSA, which could be distinguished from the major histocompatibility antigen (*6-8*). In addition, Murthy et al. (*9*) demonstrated the presence of CFA on MD lymphoblastoid cell lines and on an ALV-transformed cell line. More recently, two antigens were shown on cell lines derived from JMV, a nonproducer MD transplant (*10*), but not on other cell lines. Using monoclonal antibodies, Shearman et al. (*11*) described a metastasis-specific antigen, whereas Ikuta et al. (*12*) demonstrated the presence of Forssman antigen. The importance of these antigens for the immune response against tumor cells is not clear. It had been speculated that MATSA was an important antigen for the cell-mediated immune response against tumor cells [reviewed by Calnek (*13*)]. Schat and Murthy (*14*) and Schat et al. (*15*) demonstrated that the in vitro CMC against allogeneic MD tumor cells was not directed against MATSA but against an alloantigen also present on normal spleen cells with the same major histocompatibility complex as the tumor cell.

In other studies on the characterization of MDV-infected lymphocytes (Shek WR, Calnek BW, Schat KA, Chen CH: Submitted for publication), it was shown that the early lytic infection is initiated in vivo in a population of low-density lymphocytes that are positive for Ia, surface IgM, and Fc receptors. Later, other lymphocytes also became infected. Calnek et al. (*16*) corroborated these data by in vitro infection of splenic lymphocytes when they found that deletion of B-lymphocytes significantly reduced the extent of in vitro infection. In this paper, we characterize transformed lymphocytes by showing that they are low-density, Fc receptor-negative and μ-negative, but Ia-positive, cells.

MATERIALS AND METHODS

Experimental chickens and holding conditions.—Two specific-pathogen-free departmental flocks were sources of experimental chickens: P-2 and the highly inbred UCD-003, which are homozygous for the major histocompatibility alleles $B^{19}B^{19}$ and $B^{17}B^{17}$, respectively (*17*). Experimental chickens were held in isolation units.

Lymphoblastoid cells lines.—Thirty-three MD lymphoblastoid cells lines were used for this study. Cell line designations, inducing viruses, and characteristics of the donors of the original tumor are given in table 1. MDCC-CU1 to MDCC-CU43 and LSCC-CU10, an ALV-derived cell line, were developed and reported by Calnek et al. (*4, 18*), MDCC-MSB-1 (*19*) and MDCC-RP1 (*20*) were received from Dr. K. Nazerian (Regional Poultry Research Laboratory, East Lansing, Mich.), and RECC-UT1 (*21*) was from Dr. H. Bose, Jr. (University of Texas, Austin, Tex.).

Virus inoculation.—Passage 11 of the nononcogenic SB-1 strain of MDV was propagated in chicken embryo fibro-

---

ABBREVIATIONS USED: AbC=antibody-complement; ALV=avian leukosis virus; CFA=chicken fetal antigen; CMC=cell-mediated cytotoxicity; FITC=fluorescein isothiocyanate; HBSS-BSA=Hanks' balanced salt solution containing 1.5% bovine serum albumin and 0.1% sodium azide; IFA=indirect fluorescent antibody; LM-20=RPMI-1640 medium with 20% heat-inactivated fetal bovine serum; MATSA=Marek's disease tumor-associated surface antigen; MD=Marek's disease; MDV=MD virus; NChS=normal chicken serum; REV=reticuloendotheliosis virus; SRBC=sheep red blood cell(s).

---

[1] Received December 15, 1981; accepted April 21, 1982.

[2] Supported in part by Public Health Service research grant CA-06709-19 from the National Cancer Institute.

[3] Animals were maintained under the guidelines set forth by Cornell University.

[4] Department of Avian and Aquatic Animal Medicine, New York State College of Veterinary Medicine, Cornell University, Ithaca, N.Y. 14853.

[5] Departments of Pediatrics and Microbiology, University of Alabama in Birmingham, School of Medicine, Comprehensive Cancer Center Cellular Immunobiology Unit, University Station, Ala. 35294.

[6] We thank Mrs. Beverley Bauman and Mr. Gary Allen for excellent technical assistance and Mrs. Gwen Troise for typing the manuscript.

TABLE 1.—*Characterization of the lymphoblastoid cell lines*

Donor of original tumor						
Strain of chicken	Histocompatibility alleles[a]		Inducing agent		Cell line	Remarks
	Major *(B)*	Minor *(C)*	Virus	Strain		
P-line	$B^{19}B^{19}$	—	MDV	CU-2	MDCC-CU2	
P-2	$B^{19}B^{19}$	C^2C^2		GA-5	MDCC-CU6, 12, 14, 17	
				JM-10	MDCC-CU32	
				RB-1B	MDCC-CU39, 40, 41, 42, 43	
				BC-1	MDCC-CU24	
N-line	$B^{21}B^{21}$	—		GA-5	MDCC-CU1	Contains ALV
N-2	$B^{21}B^{21}$	C^2C^2		GA-5	MDCC-CU21, 22	
G-B1	$B^{13}B^{13}$	C^2C^2		GA-5	MDCC-CU19	
				JM-10	MDCC-CU13	
				Conn-B	MDCC-CU5	Contains herpesvirus of turkeys
UCD-003	$B^{17}B^{17}$	C^2C^2		GA-5	MDCC-CU25, 29, 36, 37, 38	UCD-003 is fixed for all other blood group antigens
UCD-336	$B^{17}B^Q$	C^2C^2		GA-5	MDCC-CU26	UCD-336 is congenic to UCD-003
UCD-253	B^6B^6	C^2C^2		GA-5	MDCC-CU30	UCD-253 is congenic to UCD-003
UCD-254	$B^{15}B^{15}$	C^2C^2		GA-5	MDCC-CU31	UCD-254 is congenic to UCD-003
UCD-335	$B^{19}B^{19}$	C^2C^2		JM-10	MDCC-CU28	UCD-335 is congenic to UCD-003
Line 7	B^2B^2	C^2C^2		JM-10	MDCC-CU20	
S-strain	—	—		BC-1	MDCC-CU16, 18	
PDR	—	—		JM	MDCC-CU3, 11	
Outbred	—	—		BC-1	MDCC-MSB-1	
Outbred	—	—		JM	MDCC-RP1	
Outbred	—	—	ALV	—	LSCC-CU10	
Outbred	—	—	REV	T-strain	RECC-UT1	

[a] — = unknown.

blasts (*22*). For the induction of cytotoxic spleen lymphocytes, 3-week-old UCD-003 chickens received 500 focus-forming units of SB-1 by intra-abdominal injection.

Antisera and complement.—Ascitic fluids from BALB/c mice, inoculated with hybridomas secreting monoclonal antibodies against either the Ia-like (referred to in this paper as Ia) antigen of the chicken or the μ-chain of chicken IgM, were diluted 1:100 and 1:50, respectively, in RPMI-1640 medium. Both monoclonal antibodies were prepared according to the method of Kearney et al. (*23*). Anti-μ was induced by injection of purified IgM and characterized by radioimmunoassay against purified chicken immunoglobulins. This antibody gave staining patterns identical to those seen with highly purified goat anti-chicken μ (*24*) in double-fluorescence staining tests. The detailed characterization of anti-Ia, which is an IgM, will be published elsewhere (Ewert DL, Munchus MS, Chen CH, Cooper MD: Manuscript in preparation).

An alloantiserum against chicken Ia was from Dr. D. Gilmour (New York University, New York, N.Y.). B/L2 was prepared against B^2B^2-linked Ia antigen (*25*) of chickens of lines 6 and 7. Anti-MATSA serum was prepared in rabbits by inoculation with MDCC-MSB-1 cells (*26*). Guinea pig serum was used as a source of complement.

Isopyknic separation of MD lymphoblastoid cell lines.—The density distribution of each of 5 cell lines (MDCC-CU25, 29, 39, 42, and 43) was characterized with the use of a continuous Percoll (Pharmacia Chemicals AB, Uppsala, Sweden) gradient. The preparation of the gradient, the separation of cells, and the determination of the density of the fractions are detailed elsewhere (Shek WR, Calnek BW, Schat KA, Chen CH: Submitted for publication). The density distribution of MD tumor cells was compared to that of normal spleen cells in each test.

Assay for Fc receptors.—Fc receptors on lymphoblastoid cell lines were detected by adherence of the cells to a monolayer of SRBC coated with chicken anti-SRBC serum or NChS (*27*). Twenty-four-well tissue culture plates (Falcon Plastics, Oxnard, Calif.) were used instead of 35-mm tissue culture dishes; otherwise, the conditions were as described elsewhere (Shek WR, Calnek BW, Schat KA, Chen CH: Submitted for publication). Each cell line was tested by the addition of 2.5×10^6 cells/well to two wells with anti-SRBC serum and to two wells with NChS. Normal spleen cells from 4- to 6-week-old chickens were included as a positive control in all tests. Adherence of cells to SRBC coated with NChS was considered as background, and specific adherence was calculated by the following formula: percent specific adherence = percent adherence to SRBC coated with anti-SRBC serum − percent adherence to SRBC coated with NChS.

IFA test.—Ia antigen and surface IgM were detected by IFA tests applied to all cell lines listed in table 1. One to two million cells were resuspended in HBSS-BSA, incubated at room temperature for 30 minutes, centrifuged, and resuspended in 20 μl of monoclonal anti-Ia or anti-μ. After 30 minutes at 4°C, cells were washed once in HBSS-BSA, resuspended in 20 μl of FITC-conjugated goat anti-mouse globulin serum (Cappel Laboratories, Cochranville, Pa.), and kept at 4°C for 30 minutes. Cells were washed once in HBSS-BSA and resuspended in 0.1 ml of HBSS-BSA. Smears of 10 μl were air dried, either fixed with methanol for 4 minutes or left unfixed, rinsed in Tris-buffered saline, and then examined for membrane fluorescence with a Leitz Dialux fluorescence microscope equipped with epi-illumination. Normal splenic lymphocytes were included in each trial to assure that the test could detect cells positive for Ia antigen or μ-chain.

At least 200 cells were scored independently by two investigators for most trials. The presence of Ia was also investigated by staining MDCC-CU20 (B^2B^2), *MDCC-CU31* ($B^{15}B^{15}$), and MDCC-CU36 ($B^{17}B^{17}$) with the B/L2 alloantisera against Ia. The procedure was exactly as above except that FITC-conjugated horse anti-chicken globulin serum (Roboz Surgical Instrument Co., Inc., Washington, D.C.) was used for staining.

Blocking assays.—For the blocking test, $1-2\times10^6$ cells were incubated with 20 μl of an appropriate "blocking" antiserum for 30 minutes. Cells were then washed in HBSS-BSA and resuspended in 20 μl of the second antiserum. After 30 minutes' incubation, cells were washed once more and then reacted with 20 μl of conjugate as above. The cell lines, antisera, and conjugates used are given in table 4.

Chromium release assays.—Labeling of lymphoblastoid cell lines with 200 μCi of $Na^{51}CrO_4$ (sp act, 200–400 Ci/mg; New England Nuclear Corp., Boston, Mass.) per 10^7 cells was done as previously reported (*28*). Labeled cells were used for AbC lysis and CMC tests.

The AbC lysis test was done as reported before (*14*). Cells were incubated for 30 minutes with monoclonal antibody against Ia and washed. Complement was added. After incubation for 30 minutes at 39°C, the supernatants and the pellets were harvested separately and each was counted for 10 minutes in a Beckman 4000 gamma counter (Beckman Instruments, Inc., Irvine, Calif.). The procedure for the 4-hour CMC test has been reported (*28*). Effector spleen cells were obtained from SB-1-inoculated or control UCD-003 chickens 7 days post inoculation. Effector cells were prepared by established procedures (*14, 28*) with one modification: Cells were separated on a Percoll three-step gradient to concentrate cytotoxic lymphocytes that have a density range of 1.057–1.068 g/ml (Schat KA: Unpublished data). A discontinuous gradient was made with 9.57 and 7.02% Percoll (Pharmacia Chemicals AB). Forty million cells in 11.7% Percoll were carefully placed on the bottom, and the cells were centrifuged for 15 minutes at 400×*g*. Cytotoxic lymphocytes were harvested from the interface formed between 9.57 and 7.02% Percoll. Target cells for the CMC test were reacted with monoclonal antibody against Ia antigen for 30 minutes just before the test or they were left untreated. Target and effector cells were resuspended for AbC and CMC assays in LM-20.

RESULTS

Isopyknic Separation of MD Lymphoblastoid Cell Lines

The results of the two trials are summarized in table 2. Most (78–91%) of the tumor cells were found in fractions 3–5 (density, 1.051–1.060 g/ml), whereas only 9–28% of normal spleen cells were in those same fractions. Small differences in density were observed between P-2-derived tumors and UCD-003-derived tumors; the density of the former was apparently slightly higher than that of the latter, since more of the cells were in the higher fractions. The same differences were observed between normal spleen cells obtained from UCD-003 and P-2 chicks. The densities of the Percoll in all recovered fractions were identical in both experiments.

Fc Receptors

In total, eight tests were done in which the following cell lines were tested for the presence of Fc receptors: MDCC-CU2, 6, 12, 13, 17, 18, 19, 20, 21, 25, 26, 31, 32, 36, 37, 38, 39, 40, 42, and 43, MDCC-RP1, and MDCC-MSB-1. Fc receptor-positive normal spleen cells could be easily demonstrated in all trials with the use of normal spleen lymphocytes (average of percent specific adherence ± SE for eight trials: 26.6±3.3). Normally, 10–40% of the tumor cells adhered nonspecifically to SRBC coated with NChS, depending on the cell line. Specific adherence of cell lines could not be demonstrated; the percentage of specific adherence varied from +8.2 to −12.1%. Four cell lines were also tested after cultivation in a medium without chicken serum to exclude a possible coverage of Fc receptors. Under these conditions we still failed to demonstrate Fc receptors.

Presence of μ and Ia on Lymphoblastoid Cell Lines

IFA test: Normally, 30–40% of the spleen cells were positive for the presence of Ia, and 10–15% of the cells were positive for μ. The intensity of the staining for μ was weak,

TABLE 2.—*Densities of cells of five MD lymphoblastoid lines fractionated on continuous Percoll gradients*

Origin of tumor or spleen cells	Cell line[a]	Passage	Percent cells in fraction indicated[b] (density[c])				
			2 (1.042)	3 (1.051)	4 (1.057)	5 (1.060)	6 (1.063)
UCD-003	Normal spleen (4 wk of age)	—	1.0	3.8	10.0	13.7	15.7
	MDCC-CU25	22	5.3	43.3	40.0	7.3	1
	MDCC-CU29	13	5.4	35.1	42.3	11.3	2.3
P-2	Normal spleen (4 wk of age)	—	0.3	1.3	3.4	4.0	8.1
	MDCC-CU39	11	2.3	19.8	31.0	24.6	7.5
	MDCC-CU42	14	2.2	9.6	44.1	24.3	8.1
	MDCC-CU43	9	5.0	18.0	32.4	28.1	5.8

[a] MDCC-CU25 and MDCC-CU29 were induced by GA-5, whereas the others were induced by RB-1B.
[b] Most tumor cells were found in fractions 2–6; thus other fractions were not reported.
[c] Density is in g/ml.

TABLE 3.—*Detection of Ia-like antigen by AbC lysis on the surface of MD lymphoblastoid cell lines (MDCC), an avian leukosis cell line (LSCC), and a reticuloendotheliosis cell line (RECC)*

Trial	Cell line	Percent release of ^{51}Cr: No treatment[a]	Percent release of ^{51}Cr following treatment with: C alone[b]	Anti-Ia alone[c]	Anti-Ia + complement
1	MDCC-CU6	2.64	2.77	6.66	43.78
	MDCC-CU20	2.99	2.19	5.99	50.47
	MDCC-CU24	5.34	4.37	13.27	39.30
	MDCC-CU26	4.09	4.77	13.48	74.84
	MDCC-CU28	3.36	8.34	27.30	77.31
	MDCC-CU30	4.36	3.89	6.02	54.71
	Splenic lymphocytes	8.89	11.31	12.25	21.22
2	MDCC-CU12	2.05	3.03	2.12	72.47
3	MDCC-CU12	0.71	0.66	0.65	43.30
4	MDCC-CU12	1.64	4.68	1.58	23.89
	MDCC-RP1	2.17	5.48	1.90	66.37
5	MDCC-RP1	3.27	15.13	3.17	30.46
	LSCC-CU10	1.90	1.73	2.01	2.15
	RECC-UT1	1.34	1.56	1.43	34.55

[a] LM-20 was added in lieu of anti-Ia and complement.

[b] C = guinea pig complement.

[c] Mouse monoclonal antibody against chicken Ia.

while the Ia stained intensively. On the one hand, all cell lines, including the avian leukosis cell line LSCC-CU10 and the reticuloendotheliosis line RECC-UT1, were negative for μ. On the other hand, all cell lines were positive for Ia with the exception of MDCC-RP1 and LSCC-CU10. Between 70 and 100% of the cells showed either patchy or complete ring fluorescence. The intensity of the staining was generally quite strong, and cell clumping was occasionally observed. Most cell lines were tested between passage levels 10 and 35. Exceptions were MDCC-CU17, tested at passages 24 and 53; MDCC-MSB-1, tested at passages 116 and 342; and MDCC-RP1, tested at passage 204. There were no detectable differences between low- and high-passage levels of MDCC-MSB-1 and MDCC-CU17 when tested for the presence of Ia.

The alloantiserum against B^2B^2-linked Ia did demonstrate the presence of Ia on MDCC-CU20, a B^2B^2-derived MD cell line, but not on MDCC-CU36 ($B^{17}B^{17}$) or MDCC-CU31 ($B^{15}B^{15}$). Both intensity of staining and number of fluorescing cells were comparable to reactions with monoclonal anti-Ia.

AbC lysis: Eight MD cell lines and RECC-UT1 (table 3) were found to be positive for Ia with the use of an AbC lysis test. The percent release of ^{51}Cr in the presence of anti-Ia and complement varied, but it was always considerably higher than the percent release with LM-20, anti-Ia, or complement. On occasion, the monoclonal anti-Ia seemed slightly toxic for certain cell lines. Interestingly, MDCC-RP1 was positive for Ia in the AbC lysis test but not in the less sensitive IFA test. Ia could not be demonstrated on LSCC-CU10, the ALV-induced cell line.

Blocking Assays

Treatment of MDCC-MSB-1 with antiserum against MATSA did not block the staining of the cells with antiserum against Ia. The reverse was also true. Monoclonal anti-Ia did not block the staining of MDCC-MSB-1 by MATSA (table 4).

Treatment of MDCC-CU20 with monoclonal anti-Ia did prevent the staining of the cells by alloantiserum. However, the alloantiserum did not prevent the recognition of the cells by the monoclonal antibody (table 4), as could be expected for two antibodies detecting a public and a private (allo-) antigenic determinant, respectively.

CMC Assays

In two trials MDCC-CU12 cells were treated either with monoclonal anti-Ia or with LM-20. The coating with anti-

TABLE 4.—*Blocking assays for MATSA versus Ia and for monoclonal Ia versus allo-Ia*

Cell line	Blocking serum[a]	Test antiserum[a]	FITC conjugate[b]	Positive cells, %
MDCC-MSB-1	M- anti-μ	Anti-MATSA	CARG	95
	Normal rabbit	M- anti-Ia	GAMG	100
	M- anti-Ia	Anti-MATSA	CARG	94
	Anti-MATSA	M- anti-Ia	GAMG	100
MDCC-CU20	M- anti-μ	A- anti-Ia	HACG	75
	Normal chicken	M- anti-Ia	GAMG	95
	M- anti-Ia	A- anti-Ia	HACG	0
	A- anti-Ia	M- anti-Ia	GAMG	70

[a] M = monoclonal antibody; A = alloantibody. Anti-μ was used as a control for ascitic fluid.

[b] CARG = chicken anti-rabbit globulin; GAMG = goat anti-mouse globulin; HACG = horse anti-chicken globulin.

TABLE 5.—*Effect of coating with anti-Ia serum on CMC against MD lymphoblastoid cells (MDCC-CU12)*[a]

Trial	Treatment of target (MDCC-CU12) cells	Percent ^{51}Cr release induced by complement	^{51}Cr in CMC assay with spleen cells from: Control donors: Mean % release ± SEM (No. of donors)	Individual SB-1-infected donors: % specific release[b] 1	2	3	4	5
1	None	2.88	7.92±0.22 (5)	22.32	3.49	20.92	8.68	20.60
	Anti-Ia	70.35	9.63±0.50 (5)	22.06	1.36*	21.45	7.34	19.82
2	None	0	8.09±0.29 (8)	3.87	23.30	2.64	31.78	11.99
	Anti-Ia	42.65	8.83±0.39 (8)	2.63	24.65	2.61	27.95	11.40

[a] Cells were incubated for 30 min in the presence of LM-20 or mouse monoclonal antibody against Ia antigen prior to their use in the CMC assay.

[b] Donors with release of ^{51}Cr outside the $P = 0.001$ confidence limits established for the control group by Student's *t*-test; * = inside the interval.

Ia was effective since the addition of complement resulted in cytolysis (table 5). A total of 10 of 15 SB-1-inoculated chickens yielded cytotoxic spleen cell preparations causing a significant percent specific release. The presence of anti-Ia on the surface of the target cells did not interfere with the percent specific release, nor did it change the percent release in the presence of lymphocytes from control birds.

DISCUSSION

An antigen comparable to the Ia antigen of the mouse and the human being has been detected on chicken B-cells (bursa-derived cells), monocytes, macrophages, and a small population of unidentified mononuclear cells prevalent in the spleen and bone marrow (*29*). The Ia-like antigen of the chicken is closely linked with the B-major histocompatibility complex (*30*). Recently, the Ia antigen has been reported to be present on important subsets of T-cells. Hämmerling et al. (*31*) found that 40% of the T-cells of the mouse carried Ia antigens, but these antigens could be detected only with a fluorescein-activated cell sorter and not by conventional IFA staining or AbC cytotoxicity. These authors calculated that the density of Ia molecules on T-cells was a hundredfold less than that on B-cells. Enhanced expression of Ia on human T-cells has been reported for T-cell leukemias (*32*) and as a result of blast transformation by antigen and mitogen stimulation (*33*).

The presence of Ia-like antigens was clearly demonstrated on all MD cell lines by IFA tests and/or complement lysis. The detection of Ia, as well as the absence of Fc receptors and IgM on the surface of the MD tumor cell lines, is compatible with the suggested T-cell nature of the MD tumor cells. In a recent paper, the question was raised whether Ia-positive T-cells of chickens might be suppressor cells (*25*), as is the case in the mouse (*34*). It would be of considerable interest to search for suppressor factors produced by MD tumor cell lines. The densities of the cell lines examined in this study were comparable to those of the spleen cells that resulted in the establishment of cell lines (Shek WR: Unpublished data).

It is not clear from the data whether MDV-transformed lymphocytes express Ia antigen as a consequence of transformation or whether the expression of the Ia antigen is a prerequisite to infection and transformation. The prerequisite theory would present an attractive explanation for transformation. Following this hypothesis, early infection of B-cells by MDV, as demonstrated elsewhere (Shek WR, Calnek BW, Schat KA, Chen CH: Submitted for publication) and by Calnek et al. (*16*), would induce blast transformation of T-cells, which then would express Ia and become susceptible to infection and neoplastic transformation. Further characterization of subpopulations of lymphocytes susceptible to in vitro infection might answer the question of whether or not Ia is present before infection of T-cells as it is on B-cells.

The finding of Ia on the tumor cells adds one more antigen to the growing list of antigens known to be present on such cells. It is unlikely that this antigen is identical to MATSA, CFA, Forssman antigen, or organ-specific metastasis antigen for the following reasons: 1) Anti-MATSA serum failed to block staining of Ia. 2) CFA was found to be present on LSCC-CU10 (previously named TLT-1) (*9*), whereas we were unable to demonstrate Ia on this cell line. 3) Forssman antigen was found only on JMV-derived cell lines and not on MDCC-MSB-1 (*12*), whereas Ia was present on all MD cell lines. Interestingly, Ia appeared to be present at a lower concentration on the JMV-derived cell line MDCC-RP1 than on the other MD cell lines. 4) A number of the cell lines positive for Ia failed to transplant (*35*), which makes it unlikely that Ia is related to an organ-specific metastasis antigen.

Recently, Schat et al. (*15*) showed that the allogeneic CMC against MD tumor cells was directed against alloantigens. They speculated that this could be against the major histocompatibility B-antigen or the Ia antigen. It now seems unlikely that the CMC was directed against Ia antigen. Coating of Ia with monoclonal antibody covered the public and private major histocompatibility complex-related antigen (blocking assay), but it did not prevent lysis of allogeneic target cells by effector cells.

The one-way blocking of Ia (table 4) by the monoclonal antibody to the reaction with the allo anti-Ia serum suggests that the determinants are situated close to each other; therefore, the large IgM molecules of the monoclonal anti-Ia may have physically blocked the attachment of the alloantiserum.

REFERENCES

(*1*) Powell PC, Payne LN, Frazier JA, Rennie M. T lymphoblastoid cell lines from Marek's disease lymphomas. Nature 1974; 251:79–80.

(*2*) Nazerian K, Sharma JM. *Brief communication:* Detection of T-cell surface antigens in a Marek's disease lymphoblastoid cell line. J Natl Cancer Inst 1975; 54:277–279.

(*3*) Matsuda H, Ikuta K, Kato S. Detection of T-cell surface determinants in three Marek's disease lymphoblastoid cell lines. Biken J 1976; 19:29–32.

(*4*) Calnek BW, Murthy KK, Schat KA. Establishment of Marek's disease lymphoblastoid cell lines from transplantable versus primary lymphomas. Int J Cancer 1978; 21:100–107.

(*5*) Ross LJ, Powell PC, Walker DJ, Rennie M, Payne LN. Expression of virus-specific antigens in lymphoblastoid cell lines derived from Marek's disease lymphomas. J Gen Virol 1977; 35:219–235.

(*6*) Murthy KK. Immunization against Marek's disease with virus- versus tumor-associated antigens and studies on the characterization of a tumor-associated surface antigen. Ph.D. thesis. Ithaca, N.Y.: Cornell University, 1979.

(*7*) Coleman RM, Schierman LW. Independence of chicken major histocompatibility antigens and tumor-associated antigen on the surface of herpesvirus-induced lymphoma cells. Infect Immun 1980; 29:1067–1072.

(*8*) Witter RL, Stephens EA, Sharma JM, Nazerian K. Demonstration of a tumor-associated surface antigen in Marek's disease. J Immunol 1975; 115:177–183.

(*9*) Murthy KK, Dietert RR, Calnek BW. Demonstration of chicken fetal antigen (CFA) on normal splenic lymphocytes, Marek's disease lymphoblastoid cell lines and other neoplasms. Int J Cancer 1979; 24:349–354.

(*10*) Stephens EA, Witter RL, Lee LF, Sharma JM, Nazerian K, Longenecker BM. Characteristics of JMV Marek's disease tumor: A nonproductively infected transplantable cell lacking in rescuable virus. J Natl Cancer Inst 1976; 57:865–874.

(*11*) Shearman PJ, Gallatin WM, Longenecker BM. Detection of a cell surface antigen correlated with organ-specific metastasis. Nature 1980; 286:267–269.

(*12*) Ikuta K, Kitamoto R, Shoji N, Kato S, Naiki M. Expression of

Forssman antigen of avian lymphoblastoid cell lines transformed by Marek's disease virus or avian leukosis virus. J Gen Virol 1981; 52:145–151.

(13) Calnek BW. Marek's disease virus and lymphoma, chapt 5. In: Rapp F, ed. Oncogenic herpesviruses. Vol I. Boca Ratton, Fla.: CRC Press, 1980:103–144.

(14) Schat KA, Murthy KK. In vitro cytotoxicity against Marek's disease lymphoblastoid cell lines after enzymatic removal of Marek's disease tumor-associated surface antigen. J Virol 1980; 34:130–135.

(15) Schat KA, Shek WR, Calnek BW, Abplanalp H. Syngeneic and allogeneic cell-mediated cytotoxicity against Marek's disease lymphoblastoid tumor cell lines. Int J Cancer 1982; 29:187–194.

(16) Calnek BW, Schat KA, Shek WR, Chen CH. In vitro infection of lymphocytes with Marek's disease virus. JNCI 1982; 69:709–713.

(17) Schat KA, Calnek BW, Fabricant J, Abplanalp H. Influence of oncogenicity of Marek's disease on evaluation of genetic resistance. Poultry Sci 1981; 60:2559–2566.

(18) Calnek BW, Shek WR, Schat KA. Spontaneous and induced herpesvirus genome expression in Marek's disease tumor cell lines. Infect Immun 1981; 34:483–491.

(19) Akiyama Y, Kato S. Two cell lines from lymphomas of Marek's disease. Biken J 1974; 17:105–116.

(20) Nazerian K, Stephens EA, Sharma JM, Lee LM, Gailitis M, Witter RL. A nonproducer T lymphoblastoid cell line from Marek's disease transplantable tumor (JMV). Avian Dis 1977; 21:69–76.

(21) Franklin RB, Maldonado RI, Bose HR. Isolation and characterization of reticuloendotheliosis virus transformed bone marrow cells. Intervirology 1974; 3:342–352.

(22) Schat KA, Calnek BW. Characterization of an apparently nononcogenic Marek's disease virus. J Natl Cancer Inst 1978; 60:1075–1082.

(23) Kearney JF, Radbruch A, Liesegang B, Rajewsky K. A new mouse myeloma cell line that has lost immunoglobulin expression but permits the construction of antibody-secreting hybrid cell lines. J Immunol 1979; 123:1548–1550.

(24) Chen CH. Ontogeny of immunoglobulin isotype diversity expressed by chicken lymphocytes. Fed Proc 1978; 37:1395

(25) Nowak JS, Vainio O, Lassila O, Toivanen P, Gilmour DG. A rosette assay for identification of Ia-like alloantigens on chicken lymphoid cells. J Immunol Methods 1981; 42:325–335.

(26) Murthy KK, Calnek BW. Pathogenesis of Marek's disease: Early appearance of Marek's disease tumor-associated surface antigen in infected chickens. JNCI 1978; 61:849–854.

(27) Kedar E, Ortiz de Landazuri M, Bonavida B. Cellular immunoadsorbents: A simplified technique for separation of lymphoid cell populations. J Immunol 1974; 112:1231–1243.

(28) Schat KA, Calnek BW. In vitro cytotoxicity of spleen lymphocytes against Marek's disease tumor cells: Induction by SB-1, an apparently nononcogenic Marek's disease virus. In: Biggs PM, ed. Resistance and immunity to Marek's disease. Luxembourg: EEC Publ, 1980:301–319.

(29) Ewert DL, Cooper MD. Ia-like alloantigens in the chicken: Serologic characterization on ontogeny of cellular expression. Immunogenetics 1978; 7:521–535.

(30) Ewert DL, Gilmour DG, Briles We, Cooper MD. Genetics of Ia-like alloantigens in chickens and linkage with *B* major histocompatibility complex. Immunogenetics 1980; 10:169–174.

(31) Hämmerling GJ, Hämmerling U, Lemke H. Isolation of twelve monoclonal antibodies against Ia and H-2 antigens. Serological characterization and reactivity with B and T lymphocytes. Immunogenetics 1979; 8:433–445.

(32) Fu SM, Chiorazzi N, Wang CY, et al. Ia-bearing T lymphocytes in man. Their identification and role in the generation of allogeneic helper activity. J Exp Med 1978; 148:1423–1428.

(33) Ko HS, Fu SM, Winchester RJ, Yu OT, Kunkel HG. Ia determinants on stimulated human T lymphocytes. Occurrence on mitogen and antigen activated T cells. J Exp Med 1979; 150:246–255.

(34) Tada T, Hayakawa K, Okumura K, Taniguchi M. Coexistence of variable region of immunoglobulin heavy chain and I region gene products on antigen-specific suppressor T cells and suppressor T cell factor. Molec Immunol 1980; 17:867–875.

(35) Fabricant J, Calnek BW, Schat KA, Murthy KK. Marek's disease virus-induced tumor transplants: Development and rejection in various genetic strains of chickens. Avian Dis 1978; 22:646–658.

Some Effects of the Tumor Promoter 12-*O*-Tetradecanoylphorbol 13-Acetate on Cell Interactions In Vitro[1, 2]

David E. Maslow,[3] **Eric G. Mayhew,**[3] *and* **Charles E. Wenner**[4, 5]

ABSTRACT—Studies were made of the effects of the potent tumor promoter 12-*O*-tetradecanoylphorbol 13-acetate (TPA), 4-*O*-methyl TPA (4-*O*-MeTPA), and 4αphorbol 12,13-didecanoate (4αPDD) on the aggregation of embryonic chick cells in gyratory shaker culture, a model system useful for the study of cell adhesion and cell interactions. TPA and, to a lesser extent, 4-*O*-MeTPA significantly reduced the neural retina aggregate size at concentrations as low as 10^{-9} *M* and 10^{-8} *M*, respectively. An inactive isomer, 4αPDD, had no effect up to 10^{-6} *M*. The reduction in aggregate size appeared related to promoter activity since dexamethasone, a steroid that inhibits tumor promotion by TPA, significantly reversed the inhibitory effect of TPA. None of the agents tested affected the sorting pattern in mixed neural retina and heart cultures. The results indicate that intercellular adhesion, as determined by extent of aggregation, is reduced in the presence of TPA. This inhibition is considered to be related to the tumor-promoting activity of TPA.—JNCI 1982; 69: 721–724.

Tumor promoters have been shown to have numerous biological and biochemical effects on normal cells in vitro, frequently resulting in the cells' acquiring characteristics usually associated with the transformed phenotype (*1*). These characteristics include increased plasminogen activator production (*2-4*), decreased fibronectin levels (*5*), stimulation of prostaglandin synthesis (*6*), enhanced cell proliferation (*7*), and altered cell morphology (*7, 8*). This mimicry of transformation is dependent on the continued presence of the promoters, without which the cells revert to their original phenotype (*9*), and such changes have not been uniformly observed in all cells studied.

There is much evidence to suggest that the cell membrane may be the major site of action of TPA, an extremely potent and widely used tumor promoter (*10-12*). TPA has also been shown to be a highly potent inhibitor of terminal differentiation in many cell systems (*9, 13-16*), although in some cases it has been shown to induce rather than inhibit differentiation (*17, 18*). TPA may also act to induce permanent phenotypic changes (*19, 20*).

The aggregation of embryonic cells in gyratory shaker culture is a model system for the study of cell interactions in which the size of the aggregates, the differentiation of the cells, and the sorting of the cell types are reproducible standards of normal cell behavior, which can act as sensors of the effects of added agents (*21*). Because of the effects of tumor promoters on cells and their surfaces, it was of interest to determine what effect TPA might have on this aspect of normal cell behavior.

MATERIALS AND METHODS

Neural retina cells were isolated from 10- to 11-day chick embryos with crystallized trypsin (Enzar-T; Armour Pharmaceutical Co., Phoenix, Ariz.) following the optimal procedure described by Barnard et al. (*22*). We isolated heart cells from 9-day-old embryos by repeatedly pipetting trypsinized, minced heart fragments. Viability determinations with trypan blue indicated that the viability of treated neural retina cells remained better than 90% up to 24 hours after treatment.

Aggregation was furthered by culture of 6×10^6 neural retina cells alone or together with 1×10^6 heart cells in 3 ml of Eagle's minimum essential medium with 10% horse serum in a 25-ml Erlenmeyer flask on a gyratory, incubator shaker rotating at 70 rpm. After 24 hours in culture the diameters of 50 neural retina aggregates from each treatment group were measured with an eyepiece micrometer (Carl Zeiss, Ober Kochen, Federal Republic of Germany). Mixed aggregates were fixed in Gendre's fixative after 72 hours in culture for periodic acid-Schiff staining to distinguish the glycogen-rich heart cells.

TPA and 4-*O*-MeTPA were obtained from Chemical Carcinogens (Eden Prairie, Minn.) dexamethasone from Sigma Chemical Co. (St. Louis, Mo.), and 4αPDD from Lifesystems Co. (Newton, Mass.). Stock solutions at 10^{-3} *M* in ethanol were diluted in culture as indicated; control cultures received ethanol equivalent to the highest dose.

Changes in diameter measurements do not accurately reflect the true extent of the differences in aggregate volume and number of cells contained. (A 20% reduction in diameter, for example, indicates a reduction in volume of ≈49%.) However, we present the data for mean diameters that were actually measured, rather than for mean volumes, which may be calculated from those measurements.

RESULTS

Table 1 gives the mean diameter of aggregates formed in neural retina cultures containing tenfold dilutions of the potent tumor promoter TPA and of an isomer with reduced activity, 4-*O*-MeTPA. A significant reduction (Student's *t*-test, $P<0.01$) in aggregate size was obtained with TPA at concentrations as low as 10^{-9} *M* and with 4-*O*-MeTPA at concentrations as low as 10^{-8} *M*. At 10^{-6} *M* and 10^{-7} *M*,

---

ABBREVIATIONS USED: 4αPDD=4αphorbol 12,13-didecanoate; TPA=12-*O*-tetradecanoylphorbol 13-acetate; 4-*O*-MeTPA=4-*O*-methyl TPA.

---

[1] Received December 23, 1981; accepted April 13, 1982.

[2] Supported by Public Health Service grants CA-14370, CA-28494, and CA-16056 from the National Cancer Institute.

[3] Department of Experimental Pathology, Roswell Park Memorial Institute, 666 Elm St., Buffalo, N.Y. 14263.

[4] Department of Experimental Biology, Roswell Park Memorial Institute.

[5] We thank Dr. L. Weiss for useful discussions and Mrs. Rita Pawlak and Mr. Gerald Johnson for technical assistance.

TABLE 1.—*Effect of TPA and its analogs on aggregation of neural retina cells*[a]

Concentration, *M*	Control		TPA	4-*O*-MeTPA	4αPDD
	−Solvent	+Ethanol, 0.01%			
0	248.9±5.2 (250)	240.1±3.9 (250)			
10^{-9}			230.9±3.5 (150)	236.2±4.0 (150)	
10^{-8}			219.7±2.7 (250)	226.2±3.6 (250)	258.7±5.4 (100)
10^{-7}			208.6±3.4 (200)	221.6±3.1 (200)	249.2±4.4 (100)
10^{-6}			198.9±2.9 (250)	218.8±4.0 (250)	242.2±3.8 (100)

[a] 6×10^6 neural retinal cells were maintained in gyratory shaker culture under conditions favoring aggregation with TPA or its analogues at concentrations up to 10^{-6} *M*. After 24 hr of culture, at least 50 aggregates from each group were measured with an eyepiece micrometer. Numbers are aggregate sizes (μm) ± SE (No. measured). Statistical significance based on Student's *t*-test is given in text.

TABLE 2.—*Effect of dexamethasone on inhibition of neural retina cell aggregation by TPA*[a]

Experimental series	Dexamethasone concentration, *M*	Control		−TPA	+TPA 10^{-7} *M*	+TPA 10^{-6} *M*
		−Solvent	+Ethanol, 0.01%			
1	0	227.9±7.3	192.8±7.0		160.1±5.1	
	10^{-8}			222.9±7.2	197.4±6.4	
	10^{-7}			224.8±6.6	193.8±6.0	
	10^{-6}			202.1±6.2	195.3±4.2	
2	0	231.6±4.4	213.6±3.8		204.1±3.1	193.3±2.2
	10^{-7}			219.9±3.4	232.5±3.8	213.6±3.1

[a] 6×10^6 neutral retina cells were maintained in gyratory shaker culture under conditions favoring aggregation with either TPA or TPA and dexamethasone. After 24 hr of culture, at least 50 aggregates from each group were measured with an eyepiece micrometer. Numbers are aggregate sizes (μm) ± SE; 250 aggregates are measured in expt 1 and 200 in expt 2. Statistical significance based on Student's *t*-test is given in text.

TPA was significantly ($P<0.01$) more inhibitory than 4-*O*-MeTPA; the differences in aggregate size at 10^{-6} *M* ($0.1>P>0.3$) were not significant. We also treated cultures with 4αPDD, an isomer with no reported promoter activity, to determine if the observed inhibition with TPA and 4-*O*-MeTPA was due to the promoter-related activity of the phorbol esters added, and the results are also shown in table 1. Aggregate diameters were not reduced at any of the concentrations of 4αPDD tested.

To further demonstrate that the reduction in aggregate size in cultures containing TPA or 4-*O*-MeTPA was not unrelated to their promoter activities, we added dexamethasone to aggregating cultures containing TPA at 10^{-6} *M* or 10^{-7} *M*. Dexamethasone is a steroid that inhibits tumor promotion by TPA (*23*). A reversal by the dexamethasone of the inhibitory action of TPA on cell aggregation would indicate that the dexamethasone is blocking one or more of the events associated with and likely required as part of the promotion process. No effect by the dexamethasone on the TPA-related inhibition of cell aggregation would suggest that its antipromoter effect is on some other aspect of the promotion process but would not rule out the inhibition as a required part of tumor promotion. The results of these experiments are summarized in table 2. The differences in the sizes of similarly treated aggregates between the former experimental group and these are within the normal range experienced with neural retina aggregates and may be due to seasonal differences in eggs or different serum lots. The addition of dexamethasone alone at these doses tested caused no decrease in aggregate size. However, dexamethasone when added to aggregating cultures containing TPA at both 10^{-6} *M* and 10^{-7} *M* caused a significant ($P<0.001$) reversal of inhibition of the TPA, although the aggregates were still smaller than those treated with dexamethasone alone at the same concentration.

We also added TPA to aggregating cultures of neural retina and heart cells and examined the sorting pattern and extent of differentiation in periodic acid–Schiff-stained aggregate sections. There was no effect of TPA up to a concentration of 10^{-6} *M* on the normal sorting pattern of a central heart area surrounded by peripheral neural retina cells compared to the pattern seen in control cultures. In addition, the frequency and appearance of retinal rosettes characteristic of neural retina aggregates did not differ in control and treated cultures. However, the aggregates formed in treated cultures were significantly smaller ($0.01>P>0.001$) than those in the control cultures.

DISCUSSION

Embryonic fibroblasts have been utilized in experiments analyzing the in vitro biological effects of tumor promoters, including their adhesion and orientation on artificial substrata (*24*), but they were usually secondary cultures and the properties studied were not related to their differentiation. The effect of TPA on the differentiation of normal cells in primary cultures has been uniformly inhibitory in contrast to less consistent results with transformed cells (*9*). The sizes of aggregates formed in cultures of primary embryonic cells can be similarly considered in vitro characteristics of differentiation related to in vivo behavior (*25*) and can serve to monitor changes in cell–cell adhesion. Aggregate size has been used by many investigators to study changes at the cell surface and effects of exogenous agents on cell interactions. Treatment with trypsin (*26*), protein synthesis inhibitors (*27*), cytoskeletal disrupters (*28, 29*), and other surface active agents (*30, 31*) has been shown to cause changes in the aggregation behavior of the cells. The size of aggregates also has been used to study the effect of the presence of metal cations (*32*) and various anticancer agents (*33*) on cell behavior. In addition, the differential inhibition of neural retina aggregates is an assay procedure useful for demonstrating the presence of small numbers of cancer cells (*34, 35*). Thus the aggregation of embryonic cells should be a useful additional in vitro tool for the study of the biological effects of tumor promoters, and the extent of inhibition observed in these experiments (20% of aggregate diameter or 49% of aggregate volume) is within the ranges reported for other studies using aggregate size as a sensor of changes in cell interactions.

Our results indicate that the presence of active tumor promoters such as TPA and, to a lesser extent, 4-*O*-MeTPA results in the formation of aggregates of reduced size, reflecting possible promoter-induced changes in the extracellular adhesion of these freshly isolated cells, whereas the nonactive isomer 4αPDD had no inhibitory effect. These results indicate that the reduction of aggregation caused by the active tumor promoters correlates with their promoter activity. The mechanisms of action of the two related compounds may differ, however, possibly related to the correlation between the presence of TPA and the induction of prostaglandin synthesis (*6*), hyperplasia, or other changes not found with 4-*O*-MeTPA (*36*) and not simply from nonspecific hindrance of adhesion caused by adsorption of the relatively small molecules to the surface of the cells. It still remains to be resolved whether these changes are obligatory or dissociable events following TPA exposure (*37, 38*). First-stage promoter activity has been reported for 4-*O*-MeTPA (*39, 40*) in contrast to the full promoter capabilities of TPA, which may also account for the smaller effect of 4-*O*-MeTPA.

The results from the experiments in which the presence of dexamethasone, a steroid shown to be highly effective in inhibiting tumor promotion by TPA (*23*), was correlated with a reversal of the inhibitory action of TPA suggest a causal relationship between the tumor-promoting activity of the TPA and reduced cell-cell adhesion. The mechanism of this inhibition of tumor promotion is unknown, although dexamethasone and other steroid anti-inflammatory agents act to reduce plasminogen activator and prostaglandin activity in treated cells (*41, 42*). Dexamethasone also inhibits the binding of TPA in vivo, but not by competitively binding to the same sites (*43, 44*). The lack of effect of TPA up to a concentration of 10^{-6} *M* on the normal sorting pattern of neural retina and heart cells indicates that the effect of tumor promoters on cell behavior in our experiments is to reduce nonspecific cell adhesion without affecting specific cell interactions. The sorted configuration formed in mixed aggregation cultures has been shown to be remarkably resistant to disruption by exogenous agents with the sole exception of cytochalasin B (*28, 29*).

There have been reports of both the enhancing (*45, 46*) and inhibitory (*20, 47*) effects of tumor promoters on cell–substrate adhesion, but we report here on their effects on cell–cell adhesion. Since the difference in the mechanisms of these two adhesive processes themselves are not yet clearly understood, it is premature to extrapolate from the effects of tumor promoters in one case to the other. However, the many changes in cells and cell surfaces caused by TPA suggest several possibilities. Reduced aggregation as a result of increased electrostatic repulsive forces is unlikely in view of the results of Wenner et al, (*11*) showing that TPA at 10^{-6} *M* caused a reduction in the electrophoretic mobility of mouse Ehrlich ascites cells, reflecting a reduced net negative surface charge density. TPA also disrupts actin filaments normally present at the cell periphery (*48*), as well as other cytoskeletal elements, which may be reflected in reduced adhesive capabilities. This observation of perturbed cytoskeletal integrity may also support the possible role of alterations in intracellular calcium ion movement in response to tumor promotion suggested by the work of Boynton and Whitfield (*49*) and is consistent with our preliminary observation of significant reductions in the size of aggregates formed in cultures containing calcium ionophore A23157 at concentrations of 1 μg/ml ($0.5>P>0.02$) and 2, 5, or 10 μg/ml ($P<0.001$). Also, tumor promoters cause a marked increase in plasminogen activator synthesis. The proteases produced may act to reduce the strength of adhesion of the cells, thereby enhancing their likelihood of separation by the shearing forces present in gyratory shaker culture. Tumor-promoting but not nonpromoting phorbol esters also produced a relatively specific decrease in the synthesis of some glycoproteins and other glycoconjugates correlated with the induction of anchorage independence; both were reversible by retinoic acid, a potent inhibitor of TPA tumor promotion (*50*). These observations are consistent with the reductions in intercellular matrix and fibronectin synthesis that have been reported (*5, 51*). Finally, any of the other reported effects of tumor promoters on cells may affect the adhesion and aggregation of the cells in a direct way or in ways not yet apparent to produce the reduction in intercellular adhesion, as measured by aggregate size, reported here.

REFERENCES

(*1*) Sivak A, Van Duuren BL. Phenotypic expression of transformation: Induction in cell culture by a phorbol ester. Science 1967; 157:1434–1444.

(*2*) Goldfarb RH, Quigley JP. Synergistic effect of tumor virus transformation and tumor promoter treatment on the production of plasminogen activator by chick embryo fibroblasts. Cancer Res 1978; 38:4601–4609.

(*3*) Wigler M, DeFeo D, Weinstein IB. Induction of plasminogen activator in cultured cells by macrocyclic plant diterpene esters and other agents related to tumor promotion. Cancer Res 1978; 38:1434–1437.

(*4*) Wigler M, Weinstein IR. Tumour promoter induces plasminogen activator. Nature 1976; 259:232–233.

(*5*) Blumberg PM, Driedger PE, Rossow PW. Effect of a phorbol ester on transformation-sensitive surface protein of chick fibroblasts. Nature 1976; 264:446–447.

(*6*) Furstenberger G, Marks F. Early prostaglandin E synthesis is an obligatory event in the induction of cell proliferation in mouse epidermis in vivo by the phorbol ester TPA. Biochem Biophys Res Commun 1980; 92:749–756.

(*7*) Diamond L, O'Brien S, Donaldson C, Shimizu Y. Growth stimulation of human diploid fibroblasts by the tumor promoter, 12-*O*-tetradecanoylphorbol-13-acetate. Int J Cancer 1974; 13:721–730.

(*8*) Boreiko C, Mondal S, Naragon KS, Heidelberger C. Effect of 12-*O*-tetradecanoylphorbol-13-acetate on the morphology and growth of C3H-10T½ mouse embryo cells. Cancer Res 1980; 40:4709–4716.

(*9*) Weinstein IB, Lee LS, Fisher PB, Mufson A, Yamasaki H. Action of phorbol esters in cell culture: Mimicry of transformation, altered differentiation, and effects on cell membranes. J Supramol Struct Cell Biochem 1979; 12:195–208.

(*10*) Berenblum I. Sequential aspects of chemical carcinogenesis: Skin. In: Becker FF, ed. Cancer: A comprehensive treatise. Vol 1. New York: Plenum, 1975:323–344.

(*11*) Wenner CE, Hackney J, Kimelberg HK, Mayhew E. Membrane effects of phorbol esters. Cancer Res 1974; 34:1731–1737.

(*12*) Wenner CE, Moroney J, Porter CW. Early membrane effects of phorbol esters in 3T3 cells. In: Slaga TJ, Sivak A, Boutwell RK, eds. Carcinogenesis: A comprehensive survey. Vol 2. New York: Raven, 1978:363–378.

(*13*) Cohen R, Pacifici M, Rubinstein N, Biehl J, Holtzer H. Effect of a tumour promoter on myogenesis. Nature 1977; 266:538–540.

(*14*) Diamond L, O'Brien TG, Rovera G. Tumor promoters inhibit terminal cell differentiation in culture. In: Slaga TJ, Sivak A, Boutwell RK, eds. Carcinogenesis: A comprehensive survey. Vol 2. New York: Raven, 1978:335–342.

(*15*) Pacifici M, Holtzer H. Effects of a tumor-promoting agent on chondrogenesis. Am J Anat 1977; 150:207–212.

(*16*) Payette R, Biehl J, Toyama Y, Holtzer S, Holtzer H. Effects of 12-*O*-tetradecanoylphorbol-13-acetate on the differentiation of avian melanocytes. Cancer Res 1980; 40:2465–2474.

(*17*) Huberman E, Callaham MF. Induction of terminal differentiation in human promyelocytic leukemia cells by tumor-promoting agents. Proc Natl Acad Sci USA 1979; 76:1293–1297.

(*18*) Huberman E, Heckman C, Langenback R. Stimulation of differentiated functions in human melanoma cells by tumor-promoting agents and dimethylsulfoxide. Cancer Res 1979; 39:2618–2624.

(*19*) Colburn NH. Tumor promoter produces anchorage independence in mouse epidermal cells by an induction mechanism. Carcinogenesis 1980; 1:951–954.

(*20*) Colburn NH, Former BF, Nelson KJ, Yuspa SH. Tumour promoter induces anchorage independence irreversibly. Nature 1979; 281:589–591.

(*21*) Maslow DE. In vitro analysis of surface specificity in embryonic cells. Cell Surface Revs 1976; 1:697–745.

(*22*) Barnard PJ, Weiss L, Ratcliffe T. Changes in the surface properties of embryonic chick neural retina cells after dissociation. Exp Cell Res 1969; 54:293–301.

(*23*) Belman S, Troll W. The inhibition of croton oil-promoted mouse skin tumorigenesis by steroid hormones. Cancer Res 1972; 32:450–454.

(*24*) Driedger PE, Blumberg, PM. The effect of phorbol diesters on chicken embryo fibroblasts. Cancer Res 1977; 37:3257–3265.

(*25*) Moscona A. Rotation mediated histogenetic aggregation of dissociated cells. Exp Cell Res 1961; 22:455–475.

(*26*) Weiss L, Maslow DE. Some effects of trypsin dissociation on the inhibition of reaggregation among embryonic chicken neural retina cells by cycloheximide. Dev Biol 1972; 29:482–485.

(*27*) Richmond JE, Glaeser RM, Todd P. Protein synthesis and aggregation of embryonic cells. Exp Cell Res 1968; 52:43–58

(*28*) Maslow DE, Mayhew E. Cytochalasin B prevents specific sorting of reaggregating embryonic cells. Science 1972; 177:281–282.

(*29*) ———. Histotypic cell aggregation in the presence of cytochalasin B. J Cell Sci 1974; 16:65[illegible]663.

(*30*) Maslow DE, Harlos JP. The effect of neuraminidase- and ribonuclease-susceptible surface anionic groups on the aggregation of embryonic chick neural retina cells. J Cell Sci 1981; 51:229–240.

(*31*) Maslow DE, Weiss L. Some effects of positively charged groups on cell aggregation. J Cell Sci 1976; 21:219–225.

(*32*) Armstrong PB. On the role of metal cations in cellular adhesion: Effect on cell surface charge. J Exp Zool 1966; 163:99–110.

(*33*) Storme G, Mareel M. Effects of anti-cancer agents on directional migration of malignant C3H mouse fibroblastic cells in vitro. Cancer Res 1980; 40:943–948.

(*34*) Maslow DE, Mayhew E. Inhibition of embryonic cell aggregation by neoplastic cells. J Natl Cancer Inst 1975; 54:1097–1102.

(*35*) Weiss L, Maslow DE. In vitro studies on the interactions of tumour and non-tumour cells. In: Richards RT, Rajan RT, eds. Tissue culture in medical research. Vol II. Oxford: Pergamon, 1980:117–124.

(*36*) Furstenberger G, Richter H, Argyris TS, Marks F. Effects of the phorbol ester 4-*O*-methyl-12-*O*-tetradecanoylphorbol-13-acetate on mouse skin in vivo: Evidence for its uselessness as a negative control compound in studies on the biological effects of phorbol ester tumor promoters. Cancer Res 1982; 42:342–348.

(*37*) Crutchley DJ, Conanan LB, Maynard JR. Induction of plasminogen activator and prostaglandin biosynthesis in HeLa cells by 12-*O*-tetradecanoylphorbol-13-acetate. Cancer Res 1980; 40:849–852.

(*38*) Lanz R, Brune K. Dissociation of tumor-promoter-induced effects of prostaglandin release, polyamine synthesis and cell proliferation of 3T3 cells. Biochem J 1981; 194:975–982.

(*39*) Slaga TJ, Fischer SM, Nelson K, Gleason GL. Studies on the mechanism of skin tumor promotion: Evidence for several stages in promotion. Proc Natl Acad Sci USA 1980; 77:3659–3663.

(*40*) Slaga TJ, Kelin-Szanto AJ, Fischer SM, Weeks CF, Nelson K, Major S. Studies on mechanism of action of anti-tumor promoting agents: Their specificity in two-stage promotion. Proc Natl Acad Sci USA 1980; 77:2251–2254.

(*41*) Slaga TJ, Fischer SM, Viaje A, et al. Inhibition of tumor promotion by anti-inflammatory agents: An approach to the biochemical mechanism of promotion. In: Slaga TJ, Sivak A, Boutwell RK, eds. Carcinogenesis: A comprehensive survey. Vol 2. New York: Raven, 1978:363–378.

(*42*) Viaje A, Slaga TJ, Wigler M, Weinstein IB. Effects of anti-inflammatory agents on mouse skin tumor promotion, epidermal DNA synthesis, phorbol ester-induced cellular proliferation and production of plasminogen activator. Cancer Res 1977; 37:1530–1536.

(*43*) Driedger PE, Blumberg PM. Specific binding of phorbol ester tumor promoters. Proc Natl Acad Sci USA 1980; 77:567–57[illegible].

(*44*) Delclos KB, Nagle DS, Blumberg PM. Specific binding of phorbol ester tumor promoters to mouse skin. Cell 1980; 19:1025–1032.

(*45*) Tomei LD, Wenner CE. Similar effects of phorbol esters and retinoids on two specific modes of cellular adhesion. Proc Am Assoc Cancer Res 1981; 22:135.

(*46*) Castagna M, Rochette-Egly C, Rosenfeld C. Tumour-promoting phorbol diester induces substrate-adhesion and growth inhibition in lymphoblastoid cells. Cancer Lett 1979; 6:227–234.

(*47*) Colburn NH. Tumor promoter produces anchorage independence in mouse epidermal cells by an induction mechanism. Carcinogenesis 1980; 1:951–954.

(*48*) Rifkin DB, Crowe RM, Pollack R. Tumor promoters induce changes in the chick embryo fibroblast cyto-skeleton. Cell 1979; 18:361–368.

(*49*) Boynton AL, Whitfield JF. Stimulation of DNA synthesis in calcium-deprived T51B liver cells by the tumor promoters phenobarbital, saccharin, and 12-*O*-tetradecanoylphorbol-13-acetate. Cancer Res 1980; 40:4541–4545.

(*50*) Dion LD, DeLuca LM, Colburn NH. Phorbol ester-induced anchorage independence and its antagonism by retinoic acid correlates with altered expression of specific glycoproteins. Carcinogenesis 1981; 2:951–958.

(*51*) Declos KB, Blumberg PM. Decrease in collagen production in normal and Rous sarcoma virus-transformed chick embryo fibroblasts induced by phorbol myristate acetate. Cancer Res 1979; 39:1667–1672.

Mouse Skin Tumor-Initiating Activity of 5-, 7-, and 12-Methyl- and Fluorine-Substituted Benz[*a*]anthracenes[1,2,3]

Alexander W. Wood,[4] Wayne Levin,[4] Richard L. Chang,[4] Allan H. Conney,[4] Thomas J. Slaga,[5] Robert F. O'Malley,[6] Melvin S. Newman,[7] Donald R. Buhler,[8,9] *and* Donald M. Jerina[8]

ABSTRACT—As an approach for elucidation of structure activity relationships that underlie the exceptionally large difference in carcinogenic activity between benz[*a*]anthracene and 7,12-dimethylbenz[*a*]anthracene (7,12-DMBA), 11 methyl- and/or fluorine-substituted benz[*a*]anthracenes were evaluated for tumor-initiating activity on mouse skin. Outbred CD-1 and outbred Sencar mice received a single topical application of the hydrocarbons followed by twice weekly applications of the tumor promoter 12-*O*-tetradecanoylphorbol 13-acetate for 16–26 weeks. 7,12-DMBA was almost two orders of magnitude more active as a tumor-initiator than 7- and 12-methylbenz[*a*]anthracene. Methyl substitution at the 7- and 7,12-positions of benz[*a*]anthracene was significantly more effective in the enhancement of tumorigenic activity than fluorine substitution at these positions. Although 7-fluorobenz[*a*]anthracene, 12-fluorobenz[*a*]anthracene, and 7,12-difluorobenz[*a*]anthracene had only 0.15, 0.26, and less than 0.005 times the tumor-initiating activity of their respective methyl-substituted derivatives, they were severalfold more active than benz[*a*]anthracene. 7-Fluorobenz[*a*]anthracene was slightly less active than 12-fluorobenz[*a*]anthracene, whereas 7-methylbenz[*a*]anthracene was about twofold more active than 12-methylbenz[*a*]anthracene. For 7,12-disubstituted benz[*a*]anthracenes, 7-methyl-12-fluorobenz[*a*]anthracene was more than twice as tumorigenic as 7-fluoro-12-methylbenz[*a*]anthracene, but each was individually more active than 7-methylbenz[*a*]anthracene and 12-methylbenz[*a*]anthracene, respectively. Both fluorinated compounds were much less active than 7,12-DMBA. Substitution of fluorine or methyl at the 5-position of 7-methylbenz[*a*]anthracene and substitution of fluorine at the 5-position of 12-methylbenz[*a*]anthracene dramatically reduced their tumorigenic activity.—JNCI 1982; 69:725–728.

The polycyclic aromatic hydrocarbons represent a particularly intriguing class of environmental carcinogens in that seemingly small changes in structure can have profound effects on biologic activity. A striking example of this phenomenon is seen from a comparison of the structure and carcinogenicity of BA and 7,12-DMBA (text-fig. 1). Whereas BA is at best a weak carcinogen and has been described as noncarcinogenic in several tumor models, 7,12-DMBA is an extremely potent carcinogen in a variety of tumor models and is the most potent of the polycyclic hydrocarbons with respect to tumor-initiating activity on mouse skin (*1*). This striking difference in biologic activity is made all the more intriguing by the fact that a significant amount of experimental (*2–17*) as well as theoretical (*18, 19*) evidence indicates that a 3,4-diol-1,2-epoxide in which the 1,2-epoxide forms part of a bay region in the metabolite is an ultimate carcinogen of both BA and 7,12-DMBA. At present, an adequate physicochemical or biochemical basis by which the large difference in biologic activity of these two hydrocarbons can be explained is unavailable. In an attempt to elucidate the structure–activity relationships that underlie the exceptionally large difference in carcinogenic activity between BA and 7,12-DMBA, we have synthesized and tested the skin tumor-initiating activity of 11 methyl- and/or fluorine-substituted derivatives of BA.

MATERIALS AND METHODS

Chemicals.—TPA was obtained from Dr. Peter Borchert, Chemical Carcinogenesis, Inc., Eden Prairee, Minn. Organic solvents were obtained from Fisher Scientific Co., Springfield, N.J., and Burdick & Jackson, Inc., Muskegon, Mich.

BA derivatives.—A sample of BA obtained from Eastman Kodak Co., Rochester, N.Y., was judged to be pure by HPLC (*17*) and was used as such. Both 7-MBA (*20*) and 12-MBA (*21*) were synthesized as previously described. 7,12-DMBA, obtained from Aldrich Chemical Co., Milwaukee, Wis., was purified by column chromatography on silica gel eluted with cyclohexane and stored in the dark before use. 5,7-DMBA was prepared as described in (*22*). 7-FBA, 12-FBA, and 7,12-DFBA were prepared by anodic fluorination of BA (*23*). Both 5-F-7-MBA (*24*) and 5-F-12-MBA (*25*)

ABBREVIATIONS USED: BA=benz[*a*]anthracene; 7,12-DFBA=7,12-difluorobenz[*a*]anthracene; 3,4-diol-1,2-epoxide=either or both diastereomerically related 3,4-dihydroxy-1,2-epoxy-1,2,3,4-tetrahydrobenz[*a*]anthracenes in which the benzylic 4-hydroxyl group and the bay-region 1,2-epoxide oxygen are either *cis* or *trans*; DMBA=dimethylbenz[*a*]anthracene; FBA=fluorobenz[*a*]anthracene; 7-M-12-FBA-7-methyl-12-FBA; HPLC-high pressure liquid chromatography; MBA=methylbenz[*a*]anthracene; 5-F-7-MBA=5-fluoro-7-MBA; 5-F-12-MBA=5-fluoro-12-MBA; 7-F-12-MBA=7-fluoro-12-MBA; TPA=12-*O*-tetradecanoylphorbol 13-acetate.

---

[1] Received December 31, 1981; accepted April 13, 1982.

[2] Supported in part by Public Health Service (PHS) grant CA-20076 from the National Cancer Institute, and by the Office of Health and Environmental Research, U.S. Department of Energy, under contract W-7405-eng-26 with Union Carbide Corporation to T. J. S.

[3] Guidelines for the care and use of laboratory animals were followed as set forth by the American Association for Accreditation of Laboratory Animal Care.

[4] Department of Biochemistry and Drug Metabolism, Hoffmann-La Roche Inc., Nutley, N.J. 07110.

[5] Biology Division, Oak Ridge National Laboratory, Oak Ridge, Tenn. 37830.

[6] Department of Chemistry, Boston College, Chestnut Hill, Mass. 02167.

[7] Department of Chemistry, The Ohio State University, Columbus, Ohio 43210.

[8] Laboratory of Bioorganic Chemistry, National Institute of Arthritis, Diabetes, and Digestive and Kidney Diseases, National Institutes of Health, PHS, U.S. Department of Health and Human Services, Bethesda, Md. 20205.

[9] D. R. B. gratefully acknowledges sabbatical leave from The Oregon State University, Corvallis, Oreg.

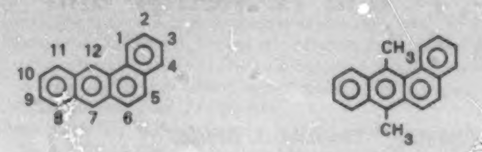

BENZ [a] ANTHRACENE (BA)

7,12-DIMETHYLBENZ[a]-ANTHRACENE (7,12-DMBA)

TEXT-FIGURE 1.—Structure of BA and 7,12-DMBA.

were obtained from fluorinated naphthalene, whereas 7-F-12-MBA and 7-M-12-FBA were synthesized (*26*) from BA-7,12-dione. All synthetic compounds were judged to be of analytic purity on the basis of microanalytic combustion data as indicated in the above references (*20–26*). Furthermore, the products obtained by anodic fluorination were free of cross-contamination as judged by HPLC.

Tumorigenicity studies.—Outbred CD-1 mice were obtained at 6 weeks of age from Charles River Breeding Laboratories, Wilmington, Mass. Outbred Sencar mice, originally obtained from Dr. R. K. Boutwell, University of Wisconsin, Madison, Wis., are presently raised at Oak Ridge National Laboratory. Only female mice were used for tumor experiments. At approximately 8 weeks of age, the dorsal surfaces of the mice were shaved with electric clippers. Two to 4 days later, mice in the resting phase of their hair cycle received a single topical application of the test compounds in 200 µl acetone. Control animals received solvent only. Each treatment group was comprised of 30 mice housed at 15 animals/cage.

The tumor promoter TPA was applied in 200 µl acetone twice weekly to each mouse, commencing 7 days after administration of the test compounds. CD-1 mice received 16 nmol TPA/application, whereas Sencar mice received 3.2 nmol/application. Incidence of papillomas was recorded once every 2 weeks. For purposes of comparison, the significance of relative tumorigenic activity was evaluated by Student's *t*-test.

RESULTS

The skin tumor-initiating activities of BA and six methyl- or fluorine-substituted derivatives at the 7- and/or 12-positions of BA in CD-1 mice after 18 and 26 weeks of tumor promotion with TPA are summarized in table 1. In agreement with numerous other studies, BA was a weak tumor initiator. A 500-nmol dose of the hydrocarbon did not significantly increase the tumor incidence above solvent control levels, whereas a 2,500-nmol dose induced tumors in 38% of the mice with an average of 0.67 papillomas/mouse at 26 weeks of promotion. In contrast, a single 10-nmol dose of 7,12-DMBA induced 3.6 tumors/mouse at 18 weeks of promotion and was thus over three orders of magnitude more active than BA. Comparison of papillomas/mouse at 26 weeks of promotion indicated that 7-FBA and 12-FBA were 4–11 times more tumorigenic than BA. 7,12-DFBA was more active than BA, but the lack of comparable doses or information on the shape of the dose-response curves makes precise comparisons difficult. All three of these fluoro-substituted BA derivatives, however, were less active than the corresponding methyl-substituted BA derivatives. Thus at 26 weeks of promotion a dose of 100 nmol of 7-MBA was six times more tumorigenic than 7-FBA, and 12-MBA was almost four times more active than 12-FBA. At 18 weeks of promotion 7,12-DMBA was at least 100 times more active than 7,12-DFBA. Whereas a 100-nmol dose of 7-MBA was not significantly more active than the same dose of 12-MBA at 26 weeks of promotion (0.87 vs. 0.67 tumors/mouse, $P>0.5$), 7-MBA was up to 4.6 times more tumorigenic than 12-MBA when higher doses were compared at 18 weeks of promotion. 7-MBA showed a linear dose response with respect to average numbers of papillomas/mouse over a tenfold dosage range, whereas tumor incidence with 12-MBA did not increase proportionately over the same dosage range. This nonproportionality in the dose-response curve of 12-MBA also explained the diminished difference in tumorigenic activity between 12-FBA and 12-MBA when higher doses of the two compounds were used.

Table 2 summarizes the skin tumor-initiating activity of eight BA derivatives in Sencar mice after 16 weeks of tumor promotion with TPA. Sencar mice were developed by inbreeding mice that had a high susceptibility to DMBA-initiated skin tumors. DiGiovanni et al. (*27*) have shown that higher tumor incidences are observed at an earlier time and with lower doses of TPA in Sencar mice compared to those in CD-1 mice. Consistent with observations in CD-1 mice (table 1), 7-MBA was about twofold more tumorigenic than 12-MBA in Sencar mice, and 7,12-DMBA was about 80 times more tumorigenic than 7-MBA. The high tumori-

TABLE 1.—*Comparison of the effects of methyl and fluorine substitution at the 7- and 12-positions on the skin tumor-initiating activity of BA in CD-1 mice*[a]

Compound	BA dose, nmol	Percent of mice with papillomas		Papillomas/mouse[b]	
		18 wk	26 wk	18 wk	26 wk
Solvent	0	0	4	0	0.04±0.04
BA	500	7	7	0.07±0.05	0.07±0.05
	1,000	7	17	0.07±0.05	0.17±0.07
	2,500	24	38	0.35±0.13	0.67±0.17
7-FBA	100	0	10	0	0.13±0.08
	500	17	30	0.20±0.09	0.50±0.16
	1,000	14	48	0.17±0.09	0.62±0.14
12-FBA	100	7	17	0.07±0.05	0.17±0.07
	500	20	38	0.33±0.14	0.79±0.23
	1,000	36	59	0.64±0.18	1.28±0.26
7,12-DFBA	10	7	ND	0.07±0.05	ND
	25	7	ND	0.07±0.05	ND
	100	10	21	0.10±0.06	0.25±0.14
7-MBA	100	35	40	0.48±0.15	0.87±0.26
	500	70	ND	2.17±0.58	ND
	1,000	76	ND	4.82±0.93	ND
12-MBA	100	30	43	0.40±0.12	0.67±0.18
	500	48	59	0.83±0.20	1.38±0.31
	1,000	40	50	1.00±0.31	1.40±0.35
7,12-DMBA	10	63	ND	3.59±0.84	ND
	25	83	ND	8.00±1.63	ND
	100	92	ND	11.64±1.90	ND

[a] Thirty female CD-1 mice received a single topical application of compound in 200 µl acetone; 7 days later the mice received twice-weekly topical applications of TPA (16 nmol/application) in 200 µl acetone. In each group 27–30 mice were alive at the end of 26 wk of tumor promotion. ND=not determined.

[b] Values are means ± SEM.

TABLE 2.—*Comparison of the effects of methyl and fluorine substitution on the skin tumor-initiating activity of 7-methyl-BA and 12-methyl-BA in Sencar mice*[a]

Compound	BA dose, nmol	Percent of mice with papillomas	Papillomas/mouse[b]
Solvent	0	0	0
7-MBA	400	86	3.00±0.52
12-MBA	400	73	1.65±0.28
7,12-DMBA	10	100	6.43±0.53
	400	100[c]	22.62±1.93[c]
7-M-12-FBA	400	100	9.00±0.94
7-F-12-MBA	400	88	3.43±0.38
5-F-7-MBA	400	33	0.44±0.08
5,7-DMBA	400	41	0.63±0.12
5-F-12-MBA	400	10	0.21±0.05

[a] Thirty female Sencar mice received a single topical application of compound in 200 µl acetone; 7 days later the mice received twice-weekly topical applications of TPA (3.2 nmol/application) in 200 µl acetone. In each group 28–30 mice were alive at the end of 16 wk of tumor promotion.

[b] Values are means ± SEM.

[c] Results were calculated at 10 wk of tumor promotion with TPA.

genicity of 7-MBA was markedly decreased by introduction of either a fluorine or a methyl group at the 5-position of 7-MBA. Similarly, the average number of papillomas/mouse with 12-MBA was reduced from 1.6 to 0.20 as the result of substitution by fluorine at the 5-position. Substitution of fluorine at position 12 of 7-MBA and at position 7 of 12-MBA significantly increased the tumorigenicity of the hydrocarbons. Thus 7-M-12-FBA was three times more active as a tumor initiator than 7-MBA (9 vs. 3 papillomas/mouse), and it was the second most active compound tested. 7-F-12-MBA was two times more active as a tumor initiator than 12-MBA (3.4 vs. 1.6 papillomas/mouse).

DISCUSSION

Although other pathways of activation may occur, studies of the mutagenicity, metabolism, tumorigenicity, and DNA binding of BA, 7-MBA, and 7,12-DMBA and their metabolites have indicated that metabolic formation of bay-region diol epoxides is the principal pathway by which these hydrocarbons are activated to ultimate carcinogens (*2–19*). Consistent with earlier reports [cf. (*1*)], the present study has found that 12-MBA is tenfold to twentyfold more active, 7-MBA is about fiftyfold more active, and 7,12-DMBA is greater than one thousandfold more active than BA as a tumor initiator. Some of the factors that could be responsible for these dramatic differences in activity consist of the steric and electronic effects of substituents in altering 1) the rate and extent to which these hydrocarbons are metabolized to reactive metabolites, 2) the effectiveness with which these metabolites bind to critical cellular nucleophiles, and 3) the rate at which such damage is repaired. In general, the electronic effect of a methyl substituent on an aromatic ring is one of activation via hyperconjugation, whereas a fluorine substituent deactivates via induction but still acts as an ortho-para director via resonance. Thus direct electronic interaction (resonance stabilization) of a C-1 carbocation derived from a bay region 3,4-diol-1,2-epoxide in the BA series can be expected for C-7 but not C-12 substituents. Since fluorine is only slightly larger than hydrogen, they should exert similar steric effects. However, a 12-methyl substituent is known to cause nonplanarity in 12-MBA and 7,12-DMBA due to adverse steric interaction with the C-1 hydrogen across the bay region. Little is presently known about the positional reactivity of nonplanar aromatic hydrocarbons compared to their planar analogues.

The fiftyfold-higher tumorigenicity of 7-MBA relative to BA is higher than might be expected on the basis solely of enhanced reactivity of the bay region diol epoxide due to the 7-methyl substituent. Some of the difference in activity may be due to the metabolism profiles suggesting that the 3,4-dihydrodiol, the immediate metabolic precursor of the bay region 3,4-diol-1,2-epoxide, is a more prominent metabolite of 7-MBA than of BA (*17, 28*). Although 7-substitution has been proposed to block a principal route of metabolic detoxification of BA, there is apparently little if any metabolism of BA at the 7-position (*17*). Comparative studies on the metabolic conversion of the 3,4-dihydrodiol of BA and 7-MBA to their respective 3,4-diol-1,2-epoxides have not been reported. However, studies with BA 3,4-dihydrodiol indicate that it is not efficiently converted to its bay region diol epoxide (*7*). Since 12-MBA is tenfold to twentyfold more active than BA, presumably due to some type of steric effect, the cumulative influence of 7- and 12-methyl substituents might account for the one thousandfold-greater activity of 7,12-DMBA over the activity of BA.

The above arguments are, however, fragile when considered in light of the tumorigenicity of the fluorinated BA's in the present study. Although fluorine at the 7-position of BA could slightly decrease the reactivity of its bay-region diol epoxide, 7-FBA is greater than threefold-more active than BA. Although a fluorine at position 12 has little steric effect relative to hydrogen, 12-FBA is greater than sevenfold-more active than BA. The cumulative effect is small since 7,12-DFBA, although more active than BA, has only 1% of the activity of 7,12-DMBA. Replacement of either methyl group by fluorine in 7,12-DMBA results in an approximately fiftyfold loss in activity, yet 7-M-12-FBA and 7-F-12-MBA are twofold- to threefold-more active than 7- and 12-MBA, respectively. Thus fluorine substitution at the 7- and/or 12-positions enhances tumorigenic activity relative to the unfluorinated compound but not as much as methyl substitution. Although the present results have not provided a basis by which substitution at the 12-position enhances the tumorigenicity of BA, they do emphasize the importance of either a methyl or a fluorine substituent in enhancing tumorigenicity when the substituent is in the bay region but not on the critical benzo-ring. This is also the case for 5-methylchrysene (*1, 29, 30*) and 11-methylbenzo[*a*]pyrene (*31*).

When formulating the bay region theory (*19*), we noted that substituents peri to the critical benzo-ring (the 5-position in BA) often decrease tumorigenic activity. This effect seems to be generally true for the BA series since 5-F-7-MBA and 5,7-DMBA have less than 20% of the activity of 7-MBA, 5-F-12-MBA has less than 15% of the activity of 12-MBA (table 2), and 5-fluro-7,12-DMBA has less than 1% of the tumor initiating activity of 7,12-DMBA (*32*). Similarly, substitution of fluorine at the 12-position (peri to the critical benzo-ring) of 5-methylchrysene markedly inhibits tumorigenic activity (*29, 30*). Although the basis of this "peri effect" is presently unknown, it is possible that certain substituents cause dihydrodiols with bay region double bonds to adopt a quasi-diaxial conformation. For some but not all dihydrodiols, this conformation results in poor conversion to bay region diol epoxides (*33–38*).

REFERENCES

(*1*) Dipple A. Polynuclear aromatic carcinogens. Chemical carcinogens. Am Chem Soc Monogr 1976; 173:245–314.

(*2*) Wislocki PG, Buening MK, Levin W, et al. Tumorigenicity of the diastereomeric benz[*a*]anthracene 3,4-diol-1,2-epoxides and the (+)- and (−)-enantiomers of benz[*a*]anthracene 3,4-dihydrodiol in newborn mice. JNCI 1979; 63:201–204.

(*3*) Levin W, Thakker DR, Wood AW, et al. Evidence that benzo[*a*]anthracene 3,4-diol-1,2-epoxide is an ultimate carcinogen on mouse skin. Cancer Res 1978; 38:1705–1710.

(*4*) Wislocki PG, Juliana MM, MacDonald JS, Chou MW, Yang SK, Lu AY. Tumorigenicity of 7,12-dimethylbenz[*a*]anthracene, its hydroxymethylated derivatives and selected dihydrodiols in the newborn mouse. Carcinogenesis 1981; 2:511–514.

(*5*) Slaga TJ, Gleason GL, DiGiovanni J, Sukumaran KB, Harvey RG. Potent tumor-initiating activity of the 3,4-dihydrodiol of 7,12-dimethylbenz[*a*]anthracene in mouse skin. Cancer Res 1979; 39:1934–1936.

(*6*) Slaga TJ, Gleason GL, DiGiovanni J, et al. Tumor initiating activities of various derivatives of benz[*a*]anthracene and 7,12-dimethylbenz[*a*]anthracene in mouse skin. In: Jones PW, Lever P, eds. Polynuclear aromatic hydrocarbons. Ann Arbor, Mich.: Ann Arbor Science Publishers, 1979:753–764.

(*7*) Thakker DR, Levin W, Yagi H., et al. Stereoselective metabolism of the (+)- and (−)-enantiomers of *trans*-3,4-dihydroxy-3,4-dihydrobenz[*a*]anthracene by rat liver microsomes and by a purified and reconstituted cytochrome P-450 system. J Biol Chem 1982; 257:5103–5110.

(*8*) Chou MW, Yang SK. Identification of four *trans*-3,4-dihydrodiol metabolites of 7,12-dimethylbenz[*a*]anthracene and their in vitro DNA-binding activities upon further metabolism. Proc Natl Acad Sci USA 1978; 75:5466–5470.

(*9*) Moschel RC, Baird WM, Dipple A. Metabolic activation of the carcinogen 7,12-dimethylbenz[*a*]anthracene for DNA binding. Biochem Biophys Res Commun 1977; 76:1091–1098.

(*10*) Slaga TJ, Huberman E, Selkirk JH, Harvey RG, Bracken WM. Carcinogenicity and mutagenicity of benz[*a*]anthracene diols and diol epoxides. Cancer Res 1978; 38:1699–1704.

(*11*) Wislocki PG, Kapitulnik J, Levin W, et al. Exceptional carcinogenic activity of benzo[*a*]anthracene 3,4-dihydrodiol in the newborn mouse and the bay region theory. Cancer Res 1978; 38:693–696.

(*12*) Wood AW, Levin W, Chang RL, et al. Tumorigenicity of five dihydrodiols of benz[*a*]anthracene 3,4-dihydrodiol. Proc Natl Acad Sci USA 1977; 74:3176–3179.

(*13*) Wislocki PG, Gadek KM, Chou MW, Yang SK, Lu AY. Carcinogenicity and mutagenicity of the 3,4-dihydrodiols and other metabolites of 7,12-dimethylbenz[*a*]anthracene and its hydroxymethyl derivatives. Cancer Res 1980; 40:3661–3664.

(*14*) Vigny P, Duquesne M, Coulomb H, Tierney B, Grover PL, Sims P. Fluorescence spectral studies on the metabolic activation of 3-methylcholanthrene and 7,12-dimethylbenz[*a*]anthracene. FEBS Lett 1977; 82:278–282.

(*15*) Huberman E, Chou MW, Yang SK. Identification of 7,12-dimethylbenz[*a*]anthracene metabolites that lead to mutagenesis in mammalian cells. Proc Natl Acad Sci USA 1979; 76:862–866.

(*16*) Wood AW, Chang RL, Levin W, et al. Mutagenicity and cytotoxicity of benz[*a*]anthracene diol epoxides and tetrahydro-epoxides: Exceptional activity of the bay region 1,2-epoxides. Proc Natl Acad Sci USA 1977; 74:2746–2750.

(*17*) Thakker DR, Levin W. Yagi H, et al. Metabolism of benzo[*a*]anthracene to its tumorigenic 3,4-dihydrodiol. Mol Pharmacol 1979; 15:138–154.

(*18*) Jerina DM, Lehr RE, Yagi H, et al. Mutagenicity of benzo[*a*]pyrene derivatives and the description of a quantum mechanical model which predicts the ease of carbonium ion formation from diol epoxide. In: de Serres JF, Fouts JR, Bend JR, Philpot RM, eds. In vitro metabolic activation in mutagenesis testing. Amsterdam: Elsevier/North Holland, 1976:157–177.

(*19*) Jerina DM, Daly JW. Oxidation at carbon. In: Parke DV, Smith RL, eds. Drug metabolism. London: Taylor and Francis, 1976:15-33.

(*20*) Wood JL, Fieser LF. Sulfhydryl and cysteine derivatives of 1,2-benzanthracene, 10-methyl-1,2-benzanthracene and 3,4-benzpyrene. J Am Chem Soc 1940; 62:2674–2681.

(*21*) Newman MS, Khanna JM. Lilje KC. Recommended syntheses for 7-methylbenz[*a*]anthracene and 7,12-dimethylbenz[*a*]anthracene. Org Prep Proc Int 1979; 11:271–274.

(*22*) Newman MS, Hart RT. A new synthesis of 1,2-benzanthracene. J Am Chem Soc 1947; 69:298–300.

(*23*) O'Malley RF, Mariani HA, Buhler DR, Jerina DM. Anodic fluorination of benzo[*a*]anthracene. J Org Chem 1981; 46:2816-2818.

(*24*) Newman MS, MacDowell D, Swaminathan S. The synthesis of some monofluoro-1,2-benzanthracenes. J Org Chem 1959; 24:509-512.

(*25*) Bergmann ED, Blum J. Fluorine-substituted 1,2-benzanthracene and 3,4-benzophenanthrene derivatives and related compounds. J Org Chem 1962; 27:527–533.

(*26*) Newman MS, Khanna JM. Synthesis of 12-fluoro-7-methylbenz[*a*]anthracene and 7-fluoro-12-methylbenz[*a*]anthracene. J Org Chem 1979; 44:866–868.

(*27*) DiGiovanni J, Slaga TJ, Boutwell RK. Comparison of the tumor initiating activity of 7,12-dimethylbenz[*a*]anthracene and benzo[*a*]pyrene in female Sencar and CD-1 mice. Carcinogenesis 1980; 1:381–389.

(*28*) Tierney B, Hewer A, Walsh C, Grover PL, Sims P. The metabolic activation of 7-methylbenz[*a*]anthracene in mouse skin. Chem Biol Interact 1977; 18:179–193.

(*29*) Hecht SS, LaVoie E, Mazzarese R, Hirota N, Ohmori T, Hoffmann D. Comparative mutagenicity, tumor-initiating activity, carcinogenicity, and in vitro metabolism of fluorinated 5-methylchrysenes. JNCI 1979; 63:855–861.

(*30*) Hecht SS, Hirota N, Loy M, Hoffmann D. Tumor-initiating activity of fluorinated 5-methylchrysenes. Cancer Res 1978; 38:1694–1698.

(*31*) Iyer RP, Lyga JW, Secrist JA, Daub GH, Slaga TJ. Comparative tumor-initiating activity of methylated benzo[*a*]pyrene derivatives in mouse skin. Cancer Res 1980; 40:1073–1076.

(*32*) Huberman E, Slaga TJ. Mutagenicity and tumor-initiating activity of fluorinated derivatives of 7,12-dimethylbenz(*a*)anthracene. Cancer Res 1979; 39:411–414.

(*33*) Wood AW, Levin W, Thakker DR, et al. Biological activity of benzo[*e*]pyrene: An assessment based on mutagenic activities and metabolic profiles of the polycyclic hydrocarbon and its derivatives. J Biol Chem 1979; 254:4408–4415.

(*34*) Thakker DR, Yagi H, Lehr RE, et al. Metabolism of *trans*-9,10-dihydroxy-9,10-dihydrobenzo[*a*]pyrene occurs primarily by arylhydroxylation rather than formation of a diol epoxide. Mol Pharmacol 1978; 14:502–513.

(*35*) Yang SK, Chou MW. Metabolism of the bay-region *trans*-1,2-dihydrodiol of benz[*a*]anthracene in rat liver microsomes occurs primarily at the 3,4-double bond. Carcinogenesis 1980; 1:803–806.

(*36*) Vyas KP, Yagi H, Levin W, Conney AH, Jerina DM. Metabolism of (−)-*trans*-(3R,4R)-dihydroxy-3,4-dihydrochrysene to diol epoxide by liver microsomes. Biochem Biophys Res Commun 1981; 98:961-968.

(*37*) Chou MW, Fu PP, Yang SK. Metabolic conversion of dibenz-[*a,h*]anthracene (±)-*trans*-1,2-dihydrodiol and chyrsene (±)-*trans*-3,4-dihydrodiol to vicinal dihydrodiol epoxides. Proc Natl Acad Sci USA 1981; 78:4270–4273.

(*38*) Cerniglia CE, Gibson DT. Fungal oxidation of (±)-9,10-dihydroxy-9-10-dihydrobenzo[*a*]pyrene: Formation of diastereomeric benzo[*a*]pyrene 9,10-diol 7,8-epoxides. Proc Natl Acad Sci USA 1980; 77:4554–4558.

Free Amino Acid Pools of Rodent Mammary Tumors[1,2,3]

Martin J. Pine,[4] Untae Kim,[5] *and* Clement Ip[6,7]

ABSTRACT—Intracellular pools of free amino acids were compared individually in mammary tumors of Wistar Furth and Sprague-Dawley rats and C3H and DBA/2 mice. Of 11 transplantable and 7,12-dimethylbenz[*a*]anthracene-induced adenocarcinomas of the rat, all nonmetastasizing tumors could be distinguished from metastasizing tumors by the accumulation of high glutamine pools and significant-to-high cystathionine pools. In primary mammary tumors of C3H mice and transplanted mammary tumors of DBA/2 mice, intracellular free arginine was frequently below that of the circulating plasma level and approached that in the arginine-destroying organ, the liver. Arginine pool depletion was also noted in normal mammary tissue, particularly in the actively lactating mouse. Individual rat or mouse mammary tumors also contained high levels of taurine, β-alanine, and γ-aminobutyric acid, which, like cystathionine, are distinctive for or are enriched in neural tissue. None of these pool enrichments were characteristic of normal rat or mouse mammary tissue. Free hydroxyproline was low in primary induced rat mammary tumors and higher in transplanted mammary tumors and in normal lactating mammary glands, particularly in the mouse. In contrast, the hydroxyproline residues of collagen, taken as an index of mesenchymal cell contribution, were very low in all tumors.—JNCI 1982; 69:729–735.

Free amino acid pools have been examined in several human and animal tumor systems. Alterations in plasma aminogram profiles have been noted in patients with leukemia (*1*), carcinoid syndrome (*2*), or malignant bone tumors (*3*). The relatively indirect cachectic effects of tumor growth on the aminogram profile of host plasma has also been studied in tumor systems of human beings (*4*) and rats (*5*). The plasma aminogram alterations found in those studies were variously attributed to characteristic properties of the tumor to adjustments in host amino acid metabolism and to the increased turnover of collagen. In minimal deviation rat hepatomas, the amino acid pools of host and tumor tissue have also been examined as potential sites of depletion by the surviving amino acid-metabolizing enzymes of the tumor (*6*). Neuroblastomas, gliomas, and other brain tumors have been compared to their metastases for retention of the distinctive profiles of taurine, cystathionine, GABA, and other amino acids found in the neural tissue (*7*, *8*).

We were initially interested in the aminogram profiles of established rat mammary adenocarcinomas (*9*) for their possible relevance to variations of tumor growth rate and metastatic potential. Our findings with these and additional rodent mammary tumors show that a tumor type in a given species can exhibit distinctive patterns of free amino acid pool content, and that these may be useful in tumor prognosis and in the design of tumor antagonists.

MATERIALS AND METHODS

Tumor systems.—Transplanted rat mammary tumor lines were carried by subcutaneous implantation in WF female rats. Each line has maintained differentiation and metastatic potential as previously described (*9*). Primary rat mammary tumors were induced by gastric intubation of 10 mg DMBA in 1 ml corn oil in 50-day-old female SD rats. The animals were fed a semisynthetic diet with 20% casein content (*10*). Tumors were harvested at intervals up to 6 months after induction. All tumors except the smallest one were examined histologically and confirmed as well-differentiated, nonmetastasizing adenocarcinomas. The SMT-F and SMT-S nonmetastasizing tumors were maintained subcutaneously in DBA/2HaDD mice grown in the West Seneca Laboratories, West Seneca, N.Y., and fed Teklad (4% fat) diet. Spontaneous mammary tumors, all histologically confirmed as moderately- to well-differentiated nonmetastasizing adenocarcinomas, were from retired C3H/St female breeders grown in the West Seneca Laboratories. The animals were anesthetized, and mice were bled from the ocular plexus and rats from the aorta, with the use of heparinized instruments. Blood was centrifuged and the plasma was inactivated within 5 minutes after bleeding, with 4 volumes of 5% sulfosalicylic acid. For milk collection, about 0.1 ml of milk was aspirated from the two posterior gland pairs of an actively nursing (BALB/c♀ × DBA/2HaDD♂)F_1 mouse that had been anesthetized with Nembutal and received an ip injection of 0.4 U of oxytocin (Parke-Davis, Morris Plains, N.J.). Tumor samples were rapidly excised at their underside and freed of necrotic tissue and capsule. Cystlike or necrotic areas, which were common only in spontaneous C3H mouse tumors, were very briefly scraped and rinsed away in phosphate-buffered saline and blotted dry. Samples were weighed and ground within 1 minute of removal with 4 volumes of 5% sulfosalicylic acid in a conical glass tissue homogenizer. The rat tumor extracts usually required high-speed centrifugation for removal of lipid particles. The deproteinized extracts of tumor and plasma were neutralized with lithium citrate buffer and LiOH to bring them to pH 2.28. For hydrolysate analysis, tumor protein was purified by being boiled in 0.5 *N* $HClO_4$ for 30 minutes and then

---

ABBREVIATIONS USED: DMBA=7,12-dimethylbenz[*a*]anthracene; GABA=γ-aminobutyric acid; SMT-F=fast-growing mouse mammary tumor(s); SMT-S=slow-growing mouse mammary tumor(s).

---

[1] Received December 31, 1981; accepted April 26, 1982.

[2] Supported in part by Public Health Service grant CA-24215 from the National Cancer Institute.

[3] Animals were maintained under the guidelines set forth by the "Guide for the Care and Use of Laboratory Animals" by the Institute of Laboratory Animal Resources, National Research Council.

[4] Department of Experimental Therapeutics, Roswell Park Memorial Institute (RPMI), 666 Elm St., Buffalo, N.Y. 14263.

[5] Department of Pathology, RPMI.

[6] Department of Breast Surgery, RPMI.

[7] We thank William H. Haile for performing the amino acid assays.

washed in 0.1 *N* $HClO_4$, acetone, and $CHCl_3$-CH_3OH at 1:2 dilution. The protein was hydrolyzed in 5 *N* HCl for 28 hours at 100°C without evacuation. Soluble calf skin collagen was also hydrolyzed and assayed for hydroxyproline as a pure collagen standard. Amino acid assays were performed with the Beckman 121M amino acid analyzer, with the use of a one-column Li^+-based physiologic program (*12*). Abbreviated programs were used to assay hydroxyproline, GABA, and arginine; also, for arginine a short column was used. To confirm the identity of GABA, the physiologic program was abbreviated to begin with the third buffer, which removed a small interfering peak. The identity of cystathionine was substantiated by its disappearance upon performic acid oxidation. A solution of 50% H_2O_2–formic acid, 1:5 dilution, was developed for 30 minutes at room temperature, and 8–20 µl were added to 200 µl of the sample. The sample was then reneutralized. This procedure did not appreciably destroy 3,4-dihydroxyphenylalanine, which comigrates with cystathionine. Amino acids were also identified from their 440- to 570-nm peak area ratios and from their unchanged peak widths upon addition of equal levels of a standard.

RESULTS

The levels of the 12 most variable amino acids found in mammary tissue and tumor pools are listed in tables 1–6. The rat representatives comprised 4 metastasizing tumors (all transplanted; table 1) and 7 nonmetastasizing tumors (2 transplanted and 5 DMBA-induced; tables 1, 2). We sampled all tumors at their primary or implantation sites. The nonmetastasizing tumors could be distinguished without overlap from the metastasizing tumors by high accumulations of free glutamine (2,623±845 vs. 765±301 nmol/g of tumor, respectively) and by significant cystathionine pools (212±196 vs. 5±7, respectively). For both amino acids these differences were of the same high significance by the Mann-Whitney test (P=0.01) and by the Wilcoxon signed rank test (P=0.009) (*13*). The high glutamine pool levels were not associated with any maxima or minima in the pool levels of asparagine or of the other nonessential amino acids.

Of the transplanted tumors, strains DMBA-4 and MT-449 are the slowest and the fastest, respectively, to appear after transplantation, SMT-2A and TMT-081 are the 2 most metastatic and least differentiated tumors, respectively, whereas MT-449 and MT-100 had been harvested in unusually small and large sizes, respectively. None of these distinctions appeared to be accompanied by major or consistent pool changes. Also, the pool profiles of the tumor centers, which would represent the most circumscribed nutritional supply and the most limited growth, showed only minimal and random statistical differences from the profiles of the tumor peripheries.

Close similarity if not near identity in pool sizes may be noted among the different-sized DMBA-induced tumors of table 2, except for the smallest, whose cellularity was unknown. These tumors had consistently low free hydroxyproline pools. This phenomenon could be due to low endogenous production or turnover of collagen, the absence of hydroxyproline in the casein diet, and poor tumor transport of hydroxyproline.

For a more consistent comparison with the transplanted tumors, the circulating level of hydroxyproline in the blood plasma of a TMT-081-bearing rat was kept at a minimal 20 nmol/ml by feeding the rat a 20% casein diet for 4 days. The hydroxyproline pool of the tumor was still moderate, at 130 nmol/g tumor tissue. Thus the basal hydroxyproline pool in at least 1 transplanted tumor was still sensibly higher than that in the induced tumors.

We further compared the amino acid pools in a relatively old, 20-g TMT-081 rat tumor with the pools of its axillary metastasis and pools in normal rat virgin and lactating mammary tissue (table 3). The postpartum mammary sample may be regarded as involuting since the newborn were probably not nursed. The original implantation site was highly necrotic, and the assayed narrow intact periphery was not firm. Nevertheless, the amino acid pool profile was not notably different from that of the 1.5-g nonnecrotic axillary metastasis, and this profile also resembled the profile of the earlier implant sample in table 1. The glutamine pool level was low, close to the plasma level, whereas the other

TABLE 1.—*Levels of selected amino acid pools of transplanted rat mammary tumors*[a]

Amino acid	DMBA-4	Metastasizing tumors		TMT-081	Nonmetastasizing tumors	
		MT-449	SMT-2A		MTW-9B	MT-100
Taurine	25,000±800	4,800	10,200±320	9,200±1,040	8,500±990	3,190±1,070
Asparagine	352±110	170	662±45	661±50	367±16	741±11
Hydroxyproline	104±15	208	279±12	279±24	182±19	329±25
Glutamate	5,400±380	5,400	3,140±284	4,500±490	4,700±294	6,000±134
Glutamine	1,270±198	700	490±12	600±40	4,100±100	3,700±420
Glycine	2,200±500	2,740	4,300±90	4,400±410	5,500±460	7,900±0
Alanine	1,500±177	2,290	2,860±286	3,870±330	3,000±89	5,700±18
Cystathionine	<1	<1	16±13	2±1	680±54	114±6
GABA	8	23	4	6	6	28
β-Alanine	600	<50	50	50	<50	50
Ornithine	89	120	89	73	131	92
Arginine	170	105	131	125	90	218
Tumor weight, g	7.4	0.62	6.1	5.6	2.2	13.5

[a] Values are means (mmol/g tissue) ± SD. A single tumor of each line was harvested from the original implantation site. The whole MT-449 tumor was assayed. For the other tumors, acidic and neutral amino acids were determined in tumor periphery and core samples, and the values were averaged. Basic amino acids were determined only in the tumor peripheries. Animals were fed Purina Laboratory Chow.

nonessential amino acid and hydroxyproline levels were high.

The nonessential amino acid pools were all relatively low in the virgin mammary tissue, but all of them rose during lactation. In all tumor and normal mammary tissue samples, the arginine level was either low or was depleted slightly below plasma levels. Such depletion would be consistent with the vigorous metabolism of arginine and ornithine noted in other species for the production of nonessential amino acids in milk proteins via the ornithine–proline pathway (*14, 15*). There was no evidence of cystathionine or of unusual levels of other nonprotein amino acids in any of the normal rat tissue samples.

In tables 4–6 the free amino acid pools of mouse tumors are compared with those of other tissues. In 2 of 3 spontaneous C3H tumors examined (table 4), the arginine pool was greatly depleted below plasma level. The tumor with the lowest arginine pool also had the highest ornithine level. In an additional experiment, we found the arginine pool levels of 5 spontaneous mammary tumors to be usually depleted, at tumor:whole blood ratios of 1.73, 1.20, 0.67, 0.64, and 0.30.

We also found arginine depletion in the poorly differentiated SMT-F tumor of the DBA/2Ha mouse. At 4 weeks after subcutaneous implantation, the arginine depletion was severe, equaling that in the arginine-destroying organ, the liver, whereas the arginine level was high in the earliest growths (large and small SMT-F tumors, table 5). It is remarkable that at 4 weeks the tumor had accumulated high GABA levels, which is characteristic of neural tissue. In an additional experiment, 6 SMT-F that weighed 0.25–0.9 g at 9 days were found to have small but consistent arginine pool depletions, with tumor-to-plasma ratios of 0.76±0.10 SD. We observed 2 SMT-F of 0.6 and 1.4 g that contained 6 and 34 nmol GABA/g, respectively, and a 3.5-g tumor at 15 days after subcutaneous implant that con-

TABLE 2.—*Levels of selected free amino acid pools of DMBA-induced primary rat mammary tumors*[a]

Amino acid	nmol amino acid/g tissue in tumors					
	#1	#2	#3	#4	#5	Mean ± SD[b]
Taurine	3,180	3,310	5,400	6,000	3,700	4,600±1,130
Asparagine	196	241	304	326	368	310±46
Hydroxyproline	17	49	45	49	44	47±2
Glutamate	2,300	3,800	3,750	4,000	3,800	3,840±100
Glutamine	1,600	1,840	2,440	2,070	2,650	2,250±310
Glycine	1,600	2,670	2,820	2,700	3,500	2,920±340
Alanine	1,110	2,310	2,110	2,110	1,840	2,090±167
Cystathionine	88	230	109	123	131	148±48
GABA	6	4	25	6	7	11±8
β-Alanine		125	450	188	219	246±173
Ornithine	119	55	78	66	56	64±9
Arginine	86	160	210	228	156	189±31
Tumor weight, g	0.16	0.20	0.37	1.1	4.6	

[a] Tumors are arranged in order of increasing size. Tumors #2 and #5 were from the same animal, and the remainder were all from different animals. Animals were maintained on a 20% casein diet. All but the first tumors were examined histologically and were characterized as well-differentiated adenocarcinomas.

[b] Tumor #1 was omitted from the means.

TABLE 3.—*Comparison of amino acid pools in TMT-081 rat mammary tumor implant and metastasis and in normal mammary tissue*

Amino acid	nmol amino acid/g or ml in:[a]					
	TMT-081-bearing Wistar Furth rat[b]				2-day postpartum Sprague-Dawley rat[c]	
	Plasma	Tumor at implant	Tumor at axilla	Mammary (uninvolved)	Plasma	Mammary
Taurine	116	6,700	10,500	2,300	208	2,500
Asparagine	66	430	470	113	116	379
Hydroxyproline	45	244	310	59	28	27
Glutamate	33	3,750	4,400	1,030	81	2,360
Glutamine	390	520	630	430	710	1,880
Glycine	223	2,350	2,950	640	398	830
Alanine	400	2,400	3,000	510	680	920
Cystathionine	1	2	2	1	<0.4	<1
GABA	<0.5	<2	<2	<2	<0.6	<2
β-Alanine	<7	<30	<30	<30	7	90
Ornithine	50	104	80	59	47	60
Arginine	188	153	173	122	183	136

[a] Values are nmol/ml of plasma or per g wet wt of tumor or gland tissue in individual samples.

[b] Animal was fed Purina Laboratory Chow.

[c] Animal was fed Teklad diet.

tained 69 and 126 nmol GABA/g in the tumor periphery and in the more friable interior, respectively. Older tumors contained 300 nmol or more GABA/g. Thus arginine pools were depleted relatively early in the SMT-F and GABA accumulation appeared much later and mainly in the older parts of the tumor.

In the more highly differentiated SMT-S tumor, arginine was not depleted materially at a large tumor size (table 5). In an additional experiment in $CD_{ha}F_1$ females, the SMT-S had depleted tumor-to-plasma arginine ratios of 0.71, 0.50, and 0.72 in 0.3-, 0.4-, and 0.6-g tumors, respectively, and undepleted ratios of 1.05 and 1.10 in 0.5- and 4.0-g tumors, respectively. Thus in this tumor arginine depletion is more characteristic of early growth. SMT-F and SMT-S had high, variable hydroxyproline pools (table 5 and additional data not shown). SMT-F and SMT-S also had slightly elevated glutamine pools, but their significance in these nonmetastasizing tumors is unclear in the absence of metastasizing examples. Cystathionine was present in more than trace quantities in SMT-S and SMT-F, and perhaps even in primary tumors (all nonmetastasizing; tables 4, 5), but it was not present at the levels encountered in the rat tumor counterparts. Cystathionine accumulation may reflect a balance between production and breakdown. Thus in sample 2, table 5, the SMT-F host was slightly cystathioninemic with elevated liver cystathionine, whereas the tumor had lower cystathionine levels than the plasma. β-Alanine, which is low in normal tissues, accumulated at significant-to-high levels in mouse and rat tumors. Taurine accumulated in the slow-growing DMBA-4 rat tumor at an unusually high level characteristic of brain or muscle tissue (*16*). The remaining acid pools were not notably different from those in spleen or liver.

In table 6 we compared the pool profiles of the normal mouse mammary gland without lactation, during lactation, and 2 days after removal of the young (at 11 days postpartum). In the sample taken 2 days after the removal of the young, the breast tissue was centrifuged for 5 minutes at low

TABLE 4.—*Levels of selected free amino acids in plasma and primary tumors of retired C3H mouse breeders*[a]

Amino acid	nmol amino acid/g or ml in mouse[b]					
	1		2		3	
	Tumor	Plasma	Tumor	Plasma	Tumor	Plasma
Taurine	5,400	356	8,400	330	9,300	360
Asparagine	219	66	308	51	195	67
Hydroxyproline	243	65	350	52	159	79
Glutamate	5,300	25	4,900	37	2,060	105
Glutamine	950	700	1,220	630	780	610
Glycine	1,200	174	3,600	360	2,180	480
Alanine	1,870	630	4,900	460	2,230	600
Cystathionine	6	2	6	<1	3	<1
GABA	2	<1	6	<1	4	2
β-Alanine	<50	<20	150	<20	75	<20
Ornithine	97	57	440	184	207	153
Arginine	130	107	47	219	117	210
Tumor weight, g	2.0		0.31		0.51	

[a] The first of the 3 tumors was hemorrhagic. Animals were maintained on Teklad (4% fat) diet.
[b] Values are nmol/ml of blood plasma or per g of tumor tissue in individual samples.

TABLE 5.—*Levels of selected free amino acids in plasma and tissue of SMT mammary tumor-bearing DBA/2Ha hosts*[a]

Amino acid	nmol amino acid/g or ml in mouse[b]						
	1—SMT-F tumor	2—SMT-F				3—SMT-S	
		Tumor	Spleen	Liver	Plasma	Tumor	Plasma
Taurine	8,600	6,700	15,500	19,500	430	17,300	293
Asparagine	199	118	259	150	33	480	65
Hydroxyproline	1,020	153	350	340	47	830	126
Glutamate	5,500	2,170	3,600	2,140	29	5,300	51
Glutamine	1,230	1,040	1,300	4,600	610	1,150	308
Glycine	4,100	3,000	4,400	2,890	350	3,763	357
Alanine	3,300	2,130	2,460	5,600	510	5,280	488
Cystathionine	39	9	5	77	20	31	2
GABA	17	620	10	59	1	17	5
β-Alanine	50	160	<50	<50	<20	160	20
Ornithine	261	379	258	1,090	261	233	176
Arginine	350	66	410	68	190	145	169
Tumor weight, g	0.36	6.0				5.0	

[a] Animals were maintained on Teklad (4% fat) diet.
[b] Values are nmol/ml of blood plasma or per g of tumor or organ tissue in individual samples.

TABLE 6.—*Free amino acid pools of the mouse mammary gland*[a]

Amino acid	nmol amino acid/g or ml in:							
	Virgin mouse		Mouse lactating 7 days		Mouse lactating 12 days		Mammary involuted 2 days	
	Breast	Plasma	Breast	Plasma	Milk	Plasma	Breast, centrifuged	Plasma
Taurine	5,900	285	2,680	285	413	333	680	560
Asparagine	47	38	93	86	25	25	263	66
Hydroxyproline	94	59	740	204	75	38	78	62
Glutamate	820	19	1,730	36	142	24	600	25
Glutamine	990	750	920	530	118	430	850	470
Glycine	690	280	1,600	590	192	135	390	188
Alanine	430	204	2,140	530	120	142	830	580
Cystathionine	<1	<0.3	<1	<0.3	<1	<0.3	<1	<1
GABA	<4	<2	<4	<2	<2	<2	<2	<1
β-Alanine	60	20	60	20	<20	20	121	12
Ornithine	32	49	378	344	23	31	48	111
Arginine	66	113	86	387	40	61	86	163

[a] (BALB/c × $DBA_2HaDD)F_1$ female mice were used; Teklad diet.

temperature to express part of its milk content. Milk has been estimated to comprise three-quarters of the mass of the actively lactating mammary gland and half of the mass after 2 days in involution (*17*). Freshly collected milk itself was depleted in arginine, but it was also low or depleted in almost every other amino acid. In addition to the amino acids shown, the branched chain, aromatic, and sulfur-containing amino acids were virtually abolished in the free form, at levels of 2–17 nmol/ml. Thus most of the free amino acids in the lactating glandular tissue per se must be several times higher than the values shown for the whole gland. The mammary arginine pools were clearly depleted at all stages, most strikingly during active lactation. Arginine breakdown in the rat mammary gland appears to be induced largely during active lactation (*15*), but in the mouse mammary gland, arginine depletion occurred even without milk production. Taurine content appears to be very variable; we observed high levels in the virgin mouse breast. The hydroxyproline pool became extremely high during active lactation. Other nonprotein amino acids were absent or unchanged.

We found all tumors to be virtually collagen-free. This was established from the hydrolysate assays of the proteins of the transplanted tumors DMBA-4, MT-449, TMT-081, MT-100, SMT-F, and SMT-S, of 3 primary DMBA-induced rat mammary tumors, and of 1 spontaneous C3H mammary tumor. Hydroxyproline residues accounted for collagen levels of only 0.1–0.2% of the tumor protein.

DISCUSSION

Intracellular Arginine Pools

Among the most noteworthy characteristics of the free amino acid pools of rodent mammary adenocarcinomas was the observation that arginine pools can be depleted, most commonly in the spontaneous C3H mouse mammary tumor (5/8 tumors). Depletion, comparable to virtual abolition as occurs in the liver, was found in 2 relatively early intact tumors less than 1 cm in diameter and without conspicious hematomatous areas. In transplanted SMT-F and SMT-S, this depletion was most apparent in established but not always in advanced growth. Arginine depletion is not unique to the tumors, because it also occurred in normal mammary tissue, particularly in the mouse, and during active lactation. In mouse mammary tumors the arginine depletion may be accompanied by heightened levels of ornithine, but this is not consistent. Arginine depletion in the mouse mammary tumor cannot be attributed to poor uptake, because of the nonspecificity of the basic amino acid transport system Ly^+ (*18*). The levels of other basic amino acids, lysine and histidine, were the same or up to twice that of the circulating plasma level in the 8 examined spontaneous tumors.

These studies thus show that some tumors can, like the liver, catabolize an amino acid faster than it can be replaced from the plasma. Arginase already present in the normal mammary tissue (*19*), may deplete arginine pools in tumors. Invading macrophages may further contribute high arginase activity as a component of host defense (*20*). In preliminary experiments we found considerable in vitro destruction of arginine in the adherent cells of minced and sieved fragments of a spontaneous C3H mammary tumor, but we found a similar activity in the nonadherent component of the SMT-F transplanted tumor. The differences remain to be resolved. The variable occurrence of spontaneous arginine depletion in mammary adenocarcinomas may explain the contradictory claims for the effectiveness of arginase treatment of these tumors (*21, 22*). Experimental tumors that are already prone to arginine depletion would be the most suitable targets for arginine antagonism, e.g., by canavanine (*23*), or for further arginine depletion by activated macrophages.

GABA and Cystathionine Levels in Rodent Mammary Tumors

GABA and cystathionine, which were found at significant-to-high levels in a number of the mammary tumors, have heretofore been considered virtually unique to neural tissue or neurally derived cells (*7, 8*). We have shown cystathionine pools to be absent at all functional stages in normal rodent mammary tissue. We have found cystathionine to be present in only relatively moderate quantities in rodent brain, at 28 and 140 nmol/g of the cerebrum and cerebellum of the rat, and at 22 and 55 nmol/g in cerebrum and cerebellum of the mouse, respectively. The cystathionine levels in rat mammary tumors are more comparable to the 400-nmol/g level in the mouse C1300 neuroblastoma (Pine MJ: Unpublished results). Cystathionine can also accumulate in plasma or urine from the reduction or loss of γ-cystathionase activity, either from drug treatment, vitamin B_6 depletion, or inborn errors of metabolism (*24*). γ-Cystathionase commonly becomes depleted or absent in tumors (*25*). This depletion, however, would not explain the association of high cystathionine pools only in the nonmetastatic rat mammary tumors. Moreover, cystathionine pools are generally absent (Pine MJ: Unpublished results) in nonneural tumors, such as L1210 leukemia and B-16 melanoma, that also lack γ-cystathionase. Elevated cystathionine in the nonmetastasizing rat tumors may possibly reflect an early disturbance in sulfur amino acid metabolism associated with tumorigenesis.

Cystathioninuria can also be associated with hepatic metastasis (*26*). Hepatic alteration from metastases could thus account for the significantly elevated cystathionine levels in host liver and plasma found in one SMT-F tumor-bearing mouse. Other less specific neural constituents such as taurine and β-alanine also occurred at unusually high levels in individual mammary tumors.

Amino Acid Markers in Rat Tumors

In the rat tumors, metastatic capacity correlated consistently with a low concentration of free glutamine and with a virtual absence of cystathionine. Many rodent tumors can concentrate glutamine to twice the plasma levels or greater (Pine MJ: Unpublished observations). This ability refutes the notion of a general depletion of glutamine pools in tumors indicated by older qualitative assays (*27*). Arginine appeared to be only marginally depleted in the TMT-081 tumor (table 3). In addition, in a TMT-081 tumor-bearing animal on a 20% casein diet the tumor-to-plasma arginine ratio was also found to be slightly depressed at 0.92. The rat mammary tissue, like that of the cow (*14*), may not rely as heavily on arginine metabolism as do other species for the production of the nonessential amino acid residues of milk protein.

Since all the tumors examined were very low in collagen content, the hydroxyproline pools are likely to reflect the relative concentrative activity of the amino acid transport system(s) for imino acids and glycine (*17, 28*). This activity may serve as a distinction between autochthonous and transplanted mammary tumors in the rat. The normal mammary gland may also augment this transport system during lactation. The virtual absence of collagen in the mouse and rat mammary tumors would suggest that mesenchymal cells do not contribute substantially to the amino acid pools determined for these tumors. The presence of some stromal material, however, is not precluded, because the SMT-S was relatively resistant to physical dissociation. The SMT-S may produce some cartilagenous component, but this would probably be a product of the tumor cell per se rather than a structure that involves mesenchymal cell participation.

The intracellular pool of nutrients would be expected to depend on, or to be affected by external supplies. The TMT-081 tumor, taken as representative of metastatic rat mammary tumors, has been found to have a lower rate of blood flow than several nonmetastatic representatives (Jirdle R, Kim U: Unpublished observations). Although the individuality of blood supply might be the underlying reason for some of the differences in intracellular pool sizes, a great dependence might be expected to produce more significant variations than those that are actually apparent in the pool profiles of TMT-081 tumor samples taken either from the tumor center, from the periphery, from intact areas, or from areas adjacent to necrosis (tables 1, 2). Rodent mammary tumors may contain large macrophage populations. In a recent study of macrophage content versus metastatic capacity (*29*), the macrophage content of the MADB-100 nonmetastasizing DMBA-induced rat mammary tumor was found not to differ greatly from that of its metastasizing MADB-105 derivative. The same was seen in other metastasizing and nonmetastasizing tumor pairs (*29*). Thus it is unlikely that changes in the macrophage population would consistently explain the amino acid pool differences that distinguish the metastasizing from the nonmetastasizing rat mammary tumors in tables 1 and 2.

Although free amino acids may be easily liberated artifactually, for example at room temperature, the effect is probably minimal on the reported tumor pool values. Thus variations in harvesting the SMT-F and several other tumors that either shortened the harvest time (e.g., exposure of the tumor periphery during anesthesia and excising of tumor directly into sulfosalicylic acid before weighing) or that prolonged harvest (e.g., 10 min of incubation on ice) produced relatively minor pool alterations. Free amino acid pools have been determined in liver and hepatoma by freezing and grinding the tissues in liquid N_2 before extraction (*29*). We have found that freezing in N_2 produced variable levels of free amino acid, equal to or much greater than those obtained by direct acid inactivation (Pine MJ: Unpublished results). The pools of free amino acids in rat liver obtained by freezing in liquid N_2 reported by Moyer and Pitot (*30*) are much higher than our own pools for liver and other organs. Therefore, N_2 freezing may produce artifacts in pool extraction rather than minimize their chances. Although necrosis might also be expected to liberate free amino acids, the similarity of pools from old and young mammary tumors and from areas adjacent to necrosis would suggest that inflammatory cells and the circulation prevent the accumulation of necrotic products. Samples from the frankly necrotic areas of neuroblastomas have reduced levels of marker amino acids such as cystathionine but without the accompaniment of conspicuous increases in other amino acids (Pine MJ: Unpublished results).

REFERENCES

(*1*) Kelly JJ, Waisman HA. Quantitative plasma amino acid values in leukemic blood. Blood 1957; 12:635-643.

(2) Feldman JM, Plonk JW, Admiraal J, Sidbury JB Jr. Plasma amino acids in patients with the carcinoid syndrome. 1976; Cancer 38:2127–2131.

(3) Zender R, Courvoisier B. Étude comparative des acides amines plasmiques libres dans les cas de tumeurs osseuses malignes et chez les sujets sains. Clin Chim Acta 1970; 27:259–265.

(4) Clarke EF, Lewis AM, Waterhouse C. Peripheral amino acid levels in patients with cancer. Cancer 1978; 42:2909–2913.

(5) Krause R, James JH, Humphrey C, Fischer JE. Plasma and brain amino acids in Walker 256 carcinoma-bearing rats. Cancer Res 1979; 39:3065–3069.

(6) Moyer GH, Pitot HC. Static and dynamic aspects of amino acid pools in rat liver and Morris hepatomas 9618A and 7800. Cancer Res 1974; 34:2647–2653.

(7) Lefauconnier JM, Portemer C, Chatagner F. Free amino acids and related substances in human glial tumors and in fetal brain—comparison with normal adult brain. Brain Res 1976; 117:105–113.

(8) Shibasaki T, Uki J, Kanoh T, Kawafuchi JI: Composition of free amino acids in brain tumors. Acta Neurol Scand 1979; 60:301–311.

(9) Kim U. Factors influencing metastasis of breast cancer. In: McGuire WL, ed. Breast cancer: Advances in research and treatment. Vol 3. New York: Plenum Press, 1979:1–49.

(10) Ip C, Ip M. Serum estrogens and estrogen responsiveness in 7,12-dimethylbenz[*a*]anthracene-induced mammary tumors as influenced by dietary fat. JNCI 1981; 66:291–295.

(11) Pavelic ZP, Porter CW, Allen LM, Mihich E. Cell population kinetics of fast- and slow-growing transplantable tumors derived from spontaneous mammary tumors of the DBA/2HaDD mouse. Cancer Res 1978; 38:1533–1538.

(12) Slocum R. Physiological fluid analysis, single column lithium. Technical Bulletin 12M-005, Beckman Instruments, Inc., 1976.

(13) Siegel S. Nonparametric statistics for the behavioral sciences. New York: McGraw-Hill, 1956:111–127.

(14) Mepham TB, Linzell JL. A quantitative assessment of the contribution of individual plasma amino acids to the synthesis of milk proteins by the goat mammary gland. Biochem J 1966; 101:76–82.

(15) Morris C, Yip Y, Knox WE. Function of arginase in lactating mammary gland. Biochem J 1972; 127:893–899.

(16) Spaeth DG, Schneider DL. Taurine metabolism: Effects of diet and bile salt metabolism. In: Huxtable R, Barbeau A, eds. Taurine. New York: Raven Press, 1976:35–44.

(17) Greenbaum AL, Slater TF. Studies on the particulate components of rat mammary gland. 1. A method for determining the composition of the retained fluid. Biochem J 1957; 66:148–155.

(18) Christensen HN. Recognition sites for material transport and information transfer. In: Bronner F, Kleinzeller A, eds. Current topics in membranes and transport. Vol 5. New York: Academic Press, 1975:227–258.

(19) Herzfeld A, Raper SM. The heterogeneity of arginases in rat tissues. Biochem J 1976; 153:469–478.

(20) Currie GA. Activated macrophages kill tumour cells by releasing arginase. Nature 1978; 273:758–759.

(21) Bach SJ, Swaine D. The effect of arginase on the retardation of tumour growth. Br J Cancer 1965; 19:379–386.

(22) Greenberg DM, Sassenrath EN. Lack of effect of high potency arginase on tumor growth. Cancer Res 1953; 13:709–715.

(23) Mendelsohn J, Howell SB, Brooks TC. Cytotoxic and antitumor activity of canavanine. Am Assoc Cancer Res Abstr 1979:260.

(24) Bremer HJ, Duran M, Kamerling JP, Przyrembel H, Wadman SK. Disturbances of amino acid metabolism: Clinical chemistry and diagnosis. Baltimore: Urban, 1981.

(25) Glode LM, Greene, HL, Bikel I. γ-Cystathionase in normal and leukemic cells. Cancer Treat Rep 1979; 63:1081–1088.

(26) Helson L, Fleisher M, Bethune V, Murphy ML, Schwartz MK. Urinary cystathionine, catecholamine and metabolites in patients with neuroblastoma. Clin Chem 1972; 18:613–615.

(27) Roberts E, Simonsen DG. Free amino acids and related substances in normal and neoplastic tissues. In: Edsall JT, ed. Amino acids proteins and cancer biochemistry. New York: Academic Press, 1960:121–145.

(28) Mohyuddin F, Scriver CR. Amino acid transport in mammalian kidney: Multiple systems for imino acids and glycine in rat kidney. Am J Physiol 1970; 219:1–8.

(29) Talmadge JE, Key M, Fidler IJ. Macrophage content of metastatic and non-metatastic rodent neoplasma. J Immunol 1981; 126:2245–2248.

(30) Moyer GH, Pitot H. Static and dynamic aspects of amino acid pools in rat liver and Morris hepatomas 9618A and 7800. Cancer Res 1974; 34:2647–2653.

blank page

Immunomodulation of the Lymphoresponsive Phases of Carcinogenesis: Mechanisms of Natural Immunity[1,2]

Charles H. Evans,[3,4] **Joseph A. DiPaolo,**[3] **Jeffrey A. Heinbaugh,**[3] *and* **Anthony J. DeMarinis**[3]

ABSTRACT—Biphasic modulation of the frequency of 3-methylcholanthrene-induced tumors in relation to increasing immunocompetence of tumor-bearing mice is indicative of lymphoresponsive stimulatory and inhibitory phases of carcinogenesis; components and mechanisms contributing to the paradoxical ability of the native or natural immune system to stimulate as well as to inhibit the development of cancer were identified with the use of an in vitro model of carcinogenesis. Normal NIH/N Syrian golden hamster spleen leukocytes caused a biphasic modulation of UV-irradiated hamster cell morphologic transformation that was dependent on the leukocyte-to-target cell (L:TC) ratio. Whereas low (<50:1) and high (>200:1) L:TC ratios inhibited the transformation frequency, intermediate ratios were less inhibitory and seemingly immunostimulatory. Inhibition alone occurred with antigen- or mitogen-activated leukocytes or with macrophages. An anticarcinogenic lymphocyte hormone, lymphotoxin, eliminated the leukocyte-mediated stimulatory phase; galactose, a lymphotoxin inhibitor, blocked the leukocyte-mediated inhibitory phases. Thus immunoinhibition was mediated through lymphotoxin, and the apparent immunostimulation possibly resulted from immune cell regulation of lymphotoxin activity during the early stages of carcinogenesis.—JNCI 1982; 69:737–740.

Lymphoresponsive stimulatory and inhibitory phases of carcinogenesis have been postulated because the number of tumors in immunologically crippled mice receiving the carcinogen 3-methylcholanthrene increases and decreases with progressive restoration of the immune capacity of the mice (*1, 2*). The same biphasic response occurs in immunoreconstituted mice that receive skin grafts from 3-methylcholanthrene-treated syngeneic mice (*3*). Thus the lymphoresponsive phases are a result of natural physiologic or homeostatic responses by the host rather than a result of carcinogen-induced systemic effects.

The frequency of carcinogen-induced morphologic transformation in cultured Syrian hamster cells can be quantitated within a week after carcinogen treatment (*4, 5*). UV light irradiation and various chemical carcinogens induce neoplasia as indicated by the ability of the transformed cells to produce tumors (*6, 7*). Transformation, moreover, can be irreversibly inhibited by the immunologic hormone lymphotoxin (a lymphokine) (*8*). In the present investigation, Syrian hamster macrophages, spleen lymphocytes, and/or lymphotoxin were cocultivated with carcinogen-treated target cells to characterize the cellular and soluble mediators modulating carcinogenesis. UV radiation was selected as the carcinogen to minimize effects of the carcinogen on the effector leukocytes. The results provide the first demonstration that the lymphoresponsive phases can occur early in carcinogenesis and that the balance between apparent immunoinhibition or immunostimulation may be mediated through lymphotoxin.

MATERIALS AND METHODS

Carcinogen-induced transformation of hamster cells.—In the quantitative HEC transformation assay, secondary culture cells derived from 13-day-gestation NIH/N Syrian golden hamster fetuses were seeded at a density of 300 cells/60-mm tissue culture dish in 4 ml D-EMEM containing 10% FBS (*9*) and 25 μg endothelial cell growth supplement (Collaborative Research Inc., Waltham, Mass.) (*10*). One day later, the cells were treated by UV irradiation and incubated in 8-ml medium–serum for 6 additional days. Dishes were fixed and stained and colonies counted and microscopically evaluated for transformed morphology. The cloning efficiency was the ratio of the colonies greater than 2 mm in diameter, and the number of cells plated was expressed as a percentage. Details regarding the administration of UV radiation to the cells were given by DiPaolo and Donovan (*7*).

Addition of leukocytes and lymphotoxin to the transformation assay.—We obtained freshly prepared spleen leukocytes from 4- to 6-month-old healthy male NIH/N Syrian golden hamsters [some having KLH immunity (*8*) and some nonimmunized] by gently teasing spleens to obtain single cell suspensions. We then washed the leukocytes with RPMI-1640 medium, and filtered them through gauze. Alveolar macrophages were obtained by bronchial lavage with 50 ml RPMI-1640 medium per hamster, washed in 50 ml RPMI-1640 medium, and cultured during the transformation assay in the presence of 50 μg gentamicin/ml D-EMEM. Peritoneal macrophages were obtained from mineral oil-induced peritoneal leukocytes (*11*). Peritoneal leukocytes were collected by lavage with 50 ml RPMI-1640 medium per hamster and cultured for 30 minutes in RPMI-1640 medium–10% FBS; the adherent cells were removed with a rubber policeman, washed two times with RPMI-1640 medium, counted, and suspended in D-EMEM. The leukocytes were added to HEC immediately after irradiation, and D-EMEM was adjusted to 8 ml. The antigen KLH at 100 μg/ml was

---

ABBREVIATIONS USED: D-EMEM=Dulbecco's modified Eagle's minimum essential medium; FBS=fetal bovine serum; HEC=hamster embryo cell(s); KLH=keyhole limpet hemocyanin; PHA=phytohemagglutinin.

---

[1] Received January 19, 1982; accepted April 13, 1982.

[2] Animals were maintained under the guidelines set forth by the National Institutes of Health Policy on Humane Care and Use of Animals and by the Animal Welfare Act.

[3] Laboratory of Biology, Division of Cancer Cause and Prevention, National Cancer Institute, National Institutes of Health, Public Health Service, U.S. Department of Health and Human Services, Bethesda, Md. 20205.

[4] *Address reprint requests to* Dr. Evans, Building 37, Room 2A17, National Institutes of Health, Bethesda, Md. 20205.

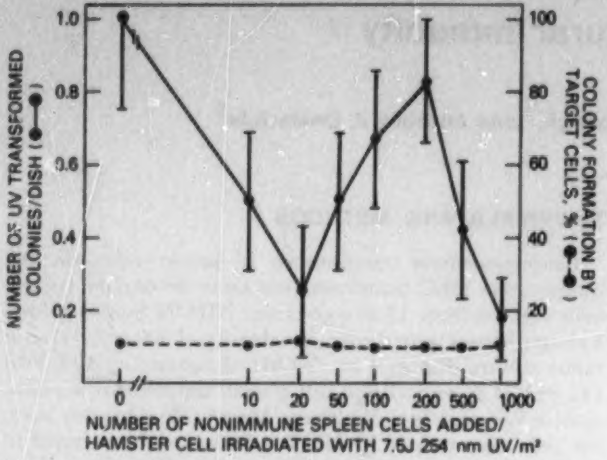

TEXT-FIGURE 1.—Inhibition of carcinogen-induced morphologic transformation ± SEM of Syrian HEC by normal spleen leukocytes. Cells (300) were seeded/60-mm dish in 4 ml D-EMEM containing 10% FBS and 25 µg endothelial cell growth supplement/ml and treated by UV irradiation 24 hr later. Freshly prepared spleen leukocytes from 4- to 6-mo-old male nonimmunized healthy NIH/N Syrian golden hamsters were added to the embryo cells immediately after irradiation, and the culture medium was adjusted to 8 ml. Cells were fixed and stained 7 days after seeding, and the colonies were counted and examined for morphologic transformation.

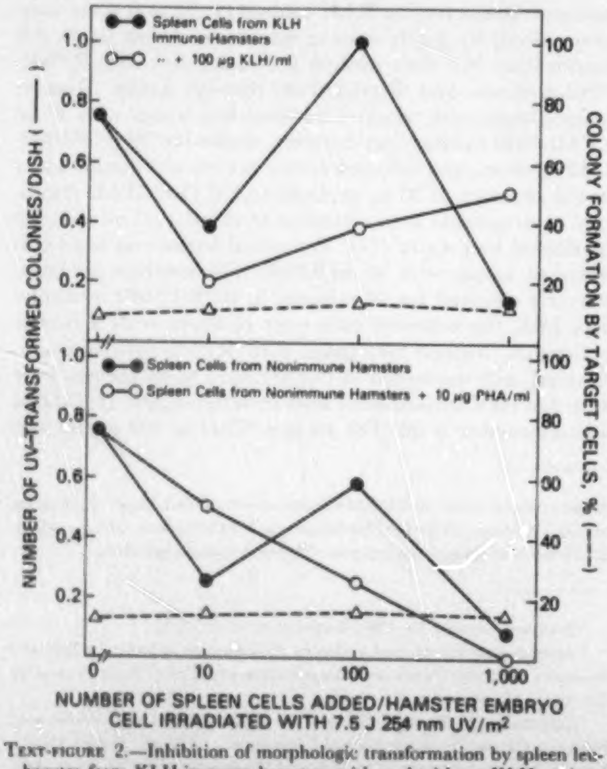

TEXT-FIGURE 2.—Inhibition of morphologic transformation by spleen leukocytes from KLH-immune hamsters with and without KLH antigen stimulation and by nonimmune leukocytes with and without mitogen (PHA) stimulation. Transformation assay was performed as described in text-fig. 1.

included in some KLH-immune spleen leukocyte–HEC cultures. The mitogen PHA at 10 µg/ml was added to some nonimmune spleen leukocyte–HEC cultures. Cells were fixed and stained 7 days after they were seeded and the colonies were counted and examined for morphologic transformation. Lymphotoxin free of detectable interferon antiviral activity was obtained from mitogen-stimulated hamster peritoneal leukocytes, was concentrated by diafiltration with the use of a YM10 membrane, and was added to the HEC immediately after irradiation (8). In each experiment, 12 dishes were set up for each carcinogen, leukocyte, chemical, and/or lymphotoxin concentration.

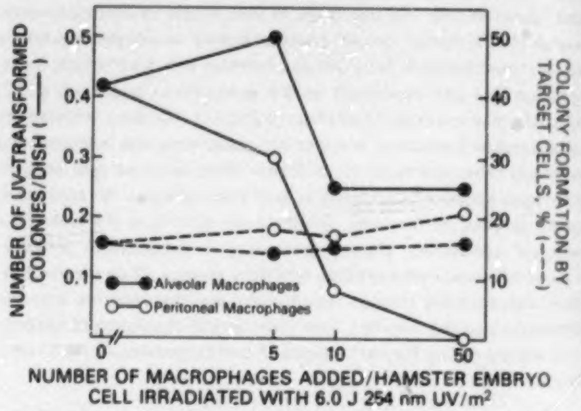

TEXT-FIGURE 3.—Inhibition of morphologic transformation by alveolar and peritoneal macrophages from nonimmune hamsters. Transformation assay was performed as described in text-fig. 1.

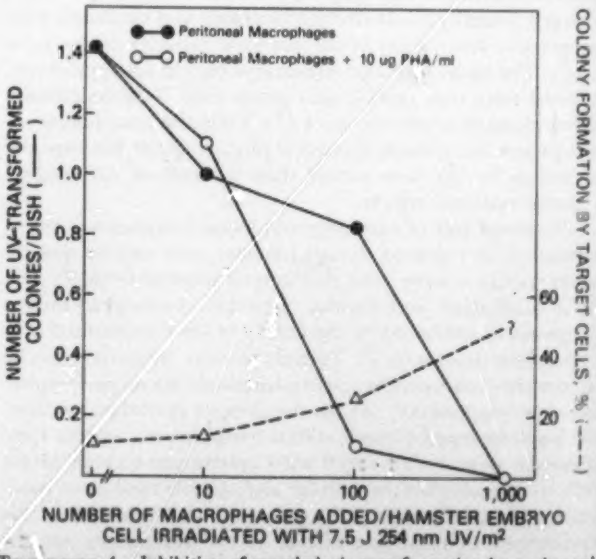

TEXT-FIGURE 4.—Inhibition of morphologic transformation by peritoneal macrophages from nonimmune hamsters with and without mitogen stimulation. Transformation assay was performed as described in text-fig. 1. *Question mark* indicates that colonies were too numerous to quantify accurately due to the macrophages serving as a feeder layer at the 1,000:1 effector-to-target cell ratios.

RESULTS

The addition of normal nonstimulated hamster spleen leukocytes to UV-irradiated hamster fibroblasts at effector-to-target cell ratios from 10:1 to 1,000:1 resulted in a biphasic modulation of the transformation frequency of UV-irradiated hamster fibroblasts (text-fig. 1). Transformation frequency was reduced at ratios less than 50:1, approached the UV irradiation only level at ratios approximately 50:1–200:1, and was reduced again at higher effector-to-target cell ratios. Spleen leukocyte modulation of the transformation frequency occurred without cell lethality since the number of colonies was independent of the number of leukocytes. Alteration of the transformation but not the colony-forming frequency demonstrated the specificity of the lymphomodulation for carcinogenesis.

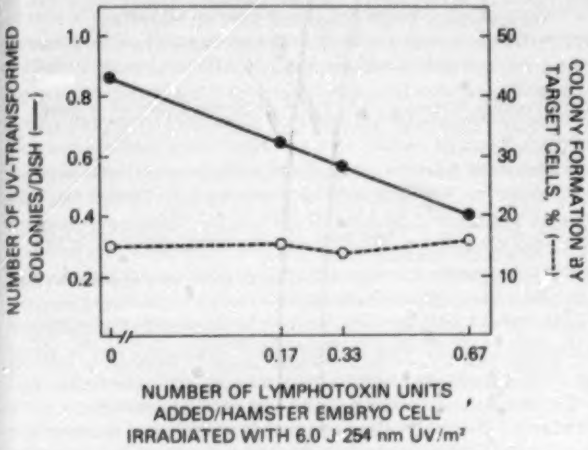

TEXT-FIGURE 5.—Inhibition of morphologic transformation by lymphotoxin. Transformation assay was performed as described in text-fig. 1.

TABLE 1.—*Modulation of normal spleen cell anticarcinogenic activity*

Treatment[a]	Absolute No. of transformed colonies/dish
UV radiation alone	2.1
UV radiation + galactose	1.8
UV radiation + lymphotoxin	0.6[b]
UV radiation + 100:1 spleen cells	1.1[b]
UV radiation + 100:1 spleen cells + galactose	2.1[c]
UV radiation + 100:1 spleen cells + lymphotoxin	0.2[b, c]
UV radiation + 200:1 spleen cells	1.4
UV radiation + 200:1 spleen cells + galactose	1.9
UV radiation + 200:1 spleen cells + lymphotoxin	0.3[b, d]

[a] HEC were UV irradiated with 4.5 J/m² and treated with nonimmune spleen leukocytes as described in text-fig. 1. Galactose (1 μ*M*), an inhibitor of lymphotoxin activity, and lymphotoxin (0.3 U/cell) were also included in the assay at the time of spleen cell addition for determination of the extent of participation of lymphotoxin in the biphasic inhibition of transformation. Results are shown for the maximum inhibitory (100:1) and stimulatory (200:1) effector-to-target cell ratios in the experiment.

[b] $P<0.05$ compared to value for UV irradiation alone, by Student's *t*-distribution two-tailed test.

[c] $P<0.05$ compared to value for UV irradiation + 100:1 administered spleen cells, by Student's *t*-distribution two-tailed test.

[d] $P<0.05$ compared to UV irradiation + 200:1 administered spleen cells, by Student's *t*-distribution two-tailed test.

Antigen or mitogen stimulation of spleen leukocytes eliminated the stimulatory phase (text-fig. 2). This suggested that the stimulatory phase was mediated through lymphocytes. This hypothesis was confirmed by macrophage modulation of the transformation frequency inasmuch as only the inhibitory phase was observed in the presence of macrophages (text-figs. 3, 4). The addition of lymphotoxin, a lymphokine that directly inhibits transformation (text-fig. 5), eliminated the immunostimulatory phase (table 1). However, galactose, a critical sugar in the glycopeptide receptor to which lymphotoxin binds (*12*), blocked the inhibitory but not the stimulatory phase (table 1). Thus: 1) Inhibition was mediated through lymphotoxin, 2) the lymphostimulatory phase resulted from modulation of lymphotoxin activity, and 3) both lymphoresponsive inhibitory and stimulatory phases were present early in carcinogenesis.

DISCUSSION

The components contributing to the lymphoresponsive phases of primary autochthonous tumor growth (*1–3*) have been cryptic as has been the carcinogenic stage(s) affected by these homeostatic responses. This is partly due to the complexity of carcinogenesis, which proceeds through many stages commencing with carcinogen exposure and culminating with the appearance of an observable tumor (*13*). During neoplastic development a multiplicity of immunobiologic alterations capable of eliciting a host response can occur at the level of the developing tumor or target cell, including antigen formation, alteration and/or deletion (*14*), and susceptibility to natural leukocyte (*15–17*) and lymphokine cytotoxicity (*18*). Some of these changes can develop very early and others quite late during carcinogenesis. For example, neoantigens have been detected as early as 18 hours after 3-methylcholanthrene exposure (*19*), whereas development of susceptibility to the growth inhibitory activity of lymphotoxin may require many months (*18*). Growth of tumor cells may also be stimulated by normal naturally or specifically immune lymphocytes, possibly due to the presence of fetal antigens or undefined components on the tumor cells (*20–22*).

Immune regulation is a complex interaction or balance among helper, suppressor, and natural cytotoxic and killer leukocytes (*23, 24*), lymphokines (*25*), and other hormone regulators (*26*). UV irradiation, for example, both induces neoplasia and enhances suppressor leukocyte activity, thus permitting the growth of highly antigenic tumors (*27, 28*). Corticosteroids are immunoinhibitory and can also directly modulate carcinogenesis at the level of the target cell (*29*). Interferon stimulates natural killer cell activity while it decreases target cell sensitivity to natural killer destruction (*30*). Interferon can inhibit carcinogenesis (*31*), but it can also stimulate morphologic transformation of the murine C3H/10T½ cell line (*32*). Lymphotoxin, in contrast, has little or no effect on the tumor inhibitory activity of macrophages, killer lymphocytes, or other naturally cytotoxic lymphocytes (*11*), but it increases target cell sensitivity during carcinogenesis to natural killer cell destruction (*33*), reversibly inhibits growth of most tumor cells (*11, 34*), and irreversibly inhibits carcinogen-induced morphologic transformation (*8*). Therefore, many points or stages in carcinogenesis are subject to homeostatic control by the normal immune system, and the apparent immunostimulation of the lymphoresponsive phases of carcinogenesis in vivo may reflect in part the immunomodulation of lymphotoxin.

REFERENCES

(*1*) Prehn RT. The immune reaction as a stimulator of tumor growth. Science 1972; 176:170–171.

(*2*) ———. Guest editorial. Immunostimulation of the lymphodependent phase of neoplastic growth. J Natl Cancer Inst 1977; 59:1043–1049.

(*3*) Outzen HC. Development of carcinogen-induced skin tumors in mice with varied states of immune capacity. Int J Cancer 1980; 26:87–92.

(*4*) Berwald Y, Sachs L. In vitro transformation of normal cells to tumor cells by carcinogenic hydrocarbons. J Natl Cancer Inst 1965; 35:641–661.

(*5*) DiPaolo JA, Donovan P, Nelson R. Quantitative studies of in vitro transformation by chemical carcinogens. J Natl Cancer Inst 1969; 42: 867–874.

(*6*) DiPaolo JA, Nelson RL, Donovan PJ. Morphological, oncogenic, and karyological characteristics of Syrian hamster embryo cells transformed in vitro by carcinogenic polycyclic hydrocarbons. Cancer Res 1971; 31:1118–1127.

(*7*) DiPaolo JA, Donovan FJ. In vitro morphological transformation of Syrian hamster cells by UV-irradiation is enhanced by X-irradiation and unaffected by chemical carcinogens. Int J Radiat Biol 1976; 30:41–53.

(*8*) Evans CH, DiPaolo JA. Lymphotoxin: An anticarcinogenic lymphokine as measured by inhibition by chemical carcinogen or ultraviolet-irradiation-induced transformation of Syrian hamster cells. Int J Cancer 1981; 27:45–49.

(*9*) DiPaolo JA. Quantitative in vitro transformation of Syrian golden hamster embryo cells with the use of frozen stored cells. J Natl Cancer Inst 1980; 64:1485–1489.

(*10*) Evans CH, DiPaolo JA. Equivalency of endothelial cell growth supplement to irradiated feeder cells in carcinogen-induced morphological transformation of Syrian hamster embryo cells. JNCI 1982; 68:127–131.

(*11*) Evans CH. The role of lymphotoxin in natural cell-mediated cytotoxicity. Cell Immunol 1981; 62:1–15.

(*12*) Kobayashi Y, Sawada J, Osawa T. Isolation and characterization of an inhibitory glycopeptide against guinea pig lymphotoxin from the surface of L cells. Immunochemistry 1978; 15:61–66.

(*13*) Berenblum I. Carcinogenesis as a biological problem. Amsterdam and Oxford: Elsevier/North-Holland, 1974.

(*14*) Baldwin RW. Immunological aspects of chemical carcinogenesis. Adv Cancer Res 1973; 18:1–76.

(*15*) Cudkowicz G, Hochman PS. Do natural killer cells engage in regulated reactions against self to ensure homeostasis? Immunol Rev 1979; 44:13–41.

(*16*) Herberman RB, Djeu JY, Kay HD, et al. Natural killer cells: Characteristics and regulation of activity. Immunol Rev 1979; 44:43–70.

(*17*) Zwilling BS, Meltzer MS, Evans CH. Differential cytotoxicity of tumorigenic and nontumorigenic strain-2 guinea pig cells as mediated by syngeneic phytohemagglutinin-stimulated peritoneal exudate cells. J Natl Cancer Inst 1975; 54:743–747.

(*18*) Evans CH, Rabin ES, DiPaolo JA. The susceptibility of guinea pig cells to the colony-inhibitory activity of lymphotoxin during carcinogenesis. Cancer Res 1977; 37:898–903.

(*19*) Embleton MJ, Baldwin RW. Tumour-related antigen specificities associated with 3-methylcholanthrene-treated rat embryo cells. Int J Cancer 1979; 23:840–845.

(*20*) Medina D, Heppner G. Cell-mediated "immunostimulation" induced by mammary tumour virus-free BALB/c mammary tumours. Nature 1973; 242:329–330.

(*21*) Fidler IJ. In vitro studies of cellular-mediated immunostimulation of tumor growth. J Natl Cancer Inst 1973; 50:1307–1312.

(*22*) Prehn LM. Immunostimulation of highly immunogenic target tumor cells by lymphoid cells in vitro. J Natl Cancer Inst 1976, 56:833–838.

(*23*) Broder S, Waldmann TA. The suppressor-cell network in cancer. N Engl J Med 1978; 299:1281–1284 and 1335–1341 (parts I and II, respectively).

(*24*) Hellström KE, Hellström I. Cell-mediated suppression of tumor immunity has a non-specific component. I. Evidence from transplantation tests. Int J Cancer 1981; 27:481–485.

(*25*) Cohen S, Pick E, Oppenheim JJ, eds. Biology of the lymphokines. New York: Academic Press, 1979.

(*26*) Hadden JW, Coffey RG, Spreafico F, eds. Immunopharmacology. New York: Plenum Press, 1977.

(*27*) Daynes RA, Spellman CW. Evidence for the generation of suppressor cells by ultraviolet irradiation. Cell Immunol 1977; 31:182–187.

(*28*) Fisher MS, Kripke ML. Systemic alteration induced in mice by ultraviolet light irradiation and its relationship to ultraviolet carcinogenesis. Proc Natl Acad Sci USA 1977; 74:1688–1692.

(*29*) Evans CH, Greiner JW. Corticosteroid prevention of carcinogenesis in benzo[*a*]pyrene or ultraviolet irradiation-treated Syrian hamster cells in vitro. Cancer Lett 1981; 12:23–27.

(*30*) Trinchieri G, Santoli D. Anti-viral activity induced by culturing lymphocytes with tumor-derived or virus-transformed cells. Enhancement of human natural killer cell activity by interferon and antagonistic inhibition of susceptibility of target cells to lysis. J Exp Med 1978; 147:1314–1333.

(*31*) Gresser I. Antitumor effects of interferon. *In* Becker FF, ed. Cancer: A comprehensive treatise. Vol 5. New York: Plenum Press, 1977:521–571.

(*32*) Brouty-Bové D, Little JB. Enhancement of X-ray-induced transformation in C3H/10T½ cells by interferon. Cancer Res 1977; 37:2714–2716.

(*33*) Ransom JH, Evans CH. Lymphotoxin enhances the susceptibility of neoplastic and preneoplastic cells to natural killer cell mediated destruction. Int J Cancer 1982; 29:451–458.

(*34*) Evans CH, Heinbaugh JA. Lymphotoxin cytotoxicity, a combination of cytolytic and cytostatic cellular responses. Immunopharmacology 1981; 3:347–359.

Lymphotoxin Prevention of Diethylnitrosamine Carcinogenesis In Vivo[1,2]

Janet H. Ransom,[3,4] Charles H. Evans,[3] *and* Joseph A. DiPaolo[3]

ABSTRACT—Development of intervention measures to control cancer would be facilitated by being able to monitor in vivo carcinogenesis by in vitro quantitation of early indices of neoplastic transformation to assess the in vivo effectiveness of preventative–therapeutic measures. Pregnant Syrian golden hamsters were used in an in vivo–in vitro transplacental model of carcinogenesis to determine the extent that in vivo administration of immunologic hormone preparations along with chemical carcinogen would prevent morphologic transformation assessed in vitro. Pregnant hamsters at 10–11 days of gestation were given injections ip of 3 mg diethylnitrosamine (DENA)/100 g body weight and were killed 2 days later when fetal cells were seeded for colony formation. The frequency of morphologically transformed colonies was assessed after 7 days of growth. Cloning efficiency and mean transformation frequency after DENA exposure were 3.6% and 1×10^{-4} per cell seeded, respectively. The ip injection of an immunologic hormone preparation reduced the transformation frequency by 46%. The hormone preparation, containing 10,000 U of lymphotoxin but no detectable interferon, was the ultrafiltered lymphokines (>10,000 mol wt) from phytohemagglutinin-stimulated hamster peritoneal leukocytes. The effect of lymphotoxin on cocarcinogenic exposure of fetal cells to DENA in vivo followed by X-irradiation in vitro was also determined. Cells exposed to 250 rad in vitro had a cloning efficiency of 0.5% and a transformation frequency of 0.4×10^{-4} per cell seeded. After DENA injection and X-irradiation, the transformation frequency increased to 1×10^{-4} and was inhibited 64% by lymphotoxin in vivo. Thus immunologic hormones (e.g., lymphotoxin) can prevent carcinogenesis in vivo. Furthermore, in vitro quantitation of transformation is a rapid means for evaluating therapeutic and autochthonous effector mechanisms for their ability to prevent or otherwise modulate carcinogenesis in vivo.—JNCI 1982; 69:741–744.

Cancer prevention may be achieved by active intervention at various stages during the carcinogenic process to prevent and/or reverse the development of neoplasia (*1*). Intervention measures, exclusive of those eliminating the causative agent, include control of carcinogen metabolism (*2, 3*) and suppression of preneoplastic cells by immunologic (*4–7*), hormonal (*8, 9*), and nutritional (*10*) factors. One type of immune mediator, the immunologic hormones (including lymphokines, monokines, interleukins, and interferons) is of particular interest as an anticarcinogenic agent inasmuch as these hormones have or mediate antitumor activity in vivo (*11–13*) and anticarcinogenic activity in vitro (*14–16*).

Two immunologic hormones with direct-acting anticarcinogenic activity are lymphotoxin (*14, 17*) and interferon (*16, 18*). Lymphotoxin may be either cytolethal or cytostatic for tumor cells (*19*), can irreversibly prevent carcinogenesis in vitro without inhibiting cell growth (*14*), and can induce a heightened susceptibility in preneoplastic and neoplastic cells to natural killer cell-mediated cytotoxicity (*20*). In this investigation lymphotoxin was administered with a chemical carcinogen in vivo for evaluation of lymphotoxin anticarcinogenic activity in vivo. A combined in vivo–in vitro method utilizing transplacental DENA exposure of pregnant Syrian golden hamsters was selected for assessment of the in vivo anticarcinogenic activity of lymphotoxin. This method was chosen because the effects of in vivo carcinogen exposure can be rapidly quantitated by measurement of morphologic transformation in vitro (*21, 22*). DENA, a known transplacental carcinogen in hamsters, causes the progeny to develop respiratory tract tumors (*23*). In the combined in vivo–in vitro assay, carcinogen-exposed fetal cells are subpassaged and plated for colony formation. Morphologically transformed colonies result that, when isolated, produce tumors in Syrian hamsters and athymic nude mice (*21, 22, 24*). Thus the extent to which lymphotoxin prevents carcinogenesis in vivo was determined by in vitro measurement of morphologic transformation of cells that had been exposed transplacentally to lymphotoxin and DENA.

MATERIALS AND METHODS

Combined in vivo–in vitro carcinogenesis assay.—Pregnant NIH/N Syrian golden hamsters at days 10–11 of gestation received ip injections of 3 mg DENA/100 g body weight (*21, 22*). Two days later fetuses were excised, the heads and viscera were removed, and the carcasses were mechanically minced and dissociated into a single cell suspension by trypsinization (*25*). Then 2,000 cells were seeded per 60-mm tissue culture dish in 8 ml of modified Dulbecco's medium containing 10% fetal bovine serum, 3×10^{-6} *M* thymidine, 3×10^{-5} *M* hypoxanthine (Calbiochem-Behring Corp., La Jolla, Calif.), and 50 µg endothelial cell growth supplement/ml (Collaborative Research Inc., Waltham, Mass.) (*26*). Cells were incubated 7 days for colony formation at 37°C in a 10% CO_2–water-saturated atmosphere of compressed air purified by PHARM-AIR (Pall Trinity Micro Corp., Cortland, N.Y.). Colonies were fixed in methanol, stained with Giemsa, enumerated on an Artek model 880 counter (Artek Systems Corp., Farmingdale, N.Y.), and examined micro-

---

ABBREVIATION USED: DENA=diethylnitrosamine.

---

[1] Received February 3, 1982; accepted May 5, 1982.

[2] Animals were maintained under the guidelines set forth by the National Institutes of Health Policy on Humane Care and Use of Animals and by the Animal Welfare Act.

[3] Laboratory of Biology, Division of Cancer Cause and Prevention, National Cancer Institute, National Institutes of Health, Public Health Service, U.S. Department of Health and Human Services, Bethesda, Md. 20205.

[4] *Address reprint requests to* Dr. Ransom, Building 37, Room 2A19, National Institutes of Health, Bethesda, Md. 20205.

scopically for morphologic transformation, a random piled-up layering of cells not observed in non-carcinogen-exposed cells (*21, 26*). For each experimental treatment 120 dishes were examined and quantitated. For some experiments 2×10^6 fetal cells suspended in 2 ml of medium/100-mm dish were X-irradiated with 250 rad, immediately before being seeded, with a Torex model 120 X-ray machine (Torr X-ray Corp., Van Nuys, Calif.) (*15*). After X-irradiation 9×10^3 cells were seeded per 60-mm dish.

Lymphotoxin preparation, assay, and in vivo administration.— Lymphotoxin was prepared by incubation of 10^7 Syrian hamster mineral oil-induced peritoneal leukocytes (*14*) in RPMI-1640 medium containing 100 µg phytohemagglutinin/ml (*7*). After 24 hours the cell-free medium was collected, aseptically diafiltered against phosphate-buffered saline, and concentrated tenfold with an Amicon diafiltration apparatus with a 10,000 nominal molecular weight including YM10 membrane (Amicon Inc., Danvers, Mass.). The number of lymphotoxin units was determined by a radionuclide released assay in which 1 U of lymphotoxin caused the release of 50% of the ^{3}H from [^{3}H]thymidine-labeled murine αL929 cells (*19*).

Lymphotoxin preparations did not contain detectable levels of interferon as assayed by Bio-Fluids, Inc., Rockville, Md., with the use of a semimicrocytopathic effect-reading method (*27*) in which interferon units represented the dilution causing a 50% inhibition of bovine vesicular stomatitis virus cytopathic effect in a benzo[*a*]pyrene-transformed Syrian hamster cell line (*14*). The sensitivity of this assay is 5 interferon units.

The anticarcinogenic activity of lymphotoxin preparations administered in vivo was determined by inhibition of morphologic transformation. At the time of DENA injection, pregnant hamsters were also given 10,000 U of lymphotoxin in 0.5 ml ip or 500 U in 0.1 ml iv. Concentrated lymphotoxin preparations at 20,000–30,000 U lymphotoxin/ml were diluted with phosphate-buffered saline to deliver the appropriate dose. Four different preparations were used.

RESULTS

Fetal cells from individual normal hamsters were seeded at various densities to determine the optimal number of colonies for examination. For each dish 60–90 colonies were desired, and with 2,000 cells per dish 70–80 colonies ordinarily result. When cells from 4 normal hamsters were seeded at this density, only nontransformed colonies were observed.

When fetal cells were exposed transplacentally to DENA, the average transformation frequency and cloning efficiency for 13 pregnant hamsters were 1.0×10^{-4} transformants/cell seeded and 3.6%, respectively (table 1). Cells from nontreated animals had the same cloning efficiency as did those from carcinogen-treated animals. An average of 23 total transformants in 120 dishes examined from each DENA-treated animal was observed. This number is sufficiently large and reproducible (an SEM of 1.3) to allow for detection of significant differences in the transformation frequency produced by in vivo intervention measures.

TABLE 1.—*Morphologic transformation frequency of Syrian hamster cells exposed transplacentally to DENA*[a]

Animal No.	Cloning efficiency, %	Total transformants/120 dishes	Transformants/colony, $\times10^{-3}$	Transformants/cell seeded, $\times10^{-4}$
81-11	4.2	26	2.6	1.1
81-12	4.2	19	1.9	0.8
81-13	3.5	28	3.3	1.2
81-14	3.5	17	2.0	0.7
81-15	3.2	21	3.0	0.9
81-16	3.8	19	2.3	0.8
81-17	2.4	24	3.5	1.0
81-18	4.4	20	1.9	0.8
81-19	3.5	18	2.2	0.7
81-20	3.5	29	3.4	1.2
81-22	3.8	18	2.0	0.7
81-32	4.0	30	3.4	1.2
81-35	3.7	29	3.2	1.2
Mean ± SE	3.6±0.23	23±1.3	2.7±0.2	1.0±0.05

[a] Pregnant hamsters at 10–11 days of gestation were given ip injections of 3 mg DENA/100 g body wt 2 days before fetuses were removed and trypsinized, and 2,000 cells were seeded per 60-mm dish.

The in vivo treatment of hamsters ip with 10,000 U or iv with 500 U of lymphotoxin simultaneously with DENA exposure resulted in 43 and 26% inhibition of the transformation frequency, respectively (table 2). The similarities in cloning efficiencies indicate that the reduction of the transformation frequency was not due to a decrease in colony formation.

The cocarcinogenic exposure of cells to DENA in vivo and X-irradiation in vitro was examined to determine whether combined treatment would enhance the transfor-

TABLE 2.—*Lymphotoxin in vivo inhibition of DENA-induced morphologic transformation*[a]

Animal No.	Total transformants/120 dishes	Transformants/cell seeded, $\times10^{-4}$	Inhibition, %[b]
Expt I—10,000 U lymphotoxin ip			
81-21	10	0.4	
81-23	13	0.5	
81-25	7	0.3	
81-30	16	0.7	
81-31	17	0.7	
Mean ± SE	13±1.9	0.5±0.1	47±18
Expt II—500 U lymphotoxin iv			
81-36	16	0.7	
81-37	18	0.8	
Mean ± SE	17±1.0	0.7±0.04	26±5

[a] Pregnant hamsters at 10–11 days of gestation were given simultaneously ip injections of 3 mg DENA/100 g body wt and either ip injections of 10,000 U of lymphotoxin in expt I or iv injections of 500 U of lymphotoxin in expt II. Two days later fetuses were removed and trypsinized, and 2,000 cells were seeded into 60-mm dishes.

[b] Determined by dividing the mean total transformants of lymphotoxin plus DENA-treated hamsters by the mean total transformants of DENA-injected hamsters (as shown in table 1) and multiplying by 100%. $P<0.05$ by Student's *t*-test (two-tailed) and by comparison of data from table 1 with those in table 2 by the Wilcoxon two-sample analysis after testing for significance by the Kruskal-Wallis nonparametric analysis of variance (*28*).

TABLE 3.—*Lymphotoxin inhibition in vivo of morphologic transformation induced by cocarcinogenic exposure to DENA and X-ray*

Treatment[a]	Animal No.	Total transformants/120 dishes	Transformants/cell seeded, $\times10^{-4}$	Inhibition, %
X-irradiation	81-34	38	0.4	
	81-40	54	0.5	
Mean ± SE		46±7.9	0.4±0.1	
Lymphotoxin + X-irradiation	81-65	44	0.4	
	81-66	60	0.6	
Mean ± SE		52±8.1	0.5±0.1	None[b]
DENA + X-irradiation	81-32	96	1.8	
	81-33	90	0.8	
	81-35	84	0.8	
Mean ± SE		90±3.5	1.1±0.3	
DENA + lymphotoxin + X-irradiation	81-30	26	0.2	
	81-31	37	0.3	
Mean ± SE		32±5.6	0.31±0.05	64±5[c]

[a] The 4 treatment groups consisted of hamsters at 10-11 days of gestation either untreated or given injections ip of 10,000 U of lymphotoxin, 3 mg DENA/100 g body wt, or both lymphotoxin and DENA. Two days later fetuses were removed, trypsinized, and X-irradiated with 250 rad, and 9,000 cells were seeded per 60-mm dish.

[b] Compared to X-irradiation.

[c] Compared to DENA + X-irradiation; $P<0.05$ by Student's *t*-test.

mation frequency and the extent to which lymphotoxin would prevent this transformation (table 3). When fetal cells were exposed to 250 rad of X-irradiation alone in vitro, the cloning efficiency was reduced to 0.5%. However, when 9×10^3 cells were seeded per dish, an equivalent number of colonies resulted as in the DENA experiments. X-irradiation alone at the time of cell seeding induced a transformation frequency of 0.4×10^{-4}/cell seeded, which was unaffected by 10,000 U of lymphotoxin ip 2 days before X-irradiation. With DENA plus X-irradiation the transformation frequency increased to 1×10^{-4} compared to that seen in cells only X-irradiated. This cocarcinogenic exposure was inhibited 64% by in vivo ip administration of 10,000 U of lymphotoxin. After lymphotoxin the transformation frequency was similar to that observed following exposure of cells to lymphotoxin and X-irradiation or to X-irradiation alone (table 3).

DISCUSSION

This investigation demonstrates two important points: *a*) Lymphotoxin is anticarcinogenic in vivo and *b*) the efficacy of potential in vivo modulators of carcinogenesis may be evaluated by in vitro measurement of morphologic transformation. The immunologic hormone preparation that inhibited carcinogenesis in this study contained lymphotoxin but no detectable interferon. Of the other possible lymphokines present, only lymphotoxin has been identified individually to be anticarcinogenic (*17*). Hamster lymphotoxin has been shown to inhibit chemical-induced and UV radiation-induced carcinogenesis in vitro (*14, 15*). Hamster lymphotoxin purified by isoelectric focusing was also anticarcinogenic in vitro, which provided additional evidence that the direct-acting anticarcinogenic activity is due to lymphotoxin (*15*).

In vivo administration of hamster lymphotoxin purified by isoelectric focusing also inhibits γ-irradiation-induced transformation, as assessed by measurement of morphologic transformation with inhibition varying directly with lymphotoxin concentration (*29*). Future investigations will be required to determine if other lymphokines also possess direct and/or indirect anticarcinogenic activities in vivo. If other lymphokines with anticarcinogenic activity are present in hamster lymphotoxin preparations, they have isoelectric pH's, stability upon storage, and fractionation characteristics similar to those of hamster lymphotoxin.

Most animal models for carcinogenesis require carcinogen treatment followed by monitoring of tumor development, a process extending from months to years. Therefore, the use of the rapid quantitative system described herein is an invaluable addition to protracted in vivo assays for identification of substances–effectors and for determination of the optimal conditions for their anticarcinogenic activity. Expression of morphologic transformation correlates with the neoplastic potential of cells, inasmuch as cells derived from isolated transformed colonies produce tumors when these cells are injected into hamsters or athymic nude mice (*21, 22, 24, 30*). Thus the reduction of the transformation frequency measures the prevention of morphologic transformation, an early step in carcinogenesis, and is a direct measure of the prevention of carcinogenesis.

One difference in the transplacental transformation procedure followed in the present investigation from the procedures used by others (*21, 22*) is that in the present investigation cells, instead of being subcultured, were seeded directly from the animal for colony formation. Quarles et al. (*22*) reported a transformation frequency of 0.01 transformant/colony on cells subcultured three to ten times before being seeded for colony formation. We observed without subculture a somewhat lower number of 0.0027 transformants/colony, a number in agreement with that of DiPaolo et al. (*21*), who reported that the transformation frequency increases with subculture of transplacentally exposed fetal cells. For these reasons the transformation frequency per cell plated directly from the fetus(es) more closely approximates the number of cells affected by the carcinogen in vivo and is a better indication of the effectiveness of in vivo intervention measures.

When DENA treatment in vivo was coupled with a cocarcinogenic X-irradiation exposure in vitro, the frequency of transformation was enhanced compared to that seen in cells treated only with X-irradiation. The cocarcinogen transformation frequency was also considerably higher than that resulting from DENA alone when the toxicity due to X-irradiation is considered (tables 1, 3). Lymphotoxin inhibited the cocarcinogen-induced transformation but had no effect on transformation induced by in vitro X-ray exposure alone. This observation suggests that there may be at least three populations of transformed cells: one transformed by in vivo DENA, one transformed by in vitro X-irradiation, and one that is initiated by in vivo DENA but transformed only after an additional in vitro cocarcinogenic insult by X-irradiation. The two populations susceptible to in vivo lymphotoxin anticarcinogenic activity are those induced in vivo by DENA. Although lymphotoxin directly inhibits X-ray-induced transformation in vitro (*15*), the in vivo lymphotoxin treatment had no effect on the in vitro X-ray transformation frequency (table 3). The temporal relationship of lymphotoxin treatment to X-ray exposure in the presence of increasing numbers of fetal target cells (in vivo growth) may be responsible for the disparity in results. Distinct carcinogen and lymphotoxin antitransformation–temporal interrelationships have been observed when cells are pulsed for varying periods with lymphotoxin in vitro before (*31*) or after (*14*) carcinogen exposure. Similar relationships most likely occur in vivo. Therefore, cells that are initiated and receptive to the appropriate cocarcinogenic insult and completely transformed cells are at this premalignant state susceptible to immune regulation. Intervention measures thus have the potential to prevent the continued development of neoplastic transformation in cells having received a complete or an initiated carcinogenic insult.

REFERENCES

(*1*) Berenblum I. Cancer prevention as a realizable goal. Cancer 1981; 47:2346–2348.

(*2*) Mirvish SS. Formation of N-nitroso compounds: Chemistry, kinetics and in vivo occurrence. Toxicol Appl Pharmacol 1975; 31:325–351.

(*3*) Wattenberg LW. Inhibition of chemical carcinogenesis by antioxidants. In: Slaga TJ, ed. Modifiers of chemical carcinogenesis: An approach to the biochemical mechanism and cancer prevention. New York: Raven Press, 1980:85–98.

(*4*) Lappé MA. Evidence for the antigenicity of papillomas induced by 3-methylcholanthrene. J Natl Cancer Inst 1968; 40:823–846.

(*5*) Baldwin RW. Immunological aspects of chemical carcinogenesis. Adv Cancer Res 1973; 18:1–75.

(*6*) Kripke ML, Borsos T. Guest editorial: Immune surveillance revisited. J Natl Cancer Inst 1974; 52:1393–1395.

(*7*) Evans CH, Rabin ES, DiPaolo JA. The susceptibility of guinea pig cells to the colony-inhibitory activity of lymphotoxin during carcinogenesis. Cancer Res 1977; 37:898–903.

(*8*) Slaga TJ. Anti-inflammatory steroids: Potent inhibitors of tumor promotion. In: Slaga TJ, ed. Modifiers of chemical carcinogenesis: An approach to the biochemical mechanism and cancer prevention. New York: Raven Press, 1980:111–126.

(*9*) Evans CH, Greiner JW. Corticosteroid prevention of carcinogenesis in benzo(*a*)pyrene or ultraviolet irradiation-treated Syrian hamster cells in vitro. Cancer Lett 1981; 12:23–27.

(*10*) Hayes JR, Campbell TC. Nutrition as a modifier of chemical carcinogenesis. In: Slaga TJ, ed. Modifiers of chemical carcinogenesis: An approach to the biochemical mechanism and cancer prevention. New York: Raven Press, 1980:207–242.

(*11*) Holterman OA, Papermaster BW, Rosner D, Klein E. Studies on local administration of material with lymphokine activity to neoplasms involving the skin. In: Fink MA, ed. The macrophage in neoplasia. New York: Academic Press, 1976:259–261.

(*12*) Papermaster BW, Guilliland CD, Smith M, et al. Tumor regression induced in mice by partially purified lymphokine factors. Ann NY Acad Sci 1979; 332:451–459.

(*13*) Fidler IJ. Therapy of spontaneous metastases by intravenous injection of liposomes containing lymphokines. Science 1980; 208:1469–1471.

(*14*) Evans CH, DiPaolo JA. Lymphotoxin: An anticarcinogenic lymphokine as measured by inhibition of chemical carcinogen or ultraviolet-irradiation-induced transformation of Syrian hamster cells. Int J Cancer 1981; 27:45–49.

(*15*) DiPaolo JA, Demarinis AJ, Evans CH, Doniger J. Expression of initiated and promoted stages of irradiation carcinogenesis in vitro. Cancer Lett 1981; 14:243–249.

(*16*) Brouty-Boyé D, Gresser I, Baldwin C. Decreased sensitivity to interferon associated with in vitro transformation of X-ray-transformed C3H/10T1/2 cells. Int J Cancer 1979; 24:261–265.

(*17*) Evans CH. Lymphotoxin—an immunologic hormone with anticarcinogenic and antitumor activity. Cancer Immunol Immunother 1982; 12:181–190.

(*18*) Gresser I. Antitumor effects of interferon. In: Becker FF, ed. Cancer: A comprehensive treatise. New York: Plenum Press, 1977:521–571.

(*19*) Evans CH, Heinbaugh JA. Lymphotoxin cytotoxicity, a combination of cytolytic and cytostatic cellular responses. Immunopharmacology 1981; 3:347–359.

(*20*) Ransom JH, Evans CH. Lymphotoxin enhances the susceptibility of neoplastic and preneoplastic cells to natural killer cell mediated destruction. Int J Cancer 1982; 29:451–458.

(*21*) DiPaolo JA, Nelson RL, Donovan PJ, Evans CH. Host-mediated in vivo–in vitro assay for chemical carcinogenesis. Arch Pathol 1973; 95:380–386.

(*22*) Quarles JM, Sega MW, Schenley CK, Lijinsky W. Transformation of hamster fetal cells by nitrosated pesticides in a transplacental assay. Cancer Res 1979; 39:4525–4533.

(*23*) Mohr V, Althoff J, Authaler A. Diaplacental effect of the carcinogen diethylnitrosamine in the golden hamster. Cancer Res 1966; 26:2349–2352.

(*24*) Evans CH, DiPaolo JA. Comparison of nude mice with the host species for evaluation of the tumorigenicity of guinea pig and hamster cells transformed in vitro by chemical carcinogens. Cancer Res 1976; 36:128–131.

(*25*) DiPaolo JA. Quantitative in vitro transformation of Syrian golden hamster embryo cells with the use of frozen stored cells. JNCI 1980; 64:1485–1489.

(*26*) Evans CH, DiPaolo JA. Equivalency of endothelial cell growth supplement to irradiated feeder cells in carcinogen-induced morphologic transformation of Syrian hamster embryo cells. JNCI 1982; 68:127–131.

(*27*) Stewart WE II. The interferon system. New York: Springer-Verlag, 1979:17–18.

(*28*) Winer BJ. Statistical principles in experimental design. New York: McGraw-Hill, 1971:848–849.

(*29*) Evans CH, Ransom JH, Jones AE, DiPaolo JA. Modulation of the carcinogenic potential of the diagnostic radionuclide 99M technetium (99MTc). Proc Am Assoc Cancer Res 1982; 23:95.

(*30*) DiPaolo JA, Nelson RL, Donovan PJ. Morphological, oncogenic, and karyological characteristics of Syrian hamster embryo cells transformed in vitro by carcinogenic polycyclic hydrocarbons. Cancer Res 1971; 31:1118–1127.

(*31*) DiPaolo JA, Evans CH, DeMarinis AJ, Ohanian SH, Doniger J. Cell surface pertubations by the immunologic hormone lymphotoxin inhibits transformation. Proc Am Assoc Cancer Res 1982; 23:74.

Announcements

The Journal *will publish notices of major meetings dealing with cancer. Submission of notices 6 months in advance is requested to permit timely publication.*

Advances in Pediatric Oncology Seminar

The Association of Pediatric Oncology Nurses will sponsor this meeting entitled "Care of the Child and Family" to be held in New York City on October 7–8, 1982. The program will focus on assessment and management of pain in children, alternative strategies of coping with pain and chronic illness, and long term psychological effects of illness in children.

For brochure and registration forms please contact Ms. N. Houlihan, APON Program, 511 E. 80th Street, New York, New York 10021.

Thirty-Sixth Annual Symposium on Fundamental Cancer Research

"Cancer Invasion and Metastasis" is the subject of this symposium to be held at the Shamrock Hilton Hotel in Houston, Texas, on March 1–4, 1983. The symposium will consider recent developments in the biology of tumor metastasis formation and investigate the possible contributions of these developments to cancer treatment. Program topics will include tumor cell properties and metastasis, tumor invasion, tumor heterogeneity, host factors and metastasis, and therapy of metastasis.

For additional information please contact the Office of Conference Services, Box 18, M. D. Anderson Hospital and Tumor Institute, 6723 Bertner Avenue, Houston, Texas 77030 (telephone: 713-792-2222).

Twenty-Fourth Postgraduate Institute for Pathologists in Clinical Cytopathology

This program, designed for pathologists who are certified (or qualified) by the American Board of Pathology (PA), or their international equivalents, will be given at The Johns Hopkins University School of Medicine and The Johns Hopkins Hospital, Baltimore, Maryland, on April 18–29, 1983. The course will provide an intensive refresher in all aspects of the field of clinical cytopathology, with time devoted to newer techniques, special problems, and recent applications. Topics will be covered in lectures, explored in small informal conferences, and discussed over the microscope with the faculty. Self-instructional material will be available to augment at individual pace. A loan set of slides with texts will be sent to each participant for home-study during March and April before the course begins.

Approval has been granted for 125 credit hours in AMA Category I. Application should be made before February 2, 1983. For additional details please write to Dr. John K. Frost, 610 Pathology Building, The Johns Hopkins Hospital, Baltimore, Maryland 21205.

Accredited Visiting Faculty Program on Colorectal Cancer

An accredited Visiting Faculty Program that will give primary care physicians around the country access to the latest clinical information on colorectal cancer was announced recently. This program is a key element of a 2-year course entitled "Colorectal Cancer: Essentials for Primary Care Physicians." The program is accredited for up to six CME credit hours and is being presented without charge by an independent group of experts in gastrointestinal and family medicine. Like other elements of the course, the Visiting Faculty Program is sponsored by the Office of Continuing Medical Education of Memorial Sloan-Kettering Cancer Center.

A five-member Editorial Board directs the course. Dr. Sidney J. Winawer, Chief of the Gastroenterology Service at Memorial Sloan-Kettering Cancer Center is Executive Editor, and 25 nationally recognized authorities comprise the balance of the Visiting Faculty. The complete program is comprised of two parts: part 1 focuses on disease and diagnosis, and part 2 focuses on case finding and management. Each part consists of a lecture supported by slides, a discussion session, and a monograph for independent study and later referral. The Visiting Faculty will address audiences comprised mostly of primary care physicians at hospitals, medical schools, and medical association meetings throughout the United States.

Developed and produced by Health Learning Systems, Inc., under an educational grant from SmithKline Diagnostics, Inc., the course is provided in cooperation with the American Cancer Society, the American Society for Gastrointestinal Endoscopy, The American Society of Colon and Rectal Surgeons, The International Workgroup on Colorectal Cancer, and the National Cancer Institute. For additional information about the program please contact Ms. Barbara Anderson, Visiting Faculty Program Coordinator, 200 Broadacres Drive, Bloomfield, New Jersey 07003 (telephone: 201-338-3615 or 800-526-6312).

☆ U.S. GOVERNMENT PRINTING OFFICE: 1982-361-145/58

JNCI (NIH Publication No. 82-13)

69/4

JNCI

Journal of the National Cancer Institute

October 1982
Volume 69
Number 4

NEWARK PUBLIC LIBRARY

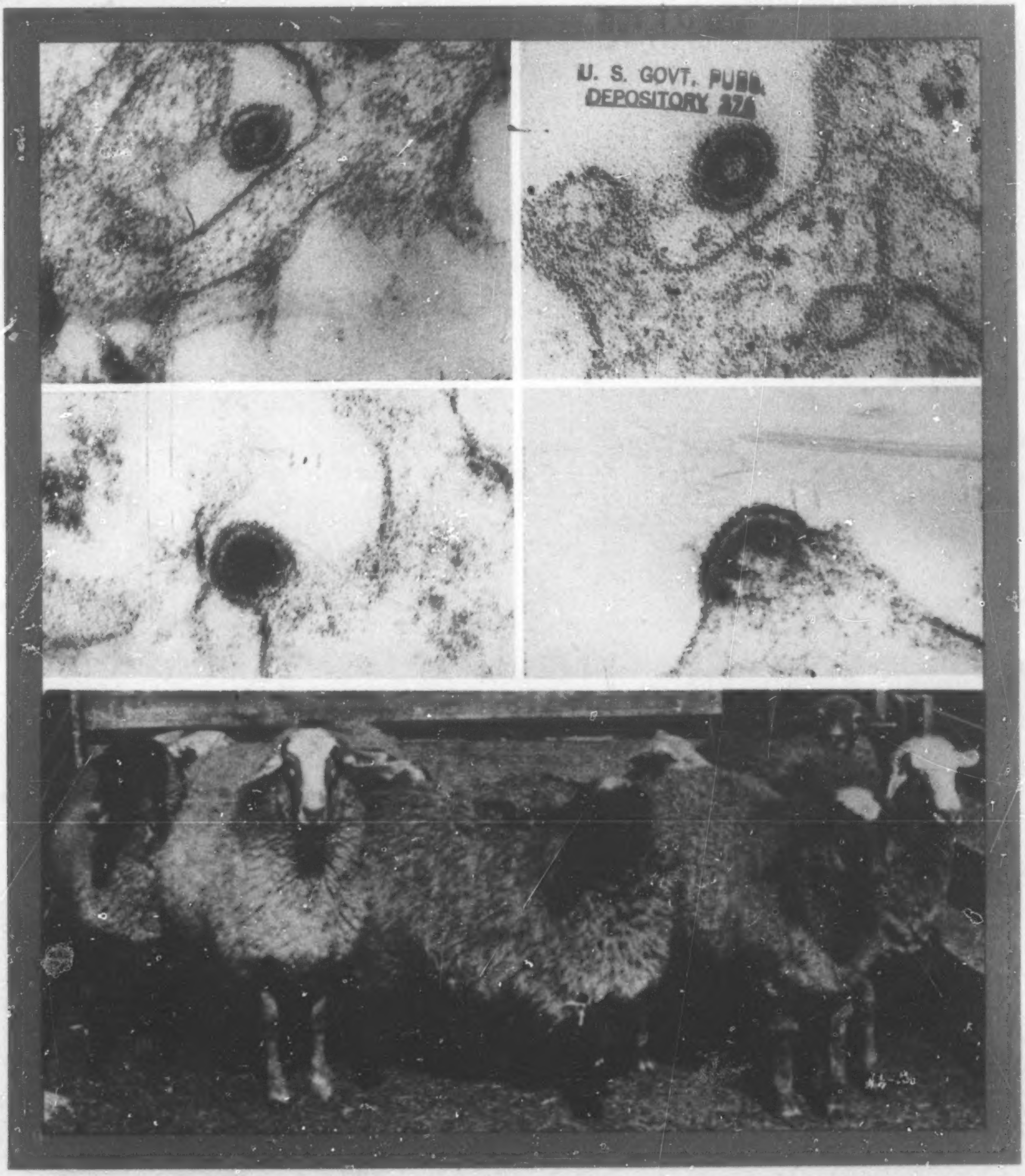

U. S. GOVT. PUBS.
DEPOSITORY 376

U.S. DEPARTMENT OF HEALTH AND HUMAN SERVICES Public Health Service National Institutes of Health

HE 20.3161:

The cover shows (*top*) the first virus particles seen by the electron microscope in a primary bronchoalveolar cell carcinoma (jaagsiekte, pulmonary adenomatosis) of sheep in 1971. The photograph (*bottom*) shows experimental animals in which bronchoalveolar cell carcinomas were successfully induced by virus preparations in 1981 (*see* guest editorial by Perk and Hod on pages 747–749).

JNCI

Journal of the National
Cancer Institute

October 1982
Volume 69
Number 4

THE JOURNAL of the National Cancer Institute solicits manuscripts on original observations in laboratory and clinical research from all scientists. A manuscript is considered for publication with the understanding that it has not been published previously and is submitted exclusively to the Journal. Opinions expressed by the authors are not necessarily those of the publisher or its editors.

THE JOURNAL is published monthly (two volumes a year). The Secretary of Health and Human Services has determined that the publication of this periodical is necessary in the transaction of the public business required by law of this Department. Use of funds for printing this periodical has been approved by the Director of the Office of Management and Budget through August 30, 1985.

A MONOGRAPH SERIES covering proceedings of scientific meetings pertaining to cancer is also published. These books may be purchased from the Superintendent of Documents. Series subscriptions are not available and monographs are not included in a subscription to the Journal.

THE JOURNAL is for sale by the Superintendent of Documents, U.S. Government Printing Office, Washington, D.C. 20402. Price per copy, $7.00. Subscription price for two volumes per year in the United States, $70.00; foreign, $87.50. Payment is required in advance, and check or money order should be made payable to the Superintendent of Documents.

All inquiries regarding purchase of subscriptions or depository library distribution, including inquiries about missing issues and change of address, should be addressed to the Government Printing Office. The Government Printing Office requires payment in advance on all orders. Inquiries regarding missing issues or change of address for official subscriptions should be addressed to the Editorial Office, Room 850, Westwood Building, 5333 Westbard Avenue, Bethesda, Md. 20816.

VINCENT T. DEVITA, JR., *Director, National Cancer Institute*

BOARD OF EDITORS

PETER GREENWALD, *Editor in Chief*

ELIZABETH K. WEISBURGER, *Assistant Editor in Chief*

STUART A. AARONSON, *Associate Editor*

CHARLES H. EVANS, *Associate Editor*

MARY A. FINK, *Associate Editor*

JANET W. HARTLEY, *Associate Editor*

DONALD HENSON, *Associate Editor*

RONALD B. HERBERMAN, *Associate Editor*

GEORGE S. JOHNSON, *Associate Editor*

KURT W. KOHN, *Associate Editor*

ARTHUR S. LEVINE, *Associate Editor*

JOHN J. MULVIHILL, *Associate Editor*

ALAN S. RABSON, *Associate Editor*

RICHARD M. SIMON, *Associate Editor*

EDITORIAL STAFF

EDWIN A. HAUGH, *Managing Editor*

PAMELA T. ALLEN, *Assistant Managing Editor*

FLORENCE I. GREGORIC, *Monograph Editor*

Editors: DOROTHY D. KATZ, MERCEDES B. LA CHARITY, I. AGNES REVESZ, JOAN O'BRIEN RODRIGUEZ, CONSTANCE P. STONESTREET, and ANNA B. WITTIG

JNCI (NIH Publication No. 83-13)

U.S. DEPARTMENT OF HEALTH AND HUMAN SERVICES Public Health Service National Institutes of Health

Instructions to Authors

Text: Send one original and two copies. **Text-figures** (graphs, charts, and line drawings): Send one original and two copies. **Figures** (photomicrographs and photographs): Send three original glossy prints, unmounted. **Tables:** Send tabular material in typewritten form; do not submit tables as glossy prints to be photographed. The entire manuscript including footnotes, legends, and references must be typed double spaced. Single-spaced portions of a manuscript will be returned to the author for retyping. The mailing address is: Journal of the National Cancer Institute, Westwood Building, Room 850, 5333 Westbard Avenue, Bethesda, Maryland 20816.

Manuscripts should be accompanied by a covering letter from the author responsible for correspondence about the manuscript. The covering letter should contain a statement that the manuscript has been seen and approved by all authors and that all persons listed as authors have made significant (not merely administrative, technical, or supervisory) contributions to the content of the paper. The letter should also state that the manuscript or substantial portions thereof have not been previously published nor are they under consideration for publication in another journal.

Data too extensive for inclusion in a manuscript, but which may be of interest to other investigators, may be deposited with the National Auxiliary Publications Service (NAPS), c/o Microfiche Publications, P.O. Box 3513, Grand Central Station, New York, New York 10017. Authors using the NAPS facilities should indicate in a footnote how their additional data may be obtained.

Approximately one-half of all manuscripts submitted to the Journal are accepted for publication. Publication of manuscripts is contingent on transfer of copyright to the Journal. Forms for this purpose will be sent to authors when a manuscript has been approved for publication. All material published in the Journal is in the public domain; therefore, permission to reproduce any portions is not necessary. As a matter of courtesy, communication should be made to the author(s) concerned.

TITLE: Be brief (no more than 14 words, if possible), but for indexing purposes include all key words. The annual subject index is prepared directly from the titles. Titles that form complete sentences are not acceptable. Do not use abbreviations or chemical formulas in titles.

BYLINE: Supply the complete first name, middle initial, and last name of each author. Avoid use of nicknames. Academic degree is optional; however, if a degree is provided for one author, it should be provided for all authors on a manuscript. Include the name of the institution, address, and zip code for each author. Indicate address for reprint requests in a footnote on the byline.

ACKNOWLEDGMENTS: Financial aid in support of research should be recognized in a footnote. Aid in technical fields, animal care, photography, stenography, and other areas may be mentioned in a separate footnote. Indicate the title (Dr., Mr., Mrs., Miss, Ms.) and affiliation of each person acknowledged.

ABSTRACT: Provide an abstract, 150 words or less, on a separate page. The abstract should describe only *results* of the work being reported. Speculation, historical background, or reference to published works will be deleted from abstracts. Any inbred strains, noninbred stocks, cell lines, or other living materials used in the work should be noted in the abstract.

TEXT: Avoid the use of laboratory jargon and abbreviations not in common usage. When possible, refrain from the use of abbreviations that form words (exceptions are PAGE, ALL). Whenever possible, write mathematical equations and chemical formulas on a single line; submit complicated chemical structures as artwork. Avoid repetition of data in the text when it is presented in tables or text-figures.

Use the following style sources: Webster's *Third New International Dictionary* and Dorland's *Illustrated Medical Dictionary* (25th ed) for spelling; *Council of Biology Editors Style Manual* (4th ed) for scientific abbreviations and symbols; *Government Printing Office Style Manual* for other abbreviations and symbols, punctuation, and hyphenation; *Biochemical Nomenclature and Related Documents* (IUB, 1978) for abbreviations of chemical substances; *Enzyme Nomenclature*, recommendations (1978) of the IUB for recommended names of enzymes and information on nomenclature of isozymes; *The Merck Index* (9th ed) for chemical compounds; "Standard Nomenclature for Inbred Strains of Mice: Seventh Listing" by Joan Staats (Cancer Res 1980;40: 2083-2128) for inbred mouse strains; "Standardized Nomenclature for Inbred Strains of Rats: Fourth Listing" by Joan Staats and Michael Festing (Transplantation 1973;16:221-245) for designations of inbred rat strains; *Animals for Research* (9th ed) prepared by the Institute of Laboratory Animal Resources, National Academy of Sciences, for designations of laboratory animal stocks and strains.

TABLES: Submit tabular material typed double spaced on a separate page. Computer print-outs of tables are acceptable only if they are double spaced and with satisfactory title, column headings, legends, and other textual material. Provide headings for all columns of a table and indicate units of measurement where applicable.

TEXT-FIGURES: Refer to graphs, charts, and line drawings as text-figures. Make the abbreviations on text-figures identical to the abbreviations used in the text and legends. Symbols and lettering should be large enough to be legible if reduced. Glossy prints or original drawings in black ink are acceptable; orient vertically instead of horizontally.

FIGURES: Refer to photomicrographs and photographs as figures. Figures and their legends should fit a 7.5- by 9-inch dimension. Calculate that nine typewritten lines of legend will require 1 inch of vertical space. Type figure legends on a separate sheet and identify in the legend any lettering used on the figure. Trim photographs to show only important areas. Do not number face of photographs; use the back or overlay to indicate the top and number of each. Printed indicators may be included on photographs; do not use hand-drawn indicators. *Insert internal scale markers on all photomicrographs.* Color photographs must be grouped as a single plate. For color reproduction, submit both color transparencies and high-quality black and white reproductions. The need for color must be documented before it will be considered.

REFERENCES: Use any recent issue of the Journal as a style guide for reference lists. Number references in order of citation in both text and reference list. For periodicals, provide author(s), title of paper, journal, year, volume, and first and last page numbers. For books, give the author(s), title, name(s) of editor(s), location and name of publisher, year, pertinent chapter or section title, and page numbers. Follow *Index Medicus* for punctuation and abbreviations. Citations of papers in preparation or submitted for publication, unpublished observations, and personal communications should be noted parenthetically in the text. Do *not* include them in the reference list. The accuracy of all references is the responsibility of the authors and not of the editorial staff.

LETTERS TO THE EDITOR should pertain to recent articles in the Journal and should not contain new data unless relevant to the discussion of a particular paper. The authors addressed will be invited to reply to comments before correspondence is published. Letters will be edited by the Staff, subject to contributor approval.

FURTHER DETAILS on the preparation of manuscripts are set forth in the document "Uniform Requirements for Manuscripts Submitted to Biomedical Journals" prepared by the International Steering Committee of medical editors (*see* Am Rev Respir Dis 1979;119:3-10/Ann Intern Med 1979;90:95-99/Br Med J 1979;1:532-535/ or Lancet 1979;1:428-430).

UNITED STATES GOVERNMENT PRINTING OFFICE, WASHINGTON, D.C.: 1982

Table of Contents

Vol. 69, No. 4—October 1982

Guest Editorial

747 Sheep lung carcinoma: An endemic analogue of a sporadic human neoplasm *K. Perk, I. Hod*

Investigations on Man

751 Studies on carcinogenesis of human prostate. II. Long-term explant culture of normal prostate and benign prostatic hyperplasia: Light microscopy *Hayato Sanefuji, Barry M. Heatfield, Benjamin F. Trump, John D. Young, Jr.*

757 Studies on carcinogenesis of human prostate. III. Long-term explant culture of normal prostate and benign prostatic hyperplasia: Transmission and scanning electron microscopy *Barry M. Heatfield, Hayato Sanefuji, Benjamin F. Trump*

767 Enhancement of growth of human colon tumor cell lines by feeder layers of murine fibroblasts *M. G. Brattain, D. E. Brattain, A. M. Sarrif, L. J. McRae, W. D. Fine, J. G. Hawkins*

773 Major histologic types of cancers of the gum and mouth, esophagus, larynx, and lung by sex and by income level *V. L. Ernster, S. Selvin, S. T. Sacks, D. W. Merrill, E. A. Holly*

777 Glycoconjugate with *Ulex europaeus* agglutinin-I-binding sites in normal mucosa, adenoma, and carcinoma of the human large bowel *Suguru Yonezawa, Takao Nakamura, Sadao Tanaka, Eiichi Sato*

787 Cerebrospinal fluid markers in African Burkitt's lymphoma with central nervous system involvement *William C. Wallen, Robert J. Biggar, Paul H. Levine, Janet Neequaye, Francis K. Nkrumah*

793 Transforming growth factors in the urine of normal, pregnant, and tumor-bearing humans *Daniel R. Twardzik, Stephen A. Sherwin, Jane Ranchalis, George J. Todaro*

799 Selective cytotoxicity of a ricin A-chain–anti-carcinoembryonic antigen antibody conjugate for human colon adenocarcinoma cell line *Thomas W. Griffin, Linda R. Haynes, Julie A. DeMartino*

807 In vitro potentiation of human natural killer cell activity by a streptococcal preparation, OK-432: Interferon and interleukin-2 participation in the stimulation with OK-432 *Hiro Wakasugi, Tadashi Kasahara, Nagahiro Minato, Junji Hamuro, Michio Miyata, Yasuhiko Morioka*

813 Carcinoembryonic antigen: Usefulness as a postsurgical method in the detection of recurrence in Dukes stage B_2 and C colorectal cancers *Maria Koch, Graeme Washer, Herta Gaedke, Thomas A. McPherson*

817 Interaction of familial and hormonal risk factors for breast cancer *Louise A. Brinton, Robert Hoover, Joseph F. Fraumeni, Jr.*

823 Imaging of human melanoma xenografts in nude mice with a radiolabeled monoclonal antibody *Tarun Ghose, Soldano Ferrone, Kohzoh Imai, Stevens T. Norvell, Jr., Steven J. Luner, Robert H. Martin, A. Huntley Blair*

827 Functional properties of human thymoma lymphocytes: Role of subcellular factors in blastic activation *Piero Musiani, Libero Lauriola, Nicola Maggiano, Pietro Tonali, Mauro Piantelli*

833 Changes in lung cancer incidence and mortality rates among Americans: 1969–78 *John W. Horm, Ardyce J. Asire*

Investigations on Nonhuman Systems

839 Simian virus 40 (SV40)-specific isoelectric point-4.7–94,000-M_r membrane glycoprotein: Major peptide homology exhibited with the nuclear and membrane-associated 94,000-M_r SV40 T-antigen in hamsters *Rupert Schmidt-Ullrich, W. Scott Thompson, Stuart J. Kahn, Maureen T. Monroe, Donald F. H. Wallach*

851 Relationship of lung adenoma prevalence and growth rate to acute urethan dose and target cell number *Michael L. Dourson, Ellen J. O'Flaherty*

859 Relationship between urethan dose rate and adenoma latency: Relevance of tumor growth rate and target cell number *Ellen J. O'Flaherty, Michael L. Dourson*

867 Tumor cell-triggered macrophage-mediated suppression of the T-cell cytotoxic response to tumor-associated antigens. I. Characterization of the cell components for induction of suppression *Chou-Chik Ting, Dennis Rodrigues*

873 Tumor cell-triggered macrophage-mediated suppression of the T-cell cytotoxic response to tumor-associated antigens. II. Mechanisms for induction of suppression *Chou-Chik Ting, Myrthel E. Hargrove*

879 Inducible macrophage cytotoxins. I. Biokinetics of activation and release in vitro *Thomas H. Reidarson, Walter E. Levy III, Jim Klostergaard, Gale A. Granger*

889 Inducible macrophage cytotoxins. II. Tumor lysis mechanism involving target cell-binding proteases *Thomas H. Reidarson, Gale A. Granger, Jim Klostergaard*

895 Squamous metaplasia in organ cultures of vitamin A-deficient hamster trachea: Cytokinetic and ultrastructural alterations *Dharam P. Chopra*

907 Primordial germ cell proliferation in fetal testes in mouse strains with high and low incidences of congenital testicular teratomas *Takehiko Noguchi, Leroy C. Stevens*

915 Epizootic neoplasms in fishes from a lake polluted by copper mining wastes — *John J. Black, Elwin D. Evans, John C. Harshbarger, Robert F. Zeigel*

927 Electron microscopic autoradiography of the trachea in fetal Syrian golden hamsters treated transplacentally with *N*-nitrosodiethylamine — *Hildegard M. Reznik-Schüller*

933 Comparison of biologic behavior and histology of transplanted mammary tumors in GR mice — *Dean H. Percy, Vincent L. Morris, Janet I. MacInnes*

939 Regulation of cell-mediated immunologic reactivity to Moloney murine sarcoma virus-induced tumors. III. Further characterization of tumor-specific serum blocking factors — *William J. Halliday, Thelma A. Koppi, Ian F. C. McKenzie*

945 Trisomy 15 and other nonrandom chromosome changes in Rauscher murine leukemia virus-induced leukemia cell lines — *Anne Hagemeijer, Elisabeth M. E. Smit, Francine Govers, Nico J. de Both*

953 Induction of gp70-specific suppressor T-cells in mice inoculated with virus-producing tumor cells — *Jeffrey A. Bluestone, Carlos Lopez*

961 Carcinogenicity test of acetoxime in MRC-Wistar rats — *Sidney S. Mirvish, Shahrokh Salmasi, Richard G. Runge*

963 β-Cyclodextrin: Promoting effect on the development of renal tubular cell tumors in rats treated with *N*-ethyl-*N*-hydroxyethylnitrosamine — *Yoshio Hiasa, Masato Ohshima, Yoshiteru Kitahori, Noboru Konishi, Toyohisa Fujita, Takashi Yuasa*

969 Secretagogue response in rat pancreatic acinar carcinoma — *John R. Warren*

975 Enhanced metastatic potential of tumor cells harvested from spontaneous metastases of heterogeneous murine tumors — *James E. Talmadge, Isaiah J. Fidler*

Meeting Highlights

981 Adult T-cell leukemia–lymphoma: Role of a human retrovirus — *Max Essex*

Corrections

987 December 1981, vol 67, No. 6 page 1328: Enhancement of Experimental Pancreatic Cancer in Syrian Golden Hamsters by Dietary Fat — *Diane F. Brit, Sharokh Salmasi, Parviz M. Pour*

987 April 1982, vol 68, No. 4, page 678: Mechanisms of Immunologic Eradication of a Syngeneic Guinea Pig Tumor — *Suyu Shu, James T. Hunter, Herbert J. Rapp, Leila S. Fonesca*

best copy available

Announcements

987 Formaldehyde Toxicology Meeting

987 Symposium on Application of Biological Markers to Carcinogen Testing

987 Eighth Annual Postgraduate Course

987 Seventh Annual Meeting of the Cell Kinetics Society

987 First International Meeting on Cell Biochemistry and Function

988 The Fourth Annual Meeting of the Society for Clinical Trials

988 Thirteenth International Congress of Chemotherapy

Guest Editorial

K. Perk[1] *and* **I. Hod**[1]

Sheep Lung Carcinoma: An Endemic Analogue of a Sporadic Human Neoplasm[2,3]

The increase in the incidence of lung tumors, which has become the leading cause of death from cancer in humans, emphasizes the importance of determining the frequency and nature of lung cancer in experimental animals. Also, the search for and the establishment of spontaneous host-lung tumor systems in other outbred species may prove to be relevant to the study of the etiology, pathogenesis, and immunologic behavior of lung cancer and the response of this cancer to clinical therapy in humans. The comparative method has, of course, long been recognized as an essential and, indeed, an unavoidable approach to the study of human diseases; the names of Koch, Pasteur, and Sigurdsson are sufficiently illustrative and convincing.

FATAL PROLIFERATIVE LUNG DISEASES IN SHEEP

In contrast to the prevalence of primary neoplasms of the lungs in humans, primary neoplasms of the lungs in domestic animals are rare. Sheep are exceptional in having two fatal proliferative lung diseases distributed worldwide. These diseases are 1) pulmonary adenomatosis, which exhibits all the criteria included in the definition of bronchoalveolar cell carcinoma, and will, therefore, be the topic of this editorial, and 2) maedi disease, manifested by typical interstitial proliferation of the lymph aggregates confined to the lungs, a disease as yet unrevealed in humans.

METASTATIC AND CONTAGIOUS PROPERTIES OF SPC

Sheep pulmonary adenomatosis, also called "jaagsiekte" (Dutch *jaag*—"to drive"; *siekte*—"sickness") or "SPC," is characterized by tumor cell growth in the lungs with metastases in the pulmonary and mediastinal lymph nodes (*1–7*). Metastases in the mesentery lymph nodes and visceral organs have also been reported (*5, 6, 8–10*). The symptomatology and macroscopic pathology of this disease were first recorded in scientific publications toward the end of the 19th century (*2*). This naturally occurring malignant disease occurs in most breeds of sheep and in most countries (*2, 8, 10, 11*). Epidemologic and experimental evidence indicates that this neoplasm is horizontally transmitted in nature (*2, 8, 11, 12*).

Most reports on SPC until 1970 (*8*) were in general agreement with respect to the clinical signs, epidemiology, and gross pathology of SPC. The variations in histopathologic interpretations can now be attributed to the stage of development of the tumor, i.e., whether the tumor is early or advanced. However, as far as the etiology was concerned, little was known then about the nature of the putative infectious agent suspected to be involved, although the evidence incriminated "a virus" (*8*).

Histopathologically, the neoplastic cells (cuboidal or columnar) may be arranged in short rows, layers, and acinar or papillary structures or clusters and appear to arise from alveoli, alveolar ducts, and bronchioles (*2, 5, 7, 8, 12–14*). Our first ultrastructural examinations of SPC (*4*) indicated that the neoplastic cells are derived from terminal bronchiolar epithelial cells and from type II alveolar epithelial cells (also called "type B alveolar cells" or "granular pneumocytes"). Our diagnosis was confirmed by others (*15*).

Metastatic lesions anywhere in the body resemble the primary lesions histologically and ultrastructurally (*5, 6, 8, 13, 16, 17*). Various stages of neoplastic expression, ranging from "alveolar epithelialization" to poorly differentiated adenocarcinoma, can be detected in the same tumorous lung of a clinically ill animal (*13, 14, 18*). Most neoplastic structures are composed of neoplastic cells that contain glycogen granules and cytosomes characteristic also of undifferentiated, embryonal lung epithelium. Apart from the alveolar epithelialization, the marginal alveoli surrounding the tumor mass are usually lined by a single layer of relatively well-differentiated cuboidal or columnar cells rich in glycogen granules. In many of these alveoli, papillary projections of the septum and the transformed epithelium into the lumina may plug the bronchoalveolar pathway within the tumor mass. Intensely proliferating cores, sheets, or nests of anaplastic epithelial cells are seen.

HUMAN BRONCHOALVEOLAR CELL CARCINOMA AND SPC SIMILARITIES

The overall tumor architecture and the ultrastructure of the neoplastic cell, including the metastasis, warranted the classification of SPC as a bronchoalveolar cell carcinoma (*7*), strikingly resembling the human bronchoalveolar carcinoma (*7, 19–21*). Both diseases originate in the periphery of the lung and tend to grow within the lung for a prolonged period, terminating in a late metastatic process. In the human tumor cell, as in the sheep tumor cell, apical mucin granules, tonofibrils, microvilli, and cytosomes are found. In domestic animals, bronchiolar and mainly peripheral ade-

---

ABBREVIATION USED: SPC=sheep pulmonary carcinoma.

---

[1] Department of Animal Science, The Levi Eshkol School of Agriculture, The Hebrew University of Jerusalem, Rehovot Campus, Rehovot 76-100, Israel.

[2] Received December 31, 1981.

[3] Supported in part by grants from the United States-Israel Binational Science Foundation (1926/79), The United States-Israel Agricultural Research and Development Fund (1-74-79), and the Bergman Foundation.

Editor's note: Periodically, the Journal publishes guest editorials as a means of transmitting to investigators in cancer research the essence of current work in a special field of study. The Board of Editors welcomes suggestions for future editorials that succinctly summarize current work toward a clearly defined hypothesis regarding the causes or cure of cancer.

nocarcinomas are undoubtedly the most prevalent lung neoplasms; epidermoid and anaplastic carcinomas are rare. Perhaps the situation regarding the type of lung tumors encountered in animals now is similar to that seen in human beings decades ago (*10*). However, at the last World Congress of Pathology, the Panel on Lung Tumors in Man discussed the cause of the recent increase in incidence of human bronchoalveolar cell carcinoma but came to no conclusions.[4]

EARLY TRANSMISSION EXPERIMENTS IN SPC

There has been general agreement that this neoplasm in sheep is horizontally transmitted. As early as 1904, Robertson (*22*) suggested that this natural disease was moderately contagious and emphasized that once it commenced in a flock, the disease was apt to continue and become more widespread. In 1929 De Kock (*1*) further substantiated these findings by exposing healthy sheep to infected animals. A number of these exposed sheep developed SPC. Dungal (*3*) and Dungal et al. (*12*) repeated this experiment in Iceland (*3, 12*). Dungal (*3*) using two methods also proved that the exhaled respiratory air of an affected sheep may contain the infectious agent. The Icelandic epizootic studies by Dungal (*3*) and Dungal et al. (*12*) and the studies by Tustin (*2*) in South Africa left little doubt that horizontal transmission occurs in nature. The disease typically appears as multiple cases in a single herd, whereas in other flocks it may be absent for many years (*2, 17*).

VIRUS DEMONSTRATION IN SPC

A decade ago, we first reported that virus particles morphologically similar to RNA tumor viruses (retroviridae, i.e., clusters of intracytoplasmic A and budding C-type particles) are present in situ in SPC (*4*). These electron microscopic findings were confirmed more recently by other authors (*23*). In addition to the retrovirus association with SPC, herpesvirus-like particles were found in tissue cultures of alveolar macrophages and lung tissues of SPC-diseased animals (*24, 25*). Furthermore, this herpesvirus could be transmitted to normal cultures (*26–28*). However, attempts to produce neoplasms with this agent have been unsuccessful (*29*). The observations of the presence of retroviruses were complemented by our findings that extracts of sheep lung tumors contain particles with a density of 1.15–1.20 g/ml, having the characteristics of a reverse transcriptase in association with a 60–70S RNA (*30*).

INDUCTION OF SPC BY VIRUS PREPARATIONS

The presence of a reverse transcriptase-producing agent in SPC (*30*) was reconfirmed (*29*). When sheep were given this fraction endobronchially, adenomas developed in 2 of 4 of these animals (*29*). More recently, pulmonary adenomatosis was transmitted to newborn lambs by inoculation of the microsomal fraction of a cytoplasmic extract of cultured SPC tumor cells or tumor tissue (*31*). We previously examined by electron microscopy aliquots of equilibrium density gradient-purified material from a primary lung tumor and normal lung tissue and tested them for the presence of reverse transcriptase and oncogenicity. We demonstrated that sections from the 1.15- to 1.20-g/ml density regions of the tumor material contained reverse transcriptase activity and possessed morphologically typical C-type "mature" and "immature" retroviruses (*30*). Normal adult sheep inoculated in the lungs last year with these virus-containing fractions developed the typical proliferating neoplasm after 1 year (*32*).

In summary, the electron microscopic observation of retrovirus in the lungs of sheep bearing SPC (*4, 14, 17, 23*) and the detection of particles with reverse transcriptase (*30, 29*) together with recent infectivity studies (*29, 31, 32*) indicate a retrovirus etiology of SPC. Notwithstanding the findings of close morphologic similarities between human bronchoalveolar carcinoma and SPC, we still do not know whether the diseases are etiologically related.

DIFFERENTIATION OF SPC AND MAEDI

Maedi (sheep progressive interstitial pneumonia), the second lung disease of sheep and frequently associated and occasionally confused with SPC, is also caused by a C-type retrovirus (*32–34*). The relationship between the C-type retrovirus of SPC and the maedi–visna C-type virus was tested by molecular hybridization, which revealed no sequence homology (*35*). This finding indicates that the maedi–visna virus is not implicated in the etiology of SPC, which complements findings in numerous earlier studies in which striking differences in clinical symptoms, pathology, serology (*32*), and histopathology were found.

COMMENTS WITH REGARD TO FUTURE STUDIES

Studies on SPC, a spontaneous, natural animal model, may aid in acquiring a better understanding of the pathogenesis, natural history, epidemiology, and host susceptibility of the disease and may lead to the selection of agents and modalities for chemotherapy in experimental animals and humans.

The etiologic demonstration of C-type retrovirus particles in this naturally occurring neoplasm extends the range of virus–tumor host systems to the ovine species and from leukemia–sarcoma and mammary tumors to lung epithelial tumors, i.e., to the epiendoderm, a major embryonal layer in human neoplasia.

REFERENCES

(*1*) De Kock G. Are the lesions of the jaagsiekte in sheep of the nature of a neoplasm? In: Fifteenth Annual Report of Director of Veterinary Services, Union of South Africa. Government publication. 1929:611–641, 1169–1183.

(*2*) Tustin, RC. Ovine jaagsiekte. J SC Afr Med Assoc 1969; 40:3–23.

(*3*) Dungal N. Experiments with jaagsiekte. Am J Pathol 1946; 22:737–759.

(*4*) Perk K, Hod I, Nobel TA. Pulmonary adenomatosis of sheep (jaagsiekte). I. Ultrastructure of the tumor. J Natl Cancer Inst 1971; 46:525–537.

(*5*) Enchev S. On malignant (metastasizing) forms of what is known as

---

[4] Eleventh Triennial World Congress of Pathology, Jerusalem, Israel, Sept. 20–25, 1981.

pulmonary adenomatosis (jaagsiekte) in sheep. C R Acad Bulg Sci 1963; 16:441–444.

(6) Nobel TA, Neumann F, Flopfer U. Histological pattern of metastases in pulmonary adenomatosis of sheep (jaagsiekte). J Comp Pathol 1969; 79:537–540.

(7) Nobel TA, Perk K. Bronchiolo-alveolar cell carcinoma. Am J Pathol 1978; 90:783–786.

(8) Wandera JG. Sheep pulmonary adenomatosis (jaagsiekte). Adv Vet Sci Comp Med 1971; 15:251–283.

(9) Cvjetanovic V, Forsek Z, Nevjestic A. Sheep pulmonary adenomatosis in SR Crna Gora, Yugloslavia. Veterinaria 1970; 19:315–320.

(10) Stunzi H, Head KW, Nielsen SW. Tumors of the lung. Bull WHO 1974; 50:9–19.

(11) Nielsen SW. Pulmonary neoplasia in domestic animals. In: Nettesheim P, Hanna MG, Deatherage JW, eds. Atomic Energy Commission symposium series. Springfield, Va.: Natl Technical Information Service, 1970:123–145.

(12) Dungal N, Gislason G, Taylor EL. Epizootic adenomatosis in the lungs of sheep—comparisons with jaagsiekte, verminous pneumonia and progressive pneumonia. J Comp Pathol 1938; 51:46–63.

(13) Perk K, Hod I, Presentey B, Nobel TA. Lung carcinoma of sheep (jaagsiekte). II. Histogenesis of the tumor. J Natl Cancer Inst 1971; 47:197–205.

(14) Hod I, Herz A, Zimber A. Pulmonary carcinoma (jaagsiekte) of sheep. Am J Pathol 1977; 86:545–558.

(15) Nisbet DK, MacKay JM, Smith W, Gray EN. Ultrastructure of sheep pulmonary adenomatosis (jaagsiekte). J Pathol 1971; 103:157–162.

(16) Perk K, Hod I, Nobel TA, Klopfer U. Some pathogenic aspects on ovine pulmonary carcinoma. Refu Vet 1972; 29:15–19.

(17) Hod I, Zimber, A, Klopfer U, Helder AW, Nobel TA, Perk K. Pulmonary carcinoma (jaagsiekte) of sheep: Pathologic findings and comparison in multiple-case and case-free herds. J Natl Cancer Inst 1974; 53:103–110

(18) Wandera JG. Sheep pulmonary adenomatosis. Ph.D. thesis. Nairobi: University of East Africa, 1970.

(19) Greenberg SD, Smith MN, Spjut HJ. Bronchiolo-alveolar carcinoma cell of origin. Am J Clin Pathol 1975; 63:153–167.

(20) Coalson JJ, Mohr JA, Pirtie JK, Dee AL, Rhoades ER. Electron microscopy of neoplasm in the lung with special emphasis on the alveolar cell carcinoma. Am Rev Respir Dis 1970; 101:181–197.

(21) Adamson JS, Senior RM, Merrill T. Alveolar cell carcinoma. An electron microscopic study. Am Rev Respir Dis 1969; 100:550–558.

(22) Robertson W. Jaagsiekte or chronic catarrhal pneumonia (sheep). J Comp Pathol Therap 1904; 17:221–224.

(23) Bucciarelli E. L-Adanomatosi pulmonare della pecora (jaagsiekte) studio ultrastructurale. Lav Ist Anat Istol Patol Univ Studi Perugia 1973; 33:99–117.

(24) Smith W, MacKay JM. Morphological observations on a virus associated with sheep pulmonary adenomatosis (jaagsiekte). J Comp Pathol 1968; 79:421–427.

(25) MacKay JM. Tissue culture studies of sheep pulmonary adenomatosis (jaagsiekte). I. Direct cultures of affected lungs. J Comp Pathol 1969; 79:141–146.

(26) ———. Tissue culture studies of sheep pulmonary adenomatosis (jaagsiekte). II. Transmission of cytopathic effects to normal cultures. J Comp Pathol 1969; 79:147–154.

(27) De Villiers EM, Els HJ, Verwoerd DW. Characteristics of an ovine herpes virus associated with pulmonary adenomatosis (jaagsiekte) in sheep. S Afr J Med Sci 1975; 49:165–175.

(28) Malmquist WA, Krauss HH, Moulton JE, Wandera JG. Morphologic study of virus infected lung cell culture from sheep pulmonary adenomatosis (jaagsiekte). Lab Invest 1972; 26:528–533.

(29) Martin WB, Scott MM, Sharp GM, Angus KW. Experimental production of sheep adenomatosis. Nature 1976; 264:183–185.

(30) Perk K, Michalides R, Spiegelman S, Schlom J. Biochemical and morphologic evidence for the presence of an RNA tumor virus in pulmonary carcinoma of sheep (jaagsiekte). J Natl Cancer Inst 1974; 53:131–135.

(31) Verwoerd DW, Williamson AL, De Villiers EM. Aetiology of jaagsiekte: Transmission by means of subcellular fractions and evidence for the involvement of a retrovirus. Onderstepoort J Vet Res 1980; 47:275–280.

(32) Perk K. Slow virus infections of ovine lung. Adv Vet Sci Comp Med 1982; 26:267–287.

(33) Sigurdardottier B, Thormar H. Isolation of a viral agent from the lungs of sheep affected with maedi. J Infect Dis 1964; 114:55–60.

(34) Takemoto KK, Aoki T, Garon C, Sturm MM. *Brief communication:* Comparative studies on visna, progressive pneumonia, and Rous sarcoma viruses by electron microscopy. J Natl Cancer Inst 1973; 50:543–547.

(35) Perk K, Yaniv A. Lack of maedi viral related RNA in pulmonary carcinoma of sheep (jaagsiekte). Res Vet Sci 1977; 23:46–49.

blank page

Studies on Carcinogenesis of Human Prostate. II. Long-Term Explant Culture of Normal Prostate and Benign Prostatic Hyperplasia: Light Microscopy[1,2,3,4]

Hayato Sanefuji,[5,6] **Barry M. Heatfield,**[5] **Benjamin F. Trump,**[5,7] *and* **John D. Young, Jr**[5,8,9]

ABSTRACT—Light microscopic and histochemical changes in normal human prostate and benign prostatic hyperplasia (BPH) during long-term explant culture were characterized. Normal human prostate obtained at immediate autopsy of young adults or BPH obtained at the time of surgery were maintained in explant culture as long as 24 weeks. Morphologic alterations in glandular epithelium and stroma in response to culture conditions were assessed by light microscopy and histochemistry of mucosubstances. The histologic and histochemical responses of normal prostate and BPH to in vitro conditions were essentially identical. Within 1 week, secretory epithelial cells became necrotic and sloughed into acinar lumina. Remaining epithelial cells proliferated, repopulated acinar structures, and migrated onto explant surfaces forming a new well-differentiated epithelium characterized by synthesis and secretion of neutral and acidic mucosubstances. During subsequent periods in vitro, synthesis and secretion of mucosubstances gradually diminished whereas the stroma and deep glandular structures became necrotic. Our observations suggest that cells comprising the new epithelium in cultured explants of normal human prostate and BPH are derived from prostatic basal cells.—JNCI 1982; 69:751–756.

Spontaneous adenocarcinoma of the prostate is the most common malignant neoplasm in the adult male and the third most common cause of death from cancer in the United States; only bronchogenic and colorectal carcinomas are more common causes of death. Despite numerous studies of the disease, little progress has been made in understanding the etiology, histogenesis, clinical behavior, and other features of this important neoplasm. Clearly, a suitable model of this disease is needed.

However, the validity of extrapolation from animal models of prostatic adenocarcinoma to the human neoplasm is questionable, and the need for models that are based on human tissues has been recently emphasized (*1–3*) despite inherent difficulties. For example, induction of adenocarcinoma in prostatic tissue of humans can only be done in vitro, with subsequent xenotransplantation for the assessment of tumorigenicity. However, one objection to this approach has been that human prostate tissue usually available for such studies is obtained from surgical specimens of BPH from older patients, which is *not* normal prostate (*1*). Moreover, numerous authors report maintenance of human prostate in explant culture for relatively short periods, usually less than 2 weeks (*4–10*); others report maintenance for periods of 6 weeks (*11*) to many months (*12*). However, few details are available with respect to morphologic or other changes occurring in glandular epithelium during short- or long-term culture. Establishment of these changes is vital as a base line for the interpretation of cellular alterations in response to agents such as hormones or chemical carcinogens in vitro.

In this paper, we provide this base-line information by describing histologic changes in normal human prostate of young adults throughout long-term explant culture as long as 24 weeks, with emphasis on epithelial cells and their responses to in vitro conditions. Further, we compare responses in normal human prostatic epithelium with those of BPH.

MATERIALS AND METHODS

Tissues.—Human prostate tissues were obtained from 8 patients, 16–31 years old, during IA after accidental death (*13*) or surgically from 30 patients, 55–82 years old, treated for BPH by transurethral resection or suprapubic prostatectomy.

Explant culture.—Complete details pertaining to culture techniques used in this study are presented elsewhere (*14*). Explants were cultured in CMRL-1066 medium (Grand Island Biological Co., Grand Island, N.Y.) supplemented with antibiotics, 5% heat-inactivated fetal bovine serum, hydrocortisone, and insulin. Cultures were incubated at 37°C on rocker platforms (Bellco Glass, Inc., Vineland, N.J.) in an atmosphere of 5% CO_2, 45% O_2, and 50% N_2. Culture medium and gas phase were changed three times each week.

Fixation.—During intervals of culture, from zero time to 24 weeks, explants were sampled and fixed in mixed alde-

---

ABBREVIATIONS USED: AB=alcian blue, pH 2.5; AF=aldehyde fuchsin, pH 1.0; BPH=benign prostatic hyperplasia; H & E=hematoxylin and eosin; IA=immediate autopsy; LM=light microscopy; PAS=periodic acid-Schiff.

---

[1] Received February 1, 1980; revised April 23, 1982; accepted May 10, 1982.

[2] Contribution #627 from the Cellular Pathobiology Laboratory, Department of Pathology, University of Maryland School of Medicine.

[3] Supported by Public Health Service grant CA-15798 from the National Cancer Institute.

[4] Research procedures were in accord with the ethical standards of the Human Volunteers Research Committee of the University of Maryland at Baltimore.

[5] Department of Pathology, University of Maryland School of Medicine, 10 South Pine St., Baltimore, Md. 21201.

[6] *Present address:* Department of Pathology, University of Occupational and Environmental Health, School of Medicine, Yahatanishi-ku, Kitakyushu 807, Japan.

[7] *Address reprint requests to* Dr. Trump.

[8] *Present address:* Department of Urology, University of Maryland School of Medicine.

[9] We thank Dr. L. Barrett and staff for aid in explant culture, Dr. E. Hillman and staff for preparation of tissues for light microscopy and for publication prints, and Mrs. E. Adelberg and staff for typing the manuscript.

hydes (4% formaldehyde–1% glutaraldehyde in 200 mos*M* phosphate buffer) (*15*) and were processed for LM and histochemistry.

LM.—Fixed tissues were dehydrated through a series of graded alcohols, embedded in paraffin, cut at a thickness of 4–5 μm, and routinely stained with H & E.

Histochemistry.—For the study of mucosubstances, serial sections were stained with PAS with and without α-amylase digestion, AB–PAS sequence, AF–AB sequence, and mucicarmine. Before being stained with PAS, tissue sections were treated with dimedone (*16*), which blocked free aldehyde groups contributed by the glutaraldehyde component of the fixative groups that would otherwise react with the Schiff reagent producing a false-positive result.

RESULTS

Explants showed good preservation of morphology in culture for as long as 24 weeks for normal prostate and as long as 20 weeks for BPH, at which times all explants had been sampled. The observations described below are characteristic of all explants of normal prostate or BPH which showed survival of epithelial cells.

Zero Time Culture

Normal glands, IA.—By LM, normal prostate consisted of numerous tubuloalveolar glands and ducts surrounded by dense eosinophilic fibromuscular stroma (fig. 1). The glandular epithelium was composed of two cell types: *a*) columnar to cuboidal secretory cells with a foamy cytoplasm and large, round nuclei and *b*) flattened basal cells which lacked foamy cytoplasm and possessed a triangular or elongated, densely staining nucleus (fig. 2). Eosinophilic corpora amylacea were occasionally present in glandular lumina (fig. 1).

Histochemically, in dimedone-blocked histologic sections, PAS-positive, α-amylase-resistant granules were seen scattered within the cytoplasm of secretory epithelial cells (fig. 3). At the cell apex, the granules appeared coarser than elsewhere. Within gland lumina, these granules appeared free or in coarse aggregates, sometimes in association with PAS-positive amorphous material. PAS-positive granules and amorphous material were negative for acidic component by the AB–PAS or AF–AB sequence. In some acini, rather large PAS-positive, α-amylase-resistant droplets of varying diameter were present, especially in basal portions of secretory cells as well as within acinar lumina.

BPH.—LM of specimens of BPH showed varying degrees of glandular and stromal hyperplasia. The acini were sometimes enlarged with numerous papillary processes projecting into the lumina. Corpora amylacea were more frequently seen in BPH than in normal prostate. Otherwise, the histology and histochemistry were essentially identical to the histology and histochemistry of normal prostate, as described above.

One Week of Culture

Normal glands, IA.—Within explants during the first 2–3 days of culture, rapid degeneration and necrosis of secretory epithelial cells were striking features, although the rate of degeneration varied from acinus to acinus (figs. 4, 5). In some acini, an occasional pyknotic nucleus was seen; in other acini, large numbers of necrotic secretory cells sloughed into the lumen. Compared to acini near the surface of explants, degeneration appeared sooner and was more extensive in acini deep within explants. Eventually, within this time, some gland lumina were filled with heterogeneous eosinophilic cellular debris (figs. 5, 6). Some acinar cells did not degenerate but remained viable and appeared to repopulate acini and ducts denuded of secretory cells. Mitotic figures were sometimes seen among these cells during and subsequent to degeneration of secretory cells.

At the same time degenerative changes were occurring within the explants, epithelial cells migrated from exposed ducts or glandular spaces over the cut surfaces of explants. By 1 week of culture, the cut surface was shown by LM to be completely covered with a sheet of migrating cells, which was continuous with the cell sheet lining the exposed ducts or glandular spaces exposed to view after sectioning had been done. In occasional explants consisting only of stromal tissue, few migrating cells were seen.

Cells repopulating acini and cut surfaces of explants formed a multilayered epithelium characterized by widened intercellular spaces. The epithelium consisted of columnar to polygonal or flattened, squamous-like cells; polygonal cells predominated (fig. 6).

By histochemistry, the surface cells of the explant as well as the cells lining the glands within explants exhibited numerous PAS-positive, α-amylase-resistant granules, particularly in the apical portion above the nucleus (fig. 7). At the cell apex, granules were dense and intensely PAS-positive and were also frequently stained with AB (fig. 8) but not with AF; these staining patterns are consistent with both neutral and sialic acid-containing mucosubstances. In the supranuclear zone within these cells, granules usually stained only with PAS. AB-positive mucosubstances also stained with mucicarmine to varying degrees. The apical surfaces of cells appeared to stain with AB, AF, and mucicarmine. Substances with similar staining properties also were present within gland lumina.

BPH.—LM and histochemical observations for BPH were essentially identical to those described above for normal prostate. Squamous metaplasia was sometimes seen in specimens of BPH (fig. 9) but was not seen in normal prostate.

Two Weeks of Culture

Normal glands, IA.—Fewer tall columnar cells were seen at this time. An occasional mitotic figure was present among acinar and surface cells of explants. Few viable cells were noted in the fibromuscular stroma.

At this time, mucosubstances were abundant in cells with markedly convex apical surfaces. This observation was especially true for columnar cells, in which the convex apical surfaces persisted. Outer surfaces of cells continued to stain with AB, AF, and mucicarmine.

BPH.—Explant surfaces were covered by a mucus-secreting multilayered epithelium (fig. 10), essentially identical to that described above for normal prostate.

Three to Twenty-Four Weeks of Culture

Normal glands, IA.—Most cultures were terminated at 12–14 weeks. However, one experiment with normal prostate was terminated at 22 weeks and another was terminated at 24 weeks. Throughout this period, the surface sheet was maintained even in 24-week explants. It differed in thickness from area to area, yet the overall organization remained virtually the same (figs. 11, 12). Intact acini were lined by polygonal, cuboidal, or squamous-like cells and were generally limited to the peripheral zones of explants. Occasional mitotic figures were seen. During this interval, mucosubstances were present but in amounts that appeared diminished when compared to amounts during earlier intervals. There were fewer apical granules present in surface or acinar cells, yet histochemical staining was qualitatively similar to staining at earlier times. The surfaces of these cells continued to show an affinity for AB and mucicarmine. Few viable cells were present within the necrotic stroma.

BPH.—Morphologic and histochemical changes occurring in explants of BPH were identical to those changes described above for normal prostate. Squamous changes persisted in some BPH explants.

DISCUSSION

The present study is the first to describe LM of long-term explant culture of normal, nonhypertrophic, nonneoplastic human prostate obtained from young adult patients, with a comparison to BPH obtained from older individuals. Previous studies of cultured human prostate have usually used BPH from older men which had been obtained surgically because of obstructive prostatic disease (*4–10, 12*). Noyes (*11*) used prostate tissue from patients 50–70 years old, which was sampled at the time of cystectomy, and concluded that it was histologically "normal." However, BPH is a common entity beyond the age of 50 and is usually unnoticed until obstructive symptoms appear. Despite the similar response of BPH and normal prostate to in vitro conditions in the present paper, Franks (*1*) has concluded that BPH is *not* normal prostate. Moreover, there is a possibility of inadvertently sampling preneoplastic or neoplastic cells in older patients, which would invalidate studies on induction of malignant transformation by carcinogenic agents (*1*).

On the basis of continuity and similarities in morphology and histochemistry of cells colonizing explant surfaces and acinar structures throughout long-term culture of normal prostate and BPH, we conclude from the present work that epithelial cells covering explant surfaces are identical to and are derived from epithelial cells of acini. In these acini, cells in a basal location appeared to remain viable during degeneration and necrosis of secretory cells. The presence of occasional mitotic figures among these basally situated cells suggests proliferation followed by repopulation of acini and migration and colonization of explant surfaces. Thus it seems likely that proliferation of basal cells accounts for repopulation of acinar structures, colonization of explant surfaces, and synthesis and secretion of mucosubstances during early periods of culture.

Previous studies of BPH or normal prostate in explant culture have reported maintenance of viability of glandular epithelium for periods of typically less than 2 weeks to periods as long as 48 months (*4–9, 11, 12*). Usually, no distinction was made in these studies between columnar secretory cells and basal cells with regard to degeneration and necrosis nor were morphologic features described in detail, as we attempted in the present study. Maintenance of secretory epithelial cells with a columnar profile has been possible for as long as 10 days (*6*), although reduction in secretory vacuoles and cell height has been reported after only a few days in vitro (*4, 10*). Squamous changes have also been seen during early periods of culture (*4, 6, 9–11*). On the basis of the present study, it is very unlikely that epithelial cells seen during long-term explant culture of human prostate in previous work are viable columnar secretory cells. Rather, we propose that cultured prostatic epithelial cells seen by previous authors were derived from basal cells we have defined ultrastructurally (*17*).

The implication for a potential role of basal cells in the genesis of adenocarcinoma of the prostate is strongly suggested by the above observations and by morphologic evidence of premalignant and malignant changes in basal cell derivatives in response to *N*-methyl-*N*′-nitro-*N*-nitosoguanidine in vitro (*18, 19*). In this regard we also find it interesting that differentiated basal cells synthesize and secrete acidic mucosubstances during explant culture, which we report in the present paper. Although acidic mucosubstances are not demonstrable histochemically in the epithelium of normal prostate, they are frequently detected in prostatic adenocarcinoma (*20, 21*) and have staining affinities (neutral and acidic components) similar to those seen in the present study. Using histochemical techniques, Noyes (*11*) also detected neutral mucosubstances in the epithelium of prostatic explants after culture for 12 days, but he did not stain for acidic components, and thereby he failed to recognize synthesis and secretion of acidic mucosubstances in vitro.

REFERENCES

(*1*) Franks LM. Tissue culture in the investigation of prostatic cancer. Urol Res 1977; 5:159–162.

(*2*) Handelsman H. The limitations of model systems in prostatic cancer. Oncology 1977; 34:96–99.

(*3*) Merchant DJ. Model systems for the study of prostatic cancer. Oncology 1977; 34:100–101.

(*4*) Schrodt GR, Foreman CD. In vitro maintenance of human hyperplastic prostate tissue. Invest Urol 1971; 9:85–94.

(*5*) Stonington OG, Hemmingsen H. Culture of cells as a monolayer derived from the epithelium of the human prostate: A new cell growth technique. J Urol 1971; 106:393–400.

(*6*) McMahon MJ, Thomas GH. Morphological changes of benign prostatic hyperplasia in culture. Br J Cancer 1973; 27:323–335.

(*7*) McRae CU, Ghanadian R, Fotherby K, Chisholm GD. The effect of testosterone on the human prostate in organ culture. Br J Urol 1973; 45:156–162.

(*8*) Harbitz TB, Falkanger B, Sander S. Benign hyperplasia of the human prostate exposed to steroid hormones in organ culture. Acta Pathol Microbiol Scand Suppl 1974; 248:89–93.

(*9*) Lasnitzki I, Whitaker RH, Withycombe JF. The effect of steroid hormones on the growth pattern and RNA synthesis in human benign prostatic hyperplasia in organ culture. Br J Cancer 1975; 32:168–178.

(*10*) Dilley WG, Birkhoff JD. Hormone response of benign hyperplastic prostate tissue in organ culture. Invest Urol 1977; 15:83–86.

(*11*) Noyes WF. Effect of 3-methylcholanthrene (NSC-21970) on human prostate in organ culture. Cancer Chemother Rep 1975; 59:67–71.

(*12*) Franks LM, Riddle PN, Carbonell AW, Gey GO. A comparative study of the ultrastructure and lack of growth capacity of adult human prostate epithelium mechanically separated from its stroma. J Pathol 1970; 100:113–119.

(*13*) Trump BF, Valigorsky JM, Jones RT, Mergner WJ, Garcia JH, Cowley RA. The application of electron microscopy and cellular biochemistry to the autopsy. Observations on cellular changes in human shock. Hum Pathol 1975; 6:499–516.

(*14*) Sanefuji H, Heatfield BM, Trump BF. Studies on carcinogenesis of human prostate. I. Technique for long-term explant culture. Tissue Cult Assoc Manual 1978; 4:855–856.

(*15*) McDowell EM, Trump BF. Histologic fixatives suitable for diagnostic light and electron microscopy. Arch Pathol Lab Med 1976; 100:405–414.

(*16*) Pearse AG. Histochemistry: Theoretical and applied. Vol I. 3d ed. Boston: Little, Brown & Co., 1968:455–456.

(*17*) Heatfield BM, Sanefuji H, Trump BF. Studies on carcinogenesis of human prostate. III. Long-term explant culture of normal prostate and benign prostatic hyperplasia: Transmission and scanning electron microscopy. JNCI 1982; 69:757–766.

(*18*) ———. Studies on carcinogenesis of human prostate. IV. Comparison of normal and neoplastic prostate during long-term explant culture. Scan Electron Microsc 1979; 3:645–656.

(*19*) Sanefuji H, Heatfield BM, Trump BF. Studies on carcinogenesis of human prostate. V. Effects of the carcinogen, *N*-methyl-*N'*-nitro-*N*-nitrosoguanidine (MNNG), on normal prostate during long-term explant culture. Scan Electron Microsc 1979; 3:657–663.

(*20*) Franks LM, O'Shea JD, Thomson AE. Mucin in the prostate: A histochemical study in normal glands, latent, clinical, and colloid cancers. Cancer 1964; 17:983–991.

(*21*) Hukill PB, Vidone RA. Histochemistry of mucus and other polysaccharides in tumors. II. Carcinoma of the prostate. Lab Invest 1967; 16:395–406.

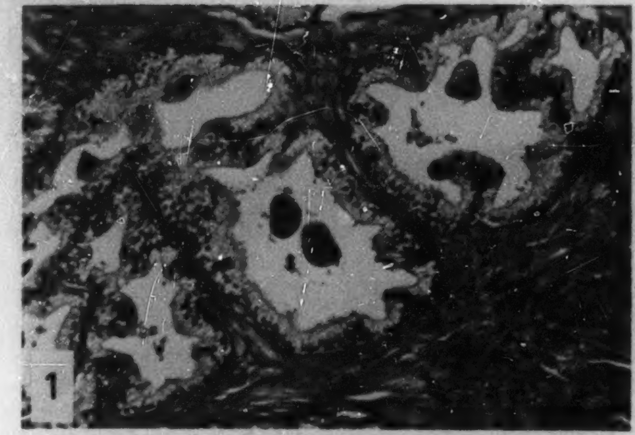

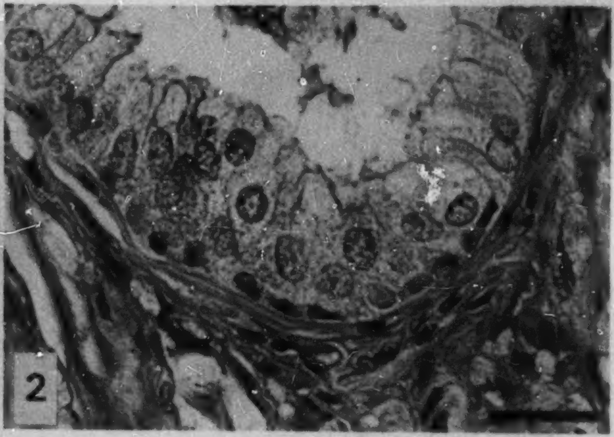

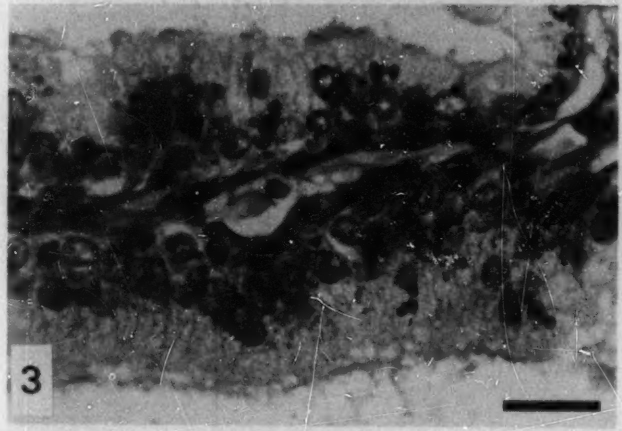

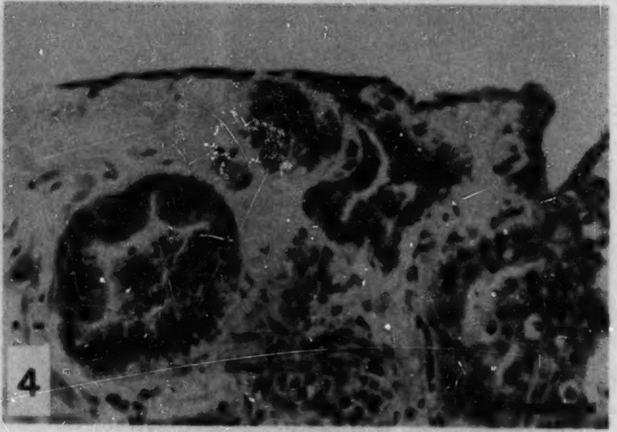

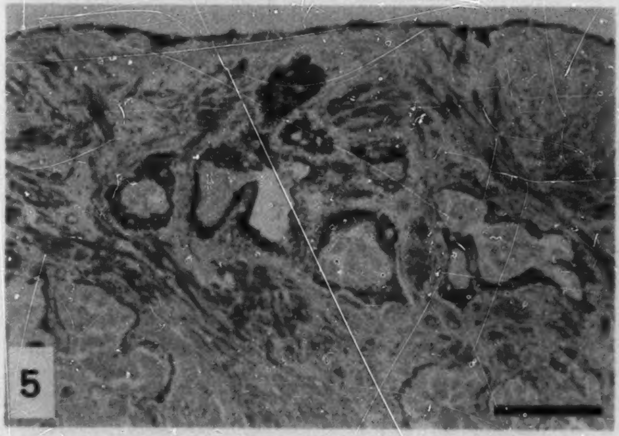

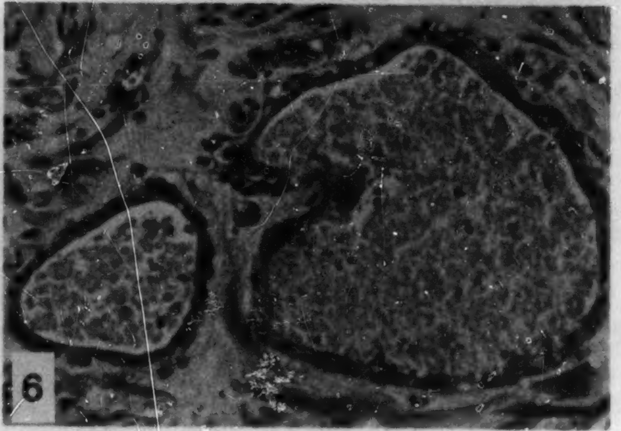

FIGURE 1.—Normal prostate, IA, zero time culture. Glandular lumina are lined by foamy-appearing epithelial cells and surrounded by fibromuscular stroma; two eosinophilic corpora amylacea appear within the central gland lumen. H & E. *Bar*=100 μm. × 120

FIGURE 2.—Higher magnification of fig. 1. Columnar secretory cells with foamy cytoplasm are oriented toward the gland lumen; basal cells beneath columnar cells are seen flattened along the basement membrane. H & E. *Bar*=25 μm. × 625

FIGURE 3.—Same tissue as in fig. 1. α-Amylase-resistant, PAS-positive fine granules are present in the cytoplasm of columnar cells. PAS after α-amylase digestion. *Bar*=25 μm. × 540

FIGURE 4.—Normal prostate, IA, 2-day culture. Epithelial cells appear on explant surfaces and adjacent glandular structures near the surface or deep within the explant. H & E. *Bar*=50 μm. × 225

FIGURE 5.—Normal prostate, IA, 1-wk culture. Viability of epithelial cells varies with distance from the explant surface. Deep within the explant, extensive necrosis and accumulation of cell debris are seen. H & E. *Bar*=250 μm. × 60

FIGURE 6.—Normal prostate, IA, 1-wk culture. Higher magnification of same explant as in fig. 5. Eosinophilic cellular debris fills glandular lumina lined by cuboidal or polygonal epithelial cells. H & E. *Bar*=50 μm. × 250

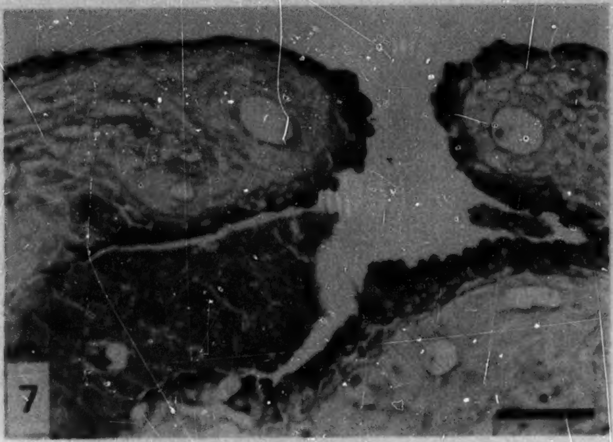
7

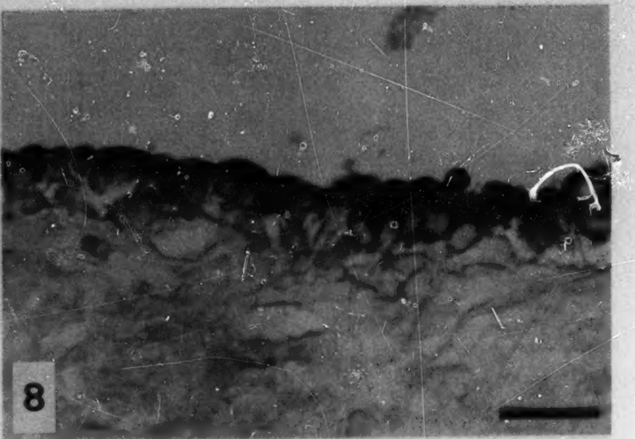
8

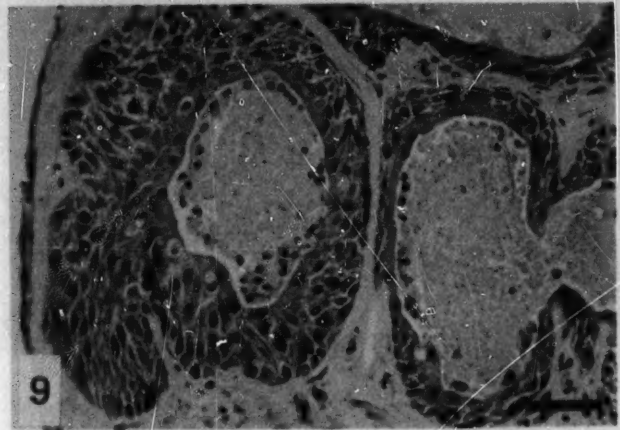
9

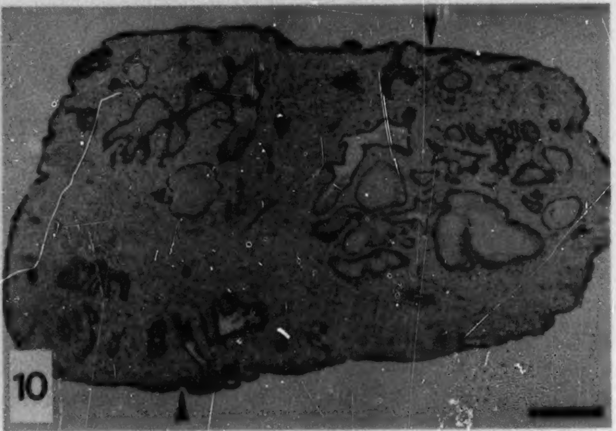
10

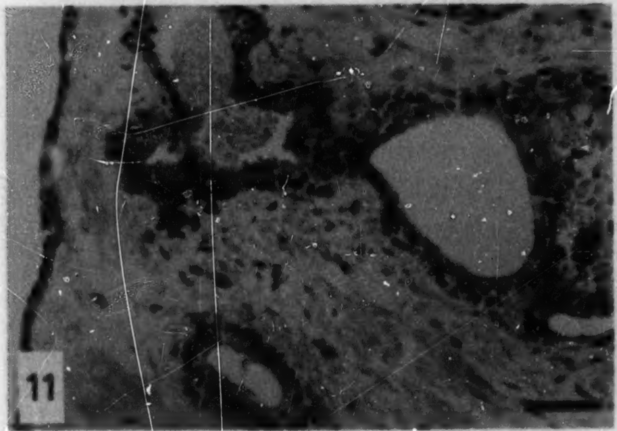
11

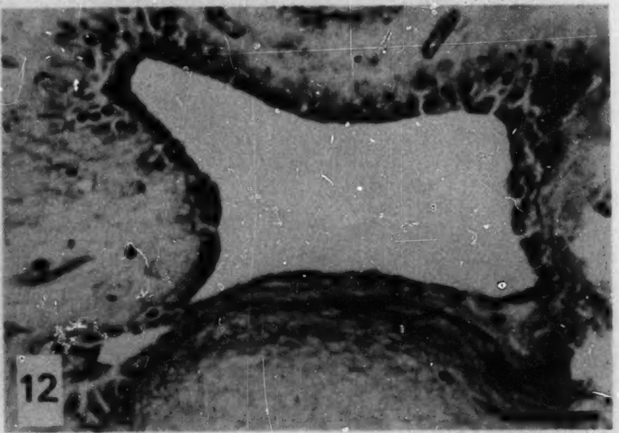
12

Figure 7.—Normal prostate, IA, 1-wk culture. PAS-positive, α-amylase-resistant material, for the most part, is restricted to the apical portion of epithelial cells. *Note* continuity of surface epithelial cells with cells of adjacent glandular structures and *note* identity of staining properties. PAS after α-amylase digestion. *Bar*=50 μm. × 280

Figure 8.—Normal prostate, IA, 1-wk culture. Mucosubstances are found in the apical portions of epithelial cells and at the outer cell surfaces. AB-PAS. *Bar*=25 μm. × 575

Figure 9.—BPH, 1-wk culture. Morphologic appearances resembling squamous metaplasia are seen. H & E. *Bar*=50 μm. × 215

Figure 10.—BPH, 2-wk culture. A thin sheet of epithelial cells covers the cut surface (*arrowheads*) of the explant and is continuous with the epithelial cell layer lining glands and ducts within the explant. H & E. *Bar*=250 μm. × 45

Figure 11.—Normal prostate, IA, 5-wk culture. Well-preserved glands are lined by epithelial cells similar to those at the explant surface. H & E. *Bar*=50 μm. × 210

Figure 12.—Normal prostate, IA, 11-wk culture. Epithelial cells lining glandular spaces are cuboidal or flattened. H & E. *Bar*=50 μm. × 285

Studies on Carcinogenesis of Human Prostate. III. Long-Term Explant Culture of Normal Prostate and Benign Prostatic Hyperplasia: Transmission and Scanning Electron Microscopy[1,2,3,4]

Barry M. Heatfield,[5] **Hayato Sanefuji,**[5,6] *and* **Benjamin F. Trump**[5,7,8]

ABSTRACT—Ultrastructural changes in normal human prostate and benign prostatic hyperplasia (BPH) during long-term explant culture were compared. Explants of normal prostate obtained at immediate autopsy of young adults or of BPH obtained at the time of surgery were maintained as long as 24 weeks in vitro. Ultrastructural changes occurring in epithelial cells during culture were monitored by transmission and scanning electron microscopy. Essentially identical results were found for normal prostate and BPH. During the first week of culture, secretory epithelial cells degenerated and sloughed into the acinar lumen, resulting in an accumulation of necrotic debris. During this period, however, epithelial cells with ultrastructural characteristics of basal cells remained viable, repopulated glandular structures, migrated from glands and ducts, and epithelialized adjacent cut surfaces, eventually covering the explant. On explant surfaces, these basal cells initially were squamous-like, but they later became typically cuboidal, polygonal, or sometimes columnar and formed an epithelium, two cells or more thick. Epithelium with similar features lined acini within explants. Epithelial cells at the surface or within explants were distinguished by the presence of microvilli, junctional complexes, multiple Golgi complexes, well-developed rough endoplasmic reticulum, polyribosomes, nuclei with prominent nucleoli, orthodox mitochondria, scattered tonofilaments, and a basal lamina. Some epithelial cells extended from the lumen to the basal lamina; others were oriented along the basal lamina and did not extend to the lumen. By 1-2 weeks in vitro, these epithelial cells began synthesis of mucus-like material. At later intervals of culture, microvilli were shortened and mucosubstances were reduced. During culture, the stroma became progressively hypocellular and necrotic. In summary, explant-cultured epithelial cells of normal human prostate or BPH were similar ultrastructurally and were found to originate from basal cells, which alone survive culture conditions.—JNCI 1982; 69:757-766.

Another paper in this series describes light microscopic and histochemical alterations in normal human prostate and BPH during long-term explant culture as long as 24 weeks (*1*). The results of this other study suggested that basal cells were responsible for epithelial recovery and growth in vitro (*1*). The present paper extends these observations to the ultrastructural level with the transmission and scanning electron microscopes and conclusively demonstrates survival and repopulation of glandular acini and colonization of explant surfaces of normal human prostate and BPH by epithelial cells having ultrastructural features identical to features of prostatic basal cells.

MATERIALS AND METHODS

Tissues.—Human prostate tissues were obtained from 8 patients, 16-31 years old, during IA after accidental death (*2*) or surgically from 30 patients, 55-82 years old, treated for BPH by transurethral resection or suprapubic prostatectomy.

Explant culture.—Complete details pertaining to explant culture techniques used in this phase of the study are presented elsewhere (*3*).

Fixation.—During intervals of culture, from zero time to 24 weeks, explants were sampled and fixed in 4% formaldehyde-1% glutaraldehyde in 200 mos*M* phosphate buffer (*4*).

Electron microscopy.—For TEM, fixed tissues were washed in three changes of 0.2 *M* cacodylate-7% sucrose buffer and postfixed in 1% OsO_4. Washed tissues were then stained en bloc with 1% uranyl acetate, dehydrated through a series of graded ethanols and propylene oxide, and embedded in Epon. For high-resolution LM, semithin sections were cut at a thickness of 1 μm and stained with toluidine blue (*5*); suitable areas were then selected for ultrathin sectioning. Ultrathin sections were stained with uranyl magnesium acetate and lead citrate and examined in a JEOL 100B electron microscope.

For SEM, fixed tissues were washed in three changes of 0.2 *M* sodium cacodylate-7% sucrose, postfixed in 2% OsO_4 for 1-2 hours, washed in 5-10 changes of 0.2 *M* sodium cacodylate-7% sucrose, and placed in saturated thiocarbo-

---

ABBREVIATIONS USED: BPH=benign prostatic hyperplasia; IA=immediate autopsy; LM=light microscopy; RER=rough endoplasmic reticulum; SEM=scanning electron microscopy; TEM=transmission electron microscopy.

---

[1] Received February 1, 1980; revised April 23, 1982; accepted May 10, 1982.

[2] Contribution #628 from the Cellular Pathobiology Laboratory, Department of Pathology, University of Maryland School of Medicine.

[3] Supported by Public Health Service grant CA-15798 from the National Cancer Institute.

[4] Research procedures were in accord with the ethical standards of the Human Volunteers Research Committee of the University of Maryland at Baltimore.

[5] Department of Pathology, University of Maryland School of Medicine, 10 South Pine St., Baltimore, Md. 21201.

[6] *Present address:* Department of Pathology, University of Occupational and Environmental Health, School of Medicine, Yahatanishi-ku, Kitakyushu 807, Japan.

[7] *Address reprint requests to* Dr. Trump.

[8] We thank Dr. L. Barrett and staff for aid in explant culture, Dr. E. Hillman and staff for preparation of tissues for light and electron microscopy and for publication prints, and Mrs. E. Adelberg and staff for typing the manuscript.

hydrazide (6) in distilled water for 20 minutes at room temperature. Specimens were then washed in 5–10 changes of distilled water, placed in OsO_4 for 30 minutes to 1 hour, dehydrated through graded ethanols, and subjected to critical-point drying (model E 3000; Polysciences, Inc., Warrington, Pa.) with liquid CO_2. Thereafter, dried specimens were mounted on aluminum stubs (E. J. Fjeld Co., Inc., Maynard, Mass.) with silver conductive paint (Acme Chemicals and Insulation Co., Division of Allied Products Corp., New Haven, Conn.), sputter-coated (Technics Inc., Alexandria, Va.) with gold–palladium for 5 minutes, and examined with an AMR-1000 scanning electron microscope.

RESULTS

Zero Time Culture

Normal glands, IA.—LM of Epon-embedded normal prostate at zero time revealed columnar to cuboidal secretory cells and nonsecretory basal cells lining glandular acini (fig. 1).

TEM of secretory cells showed a polarized distribution of cytoplasmic organelles. The most characteristic ultrastructural features of these cells were a well-developed Golgi complex and numerous vesicles and secretory vacuoles in the supranuclear zone (fig. 2). Secretory vacuoles possessed a variable number of heterogeneous inclusions including small, irregular dense bodies, small vesicles, and occasional membrane whorls. Short microvilli characterized the apical cell surface but were most numerous in narrow clefts between adjacent cells (fig. 2). Blebs on the apical surface were observed, and membrane-bound extracellular vesicles, vacuoles, and membrane-enclosed portions of the cytoplasm were often seen in contact with the outer surface of the apical plasma membrane, or they appeared free in the acinar lumen. The apical plasma membrane of some cells was disrupted or absent altogether. Lateral surfaces of adjacent cells were connected by tight junctions at the apex, with gap junctions and desmosomes present more basally between cells. Narrow intercellular spaces were crowded with interdigitating folds of the lateral plasma membrane. The basal portion of secretory cells, which abutted on the basal lamina, contained mitochondria, sparse RER, lipid droplets, free polyribosomes, and a few secretory vacuoles (figs. 2, 3). Above this portion were a few orthodox mitochondria and a round nucleus containing a single nucleolus. Lysosomes with a homogeneous, finely granular interior were scattered in all portions of the cell.

Nestled among the basal portions of columnar cells and in contact with the basal lamina were polymorphic basal cells that differed conspicuously from their secretory counterparts by the absence of secretory vacuoles and of a well-developed Golgi complex (figs. 2, 3). The nucleus was prominent in these cells, although other organelles were sparse (fig. 3). Numerous free polyribosomes were present, which contributed to an increased electron density of the cytoplasm. The basal lamina appeared as a thin, amorphous zone separating the underlying stroma from the epithelial layer (figs. 2, 3).

SEM of cut surfaces of explants showed glandular elements that were easily distinguished from stromal components. Glands were lined by epithelial cells. Epithelial cells covering folds or papillae of the gland wall projected into the acinar space in compact, grapelike masses (fig. 4). If tissues were fixed without additional trimming, glands exposed at cut surfaces were distorted and bulged outward. But when tissues were retrimmed after fixation and tissue contraction, a more normal histologic appearance of the gland was observed (fig. 4). The apical contour of epithelial cells was typically convex.

Short microvilli were distributed over the surface of each cell (fig. 5). In addition, the apical plasma membrane frequently was perforated by pores or holes (fig. 5); occasionally, the entire apical plasma membrane was absent. One interesting feature encountered to varying degrees in most glands was that of apical surface blebs. Blebs ranged from small, irregular or spherical protuberances (fig. 5) to smooth, balloon-like structures involving the entire apical plasma membrane.

BPH.—LM, TEM, and SEM of epithelial cells of BPH provided results similar to those obtained from normal glands, although morphologic integrity was not as satisfactory as it was in fresh glands obtained at immediate autopsy. In one case of BPH, lacunar separation of basal cells was observed, comparable to the separation seen during culture in vitro in normal glands and glands of BPH.

One Week of Culture

Normal glands, IA.—By 1 week of culture, most of the cut surfaces of explants of normal prostate were shown by LM to be covered by a sheet of cells continuous with the cell sheet lining ducts or glandular alveoli. Where bare areas were being covered, a single layer of flattened migratory cells was seen (fig. 6). Away from the leading edge of migrating cells, the sheet was 2–3 cells thick. Cells were either columnar (fig. 7), polygonal, cuboidal, or flattened and squamous-like. Cells were typically separated by widened intercellular spaces. In glands within the interior of explants, necrosis of columnar secretory cells was a common feature and was evident as early as 2–3 days of culture (fig. 8). The lumina were filled with cellular debris.

TEM of cells at explant surfaces showed a sheet of epithelial cells varying from one cell thick at the leading, migrating edge to 2–3 cells or more thick in more proximal locations resting on a basal lamina (fig. 9). Some cells extended from the basal lamina to the surface; others appeared intermediate in position or were flattened along the basal lamina. Typically, wide intercellular spaces separated cells (figs. 9, 10). Penetrating these spaces were microvillus-like projections, shown by SEM of exposed cell surfaces to be delicate folds of the plasma membrane (*see* fig. 14). These projections intermingled with or showed close apposition to those of neighboring cells. The outermost cells were connected to adjacent cells at the apex by tight junctions (fig. 10). Scattered along the apical surface were numerous microvilli. All cells comprising the surface sheet were attached at other points of contact by small desmosomes. Polarization of cell organelles was not conspicuous, with the exception of vacuoles as described below. Nuclei varied markedly in shape and were not restricted to basal regions of the cell. Typically, a single prominent nucleolus was present; condensed chromatin was scanty. Cells possessed multiple Golgi complexes, numerous, sometimes bizarre mitochondria, RER occasionally in whorl-like configurations, and free polyribosomes (figs. 9, 10). Other organelles present included lysosomes, occasional residual bodies, lipid droplets, microtubules, and small bands of filaments that resembled tonofilaments. In a few cells numerous myelin figures were seen. Characteristic inclusions, especially prominent in columnar cells, were membrane-bound vacuoles of variable size and number which were filled with flocculent material and frequently had a finely granular, moderately dense eccentric core. Vacuoles were closely associated with Golgi elements in some instances. The apical portion of some cells was packed with these vacuoles (fig. 10).

Deep within explants, normal prostate columnar secretory cells were seen in various stages of necrosis (fig. 11). Characteristic features of these secretory cells included numerous autophagic vacuoles, loss of organelles, disrupted cell membranes, and pyknotic nuclei. Basal cells remained viable (fig. 11), however, and lined lumina filled with cell debris. In some basal cells, numerous vacuoles were filled with dense heterogeneous material, lipid droplets, or myelin figures, suggesting heterophagy of secretory cell debris. Basal cells within explants also possessed mucus-filled vacuoles, sometimes in large numbers, and resembled or were identical to cells comprising the epithelium at explant surfaces. Microvilli varied in number.

SEM showed explant surfaces covered by tightly packed arrays of polygonal epithelial cells with flattened to convex surfaces on which numerous short microvilli were borne (figs. 12, 13), or it showed overlapping, squamous-like migratory cells with irregular surfaces and minute microvilli. When artifactual separation of surface epithelial cells occurred, petal-like lateral plasma membrane folds were revealed (fig. 14). Epithelial cells resembled normal glandular epithelium at zero time, except that microvilli were longer and covered the apical surface. Pores or holes in the apical plasma membrane were not seen. Surface blebs were uncommon. Occasionally, the cut surfaces of explants were naked; only a tangled, interlacing meshwork of collagen fibrils was seen. Encroaching on these bare areas were sheets of migratory cells, with characteristics of squamous-like epithelium.

BPH.—LM, TEM, and SEM observations of cultured BPH explants at this time were essentially identical to the observations described above for normal prostate. In some instances, degeneration of columnar secretory cells in acinar spaces within explants appeared earlier compared to normal glands.

Two Weeks of Culture

Normal glands, IA.—By LM, fewer tall columnar cells were observed at this time or at subsequent times; abundant necrotic debris was seen in acinar lumina within explants (fig. 15).

TEM revealed some reduction in height and numbers of microvilli and in apical vacuoles containing mucus-like material (fig. 16). Residual bodies, myelin figures, and lipid droplets were more numerous in epithelial cells lining acini than in those epithelial cells at the explant surfaces.

The outline and surface features of epithelial cells at the exterior of the explants were variable. Apical surfaces were polygonal and varied from flat to markedly convex, as seen by SEM (*see* fig. 18).

BPH.—Changes in cultures of BPH explants at this interval were essentially identical to the changes seen for normal glands.

Three to Twenty-Four Weeks of Culture

Normal glands, IA.—Intercellular spacing was more variable, yet the overall organization remained remarkably the same (fig. 17) when viewed by LM.

By TEM, small vacuoles enclosing mucus-like material occasionally were seen at 7 weeks' culture and were seen later, both in epithelial cells of explant surfaces and within explants. At 24 weeks, epithelial cells were similar to those at earlier times. Calcification of residual cell debris within some acini was noted.

By SEM, epithelial cells were polygonal with flattened to convex apical surfaces bearing shortened microvilli (fig. 18). In one specimen, both surface and underlying epithelial cells as well as collagen fibrils of subjacent stroma were visible. Small blebs of the apical plasma membrane were occasionally seen.

BPH.—BPH explants at 20 weeks were essentially identical in ultrastructure to explants described above for normal prostate. However, in 2 cases of BPH examined by SEM, some of the explants were covered with bizarre cells. Such cells piled up on explant surfaces, did not show close attachment to one another, but did appear loosely organized with cytoplasmic projections and filopodia contacting adjacent cells (fig. 19). There was little evidence of surface activity; only ripple-like undulations of the apical plasma membrane or tiny spherical projections were scattered over the cell surface. Cells with these features were not associated with explants derived from normal prostate.

With the exception of the bizarre alterations and occasional squamous metaplasia in BPH described above, no consistent differences were noted either in the pattern of in vitro epithelial response among the various normal prostates and cases of BPH studied or among explants of the same case of BPH in which basal cell types survived.

DISCUSSION

Before culture, the normal prostate of young adults and BPH in our study resembled BPH described in older patients (*7-16*). Two cell types were present: *a*) columnar to cuboidal secretory cells and *b*) nonsecretory basal cells. By SEM, a variety of apical surface features as well as several morphologic cell types have been described for secretory cells of BPH (*12, 13, 16, 17*) but have not been described for normal prostate. Stone et al. (*13, 16*) described *a*) microvillus cells possessing numerous microvilli (≥90% cells present), *b*) bare cells lacking membrane specializations, and *c*) ruffled cells characterized by the presence of variable numbers of tiny folds or microplicae. In addition, Clark et al. (*12*) observed numerous cells with pits or holes in the apical plasma membrane. In other cells, termed "crater cells," the entire apical portion of the plasma membrane was lost. Stone et al. (*13*, *16*) considered these features a preparative artifact, although they left open the possibility that crater cells represented active secretion. We observed microvilli on virtually all apical cell surfaces in samples of BPH and normal prostate; we did not observe naked or bare cells, and we rarely saw ruffled cells. Crater cells and cells with pits or holes were seen, however, and were especially prominent in areas of active secretion, where sometimes the entire apical cell surface formed a balloon-like bleb. Crater cells may arise by loss of this bleb during mechanical trauma and/or as a consequence of apocrine secretion. Cells with pits or holes may represent fusion of the secretory vacuole membrane with the plasma membrane, reflecting merocrine secretion. Both apocrine and merocrine secretory mechanisms appear to be operative in human prostate (*9*, *11*, *18*), which could account for these morphologic features. Similar disruptions of the plasma membrane were absent in cultured explants.

In contrast to secretory cells, basal cells are structurally undifferentiated (*7*–*11*, *19*). Little is presently known about the role of these cells in human prostate, although basal cells frequently are regarded as "reserve" cells (*7*, *9*, *11*, *18*, *19*), which implies a capacity to differentiate into secretory or transitional epithelial cell types when appropriately stimulated. In ultrastructural studies, possible transitional forms between secretory cells and basal cells have been noted (*11*, *13*). Experimental evidence also favoring this view was obtained by Dermer (*19*) who studied [^{3}H]thymidine incorporation by epithelial cells of BPH in vitro by the use of autoradiographic techniques. He observed nuclear labeling (0.1%) associated only with cells in a basal location and concluded that basal cells are capable of proliferating and may be a source of secretory cells. Our in vitro studies (*20*) of normal human prostate also have demonstrated the capacity of basal cells to divide. The factor(s) stimulating proliferation of these cells is not yet known, although death of secretory epithelial cells within a given acinus during early culture appeared to be correlated with incorporation of [^{3}H]thymidine by basal cells as determined by autoradiography. That basal cells are capable of differentiation is supported by our in vitro studies (*1*), which demonstrated mucus metaplasia in cells repopulating glands and ducts and colonizing explant surfaces. In ultrastructure, the contents of these secretory vacuoles, as described above, resembled mucus-like material. Moreover, the distribution of these vacuoles within basal cells during culture corresponds to the pattern of histochemical staining for acidic mucosubstances, as demonstrated elsewhere (*1*).

Similarity in morphology, histochemistry, and continuity of epithelia revealed by LM (*1*) together with similarities in ultrastructure described in the present paper leave little doubt that epithelial cells colonizing acini and exterior surfaces of explants and differentiating in vitro are derived from prostatic basal cells. In previous studies, Schrodt and Foreman (*21*) using TEM examined explants of BPH in short-term experiments up to 9 days in vitro. They also noted the early presence of degenerating secretory epithelial cells lining a few acini and the subsequent appearance of squamous-like epithelial cells with prominent tonofilaments, which appeared to represent altered basal cells.

Other evidence also supports the origin of cultured prostatic epithelial cells from basal cells. For example, Franks et al. (*22*) examined the role of stroma in maintenance of growth capacity of BPH in vitro. During mechanical separation of glandular epithelium from the underlying stroma, mechanical forces resulted in the apparent shearing and destruction of myoepithelial (basal) cells, as judged by adherence of nuclei of ruptured cells to the overlying secretory cells seen by TEM. Such preparations did not survive in vitro, nor did they incorporate [^{3}H]thymidine, although epithelium (probably basal cell derivatives) of intact explants could be maintained for many months in vitro. In view of the capacity of basal cells but not of secretory cells to proliferate, it is probable that destruction of basal cells was responsible for the subsequent lack of growth of mechanically separated epithelia. In related studies, Stone et al. (*23*) isolated glandular structures from BPH by enzymatic separation of epithelium and stroma. Glandular isolates were then cultured for 7 days in vitro and examined by SEM. The surface morphology of these isolates was very similar to that of explants illustrated in this paper, including the presence of features such as microvilli and convex apical surfaces.

The results of our in vitro studies so far have focused attention on prostatic basal cells, which may play an important role in neoplasia of the human prostate. The possibility that basal cells are important in the pathogenesis of BPH and prostatic carcinoma has been given little attention in the past. However, in recent in vitro studies we have demonstrated morphologic evidence of malignant transformation of basal cells of normal human prostate in response to chemical carcinogens (*24*, *25*), which strongly suggests an important role for these cells in the pathogenesis of prostatic adenocarcinoma.

In contrast to explant-cultured epithelial cells of normal prostate, bizarre cells seen on explant surfaces from 2 cases of BPH after 8 weeks' culture in the present study closely resemble epithelial cells associated with long-term cultured explants of prostate adenocarcinoma and carcinogen-exposed explants of normal prostate (*24*, *25*). The fact that similar cells were not seen on explants of normal prostate supports the contention by Franks (*26*) that BPH cannot be considered normal prostate. Thus BPH may be of limited usefulness in experimental studies in which responses of normal prostate are required, despite ultrastructural and histochemical (*1*) similarities between normal prostate and BPH in vivo and in vitro.

In conclusion, our studies have identified basal cells as those cells responsible for new epithelial growth of normal prostate and BPH in vitro. By use of an in vitro approach, secretory cell types can be eliminated, enabling further comparative studies on the characteristics of basal cells in normal and pathologic human prostate.

REFERENCES

(*1*) Sanefuji H, Heatfield BM, Trump BF, Young JD. Studies on carcinogenesis of human prostate. II. Long-term explant culture of normal prostate and benign prostatic hyperplasia: Light microscopy. JNCI 1982; 69:751-756.

(*2*) Trump BF, Valigorsky JM, Jones RT, Mergner WJ, Garcia JH, Cowley RA. The application of electron microscopy and cellular biochemistry to the autopsy. Observations on cellular changes in human shock. Hum Pathol 1975; 6:499-516.

(3) Sanefuji H, Heatfield BM, Trump BF. Studies on carcinogenesis of human prostate. I. Technique for long-term explant culture. Tissue Cult Assoc Manual 1978; 4:855-856.

(4) McDowell EM, Trump BF. Histologic fixatives suitable for diagnostic light and electron microscopy. Arch Pathol Lab Med 1976; 100:405-414.

(5) Trump BF, Smuckler EA, Benditt EP. A method for staining epoxy sections for light microscopy. J Ultrastruct Res 1961; 5:343-348.

(6) Kelley RO, Dekker RA, Bluemink JG. Ligand-mediated osmium binding: its application in coating biological specimens for scanning electron microscopy. J Ultrastruct Res 1973; 45:254-258.

(7) Brandes D, Kirchheim D, Scott WW. Ultrastructure of the human prostate: Normal and neoplastic. Lab Invest 1964; 13:1541-1560.

(8) Fisher ER, Jeffrey W. Ultrastructure of human normal and neoplastic prostate. Am J Clin Pathol 1965; 44:119-134.

(9) Mao P, Nakao K, Bora R, Geller J. Human benign prostatic hyperplasia. Arch Pathol 1965; 79:270-283.

(10) Mao P, Angrist A. The fine structure of the basal cell of human prostate. Lab Invest 1966; 15:1768-1782

(11) Fisher ER, Sieracki JC. Ultrastructure of human normal and neoplastic prostate. Pathol Annu 1970; 5:1-26.

(12) Clark MA, O'Connell KJ, Edson M. Scanning electron microscopic studies of control and hypertrophic human prostate glands. J Urol 1973; 110:558-560.

(13) Stone MP, Stone KR, Paulson DF. Scanning electron microscopy of hyperplastic and neoplastic human prostate. Urol Res 1976; 4:71-75.

(14) Burns J. Prostatic acid phosphatase in tissue sections revealed by the unlabeled antibody peroxidase-antiperoxidase method. Biomedicine 1977; 27:7-10.

(15) Serrano JA, Wasserkrug HL, Serrano AA, Paul BD, Seligman AM. The histochemical demonstration of human prostatic acid phosphatase with phosphorylcholine. Invest Urol 1977; 15:123-136.

(16) Stone MP, Stone KR, Ingram P, Mickey DD, Paulson DF. Scanning and transmission electron microscopy of human prostatic acinar cells. Urol Res 1977; 5:185-200.

(17) Mickey DD, Stone KR, Stone MP, Paulson DF. Morphologic and immunologic studies of human prostatic carcinoma. Cancer Treat Rep 1977; 61:133-138.

(18) Brandes D. The fine structure and histochemistry of prostatic glands in relation to sex hormones. Int Rev Cytol 1966; 20:207-276.

(19) Dermer GB. Basal cell proliferation in benign prostatic hyperplasia. Cancer 1978; 41:1857-1862.

(20) Heatfield BM, Sanefuji H, Trump BF. Long-term explant culture of normal human prostate. Methods Cell Biol 1980; 21:171-194.

(21) Schrodt GR, Foreman CD. In vitro maintenance of human hyperplastic prostate tissue. Invest Urol 1971; 9:85-94.

(22) Franks LM, Riddle PN, Carbonell AW, Gey GO. A comparative study of the ultrastructure and lack of growth capacity of adult human prostate epithelium mechanically separated from its stroma. J Pathol 1970; 100:113-119.

(23) Stone KR, Stone MP, Paulson DF. In vitro cultivation of prostatic epithelium. Invest Urol 1976; 14:79-82.

(24) Heatfield BM, Sanefuji H, Trump BF. Studies on carcinogenesis of human prostate. IV. Comparison of normal and neoplastic prostate during long-term explant culture. Scan Electron Microsc 1979; 3:645-656.

(25) Sanefuji H, Heatfield BM, Trump BF. Studies on carcinogenesis of human prostate. V. Effects of the carcinogen *N*-methyl-*N'*-nitro-*N*-nitrosoguanidine (MNNG), on normal prostate during long-term explant culture. Scan Electron Microsc 1979; 3:657-663.

(26) Franks LM. Tissue culture in the investigation of prostatic cancer. Urol Res 1977; 5:159-162.

Figures 1-18.—Normal human prostate obtained at IA.

Figure 1.—LM, zero time culture. Columnar to cuboidal secretory cells with basal nuclei and numerous apical vacuoles and with basal cells (*arrows*) line the gland wall. Toluidine blue. *Bar*= 10 μm. × 1,400

Figure 2.—TEM of several secretory cells with microvilli, junctional complexes, apical vacuoles, basal nuclei, lysosomes, and other organelles, zero time culture. Basal cell lacking secretory vacuoles is seen at *right*, adjacent to the basal lamina (*arrow*). *Bar*=2 μm. × 8,000

Figure 3.—TEM of a basal cell adjacent to basal lamina, zero time culture. *Note* absence of secretory vacuoles and sparsity of organelles. *Bar*=1 μm. × 10,600

Figure 4.—SEM of explant surface additionally trimmed after fixation at zero time culture. Normal architectural integrity is maintained. *Bar*=20 μm. × 440

Figure 5.—SEM of apical surface of secretory cells showing microvilli, occasional pores or holes in the plasma membrane, and small spherical blebs, zero time culture. *Bar*=3 μm. × 4,800

Figure 6.—LM of explant surface, 1-wk culture. Migratory epithelial cells and early development of a multilayered epithelium are shown. Toluidine blue. *Bar*=20 μm. × 560

Figure 7.—LM of columnar and polygonal epithelial cells comprising the multilayered epithelium, 1-wk culture. Toluidine blue. *Bar*=20 μm. × 560

Figure 8.—LM of polygonal epithelial cells lining debris-filled acini within an explant, 1-wk culture. Toluidine blue. *Bar*=20 μm. × 560

Figure 9.—TEM of basal portion of columnar epithelial cells shown in fig. 7. A basal lamina is interposed between cells and underlying stroma. Other features include widened intercellular spaces, membrane folds, mitochondria, and a prominent Golgi complex (G). *Bar*=2 μm. × 8,300

Figure 10.—TEM of the apical portion of columnar epithelial cells shown in fig. 7. Characteristic features include microvilli, junctional complexes, vacuoles containing mucus-like material, multiple Golgi complexes, and widened intercellular spaces penetrated by plasma membrane folds. *Bar*=3 μm. × 5,200

Figure 11.—TEM illustrating early degeneration of secretory cells with accumulation of necrotic debris in the gland lumen (*upper right*), 3-day culture. Secretory cells contain numerous autophagosomes. Basal cells, adjacent to the stroma (*lower-upper left*), remain viable. *Bar*=3 μm. × 4,600

Figure 12.—SEM of explant surface covered with epithelial cells, 1-wk culture. *Bar*=30 μm. × 380

Figure 13.—SEM of apical surface of epithelial cells shown in fig. 12. Numerous, short microvilli cover the surface of each cell. *Bar*=3 μm. × 3,900

Figure 14.—SEM of apical and lateral surfaces of epithelial cells similar to those shown in fig. 13. Lateral cell surfaces are characterized by many irregular folds of plasma membrane. *Bar*=2 μm. × 9,500

Figure 15.—LM of explant, 2-wk culture. A multilayered epithelium covers the surface and lines debris-filled acinar spaces within the interior. Toluidine blue. *Bar*=20 μm. × 560

Figure 16.—TEM of multilayered epithelium with widened intercellular spaces at the explant surface, 2-wk culture. Outer surface (*upper left*) bears short microvilli; inner surface (*lower right*) rests on a basal lamina. *Bar*=2 μm. × 8,000

Figure 17.—LM of explant surface, 14-wk culture. The multilayered epithelium is characterized by widened intercellular spaces typical of those seen at earlier intervals. Toluidine blue. *Bar*=20 μm. × 560

Figure 18.—SEM of an explant, 5-wk culture. Apical surface of epithelial cells ranges from flat to convex. *Bar*=3 μm. × 3,600

Figure 19.—SEM of atypical BPH, 8-wk culture. Cells are piled up, with little organizational pattern. Pseudopodial and filopodial cytoplasmic projections contact neighboring cells. Tiny spherical blebs are present on apical surfaces. *Contrast* with normal prostate in fig. 18. *Bar*=2 μm. × 6,000

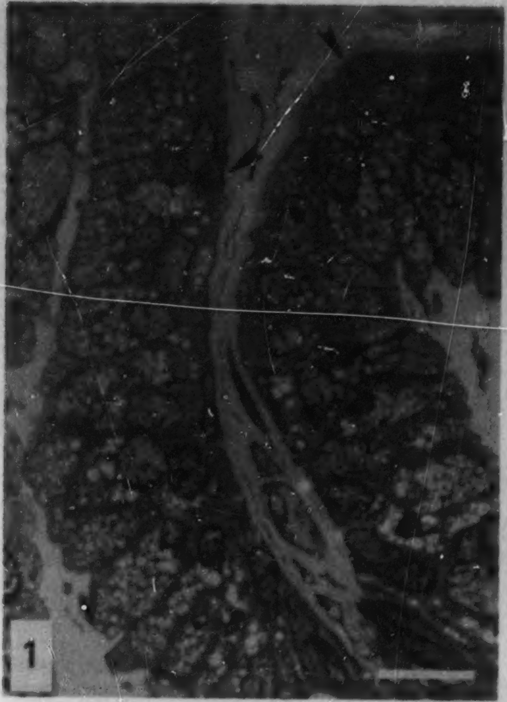

1

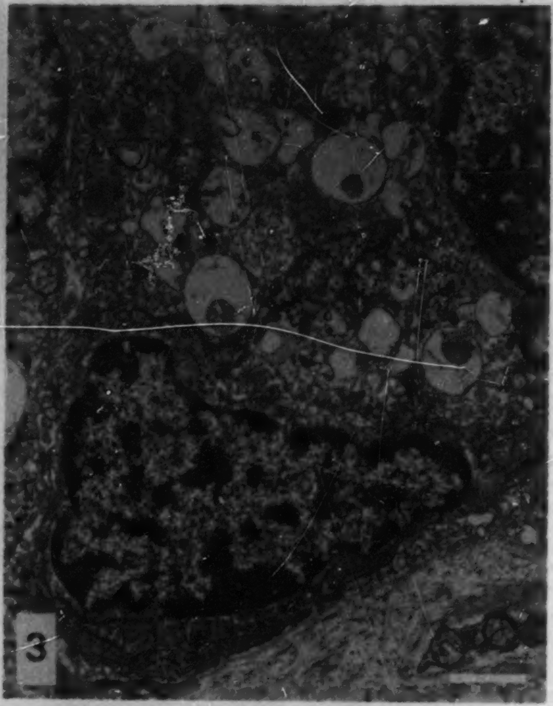

3

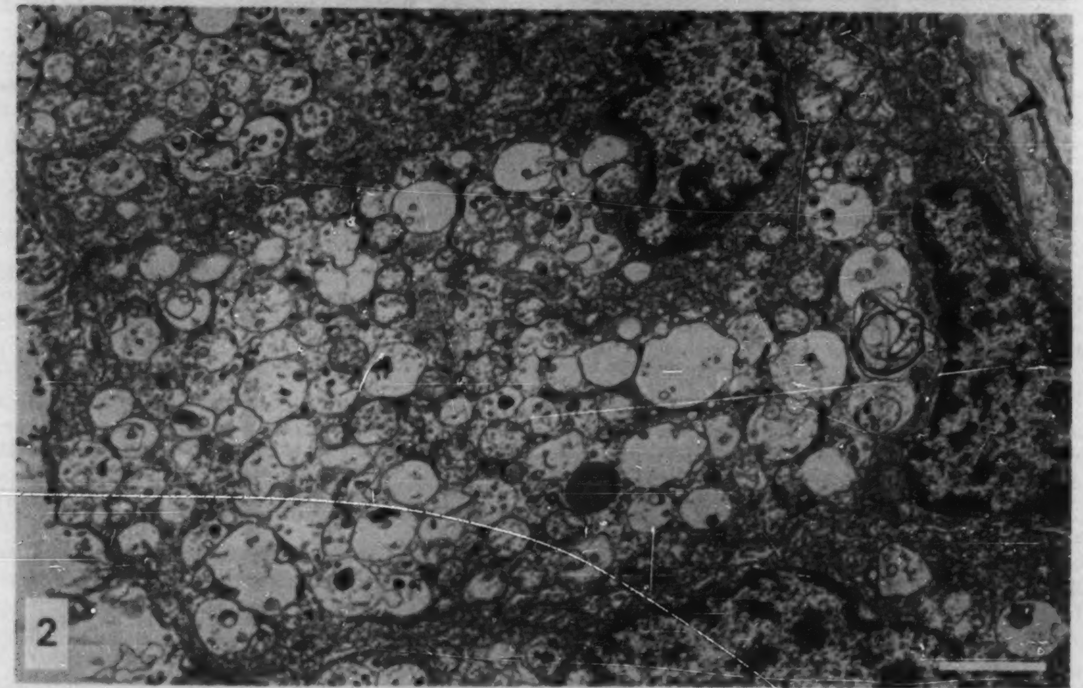

2

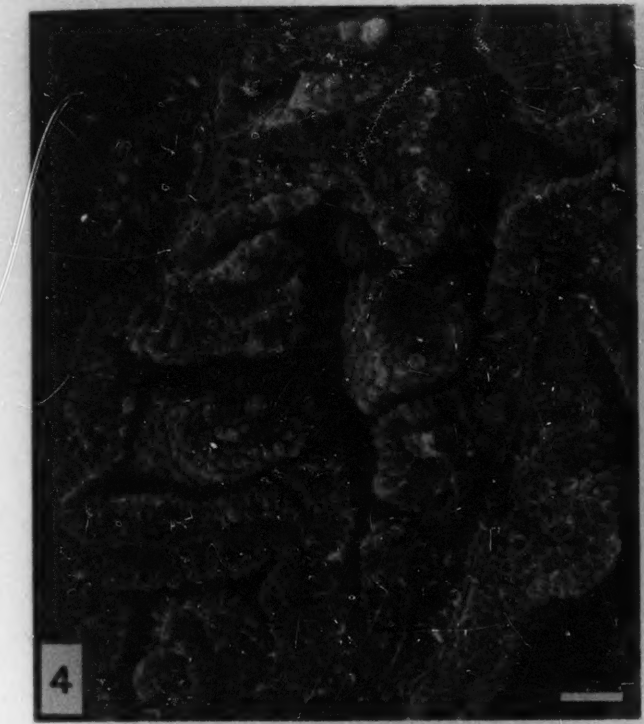
4

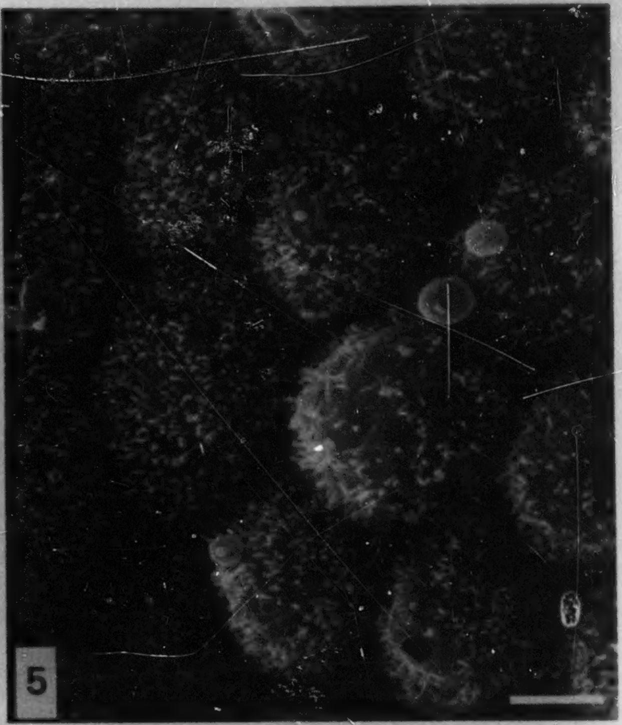
5

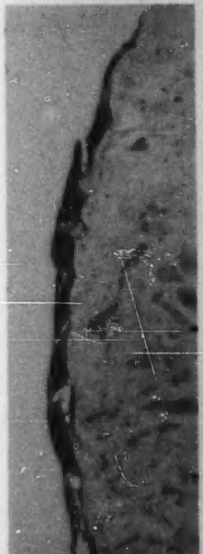
6

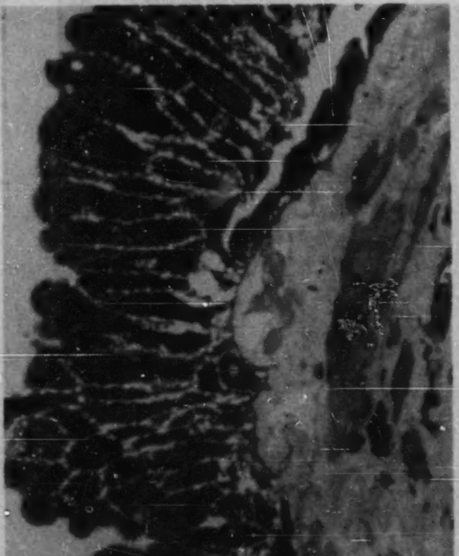
7

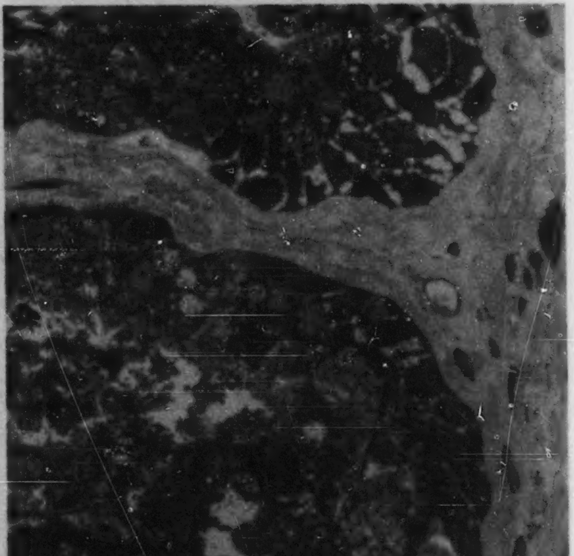
8

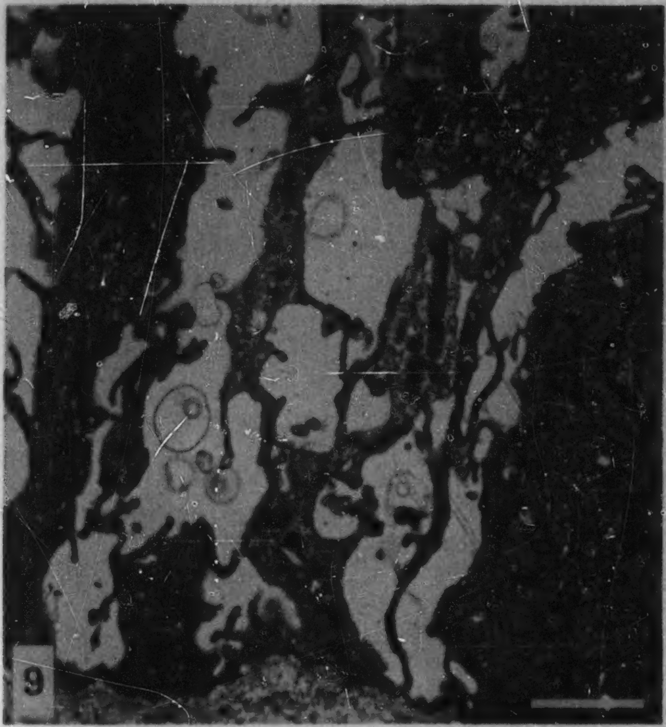

9

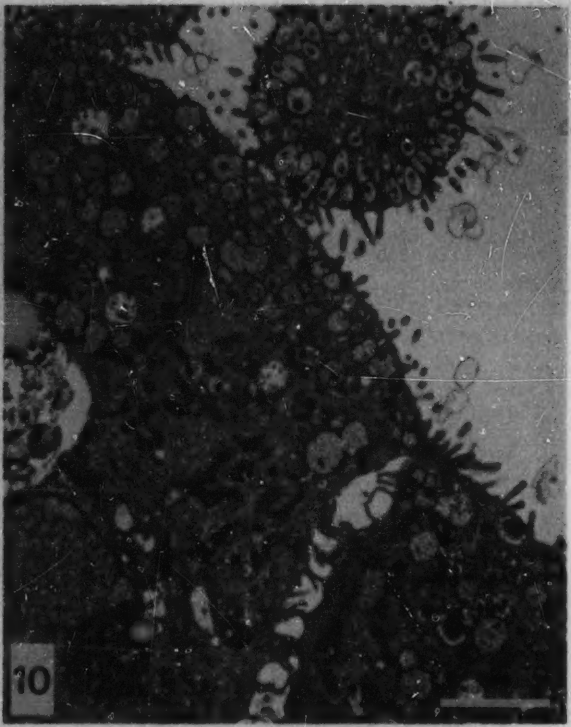

10

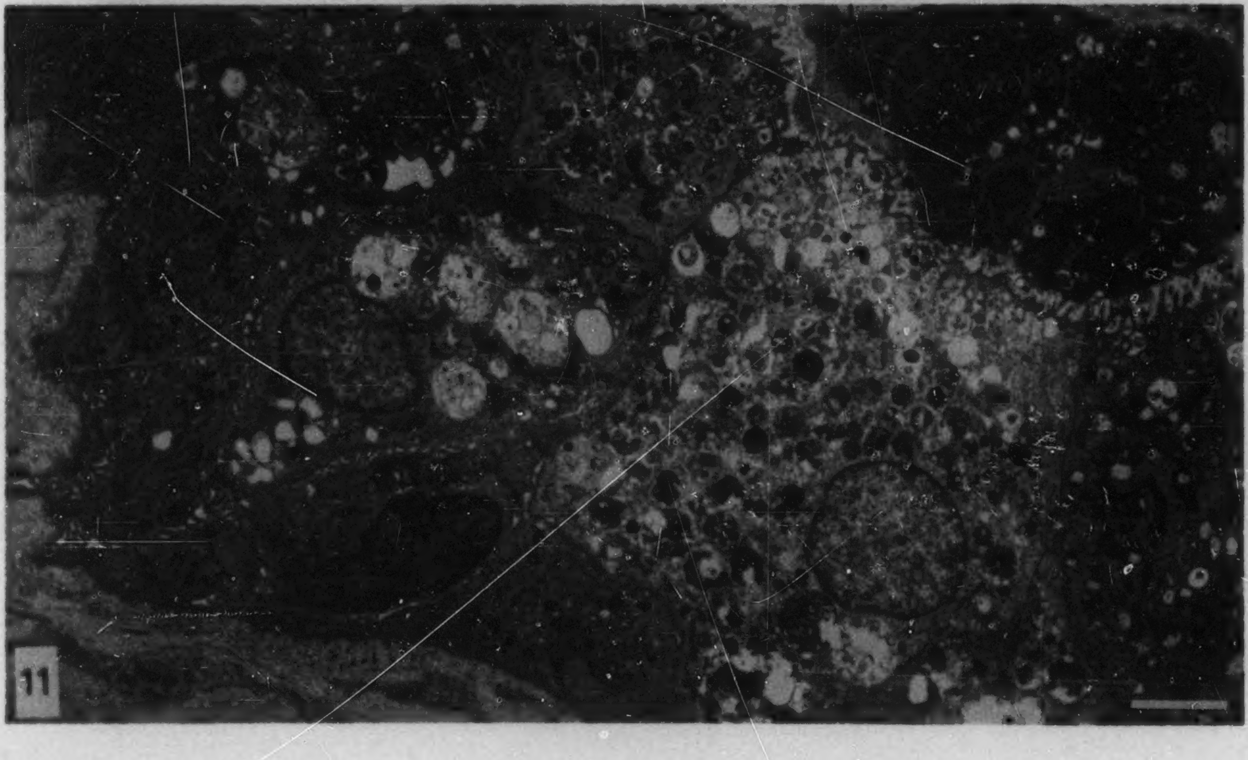

11

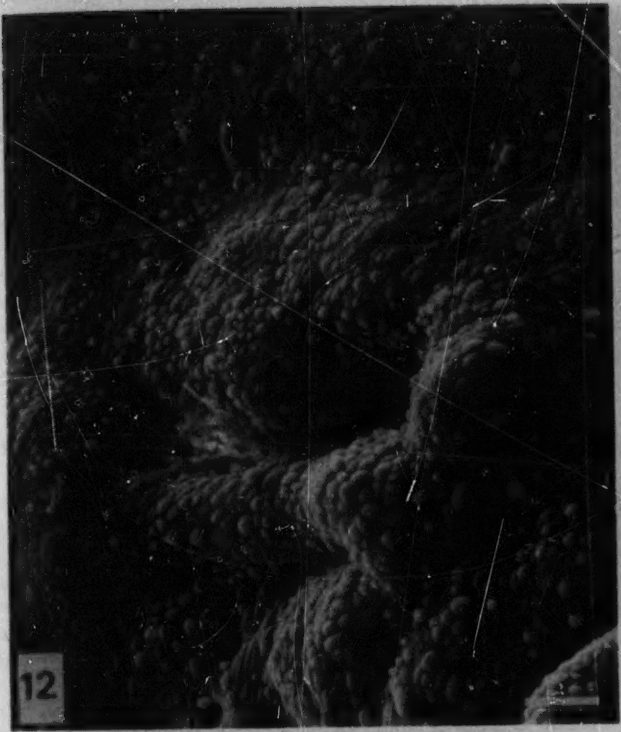
12

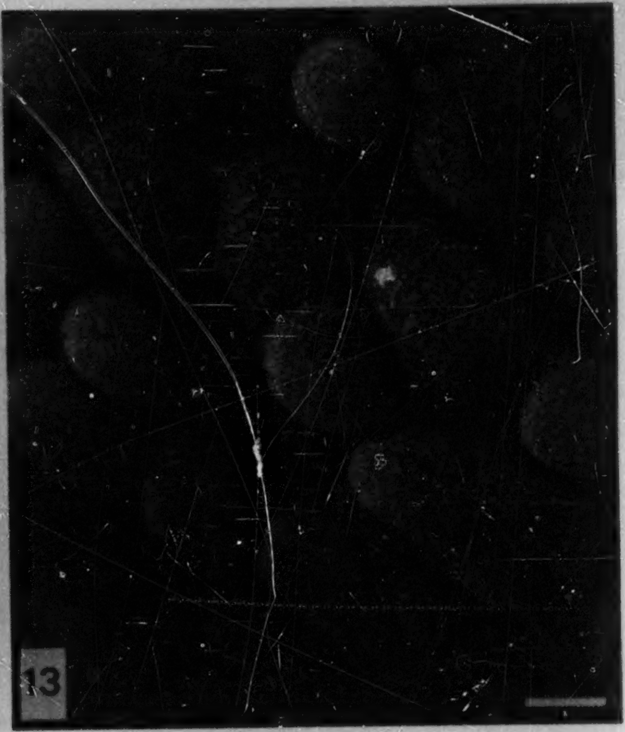
13

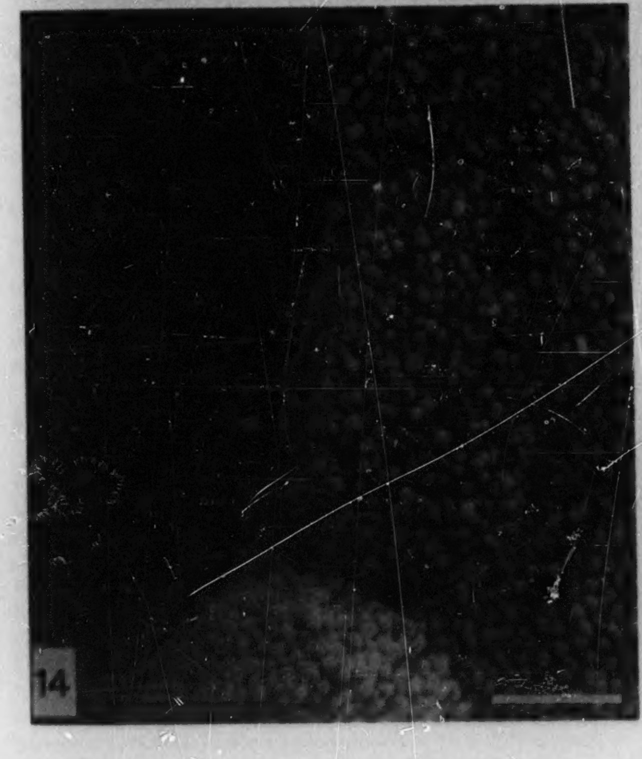
14

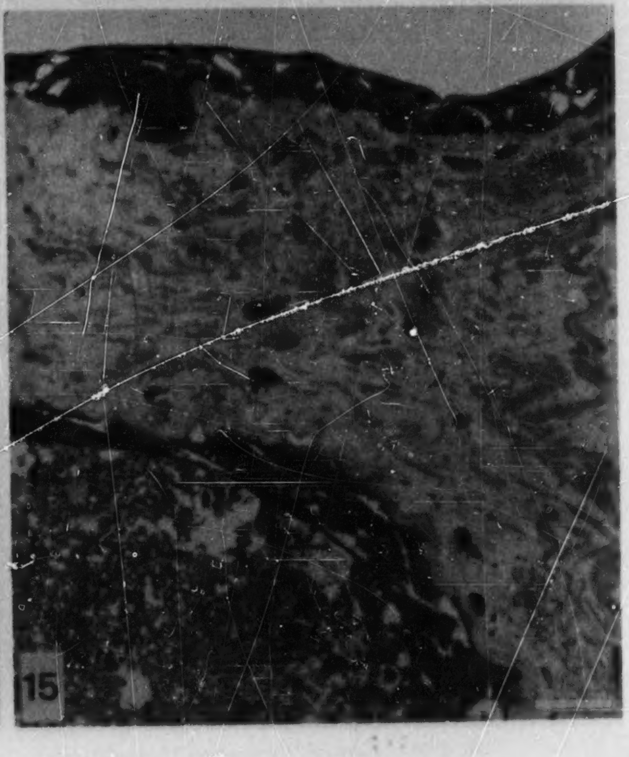
15

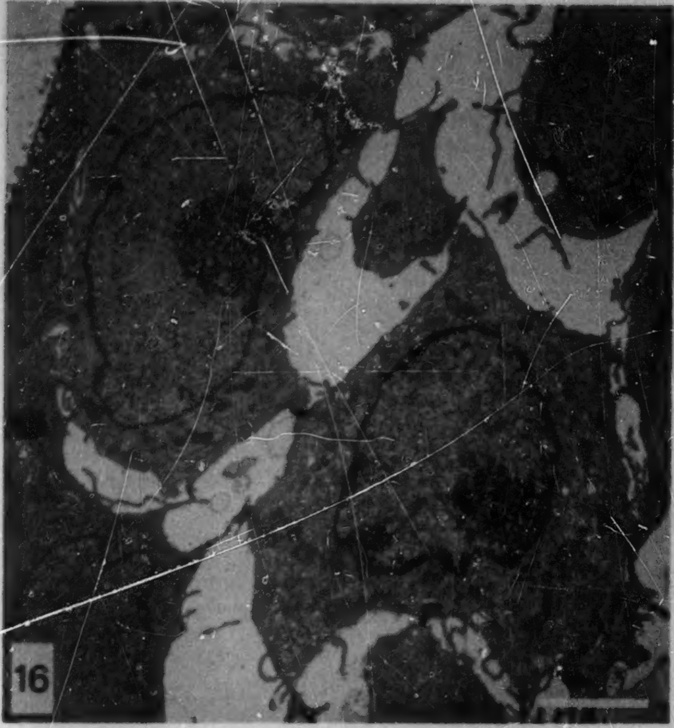

16

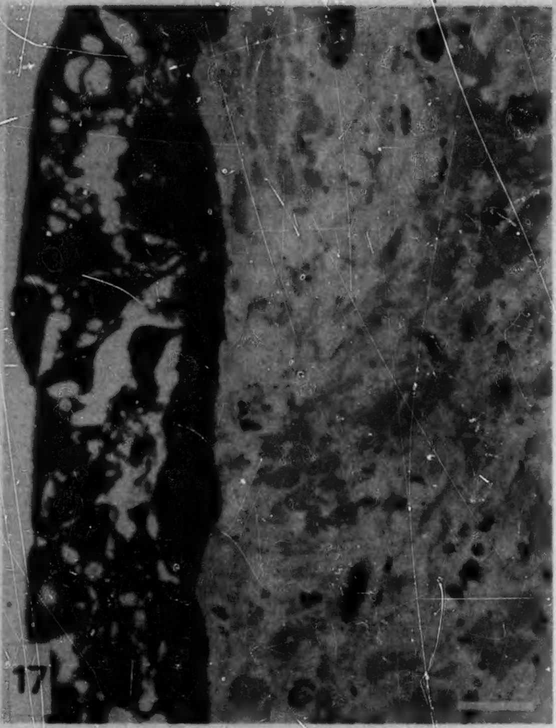

17

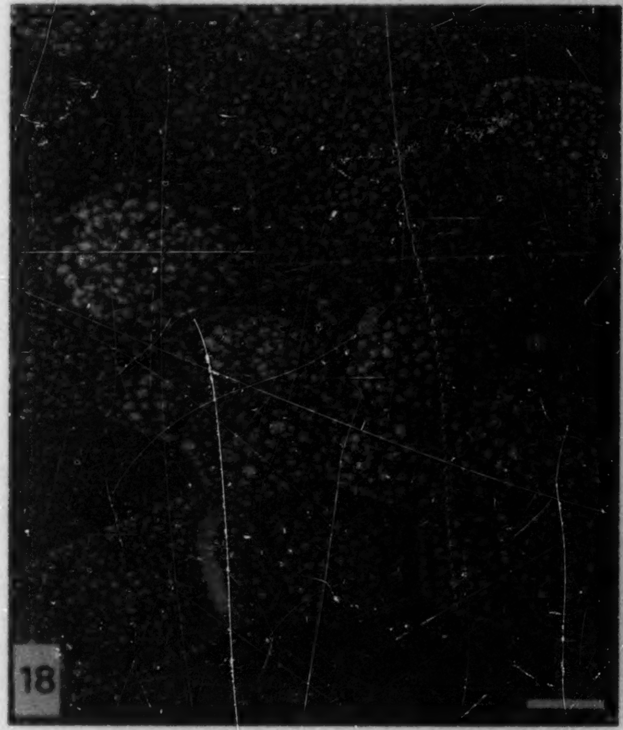

18

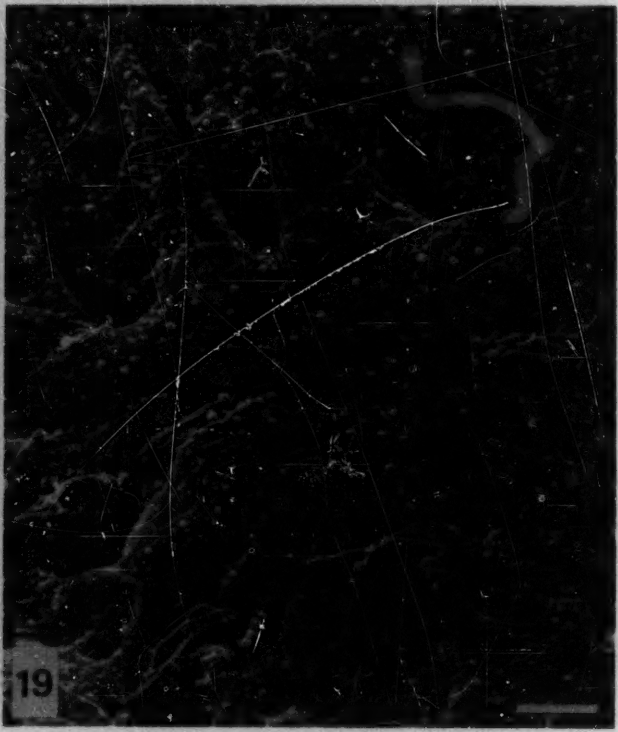

19

Enhancement of Growth of Human Colon Tumor Cell Lines by Feeder Layers of Murine Fibroblasts[1,2]

M. G. Brattain,[3,4,5] **D. E. Brattain,**[3] **A. M. Sarrif,**[5,6,7] **L. J. McRae,**[5] **W. D. Fine,**[3] *and* **J. G. Hawkins**[3]

ABSTRACT—The effects of feeder layers of C3H/10T½ cells on the growth of human and mouse cell lines were tested. Feeder layers increased colony formation by cultured cancerous cells in semisolid medium over controls grown in semisolid medium without feeder layers. Maximal colony formation was also attained at a faster rate when feeder layers were used. Plating efficiency by cancerous cells obtained directly from xenografts was increased threefold to fivefold in tissue culture when feeder cells were present as confluent monolayers.—JNCI 1982; 69:767–771.

Although some advances have been made with certain types of cancers in recent years, the cure rates for colon carcinoma have remained largely unchanged over the past two decades (*1*). This is in part due to the lack of effective chemotherapeutic agents against this disease (*2*). In vitro models would be helpful for the development of chemotherapeutic agents, but there has been little success with regard to the elucidation of routine methods for the tissue culture of colon carcinoma (*3–5*). Recently, however, we described the utilization of feeder layers of C3H/10T½ cells for the improved establishment of human colon tumors in tissue culture (*6*). Several studies have described the establishment of tissue cultures of human tumors with the use of a variety of normal cells and tissues as feeder layers for the cancerous cells (*7–12*).

The effects of C3H/10T½ cells on the growth of human colon carcinoma have not been widely studied. Therefore, we have attempted to evaluate the potential for the application of feeder layers to the tissue culture of human colon carcinoma *a*) by determining the effects of normal mouse embryo fibroblasts on the growth of established cell lines of colon carcinoma in soft agar and *b*) from xenografts. Both of these modes of culture are of potential importance in the development of suitable systems for prediction of the chemotherapeutic effects of drugs (*11, 13*).

MATERIALS AND METHODS

Cell lines.—The cell lines utilized in this study were developed from primary human colon tumors in this laboratory and are described elsewhere (*6, 14*). All five lines formed tumors in nude mice, grew in semisolid medium, and produced moderate (HCT 116, HCT 214) to large (HCT 525, HCT 116a) amounts of CEA in tissue culture, except for line HCT 116b, which produced low amounts of CEA. All cell lines were maintained at 37°C in an atmosphere of 5% CO_2, with McCoy's 5-A medium supplemented with 10% heat-inactivated FBS and antibiotics (4.3 µg gentamicin/ml, 90 µg streptomycin/ml, and 90 U penicillin/ml). Cultures were routinely subcultured weekly with 0.25% trypsin–0.1% EDTA in tissue culture medium. C3H/10T½ cells were maintained under the same conditions as the human cell lines. Benzo[*a*]pyrene-transformed cells (type III) derived from C3H/10T½ cells were also maintained under the same conditions. The properties of these cells and the C3H/10T½ cells have been described in detail in (*15, 16*). Human breast cancer cells (734B) were obtained from the Naval Bioscience Laboratory, Oakland, Calif., and human melanoma cells (designated M-21) were obtained from Dr. Charles Balch, University of Alabama, Birmingham, Ala.

Culture in semisolid medium.—Soft-agarose culture of human colon carcinoma cells was performed as described previously (*14, 17*). Other cell lines were grown by the standard soft-agar technique described by Salmon and co-workers (*13*) without feeder layers of spleen cells. In this system underlayer ingredients contained 40 ml enriched McCoy's 5-A medium, 10 ml tryptic soy broth (3%), 0.6 ml L-asparagine (6.6 mg/ml), and 0.3 ml DEAE–dextran. Enriched McCoy's 5-A medium (500 ml) contained 5% horse serum, 10% FBS, 5 ml sodium pyruvate (2.2%), 1 ml L-serine (21 mg/ml), and 5 ml (200 m*M*) glutamine. Underlayers were plated by mixing this medium with 3% agar to give a final concentration of 0.5% agar. Cells were plated into an upper layer of 0.3% agar which contained in 100 ml of CMRL-1066 medium: 15% horse serum, 4 ml (100 m*M*) $CaCl_2$, 200 U insulin, 1 ml (30 m*M*) vitamin C, and 2 ml (200 m*M*) glutamine.

In experiments testing the effects of feeder layers, 5×10^4 C3H/10T½ cells were plated into 9.6-cm^2 tissue dishes and permitted to grow to confluence in approximately 3 days. Underlayers (1 ml) of 1% agarose in McCoy's 5-A medium with 5% FBS were plated directly onto the confluent C3H/10T½ cells and incubated at 37°C in 5% CO_2 for 48 hours. Cells (5×10^4) from the colon carcinoma cells described above were suspended in growth medium containing 0.5% agarose B in McCoy's 5-A medium with 1 ml 5% FBS at

ABBREVIATIONS USED: CEA=carcinoembryonic antigen; FBS=fetal bovine serum.

---

[1] Received February 18, 1981; revised May 7, 1982; accepted May 27, 1982.

[2] Supported by Public Health Service (PHS) grant CA-21520 from the National Cancer Institute (NCI), National Large Bowel Cancer Project, by PHS grant CA-13148 from the NCI, and by American Cancer Society grant PDT-109A.

[3] Department of Biochemistry, University of Alabama, Birmingham, Ala. 35294.

[4] *Address reprint requests to* Dr. Brattain at his *present address*: Bristol-Meyer Laboratory, Department of Pharmacology, Baylor College of Medicine, Houston, Tex. 77030.

[5] Department of Pharmacology, University of Alabama.

[6] Comprehensive Cancer Center, University of Alabama.

[7] *Present address*: Haskell Laboratory for Toxicology and Industrial Medicine, E. I. du Pont de Nemours & Co., Inc., Newark, Del. 19711.

39°C and plated onto the underlayer containing 1% agarose B. This upper layer was then permitted to solidify at room temperature for approximately 30 minutes and subsequently maintained at 37°C in an atmosphere of 5% CO_2. Other cell lines were treated in the same manner except that the Salmon system (*13*) of soft-agar culture was utilized and the number of cells inoculated was varied. Control dishes were prepared in exactly the same manner except that there were no feeder layers of C3H/10T½ cells. Some cultures were fixed in glutaraldehyde immediately after solidification of the upper layer and stored at 4°C as time 0 samples (T_0) for comparison with experimental cultures at various times (1, 2, and 3 wk after plating). Each experiment was performed with a T_0 flask and three cultures for each week. Colonies of 20 cells or more were scored microscopically.

Xenograft tissue culture.—Cells from the human colon carcinoma cell lines were removed from 75-cm^2 tissue culture flasks with the trypsin-EDTA mixture described above, harvested by centrifugation at $98\times g$ for 7.5 minutes, and resuspended in tissue culture medium, and 10×10^6 cells were injected sc into BALB/c athymic nude mice bred in our own laboratory. Xenografts were allowed to grow to a diameter of approximately 2 cm. The animals were then killed, and the tumors were removed by a sterile technique and placed into sterile tissue culture medium. Tumors were prepared for tissue culture as previously described (*6, 14*). Tumors were minced to 1- to 2-mm^3 pieces, washed extensively in tissue culture medium containing 10% FBS, and subsequently disaggregated to single cell suspensions with 0.25% trypsin. Cell suspensions were harvested by centrifugation at $98\times g$, resuspended in the standard growth medium described above, and inoculated (5×10^4) into 25-cm^2 tissue culture flasks. Cells from each tumor were inoculated into six flasks, three of which contained confluent monolayers of C3H/10T½ cells. Each experiment consisted of three xenografts of each cell line. After 72 hours the entire volume of medium was changed, and colonies (≥20 cells) were scored microscopically. Colonies were scored again 6 days after plating.

RESULTS

Growth in Semisolid Medium

All five of the colon tumor cell lines formed colonies in soft agarose without feeder layers except HCT 525. Maximal colony formation was observed at 2 or 3 weeks, after which the colonies began to deteriorate through extensive disintegration of the cells. HCT 525 cells grew very poorly in soft agarose and HCT 116 and HCT 116b showed moderate colony formation relative to the other lines, whereas HCT 214 and HCT 116a grew relatively well in soft agarose without feeder layers (table 1). The addition of feeder layers to the soft-agarose system had dramatic effects on the extent of colony formation. Increases in colony formation were in the range of fivefold to ninefold for those lines that had moderate or low colony formation without feeder layers, whereas HCT 214 and HCT 116a showed an approximately twofold increase. The presence of feeder layers in the soft-agarose system also had the effect of speeding up the growth rate of the cell lines. Maximal colony formation was twofold to fourfold higher than colony formation after the first week for all of the cell lines, except HCT 525, when feeder layers were not included in this system. When feeder layers were added to the soft-agarose system, there were no significant changes in colony formation after the first week, except for HCT 116a, which showed an approximately twofold increase after 3 weeks of culture. Stimulation of proliferation of colon carcinoma cells was also demonstrated in tissue culture with conditioned medium from confluent C3H/10T½ cells grown in McCoy's 5-A medium enriched with 10% FBS (table 1). Although stimulation was observed with conditioned medium, it was generally lower than that obtained with feeder layers in the agarose system that was supplemented with 5% FBS. Reduced stimulation may have been due to the presence of 10% FBS required for optimal growth by C3H/10T½ cells in conditioned medium or possibly due to lower concentrations of conditioning factors in conditioned medium. Conditioned medium was harvested after 16-hour contact with confluent C3H/10T½ cells, whereas feeder layers were continuously present during the period of agarose culture.

The preliminary results obtained with human colon carcinoma cells raised the questions as to whether stimulation could be achieved with a more enriched medium such as the soft-agar culture system described by Salmon and coworkers (*13*), whether other types of malignant cells could be stimulated by C3H/10T½ cells, and whether the concentration of cells plated affected the obtained results. To answer these questions, we cultured different types of malignant cells at concentrations ranging from 10^3 to 5×10^3 cells in the soft-agar culture system described by Salmon et al. (*13*). The cell lines selected for this study included the HCT 116 human colon carcinoma, benzo[*a*]pyrene-transformed C3H/10T½ cells (type III), the M-21 human melanoma cell line, and the 734B human breast carcinoma cell line. All four of these cell lines were stimulated by feeder layers of C3H/10T½ cells as described below.

Cloning efficiencies for HCT 116 were considerably higher in the soft-agar culture system of Salmon et al. (*13*) than in soft agarose containing McCoy's 5-A medium enriched with 5% FBS (text-fig. 1). In addition, we observed

TABLE 1.—*Effects of C3H/10T½ cells on growth of human colon carcinoma cells in soft agarose and in tissue culture*

Cell line	Cloning efficiencies, %[a] (range): Without feeder layer	Cloning efficiencies, %[a] (range): With feeder layer	Cloning efficiencies,[b] ratio (range): With conditioned C3H/10T½ medium
HCT 214	1.5 (1.2–1.8)	2.9 (2.4–3.4)	2.2 (2.1–2.3)
HCT 525	0	1.1 (0.8–1.3)	3.0 (2.6–3.7)
HCT 116a	2.2 (1.9–2.8)	4.3 (3.8–5.1)	1.9 (1.6–2.5)
HCT 116	0.8 (0.7–1.1)	4.4 (3.7–4.8)	1.3 (1.1–1.4)
HCT 116b	0.5 (0.4–0.7)	3.7 (3.3–4.8)	1.9 (1.5–2.6)

[a] Cloning efficiencies are expressed as the percent of cells plated giving rise to colonies. The entire dish was scored for colonies. Values represent the average of three separate expts.

[b] Results are expressed as the ratio of the No. of cells grown in the presence of conditioned C3H/10T½ cell medium in 25-cm^2 flasks to the No. of cells obtained from control flasks as described in the "Materials and Methods" section. Values are the averages of ratios obtained from three expts comprising duplicate experimental and control flasks.

that the efficiency of colony formation was dependent on cell concentration, and maximal efficiency occurred in the range of 3×10³ cells plated. We observed stimulation of colony formation by feeder layers of C3H/10T½ cells at all cell concentrations tested, but the extent of this stimulation was less than that obtained from the soft-agarose culture experiments described in table 1. Stimulation of colony formation was more pronounced at lower than at higher cell concentrations.

Colony formation by chemically transformed C3H/10T½ cells was stimulated by more than twofold at low cell concentrations with feeder layers of C3H/10T½ cells, whereas at higher cell concentrations the degree of stimulation was considerably reduced (text-fig. 1). We obtained similar results with the human melanoma cell line, except that stimulation was approximately tenfold at culture inocula of 10³ cells and threefold at higher cell concentrations (text-fig. 1). Particularly striking was the stimulation observed with the mammary carcinoma cell line (text-fig. 2). Control cultures gave rise to only 5–40 colonies per plate over the range of 10³–5×10³ cells plated, whereas cultures with C3H/10T½ feeder layers were stimulated by approximately 25-fold at low inocula and 15-fold at higher inocula.

Several of the cell lines were not stimulated by C3H/10T½ cells in the soft-agar assay system. These included the previously described mouse colon carcinomas CT26 and CT51 (*17*), two human colon carcinoma cell lines, and untransformed C3H/10T½ cells.

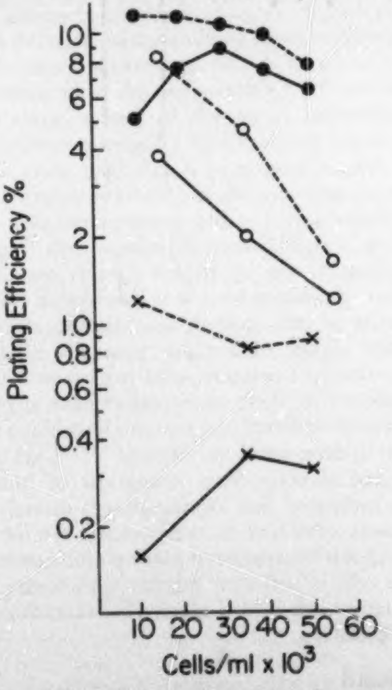

TEXT-FIGURE 1.—Effects of cell inocula on colony formation: ----, in the presence of feeder layers; ——, in the absence of feeder layers. ●, HCT 116 cells; ○, chemically transformed C3H/10T½ cells; ×, M-21 melanoma cells. Cultures were plated according to the soft-agar system described by Salmon et al. (*13*).

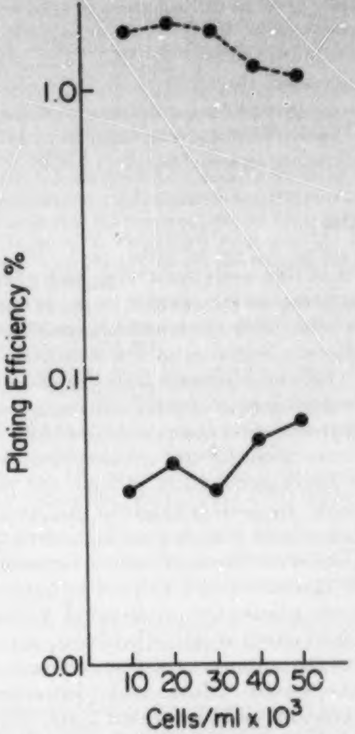

TEXT-FIGURE 2.—Effect of cell inoculum on colony formation by 734B cells: ----, in the presence of feeder layers; ——, in the absence of feeder layers. Cultures were plated according to the soft-agar system described by Salmon et al. (*13*).

TABLE 2.—*Enhancement of colony formation by cancerous cells obtained directly from xenografts on feeder layers of C3H/10T½ cells*

Cell line	Time, days	Total No. of colonies[a] (range)	
		Without feeder layer	With feeder layer
HCT 214	3	0.7 (0.5–0.8)	2.0 (1.5–2.9)
	6	1.0 (0.9–1.1)	4.1 (3.0–4.7)
HCT 525	3	0.2 (0.2–0.3)	0.3 (0.2–0.3)
	6	0.9 (0.7–1.4)	1.3 (1.2–1.5)
HCT 116a	3	0.4 (0.4–0.5)	1.8 (1.5–2.2)
	6	1.2 (0.9–1.4)	5.5 (5.1–6.1)
HCT 116	3	0.6 (0.4–0.7)	1.7 (1.1–2.1)
	6	0.9 (0.8–1.0)	3.5 (3.3–3.9)

[a] Colony formation is expressed as total No. of colonies per 25-cm² tissue culture flask. The entire flask was scored for colonies. Values represent the averages of duplicate flasks for three different xenografts of each cell line.

Effects of Feeder Layers on Colony Formation by Xenografts

All of the cell lines except HCT 116b grew as discrete epithelioid colonies when plated onto plastic or confluent monolayers of fibroblasts. Clear demarcation of the colonies permitted determination of plating efficiencies of cell suspensions obtained directly from xenografts (table 2). HCT 116b cells would form clear-cut colonies on confluent fibroblasts, but they grew as diffuse areas of cells when plated on plastic. Consequently, HCT 116b xenografts were not included in this study. Except for HCT 525, plating efficiencies were increased threefold to fivefold when cells from xenografts were plated onto confluent monolayers of C3H/10T½ cells. Colony formation by cells from HCT 525 xenografts was increased approximately 1.5-fold.

DISCUSSION

The results of this study show that feeder layers of C3H/10T½ cells enhance colony formation by human colon carcinoma cells both from tissue culture and from xenografts resulting from the injection of the cultured cells in nude mice. Other types of malignant cells can also be stimulated. Recently, we described improved initiation of human colon tumor cell lines on feeder layers of C3H/10T½ cells (*6*). The mechanism responsible for this enhancement is unknown at present, but likely possibilities include the production of "growth factors" by C3H/10T½ cells and/or increased attachment of cancerous cells due to their interaction with the fibroblasts. The stimulation of colony formation by feeder layers in soft-agarose culture and the enhancement of cell proliferation on plastic by conditioned medium strongly suggest the production of growth factors, since the feeder layer cells and the cultured cancerous cells are not in direct contact in this system. Moses and co-workers (*18*) have shown that chemically transformed C3H/10T½ cells produce a growth factor that can induce normal fibroblasts to form colonies in semisolid medium. Gallie and co-workers (*12*) have described the growth of human retinoblastoma cells with the use of C3H/10T½ cells, as well as other types of fibroblasts. These investigators found that the cancerous cells required direct contact with the fibroblasts, suggesting that "conditioning factors" for these cells may be particularly labile. Other types of fibroblasts have been found to stimulate clonal proliferation of biopsy specimens of human colon carcinoma in soft-agarose culture (*19*).

Both the growth rate and the extent of growth appear to be increased when feeder layers of C3H/10T½ cells are utilized in the soft-agarose system for human colon carcinoma. Maximal growth in semisolid medium with feeder layers is generally achieved within 1 week of inoculation. Without feeder layers, 2–3 weeks are required for a maximal level of growth, which is considerably lower than that obtained with the feeder layers. Apparently, there are many cells with the potential to form colonies in soft agarose, which for unknown reasons do not grow. The addition of feeder layers to the system enables a higher proportion of these cells to grow. However, it is not clear whether the fraction of cells that grow in soft agarose in the presence of feeder layers represents the total number of cells with the potential to form colonies and whether growth is limited by the availability of nutrients, for instance. The size of the colonies when maximal growth has been attained is not significantly different for cultures with or without feeder layers.

Recent studies described the biologic heterogeneity of malignant cell populations comprising individual tumors (*20–24*), including human colon carcinoma (*14*, *25*). The concept of heterogeneity suggests the possibility that the additional growth observed in the presence of feeder layers may represent colony formation by different cells from those that grow in the absence of feeder layers. This concept is of paramount importance to the development of in vitro assays for drug screening because those cells that do not grow in the absence of feeder layers may have significantly different drug sensitivities from those that form colonies under these conditions.

Colony formation by cancerous cells from xenografts was considerably higher than that obtained for soft-agarose culture. It is impossible to estimate the effects of the production of growth factors by feeder layer cells in this system, since cancerous cells were in direct contact with the monolayers of C3H/10T½ cells. Higher plating efficiencies with feeder layers may have been promoted by adhesive interactions between the two cell types. In general, after 6 days, colonies on feeder layers were approximately twice the surface area of colonies that resulted from plating of xenograft cells directly onto plastic. However, it is impossible to determine whether these larger colonies represented more cell growth, since it is not clear whether the surface area occupied by a cancerous cell growing on top of a fibroblastic monolayer is the same as that of a cell growing on plastic.

Another area of potential applicability of feeder layers is in the development of in vitro assay systems for drug sensitivity screening. As indicated above, this is particularly important with regard to colon cancer because of the general lack of effective chemotherapy for this disease. Currently, clonogenic assay methods have not been effective for colon carcinomas disaggregated by mechanical means (*26*). Some cluster formation from enzymatically digested tumors has been observed for solid colon carcinoma, but a suitable assay for drug sensitivity screening has yet to be developed (*27*). The enhancement of growth by feeder layers may allow sufficient colony formation of a higher percentage of specimens for drug screening in a soft-agar assay system. Recently, Smith and co-workers (*11*) have described the utilization of feeder layers in the development of a clonogenic assay system in which second-passage cells from cultured mammary carcinomas are plated directly onto fibroblasts. The number of colonies formed is linear with respect to the concentration of cells seeded, and plating efficiencies are considerably higher than those generally obtained with clonogenic assays of primary solid tumors in soft-agar culture. Consequently, these investigators have suggested that assays that involve direct plating onto fibroblasts might find application in drug-sensitivity testing (*11*). Our results with cells obtained directly from xenografts of human colon carcinoma indicated that clonal growth directly on fibroblasts is easily obtained in this system. We are currently investigating the comparative plating efficiencies of malignant colon cells in soft-agar systems with feeder layer cells and in systems with direct contact between the malignant cells and fibroblasts.

REFERENCES

(*1*) Freeman HJ, Kim YS. Membrane biochemistry and physiology of human colonic cancer. Cancer Bull 1978; 30:237–242.

(*2*) Johnson RK. Models to evaluate pharmacologic agents. Cancer Bull 1978; 30:243–245.

(*3*) Brattain MG, Pretlow TP, Pretlow TG. Cell fractionation of large bowel cancer. Cancer 1977; 40:2479–2486.

(*4*) Breborowicz J, Easty GC, Birbach M, Robertson D, Nery R, Neville AM. The monolayer and organ culture of human colorectal carcinoma and associated "normal" colonic mucosa and their production of carcinoembryonic antigens. Br J Cancer 1975; 31:557–569.

(*5*) Leibovitz A, Stinson JC, McCombs WB III, McCoy CE, Mazur KC, Mabry ND. Classification of human colorectal adenocarcinoma cell lines. Cancer Res 1976; 36:4562–4569.

(*6*) Brattain MG, Brattain DE, Fine WD, et al. Initiation and characterization of cultures of human colonic carcinoma with different biological characteristics utilizing feeder layers of confluent fibroblasts. Oncol Devel Biol Med 1981; 2:355–367.

(*7*) Taylor-Papadimitriou J, Shearer M, Stoker MG. Growth requirements of human mammary epithelial cells in culture. Int J Cancer 1977; 20:903–908.

(*8*) Armstrong RC, Roseman W. Cocultivation of human primary breast carcinomas and embryonic mesenchyme resulting in growth and maintenance on tumor cells. Cancer Res 1978; 38:894–900.

(*9*) Epstein AL, Kaplan HS. Feeder layer and nutritional requirements for the establishment and cloning of human malignant lymphoma cell lines. Cancer Res 1979; 39:1748–1759.

(*10*) Hamburger AW, Salmon SE. Primary bioassay of human tumor cells. Science 1977; 197:761–763.

(*11*) Smith HS, Lan S, Ceriani R, Hackett AJ, Stampfer MR. Clonal proliferation of cultured nonmalignant and malignant human breast epithelia. Cancer Res 1981; 41:4637–4643.

(*12*) Gallie BL, Holmes W, Phillips RA. Reproducible growth in tissue culture of retinoblastoma tumor specimens. Cancer Res 1982; 42:301–305.

(*13*) Salmon SE, Hamburger AW, Schoenlin B, Durie BG, Alberts QS, Moon TE. Quantitation of differential sensitivity of human tumor cells to anticancer drugs. N Engl J Med 1978; 298:1321–1327.

(*14*) Brattain MG, Fine WD, Khaled FM, Thompson J, Brattain DE. Heterogeneity of malignant cells from a human colonic carcinoma. Cancer Res 1981; 41:1751–1756.

(*15*) Reznikoff CA, Bertram JS, Brankow DW, Heidelberger C. Quantitative studies of chemical transformation of cloned C3H mouse embryo cells sensitive to post-confluence inhibition of cell division. Cancer Res 1973; 33:3239–3249.

(*16*) Reznikoff CA, Brankow DW, Heidelberger C. Establishment and characterization of a cloned line of C3H mouse embryo cells sensitive to post-confluence inhibition of cell division. Cancer Res 1973; 33:3231–3238.

(*17*) Brattain, MG, Strobel-Stevens J, Fine D, Webb M, Sarrif AM. Establishment of mouse colonic carcinoma cell lines with different metastatic properties. Cancer Res 1980; 40:2142–2146.

(*18*) Moses HL, Branum EL, Proper JA, Robinson RA. Transforming growth factor production by chemically transformed cells. Cancer Res 1981; 41:2842–2848.

(*19*) Laboisse CL, Augeron C, Potet F. Growth and differentiation of human gastrointestinal adenocarcinoma stem cells in soft agarose. Cancer Res 1981; 41:310–315.

(*20*) Dexter DL, Kowalski HM, Blazar BA, Fligiel Z, Vogel R, Heppner GH. Heterogeneity of tumor cells from a single mouse mammary tumor. Cancer Res 1978; 38:3174–3181.

(*21*) Fidler IJ. Tumor heterogeneity and the biology of cancer invasion and metastasis. Cancer Res 1978; 38:2651–2656.

(*22*) Fidler IJ, Kripke ML. Metastasis results from preexisting variant cells within a malignant tumor. Science 1977; 197:893–895.

(*23*) Heppner GH, Dexter DL, DeNucci T, Miller FR, Calabresi P. Heterogeneity in drug sensitivity among tumor cell subpopulations of a single mammary tumor. Cancer Res 1978; 38:3758–3763.

(*24*) Poste G, Fidler IJ. The pathogenesis of cancer metastasis. Nature 1980; 283:139–146.

(*25*) Dexter DL, Barbosa JA, Calabresi P. *N,N*-Dimethylformamide-induced alteration of cell culture characteristics and loss of tumorigenicity in cultures of human colon carcinoma cells. Cancer Res 1979; 39:1020–1025.

(*26*) Buick RN, Fry SE, Salmon SE. Application of in vitro soft agar techniques for growth of tumor cells to the study of colon cancer. Cancer 1980; 45:1238–1242.

(*27*) Kimball PM, Brattain MG, Pitts AM. A soft-agar procedure for measuring growth of human colonic carcinomas. Br J Cancer 1978; 37:1015–1019.

blank page

Major Histologic Types of Cancers of the Gum and Mouth, Esophagus, Larynx, and Lung by Sex and by Income Level[1,2]

V. L. Ernster,[3,4] S. Selvin,[5] S. T. Sacks,[3] D. W. Merrill,[6] *and* E. A. Holly[3,7]

ABSTRACT—Incidence rates by income level were computed for squamous cell carcinomas of the gum and mouth, larynx, and esophagus and for squamous cell carcinoma, small cell carcinoma, and adenocarcinoma of the lung in white males and females aged 35–64 years, with the use of data for the nine geographic areas of the Third National Cancer Survey and the 1970 U.S. census. Within sex, age, and geographic area groups, patterns of cancer incidence by income level were analyzed by use of a nonparametric statistical method. Higher rates for males than for females were found for every histologic type studied, and the ratio of male-to-female rates increased with age (especially for squamous cell carcinomas of the larynx and lung). A strong inverse relation to income level was found for all of the histologic types studied in males and for squamous cell carcinomas of the gum and mouth and esophagus and small cell carcinoma of the lung in females. These findings are discussed with reference to patterns of smoking and alcohol use by sex and social class.—JNCI 1982; 69:773–776.

Epidemiologists have long been interested in the differential distribution of disease patterns across social groups. Such patterns can suggest life-style or other associated characteristics more directly implicated in disease etiology. The relation of sex and socioeconomic status to cancer rates has therefore been examined by numerous previous investigators, although few studies have considered rates by histologic type of cancer studied. Using data from the TNCS, conducted in the United States during 1969–71, we report incidence rates by sex, age, and income level for major histologic types of the following four cancer sites: gum and mouth, larynx, esophagus, and lung. We have selected these four sites because studies using TNCS data are under way elsewhere (*1*) on the relation between socioeconomic status and cancers of other major sites and because the four sites are all strongly associated with tobacco use.

MATERIALS AND METHODS

Incidence rates by age were computed for white males and females aged 35–64 for major histologic types of cancers of the gum and mouth, esophagus, larynx, and lung. Cancer incidence data were drawn from the population-based TNCS, conducted in nine areas (population of 21 million) of the United States during 1969–71 (*2*). Denominator data for the populations at risk by sex and age for the nine survey areas came from the 1970 tapes of the U.S. Bureau of the Census. The histologic types selected include squamous cell carcinomas of the gum and mouth, larynx, and esophagus and squamous cell carcinoma, small cell carcinoma, and adenocarcinoma of the lung.

Each cancer patient was assigned to one of three income levels based on the median income of his or her census tract of residence. For each of the nine TNCS areas, income was divided into thirds using median income for each census tract within that area. When the data were analyzed across areas, an individual (and his or her census tract population at risk) remained in the same tertile, even though the precise dollar cut points of the income tertiles varied from area to area. This approach assumes that relative income distributions are similar across areas.

A nonparametric method was used to analyze the association between cancer incidence (by site and histologic type) and the three income levels and is described in "Appendix." The significance probabilities used in the presentation reflect the likelihood that observed associations occurred by chance. Of course, these *P*-values indicate the impact of random variation on a single comparison and only generally reflect the overall likelihood associated with the large number of ad hoc comparisons made within this data set.

RESULTS

Table 1 shows for white males and females the number and proportion that each histologic type under study comprised of all microscopically confirmed cancers of the gum and mouth, esophagus, larynx, and lung. For every histologic type studied, the proportion with microscopic confirmation was at least 98% in the overall TNCS data set (*2*).

We first examined incidence rates by sex and age for each of the histologic types of cancer studied (table 2). Rates for males were higher than those for females in every case, and the ratio of male-to-female rates increased with age. The relative excess in male rates at older ages was particularly marked for squamous cell carcinomas of the larynx and

Abbreviation used: TNCS=Third National Cancer Survey.

---

[1] Received September 18, 1981; revised April 13, 1982; accepted April 26, 1982.

[2] Supported in part by Public Health Service grant P01CA-13556-10 from the National Cancer Institute and by Department of Energy contract W-7405-ENG-48.

[3] Department of Epidemiology and International Health, University of California, San Francisco, Calif. 94143.

[4] *Address reprint requests to* Dr. Ernster, Department of Epidemiology and International Health, 1699 HSW, University of California, San Francisco, Calif. 94143.

[5] Department of Biomedical and Environmental Health Sciences, School of Public Health, University of California, Berkeley, Calif. 94720.

[6] Lawrence Berkeley Laboratory, Berkeley, Calif. 94720.

[7] Incidence data in the form of the Third National Cancer Survey public-use tapes were provided by Dr. John L. Young, Jr., Biometry Branch, National Cancer Institute, Bethesda, Md.

lung, with male-to-female ratios at ages 55–64 of 7.4 and 7.1, respectively.

Among males we found a strong inverse relation to income level for all of the histologic types of cancer studied (table 3). Among females we found an inverse association for squamous cell carcinomas of the gum and mouth and esophagus and for small cell carcinoma of the lung. A similar relation was seen for squamous cell carcinoma of the larynx, but this finding is of borderline significance. There was no association with income for squamous cell carcinoma

TABLE 1.—*Proportion of cases each histologic type examined comprised of the cancers studied, TNCS, 1969–71*[a]

Site and type of cancer	White males		White Females	
	No.	Percent	No.	Percent
Gum and mouth, all histologic types	925	100.0	538	100.0
Squamous cell carcinoma	843	91.1	450	83.6
Larynx, all histologic types	1,921	100.0	258	100.0
Squamous cell carcinoma	1,825	95.0	251	97.3
Esophagus, all histologic types	967	100.0	351	100.0
Squamous cell carcinoma	723	74.8	296	84.3
Lung, all histologic types	14,199	100.0	3,695	100.0
Squamous cell carcinoma	5,352	37.7	781	21.1
Small cell carcinoma	1,979	13.9	540	14.6
Adenocarcinoma[b]	2,437	17.2	1,187	32.1

[a] Values are based on microscopically confirmed cases and represent all age groups combined, not just those groups aged 35–64 examined elsewhere in this report.

[b] This category includes alveolar adenocarcinoma, papillary adenocarcinoma, mucin-producing adenocarcinoma, acinar cell carcinoma, adenosquamous carcinoma, and adenocarcinoma, not otherwise specified.

TABLE 2.—*Number of cases and incidence rates per 100,000 for selected cancers by sex and age, TNCS, 1969–71*

Site of cancer	Type of cancer	Age, yr, of patient	White males		White females		Male: female ratio
			No.	Rate	No.	Rate	
Gum and mouth	Squamous cell carcinoma	35–44	25	0.9	14	0.5	1.8
		45–54	161	5.8	100	3.4	1.7
		55–64	286	14.3	141	6.3	2.3
Larynx	Squamous cell carcinoma	35–44	62	2.2	15	0.5	4.4
		45–54	354	12.7	63	2.1	6.0
		55–64	590	29.4	89	4.0	7.4
Esophagus	Squamous cell carcinoma	35–44	8	0.3	7	0.2	1.5
		45–54	89	3.2	37	1.3	2.5
		55–64	236	11.8	93	4.2	2.8
Lung	Squamous cell carcinoma	35–44	164	5.8	43	1.5	3.9
		45–54	759	27.2	171	5.8	4.9
		55–64	1,596	79.6	251	11.2	7.1
Lung	Small cell carcinoma	35–44	72	2.6	30	1.0	2.6
		45–54	315	11.3	130	4.4	2.6
		55–64	642	32.0	191	8.5	3.8
Lung	Adenocarcinoma	35–44	145	5.2	96	3.3	1.6
		45–54	542	19.4	302	10.2	1.9
		55–64	839	41.9	342	15.3	2.7

TABLE 3.—*Incidence rates per 100,000 population for selected cancer sites by histologic type, age, and income level, TNCS, 1969–71, white males*

Age, yr	Income level[a]	Squamous cell carcinoma				Small cell carcinoma of lung	Adenocarcinoma of lung
		Gum and mouth	Larynx	Esophagus	Lung		
35–44	1	1.7	3.1	1.8	8.8	4.2	8.8
	2	1.4	2.6	0.6	7.1	3.5	4.4
	3	1.0	1.9	1.0	4.5	1.8	4.4
45–54	1	11.2	17.6	6.9	41.9	14.8	27.0
	2	5.4	14.3	2.9	30.6	12.1	20.5
	3	3.7	9.2	2.6	18.2	9.4	15.3
55–64	1	18.8	41.6	16.0	97.3	36.0	50.4
	2	13.8	29.5	11.1	83.2	32.9	43.5
	3	11.6	22.6	9.5	64.0	28.4	34.4
		$P<0.001$	$P<0.001$	$P<0.001$	$P<0.001$	$P<0.001$	$P<0.02$

[a] 1=low; 2=intermediate; 3=high.

TABLE 4.—*Incidence rates per 100,000 population for selected cancer sites by histologic type, age, and income level, TNCS, 1969–71, white females*

Age, yr	Income level[a]	Squamous cell carcinoma				Small cell carcinoma of lung	Adenocarcinoma of lung
		Gum and mouth	Larynx	Esophagus	Lung		
35–44	1	2.7	1.5	1.7	3.3	2.5	4.4
	2	0.7	0.8	1.3	1.6	1.9	4.1
	3	0.7	0.8	0.4	1.3	0.8	2.4
45–54	1	4.1	4.8	2.7	5.9	6.6	14.4
	2	4.1	2.6	1.2	5.6	4.7	9.7
	3	2.6	1.7	1.1	5.8	3.4	8.6
55–64	1	8.0	4.9	6.3	11.4	9.0	16.6
	2	6.3	4.0	3.2	11.7	8.8	14.0
	3	5.2	4.0	4.4	10.5	8.6	15.6
		$P<0.01$	$P=0.07$	$P<0.001$	$P=0.22$	$P=0.01$	$P=0.18$

[a] 1=low; 2=intermediate; 3=high.

of the lung or adenocarcinoma of the lung in females (table 4).

DISCUSSION

Our findings show that the inverse relation between income level and selected cancer sites reported in the past continues to be seen in relatively recent population-based incidence data.

Squamous cell carcinoma comprises the vast majority of cancers of the gum and mouth, larynx, and esophagus in both men and women. Thus it is not surprising that the male excess in rates and the inverse relation to social class found here replicate the work of previous investigators who have considered all histologic types of those cancers combined (*3-8*). Published reports on incidence of those cancers by social class among women are fewer and show either an inverse relation (*8, 9*) or no clear gradient (*4, 5*). Smoking has traditionally been more common in men than in women, and the association between smoking and cancers of those sites is well established (*10*). The lower male-to-female rate ratios at younger ages compared to older ages are consistent with a narrowing of smoking differences between the sexes over time, a pattern that has been documented in national smoking surveys (*10*). Alcohol use is also clearly associated with increased risks of cancers of the oral cavity, larynx, and esophagus (*10*), and rates of heavy alcohol use are much higher in men than in women in the United States (*11*). The proportion of drinkers is higher among younger than older women, although the percentage of heavy drinkers is relatively constant across age groups (*11, 12*).

The literature on smoking and drinking patterns by social class is replete with inconsistencies, and only a few of the many relevant published studies can be cited. Among men, smoking has been more common in those with relatively low levels of education and occupational status (*10*) and was also inversely related to a four-component (education, occupation, income, and rent) socioeconomic index (*13*); however, no consistent relation to income alone has been shown in national surveys (*14*). The measure of social class used here, i.e., median income of census tract of residence, may not reflect individual income as much as a more broadly defined "social environment."

Alcohol use and heavy drinking have been positively related to social class in men in some reports (*11*), which is inconsistent with the inverse income gradient that we found for cancers of the gum and mouth, larynx, and esophagus. Others (*15, 16*) have reported an inverse association between alcohol use and social class, consistent with the cancer rates reported here. One of these studies, based on a subset of the TNCS data, found cigarette smoking and alcohol use to be highly correlated with one another (*16*).

In women there has been no clear-cut association between smoking patterns and education or occupation (*10*), but there was an association with the four-component socioeconomic index (*13*) and with income (*14*). Williams and Horm (*16*) reported a strong positive relation between alcohol consumption and both education and family income in women. It is difficult, therefore, to explain the inverse association we found between income level and cancers of the gum and mouth, larynx, and esophagus in women on the basis of smoking and alcohol consumption alone.

The relative frequencies of the major histologic types of lung cancer differ between males and females. In the TNCS data, squamous cell carcinoma comprised 38% of all microscopically confirmed cases of lung cancer in men and only 21% in women, whereas small cell carcinoma comprised nearly equal proportions in the two sexes (13.9% in men and 14.6% in women) and adenocarcinoma accounted for 17% of lung cancer in men and 32% in women. We found a marked male excess in squamous cell carcinoma rates, particularly in males at the older ages, which again reflects a reduction in smoking differences between men and women over time. The strong reverse gradient between income level and both squamous cell carcinoma and adenocarcinoma in men but not in women may be due to the inverse association between smoking and social class noted for men only. However, it is then curious that small cell carcinoma of the lung is inversely related to social class in women as well as in men. Such inconsistencies suggest that some histologic types have etiologies different from others and point to the need for further investigations by histologic type.

In this regard, it has been suggested that the relation of cigarette smoking to lung cancer is stronger for squamous cell carcinoma than for other histologic types, a notion that some investigators have confirmed and others have refuted (*10*). Of interest are the preliminary results of a case-control study among Chinese women in Hong Kong; adenocarcinoma and large cell carcinomas comprised 79% of tumors among the 111 female patients studied, and more than half of these patients were nonsmokers (*17*).

The lack of consistency across studies in the United States that address the relationship between smoking, alcohol consumption, and socioeconomic status suggests that there are factors related to social class, not limited to smoking and drinking, that differentially influence rates for histologic types of the cancers we examined. Of course, it is important to take into account variations by social class in type and amount of cigarettes and alcohol consumed, patterns of smoking in relation to drinking practices, and time trends in such behaviors, which have not been explored here.

We have performed similar analyses for most of the major cancer sites and found a significant inverse relation to income level for only a few sites other than those considered here. Thus our results do not appear to reflect a general cancer susceptibility among the lower income population or to be an artifact of census underenumeration in that group.

REFERENCES

(*1*) Devesa SS, Diamond EL. Association of breast cancer and cervical cancer incidences with income and education among whites and blacks. JNCI 1980; 65:515-528.

(*2*) Cutler SJ, Young JL Jr, eds. Third National Cancer Survey: Incidence data. Natl Cancer Inst Monogr 1975; 41:1-454.

(*3*) Cohart EM, Muller C. Socioeconomic distribution of cancer of gastrointestinal tract in New Haven. Cancer 1955; 8:379-388.

(*4*) Dorn HF, Cutler SJ. Morbidity from cancer in the United States. Monograph No. 56. Washington, D.C.: U.S. Govt Print Off, 1959.

(*5*) Graham S, Levin M, Lilienfeld AM. The socioeconomic distribution of cancer of various sites in Buffalo, N.Y., 1948-1952. Cancer 1960; 13:180-191.

(*6*) Buell P, Dunn JE, Breslow L. The occupational-social class risks of cancer mortality in men. J Chronic Dis 1960; 12:600–621.

(*7*) Clemmesen J. Statistical studies in the aetiology of malignant neoplasms. Vol 1. Copenhagen: Munksgaard, 1965.

(*8*) Wynder EL, Stellman SD. Comparative epidemiology of tobacco-related cancers. Cancer Res 1977; 37:4608–4622.

(*9*) Blot WJ, Fraumeni JF Jr. Geographic patterns of oral cancer in the United States: Etiologic implications. J Chronic Dis 1977; 30:745–757.

(*10*) U.S. Department of Health, Education, and Welfare. Smoking and health. A report of the Surgeon General. Washington, D.C.: U.S. Govt Print Off, 1979 [DHEW publication No. (PHS)79-50066].

(*11*) ———. Second special report to the U.S. Congress on alcohol and health from the Secretary of Health, Education, and Welfare. Washington, D.C.: U.S. Govt Printing Off, 1974 [DHEW publication No. (ADM)75-212].

(*12*) ———. Third special report to the U.S. Congress on alcohol and health from the Secretary of Health, Education, and Welfare. Washington, D.C.: U.S. Govt Print Off, 1978 [DHEW publication No. (ADM)78-569].

(*13*) Srole L, Fischer AK. The social epidemiology of smoking behavior 1953 and 1970: The midtown Manhattan study. Soc Sci Med 1973; 7:341–358.

(*14*) Schuman LM. Patterns of smoking behavior, research on smoking behavior. In: Jarvick ME, Cullen JW, Gritz ER, Vogt TM, West LJ, eds. Research on smoking behavior. NIDA research monograph 17. Washington, D.C.: U.S. Govt Print Off, 1977:36–65.

(*15*) Wechsler H, Thurn D. Teen-age drinking, drug use and social correlates. Q J Studies Alcohol 1973; 34:1220–1227.

(*16*) Williams RR, Horm JW. Association of cancer sites with tobacco and alcohol consumption and socioeconomic status of patients: Interview study from the Third National Cancer Survey. J Natl Cancer Inst 1977; 58:525–547.

(*17*) Colbourne MJ, Ho JH. Bronchial cancer in Hong Kong, 1976–77: A preliminary report. Natl Cancer Inst Monogr 1979; 53:49–51.

APPENDIX

The scheme for assigning scores to the patterns of cancer incidence with increasing income level within each age group and geographic area is shown in appendix table 1.

For example, if incidence rates increased consistently as income levels increased, a score of +2 was assigned. Conversely, if rates decreased as income levels increased, a score of −2 was assigned. Summing over age groups within each TNCS area gives a range of possible values of −6 to +6. The expected value of the score calculated under the assumption of no association between cancer incidence and socioeconomic status is 0.0 and the variance is 2.0, since each ordering is equally likely ($P=1/6$). If a tie occurred, a probability distribution under the null hypothesis was generated that accounted for the tie. If rates for all three income levels within a given age group were identical, the age group was dropped from the analysis. This situation rarely occurred.

The scores across the nine geographic areas were then added, resulting in a single score between −54 and +54 that summarized the overall association while "controlling" for any influences due to heterogeneity in socioeconomic levels. To calculate the significance levels, we used an approximation. If X represents the summary score over m areas, then $P(X\leq -k)=P(X\geq k)=P(Z>[k-0.5]/\sqrt{6m})$, where Z has a standard normal distribution. For example, if $m=9$ and the score is 16, then $P(X\geq 16)=P(Z\geq 2.111)=0.017$.

Appendix table 1.—*Patterns of cancer incidence*

Income level[a]	Score							
	+2	+1			−1			−2
1	Low	Intermediate	*or*	Low	High	*or*	Intermediate	High
2	Intermediate	Low		High	Low		High	Intermediate
3	High	High		Intermediate	Intermediate		Low	Low

[a] 1=low; 2=intermediate; 3=high.

Glycoconjugate With *Ulex europaeus* Agglutinin-I-Binding Sites in Normal Mucosa, Adenoma, and Carcinoma of the Human Large Bowel[1,2]

Suguru Yonezawa,[3] Takao Nakamura,[3] Sadao Tanaka,[3] *and* Eiichi Sato[3,4]

ABSTRACT—Cancerous lesions and nonneoplastic mucosa of surgically extirpated specimens from 94 patients with colorectal carcinoma (of the right colon, 31 patients; of the left colon, 29 patients; and of the rectum, 34 patients) and endoscopically polypectomized specimens from 18 patients with rectal adenoma were examined with fluorescein isothiocyanate-conjugated or horse-radish peroxidase-conjugated *Ulex europaeus* agglutinin-I (UEA-I) specific to a certain terminal α-L-fucosyl residue in glycoconjugates. Of the 31 patients with right colon cancers, 22 showed positive UEA-I binding in the neoplastic cell apexes, apical luminal borders, and luminal secretions. The adjacent nonneoplastic mucosa of all 31 patients, however, demonstrated positive UEA-I binding in the goblet cell mucus. UEA-I binding was positive for 23 of the 29 left colon cancers and for 28 of the 34 rectal cancers, although UEA-I binding was not revealed in the adjacent nonneoplastic mucosa for most of the cases. Of the 18 rectal adenomas, 12 specimens showed positive UEA-I binding in the apical secretions of their adenoma cells. Marked regional differences of UEA-I binding in the nonneoplastic mucosae indicated that the constituents of glycoprotein with UEA-I binding sites in goblet cell mucus differed significantly between the human right and left large bowels. Positive UEA-I binding in many rectal cancerous and adenomatous lesions suggested that a neoplastic glycoprotein with α-L-fucosyl residue was produced or that the terminal carbohydrate structure of glycoprotein present in the nonneoplastic mucosa was altered to bind easily with UEA-I after the neoplastic transformation had occurred. A possible relation of this UEA-I binding to blood group H(O) substance is discussed.—JNCI 1982; 69:777–785.

Glycoproteins are the major components of secreted mucins and of membranes of the gastrointestinal mucosa. Histochemical studies in which stains such as periodic acid–Schiff, Alcian blue, high-iron diamine, and high-iron diamine–Alcian blue have been used have demonstrated mucosubstances in human colon mucosa. The histochemical investigations have suggested either qualitative and quantitative differences in carbohydrate content between the proximal and distal portions of the colon (*1–4*) or considerable alterations in the carbohydrate contents of mucinous glycoproteins in colorectal cancerous and adenomatous lesions (*3–6*). However, these staining procedures do not discriminate a specific carbohydrate sequence in glycoconjugates in normal mucosa or in neoplastic lesions.

Lectins derived from plants or animals have an ability to bind with specific carbohydrate residues of glycoconjugates (*7*). Recently, FITC or HRP conjugates of lectins have been used for investigation of tissue sections (*8–12*). We used lectins to study glycoprotein in nonneoplastic mucosa and neoplastic lesions of the specimens of human colorectal carcinoma, and we found specific and interesting features of binding of UEA-I specific to a certain terminal α-L-fucosyl residue (*13, 14*) in both nonneoplastic mucosa and neoplastic lesions. In this study, regional differences of glycoprotein with UEA-I receptors in nonneoplastic colorectal mucosa were noted; furthermore, alteration of glycoprotein following neoplastic change is discussed.

MATERIALS AND METHODS

Surgically extirpated specimens were examined from 94 patients with colorectal carcinoma [of the right colon (cecum and ascending colon), 31 patients; of the left colon (descending and sigmoid colons), 29 patients; and of the rectum, 34 patients], and endoscopically polypectomized specimens were examined from 18 patients with rectal adenoma.

Staining with FITC–lectins.—Surgical specimens of neoplastic or nonneoplastic portions from the patients with colorectal carcinoma and adenoma were either fixed in Formalin or frozen in Dry Ice–acetone. The Formalin-fixed specimens were embedded in paraffin, cut at 4 μm, deparaffinized, rehydrated, and washed four times in PBS (pH 7.2) for 5 minutes each. The frozen specimens were cut in a cryostat, dried in air, fixed in acetone for 1 minute, and washed four times in PBS. These tissue sections were incubated with FITC-conjugated plant lectins for 30 minutes at room temperature. The lectins used as the FITC-conjugated materials were Con A, WGA, *Bauhinia purpurea* agglutinin, *Ricinus communis* agglutinin-I, and UEA-I, all of which were purchased from E-Y Laboratories, Inc., San Mateo, Calif. The concentration of all lectins was 1 mg lectin/ml. The tissue sections were then washed four times in PBS and examined under a fluorescence microscope with epi-illumination (Olympus, model BH-RFL-LB) in which the excitation interference filter IF 490 and dichroic mirror reflector DM 500 containing absorption filter O 515 were used. Photographs were taken with Fujichrome 100 daylight film. For control inhibition studies, 0.2 *M* of the appropriate

---

ABBREVIATIONS USED: Con A=concanavalin A; FITC=fluorescein isothiocyanate; HRP=horse-radish peroxidase; PBS=phosphate-buffered saline; UEA-I=*Ulex europaeus* agglutinin-I; WGA=wheat-germ agglutinin.

---

[1] Received October 2, 1981; revised April 13, 1982; accepted May 5, 1982.

[2] Supported in part by Grant-in-Aid 401004 for Cancer Research from the Ministry of Education, Science and Culture, Japan.

[3] Second Department of Pathology, Faculty of Medicine, Kagoshima University, 1208-1 Usuki-cho, Kagoshima City, 890, Japan.

[4] We express our appreciation to Dr. Takashi Muramatsu, Department of Biochemistry, Faculty of Medicine, Kagoshima University, Kagoshima, for his valuable advice. We also thank Mr. Saburo Irifune for his technical assistance.

competing sugars was mixed in the incubation solutions (α-methyl-D-mannoside for Con A, *N*-acetyl-D-glucosamine for WGA, *N*-acetyl-D-galactosamine for *Bauhinia purpurea* agglutinin, β-lactose for *Ricinus communis* agglutinin-I, and α-L-fucose for UEA-I).

Staining with HRP-UEA-I.—The Formalin-fixed, paraffin-embedded sections were incubated with HRP-conjugated UEA-I (E-Y Laboratories, Inc.) for 30 minutes at room temperature, after endogenous peroxidase activity of the sections had been blocked by treatment of the sections with methanol and H_2O_2 (*15*). The sections were then washed four times in PBS and stained with 3,3′-diaminobenzidine as described by Graham and Karnovsky (*16*).

RESULTS

As a first experiment, we used the five FITC-conjugated lectins listed in "Materials and Methods" to do lectin-binding studies on Formalin-fixed surgical specimens of 15 human colorectal carcinomas (of the right colon, 5 cases; of the left colon, 5 cases; and of the rectum, 5 cases). The lectin-binding studies indicated that only UEA-I presented an evident difference in the labeling behavior of goblet cell mucus of nonneoplastic mucosa when the right and left large bowels were compared (figs. 1A, 1B). The other four lectins did not show regional differences in their labeling patterns. Therefore, we examined UEA-I binding further in nonneoplastic mucosa and neoplastic lesions from 112 patients, of whom 94 had carcinomas and 18 of whom had adenomas.

To elucidate the influence of Formalin fixation and paraffin embedding on UEA-I binding, we did comparative UEA-I-binding studies on both fresh (unfixed)-frozen sections and Formalin-fixed, paraffin-embedded sections prepared from adjacent tissues of the frozen sections. These specimens were obtained from nonneoplastic portions and neoplastic lesions in 6 extirpated specimens of colorectal carcinoma (from 3 cases each of the right colon and of the rectum). Fresh-frozen sections and Formalin-fixed, paraffin-embedded sections of the 6 specimens showed identical results with regard to the UEA-I binding with goblet cell mucus in the nonneoplastic mucosa or with cell apexes, apical luminal borders, and luminal secretions in the neoplastic lesions. Therefore, we concluded that conventional Formalin-fixed, paraffin-embedded specimens were useful in the UEA-I-binding study within the limits of nonneoplastic goblet cell mucus or neoplastic cell apexes, apical luminal borders, and luminal secretions.

However, we noted some discrepancies between frozen sections and paraffin sections: Fresh-frozen sections from the 6 colorectal carcinoma cases demonstrated evident UEA-I binding with capillaries and blood vessels and very weak UEA-I binding with epithelial cell membranes, but Formalin-fixed, paraffin-embedded sections from these 6 cases did not demonstrate such bindings. However, in the following series of UEA-I-binding studies of many other surgical specimens, UEA-I binding with capillaries and blood vessels was at times observed even in the Formalin-fixed, paraffin-embedded sections (fig. 6), although binding with the cell membranes was never observed in the Formalin-fixed, paraffin-embedded sections of this series.

On the basis of the above-mentioned data, we used both FITC-conjugated UEA-I and HRP-conjugated UEA-I to examine surgically extirpated specimens from 94 patients with colorectal carcinoma and endoscopically polypectomized specimens from 18 patients with rectal adenoma. Sections treated with both FITC-conjugated UEA-I and HRP-conjugated UEA-I showed identical results. The UEA-I binding was inhibited by incubation with 0.2 *M* α-L-fucose, as shown in figure 1C.

The results of UEA-I-binding studies on nonneoplastic mucosae and neoplastic lesions of the 94 patients with colorectal carcinoma are summarized in table 1. The data by case are shown in text-figure 1. The extent of cancerous lesions was not correlated with the degree of UEA-I binding.

Right colon (cecum and ascending colon).—Most of the goblet cell mucus (20 patients) and some of the goblet cell mucus (11 patients) were bound with UEA-I in the nonneoplastic mucosae of the 31 patients with right colon cancer. There was no patient from whom the goblet cell mucus of the nonneoplastic mucosa was not labeled by UEA-I.

In the cancerous lesions of these 31 patients, most of the neoplastic cell apexes, apical luminal borders, and luminal secretions were bound with UEA-I (10 patients) (fig. 2); however, some of the neoplastic cell apexes, apical luminal borders, and luminal secretions were labeled by UEA-I (12 patients). No binding of UEA-I with neoplastic cell apexes, apical luminal borders, or luminal secretions was found in the remaining 9 patients, although most if not some of their nonneoplastic goblet cell mucus revealed UEA-I binding (fig. 3). In these cases, UEA-I selectively bound with nonneoplastic goblet cell mucus but did not label neoplastic secretions (fig. 4A), although the other four lectins (i.e., excluding UEA-I) labeled both secretions of the nonneoplastic mucosa and neoplastic lesion (fig. 4B).

Left colon (descending colon and sigmoid colon).—Goblet cell mucus of the nonneoplastic mucosa of the left colon in 26 of 29 patients was never labeled by UEA-I, whereas some of the unaffected goblet cell mucus in the remaining 2 patients and most of it in the other patient was bound with UEA-I.

In the cancerous lesions, most of neoplastic cell apexes, apical luminal borders, and luminal secretions were bound with UEA-I in 14 patients, and some of the neoplastic cell

TABLE 1.—*UEA-I binding in nonneoplastic mucosa and carcinoma of the human large bowel*

Bowel tissue	UEA-I binding[a]		
	−	+	++
Right colon			
Nonneoplastic mucosa	0	11	20
Carcinoma	9	12	10
Left colon			
Nonneoplastic mucosa	26	2	1
Carcinoma	6	9	14
Rectum			
Nonneoplastic mucosa	34	0	0
Carcinoma	6	14	14

[a] −=none; +=some; ++=most.

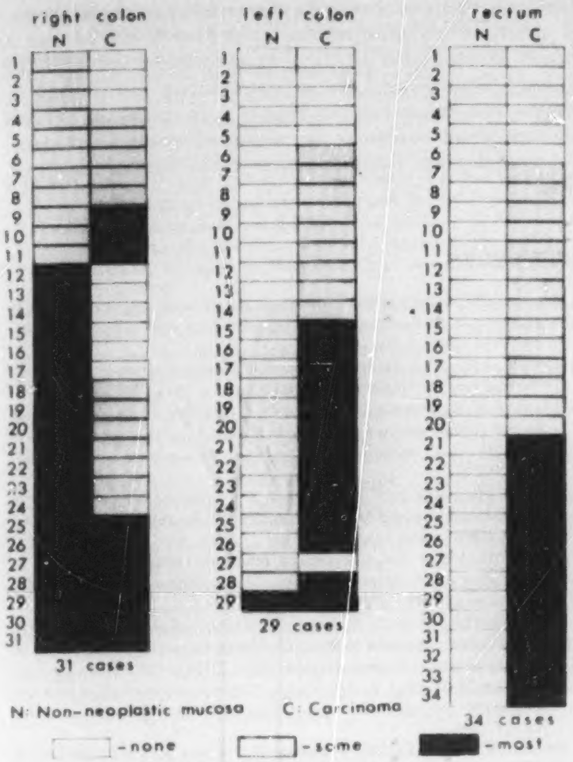

TEXT-FIGURE 1.—UEA-I binding in the nonneoplastic mucosa and in the carcinoma in specimens from each patient with colorectal carcinoma. Data are presented by case.

apexes, apical luminal borders, and luminal secretions were labeled in 9 patients. The cancerous lesions of the remaining 6 patients showed no binding of UEA-I.

Rectum.—None of the goblet cell mucus of the nonneoplastic rectal mucosa of any of the 34 patients was bound with UEA-I. In the cancerous rectal lesions, most of neoplastic cell apexes, apical luminal borders, and luminal secretions in 14 of the patients and some of the neoplastic cell apexes, apical luminal borders, and luminal secretions in 14 patients were bound with UEA-I (fig. 5). The cancerous lesions in the remaining 6 patients showed no UEA-I binding.

In the 18 polypectomized specimens of rectal adenoma, most of the neoplastic apical secretions of 2 of the patients and some of the secretions in 10 of the other patients were labeled by UEA-I. The remaining specimens of the other 6 patients showed no UEA-I binding. In addition, adenomatous lesions were combined with carcinoma in several patients with rectal cancer. In the contact points of adenomatous lesions and nonneoplastic mucosae in these patients, UEA-I labeled only the neoplastic epithelium but did not label the nonneoplastic mucosa (fig. 6).

DISCUSSION

This UEA-I-binding study of the nonneoplastic mucosa of human colon and rectum demonstrated an obvious difference between UEA-I receptors in the nonneoplastic goblet cell mucus of the right large bowel and the UEA-I receptors in the nonneoplastic goblet cell mucus of the left large bowel. In all specimens of the right colon, some if not most of the UEA-I receptor was in the nonneoplastic goblet cell mucus. However, most of the left colon and rectum specimens (from 60 of 63 patients) had no UEA-I receptor in their nonneoplastic goblet cell mucus. It is especially noteworthy that no nonneoplastic goblet cell mucus in any specimen of the rectal mucosa had the UEA-I receptor.

Terminal positions on the oligosaccharide side chains are generally occupied by sialic acid or fucose (*17, 18*). These two sugars compete with each other for occupation of the terminal positions (*19*). In chemical studies of secretions from a normal human, Hoskins and Zamcheck (*20*) showed a significantly greater sialic acid content and a lower fucose content in rectal mucus. As UEA-I is specific to a terminal fucosyl residue (*13, 14*), the lack of UEA-I binding with rectal mucus may be related to the low fucose content in the rectum.

Culling et al. (*21*) histochemically demonstrated O-acylated sialic acids in the epithelial mucins of the lower end of the gastrointestinal tract, and they also reported an increase in periodic acid–Schiff reactivity after saponification, by which the sialic acids are removed. Therefore, the differing intensity of periodic acid–Schiff stain between the proximal and the distal colon, which has been observed in previous histochemical studies (*2–4*), is probably related to the presence of the sialic acids that compete with fucose for the occupation of the terminal positions on sugar side chains; therefore, the differences in intensity may not be directly related to fucose content.

Essner et al. (*9*) used fluoresceinated lectins to study the location of carbohydrate components in the colon of rats. They studied only the descending colon; the proximal colon was not examined. Freeman et al. (*22*) used lectins to detect goblet cell glycoconjugate differences in the proximal and distal colons of rats, tissues of which had been fixed in a modified Bouin's solution containing picric acid, formaldehyde, and acetic acid. They reported an apparent regional difference in binding of Con A and *Lens culinaris* agglutinin, which are specific to mannosyl or glucosyl residues, in the goblet cell mucus of normal colon mucosae of the rats. Labeling of the two lectins with goblet cell mucus was observed only in the proximal colon and not in the distal colon, whereas UEA-I did not show regional differences in the rats examined in this study (*22*). However, in the human colorectal specimens, only UEA-I showed an apparent regional difference in the labeling behavior of goblet cell mucus between the right and left large bowels (figs. 1A, 1B), inasmuch as Con A did not reveal any regional difference. These interspecies differences must be accounted for in the comparison of experimental animal with human specimens.

Because Cazal and Lalaurie (*23*) showed that extracts of *Ulex europaeus* seed contain a protein that reacts with blood group H(O) antigen, the *Ulex* extracts have been used for studies of the blood group H(O) substance in human tissues (*24–31*). The H(O) antigen is considered to be a precursor substance of A or B antigens and is present not only in human blood group O but also in human non-O blood groups (*32*, 33). Therefore, an investigation of the H(O) antigen may be basic and valuable in studies of blood group substances in human tissues, irrespective of the A-B-O blood groups. However, as some authors described (*24–26, 28, 31*), the *Ulex* extracts used in the earlier studies had questionable specificity and sensitivity; consequently, the results are inconclusive. Also, in the earlier studies of human colon, the blood group H(O) substance had not been successfully investigated, although blood group A and B substances were well demonstrated (*24, 25, 28, 34–36*). Our present study could well detect UEA-I receptors in nonneoplastic mucosae and neoplastic lesions of human large bowels. The UEA-I receptors may be a blood group H(O) substance, because the mode of distribution of UEA-I receptors is similar to those of A or B substances (*24, 25, 28, 34–36*).

Many of the rectal cancers revealed positive UEA-I binding in their neoplastic cell apexes, apical luminal borders, and luminal secretions in spite of negative UEA-I binding in the adjacent nonneoplastic mucosa (fig. 5). Although these findings probably indicate that blood group H(O) substances appear in the cancerous lesions, it is undeniable that a neoplastic glycoprotein with terminal α-L-fucosyl residue which does not belong to the blood group H(O) substance is produced or that the terminal carbohydrate structure of glycoprotein present in the nonneoplastic mucosa is altered to a form that binds easily with UEA-I.

Kim and Isaacs (*37*) noted that the level of fucose was significantly reduced in the colon cancer tissue as compared with normal human colon mucosa. Their data are concerned with a total amount of fucose in the tissue, but the results obtained by our UEA-I binding study are concerned only with a certain terminal α-L-fucosyl residue. Therefore, the data in our study and the data of Kim and Isaacs are not comparable. However, the obvious difference between the UEA-I binding in the nonneoplastic mucosa of the human right and left large bowels must be accounted for in studies of fucose content of human colorectal mucosa.

Two-thirds of the 18 rectal adenoma patients showed positive UEA-I binding in their neoplastic epithelium, in spite of the negative UEA-I binding in the nonneoplastic rectal mucosae of the previously mentioned 34 patients with rectal cancer. In the contact points of adenomatous lesions combined with carcinoma and the adjacent nonneoplastic mucosa in the rectum, UEA-I binding clearly distinguished the adenomatous lesions from the adjacent nonneoplastic mucosa, as shown in figure 6. Because malignant potentiality of colorectal adenoma has been noted (*38–41*), we were interested to note that the solitary adenomas and the adenomatous lesions combined with carcinomas were labeled by UEA-I. This suggests either the appearance of blood group H(O) substance, the production of neoplastic glycoprotein, or the alteration of the terminal carbohydrate structure of glycoprotein in the adenomas similar to those of the cancerous lesions discussed above.

Cancerous cells or embryonic cells are known to have different spectra of glycoconjugates as compared with their normal or differentiated counterparts (*42–44*). These differences are caused either by incomplete glycosylation in cancerous cells or by formation of additional sugar chains in such cells. We are especially interested to know which mechanism operates in the altered expression of UEA-I receptors in malignant cells. Further studies on the biochemical nature of glycoconjugates labeled with UEA-I and a detailed investigation of the correspondence between the histologic findings and the glycoconjugate distribution in adenomatous and cancerous lesions may reveal the process by which glycoconjugates are alterated as an accompaniment to malignant transformation in the human colorectal region.

REFERENCES

(*1*) Filipe MI, Branfoot AC. Abnormal patterns of mucus secretion in apparently normal mucosa of large intestine with carcinoma. Cancer 1974; 34:282–290.

(*2*) Lev R, Orlic D. Histochemical and radioautographic studies of normal human fetal colon. Histochemistry 1974; 39:301–311.

(*3*) Mäkelä V, Korhonen LK, Lilius G. Carbohydrate rich compounds in the colonic mucosa of man. I. Histochemical characteristics of normal and adenomatous colonic mucosa. Cancer 1971; 27:120–127.

(*4*) Sovari TE, Lauren P. Histochemical investigation of mucins in normal intestine and intestinal carcinoma. Scand J Clin Lab Invest 1969; 108:71.

(*5*) Filipe MI. Value of histochemical reactions for mucosubstances in the diagnosis of certain pathological conditions of the colon and rectum. Gut 1969; 10:577–586

(*6*) Korhonen LK, Mäkelä V, Lilius G. Carbohydrate rich compounds in the colonic mucosa of man. II. Histochemical characteristics of colonic adenocarcinoma. Cancer 1971; 27:128–133.

(*7*) Goldstein IJ, Hayes CE. The lectins: Carbohydrate-binding proteins of plants and animals. Adv Carbohydr Chem Biochem 1978; 35:127–340.

(*8*) Brabec RK, Peters BP, Bernstein IA, Gray RH, Goldstein IJ. Differential lectin binding to cellular membranes in the epidermis of the newborn rat. Proc Natl Acad Sci USA 1980; 77:477–479.

(*9*) Essner E, Screiber J, Griewski RA. Localization of carbohydrate components in rat colon with fluoresceinated lectins. J Histochem Cytochem 1978; 26:452–458.

(*10*) Peters BP, Goldstein IJ. The use of fluorescein-conjugated *Bandeiraea implicifolia* B_4-isolation as a histochemical reagent for the detection of α-D-galactopyranosyl groups—their occurrence in basement membranes. Exp Cell Res 1972; 120:321–334.

(*11*) Thoss K, Roth J. The use of fluorescein isothiocyanate labelled lectins for immuno-histological demonstration of saccharides. III. Studies by use of *Ricinus communis* lectin and wheat germ agglutinin. Exp Pathol (Jena) 1977; 14:215–219.

(*12*) Whyte A, Loke YW, Stoddart RW. Saccharide distribution in human trophoblast demonstrated using fluorescein-labelled lectins. Histochem J 1978; 10:417–423.

(*13*) Matsumoto I, Osawa T. Purification and characterization of anti-H(O) phytohemagglutinin of *Ulex europeus*. Biochim Biophys Acta 1969; 194:180–189.

(*14*) ———. On the specificity of various heterologous anti-H hemagglutinins. Vox Sang 1971; 21:548–577.

(*15*) Taylor CR, Burns J. The demonstration of plasma cells and other immunoglobulin-containing cells in Formalin-fixed, paraffin-embedded tissues using peroxidase-labelled antibody. J Clin Pathol 1974; 27:14–20.

(*16*) Graham RC, Karnovsky MJ. The early stages of absorption of injected horseradish peroxidase in the proximal tubules of the mouse kidney: Ultrastructural cytochemistry by a new technique. J Histochem Cytochem 1966; 14:291–302.

(*17*) Gottschalk A. The basic structure of glycoproteins and problems of their chemical and physico-chemical analysis. Ann NY Acad Sci 1963; 106:168–176.

(*18*) Pigman W, Tsuiki S. The nature of the epithelial mucins. Int Dent J 1959; 9:502–516.

(*19*) Paulson JC, Prieels J-P, Glasgow LR, Hill RL. Sialyl- and fucosyltransferases in the biosynthesis of asparaginyl-linked oligosaccharide in glycoproteins: Mutally exclusive glycosylation by βgalactoside α2 → 6 sialyltransferase and *N*-acetylglucosaminide α1 → 3 fucosyltransferase. J Biol Chem 1978; 253:5617-5624.

(*20*) Hoskins LC, Zamcheck N. Studies on gastric mucins in health and disease. Ann NY Acad Sci 1963; 106:767-774.

(*21*) Culling CF, Reid PE, Clay MG, Dunn WL. The histochemical demonstration of O-acylated sialic acid in gastro-intestinal mucins: Their association with the potassium hydroxide-periodic acid-Schiff effect. J Histochem Cytochem 1974; 22:826-831.

(*22*) Freeman HJ, Lotan R, Kim YS. Application of lectins for detection of goblet cell glycoconjugate differences in proximal and distal colon of the rat. Lab Invest 1980; 42:405-412.

(*23*) Cazal P, Lalaurie M. Recherches sur quelques phyto-agglutinines spécifiques des groupes sanguins ABO. Acta Haematol (Basel) 1952; 8:73-80.

(*24*) Abdelfattah-Gad M, Denk H. Epithelial blood group antigens in human carcinomas of the distal colon: Further studies on their pathologic significance. JNCI 1980; 64:1025-1028.

(*25*) Cooper HS, Haesler WE. Blood group substances as tumor antigens in the distal colon. Am J Clin Pathol 1978; 69:594-598.

(*26*) Davidsohn I, Kovarik S, Lee CL. A, B and O substances in gastrointestinal carcinoma. Arch Pathol 1966; 81:381-390.

(*27*) Davidsohn I, Ni LY. Loss of isoantigens A, B, and H in carcinoma of the lung. Am J Pathol 1969; 57:307-334.

(*28*) Denk H, Tappeiner G, Davidovits A, Eckerstorfer R, Holzner JH. Carcinoembryonic antigen and blood group substances in carcinomas of the stomach and colon. J Natl Cancer Inst 1974; 53:933-942.

(*29*) Gupta RK. Immunocytologic losses of isoantigens A, B, and H(O) in the endometrium and brain. Am J Clin Pathol 1976; 66:390-394.

(*30*) Gupta RK, Schuster R. Isoantigens A, B and H in benign and malignant lesions of the breast. Am J Pathol 1973: 72:253-260.

(*31*) Kent SP. The demonstration and distribution of water soluble blood group O(H) antigen in tissue sections using a fluorescein labelled extract of *Ulex europaeus* seed. J Histochem Cytochem 1964; 12:591-599.

(*32*) Kobata A. Biochemical basis for blood groups. Tanpakushitsu Kakusan Koso 1973; 18:83-92 (in Japanese).

(*33*) Watkins WM. Blood group substances: In the ABO system, the genes control the arrangement of sugar residues that determines blood group specificity. Science 1966; 152:172-181.

(*34*) Cooper HS, Cox J, Patchefsky AS. Immunohistologic study of blood group substances in polyps of the distal colon: Expression of a fetal antigen. Am J Clin Pathol 1980; 73:345-350.

(*35*) Denk H, Holzner JH, Obiditsch-Mayr I. Epithelial blood group antigens in colon polyps. I. Morphologic distribution and relationship to differentiation. J Natl Cancer Inst 1975; 54:1313-1317.

(*36*) Wiley EL, Mendelsohn G, Eggleston JC. Distribution of carcinoembryonic antigens and blood group substances in adenocarcinoma of the colon. Lab Invest 1981; 44:507-513.

(*37*) Kim YS, Isaacs R. Glycoprotein metabolism in inflammatory and neoplastic diseases of the human colon. Cancer Res 1975; 35:2092-2097.

(*38*) Bockus HL, Tachdjian V, Ferguson LK, Monhran MD, Chamberline C. Adenomatous polyps of colon and rectum: Its relation to carcinoma. Gastroenterology 1961; 41:225-232.

(*39*) Enterline HT, Evans GW, Marcado-Lugo R, Miller L, Fitts WT. Malignant potential of adenoma of colon and rectum. JAMA 1962; 179:322-330.

(*40*) Morson BC. Precancerous and early malignant lesions of the large intestine. Br J Surg 1968; 55:725-731.

(*41*) Sato E. Adenomatous polyps of large intestine in autopsy and surgical material. Gann 1974; 65:295-306.

(*42*) Hakomori S. Glycosphingolipids in cellular interaction, differentiation, and oncogenesis. Ann Rev Biochem 1981; 50:733-764.

(*43*) Muramatsu T, Avner P, Fellous M, Gachelin G, Jacob F. Distinctive properties of fucosyl glycopeptides on human teratoma cells. Somatic Cell Genet 1979; 5:753-761.

(*44*) Nicolson GL, Poste G. The cancer cell: Dynamic aspects and modification in cell-surface organization (second of two parts). N Engl J Med 1976; 295:253-258.

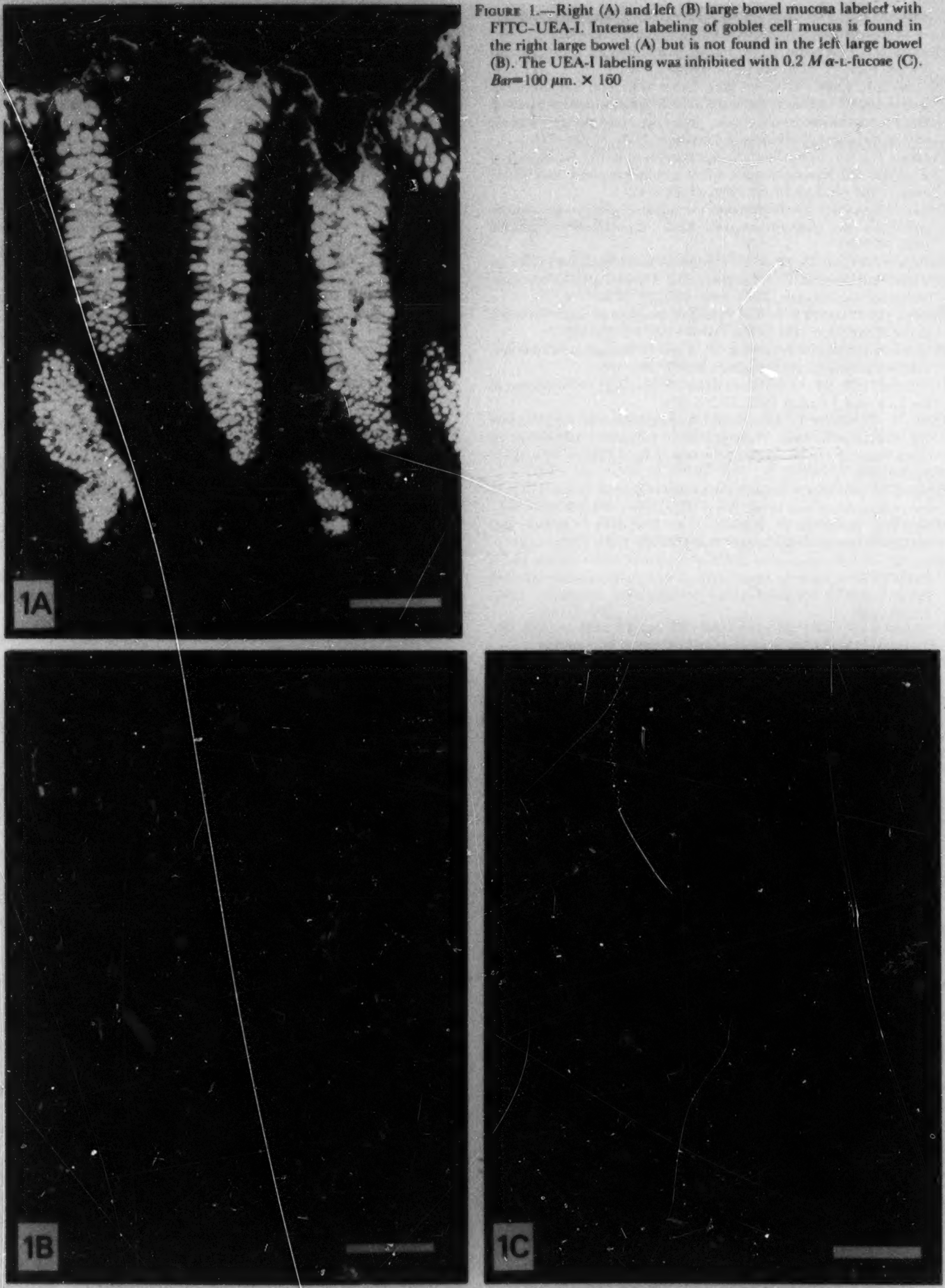

FIGURE 1.—Right (A) and left (B) large bowel mucosa labeled with FITC–UEA-I. Intense labeling of goblet cell mucus is found in the right large bowel (A) but is not found in the left large bowel (B). The UEA-I labeling was inhibited with 0.2 *M* α-L-fucose (C). *Bar*=100 μm. × 160

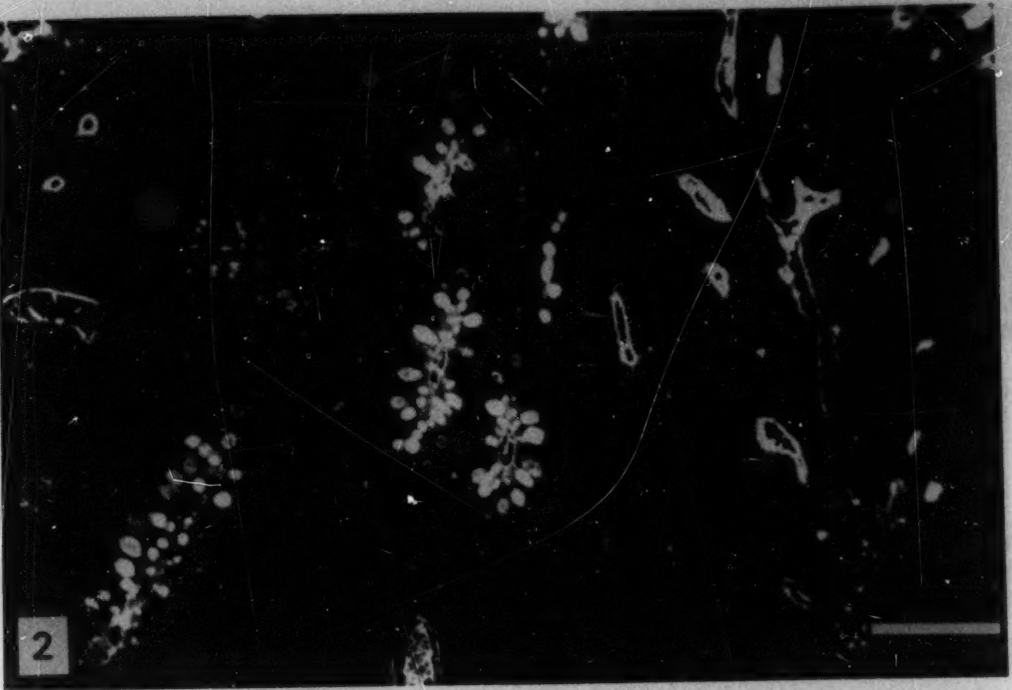

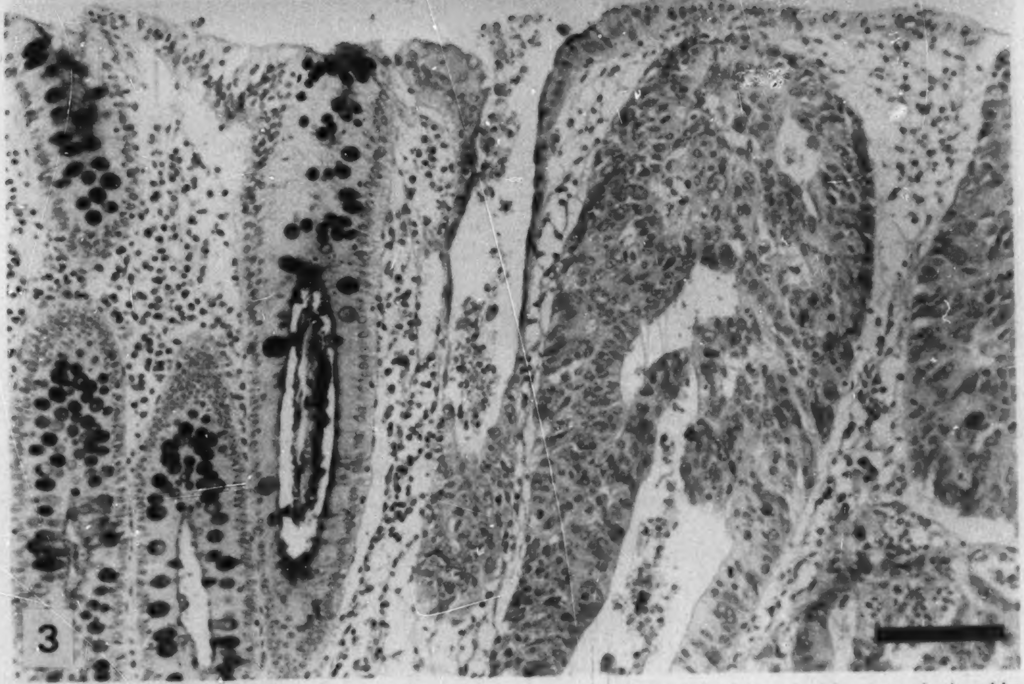

FIGURE 2.—Right colon cancer labeled with FITC–UEA-I (right colon, case #25). UEA-I bound with nonneoplastic goblet cell mucus (*left side*) and bound with neoplastic cell apexes, apical luminal borders, and luminal secretions (*right side*). Bar=100 µm. × 190

FIGURE 3.—Right colon cancer labeled with HRP–UEA-I (right colon, case #12). UEA-I bound only with nonneoplastic goblet cell mucus (*left side*) but did not bind with cancerous lesion (*right side*). Nuclear counterstain, hematoxylin. *Bar*=100 µm. × 190

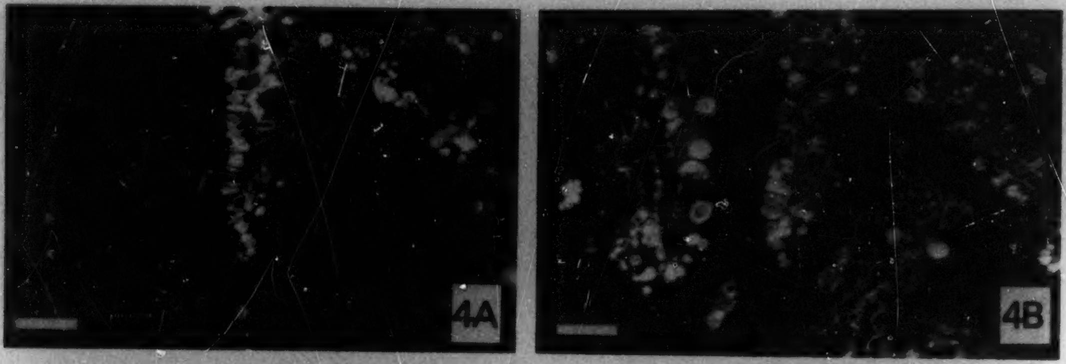

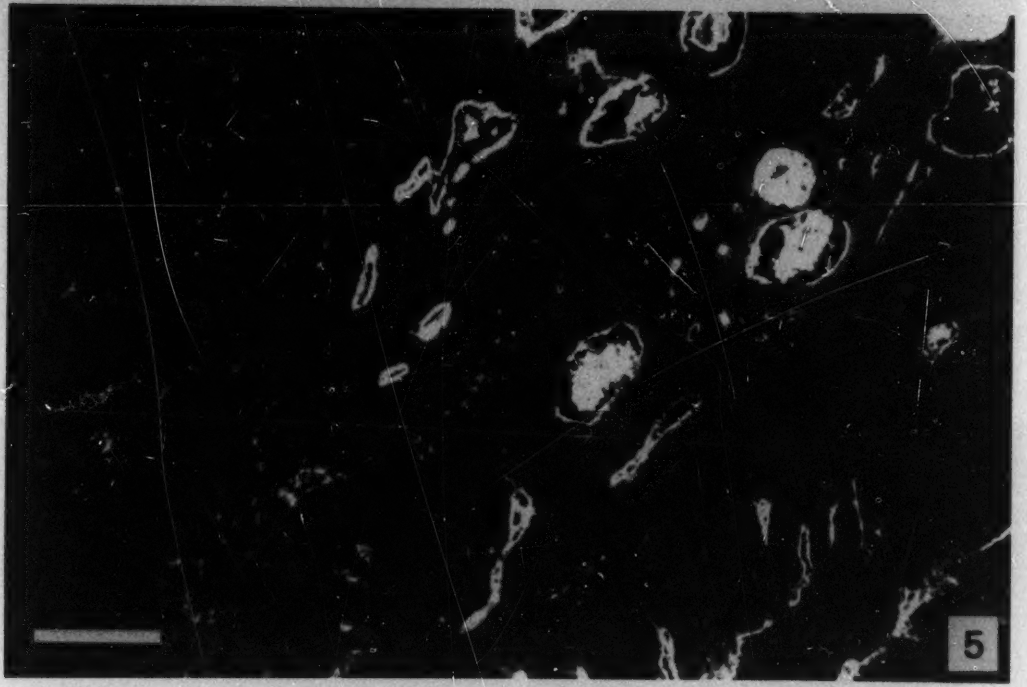

Figure 4.—Right colon cancer labeled with FITC–UEA-I (A) and FITC–WGA (B) in serial sections (right colon, case #13). UEA-I selectively bound with nonneoplastic goblet cells and did not label neoplastic secretion (A). In contrast, WGA labeled both secretions of the nonneoplastic mucosa and the cancerous lesion (B). *Bar*=100 µm. × 90

Figure 5.—Rectal cancer labeled with FITC–UEA-I (rectum, case #21). UEA-I bound only with cancerous cell apexes, apical luminal borders, and luminal secretions (*right side*) but did not bind with the nonneoplastic mucosa (*left side*). *Bar*=100 µm. × 190

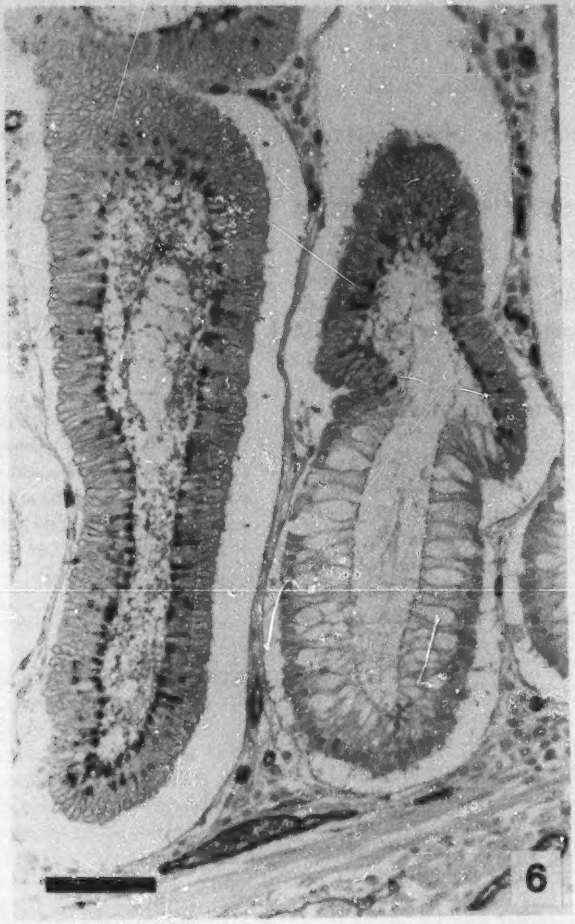

FIGURE 6.—A contact point of adenomatous lesion and nonneoplastic mucosa labeled with HRP-UEA-I in the rectum. UEA-I labeled only the adenomatous epithelium but did not label the nonneoplastic mucosa. Capillary vessels were also bound with UEA-I in this specimen, as shown near *lower corner*. Nuclear counterstain, hematoxylin. *Bar*=100 µm. × 160

blank page

Cerebrospinal Fluid Markers in African Burkitt's Lymphoma With Central Nervous System Involvement[1,2]

William C. Wallen,[3,4] Robert J. Biggar,[5] Paul H. Levine,[6] Janet Neequaye,[7] *and* Francis K. Nkrumah[7,8]

ABSTRACT—Several cerebrospinal fluid markers were found to be elevated in Burkitt's lymphoma patients with central nervous system (CNS) involvement. Antibody levels to the virus capsid antigen of the Epstein-Barr virus and to the brain cell antigens myelin and cerebroside were elevated during active CNS disease. Immune complexes were present in levels above 100 μg/ml in most patients with CNS involvement but tended to be low or negative in patients without CNS disease. Oligoclonal IgG bands were present in 12 of 13 patients with CNS disease and in only 3 of 26 patients with no clinical evidence of disease. None of these markers were present in 6 other tumor patients without CNS disease. The presence of these markers in 12 of 13 patients in whom CNS disease was involved suggests that these markers may be useful in determining the status of the tumor with regard to involvement of the CNS.—JNCI 1982; 69:787–792.

BL is a B-cell cancer endemic in Africa (*1*) and New Guinea (*2*). It typically involves the abdomen and/or facial bones of young children (*3*) and frequently involves the CNS either at initial presentation or at relapse (*4*).

The association of EBV with Burkitt's tumors has been demonstrated by serologic (*5*) and antigenic (*6*) studies and by detection of EBV DNA by nucleic acid hybridization (*7, 8*). Although the etiology of BL remains to be determined, the association of EBV with these tumor cells is well established.

The involvement of the CNS in BL may be difficult to diagnose when few cells are present or when the patient has neuropathy but no pleocytosis. When the CNS becomes involved, the prognosis is poor and treatment is generally unsuccessful (*9*). Markers that identify CNS involvement would be useful in the diagnosis and prognosis of CNS disease as well as in the monitoring of chemotherapy. Previously, we found oligoclonal IgG bands in CSF of African BL patients with CNS involvement but not in patients without CNS disease (*10*). Oligoclonal IgG bands are a variable number of abnormal discrete protein bands that appear in the γ-globulin region in polyacrylamide gel electrophoresis patterns. These bands are seen in such CNS diseases as subacute sclerosing panencephalitis (*11*), multiple sclerosis (*12*), and other virus-induced CNS diseases (*13, 14*) and have also been reported in 5 children with medulloblastoma (*15*). In this study we report our findings from an examination of CSF from African BL patients for several parameters of CNS involvement including CSF antibodies to EBV antigens, antibodies to the brain antigens myelin and cerebroside, antigen-antibody complexes, and oligoclonal IgG. We analyzed serial samples taken from BL patients with CNS involvement during their therapeutic treatment schedule. We found a good correspondence between CNS involvement by the tumor and the presence of some of these biologic markers in the CSF.

MATERIALS AND METHODS

Patients.—Patients were seen in the African Burkitt Tumor Project, University of Ghana Medical School. Each patient was examined thoroughly and his and her BL was confirmed by biopsy according to accepted criteria (*16*). Involvement of the CNS by the tumor was assessed by clinical criteria and by examination of CSF. When the patient initially presented with the disease and during therapy for each tumor occurrence, lumbar puncture was performed for evaluation and therapy (either prophylactic or therapeutic). Evaluation of the CSF included protein determinations and cytology with greater than 10 cells. The presence of blast cells was considered abnormal. Serial samples were obtained from patients undergoing treatment for CNS disease. The remaining CSF was frozen at −20°C and shipped to the National Institutes of Health where they were tested under code for biologic markers.

Of 39 African BL patients, 13 were diagnosed as having CNS involvement on the basis of symptoms (ataxia, paraplegia, ophthalmoplegia, headaches, and dizziness) and/or other signs (elevated CSF protein, increased numbers of CSF lymphocytes, and/or the presence of blast cells in the CSF). In addition, 6 patients in the same age range but having other diseases not involving the CNS served as a control group. Patients with BL routinely received a systemic therapeutic regimen that varied according to tumor extent and response but always included at least three courses of cyclophosphamide; some patients also received

---

ABBREVIATIONS USED: BL=Burkitt's lymphoma; CNS=central nervous system; CSF=cerebrospinal fluid; EBNA=Epstein-Barr virus-associated nuclear antigen; EBV=Epstein-Barr virus; SDS=sodium dodecyl sulfate; VCA=virus capsid antigen.

---

[1] Received October 27, 1981; revised April 26, 1982; accepted May 12, 1982.

[2] Research procedures were in accord with the ethical standards of the Research Review Committee, University of Ghana Medical School.

[3] Infectious Disease Branch, National Institute of Neurological and Communicative Disorders and Stroke, National Institutes of Health, Public Health Service, U.S. Department of Health and Human Services, Bethesda, Md. 20205.

[4] *Address reprint requests to* Dr. Wallen, Building 36, Room 5D06, National Institutes of Health, Bethesda, Md. 20205.

[5] Environmental Epidemiology Branch, Division of Cancer Cause and Prevention, National Cancer Institute, National Institutes of Health.

[6] Laboratory of Viral Carcinogenesis, Division of Cancer Cause and Prevention, National Cancer Institute.

[7] Department of Child Health, University of Ghana Medical School, Accra, Ghana.

[8] We thank Dr. Matti Iivanainen for assistance in running the oligoclonal IgG assay and Ms. Linda Perry and Mrs. Renee Traub for their technical assistance.

vincristine and cytosine arabinoside (dose varied with regimen). Those patients with CNS involvement received intrathecal therapy consisting of 10 mg methotrexate daily for 4 days with each course. Prophylactic intrathecal therapy for those without clinically apparent CNS involvement was 15 mg methotrexate given once with each course of septicemic chemotherapy.

Antibody assays.—The CSF samples were evaluated for antibody to EBV VCA and EBNA by indirect immunofluorescence (*5, 6*). Antibodies to myelin and cerebroside were assayed by an enzyme-linked immunosorbent assay previously described (*17*). Myelin was provided by Dr. G. DeVries (Medical College of Virginia, Richmond, Va.) and was obtained according to an established procedure from human minced white matter that was homogenized and purified on a discontinuous sucrose density gradient (*18*). The myelin had enzymatic properties consistent with those of myelin obtained by procedures of Norton and Poduslo (*19*). Cerebroside was obtained from bovine brain (Sigma Chemical Corp., St. Louis, Mo.). Each antigen was concentrated to 1 mg/ml, added to 96 flat-well microtiter plates at 100 µl/well, and absorbed for 15 hours at 4°C. We removed unabsorbed antigen by washing the wells with phosphate-buffered saline (pH 7.4). Patient CSF was added in 50-µl volumes to appropriate wells and was incubated at 37°C for 90 minutes. After the wells were washed, goat anti-human IgG conjugated with alkaline phosphatase (Sigma Chemical Co.) was added to the wells and incubated for 60 minutes at 37°C. The color reaction was obtained by the addition of *p*-nitrophenylphosphate as substrate for 30 minutes at 37°C. The reaction was halted with 3 *M* NaOH, and the optical density was read at 405 nm in an automated plate reader (Titertek Multiscan; Flow Laboratories, McLean, Va.).

Immune complexes.—The levels of immune complexes were determined by a radioimmune Raji cell assay according to the procedure of Theofilopoulos et al. (*20*). In this assay, 75 µl of CSF was mixed with 25 µl of fresh BALB/c mouse serum (diluted 1:20) and incubated at 37°C for 30 minutes. Raji cells (4×10^7 cells/ml) were added to the samples in 50-µl volumes and incubated at 37°C for 45 minutes. The mixture was then washed three times and incubated with 25 µl of ^{125}I-labeled goat anti-human IgG (Cappel Laboratories, Cochranville, Pa.) for 30 minutes at 4°C. The samples were then washed three times and enumerated in a Packard gamma counter. Samples were analyzed with the use of a standard curve of aggregated IgG to compare equivalent radioactivity bound to the Raji cells. Results are presented as microgram equivalents of bound aggregated IgG per milliliter of CSF.

Oligoclonal IgG.—The oligoclonal IgG in CSF was detected by use of an SDS-polyacrylamide gel electrophoresis procedure as previously described (*21*). Electrophoresis was performed on vertical slab gels of 7% acrylamide with a 9% separating gel for 12 hours at 4°C with a constant current of 20 milliamperes per gel. Samples of CSF (50 µl) were mixed with 50 µl of electrophoresis buffer (2 parts 70% sucrose with bromophenol blue and 1 part 10% SDS) and were incubated at 37°C for 15 minutes. Samples were then heated at 100°C for 3 minutes and electrophoresed at 50 µl/lane. The gel protein bands were then stained with Coomassie brilliant blue. Two or more distinct bands that appeared in the γ-globulin region of the gel were considered positive. The IgG nature of the bands was confirmed by surface immunofixation with an indirect immunoenzyme procedure described previously (*20*). Strips of cellulose acetate membrane coated with solid-phase absorbed goat anti-human IgG (γ-chain-specific; Cappel Laboratories, Cochranville, Pa.) were overlaid on the gel for 4 hours at 37°C. The gels were washed for 15 hours at 4°C with multiple changes. Peroxidase-conjugated rabbit anti-goat IgG (Miles-Yeda Ltd., Rehovot, Israel) was used to detect the antihuman-human IgG complex. The bands were identified by a substrate–diaminobenzidine–indicator that precipitated on the IgG bands.

RESULTS

Of the 39 BL patients, 13 had CNS disease associated with the primary tumor that occurred at presentation or developed during the course of the study. The 6 non-BL patients had no indications of CNS disease. A comparison of the antibody levels in CSF to EBV VCA and EBNA as well as the brain cell antigens myelin and cerebroside showed that most BL patients with active CNS involvement had antibody levels to EBV VCA, myelin, and cerebroside but not to EBNA. These results are presented in text-figure 1, where the highest values obtained from any of the serial samples tested were used to make up the composite graphs. Among BL patients without CNS disease, 22 of 26 (85%) had EBV VCA titers of 1:2 or less, 3 had titers of 1:4, and 1 had an elevated titer of 1:32. All 6 of the non-BL patients were negative for antibody to EBV VCA. Of the 13 BL patients with active CNS disease, 10 of 13 (77%) had elevated anti-VCA antibody (ranging from 1:8 to 1:512) in their CSF. The CSF levels of antibody to EBNA were not significant in any of the groups. Only 4 of 13 (31%) patients with CNS disease had any titer (ranging from 1:2 to 1:4), and only 1 of 26 (4%) without CNS disease had detectable EBNA antibody. None of the patients without CNS disease (BL and non-BL) had antibody to myelin, and only 1 of the BL patients had a significant titer against cerebroside (1:20). Among BL patients with active CNS disease, 11 of 13 (85%) had antibody to both myelin (ranging from 1:5 to 1:640) and cerebroside (ranging from 1:5 to 1:2560) at the time of active disease.

Immune complex levels were also elevated in the CSF of patients with CNS disease (text-fig. 2). Non-BL patients had low CSF immune complex levels, which ranged up to 32 µg with levels for 3 of 6 patients being undetectable. Among BL patients without CNS disease, none had CSF immune complex levels over 100 µg, and only 4 of 26 (15%) had levels over 50 µg. However, among 13 BL patients with active CNS involvement, all had detectable levels of immune complexes (ranging from 18 to 248 µg) and 9 of the 13 (69%) patients had immune complex levels over 100 µg.

Of the 13 BL patients with active CNS disease, 12 (92%) had oligoclonal IgG bands in their CSF that numbered from 2 to 5 (table 1). Ten cases of the 13 with CNS disease were seen prior to the development of CNS involvement, and 8

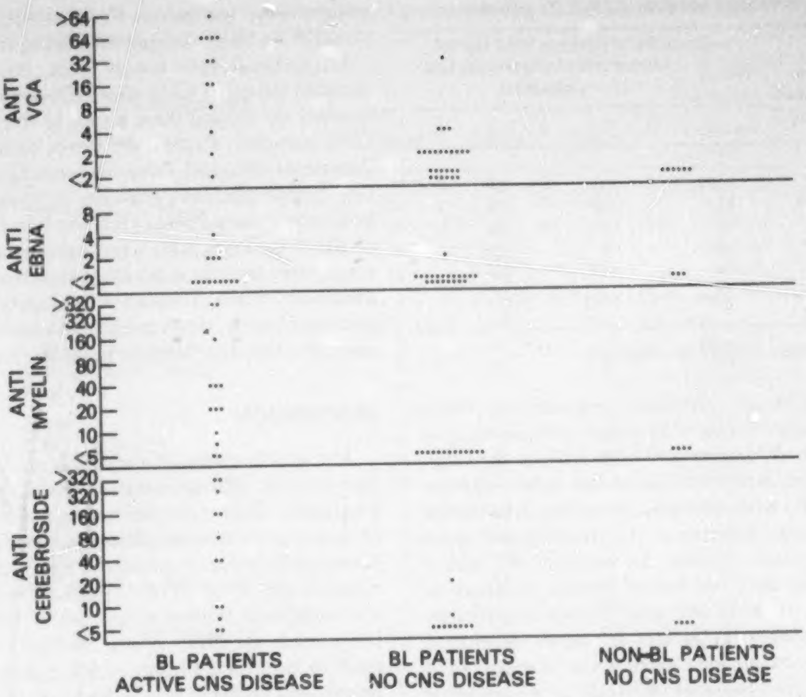

TEXT-FIGURE 1.—CSF levels to EBV VCA, EBNA, and the brain cell antigens myelin and cerebroside in BL patients with active CNS disease, in BL patients without CNS disease, and in non-BL patients without CNS disease.

of these BL cases did not have these bands upon initial sampling but developed them only at the time of CNS involvement by the tumor. Among the 26 BL patients without CNS symptoms or signs, only 3 (12%) had oligoclonal IgG (band numbers ranging from 2 to 3) and 23 were negative. None of the non-BL patients had these bands in their CSF.

The frequency of positive CNS markers is summarized in table 2. None of the non-CNS-involved non-BL patients had significant levels of CSF activity with these markers. Among BL patients without CNS involvement, a few (up to 15%) had elevated levels of one of the CSF markers. Most of the patients with CNS disease (≥69%) had positive responses with each of these CSF markers except EBNA.

Multiple samples of CSF were collected from the 13 patients with CNS disease during their chemotherapy to examine for reactivation of disease. Results from serial samples from these patients are presented in table 3 along with their clinical status. Samples were obtained from 10 patients (#1–9 and #13) prior to CNS involvement and from 3 patients (#10–12) first seen with CNS disease. In the samples from the 10 patients obtained prior to CNS disease onset, the VCA antibody was low or negative (≤2) in all except patient #7 and increased in titer as the CNS became involved except for patient #9. Patient #7 had a relatively high VCA titer and retained this level throughout the testing. Patient #9 had no clinical indication of CNS in-

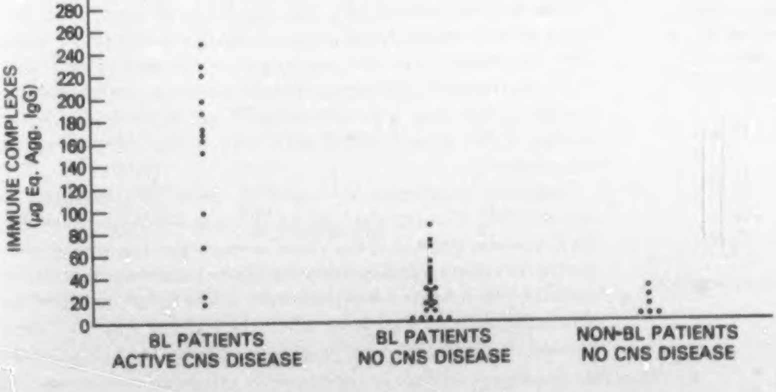

TEXT-FIGURE 2.—Immune complexes detected by Raji cell radioimmunoassay in CSF of BL patients with and without CNS disease and in non-BL patients without CNS disease. Eq. Agg.=equivalents of aggregated IgG.

TABLE 1.—*Oligoclonal IgG bands in CSF of BL patients*

Patients	CNS involvement	No. of patients	No. of patients with the following No. of oligoclonal IgG bands:				
			0	2	3	4	5
BL							
CNS disease	Prior[a]	10	8	1	0	1	0
	Active	13	1	2	5	4	1
No CNS disease	None	26	23	1	2	0	0
Non-BL							
No CNS disease	None	6	6	0	0	0	0

[a] Prior to the development of CNS involvement.

CSF antibody to VCA, no antibody responses to brain antigens, low or negative levels of immune complexes, and no oligoclonal IgG bands despite 530 blast cells in the CSF.

Antibodies to myelin and cerebroside also were negative in 5 of 8 patients tested when samples were obtained before CNS disease and became positive at the time clinical signs and/or symptoms became evident. In patients #3 and 4 antibody to myelin was detected before clinical evidence of disease was present, patients #5 and 6 had insufficient initial samples for testing, and patient #9 never developed antibody to either brain antigen during the disease. In 2 (patients #11 and 12) of 3 patients (#10–12) in whom CNS disease was already evident at the time of sampling, antibody to myelin was already present. (The third patient, #10, was not tested on the first sample because of insufficient CSF.) In general, the level of antibody did not progress with disease and often was higher during initial phases of CNS disease and frequently decreased during later attacks of the disease or when the patient was near death.

Immune complex levels were low in 7 patients (#1, 3–7, and 13) prior to CNS disease onset and progressively increased with CNS disease. In patients #2 and 8 the immune complexes were initially high, whereas the other parameters and clinical signs were negative or low. Patient #9 had low levels of immune complexes throughout the disease. Among the 3 patients initially seen with CNS disease, 2 (#11 and 12) had significant immune complex levels that remained elevated during CNS involvement and tended to subside with disease remission. Patient #10 developed barely detectable levels of complexes during the period of testing.

TABLE 2.—*CSF markers of CNS involvement in BL and other tumors at the time of active disease*[a]

Antibody responses	No. of non-CNS-involved BL patients with markers (%)[b]	No. of CNS-involved BL patients with markers (%)[c]
EBV		
VCA (≥1:4)	4 (15)	11 (85)
EBNA (≥1:2)	1 (4)	4 (31)
Myelin (≥1:5)	0 (0)	11 (85)
Cerebroside (≥1:5)	1 (4)	11 (85)
Immune complexes (≥50 μg)	4 (15)	11 (85)
Oligoclonal IgG bands (≥2)	3 (12)	12 (92)

[a] Of the 6 non-CNS-involved non-BL patients, none had significant levels of CSF activity with these markers.

[b] There were 26 non-CNS-involved BL patients.

[c] There were 13 CNS-involved BL patients.

Oligoclonal IgG bands were not detected in 8 of 10 samples prior to CNS disease onset. Seven patients subsequently developed these bands at the time, or just following, CNS invasion. Patient #9 never developed these bands. In 2 patients (#5 and 7) bands were found at initial examination before clinical signs and/or symptoms became evident and before the patients received any chemotherapy. In each of the 3 patients who were initially seen with CNS symptoms, none had these bands at that time but all subsequently developed them. Patient #4 initially was negative for oligoclonal bands, developed 3 IgG bands at the time of CNS disease onset, but became negative for the bands at death.

DISCUSSION

The involvement of the CNS by African BL results in a particularly difficult stage of the disease for diagnosis and treatment. This study demonstrated that several parameters of tumor activity were altered as the CNS became involved. Immunofluorescent antibody levels to EBV VCA became elevated (≥1:8) in 10 of 13 patients with active CNS disease and in general tended to increase in titer as the CNS disease progressed. Because serum antibody levels to EBV VCA tend to be much higher in BL patients (*5*) than in other lymphoma patients, it was impossible to determine whether the moderate levels of antibody in the CSF were due to in situ synthesis of EBV antibody or diffusion across the blood-brain barrier. Possibly, the tumor cells as they invaded the CNS altered the blood-brain barrier and caused an increased permeability for EBV VCA antibody. It is also possible that the prophylactic or therapeutic use of intrathecal methotrexate contributed to elevating some of these biomarkers. However, the findings in patients with CNS disease who were studied before any intrathecal treatment, (i.e., patient #11 and 12) were similar to those in patients who later developed CNS disease. We believe, therefore, that the biomarkers do reflect disease activity and are not simply a reaction to therapy.

Antibodies to brain cell constituents (myelin and cerebroside) were present in 12 of 13 patients with active CNS disease but rarely occurred in BL patients or non-BL patients without CNS disease. The responses to these brain antigens were frequently quite similar and could overlap inasmuch as cerebroside is an integral component of myelin. These antibody titers did not appear to progress with disease, which suggests that they indicate disruption of brain cells themselves but are unrelated to the degree of tumor cell involvement. Why individuals develop these autoantibodies at all and how much brain cell disruption occurs during CNS involvement with this tumor remain to be determined.

Immune complexes in the CSF were also elevated in active CNS disease but not in the non-CNS-involved BL and non-BL groups. The levels of immune complexes generally increased in patients with CNS disease at the time of active CNS involvement and were lower at times when no CNS disease was present or when the patient was in clinical remission. However, 3 of the patients developed CNS disease

TABLE 3.—*Antibody levels, immune complexes, and oligoclonal IgG in CSF of BL patients with CNS disease*

Patient No.	Date of sample	CNS involvement	CSF markers[a]					
			Antibody levels				Immune complexes, μg[d]	Oligoclonal IgG bands[e]
			VCA[b]	EBNA[b]	Myelin[c]	Cerebroside[c]		
1	4/15/78	None	2	<2	Neg	Neg	Neg	Neg
	10/6/78	CSF cells (141), blasts	16	<2	Neg	ND	164	Neg
	10/12/78	Tx[f]	16	<2	160	320	220	Neg
	10/23/78	CSF cells (87), blasts, Tx	4	<2	40	160	105	Pos (4)
	11/18/78	Complete remission	16	<2	ND	80	96	Pos (2)
2	1/17/79	None	4	<2	Neg	Neg	85	Neg
	2/27/79	Headaches	<2	<2	Neg	Neg	58	Neg
	3/23/79	CSF cells (15), blasts	2	<2	5	Neg	87	Pos (3)
	6/11/79	CSF cells (157), blasts	8	<2	10	20	88	Pos (4)
	7/30/79	Died	32	<2	10	40	113	Pos (4)
3	9/21/78	None	4	<2	10	Neg	43	Neg
	11/13/78	CSF cells (1,188)	64	2	20	ND	100	Neg
	2/2/79	CSF cells (383), blasts, Tx	32	<2	ND	ND	108	Pos (2)
	5/14/79	CSF cells (243), blasts, Tx	16	<2	5	10	152	Pos (3)
4	2/27/79	None	2	<2	5	Neg	78	Neg
	3/19/79	CSF cells (157), blasts, Tx	2	<2	40	10	155	Pos (3)
	4/12/79	None, Tx	4	<2	20	40	165	Pos (3)
	6/20/79	CSF cells (905), blasts, died	8	<2	10	80	102	Neg
5	3/13/78	None	<2	<2	ND	ND	Neg	Pos (4)
	6/6/78	CSF cells (1,184) blasts, Tx	4	<2	40	10	Neg	Pos (4)
	6/9/78	Tx	2	<2	20	10	18	Pos (4)
	8/11/78	Died, CNS relapse	ND	ND	ND	ND	ND	ND
6	5/23/78	None	<2	ND	ND	ND	15	Neg
	6/22/78	CSFF cells (968), blasts	8	<2	20	40	21	Neg
	7/21/78	Cranial neuropathy	4	<2	10	80	24	Neg
	8/17/78	None	32	<2	10	40	43	Pos (2)
	9/11/78	Died	64	4	5	20	67	Pos (2)
7	6/4/79	None	16	<2	Neg	Neg	67	Pos (2)
	10/2/79	CSF cells (154), blasts	64	<2	20	160	164	Pos (2)
	7/14/80	Cranial neuropathy, neuralgia, CSF cells (437), blasts	16	<2	5	320	82	Pos (2)
8	2/27/79	None	2	<2	Neg	Neg	72	Neg
	7/12/79	CSF cells (40), peripheral neuropathy, Tx[f]	32	<2	5	10	196	Pos (2)
	8/20/79	Complete remission	16	<2	Neg	40	116	Pos (2)
9	5/18/79	None	<2	ND	Neg	ND	16	Neg
	6/4/79	CSF cells (530), blasts, Tx	<2	<2	Neg	Neg	9	Neg
	6/7/79	Died	ND	ND	ND	ND	ND	Neg
10	6/13/78	CSF cells (16)	2	ND	ND	ND	Neg	Neg
	11/30/78	CSF cells (28)	4	<2	40	40	14	Pos (4)
	12/12/78	Tx	2	<2	10	40	13	Pos (3)
	12/28/78	Complete remission	4	<2	10	20	16	Pos (4)
11	12/20/78	CSF cells (155), blasts, Tx	32	<2	640	2,560	169	Neg
	1/15/79	CSF cells (16), Tx	64	<2	320	640	146	Pos (3)
	4/10/79	Complete remission	16	<2	320	80	149	Pos (3)
	5/14/79	Complete remission	16	<2	320	80	90	Pos (3)
12	3/5/79	CSF cells (34)	2	2	20	ND	40	Neg
	7/23/79	CSF cells (1,535), Tx	2	<2	10	40	124	ND
	10/24/79	CSF cells (690), Tx	2	2	20	20	170	Pos (4)
	11/16/79	Complete remission	2	2	40	20	80	Pos (4)
13	6/7/78	None	<2	ND	Neg	Neg	Neg	Neg
	9/15/78	None	16	<2	5	10	133	Neg
	10/18/78	None, Tx	8	<2	20	40	156	Neg
	10/23/78	Ophthalmoplegia, Tx	16	<2	40	160	248	Pos (3)

[a] ND = not done. Neg = negative. Pos = positive.

[b] Antibody titers to EBV VCA and EBNA.

[c] Antibody titers to brain cell antigen myelin and cerebroside.

[d] Immune complex levels in μg equivalents of aggregared IgG.

[e] The number of oligoclonal IgG bands is *in parentheses*.

[f] Patients were undergoing chemotherapy to the time sample was obtained = Tx.

and had little or no immune complexes in their CSF. Two patients died abruptly with CNS symptoms and 1 patient went into a complete remission, possibly before significant levels of complexes could form.

The relationship of oligoclonal IgG in the CSF and in CNS disease in BL patients was more consistent. Twelve of 13 patients with CNS disease developed oligoclonal bands in their CSF compared to 3 of 26 patients without CNS involvement. More important, 2 patients had the bands at initial examination before any chemotherapy, which suggested that this marker was also disease related. Finding up to 12% of the patients without overt CNS disease but with bands suggests that these patients should be watched for development of CNS involvement. No direct relationship between the numbers of bands and CNS disease progress could be determined, although most of the patients developed these bands concomitant with the development of CNS disease. Only patient #9 in this study failed to develop bands, which may have been a result of insufficient time for their production because CNS involvement was found only 3 days before this patient died.

These CSF markers were of some value for the determination of CNS involvement by African Burkitt's tumor cells in most patients with CNS disease. In these cases, however, the findings should be interpreted with the fact in mind that a virus association has been proposed for this tumor, which distinguishes it from other lymphoma forms. There was a clear distinction between the presence of antibody to EBV VCA and brain cell antigens, immune complexes of over 100 μg/ml, and oligoclonal IgG in the CSF of patients with CNS disease compared to those without any CNS involvement. Only 1 patient (#9) with CNS disease did not express any of these CSF markers, and this patient died just after CNS disease onset. Some patients may show these markers without apparent CNS signs or symptoms, but it is possible that CNS disease did occur but went undetected. Therefore, although not necessarily diagnostic, these markers would be useful in those patients in whom CNS disease is suspected and also may be useful in the monitoring of the progress of chemotherapy for CNS disease in this tumor system.

REFERENCES

(*1*) Burkitt D. A lymphoma syndrome in tropical Africa. Int Rev Exp Pathol 1963; 2:67–138.

(*2*) Ten Seldam RE, Cooke R, Atkinson L. Childhood lymphoma in the territories of Papua and New Guinea. Cancer 1966; 19:437–446.

(*3*) Biggar RJ, Nkrumah FK, Perkins IV. Presenting clinical features of Burkitt's lymphoma in Ghana, West Africa. J Trop Pediatr Environ Child Health 1979; 25:157–161.

(*4*) Burkitt D. A tumor syndrome affecting children in tropical Africa. Postgrad Med J 1962; 38:71–79.

(*5*) Henle G, Henle W. Immunofluorescence in cells derived from Burkitt's lymphoma. J Bacteriol 1966; 91:1248–1256.

(*6*) Reedman BM, Klein G, Pope JH, et al. Epstein-Barr virus associated complement-fixing and nuclear antigens in Burkitt's lymphoma biopsies. Int J Cancer 1974; 13:755–763.

(*7*) Zur Hausen H, Schulte-Holthausen H. Presence of EB virus nucleic acid homology in a "virus-free" line of Burkitt's tumour cells. Nature 1970; 227:245–248.

(*8*) Nonoyama M, Pagano J. Homology between Epstein-Barr virus DNA and viral DNA from Burkitt's lymphoma and nasopharyngeal carcinoma determined by DNA–DNA reassociation kinetics. Nature 1973; 242:44–47.

(*9*) Ziegler JL, Bluming AZ, Morrow RH, Fass L, Carbona PP. Central nervous system involvement in Burkitt's lymphoma. Blood 1970; 36:718–728.

(*10*) Wallen WC, Biggar RJ, Levine P, Iivanainen M. Oligclonal IgG in cerebrospinal fluid of patients with African Burkitt's lymphoma. Arch Neurol. In press.

(*11*) Vandvik B, Norrby E, Nordal HJ, Degre M. Oligoclonal measles-specific IgG antibodies isolated from cerebrospinal fluids, brain extracts and sera of patients with subacute sclerosing panencephalitis and multiple sclerosis. Scand J Immunol 1976; 5:979–992.

(*12*) Laterre EC, Cullewaert A, Heremans JF, Sfaello Z. Electrophoretic morphology of gamma globulins in cerebrospinal fluid of multiple sclerosis and other diseases of the nervous system. Neurology 1970; 20:982–990.

(*13*) Wolinsky JS, Berg BO, Maitland CJ. Progressive rubella panencephalitis. Arch Neurol 1976; 33:722–723.

(*14*) Vandvik B, Norrby E, Steen-Johnson J, Stensvold K. Mumps meningitis prolonged pleocytosis and occurrence of mumps virus specific oligoclonal IgG antibodies in cerebral spinal fluid. Eur Neurol 1978; 17:13–22.

(*15*) Siemes H, Siegert M, Hanefeld F. Occurrence of oligoclonal gamma globulin in the CSF of children with prolonged and chronic CNS-infections. Acta Paediatr Scand 1981; 70:91–99.

(*16*) Berard, C, O'Conor GT, Thomas LB, Torloni H. Histopathological definition of Burkitt's tumor. Bull WHO 1969; 40:601–607.

(*17*) Calabrese VP, Wallen WC, Castellano G, Ward L, Anderson MC, DeVries, GH. Enzyme-linked immunosorbent assay (ELISA) for antibodies to human myelin and axolemma-enriched fractions. Neurosci Lett 1981; 21:189–195.

(*18*) DeVries GH, Maithieu JM, Berg M, Checkeperticke R, Lazdinski M, Colivo M. Isolation and partial characterization of rat central nervous system axolemma enriched fraction. Brain Res 1978; 147:339–344.

(*19*) Norton WT, Podusko SE. Myelination in rat brain: Method of myelin isolation. J Neurochem 1973; 21:749–757.

(*20*) Theofilopoulos AN, Wilson CB, Dixon FJ. The Raji cell radioimmunoassay for detecting immune complexes in human sera. J Clin Invest 1976; 57:169–182.

(*21*) Iivanainen MV, Wallen WC, Leon ME, et al. Micromethod for detection of oligoclonal IgG in unconcentrated CSF by polyacrylamide gel electrophoresis. Arch Neurol 1981; 38:427–430.

Transforming Growth Factors in the Urine of Normal, Pregnant, and Tumor-Bearing Humans[1,2]

Daniel R. Twardzik,[3,4] **Stephen A. Sherwin,**[5] **Jane Ranchalis,**[3] *and* **George J. Todaro**[3,6]

ABSTRACT—Transforming growth factor (TGF) activities could be detected in the urine of normal, pregnant, and tumor-bearing humans. These acid- and heat-stable polypeptides competed for binding to epidermal growth factor (EGF) membrane receptors and promoted the anchorage-independent growth of nontransformed rodent cells. They differed from human EGF in their apparent molecular weights and soft-agar growth-stimulating activity. The urine from pregnant females contained TGF activities with apparent molecular weight(s) (relative) (M_r) of 10,000 and 17,000–20,000. In the case of a lung cancer patient, an additional major activity of approximately 30,000–35,000 M_r was found. All urine specimens examined also contained a "common" 8,000-M_r soft-agar growth-stimulating activity, which competed for binding to EGF membrane receptors and which was chromatographically separable from EGF (urogastrone). Thus urine may provide a convenient and readily available source for the biochemical characterization of these TGF-like activities, some of which may be clinically useful biologic markers for certain types of cancer.—JNCI 1982; 69:793–798.

Growth-promoting polypeptides have been found in the supernatants from cultures of virally transformed rodent cells (*1, 2*) and human tumor cells (*3*). Polypeptides with similar biologic activities have also been isolated directly from human tumor cells (*4*) and from early mouse embryo cells (*5*). In each case a family of heat- and acid-stable polypeptides of varying molecular weights has been identified that can reversibly stimulate the anchorage-independent growth of nontransformed rodent cells and has thus been designated TGF. For the most part, human TGF have been shown to compete with EGF for binding to EGF membrane receptors, although non-EGF-related peptides with soft-agar growth-promoting activity have also been identified (*3*). Nontransformed cells do not release detectable quantities of soft-agar growth-stimulatory factors into the culture supernatants (*1–3*). Since TGF are of low molecular weight and stable, it was thought that similar activities might also be detected in urine. We report here that the urine from pregnant and tumor-bearing humans does indeed contain TGF-like activities of varying molecular sizes.

MATERIALS AND METHODS

Urine extraction.—Normal urine pools consisted of early morning voided urine collected from 10 healthy laboratory workers ranging from 24 to 40 years of age. Pregnant donor urine pools were derived from mid- to late-term pregnant individuals of mixed child-bearing ages; the pools were collected during routine outpatient prenatal care examination. Fresh urine specimens were clarified by low-speed centrifugation, lyophilized to dryness, and extracted with the use of a modification of the procedure described by Roberts et al. (*4*) for isolation of TGF from tumor cells. The dry residue from approximately 2 liters of urine was resuspended in 375 ml of a solution containing 95% (vol/vol) ethanol, 7.5 ml concentrated HCl, 0.1 mg phenylmethylsulfonyl fluoride/ml, and 0.15 trypsin inhibitory units/ml of aprotinin from bovine lung. Distilled H_2O (185 ml) was then added, and the above suspension was extracted overnight at 4°C. Following centrifugation at 10,000×*g* for 1 hour, the supernatant was adjusted to pH 5.2 with concentrated ammonium hydroxide. One milliliter of 2 *M* ammonium acetate buffer (pH 5.2) was then added per 100 ml of extract. The resultant precipitate was discarded and the supernatant precipitated with four volumes of cold anhydrous ether and two volumes of cold ethanol (−20°C for 24 hr). The precipitate was collected by centrifugation, redissolved in 1 *M* acetic acid, and extensively dialyzed against 0.2 *M* acetic acid (Spectraphon tubing; mol wt cutoff, 3,500; Spectrum Medical Industries Inc., Los Angeles, Calif.). This extraction procedure generally yielded approximately 15–20 mg protein/liter of raw urine as determined by the method of Lowry et al. (*6*). The lyophilized protein was then resuspended in 6.5 ml of 1 *M* acetic acid, recentrifuged, and applied to a 2.5×100-cm Biogel P-100 column in 1 *M* acetic acid.

EGF binding assays.—EGF was isolated (*7*) and radiolabeled with ^{125}I (*8*) as previously described. Binding of ^{125}I-labeled EGF (*1, 2*) was measured on subconfluent monolayers of formaldehyde-fixed A431 cells in 16-mm tissue culture wells (Linbro No. 76-033-05). Competitions were initiated by the addition of 0.2 ml of binding buffer—DMEM containing 1 mg bovine serum albumin/ml and 50

ABBREVIATIONS USED: DMEM=Dulbecco's modified Eagle's minimum essential medium; DTT=dithiothreitol; EGF=epidermal growth factor; M_r=molecular weight(s) (relative); NRK=normal rat kidney; SCCL=small cell carcinoma(s) of the lung; TGF=transforming growth factor(s); UR=urogastrone.

---

[1] Received October 29, 1981; revised April 27, 1982; accepted May 20, 1982.

[2] Research procedures were in accord with the ethical standards of the Frederick Cancer Research Facility Institutional Review Board, National Cancer Institute.

[3] Laboratory of Viral Carcinogenesis, Division of Cancer Cause and Prevention, National Cancer Institute, National Institutes of Health, Public Health Service, U.S. Department of Health and Human Services, Frederick, Md. 21701.

[4] *Address reprint requests to* Dr. Twardzik at Building 560, Room 21-77, NCI-Frederick Cancer Research Facility, Frederick, Md. 21701.

[5] Biological Response Modifiers Program, Division of Cancer Treatment, National Cancer Institute.

[6] We thank Dr. D. Orth (Vanderbilt University Medical School) for the human epidermal growth factor radioimmunoassays, Dr. Joseph De Larco (NCI-Frederick Cancer Research Facility) for helpful discussions, Mr. W. Bohn for his excellent technical assistance, Ms. Patricia Johnson for editing, and Ms. Virginia Frye for help in the preparation of this manuscript.

m*M* 2-[bis(2-hydroxyethyl)amino]ethanesulfonic acid adjusted to pH 6.8—containing 2 ng ^{125}I-labeled EGF/ml with or without an aliquot of the sample to be tested. After a 1-hour incubation at 22°C, the binding buffer was removed, culture wells were washed four times with binding buffer (1 ml), and the quantity of ^{125}I-labeled EGF specifically bound was determined.

Soft-agar colony assay.—The assay for colony growth in soft agar was as previously described (*1, 3*). A 2-ml base layer of 0.5% agar (Agar Noble; Difco Laboratories, Detroit, Mich.) in DMEM containing 10% calf serum was added to 60-mm Costar petri dishes. A 2-ml overlay of 0.3% agar containing the same medium–calf serum mixture, 2×10^3 NRK cells (clone 49F), and the sample to be tested was then added. The cells were incubated at 37°C in a humidified atmosphere of 5% CO_2 in air and refed after 7 days by addition

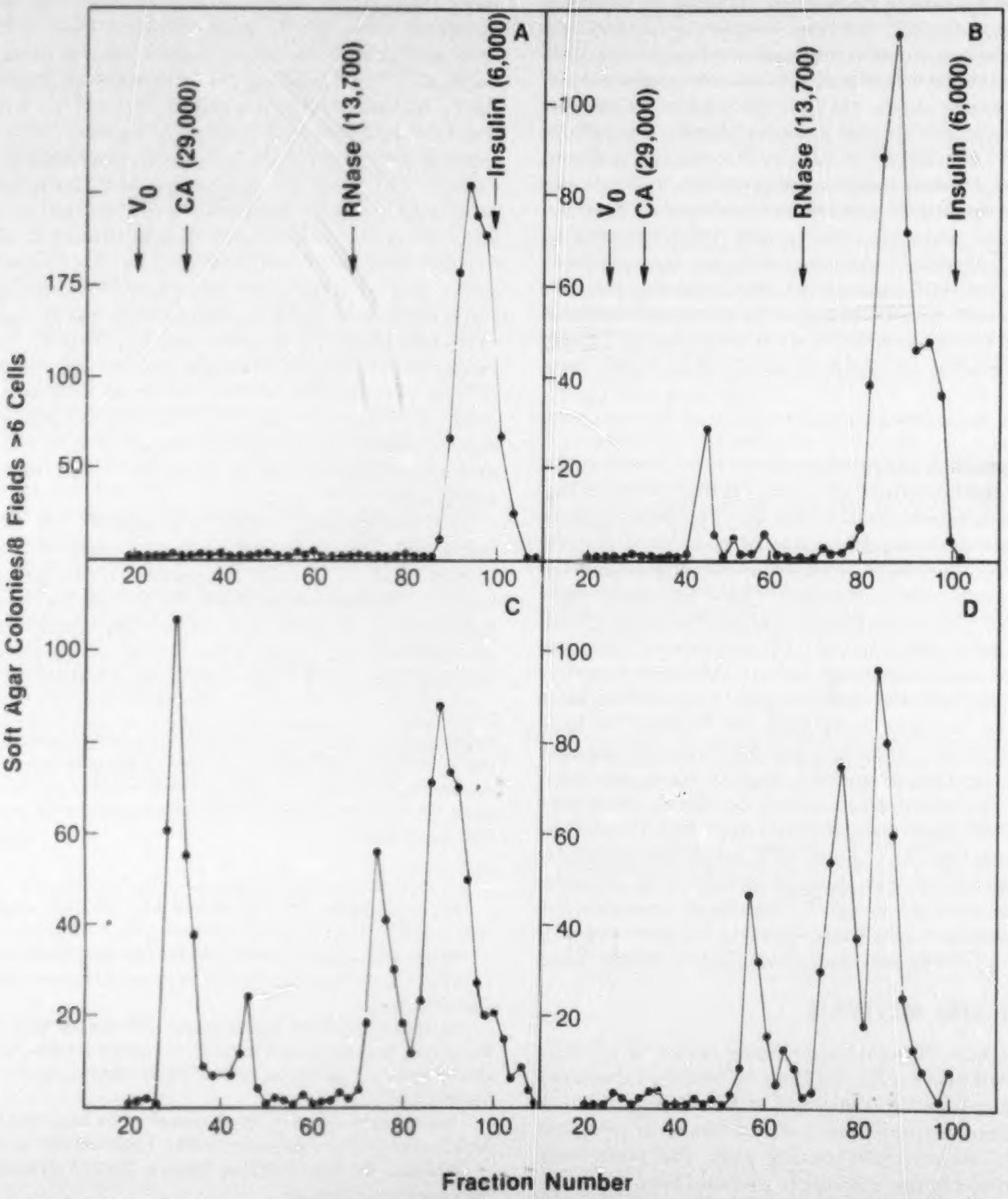

TEXT-FIGURE 1.—Biogel P-100 column chromatography of acid-ethanol-extracted human urine pools from A) normal males, 2 liters; B) normal females, 2 liters; C) untreated male SCCL patient, 0.4 liters; D) mid- to late-term pregnant females, 2 liters. Acid-ethanol-solubilized urinary peptides (15–20 mg protein/liter processed urine) were applied to a Biogel P-100 column (2.5×75 cm) equilibrated with 1 *M* acetic acid. Aliquots (1 ml) of each fraction (3.5 ml) were sterilized by lyophilization of 1-*M* acetic acid solutions in sterile tubes and assayed as described in "Materials and Methods" for the stimulation of NRK fibroblasts (clone 49F) to form progressively growing colonies in soft agar. Column markers included carbonic anhydrase, 29,000 daltons; RNase, 13,700 daltons; and insulin, 6,000 daltons. Mouse submaxillary gland EGF elutes from this column with the insulin marker.

of 2 ml of 0.3% agar containing the appropriate supplements. Colonies were measured unfixed and unstained, and the number of colonies greater than 10 cells per 8 low-power random fields was scored after 14 days. NRK fibroblasts from clone 49F showed predominantly single cells after 14 days in these assays.

RESULTS

Acid–ethanol-extracted urine polypeptides were chromatographed on Biogel P-100 columns in 1 *M* acetic acid. Individual column fractions were then tested for their ability to stimulate the growth in soft agar of NRK fibroblasts. As shown in text-figure 1A, acid–ethanol-extracted urine derived from a pool of normal males contained peptides that supported anchorage-independent cell growth. Typical colonies were round and compact and usually contained more than 20–30 cells 3 days after being seeded in soft agar. This activity eluted from these columns with an apparent M_r of 8,000, slightly larger than that of EGF, which does not stimulate anchorage-independent cell growth and elutes under these conditions in fractions 95–105. In addition, for example, as shown in text-figure 2, the 8,000-M_r soft-agar growth-stimulating activity coeluted with EGF-competing activity (fractions 80–88), whereas the major EGF-competing activity eluting later (fractions 90–110) did not stimulate similar growth in soft agar. This minor EGF-competing component could only be detected in EGF binding assays with the use of dilutions of column fractions that minimized the excess concentration of EGF, which chromatographed in this low-molecular-weight region of the column.

The 8,000-M_r component eluted from high-pressure liquid chromatographic columns at solvent concentrations different than those of human EGF and will be described in detail elsewhere. No soft-agar growth-stimulatory activity from normal urine was detected in any column fractions corresponding to a higher molecular weight, and the A_{280} absorbance profile on these regions (fractions 20–80) was similar in all urine specimens examined, indicating no evidence of proteinuria. Similar activities were seen after chromatography of acid–ethanol-extracted urine derived from a pool of normal female donors (text-fig. 1B). In addition, a minor, although reproducible, soft-agar growth-promoting activity eluting in the region of approximately 25,000 M_r (fractions 42–48) was seen in normal female urine specimens. In contrast to the elution profile of soft-agar growth-promoting activity from the urine of normal males and females, several molecular species of TGF activity were found in acid–ethanol-extracted, pooled urine obtained from mid- to late-term pregnant females (text-fig. 1D). TGF activities corresponding to apparent M_r of 10,000 (fractions 70–80) and 17,000–20,000 (fractions 52–60) were seen in addition to the 8,000-M_r (fractions 85–95) activity common to all urine specimens examined thus far.

Since continuous cell lines derived from patients with SCCL have previously been shown in vitro to produce soft-agar growth-promoting factors (*9*), the urine of a 56-year-old, previously untreated, male patient with this type of lung cancer was also examined. In contrast to the TGF activities of pooled normal male and female controls, several higher molecular weight TGF activities were detected, including activities with apparent M_r of 30,000–35,000 (fractions 26–35) and 10,000 (fractions 70–80) (text-fig. 1, *panel C*). Moreover, when the column fractions of the SCCL patient were tested for EGF-competing activity according to previously described methods (*1, 3*), the soft-agar growth-promoting activity, in particular in the 30,000- to 35,000-M_r region (fractions 25–35), coeluted with EGF-competing activity. A typical Biogel P-100 chromatograph demonstrating coelution of soft-agar growth-stimulating activity and EGF-competing activity in the 30,000- to 35,000-M_r (fractions 25–40) region is shown in text-figure 3A. The urine of this particular patient with alveolar cell soft tissue sarcoma contained approximately 250 ng EGF equivalents/liter of urine of the high-molecular-weight TGF. The soft-agar growth-stimulating and EGF-competing activities coeluted as a shoulder of the major protein peak found in fractions 20–25 and were not found in the column void volume. Other minor EGF-competing activities that also promoted anchorage-independent cell growth eluting in the 17,000- to 20,000-M_r (fractions 52–60) region and in the 10,000- to 12,000-M_r (fractions 65–75) region of the column are also seen in the urine of this previously untreated cancer patient. Text-figure 3B shows the profile of urine derived from normal individuals of both sexes. Again, the major EGF-

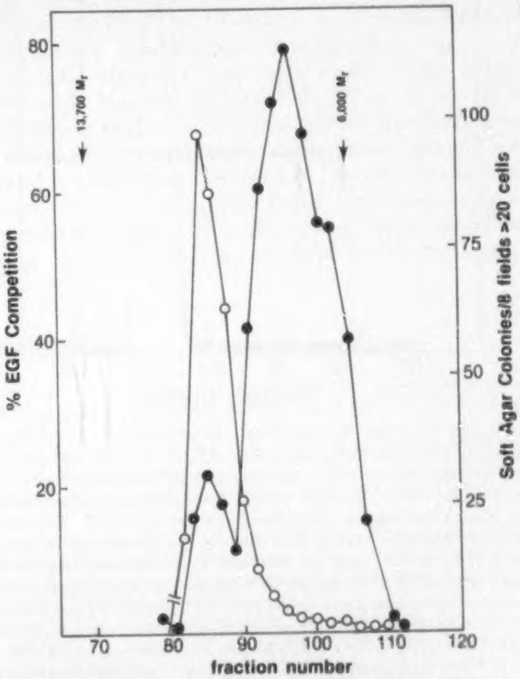

TEXT-FIGURE 2.—Biogel P-100 column chromatography of acid–ethanol-extracted urine from late-term pregnant females. Acid–ethanol-solubilized urinary peptides (30 mg protein) were applied to a Biogel P-100 column (20×70 cm) equilibrated with 1 *M* acetic acid. Aliquots of each fraction were lyophilized and tested at various dilutions for the EGF competition on receptor-rich A431 human carcinoma cells (*1, 3*) and for the stimulation of NRK cells (clone 49F) to form colonies in soft agar as described in "Materials and Methods." The minor EGF-competing activity eluting in fractions 80–88 was resolved from EGF only when tested at dilutions >1:350. ●—●, ^{125}I-labeled EGF competition; ○—○, number of NRK colonies consisting of >20 cells in 8 random low-power fields.

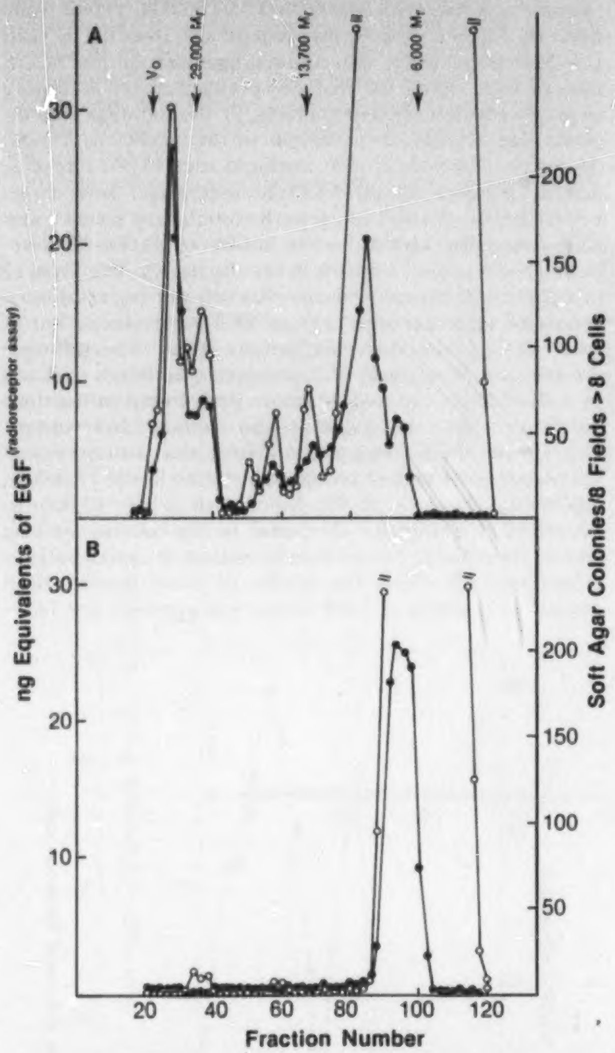

TEXT-FIGURE 3.—Biogel P-100 column chromatography of acid-ethanol-extracted urine (200 ml) polypeptides (5.5 mg protein) from A) a patient with alveolar cell soft tissue sarcoma and B) solubilized urine (1 liter) polypeptides (25.7 mg) from a pool of healthy individuals. Aliquots (1 ml) of each fraction were lyophilized and tested for EGF competition on receptor-rich A431 human cells and for the stimulation of growth of NRK cells in soft agar as described in "Materials and Methods." Equivalents of EGF in nanograms were calculated by means of an EGF competition dilution curve constructed with the use of mouse submaxillary EGF as the standard. The column calibration is as described in the legend to text-fig. 1. ○—○, ^{125}I-labeled EGF competition; ●—●, number of NRK colonies consisting of >8 cells in 8 random low-power fields.

competing activity found in all urine specimens examined was human EGF (UR), which eluted in the region of the 6,000-M_r insulin marker. This activity did not support the growth in soft agar of NRK fibroblasts and competed in a radioimmune assay for human EGF.

TABLE 1.—*Stability of the 10,000-M_r TGF activity from the urine of an SCCL patient*

Treatment[a]	No. of soft-agar colonies/8 fields >10 cells
Trypsin control	220
Trypsin	<1
DTT control	203
DTT	<5
Acetic acid control	188
Acetic acid	
4°C, 24 hr	200
22°C, 24 hr	210
37°C, 24 hr	205
Relyophilization (2×)	182

[a] The Biogel P-100 10,000-M_r TGF activity from urine derived from an SCCL patient was pooled, and equivalent aliquots were lyophilized and redissolved in 0.1 *M* NH_4HCO_3 (pH 7.8). A control solution and one containing 50 μg trypsin/ml were incubated at 37°C for 2 hr after which soybean trypsin inhibitor was added to each sample to give 100 μg/ml. For DTT treatment, a control solution and one containing 0.075 *M* DTT were incubated at 22°C for 2 hr followed by extensive dialysis against 0.2 *M* acetic acid. Each sample was then adjusted to 1 *M* in acetic acid and lyophilized. Acid stability studies were conducted in samples adjusted to 1 *M* in acetic acid prior to lyophilization. All samples were redissolved in binding buffer and assayed for soft-agar growth-promoting activity as previously described (*1, 3*).

The activity of the 10,000-M_r TGF component from the urine of pregnant donors and from a patient with SCCL was susceptible to treatment with trypsin or DTT (table 1), as reported previously for sarcoma growth factor (*1*) and TGF from human tumor cells (*3, 4*). In addition, the activity was also heat-stable in 1 *M* acetic acid and was recovered after repeated lyophilizations. Both the EGF-competing and soft-agar growth-stimulating activity for the urine-derived

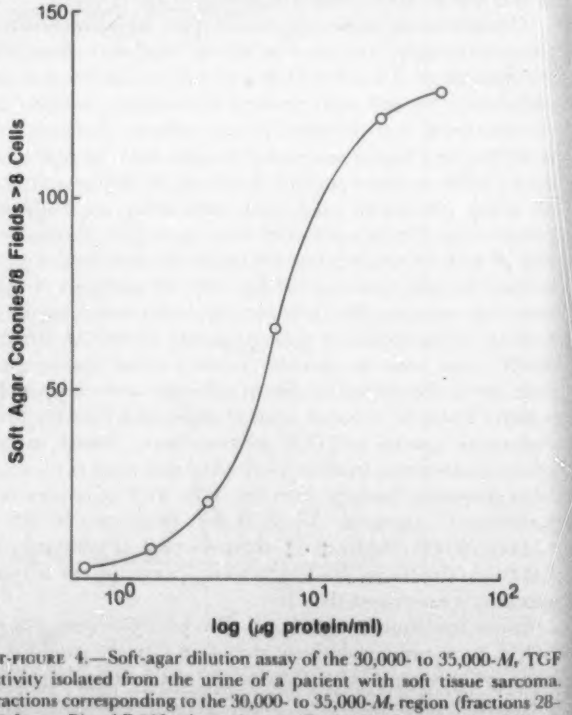

TEXT-FIGURE 4.—Soft-agar dilution assay of the 30,000- to 35,000-M_r TGF activity isolated from the urine of a patient with soft tissue sarcoma. Fractions corresponding to the 30,000- to 35,000-M_r region (fractions 28–30) from a Biogel P-100 column (*see* text-fig. 3A) were pooled, lyophilized, and tested at the protein concentration indicated above for stimulation of NRK cells to form progressively growing colonies in soft agar as previously described.

TABLE 2.—*TGF activity*

Urine source[a]	10,000 M_r	17,000–20,000 M_r	30,000 M_r
Normal male	−		−
Normal female	−	−	−
Pregnant female[b]	+	+	−
SCCL patient[c]	+	−	+

[a] With the exception of the SCCL patient, all urine samples represent a pool derived from multiple donors.

[b] Pregnant donors ranged from second to third trimester in their pregnancy.

[c] Previously untreated patient with disseminated disease.

30,000- to 35,000-M_r TGF activity from previously untreated cancer patients also exhibited a typical dose-response curve and, as with the TGF isolated from cell culture fluids, the high-molecular-weight urine TGF have both transforming and EGF-competing activities. The number of soft-agar colonies formed was proportional to the amount of protein added and, as shown in text-figure 4, approximately 100 soft-agar colonies were stimulated to grow by the addition of 10 μg input protein of TGF activity (30,000- to 35,000-M_r region) from a patient with soft tissue sarcoma. These data indicate a functional similarity between TGF-like activities found in urine from tumor-bearing humans and those identified in conditioned medium from tumor cell cultures.

DISCUSSION

The experiments described above demonstrate that the acid–ethanol extraction procedure previously used to isolate TGF from tumor cells (*4*) can be used to identify similar factors in human urine. The family of TGF-like polypeptides isolated from urine exhibited many of the biologic and biochemical characteristics of the TGF isolated from cell culture supernatants derived from mouse (*1*), rat (*2*), and human transformed cells (*3*). In addition to competing for EGF membrane receptors and stimulating anchorage-independent cell growth, these urinary peptides further resemble TGF in that they were also acid- and heat-stable and required disulfide bonds for activity. In contrast to human EGF, which did not stimulate the growth of large colonies in soft agar, the urinary TGF-like activities eluted from acidified Biogel columns with higher apparent molecular weights. The relatedness of the "common" urinary 8,000-M_r TGF-like activity to TGF isolated from tumor cell cultures remains to be determined. The possibility that this activity represents a form of UR with modified biologic activity must also be considered.

As shown in table 2, the 10,000-M_r TGF activity was found in the urine of mid- to late-term pregnant females and a patient with SCCL. These activities were not detected in urine pools derived from normal males and nonpregnant females. The 17,000- to 20,000-M_r components, however, appeared to be restricted to the urine of pregnant females. In this regard the exact source of TGF activity in the urine of pregnant females has yet to be established, but experiments with mice have identified TGF activity at 10,000 and 17,000–20,000 M_r in the 12- to 14-day mouse embryo (*5*), which suggests that the human fetus may also be capable of producing such factors.

In addition to having the 10,000-M_r factor, urine derived from previously untreated cancer patients (18 of 22) with a variety of carcinomas, including lung, breast, and colon, contained a major TGF activity with an apparent M_r of 30,000–35,000 (Sherwin SA, Twardzik DR, Bohn W, Cockley K, Todaro GJ: Manuscript submitted). This activity was not detected in the urine from an equal number of age- and sex-matched controls. Since SCCL cells in vitro have been shown to produce soft-agar growth-stimulating factors (*9*), it can also be postulated that the unusually high-molecular-weight TGF activity in the urine of the patient with SCCL is derived from his tumor cells. Furthermore, high-molecular-weight TGF activities have recently been detected (*10*) in surgically removed human tumors, including adenocarcinomas of the breast, colon, and ovary. Inasmuch as TGF are secreted into tumor cell culture fluids, we propose that these tumor cell products or TGF are released from tumor cells in vivo and subsequently cleared into the urine. We must, however, also entertain the possibility that this tumor-"associated" activity may be a host response to tumor burden. The relationship of the high-molecular-weight (30,000–35,000 M_r) TGF activity found in the urine of previously untreated cancer patients to a high-molecular-weight form of human EGF also found in urine (*11, 12*) is presently being examined. The detection of peptides with diverse biologic effects in the urine is not a novel observation because, for example, peptides that stimulate capillary endothelial cell migration have been found in the urine of patients with bladder tumors (*13*). What is interesting, nevertheless, is that this family of growth-stimulating peptides found in the urine under different physiologic states does exhibit a biologic activity; i.e., it promotes the reversion of nontransformed cells to the transformed phenotype, and high-molecular-weight forms of these growth factors may prove to be useful biologic markers in certain types of cancers.

REFERENCES

(*1*) De Larco JE, Todaro GJ. Growth factors from murine sarcoma virus transformed cells. Proc Natl Acad Sci USA 1978; 75:4001–4005.

(*2*) Twardzik DR, Todaro GJ, Marquardt H, Reynolds FH, Stephenson JR. Transformation induced by Abelson murine leukemia virus involves production of a polypeptide growth factor. Science 1982; 216:894–897.

(*3*) Todaro GJ, Fryling C, De Larco JE. Transforming growth factors produced by certain human tumor cells: Polypeptides that interact with epidermal growth factor receptors. Proc Natl Acad Sci USA 1980; 77:5258–5262.

(*4*) Roberts AB, Lamb LC, Newton DL, Sporn MB, De Larco JE, Todaro GJ. Transforming growth factors: Isolation of polypeptides from virally and chemically transformed cells by acid/ethanol extraction. Proc Natl Acad Sci USA 1980; 77:3494–3498.

(*5*) Twardzik DR, Ranchalis JE, Todaro GJ. Mouse embryos contain transforming growth factors related to those isolated from tumor cells. Cancer Res 1982; 42:590–593.

(*6*) Lowry OH, Rosebrough NJ, Farr AL, Randall RJ. Protein measurement with the Folin phenol reagent. J Biol Chem 1951; 193:265–275.

(*7*) Savage CR Jr, Cohen S. Epidermal growth factor and a new derivative. J Biol Chem 1972; 247:7609–7611.

(*8*) Greenwood FC, Hunter WM, Glover JS. The preparation of ^{131}I-labelled human growth hormone of high specific radioactivity. Biochem J 1963; 89:114–123.

(9) Sherwin SA, Minna JD, Gazdar AF, Todaro GJ. Expression of epidermal and nerve growth factor receptors and soft agar growth factor production by human lung cancer cells. Cancer Res 1981; 41:3538–3542.

(10) Nickell KA, Moses HL. Transforming growth factor (TGF)-like substances in solid human malignant neoplasms. J Cell Biol 1981; 91:204a.

(11) Hirata Y, Orth DN. Epidermal growth factor (urogastrone) in human fluids: Size heterogeneity. J Clin Endocrinol Metab 1979; 48:673–679.

(12) ———. Conversion of high molecular weight human epidermal growth factor (hEGF)/urogastrone (UR) to small molecular weight hEGF/UR by mouse EGF-associated arginine esterase. J Clin Endocrinol Metab 1979; 49:481–483.

(13) Chodak GW, Scheiner CJ, Zetter BR. Urine from patients with transitional-cell carcinoma stimulates migration of capillary endothelial cells. N Engl J Med 1981; 305:869–874.

Selective Cytotoxicity of a Ricin A-Chain–Anti-Carcinoembryonic Antigen Antibody Conjugate for a Human Colon Adenocarcinoma Cell Line[1,2]

Thomas W. Griffin,[3,4] **Linda R. Haynes,**[3] *and* **Julie A. DeMartino**[3]

ABSTRACT—Ricin A-chain, the toxic subunit of the potent plant toxin ricin, has been isolated by affinity chromatography and conjugated via a disulfide linkage to affinity-purified goat anti-carcinoembryonic antigen (CEA) antibody. Such conjugates retained the integrity of their antibody-combining site, as demonstrated by the ability to displace ^{125}I-labeled anti-CEA antibody bound to CEA-positive cell lines. In addition, such conjugates retained A-chain activity, producing inhibition of [^{14}C]leucine incorporation into a CEA-negative G-361 human melanoma cell line at concentrations similar to those of unconjugated A-chain. However, these conjugates were 40 times as potent in the inhibition of [^{14}C]leucine incorporation in the CEA-bearing WiDr human adenocarcinoma cell line as A-chain alone or as an unreacted mixture of A-chain and specific antibody. Such toxicity could be blocked by preincubation of the conjugate with fluid-phase CEA. Complete inhibition of [^{14}C]leucine incorporation as well as inhibition of cellular proliferation by the conjugate was seen at 50 n*M* concentration. Conjugates that combine the determinant specificity of an antibody with the toxicity of ricin A-chain may show promise as selective cytotoxins for cells bearing CEA.—JNCI 1982; 69:799–805.

The use of presently available antitumor agents is limited to a major extent by their nonspecific cytotoxic effect on normal cells. The concept of increasing the selectivity of antitumor agents by linkage of "antitumor" antibodies dates back nearly a century (*1*) and has been the subject of intense and imaginative investigation for the past 3 decades. These investigations have been the subject of several recent reviews (*2–4*). Although the present understanding of the genetic heterogeneity and clonal evolution of human tumor cell populations makes "magic bullet" therapy problematic, nevertheless, a combination of the selectivity of antibody with the lethal effects of toxins offers the promise of antitumor therapy with increased selectivity. Although early results gave only marginal specificity for target cells, more recent efforts that utilized improved methods of chemical coupling have demonstrated greater success. Furthermore, two recent developments have caused reassessment of the use of such "immunotoxins." The first development is the prospective availability of hybridoma-derived homogenous antibodies, with defined specificity, avidity, and class, against tumor-related antigens (*5*). The second advance is a greatly improved understanding of the structure and mechanism of action of the potent toxic proteins ricin, abrin, diphtheria toxin, and others (*6–8*).

Previous investigators have suggested that antibody delivery systems for cytotoxins are most successful when they utilize extremely toxic substances (*9–11*). The toxic proteins we used satisfy such a requirement, in that their toxic moieties act enzymatically, rather than stoichiometrically, to inhibit protein synthesis (*6–9*). Thus only a few molecules of these effector subunits are capable of producing cytotoxicity if entry is gained to the cytoplasm. However, utilization of the complete toxin incurs the risk of nonspecific toxicity. To circumvent this difficulty, we, (*12*) and other investigators (*13–17*) have explored the selective toxicity of conjugates of a specific antibody and the toxic subunit of ricin. Ricin, a potent protein inhibitor derived from the castor bean, has proved exceptionally adaptable to this approach, in that the toxin molecule shows segregation of biologic function into *a*) a binding (or B) chain that adheres to galactose moieties on the cell surface, and *b*) an activity (or A) chain that enzymatically inactivates ribosomes (*8*). These investigations have shown that it is possible to substitute specific antibody or antibody fragments as fraudulent B-chains, thereby producing conjugates of high cytotoxic potential, specific for cells that bear the appropriate antigen.

The present report extends these observations to conjugates constructed with antibodies directed against the oncofetal protein CEA. This operationally defined antigen describes a family of glycoproteins found on the surfaces of a variety of human cancers (*18*), and this family may be an appropriate target for clinically relevant immunotoxins.

MATERIALS AND METHODS

Cell lines.—The human adenocarcinoma cell line WiDr and human melanoma cell line G-361 were both obtained from the American Type Culture Collection, Rockville, Md. GM 316 fibroblasts were obtained from the Institute for Medical Research, Camden, N.J. The human adenocarcinoma cell line HT-29 was donated by Dr. J. Fogh, Sloan-Kettering Institute for Cancer Research, Rye, N.Y. Both adenocarcinoma cell lines have been shown to produce CEA in culture (*19–21*). HT-29 produces relatively small amounts of CEA in culture, whereas WiDr produces small to mod-

---

ABBREVIATIONS USED: CEA=carcinoembryonic antigen; DTT=dithiothreitol; EMEM=Eagle's minimum essential medium; FCS=fetal calf serum; IA=iodoacetamide; ID_{50}=median inhibitory dose; PAGE=polyacrylamide gel electrophoresis; PBS=phosphate-buffered saline; SDS=sodium dodecyl sulfate.

---

[1] Received October 30, 1981; revised March 24, 1982; accepted May 12, 1982.

[2] Supported in part by Public Health Service grant CA-29160-01 from the National Cancer Institute.

[3] Division of Oncology, Department of Medicine, University of Massachusetts Medical School, 55 Lake Ave. North, Worcester, Mass. 01605.

[4] Dr. Griffin is a Junior Clinical Faculty Fellow of the American Cancer Society.

erate amounts compared to amounts produced by other adenocarcinoma cell lines (*22*).

Antibody and free antigen.—High-titer, affinity-purified goat anti-CEA antibody (lot #RK-1) was a gift of Dr. H. J. Hansen, Hoffman-LaRoche, Inc., Nutley, N.J. Soluble-phase CEA (1 mg/ml in PBS) was also obtained from Dr. Hansen. ^{125}I-radiolabeled anti-CEA antibody was donated by Dr. Steven Rose, Abbott Laboratories, North Chicago, Ill. Control antibody (affinity-purified goat anti-human IgG) was obtained from Kirkegaard & Perry Laboratories, Gaithersburg, Md.

Isolation of ricin A-chain.—Ricin A-chain was isolated from the parent toxin (Sigma Chemical Co., St. Louis, Mo.; EY Laboratories, San Mateo, Calif.) by an adaptation of a previously described method (*23*). The toxin was reduced by the addition of 2-mercaptoethanol to a final concentration of 5%, incubated for 12 hours at 23°C, and centrifuged at 3,000 rpm for 15 minutes. The supernatant was then applied to a column of lactose-substituted agarose (Selectin 12; Pierce Chemical Co., Rockford, Ill.). The isolated A-chain was eluted with PBS that contained 0.1% 2-mercaptoethanol. Further traces of contaminating ricin and B-chain were then removed by passage over a Sepharose 4B column pretreated with 1 *N* acetic acid for 24 hours and washed extensively with elution buffer (*24*). After repeated elution of the A-chain, the peak tubes were pooled, dialyzed against PBS for removal of residual 2-mercaptoethanol, and concentrated by ultrafiltration (PM10 membrane; Amicon Corp., Lexington, Mass.). The resulting product was further purified by passage over a Sephadex G-25 column. The homogeneity of the A-chain prepared in this manner was assessed by SDS-PAGE by a previously described method (fig. 1.) (*25, 26*). The integrity of A-chain protein inhibition was assessed in a rabbit reticulocyte lysate system (Bethesda Research Laboratories, Inc., Gaithersburg, Md.). Successfully purified A-chain demonstrated an ID_{50} of [^{14}C]leucine incorporation of $1\text{-}5\times10^{-7}$ *M* in WiDr cells in the system described above, compared to the ID_{50} of intact ricin of 2×10^{-10} *M*. Additional ricin A-chain was obtained commercially from EY Laboratories.

Synthesis of ricin A-chain–antibody conjugates.—Affinity-purified antibody, at a concentration of 2.5 mg/ml, was dialyzed against PBS for 24 hours and then reacted with a 25-fold molar excess of the bifunctional coupling reagent *N*-succinimidyl-3-(2-pyridyldithio)propionate (Pharmacia, Fine Chemicals, Piscataway, N.J.) (*27*). Reaction continued at 23°C for 30 minutes, after which time reaction products were again dialyzed against PBS for an additional 24 hours. The resulting protein was then reacted with a two times molar excess of ricin A-chain. The progress of the reaction was monitored by release of pyridine-2-thione (increased absorbance at 343 nm). Reaction products were then separated on a molecular sizing column (Sephadex G-100). Progress of the reaction was confirmed by SDS-PAGE (fig. 1.).

^{125}I-labeled anti-CEA antibody binding assay.—To measure specific binding of ^{125}I-labeled anti-CEA antibody by the various cell lines, we performed competitive binding experiments with radioiodinated anti-CEA antibody, unreacted antibody, and conjugate in this manner: 1 ml of the designated cell line (at 4×10^4 cells/ml) was spun to a firm pellet (2,000 rpm for 10 min). The supernatant was removed, and ^{125}I-labeled anti-CEA antibody (10^5 cpm/0.05 ml) was added to the pellet. The cells were then incubated at 23°C for 30 minutes, washed twice with 1 ml of PBS, and then pelleted and counted. The absolute number of counts bound was obtained by the subtraction of counts in tubes containing radiolabeled antibody alone from counts in tubes containing label and cells. In experiments that demonstrated the integrity of the antibody combining site, cells were preincubated for 30 minutes at 23°C with unlabeled anti-CFE antibody or conjugate in the designated amount and then treated in the above manner.

Assay of protein inhibition.—Confluent WiDr cells were removed with a T-75 flask with 0.25% trypsin and 0.02% EDTA. The cells were then suspended in leucine-free medium (MEM with 10% FCS and 1% antibiotics) and seeded into microtiter wells (2×10^4 cells/well). The cells were incubated (after appropriate additions of conjugate, ricin, ricin A-chain, or unconjugated antibody to achieve the specified levels) for 16 hours at 37°C in 5% CO_2, treated with a 3-hour pulse of [^{14}C]leucine (New England Nuclear Corp., Boston, Mass.), and harvested onto filter disks with a Mash II cell harvester. Incorporation of radioactivity into the cells was measured by scintillation counting after extensive washing on a glass fiber filter.

Reversal of toxicity by free CEA.—Specific anti-CEA conjugate (2×10^{-7} *M*) was incubated for 1 hour with free CEA (2×10^{-7} *M*) and then added to WiDr cells to a final conjugate concentration of 1×10^{-8} *M*. Inhibition of [^{14}C]leucine incorporation was assayed in the manner described and was compared to that of unreacted conjugate, free antigen, or controls.

Reversal of toxicity by free antibody.—Confluent WiDr cells were removed from a T-75 flask with 0.25% trypsin in 0.02% EDTA. The cells were resuspended in leucine-free medium (EMEM, 10% FCS, and antibiotics) at a concentration of 10^5 cells/ml. The cells were then centrifuged (2,000 rpm for 5 min) to a pellet. and the supernatant was removed.

Unreacted anti-CEA antibody or nonspecific antibody was added to the pellet at a concentration of 2.0×10^{-5} *M* (2-log excess over conjugate). Similarly handled cells were treated with an equal volume of PBS alone. The cells were then incubated at 23°C for 1 hour, and conjugate (1×10^{-7} *M*) was added to PBS and antibody-treated cells. After a subsequent 1-hour incubation at 23°C, the cells were washed with medium and plated into microtiter wells. [^{14}C]leucine incorporation was then determined in the manner described above.

RESULTS

PAGE of Ricin A-Chain–Anti-CEA Antibody Conjugates

Figure 1 presents PAGE of unreacted antibody, free A-chain, conjugate, and conjugate after reduction. These dual bands of isolated A-chain (fig. 1: A, B, I, J) were seen in both A-chain preparations obtained from the parent toxin, by the above-cited method, and in that obtained commercially. The appearance of homologous A-chains of these

TABLE 1.—*Binding of ^{125}I-labeled anti-CEA antibody by cells in culture*

Culture	cpm per 2×10^4 cells ± SD
GM 316 fibroblasts	159±12
G-361 melanoma	224±12
HT-29 adenocarcinoma	1,819±232
WiDr adenocarcinoma	3,201±284

TABLE 2.—*Inhibition of binding of ^{125}I-labeled CEA antibody by conjugate and unreacted antibody*

Cell line	Concentration, *M*	cpm per 2×10^4 cells	Inhibition of binding, %
WiDr			
Control		2,686	
Conjugate	9×10^{-7}	1,236	54
	9×10^{-8}	2,112	21
Antibody	9×10^{-7}	863	67
	9×10^{-8}	1,581	41
HT-29 adenocarcinoma			
Control		2,172	
Conjugate	9×10^{-7}	691	68
	9×10^{-8}	2,098	3
Antibody	9×10^{-7}	680	68
	9×10^{-8}	1,856	14

molecular masses (30,000 and 33,000 daltons) following reduction of the parent toxin has been previously described (*28*). The affinity-isolated antibody (G) is a broad band at a molecular mass of approximately 150,000 daltons, whereas the conjugate preparation (C and E) shows an increase in the molecular mass over that of antibody alone, suggesting the addition of A-chain to the antibody. Reappearance of the free A-chain bands following DTT treatment of the conjugate (D and F) confirms successful synthesis of the conjugate.

Binding of Anti-CEA Antibody–Ricin A-Chain Conjugates by CEA-Positive Cell Lines

HT-29 adenocarcinoma cells produce small amounts of CEA during growth in vitro and have been shown to bind anti-CEA antibody, both by immunofluorescence and by the binding of radiolabeled antibody (*29, 30*). WiDr, a recently characterized cell line, produces a moderate amount of CEA (118 ng/10^6 cells in 10 days: American Type Culture Collection Information Sheet) compared to that produced by other colorectal adenocarcinoma cell lines in vitro (*22*).

Table 1 presents the degree of binding of ^{125}I-labeled anti-CEA antibody by the fibroblast line GM 316, the human melanoma G-361, and the two adenocarcinoma cell lines HT-29 and WiDr. The binding of ^{125}I-labeled anti-CEA antibody by the nonadenocarcinoma cells lines was similar to nonspecific binding to the adenocarcinoma cells, as defined by binding of radiolabeled antibody not displaceable by preincubation with 10^{-6} *M* unlabeled specific antibody. Thus by this method of analysis, these cell lines express little or no CEA on their cell membrane. In contrast, the adenocarcinoma cell lines showed specific binding of ^{125}I-labeled anti-CEA antibody. The moderate CEA producer WiDr bound more radiolabeled antibody than the low CEA producer HT-29. Similar in vitro binding of radiolabeled anti-CEA antibody by the HT-29 cell line has been previously described by Tompkins and colleagues (*30*).

To demonstrate retention of antigen-binding activity of the anti-CEA–ricin A-chain conjugates, we compared the ability of these conjugates to prevent binding of ^{125}I-labeled anti-CEA antibody to that of unreacted antibody (table 2). This displacement was concentration related, with 50% of bound counts displaced by pretreatment with a concentration of 5–7×10^{-7} *M* conjugates and 3–5×10^{-7} *M* unreacted antibody in the two adenocarcinoma cell lines. Thus the conjugate showed comparable or slightly reduced reactivity with cell surface CEA as free antibody, thereby

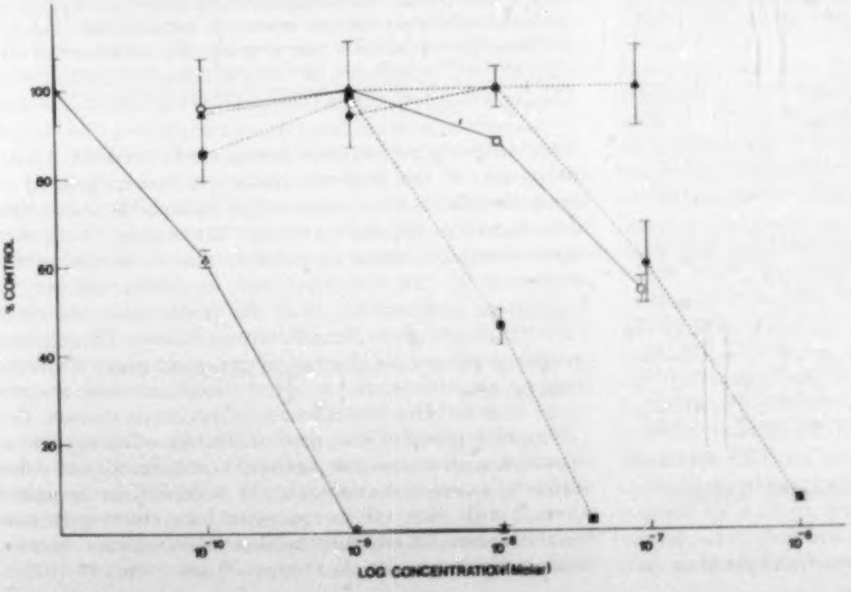

TEXT-FIGURE 1.—Inhibition of [^{14}C]leucine incorporation in WiDr cells by ricin, ricin A-chain, specific conjugate, specific antibody, or a noncovalent mixture of ricin A-chain and antibody. Cells (2×10^4/microtiter well) were incubated in leucine-free medium with 5% FCS at 37°C in 5% CO_2 for 16 hr after appropriate additions of the above compounds at the designated concentrations. At 16 hr, the cells were treated with [^{14}C]leucine (0.2 μCi/well) for 3 hr and gathered onto filter disks with a Mash II cell harvester, and the radioactivity incorporated was counted. *Each data point* represents the mean of six measurements. *Vertical bars* represent the standard deviation. ● - - ●, ricin A-chain; ○—○, anti-CEA antibody + A-chain; ▲ - - ▲, anti-CEA antibody; △—△, ricin; ■ - - ■, anti-CEA–ricin A-chain conjugate.

confirming the integrity of the antigen-combining site in the conjugate. The slightly reduced reactivity of the conjugate may be related to steric interference by A-chain with antigen–antibody interaction.

Inhibition of [^{14}C]Leucine Incorporation in Human Adenocarcinoma Cell Lines by Ricin A-Chain–Anti-CEA Antibody Conjugates

Dose-response curves of inhibition of [^{14}C]leucine incorporation in WiDr CEA-positive cells are presented in text-figure 1. The ID_{50} for intact ricin in this system was 2×10^{-10} *M*. The ID_{50} levels for whole ricin in the presence of serum proteins, which inhibit its binding, may be overestimates. Conjugates prepared in the above manner had an ID_{50} of 8×10^{-9} *M* or approximately, 2.5% that of the native toxin. Levels of 5×10^{-8} *M* completely inhibited [^{14}C]leucine incorporation. The A-chain itself, or mixed with unconjugated antibody, had an ID_{50} of 3×10^{-7} *M* or 0.1% of the parent toxin. Free antibody alone gave no inhibition of protein synthesis in this system. The conjugate was, therefore, 40 times more effective than free A-chain in producing an inhibition of protein synthesis in this system. In contrast, the conjugate was not more toxic than free A-chain in the melanoma cell line G-361, which bears no CEA.

To determine whether the inhibition of [^{14}C]leucine incorporation was associated with cytotoxic effect, we examined the effect of specific conjugate, free A-chain, and a noncovalent mixture of A-chain and antibody on adenocarcinoma proliferation in vitro. WiDr cells were seeded as above with the exception that complete medium (EMEM with leucine, 10% FCS, and 1% antibiotics) rather than leucine-free medium was used, and daily cell enumerations were obtained by a Coulter counter. The number of untreated cells increased five times over 5 days. At a level of 5×10^{-8} *M* conjugate, 50% inhibition of cellular proliferation at 5 days was seen. Similar degrees of inhibition required levels of 1×10^{-6} *M* A-chain or 1×10^{-6} *M* A-chain plus antibody. Thus the conjugate demonstrated the capacity to function as a potent cytotoxin against cells bearing the appropriate antigen.

Text-figure 2A compares protein inhibition in WiDr versus the control cell line human melanoma G-361. G-361 cells showed similar sensitivity to protein synthesis inhibition by ricin and ricin A-chain as WiDr in that system. Again, the specificity of conjugate effect was approximately eightfold at the ID_{50} concentration.

In text-figure 2B the toxicity of specific anti-CEA conjugate is compared with that of a conjugate prepared with nonspecific antibody (goat anti-human IgG, affinity purified). This nonspecific antibody was more toxic than free A-chain (three times at the ID_{50}) but still eightfold less toxic than specific conjugates at the ID_{50} level. In contrast, the nonspecific conjugate showed equivalent toxicity ($ID_{50} \approx 1 \times 10^{-7}$ *M*) to both the CEA-bearing and CEA-negative cell lines.

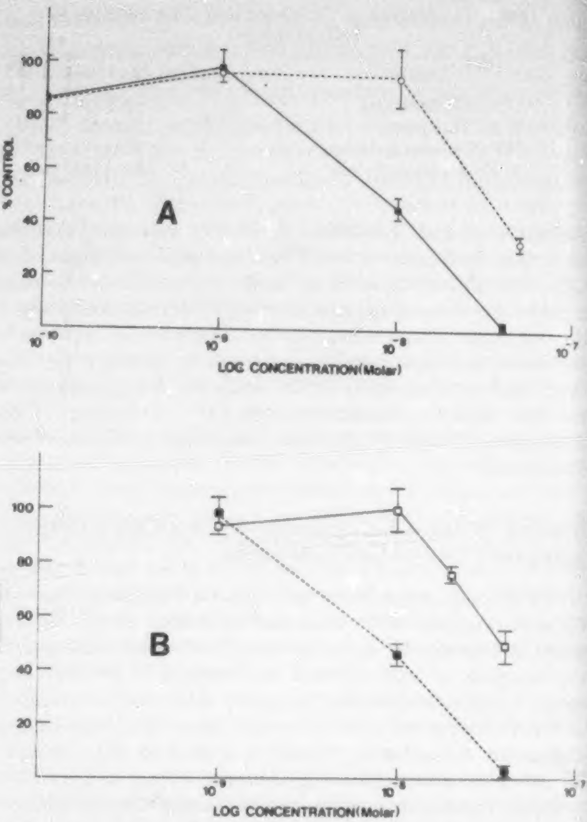

TEXT-FIGURE 2.—Specificity of conjugate action: A) Protein inhibition in the ■, specific (WiDr) cell line vs. a control cell line, ○, human melanoma G-361. The G-361 cell line bound little or no radiolabeled anti-CEA antibody and showed equivalent sensitivity to WiDr to the inhibition of [^{14}C]leucine incorporation by ricin and ricin A-chain. Dose-response curves were generated in the manner described in the legend to text-fig. 1. B) Comparison between the inhibition of [^{14}C]leucine incorporation by ■, specific (affinity-isolated goat anti-CEA antiserum) conjugate, vs. □, control (affinity-purified goat anti-human IgG antiserum) conjugate in WiDr colorectal cells. The same degree of molar substitution of ricin A-chain/mole antibody was observed in both preparations. Dose-response curves were generated as described in the legend to text-fig. 1.

Reversal of Conjugate Toxicity by Specific Antigen and Specific Antibody

To demonstrate that the increased toxicity of the ricin A-chain–antibody conjugate was mediated by the CEA combining site of the antibody moiety of the conjugate, we showed reversal of cytotoxic effect with both fluid-phase antigen and excess free antibody. Text-figure 3A demonstrates complete reversal of the inhibitory action of the conjugates by preincubation with equimolar amount of fluid-phase antigen for 1 hour. No precipitation occurred during this incubation. Simultaneous addition of fluid-phase antigen produced no reversal of cytotoxic effect. Preincubation of the nonspecific conjugate with fluid-phase antigen under identical conditions had no effect on its toxicity.

Similar reversal of conjugate inhibitory effect was demonstrated with excess free antibody (text-fig. 3B). A 2-log antibody excess pretreatment was required for complete reversal, with lesser effects seen with 1-log excess and equimolar amounts. Nonspecific antibody pretreatment had no effect on conjugate action.

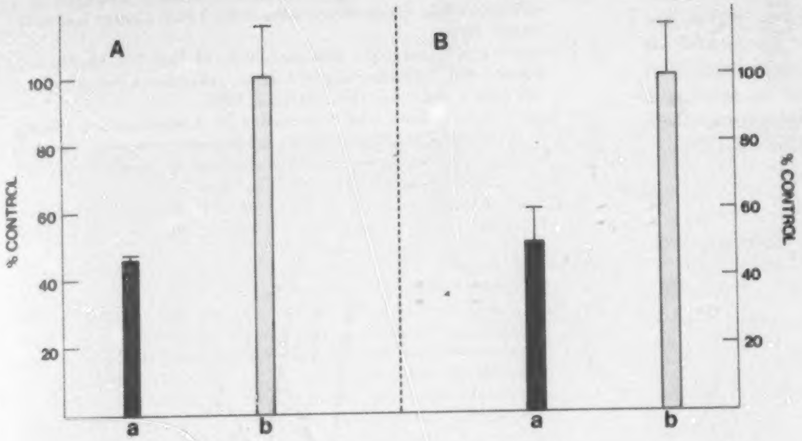

TEXT-FIGURE 3.—Blockage of inhibitory action of conjugate by preincubation with free antigen or antibody. A) The inhibitory action of the (a) specific conjugate can be blocked by preincubation of the conjugate with (b), equimolar amounts of fluid-phase antigen. The assay for protein inhibition was performed as described, with conjugate CEA reaction mixture at a concentration of 1×10^{-8} *M*. B) The inhibition of [^{14}C]leucine incorporation by (a), specific conjugate can also be reversed by pretreatment with (b), specific (anti-CEA) antibody. In these experiments the WiDr adenocarcinoma cells were incubated for 1 hr at 23°C with a 2-log excess (10^{-5} *M*) of anti-CEA antibody, before a 1 hr incubation with 10^{-7} *M* conjugate. The cells were washed twice with PBS before being resuspended in leucine-free medium with 5% FCS, and seeded into microtiter wells at a concentration of 2×10^{4} cells/well. The remainder of the experiments was conducted in the manner described in the legend to text-fig. 1.

DISCUSSION

The demonstration that specific antibody or antibody fragments can serve as alternate binding units for the toxic A-chains of ricin and diphtheria toxin (*12–16*) and impart antigen-dictated selective cytotoxicity to these conjugates has rekindled interest in such immunotoxins as selective antitumor agents. Most attempts to date have focused on lymphocyte-differentiation antigens (*16*), surface IgG on B-lymphocytes (*12, 13*), or artificially introduced antigens (*15*), except one study that described the use of a monoclonal antibody directed against an antigen that was reported specific for colorectal adenocarcinoma (*14*).

CEA was first described by Gold and Freedman (*31*) in 1965 as an antigen associated with embryonic and neoplastic gastrointestinal tissues. A radioimmunoassay for CEA was reported in 1969. The presence of detectable quantities of CEA in adult serum was originally thought to be specific for the presence of cancer, but recent evidence indicates that CEA may be elevated in many benign conditions as well (*18*). In addition, CEA levels are commonly elevated in many cancers of nondigestive tract origin (*32*). CEA is operationally defined by reagents similar to those originally used by Gold and Freedman (*31*) and is immunochemically complex. Evidence now suggests that CEA describes a family of related glycoproteins, with a wide range of molecular weights and carbohydrate content (*33*). Polar redistribution of CEA expressed on the surfaces of human intestinal carcinoma cells in culture induced by specific antibody has been described (*29*).

The inhomogeneity of the CEA, its shedding by malignant cells, and its wide distribution may limit the usefulness of such conjugates as described here. However, an extensive literature has documented the successful in vivo tumor localization of radiolabeled anti-CEA antisera in both animal and clinical models (*34*) and possible therapeutic utility of such conjugates (*35*). Therefore, despite the limitations of this system noted above, CEA remains an attractive antigenic "target" for immunotoxins.

Previous investigators have described CEA antiserum as a carrier of cytotoxins. Shearer et al. (*36*) reported specific cytotoxicity of glucose oxidase–anti-CEA antisera for human colon carcinoma cells (HT-29). This system required subsequent treatment with glucose, iodide, and lactoperioxidase for production of specific iodination of cell membranes, and, therefore, is much more cumbersome than the system described here. Belles-Isles and Page (*37*) have described selective cytotoxicity of daunomycin–anti-CEA conjugates for a human colon carcinoma cell line. Similarly, Johnson et al. (*38*) have recently described a conjugate of sheep anti-CEA immunoglobulin and the anticancer drug vindesine, which was cytotoxic for human cancer cells in vitro. The optimal cytotoxin for antibody conjugation will require further study, but the relative lack of cytotoxicity of isolated ricin A-chain makes it an attractive candidate.

The increased toxicity of ricin A-chain after conjugation to anti-CEA heteroantibody toward human adenocarcinoma cells is significantly less than that described with other tumor systems. For example, Raso et al. (*23*) have recently reported a conjugate of ricin A-chain and monoclonal antibody directed against the common antigen expressed on human lymphoblastic leukemia cells. This conjugate produced 50% inhibition of proliferation in culture of a human leukemia cell line bearing the appropriate antigen at levels of 2×10^{-10} *M*. Similarly, Blythman et al. (*16*) have described the construction of a conjugate of ricin A-chain and monoclonal IgM antibody directed against the Thy 1.2 differentiation antigen of mouse T-cells. This conjugate's specificity factor (conjugate:ricin A-chain) was 5,000, more than 100 times that described in our system.

The explanation for the relative lack of potency of our conjugate is unclear but may be related to a variety of factors. First, the use of heteroantibody as compared to monoclonal antibody may decrease the molar potency of the conjugates. With this prospect in mind, the use of monoclonal anti-CEA antibody in our system would be of interest. Second, and perhaps most important, CEA may be much less efficient in mediating A-chain entry into the cytoplasm than the above-cited antigens. Finally, our method of A-chain coupling may not be the optimal approach, and alternate methods of conjugation or delivery may yield superior results (*3*).

Human colorectal cancers have proved extremely resistant to conventional chemotherapeutic agents, which are directed primarily against DNA synthesis. Ricin and its toxic subunit exert their cytotoxic effect through inhibition of protein synthesis and therefore may present an attractive alternate therapeutic approach, especially if the toxic effect can be targeted by specific antitumor antibody.

REFERENCES

(*1*) Ehrlich P. Collected studies on immunity. New York: Wiley, 1906.

(*2*) Ghose T, Blair AH. Antibody-linked cytotoxic agents in the treatment of cancer: Current status and future prospects. JNCI 1978; 61:657–676.

(*3*) Gregoriades G. Targeting of drugs. Nature 1977; 265:407–411.

(*4*) Rubens, RD. Antibodies as carriers of anticancer agents. Lancet 1974; 1:498–499.

(*5*) Kohler G, Milstein C. Continuous cultures of fused cells secreting antibody of predefined specificity. Nature 1975; 256:495–497.

(*6*) Pappenheimer AM, Gill PM. Diphtheria. Science 1973; 182:353–55.

(*7*) Olsnes S, Haylett T, Refsnes K. Purification and characterization of the highly toxic lectin modeccin. J Biol Chem 1978; 253:5069–5073.

(*8*) Olsnes S, Refnes K, Pihl A. Mechanism of action of the toxic lectins abrin and ricin. Nature 1974; 249:627–631.

(*9*) Thorpe PE, Ross WC, Cumber AJ, Hinson CA, Edwards DC, Davies AJ. Toxicity of diphtheria toxin for lymphoblastoid cells is increased by conjugation to antilymphocytic globulin. Nature 1978; 271:752–755.

(*10*) Moolten FL, Cooperband SR. Selective destruction of target cells by diphtheria toxin conjugated to antibody directed against antigens on the cells. Science 1970; 169:68–70.

(*11*) Moolten F. Zajdel S, Cooperband S. Immunotherapy of experimental animal tumors with antitumor antibodies conjugated to diphtheria toxin or ricin. Ann NY Acad Sci 1976; 277:690–699.

(*12*) Raso V, Griffin TW. Specific cytotoxicity of a human immunoglobulin directed Fab′-ricin A chain conjugate. J Immunol 1980; 125:2610–2616.

(*13*) Krolick KA, Villemez C, Isakson PL, Uhr JW, Vittetta ES. Selective killing of normal or neoplastic B cells coupled to the A chain of ricin. Proc Natl Acad Sci USA 1980; 77:5419–5423.

(*14*) Gilliland DG, Stephlewski Z, Collier RJ, Mitchell KF, Chang TH, Koprowski H. Antibody directed cytotoxic agents; use of monoclonal antibodies to direct the action of toxic A chains to colorectal carcinoma cells. Proc Natl Acad Sci USA 1980; 77:4539–4543.

(*15*) Jansen FK, Blythman HE, Carriere D, et al. High specific cytotoxicity of antibody–toxin hybrid molecules (immunotoxins) for target cells. Immunol Lett 1980; 2:97–102.

(*16*) Blythman HE, Casellas P, Gros O, et al. Immunotoxins: Hybrid molecules of monoclonal antibodies and a toxin subunit specifically kill tumour cells. Nature 1981; 290:145–146.

(*17*) Masuho Y, Hara T. Target-cell cytotoxicity of a hybrid of Fab′ of immunoglobulin and A-chain of ricin. Gan 1980; 71:759–765.

(*18*) Gold P, Shurster J, Freedman SO. Carcinoembryonic antigen (CEA) in clinical medicine. Cancer 1978; 42:1399–1405.

(*19*) Noguchi P, Wallace R, Johnston J, et al. Characterization of WiDr: A human colon carcinoma cell line. In Vitro 1979; 15:401–408.

(*20*) Fogh J, Fogh JM, Orfeo T. One hundred and twenty-seven cultured human tumor cell lines producing tumors in nude mice. J Natl Cancer Inst 1977; 59:221–225.

(*21*) Egan ML, Todd CW. Carcinoembryonic antigen: Synthesis by a continuous line of adenocarcinoma cells. J Natl Cancer Inst 1972; 49:887–889.

(*22*) Leibovitz A, Stinson JC, McCombs WB, McCoy CE, Mazur KC, Mabry ND. Classification of human colorectal adenocarcinoma cell lines. Cancer Res 1976; 36:4562–4569.

(*23*) Raso V, Ritz J, Basala M, Schlossman JF. A monoclonal antibody-ricin A chain conjugate which is selectivity cytotoxic for cells bearing the common acute lymphoblastic leukemia antigen (CALLA). Cancer Res 1982; 42:457–464.

(*24*) Funatsu G, Mise T, Matsuda H, Funatsu M. Isolation and characterization of two constituent polypeptide chains of ricin E. Agric Biol Chem 1978; 42:851–859.

(*25*) King J, Laemmli VK. Polypeptides of the tail fibres of bacteriophage T_4. J Mol Biol 1971; 62:465–477.

(*26*) Rogan FM, Faldette TJ, Boto W, et al. Heterogeneity in the membrane proteins of human lymphoid cell lines as seen in sodium dodecyl sulfate–polyacrylamide electrophoresis slab gels. Cancer Res 1978; 38:3604–3610.

(*27*) Carlsson J, Drevin H, Axen R. Protein thiolation and reversible protein conjugation. *N*-Succinimidyl-3-(2-pyridyldithio)propionate: A new heterobifunctional reagent. Biochem J 1978; 173:723–737.

(*28*) Cawley DA, Hedblom ML, Houston LL. Homology between ricin and ricins communis agglutinin: Amino terminal sequence analysis and protein synthesis inhibition studies. Arch Biochem Biophys 1978; 190:744–755.

(*29*) Rosenthal KL, Palmer JL, Harris JA, Rawls WE, Tompkins WA. Antibody-induced redistribution of CEA on the cell surface: Utilization in separation of CEA and isoantigen A. J Immunol 1975; 115:1049–1053.

(*30*) Tompkins WA, Schmale JD, Mock R, et al. Neuraminidase-augmented anticarcinoembryonic antigen (CEA)-complement lysis of human colon tumor cells: Lack of correlation with anti-CEA-mediated K-cell lysis and iodine-125 binding. JNCI 1979; 62:503–511.

(*31*) Gold P, Freedman SO. Demonstration of tumor specific antigens in human colonic carcinoma by immunological tolerance and absorption techniques. J Exp Med 1965; 122:439–443.

(*32*) Van Nagell JR Jr, Donaldson ES, Wood EG, Goldenberg DM. The clinical significance of carcinoembryonic antigen in the plasma and tumors of patients with gynecologic malignancies. Cancer 1978; 42:1527–1532.

(*33*) Alpert E. The immunochemical complexity of CEA: A golden dream or molecular nightmare. Cancer 1978; 42:1585–1594.

(*34*) Goldenberg DM, DeLand F, Kim E, et al. Use of radiolabeled antibodies to carcinoembryonic antigen for the detection and localization of diverse cancers by external photoscanning. N Engl J Med 1978; 258:1384–1388.

(*35*) Leibal SA, Klein JL, Syagias M, Leichmer P, Order SE. The integration of tumor associated antigens in cancer management. Semin Oncol 1981; 8:92–102.

(*36*) Shearer WT, Turabaugh TR, Coleman WE, Arch RO, Philpott GW, Parker LW. Cytotoxicity with antibody glucose oxidase conjugates specific for a human colonic cancer and carcinoembryonic antigen. Int J Cancer 1974; 14:539–547.

(*37*) Belles-Isles M, Page M. Anti-oncofetal proteins for targeting cytotoxic drugs. Int J Immunopharmacol 1981; 3:97–102.

(*38*) Johnson JR, Ford CM, Newman CE, Woodhouse CS, Rowland GF, et al. A vindesine-anti-CEA conjugate cytotoxic for human cancer cells in vitro. Br J Cancer 1981; 44:472–475.

(*39*) Raso V, Griffin TW. Hybrid antibodies with dual specificity for the delivery of ricin to immunoglobulin-bearing target cells. Cancer Res 1981; 41:2073–2078.

Figure 1.—SDS-PAGE of anti-CEA conjugate and components. Electrophoresis was performed according to King and Laemmli (*25*) with modification as per Rogan et al. (*26*) with the use of a slab gel of 10% acrylamide (0.1% SDS) and with a stacking gel of 5% acrylamide (0.1% SDS). Samples B, D, F, and H were reduced and alkylated by incubation with DTT (final concentration 5 m*M*) for 10 min at 37°C with the subsequent addition of IA (final concentration 60 n*M*). A) 3 μg ricin A-chain; B) 3 μg ricin A-chain reduced with DTT and alkylated with IA; C) 3.5 μg anti-CEA antibody–ricin A-chain conjugate; D) 3.5 μg reduced and alkylated anti-CEA antibody–ricin A-chain conjugate; E) and F) repeat of C and D; G) 3.5 μg anti-CEA antibody; H) 3.5 μg reduced and alkylated anti-CEA antibody; I) 5 μg ricin A-chain; J) 5 μg reduced and alkylated ricin A-chain. Molecular mass standards are indicated on the *ordinate*.

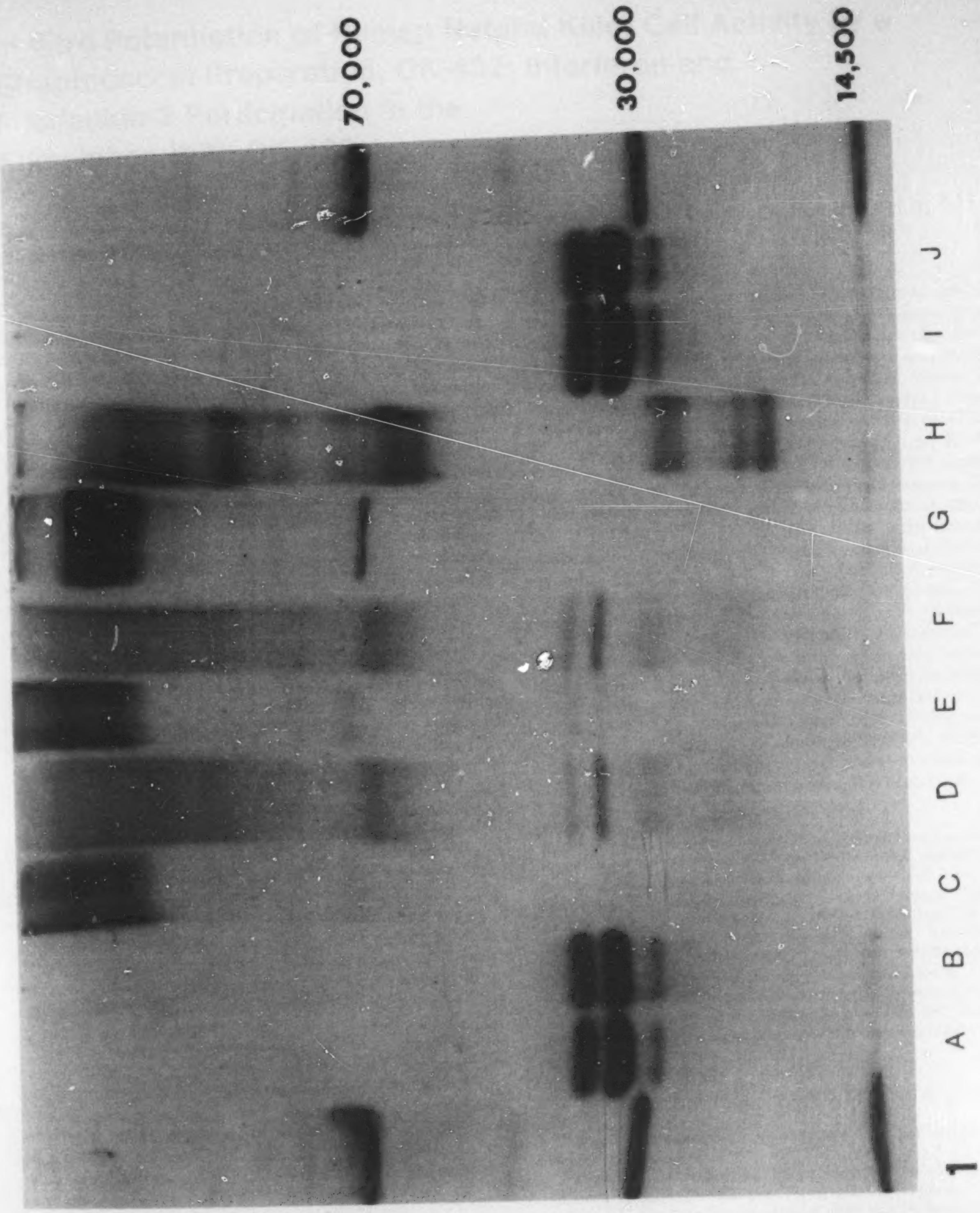
70,000
30,000
14,500
1
A
B
C
D
E
F
G
H
I
J

blank page

In Vitro Potentiation of Human Natural Killer Cell Activity by a Streptococcal Preparation, OK-432: Interferon and Interleukin-2 Participation in the Stimulation With OK-432[1,2]

Hiro Wakasugi, *M.D.*,[3] Tadashi Kasahara, *Ph.D.*,[4] Nagahiro Minato, *M.D.*,[5] Junji Hamuro, *Ph.D.*,[6] Michio Miyata, *M.D.*,[3] *and* Yasuhiko Morioka, *M.D.*[3,7]

ABSTRACT—Inasmuch as human natural killer (NK) cell activity was markedly augmented by a streptococcal immunopotentiator, OK-432, both in vivo and in vitro, the mechanism in which OK-432 augmented human NK cell activity was analyzed. Culture supernatants of nonadherent lymphocytes stimulated with OK-432 significantly augmented NK cell activity. Significant activity of both interferon (IFN) (both α- and γ-types) and interleukin-2 (IL-2) was detected in the culture supernatants from nonadherent lymphocytes. Concomitant treatment of supernatants with anti-IFN-α antiserum and pH-2 glycine–HCl buffer or the absorption of supernatants with an IL-2-dependent cell line completely abrogated the NK-augmenting activity, whereas the treatment with either one of these resulted in only partial elimination of the activity. These results indicate that OK-432 stimulates human nonadherent lymphocytes to produce IFN and IL-2 and that both factors are primarily responsible for the NK augmentation by OK-432.—JNCI 1982; 69:807–812.

Lymphoid cells from healthy, previously unsensitized experimental animals and humans are capable of mediating cytotoxicity against a variety of tumors and virus-infected cells. This phenomenon has been called "natural killing" (*1*, *2*). NK effector cells in humans have been characterized as NAdL expressing low-affinity receptors for SRBC and Fc-γR (*3*, *4*). NK cells have received considerable attention because of their potential role in resistance to cancer (*5*). NK cell activity has been reported to be augmented by a number of agents such as virus (*6*), tumor cells (*7*), BCG (*8*), *Corynebacterium parvum* (*9*), and IFN (*10*). Because most of these agents are also known to be able to induce IFN, the augmentation of NK cell activity by these agents has been proposed to be mediated by IFN production (*6*, *7*, *9*). More recently, however, IL-2, which is primarily involved in T-cell growth regulation, also has been shown to be able to augment NK cell activity (*11*).

Some of us have reported (*12*, *13*) that a streptococcal preparation, OK-432, which is widely used as an immunopotentiator with considerable success in patients with malignant diseases in Japan, strongly augmented human NK cell activity in vivo (*12*) as well as in vitro (*13*). In this paper we present evidence that both IFN and IL-2 produced by the lymphocytes stimulated with OK-432 play an essential role in the augmentation of NK cell activity.

MATERIALS AND METHODS

Cell separation.—Cell-separation procedures have been described in (*13*). Peripheral blood from normal donors was diluted with equal volumes of phosphate-buffered saline, and UFC were separated by the Ficoll-Conrey (d=1.078; Daiichi Seiyaku Co., Ltd., Tokyo, Japan) density gradient centrifugation method. Monocyte-rich and lymphocyte-rich cell fractions were separated with adherent properties. UFC suspended in a RPMI-1640 tissue culture medium (Flow Laboratories, Inc., Rockville, Md.) supplemented with 6% FCS (Flow Laboratories, Inc.,) were incubated at 37°C for 12 hours in plastic dishes (LUX Scientific Corp., Newburg Park, Calif.). NAdC were harvested with gentle pipetting and further purified on a Sephadex G-10 column. These procedures reduced the number of monocytes to less than 2%. After harvesting NAdC, the dishes were repeatedly washed, and remaining AdC were detached from the dishes by rubber policemen. AdC usually contained nearly 90% peroxidase-positive monocytes. In some experiments, T-cells (erythrocyte rosette-positive) and non-T-cells (erythrocyte rosette-negative) were separated by being rosetted with AET (2-aminoethylisothiouronium bromide hydrobromide)-treated SRBC. FcγR-positive (erythrocyte–antibody rosette-positive) and FcγR-negative (erythrocyte–antibody rosette-negative) cells were also separated by being rosetted with rabbit IgG anti-SRBC-sensitized SRBC. Cells thus obtained were usually treated with distilled water for 20 seconds for removal of contaminating red blood cells. In all

---

ABBREVIATIONS USED: AdC=adherent cell(s); AdL=adherent population(s) of peripheral blood lymphocytes; DMEM=Dulbecco's modified Eagle's minimum essential medium; E:T=effector-to-target cell ratio; FcγR= receptor for Fc portion of IgG; FCS=fetal calf serum; [^{3}H]dThd= tritiated thymidine; IFN=interferon(s); IFN-α=IFN, α-type; IFN-γ=IFN, γ-type; IL-2=interleukin-2; KE=Klinische Einheit (clinical unit); NAdC=nonadherent cell(s); NAdL=nonadherent lymphocytes; NK= natural killer; OK-432=streptococcal immunopotentiator; PBL=peripheral blood lymphocyte(s); SpA=staphylococcal protein A; SpA-CoI= *Staphylococcus aureus* Cowan I strain; SRBC=sheep red blood cells; UFC=unfractionated mononuclear cells; UFL=unfractionated PBL.

---

[1] Received November 9, 1981; revised April 23, 1982; accepted May 20, 1982.

[2] Research procedures were in accord with the ethical standards of the Helsinki Declaration of 1975.

[3] Department of Surgery, Jichi Medical School, 3311-1, Yakushiji, Minamikawachi-machi, Kawachi-gun, Tochigi-ken 329-04, Japan.

[4] Department of Medical Parasitology, Jichi Medical School.

[5] Department of Internal Medicine, Jichi Medical School.

[6] Central Research Laboratories, Ajinomoto Co. Inc., Kanagawa, 244, Japan.

[7] We thank Dr. Mitsunobu Imai, Department of Immunology, Jichi Medical School, for his preparation of the anti-interferon-α serum.

experiments, viability of the preparations before and after incubation was tested by trypan blue exclusion. The viability of the cells exceeded 90% in every fraction.

Preparation of culture supernatants.—The incubation of 2×10^6 UFC, NAdC, or AdC/ml with 0.2 KE OK-432/ml, 10 μg SpA/ml, 0.005% SpA-CoI bacteria, or 1×10^3IU IFN-α/ml was in RPMI-1640 medium supplemented with 6% FCS. After a 24-hour incubation, the culture supernatants were collected by centrifugation at 2,000 rpm for 5 minutes, were then filtered through a Millipore membrane (0.45 μm; Millipore Corp., Bedford, Mass.) for removal of the streptococcal or staphylococcal bacteria, and were stored at 4°C for later use. In all experiments, supernatants from unstimulated cultures were used as a control.

Assay of cytotoxic activity.—An erythroleukemic cell line, K562, was maintained in RPMI-1640 medium containing 7% FCS. Cells were labeled with 100 μCi of $Na_2{}^{51}CrO_4$ (300–400 μCi/mg; New England Nuclear Corp., Boston, Mass.) by incubation at 37°C for 90 minutes. After being washed four times, the serially diluted lymphoid cells (0.1 ml) and the ^{51}Cr-labeled K562 target cells (10^4 cells/0.1 ml) were mixed in a round-bottom tissue culture plate (Linbro Scientific Inc., Hamden, Conn.) and were incubated for 5 hours in a 5% CO_2–air incubator at 37°C. After incubation, the plates were centrifuged, and 0.1 ml of the supernatants was removed. The radioactivity in the supernatants was counted in a gamma well counter. The specific ^{51}Cr release was calculated as decribed in (*13*).

Determination of antiviral (*IFN*) *activity.*—The culture supernatants were assayed for antiviral activity by the cytopathic effect inhibition method in which FL cells were used as indicator cells and vesicular stomatitis virus (New Jersey strain) was used as challenge virus (*14*). IFN titer expressed in IU was determined by comparison with a standard international reference IFN-α (NIH human reference IFN-G-023-901-527).

Acid treatment of cultured supernatants.—The samples were dialyzed in 0.05 *M* pH 2.0 glycine-HCl buffer at 4°C for 24 hours. An additional dialysis in RPMI-1640 medium at 4°C for 24 hours brought the pH of the samples back to 7.2. Samples were stored at 4°C for later use.

Anti-IFN antiserum.—Sheep anti-human-IFN-α antiserum was provided by Dr. M. Imai. Anti-IFN-α serum at a 1:10,000 dilution was capable of neutralizing 10 IU of IFN-α.

Determination of IL-2 activity.—IL-2 activity in the cultured supernatants was determined according to the methods of Baker et al. (*15*) and Gillis et al. (*16*). Murine (C57BL/6) tumor-specific cytotoxic T-lymphocyte line (CTLL-2) was used as an indicator cell in IL-2 microassays. The cells were washed extensively three times with DMEM (GIBCO, Grand Island, N.Y.) and were resuspended in the DMEM supplemented with 2% FCS. Cells (0.1 ml) were placed in 96-well Microplates, and serial dilutions of the IL-2 sample (0.1 ml) to be assayed were then added. Microplates were incubated at 37°C in an atmosphere of 5% CO_2 in air. Following a 24-hour incubation, 0.5 μCi of [^{3}H]dThd (5 mCi/mmol; New England Nuclear Corp.) was added to each well and incubated for an additional 4 hours. Cultures were harvested, and [^{3}H]dThd incorporation was determined by a scintillation counter.

Preparation of IL-2-absorbed supernatants.—The IL-2-dependent cell line CTLL-2 was washed repeatedly with IL-2-free, fresh RPMI-1640 medium, which removed the remaining IL-2. Then 1×10^7 CTLL-2 cells were incubated with 1 ml of the cultured supernatants at 4°C for 24 hours. The supernatants were collected by sedimentation, filtered through a Millipore membrane (0.45 μm), and stored at 4°C for later use. The procedure completely eliminated IL-2 activity in the culture supernatants.

Stimulants.—OK-432, a penicillin- and heat-treated lyophilized preparation of the low-virulence strain SU of *Streptococcus pyogenes* (group A3), was provided by Chugai Seiyaku (Tokyo, Japan). One KE of OK-432 contained 0.1 mg of dried cocci (10^7–10^8), which was used as a suspension in physiologic saline. SpA-CoI bacteria killed by 0.5% of formaldehyde and heat treatment at 80°C for 5 minutes were used as a stimulant of IFN-α induction (*17*). SpA (Pharmacia Chemicals AB, Uppsala, Sweden) was purchased commercially.

RESULTS

Effect of OK-432-Stimulated Supernatants on the NK Cell Activity

Some of us have previously reported (*12*) that OK-432

TABLE 1.—*OK-432-stimulated supernatants and NK cell activity: Supernatant effectivity on both autologous and allogeneic effector cells*[a]

Effector cells	Added supernatant	Percent cytotoxicity						Mean percent cytotoxicity ± SD, E:T	
		Expt 1, E:T		Expt 2, E:T		Expt 3, E:T			
		20:1	10:1	20:1	10:1	20:1	10:1	20:1	10:1
Autologous	Medium	16.7	9.2	21.7	15.0	23.2	15.2	20.5±3.4	13.1±3.4
	Unstimulated	14.6	9.4	23.2	18.0	22.7	14.2	20.2±4.8	13.9±4.3
	OK-432 stimulated	32.3	23.4	42.8	30.6	37.8	27.6	37.6±5.3[b]	27.2±3.6[c]
Allogeneic	Medium	69.3	42.7	57.0	45.1	45.0	40.2	57.1±12.2	42.6±2.5
	Unstimulated	64.7	40.5	55.4	44.0	49.4	42.7	56.5±7.7	42.4±1.8
	OK-432 stimulated	90.4	59.4	82.0	69.2	73.2	66.0	81.8±8.6	65.5±5.3

[a] Effect of OK-432-stimulated PBL supernatants on the cytotoxicity of both autologous and allogeneic cells was examined with K562 target cells. Fresh autologous or allogeneic PBL were incubated for 24 hr with medium alone, culture supernatants from unstimulated PBL (supernatants at a final concentration of 50%), or with culture supernatants from OK-432-stimulated PBL (supernatants at a final concentration of 50%). Cells were washed and assayed for the cytotoxicity against ^{51}Cr-labeled K562 cells in the 4-hr ^{51}Cr release assay.

[b] $P<0.01$, when compared with above two values.

[c] $P<0.001$, when compared with above two values.

TABLE 2.—*OK-432-stimulated supernatants and NK cell activity: AdC-independent production of NK-augmenting factor(s)*[a]

Added supernatant		Percent cytotoxicity					
Origin	Supernatant	Expt 1, E:T		Expt 2, E:T		Expt 3, E:T	
		10:1	5:1	10:1	5:1	10:1	5:1
UFC	Medium	35.2	18.6	14.8	8.6	42.0	30.1
	Unstimulated	29.2	17.0	17.6	7.3	52.7	32.2
	OK-432 stimulated	54.0	30.4	40.2	20.2	61.0	41.3
NAdC	Unstimulated	31.0	18.8	17.3	7.8	57.8	40.0
	OK-432 stimulated	50.7	28.4	45.0	23.1	75.1	60.4
AdC	Unstimulated	31.9	14.4	15.8	6.8	51.3	43.2
	OK-432 stimulated	44.4	25.9	15.1	7.8	56.3	50.5

[a] Effector cells were all allogeneic UFC. Fresh PBL were separated into AdL and NAdL fractions as described in "Materials and Methods." UFC, NAdC, or AdC were then cultured with or without OK-432, and the culture supernatants were harvested 24 hr later. The effect of each supernatant on NK activity was examined as described in table 1.

strongly augmented cytotoxic activity against K562 target cells in vitro. The augmented cytotoxic activity was considered to be mainly mediated by nonadherent, FcγR-positive, and non-erythrocyte-rosetting lymphocytes, which were the same characteristics as the characteristics of endogenous NK cells. Our preliminary results indicated that AdC were not required for NK cell augmentation (data not shown).

We thus first investigated the possibility that augmentation of cytotoxicity by OK-432 was mediated by soluble factors. UFC were cultured with or without 0.2 KE OK-432/ml for 24 hours, and the culture supernatants were harvested and centrifuged to eliminate OK-432. Fresh autologous or allogeneic PBL were then incubated with medium or with these supernatants (supernatants at a final concentration of 50%) for 24 hours, and the cytotoxicity was assayed against K562 cells. As shown in table 1, cytotoxic activity of both autologous and allogeneic cells was significantly augmented by OK-432-stimulated supernatants, suggesting that some soluble factors were responsible for the augmentation of NK cell activity.

To examine whether NK cell-enhancing activity derived from NadC or AdC, we tested the effect of the supernatants from each fraction. As shown in table 2, supernatants derived from NAdL significantly enhanced NK cell activity, whereas supernatants from AdC did not.

TABLE 3.—*IFN induction by various bacterial agents*[a]

Origin of supernatants	Agents[b]	IFN titer, IU/0.1 ml		
		Expt 1	Expt 2	Expt 3
UFC	Control	<2	<2	<2
	OK-432	64	32	256
	SpA	<2	<2	<2
	SpA-CoI	128	64	16
NAdC	Control	2	<2	<2
	OK-432	128	32	256
	SpA	<2	<2	<2
	SpA-CoI	256	64	32
AdC	Control	<2	<2	<2
	OK-432	<2	<2	<2
	SpA	<2	<2	<2
	SpA-CoI	128	128	16

[a] Various agents were incubated with 2×10^6 mononuclear cells/ml from three donors for 24 hr. Culture supernatants were then collected, passed through a Millipore membrane, and immediately tested for their antiviral activity. Optimal incubation times, cell concentrations, and concentrations of the agents were determined in the preliminary experiments.

[b] Concentrations of the agents were 0.2 KE OK-432/ml, 10 μg SpA/ml, and 0.005% SpA-CoI.

Production of IFN and IL-2 by Stimulation With OK-432

IFN and, more recently, IL-2 are well-established molecules involved in the regulation of NK activity in both murine and human systems (*6, 10, 11*). Thus to characterize the NK-augmenting factor(s) in the supernatants of OK-432-stimulated cultures, we first examined whether OK-432 could stimulate the production of these factors, namely, IFN and IL-2, in human PBL. Normal UFL, NAdL, or AdL were cultured in the presence of OK-432. At various culture intervals, culture supernatants as well as cultured cells were harvested and assayed first for IFN and IL-2 activity and then for NK activity. The results are summarized in text-figure 1. Significant IL-2 activity was detected in the culture supernatants as early as 6 hours of culture; IL-2 activity reached the peak level at 24 hours and progressively declined thereafter (text-fig. 1A). Antiviral (IFN) activity was also detected in OK-432-stimulated culture supernatants. The kinetics of IFN production, however, were quite different from the kinetics of IL-2. Thus a progressive increase of IFN activity was observed up to 96 hours. Augmented NK

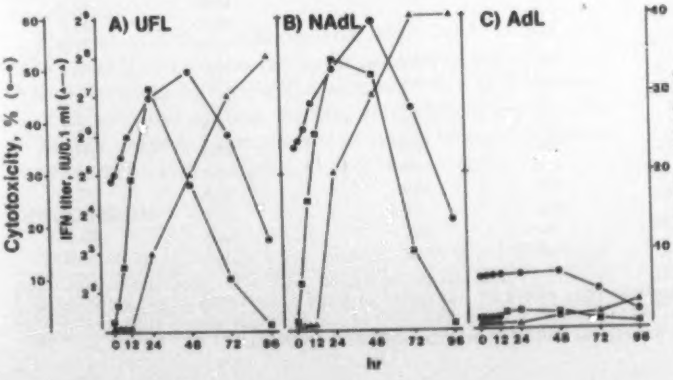

TEXT-FIGURE 1.—Kinetics of development of cytotoxic activity, induction of IFN, and IL-2 production by OK-432 in culture. Fresh UFL (2×10^6) or separated AdL were incubated for 0–96 hr with 0.2 KE OK-432/ml. At various intervals, NK cell activity of the cells (E:T=10:1) as well as IFN and IL-2 activity in the supernatants were assayed.

TABLE 4.—*IL-2 induction by various bacterial agents*[a]

Origin of supernatants	Agents[b]	IL-2 titer, U/ml		
		Expt 1[c]	Expt 2[c]	Expt 3
UFC	Control	<1	<1	<1
	OK-432	32	6	10
	SpA	50	NT	50
	SpA-CoI	4	<1	<1
	PHA	NT	NT	10
NAdC	Control	<1	2	<1
	OK-432	32	32	20
	SpA	50	NT	50
	SpA-CoI	8	8	<1
AdC	Control	<1	<1	<1
	OK-432	<1	<1	<1
	SpA	<1	NT	<1
	SpA-CoI	<1	<1	<1

[a] Various agents were incubated with 2×10^6 mononuclear cells/ml from separate donors for 24 hr. Culture supernatants were collected and passed through a Millipore membrane, and IL-2 activity in the supernatants was tested.

[b] Concentrations of the agents were 0.02 KE OK-432/ml, 10 μg SpA/ml, 0.005% SpA-CoI, and 5 μg phytohemagglutinin (PHA)/ml. PHA served as a control for the induction of IL-2 activity.

[c] NT=not tested.

activity was observed between 6 and 72 hours, the highest level being around 48 hours.

Essentially similar results were obtained for NAdL, except that both IFN and IL-2 titers as well as the degree of NK augmentation were consistently higher in NAdL cultures than in UFL cultures (text-fig. 1B). In contrast, neither IFN nor IL-2 activity was detected in the cultures of AdL throughout the culture period, nor was any significant NK augmentation noted (text-fig. 1C).

The stimulation capacity of IFN and IL-2 of OK-432 was compared with the stimulation capacity of other bacterial preparations, SpA and SpA-CoI, which were also shown to be able to augment NK activity of human PBL (*13*, *14*). These results are summarized in tables 3 and 4. SpA-CoI induced a level of IFN in UFC population comparable to the level induced by OK-432, whereas SpA did not stimulate a detectable level of IFN in 24 hours. SpA-CoI stimulated IFN production in both NAdL and AdL equally, whereas OK-432 induced IFN production only in the NAdL. In contrast, SpA was found to be a very potent IL-2 inducer, and SpA-CoI was found to be a poor inducer. IL-2 was produced by the NAdL, and no detectable IL-2 activity was found in the AdL fraction by any of the stimulants.

Thus we addressed the next question: Is the production of IFN or IL-2 by OK-432 stimulation really responsible for NK cell augmentation? First, to elucidate the role of IFN, we examined the effect of anti-IFN-α serum on the NK cell-enhancing activity of the OK-432-stimulated culture supernatants of UFC. The supernatants, which had been neutralized with anti-IFN-α antibody (antibody dilution, 1:100; incubation, 37°C for 2 hr) and/or acid treatment (at pH 2 and 4°C for 24 hr) were added to the fresh PBL cultures and then tested for their NK cell-augmenting effects. As shown in table 5, the NK cell-augmenting effect of both IFN-stimulated and SpA-CoI bacteria-stimulated supernatants was completely eliminated by treatment with a 1:100 dilution of anti-IFN-α antibody. In contrast, only partial reduction of such activity was observed in both SpA-stimulated and OK-432-stimulated supernatants. Similar results were obtained even when acid treatment was added to the anti-IFN-α antibody for the neutralization of IFN.

Second, we investigated the effect of absorption of IL-2 activity in the supernatants. The supernatants, which had been preabsorbed with CTLL-2 cells, were added to the fresh PBL cultures and tested for their NK cell-enhancing

TABLE 5.—*Inactivation of antiviral activity of culture supernatants and NK-enhancing activity*[a]

Stimulants	Treatments[b]	IFN titer, IU/0.1 ml		NK cell activity, %	
		Expt 1	Expt 2	Expt 1	Expt 2
None	—	<2	<2	30.0	21.2
	Anti-IFN-α	<2	<2	28.5	20.6
	pH 2	<2	<2	28.0	20.0
	pH 2 + anti-IFN-α	<2	<2	18.2	18.3
SpA, 10 μg/ml	—	<2	<2	66.7	44.2
	Anti-IFN-α	<2	<2	59.4	37.5
	pH 2	<2	<2	63.0	40.1
	pH 2 + anti-IFN-α	<2	<2	45.6	30.9
OK-432, 0.2 KE/ml	—	256	128	60.9	46.0
	Anti-IFN-α	4	2	47.0	31.3
	pH 2	64	64	52.5	40.1
	pH 2 + anti-IFN-α	<2	<2	27.0	25.6
SpA-CoI, 0.005%	—	64	128	51.3	35.7
	Anti-IFN-α	<2	<2	16.2	18.7
	pH 2	64	64	46.6	30.2
	pH 2 + anti-IFN-α	<2	<2	14.0	16.4
IFN-α, 1×10^3 IU/ml	—	128	128	55.3	37.8
	Anti-IFN-α	<2	<2	15.7	17.4
	pH 2	64	128	54.1	35.9
	pH 2 + anti-IFN-α	<2	<2	16.4	17.3

[a] PBL were cultured with various agents for 24 hr. Culture supernatants were either left untreated or were treated with *a*) pH 2 glycine-HCl buffer for 24 hr at 4°C, with *b*) anti-IFN-α antiserum (final dilution, 1:100) for 2 hr at 37°C, or with both *a*) and *b*). Supernatants thus treated were then assayed for NK-enhancing activity as well as for antiviral (IFN) activity as described in "Materials and Methods."

[b] —=none.

TABLE 6.—*IL-2 absorption combined with IFN inactivation and the NK-enhancing activity of culture supernatants*[a]

Stimulants	Treatments[b]	IL-2 titer, U/ml[c]	IFN titer, IU/0.1 ml	NK cell activity, %
None	—	<1	<2	31.7
	CTLL-2	<1	<2	29.8
	CTLL-2 + pH 2 + anti-IFN-α	NT	<2	28.1
SpA, 10 μg/ml	—	50	<2	69.2
	CTLL-2	<1	<2	58.4
	CTLL-2 + pH 2 + anti-IFN-α	NT	<2	41.6
OK-432, 0.2 KE/ml	—	10	128	66.3
	CTLL-2	<1	128	52.5
	CTLL-2 + pH 2 + anti-IFN-α	NT	<2	25.7
SpA-Col, 0.005%	—	<1	64	58.5
	CTLL-2	<1	64	56.7
	CTLL-2 + pH 2 + anti-IFN-α	NT	<2	27.2
IFN-α, 1×10^3 IU/ml	—	<1	128	55.0
	CTLL-2	NT	128	54.3
	CTLL-2 + pH 2 + anti-IFN-α	NT	<2	24.9

[a] Supernatants previously IL-2 absorbed with CTLL-2 cells (4°C, 24 hr) were treated with or without the combined treatments of pH 2 glycine–HCl buffer for 24 hr at 4°C and of incubation with an equal volume of anti-IFN antibody (1:100 diluted) for 2 hr at 37°C. Supernatants were then tested for IL-2 and IFN titers. After these treatments, fresh PBL (3×10^5/30 μl) were mixed with the supernatants (300 μl, 50% of final concentration) and were incubated for 24 hr. Finally, NK cell activity was assayed. E:T=10:1. Representative data from three similar experiments are shown.

[b] —=none.

[c] NT=not tested.

effects. As shown in table 6, such treatment completely eliminated IL-2 activity in the supernatants. A significant but again partial reduction of cytotoxic activity was observed both in SpA-stimulated and OK-432-stimulated supernatants, whereas the cytotoxicity in IFN-α-stimulated and SpA-CoI-stimulated supernants remained unaffected. Finally, when both anti-IFN-α serum and acid treatment were combined with absorption by CTLL-2 cells, the cytotoxicity in OK-432-stimulated supernatants was completely eliminated.

These results thus indicate that IFN, both IFN-α and IFN-γ, *and* IL-2 are involved in the augmentation of human NK cell activity by OK-432. However, either IFN alone or IL-2 alone could explain the NK cell-augmenting activity of further degraded components of staphylococcal preparations, namely, IFN in SpA-CoI and IL-2 in SpA.

DISCUSSION

Some of us (*12*, *13*) have shown that a streptococcal immunopotentiator, OK-432, augmented natural cytotoxic activity of human PBL from healthy donors as well as from donors with cancer. In the present paper, we tried to analyze the mechanisms by which OK-432 as well as other staphylococcal preparations augment human NK activity in vitro. A number of reports indicate that OK-432 can activate the monocyte–macrophage system (*18*, *19*). The first question we thus addressed was whether monocytes–macrophages were required for augmentation of NK activity by OK-432. Our preliminary study, however, indicated that monocytes–macrophages were not required for NK augmentation by OK-432. Thus equivalent or even greater augmentation of NK activity was obtained in AdC-depleted mononuclear cells by OK-432, as compared with NK activity in UFC, and no significant NK cell augmentation was observed in AdC by OK-432.

The next question we addressed was whether OK-432 acted directly on NK effector cells to potentiate their NK activity or if OK-432 stimulated the production of some mediators, which in turn stimulated NK cells. As was clearly shown in table 1, supernatants of OK-432-stimulated cultures, which were absolutely free of OK-432 particles, strongly augmented the NK activity of fresh UFC at a comparable degree of augmentation as if OK-432 particles were present. These results clearly indicate that OK-432 can stimulate the production of secondary NK-enhancing factors, although the results do not completely eliminate the possibility that OK-432 also can directly stimulate NK effector cells.

As chemically defined molecules, IFN and most recently IL-2 are the only molecules so far known that directly stimulate NK cells (*6*, *10*, *11*), although the ways in which they act seem to vary considerably between them (*10*, *20*, *21*). Indeed, a number of agents known to augment NK activity, agents such as various mitogens, bacteria, chemicals, viruses, and allogeneic and virus-infected as well as various tumor cells are also shown to stimulate either IFN or IL-2 (*6*, *7*, *9*, *22*). Our present results indicate that, in fact, OK-432 stimulated both IFN and IL-2 simultaneously in normal human PBL.

Using a murine system, Matsubara et al. (*23*) reported that OK-432 could strongly induce IFN-γ. In the present study, we showed that IFN produced by OK-432 in human PBL was partially inactivated either by anti-IFN-α serum or by pH 2.0 treatment and was almost completely eliminated by both treatments, suggesting that both IFN-α and IFN-γ were included. Conforming to this observation, preliminary experiments showed that IFN was derived from both T-cell and non-T-cell populations of NAdC by OK-432 stimulation (data not shown). Interestingly, IFN induction by OK-432 seems to be independent of the presence of adherent accessory cells, although the possible involvement of small numbers (<2%) of contaminant accessory cells in our NAdL population could not be completely eliminated.

Other soluble IFN inducers such as polyinosinic-polycytidylic acid, phytohemagglutinin, and concanavalin A have been shown to be dependent on the presence of AdC for their action (*24*, *25*). Because OK-432 is a particulate material, the difference may well be due to the differences in the physical forms of these IFN inducers. At present, we do not know whether the same structure on OK-432 is responsible for both IFN and IL-2 production or if separate structures are involved. In this context, it is noteworthy that purified SpA, which is derived from a staphylococcal preparation, preferentially stimulated IL-2 in human PBL, whereas SpA-CoI strongly induced IFN with less IL-2 as compared to the amount of IL-2 in the SpA-stimulated preparation. Thus it seems very likely that different structures on OK-432 particles are responsible for IFN and IL-2 stimulation in human lymphocytes.

That both IFN and IL-2 are truly responsible for the OK-432-induced NK cell augmentation was undoubtedly proved by the following experiments: 1) Treatment of the OK-432-stimulated culture supernatants with anti-IFN-α serum, with pH 2.0 treatment, or with both resulted in a partial but significant reduction in the NK cell-augmenting activity; 2) absorption of the supernatants with CTLL-2 cells, which completely eliminated IL-2 activity, also resulted in a partial reduction in the NK cell-augmenting activity; and finally, 3) combined treatment of the supernatants with both procedures completely eliminated the NK cell-augmenting activity. As to how IFN and IL-2 stimulate NK activity, two basic explanations seem possible: 1) IL-2 and IFN stimulate NK activity absolutely independently of each other and 2) IL-2 stimulates IFN production, which finally stimulates NK cell activity. Study of the kinetics of these modes of production indicated that IL-2 production by OK-432 stimulation preceded the IFN production in the culture (text-fig. 1). In the murine system, it was indeed shown that partially purified IL-2 freed from IFN activity could stimulate IFN production in the normal PBL population (*26*). These observations seem to favor, but do not prove, the second possibility, that of a stepwise stimulation of NK cell activity. Recently, Farrar et al. (*27*) reported that IFN-γ produced by the stimulation with IL-2 in mixed PBL cultures was the essential signal for the generation of alloreactive, cytotoxic T-lymphocytes. The exact interrelationship between IL-2 and IFN in the NK cell system, however, remains to be further elucidated.

REFERENCES

(*1*) Herberman RB, Nunn ME, Holden HT, Laurin DH. Natural cytotoxic reactivity of mouse lymphoid cells against syngeneic and allogeneic tumors. II. Characterization of effector cells. Int J Cancer 1975; 16:230–239.

(*2*) Kiessling R, Klein E, Wigzell H. "Natural" killer cells in the mouse. I. Cytotoxic cells with specificity for mouse Moloney leukemia cells. Specificity and distribution according to genotype. Eur J Immunol 1975; 5:112–117.

(*3*) West WH, Cannon GB, Kay HD, Bonnard GD, Herberman RB. Natural cytotoxic reactibility of human lymphocytes against a myeloid cell line. Characterization of effector cells. J Immunol 1977; 118:355–361.

(*4*) Cooper SM, Hirsen DJ, Friou GJ. Spontaneous cell-mediated cytotoxicity against Chang cells by nonadherent, non-thymus-derived, Fc receptor-bearing lymphocytes. Cell Immunol 1977; 32:135–145.

(*5*) Santoli D, Koprowski H. Mechanism of activation of human natural killer cells against tumour and virus-infected cells. Immunol Rev 1979; 44:125–163.

(*6*) Trinchieri G, Santoli D, Dee RR, Knowles BB. Antiviral activity induced by culturing lymphocytes with tumor-derived or virus-transformed cells. Identification of the anti-viral activity as interferon and characterization of the human effector lymphocyte subpopulation. J Exp Med 1978; 147:1299–1313.

(*7*) Dieu JY, Huang KY, Herberman RB. Augmentation of mouse natural killer activity and induction of interferon by tumor cells in vivo. J Exp Med 1980; 151:781–789.

(*8*) Wolfe SA, Tracey DE, Henny CS. BCG-induced murine effector cells. II. Characterization of natural killer cells in peritoneal exudates. J Immunol 1977; 119:1152–1158.

(*9*) Macfarlan RI, Ceredig R, White DO. Comparison of natural killer cells induced by Kunjin virus and *Corynebacterium parvum* with those occurring naturally in nude mice. Infect Immun 1979; 26:832–836.

(*10*) Gidlund M, Örn A, Wigzell H, Senik A, Gresser I. Enhanced NK cell activity in mice injected with interferon and interferon inducers. Nature 1978; 273:759–761.

(*11*) Henny CS, Kuribayashi K, Kern DE, Gillis S. Interleukin-2 augments natural killer cell activity. Nature 1981; 291:335–338.

(*12*) Wakasugi H, Oshimi K, Miyata M, Morioka Y. Augmentation of natural killer (NK) cell activity by a streptococcal preparation, OK-432, in patients with malignant tumors. J Clin Immunol 1981; 1:154–162.

(*13*) Wakasugi H, Oshimi K, Kasahara T, Miyata M, Morioka Y. In vitro augmentation of human natural killer (NK) cell activity by a streptococcal preparation and its extracts, protein A and polysaccharides. Int Arch Allergy Appl Immunol 1982; 67:322–328.

(*14*) Kasahara T, Harada H, Shioiri-Nakano K, Imai M, Sano T. Potentiation of natural killer activity of human lymphocytes by *Staphylococcus aureus* bacteria and its protein A. Immunology 1981; 42:175–183.

(*15*) Baker PE, Gillis S, Smith KA. Monoclonal cytotolytic T-cell lines. J Exp Med 1979; 149:273–278.

(*16*) Gillis S, Feron MM, Ou W, Smith KA. T cell growth factor: Parameters of production and a quantative microassay for activity. J Immunol 1978; 120:2027–2032.

(*17*) Kasahara T, Harada H, Shioiri-Nakano K, et al. Potentiation of natural killer cell activity of human lymphocytes in vitro: The participation of interferon in the stimulation with *Staphylococcus aureus* CoI bacteria but not protein A. Immunology 1982. In press.

(*18*) Ishii Y, Yamaoka H, Toh K, Kikuchi K. Inhibition of tumor growth in vivo and in vitro by macrophages from rats treated with a streptococcal preparation, OK-432. Gan 1976; 67:115–119.

(*19*) Yamashita A, Hattori Y, Fukumoto T. Augmenting effect of exogenous macrophages on the rat graft-versus-host reaction in F_1 hybrids depleted of macrophages. Transplantation 1980; 30:122–127.

(*20*) Minato N, Reid LM, Bloom BR. On the heterogeneity of murine natural killer (NK) cells. J Exp Med 1981; 154:750–762.

(*21*) Kuribayashi K, Gillis S, Kern DE, Henny CS. Murine NK cell cultures: Effect of interleukin-2 and interferon on cell growth and cytotoxic reactivity. J Immunol 1981; 126:2321–2327.

(*22*) Minato N, Bloom BR, Jones C, Holland J, Reid LM. Mechanism of rejection of virus persistently infected tumor cells by athymic nude mice. J Exp Med 1979; 149:1117–1133.

(*23*) Matsubara S, Suzuki F, Ishida N. Induction of immune interferon in mice treated with a bacterial immunopotentiator, OK-432. Cancer Immunol Immunother 1979; 6:41–45.

(*24*) Oehler JR, Lindsay LR, Nunn ME, Holden HT, Herberman RB. Natural cell-mediated cytotoxicity in rats. II. In vivo augmentation of NK-cell activity. Int J Cancer 1978; 21:210–220.

(*25*) Djeu JY, Heinbaugh JA, Holden HT, Herberman RB. Role of macrophages in the augmentation of mouse natural killer cell activity by poly I:C and interferon. J Immunol 1979; 122:182–188.

(*26*) Minato N, Bloom BR. Heterogeneity and regulation of the natural killer cell system. In: Herberman RB, ed. Natural cell-mediated immunity against tumors. Vol 2. New York: Academic Press, 1982. In press.

(*27*) Farrar WL, Johnson HM, Farrar JJ. Regulation of the production of immune interferon and cytotoxic T lymphocytes by interleukin-2. J Immunol 1981; 126:1120–1125.

Carcinoembryonic Antigen: Usefulness as a Postsurgical Method in the Detection of Recurrence in Dukes Stages B_2 and C Colorectal Cancers[1,2]

Maria Koch,[3] Graeme Washer,[4] Herta Gaedke,[3] *and* Thomas A. McPherson[4,5]

ABSTRACT—Sequential carcinoembryonic antigen (CEA) plasma levels were obtained postoperatively in 181 patients with colorectal Dukes stages B_2 and C colorectal cancers to assess their usefulness as part of a follow-up program designed to detect disease progression. In all, 1,684 determinations were obtained in patients who were, at the time, free of any clinical or radiologic evidence of disease. If individual CEA determinations are considered and if 10 ng/ml is specified as the limit between normal and elevated CEA levels, both sensitivity (45.0%) and specificity (93.4%) make determination of CEA levels an acceptable screening test in this well-defined population, especially as it also fulfills the criteria of patient acceptance, potential benefit to the patient, and low cost. Preoperative CEA levels were also determined in 93 of the 181 patients, and these results confirm the prognostic value of the slope between preoperative and postoperative CEA levels.—JNCI 1982; 69:813–815.

In the fall of 1980, the Consensus Development Conference was held at the National Institutes of Health, Bethesda, Md., on the role of CEA as a marker in the management of cancer (*1*). For patients with colorectal cancer, the Conference panel recommended obtaining CEA plasma levels before surgery, 4–6 weeks after surgery, and at regular intervals thereafter. Determination of CEA plasma levels is considered to be "the best presently available noninvasive technique for postoperative surveillance" of these patients.

Low preoperative levels of CEA are correlated with better survival rates (*2*) and have been proposed as a stratifying factor in adjuvant chemotherapy protocols (*3*). Postoperative elevated CEA titers are often an indication of residual disease (*4, 5*), just as rising CEA levels in general are an indication of disease progression (*6, 7*). In some patients, CEA levels never rise above normal even in the presence of extended disease (*8*), but a normal preoperative CEA level does not preclude the possibility of rising titers if disease progression occurs (*9*).

According to Möschl et al. (*10*), patients with colorectal cancer can be divided into the following 2 groups according to the change in their CEA levels: patients whose CEA concentrations decreased postoperatively and remained normal for a year or more (recurrence rate, 9%) and patients whose postoperative CEA levels showed little or no decrease and later increased (recurrence rate, 86%).

When CEA plasma levels are utilized to monitor colorectal cancer in patients who are apparently free of disease, they must be considered as a surveillance or screening test, rather than as a diagnostic test, applied to a select population at risk and should fulfill the criteria generally accepted for screening tests (*11*): sensitivity, specificity, acceptance, low cost, and potential possible benefits to the patients. The usefulness of a screening test depends on a combination of all these factors as they relate to the population being screened.

To test the efficacy of CEA levels as a postoperative screening method, we have chosen patients with Dukes stages B_2 and C colorectal cancers, since these patients have a high probability of developing recurrent disease postoperatively (*12*).

The prognostic value of any single CEA determination in apparently disease-free patients as well as the prognostic value of the slope between presurgical and postsurgical CEA levels was analyzed.

MATERIALS AND METHODS

All CEA determinations were done by the Ziconyl-phosphate method (Z-gel) developed by Hansen et al. (*13*) as modified in our laboratory (*14*). Although for diagnostic purposes CEA plasma levels from 0 to 5.0 ng/ml are considered within normal limits and levels between 5.1 and 10.0 ng/ml are considered borderline, for screening purposes we define levels up to 10.0 ng/ml as normal. CEA slopes were obtained by the following formula: [Postoperative CEA level (ng/ml)−preoperative CEA level (ng/ml)]/interval in months. The interval ranged from 1.0 to 4.2 months. The first CEA level available 30 days or more after surgery was considered for the slope calculation.

Of the patients who presented at the Cross Cancer Institute between January 1, 1976 and December 31, 1980 with Dukes stage B_2 or C colorectal cancer as part of an adjuvant therapy program, 181 were considered in this study: All of these 181 patients had a CEA determination shortly (1–3 wk) after surgical excision of the tumor as well as one determination every 3 months. A preoperative CEA level was also available in 93 of these 181 patients.

A base-line chest X-ray and liver scan were part of the patient's postoperative clinical evaluation. On successive clinic attendances, the chest X-ray and liver scan were repeated every 6 months and a double-contrast barium enema was obtained once a year.

ABBREVIATION USED: CEA=carcinoembryonic antigen.

---

[1] Received November 27, 1981; accepted April 19, 1982.

[2] Research procedures were in accord with the ethical standards of the Research Committee of the Alberta Cancer Board.

[3] Department of Epidemiology, Provincial Cancer Hospitals Board, 11560 University Ave., Edmonton, Alberta, Canada T6G 1Z2.

[4] Department of Medicine, Cross Cancer Institute, 11560 University Ave., Edmonton, Alberta, Canada T6G 1Z2.

[5] We gratefully acknowledge Hoffmann-La Roche Inc., Nutley, N.J., for providing financial assistance needed to complete this study.

Factors known to affect CEA values such as concomitant ulcerative colitis were considered in patient management. However, all 1,684 CEA levels obtained in patients who were at the time free of clinical and/or radiologic evidence of cancer have been included in our analysis.

To calculate the sensitivity and the specificity of the test as a screening method, we used the classical definitions (*13*). Sensitivity is the probability that the test will correctly identify a diseased person: It is equal to the number of persons diseased with a positive test divided by the number of all diseased. Specificity is the probability that the test will correctly identify a nondiseased person: It is equal to the number of persons nondiseased with a negative test divided by all the nondiseased who were screened.

TABLE 1.—*CEA levels measured at different times: Correlation with eventual disease progression*

Measurement times	CEA plasma levels, ng/ml	Total No. of tests	No. of tests in patients who later showed disease progression (%)
Preoperative	0–5.0	49	7 (14.3)
	5.1–10.0	22	5 (22.7)
	10.1–25.0	15	5 (33.3)
	>25.0	7	4 (57.1)
Total		93	21 (22.6)
Postoperative	0–5.0	122	16 (13.1)
	5.1–10.0	42	8 (19.0)
	10.1–25.0	13	7 (53.8)
	>25.0	4	4 (100.0)
Total		181	35 (19.3)
Any test in a "disease-free" patient (includes postoperative values)	0–5.0	1,070	60 (5.6)
	5.1–10.0	429	45 (10.5)
	10.1–25.0	147	52 (35.4)
	>25.0	38	34 (89.5)
Total		1,684	191 (11.3)

TABLE 2.—*Sensitivity and specificity of CEA determinations measured at different times*[a]

Measurement times	Sensitivity, %[b]	Specificity, %[c]
Preoperative CEA, $n=93$	42.8	81.9
Postoperative CEA, $n=181$	31.4	95.9
All CEA in patients apparently free of disease, $n=1{,}684$	45.0	93.4

[a] Levels 10 ng/ml were considered as normal.
[b] Sensitivity=(true positives/all diseased) × 100.
[c] Specificity=(true negatives/all health) × 100.

TABLE 4.—*Distribution of false-positive CEA values in patients who remained free of disease*

Parameter	No. of patients	No. of tests
Single elevated value	27	27
Chronic alcoholism	2	15
Short follow-up	4	11
Unexplained	12	132
Total	45	185

RESULTS

The 181 patients with postsurgical follow-up ranging from 6 to 64 months included 115 patients with Dukes stage B_2 colorectal cancers and 66 patients with Dukes stage C colorectal cancers. Of these, 35 patients (12 with B_2 cancers and 23 with C cancers) developed disease progression.

CEA levels obtained before surgery ($n=93$), after surgery ($n=181$), or at any time the patient was considered free of disease ($n=1{,}684$) were correlated with eventual disease progression (table 1).

According to these results, the predictive value of CEA determinations in patients apparently free of disease measured either within 3 weeks of surgery for cure or at any time during their follow-up is much more specific when the limit between normal and elevated is set at 10 ng/ml. This was the level chosen to calculate the sensitivity and specificity of the test (table 2).

The slope between preoperative and postoperative CEA levels as described by Staab et al. (*7*) was positive (rising) in 38 patients and negative (decreasing) in 54 patients (table 3).

Table 1 shows that there were 105 instances of normal CEA values in patients who eventually showed disease progression ("false-negative" values). These 105 tests belonged to 25 of the 35 patients who had disease recurrence. Of these 25 patients, CEA values remained consistently low in 7 patients and these values account for 47 negative tests. If an arbitrary time lag of 3 months is chosen as the minimum useful time by which CEA level elevations should precede the clinical and/or radiologic evidence of disease progression, another 14 tests would also qualify as false-negative. Conversely, 54 normal tests that occurred in patients who remained free of disease for at least the following 3 months should no longer be so considered. This correction improves the sensitivity of the test to 62.8 from 45.0%.

Also according to table 4, there were 185 instances of elevated CEA (>10 ng/ml) occurring in 45 patients who remained free of disease (false-positive values). Table 4 shows that in 27 cases this was an isolated CEA value in a

TABLE 3.—*Analysis of slopes between preoperative and postoperative CEA values*

Parameter	CEA levels		Slope[a]		
	No. decreasing	No. rising	Mean	SD	Range
Patients free of disease, $n=72$	43	29	−2.02	5.5[b]	−29.0 to +5.8
Patients who showed disease progression, $n=21$	12	9	+9.97	36.7[b]	−52.0 to +110.0
Total, $n=93$	55	38	0.70		−52.0 to +110.0

[a] Slope=(postoperative CEA−preoperative CEA)/time in mo.
[b] Unpaired t-value is 2.71, $P>0.01$.

sequence of normal ones. Two patients (accounting for 15 determinations) were suffering from hepatocellular disease due to chronic alcoholism, and in 4 cases (11 determinations) the follow-up was under 1 year (table 4).

DISCUSSION

The controversy over the potential usefulness of CEA testing has caused enough concern to assemble a panel of experts to discuss the issue (*1*), and although the panel's conclusions were favorable to the continued use of CEA plasma levels to monitor colorectal cancer patients, their recommendations are not very specific in that area.

A preoperative CEA level is most useful when assessed in conjunction with the postoperative one: High preoperative values that remain high for over 3 months after resection for cure probably indicate more advanced disease at the time of surgery and should be taken into consideration along with the preoperative value alone when one is randomizing patients to treatment protocols (*3*).

The calculation of the slope between preoperative and postoperative CEA levels showed a tendency for CEA levels to fall in those patients who remained free of disease and to rise in those patients who developed disease progression. The more abrupt rises belong to those patients whose CEA remained elevated and whose disease may have been understaged at diagnosis.

When only those patients who are seemingly free of disease are considered and 10 ng/ml is set as the limit between normal and elevated CEA levels, any particular individual test proved to be highly specific and of acceptable sensitivity. Sequential tests further increased the specificity by avoiding the error introduced by a single elevated level. Other conditions known to affect CEA levels must also be considered.

CEA testing also fulfills the other criteria for a good screening test: 1) The probability of recurrence or metastases in B_2 and C colorectal cancer patients is high, making this group a high-risk population and well worth screening. 2) In many cases the recurrences or metastases are amenable to further surgical treatment (*15, 16*). 3) CEA determination is a noninvasive test well accepted by the patients. 4) The cost of a CEA determination is only a fraction of that of liver scans and barium enemas.

In conclusion, and when the limitations of all screening tests are considered, determination of individual CEA levels in patients apparently free of disease is useful, but improvement in sensitivity can be obtained when sequential tests are considered. However, and as with many other clinical laboratory tests, CEA levels in individual patients must be given a probabilistic interpretation.

A definite assessment of CEA as a screening test in postoperative patients with colorectal cancer can be the result only of a randomized prospective trial, since the CEA values tend to affect patient management. However, it is doubtful if such a trial would now be acceptable on ethical grounds.

REFERENCES

(*1*) Consensus Development Conference. Carcinoembryonic antigen: Its role as a marker in the management of cancer. Summary of an NIH consensus statement. Br Med J 1981; 282:373–375.

(*2*) Koch M, McPherson TA, Morrish DW. Carcinoembryonic antigen: Three years experience in a cancer clinic. Can Med Assoc J 1977; 116:769–771.

(*3*) Goslin R, Steele G, MacIntyre J, et al. The use of preoperative plasma CEA levels for the stratification of patients after the curative resection of colorectal cancers. Ann Surg 1980; 192:747–751.

(*4*) Alsabti E. Carcinoembryonic antigen (CEA) as prognostic marker in colonic cancer. J Surg Oncol 1979; 12:127–129.

(*5*) Koch M, McPherson TA. Predictive value of plasma CEA in patients with colorectal carcinoma. J Surg Oncol 1979; 12:319–325.

(*6*) Lim CN, McPherson TA, McClelland AR, McCoy L, Koch M. Value of serial CEA determinations in a surgical adjuvant trial of colorectal and gastric carcinoma. J Surg Oncol 1980; 14:275–280.

(*7*) Staab HJ, Anderer FA, Stumph E, Fisher R. Slope analysis of the post-operative CEA time course and its possible application as an aid in diagnosis of disease progression in gastrointestinal cancer. Am J Surg 1978; 136:322–327.

(*8*) Moertel CG, Schutt AJ, Go VL. Carcinoembryonic antigen test for recurrent colorectal carcinoma. JAMA 1978; 239:1065–1066.

(*9*) Mariani G, Carmellini M, Bonaguidi F, Benelli MA, Toni MG. Serum CEA monitoring in the follow-up of colorectal cancer patients with negative preoperative serum CEA. Eur J Cancer 1980; 16:1099–1104.

(*10*) Möschl P, Staritz C, Keiler A, Kreuzer W, Faschino W. Das karzinoembryonale Antigen als Screeningprotein in der Nachkontrolle chirurgisch behandelter Patienten mit gastrointestinalem Karzinom. Wien Klin Wochenschr 1980; 92:128–130.

(*11*) Grant JA. Quantitative evaluation of a screening program. Am J Public Health 1974; 64:66–71.

(*12*) Cass AW, Million RR, Pfaff WW. Patterns of recurrence following surgery alone for adenocarcinoma of the colon and rectum. Cancer 1976; 37:2861–2865.

(*13*) Hansen HJ, Snyder JJ, Miller E, et al. Carcinoembryonic antigen (CEA) assay. A laboratory adjunct in the diagnosis and management of cancer. Hum Pathol 1974; 5:139–147.

(*14*) McPherson TA, Coates JE, Koch M. Evaluation of a direct radioimmunoassay for carcinoembryonic antigen. Clin Biochem 1978; 11:169–171.

(*15*) Martin EW, James KK, Hurtubise PE, Catalano P, Minton JP. The use of CEA as an early indication for gastrointestinal tumor recurrence and second look procedures. Cancer 1977; 39:440–446.

(*16*) Attiyeh FF, Stearns MW. Second look laparotomy based on CEA elevations in colorectal cancer. Cancer 1981; 47:2119–2125.

blank page

Interaction of Familial and Hormonal Risk Factors for Breast Cancer[1]

Louise A. Brinton,[2,3] Robert Hoover,[2] *and* Joseph F. Fraumeni, Jr.[2]

ABSTRACT—A case–control study, conducted among participants in the Breast Cancer Detection Demonstration Project, obtained detailed information on family history of breast cancer and other risk factors from 1,362 breast cancer patients and 1,250 control subjects. An affected first-degree relative was reported by 22.4% of the patients and 12.2% of the control subjects. This finding was associated with a twofold increased risk of breast cancer, although greater elevations in risk were seen in younger study subjects and in those reporting both an affected mother and a sister. Analysis of other risk factors showed that, compared to women without a family history of breast cancer, control subjects with a family history of breast cancer tended to have early or late menarche, were older at first childbirth, and were younger at oophorectomy. In addition, the effect of family history on breast cancer risk was modified by age at menarche, but not by age at first birth or type of menopause. These findings suggest that familial susceptibility to breast cancer may be mediated through hormonal factors that operate early in a woman's life. A synergistic relationship was also observed between family history of breast cancer and the occurrence of multiple biopsies for benign breast disease, although the mechanisms for this relationship remain to be elucidated.—JNCI 1982; 69:817–822.

The familial aggregation of breast cancer has been well established (*1–7*). However, apart from examining differential effects according to age at diagnosis and/or menopause status (*8–12*), few studies have assessed the interaction of familial susceptibility with other risk factors for breast cancer. Bain et al. (*13*) examined family history in relation to a variety of risk factors and found the effects most pronounced in women with younger ages at disease onset and in those who had menstruated for more than 35 years. However, this study included few older women and was not able to assess fully the effects of family history according to cessation of menstrual function. An understanding of how hormonally related factors interact with familial occurrence is of particular interest, given the strong relationship of ovarian function to breast cancer risk (*14*) and laboratory evidence suggesting that familial predisposition to breast cancer is mediated through hormonal mechanisms (*15–18*).

With the use of data collected from participants in the BCDDP, we had the opportunity to evaluate family history of breast cancer as a risk indicator in the presence and absence of a variety of hormonally related risk factors. This population was particularly amenable to the study of the effects of familial factors on breast cancer risk, since a relatively large proportion of the women who volunteered for the program had a family history of breast cancer.

METHODS

Study subjects were selected from the BCDDP, a multicenter breast cancer-screening program involving over 280,000 women at 29 widely dispersed centers. This program, jointly sponsored by the American Cancer Society and the National Cancer Institute, recruited women between 1973 and 1975 for a 5-year program of annual breast examinations by combined modalities of physical examination, mammography, and thermography. The present investigation used the case–control approach, with cases consisting of participants at 28 of the centers whose breast cancer was detected during the period July 1973 to May 1977. Control subjects were selected from participants who had not received a recommendation for biopsy or a biopsy during the course of the screening. These control subjects were chosen to be comparable to the cases on the following factors: screening center, race (white, black, oriental, other), age (same 5-yr group), time of entry (same 6-mo period), and length of continuation in the program (controls had to have had at least as many years of screening as comparable cases).

Home interviews were conducted by nurse interviewers who had been standardly trained. Completed interviews were obtained from 1,375 controls (74.2% of eligible subjects) and 1,552 cases (86.1%). The lower response rate for controls than for cases was primarily due to the fact that controls had moved and were unavailable for interviews (12.9% controls vs. 5.0% cases unavailable) and to their more frequent refusals to be interviewed (10.5% controls vs. 4.6% cases). In addition, 2.4% of the controls and 4.3% of the cases had died, and interviews were not attempted with proxy respondents. Women who were interviewed, however, did not differ significantly from those not interviewed with regard to a number of factors determined for each woman at entry to the BCDDP—including age, race, family income, and history of surgery for benign breast disease.

The cases were interviewed at various intervals after diagnosis. However, in the analyses, exposure information was truncated at the time of diagnosis for cases or the equivalent period for controls. A number of women (60 cases and 11 controls) reported a history of breast cancer prior to entering the BCDDP and were excluded from the present analysis. We also restricted this analysis to white subjects (who comprised 91% of the entire study population). The final study group consisted of 1,362 cases and 1,250 controls.

The measure of association used for the evaluation of effects of an exposure factor is the RR, as estimated by the

---

ABBREVIATIONS USED: BCDDP=Breast Cancer Detection Demonstration Project; CI=confidence interval; RR=relative risk(s).

---

[1] Received December 14, 1981; accepted May 5, 1982.

[2] Environmental Epidemiology Branch, Field Studies and Statistics Program, Division of Cancer Cause and Prevention, National Cancer Institute, National Institutes of Health, Public Health Service, U.S. Department of Health and Human Services, Bethesda, Md. 20205.

[3] *Address reprint requests to* Dr. Brinton, Environmental Epidemiology Branch, Landow Building, Room 3C06, National Institutes of Health, Bethesda, Md. 20205.

odds ratio. Confounding variables were evaluated by stratified techniques, with maximum likelihood estimates of combined ratios and 95% CI derived (*19*). For multiple levels of exposure, significance was assessed with the use of a one-tailed linear trend test (*20*). For assessment of the effects of interactions of variables, factors were cross-tabulated and risks computed in relation to women who did not possess either factor (i.e., the referent group). Interactive effects of factors were further assessed with the use of a disease probability (prospective) logistic model (*21*), which entered family history as an independent factor (exposure variable) and the potential interactive factor as both an independent variable and an interaction term, i.e., as both a confounding variable and an effect modifier. These interactive factors, as well as other potential confounding variables, were considered to contribute significantly to the model if the absolute value of the *T*-statistic was greater than 1.96.

RESULTS

Risks associated with having various relatives affected with breast cancer are shown in table 1. A history of breast cancer in a first-degree relative (mother, sister, or daughter) was reported by 304 patients (22.4%) as compared to 152 controls (12.2%). This resulted in an RR of 2.1 (95% CI: 1.7–2.6). Of the cases, 170 (12.5%) reported a mother and 159 (11.7%) a sister with breast cancer. The RR associated with having a mother with breast cancer was 2.1 (1.6–2.8), whereas the RR associated with having an affected sister was 2.3 (1.7–3.1). The estimate associated with having an affected sister was not confounded by women with breast cancer having more sisters than those without cancer. A small proportion of cases (2.1%) reported having both a mother and a sister affected, a condition associated with an excessively high risk (5.8; 95% CI: 2.5–13.5).

Information was also collected on history of breast cancer in paternal and maternal grandmothers. A substantial proportion of the subjects were unable to recall such information (21.2% unknown response for question regarding paternal grandmother and 13.2% for maternal grandmother). An unknown response initially appeared to be associated with significantly elevated risks; however, adjustment for history of breast cancer in a first-degree relative abolished this association. Analysis of provided information revealed nonsignificant risks associated with having affected grandmothers. The risks were similar for either ancestral line, with the RR being 1.3 (0.7–2.5) for a positive history in a paternal grandmother and 1.4 (0.9–2.4) in a maternal grandmother.

TABLE 1.—*RR associated with history of breast cancer in various first- and second-degree relatives*[a]

Family history of breast cancer	Cases	Controls	RR[b]	95% CI
None in first-degree relative	1,054	1,094	1.00	—
In first-degree relative	304	152	2.08	1.7–2.6
Mother	170	84	2.10	1.6–2.8
Sister	159	71	2.32	1.7–3.1
Mother or sister	301	150	2.08	1.7–2.6
Mother and sister	28	5	5.81	2.5–13.5
In paternal grandmother				
No	1,067	947	1.00	—
Yes	28	19	1.30	0.7–2.5
Unknown	273	280	0.84	0.7–1.0
In maternal grandmother				
No	1,126	1,059	1.00	—
Yes	48	28	1.44	0.9–2.4
Unknown	184	159	1.04	0.8–1.3

[a] Unknown responses with regard to breast cancer in first-degree relatives were excluded from the analysis.

[b] RR associated with family history in grandmothers were adjusted by family history in a first-degree relative.

TABLE 2.—*RR associated with breast cancer in a first-degree relative by age at diagnosis of study subjects*[a]

Age at diagnosis, yr	Cases	Controls	RR	95% CI
<40	11	3	5.26	1.4–20.5
40–44	20	11	1.87	0.8–4.1
45–49	46	28	1.54	0.9–2.6
50–54	70	34	2.08	1.3–3.2
55–59	54	25	2.23	1.3–3.7
≥60	103	51	2.21	1.5–3.2
Total (age-adjusted)	304	152	2.08	1.7–2.6

[a] Unknown responses with regard to breast cancer in first-degree relatives were excluded from the analysis.

TABLE 3.—*RR of breast cancer by characteristics of breast cancer in mother*[a]

Characteristics of breast cancer in mother	Cases	Controls	RR[b]	95% CI
No history in mother	1,167	1,156	1.00	—
Age at diagnosis, yr				
<50	31	22	1.39	0.8–2.5
≥50	127	59	2.13	1.5–3.0
Unknown	12	3	4.01	1.0–17.9
Bilaterality				
Bilateral	17	19	0.88	0.4–1.8
Unilateral	143	62	2.28	1.7–3.2
Unknown	10	3	3.29	0.8–15.1

[a] Unknown responses with regard to breast cancer in the mother were excluded from the analysis.

[b] RR were adjusted by age at diagnosis of study subjects.

Information on first-degree relatives was further examined according to age at diagnosis of the study subjects. The highest RR occurred among women whose breast cancer was diagnosed before the age of 40 (table 2). For these women, the RR was 5.3 (1.4–20.5). This excess derived primarily from patients having an affected mother. However, risks were also elevated for younger women who reported a sister with breast cancer.

The relationship of a maternal history of breast cancer was examined further according to age at onset of the mothers' breast cancer and to whether or not the disease was bilateral. Risks were dichotomized according to whether the mothers' disease was detected before or after age 50, an age selected because of its approximate correspondence with the onset of menopause. As seen in table 3, the RR was 1.4 for women whose mothers' disease was diagnosed prior to the age of 50 and 2.1 for women whose mothers' disease had a later onset. However, significantly more cases than controls were unable to provide information on their mothers' age at onset of breast cancer. A similar pattern of risk emerged when data on bilaterality were examined. Women whose mothers' disease was bilateral demonstrated no excess RR (0.9), whereas a significant excess RR (2.3) was associated with unilateral disease in the mother. An unknown response to whether the mother's disease was bilateral or not was also associated with a nonsignificant increase in risk (3.3). These same patterns of risk were seen in relation to characteristics of the mothers' breast cancer when analysis considered age and menopause status of the study subjects.

For assessment of possible confounding effects, correlations of familial occurrence with other breast cancer risk factors were examined among the control subjects (table 4). This analysis demonstrated that women with a family history of breast cancer in a first-degree relative had a different distribution of age at menarche than women without a family history; i.e., women with a family history tended to have either early or late menarche. In addition, those with a family history had a significantly later age at first live birth than those without affected relatives, as well as an earlier age at oophorectomy when this procedure was performed. The variable of age at oophorectomy, however, did not differ significantly between women with and without a family history of breast cancer. Other factors, including age, parity, number of miscarriages, menopause status, number of previous breast biopsies, weight, height, oral contraceptive use, menopausal estrogen use, and family income or education, did not differ between women with a family history of breast cancer and those without such a history.

TABLE 4.—*Distribution of selected breast cancer risk factors among control subjects by family history of breast cancer in a first-degree relative*[a]

Characteristics of control subjects	Family history of breast cancer[b] No.	Family history of breast cancer[b] Percent	No family history of breast cancer[c] No.	No family history of breast cancer[c] Percent
Age at menarche, yr				
<12	27	17.9	167	15.3
12	33	21.8	259	23.8
13	33	21.8	342	31.4
14	30	19.9	165	15.2
≥15	28	18.5	156	14.3
Chi-square test		χ^2_4=8.22 (P=0.08)		
Age at first live birth, yr				
Nulliparous	24	15.8	169	15.4
<20	14	9.2	132	12.1
20–24	43	28.3	419	38.3
25–29	51	33.6	278	25.4
≥30	20	13.2	96	8.8
Chi-square test		χ^2_4=10.65 (P=0.03)		
Menopause status				
Premenopausal	41	27.3	338	31.3
Ovaries retained	85	56.7	591	54.7
Ovaries removed	24	16.0	152	14.1
Chi-square test		χ^2_2=1.10 (P=0.58)		
Age at menopause–ovaries retained, yr				
<45	23	27.4	176	30.2
45–49	28	33.3	173	29.7
50–54	26	31.0	194	33.3
≥55	7	8.3	40	6.9
Chi-square test		χ^2_3=0.87 (P=0.83)		
Age at menopause–ovaries removed, yr				
<40	10	41.7	45	29.6
40–44	5	20.8	45	29.6
45–49	5	20.8	37	24.3
≥50	4	16.7	25	16.4
Chi-square test		χ^2_3=1.63 (P=0.65)		

[a] Unknown responses were excluded from the analysis.

[b] Total No.: 152.

[c] Total No.: 1,094.

TABLE 5.—*Breast cancer risk by history of breast cancer in a first degree relative and age at menarche*[a]

Family history of breast cancer	Age at menarche, yr	Cases	Controls	RR[b]	95% CI
No	<12	194	167	1.00	—
	12	255	259	0.85	0.6–1.1
	13	313	342	0.78	0.6–1.0
	≥14	280	321	0.74	0.6–0.9
Yes	<12	55	27	1.76	1.1–2.9
	12	73	33	1.89	1.2–3.0
	13	83	33	2.22	1.4–3.5
	≥14	89	58	1.34	0.9–2.0

[a] Unknown responses were excluded from the analysis.

[b] RR were adjusted by age at diagnosis of study subjects. χ_1 for linear trend: without family history=−2.23 (P=0.01) and with family history=−0.92 (P=0.18).

Because of the differences observed, risk estimates associated with having various relatives affected with breast cancer were adjusted for possible confounding effects of age at menarche, age at first live birth, and age at bilateral oophorectomy. Control for these factors did not substantially alter the risk estimates associated with a family history in any first-degree relative. In addition, use of multivariate models with simultaneous control for a number of factors did not alter the previously derived crude estimates associated with a family history of breast cancer or those associated with specific attributes of family history, such as bilaterality and young age at onset of mothers' breast cancer.

Further analysis pursued the effects of a family history in relation to the presence and absence of a variety of breast cancer risk factors.

Effects of varying ages at menarche according to the presence or absence of a family history of breast cancer are shown in table 5. There was a significant decreasing trend (P=0.01) in risk with increasing age at menarche among women without a family history. Although the lowest risk occurred in the oldest age at menarche grouping among those with a family history, there was no consistent or significant trend in the RR. In fact, prior to the last grouping, the RR actually increased with increasing ages at menarche.

In contrast to age at menarche, parity and age at first live birth showed similar effects in both the presence and absence of a family history of breast cancer (table 6). In both groups, there was evidence of increasing risk with later ages at first childbirth. For women without a history of breast cancer, the RR increased significantly (P<0.01) with increasing age at first birth. Women who delayed their first childbirth until 30 years of age or later showed a 2.7-fold increased risk compared to those who had their first child before the age of 20. Nulliparous women had risks similar to those who had their first childbirth between the ages of 25 and 29. (RR compared to RR of women with a live birth prior to age 20 were 1.8 and 2.0, respectively.) Among women with a family history of breast cancer, those with a birth after the age of 30 were at highest risk, five times (95% CI: 2.8–9.1) that of the referent group (women without a family history of breast cancer and who had their first childbirth prior to the age of 20).

Table 7 shows the RR associated with family history of breast cancer and history of biopsies for benign breast disease. Among those without a family history, risk increased slightly with the number of previous biopsies for benign breast disease. Those who reported two or more biopsies had a risk 1.5 times that of women without any previous biopsies. A similar increasing trend in risk with number of benign breast disease biopsies was seen for those with a family history of breast cancer. As compared to the referent group, those with a family history and no biopsies had a risk of 2.0, those with one biopsy had a risk of 2.3, and those with two or more biopsies had a risk of 5.6.

The examination of risks according to menopause status is presented in table 8. In this analysis, it was necessary to adjust estimates among the menopausal woman by age at menopause and by hormone usage, since these variables acted as negative confounders. Women with a family history of breast cancer who had undergone a bilateral oophorectomy demonstrated an RR of 1.8 compared to nonfamilial subjects with other types of menopause (the referent group). Risks among those with a family history were similar to those among the other menopause groups, with the RR being 2.6 for premenopausal subjects and 2.2 for those who retained their ovaries during surgical menopause. Women who had a bilateral oophorectomy but no family history of breast cancer were at a slightly lower risk (0.8) than those with other types of menopause.

TABLE 6.—*Breast cancer risk by history of breast cancer in a first-degree relative and age at first live birth*[a]

Family history of breast cancer	Age at first live birth, yr	Cases	Controls	RR[b]	95% CI
No	<20	78	132	1.00	—
	20–24	337	419	1.34	0.9–1.8
	25–29	320	278	1.96	1.4–2.7
	≥30	151	96	2.66	1.8–3.9
	Nulliparous	166	169	1.77	1.2–2.6
Yes	<20	20	14	2.41	1.2–5.0
	20–24	99	43	3.79	2.4–5.9
	25–29	78	51	2.65	1.7–4.2
	≥30	54	20	5.04	2.8–9.1
	Nulliparous	51	24	3.82	2.1–6.8

[a] Unknown responses were excluded from the analysis.

[b] RR were adjusted by age at diagnosis of study subjects. χ_1 for linear trend: Without family history=6.13 ($P<0.01$) (nulliparas excluded) and with family history=0.62 ($P=0.27$).

TABLE 7.—*Breast cancer risk by history of breast cancer in a first-degree relative and number of previous biopsies for benign breast disease*[a]

Family history of breast cancer	Previous biopsies for benign breast disease	Cases	Controls	RR[b]	95% CI
No	None	815	887	1.00	—
	1	159	149	1.16	0.9–1.5
	≥2	80	58	1.49	1.0–2.1
Yes	None	230	126	1.98	1.6–2.5
	1	43	20	2.32	1.4–3.9
	≥2	31	6	5.63	2.6–12.3

[a] Unknown responses were excluded from the analysis.

[b] RR were adjusted by age at diagnosis of study subjects. χ_1 for linear trend: Without family history=2.42 ($P=0.01$) and with family history=2.04 ($P=0.02$).

TABLE 8.—*Breast cancer risk by history of breast cancer in a first-degree relative and menopause status*[a]

Family history of breast cancer	Menopause status	Cases	Controls	RR[b]	95% CI
No	Ovaries retained	539	583	1.00	—
	Ovaries removed	115	152	0.81	0.6–1.1
	Premenopausal	371	338	1.30	0.9–1.7
Yes	Ovaries retained	165	84	2.15	1.6–2.8
	Ovaries removed	43	24	1.90	1.1–3.2
	Premenopausal	87	41	2.62	1.7–4.0

[a] Unknowa responses were excluded from the analysis.

[b] RR for premenopausal women were adjusted by age at diagnosis of study subjects; RR for menopausal women were adjusted by age at menopause and menopausal hormone usage.

Logistic analyses were also conducted to examine interactive effects of family history with other breast cancer risk factors. These analyses, which controlled for the influence of confounding variables on interactive effects, showed findings in close concordance with stratified analyses, i.e., no clear interaction with age at first live birth or menopause status, but an interaction of family history with multiple previous benign breast disease biopsies (RR=4.0). In addition, differential effects of age at menarche were seen according to the presence or absence of a family history of breast cancer.

DISCUSSION

In this study, we found that women who reported to have either a mother or a sister with breast cancer experienced approximately a twofold excess risk of breast cancer, an estimate that agrees with estimates given in previous reports (*2, 10–13*). Our estimates are somewhat lower than those previously derived in a study of BCDDP participants (*22*), possibly as a result of different data collection techniques (mailed questionnaire in previous study vs. home interview in this study). In the present investigation, women who reported both a mother and a sister with breast cancer had an especially high risk, and the effects of family history were greatest for women under age 40 at diagnosis. These findings are also consistent with previous observations (*9, 10, 13*). Women whose mothers had bilateral disease and/or disease at premenopausal ages were not at high risk, a finding for which we have no ready explanation. Our findings may be influenced by the higher proportion of cases than controls who were unable to provide information on the bilaterality of their mothers' breast cancer or on the age of their mothers at diagnosis.

The analysis of interactions between family history of breast cancer and other breast cancer risk factors seemed to be a useful approach toward the understanding of the mechanisms of breast carcinogenesis, since those factors that modify the effects of family history may act through common pathways. Also, since family history is likely to reflect genetic determinants, whereas other factors arise at different times in a woman's life, there was a potential for discernment of periods when familial effects tend to operate.

We observed no modification of the effects of parity, age at first live birth, or age at oophorectomy according to the presence of a family history of breast cancer. For all of these factors, effects among women with a family history were those that would have been predicted on a basis of additivity of RR; i.e., there was no evidence of any multiplicative effects or synergy. For example, additivity would have predicted that women with bilateral oophorectomy and a family history of breast cancer would exhibit a risk approximately 96% greater than that of other menopausal women without a family history; in fact, we actually observed a 90% elevation in risk. However, the effect of age at menarche seemed to be modified by a family history of breast cancer. Among women without a family history, we observed a significant linear trend of decreasing risk with increasing age at menarche, a result consistent with the pattern generally seen in studies that have examined menarche effects without reference to family history (*14*, *23*). This effect, however, was not observed in the presence of a family history. Although this difference could be due to chance, we think it may reflect some biologic interaction, since there was some evidence that risk actually rose with increasing age at menarche up to age 14.

Taken together, our findings suggest that the familial predisposition to breast cancer exerts an influence early in a woman's life. This speculation is based on the observation that familial effects were not modified by age at first live birth or oophorectomy but were modified by age at menarche. In addition, we believe that the effect is probably mediated through a hormonal mechanism, rather than a structural defect in breast tissue. This impression is supported by the observation that control subjects with a family history of breast cancer tended to have early or late menarche, a late first childbirth and a young age at oophorectomy compared to controls without such a family history.

Laboratory studies of high-risk women support the notion that familial predisposition may be mediated through hormonal mechanisms in early reproductive life. Alterations of hormonal profiles have been described among daughters (*24-26*) and among younger rather than older sisters (*27*) of women with breast cancer. This idea is also consistent with the view that breast cancer risk factors can operate at different periods in women's lives (*14*)—in this case, early in reproductive life rather than later in life.

Of special interest was the interaction observed between a history of surgery for benign breast disease and familial occurrence of breast cancer. Among women with and without a family history of breast cancer, a history of only one biopsy was a weak risk indicator; this is consistent with a previous study of BCDDP participants and may reflect the self-selection of women into this screening program (*22*). Women with two or more biopsies, however, were at excess risk: Those without a family history exhibited a 1.5-fold excess risk, whereas those with a family history had a risk of 5.6. The RR of 5.6 is greater than the product achieved by the multiplication of the RR of the individual risk factors: family history in the absence of breast surgery (2.0) and multiple biopsies in the absence of family history (1.5). This synergy seems to imply a common mechanistic pathway of carcinogenesis involved with a family history of breast cancer and with multiple surgeries for benign breast disease.

Thus we conclude that the familial excess of breast cancer is established by early adolescence and is uninfluenced by protective factors introduced later. In addition, although more speculative, the evidence also seems to imply that these familial effects are mediated through a hormonal mechanism. Although there is previous support for this hypothesis, further studies are needed that specifically address the issue. Further assessment and elucidation of mechanisms are also needed for the synergy that we observed between a family history of breast cancer and the occurrence of multiple benign breast disease biopsies.

REFERENCES

(*1*) Penrose LS, MacKenzie HJ, Karn MN. A genetical study of human mammary cancer. Br J Cancer 1948; 2:168-176.

(*2*) Macklin MT. Comparison of the number of breast cancer deaths observed in relatives of breast-cancer patients and the number expected on the basis of mortality rates. J Natl Cancer Inst 1959; 22:927-951.

(*3*) Lilienfeld AM. The epidemiology of breast cancer. Cancer Res 1963; 23:1503-1513.

(*4*) Tokuhata GK. Morbidity and mortality among offspring of breast cancer mothers. Am J Epidemiol 1969; 89:139-153.

(*5*) Lynch HT, Guirgis H, Albert S, Brennan M. Familial breast cancer in a normal population. Cancer 1974; 34:2080-2086.

(*6*) Morgan RW, Vakil DV, Chipman ML. Breast feeding, family history, and breast disease. Am J Epidemiol 1974; 99:117-122.

(*7*) Petrakis NL. Genetic factors in the etiology of breast cancer. Cancer 1977; 39:2709-2715.

(*8*) Anderson DE. A genetic study of breast cancer. J Natl Cancer Inst 1972; 48:1029-1034.

(*9*) ———. Genetic study of breast cancer. Identification of a high risk group. Cancer 1974; 34:1090-1097.

(*10*) Henderson BE, Powell D, Rosario I, et al. An epidemiologic study of breast cancer. J Natl Cancer Inst 1974; 53:609-614.

(*11*) Adami HO, Hansen J, Jung B, Rimsten A. Familiality in breast cancer: A case-control study in a Swedish population. Br J Cancer 1980; 42:71-77.

(*12*) Paffenbarger RS, Kampert JB, Chang H. Characteristics that predict risk of breast cancer before and after the menopause. Am J Epidemiol 1980; 112:258-268.

(*13*) Bain C, Speizer FE, Rosner B, Belanger C, Hennekens CH. Family history of breast cancer as a risk indicator for the disease. Am J Epidemiol 1980; 111:301-308.

(*14*) MacMahon B, Cole P, Brown J. Etiology of human breast cancer: A review. J Natl Cancer Inst 1973; 50:21-42.

(*15*) Kwa HG, Cleton F, de Jong-Bakker M, Bulbrook RD, Hayward JL, Wang DY. Plasma prolactin and its relationship to risk factors in human breast cancer. Int J Cancer 1976; 17:441-447.

(*16*) Henderson BE, Pike MC, Gerkins VR, Casagrande JT. The hormonal basis of breast cancer: Elevated plasma levels of estrogen, prolactin, and progesterone. In: Hiatt HH, Watson JD, Winston JA, eds. Origins of human cancer. Cold Spring Harbor, N.Y.: Cold Spring Harbor Laboratory, 1977:77-86.

(*17*) Bulbrook RD, Moore JW, Clark GM, et al. Plasma oestradiol and progesterone levels in women with varying degrees of risk of breast cancer. Eur J Cancer 1978; 14:1369-1375.

(*18*) Fishman J, Fukushima DK, O'Connor J, Lynch HT. Low urinary estrogen glucuronides in women at risk for familial breast cancer. Science 1979; 204:1089-1091.

(*19*) Gart JJ. Point and interval estimation of the common odds ratio in the combination of 2×2 tables with fixed marginals. Biometrika 1970; 57:471–475.

(20) Mantel N. Chi-square tests with one degree of freedom, extensions of the Mantel-Haenszel procedure. J Am Stat Assoc 1963; 58:690–700.

(21) Breslow N, Powers W. Are there two logistic regressions for retrospective studies? Biometrics 1978; 34:100–105.

(22) Brinton LA, Williams RR, Hoover RN, Stegens NL, Feinleib M, Fraumeni JF Jr. Breast cancer risk factors among screening program participants. JNCI 1979; 62:37–44.

(23) Staszewski J. Age at menarche and breast cancer. J Natl Cancer Inst 1971; 47:935–940.

(24) Henderson BE, Gerkins V, Rosario I, Casagrande J, Pike MC. Elevated serum levels of estrogen and prolactin in daughters of patients with breast cancer. N Engl J Med 1975; 293:790–795.

(25) Pike MC, Casagrande JT, Brown JB, Gerkins V, Henderson BE. Comparison of urinary and plasma hormone levels in daughters of breast cancer patients and controls. J Natl Cancer Inst 1977; 59:1351–1355.

(26) Trichopoulos D, Brown, JB, Garas J, Papaioannou A, MacMahon B. Elevated urine estrogen and pregnanediol levels in daughters of breast cancer patients. JNCI 1981; 67:603–606.

(27) Bulbrook RD. Endocrine, genetic and viral factors in the etiology of breast cancer. Proc R Soc Med 1972; 65:646–648.

Imaging of Human Melanoma Xenografts in Nude Mice With a Radiolabeled Monoclonal Antibody[1,2,3]

Tarun Ghose,[4] Soldano Ferrone,[5] Kohzoh Imai,[5] Stevens T. Norvell, Jr.,[6] Steven J. Luner,[4] Robert H. Martin,[7] *and* A. Huntley Blair[8,9]

ABSTRACT—External photoscanning with display of radioactivity data as a color-scaled image detected xenografts of human melanoma in male nude inbred mice of BALB/c background 48 hours after injection of ^{131}I-labeled monoclonal IgG 225.28S that is specific for human melanoma. A ^{131}I-labeled polyclonal goat IgG against human melanoma-associated antigens could also image the tumor, but with this preparation there was considerable localization of radioactivity in normal tissues, resulting in less satisfactory tumor definition. Labeled normal mouse IgG did not image the melanoma grafts. Assay of radioactivity in tissues of melanoma-grafted mice confirmed tumor-specific localization of the antimelanoma antibodies. The tumor:blood ratio of radioactivity was 6.55 with the monoclonal antimelanoma IgG and 0.45 with the polyclonal IgG.—JNCI 1981; 69:823–826.

We have successfully imaged several mouse and human tumors including human malignant melanomas and renal cell carcinomas by using ^{131}I-labeled polyclonal IgG from rabbit and goat antisera rendered specific against tumor-associated antigens by repeated absorptions with appropriate normal tissues (*1–5*). There is considerable loss of specific antibodies during absorptions, and a proportion of immunoglobulins without tumor specificity persists in absorbed antisera and even in the IgG fraction therefrom after its further purification by affinity techniques (*6–8*). Radiolabeled non-tumor-specific IgG molecules in imaging preparations contribute to high background activity that obscures small lesions and lesions with low uptake of the agent. One approach to overcoming this problem has been the application of subtraction methodology, i.e., injection of radiolabeled non-tumor-specific serum proteins (or other radiopharmaceuticals that measure blood volume) and then subtraction of the radioactivity contributed by the nonspecific agent from that of the specific antibody (*8*). However, it should be possible to substantially overcome this limitation of polyclonal antibody by use of the monoclonal antibodies against membrane-associated antigen(s), since such antibodies are homogeneous and can be obtained free from contaminating nonspecific immunoglobulin molecules (*9*). In this study we have investigated the monoclonal antibody 225.28S against human melanoma-associated antigens for imaging xenografts of human melanoma in nude mice and have compared its efficiency with that of a polyclonal antimelanoma IgG preparation derived from immune goat serum rendered specific by repeated absorptions with normal human tissues (*10, 11*).

MATERIALS AND METHODS

Tumors and cell lines.—For localization studies, the human melanoma cell line M1, obtained from Dr. P. B. Dent, McMaster University, Hamilton, Ontario, Canada, was xenografted sc (10^6 cells/mouse) into the flank of 8-week-old male nude inbred mice of BALB/c background (Harlan Sprague-Dawley, Inc., Madison, Wis.). The tumors were 1.8–2 cm in diameter at the commencement of scanning. Five other human melanoma cell lines, 4 human renal adenocarcinoma lines, HeLa cells, and human foreskin fibroblasts were maintained in RPMI-1640 supplemented with 10% fetal calf serum.

Monoclonal antibody 225.28S and goat anti-human melanoma sera.—The monoclonal antibody 225.28S, an IgG2a, is secreted by a hybridoma constructed with splenocytes from a BALB/c mouse immunized with cultured human melanoma M21 cells. Testing of this antibody with a large variety of tumor cell lines and of surgically removed normal and malignant tissues by ourselves and several other investigators (*12*) has shown that this antibody recognizes a determinant preferentially expressed on melanoma and nevi cells (*13*).

Details of production and serologic analysis of the specificity of goat anti-human melanoma IgG have been described elsewhere (*10, 11*). Viable malignant melanoma cells, 4×10^6, from fresh, surgically excised specimens, mixed with 2 ml of Freund's complete adjuvant (Difco Laboratories, Detroit, Mich.) were injected im into adult goats. Eleven subsequent injections of tumor cells were given without Freund's adjuvant. Immune sera were heat inactivated and repeatedly absorbed with group AB, Rh^+ red blood cells and homogenates of normal human liver, lung, kidney, and spleen. The absorptions were repeated until the sera would react only with the immunizing melanoma cells and not with the patient's normal skin fibroblasts, peripheral blood lymphocytes, or other normal adult human tissues. These xenogeneic antimelanoma sera have been shown to

---

ABBREVIATIONS USED: NMG=normal mouse IgG; PBS=0.01 *M* sodium phosphate (pH 7.1) containing 0.145 *M* sodium chloride.

---

[1] Received December 31, 1981; accepted May 20, 1982.

[2] Supported by grants from the Medical Research Council and the Kidney Foundation of Canada and by Public Health Service grants CA-24239 and CA-16069 from the National Cancer Institute.

[3] The animals used in this research were maintained under conditions promulgated by the Canadian Council for Animal Care.

[4] Department of Pathology, Dalhousie University, Halifax, Nova Scotia, Canada B3H 4H7.

[5] Department of Pathology, College of Physicians and Surgeons, Columbia University, New York, N.Y. 10032.

[6] Department of Surgery, Dalhousie University.

[7] Department of Diagnostic Radiology and Nuclear Medicine, Dalhousie University.

[8] Department of Biochemistry, Dalhousie University.

[9] We are grateful to Ms. M. Mammen and Mr. D. Sadi for technical assistance.

cross-react with surface and cytoplasmic antigens of melanoma cells from several patients (*10*).

Immunofluorescence assay.—Cytoplasmic immunofluorescence was performed either on 5-μm cryostat sections of snap-frozen (−176°C) human and mouse tissues or on smears of acetone-fixed tumor cells. The sandwich method with rabbit antigoat 7S globulin or rabbit antimouse 7S globulin both labeled with fluorescein was used with appropriate controls. Membrane immunofluorescence was performed on viable cells with appropriate conjugate and normal serum controls (*10, 11*).

^{125}I-labeled protein A assay.—Aliquots of 5×10^5 melanoma cells, human neonatal fibroblasts or HeLa cells, were first incubated with 250 μg of monoclonal IgG for 30 minutes at 37°C, washed with PBS, and then incubated with ^{125}I-labeled protein A (21,000 cpm; New England Nuclear Corp., Boston, Mass.). For blocking experiments, suspensions of melanoma cells were first exposed to 250 μg, 500 μg, 1 mg, or 2 mg of goat antimelanoma IgG (which does not bind protein A) and then sequentially to 250 μg monoclonal IgG and ^{125}I-labeled protein A.

Preparation of labeled immunoglobulins, scanning, and assay of radioactivity.—We obtained NMG and goat IgG fractions by using protein A Sepharose and Sephadex G200 [Pharmacia (Canada) Ltd., Dorval, Quebec] chromatography, respectively. We labeled monoclonal IgG 225.28S, goat antimelanoma IgG, and NMG with carrier-free and reductant-free ^{131}I (New England Nuclear Corp.) by the chloramine T method (*14*) to yield approximately 1 μCi of ^{131}I bound to 3 μg of each IgG. The same method was used to bind 1 μCi ^{125}I (New England Nuclear Corp.) to 15 μg NMG.

For scanning experiments, melanoma-bearing mice in groups of 4 were each given iv injections of 150 μg (50 μCi) of ^{131}I-labeled monoclonal antimelanoma IgG, goat antimelanoma IgG, or NMG. For paired label studies, animals received injections of a mixture containing 150 μg each of ^{131}I-labeled monoclonal IgG and ^{125}I-labeled NMG. In all cases, mice were given Lugol's iodine in drinking water, starting 3 days before administration of the scanning agent. Animals under sodium pentobarbital anesthesia (35 mg/kg, ip) were scanned every 24 hours with a Nuclear Chicago Pho-Dot rectilinear scanner and a large-field-of-view scintillation camera interfaced to a PDP 11/34 computer.

For assay of radioactivity in tissues, groups of 3 melanoma-bearing mice were killed 6 days after iv injections of 150 μg of ^{131}I-labeled monoclonal antimelanoma IgG, goat antimelanoma IgG, or NMG. A 0.5-ml sample of blood was obtained by cardiac puncture from each anesthetized mouse. The axillary vessels were then severed and blood was flushed out of the organs by injection of 50 ml of warm PBS into the heart (*5*). Aliquots of tissue were washed in PBS, blotted dry, weighed, and individually digested in concentrated sulfuric acid. We determined radioactivity in duplicate aliquots by using at least 2 different dilutions of each tissue digest. In analysis of tissues from the mice given both ^{131}I- and ^{125}I-labeled IgG, appropriate windows were used for separate assays of ^{131}I and ^{125}I activities, corrections being made for the counts contributed by ^{125}I to the ^{131}I window. We assayed ^{125}I activity in these digests after allowing ^{131}I activity to decay for 50 days (≈6 half-lives).

RESULTS

Establishment of Antibody Specificity by Immunofluorescence Assay

The monoclonal IgG 225.28S and goat anti-human melanoma IgG reacted on indirect immunofluorescence with 5 human melanoma lines in long-term culture and with viable melanoma cells isolated from biopsy specimens obtained from 8 patients. Both types of antibodies were shown not to react with murine melanoma B16 cells, peripheral blood lymphocytes from melanoma patients, human neonatal foreskin fibroblasts, HeLa cells, four human renal carcinoma cell lines in long-term culture, and cryostat sections of the following adult humans tissues: skin, breast, brain, lung, liver, pancreas, large and small intestines, spleen, heart, kidney, bladder, and prostate glands.

Antibody Specificity by ^{125}I-Labeled Protein A Assay

Melanoma cells, exposed first to the monoclonal IgG and then to ^{125}I-labeled protein A, bound 30% of the protein A activity, whereas similarly exposed HeLa cells and human neonatal fibroblasts bound 10% of the protein A activity. The goat antimelanoma IgG or sera from mice bearing grafts of human melanoma did not interfere with the binding of monoclonal IgG to the M1 melanoma cells.

Scanning and Assay of Radioactivity

External scanning at 48 hours visualized the melanoma grafts in all tumor-bearing mice given either the labeled monoclonal IgG or goat antimelanoma IgG, particularly when scintigraphic data were displayed as linear color-scaled television images (fig. 1). Tumors were less distinct in the mice given ^{131}I-labeled goat antimelanoma IgG than in mice given monoclonal antimelanoma IgG, a finding consistent with the lower tumor:blood ratio of radioactivity in the former group (table 1). Tumors could not be visualized in the mice given ^{131}I-labeled NMG. Scanning at 24 hours after administration of ^{131}I-labeled 225.28S IgG showed substantial amounts of radioactivity in the thoracic cavity, liver, and spleen, resulting in variable tumor delineation from mouse to mouse at this time.

The results of assay of radioactivity in tissues of mice killed 6 days after injection of radiolabeled antibodies and NMG are presented in table 1. The mice given ^{131}I-labeled monoclonal antimelanoma IgG showed higher localization of radioactivity in the tumor than in all other tissues including blood (tumor:blood ratio=6.55). Animals given the goat polyclonal antimelanoma IgG showed higher localization in the tumor than in all other tissues except blood (tumor:blood ratio=0.45). Administration of ^{131}I-labeled NMG led to uniformly lower tumor:nontumor tissue ratios of radioactivity than those obtained with either ^{131}I-labeled monoclonal or polyclonal antimelanoma IgG. However, even NMG showed more localization in tumor than in normal tissues, with the exceptions of liver and blood.

In a separate experiment, melanoma-bearing mice were given a mixture of ^{131}I-labeled monoclonal antimelanoma IgG and ^{125}I-labeled NMG. Tumor:blood ratios of radioac-

TABLE 1.—*Melanoma:mouse tissue ratios of radioactivity in xenografted nude mice 6 days after injection of* ^{131}*I-labeled IgG*[a]

Tissue	Monoclonal IgG2a 225.28S against melanoma-associated antigen	Goat polyclonal anti-human melanoma IgG	NMG
Normal muscle adjacent to tumor	7.20	6.22	4.27
Heart muscle	13.54	9.69	3.89
Kidneys	4.10	8.24	1.70
Lungs	16.04	9.27	8.69
Spleen	4.21	5.80	2.37
Bone marrow	8.48	4.26	3.59
Liver	2.63	2.93	0.48
Blood	6.55	0.45	0.35

[a] Human melanoma-bearing nude mice weighing 18–22 g received iv injections of 50 μCi ^{131}I bound to 150 μg monoclonal anti-human melanoma IgG, goat anti-human melanoma IgG, or NMG. Each group contained 3 mice that were killed 6 days after receiving labeled IgG. Tumor weight at killing varied from 1.2 to 1.6 g. Ratios were calculated as follows: (μCi/g tumor tissue)/(μCi/g specified tissue).

tivity (2 mice/group) at 24 hours were 0.32 for ^{131}I and 0.28 for ^{125}I; at 48 hours the respective ratios were 1.2 and 0.3. Thus at 48 hours ^{131}I accumulated to a greater extent in tumor tissue than in blood but ^{125}I failed to do so.

DISCUSSION

This study shows for the first time that radiolabeled monoclonal antibody 225.28S against a human melanoma-associated antigen can efficiently image melanoma grafts in nude mice. Although goat antimelanoma IgG also imaged these grafts as expected, the tumor:blood ratio of radioactivity was much lower with this polyclonal antibody. The failure of the goat antimelanoma IgG to block binding of the monoclonal IgG to M1 melanoma cells suggests that these two antibodies have different antigenic specificities. However, since the polyclonal preparation is likely to include multiple specificities, the presence in it of a small amount of IgG directed toward the same determinant as the monoclonal IgG cannot be ruled out.

Table 1 shows that all tumor:normal tissue ratios (radioactivity per gram of tumor tissue/radioactivity per gram of normal tissue) for both antibodies were greater than the corresponding ratios of NMG. A comparison between the groups given monoclonal and polyclonal antibodies shows that the tumor:blood ratio of ^{131}I activity achieved with the polyclonal IgG was fifteenfold lower than the corresponding ratio for monoclonal IgG even though the goat IgG as a foreign protein would be expected to have the shorter half-life in the circulation. Furthermore, the tumor:normal tissue ratios of localization of the monoclonal IgG were generally greater than those of the polyclonal IgG, the chief exception being the greater amounts of ^{131}I activity in kidneys of mice given the monoclonal IgG (table 1). These differences may reflect greater serum clearance of non-tumor-bound ^{131}I through the kidneys in mice given the labeled monoclonal IgG. It is unlikely that rapid clearance resulted from formation of immune complexes, since antigens reacting with the monoclonal antibody could not be detected in sera of human melanoma-bearing nude mice. Evidence suggests that the slow clearance of labeled polyclonal IgG rendered tumor-specific solely by absorptions with normal tissues may reflect the persistence in these preparations of contaminating antibodies that cross-react and bind to normal mouse tissues (more radioactivity being found in muscle, lungs, and bone marrow of mice given ^{131}I-labeled polyclonal goat globulin than in the same organs of mice given ^{131}I-labeled NMG). The tumor:normal tissue radioactivity ratios after injection of polyclonal antimelanoma IgG were lower than those after injection of the monoclonal IgG. Also, previous studies (*5*) have shown that further purification of normal tissue absorbed polyclonal antitumor IgG by absorption and elution with the use of glutaraldehyde-fixed tumor cells reduces localization in normal tissues and accelerates the serum clearance of these purified IgG preparations. Contaminating antibodies (against normal tissue components) in amounts not manifestly toxic can give rise to background radioactivity in nonneoplastic tissues after systemic administration of preparations that have been radiolabeled. When such antibody preparations are used as carriers of cytotoxic drugs, these amounts of antinormal tissue antibodies may contribute to the systemic toxicity of conjugates (*15*).

The tumor:normal tissue and tumor:blood ratios of radioactivity were higher for both antimelanoma IgG preparations than for NMG. Results at 48 hours of the paired labeled experiment comparing monoclonal antimelanoma IgG and NMG also demonstrated the increased tumor-localizing potential of the monoclonal antimelanoma IgG. These findings are in keeping with the observation that only labeled antibody preparations could produce sufficient contrast for successful imaging. Thus the presence of specific antimelanoma antibody was clearly essential for imaging, but imaging may well have been aided by nonspecific tumor localization of radioiodinated immunoglobulin that was not bound to target tumor antigen. Increased localization of normal serum proteins in tumor tissue has been reported before by our laboratory (*16*) and by Peterson (*17*).

The best image was provided by the monoclonal IgG at all scanning times, and this finding correlates with the observed tumor:normal tissue radioactivity ratios. The tumor:adjacent muscle ratio was somewhat higher for the monoclonal IgG than for the polyclonal IgG, but the most dramatic difference between these two was observed on comparison of tumor:blood ratios. A ratio of 6.55 was obtained for the monoclonal IgG but only 0.45 for the polyclonal IgG and 0.35 for NMG, showing the importance of elimination of irrelevant IgG molecules. Before this report, in vivo preferential localization of injected monoclonal antibodies in target antigen-bearing normal tissues or tumor tissues was reported by several groups (*9, 18–20*). High tumor:blood ratios of localization, comparable to those we observed in melanoma-grafted mice given the monoclonal IgG, were seen after injections of radioiodine-labeled monoclonal antitumor antibody in MH15 teratocarcinoma-bearing BALB/c mice (*9*) and in immunosuppressed CBA mice bearing a human teratocarcinoma (*20*). Monoclonal antibodies against tumor-associated antigens may thus provide us with specific carriers for radioimmunodetection of primary and metastatic cancers.

REFERENCES

(1) Ghose T, Tai J, Aquino J, Guclu A, Norvell ST, MacDonald AS. Tumor localization of 131-I-labeled antibodies by radionuclide imaging. Radiology 1975; 116:445–448.

(2) Ghose T, Guclu A, Tai J, MacDonald AS, Novell ST, Aquino J. Antibody as carrier of ^{131}I in cancer diagnosis and treatment. Cancer 1975; 36:1646–1657.

(3) Belitsky P, Ghose T, Aquino J, Norvell ST, Blair AH. Radionuclide imaging of primary renal cell carcinoma by ^{131}I-labelled antitumor antibody. J Nucl Med 1978; 19:427–430.

(4) Belitsky P, Ghose T, Aquino J, Tai J, MacDonald AS. Radionuclide imaging of metastases in renal cell carcinoma patients by ^{131}I-labelled antitumor antibody. Radiology 1978; 126:515–517.

(5) Ghose T, Norvell ST, Aquino J, et al. Localization of ^{131}I-labeled antibodies in human renal cell carcinoma and a mouse hepatoma: Correlation with tumor detection by photoscanning. Cancer Res 1980; 40:3018–3031.

(6) Ghose T, Tai J, Norvell ST, Guclu A, MacDonald AS. Antibodies as carriers of radionuclides and cytotoxic drugs in the treatment and diagnosis of cancer. Ann NY Acad Sci 1976; 277:671–689.

(7) Guclu A, Tai J, Ghose T. Endocytosis of chlorambucil bound antitumor globulin following "capping" in EL4 lymphoma cells. Immunol Commun 1975; 4:229–242.

(8) Goldenberg DM, Deland F, Kim E, et al. Use of radiolabeled antibodies to carcinoembryonic antigen for the detection and localization of diverse cancers by external photoscanning. N Engl J Med 1978; 298:1384–1388.

(9) Ballou B, Levine G, Hakala TR, Solter D. Tumor location detected with radioactivity labeled monoclonal antibody and external scintigraphy. Science 1979; 206:844–847.

(10) Ghose T, Norvell ST, Guclu A, Bodurtha A, Tai J, MacDonald AS. Immunochemotherapy of human malignant melanoma with chlorambucil-carrying antibody. Eur J Cancer 1975; 11:321–326.

(11) ———. Immunochemotherapy of malignant melanoma with chlorambucil-bound antimelanoma globulins: Preliminary results in patients with disseminated disease. J Natl Cancer Inst 1977; 58:845–852.

(12) Imai K, NG A-K, Ferrone S. Characterization of monoclonal antibodies to human melanoma-associated antigens. JNCI 1981; 66:489–496.

(13) Wilson BS, Kohzoh I, Natali PG, Ferrone S. Distribution and molecular characterization of a cell-surface and a cytoplasmic antigen detectable in human melanoma cells with monoclonal antibodies. Int J Cancer 1981; 28:293–300.

(14) Ghose T, Guclu A. Cure of a mouse lymphoma with radioiodinated antibody. Eur J Cancer 1974; 10:787–792.

(15) Hurwitz E, Maron R, Bernstein A, Wilchek M, Sela M, Arnon R. The effect in vivo of chemotherapeutic drug—antibody conjugates in two murine experimental tumor systems. Int J Cancer 1978; 21:747–755.

(16) Ghose T, Nairn RC, Fothergill JH. Uptake of proteins by malignant cells. Nature 1962; 196:1108–1109.

(17) Peterson H. Vascular and extravascular spaces in tumors: Tumor vascular permeability. In: Peterson J, ed. Tumor blood circulation. Boca Raton, Fla. CRC Press, 1979:77–85.

(18) Houston LL, Nowinski RC, Bernstein ID. Specific in vivo localization of monoclonal antibodies directed against the Thy 1.1 antigen. J Immunol 1980; 125:837–843.

(19) Herlyn DM, Steplewski A, Herlyn MF, Koprowski H. Inhibition of growth of colorectal carcinoma in nude mice by monoclonal antibody. Cancer Res 1980; 40:717–721.

(20) Moshakis V, McIlhinney RA, Raghavan D, Neville AM. Localization of human tumor xenografts after i.v. administration of radiolabelled monoclonal antibodies. Br J Cancer 1981; 44:91–99.

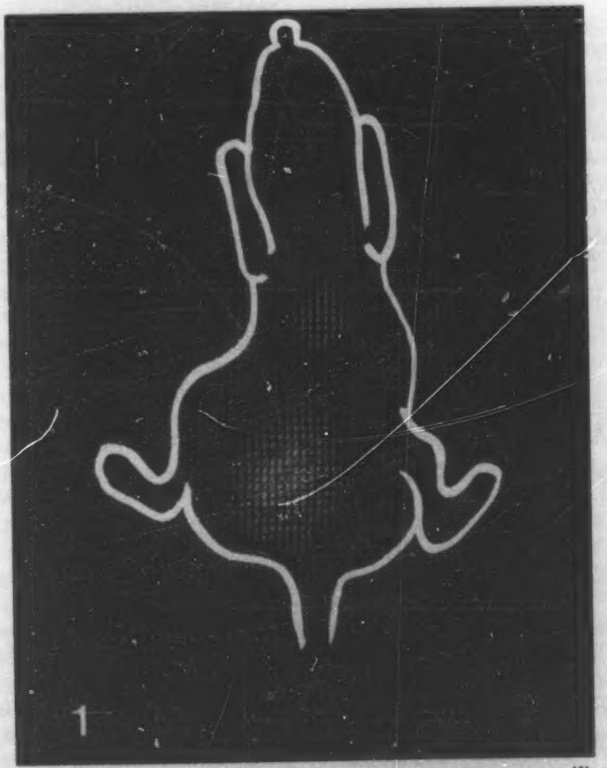

Figure 1.—Scintiscan of a human melanoma xenograft-bearing nude mouse 48 hr after iv injection of 50 μCi ^{131}I bound to 150 μg monoclonal anti-human melanoma IgG. The mouse was scanned with a large-field-of-view scintillation camera interfaced to a PDP 11/34 computer. The scan of ^{131}I distribution was obtained at 364 KeV with a 20% window, stored in the computer, and then displayed in a linear color scale from dark blue (lowest activity) to white (highest activity). Localization of radioactivity in excess of the background can be seen in the melanoma.

Functional Properties of Human Thymoma Lymphocytes: Role of Subcellular Factors in Blastic Activation[1,2]

Piero Musiani,[3] Libero Lauriola,[3] Nicola Maggiano,[3] Pietro Tonali,[4] *and* **Mauro Piantelli[3,5]**

ABSTRACT—The proliferative responses to phytohemagglutinin and the role of subcellular factors in the modulation of blastogenesis of thymoma lymphocytes from 5 thymoma patients were investigated. The addition of exogenous interleukin 1, a macrophage product, strongly augmented the blastic transformation of cultured thymocytes from both normal and neoplastic glands by influencing the production of interleukin 2 (IL-2) by a well-defined T-cell subset. The magnitudes of the blastic responses were ultimately modulated by the amount of IL-2 released in culture. The higher proliferative responses exhibited by thymocytes from thymoma were effectively sustained by a higher production of IL-2 in culture. In addition to having distinctive surface membrane receptors in common with normal thymocytes, thymoma lymphocytes were also under the influence of the same subcellular factors involved in T-cell blastic activation as thymocytes. These observations imply the presence of functionally distinct subpopulations in the thymoma lymphocyte component and add arguments in favor of their nonneoplastic nature.—JNCI 1982; 69:827–831.

Human thymomas are neoplasms composed of a mixture of thymic epithelial cells and lymphocytes, with a variation in the relative proportions from case to case and within different areas of the same tumor. The epithelial cells of thymomas display morphologic and biologic properties of neoplastic cells (*1*), whereas the morphologic and the biologic properties of thymoma lymphocytes do not suggest their neoplastic origin. The precise nature, role, and functional attributes of the lymphocytic component of thymomas remain undefined.

In previous papers we have pointed out some immunologic similarities between lymphocytes from both the neoplastic and the normal thymus (*2, 3*). In the normal human thymus, various lymphocyte subpopulations have been identified and separated on the basis of their different expression of surface membrane receptors. The majority of thymocytes from the normal thymus exhibit receptors for PNA. These PNA$^+$ cells (mainly cortical thymocytes) respond poorly to phytohemagglutinin and when tested in mixed lymphocyte culture, whereas the minor PNA$^-$ subset (mainly composed of medullary thymocytes) responds to both stimuli (*4*). Lymphocytes from thymomas with moderate or predominant lymphocytic infiltrate exhibited surface membrane receptors at numbers close to those found in the normal thymus. Furthermore, in our experiments lymphocytes from thymomas with scant lymphocyte components showed surface membrane receptors and displayed proliferative responses to phytohemagglutinin comparable to those of the more mature pool of normal medullary thymocytes (*2, 3*).

Recent studies on T-lymphocytes activation by mitogens or antigens in both experimental animals and humans have demonstrated a monocyte dependence for optimal initial mitogenesis (*5–10*). It has been postulated that monocytes exert their effect, at least in part, through the production of IL-1 (*11*) which facilitates the release of IL-2 by a T-cell subset (*12–14*). IL-2 is the obligatory modulator of T-cell blastic activation (*15*).

In the present paper we describe the study of the proliferative responses of thymoma lymphocytes to phytohemagglutinin and the role of the interleukins in the modulation of their blastogenesis. Our data indicate that thymoma lymphocytes are characterized by a distinctive surface receptor pattern similar to that of normal thymocytes. Moreover, thymoma lymphocytes are under the influence of the same subcellular factors that are involved in the blastic activation of both normal thymocytes and peripheral lymphocytes. This implies the presence of functionally distinct subpopulations in thymoma lymphocyte suspensions and argues in favor of their nonneoplastic origin.

MATERIALS AND METHODS

Thymocyte preparation.—Cell suspensions were prepared of neoplastic tissue from 5 thymoma patients with myasthenia gravis and of normal tissue from 10 children, 4 months to 7 years old, undergoing open-heart surgery. The tissues were gently teased and washed three times in Hanks' balanced salt solution. The cells were more than 95% viable as assessed by trypan blue exclusion. Monocytes within the thymic cell suspensions were assessed by nonspecific esterase staining (*16*). Tissue specimens taken for light microscopic examination were classified according to the shape of the epithelial cells, i.e., round-oval, spindle, or mixed, and the degree of lymphocytic infiltration, i.e., absent, scant, moderate, or predominant as suggested by Rosai and Levine (*1*). Tumors were also divided into two major categories, invasive and noninvasive, on the basis of the surgical and gross findings (*1*).

ABBREVIATIONS USED: E$_N$-RFC=E-neuraminidase rosette-forming cell(s); FCS=fetal calf serum; FITC=fluorescein isothiocyanate; $[^3H]$dThd=tritiated thymidine; IL-1=interleukin 1; IL-2=interleukin 2; PNA=peanut agglutinin; PNA$^-$=PNA-negative; PNA$^+$=PNA-positive; SmIg$^+$ cells=surface membrane immunoglobulin-bearing cells; T$_G$=T-cell(s) with receptors for the Fc portion of IgG; T$_M$=T-cell(s) with receptors for the Fc portion of IgM.

---

[1] Received January 22, 1982; accepted May 12, 1982.

[2] Supported by the Consiglio Nazionale delle Ricerche (Progetto Finalizzato "Controllo della Crescita Neoplastica"), Rome, Italy.

[3] Instituto di Anatomia e Istologia Patologica, Università Cattolica del Sacro Cuore, Via della Pineta Sacchetti 644, 00168 Rome, Italy.

[4] Department of Neurology, Università Cattolica del Sacro Cuore, Largo Gemelli 1, 00168 Rome, Italy.

[5] We thank Mr. Paolo Baldassarri of the Università Cattolica del Sacro Cuore for the manuscript preparation.

Separation of thymocyte subpopulations by PNA agglutination.—PNA was purified from fresh, unpeeled, shelled peanuts with the use of a sialic acid-less fetuin–Sepharose column (*17*). The thymocyte suspensions were separated in PNA$^+$ and PNA$^-$ subsets by the agglutination technique reported by Reisner et al. (*4*). The agglutinated cells were virtually all (>97%) FITC-PNA$^+$; however, the nonagglutinated fraction contained about one-third of weakly FITC–PNA$^+$ cells.

Detection of surface membrane markers.—We determined E$_N$-RFC in lymphocyte suspension as reported earlier (*2*) and scored SmIg$^+$ cells by a direct immunofluorescence test, as described by us previously (*18*). To detect the presence of T$_G$ and T$_M$, we cultured thymocytes for 24 hours in medium 199 (Gibco Bio-Cult Ltd., Paisley, Scotland) with 20% selected FCS in a humidified incubator with 5% CO_2 according to the procedure reported by Moretta et al. (*19*). We counted T$_G$ and T$_M$ after rosetting thymocytes with ox erythrocytes coated with purified rabbit IgG or IgM antibodies. Detailed descriptions of the procedures used were reported by us elsewhere (*20*). For FITC–PNA binding assay, we incubated thymocytes (0.1 ml, 3×10^6 cells) with FITC–PNA (0.1 ml, 350 μg/ml) for 20 minutes at room temperature.

Preparation of IL-1.—IL-1 was obtained following the procedure reported by Blyden and Handschumacher (*21*). IL-1-containing supernatants demonstrated an augmenting activity on lectin-stimulated thymocyte blastogenesis. In our culture conditions IL-1 dilutions capable of sustaining maximal blastogenic responses ranged between 1:5 and 1:10. Detectable activity was still found in most of these supernatants even at 1:160 dilutions. We screened all IL-1 preparations for IL-2 activity as described below and found them to be negative.

Preparation of conditioned medium containing IL-2.—We prepared IL-2-containing supernatants from peripheral blood lymphocytes from single donors or from thymocytes from both neoplastic and normal thymus tissues. We incubated peripheral blood lymphocytes or thymocytes at 37°C in RPMI-1640 medium with 3% FCS. Phytohemagglutinin was added to the culture at 0.5 μg/ml for peripheral blood lymphocyte culture and 5 μg/ml for thymocyte culture. After 48 hours, cells were removed by centrifugation at 400×*g* for 10 minutes.

Quantitative microtiter-well assay for IL-2 activity.—We assayed IL-2 activity according to the procedure described by Bonnard et al. (*22*) with minor modifications. Sensitized cells from 7-day primary one-way-mixed lymphocyte culture were resuspended at 5×10^5 cells/ml in RPMI-1640 and 10% FCS, with 10–25% of IL-2-containing conditioned medium. By day 3 or 4, the cultured T-cells reached 10^6/ml and were fed by dilution with fresh medium to 5×10^5/ml. Every 3 days thereafter, the cells were split in a similar manner. Serial 1:3 dilutions of various preparations of conditioned media were assayed for ability to stimulate proliferation of third passage (≈14-day-old) cultured T-cells (10^6) during 3 days of incubation in microtiter wells. The degree of proliferative activity was measured by incorporation of [^{3}H]dThd added during the last 4 hours of culture (sp act, 5 Ci/mmol; Amersham International Ltd., Amersham, England). As a control, 0.5 μg phytohemagglutinin/ml was also used in all experiments. Cultured T-cells were only weakly stimulated by the phytomitogen. The observed proliferative responses represent a quantitative measure of IL-2 in a given supernatant. By determination of the dilutions of supernatants needed to produce a similar stimulatory effect, it was possible to estimate graphically the relative IL-2 activities of various supernatants. An excellent correlation has been reported between the results of the assays in microtiter plates and the abilities of the various conditioned media to promote actual T-cell growth (*22*).

Thymocyte responses to mitogen.—Cell response to phytohemagglutinin was determined as previously reported (*2, 3*) with some modifications. We suspended unfractionated, PNA$^+$ and PNA$^-$ thymocytes in RPMI-1640 medium, supplemented with 10% heat-inactivated FCS. Cultures were established in flat-bottomed microtiter plates (MicroTest II, Falcon 3040; Falcon Plastics, Oxnard, Calif.) in triplicate and consisted of 0.2 ml of culture medium containing thymocytes at concentrations ranging from 5×10^5 to 2×10^6 cells/ml. Phytohemagglutinin at 5 μg/ml end concentration was added to each well. Cultures were incubated for 84 hours in a humidified environment that contained 5% CO_2; for the last 16 hours of the culture period, 0.5 μCi of [^{3}H]-dThd was added to each culture well. The cultures were then harvested for scintillation spectrometery.

RESULTS

The morphologic features of the neoplastic epithelial cells, the proportion of lymphocytes in the neoplastic tissue, and the invasiveness of each tumor are reported in table 1. The contamination of the cell suspensions with peripheral blood mononuclear cells was negligible as assessed according to Galili and Schlesinger (*23*). The percentages of E$_N$-RFC, SmIg$^+$ cells, FITC–PNA$^+$, T$_M$, and T$_G$ and the mean values plus or minus standard deviation for the control thymuses are reported in table 2.

The great majority of the lymphocytes from thymomas with abundant lymphocytic components, as well as from normal thymus, showed surface membrane receptors for PNA. Alternatively, lower numbers of PNA$^+$ cells were observed in the lymphocyte population from thymomas with a low lymphocyte-to-epithelial cell ratio.

T$_G$ were absent or very exiguous in all thymocyte suspensions. Moreover, the percentage of T$_M$ lymphocytes present in thymomas with scant lymphocytic component substantially exceeded the percentages exhibited by both the normal

TABLE 1.—*Histologic appearance and invasiveness of thymomas from 5 patients*

Patient	Age, yr	Sex	Shape of neoplastic epithelial cells	Degree of lymphocytic infiltration	Invasiveness
#1	57	♂	Round–oval	Predominant	Not invasive
#2	44	♀	Round–oval	Predominant	Invasive
#3	55	♀	Round–oval	Moderate	Not invasive
#4	59	♀	Spindle	Scant	Not invasive
#5	54	♂	Round–oval	Scant	Invasive

TABLE 2.—*Percentages of lymphocyte subpopulations in 5 thymomas and in 10 normal thymuses*[a]

Thymoma patient	E_{ox}-RFC, %	SmIg$^+$ cells, %	FITC-PNA$^+$ cells, %	T_M, %	T_G, %
#1	98	0	75	28	0
#2	96	1	63	33	0
#3	98	1	69	32	1
#4	95	1	34	49	0
#5	92	2	21	56	2
10 control patients	98.0±2.1	<1	79.1±4.9	24.8±4.2	<1

[a] Nonspecific esterase-positive cells were <1% in all the thymocyte preparations. Values for the control thymuses are means ± SD.

thymus and thymomas with predominant or moderate lymphocytic component. These findings are in accord with those previously reported by us (*3*).

Results concerning the proliferative responses of unfractionated, PNA$^+$, and PNA$^-$ thymocytes from both normal thymus and thymomas are shown in text-figure 1. Thymoma lymphocytes exhibit higher proliferative responses than their normal counterparts. For increasing cell concentrations up to 2×10^6/ml, [^{3}H]dThd incorporation per cell strongly increases in all preparations. The differences in mitogen responsiveness between lymphocytes from normal and neoplastic thymuses evident at low cell densities become more prominent at higher cell concentrations. At any cellular concentration the highest responses are exhibited by PNA$^-$ fractions, whereas PNA$^+$ cells are always unresponsive whether the lymphocytes are from normal or from neoplastic glands. It is significant that lymphocyte preparations from thymomas with predominant epithelial components not only show the highest percentages of PNA$^-$ cells (table 2) but also exhibit the highest proliferative response to phytohemagglutinin (text-fig. 1).

Because of the essential role of macrophages and their product IL-1 in the initiation of T-cell blastic activation, we evaluated the effect of IL-1 on the thymocyte mitogenic responses. Addition of IL-1-containing medium strongly

TABLE 3.—*Proliferative response of thymoma lymphocytes in culture to phytohemagglutinin with the addition of exogenous IL-1*[a]

Lymphocyte characteristics	[^{3}H]dThd incorporation, cpm × 10^5 cells: Without IL-1 addition	[^{3}H]dThd incorporation, cpm × 10^5 cells: With IL-1 addition[b]
Normal thymus		
Unfractionated	3,000	6,900
PNA$^-$	6,900	17,100
PNA$^+$	600	700
Thymomas with abundant lymphocyte component		
Patient #1—Unfractionated	6,300	11,100
PNA$^-$	15,700	31,600
PNA$^+$	700	800
Patient #2—Unfractionated	8,200	14,200
PNA$^-$	19,900	33,300
PNA$^+$	550	2,100
Patient #3—Unfractionated	9,300	15,600
PNA$^-$	21,000	39,000
PNA$^+$	600	1,900
Thymomas with scant lymphocyte component		
Patient #4—Unfractionated	33,000	51,000
PNA$^-$	47,000	56,700
PNA$^+$	790	3,000
Patient #5—Unfractionated	38,400	54,000
PNA$^-$	56,000	61,000
PNA$^+$	760	3,100

[a] 1 µg of phytohemagglutinin was added to each well containing 1.0×10^5 cells in a final volume of 200 µl.

[b] 30 µl of IL-1-containing supernatant was added to each well; preliminary data indicated that this conditioned medium concentration yielded optimum mitogenesis.

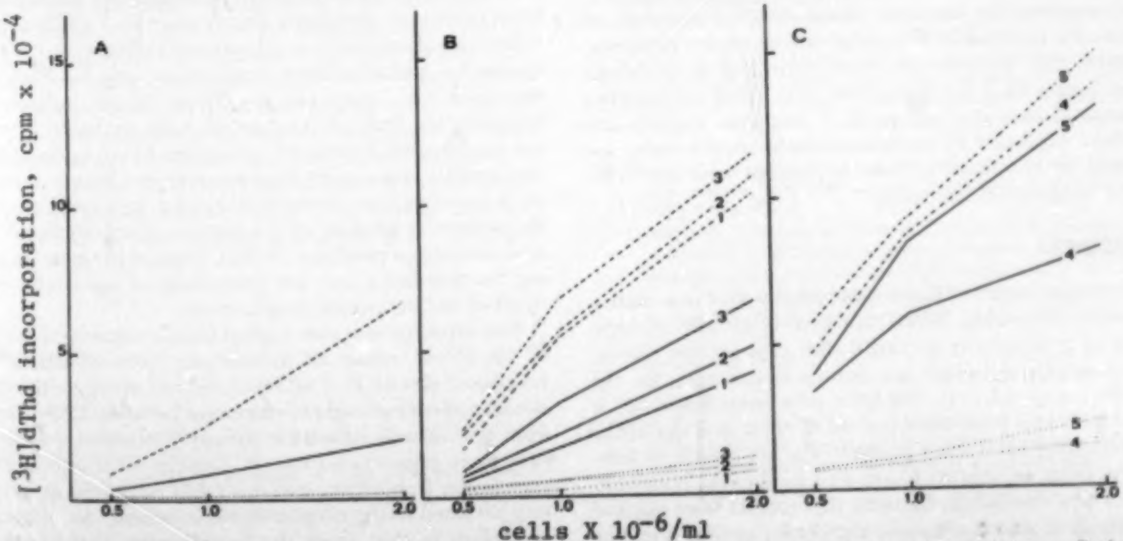

TEXT-FIGURE 1.—Proliferative responses of unfractionated (——), PNA$^-$ (-----), and PNA$^+$ (·····) lymphocytes from A) normal thymus, B) thymomas with abundant lymphocyte components, and C) thymomas with scant lymphocyte components. Lymphocytes were cultured for 84 hr at various cell:volume ratios in microtiter wells. One µg of phytohemagglutinin was added to each well containing a final volume of 200 µl.

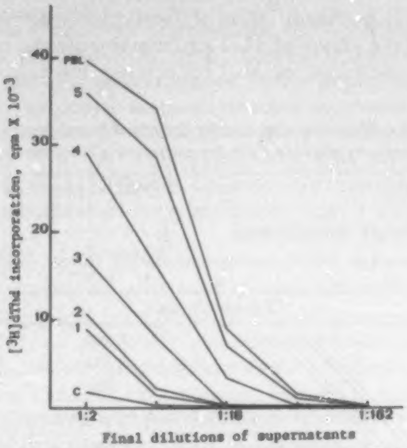

TEXT-FIGURE 2.—Quantitative microtiter-well assay for IL-2 activity. T-cells (1.0×10^6 cells/ml) were cultured for 48 hr with the addition of various dilutions of culture supernatants from peripheral blood mononuclear cells (PBL), thymomas (1, 2, 3, 4, 5), and normal thymus lymphocytes (C).

augments the blastic transformation of lymphocytes from both normal and neoplastic glands cultured at low cell densities (table 3). The highest [^{3}H]dThd-incorporation values are exhibited by thymoma lymphocytes, particularly by those with low lymphocyte-to-epithelial cell ratios.

The magnitude of the blastic response is ultimately modulated by the amount of endogenous IL-2 produced by a T-cell subset under the influence of IL-1 (*12–15*). Therefore, we have evaluated the capacity of the lymphocytes from normal and neoplastic glands to produce IL-2. We assayed conditioned media from phytohemagglutinin-stimulated thymocytes for their ability to stimulate the proliferation of cultured T-cells from mixed lymphocyte culture. Proliferative responses of cultured T-cells to the various supernatants in the IL-2 microtiter-well assay are shown in text-figure 2. For comparison, we also determined the IL-2 activities of supernatants generated from peripheral blood lymphocytes. We found that supernatants from thymoma lymphocytes contain higher IL-2 activities than those from normal thymocytes and that the highest IL-2 amounts, slightly less than those produced by peripheral blood lymphocytes, are generated by lymphocytes from thymomas with low lymphocyte-to-epithelial cell ratios.

DISCUSSION

The precise nature of thymoma lymphocytes is a matter still open to discussion. Based on morphologic and biologic features of lymphocytes and epithelial cells present in thymomas, neoplastic nature has been assumed only for the epithelial component (*1*). We have previously found (*2, 3*) that lymphocytes from both normal thymus and thymoma bear distinctive membrane markers that are absent in lymphocytes from peripheral blood and peripheral lymphoid tissues. These similarities between thymocytes from normal and neoplastic glands are valid arguments against a theory of thymoma lymphocytes originating in the lymphoid periphery.

We have previously investigated the lectin-stimulated mitogenesis of normal unfractionated thymocytes and PNA$^+$ and PNA$^-$ subsets and showed that only PNA$^-$ thymocytes, the minor pool of more mature medullary cells, are capable of responding to the mitogen as described by Reisner et al. (*4*). To clarify the steps of mitogen-induced activation and the role of subcellular factors in the promotion and regulation of the blastogenesis of thymoma lymphocytes, we have investigated the in vitro [^{3}H]dThd incorporation of total, PNA$^+$, and PNA$^-$ lymphocytes from neoplastic thymuses in comparison with thymocytes from normal thymus under several different experimental conditions. Unfractionated thymoma lymphocytes exhibit higher mitogen-induced blastogenesis than normal thymocytes. Total lymphocyte suspensions from thymomas with low lymphocyte-to-epithelial cell ratios show the highest blastic responses upon phytohemagglutinin stimulation. As in the normal thymus, only PNA$^+$ lymphocyte preparations from thymomas are able to respond to phytohemagglutinin, whereas PNA$^+$ lymphocytes are practically unresponsive. The PNA$^-$ subset from thymomas with a low lymphocyte-to-epithelial cell ratio shows maximal blastic responses clearly higher than those exhibited by equal numbers of PNA$^-$ normal thymocytes.

At this point, it could be suspected that variable percentages of macrophages and, consequently, variable concentrations of their products could be present in the thymocyte preparations from normal thymus or thymoma, thereby influencing their response capacity. The role of accessory cells and of IL-1, a macrophage product, for the release of IL-2 by some T-lymphocyte subsets and the obligatory role of IL-2 for the blastogenesis of lectin-activated T-cells are presently widely accepted. Consequently, we added a saturating concentration of exogenous IL-1 to each thymocyte culture to overcome potential experimental artifacts and to be able to better evaluate the intrinsic blastogenic capacity of each thymocyte population. In effect, the data concerning the blastic proliferation of thymocytes from normal or neoplastic glands after IL-1 addition to the culture medium show a substantial increase in blastic response by unfractionated populations and by PNA$^-$, but not by PNA$^+$, preparations. These results indicate that lymphocytes from thymomas as well as those from the normal thymus depend on monocytes for an optimal initial mitogenesis and suggest that the inherent blastic capacities of thymocytes from both normal and neoplastic thymuses are ordinarily masked by the scarcity of macrophages and/or macrophage products. In fact, nonspecific esterase staining has revealed a very low percentage of monocytes (<1%) in all of the thymocyte preparations.

The capacity to mount a good blastic response is confined to the PNA$^-$ subset of thymocytes, both in normal and neoplastic glands. IL-1 addition did not abrogate the differences in the amplitude of responses between PNA$^-$ subsets from normal and neoplastic tissues. This effect may be due to a more pronounced blastic capacity of the total PNA$^-$ population from thymomas due to an advanced maturative step attained in the neoplastic environment. An alternative possibility is that since the lymphocytes that cannot be agglutinated by peanut lectin could represent a heterogeneous population, variable percentages of mitogen-responsive cells may be present in the PNA⁻ preparations from the various sources.

To better evaluate the subcellular factors that regulate blastic activation of thymocytes both from normal and pathologic tissues, we then investigated the effective in vitro IL-2 production by the various thymocyte preparations after phytohemagglutinin stimulation. In lymphocyte cultures from peripheral blood lymphocytes and from peripheral lymphoid tissue, both in experimental animal and human systems, a subset of T-lymphocytes produces IL-2 under the influence of IL-1. IL-2 then is taken up by antigen-or mitogen-activated T-lymphocytes and switches them to proliferative activities. In our experiments, lymphocytes from both normal and neoplastic thymuses produced IL-2 in detectable amounts. Moreover, thymoma lymphocytes produced IL-2 in significantly higher quantities than did normal thymocytes. The production of and the assumption of subcellular factors by distinct cell subpopulations are then effective in the promotion and regulation of blastic activation of lymphocytes from both thymus and thymoma, as well as from peripheral blood. The existence of such a complex system of stepwise blastogenesis control in thymoma lymphocytes implies that thymoma lymphocytes are not a homogeneous population; therefore, they are likely to be of nonneoplastic nature.

The greater than expected increase of [^{3}H]dThd incorporation in thymocytes attained by augmenting cell concentration in thymocyte cultures from normal and neoplastic glands suggests a role for subcellular factors in the regulation of blastic response in these suspensions. It is conceivable that, at the highest cell concentration per culture volume, IL-1 and the produced IL-2 are no longer diluted out in the medium and their effects can become fully manifested. However, on the basis of our experiments, the influence on mitogenesis of an increased, intimate cell-to-cell contact in culture at high cell concentration cannot be ruled out.

In conclusion, our data indicate that thymoma lymphocytes are functionally heterogeneous and functionally superior to normal thymocytes, particularly when obtained from tumors with the scantest lymphocyte component. Furthermore, the heterogeneity of thymoma lymphocytes in terms of surface marker expression and functional capacities, as well as the substantial similarities between the mechanisms that regulate mitogenesis of T-cells from normal and neoplastic glands, further suggests a nonneoplastic nature of thymoma lymphocytes.

REFERENCES

(*1*) Rosai J, Levine GD. Tumors of the thymus. In: Firminger HI, ed. Atlas of tumor pathology. Washington, D.C.: Armed Forces Institute of Pathology, 1976:34–150.

(*2*) Lauriola L, Piantelli M, Carbone A, Dina MA, Scoppetta C, Musiani P. Subpopulations of lymphocytes in human thymomas. Clin Exp Immunol 1979; 37:502–506.

(*3*) Lauriola L, Maggiano N, Marino M, Carbone A, Piantelli M, Musiani P. Human thymoma: Immunological characteristics of the lymphocytic component. Cancer 1981; 48:1992–1995.

(*4*) Reisner Y, Biniaminov M, Rosenthal E, Sharon N, Ramot B. Interaction of peanut agglutinin with normal human lymphocytes and with leukemic cells. Proc Natl Acad Sci USA 1979; 76:447–451.

(*5*) Rosenstreich DL, Mizel SB. The participation of macrophage and macrophage cell lines in the activation of T lymphocytes by mitogens. Immunol Rev 1978; 40:102–135.

(*6*) Rosenstreich DL, Farrar JJ, Dougherty S. Absolute macrophage dependency of T lymphocyte activation by mitogens. J Immunol 1976; 116:131–139.

(*7*) Arala-Chaves MP, Hope L, Korn JH, Fudemberg H. Role of adherent cells in immune responses to phytohaemagglutinin and concanavalin A. Eur J Immunol 1978; 8:77–81.

(*8*) Maizel AL, Mehta S, Ford RJ. Monocyte enhancement of human T-cell proliferation dependent upon conditioned media. J Reticuloendothel Soc 1980; 28:357–366.

(*9*) Twomey JJ, Sharkey O, Brown JA, Laugher AH, Jordan PH. Cellular requirements for the mitotic response in allogeneic leukocyte cultures. J Immunol 1970; 104:845–853.

(*10*) Waldron JA, Horn RG, Rosenthal AS. Antigen-induced proliferation of guinea pig lymphocytes in vitro: Obligatory role of macrophages in the recognition of antigen by immune T-lymphocytes. J Immunol 1973; 111:58–64.

(*11*) Mizel SB, Farrar JJ. Revised nomenclature for antigen-nonspecific T-cell proliferation and helper factors. Cell Immunol 1979; 48:433–436.

(*12*) Smith KA, Lachman LB, Oppenheim JJ, Favata MF. The functional relationship of the interleukins. J Exp Med 1980; 151:1551–1556.

(*13*) Shaw J, Caplan B, Paetkau V, Pilarski LM, Delovitch TL, McKenzie IF. Cellular origins of costimulator (IL-2) and its activity on cytotoxic T lymphocyte responses. J Immunol 1980; 124:2231–2239.

(*14*) Maizel AL, Mehta SR, Ford RJ, Lachman LB. Effect of interleukin 1 on human thymocytes and purified human T cells. J Exp Med 1981; 153:470–475.

(*15*) Smith KA, Gillis S, Baker PE. The role of soluble factors in the regulation of T-cell immune reactivity. In: Kaplan JG, ed. The molecular basis of immune cell functions. Amsterdam: Elsevier/North-Holland, 1979:223.

(*16*) Yam LT, Li CY, Crosby WH. Cytochemical identification of monocytes and granulocytes. Am J Clin Pathol 1971; 55:283–291.

(*17*) Irlé C. Rapid purification of peanut agglutinin by sialic acid-less fetuin-Sepharose column. J Immunol Methods 1977; 17:117–121.

(*18*) Salsano F, Pisarri-Salsano S, Ciancarelli MP, Piantelli M, Lauriola L, Musiani P. Structural and functional characteristics of hairy cells. Acta Haematol (Basel) 1979; 61:184–193.

(*19*) Moretta L, Ferrarini M, Durante ML, Mingari MC. Expression of a receptor for IgM by human T cells in vitro. Eur J Immunol 1975; 5:565–569.

(*20*) Carbone A, Piantelli M, Musiani P, Pozzuoli R, Lauriola L. Fc receptor for IgM: Factors influencing detection on human T lymphocytes. J Immunol Methods 1979; 29:245–251.

(*21*) Blyden G, Handschumacher RE. Purification and properties of human lymphocyte activating factor (LAF). J Immunol 1977; 118:1631–1638.

(*22*) Bonnard GD, Yasaka K, Maca RA. Continued growth of functional human T lymphocytes: Production of human T-cell growth factor. Cell Immunol 1980; 51:390–401.

(*23*) Galili U, Schlesinger M. Subpopulations of human thymus cells differing in their capacity to form stable E-rosettes and in their immunologic reactivity. J Immunol 1975; 115:827–833.

blank page

Changes in Lung Cancer Incidence and Mortality Rates Among Americans: 1969–78[1]

John W. Horm[2, 3] *and* Ardyce J. Asire[2]

ABSTRACT—Cancer incidence data from two large cancer surveys and cancer mortality data for the entire United States were used to estimate trends in lung cancer incidence and mortality rates among whites for specific age groups during the 10 years 1969–78. Data for the Third National Cancer Survey were from 1969 to 1971; data for the Surveillance, Epidemiology, and End Results Program were from 1973 to 1978. For both incidence and mortality, the rates for women increased much more rapidly than the rates for men, except in the oldest age group (≥85). For both men and women, there was a striking similarity between the average annual percent changes for age-specific incidence rates and those for age-specific mortality rates. For the first time women and men had a similar incidence rate for the youngest (35–44) age group in 1978. If these trends continue, the data suggest that the total incidence rates for men and women will be equal by the year 2000.—JNCI 1982; 69:833–837.

Lung cancer comprises about 21% of all newly diagnosed cancer cases and 32% of all cancer deaths in white men. In white women, this cancer accounts for about 8% of all new cancers and 13% of all cancer deaths (*1*). For all patients diagnosed with lung cancer in 1970–73, the 5-year survival rate was 9% for white men and 14% for white women (*2*). Because this disease accounts for a large proportion of all cancers and results in poor survival, it is important to assess trends in the incidence of and mortality from lung cancer.

In recent years, several investigators have indicated that lung cancer incidence and mortality rates in the United States have been increasing dramatically. In particular, Cutler and Devesa (*3*) found that from 1937 to 1969 the incidence rates increased by over 400% in white men and 200% in white women. In their analysis of mortality, these authors indicated that from 1935 to 1965 lung cancer mortality rates increased by over 500% in white men and 100% in white women. Among the 11 cancer sites investigated for whites, lung cancer showed the largest increases. In a more comprehensive analysis of trends from 1935 to 1974, Devesa and Silverman (*4*) showed that lung cancer again had the largest increases in both incidence and mortality among whites. In addition, they noted that the mortality rates from lung cancer in white women had increased only since the mid-1950's, but those for white men had increased over the entire time period.

In an analysis of cancer incidence and mortality trends from 1969 to 1976, Pollack and Horm (*5*) determined that among whites lung cancer incidence increased by 1.4% per year for men and 8.6% per year for women. Mortality from lung cancer in the entire United States increased by 2.6 and 7.1% per year for white men and women, respectively. Thus, whereas the earlier studies indicated that the lung cancer incidence and mortality rates were increasing more rapidly in men than in women, the more recent Pollack and Horm study found that the rates for women were increasing more rapidly than were the rates for men.

The above-mentioned studies dealt solely with the trends in the overall age-adjusted lung cancer incidence and mortality rates. This investigation focuses on the age-specific trends in lung cancer incidence and mortality rates occurring between 1969 and 1978 in men and women in the United States.

MATERIALS AND METHODS

In recent years the National Cancer Institute has conducted two programs to assess cancer incidence in the United States: the TNCS and the SEER Program. The TNCS was conducted for the finite period of 1969–71 (*6*). The SEER Program was begun in 1973 as a continuous source of population-based cancer incidence and patient survival data in the United States. Data are now available for the years 1973–79 (*7*).

These two programs monitored approximately 10% of the U.S. population; only four registry areas, however, were common to both. In addition, the State of Connecticut has conducted a statewide cancer registry system since 1935 (*7*) and is now a participant in the SEER Program. Although the Atlanta registry was common to both programs, it did not participate in the SEER Program until 1975. Thus this analysis is restricted to the years 1969–71 and 1975–78 and to the four TNCS–SEER Program common areas plus Connecticut.

The five areas with their total populations for 1970 are the States of Connecticut (3,021,709) and Iowa (2,824,376) and the metropolitan areas of Atlanta (1,390,164), Detroit (4,199,931), and San Francisco–Oakland (3,109,519). These areas included about 7% of the 1970 U.S. population. The total black population in these areas was too small to permit an accurate evaluation of incidence trends among blacks. Therefore, the incidence rates of lung cancer discussed here have been determined for whites only from the data for these five areas.

The mortality data used in this report are from computer tapes made available to the public annually by the National Center for Health Statistics. The most recent year for which

---

ABBREVIATIONS USED: SEER=Surveillance, Epidemiology, and End Results; TNCS=Third National Cancer Survey.

---

[1] Received February 10, 1982; accepted June 17, 1982.

[2] Demographic Analysis Section, Biometry Branch, Division of Cancer Cause and Prevention, National Cancer Institute, National Institutes of Health, Public Health Service, U.S. Department of Health and Human Services, Bethesda, Md. 20205.

[3] *Address reprint requests to* J. W. Horm, Landow Building, Room 5B06, National Institutes of Health, Bethesda, Md. 20205.

such public-use tapes are currently available is 1978.

The populations used as denominators for computation of the incidence and mortality rates for 1969–71 are from the 1970 U.S. census. The populations for the years 1973–78 are based on projections prepared by the Bureau of the Census. For Connecticut, however, the population estimates were made by the Department of Health Services of that state.

The trends for both incidence and mortality are expressed in terms of average annual percent changes, convenient measures for trends over the 10-year period covered in this report. The measure was derived by an exponential model of the form $Y = ae^{bt}$ being fitted to the annual incidence and mortality rates by means of a regression technique. The advantage of an exponential model being used rather than a linear model is that the exponential model allows for a direct interpretation of the average annual percent change, whereas a linear model does not. The average annual percent change from the exponential model is then $(e^{b-1}) \cdot 100$.

Both the incidence and mortality rates were computed according to six 10-year age groups: 35–44, 45–54, 55–64, 65–74, 75–84, and 85 and older. An analysis was not performed for persons under age 35 because the small numbers did not permit a reasonable assessment of trends.

RESULTS

Table 1 presents the age-specific incidence rates for white men and women. The incidence rates increased with age for men, except that the rate for the oldest age group (≥85) was lower than that for the age group 65–74. A similar pattern is seen for women, but the rates for 2 age groups (75–84 and ≥85) were lower than the rate for the age group 55–64. Most noteworthy is the fact that for the first time women and men had a similar incidence rate for the youngest (35–44) age group in 1978—a direct result of the decreasing rate for men and the increasing rate for women during the 10 years covered by this study.

Age-specific mortality rates for white men and women in the entire United States are shown in table 2. The mortality patterns are seen to be generally similar to the incidence patterns. The major difference is that the mortality rate for women in the age group 35–44 did not increase as rapidly as did the incidence rate. Thus, in contrast to incidence, the

TABLE 1.—*Age-specific and age-adjusted lung cancer incidence rates by sex and year, average annual percent change, and 95% confidence interval for percent change, five common areas, 1969–78: Whites*

Age, yr	Sex	Incidence rate per 100,000 population							Average annual change, %	95% confidence interval	
		1969	1970	1971	1975	1976	1977	1978			
All ages[a]	♂	70.3	70.4	69.0	78.5	81.3	83.4	83.6	2.3	1.8	2.8
	♀	13.5	14.5	16.4	22.3	24.1	25.4	27.2	8.2	7.7	8.7
35–44	♂	20.3	20.9	16.7	15.8	16.2	17.8	17.2	−2.0	−4.0	0.0
	♀	8.9	8.7	8.2	11.4	12.4	12.9	16.3	6.8	4.8	8.8
45–54	♂	79.1	78.7	74.8	88.0	84.9	85.2	87.0	1.4	0.6	2.2
	♀	26.5	29.7	30.5	37.5	43.1	39.2	46.5	5.8	4.6	7.0
55–64	♂	217.1	231.0	218.3	236.7	245.3	237.7	246.5	1.2	0.6	1.8
	♀	43.7	48.2	58.4	86.2	78.5	94.9	100.9	9.5	7.9	11.1
65–74	♂	405.6	383.2	396.6	441.9	452.6	487.9	480.9	2.5	1.7	3.3
	♀	50.5	53.4	62.8	89.1	111.8	117.8	118.6	10.9	9.6	12.2
75–84	♂	409.1	404.5	405.5	500.8	558.9	557.2	555.6	4.3	3.3	5.3
	♀	58.8	58.1	72.7	85.7	98.3	90.7	93.6	5.9	4.2	7.6
≥85	♂	228.6	276.8	252.7	360.2	356.7	402.0	380.6	6.0	4.5	7.5
	♀	46.2	58.5	61.6	75.5	70.9	88.7	70.6	5.1	2.5	7.7

[a] Age adjusted to the 1970 U.S. population.

TABLE 2.—*Age-specific and age-adjusted lung cancer mortality rates by sex and year, average annual percent change, and 95% confidence interval for percent change, United States, 1969–78: Whites*

Age, yr	Sex	Mortality rate per 100,000 population							Average annual change, %	95% confidence interval	
		1969	1970	1971	1975	1976	1977	1978			
All ages[a]	♂	55.0	57.6	60.2	64.6	66.3	67.6	69.1	2.4	2.1	2.7
	♀	10.2	11.1	12.2	15.5	16.7	17.6	19.1	7.0	6.7	7.3
35–44	♂	14.9	14.7	13.9	12.6	12.8	11.8	11.1	−2.9	−3.6	−2.2
	♀	5.6	5.8	5.8	6.8	6.4	6.9	6.7	2.3	1.7	2.9
45–54	♂	60.9	63.3	64.1	69.2	69.2	70.2	71.0	1.7	1.4	2.0
	♀	18.4	20.9	22.5	26.5	28.1	29.6	31.6	5.6	4.9	6.3
55–64	♂	178.6	186.8	186.7	194.6	197.9	197.5	204.1	1.2	0.9	1.5
	♀	33.2	37.2	40.3	56.1	60.1	62.6	67.3	8.1	7.6	8.6
65–74	♂	313.8	325.0	345.0	366.0	372.4	381.1	388.1	2.2	1.9	2.5
	♀	41.6	42.9	49.3	64.9	72.6	77.7	86.6	8.5	8.0	9.0
75–84	♂	310.5	336.7	369.3	425.8	452.0	474.3	485.1	4.9	4.4	5.4
	♀	47.0	52.6	57.6	67.4	75.6	79.8	87.1	6.5	5.8	7.2
≥85	♂	177.0	199.6	233.5	273.8	298.0	314.2	333.3	6.7	5.7	7.7
	♀	46.4	50.3	61.6	66.9	70.6	72.1	71.9	7.0	6.7	7.3

[a] Age adjusted to the 1970 U.S. population.

mortality rate for women in this youngest age group was still lower than that for men.

The age-specific mortality rates for black men and women in the United States are given in table 3. The rates for men are higher than the rates for women in each year and age group. In addition, the rates for black men are higher than the rates for white men in every age group except the 2 oldest groups (75–84 and ≥85). The rates for black women are higher than the rates for white women in the 2 youngest age groups only.

Average annual percent changes, computed for the age-specific incidence and mortality rates shown in tables 1–3, are displayed graphically in text-figure 1 (incidence) and text-figure 2 (mortality) for whites and in text-figure 3 (mortality) for blacks. These graphs show that for both incidence and mortality the rates for white women increased much more rapidly than the rates for white men except in the oldest age group (≥85). The mortality rates for black women, however, increased more rapidly than did the rates for black men in every age group except the 2 oldest groups (75–84 and ≥85). For both white men and women, there was a striking similarity between the average annual percent changes for age-specific incidence rates and those for age-specific mortality rates. This similarity reflects the poor survival experience of lung cancer patients. With a median survival time of about 6 months, these patients often died in the same year they were diagnosed. The only exception to this similarity is among women between the ages of 35 and 44; the incidence rate for these women increased at about 7% per year, whereas their mortality rate increased at about

TABLE 3.—*Age-specific and age-adjusted lung cancer mortality rates by sex and year, average annual percent change, and 95% confidence interval for percent change, United States, 1969–78: Blacks*

Age	Sex	Mortality rate per 100,000 population							Average annual change, %	95% confidence interval	
		1969	1970	1971	1975	1976	1977	1978			
All ages[a]	♂	63.0	66.0	68.7	80.5	82.9	88.8	89.5	4.1	3.7	4.5
	♀	10.4	11.6	13.0	15.2	16.2	18.0	18.7	6.2	5.5	6.9
35–44	♂	19.8	29.7	28.9	27.7	24.0	25.8	25.3	0.3	−2.7	3.3
	♀	6.4	9.6	9.5	9.1	8.7	10.9	7.8	1.4	−2.0	4.8
45–54	♂	114.9	115.1	116.7	127.4	131.6	137.3	136.9	2.2	1.5	2.9
	♀	20.6	23.9	28.9	30.8	35.6	38.4	38.7	6.5	4.9	8.1
55–64	♂	223.5	233.6	243.9	292.6	300.6	310.6	318.2	4.1	3.6	4.6
	♀	34.1	33.4	38.7	50.7	54.0	62.6	65.3	8.0	7.0	9.0
65–74	♂	293.5	300.0	309.6	380.0	384.9	414.0	414.8	4.3	3.7	4.9
	♀	40.7	46.1	50.7	60.7	60.8	67.1	67.4	5.4	4.4	6.4
75–84	♂	228.9	271.0	314.9	350.3	376.6	442.9	459.6	7.0	5.6	8.4
	♀	43.1	49.2	49.2	60.0	68.6	62.7	86.9	6.4	4.4	8.4
≥85	♂	134.8	137.0	123.9	207.6	219.6	230.0	195.4	6.7	3.8	9.6
	♀	28.0	44.8	39.2	50.5	45.9	42.9	50.0	3.9	0.7	7.1

[a] Age adjusted to the 1970 U.S. population.

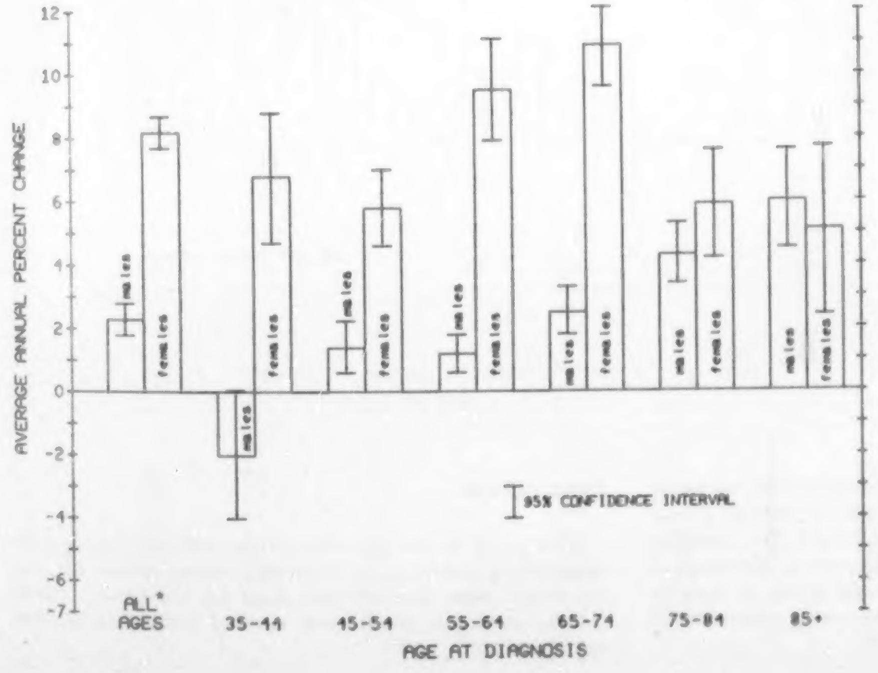

TEXT-FIGURE 1.—Average annual percent change in lung cancer incidence rates in whites in the United States from 1969 to 1978. *=all ages were based on rates adjusted to the 1970 U.S. standard population.

TEXT-FIGURE 2.—Average annual percent change in lung cancer mortality rates in whites in the United States from 1969 to 1978. *=all ages were based on rates adjusted to the 1970 U.S. standard population.

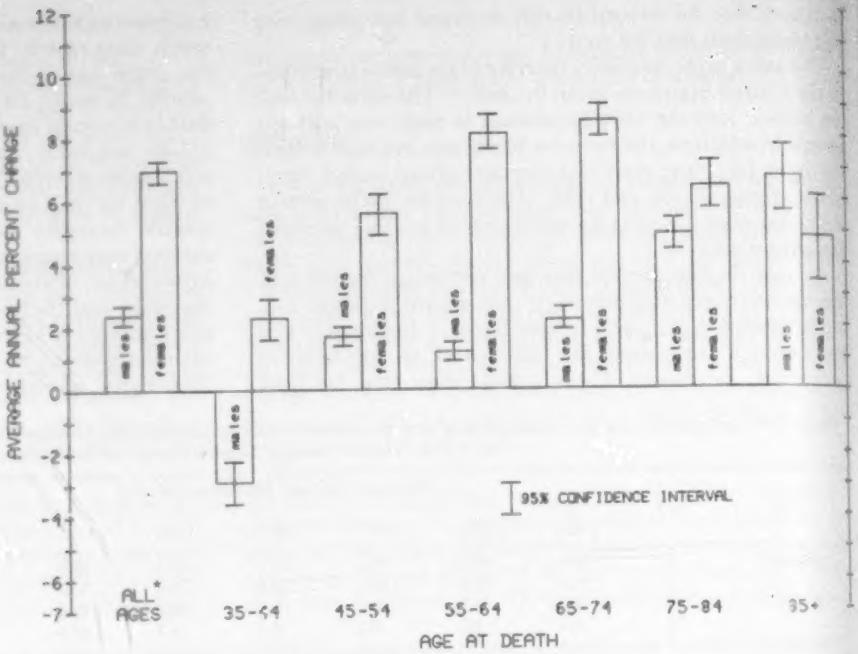

TEXT-FIGURE 3.—Average annual percent change in lung cancer mortality rates in blacks in the United States from 1969 to 1978. *=all ages were based on rates adjusted to the 1970 U.S. standard population.

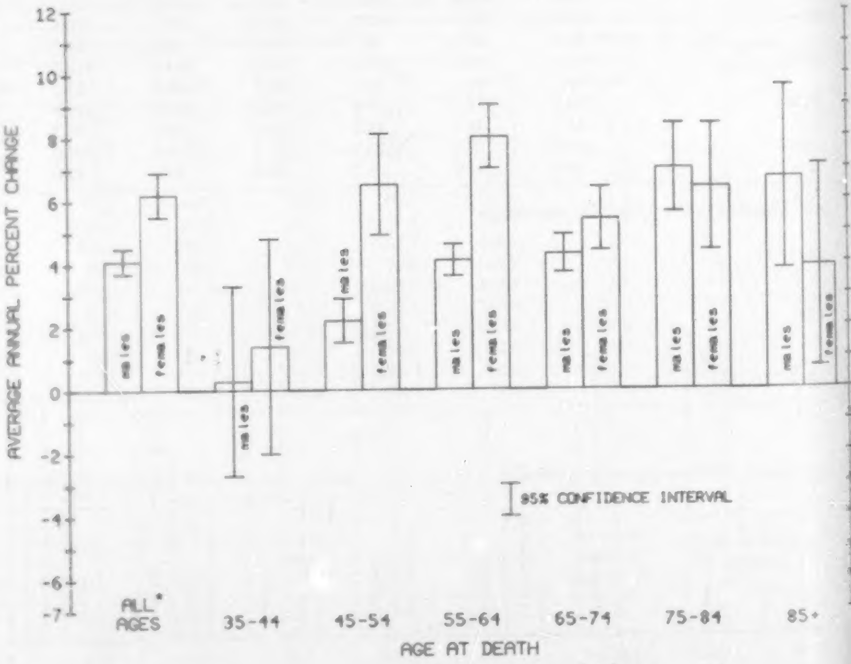

only 2% per year. This difference could be accounted for by variability due to small numbers of cases in this age group; there were less than 100 cases/year in the five common areas. It is also possible that this difference is the result of the better survival of women in this age group. It may be that in the most recent years these young women were diagnosed with more localized disease.

DISCUSSION

This paper investigates the current trends in age-specifi lung cancer incidence and mortality among whites. Morta ity trends were derived from data for the entire Unite States; incidence trends were derived from data for fi specific areas.

Although no formal analysis of lung cancer incidence trends among blacks is shown here, the data were analyzed for changes in incidence for black men and women. The trends in the age-adjusted rates for blacks were similar to those for whites. Because of a large variation in the yearly rates, readily discernible trends were not apparent among black men for any of the 6 age groups analyzed. Among black women, the trends did seem to follow closely those for white women.

It is with concern that we view the increasing lung cancer incidence and mortality trends for women. If these trends continue, the data suggest that the total incidence rates for men and women will be equal by the year 2000. In fact, as stated above, the incidence rates for men and women are already at a similar level for the age group 35–44. Lung cancer incidence and mortality should be monitored often and completely because of the rapid changes that have occurred and are expected to occur.

REFERENCES

(*1*) Young JL Jr, Asire AJ, Pollack ES. Cancer incidence and mortality in the United States, 1973–76. Bethesda, Md.: National Institutes of Health, 1978 [DHEW publication no. (NIH)78-1837].

(*2*) Myers MH, Hankey BF. Cancer patient survival experience. Bethesda, Md.: National Institutes of Health, 1980. NIH publication No. 80-2148.

(*3*) Cutler SJ, Devesa SS. Trends in cancer incidence and mortality in the U.S.A. In: Doll R, Vodopija I, eds. Host environment interactions in the etiology of cancer in man. IARC Sci Publ 1973; 7:15–43.

(*4*) Devesa SS, Silverman DT. Cancer incidence and mortality trends in the United States: 1935–74. J Natl Cancer Inst 1978; 60:545–571.

(*5*) Pollack ES, Horm JW. Trends in cancer incidence and mortality in the United States, 1969–76. JNCI 1980; 64:1091–1103.

(*6*) Cutler SJ, Young JL Jr, eds. Third National Cancer Survey: Incidence data. Natl Cancer Inst Monogr 1975; 41:1–454.

(*7*) Young JL Jr, Percy CL, Asire AJ, eds. Surveillance, Epidemiology, and End Results Program: Incidence and mortality data, 1973–77. Natl Cancer Inst Monogr 1981; 57:1–1082.

blank page

Simian Virus 40 (SV40)-Specific Isoelectric Point-4.7–94,000-*M*$_r$ Membrane Glycoprotein: Major Peptide Homology Exhibited With the Nuclear and Membrane-Associated 94,000-*M*$_r$ SV40 T-Antigen in Hamsters[1,2,3]

Rupert Schmidt-Ullrich,[4] W. Scott Thompson,[4] Stuart J. Kahn,[4] Maureen T. Monroe,[4] *and* Donald F. H. Wallach[4]

ABSTRACT—Tryptic peptide maps of electrophoretically purified 94,000-molecular weight (relative) (M_r) nuclear and membrane-associated simian virus 40 (SV40) T-antigens, T_N and T_M, respectively, were compared to those of the SV40-specific isoelectric point (pI)-4.7–94,000-M_r plasma membrane component reactive with anti-T-sera from Syrian golden hamsters. Bidimensional thin-layer electrophoresis and chromatography of T_N labeled with ^{125}I revealed about 27 tryptic peptides. A similar number of peptides was identified for T_M and the pI-4.7–94,000-M_r component. A peptide homology between T_N and T_M or T_N and the pI-4.7–94,000-M_r protein exists and indicates that the previously described pI-4.7–94,000-M_r membrane component represents T_M. Only 4 of 27 peptides were labeled when T_M was subjected to lactoperoxidase-catalyzed radioiodination from the outer surface of the plasma membrane. One of these T_M peptides was metabolically labeled with [^{14}C]glucosamine. The data indicate that T_M is partially exposed on the cell surface and represents a glycosylated form of T_N. Closely associated with T_M is a pI-4.5–55,000-M_r membrane component. This component does not exhibit significant peptide homology with the 94,000-M_r SV40 protein and, therefore, appears to be coded for by the host cell genome.—JNCI 1982; 69:839–849.

Mammalian cells neoplastically transformed by SV40 express virus-specific proteins on their surface membrane. These proteins are defined as TSTA or TSSA (*1–5*). Recent evidence indicates that TSTA and TSSA may represent identical antigens that are monitored by in vivo and in vitro test systems, respectively (*6*). The two antigens also exist in a close relationship with the 94,000-M_r SV40 T-antigen. This relationship is indicated by copurification of TSTA-TSSA and T-antigen during biochemical fractionation (*4*), similar subcellular distribution of the 2 groups of antigens (*2, 7*), and their concordant expression at permissive and nonpermissive temperatures in cells transformed by nondefective tsA mutants (*8, 9*). Other data indicate that purified T-antigen can induce a TSTA response in vivo (*10*), and this finding is concordant with recent findings that a 94,000-M_r T-antigen, immunochemically indistinguishable from nuclear T-antigen, can be immunoprecipitated from membranes of SV40-transformed cells (*7, 11, 12*). That SV40 T-antigen is expressed at the plasma membrane of SV40-transformed cells is further suggested by studies in which rabbit immune serum against purified T-antigen reveals a specific indirect immunofluorescence reaction at the surface of SV40-transformed cells (*11, 13*). In previous work we have identified and partially characterized two SV40-specific proteins in membranes of SV40-transformed cells (*14–16*). Using highly purified plasma membranes of SV40-transformed GD248 hamster lymphoid cells (*14, 15*) and SV80 human fibroblasts (*15*), we presented evidence that the SV40-specific pI-4.7–94,00-M_r membrane glycoprotein of these cells represents a host-modified, glycosylated T-antigen (*15, 16*). We have now obtained tryptic peptide maps of ^{125}I-labeled SV40 proteins showing that the SV40-specific pI-4.7–94,000-M_r glycoprotein exhibits a major tryptic peptide homology with the T_N. This similar peptide homology exists when the T_M or pI-4.7–94,000-M_r protein is compared with T_N. T_M represents maximally 1% of the total cellular T-antigen. Like the 94,000-M_r intracellular T-antigen (*12, 17–19*), T_M is associated with a 55,000-M_r host cell protein. This protein does not react with anti-T serum and, on the basis of tryptic peptide analyses, does not share peptides with T_N or T_M (*20–22*).

MATERIALS AND METHODS

Chemicals, media, and materials.—Triton X-100, HEPES, DTT, BSA, and PMSF were obtained from Sigma Chemical Co. (St. Louis, Mo.); Chloramine-T was from Eastman Kodak Co. (Rochester, N.Y.); SDS and urea were from Fisher Chemical Co. (Fair Lawn, N.J.); acrylamide, *N,N'*-methylenebisacrylamide, *N,N,N',N'*-tetramethylethylenediamine, ammonium persulfate, and Coomassie brilliant blue were from Bio-Rad Laboratories (Richmond, Calif.); and ampholytes (Ampholine, pH 3.5–10.0) were from LKB In-

---

Abbreviations used: BSA=bovine serum albumin; DMEM=Dulbecco's modified Eagle's minimum essential medium; DTT=dithiothreitol; EMEM=Eagle's minimum essential medium; FCS=fetal calf serum; HEPES=4-(2-hydroxyethyl)-1-piperazine ethanesulfonic acid; IEF=isoelectric focusing; M_r=molecular weight (relative); PAGE=polyacrylamide gel electrophoresis; pI=isoelectric point; PMSF=phenylmethylsulfonyl fluoride; SDS=sodium dodecyl sulfate; SV40=simian virus 40; T_M=membrane-associated 94,000-M_r T-antigen; T_N=nuclear 94,000-M_r T-antigen; TPCK=L-1-tosylamide-2-phenylethyl chloromethyl ketone; TSSA=tumor-specific surface antigen; TSTA=tumor-specific transplantation antigen.

---

[1] Received May 13, 1980; revised April 28, 1982; accepted May 10, 1982.

[2] Supported by Public Health Service grants CA-23642 and CA-12178 from the National Cancer Institute.

[3] Animals were maintained under the guidelines set forth in the "Guide for the Care and Use of Laboratory Animals" by the Institute of Laboratory Animal Resources, National Research Council.

[4] Radiobiology Division, Department of Therapeutic Radiology, Tufts-New England Medical Center, 171 Harrison Ave., Boston, Mass. 02111.

struments, Inc. (Uppsala, Sweden). Lactoperoxidase, from Boehringer Mannheim Biochemicals (Indianapolis, Ind.), in 3.2 *M* $(NH_4)_2SO_4$ was freed of ammonium sulfate by dialysis against the buffer used for labeling. TPCK-trypsin was from Worthington Biochemical Corp. (Freehold, N.J.). Protein A-Sepharose CL-4B beads, used as immune adsorbent, were obtained from Pharmacia Chemicals AB (Uppsala, Sweden) and hydrated in an equal volume of water (50%, vol/vol, suspension) prior to use. $Na^{125}I$ (carrier-free in 0.1 *M* NaOH, 17 Ci/mg), [^{35}S]methionine (>400 Ci/mmol), and [^{14}C]glucosamine hydrochloride (250-350 mCi/mmol) were obtained from New England Nuclear Corp. (Boston, Mass.). DMEM and EMEM were obtained from the Cancer Research Center, Tufts University School of Medicine; FCS was purchased from GIBCO (Grand Island, N.Y.) and heat inactivated prior to use. Cellulose thin-layer plates, Polygram Cell 300, were from Brinkman Instruments, Inc. (Westbury, N.Y.), and nitrocellulose sheets were from Beckman Instruments, Inc. (Palo Alto, Calif.).

Cells.—SV40-transformed human fibroblasts, SV80 cells, were grown in DMEM containing 10% FCS and were metabolically labeled during the logarithmic growth phase (*23*). Cultures of SV80 cells were grown to subconfluence in 850-cm^2 roller bottles (Corning Glass Works, Corning, N.Y.), starved in methionine-deficient EMEM containing 10% dialyzed FCS, and metabolically labeled with the use of 5 ml of the same medium containing [^{35}S]methionine (0.2 mCi/ml). The initial labeling was for 5 hours and was continued overnight after addition of 15 ml EMEM-10% FCS. Metabolic labeling with [^{14}C]glucosamine at a concentration of 0.2 mCi/ml was in EMEM-10% dialyzed FCS. After a 2-hour pulse the cultures were chased with 2 m*M* unlabeled glucosamine for 4 hours. After labeling, the cells were detached from the culture flasks with the use of phosphate-buffered saline (0.13 *M* NaCl-0.02 *M* Na phosphate; pH 7.2) containing 5×10^{-4} *M* EDTA.

SV40-transformed hamster skin fibroblasts [SK, line B (24)] were cultivated in EMEM fortified with 10% heat-inactivated FCS. At confluence, the cells were harvested by trypsinization and washed twice in EMEM free of serum. For tumor production, about 10^8 SK cells, suspended in 0.2 ml of EMEM without FCS, were injected im into the hind legs of 6- to 8-week-old outbred Syrian golden hamsters.

Membranes, nuclei.—SV80 cells were disrupted by nitrogen decompression (*25*). Nuclei were collected at 1.5×10^4 g/minute, washed twice in 0.065 *M* NaCl, 0.075 *M* KCl, 0.02 *M* HEPES, and 0.005 *M* $MgCl_2$ (pH 6.5) prior to extraction with 1% Triton X-100. Plasma membranes were isolated as small vesicles (*25, 26*).

Solubilization.—Prior to fractionation by bidimensional IEF-SDS-PAGE, purified membranes were solubilized in HEPES-Triton X-100 (0.001 *M*/1%, vol/vol), pH 8.5 (*27, 28*), and assayed for protein with the use of BSA as a standard (*29*). SV40 T-antigen was extracted from nuclei and plasma membrane purified from [^{35}S]methionine and [^{14}C]glucosamine-labeled SV80 cells. The extraction for immunoprecipitation was in 0.137 *M* NaCl, 0.02 *M* Tris-HCl, 0.001 *M* $CaCl_2$, and 0.001 *M* $MgCl_2$ (pH 9.0), 1% (vol/vol) in Triton X-100 and 10% (vol/vol) in glycerol, adjusted to 0.002 *M* PMSF (*23*). After extraction at 4°C for 1 hour, nuclear and membrane-associated debris was removed at 4×10^5 g/minute (*23*).

Antisera—Sera from SK (line B) sarcoma-bearing hamsters were obtained at the time of highest T-antigen reactivity, i.e., 5-7 weeks after im inoculation of 10^6 cells per site (*24*). At this time, the tumors were at least 0.5 cm in diameter. The T-antigen-reactive sera (anti-T-sera) were tested by indirect immunofluorescence by means of serial dilutions up to 512-fold. Sera positive at this titer were used for immunoprecipitation of membrane antigens. As controls, pooled sera from normal hamsters were used. Preabsorption of antigen was with normal sheep serum (*23*).

Isolation of SV40 transformation-associated proteins.—The 94,000-M_r SV40 T-antigen was precipitated from Triton X-100-solubilized plasma membranes and nuclei, both isolated from [^{35}S]methionine-labeled SV80 cells. For this procedure, solubilized plasma membranes and nuclei were adjusted to a protein concentration of 1 mg and 3 mg/ml, respectively, with the use of 0.137 *M* NaCl, 0.02 *M* Tris-HCl, 0.001 *M* $CaCl_2$, and 0.001 *M* $MgCl_2$ (pH 9.0), 1% (vol/vol) in Triton X-100 and 0.002 *M* in PMSF. The antigen (1 ml each) was preincubated with 0.01 ml of normal sheep serum and 0.08 ml of 50% (vol/vol) protein A-Sepharose immune adsorbent. Specific immunoprecipitation was then performed after addition of 0.01 ml of antigen-T-serum (and normal hamster serum as control) and 0.08 ml protein A-Sepharose at 4°C for 60 minutes (*23*). The protein A-Sepharose beads were washed three times in 0.5 ml of 0.1 *M* Tris-HCl, 0.5 *M* LiCl, and 0.14 *M* β-mercaptoethanol (pH 9.0) for removal of nonspecifically adsorbed protein. Specifically bound proteins were released by incubation in 0.05 ml of 0.02 *M* Tris-HCl and 0.7 *M* β-mercaptoethanol (pH 9.0), 5 and 20% (vol/vol), respectively, in SDS and glycerol at 80°C for 30 minutes.

After SDS-PAGE fractionation of immunoprecipitated SV40 T_M and T_N (*31*), the antigens were identified by ^{35}S autoradiography of dried gels. Bidimensional IEF-SDS-PAGE was as in (*15, 16*). The pI-4.7-94,000-M_r membrane component was isolated after protein staining of the slab gels with Coomassie blue (*31*). For peptide mapping the immunoprecipitated 55,000-M_r protein was used. The 94,000- and 55,000-M_r membrane proteins specifically bound to protein A-Sepharose were desorbed from the beads and separated from heavy- and light-chain immunoglobulins by means of IEF (*32*). The [^{35}S]methionine-labeled 94,000- and 55,000-M_r components focusing near pI 4.5 were isolated from the IEF gel, subfractionated by DS-PAGE, and identified by ^{35}S autoradiography. Gels run in parallel were stained with Coomassie blue to assure quantitative separation of immunoglobulin and the SV40 membrane proteins.

The reactivity of the pI-4.7-94,000-M_r and pI-4.5-55,000-M_r components with anti-T-sera was investigated by an electrophoretic blotting procedure (*33*). After IEF-DS-PAGE, plasma membrane proteins from SV80 cells, focusing between the pI-5.5 and pI-4.0 regions, were electrophoretically transferred from the slab gel onto nitrocellulose sheets. These were soaked in NaCl-BSA (0.15 *M*/3%, wt/vol) and reacted with hamster anti-T-serum (0.02 ml/ml of NaCl-BSA-0.001 *M* NaN_3) for 16 hours at 20°C. The nitrocellulose sheets were then soaked in NaCl (0.15 *M*) as in (*33*) for removal of unbound serum proteins. Specifically bound hamster immunoglobulin was identified by equilibration with ^{125}I-labeled protein A (5×10^7 cpm/mg protein) for 6 hours at 20°C followed by autoradiography.

^{125}I labeling of SV40-specific proteins.—The chloramine-T technique (*34*) was used to achieve iodination of T_N and SV40 membrane proteins to specific activities of about 10^8 cpm/mg protein. T_N, T_M, the pI-4.7–94,000-M_r protein, and the pI-4.5–55,000-M_r protein were localized by [^{35}S]methionine autoradiography and then iodinated in polyacrylamide gel pieces according to the procedure of Elder et al. (*35*). The protein-containing gel pieces were lyophilized in siliconized test tubes and rehydrated in about 0.05 ml of 0.5 *M* sodium phosphate (pH 8.5). After an additional 0.02 ml of chloramine-T (1 mg/ml in H_2O) and 0.3 mCi of Na^{125}I in 0.005 ml, iodination was allowed to proceed for 30 minutes at 20°C. The reaction was then quenched by addition of 0.02 ml sodium bisulfate (1 mg/ml in H_2O). Unreacted ^{125}I was removed by extensive dialysis against methanol (10%, vol/vol).

To identify the peptide moieties of T_M exposed at the cell surface, we ^{125}I labeled sealed plasma membrane vesicles by using lactoperoxidase-catalyzed radioiodination (*36*). In control experiments, plasma membranes were solubilized in Triton X-100 (1%, vol/vol) and subjected to the same iodination procedure. Immunoprecipitation and electrophoretic isolation of ^{125}I-labeled T_M were as for metabolically labeled proteins, except that the chloramine-T-mediated iodination prior to tryptic peptide mapping was omitted.

Trypsin treatment of SV40-specific proteins.—For cleavage with TPCK-trypsin, dried gel pieces containing ^{125}I-labeled SV40-specific proteins were hydrated with 0.02–0.05 ml of 0.05 *M* NH_4HCO_3; so TPCK-trypsin (0.5 mg/ml) was then added in the volume of 0.05 *M* NH_4HCO_3 required for complete hydration of the gel piece. Trypsinization was for 40 hours at 37°C with a second addition of 0.05 mg TPCK-trypsin after 16 hours. To assure that only peptides of the SV40 proteins were detected, we performed several control experiments under identical conditions: *a*) TPCK-trypsin was incubated alone in the presence of ^{125}I (2×10^6 cpm); *b*) [^{125}I]BSA, a protein completely unrelated to T-antigen, was subjected to cleavage by TPCK-trypsin, and *c*) a gel piece corresponding to the 94,000-M_r region, obtained from a sample precipitated with normal hamster serum, was trypsinized. The supernatant containing TPCK-trypsin and ^{125}I-labeled peptides was lyophilized, and the residue was solubilized in acetic acid–formic acid (15%/5%, vol/vol) for peptide mapping by electrophoresis and chromatography on cellulose thin-layer plates (*35*).

Peptide mapping—Bidimensional thin-layer peptide mapping was used to define the positions of peptides–glycopeptides in a two-dimensional grid (*35*). In addition, the "grouping" of peptides and the relative intensities of the peptide spots were evaluated. Finally, we investigated the identities of peptides from T_N and T_M and the pI-4.7–94,000-M_r component by mixing peptides of T_M with T_N, or the pI-4.7–94,000-M_r component, or all three proteins prior to bidimensional thin-layer electrophoresis and chromatography.

About 5×10^5 cpm ^{125}I-labeled or 10^4 cpm [^{14}C]glucosamine-labeled peptides were applied to a 10×10-cm thin-layer chromatography plate near the cathode. The plate was then moistened with acetic acid–formic acid (15%/5%, vol/vol) and a dye mixture of Orange G–acid fuchsin (2%/1%, wt/vol) spotted near the anode. Electrophoresis in the first dimension, at 1,000 V, was terminated when the dye had reached the sample spot. The plates were dried under cold air. Chromatography in butanol–pyridine–acetic acid–water (32.5/25/5/20, vol/vol) was at right angles to the first dimension. After drying, the peptide maps were obtained by autoradiography on Kodak no-screen X-ray film.

To prove the identity of peptides derived from T_N, T_M, and the pI-4.7–94,000-M_r protein, we localized individual peptides by using ^{125}I autoradiography. The peptides were scraped off the cellulose thin-layer plates and eluted by acetic acid–formic acid–water (15%/5%/80%, vol/vol). In all reelectrophoresis–rechromatography experiments, identical amounts, as determined by ^{125}I cpm, of peptides from the three SV40 proteins were rerun on thin-layer plates.

RESULTS

SV40-specific membrane proteins.—The present data were obtained with the use of SV80 cells that produce large quantities of SV40 T-antigen (*23*). As shown in figure 1A, plasma membranes of SV80 cells, purified and freed of nuclear contaminants according to the procedure described for GD248 hamster lymphoid cells and other SV40-transformed fibroblasts (*16, 25*), contain two membrane proteins characteristic for SV40-transformed cells—the pI-4.7–94,000-M_r and pI-4.5–55,000-M_r components. These proteins correspond to entities identified by us in plasma membranes of other SV40-transformed cells (*14, 16, 37*). Of SDS-denatured components, only the pI-4.7–94,000-M_r protein reacts with anti-T-serum after transfer from polyacrylamide to nitrocellulose (fig. 1B).

When Triton X-100-solubilized membrane proteins of SV80 cells are reacted with anti-T-serum, a 94,000-M_r protein and a 55,000-M_r protein are specifically precipitated (fig. 2). No proteins of this molecular mass are deposited when normal serum is used for precipitation of membrane-associated antigens (fig. 2). We have previously shown that the 94,000-M_r protein isolated by SDS-PAGE focuses between pI 5.5 and 4.5, with a major protein peak at pI 4.7 (*16*). Our data indicate that the 94,000-M_r T_M is associated with the 55,000-M_r component as has been reported for the total cellular T-antigen (*12, 17, 18, 20, 22, 38–40*). Whereas with the T_N a prominent 55,000-M_r component is deposited, this protein reproducibly precipitates to a lesser amount when plasma membranes are reacted with anti-T-serum. However, the 55,000-M_r protein per se does not react with anti-T-antibodies (*39, 41*). In agreement with others' results (*12*), the anti-T-serum does not precipitate possible 20,000-M_r T-antigen from plasma membranes.

Tryptic peptides of the SV40-specific membrane proteins.—Figures 3A–3F compare the tryptic peptide maps of T-antigen isolated by immunoprecipitation from purified plasma membranes, T_M, and from isolated nuclei, T_N, with those of the SV40-specific, pI-4.7–94,000-M_r plasma membrane protein.

The sensitivity of bidimensional thin-layer peptide mapping of ^{125}I-labeled peptides is sufficient for the resolution of at least 27 T_N peptides (figs. 3A, 3D). This peptide resolution appears to be superior to [^{35}S]methionine ion-exchange peptide mapping, which yielded maximally 19 peptides for the 94,000-M_rT-antigen (*21*). None of the ^{125}I-labeled peptides are contributed by trypsin itself, because no peptides were revealed when trypsin was incubated in the presence of free ^{125}I. Further, there was no peptide homology between ^{125}I-labeled BSA and ^{125}I-labeled T_N, both digested with identical quantities of TPCK–trypsin; no peptides could be identified when gel pieces of the 94,000-M_r and 55,000-M_r regions were processed from gels in which material, precipitated with normal hamster serum, was fractionated.

The numbering of peptides was based on the pattern obtained with SV40 T_N. Peptides with identical position and grouping in T_N, on the one hand, and T_M or the pI-4.7–94,000-M_r component, on the other hand, carry the same numbers. Peptides apparently deviating in position were assigned the numbers of the corresponding T_N peptide plus the letters *N* or *M*, depending on their characteristic appearance in the T_N or T_M peptide maps. Peptides from T_M and the pI-4.7–94,000-M_r component, not corresponding to those of T_N, were assigned letters (in alphabetical order).

Of the 27 peptides obtained by tryptic cleavage of ^{125}I-labeled T_N (figs. 3A, 3D), a significant number occur also in the maps obtained from both the 94,000-M_r T_M, isolated by immunoprecipitation from Triton X-100-solubilized membranes, and the pI-4.7–94,000-M_r protein. The two membrane proteins exhibit a major peptide homology between each other and with T_N (figs. 3B, 3C, 3E, 3F). The qualitative peptide pattern and the peptide intensity shown in figures 3A–3C are highly reproducible. On the basis of these observations, peptides 3, 7, 8, 9, and 16 exhibit different migrations and/or intensities when T_N and the SV40 membrane components are compared. Although a minor peptide of T_M is found in the area of peptide 7N, the displacement of the major peptide 7M relative to the positions of peptides 3, 8, and 9 is significant. New peptides, A and B, are found only in T_M and the pI-4.7–94,000-M_r component (figs. 3B, 3C, 3E, 3F). On the basis of the comparisons of figures 3A–3C, the distinctions between T_N and T_M appear to be confined to different migration and/or different intensities of peptides 3, 7, 8, 9, and 16 and the presence of additional peptides, A and B in T_M. Peptides 3, 7–9, and 16 are investigated in more detail by reelectrophoresis–rechromatography of groups of isolated peptides (figs. 4A–4D). Peptides 6, 14, and 16–19 obtained from T_M and the pI 4.7–94,000-M_r component comigrate (fig. 4B). Analyses of peptides 3, 7, 8, 9, and 21–23 (fig. 4C) and peptides 1, 2, 16, 18, and 19 (figs. 4D) reveal apparent identity of peptides 1, 2, 14, 17–19, and 21–23. This identity is confirmed by mixing experiments in which individual peptides from all three 94,000-M_r proteins are rerun (figs. 5A–5E). As shown in figure 5A, a mixture of peptides, three from T_M and the pI-4.7–94,000-M_r component comigrate as essentially one spot. Peptide 3 of T_N moves with a lower electrophoretic mobility (fig. 5B), which results in a lower intensity peptide from T_N and the more intense spot due to comigration of peptide 3 from T_M and the pI-4.7–94,000-M_r component. Due to some heterogeneity, peptides 7 of T_M and T_N migrate as two distinct spots. Peptide 16 (fig. 5F) migrates as three spots, indicating that this protein moiety may be different in T_N, T_M, and the pI-4.7–94,000-M_r component. Peptides 8 and 9 (figs. 5D, 5E) are identical in T_N and T_M.

Exposure of T_M at the membrane surface.—The peptide maps of the 94,000-M_r T_M, subjected to vectorial lactoperoxidase-catalyzed radioiodination (*36*), are shown in figure 6. Selective iodination of peptides 3, 7, 8, 9, and possibly 16 indicates that only these portions of T_M are exposed at the surface of the plasma membrane and accessibie to lactoperoxidase-catalyzed radioiodination. Peptides 3 and 7 are characteristic for T_M. A peptide pattern closely resembling that of T_M (fig. 3B) is obtained when T_M is isolated from plasma membranes that have been iodinated in the presence of 1% Triton X-100.

Glycosylation of T_M.—T_M isolated from SV80 cells pulse labeled with [^{14}C]glucosamine and subjected to tryptic peptide mapping reveals five peptides that selectively incorporate this sugar. The most prominent labeling occurs in peptide 7 (fig. 7). Peptides 9, 13, and 15 are weakly labeled. The different mobility of the prominent peptide 7 from T_N and T_M is at least in part due to glycosylation of this portion of T_M. These data indicate that some of the differences between T_N and T_M are due to posttranslational glycosylation of the membrane-associated SV40 T-antigen and suggest that peptide 7M represents a glycosylated polypeptide moiety. The persistence of a low-intensity peptide in the area of 7N of T_M may indicate microheterogeneity in the carbohydate residues or glycosylation of only a part of T_M.

T_M-associated 55,000-M_r membrane protein.—The peptide maps of T_N, T_M, and the pI-4.7–94,000-M_r protein reveal no apparent homology with that of the pI-4.5–55,000-M_r protein (fig. 8). Our data are in agreement with findings by others indicating that the 55,000-M_r protein represents a protein associated with T-antigen but encoded for by the host cell genome (*42, 43*).

DISCUSSION

Tryptic peptide mapping of the SV40 94,000-M_r T-antigen associated with the nucleus T_N, surface membrane T_M, and the pI 4.7–94,000-M_r membrane component, all labeled with ^{125}I, revealed at least 27 ^{125}I-labeled peptides for T_N and a similar number for the membrane protein. Significant peptide homology was observed between T_N and T_M or the pI-4.7–94,000-M_r protein and an apparently higher homology was observed between the two latter proteins. This analysis and our immunochemical analyses indicate that the pI-4.7–94,000-M_r glycoprotein (*14*) represents the membrane-associated T-antigen T_M. The glycosylation of T_M might easily be missed, unless purified plasma membranes are investigated, because T_M represents less than 1% of the total cellular T-antigen.

At least three major peptides, peptides 3, 7, and 16 (figs. 3, 4, 5), occupy different positions in peptide maps of T_N or T_M. The differences in peptides 3 and 16 could mean that the two proteins differ in their primary protein structure. Such a possibility is suggested by data of Mark and Berg (*44*) according to which a third splice site in the early messenger RNA would result in synthesis of a 94,000-M_r T-antigen with a more hydrophobic region near its carboxy terminus. Such a protein might qualify as a protein with high membrane affinity.

Posttranslational modification of T_M is indicated by our finding that T_M represents a glycosylated T_N. Data of others (*7*) and our own unpublished data indicate that T_M is also phosphorylated. It remains to be shown, however, whether the phosphate residue(s) in T_M are bound to the same residues as in T_N (*45*). A combination of translational and posttranslational modifications is conceivable.

Changes in the immunologic reactivity of the pI-4.7–94,000-M_r component after trypsin and neuraminidase treatment of intact isolated membranes from GD248 cells (*14*) and surface iodination of plasma membranes of SV80 cells indicate that portions of the T_M are exposed at the membrane surface. Serologic analyses by Soule et al. (*11*) have led to similar conclusions. Using immunofluorescence analyses and radioimmunoassays with sera against denatured isolated total cellular T-antigen, sera of tumor-bearing animals and surface-reactive anti-T-sera (all sera precipitated a 96,000-M_r T-antigen), these workers found differential reactivities of the membrane-associated T-antigen and the nuclear T-antigen. Soule et al. (*11*) concluded that membrane-bound T-antigen expresses antigenic sites absent on T_M or that, due to the conformation of T-antigen in the nucleus, certain antigenic sites are masked (*11*). The data on antigenicity and immunogenicity of T_M fit our own findings, which indicate that the heterologous guinea pig anti-GD248 membrane sera recognize neuraminidase-sensitive antigenic sites on the T_M molecule and that these sites are distinct from sites that react with anti-T-serum (*16*). Conversely, the anti-GD248 membrane serum does not react with T_N antigen (*14*).

The peptide homologies between T_N and T_M are in accord with previous data showing biochemical and immunologic similarities between T_N and the surface membrane-associated SV40 protein(s) described as TSTA–TSSA (*1–6*). However, the full relationship between TSTA and/or TSSA and T_M cannot yet be established, because there is another group of proteins that appear to be associated with SV40-induced transformation but not encoded by the SV40 genome. This group represents the 53,000- to 56,000-M_r phosphorylation proteins [e.g., (*19, 46*)] that do not react with anti-T-immunoglobulin intrinsically but can be immunogenic in some hosts bearing SV40-induced tumors (*41*). While our peptide analyses suggest, in agreement with data of others (*39, 40*), that this protein represents a host cell protein, data from other groups (*20, 22*) seem to indicate that this category of proteins exhibits partial peptide homology with SV40 T-antigen. A functional relationship between T_M and the 55,000-M_r protein is suggested because the two proteins are associated in the plasma membrane and the intracellular space (*12, 17, 18, 20–22, 38–40, 42*) and because they selectively associated in vitro (*19*).

REFERENCES

(*1*) Tevethia SS, Katz M, Rapp F. New surface antigen in cells transformed by simian papovavirus SV40. Proc Soc Exp Biol Med 1975; 119:896–901.

(*2*) Anderson JL, Martin RC, Chang C, Mora PT. Tumor-specific transplantation antigen is expressed during SV40 lytic infection with wild-type and tsA mutant viruses. Virology 1977; 76:254–262.

(*3*) Law LW, Takemoto KK, Rogers MJ, Ting RC. Induction of simian virus 40 (SV40) transplantation immunity in mice by SV40-transformed cells of various species. J Natl Cancer Inst 1977; 59:1523–1526.

(*4*) Luborsky SW, Chang C, Pancake SJ, Mora PT. Comparative behavior of simian virus 40 T-antigen or of tumor-specific surface and transplantation antigens during partial purification. Cancer Res 1978; 38:2367–2371.

(*5*) Pancake SJ, Mora PT. Comparison of SV40-induced antigens on the surface of cultivated cells by a cytolytic microassay. Virology 1974; 59:323–327.

(*6*) Chang C, Pancake SJ, Luborsky SW, Mora PT. Detergent solubilization and partial purification of tumor specific surface and transplantation antigens from SV40-virus-transformed mouse cells. Int J Cancer 1977; 19:258–266.

(*7*) Soule HR, Butel JS. Subcellular localization of simian virus 40 large tumor antigen. J Virol 1979; 30:523–532.

(*8*) Tenen DG, Martin RG, Anderson J, Livingston DM. Biological and biochemical studies of cells transformed by simian virus 40 temperature-sensitive gene A mutants and A mutant remutants. J Virol 1977; 22:210–218.

(*9*) Anderson JL, Chang C, Mora PT, Martin RG. Expression and thermal stability of simian virus 40 tumor-specific transplantation antigen and tumor-antigen in wild-type- and tsA mutant transformed cells. J Virol 1976; 21:459–467.

(*10*) Chang C, Martin RG, Livingston DM, Luborsky SW, Hu C-P, Mora PT. Relationship between T-antigen and tumor-specific transplantation antigen in simian virus 40-transformed cells. J Virol 1979; 29:69–75.

(*11*) Soule HR, Lanford RE, Butel JS. Antigenic and immunogenic characteristics of nuclear and membrane-associated simian virus 40 T antigen. J Virol 1980; 33:887–901.

(*12*) Chandrasekaran K, Winterbourne DJ, Luborsky SW, Mora PT. Surface proteins of simian virus 40-transformed cells. Int J Cancer 1981; 27:397–407.

(*13*) Lanford RE, Butel JS. Antigenic relationship of SV40 early proteins to purified large T polypeptide. J Virol 1979; 97:295–306.

(*14*) Schmidt-Ullrich R, Thompson WS, Lin P-S, Wallach DF. Simian virus 40-specific proteins in membranes of simian virus 40-transformed hamster and mouse cells. Proc Natl Acad Sci USA 1977; 74:5069–5072.

(*15*) Schmidt-Ullrich R, Thompson WS, Wallach DF. Biochemical and immunochemical characterization of two simian virus 40 (SV40)-specific glycoproteins in nuclear and surface membranes of SV40-transformed cells. Biochem Biophys Res Commun 1979; 88:887–894.

(*16*) Schmidt-Ullrich R, Kahn SJ, Thompson WS, Wallach DF. Host cell-modified T-antigen in membranes of simian virus 40-transformed hamster cells. JNCI 1980; 65:585–593.

(*17*) Harlow E, Pim DC, Crawford LV. Complex of simian virus 40 large-T antigen and host 53,000-molecular weight protein in monkey cells. J Virol 1981; 37:564–573.

(*18*) McCormick F, Clark R, Harlow E, Tijan R. SV40 T antigen binds specifically to a cellular 53 K protein in vitro. Nature 1981; 292:63–65.

(*19*) McCormick F, Harlow E. Association of a murine 53,000-dalton phosphoprotein with simian virus 40 large-T antigen in transformed cells. J Virol 1980; 34:213–224.

(*20*) Chang C, Simmons DT, Martin MA, Mora PT. Identification and partial characterization of new antigens from simian virus 40-transformed mouse cells. J Virol 1979; 31:463–471.

(*21*) Melero JA, Stitt DT, Mangel WR, Carroll RB. Identification of new polypeptide species (48–55K) immunoprecipitable by antiserum to purified large T antigen and present in SV40-infected and -transformed cells. Virology 1979; 93:466–480.

(*22*) Kress M, May E, Cassingena R, May P. Simian virus 40-transformed cells express new species of proteins precipitable by anti-simian virus 40 tumor serum. J Virol 1980: 31:472–483.

(*23*) Griffin JD, Light S, Livingston DM. Measurement of the molecular size of the simian virus 40 large T antigen. J Virol 1978; 27:218–226.

best copy available

(*24*) Diamandopoulos GT, Dalton-Tucker MF. Induction in hamsters of various carcinomas and sarcomas by in vitro SV40-transformed homologous embryonic skin and subcutaneous tissue cells. Am J Pathol 1969; 56:59–77.

(*25*) Schmidt-Ullrich R, Wallach DF, Davis FD II. Membranes of normal hamster lymphocytes and lymphoid cells neoplastically transformed by simian virus 40. I. High-yield purification of plasma membrane fragments. J Natl Cancer Inst 1976; 57:1107–1116.

(*26*) Wallach DF, Schmidt-Ullrich R. Isolation of plasma membrane vesicles from animal cells. Methods Cell Biol 1977; 15:235–276.

(*27*) Schmidt-Ullrich R, Verma SP, Wallach DF. Increased side chain amidation of hamster lymphocyte plasma membranes after transformation with simian virus 40 is revealed by isoelectric focusing and laser Raman spectroscopy. Biochem Biophys Res Commun 1975; 67:1062–1069.

(*28*) Schmidt-Ullrich R, Wallach DF, Davis FD II. Membranes of normal hamster lymphocytes and lymphoid cells neoplastically transformed by simian virus 40. II. Plasma membrane proteins analyzed by dodecyl sulfate–polyacrylamide gel electrophoresis and two-dimensional immune electrophoresis. J Natl Cancer Inst 1976; 57:1117–1126.

(*29*) Moore S, Stein WG. Photometric ninhydrin method for use in chromatography of amino acids. J Biol Chem 1948; 116:367–388.

(*30*) Laemmli UK. Cleavage of structural proteins during the assembly of the head of bacteriophage T4. Nature 1970; 227:680–685.

(*31*) Fairbanks G, Steck TL, Wallach DF. Electrophoretic analysis of major polypeptides of the human erythrocyte membrane. Biochemistry 1981; 10:2606–2616.

(*32*) Maidment RW, Papsidero LD, Gamarra M, Nemoto T, Chu TM. Isoelectric focussing analysis of immune complexes bound to protein A-sepharose. Anal Biochem 1981: 3:336–342.

(*33*) Towbin H, Staehelin T, Gordon J. Electrophoretic transfer of proteins from polyacrylamide gels to nitrocellulose sheets: Procedure and some applications. Proc Natl Acad Sci USA 1979; 76:4350–4354.

(*34*) Greenwood FC, Hunter WM, Glover JS. The preparation of I-131-labelled growth hormone of high specific radioactivity. Biochem J 1963; 89:114–123.

(*35*) Elder JW, Pickett RA II, Hampton J, Lerner RA. Radioiodination of proteins in single polyacrylamide gel slices. J Biol Chem 1977; 252:6510–6515.

(*36*) Schmidt-Ullrich R, Mikkelsen RB, Wallach DF. Transmembrane disposition of the 55,000-dalton concanavalin A receptor protein of thymocyte plasma membranes. J Biol Chem 1978; 253:6973–6978.

(*37*) Schmidt-Ullrich R, Thompson WS, Wallach DF. Antigenic distinctions of glycoproteins in plasma membranes and mitochondrial membranes of lymphoid cells neoplastically transformed by simian virus 40. Proc Natl Acad Sci USA 1977; 74:643–647.

(*38*) Luborsky SW, Chandrasekaran K. Subcellular distribution of simian virus T antigen species in various cell lines: The 56 K protein. Int J Cancer 1980; 25:517–527.

(*39*) Lane DP, Crawford LV. T antigen is bound to a host protein in SV40-transformed cells. Nature 1979; 278:261–263.

(*40*) Linzer DI, Levine AJ. Characterization of a 54K dalton cellular SV40 tumor antigen present in SV40-transformed cells and uninfected embryonal cells. Cell 1979; 17:43–52.

(*41*) Harlow E, Crawford LV, Pim DC, Williamson NM. Monoclonal antibodies specific for simian virus 40 tumor antigen. J Virol 1981; 39:861–869.

(*42*) Greenspan DS, Carrel RB. Complex of simian virus 40 large tumor antigen and 48,000-dalton host tumor antigen. Proc Natl Acad Sci USA 1981; 78:105–107.

(*43*) Crawford CV, Pim DC, Gurney EG, Goodfellow P, Taylor-Papadimitriou J. Detection of a common feature in several human tumor cell lines—a 53,000-dalton protein. Proc Natl Acad Sci USA 1981; 78:41–45.

(*44*) Mark DF, Berg P. A third splice site in the SV40 early mRNA. Cold Spring Harbor Symp Quant Biol 1980; 44:55–62.

(*45*) Rundell K, Collins JK, Tegtmeyer P, Ozer HL, Lai C-J, Nathans D. Identification of a simian virus 40 protein A. J Virol 1977; 21:636–646.

(*46*) Jay G, Khoury G, DeLeo AB, Dippold WG, Oza LJ. P53 transformation-related protein. Detection of an associated phosphotransferase activity. Proc Natl Acad Sci USA 1981; 78:2932–2936.

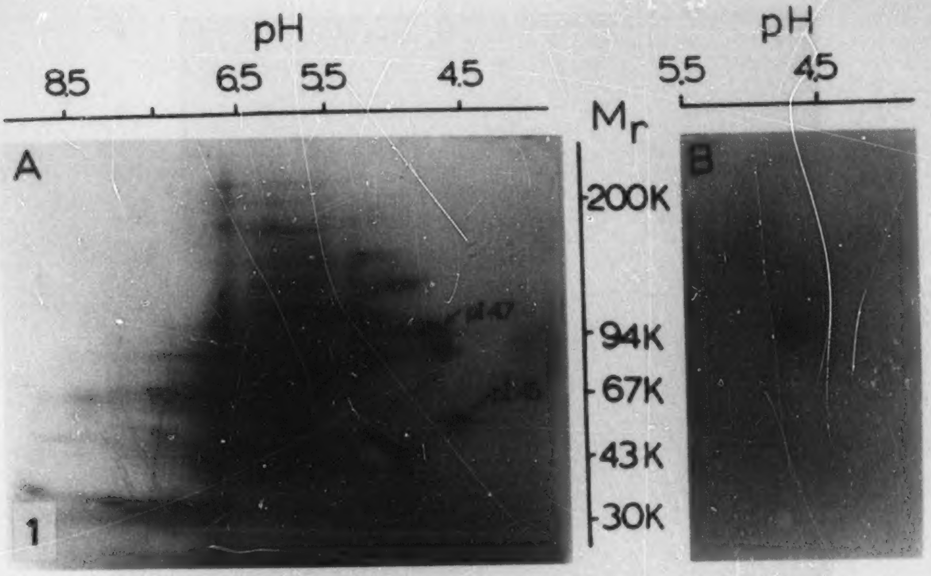

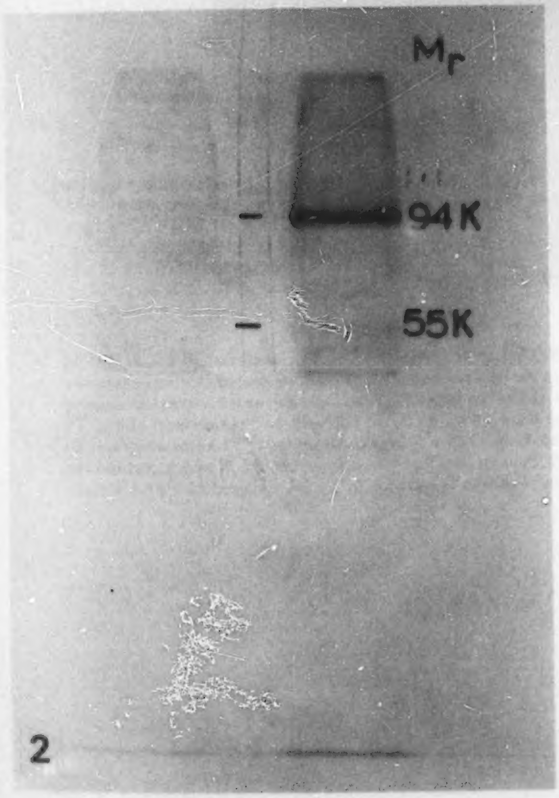

FIGURE 1.—Bidimensional IFF-SDS-PAGE of plasma membranes from SV80 cells. Triton X-100-solubilized protein (≈0.4 mg) was separated by IEF in the first dimension and then, at right angles, fractionated according to M_r in the presence of SDS and DTT. A) Coomassie blue protein staining. The SV40-specific pI-4.7-94,000-M_r and pI-4.5-55,000-M_r membrane components are identified by *arrows*. B) Electrophoretic blot of the slab gel in the pI-5.5-4.0 range after reaction with anti-T-serum and ^{125}I-labeled protein A. ^{125}I autoradiogram. The *abscissa* gives the pH gradient, and the *ordinate* gives the $M_r \times 10^3$ (K).

FIGURE 2.—SDS-PAGE of [^{35}S]methionine-labeled membrane-associated SV40 T-antigen, T_M, immunoprecipitated from Triton X-100-solubilized SV80 plasma membranes. ^{35}S autoradiogram. *Right lane:* Hamster anti-T-serum reacted with SV80 membrane proteins. *Left lane:* Normal hamster serum reacted with an identical quantity of membrane protein. $M_r \times 10^3$ (K).

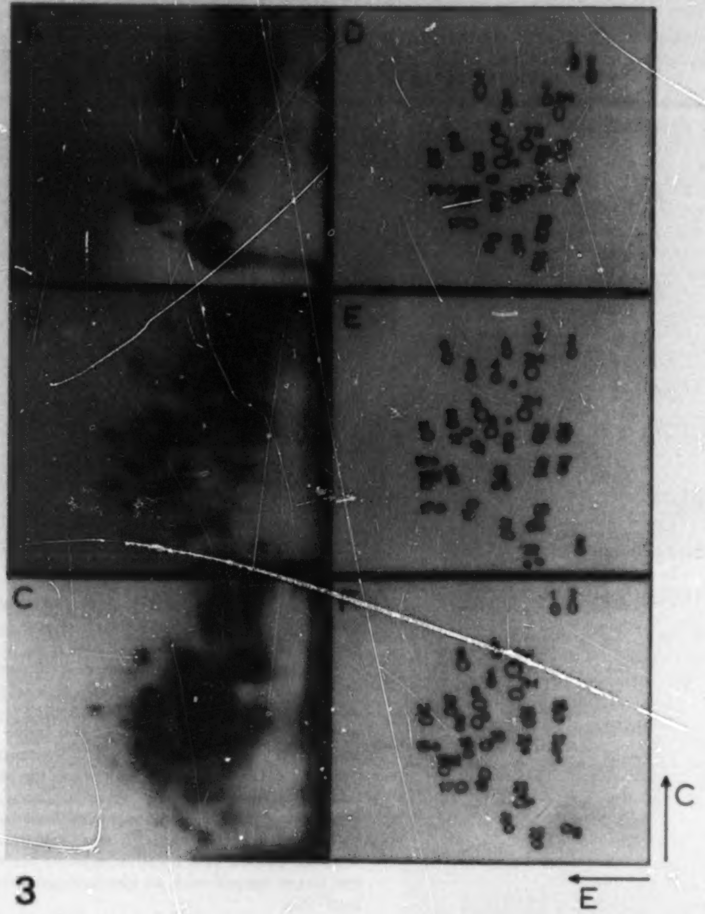

3

FIGURE 3.—Bidimensional tryptic peptide maps of the 94,000-M_r SV40-specific proteins. T_N, T_M, and the pI-4.7-94,000-M_r component were labeled with ^{125}I, digested with TPCK-trypsin, and, in the first dimension (*horizontal*), separated electrophoretically (E) on thin-layer chromatography plates in acetic acid-formic acid (15%/5%, vol/vol). Fractionation in the second dimension (*vertical*) was by chromatography (C) in butanol-pyridine-acetic acid-water (32.5/25/5/20, vol/vol). A) Peptide map of T_N; ^{125}I autoradiogram. B) Peptide map of T_M; ^{125}I autoradiogram. C) Peptide map of pI-4.7-94,000-M_r protein; ^{125}I autoradiogram. D) Schematic of map A. E) Schematic of map B. F) Schematic of map C. Peptides are numbered from 1 to 27. N and M behind the numbers indicate the peptide characteristic for T_N and T_M, respectively. Peptides found only in T_M are assigned by letters. Results represent four independent experiments.

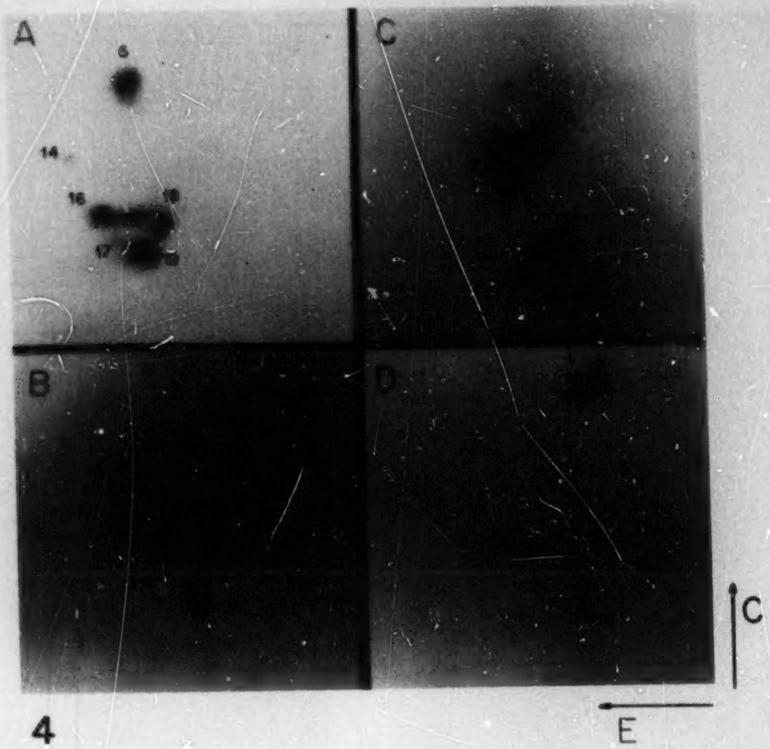

4

FIGURE 4.—Bidimensional mapping of tryptic peptides isolated from maps of ^{125}I-labeled T$_N$, T$_M$, and the pI-4.7–94,000-*M*$_r$ component. Separation in the first dimension (*horizontal*) was electrophoretically (E) on thin-layer chromatography plates in acetic acid–formic acid (15%/5%, vol/vol). Fractionation in the second dimension (*vertical*) was by chromatography (C) in butanol–pyridine–acetic acid–water (32.5/25/5/20, vol/vol). ^{125}I autoradiograms. A) Peptides 6, 14, and 16–19 combined of T$_N$, T$_M$, and the pI-4.7–94,000-*M*$_r$ component. B) Peptides 6, 14, and 16–19 combined of T$_M$ and the pI-4.7–94,000-*M*$_r$ component. C) Peptides 3, 7, 8, 9, and 21–23 combined of T$_N$, T$_M$, and the pI-4.7–94,000-*M*$_r$ component. D) Peptides 1, 2, 16, 18, and 19 combined of T$_M$ and the pI-4.7–94,000-*M*$_r$ component.

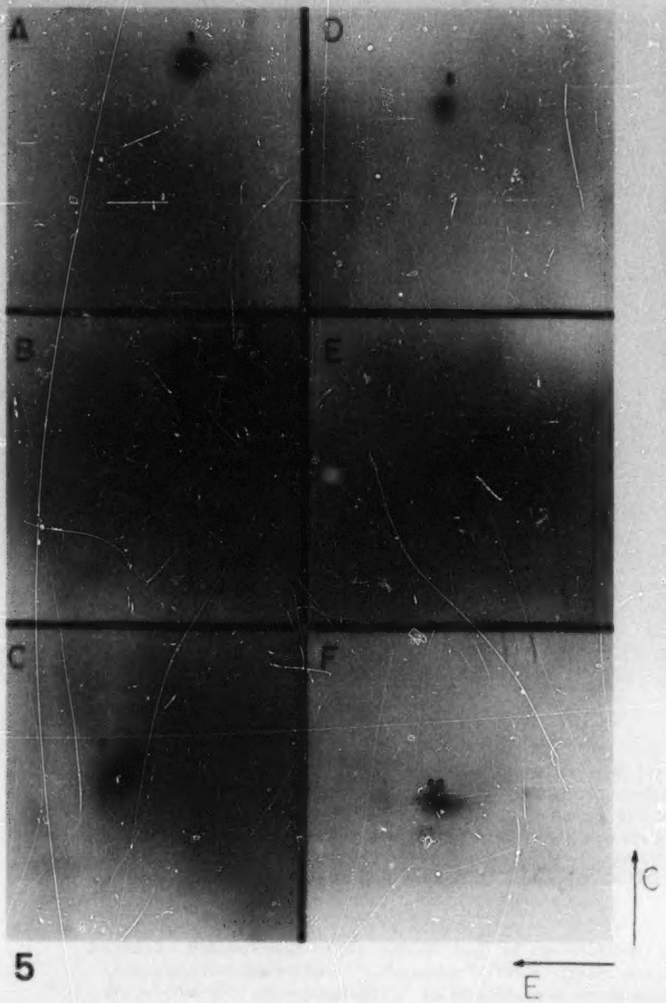

5

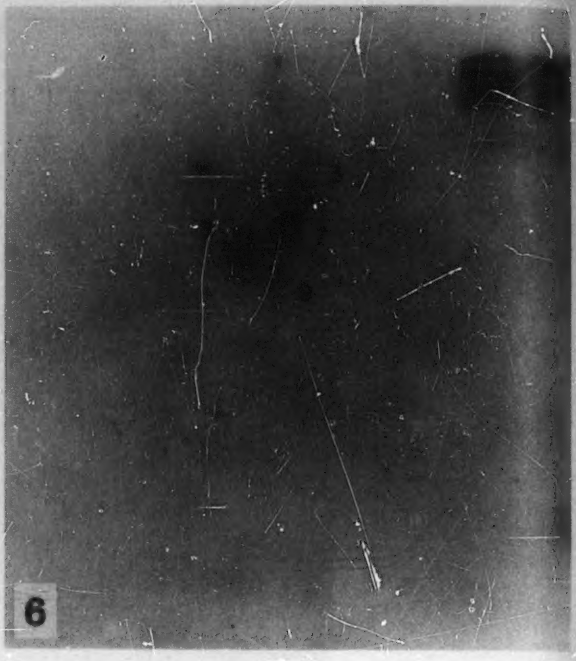

FIGURE 5.—Bidimensional mapping of tryptic peptides isolated from maps of ^{125}I-labeled T_N, T_M, and the pI-4.7-94,000-*M*$_r$ component. Separation in the first dimension (*horizontal*) was electrophoretically (E) on thin-layer chromatography plates in acetic–formic acid (15%/5%, vol/vol). Fractionation in the second dimension (*vertical*) was by chromatography (C) in butanol–pyridine–acetic acid–water (32.5/25/5/20, vol/vol). ^{125}I autoradiograms. A) Peptides 3 combined of T_M and the pI-4.7-94,000-*M*$_r$ component. B) Peptides 3 combined of T_N, T_M, and the pI-4.7-94,000-*M*$_r$ component. C) Peptides 7 combined of T_N and T_M. D) Peptides 8 combined of T_N, T_M, and the pI-4.7-94,000-*M*$_r$ component. E) Peptides 9 combined of T_N, T_M, and the pI-4.7-94,000-*M*$_r$ component. F) Peptides 16 combined of T_N, T_M, and the pI-4.7-94,000-*M*$_r$ component.

FIGURE 6.—Bidimensional tryptic peptide maps of the SV40 T_M, surface iodinated in plasma membranes of SV80 cells with the use of lactoperoxidase-catalyzed radioiodination. After digestion with TPCK-trypsin, the peptides were separated electrophoretically in the first dimension (*horizontal*) on thin-layer chromatography plates in acetic acid–formic acid (15%/5%, vol/vol). Fractionation in the second dimension (*vertical*) was by chromatography in butanol–pyridine–acetic acid–water (32.5/25/5/20, vol/vol). ^{125}I autoradiogram. Numbering of the peptides is as in fig. 3B. Results are of three independent experiments.

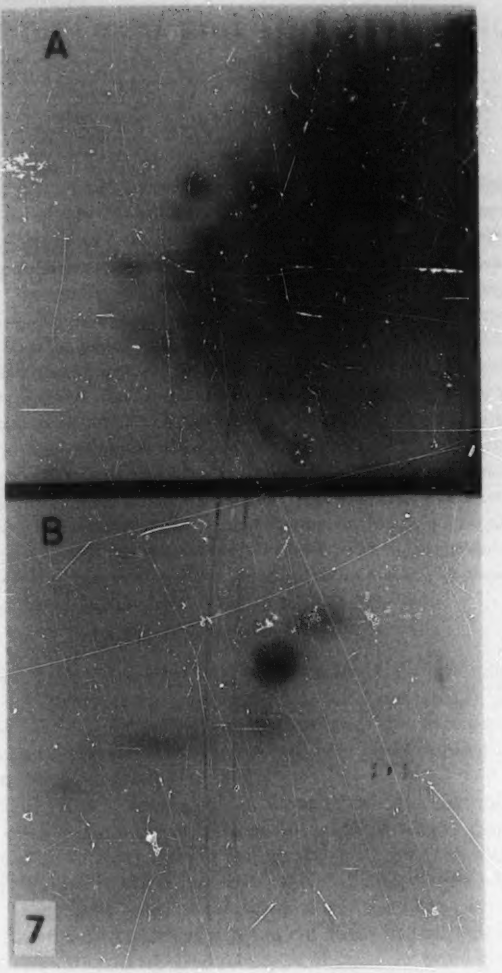

7

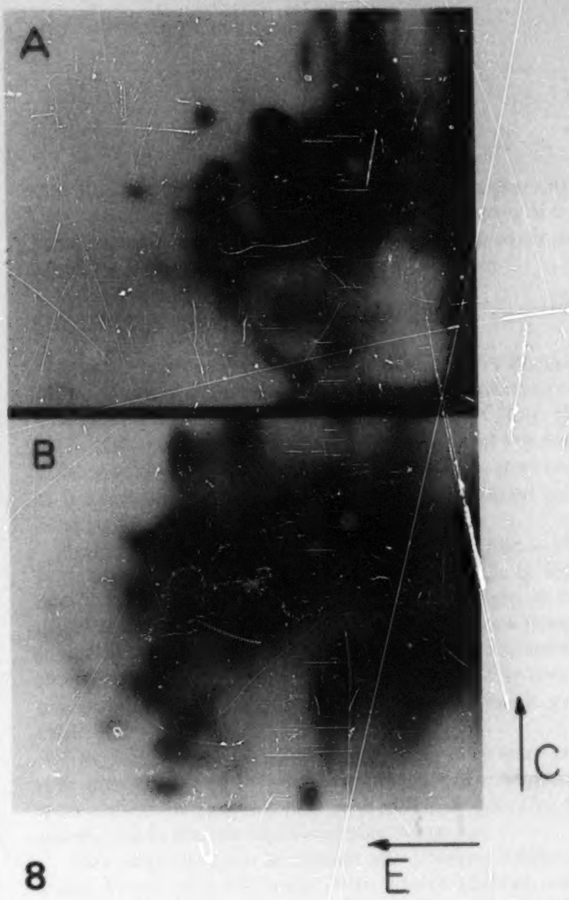

8

Figure 7.—Bidimensional tryptic peptide maps of SV40 T$_{\text{M}}$. After digestion with TPCK-trypsin, the peptides were separated electrophoretically in the first dimension (*horizontal*) on thin-layer chromatography plates in acetic acid-formic acid (15%/5%, vol/vol). Fractionation in the second dimension (*vertical*) was by chromatography in butanol-pyridine-acetic acid-water (32.5/25/5/20, vol/vol). A) Peptide map of T$_{\text{M}}$; ^{125}I autoradiogram. B) Peptide map of T$_{\text{M}}$; ^{14}C autogram of T$_{\text{M}}$ metabolically labeled with [^{14}C]glucosamine. Results of two independent experiments.

Figure 8.—Bidimensional tryptic peptide maps of SV40 T$_{\text{M}}$ and the 55,000-M_r membrane component. After digestion with TPCK-trypsin, the peptides were separated electrophoretically (E) in the first dimension (*horizontal*) on thin-layer chromatography plates in acetic acid-formic acid (15%/5%, vol/vol). Fractionation in the second dimension (*vertical*) was by chromatography (C) in butanol-pyridine-acetic acid-water (32.5/25/5/20, vol/vol). ^{125}I autoradiograms. A) Peptide map of T$_{\text{M}}$. B) Peptide map of the 55,000-M_r component. Results are of three independent experiments.

blank page

Relationship of Lung Adenoma Prevalence and Growth Rate to Acute Urethan Dose and Target Cell Number[1,2,3,4]

Michael L. Dourson[5,6] *and* Ellen J. O'Flaherty[5,7,8]

ABSTRACT—Outbred Swiss Cox mice of both sexes were given single ip injections of 0.5–2.0 mg urethan/g body weight. Lung adenomas began to grow about 7 days after urethan administration. The relationship of plateau tumor level to dose was slightly concave upward. However, the relationship of average tumor number per 10^6 surviving target cells or alveolar type II cells to dose was markedly concave upward. Thus the definition of the urethan dose–lung adenoma prevalence curve should take into account the urethan cytotoxicity. Tumor diameters followed a log normal distribution pattern. The rate of change of geometric mean tumor diameter was independent of sex and urethan dose. In another experiment Swiss Cox mice received ip injections of 1.5 mg urethan/g body weight, and 4 weeks later chronic exposure to urethan in the drinking water was begun. The growth rate of adenomas induced by the single urethan injection was unaffected by subsequent chronic urethan administration. The results support the common assumption that tumor growth rate is independent of the rate of chronic administration of a carcinogen.—JNCI 1982; 69:851–857.

Mouse lung adenoma has been induced by all major groups of chemical carcinogens except hormones (*1*). Because of the ease of tumor induction and the rapidity of tumor appearance, this model has enjoyed wide application in carcinogenesis studies.

Urethan (ethyl carbamate) is a water-soluble carinogen with a simple chemical structure. Its administration causes adenomas of alveolar type II cell origin to appear randomly throughout the lungs of sensitive mice (*2*). Given in sufficiently large amounts, urethan is cytotoxic. Qualitative studies have demonstrated a transient drop in the number of lung cells, including alveolar type II cells, in mice given a single injection of urethan (*3, 4*). Therefore, the total number of adenomas induced by a single dose of urethan will be determined by both the carcinogenic action of urethan and its effect on the number of target cells. Although urethan dose–adenoma prevalence relationships have been investigated (*5–8*), the relative importance of the cytotoxic effects of urethan in determining the shapes of these curves is not known.

The growth rate of lung adenomas induced by single urethan injections has been studied in several mouse strains (*8–12*). Shimkin and Polissar (*10*) concluded that the initiating dose did not affect the geometric mean lung adenoma diameter. Rogers (*8*) also found that tumor size distribution was independent of the size of a single urethan dose. In addition, Rogers observed that multiple identical urethan doses did not significantly alter either the maximum tumor size or the tumor size distribution. However, neither of these studies addressed the question of the effect of chronic urethan exposure on adenoma growth rate.

The purposes of this investigation were to define the acute urethan dose–adenoma prevalence relationship to express prevalence based on the size of the viable alveolar type II cell population, to establish the growth rate of lung adenomas after single urethan injections at different doses in Swiss Cox mice, and to determine whether the growth rate of adenomas previously induced by single urethan injections could be affected by chronic urethan exposure.

MATERIALS AND METHODS

Mice.—Outbred Swiss Cox mice (Laboratory Supply Co., Indianapolis, Ind.) were used to establish a breeding colony. The animals were fed Rodent Laboratory Chow (Purina 5001; Ralston Purina Co., St. Louis, Mo.) and tap water ad libitum and were housed in standard stainless steel cages up to 5 mice per cage. All animals were maintained on a 12-hour light–12-hour dark cycle.

Acute study—adenoma prevalence and growth rate.—Mice of both sexes, 41–45 days old, were given a single ip injection of 0.5, 1.0, 1.5, or 2.0 mg urethan/g body weight in 10 µl of distilled waer. The mice were killed at various times after injection as described (*13*). Twenty controls received injections of 10 µl distilled water/g body weight. The number of exposed animals killed at each dose and time is given in table 1.

The lungs were prepared, and adenomas were counted and measured as previously described (*13*). Several lungs were chosen at random and embedded in paraffin for histologic confirmation of pulmonary adenoma.

Acute study—response of alveolar type II cells.—Mice of both sexes, 41–45 days old were treated with identical doses of urethan as before and were killed at either 6, 12, 18, or 42 hours after injection. Four animals that received identical doses were killed at each time. There were 14 controls.

At the time of killing, 2 mice of each sex at each dose level were anesthetized as before. Lungs were collapsed by opening the chest, excised, placed in cold (≈4–5°C) isotonic

---

[1] Received August 1, 1980; revised April 5, 1982; accepted April 27, 1982.

[2] Supported by Public Health Service grant ES-07073, training program in toxicology, from the National Institute of Environmental Health Sciences.

[3] Animals were maintained under the guidelines set forth in the "Guide for the Care and Use of Laboratory Animals" by the Institute of Laboratory Animal Resources, National Research Council.

[4] Parts of the investigation were performed in partial fulfillment of the requirements of a Ph.D. degree (M. L. D.).

[5] Department of Environmental Health, College of Medicine, University of Cincinnati, 3223 Eden Ave., Cincinnati, Ohio 45267.

[6] *Present address*: Environmental Protection Agency, 26 West St. Clair St., Cincinnati, Ohio 45268.

[7] *Address reprint requests to* Dr. O'Flaherty.

[8] We thank Klaus L. Stemmer, *M.D.*, Cincinnati College of Medicine, for the identification of pulmonary adenomas; and Dr. Peter S. Gartside for his assistance with the method used to calculate geometric mean tumor diameter.

TABLE 1.—*No. of mice killed at various doses and times in the acute study, and No. of adenomas measured*[a]

Time of killing, wk post injection	Urethan dose, mg/g body wt[b]							
	0.5		1.0		1.5		2.0	
	No. of tumors	No. of mice	No. of tumors	No. of mice	No. of tumors	No. of mice	No. of tumors	No. of mice
3	—	—	—	—	31	12	—	—
4	—	—	—	—	56	11	—	—
6	18	9	48	10	87	8	149	7
8	29	9	63	9	176	10	148	4
10	31	10	66	8	269	10	316	7
12	43	8	139	11	288	10	184	5
14	61	10	164	9	301	10	150	5
16	—	—	401	16	—	—	—	—

[a] Data of male and female mice were combined.

[b] — = no mice killed at this dose and time.

saline, stripped of excess tissue, weighed, and expanded with cold (~10°C) double aldehyde fixative (*14*) at 20 cm of solution pressure for 2–3 minutes. Lung volume was determined by fluid displacement, and lungs were refrigerated in double aldehyde fixative for 24–48 hours.

After the refrigeration period, lung lobes were separated and 10–15 1-mm cubes were cut from the thickest portions of the three major lobes (left, apical, and posterior). Cubes were washed in Millonig's phosphate buffer (*15*) and post fixed in 2% OsO_4–Millonig's buffer solution (1:1) for 2 hours at 4°C. The cubes were dehydrated through a sequence of increasingly concentrated alcohol solutions and then by propylene oxide and embedded in Spurr plastic (*16*).

Eight different 1- to 2-μm sections of lung tissue were stained with toluidine blue for 2 minutes at 56°C. Slides were made and viewed blindly under oil immersion at 1,250×. Five fields per section were sampled at random, and dead, borderline, and live type II cells were scored based on the following criteria: Dead type II cells were identified by loss of nuclear detail, which included lack of staining of nuclear membrane and hyperchromicity of nucleus, and accumulation of large lamellar bodies in the cytoplasm (*17*); borderline cells were identified by either, but only one, of the above criteria; live type II cells had neither of these characteristics. All eight tissue sections were viewed to give 40 sampled fields. Each field enclosed an area of 15,840.0 μm^2. Approximately 80 type II cells were counted in 40 fields in control animals.

Lung parenchymal volume is 80% of the total lung lobe volume in outbred Swiss mice (*18*). Lung lobe volume in the Swiss Cox mice used in this study was 93.8% of total lung volume. Therefore, we used a factor of 0.8×93.8% or 75.0% to convert total lung volume to lung parenchymal volume.

The total number of live type II cells in the lung was calculated by multiplying the total lung parenchymal volume by the density of live type II cells in the lung parenchyma. This density was estimated by the division of the number of type II cell nuclei in 40 microscopic fields by the area of these 40 fields and then by the nuclear diameter 6 μm (*4*, *18*).

Acute-chronic study.—Mice of both sexes, 41–45 days old, were given single ip injections of 1.5 mg urethan/g body weight and returned to standard animal room conditions. Four or 6 weeks later chronic exposure was started by giving the animals distilled water ad libitum to which urethan was added to yield a 0.10 or 0.02% concentration by weight. The higher concentration has been used in studies of hyperplasia during chronic urethan exposure (*17*, *18*), but both dose schedules are able to increase the incidence of pulmonary adenoma in mice. Controls were also given injections of 1.5 mg urethan/g body weight but were given distilled water ad libitum throughout the study. The number of mice in each group is given in table 2.

All the animals were killed 4 weeks after the start of chronic urethan administration, their lungs were prepared, and adenomas were counted and measured as before. The times of killings were selected so that adenomas induced by chronic exposure to urethan should not have attained a large enough size to interfere with the count and measurement of the original adenoma population. In this way it was possible to evaluate any effect of urethan on tumor growth rate independently of its tumor-inducing action.

TABLE 2.—*Geometric mean tumor diameter with various urethan treatments in the acute–chronic study*

Acute urethan dose, mg/g body wt	Chronic urethan dose, % drinking water	No. of animals killed	No. of tumors measured	Geometric mean tumor diameter, 10^{-4} m	Logarithm of tumor diameter, mean±SD
Killing time: 8 wk post injection[a]					
All doses[b]	0.0	32	416	3.55	0.55±0.25
1.5	0.0	9	186	4.07	0.61±0.25
1.5	1.10	21	331	4.07	0.61±0.20
1.5	0.02	—	—	—	—
Killing time: 10 wk post injection[a]					
All doses[b]	0.0	35	682	4.27	0.63±0.27
1.5	0.0	—	—	—	—
1.5	0.10	—	—	—	—
1.5	0.02	21	413	4.79	0.68±0.22

[a] — = no animals killed at this time.

[b] Data from tables 1 and 3, all doses (0.5, 1.0, 1.5, and 2.0 mg/g body wt) were combined, as well as data for male and female mice.

RESULTS

Adenoma Prevalence

Average tumor number was dependent on both time and dose (text-fig. 1). These averages were about half of those

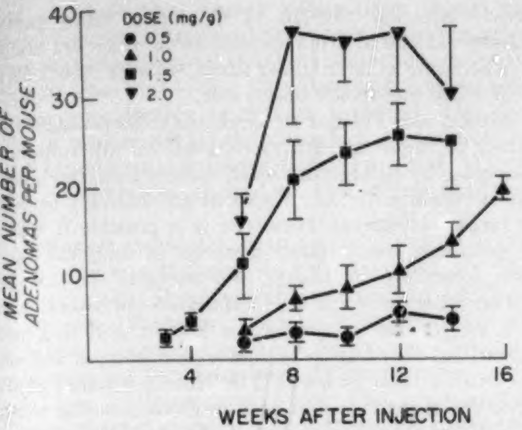

TEXT-FIGURE 1.—Mean tumor No. per animal at different times after different single urethan doses. *Bars* indicate ±SEM. Data of animals that had a number of tumors in excess of 2 SD were disregarded.

expected for A mice, the common strain used in such studies (*1*). In agreement with other reports for small groups of animals (*1*, *2*), there were no consistent sex-related differences in average tumor numbers. As a result, data from both sexes were combined as shown.

Average tumor numbers appear to reach a plateau between 10 and 14 weeks at three of the four doses (0.5, 1.5, and 2.0 mg/kg). These findings are consistent with previous observations in other mouse strains. Shimkin and Stoner (*1*), in a summary of several studies, stated that average tumor numbers reach a plateau by 7 weeks if histologic methods are used to identify the adenomas, or by 16 weeks if only the surface tumors are counted. The present method of adenoma identification is apparently intermediate in its sensitivity. The anomalous behavior of the 1.0-mg/g dose group at 16 weeks is perhaps due to sampling variability, because in other measured variables (e.g., tumor growth rate and lung weights) this group was consistent with other doses. Plateau values were estimated at each dose in this study as the mean of the three highest adenoma averages. The relationship between plateau tumor level and dose was slightly concave upward (text-fig. 2).

Average Number of Live Type II Cells

There were no differences between sexes in the average number of live type II cells per lung; therefore, data from both sexes were combined. The average number of live alveolar type II cells showed a transient decrease that was dose and time related. The largest decreases were seen at the highest doses and shortest times (text-fig. 3). Increases in dead and borderline type II cells, in general, reflected the decreases in live type II cells. When 6-, 12-, and 18-hour data for each dose were averaged, the percent decrease in live type II cells was linear with respect to dose.

From the estimated plateau tumor level and the 6- to 18-hour averaged number of live type II cells (text-fig. 3), the mean tumor number per 10^6 surviving alveolar type II cells at each dose was calculated. The relationship between this measure of prevalence and dose is shown in text-figure 4.

Adenoma Growth—Acute Study

Variations in tumor diameters have been shown to be greater within the same mouse rather than among mice given an acute dose of urethan (*10*) and to be independent of sex (*11*). Our results duplicated these observations. Independence of adenoma growth rate from size of the urethan dose has also been reported by others (*8*, *10*). Although there were statistically significant differences among the geometric mean tumor diameters observed in this study in mice killed at the same time but given different doses of urethan (table 3), such differences occurred randomly and were not dose

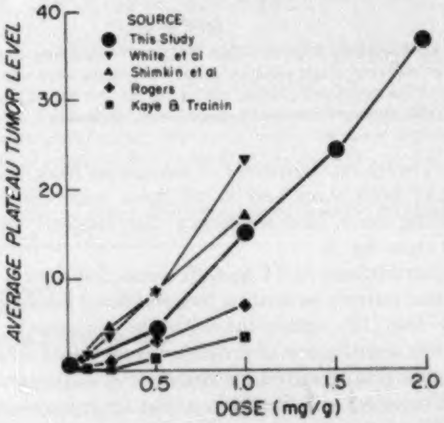

TEXT-FIGURE 2.—Mean plateau tumor No. per animal at various single doses of urethan. Plateau tumor levels have been estimated by averaging the 3 highest averages of adenoma No. at each dose. The estimated plateau tumor levels in this study were: 0.0 mg/g, 0.2; 0.5 mg/g, 4.3; 1.0 mg/g, 15; 1.5 mg/g, 25; and 2.0 mg/g, 37. Experimental prevalence taken from the literature has been adjusted for control prevalence wherever possible. Data from White et al. (*6*) on animals given injections on the 1st and last days of the study were combined and averaged.

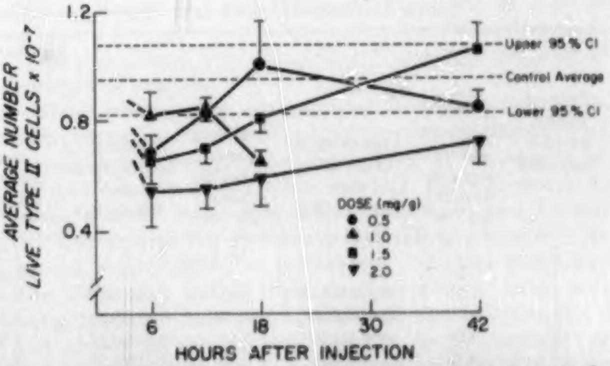

TEXT-FIGURE 3.—Average No. of live alveolar type II cells per lung ($\times 10^{-7}$) at different times after various single doses of urethan; *each point* represents 4 animals. *Bars* indicate ±SEM. Control level of live type II cells was 0.96×10^7 cells/lung based on 12 animals; the 95% confidence interval on the control mean is indicated in the figure. The No. of live cells is assumed to be normally distributed among animals. Mice given 1.0 mg urethan/g body wt were not examined at 42 hr.

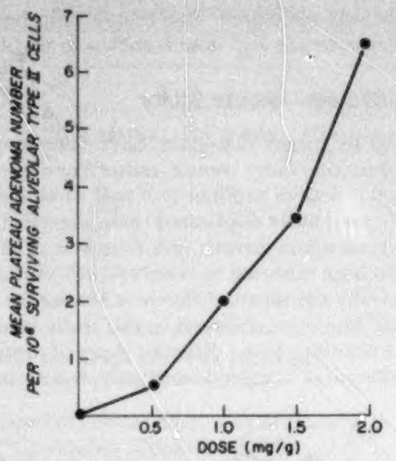

TEXT-FIGURE 4.—Mean plateau tumor No. per 10^6 surviving alveolar type II cells at different single urethan doses. The means were calculated by division of the estimated plateau tumor No. by the No. of live alveolar type II cells, averaged over 6, 12, and 18 hr at each dose.

related. Therefore, diameters of adenomas from individual animals of both sexes and at all doses were combined at each killing time, and frequency distributions were constructed (text-fig. 5).

The distributions at 14 and 16 weeks followed a normal logarithmic pattern according to a modified Kolmogorov—Smirnov test (*19*), consistent with the apparently normal logarithmic distribution of tumor cross-sectional area (*9–11*) and volume (*12*) reported previously. An important aspect of these frequency distributions is that large fractions of the induced tumors are unobservable 3 and 4 weeks after urethan injection. The fraction of total tumors that is unobservable decreases steadily with increasing time before killing so that by 10–12 weeks virtually all tumors are observable. This phenomenon is consistent with the time needed to reach a plateau, between 10 and 14 weeks, when average tumor numbers were plotted as a function of time after urethan injection (text-fig. 1). Geometric mean tumor diameters calculated from experimental data are therefore more accurate at later killing times, because relatively more of the small tumors are observable.

Shimkin and Polissar (*9*) dealt with the problem of estimation of tumor growth rates when not all tumors were observable by eliminating small tumors from consideration and calculating the mean area of an arbitrary number of the largest adenomas. However, it is possible to calculate the geometric mean tumor diameter at early killing times more accurately by taking into account the number of unobservable tumors, if the total number of tumors induced by a single dose of urethan is known and if a normal logarithmic distribution of tumor diameters is assumed at times earlier than 14 weeks. The plateau number of adenomas induced per mouse at each urethan dose was estimated by averaging the three largest mean numbers of adenomas per mouse counted at that dose (text-fig. 2). Since construction of the frequency distributions was done without regard to dose, the total number of tumors expected in the mice sampled for tumor size at each killing time was calculated by multiplying the number of mice on each dose by the plateau number of adenomas per mouse induced by that dose and summing the products. The number of tumors observed at each killing time was then divided by this expected number of tumors to give the fraction of tumors observable at that time; that is, the probability that any given tumor would have a diameter equal to or greater than 0.1 mm—the lower limit of visible tumor diameters. The value of the expression $Z=(x-d)/\sigma$ corresponding to each observed probability was obtained directly from a standard normal distribution table. In this expression d is the mean log tumor diameter in millimeters, σ is the standard deviation of the log tumor diameter, and x in this case equals log 0.1.

The standard deviation of the log tumor diameter was estimated by averaging all experimental standard deviations. These should represent accurately the true standard deviation σ only at late killing times when virtually all

TABLE 3.—*Geometric mean tumor diameter as a function of urethan dose and killing time in the acute study*[a]

Time of killing, wk post injection	Urethan dose, mg/g body wt[b]									
	0.5		1.0		1.5		2.0		All doses combined	
	Geometric mean tumor diameter, 10^{-4} m	Logarithm of tumor diameter mean±SD	Geometric mean tumor diameter, 10^{-4} m	Logarithm of tumor diameter, mean±SD	Geometric mean tumor diameter, 10^{-4} m	Logarithm of tumor diameter, mean±SD	Geometric mean tumor diameter, 10^{-4} m	Logarithm of tumor diameter, mean±SD	Geometric mean tumor diameter, 10^{-4} m	Logarithm of tumor diameter, mean±SD
3	—	—	—	—	1.20	0.98±0.14	—	—	1.20	0.08±0.15
4	—	—	—	—	1.86	0.27±0.25	—	—	1.86	0.27±0.25
6	1.95	0.29±0.27	2.75	0.44±0.23	2.88	0.46±0.21	2.69	0.43±0.22	2.75	0.44±0.23
8	4.47	0.65±0.20[c]	3.39	0.53±0.30	3.31	0.52±0.25[c,d]	4.17	0.62±0.23[d]	3.55	0.55±0.25
10	4.90	0.69±0.16	3.89	0.59±0.27	3.98	0.60±0.29	4.57	0.66±0.25	4.27	0.63±0.27
12	4.37	0.64±0.32	5.13	0.71±0.28	5.75	0.76±0.22[e]	5.01	0.70±0.20[e]	5.25	0.72±0.24
14	6.17	0.79±0.26[c]	6.76	0.83±0.23[d,e]	5.37	0.73±0.21[e,f]	4.57	0.66±0.21[c,d,f]	5.50	0.74±0.23
16	—	—	6.31	0.80±0.22	—	—	—	—	6.31	0.80±0.22

[a] Logarithms of tumor diameters were normally distributed according to the Kolmogorov-Smirnov test. Data of male and female mice have been combined.

[b] — = no mice killed at this dose and time.

[c,d,e,f] Means with identical superscripts at the same killing time are significantly different at $P=0.05$ (95% confidence interval exclusion).

tumors are observable. Earlier killing times should yield smaller experimental standard deviations. However, table 3 suggests that experimental standard deviations varied randomly with dose and killing time except at 3 weeks where they were considerably smaller as expected. This small number of tumors (n=31) did not affect the estimate of σ when all experimental standard deviations, weighted by the number of tumors at each dose and killing time, were averaged.

The adjusted geometric mean tumor diameter at each killing time was calculated by the equation: μ=antilog d=antilog ($x-\sigma Z$). There are other methods by which true geometric mean diameter could be estimated. This technique, which utilizes not only the tumor size distribution measurements but also the estimated plateau tumor number at each dose, is simple and direct. The adjusted mean diameter calculated in this way should provide a reasonable estimate of the true geometric mean.

When these adjusted mean diameters were plotted as a function of time after injection in a double logarithmic coordinate system, the transformation gave the straight line in text-figure 6.

Adenoma Growth—Acute-Chronic Study

Geometric mean tumor diameters (not adjusted for unobservable tumors at early times) for the acute-chronic experimental groups are shown in table 2, where they are compared with the corresponding unadjusted means from table 3 for groups given only single urethan injections. These data indicate that chronic urethan administration to mice at drinking water concentrations up to 0.1% did not affect the growth rate of lung adenomas previously established by single urethan injections.

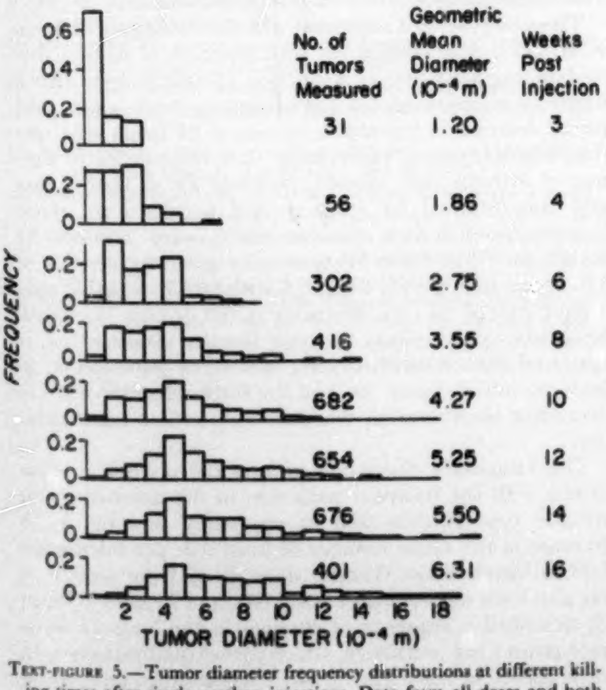

No. of Tumors Measured	Geometric Mean Diameter (10^{-4}m)	Weeks Post Injection
31	1.20	3
56	1.86	4
302	2.75	6
416	3.55	8
682	4.27	10
654	5.25	12
676	5.50	14
401	6.31	16

TEXT-FIGURE 5.—Tumor diameter frequency distributions at different killing times after single urethan injections. Data from all doses and both sexes have been combined.

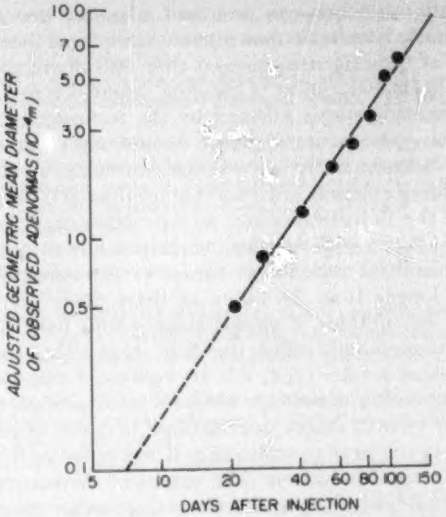

TEXT-FIGURE 6.—Increase in adjusted geometric mean adenoma diameter after single urethan dose. The *line* is drawn by linear regression. The diameter of 1 tumor cell is 10 µm (0.1×10^{-4} m) (*10*).

DISCUSSION

Adenoma Prevalence

The relationship between acute urethan dose and lung adenoma prevalence has been investigated previously. Kaye and Trainin (*7*) observed no tumors in groups of mice 12 weeks after ip injection of 0.1 or 0.25 mg urethan/g body weight. Above this experimental threshold, prevalence appeared to increase linearly with doses of 0.5 and 1.0 mg urethan/g. Shimkin et al. (*5*) also observed what appeared to be a linear response, but without threshold, in mice 18.7–22 weeks after ip injection of 0.25, 0.5, or 1.0 mg urethan/g body weight. Alternatively, within the same dose range the data of Rogers (*8*) and White et al. (*6*) can be used to construct dose-prevalence curves that are concave upward. These prevalences were observed at 9 and 24 weeks after ip injection of urethan.

These relationships are included in text-figure 2. The adenoma prevalences recorded in this study are intermediate between the higher prevalences observed by Shimkin et al. (*5*) and White et al. (*6*) in mice of the highly susceptible A-strain, and the lower ones observed by Kaye and Trainin (*7*) and Rogers (*8*) in Swiss mice lacking selectively enhanced susceptibility to pulmonary adenoma induction. The differences among these dose-prevalence curves presumably are due both to strain differences and the sensitivity and timing of the methods used to detect tumors. For example, tumors in Rogers' mice were counted at an early time and with the use of a technique that detected only surface tumors, which suggests that not all tumors may have been counted.

Urethan cytotoxicity was not considered in these studies. When cytotoxicity is taken into account, as in text-figure 4, the relationship between dose and adenoma prevalence is more nearly quadratic than linear. Since most mechanistic models of tumorigenesis suggest that prevalence should be related to the *m*th power of the dose, where *m* is the number of mechanistic stages affected by the tumorigen (*20*), the relationship shown in text-figure 4 could imply that urethan induces adenomas by a two-stage mechanism. However, independent evidence suggests that urethan acts only at one stage in the induction of mouse lung adenomas. To begin with, one dose is sufficient for the induction of tumors. Since urethan and its metabolites persist in the mouse for only slightly longer than 24 hours at these doses (*21*), to be affected by urethan, a second stage would have to occur almost immediately after the first stage. The results of divided-dose studies (*5*, *6*, *22*) are equivocal and would be consistent with a multistage mechanism of urethan tumorigenesis if cells in stages intermediate between normal cell and tumor cell were to replicate at a rate different from that of their normal neighbors. The results of chronic exposure studies, (*23*) however, provide direct support for the concept that urethan affects only one stage in murine adenogenesis.

Factors other than the mechanism of action may also contribute to nonlinearity in the dose-prevalence relationship. Stochastic models of tumorigenesis generally do not take into account interindividual variability in susceptibility to a carcinogen. Heston and Schneiderman (*24*) pointed out that variation in individual "thresholds" should confer concave upward curvature on dose-prevalence curves in low dose ranges. Regardless of the mechanism of action, therefore, some degree of upward curvature in the dose-prevalence relationship is to be expected for all carcinogens in low dose ranges. This curvilinearity should be less pronounced for dose-prevalence curves obtained with the use of highly inbred test strains and more pronounced when the test population is genetically heterogeneous. Some of the differences among dose-prevalence curves in text-figure 2 may therefore be attributable to the greater genetic heterogeneity of the Swiss mouse test groups than of the inbred A-strain test groups. Furthermore, the urethan dose range where this curvilinearity occurs is a range associated with only mild and transient urethan cytotoxicity (text-fig. 3). Therefore, it is reasonable to speculate that part of the curvilinearity in the urethan dose-lung adenoma-prevalence relationship results from variability in individual thresholds for carcinogen action.

Another explanation must be sought, however, for the curvilinearity in the dose-prevalence relationship in text-figure 4 at urethan doses greater than 0.5 mg/g, because all mice given 0.5 mg urethan or more per gram body weight developed adenomas. White (*21*) has shown that the rate of urethan metabolism in female A-strain mice is not directly proportional to dose. At doses as low as 0.25 mg urethan/g, metabolism shows signs of approaching saturation indicated by increasing persistence of radiolabel with increasing dose and by a curvilinear relationship between integrated internal dose of radiolabel and injected dose of urethan. Since only the radiolabel was monitored, it was not possible in this study to relate adenoma prevalence to persistence of either individual metabolic products or parent urethan. However, prevalence was found to be more linearly related to integrated internal exposure to radiolabel than to administered dose, at least at tumor prevalences of less than about 35 adenomas per mouse which were associated with exposures up to 1.0 mg/g in this sensitive strain.

White's data for internal dose as a function of administered dose cannot be used to transform our administered dose to internal dose because they do not extend beyond an administered dose of 1.0 mg/g and because different strains of mice were used in the two studies. Nevertheless, comparison of White's data with the data in text-figure 4 shows that the dependence of tumor prevalence on administered dose is similar in the dose range of coincidence. Thus curvilinearity in the dose-prevalence relationship at doses greater than about 0.5 mg/g may be attributable partly to nonlinearities of urethan metabolism.

Adenoma Growth Rate

Based on the fit by linear regression of the data points in text-figure 6, μ (the adjusted mean diameter) is 1.0×10^{-4} m, the size of the smallest visible tumor, at 33 days post injection. This time agrees closely with that found by Shimkin and Polissar (*9*, *10*), who observed histologically a geometric mean tumor diameter of 1.0×10^{-4} m in strain A mice and (by extrapolation) in C3H mice at about 28 days after acute urethan injection.

Extrapolation from text-figure 6 indicates that μ is 0.1×10^{-4} m, the diameter of one tumor cell (*10*), at about 7 days after urethan injection. If the extrapolated portion of the line is a good approximation to the true growth curve in the range of unobservable tumor sizes, then tumors induced by single urethan injections do not enter a phase of significant growth until several days after induction.

This observation is consistent with the findings of Shimkin et al. (*25*), who studied the incorporation of labeled thymidine into lung cells as a function of time in mice after a single ip injection of 1.0 mg urethan/g body weight. An initial decrease in thymidine uptake at 24 hours after urethan administration, expressed as thymidine index, or fraction of alveolar cells labeled, persisted for at least 3 days and was followed by recovery and a subsequent sharp increase by 5-7 days. Similar results were obtained by Kauffman (*4*) in Swiss Webster mice given ip injection of 1.0 mg urethan/g body weight. Kauffman showed that only a small part of the total alteration in cell division rate could be attributed to effects on type II cells. Nevertheless, it appeared that individual lung cell types participated in both the initial depression and the subsequent elevation of thymidine incorporation that followed urethan administration.

This temporary depression of lung cell division rate coincides with the transient reduction in the number of live alveolar type II cells seen in our study (text-fig. 3). A decrease in the mean number of lung cells per microscope field in female Swiss Webster mice given 1 mg urethan/g has also been reported previously (*4*), and Brachetto-Brian (*3*) described a sequence of changes in the lungs of Swiss mice given 1 mg urethan/g, which agrees qualitatively with the sequence in text-figure 3. Since we observed an increase in the number of dead alveolar type II cells at the same time that live type II cells were reduced in number, the reduction in live type II cells must be attributable partly to urethan cytotoxicity. However, the persistence of live type II cell reduction for several days may be related to inability of the lung to respond to the deficit with an increase in the rate of cell division during this period. Thus it is reasonable to speculate that, although single adenoma cells appear shortly after urethan injection in mice, their period of rapid replication with consequent measurable adenoma growth does not begin, on the average, until several days later. This lag time is associated with inhibition of cell division, a cytotoxic effect of urethan probably not directly related to its tumorigenic action (*25*).

Rogers (*8*) gave multiple urethan doses to Swiss mice 7 weeks apart to avoid any possible extension of influence of the first urethan dose to the time of the second, but he did not sample the lungs until 8 weeks after the last injection. His conclusion that multiple injections did not result in adenomas of generally larger size was based on the largest observed tumor size coupled with a crude tumor diameter breakdown. Other investigators (*5, 6*) have also given multiple injections of urethan to mice. In none of these studies has the effect of total urethan dose, as related to the total number of adenomas and the timing of their appearance, been distinguishable from an effect of urethan on adenoma growth rate. The experimental design utilized in our study allows such a distinction to be made and indicates that adenoma growth rate in mice is independent of chronic urethan exposures of up to 0.1% in the drinking water.

REFERENCES

(*1*) Shimkin MB, Stoner GD. Lung tumors in mice: Application to carcinogenesis bioassay. Adv Cancer Res 1975; 21:1–58.

(*2*) Mirvish SS. The carcinogenic action and metabolism of urethan and *N*-hydroxyurethan. Adv Cancer Res 1968; 11:1–42.

(*3*) Brachetto-Brian D. Histology of pulmonary tumors induced in the mouse by urethane (ethyl carbamate). Acta UICC 1951; 7:660–667.

(*4*) Kauffman SL. Alterations in cell proliferation in mouse lung following urethane exposure. Am J Pathol 1969; 54:83–93.

(*5*) Shimkin MB, Wieder R, Marzi D, Gubareff N, Suntzeff V. Lung tumors in mice receiving different schedules of urethane. In: Le Cam LM, Neyman J, eds. Proceedings of the fifth Berkeley symposium on mathematical statistics and probability. Dec 27, 1965–Jan 7, 1966. Berkeley: Univ Calif Press, 1967:707–719.

(*6*) White M, Grendon A, Jones HB. Effects of urethane dose and time patterns on tumor formation. In: Le Cam LM, Neyman J, eds. Proceedings of the fifth Berkeley symposium on mathematical statistics and probability. Dec 27, 1965–Jan 7, 1966. Berkeley: Univ Calif Press, 1967:721–743.

(*7*) Kaye AM, Trainin N. Urethan carcinogenesis and nucleic acid metabolism: Factors influencing lung adenoma induction. Cancer Res 1966; 26:2206–2212.

(*8*) Rogers S. Age of the host and other factors affecting the production with urethane of pulmonary adenomas in mice. J Exp Med 1951; 93:427–449.

(*9*) Shimkin MB, Polissar MJ. Some quantitative observations on the induction and growth of primary pulmonary tumors in strain A mice receiving urethane. J Natl Cancer Inst 1955; 16:75–97.

(*10*) ———. Growth of pulmonary tumors in mice of strains A and C3H. J Natl Cancer Inst 1958; 21:595–610.

(*11*) Dyson P, Heppleston AG. Cell kinetics of urethane-induced murine pulmonary adenomata. I. The growth rate. Br J Cancer 1975; 31:405–415.

(*12*) Yuhas JM. Radiotherapy of experimental lung tumors in the presence and absence of a radioprotective drug, S-2-(3-aminopropylamino)-ethylphosphorothioic acid (WR-2721). J Natl Cancer Inst 1973; 50:69–78.

(*13*) Dourson ML, Baxter CS. Reduced prevalence and growth rate of urethane-induced lung adenomas in ageing adult strain A mice. Toxicology 1981; 20:165–172.

(*14*) Hayat MA. Principles and techniques of electron microscopy. Vol 1. Baltimore: Univ Park Press, 1981:57.

(*15*) Millonig G. Further observations on a phosphate buffer for osmium solutions in fixation. In: Breese SS, Jr, ed. Proceedings of the fifth international congress for electron microscopy. Philadelphia, Aug. 9–Sept 5, 1962. Vol 2. New York: Academic Press, 1962:8.

(*16*) Spurr AR. A low-viscosity epoxy resin embedding medium for electron microscopy. J Ultrastruct Res 1969; 26:31–43.

(*17*) Kauffman SL. Autoradiographic study of type II-cell hyperplasia in lungs of mice chronically exposed to urethane. Cell Tissue Kinet 1976; 9:489–497.

(*18*) ———. Kinetics of alveolar epithelial hyperplasia in lungs of mice exposed to urethane. I. Quantitative analysis of cell populations. Lab Invest 1974; 30:170–175.

(*19*) Lilliefors HW. On the Kolmogorov-Smirnov test for normality with mean and variance unknown. Am Stat Assoc J 1967; 62:399–402.

(*20*) Whittemore J. Quantitative theories of oncogenesis. Adv Cancer Res 1978; 27:55–58.

(*21*) White M. Studies of the mechanism of induction of pulmonary adenomas in mice. In: Le Cam LM, Neyman J, Scott EL, eds. Proceedings of the sixth Berkeley symposium on mathematical statistics and probability. Jun 21–July 18, 1970. Berkeley: Univ Calif Press, 1971:287–307.

(*22*) Neyman J, Scott EL. Statistical aspect of the problem of carcinogenesis. In: LeCam LM, Neyman J, eds. Proceedings of the fifth Berkeley symposium on mathematical statistics and probability. Jun 21–July 18, 1965. Berkeley: Univ Calif Press, 1967:745–776.

(*23*) O'Flaherty EJ, Dourson ML. Relationship between urethan dose rate and adenoma latency: Relevance of tumor growth rate and target cell number. JNCI, 1982; 69:859–865.

(*24*) Heston WE, Schneiderman MA. Analysis of dose-response in relation to mechanism of pulmonary tumor induction in mice. Science 1953; 117:109–111.

(*25*) Shimkin MB, Sasaki T, McDonough M, Baserga R, Thatcher D, Wieder R. Relation of thymidine index to pulmonary tumor response in mice receiving urethane and other carcinogens. Cancer Res 1969; 29:994–998.

blank page

Relationship Between Urethan Dose Rate and Adenoma Latency: Relevance of Tumor Growth Rate and Target Cell Number[1,2,3,4]

Ellen J. O'Flaherty[5] *and* Michael L. Dourson[5,6]

ABSTRACT—Outbred Swiss Cox mice of both sexes were chronically exposed to urethan added to their drinking water at levels of 0.02–0.10% by weight. The number and sizes of lung adenomas that developed as a result were monitored as functions of time and dose rate (DR). The relationship between dose per unit time, or DR, and time (t_1) needed for the development of a mean of one observable tumor per mouse was: $DR \times t_1^n = K$, where K and n are constants. The value of n was 2.75. This value could be largely accounted for by the DR-independent tumor growth time, although an increase in the number of target cells at higher urethan dose rates may also be a factor in the relationship between DR and t_1. Examination of the relationships between cumulative incidence and DR and between cumulative incidence and adenoma induction time suggests that urethan acts at one stage of a two-stage mechanism in the induction of mouse lung adenomas.—JNCI 1982; 69:859–865.

It has been firmly established that for chronic exposure to chemical carcinogens in general, the effects of DR and time are not equivalent; that is, cumulative tumor incidence associated with a given total carcinogen exposure is not constant but is dependent on whether exposure was low and continued over a long period of time, or was high and took place over a short period. The relationship was expressed by Druckrey (*1*) as: $DR \times T_{50}^n = K$, where DR is dose rate, T_{50} is the time to reach 50% tumor prevalence in the study population, K is a constant, and n is a constant but not necessarily an integer. The value of n varies among carcinogens. If n were equal to 1, prevalence would be directly proportional to total dose. For chemical carcinogens, $n>1$; that is, the effect of time dominates the effect of dose (*1, 2*).

With the exclusion of any contributions by nonlinearities of metabolism or by age-related changes in the host, the Druckrey effect might be the result of either alteration in size of the target cell population at higher dose rates as a result of cytotoxicity, or of dose-independent tumor growth rate. The second hypothesis is particularly interesting since it deals with tumor latency, a feature of carcinogenesis whose incorporation into regulatory decision-making processes is still a subject of controversy.

Latent period is the time from initial administration of the carcinogen to initial observation of the neoplasm. It consists of the induction time, or time needed to transform a normal cell into a tumor cell, and the growth time, the time until the tumor reaches minimum detectable size. Direct proportionality between cumulative incidence, expressed as mean number of tumors per mouse, and total dose would require both induction time and growth time to be inversely proportional to DR. This is, however, not likely to be the case. In particular, most investigators assume that mean tumor growth rate is independent of DR (*3*). The specific test system of interest to us is the urethan-induced mouse lung adenoma. For this test system there is experimental support for the independence of tumor growth rate from DR. The growth rate of adenomas induced by urethan exposure is independent of either acute dose (*4, 5*) or chronic DR (*5*).

The specific aims of this study were to determine whether in the urethan-induced mouse lung adenoma test system the Druckrey effect can be accounted for on the basis of DR independence of tumor growth rate and/or an alteration in size of the target cell population at higher DR of urethan. Some of the data accumulated in the course of this work also have direct bearing on the kinetics of the mechanism of urethan adenogenesis.

MATERIALS AND METHODS

Mice.—Outbred Swiss Cox mice (Laboratory Supply Co., Indianapolis, Ind.) were used to establish a breeding colony. The animals were fed Rodent Laboratory Chow (Purina 5001; Ralston Purina Co., St. Louis, Mo.) and tap water ad libitum and were housed in standard stainless steel cages, up to 5 mice per cage. The animals were maintained on a 12 hour light–12 hour dark cycle.

Chronic study—rate of appearance and growth of lung adenomas.—Mice of both sexes, 41–45 days old, were given distilled water ad libitum to which different amounts of urethan were added to yield several concentrations by weight (0.02, 0.05, or 0.10%). Five males and 5 females from each dose rate group were killed at 4, 6, 8, 10, 12, or 14 weeks after the start of treatment. The 31 controls were given distilled water ad libitum, and the intake was monitored regularly. Immediately after the mice were killed, their lungs were excised

---

ABBREVIATIONS USED: DR=dose rate(s) [dose(s) per unit time]; t_1=time(s) of appearance of a mean of 1 observable adenoma per mouse; t_g=growth time from one adenoma cell to a mean of 1 observable adenoma per mouse; t_i=time(s) required for induction of a mean of one adenoma cell per mouse; T_{50}=time to reach 50% tumor prevalence in a study population; TD_1=total dose(s) at t_1; TD_i=total dose(s) at t_i.

---

[1] Received August 1, 1980; revised April 5, 1982; accepted April 27, 1982.

[2] Supported by Public Health Service grant ES-07073, training program in toxicology, from the National Institute of Environmental Health Sciences.

[3] Animals were maintained under the guidelines set forth in the "Guide for the Care and Use of Laboratory Animals" by the Institute of Laboratory Animal Resources, National Research Council.

[4] Parts of the investigation were performed in partial fulfillment of the requirements of a Ph.D. degree (M. L. D.).

[5] Department of Environmental Health, College of Medicine, University of Cincinnati, 3223 Eden Ave., Cincinnati, Ohio 45267.

[6] *Present address*: Environmental Protection Agency, 26 West St. Clair St., Cincinnati, Ohio 45268.

and expanded with Tellyesniczky's fixative. The expanded lobes were later separated and cleaned and viewed on a lightbox for counting and sizing of adenomas according to the procedure described previously (*6*).

Chronic study—lung type II cell population size response.—Mice of both sexes, 41–45 days old, were given distilled water ad libitum to which different amounts of urethan were added to yield 0.02, 0.05, or 0.10% concentrations by weight. Three to 6 mice from each DR group were killed at 2, 6, 8, 10, 11, or 12 weeks after initiation of treatment. There were 8 control mice.

For the purpose of this study, the lungs were expanded with cold double aldehyde fixative before being embedded in plastic and sectioned at 1–2 µm to observe the number of live, borderline, or dead type II cells after the various treatments. The techniques have been given previously (*5*).

RESULTS

Dose rates.—The total amount of urethan ingested per gram of body weight increased linearly with the length of time of continuous urethan administration in the drinking water (text-fig. 1). The slopes of the lines are expressed in milligrams of urethan per gram body weight per week; that is, they are the DR. These DR are not directly proportional to concentration in these drinking water because the mice drank less water when the urethan concentration was high.

Mean tumor number.—The tumor number per animal had a normal distribution among experimental animals. Accordingly, we used arithmetic means in all calculations that involved tumor number. Mean tumor numbers were related to both dose and time during chronic urethan administration. An average of 0.03 adenomas/mouse was observed for control mice at all killing times. This value was so low that mean tumor numbers at other dose rates were not corrected for control prevalence. Text-figure 2 shows that the relationship between mean tumor number per animal and time was linear in a log–log coordinate system and that the lines for the three DR appeared to be parallel.

Mean tumor growth rate.—Comparison of the geometric mean diameters of observed adenomas at different single killing times showed that there was no significant systematic

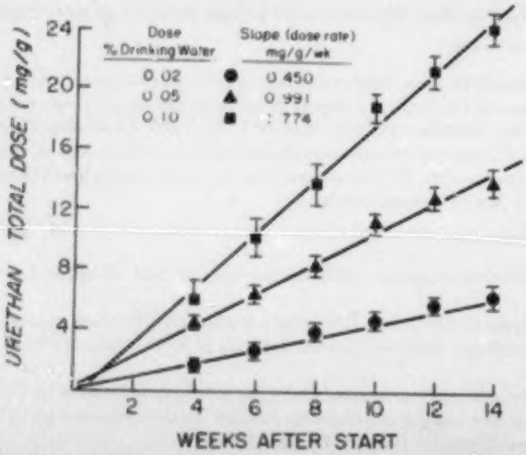

TEXT-FIGURE 1.—Total urethan dose as a function of time after the start of chronic administration to mice. Total doses were calculated from water consumption rates of individual mice. *Each point* represents data from 10 animals. *Bars* indicate the 95% confidence interval. Lines are fit by linear regression. Slopes of these lines represent the urethan dose rates in mg/g body wt/wk.

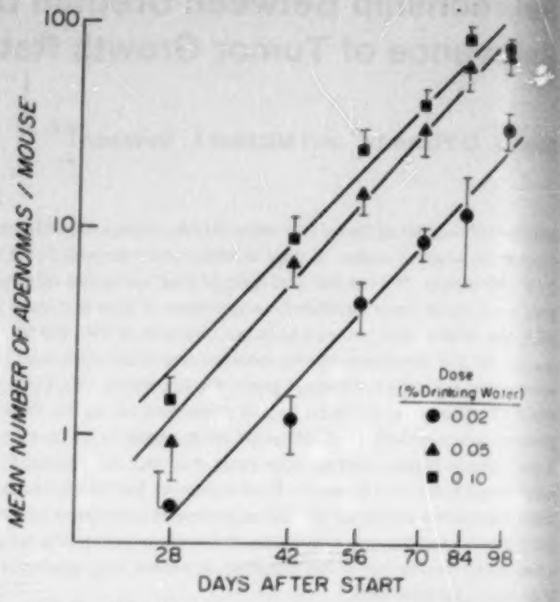

TEXT-FIGURE 2.—Mean No. of lung adenomas/mouse at different times during chronic exposure to urethan. Data are plotted in a log–log coordinate system. *Each point* represents data from 10 animals. *Bars* indicate ±SEM. Lines are fit by linear regression. From these lines, extrapolated in the case of the highest DR, the times to the appearance of a mean of 1 adenoma/mouse are estimated.

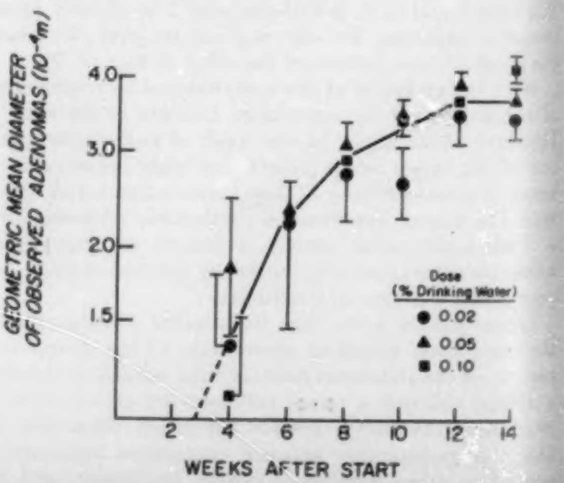

TEXT-FIGURE 3.—Geometric mean diameters of observed lung adenomas at different times during chronic exposure of mice to urethan are plotted in a log linear coordinate system. The 95% confidence intervals for the points are shown where possible. *Solid line* connects geometric means calculated over all doses. *Dashed line* shows the extrapolation to a geometric mean diameter of 0.1 mm, the size of the smallest observable adenoma.

dependence of geometric mean tumor diameter on DR (text-fig. 3). Accordingly, we combined tumor diameter data for all DR at each killing time. Tumor diameters appeared to have a normal logarithmic distribution at intermediate killing times (text-fig. 4) (*5*). At earlier or later killing times, these distributions were skewed to the left, presumably due either to the large fraction of unobservable (<0.1 mm in diameter) tumors (at early times) or to the continual influx of smaller tumors (at later killing times).

Number of live type II cells.—The number of live alveolar type II cells per lung increased by 50% between 2 and 6 weeks after the initiation of chronic urethan administration at 0.1% in the drinking water. After this time the number of live type II cells per lung reached a plateau at 1.83×10^7 (text-fig. 5). In mice given 0.02% urethan in the drinking water, the number of live alveolar type II cells per lung also showed a time-related increase (text-fig. 5), reaching 1.57×10^7, 28% above control values, at 10 weeks after the start of urethan administration. The number of live alveolar type II cells per lung in mice given 0.05% urethan, however, remained within the control range instead of reaching an intermediate level between the numbers associated with the other two DR.

The number of dead and borderline type II cells also increased relative to control values during chronic administration of urethan.

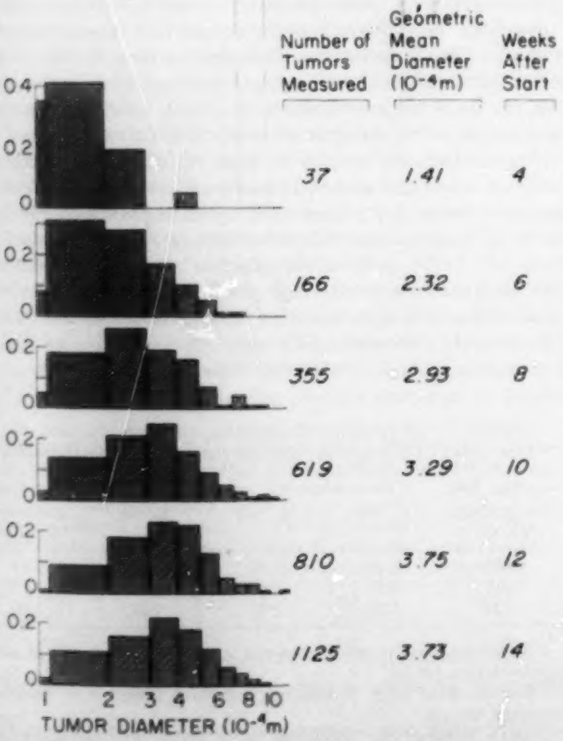

TEXT-FIGURE 4.—Lung adenoma diameter frequency distributions at various killing times after the start of chronic urethan treatment. Data from all dose groups were combined for the purpose of calculation. Killing time, in wk after start of treatment, is given with each distribution.

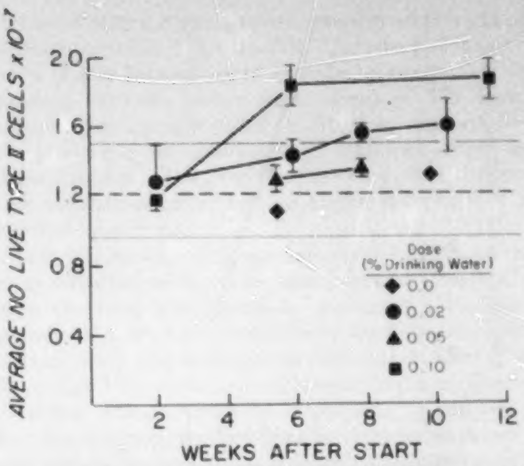

TEXT-FIGURE 5.—Average No. of live alveolar type II cells/lung at different times during chronic exposure to urethan. *Each point* represents data from an average of 4–5 mice. *Bars* indicate ±SEM. *Dashed line* represents the control mean of 1.23×10^7 cells; *horizontal, solid lines* indicate the 95% confidence interval around the control value. No. of live cells is assumed to be normally distributed among animals.

DISCUSSION

The data for mouse lung adenoma induction by urethan exemplify the Druckrey effect. When total dose is calculated by multiplying the observed time to a mean of 1 adenoma, t_1 (text-fig. 2), by the DR (text-fig. 1), it is found not to be constant for the selected prevalence of 1 observable adenoma per mouse (table 1). Therefore, prevalence is not directly proportional to total dose, and n is not equal to 1.

One can find the value of n for this test system by taking advantage of the Druckrey equation $\log \text{DR} = \log K - n \log t_1$ and by plotting log DR against log t_1 as shown in text-figure 6. Note that time to a mean of 1 tumor, from text-figure 2, is used here as the equivalent of T_{50}, the time to occurrence of 1 tumor in 50% of the study population. As long as tumor numbers are normally distributed, this alternative is justified. Furthermore, since the lines in text-figure 2 are roughly parallel, and since total urethan dose is linearly related to time (text-fig. 1), values of n calculated from times to different mean numbers of tumors should be about the same. If the lines in text-figure 2 were parallel, the choice of the number of tumors would not affect the value of n at all. The value of n (text-fig. 6) is 2.75. This value is consistent

TABLE 1.—*Latent period, DR, and TD$_1$ during chronic urethan administration*

Urethan dose, %, in drinking water	DR, mg/g body wt/wk	t_1,[a] wk	TD$_1$,[b] mg urethan/g body wt
0.02	0.450	5.28	2.37
0.05	0.991	3.79	3.75
0.10	1.774	3.25	5.76

[a] Time required for appearance of a mean of 1 observable adenoma/mouse=latent period.

[b] Total exposure at the time of appearance of a mean of 1 observable adenoma/animal; DR×t_1.

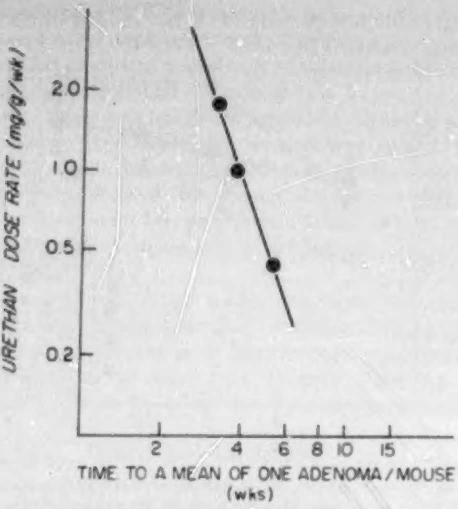

TEXT-FIGURE 6.—Relationship of urethan dose rate to the latent period, or time to a mean of 1 observable adenoma/mouse. The line was fit by linear regression; absolute value of its slope, 2.75, equals the value of *n*.

with those calculated for other chemical carcinogens, most of which fall in the range 2–4 (*2*).

Text-figure 3 shows that adenoma growth rate is independent of urethan DR in these mice rather than being inversely proportional to DR as would be required if *n* in the Druckrey equation were equal to 1. Therefore, it is of interest to determine whether adenoma prevalence is proportional to total dose calculated to the time of appearance of a mean of one adenoma cell per mouse, rather than to the time of appearance of a mean of 1 observable adenoma per mouse. One can estimate the time of appearance of a mean of one adenoma cell per mouse by subtracting from the total latent periods (table 1) the mean growth time from 1 adenoma cell to 1 observable adenoma per mouse, which can be approximated from the adenoma growth rate data (text-fig. 3).

As noted, tumor diameter distributions reflecting adenoma growth rates were generally not of a normal logarithmic nature but were skewed to the left, particularly at earlier and later killing times, as a result of both the left truncated nature of these distributions and the continual influx of small tumors. There is some question regarding the most appropriate measurement of the central tendency of these skewed distributions, and as to whether these measurements should be adjusted either because the distributions are skewed or because of the presence of unobservable (<0.1 mm) tumors, as was done previously (*5*). The geometric mean appears to be a reasonable measure. In this case, however, we did not make adjustments to the geometric means for unobservable tumors because we could not determine the total number of tumors induced by urethan in this experimental design, and, therefore, the ratios of unobservable tumors to total tumors at different killing times were unknown. The means also were not adjusted for the continued influx of induced tumors either. This influx affected the geometric means of tumors principally at later killing times. As described below, we used adenoma size data only of groups that were killed early in the approximation of the mean adenoma growth rate from 1 adenoma cell to 1 observable adenoma per mouse.

Originally, it was thought that the adenoma growth curve from the acute study (*5*), which was adjusted for the fraction of unobservable tumors, could be used to approximate the adenoma growth rate from 1 adenoma cell to 1 observable adenoma per mouse. This seemed quite reasonable in light of the fact that adenoma growth rate is independent of both acute and chronic urethan dose (*5*). This approximation, however, failed to take into account that the total latent periods observed in this study were almost certainly determined by a subpopulation of fast-growing tumors. Therefore, the average adenoma growth rate obtained in the acute study, which adequately described the data for all tumors (whether observable or not), should not be expected to be applicable in this situation. Additional work is being done to characterize the growth rates of adenomas during chronic urethan exposure.

The chronic adenoma growth curve (text-fig. 3) is not linear in any of the common coordinate systems. Since there is no theoretical reason to give preference to any of these transformations, a growth time of 18.6 days or 2.65 weeks from one cell to a mean of 1 observable tumor was approximated by extrapolation of the line determined by the geometric mean values at 4 and 6 weeks in text-figure 3. As a practical matter, it is not particularly important whether this extrapolation is done in a log linear (as done here), in a log–log, or in a linear coordinate system. Extrapolation of a log–log plot yields a growth time of 17.5 days; extrapolation of a linear (arithmetic) plot yields a growth time of 19.3 days. Although the magnitude of these differences does alter the results of the calculations in the following paragraphs, it does not affect the general conclusions of this study.

Subtraction of the growth time of 2.65 weeks from one cell to a mean of 1 observable tumor from the latent periods given in table 1 results in the times to development of a mean of 1 adenoma cell per mouse, or induction times, at each DR (table 2). When the appropriate DR and induction times are multiplied with each other, the resulting calculated total doses (TD_i) associated with one transformed type II cell actually decrease, although very slightly, as DR is increased. Table 2 summarizes these calculations.

TABLE 2.—*Dependence of adenoma induction time and the associated TD_i on urethan DR during chronic administration*

Urethan DR, mg/g body wt/wk	t_l,[a] wk	t_g,[b] wk	t_i,[c] wk	TD_i,[d] mg urethan/g body wt
0.450	5.28	2.65	2.63	1.18
0.991	3.79	2.65	1.14	1.13
1.774	3.25	2.65	0.60	1.06

[a] Time required for appearance of a mean of 1 observable adenoma/mouse=latent period.

[b] Growth time from 1 adenoma cell to a mean of 1 observable adenoma/mouse.

[c] Time required for induction of a mean of 1 adenoma cell/mouse=induction time.

[d] Total exposure at the time of appearance of a mean of 1 adenoma cell/mouse; DR×t_i. The relationship among the three time periods is $t_l=t_g+t_i$.

However, the effect of urethan on the number of type II lung cells should also be taken into account in this calculation. If it is assumed that the probability of tumor induction by a given amount of carcinogen is directly proportional to the number of susceptible cells, then, when more cells are present, a relatively smaller total amount of carcinogen should be required on the average to induce the same number of tumors. Therefore, as target cells increase in number at higher dose rates, the TD_i would be expected to decrease. This is, in fact, the direction of the trend in the calculated TD_i values in table 2. Any adjustment to TD_i made on the basis of the plateau number of type II cells in the lung cannot be better than an approximation, since plateau levels of type II cells were not reached before the 6th or 8th week of chronic urethan administration (text-fig. 5), although many of the adenomas registered had been induced well before this time. Nevertheless, it is worthwhile to determine whether an adjustment with the use of plateau numbers of target cells would be of the right order of magnitude to account for the rather slight trend in TD_i in table 2.

Adjustment for the plateau number of target cells presents the problem that the intermediate urethan dose, 0.991 mg/g body weight/week, showed anomalous behavior with respect to type II cell induction; that is, it did not appear to increase the number of type II cells at all. This behavior is inconsistent with the effect of this DR on the more general index of increased cellularity, percent increase in lung weight, which was intermediate between the effects of the other two doses. The degree of type II cell induction by the highest DR of urethan appears to be a reliable figure since it is very close to the value reported by Kauffman (*7*), who observed a 60% increase in the number of live type II cells per lung between 3 and 8 weeks after the start of chronic urethan administration at 0.1% in the drinking water of Swiss Webster mice. The number of cells reached a plateau at about 1.8×10^7 per lung. Therefore, a fractional increase in the number of type II cells was interpolated for the intermediate dose rate as indicated in table 3.

The fractional increases in target cell numbers at different DR of urethan can be used to adjust calculated TD_i to a control number of target cells. These calculations are summarized for all urethan DR in table 3. They demonstrate that adjustment of TD_i to the plateau numbers of target cells causes only a slight alteration in the magnitude of any systematic trend in TD_i with DR. The effect of the number of type II cells is therefore of an order of magnitude that is consistent with the rather slight trend in TD_i with DR observed in this study (table 2). Thus it appears that the value of *n* in this test system can be explained largely by the independence of DR of tumor growth time, with the increase in the number of target cells at higher urethan DR being much less important.

TABLE 3.—*Dependence of TD_i adjusted for the urethan dose-related increase in steady state type II cell population, on urethan DR during chronic administration*

Urethan DR, mg/g body wt/wk	TD_i,[a] mg urethan/g body wt	Plateau level of type II cells relative to control	TD_{ic},[b] mg urethan/g body wt
0.450	1.18	1.285	1.52
0.991	1.13	1.407[c]	1.59
1.774	1.06	1.496	1.59

[a] Required to induce a mean of 1 adenoma cell/mouse (from table 2).

[b] Needed if type II cells had not increased with higher DR (i.e., adjusted to control level of type II cells).

[c] This value is not an experimental value. It was interpolated from an analysis of lung weights at all DR and plateau levels of type II cells at the other two values.

Other factors, such as dose-dependent kinetics of carcinogen metabolism or excretion, alterations in host sensitivity during the long latent periods associated with very low exposure rates, or severe cytotoxicity leading to uncompensated cell death and reduction in the total number of target cells at high DR, could also contribute to the production of a Druckrey effect. Aging, as it pertains to the Druckrey effect, has not been studied directly. Studies of tumor incidence and tumor growth in animals of different ages have produced ambiguous and sometimes conflicting results (*6, 8, 9*).

Some of these factors could operate to reduce, rather than increase, the value of *n*. For example, an increase in the number of target cells with increasing DR, as shown in this experiment, would produce a value of $n<1$ in the absence of any other contributory factors. Similarly, *n* should be less than 1 if metabolism of the active carcinogen to inactive forms approached saturation at higher chronic exposure rates. The observation that generally $n\geq1$ with chemical carcinogens may provide some insight into the relative importance of factors that would tend to decrease the value of *n*.

Selective growth of transformed but precancerous cells is an additional factor that has received much attention. Selective growth advantage is a mechanistic equivalent of the "reinforcing action" to which Druckrey attributed the effect he observed. The idea that a clone of precancerous cells might enjoy a selective growth advantage was given mathematical form by Armitage and Doll (10) so that the observed age dependence of human cancer incidence, which in many cases suggests a five- or six-stage mechanism, could be reconciled with the absence of direct experimental support for mechanisms of more than two stages. Since selective growth as a factor in the Druckrey effect is restricted to carcinogens that act in multistage mechanisms, it is of interest to examine the kinetics of the mechanism of urethan tumorigenesis as expressed in the results of the present study.

Armitage and Doll (*11*) showed that development of the model for a multistage mechanism of tumorigenesis, with *r* number of stages and constant (but not necessarily equal) probabilities $p_1 \ldots p_r$ of occurrence of each of the *r* stages, leads to the predicted relationship: $I = Np_1p_2 \ldots p_r\, t_i^r/r! = k\, t_i^r$ or $\log I = \log k + r \log t_i$, where *I* is tumor prevalence or mean tumor number per animal, *N* is the total number of cells exposed to the risk of a first transformation, t_i is the induction time, and *k* is a constant, at fixed DR, characteristic of a particular value of *r* with its associated product of probabilities. The *r* can be equated with the number of stages in the tumorigenesis mechanism only if there is no Druckrey effect (i.e., if $n=1$).

A linear relationship between log *I* and log *t* has been demonstrated in many other studies of the occurrence of cancer in human (*11*) and experimental animal (*2*) populations, although generally in these analyses tumor growth time has been assumed to be negligible, and t_i has been taken to be equivalent to the time t at which the tumors induced by time t_i were actually observed. Induction times can be estimated for the cumulative tumor incidence measurements of the present study, however, by subtraction from each killing time of the growth time from 1 adenoma cell to a mean of 1 observable adenoma per mouse, 2.65 weeks (table 2). When this is done, the log t_i–log I relationships take the form shown in text-figure 7. Since this transformation of the data effectively eliminates the Druckrey effect in this test system, the slopes of these lines should represent the value of r, the number of stages in the tumorigenesis mechanism. The mean slope of the three lines in text-figure 7 is 1.97. Thus the value of r is consistent with the premise that there are two stages in the mouse lung adenogenesis mechanism.

Urethan, however, need not act at both of these stages. Whatever the total number of stages in a multistage mechanism, the number m induced by the carcinogen should be given by the slope of a graph of log cumulative incidence against log DR at a fixed time: log I=log k_t+m log DR, where k_t is a constant, as shown by Whittemore (*3*). The value of m can therefore be determined directly from plots of log I, log DR at a fixed time. When the three data points for the three DR at each of the six killing times of the present study are fit by linear regression and the slopes are calculated and averaged, the value of the mean slope is found to be 1.1. Thus these data suggest that urethan acts at only one stage of the adenogenesis mechanism. The kinetic data are therefore in agreement with independent evidence that has led to the consensus that urethan acts at only one stage in the induction of mouse lung adenomas. This evidence, principally from acute studies, includes both the observation that urethan and its metabolites persist in the body only for a short period of time and the nature of the relationship between cumulative adenoma incidence and total acute dose. Deviations from linearity in the acute dose, cumulative incidence relationships reported by us (*5*) and by others may be explained by variations in susceptibility to the tumorigenic action of urethan and by dose-dependent urethan elimination kinetics. The mouse lung adenoma may be considered a special case with regard to the order of the tumor induction mechanism since mice display a high spontaneous incidence, which suggests that the transformation effected by urethan may occur in conjunction with a spontaneously occurring transformation.

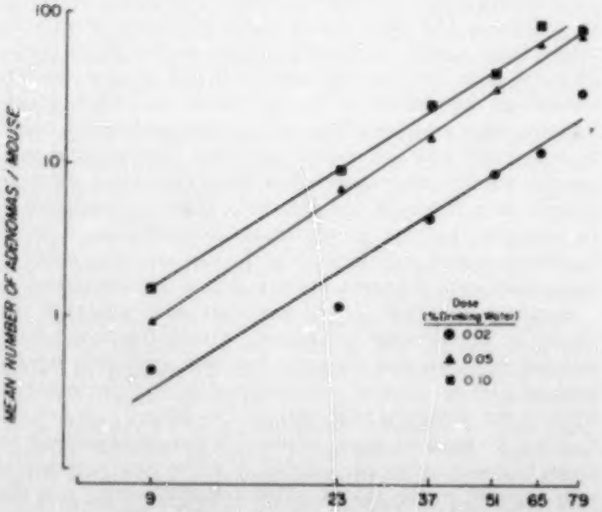

TEXT-FIGURE 7.—Mean No. of lung adenomas/mouse plotted in a log–log coordinate system as a function of the mean induction time, or the time at which that No. of tumors had been induced as single adenoma cells. *Each point* represents data from 10 mice. Lines are fit by linear regression; mean value of their slopes is 1.97.

The urethan-induced mouse lung adenoma lends itself to this type of investigation because, first, urethan affects only one stage of the adenogenesis mechanism; and second, a large fraction of the latent period can be assigned to tumor growth. It would be of interest to extend this type of analysis to a tumor test system for which induction, not growth, represents the greater part of the latent period. Rat liver carcinogenesis by diethylnitrosamine is one example. This test system is apparently analogous to the lung adenoma test system in that development of identifiable hyperplastic foci of altered cells precedes the appearance of liver carcinoma. For induction of these hyperplastic foci, m is apparently equal to 1 (*12*).

Additional possibilities present themselves with test systems whose mechanisms involve more than one carcinogen-related stage. The diethylnitrosamine-induced liver carcinoma and urethan-induced lung adenocarcinoma are interesting in this context, since induction of rat hepatic carcinoma requires continuing exposure to diethylnitrosamine while mouse lung adenocarcinomas appear after a long latent period following a single exposure to urethan.

REFERENCES

(*1*) DRUCKREY H. Quantitative aspects in chemical carcinogenesis. In: Truhaut R, ed. Potential carcinogenic hazards from drugs. Geneva: UICC, 1977:60–78 (Technical Report Series 7).

(*2*) SCHERER E, EMMELOT P. Multihit kinetics of tumor cell formation and risk assessment of low doses of carcinogen. In: Griffin AC, Shaw CR, eds. Carcinogens: Identification and mechanisms of action. New York: Raven Press, 1979:337–365.

(*3*) WHITTEMORE AS. Quantitative theories of oncogenesis. Adv Cancer Res 1978; 27:55–88.

(*4*) ROGERS S. Age of the host and other factors affecting the production with urethane of pulmonary adenomas in mice. J Exp Med 1951; 93:427–449.

(*5*) DOURSON ML, O'FLAHERTY EJ. Relationship of lung adenoma prevalence and growth rate to acute urethan dose and target cell number. JNCI 1982; 69:851–857.

(*6*) DOURSON ML, BAXTER CS. Reduced prevalence and growth rate of urethane-induced lung adenomas in aging adult strain A mice. Toxicology 1981; 20:165–172.

(*7*) KAUFFMAN SL. Autoradiographic study of type II cell hyperplasia in lungs of mice chronically exposed to urethane. Cell Tissue Kinet 1976; 9:489–497.

(*8*) DOLL R. Cancer and aging: The epidemiologic evidence. S Afr Cancer Bull 1971; 15:51–52.

(*9*) Peto R, Roe FJ, Lee PN, Levy L, Clack J. Cancer and aging in mice and men. Br J Cancer 1975; 32:411–426.

(*10*) Armitage P, Doll R. A two-stage theory of carcinogenesis in relation to the age distribution of human cancer. Br J Cancer 1957; 11:161–169.

(*11*) ———. The age distribution of cancer and a multistage theory of carcinogenesis. Br J Cancer 1954; 8:1–12.

(*12*) Scherer E, Emmelot P. Kinetics of induction and growth of precancerous liver cell foci, and liver tumour formation by diethylnitrosamine in the rat. Eur J Cancer 1975; 11:689–696.

blank page

Tumor Cell-Triggered Macrophage-Mediated Suppression of the T-Cell Cytotoxic Response to Tumor-Associated Antigens.

I. Characterization of the Cell Components for Induction of Suppression[1,2]

Chou-Chik Ting[3,4] *and* **Dennis Rodrigues**[3,5]

ABSTRACT—A tumor cell-triggered macrophage-mediated suppressor mechanism was demonstrated. It suppressed the induction of specific tumor immunity in the syngeneic, primary mixed lymphocyte tumor cell culture reactions. Preexposure of splenic adherent cells (SAC) to syngeneic FBL-3 tumor cells induced complete suppression of the generation of cytotoxic T-cells. The SAC responsible for inducing suppression were consistent with being macrophages. They were resistant to the treatment of anti-Thy-1.2 antibody plus complement and were relatively radioresistant (at least ≤750 R X-radiation). Adherent cells obtained from lymph nodes or thymuses acted in the same way as SAC. However, preexposure of peritoneal adherent cells to tumor cells failed to induce suppression. In contrast, the simultaneous presence of peritoneal adherent cells with SAC upon exposure to tumor cells prevented the induction of suppression. These peritoneal cells were also consistent with being macrophages. These results confirmed our previous observations obtained with experiments performed in the allogeneic system. An immunoregulatory circuit existed between two subsets of macrophages that were derived from the population of cells in the peritoneal cavity and from spleen, lymph nodes, or thymus. In the presence of tumor cells, these macrophages produced both positive regulation and negative regulation of the T-cell-mediated cytotoxic response against syngeneic tumor cells. The tumor cells may have utilized the host's own immune network to activate the suppressor mechanisms, thus successfully evading the host's immune surveillance.—JNCI 1982; 69:867–872.

It has been demonstrated in various systems that tumor cells or their products can be immunosuppressive (*1*). The mechanisms for the induction of suppression by tumor cells are still not well understood. In our recent studies we have demonstrated that there may be a unique suppressor mechanism that is mediated by tumor cells via macrophages (*2*, *3*). When a population of macrophages of splenic origin is preexposed to a nonsuppressive dose of tumor cells, generation of CTL in the allogeneic MLC reactions is completely suppressed by further addition of another population of macrophages derived from the peritoneal cavity. There is a strict requirement for the preexposure of splenic macrophages to tumor cells for the induction of suppression. Not only does preexposure of PM to tumor cells fail to induce suppression but also the simultaneous presence of PM with SAC will preclude the induction of suppression by tumor cells (*3*).

To further determine whether this tumor cell-triggered macrophage-mediated suppressor mechanism may operate in the induction of specific tumor immunity, we extended the study to the syngeneic system. We have examined the interactions between two subsets of macrophages (splenic and peritoneal) and tumor cells and their effect on the generation of a T-cell-mediated cytotoxic response in the primary syngeneic MLTC reactions.

MATERIALS AND METHODS

Mice.—Female C57BL/6 (B6) mice 2–5 months of age were obtained from the Small Animal Section, Veterinary Resources Branch, Division of Research Services, National Institutes of Health.

Tumor cells.—Four cultured tumor lines were used: a Friend virus-induced leukemia FBL-3 (*4*) and a benzo[*a*]pyrene-induced leukosis EL-4 (*5*), both of $H\text{-}2^b$ haplotype, and a Friend virus-induced leukemia HFL/d (*6*) and a 3-methylcholanthrene-induced sarcoma Meth A (*7*), both of $H\text{-}2^d$ haplotype. All tumor lines were adapted to grow in suspension tissue culture and were maintained in RPMI-1640 medium containing 5% FBS (Grand Island Biological Co., Grand Island, N.Y.).

MLTC reactions.—MLTC reactions were performed by a technique similar to that developed by Nabholz et al. (*8*). The culture medium was RPMI-1640 containing 5% FBS, 5×10^{-5} *M* 2-mercaptoethanol (Sigma Chemical Co., St. Louis, Mo.), and 2×10^{-2} *M* HEPES[6] buffer solution (Media Unit, National Institutes of Health). The responding cells (responders) were spleen cells obtained from normal B6 mice. The stimulators were 10,000-R X-irradiated B6 FBL-3 tumor cells. The spleen cells were pressed gently in HBSS containing 5% FBS and passed through two layers of cotton gauze for preparation of single cell suspensions. They were

---

ABBREVIATIONS USED: CTL=cytotoxic T-lymphocytes; E:T=effector-to-target cell ratio; FBS=fetal bovine serum; HBSS=Hanks' balanced salt solution; [^{125}I]IdUrd=[^{125}I]5-iodo-2′-deoxyuridine; MLC=mixed lymphocyte culture; MLTC=mixed lymphocyte tumor cell culture(s); PC=peritoneal cell(s); PM=peritoneal macrophage(s); R:S=responder-to-stimulator cell ratio(s); SAC=splenic adherent cells.

---

[1] Received February 12, 1981; revised April 22, 1982; accepted May 5, 1982.

[2] Animals were maintained under the guidelines set forth by the National Institutes of Health, Bethesda, Md.

[3] Laboratory of Cell Biology, Division of Cancer Biology and Diagnosis, National Cancer Institute, National Institutes of Health, Public Health Service, U.S. Department of Health and Human Services, Bethesda, Md. 20205.

[4] *Address reprint requests to* Dr. Ting at Building 8, Room 219, National Institutes of Health, Bethesda, Md. 20205.

[5] We are grateful to Ms. Victoria Armstrong for her valuable help in the preparation of this manuscript.

[6] 4-(2-Hydroxyethyl)-1-piperazine ethanesulfonic acid.

treated with ammonium chloride–potassium lysing buffer (NH_4Cl, 0.155 M; Na_2EDTA, 0.1 m*M*; $KHCO_3$, 0.01 *M*) for 2 minutes at 4°C for removal of erythrocytes. The responders were always suspended in culture medium at a final concentration of 1.5×10^6/ml. They were incubated either alone (control culture) or with stimulators at an R:S of 150:1. Each flask usually contained 10 ml of cultured cells. All cultures were established in 30-ml tissue culture flasks (Falcon Plastics, Oxnard, Calif.) and incubated in an upright position at 37°C in a humidified atmosphere containing 5% CO_2. After 6 days of being cultured, the cells were counted, washed once, and resuspended in RPMI-1640–10% FBS at the appropriate concentrations to be tested in the $[^{125}I]$IdUrd release assay for cell-mediated cytotoxicity.

Preparation of adherent cells from spleen, lymph nodes, or thymus.—The adherent cells were obtained by the method described by Cowing et al. (*9*) with some modification. Spleen cells, pooled lymph node cells (cervical, axillary, and inguinal), or thymocytes at 1×10^7/ml in RPMI-1640 medium–5% FBS were incubated in T30 flasks in an upright position at 37°C for 2 hours in a 5% CO_2 atmosphere. The nonadherent cells were removed by three washings with HBSS containing 5% FBS.

Preparation of PC.—The PC were obtained by irrigation of the peritoneal cavity with HBSS containing 5% FBS.

Removal of phagocytes by the carbonyl iron and magnet technique.—PC (1–3×10^7) were preincubated with carbonyl iron particles (Technicon Instruments Corp., Tarrytown, N.Y.) for 1 hour at 37°C; the phagocytes were then removed with a magnet. This treatment could remove over 99% of the phagocytes as shown by the latex bead ingestion assay.

Treatment with anti-Thy-1.2 antibody.—Monoclonal anti-Thy 1.2 antibody was purchased from New England Nuclear Corp. (Boston, Mass.) and was designated as "NE001." Usually, each 1×10^7 spleen cell was incubated with 0.1 ml of the anti-Thy 1.2 antibody at a 1:100 dilution for 30 minutes at room temperature. The spleen cells were washed and then incubated a second time with 0.1 ml of a nontoxic rabbit serum at a 1:5 to 1:10 dilution as the source of complement. They were then washed, counted, and resuspended to the appropriate concentration. This treatment eliminates all the proliferative response to the T-cell mitogens concanavalin A and phytohemagglutinin, with increases of twofold to threefold of proliferative response to the B-cell mitogen lipopolysaccharide.

Cell-mediated cytotoxicity assay.—The $[^{125}I]$IdUrd release assay was used to measure cell-mediated cytotoxicity. The details of the technique have been described elsewhere (*10*). $[^{125}I]$IdUrd-labeled FBL-3 target cells (0.05 ml) at 1×10^5/ml and effector cells (0.15 ml) at an appropriate concentration were added to the wells of MicroTest II plates. All effector cells were adjusted to contain the same number of viable cells for each E:T. Incubation was done at 37°C in a 5% CO_2 atmosphere for 18–24 hours. Then the cells and supernatants were harvested by MASH II (M.A. Bioproducts, Walkersville, Md.). The supernatants and cell pellets were collected separately, and their radioactivity was determined in a well-type gamma scintillation counter. The results were expressed as total percentage of lysis and net percentage of lysis according to the following formulas: Total percent lysis=[cpm in supernatant/ (cpm in supernatant + cpm in cells)] × 100, and net percent lysis=total percent lysis obtained with responders incubated with stimulators − total percent lysis obtained with responders incubated alone. The standard errors obtained with total percent lysis were usually between 0.5 and 3%.

RESULTS

Restoration by PC of the T-cell-mediated cytotoxic response in primary, syngeneic MLTC reactions.—It has been demonstrated that FBL-3 cells have persistently failed to induce primary cytotoxic response both in the allogeneic and syngeneic MLTC reactions. However, the immunogenicity of FBL-3 cells could be restored by the addition of small amounts of PC syngeneic to the responders (*11–13*). When studying the time course relationship between the addition of PC and the restoration of cytotoxic response, we have found that if PC were added at 4 hours or later after starting the MLTC, the cytotoxic response could no longer be restored. Two representative experiments are shown in table 1. This finding is consistent with our results obtained in the allogeneic MLC experiments. In the presence of a nonsuppressive dose of tumor cells, addition of PC at a later time (1 day after MLC was started) induced suppression (*2*). Therefore, we performed further experiments to determine whether the same mechanism also operates in the syngeneic system, i.e., cytotoxic response against tumor-associated antigens.

Suppression of T-cell-mediated cytotoxic response by preexposure of SAC to FBL-3 tumor cells.—Experiments performed in the allogeneic MLC have shown that the macrophage-mediated suppression requires the collaboration of two subsets of macrophages (splenic and peritoneal) and the preexposure of splenic macrophages to tumor cells (*2, 3*). Similar experiments were performed to determine whether this was also true in the syngeneic MLTC. Results obtained from four representative experiments are shown in table 2. With addition of 10% syngeneic PC, primary MLTC could generate 20–50% of cytotoxicity against syngeneic FBL-3 tumor cells (group 2). However, if SAC were first prepared and preexposed to FBL-3 cells prior to the MLTC reactions (group

TABLE 1.—*Restoration by PC of the T-cell-mediated cytotoxic response in primary syngeneic MLTC reactions*[a]

Stimulators[b]	Time PC added, hr[c]	Net % lysis[d]	
		Expt 1	Expt 2
XFBL-3	—	4	1
XFBL-3	0	22	29
XFBL-3	1	29	ND
XFBL-3	2	23	32
XFBL-3	4	12	4
XFBL-3	7	ND	−5
XFBL-3	24	−1	−3
—	0	3	5

[a] All responders were normal B6 spleen cells.

[b] 10,000-R X-irradiated FBL-3 tumor cells (XFBL-3) were added at an R:S of 150:1; — = not added.

[c] 10% of syngeneic B6 PC were added at indicated time after the MLTC reactions were started; — = not added.

[d] Target cells were FBL-3; E:T = 100:1. ND=not determined.

TABLE 2.—*Suppression of T-cell-mediated cytotoxic response by preexposure of SAC to FBL-3*

Group	Different cell components added at:			Net % lysis[d]			
	0 hr[a]	2 hr[b]	6 hr[c]	Expt 1	Expt 2	Expt 3	Expt 4
1			NS+XFBL-3	1	−4	3	−2
2			NS+XFBL-3+PC	21	24	41	53
3	SAC		NS+XFBL-3+PC	25	20	42	52
4	SAC	XFBL-3	NS+PC	−2	−4	7	−2
5			NS+PC	3	4	−4	−1

[a] At 0 hr SAC were prepared by incubation of 1×10^7 normal B6 spleen cells in T30 flasks in an upright position.

[b] After 2 hr the nonadherent cells were removed by three washings with HBSS containing 5% FBS. In group 3, 2 ml lymphocyte culture medium was added to the T30 flask containing SAC. In group 4, 10,000-R X-irradiated FBL-3 tumor cells (XFBL-3) were added at 1.0×10^5/2 ml (equivalent to an R:S of 150:1, *see* footnote c).

[c] Primary syngeneic MLTC was performed by addition of 1.5×10^7 normal B6 spleen cells (NS) and 1.0×10^5 10,000-R X-irradiated FBL-3 cells (XFBL-3) (group 1); 10% syngeneic PC obtained from normal B6 mice were also added in groups 2 and 3; only NS and PC were added in groups 4 and 5. The final volume in each T30 flask was 10 ml.

[d] After 6 days of MLTC reactions, the effectors were washed, counted, and tested in the [^{125}I]IdUrd release assay at an E:T of 100:1. The target cells were FBL-3.

TABLE 3.—*Characterization of SAC involved in suppression*[a]

Treatment of SAC[b]	Time of addition of stimulators, hr[c]	PC[d]	Net % lysis
—	0	−	−4
—	0	+	24
SAC	0	+	20
SAC	−4	+	−4
SAC+anti-Thy 1.2+C	0	+	23
SAC+anti-Thy 1.2+C	−4	+	−6
SAC+X-radiation	0	+	22
SAC+X-radiation	−4	+	−5
—	—	+	4

[a] All responders were normal B6 spleen cells.

[b] Spleen cells, untreated (—) or treated with anti-Thy 1.2 antibody plus complement (C) or with 750 R X-radiation, were incubated at 1×10^7 cells in 2 ml in a T30 tissue culture flask in an upright position, at 37°C in a 5% CO_2 atmosphere. After 2 hr they were washed and the nonadherent cells were removed. These SAC were then incubated alone in medium or were incubated with 10,000-R X-irradiated FBL-3 tumor cells at a dose that was equivalent to an R:S of 150:1. After 4 hr of further incubation, MLTC were set up in these flasks.

[c] It is relevant to the time when MLTC was set up. X-irradiated FBL-3 cells were added at an R:S of 150:1; — = no addition of stimulators.

[d] 10% syngeneic PC were added at the onset (0 hr) of the MLTC; — = not added; + = added.

4), the cytotoxic response was completely suppressed, whereas the presence of extra amounts of SAC without preexposure to FBL-3 cells (group 3) gave the same degree of cytotoxic response as the control group (group 2). The amount of X-irradiated FBL-3 cells added in each group was exactly the same (1×10^5). In group 4, the FBL-3 cells were added in the presence of SAC at 4 hours prior to MLTC. In some experiments, addition of PC to responders (group 5) could generate 15–30% cytotoxicity above that of responders cultured alone. These experiments were excluded because the results were difficult to interpret.

Characterization of SAC responsible for inducing suppression.—To determine the nature of SAC responsible for inducing suppression, we pretreated the spleen cells with excess amounts of anti-Thy-1.2 antibody plus complement to remove T-cells, or we gave 750 R X-radiation to remove radiosensitive lymphocytes. These treated spleen cells were then incubated in T30 flasks to prepare adherent cells. The SAC obtained after such treatments were fully capable of inducing suppression (table 3). Thus they were consistent with being macrophages.

Characterization of PC responsible for inducing suppression.—The PC were subjected to the same treatments as the SAC in the preceding experiment. Their effects on the induction of suppression were tested. The results are summarized in table 4. These cells were also consistent with being macrophages: They were adherent to plastics, relatively radioresistant, and resistant to anti-Thy-1.2 antibody lysis.

Induction of suppression by tumor cells of various origins.—Two chemically induced tumors (EL-4 and Meth A) and two Friend virus-induced tumors (FBL-3 and HFL/d) were used in these experiments. EL-4 and FBL-3 are of syngeneic origin and are of the *H-2*^{b} haplotype. Meth A and HFL/d are of allogeneic origin and are of the *H-2*^{d} haplotype.

TABLE 4.—*Characterization of PC involved in suppression*

Group	Different cell components added at:			Net % lysis[d]
	0 hr[a]	2 hr[b]	6 hr[c]	
1			NS+XFBL-3	5
2			NS+XFBL-3+uPC	21
3			NS+XFBL-3+PC-NT	18
4			NS+XFBL-3+uPC-AD	17
5	SAC	XFBL-3	NS+uPC	−1
6	SAC	XFBL-3	NS+PC-NT	−1
7	SAC	XFBL-3	NS+uPC-AD	−5

[a] At 0 hr SAC were prepared by incubation of 1×10^7 normal B6 spleen cells in a T30 flask in an upright position.

[b] After 2 hr the nonadherent cells were removed by three washings with HBSS containing 5% FBS. In groups 5–7, 10,000-R X-irradiated FBL-3 tumor cells (XFBL-3) were added at 1.0×10^5/2 ml (equivalent to an R:S of 150:1; *see* footnote *c*).

[c] Primary syngeneic MLTC was performed by addition of 1.5×10^7 normal B6 spleen cells (NS) and 1.0×10^5 10,000-R X-irradiated FBL-3 cells (XFBL-3) (group 1); 10% syngeneic PC obtained from normal B6 mice were also added in groups 2–4; only NS and PC were added in groups 5–7. The final volume in each T30 flask was 10 ml. uPC=untreated PC, PC-NT=PC treated with anti-Thy 1.2 antibody plus complement and then with 750 R X-radiation, and uPC-AD=adherent uPC.

[d] Target cells were FBL-3; E:T = 100:1.

TABLE 5.—*Induction of suppression by tumor cells of various origins*

Group	Different cell components added at: 0 hr[a]	2 hr[b]	6 hr[c]	Net % lysis[d]	P[e]
1			NS+XFBL-3	3	
2			NS+XFBL-3+PC	43	
3	SAC		NS+XFBL-3+PC	40	
4	SAC	XFBL-3	NS+XFBL-3+PC	19	<0.01
5	SAC	XEL-4	NS+XFBL-3+PC	9	<0.01
6	SAC	XHFL/d	NS+XFBL-3+PC	16	<0.01
7	SAC	XMeth A	NS+XFBL-3+PC	−3	<0.01
8	SAC	XNS	NS+XFBL-3+PC	41	
9		XEL-4	NS+XFBL-3+PC	30	<0.01
10		XHFL/d	NS+XFBL-3+PC	38	
11		XMeth A	NS+XFBL-3+PC	39	
12			NS+PC	−4	

[a] At 0 hr SAC were prepared by incubation of 1×10^7 normal B6 spleen cells in a T30 flask in an upright position.

[b] After SAC were prepared, 10,000-R X-irradiated tumor cells were added at 5×10^4 cells/2 ml. Some T30 flasks contained only tumor cells without SAC (groups 9–11).

[c] After another 4 hr primary MLTC were performed by addition of 1.5×10^7 normal B6 spleen cells (NS) and 1×10^5 X-irradiated FBL-3 cells (XFBL-3) at an R:S of 150:1. Syngeneic PC were also added in groups 2–11. They were incubated for 6 days.

[d] Target cells were FBL-3; E:T = 100:1.

[e] Groups 4–8 were compared to group 3, and groups 9–11 were compared to group 2. The statistics were evaluated by the Welch distribution *t*-test.

TABLE 6.—*Induction of suppression by adherent cells from lymph nodes and thymus*

Different cell components added at: 0 hr[a]	2 hr[b]	6 hr[c]	Net % lysis[d]
		NS+XFBL-3	3
		NS+XFBL-3+PC	26
SAC		NS+XFBL-3+PC	28
SAC	XFBL-3	NS+PC	−1
LAC		NS+XFBL-3+PC	29
LAC	XFBL-3	NS+PC	1
TAC		NS+XFBL-3+PC	29
TAC	XFBL-3	NS+PC	5
PAC		NS+XFBL-3+PC	39
PAC	XFBL-3	NS+PC	31
		NS+PC	3

[a] 1×10^7 normal SAC, pooled lymph node cells (LAC) or thymocytes (TAC), or 1.5×10^6 normal PC (PAC) were incubated in T30 flasks for 2 hr. The nonadherent cells were removed by three washings with HBSS containing 5% FBS. Each flask contained ≈$5–10\times10^5$ adherent cells.

[b] 1×10^5 of 10,000-R X-irradiated FBL-3 cells (XFBL-3).

[c] Primary syngeneic MLTC was performed by addition of 1.5×10^7 normal B6 spleen cells (NS) and 1.0×10^5 10,000-R X-irradiated FBL-3 cells (XFBL-3) with or without PC. The final volume in each T30 flask was 10 ml.

[d] Target cells were FBL-3; E:T=100:1.

If SAC were preexposed to these tumor cells, significant suppression was induced (table 5, groups 4–7). In contrast, preexposure of SAC to X-irradiated normal spleen cells gave no suppression. Among these four tumor lines, only EL-4 cells were suppressive without being preexposed to SAC (group 9), but the degree of suppression was much lower than that of the group (group 5) that was preexposed to SAC.

Induction of suppression by adherent cells from lymph nodes and thymus.—To determine whether the macrophage-mediated suppression is unique to the SAC, we performed experiments using adherent cells obtained from other origins: pooled lymph nodes (cervical, axillary, and inguinal), thymus, and peritoneal cavity. We found that adherent cells obtained

TABLE 7.—*Preclusion of suppression by simultaneous presence of PM*

Group	Different cell components added at: 0 hr[a]	2 hr[b]	6 hr[c]	Net % lysis at E:T[d] 100:1	30:1
			Experiment 1		
1			NS+XFBL-3	−2	3
2			NS+XFBL-3+uPC	53	29
3	SAC		NS+XFBL-3+uPC	52	26
4	SAC	XFBL-3	NS+uPC	−2	1
5	SAC, PM	XFBL-3	NS+uPC	60	26
6			NS+uPC	−1	0
			Experiment 2		
1			NS+XFBL-3	−2	
2			NS+XFBL-3+uPC	28	
3	SAC		NS+XFBL-3+uPC	31	
4	SAC	XFBL-3	NS+uPC	3	
5	SAC, PM	XFBL-3	NS+uPC	23	
6	SAC	uPC+XFBL-3	NS+uPC	31	
7	SAC	PC-NT+XFBL-3	NS+uPC	36	
8	SAC	PC-CIM+XFBL-3	NS+uPC	0	

[a] PM and SAC mixture (group 5) was prepared by incubation of 1.5×10^6 PC with 1×10^7 spleen cells for 2 hr in T30 flasks. The nonadherent cells were removed by three washings with HBSS containing 5% FBS.

[b] At 1×10^5 of 10,000-R X-irradiated FBL-3 cells (XFBL-3). uPC = untreated PC, PC-NT=PC treated with anti-Thy 1.2 antibody plus complement and then with 750 R X-radiation, and PC-CIM=PC treated with carbonyl iron and magnet. All PC were added at 1.5×10^6 cells/flask.

[c] Primary syngeneic MLTC was performed by addition of 1.5×10^7 normal B6 spleen cells (NS) and 1.0×10^5 10,000-R X-irradiated FBL-3 cells (XFBL-3) (group 1); 10% syngeneic uPC (untreated PC) obtained from normal B6 mice were also added in groups 2 and 3; only NS and uPc were added in groups 4–6 in expt 1 or groups 4–8 in expt 2. The final volume in each T30 flask was 10 ml.

[d] Target cells were FBL-3.

from lymph nodes or thymus induce the same degree of suppression as the SAC (table 6). In contrast, preexposure of peritoneal adherent cells to tumor cells does not induce suppression. This result is consistent with our results obtained in the allogeneic MLC reactions (*2, 3*).

Preclusion of suppression by PM.—In the allogeneic MLC experiments, not only did preexposure of PM to tumor cells fail to induce suppression but also their simultaneous presence could preclude the induction of suppression by preexposure of SAC to tumor cells (*3*). We performed similar experiments to determine whether this was also true in syngeneic MLTC. The results are summarized in table 7. We found that the simultaneous presence of PM indeed precluded the suppression (group 5, expt 1). In this experiment, PM and SAC were prepared by incubation of PC and spleen cells together. To rule out the possibility that the adherence of SAC might be inhibited by the presence of PC, we performed additional experiments to obtain SAC and then we added PC 2 hours later (expt 2). When X-irradiated FBL-3 cells were added to trigger the suppression, suppression was precluded (group 6, expt 2), indicating that the preclusion was not due to the inhibition by PC of the SAC adherence. Furthermore, removal of T-cells from the PC populations did not affect its ability to prevent the suppression (group 7, expt 2). However, if phagocytes were removed from the PC, they were no longer able to prevent the suppression (group 8, expt 2).

DISCUSSION

Macrophages are heterogeneous in nature and so are their functions (*14-16*). Being the antigen-presenting cells or producers of various humoral mediators (e.g., macrokines), they are essential for the initiation of many immune responses to antigenic or mitogenic stimulation. Contrarily, macrophages exert suppressive effects on many immune functions, including antibody production (*17*), lymphoproliferative response (*18-20*), generation of cytotoxic T-cells (*19, 21, 22*), and T-cell-mediated hypersensitivity reaction (*23*). In tumor-bearing hosts, macrophages have been demonstrated to be one of the major components for inducing immunosuppression (*17, 18, 20*). In the present study, we have described a unique suppressor mechanism which was triggered by tumor cells and was mediated through the collaboration of two populations of macrophages. This suppressor mechanism restrained the generation of CTL in syngeneic MLTC reactions.

Our previous study demonstrated that the syngeneic MLTC reactions induced by FBL-3 cells are antigenically specific and are T-cell-dependent (*24*). The cytotoxic responses generated in the in vitro MLTC reactions are generally much weaker than those generated in vivo. This is especially true for the primary MLTC (*25*). The major reason for the weak in vitro response was found to be due to the tumor cell-induced immunosuppression, which can be overcome by the addition of exogenous PM [(*12, 26*), table 1]. In previous reports (*11, 13, 24*) we have shown that T-cells were the effectors for mediating the cytotoxic reactions generated in the syngeneic, primary MLTC reactions. The cytotoxic reactions was also specific for the Friend–Moloney–Rauscher tumor-associated antigens (*11, 13, 24*). This was true for the weak primary MLTC without addition of PC (*24*) and for the augmented primary MLTC with addition of PC (*11, 13*). We have also shown that in the PC-augmented MLTC, the cytotoxic reactions were mediated by T-cells and PM did not participate in the cytotoxic phase of the reactions (*13*).

In this study, there are several unique features in the tumor cell-triggered macrophage-mediated suppression. Three major cellular components are involved and they have to be interacted in a specific manner. These cellular components are: tumor cells, SAC, and PC. One critical requirement for induction of suppression is the preexposure of SAC to tumor cells (table 2). If peritoneal adherent cells are preexposed to tumor cells, there is no suppression (table 6), whereas adherent cells from lymph nodes or thymuses act in the same manner as SAC (table 6). Furthermore, the simultaneous presence of PC and SAC prevents the induction of suppression (table 7). These findings indicate that there are at least two populations of macrophages involved here, one from the peritoneal cavity and the other from spleen, lymph nodes, or thymuses. At present, there are no cell surface markers to distinguish these two populations. Both appeared to be macrophages (tables 3, 4, 7) and lacked the Ia antigen (not shown). In the SAC population, especially that prepared from T-cell-depleted spleen cells (table 3), almost all of the cells were macrophages as shown by their morphology and their phagocytic activity. In the PC population (table 4), the T-cell-depleted preparation also contained more than 90% macrophages.

Tumor cells are also a critical component for triggering of the suppressor mechanism. The origin of tumor cells is not critical. They can be from tumors induced by a different etiologic agent or from tumors of different *H-2* haplotype (table 5). In contrast, normal spleen cells treated in the same manner fail to induce suppression (table 5). Since the suppression could be induced by tumor cells of different etiologic origins, it was evident that the suppression of T-cell response was not antigen-specific; i.e., the effect of the mechanism is a general suppression of CTL induction. In previous reports (*2, 3*) we have demonstrated that this mechanism suppressed the induction of CTL against alloantigen. In the present study, we have shown that similar mechanisms suppressed the induction of CTL against the tumor-associated antigen(s).

Therefore, the macrophage-mediated suppressor mechanism described here is quite different from the mechanisms reported by other investigators (*17-23, 27, 28*). In other systems, either there was no need for the presence of tumor cells, or one source of macrophages (splenic or peritoneal) was sufficient. In our experiments, the exact reason for the need for two populations of macrophages is still not clear. Experiments performed in the allogeneic systems had clearly shown that both populations were needed for triggering of suppression. In regard to the preclusion of suppression by PC (table 7), it is possible that PM do not prevent suppression but provide help. This help overcomes the suppression induced by SAC and thus shifts the balance from suppression to assistance.

In this study, all experiments were performed strictly in the syngeneic system. We have found that tumor cells can indeed activate a suppressor mechanism via macrophages. This suppression may be mediated through three pathways: 1) generation of suppressor cells (suppressor macrophages or suppressor T-cells), 2) inactivation of helper T-cells, or 3) production of suppressive factors. Because suppressor cells and suppressive factors have been demonstrated in various tumor models (*27–31*), it is very likely that tumor cells can utilize different mechanisms to evade host immune surveillance. These issues will be examined in the accompanying paper (*32*).

REFERENCES

(*1*) Stutman O. Immunosuppression and malignancy. Adv Cancer Res 1975; 22:261–422.

(*2*) Ting CC, Rodrigues D. Immunoregulatory circuit among macrophage subsets for T cell-mediated cytotoxic response to tumor cells. J Immunol 1980; 124:1039–1044.

(*3*) — — —. Switching on the macrophage-mediated suppressor mechanism by tumor cells to evade host immune surveillance. Proc Natl Acad Sci USA 1980; 77:4265–4269.

(*4*) Glynn JP, McCoy JL, Fefer A. Cross-resistance to the transplantation of syngeneic Friend, Moloney and Rauscher virus-induced tumors. Cancer Res 1968; 28:434–439.

(*5*) Gorer PA. Studies in antibody response of mice to tumour inoculation. Br J Cancer 1950; 4:372–379.

(*6*) Freeman HA, Lilly F. Properties of cell lines derived from tumors induced by Friend virus in BALB/c and BALB/c-*H-2*^{b} mice. J Exp Med 1975; 142:122–223.

(*7*) Old LJ, Boyse EA, Clarke DA, Carswell EA. Antigenic properties of chemically induced tumors. Ann NY Acad Sci 1962; 101:80–106.

(*8*) Nabholz M, Vives J, Yong HM, Miggiono Y, Rijnbeck A, Shreffler DC. Cell-mediated lysis in vitro: Genetic control of killer cell production and target specificities in the mouse. Eur J Immunol 1974; 4:378–387.

(*9*) Cowing C, Pincus SH, Sachs DH, Dickler HB. A subpopulation of adherent accessory cells bearing I-A and I-E or C subregion antigens is required for antigen-specific murine T lymphocyte proliferation. J Immunol 1978; 121:1680–1686.

(*10*) Ting CC, Bushar GS, Rodrigues D, Herberman RB. Cell-mediated immunity to Friend virus-induced leukemia. I. Modification of ^{125}I-IUdR release cytotoxicity assay for use with suspension target cells. J Immunol 1975; 115:1351–1356.

(*11*) Igarashi T, Rodrigues D, Ting CC. Studies on the mechanisms for the induction of in vivo tumor immunity. IV. Enhancement of the in vitro generation of secondary cell-mediated cytotoxic response by normal peritoneal macrophages and their culture supernatants. J Immunol 1979; 122:1519–1527.

(*12*) Ting CC, Rodrigues D. Reversal by peritoneal adherent cells of tumor cell suppression of T cell-mediated immunity. J Immunol 1979; 123:801–807.

(*13*) Rodrigues D, Ting CC. Studies on the mechanisms for the induction of in vivo tumor immunity. V. A comparison of the generation of the primary cell-mediated cytotoxic response using in vitro mixed lymphocyte tumor cell culture and an in vivo technique. Cell Immunol 1981; 59:127–137.

(*14*) William SW. Functional heterogeneity of macrophages. In: Nelson DS, ed. Immunobiology of the macrophages. New York: Academic Press, 1976:91–109.

(*15*) Kavai M, Laczko J, Csaba B. Functional heterogeneity of macrophage. Immunology 1979; 36:729–732.

(*16*) Stenson WF, Parker CW. Prostaglandin, macrophages, and immunityy. J Immunol 1980; 125:1–5.

(*17*) Kennard J, Zolla-Pazner S. Origin and function of suppressor macrophages in myeloma. J Immunol 1980; 124:268–273.

(*18*) Kirchner H, Herberman RB, Glaser M, Lavrin DH. Suppression of in vitro lymphocyte stimulation in mice bearing primary Moloney sarcoma virus-induced tumors. Cell Immunol 1974; 13:32–40.

(*19*) Oehler JR, Herberman RB, Campbell DA, Djeu JY. Inhibition of rat mixed lymphocyte cultures by suppressor macrophages. Cell Immunol 1977; 29:238–250.

(*20*) Padarathsingh ML, Dean JH, Jerrells TR, McCoy JL, Lewis DD, Northing JW. Evidence for and characterization of suppressor cells in BALB/c mice bearing ADJ-PC5 plasmacytomas. JNCI 1979; 62:1235–1241.

(*21*) Fernbach BR, Kirchner H, Herberman RB. Inhibition of the mixed lymphocyte culture by peritoneal exudate cells. Cell Immunol 1976; 22:399–403.

(*22*) Truitt GA, Dennison DK, Rich RR, Rich SS. Interaction between T cells and non-T cells in suppression of cytotoxic lymphocyte response. J Immunol 1979; 123:745–750.

(*23*) Ptak W, Zembala M, Gershon RK. Intermediary role of macrophages in the passage of suppressor signals between T-cell subsets. J Exp Med 1978; 148:424–434.

(*24*) Ting CC, Bonnard GD. Cell-mediated immunity to Friend virus-induced leukemia. IV. In vitro generation of primary and secondary cell-mediated cytotoxic responses. J Immunol 1976; 116:1419–1425.

(*25*) Ting CC. Studies of the mechanisms for the induction of in vivo tumor immunity. I. Induction of primary and secondary cell-mediated cytotoxic response by adoptive transfer of lymphocytes. Cell Immunol 1976; 27:71–81.

(*26*) Ting CC, Rodrigues D, Ting RC, Wivel N, Collins MJ. Suppression of T cell-mediated immunity by tumor cells: Immunogenicity versus immunosuppression and preliminary characterization of the suppressive factors. Int J Cancer 1979; 24:644–655.

(*27*) Kirchner H, Chused TM, Herberman RB, Holden HT, Lavrin DH. Evidence of suppressor-cell activity in spleens of mice bearing primary tumors induced by Moloney sarcoma virus. J Exp Med 1974; 139:1473–1487.

(*28*) Connolly KM, Elgert KD. Regulation of T-cell mixed lymphocyte reaction reactivity: Demonstration of enhancing and inhibitory activity in tumor bearing host macrophages supernatants. Cell Immunol 1979; 45:94–107.

(*29*) Ting CC, Rodrigues D. Increased susceptibility to tumor cell immunosuppressive effect in tumor-bearing mice. JNCI 1980; 65:205–209.

(*30*) Yamanch K, Fujimoto S, Tada T. Differential activation of cytotoxic and suppressor T cells against syngeneic tumors in the mouse. J Immunol 1979; 123:1653–1658.

(*31*) Nelson K, Cory J, Hellström I, Hellström KE. T-T hybridoma product specifically suppresses tumor immunity. Proc Natl Acad Sci USA 1980; 77:2866–2870.

(*32*) Ting CC, Hargrove ME. Tumor cell-triggered macrophage-mediated suppression of the T-cell cytotoxic response to tumor-associated antigens. II. Mechanisms for induction of suppression. JNCI 1982; 69:873–878.

Tumor Cell-Triggered Macrophage-Mediated Suppression of the T-Cell Cytotoxic Response to Tumor-Associated Antigens.
II. Mechanisms for Induction of Suppression[1,2]

Chou-Chik Ting[3,4] *and* **Myrthel E. Hargrove**[3,5]

ABSTRACT—The mechanisms were investigated for the tumor cell-triggered macrophage-induced suppression of T-cell-mediated tumor immunity. Interaction between tumor cells and macrophages triggered the production of prostaglandin(s) (PG) that initiated the suppressor events. In our experiments, PGE_1 or PGE_2 suppressed the generation of cytotoxic T-lymphocytes in the syngeneic mixed lymphocyte tumor cell cultures. Indomethacin, a PG synthetase inhibitor, blocked the induction of the macrophage-mediated suppression, which suggested that suppression was caused by endogenous PG. This suppression might be further mediated by the generation of suppressor T-cells. Significant reduction in the levels of macrophage-induced suppression was seen in hosts receiving cyclophosphamide treatment, which could eliminate the precursors of suppressor T-cells. These findings indicated that tumor cells may trigger a chain of reactions, through the generation of suppressor factors or suppressor cells, to subvert the host's immune surveillance.—JNCI 1982; 69:873–878.

We have demonstrated a unique mechanism for tumor cell-induced suppression. This mechanism was mediated through the participation of two populations of macrophages. It was first demonstrated in the allogeneic system—suppression of the generation of CTL against alloantigen (*1*, *2*). This observation was extended to the syngeneic system—suppression of CTL against tumor-associated antigen (*3*). In this study, we have further examined the mechanisms involved in this tumor cell-triggered macrophage-mediated suppression.

It has been reported that macrophage-mediated suppression could be attributed to the production of PG (*4–8*). In some systems, PG further triggered the generation of suppressor T-cells (*6*) or inactivation of TCGF (*7*). The net result was the suppression of immune response. We have performed experiments to determine whether these mechanisms were involved in the generation of a specific T-cell-mediated tumor immunity.

MATERIALS AND METHODS

Mice.—Female C57BL/6 (B6) mice 2–5 months of age were obtained from the Small Animal Section, Veterinary Resources Branch, Division of Research Services, National Institutes of Health.

Tumor cells.—FBL-3, a Friend virus-induced leukemia in B6 mice (*9*) was adapted to grow in suspension tissue culture and was maintained in RPMI-1640 medium containing 5% FBS (Grand Island Biological Co., Grand Island, N.Y.).

MLTC reactions.—MLTC reactions were performed by a technique similar to that developed by Nabholz et al. (*10*). The culture medium was RPMI-1640 containing 5% FBS, 5×10^{-5} *M* 2-mercaptoethanol (Sigma Chemical Co., St. Louis, Mo.), and 2×10^{-2} *M* HEPES[6] buffer solution (Media Unit, National Institutes of Health). The responding cells (responders) were spleen cells obtained from normal B6 mice. The stimulators were 10,000-R X-irradiated B6 FBL-3 tumor cells. The spleen cells were pressed gently in HBSS containing 5% FBS and passed through two layers of cotton gauze for preparation of single cell suspensions. They were treated with ammonium chloride–potassium lysing buffer (NH_4Cl, 0.155 *M*; Na_2EDTA, 0.1 m*M*; $KHCO_3$, 0.01 *M*) for 2 minutes at 4°C for removal of erythrocytes. The responders were always suspended in culture medium at a final concentration of 1.5×10^6/ml. They were incubated either alone (control culture) or with stimulators at an R:S of 150:1. Each flask usually contained 10 ml of cultured cells. All cultures were established in 30-ml tissue culture flasks (Falcon Plastics, Oxnard, Calif.) and incubated in an upright position at 37°C in a humidified atmosphere containing 5% CO_2. After 6 days of being cultured, the cells were counted, washed once, and resuspended in RPMI-1640–10% FBS at the appropriate concentration.

Preparation of SAC.—The SAC were obtained by the method described by Cowing et al. (*11*) with some modification. Spleen cells at 1×10^7/ml in RPMI-1640 medium containing 5% FBS were incubated in T30 flasks in an upright position at 37°C for 2 hours in a 5% CO_2 atmosphere. The nonadherent cells were removed by three washings with HBSS containing 5% FBS.

Preparation of PC.—The PC were obtained from normal mice by irrigation of the peritoneal cavity with HBSS containing 5% FBS.

Cell-mediated cytotoxicity assay.—The [^{125}I]IdUrd release as-

---

ABBREVIATIONS USED: CTL=cytotoxic T-lymphocytes; E:T=effector-to-target cell ratio; FBS=fetal bovine serum; HBSS=Hanks' balanced salt solution; [^{125}I]IdUrd=[^{125}I]5-iodo-2′-deoxyuridine; MLTC=mixed lymphocyte tumor cell culture(s); PC=peritoneal cell(s); PG=prostaglandin(s); R:S=responder-to-stimulator cell ratio(s); SAC=splenic adherent cells; TCGF=T-cell growth factor or interleukin 2.

---

[1] Received February 12, 1981; revised April 22, 1982; accepted May 5, 1982.

[2] Animals were maintained under the guidelines set forth by the National Institutes of Health, Bethesda, Md.

[3] Laboratory of Cell Biology, Division of Cancer Biology and Diagnosis, National Cancer Institute, National Institutes of Health, Public Health Service, U.S. Department of Health and Human Services, Bethesda, Md. 20205.

[4] *Address reprint requests to* Dr. Ting at Building 8, Room 219, National Institues of Health, Bethesda, Md. 20205.

[5] We are grateful to Ms. Victoria Armstrong for her valuable help in the preparation of this manuscript.

[6] 4-(2-Hydroxyethyl)-1-piperazine ethanesulfonic acid.

say was used to measure cell-mediated cytotoxicity. The details of the technique have been described elsewhere (*12*). [^{125}I]IdUrd-labeled FBL-3 target cells (0.05 ml) at 1×10^5/ml and effector cells (0.15 ml) at an appropriate concentration were added to the wells of MicroTest II plates. All effector cells were adjusted to contain the same number of viable cells for each E:T. Incubation was done at 37°C in a 5% CO_2 atmosphere for 18–24 hours. Then the cells and supernatants were harvested by MASH II (M.A. Bioproducts, Walkersville, Md.). The supernatants and cell pellets were collected separately, and their radioactivity was determined in a well-type gamma scintillation counter. The results were expressed as total percentage of lysis and net percentage of lysis according to the following formulas: Total percent lysis=[cpm in supernatant/(cpm in supernatant+cpm in cells)]×100, and net percent lysis=(total percent lysis obtained with responders incubated with stimulators−total percent lysis obtained with responders incubated alone).

The standard errors obtained with total percent lysis were usually between 0.5 and 3%.

PG and PG synthetase inhibitors.—PGE_1, PGE_2, and $PGF_{1\alpha}$ (Sigma Chemical Co.) were dissolved in 95% ethanol alcohol at 5×10^2 *M* and stored at −20°C. The PG synthetase inhibitor indomethacin (Sigma Chemical Co.) was stored in dry form at 4°C. Immediately before use, indomethacin was dissolved in 95% ethanol alcohol at a 1×10^{-2} *M* concentration and was then diluted in RPMI-1640–5% FBS at an appropriate concentration.

Cyclophosphamide.—Cyclophosphamide was purchased from ICN Pharmaceuticals, Inc. (Plainview, N.Y.). It was dissolved in phosphate-buffered saline before use.

TCGF.—Two preparations of TCGF were used. One preparation (TCGF-R) was made according to the method of Gills et al. (*13*) by coculturing of inbred W/Fu rat spleen cells with the T-cell mitogen concanavalin A (Calbiochem-Behring, San Diego, Calif.). Rat spleen cells at 5×10^6/ml were cultured with concanavalin A at 5 µg/ml for 2 days. The supernatants were harvested, passed through 0.20-µm Millipore filters (Nalge Co., Rochester, N.Y.), and stored at −70°C. The optimal concentration of TCGF-R for supporting the T-cell growth was at 7.5–10%. Another preparation (TCGF-M or IL2) was obtained from a TCGF-producing EL-4 clones (*14*). This preparation was free of lectin or FBS.

RESULTS

Effect of PG on generation of T-cell-mediated cytotoxic response in syngeneic MLTC.—PG have been shown to suppress cell-mediated cytotoxic reactions (*5*, *16*). We performed experiments to determine the direct suppressive effect of PG in the generation of cytotoxic T-cells against tumor-associated antigens. The results are summarized in table 1. We found that 5×10^{-6} *M* of PGE_2 completely suppressed the MLTC cytotoxic response (expt 1); this suppressive effect was also seen at 5×10^{-7} *M* of PGE_2 (expt 2). In other experiments, 1-5×10^{-7} *M* of PGE_2 gave complete suppression (not shown). Indomethacin, PG synthetase inhibitor, did not alter the direct suppressive effect of PG. PGE_1, which had a chemical structure similar to that of PGE_2, also gave strong suppression. $PGF_{1\alpha}$ had no suppressive effect. If PGE_2 was added at the effector phase of the cytotoxic reaction (on days 5, 6), no suppression was seen (not shown). These results indicated that PGE can suppress the induction of a T-cell-mediated cytotoxic response. Addition of PGE_2 or PGE_1 into MLTC cultures was not always associated with reduction of cell viability, yet strong suppression of cytotoxic response was always seen. Furthermore, during the cytotoxicity test, all the effector preparations have been adjusted to contain the same number of viable cells (*see* "Materials and Methods"). Thus the PG-induced suppression could not be attributed to its cellular toxicity.

TABLE 1.—*Effect of PG and indomethacin on generation of T-cell-mediated cytotoxic response in syngeneic MLTC*[a]

Group	PC[b]	PG	Final concentration, *M*[c]	Indomethacin[d]	Net % lysis[e]	Suppression, %[f]	P[g]
			Experiment 1				
1					6		
2	+				21		
3	+	E_2	5×10^{-6}		3	86	<0.01
			Experiment 2				
1					0		
2	+				29		
3	+			+	36	−24	<0.05
4	+	E_2	5×10^{-6}		1	97	<0.01
5	+	E_2	5×10^{-7}		22	24	<0.05
6	+	E_2	5×10^{-8}		25	14	
7	+	E_2	5×10^{-6}	+	0	100	<0.01
8	+	E_2	5×10^{-7}	+	16	45	<0.01
9	+	E_2	5×10^{-8}	+	13	55	<0.01
			Experiment 3				
1					3		
2	+				24		
3	+	E_2	5×10^{-6}		0	100	<0.01
4	+	E_1	5×10^{-6}		0	100	<0.01
5	+	$F_{1\alpha}$	5×10^{-6}		25	−4	

[a] All responders in all groups were normal B6 spleen cells. Stimulators in all groups were 10,000-R X-irradiated FBL-3 tumor cells added at an R:S of 150:1.

[b] Ten percent syngeneic PC. + = PC were added.

[c] PGE_2, PGE_1, or $PGF_{1\alpha}$.

[d] Indomethacin was added (+) at a final concentration of 1×10^{-5} *M*.

[e] Target cells were FBL-3; E:T=100:1.

[f] [(Net % lysis obtained with group 2−net % lysis obtained with other group)/net % lysis obtained with group 2] ×100.

[g] Statistics were evaluated by the Welch distribution *t*-test by comparison with group 2.

Reversal by indomethacin of the macrophage-mediated suppression.—Experiments were performed to further determine whether endogenous PG was produced in our experiments, i.e., the macrophage-mediated suppression of specific T-cell-mediated tumor immunity (*3*). It has been shown in several experimental systems that macrophage-mediated suppression was attributed to the production of PG (*6*, *7*). This PG-induced suppression was blocked by a PG synthetase inhibitor, e.g., indomethacin (*6*, *7*, *16*). This was found to be the case in our experiments (table 2). As noted before (*3*), preexposure of FBL-3 cells to SAC induced suppression of the MLTC cytotoxic response (group 4). Addition of 1×10^{-5} *M* of indomethacin completely blocked the macro-

TABLE 2.—*Reversal by indomethacin of the macrophage-mediated suppression*

Group	Different cell components added at: 0 hr[a]	2 hr[b]	6 hr[c]	Indomethacin concentration, *M*[d]	Net % lysis[e] Expt 1	Expt 2	Expt 3
1			NS+XFBL-3		−4	−3	3
2			NS+XFBL-3+PC		40	31	25
3	SAC		NS+XFBL-3+PC		37	30	27
4	SAC	XFBL-3	NS+PC		9	9	0
5	SAC	XFBL-3	NS+PC	1×10^{-5}	53	31	32
6	SAC	XFBL-3	NS+PC	1×10^{-6}	33	23	29
7	SAC	XFBL-3	NS+PC	1×10^{-7}	23	15	25

[a] At 0 hr SAC were prepared by incubation of 1×10^7 normal B6 spleen cells in T30 flasks in an upright position.

[b] After 2 hr the nonadherent cells were removed by three washings with HBSS containing 5% FBS. In group 3, lymphocyte culture medium was added to the T30 flasks containing SAC. In groups 4–7, 10,000-R X-irradiated FBL-3 tumor cells (XFBL-3) were added at 1.0×10^5/2 ml (equivalent to an R:S of 150:1; *see* footnote *c*).

[c] Primary syngeneic MLTC was performed by addition of 1.5×10^7 normal B6 spleen cells (NS) and 1.0×10^5 10,000-R X-irradiated FBL-3 cells (XFBL-3) (group 1); 10% syngeneic PC obtained from normal B6 mice were also added in groups 2 and 3; only NS and PC were added in groups 4–7. Final vol in each T30 flask was 10 ml.

[d] Final concentration of indomethacin added.

[e] After 6 days the effectors were washed, counted, and tested in the [^{125}I]IdUrd release assay at an E:T of 100:1. Target cells were FBL-3.

phage-induced suppression, and the effect could be seen with a concentration of 1×10^{-7} *M* indomethacin (groups 5–7). These findings strongly suggest that endogenous PG is being produced and that endogenous PG accounted for the suppression of T-cell immunity.

Effect of indomethacin added at different times after MLTC reactions.—To determine how early indomethacin was needed to block the suppression, we performed a kinetic study. The results are summarized in table 3. We found that if indomethacin was added within the first 48 hours of the MLTC reaction, the macrophage-induced suppression was completely blocked. If it was added after that time, indomethacin was no longer able to block the suppression. This finding further confirmed that sufficient amounts of endogenous PG were produced in the first 48 hours to suppress the induction of cytotoxic T-cells, and indomethacin had no effect on the preformed PG.

TABLE 3.—*Effect of indomethacin added at different times of MLTC*

Group	Different cell components added at: 0 hr[a]	2 hr[b]	6 hr[c]	Indomethacin[d] added at:	Lysis, %[e]
1			NS+XFBL-3		3
2			NS+XFBL-3+PC		29
3	SAC		NS+XFBL-3+PC		27
4	SAC	XFBL-3	NS+PC		1
5	SAC	XFBL-3	NS+PC	Day 0	29
6	SAC	XFBL-3	NS+PC	Day 1	32
7	SAC	XFBL-3	NS+PC	Day 3	8
8	SAC	XFBL-3	NS+PC	Day 5	1

[a] At 0 hr SAC were prepared by incubation of 1×10^7 normal B6 spleen cells in T30 flasks in an upright position.

[b] After 2 hr the nonadherent cells were removed by three washings with HBSS containing 5% FBS. In group 3, lymphocyte culture medium was added to the T30 flasks containing SAC. In groups 4–8, 10,000-R X-irradiated FBL-3 tumor cells (XFBL-3) were added at 1.0×10^5/2 ml (equivalent to an R:S of 150:1; *see* footnote *c*).

[c] Primary syngeneic MLTC was performed by addition of 1.5×10^7 normal B6 spleen cells (NS) and 1.0×10^5 10,000-R X-irradiated FBL-3 cells (XFBL-3) (group 1); 10% syngenic PC obtained from normal B6 mice were also added in groups 2, 3; only NS and PC were added in groups 4–8. Final vol in each T30 flask was 10 ml.

[d] Indomethacin was added at a final concentration of 1×10^{-5} *M*, at indicated time of MLTC.

[e] Target cells were FBL-3; E:T = 100:1.

Effect of cyclophosphamide treatment on the macrophage-mediated suppression.—In some systems it has been reported that the suppressive effect produced by PG was attributed to the generation of suppressor T-cells (*5, 6*). It has also been demonstrated that the precursors of the suppressor T-cells could be effectively removed by pretreatment of the hosts with cyclophosphamide (*17*). We had taken this approach to determine whether the mechanism for macrophage-mediated suppression was due to the induction of suppressor T-cells. In these experiments, some mice were given 100 mg cyclophosphamide/kg body weight 2 days before the experiments, and then their spleens and PC were removed. The effect of cyclophosphamide treatment on the macrophage-mediated suppression was then tested. The yield of spleen cells in cyclophosphamide-treated mice was usually between 20 and 30% of that in the untreated mice. There was a slight reduction (10–20%) in the yield of PC. The results are summarized in table 4. The PC from both the cyclophosphamide-treated hosts and the normal hosts could restore the same levels of cytotoxic response in the syngeneic MLTC (group 6 vs. group 2). Addition of extra amounts of SAC into the MLTC did not alter these responses (groups 3, 7). However, if SAC were preexposed to tumor cells before the MLTC were started, significant suppression was induced in the untreated host (group 4) but not in the cyclophosphamide-treated host (group 8), in which only a marginal suppression occurred in one experiment (expt 2).

Effect of TCGF and indomethacin on MLTC and macrophage-mediated suppression.—It has been shown that PG could inhibit the production or reduce the activity of TCGF (*18*). To determine this possibility, we supplemented exogenous TCGF in the cultures to determine its effect on MLTC or macrophage-mediated suppression. The results are summarized in table 5. Two different preparations of TCGF were used. Rat TCGF (TCGF-R) was used in experiment 1; it contained lectin (concanavalin A). TCGF-M or IL-2 (*13*) was used in experiment 2; it was obtained from a TCGF-producing EL-4 cell line and was lectin-free. Without the

TABLE 4.—*Effect of cyclophosphamide treatment on the macrophage-mediated suppression*

Group	Different cell components added at:[a]			Net % lysis[e]		
	0 hr[b]	2 hr[c]	6 hr[d]	Expt 1	Expt 2	Expt 3
1			NS+XFBL-3	−3	−1	3
2			NS+XFBL-3+NPC	31	13	25
3	NSAC		NS+XFBL-3+NPC	30	14	27
4	NSAC	XFBL-3	NS+NPC	9[f]	2[f]	0[f]
5			CP-S+XFBL-3	0	0	3
6			CP-S+XFBL-3+CP-PC	34	20	18
7	CP-SAC		CP-S+XFBL-3+CP-PC	40	19	17
8	CP-SAC	XFBL-3	CP-S+CP-PC	36	14[g]	15

[a] NSAC, CP-SAC=normal SAC or SAC from cyclophosphamide-treated mice, respectively. NS, NPC=normal spleen cells or normal PC, respectively. CP-S, CP-PC=spleen cells or PC from cyclophosphamide-treated mice, respectively. XFBL-3=10,000-R X-irradiated FBL-3 tumor cells.

[b] At 0 hr SAC were prepared by incubation of 1×10^7 normal B6 spleen cells in T30 flasks in an upright position.

[c] After 2 hr the nonadherent cells were removed by three washings with HBSS containing 5% FBS. In group 3, lymphocyte culture medium was added to the T30 flasks containing SAC. In groups 4–7, XFBL-3 were added at 1.0×10^5/2 ml (equivalent to an R:S of 150:1; *see* footnote *c*).

[d] Primary syngeneic MLTC was performed by addition of 1.5×10^7 NS or CP-S and 1.0×10^5 XFBL-3 cells (groups 1, 4); 10% syngeneic NPC or CP-PC were also added in groups 2, 3 or groups 6, 7, respectively; only spleen cells and PC were added in groups 4, 8. Final vol in each T30 flask was 10 ml.

[e] Target cells were FBL-3; E:T=100:1.

[f] $P<0.01$.

[g] $P<0.05$.

TABLE 5.—*Effect of TCGF and indomethacin on syngeneic MLTC and macrophage-mediated suppression*

Group	Different cell component added at:			TCGF[d]	Indomethacin, *M*[e]	Net % lysis[f]	
	0 hr[a]	2 hr[b]	6 hr[c]			Expt 1	Expt 2
1			NS+XFBL-3			−2	0
2			NS+XFBL-3	1×		−3	9
3			NS+XFBL-3	3×		2	2
4			NS+XFBL-3		1×10^{-5}	1	2
5			NS+XFBL-3		1×10^{-6}	3	−1
6			NS+XFBL-3+PC			35	26
7	SAC		NS+XFBL-3+PC			31	24
8	SAC	XFBL-3	NS+PC			11	1
9	SAC	XFBL-3	NS+PC	1×		0	2
10	SAC	XFBL-3	NS+PC	3×		0	4
11	SAC	XFBL-3	NS+PC		1×10^{-5}	51	30
12	SAC	XFBL-3	NS+PC		1×10^{-6}	55	25

[a] At 0 hr SAC were prepared by incubation of 1×10^7 normal B6 spleen cells in T30 flasks in an upright position.

[b] After 2 hr the nonadherent cells were removed by three washings with HBSS containing 5% FBS. In group 7, lymphocyte culture medium was added into the T30 flasks containing SAC. In groups 8–12, 10,000-R X-irradiated FBL-3 tumor cells (XFBL-3) were added at 1.0×10^5/2 ml (equivalent to an R:S of 150:1; *see* footnote *c*).

[c] Primary syngeneic MLTC was performed by addition of 1.5×10^7 normal B6 spleen cells (NS) and 1.0×10^5 10,000-R X-irradiated FBL-3 cells (XFBL-3) (groups 1–5); 10% syngeneic PC obtained from normal B6 mice were also added in groups 6, 7; only NS and PC were added in groups 8–12. Final vol in each T30 flask was 10 ml.

[d] Ten percent TCGF was added at day 0 (1 time) or day 0, 1, or 2 (3 times). Rat TCGF was used in expt 1, and IL-2 was used in expt 2.

[e] Indomethacin was added at indicated final concentration.

[f] Target cells were FBL-3; E:T=100:1.

addition of exogenous PC, neither preparation restored the cytotoxic response of the syngeneic MLTC (groups 2, 3). Addition of indomethacin alone also failed to restore the cytotoxic response (groups 4, 5). In the macrophage-mediated suppression (group 8), addition of TCGF failed to inhibit the suppressive effect (groups 9, 10), whereas indomethacin could effectively block the suppression (groups 11, 12).

DISCUSSION

Macrophages can induce suppression in a variety of immune responses. In most cases, the suppressive effect appears to be more pronounced at the induction phase of the immune response. Generally, the effector phase is not affected. This has been noted, for example, in the generation of cytotoxic responses (*19–21*), lymphoproliferative responses (*19, 22, 23*), and production of lymphokines (*24*).

In this study, the tumor cell-triggered macrophage-mediated suppression is initiated in the first 4–6 hours of the immune response [(*3*), table 2]. Three critical components are involved: tumor cells, SAC, and peritoneal macrophages. The unique feature of this suppressor mechanism is the requirement of preexposure of the SAC to tumor cells [(*3*), table 2], indicating that preexposure is the first key element in the initiation of the suppressor events.

In several macrophage-mediated suppression systems, PG have been identified as the humoral mediators for induction of suppression (*4–9*). PG have also been proposed to modulate the extent or severity of numerous immune responses (*25, 26*). The E-type PG (E_1 or E_2) have been shown to suppress a variety of immune functions, such as T-cell-mediated cytotoxicity (*16*), lymphoproliferative responses (*5, 27*), lymphokine production (*24, 28*), and antibody response (*29*). The PG-induced suppression generally follows the same spectrum as that of the macrophage-mediated suppression.

Our experiments clearly demonstrated that PGE_1 and PGE_2 but not $PGF_{1\alpha}$ suppress the generation of cytotoxic T-cells against tumor-associated antigens (table 1). The macrophage-mediated suppression is blocked by indomethacin, a PG synthetase inhibitor (table 2). However, indomethacin has no effect on the preformed PG (tables 1, 3). Taken together, these findings strongly suggest that the macrophage-induced suppression is mediated by the endogenous production of PG, which act on the induction phase of the cytotoxic responses.

The exact immunoregulatory role of the PG remains to be determined. It has been shown that at least in some systems PG-induced suppression can be attributed to the generation of suppressor T-cells (*5, 6*).

Approaches were taken to eliminate the precursors of suppressor T-cells by treatment of the host with cyclophosphamide (*17*). Then the host's ability to induce macrophage-mediated suppression was examined (table 4). It was shown that cyclophosphamide treatment significantly reduced the host's ability to induce the macrophage-mediated suppression, which suggests that this suppressor mechanism was mediated by the generation of suppressor T-cells

TCGF does not seem to play a role here. It fails to restore the cytotoxic response to tumor-associated antigen (groups 2, 3; table 5), and it cannot block the suppressive effect of macrophage-induced suppression (groups 9, 10; table 5). However, these experiments cannot rule out the possibility that PG may interfere with the activity of TCGF rather than with its production.

In the present study, we have demonstrated that the tumor cell-triggered macrophage-mediated suppression is very likely caused by the increased production of E-type PG. The PG may further trigger the generation of suppressor T-cells that suppress the generation of cytotoxic T-cells. This mechanism may be normally operative in the hosts for the regulation of immune response. However, tumor cells may trigger the early production of PG and thus cause premature termination of the T-cell response. It has been shown that subversion of the in vivo immune response by tumor cells may also be attributed to the PG (*30*). Therefore, understanding these underlying mechanisms may help to design an effective strategy to prevent the tumor cells from evading the host's immune surveillance.

REFERENCES

(*1*) Ting CC, Rodrigues D. Immunoregulatory circuit among macrophage subsets for T cell-mediated cytotoxic response to tumor cells. J Immunol 1980; 124:1039–1044.

(*2*) ———. Switching on the macrophage-mediated suppressor mechanism by tumor cells to evade host immune surveillance. Proc Natl Acad Sci USA 1980; 77:4265–4269.

(*3*) ———. Tumor cell-triggered macrophage-mediated suppression of the T-cell cytotoxic response to tumor-associated antigens. I. Characterization of the cell components for induction of suppression. JNCI 1982; 69:867–872.

(*4*) Webb DR, Jamieson AT. Control of mitogen-induced transformation: Characterization of a splenic suppressor cell and its mode of action. Cell Immunol 1976; 24:45–57.

(*5*) Webb DR, Nowowiejski I. Mitogen-induced changes in lymphocyte prostaglandin levels: A signal for the induction of suppressor cell activity. Cell Immunol 1978; 41:72–85.

(*6*) ———. Control of suppressor cell activation via endogenous prostaglandin synthesis: The role of T cells and macrophages. Cell Immunol 1981; 63:321–328.

(*7*) Taffect SM, Russell SW. Macrophage-mediated tumor cell killing: Regulation of expression of cytolytic activity by prostaglandin E. J Immunol 1981; 126:424–427.

(*8*) Stenson WF, Parker CW. Opinion. Prostaglandins, macrophage and immunity. J Immunol 1980; 125:1–5.

(*9*) Glynn JP, McCoy JL, Fefer A. Cross-resistance to the transplantation of syngeneic Friend, Moloney and Rauscher virus-induced tumors. Cancer Res 1968; 28:434–439.

(*10*) Nabholz M, Vives J, Yong HM, Miggiono Y, Rijnbeck A, Shreffler DC. Cell-mediated lysis in vitro: Genetic control of killer cells production and target specificities in the mouse. Eur J Immunol 1974; 4:378–387.

(*11*) Cowing C, Pincus SH, Sachs DH, Dickler HB. A subpopulation of adherent accessory cells bearing I-A and I-E or C subregion antigens is required for antigen-specific murine T lymphocyte proliferation. J Immunol 1978; 121:1680–1686.

(*12*) Ting CC, Bushar GS, Rodrigues D, Herberman RB. Cell-mediated immunity to Friend virus-induced leukemia. I. Modification of ^{125}IUdR release cytotoxicity assay for use with suspension target cells. J Immunol 1976; 115:1351–1356.

(*13*) Gills S, Smith KA, Watson J. Biochemical and biological characterization of lymphocyte regulatory molecules. II. Purification of a class of rat and human lymphokines. J Immunol 1980; 124:1954–1962.

(*14*) Gills S, Scheid M, Watson J. Biochemical and biological characterization of lymphocyte regulatory molecules. III. The isolation and phenotype characterization of interleukin-2 producing T cell lymphomas. J Immunol 1980; 125:2570–2578.

(*15*) Droller MJ, Schneider MU, Perlmann P. A possible role of prostaglandins in the inhibition of natural and antibody-dependent cell-mediated cytotoxicity against tumor cells. Cell Immunol 1978; 39:165–177.

(*16*) Leung KH, Mihich E. Prostaglandin modulation of development of cell-mediated immunity in culture. Nature 1980; 288:597–600.

(*17*) Rollinghoff M, Starzinski-Powitz A, Pfizenmaier K, Wagner H. Cyclophosphamide-sensitive T lymphocytes suppress the in vivo generation of antigen specific cytotoxic T lymphocytes. J Exp Med 1977; 145:455–459.

(*18*) Baker PE, Fahey JV, Munck A. Prostaglandin inhibition of T-cell proliferation is mediated at two levels. Cell Immunol 1981; 61:52–61.

(*19*) Oehler JR, Herberman RB, Campbell DA, Djeu JY. Inhibition of rat mixed lymphocyte cultures by suppressor macrophages. Cell Immunol 1977; 29:238–250.

(*20*) Fernbach BR, Kirchner H, Herberman RB. Inhibition of the mixed lymphocyte culture by peritoneal exudate cells. Cell Immunol 1976; 22:399–403.

(*21*) Truitt GA, Dennison DK, Rich RR, Rich SS. Interaction between T cells and non-T cells in suppression of cytotoxic lymphocyte response. J Immunol 1979; 123:745–750.

(*22*) Kirchner H, Herberman RB, Glaser M, Lavrin DH. Suppression of in vitro lymphocyte stimulation in mice bearing primary Moloney sarcoma virus-induced tumors. Cell Immunol 1974; 13:32–40.

(*23*) Padarthsingh ML, Dean JH, Jerrells TR, McCoy JL, Lewis DD, Northing JW. Evidence and characterization of suppressor cells in BALB/c mice bearing ADJ-PC5 plasmacytomas. JNCI 1979; 62:1235–1241.

(*24*) Varesio L, Holden HT, Taramelli D. Suppression of lymphokine production. II. Macrophage-dependent inhibition of production of macrophage activating factor. Cell Immunol 1981; 63:279–292.

(*25*) Goodwin JS, Webb DR. Review. Regulation of the immune responses by prostaglandins. Clin Immunol Immunopathol 1980; 15:106–122.

(26) Pelus LM, Strausser HR. Minireview. Prostaglandins and the immune response. Life Sci 1977; 20:903–914.

(27) Metzger Z, Hoffeld JT, Oppenheim JJ. Macrophage-mediated suppression. I. Evidence for participation of both hydrogen peroxide and prostaglandins in suppression of murine lymphocyte proliferation. J Immunol 1980; 124:983–988.

(28) Gordon, D, Bray MA, Morley J. Control of lymphokine secretion by prostaglandins. Nature 1976; 262:401–402.

(29) Zimecki M, Webb DR. The role of prostaglandins in the control of the immune response to an autologous red blood cell antigen (Hb). Clin Immunol Immunopathol 1977; 8:420–429.

(30) Plescia OT, Smith AH, Grinwich K. Subversion of immune system by tumor cells and role of prostaglandins. Proc Natl Acad Sci USA 1975; 72:1848–1851.

Inducible Macrophage Cytotoxins. I. Biokinetics of Activation and Release In Vitro[1,2]

Thomas H. Reidarson,[3] Walter E. Levy III,[3] Jim Klostergaard,[3,4,5] *and* **Gale A. Granger**[3,6]

ABSTRACT—Peritoneal exudate macrophage monolayers (PEMM) from C57BL/6 and DBA/2 mice inoculated ip with tumor allografts were induced to release in vitro labile cell toxin(s), herein called "macrophage cytotoxin(s)" (MCT). Macrophages released MCT spontaneously for a short interval when initially established as monolayers, and they were reinduced to secrete MCT by exposure to allogeneic and syngeneic tumor cells (but not to normal cells) and by exposure to polyinosinic-polycytidylic acid (poly I·poly C) and lipopolysaccharide (LPS). PEMM from normal mice treated ip 3 days previously with thioglycollate were also induced to release toxins in vitro. These cells did not release MCT spontaneously before or after treatment with neoplastic cells but were induced to release MCT by exposure to poly I·poly C or LPS. Resident peritoneal macrophages did not release MCT either spontaneously or after treatment with tumor cells, poly I·poly C, or LPS. MCT released from alloimmune mice stimulated with syngeneic or allogeneic tumor cells were resolved by molecular sieving into a major peak at 140,000–160,000 daltons, called "α-MCT," and into a minor peak at 60,000 daltons, called "β-MCT." However, supernatants from thioglycollate-induced PEMM, stimulated with poly I·poly C or LPS, appeared to be composed entirely of the α-class. α-MCT from poly I·poly C-stimulated PEMM caused 31–56% lysis of syngeneic EL-4 and allogeneic L-929, NS-1, and YAC-1 tumor cells in vitro but was not cytotoxic for normal cells. Secretion of the MCT by PEMM derived from thioglycollate-treated animals stimulated with poly I·poly C was inhibited by colchicine, emetine, iodoacetic acid, trypan blue, and cytochalasin B.—JNCI 1982; 69:879–887.

The activated state of a murine PEM is characterized by increases in size, in motility, in phagocytic capacity, and in production of lysosome enzymes; by greater adherence to glass; and by an increased ability to nonspecifically destroy allogeneic and syngeneic neoplastic cells over normal cells in vitro (*1–8*). The mechanism by which the activated murine PEM destroy tumors is not known. However, in vitro evidence suggests that this mechanism requires contact between effector and target cells, occurs in 24–72 hours, and does not involve phagocytosis (*9–12*).

In a recent review, Hibbs Jr. et al. (*13*) described various treatments that induce the activation of murine PEM to tumoricidal activity in vitro. The first treatment induces the macrophage to a "stimulated" but nontumoricidal stage. This inducement can be brought about by ip injection of thioglycollate before harvest of the PEM or by maintenance of the macrophage in vitro. Secondary stimulation in vitro is initiated by addition of LPS, macrophage activating factor, or various "serum factors," which raise the PEM to the final tumoricidal stage. Most investigators believe that activated macrophages selectively destroy neoplastic over normal cells (*1, 5–7, 11–13*); however, evidence indicates that such macrophages may also destroy normal cells (*14*).

The destruction of neoplastic cells by activated macrophages normally requires contact between effector and target cells. Several investigators (*15*) have suggested that tumor cell lysis subsequent to contact with the effector is mediated by materials derived from the activated macrophage lysosome system. It has been demonstrated that PEM from BCG-immune mice, obtained with or without purified protein derivative challenge, or that PEM from normal mice stimulated with LPS and poly I·poly C release cell toxins in vitro (*16–19*). These toxins have not been well characterized; however, their involvement in the lytic event has been suggested.

The present study describes an inducible system of cell lytic molecule(s) called "MCT" that are released by activated murine PEM in response to different in vitro stimuli.

MATERIALS AND METHODS

Culture media and cell lines.—Culture media used in these studies consisted of RPMI-1640 supplemented with 3 or 10% heat-inactivated (56°C, 60 min) FCS (GIBCO, Grand Island, N.Y.) or NBCS (GIBCO), 100 μg streptomycin/ml, and 100 U penicillin/ml. Murine α-L-929 (C3H-H-2^k) transformed fibroblasts, which had previously been selected in our laboratory from a number of L-cell strains for extreme sensitivity to lysis by human lymphotoxins, were grown in 32-oz prescription bottles in RPMI-1640 with 3% NBCS at 37°C in a 95% air–5% CO_2 atmosphere and passed twice a week, indefinitely. Murine C57BL/6 EL 4 (H-2^b) lymphoma, Balb/c NS-1 (H-2^d) myeloma, P815 DBA/2 (H-2^d) mastocytoma, A/Sn YAC-1 (H-2^a) lymphoma, and human K562 erythroid leukemia cell lines were grown in RPMI-

---

Abbreviations used: Con A=concanavalin A; EMEM-Eagle's minimum essential medium; FCS=fetal calf serum; HBSS=Hanks' balanced salt solution; LAH=lactalbumin hydrolysate; LPS=lipopolysaccharide; MCT=macrophage cytotoxin(s); α=MCT=MCT detectable at 140,000–160,000 daltons; β-MCT=MCT detectable at 60,000 daltons; NBCS=newborn calf serum; OD_{600}=optical density at 600 nm; PBS=phosphate-buffered saline; PEC=peritoneal exudate cell(s); PEM=peritoneal exudate macrophage(s); PEMM=PEM monolayers; PHA=phytohemagglutinin; PHA-P=aglycan protein form of PHA; poly I·poly C=polyinosinic-polycytidylic acid; SBTI=soybean trypsin inhibitor; SDS=sodium dodecyl sulfate.

---

[1] Received July 23, 1981; revised January 20, 1982; accepted April 19, 1982.

[2] Guidelines for the care and use of laboratory animals were followed as set forth by the National Research Council.

[3] Department of Molecular Biology and Biochemistry, School of Biological Sciences, University of California at Irvine, Irvine, Calif. 92717.

[4] Recipient of Senior Postdoctoral Fellowship S-25-81 from the American Cancer Society, California Division.

[5] *Address reprint requests to* Dr. Klostergaard.

[6] We are grateful to Mr. Robert Yamamoto for excellent technical assistance. We also thank Mrs. Gloria Heidenfelder and Ms. Virginia Baker for preparation of this manuscript and L. T. Furbrush for his inspiration.

1640 supplemented with 10% FCS. Naive BALB/c (H-2^d) spleens were asceptically removed and prepared on the day of the experiment. Spleens were minced, and a single cell suspension was formed and then transferred to a T-25 culture flask (Corning Glass Works, Corning, N.Y.) at 4×10^6 cells/ml in RPMI-1640 supplemented with 10% FCS. The cells were allowed to incubate for 1 hour at 37°C for removal of adherent cells. Viability was 93–98% as determined by eosin Y dye exclusion. Blasts were induced by Con A (1 μg/ml) treatment of normal nonadherent splenocytes for 4 hours at 37°C.

Induction of PEC.—PEC were obtained by three methods: *a*) P815 mastocytoma cells (10^7) suspended in RPMI-1640 or PBS were injected ip into C57BL/6 mice; 10–14 days later the PEC were harvested as previously described (*20*). PEC induction was similarly performed by ip injection of EL 4 lymphoma cells into DBA/2 mice. Thioglycollate (3 ml) (BBL, Cockeysville, Md.) was prepared and injected ip into C57BL/6 mice. Approximately 15–20×10^6 PEC/mouse was harvested 3 days later. *c*) Resident PEC (2–4×10^6/mouse) from nonmanipulated C57BL/6 or DBA/2 mice were harvested by peritoneal lavage 24 hours before in vitro stimulation.

Preparation of PEMM.—PEMM were obtained from C56BL/6 (Kingston Colony, Charles River Breeding Laboratories, Wilmington, Mass.) and DBA/2 (ARS, San Diego, Calif.) mice 6–8 weeks old. Mice were killed by cervical dislocation, and each peritoneal cavity was irrigated aseptically with 7–8 ml cold PBS (pH 6.9). The exudate was pooled and centrifuged for 5 minutes at 1,500×*g* at 4°C. The cell pellet was resuspended in 5–10 ml of either cold-modified EMEM in HBSS or RPMI-1640 (GIBCO) supplemented with 10% FCS or NBCS, 100 U penicillin/ml, and 100 μg streptomycin/ml. The PEC were then suspended in either EMEM in HBSS or RPMI-1640 and placed in T-culture flasks at $1\times10^6/5$ cm^2/ml. The flasks were incubated at 37°C in 95% air–5% CO$_2$ for 2 hours and then washed four times with serum-free RPMI-1640 or sterile PBS to remove nonadherent cells. Monolayers were maintained in RPMI-1640 at 37°C. The composition of the adherent cells was determined by examination of tetrachrome-, eosin Y-, and neutral red-stained cover slip PEMM. The monolayers were 99% or more macrophages and 100% viable.

Assay for direct macrophage-mediated cytolysis.—PEC obtained as described above were pelleted by centrifugation, resuspended in RPMI-1640 supplemented with 10% heat-inactivated NBCS, and plated in 16-mm diameter Costar plates (Costar, Cambridge, Mass.) at a density of 0.5×10^6 cells/well. After 2 hours, the monolayers were washed and allowed to incubate for an additional 24 hours in RPMI-1640 supplemented with 10% FCS before use.

The PEMM were then treated with 40 μg poly I·poly C/ml (P-L Biochemicals, Inc., Milwaukee, Wis.) in RPMI-1640 containing 10% NBCS, incubated for 1 hour, and washed four times with serum-free media. Various tumor target cells were added at a 10:1 effector-to-target cell ratio (total vol, 0.5 ml). After 12 and 36 hours of incubation at 37°C, we removed the remaining target cells from the monolayers by aspirating five to seven times, followed by a short trypsinization. Upon visual inspection, less than 5% of the tumor cells remained associated with the monolayers after this treatment. The washes and trypsin supernatant were then pooled and centrifuged. The pelleted tumor cells were resuspended in 0.1% eosin Y in PBS solution, and viable cells were enumerated in a hemacytometer. All targets were nonadherent cells.

Production of MCT.—Alloinduced PEMM were incubated in RPMI-1640 containing either 10% FCS, 10% NBCS, or 0.01% LAH (GIBCO) for various lengths of time. Supernatants were then collected, rendered cell-free by centrifugation, and assayed for MCT activity. We attempted restimulation of alloinduced macrophages by adding 2.5×10^6 EL 4 or P815 tumor cells, poly I·poly C (P-L Biochemicals, Inc.), LPS (Sigma Chemical Co., St. Louis, Mo.), Con A (Sigma), or PHA-P (Difco Laboratories, Detroit, Mich.) to PEMM in serum-free RPMI-1640. After incubation for 1–2 hours, the PEMM were washed thoroughly with serum-free medium and then the medium was replaced; the supernatant was assayed for MCT activity as described later.

Thioglycollate-elicited or resident macrophages were treated in a similar fashion with either EL 4 or NS-1 tumor cells, poly I·poly C, LPS, Con A, or PHA-P for 1–2 hours; cultured; and assayed for MCT activity. Media were either assayed for MCT immediately or frozen at −20°C and analyzed within 48 hours.

Assay for MCT and determination of the number of units of activity in a supernatant.—Methods are detailed in (*20*). Serial dilutions of MCT-containing or control supernatants in RPMI-1640 were added to duplicate 1-ml slant-tube cultures, which were seeded with 10^5 mitomycin C-treated α-L-929 cell targets. These nondividing targets were used for evaluation of cytolysis only and not cytostasis. After 14–24 hours at 37°C, the remaining viable adherent cell number was then enumerated on a model F Coulter counter. Nonattached cells were determined to be greater than 95% nonviable by eosin Y staining. One unit of MCT activity is defined as that amount of material that destroys 50% of the target L-cells (50,000). The reciprocal of the highest dilution that destroys 50% of the target L-cells denotes the number of MCT unit per milliliter in a given supernatant.

Generation of activated macrophage supernatants, molecular sieving fractions containing α-MCT, and assay for MCT-induced tumor cell cytolysis.—The 10×10^6 thioglycollate-elicited PEC were established as monolayers in T-75 culture flasks as described above. The PEMM were washed and stimulated with 40 μg poly I·poly C/ml. Following the last wash, 10 ml RPMI-1640 supplemented with 0.01% LAH was added, and the monolayers were incubated for 2 hours at 37°C. The supernatant was collected and either: *a*) immediately assayed for units of lytic activity on L-929 cells or *b*) concentrated 20 times by ultrafiltration on an Amicon PM10 membrane and passed through an Ultrogel AcA 44 column. We applied 2 ml of twentyfold to thirtyfold concentrates of MCT supernatants to an Ultrogel AcA 44 column (2.5×60 cm) equilibrated in 10 m*M* potassium phosphate (pH 7.2) and 10^{-4} *M* EDTA. Fractions of 4 ml were collected at a flow rate of 40 ml/hour. The peak of cytolytic activity detectable on murine L-929 cells at 140,000–160,000 daltons, called "α-MCT," was pooled and concentrated as described above. The α-MCT was filtered through a cellulose nitrate membrane with a 0.2-μm pore (Sartorious membrane filter; Science Essentials, Fullerton, Calif.) and then added to the various tumor targets. Following 12 and 36 hours of incubation at 37°C, the remaining cells were removed and viable cells enumerated as described previously.

Determination of macrophage viability.—We added 25 μCi $Na_2{}^{51}CrO_4$/ml RPMI-1640 to 0.5×10^6 macrophages seeded in 16-mm Costar plates (Costar) and incubated them for the release period (4–6 hr) at 37°C. PEMM were then washed thoroughly for removal of the nonincorporated counts, solubilized with 0.5 ml 10% SDS in PBS, and enumerated in a Beckman biogamma counter.

Inhibitors.—The inhibitors colchicine, emetine, iodoacetic acid, SBTI, and trypan blue were dissolved directly in RPMI-1640. Trypan blue was dialyzed against 500 vol PBS before use. Inhibitor cytochalasin B was first dissolved in dimethyl sulfoxide and then diluted with RPMI-1640. All inhibitors here came from Sigma.

Use of trypan blue.—Thioglycollate-elicited macrophage monolayers were established as described previously. Trypan blue was added to monolayers at various concentrations as described by Hibbs Jr. (*15*). After 24 hours, the monolayers were washed four times; then they were incubated for 2 hours in 0.01% LAH, after 1 hour of poly I·poly C stimulation. The supernatant was removed and assayed for lytic activity. To evaluate the amount of trypan blue incorporated by the macrophages, we solubilized the monolayer with 10% SDS in PBS and determined the light absorption at 600 nm with a Beckman model 25 spectrophotometer.

RESULTS

Spontaneous MCT release in vitro from PEMM obtained from C57BL/6 allografted mice.—PEMM, from C57BL/6 mice that had received an ip injection of P815 tumor, were established as described in "Materials and Methods." Samples of medium were removed at various intervals and tested for MCT activity on L-929 cells. As seen in text-figure 1, low levels of MCT activity were detected in the initial 1- to 4-hour culture; then between 4 and 6 hours, activity climbed to a peak, followed by a decline to less than 6 U MCT by 24 hours. While the data are not shown, additional experiments revealed that release of MCT rapidly ceased after 6–8 hours in these cultures. Resident macrophages released less than 6 U MCT/ml during the same culture period.

Restimulation of MCT release in vitro from C57BL/6 and DBA/2 alloimmune PEMM after a short exposure to P815 or EL 4 tumors.—PEMM from alloimmune C57BL/6 or DBA/2 mice were cultured in vitro for 6–8 hours, as described in "Materials and Methods." The monolayers were then washed thoroughly and reexposed to allogeneic or syngeneic tumor cells for 1 hour. The data shown in table 1 reveal that alloimmune macrophages released from 75–110 U MCT/ml in 4–6 hours when reexposed to EL 4 or P815 tumors for 1 hour. Resident or naive macrophages, however, did not release detectable levels of activity under the same conditions. Moreover, when exposed to allogeneic or syngeneic normal lymphocytes, these alloimmune macrophages did not release detectable levels of activity (data not shown). Exposure of alloimmune macrophages to Con A lymphoblasts caused the release of low levels (10–15 U/ml; data not shown) of a toxin into the supernatant. However, the nature of this toxin is currently unclear (*see* "Discussion").

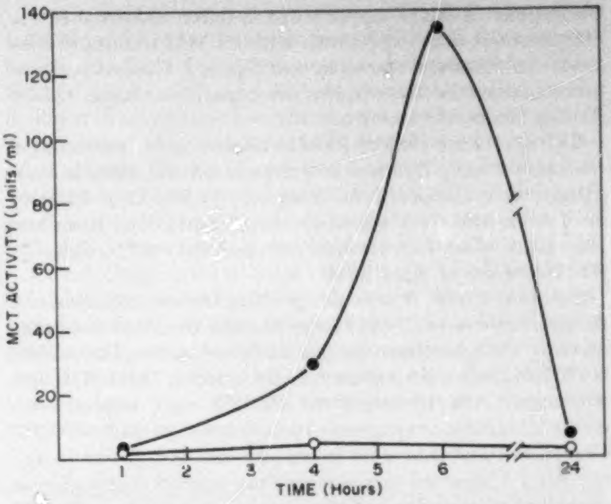

TEXT-FIGURE 1.—Spontaneous release of MCT from alloimmune and resident PEMM. Alloimmune (●——●) and resident (○——○) C57BL/6 PEM were collected, cultured as monolayers, and then allowed to release MCT up to 24 hr. Supernatants were collected at various intervals of time and assayed for lytic activity as described in "Materials and Methods."

Next, experiments were designed to determine if MCT could be induced from alloimmune and thioglycollate-elicited PEMM maintained in culture for various periods of time without stimulation. In numerous experiments, we were able to restimulate alloimmune cells up to 12 days in culture by reexposure to tumor cells for 1 hour. Moreover,

TABLE 1.—*Release of MCT by PEMM[a] obtained from alloimmune and normal C57BL/6 and DBA/2 mice following a 1-hour exposure to allogeneic and syngeneic tumor cells*

PEMM	Treatment	MCT U/ml
Alloimmune		
C57BL/6 immunized with P815	EL 4	110±60[b]
	P815	90±30[b]
	None	12±3[b]
DBA/2 immunized with EL 4	EL 4	80±40[b]
	P815	75±25[b]
	None	8±4[b]
Resident[c]		
C57BL/6	EL 4	<6
	P815	<6
	None	<6
DBA/2	EL 4	<6
	P815	<6
	None	<6

[a] PEMM were obtained from C57BL/6 and DBA/2 mice 10–15 days after intraperitoneal allografts of P815 and EL 4 tumors, respectively. PEMM were treated as described in "Materials and Methods" and supernatants were collected 6 hr after exposure to tumor cells and tested for MCT activity.

[b] Values are means ± range.

[c] Resident PEMM were obtained from nonimmunized mice and treated as stated in *footnote a*.

the release of MCT approached original maximal levels. One restimulation experiment with PEMM maintained for 5 days in culture is shown in text-figure 2. Control resident macrophages did not acquire the capacity to release MCT during this period in vitro.

Thioglycollate-elicited PEMM could also be restimulated with poly I·poly C. After 3–4 days in culture, these macrophages were reexposed to 40 μg poly I·poly C or LPS/ml for 1 hour and then allowed to release MCT as described previously (data not shown). We observed MCT release to 90–95% of the original level.

Induction of MCT secretion by PEMM from alloimmune or thioglycollate-treated C57BL/6 mice treated with various stimulating agents.—Thioglycollate- or tumor-elicited macrophages from C57BL/6 mice were cultured as described in "Materials and Methods." After 8 hours, the PEMM were treated with either allogeneic or syngeneic tumors or poly I·poly C, LPS, Con A, or PHA that were tested at levels from 0.1 to 75 μg/ml. After 1 hour the monolayers were washed thoroughly as described previously, and then supernatants were collected after 4 hours and assayed for lytic activity. As seen in table 2, syngeneic or allogeneic tumor cells stimulated release from PEMM from allografted animals but not thioglycollate-elicited PEMM. However, poly I·poly C and LPS were capable of inducing the release of cell-lytic material from thioglycollate-elicited and alloinduced macrophages. In contrast, the lectins Con A and PHA did not induce MCT release in any of these cultures. While not shown, release by poly I·poly C and LPS was dose dependent; maximal activity was observed with 40 μg of either agent/ml; however, as little as 0.1 μg LPS/ml was sufficient to achieve a comparable response. Finally, resident macrophages could not be stimulated to release cell lytic molecules with any stimulating agent or treatment used.

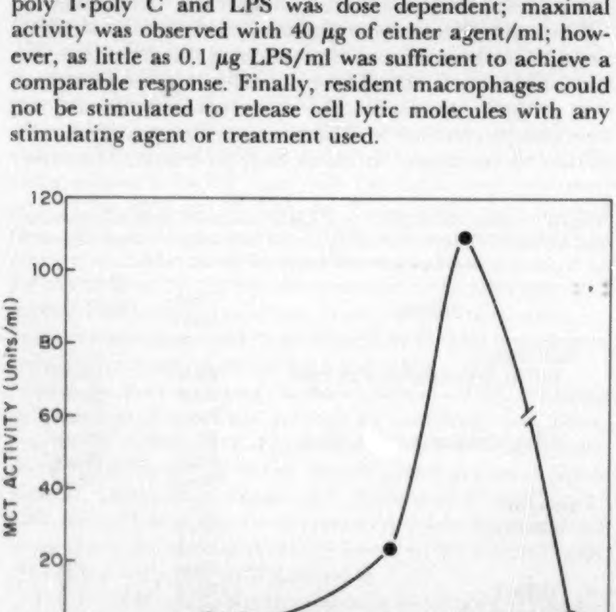

TEXT-FIGURE 2.—Restimulation of C57BL/6 alloimmune PEMM by short exposure to allogeneic tumor cells. Alloimmune (●——●) and resident (○——○) C57BL/6 macrophages were cultured for 5 days, exposed to P815 allogeneic tumors for 1 hr, washed free of tumors, and then allowed to release material for 24 hr. Supernatants were collected at various times and assayed for MCT activity as described in "Materials and Methods."

TABLE 2.—*Release of MCT by C57BL/6 PEMM treated in vitro with different stimulating agents*[a]

PEMM	Treatment[b]	MCT released in U/ml
Alloinduced, immunized with P815	EL 4	70±35[c]
	P815	85±40[c]
	NS-1	65±30[c]
	Poly I·poly C	143±50[c]
	LPS	125±25[c]
	PHA	<15
	Con A	<15
	None	<15
Thioglycollate elicited	EL 4	<6
	NS-1	<6
	Poly I·poly C	47±25[c]
	LPS	33±5[c]
	PHA	<6
	Con A	<6
	None	<6
Resident	EL 4	<6
	NS-1	<6
	Poly I·poly C	9±3[c]
	LPS	<6
	PHA	<6
	Con A	<6
	None	<6

[a] PEMM were established and 8 hr later were treated with various stimulating agents as described in "Materials and Methods." Each culture was then thoroughly rinsed and fresh RPMI-1640 containing 10% FCS added. After 2–4 hr, supernatants were removed and assayed for MCT activity.

[b] Poly I·poly C, LPS, PHA, and Con A were used at 40 μg/ml.

[c] Values are means ± range.

Kinetics of MCT release from thioglycollate-elicited C57BL/6 PEMM in vitro under various stimulation and culture conditions.—Thioglycollate-elicited PEMM were treated with poly I·poly C or LPS for 1 hour and placed in fresh medium, and MCT release was measured at various time intervals as described in "Materials and Methods." As seen in text-figure 3, there was a lag period of 30–60 minutes following poly I·

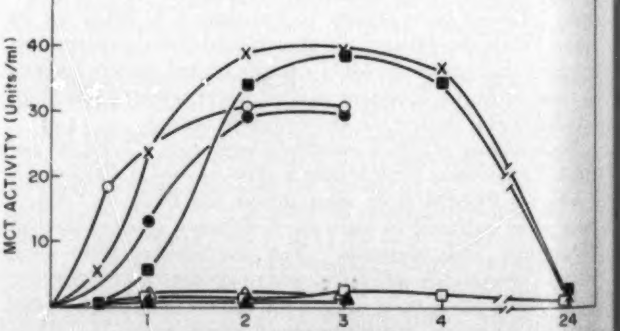

TEXT-FIGURE 3.—Kinetics of MCT release from C57BL/6 poly I·poly C-stimulated PEMM in vitro. Thioglycollate-elicited C57BL/6 PEMM were stimulated with 40 μg poly I·poly C/ml for various lengths of time (■——■, 30 min; ×——×, 60 min; ●——●, 90 min; ○——○, 120 min; ▲——▲, 180 min; △——△, 240 min) and then allowed to release MCT over 24 hr. Resident PEMM (□——□) was treated similarly. Supernatants were collected at various time intervals and assayed for lytic activity as described in "Materials and Methods."

poly C stimulation, and maximal levels of MCT were detected after 2 hours of culture. When macrophages were exposed to poly I·poly C for either 90 or 120 minutes, the lag period disappeared; if exposed for greater than 180 or 240 minutes, no release was observed.

Production of MCT from thioglycollate-elicited C57BL/6 PEMM under various culture conditions.—To generate quantities of MCT for biochemical characterization, we explored the capacity of thioglycollate-elicited PEMM monolayers to release MCT under various in vitro conditions. When poly I·poly C-stimulated macrophages were allowed to release MCT in medium containing 10% FCS, 10% NBCS, 0.01% LAH, 200 μg serum albumin/ml, or 200 μg ovalbumin/ml, levels of lytic activity were comparable, averaging between 21 and 48 U MCT/ml (data not shown). Only under protein-free conditions were both MCT activity levels and macrophage viability lowered.

Definition of the molecular classes of murine MCT.—Supernatants from PEMM obtained from C57BL/6 mice immunized with EL 4 lymphoma were concentrated and chromatographed on Ultrogel AcA 44. A typical elution profile is shown in text-figure 4A. Also shown are elution profiles of supernatants obtained from LPS or poly I·poly C-stimulated thioglycollate-induced macrophages as described in "Materials and Methods" (text-figs. 4B, 4C). The elution profiles of the various molecular weight markers blue dextran, IgG, α-hemoglobin, and phenol red are also indicated.

Clearly, supernatant MCT stimulated by all induction methods can be resolved into one major class of approximately 140,000–160,000 daltons known as α-MCT and a smaller class of activity of approximately 60,000 daltons called "β-MCT." The β-MCT class was only observed when supernatants from PEMM from alloimmune mice were stimulated by tumor cells.

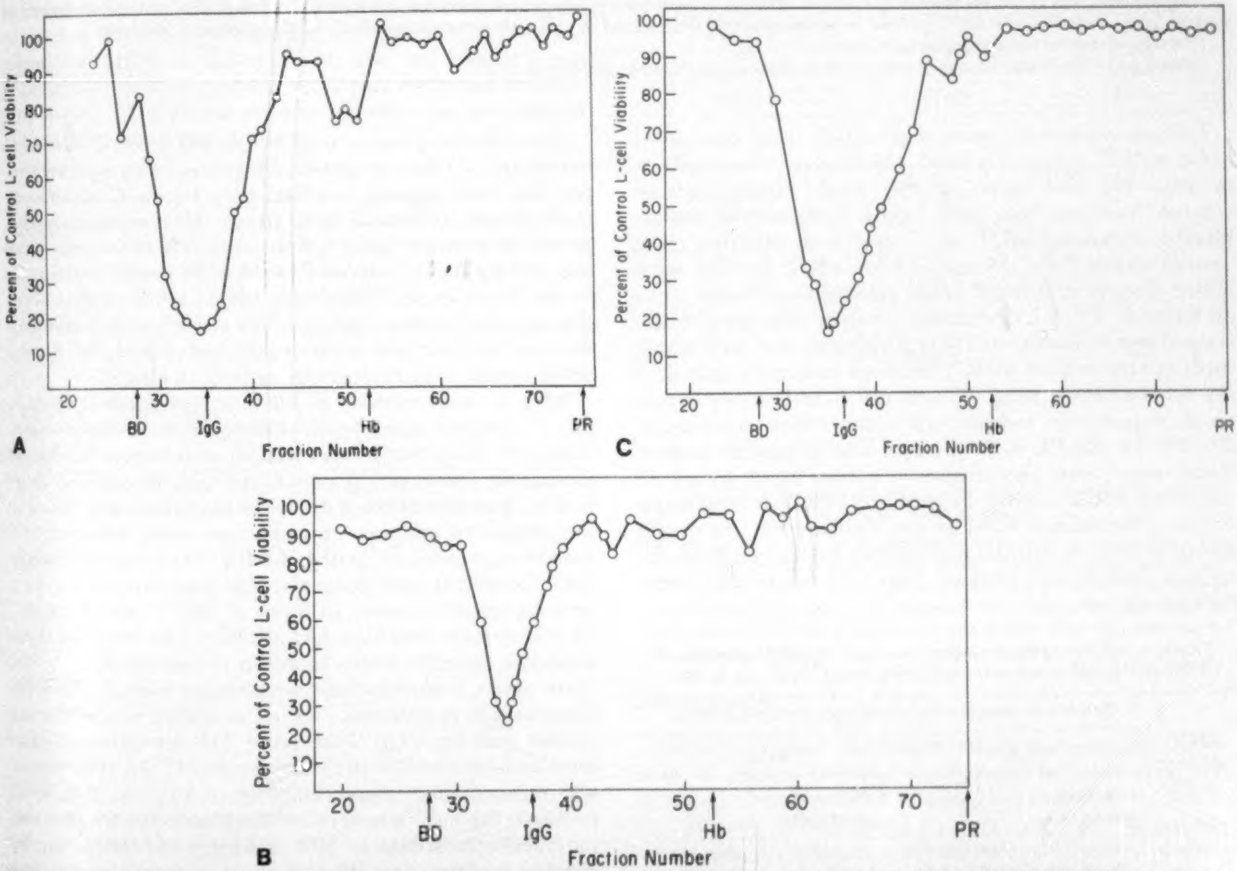

TEXT-FIGURE 4.—Ultrogel AcA 44 chromatography of MCT-containing supernatants obtained from C57BL/6 PEMM stimulated in various ways. Molecular mass markers: Blue dextran (BD), $>2\times10^6$ daltons; IgG, 140,000–160,000 daltons; hemoglobin (Hb), 64,000 daltons; and phenol red (PR), 354 daltons. Columns were equilibrated and eluted with 10 m*M* phosphate (pH 7.2) containing 10^{-4} EDTA. A) Alloinduced: A 1-ml sample of a twentyfold-concentrated supernatant generated by incubation of PEMM from P815 alloimmune C57BL/6 mice stimulated with P815 cells was chromatographed over a 60-cm gel bed on Ultrogel AcA 44 in a 2.5×75-cm column. Four-ml fractions were collected at 40 ml/hr, and 200-μl samples were tested from every other fraction for MCT activity. For details, see "Materials and Methods." Toxic activity of each sample is expressed as percent viability. B) LPS induced: A 1-ml sample of a twentyfold-concentrated supernatant generated by LPS stimulation of PEMM from thioglycollate-induced C57BL/6 mice was chromatographed as above. Samples were collected and tested, and results were expressed in a manner identical to those in text-fig. 4A. C) Poly I·poly C induced: A 1-ml sample of a thirty-fold-concentrated supernatant generated by poly I·poly C stimulation of PEMM from thioglycollate-induced C57BL/6 mice was chromatographed and tested for MCT activity as described in text-fig. 4A.

TABLE 3.—*Effect of whole supernatants and ultrogel AcA-44 fractions containing MCT activity from poly I·poly C-stimulated C57BL/6 PEMM on different tumor targets in vitro*[a]

MCT preparation	Percent of control cells remaining; incubation time:							
	12 hr				36 hr			
	EL 4	NS-1	YAC-1	K562	EL 4	NS-1	YAC-1	K562
Whole supernatant, U/ml[b]								
175	90[c] (82±3)	91±2 (90±4)	92±2 (96±2)	104±3 (96±2)	55±3 (73±4)	44±5 (63±3)	53±2 (84±2)	96±0.7 99±2
17.5	97±6 (84±1.9)	98±0.7 (93±12)	94±4 (99±6)	98±4 (102±3)	74±3 (93±2)	80±7 (91±2)	77±5 (89±2)	103±8.0 (99±2)
α-MCT, U/ml[d]								
150	90±6 (90±2)	88±4 (93±2)	94±2 (97±1)	99±3 (101±0.4)	53±2 (72±0.5)	48±3 (67±2)	69±3 (83±2)	100±5 (103±2)
15	94±2 (95±6)	93±1 (97±7)	98±3 (94±1)	105±6 (98±3)	79±3 (97±3)	76±2 (83±1)	79±2 (92±0.1)	100±6 (100±2)

[a] Target cells, 0.5×10^6, were added to supernatants containing various MCT lytic activities (total vol, 0.5 ml). After 12 and 36 hr, the remaining cells were removed and enumerated on a hemacytometer, as described in "Materials and Methods." These data are representative of two expts. Values are means ± range. *Values in parentheses* represent viabilities of the remaining tumor targets ± range.

[b] Supernatant was generated from poly I·poly C-stimulated peritoneal macrophages, rendered cell-free by centrifugation, and added directly to various target cells. Units of MCT in these supernatants were determined by an L-cell assay as described in "Materials and Methods."

[c] Percent of control number, untreated targets.

[d] Prepared by molecular sieving of supernatants obtained as stated in *footnote b*.

Cytolysis–cytostasis of various target cells by whole supernatants and by α-MCT elaborated by poly I·poly C-stimulated macrophages in vitro.—We next tested whether whole supernatants or column fractions from poly I·poly C-stimulated macrophages containing MCT were capable of affecting these various tumor cells. Materials with MCT activity were added directly to 0.5×10^6 target cells and incubated up to 36 hours at 37°C. The remaining tumor cells were vitally stained and enumerated. Table 3 indicates that both whole supernatants and the α-MCT fractions from molecular sieving columns containing 175 and 150 U of L-cell-lytic material, respectively, reduced cell number from controls by 20–52% for the EL 4, NS-1, and YAC-1 murine targets. These targets were also affected to a lesser extent by a 1:10 dilution of MCT activity. Interestingly, MCT at these levels did not affect human K562 targets. Furthermore, the results shown in table 4 indicate that murine spleen lymphocytes, normal counterparts of these lymphoid tumor cells, were resistant to lysis.

TABLE 4.—*Effect of supernatants from poly I·poly C-stimulated C57BL/6 PEMM on normal and transformed NS-1 cells in vitro*[a]

MCT activity, U/ml[b]	Percent of control cells remaining;[c] incubation time:			
	12 hr		36 hr	
	Normal spleen cells	NS-1	Normal spleen cells	NS-1
50	102±7.3 (101±4.9)	98.2±3.2 (92.5±2.6)	95.5±2 (98.9±9.4)	48.9±6.4 (78.9±4.8)
5	97±3.1 (100±3.0)	99.6±2.0 (95.6±3.4)	102.2±6.8 (104±9.8)	84.5±5.1 (87.7±1.6)

[a] *See footnote a* in table 3.

[b] *See footnote b* in table 3.

[c] Values are means ± range of viable treated cells as compared to values for untreated controls. *Values in parentheses* represent mean viabilities ± range of treated cells as compared to viabilities of untreated controls.

Direct cytolysis of various target cells by poly I·poly C-stimulated macrophages.—When syngeneic, allogeneic, or xenogeneic target cells were exposed to intact poly I·poly C-stimulated macrophages, reduction in all tumor cell numbers was observed. As shown in table 5, from 23 to 70% of the cells were removed by the stimulated PEMM at 36 hours. In contrast to the above experiments with MCT, K562 targets were destroyed by the macrophages. The reduction in tumor cell numbers in these and the previous studies could be due to either cytostasis or cytotoxicity or to both effects.

Effect of various inhibitors on MCT secretion in vitro by poly I·poly C-stimulated macrophages.—PEMM from thioglycollate-induced C57BL/6 mice were treated with various inhibitors during the 1-hour poly I·poly C stimulation, washed thoroughly, and then allowed to release materials for 2 hours in the absence of inhibitors. Supernatants were collected and tested for cytotoxicity, as described in "Materials and Methods." Colchicine and iodoacetic acid inhibited release, in a dose-dependent manner, at levels of 5×10^{-5} and 1.2×10^{-4} M, respectively (text-figs. 5A, 5B, 5C). The effect of these inhibitors on cell viability is shown in text-figure 5. At the above levels, these inhibitors were not toxic to the PEMM. Cytochalasin B, however, was not as effective in inhibiting release (text-fig. 5C). Text-figure 5D demonstrates that emetine inhibited 75% of the release at 10^{-5} M. However, it also reduced macrophage viability to 83%. At this level, protein synthesis (^{75}selenium–methionine incorporation) was inhibited approximately 30%. Further, the inhibition by emetine was not dose dependent; at a concentration two orders of magnitude higher, 10^{-3} M, MCT release was inhibited only 80%, whereas viability was reduced to 57%. An inhibitor of trypsin-like proteases, SBTI, was also tested. Neither viability nor release was significantly affected at a concentration of 10^{-4} M (data not shown).

Finally, trypan blue, a vital stain reported to be an inhibitor of lysosomal hydrolysis (*15*), was tested. Macrophages were pretreated with various concentrations of try-

Table 5.—*Direct cytolysis and/or cytostasis of target cells by poly I·poly C-stimulated C57BL/6 PEMM*[a]

Expt No.	Percent of control cells remaining; incubation time:							
	12 hr				36 hr			
	EL 4	NS-1	YAC-1	K562	EL 4	NS-1	YAC-1	K562
1	78.9±15.4	97.3±5.6	81.4±6.2	91.6±8.4	55.2±8.4	77.2±8.7	30.7±5.9	39.1±13.7
2	85.6±14.4	102.5±3.9	96.1±8.3	105.6±8.8	64.7±1.4	65.1±2.7	60.2±6.2	76.5±1.9

[a] Target cells, 0.5×10^6, were added to 5×10^5 poly I·poly C-stimulated C57BL/6 PEMM (10:1 effector-to-target cell ratio). After 12 and 36 hr, the remaining tumor cells were removed, and total viable cells were enumerated on a hemacytometer, as described in "Materials and Methods." Values are means ± range.

pan blue. After 24 hours, the residual vital stain was washed from the macrophages, poly I·poly C was added, and release was allowed to proceed, as described in "Materials and Methods." The incorporation of trypan blue by the macrophages, as determined by OD_{600}, is shown in table 6. Clearly, incorporation was inhanced with increasing concentrations of the dye. Trypan blue inhibited approximately 50% of the release of MCT at 2.2×10^{-3} *M*, and cell viability was approximately 70% (text-fig. 6). Upon restimulation with poly I·poly C, a similar pattern of inhibition and effector cell viability was observed.

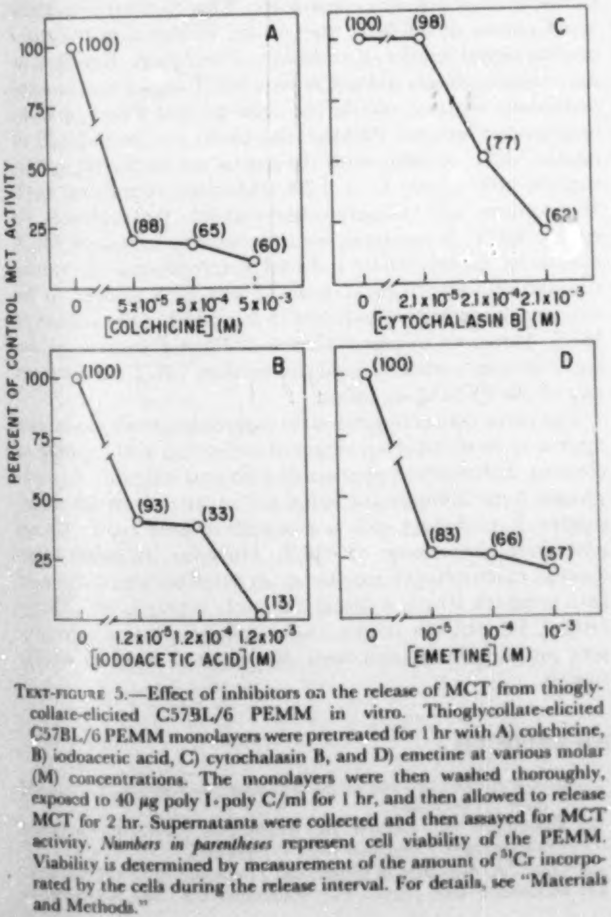

Text-figure 5.—Effect of inhibitors on the release of MCT from thioglycollate-elicited C57BL/6 PEMM in vitro. Thioglycollate-elicited C57BL/6 PEMM monolayers were pretreated for 1 hr with A) colchicine, B) iodoacetic acid, C) cytochalasin B, and D) emetine at various molar (M) concentrations. The monolayers were then washed thoroughly, exposed to 40 μg poly I·poly C/ml for 1 hr, and then allowed to release MCT for 2 hr. Supernatants were collected and then assayed for MCT activity. *Numbers in parentheses* represent cell viability of the PEMM. Viability is determined by measurement of the amount of ^{51}Cr incorporated by the cells during the release interval. For details, see "Materials and Methods."

Table 6.—*Incorporation of trypan blue by thioglycollate-elicited C57BL/6 PEMM after primary and secondary stimulation by poly I·poly C*

Trypan blue concentration, *M*	OD_{600}	
	Primary	Secondary
5.5×10^{-4}	0.075	0.069
1.1×10^{-3}	0.082	0.080
2.2×10^{-3}	0.093	0.093
4.4×10^{-3}	0.120	0.118

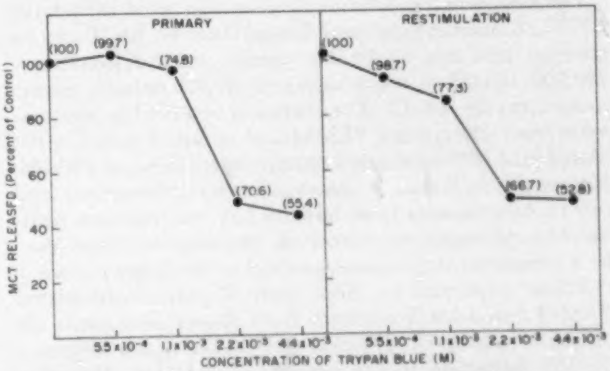

Text-figure 6.—Effect of incorporated trypan blue on the primary and secondary stimulation and release of MCT from thioglycollate-elicited C56BL/6 PEMM in vitro. Following solubilization of the monolayer as described in "Materials and Methods," the PEMM were examined for cell viability by ^{51}Cr incorporation and trypan blue incorporation by absorbance at 600 nm.

DISCUSSION

PEMM obtained from alloimmune mice can be stimulated to release cell-lytic molecule(s) in vitro. The cell toxin(s) are herein termed "macrophage cytotoxin(s)" MCT. Furthermore, PEMM from animals that had rejected the tumor allograft spontaneously released MCT when initially established as monolayers, whereas PEMM from an occasional animal that did not reject the tumor did not release detectable levels of MCT. Release in vitro from PEMM begins 4 hours after a 1-hour contact with tumor cells. Release ceases at 4–6 hours; in cultures left at 37°C, activity declines by 12–24 hours. After 6–8 hours, or even 4–5 days in culture, release can be reinitiated by a 1-hour exposure to fresh allogeneic or syngeneic tumor cells but *not* by exposure to normal allogeneic or syngeneic lymphocytes. Moreover, the second round of release follows similar patterns of kinetics. Treatment of the alloimmune macrophages with Con A lymphoblasts caused release of low levels of a cytotoxin. However, the treated PEMM were associated with bound lymphoblasts (presumably binding via free valences of lectin) during the release period, and in this case the toxin may in fact be lymphocyte derived. This is clearly an inducible system of cell-lytic molecules. No MCT is detectable in these cultures if the tumor cells are not removed, which will be discussed later. In contrast to the response of alloimmune macrophages, resident macrophages release negligible MCT under all conditions.

Although we were able to generate significant levels of lytic activity from alloimmune macrophages, other methods were examined for induction of these molecules for further study. We found that thioglycollate-elicited PEMM treated with 40 μg poly I·poly C/ml responded quite uniformly and released high levels of MCT. Following the removal of poly I·poly C, there was a 30- to 60-minute lag period, after which the levels climbed to a peak by 2 hours and then declined to very low levels by 24 hours. The loss of MCT activity in the supernatant is clearly due to two effects: *a*) cessation of biosynthesis and secretion and *b*) degradation of already secreted forms.

Upon chromatography of supernatants from stimulated C57BL/6 macrophages on Ultrogel AcA 44, MCT can be resolved into two molecular species: α- and β-classes—140,000–160,000 and approximately 60,000 daltons, respectively (text-fig. 4A–C). The α-class is observed in supernatants from alloimmune PEMM and in poly I·poly C-stimulated and LPS-stimulated thioglycollate-induced PEMM. However, the β-class is observed rather infrequently and *only* in supernatants from alloimmune macrophages (text-fig. 4A). Although not examined, this smaller β-form may be a subunit or degradation product of the larger α-class.

When supernatants from poly I·poly C-stimulated PEMM and α-MCT obtained from these supernatants are added to murine EL 4, NS-1, and YAC-1 tumor targets, a 30–55% reduction in cell number is observed. However, there was little or no effect either on the human K562 tumor or on normal BALB/c spleen cells. When the above transformed cells are added to poly I·poly C-stimulated thioglycollate-elicited PEMM at a 10:1 ratio, 24–70% of the targets are removed. Whether cytolysis or cytostasis is occurring is difficult to prove unequivocally. As observed in table 3, the reduction in cell number does not directly correlate with the reduction of cell viability, which would suggest cytostasis occuring. An appropriate suggestion is that both cytolysis and cytostasis are occurring simultaneously.

A common feature of MCT and previously described macrophage-derived cell-lytic materials is their instability in supernatants (*7, 21, 22*). Once released, MCT is unstable at 37°C, which might contribute to the fall in supernatant activity levels. At −20 or 4°C, activity is partially preserved for an additional 2–4 days (data not shown). However, the activity is stable enough for various parameters of production and release from the PEMM to be examined.

The release of MCT after stimulation appears to require cellular protein synthesis and an active secretory system, because treatment of stimulated PEMM with emetine (to block protein synthesis), colchicine (to disrupt microtubules), and iodoacetic acid (an alkylating agent to block phagocytosis) at levels that were shown not to significantly affect cell viability in a 3-hour period dramatically affected the secretion of MCT. Treatment with cytochalasin B affected release to a lesser extent, and SBTI had no measurable effect. However, trypan blue at a concentration of 2.2×10^{-3} *M* inhibited release by approximately 55% while decreasing macrophage viability to 70%. With a twofold-higher concentration, release of MCT was still approximately 50% while cell viability dropped to 55%; these results obtained with trypan blue might indicate existence of both lysosomal and nonlysosomal release mechanism(s). In other words, the inhibition by trypan blue would indicate that an alternative secretory route might exist—possibly one that does not require a vacuolar system.

There are several parameters that are operative and control the in vitro release of MCT by murine PEMM. The first raises macrophages to a particular state of activation, which permits them to respond to further stimulation. In our experiments this is represented as an ip injection of tumor cells or thioglycollate. As an alternative explanation, these treatments may induce responsive cells to migrate into the peritoneum from other tissue sites. The second is a stimulating signal in vitro represented in our studies by tumor or poly I·poly C treatment. This treatment induces rapid release of cell-lytic material(s). Removal of the stimulating signal results in cessation of secretion. Resident or naive macrophages did not release MCT under any in vitro conditions we used. While the data are not shown, starch- or glycogen-induced PEMM also could not be induced to release MCT, in vitro, with the agents we employed. In our studies, poly I·poly C or LPS treatment stimulated both alloimmune and thioglycollate-elicited macrophages to release MCT. In contrast, we were unable to induce MCT release by thioglycollate-induced macrophages via tumor stimulation. Thus poly I·poly C and LPS appear to be stronger, less-selective inducers in stimulating the release of MCT. However, mitogens Con-A or PHA-P cannot apparently serve as a second signal to stimulate MCT release from any of the PEMM we tested.

The three classes of peritoneal macrophages we examined appear to be at different stages of activation and capable of eliciting differential responses to a second stimulus. Macrophages from alloimmune mice are at an advanced stage, inasmuch as contact with tumor cells or poly I·poly C can potentiate the release of MCT. However, thioglycollate-elicited macrophages may be at an intermediate stage and thus require a stronger signal (i.e., poly I·poly C or LPS) to release. Finally, the resident macrophage appears to represent an early stage and does not respond even to strong signals.

REFERENCES

(*1*) North R. The concept of the activated macrophage. J Immunol 1978; 121:806–1809.

(*2*) Karnovsky ML, Lazdins JK. Biochemical criteria for activated macrophages. J Immunol 1980; 121:809–813.

(*3*) Cohn ZA. Activation of phagocytes. J Immunol 1978; 121:813–816.

(*4*) McGregor DD, Foster FT, Machaness GB. The mediation of cellular immunity. J Exp Med 1971; 113:389–399.

(5) Bennett B, Old LJ, Boyse EA. The phagocytosis of tumor cells in vitro. Transplantation 1964; 2:183–202.

(6) Granger GA, Weiser RS. Homograft target cells: Specific destruction in vitro by contact interaction with immune macrophages. Science 1964; 145:1427–1429.

(7) Evans R, Alexander P. Mechanism of immunologically specific killing of tumour cells by macrophages. Nature 1972; 236:168–170.

(8) Piper CE, McIvor KL. Alloimmune peritoneal macrophages as specific effector cells: Characterization of specific macrophage cytotoxin. Cell Immunol 1975; 17:423–430.

(9) Marino PA, Adams DO. Interaction of Bacillus Calmette-Guerin activated macrophages and neoplastic cells in vitro. I. Condition of binding and its selectivity. Cell Immunol. 1980; 54:11–25.

(10) ———. Interaction of Bacillus Calmette-Guerin activated macrophages and neoplastic cells in vitro. II. Relationship of selective binding to cytolysis. Cell Immunol 1980; 54:26–35.

(11) Fidler IJ, Gensler DM, Hart IR. The biology of cancer invasion and metastasis. Adv Cancer Res 1978; 28:149–250.

(12) Tagliabue A, Mantovani A, Kilgallen M, Herberman RB, McCoy JL. Natural cytotoxicity of mouse monocytes and macrophages. J Immunol 1979; 122:2363–2370.

(13) Hibbs JB Jr, Chapman HA Jr, Weinberg JB. The macrophage as an antineoplastic surveillance cell: Biological perspectives. J Reticuloendothel Soc 1978; 24:549–570.

(14) Keller R. Promotion of tumor growth in vivo by antimacrophage agents. J Natl Cancer Inst 1976; 57:1355–1361.

(15) Hibbs JB Jr. Heterocytolysis by macrophages activated by Bacillus Calmette-Guerin: Lysosome exocytosis into tumor. Science 1974; 184:468–471.

(16) Alexander P, Evans R. Endotoxin and double stranded RNA render macrophages cytotoxic. Nature [New Biol] 1971; 232:76–78.

(17) Unanue ER. Secretory function of mononuclear phagocytes. Am J Pathol 1976; 83:397–417.

(18) Page R, Davis P, Allison AC. The macrophage as a secretory cell. Int Rev Cytol 1978; 52:119–157.

(19) Adams DO. Effector mechanisms of cytolytically activated macrophages. I. Secretion of neutral proteases and effect of protease inhibitors. J Immunol 1980; 124:286–292.

(20) Kramer JJ, Granger GA. The in vitro induction and induction and release of cell toxins by immune C57BL/6 mouse peritoneal macrophages. Cell Immunol 1972; 3:88–100.

(21) Helsom H, Sanner T, Seljelid R. Macrophage cytolytic factor. Exp Cell Res 1975; 94:221–226.

(22) Currie GA, Basham C. Activated macrophages release a factor which lyses malignant but not normal cells. J Exp Med 1975; 142:1975.

blank page

Inducible Macrophage Cytotoxins. II. Tumor Lysis Mechanism Involving Target Cell-Binding Proteases[1,2]

Thomas H. Reidarson,[3] Gale A. Granger,[3] *and* Jim Klostergaard[3,4,5,6]

ABSTRACT—Thioglycollate-elicited C57BL/6 peritoneal exudate macrophage monolayers (PEMM) stimulated with poly I·poly C or LPS released a macrophage cytotoxin (MCT) that rapidly bound to syngeneic (EL 4) or allogeneic (NS-1, YAC-1) tumor cells but did not bind to normal splenocytes. No binding to human (K562) tumor cells was observed. PEMM stimulated with poly I·poly C destroyed allogeneic tumor cells (NS-1) when separated by cell-impermeable Millipore filters in vitro; in contrast, PEMM *not* stimulated with poly I·poly C were incapable of lysing targets when separated by membranes. The reversible inhibitors *Nα-p*-tosyl-L-arginine methyl ester and soybean trypsin inhibitor and the irreversible inhibitors *Nα-p*-tosyl-L-lysine chloromethyl ketone and phenylmethylsulfonyl fluoride, of trypsin-like proteases, significantly or totally inhibited MCT cell-lytic activity for L-929 cells in vitro. Furthermore, modification of MCT-associated arginine residues by 1,2-cyclohexanedione completely blocked lytic activity. MCT was concluded to be an inducible nonspecific cell-lytic effector molecule elaborated by activated macrophages, which could bind to potential target cells, and was itself or was associated with a protease.—JNCI 1982; 69:889–894.

Activated peritoneal macrophages from mice are capable of inducing nonspecific cytotoxicity to a variety of syngeneic, allogeneic, and xenogeneic tumor targets in vitro (*1–3*). The cytotoxic reaction occurs within a microenvironment existing at the contact region(s) between the effector and the target. One mechanism of lysis has been proposed to involve a vectorial release of a monokine (e.g., lysosomal enzymes) from the macrophage to the target cell (*4–5*). Yet very little is known about the putative cytotoxic molecule(s) involved in this reaction and the mechanism by which they act on tumor cells.

In the previous manuscript of this series (*6*) we demonstrated that PEMM from alloimmune C57BL/6 mice and thioglycollate-elicited macrophages from nonimmune C57BL/6 mice can be induced in vitro to release a cell-lytic material known as MCT. This is an inducible toxin, and activated macrophages can be stimulated to release MCT when briefly exposed to tumor cells or poly I·poly C in vitro. Release begins within a few hours after stimulation and then rapidly ceases. Physical studies have indicated that MCT from macrophages obtained from alloimmune or thioglycollate-induced mice appears on molecular sieving columns principally as one species of 140,000–160,000 daltons. Biochemical studies indicated that MCT is homogeneous with respect to charge and is heat- and pH-labile (Klostergaard J, Reidarson TH, Granger GA: Manuscript in preparation).

We report here that MCT binds rapidly to murine tumor targets but not to normal cells. Additional studies reveal that stimulated PEMM can destroy NS-1 allogeneic targets in the absence of effector-to-target cell contact. Both reversible and irreversible inhibitors of trypsin-like proteases block MCT activity. Modification of MCT arginine but not lysine residues also blocks lytic activity. These findings suggest that a proteolytic reaction is necessary for the cell-lytic event. Several model(s) are proposed to explain how MCT may act as an effector of in vitro tumor cell lysis mediated by macrophages.

MATERIALS AND METHODS

Culture media and cell lines.—Culture media consisted of RPMI-1640 medium supplemented with 3 or 10% heat-inactivated (56°C, 60 min) FCS (GIBCO, Grand Island, N.Y.) or newborn calf serum (GIBCO), 100 μg streptomycin/ml, and 100 U penicillin/ml. Murine C3H L-929 (H-2^k) transformed fibroblasts were grown in 32-oz prescription bottles in RPMI-1640 with 3% serum at 37°C in 95% air and 5% CO_2 atmosphere and passed twice a week. C57BL/6 EL 4 (H-2^b) lymphoma, BALB/c NS-1 (H-2^d) myeloma, A-Sn YAC-1 (H-2^a) lymphoma, and human K562 erythroid leukemia cell lines were grown in RPMI-1640 supplemented with 10% FCS. Naive BALB/c (H-2^d) spleens were asceptically removed and prepared on the day of the experiment as previously described (*6*).

Binding of MCT to target cells.—Tumor and normal cells, 15×10^6 and 3×10^6, respectively, which were 93–98% viable, were pelleted by centrifugation at 300×*g* for 5 minutes and washed four additional times with serum-free RPMI-1640. The cells were then resuspended in 300 μl MCT obtained from supernatants of poly I·poly C-stimulated PEMM containing 39–62 U lytic activity and incubated at 4°C. After 30 minutes the cells were pelleted by centrifugation, and

---

Abbreviations used: ALME=*Nα*-acetyl-L-lysine methyl ester; CF=cytolytic factor; CHD=1,2-cyclohexanedione; FCS=fetal calf serum; IAM=iodoacetamide; MA=maleic anhydride; MAI=methylacetimidate hydrochloride; MCT=macrophage cytotoxin; α-MCT=MCT detectable at 140,000–160,000 daltons; PBS=phosphate-buffered saline; PEMM=peritoneal exudate macrophage monolayers; PMSF=phenylmethylsulfonyl fluoride; poly I·poly C=polyinosinic-polycytidylic acid; SBTI=soybean trypsin inhibitor; TAME=*Nα-p*-tosyl-L-arginine methyl ester; TLCK=*Nα-p*-tosyl-L-lysine chloromethyl ketone.

---

[1] Received July 23, 1981; revised January 20, 1982; accepted April 19, 1982.

[2] Guidelines for the care and use of laboratory animals were followed as set forth by the National Research Council.

[3] Department of Molecular Biology and Biochemistry, School of Biological Sciences, University of California at Irvine, Irvine, Calif. 92717.

[4] Recipient of Senior Postdoctoral Fellowship S-25-81 from the American Cancer Society, California Division.

[5] *Address reprint requests to* Dr. Klostergaard.

[6] We are grateful to Mr. Robert Yamamoto for excellent technical assistance. We also thank Mrs. Gloria Heidenfelder and Ms. Virginia Baker for the preparation of this manuscript.

250 µl supernatant was removed and then assayed for lytic activity on L-929 cells. Percent adsorption or removal of units of activity was determined by comparison of the control level of activity with the activity remaining after the supernatants were removed from the target cells.

Lysis of NS-1 targets by poly I·poly C-activated macrophages through membrane filters.—Cellulose nitrate membranes with 0.2 µm-pores (Sartorius membrane filter; Science Essentials, Fullerton, Calif.) were cut into circles and washed with sterile PBS, and then one or two were fitted tightly over 0.5×10^6 adherent macrophages in wells of Costar plates 15 minutes before 50×10^3 target cells were added. After 12- and 36-hour incubation periods at 37°C in a CO_2 incubator, the remaining tumor cells were enumerated and viability was determined by eosin Y exclusion in a hemacytometer.

Protein modification reactions.—MCT partially purified by molecular sieving, as previously described (*6*), was used for protein modification studies. The active fractions were pooled, concentrated on an Amicon PM10 membrane to 5 ml, and then dialyzed overnight against more than 100 volumes of approximately 0.2 *M* (pH 9) carbonate buffer. Aliquots of this pool (250–1,500 µl) were used in the chemical modification reactions described below.

MA (0.2–4.0 mg; Aldrich Chemical Co., Milwaukee, Wis.) was dissolved directly in the MCT preparation. The solution was agitated until dissolution was complete (≈60 sec). After 30 minutes at room temperature, the preparation was dialyzed against approximately 1,000 volumes of PBS for 4–16 hours. The dialyzed preparation was then assayed for toxicity on L-cells.

MAI (Pierce Chemical Co., Rockford, Ill.) was either added directly to the buffered MCT or first diluted in PBS and then an aliquot was added to the MCT. The final level was 0.1–11 mg/ml. After 30 minutes at room temperature, the preparation was dialyzed and assayed as above.

We reacted MCT with CHD (Pierce Chemical Co.) by making the MCT preparation 0.06 *M* in CHD. The reaction was quenched at various times (30 min–5 hr) by dialysis; after dialysis against more than 1,000 volumes of PBS for 4–16 hours, cytotoxic activity of the modified MCT was determined by assay on L-cells, as above.

Protease inhibitors.—MCT was purified as described before. Similarly, the active fractions were pooled, concentrated, and dialyzed overnight against 100 m*M* (pH 7.2) phosphate buffer. Aliquots (250–1,500 µl) were employed in the reaction described below.

SBTI at 0.1 and 1.0 m*M* (Sigma Chemical Co., St. Louis, Mo.) was dissolved in the MCT preparation of 6–15 U/ml. After 30 minutes at room temperature, the sample was assayed directly on L-cells. As a toxicity control, SBTI was diluted in PBS to the concentration used for the protease-inhibition experiments and added directly to L-cells.

Modification of MCT by TLCK and PMSF (Sigma Chemical Co.) was conducted according to the following protocol. Aliquots (400–1,500 µl) of MCT corresponding to approximately 10–40 U/ml *were reacted directly* with TLCK at final levels of 0.4–10 m*M*. The modification was performed at 37°C for 1 hour. The samples were then dialyzed against approximately 1,000 volumes of PBS for 4–6 hours at room temperature. After dialysis, the lytic activity of each sample was determined by assay on L-cells, as previously described.

TAME and ALME (Sigma Chemical Co.) were used in inhibition studies by *concurrent incubation* of MCT prepared as above, with various levels (10^{-4} to 10^{-2} *M*) of the inhibitor on L-cells. After 20 hours, the level of MCT lysis in the presence of TAME was compared to the level of control MCT lysis. TAME was not toxic to L-cells at levels up to 10^{-2} *M*; ALME was occasionally toxic at this level.

MCT was prepared as above and treated with various levels (1–10 m*M*) of IAM (Sigma Chemical Co.) for 2 hours at room temperature. After dialysis against 500 vol PBS for 24 hours, the samples were assayed on L-cells and their titers determined.

The percent inhibition of MCT by MA, MAI, CHD, PMSF, and TLCK was calculated according to the following equation: Percent inhibition=[(control MCT, U/ml − experimental MCT, U/ml)/control MCT, U/ml]×100%. The percent inhibition of MCT by SBTI, TAME, or IAM was expressed as follows: Percent inhibition=1−[(control L-cell No. − experimental MCT L-cell No.)/(control L-cell No. − MCT L-cell No.)]×100%.

RESULTS

Reduction of MCT activity by adsorption of whole macrophage supernatant on various target cells.—Cell-free whole supernatants containing approximately 39–102 U L-cell lytic activity ml were collected from poly I·poly C-stimulated macrophages as described in "Materials and Methods" and treated as follows: Supernatant, 300 µl, was incubated with various targets or left untreated for 30 minutes at 4°C. The cells were then removed by centrifugation, and supernatants were retested for lytic activity. Shown in tables 1 and 2 are four separate experiments. Both EL 4 and NS-1 removed approximately the same amount of MCT (40–50%), and YAC-1 adsorbed an even greater amount (≈60%). In contrast, the human K562 targets and normal BALB/c spleen

TABLE 1.—*Removal of supernatant MCT activity from poly I·poly C-stimulated C57BL/6 PEMM on normal BALB/c spleen cells in vitro*[a]

Expt No.[b]	Target cell	Percentage of MCT activity adsorbed on targets:	
		3×10^6	15×10^6
1	Normal BALB/c spleen	15.7	12.1
	NS-1	18.7	54.2
2	Normal BALB/c spleen	−2.4	7.9
	NS-1	27.4	38.6

[a] A 300-µl sample of whole supernatant from poly I·poly C-stimulated PEMM containing various levels of MCT activity was added to 3×10^6 and 15×10^6 target cells, allowed to incubate at 4°C for 30 min, and then rendered cell-free. A 250-µl sample of this cell-free supernatant was collected and assayed for MCT as described in "Materials and Methods."

[b] Total numbers of MCT (U/ml) in supernatant were 52 for expt 1 and 102 for expt 2.

TABLE 2.—*Removal of supernatant MCT activity from poly I·poly C-stimulated C57BL/6 PEMM on various target cells in vitro*[a]

Expt No.[b]	Target cell	Percentage of MCT activity adsorbed on targets:	
		3×10^6	15×10^6
1	EL 4	27.8	43.9
	NS-1	20.8	42.8
	YAC-1	22.2	62.5
	K562	13.0	10.8
2	EL 4	24.3	52.8
	NS-1	25.1	38.8
	YAC-1	19.7	54.3
	K562	6.7	7.2

[a] *Refer to* table 1 for details.

[b] Total numbers of MCT (U/ml) in supernatants were 62 for expt 1 and 39 for expt 2.

cells had little effect; neither target cell type removed greater than 16% of the MCT activity.

Cytolysis and/or cytostasis of allogeneic NS-1 target cells in vitro through Millipore membranes by poly I·poly C-stimulated macrophages.—The preceding results raised the question of whether stimulated macrophages could inhibit growth or kill tumors in the absence of direct cellular contact. We separated effector macrophages and target tumor cells by a 0.2-μm Millipore membrane. After the macrophages were stimulated with poly I·poly C, as described in "Materials and Methods," the filter was placed over the macrophage monolayer and tumor targets were added at a 10:1 effector-to-target cell ratio. In both experiments shown in table 3, little effect was seen after 12 hours, whether or not effectors and targets were separated by filters. However, after 36 hours, reduction in the number of viable tumor cells was evident in control cultures without filters (47–75%) as well as in tests separated by filters (40–55%).

Effect of protease inhibitors on MCT activity.—Several investigators have suggested that serine proteases are involved in the expression of lytic activity by activated macrophages (*5, 7-9*). We tested the effects of several inhibitors of trypsin-like proteases: SBTI, TLCK, PMSF, TAME, and ALME on α-MCT-containing fractions, as described in "Materials and Methods." The results are presented in table 4. α-MCT showed a very striking susceptibility to direct treatment with TLCK. Although TLCK blocked MCT activity, it was important for us to establish whether this blockage occurred by inactivation of a trypsin-like protease or by modification of a vital sulfhydryl group (*10-13*). IAM at levels as high as 10 m*M* was totally without effect on the lytic activity (table 4), which suggested that the former mechanism (trypsin-like protease) and not the latter (vital sulfhydryl group) was operative. This probability was further supported by the blocking observed with PMSF. Higher doses of PMSF (>2.5 m*M*) could not be examined due to insolubility of the drug.

When MCT was incubated with TAME during target cell lysis, as described in "Materials and Methods," a dose-dependent inhibition of lysis was observed (table 4). When MCT was co-incubated with SBTI during target cell lysis, as described in "Materials and Methods," there was a decrease in lytic activity (table 4). If inhibition were occurring at the same active site as that affected by TLCK and TAME, inhibition beyond that seen at 0.1 m*M* (40%) should be attainable. However, at levels higher than this (table 4), toxicity of SBTI for the cells was apparent, thereby overriding the effect of MCT-mediated cytolysis being inhibited. The specificity of the protease was further probed with ALME. No blocking could be observed up to 10^{-2} *M*, the highest dose usually nontoxic for the L-cell (table 4).

Protein modification of MCT.—The effects of modification of MCT partially purified by being sieved on Ultrogel AcA 44 with amino acid side chain-specific reagents MA (which modifies lysine and tyrosine), MAI (which modifies lysine), and CHD (which modifies arginine) are presented in table 5. In none of these modification experiments were we able to quantitate the extent of reaction with a particular type of amino acid side chain, because the MCT preparation was impure and the lytic moiety present was in extremely low amounts; these factors precluded the necessary total amino

TABLE 3.—*Cytolysis and/or cytostasis of NS-1 tumor cells by poly I·poly C-stimulated C57BL/6 PEMM through Millipore membranes*[a]

Expt No.	Treatment	Percent targets[b] remaining after incubation time[c]:	
		12 hr	36 hr
1	Macrophages	93.6±3.2	53.4±4.8
	Macrophages + filters	96.7±1.2	59.8±3.9
2	Macrophages	92.1±1.8	25.6±5.8
	Macrophages + filters	91.3±10.0	44.8±5.6

[a] NS-1 target cells, 5×10^4, were added to 5.0×10^5 PEMM (poly I·poly C treatment described in "Materials and Methods"). An intact Millipore filter with 0.2-μm pores was placed over the macrophages 15 min before the targets were added.

[b] Expressed as percent of tumor targets incubated in the presence of untreated macrophages.

[c] After 12 and 36 hr, the remaining cells were removed and enumerated on a hemacytometer, as described in "Materials and Methods."

TABLE 4.—*Effect of protease inhibitors on lytic activity of α-MCT*[a]

Inhibitor	Concentration, m*M*	Reaction factors	Percent of inhibition[b]
TLCK	0.4	1 hr, 37°C	2
	2		96
	10		100
IAM	1	3 hr, ambient temperature	0
	10		0
PMSF	1	1 hr, 37°C	53
	2.5		61
TAME	0.1	Simultaneous incubation on L-cells	10
	1		52
	10		100
SBTI	0.1	Simultaneous incubation on L-cells	41
	1		23[c]
ALME	0.4	Simultaneous incubation on L-cells	0
	2		0
	10		0

[a] α-MCT was purified by molecular sieving, as described in "Materials and Methods." Concentrated, pooled fractions were dialyzed against 100 m*M* (pH 7.2) phosphate buffer and then treated with the reagents.

[b] Calculated as described in "Materials and Methods."

[c] Toxicity of SBTI on L-cells reduced apparent inhibition of MCT.

TABLE 5.—*Effect of chemical modification on lytic activity of α-MCT*[a]

Reagent	Amino acid modified	Reagent concentration	Reaction time	Percent inhibition[b]
MA	Lysine and tyrosine	0.2 mg/ml	30 min	88.8
		4 mg/ml		98.7
MAI	Lysine	0.1 mg/ml	30 min	15.1
		0.4 mg/ml		39.2
		1.0 mg/ml		43.1
		11 mg/ml		59.1
CHD	Arginine	60 m*M*	30 min	65.6
			3 hr	75.7
			5 hr	89.3

[a] α-MCT purified by molecular sieving was used. The active fractions were pooled, concentrated, and dialyzed overnight against 0.2 *M* (pH 9) carbonate buffer. Various protein modifiers were dissolved directly in the MCT preparation and then assayed for lytic activity, as described in "Materials and Methods."

[b] Various percentages are representative of several experiments in which 10–70 U control MCT activity/ml was observed.

acid analysis for determination of the extent of modification. However, in an attempt to obtain reasonable levels of substitution, we used wide ranges of exposure to the reagents.

Modification of MCT with MA was achieved with the use of a twentyfold range of MA (0.2–4.0 mg). Although multiple experiments were performed, only the results from the extremes of reagent concentration are shown. In every case, total, or nearly total, abrogation of lytic activity was observed (table 5).

When MCT was allowed to react with the lysine-specific reagent MAI, there was an initially progressive loss of lytic activity, which tended to plateau. However, even at extremely high reagent concentrations, blocking of lysis was incomplete.

The guanido-specific reagent CHD caused progressive loss of MCT lytic activity. Loss of activity corresponded to increased time of exposure to and reaction with the CHD, until after 5 hours when lytic activity was abolished. This was a remarkable rate of modification, when one considers that the pH of the reaction (9) was at least 3 U lower than the pK of arginine side chains (≈12).

DISCUSSION

In the first manuscript of this series (*6*), we demonstrated that alloimmune macrophages stimulated with tumor cells, poly I·poly C, or lipopolysaccharide release MCT in vitro. The principal form of MCT from this source appeared to have biochemical and functional characteristics indistinguishable from those of MCT obtained by poly I·poly C or LPS stimulation of thioglycollate-elicited macrophages. MCT had selective cytotoxic effects for murine tumor cells when compared to normal cells.

In this report, we demonstrate that when supernatants from C57BL/6 (*H-2*^{b}) thioglycollate-elicited PEMM stimulated with poly I·poly C are added to normal BALB/c (*H-2*^{d}) spleen cells, syngeneic EL 4 (*H-2*^{b}) lymphoma, allogeneic NS-1 (*H-2*^{d}) myeloma, YAC-1 (*H-2*^{a}), and human K562 erythroid leukemia targets, approximately 10, 48, 44, 57, and 9%, respectively, of the MCT activity is removed (tables 1, 2). This removal occurs rapidly at 30 minutes and 4°C, suggesting that adsorption, rather than degradation, has occurred. Adsorption of MCT to the target cell appears to be a prerequisite for cell cytotoxicity. That the human K562 targets were not affected by the levels of MCT used in these studies might be explained by either target insensitivity or target selectivity on the part of MCT. Target insensitivity is most likely, in view of the work by Kramer and Granger (*14*), who have demonstrated that another human target cell (HeLa) was destroyed by activated murine macrophage supernatants. It is also possible that a mechanism not involving MCT is used by the macrophage in cytolysis of K562.

Although direct cell-to-cell contact is considered necessary for cytolysis of targets by activated macrophages (*1–5, 7–9, 15–17*), this contact appears not to be necessary in certain situations, provided the effectors are appropriately activated. We separated poly I·poly C-stimulated macrophages from the NS-1 targets by a membrane filter with a 0.2-μm pore and found that normal levels of cytolysis and/or cytostasis are observed in 36 hours (table 3). To control for the possibility that effector macrophages could project a cytoplasmic process(es) through the filter and affect target cells through direct contact, we separated the cells by two filters and observed identical results (data not shown). Clearly, the signal presented to the macrophage by poly I·poly C overrides the necessity for contact with the tumor in this system. In contrast, when non-poly I·poly C-stimulated macrophages were employed, they were unable to induce cell lysis through the filter. If MCT is involved in tumor cell lysis, these studies suggest that contact between a tumor and effector macrophage is a necessary first step to provide the inducing signal for MCT release, followed by rapid binding of MCT to the target. However, poly I·poly C alone is capable of triggering; once induced, effector macrophages may not require contact with the target cell to induce lysis. The rapidity with which the MCT binds to the tumor target might explain why MCT was not observed to be spontaneously released into the supernatant from alloimmune macrophages if residual tumor cells were present in the exudate (*6*). This rapid binding is compatible with a role for MCT only in the immediate microenvironment between a macrophage and its conjugated tumor target.

Our evidence further suggests that the manner in which MCT expresses cell-lytic activity involves protease-dependent steps. Previous in vitro studies by Hibbs and co-workers (*5*) and by other groups (*7–9*) have suggested a role for serine proteases in the expression of cytolysis by activated macrophages. In particular, the reagent TLCK, which alkylates proteases with trypsin-like specificity, has been shown to effectively block cytolysis in these cell-lytic reactions. This blockage suggested to us that, if MCT were in fact a toxic mediator employed by the activated macrophage in cytolysis, MCT's activity might also be protease dependent. Experiments with partially purified MCT and TLCK do show that this alkylating reagent destroys lytic activity of the soluble molecule (table 4). The blocking of MCT activity also observed with TAME, PMSF, and SBTI and the lack of effect of the sulfhydryl alkylating agent IAM (table 4) further suggest the vital role of a trypsin-like protease in the expression of lytic activity.

On the basis of these results, we attempted to determine the nature of the specific substrate of this protease. We believe that MCT could either be a protease or be associated with a protease. Although a reasonable model for the mechanism of MCT-induced lysis could invoke direct protease action on the target cell, we favor a second model. In this model, the substrate for the protease is within the MCT itself, and it must itself be cleaved for lytic activity to be expressed. Since inactivation of MCT by TLCK suggested the protease has trypsin-like specificity, we approached the chemical characterization of the substrate by using reagents capable of modification of positively charged amino acid side chains. If the protease were juxtaposed in the MCT in such a way as to cleave an arginine- or lysine-containing loop of the polypeptide chain, then chemical modification of the arginine or lysine residue should prevent "activation" by the protease and therefore block cell lysis. We used the reagents MA (which acylates lysine and tyrosine residues), MAI (which modifies lysine), and CHD (which reacts with arginine).

Our results suggest that if MCT were associated with a protease, the protease would cleave an MCT-associated polypeptide chain containing arginine regions. The most compelling evidence for this supposition is the time-dependent reaction of MCT with CHD, which results in a progressive and virtually complete loss of lytic activity (table 5). The kinetics of this reaction appear to be similar to that reported by Toi et al. (*18*) for CHD and hemoglobin. Their studies were conducted in strongly alkaline conditions (0.05–0.10 *N* NaOH), whereas extensive modification of the MCT was successful for us in 0.2 *M* (pH 9) carbonate buffer. This hyperreactivity is fortuitous because we could not subject the MCT to such extremes of pH to promote chemical modification since the biologic activity would be lost at this pH (Klostergaard J, Reidarson TH, Granger GA: Manuscript in preparation).

In contrast to our results from modifying arginine, attempts to ascertain a role for a lysine-containing region of the protein were equivocal. MAI, which modifies lysine side chains while preserving the positive charge, showed some blocking effect on the lytic activity of MCT when a wide range of reagent levels was used (table 5). This effect appears to plateau at high reagent levels. Had, in fact, a lysine residue been the target of the protease, lytic activity should have been *totally* blocked, when the extremely high levels of MAI were used. The partial effect observed might be explained by a general denaturation effect upon modification of MCT lysine residues with MAI. In view of the report by Hunter and Ludwig (*19*), side reactions with other amino acid side chains and MAI are not likely.

In this light, the blocking of MCT by MA (table 5) does not suggest a role for lysine. On the contrary, two alternate explanations are more tenable. First, MA also modifies tyrosine and possibly serine. Thus these residues might be of importance, not as substrates, but as contact or catalytic residues in the protease. Serine is an important catalytic residue in some extensively characterized enzymes [for review, *see* (*20*)]. The other distinct and reasonable explanation for the MA inactivation of MCT is the electrostatic repulsion introduced by the negatively charged maleyl-lysine adducts where previously positively charged lysine side chains had been. This repulsion, which is widely reported for proteins reacting with dicarboxylic anhydrides (*27–33*), could easily lead to perturbation of critical tertiary or quarternary structure.

Although it is also possible that CHD and MAI react directly with the protease active site rather than the protease's substrate to inactivate MCT, we believe this model is less likely, since basic amino acids are poor candidates to occupy binding or catalytic regions of a trypsin-like protease [for review, *see* (*20*)].

The distinct effects of the two reversible inhibitors TAME and ALME further suggest that the protease cleaves at an arginine rather than lysine residue. TAME, an arginine derivative, was a very effective inhibitor (table 4), whereas ALME, a lysine derivative, had no measurable effect. We cannot discount, however, that TAME may be superior at least in part due to its hydrophobic binding in the ρ_1 region of the protease active site (*21, 22*). This hydrophobicity could account for the blocking observed by TLCK, a lysine derivative. However, TLCK and the protease may initially form complexes with only a low association constant, comparable to the poor association with ALME; the subsequent covalent bond-forming step with TLCK would then serve to effectively block the active site.

Contrast of the characteristics of MCT with those of CF described by Adams and co-workers (*8*) is noteworthy. They described CF found in the supernatants of peritoneal macrophages from BCG- or thioglycollate-treated mice, following endotoxin stimulation, to be principally approximately 40,000 daltons (*7, 8*), whereas MCT is approximately 150,000 daltons. Furthermore, the lytic activity CF is strongly blocked by serum (*17, 23*), whereas MCT can lyse all susceptible tumor targets in the presence of 3–10% bovine serum. This difference may reside in the inability of α_2-macroglobulin to effectively "bury" MCT in its cleft(s) (*24–26*). Both CF (*8*) and MCT are dependent on protease activity for expression of their tumoricidal function. Further studies for characterization and comparison of CF and MCT are warranted and their possible subunit relationship should be considered.

Finally, these reports provide initial documentation of a molecular mechanism that may be operative in the target-injury phase of macrophage-mediated cytolysis. Further aspects of this possible mechanism can be only elucidated pending the purification and characterization of the MCT itself.

REFERENCES

(*1*) Evans R, Alexander P. Mechanism of extracellular killing of nucleated mammalian cells by macrophages. In: Nelson DS, ed. Immunobiology of the macrophage. New York: Academic Press, 1976:536–576.

(*2*) Hibbs JB Jr. The macrophage as a tumoricidal effector cell: A review of in vivo and in vitro studies on the mechanism of the activated macrophage nonspecific cytotoxic reaction. In: Fink MA, ed. Macrophage in neoplasia. New York: Academic Press, 1976:83–111.

(*3*) Keller R. Cytostatic and cytocidal effects of activated macrophages. In: Nelson DS, ed. Immunobiology of the macrophage. New York: Academic Press, 1976:487–508.

(4) Hibbs JB Jr. Heterocytolysis by macrophages activated by Bacillus Calmette-Guerin: Lysosome exocytosis into tumor cells. Science 1974; 184:468–471.

(5) Hibbs JB Jr, Taintor RR, Chapman HA, Weinberg JB. Macrophage tumor killing: Influence of the local environment. Science 1977; 197:279–282.

(6) Reidarson TH, Levy W, Klostergaard J, Granger GA. Inducible macrophage cytotoxins. I. Biokinetics of activation and release in vitro. JNCI 1982; 69:879–887.

(7) Adams DO. Effector mechanisms of cytolytically activated macrophages: I. Section of neutral proteases and effect of protein inhibitors. J Immunol 1980; 124:286–292.

(8) Adams DO, Kao KJ, Farb R, Pizzo SV. Effector mechanisms of cytolytically activated macrophages. II. Secretion of a cytolytic factor by activated macrophages and its relationship to secreted neutral proteases. J Immunol 1980; 124:293–300.

(9) Piessens WF, Sharma SO. Tumor cell killing by macrophages activated in vitro with lymphocyte mediators: Role of proteases, inhibitors, and substrates. Cell Immunol 1981; 56:286–291.

(10) Shaw E, Mares-Guia M, Cohen W. Evidence for an active center histidine in trypsin through use of a reagent, 1-chloro-3-tosylamido-7-aminoheptanone, the chloromethyl ketone derived from *N*-alpha-tosyl-L-lysine. Biochemistry 1965; 4:2219–2224.

(11) Amon R. Papain. Methods Enzymol 1970; 19:226–244.

(12) Glazer AM, Smith EL. Papain and other plant sulfhydryl proteolytic enzymes. In: Boyer PD, ed. The enzymes. Vol III. 3d ed. New York: Academic Press, 1971:502–546.

(13) Barrett AJ. Human cathepsin B1. Purification and some properties of the enzyme. Biochem J 1973; 131:809–822.

(14) Kramer JJ, Granger GA. Induction and release of cell toxins by immune C57BL/6 mouse peritoneal macrophages. Cell Immunol 1972; 3:88–100.

(15) Alexander P, Evans R. 1971 Endotoxin and double stranded RNA render macrophages cytotoxic. Nature [New Biol] 1971; 237:76–78.

(16) Doe WF, Henson PM. Macrophage stimulation by bacterial lipopolysaccharides. I. Cytolytic effect on tumor target cells. J Exp Med 1978; 148:553–567.

(17) Marino PA, Adams DO. Interaction of Bacillus Calmette-Guerin-activated macrophages and neoplastic cells in vitro. II. The relationships of selective binding to cytolysis. Cell Immunol 1980; 54:26–35.

(18) Toi K, Bynum E, Norris E, Itano HA. Studies on the chemical modification of arginine. I. The reactions of 1,2-cyclohexamidione with arginine and arginyl residues of proteins. J Biol Chem 1967; 242:1036–1043.

(19) Hunter MJ, Ludwig ML. The reaction of imidoesters with proteins and related small molecules. J Am Chem Soc 1962; 84:3491–3504.

(20) Perlmann GE, Lorand L, eds. Proteolytic enzymes. Methods Enzymol 1970; 19:31–225.

(21) Hein GE, Niemann C. Steric course and specificity of α-chymotrypsin-catalyzed reactions. II. J Am Chem Soc 1962; 84:4495–4503.

(22) Jones JB, Niemann C, Hein GE. The primary specificity of α-chymotrypsin. Interaction with acylated derivatives of D-valine methy ester and D-norvaline methyl ester. Biochemistry 1965; 4:1735-1739.

(23) Adams DO, Marino PA. Evidence for a multistep mechanism of cytolysis by BCG-activated macrophages: The interrelationship between the capacity for cytolysis, target binding, and secretion of cytolytic factor. J Immunol 1981; 126:981–987.

(24) Barrett AJ, Starkey PM. The interaction of α_2-macroglobulin with proteinases. Characteristics and specificity of the reaction, and a hypothesis concerning its molecular mechanism. Biochem J 1973; 133:709–724.

(25) Harpel PC, Hayes MB, Habli TE. Heat-induced fragmentation of human α_2-macroglobulin. J Biol Chem 1979; 254:8669–8678.

(26) Katayama RK, Fujita T. Studies on biotransformation of elastase. III. Effects of elastase-binding proteins in serum on the disappearance of ^{131}I-labelled elastase from blood. Biochim Biophys Acta 1974; 336:165–177.

(27) Hass LF. Aldolase dissociation into subunits by reaction with succinic anhydride. Biochemistry 1964; 3:535–541.

(28) Habeeb AF, Cassidy HG, Singer SJ. Molecular structural effects produced in proteins by reaction with succinic anhydride. Biochim Biophys Acta 1958; 29:587–593.

(29) Habeeb AF. Evaluation of conformational changes in chemically modified bovine serum albumins on a column of Sephadex. Biochim Biophys Acta 1966; 121:21–25.

(30) Jonas A, Weber G. Partial modification of bovine serum albumin with dicarboxylic anhydrides: Physical properties of the modified species. Biochemistry 1970; 9:4729–4735.

(31) Bezkorovainy A, Zschocke R, Grohlich D. Some physical–chemical properties of succinylated transferrin, conalbumin and orosomucoid. Biochim Biophys Acta 1969; 181:295–304.

(32) Lockhart WE, Smith DB. Effect of maleylation and amidination of hemoglobin on its haptoglobin and oxygen reactions. Can J Biochem 1971; 49:148–153.

(33) Klostergaard J, Grossberg AL, Krausz LM, Pressman D. Absence of lysine from the DNP–lysine binding site of protein 315; designation of lysine 52 of the heavy chain as a peripheral residue. Immunochemistry 1977; 14:37–44.

Squamous Metaplasia in Organ Cultures of Vitamin A-Deficient Hamster Trachea: Cytokinetic and Ultrastructural Alterations[1,2,3]

Dharam P. Chopra[4,5]

ABSTRACT—Cytokinetic and morphologic studies were performed to elucidate the origin of epidermoid metaplasia in organ cultures of tracheas derived from vitamin A-deficient Syrian golden hamsters. Focal areas of squamous metaplasia were observed 2 days after explantation, and extensive epidermoid metaplasia and cornification were present in approximately 89% of the explants at day 10. During the first 2 days, both basal and mucous cells proliferated actively. By day 3, the total mucous cell [^{3}H]thymidine labeling index (LI) had declined and remained at very low levels during the remaining culture period. The basal cell LI also declined from its higher level, but it remained at relatively higher levels than those of the mucous cells between days 3 and 9 after culture. In the lesions, labeled cells were generally confined to the basal layer, and the LI was about thirtyfold greater than the total basal cell LI. As the lesions progressed, the surface layer containing the mucous and ciliated cells was exfoliated as a result of population pressure from the underlying actively proliferating basal cells and subsequent epidermoid differentiation of the daughter cells. These data support the hypothesis that epidermoid metaplasia of tracheobronchial epithelium caused by vitamin A deficiency originates from the generative or basal cells—JNCI 1982; 69:895–905.

Vitamin A plays an important role in the control of cellular proliferation and differentiation in a variety of epithelia. Deficiency of vitamin A in experimental animals leads to the development of keratinizing squamous metaplasia in the urinary bladder and tracheobronchial mucosa (*1–3*). In the tracheobronchial epithelium, squamous metaplasia consists of an epidermoid transformation of pseudostratified normal epithelium (*2–3*). This process can also be demonstrated in vitro. Organ cultures of trachea obtained from vitamin A-deficient hamsters and cultured in chemically defined medium for 10 days without vitamin A become squamous and keratinize. Supplementing the medium with vitamin A or an active retinoid, however, prevents the development of the lesions (*4*).

Exposure of the respiratory epithelium to carcinogens and to certain toxic inhalants also causes squamous metaplasia (*5–11*). Although histogenesis of squamous metaplasia induced by different agents including injury and infection with mycoplasma and paramyxovirus (*12–14*) have been extensively studied in experimental animals, there is a wide gap in cytokinetic evidence to define the origin of the lesions. Cytokinetic information is important since a very large fraction of squamous metaplasias and squamous cell carcinomas are generally considered mucous cell lesions (*12*), but there is evidence to indicate that certain types of squamous metaplasias in experimental animals arise from the basal cells (*2, 3, 10*). In the present study, organ cultures of tracheas obtained from hamsters that were maintained on vitamin A-sufficient and vitamin A-deficient diets were used to define the origin of squamous metaplasias caused by the deficiency. The results indicate that the lesions produced by vitamin A deficiency originate in the basal cells.

MATERIALS AND METHODS

Hamsters.—To induce vitamin A deficiency, we fed Syrian golden hamsters 11–12 days pregnant (Harlan Industries, Inc., Madison, Wis.) in individual cages a mixed diet of one part laboratory chow (Ralston Purina Co., St. Louis, Mo.) and one part vitamin A-deficient diet (Teklad, Inc., Madison, Wis.). After birth of the litters, the mothers were fed only on the vitamin A-deficient diet. The young hamsters were weaned at 21 days after birth and thereafter kept entirely on the vitamin A-deficient diet until utilized (27–30 days after birth). Six young hamsters were housed in each cage (14×12×7 inches). All animals were housed in a semi-isolated room maintained at 23–24°C with a 12-hour light–dark cycle.

All batches of vitamin A-deficient diets were checked for the deficiency before use by a group of 8 vitamin A-deficient hamsters being kept on the new diet. If the animals continued to lose weight, developed dull-matted fur and impaired vision, and subsequently died, the diet was considered deficient in vitamin A.

Normal hamsters were similarly raised except that they were fed a diet supplemented with 15,000 U of vitamin A (vitamin A–palmitate)/kg diet. Animals maintained on this diet continued to grow and reached maturity. All diets were stored at 4°C and used within 2 months after they were received.

Organ culture.—Animals with body weights between 48

ABBREVIATIONS USED: BP=benzo[*a*]pyrene; DH=hamsters fed vitamin A-deficient diet; H & E=hematoxylin and eosin; [^{3}H]dThd=tritiated thymidine; LI=labeling index (indices); MCA=3-methylcholanthrene; MGC=mean grain count; NH=normal hamsters fed vitamin A-supplemented diet; PAS=periodic acid–Schiff; AB–PAS=Alcian blue–PAS; RER=rough endoplasmic reticulum.

---

[1] Received July 28, 1981; revised April 9, 1982; accepted May 10, 1982.

[2] Supported by Public Health Service grant 1-R01CA-26696-01A from the National Cancer Institute.

[3] Animals were maintained under the guidelines set forth by the Animal Care Committee of the Southern Research Institute.

[4] Cell Structure and Differentiation Section, Kettering-Meyer Laboratory, Southern Research Institute, P.O. Box 3307-A, 2000 Ninth Ave. South, Birmingham, Ala. 35255.

[5] I thank Mr. Lawrence R. Melsen of the Electron Microscope Core Facility, Comprehensive Cancer Center, University of Alabama, for his technical assistance in the electron microscope work.

and 58 g were used. At this stage most animals were gaining weight, and DH showed no external sign of vitamin A deficiency. Animals were killed with 0.5 ml of a 1% solution of Brevital Sodium (methohexital sodium; Eli Lilly & Co., Indianapolis, Ind.) injected ip, and their tracheas were excised aseptically. The tracheas were kept in the cold serum-free "holding medium" L-15, supplemented with 100 U penicillin/ml and 100 µg streptomycin/ml (Grand Island Biological Co., Grand Island, N.Y.). Each trachea was cleaned to remove any adherent tissue, opened longitudinally along the membraneous dorsal wall, and cultured individually in 60-mm plastic culture dishes (Falcon Plastics, Oxnard, Calif.). Each dish contained 2 ml of CMRL-1066 serum-free medium (Grand Island Biological Co.), supplemented with 1.0 µg crystalline bovine insulin/ml (Sigma Chemical Co., St. Louis, Mo.), 0.1 µg hydrocortisone hemisuccinate /ml (The Upjohn Co., Kalamazoo, Mich.), 2 m*M* glutamine, 100 U penicillin/ml, and 100 µg streptomycin/ml (Grand Island Biological Co.) (*4*). The cultures were gassed with a mixture of 50% O_2+45% N_2+5% CO_2 (Matheson Gas Products, Morrow, Ga.) in a rocker chamber (Bellco Glass, Vineland, N.J.) at 35-36°C and rocked approximately 8-10 times per minute. Each experiment was repeated and the data were pooled.

Morphologic observations.—For each experiment 45-50 tracheal organ cultures were prepared. To follow the development of squamous metaplasia and keratinization, we terminated groups of seven cultures at different intervals. Each explant was cut into two pieces, one to be processed for light microscopy and one for electron microscopy. For light microscopy, explants were fixed in 10% neutral buffered Formalin and embedded in paraffin. Serial sections (4 µm each) were cut through the middle of each trachea and stained in AB-PAS or H & E. Sections were analyzed according to the degree of squamous metaplasia and the presence or absence of keratohyalin granules and keratin as described previously by Sporn et al. (*4*).

For electron microscopy, specimens were fixed in 3% glutaraldehyde in phosphate buffer at pH 7.3. These specimens were cut into 1×2-mm pieces, postfixed in osmium, dehydrated in acetone, and embedded in polybed 812 (Polysciences Inc., Warrington, Pa.). Sections (1 µm each) were cut and pertinent areas localized by the examination of thick sections with a light microscope. Thin sections were cut with a diamond knife in a Porter-Blum ultramicrotome, stained with uranyl acetate and lead citrate, and examined with a Philips-300 or Hitachi HU12 electron microscope.

LI at different times after culture.—Twentyfive to 30 organ cultures were prepared. At different times after culture groups of three cultures each were pulse labeled with [^{3}H]-dThd (sp act, 6.7 Ci/mmol, 2 µCi/ml) for 1 hour and fixed in Formalin for histologic examination. From these specimens 4-µm sections were cut, deparaffinized, stained in PAS, and dipped in Kodak NTB2 emulsion diluted 1:1 with distilled water. Autoradiograms were exposed for 2 weeks at 4°C, developed in D-19, and counter stained in hematoxylin (*15*). The number of mucous (PAS-positive) and basal (PAS-negative) cells with four grains or more over their nuclei were counted in two sections (covering ≈6 mm mucosal surface) from each trachea. The LI were expressed as the number of labeled cells per centimeter length of epithelial surface.

The identification of basal and mucous cells was essentially based on the stainability of cells with AB-PAS reagents. Although this method is extensively used for identification of cells containing mucopolysaccharides, some cells that stain negatively may contain very small amounts of mucin and are not detected at this level. In the present study, basal cells were identified by the PAS-negative cytoplasm and their distribution along the basal lamina. The apexes of basal cells did not reach the tracheal lumen. These observations correlated with the ultrastructural findings.

In addition to analysis of total LI (labeled cells in the epithelial mucosa, including areas of squamous metaplasia), LI was also determined exclusively in areas exhibiting squamous metaplasia and keratinization in explants derived from the DH.

Changes in MGC at different intervals after a single [^{3}H]dThd pulse.—For each experiment 25-30 cultures were prepared. Twenty-four hours later, all cultures were pulse labeled with [^{3}H]dThd (2 µCi/ml) for 1 hour, thoroughly rinsed by three changes of fresh medium to displace free [^{3}H]dThd, and reincubated in the fresh culture medium. Groups of three cultures each were terminated at 1 hour and at 1, 2, 3, 4, and 5 days after the pulse labeling and processed for autoradiography. To estimate their proliferative potential, we enumerated the numbers of grains over mucous and basal cell nuclei. In these experiments allowance had to be made for halving of grain counts that would occur at the division of labeled nuclei. Nuclei with two grains above the background level were classified as labeled. Background count was approximately one grain per nucleus. Groups of 25 labeled basal or mucous cells were scored from each trachea, and the mean value and the standard error were calculated for each group. The significance of the difference between two groups was determined by Student's *t*-test.

RESULTS

Normal Hamster Trachea

The detailed structure of the tracheobronchial epithelium of normal hamster trachea has been described in (*2, 3, 9, 16*). Organ culture of the NH trachea for 10 days maintained typical morphology. The pseudostratified epithelium contained a row of PAS-positive columnar-cuboidal mucous and ciliated cells that extend from the basal lamina to the tracheal lumen and an intercalated row of PAS-negative basal cells that lie on the basal lamina and do not reach the lumen (fig. 1). At the ultrastructural level, the basal cells contained large, centrally located nuclei and prominent nucleoli (fig. 2). Their cytoplasm was electron-dense and contained polysomes, scant RER, and a few small mitochondria (fig. 3). Microfilaments were scant and were not commonly seen in the basal cells. The mucous cells that varied somewhat in structure according to the degree of mucus secretion showed microvilli facing lumen and their cytoplasms contained extensive RER and mucus droplets (fig. 2). Adjacent luminal cells showed junctional complexes between them. Desmosomal junctions were present, but their number was reduced after 10 days of culture. The ciliated cells showed irregular nuclei, numerous mitochondria, and RER.

Development of Squamous Metaplasia in vitamin A-Deficient Hamsters

At the initiation of cultures, the morphology of the DH trachea was essentially similar to that of the NH trachea. Organ culture of the vitamin A-deficient hamster trachea showed rapid alterations in the structure of the epithelial mucosa. Within 48 hours, focal areas of altered epithelium consisting of two distinct rows of cells were present (fig. 4). The ciliated and mucous cells of the upper row characterized by PAS-positive cytoplasms were cuboidal-flat, whereas the basal cells were round and contained large basophilic nuclei. Cells with squamous morphology extruding from the basal layer were frequently observed in the altered epithelium. At 72 hours after culture, the mucosa contained several dome-shaped structures (fig. 5) consisting of a basal layer of large, round cells, two to three layers of squamous cells, and an overlying layer of cells with PAS-positive cytoplasm. We did not see the ciliated cells in these areas. The basal and squamous cells contained PAS-negative cytoplasm. Mitotic cells were frequently observed in the basal cell layer. Subsequently, the population pressure caused by the continued proliferation of the basal cells associated with squamous differentiation resulted in rupture and, consequently, exfoliation of the surface layer of the PAS-positive cells (fig. 6).

The light-microscopic observations associated with the squamous metaplasia correlated well with alterations at the ultrastructural level. We observed the earliest sign of squamous metaplasia in a group of three to four basal cells comprising electron-dense cytoplasms that appeared to be displacing overlying mucous and ciliated cells (fig. 7). The basal cells exhibited features of active proliferation but also contained bundles of tonofilaments occasionally referred to as 'keratin' filaments (fig. 8). The presence of keratin filaments in the basal cells indicates early keratinization, since the filaments were not commonly present in the basal cells of cultures derived from NH trachea. The mucous and ciliated cells exhibited typical morphologies. We occasionally saw degenerative cells overlying metaplastic cells (fig. 7).

As the lesions progressed, metaplastic epithelium consisted of two to three layers of electron-dense squamous cells and a distinct superficial layer of cells that were electron-lucent (fig. 9). The electron-dense cells had little resemblance to the normal respiratory epithelium. The basal cells were cuboidal with large, round nuclei, predominant nucleoli, abundant polysomes, and a few bundles of keratin filament. Numerous interdigitating cytoplasmic processes occasionally ending in desmosomes projected into intercellular spaces. We frequently saw mitoses in the basal cell layer. One to two layers of electron-dense cells were in the intermediate position and resembled basal cells except that they were somewhat flatter and contained greater amounts of keratin filament. A large number of well-developed desmosomes were present between the electron-dense cells. Such a large number of well-developed desmosomes are generally observed in differentiating epidermal cells. Furthermore, vesicles containing mucous granules were not usually seen in the metaplastic basal cells.

In contrast to electron-dense metaplastic cells, the superficial electron-lucent cells continued to exhibit features characteristic of respiratory cells, although the amount of mucus granules had decreased. The boundary between the metaplastic and nonmetaplastic cells was distinct (fig. 9). The cytoplasm of superficial cells contained extensive RER, Golgi complexes, and occasionally tonofilaments. These cells had short, stubby, irregularly placed microvilli on the luminal surface. Junctional complexes were present between adjacent surface cells. Intermittent desmosomes were also present at the boundary between the electron-dense metaplastic cells and surface cells.

Continued proliferation of the basal cells and their subsequent differentiation into squamous metaplastic cells resulted in exfoliation of the surface cells. The cells at the advancing edge of metaplastic lesions contained large bundles of keratin filaments (fig. 10) and appeared to displace the overlying surface cells. Subsequently keratohyaline granules were formed in the metaplastic cells followed by cornification (fig. 11).

The percentages of explants showing various degrees of metaplasia and keratinization as a function of time are shown in table 1. Cornified squamous metaplastic areas were present after 3 days in approximately 50% of the explants. The degree and severity of the lesions progressed with the length of culture period. Keratinized lesions were present in approximately 89% of the explants after 10 days.

Comparison of LI of Basal and Mucous Cells at Different Times after Culture

Text-figure 1 shows total basal and mucous cell LI at different intervals after culture of tracheas from the NH and DH. The total basal and mucous cell LI refers to their respective LI in the entire epithelial mucosa including areas of squamous metaplasia that occurred only in the explants of DH trachea. Culture of NH trachea resulted in hyperplasia of both the basal and mucous cells. However, between 72 and 96 hours, the LI of both cell types returned to the original levels that were maintained for the remaining culture period (text-fig. 1A).

TABLE 1.—*Explants with different degrees of squamous metaplasia, keratohyaline granules, and keratin at different times after culture*[a]

Days in culture	Percentages of explants showing:						
	Squamous metaplasia, %					Keratohyaline granules	Keratin
	None	0–2	2–10	10–40	40		
1	42	29	29	0	0	0	0
2	28	18	14	40	0	0	0
3	8	12	40	20	20	49	43
4	0	18	62	12	8	62	62
6	0	17	50	33	0	67	67
8	0	13	25	26	36	88	58
10	0	12	13	29	46	89	89

[a] Tracheal organ cultures were prepared. Groups of explants were terminated at different intervals after incubation and processed for histologic examinations.

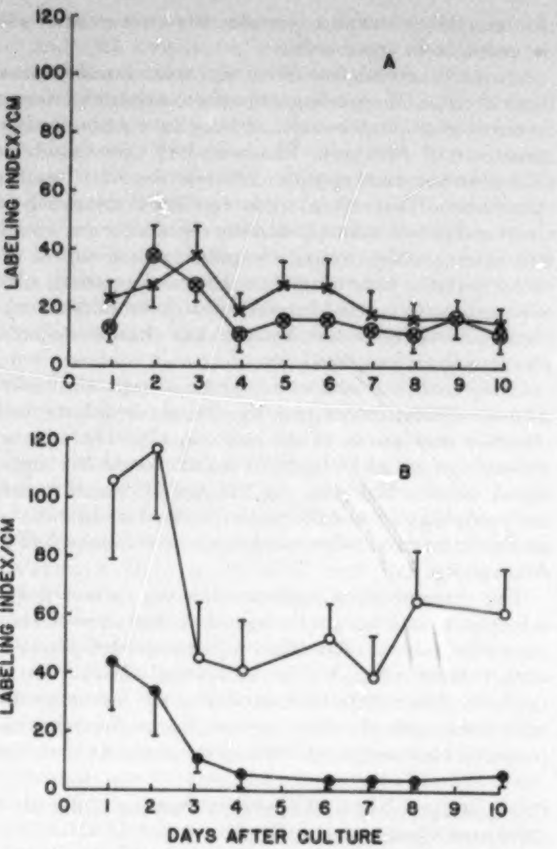

Text-figure 1.—Total LI±SD in basal and mucous cells at different intervals after culture. A) Explants of NH trachea, (X), basal cells; (⊗), mucous cells. B) Explants of DH trachea, (○), basal cells; (●), mucous cells.

Explantation of DH trachea also resulted in hyperplasia of both the basal and mucous cells, although basal cells proliferated more actively than the mucous cells (text-fig. 1B). During the first 48 hours the basal cell LI was at least twofold higher than the mucous cell LI. The mucous cell LI declined gradually after 24 hours, reached a very low level at 6 days, and remained unchanged thereafter. The basal cell LI also began to decline after 48 hours but remained at relatively higher levels between 3 and 9 days after culture. During this time the basal cell LI was approximately forty-fold greater than the mucous cell LI. The high degrees of standard deviation of total mucous and basal cell LI are caused by the variable degrees of squamous metaplasia in different explants within the same group.

Since squamous metaplasia occurs at least initially in focal areas, the LI was also determined exclusively in the lesions. Text-figure 2 shows that cells in the lesions that stained negatively with PAS proliferated actively and mainly in the basal cell layer. The basal cell LI in the lesions between 6 and 9 days after culture was approximately thirtyfold and a thousandfold greater than the total LI of basal and mucous cells, respectively (text-fig. 1).

Although squamous metaplasia originates in focal areas, it expands to involve a large part of the epithelium. The expansion of lesions appears to be associated with the expansion of the proliferative zones, since cohorts of [^{3}H]dThd-labeled cells were frequently seen at the edges of lesions (fig. 12). Furthermore, a majority of the [^{3}H]dThd-labeled cells were concentrated in the basal cell layer (fig. 13).

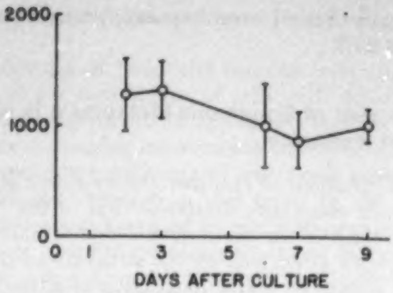

Text-figure 2.—LI±SD of PAS-negative cells in areas exhibiting squamous metaplasia of DH explants. The PAS-positive cells did not incorporate [^{3}H]dThd.

The proliferative activity of PAS-positive or PAS-negative cells in areas of normal morphology was very low.

MGC in Basal and Mucous Cells as a Function of Time After a Single [^{3}H]dThd Pulse

To determine the proliferative potential of the mucous and basal cells, explants were pulse labeled 24 hours after initiation with [^{3}H]dThd for 1 hour and terminated at different intervals thereafter. The basal and mucous cell MGC in the NH tracheal explants declined by approximately 51 and 53%, respectively, at 24 hours after the pulse labeling and remained stable thereafter for at least 5 days (text-figs. 3A, 3B). This result indicates that the basal and

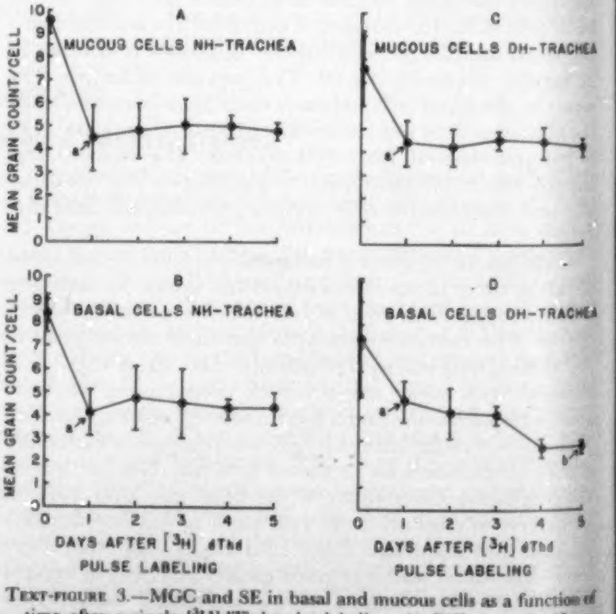

Text-figure 3.—MGC and SE in basal and mucous cells as a function of time after a single [^{3}H]dThd pulse labeling. A) Difference significant ($P<0.05$) compared to the corresponding value at 1 hr after the pulse. B) Difference significant ($P<0.05$) compared to the corresponding value on day 1.

mucous cells of NH trachea have divided only once during this period.

In the explants of DH tracheas, the MGC of mucous cells dropped nearly 42% in the first 24 hours after the pulse and remained relatively constant thereafter (text-fig. 3C). In contrast, the basal cell MGC declined by 36% in the first 24 hours and again by another 43% between 24 and 96 hours after the pulse labeling (text-fig. 3D). This suggests that the basal cell population have undergone division twice, once during the first 24 hours and again between 24 and 96 hours.

DISCUSSION

Epidermoid metaplasia of the respiratory epithelium, generally considered a preneoplastic lesion (*17–19*), may be induced by different treatments (*5–11*). In tracheobronchial epithelium, metaplasias induced by various agents exhibit certain morphologic similarities; however, there apparently are some inherent differences. For instance, metaplasia induced by carcinogenic insults proceeds to develop into squamous cell carcinoma (*3, 5, 8, 9, 20*), whereas the lesions induced by vitamin A deficiency (*2, 3*), noxious gases (*6, 21*), mechanical trauma (*10, 12*), or infections (*13, 14, 22*) are merely benign states that are generally reversible. The variable characteristics of metaplasia may be associated with the nature of insults and the origin of metaplasia. Most investigators believe that the epidermoid metaplasia in tracheobronchial epithelium arises as a result of the replacement of ciliated and mucous cells by epidermoid cells that originate from the basal cells (*2, 3, 10*). For instance, on the basis of ultrastructural observations of tracheobronchial epithelium of rats maintained on a vitamin A-deficient diet, Wong and Buck (*2*) proposed that the epidermoid metaplasia involved differentiation of basal or generative cells into squamous metaplastic epithelium. In the hamster, Harris et al. (*3*) showed that metaplasia caused by vitamin A deficiency or BP–Fe_2O_3 treatment also originates from the basal cells, although the ultrastructural characteristics of lesions produced by the two treatments differed. Recently, the origin of metaplasia in the basal cells of tracheobronchial epithelium was reevaluated. On the basis of the ultrastructural observations, McDowell et al. (*23*) have proposed that epidermoid metaplasia caused by BP–Fe_2O_3 (*9*) or mechanical trauma (*23*) may originate from the mucous cells (small mucous granular cells), although several characteristic features of the mucous cells were also noted in the basal cells. In the present study cytokinetic and ultrastructural features in tracheal organ cultures derived from NH and DH were compared in an effort to define the origin of the squamous metaplasia. The results indicate that these lesions originated in the basal cells, i.e., the epithelial cells that lie along the basal lamina and do not reach the tracheal lumen.

The tracheas of animals fed vitamin A-deficient and vitamin A-supplemented diets exhibited similar morphologic characteristics at the initiation of organ cultures. However, they exhibited different patterns of proliferation and differentiation in culture. During the 10-day culture period, while the NH trachea maintained morphologic integrity typical of normal tissue, the tracheas derived from the DH developed extensive squamous keratinizing metaplasia. Accordingly, the epithelial cell composition of the NH trachea changed little in organ culture, but in the tracheal explants of DH, the differentiation of ciliated and mucous cells was inhibited while the production of squamous cells characteristic of epidermoid metaplasia was enhanced. Similar results have previously been reported in the respiratory epithelium of animals maintained on the deficient diet for prolonged periods (*2, 3*). Furthermore, the transitory regenerative hyperplasia that occurs in many tissues after injury or on organ culture (*24–27*) also occurred in the basal and mucous cells of normal and deficient animal tracheas. However, whereas the hyperplasia of basal and mucous cells in NH and of the mucous cells in DH tracheas subsided after 3 days of culture, hyperproliferation of basal cells in the DH trachea continued during the entire culture period. Higher LI in the tracheobronchial epithelium of vitamin A-deficient hamsters than that of the normal hamster has been reported previously (*28*). Thus the data suggest that the variable patterns of proliferation and differentiation exhibited by tracheal cultures derived from the NH and DH animals are related to the vitamin A status of the donor prior to organ culture.

The ultrastructural observations on organ cultures showed that the basal, mucous, and ciliated cells of NH and the mucous and ciliated cells of DH trachea retain typical characteristics of the respiratory epithelium. In contrast, the hyperplastic foci of basal cells in the DH trachea showed epidermoid characteristics, such as keratin filaments in the cytoplasm and well-developed desmosomes between cells. These epidermoid characteristics were not seen in the tracheal cultures of NH. The hyperplastic epidermoid foci then spread over a larger area, and the superficial layer that consisted of cells distinctly different from the basal cells in ultrastructure and staining properties was undercut and subsequently sloughed off. The secretory cells may have discharged mucous granules at organ culture (*29*), but these cells were not responsible for the induction of lesions since the ultrastructural characteristics of the electron-dense metaplastic cells differed from those of the electron-lucent surface cells right from the initiation of the cultures. In addition, squamous lesions were not present in cultures of NH tracheas. The hyperplastic basal cells differentiated into flatter cells toward the surface, and these exhibited more prominent features of epidermoid lesions. The development of lesions occurs by altered differentiation beginning in the basal cells, which apparently have the capability to divide and flexibility for variable differentiation. The result that mucous and ciliated cells showed no tendency to keratinization indicates that their potential for keratinization was absent or not expressed. The observation that fully differentiated mucous cells exhibit transitory proliferative potential in the tracheal organ culture is consistent with other reports (*30–33*).

Tracheal grafts in isogenic rats exposed to pellets of BP or MCA resulted in the induction of hyperproliferation of the basal cells, which remained elevated as squamous metaplasia progressed (*34*). In the present study, hyperplasia of basal cells after 72 hours of culture of DH trachea was mainly confined to the areas that exhibited squamous metaplasia. Labeling data showed that $[^3H]$dThd incorporation in the lesions was approximately fortyfold greater than in the epithelium that exhibited normal morphology. When the LI in the metaplastic lesions was compared with that of the mucous cells, the former was almost a thousandfold greater than the latter. The MGC data further showed that unlike basal and mucous cells of NH trachea and mucous cells of DH tracheas that divided only once, basal cells of DH trachea divided repeatedly. These results thus support the hypothesis that basal cells with their extraordinary proliferative potential in the areas that exhibit lesions are responsible for the development and progression of the lesions. The factors that cause these cells to alter their differentiation pathway remains to be defined.

The increase in the number of basal cells in areas that exhibit epidermoid lesions is most likely to occur as a result of the division of basal cells and retention of daughter cells in the basal layer, although the possibility of dedifferentiation of mucous cells cannot be ruled out (*9*). However, the division of a mucous cell is likely to produce daughter mucous cells, and the result that mucous cells in the tracheal organ cultures only divide once strongly indicates that squamous lesions originate as a result of continued proliferation of the basal cells and subsequent differentiation of daughter cells into keratinizing cells. In addition, metaplastic cells did not exhibit any feature characteristic of the secretory cells. We frequently saw exfoliation of an overlying layer of mucous cells in metaplastic areas.

An increase in the number of basal cells has been observed commonly in tracheobronchial epithelium of human smokers (*6, 35*) and in tracheas of hamsters treated with BP-Fe_2O_3 (*3*) or 7,12-dimethylbenz[*a*]anthracene (*36*). However, recently Becci et al. (*9*) were unable to detect any significant increase in the basal cell population after exposure of hamster tracheal epithelium to BP-Fe_2O_3. The reason for this discrepancy is not clear, although it may be related to differences in specific definitions of various cell types used by different authors. In the present study, a continuous layer of basal cells (cells overlying the basal lamina, not reaching the lumen, and containing PAS-negative cytoplasm) was regularly observed in areas of epidermoid lesions, whereas the uninvolved epithelium exhibited typical pseudostratified morphology. Although squamous metaplasia starts in focal areas, the lesions progress as a result of expansion of proliferative zones, since cohorts of labeled cells were frequently observed at the edges of lesions. Expansion of proliferative zones has been reported in the gastrointestinal epithelium after treatment of mice with 1,2-dimethylhydrazine (*37*).

Vitamin A deficiency and other manipulations of tracheal epithelium with carcinogenic and noncarcinogenic insults have inherent differences and may therefore elicit variable responses by the tissue. Whereas vitamin A deficiency does not cause any physical damage to the tissue, other treatments, such as BP-Fe_2O_3 instillation, inhalation of noxious gases, or mechanical trauma, inflict direct damage to the superficial and, probably, to the deeper components of the mucosa. Vitamin A deficiency that involves sequential alterations probably allows the tissue sufficient time to respond by the initiation of programmed changes in the generative cells as has been shown by the present and other investigations (*2, 3*). Alternatively, direct insults that cause tissue damage may require immediate response involving both the basal and mucosa cells (*9, 11*). Hyperproliferation of both the mucous and basal cells after carcinogenic treatment may render them more susceptible to neoplastic transformation.

In conclusion, the present study indicates that although both the mucous and basal cells are capable of proliferation when suitably stimulated, epidermoid metaplasia in the organ cultures of vitamin A-deficient hamster trachea is produced mainly as a result of repeated proliferation of basal cells and subsequent epidermoid differentiation of daughter cells. The cytokinetic data associated with the squamous metaplasia correlated well with alterations at the ultrastructural level.

REFERENCES

(*1*) Hicks RM. Hyperplasia and cornification of the transitional epithelium in the vitamin A-deficient rat: Changes in the fine structure of the cells. J Ultrast Res 1968, 22:206–230.

(*2*) Wong Y, Buck R. An electron microscopic study of metaplasia of the rat tracheal epithelium in vitamin A deficiency. Lab Invest 1971, 24:55–66.

(*3*) Harris CC, Sporn MB, Kaufman DG, Smith JM, Jackson FE, Saffiotti U. Histogenesis of squamous metaplasia in the hamster tracheal epithelium caused by vitamin A deficiency or benzo[*a*]pyrene-ferric oxide. J Natl Cancer Inst 1972; 48:743–761.

(*4*) Sporn MB, Dunlop NM, Newton DL, Henderson WR. Relationships between structure and activity of retinoids. Nature 1976; 263:110–113.

(*5*) Harris CC, Sporn MB, Kaufman DG, Smith JM, Baker MS, Saffiotti U. Acute ultrastructural effects of benzo[*a*]pyrene and ferric oxide on the hamster tracheobronchial epithelium. Cancer Res 1971; 31:1977–1989.

(*6*) Auerbach O, Stout AP, Hammond EC, Garfinkel L. Changes in bronchial epithelium in relation to cigarette smoking and in relation to lung cancer. N Engl J Med 1961; 265:253–267.

(*7*) Nettesheim P. Respiratory carcinogenesis studies with the Syrian golden hamsters: A review. Prog Exp Tumor Res 1972; 16:185-200.

(*8*) Saffiotti U, Montesano R, Sellakumar AR, Cefis F, Kaufman DG. Respiratory tract carcinogenesis in hamsters induced by different numbers of administrations of benzo(*a*)pyrene and ferric oxide. Cancer Res 1972; 32:1073–1081.

(*9*) Becci PJ, McDowell EM, Trump BF. The respiratory epithelium. IV. Histogenesis of epidermoid metaplasia and carcinoma in situ in the hamster. JNCI 1978; 61:577–586.

(*10*) Lane BP, Gordon R. Regeneration of rat tracheal epithelium after mechanical injury. I. The relationship between mitotic activity and cellular differentiation. Proc Soc Exp Biol Med 1974; 145:1139-1144.

(*11*) Dirksen ER, Crocker TT. Ultrastructural alterations produced by polycyclic aromatic hydrocarbons on rat tracheal epithelium in organ culture. Cancer Res 1968; 28:906–923.

(*12*) McDowell EM, Becci PJ, Barrett LA, Trump BF. Morphogenesis and classification of lung cancer. In: Harris CC, ed. Pathogenesis and therapy of lung cancer. New York and Basel: Marcel Dekker 1978:445–519.

(*13*) Woodruff KH, Schneider E, Unger L, Coalson JJ. Ultrastructural changes in hamster tracheal ring cultures exposed to *Mycoplasma pneumoniae*. Am J Pathol 1973; 72:91–102.

(*14*) Murphy GF, Brody AR, Craighead JE. Exfoliation of respiratory epithelium in hamster tracheal organ cultures infected with *Mycoplasma pneumoniae*. Virchows Arch [Pathol Anat] 1980; 389:93–102.

(*15*) Thurston JM, Joftes, DL. Stains compatible with dipping radioautography. Stain Technol 1963; 38:231–235.

(*16*) Becci PJ, McDowell EM, Trump BF. The respiratory epithelium. II. Hamster trachea, bronchus, and bronchioles. JNCI 1978, 61:551–561.

(17) Black H, Ackerman LV. The importance of epidermoid carcinoma in situ in the histogenesis of carcinoma of the lung. Ann Surg 1952; 136:44–55.

(18) Valentine EH. Squamous metaplasia of the bronchus. A study of metaplastic changes occurring in the epithelium of the major bronchi in cancerous and noncancerous cases. Cancer 1957; 10:272–279.

(19) Carroll R. Changes in the bronchial epithelium in primary lung cancer. Br J Cancer 1961; 15:215–219.

(20) Saffiotti U, Montesano R, Sellakumar AR, Kaufman DG. Respiratory tract carcinogenesis induced in hamsters by different dose levels of benzo[*a*]pyrene and ferric oxide. J Natl Cancer Inst 1972; 49:1199–1204.

(21) Amundsson T, Kilburn KH, McKenzie WN. Injury and metaplasia of airway cells due to SO_2. Lab Invest 1973; 29:41–53.

(22) Collier AM, Clyde WA Jr, Denny FW. Biological effects of *Mycoplasma pneumoniae* and other mycoplasmas from man on hamster tracheal organ culture. Proc Soc Exp Biol Med 1969; 132:1153–1158.

(23) McDowell EM, Becci PJ, Schürch W, Trump BF. The respiratory epithelium. VII. Epidermoid metaplasia of hamster tracheal epithelium during regeneration following mechanical injury. JNCI 1979; 62:995–1008.

(24) Epstein WL, Sullivan DJ. Epidermal mitotic activity in wounded human skin. In: Montagna W, Billingham RE, eds. Advances in biology of skin. Vol 5. New York: Pergamon Press, 1964:68–75.

(25) Gross RJ. The strategy of growth. In: Teir H, Rytomaa T, eds. Control of cellular growth in adult organisms. London and New York: Academic Press, 1967:5–27.

(26) Franks LM. Nutritional and other factors influencing the balance between function and proliferation in organ culture. Natl Cancer Inst Monogr 1963; 11:83–94.

(27) Simnett JD, Morley AR. Factors controlling growth of prostatic epithelium. Exp Cell Res 1967; 46:29–36.

(28) Harris CC, Silverman T, Smith JM, Jackson F, Boren HG. Proliferation of tracheal epithelial cells in normal and vitamin A-deficient Syrian golden hamsters. J Natl Cancer Inst 1973; 51:1059–1062.

(29) Barrett LA, McDowell EM, Frank AL, Harris CC, Trump BF. Long-term organ culture of human bronchial epithelium. Cancer Res 1976; 36:1003–1010.

(30) Boren HG, Paradise LJ. Cytokinetics of lung. In: Harris CC, ed. Pathogenesis and therapy of lung cancer. New York: Marcel Dekker. 1978:368–418.

(31) Blenkinsopp WK. Proliferation of respiratory tract epithelium in the rat. Exp Cell Res 1967; 46:144–154.

(32) Bindreiter M, Schuppler J, Stockinger L. Zellproliferation und Differenzierung im Trachealepithel der Ratte. Exp Cell Res 1968; 50:377–382.

(33) Harris C, Frank A, Barrett L, et al. Cytokinetics in the respiratory epithelium of the hamster, cow and man. J Cell Biol 1975; 67:158a.

(34) Kendrick J, Nettesheim P, Hammons AS. Tumor induction in tracheal grafts: A new experimental model for respiratory carcinogenesis studies. J Natl Cancer Inst 1974; 52:1317–1325.

(35) Trump BF, McDowell EM, Glavin F, et al. The respiratory epithelium. III. Histogenesis of epidermoid metaplasia and carcinoma in situ in the human. JNCI 1978; 61:563–575.

(36) Stenback F, Sellakumar A. Squamous metaplasia and respiratory tumors induced by intratracheal installations of 7,12 dimethylbenz(*a*)anthracene in Syrian golden hamsters. Eur J Cancer 1974; 10:483–486.

(37) Thurnherr N, Deschner EE, Stonehill EH, Lipkin M. Induction of adenocarcinomas of the colon in mice by weekly injections of 1,2-dimethylhydrazine. Cancer Res 1973; 33:940–945.

Figure 1.—NH tracheal epithelium at inception of organ culture. Hamsters were ≈4 wk old. Epithelium of DH exhibited similar morphology. *Arrows* show basal cells. H & E. × 300

Figure 2.—NH trachea maintained in organ culture for 10 days. Epithelium shows typical structure of the respiratory epithelium. BC, basal cell; BL, basal lamina; MC, mucous cell; MV, microvilli; JC, junctional complexes. *Bar*=1 μm. × 5,000

Figure 3.—Basal cell of NH trachea cultured for 10 days. *Note* characteristics of an undifferentiated cell such as scant RER. BL, basal lamina. *Bar*=1 μm. × 20,000

Figure 4.—Tracheal epithelium of DH cultured for 3 days. *Note* the continuous row of basal cells and overlying layer of PAS-positive cells. *Arrow* indicates cells with squamous morphology that appear to extrude from the basal layer. AB–PAS. × 300

Figure 5.—A patch of squamous metaplasia during early stages of development. Epithelium consists of a basal layer of large, round cells, 2–3 layers of squamous cells, and an overlying layer of PAS-positive cells. *Arrow* indicates PAS-positive cells as they are pushed out by underlying cells producing a dome-shaped structure. AB–PAS. × 300

Figure 6.—An area of squamous metaplasia showing exfoliation of the outer PAS-positive layer of cells caused by active proliferation and squamoid differentiation of underlying epithelial cell population. AB–PAS. × 300

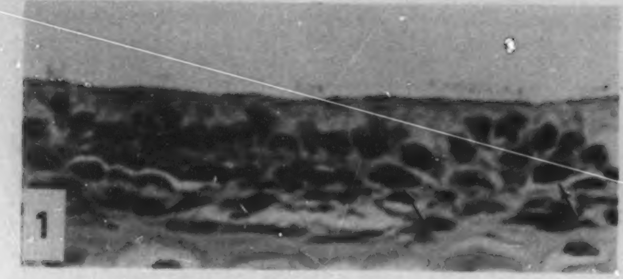
1

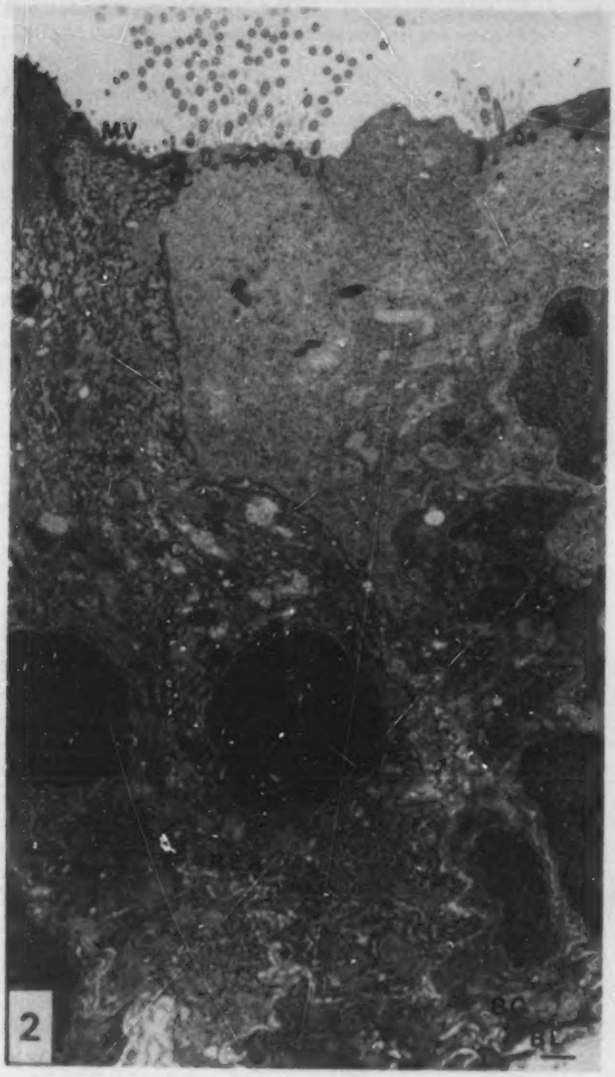
2

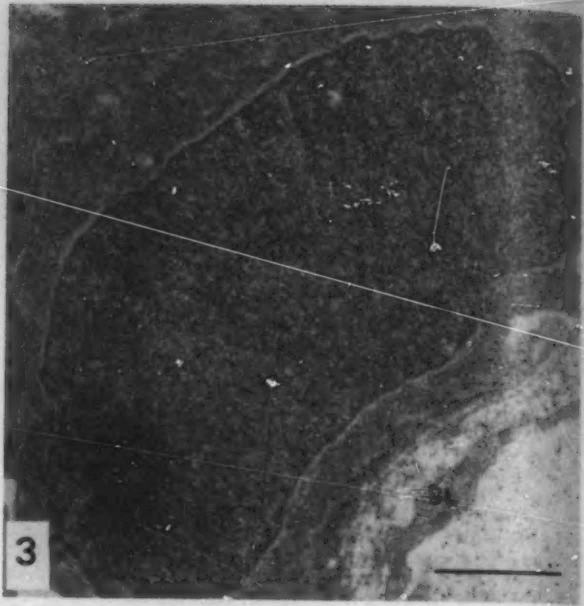
3

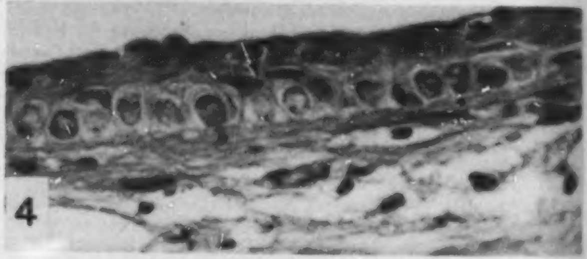
4

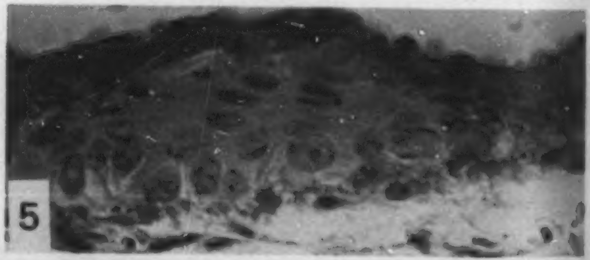
5

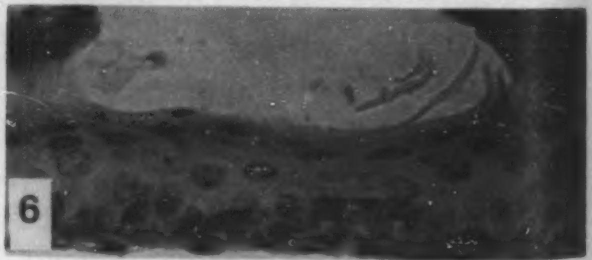
6

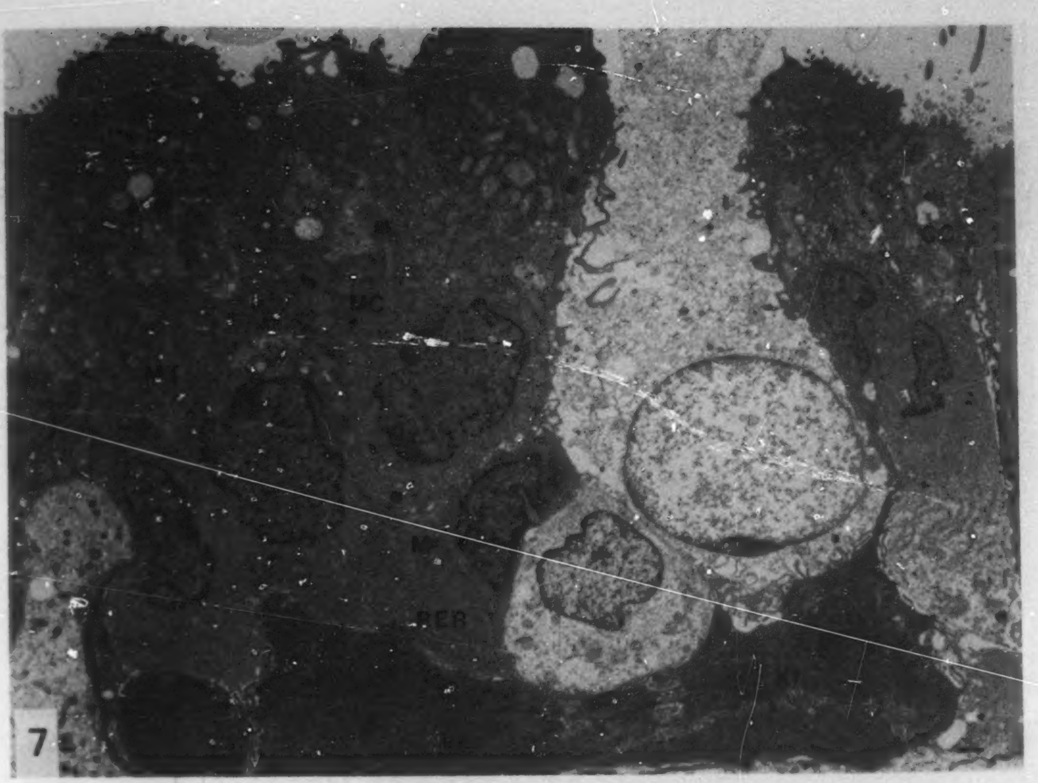

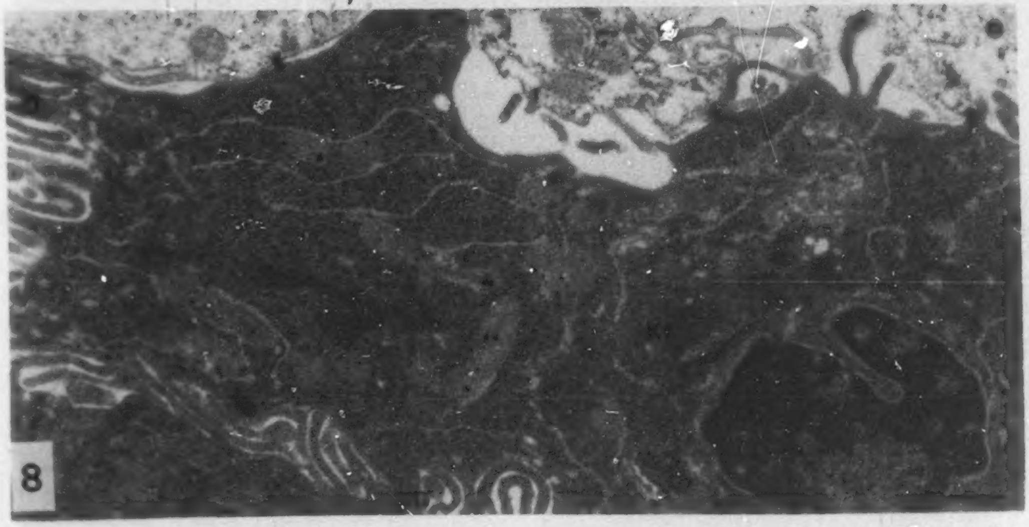

FIGURE 7.—DH trachea cultured for 3 days. Mucous and ciliated cells show normal ultrastructural features. Basal cells are electron-dense and contain bundles of keratin filament and abundant free ribosomes. Numerous interdigitating cytoplasmic processes are present between basal cells. Degenerating cells are seen overlying the metaplastic basal cells. MC, mucous cells; CC, ciliated cell; BC, basal cell; MT, mitochondria; M, mucous droplets; Kf, keratin filaments. *Bar*=1 µm. × 3,300

FIGURE 8.—Basal cells shown in fig, 7. They contain bundles of keratin filaments. *Note* extensive network of cytoplasmic processes between basal cells. Desomosomes are prominent. Kf, keratin filaments; D, desomosomes. *Bar*=1 µm. × 9,400

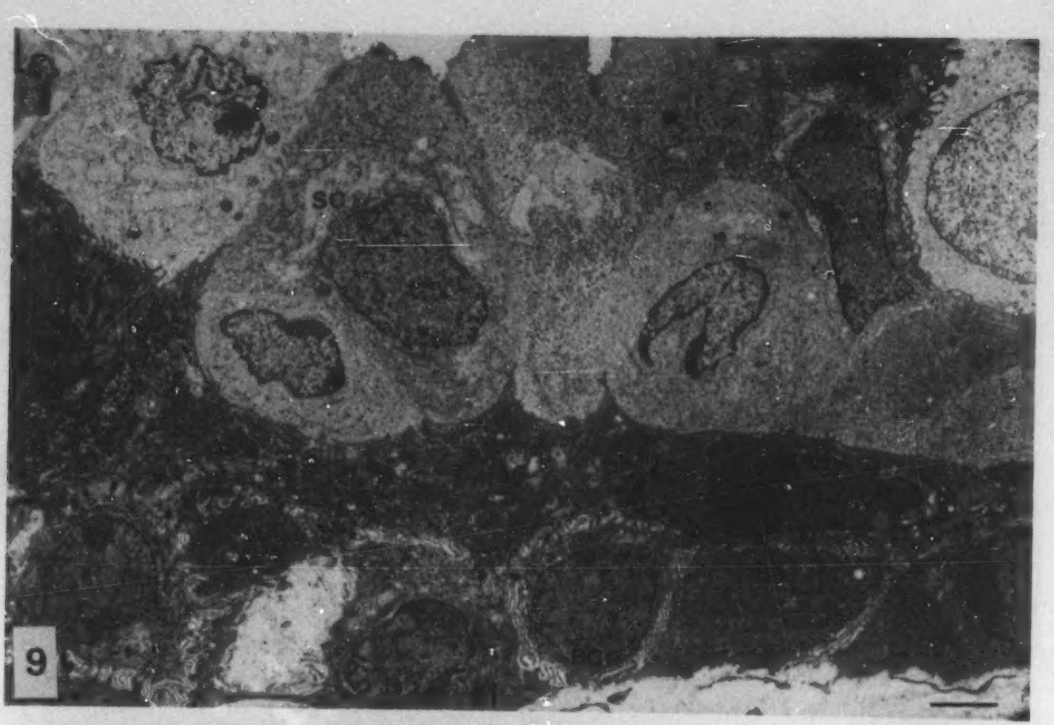

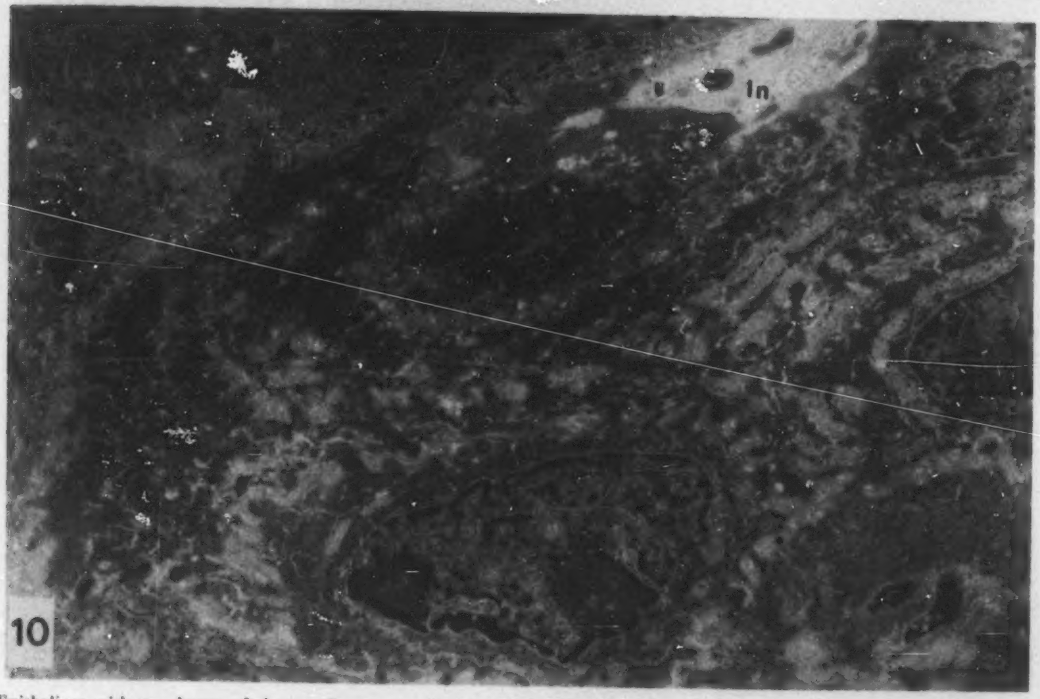

FIGURE 9.—Epithelium with two layers of electron-dense metaplastic epidermoid cells and an overlying layer of secretory cells. Metaplastic cells are distinctly different from the secretory cells in ultrastructure and staining properties. BC, basal cell; SC, secretory cell; Kf, keratin filament. *Bar*=1 µm. × 10,000

FIGURE 10.—An advancing edge of metaplastic lesion shown to be displacing the overlying electron-lucent mucous cell. Large intercellular spaces are seen at the boundary of metaplastic and nonmetaplastic cells. In, intercellular space. *Bar*=1 µm. × 7,300

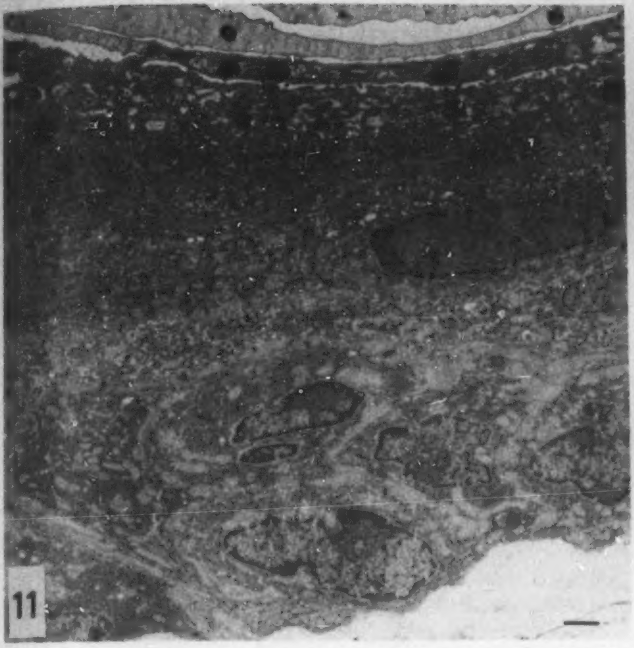

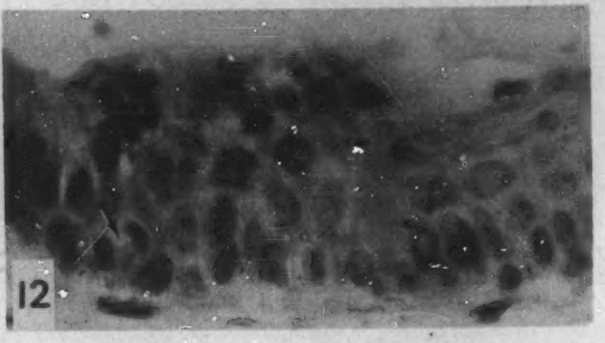

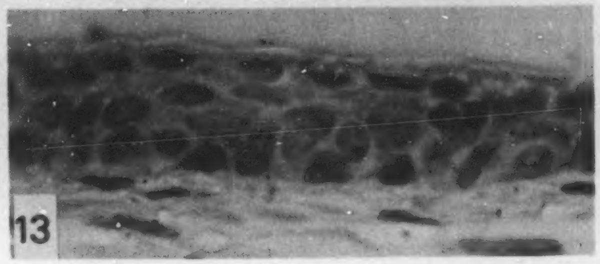

FIGURE 11.—Cornified epithelium. Explant from DH trachea cultured for 10 days. kg, keratohyaline granules. *Bar*=1 μm. × 5,300

FIGURE 12.—Autoradiograph showing cohort of labeled cells at the edge of a squamoid lesion. *Arrow* indicates a dividing cell also present. Photograph is focused on the silver grains in the overlying emulsion so that the tissue is slightly out of focus. PAS-hematoxylin. × 1,500

FIGURE 13.—Autoradiograph showing extensive [^{3}H]dThd incorporation in the basal cell layer during early stages of the development of squamous metaplasia. PAS-hematoxylin. × 1,500

blank page

Primordial Germ Cell Proliferation in Fetal Testes in Mouse Strains With High and Low Incidences of Congenital Testicular Teratomas[1,2,3]

Takehiko Noguchi[4,5] *and* **Leroy C. Stevens**[6,7]

ABSTRACT—The development of genital ridges in mouse strains was compared with high and low susceptibility to teratocarcinogenesis. The number of dividing primordial germ cells (PGC) was low at 12 days of gestation. The number increased sharply at 13 days and decreased precipitously by 15 days of gestation. The period of high mitotic activity closely paralleled the period of susceptibility to experimentally induced teratocarcinogenesis. Testes that had a long proliferative period had a higher incidence of teratomas than those that had a short proliferative period. A group of fetuses was identified that had markedly fewer than normal PGC. The incidence of teratomas in this group was very high, and nearly all growths were bilateral.—JNCI 1982; 69:907–913.

Spontaneous testicular teratomas are common only in inbred strain 129 mice and in congenic and recombinant inbred strains derived from it (*1–5*). The incidence is high in strain 129/Sv-*ter* (*4*) and low in strains 129 (*2*) and A^y.

Testicular teratomas are derived from PGC (*6*) that begin to develop as a result of a process akin to parthenogenesis within the seminiferous tubules of fetuses of about 12 days of gestation (*7*). The earliest recognizable foci were observed in 15-day fetuses for strain 129 and in 16-day fetuses for strain 129/Sv-*ter*. It seems likely that the initiation of teratocarcinogenesis occurs about 2 or 3 days earlier. PGC can first be observed at the base of the allantois at 8.5 days of gestation (*8*). PGC proliferate at a high rate during migration to the genital ridge (*9*) and for a short time after arrival on about the 12th day of gestation. After that, PGC enter a mitotically quiescent stage (*10*).

Several genetic and environmental factors influence susceptibility to teratocarcinogenesis (*2, 3, 5*). In strain 129 (*2*) there are twice as many teratomas in the left testis as in the right one. Bilateral teratomas are rare. Teratomas are also twice as frequent in the left testes (13%) as in the right one (7%) in strain 129/Sv-*ter*; however, they occur bilaterally (12%) as frequently as in the left testes (*4*). If teratocarcinogenesis in the left testis is independent of that in the right one, then the frequency of bilateral tumors should be the product of the frequencies of unilaterality: $0.13 \times 0.07 = 0.0091$ or 0.9%. A partial explanation for the unexpected high incidence of bilateral teratomas in 129/Sv-*ter* is presented here.

Testicular teratomas can be experimentally induced in some strains of mice by grafting of male genital ridges into the testes of adults (*11, 12*). The grafted genital ridges develop into testes, and teratomas were observed in most of them 5–6 days after grafting. The age of the genital ridge is crucial (*13*). For strain 129, when 11- or 12-day genital ridges were grafted, about 80% of them developed into testes with teratomas; with 13-day genital ridges 16% developed teratomas, and with 14-day ridges 8% developed them. For 129/Sv-*ter*, about 85% of grafted 11- and 12-day genital ridges developed into testes with teratomas. The incidence dropped to 61% for 13-day genital ridges and to 0.0% for 14-day ridges (*4*).

We compared the development of genital ridges in strains with high and low susceptibility to teratocarcinogenesis. We found that, in general, the absolute number of dividing PGC in a testis was low at 12 days of gestation, but shortly thereafter the number increased sharply. The number peaked at 13 days and decreased precipitously by 15 days of gestation. The mitotic activity of PGC, as revealed by MI, closely paralleled the susceptibility to experimental teratocarcinogenesis. We also found that low numbers of PGC and a prolonged proliferative period correlated well with a high incidence of spontaneous testicular teratomas.

MATERIALS AND METHODS

Mice.—Strain 129/Sv-*ter* males have a higher incidence of spontaneous teratomas (33%) than any other strain (*4*). Even though this subline has been inbred for more than 30 generations of brother×sister matings, some matings produce offspring with fewer teratomas (10%) than others. All descendants of these matings retain the low incidence and will be referred to as the "Lo-line." Families with a high incidence (33%) will be referred to as "Hi-line." To maintain the incidence of 33% in the 129/Sv-*ter* colony, it is necessary to select for Hi-line families.

Three percent of strain 129 and 0.7% of strain A^y males had teratomas. The A^y colony was maintained by $A^y/+ \times +/+$ matings.

Determination of developmental stage of fetuses.—To detect

ABBREVIATIONS USED: A^y=129/Sv-A^yCP with <1% teratomas; Hi-line=strain 129/Sv-*ter* with ≈33% teratomas; Lo-line=strain 129/Sv-*ter* with ≈10% teratomas; MI=mitotic index (indices); PGC=primordial germ cell(s); 129=129/Sv with 3% teratomas.

---

[1] Received October 27, 1981; revised April 28, 1982; accepted May 6, 1982.

[2] Supported in part by Public Health Service grant CA-02662 from the National Cancer Institute and in part by Grants-in-Aid for Special Project Research and for Cancer Research from the Ministry of Education, Science and Culture, Japan.

[3] Animals were maintained under the guidelines set forth by The Jackson Laboratory, Bar Harbor, Maine.

[4] National Institute of Genetics, Mishima, Schizuoka-ken 411 Japan.

[5] Recipient of a fellowship spent at The Jackson Laboratory from the Science and Technology Agency of Japan.

[6] The Jackson Laboratory, Bar Harbor, Maine 04609.

[7] We thank Mr. D. S. Varnum, Mrs. S. Murphy, Mrs. Y. T. Wada, and Mrs. Yoneyama for their excellent technical assistance.

differences in mitotic activity in PGC between fetuses in strains with high and low incidences of teratomas, we had to determine their developmental stage more precisely than by the number of days of gestation. In addition to gestational days, we used the maximum length of the head as a criterion of developmental stage. Head length was measured as shown in text-figure 1 with a micrometer accurate to 0.01 mm. Two stainless steel microsyringe needles were glued parallel to the beaks of the micrometer. Text-figure 2 shows the relationship between head length and days of gestation. A head length of 4.0 mm corresponded to early (12 days) gestation. The head length increased by 1 mm/day of gestation thereafter.

Dissection of specimens.—After dislocation of cervical vertebrae of pregnant females, fetuses were dissected from the uterus, washed with Hanks' balanced salt solution that contained 1% glucose, and transferred to a petri dish with Hanks' solution. Fetuses were secured ventral side up by insect pins on a paraffin bed stained with Sudan black. The gonads were removed with watchmakers forceps. The sex of the gonad could be identified in fetuses with head lengths of 4.5 mm and longer.

Histology.—Gonads were fixed in Vandegrift's solution, embedded in paraffin, serially sectioned at 7 µm, and stained with hematoxylin and eosin.

Identification of PGC.—The criteria adopted for the discrimination of PGC from supporting cells in the seminiferous tubules were similar to those described for the rat by Clermont and Perey (*14*). Dividing PGC could easily be discriminated from supporting cells at the head length stage of 4.5 mm. Identification of nondividing PGC and supporting cells was more difficult in fetuses at stages of up to 5.5-mm head length. In fetuses of 6.5-mm head length and larger, however, most of the supporting cells were located near the periphery of the seminiferous tubules and identification was easy. Nondividing PGC were larger than most of the supporting cells and had lightly stained spherical nuclei with two nucleoli or more. The supporting cells had darkly stained oval or coffee bean-shaped nuclei and most were smaller than those of PGC.

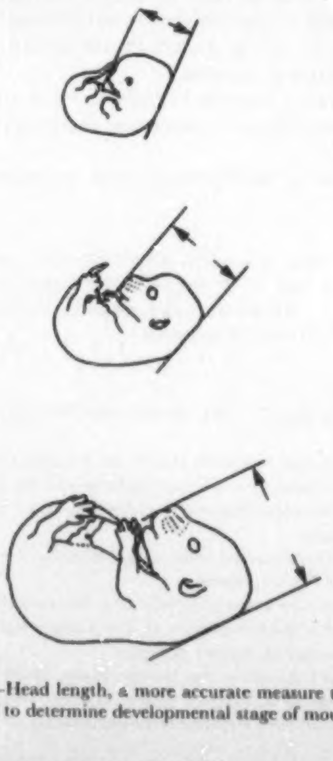

TEXT-FIGURE 1.—Head length, a more accurate measure than gestational days, was used to determine developmental stage of mouse fetuses.

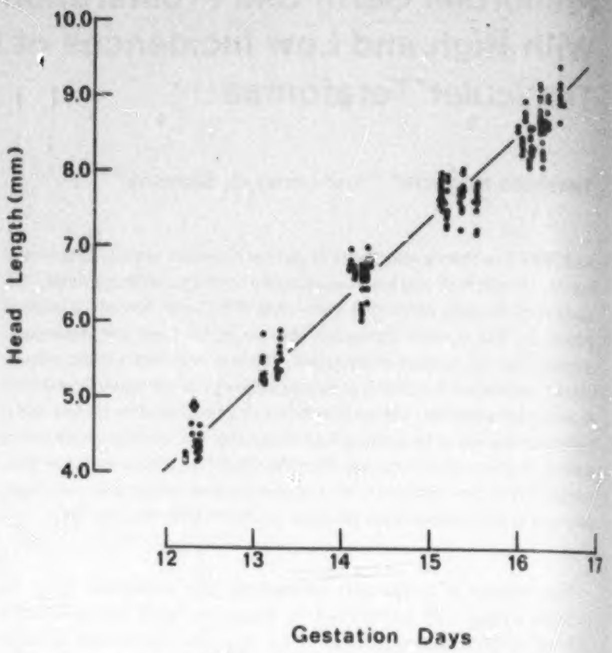

TEXT-FIGURE 2.—Relationship between head length and days of gestation.

Sl^J/Sl^J fetuses have very few or no PGC (*15*); they were used as reference to help identify supporting cells.

Determination of proliferative activity of PGC.—The proliferative activity of PGC was determined by two methods: 1) by counting the number of PGC in every other histologic section of each testis and 2) by the MI (dividing cells:dividing plus nondividing cells).

In some fetuses the seminiferous tubules in both testes were very sparsely populated with PGC. There were only about 200 PGC determined by counting in each or in every other section. When testes appeared normal, the number of PGC estimated were 800–3,500 by counting in every four to six sections. Cells were counted by slides being projected onto a high-resolution glass screen.

In fetuses with head lengths greater than 7 mm, the number of dividing PGC was so small and the total number of PGC was so large (30,000–50,000) that the MI could not be precisely determined.

RESULTS

Developmental Change in the Proliferative Activity of PGC

The dividing PGC in serial sections of 547 testes were counted in fetuses with head lengths ranging from 4.2 to 9.0

mm. Text-figure 3 shows the pattern of PGC proliferation in 111 testes in A^y fetuses. There was a sharp increase in the number of dividing PGC in testes of fetuses from 4- to 6-mm head length. The number of dividing PGC peaked between 5.0 and 6.0 mm of head length and then decreased precipitously. Most PGC became mitotically quiescent at the head length stage of about 7 mm.

Text-figure 4 shows the proliferative pattern of 142 testes of Lo-line fetuses. The pattern was approximately the same as for the A^y except that the peak at 5.0–6.0 mm appeared lower.

Text-figure 5 shows the proliferative pattern of PGC in 294 testes of Hi-line fetuses. The counts were more broadly scattered than those for the A^y and Lo-line fetuses.

At the peak of mitotic activity (5.0- to 6.0-mm head length), the average number of dividing PGC was highest in A^y testes (381), intermediate in Lo-line testes (267), and lowest in Hi-line testes (196) (table 1). The differences between A^y and Lo-line and between A^y and Hi-line were significant ($P<0.001$) as well as the difference between Lo-line and Hi-line ($P<0.005$), as determined by Student's t-test.

The pattern of change in MI in 160 developing Hi-line testes was compared with 55 A^y and 48 Lo-line testes (text-fig. 6). The rate of decline in MI was similar in A^y and Lo-

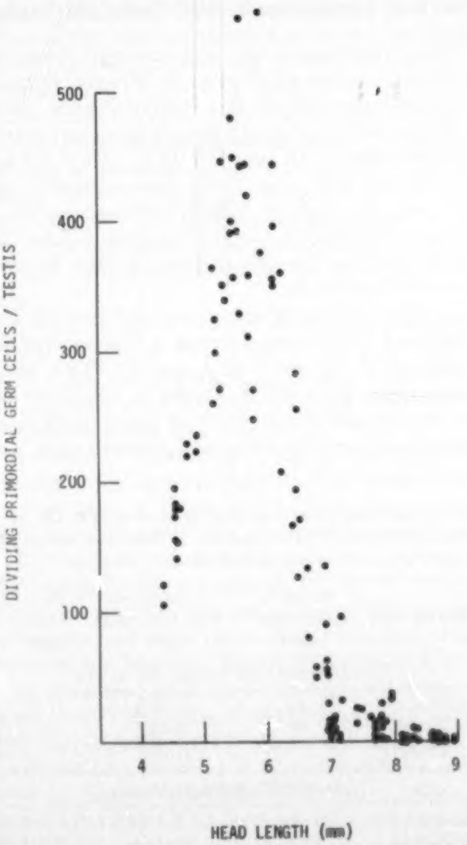

TEXT-FIGURE 3.—Pattern of PGC proliferation in testes of fetuses of strain A^y.

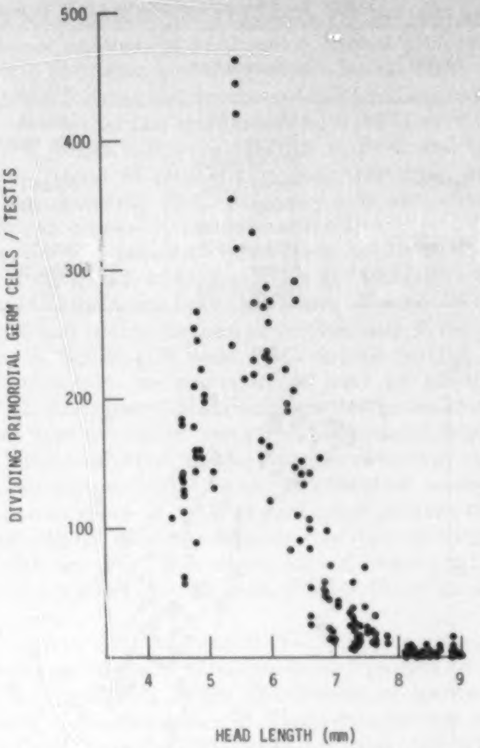

TEXT-FIGURE 4.—Proliferative pattern of PGC in testes in Lo-line fetuses.

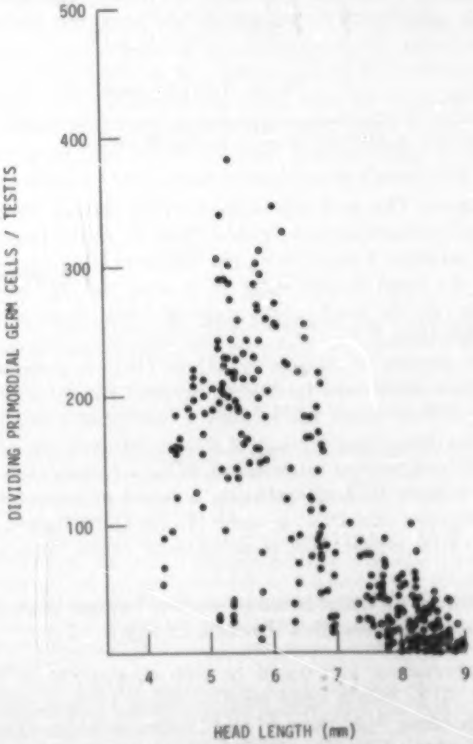

TEXT-FIGURE 5.—Proliferative pattern of PGC in testes of Hi-line fetuses.

TABLE 1.—*Numbers of dividing PGC in testes of mouse fetuses with increasing head length in the 129 sublines*

Strain	Parameters	No. of dividing PGC in testes of mouse fetuses with head length, mm:				
		4.0–5.0	5.0–6.0	6.0–7.0	7.0–8.0	8.0–9.0
A^y	Mean ± SD	183±44	381±96	177±127	21±20	1.9±3.4
	Range	106–234	212–628	16–446	2–98	0–12
	No. of testes	10	28	23	22	20
Lo-line	Mean ± SD	161±54	267±91	121±82	23±15	4.1±4.0
	Range	58–268	130–462	20–296	6–68	0–16
	No. of testes	25	23	38	30	28
Hi-line	Mean ± SD	156±51	196±81	129±84	32±25	17.7±17.5
	Range	48–222	10–384	20–348	0–88	0–100
	No. of testes	26	72	53	23	96

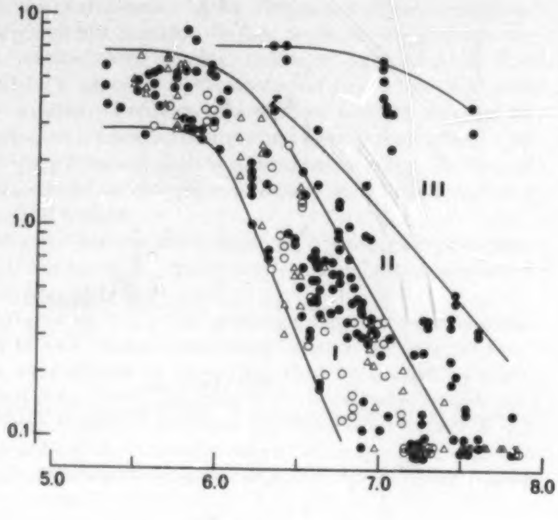

TEXT-FIGURE 6.—Developmental change in MI of PGC in fetal testes of A^y, Lo-line, and Hi-line. △, A^y; ○, Lo-line; ●, Hi-line.

line testes. The area where most of the values fell is schematically shown in text-figure 6 (zone I). In the head length stage between 5 and 6 mm, the MI were high (3–6%), and after the head length stage of 6 mm, the MI decreased sharply. At the head length stage of 7 mm, most of the MI were less than 0.5%.

The pattern of change in MI in Hi-line testes differed from that in A^y and Lo-line testes (text-fig. 6). The MI of many Hi-line testes fell in zone I, but others were higher after the head length stage of 6 mm. Most of the testes in zone II had normal numbers of PGC, whereas most of the testes in zone III had markedly reduced numbers of PGC. This suggests that PGC in some Hi-line testes have a longer proliferative period than those in testes of the other strains.

Incidences of Teratomas in Hi-line Testes With Short and Long Proliferative Periods of PGC

Teratomatous foci could be first recgonized in 16-day fetuses (8- to 9-mm head length). Some Hi-line testes had more dividing PGC than A^y and Lo-line as late as this stage. The number of dividing PGC in A^y testes ranged from 0 to 12 (average=1.9; SD=3.4), in Lo-line testes from 0 to 16 (average=4.1; SD=4.0), and in Hi-line from 0 to 100 (average=17.7; SD=17).

Hi-line testes with teratomatous foci tended to have more dividing PGC than those without foci. For example, 7% (3/41) of testes with 0–9 dividing cells had teratomatous foci; 17% (6/35) of testes with 10–29 dividing cells had teratomas, and 60% (12/20) of those with 30–100 dividing cells had teratomas. These figures indicate that testes with prolonged proliferative periods had a much higher incidence of tumors than those with shorter proliferative periods.

Incidence of Teratomas in PGC-Deficient Testes

A striking observation was independently made both at the National Institute of Genetics in Misima, Japan, and at The Jackson Laboratory in Bar Harbor, Maine. About 12% of the Hi-line fetuses of 16–18 days of gestation examined in Misima had testes with very few PGC. All of these fetuses had teratomas, and most (5/6) were bilateral (table 2). Fourteen percent of strain 129/Sv-*ter* fetuses at 16–18 days of gestation examined in Bar Harbor were deficient in PGC, and all of them had teratomas. Most of these fetuses (8/10) had bilateral teratomas.

Only strain 129/Sv-*ter* testes were deficient in PGC. No PGC-deficient testes were observed in 419 testes of fetuses of other sublines of 129 and in 80 testes of 129×A/HeF$_1$ mice.

In some cases, germ cell deficiency in 129/Sv-*ter* persisted at least until weaning age. Parts of testes of 16 males with bilateral teratomas were examined histologically, and both

TABLE 2.—*Incidence and laterality of teratomas in Hi-line fetuses with testes with normal numbers of PGC and with PGC-deficient testes*

Location of expt	No. of fetuses examined	No. of fetuses with teratomas (%)	No. of fetuses with bilateral teratomas (%)
No. of fetuses with normal No. of PGC			
Mishima	44	13 (30)	6 (14)
Bar Harbor	60	18 (30)	3 (5)
Total		31 (30)	9 (9)
No. of PGC-deficient fetuses			
Mishima	6	6 (100)	5 (83)
Bar Harbor	10	10 (100)	8 (80)
Total		16 (100)	13 (81)

testes in 10 were found to be germ cell-deficient. PGC-deficient testes in weaning age males were always affected bilaterally, whereas their littermates usually had normal numbers of PGC. Photomicrographs of PGC-deficient and normal testes are shown in figure 1.

DISCUSSION

The proliferative activity of PGC was determined in 3 groups of inbred mice derived from strain 129, that differed in susceptibility to testicular teratocarcinogenesis. About 0.07% of the males in one group, designated A^y, had teratomas. Ten percent of the Lo-line and 33% of the Hi-line mice had teratomas. The mitotic activity remained high until late (13th-day) gestation and decreased precipitously therafter. By day 15 or 16 the PGC in most testes were mitotically quiescent.

This decline in mitotic activity paralleled exactly the decline with age in susceptibility to experimentally induced teratocarcinogenesis. When male genital ridges from strain 129 fetuses of 12.5 days of gestation were grafted to adult testes, about 80% of them developed into testes with teratomas (*12*). When genital ridges from 13.5- to 14.5-day fetuses were grafted to adult testes, the incidence of teratomas in testes that developed from the grafts declined to about 15 and 8%, respectively (the incidence of spontaneous teratomas in this strain) (*13*). Apparently, as the PGC cease to proliferate, they lose susceptibility to teratocarcinogenesis.

The PGC in the Hi-line mice proliferated for a longer period than in the groups with lower incidences of teratomas. A significant fraction of the PGC in the testes of many of these mice continued to proliferate even through the 15th and 16th day of gestation, whereas nearly all of the PGC in the testes of the two strains with lower incidences of teratomas had stopped proliferation by the end of the 14th day of gestation. The extension of the proliferative period in the Hi-line PGC correlated well with the higher incidence of teratomas.

Compared to A^y, the extension of the proliferative period of the PGC in Hi-line fetuses became apparent from the 14th to 16th days of gestation (6- to 8-mm head lengths). Another phenomenon that correlated with high incidence of teratocarcinogenesis was observed in fetuses at the 13th day of gestation (5.5-mm head length) when proliferation was at its peak. The testes of some Hi-line fetuses had fewer dividing PGC than A^y testes. These Hi-line fetuses included both PGC-deficient testes and testes with normal numbers of PGC. Perhaps the period of high proliferation began later and lasted longer in Hi-line testes.

Independent observations on the correlation between PGC deficiency and high incidence of bilateral teratomas were made at the National Institute of Genetics in Japan and at The Jackson Laboratory in the United States. Serial sections of testes of 70 fetuses of 16–19 days of gestation were examined histologically at The Jackson Laboratory. Of 60 fetuses with normal numbers of PGC, 18 (30%) had teratomas (table 1). Fifteen teratomas (25%) were unilateral and 3 (5%) were bilateral. Of 10 fetuses with markedly reduced numbers of PGC, all had teratomas, 2 were unilateral, and 8 bilateral. In all cases, the deficiency in PGC was bilateral. MI were not determined.

At the National Institute of Genetics, 4 of 29 (14%) fetuses with normal numbers of PGC and a normal proliferative period had teratomas and none were bilateral. Nine of 15 (60%) fetuses with normal numbers of PGC and a prolonged proliferative period had teratomas, and 6 (40%) were bilateral. All 6 fetuses that were deficient in PGC and had a prolonged period of proliferation had teratomas, and 5 (83%) were bilateral. PGC deficiency was also observed bilaterally in ovaries of some Hi-line females.

These are four possible explanations for the PGC deficiency in the gonads of Hi-line mice: 1) PGC fail to form; 2) some PGC form, but fail to proliferate; 3) some PGC are abnormal and cannot migrate or survive; and 4) the environment is hostile and some PGC do not survive. It is possible that PGC are damaged and most are killed, but some PGC that survive the damaging influence are changed in a way that transforms them into embryonal carcinoma cells. That this might be the case is suggested by the response of PGC to transplantation in the experimental production of teratomas. When 12.5-day genital ridges of some strains are grafted to the testes of adults, most of them develop into testes with few PGC and many foci of teratomas. They appear histologically similar to the PGC-deficient gonads of Hi-line mice.

This high correlation between PGC-deficient testes and a high incidence of bilateral teratomas may partially explain an unusual laterality in the distribution of spontaneous teratomas in Hi-line mice (*4*). Thirty-two percent of the males of this strain had teratomas. Of these, 13% were in the left testis, 7% in the right, and 12% were bilateral. If teratocarcinogenesis in the right testis was independent from that in the left, then the frequency of bilaterality should have been the product of the frequencies of unilaterality. This product, 0.9%, is far below the 12.5% observed for bilaterality. Our observations show that for PGC-deficient testes, teratocarcinogenesis in the right testis is not independent from that in the left one. Susceptibility to teratocarcinogenesis in both testes is highly correlated with PGC deficiency.

REFERENCES

(1) Stevens LC, Little CC. Spontaneous testicular teratomas in an inbred strain of mice. Proc Natl Acad Sci USA 1954; 40:1080–1087.

(*2*) Stevens LC, Mackensen JA. Genetic and environmental influences on teratocarcinogenesis in mice. J Natl Cancer Inst 1961; 27:443–453.

(*3*) Stevens LC. The biology of teratomas. Adv Morphol 1967; 6:1–31.

(*4*) ———. A new inbred subline of mice (129/*ter*-Sv) with a high incidence of spontaneous congenital testicular teratomas. J Natl Cancer Inst 1973; 50:235–242.

(*5*) ———. Developmental biology of teratomas in mice. In: McMahon D, Fox FC, eds. ICN-UCLA symposia on molecular and cellular biology. Vol 2. London and Sydney: Benjamin, 1975:186–204.

(*6*) ———. Origin of testicular teratomas from primordial germ cells in mice. J Natl Cancer Inst 1967; 38:549–552.

(*7*) ———. Testicular teratomas in fetal mice. J Natl Cancer Inst 1962; 28:247–267.

(*8*) Chiquoine AD. The identification, origin and migration of the primordial germ cells in the mouse embryo. Anat Rec 1954; 118:135–146.

(*9*) Mintz B, Russell ES. Gene-induced embryological modifications of primordial germ cells in the mouse. J Exp Zool 1957; 124:207–237.

(10) PETERS H. Intrauterine gonadal development. Fertil Steril 1976; 27:493–500.

(11) STEVENS LC. Experimental production of testicular teratomas in mice. Proc Natl Acad Sci USA 1964; 52:654–661.

(12) ———. Experimental production of testicular teratomas in mice of strain 129, A/He and their F_1 hybrids. J Natl Cancer Inst 1970; 44:923–929.

(13) ———. Development of resistance to teratocarcinogenesis by primordial germ cells in mice. J Natl Cancer Inst 1966; 37:859–867.

(14) CLERMONT Y, PEREY B. Quantitative study of the cell population of the seminiferous tubules in immature rats. Am J Anat 1957; 100:241–267.

(15) BENNETT D. Developmental analysis of a mutation with pleiotropic effects in the mouse. J Morphol 1956; 98:199–233.

FIGURE 1.—A) PGC-deficient testis in Hi-line mouse fetus with 6.8-mm head length. 1B) Normal testis in Hi-line littermate with 6.9-mm head length

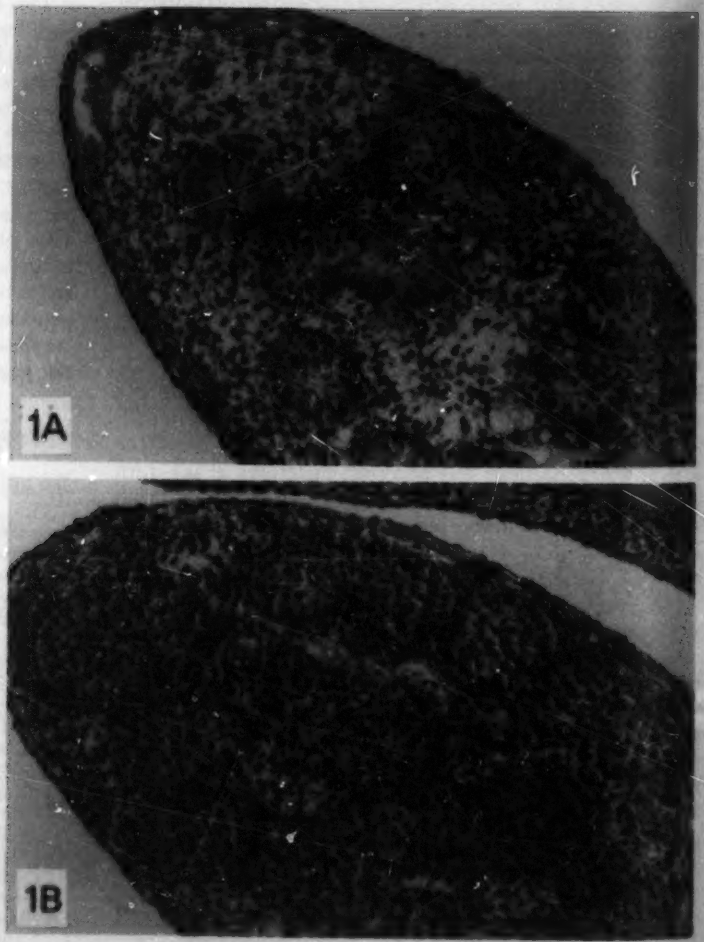

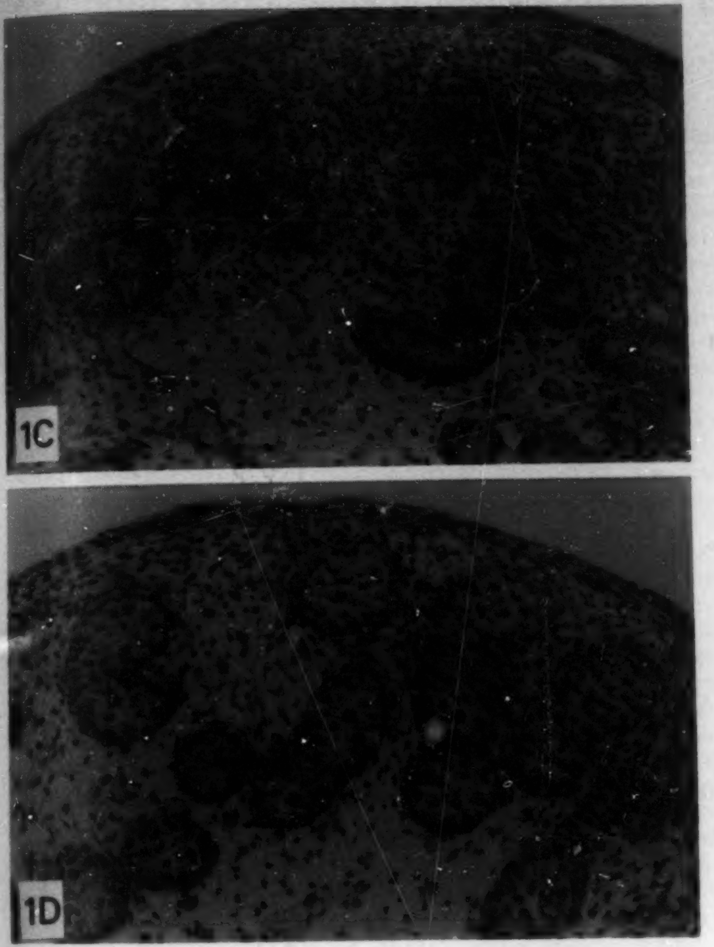

FIGURE 1—C) PGC-deficient testis in mouse fetus with 10.5-mm head length; *arrows* indicate 2 teratomatous foci. 1D) Normal testis in littermate of C with 10.9-mm head length.

blank page

Epizootic Neoplasms in Fishes From a Lake Polluted by Copper Mining Wastes[1,2]

John J. Black,[3] Elwin D. Evans,[4] John C. Harshbarger,[5] *and* **Robert F. Zeigel[6,7]**

ABSTRACT—Examination of fishes from Torch Lake, Houghton County, Mich., revealed epizootic neoplasms of several types in two closely related species. Saugers, *Stizostedion canadense*, and walleyes, *Stizostedion vitreum*, were commonly affected with hepatocellular carcinomas, dermal ossifying fibromas, and perivisceral masses resembling mesotheliomas that were usually associated with the mesenteric capsule of the spleen. Saugers were 100% affected with liver neoplasms. Histopathologic and ultrastructural aspects of the neoplasms are described. Torch Lake has been used as a repository for copper mining waste to the extent that an estimated 20% of the original lake volume has been filled in by these materials. Several direct and indirect etiologic roles for the mine waste as causative agents of the fish tumors are discussed.—JNCI 1982; 69:915–926.

Torch Lake is a large, deep lake (surface area, 1077 ha; mean depth, 17 m; maximum depth, 35 m) located near the middle of the Keweenaw Peninsula of Michigan in Houghton County (Lat 40° N, Long 88° W) and is a tributary to Portage Lake and thus to Lake Superior (*see* text-fig. 1). The watershed is about 300 km^2 and mostly covered with second-growth hardwoods. Soils are predominantly spodosals, with agriculture limited to a few dairy and potato farms.

Copper associated with ancient metamorphic and igneous bedrocks of this region once supported a major copper mining industry. Since the turn of the century, copper ore extracted from mines northeast of Torch Lake was crushed at mills along the lake's shoreline. The almost pure native copper was separated from the ore, processed, and shipped by rail or barge. Tailings were dumped into the lake near the mills. Finer tailings were dispersed by currents throughout Torch Lake and into much of Portage Lake. During the latter part of this mining period, as it became profitable, the tailings or coarse stampsands that settled near the shore were dredged from the lake, ground to a powder, and leached with cupric ammonium carbonate to remove additional copper. The remaining very fine tailings were again discharged into Torch Lake.

At least 20% of the original volume of Torch Lake has been filled with copper tailings. In addition to the discharge of tailings, mine water pumpage and raw municipal sewage were discharged into the lake for years. Chloride concentrations in tributary streams receiving mine water has been as high as 5,000 mg/liter, with lake concentrations exceeding 200 mg/liter before mine dewatering ceased.

Municipal sewage from the small communities along the lake is now collected and treated in lagoons and spray irrigated on grass established on mine tailings. Water quality in Torch Lake has improved since mining ceased and municipal sewage receives better treatment. The water has changed from turbid reddish-brown to a clear brown, with a concurrent increase in transparency (secchi disk, ≈3.0 m). The lake presently has soft water and low concentrations of dissolved substances. Nutrients are not sufficient to result in depletion of hypolimnetic oxygen. An orthograde dissolved oxygen curve exists, and the lake would be considered oligotrophic. Average total phosphorous concentrations are about 0.02 mg/liter. Nitrate nitrogen concentrations range from 0.2 to 0.4 mg/liter, and they increase with water depth. Chlorophyll a concentrations are generally less than 3.0 µg/liter.

Cadmium, nickel, and lead in the water column are at or near the levels of detectability. Zinc ranges from 5.0 to 25.0 µg/liter. Copper is markedly elevated over Lake Superior average concentrations of 3.4 µg/liter. Total copper ranges from 30 to 45 µg/liter, with higher concentrations near the lake bottom.

Copper concentrations as high as 910 µg/liter were found in an embayment that received a large but unknown amount of cupric ammonium carbonate during the fall of 1971 and the early summer of 1972 (*1*). Although copper concentrations remain high in Torch Lake at the present time, obvious lethal conditions are not apparent. Dissolved humic substances—as indicated by water color and total organic carbon concentrations—moderate alkalinity, and circumneutral pH's may contribute to the formation of copper complexes that greatly alter copper toxicity.

Sediments in Torch Lake and Portage Lake are largely composed of extremely fine, reddish, clay-like tailings covered with a dark-brown compacted layer of organic material approximately 4 cm thick. In 1970, a flocculent, light-brown ooze covered the reddish tailings (*2*). Copper concentrations in this upper dark-brown layer range from 1,700 to 2,400 mg/liter dry weight. Lower concentrations, found beneath the upper layer, range from 300 to 1,700 mg/kg. Lead (80–270 mg/kg) and zinc (≤180 mg/kg) in the upper dark-

---

ABBREVIATIONS USED: H & E=hematoxylin and eosin; MDNR=Michigan Department of Natural Resources.

---

[1] Received November 5, 1981; accepted March 24, 1982.

[2] Supported in part by grant PFR78-22625 from the National Science Foundation and by Public Health Service contract N01CP-33874 from the Division of Cancer Cause and Prevention, National Cancer Institute.

[3] Department of Experimental Biology, Roswell Park Memorial Institute, 666 Elm St., Buffalo, N.Y. 14263.

[4] Michigan Department of Natural Resources (MDNR), Steven T. Mason Building, Lansing, Mich. 48926.

[5] Registry of Tumors in Lower Animals, Museum of Natural History, The Smithsonian Institution, Washington, D.C. 20560.

[6] Department of Experimental Pathology, Roswell Park Memorial Institute.

[7] We acknowledge the capable assistance of Ms. P. Black and Mr. J. Dinchuk. We are indebted to Ms. Ruth Weaver for histologic specimen preparation and to Mr. Ray Juetten, Fisheries Division, MDNR, for sample collection.

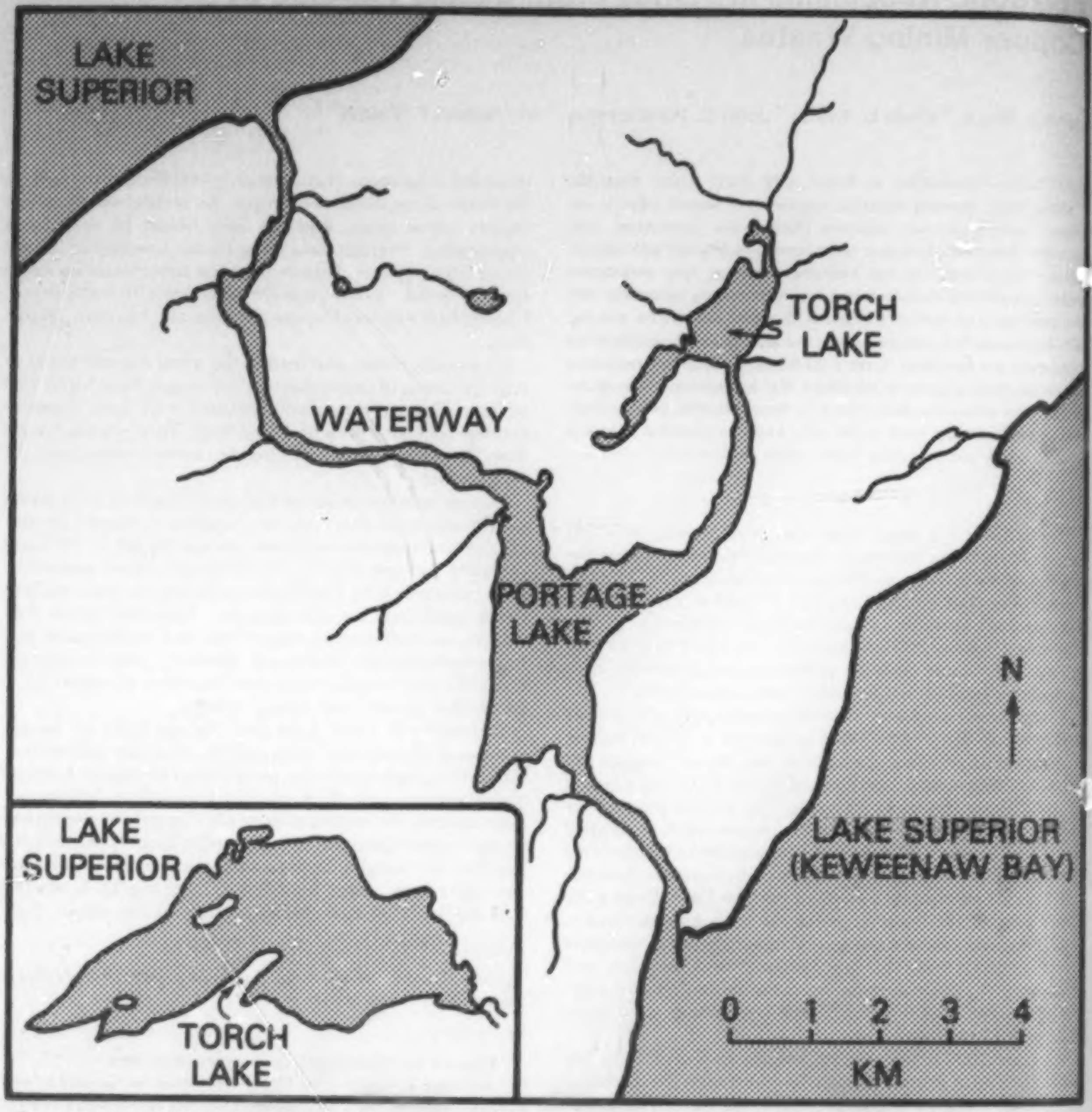

Text-figure 1.—Outline map of the Keweenaw Waterway. *Inset* locates Keweenaw Peninsula jutting into Lake Superior from the southcentral shore.

brown layer follow a similar pattern to that of copper in their distribution in sediments. Chromium (30–40 mg/kg) and nickel (90–120 mg/kg) had higher concentrations in the reddish clay-like layer. Cadmium was less than 2 mg/kg sediments. Apparently, copper, lead, and zinc still are entering this aquatic ecosystem, being bound by biota or particulate materials, and are settling to the bottom. Mineral recycling—from sediments, erosion, and percolation of water through shoreline soils—and deposited tailings are probable continuing sources of heavy metals within the watershed.

Except for low densities of benthic macroinvertebrates, Torch Lake does not appear to be an extremely disturbed aquatic system. Only very low densities of midge larva and aquatic worms were found in most bottom samples (*2*). Diatoms dominate the phytoplankton community, but blooms of green and blue-green algae have been observed (*1*). A rather diverse zooplankton community exists. Macrophytes are present in some littoral areas of the lake and reach greatest densities where tributaries deposit organic materials.

A diverse fish population is present. Walleye, sauger, and northern pike are the dominant species in terms of weight. Smallmouth bass, yellow perch, lake sturgeon, sea lamprey, brook trout, rainbow trout, burbot, alewife, smelt, cisco, white sucker, bullhead, trout-perch, sculpin, coho salmon, bluegill, rock bass, and redhorse sucker also have been collected in Torch Lake since 1970. Both Torch Lake and Portage Lake have supported a productive sauger fishery since the 1930's. Since the time that mining ceased, walleye and northern pike appear to be replacing sauger as the dominant larger predator species. In records maintained by the Fisheries Division, MDNR, the average ages of saugers, walleyes, and northern pike collected in 1979 were 11, 6, and 5 years, respectively (Juetten R: Personal communication). Reproduction of the sauger population as evidenced by the presence of juveniles has not been noted for at least 10 years (Juetten R: Personal communication). Whether recent changes in water quality or critical habitat destruction during the 1960's caused the decline in sauger population is not known.

Reports of abnormalities in fishes from this lake, including tumors in saugers and walleyes, prompted us to initiate a preliminary study of the light microscopic histology and ultrastructure of three different neoplasms that were found to be epizootic in these two fish populations.[8] In summary: Compelling circumstantial evidence exists that mine-waste pollution plays a causal role.

MATERIALS AND METHODS

Fishes were collected by gill nets in September 1979 and July 1980. They were examined externally and after a lengthwise incision was made in the left flank, the internal organs were removed and examined for gross signs of neoplasms.

For light microscopy, samples of tissue from organs exhibiting evidence of gross pathology were fixed in 10% buffered Formalin. After fixation and dehydration, specimens were embedded in paraffin, sectioned at 5-μm thickness, and stained with H & E. The following special stains were used: oil red-O for lipids, Mayer's mucicarmine for mucus, and periodic acid–Schiff for carbohydrates (*4, 5*).

For electron microscopy, tissues were minced with a razor blade to 1.0-mm^3 pieces or smaller. Aliquots were transferred to vials containing 2.0 ml cacodylate-buffered 2.0% glutaraldehyde (*6*). This prefixation was performed in the field, and specimens were kept on ice for 48 hours. When the specimens arrived at the laboratory, the glutaraldehyde was removed and the tissues were rinsed briefly in cold cacodylate buffer before fixation in Dalton's chrome–osmium fixative (*7*). After fixation, tissues were rapidly dehydrated, embedded in Epon–Araldite, and sectioned at 0.05- to 0.9-μm thickness on diamond or glass knives with an LKB model 3 ultramicrotome. Thin sections were picked up on 200-mesh carbon-coated or bare grids and were stained with lead citrate and uranyl acetate (*8*). Specimens were examined by transmission microscopy in a Siemens 1A electron microscope.

RESULTS

Various fish species from Torch Lake were necropsied and examined for tumors. In 8 northern pike (*Esox lucius*), 8 white suckers (*Catostomus commersoni*), 5 smallmouth bass (*Micropterus dolomieu*), 4 rainbow trout (*Salmo gairdneri*), and 1 brook trout (*Salvelinus fontinalis*), no tumors, either internal or external, were observed. In saugers and walleyes several types of abnormal growths were present. Although a statistical survey per se of the incidence of neoplasms was not made among the 20 saugers and 11 walleyes necropsied and examined in 1979, the most striking and consistent finding involved the livers of the saugers, which universally exhibited widely varied gross signs of neoplastic disease. The livers, ranging in color from pale yellow with a slightly greenish tinge to a normal reddish-tan, contained variably sized, raised nodules, and some were simultaneously affected with multiple, subcapsular, fluid-filled cysts (figs. 1, 2). Nodules ranged from single foci, barely discernible with the naked eye (≈2 mm in diameter), to large, raised (1- to 8-mm) neoplastic-appearing nodules (>2 cm in diameter) (fig. 1). Nodule color varied from reddish-brown to grayish-tan to gray. On fixation, the neoplastic nodules were paler than the surrounding liver tissue. On the basis of the presence of nodules found at gross examination, liver neoplasms apparently were present in every sauger examined, i.e., 100%. Similar nodules were present in some of the walleye livers, but nodule prevalence in walleyes was not determined in 1979.

Affected livers from 8 saugers and 3 walleyes were examined microscopically. The livers were all similar in their histologic appearance, with neoplasms appearing as single-to-multiple nodules that exhibited increased basophilia and moderate anaplasia (fig. 3). Cord structure was typically many cells thick and in some areas was replaced by a cobblestone type of growth pattern. Tumors were composed of hepatocytes that exhibited only mild pleomorphism. Tumor cells had large nuclei with prominent nuclear membranes, marginated chromatin, and large nucleoli (fig. 4). Few mitoses were present, and tumors appeared to be slow growing with only slight bands of compression atrophy surrounding the liver nodules. Fibrosis was not a prominent finding, but parasitic cysts and melanin macrophage centers were present in most sections. The tumors were diagnosed as hepatocellular carcinomas, a well-differentiated type.

In addition to hepatocellular carcinomas, dermal neoplasms were also present in saugers and walleyes. Three of these neoplasms (2 from saugers, 1 from a walleye) were examined microscopically, and all appeared as unencapsulated dermal fibromas with variable degrees of ossification (fig. 5). Some sections had an inflammatory infiltrate, usually more prominent in the area of the dermis. Examination of thin sections by electron microscopy did not indicate any obvious virus particles as reported in walleye dermal fibromas by Walker (*9*).

---

[8] Abnormalities diagnosed as lipogranulomas and ossifying fibromas in Torch Lake fishes were initially discovered and subsequently reported to the MDNR by Mr. David A. Tomljanovich, a graduate student at Michigan Technological Institute, Houghton, Mich. [*see* (*3*)]. The present follow-up study resulted when one of the authors (E. D. E) requested the assistance of the senior author in confirming the nature of the abnormalities.

A third type of growth observed in these two species frequently took the form of large perivisceral masses that were frequently attached to the spleen but sometimes appeared to be attached to mesenteric fat and/or mesenteries (fig. 6). On palpation, these masses were somewhat gelatinous or rubbery, and when cut they exuded a scant amount of clear viscous fluid. These perivisceral neoplasms varied in size and color. Sizes ranged from large polypoid growths (4–6 cm in diameter) to smaller, solitary pedunculated nodules (≥1 cm in diameter). Colors ranged from an opaque tan through a translucent pinkish-tan to a colorless, somewhat hyaline appearance. Within the masses were grossly visible septa that partitioned the masses into multiple microcystic structures that corresponded to the larger follicles seen by light microscopy. An occasional fish had more than one mass arising from different parts of the viscera, e.g., mesentery versus spleen (fig. 6).

Recognition was not immediate that these masses were sometimes hidden by large accumulations of visceral fat and, therefore, no figure can be advanced for their prevalence in the 1979 fish sampling. However, they may have been common, inasmuch as several masses were sufficiently exposed so that they were detected in viscera examined in the field. In one other case, later dissection of viscera preserved en bloc in 10% Formalin revealed the presence of a large mass attached to the spleen.

By light microscopy, these growths were seen to be composed of large follicles (figs. 7, 8) that contained a pale-staining (H & E), proteinaceous-appearing material. This material was negative for both lipid and mucin but was weakly positive in some areas for the periodic acid–Schiff reaction. When associated with the spleen, the neoplasms were covered by a thin capsule that appeared continuous with that of the spleen capsule. In some sections, a distinct subcapsular layer of large uniform follicles was present (fig. 8). In this area, tumor cells frequently appeared to be continuous with the cells of the spleen capsule (fig. 9), suggesting that the neoplasms may have originated from the spleen component of the visceral mesentery.

Electron microscopy of these neoplasms indicated several types of cells. Those bordering the follicles were extremely elongated epithelioid cells with obvious tonofibrillae. Evidence of secretion by these cells was seen. Elements of rough endoplasmic reticulum were found near the cell surface, appearing in some sections to be emptying their contents directly into the large colloid-like areas contained within the follicles (fig. 10). Cellular elements of the blood system, perhaps sequestered from the spleen, plus neuronal elements and connective tissue were observed in areas between the secretory cells. Although with the light microscope the appearance of these masses resembled myxoma, the combination of morphology and secretory activity in the elongate epithelioid cells of possible visceral mesenteric origin suggested a diagnosis of mesothelioma. Differential diagnosis also included lymphangioma.

Idiopathic intercellular and intracellular crystalloid profiles, similar in appearance to Auer bodies (*10*), were observed in some sections. These were variably shaped rhomboid and rod-like forms up to 2.0 µm in length, usually enclosed by a membrane (fig. 11). They appeared within or in association with cells that resembled granulocytes and lymphocytes. The suggestion has been advanced that the crystalloids are generated in the cisternal region of the rough-surfaced endoplasmic reticulum. Crystalloids were not observed in the elongate follicular cells of these tumors and were not observed in either hepatomas or the dermal ossifying fibromas.

TABLE 1.—*Neoplasms in Torch Lake saugers and walleyes, 1980*

Neoplasm	No. of lesions/total No. of fish	
	Sauger	Walleye
Hepatocellular carcinoma	3/3	3/11
Dermal ossifying fibroma	1/3	2/11
Perivisceral masses	2/3	2/11

To quantify the incidence of the various types of neoplasms, an additional sampling of Torch Lake fishes was made in July 1980. The numbers and kinds of tumors present in the saugers and walleyes from this collection are shown in table 1. Some of the saugers and walleyes examined in 1980 had more than one type of tumor in the same individual; e.g., 1 sauger and 1 walleye had both hepatocellular neoplasms and the mesothelioma-like spleen masses, 1 sauger had both hepatocellular and dermal neoplasms, and 1 sauger had all 3 types of neoplasms. Occasional fishes with multiple neoplasms were also observed among the 1979 group, but the frequency with which multiple neoplasms occurred was not determined.

DISCUSSION

The data from numerous investigations have indicated an association between water pollution and elevated tumor frequencies in fishes (*11–18*). Although direct proof of a causal role for pollutants is presently lacking for any spontaneous tumors in teleosts, a pollutant chemical hypothesis is supported indirectly by laboratory experiments which indicate that a number of chemical carcinogens readily cause tumors in fishes (*19–24*). In addition, most teleosts also appear to activate chemical carcinogens by enzymatic reactions similar to those of higher vertebrates (*25–28*). However, not all fish tumors are caused solely by exposure to chemicals. Strong experimental evidence exists that viruses are causative agents for lymphosarcoma in northern pike, and virus particles have been observed in several other fish neoplasms (*9, 29, 30*).

Sauger and walleye are important Great Lakes predator species that are valued as food and as sport fishes. Preliminary examination of two modest samples of these two species from Torch Lake indicated that they were commonly affected with three types of neoplasms: hepatomas, dermal fibromas, and multiloculated gelatinous masses possibly originating from the visceral peritoneum. The precise classification of the perivisceral lesions is unknown, but myxoma, lymphangioma, and mesothelioma were included in the differential diagnosis. No virus particles were observed in any of the tumor tissues when examined by electron microscopy. Livers were heavily parasitized with trematodes, but any relationship these organisms may have had to the liver tumors was inapparent.

Tomljanovich (3) described numerous lesions in Torch Lake saugers, including dermal fibromas and the mesothelioma-like lesions that were interpreted variously as lipomas and fat necroses. The hepatomas were not reported. Although hepatic neoplasms possibly were not present then (1974), more likely the liver tumors were missed inasmuch as the prevalence of hepatomas in saugers appeared to be 100% in our samples that were taken only 5 and 6 years later. This constitutes the highest frequency of spontaneous tumors occurring in any species and is seldom achieved even in laboratory attempts to induce hepatomas.

Tomljanovich (3) thought that the high concentration of copper very possibly was responsible for the neoplasms. We accept the hypothesis that the observed fish pathology is related to the presence of mining wastes; however, at present no evidence is available that copper is carcinogenic intrinsically. Conversely, copper ores may contain metals, such as selenium and arsenic (31), that are considered carcinogenic. Despite a lack of evidence of copper carcinogenicity, conceivably there is a link through cirrhosis to copper as a possible causative agent of liver tumors, in that human patients with cirrhosis are predisposed to develop liver cancer (32). Cirrhosis is a component of two metal-induced diseases (33, 34), i.e., hemochromatosis (excessive loading of iron in tissues, especially the liver) and Wilson's disease (excessive storage of copper in the liver and brain due to a metabolic defect). Against this line of reasoning is the fact that relatively few cases of Wilson's disease eventuate in liver tumors, and none of the sauger and walleye livers were cirrhotic.

A possible carcinogenic role for the physical nature of the mining waste might also be considered. These copper tailings are extremely fine particles that readily suspend in water; however, their exact physical form and their possible relationship to any of the observed neoplasms are presently unknown. Other mining-related physical agents, such as hematite, silica dust, and asbestos, have been implicated in health problems and in some kinds of cancer (35–37). Among these agents, asbestos has been shown to cause mesothelioma in laboratory animals and is implicated by epidemiologic evidence in human cancers of this type (38, 39). Although some mineral-bearing ores found in the North Central United States contain asbestos, the presence of this mineral fiber in Torch Lake has not been ascertained. No obvious asbestos bodies or birefringent asbestos-like crystals were seen in the spleen tumors.

An alternative indirect action may also be postulated for mine waste pollution. Copper or other metals may be acting to catalyze the formation of a new compound(s) that is carcinogenic in fishes. One possible route may be the metal-catalyzed formation of carcinogenic nitrosamines from secondary amine compounds contained in domestic sewage effluent or perhaps from naturally occurring amines (40). As stated previously, the lake has received some domestic sewage which may have provided precursor molecules. Nitrosamines may be plausible candidates for the putative agents inasmuch as they are potent liver carcinogens (41–43).

Another interesting aspect of the problem is that Torch Lake saugers are extremely old fish. The average length of specimens examined in our preliminary survey was in excess of 20 inches. Specimens from Torch Lake have been estimated to exceed 12 years in age (Juetten R: Personal communication), and no small saugers were reported in recent surveys conducted by the MDNR. Presently, considerable doubt exists that any sauger reproduction is occurring. This observation is consistent with our pathology studies in which gonads in this species frequently appeared atrophic. In addition, some gonads were heavily infiltrated with lipogranuloma-like lesions that consisted of aggregations of macrophage-like cells containing a yellow crystalloid-appearing material. Our pathology findings, though preliminary, indicated that a similar pattern of lesions was occurring in Torch Lake walleyes but at a lower incidence. It would not be surprising, therefore, if survival of the walleye population also will be effected.

Although the tumors in Torch Lake fishes circumstantially appear to be related to the presence of copper-mining wastes, further study will be required to determine the precise identity of the causative factor(s). The extent of this problem beyond the immediate waters of Torch Lake is presently unknown. The scientific, human health, and economic implications of these findings argue strongly for further study.

REFERENCES

(1) Evans ED. An evaluation of a cupric ammonium carbonate spill into Torch Lake, Houghton County, Michigan. Lansing, Mich.: Michigan Department of Natural Resources, 1973.

(2) Wright T, Leddy D, Brandt D, Virnig T. Water quality alteration of Torch Lake, Michigan, by copper leach liquor. In: Proceedings of the sixteenth conference of the Association of Great Lakes Research, Huron, Ohio, Apr. 16–18. Shelbourne, Ontario: Assoc Great Lakes Res, 1973:329–344.

(3) Tomljanovich DA. Growth phenomena and abnormalities of the sauger, *Stizostedion canadense* (Smith), of the Keweenaw Waterway. M.S. thesis. Houghton, Mich.: Michigan Technological Institute, 1974.

(4) Lillie RD. Histopathological technique and practical histochemistry. New York: Blakiston, 1954:501.

(5) Davenport HA. Histological and histochemical techniques. Philadelphia: Saunders, 1960:401.

(6) Sabatini DD, Miller F, Barrnett RJ. Aldehyde fixation for morphological and enzyme histochemical studies with the electron microscope. J Histochem Cytochem 1964; 12:57–71.

(7) Dalton AJ. A chrome-osmium fixative for electron microscopy. Anat Rec 1955; 121:281.

(8) Reynolds ES. The use of lead citrate at high pH as an electron opaque stain in electron microscopy. J Cell Biol 1963; 17:208–212.

(9) Walker R. Virus associated with epidermal hyperplasia in fish. Natl Cancer Inst Monogr 1967; 31:195–207.

(10) Bessis M. Living blood cells and their ultrastructure. Weed RI, translator. New York, Heidelberg, and Berlin: Springer-Verlag, 1973:767.

(11) Dawe CJ, Stanton MF, Schwartz FJ. Hepatic neoplasms in native bottom-feeding fish of Deep Creek Lake, Maryland. Cancer Res 1964; 24:1194–1201.

(12) Brown ER, Hazdra JJ, Keith L, Greenspan I, Kwapinski JB, Beamer P. Frequency of fish tumors found in a polluted watershed as compared to nonpolluted Canadian waters. Cancer Res 1973; 33:189–198.

(13) Black JJ, Simpson CL. Thyroid enlargement in Lake Erie coho salmon. J Natl Cancer Inst 1974; 53:725–729.

(14) Falkmer S, Emdin SO, Östberg Y, Mattisson A, Johansson-Sjöbeck

M-L, Fänge R. Tumor pathology of the hagfish, *Myxine glutinosa*, and the river lamprey, *Lamprey fluviatilis*. Prog Exp Tumor Res 1976; 20:217–250.

(*15*) Sonstegard RA. Environmental carcinogenesis studies in fishes of the Great Lakes of North America. Ann NY Acad Sci 1977; 298:261–269.

(*16*) Pierce KV, McCain BB, Wellings SR. Pathology of hepatomas and other liver abnormalities in English sole (*Parophrys vetulis*) from the Duwamish River Estuary, Seattle, Washington. J Natl Cancer Inst 1978; 60:1445–1453.

(*17*) Smith CE, Peck TH, Klauda RJ, McLaren JB. Hepatomas in Atlantic tomcod, *Microgadus tomcod* (Walbaum), collected in the Hudson River Estuary in New York. J Fish Dis 1979; 2:313–319.

(*18*) Black JJ, Holmes M, Dymerski PP, Zapisek WF. Fish tumor pathology and aromatic hydrocarbon pollution in a Great Lakes Estuary. In: Afghan BK, McKay, eds. Hydrocarbons and halogenated hydrocarbons in the aquatic environment. New York: Plenum Press, 1980:559–565.

(*19*) Stanton MF. Dimethylnitrosamine-induced hepatic degeneration and neoplasia in the aquarium fish, *Brachydanio rerio*. J Natl Cancer Inst 1965; 34:117–130.

(*20*) Halver JE. Crystalline aflatoxin and other vectors for trout hepatoma. In: Halver JE, Mitchell IA, eds. Trout Hepatoma Research Conference papers research report 70. Washington, D.C.: U.S. Govt Print Off, 1967.

(*21*) Ashley LM, Halver JE. Dimethylnitrosamine-induced hepatic cell carcinoma in rainbow trout. J Natl Cancer Inst 1968; 41:531–552.

(*22*) Sato S, Matsushima T, Tanaka N, Sugimura T, Takashima F. Hepatic tumors in the guppy (*Lebistes reticulatus*) induced by aflatoxin B_1, dimethylnitrosamine, and 2-acetylaminofluorene. J Natl Cancer Inst 1973; 50:765–778.

(*23*) Matsushima T, Sugimura T. Experimental carcinogenesis in small aquarium fishes. Prog Exp Tumor Res 1976; 20:367–379.

(*24*) Khudoley VV. Induction of liver tumors by some azo compounds in aquarium guppies (*Lebistes reticulatus* Peters). J Ichtly 1972; 12:319–324.

(*25*) Adamson RH. Drug metabolism in marine vertebrates. Fed Proc 1976; 26:1047–1054.

(*26*) Pedersen MG, Hershberger WK, Juchau MR. Metabolism of 3,4-benzpyrene in rainbow trout. Bull Environ Contam Toxicol 1974; 12:481–486.

(*27*) Walton DG, Penrose WR, Green JM. The petroleum inducible mixed function oxidase of cunner (*Tautogolabrus adspersus* Walbaum, 1792): Some characteristics relevant to hydrocarbon monitoring. J Fish Res Bd Canada 1978; 35:1547–1552.

(*28*) Tan B, Melius P, Grizzle J. Hepatic enzymes and tumor histopathology of black bullheads. In: Cooke M, Dennis AJ, eds. Chemical analysis and biological fate: Polynuclear aromatic hydrocarbons. Columbus: Battelle, 1980.

(*29*) Mulcahy MF, O'Leary A. Cell-free transmission of lymphosarcoma in the northern pike, (*Esox lucius* L.). Experientia 1970; 26:891.

(*30*) Sonstegard R. Studies of the etiology and epizootiology of lymphosarcoma in Esox (*Esox lucius* L.) and (*Esox masquinongy*). Prog Exp Tumor Res 1976; 20:141–155.

(*31*) Germani MS, Small M, Zoller WH. Fractionation of elements during copper smelting. Environ Sci Technol 1981; 15:299–305.

(*32*) Shikota T. Primary liver carcinoma and liver cirrhosis. In: Kunio O, Peters RL, eds. Hepatocellular carcinoma. New York: Wiley, 1976:53–71.

(*33*) Robbins SL. Pathologic basis of disease. Philadelphia: Saunders, 1974:1598.

(*34*) Goldfischer S, Sternlieb I. Changes in the distribution of hepatic copper in relation to the progression of Wilson's disease (hepatolenticular degeneration). Am J Pathol 1968; 53:883–899.

(*35*) Boyd JT, Doll R, Faulds JS, Leiper J. Cancer of the lung in iron ore (hematite) miners. Br J Ind Med 1970; 27:97–105.

(*36*) David A, Hurych J, Effenbergerova J, Holusa R, Simecek J. Laboratory testing of biological activity of ore mine dust: Fibrogenicity, cytotoxicity and hemolytic activity. Environ Res 1981; 24:140–151.

(*37*) Selikoff I, Churg J, Hammond EC. Relation between exposure to asbestos and mesothelioma. N Engl J Med 1965; 272:560–565.

(*38*) Shin ML, Firminger HI. Acute and chronic effects of intraperitoneal injection of two types of asbestos in rats with a study of the histopathogenesis and ultrastructure of resulting mesotheliomas. Am J Pathol 1973; 70:291–313.

(*39*) Becklake MR. Asbestos-related diseases of the lung and other organs: Their epidemiology and implications for clinical practice. Am Rev Resp Dis 1976; 114:187–227.

(*40*) Croisy AF, Fanning JC, Keefer LK, Slavin BW, Uhm SJ. Methyl complexes as promoters of N-nitrosation reactions: A progress report. Reprinted from: Walker EA, Castegnaro L, Griciute L, Borzsonyi M, eds. N-nitroso-compounds: Analysis, formation and occurrence. Lyon: IARC Sci Publ, 1980 (publication No. 31).

(*41*) Miller JA. Carcinogenesis by chemicals: An overview—G. H. A. Clowes memorial lecture. Cancer Res 1970; 30:559–576.

(*42*) National Cancer Institute, National Institutes of Health. Survey of compounds which have been tested for carcinogenic activity. Washington, D.C.: U.S. Govt Print Off, 1978 [DHEW publication No. (NIH)80–453].

(*43*) Kimura I, Miyake I, Yoshizaki K. Induction of tumors of the stomach, of the liver and of the kidney in rainbow trout by intrastomach administration of *N*-methyl-*N'*-nitro-*N*-nitrosoguanidine (MNNG). Proc Jpn Cancer Assoc 1976; 35:16.

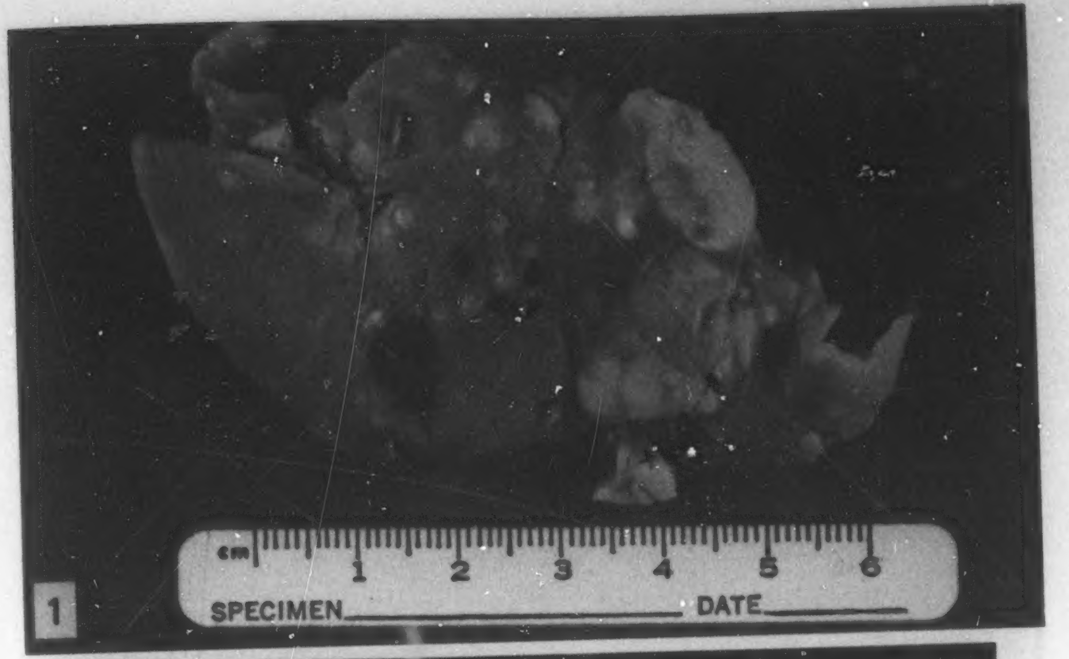
1
cm 1 2 3 4 5 6
SPECIMEN
DATE

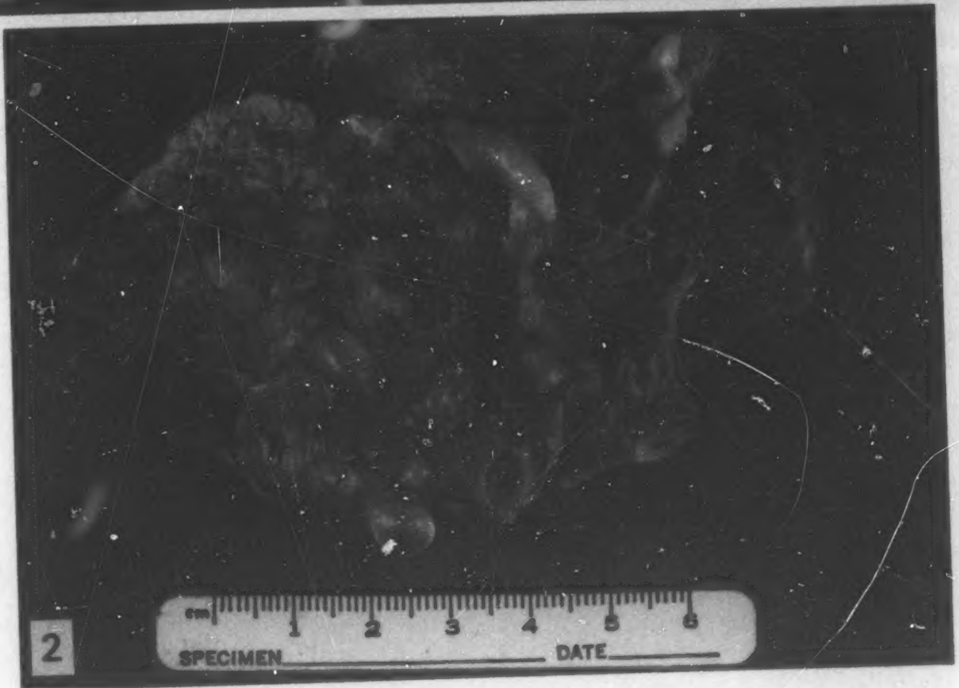
2
cm 1 2 3 4 5 6
SPECIMEN
DATE

FIGURE 1.—Liver with hepatoma nodules (H) and parasitic cysts (P).
FIGURE 2.—Liver with hepatomas (H) and serous cysts (S).

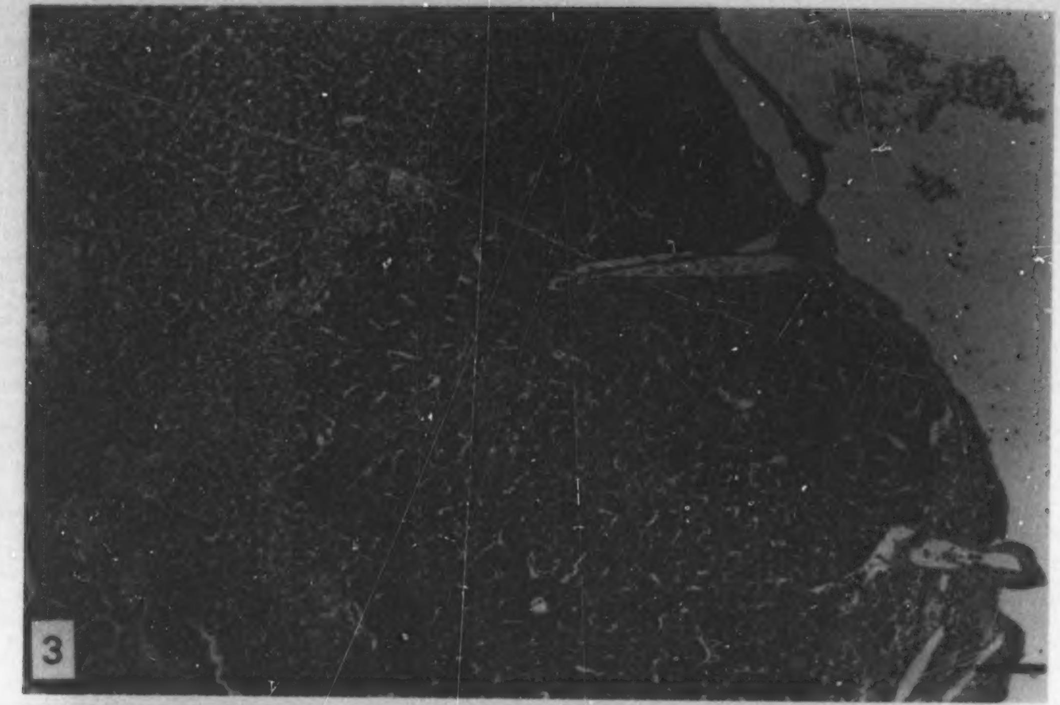

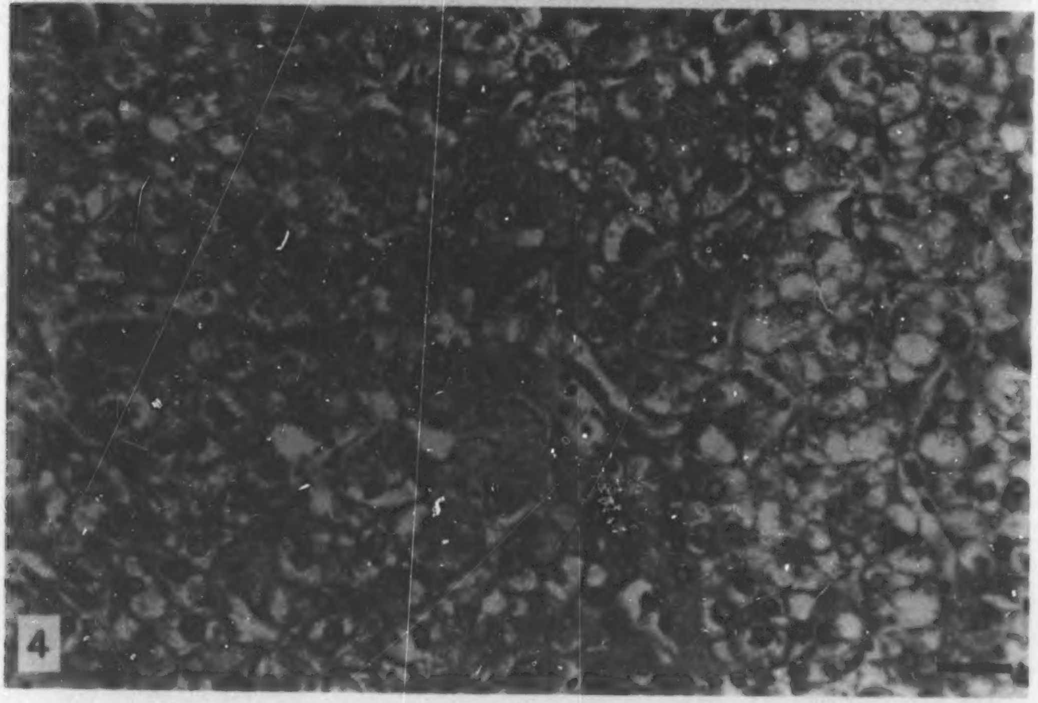

FIGURE 3.—Liver hepatoma. Small basophilic nodule can be seen *at right*. *Note* lack of capsule. *Bar*=120 µm. × 85

FIGURE 4.—Hepatoma cells with large basophilic cytoplasms and enlarged nuclei, in contrast to normal hepatocytes *at right*. *Bar*=20 µm. × 480

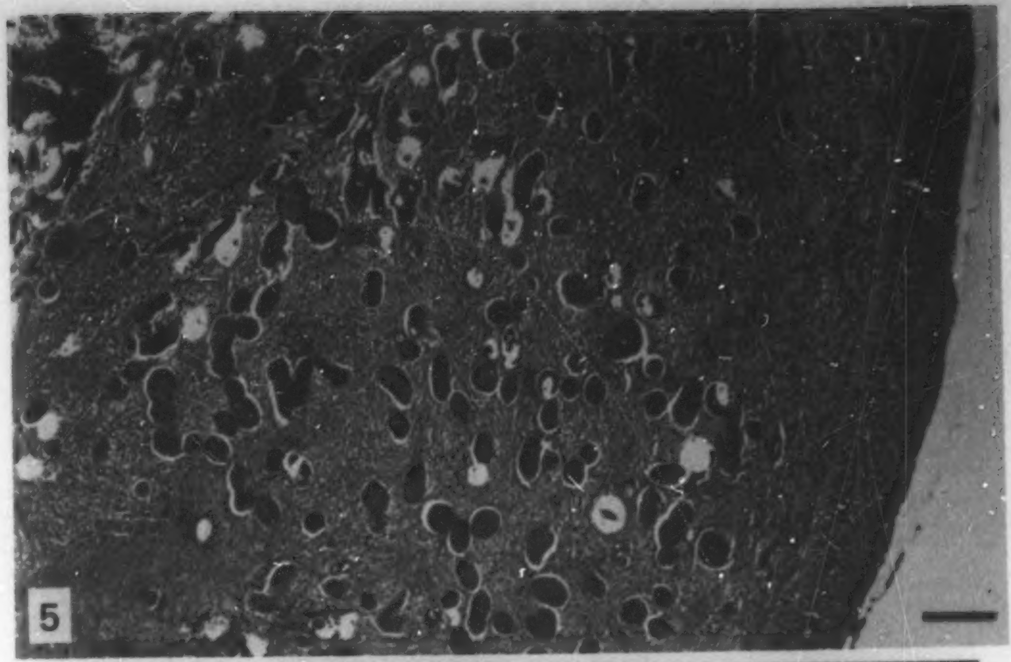

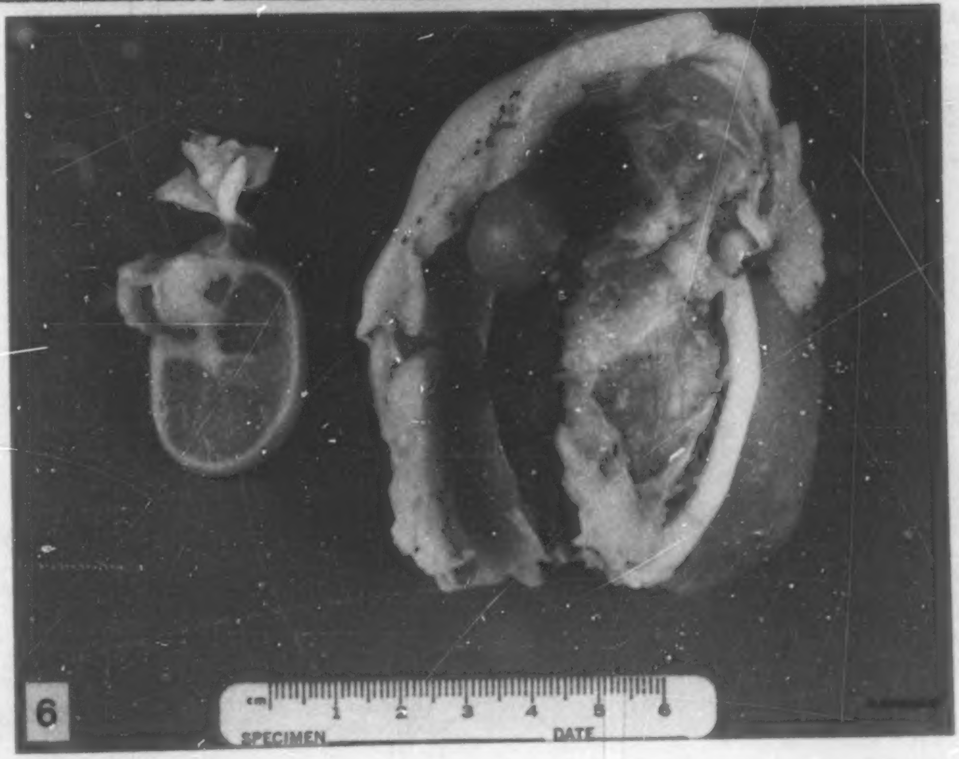

FIGURE 5.—Dermal fibroma showing numerous ossification foci. *Bar*=54 µm. × 85

FIGURE 6.—Gross aspect of visceral masses (actual size). Mass *at left* was attached by peduncle to the surface of mesenteric fat. Larger mass *at right* was associated with spleen.

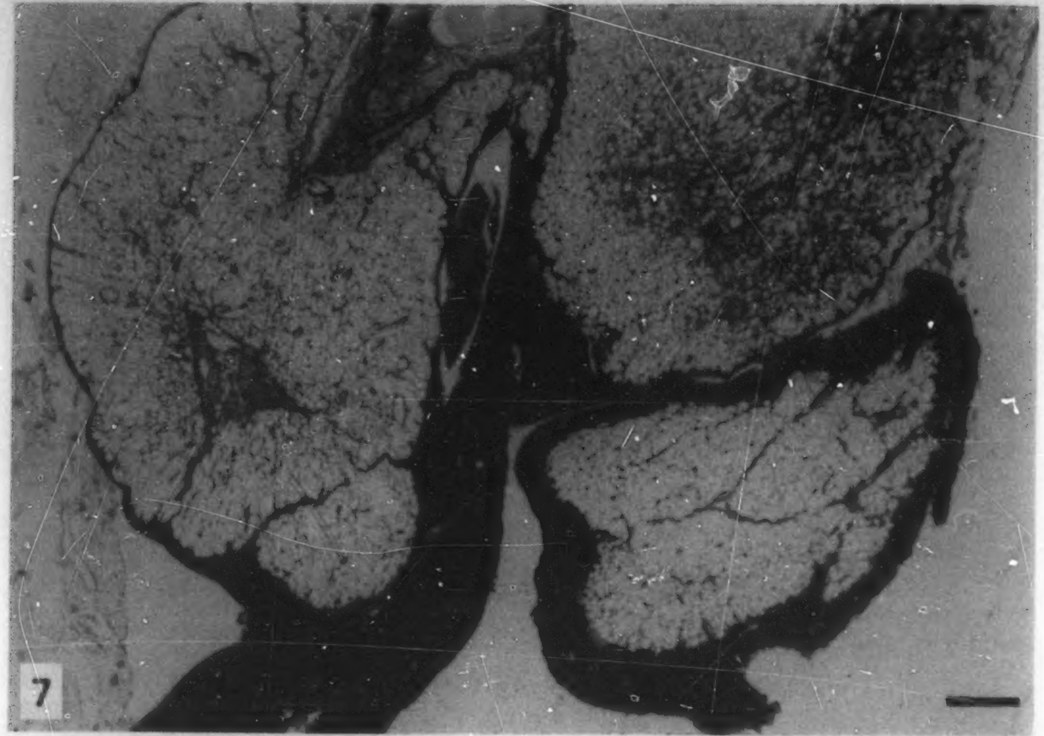

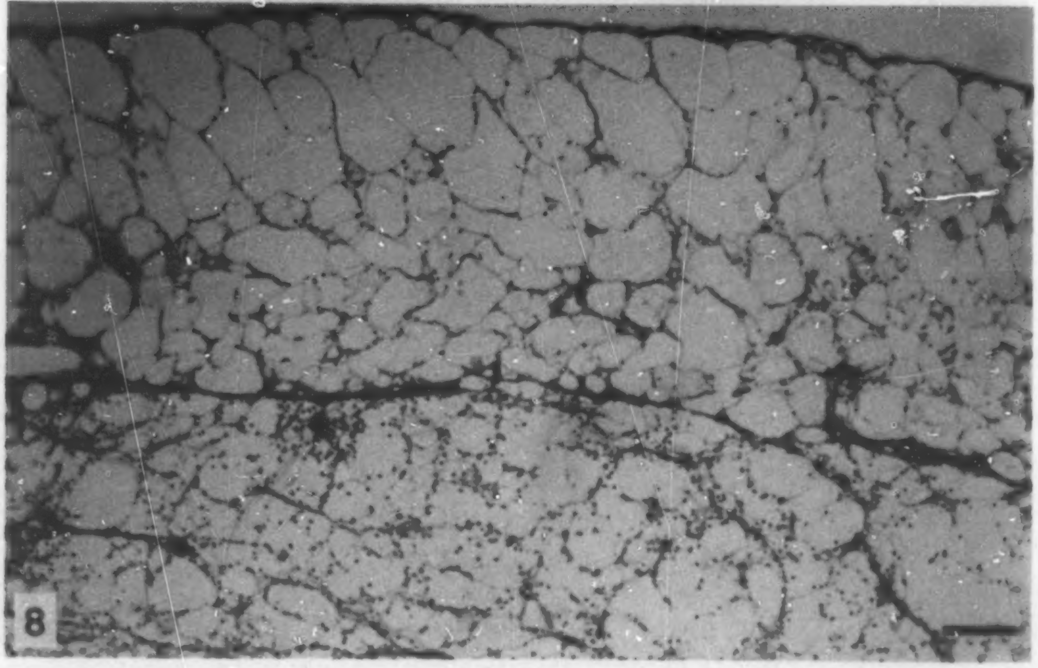

FIGURE 7.—Microscopic overview of spleen mass. Spleen tissue is represented by *dark areas. Bar*=1 mm. × 10

FIGURE 8.—Spleen mass showing outer large follicular layer and inner small follicular zone. *Bar*=120 μm. × 85

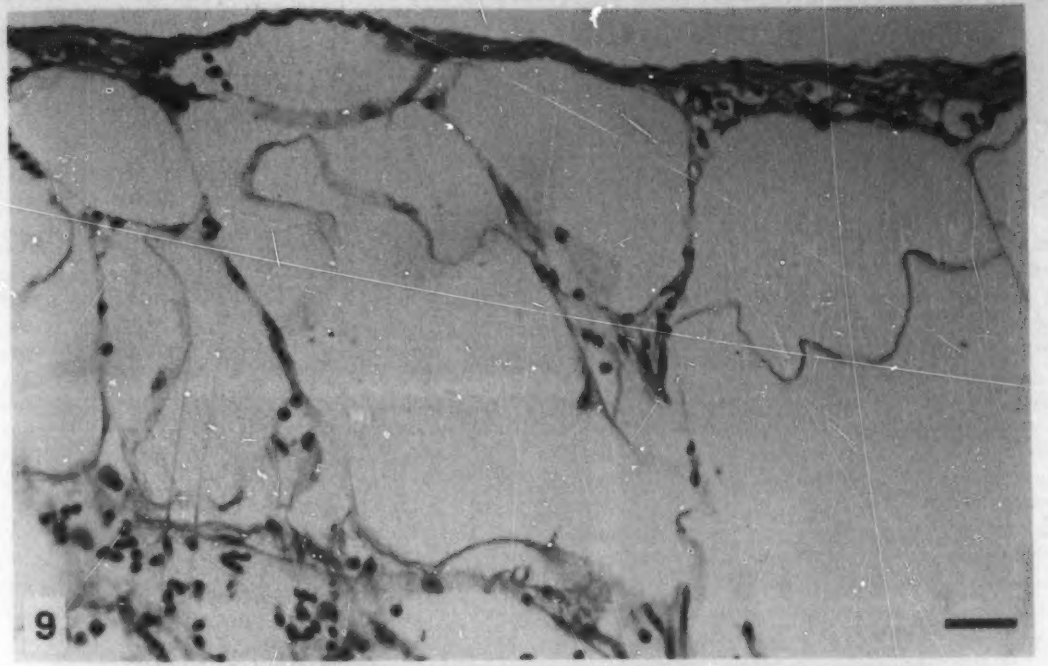

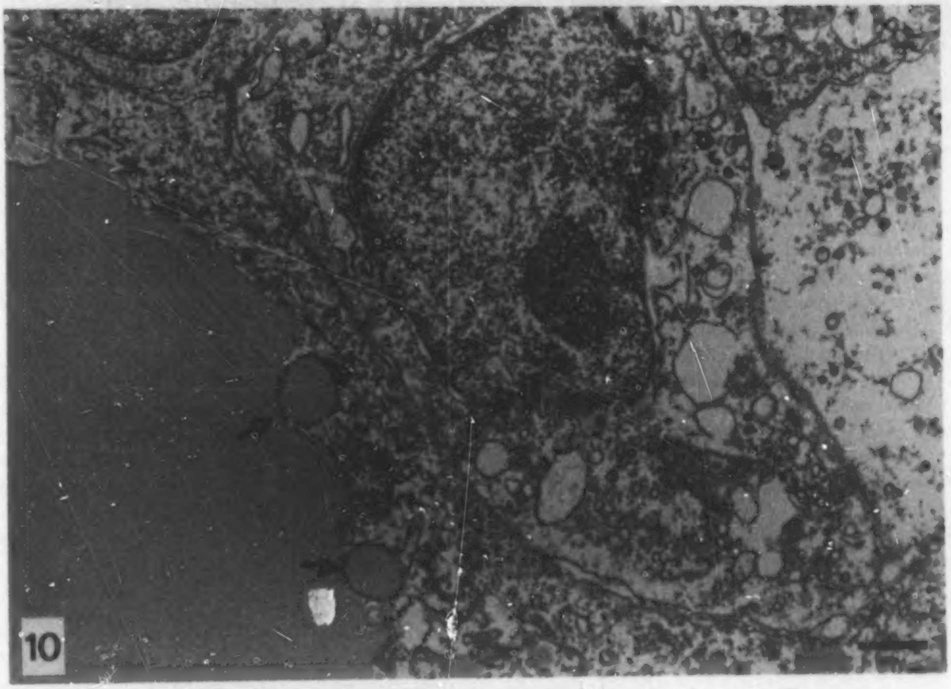

FIGURE 9.—Spleen mass showing detail of capsule and underlying follicular structures of tumor. *Bar* = 55 µm. × 180

FIGURE 10.—Electron micrograph of spleen tumor showing morphology of cells adjoining a follicle. Vesicles (*arrows*) formed by elements of the rough-surfaced endoplasmic reticulum can be seen at the cell surface, appearing to empty their contents into the follicle lumen. *Bar*=0.2 µm. × 41,000

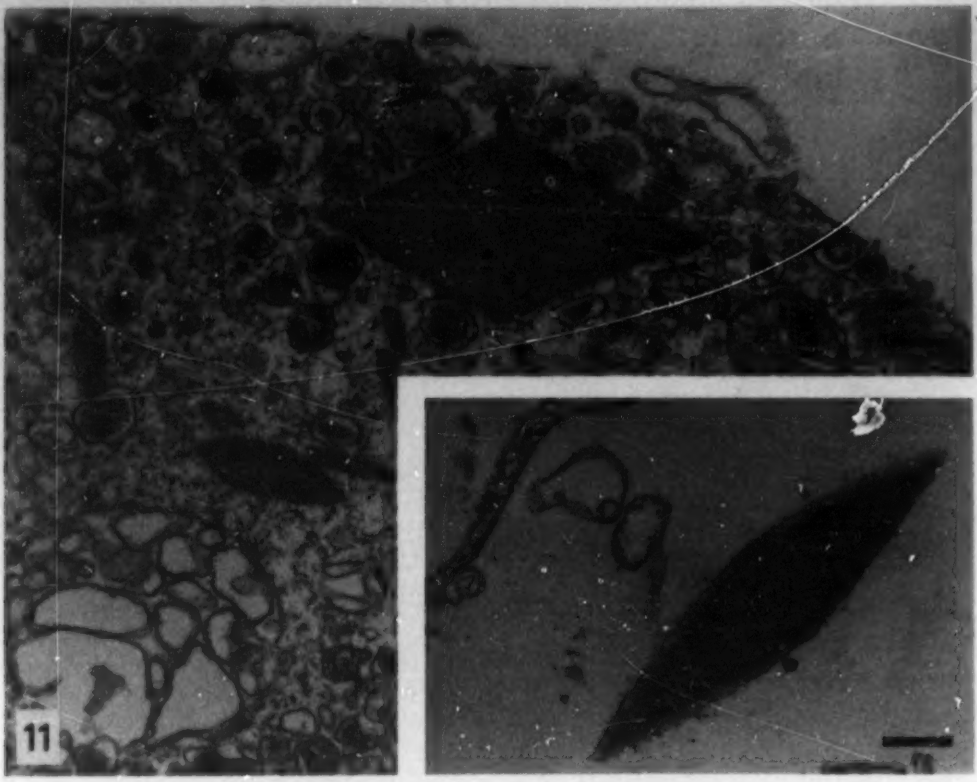

FIGURE 11.—Electron micrograph of crystalloid inclusions within the cell and in extracellular space (*inset*). *Note* membrane enclosure. *Bar*=0.2 µm. × 41,000. *Inset: Bar*=0.3 µm. × 30,600

Electron Microscopic Autoradiography of the Trachea in Fetal Syrian Golden Hamsters Treated Transplacentally With *N*-Nitrosodiethylamine[1,2]

Hildegard M. Reznik-Schüller[3,4]

ABSTRACT—Tritiated *N*-nitrosodiethylamine (DENA) was administered to female Syrian golden hamsters on each of the last 4 days (days 12–15) of pregnancy. The intracellular distribution of bound radioactivity was monitored by electron microscopic autoradiography in the epithelium of the fetal tracheas, from which transplacentally induced tumors arise in this system. Most of the bound radioactivity was concentrated in the rough endoplasmic reticulum of undifferentiated stem cells and mucous cells. The level of binding on the various days of pregnancy appeared to reflect the degree of differentiation of the endoplasmic reticulum in these cells. Basal cells, which were identified as the origin of DENA-induced tracheal tumors in adult hamsters by one of our earlier studies, demonstrated only little bound radioactivity in the fetal tracheas. The pathogenesis of DENA-induced tracheal tumors in this transplacental system may hence be different from that in adult animals.—JNCI 1982; 69:927–931.

DENA, a potent respiratory tract carcinogen in Syrian golden hamsters (*1–8*), induces tumors in the trachea, nasal cavities, and lungs of adult animals. When administered to pregnant hamsters, it crosses the placenta and induces neoplasms of the trachea in up to 100% of the offspring (*9, 10*). Such a transplacental carcinogenic effect does occur, however, only if the compound is administered to the mother on one of the last 4 days of gestation. Treatment at an earlier time does not induce any such tumors (*10*). Using liquid scintillation counting after transplacental administration of tritiated DENA on different days of gestation, we found no binding in the fetal tracheas before day 12, whereas binding was high (*11*) on the last 4 days (days *12–15*). By light microscopic autoradiography, we were later able to demonstrate that mucous cells and their precursors, as well as undifferentiated stem cells, contained most of the bound radioactivity in the fetal tracheas (*12*). We have now investigated the subcellular distribution of [^{3}H]DENA in target cells by electron microscopic autoradiography. Our data show that the amount of binding is clearly linked to the level of differentiation of selected organelles in the target cell types.

MATERIALS AND METHODS

[^{3}H]DENA was prepared as reported (*13*). It had a specific activity of 48 mCi/mmol. We used a concentration of 2 mCi/ml dissolved in 1 ml ethanol (2 mg). Syrian golden hamsters mated at 3 months of age were given the compound on days 12–15 of the pregnancy. On each of these days, 2 animals received a single intragastric dose by intubation of 0.5 ml DENA in alcohol (1 mCi/animal). Under pentobarbital sodium anesthesia (Diabutal; Diamond Laboratories, Inc., Des Moines, Iowa), the animals were exsanguinated 1 hour after treatment. They were then fixed in situ by vascular perfusion with 2% cacodylate-buffered glutaraldehyde (pH 7.4). The uteri were removed and immersed in the fixative. With the use of a stereomicroscope the fetal tracheas (8–14 fetuses/mother) were excised and processed for electron microscopic autoradiography (for detection of bound radioactivity) as previously described (*14*). Quantitative evaluation of electron microscopic autoradiographs was done by the method of Williams (*15*). Twenty-five cells of each type per animal (trachea: nonciliated stem cells, ciliated cells, basal cells, mucous cells) were examined. To ensure that different cells and not merely serial sections of the same cell were examined, we used only one section per tissue block in the evaluation. To check the validity of the autoradiographic findings, we compared grain counts with the percent distribution of the various organelles in the cells. Labeling was considered significant when grain counts on an organelle were significantly higher (Student's *t*-test) than the percent amount of this organelle per cell (*15*). The percent distribution of organelles per cell and the percent distribution of the grains over various organelles in the cells were measured with the aid of an image analysis system (A.S.M. Image Analysis System; E. Leitz, Inc., Rockleigh, N.J.).

RESULTS

Our grain count results and morphometry data are summarized in table 1. On day 12 of gestation, the epithelium of the fetal hamster trachea consisted of a single layer of tall columnar undifferentiated stem cells (fig. 1). The cytoplasm of these cells was deficient in organelles; the ER was especially scanty and present only in its earliest developmental form as short individual tubules. The nuclei contained little heterochromatin. On this day, the level of radioactive labeling was low and the few autoradiographic grains present were localized on the short ER tubules (fig. 2) and peripheral areas of the nuclei (fig. 3). Whether this labeling in the nuclei was attributable to radioactivity bound to heterochromatin or to the nuclear membrane was not clear.

ABBREVIATIONS USED: DENA=*N*-nitrosodiethylamine; ER=endoplasmic reticulum.

---

[1] Received November 9, 1981; revised April 29, 1982; accepted May 20, 1982.

[2] Supported by Public Health Service contract No. N01CO-75380 from the Office of the Director, National Cancer Institute.

[3] Chemical Carcinogenesis Program, NCI-Frederick Cancer Research Facility, P.O. Box B, Frederick, Md. 21701.

[4] I thank M. Gregg and M. Sherman for their excellent technical assistance.

TABLE 1.—*Area, in percent of total cell, of organelles and intracellular distribution of autoradiographic grains, in percent of total grains/cell, in tracheal epithelia of fetal Syrian golden hamsters treated transplacentally with [^{3}H]DENA*

Day of gestation	Cell type	Cell size area, µm^2	Grains/cell, mean ± SD	Euchromatin, %		Heterochromatin/nuclear membrane, %		Rough ER, %		Mitochondria, %		Mucus droplets, %	
				Area	Grains	Area	Grains	Area	Grains	Area	Grains	Area	Grains
12	Stem	88.8	2.3±0.4	40	0	40	20	1	80	1.5	0	0	0
13	Stem	111.6	4.5±0.6	36.8	1.5	5.0	18.2	7.2	79	3.4	0	0	0
	Basal	65.7	1.5±0.2	55	92	4.2	6.0	2	1.5	3	0	0	0
14	Stem	92.8	8.5±1.2	30.4	20.2	11.5	22.4	13.5	48.7	3.2	2.8	0	0
	Basal	57.8	2.2±0.4	43.2	82.8	12.7	11.2	0.8	1.0	0.9	1.1	0	0
	Ciliated	78.8	3.0±0.4	20.1	0	16.2	0	6.7	0	8.3	0	0	0
15	Stem	94.7	13.5±2.0	28.8	17.1	13.4	20.5	28.9	56.2	3.9	7.1	0	0
	Basal	34.8	2.7±0.4	41.8	80.5	15.1	10.4	1.7	1.2	1.1	0.8	0	0
	Ciliated	93.4	4.7±0.3	18.2	0	15.3	0	10.3	0	11.3	0	0	0
	Mucous	71.9	17.7±4.3	16.0	3.4	14.2	0.4	30.7	50.2	9.4	15.1	5.7	30.4

On day 13, the epithelium of the fetal hamster trachea consisted of nonciliated stem cells and basal cells. At this time, the differentiation of cytoplasmic organelles in the stem cells appeared improved, whereas the cytoplasm of basal cells contained few organelles. Radioactive labeling was still low, although higher than on day 12. In the stem cells, autoradiographic grains were again mainly associated with the ER and areas of the nuclear periphery, whereas in the basal cells grains were restricted to the nuclei, mainly the euchromatin.

On day 14, epithelial differentiation in the fetal tracheas had progressed further with a few short cilia becoming noticeable. However, such ciliated cells contained so few grains that quantification was not possible. In basal cells and nonciliated stem cells, more bound radioactivity was seen than on the 2 earlier days. Generally, the distribution of grains within these cells was much as before, with the only difference being that the mitochondria were now also labeled in the stem cells.

One day before birth (day 15), mucous cells were discernible in addition to ciliated, basal, and stem cells in the fetal tracheas. These mucous cells contained mucus droplets in their apical cytoplasm and demonstrated a well-developed rough ER. Mucous cells were the most heavily labeled at that time. Autoradiographic grains in their cytoplasm were associated mainly with mucus droplets and ER (fig. 4). In the other cell types, the grain distribution over the various organelles was similar to that seen on the preceding days of gestation, but labeling in general had increased (table 1).

DISCUSSION

Our data suggest that transplacental carcinogenicity of DENA in the fetal Syrian hamster trachea depends on the level of functional competence of enzyme systems necessary for the metabolic activation of this compound in the target fetal organ. Before day 12 of gestation, when DENA is noncarcinogenic in this system (*10*), the poorly differentiated epithelia of the fetal tracheas do not yet possess any ER (*12, 16*) and accordingly do not bind DENA and/or its metabolites (*11*). When administered to hamsters on day 12 of pregnancy, DENA induces tracheal tumors in 43% of the offspring (*10*). At this time, the first short tubules of rough ER were reported to develop from blebbings of the nuclear membranes in the epithelia of the fetal tracheas (*17*). Our study showed that transplacental administration of [^{3}H]-DENA on this day resulted in binding of radioactivity only to the few ER tubules and periphery of nuclei in the target epithelia. Since nitrosamines are carcinogenic only after metabolic activation (*18, 19*), a reasonable assumption is that these areas are the site of intracellular activation of these compounds. Although this method does not identify the nuclear membrane (with certainty) as one of the binding sites (autoradiographic grains on the nuclear periphery could indicate binding of radioactivity to nuclear membrane or to marginally condensed heterochromatin), the development of ER tubules from this organelle described above (*17*) suggests that the nuclear membrane may possess some of the enzymes generally associated with the ER. Our results are supported by several biochemical studies (*20–22*), which found cytochrome P_{450}-related enzyme systems in nuclear fractions of liver cells and demonstrated their localization in the nuclear envelope (*23*). Together with an increase of transplacental carcinogenicity of DENA for the fetal hamster tracheas during later stages of gestation (*10*), the amount of binding in the target epithelia increased when [^{3}H]DENA was given on one of the last 2 days (days 14, 15) before birth. The increase in binding probably reflects only the increase in ER in stem cells and mucous cells. In addition, basal cells were now also labeled; but in agreement with their known low levels of metabolic competence (*24*), only their nuclei demonstrated autoradiographic grains, whereas their cytoplasm remained unlabeled. Serial sacrifice studies of DENA-induced tracheal carcinogenesis have shown that it is in the basal cells of the respiratory epithelium from which tumors arise, whereas the mucous cells develop intracytoplasmic changes that suggest they can activate the compound (*8*). Our autoradiographic data support this interpretation by showing that the ER is the principal site of binding in the mucous cells and their precursors. The presence of bound radioactivity in mucus droplets suggests that the labeled compound and/or its products are incorporated in the synthesis of mucus.

The low level of binding found in the basal cells appears to contradict the role of this cell type as progenitor cell of DENA-induced tracheal tumors, as revealed in our pathogenesis study in DENA-treated *adult* hamsters (*8*). The histogenesis of tumors in this transplacental system may hence be different from the pathways followed in the adult animal. However, we found in an autoradiographic study with [^{3}H]DENA in adult hamsters that binding to basal cells was substantially lower than that in mucous and ciliated cells (*25*). In that paper (*25*) we suggested that the compound may be metabolically activated in those cells with high levels of binding, whereas the adjacent basal cells are later transformed into tumor cells. It still remains to be clarified if such a transformation is caused by the binding of an active metabolite to macromolecules of basal cells at a time different from the 1-hour interval after administration of [^{3}H]DENA, as selected in our experiment, or if perhaps some yet unknown indirect mechanisms (e.g., feedback between basal cells and mucous cells) are involved.

REFERENCES

(*1*) Dontenwill W, Mohr U. Carcinome des Respirationstraktes nach Behandlung von Goldhamstern mit Diaethylnitrosamin. Z Krebsforsch 1961; 64:305-312.

(*2*) Dontenwill W, Mohr U, Zagel M. Über die unterschiedliche lungencarcinogene Wirkung von Diaethylnitrosamin bei Hamster und Ratte. Z Krebsforsch 1962; 64:499-502.

(*3*) Herrold KM, Dunham L. Induction of tumors in the Syrian golden hamster with diethylnitrosamine (*N,N*-nitrosodiethylamine). Cancer Res 1963; 23:773-777.

(*4*) Montesano R, Saffiotti U. Carcinogenic response of the respiratory tract of Syrian golden hamsters to different doses of diethylnitrosamine. Cancer Res 1968; 28:2197-2210.

(*5*) Reznik-Schüller H. Proliferation of endocrine (APUD-type) cells during early *N*-diethylnitrosamine-induced lung carcinogenesis in hamsters. Cancer Lett 1 1976; 1:255-258.

(*6*) ———. Ultrastructural alterations of nonciliated cells after nitrosamine treatment and their significance for pulmonary carcinogenesis. Am J Pathol 1976; 85:549-552.

(*7*) ———. Ultrastructural alterations of APUD cells during nitrosamine-induced lung carcinogenesis. J Pathol 1977; 121:79-82.

(*8*) ———. Pathogenesis of diethylnitrosamine-induced tumors in the trachea of the Syrian golden hamster. Pathol Res Pract 1980; 168:185-192.

(*9*) Mohr U, Althoff J, Wrba H. Diaplacentare Wirkung des Carcinogens Diaethylnitrosamin beim Goldhamster. Z Krebsforsch 1965; 66:536-540.

(*10*) Mohr U, Reznik-Schüller H, Reznik G, Hilfrich J. Transplacental effects of diethylnitrosamine in Syrian hamsters as related to different days of administration during pregnancy. J Natl Cancer Inst 1975; 55:681-683.

(*11*) Reznik-Schüller H, Tomaszewski JE. Binding of radioactivity after transplacental administration of tritiated *N*-nitrosodiethylamine to Syrian golden hamsters. JNCI 1980; 64:373-375.

(*12*) Reznik-Schüller HM, Hague BF Jr. Autoradiography in fetal Syrian golden hamsters treated with tritiated diethylnitrosamine. JNCI 1981; 66:773-777.

(*13*) Lijinsky W. The preparation of tritium labeled nitrosamines. J Labeled Compounds 1966; 2:384-390.

(*14*) Reznik-Schüller HM, Lijinsky W, Hague BF Jr. Electron microscopic autoradiography of the pancreas in the hamster treated with tritiated *N*-nitroso-2,6-dimethylmorpholine. Cancer Res 1980; 40:2245-2251.

(*15*) Williams MA. Assessment of electron microscopic autoradiograms. Adv Opt Electr Microsc 1969; 3:219-272.

(*16*) Mohr U, Reznik-Schüller HM, Emara M. Tissue differentiation as a prerequisite for transplacental carcinogenesis in the hamster respiratory system with specific respect to the trachea. Natl Cancer Inst Monogr 1979; 51:117-122.

(*17*) Emura M. Praenatale Entwicklung der Hamstertrachea. Ph.D. thesis. Hannover: Technische Hochschule, 1977.

(*18*) Magee PN, Pegg AE, Swann PF. Molecular mechanisms of chemical carcinogenesis. In: Grundmann E, ed. Handbuch der allgemeinen Pathologie. Bänd 6. Tumors. II: Viral and chemical carcinogenesis. Berlin: Springer-Verlag, 1975:329-419.

(*19*) Lijinsky W. Carcinogenic and mutagenic N-nitroso compounds. Chem Mutagens 1976; 4:193-217.

(*20*) Bresnick, E, Vaught JB, Chuang AH, Stoming TA, Bockman D, Mukhtar H. Nuclear aryl hydrocarbon hydroxylase and interaction of polycyclic hydrocarbons with nuclear components. Arch Biochem Biophys 1977; 181:257-269.

(*21*) Pezzuto JM, Lea MA, Yang CS. The role of microsomes and nuclear envelope in the metabolic activation of benzo(*a*)pyrene leading to binding with nuclear macromolecules. Cancer Res 1977; 37:3427-3433.

(*22*) Sagara Y, Harano T, Omura T. Characterization of electron transport enzymes in the envelope of rat liver nuclei. J Biochem 1978; 83:807-812.

(*23*) Fahl WE, Jefcoate CR, Kasper CB. Characteristics of benzo(*a*)pyrene metabolism and cytochrome P-450 heterogeneity in rat liver nuclear envelope and comparison to microsomal membrane. J Biol Chem 1978; 253:3106-3113.

(*24*) Kuhn CH III. The cells of the lung and their organelles. In: Crystal RG, ed. Lung biology in health and disease. Vol 2. The biochemical basis of pulmonary function. New York: Marcel-Dekker, 1976:3-48.

(*25*) Reznik-Schüller HM, Hague BF Jr. Autoradiographic study of the distribution of bound radioactivity in the respiratory tract of Syrian hamsters given *N*-[^{3}H]nitrosodiethylamine. Cancer Res 1981; 41:2147-2150.

FIGURE 1.—Light micrograph of fetal Syrian hamster trachea on day 12 of gestation: The epithelium consists of a single layer of tall columnar undifferentiated stem cells. Mitosis (*arrow*) is common. Semithin section stained with toluidine blue. *Bar*=5 µm. × 1,200

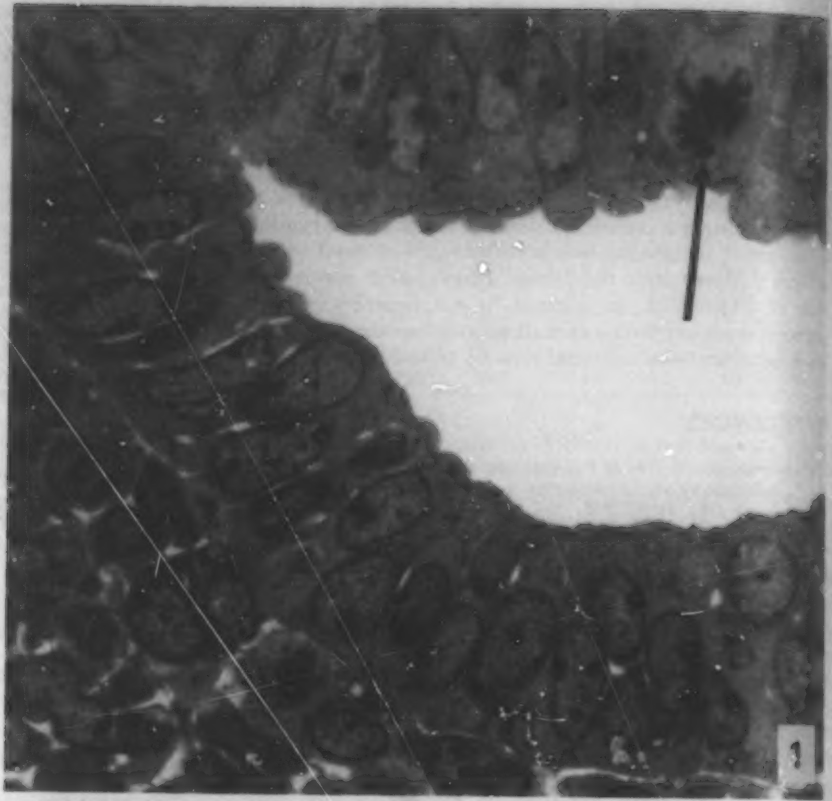

FIGURE 2.—Electron microscopic autoradiograph of cytoplasmic area in epithelium of fetal Syrian hamster trachea 1 hr after transplacental administration of [^{3}H]DENA on day 12 of gestation: Autoradiographic grains are scanty at this time and localized on short tubules of rough ER (*arrow*). Ilford L4 emulsion, stained with uranyl acetate and lead citrate. *Bar*=0.8 µm. × 12,500

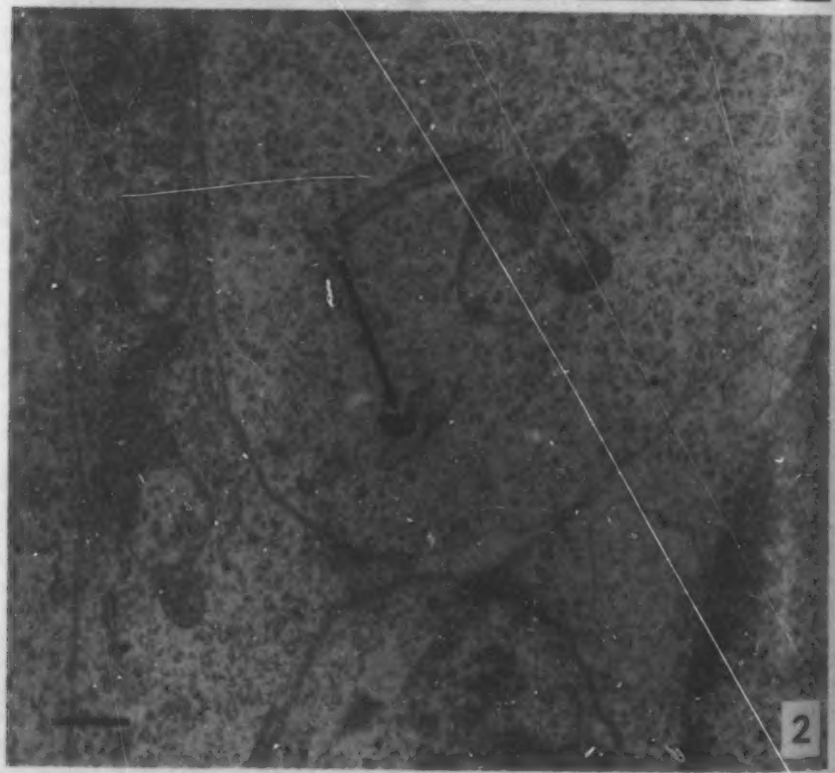

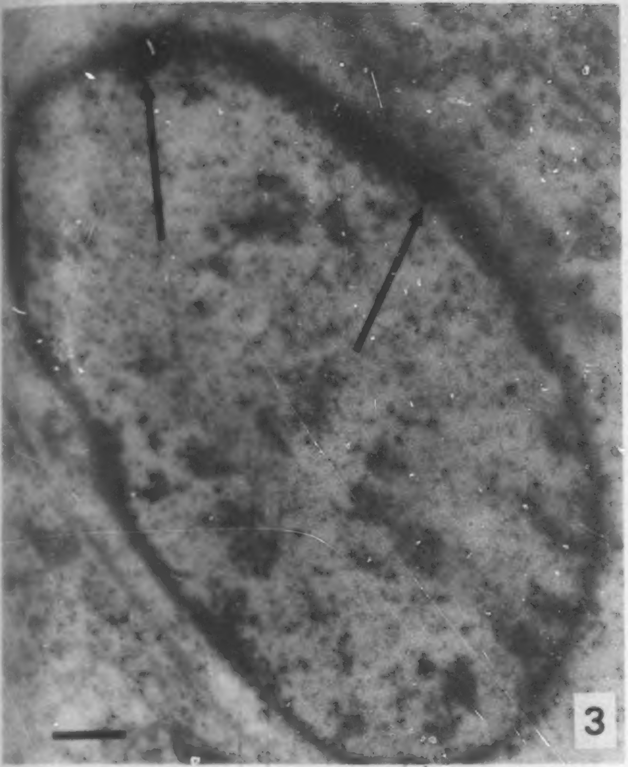

FIGURE 3.—Electron microscopic autoradiograph of nucleus in epithelium of fetal Syrian hamster trachea 1 hr after transplacental administration of [^{3}H]DENA on day 12 of gestation: Autoradiographic grains (*arrows*) are localized on marginal areas of nucleus, indicating bound radioactivity in nuclear membrane or marginally condensed heterochromatin. Ilford L4 emulsion, stained with uranyl acetate and lead citrate. *Bar*=0.65 µm. × 15,000

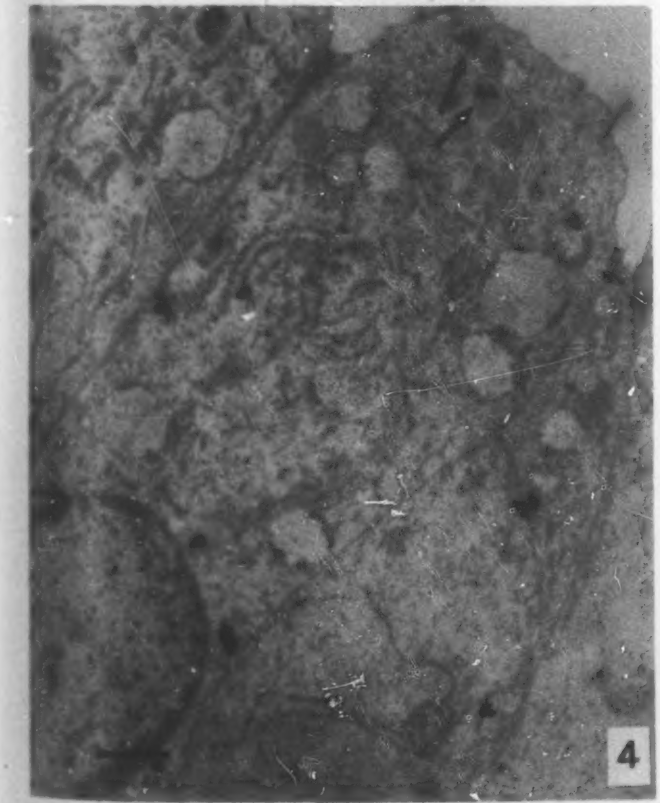

FIGURE 4.—Electron microscopic autoradiograph of mucous cell in epithelium of fetal Syrian hamster trachea 1 hr after transplacental administration of [^{3}H]DENA on day 15 of gestation: Autoradiographic grains are predominantly localized on rough ER and mucus droplets (*arrows*). Ilford L4 emulsion, stained with uranyl acetate and lead citrate. *Bar*=1.25 µm. × 7,900

blank page

Comparison of Biologic Behavior and Histology of Transplanted Mammary Tumors in GR Mice[1,2,3]

Dean H. Percy,[4,5] Vincent L. Morris,[4,6] *and* Janet I. MacInnes[4,7,8,9]

ABSTRACT—Mammary tumors that arose spontaneously in inbred GR mice were transplanted into syngeneic castrated males. The hormone responsiveness of the transplants was studied in mice treated with estrone and progesterone and was compared with the hormone responsiveness in mice that received no hormone treatment. Microscopic examination of hormone-responsive and hormone-independent tumors revealed similar histologic patterns in both groups. It was evident that pale cells, which are classically associated with hormone-responsive tumors, may also be present in transplanted hormone-independent tumors in this strain. No correlation was found between the histologic pattern of these transplanted tumors and the biologic behavior, hormonal status, or presence of a specific murine mammary tumor virus (MuMTV) proviral fragment. Mammary tumors also appeared capable of undergoing differentiation into more than one morphologic type. Two cotransplanted tumors (derived from the same parental tumor) had markedly different histologic patterns; however, analysis of MuMTV proviral fragments indicated that the MuMTV-infected cells were of the same parentage.—JNCI 1982; 69:933–938.

MuMTV is associated with mammary carcinomas in high-tumor-incidence strains of mice such as GR and C3H (*1*). Examination of GR mammary tumor DNA reveals that, in addition to ten endogenous MuMTV copies per diploid cell, there are from one to approximately ten acquired proviral copies stably integrated into the genome (*2, 3*). It has been observed that DNA's extracted from spontaneous mammary tumors produce a unique pattern of MuMTV-specific fragments for each tumor when digested with restriction endonucleases (*4*). This result indicates that while there are many possible integration sites for acquired MuMTV copies, none of these sites appear to be strongly preferred (*4*).

Hormone-responsive tumors rarely occur in most strains of mice (*1, 5*). However, in the GR strain, as in the human counterpart, both hormone-independent and hormone-responsive neoplasms are found (*6–8*). To evaluate the biologic behavior of tumors arising spontaneously in GR mice, we transplanted tumor cell suspensions into pairs of syngeneic castrated male recipients (*7, 9*). Estrone and progesterone were administered to one group to determine whether the transplanted tumor was hormone-independent or hormone-responsive (*7, 9*). On the basis of the work of Sluyser and van Nie (*9*), a tumor was deemed hormone-responsive if transplanted cells gave rise to a palpable tumor at least 14 days earlier in the hormone-treated animal.

In a previous study, analysis of acquired MuMTV proviral copies in transplanted mammary tumor from GR mice revealed differences between hormone-responsive and hormone-independent cells derived from the same tumor (*7*). It was concluded that the spontaneous tumors were composed of a limited number of populations of hormone-responsive and hormone-independent cells; however, specific MuMTV fragments could not necessarily be correlated with the hormone responsiveness of the tumor (*7*).

In this study, we were interested in determining whether the histologic patterns of the tumors were related to their hormone responsiveness or to other factors, such as the presence of specifically acquired MuMTV proviral fragments. Like Dunn and others (*10, 11*), we found that the tumors displayed a significant degree of histologic heterogeneity. In contrast to reports by Strum and others (*5, 11, 12*), though, we found that many pale cell carcinomas were not hormonally responsive. Our data suggest that the histology of these tumors is very complex and might be influenced by many factors. The histologic pattern was not directly related to the hormone status of the tumor or to the presence or absence of hormone treatment. In addition, using the acquired MuMTV proviral fragments as markers for cell populations, we have evidence that neoplastic epithelial cells may be able to undergo differentiation into more than one morphologic type.

MATERIALS AND METHODS

Source of animals and tumor transplantation scheme.—Inbred GR mice used in this study were obtained from Dr. E. Y. Lasfargues. The methods of tumor collection and transplantation have been described previously (*7*). Spontaneous tumors from multiparous GR females were aseptically removed and homogenized, and approximately 2×10^6 cells were administered sc into the lower flank of pairs of synge-

---

ABBREVIATIONS USED: cDNA=complementary DNA; Kb=kilobase pair; MuMTV=murine mammary tumor virus.

---

[1] Received November 10, 1981; accepted May 10, 1982.

[2] Supported by a National Cancer Institute of Canada grant awarded to V. L. M.

[3] Animals were maintained under the guidelines set forth by the University of Western Ontario in accordance with the recommendations of the Canadian Council on Animal Care.

[4] Department of Microbiology and Immunology, University of Western Ontario, London, Ontario, N6A 5C1, Canada.

[5] *Present address*: Department of Pathology, O.V.C., University of Guelph, Guelph, Ontario, N1G 2W1, Canada.

[6] *Address reprint requests to* Dr. Morris.

[7] *Present address*: Cold Spring Harbor Laboratory, Cold Spring Harbor, N.Y. 11724.

[8] Recipient of an Ontario Graduate Scholarship.

[9] We thank Dr. E. Y. Lasfargues and Dr. G. Mackie for materials cited in the text and Dr. B. Sass for examining the histologic slides of some of the tumors discussed in this paper. Murine mammary tumor virus (C3H) RNA and avian myeloblastosis virus DNA polymerase were supplied by the Office of Program Resources and Logistics, National Cancer Institute. We also thank Mr. E. C. M. Lee Chan, Ms. U. Jorch, Ms. A. Orosz, and Ms. E. M. Seaman for their technical assistance.

neic castrated male mice. One mouse was given an injection weekly of 3×10^{-3} g progesterone (Sigma Chemical Co.), and estrone at 0.5×10^{-6} g/ml was administered in the drinking water. The other hormone-untreated mouse was housed under identical conditions. With each passage, the histology and hormone responsiveness of the tumors were assessed. Following the criterion of Sluyser and van Nie (*9*), a tumor was deemed hormone-responsive if it appeared at least 14 days earlier in the hormone-treated animal. Most hormone-responsive tumors, however, appeared 8–30 weeks earlier in the hormone-treated animals.

Restriction endonuclease analysis of tumor DNA's.—DNA was extracted from tumors at selected passages, digested with restriction endonucleases Eco RI or Bam HI, and separated by electrophoresis in agarose gels (*7, 13*). Eco RI cuts the provirus approximately midway in the genome and at the nearest Eco RI site in the flanking cell sequences (*2, 14*). Since integration of MuMTV appears to occur in general at different sites in the genome, a proviral copy cut with Eco RI generates two unique-sized fragments (*4*). In a similar manner, digestion with Bam HI generates two unique fragments in addition to a 1.1-Kb internal piece (*14*). These enzymes, therefore, can be conveniently used to determine the number of integrated proviral copies. After transfer of fragments from the agarose gels to nitrocellulose filters (*7, 13*), the MuMTV-specific sequences were annealed with MuMTV ^{32}P cDNA (*7*). Unhybridized cDNA was washed away, and the MuMTV-specific sequences were visualized by autoradiography (*15*). The details of the procedures for the restriction endonuclease analysis, Southern transfer procedure, and hydridization reactions have been described previously (*7*).

Histologic and ultrastructural studies.—Tissues collected for light microscopy were fixed in Bouin's fluid, embedded in paraffin, sectioned at 6 µm, and stained with hematoxylin and eosin and periodic acid–Schiff (*16*). Selected specimens were collected for electron microscopy. Tissues were fixed in 3% glutaraldehyde, minced, dehydrated, and embedded in Spurr's medium. Sections (1 µm) were stained with toluidine blue for light microscopic examination. Thin sections were stained with uranyl acetate and Reynold's lead citrate and examined in a Zeiss EM 9S electron microscope.

RESULTS

Morphologic Studies

The histologic characterization of mammary tumors seen in most strains of mice has been described in detail by Dunn, Sass, and others (*10–12*). In this study, particular emphasis was placed on the identification of pale cell tumors that are associated with GR mice (*5, 11, 12*). Most of the tumors examined were classified as either type B adenocarcinomas (*10*) or pale cell carcinomas (*11*). The type B tumors demonstrated a variety of architectural features ranging from acinar structures to anastomosing trabeculae or solid sheets of cells. In the pale cell tumors, characteristically, cords or nests of pale cells were found close to clusters of dark cells (fig. 1). Occasionally, glandular structures were observed. Electron microscopic examination of pale cell tumors revealed large cells with electron-lucent cytoplasm and scattered cytoplasmic organelles (figs. 4A, 4B). In addition to the pale cells, there were darkly staining cells with electron-dense cytoplasm, closely packed cytoplasmic organelles, and clearly delineated cell outlines (figs. 4A, 4B). Intercellular desmosomes were observed (fig. 4A), and typical A-type MuMTV particles were frequently demonstrated, particularly in the cytoplasm of the dark cells (fig. 4B).

In many cases, the tumors displayed some heterogeneity with respect to cell and architectural types. In some tumors that were predominantly type B adenocarcinomas, isolated islands of pale cells could be detected. Similarly, in pale cell tumors, scattered areas of cells typical of those of type B tumors were observed in some cases. This heterogeneity is consistent with the fact that spontaneous tumors contain multiple populations of cells; however, the presence of a particular cell type cannot necessarily be correlated with any biologic property.

Pale cell tumors in the GR mouse are classically considered to be hormone-responsive (*5, 11, 12*). Hormone-treated mice, however, did not always develop hormone-responsive tumors. We were unable to correlate the histologic type with hormone responsiveness or hormone treatment (table 1). In general, there were no obvious differences seen in the histologic pattern of those tumors passaged in the presence of hormones (76 vs. 74%) or in tumors determined to be hormone-responsive or hormone-independent (74 vs. 82%).

Relationship of Carcinoma and Myoepithelial Tumor

We have examined approximately 170 transplanted GR tumors in this study and in related studies. In one instance we found that 2 transplanted tumors derived from the same hormone-independent parental neoplasm had distinctly different histologic patterns. On the basis of the criteria previously described (*5, 11, 12*), transplant 4483 D (passaged in a hormone-treated recipient) was classified as a pale cell carcinoma (fig. 2). Conversely, the cotransplant 4525D (passaged in a recipient without hormone treatment) contained interlacing bands of fusiform cells. Individual cells had flattened nuclei with rounded poles and finely fibrillar, elongated cytoplasmic outlines (fig. 3). With the use of Hamperl's criteria (*17*), this neoplasm was interpreted to be of myoepithelial origin. The architecture and cell type were

TABLE 1.—*Morphologic classification of transplanted mammary tumors in GR mice according to treatment with, and response to, hormones*

Parameter	No. of animals so classified/total No. of animals (%)		
	Pale cell tumor	Type B adenocarcinoma	Myoepithelial tumor
Treatment:			
Passage with hormones[a]	29/38 (76)	9/38 (24)	0/38 (0)
Passage without hormones	25/34 (74)	8/34 (23)	1/34 (3)
Response to hormones:			
Responsive	14/19 (74)	5/19 (26)	0/19 (0)
Independent	14/17 (82)	3/17 (18)	0/17 (0)

[a] Estrone and progesterone (*see* "Materials and Methods").

consistent throughout, and no typical epithelial elements were observed. Despite the differences in histologic type, the time of appearance and gross morphology of the 2 tumors were very similar. The myoepithelial tumor was palpable 37 days post injection in the animal that did not receive hormone treatment; the pale cell tumor appeared 34 days post injection in the hormone-treated corecipient.

Examination of the 2 tumors with the Southern transfer procedure revealed that both tumors contained the same pattern of acquired proviral Eco RI fragments (fig. 5). Similar results were obtained with Bam HI analysis. Since both tumors gave identical patterns, we concluded that the MuMTV-infected cells in the myoepithelial tumor and the pale cell carcinoma very likely originated from the same parental tumor cells. If the myoepithelial tumor had arisen independently, then the pattern of MuMTV-specific fragments would have been different because, to date, data indicate that none of the many possible sites of integration for acquired MuMTV DNA copies appear to be preferred (*4*).

The parental spontaneous tumor has a pattern of major MuMTV-specific, acquired DNA sequences that differs from the pattern seen in the transplanted tumors 4525D and 4483D (fig. 5); this observation occurs because spontaneous GR mammary tumors are made up of more than one population of cells that can be distinguished by their MuMTV proviral restriction fragments (*7*). The relative proportion of these cells can vary as the tumor is passaged in mice in the presence or absence of hormones (*7*).

DISCUSSION

The distinctive pale cell mammary tumors seen in GR mice have been reported to be hormone-responsive (*5*, *11*, *12*). However, in our transplantation study, both hormone-responsive and hormone-independent neoplasms were of the pale cell type. In fact, no distinctive differences could be detected between the histologic patterns seen in hormone-responsive and hormone-independent mammary tumors (table 1). Similarly, the histologic findings were comparable in the transplanted tumors whether or not the recipient mice were treated with hormones. These data suggest that pale cells may persist in hormone-independent tumors and that their presence is a reflection of a coincidental or obligatory cell heterogeneity in these tumors. Alternatively, the degree of hormone responsiveness of a tumor may have little or no bearing on the histology of the tumor. Studies of human breast carcinomas indicate that the histologic type is generally a poor prognosticator of hormone responsiveness (*18*). Thus many influences, including genetic, immunologic, hormonal, and physiologic factors, may determine the histologic pattern of a neoplasm.

Our data also suggest that mammary tumor cells may be able to undergo differentiation into more than one morphologic type. In this study, 2 transplanted tumors derived from the same parental tumor had distinctly different histologic patterns. Transplant 4483D was classified as a pale cell carcinoma, whereas the cotransplant 4525D was interpreted to be a myoepithelial tumor (figs. 2, 3). Despite their differences in histology, both tumors shared the same pattern of acquired MuMTV proviral fragments (fig. 5). Since both tumors appeared within 4 days of each other and within 37 days post injection, selection of a single mutated cell would not likely account for the appearance of the myoepithelial tumor. In addition, it is unlikely that the appearance of the myoepithelial tumor was due to the selection of preexisting cells with the same pattern of acquired MuMTV proviral fragments since there appears to be no strongly preferred integration sites (*4*). The role of hormone treatment or, in the case of the myoepithelial tumor, lack of treatment is not clear, but hormonal influences are likely important under certain conditions for the selection of different morphologic types.

This observation provides molecular evidence to support the contentions of Hamperl (*17*) and Foulds (*19*) that the varied types of epithelium (seen in mammary tumors) may be different growth forms of divergent differentiations in cells of a common ancestry. In our experiments, however, this differentiation may be a relatively rare event in vivo. Dulbecco et al. (*20*) have reported a similar differentiation process in vitro in Rama 25 cells derived from a chemically induced rat mammary carcinoma. They were able to isolate fusiform myoepithelial-like cells from rapidly differentiating F-precursor cells. They suggested that the differentiation of the F-precursor cells in vitro into various cell types (including myoepithelial-like elements) may correspond to processes occurring in vivo.

REFERENCES

(*1*) Nandi S, McGrath CM. Mammary neoplasia in mice. Adv Cancer Res 1973; 17:353–414.

(*2*) Cohen JC, Varmus HE. Proviruses of mouse mammary tumor virus in normal and neoplastic tissues from GR and C3Hf mouse strains. J Virol 1980; 35:298–305.

(*3*) Groner B, Hynes N. Number and location of mouse mammary tumor virus proviral DNA in mouse DNA of normal tissue and of mammary tumors. J Virol 1980; 33:1013–1025.

(*4*) Cohen JC, Shank PR, Morris VL, Cardiff R, Varmus HE. Integration of the DNA of mouse mammary tumor virus in virus-infected normal and neoplastic tissues of the mouse. Cell 1979; 16:333–345.

(*5*) Strum JM. Pale cell carcinoma. Ultrastructure of a hormone-dependent mammary tumor in GR mice. Am J Pathol 1981; 103:283–291.

(*6*) Sluyser M, Evers SG, DeGroeij CC. Sex hormone receptors in mammary tumours of GR mice. Nature 1976; 263:386–389.

(*7*) MacInnes JI, Lee Chan EC, Percy DH, Morris VL. Mammary tumors from GR mice contain more than one population of mouse mammary tumor virus-infected cells. Virology 1981; 113:119–129.

(*8*) Donegan WL, Spratt JS. Cancer of the breast. Toronto: Saunders, 1979.

(*9*) Sluyser M, van Nie R. Estrogen receptor content and hormone-responsive growth of mouse mammary tumors. Cancer Res 1974; 34:3253–3257.

(*10*) Dunn TB. Morphology of mammary tumors in mice. In: Homburger F, ed. Physiopathology of cancer. 2d ed. New York: Hoeber-Harper, 1959:38–84.

(*11*) Sass B, Dunn TB. Classification of mouse mammary tumors in Dunn's miscellaneous group including recently reported types. JNCI 1979; 62:1287–1293.

(*12*) Van Nie R, Dux A. Biological and morphological characteristics of mammary tumors in GR mice. J Natl Cancer Inst 1971; 46:885–897.

(*13*) Southern EM. Detection of specific sequences among DNA fragments separated by gel electrophoresis. J Mol Biol 1975; 98:503–517.

(*14*) Shank PR, Cohen JC, Varmus HE, Yamamoto KR, Ringold GM.

Mapping of linear and circular forms of mouse mammary tumor virus DNA with restriction endonucleases: Evidence for a large specific detection occurring at high frequency during circularization. Proc Natl Acad Sci USA 1978; 75:2112–2116.

(*15*) SWANSTROM R, SHANK PR. X-ray intensifying screens greatly enhance the detection by autoradiography of the radioisotopes ^{32}P and ^{125}I. Anal Biochem 1978; 86:184–192.

(*16*) LUNA LG, ed. Manual of histologic staining methods of the Armed Forces Institute of Pathology. 3d ed. Toronto: McGraw-Hill, 1968.

(*17*) HAMPERL H. The myothelia (myoepithelial cells). Normal state; regressive change; hyperplasia; tumors. Curr Top Pathol 1970; 53:161–220.

(*18*) MCGUIRE WL. Current status of estrogen receptors in human breast cancer. Cancer 1975; 36:638–644.

(*19*) FOULDS L. The histologic analysis of mammary tumors of mice. I. Scope of investigations and general principles of analysis. J Natl Cancer Inst 1956; 17:701–711.

(*20*) DULBECCO R, BOLOGNA M, UNGER M. Differentiation of a rat mammary cell line in vitro. Proc Natl Acad Sci USA 1979, 76:1256–1260.

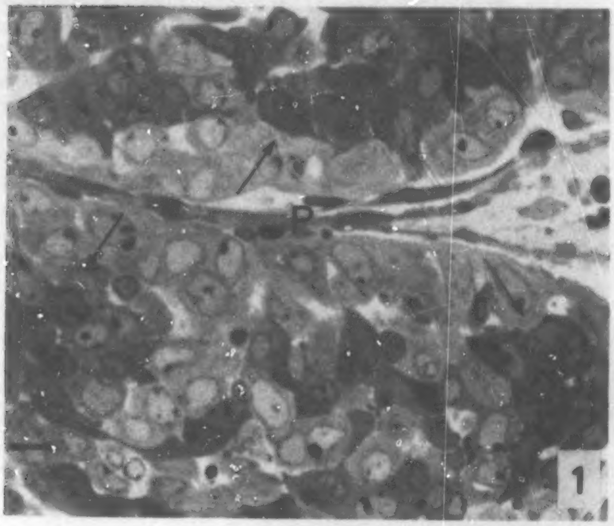

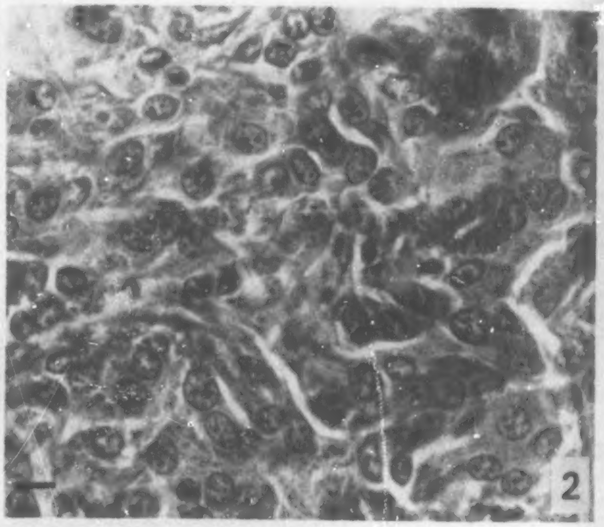

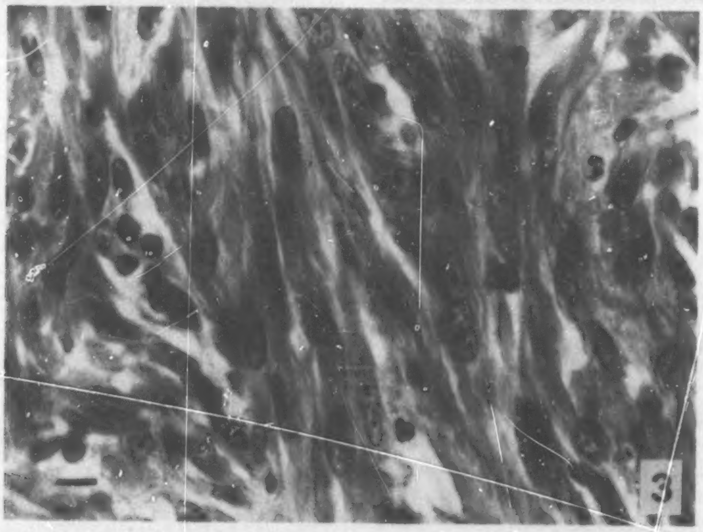

FIGURE 1.—Transplant 4616C. Light micrograph of a pale cell tumor that was passaged in a castrated GR male mouse in the absence of hormones (*see* "Materials and Methods"). *Note* sheets of pale cells (P) with large nuclei and light-staining cytoplasm and adjacent dark cells (*arrows*). Toluidine blue. *Bar*=10 µm.

FIGURE 2.—Transplant 4483D. Light micrograph of a pale cell carcinoma transplanted into a hormone-treated animal (*see* "Materials and Methods"). *Note* the sheets of epithelial cells with some tendency to form acinar structures. Hematoxylin and eosin. *Bar*=10 µm.

FIGURE 3.—Cotransplant 4525D. Light micrograph of a mammary tumor of the same parental origin as the tumor shown in fig. 2, but which was transplanted into an animal that did not receive hormones. The finely fibrillar, elongated cytoplasmic outlines and the general architecture are compatible with a tumor of the myoepithelial type. Hematoxylin and eosin. *Bar*=10 µm.

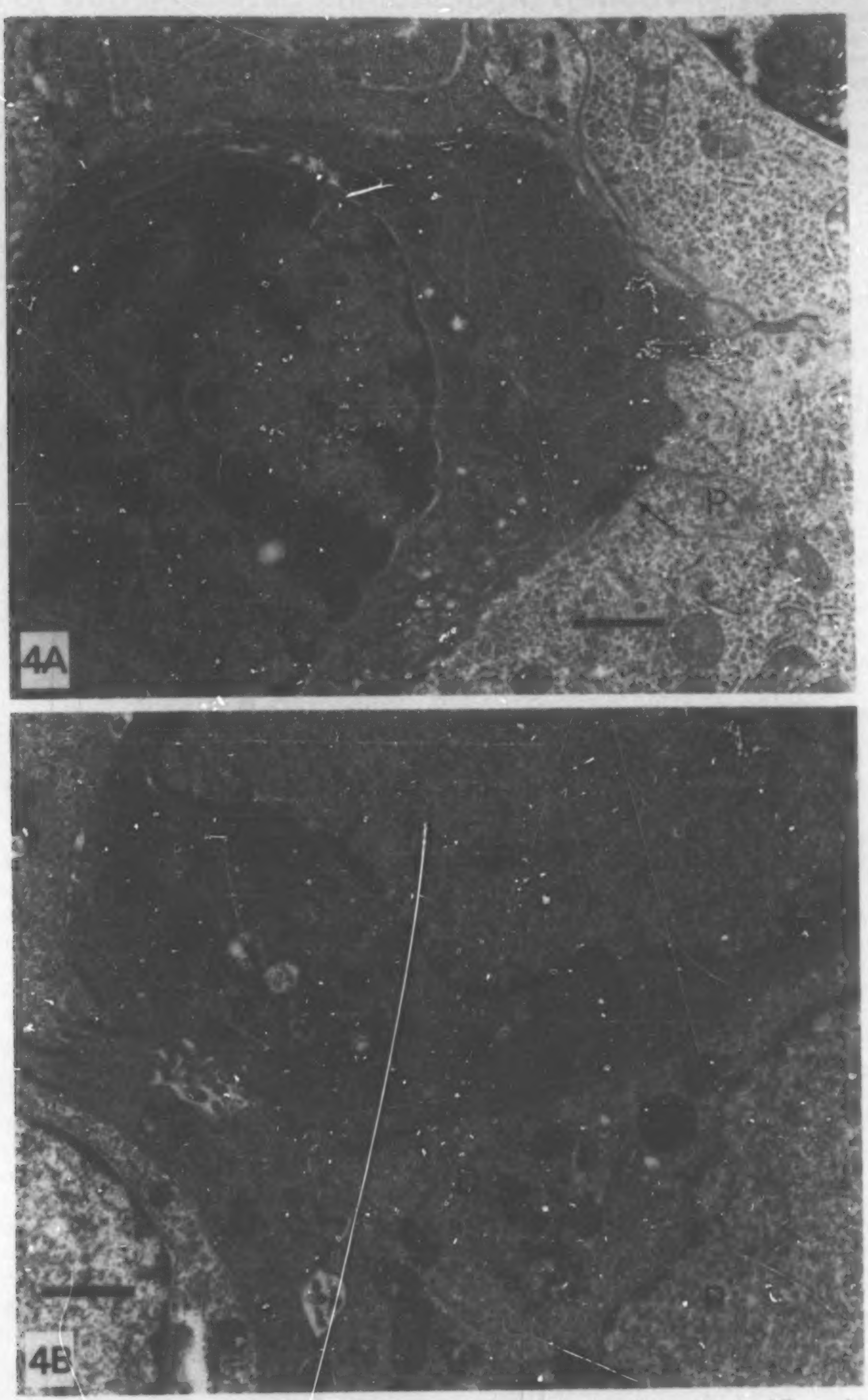

FIGURE 4A.—Transplant 4616B. Electron micrograph of transplanted mammary tumor of the pale cell type. *Note* the difference between the cytoplasm of the pale cells (P) and the dark cell (D). There are abundant organelles including densely packed ribosomes in the cytoplasm of the dark cell in contrast to the scattered ribosomes in the pale cells. Desmosomes (*arrow*) are evident between the dark cell and an adjacent pale cell. FIGURE 4B: Transplant 4616A. Electron micrograph of transplanted mammary tumor of the pale cell type. Dark cells (D) are close to two pale cells (P). Typical MuMTV particles are scattered in the cytoplasm and are oriented around and within the cytoplasmic lumens in the dark cells. Lead citrate and uranyl acetate. *Bar*=0.1 μm.

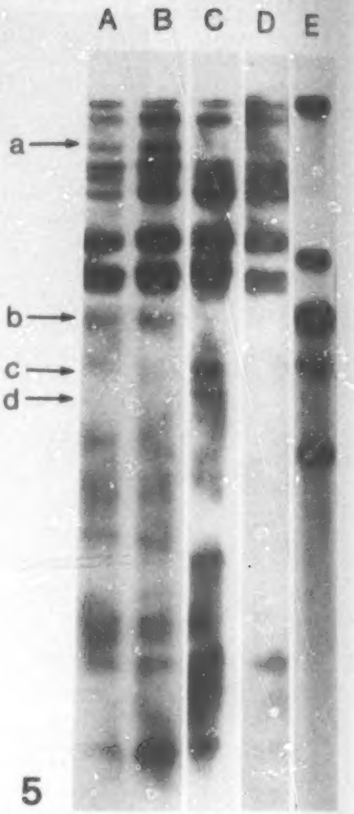

5

FIGURE 5.—MuMTV-specific proviral sequences in transplanted tumor series. Mammary tumors grafted into castrated GR male mice were extracted, and 5 µg of DNA was digested with Eco RI. After complete digestion, MuMTV-specific sequences were separated and visualized as described in "Materials and Methods." The major acquired MuMTV fragments are indicated by a lower-case letter. *Lane A* (4525D), myoepithelia tumor with predominant acquired MuMTV fragments a and b; *lane B* (4483D), cotransplant with predominant acquired MuMTV fragments a and b; *lane C*, original spontaneous tumor with predominant acquired proviral fragments c and d; and *lane D*, GR normal organs (heart, liver, spleen, lungs, and kidneys). Molecular weights of the MuMTV-specific fragments were determined by comparison with those of Eco RI fragments of ^{32}P lambda DNA, *lane E* (provided by Dr. G. Mackie).

Regulation of Cell-Mediated Immunologic Reactivity to Moloney Murine Sarcoma Virus-Induced Tumors.
III. Further Characterization of Tumor-Specific Serum Blocking Factors[1,2,3]

William J. Halliday,[4] **Thelma A. Koppi,**[4] *and* **Ian F. C. McKenzie**[5]

ABSTRACT—Blocking factors in the sera of inbred CBA mice bearing either Moloney murine sarcoma virus-induced tumors or transplanted 3-methylcholanthrene-induced tumors specifically blocked in the leukocyte adherence inhibition reaction between tumor-sensitized peritoneal cells and tumor antigens. These factors were absorbed from serum by treatment with anti-Ia antibodies and could be eluted in a partially purified form. Chromatography on Sephacryl S-200 columns demonstrated blocking activity in fractions of high and low molecular weight (>100,000 and 40,000–50,000, respectively) derived from whole sera or eluates. Active fractions from serum appeared to retain the tumor specificity of the original material.—JNCI 1982; 69:939–944.

Specific BF have been defined as any humoral factors that can in a specific way impair an immune response to tumor antigens independently of their site of action (central, afferent, or efferent) and their molecular composition (*1*). The most intensively studied BF are those found in the sera of tumor-bearing hosts and that block in vitro reactions of specific cell-mediated antitumor immunity by an efferent mechanism. These BF were first detected by the lymphocyte cytotoxicity reaction, the destructive effect of immune lymphocytes on tumor cells being abrogated by the sera of subjects bearing the same type of tumor (*2*).

The earliest assumption that BF were antibodies (*3*) was soon supplanted by the hypothesis that BF were antigen-antibody complexes, derived at least in part from the tumor. Much of the more recent work on the nature of BF supports this concept. Investigations by the Hellström group (*4*) showed that BF could be split into low and high MW fractions, and activity was reconstituted when these fractions were combined. Baldwin and co-workers (*5*) prepared artificial BF by mixing tumor antigen with antibody in suitable proportions. Free tumor antigen was also found to interfere with cell-mediated cytotoxicity under some conditions (*6*).

Further evidence for the existence of BF distinct from antibodies came from studies with sera of mice bearing MCA-induced sarcomas. Fractionation of these sera on immunoadsorbent columns and by gel filtration on Sephadex G-200 yielded specific BF of MW 56,000. These materials had affinity for the corresponding tumor cells and properties of glycoproteins (*7*). The existence of this form of BF was reconciled with evidence for antigen–antibody complexes with blocking properties by the proposition that the 56,000-MW factor may exist in serum as a complex with immunoglobulin or that it may be formed by cells stimulated by specific immune complexes (*1*).

Serum BF have obvious affinities with antigen-specific suppressor factors found in other circumstances. A relevant example is the factor extracted from thymuses of tumor-bearing mice (*8*); this factor enhanced tumor growth in vivo and contained determinants coded by the I-J subregion of the MHC.

Several in vitro reactions other than lymphocyte cytotoxicity are susceptible to blocking by serum factors. The BF in different systems may be identical, but this is not necessarily so. LAI with soluble tumor antigens can be blocked by sera from the appropriate tumor-bearing subjects (*9–12*). Specific BF related to M-MuSV-induced tumors were recently shown to contain Ia determinants related to the I-J subregion of the MHC (*13*). These BF were removed specifically from serum by anti-Ia antibodies. Similar studies have now been conducted with MCA-induced tumors, the BF suppressing LAI have been partially purified by immunoadsorption with anti-Ia antibodies followed by elution, and the molecular size distribution of BF in sera and eluates has been determined.

MATERIALS AND METHODS

Mice.—Inbred CBA mice were procured from the Central Animal Breeding House, University of Queensland. They were 2–6 months old when used.

MCA-induced tumor.—Fibrosarcomas were induced in CBA mice by sc injection of MCA as previously described (*9*). One of these tumors was passaged by serial sc transplantation in syngeneic mice and had passed through 12 generations before this study was done. Tumors grew to 10 mm in diameter in 10–15 days. Tumor tissue for extraction was removed when the tumors reached 10 mm in diameter and was frozen at −50°C until required.

Virus-induced tumor.—M-MuSV (lot #B-156, #110, and

ABBREVIATIONS USED: BF=blocking factor(s); HLA=human leukocyte antigen; LAI=leukocyte adherence inhibition; MCA=3-methylcholanthrene; MHC=major histocompatibility complex; M-MuSV=Moloney murine sarcoma virus; MW=molecular weight(s); PBS=phosphate-buffered saline; PC=peritoneal cells.

---

[1] Received November 23, 1981; accepted May 10, 1982.

[2] Supported by the Queensland Cancer Fund.

[3] Research procedures were in accord with the ethical standards of the Human and Animal Experimentation Ethical Review Committee, University of Queensland.

[4] Department of Microbiology, University of Queensland, St. Lucia, Queensland, Australia 4067.

[5] Department of Pathology, University of Melbourne, Parkville, Australia 3052.

#160) was donated by the National Cancer Institute (Bethesda, Md.) through M.A. Bioproducts (Walkersville, Md.). The undiluted material (0.1 ml) was injected im into the thighs of mice to produce regressing tumors as previously described (*12, 14*). Tissue for extraction was removed at the height of tumor growth and frozen as detailed above.

Tumor extracts (antigens).—Fresh or frozen tumor tissue was homogenized in PBS (pH 7.2), and a soluble extract was prepared according to the published procedure (*9, 12*). Before use the extracts were titrated and diluted to give optimal LAI reactions (final dilutions of 1:20 in the reaction mixtures) (*12*).

PC.—We killed donor mice with ether and obtained PC by injecting heparinized Hanks' solution into the peritoneal cavity and then collecting the fluid after opening the cavity. The fluid was centrifuged at $200\times g$ for 5 minutes, and the erythrocytes in the pellet were lysed with $0.15\ M$ ammonium chloride solution. The PC were washed three times with Eagle's basal medium containing 10% fetal calf serum (Commonwealth Serum Laboratories, Melbourne, Australia). The cell concentration was adjusted to 1×10^7/ml for use in LAI. PC were obtained from M-MuSV-inoculated mice (5–10 days after inoculation) and from mice with MCA-induced tumors (10–12 days after transplantation).

Mouse serum.—Mice were anesthetized and bled from the tail, the blood was allowed to clot, and the serum was either used fresh on the same day or stored frozen at −20°C for a few days. Serum was obtained from normal mice and from mice bearing either M-MuSV-induced tumors (5 days after inoculation) or MCA-induced tumors (10–12 days after transplantation).

Preparation of anti-Ia antibodies.—Antiserum was prepared by the alloimmunization of suitable mouse strains (A.TH anti-A.TL) and is described elsewhere (*13*). The Ia antibodies recognized products of the I-region (*k*-haplotype as in the MHC of CBA mice).

Absorption of serum with anti-Ia antibodies and elution of serum factors.—Anti-Ia antiserum was coupled to Sepharose 4B (Pharmacia Fine Chemicals, Uppsala, Sweden) as described (*13*). The coupled gel was used to absorb CBA mouse serum (normal mouse and tumor-bearing mouse) by the column method. The gel (3 ml) was poured into a 5-ml plastic syringe barrel, and the serum (3–4 ml) was poured into the resulting column. The serum was washed through with 3–4 ml of PBS, and the effluent was collected. The column was washed with about 20 ml of PBS. To elute the absorbed material on the gel, we poured $0.1\ M$ glycine-HCl buffer at pH 2 through the column until the eluate became acidic. This eluate was collected and neutralized with saturated sodium bicarbonate solution. The neutralized eluate (Ia eluate) and the initial effluent (Ia effluent) were concentrated to one-third of the original serum volume on Minicon B-15 concentrators (Amicon Corp., Lexington, Mass.).

Column chromatography (gel filtration).—A column (90×2.5 cm) of Sephacryl S-200 superfine (Pharmacia Fine Chemicals) was equilibrated with PBS and calibrated with proteins of known MW. The material to be fractionated (2 ml) was run into the column, and 5-ml fractions were collected and then stored frozen at −20°C until required to be assayed for BF. The fractions were then thawed and 2-ml quantities of each fraction were pooled as specified below. The fraction pools and some individual fractions were finally concentrated to 1/100 volume with Minicon B15 concentrators. Fractions were collected in this way from sera (normal mouse and tumor-bearing mouse) and Ia eluates (normal mouse and tumor-bearing mouse).

LAI technique.—The hemacytometer method was used throughout (*9–12*). Mixtures for the determination of leukocyte adherence contained 10^6 PC, diluted tumor extract as antigen (or medium only as control), and 25% mouse serum (normal serum or material to be tested for BF), all in a total volume of 0.2 ml. These mixtures, in duplicate, were coded, preincubated at 37°C for 30 minutes, then introduced into hemacytometers. After incubation at 37°C for 1 hour the cells were counted, the hemacytometer slides were washed to remove nonadherent cells, and the remaining cells were recounted. A significant reduction in mean percent adherence, consequent upon the inclusion of tumor extract in a mixture of PC and normal serum, was interpreted as a positive LAI reaction.

The quantitative expression of LAI in the tables of results was calculated by simple subtraction of the relevant mean percent adherence from the control mean; the statistical significance of the difference between these means was then determined by Student's *t*-test (modified for unequal variances), inasmuch as the individual values of percent adherence were normally distributed. An LAI value of 10 or greater was usually significant ($P<0.05$).

We determined the ability of a test material (serum or some derivative) to block LAI by comparing the adherence (X) of sensitized PC incubated in the presence of antigen and this test material with the adherence (Y) of the same PC incubated in the presence of antigen and a control material. The difference (X−Y) was the blocking value, and the statistical significance of the difference was determined as above. When the test material was whole tumor-bearing mouse serum, the control was whole normal mouse serum. When the test material was a fraction or derivative of tumor-bearing mouse serum, the control was a similarly derived material from normal mouse serum. In this case, inasmuch as the material was often deficient in serum protein, normal mouse serum was added to the incubation mixtures.

RESULTS

Specific serum effects on LAI.—When PC from tumor-bearing mice were incubated with normal mouse serum, a normal adherence to glass was determined (table 1, mixtures 1 and 5). Addition of the corresponding tumor extract induced significant LAI (mixtures 2 and 6). With the same mixtures of PC and extract, LAI was blocked by the corresponding tumor-bearing mouse serum (mixtures 3 and 7) but not by unrelated tumor-bearing mouse serum (mixtures 4 and 8). The results presented in table 1 establish the tumor specificity of BF in serum and illustrate the procedures and calculations used throughout the present investigation. Substantial negative blocking values (as in mixture 4) were occasionally observed.

Absorption and elution of BF.—In table 2 are shown the data

TABLE 1.—*Specificity of blocking serum activity in LAI as related to tumor type*

Mixture No.	Source of PC[a]	Tumor extract	Source of serum[a]	Percent adherence, mean ± SE	LAI value[b]	Blocking value[b]
1	Mouse with M-MuSV-induced tumor	None	Normal mouse	76.4±2.7		
2	"	M-MuSV-induced tumor	"	58.0±2.8	18.4***	
3	"	"	Mouse with M-MuSV-induced tumor	68.2±2.9	8.2	10.2*
4	"	"	Mouse with MCA-induced tumor	43.8±3.6	32.6***	−14.2
5	Mouse with MCA-induced tumor	None	Normal mouse	71.1±4.5		
6	"	MCA-induced tumor	"	54.2±1.9	16.9**	
7	"	"	Mouse with MCA-induced tumor	83.6±4.1	−12.5	29.4***
8	"	"	Mouse with M-MuSV-induced tumor	49.6±3.5	21.5***	−4.8

[a] PC and sera from mice with M-MuSV-induced tumors were obtained 6 and 5 days, respectively, after M-MuSV inoculation; PC and sera from mice with MCA-induced tumors were obtained 12 and 10 days, respectively, after transplantation of MCA-induced tumors.

[b] *** $P<0.001$; ** $P<0.01$; * $P<0.05$; unmarked values are not significant.

TABLE 2.—*Demonstration of blocking of LAI by whole tumor-bearing mouse serum but not by effluent from an anti-Ia column and recovery of blocking factors in pH-2 eluate*

Mixture No.	Source of PC[a]	Tumor extract	Source of serum or derivative[a]	Percent adherence, mean ± SE	Blocking value[b]
1	Mouse with MCA-induced tumor	None	Normal mouse serum	88.1±3.5	
2	"	MCA-induced tumor	"	57.6±4.4	
3	"	"	Serum from mouse with MCA-induced tumor	78.6±3.7	21.0***
4	"	"	Normal mouse effluent	78.8±4.5	
5	"	"	Effluent from mouse with MCA-induced tumor	67.5±4.8	−11.3
6	"	"	Normal mouse eluate	65.2±2.9	
7	"	"	Eluate from mouse with MCA-induced tumor	83.2±3.5	18.0***
8	Mouse with M-MuSV-induced tumor	None	Normal mouse serum	78.9±3.3	
9	"	M-MuSV-induced tumor	"	66.0±1.8	
10	"	"	Serum from mouse with M-MuSV-induced tumor	84.0±3.2	18.0***
11	"	"	Normal mouse effluent	76.8±3.7	
12	"	"	Effluent from mouse with M-MuSV-induced tumor	70.8±3.5	−6.0
13	"	"	Normal mouse eluate	52.3±2.4	
14	"	"	Eluate from mouse with M-MuSV-induced tumor	63.8±3.0	11.5*

[a] PC and sera from mice with MCA-induced tumors were obtained 12 and 10 days, respectively, after transplantation of MCA-induced tumors; PC and sera from mice with M-MuSV-induced tumors were obtained 9 and 5 days, respectively, after M-MuSV inoculation.

[b] *** $P<0.001$; ** $P<0.01$; * $P<0.05$; unmarked values are not significant.

for blocking activity of whole sera from tumor-bearing mice (mixtures 3 and 10) and materials derived from these sera by treatment with anti-Ia antibody coupled to Sepharose 4B. The absorbed sera (anti-Ia column effluents, mixtures 5 and 12) were no longer blocking when compared with the relevant controls (mixtures 4 and 11, respectively). BF were recovered by treatment of the columns with pH-2 buffer as demonstrated by the significant blocking activity of Ia eluates (mixtures 7 and 14, compared with mixtures 6 and 13, respectively). In all experiments the Ia effluents (absorbed sera) had no residual blocking activity (table 2).

Molecular size distribution of serum and eluate BF.—Sera from mice bearing either M-MuSV-induced or MCA-induced tumors were passed through columns of Sephacryl S-200; fractions were collected, pooled as required, and assayed for BF (by comparison with equivalent fractions from normal serum). Concurrently, Ia eluates were prepared from the same sera by absorption to and elution from immobilized anti-Ia antibody; these eluates were fractionated, pooled as required, and assayed for BF (by comparison with equivalent fractions from Ia eluates of normal serum).

The results are expressed diagrammatically for the original unfractionated materials and the column fractions in which BF were found. Text-figure 1 illustrates the results for whole serum and Ia eluate before being placed on the column (original) and the fraction pools where blocking activity was detected. These materials are related to mice bearing the MCA-induced tumor. In the upper part of text-

best copy available

figure 1 there is a UV transmittance curve for the serum fractions with calibrated MW marked. The whole serum (original) was significantly blocking. After fractionation, high (>100,000) and low (<50,000) MW pools were blocking. In the lower part, the text-figure shows the properties of the Ia eluate and its fractions. The Ia effluent was not blocking (data not shown), which indicated that the active factor was absorbed completely by anti-Ia antibody. The pH-2 eluate (original) was blocking, and the active factor appeared in the fraction pools at an approximate MW of 100,000 and 50,000. There was not enough protein in the eluate to give a transmittance curve.

Examination of pairs of fractions from the same serum as in text-figure 1 confirmed the presence of BF of two different molecular sizes in sera from mice with MCA-induced tumors. This is illustrated in text-figure 2 (upper part). The lower part of text-figure 2 shows the analysis of single fractions from the Ia eluate in the low MW area (fractions 48–55) rather than pools. The smaller factor had an apparent MW of about 40,000. The reason for the absence of activity from fraction 54 is not known.

Text-figures 3 and 4 show the blocking of LAI by sera from mice bearing M-MuSV-induced tumors, the corresponding Ia eluates, and their Sephacryl S-200 fractions. With the first serum (text-fig. 3), both high and low MW activities were found when the whole serum was fractionated, but the original Ia eluate was not significantly blocking. On fractionation of this eluate, high MW blocking material was detected, but there was no significant blocking activity in other fraction pools.

With a second serum of the same type, both the whole serum and Ia eluate were blocking, but only low MW fraction pools had significant activity (text-fig. 4).

Tumor specificity of BF in serum fractions.—To confirm that the blocking fractions found above were specific for tumor type (as previously demonstrated for whole serum), we tested known blocking fractions related to the MCA-induced tumor on PC from mice bearing M-MuSV-induced tumors. The three fractions used were those from serum that showed blocking in text-figure 1; blocking values of 19.8, 9.9, and 11.3, as in the text-figure, were obtained with PC from mice bearing the corresponding tumor. Table 3 presents the results of testing the same pooled fractions on M-MuSV tumor-sensitized PC. These cells gave significant LAI in the presence of normal serum (data not shown) and could be blocked by whole serum from mice with M-MuSV-induced tumors. When the three fraction pools related to the MCA-induced tumor were tested, no blocking reactions occurred. Thus blocking activity of both the high and low MW fractions appeared to be antigen-specific. The reverse test (for nonspecific blocking by serum fractions related to M-MuSV-induced tumors) was not done.

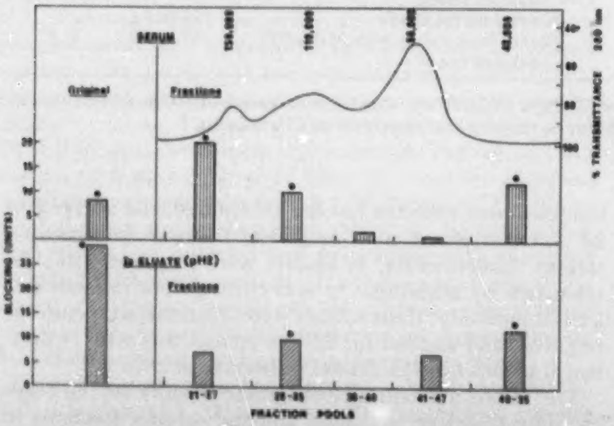

TEXT-FIGURE 1.—Blocking of LAI by sera of mice bearing MCA-induced tumors, by Ia eluate, and by Sephacryl S-200 fraction pools. Tests were performed with PC from similar mice and MCA-induced tumor extracts. A UV transmittance curve for serum fractions is shown, and MW of known proteins are marked. *=significant blocking. Pool 36–40 (eluate) had no blocking activity.

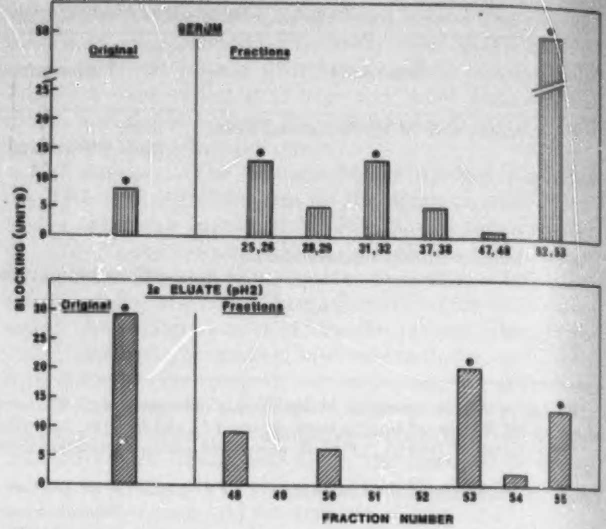

TEXT-FIGURE 2.—Blocking of LAI for certain fraction pairs (from serum) and single fractions (from Ia eluate), from the same experiment as for text-fig. 1. *=significant blocking. Fractions 49, 51, and 52 had no blocking activity.

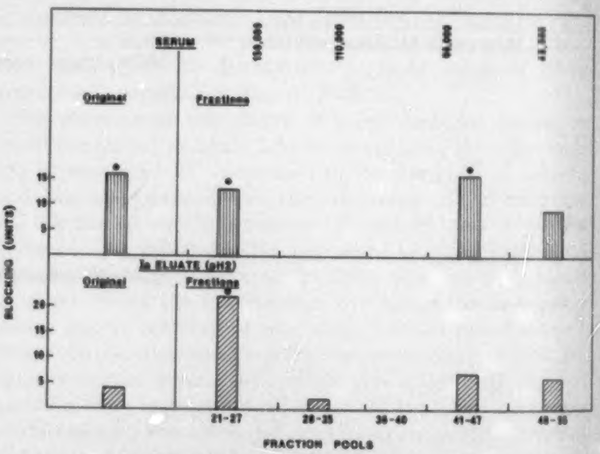

TEXT-FIGURE 3.—Blocking of LAI by sera of mice bearing M-MuSV-induced tumors, by Ia eluate, and by Sephacryl S-200 fraction pools. Tests were performed with PC from similar mice and M-MuSV-induced tumor extracts. *=significant blocking. Pools 28–35 and 36–40 (serum) and 36–40 (eluate) had no blocking activity.

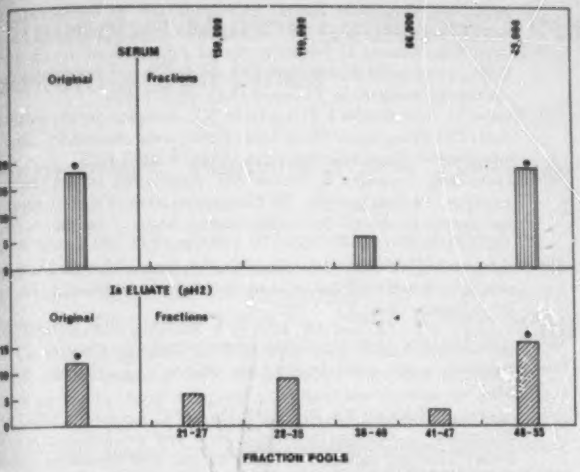

TEXT-FIGURE 4.—Blocking of LAI by sera of mice bearing M-MuSV-induced tumors, by Ia eluate, and by Sephacryl S-200 fraction pools. Text-figs. 3 and 4 show data from different experiments. *=significant blocking. Pools 21–27, 28–35, and 41–47 (serum) and 36–40 (eluate) had no blocking activity.

TABLE 3.—*Tumor specificity of BF in serum fractions from mice bearing MCA-induced tumors*[a]

Serum or fractions[b]	Percent adherence, mean±SE[c]	Blocking value[d]
Whole serum from:		
Normal mouse	63.5±2.9	20.4***
Mouse with M-MuSV-induced tumor	83.9±3.3	
Fraction pools 21–27 from:		
Normal mouse	69.1±5.1	−13.1
Mouse with MCA-induced tumor	56.0±5.0	
Fraction pools 28–35 from:		
Normal mouse	69.7±3.2	−6.5
Mouse with MCA-induced tumor	63.2±4.1	
Fraction pools 48–55 from:		
Normal mouse	64.6±4.7	−3.6
Mouse with MCA-induced tumor	61.0±2.6	

[a] The same serum fraction pools were significantly blocking when tested with PC and antigen related to MCA-induced tumor (text-fig. 1).

[b] Sera from mice with M-MuSV-induced tumors were obtained 5 days after M-MuSV inoculation. Sera from mice with MCA-induced tumors were obtained 10 days after tumor transplantation and fractionated as for text-fig. 1. Corresponding fractions were obtained from normal serum.

[c] Adherence of PC from mice with M-MuSV-induced tumors; the PC were incubated with M-MuSV-induced tumor extract and the serum or fractions specified.

[d] *** $P<0.001$; unmarked values are not significantly blocking.

DISCUSSION

The LAI assay has previously been shown to be susceptible to blocking by serum factors (*9–13*). BF are detectable in tumor-bearing subjects and have a specificity similar to that of the tumor antigens employed in the assay. When added to PC whose adherence has been inhibited through reaction with antigen, BF restore the adherence toward the normal level. This effect is a result of the prevention of lymphocyte activation, rather than a direct modification of cellular adherence (*12*). Sera from tumor-bearing animals nevertheless often have a nonspecific depressing effect on adherence, as revealed in situations in which BF have been removed or cannot operate; examples of this phenomenon are seen in tables 1–3 of this paper as negative blocking values and also in our other publications [e.g., (*12*)].

Previous studies of the molecular size of tumor-specific BF have yielded conflicting data. Early estimates (*14*) indicated that BF accompanied 7S immunoglobulins when serum was fractionated; more recently (*7*), molecules of MW 56,000 were isolated. The present results are compatible with both observations in that high (>100,000) and low (40,000–50,000) MW forms of BF were obtained from serum, either singly or together. Both tumor types studied (M-MuSV-induced and MCA-induced) gave comparable results. The active fractions of serum from mice with MCA-induced tumors appeared to be tumor-specific (as was the original serum) in their blocking action.

Low and high MW fractions of BF (detected by their effect on lymphocyte cytotoxicity) were previously described (*4*) as the products of dissociation at acidic pH; only the lower MW material (<100,000) had any blocking effect alone, and full activity was restored only when the fractions were recombined. The active factors reported in the present work appeared to exist individually in serum and required only gel filtration and not low pH treatment for their separation; each had independent blocking activity.

An additional distinctive property of at least some BF, their possession of Ia antigenic determinants (*13*), permitted a selective immunoadsorption of BF from serum. These determinants were shown previously to be related to the I-J subregion (*13*). Within the limits of the assay methods, it appeared that all BF were removed from serum by combination with anti-Ia antibodies. Other kinds of BF, if present at all, must have been in small amounts or not detectable by the assay system. Elution of BF with an acidic buffer yielded material with blocking activity; these eluted BF were then shown to have an MW distribution broadly similar to that of the serum BF from which they were derived. An exception was found in one instance (text-fig. 3) in which BF of low MW were not recovered in the eluate. The tumor specificity of active eluate fractions was not determined, nor was it shown that all recovered active fractions retained Ia determinants. It is possible that acid elution dissociated some of the BF, but this seems unlikely since both high and low MW forms were recovered after neutralization and fractionation.

The estimate of MW for BF in fractions from a Sephacryl S-200 column is tentative, inasmuch as the shape of the molecule influences its chromatographic behavior and the protein standards used may not have been ideal for calibration. There was lack of agreement in some details between the results for the same tumor on different occasions (text-figs. 3, 4). It seems that BF in distinct molecular forms can have similar biological activity.

The low MW factors resemble antigen-specific T-cell suppressor factors (*8*) in possessing Ia determinants and a molecular size of approximately the same range. They may also correspond with the factor of Nepom et al. (*7*). The larger factors may be the complexes described by earlier workers. As suggested previously (*1, 13*), the smaller factor might be expected to combine with tumor antigen and then with antibody. The contribution of these entities to the composition of Ia-containing BF remains to be studied.

An area of current interest concerns the cellular origin of BF. It is already known that BF are produced in cultures of spleen cells from tumor-bearing mice and that the responsible cells are T-lymphocytes (*15*). We have further characterized the markers on BF-producing spleen cells and have identified Thy-1, Ly-2, and I-J (Koppi TA, Halliday WJ: Unpublished data). These cells therefore resemble the T-suppressor cells found in other situations.

The regulatory molecules revealed in serum by the present investigation probably have their counterpart in human cancer, where LAI techniques have consistently detected specific BF (*11*). Whether human BF are HLA related is not yet known.

REFERENCES

(*1*) Hellström KE, Hellström I, Nepom JT. Specific blocking factors—are they important? Biochim Biophys Acta 1977; 473:121–148.

(*2*) Hellström I, Hellström KE, Evans CA, Heppner GH, Pierce GE, Yano JP. Serum-mediated protection of neoplastic cells from inhibition by lymphocytes immune to their tumor-specific antigens. Proc Natl Acad Sci USA 1969; 62:362–368.

(*3*) Hellström KE, Hellström I. Cellular immunity against tumor antigens. Adv Cancer Res 1969; 12:167–223.

(*4*) Sjögren HO, Hellström I, Bansal SC, Hellström KE. Suggestive evidence that the blocking antibodies of tumor-bearing individuals may be antigen-antibody complexes. Proc Natl Acad Sci USA 1971; 68:1372–1375.

(*5*) Baldwin RW, Price MR, Robins RA. Blocking of lymphocyte-mediated cytotoxicity for rat hepatoma cells by tumour-specific antigen-antibody complexes. Nature 1972; 238:185–187.

(*6*) Currie GA, Basham G. Serum-mediated inhibition of the immunological reaction of a patient to his own tumour: A possible role for circulating antigen. Br J Cancer 1972; 26:427–438.

(*7*) Nepom JT, Hellström I, Hellström KE. Antigen-specific purification of blocking factors from sera of mice with chemically induced tumors. Proc Natl Acad Sci USA 1977; 74:4605–4609.

(*8*) Greene MI, Fujimoto S, Sehon AH. Regulation of the immune response to tumor antigen. III. Characterization of thymic suppressor factors produced by tumor-bearing hosts. J Immunol 1977; 119:757–764.

(*9*) Halliday WJ, Miller S. Leukocyte adherence inhibition: A simple test for cell-mediated tumor immunity and serum blocking factors. Int J Cancer 1972; 9:477–483.

(*10*) Halliday WJ, Maluish AE, Miller S. Blocking and unblocking of cell-mediated anti-tumor immunity in mice, as detected by the leukocyte adherence inhibition test. Cell Immunol 1974; 10:467-475.

(*11*) Halliday WJ, Koppi TA, Khan JM, Davis NC. Leukocyte adherence inhibition: Tumor specificity of cellular and serum-blocking reactions in human melanoma, breast cancer, and colorectal cancer. JNCI 1980; 65:327–335.

(*12*) Koppi TA, Halliday WJ. Regulation of cell-mediated immunologic reactivity to Moloney murine sarcoma virus-induced tumors. I. Cell and serum activity detected by leukocyte adherence inhibition. JNCI 1981; 66:1089–1096.

(*13*) Koppi TA, Halliday WJ, McKenzie IF. Regulation of cell-mediated immunologic reactivity to Moloney murine sarcoma virus-induced tumors. II. Nature of blocking and unblocking factors in serum. JNCI 1981; 66:1097–1102.

(*14*) Hellström I, Hellström KE. Studies on cellular immunity and its serum-mediated inhibition in Moloney-virus-induced mouse sarcomas. Int J Cancer 1969; 4:587–600.

(*15*) Nelson K, Pollack S, Hellström KE. Specific anti-tumor responses of cultured immune spleen cells. III. Further characterization of cells which synthesize factors with blocking and antiserum dependent cellular cytotoxic (ADC) activities. Int J Cancer 1975; 16:539-549.

Trisomy 15 and Other Nonrandom Chromosome Changes in Rauscher Murine Leukemia Virus-Induced Leukemia Cell Lines[1,2]

Anne Hagemeijer,[3] Elisabeth M. E. Smit,[3] Francine Govers,[4] *and* Nico J. de Both[4]

ABSTRACT—The cytogenetics of Rauscher murine leukemia virus-induced erythroid, myeloid, and lymphatic leukemias were studied in BALB/c and DBA/2 mice. In primary virus-induced leukemias, no chromosome abnormalities were found. However, in tumors derived from transplanted leukemia tissue and in cell lines obtained from these tumors, euploidy and mostly aneuploidy were observed that varied according to the type of tumor cells and the number of passages. Eleven erythroleukemia cell lines showed aneuploidy from the first in vivo transplant stage on. Nonrandom abnormalities were found: trisomy 15 in 9 of 11 lines, followed by trisomy 3 in 8 of 11 lines and monosomy 6 in 5 of 11 lines. Subsequent evolution of the karyotypes was frequent (10 of 11 lines) and rapid. In vivo cell lines established from these tumors showed many structural rearrangements. Three myeloid lines revealed a stable karyotype with no or only minor changes: trisomy 15 in 1 line and normal diploid in 2 lines. One lymphatic leukemia cell line established in vitro presented with a very stable karyotype: trisomies 14 and 15. Another in vivo transplantable line showed trisomies 11, 9, and 17. These results suggest that trisomy of chromosome 15 plays a significant role in tumors derived from different types of mouse leukemias.—JNCI 1982; 69:945–951.

Cytogenetic abnormalities are a common feature in cancer cells, but so far the role of these chromosome aberrations in cancer has remained elusive and is the source of controversial hypotheses. During the last decade, studies of human leukemias have shown *a*) that a few chromosomes were preferentially involved in abnormal karyotypes, *b*) that additional cytogenetic changes occurred with progression of the disease, and *c*) that some chromosome translocations were specifically associated with certain types of leukemia, e.g., the t(9;22) in chronic myeloid leukemia, the t(8;21) and t(15;17) in acute myeloid and promyelocytic leukemias, respectively, and the 14q+, often resulting from a t(8;14) in B-cell lymphomas (*1–4*). Solid tumors, like meningiomas or breast carcinomas, also showed nonrandom occurrences of chromosome abnormalities (*4*). Animals with experimentally induced tumors were also studied. In the rat, it was found that chromosome aberrations tended to be specific for the oncogenic agent rather than for the histologic type of tumor; i.e., chemically induced sarcomas and leukemias were characterized by trisomy of chromosome 2, whereas similar sarcomas virally induced showed trisomies 7, 12, and 13 (*5–7*). In contrast, in the mouse, there was a tendency to relate the type of aneuploidy with the cytologic type of leukemia: Plasmacytomas and B-cell leukemias showed a specific translocation of #15 with #12 or with #6 (*8, 9*), myeloid leukemia showed a deletion of #2 (*10, 11*), and thymomas were characterized by trisomy 15 (*12–16*).

Trisomy of chromosome 15 is claimed to be highly specific for murine T-cell lymphomas, and its specificity is independent of whether the lymphoma occurs spontaneously as in the AKR mouse (*12*) or is induced by exposure to virus, radiation, or carcinogens (*13–16*). In a previous study (*17*) we found that in a myeloid cell line derived from a myeloid leukemia induced by R-MuLV, trisomy of chromosome 15 was the only karyotypic abnormality. Since the same oncogenic virus under appropriate experimental conditions can induce different types of leukemia, we decided to analyze cytogenetically these cytologically different leukemias.

We report here the cytogenetics of Rauscher virus complex-induced erythroid, myeloid, and lymphatic leukemias, of tumors derived from transplantation of the corresponding leukemias, and of in vitro cell lines derived from transplantable leukemia cells. We found that trisomy 15 was the most frequent aberration among the different types of leukemia blast cells after at least one in vivo transfer.

MATERIALS AND METHODS

Virus and animals.—The Rauscher virus complex was obtained both from cell-free extracts of hyperplastic leukemic spleens of BALB/c mice with erythroid leukemia and from cultured JLS-V5 cells that by their constitution produce large amounts of virus (*18*). The Rauscher virus complex consists of the helper independent component (R-MuLV) that induces a lymphatic leukemia and the replication-defective R-SFFV associated with erythroid leukemia. In some experiments mice were infected with the cloned lymphatic leukemia-inducing component (R-MuLV). This component was obtained by end-point dilution and infection of 3T3 cells (Stoof TJ: Unpublished data). BALB/c and DBA/2 mice 6–8 weeks old were used for infection and transformation studies. As a rule, tumors were serially transplanted into animals of the opposite sex from the one in which the leukemia had been induced. In most cases leukemia induction occurred in female mice and tumor transplantation occurred in male mice.

Induction and characterization of primary leukemias.—Erythroid leukemias were induced as previously described (*19*). The infection is always lethal within 30 days for BALB/c mice and within 45 days for DBA/2 mice. The leukemia blast

---

ABBREVIATIONS USED: DMSO=dimethyl sulfoxide; EP=erythropoietin; R-MuLV=Rauscher murine leukemia virus; R-SFFV=Rauscher spleen focus-forming virus.

---

[1] Received December 16, 1981; accepted May 5, 1982.

[2] Supported by the Netherlands Cancer Institute Koningin Wilhelmina Fonds.

[3] Department of Cell Biology and Genetics, Erasmus University, P.O. Box 1738, 3000 DR Rotterdam, The Netherlands.

[4] Department of Pathology, Erasmus University.

cells showed the features of proerythroblasts and basophilic erythroblasts (*20, 21*). Myeloid and lymphatic leukemias were induced by the injection of 0.5 ml of supernatants of subconfluent cultures of JLS-V5 cells or infected 3T3 cells harvested 24 hours after renewal of the culture fluid. After a latent period of about half a year, most of the animals became leukemic. The most frequent leukemia was lymphatic leukemia, but occasionally myeloid leukemia was induced. The myeloid leukemia was identified by the greenish color of the lymph nodes (chloroleukemia). The blast cells showed horseshoe-shaped nuclei and in their cytoplasm azurophilic granules stained peroxidase-positive. Organs affected by lymphatic leukemia appeared white, and the cells could be classified as T-cells and B-cells with the use of the binding of fluorescein-conjugated antibodies directed against theta antigens or against membrane-bound immunoglobulins (Nordic Immunological Laboratories, Tilburg, The Netherlands).

Transplantations of leukemia tissue.—Infiltrated hyperplastic spleens, livers, or lymph nodes from primary leukemic animals were removed, dissected in small pieces, and transplanted sc into syngeneic mice of the opposite sex from the mice in which the leukemia had been induced. A few weeks later, tumors appeared at the injection sites. We removed these tumors aseptically, and we obtained single cell suspensions by mincing the tissues and filtering them through nylon gauze. We used these cells suspensions 1) for serial tumor transplantation by injection of 5×10^6 cells sc, 2) for cytogenetic analysis, 3) for long-term in vitro culture in order to establish permanent cell lines, and 4) for morphologic characterization of these leukemia lines. Sometimes in erythroid leukemias, not all studies could be done satisfactorily on the first tumor due to simultaneous transfer of virus which shortens the life-span of the host mouse. In such instances, the analyses were done on the second or third tumor obtained by serial in vivo transplantation and/or on the derived permanent cell lines. In a few instances, serial cytogenetic analysis was done to study sequential chromosome changes during in vivo and in vitro passages.

Long-term cultures.—We initiated long-term cultures by placing about 2×10^6 tumor cells in petri dishes in RPMI-1640 medium or in Dulbecco's medium (Flow Laboratories Ltd., Irvine, Scotland) supplemented with 20% fetal calf serum. We incubated the mixture at 37°C in a humidified atmosphere of 5% CO_2 in air. When growth occurred, the cells were initially passaged once a week and later, depending on their growth rate, twice a week.

Cytogenetic analysis.—We analyzed tumor cells and the cell lines after 24 hours of culture by using methotrexate treatment as described previously for human leukemia cells (*22*). Colcemid instead of colchicine was used for mitotic arrest. The harvesting method was standard—hypotonic shock with 0.075 *M* KCl, three successive fixations in methanol:acetic acid (3:1), and spreads on dry slides. A few lymphoid tumors could not be cultured. To obtain metaphase plates, we gave mice bearing these tumors ip injections of 100 μg colchicine and removed the tumors after 1 and 4 hours for direct analysis.

All metaphases were analyzed with the use of banding techniques: R-banding with acridine orange and G-banding with trypsin-Giemsa staining. Karyotyping was done according to the recommendations of the Committee on Standardized Genetic Nomenclature for Mice (1972) (*23*) and the system proposed by Nesbitt and Francke (1973) (*24*).

Differentiation lineage.—We verified the differentiation lineage of the cell lines established from transplanted tumors by using different specific markers. Erythroid cell lines were cultured in a plasma clot assay (*25*) and tested for their ability to form benzidine-positive colonies after treatment with EP and/or DMSO (*26, 27*). Myeloid cell lines were identified by a number of properties described earlier (*17, 28*). Lymphatic cell lines were characterized by the presence of Thy 1 antigens (T-cells) or by the presence of immunoglobulins on their plasma membranes (B-cells).

Designation of the different leukemia cell lines.—This designation followed a code that summarized the cell line's origin, differentiation lineage, and the mouse strain from which it was derived, e.g., RED- (*R*auscher MuLV, *E*rythroid leukemia, *D*BA/2 mouse strain), followed by the number of sequential cell lines. In this study the beginning of a line is at the first transplant stage (T1). Tumors that originated from a transplant of the same primary leukemia tissue in different animals are indicated as clusters in the tables.

RESULTS

Primary Leukemias

Cytogenetic analysis of the erythroleukemic spleens and of enlarged lymph nodes appearing in the animals given injections of R-MuLV or of R-MuLV plus R-SFFV was done repeatedly. The karyotype of these cells was always found to be normal diploid without deviation (table 1). Many attempts at karyotyping the primary lymphoid leukemias with the use of short-term cultures failed to produce metaphase plates suitable for analysis. The few cells studied were also normal diploid.

Erythroleukemia Cell Lines

Twelve erythroleukemia cell lines were isolated at T1 after sc transplantation of spleen or liver cells from erythroleukemic mice. With the exception of RED-3, all tumors were serially transplanted, established as permanent in vitro cell lines, and kept frozen in liquid nitrogen. The origin of the cell lines and their differentiation characteristics are given in table 2. Results of cytogenetic analysis are given in table 3. RED-4, RED-5, and RED-6 and RED-7, RED-8,

TABLE 1.—*Cytogenetic analysis of Rauscher virus complex-induced primary leukemias*[a]

Mouse strain	Organ	Leukemia type	No. of cells analyzed
BALB/c	Spleen	Erythroid	200
DBA/2	Spleen	Erythroid	16
DBA/2	Spleen	Erythroid	20
BALB/c	Lymph node	Myeloid	20
BALB/c	Lymph node	Myeloid	30
BALB/c	Lymph node	Lymphoid	2

[a] In all instances, the karyotype was 40,XX.

and RED-9 are clusters, which means that they originated from the same leukemia tissue but that they developed first as subcutaneous tumors on different hosts. All cell lines except one (RED-12) were still able to form benzidine-positive colonies in plasma clot assays when stimulated with either EP or DMSO or both in combination. RED-12 proliferated in vitro as undifferentiated blast cells.

TABLE 2.—*Origin and differentiation response of the Rauscher virus complex-induced erythroid lines*

Erythroid lines	Origin of primary leukemia		Differentiation response of cell lines[a]			
	Sex of animal	Organ transplanted	In vitro passage	Inducers[b]		
				EP	DMSO	EP + DMSO
RED-1	♀	Liver	28, 60	+	+	++
RED-2	♂	Liver	19	+	±	±
RED-4			10	−	−	±
RED-5	♀	Liver	25	+	±	++
RED-6			29	+	−	+
RED-7			35	+	±	+
RED-8	♀	Liver	33	+	+	++
RED-9			58	±	−	+
RED-10	♀	Liver	14	+	−	++
RED-11	♀	Liver	12	−	−	±
RED-12	♀	Spleen	12	−	−	−

[a] Percentage of benzidine-positive colonies in a plasma clot assay: −=0%, ±=1-10%, +=10-40%, and ++=>40%.

[b] EP=0.25 U EP/ml, DMSO=0.5% DMSO, and EP + DMSO=0.25 U EP/ml + 0.5% DMSO.

Cytogenetic analyses were done mainly at T1 and T2 or on the in vitro cell lines. More than 270 metaphases obtained from freshly harvested tumors were analyzed, and only one cell showed the karyotype of the host (40,XY in RED-7 T1); all others showed sex chromosomes consistent with those of the donor of the leukemia cells. An abnormal karyotype was found in all the erythroid lines studied. The most frequent abnormality observed was trisomy 15, either as isochromosome 15 or as an extra chromosome, which was found in 9 of the 11 lines. Trisomy 3 [either as iso(3) or +3] came a close second most frequent (eight times) and monosomy 6 a third most frequent (five times). Random additional aberrations were particularly frequent in the in vitro cell lines with many structural rearrangements (RED-1 and RED-9) and in the two lines that were mainly hypotetraploid (RED-6 and RED-11). In some of the lines many endoreduplications and tetraploid and octoploid mitotic cells were observed. Clonal progression was also very common (RED-4, RED-7, RED-10, RED-11, and RED-12).

From RED-12, 2×10^6 cells were transplanted at each in

TABLE 3.—*Karyotype of the Rauscher virus complex-induced erythroid lines*

Lines[a]	Tissue[b]	Range of chromosome No.	Stemline karyotype[c]	Cells with random additional changes, %[d]	Cells showing polyploidization, %[e]
RED-1 (30)	Cell line	38–40	39,X,Rb(X.1),+3,5L+,−6,T(15;6)	80	3
RED-2 (16)	T1 transplant	41	41,XY,+15	5	0
(20)	Cell line	40–42	41,XY,+15	25	0
RED-4 (16)	T2 transplant	40–41	40,XX,Df(2EF),I(15),(20%)//40,XX,Df(2EF),I(15),11L+(45%)//40 or 41,XX,Df(2EF),I(15),11L+,+3 or I(3)	25	5
RED-5 (10)	T2 transplant	40–42	41,XX,+Df(X),+3,−6,I(15)	40	0
(10)	Cell line	41–42	42,XXX,−6,+8L+,+14,I(15),19L+,+mar	70	50
RED-6 (15)	Cell line	69–75, hypotetraploid	73,XXXX,−2,−6,−6,−8,−8,−10,−11,12L+,T(12;14),−14,−19,+2 markers	70	5
RED-7 (20)	T1 transplant	40–45	41,XX,+15(70%)//45,XX,+3,+8,+14,+15,+16(30%)	40[f]	10
RED-8 (16)	T2 transplant	45–46	46,XXX,+3,+4,+15,+15,+17	20	0
RED-9 (19)	Cell line	34–47	35,XL+,XL−, complex changes with many translocations: Rb(1.2),I(3),T(6;4;6C),7S+,T(9;15),+15,T(11;12),T(13;8;3), etc.	80	10
RED-10 (20)	T1 transplant	41–42	41,XX,+14,I(15)(30%)//42,XX,+14,+15(70%)	5	0
(17)	T2 transplant	41–44	43,XX,+3,+14,+15	35	0
RED-11 (30)	T1 transplant	38–39	38,XX,−6,Rb(16.19)	20	15
(26)	T2 transplant	38–40	39,XX,−6,+15,Rb(16.19)(50%)//40,XX,−6,+15,+15,Rb(16.19)(50%)	90	70
RED-12 (97)	T1 transplant	40–41	40,XX(60%)//41,XX,+15(40%)	0	0
	T2 transplant	41–51	41,XX,+15(10%)//51,XXX,+2,+3,+4,+4,+9,+14,+15,+16,+17,+18(40%)//43→50(50%)[g]	50	5
	T3, T4, and T5 transplants	48–51	50,XXX,+3,+4,+9,+10,+14,+15,+16,+18,4L+,T(4;14),10L+,+17L+	80	25

[a] Number of cells analyzed is indicated *in parentheses*.

[b] Cell lines were established in vitro.

[c] Cytogenetic abnormalities were present in all metaphases analyzed, including cells with additional random changes. In cases of multiple stem cell lines, the percentages of cells are given *in parentheses. Symbols* used are the following: T=translocation, L=long arm, S=short arm, I=isochromosome, Df=deletion, and Rb=Robertsonian translocation.

[d] Random changes consisted either in occasional translocation or in intermediate forms between the diploid and hyperdiploid stemline karyotypes.

[e] Endoreduplications and tetraploid and octoploid mitotic figures.

[f] One cell with 40,XY karyotype of the host.

[g] Intermediate forms between the 41 and the 51 chromosome karyotypes described.

TABLE 4.—*Cytogenetic analysis of R-MuLV-induced myeloid and lymphatic leukemias*

Leukemia	Lines	Tissue	No. of cells analyzed	Karyotype
Myeloid	RMB-1	Cell line	90	41,XY,+15
	RMB-1	$HPRT^-$ mutant	10	41,XY,+15
	RMB-2	T1 transplant	16	40,XX
	RMB-3	T1 transplant	8	40,XX
		T2 transplant	20	40,XX
		T3 transplant	10	40,XX
		T4 transplant	16	40,XX
		T6 transplant	30	40,XX
Lymphatic	RLD-1	Cell line	22	42,XX,+14,+15
	RLB-2	T4 mouse 1[a]	23	40,XX

		T4 mouse 2[a]	21	41,XX,+11(60%)//
				42,XX,+9,+11(20%)//
				43,XX,+9,+11,+17(20%)

[a] Animals were given injections of cell suspension from the same T3 tumor and inoculated with colchicine 1 and 4 hr before the T4 tumors were harvested.

vivo passage and cytogenetic analysis of the successive tumors was performed so that we could follow the chromosome evolution and the eventual increase in the tumor growth rate. In this experiment, the karyotype of the primary leukemia (erythroblastic spleen) was studied and was found to be normal diploid: 40,XX as always. The time required to obtain the first subcutaneous tumor with a diameter of approximately 2 cm was 62 days. The cell karyotypes at T1 were 40,XX(60%) and 41,XX,+15(40%). After 49 days the cells at T2 were harvested. The karyotype had become hyperdiploid with trisomies of chromosomes X, 3, 4, 9, 10, 14, 15, 16, 17, and 18. Subsequent transplants from T3, T4, and T5 were obtained after a delay of about 3 weeks after sc injection of 2×10^6 cells. Their karyotypes were essentially similar to the T2 karyotype. The T3, T4, and T5 transplants had, in addition, some structural rearrangements [t(4;14),10L+,17L+,Df(2)], random variation around the main karyotype in about 80% of the metaphases, and an increased percentage of tetraploid cells (25%).

Myeloid Lines

Three myeloid lines were studied (table 4). The karyotype and differentiation characteristics of the RMB-1 cell line have already been reported (*17*). The RMB-2 and RMB-3 lines constituted a cluster, meaning that they originated from the same chloroleukemia injected in 2 animals that developed tumors. RMB-2 could not be further transplanted, whereas RMB-3 was serially transplanted in the male syngeneic host and remained female diploid (40,XX) as did the original tissue. In contrast to the karyotypes of the erythroid lines, the karyotypes of the myeloid lines appeared stable: Clonal progression and random changes were not seen. The myeloid tumors also remained slow-growing, and 2–4 months were necessary for tumors to arise at the sc injection site.

Lymphoid Lines

One line induced in the DBA/2 mouse was serially transplanted and was also established as a permanent cell line in vitro (table 4). It showed membrane characteristics of T-cells (Thy 1 and Lyt 1 binding). The karyotype appeared very stable: 42,XX,+14,+15. Two other lines were induced in BALB/c mice. They were readily transplantable and very rapidly formed tumors on the host, but the tumor cells could not be cultured in vitro. Even short-term cultures for cytogenetic analysis failed. To obtain mitoses, we gave animals bearing tumors (T4 of RLB-2 line) injections of colchicine in vivo and harvested the tumors 1 and 4 hours after injection. In 1 animal the tumor had a female diploid karyotype: 40,XX. In the other animal the main karyotype showed trisomy of chromosome 11 with two sublines showing, in addition, trisomies 9 and 17.

DISCUSSION

The Rauscher virus complex consists of R-SFFV and a lymphatic leukemia helper virus (R-MuLV), which together induce an erythroid leukemia in 100% of infected susceptible mice (*21, 29*). When virus preparations are used from cell lines that by their constitution produce virus, the R-MuLV may predominate and infection results after a long latent period in lymphoid leukemia in most of the animals or in myeloid leukemia in a few animals. The same is true when cloned R-MuLV is used. For these reasons the number of erythroid leukemias analyzed surpasses the number of lymphoid and myeloid leukemias. In primary leukemias, only normal diploid numbers of chromosomes were found. In contrast, in tumors obtained after transplantation, diploid and aneuploid karyotypes were observed. Especially in the tumor obtained from transplanted erythroid leukemia tissue, there was a rapidly changing karyotype during in vivo and in vitro passages. However, in these abnormal leukemia karyotypes there was a nonrandom involvement of some chromosomes, particularly trisomy of #15 (11x) followed by trisomy of #3 (8x), then monosomy of #6, and trisomies or rearrangements in #14, 4, 8, 12, 16, and 17 and X. The myeloid lines were slow-growing, with a very stable karyotype, and RMB-3 with a 40,XX diploid karyotype has not yet been successfully established in vitro but is continuously passaged in vivo.

Despite their rapid growth in vivo, the lymphatic lines induced in BALB/c mice could not be maintained in vitro. They produced few, poorly spread metaphases with contracted, fuzzy chromosomes, not suitable for banding analysis, and reminded us of the metaphases usually obtained in cases of human acute lymphocytic leukemia.

Absence of host metaphases in the subcutaneous transplants tends to minimize the role of viral infection and induction of leukemia in host cells; clearly, there is continuous proliferation of leukemia cells from the donor.

The finding of a normal diploid karyotype in the different primary leukemias implies that although the virus causes hyperplasia of its target cells, it does not necessarily induce chromosome abnormalities. This diploid character of leukemia cells has already been reported by others for Rauscher and Friend leukemias with, however, the presence of cytogenetically abnormal cells in the late stage of the diseases (*30, 31*). The same diploid character of leukemia cells holds for infection of lymphoid target cells by Abelson and Moloney viruses (*32, 33*).

Our observations are in line with the concept that virally induced murine leukemias are "multiple-step" diseases (*34*). In the terminal phase of Rauscher virus-induced leukemias, the proliferating erythroblasts are infiltrating all hematopoietic organs, which increase dramatically in size. Most of these cells can proliferate in vitro only for a limited time (data not shown). Nevertheless, 11 of the 12 erythroblastic tissues transplanted in syngeneic hosts gave rise to transplantable leukemia cell lines. These cell lines were all aneuploid, which suggests that *a*) among the many diploid erythroblastic cells, a few develop chromosome aberrations and *b*) in vivo passaging selects for these cells which are presumably more tumorigenic or exhibit marked growth advantages.

However, as seen in the myeloid lines, permanently transformed tumor cells can be of diploid karyotype with no detectable chromosome aberrations, which indicates that chromosome changes are not a prerequisite for the induction of transformation or its maintenance.

Chromosome analysis of the erythroid tumor transplants demonstrates in all cases the presence of "stemlines" that suggest either clonal origin or in vivo selection in favor of cells carrying the same type of chromosome rearrangement. In erythroleukemia lines, clonal progression occurred rapidly (table 3, RED-4, RED-7, RED-10, RED-11, and RED-12).

Extensive chromosome rearrangements have also been reported in Friend virus-induced mouse erythroleukemia cell lines that had been maintained in vitro for long periods (*35*). The erythroleukemia cell lines RED-1, RED-6, and RED-9 that we studied after in vitro passaging were also characterized by many structural rearrangements involving, among others, chromosome 15. In contrast, RED-2 was very stable: The only deviation observed was the number of Y-chromosomes: 0 or 2 in a minority of cells.

The high specificity of trisomy 15 for T-cell lymphomas (*12-16, 33, 34*) is not supported by this study in which it was found in 9 of 11 erythroid lines: Frequently, it was the first and earliest change to appear in the leukemia karyotypes (table 3, RED-2, RED-3, RED-5, RED-7, RED-10, and RED-12). Analysis of proviral integration sites with the use of radioactively labeled copy DNA and the Southern blotting technique (*36*) showed that multiple and, in each tumor, different integration sites exist (data not shown). These results were not conclusive regarding preferential integration in a particular chromosome.

Our results stress the significant role played by trisomy of chromosome 15 in mouse cancers. In mouse leukemia, trisomy 15 could possibly occur preferentially to other karyotypic changes, as does trisomy of chromosome 8 in human myeloproliferative disorders. If, in addition, trisomy 15 leukemia cells have a much higher take in syngeneic host, they will overgrow the diploid (or non-trisomy 15) cells. The current method of in vivo passaging is probably selecting for trisomy 15 leukemia cells either from T-lymphoma or from another, e.g., erythroleukemia origin.

REFERENCES

(*1*) Rowley JD, De La Chapelle A. General report on the first international workshop on chromosomes in leukemia. Int J Cancer 1978; 21:307-308.

(*2*) Second international workshop on chromosomes in leukemia, Leuven, Belgium, Oct. 2-6, 1979. Cancer Genet Cytogenet 1980; 2:89-113.

(*3*) Manolova Y, Manolov G, Kieler G, Levan A, Klein G. Genesis of the 14q+ marker in Burkitt's lymphoma. Hereditas 1979; 90:5-10.

(*4*) Mitelman F, Levan G. Clustering of aberrations to specific chromosomes in human neoplasms. III. Incidence and geographic distribution of chromosome aberrations in 856 cases. Hereditas 1978; 89:207-232.

(*5*) Levan G, Mitelman F. G-banding in Rous rat sarcomas during serial transfer: Significant chromosome aberrations and incidence of stromal mitoses. Hereditas 1976; 84:1-14.

(*6*) Sugiyama T, Uenaka H, Ueda N, Fukuhara S, Maeda S. Reproducible chromosome changes of polycyclic hydrocarbon-induced rat leukemia: Incidence and chromosome banding pattern. J Natl Cancer Inst 1978; 60:153-160.

(*7*) Mitelman F. Cytogenetics of experimental neoplasms and non-random chromosome correlations in man. Clin Haematol 1980; 9:195-219.

(*8*) Shepard JS, Pettengill OS, Wurster-Hill DH, Sorenson GD. A specific breakpoint associated with mouse plasmacytomas. JNCI 1978; 61:255-258.

(*9*) Voss R, Magyozir G, Slavin S. Cytogenetic analysis of the spontaneous murine B-cell leukemia (BCL1). Leuk Res 1980; 4:325-332.

(*10*) Azumi JI, Sachs L. Chromosome mapping of the genes that control differentiation and malignancy in myeloid leukemic cells. Proc Natl Acad Sci USA 1977; 74:253-257.

(*11*) Hayata I, Ishihara T, Hirashima K, Sado T, Yamagiwa J. Partial deletion of chromosome #2 in myelocytic leukemias of irradiated C3H/He and RFM mice JNCI 1979; 63:843-848.

(*12*) Dofuku R, Biedler JL, Spengler BA, Old LJ. Trisomy of chromosome 15 in spontaneous leukemia in AKR mice. Proc Natl Acad Sci USA 1975; 72:1515-1517.

(*13*) Chan FP, Ball JK, Sergovich FR. Trisomy #15 in murine thymomas induced by chemical carcinogens, X-irradiation, and an endogenous murine leukemia virus. JNCI 1979; 62:605-610.

(*14*) Wiener F, Ohno S, Spira J, Haran-Ghera N, Klein G. Chromosome changes (trisomy #15 and 17) associated with tumor progression in leukemias induced by radiation leukemia virus. JNCI 1978; 61:227-237.

(*15*) Wiener F, Spira J, Ohno S, Haran-Ghera N, Klein G. Chromosome changes (trisomy 15) in murine T-cell leukemia induced by 7,12-dimethylbenz(*a*)anthracene (DMBA). Int J Cancer 1978; 22:447-453.

(*16*) Spira J, Wiener F, Ohno S, Klein G. Is trisomy cause or consequence of murine T-cell leukemia development? Studies in Robertsonian translocation mice. Proc Natl Acad Sci USA 1979; 76:6619-6621.

(*17*) de Both NJ, Hagemeijer A, Rhijnsburger EH, Vermey M, van 't Hull E, Smit EM. DMSO-induced terminal differentiation and trisomy 15 in myeloid cell line transformed by Rauscher murine leukemia virus. Cell Differ 1981; 10:13-21.

(*18*) Wright BS, Lasfargues JC. Long term propagation of the Rauscher murine leukemia virus in tissue culture. J Natl Cancer Inst 1965; 35:319-327.

(19) de Both NJ, Vermey M, van Griensven LJ. The effect of Rauscher murine leukemia virus infection on the hemopoietic system of BALB/c mice: Cell proliferation and cell loss. Exp Hematol 1978; 6:515–527.

(20) Rauscher FJ. A virus-induced disease of mice characterized by erythrocytopoiesis and lymphoid leukemia. J Natl Cancer Inst 1962; 29:515–543.

(21) Pluznik DH, Sachs L, Resnitsky P. The mechanism of leukemogenesis by Rauscher virus infection. Natl Cancer Inst Monogr 1966; 22:3–13.

(22) Hagemeijer A, Smit EM, Bootsma D. Improved identification of chromosomes of leukemic cells in methotrexate-treated cultures. Cytogenet Cell Genet 1979; 23:208–212.

(23) Committee on Standardized Genetic Nomenclature for Mice. J Hered 1972; 63:69–72.

(24) Nesbitt MN, Francke U. A system of nomenclature for band patterns of mouse chromosomes. Chromosoma 1973; 41:145–158.

(25) McLeod DL, Shreeve MM, Axelrad AA. Improved plasma culture system for production of erythrocytic colonies in vitro. Quantitative assay method for CFU-E. Blood 1974; 44:517–534.

(26) de Both NJ, Vermey M, van 't Hull E, et al. A new erythroid cell line induced by Rauscher murine leukaemia virus. Nature 1978; 272:626–628.

(27) Sytkowski AJ, Salvado AJ, Smith GM, McIntyre CJ, de Both NJ. Erythroid differentiation of clonal Rauscher erythroleukemic cells in response to erythropoietin or dimethylsulfoxide. Science 1980; 210:74–76.

(28) Sachs L. Control of normal differentiation and the phenotypic reversion of malignancy in myeloid leukaemia. Nature 1978; 274:535–539.

(29) Steeves RA. Guest Editorial: Spleen focus-forming virus in Friend and Rauscher leukemia virus preparations. J Natl Cancer Ins 1975; 54:289–297.

(30) Tsuchida R, Rich MA. Chromosomal aberrations in viral leukemogenesis. I. Friend and Rauscher leukemia. J Natl Cancer Inst 1964; 33:33–47.

(31) Majumbar SK, Bilenker JD. *Brief communication:* Failure to detect chromosome damage in vivo in Friend virus-infected leukemic mice. J Natl Cancer Inst 1975; 54:503–505.

(32) Klein G, Ohno S, Rosenberg N, Wiener F, Spira J, Baltimore D. Cytogenetic studies in Abelson-virus induced mouse leukemias. Int J Cancer 1980; 25:805–811.

(33) Spira J, Åsjö B, Cochran A, Shen FW, Wiener F, Klein G. Chromosomal, histopathological and cell surface marker studies on Moloney virus induced lymphomas. Leuk Res 1981; 5:113–121.

(34) Klein G. Lymphoma development in mice and humans: Diversity of initiation is followed by convergent cytogenetic evolution. Proc Natl Acad Sci USA 1979; 76:2442–2446.

(35) Miller DA, Tantravahi R, Newman B, Dev VG, Miller OJ. Karyotype of Friend-virus mouse erythroleukemia cells. Cancer Genet Cytogenet 1979; 1:103–113.

(36) Southern EM. Detection of specific sequences among DNA fragments separated by gel electrophoresis. J Mol Biol 1975; 98:503–517.

Figure 1.—Karyotype of the RED-4 cell line at T2: 40,XX,Df(2EF),I(3),11L+,I(15). R-bands with acridine orange.

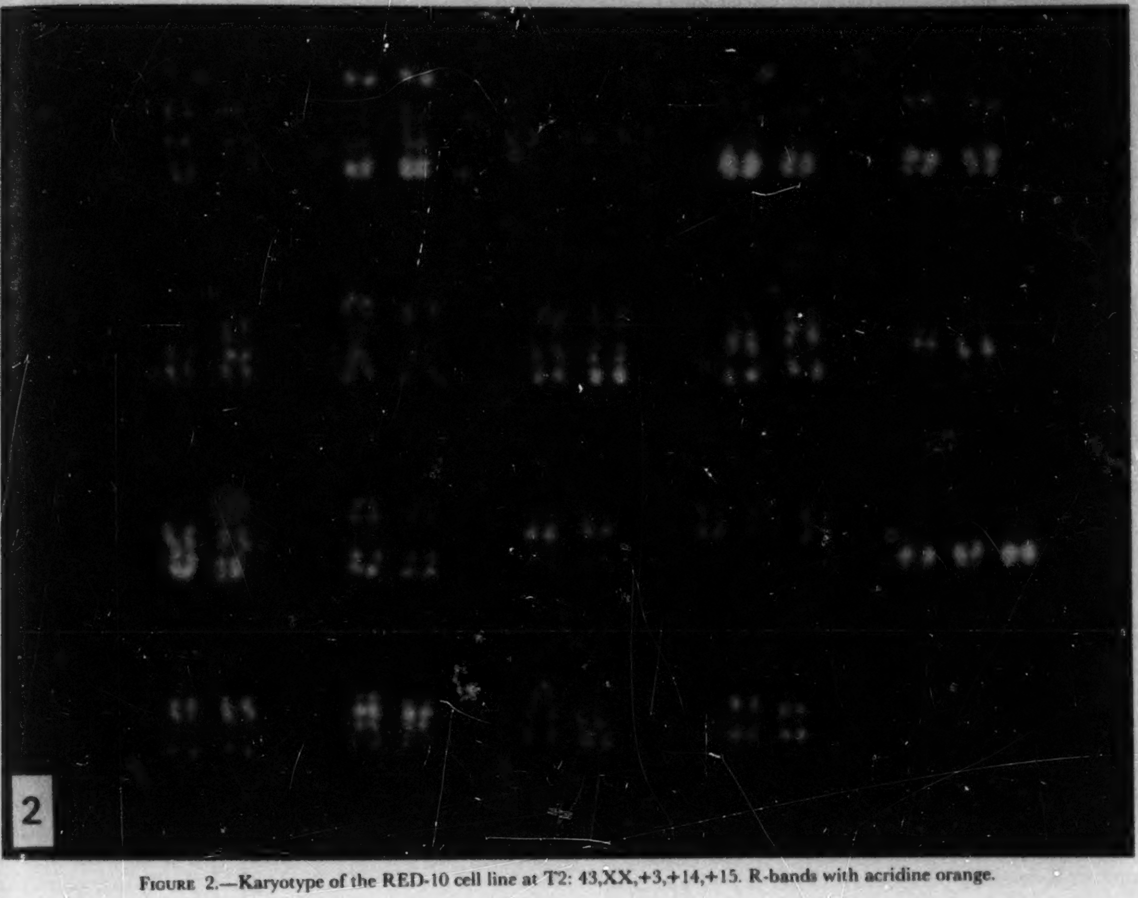

FIGURE 2.—Karyotype of the RED-10 cell line at T2: 43,XX,+3,+14,+15. R-bands with acridine orange.

blank page

Induction of gp70-Specific Suppressor T-Cells in Mice Inoculated With Virus-Producing Tumor Cells[1,2,3]

Jeffrey A. Bluestone[4,5] *and* **Carlos Lopez**[4,6,7]

ABSTRACT—Inoculation of BALB/c mice with syngeneic, murine leukemia virus (MuLV)-producing (murine sarcoma virus-transformed) Balb/3T3 tumor cells resulted in diminution of alloreactivity as measured in the mixed leukocyte culture (MLC) reaction. Cells that suppressed this response were identified in the spleens of tumor-bearing mice 10–14 days after inoculation. The suppressor cells were adherent, radiosensitive T-lymphocytes of the Lyt 1^-, 2, 3^+ phenotype. Mice inoculated with Gross MuLV (G-MuLV)-producing tumor cells, but not those inoculated with a nonproducing subclone of the same tumor cells, developed suppressor T-cells. The T-cell-mediated suppression of the MLC could be augmented by the admixture of G-MuLV antigen, similar to that replicated by the tumor cell, but not by the admixture of a Rauscher-type MuLV antigen which lacked the cross-reactive, type-specific antigens of the G-MuLV. Furthermore, this augmented suppression could be abrogated by the addition of monoclonal anti-gp70 antibody. These findings indicated that antigen-specific suppressor T-cells were induced in response to leukemia virus antigen shed from and/or expressed on tumor cells and that the suppressive activity involved the specific recognition of the gp70 portion of the virus.—JNCI 1982; 69:953–959.

Suppressor cells have been shown to be a factor in the ability of a tumor to escape host antitumor responses (*1–3*) by inhibiting both nonspecific (*4, 5*) and specific (*6–8*) immune capacities. In several studies, suppressor T-cells were identified in MuSV-inoculated TBM and were reported to be antigen-specific (*7–10*). However, the precise nature of the antigen(s) responsible for triggering the suppression has not been determined.

We have recently identified suppressor T-cells induced in mice inoculated 10–14 days previously with MuSV-transformed tumor cells, which were capable of inhibiting alloreactivity in vitro (*11*). Suppressor T-cell induction was shown to be virus antigen-dependent inasmuch as subclones of the MuSV-transformed tumor cells not expressing the ecotropic virus failed to induce this early suppression.

In this report, we present further studies of the suppressor T-cells induced in mice inoculated with MuSV-transformed Balb/3T3 cells (11A-VP). Our studies indicate that the cells responsible for suppression were of the Lyt 1^-, 2, 3^+ phenotype and that these cells were induced by the major virus glycoprotein gp70, which was also expressed by these tumor cells.

MATERIALS AND METHODS

Mice.—BALB/c (H-2^d) and C57BL/6 (B6) (H-2^b) mice were obtained from Charles River Breeding Laboratories (North Wilmington, Mass.). All mice used were male, 6–12 weeks of age, and were kept under relatively clean conditions in the Sloan-Kettering Institute animal facilities.

Tumor cell lines.—The cell lines used in this study were tissue culture-grown Balb/3T3 cell lines previously transformed in the absence of virus production by a Moloney MuSV. The parent cell line, designated "11A," was provided by Dr. George Todaro (*12*), National Cancer Institute, Frederick, Md. These cells lacked detectable transplantation or Moloney serotype viral structural antigens (*13, 14*). During in vitro cultivation, the 11A cell line was found to have begun spontaneously expressing virus and virally coded cell surface antigens. Subsequent cloning of the cell line has resulted in the two sublines (11A-NP and 11A-VP) used in this study. Subline 11A-NP lacked any detectable viral antigens on the cell surface and closely resembled the nonproducer parental cell line 11A. Alternatively, subline 11A-VP was shown to be a G-MuLV VP cell by the methods discussed below.

Virus antigen preparation.—Clonal strains of R-MuLV was obtained commercially (Litton Bionetics, Kensington, Md.). The R-MuLV was propagated in BALB/c bone marrow cells (JLSV-9). AKR leukemia virus and G-MuLV preparations, propagated in Sc-1 cells, were provided by Dr. A. Pinter, Sloan-Kettering Institute. All virus preparations were double-band purified with the use of sucrose gradient zonal centrifugation (*15*) and diluted in PBS to a final concentration of 10^{10} particles/ml. Aliquots (1 ml) of each preparation were placed in 60-mm petri dishes, exposed to UV radiation (GE G8T5 lamp) for 15 minutes at a distance of 10 cm, and stored at −70°C prior to use.

Antisera and C.—Monoclonal anti-Thy 1.2 antiserum was provided by Dr. Ulrich Hämmerling, Sloan-Kettering Insti-

---

ABBREVIATIONS USED: C=complement; FMR=Friend, Moloney, Rauscher cell surface antigen; GCSA=Gross cell surface antigen; IRR=irradiated; Lyt=T-lymphocyte differentiation antigen(s); MLC=mixed leukocyte culture(s); MuLV=murine leukemia virus(es); G-MuLV=Gross MuLV; M-MuLV=Moloney MuLV; R-MuLV=Rauscher MuLV; MuSV=murine sarcoma virus; NP=non-virus-producing; PBS=phosphate-buffered saline; PI=post inoculation; RR=relative response; TBM=tumor-bearing mouse (mice); VP=virus-producing.

---

[1] Received January 18, 1982; accepted May 20, 1982.

[2] Supported in part by Public Health Service grants CA-08748 and CA-16599 from the National Cancer Institute.

[3] Animals were maintained under the guidelines set forth by the Sloan-Kettering Institute for Cancer Research and in the "Guide for the Care and Use of Laboratory Animals" by the Institute of Laboratory Animal Resources, National Research Council.

[4] Memorial Sloan-Kettering Cancer Center, 1275 York Ave., New York, N.Y. 10021.

[5] *Present address:* Transplantation Biology Section, Immunology Branch, Division of Cancer Biology and Diagnosis, National Cancer Institute, National Institutes of Health, Public Health Service, U.S. Department of Health and Human Services, Bethesda, Md. 20205.

[6] Recipient of Faculty Research Award 193 from the American Cancer Society.

[7] *Address reprint requests to* Dr. Lopez.

tute. This antiserum plus rabbit C specifically lysed 95% of BALB/c thymocytes at a dilution of 1:200 and reduced the T-cell mitogenic response to phytohemagglutinin (HA-16; Burroughs-Wellcome Co., Research Triangle Park, N.C.) by more than 90%. Antiserum directed against Lyt were obtained from Dr. E. A. Boyse, Sloan-Kettering Institute. The two antisera anti-Lyt 1.2 and anti-Lyt 2.2 were used in this study.

Several antivirus antibodies were also used in this study. Purified monoclonal anti-gp70 (35/56, 35/299, 42/94), anti-p30 (60/35, 35/270), and anti-p15(E) (42/114) were provided by Dr. Ulrich Hämmerling. These monoclonal antibodies have been described in detail elsewhere (*16*). In addition, hyperimmune anti-p30 and anti-p15(E) antisera were provided by Dr. A. Pinter.

Both prescreened rabbit C and guinea pig C were used at a dilution of 1:15. These preparations were shown to be cytotoxic for less than 10% of BALB/c spleen cells.

Characteristics of monoclonal antibodies.—Characteristics of the monoclonal antivirus antibodies used in this study are presented in table 1. In radioimmune precipitation assays, performed by Dr. P. O'Donnell, Sloan-Kettering Institute, antibodies 35/56, 42/94, and 35/299 were found to precipitate gp70 and recognize cell-associated MuLV G_{IX} antigen, whereas antibodies 60/35 and 35/270 precipitated p30 and antibody 42/114 precipitated p15(E) (*16*).

Removal of adherent spleen cells by Sephadex G-10.—Adherent spleen cells were removed by filtration through Sephadex G-10 columns (Pharmacia Fine Chemicals, Piscataway, N.J.) with the use of the method of Ly and Mishell (*17*) as modified by us (*18*).

Serologic detection of MuLV-related antigens on tumor cells.—The transformed cell lines were evaluated for the expression of MuLV antigens by two techniques: First, microcytotoxicity assays, with the use of polyvalent and monovalent anti-MuLV antisera, were performed by Dr. Albert DeLeo, Sloan-Kettering Institute, as described in (*19*). Second, absorption tests were performed by Dr. DeLeo to examine expression on the tumor cells of G_{IX} and GCSA (*20*), type-specific cell surface antigens specified by G-MuLV.

Tumor induction.—BALB/c mice were inoculated sc with 0.5×10^6 viable, VP or NP tumor cells in 0.1 ml PBS, dorsal into the deltopectoral girdle. Palpable, nonmetastasizing fibrosarcomas were detected at the site of inoculation 9–12 days PI. The tumors never spontaneously regressed and eventually caused the death of the mice 25–40 days PI.

MLC.—The preparation of mononuclear spleen cell suspensions and MLC conditions have been described (*11*). Suppressor cell function was assayed in a three-cell MLC in which 3×10^5 spleen cells from normal mice or TBM were added to an MLC between 3×10^5 syngeneic (BALB/c) responder and 3×10^5 allogeneic (B6) stimulator cells (1,500 rad of radiation).

Elimination of Lyt subclasses.—Spleen cells ($20\text{–}50 \times 10^6$/ml) were pelleted, washed, and resuspended in 1 ml of antiserum (diluted 1:20 for anti-Lyt 1.2 and 1:40 for anti-Lyt 2.2 antiserum). The suspension was incubated for 30 minutes at room temperature and washed. The packed cells were brought up in 1 ml of freshly thawed rabbit C (diluted 1:15) and incubated for 30 minutes at 37°C. Cells were washed three times, and viable counts were determined by trypan blue dye-exclusion analyses. Generally, anti-Lyt 1.2 antiserum plus C eliminated about 40% of the T-cells, whereas anti-Lyt 2.2 antiserum plus C eliminated about 25% of the splenic T-cells. All antisera were prepared and absorbed for removal of autoantibodies as described by Shen et al. (*21*).

Statistical evaluation.—Mean values and standard errors were estimated from triplicate cultures. Significance was determined by a two-tailed Student's *t*-test.

RESULTS

Induction of Suppressor Cells in 11A-VP TBM

In an earlier study, we showed that spleen cells isolated from BALB/c mice inoculated 10–14 days earlier with VP tumor cells had a depressed MLC response (*11*). Mice inoculated with a nonproducer subclone of these tumor cells failed to induce this early suppression. Cocultivation studies were undertaken here for confirmation that the low MLC responses were due to suppressor cells and for development of an assay system with which to characterize these cells.

The addition of increasing concentrations of spleen cells from TBM to an MLC between normal BALB/c (responder) and irradiated B6 (stimulator) cells resulted in the progressive depression of the response (text-fig. 1). In contrast, addition of up to 1×10^6 normal BALB/c spleen cells augmented the response. However, addition of more than 1×10^6 normal cells depressed alloreactivity. Removal of adherent cells from the normal BALB/c responder population abrogated the suppression found with high concentrations of added normal cells without diminishing the suppression caused by the addition of spleen cells from TBM (data not presented). Therefore, experiments to characterize the effectors of early suppression were done with the use of 3×10^5 (TBM or control BALB/c spleen) cells added to an MLC in which the adherent cells had been removed from the responder (BALB/c) population by filtration over Sephadex G-10 (*18*). Addition of 3×10^5 normal BALB/c spleen cells

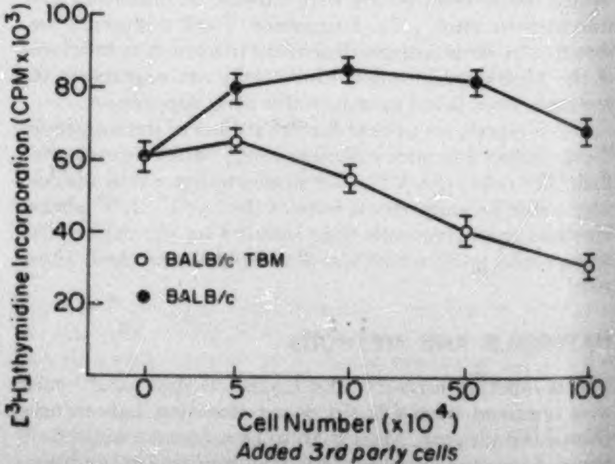

TEXT-FIGURE 1.—Increasing concentrations of spleen cells from normal mice and from TBM were added to a normal MLC [BALB/c × $B6_{(irr)}$] for study of suppression in the three-cell assay.

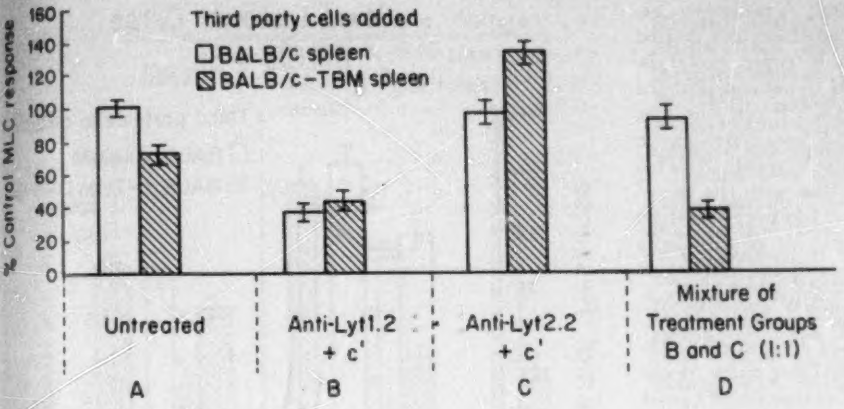

TEXT-FIGURE 2.—Spleen cells from normal mice (*open bars*) and TBM (*cross-hatched bars*) were treated with anti-Lyt 1.2 or anti-Lyt 2.2 plus C for analysis of the phenotype of the suppressor cells. Treated and control spleen cells were evaluated for their capacity to suppress a normal MLC response [BALB/c × $B6_{\text{irrad}}$]. MLC responses are expressed as percent normal MLC response (BALB/c × $B6_{\text{irrad}}$ + BALB/c) ± SEM. *Panel A* refers to control untreated cells. *Panel B* depicts results with Lyt 1.2 antiserum plus C-treated cells. Such treatment reduced the normal control response, probably because of a decrease of responder cells. *Panel C* shows that elimination of Lyt 2^+ cells from TBM spleen cells eliminated suppression. *Panel D* presents data obtained by the mixture of equal numbers of Lyt 1.2 antiserum plus C and Lyt 2.2 antiserum plus C-treated spleen cells. Elimination of Lyt 1, 2, 3^+ cells did not diminish suppression.

to such an assay resulted in a 20–40% increase in response over the MLC without the added cells.

Cell Surface Markers of Suppressor Cells

We previously showed that suppressor cells induced 10–14 days PI with VP tumor cells were probably T-cells since they were γ-irradiation-sensitive, were absent in athymic nude mice, and could be eliminated with anti-Thy 1.2 plus C (*11*). Further studies were therefore done with the use of antisera against specific Lyt antigens to determine the subpopulation of T-cells involved (text-fig. 2). Spleen cells from normal mice and from TBM were treated with anti-Lyt 1.2 or anti-Lyt 2.2 antiserum plus C, and aliquots of the remaining viable cells were added to a normal MLC reaction. As stated previously, the addition of normal spleen cells can result in a 20–40% increase in MLC response. Treatment of spleen cells from TBM with anti-Lyt 2.2 antiserum plus C resulted in the complete abrogation of suppression (text-fig. 2) and some increase in MLC, whereas similar treatment of control spleen cells had no significant effect on the MLC response. Treatment of spleen cells from TBM with anti-Lyt 1.2 antiserum plus C did not eliminate the suppression of the MLC response. However, treatment of normal BALB/c spleen cells with anti-Lyt 1.2 antiserum plus C abrogated the 20–40% increase in response usually found with the addition of these cells to an MLC reaction. In retrospect, this observation indicated that if Lyt 1, 2, 3^+ cells were suppressive, treatment of TBM spleen cells with anti-Lyt 1.2 plus C would have abrogated the responder cells as well as suppressor cells and Lyt 1, 2, 3^+ suppressor cells would not have been recognized. This possibility was evaluated in experiments in which normal or TBM spleen cells treated with Lyt 1.2 antiserum plus C were reconstituted with an equal number of normal BALB/c spleen cells treated with Lyt 2.2 antiserum plus C. Clearly, normal BALB/c spleen cells treated with Lyt 1.2 antiserum plus C and then reconstituted with normal spleen cells treated with Lyt 2.2 antiserum plus C showed normal responses (text-fig. 2), indicating that the treatment of added normal cells with Lyt 1.2 antiserum plus C had depressed the response by reducing the number of responding cells. Reconstitution of Lyt 1.2 antiserum plus C-treated TBM spleen cells with Lyt 2.2 antiserum plus C-treated TBM spleen cells continued to show a depressed response (text-fig. 2).

Clearly, Lyt 1, 2, 3^+ cells, absent from this mixture, did not participate in suppression since their absence failed to diminish suppression. We therefore concluded that the T-cells responsible for the suppressed MLC responses in TBM were of the Lyt 1^-, 2, 3^+ phenotype.

Association of Viral Antigens With Tumor-Induced Hyporesponsiveness: In Vivo Studies

Although the parental tumor cell line (11A) had been a virus nonproducer (*12*), it spontaneously began producing

TABLE 1.—*Characteristics of monoclonal antibody products from hybridoma cell lines*

Monoclonal antibody	Antigen specificity	Characteristics and distribution of the antigenic specificity in murine oncoviruses	G-MuLV-AKR leukemia virus	FMR
35/299	gp70	Type-specific antigen: Endogenous, ecotropic MuLV	+	−
35/56	gp70	Type-specific antigen: Endogenous, ecotropic MuLV (G_{IX}^+)	+	−
42/94	gp70	Type-specific antigen: Endogenous, ecotropic MuLV (Gross passage A-negative)	−/+	−
35/270	p30	Type-specific antigen: Endogenous, ecotropic MuLV ($GCSA^+$)	+	−
60/35	p30	Group-specific antigen: Fv-1 tropism N^+, B^-; endogenous and exogenous, ecotropic MuLV	+	+
42/114	p15(E)	Group-specific antigen: Endogenous and exogenous, ecotropic MuLV	+	+

virus during the course of in vitro passage. A microcytotoxicity assay was used to show that one subclone (designated "11A-VP") of these cells produced a B-tropic, ecotropic virus and expressed gp70 and p30 viral structural proteins on its cell surface. In addition, the 11A-VP cell line was shown to express G_{IX} antigen and GCSA, two type-specific cell surface antigens specified by G-MuLV (table 1). This cell line has been extensively characterized with the use of the monoclonal anti-gp70 antibodies and has been shown to be expressing serologically detected proteins of the Gross serotype. These results suggested that the cell line had begun expressing an endogenous Gross-type retrovirus. In contrast, a second such clone was shown to lack demonstrable evidence of MuLV production and was thus designated "11A-NP." Our earlier study showed that BALB/c mice inoculated with the 11A-NP clone of MuLV-transformed tumor cells failed to induce the T-cell-mediated suppression. A compendium of mice inoculated with 11A-NP and 11A-VP is presented in text-figure 3. Only mice inoculated with 11A-VP demonstrated suppressor cell activity 10–14 days PI (mean RR=70±6%, $P<0.01$).

Since the T-cell suppression might have been caused by a systemic MuLV viremia, DEAE–dextran-treated Sc-1 monolayers were cocultivated with spleen cells from TBM, passaged blindly three times, and evaluated with the use of anti-p30 antiserum for the presence of an oncovirus by indirect immunofluorescence. The Sc-1 cells are very susceptible to ecotropic virus infection and successfully detected the MuLV infection of 11A-VP tumor cells excised from these mice. In three experiments, we failed to detect virus in the spleens of TBM, indicating that an MuLV viremia was probably not present and that viral structural antigens, expressed by or released from the tumor cells, were probably responsible for inducing the suppressor T-cells.

Augmentation of Suppressor T-Cell Activity in Vitro With Viral Antigens

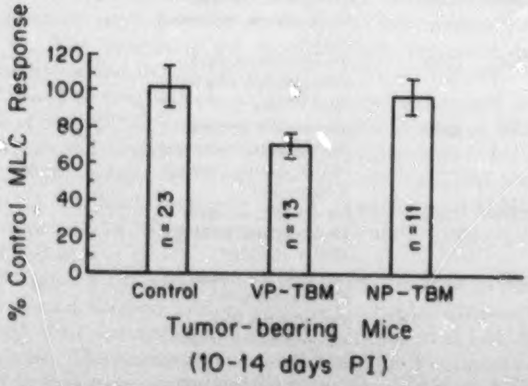

TEXT-FIGURE 3.—Role of virus in the induction of suppressor T-cells. The MLC response of a compendium of mice inoculated with either VP or NP tumor cells (10-14 days PI) is presented. Suppressor T cells were identified only in mice inoculated with VP tumor cells ($P<0.005$) (*11*).

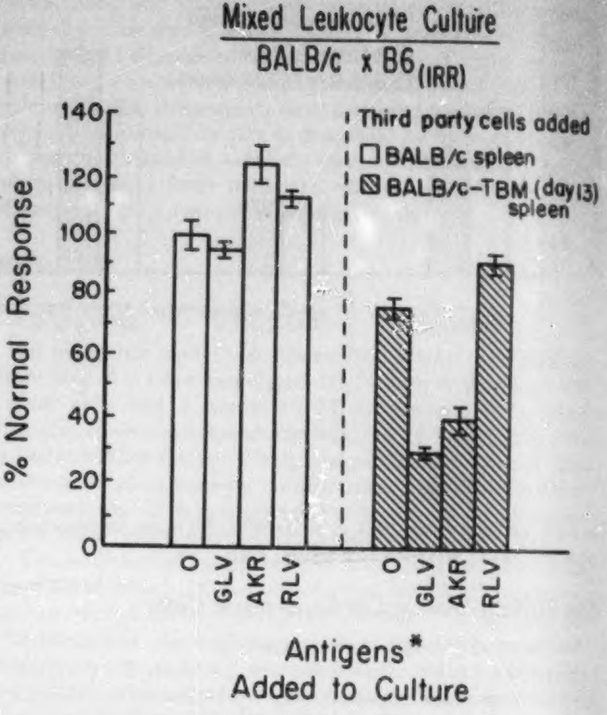

* All antigens UV-irradiated and adjusted to 10^8 particles/10 λ

TEXT-FIGURE 4.—Augmentation of suppressor cell activity by addition of specific viral antigens. Spleen cells from normal BALB/c and BALB/c mice inoculated with syngeneic VP tumor cells were added to a normal allogeneic MLC. The effects of the addition of G-MuLV–AKR leukemia virus antigen, R-MuLV antigen, or PBS without antigen were compared. Only the addition of G-MuLV–AKR leukemia virus antigen enhanced the suppressive activity of the suppressive T-cells ($P<0.001$). Neither antigen had a significant effect on the response of normal spleen cells in the third-party MLC ($P>0.1$).

Experiments were undertaken to evaluate further the role of viral antigens in the induction of suppressor T-cells. UV-irradiated preparations of virus (10^8 virus particles) were added to normal MLC reactions [BALB/c × $B6_{(IRR)}$] to which had been added either normal BALB/c mouse spleen cells or TBM spleen cells. G-MuLV and AKR leukemia virus, both B-tropic, ecotropic viruses that share type-specific antigens with the virus shed by the 11A-VP tumor cells, had no significant effect on the response of normal cells. When added to an MLC reaction containing suppressor T-cells from a TBM, both G-MuLV and AKR leukemia virus antigen preparations significantly augmented suppression from an RR of 76% to 31 and 41%, respectively ($P<0.001$; text-fig. 4). In contrast, addition of R-MuLV, a member of the FMR^+ group of MuLV that does not share type-specific antigens with the virus shed by the 11A-VP tumor cells, resulted in no augmentation of the suppression (text-fig. 4). In other experiments, virus preparations that had been disrupted by repeated freezing and thawing gave similar results (data not shown).

Identification of Specific Viral Antigen Responsible for Augmenting Suppressor T-Cell Function

Our results suggested that a specific viral antigen, ex-

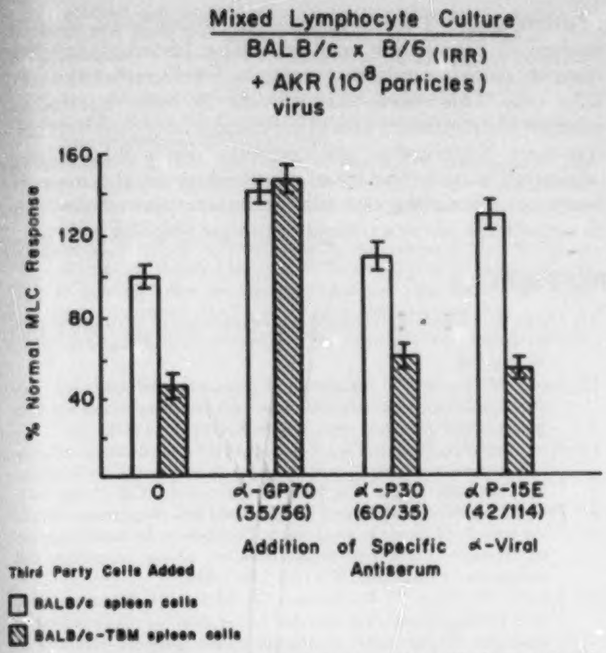

TEXT-FIGURE 5.—Blocking of suppressor cell activity with the use of antisera directed against specific viral structural proteins. Spleen cells from normal mice and from TBM were added in conjunction with UV-inactivated AKR leukemia virus (10^8 particles) to a normal third-party MLC. Several antisera directed against specific viral structural proteins were added to the assay. Only the antiserum directed against the gp70 glycoprotein present on G-MuLV–AKR leukemia virus was able to block suppressor cell activity ($P<0.005$). GLV=G-MuLV; AKR=AKR leukemia virus; RLV=R-MuLV; λ=μl.

pressed on G-MuLV but not on FMR$^+$-type MuLV, triggered suppressor cell activity in vitro. If so, then addition of specific antibodies directed at these structural antigen(s) might block the augmented suppression of the MLC reaction induced by viral antigen. Text-figure 5 illustrates the effect of monoclonal antiviral antibodies on normal and suppressed MLC responses. Monoclonal anti-p30 antibody (60/35) and monoclonal anti-p15(E) antibody (42/114) had no significant effect on either the normal or the suppressed MLC responses, even in experiments in which disrupted virus preparations were used. Only monoclonal antibodies directed against gp70, the glycoprotein present on G-MuLV–AKR leukemia virus, were able to block AKR leukemia virus antigen-augmented suppression (RR=147%; $P<0.005$). Several additional monoclonal antibodies directed against gp70 (35/299, 42/94) and monovalent hyperimmune sera yielded similar results (data not shown).

TABLE 2.—*Abrogation of suppressor T-cell activity with anti-gp70 antibodies*

Responders	Stimulators	Anti-gp70	Mean ± SE	RR, %
BALB/c	BALB/c	–	2,047±142	—
BALB/c TBM	BALB/c TBM	–	2,438±263	—
BALB/c	B6	–	47,813±938	100
BALB/c TBM	B6	–	29,011±1,096[a]	61[a]
BALB/c	BALB/c	+	1,873±64	—
BALB/c TBM	BALB/c TBM	+	6,832±718	—
BALB/c	B6	+	50,291±4,873	105
BALB/c TBM	B6	+	52,433±2,518	181[b]

[a] $P<0.05$.
[b] $P<0.001$.

Studies were also done to evaluate the effect of monoclonal anti-gp70 antibodies on the capacity of spleen cells from normal mice or TBM to respond in a one-way MLC in the absence of additional AKR leukemia virus antigen (table 2). Once again, the anti-gp70 antibodies were able to significantly augment the lymphoproliferative response of spleen cells from TBM (RR=181%; $P<0.05$). In contrast, there was no significant augmentation by anti-gp70 of the normal MLC in the absence of additional viral antigen.

DISCUSSION

Antigen-specific suppressor T-cells have been identified in a number of model systems with the use of synthetic antigens (*22, 23*). Administration of certain simple antigens, such as GAT or GT, and some more complex antigens under certain conditions, has been shown to lead to the almost exclusive development of suppressor T-cells (*24*). Induction of such responses has allowed the evaluation of the specific determinants on the antigen necessary for induction, the genetics of the host immune response that dictates this response, and the cellular interactions required for this response to be expressed (*22, 23*). Tumors have also been shown to activate suppressor cells, often T-cells, operative in a variety of in vivo and in vitro assay systems (*3, 7, 8*). However, although the study of the well-defined antigens' capacity to induce suppressor T-cells has led to a much better understanding of this phenomenon, little has been learned about suppressor T-cells induced naturally, e.g., by a syngeneic tumor. The model system that we have described clearly offers the opportunity to study such a natural situation. The MuSV-transformed Balb/3T3 cells spontaneously began to produce a Gross-like MuLV during passage in culture, and subclones with and without virus expression have been selected and used. These cells have subsequently been evaluated regularly to assure that they remain either virus producers or not, since our studies have clearly shown that expression of viral antigens by the tumor cells was required for the induction of T-suppressor cells. As was found with the T-suppressor cells induced by synthetic antigens (*22*), the cells induced by the clone of VP tumor cells were of the Lyt 1^-, 2, 3^+ phenotype.

The absolute requirement for virus antigen on the tumor cells for the induction of suppressor T-cells prompted us to develop an in vitro assay system to further evaluate this association. Adding UV-inactivated, band-purified virus to MLC containing suppressor T-cells augmented suppression significantly. The specificity of this augmentation was impressive; MuLV that shared type-specific antigens with the virus produced by the tumor cells clearly augmented suppression, whereas a closely related R-MuLV or M-MuLV (data not shown), both of which belong to the FMR$^+$ group and therefore do not share type-specific antigens, failed to augment suppression. Neither viral antigen preparation induced suppression of normal BALB/c responses. These studies suggest that the type-specific, Gross-like viral antigens on the tumor cells were responsible for inducing the suppressor T-cells and that sensitized cells were triggered in vitro by the addition of the specific antigen.

Since soluble viral structural antigens were not available, the specific structural antigen of the virus responsible for the induction of suppression was delineated with the help of a series of monoclonal antibodies to G-MuLV-AKR leukemia virus proteins. When added to MLC containing T-suppressor cells and augmenting antigen only antiserum directed against the major cell surface glycoprotein gp70 blocked the induction of suppression. Thus the amplification of suppression in vitro and, perhaps, the induction of suppression in vivo were mediated by gp70. This is an interesting observation since gp70 has been found in bone marrow cells of several mouse strains tested (including BALB/c (*25*) and may indicate that the mice had been previously exposed to the gp70 molecule. Thus inoculation of tumor cells expressing the same viral antigen might result in amplification of suppressor cells or their suppressive function.

These observations of gp70-induced immunosuppression are clearly different from those of Mathes et al. (*26*), who showed suppression of concanavalin A-induced lymphocyte proliferation by p15 of feline leukemia virus. In the Mathes study, sensitization to the viral antigen did not appear to be a requirement, whereas in our study sensitization was required. In addition, anti-15E failed to inhibit the immunosuppression induced by disrupted virus particles, clearly indicating that this viral polypeptide was not required for this function.

Of great interest was the finding that two monoclonal anti-gp70's were able to augment MLC reactivity of spleen cells from TBM even in the absence of additional viral antigens. These results suggest that viral antigens, perhaps expressed by activated normal spleen cells (*27*) or shed by the tumor cells and processed by TBM host antigen-presenting cells, were present in the spleen cell suspensions. Since gp70 antigen is present in large quantities on the surface of the tumor cells, it is reasonable to assume that the antigen might have been shed and be present in the spleens of TBM and therefore carried over to the MLC. The anti-gp70 antibodies might interact with these antigen-presenting cells to prevent the induction of suppression. Preliminary experiments showed that anti-gp70 and C abrogated the gp70-augmentable function of suppressor T-cells, suggesting that this treatment might have eliminated an antigen-bearing spleen cell population. However, in several experiments treatment of spleen cells with anti-gp70 plus C had no effect on the response of these cells in the absence of additional antigen, perhaps due to a relatively low expression of the viral antigen on the spleen cells (data not shown). More extensive studies will be required to delineate these cellular interactions.

Finally, it should be reemphasized that the model of immunoregulation described in this study used a naturally occurring cell surface-associated viral antigen. Preliminary studies suggest that, like T-cell-mediated cytotoxicity of virus-infected cells (*28*), our suppressor T-cells are also genetically restricted (Bluestone JA, Lopez C: Manuscript in preparation). This may mean that presentation of gp70 antigen in conjunction with self-major histocompatibility complex antigen results in suppressor T-cells rather than T-killer cells. This system may provide the tools required to examine the regulatory arm of genetically restricted immune responses. Experiments are currently under way in our laboratory to examine these relationships in the hope of better understanding the cellular interactions involved in the regulation of the antitumor immune response.

REFERENCES

(*1*) Umiel T, Trainin N. Immunological enhancement of tumor growth by syngeneic thymus-derived lymphocytes. Transplantation 1974; 18:244–250.

(*2*) Small M, Trainin N. Separation of populations of sensitized lymphoid cells into fractions inhibiting and fractions enhancing syngeneic tumor growth in vivo. J Immunol 1976; 117:292–297.

(*3*) Hellström KE, Hellström I. Evidence that tumor antigens enhance tumor growth in vivo by interacting with radiosensitive (suppressor?) cell populations. Proc Natl Acad Sci USA 1978; 75:436–440.

(*4*) Pope BL, Whitney RB, Levy JG, Kilburn DG. Suppressor cells in the spleens of tumor-bearing mice: Enrichment by centrifugation on Hypaque–Ficoll and characterization of the suppressor cell population. J Immunol 1976; 116:1342–1346.

(*5*) Jerrells TR, Dean JH, Richardson GL, McCoy JL, Herberman RB. Role of suppressor cells in depression of in vitro lymphoproliferative responses of lung cancer and breast cancer patients. JNCI 1978; 61:1001–1009.

(*6*) Schaaf-LaFontaine N. Separation of lymphoid cells with a suppressor effect on the activity of cytotoxic cells in vitro during the growth of syngeneic mouse tumor. Int J Cancer 1978; 21:329–333.

(*7*) Fujimoto S, Green MI, Sebon AH. Regulation of the immune response to tumor antigens. I. Immunosuppressor cells in tumor-bearing hosts. J Immunol 1976; 116:791–799.

(*8*) ———. Regulation of the immune response to tumor antigens. II. The nature of the suppressor cells. J Immunol 1976; 116:800–806.

(*9*) Hellström KE, Hellström I, Kant JA, Tamerius JD. Regression and inhibition of sarcoma growth by interference with a radiosensitive T-cell population. J Exp Med 1978; 148:799–804.

(*10*) Plata F, MacDonald HR, Shain B. Suppressor T-cells regulate the cytotoxic T lymphocyte response to syngeneic tumors induced by murine sarcoma virus (MSV) in the mouse. J Immunol 1979; 123:852–860.

(*11*) Bluestone JA, Lopez C. Suppression of the immune response in tumor-bearing mice. I. Response to virus-producing tumor cells and non-virus-producing tumor cells. JNCI 1979; 63:1215–1220.

(*12*) Todaro GH, Aaronson SA. Properties of clonal lines of murine sarcoma virus transformed BALB/3T3 cells. Virology 1969; 38:174–179.

(*13*) Strouk V, Frunder G, Fenyö CM, Lamon E, Skurnyak H, Klein G. Lack of a distinctive surface antigen on cells transformed by murine sarcoma virus. J Exp Med 1972; 136:344–352.

(*14*) Greenberger JS, Stephenson JR, Aoki T, Aaronson SA. Cell-surface antigens of murine sarcoma-virus-transformed non-producer cells: Further evidence for lack of transplantation immunity. Int J Cancer 1974; 14:145–152.

(*15*) Toplin M, Sottong P. Large volume purification of tumor viruses by use of zonal centrifuges. Appl Microbiol 1972; 23:1010–1014.

(*16*) O'Donnell PV, Nowinski RC. Serological analysis of antigenic determinants on the *env* gene products of AKR dualtropic (MCF) murine leukemia viruses. Virology 1980; 107:81–88.

(*17*) Ly IA, Mishell RI. Separation of mouse spleen cells by passage through columns of Sephadex G-10. J Immunol Methods 1974; 5:239–247.

(*18*) Bluestone JA, Lopez C. Suppression of the immune response in tumor-bearing mice. II. Characterization of adherent suppressor cells. JNCI 1979; 63:1221–1227.

(*19*) DeLeo AB, Shiku H, Takahashi T, John J, Old LJ. Cell surface antigens of chemically-induced sarcoma of the mouse. I. Murine leukemia virus-related antigens and alloantigens on cultured fibroblasts and sarcoma cells: Description of a unique antigen in BALB/c Meth A sarcoma. J Exp Med 1977; 146:720–734.

(20) O'Donnell PV, Stockert E. Induction of G_{IX} antigen and Gross cell surface antigen after infection by ecotropic and xenotropic murine leukemia viruses in vitro. J Virol 1976; 20:545–554.

(21) Shen FW, Boyse EA, Cantor H. Preparation and use of Ly antisera. Immunogenetics 1975; 2:591–595.

(22) Benacerraf B, Kapp JA, Debre P, Pierce CW, Delacroix F. The stimulation of specific suppressor T-cells in genetic nonresponder mice by linear random copolymers of L-amino acids. Trans Rev 1975; 26:21–38.

(23) Kapp JA, Pierce CW, Schlossman S, Benacerraf B. Genetic control of immune response in vitro. V. Stimulation of suppressor T-cells in non-responder mice by the tripolymer L-glutamic acid^{60}-L-alanine L-tyrosine^{10} (GAT). J Exp Med 1974; 140:648–659.

(24) Liew FY. Regulation of delayed-type hypersensitivity. I. T-suppressor cells for delayed-type hypersensitivity to sheep erythrocytes in mice. Eur J Immunol 1977; 7:714–718.

(25) McClintock RP, Ihle JN, Joseph DR. Expression of AKR murine leukemia virus gp70-like and BALB (X) gp71-like antigens in normal tissues in the absence of overt virus expression. J Exp Med 1977; 146:422–434.

(26) Mathes LE, Olsen RG, Hilebrand LC, et al. Immunosuppressive properties of a virion polypeptide, a 15,000-dalton protein, from feline leukemia virus. Cancer Res 1979; 39:950–955.

(27) Wecker E, Schimpl A, Hunig T. Expression of MuLV gp71-like antigen in normal mouse spleen cells induced by antigenic stimulation. Nature 1977; 269:598–600.

(28) Zinkernagel RM. Thymus and lymphohemopoietic cells: Their role in T-cell maturation in selection of T-cells' H-2-restriction-specificity and in H-2 linked *Ir* gene control. Immunol Rev 1979; 42:224–270.

blank page

Carcinogenicity Test of Acetoxime in MRC-Wistar Rats[1,2,3]

Sidney S. Mirvish,[4] Shahrokh Salmasi,[4] *and* **Richard G. Runge**[4,5]

ABSTRACT—Acetoxime was tested for carcinogenicity by chronic administration in the drinking water to male and female outbred MRC-Wistar rats. The dose of 1.0 g/liter was administered 5 days/week for 18 months (total dose, 6.2–7.0 g/rat). The test compound induced benign hepatocellular adenomas in 80% of the males but did not produce tumors in the females. This is the first report that oximes, which are fairly widely used in industry, are tumorigenic.—JNCI 1982; 69:961–962.

We previously tested a series of nitrosamides and related compounds for carcinogenicity in MRC-Wistar rats, mostly by administration in the drinking water (*1–4*). In continuation of this series, we report here a carcinogenicity test on acetoxime [acetone oxime, $(CH_3)_2C{=}NOH$] given in the drinking water. This compound was tested because of the resemblance of its *C*-nitroso tautomer to the carcinogen dimethylnitrosamine. We made this comparison although the generally accepted mechanism of nitrosamine activation (*1*) could not apply to the activation of acetoxime, which could not lose N_2 to generate a carbonium ion: $(CH_3)_2C{=}NOH \rightleftharpoons (CH_3)_2CHN{=}O$, compare to $(CH_3)_2N{-}N{=}O$.

MATERIALS AND METHODS

Acetoxime (Aldrich Chemical Co., Milwaukee, Wis.) was recrystallized twice from hot methanol (cooled to −20°C) to yield white crystals, mp 59.5–61.5°C (literature mp, 61°C). Analysis indicated: *a*) calculated: C, 49.3; H, 9.65; and N, 19.2% and *b*) found: C, 49.1; H, 9.88; and N, 19.3%. Solutions in water were stable for 1 day at 22°C and for 3 days at 4°C, as determined by their UV absorption at 195 nm.

Outbred MRC (Medical Research Council) Wistar rats from the breeding colony of The Eppley Institute were maintained 4 or 5/cage on Wayne Lab Blox pellets (Allied Mills, Inc., Chicago, Ill.) and were kept in the same room. The treated and untreated groups were started 8 months apart, because the untreated rats also served as controls for other treated groups not reported here. Acetoxime was weighed out twice weekly in a ventilated glove box and dissolved in distilled water. The solutions were stored at 6°C for not more than 2 days. Rats were given the test solution as drinking water (20 ml/rat/day) in brown bottles at 1–3 p.m. 5 days/week. Tap water was given when the compounds were not being administered and to the untreated rats. Treatment was started on rats from 8 to 10 weeks of age.

For selected cages, the rate of consumption of test solution per cage was measured over 24-hour periods every month. The rats were weighed monthly and maintained until they were moribund or died. After complete necropsies, organs were fixed in 10% buffered Formalin and sections were prepared of the principal organs and apparent tumors, stained with hematoxylin and eosin, and examined. For each organ, the incidence of tumor-bearing animals was compared with that for the untreated controls of the same sex by the use of the life table method (*2*), which is based on the number of rats at risk when each tumor develops. The acute LD_{50} was determined as before (*3*) after ip injection of test compound solutions in distilled water. The 7-day survival was recorded.

RESULTS

The acute LD_{50} of acetoxime was 840 mg/kg. Tables 1 and 2 show the results of the carcinogenicity test. Mean body weights reached maximum values of 650 g for the male and 400 g for the female untreated rats. The groups receiving acetoxime showed body weight curves similar to those of the controls but achieved maximum mean body weights of only 520 g for the males and 320 g for the females. In the following descriptions, mean survival periods (in wk) for tumors at each site are given *in parentheses*.

Untreated controls.—The males had a 43% tumor incidence at all sites. The females had incidences of 50% for pituitary adenomas (95 wk) and 30% for mammary gland tumors [2 adenocarcinomas and 4 fibroadenomas (105 wk)]. No liver tumors were observed. These results are similar to those for previous untreated groups of Eppley Institute MRC-Wistar rats (*3*).

Acetoxime.—Liver tumors were present, chiefly in the male rats [80% incidence (93 wk)] but also in the females [17% incidence (111 wk)]. For males only, the liver tumor incidence was significantly greater than the 0% incidence in the controls. All rats with liver tumors had hepatocellular adenomas, mostly 1–4 cm in diameter. These were composed of circumscribed masses of cells, having abundant cytoplasm and small, round nuclei. All these tumors had benign histologic criteria despite occasional differences in nuclear size, except in 1 male rat in which focal malignant degeneration was noted. Three rats (including 2 males) had liver hemangiomas in addition to the adenomas.

The male rats had a 20% incidence of squamous cell papillomas of the forestomach (98 wk), but this was not significantly raised from the control incidence of 0%. In the females, the incidences of pituitary adenomas [19% (83 wk)]

ABBREVIATIONS USED: LD_{50}=median lethal dose; mp=melting point.

---

[1] Received January 22, 1982; accepted May 20, 1982.

[2] Supported by Public Health Service contract N01CP-33278 and grant P01CA-25100 from the National Cancer Institute.

[3] Guidelines for the care and use of laboratory animals were followed as set forth by the National Research Council.

[4] The Eppley Institute for Research in Cancer, University of Nebraska Medical Center, 42d and Dewey Ave., Omaha, Nebr. 68105.

[5] We thank Dr. K. Patil (Family Practice Department, University of Nebraska Medical Center) for the statistical evaluations, Dr. K. E. McCaleb (Chemical-Environmental Program, SRI International, Menlo Park, Calif.) for information on the industrial uses of oximes, and Mr. J. Sams, Ms. F. Goldenberg, and Mr. R. Feldman for technical assistance.

TABLE 1.—*Treatment and survival data*

Test compound	Sex	Dose level, mg/liter water	Mean vol drunk, ml/rat/day	Treatment time, mo	Total dose, g/rat[a]	No. of rats surviving at wk:					
						40	60	80	100	120	140
None	♂	—	—	—	—	23	21	8	1	0	
None	♀	—	—	—	—	20	20	19	9	0	
Acetoxime	♂	1,000	18	18	7.0	15	15	11	2	0	
Acetoxime	♀	1,000	16	18	6.2	16	15	12	8	2	0

[a] Based on data in preceding three columns.

TABLE 2.—*Tumors in each group of rats*

Test compound	Sex	Effective No. of rats[a]	No. of tumor-bearing rats	No. of rats with tumors of:								No. of other tumors[b]
				Forestomach	Liver	Kidney	Testis	Pituitary gland	Adrenal gland	Mammary gland	Nervous system	
None	♂	23	9	—	—	2	1	1	1	1	1	3
None	♀	20	15	—	—	—	—	10	2	6	1	5
Acetoxime	♂	15	13	3	12	—	2	—	2	—	1	—
Acetoxime	♀	16	13	1	3	1	—	3	4	—	1	2

[a] Number of rats alive when first tumor-bearing rat died.
[b] ≤2 tumors/site.

and adrenal tumors [25%, mostly pheochromocytomas (108 wk)] were not significantly different from those in the controls. Hence acetoxime was a potent liver tumorigen in the male rats but was not significantly tumorigenic in the females.

DISCUSSION

The induction of benign hepatocellular adenomas by acetoxime is the first report of the tumorigenicity of oximes. The greater incidence in male rats is characteristic of several liver carcinogens, e.g., 4-*N*-dimethylaminoazobenzene (*4*). Previous research on the toxicology of oximes was connected with their ability to reactivate cholinesterase after animals were poisoned with organophosphorus compounds (*5, 6*). The LD_{50} of acetoxime was reported to be 4,000 mg/kg in mice (*5*), which is five times higher than what we observed in rats. The related compounds hydroxylamine (NH_2OH) and hydroxyurea ($NH_2 \cdot CO \cdot NHOH$) were not carcinogenic to mice (*7*). Aromatic hydroxamic acids ($ArNHO \cdot COR$),[6] such as *N*-acetoxy-2-aminofluorene, are strong carcinogens (*8*). Several O-acyl hydroxamic acids ($RCO \cdot NHO \cdot COR'$), but not the corresponding hydroxamic acids ($RCO \cdot NHOH$), were mutagenic to bacteria, possibly because they rearranged to form isocyanates (*9*).

The tumorigenicity of acetoxime is important because oximes are rather widely used in industry. Cyclohexanone oxime is produced (1.2×10^9 lb/yr) in situ as an intermediate in the synthesis of caprolactam, used to manufacture nylon. About 3×10^6 pounds/year of oximes, including methyl ethyl ketone oxime (2-pentanone oxime), butyraldehyde oxime, and cyclohexanone oxime, are used as antiskinning agents in paints and coatings, in which they constitute 0.1–0.4% of the total weight. A mixture of hydroxy-oximes is marketed for the solvent extraction of copper. Oximes are also used by organic chemists as derivatives of aldehydes and ketones.

A possible mechanism for acetoxime activation involves oxidation to 2-nitropropane: $(CH_3)_2C{=}NOH + O \rightarrow (CH_3)_2CHNO_2$. This last compound was reported (*10*) to induce hepatocellular carcinomas in 100% incidence when administered by inhalation (207 ppm for 6 mo, 7 hr/day, 5 days/wk). No tumors were induced by exposure to 25 ppm of the compound. A later test (*11*) also failed to induce tumors with 25 ppm 2-nitropropane.

REFERENCES

(*1*) MAGEE PN, BARNES JM. Carcinogenic nitroso compounds. Adv Cancer Res 1967; 10:163–246.

(*2*) PETO R. Guidelines on the analysis of tumour rates and death rates in experimental animals. Br J Cancer 1974; 29:101–105.

(*3*) BULAY O, MIRVISH SS, GARCIA H, PELFRENE AF, GOLD B, EAGEN M. Carcinogenicity test of six nitrosamides and a nitrosocyanamide administered orally to rats. JNCI 1979; 62:1523–1528.

(*4*) MULAY AS, O'GARA RW. Incidence of liver tumors in male and female rats fed carcinogenic azo dyes. Proc Soc Exp Biol Med 1959; 100:320–322.

(*5*) DULTZ L, EPSTEIN MA, FREEMAN G, GRAY EH, WEIL WB. Studies on a group of oximes as therapeutic compounds in sarin poisoning. J Pharmacol Exp Ther 1957; 119:522–531.

(*6*) COLEMAN IW, LITTLE PE, GRANT GA. Oxime mixtures and atropine in the protection of mice and rats from sarin poisoning. Can J Biochem 1969; 38:1035–1043.

(*7*) YAMAMOTO RS, WEISBURGER EK, KORZIS J. Chronic administration of hydroxylamine and derivatives in mice. Proc Soc Exp Biol Med 1967; 124:1217–1220.

(*8*) CLAYSON DB, GARNER RC. Carcinogenic aromatic amines and related compounds. In: Searle CE, ed. Chemical carcinogens. ACS monograph 173. Washington, D.C.: American Chemical Society, 1976:366–401.

(*9*) SKIPPER PL, TANNENBAUM SR, THILLY WG, FURTH EE, BISHOP WW. Mutagenicity of hydroxamic acids and the probable involvement of carbamoylation. Cancer Res 1980; 40:4704–4708.

(*10*) LEWIS TR, ULRICH CE, BUSEY WM. Subchronic inhalation toxicity of nitromethane and 2-nitropropane. J Environ Pathol Toxicol 1979; 2:233–249.

(*11*) GRIFFIN TB, COULSTON F, STEIN AA. Chronic inhalation exposure of rats to vapors of 2-nitropropane at 25 ppm. Ecotoxicol Environ Safety 1980; 4:267–281.

---

[6] Ar=aryl; R=alkyl.

β-Cyclodextrin: Promoting Effect on the Development of Renal Tubular Cell Tumors in Rats Treated With *N*-Ethyl-*N*-hydroxyethylnitrosamine[1]

Yoshio Hiasa,[2] **Masato Ohshima,**[2] **Yoshiteru Kitahori,**[2] **Noboru Konishi,**[2] **Toyohisa Fujita,**[2] *and* **Takashi Yuasa**[2,3]

ABSTRACT—Injection (sc) of β-cyclodextrin (β-C) increased the number and size of renal tubular cell tumors in inbred Wistar (W) rats treated with 1,000 ppm of *N*-ethyl-*N*-hydroxyethylnitrosamine (EHEN). The incidence of renal tumors at the end of the 32-week experiment was 50% in rats treated with 1,000 ppm EHEN for 2 weeks and 100% in rats treated with 1,000 ppm EHEN for 2 weeks and then given daily sc injections of β-C for 1 week. The incidence of renal tumors more than 3 mm in diameter was 70% in rats treated with 1,000 ppm EHEN before β-C but 0% in rats treated with EHEN alone. In addition, β-C promoted the development of renal tumors in rats treated with 500 ppm EHEN, which is a subthreshold dose for renal tubular cell tumorigenesis. These results show that β-C promotes EHEN-induced renal tubular cell tumorigenesis.—JNCI 1982; 69:963–967.

Since Berenblum (*1*) in 1941 discovered the promoting property of croton oil in skin carcinogenesis, many investigators have reported on promotion of chemical carcinogenesis (*2–21*). Croton oil was considered to be the most effective promoter and was initially judged to be noncarcinogenic (*1–6*). However, since a high incidence of skin tumors was observed in mice treated with croton oil alone, croton oil was concluded to be not merely a promoter but also an initiator of tumor formation. Boutwell et al. (*22*) and Roe (*23*) reported that croton oil is a weak carcinogen and a strong promoter.

Recently, there have been reports about promoting agents in the liver (*7–12*), lung (*13*), intestine (*14, 15*), and urinary bladder (*16–21*). However, there are few reports about promoters of renal tubular cell tumorigenesis (*24–29*). β-C is a nephrotoxic agent and is not a carcinogen (*30, 31*).

EHEN is a strong carcinogen in the rat kidney, where it induces only renal tubular cell tumors. The dose response in rats to EHEN in renal tubular cell tumorigenesis has been reported (*32*).

In the present work we tested whether β-C is a promoter of EHEN-induced renal tubular cell tumorigenesis in rats.

MATERIALS AND METHODS

Chemicals and diet.—EHEN was purchased from Nakarai Chemical Co., Kyoto, Japan, and was added to the basal diet (*33*) at a concentration of 1,000 ppm for groups 1 and 3 and 500 ppm for groups 2 and 4 for the first 2 weeks. β-C was purchased from Nakarai Chemical Co., Kyoto, and was injected sc at a dose of 45 mg/100 g body weight once a day for 7 days in week 3 of the experiment. Commercial diet (Oriental M) was purchased from Oriental Kobo Co., Osaka, Japan, and given to all rats for 30 weeks from week 3 to week 32.

Animals.—A total of 120 male W rats (Kitayama Labes Animal Co., Kyoto) 6 weeks old and weighing 150–170 g were divided into 6 groups of 20 rats each. These groups received the following diets and treatments: group 1, 1,000 ppm EHEN in basal diet; group 2, 500 ppm EHEN in basal diet; group 3, 1,000 ppm EHEN in basal diet and β-C; group 4, 500 ppm EHEN in basal diet and β-C; group 5, basal diet and β-C; and group 6, basal diet. The experimental design is shown in text-figure 1.

The animals were housed in wire cages in an air-conditioned room at 24°C and weighed weekly. Two rats in group 1 and 1 rat in group 3 died of pneumonia, and 2 rats in group 3 died of pulmonary hemorrhage and acute nephrosis due to β-C before the end of the experiment and were not included in effective numbers. Animals that survived for 32 weeks were killed with ether after food was withheld for 16 hours. Their kidneys were weighed, and the number and the diameters of the tumors on the surfaces of the kidneys were determined macroscopically. Serial cross sections of the right kidneys and serial horizontal sections of the left kidneys were embedded in paraffin. The number of tumors was also counted microscopically in serial sections and compared with that determined macroscopically. Other organs that appeared grossly abnormal were also examined histologically.

RESULTS

Body and kidney weights.—The mean weights of the body and kidneys in each group are shown in table 1. The mean final body weights in different groups were not significantly different. The right kidneys were significantly larger in group 2 than in group 4 and smaller than those in groups 1 and 5. In group 3, the weights of the right kidneys varied between 1.42 and 2.48 g except for one kidney with a large renal tubular cell tumor that weighed 8.93 g.

Incidences of renal tumors.—The incidences of renal tumors in the groups are shown in table 2. The sizes of the renal tumors shown in table 2 are diameters of the largest tumor in either kidney. In group 1, there were 12 renal tumors in 9 (50%) of 18 rats; these tumors were small (<3 mm in

---

ABBREVIATIONS USED: β-C=β-cyclodextrin; DMN=dimethylnitrosamine; EHEN=*N*-ethyl-*N*-hydroxyethylnitrosamine; H & E=hematoxylin and eosin; NDPS=*N*-(3,5-dichlorophenyl)succinimide.

---

[1] Received February 5, 1982; accepted May 5, 1982.

[2] 1st Department of Pathology, Nara Medical University, Kashihara, Nara 634, Japan.

[3] We thank Ms. Kyoko Khono for typing the manuscript.

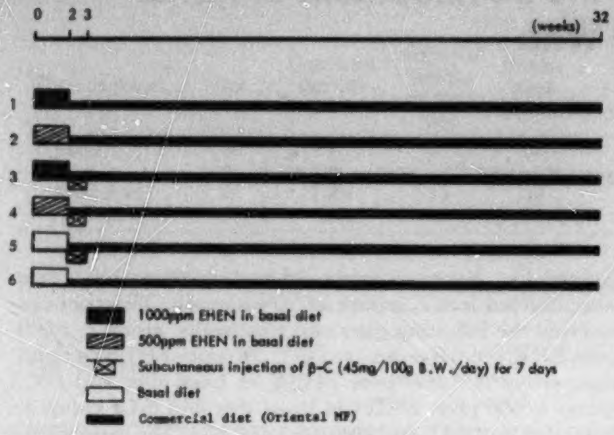
0
2 3
(weeks) 32
1
2
3
4
5
6
1000ppm EHEN in basal diet
500ppm EHEN in basal diet
Subcutaneous injection of β-C (45mg/100g B.W./day) for 7 days
Basal diet
Commercial diet (Oriental MF)

TEXT-FIGURE 1.—Experimental design.

diameter). In group 3, there were 32 renal tumors. Of the 17 rats in group 3, all had tumors, 15 had renal tumors in both kidneys, and 12 had renal tumors of more than 3 mm in diameter. In group 4, there were 8 renal tumors all less than 3 mm in diameter in 6 (30%) of 20 rats. No renal tumors were found in group 2, 5, or 6. Two of 12 renal tumors in group 1, 5 of 32 renal tumors in group 3, and 1 of 8 renal tumors in group 4 were clear cell tumors. These clear cell tumors were small (<3 mm in diameter). Other renal tumors were dark cell tumors.

Macroscopic findings.—Most renal tumors in groups 1, 3, and 4 were round and were present in the cortex. A few tumors were in the medulla but not in the pelvis. These tumors were yellowish, and there was a clear border between the tumor and surrounding nontumorous tissue. A section of a large renal tumor showed necrotic and hemorrhagic changes in the central area (fig. 1).

Microscopic findings.—Histologically, the renal tumors were composed of tubular cords or papillary structures and may have been cystic. Tumors were classified into two types, dark and clear cell tumors. The cells in dark cell tumors had a large round nucleus with light nucleoplasm and abundant light or dark basophilic cytoplasm (fig. 2). The cells in clear cell tumors had a small round nucleus and abundant clear cytoplasm (fig. 3). The cells in small and large renal tumors did not differ morphologically. Hemorrhage and necrosis were seen in the central areas of large renal tumors. There was no invasive growth or metastasis of renal tumor in any rats.

Microscopic findings in nontumorous areas of the kidneys.—Histologic findings in nontumorous areas of the kidneys of each group are summarized in table 3. Dark cell dysplasias were composed of cells similar to those of dark cell tumors (fig. 4A), and clear cell dysplasias were composed of cells similar to those of clear cell tumors (fig. 4B). These dysplasias were composed of tubular structures. Dysplasia of the kidney was seen in 13 of 18 rats in group 1, in all rats in group 3, and in 10 of 20 rats in group 4. Slight cystic dilatation of tubules, tubular casts, and interstitial fibrosis were seen focally in the kidneys of a few rats treated with β-C.

Tumors in other organs.—Two of 18 rats in group 1 and 2 of 20 rats in group 3 had hepatocellular carcinomas. There were no hepatocellular carcinomas in other groups.

DISCUSSION

Renal tubular cell tumors were induced by week 32 in all 17 rats treated with 1,000 ppm of EHEN for 2 weeks and

TABLE 1.—*Mean body and kidney weights of rats treated with EHEN and β-C*[a]

Experimental group (ppm)	Effective No. of rats	Final body weight, g	Right kidney weight, g (% of body weight)	Left kidney weight, g (% of body weight)
1. EHEN (1,000)	18	561	2.0±0.3[b] (0.36)	2.0±0.2[b] (0.36)
2. EHEN (500)	20	626	1.7±0.4 (0.27)	1.7±0.4 (0.27)
3. EHEN (1,000)+β-C	17	618	2.8±2.3 (0.45)	2.0±0.5 (0.32)
4. EHEN (500)+β-C	20	607	1.5±0.2[b,c] (0.25)	1.6±0.2 (0.27)
5. Basal diet+β-C	20	636	2.0±0.2[b] (0.31)	2.0±0.2[b] (0.31)
6. Basal diet	20	621	1.7±0.2 (0.27)	1.7±0.2 (0.27)

[a] Analysis of relative significance was done with Students' *t*-test. Kidney weights are means ± SD.
[b] Difference from group 6 was significant at $P<0.05$.
[c] Difference from group 2 was significant at $P<0.05$.

TABLE 2.—*Incidences of renal tumors in rats treated with EHEN and β-C*[a]

Experimental group (ppm)	Effective No. of rats	No of tumor-bearing rats (%)	No. of tumors			No. of rats with tumor sizes of:		
			Total	Dark cell	Clear cell	<3 mm	3–10 mm	>10 mm
1. EHEN (1,000)	18	9 (50)[b]	12	10	2	9	0	0
2. EHEN (500)	20	0	0	0	0	0	0	0
3. EHEN (1,000)+β-C	17	17 (100)[c]	32	27	5	5	6	6
4. EHEN (500)+β-C	20	6 (30)[d]	8	7	1	6	0	0
5. Basal diet+β-C	20	0	0	0	0	0	0	0
6. Basal diet	20	0	0	0	0	0	0	0

[a] Analysis of relative significance was by the χ^2-test.
[b] Difference from group 6 was significant at $P<0.05$.
[c] Difference from group 1 was significant at $P<0.05$.
[d] Difference from group 2 was significant at $P<0.05$.

TABLE 3.—*Histologic changes induced by EHEN and β-C in nontumorous areas of rat kidneys*[a]

Experimental group (ppm)	Tubules			Interstitial fibrosis[b]
	Dysplasia (%)	Cystic dilatation[b]	Cast[b]	
1. EHEN (1,000)	13 (72)[c]	–	–	–
2. EHEN (500)	0	–	–	–
3. EHEN (1,000)+β-C	17 (100)	±	±	±
4. EHEN (500)+β-C	10 (50)[d]	±	±	±
5. Basal diet+β-C	0	±	±	±
6. Basal diet	0	–	–	–

[a] Analysis of relative significance was done by χ^2 test.

[b] –: none, ±: a few.

[c] Difference from group 6 was significant at $P<0.05$.

[d] Difference from group 2 was significant at $P<0.05$.

then given sc injections of 45 mg β-C/100 g body weight daily for 7 days. Twelve of these 17 rats had kidney tumors of more than 3 mm in diameter. Treatment with 1,000 ppm of EHEN alone for 2 weeks induced renal tubular cell tumors in 9 of 18 rats by week 40, as reported previously (*32*), but these tumors were less than 3 mm in diameter. Injection (sc) of 45 mg of β-C/100 g body weight daily for 7 days alone did not induce any tumors or any remarkable histologic changes in the kidney by week 32. β-C is a nephrotoxin that induces polyuria and decreases the activities of some enzymes in the proximal convoluted tubules (*30, 31*). β-C induces degeneration and necrosis of the epithelium in the proximal convoluted tubules (30). In the present study these histologic changes induced in the kidneys by daily sc injections of 45 mg β-C/100 g body weight for 7 days had almost disappeared by week 32, but this treatment enhanced the development of renal tubular cell tumors but not of tumors in other organs in rats treated with 1,000 ppm EHEN. Thus the histologic changes induced by β-C in the kidneys may enhance the development of renal tubular cell tumors in rats treated with 1,000 ppm EHEN.

Renal tubular cell tumors were induced by week 32 in 6 of 20 rats fed diets containing 500 ppm of EHEN for 2 weeks and then given sc injections of 45 mg β-C/100 g body weight daily for 7 days. A dose of 500 ppm EHEN in the diet for 2 weeks was subthreshold for renal tumorigenesis, as reported previously (32). No renal tubular cell tumors were induced by week 32 in rats fed diets containing 500 ppm EHEN alone for 2 weeks, and there were few histologic changes in the kidneys by week 32 among rats treated with 500 ppm EHEN for 2 weeks. Thus the fact that treatment with β-C after this subcarcinogenic dose of EHEN induced tumors in 6 of 20 rats confirms the theory that β-C is a promoter in EHEN-induced renal tubular cell tumorigenesis.

There are a few reports on the effects of various compounds on the development of renal tumors in rats treated with DMN (*25-28, 32*), streptozotocin (*29, 34*), and EHEN (*24*). NDPS (*27, 29*) and citrinin (*28*) enhanced the development of renal tubular cell tumors in rats treated with DMN. NDPS and citrinin induced interstitial nephritis following degeneration of the proximal convoluted tubules (*27-29*). However, β-C is a stronger promoter than NDPS or citrinin in renal tubular cell tumorigenesis, possibly because it directly injures the proximal convoluted tubular epithelium. Lead acetate is also a strong promoter in EHEN-induced tumorigenesis (*24*) and is a weak carcinogen (*35-38*). Lead acetate, like β-C, injures the proximal convoluted tubules (*39, 41*). Thus prolonged or temporary injury of the proximal convoluted tubules may enhance or promote the development of renal tubular cell tumors in rats treated with a chemical carcinogen.

The promoting effect of 12-*O*-tetradecanonylphorbol 13-acetate is reported to be due to changes in the cell membrane (*42*). Changes in the cell membrane of the proximal convoluted tubular cells induced by β-C may explain the promoting effect of this compound on induction of renal tubular cell tumors by EHEN.

Further studies are required on changes induced by β-C in the cell membrane. DMN induced both renal tubular cell tumors and nephroblastomas in rats, the incidence of the nephroblastomas being higher (*33*). Streptozotocin induced renal tubular cell tumors without nephroblastomas in rats, but these renal tubular cell tumors took a long time to develop (*34*). Inasmuch as EHEN, which also induces only renal tubular cell tumors, induces tumors more rapidly than streptozotocin in rats, EHEN is a better initiator for use in tests on promoters of renal tubular cell tumorigenesis.

Some renal tubular cell tumors induced by EHEN are malignant because some had areas of necrosis and hemorrhage and because some were transplantable (Hiasa Y: Unpublished observations). Histologically, there was no difference between the cells in small and large renal tumors induced by EHEN and the cells in small and large renal tumors induced by other chemical carcinogens. Therefore, it was very difficult to distinguish cancers from renal tubular cell tumors, and the term "tumor" is used instead of "cancer" in the present paper.

REFERENCES

(*1*) Berenblum I. The carcinogenic action of croton resin. Cancer Res 1941; 1:44–48.

(*2*) Mottram JC. A developing factor in experimental blastogenesis. J Pathol 1944; 54:181–187.

(*3*) Berenblum I, Shubik P. The persistence of latent tumor cells induced in the mouse's skin by single application of 9,10-dimethyl-1,2-benzanthracene. Br J Cancer 1949; 3:384–386.

(*4*) Berenblum I. The probable nature of promoting action and its significance in the understanding of the mechanism of carcinogenesis. Cancer Res 1954; 14:471–477.

(*5*) Roe FJ, Salaman MH. Further studies on incomplete carcinogenesis: Triethylene melamine (T.E.M.), 1,2-benzanthracene and β-propiolactone as initiators of skin tumour formation in the mouse. Br J Cancer 1955; 9:177–203.

(*6*) Saffiotti U, Shubik P. The effects of low concentration of carcinogen in epidermal carcinogenesis. A comparison with promoting agents. J Natl Cancer Inst 1956; 16:961–969.

(*7*) Ito N, Tatematsu M, Nakanishi K, et al. The effects of various chemicals on the development of hyperplastic liver nodules in hepatectomized rats treated with *N*-nitrosodiethylamine or *N*-2-fluorenylacetamide. Gan 1980; 71:832–842.

(*8*) Kimura NT, Kanematsu T, Baba T. Polychlorinated biphenyl as a promoter in experimental hepatocarcinogenesis in rats. Z Krebsforsch 1976; 87:256–266.

(*9*) Nishizu M. Effects of phenobarbital, dichlorodiphenyltrichloroethane (DDT), and polychlorinated biphenyls (PCB) on diethylnitrosoamine-induced hepatocarcinogenesis. Gan 1979; 70:835–837.

(*10*) Peraino C, Fry RJ, Staffeldt E, Kisieleski WE. Effects of varying the exposure to phenobarbital on its enhancement of 2-acetylaminofluorene-induced hepatic tumorigenesis in rats. Cancer Res 1973; 33:2701–2705.

(*11*) Peraino C, Fry RJ, Staffeldt E, Christopher JP. Comparative enhancing effects of phenobarbital, amobarbital, diphenylhydantoin, and dichlorodiphenylchloroethane on 2-acetylaminofluorene-induced hepatic tumorigenesis in rats. Cancer Res 1975; 35:2884–2890.

(*12*) Peraino C, Fry RJ, Staffeldt E. Reduction and enhancement by phenobarbital of hepatocarcinogenesis induced in the rat by 2-acetylaminofluorene. Cancer Res 1971; 31:1506–1512.

(*13*) Witschi H, Williamson D, Lock S. Enhancement of urethan tumorigenesis in mouse lung by butylated hydroxytoluene. J Natl Cancer Inst 1977; 58:301–305.

(*14*) Pollard M, Luckert PH. Promotional effect of sodium barbiturate on intestinal tumors induced in rats by dimethylhydrazine. JNCI 1979; 63:1089–1092.

(*15*) Reddy BS, Watanabe K, Weisburger JH. Promoting effect of bile acids in colon carcinogenesis in germfree and conventional F344 rats. Cancer Res 1977; 37:3238–3242.

(*16*) Bryan GT, Erturk E, Yoshida O. Production of urinary bladder carcinomas in mice by sodium saccharin. Science 1970; 168:1238–1240.

(*17*) Cohen SM, Arai M, Jacobs JB, Friedell GH. Promoting effects of saccharin and DL-tryptophan in urinary bladder carcinogenesis. Cancer Res 1979; 39:1207–1217.

(*18*) Fukushima S, Friedell GH, Jacobs JB, Cohen SH. Effects of L-tryptophan and sodium saccharin on urinary tract carcinogenesis initiated by *N*-[4-(5-nitro-2-furyl)-2-thiazolyl]formamide. Cancer Res 1981; 41:3100–3103.

(*19*) Hicks RM, Wakefield J, Chowaniec J. Evaluation of a new model to detect bladder carcinogens or co-carcinogens; results obtained with saccharin, cyclamate and cyclophosphamide. Chem Biol Interact 1975; 11:225–233.

(*20*) Hicks RM, Chowaniec J. The importance of synergy between weak carcinogens in the induction of bladder cancer in experimental animals and humans. Cancer Res 1977; 37:2943–2949.

(*21*) Hicks RM, Wakefield JS, Chowaniec J. Letter: Co-carcinogenic action of saccharin in the chemical induction of bladder cancer. Nature 1973; 243:347–349.

(*22*) Boutwell RK, Bosch DK, Rusch MP. On the role of croton oil in tumor formation. Cancer Res 1957; 17:71–75.

(*23*) Roe FJ. The development of malignant tumours of mouse skin after "initiating" and "promoting" stimuli. III. The carcinogenic action of croton oil. Br J Cancer 1956; 10:72–78.

(*24*) Hiasa Y, Kitahori Y, Ohshima M, et al. Effects of β-cyclodextrin and lead acetate on the development of renal tubular cell tumor in rats treated with different doses of *N*-ethyl-*N*-hydroxyethylnitrosamine. Proc Jpn Cancer Assoc 1981; 40:74.

(*25*) Ito N, Hiasa Y, Tamai A, Kamamoto Y, Makiura S, Kondo Y. The influence of unilateral nephrectomy on the development of renal tumors in rats treated with dimethylnitrosamine and basic lead acetate. In: Abstracts of papers from the tenth International Cancer Congress, 1970:12.

(*26*) Ito N, Hiasa Y, Tamai A, Yoshida K. Effect of unilateral nephrectomy on the development of kidney tumors in rats treated with *N*-nitrosodimethylamine. Gan 1969; 60:319–327.

(*27*) Ito N, Sugihara S, Makiura S, et al. Effect of *N*-(3,5-dichlorophenyl)-succinimide on the histological pattern and incidence of kidney tumors in rats induced by dimethylnitrosamine. Gan 1974; 65:131–138.

(*28*) Shinohara Y, Arai M, Hirao K, et al. Combination effect of citrinin and other chemicals on rat kidney tumorigenesis. Gan 1976; 67:147–156.

(*29*) Shinohara Y, Miyata Y, Murasaki G, Nakanishi K, Yoshimura T, Ito N. Effect of *N*-(3,5-dichlorophenyl)succinimide on the histological pattern and incidence of kidney tumors induced by streptozotocin in rats. Gan 1977; 68:397–404.

(*30*) Hiasa Y, Ohshima M, Kitahori Y, et al. Histochemical studies of β-cyclodextrin nephrosis in rats. J Nara Med Assoc 1981; 32:316–321.

(*31*) Frank DW, Gray JE, Weaver RN. Cyclodextrin nephrosis in the rat. Am J Pathol 1976; 83:367–374.

(*32*) Hiasa Y, Ohshima M, Iwata C, Tanikake T. Histopathological studies on renal tubular cell tumors in rats treated with *N*-ethyl-*N*-hydroxyethylnitrosamine. Gan 1979; 70:817–820.

(*33*) Ito N, Johno I, Marugami M, Konishi Y, Hiasa Y. Histopathological and autoradiographic studies on kidney tumors induced by *N*-nitrosomethylamine in rats. Gan 1966; 57:595–604.

(*34*) Mauer SM, Lee CS, Najarian JS, Brown DM. Induction of malignant kidney tumors in rats with streptozotocin. Cancer Res 1974; 34:158–160.

(*35*) Boyland E, Dukes CE, Grover PL, Mitchley BC. The induction of renal tumours by feeding lead acetate to rats. Br J Cancer 1962; 16:283–288.

(*36*) Ito N, Hiasa Y, Kamamoto T, Makiura S, Sugihara S, Marugami M. Histopathological analysis of kidney tumors in rats induced by chemical carcinogens. Gan 1971; 62:435–444.

(*37*) Mao P, Molnar JJ. The fine structure and histochemistry of lead-induced renal tumors in rats. Am J Pathol 1967; 50:571–603.

(*38*) Van Esch GJ, Van Genderen H, An Vink HH. The induction of renal tumours by feeding of basic lead acetate to rats. Br J Cancer 1962; 16:289–297.

(*39*) Fairhall LT, Miller JW. Study of relative toxicity of molecular components of lead arsenate. Public Health Rep 1941; 56:1610–1625.

(*40*) Fowler BA, Kimmel CA, Woods JS, McConnell EE, Grant LD. Chronic low-level lead toxicity in the rat. III. An integrated assessment of long-term toxicity with special reference to the kidney. Toxicol Appl Pharmacol 1980; 56:59–77.

(*41*) Muro LA, Goyer RA. Chromosome damage in experimental lead poisoning. Arch Pathol 1969; 87:660–668.

(*42*) Driedger PE, Blumberg PM. Specific binding of phorbol ester tumor promoters. Proc Natl Acad Sci USA 1980; 77:567–571.

Figure 1.—Section of a kidney in group 3, showing a renal tubular cell tumor with necrotic and hemorrhagic changes in the central area.

Figure 2.—Renal dark cell tumor in group 3, consisting of cells with large round nuclei and dark cytoplasm. H & E. × 100

Figure 3.—Renal clear cell tumor in group 4, consisting of small round nuclei and clear cytoplasm. H & E. × 100

Figure 4A.—Dark cell dysplasia of a kidney in group 4 is composed of cells similar to those of dark cell tumors. H & E. × 200

Figure 4B.—Clear cell dysplasia of a kidney in group 4 is composed of cells similar to those of clear cell tumors. H & E. × 200

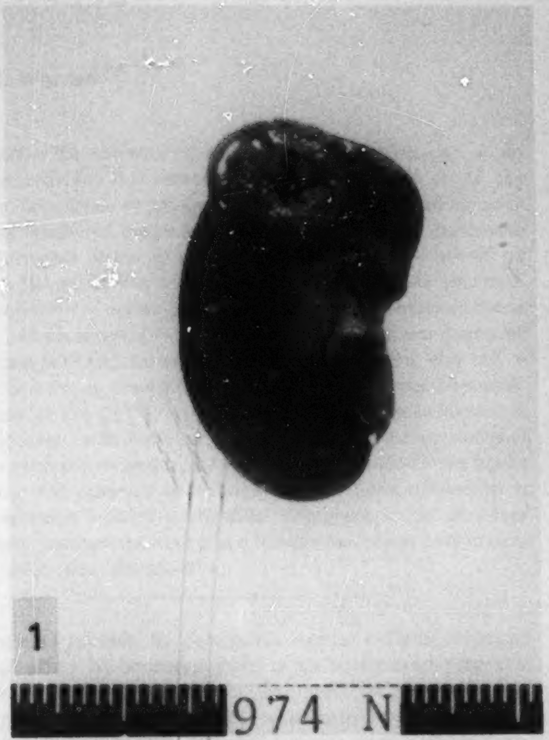
1

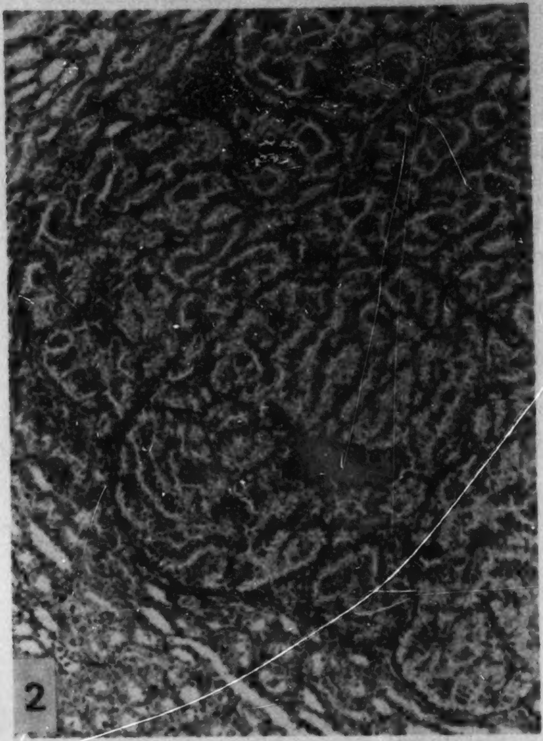
2

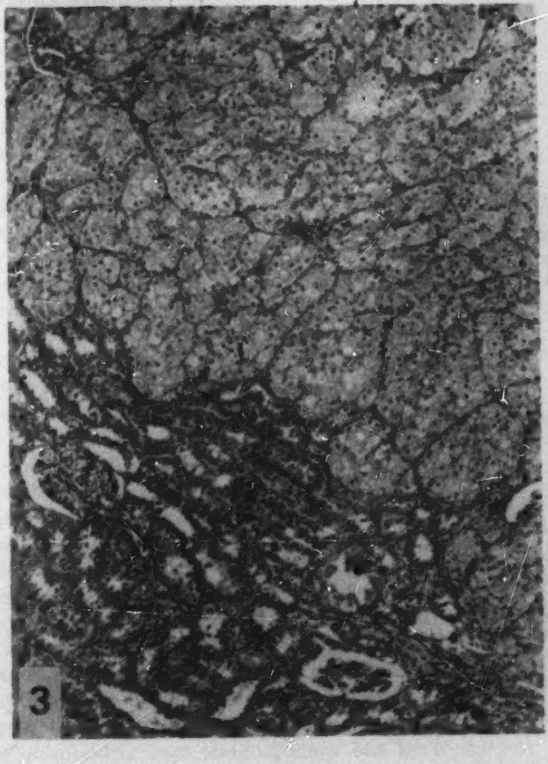
3

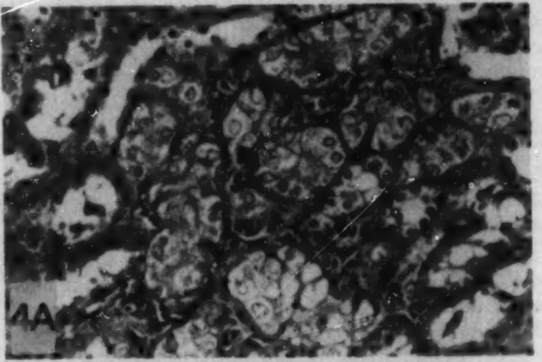
4A

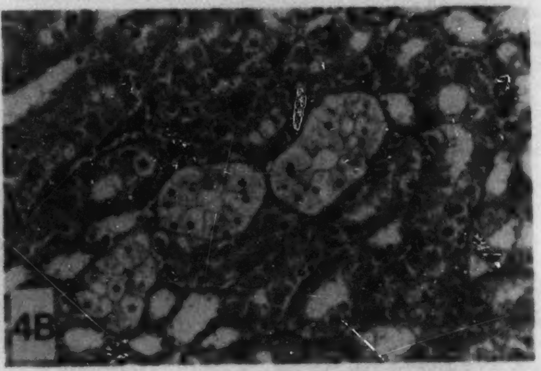
4B

blank page

Secretagogue Response in Rat Pancreatic Acinar Carcinoma [1,2,3]

John R. Warren [4,5]

ABSTRACT—The secretion of protein, like cell proliferation, is an integrated response that reflects structural organization of the cell periphery. Stimulation of protein secretion was thus utilized for comparison of integrated responses of the cell periphery in pancreatic acinar carcinoma of the rat and integrated responses in normal rat pancreas. Results of this comparison include: *a*) The stimulation of protein secretion in acinar carcinoma fragments by carbamylcholine chloride and cholecystokinin octapeptide, pancreatic secretagogues that interact with specific plasma membrane receptors, was only a fraction (one-fifth to one-half) of that observed in normal pancreatic minilobules. *b*) The Ca^{2+} ionophore A23187 and the cyclic nucleotide $N^6,O^{2'}$-dibutyryl cyclic AMP, secretagogues that act independently of specific membrane receptors, did not stimulate secretion in the acinar carcinoma. The observed quantitative and qualitative differences in protein secretion indicate fundamental differences in cell periphery organization between the normal and transformed acinar cells of pancreas.—JNCI 1982; 69:969–974.

Release of protein by pancreatic acinar cells in response to stimulation by secretagogues is an integrated response involving membrane structures of the cell periphery (*1*). For the peptide secretagogue cholecystokinin and muscarinic cholinergic agents such as the agonist carbamylcholine, initial secretagogue binding to specific plasma membrane receptors results in displacement into the cell of Ca^{2+} from membrane-bound stores (*1, 2*). The displacement of intracellular membranous Ca^{2+} stores by carbamylcholine and cholecystokinin activates protein secretion by acinar cells. Another important group of secretagogues, including the Ca^{2+} ionophore A23187 and the cyclic nucleotide derivative db-cAMP, stimulates pancreatic acinar cell secretion in the absence of specific interactions with plasma membrane receptors. The ionophore A23187 forms channels for increased Ca^{2+} flux across cell membranes and thereby stimulates Ca^{2+}-dependent protein secretion by acinar cells (*3*). The cyclic nucleotide db-cAMP activates cAMP-dependent protein kinase, and activation of cAMP-dependent kinase is thought to result in acinar cell secretion (*4, 5*).

For the comparison of properties of the periphery of normal acinar cells and acinar carcinoma cells, the responsiveness of normal pancreas and pancreatic acinar carcinoma to these four secretagogues has been contrasted. The nafenopin-induced pancreatic acinar cell carcinoma of the F344 rat has been utilized for these experiments (*6*). In initial studies, the acinar carcinoma of the rat was observed to secrete protein in response to the cholinergic agonist carbamylcholine chloride, but at a rate less than that observed with normal rat pancreatic minilobules under identical experimental conditions (*7*). For the examination of the significance of diminutive responsiveness of the acinar carcinoma to carbamylcholine, the responsiveness of the carcinoma to additional secretagogues has been investigated. The C-terminal octapeptide of the protein hormone cholecystokinin stimulated protein secretion in the acinar carcinoma. Again, however, the rate of cholecystokinin octapeptide-stimulated protein secretion in the carcinoma was only a fraction of the rate detected in normal pancreatic minilobules. The secretagogues A23187 and db-cAMP were without stimulatory action in the pancreatic carcinoma under conditions stimulatory for normal pancreas. These differences in secretagogue responsiveness between the acinar carcinoma and normal pancreas indicate fundamental alteration in integrated responses involving the acinar carcinoma cell periphery. Directly testable mechanisms (insensitivity to extracellular Ca^{2+}, defective protein kinase) are discussed that could explain the observed differences in secretagogue responsiveness. In addition, implications of secretagogue responsiveness for pathways of cellular differentiation in the pancreatic acinar carcinoma are reviewed. A preliminary report of this work has been presented (*8*).

MATERIALS AND METHODS

Chemicals and incubation medium.—The secretagogues utilized in these experiments were obtained as follows: carbamylcholine chloride (carbachol) and db-cAMP (monosodium salt) from the Sigma Chemical Co., St. Louis, Mo.; the synthetic C-terminal octapeptide of cholecystokinin from E. R. Squibb & Sons, Inc., Princeton, N.J.; and the Ca^{2+} ionophore A23187 from Calbiochem-Behring, La Jolla, Calif. Normal pancreas was dissociated with the use of a commercially purified preparation of collagenase (CLSPA, lot #51 A 599) from Worthington Biochemical Corp., Freehold, N.J. The incubation medium utilized in all experiments contained 123 m*M* NaCl, 6.2 m*M* KCl, 33 m*M* $NaHCO_3$, 1.5 m*M* KH_2PO_4, 3.3 m*M* $CaCl_2$, 0.6 m*M* $MgSO_4$, 18 m*M* glucose, 0.1 mg soybean trypsin inhibitor/ml (Sigma Chemical Co.), 1.0% (vol/vol) complete amino acid mixture (catalog #LM-112; Kansas City Biologicals, Lenexa, Kans.), 2 m*M* glutamine (Kansas City Biologicals), 0.2% (wt/vol) fraction V bovine albumin (Sigma Chemical Co.), and antibiotics (100 U penicillin/ml and 100 μg streptomycin/ml). The osmolality of this incubation medium was 352 mosmol/kg water. The fraction V albumin was extensively dialyzed against distilled water and then

ABBREVIATIONS USED: cAMP=cyclic AMP; db-cAMP=$N^6,O^{2'}$-dibutyryl cAMP; LDH=lactate dehydrogenase.

---

[1] Received February 9, 1982; accepted May 10, 1982.

[2] Supported by Public Health Service grant CA-27443 from the National Cancer Institute.

[3] Animals were maintained under the guidelines set forth by Northwestern University.

[4] Department of Pathology, Northwestern University Medical School, 303 East Chicago Ave., Chicago, Ill. 60611.

[5] The technical assistance of Ms. Rosetta Young Kale is gratefully acknowledged.

lyophilized before use in the incubation medium. Pulse-chase labeling of carcinoma or pancreas protein for secretion measurements was accomplished with L-[3,4,5-^{3}H]leucine (50 Ci/mmol) from Research Products International Corp., Elk Grove Village, Ill. The 3,5-dinitrosalicylic acid and D-(+)-maltose for the determination of amylase activity were from Eastman Kodak Co., Rochester, N.Y., and the soluble starch substrate was from Schwarz/Mann Div., Becton, Dickinson & Co., Orangeburg, N.Y. Sodium pyruvate, reduced β-nicotinamide adenine dinucleotide, and the 2,4-dinitrophenylhydrazine color reagent for measurement of LDH activity were purchased from Sigma Chemical Co.

Measurement of [^{3}H]leucine-labeled protein release by acinar carcinoma and normal pancreas.—Fragments of the pancreatic acinar carcinoma were mechanically prepared by being sieved through stainless steel screens, and minilobules were obtained by collagenase dissociation of pancreas (200- to 250-g F344 rats fasted for 48 hr) exactly as described previously (*9*, *10*). The acinar carcinoma fragments varied in size, consisted of sheets of neoplastic cells, contained abundant, large, endothelium-lined vascular channels, and in wet preparation completely excluded the vital dye trypan blue. Pancreatic minilobules consisted of groups of acini and occasional small ducts and also completely excluded trypan blue in wet preparation. The carcinoma fragments and normal pancreatic minilobules were pulse-chase labeled at 37°C by L-[3,4,5-^{3}H]leucine (*7*, *9*). Labeling of cell protein was accomplished by incubation for 15 minutes at 37°C with 60 μCi [^{3}H]leucine/ml in incubation medium containing 0.4 m*M* [^{1}H]leucine (*7*, *9*). The fragments or minilobules were then washed once, and the [^{3}H]leucine label was chased by incubation for 60 minutes at 37°C without [^{3}H]leucine in incubation medium containing 4.0 m*M* [^{1}H]leucine. Appearance of radioactive label in zymogen granules has been demonstrated under these conditions of pulse-chase labeling for both acinar carcinoma and normal pancreatic acinar cells (*9*, *11*). For experiments in which protein release was measured at both 37 and 4°C the pulse-chase-labeled carcinoma fragments or pancreatic minilobules were incubated for an additional 30 minutes at 37 or 4°C without secretagogue. The fragments or minilobules were then washed by centrifugation and incubated without or with secretagogue for 3 hours at 37 or 4°C in 12×75-mm polypropylene culture tubes (2.0 ml of a 2.0% vol/vol fragment or minilobule suspension/tube) for measurement of protein release. Tubes and solutions were precooled to 4°C before use with fragments and minilobules at 4°C. Three replicate tubes were prepared at each secretagogue concentration and temperature examined. Ethanol was used as a carrier solvent for A23187 and db-cAMP. Ethanol alone at the concentrations utilized (0.5–1.0% vol/vol) had no effect on protein release. In experiments performed with db-cAMP, 5 m*M* theophylline was also added to the incubation medium. All incubations were performed under a 95% O_2–5% CO_2 gas phase. The pH of the incubation medium as measured by a Beckman model 3550 digital pH meter with the use of a 39501 pH combination electrode was maintained at 7.4 when the medium was supplemented with 2 m*M* HEPES.[6] Incubation tubes were placed at a 5° slant (model ATR-100 Virglass tube rack; VirTis Co., Gardiner, N.Y.) on a rocker platform (Bellco Glass, Inc., Vineland, N.J.). The radioactivity present in acid-precipitable protein (1.0 *N* perchloric acid at 4°C overnight) was measured in fragments or minilobules and in incubation medium by liquid scintillation counting (Beckman LS-9000 liquid scintillation spectrometer) of perchloric acid precipitates digested in 0.6 *N* NaOH at 37°C. The amount of [^{3}H]leucine-labeled protein present in incubation medium was calculated for all experiments as a percent of total labeled protein (incubation medium plus fragments or minilobules). Where indicated, statistical analysis of protein release was accomplished by Student's *t*-test for carcinoma fragments (or pancreatic minilobules) incubated at 37°C as compared to 4°C and for carcinoma fragments as compared to pancreatic minilobules.

Measurement of amylase release.—Acinar carcinoma fragments were incubated without or with carbamylcholine for 3 hours at 37 or 4°C under experimental conditions identical to those utilized to follow [^{3}H]leucine-labeled protein release. After the 3-hour incubation, carcinoma fragments were separated from incubation medium by centrifugation and were frozen-thawed five times in distilled water. Amylase activity in the incubation medium and amylase activity released from frozen-thawed fragments were measured with the use of soluble starch as a substrate (*12*).

Measurement of LDH release.—Possible damage of acinar carcinoma cells by carbamylcholine or A23187 and of normal pancreatic acinar cells by A23187 was assessed by measurement of passive leakage of the cytosolic enzyme LDH into incubation medium. The LDH activity in incubation medium and LDH released from frozen–thawed carcinoma fragments or pancreatic minilobules were determined by colorimetric measurement of pyruvate reduction (Sigma technical bulletin No. 500).

RESULTS

When the amount of [^{3}H]leucine-labeled protein present in the incubation medium was measured as a percent of total labeled protein (incubation medium plus carcinoma fragments), 14.2±1.7% (mean ± SD, *n*=3 experiments) of total labeled protein was released by carcinoma fragments incubated at 37°C without carbamylcholine, and 16.7±3.0, 17.6±3.2, 18.3±3.1, 21.2±2.3, 22.0±3.5, or 21.1±2.6% of total labeled protein was released by carcinoma fragments incubated with 10^{-8}, 10^{-7}, 10^{-6}, 10^{-5}, 10^{-4}, or 10^{-3} *M* carbamylcholine, respectively. The same preparations of carcinoma fragments incubated at 4°C without and with carbamylcholine (10^{-8}–10^{-3} *M*) released 4.9±2.0, 4.7±1.8, 4.4±2.2, 4.6±1.5, 5.4±2.7, 6.0±1.5, and 5.6±1.9% of the total labeled protein. In a separate group of experiments, the amount of [^{3}H]leucine-labeled protein and the cytosolic enzyme LDH present in incubation medium was concomitantly measured as a percent of total labeled protein or LDH activity. Carcinoma fragments incubated at 37°C without or with 10^{-8}, 10^{-7}, 10^{-6}, 10^{-5}, 10^{-4}, and 10^{-3} *M* carbamylcholine released 20.9±1.7, 21.2±0.5, 23.7±1.1, 25.7±1.8, 29.3±1.6, 28.4±1.4, and 27.2±2.8%, respectively, of the total labeled protein, whereas in the same experiments (n=3) the fragments released 14.4±5.9, 13.1±4.2, 14.1±3.7, 15.4±4.7, 14.6±3.1, 16.8±5.0, and 15.5±2.3% of the total LDH activity. These results show that the concentration-dependent increase in the amount of [^{3}H]-leucine-labeled protein in incubation medium stimulated by carbamylcholine at 37°C was not accompanied by an increase in the amount of LDH in the incubation medium. We conclude that the increased release of [^{3}H]leucine-labeled protein by carcinoma fragments induced with carbamylcholine at 37°C was not due to passive membrane leakage of cytosolic protein. When the release of [^{3}H]leucine-labeled protein at 37 and 4°C was calculated at each carbamylcholine concentration as net release (protein release observed with carbamylcholine − protein release observed without carbamylcholine), both dependence of net protein release at 37°C ($\Delta_{t=37°}$) on carbamylcholine concentration and absence of stimulation of net release at 4°C ($\Delta_{t=4°}$) were apparent (text-fig. 1A). Carbamylcholine was also observed to stimulate a concentration-dependent net release of amylase from carcinoma fragments at 37°C (−0.1±0.7, +3.6±0.2, +3.6±2.3, +6.8±0.6, and +4.4±1.5% at 10^{-8}, 10^{-7}, 10^{-6}, 10^{-5}, and 10^{-4} *M* carbamylcholine, respectively) but not at 4°C (−0.5±1.0, +0.1±0.7, +0.9±1.2, +1.1±1.7, and +0.9±1.8% at the same carbamylcholine concentrations) (n=3 experiments). We conclude, therefore, that carbamylcholine induces protein secretion in metabolically active acinar carcinoma fragments.

---

[6] 4-(2-Hydroxyethyl)-1-piperazine ethanesulfonic acid.

Minilobules were prepared from normal pancreas by collagenase dissociation (*10*) and were incubated under identical conditions without or with carbamylcholine. An increase in the amount of [^{3}H]leucine-labeled protein released into the incubation medium was detected for normal pancreas minilobules incubated with carbamylcholine at 37°C (8.8±2.1% of total labeled protein released without carbamylcholine and 11.1±1.6, 11.2±2.6, 14.7±3.2, 21.3±4.0, 23.2±2.7, and 22.5±3.1% with 10^{-8}, 10^{-7}, 10^{-6}, 10^{-5}, 10^{-4}, and 10^{-3} *M* carbamylcholine, respectively) but not for minilobules incubated with carbamylcholine at 4°C (1.3 ± 0.5% without carbamylcholine and 1.3±0.6, 1.5±0.4, 1.2±0.3, 1.5±0.4, 1.6±0.8, and 1.5±0.5% with 10^{-8}–10^{-3} *M* carbamylcholine) (n=3 experiments). Dependence of net [^{3}H]leucine-labeled protein release on carbamylcholine concentration was clearly present with normal pancreas minilobules incubated at 37°C (text-fig. 1B). Maximal stimulation of [^{3}H]leucine-labeled protein release in the pancreas minilobules was achieved at 10^{-5} *M* carbamylcholine, a value identical to that obtained by other laboratories for in vitro preparations of normal pancreas (*1*). The rate of stimulated protein secretion in normal pancreatic minilobules at maximal carbamylcholine concentrations (≥10^{-5} *M*) (text-fig. 1B) was significantly greater than rates of stimulated protein secretion in acinar carcinoma fragments (text-fig. 1A). At 10^{-5} *M* carbamylcholine, the rate of stimulated protein secretion in pancreatic minilobules was 1.9-fold greater than the rate of secretion in carcinoma fragments (P<0.02), at 10^{-4} *M* carbamylcholine 2.2-fold greater (P<0.05), and at 10^{-3} *M* carbamylcholine 2.2-fold greater (P<0.01).

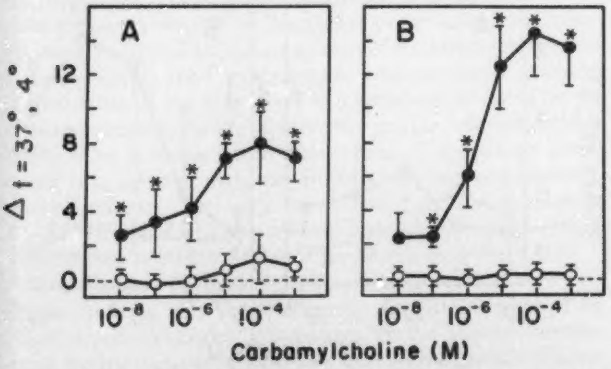

TEXT-FIGURE 1.— Effect of carbamylcholine on net [^{3}H]leucine-labeled protein release ($\Delta_{t=37°,4°}$) by acinar carcinoma fragments (A) or normal pancreas minilobules (B) at 37 (●) or 4°C (○). Release of [^{3}H]leucine-labeled protein into the incubation medium was measured as the percent of total [^{3}H]leucine-labeled protein present in incubation medium and carcinoma fragments or pancreas minilobules. *Each point* reported for $\Delta_{t=37°,4°}$ is corrected for [^{3}H]leucine-labeled protein release detected in the absence of carbamylcholine and represents the mean ± SD (*vertical bars*, SD) obtained in three experiments. Statistically significant differences (P<0.05) in net [^{3}H]leucine-labeled protein release between 37 and 4°C are denoted by *asterisks.*

The peptide secretagogue cholecystokinin octapeptide also stimulated net release into buffer of [^{3}H]leucine-labeled protein with normal pancreatic minilobules incubated at 37°C (text-fig. 2B), and rates of stimulated protein secretion in normal pancreatic minilobules demonstrated a biphasic dependence on cholecystokinin octapeptide concentration identical to that reported by other groups (*1*). Compared to the stimulation seen with the normal pancreatic minilobules, less stimulation of net [^{3}H]leucine-labeled protein release occurred with acinar carcinoma fragments incubated at 37°C in the presence of cholecystokinin octapeptide (text-fig. 2A). Significant stimulation of protein secretion in acinar carcinoma fragments occurred only at 10^{-9} and 10^{-8} *M* cholecystokinin octapeptide. The rate of stimulated protein secretion in pancreas minilobules was fivefold greater (P<0.01) at 10^{-9} *M* cholecystokinin than the rate of secretion in acinar carcinoma fragments and 2.5-fold greater (P<0.02) at 10^{-8} *M* cholecystokinin octapeptide.

The ionophore A23187 acts on pancreatic acinar cells to increase transmembrane Ca^{2+} flux and thereby stimulates protein secretion by the acinar cells (*2*). At A23187 concentrations greater than 10^{-7} *M*, significant stimulation of net [^{3}H]leucine-labeled protein release was detected with pancreatic minilobules incubated at 37°C (text-fig. 3B) with a maximal response obtained at approximately 10^{-6}–5×10^{-6} *M* A23187. Maximal net release of [^{3}H]leucine-labeled protein stimulated by A23187 occurred without increased passive leakage of LDH in the pancreatic minilobules (a value of −0.6±2.6% was measured for net LDH release at 5×10^{-6} *M* A23187), without increased net release of [^{3}H]leucine-labeled protein in the pancreatic minilobules incubated at 4°C (text-fig. 3B), and closely resembled the dependence on A23187 concentration reported elsewhere for in vitro preparations of normal pancreas (*11*). Under the same conditions that were stimulatory for pancreatic minilobules, a significant increase of net [^{3}H]leucine-labeled protein release was not detected in acinar carcinoma fragments incubated with

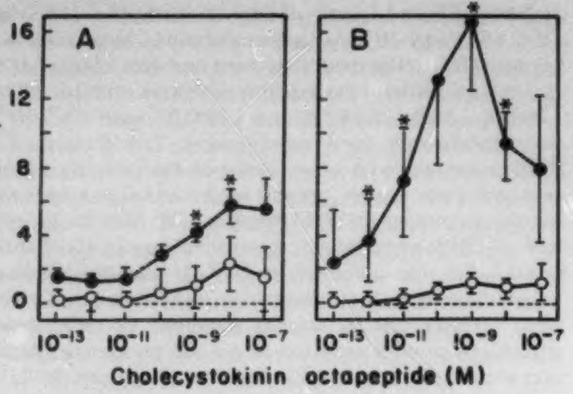

TEXT-FIGURE 2.—Effect of cholecystokinin octapeptide on net [^{3}H]leucine-labeled protein release ($\Delta_{t=37^\circ,4^\circ}$) by acinar carcinoma fragments (A) or normal pancreas minilobules (B) at 37 (●) or 4°C (○). Release of [^{3}H]leucine-labeled protein into the incubation medium was measured as the percent of total [^{3}H]leucine-labeled protein present in incubation medium and carcinoma fragments or pancreas minilobules. *Each point* reported for $\Delta_{t=37^\circ,4^\circ}$ is corrected for [^{3}H]leucine-labeled protein release detected in the absence of cholecystokinin octapeptide and represents the mean ± SD (*vertical bars*, SD) obtained in three experiments. Statistically significant differences ($P<0.05$) in net [^{3}H]leucine-labeled protein release between 37 and 4°C are denoted by *asterisks*.

A23187 (text-fig. 3A). The small increase of [^{3}H]leucine-labeled protein release present in carcinoma fragments at 37°C was not significantly different than that observed at 4°C. At A23187 concentrations greater than 10^{-5} *M*, the ionophore induced a concentration-dependent leakage of LDH in carcinoma fragments. (Values of +15.5±6.5, +21.4±2.5, and +37.5±11.8% were measured for net LDH release at 37°C and 5×10^{-5}, 7.5×10^{-5}, and 10^{-4} *M* A23187, respectively.)

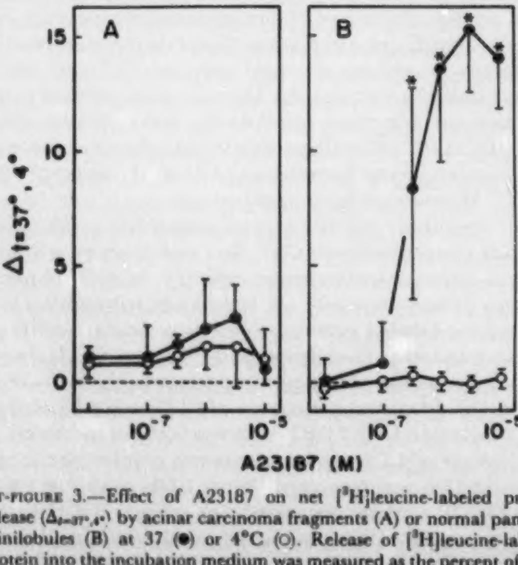

TEXT-FIGURE 3.—Effect of A23187 on net [^{3}H]leucine-labeled protein release ($\Delta_{t=37^\circ,4^\circ}$) by acinar carcinoma fragments (A) or normal pancreas minilobules (B) at 37 (●) or 4°C (○). Release of [^{3}H]leucine-labeled protein into the incubation medium was measured as the percent of total [^{3}H]leucine-labeled protein present in incubation medium and carcinoma fragments or pancreas minilobules. *Each point* reported for $\Delta_{t=37^\circ,4^\circ}$ is corrected for [^{3}H]leucine-labeled protein release detected in the absence of A23187 and represents the mean ± SD (*vertical bars*, SD) obtained in three experiments. Statistically significant differences ($P<0.05$) in net [^{3}H]leucine-labeled protein release between 37 and 4°C are denoted by *asterisks*.

The fourth secretagogue included in this study, db-cAMP, is thought to stimulate pancreatic acinar cell secretion by direct activation of cAMP-dependent protein kinase (*4, 5*). Significant stimulation of net [^{3}H]leucine-labeled protein release was observed in pancreatic minilobules incubated at 37°C with 10^{-4} and 10^{-3} *M* db-cAMP (text-fig. 4B). Bauduin et al. (*13*) have previously observed in vitro stimulation of rat pancreas at approximately 10^{-4}–10^{-3} *M* db-cAMP. As was reported by Bauduin et al. for rat pancreas pieces (*13*), maximal stimulation of protein secretion in the pancreatic minilobules by db-cAMP was considerably less than maximal stimulation obtained with carbamylcholine and cholecystokinin. More importantly, no significant stimulation of protein secretion was seen in acinar carcinoma fragments incubated with db-cAMP (text-fig. 4A).

In repeated experiments ($n=12$) the amount of [^{3}H]leucine-labeled protein released into the incubation medium as a percent of total labeled protein was 12.8±3.5% at 37°C and 4.9±2.3% at 4°C when the acinar carcinoma fragments were incubated without secretagogues. Likewise, with pancreatic minilobules incubated in the absence of secretagogue, the amount of labeled protein released into the incubation medium as a percent of total protein was 8.8±2.9% at 37°C and 1.4±0.4% at 4°C ($n=12$ experiments). From these results one may calculate the basal (unstimulated) rate of [^{3}H]-leucine-labeled protein release by metabolically active carcinoma fragments or pancreatic minilobules by subtracting the amount of labeled protein present in incubation medium at 4°C from the amount present in incubation medium at 37°C. A basal rate of protein release in acinar carcinoma fragments of 7.9±3.6% and in normal pancreatic minilobules of 7.5±2.7% was observed. These values for basal rates

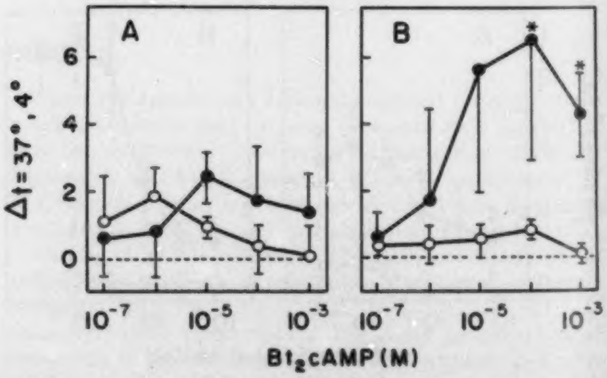

TEXT-FIGURE 4.—Effect of db-cAMP (Bt_2cAMP) on net [^{3}H]leucine-labeled protein release ($\Delta_{t=37^\circ,4^\circ}$) by acinar carcinoma fragments (A) or normal pancreas minilobules (B) at 37 (●) or 4°C (○). Release of [^{3}H]-leucine-labeled protein into the incubation medium was measured as the percent of total [^{3}H]leucine-labeled protein present in incubation medium and carcinoma fragments or pancreas minilobules. *Each point* reported for $\Delta_{t=37^\circ,4^\circ}$ is corrected for [^{3}H]leucine-labeled protein release detected in the absence of db-cAMP and represents the mean ± SD (*vertical bars*, SD) obtained in three experiments. Statistically significant differences ($P<0.05$) in net [^{3}H]leucine-labeled protein release between 37 and 4°C are denoted by *asterisks*.

of [^{3}H]leucine-labeled protein release are very similar to in vitro basal rates of secretion reported by other investigators for normal pancreas (*14*). Two conclusions are drawn from the observed rates of protein release in the absence of secretagogue: 1) In contrast to the large differences observed for the secretagogue-stimulated rates of protein secretion by the carcinoma and normal pancreas, no significant difference existed between basal (unstimulated) rates of [^{3}H]leucine-labeled protein release by metabolically active cells in the acinar carcinoma fragments and in the normal pancreatic minilobules. 2) Rates of [^{3}H]leucine-labeled protein release at 4°C indicate that at most only 5% of labeled cells in the carcinoma fragments and 1% of labeled cells in the pancreatic minilobules were sufficiently damaged during preparation of fragments and minilobules to passively leak radioactive protein.

DISCUSSION

Two important differences were observed between the stimulation of protein secretion in the pancreatic acinar carcinoma and the stimulation of protein secretion in normal pancreas: 1) The rate of cholecystokinin octapeptide- and carbamylcholine-stimulated secretion in acinar carcinoma was only a fraction (one-fifth to one-half) of the rate of stimulated secretion in normal pancreas. 2) A23187 and db-cAMP did not stimulate protein secretion in the acinar carcinoma but, under identical experimental conditions, did stimulate secretion in normal pancreas. The major difference between techniques used to prepare the carcinoma fragments and normal pancreatic minilobules was the use of collagenase to obtain minilobules. In previous work we have found that treatment of carcinoma fragments with collagenase under conditions comparable to those used to prepare minilobules diminished carbamylcholine stimulation by the fragments to 50–60% of the rate observed for carcinoma fragments not treated with collagenase (*7*). Thus mechanically prepared carcinoma fragments not treated with collagenase are optimal for measurement of secretagogue responsiveness. Diminished secretagogue responsiveness detected with the use of the fragments is considered by us to be an intrinsic property of the pancreatic acinar cell carcinoma. Diminutive secretagogue responsiveness of the acinar carcinoma is consistent with our electron microscopic analysis, which indicates that, at a maximum, only approximately 30–50% of the carcinoma cells are capable of incorporating protein into zymogen granules for discharge (*15*).

Stimulation of protein secretion by the peptide hormone cholecystokinin and the cholinergic agonists consists of an afferent and an efferent component. In the afferent component, the hormone or agonist interacts with a specific plasma membrane receptor (*1*). Interaction of cholecystokinin or carbamylcholine with their specific receptors is followed by displacement of membrane-bound Ca^{2+} into the cell interior which activates the cell for secretion (*2*). The efferent limb consists of zymogen granule migration to the plasma membrane, fusion of granule and plasma membranes, and discharge of zymogen protein to the cell exterior. The ionophore A23187 activates the efferent component of protein secretion without interacting with specific plasma membrane receptors (*2*). The absence of responsiveness of acinar carcinoma fragments to A23187 indicates that the efferent limb of stimulated protein secretion sensitive to extracellular Ca^{2+} (*16, 17*) is defective in acinar carcinoma cells. Absence of A23187-stimulated protein secretion in acinar carcinoma fragments was an unexpected observation. Both carbamylcholine stimulation and A23187 stimulation of pancreatic acinar cell secretion are Ca^{2+}-dependent processes (*2*). Thus since carbamylcholine had been found in our initial group of experiments to stimulate acinar carcinoma secretion (*7, 9*), it was expected that A23187 would also stimulate secretion in the carcinoma. A possible explanation for this discrepancy is the ability of intracellular Ca^{2+} stores to support stimulation by carbamylcholine of secretory protein discharge in normal pancreas (*2, 17*). It can be proposed that carbamylcholine stimulates protein secretion in the acinar carcinoma by mobilization of intracellular Ca^{2+} stores. However, if secretion in the acinar carcinoma were refractory toward influx of extracellular Ca^{2+} into carcinoma cells, absence of A23187 stimulation of protein secretion in the acinar carcinoma would be explained. In addition, it has been demonstrated that release of Ca^{2+} from intracellular stores is responsible for only a fraction of the secretory protein discharge in normal pancreas stimulated by carbamylcholine in the presence of physiologic extracellular Ca^{2+} concentration (*17*). Stimulation of sustained secretion by carbamylcholine appears to require influx of extracellular Ca^{2+} into the pancreatic acinar cell (*17*). We can speculate, therefore, that the diminutive responses of the acinar carcinoma to carbamylcholine (and to cholecystokinin octapeptide) also reflect insensitivity of carcinoma secretion to extracellular Ca^{2+}. The proposed insensitivity of the acinar carcinoma to extracellular Ca^{2+} will be directly tested by measurement of the dependence of carbamylcholine and cholecystokinin octapeptide stimulation of protein secretion in carcinoma fragments on extracellular Ca^{2+} concentration. The proliferative insensitivity of neoplastically transformed cells to extracellular ionized calcium has recently been observed (*18*). Further examination of Ca^{2+} homeostasis should yield important information on the regulation by Ca^{2+} of integrated cellular responses, including proliferation as well as protein secretion, in the acinar carcinoma. In addition, db-cAMP has been observed to activate protein phosphorylation in normal pancreatic acinar cells (*4*), activation of protein phosphorylation appears to be coupled to stimulation of acinar cell secretion by db-cAMP (*4*), and cAMP-dependent protein kinase has been identified in normal acinar cells (*5*). The inability of db-cAMP to stimulate protein secretion by acinar carcinoma cells indicates a deficiency of the cAMP-dependent protein kinase system. Like Ca^{2+}, cAMP is an important regulator of integrated cell function, and it will be important to elucidate why cAMP-dependent responses are deficient in the carcinoma.

Finally, discussion is required as to whether diminished secretagogue responsiveness of the acinar carcinoma is or is not an expression of maturational arrest in the carcinoma. Rat pancreas during normal embryogenesis becomes highly responsive to the secretagogues A23187 and db-cAMP several days prior to becoming responsive to cholinergic and peptide secretagogues (*19, 20*). It appears, therefore, that maturation of the efferent component occurs prior to maturation of the afferent component in pancreatic embryogenesis. If secretagogue responsiveness in the acinar carcinoma reflects arrest of carcinoma cells at a stage corresponding to immature normal acinar cell development, then responsiveness of the acinar carcinoma to A23187 and db-cAMP should be comparable to or exceed carcinoma responsiveness to carbamylcholine and cholecystokinin octapeptide. This was not the case, and diminished secretagogue responsiveness is, therefore, not adequately explained as immaturity of acinar differentiation in the pancreatic carcinoma. We have recently reported that, unlike normal embryonic pancreas, the presence of plasmalemma receptors for the lectin concanavalin A is not a specific membrane marker for pancreatic acinar carcinoma cells containing mature cytoplasmic zymogen granules (*21*). These lectin binding data also suggest that cellular differentiation in the acinar carcinoma does not mimic stages of acinar cytodifferentiation in normal pancreatic embryogenesis. Morphologic evidence has been obtained in other studies (*22*) that the direction of cellular differentiation in pancreatic carcinoma is from cells with zymogen maturation to ductlike cells lacking such maturation (retrodifferentiation), rather than from undifferentiated cells lacking zymogen maturation to cells with such maturation (stem cell differentiation). Both mitotic activity and DNA synthesis have been observed in the nafenopin-induced acinar carcinoma in cells containing mature zymogen granules (*15*). Therefore, granule-containing carcinoma cells could theoretically serve as a proliferative pool for the generation of carcinoma cells lacking zymogen maturation.

REFERENCES

(*1*) Jensen RT, Gardner JD. Identification and characterization of receptors for secretagogues on pancreatic acinar cells. Fed Proc 1981; 40:2486–2496.

(*2*) Williams JA. Regulation of pancreatic acinar cell function by intracellular calcium. Am J Physiol 1980; 238:G269–G279.

(*3*) Scheele G, Haymovits A. Potassium- and ionophore A23187-induced discharge of secretory protein in guinea pig pancreatic lobules. Role of extracellular calcium. J Biol Chem 1980; 225:4918–4927.

(*4*) Lambert M, Camus J, Christophe J. Phosphorylation in vitro of proteins in the pancreas and parotids of rats: Effects of hormonal secretagogues and cyclic nucleotides. Biochem Pharmacol 1975; 24:1755–1758.

(*5*) Jensen RT, Gardner JD. Cyclic nucleotide-dependent protein kinase activity in acinar cells from guinea pig pancreas. Gastroenterology 1978; 75:806–817.

(*6*) Reddy JK, Rao MS. Transplantable pancreatic carcinoma of the rat. Science 1977; 198:78–80.

(*7*) Warren JR, Trump MJ, Reddy JK, Becich MJ. Carbamylcholine stimulation of protein secretion in pancreatic acinar carcinoma of rat. Cancer Lett 1982; 15:245–253.

(*8*) Warren JR. Differentiation of secretory responses in pancreatic acinar carcinoma. Joint Meeting, Pancreatic Association Inc. and National Pancreatic Cancer Project. Newsletter, National Pancreatic Cancer Project. New Orleans: Louisiana State Univ, 1981; 6:64.

(*9*) Warren JR, Reddy JK. Transplantable pancreatic acinar carcinoma. Cancer 1981; 47:1535–1542.

(*10*) Amsterdam A, Solomon TE, Jamieson JD. Sequential dissociation of the exocrine pancreas into lobules, acini, and individual cells. Methods Cell Biol 1978; 361–378.

(*11*) Amsterdam A, Jamieson JD. Studies on dispersed pancreatic exocrine cells. II. Functional characteristics of separated cells. J Cell Biol 1974; 63:1057–1073.

(*12*) Bernfeld P. Amylases, α and β. Methods Enzymol 1955; 1:149–158.

(*13*) Bauduin H, Rochus L, Vincent D, Dumont JE. Role of cyclic 3′,5′-AMP in the action of physiological secretagogues on the metabolism of rat pancreas in vitro. Biochim Biophys Acta 1971; 252:171–183.

(*14*) Schultz GS, Sarras MP Jr, Gunther GR, et al. Guinea pig pancreatic acini prepared with purified collagenase. Exp Cell Res 1980; 130:49–62.

(*15*) Reddy JK, Rao MS, Warren JR, Qureshi SA, Christensen EI. Differentiation and DNA synthesis in pancreatic acinar carcinoma of rat. Cancer Res 1980; 40:3443–3454.

(*16*) Chandler DE, Williams JA. Intracellular uptake and α-amylase and lactate dehydrogenase releasing actions of the divalent cation ionophore A23187 in dissociated pancreatic acinar cells. J Membrane Biol 1977; 32:201–230.

(*17*) Scheele G, Haymovits A. Cholinergic and peptide-stimulated discharge of secretory protein in guinea pig pancreatic lobules. Role of intracellular and extracellular calcium. J Biol Chem 1979; 254:10346–10353.

(*18*) Boynton AL, Whitfield JF. Different calcium requirements for proliferation of conditionally and unconditionally tumorigenic mouse cells. Proc Natl Acad Sci USA 1976; 73:1651–1654.

(*19*) Doyle CM, Jamieson JD. Development of secretagogue response in rat pancreatic acinar cells. Dev Biol 1978; 65:11–27.

(*20*) Werlin SL, Grand RJ. Development of secretory mechanisms in rat pancreas. Am J Physiol 1979; 236:E446–E450.

(*21*) Warren JR, Trump MJ, Reddy JK. Concanavalin A binding and cytodifferentiation in pancreatic acinar carcinoma of rat Biochim Biophys Acta. In press.

(*22*) Reddy JK, Scarpelli DG, Rao MA. Experimental pancreatic carcinogenesis. In: Thatcher N, ed. Advances in medical oncology, research and education. Vol 9. Digestive cancer. Oxford and New York: Pergamon Press, 1979:99–109.

Enhanced Metastatic Potential of Tumor Cells Harvested From Spontaneous Metastases of Heterogeneous Murine Tumors[1,2,3,4]

James E. Talmadge[5] *and* **Isaiah J. Fidler**[5]

ABSTRACT—These studies demonstrated that cells populating spontaneous metastases are, in general, more metastatic than the cells populating the parent neoplasm, thereby providing direct evidence that the process of metastasis is selective and not random. The tumors used in these studies were the UV-2237 fibrosarcoma, an in vitro cloned line (C-40) from the UV-2237 tumor, and the K-1735 melanoma, all of which are syngeneic to the C3H/HeN (mammary tumor virus-negative) mouse strain; the M5076 reticulum cell sarcoma and the Lewis lung carcinoma 3LL, which are syngeneic to the C57BL/6 mouse strain, were also used. All tumors were implanted sc into the footpads of syngeneic mice, and several resulting spontaneous metastases were isolated and established in culture as individual cell lines. For each tumor system, comparison was made of the ability of parent tumor cells and cells isolated from several spontaneous metastases to produce either experimental or spontaneous metastases. Cells populating spontaneous metastases produced by heterogeneous and poorly metastatic tumors were significantly more metastatic than the cells of their respective parent tumors. In contrast, cells populating metastases produced by previously selected tumors did not differ significantly in metastatic potential from cells populating their parent tumors. In such systems, metastasis appeared to be random.—JNCI 1982; 69:975–980.

A growing body of data suggests that malignant, metastatic neoplasms are heterogeneous and that metastases result from the proliferation of a minor subpopulation of cells that preexist within the parent neoplasm (*1–3*). Only a few (<0.1%) tumor cells survive the multistep process to produce metastases (*4–6*), which raises the question of whether the metastatic process is random (*7–9*) or selective (*10, 11*). Selection could only take place under certain conditions. The starting tumor population would have to be unselected and heterogeneous with regard to metastatic potential, and the metastatic process per se would have to exert selective pressures on the participating tumor cells (*2, 11*). We investigated this issue further by determining whether cells populating a spontaneous metastasis are more metastatic than cells populating the parent neoplasm. A finding that the cells of the metastases were more metastatic would constitute direct evidence that the metastatic process is selective. To rule out the possibility that our results were unique to one tumor system or another, we used four different murine tumor systems and found in each system that tumor cells harvested from spontaneous metastases have a greater propensity to metastasize than cells harvested from their respective heterogeneous parent tumors. However, when the starting "parent tumor" consisted of an already selected cell line or a cloned, presumably homogeneous, population, the cells from metastases did not differ significantly in metastatic potential from the parent tumor cells.

MATERIALS AND METHODS

Mice.—Specific-pathogen-free mice of the inbred strains C3H⁻ and C57BL/6N were obtained from the Animal Production Area, NCI-Frederick Cancer Research Facility. Within a single experiment, all mice were matched for age and sex.

Tumors.—Tumors syngeneic to the C57BL/6 mouse were the Lewis lung carcinoma 3LL (obtained from Dr. J. Mayo, NCI-Frederick Cancer Research Facility) and the M5076 reticulum cell sarcoma of histiocytic origin (high metastatic potential) (*12, 13*). Tumors syngeneic to the C3H⁻ mouse were the UV radiation-induced fibrosarcoma UV-2237 (*14*), a metastatic clone (C-40) isolated in vitro from the parent UV-2237 tumor, and the metastatic, UV radiation-induced, croton oil-promoted malignant melanoma K-1735 (obtained from Dr. Margaret Kripke, NCI-Frederick Cancer Research Facility) (*15, 16*).

All adherent tumors were adapted to growth in culture as described previously (*12, 16, 17*). Cell cultures were maintained on tissue culture plastic in Eagle's minimum essential medium supplemented with 5% fetal bovine serum, sodium pyruvate, nonessential amino acids, L-glutamine, and a twofold vitamin solution (Flow Laboratories, Inc., Rockville, Md.). The M5076 cells were grown in RPMI-1640 medium (Grand Island Biological Co., Grand Island, N.Y.) supplemented with 10% heat-inactivated equine serum (Flow Laboratories), L-glutamine, sodium pyruvate, and 50 µg gentamicin/ml. All cell lines were free of mycoplasma and the following murine viruses: reovirus type 3, pneumonia virus of mice, K-virus, Theiler's virus, Sendai virus, minute virus of mice, mouse adenovirus, mouse hepatitis virus, lymphocytic choriomeningitis virus, ectromelia virus, and lactate

ABBREVIATIONS USED: C3H⁻=C3H/HeN mammary tumor virus-negative; HBSS=Hanks' balanced salt solution.

---

[1] Received February 10, 1982; accepted May 12, 1982.

[2] Supported by Public Health Service contract N01CO-75380 from the Office of the Director, National Cancer Institute, with Litton Bionetics, Inc.

[3] Animals were maintained under the guidelines set forth by the National Institutes of Health Policy on Humane Care and Use of Animals and the Animal Welfare Act in facilities accredited by the American Association for Accreditation of Laboratory Animal Care.

[4] The contents of this publication do not necessarily reflect the views or policies of the U.S. Department of Health and Human Services, nor does mention of trade names, commercial products, or organizations imply endorsement by the U.S. Government.

[5] Cancer Metastasis and Treatment Laboratory, NCI-Frederick Cancer Research Facility, P.O. Box B, Frederick, Md. 21701.

dehydrogenase virus (M.A. Bioproducts, Walkersville, Md.). We avoided using cell lines that had been cultured for long periods of time; to assure that our results would be reproducible, we renewed the cultures from frozen stocks every 2–3 months and maintained them without antibiotics.

Preparation of tumor cells for injection.—We harvested the tumor cells from subconfluent cultures (50–70% confluence) by rinsing the monolayers with 0.25% trypsin and 0.02% Versene. After 1 minute, the flasks were tapped sharply to dislodge the monolayer, and the cells were washed in medium with fetal bovine serum. The suspension cultures of M5076 cells were harvested as previously described (*13*). The cells were resuspended in Ca^{2+}- and Mg^{2+}-free HBSS. Only suspensions containing single cells of greater than 90% viability (determined by the trypan blue exclusion test) were used.

Isolation and culture of spontaneous metastases.—To obtain spontaneous metastases, we injected tumor cells into the posterior footpads of syngeneic mice. The limbs bearing tumors were amputated at the midfemur when the tumors reached 1.2–1.5 cm in diameter. Mice were killed 4–8 weeks thereafter, and single pulmonary or hepatic (M5076) metastases were isolated in an aseptic manner. Individual lines were established in culture from single metastases.

Assay for experimental pulmonary metastasis.—Unanesthetized mice received injections in the lateral tail vein of 0.2 ml HBSS containing tumor cells. The cell inoculum varied among the different tumor systems (*see* "Results"). The mice were killed 21–35 days later, and the lungs or livers were removed, rinsed in water, and fixed in Bouin's solution to facilitate observation of tumor colonies (*17*). After this treatment, tumor colonies were visible as raised opaque foci. They were counted under a dissecting microscope.

Spontaneous metastasis assay.—Viable tumor cells in a volume of 0.05 ml HBSS were injected into the mouse posterior footpad at cell doses previously determined to yield tumors in most recipient mice. When the tumors reached 1.2–1.5 cm in diameter, the legs bearing tumors were amputated at the midfemur. The mice were killed 6–8 weeks later and necropsied; the presence of metastases was determined. In studies of the M5076 tumor, the local tumors were not excised. Because this tumor is very invasive, mice bearing the M5076 sarcoma were necropsied 42 days after intrafootpad injection.

Statistical analyses.—Differences in the number of metastases among test groups were analyzed with the Mann-Whitney *U* test.

RESULTS

K-1735 Melanoma

We compared the metastatic potential (experimental and spontaneous) of cells from the parent K-1735 melanoma and four spontaneous metastases produced by parent tumors growing at a primary site. The data are shown in table 1. The iv injection of 25,000 viable tumor cells from spontaneous metastases into syngeneic $C3H^-$ mice produced significantly more lung tumor colonies than the same input of parent K-1735 cells. However, when the inoculum dose of cells was increased to 100,000/mouse, the lungs became saturated with tumor colonies, thus obscuring differences in the metastatic potential of the cell lines (*17*).

Because of several reports that excision of primary tumors can affect the production of spontaneous metastases (*18–20*), we examined the incidence of spontaneous metastasis in mice in which the primary tumor was excised and in mice in which the primary tumor was left intact. Either 10^5 K-1735 parent cells or cells from spontaneous metastases were injected into the footpads of $C3H^-$ mice. This dose of cells was tumorigenic in 100% of the mice, but the growth rate of the tumors varied: The parent tumor reached 9 mm in diameter in 43 days, whereas the tumors established from metastases reached this size in 22 days. When tumors reached diameters of 12–15 mm, the leg bearing the tumor was amputated at the midfemur (including the popliteal lymph node) from one group of mice. The mice were

TABLE 1.—*Metastatic potential of cells from the K-1735 melanoma parent and lines established from its spontaneous pulmonary metastases*

Source of tumor cells[a]	Experimental metastasis[b]				Spontaneous metastasis		
	Median No. of pulmonary metastases from 25,000 tumor cells (range)	P[c]	Median No. of pulmonary metastases from 100,000 tumor cells (range)	P[c]	Tumor excised,[d] No. of mice with metastases/total No. of mice	Tumor intact,[e] No. of mice with metastases/total No. of mice	Both groups, No. of mice with metastases/total No. of mice
Parent	44 (4–265)		198 (18–>300)		0/7	2/10	2/17
Met-4	252 (55–>500)	<0.001	>300 (36–>300)	<0.005	1/7	6/10	7/17
Met-5	376 (1–>500)	<0.001	>300 (267–>300)	<0.005	1/8	9/9	10/17
Met-3	143 (11–315)	<0.005	176 (8–>300)	NS	3/7	6/8	9/15
Met-2	91 (6–>500)	<0.01	>300 (1–>300)	<0.05	5/10	7/9	12/19

[a] Cells injected into syngeneic mice were from in vitro cultures of parent tumors or of tumors established from spontaneous metastases. Met=metastasis.

[b] Mice were given iv injections of the indicated cell inoculum and killed 35 days later ($n=10$).

[c] Probability of no difference compared to the value for the parent tumor as determined by the Mann-Whitney *U* test. NS=not significant.

[d] Mice were given intrafootpad injections of viable cells. When tumors reached 1–1.2 cm in diameter (44 days for the parent tumors and 22 days for the spontaneous metastases), the leg bearing the tumor was amputated at the midfemur. Mice were necropsied 68 days after the implantation of tumor cells.

[e] Mice were given intrafootpad injections of viable cells. Mice were necropsied when moribund (57–84 days after tumor implantation).

necropsied 8–9 weeks later. In the other group, the tumors were allowed to grow progressively. None of the mice inoculated with K-1735 parent tumor cells and in which the tumor was excised developed spontaneous metastases.

In contrast, 1 of 7, 1 of 8, 3 of 7, and 5 of 10 mice inoculated with cells from the four spontaneous metastases and in which primary tumors were excised developed spontaneous metastases. Differences in survival were recorded between mice bearing parent K-1735 tumors and those bearing primary tumors established from metastatic cell lines. The mean survival time of mice bearing the parent K-1735 melanoma was 84 days. Spontaneous metastases developed in only 2 of 10 mice; the other 8 mice died without evidence of systemic disease. In contrast, when the cells from each of four spontaneous metastases were implanted into groups of mice, the 4 groups survived a mean of 57, 64, 68, and 63 days, respectively. Spontaneous metastases were clearly visible in 6 of 10, 9 of 9, 6 of 8, and 7 of 9 mice. In this tumor system, when the primary tumor was excised, the incidence of metastasis was lower than that when the primary neoplasm was not excised. Nonetheless, in the K-1735 tumor system, cells obtained from spontaneous metastases were more metastatic than their parent tumor cells.

Qualitative differences were also noticeable in the gross morphology of the metastases produced by parent cells and cells isolated from the various spontaneous metastases. Whereas parent cells produced experimental metastases of various sizes and pigmentation, cells from individual metastatic lines produced more uniform lung tumor colonies. The gross appearance of spontaneous lung metastases produced from the parent K-1735 melanoma or metastatic lines growing in the footpad is shown in figure 1. Distinct differences in the size and pigmentation of the metastases are visible. Figure 1 also shows the size of the primary tumors at the time of excision, as well as the presence of a secondary tumor mass in the popliteal node.

M5076 Reticulum Cell Sarcoma

In these experiments, we examined the metastatic potential of cells from the highly metastatic M5076 reticulum cell sarcoma (*12, 13*) and five of its hepatic metastases. Following iv or intrafootpad injection into syngeneic C57BL/6 mice, M5076 cells produced peritoneal, but not pulmonary, metastases in all recipients (*13*). Cells harvested from hepatic metastases produced experimental metastases more efficiently than did cells of the parent M5076 (table 2). The mice were necropsied 21 days after the iv injection of 2×10^4 viable cells, at which time the hepatic tumor nodules were visible. Since this highly metastatic tumor produced spontaneous metastases in practically all of the mice, differences between cells of the parent M5076 and the five metastases could not be measured by examination of the incidence of spontaneous metastases; therefore, we assessed differences in metastatic potential by comparing the number of nodules per mouse. By these criteria, mice given intrafootpad injections of cells obtained from spontaneous M5076 metastases developed significantly more hepatic tumor foci (spontaneous) than did mice given injections of cells from the parent tumor ($P<0.01$). As shown in table 2, there is no apparent correlation between the size of the subcutaneous tumor at necropsy and the median number of hepatic metastases. Therefore, the increase in the number of spontaneous metastases could not be attributed to differences in the growth rate or size of the tumor in the footpad.

UV-2237 Fibrosarcoma Parent Tumor

In studies of the heterogeneous parent UV-2237 tumor (*14*) and nine spontaneous pulmonary metastases, we found that cells obtained from metastases produced more experimental metastases than did cells from the parent tumor (table 3). This finding extended and confirmed a previous study on the ability of the parent UV-2237 tumor and its metastases to form experimental metastases (*11*).

Cloned Cell Line of UV-2237 Fibrosarcoma

Studies of an in vitro cloned, presumably homogeneous, line of the UV-2237 fibrosarcoma (C-40) and four spontaneous metastases produced from this clone demonstrated that cells harvested from the spontaneous metastases varied only slightly from the parent tumor; as compared to the parent (cloned) line, they did not show an increased propensity to produce experimental metastases (table 4).

3LL Carcinoma

The variant 3LL carcinoma examined in this study was far less metastatic than were the other 3LL tumor variants

TABLE 2.—*Metastatic potential of cells from the reticulum cell sarcoma M5076 and lines established from its spontaneous hepatic metastases*

Source of tumor cells[a]	Experimental metastasis[b]		Spontaneous metastasis[c]		Mean size of local tumor in $mm^3 \pm SD$
	Median No. of hepatic metastases (range)	P[d]	Median No. of hepatic metastases (range)	P[d]	
Parent	24 (3–68)		28 (0–40)		118±43
HMet-1	91 (31–133)	<0.01	146 (10–455)	<0.001	201±74
HMet-2	153 (108–>300)	<0.005	257 (12–>500)	<0.001	92±32
HMet-3	51 (27–>300)	<0.01	20 (2–>500)	<0.01	119±44
HMet-5	59 (28–128)	<0.01	163 (26–>500)	<0.005	125±61
HMet-6	101 (56–153)	<0.01	37 (4–>500)	<0.01	209±106

[a] HMet=hepatic metastasis.

[b] Mice were given iv injections of 2×10^4 viable tumor cells and killed 21 days later ($n=10$).

[c] Mice were given intrafootpad injections of 5×10^4 tumor cells and killed 42 days later. All mice were positive for both local tumor and metastases.

[d] Probability of no difference compared to the value for the parent tumor as determined by the Mann-Whitney *U* test.

Table 3.—*Metastatic potential of the UV-2237 fibrosarcoma parent cell and cell lines established from individual spontaneous pulmonary metastases*

Source of cells[a]	Median No. of pulmonary metastases (range)[b]	P[c]
Parent	3 (0-9)	
Met-3	24 (10–104)	<0.01
Met-6	38 (0->300)	<0.01
Met-1	165 (68->300)	<0.005
Met-4	178 (120–237)	<0.005
Met-8	197 (0->300)	<0.005
Met-9	215 (192->300)	<0.001
Met-2	235 (100->300)	<0.001
Met-5	>300 (143->300)	<0.001
Met-7	>300 (>300)	<0.001

[a] Met=metastasis.

[b] Mice were given iv injections of 2×10^4 tumor cells and killed 21 days later (n=10).

[c] Probability of no difference compared to the value for the parent tumor as determined by the Mann-Whitney *U* test.

reported elsewhere (*20*). Cells from the 3LL tumor were implanted into the footpads of mice, and the tumor-bearing leg of each mouse was amputated when the tumor reached 1.2–1.5 cm in diameter. Five weeks later only 3 of 20 mice had developed lung metastases. These metastases were harvested, pooled, and established in culture as 3LL-Met-1 line. This selection procedure was repeated a second time, with the 3LL-Met-1 tumor, to yield tumor line 3LL-Met-2. Thereafter, the three tumor variants (3LL parent, 3LL-Met-1, and 3LL-Met-2) were examined to determine their potential for production of experimental and spontaneous metastases.

The ability of these lines to form experimental lung colonies was determined in the following manner: Viable tumor cells (100,000/mouse) were injected iv into the lateral tail vein of each C57BL/6 mouse (10/group). The mice were necropsied 3 weeks later and their lung metastases were counted. Mice inoculated with 3LL parent tumor cells had a median of 0 pulmonary colonies (range, 0–1), cells of the 3LL-Met-1 variant produced a median of 1 pulmonary colony (range, 0–4), and cells of the 3LL-Met-2 variant produced a median of 23 pulmonary colonies (range, 12–56). Thus the incidence of metastasis of the 3LL-Met-2 line was significantly higher than that of the 3LL parent and 3LL-Met-1 (P=0.001). Cells from the parent 3LL and the 3LL-Met-2 cell lines were injected im into the thighs of mice. The 3LL-Met-2 tumors grew to an average of 6.8±1.36 cm^3 and produced numerous metastases. Although the parent 3LL tumor also grew to a similar size (6.73±1.23 cm^3), it produced only a few pulmonary foci. The 3LL-Met-1 cell line (data not shown) exhibited a metastatic ability that was intermediate between that of the 3LL parent and 3LL-Met-2 lines.

Table 4.—*Incidence of experimental metastasis of cells from the C-40 cloned line of UV-2237 fibrosarcoma and individual spontaneous pulmonary metastases*

Source of cells[a]	Median No. of pulmonary metastases (range)[b]
Parent	5 (0–17)
Met-2	1.5 (0–6)
Met-3	2.5 (0–9)
Met-1	3 (0–13)
Met-4	4 (0–11)

[a] Met=metastasis.

[b] Mice were given iv injections of 5×10^4 viable tumor cells and killed 21 days later (n=10). Incidence of metastasis produced by any of the cell lines was indistinguishable from that of parent UV-2237 C-40 (Mann-Whitney *U* test).

DISCUSSION

Work from our laboratory (*16*) and from other laboratories (*21–26*) has suggested that the process of metastasis is not random but represents the survival and growth of selected subpopulations of cells that preexist in parent neoplasms. Our present results demonstrate that cells harvested from spontaneous metastases are in general more metastatic than their respective heterogeneous parent cells and thus provide further evidence of the selective nature of the metastatic process. Our findings were not affected by the anatomic location of the metastases, i.e., lung for metastases of the K-1735 melanoma, UV-2237 fibrosarcoma, and 3LL carcinoma and liver for metastases of the M5076 reticulum cell sarcoma. Thus the increased metastatic potential associated with cells from spontaneous metastases does not appear to be an organ-specific phenomenon (*11*). The metastatic potential of tumor cells was determined by two different assays. In the first assay, tumor cells were injected iv and the number of experimental metastases was determined. In the second assay, tumor cells were injected into a subcutaneous site and the incidence of spontaneous metastasis was determined. These two assays are well correlated as was demonstrated earlier by Kripke et al.(*14*).

Recent studies have demonstrated that many rodent and human neoplasms consist of subpopulations of cells with different growth rates, antigenicity, immunogenicity, susceptibility to cytotoxic drugs, and potential for invasion and metastasis (*1–3*). Moreover, in some rodent and human tumors, cells from various metastases have been shown to differ from cells residing within the primary neoplasm in their antigenicity (*27, 28*), biochemical properties (*29*), and response to cytotoxic drugs (*30–34*). Our data confirm these observations of tumor heterogeneity and show that the successful selection of cells with enhanced metastatic properties could occur, in a one-step procedure, during the process of metastasis. Thus spontaneous metastases of a primary tumor contain cells with enhanced metastatic properties. However, multiple selection procedures may be needed to obtain tumor variants with extremely high metastatic properties (*24–26, 35*), as evidenced in our study of the 3LL carcinoma. The parent tumor variant was poorly metastatic; although pooled metastases produced by the parent tumor (3LL-Met-1) exhibited increased metastatic potential, a second cycle of selection was needed to obtain a line with a highly metastatic phenotype. Although the process of metastasis selects for metastatic variants, spontaneous metastases per se may vary in their metastatic ability. Therefore, some spontaneous metastases from a poorly metastatic parent tumor population such as the 3LL carcinoma used here or the B16 melanoma (*25*) may not be as highly metastatic as cell populations enriched by multiple selection cycles (*25, 35*).

Evidence that a heterogeneous starting population is required for the selection of metastatic variants is provided by the finding that the cloned, presumably homogeneous, tumor failed to produce metastases with increased metastatic potential (table 4). This observation reemphasizes that growth per se in a metastatic site (lungs) does not confer metastatic properties on tumor cells; i.e., adaptive processes do not play a major role in the development of metastases (*11, 35*).

Several factors can influence the outcome of studies on experimental and spontaneous metastasis (*17*). To obtain reproducible results in assays of metastasis, one must take great care to ascertain that the procedures used to prepare tumor cells for injection do not extensively modify cell membrane characteristics because such modifications may reduce the metastatic capabilities of the injected cells (*17, 35–37*). This situation may partially explain why, in some recent studies, tumor cells obtained after extensive trypsinization of neoplasms produced few metastases when they were implanted iv; these results suggested that metastasis was not a selective process (*7, 8*).

Furthermore, as already stated, to demonstrate a selection process in metastasis, the starting parent tumor must be heterogeneous. Trope (*38*) recently hypothesized [subsequently confirmed by Fidler and Hart (*39*)] that the repeated passage of tumors by trocar implantation of fragments produces tumors that are no longer populated by diverse subpopulations but rather exhibit cellular uniformity. Because the methods of transplantation and culture can profoundly influence the composition of a tumor population, a tumor in one laboratory may not have the same characteristics as the presumably identical tumor in another laboratory. A case in point is the 3LL carcinoma. This tumor has been reported by most investigators to be highly malignant and metastatic (*9, 20*). Yet the 3LL carcinoma variant that we recently obtained was neither. Nonetheless, when metastases produced by this parent tumor were isolated and repeatedly passaged, an increasingly metastatic cell population was produced that may well approximate the variant population used in other laboratories. Because the 3LL carcinoma variant that we obtained was poorly metastatic, we succeeded in demonstrating that the process of metastasis selects for cells with increased metastatic potential (table 4). However, if we had used an already highly metastatic 3LL variant (*9, 20*) as a starting population, further selection for metastasis would have been difficult (*7*).

In conclusion, we have demonstrated that, compared to parent tumor cells, tumor cells from spontaneous metastases, obtained from unselected tumors that are heterogeneous with regard to a metastatic phenotype, have an increased potential to develop experimental and spontaneous metastases. In contrast, metastases from homogeneous (cloned) or already selected tumors vary only slightly from the parent tumor in their ability to form lung colonies. These findings provide direct evidence that the process of metastasis is selective.

REFERENCES

(*1*) Fidler IJ, Gersten DM, Hart IR. The biology of cancer invasion and metastasis. Adv Cancer Res 1978; 28:149–250.

(*2*) Poste G, Fidler IJ. The pathogenesis of cancer metastasis. Nature 1980; 283:139–146.

(*3*) Hart IR, Fidler IJ. Cancer invasion and metastasis. Q Rev Biol 1980; 55:121–142.

(*4*) Fidler IJ. Metastasis: Quantitative analysis of distribution and fate of tumor emboli labeled with ^{125}I-5-iodo-2′-deoxyuridine. J Natl Cancer Inst 1970; 45:773–782.

(*5*) Weiss L. Cancer cell traffic from the lungs to the liver: An example of metastatic inefficiency. Int J Cancer 1980; 25:385–392.

(*6*) Fisher B, Fisher ER. The organ distribution of disseminated ^{51}Cr-labeled tumor cells. Cancer Res 1967; 27:412–420.

(*7*) Giavazzi R, Alessandri G, Spreafico F, Garattini S, Mantovani A. Metastasizing capacity of tumour cells from spontaneous metastases of transplanted murine tumours. Br J Cancer 1980; 42:462–472.

(*8*) Mantovani A, Giavazzi R, Alessandri G, Spreafico F, Garattini S. Characterization of tumor lines derived from spontaneous metastases of a transplantable murine sarcoma. Eur J Cancer 1981; 17:71–76.

(*9*) Eccles SA, Heckford SE, Alexander P. Effect of cyclosporin A on the growth and spontaneous metastasis of syngeneic animal tumours. Br J Cancer 1980; 42:252–259.

(*10*) Stackpole CW. Distinct lung-colonising and lung-metastasising cell populations in B16-mouse melanoma. Nature 1981; 289:298–300.

(*11*) Raz A, Hanna N, Fidler IJ. In vivo isolation of a metastatic tumor cell variant involving selective and nonadaptive processes. JNCI 1981; 66:183–189.

(*12*) Talmadge JE, Key ME, Hart IR. Characterization of a murine ovarian reticulum cell sarcoma of histiocytic origin. Cancer Res 1981; 41:1271–1280.

(*13*) Hart IR, Talmadge JE, Fidler IJ. Metastatic behavior of a murine reticulum cell sarcoma exhibiting organ-specific growth. Cancer Res 1981; 41:1281–1287.

(*14*) Kripke ML, Gruys E, Fidler IJ. Metastatic heterogeneity of cells from an ultraviolet light-induced murine fibrosarcoma of recent origin. Cancer Res 1978; 38:2962–2967.

(*15*) Kripke ML. Speculations on the role of ultraviolet radiation in the development of malignant melanoma. JNCI 1979; 63:541–548.

(*16*) Fidler IJ, Gruys E, Cifone M, Barnes Z, Bucana C. Demonstration of multiple phenotypic diversity in a murine melanoma of recent origin. JNCI 1981; 67:947–956.

(*17*) Fidler IJ. General considerations for studies of experimental cancer metastasis. Methods Cancer Res 1978; 15:399–439.

(*18*) Ketcham AS, Wexler H, Mantel N. The effect of removal of a "primary" tumor on the development of spontaneous metastases. Cancer Res 1959; 19:940–944.

(*19*) Sugarbaker EV, Thornthwaite J, Ketcham AS. Inhibitory effect of a primary tumor on metastasis. In: Day SB, Laird WP, Stansly P, et al., eds. Cancer invasion and metastasis: Biological mechanisms and therapy. New York: Raven Press, 1977:227–240.

(*20*) Gorelik E, Segal S, Feldman M. Control of lung metastasis progression in mice: Role of growth kinetics of 3LL Lewis lung carcinoma and host immune reactivity. JNCI 1980; 65:1257–1264.

(*21*) Kerbel RS, Twiddy RR, Robertson DM. Induction of a tumor with greatly increased metastatic growth potential. Int J Cancer 1978; 22:583–594.

(*22*) Nicolson GL, Brunson KW, Fidler IJ. Specificity of arrest, survival and growth of selected metastatic variant cell lines. Cancer Res 1978; 38:4105–4111.

(*23*) Schirrmacher U, Bosslet K, Shantz G, Clauer K, Hubsch D. Tumor-mediated immunity in a model system in DBA/2 mice. IV. Antigenic differences between a metastasizing variant and the parental tumor revealed by cytotoxic T lymphocytes. Int J Cancer 1979; 23:245–252.

(*24*) Brunson KW, Nicolson GL. Selection of malignant melanoma variant cell lines for ovary colonization. J Supramol Struct 1979; 11:517–528.

(*25*) Fidler IJ. Selection of successive tumor lines for metastasis. Nature [New Biol] 1973; 242:148–149.

(*26*) Koch FE. Zur Frage der Metastazenbidung bei Impfhomoren. Z

Krebsforsch 1939; 48:495.

(27) Pimm MV, Embleton MJ, Baldwin RW. Multiple antigenic specificities within primary 3-methylcholanthrene-induced rat sarcomas and metastases. Int J Cancer 1980; 25:621–629.

(28) Gorelik E, Fogel M, Segal S, Feldman M. Tumor-associated antigenic differences between the primary and the descendant metastatic tumor cell populations. J Supramol Struct 1979; 12:385–402.

(29) Baylin SD, Weisburger WR, Eggleston JC, et al. Variable content of histaminase, L-DOPA decarboxylase and calcitonin in small cell carcinoma of the lung. N Engl J Med 1978; 299:105–110.

(30) Houghton PJ, Tew KD, Taylor DM. Some studies on the distribution and effects of cyclophosphamide in normal and neoplastic tissue. Cancer Treat Rep 1976; 60:459–464.

(31) Donelli MG, Colombo T, Broggini M, Garattini S. Differential distribution of antitumor agents in primary and secondary tumors. Cancer Treat Rep 1977; 61:1319–1324.

(32) Trope C. Different sensitivity to cytostatic drugs of primary tumor and metastasis of the Lewis carcinoma. Neoplasma 1975; 22:171–177.

(33) Steel GG, Adams K. Stem cell survival and tumor control in the Lewis lung carcinoma. Cancer Res 1975; 35:1530–1535.

(34) Hay KA, Lausch RN. Uninhibited growth and metastases of herpes simplex virus-transformed cells in virus-sensitized hosts. Int J Cancer 1979; 23:337–343.

(35) Nicolson GL, Custead SE. Tumor metastasis is not due to adaptation of cells to a new organ environment. Science 1982; 215:176–178.

(36) Slocum HK, Pavelic ZP, Rustum YM, et al. Characterization of cells obtained by mechanical and enzymatic means from human melanoma, sarcoma and lung tumors. Cancer Res 1981; 41:1428–1434.

(37) Poste G, Nicolson GL. Arrest and metastasis of blood-borne tumor cells are modified by fusion of plasma membrane vesicles from highly metastatic cells. Proc Natl Acad Sci USA 1980; 77:399–402.

(38) Trope C. Different susceptibilities of tumor cell subpopulations to cytotoxic agents. In: Fidler IJ, White RJ, eds. Design of models for testing cancer therapeutic agents. New York: Van Nostrand, 1981:62–79.

(39) Fidler IJ, Hart IR. Biological and experimental consequences of the zonal composition of solid tumors. Cancer Res 1981; 41:3266–3267.

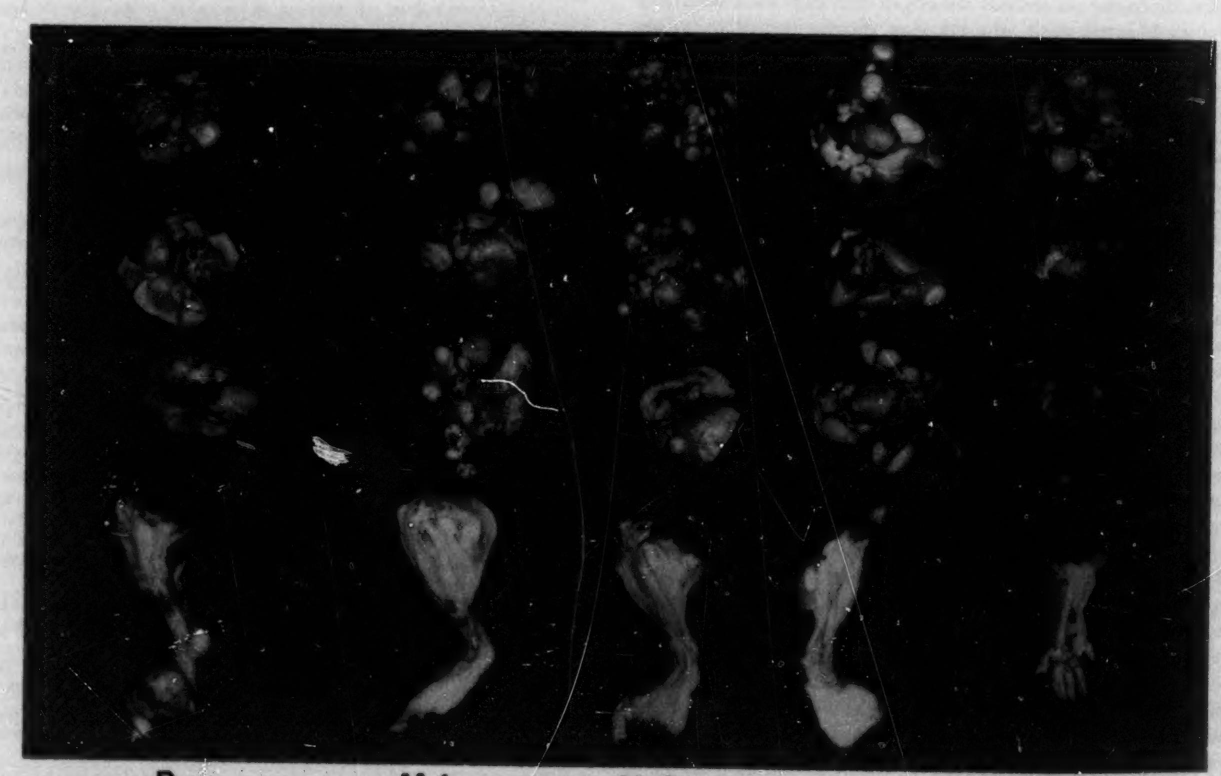

1

Figure 1.—Gross appearance of lungs from mice given an intrafootpad injection of tumor cells from the parent K-1735 cell line (P) or spontaneous metastases (M1–M4) obtained from mice bearing primary K-1735 tumors. Mice were necropsied 8–9 wk after the excision of the primary tumor. Tissues were fixed in Bouin's solution. Representative tumor-bearing legs demonstrate the size of the primary tumor.

Meeting Highlights

Adult T-Cell Leukemia–Lymphoma: Role of a Human Retrovirus[1]

A brief overview was given by Dr. Essex about viruses as potential causes for leukemia and lymphoma in humans, about retroviruses that cause leukemia or lymphoma in animals under natural conditions, and about the general biology of retroviruses. Thus far the only virus that has been clearly shown to be reproducibly associated with any form of human leukemia or lymphoma is the Epstein-Barr herpesvirus (EBV), an agent that has been associated with Burkitt's lymphoma (BL). BL is a monoclonal cancer of B-cells that occurs at elevated rates in children in certain regions of Africa. As with other B-cell tumors, the involved cells of BL have chromosomal abnormalities, usually in the form of a chromosome 8 to chromosome 14 translocation. EBV genome can usually be found in tumor cells taken from African BL patients, but its DNA is primarily in an episomal form rather than in an integrated form.

Several viruses have been shown to cause leukemia or lymphoma in animals. In chickens, mice, cats, cattle, and gibbon apes, retroviruses have been shown to cause one or more forms of lymphoproliferative cancers under natural conditions. In chickens and cattle the lymphoid tumors are primarily of B-lymphocyte origin, whereas in cats and mice they are primarily cancers of T-lymphocytes. In most, and perhaps all, of these cancers the tumors are monoclonal, and analysis by Southern blotting hybridization shows integration of the retrovirus proviral genome at a single site in all cells from the same tumor but at different sites in tumor cells from different individuals whose tumors were caused by the same virus. In all of these species the retroviruses that cause the diseases in question are acquired by horizontal or contagious transmission rather than by genetic inheritance. In selected cases, such as in lymphoid tumors of chickens, the viruses are congenitally transmitted, and in most species it appears that acquisition of the virus very early in life is most likely to result in the establishment of persistent infection.

Most retroviruses have a distinctive "C-type" appearance by electron microscopic evaluation, and they bud from the cytoplasmic membrane of productively infected cells. Their genome containing two complete copies of single-stranded RNA is about 70S, and the buoyant density of the virions is 1.14–1.16 g/ml in sucrose. The RNA replicates through a DNA proviral stage in which virus-encoded reverse transcriptase is used, and integration of proviral DNA into the DNA of the infected cell routinely occurs. The typical retroviral genome is 8–10 kilobases in length, and each end has a "long terminal repeat" sequence which can act as an efficient promoter. Retroviruses have a structure that is characteristic of transposons, and they apparently represent one of the most efficient ways for the natural activation and/or transduction of genes in animal cells. The typical genome has three genes: *a*) *gag*, which is at the 5′ end of the RNA and encodes for a polyprotein that undergoes post-translational cleavage to make the four peptides composing the core of the virion, *b*) *pol*, which encodes for the reverse transcriptase, and *c*) *env*, which encodes for the major virion envelope glycoprotein that protrudes at the surface of the virus, allows adsorption to receptor-containing cells, and serves as a target for virus-neutralizing antibodies.

Little is known about how retroviruses cause leukemia at the molecular level. Replication-defective forms of many retroviruses have been isolated and characterized. Such recombinants have usually acquired or transduced one of a series of highly conserved cell "*onc*" (*c-onc*) genes, which usually allow the virus to transform cultured fibroblasts and cause polyclonal tumors in vivo after very brief latent periods. One possible mechanism by which retroviruses might cause cancer under natural conditions is by the de novo generation of recombinants by replicating competent "helper" viruses. Another possible mechanism, for which some evidence is available in the avian system, is "promoter insertion." In this case, the promoter of the replicating helper virus integrates adjacent to a *c-onc* gene, transcriptionally activates that gene, and the presumed product (demonstrated to be a tyrosine-specific protein kinase in some instances) causes the phenotypic alteration characteristic for the given type of cancer.

Development and Characterization of Human T-Cell Lines

Recognition and characterization of the new human retrovirus, which apparently causes a cancer of mature T-lymphocytes, were made possible by the identification of human T-cell growth factor (TCGF) by Dr. Gallo and his colleagues. TCGF, which was also subsequently isolated in mice (and is referred to as interleukin-2 by some investigators) will allow the continuous proliferation of mature T-cells. This molecule, as purified by Mier and Gallo, is a 13,000-dalton protein that binds to receptors on mature terminal transferase (Tdt)-negative T-cells of the erythrocyte rosette-positive and OKT 4 (helper) positive lineage. TCGF can be used to maintain cultures from tumors of the mature T-cell type, including some cases diagnosed as mycosis fungoides (MF) or Sézary syndrome (SS) and many cases that are classified as adult T-cell leukemia (ATL). Some of the cultures from such tumors subsequently become constitutive producers of TCGF, and in such cell cultures the molecule is present both in the media and on the cytoplasmic membrane. Receptors for TCGF are preferentially expressed after stimulation of the target cells by antigen and/or lectins. The first isolation of the human T-cell leukemia virus (HTLV) was made in Dr. Gallo's laboratory in two lymphoblastoid cell lines established from a patient with a tumor composed of mature T-cells of the characteristic type (*see* below). With the use of TCGF, many lines have now been established in the Gallo laboratory, and at least three established lines are constitutive producers of TCGF.

---

[1] Proceedings of a workshop held at Fred Hutchinson Cancer Center, Seattle, Washington, March 10, 11, 1982.

Dr. Miyoshi described his work on the derivation and characterization of human T-cell lines that contain a type C virus, which is apparently the same virus as or is in the same virus family as is HTLV.[2] Several cell lines were established, usually by the procedure of cocultivating patient's cells with normal cord blood leukocytes. Some cell lines, such as MT-1, are of patient origin, while other lines, such as MT-2, are apparently derived from the infected cord blood cells. Four such lines were described (MT-1 through MT-4). Most grew efficiently as tumors when transplanted into immunosuppressed hamsters. One line that was clearly patient derived had a 14q+ chromosome aberration, whereas another that was clearly of cord blood origin (MT-2) had a normal karyotype. These observations are compatible with a situation in which only the tumor-derived lines have distinct karyotype abnormalities, whereas cultures derived from in vitro immortalization by HTLV would not be expected to have analogous chromosome translocations, at least not until after long-term in vitro cultivation. Although neither TCGF nor mitogens were added to these cultures, it appears likely that most cultures that were maintained on a long-term basis became constitutive producers of TCGF. Such cultures regularly contain virus-related antigens such as the ATL antigen (ATLA), the cytoplasmic antigen (or antigen complex) initially described by Dr. Hinuma using acetone-fixed cell immunofluorescence.

Isolation and Characterization of HTLV

The isolation and identification of HTLV was then discussed in further detail by Dr. Gallo. It appears that, although the virus is T-cell tropic, only a subpopulation of T-cells can be infected and/or transformed by this agent. Thus the types of tumors associated with HTLV are invariably of the mature Tdt-negative, T-cell type, and many cases of tumors diagnosed as MF or SS are not typical of the tumor type that is related to HTLV. Those cases of MF or SS that are related to HTLV appear to be very similar to ATL, are highly malignant, and characteristically involve the skin. Hypercalcemia may also be present, presumably because of osteoclastic factors that are released by the tumor cells.

Features that are characteristic of HTLV include "budding" from the cell surface, a typical 70S RNA, a reverse transcriptase that prefers Mg^{2+} over Mn^{2+}, and characteristic virus structural proteins of about 10,000, 13,000, 19,000, 24,000, 42,000, and 52,000 daltons. The proteins that have been best characterized are the 19,000-dalton proteins, designated p19, for which a monoclonal antibody is available, and the major core protein designated p24. It has apparently been quite difficult to characterize the major envelope glycoprotein of the virion; presumably, the difficulty is because of its extreme instability. This observation may be associated with observations of low infectivity observed for typical virus activity when the preparations are from cell culture supernatants.

By serologic analysis of the virion structural proteins and reverse transcriptase activity as well as by nucleic acid hybridization, HTLV is clearly distinct from other known retroviruses, both ecotropic and xenotropic. This list includes various other primate retroviruses, such as the gibbon ape leukemia viruses and the endogenous retroviruses of baboons. Clearly, p24 and p19 are viral proteins in that they co-purify with viral cores and have characteristics similar to those of other retroviral *gag* proteins, such as the distinctive primary amino acid sequence that begins with proline and ends with isoleucine, as is true for p24. Antisera to p19 and/or p24 react efficiently with HTLV-infected lines, including the MT-1 line of Miyoshi, but such antibodies do not react with other noninfected human cells.

The retrovirus that is apparently the closest known relative to HTLV is the bovine leukemia virus (BLV), which causes enzootic leukosis, a B-cell tumor that occurs in cattle throughout the world. Although BLV and HTLV are clearly only related in a very distant sense, common characteristics include *a*) a *gag* protein (i.e., p24) that is comparable in size for BLV and HTLV but is somewhat different in size from most other retroviruses, *b*) a reverse transcriptase that prefers Mg^{2+} over Mn^{2+}, and c) a relative inefficiency for production as extracellular virus, at least in relation to other ecotropic (as compared to xenotropic) retroviruses. Finally, recent studies by Oroszlan, Gallo, and their coworkers indicate distant relatedness between the primary amino acid sequences of the major core protein (p24) of HTLV and BLV.

One of the most important features of HTLV, as stressed by Dr. Gallo, is the fact that it is not genetically inherited because normal human cells (including uninfected tissues from infected patients) do not contain any recognizable sequences related to the virus. This implies that the virus must be acquired horizontally, i.e., as a contagion. The presence of antibodies to HTLV both in patients and in healthy controls that are known either to have been exposed to cases of ATL or to have been exposed to endemic ATL regions and the absence of antibodies in people from nonendemic regions are also compatible with this observation.

Dr. Yoshida then described his studies on the isolation and identification of the HTLV-related virus found in the two cell cultures designated MT-1 and MT-2. As indicated above, these viruses all appear to be either closely related or identical. Dr. Yoshida presented comparable data on the biochemical and biophysical characteristics of the Japanese isolate from MT-2, as well as presented preliminary data on the preparation of a molecular clone of a provirus from the MT-1 cell in the Charon 4a vector. An exciting observation made by Dr. Yoshida was that provirus is apparently found integrated in a single site for all the cells in a given tumor, but provirus is integrated in different sites in tumors taken from different individuals. Those experiments, done by Southern blotting hybridization, yielded results similar to those seen when avian or bovine retroviruses caused long latent-period lymphomas or leukemias that also appeared to arise as a clone of a single altered cell. Using a DNA probe made from virion RNA, Dr. Yoshida found single-copy integration in T-tumor cells from 5 cases of ATL. Although only one DNA band was seen in each tumor, the bands varied in size from one tumor or patient to the next, indicating that the site of integration was different in each case. In some cases, cells from both parents of the patient were also examined and found to be negative, which is compatible with the observation that the virus is not even genetically transmitted in restricted families. In most instances, control (non-T) cells from the same patients did not reveal evidence of provirus, but in one patient the granulocytes also appeared to be infected. The virus was found in multiple sites in the MT-1 and MT-2 cell cultures. The observation that HTLV is integrated in a single site in all the cells of a given tumor implies that the virus was present before the tumorous process began, and the observation contributes substantially to the argument that this virus may be the causative agent of ATL.

---

[2] For simplification, the term HTLV will be used in this report for the designation of all the different human retrovirus isolates found in tumors of the mature T-cell type. Although it is recognized that all of these isolates have not been cross-checked by serologic and/or molecular hybridization, those that have been checked appear to be closely related to the original isolate which was designated HTLV. It is also recognized that some investigators may prefer a different designation for some of the agents subsequently identified by the Japanese investigators, but it appears that such wording would introduce unnecessary confusion in this report, which is *not* intended as a policy statement on issues of nomenclature.

Dr. Reitz then presented nucleic acid hybridization data on various human preparations. Using HTLV–cDNA to explore HUT-102 cells, Dr. Reitz described the first T-cell tumor line of this type as having 2 or 3 copies of proviral DNA per cell. No comparable sequences were found in B-cells or in other tissues from either the patient or other healthy people, indicating a horizontal infection. High levels of mRNA are also found to be expressed in the tumor cells. Using hybridization kinetics, Dr. Reitz found that the HTLV sequences present in HUT-102 were very similar or identical to those in the MT-1 cell culture derived by Dr. Miyoshi from a Japanese ATL patient. The patient that yielded HUT-102 was a 28-year-old black from the Southeastern United States. Using nucleic acid hybridization, Dr. Reitz and his colleagues found comparable closely related viral sequences in tissues from several other non-Japanese patients with the same tumor type including a black male from the Caribbean and a white male from Boston. Using both serologic procedures and nucleic acid hybridization, members of Dr. Gallo's group have now identified tumor cases from various areas of the world in which infection with HTLV has occurred. These include, in addition to Japan, the Eastern United States and the Caribbean, the Western United States, the Middle East, and South America. Dr. Reitz also briefly presented preliminary information from Dr. Manzari and Dr. Wong-Staal in Dr. Gallo's laboratory about the molecular cloning of the 5′ proximal viral sequences, representative of the U5, R, and *gag* gene regions, in the PBR-322 plasmid.

In Vitro Immortalization

Dr. Miyoshi then reviewed his studies on "transformation" or "immortalization" of human cord blood lymphocytes with HTLV. His results were that both adult and cord blood lymphocytes could be immortalized with a very high rate of success if they were cocultivated with MT-2 cells that had been lethally irradiated. The infected target cells subsequently became immortalized but did not show karyotypic changes, at least not soon after establishment of the new cultures. Most of the newly infected cells were positive for the ATLA; the proportion of cells positive for this antigen increased from between only 2 and 3% soon after cocultivation to nearly 100% after a month of cultivation. Whether this was because of a selective growth advantage of the cells that were initially infected or because of subsequent infection of uninfected cells is unclear. It was clear, however, that high efficiency of infection or immortalization could only be achieved by cocultivation as opposed to inoculation with "cell-free" virus and that the MT-2 culture appeared to be the best donor cell for these experiments. Some of the newly established cultures revealed "hairy cell" processes, suggesting that alterations in phenotype had also occurred.

Dr. Hinuma then presented related studies on in vitro immortalization of peripheral blood lymphocytes in which he also found that a high degree of successful immortalization could be effected with MT-2 as the donor. More than 90% of the cells were positive for HTLV antigens 2–4 weeks after cocultivation with lethally irradiated donor cells. The infected recipient cells had a phenotype of positivity for Leu 1, Leu 3a, and Leu 4 and of negativity for Leu 2a. About 50% of the cells were positive for Ia antigens, and cell fusions could be observed in the cultures, which is compatible with the possibility that transmission of this virus might only occur with high efficiency during cell-to-cell contact. This manner of infection with HTLV might also be analogous to that seen with BLV because BLV is known to be poorly infectious when in the cell-free form but is efficient at inducing a syncitial-type effect in sensitive target cells. It seemed likely that two key elements of the successful infection and immortalization of cord blood cells was the virus of MT-2 origin and the cocultivation procedure. Dr. Gallo also mentioned that some of the more recent isolates in his laboratory have a greater potential for infectivity than has the original HUT-102 isolate.

Clinical Pathologic and Cytogenetic Aspects

The syndrome called ATL was initially recognized as a distinct clinical entity and was described as such by Dr. Takatsuki. He briefly described the syndrome at this meeting. It is characterized by mature T-cells but is distinct from many cases of SS. ATL occurs in adults whose mean age is about 50 years. Cutaneous infiltration is frequent, the rate of disease progression is rapid, and the survival rate is low. The disease clearly occurs most frequently in Kyushu, and many Japanese cases that occur outside this area can be traced back to an origin (i.e., of virus exposure) in Kyushu. Most but not all cases are characterized by hepatomegaly, splenomegaly, and lymphadenopathy. Anemia is not a characteristic feature of this disease, and immunoglobulins are usually within normal limits. Although the rates of ATL are not high (perhaps 100 cases/year in all of Japan), the proportion of adult leukemias that are T-cell is higher in Japan than in most other areas of the world.

Cytogenetic abnormalities are seen in many cases of ATL. These abnormalities were described by Dr. Takatsuki and Dr. Miyoshi and include nonrandom occurrences of trisomy 7 and of translocations producing a 14q+. Dr. Nowell pointed out that trisomy 7 does not appear to occur nonrandomly in other human tumors, including cutaneous T-cell lymphomas in the United States. Translocations involving chromosome 14, producing a 14q+ anomaly, however, are common in B-cell neoplasms and are present in some cases of T-cell chronic lymphocytic leukemia. They apparently involve the immunoglobulin heavy chain gene. Detailed chromosome data are not available on non-Japanese T-cell tumors that are HTLV-positive.

The most consistent surface phenotype is OKT $1^+3^+4^+$-$10^+11^+5^-6^-8^-$ and Ia^+ or Ia^-. Although this antigenic phenotype is normally associated with helper–inducer T-cells, in vitro some ATL cells show a suppression of immunoglobulin synthesis by normal B-cells.

Histopathologic and cytologic criteria for the recognition of ATL were discussed by Dr. Hanaoka, Dr. Jaffe, and Dr. Kadin. The presence of at least 10% multiply lobate or pleomorphic cells in the peripheral blood is characteristic, but a leukemic component may be absent in as many as 40% of the cases. The histopathology in lymph nodes is varied, but a similar spectrum was encountered in cases from Southwestern Japan, the Caribbean, and the United States. Histologic forms of ATL documented as occurring in association with positive serology for HTLV include *a*) the pleomorphic type, which is most frequent; *b*) the large cell type; *c*) the mixed cell type; and *d*) the medium-sized cell type. At this time, however, no cytologic or histologic features pathognomonic of viral association have been demonstrated.

In nearly all instances, ATL can be distinguished clinically and pathologically from the cutaneous T-cell lymphomas (CTCL), i.e., MF and SS. Still cases are unquestionably positive for HTLV, both by serology and viral isolation, in which, clinically and pathologically, the disease is more compatible with CTCL. Further studies correlating virology, histopathology, immunology, and clinical features will be necessary for further definition of the spectrum of HTLV-associated T-cell cancers.

Epidemiology

Dr. Blattner discussed seroepidemiologic studies with patients and controls from various areas of the world. He described about 10 cases of ATL from the West Indies from a study conducted with Dr. Catovsky and his co-workers. In most if not all cases, antibodies that reacted with HTLV antigens were found in sera from such patients. In most cases antibody titers were determined by radioimmunoassay to the p24 and p19 gag antigens and to cell-surface antigens by immunofluorescence. In essentially all cases there was agreement among the different procedures, and, if antibodies were present at all, they were usually present for all the antigens.

Dr. Gallo and Dr. Blattner subsequently presented serologic data for a large series of ATL and other tumor cases as well as for numerous controls. More than 90% (32/35) of the cases of typical ATL appeared to have antibodies to HTLV. Individuals with other forms of lyphoreticular neoplasms were sometimes positive for such antibodies, with various forms of T-cell cancers of a similar type having the next most frequent rate of positivity. Samples from 86 U.S. individuals with other types of neoplasms were negative. Natural antibodies to p24 were found in about 30% of the healthy relatives of ATL patients and in about 12% of the healthy donors from endemic ATL regions of Japan. About 3–5% of the healthy donors from the Caribbean area had such antibodies. Sera from approximately 180 healthy U.S. donors and approximately 800 healthy European donors were negative for such antibodies. The geometric mean antibody titers to the HTLV p24 were about the same for the antibody-positive ATL patients when compared to the antibody-positive healthy people, whether these antibody-positive people were ATL-exposed relatives of patients or were people from the endemic ATL regions.

Dr. Hinuma also presented data on the serologic screening of ATL patients and healthy controls for antibodies to ATLA, the cytoplasmic antigen that is specific for HTLV as expressed on MT-1 cells. Dr. Hinuma found that sera from 140 of 142 patients with ATL had antibodies to ATLA and that most cases of other T-cell cancers from the endemic ATL area also had such antibodies. When sera from healthy controls older than 40 years and from various areas of Japan were checked, a close association was found geographically for the Kyushu area and the presence of ATLA antibodies. Although very few of the healthy people were antibody-positive in most areas distant from Kyushu (i.e., 0/74 in Sendai, 0/60 in Yamagata, 0/74 in Kyoto, and 1/56 in Sapporo), about 25% of the healthy people from the Kyushu region had such antibodies. These results indicate a close correlation between ATL in Japan and the presence of antibodies to ATLA. A limited number of samples from healthy adults of several other countries were also screened. With the exception of Taiwan, where 2 of 40 healthy people were ATLA antibody-positive, individuals from most other areas in the Orient appeared to be negative for such antibody activity.

Finally, results presented by Dr. Miyoshi and Dr. Hinuma suggested that HTLV antigen-positive cells and/or that active virus was present in the small number of antibody-positive people who were analyzed for ATLA and/or for the ability of their cells to infect cord blood lymphocytes by cocultivation. Although these results are preliminary, they obviously raise the possibility that most antibody-positive healthy people may be virus carriers.

Summary and Conclusions

Clearly, HTLV is highly associated with the development of an extremely malignant leukemia of mature T-lymphocytes, which has been classified as ATL in Japan but has not been as clearly and consistently classified as a distinct clinical entity by other reporting countries. HTLV, the agent initially discovered by Dr. Gallo and his colleagues, appears likely to be the cause of this disease. On the basis of both epidemiologic and molecular considerations, the association between HTLV and this particular clinical entity appears at least as strong as, and probably stronger than, the association between any other human cancer and a particular viral agent (including the association between EBV and BL or the association between hepatitis B-virus and primary liver cancer). Although the disease associated with HTLV is clustered in southern Japan and in the Caribbean, both the disease and the agent have been found in various areas of the world. The virus is clearly contagious, even though it has a low degree of infectivity by cell culture analysis. The exact mechanism of infection and the source of virus are unknown. The possibility of transmission by blood transfusion has been suggested, but the frequency of exposure in the population of endemic areas (≤25% of the adults) is obviously too high to be explained solely as a transfusion-related event. The possibility that an animal reservoir may exist has also been suggested. If, however, a significant number of the antibody-positive healthy people are indeed carriers with latent infections, this carrier population would be an adequate reservoir for the maintenance of HTLV in the human population, and no vector or outside animal reservoir would be needed.

Max Essex
Department of Microbiology
Harvard University School of Public Health
Boston, Massachusetts 02115

PARTICIPANTS

Organizers and Moderators

Dr. Gregory T. O'Conor
Office of International Affairs
National Cancer Institute
Bethesda, Maryland 20205

Dr. Haruo Sugano
Cancer Institute
Japanese Foundation for Cancer Research
Tokyo 170, Japan

U.S. Participants

Dr. William Blattner (Epidemiology)
Division of Cancer Cause and Prevention
National Cancer Institute
Bethesda, Maryland 20205

Dr. Max Essex (Virology)
Department of Microbiology
Harvard University School of Public Health
Boston, Massachusetts 02115

Dr. Robert Gallo (Virology)
Division of Cancer Treatment
National Cancer Institute
Bethesda, Maryland 20205

Dr. Elaine Jaffe (Pathology–Immunology)
Division of Cancer Biology and Diagnosis
National Cancer Institute
Bethesda, Maryland 20205

Dr. Marshall Kadin (Pathology–Immunology)
Fred Hutchinson Cancer Research Center
Seattle, Washington 98104

Dr. Peter Nowell (Genetics)
Department of Pathology
University of Pennsylvania School of Medicine
Philadelphia, Pennsylvania 19104

Dr. Marvin Reitz (Virology)
Division of Cancer Treatment
National Cancer Institute
Bethesda, Maryland 20205

Japanese Participants

Dr. Masao Hanaoka (Patho-immunology)
Institute for Virus Research
Kyoto University
Shogoin, Sakyo-ku, Kyoto 606, Japan

Dr. Yorio Hinuma (Virology)
Institute for Virus Research
Kyoto University
Shogoin, Sakyo-ku, Kyoto 606, Japan

Dr. Isao Miyoshi (Medicine, Cell Biology)
Department of Internal Medicine
Kochi Medical School
Kochi 781-51, Japan

Dr. Kiyoshi Takatsuki (Medicine and Hematology)
Department of Internal Medicine
Kumamoto University School of Medicine
Honjo 2-2-1, Kumamoto 860, Japan

Dr. Kumao Toyoshima (Virology)
Institute for Medical Sciences
University of Tokyo
Shirogane-dai, Minato-ku, Tokyo 108, Japan

Dr. Mitsuaki Yoshida (Virology, Molecular Biology)
Department of Viral Oncology
Cancer Institute
Tokyo 170, Japan

blank page

Corrections

December 1981, vol 67, No. 6

In "Enhancement of Experimental Pancreatic Cancer in Syrian Golden Hamsters by Dietary Fat," by Diane F. Birt, Shahrokh Salmasi, and Parviz M. Pour, page 1328, footnote *b* in table 2 should read: Teklad vitamin mix (catalog #40060) at 1.5 g/385 kcal supplies in the final diet in mg/385 kcal: 16 *p*-aminobenzoic acid; 149 ascorbic acid; 0.07 biotin; 0.0045 vitamin B_{12}; 10 calcium pantothenate; 214 choline; 0.3 folic acid; 16 inositol; 7.4 menadione; 15 niacin; 3 pyridoxine HCl; 3 riboflavin; 8 thiamine HCl; and in units/385 kcal: 2,974 vitamin A palmitate; 330 vitamin D_2; 18 vitamin E acetate.

April 1982, vol 68, No. 4

In "Mechanisms of Immunologic Eradication of a Syngeneic Guinea Pig Tumor. I. Quantitative Analysis of Adoptive Immunity," by Suyu Shu, James T. Hunter, Herbert J. Rapp, and Leila S. Fonseca, page 678, second column, the period should be deleted at the end of line 6 and lines 7–11 should read, ". . . rejected. These data suggest that suppression of id line-10 tumor challenges by the transferred immunity in guinea pigs was independent of development of systemic immunity in the recipients. However, ..." Also, near the end of line 16 in the second column, "py" should read "by."

Announcements

The Journal *will publish notices of major meetings dealing with cancer. Submission of notices 6 months in advance is requested to permit timely publication.*

Formaldehyde Toxicology Meeting

Washington, D. C., will be the site of this meeting to be held at the Washington Hilton Hotel on November 3, 1982. The meeting will enable scientists to present work on formaldehyde toxicology research that has been carried out since the 1980 CIIT conference. Scheduled speakers will present recent research in the areas of mechanisms of toxicity, protective mechanisms, epidemiology, classical toxicology, and risk assessment.

For additional information, complete program, and registration materials please contact the Formaldehyde Institute, 1075 Central Park Avenue, Scarsdale, New York 10583 (telephone: 914-725-1492).

Symposium on Application of Biological Markers to Carcinogen Testing

The U. S. Environmental Protection Agency will sponsor this symposium to be held at the Holiday Inn, Bethesda, Maryland, on November 15–19, 1982. This symposium will discuss the current status of biochemical and immunological markers to carcinogenicity with three main objectives: to review and update specific markers, to identify data gaps, and to recommend research goals. Sessions will encompass in vivo and in vitro antibodies, viruses, and DNA-adducts. Abstracts for poster sessions will be accepted until October 15, 1982.

For additional details please contact Ms. Claire M. Wilson, Associated Universities, Inc., Suite 603, 1717 Massachusetts Avenue, N. W., Washington, D. C. 20036 (telephone: 202-462-4475).

Eighth Annual Postgraduate Course

"Ultrasound for Clinicians" is the title of this course being offered by the Department of Radiology, Brigham and Women's Hospital, and the Department of Continuing Education, Harvard Medical School, on February 28–March 2, 1983. AMA Category I Credit is for 22.5 hours; Dr. David C. Grant is Program Director.

For additional information please contact the Department of Continuing Education, Harvard Medical School, 25 Shattuck Street, Boston, Massachusetts 02115 (telephone: 617-732-1525).

Seventh Annual Meeting of the Cell Kinetics Society

The Hilton Hotel in Baltimore, Maryland, will be the site of this meeting to be held on March 16–19, 1983. The Cell Kinetics Society has an international membership of approximately 300 experimentalists, clinicians, and mathematical modelers who share an interest in the cell proliferation patterns of normal and abnormal tissues.

Inquiries concerning this meeting or membership should be directed to Dr. Bruce F. Kimler, Secretary, Cell Kinetics Society, Department of Radiation Therapy, University of Kansas Medical Center, Rainbow Boulevard at 39th Street, Kansas City, Kansas 66103.

First International Meeting on Cell Biochemistry and Function

The new journal entitled *Cell Biochemistry and Function* (first issue April 1983) will sponsor this meeting to be held at the University of Surrey, Guildford, England, on March 23–25, 1983. The scientific program will include lectures by invited speakers and poster papers covering the following topics: enzymes and receptors in context; cellular transport; special techniques for the investigation of materials and activities within functioning whole cells; diagnostic procedures involving whole cell preparations; carcinogenesis; and pharmacology and toxicology.

For further details please write to Ms. Stella A. Dutton, Butterworth Scientific Limited—Journals Division, P.O. Box 63, Westbury House, Bury Street, Guildford, Surrey GU25BH, England.

The Fourth Annual Meeting of the Society for Clinical Trials

The organization of the Society for Clinical Trials will sponsor this scientific session to be held in St. Louis, Missouri, on May 8–11, 1983. The sessions will focus on the design, organization, management, and analyses of clinical trials. Abstracts for contributed papers must be received by January 1, 1983.

For additional information please write to Dr. Christian R. Klimt, Secretary, Society for Clinical Trials, Inc., 600 Wyndhurst Avenue, Baltimore, Maryland 21210.

Thirteenth International Congress of Chemotherapy

Vienna, Austria, will be the site of this meeting to be held at the Kongresszentrum-Hofburg on August 28–September 2, 1983. The scientific program will consist of lectures, symposia, round table sessions, and free papers with posters focusing on antimicrobial and anticancer topics.

December 31, 1982, is the deadline for registration. The deadline for submitting manuscripts for final publication is April 30, 1983. For further information please contact Professor K. Karrer, Institute for Cancer Research, University of Vienna, Borschkegasse 8a, A-1090 Vienna, Austria, or Secretariat of the Thirteenth International Congress of Chemotherapy, % Wiener Medizinische Akademie, Alser Strasse 4, A-1090 Vienna, Austria.

★U.S. GOVERNMENT PRINTING OFFICE: 1982-361-145/59

JNCI (NIH Publication No. 82-13)

69/5

NEWARK PUBLIC LIBRARY

DEC 3 1982

U. S. GOVT. PUBS.
DEPOSITORY 376

JNCI

Journal of the National
Cancer Institute

November 1982
Volume 69
Number 5

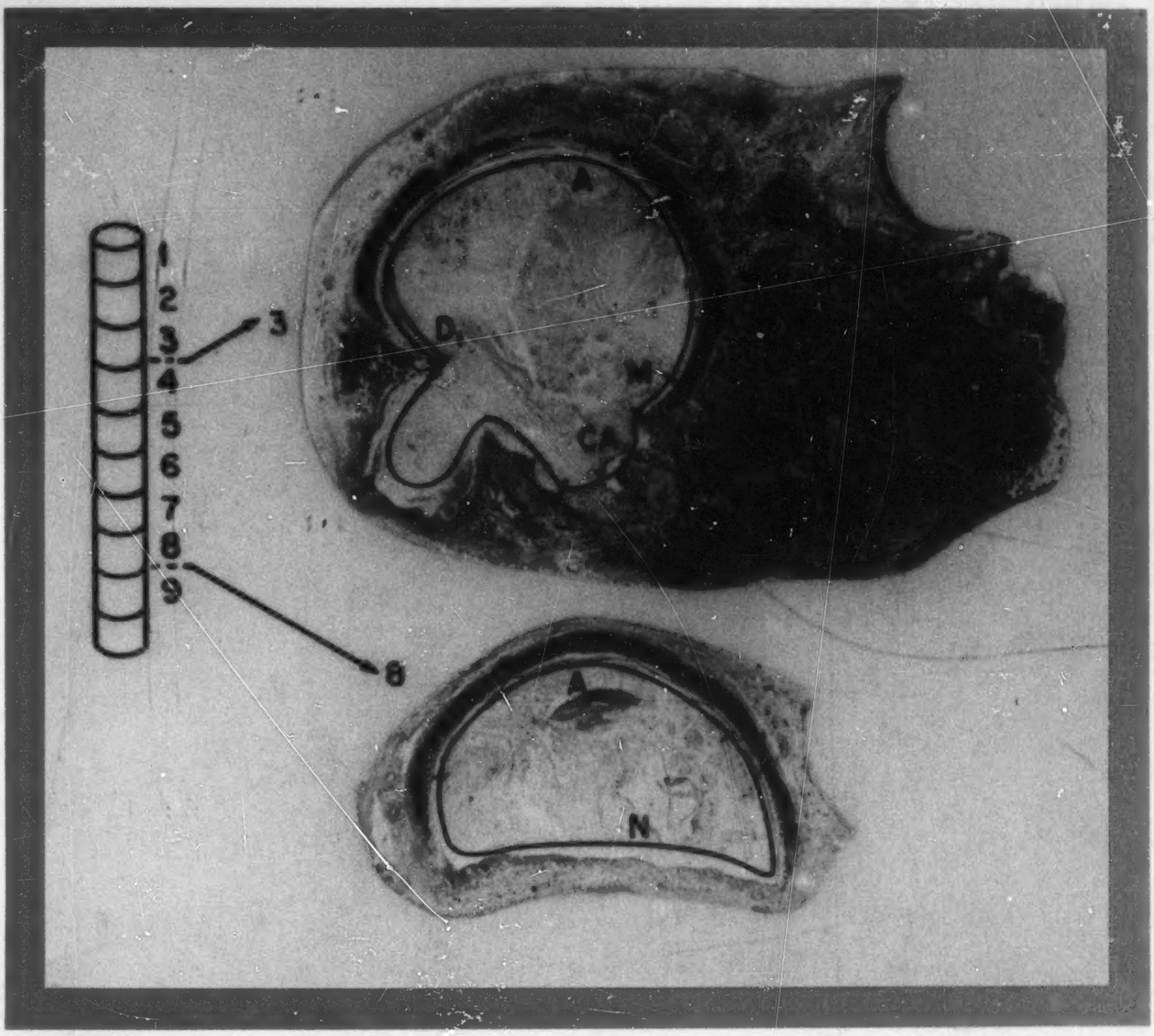

U.S. DEPARTMENT OF HEALTH AND HUMAN SERVICES Public Health Service National Institutes of Health

HE 20.3161:

This month's cover highlights the morphometric method for studying dysplasia and neoplasia in carcinogen-exposed tracheal transplants. Shiba et al. (*see* paper on pages 1155–1161) found that lower doses of 7,12-dimethylbenz[*a*]-anthracene delivered at slow dose rates were more effective in producing dysplastic plus neoplastic lesions than higher doses delivered rapidly.

JNCI

Journal of the National Cancer Institute

November 1982
Volume 69
Number 5

THE JOURNAL of the National Cancer Institute solicits manuscripts on original observations in laboratory and clinical research from all scientists. A manuscript is considered for publication with the understanding that it has not been published previously and is submitted exclusively to the Journal. Opinions expressed by the authors are not necessarily those of the publisher or its editors.

THE JOURNAL is published monthly (two volumes a year). The Secretary of Health and Human Services has determined that the publication of this periodical is necessary in the transaction of the public business required by law of this Department. Use of funds for printing this periodical has been approved by the Director of the Office of Management and Budget through August 30, 1985.

A MONOGRAPH SERIES covering proceedings of scientific meetings pertaining to cancer is also published. These books may be purchased from the Superintendent of Documents. Series subscriptions are not available and monographs are not included in a subscription to the Journal.

THE JOURNAL is for sale by the Superintendent of Documents, U.S. Government Printing Office, Washington, D.C. 20402. Price per copy, $7.00. Subscription price for two volumes per year in the United States, $70.00; foreign, $87.50. Payment is required in advance, and check or money order should be made payable to the Superintendent of Documents.

All inquiries regarding purchase of subscriptions or depository library distribution, including inquiries about missing issues and change of address, should be addressed to the Government Printing Office. The Government Printing Office requires payment in advance on all orders. Inquiries regarding missing issues or change of address for official subscriptions should be addressed to the Editorial Office, Room 850, Westwood Building, 5333 Westbard Avenue, Bethesda, Md. 20816.

VINCENT T. DEVITA, JR., *Director, National Cancer Institute*

BOARD OF EDITORS

PETER GREENWALD, *Editor in Chief*

ELIZABETH K. WEISBURGER, *Assistant Editor in Chief*

STUART A. AARONSON, *Associate Editor*

JOSEPH W. CULLEN, *Associate Editor*

CHARLES H. EVANS, *Associate Editor*

MARY A. FINK, *Associate Editor*

JANET W. HARTLEY, *Associate Editor*

DONALD HENSON, *Associate Editor*

RONALD B. HERBERMAN, *Associate Editor*

GEORGE S. JOHNSON, *Associate Editor*

KURT W. KOHN, *Associate Editor*

ARTHUR S. LEVINE, *Associate Editor*

JOHN J. MULVIHILL, *Associate Editor*

ALAN S. RABSON, *Associate Editor*

RICHARD M. SIMON, *Associate Editor*

JEROME W. YATES, *Associate Editor*

EDITORIAL STAFF

EDWIN A. HAUGH, *Managing Editor*

PAMELA T. ALLEN, *Assistant Managing Editor*

FLORENCE I. GREGORIC, *Monograph Editor*

Editors: DOROTHY D. KATZ, MERCEDES B. LA CHARITY, I. AGNES REVESZ, JOAN O'BRIEN RODRIGUEZ, CONSTANCE R. STONESTREET, and ANNA B. WITTIG

JNCI (NIH Publication No. 83-13)

U.S. DEPARTMENT OF HEALTH AND HUMAN SERVICES Public Health Service National Institutes of Health

Instructions to Authors

Text: Send one original and two copies. **Text-figures** (graphs, charts, and line drawings): Send one original and two copies. **Figures** (photomicrographs and photographs): Send three original glossy prints, unmounted. **Tables:** Send tabular material in typewritten form; do not submit tables as glossy prints to be photographed. The entire manuscript including footnotes, legends, and references must be typed double spaced. Single-spaced portions of a manuscript will be returned to the author for retyping. The mailing address is: Journal of the National Cancer Institute, Westwood Building, Room 850, 5333 Westbard Avenue, Bethesda, Maryland 20816.

Manuscripts should be accompanied by a covering letter from the author responsible for correspondence about the manuscript. The covering letter should contain a statement that the manuscript has been seen and approved by all authors and that all persons listed as authors have made significant (not merely administrative, technical, or supervisory) contributions to the content of the paper. The letter should also state that the manuscript or substantial portions thereof have not been previously published nor are they under consideration for publication in another journal.

Data too extensive for inclusion in a manuscript, but which may be of interest to other investigators, may be deposited with the National Auxiliary Publications Service (NAPS), c/o Microfiche Publications, P.O. Box 3513, Grand Central Station, New York, New York 10017. Authors using the NAPS facilities should indicate in a footnote how their additional data may be obtained.

Approximately one-half of all manuscripts submitted to the Journal are accepted for publication. Publication of manuscripts is contingent on transfer of copyright to the Journal. Forms for this purpose will be sent to authors when a manuscript has been approved for publication. All material published in the Journal is in the public domain; therefore, permission to reproduce any portions is not necessary. As a matter of courtesy, communication should be made to the author(s) concerned.

TITLE: Be brief (no more than 14 words, if possible), but for indexing purposes include all key words. The annual subject index is prepared directly from the titles. Titles that form complete sentences are not acceptable. Do not use abbreviations or chemical formulas in titles.

BYLINE: Supply the complete first name, middle initial, and last name of each author. Avoid use of nicknames. Academic degree is optional; however, if a degree is provided for one author, it should be provided for all authors on a manuscript. Include the name of the institution, address, and zip code for each author. Indicate address for reprint requests in a footnote on the byline.

ACKNOWLEDGMENTS: Financial aid in support of research should be recognized in a footnote. Aid in technical fields, animal care, photography, stenography, and other areas may be mentioned in a separate footnote. Indicate the title (Dr., Mr., Mrs., Miss, Ms.) and affiliation of each person acknowledged.

ABSTRACT: Provide an abstract, 150 words or less, on a separate page. The abstract should describe only *results* of the work being reported. Speculation, historical background, or reference to published works will be deleted from abstracts. Any inbred strains, noninbred stocks, cell lines, or other living materials used in the work should be noted in the abstract.

TEXT: Avoid the use of laboratory jargon and abbreviations not in common usage. When possible, refrain from the use of abbreviations that form words (exceptions are PAGE, ALL). Whenever possible, write mathematical equations and chemical formulas on a single line; submit complicated chemical structures as artwork. Avoid repetition of data in the text when it is presented in tables or text-figures.

Use the following style sources: Webster's *Third New International Dictionary* and Dorland's *Illustrated Medical Dictionary* (25th ed) for spelling; *Council of Biology Editors Style Manual* (4th ed) for scientific abbreviations and symbols; *Government Printing Office Style Manual* for other abbreviations and symbols, punctuation, and hyphenation; *Biochemical Nomenclature and Related Documents* (IUB, 1978) for abbreviations of chemical substances; *Enzyme Nomenclature*, recommendations (1978) of the IUB for recommended names of enzymes and information on nomenclature of isozymes; *The Merck Index* (9th ed) for chemical compounds; "Standard Nomenclature for Inbred Strains of Mice: Seventh Listing" by Joan Staats (Cancer Res 1980;40: 2083–2128) for inbred mouse strains; "Standardized Nomenclature for Inbred Strains of Rats: Fourth Listing" by Joan Staats and Michael Festing (Transplantation 1973;16:221–245) for designations of inbred rat strains; *Animals for Research* (9th ed) prepared by the Institute of Laboratory Animal Resources, National Academy of Sciences, for designations of laboratory animal stocks and strains.

TABLES: Submit tabular material typed double spaced on a separate page. Computer print-outs of tables are acceptable only if they are double spaced and with satisfactory title, column headings, legends, and other textual material. Provide headings for all columns of a table and indicate units of measurement where applicable.

TEXT-FIGURES: Refer to graphs, charts, and line drawings as text-figures. Make the abbreviations on text-figures identical to the abbreviations used in the text and legends. Symbols and lettering should be large enough to be legible if reduced. Glossy prints or original drawings in black ink are acceptable; orient vertically instead of horizontally.

FIGURES: Refer to photomicrographs and photographs as figures. Figures and their legends should fit a 7.5- by 9-inch dimension. Calculate that nine typewritten lines of legend will require 1 inch of vertical space. Type figure legends on a separate sheet and identify in the legend any lettering used on the figure. Trim photographs to show only important areas. Do not number face of photographs; use the back or overlay to indicate the top and number of each. Printed indicators may be included on photographs; do not use hand-drawn indicators. *Insert internal scale markers on all photomicrographs.* Color photographs must be grouped as a single plate. For color reproduction, submit both color transparencies and high-quality black and white reproductions. The need for color must be documented before it will be considered.

REFERENCES: Use any recent issue of the Journal as a style guide for reference lists. Number references in order of citation in both text and reference list. For periodicals, provide author(s), title of paper, journal, year, volume, and first and last page numbers. For books, give the author(s), title, name(s) of editor(s), location and name of publisher, year, pertinent chapter or section title, and page numbers. Follow *Index Medicus* for punctuation and abbreviations. Citations of papers in preparation or submitted for publication, unpublished observations, and personal communications should be noted parenthetically in the text. Do *not* include them in the reference list. The accuracy of all references is the responsibility of the authors and not of the editorial staff.

LETTERS TO THE EDITOR should pertain to recent articles in the Journal and should not contain new data unless relevant to the discussion of a particular paper. The authors addressed will be invited to reply to comments before correspondence is published. Letters will be edited by the Staff, subject to contributor approval.

FURTHER DETAILS on the preparation of manuscripts are set forth in the document "Uniform Requirements for Manuscripts Submitted to Biomedical Journals" prepared by the International Steering Committee of medical editors (*see* Am Rev Respir Dis 1979;119:3–10/Ann Intern Med 1979;90:95–99/Br Med J 1979;1:532–535/ or Lancet 1979;1:428–430).

UNITED STATES GOVERNMENT PRINTING OFFICE, WASHINGTON, D.C.: 1982

Table of Contents

Vol. 69, No. 5—November 1982

Investigations on Man

989	The serum cholesterol–cancer relationship: An analysis of time trends in the Framingham Study	*Paul D. Sorlie, Manning Feinleib*
997	Reactivity in neoplasia, preneoplasia, and pregnancy of lymphocytes against fetal extracts: Cross-reactions between man and mouse	*Günter Pasternak, Bernhard Schlott, Jürgen Reinhöfer, Günter Gryschek, Bodo von Broen, Sybille Albrecht*
1005	Cancers of the gallbladder and biliary tract in Alaskan Natives: 1970–79	*Leslie P. Boss, Anne P. Lanier, Peter H. Dohan, Thomas R. Bender*
1009	Collagen polymorphism in extracellular matrix of human osteosarcoma	*Frederic D. Shapiro, David R. Eyre*
1017	Exogenous estrogens and other risk factors for breast cancer in women with benign breast diseases	*David B. Thomas, Joyce P. Persing, William B. Hutchinson*
1027	Second cancers following radiotherapy for cervical cancer	*Ruth A. Kleinerman, Rochelle E. Curtis, John D. Boice, Jr., John T. Flannery, Joseph F. Fraumeni, Jr.*
1035	Association of breast cancer risk with age at first and subsequent births: A study in the population of the Estonian Republic	*Brian MacMahon, Maret Purde, Daniel Cramer, Evi Hint*
1039	In vitro growth stimulation of human ovarian cancer cells by xenogeneic peritoneal macrophages	*Charles E. Welander, Ronald B. Natale, John L. Lewis, Jr.*
1049	Effect of natural protease inhibitors and a chemoattractant on tumor cell invasion in vitro	*U. P. Thorgeirsson, L. A. Liotta, T. Kalebic, I. M. Margulies, K. Thomas, M. Rios-Candelore, R. G. Russo*
1055	Androgen conjugates in human breast cyst fluids	*W. R. Miller, M. M. Roberts, R. J. Creel, P. L. Yap, R. W. Kelly, A. P. M. Forrest*
1059	Parity and colorectal cancer risk in women	*Tim Byers, Saxon Graham, Mya Swanson*
1063	Correlation between cancers of the uterine cervix and penis in China	*Jun-Yao Li, Frederick P. Li, William J. Blot, Robert W. Miller, Joseph F. Fraumeni, Jr.*
1067	Use of circulating pregnancy-specific β_1 glycoprotein as a marker in carcinoma of the breast in women	*Saul W. Rosen, Mitchell H. Gail, Douglass C. Tormey*

Investigations on Nonhuman Systems

1073 Carcinoembryonic antigen in nonhuman primates *Darrow E. Haagensen, Jr., Richard S. Metzgar, Brent Swenson, William G. Dilley, Charles E. Cox, Sarah Davis, Janet Murdoch, Norman Zamcheck, Samuel A. Wells, Jr.*

1077 Spontaneous leukemia viruses: Lymphomagenic ecotropic viruses of AKR mice *Esther F. Hays, Nadine Margaretten, Stephen K. Swanson*

1083 Prostaglandin-induced differentiation or dimethyl sulfoxide-induced differentiation: Reduction of the neoplastic potential of a rat mammary tumor stem-cell line *Philip S. Rudland, Anna Twiston Davies, Michael J. Warburton*

1095 Immunotherapy by intralesional injection of BCG cell walls or live BCG in bovine ocular squamous cell carcinoma: A preliminary report *Wim R. Klein, E. Joost Ruitenberg, Peter A. Steerenberg, Wim H. de Jong, Wim Kruizinga, Wim Misdorp, Jürgen Bier, Rudy H. Tiesjema, Johan G. Kreeftenberg, Jacob S. Teppema, Herbert J. Rapp*

1105 Expression of fibronectin and laminin in the rat liver after partial hepatectomy, during carcinogenesis, and in transplantable hepatocellular carcinomas *Stewart Sell, Erkki Ruoslahti*

1115 Effects of isoproterenol on mammary gland tumors induced by *N*-nitroso-*N*-methylurea and salivary gland tumors induced by 7,12-dimethylbenz[*a*]anthracene *Tibor Barka*

1121 Immunotherapeutic effects of partially purified tumor-specific transplantation antigens on pulmonary metastases of a 3-methylcholanthrene-induced sarcoma in mice: A preliminary report *Tsuguo Tanaka, Neal R. Pellis, Barry D. Kahan*

1127 Dose-response studies with nitrosoheptamethyleneimine and its α-deuterium-labeled derivative in F344 rats *W. Lijinsky, M. D. Reuber, T. S. Davies, C. W. Riggs*

1135 Induction of mammary neoplasms in the ACI rat by 430-keV neutrons, X-rays, and diethylstilbestrol *Claire J. Shellabarger, Danielle Chmelevsky, Albrecht M. Kellerer, J. Patrick Stone, Seymour Holtzman*

1147 Inhibition by tumor-promoting phorbol esters of procollagen synthesis in promotable JB6 mouse epidermal cells *L. David Dion, Jenifer Bear, John Bateman, Luigi M. De Luca, Nancy H. Colburn*

1155 Effect of carcinogen release rate on the incidence of preneoplastic and neoplastic lesions of the respiratory tract epithelium in rats *Mitsutoshi Shiba, Andres J. P. Klein-Szanto, Ann C. Marchok, Bimal C. Pal, Paul Nettesheim*

1163 Exclusive binding of immunoglobulin to Fcγ receptors on macrophages in 3-methylcholanthrene-induced murine tumors *John M. Lindsay, Linda Manning, Gary W. Wood*

1175 Independent expression of chemical carcinogen-induced phenotypic properties frequently associated with the neoplastic state in a cultured guinea pig cell line *Charles H. Evans, Joseph A. DiPaolo*

1183 Ceruloplasmin, copper ions, and angiogenesis *Katari S. Raju, Giulio Alessandri, Marina Ziche, Pietro M. Gullino*

1189 Isolation of tumoricidal macrophages from lung melanoma metastases of mice treated systemically with liposomes containing a lipophilic derivative of muramyl dipeptide *M. E. Key, J. E. Talmadge, W. E. Fogler, C. Bucana, I. J. Fidler*

1199 Induction of mammary tumors in virgin female BALB/c mice by single low doses of 7,12-dimethylbenz[*a*]anthracene *Stephen P. Ethier, Robert L. Ullrich*

Announcements

1205 New NIH Biotechnology High Voltage Electron Microscope (HVEM) Resource Available to Biological and Medical Researchers

1205 Harvard Medical School Continuing Education Program

1205 The 1983 Oncology Update Symposium

1205 Sixty-fifth Annual Meeting of the American Radium Society

1205 Eighth Summer Program in Methods of Immunologic Research and Diagnosis

1206 Eighth International Congress of Cytology

1206 E.O.R.T.C. Symposium on Treatment of Advanced Gastrointestinal Cancer

The Serum Cholesterol–Cancer Relationship: An Analysis of Time Trends in the Framingham Study[1]

Paul D. Sorlie, *M.S.*,[2] *and* **Manning Feinleib**, *M.D., Dr. P.H.*[2,3,4]

ABSTRACT—Time trends in serum cholesterol were analyzed in the Framingham Study data to determine whether low serum cholesterol, which appears to be associated with increased cancer risk, can truly be called a precursor to the development of the disease. Serum cholesterol measured at base line was found to be associated with the risk of both fatal cancer and all cancers occurring in the subsequent 18 years in men ($P<0.05$). This inverse association seems particularly strong for colon cancer in men. Analysis of time trends in the Framingham data did not yield consistent results for all ages. Men 50–59 years old had a statistically significant lower serum cholesterol measured 16–18 years before cancer diagnosis. For men 60–65 years old, a statistically significant trend toward lower serum cholesterol was apparent as measurement was made closer to the time of cancer diagnosis. Although the Framingham data are not conclusive, they do suggest that in some cancer cases where the serum cholesterol level was lower than that expected at as much as 16–18 years before cancer diagnosis, the depressed level was likely to be a precursor to the tumor growth. However, consistent with the metabolic consequences of tumor growth, the data show that in some cancer cases, serum cholesterol had decreased at measurements made close to the time of cancer diagnosis.—JNCI 1982; 69:989–996.

Of the many analytical complexities encountered in the study of the relationship between serum cholesterol and cancer, one of the most difficult is the ascertainment of the temporal relationship between the presence of low serum cholesterol and the onset of the clinical manifestations of cancer. The relationship between the level of base-line serum cholesterol and subsequent cancer death has been described in recent publications (*1–10*). Two of them present evidence suggesting that low serum cholesterol is caused by metabolic disturbances resulting from the cancer process, inasmuch as the relationship seemed strongest when death occurred shortly after the measurement of cholesterol (*1, 2*). To accurately understand the changes in serum cholesterol that precede cancer, we would need to know the time and course of cancer from its beginning as abnormal cell division to its discovery as a malignant tumor. Because this early process is largely unknown, the interpretation of the observed cholesterol changes with time is largely subjective. Does the low serum cholesterol "precede" the cancer if the cholesterol level is found to be lower 2 years, 5 years, or 10 years before clinical onset of disease? Perhaps a lower level for 20 years is required before it can be reasonably determined to be a precursor.

In one respect, the Framingham data are quite well suited for analysis of serum cholesterol in the preclinical stage of cancer. Data are available for nine repeat measurements of serum cholesterol up to 18 years before cancer diagnosis. In another respect, however, the Framingham data are lacking. Inasmuch as the Framingham Study was designed to collect data on coronary heart disease cases, the number of subjects who developed cancer was generally small, particularly when analysis by specific site is required.

MATERIALS AND METHODS

The Framingham Study examined a cohort of 5,209 men and women at biennial intervals, with the first examination covering the period 1948–52 (*11*). Serum cholesterol was routinely measured by the method of Abell-Kendall for examinations 2–10. At examination 1 a colorimetric method was used, at examination 11 the analysis was made on plasma and not serum, and at examination 12 blood was not drawn. For analysis of time trends in serum cholesterol, the cholesterol values determined at examinations 2–10 were used. At examination 4, alcohol usage and smoking histories were recorded in addition to the routine data collection. Thus some of the analyses in this paper use examination 4 records as the base-line data.

To determine which subjects developed cancer in the course of our study, a detailed review of all 5,209 records was undertaken, and any record that contained mention of a tumor or cancer was reviewed extensively by a physician. Information was then abstracted on cancer site, histologic type, date of diagnosis, method of diagnosis, and other relevant information. Pathology data were requested by mail, telephone calls, or personal visits. As reported earlier (*5*), histologic confirmation was available for 94% of the cancer cases. The distribution by cancer site was similar to that found in the Third National Cancer Survey (*12*). A total of 691 cancer cases were detected up to the 13th cycle of examinations, 629 by histologic confirmation, 39 by nonhistologic confirmation, and 23 with uncertain confirmation. (The 23 cases were not included in the analysis.) The number of cancer cases in each table varies depending on which base line and follow-up was required for the analysis. Cancer incidence cases consist of fatal and nonfatal cases, and cancer mortality was determined from the number of cases in which the underlying cause of death was ascribed to cancer.

Incidence rates of cancer in 18 years were calculated by five levels of serum cholesterol (not quintiles) and by sex and age groups [35–44, 45–54, 55–64, and 65–69 yr (tables 1, 2)]. These rates were age adjusted by the indirect method,

---

[1] Received October 21, 1981; revised June 24, 1982; accepted July 6, 1982.

[2] Epidemiology and Biometry Program, National Heart, Lung, and Blood Institute, National Institutes of Health, Public Health Service, U.S. Department of Health and Human Services, Bethesda, Md. 20205.

[3] *Address reprint requests to* Dr. Feinleib, Federal Building, Room 2C08, National Institutes of Health, Bethesda, Md. 20205.

[4] We are grateful to Dr. Roger Williams, Ms. Patricia McNamara, and Ms. Adele Rosenthal for their thorough collection and review of the Framingham records for cancer.

with the total Framingham cohort used as the standard population. Trends in these rates were estimated according to the maximum likelihood estimates of the logistic function regression (*13*). To examine time trends in serum cholesterol in relation to the onset of cancer, mean differences between cancer cases and noncases were calculated for each examination. The mean difference by time before cancer diagnosis was estimated by a crude pooling of the separate mean differences and by a maximum likelihood method to combine differences, as described by Truett and Sorlie (*14*). With the Truett method, statistical testing of overall differences and time trends in the differences can be made.

RESULTS

The age-adjusted relationship between serum cholesterol and cancer morbidity and mortality is shown in table 1. From values for base-line serum cholesterol at examination 4 and from data on 18 years of subsequent cancer incidence (through examination 13), a significant inverse relationship is seen in cancer mortality for men in particular and for all cancer cases in general. The population at risk in tables 1 and 2 was free of any clinical evidence of cancer at examination 4. The principal elevation in risk occurs in those men with serum cholesterol below 190 mg/dl. Although this trend is not statistically significant in women, they, too, show an elevation in risk when the cholesterol level goes below 190 mg/dl. The trends are similar for fatal cancer and for all cancer in the 18-year follow-up from examination 4.

The difficulties in using a cardiovascular study to analyze cancer incidence become obvious when specific cancer sites are investigated. Only cancers of the three major sites (breast, lung, and colon) approached the number required for meaningful analysis. The age-adjusted cancer incidence rates by site are presented in table 2. Only colon cancer in men shows a statistically significant inverse gradient of risk. Again, the data for women do not show this relationship.

TABLE 1.—*Cancer mortality and morbidity rates,*[a] *by serum cholesterol level, age adjusted for men and women aged 35–69 years: Framingham Study*

Serum cholesterol, mg/dl	Men			Women		
	No. at risk	Cancer death rate, %	Cancer incidence rate, %	No. at risk	Cancer death rate, %	Cancer incidence rate, %
126–189	242	11.8	18.0	294	6.6	12.9
190–219	481	6.9	12.1	490	5.0	9.9
220–249	570	6.6	11.0	604	6.0	10.4
250–279	403	7.2	10.7	470	5.7	10.5
280–545	250	5.6	7.6	459	4.0	8.9
Unknown	276	5.8	9.0	455	3.5	7.2
Total	2,222	7.2	11.3	2,772	5.0	9.7
Total No. of cases		157	250		139	270
Trend in rates[b]		$P<0.05$	$P<0.05$		NS	NS

[a] Rates 18 yr after examination 4 serum cholesterol determination; adjusted by indirect method.

[b] Tested by means of logistic function coefficients; serum cholesterol level and age were the independent variables. NS=not significant.

TABLE 2.—*Cancer incidence (%) at specific sites, by serum cholesterol level, age adjusted*[a] *for men and women aged 35–69 years: Framingham Study*

Serum cholesterol, mg/dl	Men		Women	
	Lung cancer	Colon cancer	Breast cancer	Colon cancer
126–189	2.6	4.6	3.8	0.6
190–219	2.1	1.7	3.1	1.8
220–249	2.9	1.3	2.5	1.7
250–279	2.5	1.5	3.5	1.6
280–545	1.2	0.4	2.3	0.9
Unknown	1.1	1.1	2.9	1.7
Total rates	2.2	1.7	2.9	1.5
Total No. of cases	49	36	81	40
Trend in rates[b]	NS	$P<0.05$	NS	NS

[a] Age-specific incidence rates 18 yr after examination 4; adjusted by indirect method.

[b] Trend tested by means of logistic function coefficients; serum cholesterol level and age were the independent variables. NS=not significant.

In an earlier publication on cancer in Framingham (*5*), multiple logistic function coefficients were presented to show that the relationship between serum cholesterol and cancer persisted even after multivariate adjustment for age, alcohol, cigarette consumption, education, systolic blood pressure, and relative weight.

In the preceding analysis, several factors could be presented to refute the hypothesis that low serum cholesterol merely reflects existing disease: 1) The analyses were all performed on data for a population free of any clinically recognizable cancer. Furthermore, cancer cases diagnosed within 3 months after the routine examination were excluded as prevalence cases because the initial suspicion of cancer may have originated at the examination. 2) The analysis used incidence cases that occurred up to 18 years after base-line measurements of cholesterol. Very few cases occurred in the first 4 years of the follow-up. 3) The lack of a relationship between cholesterol level and cancer incidence in women would argue against the above hypothesis, because the assumption reasonably can be made that once the cancer process begins, the metabolic consequences for men and women would be similar, particularly for the same cancer site, e.g., colon cancer.

To describe the time at which cancer subjects began to show lower than average serum cholesterol values, mean values of cholesterol were tabulated for subjects with and without cancer at all examinations between 2 and 10. Detailed tables for all age and sex groups are presented in tables 3–10. The data are presented in detail so that the reader can evaluate the unadjusted as well as the adjusted results.

Tables 3–10 have the following format: The mean value and standard deviation of serum cholesterol (first row) are shown for measurements made at examinations 2–10 for those subjects who were free of cancer throughout the time period. All subsequent rows show the difference in mean serum cholesterol between subjects with and without cancer. The second row shows the mean difference for those subjects who developed cancer at examination 3 (i.e., between ex-

TABLE 3.—*Mean serum cholesterol level in subjects without cancer and mean difference in serum cholesterol level between subjects with and without cancer: Men aged 30–39 years*

Examination of cancer diagnosis	No. of subjects	Mean value and difference for measurement at examination								
		2	3	4	5	6	7	8	9	10
		Mean value of noncases (SD)								
—	369	221 (42)	222 (39)	233 (41)	235 (42)	242 (41)	246 (42)	240 (39)	233 (42)	223 (38)
		Mean difference, cases−noncases, at examinations before cancer diagnosis								
3	0	—								
4	0	—	—							
5	0	—	—	—						
6	2	54	37	18	9					
7	2	−5	9	3	8	6				
8	1	0	−39	−59	−44	−43	−50			
9	6	5	−4	−12	−25	−4	−5	−14		
10	0	—	—	—	—	—	—	—	—	
11	2	−14	−18	−7	−26	−32	−21	−36	−45	−38

TABLE 4.—*Mean serum cholesterol level in subjects without cancer and mean difference in serum cholesterol level between subjects with and without cancer: Men aged 40–49 years*

Examination of cancer diagnosis	No. of subjects	Mean value and difference for measurement at examination								
		2	3	4	5	6	7	8	9	10
		Mean value of noncases (SD)								
—	379	228 (39)	229 (39)	235 (37)	238 (45)	241 (40)	245 (39)	238 (44)	230 (43)	223 (40)
		Mean difference, cases−noncases, at examinations before cancer diagnosis								
3	1	48								
4	4	26	26							
5	1	−43	−48	−10						
6	3	−7	−47	−28	−29					
7	5	−8	7	−13	−9	−5				
8	4	−4	−3	−15	−4	1	−17			
9	2	21	−10	−4	−4	29	7	15		
10	7	−13	−6	−1	−8	−12	−17	0	10	
11	8	−5	−7	10	6	11	3	16	15	−4

TABLE 5.—*Mean serum cholesterol level in subjects without cancer and mean difference in serum cholesterol level between subjects with and without cancer: Men aged 50–59 years*

Examination of cancer diagnosis	No. of subjects	Mean value and difference for measurement at examination								
		2	3	4	5	6	7	8	9	10
		Mean value of noncases (SD)								
—	234	231 (38)	232 (38)	238 (41)	240 (40)	244 (38)	247 (41)	241 (39)	234 (42)	224 (40)
		Mean difference, cases−noncases, at examinations before cancer diagnosis								
3	3	20								
4	5	−11	−8							
5	5	−9	−19	−26						
6	3	−11	−18	2	−24					
7	6	−28	−30	−40	−39	−31				
8	4	−9	−6	−21	5	5	−29			
9	5	0	−30	−31	−39	−24	−45	−37		
10	7	25	10	9	12	11	15	8	−7	
11	14	−27	−20	−23	−18	−22	−16	−16	−16	−29

aminations 2 and 3) and for these subjects only the difference in cholesterol at examination 2 is tabulated. The third row gives data for those who developed cancer at examination 4, and their differences at examinations 2 and 3 are tabulated. This sequence proceeds to the last row, which shows the differences (cases minus noncases) at examinations 2–10 for those individuals who developed cancer between examinations 10 and 11. All of these subjects had to have known serum cholesterol levels at all examinations prior to evidence of cancer. Thus a row, from left to right, will show the change in cholesterol in exactly the same cohort of individuals as it was measured closer to the time of the cancer diagnosis. A column, from top to bottom, will show the variation in a measurement at a single examination for individuals in whom cancer became evident at a time more distant from the examination.

Because the largest cohort of cases is only 14 cases (table 5) and because there is considerable inter- and intra-individual variability, the mean differences need to be combined to make more stable estimates. Those mean differences on the diagonal, from upper left to lower right, form those measurements that were made just before the discovery of cancer, i.e., within 0–2 years. On the next diagonal are those differences in measurements made 2–4 years before diagnosis

TABLE 6.—*Mean serum cholesterol level in subjects without cancer and mean difference in serum cholesterol level between subjects with and without cancer: Men aged 60–65 years*

Examination of cancer diagnosis	No. of subjects	Mean value and difference for measurement at examination								
		2	3	4	5	6	7	8	9	10
		Mean value of noncases (SD)								
—	27	216 (31)	213 (32)	226 (31)	231 (32)	229 (32)	234 (33)	232 (33)	218 (34)	221 (35)
		Mean difference, cases−noncases, at examinations before cancer diagnosis								
3	2	8								
4	1	37	53							
5	2	29	23	−4						
6	2	6	8	12	−11					
7	0	—	—	—	—	—				
8	3	11	22	1	11	16	−6			
9	3	59	53	45	41	30	3	0		
10	4	−14	−3	−5	−7	−4	−7	−8	−11	
11	2	63	17	28	37	4	41	27	26	−21

TABLE 7.—*Mean serum cholesterol level in subjects without cancer and mean difference in serum cholesterol level between subjects with and without cancer: Women aged 30–39 years*

Examination of cancer diagnosis	No. of subjects	Mean value and difference for measurement at examination								
		2	3	4	5	6	7	8	9	10
		Mean value of noncases (SD)								
—	350	202 (37)	204 (37)	214 (39)	219 (40)	229 (46)	239 (65)	236 (44)	233 (43)	232 (43)
		Mean difference, cases−noncases, at examinations before cancer diagnosis								
3	1	−52								
4	4	−16	−6							
5	2	28	24	−8						
6	2	−4	3	−4	−29					
7	4	−36	−26	−40	−25	−31				
8	3	10	−31	−24	−11	−31	−40			
9	2	4	−25	7	−33	−11	−39	−25		
10	3	13	37	22	53	59	33	35	17	
11	5	−11	−25	−23	−7	−4	2	−6	9	−12

TABLE 8.—*Mean serum cholesterol level in subjects without cancer and mean difference in serum cholesterol level between subjects with and without cancer: Women aged 40–49 years*

Examination of cancer diagnosis	No. of subjects	Mean value and difference for measurement at examination								
		2	3	4	5	6	7	8	9	10
		Mean value of noncases (SD)								
—	396	224 (42)	231 (41)	245 (44)	250 (44)	261 (46)	267 (48)	262 (45)	256 (47)	250 (44)
		Mean difference, cases−noncases, at examinations before cancer diagnosis								
3	4	18								
4	6	0	3							
5	5	5	1	−3						
6	1	−7	−31	13	2					
7	4	−5	−29	−30	−31	−32				
8	8	18	−8	8	0	1	−7			
9	2	12	9	−21	−20	−10	34	9		
10	8	40	32	21	18	14	22	10	16	
11	7	9	13	17	−2	10	14	20	8	4

TABLE 9.—*Mean serum cholesterol level in subjects without cancer and mean difference in serum cholesterol level between subjects with and without cancer: Women aged 50–59 years*

Examination of cancer diagnosis	No. of subjects	Mean value and difference for measurement at examination								
		2	3	4	5	6	7	8	9	10
		Mean value of noncases (SD)								
—	281	250 (44)	253 (45)	263 (46)	265 (46)	271 (46)	272 (46)	266 (45)	261 (51)	249 (42)
		Mean difference, cases−noncases, at examinations before cancer diagnosis								
3	5	3								
4	6	−15	0							
5	11	−6	3	−12						
6	10	11	19	5	12					
7	9	−4	6	4	10	3				
8	3	−15	−39	−38	−25	−14	−4			
9	7	−3	−32	−33	−27	−14	−21	−30		
10	8	17	3	2	−5	7	2	13	18	
11	9	−7	6	−6	−20	−11	−5	−11	−21	−24

of cancer. Finally, the last mean difference is shown in the lower left hand corner—the difference determined 16–18 years before the cancer event.

In a crude sense, an overall mean difference can be determined by combining the mean differences along the diagonal, multiplying the number of cases by the mean value, adding these products, and then dividing by the total number of cases. This yields a rough estimate of the differences between cases and noncases by distance from the event. These differences are shown in tables 11 and 12 under the heading "crude estimates." Another method for combining these differences was described by Truett and Sorlie (*14*) and derives maximum likelihood estimates by means of a more elaborate weighting by the variance-covariance matrix. These estimates are also presented in tables 11 and 12 and were computed from mean differences when at least 2 cancer cases were among the cohorts (indicated by the rows in tables 3–10).

The Truett method also includes statistical tests of the estimated differences and also tests whether a trend exists in the differences as a function of time to the event (tables 11, 12). Differences at each interval before diagnosis were tested for statistical significance from zero and are indicated in tables 11 and 12 by asterisks. The statistic for heterogeneity indicates whether significant variation occurs in the differences by interval of diagnosis, and the trend statistic tests indicate whether a linear trend is present in the differences by time interval to diagnosis.

For younger men aged 30–39 years, there appears to be a trend from positive differences to negative differences as the measurement was made closer to the time of cancer diagnosis. This trend is not statistically significant ($P<0.10$). For men aged 50–59 years, a statistically significant difference is seen between those with and without cancer at as much as 16–18 years before cancer diagnosis. No evidence of a trend is apparent in the difference as these men were measured closer to the time of cancer diagnosis. For older men aged 60–65 years, there is a significant trend for differences that change from a large positive difference 18 years before cancer diagnosis to a slightly negative difference just before the event.

For women the results are quite mixed. Women 30–39 years old had significantly lower cholesterol levels when measured 14–16 years before cancer diagnosis. In the age group 40–49 years a significant trend from large differences to small differences was apparent. In the older women, 60–65 years old, 2 subjects showed markedly reduced cholesterol levels.

TABLE 10.—*Mean serum cholesterol level in subjects without cancer and mean difference in serum cholesterol level between subjects with and without cancer: Women aged 60–65 years*

Examination of cancer diagnosis	No. of subjects	Mean value and difference for measurement at examination								
		2	3	4	5	6	7	8	9	10
		Mean value of noncases (SD)								
—	52	255 (39)	252 (40)	252 (34)	254 (39)	261 (43)	264 (37)	261 (40)	250 (42)	241 (40)
		Mean difference, cases−noncases, at examinations before cancer diagnosis								
3	1	−19								
4	1	−39	−52							
5	1	−15	−29	−1						
6	1	−5	39	10	−5					
7	1	−38	−50	−61	−17	−42				
8	2	−77	−68	−48	−63	−64	−45			
9	0	—	—	—	—	—	—	—		
10	1	45	−62	38	27	42	−17	−42	−27	
11	1	−9	5	4	34	43	27	31	−7	35

TABLE 11.—*Mean difference between subjects with and without cancer, estimated by two methods: Men aged 30-65 years*[a]

Estimate	Mean difference, cases−noncases, at following No. of yr before cancer diagnosis									Chi-square Truett statistics[b]	
	16–18	14–16	12–14	10–12	8–10	6–8	4–6	2–4	0–2	Heterogeneity, 8 df	Trend, 1 df
Men aged 30–39											
Crude estimates	−14	−18	2	−10	−15	−5	−1	−6	−11	7.36	3.14
Truett estimates	9	4	13	2	−7	−6	0	−4	−11		
No. of cancer cases in estimate	2	2	8	8	10	12	12	12	12		
Men aged 40–49											
Crude estimates	−6	−10	5	0	−1	−4	−6	4	0	7.76	1.41
Truett estimates	−12	−13	2	−3	−3	−3	−5	3	0		
No. of cancer cases in estimate	8	15	17	21	26	29	29	33	33		
Men aged 50–59											
Crude estimates	−28	−5	−10	−13	−16	−17	−13	−15	−22	13.50	2.02
Truett estimates[c]	−19**	−6	−9	−11	−12*	−13*	−8	−12*	−20**		
No. of cancer cases in estimate	14	21	26	30	36	39	44	49	52		
Men aged 60–65											
Crude estimates	63	−4	24	21	15	15	14	9	−7	28.31	14.64
Truett estimates[c]	55*	16	22*	15	10	12	9	7	−5		
No. of cancer cases in estimate	2	6	9	12	12	14	16	16	18		

[a] Calculations were rounded to nearest whole number.

[b] df=degrees of freedom. Chi-square (0.05, 8 df)=15.51; chi-square (0.05, 1df)=3.84.

[c] Difference between cases and noncases was statistically different from zero for Truett estimates only: *, $P<0.05$; **, $P<0.01$.

TABLE 12.—*Mean difference between subjects with and without cancer, estimated by two methods: Women aged 30-65 years*[a]

Estimate	Mean difference, cases−noncases, at following No. of yr before cancer diagnosis									Chi-square Truett statistics[b]	
	16–18	14–16	12–14	10–12	8–10	6–8	4–6	2–4	0–2	Heterogeneity, 8 df	Trend, 1 df
Women aged 30–39											
Crude estimates	−11	−11	1	1	−5	−4	−4	−6	−16	8.20	0.03
Truett estimates[c]	−5	−20*	−7	−4	−3	−4	−3	−3	−15		
No. of cancer cases in estimate	5	8	10	13	17	19	21	25	25		
Women aged 40–49											
Crude estimates	9	27	23	13	3	4	6	2	1	11.32	5.02
Truett estimates[c]	11	23**	20*	10	4	4	7	3	2		
No. of cancer cases in estimate	7	15	17	25	29	29	34	40	44		
Women aged 50–59											
Crude estimates	−7	11	−2	−16	−14	−3	−2	−3	−4	15.51	0.46
Truett estimates	−2	12	1	−11	−12	−4	−1	−2	−5		
No. of cancer cases in estimate	9	17	24	27	36	46	57	63	68		
Women aged 60–65											
Crude estimates	—	—	—	−77	−68	−48	−63	−64	−45	2.88	0.86
Truett estimates[c]	—	—	—	−77**	−68**	−48*	−63*	−64*	−45		
No. of cancer cases in estimate				2	2	2	2	2	2		

[a] Calculations were rounded to nearest whole number.

[b] df=degrees of freedom. Chi-square (0.05, 8 df)=15.51; chi-square (0.05, 1 df)=3.84.

[c] Difference between cases and noncases was statistically different from zero for Truett estimates only: *, $P<0.05$; **, $P<0.01$.

The Truett method of analysis has a fairly stringent requirement that all measurements before cancer diagnosis be known. A bias could be caused if the measurements for cancer subjects who missed examinations were different from the measurements for those who took the examinations. The mean differences were compared for those subjects with known cholesterol values for all measurements before the disease and for all subjects without these requirements. However, aside from variation due to the small number of cases, no evidence exists that exclusion of those cancer cases with missing values would bias the results in any appreciable way.

The analyses by Cambien et al. (*1*) and Rose and Shipley (*2*), which show that the relationship disappears after removing cancer cases that occurred soon after measurement, are investigating the effect of the first vertical column of tables 3–10. In the Framingham data, removal of the cancer cases that became evident at examinations 3 and 4 in any of the age–sex groups would have no real effect on the overall difference computed from the vertical column. One difficulty in analyzing the columns is that they are composed of single individuals, thus emphasizing the inter-individual variability. The rows, however, contain only the variability from intra-individual and examination sources.

DISCUSSION

The data from the Framingham Study presented in this paper show elevations in cancer incidence primarily at low levels of serum cholesterol (<190 mg/dl) (table 1). There appears to be a gradient in incidence above that level, but it is very slight. Women also show an elevation in incidence at these low levels, but the gradient is not statistically significant. The evidence of a threshold effect and its precise location in other studies are difficult to quantify inasmuch as the methods for cholesterol measurement are so variable. However, a strong impression is conveyed that the largest elevation in risk appears for those with serum cholesterol below 190 mg/dl in the Paris study (*1*), those below 193 mg/dl in the Maoris–New Zealand study (*3*), those below 195 mg/dl in the Puerto Rico study (*7*), and those below 180 mg/dl in the Hawaii study (*8*). The studies from Sweden (*6*) and Whitehall, England, (*2*) show a more steady gradient of risk. All of these studies used the determination of cholesterol in the serum, with the exception of the Whitehall study which used plasma cholesterol.

As stated earlier, the findings of two of those studies show that the gradient of risk is largely attenuated when adjustment is made for mortality occurring soon after the baseline cholesterol measurement (*1, 2*). However, several other studies have analyzed the data by time between measurement and cancer death and found that the relationship still exists (*3, 4, 7, 8*). The Framingham data provide evidence that both hypotheses are true to some extent. Low cholesterol is likely to be both a precursor and a response to the cancer process. In some age–sex groups, the Framingham data show clear evidence that cholesterol levels are depressed in cancer cases at as much as 18 years before cancer diagnosis. In other age groups, a trend is apparent for the cholesterol level to become more depressed as the subjects were measured closer to time of cancer diagnosis. Whether these age differences represent real age effects or sampling variability is difficult to say.

Although the lack of consistent results between studies is disconcerting, it should not be too surprising. These studies were not designed in size to study cancer. Obviously, this will result in greater variability of the estimated relationships and less consistent results. Variations in the nature of the studies may also explain the differences. Some of the studies used the cause of death coding of the death certificate, others reviewed all available information to determine cause of deaths, and in others ascertainment of nonfatal cancer was also made. Some of the studies used a fairly representative population sample, but others used occupational cohorts that would have been selected more likely according to healthy status.

There are several possible explanations for the cancer–cholesterol relationship. The first is that low serum cholesterol is a result of existing cancer in the preclinical stages. In the Framingham Study and in several other studies there is evidence that cholesterol levels *in part* are related to the time course of the disease, and this evidence is consistent with the alteration of the cholesterol level by cancer. This consistency is contingent, however, on a model of cancer pathogenesis that describes cancer as a long-term insidious process that may linger in a preclinical state for many years. In that event, low serum cholesterol might serve as a "marker" for preclinical malignant tumor growth. However, most oncologists would be reluctant to accept that a metabolically active lesion would remain preclinical for 10 or more years.

A second possible explanation is that serum cholesterol is a covariate to some other factor that plays a more primary role in cancer development. If there is such a factor, it apparently would not be any of the variables analyzed in the studies listed above. The factors of smoking, alcohol consumption, relative weight, or socioeconomic status do not explain the cholesterol relationship. Possibly, the one consistency in these studies is that the results are still strong after multivariate adjustment. Other important covariates have been postulated, including the relationship between vitamin A, cholesterol, and cancer (*15*).

A third possible explanation is that low cholesterol has a direct etiologic relationship with cancer. At present, however, the biologic plausibility of the cholesterol relationship is moot. A sound hypothesis implicating low serum cholesterol as an initiator or promoter of carcinogenesis has yet to be found. However, the population studies described above present sufficient positive evidence to encourage researchers to evaluate the role that cholesterol may play, if any, in the genesis or promotion of malignant tumor growth.

REFERENCES

(*1*) Cambien F, Ducimetière P, Richard J. Total serum cholesterol and cancer mortality in a middle-aged male population. Am J Epidemiol 1980; 112:388–394.

(*2*) Rose G, Shipley MJ. Plasma lipids and mortality: A source of error. Lancet 1980; 1:523–526.

(*3*) Beaglehole R, Foulkes MA, Prior IAM, Eyles EF. Cholesterol and mortality in New Zealand Maoris. Br Med J 1980; 1:285–287.

(*4*) Kark JD, Smith AH, Hames CG. The relationship of serum cholesterol to the incidence of cancer in Evans County, Georgia. J Chronic Dis 1980; 33:311–322.

(*5*) Williams RR, Sorlie PD, Feinleib M, McNamara PM, Kannel WB, Dawber TR. Cancer incidence by levels of cholesterol. JAMA 1981; 245:247-252.

(*6*) Peterson B, Trell E, Sternby NH. Low cholesterol level as a risk factor for noncoronary death in middle-aged men. JAMA 1981; 245:2056-2057.

(*7*) Garcia-Palmieri MR, Sorlie PD, Costas R Jr, Havlik RJ. An apparent inverse relationship between serum cholesterol and cancer mortality in Puerto Rico. Am J Epidemiol 1981; 114:29-40.

(*8*) Kagan A, McGee DL, Yano K, Rhoads GG, Nomura A. Serum cholesterol and mortality in a Japanese-American population: The Honolulu Heart Program. Am J Epidemiol 1981; 114:11-20.

(*9*) Kozarevic D, McGee D, Vojvodic N, et al. Serum cholesterol and mortality: The Yugoslavia cardiovascular disease study. Am J Epidemiol 1981; 114:21-28.

(*10*) Feinleib M. On a possible inverse relationship between serum cholesterol and cancer mortality. Am J Epidemiol 1981; 114:5-10.

(*11*) Dawber TR, Meadors GP, Moore FE Jr. Epidemiological approaches to heart disease: Framingham Study. Am J Public Health 1951; 41:279-286.

(*12*) Cutler SJ, Young JL Jr, eds. Third National Cancer Survey: Incidence data. Natl Cancer Inst Monogr 1975; 41:1-454.

(*13*) Walker SH, Duncan DB. Estimation of the probability of an event as a function of several independent variables. Biometrika 1967; 54:167-179.

(*14*) Truett J, Sorlie P. Changes in successive measurements and the development of disease: The Framingham Study. J Chronic Dis 1971; 24:349-361.

(*15*) Wald N, Idle M, Boreham J, Bailey A. Low serum vitamin A and subsequent risk of cancer. Lancet 1980; 2:813-815.

Reactivity in Neoplasia, Preneoplasia, and Pregnancy of Lymphocytes Against Fetal Extracts: Cross-Reactions Between Man and Mouse[1, 2]

Günter Pasternak,[3] Bernhard Schlott,[3] Jürgen Reinhöfer,[3] Günter Gryschek,[3] Bodo von Broen,[3] *and* **Sybille Albrecht[3, 4]**

ABSTRACT—KCl extracts (3 *M*) from human fetuses were tested by macrophage electrophoretic mobility (MEMB), leukocyte migration inhibition, and/or leukocyte adherence inhibition techniques against lymphocytes-leukocytes from tumor-bearing humans and control persons. A positive MEMB test was found in 209 of 284 (73%) patients with various types of clinically manifest tumors. Only 15 of 134 (11%) controls gave a positive reaction by the MEMB test. Leukocyte migration was significantly inhibited in 48 of 64 (75%) tumor patients, and leukocyte adherence was significantly inhibited in 40 of 50 (80%) tumor patients versus 7 of 50 (14%) and 10 of 54 (19%) in the corresponding controls. Lymphocyte reactivity to fetal extracts is also detectable in inbred XVII/Bln, CBA/Bln, and C3H/Bln mice bearing spontaneous or transplanted tumors of different etiology. Human and mouse fetal extracts gave cross-reactions. Lymphocytes from tumor-bearing mice were reactive against fetal extracts from the cow, pig, sheep, guinea pig, cat, and chicken. Mice bearing benign skin warts induced by 7,12-dimethylbenz[*a*]anthracene (DMBA) as well as DMBA-treated mice without visible skin lesions gave a positive MEMB test. Likewise, pregnancy is associated with lymphocyte reactivity to fetal extracts.—JNCI 1982; 69: 997–1004.

Malignant transformation is associated with changes in gene expression that result in the production of antigens characteristic of those of fetal origin. These TAFA have been found in various tumor-host systems and species including humans (*1–4*). There are TAFA such as AFP or CEA that may appear in the sera of tumor bearers in high concentration. Their detection is dependent on xenogeneic antibodies (*5–7*). Conversely, there are TAFA not detectable in the serum that induce an immune response in the autochthonous tumor host. In this case antibodies and/or cellular reactivity to fetal and tumor cells are the indicators of fetal antigen production in the tumor bearer (*8–15*). TAFA specific for certain types of tumor (*10, 16*) and those shared by many, if not all, of the tumors (*17–19*) may be distinguished. Apparently, TAFA include a variety of molecular structures (*20*).

The existence of cross-reacting TAFA in experimental tumors is indicated by the fact that, under certain conditions, fetal tissue immunizes against syngeneically transplanted tumors of different etiology and histology. Thus transplantation resistance was shown against simian virus 40- (*21*), adenovirus- (*17*), and polyomavirus-induced sarcomas of hamsters (*22*) as well as against chemically induced sarcomas (*23, 24*) and adenocarcinomas (*25*). Likewise, lymphoid cells or sera from multiparous or fetal tissue-immunized donors can be cytotoxic for tumor cells in vitro (*10, 18, 26–29*). At least one or a few of the antigenic determinants involved seem to be expressed in various species, since mouse and human fetal tissue may immunize against hamster tumors (*22, 30*) and antibodies occur against human and mouse fetal liver cells in the sera from patients with carcinomas of the breast, colon, and lung and with malignant melanoma (*13*).

The role played by the antifetal reactivity developing in pregnancy and malignant tumors is still debatable (*3, 31*). Expression of fetal antigens is associated with cell-mediated immunity in pregnancy (*26, 32–34*). Apparently, due to sensitization against fetal antigens, tumor-bearing women with previous pregnancies had a significantly improved survival over women with no history of pregnancy (*35, 36*). Furthermore, melanoma patients with elevated IgM antibody to an oncofetal antigen showed a prolonged disease-free interval and survival (*37*). Conversely, tumors may develop and grow progressively in the presence of antifetal reactivity. T-suppressor cells have been considered a causative factor (*38–40*).

If antifetal reactivity in pregnancy and neoplasia to a species-independent antigen is a widely distributed phenomenon, then techniques other than graft rejection and antibody- or cell-mediated cytotoxicity might also allow reactivity detection and characterization.

There are a number of indirect immunologic assays, mainly based on lymphokines, that are released from lymphoid cells in the process of a specific reaction with antigen. Among these assays, the LMI and LAI tests are now generally used in tumor immunology. In addition, MEMB test may show the same degree of sensitivity and specificity, depending on the test conditions chosen. However, controversial experiences have been reported with the MEMB test, particularly with respect to its diagnostic value in cancer

---

ABBREVIATIONS USED: AFP=α-fetoprotein; CEA=carcinoembryonic antigen; DMBA=7,12-dimethylbenz[*a*]anthracene; EMEM=Eagle's minimum essential medium; FRG=Federal Republic of Germany; GDR=German Democratic Republic; LAI=leukocyte adherence inhibition; LMI=leukocyte migration inhibition; MEMB=macrophage electrophoretic mobility; MI=migration index; MSF=macrophage slowing factor; TAFA=tumor-associated fetal antigen(s).

---

[1] Received November 6, 1981; accepted April 30, 1982.

[2] Animals were maintained under the guidelines set forth by the Research Center of Molecular Biology and Medicine. Research procedures were in accord with the ethical standards of the Helsinki Declaration of 1975.

[3] Department of Experimental and Clinical Immunology, Central Institute of Cancer Research, DDR-1115 Berlin-Buch, German Democratic Republic.

[4] We acknowledge the excellent technical assistance of Mrs. K. Strecker.

(*41, 42*). In our hands, the three assays were likewise applicable to the measurement in tumor patients and tumor-bearing mice of leukocyte sensitization to 3-*M* KCl extracts from fetal organs. The results were closely correlated (*14*).

In the present investigation, we completed our data on the interspecies cross-reactivity of fetal extracts and tested the lymphocyte reactivity in mice and humans during pregnancy and under preneoplastic conditions.

MATERIALS AND METHODS

Extracts.—Liver, spleen, kidney, lung, and heart from human fetuses obtained from therapeutic or spontaneous abortion were pooled and stored at −20°C. The ages of the fetuses ranged from 2 to 7 months of gestation. Extracts were prepared by the 3-*M* KCl method of Meltzer et al. (*43*) modified according to Pellis et al. (*44*). Fetal organs were minced with scissors and mixed for 2 minutes in a 3-*M* KCl solution (1;10 wt/vol) containing 0.01 *M* Tris buffer at pH 7.3–7.4 in an Ultraturrax homogenizer (Janke and Kunkel Co., Staufen im Breisgau, FRG). After being further stirred (16 hr at 4°C), the suspension was centrifuged at 100,000×*g* for 1 hour. The clear supernatant was dialyzed against distilled water or 10 m*M* Tris in 0.15 *M* NaCl at pH 7.4. Then the material was again centrifuged at 100,000×*g* for 15 minutes and concentrated to about one-tenth of the original volume by an Amicon filter RM 10, dextran 75,000 (VEB Serumwerk, Bernburg, GDR), or the hollow fiber system DC-2a (Amicon Corp., Lexington, Mass.). The concentrated material was then precipitated with 1 volume of a cold 4-*M* $(NH_4)_2SO_4$ solution. After centrifugation (100,000×*g* for 30 min), the precipitate was solubilized in Tris-buffered saline and dialyzed until sulfate ions were no longer detectable. Finally, the protein content of the extract was determined by the method of Lowry et al. (*45*). Samples of the fetal extract were stored in liquid nitrogen until used.

In the same manner extracts were prepared from the liver, spleen, kidney, lung, and heart of adult tumor-free persons who died by accident and of fetuses from the cow, sheep, cat, and guinea pig. For the preparation of mouse and chicken fetal extracts, whole fetuses were used. In general, fetuses were derived at various times during the final third of the pregnancy period. Donors of mouse fetuses were XVII/Bln mice. Fetuses were of primiparous as well as multiparous origin.

Blood samples.—Blood was obtained from patients with clinically manifest tumors of different histology, organ localization, and stage. In one of the test groups, gynecologic patients particularly were studied. This group included patients with dysplasia of the cervical squamous epithelium and carcinoma in situ.

Blood from tumor patients was taken before surgical, radiologic, or cytostatic therapy. Control blood was obtained from normal blood bank donors, voluntary persons of the laboratory and clinical staff, and patients with nonmalignant diseases.

Heparinized whole blood (30 ml with 3,500 U heparin; Spofa, Prague, Czechoslovakia) was used as a source of leukocytes or lymphocytes. All blood samples were coded.

Leukocyte and lymphocyte preparation.—The techniques described below have been published previously (*46*). For leukocyte isolation the heparinized human blood was mixed 4:1 (vol/vol) with a 6% dextran solution (Infukoll; VEB Serumwerk) and incubated for 30 minutes at 37°C. Cells in the supernatant were repeatedly washed by centrifugation (10 min each at 250×*g*). After the red blood cells were lysed by distilled water, the leukocytes were suspended in EMEM (Staatliches Institut für Immunpräparate und Nährmedien, Berlin, GDR).

Lymphocytes were isolated according to the method of Bøyum (*47*). After spontaneous sedimentation of red blood cells (30 min at room temperature), the supernatant leukocyte-containing plasma layer was pipetted off and put on a 5-ml sample of Lymphoprep (Nyegaard & Co., Oslo, Norway) in a tube. After centrifugation for 20 minutes at 580×*g*, the lymphocyte-containing layer between the supernatant and Lymphoprep was isolated and washed three times in EMEM.

Mouse lymphocytes were obtained from axillary, inguinal, and lumbar lymph nodes. Alternatively, spleen cells were used. Cell suspensions were prepared by means of a Potter glass homogenizer. Cell aggregates were removed by filtration of the suspension through gauze. After the suspension was washed three times in EMEM, the cell concentration was adjusted to 10^7 cells/ml. According to the trypan blue dye exclusion test, lymphocytes of human and mouse origins contained more than 90% viable cells.

Peritoneal macrophages.—Guinea pigs received ip injections of 20 ml paraffin oil each. After 7–21 days, the peritoneal cavities of the animals were washed with a 150- to 200-ml isotonic NaCl solution. As controlled by cell smears, this solution contained mainly macrophages (60–80%), which were repeatedly washed, and the solution was finally suspended in EMEM at a dose of 7×10^6 cells/ml.

Mouse strains and tumors.—Lymphocyte donors were inbred mice of the following strains: XVII/Bln, CBA/Bln, and C3H/Bln. UV 15264 is a UV light-induced sarcoma, and Gr 101 is a Graffi virus-induced leukemia. Both tumors originate from XVII mice and have a long transplantation history. They are generally transferred by im inoculation of cells, and they grow as solid tumors. MCa 21224 is a transplanted mammary carcinoma, which recently developed spontaneously in a CBA mouse. Furthermore, C3H mice with spontaneous mammary cancer served as spleen or lymph node donors.

MEMB test.—Incubation of lymphocytes with fetal extracts was done according to the split method of Pritchard et al. (*48*). In the first step of incubation, 10^6 lymphocytes in 2 ml EMEM were mixed with an aliquot of fetal extract generally containing 300 µg protein. After 70 minutes at 37°C, the lymphocytes were removed by centrifugation (5 min at 1,300×*g*). The supernatants were stored at −20°C until used. Controls were supernatants after lymphocyte incubation in the absence of antigen ("lymphocyte blank").

We assumed that sensitized lymphocytes when in contact in vitro with the corresponding antigens release the MSF.

In the second step, 7×10^6 macrophages were added to each supernatant, and the mixture was incubated for 90 minutes at 23°C. MEMB and its reduction after MSF were then measured by the cytopherometric test. Controls included macrophage samples in EMEM alone ("macrophage blank") and samples with supernatant from lymphocyte blank. At the concentration used, the fetal extracts did not influence the MEMB.

For measurements, two Opton cytopherometers (Zeiss, Oberkochen, FRG) and the Parmoquant 2 cytopherometer (Zeiss, Jena, GDR) were used. The Opton instruments were equipped with television monitors, electronic timing, data processing by computer, and an alphanumeric display. In the Parmoquant 2, which is based on the same principle of cell electrophoresis, the additional elements are a presumptive part of the instrument (*49, 50*). Both types of equipment allow the manual and automatic modes of operation. Data analyses by the computer include estimation of mean mobility, standard deviation, and significance of results in comparison with those of control samples. Irregularities of the measurement, i.e., excessive drifting and exceeding of expected values and tolerance limits, are signalized. An experiment was considered positive when the difference of the electrophoretic mobility between control and test cells was statistically significant according to Student's *t*-test ($P \leq 0.05$).

LMI test.—The assay corresponded with that of Clausen (*51*). Leukocytes at a dose of 9×10^6 were incubated with 60 μg fetal extract in a volume of 60 μl for 30 minutes at 37°C. Then four 10-μl samples of this suspension and corresponding control samples were put into holes of an agarose layer on Partigen plates (Behringwerke, Marburg, FRG). After incubation for 18 hours at 37°C in a humidified CO_2 incubator, the agarose plates were fixed with methanol and Formalin and the migration areas were measured by planimetry. An MI was calculated as follows: MI=average area of migration in the presence of antigen/average area of migration in the absence of antigen. An MI of ≤ 0.7 was arbitrarily considered positive (*46*).

LAI test.—The tube LAI assay was done according to the technique of Holáň et al. (*52*). Leukocytes at a dose of 10^6 in 0.5 ml were placed in a glass tube that had a plane area of 1.5×3.0 cm at the bottom. Test samples also containing the fetal extract (≈250 μg protein) and controls (without extract) were incubated for 2 hours at 37°C. During this time the tubes were held in a horizontal position to allow the cells to adhere to the plane area. Nonadherent cells were finally counted in a hemacytometer. Adherence inhibition was expressed in percent. A value of more than 30% was arbitrarily considered positive (*46*).

Statistical analysis.—Individuals were grouped according to the clinical diagnosis. After the test samples were decoded, the results were listed in the corresponding group. Groups were compared by the chi-square test with Yates' correction ($P \leq 0.01$).

RESULTS

Fetal extracts prepared by the 3-*M* KCl method from the liver, spleen, kidney, lung, and heart of 2- to 7-month-old human fetuses induce effects on peripheral blood leukocytes and lymphocytes of human tumor patients that imply an immunologic sensitization to fetal antigens in this particular group. Supernatants obtained after incubation of the lymphocytes with fetal extract inhibit the electrophoretic mobility of guinea pig macrophages and thus show the presence of MSF, characteristic of a positive MEMB test. Altogether, the positive MEMB test was found in 209 of 284 (73%) cases with various types of tumor (table 1).

Fetal extracts were likewise active when tested by LMI and LAI. Leukocyte migration was significantly inhibited in 48 of 64 (75%) tumor patients investigated, and leukocyte adherence was significantly inhibited in 40 of 50 (80%) tumor patients investigated. The data represent a summary of different series of experiments. In general, the proportion of positive cases ranged from 70 to 80% (table 1).

In most cases leukocytes or lymphocytes from clinically healthy persons did not react with the fetal extracts. Only 15 of 134 (11%) persons were positive by MEMB, 7 of 50 (14%) by LMI, and 10 of 54 (19%) by LAI. The differences between the groups of tumor patients and clinically healthy persons are statistically significant ($P \leq 0.01$) for each test (table 1). Extracts from normal, adult human organs were active in 8 of 28 (29%) tumor patients when tested by MEMB (not in the table). However, 22 of these 28 (79%) patients reacted positively against fetal extract.

Preparations of fetal extract were of different qualitites. Some of them had to be eliminated because of total absence of activity. A discrimination by the MEMB test between tumor and control groups was possible with 9 of 18 extracts prepared.

Fetal extracts suitable for discrimination between tumor and control groups were tested by MEMB against lymphocytes from patients with various types of tumor. Table 2 presents the data obtained from these experiments. Obviously, reactivity to fetal extracts is independent of tumor localization and histology. However, certain groups might differ with respect to the rate of positivity. While 16 of 17 patients with lung cancers were positive, only 12 of 22 cases with melanomas reacted by MEMB. When comparing the data of the control group with those of each one of the tumor groups, we obtained statistically significant differences ($P < 0.01$).

Preliminary results indicate no correlation between tumor stage and MEMB result. However, positive reactions seem to be less frequent in tumor patients over 70 years of age. The same pattern of reactivity was found when 3-*M* KCl extracts from the fetal brain or gut were tested against a panel of lymphocytes from patients with various tumors.

Lymphocyte reactivity to fetal extracts is comparably detectable in mice bearing spontaneous or transplanted tumors (table 3). For example, C3H mice with spontaneous mammary cancers were positive against mouse fetal extract

TABLE 1.—*Reactivity of lymphocytes-leukocytes from tumor patients and controls to human fetal extract: Summary of experiments*

Lymphocytes-leukocytes from:	No. of positive cases/total No. tested[a]		
	MEMB	LMI	LAI
Tumor patients	209/284 (73)	48/64 (75)	40/50 (80)
Clinically healthy persons	15/134 (11)	7/50 (14)	10/54 (19)

[a] Significant difference between tumor patients and clinically healthy persons ($P < 0.01$). *Numbers in parentheses* are percentages of positive cases.

TABLE 2.—*Reactivity of lymphocytes to fetal extracts as measured by MEMB: Studies on groups of patients bearing distinct tumor types*

Clinical diagnosis	No. of positive cases/total No. tested[a]								Percentage
	E-4	N-39	N-60	N-73	N-75	N-90	N-91	Total[b]	
Gastric cancer	11/15	4/4	4/7	3/3	10/16	8/12	5/5	45/62	73
Carcinoma of colon, sigmoid colon, and rectum	11/13	1/1	8/10	NT	5/9	8/12	4/4	37/49	75
Mammary cancer	16/21	9/11	4/7	2/2	3/7	9/9	3/3	46/60	77
Lung cancer	3/3	7/7	2/2	NT	4/4	0/1	NT	16/17	≈94
Gynecologic cancer	3/3	1/1	2/2	4/4	1/1	0/1	NT	11/12	≈92
Sarcoma	5/6	2/3	4/4	NT	1/2	NT	NT	12/15	≈80
Melanoma	10/17	NT	1/4	NT	1/1	NT	NT	12/22	≈54
Other tumors	8/11	4/6	5/5	3/5	5/13	4/6	1/2	30/48	62
Clinically healthy persons	1/16	8/23	0/1	1/5	2/38	2/31	1/20	15/134	11

[a] Columns 2–8 are code numbers of fetal extracts. NT=not tested.

[b] Significant difference between tumor patients and clinically healthy persons ($P<0.01$).

TABLE 3.—*Lymphocyte reactivity as measured by MEMB to mouse and human fetal extracts in mice bearing spontaneous or transplanted tumors*

Lymph node cells from:	No. of positive cases/total No. tested[a]	
	Mouse fetal extract	Human fetal extract[b]
C3H mice bearing spontaneous mammary cancer	27/32	19/21
Normal C3H mice	2/28	1/12
XVII mice bearing transplanted sarcoma UV 15264	18/36	29/54
Normal XVII mice	0/16	2/25
CBA mice bearing transplanted mammary cancer MCa 21224	15/16	NT
Normal CBA mice	2/21	
XVII mice bearing transplanted Graffi virus-induced leukemia Gr 101	12/12	NT
Normal XVII mice	4/34	

[a] Significant difference between tumor and control groups ($P<0.01$).

[b] NT=not tested.

(27 of 32 cases) and human fetal extract (19 of 21 cases). Only 2 of 28 and 1 of 12, respectively, normal C3H mice showed a positive reaction when tested by MEMB. Mice bearing the transplantable tumors sarcoma UV 15264, mammary cancer MCa 21224, or Graffi virus-induced leukemia Gr 101 were likewise reactive. At the time of the tests, the tumors had diameters of 10–20 mm.

Text-figure 1 shows the data obtained with lymphocytes from each mouse. This experiment is already summarized in table 3. In text-figure 1, the results are expressed as average inhibition of macrophage electrophoretic mobility in percent as compared with that of controls. A wide range of test results can be stated. However, a clear distinction is possible between the groups of tumor bearers and controls. Macrophages exposed to extract-containing supernatants from control lymphocytes frequently had increased electrophoretic mobility.

Extracts from normal adult mouse tissue were ineffective. Only 1 of 15 tumor-bearing mice gave a positive MEMB test.

Lymphocytes from human tumor patients were reactive against mouse fetal extract (text-fig. 2). As indicated by the proportion of positive cases, there was no difference between the groups of lymphocytes that were exposed to human or mouse fetal extract. Apparently, human and mouse fetal extracts share common components.

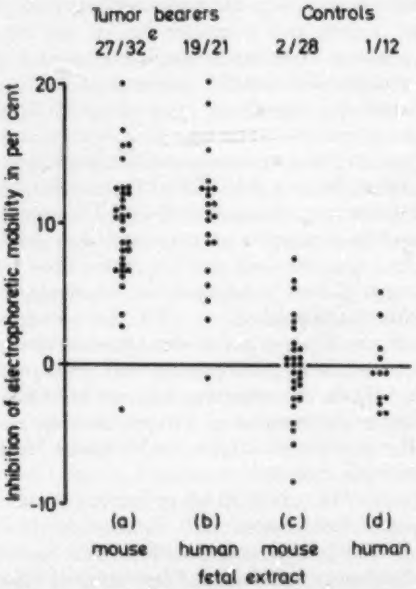

TEXT-FIGURE 1.—Lymphocyte reactivity as measured by MEMB to mouse and human fetal extracts in C3H mice bearing spontaneous mammary cancers and in C3H control mice: a and b represent the tumor-bearing groups, c and d are controls, and e is number of positive cases/total number tested.

According to the MEMB test, this common component seems to be present in fetal extracts of various species. Fetal extracts from the cow, pig, sheep, guinea pig, cat, and chicken may distinguish between groups of tumor-bearing and control mice (table 4). The clear-cut difference between the groups is striking.

Reactivity to fetal extracts is not limited to cancer. Mice bearing benign skin warts induced by DMBA as well as mice from the same DMBA-treated group having no visible skin lesions were reactive against mouse and human fetal extracts (text-fig. 3). Although the number of animals included in this experiment is relatively low, the results allow a clear distinction between the experimental groups and the controls.

Preliminary results of studies on preneoplastic conditions in humans indicate a similar situation. Gynecologic patients with dysplasia of the cervical squamous epithelium were reactive against human fetal extract in 20 of 40 (50%) cases. When patients with carcinomas in situ were tested, 10 of 21 (38%) showed a positive reaction. In the control group, 6 of 26 (23%) women were reactive (our unpublished results).

Pregnancy is also associated with lymphocyte reactivity to fetal extracts. However, the proportion of positive cases is lower in comparison with that of the tumor group. Furthermore, it is striking that the difference between the groups of pregnant women and controls is detectable only during the first and second trimesters of pregnancy. After delivery (within 2-13 wk) all 22 women tested were unreactive (table 5). Mouse and human fetal extracts gave identical results.

Finally, lymphocytes from pregnant multiparous mice were tested by MEMB against mouse fetal extract at two

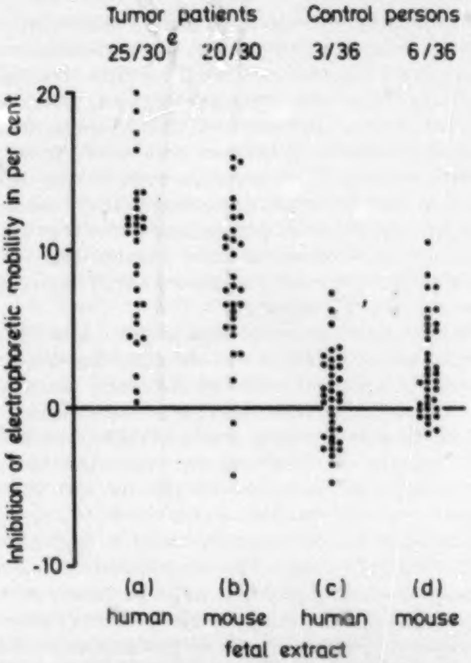

Text-figure 2.—Lymphocyte reactivity as measured by MEMB to human and mouse fetal extracts in tumor patients and controls: a and b include 21 patients with gastrointestinal tumors, 2 with mammary cancer, and 7 with tumors of other sites; c and d are blood donors, and e is number of positive cases/total number tested.

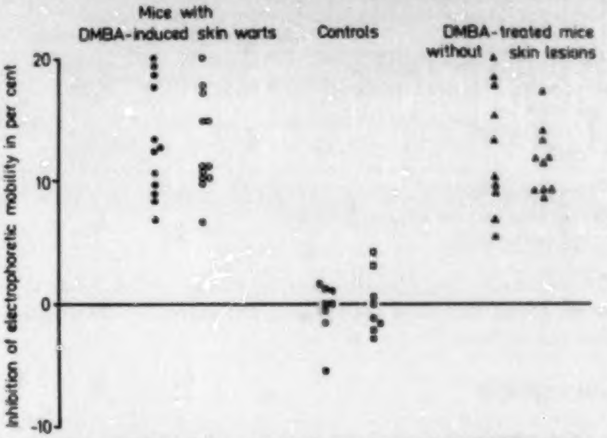

Text-figure 3.—Lymphocyte reactivity as measured by MEMB to mouse and human fetal extracts in XVII mice given a total dose of 120 μg DMBA to the dorsal skin. Each animal received 20 doses of 6 μg DMBA in acetone within 10 wk. DMBA-treated mice without skin lesions were studied at the same time and after the same dose of DMBA as were the animals with skin warts. ●, ■, ▲: tests with mouse fetal extract. ○, □, △: tests with human fetal extract. *Each dot* represents the mean value in percent of the inhibition of electrophoretic mobility of macrophages from one single test sample as compared with the control. The lymphocytes of each animal were doubly tested against the mouse as well as the human fetal extracts.

Table 5.—*Lymphocyte reactivity as measured by MEMB to human and mouse fetal extracts in women during and after pregnancy*

Peripheral blood lymphocytes from:	No. of positive cases/total No. tested	
	Human fetal extract	Mouse fetal extract
Control persons	1/19	3/19
Pregnant women		
First trimester	6/23	5/23
Second trimester	9/19[a]	7/18
Third trimester	2/32	1/32
Women after delivery	0/22	0/22
Tumor patients	19/21[a]	15/21[a]

[a] Significant difference between the test groups (pregnant women or tumor patients) and the control group ($P<0.01$).

Table 4.—*Lymphocyte reactivity as measured by MEMB to fetal extracts of different species of origin in tumor-bearing and control mice*

Lymph node cells from:	No. of positive cases/total No. tested in fetal extract[a] from:[b]					
	Cow	Pig	Sheep	Guinea pig	Cat	Chicken
Tumor-bearing C3H mice or	19/23	13/13	13/13	24/25	13/13	13/13
XVII mice[c]	12/13	13/13	13/13	13/13	12/13	13/13
Normal C3H mice or	1/22	0/7	0/7	1/22	0/7	0/7
XVII mice	0/7	0/7	0/7	0/7	0/7	0/7

[a] Fetuses were derived at the time of the third part of pregnancy period.

[b] Lymphocytes from mice of the same group were simultaneously tested against a second preparation of fetal extract from each one of the species. Significant difference between tumor-bearing mice and control mice ($P<0.01$).

[c] Mice with spontaneous or transplanted mammary cancer and with sarcoma UV 15264 were included in the tests.

TABLE 6.—*Lymphocyte reactivity as measured by MEMB in pregnant multiparous mice to mouse fetal extract*

Lymphocytes from XVII mice	No. of positive cases/total No. tested at following extract dose per test:[a]	
	150 μg protein[b]	300 μg protein
Before the 15th day of gestation	8/20	18/20
Between the 15th and 21st day of gestation	14/24	22/24
1 mo post partum	1/16	7/16
Controls	NT	0/23

[a] Significant difference between test groups (pregnant mice or mice post partum) and the controls ($P<0.01$).

[b] NT=not tested.

different doses. The results are presented in table 6. Most of the pregnant mice were reactive and the reactivity decreased after parturition.

DISCUSSION

That neoplasia, preneoplasia, and pregnancy are associated with lymphocyte sensitization to fetal antigens is the conclusion deduced from the present investigation, provided that MEMB, LMI, and LAI measure cellular immunity. LMI and LAI are widely accepted as cellular immunologic tests. In our hands all three techniques gave corresponding results so that there is no reason to doubt the immunologic background of the MEMB technique too. Moreover, data of Zöller et al. (*15*) support the concept that cancer patients are sensitized against fetal antigens and that sensitization is detectable by indirect cellular immune methods such as LMI. In these studies, similarly, 3-*M* KCl extracts from human fetuses of about the same age of gestation were used.

Information on the antigens involved in the lymphocyte reaction is poor. AFP was excluded as an active component. After its complete removal by immunoadsorption the fetal extract was still active when tested with lymphocytes from tumor patients as has been shown by MEMB. The purified AFP did not react (*14, 53*).

CEA was also inactive by MEMB (our unpublished results) and LMI (*54*). Our experiments on the concentration and isolation of the antigenic material by Sephadex G-200, DEAE-cellulose chromatography, or immunoadsorption techniques have been unsuccessful so far. Thus it is still an open question whether one or several antigenic components are responsible for the cross-reactions obtained when the lymphocytes of patients suffering from tumors of different organ localization were exposed to fetal extract.

Zöller et al. (*15*) assumed that 3-*M* KCl extracts of whole human fetuses contain a complex mixture of specificities that may have represented counterparts to most of the tumor-associated specificities. The same group (*55*) attempted to support this hypothesis experimentally by using organ-related fetal extracts. Although some of their data are in favor of this hypothesis, i.e., extracts from fetal gut preferentially reacted with leukocytes from patients who had colorectal cancer, there was still extensive cross-reactivity among the organ-related fetal antigens. Our extract from fetal gut was active in cases with different types of tumor (our unpublished result).

In previous studies by using LMI we have also shown such organ-related or tumor type-specific antigens (*56*). There was extensive immunologic cross-reactivity among mammary cancers when the leukocytes of the patients were exposed to mammary cancer extract. Generally, extracts from other tumors did not react. The same tumor type-specific pattern or reactivity was obtained by MEMB (*57*). This finding does not exclude the existence of a specific cross-reacting fetal component common to all tumors in addition to the type-specific antigen. It has been shown that chemically induced rat tumors possess individually distinct tumor antigens as well as fetal cross-reacting antigens (*58*). That a common fetal antigen that immunizes against tumors of different origin does exist has been shown by Coggin and Ambrose (*22*). Whether MEMB, LMI, or LAI measures such a cross-reacting antigen of the rejection type is not known.

Surprisingly, fetal extracts from various species including the cow, pig, sheep, cat, guinea pig, rat, and chicken share a common fetal component. A complete cross-combination of experiments that was arranged between human and mouse tumor systems demonstrated that lymphocytes from tumor-bearing individuals reacted both with human and mouse fetal extracts. The presence even in the chicken indicates that the component is phylogenetically conserved. A similar pattern of species distribution is also true for AFP (*59*). It would be of interest to know whether fetal extracts from the species mentioned also induce a rejection response against transplanted tumors.

Lymphocyte sensitization to fetal extracts is not limited to cancer. Clear-cut evidence was obtained that mice bearing benign skin warts after DMBA treatment are reactive. Their counterparts, i.e., mice showing no visible skin lesions after treatment with the same dose of DMBA, are likewise reactive. However, it is well known that there are early histologic changes in the mouse skin painted with chemical carcinogen even in the absence of skin warts (*60*). Lymphocyte sensitization is also frequently seen in patients with dysplasia of the cervix uteri. This observation raises a number of questions which, however, cannot be answered as yet. In the first place it is important to know whether reactivity to fetal extracts is characteristic of preneoplastic changes after certain carcinogens or is associated with cell proliferation in general. We have tested patients with inflammatory diseases and found that these patients as compared with a group of clinically healthy persons had a higher proportion of reactivity (our unpublished results). However, results of these experiments are not yet decisive. Furthermore, the time of appearance of this reactivity after carcinogen treatment would be interesting to know.

In mice transplanted with tumor cells, reactivity is detectable about 5–7 days after grafting (*14*). Apparently, lymphocyte sensitization occurs rapidly.

Another question is whether reactivity may develop after oncogenic or nononcogenic viruses. Several conditions such as partial hepatectomy and inflammatory lesions in experimental animals would help to resolve the question of whether differentiation and/or cell proliferation in certain organs are causally related to lymphocyte sensitization.

Another problem is lymphocyte reactivity after surgery. If reactivity is no longer detectable in women after delivery, does the tumor patient who has been successfully treated also show a loss of reactivity? Studies on patients with mammary cancers are in progress to answer this question.

That lymphocyte sensitization to fetal antigens develops under normal conditions is shown in pregnant women. However, the proportion of reactive persons is lower as compared with the proportion in tumor patients. Sensitization seems to be independent of the number of pregnancies. There were positive cases among women with first pregnancies as well as negative ones among multipara. The reason for this is not yet known. Quantitative rather than qualitative aspects have to be considered. The conclusion can be drawn from mouse experiments that the reactive cells not only disappear from the blood circulation but also are absent from the lymph nodes. Cells from the nodes of a high proportion of mice in the postnatal period did not react with fetal extracts. If memory cells are present, they are obviously inactive with respect to lymphokine release.

It has been shown recently by LMI (*61*) that persons in close contact with lung cancer patients or lung cancer materials are sensitized to lung tumor-associated antigen. We have repeatedly tested persons of our laboratory staff who are in permanent contact with the fetal materials and did not find any lymphocyte sensitization.

Detection of lymphocyte sensitization to fetal extracts as a tumor-diagnostic test appears to be problematic for two reasons: 1) The accuracy of the test is not high enough and, therefore, it allows only a grouping of individuals, and 2) neoplasia and preneoplasia cannot be distinguished on the basis of lymphocyte reactivity. Stability of fetal antigen expression on fetal cells was found to be an important factor (*3, 31*). In hamsters and rats immunogenicity of fetal tissue was limited to certain phases during embryogenesis. In our studies fetal extracts were prepared from organs of human fetuses at an age between the 4th and 7th months of pregnancy. Extracts from 2- to 3-month whole fetuses were likewise active (our unpublished results). However, it cannot be excluded that the active components in the materials from fetuses and embryos are different.

At present a classification of the fetal antigen(s) in the extract is almost impossible. Besides AFP and CEA, the human encephalitogenic protein (or myelin basic protein) (*62*) can also be excluded as a reactive component. The isolation procedure for the encephalitogenic protein differs considerably from the 3-*M* KCl method. Furthermore, comparative studies have shown that the number of "false-positives" in the control group is higher if the encephalitogenic protein is used as antigen in place of the fetal extract (*14*).

A similar cross-reactivity of fetal and tumor antigens has been reported by Salinas et al. (*13*). Cross-reactivity was demonstrated by antibodies that appear in sera from patients with tumors of various histologies. Moreover, antibodies of human and mouse origins had the same specificity. There seems to be a close correlation between these findings and our studies on lymphocyte reactivity. Antigen isolation is necessary for direct comparison of the humoral and cellular immune methods.

REFERENCES

(*1*) Alexander P. Foetal "antigens" in cancer. Nature 1972; 235:137-140.

(*2*) Laurence DJ, Neville AM. Foetal antigens and their role in the diagnosis and clinical management of human neoplasms: A review. Br J Cancer 1972; 26:335-355.

(*3*) Coggin JH Jr, Anderson NG. Cancer, differentiation and embryonic antigens: Some central problems. Adv Cancer Res 19[illegible]4; 19:105-165.

(*4*) Rees RC, Price MR, Baldwin RW. Oncodevelopmental antigen expression in chemical carcinogenesis. Methods Cancer Res 1979; 17:94-133.

(*5*) Abelev GI, Perova SD, Khramkova NI, Postnikova ZA, Irlin IS. Production of embryonal α-globulin by transplantable mouse hepatomas. Transplantation 1963; 1:174-180.

(*6*) Abelev GI, Assecritowa NA, Kraevsky NA, Perova SD, Perevodschikova NI. Embryonal serum α-globulin in cancer patients: Diagnostic value. Int J Cancer 1967; 2:551-558.

(*7*) Gold P, Freedman SO. Specific carcinoembryonic antigen of the human digestive system. J Exp Med 1965; 122:467-481.

(*8*) Hellström I, Hellström KE, Shepard TH. Cell-mediated immunity against antigens common to human colonic carcinomas and fetal gut epithelium. Int J Cancer 1970; 6:346-351.

(*9*) Della Porta G, Canevari S, Fossati G. Immune response to tumour and embryo cells in patients with mammary carcinoma. Br J Cancer 1973; 28 (suppl I):103-107.

(*10*) Steele G, Sjögren HO. Embryonic antigens associated with chemically induced colon carcinomas in rats. Int J Cancer 1974; 14:435-444.

(*11*) Irie RF, Irie K, Morton DL. A membrane antigen common to human cancer and fetal tissues. Cancer Res 1976; 36:3510-3517.

(*12*) Hellström I, Hellström KE, Shantz G. Demonstration of tumor-associated immunity with a leukocyte adherence inhibition (LAI) assay. Int J Cancer 1976; 18:354-361.

(*13*) Salinas FA, Sheikh KM, Chandor SB. Serological reactivity in cancer patients to human and mouse fetal liver cells. Cancer Res 1978; 38:401-407.

(*14*) Pasternak G, von Broen B, Schlott B, et al. Lymphocyte reactivity in animal and human tumor systems to fetal antigens as detected by MEM, LAI and LMI techniques. In: Preece AW, Sabolovic D, eds. Cell electrophoresis: Clinical application and methodology. INSERM symposium No. 11. Amsterdam: Elsevier/North-Holland, 1979:225-234.

(*15*) Zöller M, Matzku S, Schulz U, Price MR. Sensitization of leukocytes of cancer patients against fetal antigens: Leukocyte migration studies. JNCI 1979; 63:285-293.

(*16*) Häkkinen I, Järvi O, Gironos J. Sulphoglycoprotein antigens in the human alimentary canal and gastric cancer. An immunohistological study. Int J Cancer 1968; 3:572-581.

(*17*) Coggin JH Jr, Ambrose KR, Bellomy BB, Anderson NG. Tumor immunity in hamsters immunized with fetal tissues. J Immunol 1971; 107:526-533.

(*18*) Baldwin RW, Glaves D, Vose BM. Embryonic antigen expression in chemically induced rat hepatomas and sarcomas. Int J Cancer 1972; 10:233-243.

(*19*) Avis P, Lewis MG. *Brief communication*: Tumor-associated fetal antigens in human tumors. J Natl Cancer Inst 1973; 51:1063-1066.

(*20*) Evans DL, Parker DV, Frank MK. Biochemical and physical characterizations of tumor-associated fetal antigens. Cancer Res 1979; 39:2006-2015.

(*21*) Coggin JH Jr, Ambrose KR, Anderson NG. Fetal antigen capable of inducing transplantation immunity against SV 40 hamster tumor cells. J Immunol 1970; 105:524-526.

(*22*) Coggin JH Jr, Ambrose KR. Embryonic and fetal determinants on virally and chemically induced tumors. Methods Cancer Res 1979; 18:371-389.

(*23*) Bendich A, Borenfreund E, Stonehill EH. Protection of adult mice against tumor challenge by immunization with irradiated adult skin or embryo cells. J Immunol 1973; 111:284-285.

(*24*) Le Mevel BP, Wells SA. Foetal antigens cross-reactive with tumour-specific transplantation antigens. Nature [New Biol] 1973;

244:183–184.

(25) Hedlund G, Sjögren HO. Induction of transplantation immunity to rat colon carcinoma isograft by implantation of intact fetal colon tissue. Int J Cancer 1980; 26:71–73.

(26) Brawn RJ. Possible association of embryonal antigen(s) with several primary 3-methylcholanthrene-induced murine sarcomas. Int J Cancer 1970; 6:245–249.

(27) Menard S, Colnaghi MI, Della Porta G. In vitro demonstration of tumor-specific common antigens and embryonal antigens in murine fibrosarcomas induced by 7,12-dimethylbenz(*a*)anthracene. Cancer Res 1973; 33:478–481.

(28) Hellström I, Hellström KE. Cytotoxic effect of lymphocytes from pregnant mice on cultivated tumor cells. I. Specificity, nature of effector cells and blocking by serum. Int J Cancer 1975; 15:1–16.

(29) Shah LP, Rees RC, Baldwin RW. Tumour rejection in rats sensitized to embryonic tissue. I. Rejection of tumour cells implanted s.c. and detection of cytotoxic lymphoid cells. Br J Cancer 1976; 33:577–583.

(30) Coggin JH Jr, Adkinson L, Anderson NG. Fetal antigens shared as transplantation rejection antigens on chemically induced mouse and hamster sarcomas. Cancer Res 1980; 40:1568–1573.

(31) Baldwin RW, Embleton HJ, Price MR, Vose BM. Embryonic antigen expression on experimental rat tumors. Transplant Rev 1974; 20:77–99.

(32) Girardi AJ, Reppucci P, Dierlam P, Rutala W, Coggin JH Jr. Prevention of simian virus 40 tumors by hamster fetal tissue: Influence of parity status of donor females on immunogenicity of fetal tissue and on immune cell cytotoxicity. Proc Natl Acad Sci USA 1973; 70:183–186.

(33) Baldwin RW, Vose BM. The expression of a phase-specific foetal antigen on rat embryo cells. Transplantation 1974; 18:525–530.

(34) Rocklin RE, Zuckerman JE, Alpert E, David JR. Effect of multiparity on human maternal hypersensitivity to foetal antigen. Nature 1973; 241:130–131.

(35) Jones PC, Sidell N, Irie RF. Embryonic antigens and tumor cell cytolysis. Cancer Immunol Immunother 1980; 8:211–214.

(36) Hersey P, Stone DE, Morgan G, McCarthy WM, Milton GW. Previous pregnancy as a protective factor against death from melanoma. Lancet 1977; 1:451–452.

(37) Jones PC, Sze LL, Liu PY, Morton DL, Irie RF. Prolonged survival for melanoma patients with elevated IgM antibody to oncofetal antigen. JNCI 1981; 66:249–254.

(38) Beer AE, Billingham RE. Immunregulatory aspects of pregnancy. Fed Proc 1978; 37:2374–2378.

(39) Gorczynski RM. Response of tumour-related and normal lymphocytes to antigens on fibroblasts from embryos of varying age. Br J Cancer 1978; 37:786–796.

(40) Weppner WA, Adkinson LR, Coggin JH Jr. Suppression of hamster lymphocyte reactivity to simian virus 40 tumor surface antigens by spleen cells from pregnant hamsters. Cell Immunol 1980; 54:445–454.

(41) Hoffmann W, Werner W, Steiner R, Kaufmann R. Cell electrophoresis for diagnostic purposes. I. Diagnostic value of the electrophoretic mobility test (EMT) for the detection of gynecological malignancies. Br J Cancer 1981; 43:588–597.

(42) Hoffmann W, Kaufmann R, Steiner R, Werner W. Cell electrophoresis for diagnostic purposes. II. Critical evaluation of conventional cytopherometry. Br J Cancer 1981; 43:598–609.

(43) Meltzer MS, Leonard EJ, Rapp HJ, Borsos T. Tumor-specific antigen solubilized by hypertonic potassium chloride. J Natl Cancer Inst 1971; 47:703–709.

(44) Pellis NR, Shulan DJ, Kahan BD. Specific tumor immunity induced with soluble materials. Purification of antigens inducing tumor resistance. Biochem Biophys Res Commun 1976; 71:1251–1258.

(45) Lowry OH, Rosebrough NJ, Farr AL, Randall RJ. Protein measurement with the Folin phenol reagent. J Biol Chem 1951; 193:265–275.

(46) Albrecht S, Thanh Thuy L, Pasternak G, et al. Leukozytenmigrationsinhibitions-(LMI-)-und Leukozytenadhärenzinhibitions-(LAI-)-Tests bei Patienten mit Tumoren unter Verwendung von Fetalantigenpräparation. Acta Biol Med Germ 1978; 37:1747–1757.

(47) Bøyum A. Isolation of mononuclear cells and granulocytes from human blood. Isolation of mononuclear cells by one centrifugation, and of granulocytes by combining centrifugation and sedimentation at 1 *g*. Scand J Clin Lab Invest 1968; 21 (suppl 97):77–89.

(48) Pritchard JA, Moore JL, Sutherland WH, Joslin CA. Evaluation and development of the macrophage electrophoretic mobility (MEM) test for malignant disease. Br J Cancer 1973; 27 (suppl I):229–236.

(49) Pohl HJ, Schütt W. Increased reliability and productivity of the EM test by objectivated cell electrophoresis. Automated measurements and data processing. In: Proceedings of the symposium on modern trends in cell electrophoresis with particular regard to immunological tumor diagnostics, Dresden, March 12–16, 1978. Dresden: Carus, 1978:92–104.

(50) Unger R, Schoeppe G, Schütt W, Jenssen HL. Automatic measuring microscope Parmoquant 2—a modern concept for cell electrophoresis. In: Preece AW, Sabolovic D, eds. Cell electrophoresis: Clinical application and methodology. INSERM symposium No. 11. Amsterdam: Elsevier/North-Holland, 1979:399–407.

(51) Clausen JE. Migration inhibitory effect of cell-free supernatants from tuberculin-stimulated cultures of human mononuclear leukocytes demonstrated by two-step MIF agarose assay. J Immunol 1971; 107:526–533.

(52) Holáň V, Hasek M, Bubenik J, Chutna J. Antigen-mediated macrophage adherence inhibition. Cell Immunol 1974; 13:107–116.

(53) Pasternak G, Schlott B, Albrecht S, Gryschek G, Reinhöfer J, von Broen B. Cellular immune reactions to fetal extracts in patients with malignant tumours. In: Biology of the cancer cell. Proceedings of the fifth meeting of the European Association for Cancer Research. Amsterdam: Kugler 1980:173–178.

(54) Matzku S, Zöller M, Schulz U, et al. Lack of correlation between carcinoembryonic antigen content of tumor extracts and leukocyte migration reactivity of tumor patients. JNCI 1980; 64:[illegible]1348.

(55) Matzku S, Zöller M, Iking RU, Price MR. Organ-related and malignancy-associated reactivity of cancer patients' leukocytes: A leukocyte migration study with tumour and foetal extracts. Br J Cancer 1980; 39:516–523.

(56) Rieche K, Arndt A, Pasternak G. Cellular immunity in mammary cancer patients as measured by the leukocyte migration test (LMT). A follow-up study. Int J Cancer 1976; 17:212–218.

(57) Müller M, Irmscher J, Fischer R, Heidl G, Grossmann H. Immunological tumour-profile: Organ-specific carcinoma diagnosis in patients employing the macrophage electrophoretic mobility test. Cancer Lett 1977; 2:139–145.

(58) Baldwin RW, Price MR. Immunobiology of rat neoplasia. Ann NY Acad Sci 1976; 276:3–10.

(59) Laurence DJ, Munro Neville A. Foetal antigens and their role in the diagnosis and clinical management of human neoplasms: A review. Br J Cancer 1972; 26:335–355.

(60) Graffi A, Bielka H. Probleme der experimentellen Krebsforschung. Leipzig: Geest and Portig, 1959.

(61) Suslov IM, McCoy JL, Cannon GB, Herberman RB. High incidence of migration inhibition reactivity to lung tumor-associated antigen by normal donors in close contact with lung cancer patients or materials. JNCI 1980; 65:709–713.

(62) Field EJ, Caspary EA. Lymphocyte sensitization: An in vitro test for cancer? Lancet 1970; 2:1337–1341.

Cancers of the Gallbladder and Biliary Tract in Alaskan Natives: 1970–79[1,2]

Leslie P. Boss, *M.P.H., Ph.D.*,[3] **Anne P. Lanier**, *M.D., M.P.H.*,[3,4] **Peter H. Dohan**, *M.D.*,[3] *and* **Thomas R. Bender**, *M.D., M.P.H.*[3]

ABSTRACT—The records of Alaskan Native patients with gallbladder and extrahepatic bile duct cancers diagnosed during 1970–79 were reviewed. Of 34 cases identified, the primary cancer was in the gallbladder in 29, resulting in age-adjusted incidence rates for gallbladder cancer of 4.4 for males and 17.6 for females. On the basis of calculations applying cancer incidence rates for U.S. whites to the Alaska Native population, a greater than expected number of both Eskimo and Indian patients were diagnosed. A 5-year review of cholecystectomies indicated that nonmalignant gallbladder disease was also elevated in both Indians and Eskimos.—JNCI 1982; 69:1005–1007.

The incidence rates for GBC vary worldwide (*1*). The variation of GBC rates among ethnic groups in the United States is almost as great as the variation reported worldwide. In the United States, the highest rates are reported for American Indians, followed by Spanish Americans (New Mexico), Mexican Americans (Los Angeles, Calif.), whites, and blacks (*2–5*). Among most U.S. ethnic groups, the rates for GBC are higher among females than males. The female-to-male ratio, roughly twofold in both whites and blacks (*2, 6*), is even higher in American Indians and Spanish Americans (*3–5*).

The etiology of GBC is not known; however, cholelithiasis and cholecystitis are thought to be important factors in its development. Gallstones are found in approximately 80% of patients with GBC, and populations at high risk for gallbladder disease also have high rates of GBC (*2, 7–10*).

The etiology of BDC may differ from that of GBC, since the sex ratio is reversed (males predominate) and fewer patients have gallstones (*2, 8*). Studies of the epidemiology of GBC and BDC have been complicated by the fact that these cancers as well as cancer of the ampulla of Vater have been grouped under a single three-digit code (156) in the ICDA (*11*).

A 5-year survey revealed high incidence rates for cancers of the gallbladder and other biliary passages among the major groups of Alaskan Natives: Eskimo-Aleuts and Indians (*12, 13*). Although American Indians are known to be at increased risk for GBC, Eskimos living outside Alaska have not been reported to be at increased risk. This paper describes the results of a review of records of Alaskan Natives with GBC and extrahepatic BDC diagnosed in a recent 10-year period, 1970–79. Because of the putative association of GBC with gallstones, these results are compared with those from a separate review of patients from this population who had undergone cholecystectomy.

METHODS

Study population.—The Alaskan Native population was estimated to be 65,000 in 1977. All 3 subgroups, Eskimo, Aleut, and Indian, are thought to have originated in Asia (*14*). On the basis of linguistic studies, two types of Eskimos are recognized: Yupik-speaking Eskimos, who live in southwestern Alaska, and Inupiat-speaking Eskimos, who live in northwestern Alaska and across the Canadian Arctic as far east as Greenland (*15*). Linguistic studies also indicate that Aleuts and Eskimos are related and that Aleuts are most like Yupik-speaking Eskimos. Most Aleuts live on the Alaskan peninsula and the Aleutian Island chain. The Eskimos and Aleuts represent 69% of the total Alaskan Native population. Seventeen percent of Alaskan Natives are Tlingit, Haida, and Tsimshian Indians of southeastern Alaska. These Indians are members of the Northwest Coast Indian tribes also found in Canada and the northwestern United States. Athapaskan Indians, who live mainly in the interior of Alaska, make up 14% of the total Alaskan Native population and appear to be linguistically related to the Navajo and Apache Indians of the southwestern United States (*15*).

Total Native population figures used were the IHS projections for fiscal year 1977. We calculated estimates of population by ethnic group by imposing the age, sex, and ethnic distributions determined by Kraus and Buffler (*16*) on the IHS projected population figures.

Identification of cases.—All Alaskan Native patients with a diagnosis of GBC or cancer of related structures (ICDA No. 156) during the 10-year period 1970–79 were identified from death certificates and records of discharge diagnoses, surgical pathology files, and the tumor registries of the referral hospital of the Alaska Area Native Health Service and other hospitals in the state. In addition, a separate review of cholecystectomies performed on Alaskan Natives during 1975–79 provided data on gallbladder disease.

Verification of cases.—To verify the diagnosis in each cancer patient, we reviewed pathology slides, pathology and autopsy reports, and clinical data. The classifications of cancer were similar to those of the ICDA: GBC, cancer in the extrahepatic bile ducts, cancer of the ampulla of Vater, and cancer of the biliary tract, unspecified. Patients assigned to the GBC category were those with early disease confined to

---

ABBREVIATIONS USED: BDC=bile duct cancer; GBC=gallbladder cancer; ICDA=International Classification of Diseases, adapted; IHS=Indian Health Service.

---

[1] Received December 2, 1981; accepted May 27, 1982.

[2] Supported in part by Public Health Service Interagency agreement Y01CP-00500 between the Centers for Disease Control and the Division of Cancer Cause and Prevention, National Cancer Institute.

[3] Centers for Disease Control, Center for Infectious Disease, Arctic Investigations Activity, 225 Eagle St., Anchorage, Alaska 99501-2692.

[4] *Address reprint requests to* Dr. Lanier.

the gallbladder and those with more extensive disease in which the center of the tumor mass appeared to be the gallbladder and in which there was direct liver invasion, minimal ductal dilation, and late onset of clinical jaundice. Patients were assigned to the extrahepatic BDC category if the cancer obviously arose in the hepatic, cystic, or common bile ducts. Cancer in the ampulla of Vater was categorized separately. Patients included in the category of cancer of the biliary tract, unspecified, were those with such extensive disease or atypical histology as to render precise classification impossible.

Calculation of rates.—Cancer incidence rates were standardized to the U.S. population of 1970. The number of observed patients with cancer was compared as a ratio to the number expected. We calculated the number of expected cases by using the Third National Cancer Survey incidence rates for U.S. whites and applying them to estimates of the Alaskan Native population derived from the 1970 U.S. census. The statistical significance of the deviation of the ratios from one was tested by the method of Bailar and Ederer (*17*).

RESULTS

Thirty-four patients with biliary tract cancer were identified. For 31 of these patients, both slides and medical records were available for review. Original pathology and surgery reports were available on the remaining 3. All but 5 of the 34 patients had GBC; 1 male had BDC, another male had cancer of the ampulla of Vater, and 1 male and 2 females had cancer of the biliary tract, unspecified.

Among the 29 patients with GBC, 23 were female and 6 were male, for a female-to-male ratio of 3.8:1 (table 1). Patients ranged in age from 53 to 82 years, with a mean age of 71 years. Half the female patients were diagnosed under the age of 70 years, whereas all male patients were over 70 years of age at diagnosis.

There was no obvious geographic clustering of GBC patients by birthplace or residence at diagnosis. Two members of one family, a sister and a brother, diagnosed in 1977 and 1979 at ages 77 and 72, respectively, were among the 29 patients. The rest of the patients were not known to be related.

Annual crude and adjusted rates per 100,000 for GBC were, respectively, 1.8 and 4.4 for males and 7.1 and 17.6 for females. Corresponding rates for total GBC and bile duct cancer based on all 34 cases were 2.7 and 6.2 in males and 7.7 and 18.6 in females. When standardized rates for GBC were compared with those of other U.S. ethnic groups, Alaskan Natives were found to have high rates, exceeded only by the incidence in American Indians living in New Mexico (table 2).

TABLE 1.—*Number of cases and annual age- and sex-specific incidence rates of GBC per 100,000, Alaskan Natives, 1970–79*

Age at diagnosis, yr	Males		Females	
	No.	Rate	No.	Rate
50–59	0	—	3	13.7
60–69	0	—	8	63.6
≥70	6	68.0	12	171.9
Total	6	1.8	23	7.1

TABLE 2.—*Annual incidence rates of GBC per 100,000 population*[a]

Racial and ethnic groups	Male	Female
United States (1969–71)		
All races	1.1	2.1
White	1.1	2.2
Black	0.7	1.6
New Mexico (1969–75)		
Spanish American	2.0	10.5
American Indian	5.1	21.1
Alaskan Natives (1970–79)	4.4	17.6

[a] Age adjusted to the 1970 U.S. population.

TABLE 3.—*Number of patients observed (O) with GBC and ratios of observed-to-expected cases (O/E) by sex and ethnic group, Alaskan Natives, 1970–79*

Ethnic group	Males		Females	
	O	O/E	O	O/E
Indian				
Athapaskan	0	—	3	7.5[a]
Southeastern	3	10.0[b]	5	10.0[b]
Eskimo				
Inupiat	2	6.7	6	10.0[b]
Yupik-Aleut	1	1.2	9	6.4[b]
Total	6	3.5[a]	23	8.2[b]

[a] $P < 0.05$.
[b] $P < 0.01$.

Table 3 shows the ethnic distribution of the GBC patients and the ratio of observed-to-expected cases. Twenty-two of the GBC patients were full Native, 5 were probably full Native, and only 2 were known to be of mixed ancestry. Although the number of cases are small, the ratios indicate that females of all 4 ethnic groups (Inupiat- and Yupik-speaking Eskimo, as well as Athapaskan and southeastern Alaskan Indian) are at significantly increased risk. The ratio was significantly increased in males only for Alaska's southeastern Indians, although Inupiat Eskimo males also had a high ratio. Inclusion of the 3 patients categorized as having unspecified cancer of the biliary tract does not change the conclusions regarding ethnic distribution.

The type of cancer in all 29 patients with GBC was adenocarcinoma, classified as well differentiated in 17 patients, poorly differentiated in 11 patients, and adenosquamous in 1 patient. Gallstones were present in 23 patients (79%), and all but 3 of these patients had stones of cholesterol or mixed composition.

During the 5-year period 1975–79, 607 cholecystectomies or cholecystostomies were performed on Alaskan Natives. Sixteen patients were diagnosed with GBC during the same period: 13 during cholecystectomy for symptoms of cholelithiasis, 2 during laparotomy for suspected cancer, and 1 at autopsy. Therefore, GBC was diagnosed in 13 of 607 patients (2.1%) who had gallbladder surgery. In women who had gallbladder surgery, 14% of those 60 years of age or older and 26% of those 70 years or older were found to have GBC.

Only 3 of the 29 patients were alive as of January 1981: 2 patients diagnosed in 1979 and 1 patient diagnosed in 1970. The median postsurgical survival for the other 26 patients was 3 months.

DISCUSSION

GBC is the fifth most frequently diagnosed invasive cancer among Alaskan Native females and accounts for 4% of all cancers in Native females and 1.2% of all cancers in Native males. The female-to-male ratio (3.8:1) of GBC in this population is higher than the 2:1 ratio reported among U.S. whites and blacks but similar to that reported for American Indians of the southwestern United States (*3, 6, 18*).

Incidence rates of GBC based on this report indicate that GBC develops in Alaskan Native males and females nearly as often as in Indians in New Mexico. Because of the reported high rates of GBC among American Indians, elevated rates among Alaskan Indians were expected. Indeed, rates were significantly high in females both among Athapaskans, who are thought to be related to the Navajo and Apache of the southwestern United States, and among southeastern Alaskan Indian females, members of the Northwest Coast Indian tribes. Among males, rates were high for southeastern Alaskan Indians.

Of some surprise, however, was the finding of elevated rates of GBC among Alaskan Eskimos. Rates were elevated in both Inupiat- and Yupik-speaking female Eskimo subgroups. Among males, rates were elevated, although not significantly, in Inupiat-speaking Eskimos.

High rates of GBC have not been reported among Eskimos living outside Alaska. In a report of cancer in 180 Canadian Eskimos, 7 patients with biliary tract cancer were identified; 5 of these had cancer originating in the ampulla of Vater, and only 2 had cancer that had localized in the gallbladder (*19*). Among Greenland Eskimos, 5.5% of all types of cancer arose in the liver or biliary tract, in contrast to 2% in Danish cancer patients (*20*). However, no data on GBC alone have been reported.

Alaskan Indians and Eskimos differ genetically, and there has been little intermarriage. These groups also differ in diet, life-style, and area of residence. Both Alaskan Indians and Eskimos differ in many ways from other Native American groups.

Gallbladder disease (cholelithiasis and cholecystitis) appears to be an important risk factor for the development of GBC. Our investigation of gallbladder surgery among Alaskan Natives for 1975–79 suggested that gallbladder disease was increased in both Eskimo and Indian females when compared with the incidence in the U.S. white population. Rates of gallbladder disease for Native males were not higher than those for U.S. white males, although within Alaska rates for Indian males were higher than those for Eskimo males (*21*).

Therefore, among females in this population, rates for both gallbladder disease and GBC appear to be increased, which supports the reported association of the two. Among males, the numbers of cancers are too small to be conclusive, but southeastern Alaskan Indian males had the highest rates of both gallbladder disease and GBC.

This review provides additional data to support the earlier report of elevated rates of GBC among Eskimo–Aleuts. Although rates of gallbladder disease are also high, the association of gallbladder disease and GBC among Alaskan ethnic groups deserves further study. In view of the marked differences in life-style of Alaskan Natives and other ethnic groups, additional studies should be done to identify common risk factors for gallbladder disease and GBC among the various populations with increased rates.

REFERENCES

(*1*) Waterhouse J, Muir C, Correa P, Powell J, eds. Cancer incidence in five continents. IARC Sci Publ 1976; 3:470–473.

(*2*) Fraumeni JF Jr. Cancers of the pancreas and biliary tract: Epidemiological considerations. Cancer Res 1975; 35:3437–3446.

(*3*) Morris DL, Buechley RW, Key CR, Morgan MV. Gallbladder disease and gallbladder cancer among American Indians in tricultural New Mexico. Cancer 1978; 42:242–247.

(*4*) Devor EJ, Buechley RW. Gallbladder cancer in Hispanic New Mexicans. I. General Population, 1957–1977. Cancer 1980; 45:1705–1712.

(*5*) Menck HR, Mack TM. Incidence of biliary tract cancer in Los Angeles. Natl Cancer Inst Monogr 1982; 62. In press.

(*6*) Cutler SJ, Young JL Jr., eds. Third National Cancer Survey: Incidence data. Natl Cancer Inst Monogr 1975; 41:22.

(*7*) Piehler JM, Crichlow RW. Primary carcinoma of the gallbladder. Surg Gynecol Obstet 1978; 147:929–942.

(*8*) Hart J, Shani M, Modan B. Epidemiological aspects of gallbladder and biliary tract neoplasm. Am J Public Health 1972; 62:36–39.

(*9*) Maram ES, Ludwig J, Kurland L, Brian D. Carcinoma of the gallbladder and extrahepatic biliary ducts in Rochester, Minnesota, 1935–1971. Am J Epidemiol 1979; 109:152–157.

(*10*) Diehl AK. Guest editorial: Epidemiology of gallbladder cancer: A synthesis of recent data. JNCI 1980; 65:1209–1214.

(*11*) National Center for Health Statistics. International Classification of Diseases, adapted for use in the United States. Eighth revision. Washingon, D.C.: U.S. Govt Print Off, 1967:107 (PHS publication No. 1693).

(*12*) Lanier AP, Bender TR, Blot WJ, Fraumeni JF Jr, Hurlburt WB. Cancer incidence in Alaska Natives. Int J Cancer 1976; 18:409–412.

(*13*) Lanier AP, Blot WJ, Bender TR, Fraumeni JF Jr. Cancer in Alaskan Indians, Eskimos, and Aleuts. JNCI 1980; 65:1157–1159.

(*14*) Bandi HG. Eskimo prehistory. College, Alaska: Univ Alaska Press, 1972.

(*15*) Krauss ME. Alaska Native languages: Past, present, and future. In: Alaska Native Language Center research papers. Vol. 4. Fairbanks, Alaska: Alaska Native Language Center, 1980:8.

(*16*) Kraus RF, Buffler PA. Sociocultural stress and the American Native in Alaska: An analysis of changing patterns of psychiatric illness and alcohol abuse among Alaska Natives. Cult Med Psychiatry 1979; 3:111–151.

(*17*) Bailar JC III, Ederer F. Significance factors for the ratio of a Poisson variable to its expectation. Biometrics 1964; 20:639–642.

(*18*) Black W, Key C, Carmany T, Herman D. Carcinoma of the gallbladder in a population of Southwestern American Indians. Cancer 1977; 39:1267–1279.

(*19*) Schaefer O, Hildes JA, Medd LM, Cameron DG. The changing pattern of neoplastic disease in Canadian Eskimos. Can Med Assoc J 1975; 112: 1399–1404.

(*20*) Hart Hansen JP, Nielsen NH, Mikkelsen F. Malignant diseases in Greenland. Nordic Council Arctic Medical Research Report 1977; 18:76–81.

(*21*) Boss LP. Gallbladder disease in the Alaskan Native population. Ph.D. dissertation. Honolulu: Univ Hawaii, 1981.

blank page

Collagen Polymorphism in Extracellular Matrix of Human Osteosarcoma[1,2,3]

Frederic D. Shapiro[4] *and* **David R. Eyre**[4,5,6]

ABSTRACT—The collagenous matrix of human osteosarcoma was characterized biochemically and ultrastructurally. The highly cellular regions of the tumors contained many osteoblast-like cells filled with dilated rough endoplasmic reticulum. The extracellular matrix displayed a random weave of banded collagen fibrils (30–90 nm in diameter) interspersed with thinner, unbanded fibrils (15 nm in diameter). Tumors from 9 patients were analyzed for collagen composition. All gave a similar collagen profile. Three main molecular species of collagen were abundant: type I, type III, and type V, which occurred in the approximate proportions of 65:25:10. A high ratio of $\alpha1$(I) to $\alpha2$(I) chains suggested that one-third of the type I collagen was present as a type I trimer molecule. In contrast, normal bone matrix consisted almost exclusively of type I collagen. The fibrillar collagens in the soft tumor seemed unusually rich in hydroxylysine and hydroxylysine glycosides; type I collagen had two to three times the hydroxylysine content of normal bone collagen.—JNCI 1982; 69:1009–1016.

By light microscopy, the extracellular matrix of human osteosarcomas resembles the woven osteoid laid down by osteoblasts during early bone development or in fracture healing (*1–3*). Although collagen is the most prominent component of the tumor matrix, its chemical characteristics have not been defined. Chemical definition of the collagen seemed an important task because collagen typing may be of value in assessing the clinical prognosis of osteosarcomas.

Five genetically distinct types of collagen molecule have been firmly identified and can be grouped into two families: fibrillar collagens (I, II, III) and basement membrane or pericellular collagens (IV, V) (*4, 5*). Type I is the commonest collagen; it is abundant in skin, tendon, bone, and other coarsely fibered connective tissues. Type II is found mainly in cartilage, and type III seems to be the collagen constituent of reticulin fibers. Within each type of collagen, further chemical heterogeneity is also evident because of variations in the degree of certain post-translational modifications that include hydroxylation of lysine residues, glycosylation of hydroxylysine residues, and the quantity and quality of intermolecular cross-links. Type I collagen, for example, is two to three times richer in hydroxylysine in young developing bone than in the mature tissue (*6, 7*). In this paper we report the biochemical characteristics and ultrastructure of collagen in the matrix of human osteosarcoma.

MATERIALS AND METHODS

Tissue selection.—Specimens of osteosarcoma tissue were sampled immediately after surgical resection or amputation. The patients ranged in age from 10 to 19 years. The lesions studied came from the distal femur, proximal tibia, proximal humerus, and ilium. Tissues from parosteal, periosteal, or secondary osteosarcomas were excluded. None of the patients had been subjected to chemotherapy or radiation therapy before surgery. Because osteosarcoma lesions are usually heterogeneous in cell and matrix composition, care was taken to dissect for analysis subregions that appeared uniform. The subregions assessed were 1) soft tumor tissue which was highly cellular and included early tumor osteoid, 2) tumorous bone (i.e., the hard, mineralized tissue within the tumor mass itself), and 3) normal cortical bone. Care was taken to exclude cartilaginous areas from the specimens taken for analysis. Tissue samples from each of the regions were subjected to light microscopy and biochemical analysis, and soft tumor samples were examined by electron microscopy. Collagen analyses were performed on those specimens that appeared grossly and histologically most uniform. In all, tumors from 9 patients were analyzed separately.

Histologic examination.—Tissue for light microscopy was fixed in neutral buffered Formalin, decalcified when necessary in 25% formic acid, embedded in paraffin, cut at 6 μm, and stained with either hematoxylin and eosin or safranin O and fast green (*8*). Tissue for electron microscopy was dissected into 1-mm cubes, fixed in a mixture of one part 2.5% glutaraldehyde and two parts 1% osmium tetroxide, and embedded in Epon (*8*). Sections of 1 μm were stained with toluidine blue for light microscopic assessment and, if satisfactory, 60-nm sections were then stained with lead citrate and uranyl acetate for examination on a JEOL 100C electron microscope operated at 60 kV.

Collagen analyses.—Calcified samples of normal bone and tumorous bone were decalcified in 0.5 M EDTA (pH 7.4) for 4–8 days at 4°C, washed with water, and freeze dried. Soft tumor tissue was analyzed without decalcification.

Amino acid analyses.—Tissue samples were hydrolyzed in 6 M HCl under N_2 for 24 hours at 108°C. Amino acids were quantified by a single column procedure (Beckman 121MB amino acid analyzer) that resolved hydroxyproline and hydroxylysine.

Hydroxylysine glycoside analysis.—Tissue samples were hydrolyzed in 2 M NaOH for 24 hours at 108°C. Glucosylga-

---

ABBREVIATIONS USED: CNBr=cyanogen bromide; RER=rough endoplasmic reticulum; SDS=sodium dodecyl sulfate.

---

[1] Received December 28, 1981; accepted May 27, 1982.

[2] Supported by Public Health Service grants AM-00805, AM-26489, and AM-15671 from the National Institute of Arthritis, Diabetes, and Digestive and Kidney Diseases.

[3] Research procedures were in accord with the ethical standards of the Committee on Clinical Investigation of The Children's Hospital Medical Center.

[4] Department of Orthopaedic Surgery, Harvard Medical School, The Children's Hospital Medical Center, 300 Longwood Ave., Boston, Mass. 02115.

[5] Department of Biological Chemistry, Harvard Medical School.

[6] We thank Ms. Linda Lewi and Ms. Lena Ellezian for their expert technical assistance.

lactosylhydroxylysine, galactosylhydroxylysine, and nonglycosylated hydroxylysine were quantified on the Beckman 121MB analyzer, as previously described (*9*).

CNBr Digestion.—Whole tissue samples and salt-fractionated collagens from pepsin digests were reacted with equal weights of CNBr in 70% formic acid for 16 hours at room temperature. The principal type of collagen in the sample was assessed by electrophoresis of the collagen CNBr–peptides in 10% polyacrylamide slab gels (*10*).

Pepsin digestion.—Samples of soft tumor tissue were homogenized in 0.5 *M* acetic acid (100 mg wet wt tissue/5 ml) and stirred with pepsin (3 mg/5 ml; Boehringer Mannheim Biochemicals) for 20 hours at 4°C. Insoluble material was removed by centrifugation. The supernatant was neutralized with solid Na_2HPO_4 and dialyzed overnight at 4°C against 0.02 *M* Na_2HPO_4. The collagen precipitate was collected by centrifugation. For each tumor, a portion of this material was analyzed directly by gel electrophoresis in 5% polyacrylamide. From selected large tumors, the collagen was fractionated by salt precipitation as follows: The pellet was redissolved in 1 *M* NaCl containing 0.05 *M* Tris (pH 7.5) by stirring at 4°C overnight. Successive precipitates were then collected by centrifugation at NaCl concentrations of 1.7, 2.5, and 4.0 *M*, stirring for 1 hour after each increase in salt concentration. Each precipitate was dissolved in 0.1 *M* acetic acid and was then freeze dried.

SDS-polyacrylamide gel electrophoresis.—We applied the method of Neville and Glossman (*11*) and used 1.5-mm thick slabs. Protein bands were stained overnight with 0.4% Coomassie blue R250 in 10% acetic acid, 20% isopropanol, and 70% water; the gels were destained in 7% acetic acid. Tracks of pepsin-digested collagen were scanned densitometrically (E-C Apparatus Corporation densitometer), and the relative amounts of $\alpha 1(I)$, $\alpha 2$, αA, and αB chains were quantified. Because the $\alpha 1(III)$ chain was partially resolved from $\alpha 1(I)$ but overlapped αA, the amount of type III collagen in a pepsin digest was estimated from the weight of collagen recovered in the 1.7-*M* NaCl precipitate and the proportion of $\alpha 1(III)$ in this fraction, as determined by gel electrophoresis.

RESULTS

Electron Microscopy

The cell and matrix ultrastructure of tumors from all patients showed a similar spectrum. The cell nuclei varied markedly in size and shape, and the chromatin was usually marginated. The nucleoli were prominent in number, size, and density. The most impressive ultrastructural features of the cellular, early osteoid region of the tumors were malignant osteoblasts rich in dilated RER frequently present in confluent lakes. The RER was intact and filled with a moderately dense homogeneous material (fig. 1). Intracellular filaments 5–7 nm in diameter were often present in the malignant osteoblast-like cells, although they were rarely packed densely. Glycogen granules were uncommon; lipid inclusions were seen on occasion. Most of the tumors contained other less well-differentiated cells with sparse flattened RER arrayed as circumferential or stacked lamellae. Multinucleated cells were frequent, some having cytoplasm similar to that of mononuclear tumor cells and others having abundant mitochondria characteristic of giant cells.

The extracellular matrix (figs. 2A–2D) was composed of crossbanded collagen in a relatively random weave. In some areas, the fibrils were parallel. Fibrils ranged from 30 to 90 nm in width, with the crossbanding periodicity from 58 to 62 nm. Parallel clusters of thin (≈15 nm in diameter), unbanded fibrils were also seen intermixed with the larger crossbanded fibrils. Further ultrastructural assessments have been made (*12*).

Collagen Chemistry

Light microscopy was used as the basis for selecting uniform specimens for biochemical analysis.

Hydroxylysine content.—The hydroxylysine content of total collagen in the soft tumor was twofold to threefold greater than that of normal bone collagen (table 1). A higher proportion of the hydroxylysine residues of the soft tumor collagen was glycosylated and the glucosylgalactosylhydroxylysine:galactosylhydroxylysine ratio was much higher than the ratio in normal bone (table 1). Intermediate levels of hydroxylysine and hydroxylysine glycosides were found in the tumorous bone. It may be significant that of the 7 tumors analyzed, 5 had closely grouped glucosylgalactosylhydroxylysine:galactosylhydroxylysine ratios at 3.3, whereas the other 2 both had low ratios around 1.0 (table 1).

Collagen types.—Electrophoresis of pepsin-solubilized tumor collagen (fig. 3) and derived CNBr peptides (fig. 4) showed that type I collagen was the prominent collagen in all specimens of osteosarcoma. However, all specimens of soft tumor tissue were relatively rich in type III (25% of total) and type V collagens (10% of total). In normal bone, less than 2% of the collagen is type V, and no type III has been detected. Type I trimer collagen also seemed abundant as judged by the high ratio of $\alpha 1(I)$ to $\alpha 2(I)$ (table 2). The identification of type I trimer collagen must remain tentative, however, because most of the $\alpha 1(I)$-rich material was precipitated in the 1.7-*M* NaCl fraction rather than in the 4.0-*M* NaCl fraction, as others have found (*19, 20*). One possible explanation is that the pepsin-extracted collagen studied here has different solubility properties than those of the type I trimer collagen studied elsewhere in which lathyritic tissue was used, thereby avoiding pepsin. Alternatively, the high ratio of $\alpha 1(I)$ to $\alpha 2(I)$ chains in the 1.7-*M* NaCl fraction may be due to selective breakdown of the

TABLE 1.—*Hydroxylysine (Hyl) and Hyl glycoside contents of osteosarcoma collagen*

Subregions	Molar ratio ± SEM Hyl/100 Hyp[a] (*n*)	Percent ± SEM Hyl glycosylated (*n*)	Molar ratio ± SEM GlcGalHyl/GalHyl[b] (*n*)
Normal bone	4.8±0.2 (5)	26.5±1.2 (5)	0.38±0.02 (4)
Tumorous bone	9.0±0.6 (5)	33.4±3.3 (5)	1.2±0.3 (5)
Soft tumor tissue	13.4±0.4 (9)	35.3±1.7 (7)	2.7±0.4 (7)[c]

[a] Hyp=hydroxyproline.

[b] GlcGalHyl=glucosylgalactosylHyl; GalHyl=galactosylHyl.

[c] Five specimens had similar ratios that grouped at 3.3±0.15; the remaining two specimens had distinct ratios at 0.9 and 1.3.

TABLE 2.—*Collagen species per total pepsin-solubilized collagen recovered from soft tumor*

Collagen type	Normal bone, %	Soft tumor, %
Type I	>90	≥40
Type I trimer	≤10	≤25
Type III	Not detected	25
Type V	<2	10

$\alpha 2(\mathrm{I})$ chain by overdigestion with pepsin, though normal bone type I showed little evidence for similar destruction under the same conditions. Gel electrophoresis of the 1.7-*M* NaCl fraction after CNBr digestion (fig. 5) confirmed that about one-half of the material was type III collagen, the remainder consisting of $\alpha 1(\mathrm{I})$ and $\alpha 2(\mathrm{I})$ chains. The apparent content of type I trimer collagen was quantified from the ratio of $\alpha 1(\mathrm{I})$ to $\alpha 2(\mathrm{I})$ in the total pepsin digests.

Another apparent anomaly should be commented on. In figure 5, the chain identified as $\alpha 1(\mathrm{III})$ runs as a monomer both with and without disulfide-bond cleavage. The disulfide-bonded trimer (γ-chain), a species usually prominent in many preparations of type III collagen before reduction of cystine disulfides, was virtually absent. This behavior seems peculiar to the gel electrophoresis system we use; purified preparations of type III collagen from fetal skin, for example, behave in the same way. We established the identity of the slow α-chain as $\alpha 1(\mathrm{III})$ by CNBr–peptide mapping (fig. 5).

This profile of collagen types was shown by 2 individual tumors for which the pepsin-solubilized collagen was fractionated by salt precipitation. For 9 tumors, the gel electrophoresis profiles of the total pepsin-solubilized collagen all gave essentially the same distribution, with similarly high ratios of αB to $\alpha 1(\mathrm{I})$ and $\alpha 1(\mathrm{I})$ to $\alpha 2(\mathrm{I})$. Type III CNBr peptides were always evident as components of whole CNBr digests of soft tumor (fig. 5).

The high content of hydroxylysine in the tumor collagen as a whole was not due solely to the abundance of type V collagen, which is known to be particularly rich in hydroxylysine. The individual salt-precipitated fractions that contained types I and III (and perhaps type I trimer) collagens all had unusually high contents of hydroxylysine (table 3). No type II collagen was detected in any specimen, confirming the absence of cartilaginous tissue. Although small amounts of type IV collagen from basal laminae would be difficult to detect by the present methods, the electrophoretic analyses of pepsin digests ruled out significant quantities.

Analysis of pepsin digests of tumorous bone showed more type I collagen and less type III, type I trimer, and type V collagens (data not shown), suggesting that the latter three collagen types are primarily associated with the neoplasm itself.

TABLE 3.—*Hydroxylysine content of salt-precipitated collagen fractions from soft tumor tissue*

Fraction	Collagen type, electrophoretic analysis	Hydroxylysine content,[a] residues/α-chain
1.7 *M* NaCl	Type III, type I, type I trimer	10.2
2.5 *M* NaCl	Type I	11.6
3.0 *M* NaCl	Type I, type V	14.7
4.0 *M* NaCl	Type V	23.1

[a] Calculated from amino acid analyses on the basis of 333 glycines/α-chain.

DISCUSSION

The ultrastructural studies of the highly cellular, early osteoid regions demonstrated malignant osteoblasts with abundant dilated RER. Similar findings on osteosarcoma ultrastructure have been reported by others (*1–3*). The primary matrix component was collagen, seen both in parallel and more frequently in woven conformations. In general the collagen was ultrastructurally unremarkable in comparison to collagen seen in developing or repairing bone. Our ultrastructural findings of osteosarcoma tissue have been detailed elsewhere (*12*).

Biochemically, an unusual mix of collagen types has been identified in the soft tumor matrix of osteosarcoma. Three main collagens are abundant—type I, type III, and type V—which is in contrast to the distribution in normal bone matrix, which consists almost exclusively of type I collagen. The evidence suggests that a type I trimer molecule—$[\alpha 1(\mathrm{I})]_3$—may also be abundant. Type II collagen was not detected, although it will be recalled that regions demonstrating cartilage either as seen by gross examination or by light microscopy were specifically avoided. In sarcomas, the type I collagen contained two to three times more hydroxylysine and more hydroxylysine glycosides than did type I collagen of normal adult bone. All 9 tumors showed this characteristic collagen composition. The only property that showed any evidence for subgrouping was the degree of glycosylation of hydroxylysine. However, the 2 patients distinguished by having the lower ratio of glucosylgalactosylhydroxylysine to galactosylhydroxylysine did not stand out in any other way, either in clinical course of the disease or in morphology or chemistry of the tumor.

Type I trimer collagen is still a poorly characterized molecule whose polymeric form and function are unknown. It seems most prominent in young, developing tissues, e.g., embryonic bone and tendon (*13*). It was also found in a virus-induced mouse tumor, originating from epithelial cells of the salivary glands, that produces bone and cartilage (*14*). This mouse tumor produced type I collagen—$[\alpha 1(\mathrm{I})]_2\alpha 2(\mathrm{I})$—and type I trimer collagen—$[\alpha 1(\mathrm{I})]_3$. An abundance of type I trimer collagen in the osteosarcoma matrix may, therefore, be another example of a neoplasm expressing a protein that is prominent normally only during development. Fetal proteins, such as carcinoembryonic antigen and α-fetoprotein, are synthesized actively by various human neoplasms (*15*).

Although blood vessels might be a source of some of these collagens, particularly of type III, light microscopy showed that vessel walls could contribute only a minor portion of the total matrix collagen. Type III collagen seems to be the collagen component of reticulin fibers found in many tissues (*16*), though it is not yet clear whether type III collagen is restricted in distribution to reticulin. Type III is prominent in human leiomyomas (*17*), and a rhabdomyosarcoma cell line (*18*) has been shown to produce predominantly type III and much smaller amounts of type IV collagens.

Type V collagen seems to be present in most connective tissues in small amounts and is synthesized together with types I and III collagens by fibroblasts in culture (*19*). It is believed to be concentrated pericellularly, so its relative abundance in the soft tumor specimens may be directly related to the high cellularity of the tissue.

Other matrix-rich tumors have been shown to make predominantly a single collagen product. A transplantable chondrosarcoma in the rat produced type II collagen exclusively (*20*), cartilaginous portions of a human osteosarcoma synthesized procollagen type II in organ culture (*21*), and a poorly differentiated murine chondrosarcoma produced type IV collagen (*22*).

At present, the histologically defined subtype of osteosarcoma appears to be of no value in predicting clinical outcome (*23*). Osteoblastic, chondroblastic, fibroblastic, and telangiectatic (*24*) variants show no predictable differences in prognosis, and the choice between chemotherapy and surgery is not based on the dominant tissue component. Thus at present, collagen typing would appear to be of limited clinical value although more specific therapies might eventually make such information useful. Collagen typing has potential value in differentiating between highly anaplastic osteosarcomas that show no distinct osteoid histologically and that often require the implementation of varying therapies. Of potential value is the observation that Ewing's sarcoma may be rich in type IV collagen (*25*).

Questions on the properties of osteosarcoma extracellular matrix remain. Is all the collagen made by the malignant osteoblast-like cells, those cells most obviously active in protein synthesis, or is the bone formed partially or even exclusively as a secondary, reactive phenomenon of nonmalignant host cells? Undifferentiated mesenchymal cells can be induced to form bone, for example, in response to implants of decalcified bone matrix (*26, 27*). Irrespective of the origin of osteosarcoma bone, special properties of the early tumor matrix seem indicated.

REFERENCES

(*1*) Paschall HA, Paschall MM. Electron microscopic observations of 20 human osteosarcomas. Clin Orthop 1975; 111:42–56.

(*2*) Williams AH, Schwinn CP, Parker JW. The ultrastructure of osteosarcoma. Cancer 1976; 37:1293–1301.

(*3*) Reddick RL, Michelitch HJ, Levine AM, Triche TJ. Osteogenic sarcoma. A study of the ultrastructure. Cancer 1980; 45:64–71.

(*4*) Prockop DJ, Kivirikko KJ, Tuderman L, Guzman NA. The biosynthesis of collagen and its disorders. N Engl J Med 1979; 301:13, 77.

(*5*) Eyre DR. Collagen: Molecular diversity in the body's protein scaffold. Science 1980; 207:1315–1322.

(*6*) Miller EJ, Martin GR, Piez KA, Powers MJ. Characterization of chick bone collagen and compositional changes associated with maturation. J Biol Chem 1967; 242:5481–5489.

(*7*) Glimcher MJ, Shapiro F, Ellis RD, Eyre DR. Changes in tissue morphology and collagen composition during the repair of cortical bone in the adult chicken. J Bone Joint Surg [Am] 1980; 62A:964-973.

(*8*) Shapiro F, Holtrop ME, Glimcher MJ. Organization and cellula biology of the perichondrial ossification groove of Ranvier. J Bo Joint Surg [Am] 1977; 59:703–723.

(*9*) Furukawa T, Eyre DR, Koide S, Glimcher MJ. Biochemical studies of repair cartilage resurfacing experimental defects in the rabbi knee. J Bone Joint Surg [Am] 1980; 62:79–89.

(*10*) Eyre DR, McDevitt CA, Billingham ME, Muir H. Biosynthesis collagen and other matrix proteins by articular cartilage in expe imental osteoarthrosis. Biochem J 1980; 188:823–837.

(*11*) Neville DM Jr, Glossman H. Molecular weight determination o membrane protein and glycoprotein subunits by discontinuous g electrophoresis in dodecyl sulfate. Methods Enzymol 1974; 32 (pt B):92–102.

(*12*) Shapiro F. Ultrastructural observations on osteosarcoma tissue. A study of ten cases. Ultrastruct Pathol. In press.

(*13*) Jimenez SA, Bashey RJ, Binditt M, Yankowski R. Identification of collagen α1(I) trimer in embryonic chick tendons and calvaria. Biochem Biophys Res Commun 1977; 78:1354–1361.

(*14*) Moro L, Smith BD. Identification of collagen α1(I) trimer and normal type I collagen in a polyoma virus-induced mouse tumor. Arch Biochem Biophys 1977; 182:33–41.

(*15*) Ruddon RW. Role of biological markers in cancer diagnosis and treatment. In: Ruddon RW, ed. Biological markers of neoplasm: Basic and applied aspects. Amsterdam: Elsevier/North-Holland, 1978:1–7.

(*16*) Gay S. Immunohistological studies on collagen type distribution in tissues. In: Gastpar H, Kuhn K, Marx R, eds. Collagen–platelet interaction. New York: Schattauer Verlag, 1978:171–179.

(*17*) Chung E, Miller EJ. Collagen polymorphism: Characterization of molecule with the chain composition $[\alpha 1(\mathrm{III})]_3$ in human tissues. Science 1974; 183:1200–1201.

(*18*) Krieg T, Timpl R, Alitalo K, Kurkinen M, Vaheri A. Type III procollagen is the major collagenous component produced by a continuous rhabdomyosarcoma cell line. FEBS Lett 1979; 104:40 409.

(*19*) Gay R, Buckingham RB, Prince RK, Gay S, Rodnan GP, Miller EJ. Collagen types synthesized in dermal fibroblast cultures from patients with early progressive systemic sclerosis. Arthritis Rheum 1980; 23:190–196.

(*20*) Smith BD, Martin GR, Miller EJ, Dorfman A, Swarm R. Nature of the collagen synthesized by a transplanted chondrosarcoma. Arch Biochem Biophys 1975; 166:181–186.

(*21*) Lanzer WL, Liotta LA, Yee C, Azar HA, Costa J. Synthesis of procollagen type II by a xenotransplanted human chondroblastic osteosarcoma. Am J Pathol 1981; 104:217–226.

(*22*) Orkin RW, Gehron P, McGoodwin EB, Martin GR, Valentine T, Swarm R. A murine tumor producing a matrix of basement membrane. J Exp Med 1977; 145:204–220.

(*23*) Schajowicz F. Tumors and tumorlike lesions of bone and joints. Berlin: Springer-Verlag, 1981.

(*24*) Huvos AG, Rosen G, Bretsky SS, Butler A. Telangiectatic osteogenic sarcoma. Cancer 1982; 49:1679–1689.

(*25*) Maale G, Pantazis C, Balian G. Production of basement membrane collagen type IV by Ewing's sarcoma cells. Trans Orthop Res Soc 1982; 7:101.

(*26*) Urist MR. Bone: Formation by autoinduction. Science 196 150:893–899.

(*27*) Reddi AH, Anderson WA. Collagenous bone matrix-induced endochondral ossification and hemopoiesis. J Cell Biol 1976; 69:557-572.

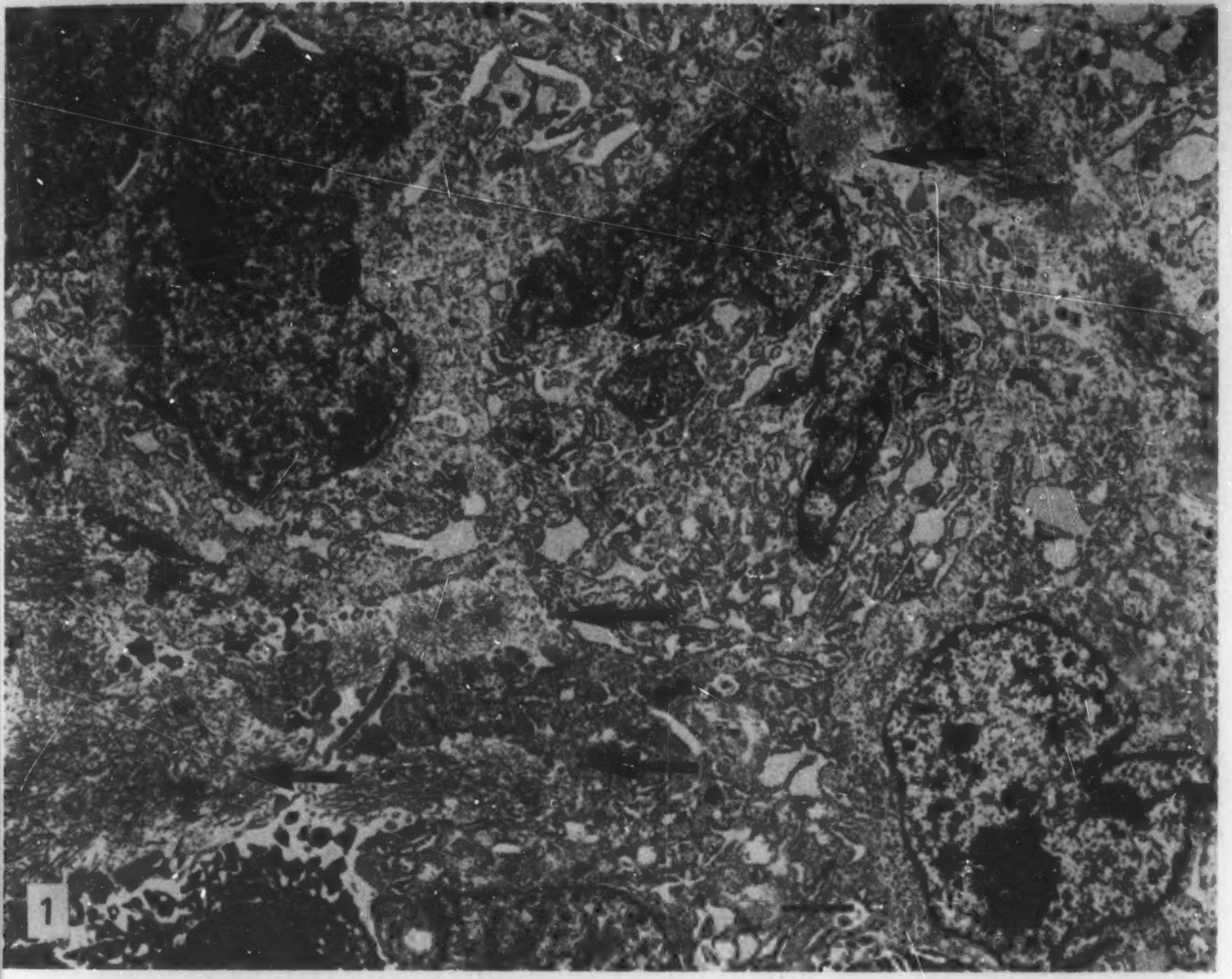

FIGURE 1.—Electron micrograph demonstrating representative section of highly cellular, early osteoid regions. Cells are characterized by irregularly shaped nuclei with prominent nucleoli and prominent collections of dilated RER. *Arrows* indicate areas of collagen. Lead citrate and uranyl acetate. *Bcr*=1.74 μm. × 5,875

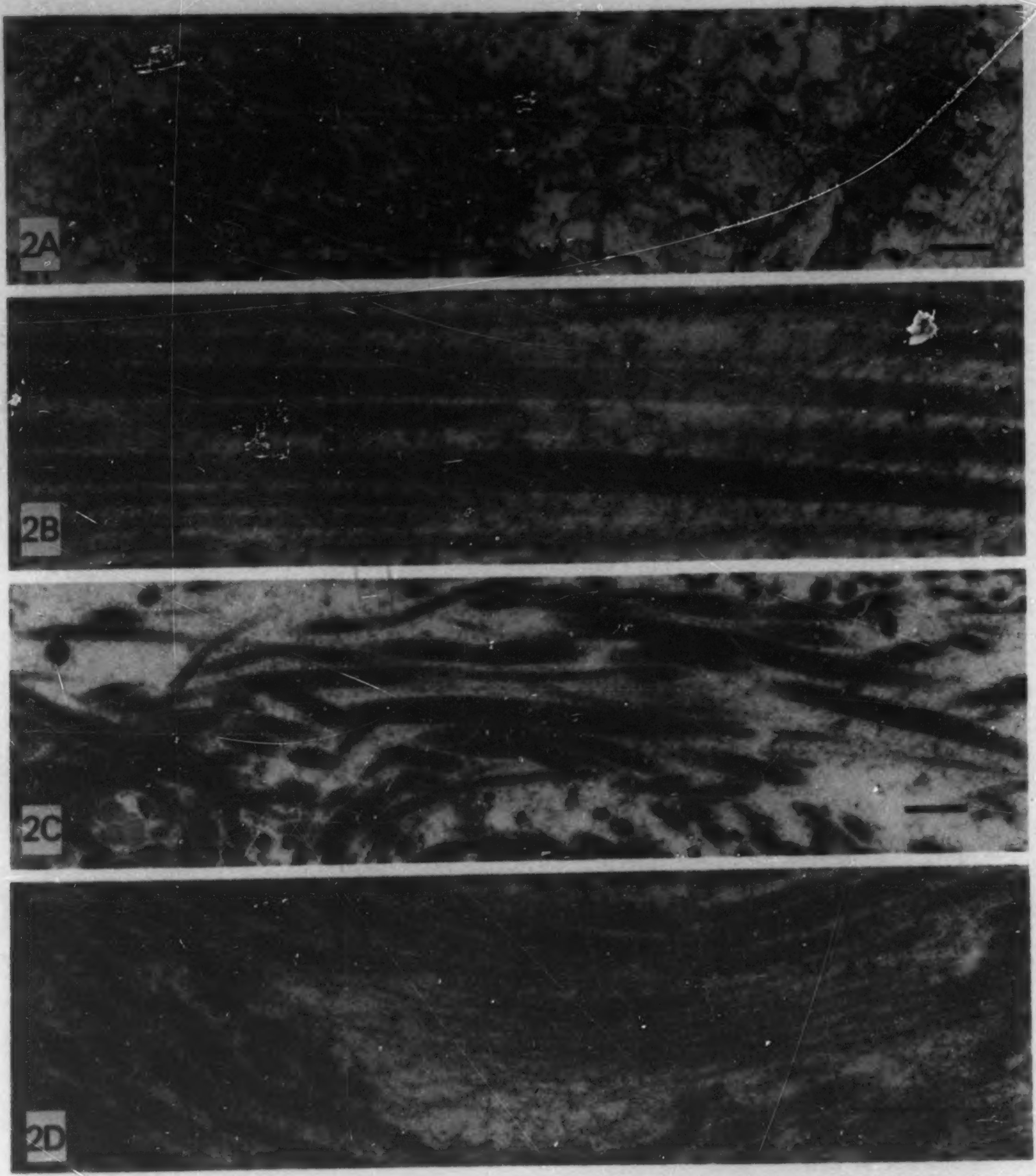

Figure 2.—Electron micrographs demonstrating the collagenous matrix seen in the osteosarcoma lesions. Lead citrate and uranyl acetate.

Figure 2A.—Low-power electron micrograph demonstrating collagen fibrils at *left* interspersed with thinner, nonbanded fibrils. Thinner fibrils are ≈15 nm wide. At *far right* a few scattered intracellular filaments are seen in a region of dilated RER. *Bar*=0.38 μm. × 26,250

Figure 2B.—Mature collagen fibrils in parallel conformation. Diameter of largest fibril is 90 nm. *Bar*=0.15 μm. × 65,000

Figure 2C.—Crossbanded collagen fibrils in woven conformation. *Bar*=0.29 μm. × 34,500

Figure 2D.—Thin, nonbanded fibrils intermixed with thicker crossbanded collagen fibrils. Diameter of thinner fibrils is 15 nm. *Bar*=0.15 μm. × 65,000

3

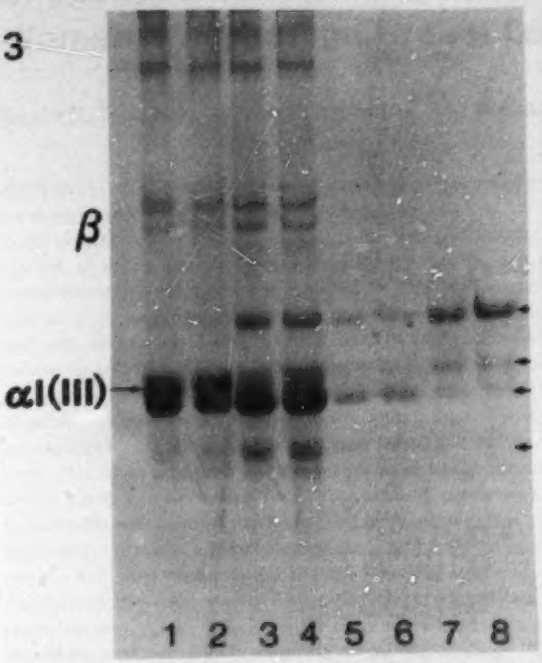

4

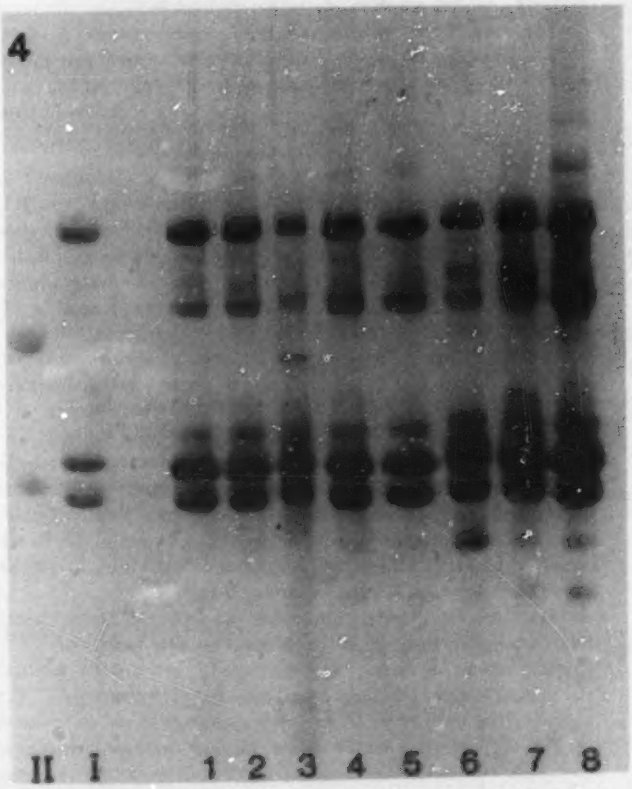

FIGURE 3.—SDS-polyacrylamide gel electrophoresis of collagen fractions from a pepsin digest of osteosarcoma soft tissue. Lanes 1, 3, 5, and 7 are respectively 1.7-, 2.5-, 3.0-, and 4.0-*M* NaCl precipitates run without dithiothreitol. Lanes 2, 4, 6, and 8 are the same samples run after being reduced with dithiothreitol. Coomassie blue R250.

FIGURE 4.—SDS-polyacrylamide gel electrophoresis of CNBr digests of whole decalcified tissue dissected from 3 osteosarcomas. Standard CNBr digests of types I and II collagens were run at the *left side* of the gel, as indicated. Patient C: tumorous bone (1), normal bone (2); Patient G: soft tumor (3), tumorous bone (4), normal bone (5); Patient L: soft tumor (6), tumorous bone (7), normal bone (8). All samples show type I collagen as their predominant collagen species. Soft tumors in lanes (3) and (6) all showed specific peptide bands of type III collagen. No type II collagen was detected. Coomassie blue R250.

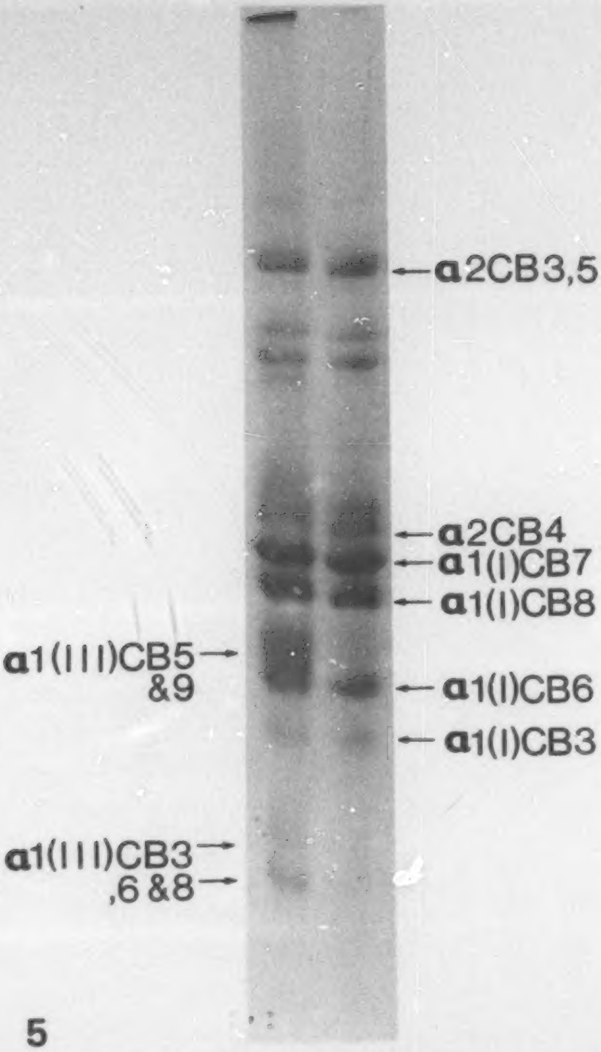
α2CB3,5
α2CB4
α1(I)CB7
α1(I)CB8
α1(III)CB5 &9
α1(I)CB6
α1(I)CB3
α1(III)CB3 ,6 &8

5

FIGURE 5.—SDS-polyacrylamide gel electrophoresis of CNBr-derived peptides of collagen fractions from pepsin-digested soft tumor. *Left lane*: 1.7-*M* NaCl fraction; *right lane*: 2.5-*M* NaCl fraction. Samples before their CNBr digestion were those analyzed in fig. 3. Coomassie blue R250.

Exogenous Estrogens and Other Risk Factors for Breast Cancer in Women With Benign Breast Diseases[1,2,3]

David B. Thomas,[4] **Joyce P. Persing,**[5] *and* **William B. Hutchinson**[6,7]

ABSTRACT—A group of 1,439 white women who were initially treated for biopsy-proved benign breast diseases from 1942 to 1975 in a single private surgery practice were followed through 1976 for development of breast cancer. Information on age, parity, and use of noncontraceptive estrogens was collected on all women at the time of their initial benign lesion. At follow-up, ages at menarche, menopause, and birth of first child were obtained, as was information on use of estrogens after the initial lesion. Slides from the initial lesion were reinterpreted and classified by a panel of pathologists. The influence of gross and microscopic features of the initial benign conditions on subsequent risk of breast cancer was ascertained and reported previously. This paper presents results of additional analyses based largely on Cox's proportional hazards model. Risk of breast cancer was related to nulliparity and ages at menarche and birth of first child and to a lesser extent to age at artificial menopause. Exogenous estrogen taken prior to the initial benign lesion did not alter risk of breast cancer. Subsequent use, primarily of conjugated estrogens, eliminated the protective effect of an artificial menopause and appeared to act synergistically with epithelial hyperplasia or papillomatosis in the initial lesion and calcification of that lesion to increase the risk of breast cancer. A marked increase in risk of breast cancer in succeeding birth cohorts was unexpectedly found that could not be explained by temporal changes in any of the other risk factors considered.—JNCI 1982; 69:1017–1025.

Risk of breast cancer is approximately doubled in women with benign breast diseases (*1–5*). The present study was initially conducted to identify specific histologic features of benign breast lesions that distinguish women at increased risk of breast cancer. Results of that aspect of the study have been published (*5*). They, along with those of Page et al. (*4*), showed risk of breast cancer to be particularly related to proliferative lesions of the ductal epithelium.

A number of case-control (*6–13*) and prospective (*14–18*) studies have been conducted to determine whether exogenous, noncontraceptive estrogens alter the risk of breast cancer. The results are generally inconsistent. Some studies showed risk of breast cancer to be increased long after initial use of estrogens (*13, 15, 16, 18*) in women exposed to high doses (*12, 13, 16, 18*), in women with an artificial menopause (*13, 15*), and in women with such risk factors for breast cancer as nulliparity (*13*) and family history of breast cancer (*13*); but other studies showed no such results. A consistent finding among one prospective (*15*) and two case-control (*12, 13*) studies is an increased risk of breast cancer in relation to use of exogenous estrogens in women with benign breast lesions; no results contradicting these have been published.

The results of additional analyses of data from our follow-up study of women with benign breast disease (*5*) are presented in this paper. These analyses were performed primarily to investigate further the influence of exogenous estrogens on risk of breast cancer in women with benign breast lesions. Risk associated with estrogen use in women with various histologic types of benign lesions is considered for the first time. Analyses were also performed to ascertain whether menstrual and reproductive risk factors for breast cancer are operative in women with benign mammary conditions and to investigate temporal trends in breast cancer incidence in such women.

METHODS

Details of the study design and data collection have been reported previously (*5*). White women (1,439) initially seen in a private surgery practice from 1942 to 1975 for benign breast lesions were followed through 1976 to ascertain whether they had developed breast cancer. Methods of follow-up included letters and phone calls to the study subjects, review of office records, and the obtaining of death certificates for women who had died.

When the patient made her initial visit for a benign lesion, information was obtained and recorded on age, parity, and prior use of noncontraceptive estrogens. Information on prior use of noncontraceptive estrogens was limited to yes–no responses. Additional data on age at menarche, age at birth of first child, type of and age at menopause, and use of exogenous estrogens since the initial episode of benign breast disease were ascertained at follow-up for development of breast cancer. Information on the use of estrogens included the type of estrogen (recorded as oral contraceptives, Premarin, other estrogens, and hormones of an unidentified type), date and age at first use, and duration of use. Infor-

---

ABBREVIATIONS USED: CI=confidence interval(s); RR=relative risk(s).

---

[1] Received January 5, 1982; accepted June 3, 1982.

[2] Supported in part by Public Health Service (PHS) grant 5-S07RR-05520 from the Division of Research Resources, National Institutes of Health; and in part by PHS grants 5-P30CA-15704 and 5T32CA-09168 from the National Cancer Institute.

[3] Research procedures were in accord with the ethical standards of the Human Research Committee of The Fred Hutchinson Cancer Research Center.

[4] Program in Epidemiology and Biostatistics, The Fred Hutchinson Cancer Research Center, 1124 Columbia St., Seattle, Wash. 98104.

[5] Department of Biostatistics, University of Washington, Seattle, Wash. 98195.

[6] The Fred Hutchinson Cancer Research Center.

[7] We thank Drs. William B. Hamlin and Gilbert J. Roth, Department of Pathology, Swedish Hospital Medical Center, for review of slides; Dr. Norman E. Breslow, University of Washington, for statistical advice; Dr. L. B. Kiriluk, Seattle, Wash., for contribution of cases; Ms. Mary DuPhorne and Ms. Jeanne-Marie Smith for their data-collection efforts; and Ms. Joy Dycus for assistance in manuscript preparation.

mation was not obtained on treatment schedules, strength of preparation, or reasons for use. Of the 504 women who used estrogens after their initial benign breast lesion, 419 used Premarin or other estrogens, 47 used only oral contraceptives, and 38 used only hormones of an unidentified type. Most users of Premarin, other estrogens, and hormones of an unidentified type used them during and after the perimenopausal period. Thus use of all these hormones probably largely represents use of estrogens for menopausal symptoms, and these users were grouped together in the analyses. Oral contraceptives tended to be used at earlier ages but by too few women to analyze as a separate group. In the analysis presented, the oral contraceptive users are grouped with the menopausal estrogen users because results of one previous study have suggested that oral contraceptives (*19*), like menopausal estrogens, may increase the risk of breast cancer in women with prior benign breast lesions.

Slides from the initial benign lesions and any subsequent breast cancers were reread and classified according to a standard protocol. Five major types of benign breast diseases were distinguished (inflammatory disease, fibrocystic disease, fibroadenoma, nipple adenoma, and intraductal papilloma). Women with fibrocystic disease were further classified with respect to the components present (apocrine metaplasia, adenosis, sclerosing adenosis, epithelial hyperplasia or papillomatosis, calcifications, inflammation, and atypia).

The data were analyzed by means of Cox's proportional hazards model (*20*), which specifies that the instantaneous incidence of breast cancer at age t for a woman with covariables $z(t)$ is given by $\lambda[t,z(t)] = \lambda_0(t) \cdot e^{\beta' z(t)}$. In this expression, $\lambda_0(t)$ represents the unknown age-specific incidence function for a base-line individual $[z(t)=0]$. A consequence of the model is that the breast cancer age incidence functions for individuals characterized by explanatory variables $z_1=z_1(t)$ and $z_0=z_0(t)$ at age t are proportional: $e^{\beta'(z_1-z_0)}$ is the ratio of their disease incidence rates and defines an RR function measured relative to that of individuals characterized by z_0.

The model is partially nonparametric in that no assumptions are made regarding the functional form of the breast cancer incidence function for base-line individuals. Statistical inference is based on asymptotic likelihood theory.

The proportional hazards model was used because of the flexibility it permits in handling large numbers of variables whose values may change over the course of the study (time-dependent covariates). Factors in this study that were time-dependent include estrogen use, parity, and menopausal status. This technique was also used to measure exposures that accumulated over time (e.g., duration of estrogen use) and latency effects (i.e., effects that depend on the elapsed time since some event).

The proportional hazards model assumes that the covariates act multiplicatively on the underlying base-line incidence (hazard) of breast cancer. The consistency of our data with this specification was examined in several ways. Marked departures from the proportional hazards assumption were assessed by the inclusion of additional time-dependent covariates in the model and tests of their statistical significance. Such factors allow the RR to be a time-dependent, rather than a constant, multiple of the base-line incidence of breast cancer (*20*). For example, this technique enabled us to determine whether the effect of an early menarche on breast cancer risk is greater during the premenopausal and perimenopausal years than in the years following menopause. Graphical methods provided additional means for assessment of the goodness of fit of the proportional hazards model to the data (*21*).

RESULTS

The total study group consists of 1,439 women with biopsy-proved benign breast disease who contributed a total of 18,542 person-years of observation for an average of 12.9 years per person. Forty-one percent of the women were followed for 15 years or more and 25% for 20 years or more. Table 1 characterizes the study group according to follow-up status. Fifteen percent of the women were not contacted at the time of follow-up. These women are included in the study until the date of their last visit for benign breast disease and contribute an average of 3.8 person-years of observation per person. The only follow-up data available from them are a small amount of information abstracted from the physician's records. The remaining 1,221 women were followed through 1976. Of these, 66 were found to have developed breast cancer, 37 had bilateral mastectomies for benign lesions, and 87 had died of causes unrelated to breast cancer. Cardiovascular diseases were the most common causes of death. The women with bilateral mastectomies were considered at risk of breast cancer until the time of their second mastectomy. The remaining 1,031 women were contacted at follow-up, as were 53 of the 66 women who developed breast cancer. Of the 13 deceased women with breast cancer, some follow-up information was obtained on 7 of them from next-of-kin.

In the analyses that follow, 86 of the breast cancer-free women (6.3%) have been eliminated: 84 because they were less than 30 years of age at the time of their last contact or at follow-up and 2 because they were older than 82 years of age at their initial diagnosis of benign breast disease. Since the youngest breast cancer case occurred at age 30 and the oldest at age 82, person-years of observation on these 86 women contribute no useful information. The analyses are, therefore, based on a maximum of 1,353 women, 66 of whom developed breast cancer. Women with no information

TABLE 1.—*Distribution of study population by status at follow-up*

Subgroups of women	Distribution of women		Average person-years of observation per person
	Number	Percent	
Complete follow-up	1,221	84.9	14.5
No breast cancer by 1976	1,031	71.7	15.0
Bilateral mastectomy for benign lesion before 1976	37	2.6	3.8
Died prior to 1976	87	6.0	14.2
Developed breast cancer by 1976	66	4.6	13.0
Incomplete follow-up	218	15.1	3.8
Total	1,439	100.0	12.9

regarding particular variables were excluded from analyses involving those variables.

Women who developed breast cancer did not differ from the others by age at diagnosis of initial benign lesion, duration of follow-up, or age at follow-up (equivalent to age at diagnosis of breast cancer for women who developed breast cancer).

Results of detailed analyses regarding specific histologic types of benign breast disease and breast cancer risk have been published (*5*). Excess risk of breast cancer was related to the presence of fibrocystic disease and particularly so if there was evidence of epithelial hyperplasia or papillomatosis and calcification. Fibroadenoma was not associated with any increased risk except in women with concomitant fibrocystic disease.

The influence of four reproductive and menstral factors on risk of breast cancer is shown in table 2. For each factor, estimates of the RR were obtained by division of the relevant data into appropriate categories (age at event) and estimation of separate, age-adjusted RR for each category. This was done with the use of the proportional hazards model with dummy variables. This technique makes no apriori assumptions regarding the direction of the relationship between risk of breast cancer and these factors. Virtually identical results were obtained by means of the Mantel-Haenszel approach (*22*) and a person-years analysis. Age at menarche and age at birth of first child showed relationships to breast cancer risk similar to those from previous studies (*23*).

As expected, the age-adjusted RR of breast cancer was lowest in women with a surgical menopause before age 45, slightly higher in premenopausal women and women with a natural menopause before age 45, and higher yet in women with a surgical menopause after age 45. However, the RR in women with a natural menopause after age 45 was unexpectedly low. There was no evidence that the apparent protective effect of a surgical menopause increased with advancing age. In these analyses, women with surgical menopause included both oophorectomized and nonoophorectomized women. In addition, this analyses does not take account of the possible influence of menopausal estrogen use.

The estimated RR of breast cancer in relation to each of the four factors shown in table 2 were also estimated by modeling the associated factors as linear functions of the log-breast cancer incidence function—i.e., $\log\lambda[t;z(t)] = \log\lambda_0(t) + \beta' z(t)$. The linear modeling was found to explain the variation in risk as well as the nonrestrictive models. Moreover, these estimates were not appreciably altered by simultaneous adjustment for each of the other variables in the table and for various features of the benign lesions. Therefore, the linear models were used to adjust for these four variables in subsequent analyses.

In the analyses of estrogen use following benign breast disease, women using estrogens contributed person-years of observation to the users category for each year subsequent to their initial use. Prior to then, they were considered nonusers. Using the proportional hazards model and not adjusting for any other factors, we estimated the RR associated with such use to be 1.80 (95% CI = 1.04–3.10; χ_1^2 = 4.51).

The RR associated with estrogen use was also estimated by the construction of a series of 2×2 tables based on the ages t_k at which breast cancer was diagnosed. Among women whose use or nonuse of estrogens was ascertained, breast cancer occurred at 23 ages between 30 and 76, so there were 23 possible 2×2 tables. The data in each of these tables are shown on a separate line in table 3. Women are only considered at risk of breast cancer subsequent to their initial benign breast lesion. The number of women at risk thus changes with age, not only due to the loss of individuals from further observation but also due to the addition of women at their age of initial benign breast disease (*24*). Within each line of the table, individuals are classified with respect to their breast cancer status at age t_k and according to whether or not they had used estrogens by that age. Individuals may be reclassified in different groups at different ages. These data were analyzed by means of technique of Mantel and Haenszel (*22*) and gave an estimated RR of 1.84, with a corresponding chi-square statistic (without con-

TABLE 2.—*RR of breast cancer in relation to age at various reproductive events: Results of proportional hazards nonrestrictive analyses*

Event	Age at event, yr	No. of women[a]		RR	95% CI	χ_1^2	*P*-value[b]
		Breast cancer	Nonbreast cancer				
Menarche	≤12	20	345	1.34	0.74–2.43	4.0	0.05
	13–14	25	491	1.00			
	≥15	3	134	0.41	0.12–1.37		
First child	≤24	16	400	1.00		2.4	0.12
	25–29	12	269	1.02	0.48–2.16		
	≥30	7	129	1.16	0.48–2.83		
	Nulliparous	20	276	1.65	0.85–3.20		
Menopausal status							
Premenopausal	—	21	323	0.98	0.32–3.00	—	
Surgical menopause	≤45	10	221	0.74	0.25–2.20		
	≥46	8	117	1.54	0.49–4.77		
Natural menopause	≤45	5	68	1.00			
	≥46	13	330	0.75	0.26–2.16		

[a] The numbers shown cannot be used to construct valid RR estimates; the RR are adjusted for age at initial benign breast lesion and age at follow-up.

[b] Score test for linear trend.

TABLE 3.—*Use of estrogens since initial benign breast disease in relation to age at diagnosis of breast cancer*[a]

Age at breast cancer, yr	No. of women at risk	Breast cancer		Nonbreast cancer	
		Estrogen users	Nonusers	Estrogen users	Nonusers
30	148	0	1	27	120
37	279	0	1	38	240
38	304	1	2	40	261
41	409	0	2	58	349
44	507	1	2	99	405
45	528	2	2	109	415
46	567	1	3	135	428
48	602	1	3	154	444
49	602	0	1	178	423
50	610	2	1	196	411
51	598	0	3	216	379
52	577	2	2	226	347
54	520	1	1	221	297
58	389	4	0	158	227
60	348	2	0	147	199
61	313	1	1	124	187
62	285	1	1	100	183
64	234	2	1	73	158
65	200	1	0	55	144
67	159	0	1	40	118
68	137	1	1	29	106
69	121	0	3	27	91
76	37	0	1	5	31

[a] Based on 1,036 women, 56 of whom developed breast cancer. Mantel-Haenszel estimate of the RR is 1.84 (95% CI=1.05–3.23).

tinuity correction) of 4.53 (P=0.03). Using Miettinen's test-based procedure (*25*), we estimated the 95% CI of the RR to be from 1.05 to 3.23.

When a single dichotomous variable is considered, the proportional hazards model is mathematically equivalent to the Mantel-Haenszel procedure (*26*). The similarity of the above results demonstrates this common conceptual framework. The advantage of the model is that it permits extensions to multiple continuous variables which are not easily handled by the Mantel-Haenszel stratification procedure.

Text-figure 1 shows Kaplan-Meier (*27*) estimates of the cumulative lifetime probability of developing breast cancer for estrogen users and nonusers. As in table 3 the compositions of the 2 groups are time-dependent since the factor defining them (estrogen use) is itself time-dependent. For example, a woman who enters the study at age 35 and begins using etrogens at age 50 would be in the nonusers category from ages 30 to 49 and in the users category from age 50 on. The text-figure illustrates that the effect of exogenous estrogens does not become apparent until after the usual age of menopause. Moreover, the estrogen effect appears to become more pronounced with the passage of time, although this tendency is not statistically significant.

The use of estrogens *prior* to diagnosis of benign breast disease did not affect subsequent breast cancer risk, and the RR associated with use of estrogens after the initial benign breast lesion was not altered by any earlier use.

The RR associated with use of exogenous estrogens after benign breast disease did not vary significantly with age or year of first use or interval of time from the initial benign breast lesion to first use. There was also no evidence of an increase in RR with increases in duration of use. The RR for users of less than 5 years was 1.87 (95% CI = 0.98–3.53), whereas that for users of 5 or more was 1.91 (95% CI = 0.90–4.03). When duration of use was dichotomized at 3 and 4 years of use, RR of breast cancer were actually slightly greater for those in the shorter duration category.

Because follow-up occurred over 34 years, we were able to investigate temporal trends in the incidence of breast cancer by including a linear term for year of birth in the regression equation. As table 4 demonstrates, there appears to have been large increases in breast cancer risk in successive birth cohorts. This trend is the strongest of any in these data ($P < 0.001$) and represents over a fourfold increase in risk between the 1905 and the 1925 cohorts.

We attempted to validate this observation using two other techniques. First, we plotted separate age incidence curves for various birth cohorts. This method was of limited utility because the curves for different cohorts were based on small numbers of cases and did not cover common ages sufficiently to allow one to draw conclusions on inspection. Second, we constructed risk sets at each age at which breast cancer occurred, in the same manner as was shown in table 3 for estrogen use, and compared the average year of birth for women who developed breast cancer with that for those who did not. As shown in table 5, on the average, compared to women of the same age who did not develop breast

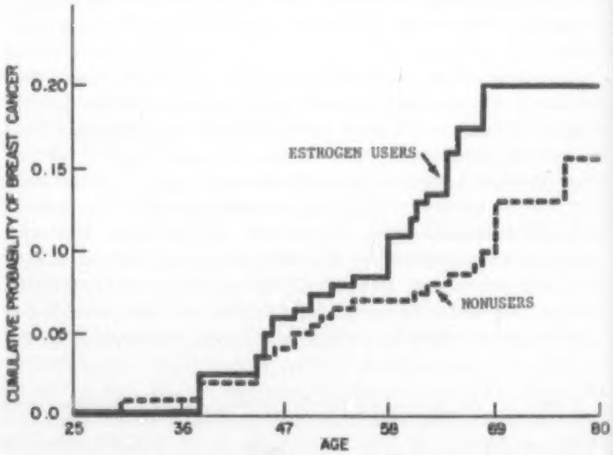

TEXT-FIGURE 1.—Cumulative lifetime probability of breast cancer for 2 time-dependent groups representing estrogen users and nonusers. Estrogen users are counted as nonusers until the age at which they first began to use estrogens.

TABLE 4.—*RR of breast cancer in relation to year of birth: Results of proportional hazards analysis*[a]

Year of birth	RR[b] (95% CI)
1905	1.00
1910	1.45 (1.17–1.80)
1915	2.11 (1.37–3.24)
1920	3.06 (1.60–5.83)
1925	4.43 (1.87–10.50)

[a] Based on 1,353 women.

[b] RR per year=1.08 (1.03–1.12); $\beta \pm SE = 0.0745 \pm 0.0220$; score test for linear trend: $\chi_1^2 = 11.8$, $P<0.001$.

TABLE 5.—*Year of birth in relation to age at diagnosis of breast cancer*

Age at breast cancer, yr	Average No. of women at risk	Average year of birth	
		Breast cancer	Nonbreast cancer
≤49	520	1922.1	1919.2
50–59	617	1916.6	1913.4
60–69	279	1907.6	1905.7
≥70	54	1894.3	1893.6

TABLE 6.—*Comparisons of the RR for year of birth by means of nonrestrictive and linear models: Results of proportional hazards analyses, grouped data*[a]

Year of birth	RR estimates	
	Nonrestrictive model	Linear model[b]
≤1909	0.50	0.59
1910–1919	1.00	1.00
1920–1929	1.48	1.68
≥1930	2.54	2.84

[a] Based on 1,353 women.

[b] The linear model was fit to the midpoints of the intervals defining cohorts. The years 1905 and 1935 were used for the two open-ended intervals. Score test for linear trend: $\chi_1^2=6.3$, $P=0.01$.

cancer, those who did tended to be born in more recent cohorts.

To determine whether the assumption of a linear year of birth trend used in the model to obtain the estimates in table 4 was reasonable, we divided the data into four approximate 10-year birth cohorts. Separate estimates of the RR were made independently from each cohort rather than with the asumption of a linear trend. These RR estimates are shown in column 2 of table 6. The 1910–19 cohort was used as the base line. Column 3 shows estimates of the RR obtained by our assigning a year of birth to all women in each interval equal to the midpoint of the interval and assuming a linear model. The departure of the RR in column 2 from the linear trend in column 3 was minor ($\chi_2^2=0.25$; $P=0.88$) whereas the trend itself was highly significant ($\chi_1^2=6.3$; $P=0.01$).

Most of the women in this study were at risk of breast cancer at ages over 45. This fact makes it difficult to compare the shape of the breast cancer age incidence curves with those of other studies. Nonetheless, by including an interaction term between age and year of birth in the model, we were able to test for differences in the shape of the age incidence curves for the various birth cohorts. There was no evidence that the increase in risk with age varied with year of birth ($\chi_1^2=1.20$; $P=0.27$). Although age at diagnosis of initial benign breast lesion was related to year of birth, adjusting for it did not influence the effect of birth cohort on breast cancer risk.

Table 7 shows that temporal changes in the ages at menarche, birth of first child, natural menopause, or surgical menopause cannot account for the large cohort effect, nor can changes in the histologic characteristics of benign lesions. Estrogen use in both women with natural and surgical menopause, on the other hand, was strongly related to year of birth (table 7). The proportion of users by age 48 in more recent cohorts was more than three times that in earlier cohorts. This finding is not surprising because use of estrogens in our area (*28*), as well as in the United States (*29*), has increased severalfold since the mid-1960's.

To determine whether this change in estrogen use could explain the cohort effect, we adjusted for estrogen use when evaluating the year of birth trend. Women with no information regarding estrogen use were excluded from this analysis. The sample size is, therefore, different from that of table 4. To compare the adjusted and unadjusted results, we also performed the same analysis as represented in table 4 on the reduced data set. These two sets of RR estimates are presented in table 8. The cohort effect was only slightly reduced after we controlled for differences in breast cancer risk due to estrogen use.

Table 9 shows estimated RR of breast cancer in estrogen users adjusted for various combinations of reproductive factors and features of the initial benign breast lesion, with and without adjustment for the cohort effect. Estimates of the RR associated with estrogen use were not appreciably altered by adjustment for reproductive factors or features of the benign lesions and are generally significantly larger than

TABLE 7.—*Known and potential risk factors for breast cancer in women in succeeding birth cohorts*

Risk factor	Year of birth			
	≤1909	1910–1919	1920–1929	≥1930
Average age at menarche	13.3	13.0	13.0	12.7
Average age at birth of first child	25.3	25.8	24.5	24.0
Average age at natural menopause	49.3	50.3	48.3	—
Percent with surgical menopause by age 46	22.9	25.4	25.1	22.2
Percent with fibrocystic disease characterized by epithelial hyperplasia or papillomatosis (age adjusted)	28.2	37.1	34.0	35.6
Percent who used estrogens by age 48				
Total women	11.3	15.7	39.8	—
With natural menopause	11.1	12.3	32.2	—
With surgical menopause	20.8	28.6	58.7	—

TABLE 8.—*RR of breast cancer in relation to year of birth, unadjusted and adjusted for estrogen use: Results of proportional hazards analyses*[a]

Year of birth	RR (95% CI)	
	Unadjusted for estrogen use[b]	Adjusted for estrogen use[c]
1905	1.00	1.00
1910	1.34 (1.06–1.69)	1.28 (1.00–1.63)
1915	1.79 (1.13–2.86)	1.63 (1.00–2.65)
1920	2.40 (1.19–4.84)	2.08 (1.01–4.32)
1925	3.22 (1.27–8.18)	2.66 (1.01–7.04)

[a] No.=1,036.

[b] RR per year=1.06 (1.01–1.11); $\beta \pm SE=0.0585 \pm 0.0238$; score test for linear trend: $\chi_1^2=6.2$, $P=0.01$.

[c] RR per year=1.05 (1.00–1.10); $\beta \pm SE=0.0490 \pm 0.0248$; score test for linear trend: $\chi_1^2=3.9$, $P=0.05$.

1.0 (column 3). However, after taking account of the cohort effect, we reduced the magnitude of the RR associated with estrogen use to a nonsignificant level irrespective of adjustments for any other factors (column 4). Thus it appears that at least part of the apparent association of breast cancer risk with estrogen use may be due to the confounding influence of birth cohort.

No interactions were observed between estrogen use and parity or ages at first birth, menarche, or natural menopause. The RR of breast cancer associated with estrogen use also did not vary with year of birth: RR were 1.70 in women born prior to 1910, 1.38 in women born between 1910 and 1919, and 1.45 in women born after 1919.

The possible interaction of exogenous estrogen use and surgical menopause is shown in table 10. Estimates of the RR shown are adjusted for year of birth. Estrogens did not increase the risk of breast cancer in women with intact ovaries (RR=1.02). The expected protective effect of a surgical menopause is evident in women who did not receive estrogens (RR=0.85), and estrogens appear to have eliminated that protection. It is uncertain whether the RR of breast cancer in estrogen users with an artificial menopause was greater than that of nonusers with intact ovaries.

Table 11 shows estimated RR of breast cancer in relation to estrogen use and characteristics of fibrocystic disease that were found to alter risk of breast cancer (*5*). This analysis is restricted to women who had fibrocystic disease and no other type of benign lesion and is thus based on only 524 individuals. Although none of the RR differ significantly from unity, noteworthy trends are evident. For each of the four categories shown, estrogen use appears to have increased breast cancer risk. Except in women with epithelial hyperplasia or papillomatosis with calcification, this effect was limited to women with a surgical menopause (not shown). In women with epithelial hyperplasia or papillomatosis, but not in women without these conditions, the presence of calcifications in the benign lesion and subsequent use of estrogen appear to act synergistically (on a multiplicative scale) to increase risk. This synergism was most apparent in women with a surgical menopause, but it was also observed to a lesser extent in women with intact ovaries.

TABLE 9.—*RR of breast cancer in relation to estrogen use, unadjusted and adjusted for year of birth and various other potential confounders: Results of proportional hazards analyses*

Potential confounders	No. of women	RR (95% CI)	
		Unadjusted for year of birth	Adjusted for year of birth
None	1,036	1.80 (1.04–3.10)	1.49 (0.84–2.63)
Fibrocystic disease	977	1.80 (1.03–3.15)	1.48 (0.83–2.65)
Age at menarche, birth of first child, and menopause[a]	857	1.80 (0.96–3.38)	1.38 (0.72–2.65)

[a] Includes both natural and surgical menopause.

TABLE 10.—*RR of breast cancer in relation to surgical menopause and estrogen use, adjusted for year of birth: Results of proportional hazards analyses*[a]

Surgical menopause	Estrogen use	RR (95% CI)
No	No	1.00
	Yes	1.02 (0.48–2.14)
Yes	No	0.85 (0.36–2.00)
	Yes	1.40 (0.63–3.11)

[a] No.=889.

TABLE 11.—*RR of breast cancer in women with fibrocystic disease in relation to various characteristics of the disease and estrogen use: Results of proportional hazards analysis*[a]

Epithelial hyperplasia or papillomatosis	Calcification	Estrogen use[b]	
		No	Yes
Absent	Absent	1.00	1.68
	Present	0.97	1.63
Present	Absent	1.48	2.49
	Present	3.20	7.65

[a] No.=524.

[b] Risks relative to that of nonestrogen users without epithelial hyperplasia or papillomatosis or calcifications.

DISCUSSION

The subjects of this study were largely middle and upper class white women who received care for their benign breast conditions in a single private practice. Actual rates of breast cancer in this population may, therefore, not accurately represent rates in all women with benign breast lesions. However, the RR that have been estimated are based on comparisons of subgroups within the study population and, as previously discussed (*5*), are not likely to have been affected by the self-selected nature of women in the study. For example, for differential selection to have caused a spuriously elevated RR of breast cancer in users of estrogens, women with benign lesions who later used estrogens and then went on to develop breast cancer would have to have been more likely to seek care for their initial lesion than future users who did not develop breast cancer. This seems an unlikely possibility.

The incompleteness of follow-up is also not likely to have resulted in spurious findings. For this to have erroneously resulted in an elevated RR of breast cancer in estrogen users, those users lost to follow-up would have had to have been at a lower risk of subsequent breast cancer than users who were completely followed. Furthermore, because those lost to follow-up were a small proportion of the total study population, the difference in their risks would have to have been large. This is unlikely because the differences in the completely and incompletely followed women with respect to parity and type of benign breast lesion were small (*5*), and although more of those lost to follow-up were younger and had fibroadenomas (lower risk), more of them also were nulliparous (higher risk).

The incomplete nature of the information on estrogen use is a true limitation of this study. The only formation on use prior to the initial benign lesion was a yes or no response to a query at the time the woman was initially evaluated for her benign condition. Use subsequent to the initial lesion was largely ascertained from the study subject at the time of follow-up, when detailed questions regarding use after her most recent office visit for a benign lesion were asked. For the 184 women with more than one benign lesion who used estrogens, use between the first and most recent lesion was obtained only from medical records, and like use subsequent to the first benign lesion was limited to a yes or no response. Fortunately, these women constituted only 13% of the study population, and risk of subsequent breast cancer was not related to number of episodes of benign breast disease. This incomplete information is thus not likely to have resulted in a spurious association between estrogen use and breast cancer. It could, however, have reduced the probability of finding a true increase in risk associated with exogenous estrogens.

The well-documented (*23*) adverse effects of early menarche, late first birth, and nulliparity, and the protective effect of a premenopausal oophorectomy were all found operative in this study population. This suggests that the increased risk of breast cancer associated with benign breast lesions is not due to women with such lesions simply having these risk factors; i.e., these risk factors and benign breast lesions independently alter risk of breast cancer. Results of case-control studies of breast cancer (*23*) are consistent with this conclusion as are findings from case-control studies of benign breast disease that show that risk factors for breast cancer do not consistently distinguish women with benign lesions (*30*). Women with benign breast lesions who have the menstrual and reproductive risk factors for breast cancer are thus at particularly high risk.

Two case-control studies (*12, 13*) have shown use of menopausal estrogens to enhance risk of breast cancer to a greater extent in women with than without a history of benign breast disease, and, consistent with our findings, in one study (*13*) this was only observed in women with a bilateral oophorectomy. The effect on breast cancer risk of estrogen use before versus after the benign lesion was not addressed in either of these studies, but it was in a prospective study by Hoover et al. (*15*). These investigators found the RR of breast cancer to be 4.0 in women who received estrogens prior to their benign lesions, as opposed to 2.1 in women who took estrogen after their lesion was diagnosed. The latter value is close to the RR of 1.8 observed for women in the present study who used estrogens after their initial benign lesion. However, we did not find estrogen use prior to a benign lesion to alter risk of breast cancer. A partial explanation for this discrepancy may be the rudimentary nature of our information on such usage. On the other hand, this information was ascertained at the time of the benign lesion and not years later at follow-up; and it is unlikely that the misclassification of usage could have been of sufficient magnitude to have totally obscured a true fourfold increase in risk.

The risk of breast cancer in women who used estrogens after their initial benign breast lesion was not significantly increased prior to menopause. Risk was elevated after menopause and showed a slight tendency to increase with age. The premenopausal estrogen users include a small number of women who took oral contraceptives plus others whose estrogen use was for unknown reasons. The postmenopausal increase in risk with age is compatible with the latent period between exposure to estrogens and increased risk of breast cancer observed by others (*15, 16, 18*) and not supportive of the results of Jick et al. (*11*), who reported an increased risk of breast cancer in current and recent users of estrogens.

Fibrocystic disease characterized by epithelial hyperplasia or papillomatosis was found to distinguish women in this study who were at particularly high risk of breast cancer, and their risk was elevated even more if their lesions had histologic evidence of calcification (*5*). The influence of estrogens on risk of breast cancer was not related to the presence of epithelial hyperplasia or papillomatosis. However, in women whose lesions had these features, the RR of breast cancer in estrogen users was greatest in women whose lesions had calcifications. Thus in women with fibrocystic disease, the presence of proliferative lesions of the ductal epithelium, calcification of these lesions, and exogenous estrogens all appear to interact to increase the risk of breast cancer. Women with all three of these factors were observed to have a risk of breast cancer that was 7.85 times greater than that of women with none of them. This effect was greatest in women with a surgical menopause. However, these observations are based on small numbers of cases, and the 95% confidence limits of the RR estimates include one. Independent confirmation of these findings is thus needed.

Many previous studies have shown premenopausal oophorectomy to reduce the risk of breast cancer (*22*). This result was noted in the present study, but not in women who had used estrogens. Elimination of the protective effect of an oophorectomy by exogenous estrogens is also evident from the reports of Hoover et al. (*15*) and Brinton et al. (*13*) and is probably a real phenomenon, although it was not demonstrated in the study by Ross et al. (*12*).

In the present study group the influence of estrogens on risk of breast cancer was largely confined to women with an artificial menopause. Compatible with our observations, Brinton et al. (*13*) found the risk associated with estrogens to be greater in women with an artificial menopause than in women with intact ovaries, but unlike us, they also observed some increase in risk in women with a natural menopause. Hoover et al. (*15*) found the increment in risk associated with estrogen use to be unrelated to ovarian status, whereas Ross et al. (*12*) found it to be confined to women with intact ovaries. These discrepant results indicate the need for additional studies of breast cancer in relation to oophorectomy and exogenous estrogen.

Evidence that the observed association between breast cancer and exogenous estrogens is causal would be strengthened if risk was found to increase with the amount of estrogen received. Ross et al. (*12*) found risk to be directly related to total cumulative dose, and Brinton et al. (*13*) found a weak (but statistically significant) increase in risk with duration of use. Hoover et al. (*15*) observed risk to increase with the strength of the preparation, but, paradoxically, to be lower in women who took estrogens daily than in women who took them less frequently. Women in these studies, like those in the present one, were largely users of conjugated estrogens for treatment of menopausal symptoms. Additional evidence for a dose response comes from three studies of women treated with diethylstilbestrol during pregnancy for threatened abortion (*16–18*). The excess risk was greatest in the study in which the mean dose of diethylstilbestrol was 16.3 g (*18*) and smaller in the study in which the mean dose was 11 g (*16*); no excess risk was observed in the study in which women received an average of 1.5 g (*17*). In the present study, risk of breast cancer did not increase with duration of estrogen use. A possible explanation for this finding is the limited accuracy of our information on dosage, which was based solely on responses to questions at the time of follow-up.

As discussed below, an unexpected finding in this study was the marked increase in risk of breast cancer in women in succeeding birth cohorts. Use of estrogens was also more common among women in later than earlier years. Year of birth was thus related to both breast cancer risk and estrogen use. However, it is unclear whether this factor should be considered a possible confounding variable which should be controlled when one is estimating the RR of breast cancer in estrogen users. This depends on the mechanisms responsible for the observed associations.

If some factor other than estrogen use is responsible for the year of birth effect on breast cancer risk, then year of birth can be considered a surrogate for this unknown factor and should be adjusted for as a confounding variable (*31*). However, if year of birth only influences estrogen use, and estrogen use in turn increases the risk of breast cancer, then year of birth is not a confounder and should not be controlled for in the analysis. Because we have no way of knowing which of the above possibilities is correct, we chose to present estimators of RR of breast cancer in estrogen users both adjusted and unadjusted for year of birth (table 9).

Forty-seven women whose only source of exogenous estrogens was oral contraceptives were considered estrogen users in the above analyses. Estimated values of RR in estrogen users were slightly lower when these women were treated as nonusers, but they were not changed sufficiently to alter any conclusions regarding the effects of exogenous estrogens on breast cancer risk.

There was approximately a fourfold increase in risk of breast cancer in birth cohorts spanning a 20-year period. Cohort-specific increases in breast cancer incidence and mortality rates have been reported in the general female populations of Iceland (*32*), Israel (*33*), Japan (*34*), Canada (*35*), England and Wales (*36, 37*), and the United States (*36*), as well as among Japanese immigrants to the United States (*38, 39*). Rather small cohort-specific increases have been related to change in fertility in such high-risk countries as Canada (*35, 40*), the United States (*36*), and England and Wales (*36*), although another study in England and Wales did not confirm this relationship (*37*). The larger cohort-specific increases in incidence in the initially low-risk country of Iceland (*41*) and in Japan (*42*), where rates are still low, have been found not to be related to changes in child-bearing practices. In Japan, they have been correlated with changes in dietary intake of fats and other nutrients (*42*). Rates of breast cancer among various countries have been correlated with these same dietary factors (*43, 44*). The cohort-specific increase in breast cancer risk observed in this study was of the same high order of magnitude as that in Iceland and, like the increases in Iceland and Japan, was not related to changes in child-bearing practices or to changes in ages at menarche or menopause. Also, the shape of the age-incidence curve in the present study did not vary with year of birth, which is consistent with similar observations in succeeding birth cohorts in Iceland and Japan, as well as in Denmark, Slovenia, Connecticut, and Finland (*45*).

In this study, there was a threefold greater use of estrogens in earlier than later birth cohorts, and a relationship between estrogen use and breast cancer was found. However, adjustment for estrogen use only reduced the cohort effect by a small amount. There are two possible explanations for this: 1) Either the cohort effect is largely due to factors unrelated to estrogen use or 2) the information on estrogen use was inadequate, and if it had been more complete, more of the cohort effect would have been explained by the temporal changes in estrogen use. There is no way of determining from analyses of the existing data which of these explanations is correct. If it is the second, then this would, of course, be additional evidence that exogenous estrogens can increase the risk of breast cancer.

Our interpretation of the available evidence is that estrogens may be responsible for a portion of the observed cohort effect but not all of it. The cohort effect *was* reduced by controlling for estrogen use and perhaps would have been reduced more if we had had more precise information on estrogen use. However, it is unlikely that all of the fourfold increase in breast cancer risk with succeeding birth cohorts could be explained on this basis. Other explanations would be conjectural. Dietary factors such those considered in national and international investigations were not studied. If the mechanisms for the large cohort difference observed in this population of women with benign breast lesions are the same as those in countries undergoing "westernization," then detailed studies of breast cancer in women with such lesions may help provide an explanation for large temporal changes in national rates and differences in risk among countries.

REFERENCES

(*1*) Donnelly PK, Baker KW, Carney NA, O'Fallon WM. Benign breast lesions and subsequent breast carcinoma in Rochester, Minnesota. Mayo Clin Proc 1975; 50:650–656.

(*2*) Monson RR, Yen S, MacMahon B, Warren S. Chronic mastitis and carcinoma of the breast. Lancet 1976; 2:224–226.

(*3*) Kodlin D, Winger EE, Morgenstern NL, Chen U. Chronic mastopathy and breast cancer. A follow-up study. Cancer 1977; 39:2603–2607.

(*4*) Page DL, Zwaag RV, Rogers LW, Williams LT, Walker WE, Hartmann WH. Relation between component parts of fibrocystic disease complex and breast cancer. JNCI 1978; 61:1055–1063.

(*5*) Hutchinson WB, Thomas DB, Hamlin WB, Roth GJ, Peterson AV, Williams B. Risk of breast cancer in women with benign breast disease. JNCI 1980; 65:13–20.

(*6*) Craig TJ, Comstock GW, Geiser PB. Epidemiologic comparison of breast cancer patients with early and late onset of malignancy and general population controls. J Natl Cancer Inst 1974; 53:1577–1581.

(*7*) Boston Collaborative Drug Surveillance Program, Boston University Medical Center. Surgically confirmed gallbladder disease, venous thromboembolism, and breast tumors in relation to postmenopausal estrogen therapy. N Engl J Med 1974; 290:15–19.

(*8*) Casagrande J, Gerkins V, Henderson BE, Mack T, Pike MC. *Brief communication*: Exogenous estrogens and breast cancer in women with natural menopause. J Natl Cancer Inst 1976; 56:839–841.

(*9*) Sartwell PE, Arthes FG, Tonascia JA. Exogenous hormones, reproductive history, and breast cancer. J Natl Cancer Inst 1977; 59:1589–1592.

(*10*) Ravnihar B, Seigel DG, Lindtner J. An epidemiologic study of breast cancer and benign breast neoplasias in relation to the oral contraceptive and estrogen use. Eur J Cancer 1979; 15:395–405.

(*11*) Jick H, Walker AM, Watkins RN, et al. Replacement estrogens and breast cancer. Am J Epidemiol 1980; 112:586–594.

(*12*) Ross RK, Paganini-Hill A, Gerkins VR, et al. A case–control study of menopausal estrogen therapy and breast cancer. JAMA 1980; 243:1635–1658.

(*13*) Brinton LA, Hoover RN, Szklo M, Fraumeni JF Jr. Menopausal estrogen use and risk of breast cancer. Cancer 1981; 47:2517–2522.

(*14*) Byrd BF, Burch JC, Vaughn WK. The impact of long term estrogen support after hysterectomy. Ann Surg 1977; 185:574–580.

(*15*) Hoover R, Gray LA, Cole P, MacMahon B. Menopausal estrogens and breast cancer. N Engl J Med 1976; 295:401–405.

(*16*) Bibbo M, Haenszel WM, Wied GL, Hubby M, Herbst AL. A twenty-five-year follow-up study of women exposed to diethylstilbestrol during pregnancy. N Engl J Med 1978; 298:763–767.

(*17*) Brian DD, Tilley BC, Labarthe DR, O'Fallon WM, Noller KL, Kurland LT. Breast cancer in DES-exposed mothers. Absence of association. Mayo Clin Proc 1980; 55:89–93.

(*18*) Beral V, Colwell L. Randomised trial of high doses of stilboestrol and ethisterone in pregnancy: Long-term follow-up of mothers. Br J Med 1980; 281:1098–1101.

(*19*) Fasal E, Paffenbarger RS Jr. Oral contraceptives as related to cancer and benign lesions of the breast. J Natl Cancer Inst 1975; 55:767–773.

(*20*) Cox DR. Regression models and life tables. J R Stat Soc (B) 1972; 34:187–220.

(*21*) Kalbfleisch JD, Prentice RL. The proportional hazards model, chapt 4. The statistical analysis of failure time data. New York: Wiley, 1980; 70–118.

(*22*) Mantel N. Evaluation of survival data and two new rank order statistics arising in its consideration. Cancer Chemother 1966; 50:163–170.

(*23*) Thomas DB. Epidemiologic and related studies of breast cancer etiology. In: Lilienfeld AM, ed. Reviews in cancer epidemiology. Vol 1. Elsevier/North Holland, 1980:153–217.

(*24*) Breslow NB. The proportional hazards model: Applications in epidemiology. Comm Stat Theor Meth 1978; A7:315–332.

(*25*) Miettinen OS. Estimability and estimation in case-referrent studies. Am J Epidemiol 1976; 103:226–235.

(*26*) Day NE, Byar DP. Testing hypothesis in case–control studies—equivalence of Mantel-Haenszel statistics and logit score tests. Biometrics 1979; 35:623–630.

(*27*) Kaplan EL, Meier P. Nonparametric estimation from incomplete observations. J Am Stat Assoc 1958; 53:457–481.

(*28*) Stadel BV, Weiss N. Characteristics of menopausal women: A survey of King and Pierce Counties in Washington. Am J Epidemiol 1975; 102:209–216.

(*29*) Weiss NS, Szekely DR, Austin DF. Increasing incidence of endometrial cancer in the United States. N Eng J Med 1976; 294:1259–1262.

(*30*) Ernster VL. The epidemiology of benign breast disease. Epidemiol Rev 1981; 3:184–202.

(*31*) Breslow NE, Day NE. Statistical methods in cancer research. Vol 1. The analysis of case–control studies. Lyon: IARC, 1980.

(*32*) Bjarnason O, Day N, Snaedal G, Tulinius H. The effect of year of birth on the breast cancer age–incidence curve in Iceland. Int J Cancer 1974; 13:689–696.

(*33*) Logan WP. Cancer of the female breast, international mortality trends. World Health Stat Rep 1975; 28:232–251.

(*34*) Moolgavkar SH, Stevens RG, Lee JA. Effect of age on incidence of breast cancer in females. JNCI 1979; 62:493–501.

(*35*) Wigle DT. Breast cancer and fertility trends in Canada. Am J Epidemiol 1977; 105:428–438.

(*36*) Armstrong B. Recent trends in breast-cancer incidence and mortality in relation to changes in possible risk factors. Int J Cancer 1976; 17:204–211.

(*37*) Hems G. Associations between breast-cancer mortality rates, childbearing and diet in the United Kingdom. Br J Cancer 1980; 41:429–437.

(*38*) Buell P. Changing incidence of breast cancer in Japanese–American women. J Natl Cancer Inst. 1973; 51:1479–1483.

(*39*) Dewaard F. Recent time trends in breast cancer incidence. Prev Med 1978; 7:160–167.

(*40*) Fabia J, Bernard PM, Hill G. Recent time-trends of age-specific death rates for breast cancer: Quebec and other provinces, 1965 through 1974. Can Med Assoc J 1977; 116:1135–1138.

(*41*) Tulinius H, Day NE, Johannesson G, Bjarnason O, Gonzales M. Reproductive factors and risk for breast cancer in Iceland. Int J Cancer 1978; 21:724–730.

(*42*) Hirayama T. Epidemiology of breast cancer with special reference to the role of diet. Prev Med 1978; 7:173–195.

(*43*) Armstrong B, Doll R. Environmental factors and cancer incidence and mortality in different countries, with special reference to dietary practices. Int J Cancer 1975; 15:617–631.

(*44*) Gray GE, Pike MC, Henderson BE. Breast-cancer incidence and mortality rates in different countries in relation to known risk factors and dietary practices. Br J Cancer 1979; 39:1–7.

(*45*) Moolgavkar SH, Day NE, Stevens RG. Two-stage model for carcinogenesis: Epidemiology of breast cancer in females. JNCI 1980; 65:559–569.

blank page

Second Cancers Following Radiotherapy for Cervical Cancer[1]

Ruth A. Kleinerman,[2,3] **Rochelle E. Curtis,**[4] **John D. Boice, Jr.,**[2] **John T. Flannery,**[5]
and **Joseph F. Fraumeni, Jr.**[2]

ABSTRACT—Incidence of second primary cancers was evaluated in 7,127 women with invasive cancer of the cervix uteri, diagnosed between 1935 and 1978, and followed up to 38 years (average, 8.9 yr) in Connecticut. Among 5,997 women treated with radiation, 449 developed second primary cancers compared with 313 expected (relative risk=1.4) on the basis of rates from the Connecticut Tumor Registry. Excess incidence was noticeable 15 years or more after radiotherapy and attributed mostly to cancers of sites in or near the radiation field, especially the bladder, kidneys, rectum, corpus uteri, and ovaries. No excess was found for these sites among the 1,130 nonirradiated women. The ratio of observed to expected cancers for these sites did not vary appreciably by age at irradiation. The data suggested that high-dose pelvic irradiation was associated with increase in cancers of the bladder, kidneys, rectum, ovaries, corpus uteri, and non-Hodgkin's lymphoma but, apparently, not leukemia, Hodgkin's disease, breast cancer, or colon cancer.—JNCI 1982; 69:1027–1033.

Conflicting data on risk of second primary cancers following radiotherapy for cervical cancer have been reported. Increased rate has been suggested for urinary bladder cancer (*1–5*), uterine cancer (*1, 2*), uterine sarcoma (*6*), rectal cancer (*2, 7*), lung cancer (*1–3, 8*), and osteosarcoma (*9*). However, no excess of leukemia has been reported in several studies (*1, 2, 6, 10–13*). To further investigate risk of second cancers, we evaluated data reported since 1935 to the Connecticut Tumor Registry. Previously, these data were analyzed through 1951 (*4*) and 1964 (*14*). The present evaluation is through 1978, increasing the number of cervical cancer patients and years of observation.

SUBJECTS AND METHODS

Of 8,247 women with primary diagnosis of invasive cancer of the cervix uteri, 7,127 women were eligible for study. Patients were excluded for any of the following reasons: unknown treatment (442), identification by death certificate or autopsy only (349), survival less than 3 months (236), occurrence of a second primary cancer within 3 months of cervical cancer diagnosis (48), or incomplete follow-up (45). Women were classified as radiotherapy patients if treatment occurred within 4 months of cervical cancer diagnosis.

Histologic confirmation was available for 96% of cervical cancers and 85% of all second primary cancers. Confirmation varied only slightly by calendar year. Cancer diagnoses were coded according to the eighth revision of the International Classification of Diseases (ICD) (*15*). Digestive cancers (ICD8 150–158) were not confirmed as often as other second primary cancers (75 vs. 89%). All second primary cancers were determined by a pathologist at the hospital where the cancer was diagnosed.

We calculated WY 3 months from date of cervical cancer diagnosis to date of diagnosis of second primary cancer; death; date lost to follow-up; or December 31, 1978, whichever occurred first. At the closing date of the study, 65% of the cervical cancer patients had died, and 13% had been reported lost to follow-up.

We derived expected numbers of cancers by multiplying age-, sex-, and calendar time-specific incidence rates by appropriate WY (*16*). RR was measured as ratio of observed to expected incident cancers. Absolute risk was computed as the difference between observed and expected events divided by the WY. Exact and approximate confidence limits were calculated with the use of the Poisson model for the observed number of cancers (*17*).

We decided not to compare incident cancers in the 2 treatment groups but to compare each group with the general population for two reasons. First, number of second primary cancers in the nonirradiated group was too small to provide stable rates, especially for evaluation of latency and effect of age at exposure to radiotherapy. Second, except for breast cancer and other genital cancer, the rate of second cancers in the nonirradiated group did not differ significantly from the rate in the general population. We stress that this analysis cannot be used to evaluate the therapeutic efficacy of different treatment regimens for cervical cancer.

Although individual dose data were not available from the registry, risk of cancer could be crudely evaluated for organs proximal, intermediate, and remote to the pelvis. Bladder, colon, rectum, uterine corpus, ovaries, bone and connective tissue, bone marrow, and lymphatics were considered proximal sites and thus heavily irradiated. Stomach, pancreas, kidneys, and liver were designated intermediate sites. Buccal cavity, lungs, breasts, brain, and thyroid gland were classified remote sites. Nonmelanoma skin cancers were excluded from all analyses.

RESULTS

Comparability of treatment groups.—Among the 7,127 women eligible for study with invasive cancer of the cervix uteri, 5,997 (84%) were treated with radiation and 1,130 (16%)

ABBREVIATIONS USED: CI=confidence interval; RR=relative risk; WY=woman-years at risk.

---

[1] Received January 18, 1982; accepted June 30, 1982.

[2] Environmental Epidemiology Branch, Division of Cancer Cause and Prevention, National Cancer Institute, National Institutes of Health, Public Health Service, U. S. Department of Health and Human Services, Bethesda, Md. 20205.

[3] *Address reprint requests to* Ms. Kleinerman at the Landow Building, Room 3C16, Bethesda, Md. 20205.

[4] Biometry Branch, Division of Cancer Cause and Prevention, National Cancer Institute.

[5] Connecticut Tumor Registry, State of Connecticut Department of Health, Hartford, Conn. 06115.

TABLE 1.—*Number of women by age at diagnosis of cervical cancer and type of treatment*

Age at diagnosis, yr	Radiotherapy	No radiotherapy	Total
<40	961	426	1,387
40–49	1,550	343	1,893
50–59	1,667	209	1,876
≥60	1,819	152	1,971
Total	5,997	1,130	7,127

were not. Irradiated women received either radiation only (86%); radiation and surgery (6%); radiation, surgery, and either hormones or chemotherapy (6%); or radiation and either chemotherapy or hormones (2%). Radiation treatment was external beam (22%), radium implant (20%), or a combination of both (58%). Women in the nonirradiated group received surgery alone (52%), surgery and either chemotherapy or hormones (46%), or either chemotherapy or hormones or both (2%).

Tables 1 and 2 compare age distributions and WY for the 2 treatment groups. Mean ages at diagnosis of cervical cancer for the irradiated and nonirradiated groups were 53 and 45 years, respectively. Maximum follow-up was 38 years for both. Mean follow-up was 7.8 years (45,392 WY) for irradiated women and 9.9 years (11,041 WY) for nonirradiated women.

All sites.—An excess of cancer occurred in both treatment groups (table 3). The observed-to-expected ratio for the irradiated group was 1.44, a statistically significant 44% excess over expectation. The ratio for the nonirradiated group was 1.30, a significant 30% excess. With the exception of breast cancer and other genital cancer, second cancer incidence in the nonirradiated group was not substantially different from that expected in the general population.

Lymphatic and hematopoietic system.—Nine leukemias were

TABLE 2.—*WY by time since diagnosis of cervical cancer and type of treatment*

Time since diagnosis, yr	Radiotherapy	No radiotherapy	Total
<1	5,257	1,064	6,321
1–4	12,896	3,152	16,048
5–9	10,548	2,658	13,206
10–14	7,205	1,849	9,054
15–19	4,698	1,282	5,980
20–24	2,714	686	3,400
25–29	1,344	262	1,606
≥30	730	88	818
Total	45,392	11,041	56,433

TABLE 3.—*Observed (O) and expected (E) second primary cancers by type of treatment*

ICD8 code	Site	No. of cancers					
		Radiotherapy			No radiotherapy		
		O	E	O/E	O	E	O/E
140–209[a]	All sites	449	312.3	1.4[b]	79	60.8	1.3[b]
140–149	Buccal cavity	13	5.7	2.3[b]	4	1.2	3.3[b]
150	Esophagus	6	2.0	3.0[b]	0	0.4	0
151	Stomach	19	14.2	1.3	2	2.1	1.0
153	Colon	47	45.1	1.0	9	7.8	1.2
154	Rectum	30	18.3	1.6[b]	5	3.2	1.6
155, 156	Liver & biliary tract	5	7.3	0.7	2	1.1	1.8
157	Pancreas	10	9.4	1.1	0	1.6	0
161	Larynx	4	1.0	4.0[b]	3	0.2	15.0[b]
162, 163	Bronchus & lungs	64	12.6	5.1[b]	3	2.8	1.1
170	Bone	2	0.7	3.0	0	0.1	0
171	Connective tissues	5	1.5	3.3[b]	1	0.3	3.3
172	Melanoma	3	3.1	1.0	2	0.8	2.5
174	Breasts	58	86.2	0.7[b]	27	18.7	1.4[b]
182	Corpus uteri	39	27.7	1.4[b]	0	5.6	0
183	Ovaries	25	16.0	1.6[b]	2	3.3	0.6
184	Other genitals	19	10.8	1.8[b]	8	1.8	4.4[b]
188	Bladder	26	7.7	3.4[b]	0	1.3	0
189	Kidneys	14	4.9	2.8[b]	0	0.9	0
191–192	Brain	3	3.5	0.9	0	0.8	0
193	Thyroid gland	0	2.3	0	0	0.5	0
201	Hodgkin's disease	1	2.2	0.5	0	0.6	0
200, 202	Reticulum cell sarcoma, lymphosarcoma	12	4.7	2.6[b]	2	1.2	1.7
203	Multiple myeloma	4	3.4	1.2	0	0.7	0
204–207	All leukemia	9	7.4	1.2	1	1.3	0.8
199	Unknown	24	11.7	2.1[b]	7	2.1	3.3[b]
152, 158, 190, 194	Other	7	2.9	2.4[b]	1	0.4	2.5
151, 153–157, 182–183, 188–189	Proximal and intermediate	215	150.6	1.4[b]	20	26.9	0.7

[a] Excludes 180.

[b] $P<0.05$, one-sided test.

TABLE 4.—*Observed (O) and expected (E) second primary cancers by time since radiotherapy for cervical cancer*

ICD8 code	Site	Parameter	No. of cancers by time since radiotherapy, yr[a]								
			<1 (5,997)	1–4 (4,518)	5–9 (2,580)	10–14 (1,736)	15–19 (1,176)	20–24 (727)	25–29 (386)	≥30 (180)	Total
140–209	All	O	30	100	90	91	59	39	20	20	449
		E	26.5	71.3	66.9	54.2	41.1	27.3	15.5	9.5	312.3
		O/E	1.1	1.4[b]	1.4[b]	1.7[b]	1.4[b]	1.4[b]	1.3	2.1[b]	1.4[b]
140–149	Buccal cavity	O	1	4	3	3	2	0	0	0	13
		E	0.5	1.2	1.2	1.0	0.8	0.5	0.3	0.2	5.7
		O/E	2.2	3.3[b]	2.5	3	2.6	0	0	0	2.3[b]
150–159	Digestive system	O	8	20	24	26	22	10	5	5	120
		E	8.2	21.8	20.7	17.0	13.6	9.5	5.7	3.7	100.6
		O/E	0.9	0.9	1.2	1.5[b]	1.6[b]	1.1	0.9	1.4	1.2
150	Esophagus	O	1	2	1	1	1	0	0	0	6
		E	0.2	0.4	0.4	0.4	0.3	0.2	0.1	0.1	2.0
		O/E	5.0	5.0	2.5	2.5	3.3	0	0	0	3.0[b]
151	Stomach	O	3	5	2	6	2.0	0	1	0	19
		E	1.4	3.4	3.1	2.4	1.8	1.2	0.7	0.4	14.2
		O/E	2.1	1.5	0.7	2.5[b]	1.1	0	1.5	0	1.3
153	Colon	O	3	5	10	12	8	4	3	2	47
		E	3.4	9.4	9.1	8.4	6.3	4.5	2.7	1.8	45.1
		O/E	0.9	0.5	1.1	1.4	1.3	0.9	1.1	1.1	1.0
154	Rectum	O	1	4	5	4	9	4	1	2	30
		E	1.5	4.1	3.9	3.2	2.4	1.6	0.9	0.6	18.3
		O/E	0.7	0.9	1.3	1.3	3.7[b]	2.5	1.1	3.3	1.6[b]
155, 156	Liver & biliary tract	O	0	0	3	0	0	1	0	1	5
		E	0.7	1.6	1.5	1.2	1.0	0.6	0.4	0.2	7.3
		O/E	0	0	2.0	0	0	1.7	0	5.0	0.7
157	Pancreas	O	0	4	2	1	2	1	0	0	10
		E	0.7	2.0	1.9	1.6	1.3	1.0	0.6	0.4	9.4
		O/E	0	2.0	1.1	0.6	1.5	1	0	0	1.1
162, 163	Bronchus & lungs	O	5	18	17	16	6	0	1	1	64
		E	0.9	2.6	2.6	2.3	1.8	1.3	0.7	0.4	12.6
		O/E	5.5[b]	6.9[b]	6.5[b]	7.0[b]	3.3[b]	0	1.4	2.5	5.1[b]
170	Bone	O	0	1	1	0	0	0	0	0	2
		E	0.1	0.2	0.2	0.1	0.1	0.1	0.02	0.01	0.7
		O/E	0	5.0	5.0	0	0	0	0	0	3.0
171	Connective tissues	O	0	1	1	1	1	1	0	0	5
		E	0.1	0.4	0.3	0.3	0.2	0.1	0.1	0.004	1.5
		O/E	0	2.5	3.3	3.3	5.0	10.0	0	0	3.3[b]
172, 173	Melanoma	O	1	2	0	0	0	0	0	0	3
		E	0.3	0.7	0.7	0.5	0.4	0.3	0.1	0.1	3.1
		O/E	3.3	2.9	0	0	0	0	0	0	1.0
174	Breasts	O	4	16	11	12	5	6	1	3	58
		E	7.8	20.8	19.1	14.8	10.7	6.9	3.8	2.3	86.2
		O/E	0.5	0.8	0.6[b]	0.8	0.5[b]	0.9	0.3	1.3	0.7[b]
182	Corpus uteri	O	2	4	11	7	5	5	3	2	39
		E	2.5	6.7	6.2	4.9	3.5	2.2	1.1	0.6	27.7
		O/E	0.8	0.6	1.8	1.4	1.4	2.3	2.7	3.3	1.4[b]
183	Ovaries	O	2	4	6	3	3	4	0	3	25
		E	1.5	4.1	3.6	2.7	1.9	1.2	0.6	0.4	16.0
		O/E	1.3	1.0	1.7	1.1	1.6	3.3[b]	0	7.5[b]	1.6[b]
188	Bladder	O	3	3	4	7	3	1	3	2	26
		E	0.6	1.5	1.5	1.3	1.1	0.8	0.5	0.4	7.7
		O/E	5.0[b]	2.0	2.7	5.4[b]	2.7	1.3	6.0[b]	5.0	3.4[b]
189	Kidneys	O	1	3	0	1	1	5	1	2	14
		E	0.4	1.1	1.1	0.9	0.7	0.5	0.3	0.2	4.9
		O/E	2.5	2.7	0	1.1	1.4	10.0[b]	3.3	10.0[b]	2.8[b]

[a] *Numbers in parentheses* are numbers of women at start of intervals.

[b] *P*<0.05, one-sided test.

pages tightly bound

best copy available

TABLE 4 (continued).—*Observed (O) and expected (E) second primary cancers by time since radiotherapy for cervical cancer*

ICD8 code	Site	Parameter	No. of cancers by time since radiotherapy, yr[a] <1 (5,997)	1–4 (4,518)	5–9 (2,580)	10–14 (1,736)	15–19 (1,176)	20–24 (727)	25–29 (386)	≥30 (180)	Total
191, 192	Brain, central nervous system	O	0	2	0	0	1	0	0	0	3
		E	0.3	0.9	0.8	0.6	0.4	0.3	0.1	0.1	3.5
		O/E	0	2.2	0	0	2.5	0	0	0	0.9
194	Thyroid gland	O	0	0	0	0	0	0	0	0	0
		E	0.2	0.6	0.6	0.4	0.3	0.2	0.1	0.1	2.3
		O/E	0	0	0	0	0	0	0	0	0
201	Hodgkin's disease	O	0	1	0	0	0	0	0	0	1
		E	0.2	0.5	0.7	0.4	0.3	0.2	0.1	0.1	2.2
		O/E	0	2.0	0	0	0	0	0	0	0.5
200, 202	Reticulum cell sarcoma, lymphosarcoma	O	1	4	3	2	1	1	0	0	12
		E	0.4	1.1	0.8	0.9	0.6	0.5	0.5	0.3	4.7
		O/E	1.7	3.6[b]	3.8[b]	2.2	1.7	2.0	0	0	2.6[b]
203	Multiple myeloma	O	0	0	0	1	0	0	1	2	4
		E	0.2	0.6	0.6	0.6	0.5	0.4	0.2	0.2	3.4
		O/E	0	0	0	1.7	0	0	5.0	10.0[b]	1.2
204–207	Leukemia	O	0	1	3	2	1	2	0	0	9
		E	0.6	1.5	1.5	1.3	1.0	0.7	0.4	0.3	7.4
		O/E	0	0.7	2.0	1.5	1.0	2.9	0	0	1.2
151, 153–157, 182–183, 188–189	Proximal & intermediate	O	15	32	41	41	33	25	12	14	215
		E	12.7	33.9	31.9	26.0	20.0	13.6	7.8	5.0	150.6
		O/E	1.2	0.9	1.3	1.6[b]	1.7[b]	1.8[b]	1.5[b]	2.8[b]	1.4[b]

[a] *Numbers in parentheses* are numbers of women at start of intervals.
[b] *P*<0.05, one-sided test.

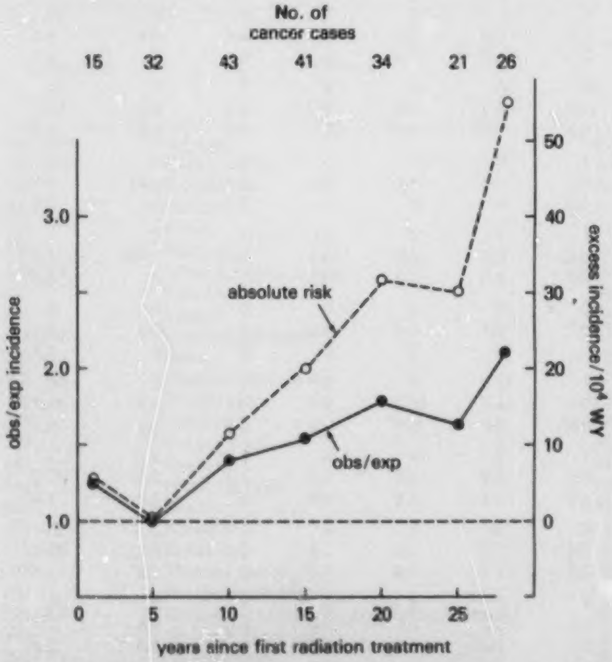

TEXT-FIGURE 1.—Ratio of observed (obs) and expected (exp) incident cancers and absolute risk [(obs−exp)/WY] of proximal and intermediate sites by years since first radiation treatment.

diagnosed compared with 7.4 expected (RR=1.2, 95% CI=0.6–2.3) in the radiotherapy group. Incidence of reticulum cell sarcoma and lymphosarcoma in that group was also greater than expected (12 observed vs. 4.7 expected). Multiple myeloma, however, was not in excess (4 observed vs. 3.4 expected) nor was Hodgkin's disease (1 observed vs. 2.2 expected). No excess of lymphatic or hematopoietic cancers was found in the women treated without radiation.

Proximal sites.—With the exception of the colon, excess cancers occurred for all heavily irradiated proximal organs. The greatest excess was for cancer of the bladder: 26 observed compared with 7.7 expected (RR=3.4, 95% CI=2.2–5.0). Risks were elevated for cancers of the uterine corpus (RR=1.4, 95% CI=1.0–2.0), rectum (RR=1.6, 95% CI=1.1–2.3), and ovaries (RR=1.6, 95% CI=1.0–2.3). Two bone cancers of the pelvis were diagnosed, and less than 1 cancer was expected. A significant excess of cancer of the connective tissues occurred (RR=3.3, 95% CI=1.1–7.8). Of the 5 connective tissue cancers, 2 were in the trunk and 1 was in the hip; the site was not specified for the other 2 cancers.

Intermediate sites.—Among irradiated women, a definite excess of kidney cancer and a slight excess of stomach cancer were found. Fourteen kidney cancers were diagnosed versus 4.9 expected (RR=2.8, 95% CI=1.6–4.8). For all proximal and intermediate sites combined, there was a significant excess of cancer among radiotherapy patients (215 vs. 151), but this excess did not occur among the nonirradiated women (20 vs. 26.9).

Remote sites.—There were 64 cancers of the lungs, whereas 12.6 were expected (RR=5.1, 95% CI=4.0–6.5). No excess of pancreas cancer was seen (10 observed vs. 9.4 expected). A deficit of breast cancer occurred in the irradiated group (RR=0.7, 95% CI=0.5–0.9), compared with an excess of breast cancer in the nonirradiated group (RR=1.4, 95% CI=1.0–2.1). Thyroid cancer was not observed in either treatment group.

Time since radiotherapy.—For several organs, a substantial

TABLE 5.—*Observed and expected cancers of proximal and intermediate sites[a] by age at radiotherapy among 10-year survivors*

Category	No. of cancers at age at exposure, yr				
	<40	40–49	50–59	≥60	Total
No. of women	369	567	469	331	1,736
Observed	19	40	37	25	121
Expected	8.7	25.3	23.4	16.0	73.4
Observed/expected	2.18	1.58	1.58	1.56	1.65
Woman-years of observation[b]	4,169	6,363	4,142	2,019	16,693
Absolute risk[c]	24.7	23.1	32.8	44.6	28.5

[a] Colon, rectum, liver, gallbladder, corpus uteri, ovaries, bladder, kidneys, pancreas, and stomach.

[b] Discrepancy between totals of WY in this table and in table 2 is due to rounding.

[c] $[(\text{Observed}-\text{expected})/\text{WY}]\times 10^4$.

excess of cancer occurred 15 years or more after radiotherapy (table 4). These included bladder (9 vs. 2.8), kidneys (9 vs. 1.7), ovaries (10 vs. 4.1), and corpus uteri (15 vs. 7.4). For women receiving radiotherapy, both the ratio of observed to expected cancers and the absolute risk of cancers of proximal and intermediate sites increased substantially after 10 years since exposure (text-fig. 1). The small risk observed in the early years might be related to close medical surveillance or metastases. Lung cancer rates were elevated during the first 19 years following radiotherapy (RR=6.1, 95% CI=4.7–7.8), but they decreased to normal levels thereafter. Breast cancer rates were lower than expected during each interval after radiotherapy.

Age at radiotherapy.—RR of cancer of irradiated proximal and intermediate sites did not vary appreciably by age at initial exposure (table 5, text-fig. 2), although those under 40 years of age had a slightly higher RR than did older women. Since the incidence of cancer generally increases with age, the constant RR implied a substantial increase in the number of cancers attributable to radiation exposure (text-fig. 2). Breast cancer rates were lower than expected for all ages, including women irradiated after 60.

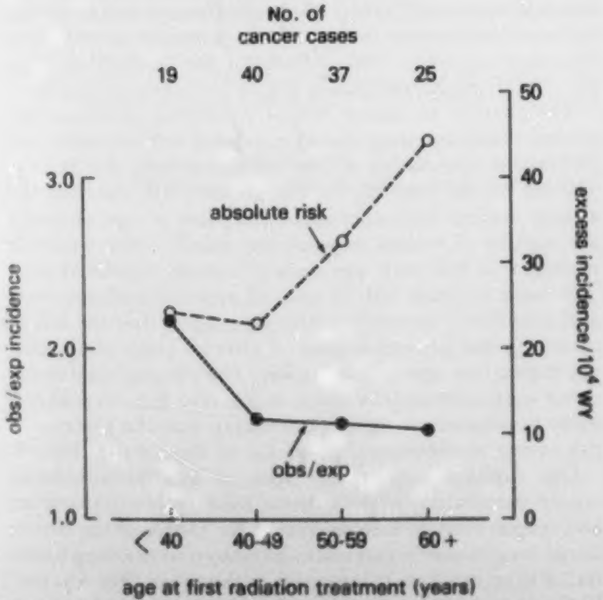

TEXT-FIGURE 2.—Ratio of observed (obs) and expected (exp) incident cancers and absolute risk [(obs−exp)/WY] of proximal and intermediate sites 10 yr or more after first treatment by age at first radiation treatment.

DISCUSSION

This study of cervical cancer patients revealed an increased incidence of second primary cancers arising in several irradiated proximal organs. However, we found surprising that no excess of leukemia occurred in the radiation group because the dose to the bone marrow was large and leukemia is frequently seen as an irradiation effect.

Published risk estimates for leukemia, on the basis of studies of atomic bomb survivors and patients irradiated for ankylosing spondylitis, are about 2 leukemia cases per million persons/year/rad (*18*). Assuming an average dose of 750 rad to the total body bone marrow, we expected an excess of 68 cases in addition to the 7–8 cases anticipated from nonirradiation causes; a total of only 9 leukemias occurred. These results, however, are consistent with other large studies of cervical cancer patients (*10, 11*).

The radiation doses used to treat cervical cancer patients have been suggested as being too large to be leukemogenic. High doses to small volumes of bone marrow may sterilize cells rather than transform them, thereby reducing the number of cells available for cancer induction (*19*). In experimental studies, large doses of radiation can kill or inactivate cells in culture, and the incidence of myeloid leukemia in mice decreases at high doses (*20*). The bone marrow outside the pelvic region received an intermediate dose of radiation; why this dose did not increase the incidence of leukemia is yet to be explained. If the smaller dose received by the bone marrow outside the pelvis is the primary determinant for leukemogenesis, then the number of women exposed to radiation in our study may not be large enough for detection of the possible low risk involved.

Radiation dose to the lymphatic system was large, and an excess of reticulum cell sarcoma and lymphosarcoma but not Hodgkin's disease was observed. This finding is consistent with previous reports (*18*).

Because cervical cancer patients are more likely to smoke cigarettes compared with other women (*21*), the smoking-related sites have to be evaluated carefully. Cancers of the bladder, lungs, buccal cavity, and the esophagus but not the pancreas were increased. Bladder cancer was increased in the first 5 years after diagnosis of cervical cancer and again at 15 years or more after treatment. Early bladder cancer risk may be related to smoking habits or metastases misclassified as primary tumors. The nine bladder cancers diagnosed 15 years after treatment are consistent with the expected latent period for irradiation-related neoplasms. Interestingly, the temporal pattern of risk for bladder cancer differs from the risk for lung cancer. Risk for bladder cancer increased over time, whereas risk for lung cancer decreased. No increase in cancer of these smoking-related sites, except for the buccal cavities, was observed in the nonirradiated group.

Lung cancer excess occurred within the first 19 years after diagnosis of cervical cancer. This pattern might be explained by cigarette smoking habits, in view of the low radiation dose to the lungs and of cervical cancer patients possibly smoking more than other women. Misclassification is also possible, because the lungs are a common site of extrapelvic spread in cervical cancer patients (*22*). Why no excess of lung cancer was observed among the nonirradiated women is difficult to explain. However, social class differences (*23*), which may be related to smoking habits, are probably associated with the stage of disease and in turn to the use of radiotherapy.

Kidney cancer has been weakly associated with smoking, mainly in men (*24*). An excess of this cancer occurred in the irradiated group only, especially 15 years after radiation exposure. Kidney cancer has not been prominently linked to irradiation, and only a slight excess in mortality was seen in one follow-up study of patients irradiated for ankylosing spondylitis (8 observed vs. 4.1 expected) (*18, 25*). In the spondylitis study, the kidneys were thought to be lightly irradiated and not directly in the radiation field. In our series, the kidneys were designated an intermediate site, but during external beam therapy the kidneys may have occasionally received substantial doses of radiation.

A deficit of breast cancer was found among irradiated women (58 vs. 86), whereas a slight excess appeared among nonirradiated patients (27 vs. 19). Ablation of the ovaries by radiotherapy may have lowered the risk of breast cancer in prememopausal women (*26, 27*), but how this disruption of ovarian function in older women would also be equally protective is not clear. A protective effect, independent of age at irradiation, however, was suggested also by Smith and Doll (*28*) in their study of 2,000 women whose ovaries were irradiated for treatment of benign gynecologic disease. Cervical cancer patients who had received radiotherapy may be at low risk of breast cancer due to greater parity and lower socioeconomic status than women in the general population. If so, the expected number of breast cancer cases from the general population would lead to overestimation of the true expected number. Unfortunately, we had no information on menopause status that could have affected breast cancer risk. Thus irradiation-induced menopause, reproductive history, and socioeconomic factors may all contribute to the observed deficit of breast cancer. Slightly elevated breast cancer risk in the nonexposed group of cervical cancer patients is difficult to be explained, although the numbers are comparatively small. Breast cancer risk was increased only within the first 5 years after exposure, and the early detection due to medical surveillance may have contributed to this excess.

Radiation doses to all pelvic organs were large. Risk of rectal cancer was increased 15 years or more after treatment, but no increase was seen for colon cancer. Socioeconomic status has been correlated positively with colon cancer (*29*) and inversely with cervical cancer, so that use of general population rates for colon cancer may have somewhat underestimated the risks of radiogenic colon cancer in this population. However, no convincing evidence was seen that the colon is particularly radiosensitive on the basis of data from the A-bomb survivors (*18*).

Excess of cancers of the corpus uteri and ovaries occurring 15 years post treatment is consistent with a radiation etiology, but one finds difficult to exclude the possibility of metastatic lesions. At least 12% of the irradiated women also had surgical treatment, and they may not have been at risk of developing these 2 cancers. Therefore, the expected number may have been too large, which would result in an underestimate of risk. Other genital cancers also occurred in excess in both treatment groups, but again the possibility of mestastases cannot be discounted. Unfortunately, information on hysterectomy and oophorectomy status was unavailable.

Ionizing radiation is the only environmental agent known to cause bone cancer, and both osteosarcomas in our series occurred in the radiation field. Cumulative incidence of bone cancer was 0.04% and is consistent with other data (*30*). Of the 5 connective tissue cancers, 3 arose in heavily irradiated proximal areas as well. Although very little quantitative data are available on the association between soft tissue sarcoma and radiation exposure, evidence of irradiation effect appears only after very high-dose therapeutic exposures (*6, 31*).

Pattern of cancer risk over time for irradiated proximal and intermediate organs (text-fig. 1) is consistent with studies of atomic bomb survivors (*32*) and ankylosing spondylitis patients (*25*). Among cervical patients, cancer risk for other sites was increased 10 years after radiotherapy and remained elevated. Metastases may account partially for the early increased incidence, but metastases are unlikely to have greatly influenced the cancer risk in long-term survivors.

The pattern of cancer risk of irradiated proximal and intermediate organs by age at exposure, excluding the first 10 years of observation, is also consistent with the findings of other studies (text-fig. 2). The greatest RR was observed among women irradiated under 40 years of age, although the number of women exposed was small. There was little variation in RR with age among women irradiated after they were 40 years old. Studies of atomic bomb survivors and ankylosing spondylitis patients suggest that the RR of cancer among persons irradiated after 20 years of age does not depend on age at irradiation. The cervical cancer patients were substantially older as a group than the other 2 study populations, and it is interesting that the patterns of risk by age at exposure were similar in these 3 populations.

Our findings suggest an excess of irradiation-induced cancer, particularly of the kidneys, bladder, rectum, ovaries, and corpus uteri in women treated for cancer of the cervix. Large lung cancer excess could be related to smoking habits rather than irradiation inasmuch as the organ dose was low. Risk of breast cancer may have been diminished by ovarian ablation or by reproductive and socioeconomic characteristics that may be protective. No increased risk was found for leukemia, Hodgkin's disease, or colon cancer. Most, but not all, inferences were based on comparisons with the general population, and they should be viewed cautiously. Additional studies of cervical cancer patients should determine to what extent the risk of second cancers may be influenced by differences in radiation dose, smoking, endocrine status, and other host and environmental factors.

REFERENCES

(*1*) Morton RF, Villasanta U. New cancers arising in 1,563 patients with carcinoma of the cervix treated by irradiation. Am J Obstet Gynecol 1973; 115:462-466.

(*2*) Dickson RJ. Late results of radium treatment of carcinoma of the cervix. Clin Radiol 1972; 23:528-535.

(*3*) Newell GR, Krementz ET. Multiple malignant neoplasms in the Charity Hospital Tumor Registry. Cancer 1977; 40:1812-1820.

(*4*) Bailar JC III. The incidence of independent tumors among uterine cancer patients. Cancer 1963; 16:842-853.

(*5*) McIntyre D, Pointon RC. Vesical neoplasms occurring after radiation treatment for carcinoma of the uterine cervix. J Roy Coll Surg (E) 1971; 16:141-146.

(*6*) Czesnin K, Wronkowski Z. Second malignancies of the irradiated area in patients treated for uterine cervix cancer. Gynecol Oncol 1978; 6:309-315.

(*7*) Schoenberg BS, Greenberg RA, Eisenberg H. Occurrence of certain multiple primary cancers in females. J Natl Cancer Inst 1969; 43:15-32.

(*8*) Schottenfeld D, Berg J. Incidence of multiple primary cancers. IV. Cancers of the female breast and genital organs. J Natl Cancer Inst 1971; 46:161-170.

(*9*) Fehr PE, Prem KA. Post-irradiation sarcoma of the pelvic girdle following therapy for squamous cell carcinoma of the cervix. Am J Obstet Gynecol 1973; 116:192-200.

(*10*) Boice JD, Hutchison GB. Leukemia in women following radiotherapy for cervical cancer: Ten-year follow-up of an international study. JNCI 1980; 65:115-129.

(*11*) Simon N, Brucer M, Hayes R. Radiation and leukemia in carcinoma of the cervix. Radiology 1960; 74:905-911.

(*12*) Zippin C, Bailar JC III, Kohn HI, Lum D, Eisenberg H. Radiation therapy for cervical cancer: Late effects on life span and on leukemia incidence. Cancer 1971; 28:937-942.

(*13*) Palmer JP, Spratt DW. Pelvic carcinoma following irradiation for benign gynecological diseases. Am J Obstet Gynecol 1956; 72:497-505.

(*14*) Schoenberg BS. Multiple primary malignant neoplasms, the Connecticut experience, 1935-1964. New York: Springer-Verlag, 1977.

(*15*) World Health Organization. Manual of the international statistical classification of disease, injuries and causes of death, 1965. Eighth revision. Geneva: WHO, 1969.

(*16*) Monson RR. Analysis of relative survival and proportional mortality. Comput Biomed Res 1974; 7:325-332.

(*17*) Rothman KJ, Boice JD Jr. Epidemiologic analysis with a programmable calculator. Washington, D.C.: U. S. Govt Print Off, 1979 (NIH publication No. 79-1649).

(*18*) Committee on the Biological Effects of Ionizing Radiations (BEIR III). The effects on populations of exposure to low levels of ionizing radiation: 1980. Washington, D. C.: Natl Acad Sci, 1980.

(*19*) Hutchison GB. Leukemia in patients with cancer of the cervix uteri treated with radiation. A report covering the first 5 years of an international study. J Natl Cancer Inst 1968; 40:951-982.

(*20*) Major IR, Mole RH. Myeloid leukemia in x-ray irradiated CBA mice. Nature 1978; 272:455-456.

(*21*) Wright NH, Vessey MP, Kenward B, McPherson K, Doll R. Neoplasia and dysplasia of the cervix uteri and contraception: A possible protective effect of the diaphragm. Br J Cancer 1978; 38:273-279.

(*22*) Van Nagell JR, Rayburn W, Donaldson ES, et al. Therapeutic implications of patterns of recurrence in cancer of the cervix. Cancer 1979; 44:2354-2361.

(*23*) Devesa SS, Diamond EL. Association of breast cancer and cervical cancer incidences with income and education among whites and blacks. JNCI 1980; 65:515-528.

(*24*) Office on Smoking and Health, Office of the Assistant Secretary for Health. Smoking and health, a report of the Surgeon General. Washington, D. C.: Public Health Service, DHEW, 1979:15-17.

(*25*) Smith PG, Doll R. Mortality among patients with ankylosing spondylitis after a single treatment course with x rays. Br Med J 1982; 284:449-460.

(*26*) Trichopoulos D, MacMahon B, Cole P. Menopause and breast cancer risk. J Natl Cancer Inst 1972; 48:605-613.

(*27*) Boice JD, Hoover RN. Radiogenic breast cancer: Age effects and implications for models of human carcinogenesis. In: Burchenal JH, Oettgen HF, eds. Cancer: Achievements, challenges, and prospects for the 1980's. Vol 1. New York: Grune & Stratton, 1981:209-221.

(*28*) Smith PG, Doll R. Late effects of x irradiation in patients treated for metropathia haemorrhagica. Br J Radiol 1976; 49:224-232.

(*29*) Correa P, Haenszel W. The epidemiology of large bowel cancer. Adv Cancer Res 1978; 26:1-141.

(*30*) Fraumeni JF Jr, Boice JD Jr. Bone. In: Schottenfeld D, Fraumeni JF Jr, eds. Cancer epidemiology and prevention. Philadelphia: Saunders, 1982:814-826.

(*31*) Kim JH, Chu FC, Woodard HQ, Melamed MR, Huvos A, Cantin J. Radiation-induced soft tissue and bone sarcoma. Radiology 1978; 129:501-508.

(*32*) Beebe GW, Kato H, Land CE. Studies of the mortality of A-bomb survivors. 6. Mortality and radiation dose, 1950-1974. Radiat Res 1978; 75:138-201.

blank page

Association of Breast Cancer Risk With Age at First and Subsequent Births: A Study in the Population of the Estonian Republic[1,2]

Brian MacMahon,[3] Maret Purde,[4] Daniel Cramer,[3] *and* Evi Hint[4]

ABSTRACT—Information on reproductive history was obtained from 362 urban breast cancer patients attending the oncological dispensaries at Tallinn and Tartu, Estonian Republic, and from 694 urban women participating in gynecologic screening programs offered by the same centers. The 2 groups were compared by means of Mantel-Haenszel and logistic regression procedures to estimate age-adjusted odds ratios. Women whose first birth occurred before 20 years of age had a breast cancer risk less than one-third the risk of nulliparous women. Risk increased with increase in age at first birth (AFB) but remained below 1.0 (relative to nulliparae), even in the highest AFB categories. The fertility rate in Estonia during the period of this study was relatively low, which facilitated an evaluation of the effect of births subsequent to the first. After adjustment for AFB, it appeared that in this population subsequent births had a protective effect additional to that conferred by the first birth. Moreover, for women who had only 2 children, the age at the time of birth of the second child was a determinant of that effect. Compared to nulliparous women, the breast cancer odds ratio for uniparous women who had their child before age 25 was 0.62, and the ratio for duoparous women who had both their children under that age was 0.18. Neither lactation nor menarche was a risk factor for breast cancer in this population.—JNCI 1982; 69:1035-1038.

Cooperation between the United States and the Soviet Union in the fields of medicine and public health was pledged by both governments in 1960 and reaffirmed in 1972. The development of this cooperation in the area of cancer research has been documented by Saunders (*1*).

A U.S.-U.S.S.R. working group on the epidemiology of cancer was established in 1974. One of the first cancer sites to be selected for cooperative activity was cancer of the breast—a dominant cancer in the United States as well as in certain parts of the Soviet Union. The Epidemiology Group of the Institute of Experimental and Clinical Medicine of Estonia had been designated by the Cancer Epidemiology Council of the U.S.S.R. Academy of Medical Sciences as the All-Union Center for the Epidemiologic Study of Breast Cancer. This group had undertaken case-control studies in several parts of the Soviet Union, but it had just completed a particularly large study in Estonia. Analyses of these data have appeared in the Soviet literature (*2*). It was agreed that the data from this study would be made available to U.S. epidemiologists for comparison with similar data that had been collected in other areas of the world.

Some results of this analysis are presented in this paper.

MATERIALS AND METHODS

Cases were breast cancer patients diagnosed between 1968 and 1973 and referred to the oncological dispensaries at Tallinn and Tartu. These are the only two oncological dispensaries in Estonia. While most breast cancer patients residing in Estonia would be seen at one of these dispensaries, only about one-third are included in the study. The reasons for including some patients and not others were logistical (especially, shortage of staff); there is no reason to suspect bias in the selection of cases for inclusion. Controls were systematically selected from women participating in the gynecologic cancer screening programs offered by the same centers. These programs were targeted on particular subpopulations of women (such as employees) and attendance rates among those asked to attend were very high—generally over 90%. Control subjects who were found to have benign breast disease at the time of their screening were excluded. Since 27% of the cases but only 8% of the controls were from rural areas, this analysis is restricted to urban subjects.

All subjects were interviewed at the dispensary, and questions were asked on a variety of factors including parity, AFB, breast-feeding experience (only for the first 2 children), menstrual history, current weight and height, and medical history.

Table 1 shows the distribution of subjects by age. Only 1 cancer patient under 30 years of age was interviewed, and she has been excluded along with controls below the same age. Even after these exclusions, the cases and controls show different age distributions, the cancer cases being older than the controls. For this reason, all comparisons stratify on age. Associations were evaluated by means of the crude and adjusted OR, the adjusted ratios being adjusted for age in decades, and other variables as specified in context by the method of MH (*3*) and its extension for trend in polychotomous exposure variables (*4*). Computations utilized the programs developed by Rothman and Boice (*5*) as well as standard computer programs for logistic regression. The CL of OR are 95% limits based on logarithmically transformed values.

RESULTS

Reproductive History

The proportion of nulliparous women among the cases (25.1%) was significantly higher than among the controls

---

ABBREVIATIONS USED: AFB=age at first birth; CL=confidence limits; MH=Mantel-Haenszel; OR=odds ratio(s).

---

[1] Received February 11, 1982; accepted June 3, 1982.

[2] Supported by Public Health Service (PHS) contract N01CP-71024 from the Division of Cancer Cause and Prevention, National Cancer Institute (NCI); and by PHS program project grant 5-P01CA-06373 from the NCI.

[3] Department of Epidemiology, School of Public Health, Harvard University, 677 Huntington Ave., Boston, Mass. 02115.

[4] Institute of Experimental and Clinical Medicine, Ministry of Health, Tallinn, Estonian S.S.R.

(16.9%). The crude OR associated with being nulliparous was 1.7, and the MH estimate was 1.6 with CL of 1.2–2.0. Table 2 gives data on risk associated with AFB. The similarity of the crude and age-adjusted OR suggests that age at interview is not an important confounding variable in this relationship. Breast cancer risk was lowest for women whose first birth occurred at ages below 20. Such women had less than one-third the risk of nulliparous women. The OR for the three categories of AFB over 25 were similar, i.e., there was no further increase in risk with increasing AFB over that age. Furthermore, OR for the highest AFB categories remained well below 1.0. These data show no excess of risk, relative to that of nulliparae, for women whose first birth is delayed until over 30 years of age.

The fertility rate in Estonia during the period of this study was relatively low. Fifty percent of the parous cases and 42 percent of the parous controls in this study had only 1 child; only 17% of the parous women in both groups had more than 2 children. This low fertility provides a favorable opportunity to examine the effect on breast cancer risk of births subsequent to the first. These data indicate that there is a substantial reduction in risk associated with having children subsequent to the first, even when one takes into account the fact that women who have their first child early are more likely to have subsequent children. A multiple logistic regression analysis comparing women of parity 1 with women of parity 2+, with adjustment for AFB in individual years and age at interview in decades, gives a point estimate of the breast cancer OR for women of parity 2+ of 0.78 with CL of 0.58–1.07. This is of the same order of magnitude as the OR for primiparous women compared to the OR for nulliparous—0.71 with CL of 0.51–1.01.

Table 1.—*Distribution of cases and controls by age*

Age, yr	No. of women		Percent	
	Cases	Controls	Cases	Controls
30–39	50	146	13.8	21.0
40–49	111	239	30.7	34.4
50–59	84	198	23.2	28.5
60–69	80	86	22.1	12.4
≥70	37	25	10.2	3.6
Total	362	694	100.0	99.9

Table 2.—*Distribution of cases and controls by AFB and estimates of OR and CL*

AFB, yr	No. of women		Crude OR[a]	MH estimates[b]	
	Cases	Controls		OR[a]	CL[c]
<20	7	33	0.27	0.29	0.13–0.66
20–24	109	248	0.57	0.52	0.36–0.75
25–29	99	192	0.66	0.70	0.48–1.01
30–34	36	72	0.54	0.70	0.42–1.15
≥35	20	32	0.81	0.71	0.37–1.36
Nulliparous	91	117	1.00	1.00	— —
Total	362	694	—	—	— —

[a] OR are expressed relative to a referent of 1.0 for nulliparous women.
[b] MH estimates are stratified over age at interview in decades.
[c] 95% CL.

Table 3.—*OR for women of parity 2, relative to those of parity 1, by AFB and age at second birth*[a]

AFB, yr	Age at second birth, yr			Total
	<25	25–29	≥30	
<25	0.29 (0.09–0.92)	0.98 (0.51–1.90)	1.04 (0.47–2.32)	0.68 (0.40–1.14)
25–29	—	0.49 (0.20–1.24)	0.70 (0.40–1.23)	0.64 (0.38–1.08)
≥30	—	—	0.91 (0.43–1.92)	0.91 (0.43–1.92)

[a] Within each category of AFB, data are stratified by single years of AFB, except that categories ≥35 yr are combined. OR are expressed relative to the risk for uniparous women whose first birth occurred in the same AFB category. *Numbers in parentheses* are 95% CL.

Table 4.—*Number of cases and controls and estimates of OR by total parity*

Total parity	No. of women		Crude OR	Adjusted OR[a]
	Cases	Controls		
0	91	117	1.00	1.00
1	136	245	0.71	0.71
2	90	236	0.49	0.50
3	28	69	0.52	0.41
4+	17	27	0.81	0.95
Total	362	694	—	—

[a] OR for parities 2, 3, and 4+ are adjusted for age at first birth in single years of age to the distribution of the first births.

We can further inquire whether the age at which births occur after the first one is a relevant factor. Since, in addition to AFB, data are available only for age at the last birth, we confine ourselves to women of parity 2, the age at last birth being then the age of the mother when the second child was born. An analysis of this group is shown in table 3. The pattern is somewhat similar to that shown for AFB in table 2. That is, the OR associated with second births over the age of 25 is somewhat, though not significantly, below 1, indicating some relatively small additional protection associated with a second birth over that age. However, a second birth below the age of 25 is associated with a substantial and statistically significant reduction in risk—to one-third of the risk for a uniparous woman who does not have a second child before that age. Note that the referent risk in table 3 is not that of nulliparous women but that of uniparous women whose childbirth occurred in the same age range. Compared to the breast cancer OR for *nulliparous* women, the breast cancer OR for women who have 2 children before they are 25 is 0.18 with CL of 0.07–0.49.

Table 4 gives the distributions of cases and controls and estimates of OR by total parity. There is no evidence of any additional protective effect for births after the second.

Lactation

Data were collected on breast feeding only for the first two live births. our analysis was restricted to women who had only one or two live births so that their total lactation experience is represented. The distributions of cases and controls are compared in table 5. For no category of duration of lactation does the OR differ significantly from that for those who did not lactate. Although the OR for all women

TABLE 5.—*Distribution of cases and controls by duration of lactation and estimates of OR and CL*[a]

Duration of lactation, mo	No. of women		Crude OR	MH estimates[b]	
	Cases	Controls		OR	CL_{95}[c]
0	24	37	1.00	1.00	—
1–6	71	185	0.59	0.60	0.32–1.11
7–12	54	138	0.60	0.64	0.35–1.17
13–24	60	107	0.86	0.80	0.43–1.49
≥25	17	15	1.75	1.35	0.56–3.25
Total	226	482	—	—	—

[a] Restricted to women with one or two live births.

[b] MH estimates are stratified over age at interview in decades and are expressed relative to a risk of 1.0 for women who did not lactate.

[c] 95% CL.

TABLE 6.—*Number of cases and controls and estimates of OR and CL by reported age at menarche*

Age at menarche	No. of women		Crude OR	MH estimates[a]	
	Cases	Controls		OR	CL_{95}[b]
≤12	47	92	1.00	1.00	—
13	74	193	0.75	0.71	0.45–1.12
14	107	177	1.18	1.27	0.81–1.98
15	53	79	1.31	1.25	0.75–2.10
16	39	89	0.86	0.74	0.43–1.26
≥17	42	64	1.28	1.07	0.62–1.84
Total	362	694	—	—	—

[a] Estimates stratified over age in decades, with the odds for women reporting age at menarche ≤12 yr as the referent.

[b] 95% CL.

who lactated relative to those who did not—0.69—is below 1.0, it is not significantly so (CL, 0.40–1.21). Further, the lower OR are seen in the shorter categories of duration of lactation, a direction of relationship that seems inconsistent with their being a true reduction in breast cancer risk associated with lactation. The data in table 3 include women of both parity 1 and parity 2 which may introduce some confounding by parity. The analysis was therefore repeated, with the data being confined to women of parity 1. The patterns were essentially identical.

Age at Menarche

Despite a wide range in the ages at menarche reported by cases and controls (table 6), there is no evidence of association of breast cancer risk with variation in age at menarche. The mean age at menarche was 14.24 years for cases and 14.12 years for controls. The difference (0.12 ± 0.12) is not statistically significant. An analysis limited to women in the two youngest decades (30–49 yr) did not alter this conclusion.

DISCUSSION

The striking reduction of breast cancer risk associated with having a full-term pregnancy early in reproductive life was first observed in data from a case-control study of some 4,000 breast cancer cases and 12,000 controls from seven areas of the world (*6*). In these data almost the entire association between breast cancer risk and parity was explained in terms of the association with early first birth, and births subsequent to the first appeared to have little or no additional protective effect when consideration was given to the fact that women whose first birth occurs at an early age tend to become of higher total parity than those whose first birth is delayed.

The inverse association of risk with early first birth has been widely confirmed. However, in studies from Burma (*7*), Iceland (*8*), Sweden (*9*), and Buffalo, New York (*10*), women of high parity appeared to have additional protection independent of AFB. Looked at retrospectively in the light of these later studies, the data from the international study suggested to one observer that there was an additional protective effect of parity in two of the seven centers (*11*).

The only previous attempt to examine the effect of age at births other than the first was in the seven-center study (*6*). The risk for women having 2 births or more under the age of 25 years, after adjustment for AFB, was estimated to be 13% lower than that for women who only had one birth under that age. In contrast, the reduction in risk for a woman having a first birth at age 22, which was the mean age at which the second births under 25 occurred, was 40%. Also, in the smaller group of women having a first birth under age 20, no additional protective effect of having a second birth under that age could be detected.

Contrarily, in the data for Estonia presented here, the protective effect of a second birth, after adjustment for AFB, was almost as great as that of the first birth. Moreover, if the second birth occurred under the age of 25, the risk of breast cancer was only one-third that of uniparous women whose only birth occurred under that age. Compared to nulliparous women, the breast cancer OR for uniparous women who had their child before age 25 was 0.62, and that for duoparous women who had both their children under that age (with adjustment for age at first birth) was 0.18. We conclude that, in this population, not only are births after the first associated with additional protection but also, as with the first birth, the extent of protection depends on the subject's age at the time of the birth.

This conclusion is, as noted, contrary to that suggested by the data in at least most of the centers in the seven-center study. The number of cases and controls was substantial in all but one of these centers, and we believe the analysis was sufficiently detailed to detect an association with births after the first, had one been present. It seems to us that these differences are not due to the common vagaries of observational data, but they reflect real differences between populations in the effect of births after the first. Conceivably, birth spacing is a factor that in some as yet unidentified way changes the influence of the second pregnancy. However, populations with a wide divergence of total female parity, in Burma and Estonia, are both among those populations that show an effect of births after the first. We believe it more likely that nutritional or other environmental circumstances produce real biological differences in susceptibility to the effect of pregnancy. The effect of early first birth, in relative terms, appears to be as great in populations that show an additional effect of births subsequent to the first as in those that do not. It seems, therefore, that the difference is not a matter of the first pregnancy not exerting its full effect in certain populations, and thus leaving more of the protective mechanism of pregnancy to be stimulated by subsequent pregnancies, but is rather a matter of a difference between populations in the overall level of protection that can be achieved by the pregancy mechanism.

There also appears to be a difference between the Estonian data and most previous observations with respect to the effect of having a first birth in the second half of reproductive life. In the seven-center study (*6*), women whose first birth occurred at 30–34 years of age had approximately the same risk as nulliparae (OR, 0.9), and those whose first birth occurred at age 35 or later actually had higher risks than nulliparae (OR, 1.2). In Estonia, both these groups had OR lower than 1.0 (0.6 and 0.8, respectively). However, neither OR is significantly below 1.0, and in both instances the confidence interval of the estimate includes the point estimate from the seven-center study. Although it is possible that differences also exist among populations with respect to this characteristic, these differences cannot be said to have been established on the basis of the present data.

We have no explanation for the absence of an association with age at menarche in these data. Most, though not all, previous studies have shown an inverse association between age at menarche and breast cancer risk (*11*).

REFERENCES

(*1*) Saunders JF. Communication in cancer research. Biosci Commun 1976; 2:98–125.

(*2*) Purde M. Epidemiology of malignant tumors in the Estonian S.S.R. Tallinn: Valgus, 1974 (in Russian).

(*3*) Mantel N. Haenszel W. Statistical aspects of the analysis of data from retrospective studies of disease. J Natl Cancer Inst 1959; 22:719–748.

(*4*) Mantel N. Chi-square tests with one degree of freedom: Extensions of the Mantel–Haenszel procedure. J Am Stat Assoc 1963; 58:690–700.

(*5*) Rothman K, Boice JD Jr. Epidemiologic analysis with a programmable calculator. Washington, D.C.: U.S. Govt Print Off, 1979 [DHEW publication No. (NIH)79-1649].

(*6*) MacMahon B, Cole P, Lin TM, et al. Age at first birth and breast cancer risk. Bull WHO 1970; 43:209:221.

(*7*) Thein-Hlaing, Thein-Maung-Myint. Risk factors of breast cancer in Burma. Int J Cancer 1978; 21:432–437.

(*8*) Tulinius H, Day NE, Johannesson G, Bjarnason O, Gonzales M. Reproductive factors and risk for breast cancer in Iceland. Int J Cancer 1978; 21:724–730.

(*9*) Adami HO, Rimsten A, Stenkvist B, Vegelius J. Reproductive history and breast cancer. Cancer 1978; 41:747–757.

(*10*) Lilienfeld AM, Coombs J, Bross ID, Chamberlain A. Marital and reproductive experience in a community-wide epidemiological study of breast cancer. Johns Hopkins Med J 1975; 136:157–162.

(*11*) Kelsey JL. A review of the epidemiology of human breast cancer. Epidemiol Rev 1979; 1:74–109.

In Vitro Growth Stimulation of Human Ovarian Cancer Cells by Xenogeneic Peritoneal Macrophages[1,2,3,4]

Charles E. Welander, *M.D.*,[5,6] **Ronald B. Natale,** *M.D.*,[5,7] *and* **John L. Lewis, Jr.,** *M.D.*[5]

ABSTRACT—For improvement of the in vitro growth rate of human ovarian tumors, an irradiated xenogeneic feeder layer of adherent peritoneal cells was added to such cultures. This adherent peritoneal cell population was obtained from oil-primed adult (C57BL/6J × DBA/2J)F_1 mice and contained predominantly macrophages. After irradiation of the feeder layer with 3,000 rad ^{137}Cs, cell suspensions prepared from fresh, solid human ovarian cancers were cocultivated with the feeder cells. Two end points were used to evaluate the growth enhancement added by such a feeder layer: 1) Primary monolayer cultures of ovarian tumors were successfully grown in continuous culture through five or more serial subcultures in 25 of 64 different patient specimens studied. Control cultures without the feeder layers did not continue growing through serial subcultures. 2) With the use of the soft agar clonogenic assay, addition of the feeder layer to the petri dishes increased the number of tumor cell colonies in each of six separate experiments, compared to the number seen in control plates without the feeder layer.—JNCI 1982; 69:1039–1047.

One of the difficult problems in tissue culture has been to grow human tumors in vitro and to subsequently establish these tumors in long-term culture. It is not known how often attempts have been made to grow human cancers in vitro; published results of successful attempts are only anecdotal (*1*). We have been concerned in particular with the difficulties encountered when attempting to culture human ovarian cancers. A review of the literature of the past 10 years reveals descriptions of only 15 long-term established ovarian cancer cell lines (*1–7*). At the Memorial Sloan-Kettering Cancer Center, efforts to establish ovarian cancers in tissue culture between the years 1973 and 1978 resulted in only one established cell line out of 72 attempts (Resnick LA, Kim WS: Unpublished data).

To improve the past experience with tissue culture of ovarian cancers, we have investigated the effects of incorporating a feeder layer into cultures of ovarian tumors. The feeder layer consists of adherent murine peritoneal cells—predominantly macrophages. In this report we describe two specific methods to determine the role of such a feeder layer in the alteration of tumor cell growth. The first method has been to incorporate an irradiated feeder layer into primary monolayer cultures prepared from solid tumor specimens of ovarian cancers. The second method is the short-term agar clonogenic assay technique that uses primary solid tumor specimens of ovarian cancers. We present data describing increased tumor cell growth through five or more serial subcultures in the monolayer cultures as well as enhanced tumor cell colony growth in the agar cultures.

MATERIALS AND METHODS

Tumor procurement.—The monolayer culture experiments were done between March 1978 and December 1979, with the use of specimens of human ovarian epithelial tumors obtained from 64 patients undergoing treatment at Memorial Sloan-Kettering Cancer Center. Of the specimens, 51 were solid tumors and 13 were malignant effusions. All of the specimens were adenocarcinomas, with only 4 reported as poorly differentiated. Subsequent to these monolayer culture experiments, selected solid ovarian tumor specimens, obtained between April and December 1980, were used for growth in soft agar. These 6 ovarian adenocarcinomas were chosen for use in the agar clonogenic assay because of their high viability.

Specimens were transferred from the operating room to the laboratory in a sterile container without any culture medium or saline solution. The time from surgical removal until processing in the laboratory was less than 1 hour.

Monolayer culture preparation.—Solid tumor specimens were washed in HBSS containing antibiotics and then minced with scalpels into small fragments. The single cells and cell clusters released by this mechanical means were stained with trypan blue for viability determination (trypan blue exclusion test), and all the viable nucleated cells were counted. Cell aggregates were counted as one cell. Viability ranged from 30 to 90% after mechanical disaggregation; the majority of specimens had more than 70% viable cells. After disaggregation, the tumor cells were resuspended in EMEM enriched with 2 m*M* glutamine, 1% nonessential amino acids, 100 IU penicillin/ml, 100 μg streptomycin/ml (all obtained from Grand Island Biological Co., Grand Island, N.Y.), 10% fetal calf serum, 10% human cord serum, and 0.1 U insulin/ml (Eli Lilly & Co., Indianapolis, Ind.). The cells were then ready for plating.

Malignant effusions are peritoneal or pleural fluids that contain tumor cells. These cells were concentrated by centrifugation (1,000 rpm for 10 min). When erythrocytes were present in the cell pellet, we used sterile distilled water to lyse the red blood cells. Viability staining was done and the

---

ABBREVIATIONS USED: EMEM=Eagle's minimum essential medium; HBSS=Hanks' balanced salt solution.

---

[1] Received February 17, 1982; accepted June 30, 1982.

[2] Supported in part by the Paul Garret Fund and by the Borden Cancer Fund, Memorial Sloan-Kettering Cancer Center.

[3] Animals were maintained under the guidelines set forth in the "Guide for the Care and Use of Laboratory Animals" by the Institute of Laboratory Animal Resources, National Research Council.

[4] Presented in part at the 12th annual meeting of the Society of Gynecologic Oncologists, Marco Island, Fla., Jan. 11–14, 1981.

[5] Memorial Sloan-Kettering Cancer Center, New York, N.Y. 10021.

[6] *Address reprint requests* to Dr. Welander at his *present address*: Bowman Gray School of Medicine, Wake Forest University, 300 South Hawthorne Rd., Winston-Salem, N.C. 27103.

[7] *Present address:* University Hospital, University of Michigan, 1405 East Ann St., Ann Arbor, Mich. 48109.

cells were resuspended in EMEM and were ready for plating.

The above methods of cell preparation are adequate for monolayer cultures, but soft agar cultures require a single cell suspension. To prepare a single cell suspension, we incubated the mechanically dissociated tumor fragments for 2 hours at 37°C in a stirring flask that contained 0.5% collagenase Type II (Worthington Biochemical Corp., Freehold, N.J.) in HBSS. The suspension was then passed sequentially through 45- and 27-µm Swinnex filters (Millipore Corp., Bedford, Mass.) to remove cell clumps. After viability staining with trypan blue, viable nucleated cells were again counted before plating.

Macrophage feeder layer preparation.—The feeder layer consisted of xenogeneic macrophages obtained from peritoneal washings of oil-primed mice. Adult (C57BL/6J × DBA/2J)F_1 mice (The Jackson Laboratory, Bar Harbor, Maine) were used. Each mouse received an ip injection of 0.5 ml Pristine (2,6,10,14-tetramethylpentadecane; Aldrich Chemical Co., Milwaukee, Wis.) at least 2 weeks before treatment. Peritoneal cells were harvested by irrigation of the peritoneal cavity with HBSS containing 5 U heparin/ml. After the cells were washed two times in HBSS, they were plated at a density of $5–8\times10^6$ cells per 25-cm^2 flask for monolayer cultures or 1×10^5 cells per 35-mm petri dish for the agar cultures. Standard EMEM was added with the same additives as used for monolayer cultures. After 2 hours of incubation at 37°C to allow macrophage attachment to the flask or petri dish, the cultures were washed two times with HBSS to remove nonadherent cells. The feeder layer was then irradiated with 3,000-rad cesium-137 teletherapy given in one fraction to prevent replication of any of the adherent peritoneal cells. The morphology of the adherent cells and the relative plating density are illustrated in figure 1. This feeder layer does not form a confluent monolayer, as is commonly seen with fibroblast feeder layers.

Plating and maintenance of cultures.—Monolayer cultures: The cell suspension obtained from the solid tumor specimens was plated over a newly prepared feeder layer as well as in control flasks without the xenogeneic feeder cells and was fed our enriched EMEM. Plating density of tumor cells was 1×10^6 cells and/or cell clusters per 25-cm^2 flask. The flasks were incubated at 37°C with 5% CO_2. Cultures prepared from malignant effusions were plated in the same fashion, but without a xenogeneic feeder layer.

When the tumor cell growth reached confluence, we subcultured the monolayer cultures with the use of 0.1% trypsin in Puck's saline A. We prepared duplicate sets of flasks with each subculture to receive the cells—one set of flasks with a fresh irradiated feeder layer and one set without feeder layer.

Soft agar cultures: After the macrophage feeder layer was attached to the bottom of the 35-mm petri dish, an agar underlayer of 0.5% molten Bacto-agar (Difco Laboratories, Detroit, Mich.) was poured over the feeder layer cells, effectively separating them from the tumor cell plating layer, which was poured over the top. Tumor cell plating density was 5×10^5 cells per petri dish, suspended in 0.3% molten Bacto-agar. The culture medium added to the agar underlayer and to the tumor cell plating layer was similar to that described by Hamburger and Salmon (*8*), except for our deletion of conditioned medium and 2-mercaptoethanol. We incubated these plates in a humidified incubator at 37°C with 7.5% CO_2.

After 7–14 days, colonies were visible and were defined as aggregates of greater than 50 cells. Colony numbers in control plates without feeder layer were compared to numbers of colonies growing in the cultures with a feeder layer.

Nude mouse heterotransplantation.—Six-week-old female nude mice of Swiss/*nu/nu* (ICR/*nu/nu*) background were obtained from the Animal Facility of the Sloan-Kettering Institute. These animals have been bred in a pathogen-free environment but were transferred to limited-access conventional animal facilities for tumor transplantation and subsequent maintenance. Each mouse received approximately 3×10^6 tissue-cultured tumor cells by sc injection and was subsequently observed twice weekly for tumor growth. We considered an enlarging palpable nodule that reached greater than 5×5 mm in size as a successful heterograft.

RESULTS

Monolayer Cultures

Each of the 51 separate specimens of solid ovarian tumors received in the laboratory was grown over a feeder layer of irradiated peritoneal macrophages as well as in control flasks without the feeder layer. During each subculture of the confluent monolayers, duplicate flasks were made to receive the cells, one with a feeder layer and one without. When the cells showed equal growth with or without a feeder layer, the feeder layer was discontinued. None of the cell lines required continuation of the feeder layer beyond passage 5, by which time each line had successfully adapted to growth in vitro without the requirements for continued macrophage presence.

From this group of 51 solid adenocarcinoma specimens, 21 tumors (41%) could be grown past passage 5. Only 1 of these 21 tumors was poorly differentiated histologically. Comparing cultures grown in the presence or absence of the feeder layer (figs. 2A, 2B), we noted two differences: 1) In flasks with the feeder layer there was an increase in the initial attachment of epithelial cells during the first 24 hours after plating primary cultures and 2) in flasks with the feeder layer there was persistence of "epithelial-looking" cells in the first few passages. None of the cell lines growing past passage 5 were successfully grown without feeder layers. Each required feeder cells during the first few culture passages. Our experience has been that 6 of the 23 primary solid ovarian tumors have grown past passage 5 in culture, whereas 15 of 28 metastatic nodules grew successfully past passage 5.

We studied 13 specimens of malignant effusions as well. Ascitic and pleural fluids were grown without feeder layers, on the basis of the observation that abundant autologous macrophages are contained in the effusion. We presumed that these autologous adherent cells (presumably the macrophages) would provide a feeder layer effect in these cultures. From these 13 specimens, 4 resulted in tumor cell growth past passage 5 (table 1).

Of the 25 tumor specimens that grew past passage 5, 7 grew successfully past passage 20. Of this group, 3 originated from primary ovarian adenocarcinomas, 3 from ovarian tumors metastatic to other sites, and 1 from ascitic fluid. Each of them was a papillary adenocarcinoma.

Soft Agar Cultures

Two groups of primary tumor cell suspensions were plated in soft agar for comparative purposes. One group of plates was prepared without a feeder layer and the other group with it. The end point measured was the difference in tumor cell colony formation between the 2 groups. The results of the colony counts are shown in table 2, reported as an average of triplicate plates in each group. The *P*-value was calculated by Fisher's exact probability test. Although the end point of tumor cell colony formation was not an all or nothing result, colony growth seemed to be enhanced by the macrophage feeder layer. Figures 3A and 3B illustrate ovarian carcinoma colony formation in soft agar.

Nude Mouse Heterotransplantation

Demonstration of the continued malignant nature of the cultured cells requires criteria other than cell morphology and growth through serial subcultures. Two criteria of the transformed phenotype are the ability of cells to grow in soft agar (*9*) and the ability of cells to grow as a heterograft in nude mice (*10*). From this group of 25 monolayer cultures grown past passage 5, 22 were injected into nude mice. Of these 22 attempts, 10 (45%) resulted in successful progressive growth as a heterograft in the mice.

TABLE 1.—*Sources of tumor cells for monolayer cultures to test the feeder layer*[a]

Tumor type	No. of specimens attempted	No. of cell lines growing past passage 5	No. of attempted specimens/No. of successes, %
Primary ovarian adenocarcinoma	23	6	26
Metastatic ovarian adenocarcinoma	28	15	54
Malignant effusions	13	4	31
Total	64	25	39

[a] Feeder layers were required for all of the primary and metastatic ovarian adenocarcinomas but were not used with malignant effusions.

TABLE 2.—*Soft agar clonogenic assays to test the feeder cell layers*

Expt No.	No. of colonies formed[a]		Growth increase, %
	Without feeder layer	With macrophage feeder layer	
1	102	133	30.4
2	26	73	180.8
3	48	51	6.3
4	22	50	127.3
5	1,464	2,528	72.7
6	129	204	58.1

[a] No. of colonies formed is an average of three plates in each group. $P<0.01$.

DISCUSSION

Cell-to-cell interactions between both benign and malignant cells can stimulate substances produced by one cell population that affect the growth of other cells, not only in vitro but also in vivo (*11, 12*). Although tumor cell populations escape from normal homeostatic growth control mechanisms, the rate of tumor cell division can often be affected by growth factors (*13, 14*). Recently, evidence has been published suggesting that a soluble substance is produced by adherent phagocytic cells from effusions (presumably macrophages) that can enhance the growth of human tumor cells in vitro (*15*). One experiment that supports this conclusion involved the addition of conditioned medium obtained from the supernatant of adherent spleen cell cultures (a majority of which are macrophages) to cultures of human tumor cells, which resulted in a notable augmentation of tumor cell growth (*8*). Another experimental method has been to deplete malignant effusions of autologous macrophages with a resulting decrease in tumor cell growth, which can be restored by replacement of the macrophages (*16*). The demonstration in this report that macrophages produce some soluble substance which enhances in vitro tumor cell growth is in keeping with these other published observations.

We have raised the question of macrophage proliferation in culture flasks with the feeder layer. We believe that the xenogeneic macrophages do not proliferate when cocultivated with human cells. However, the adherent mouse peritoneal cell population does include morphologically apparent mesothelial cells which do proliferate in the cultures and can contaminate the human cell lines. Therefore, to avoid such contamination problems, we elected to administer 3,000 rad of cesium teletherapy in one fraction to the macrophage feeder layer after the adherent peritoneal cells had attached to the flask. This dose effectively rendered any mouse mesothelial cell incapable of division but did not destroy the short-term metabolic and secretory functions of the feeder layer cells.

With regard to the preparation of the peritoneal exudate cells, we initially used peritoneal washings from normal, non-oil-primed mice. Although such cells did provide a degree of stimulation of human tumor cell growth, up to a tenfold increase in the number of peritoneal exudate cells could be recovered after oil priming of the mice.

Criteria of malignancy must be applied to tumor cell growth in agar. Growth in an unanchored state is one of the manifestations of the transformed phenotype. To form tumor colonies that arise from a single cell suspension in agar, viable clonogenic cells must be present. Stromal fibroblasts, a constant contamination in monolayer cultures, will not grow in soft agar.

Growth of tissue-cultured cell lines in nude mice as a demonstration of malignant phenotype has been a goal, but there are reasons reported in the literature by others why nude mouse heterotransplantation is not always successful. Such reasons include subthreshold cell inoculum size, inadequate length of observation, and varying levels of immunodeficiency in nude mice (*17*). Because of lack of time we have not done multiple repeated attempts at heterotransplantation of tissue-cultured cells and have achieved successful growth in nude mice in only 10 of these 22 attempts.

The observations reported here are only preliminary and empiric. They must be followed by attempts to identify and characterize the substance produced by the adherent peritoneal cell population that enhances ovarian tumor cell growth in vitro.

REFERENCES

(*1*) Fogh J, Trempe G. New human tumor cell lines. In: Fogh J, ed. Human tumor cells in vitro. New York: Plenum Press, 1975:115–159.

(*2*) DiSaia PJ, Morrow M, Kanabus J, Piechal W, Townsend DE. Two new tissue culture lines from ovarian cancer. Gynecol Oncol 1975; 3:215–219.

(*3*) Sinna GA, Beckman G, Lundgren E, Nordenson I, Roos G. Characterization of two new human ovarian carcinoma cell lines. Gynecol Oncol 1979; 7:267–280.

(*4*) Kimoto T, Ueki A, Nishitani K. A human malignant cell line established from ascites of patient with embryonal carcinoma of ovarium. Acta Pathol Jpn 1975; 25:89–98.

(*5*) Freedman RS, Pihl E, Kusyk C, Gallagher HS, Rutledge F. Characterization of an ovarian carcinoma cell line. Cancer 1978; 42:2352–2359.

(*6*) Yamada T. The cellular biology of a newly established cell line of human ovarian adenocarcinoma in vitro. Keio J Med 1974; 23:53–70.

(*7*) Woods LK, Morgan RT, Quinn LA, Moore GE, Semple TU, Stedman KE. Comparison of four new cell lines from patients with adenocarcinoma of the ovary. Cancer Res 1979; 39:4449–4459.

(*8*) Hamburger AW, Salmon SE. Primary bioassay of human tumor stem cells. Science 1977; 197:461–463.

(*9*) Shin SI, Freedman VH, Risser R, Pollack R. Tumorigenicity of virus-transformed cells in nude mice is correlated specifically with anchorage independent growth in vitro. Proc Natl Acad Sci USA 1975; 72:4435–4439.

(*10*) Giovanella BC, Stehlin JS, Wiliams LJ Jr. Heterotransplantation of human malignant tumors in "nude" thymusless mice. II. Malignant tumors induced by injection of cell cultures derived from human solid tumors. J Natl Cancer Inst 1974; 52:921–930.

(*11*) Halley RW. Control of growth of mammalian cells in culture. Nature 1975; 258:487–490.

(*12*) Puck T, Marcus PI. A rapid method for viable cell titration and clone production with HeLa cells in tissue culture: The use of x-irradiated cells to supply conditioning factors. Proc Natl Acad Sci USA 1955; 41:432–437.

(*13*) Sporn MB, Todaro GJ. Autocrine secretion and malignant transformation of cells. N Engl J Med 1980; 303:878–880.

(*14*) Salmon SE, Hamburger AW. Immunoproliferation and cancer: A common macrophage-derived promoter substance. Lancet 1978; 1:1289–1290.

(*15*) Buick RN, Fry SE, Salmon SE. Effect of host cell interactions on clonogenic carcinoma cells in human malignant effusions. Br J Cancer 1980; 41:695–704.

(*16*) Hamburger AW, Salmon SE, Kim MB, et al. Direct cloning of human ovarian carcinoma cells in agar. Cancer Res 1978; 38:3438–3444.

(*17*) Fogh J, Fogh JM, Orfeo T. One hundred and twenty-seven cultured human tumor cell lines producing tumors in nude mice. J Natl Cancer Inst 1977; 59:221–225.

FIGURE 1.—Feeder layer irradiated with 3,000 rad showing relative plating density of adherent cells. *Bar* = 30 µm. × 160

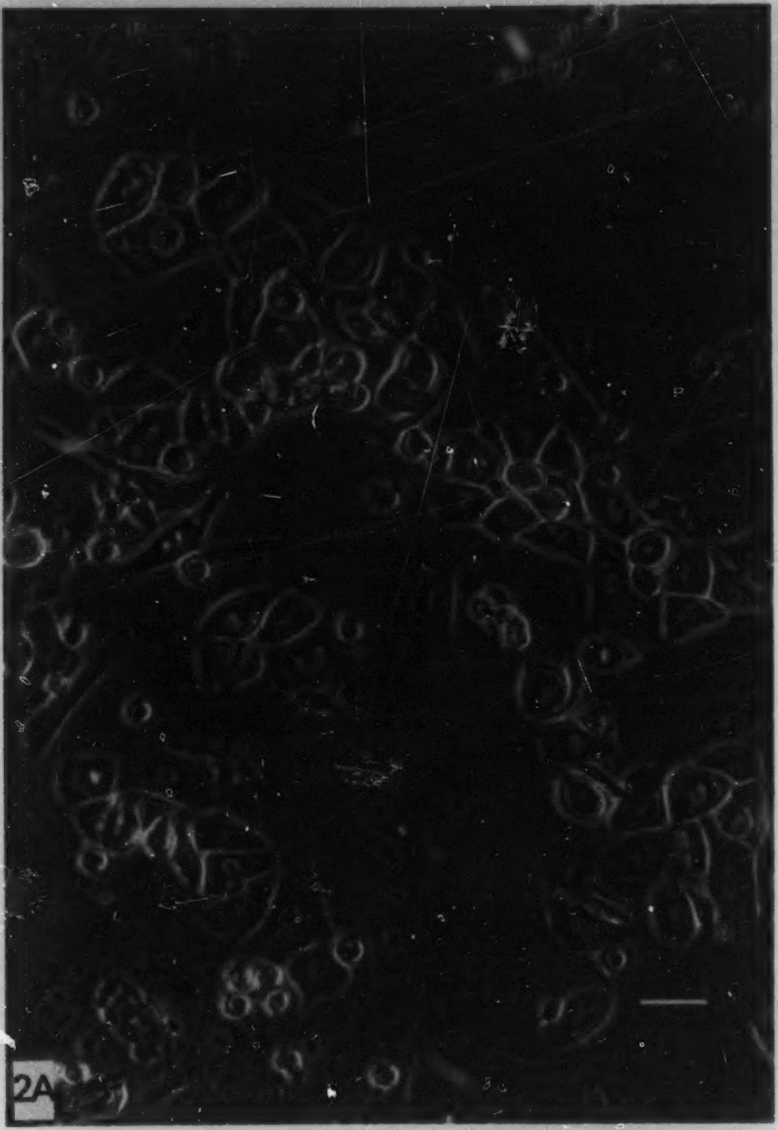

FIGURE 2A.—Ovarian carcinoma culture during passage 3, with feeder cell layer. *Bar* = 30 µm. × 160

FIGURE 2B.—Ovarian carcinoma culture during passage 3, without feeder cell layer. *Bar* = 30 µm. × 160

FIGURE 3A.—Ovarian carcinoma cell colonies in soft agar on the 14th day of growth. Bar = 200 µm. × 25

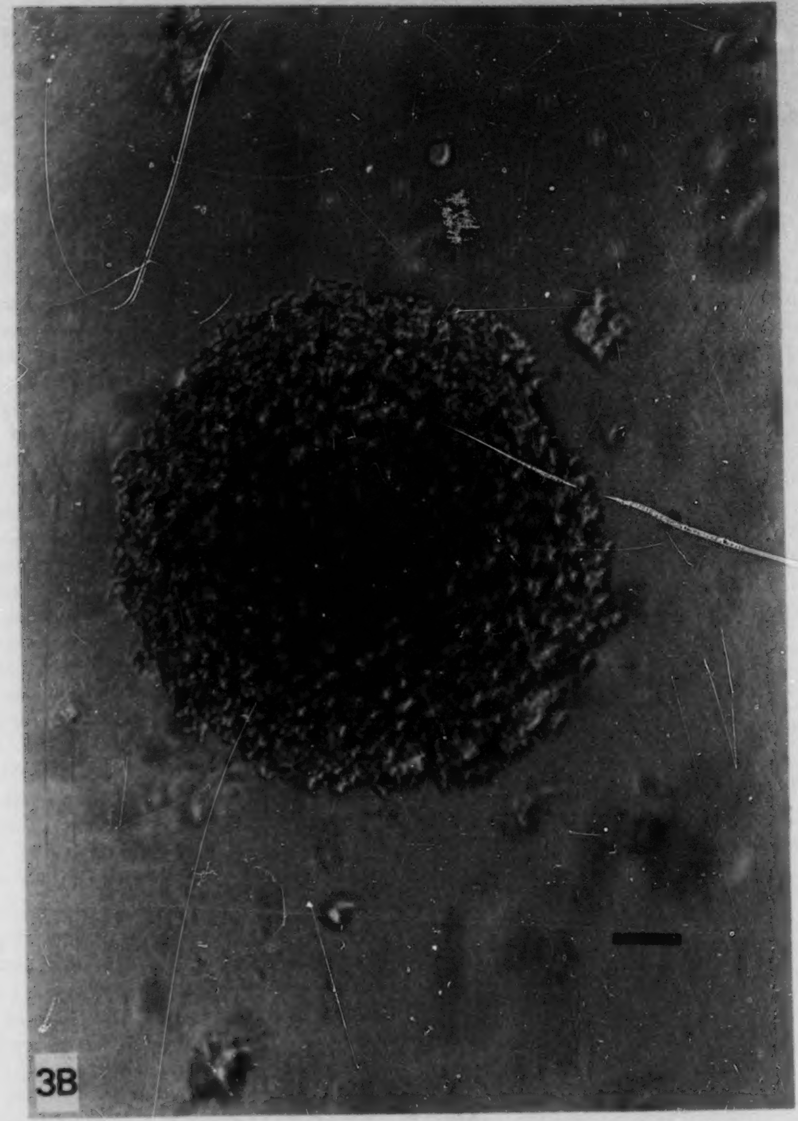

FIGURE 3B.—Ovarian carcinoma cell colonies in soft agar on the 14th day of growth. *Bar* = 30 μm. × 160

blank page

Effect of Natural Protease Inhibitors and a Chemoattractant on Tumor Cell Invasion In Vitro[1]

U. P. Thorgeirsson,[2,3] **L. A. Liotta,**[4] **T. Kalebic,**[4] **I. M. Margulies,**[4] **K. Thomas,**[5] **M. Rios-Candelore,**[5] *and* **R. G. Russo**[4, 6]

ABSTRACT—The effects of natural protease inhibitors and a chemoattractant on tumor cell invasion were studied with the use of a new in vitro quantitative assay of tumor cell penetration of native connective tissue. Human amnion membrane denuded of its epithelium is composed of a continuous basement membrane (BM) attached to a dense avascular collagenous stroma. M5076 reticulum sarcoma cells, known to be highly invasive in vivo, were placed on the BM side of the amnion connective tissue. Tumor cells penetrating the full thickness of the connective tissue barrier were collected on the stromal side with a Millipore filter. *N*-Formylmethionyl-leucyl-phenylalanine (FMLP) at an optimal concentration of 10^{-7} M stimulated the penetration of up to 600% more tumor cells into the connective tissue after 20 hours in comparison to the number of tumor cells spontaneously penetrating in serum-free media. Natural protease inhibitors blocked both FMLP-stimulated and spontaneous invasion. A bovine cartilage extract containing inhibitors of both serine proteinases and metalloproteinases caused a 500% decrease in invasion. Furthermore, a 500% inhibition of invasion was produced by a purified collagenase (metalloproteinase) inhibitor. In contrast, soybean trypsin inhibitor and bovine serum albumin did not significantly alter the invasion rate. The protease inhibitors were nontoxic and did not reduce tumor cell proliferation, attachment to the amnion, and the rate of tumor cell migration through Nuclepore filters. These data support the hypothesis that collagenolytic metalloproteinases play a necessary role in tumor cell invasion of native connective tissue.—JNCI 1982; 69:1049–1054.

Many investigators have suggested that proteases may play a role in tumor cell invasion of connective tissue (*1–8*). This supposition is based largely on the finding that tumor cells elaborate a variety of proteases (*1, 3, 7, 9*). Connective tissue barriers such as BM and interstitial collagenous stroma do not normally contain passageways for cell movement. Therefore, it is logical that localized disruption of connective tissue by proteases may play a role in tumor invasion. However, it is still possible that tumor cells penetrate connective tissue barriers by a mechanical means not requiring any proteases. Therefore, the objective of the present study was to test whether proteases actually played a necessary role during tumor cell penetration of native connective tissue barriers.

We utilized our recently described (*10–12*) amnion invasion system for counting the number of tumor cells penetrating human BM and collagenous stroma in vitro. A variety of neoplastic and normal cells have been previously tested in this system (*10, 12*). Epithelial cells, fibroblasts, and endothelial cells fail to invade the amnion. Polymorphonuclear leukocytes, macrophages, and different types of malignant cells, however, do invade the amnion (*11, 12*). In the present study we focused on the mechanism of invasion by a specific well-characterized tumor cell line (M5076) known to be highly invasive in vivo (*13, 14*). This reticulum cell sarcoma elaborates collagenolytic proteases capable of degrading all the genetically distinct types of collagens (*8*). We tested the capacity of this tumor cell to invade connective tissue with and without the addition of a synthetic peptide chemoattractant and protease inhibitors in an attempt to assess which classes of proteases were most important. The first inhibitor was a CE that contains inhibitors of both serine proteinases (such as trypsin and plasmin) and metalloproteinases (such as collagenase). CE have previously been shown to inhibit tumor cell collagenase (*15, 16*), to block neovascularization (*17*), and to prevent tumor cell invasion of extracted cartilage as determined by histologic tests (*18*). The second natural inhibitor tested for its effects on invasion was TIMP. TIMP (*19, 20*) specifically inhibits all types of metalloproteinases. The third inhibitor used was SBTI that blocks serine proteinases. These inhibitors differed markedly in their effects on tumor cell invasion in the present system.

MATERIALS AND METHODS

Cell cultures and media.—The M5076 reticulum sarcoma cells (*13, 14*) were supplied by Dr. Ian R. Hart, NCI-Frederick Cancer Research Facility, Frederick, Md. M5076 cells were grown in RPMI-1640 medium supplemented with 2 mM L-glutamine, 1 mM sodium pyruvate, 50 U penicillin/ml, 50 µg streptomycin/ml, and 10% equine serum (all purchased from Flow Laboratories, Inc., McLean, Va.). The cells were subcultured at a ratio of 1:2 twice weekly and grown at 37°C in humidified air containing 5% CO_2. Viability was determined by trypan blue exclusion.

Protease inhibitors.—We prepared the CE from bovine nasal

ABBREVIATIONS USED: BM=basement membrane; BSA=bovine serum albumin; CE=cartilage extract(s); FMLP=*N*-formylmethionyl-leucyl-phenylalanine; H & E=hematoxylin and eosin; MW=molecular weight; SBTI=soybean trypsin inhibitor; TIMP=tissue inhibitor of metalloproteinases.

---

[1] Received March 3, 1982; accepted June 3, 1982.

[2] Laboratory of Pathology, Division of Cancer Biology and Diagnosis, National Cancer Institute, National Institutes of Health, Public Health Service, U.S. Department of Health and Human Services, Bethesda, Md. 20205.

[3] *Address reprint requests to* Dr. Thorgeirsson, Building 10, Room 8B19, National Institutes of Health, Bethesda, Md. 20205.

[4] Laboratory of Pathophysiology, Division of Cancer Biology and Diagnosis, National Cancer Institute.

[5] Department of Biochemistry, Merck Institute of Therapeutic Research, Rahway, N.J. 07065.

[6] We are grateful for the editorial assistance of Ms. Pattie Moyer and for the placentas for the amnion invasion assays supplied by the nursing staff at the Bethesda Naval Hospital.

septum cartilage that was obtained from Pel-Freez Biologicals, Inc., Rogers, Ark. The noncartilage tissue was removed, and pieces of cleared cartilage (400 g) were cut into 1-mm-thick slices and stirred in 1 liter of 20 m*M* 2-(*N*-morpholino)ethane sulfonic acid (pH 6.0) containing 1 *M* guanidine chloride at room temperature for 20 hours. The extract was spun at 12,000×*g* for 20 minutes and the supernatant passed through a coarse-porosity paper filter. The filtered supernatant was dialyzed in 3,500 molecular ratio exclusion membranes against three changes of 15 liters of distilled water at 4°C over a 3-day period. The final lyophilized extract was 1% by weight of the original tissue.

We used a purified TIMP that was supplied by Dr. J. Reynolds (Strangeways Research Laboratory, Cambridge, England). The method of purification has been previously described (*19, 20*). TIMP has an MW of 28,000 (*20*). We verified that this inhibitor markedly reduces the degradation of type I collagen, type IV collagen, and type V collagen by tumor cell-derived metalloproteinases. TIMP failed to reduce the activities of the serine proteinase human urokinase or human plasmin.

SBTI, pancreatic trypsin inhibitor, and BSA were all purchased from Sigma Chemical Co., St. Louis, Mo. The serine proteinase inhibitors abolished the activity of human plasmin (*9*) but had no effect on the tumor cell metalloproteinases (*21*).

FMLP was purchased from Peninsula Laboratories, San Carlos, Calif. This chemotactic peptide (MW=437.6) was solubilized in dimethyl sulfoxide (Sigma Chemical Co.) at a stock concentration of 2 m*M* and then made up to the desired concentration (10^{-4}–10^{-8} *M*) in RPMI-1640 medium.

Amnion invasion system.—Fresh human amnion was obtained from placentas of normal term deliveries as described previously (*10–12*). The amnion membrane is highly uniform in composition and contains a single layer of epithelium attached to a continuous BM overlying a dense nonvascular collagenous stroma (*10*). The epithelium was rendered nonviable and was removed after a 30-minute treatment with 0.1 *M* ammonium hydroxide (*9, 11*). Colloidal carbon (size, 0.5–5 μm), applied to the continuous BM surface or to the stromal surface, failed to diffuse into the stroma even when it was applied after a 20-day incubation of the amnion. The amnion was also impermeable to labeled high-MW glycoproteins (*10, 22*). The nonviable amnion connective tissue was clamped in a chemotaxis chamber in a serum-free tissue culture medium as described previously (*11*). The connective tissue separated two chambers without hydrostatic pressure difference (*11, 12*). Tumor cells were applied to the upper side of the chamber facing the BM, and an 8-μm pore size Millipore filter (Millipore Corp., Bedford, Mass.) was placed in contact with the opposite stromal surface (*11, 12*) (text-fig. 1). The chemoattractant FMLP was routinely placed in the lower chamber facing the filter. In some experiments FMLP was placed only in the top chamber or in both top and bottom chambers. Tumor cells penetrating the full thickness of the BM and collagenous stroma were collected on the filter. At the end of a 20-hour incubation at 37°C, amnion and filter were fixed in 70% ethanol overnight, stained with H & E, dehydrated in ethanol, and cleared in xylene. Lastly, the filter was peeled away from the stroma and both the amnion and filter were mounted on the same microscopic slide (text-fig. 1). For each assay the total number of tumor cells attached to the BM surface (0.76 cm^2) and the total number of tumor cells in the Millipore filter were counted at 400× magnification. The reproducibility and variability of this assay have been documented previously (*11, 12*). Histologic studies of the M5076 cells penetrating the amnion connective tissue have also been presented previously (*12*).

Protease inhibitor assays.—In the second group of tests, the following agents were dissolved in culture medium and incubated with the M5076 cells at 37°C for 30 minutes before introduction into the assay: 10 μg or 100 μg bovine CE/ml, 10 μg purified metalloproteinase inhibitors/ml, 100 μg SBTI/ml, and 100 μg BSA/ml. Individual assays were performed in triplicates. Tumor cells were incubated on the amnion for 20 hours.

To assess the migratory capacity of the tumor cells separately, an 8-μm pore size Nuclepore filter (Nuclepore Corp., Pleasanton, Calif.) was used in place of the amnion. The migration assay was therefore a modification of that used by Varani et al. (*23*). Tumor cells were placed on the surface of the Nuclepore filter in the presence of 10^{-7} *M* FMLP in the lower compartment of the amnion chamber. Cells that migrated through the Nuclepore filter were collected on the lower Millipore filter. The filters were fixed and stained, and 10 fields were counted at 250× magnification on each of the triplicate Millipore filters. The data were expressed as average number of cells per field.

The inhibitory effect of the protease inhibitors was tested on the collagenolytic enzymes secreted into the culture supernatant by M5076 cells. The assay method for determining proteolysis of ^{14}C-labeled type IV collagen, type V collagen, and type I collagen was used as described previously (*8*). The CE inhibitors or TIMP was preincubated with the enzyme for 30 minutes prior to addition of the substrate.

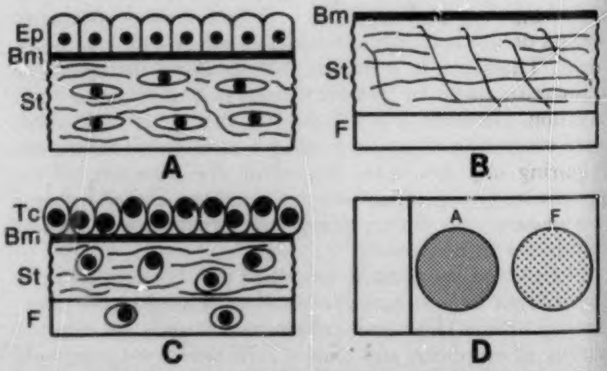

TEXT-FIGURE 1.—Diagrammatic illustration of the amnion invasion assay. A) Normal human amnion has a single layer of epithelium (Ep), a continuous BM (Bm), and a nonvascular collagenous stroma (St). B) The amnion is divested of its epithelium and a Millipore filter (F) is placed against the stromal surface. C) The amnion and filter are held in a chemotaxis chamber. Tumor cells (Tc) attach to the BM surface and a small proportion of cells penetrates the BM and stroma and is collected on the filter. D) The H & E-stained amnion (A) and filter (F) are mounted on a microscopic slide.

RESULTS

Stimulation of M5076 Tumor Cell Invasion of Amnion Connective Tissue in Vitro by FMLP

A small fraction (<1%) of the tumor cells attached to the BM surface of the amnion migrated through the entire thickness of amnion within 20 hours and entered the Millipore filter. Many more tumor cells were identified within the amnion stroma by light microscopy focusing at various levels. These cells were in various stages of migration through the stroma and could not be easily quantified.

The chemoattractant FMLP was added to the lower compartment of the amnion invasion chamber. A series of FMLP concentrations were chosen to cover the range used previously (*11*) for FMLP chemoattraction of inflammatory cells and tumor cells through porous filters (*24*). Previous experiments with labeled FMLP diffusion across the amnion system had shown that an equilibrium of the FMLP gradient across the amnion was reached in 17 hours at 37°C (*11*). Time course invasion assays demonstrated that 78% of the tumor cells had migrated through the amnion at 17 hours compared with the 20-hour incubation time used in subsequent experiments. After a 20-hour incubation there was a 400–600% increase in tumor cell migration in response to the optimal concentration of 10^{-7} *M* FMLP (text-fig. 2). At high concentrations of FMLP (10^{-4} *M*), the cell migration was actually slightly decreased. When FMLP (10^{-7} *M*) was placed in the upper chamber alone or in both the upper and lower chambers, there was no stimulation of tumor cell migration compared to that seen in controls with no FMLP. As shown in tables 1 and 2, 10^{-7} *M* FMLP had no effect on cell proliferation, either in tissue culture wells or on the amnion BM, and did not significantly increase the amount of collagenase produced. It can be concluded that the major effect of FMLP in this system was to stimulate directed locomotion of M5076 tumor cells. It is also evident from table 1 that the M5076 cells do not replicate in serum-free medium during the 20-hour incubation time.

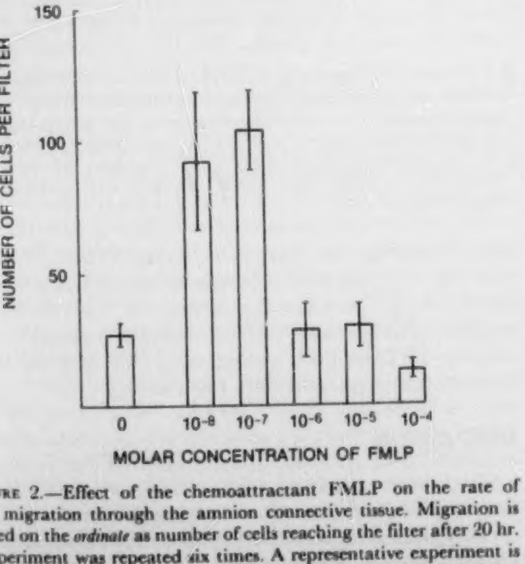

TEXT-FIGURE 2.—Effect of the chemoattractant FMLP on the rate of M5076 migration through the amnion connective tissue. Migration is expressed on the *ordinate* as number of cells reaching the filter after 20 hr. The experiment was repeated six times. A representative experiment is shown. On the *abscissa*, spontaneous cell migration is labeled as 0 (no FMLP). FMLP in concentrations ranging from 10^{-4} to 10^{-8} *M* was placed in the lower chamber. *Bars* represent standard error of the mean. The value for 10^{-7} *M* (No.=9) FMLP was significantly different from that for spontaneous migration (No.=12) ($P<0.005$); 10^{-4} *M* FMLP was different from spontaneous migration ($P<0.1$).

TABLE 1.—*Effect of FMLP on the survival and type IV collagenase secretion of M5076 tumor cells*[a]

Expt No.	Mean No., $\times 10^6$, of viable M5076 tumor cells/well after 20 hr	Presence or absence of FMLP	Type IV collagenolytic activity, mean %[b]
1	2.0	–	49.3
	2.0	+	37.0
2	2.5	–	51.0
	2.9	+	50.3

[a] Tumor cells were suspended in serum-free RPMI-1640 medium with penicillin, streptomycin, and sodium pyruvate. Duplicate samples of 2.0×10^6 viable cells in 20-ml volume were seeded in T75 tissue culture flasks and incubated at 37°C for 20 hr in the presence (+) or absence (–) of 10^{-7} *M* FMLP. At the end of the incubation, the total number of viable cells were counted and the type IV collagenolytic activity of the conditioned medium was assayed in duplicate (*4*). The cells failed to proliferate or grew slowly in serum-free medium, and FMLP did not alter their collagenase activity.

[b] Linear range of assay is between 0 and 60% of maximum substrate degraded by bacterial collagenase (*4*).

TABLE 2.—*Effect of FMLP and CE on growth of M5076 cells on the amnion BM surface*[a]

Treatment	Attached M5076 cells/amnion surface, mean No., $\times 10^5$, ± SEM
M5076 untreated	1.86±0.4
M5076 + FMLP	1.71±0.24
M5076 + CE	1.97±0.16
M5076 + FMLP + CE	1.67±0.11

[a] The tumor cells were suspended in serum-free medium as in table 1 and 5×10^5 cells inoculated in triplicate samples onto the amnion BM surface (0.76 cm^2), in the presence or absence of 10^{-7} *M* FMLP or 100 µg CE/ml. After incubation for 20 hr at 37°C, the surface was washed and the total number of attached cells was counted in 10 fields of each sample.

Inhibition of Tumor Cell Invasion of the Amnion by Bovine CE

Resistance of normal cartilage to tumor invasion has been observed in vivo. Hyaline cartilage contains a variety of different protease inhibitors as well as an antiangiogenesis factor (*17*). Therefore, we studied the effect of a CE on in vitro invasion measured in the amnion system. The extract was determined to have a metalloproteinase inhibitor (table 3) and inhibitors for chymotrypsin, trypsin, and plasmin. The trypsin inhibitors are of two sizes, one at an MW of about 13,000 by gel filtration and a second at an MW of 60,000. The bovine CE in two concentrations was tested for inhibitory effect on M5076 invasion of the amnion. The entire series of experiments with CE were repeated three times. The data were combined and are shown in text-figure 3. The lower concentration (10 μg/ml) without FMLP had no effect, and the higher concentration (100 μg/ml) caused 250% inhibition (text-fig. 3A). In the presence of FMLP a 250% inhibition was observed with the lower concentration, and a 450% inhibition with the higher concentration (text-fig. 3B). In some individual assays the CE completely abolished invasion of M5076 cells through the amnion connective tissue. The number of cells on the amnion at the end of the 20-hour incubation was not affected by the CE at concentrations that markedly inhibited in vitro invasion (table 2). Furthermore, CE had no effect on number of viable cells after a 20-hour incubation in serum-free medium in T75 flasks (data not shown). The extract was a potent inhibitor of tumor cell-derived proteases (table 3). Since the extract may have directly interfered with the FMLP chemotactic process or may have reduced tumor cell locomotion, we studied the effect of the extract on tumor cell migration through 8-μm Nuclepore filters used in place of the amnion. As shown in text-figure 3C, the CE failed to significantly inhibit locomotion of the tumor cells through Nuclepore filters in the presence of 10^{-7} FMLP. These data indicate that inhibition of tumor cell invasion by the CE in this system was not due to a direct effect on tumor cell viability, attachment, or locomotion.

Effects of Purified Protease Inhibitors

To assess separately the importance of metalloproteinases and serine proteinases in the amnion invasion system, we used two types of purified inhibitors. A purified metalloproteinase inhibitor was compared with a serine proteinase inhibitor, SBTI. BSA was used as a negative control. The TIMP had an MW of approximately 28,000, measured by molecular sieve chromatography, and is conceivably similar to the TIMP of similar MW found in the bovine CE. The data are shown in text-figure 4. The TIMP reduced invasion of the M5076 tumor cells 450% in the presence of 10^{-7} *M* FMLP (text-fig. 4B). In contrast to the TIMP, SBTI or BSA (text-fig. 4A) had no significant effect on invasive capacity either in the presence or absence of FMLP. Pancreatic trypsin inhibitor also did not inhibit invasion (data not shown). SBTI or BSA was not cytotoxic and did not affect attachment or growth (data not shown).

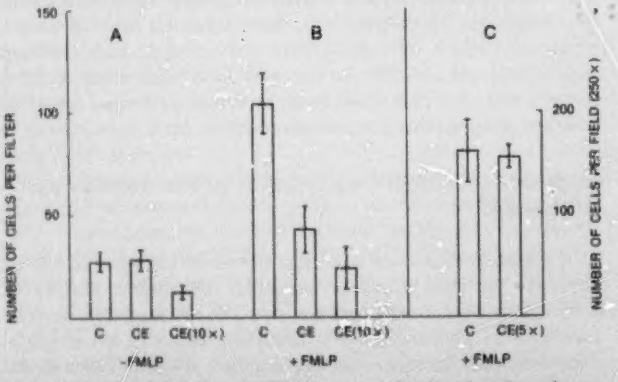

TEXT-FIGURE 3.—Inhibition of M5076 tumor cell migration through amnion by bovine CE. Each assay was performed in triplicate, and the mean value determined. Data are combined from three separate experiments (No.=9). Compared to untreated M5076 cells (C), the CE, 10 μg/ml (CE) and 100 μg/ml [CE(10×)] without (*panel A*) and with (*panel B*) 10^{-7} *M* FMLP, inhibits cell migration. CE(10×) was significantly different from control ($P<0.05$). *Panel C* shows the effect of CE on the migration of M5076 cells through Nuclepore filters in the presence of 10^{-7} *M* FMLP. *Bars*=SEM.

TABLE 3.—*Effect of 10 μg CE/ml and 1 μg TIMP/ml on type I, type IV, and type V collagenolytic activities of tumor cells*[a]

Treatment	Collagen-type substrate	Collagenolytic activity, cpm[b]
Metalloproteinase alone	I	3,050
+ CE	I	540
+ TIMP	I	—
Metalloproteinase alone	IV	2,800
+ CE	IV	410
+ TIMP	IV	620
Metalloproteinase alone	V	1,250
+ CE	V	230
+ TIMP	V	375

[a] The enzymes were extracted and assayed as described previously (*8*). Means of duplicate assays.

[b] Substrate degraded at 35.5°C during 6 hr.

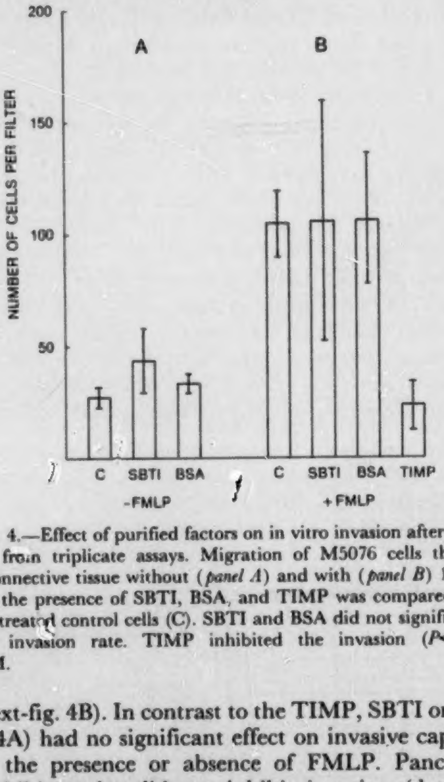

TEXT-FIGURE 4.—Effect of purified factors on in vitro invasion after 20 hr. Data are from triplicate assays. Migration of M5076 cells through amnion connective tissue without (*panel A*) and with (*panel B*) 10^{-7} *M* FMLP in the presence of SBTI, BSA, and TIMP was compared with that of untreated control cells (C). SBTI and BSA did not significantly alter the invasion rate. TIMP inhibited the invasion ($P<0.05$). *Bars*=SEM.

DISCUSSION

The present report on the in vitro invasion of a tumor cell line, M5076, indicates that metalloproteinases and chemotactic agents play an important role in the invasive process. Human amnion, which is used as a connective tissue barrier in our in vitro invasion system, contains a continuous BM, comparable in structure and composition to BM elsewhere in the body. It is a uniform, transparent membrane devoid of vessels, nerves, and host immune cells. The amnion invasion system provides a means for quantitative measurement of the rate of tumor cell migration in contrast to previous in vitro assays that consisted of histologic evaluation of either tumor cell invasion of cultured organ fragments (*25–29*) or penetration of radiolabeled tumor cells through thick complex structures such as a chorioallantoic membrane or a canine large vessel (*30, 31*). We have found that only a few (<1%) of the attached M5076 cells went through the amnion. This phenomenon is possibly analogous to the low proportion of iv injected tumor cells that initiate metastatic foci (*32*).

A variety of substances induce chemokinesis and chemotaxis of inflammatory cells (*33, 34*). Such substances are thought to direct polymorphonuclear leukocytes or macrophages out of the circulation, across the vessel wall, and into the site of an inflammation. Since the extravasation of inflammatory cells is analogous in some respects to the hematogenous metastatic process, investigators such as Ward and Varani (*23, 24, 35, 36*) have searched for chemotactic agents that attract tumor cells. FMLP is a synthetic tripeptide that is one of the most potent chemoattractants for phagocytic cells (*31, 32*). Wass et al. (*24*) reported that FMLP is also a chemoattractant for Walker tumor cells. Since FMLP is of low enough MW to diffuse through native connective tissue (*11*), we studied whether it could attract the M5076 tumor cells through the amnion in serum-free conditions. All previous in vitro studies of tumor cell chemotaxis were performed in the Boyden chamber with the use of a porous artificial filter (Millipore or Nuclepore) as a barrier. No previous chemotaxis assay was performed with native connective tissue as the migration barrier. As shown in text-figure 2, FMLP significantly stimulated the migration of M5076 tumor cells through the amnion connective tissue at an optimal concentration of 10^{-7} *M*. This concentration is similar to that found optimal for stimulating migration of phagocytes and tumor cells across artificial porous filters (*11, 24, 34*). FMLP did not elicit its effect through a change in cell number in serum-free medium (table 1). At the concentration of FMLP that was optimal for stimulation of cell migration, there was no increase in collagenolytic activity produced per tumor cell. Since the major effect of FMLP was not an increased secretion of collagenolytic enzymes, it might therefore stimulate directed invasion through an enhancement of cell locomotion. However, a tumor cell, enhanced in its tendency to migrate, may still require a proteolytic mechanism to penetrate connective tissue barriers. Therefore, we tested the effect of natural protease inhibitors on tumor cell invasion in this system with and without FMLP.

A CE containing inhibitors for both metalloproteinases and serine proteinases blocked both spontaneous and FMLP-stimulated M5076 cell invasion through the amnion (text-fig. 3). The CE inhibition was dose-dependent and was not due to an effect on cell proliferation or cytotoxicity. The CE was not a purified substance. Therefore, it was impossible to distinguish which of the factors were responsible for the observed blocking effect. To further distinguish the classes of proteases relevant in this system, purified TIMP and a serine proteinase inhibitor were also tested. The metalloproteinase inhibitor reduced migration through the amnion 450% (text-fig. 4B). In contrast, SBTI and BSA had no significant effect on invasion (text-fig. 4). The M5076 tumor cells and many other types of tumor cells have been found to elaborate metalloproteinases that degrade collagen (*8*). A subset of the family of metalloproteinases is classic mammalian collagenase, which makes a single cleavage of stromal collagens I, II, and III (*5*). Separate types of metalloproteinases produced by tumor cells (and nonneoplastic cells) can degrade collagen type IV found exclusively in the BM and collagen type V associated with stromal–BM interface (*8, 37*). Except for type II collagen, which is predominant in cartilage, all the above types of collagens have been localized in the amnion by extraction and by immunohistologic tests (*3, 8, 21, 37, 38*). The ability of the M5076 cell to elaborate metalloproteinases may play a major role in its ability to move through the amnion connective tissue. Whether this requirement is true for other types of tumor cells remains to be determined.

Tumor cells can also elaborate serine proteinases such as plasminogen activator and chymotrypsin-like enzymes (*39*). These enzymes may be associated with the cell surface and have been implicated in tumor invasion (*39*). At least one form of plasminogen activator, urokinase, does not significantly degrade any type of collagen (*9*). Plasminogen activator can generate plasmin from plasminogen (*9, 39*). Plasmin can go on to degrade glycoprotein components of connective tissue (*9*). In the present in vitro system, tumor cells invaded the amnion connective tissue in the absence of exogenous plasminogen. SBTI, a potent inhibitor of plasmin, failed to reduce invasion. This effect is not unexpected, since plasminogen was not present to generate plasmin. However, it can be concluded that in this system enzymes susceptible to inhibition by SBTI do not play a major role in invasion. SBTI is not an optimal inhibitor for plasminogen activator, and therefore the importance of this enzyme is unknown in the present invasion system.

The process of tumor invasion is complex with multiple sequential steps and a variety of possible interactions between the tumor cells and the host cellular and extracellular components. Any type of in vitro assay is obviously not equivalent to the metastatic process in vivo. Furthermore, in vitro invasion mechanisms used by one specific type of tumor cell may not necessarily relate to a general mechanism used by all types of tumors in vivo. Nevertheless, one approach to the study of tumor invasion is to break it down into defined steps upon which to focus experimental studies. The present in vitro system is designed to study one defined step of tumor invasion, i.e., the penetration of tumor cells through whole native BM and collagenous stroma. These data indicate that collagenolytic metalloproteinases play an important, and possibly even a necessary, role in tumor invasion.

REFERENCES

(*1*) ROBERTSON DM, WILLIAMS DC. In vitro evidence of neutral collagenase activity in an invasive mammalian tumour. Nature 1969; 221:259–260.

(*2*) DRESDEN MH, HEILMAN SA, SCHMIDT JD. Collagenolytic enzymes in human neoplasms. Cancer Res 1972; 32:993–996.

(*3*) LIOTTA LA, KLEINERMAN J, CATANZARO P, RYNBRANDT D. Degradation of basement membrane collagen by murine tumor cells. J Natl Cancer Inst 1977; 58:1427–1431.

(4) Liotta LA, Tryggvason K, Garbisa S, Hart IR, Foltz C, Shafie S. Metastatic potential correlates with enzymatic degradation of basement membrane collagen. Nature 1980; 284:67–68.

(5) Gross J, Highberger JH, Johnson-Wint B, Biswas C. Mode of action and regulation of tissue collagenases. In: Woolley DE, Evanson JM, eds. Collagenase in normal and pathological connective tissues. New York: Wiley, 1980:11–35.

(6) Woolley DE, Tetlow LC, Mooney CJ, Evanson JM. Human collagenase and its extracellular inhibitors in relation to tumor invasiveness. In: Strauli P, Barrett AJ, Baiei A, eds. Proteinases and tumor invasion. New York: Raven Press, 1980:97–113.

(7) Jones PA, DeClark YA. Destruction of extracellular matrices containing glycoproteins, elastin and collagen by metastatic human tumor cells. Cancer Res 1980; 40:3222–3227.

(8) Liotta LA, Lanzer WL, Garbisa S. Identification of a type V collagenolytic enzyme. Biochem Biophys Res Commun 1981; 98:184–190.

(9) Liotta LA, Goldfarb RH, Brundage R, Siegal GP, Terranova V, Garbisa S. Effect of plasminogen activator (urokinase), plasmin and thrombin on glycoprotein and collagenous components of basement membrane. Cancer Res 1981; 41:4629–4636.

(10) Liotta LA, Lee CW, Morakis DJ. New method for preparing large surfaces of intact human basement membrane for tumor invasion studies. Cancer Lett 1980; 11:141.

(11) Russo RG, Liotta LA, Thorgeirsson U, Brundage R, Schiffman E. Polymorphonuclear leukocyte migration through human amnion membrane. J Cell Biol 1981; 91:459–467.

(12) Russo RG, Thorgeirsson U, Liotta LA. In vitro quantitative assay of invasion using human amnion. In: Liotta LA, Hart IR, eds. Biology of cancer invasion and metastases. New York: Martinus and Ninjhoff. In press.

(13) Talmage JE, Kay ME, Hart IR. Characterization of a murine ovarian reticulum cell sarcoma of histiocytic origin. Cancer Res 1981; 41:1271–1280.

(14) Hart IR, Talmage JE, Fidler IJ. Metastatic behavior of a murine reticulum cell sarcoma exhibiting organ specific growth. Cancer Res 1981; 41:1281–1287.

(15) Kuettner KE, Soble L, Croxen RL, Marezynska B, Hiti J, Harper E. Tumor cell collagenase and its inhibition by cartilage-derived protease inhibitor. Science 1977; 196:653–654.

(16) Hatcher VB., Tsien G, Oberman MS, Burk PG. Inhibition of cell proliferation and protease activity by cartilage factors and heparin. J Supramol Struct 1980; 14:33–46.

(17) Langer R, Brem H, Folterman K, Klein M, Folkman J. Isolation of a cartilage factor that inhibits tumor neovascularization. Science 1976; 193:70–72.

(18) Pauli BU, Memoli VH, Kuettner KE. In vitro determination of tumor invasiveness using extracted hyaline cartilage. Cancer Res 1981; 41:2084–2091.

(19) Cawston TE, Galloway WA, Merger E, Murphy G, Reynolds JJ. Purification of rabbit bone inhibitor of collagenase. Biochem J 1981; 195:159–165.

(20) Murphy G, Cawston TE, Reynolds JJ. An inhibitor of collagenase from human amniotic fluid. Biochem J 1981; 195:167–170.

(21) Liotta LA, Abe S, Gehron-Robey P, Martin GR. Preferential digestion of basement membrane collagen by an enzyme derived from a metastatic murine tumor. Proc Natl Acad Sci USA 1979; 76:2268–2274.

(22) Pearce RH, Laurent TC. Exclusion of dextrans by meshworks of collagenous fibers. Biochem J 1977; 163:617–625.

(23) Varani J, Orr W, Ward PA. A comparison of the migration patterns of normal and malignant cells in two assay systems. Am J Pathol 1978; 90:159–171.

(24) Wass JA, Varani J, Piontek GE, Goff D, Ward PA. Characteristics of the chemotactic factor-mediated cell swelling response of tumor cells. JNCI 1981; 66:927–933.

(25) Schleich AB, Frick M, Mayer A. Patterns of invasive growth in vitro. Human decidua graviditatis confronted with established human cell lines and primary human explants. J Natl Cancer Inst 1976; 56:221–225.

(26) Scher CD, Haudenschild C, Klagsbrun M. The chick chorioallantoic membrane as a model system for the study of tissue invasion by viral transformed cells. Cell 1976; 8:373–382.

(27) Noguchi PD, Johnson JB, O'Donnel R, Petricciani JC. Chick embryonic skin as a rapid organ culture assay for cellular neoplasia. Science 1978; 199:1980–1983.

(28) Mareel M, Kint J, Meyvisch C. Methods of study of the invasion of malignant C3H mouse fibroblasts into embryonic chick heart in vitro. Virchows Arch [Cell Pathol] 1979; 30:95–111.

(29) Roos E, Van De Pavert IV, Middlekoop OP. Infiltration of tumor cells into cultures of isolated hepatocytes. J Cell Sci 1981; 47:385–397.

(30) Hart IR, Fidler IJ. An in vitro quantitative assay for tumor cell invasion. Cancer Res 1978; 38:3218–3224.

(31) Poste G, Doll J, Hart IR, Fidler IJ. In vitro selection of murine B16 melanoma variants with enhanced tissue invasive properties. Cancer Res 1980; 40:1636–1644.

(32) Fidler IJ. Tumor heterogeneity and the biology of cancer invasion and metastases. Cancer Res 1978; 38:2651–2660.

(33) Showell HJ, Freer RJ, Zigmond SH, et al. The structure activity relationship of synthetic peptides as chemotactic factors and inducers of lysosomal enzyme secretion for neutrophils. J Exp Med 1976; 143:1154–1169.

(34) Niedel JE, Cuatrecasas P. Formyl peptide chemotactic receptors of leukocytes and macrophages. Curr Top Cell Regul 1980; 17:137–170.

(35) Yoshida K, Ozaki T, Ushijima K, Hayashi H. Studies on the mechanism of invasion in cancer. Isolation and purification of a factor chemotactic for cancer cells. Int J Cancer 1970; 6:123–132.

(36) Romualdez AG, Ward PA. A unique complement derived chemotactic factor for tumor cells. Proc Natl Acad Sci USA 1975; 172:4128–4132.

(37) Liotta LA, Garbisa S, Tryggvason K. Biochemical mechanisms involved in tumor cell penetration of the basement membrane. In: Liotta LA, Hart IR, eds. Biology of cancer invasion and metastases. New York: Martinus and Ninjhoff. In press.

(38) Alitalo K, Kurkinen M, Vaheri A. Extracellular matrix components synthesized by human amniotic epithelial cells in culture. Cell 1980; 19:1053–1062.

(39) Quigley JP, Martin BM, Goldfarb RH, Scheiner CJ, Muller WD. Involvement of serine proteases in growth control and malignant transformation. Hormones and cell culture. In: Cold Spring Harbor conferences on cell proliferation. Vol 6. New York: Cold Spring Harbor Press, 1979:219–238.

Androgen Conjugates in Human Breast Cyst Fluids[1,2]

W. R. Miller,[3] M. M. Roberts,[3] R. J. Creel,[3] P. L. Yap,[4] R. W. Kelly,[5] *and* A. P. M. Forrest[3]

ABSTRACT—Dehydroepiandrosterone sulfate (DHAS) has been measured by radioimmunoassay in 100 breast cyst fluids obtained from 82 women. Values ranged from 1.5 to 1,155 μM with a median of 140 μM. These concentrations are in excess of those for plasma but are comparable or less than values for breast secretions obtained by nipple aspiration. Levels of DHAS in cyst fluid were not significantly affected by age, menopausal status, or parity of the subject or by the volume of cyst fluid obtained. In patients with multiple cysts, DHAS values from cysts aspirated from the same breast on the same date were relatively comparable, but wide variations were frequently observed between cysts aspirated on different occasions from the same breast and between cysts from different breasts of the same patient, whether sampled simultaneously or sequentially. Such variability must complicate comparative studies among women.—JNCI 1982, 69:1055–1058.

Evidence that the hormonal milieu of a woman may influence her risk of breast cancer has been reviewed by Vorheer and Messer (*1*). Most investigations on endocrine profiles have centered on levels of circulating or excreted hormone; the immediate hormonal environment of the breast has been relatively ignored. Recently, we reported that breast secretions collected by nipple aspiration from nonlactating women may contain remarkably high levels of DHAS, which are much in excess of those in the circulation (*2*).

We now report on measurements of DHAS in breast cyst fluids and factors that might influence its concentration.

MATERIALS AND METHODS

Collection of breast fluids and plasma.—A total of 100 cyst fluids were obtained by needle aspiration from 82 women who presented with tension cysts of the breast. Multiple cysts were aspirated in 10 women, and 5 patients had cysts aspirated on more than one occasion. Menopausal status was documented for 77 of the women, and volume of aspirated fluid was measured in the last consecutive 32 women studied. In 4 women, secretions were also collected by application of negative pressure to the nipple (*3*) of a breast containing a cyst, which was also immediately aspirated.

Peripheral blood was taken by venipuncture immediately before aspiration of breast fluids and collected in heparinized tubes. Plasma was separated within 30 minutes by centrifugation. All samples were stored at −20°C until assayed.

Radioimmunoassay of DHAS.—Radioimmunoassay was performed directly on diluted cyst fluids, secretions, and plasmas with the use of the method of Buster and Abrahams (*4*). The antibody was supplied by Mr. B. A. Morris, Department of Biochemistry, University of Surrey, England. The specificity of this antibody has been described previously (*2*).

GLC-MS analysis of cyst fluids.—Aliquots of six cyst fluids were diluted to 10 ml with distilled water. $[7\text{-}\alpha\text{-}^{3}\text{H}]$DHAS (25,000 cpm, ≈5 pmol) was added, and the diluted cyst fluid was extracted with an equal volume of diethyl ether for removal of unconjugated steroids. The aqueous fraction was then solvolyzed as described previously (*2*). An aliquot was removed for estimation of radioactivity for measurement of procedural losses. The remainder was derivatized as tertiary butyl dimethyl silyl ethers as described previously (*2*) with the use of deuterated epiandrosterone as internal standard. Steroids and internal standards were measured in a Dupont 490B mass spectrometer coupled through a glass jet separator to a Varian 1400 gas chromatograph. A 10-m SE 30 support-coated open tubular column maintained at 200°C was used. Transfer lines were maintained at 250°C, and the source temperature was 240°C. Steroids were quantitated by measurement of peak heights of the M-57 peaks (m/z 345 for DHA, m/z 347 for androsterone and epiandrosterone, and m/z 349 for the tetradeutero-epiandrosterone internal standard). Standard mixtures derivatized with samples were used for construction of a ratio-mass plot from which the mass of the various steroids was read.

RESULTS

Radioimmunoassay of DHAS—All 100 cyst fluids contained material that cross-reacted with the antibody to DHA and its sulfate. Concentrations ranged from 1.5 to 1,155 μM with a median value of 140 μM (text fig. 1).

GLC-MS.—Six cyst fluids were analyzed by MS, and the values are shown in table 1. Levels of DHA conjugate were detected in all, but in only two was there a good correlation with results from radioimmunoassay; in the remainder values obtained by GLC-MS were lower, although the dimensions were similar. Significant amounts of androsterone and epiandrosterone were also detected by GLC-MS in solvolyzed extracts of cyst fluids. Extracts that contained the highest proportion of epiandrosterone were derived from cyst fluids showing the greatest disparity between GLC-MS and radioimmunoassay (table 1). It is thus pertinent that

ABBREVIATIONS USED: DHA=dehydroepiandrosterone; DHAS=dehydroepiandrosterone sulfate; GLC=gas-liquid chromatography; MS=mass spectrometry; m/z=mass divided by elementary charge.

---

[1] Received March 10, 1982; accepted May 20, 1982.

[2] Research procedures were in accord with the ethical standards of the South Lothian Division of Surgery, Royal Infirmary, Edinburgh.

[3] University Department of Clinical Surgery, Medical School, Royal Infirmary, Edinburgh EH3 9YW Scotland.

[4] Blood Transfusion Service, Royal Infirmary, Edinburgh EH3 9YM Scotland.

[5] Medical Research Council Unit of Reproductive Biology, Chalmers St., Edinburgh, Scotland.

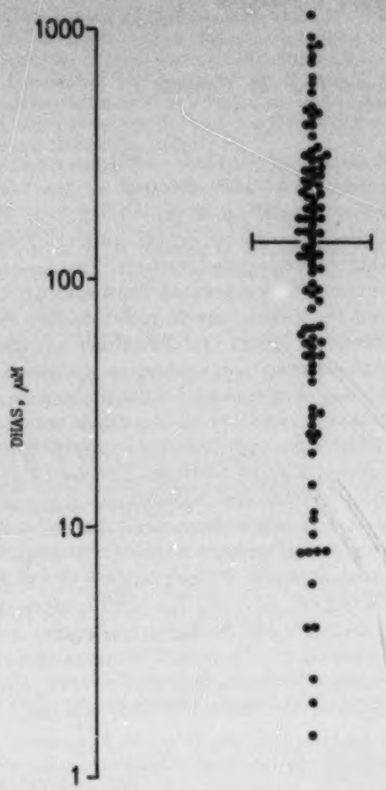

TEXT-FIGURE 1.—DHAS levels as estimated by radioimmunoassay in human breast cyst fluids. *Horizontal line* represents median value.

the antibody used in the radioimmunoassay also cross-reacted significantly with epiandrosterone sulfate (*2*). Values from radioimmunoassay probably reflect levels of both DHAS and closely related 17-oxosteroid conjugates, although for simplicity, in the text, we shall refer to them as concentrations of DHAS.

Effects of age, menopausal status, and parity.—The median age of the 82 women studied was 45 years (range 31–55). There was no significant correlation between DHAS levels in cyst fluid (as measured by radioimmunoassay) and the age of the patient from whom it was derived.

Menopausal status was known in 77 women; 64 of those were experiencing regular periods, and the remainder were perimenopausal. The median value for DHAS was lower in cysts from perimenopausal patients, but the difference between the 2 groups failed to reach statistical significance by the Wilcoxon rank sum test (text-fig. 2).

Parity was documented in 67 women; 28 were nulliparous, the remainder parous. There was no significant difference between DHAS levels in cyst fluids from nulliparous and parous women (text-fig. 3) and, within the parous group, between DHAS levels and the number of full-term pregnancies.

Effects of volume of cyst fluid.—Volume of aspirated fluid was measured in 32 cysts and varied from 1.5 to 25 ml. There was, however, no significant correlation between levels of DHAS and volume of fluid aspirated from the cysts (text-fig. 4).

Multiple cysts.—Among the patients, 10 had multiple cysts aspirated on the same visit to the clinic. In 6 women fluid was obtained from different cysts in the same breast and, in 5, cysts were obtained from both breasts (table 2). Generally, levels of DHAS were similar in cysts from the same breast, but the variation between cysts became more marked when they were derived from different breasts in the same women. (In 1 woman DHAS concentrations were completely different in cysts from the left and right breasts.)

Five women had cysts aspirated on more than one occasion at intervals that varied between 3 and 76 weeks. Large

TABLE 1.—*GLC-MS analysis of cyst fluids*

Cyst fluid sample No.	Concentration DHA conjugate, μM		Ratio of conjugates in solvolyzed extracts measured by GLC-MS
	By radioimmunoassay[a]	By GLC-MS[b]	DHA:epiandrosterone:androsterone
66	856	413	1:1.38:0.86
69	253	247	1:0.36:0.30
71	77	18	1:3.08:1.33
73	1,155	1,142	1:0.84:0.39
82	5	3	1:3.33:1.67
83	883	272	1:3.25:0.58

[a] Radioimmunoassay performed directly on diluted cyst fluids.

[b] Calculated estimations of DHA in solvolyzed extracts after correction for losses during solvolysis by recovery of labeled DHAS.

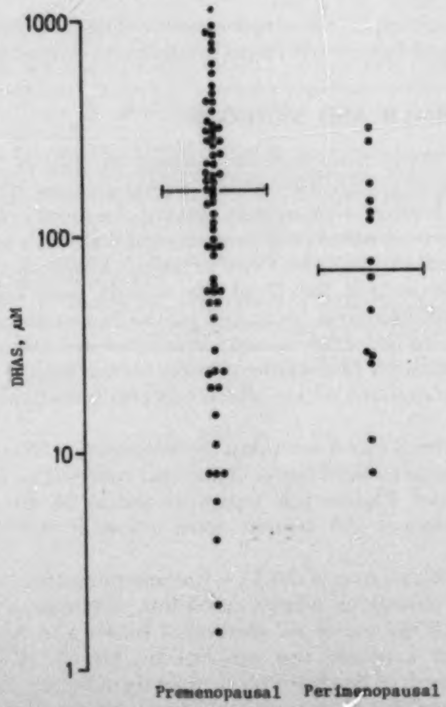

TEXT-FIGURE 2.—DHAS levels in cyst fluids from premenopausal and perimenopausal women. *Horizontal lines* represent median values.

variations in DHAS levels were frequently observed between cysts aspirated from the same breast at different times (table 2).

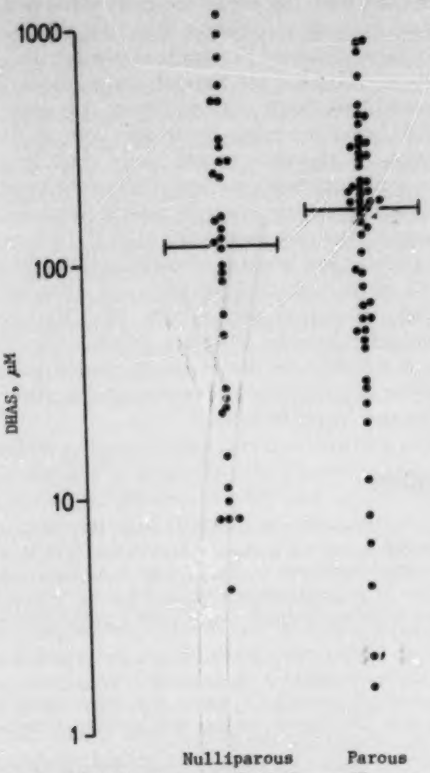

TEXT-FIGURE 3.—DHAS levels in cyst fluids from nulliparous and parous women. *Horizontal lines* represent median values.

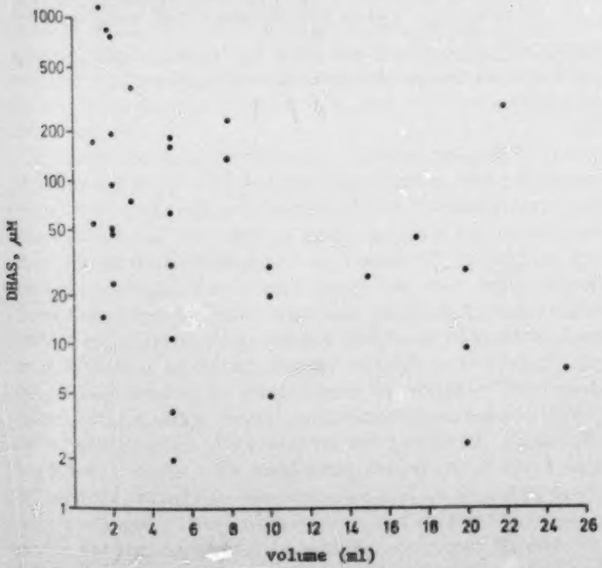

TEXT-FIGURE 4.—Relationship between DHAS concentrations and volumes of aspirated cyst fluid.

TABLE 2.—*DHAS concentrations in multiple cysts from the same individuals*

Mode of aspiration	Patient No.	DHAS concentration, µM		Time interval, wk
		Left breast	Right breast	
Simultaneous	7	187		
		217		
	8	217		
		145		
	9		156	
			152	
	10		54	
			58	
	12		64	
			63	
	5	130	250	
			288	
	3	421	307	
	6	215	128	
	37	240	8	
	53	340	277	
Sequential	6	215	128	
			279	65
			313	3
	28		49	
			492	26
	32	4		
		380		3
	69		64	
			253	76
			136	3
	74	731		
		946		3

TABLE 3.—*Comparative levels of DHAS in cyst fluids, plasma, and breast secretions*

Patient No.	DHAS, µM,[a] in:		
	Cyst fluid	Plasma	Secretion
28	492	10	—
31	90	2	—
26	421	4	425
30	10	1	45
29	24	—	747
33	60	—	380

[a] — = not measured.

Comparative levels in cyst fluids, breast secretions, and plasma.—Blood was taken from 4 women at the same time as their cysts were aspirated. In each case levels of DHAS in the cyst fluid were much in excess of those in the plasma (table 3). In 4 women nipple secretions were obtained from breasts containing cysts immediately before cyst aspiration. In 1 woman, the concentrations of DHAS in the cyst fluid and breast secretion were remarkably similar, but in the remaining 3 patients DHAS values in breast secretions were much higher than in the corresponding cyst fluids.

DISCUSSION

In a recent study, Bradlow et al. (*5*) have shown that human breast cyst fluids may contain high levels of DHA and androsterone sulfates much in excess of those in plasma and that the amount of these steroids in cyst fluid is not correlated with the volume of the cyst. The results of the present study would confirm these findings. Most cyst fluids contained large quantities of DHAS, but there was an extensive range of concentrations present in different cysts. In addition, GLC–MS confirmed the presence of large amounts of androsterone conjugate. Epiandrosterone conjugates were also present, and their high concentration probably accounts for the inconsistencies sometimes observed between the methods of radioimmunoassay and GLC–MS in the estimation of DHAS in cyst fluids. The antibody used in the radioimmunoassay cross-reacts significantly with epiandrosterone sulfate (*2*). It thus seems likely that in some cyst fluids, results from radioimmunoassay represent not only DHAS but also a contribution from other closely related steroid conjugates.

Because of the broad range of DHAS found in cyst fluids, it was of interest to examine factors that might influence these levels. Although most cyst fluids were obtained from premenopausal patients, no account was taken of the stage of the menstrual cycle in which they were collected. No cyclic pattern has been observed for DHAS levels in either plasma (*6*) or breast secretions (*7*). We could detect no significant correlation between cyst fluid concentration of DHAS and age, menopausal status, or parity of the patients. A similar lack of correlation has been reported by Bradlow et al. (*5*).

In a small number of cases we were able to analyze several cysts from the same women. There was a good correlation between DHAS levels in cysts aspirated from the same breast at the time, but larger variations were apparent between cysts from different breasts of the same women even when these were sampled at the same time. Cysts aspirated from the same women on sequential visits showed broad differences in DHAS concentrations, even though they may have been derived from the same breast. Similar observations have been made by others (*7*). The widely different values that may be observed in cysts aspirated from the same breast on separate occasions and, indeed, from both breasts of the same women when studied at the same time, makes comparative studies between different groups of women very difficult. It will be necessary to discover why such variations exist and the mechanism by which steroid conjugates accumulate in breast cysts. They may be derived from the breast secretory units or represent a transudate from the circulation. It is thus significant that breast secretions obtained by nipple aspiration also contain high levels of DHAS. Our limited comparison of breast secretions and cyst fluids obtained from the same women suggests that breast secretions invariably contain the higher concentration. It therefore seems likely that certain cyst fluids represent accumulation and dilution of breast secretions by blockage of the ducts in which they reside. Our observation (*8*) that cyst fluids with high DHAS concentrations contain only low levels of albumin, whereas those with low DHAS have high concentrations of albumin would support this contention and suggest that the diluent is plasma derived. It may be necessary to subdivide cyst fluids according to whether the derivation of their major constituents is breast or plasma before meaningful studies on their composition can be performed.

REFERENCES

(*1*) Vorheer H, Messer RH. Breast cancer: Potentially predisposing and protecting factors. Am J Obstet Gynecol 1978; 130:335–358.

(*2*) Miller WR, Humeniuk V, Kelly RW. Dehydroepiandrosterone sulphate in breast secretions. J Steroid Biochem 1980; 13:145–151.

(*3*) Sartorius O. Breast fluid cells—help in early cancer detection. JAMA 1973; 224:824–827.

(*4*) Buster JE, Abraham GE. Radioimmunoassay of plasma dehydroepiandrosterone sulphate. Anal Lett 1972; 5:543–551.

(*5*) Bradlow HL, Rosenfeld RS, Kream J, Fleisher M, O'Connor J, Schwartz MK. Steroid hormone accumulation in human breast cyst fluid. Cancer Res 1981; 41:105–107.

(*6*) Abraham GE. Ovarian and adrenal contribution to peripheral androgens during the menstrual cycle. J Clin Endocrinol Metab 1974; 39:340–346.

(*7*) Miller WR, Humeniuk V, Forrest AP. Factors affecting dehydroepiandrosterone sulphate levels in human breast secretions. Breast Cancer Res Treat 1981; 1:267–272.

(*8*) Yap PL, Miller WR, Roberts MM, et al. Studies on the composition of human breast cyst fluid. Br J Cancer. In press.

Parity and Colorectal Cancer Risk in Women[1,2]

Tim Byers, *M.D., M.P.H.*,[3,4] **Saxon Graham**, *Ph.D.*,[3,4] *and* **Mya Swanson**, *B.A.*[3]

ABSTRACT—A case-control study is reported of reproductive history and colorectal cancer risk based on information obtained from interviews with white women 40–79 years old who were admitted to Roswell Park Memorial Institute between the years 1957 and 1965. Women with the primary diagnosis of carcinoma of the colon (*n*=284) and carcinoma of the rectum (*n*=270) did not differ significantly in their prior reproductive histories as compared to those of a control group of women (*n*=1,763) with nonneoplastic diseases not affecting the breast or reproductive sites. The pertinent literature suggesting a parity-colorectal cancer association in women is reviewed. The conclusion reached is that the evidence for a parity-colorectal cancer association is equivocal; but that if such an association exists, it is probably weaker than that seen for cancers of the breast, ovary, and uterine corpus.—JNCI 1982; 69:1059–1062.

Several investigators have noted similarities in the epidemiologic features of breast, ovarian, endometrial, and colorectal cancers in women. Colon and breast cancers are positively correlated in international mortality statistics (*1*). Cancers of the colon have appeared more frequently than expected as second primary neoplasms in women with previous cancers of the breast or genital organs, and second primary neoplasms of the breast and genital organs have appeared more frequently than expected in women with previous cancers of the colon (*2, 3*). Nuns, who have experienced higher than expected mortality rates for cancers of the breast, ovary, and uterine corpus, have also been reported to have higher than expected rates of colon cancer (*4*). In the Third National Cancer Survey, single women experienced a higher incidence rate of colon cancer than did married women, a phenomenon also seen in women with cancers of various other sites including breast, ovary, and uterine corpus (*5*). All of these studies considered together suggest that cancer of the colon may share common etiologic factors with cancers of the breast and reproductive organs in women (*6*).

If there are specific common etiologic factors, however, they are yet to be clearly identified. Parity, being inversely associated with risk of cancers of the breast, ovary, and uterine corpus, has been a prime suspect for a common etiologic factor. McMichael and Potter (*7*), noting the evidence presented above and observing that birth cohort decreases in fertility have been followed later by subsequent cohort increases in colon cancer incidence in women, have suggested that hormonal factors related to pregnancy may be causally related to colon cancer in women. Three case-control studies have directly examined reproductive history as a risk factor for colorectal cancer in women. Bjelke (*8*), studying women with colorectal cancer in Norway and Minnesota, found that women with three or more live births had a reduced risk of colon cancer, but an increased risk of rectal cancer, compared to women with zero to two live births. Dales et al. (*9*), studying colorectal cancer in 52 black women in the San Francisco area, found that nulliparous women showed an apparent doubling of risk as compared to the risk for parous women. Weiss et al. (*10*), studying 148 women with colorectal cancer in the Seattle area showed an approximate doubling of risk for nulliparous women as compared to the risk for women with three or more children, but this finding was limited to the 94 women with colon cancer and was not seen in the 49 women who had rectal cancer.

The purpose of this paper is to present findings from our study of the pregnancy history of a much larger series of women with cancers of the colon and rectum, studied separately, and to review the evidence of a parity risk factor for female colorectal cancer as presented in the literature to date.

METHODS

This is a case-control study. Cases were all white women 40–79 years of age who were admitted to RPMI (Buffalo, N.Y.) between the years 1957 and 1965 with the primary diagnosis of cancer of the colon (*n*=284) or rectum (*n*=270). Although RPMI is a referral center for cancer treatment, most of these patients were admitted before definitive diagnosis or soon after their diagnosis was made. Ninety-two percent of the rectal cancer cases and 88% of the colon cancer cases were admitted within 2 years of the date of their initial diagnosis. Controls were 1,763 white women 40–79 years of age who were admitted to RPMI for nonneoplastic disease during the same years. Women with diseases of the breast or reproductive systems were excluded because of the well-established associations between diseases of these sites and prior pregnancy history. Table 1 lists the diagnoses of the women comprising the control group. Information on cancer risk factors as well as other health information, including pregnancy history, was routinely ascertained from all patients admitted to RPMI by mailed questionnaire prior to admission. This information was then verified with the patient by personal interview at the time of admission. Statistical analysis of these data was conducted controlling for age by the method described by Mantel and Haenszel (*11*) with the use of 5-year age groups. Analyses are presented separately for colon and rectal cancer cases.

ABBREVIATIONS USED: ICD=International Classification of Diseases; RPMI=Roswell Park Memorial Institute; SMSA=standard metropolitan statistical area.

---

[1] Received March 12, 1982; accepted June 6, 1982.

[2] Supported in part by Public Health Service grant CA-11535 from the National Cancer Institute.

[3] Department of Social and Preventive Medicine, Faculty of Health Sciences, School of Medicine, State University of New York at Buffalo, 2211 Main St., Buffalo, N.Y. 14214.

[4] Roswell Park Memorial Institute, Buffalo, N.Y.

TABLE 1.—*Frequency distribution of discharge diagnosis (ICD 7) for the 1,763 women comprising the RFMI control series used in this study*

System of disorder	ICD 7 code	Percent
No diagnosis made or no pathology found		18.9
Upper GI tract	530–570, 581–587	18.3
Skin	690–716	12.8
Allergic or endocrine	240–289	9.1
Circulatory	410–468	7.5
Respiratory	471–527	7.0
Lower GI tract	571–578	6.8
Urological	593–617	3.2
Skeletal	722–744	3.1
Neurological	332–396	2.2
Infectious	002–138	2.2
Miscellaneous (34 diagnoses, each under 2% of total)		8.9
		100.0

TABLE 2.—*Marital status and number of live births of colon cancer cases as compared to those of controls*

Parameter	Percent of colon cancer patients (n=284)[a]	Percent of controls (n=1,763)	Relative risk[b]	P
Marital status				
Ever-married	94.6	92.5	1.00	
Never-married	5.4	7.5	1.42	0.23
No. of live births				
0[c]	20.1	24.4	1.00	
1–2	36.4	34.3	1.29	0.16
≥3	43.5	41.3	1.25	0.20

[a] Age adjusted to that of control group.
[b] By method of Mantel–Haenszel.
[c] Includes never-married women.

TABLE 3.—*Marital status and number of live births of rectal cancer cases as compared to those of controls*

Parameter	Percent of rectal cancer patients (n=270)[a]	Percent of controls (n=1,763)	Relative risk[b]	P
Marital status				
Ever-married	91.7	92.5	1.00	
Never-married	8.3	7.5	1.27	0.32
No. of live births				
0[c]	23.9	24.4	1.00	
1–2	40.7	34.3	1.10	0.62
≥3	35.4	41.3	0.82	0.27

[a] Age adjusted to that of control group.
[b] By method of Mantel–Haenszel.
[c] Includes never-married women.

RESULTS

Tables 2 and 3 present the essential findings of the study. They show no significant differences between either the colon or rectal cancer cases and the controls with regard to marital status or the number of live births. Although the ages are pooled in the data as presented, detailed analysis revealed no pattern of association between either colon cancer or rectal cancer and marital status or parity across the various levels of age. Other reproduction variables were also examined. When patients with both colon and rectal cancers were compared to controls, no association was seen between disease status and the total number of pregnancies, the total number of miscarriages and stillbirths, or the age at first marriage. Age at first pregnancy was not examined since this information is yet to be coded from the questionnaire.

DISCUSSION

Hospital-based case-control studies may be affected by subtle biases either in the selection of cases or in the selection of controls or in both. Although a previous study has demonstrated that cases referred to RPMI during the 1957–65 era closely resemble those seen in the surrounding community with regard to such factors as socioeconomic status, marital status, religion, and tobacco use, there is the possibility that other unidentified case selection factors may in some way result in a relative underrepresentation of nulliparous cases in this series.

However, because RPMI is primarily a cancer treatment center, of more concern would be possible selection factors relative to the control group that might tend to make it not representative of the general reference population from which the cases are drawn. To test the representativeness of the control group relative to pregnancy history, we examined data from the 1960 U.S. census (collected within the study period) (*12*). Eighty-seven percent of the control series resided in the eight western-most counties of New York State and 62% resided in the two-county Buffalo, N.Y., SMSA. There were no significant differences in numbers of live births reported for those women who resided within as compared to those who resided outside the Buffalo SMSA. Parity of the 1960 census population of white women in the Buffalo SMSA is compared in an age-adjusted analysis in table 4 with that of the RPMI control group used in this study. This comparison demonstrates that, although the controls are a hospital-based series, the parity of the controls used in this study nonetheless closely resembles that of the general reference population, thus strengthening our confidence that there were not significant selection biases in the control group associated with our major independent study variable. An additional way to assess the representativeness of the control group is to compare the group to patients with other diagnoses known to be related to parity. Cancers of the breast, uterine corpus, and ovary have well-established associations with pregnancy history (*13–15*). All white women admitted to RPMI during this same 1957–65 study period with diagnoses of cancer of the breast, uterine corpus, or ovary are compared in table 5 to the same control group used in the current study. The expected finding of statistically significant associations between the reported number of live births and cancers of these three sites further strengthens our confidence in the validity of the negative findings of the colorectal cancer study presented here.

That colon cancer and cancers of the reproductive organs are by some means associated in women seems likely, though the precise determinants of this association are unclear. The

TABLE 4.—*Distribution of live births as reported by RPMI control series (1957-65) compared to that of Buffalo SMSA white female census population (1960)*

No. of live births	RPMI controls, %	1960 census, %[a]
0[b]	24.4	26.5
1-2	34.3	36.3
≥3	41.3	37.2
Total	100.0	100.0

[a] Age adjusted to that of control group.
[b] Includes never-married women.

TABLE 5.—*Relative risk estimates[a] for selected numbers of live births for RPMI patients, age 40-79, with cancers of the breast, uterine corpus, and ovary as compared to the 1,763 RPMI controls used in this study*

No. of live births	Cancer site		
	Breast (*n*=1,[illegible]65)	Uterine corpus (*n*=449)	Ovary (*n*=293)
0[b]	1.00	1.00	1.00
1-2	0.97	0.90	0.80
≥3	0.69[c]	0.66[c]	0.47[c]

[a] Age adjusted by method of Mantel-Haenszel.
[b] Includes never-married.
[c] *P*<0.01.

same type of correlation noted between female colon and breast cancer rates in international mortality statistics can also be seen between female breast cancer and male colon cancer rates (*1*). This correlation argues for a common etiologic factor for colon and breast cancers that is unrelated to pregnancy. The studies demonstrating an association between colon, breast, ovarian, and uterine corpus cancers in women with second primary cancers (*2, 3*), though also suggesting common etiologic factors (assuming the excess second primary neoplasms are not iatrogenic), do not, by design, specify those factors. It would be of interest to examine the pregnancy histories of women with these associated multiple primary cancers to determine the extent to which the observed association might be attributed to parity. The increase in risk of colon cancer among never-married women as compared to married women in the Third National Cancer Survey (a finding not seen in our data) suggests a marital status-associated risk factor, but the observation of a similar association in men in the same survey (*5*) would argue against prior pregnancy history as the specific etiologic component of the marital status risk. The reported excess of mortality rates from cancers of the colon and breast in nuns (*4*) could, of course, in addition to differences in pregnancy history, be a result of various other potential etiologic factors associated with this particular life role. It is important to note also that the excess in "intestinal" cancer in nuns was observed only in those women over 70 years of age (23 expected and 39 observed), whereas at younger ages, there was actually a lower than expected mortality rate for gastrointestinal cancers (site not specified).

The case-control study by Bjelke (*8*) demonstrated a decreased risk of colon cancer for multiparous women, but this finding was limited only to women with blood type O, and an actual increase in risk of rectal cancer for multiparous women was noted. Case-control studies by Dales et al. (*9*) and by Weiss et al. (*10*), though studies of defined populations, were both limited by small numbers of study subjects and low response rates (40% for Dales et al. and 61% for Weiss et al.). Thus case selection biases might have significantly affected the estimates of relative risk, inasmuch as these studies were of small numbers of cases and controls (resulting in relatively small contingency table cell sizes). The failure of our study to replicate the same parity-colorectal cancer association shown in these previous case-control studies might be due as well to various other factors, including a birth cohort effect. Our study (1957-65) was based on data collected on the average of 14 years previous to the more recent studies (1973-77). During these years, there were changes in the reproductive experiences of women that might account for the discordant findings. The more prevalent usage of oral contraceptives, for instance, in more recent cohorts of women could be such a change. Though not statistically significant, possibly because of small numbers of cases, Weiss' data do suggest an oral contraceptive risk factor acting in rectal cancer. Whether oral contraceptive usage is in fact related to rectal cancer risk has not been determined, however.

In summary, we have presented a case-control study that demonstrates no apparent association between prior pregnancy history and colon or rectal cancer risk in women who were diagnosed in the 1957-65 era. We conclude that the evidence for such an association is equivocal. If there is such an association, it appears to be weaker than that seen in cancers of the breast, ovary, and uterine corpus. Other possible etiologic factors that might be common to colon, breast, ovarian, and uterine corpus cancers in women should be further considered, such as diet, prior use of medications, the activity of gut flora (*16*), and, more likely, as yet unidentified common etiologic factors. In the future, the more prevalent clinical use of hormone receptor assays of colorectal neoplasms (*17*) and a more detailed study of the determinants of cancer risk for subsites of the colon (e.g., proximal vs. distal) might allow us to better define specific subsets of women with colorectal cancers of hormone-related etiologies.

REFERENCES

(*1*) WYNDER EL, HYAMS L, SHIGEMATSU T. Correlations of international cancer death rates: An epidemiological exercise. Cancer 1967; 20:113-126.

(*2*) SCHOENBERG BS, GREENBERG RA, EISENBERG H. Occurrence of certain multiple primary cancers in females. J Natl Cancer Inst 1969; 43:15-32.

(*3*) SCHOTTENFELD D, BERG JW, VITSKY B. Incidence of multiple primary cancers. II. Index cancers arising in the stomach and lower digestive system. J Natl Cancer Inst 1969; 43:77-86.

(*4*) FRAUMENI JF JR, LLOYD JW, SMITH EM, WAGONER JK. Cancer mortality among nuns: Role of marital status in etiology of neoplastic disease in women. J Natl Cancer Inst 1969; 42:455-468.

(*5*) ERNSTER VL, SACKS ST, SELVIN S, PETRAKIS NL. Cancer incidence by marital status: U.S. Third National Cancer Survey. JNCI 1979; 63:567-585.

(*6*) HOWELL MA. The association between colorectal cancer and breast cancer. J Chronic Dis 1976; 29:243-261.

(*7*) MCMICHAEL AJ, POTTER JD. Reproduction, endogenous and exogenous sex hormones, and colon cancer: A review and hypothesis. JNCI 1980; 65:1201–1207.

(8) Bjelke E. Colorectal cancer: Clues from epidemiology. In: Proceedings of the eleventh international cancer congress. Vol 6. Excerpta Med Foundation Int Congress. New York: Elsevier, 1975; 324–330.

(9) Dales LG, Friedman GD, Ury HK, Grossman S, Williams SR. A case-control study of relationships of diet and other traits to colorectal cancer in American blacks. Am J Epidemiol 1978; 9:132–144.

(10) Weiss NS, Daling JR, Chow WH. Incidence of cancer of the large bowel in women in relation to reproductive and hormonal factors. JNCI 1981; 67:57–67.

(11) Mantel N, Haenszel W. Statistical aspects of the analysis of data from retrospective studies of disease. J Natl Cancer Inst 1959; 22:719–748.

(12) U.S. Bureau of Census. U.S. Census of population: 1960. Detailed characteristics. New York. Final report PC(1)-34D. P531-2. Washington, D.C.: U.S. Govt Print Off, 1962.

(13) Kelsey JL. A review of the epidemiology of human breast cancer. Epidemiol Rev 1979; 1:74–109.

(14) Elwood JM, Cole P, Rothman KJ, Kaplan SD. Epidemiology of endometrial cancer. J Natl Cancer Inst 1977; 59:1055–1060.

(15) Hildreth NG, Kelsey JL, LiVolsi VA, et al. An epidemiologic study of epithelial carcinoma of the ovary. Am J Epidemiol 1981; 1:398–405.

(16) Hill MJ, Goddard P, Williams RE. Gut bacteria and aetiology of cancer of the breast. Lancet 1971; 2:472–473.

(17) Alford TC, Do H, Geelhoed GN, Tsangaris NT, Lippman ME. Steroid hormone receptors in human colon cancers. Cancer 1979; 43:980–984.

Correlation Between Cancers of the Uterine Cervix and Penis in China[1]

Jun-Yao Li,[2,3] Frederick P. Li,[4] William J. Blot,[2,5] Robert W. Miller,[4] *and* Joseph F. Fraumeni, Jr.[2]

ABSTRACT—A national survey of cancer mortality in the People's Republic of China during 1973–75 revealed concurrent geographic variation for cancers of the uterine cervix and penis, including clustering of both tumors in central parts of the country. The findings are consistent with recent reports from other countries that the cancers tend to aggregate in spouses and with the hypothesis of an etiologic factor in common.—JNCI 1982; 69:1063–1065.

In the People's Republic of China, cancer of the uterine cervix is one of the most common cancers among Chinese women, and several older reports have noted exceptionally high frequencies of penis cancer in autopsy and biopsy series of men (*1–6*). Using data collected in a nationwide survey of mortality from cancer during 1973–75 (*7–10*), we examined the geographic patterns of the two cancers within China. Particular attention was paid to the correlation between the cervical and penis cancer rates, in view of recent literature suggesting that the two diseases may be etiologically related (*11–16*).

METHODS

The National Cancer Control office of the Ministry of Health, Beijing, organized a survey to gather data on mortality from cancer and other causes among a population of over 800,000,000 Chinese over the 3-year period 1973–75. Details of the survey have been described elsewhere (*7–10*). Nearly 1 million workers (barefoot doctors, physicians, and community representatives) were mobilized to identify systematically all deaths attributed to cancer and to determine age-specific population estimates. The diagnosis of cancer was made at a commune hospital or higher level for 93% of all deaths. The determination was based on pathologic or cytologic examination for 17%; radiology, endoscopy, or other laboratory tests for 54%; clinical examination alone for 23%; and history of symptoms given by relatives after death for 6%. From the collected information, age-specific and age-adjusted [world standard (*17*)] rates of mortality for 15 cancers were calculated for 29 provinces, 396 prefectures and independent cities, and 2,136 counties of China during 1973–75. For 24 of the provinces in China and their 324 prefectures and independent cities, mortality rates for cancer of the penis, a rare tumor in the general population, were listed separately from rates for other genital cancers. Using the 324 areas as sampling units, we calculated the correlation between the age-adjusted rates for cancers of the cervix and penis and prepared maps of the relative distributions of the two cancers.

RESULTS

National Rates

There were approximately 53,000 deaths per year from cancer of the cervix and 4,000 deaths per year from cancer of the penis in China during 1973–75. The average annual age-adjusted national rates per 100,000 population were 14.6 and 0.64, respectively. Cervical cancer ranked third behind cancers of the stomach (15.9/100,000) and esophagus (15.9/100,000) as the leading causes of cancer death among females, whereas penis cancer was the eleventh most common cause of fatal cancer among males. Cervical cancer accounted for 18.1% of all cancer deaths among women, and penis cancer accounted for 0.5% of all cancer deaths among men. The age-specific rates of mortality for cervical cancer increased steadily with age before they began to plateau after age 50, whereas penis cancer rates increased monotonically with advancing age.

Geographic Variation Within China

Age-adjusted rates of mortality from cervical cancer ranged from a low of 4.1 per 100,000 for Xizang province to a high of 29.4 in Shanxi province, a sevenfold difference. Rates in several prefectures exceeded 40. The penis cancer rates ranged from a low of 0.11 in Xizang to a high of 0.93 in Hunan, an eightfold gradient among the 24 provinces. Prefectural rates in certain provinces often exceeded 1.0. In contrast, differences in the total cancer mortality rates between these high- and low-risk areas were small. Text-figure 1 identifies prefectures with rates for either cancer that were in the highest 10% of all prefectures and significantly ($P<0.05$) higher than the national rate. High rates for both cancers tended to cluster in central China, notably in the provinces of Jiangxi, Nei Mongol, Shanxi, and Hunan.

Table 1 shows that the average penis cancer rate was about 50% higher in prefectures with high (top quartile) compared to low (bottom quartile) cervical cancer rates. A regression analysis, with the use of the rates for the 324 prefectures, showed a highly significant ($P<.0001$) linear gradient between the cervical and penis cancer rates. The correlation coefficient was $r=0.25$. Text-figure 2 illustrates the scatter relationship between the more stable rates for the 24 provinces, where the correlation was $r=0.41$.

Penis cancer rates tended to be higher in rural than in urban prefectures. When the 324 areas were divided into

---

[1] Received March 26, 1982; accepted June 30, 1982

[2] Environmental Epidemiology Branch, Division of Cancer Cause and Prevention, National Cancer Institute, National Institutes of Health, Public Health Service, U.S. Department of Health and Human Services, Bethesda, Md. 20205.

[3] Recipient of a fellowship from the International Agency for Research on Cancer, Lyon, France.

[4] Clinical Epidemiology Branch, Division of Cancer Cause and Prevention, National Cancer Institute.

[5] *Address reprint requests to* Dr. Blot at the Landow Building, Room C307, National Institutes of Health, Bethesda, Md. 20205.

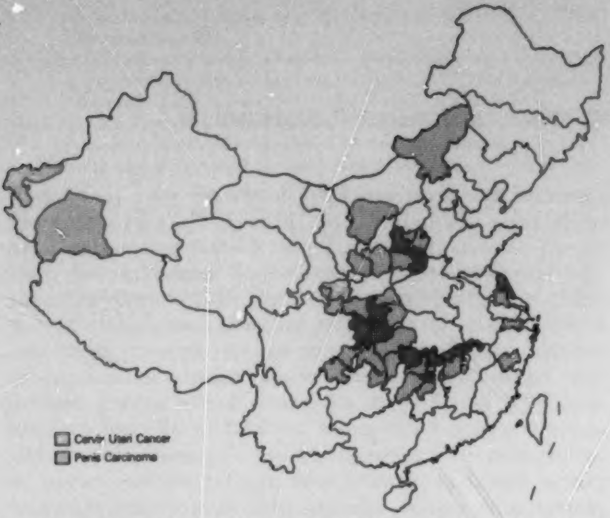

TEXT-FIGURE 1.—Prefectures in China with elevated mortality (i.e., rates in upper decile and statistically significantly higher than the national rate) from cancers of the uterine cervix and penis, 1973–75.

those encompassing independent cities and those not, the average annual penis cancer rate was 0.45 per 100,000 population in the cities, significantly ($P<0.01$ based on a *t*-test comparison of means) lower than the corresponding rate of 0.60 in the rural prefectures. No clear-cut urban–rural differences were observed for cervical cancer. On the average, death rates were somewhat higher in the urban than in the rural prefectures (16.5 vs. 14.9), but they were lowest in the major urban provinces of Beijing (10.9), Tianjin (13.1), and Shanghai (7.9).

DISCUSSION

The 1973–75 survey provided the first comprehensive and standardized determination of cancer mortality rates in China. The survey revealed the national rate of cervical cancer to be one of the highest in the world (*18*). The risk of death from cervical cancer exceeded the similarly adjusted U.S. rate for 1973–77 (*19*) by more than fourfold, as did the death rate for cancer of the penis. Penis cancer mortality figures are not reported in many countries, but incidence data have been reported for certain cancer registries around the world (*17*). Although we have only mortality information, it appears that the penis cancer rates in certain central Chinese prefectures may approach those reported in high-incidence areas of Latin America, Africa, and India.

TABLE 1.—*Average annual age-adjusted penis cancer mortality rates (per 100,000), among prefectures grouped according to percentile rank of the cervical cancer mortality rates, 1973–75*

Quartile rank[a] of cervical cancer rate	Penis cancer rate[b]
1—low	0.43±0.04
2	0.51±0.04
3	0.52±0.05
4—high	0.68±0.06

[a] The 4 groups consisted of prefectures with average annual age-adjusted cervical cancer mortality rates per 100,000 population of 1) <10.8, 2) 10.8–14.4, 3) 14.5–18.8, and 4) >18.8.

[b] Values are means ± SE.

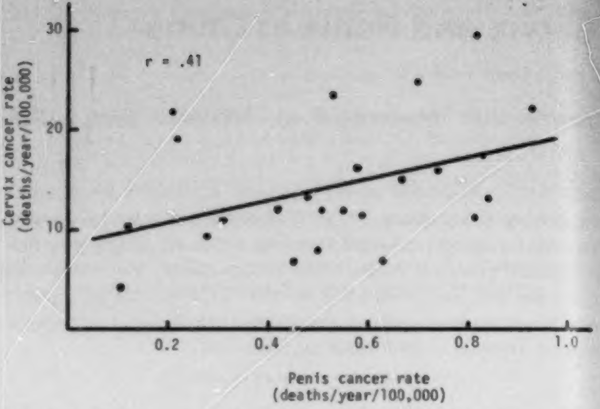

TEXT-FIGURE 2.—Average annual age-adjusted (world standard) mortality rates for cancers of the uterine cervix and penis among 24 Chinese provinces, 1973–75.

National data are not available to examine trends in mortality over time in China, but evidence from specific locales within the country suggests that rates for both cancers are declining. Hospital surveys in the 1950's and earlier listed cancer of the uterus (mostly cervical cancer) as the most common cause of cancer death among women (*1–3*), and the Shanghai cancer registry has recorded death rates for uterine cancer in 1976–77 to be only one-half those in 1963–65 (*20*). In the 1930's to 1950's, penis cancer was reported to account for 9–22% of all male cancers identified at selected hospitals in some cities (*2–6*), including Beijing where the tumor now represents only 0.2% of all cancers.

In addition to the high rates by world standards and the apparent decline in mortality, cervical and penis cancers show other similarities in China. Most striking is the geographic correlation in mortality from both tumors throughout the country, highlighted by the concurrence of elevated rates in central China. Since the findings are based on considerably larger numbers of deaths than reported elsewhere, they provide the strongest descriptive evidence to date that the diseases vary concomitantly. Some clustering has been reported within Japan (*21*) and Puerto Rico (*22*), and international correlation of the incidence rates between the two cancers has been reported, particularly in nonwhite populations (*23*). The data from China are also consistent with recent epidemiologic studies in other countries indicating an excess risk of cervical cancer among the wives of men with penis cancer (*11–16*).

Reasons for the association between cervical and penis cancers are not clear. Although penis cancer has not been extensively studied, personal hygiene, early circumcision, and the early management of phimosis appear to be protective factors (*24*). Both penis and cervical cancers occur excessively in persons with poor hygiene, a history of venereal disease, and low socioeconomic status (*24, 25*). In the United States both cancers are more common in blacks and Hispanics than in whites, with intermediate rates among

Chinese Americans (*19*). Since venereal transmission of herpes simplex virus type 2, or a human papilloma virus, is suspected in the etiology of cervical cancer (*25,27*), it is possible that the same agents may be responsible for penis cancer. To further elucidate the origins of cervical and penis cancers, investigations are planned in areas of China where rates for both cancers are high. If concurrence of the two cancers in spouses was found in China, early detection might be achieved by examination of partners of patients with cervical or penis cancer.

REFERENCES

(*1*) Tseng MT. Carcinoma of uterine cervix; clinical analysis of 651 cases. Zhong Fuchanke 1958; 6:454.

(*2*) Ku SY, Liu SL. A statistical analysis of 14,300 cases of tumors in the Shanghai tumor registry in 1958. Chinese J Pathol 1959; 5:177-183.

(*3*) The Youth Anticancer Shock Brigade, The Chinese Academy of Medical Sciences. A statistical study of 27,149 tumors. Chinese J Pathol 1958; 4:258-260.

(*4*) Yu CF. Penile carcinoma: Clinical analysis of 60 cases. Chinese J Surg 1959; 7:263-267.

(*5*) Ngai SK. Etiological and pathological aspects of squamous-cell carcinoma of penis among Chinese; analytical study of 107 cases. Am J Cancer 1933; 19:259-284.

(*6*) Bercovitz N. Cancer in Hainan China: A preliminary statistical study of 131 operations with special references to age, residence, anatomical distribution and etiology. Chinese Med J 1920; 34:119-123.

(*7*) Li FP, Shiang EL. Cancer mortality in China. JNCI 1980; 65:217-221.

(*8*) Editorial Committee. Atlas of cancer mortality in the People's Republic of China. Shanghai: China Map Press, 1979.

(*9*) Li JY, Liu BQ, Li GY, Chen ZJ, Sun XD, Rong SD. Atlas of cancer mortality in the People's Republic of China. An aid for cancer control and research. Int J Epidemiol 1981; 10:127-134.

(*10*) Li P, Li JY. National survey of cancer mortality in China. In: Marks PA, ed. Cancer research in the People's Republic of China and the United States of America. Epidemiology, causation and approaches to therapy. New York: Grune, 1981:43-64.

(*11*) Cartwright RA, Sinson JD. Carcinoma of penis and cervix. Lancet 1980; 1:97.

(*12*) Maccregor JE, Innes G. Carcinoma of penis and cervix. Lancet 1980; 1:1246-1247.

(*13*) Smith PG, Kinlen LJ, White GC, Adelstein AM, Fox AJ. Carcinoma of penis and cervix. Lancet 1980; 2:417.

(*14*) ———. Mortality of wives of men dying with cancer of the penis. Br J Med 1980; 41:422-428.

(*15*) Graham S, Priore R, Graham M, Browne R, Burnett W, West D. Genital cancer in wives of penile cancer patients. Cancer 1980; 44:1870-1874.

(*16*) Goldberg HM. Concurrent squamous cell carcinoma of the cervix and penis in a married couple. Br J Obstet Gyneacol 1979; 86:585-586.

(*17*) Waterhouse JA, Muir C, Correa P, Doll R. Cancer incidence in five continents. Vol III. IARC Sci Publ 1976; 15:512-515.

(*18*) World Health Organization. World health statistics, Annual 1978. Vol I. Vital statistics and causes of death. Geneva: WHO, 1978.

(*19*) Young JL Jr., Percy CL, Asire AJ. Surveillance, Epidemiology, and End Results Program: Incidence and mortality data: 1973-77. Natl Cancer Inst Mongr 1981; 57:34-37, 46-49.

(*20*) Gao YT, Tu JF, Jin F, Gao RN. Cancer mortality in Shanghai during the period 1963-77. Br J Cancer 1981; 43:183-195.

(*21*) Kurihara M, Asano K. The correlation between cancer of uterus and cancer of penis. Tokoho J Exp Med 1956; 64:104.

(*22*) Martinez I. Relationship of squamous cell carcinoma of the cervix to squamous cell carcinoma of the penis. Cancer 1969; 24:777-780.

(*23*) Sorahan T, Crombie IK. Cancer of the cervix and cancer of the penis. Lancet 1981: 2:1419-1420.

(*24*) Muir CS, Nectoux J. Epidemiology of cancer of the testis and penis. Natl Cancer Inst Mongr 1979; 53:157-164.

(*25*) Cramer DW. Uterine cervix. In: Schottenfeld D, Fraumeni JF Jr, eds. Cancer epidemiology and prevention. Philadelphia: Saunders, 1982:881-900.

(*26*) Kessler II. Perspectives on the epidemiology of cervical cancer with special reference to the herpes virus hypothesis. Cancer Res 1974; 34:1091-1110.

(*27*) Smith JW, Torres JE, Holmquist ND. Herpes simplex virus type 2 and human cervical cancer: Relationship between cellular and humoral immune assays for the detection of previous infection. JNCI 1981; 66:1031-1036.

blank page

Use of Circulating Pregnancy-Specific β_1 Glycoprotein as a Marker in Carcinoma of the Breast in Women[1,2]

Saul W. Rosen, *Ph.D., M.D.*,[3,4] **Mitchell H. Gail**, *M.D., Ph.D.*,[5] *and* **Douglass C. Tormey**, *M.D., Ph.D.*[6,7]

ABSTRACT—Pregnancy-specific β_1 glycoprotein (SP_1) was determined by radioimmunoassay in sera from 27 normal women, 33 women with benign breast disease, and 191 women with carcinoma of the breast, staged for extent of the disease. All diagnostic groups exhibited substantial overlap in SP_1 values. Those with benign breast diseases tended to have values at least as high as those with cancer. Normal patients tended to have slightly lower values, but this difference may well have been due to the younger ages of the normal patients in our sample, because SP_1 values tended to increase with age. Immunochemical dilutions of SP_1 in the serum with the highest value (10.2 ng/ml) did not differ significantly from standard placental SP_1.—JNCI 1982; 69:1067–1071.

The use of placental and fetal proteins as cancer markers has been well established since the pioneer studies of Li et al. (*1*) with chorionic gonadotropin in trophoblastic neoplasia, Abelev (*2*) and Tatarinov (*3*) with α-fetoprotein in hepatoma, and Gold and Freedman (*4*) with carcinoembryonic antigen in adenocarcinoma of the colon.

During the past decade, 2 groups (*5–7*) isolated and purified a new placental glycoprotein, originally detected in pregnancy plasma by Tatarinov and Masyukçvich (*8*). Following Bohn's suggestion (*5*), we refer to this material as SP_1, although it has been given a variety of names in the literature (*9*). SP_1 appears to be produced by the syncytiotrophoblast in pregnancy (*10*). Its concentration in plasma, like that of placental lactogen,[8] increases as gestation proceeds and at term reaches levels as high as 100,000–400,000 ng/ml (*11*). This increase is due, in part, to the relatively long half-time of disappearance of SP_1 from the circulation ($\approx$34 hr) (*12*). Measurements of SP_1 in the sera of nonpregnant women, or of men, reveal very low concentrations—a few nanograms per milliliter at most (*13–18*). Placental lactogen (*19*) and chorionic gonadotropin (*20*), two other placental proteins, also circulate at low or undetectable concentrations in nonpregnant individuals. Like the concentrations of both placental lactogen and chorionic gonadotropin, the concentration of SP_1 is increased in the sera of most women with gestational choriocarcinoma (*14, 21, 22*) and in many men with nonseminomatous germ cell cancers of the testis (*14, 23, 24*).

Several workers have explored the possibility that SP_1 might be useful as a marker in carcinoma of the breast. Results have been conflicting. Some workers propose that SP_1 may be a useful marker in breast cancer (*14, 17, 25*), whereas others have suggested that SP_1 measurements, at least in the circulation, have little or no value in the diagnosis of this disease (*26, 27*). We have looked at this question with a sensitive and specific radioimmunoassay for SP_1 (*16*) applied to sera from a large group of women with breast cancer at various stages and to sera from normal women and women with benign diseases of the breast.

MATERIALS AND METHODS

Patients and sera.—Blood was drawn from 251 women, all of whom lived within a few hundred mile radius of Madison, Wis. Twenty-seven normal women were blood bank volunteers. Thirty-three women had benign diseases of the breast, and histologic diagnoses were obtained in 30; these included 18 with fibrocystic disease, 7 with epithelial dysplasia, 4 with adenoma, fibroadenoma, or papilloma, and 1 with lipoma. Of the 191 women with breast cancer, blood samples were taken from 12 women 1–3 weeks before operation. None of these 12 had evidence of metastatic disease, but 7 were later found to have ipsilateral axillary nodes. Blood samples were taken from the remaining 179 cancer patients 3 weeks to 6 months after completion of local therapy (radical or modified radical mastectomy, followed in a few cases by radiotherapy); the cancers were staged according to standard criteria (*28*), and patients with T_1, T_2, and T_3A lesions were represented. Of these 179 women, 84 had no evidence of distant metastases. Sixty-nine of these 84 women had positive axillary nodes, and 15 had negative nodes; blood samples were taken from all these women before any systemic therapy. The remaining 95 women had stage IV (*28*) metastatic disease; blood samples were taken from 68 women before chemotherapy and from 27 women who had failed (*29*) at least one chemotherapeutic regimen, one hormonal regimen, or both. The previously published therapeutic regimens for metastatic disease and the sampling

---

ABBREVIATION USED: SP_1=pregnancy-specific β_1 glycoprotein.

---

[1] Received April 14, 1982; accepted June 17, 1982.

[2] Research procedures were in accord with the ethical standards of the Committee for the Protection of Human Subjects, Wisconsin Clinical Cancer Center.

[3] Clinical Endocrinology Branch, National Institute of Arthritis, Diabetes, and Digestive and Kidney Diseases, National Institutes of Health, Public Health Service, U.S. Department of Health and Human Services, Bethesda, Md. 20205.

[4] *Address reprint requests to* Dr. Rosen, Building 10, Room 8N315, National Institutes of Health, Bethesda, Md. 20205.

[5] Field Studies and Statistics Program, Biometry Branch, Division of Cancer Cause and Prevention, National Cancer Institute, National Institutes of Health.

[6] Division of Clinical Oncology, Department of Human Oncology, Wisconsin Clinical Cancer Center, University of Wisconsin, Madison, Wis. 53792.

[7] We thank Ms. Ida Calvert and Mr. Norman Beaudry for expert technical aid in performing the radioimmunoassays, Dr. Hans Bohn for the gift of purified pregnancy-specific β_1 glycoprotein, and Ms. Jane Wegenke for aid in procuring the clinical samples.

[8] But unlike that of chorionic gonadotropin, whose plasma concentration peaks in the first trimester.

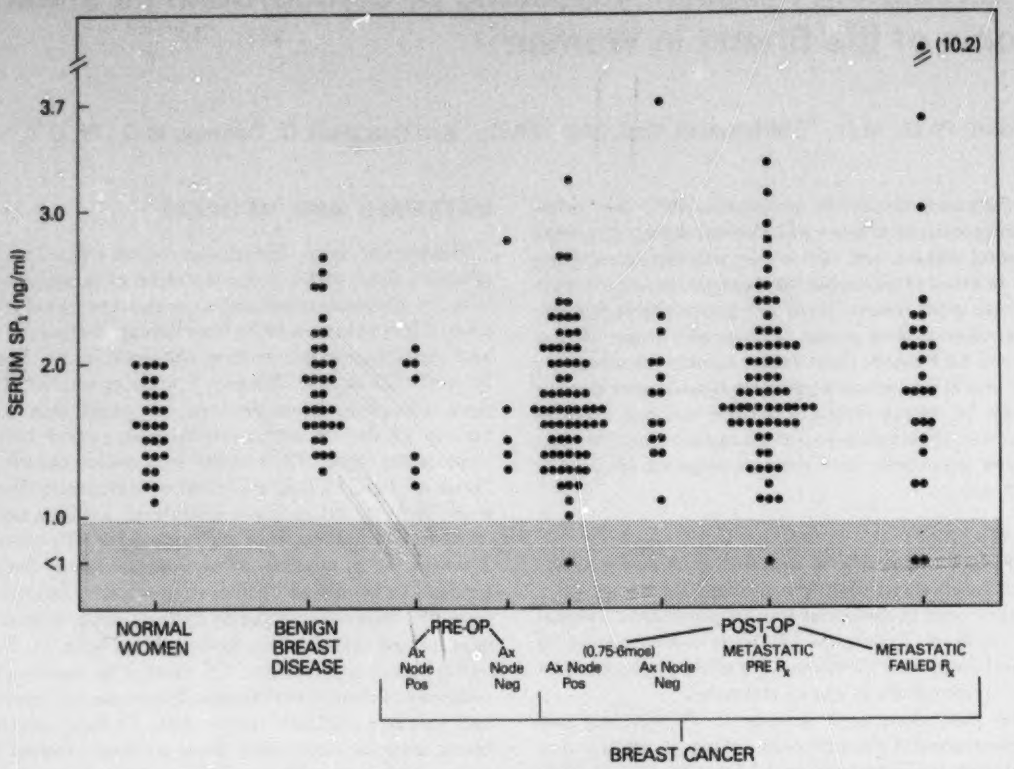

TEXT-FIGURE 1.—Distribution of serum concentrations of SP_1 in normal women, women with benign disorders of the breast, and women with breast cancer at various stages.

schedule in relation to drug dose (*30*) were followed with minor modification.

Blood samples were drawn at the Wisconsin Clinical Cancer Center; the serum was separated promptly and stored at −70°C. Coded samples were sent in Dry Ice to the National Institute of Arthritis, Diabetes, and Digestive and Kidney Diseases for radioimmunoassay.

Radioimmunoassay of SP_1.—Serum concentrations of SP_1 were determined in duplicate in a double antibody radioimmunoassay as previously reported (*16*). To eliminate interassay variation, we examined all serum samples in the same assay. Each serum sample containing more than 2.9 ng of SP_1/ml was incubated with labeled SP_1 and excess anti-SP_1, in a separate experiment, to exclude nonspecific damage to the radioligand as the cause of the high value; in every instance, more than 93% of tracer was bound.

Statistical methods.—Simple descriptive statistics, including sample percentiles, were computed by standard methods (*31*). For adjustment for differences in age distribution, analysis of covariance (*31*) was performed with the SPSS regression procedure (*32*). The model used had expectation (α) (age)$+\beta_j$, where the β_j's were disease category param-

TABLE 1.—*SP_1 distribution and mean age for various disease categories*

Diagnostic category	No. of subjects	SP_1 distribution, ng/ml					Mean age, yr
		Mean	Sample standard deviation	Percentiles		Maximum	
				50th	95th		
Normal	27	1.61	0.27	1.6	2.0	2.0	32.4
Benign breast disease	33	1.87	0.37	1.8	2.6	2.7	43.7
Preoperatively in patients with negative nodes	5	1.74	0.61	1.5	2.8	2.8	50.0
Preoperatively in patients with positive nodes	7	1.70	0.38	1.9	2.1	2.1	55.4
Postoperatively in patients with completely resected disease and negative nodes	15	1.85	0.61	1.8	3.7	3.7	43.1
Postoperatively in patients with completely resected disease and positive nodes	69	1.75	0.43	1.7	2.4	3.2	50.2
Prior to treatment in patients with metastatic disease	68	1.87	0.48	1.8	2.8	3.3	57.3
Following treatment failure in patients with metastatic disease	27	2.21	1.69	1.9	3.6	10.2	54.2

eters. Only 3 of the 251 SP_1 measurements fell below the sensitivity threshold of the assay (1.0 ng/ml), and these measurements were assigned the value 1.0 ng/ml; the percentiles used were unaffected by this convention.

RESULTS

The distribution of SP_1 measurements is indicated in text figure 1 and table 1 for each of the patient categories shown. The categories, which define when the sample was taken in relation to breast cancer status, are preoperatively in patients with negative nodes, preoperatively in patients with positive nodes, postoperatively in patients with completely resected disease and negative nodes, postoperatively in patients with completely resected disease and positive nodes, prior to treatment in patients with metastatic disease, and following treatment failure in patients with metastatic disease. Normal women and women with benign breast diseases are included for comparison.

The distributions were reasonably symmetrical and exhibited substantial overlap among the disease categories. Women with benign breast disease had a mean value of 1.87 ng/ml, which was as large as mean values found in all the cancer groups except those who failed treatment and had metastatic disease (mean, 2.21 ng/ml). If the patient with value 10.2 ng/ml was excluded from the group with treatment failure and metastatic disease, the group mean fell to 1.91.

TABLE 2.—*Unadjusted and age-adjusted differences in mean SP_1 values*

Diagnostic category	Unadjusted, ng/ml, disease group−normal group	Age adjusted, ng/ml, disease group−normal group
Benign breast disease	0.26	0.14
Preoperatively in patients with negative nodes	0.13	0.14
Preoperatively in patients with positive nodes	0.09	0.08
Postoperatively in patients with completely resected disease and negative nodes	0.24	0.18
Postoperatively in patients with completely resected disease and positive nodes	0.14	0.04
Prior to treatment in patients with metastatic disease	0.26	0.09
Following treatment failure in patients with metastatic disease	0.60	−0.04

Normal women had slightly lower mean serum SP_1 concentrations than the diseased groups. The 95th percentile of the normal group was 2.0 ng/ml, which was exceeded by 9 of 33 patients with benign disease, 1 of 5 in the preoperative-negative node group, 1 of 7 in the preoperative-positive node group, 3 of 15 in the postoperative-negative node group, 17 of 69 in the postoperative-positive node group, 22 of 68 in the pretreatment-metastatic disease group, and 12 of 27 in the treatment failure-metastatic disease group. However, as we discuss below, much of the difference between normal women and women with disease was accounted for by the younger age distribution in normal patients. Moreover, values above 2.0 ng/ml were found about as often among women with benign breast disease as among those with cancer.

The patients from whom blood samples were taken tended to be younger in the normal, benign disease, and postoperative-negative node groups and older in the 2 metastatic disease groups and the preoperative-positive node group (*see* table 1). Regression analysis indicated that SP_1 values tended to increase by roughly 0.007 ng/ml per year for each diagnostic group except the 2 preoperative cancer groups, which had very few cases and were subject to large sampling variation. Because normal women were about 20.5 years younger than cancer patients on the average, an adjusted mean SP_1 value for the normal group would have been roughly $1.61+(20.5\times 0.007)=1.75$ ng/ml; this value is in line with values for other diagnostic groups. Table 2 contains both unadjusted and adjusted differences in mean SP_1

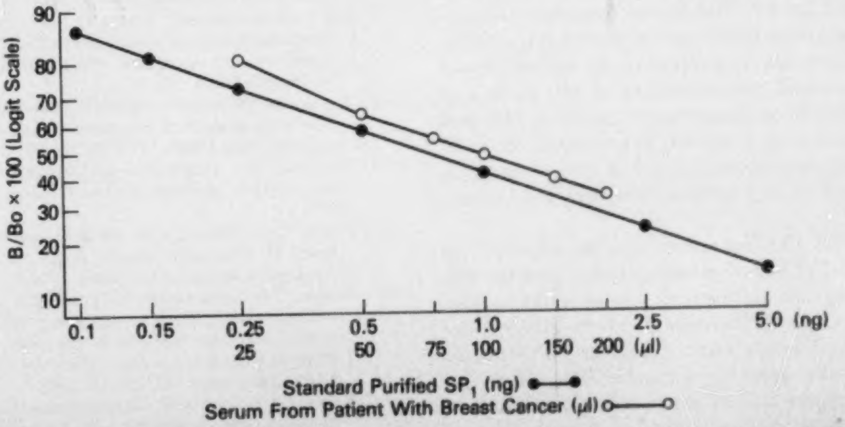

TEXT-FIGURE 2.—Immunochemical behavior of placental SP_1 and serum SP_1 from patient #1 with metastatic breast cancer. Serial dilutions of serum were compared to highly purified placental SP_1 (supplied by Dr. Hans Bohn, preparation #13) in their ability to displace ^{125}I-labeled SP_1 (Bohn preparation #17, 75 μCi/μg, 20 pg) from rabbit anti-SP_1 (#184; bleeding of Aug. 12, 1977; final dilution, 1:950,000). Relative percentage of radioligand bound ($B/B_0\times 100$) has been corrected for nonspecific binding (4.7%).

values between each disease group and the normal group. A separate analysis of covariance was performed on each disease group and the normal group for estimation of the adjusted group difference for each row in table 2. The unadjusted differences were obtained by simple subtraction of means in table 1. For example, 1.74−1.61=0.13 is the difference between the mean of the preoperative–negative node group and the mean of the normal women in table 1. In most cases, age adjustment reduced the apparent difference in mean SP_1 values between the disease groups and the normal group. This was especially true in the comparison of patients with metastatic disease, who tended to be older, with normal women, who tended to be younger.

We looked more closely at sera from patient #1, a 68-year-old woman who had undergone left radical mastectomy 7 years before she presented with metastases in the liver and lungs. She failed to respond to combination chemotherapy with cyclophosphamide, doxorubicin, 5-fluorouracil, fluoxymesterone, and prednisone. The serum concentration of SP_1 before this course of chemotherapy was 10.2 ng/ml, the highest value we have encountered among all the patients reported here. Serial dilutions of serum from patient #1, over an eightfold range, were not recognized by our anti-SP_1 serum as significantly different from standard SP_1 purified from placenta (text-fig. 2). We obtained a second serum sample 3 weeks after she had completed her first therapy course, and the SP_1 level had fallen to 5.9 ng/ml. The patient received a second course of therapy and, 3 weeks after its completion, another serum sample was obtained. This time, the SP_1 had risen to 8.4 ng/ml; she died 3 weeks later.

DISCUSSION

In a retrospective examination of tissues by an immunoperoxidase method, Horne et al. (*25*) detected SP_1 in 38 of 50 sections from patients with breast cancer but in none of 12 sections from patients with benign breast diseases. Moreover, women whose breast cancers were negative for SP_1 had significantly longer survival times than women whose cancers showed positive staining for SP_1. Searle et al. (*14*) used a radioimmunoassay for SP_1 and found increased concentrations in 6 of 21 sera from breast cancer patients, including two sera with concentrations exceeding 20 ng/ml. Wurz (*17*) also found increased concentrations of SP_1 in 18% of the 82 sera she studied from breast cancer patients; 11% had SP_1 levels between 10 and 50 ng/ml. Wurz noted, in addition, that the SP_1 concentration rose in 7 of 10 patients with recurrent disease and fell in 5 patients who received chemotherapy.

In contrast, Engvall and Yonemoto (*26*) detected SP_1 in the serum of only 1 of 22 breast cancer patients, and the SP_1 concentration in this case (1.0 ng/ml) was near the extinction of their assay. Indeed, Bremner et al. in Horne's department also assayed breast cancer sera for SP_1 and, in contradistinction to the conclusions reached from their immunocytochemical study (*25*) of tissue (mentioned above), found "little relation to disease spread in the majority of cases" (*27*).

Our data, likewise, do not support the usefulness of circulating SP_1 as a marker in carcinoma of the female breast. Although the mean serum SP_1 in a group of normal women was slightly lower than that in women with breast cancer, we found values above 2.0 ng/ml (95th percentile for the normal women) with equal prevalence in women with benign disease of the breast as in women with breast cancer. Moreover, there was no clear-cut tendency toward higher levels of SP_1 as the body burden of tumor increased.

Serum SP_1 from a breast cancer patient with the highest value in this series was immunochemically similar to standard SP_1 of normal placenta. Although we have yet to find a single instance of eutopic or ectopic SP_1 that differed from standard (Rosen SW, Calvert I: Unpublished data), one such case has been noted briefly (*14*).

Data for circulating SP_1 in the normal women reported herein agree well with those we reported earlier (*16*) in a different population of mixed normal men and women 18–70 years of age. Our finding that SP_1 values tended to increase with age was unexpected but was also noted in a group of normal men (data not shown). We are unaware of similar analyses of the effect of age on serum concentrations of other placental proteins. SP_1 has been detected in cultured human fibroblasts (*33–35*), but its physiologic role in the normal person—much less the gravid woman—remains unknown.

REFERENCES

(*1*) Li MC, Hertz R, Spencer DB. Effect of methotrexate therapy upon choriocarcinoma and chorioadenoma. Proc Soc Exp Biol Med 1956; 93:361–366.

(*2*) Abelev GI. Alpha-fetoprotein in ontogenesis and its association with malignant tumors. Adv Cancer Res 1971; 14:295–358.

(*3*) Tatarinov YS, Nogaller AM. Diagnostic importance of the embryospecific α-globulin detection in the blood serum of hepatoma patients. Vopr Onkol 1966; 12:26–29.

(*4*) Gold P, Freedman SO. Demonstration of tumor-specific antigens in human colonic carcinoma by immunological tolerance and absorption techniques. J Exp Med 1965: 121:439–462.

(*5*) Bohn H. Isolierung und Charakteriserung des schwangerschafts-spezifischen β_1-Glykoproteins. Blut 1972; 24:292–302.

(*6*) Bohn H, Schmidtberger R, Zilg H. Isolierung des schwangerschafts-spezifischen β_1-Glykoproteins (SP_1) und antigenverwandter Proteine durch Immunoadsorption. Blut 1976; 32:103–113.

(*7*) Lin T-M, Halbert SP, Kiefer D, Spellacy WN. Three pregnancy-associated human plasma proteins: Purification, monospecific antisera and immunological identification. Int Arch Allergy Appl Immunol 1974; 47:35–53.

(*8*) Tatarinov YS, Masyukevich VN. Immunological identification of a new beta$_1$-globulin in the blood serum of pregnant women. Bull Exp Biol Med USSR 1970; 69:666–668 (English translation).

(*9*) Tatarinov YS. Trophoblast-specific beta$_1$-glycoprotein as a marker for pregnancy and malignancies. Gynecol Obstet Invest 1978; 9:65–97.

(*10*) Horne CH, Towler CM, Pugh-Humphreys RG, Thomson AW, Bohn H. Pregnancy specific β_1-glycoprotein—a product of the syncytiotrophoblast. Experientia 1976; 32:1197–1199.

(*11*) Gordon YB, Grudzinskas JG, Lewis JD, Jeffrey, D, Letchworth AT. Circulating levels of pregnancy-specific β_1-glycoprotein and human placental lactogen in the third trimester of pregnancy: Their relationship to parity, birth weight, and placental weight. Br J Obstet Gynaecol 1977; 84:642–647.

(*12*) Tatra G, Placheta P, Breitenecker G. Schwangerschaftsspezifisches β_1-Glykoprotein (SP_1): Klinische Aspecte. Wien Klin Wochenschr 1975; 87:279–281.

(*13*) Towler CM, Horne CH, Jandial V, Chesworth JM. A simple and sensitive radioimmunoassay for pregnancy-specific β_1-glycoprotein.

Br J Obstet Gynaecol 1977; 84:580–584.

(14) Searle F, Leake BA, Bagshawe KD, Dent J. Serum-SP$_1$-pregnancy-specific-β_1-glycoprotein in choriocarcinoma and other neoplastic diseases. Lancet 1978; 1:579–581.

(15) Crowther ME, Grudzinskas JG, Poulton TA, Gordon YB. Trophoblastic proteins in ovarian carcinoma. Obstet Gynecol 1979; 53:59–61.

(16) Kaminska J, Calvert I, Rosen SW. Radioimmunoassay of "pregnancy-specific"-β_1-glycoprotein (SP$_1$). Clin Chem 1979; 25:577–580.

(17) Wurz H. Serum concentrations of SP$_1$ (pregnancy-specific-β_1-glycoprotein) in healthy nonpregnant individuals and in patients with nontrophoblastic malignant neoplasms. Arch Gynecol 1979; 227:1–6.

(18) Rutanen E-M, Seppala M. Pregnancy-specific β_1-glycoprotein in trophoblastic disease. J Clin Endocrinol Metab 1980; 50:57–61.

(19) Weintraub BD, Rosen SW. Ectopic production of human chorionic somatomammotropin by non-trophoblastic cancers. J Clin Endocrinol Metab 1971; 32:94–101.

(20) Vaitukaitis JL, Ross GT, Braunstein GD, Rayford PL. Gonadotropins and their subunits: Basic and clinical studies. Recent Prog Horm Res 1976; 32:289–321.

(21) Tatarinov YS, Mesnyankina NV, Nikoulina DM, Novikova LA, Toloknov BO, Falaleeva DM. Identification immunochimque de la bêta$_1$ globuline de la "zone de grossesse" dans le sérum de malades atteintes de tumeurs trophoblastiques. Int J Cancer 1974; 14:548–554.

(22) Seppala M, Rutanen E-M, Heikinheimo M, Jalanko H, Engvall E. Detection of trophoblastic tumor activity by pregnancy-specific beta$_1$-glycoprotein. Int J Cancer 1978; 21:265–267.

(23) Rosen SW, Javadpour N, Calvert I, Kaminska J. Increased "pregnancy-specific" beta$_1$-glycoprotein in certain nonseminomatous germ cell tumors. JNCI 1979; 62:1439–1441.

(24) Lange PH, Bremner RD, Horne CH, Vessella RL, Fraley EE. Is SP$_1$ a marker for testicular cancer? Urology 1980; 15:251–255.

(25) Horne CH, Reid IN, Milne GD. Prognostic significance of inappropriate production of pregnancy proteins by breast cancers. Lancet 1976; 2:279–282.

(26) Engvall E, Yonemoto RH. Is SP$_1$ (pregnancy specific β_1 glycoprotein) elevated in cancer patients? Int J Cancer 1979; 23:759–761.

(27) Bremner RD, Nisbet AD, Herriot R, et al. Detection of placental protein five (PP5) and pregnancy-specific glycoprotein (SP1) in benign and malignant breast disease. Onocodevel Biol Med 1981; 2:55–62.

(28) American Joint Committee for Cancer Staging and End-Results Reporting. The manual for staging of cancer. Chicago: American Joint Committee, 1977:101–107.

(29) Hoogstraten G, Irwin L, Ahmann D. Breast cancer: Proposed guidelines—report from the combination chemotherapy trials working group in breast cancer: Suggested protocol guidelines for combination chemotherapy trials and for combined modality trials (Carbone PP, Sears ME, eds.). Bethesda, Md.: National Cancer Institute, 1977 [DHEW publication No. (NIH)77-1192].

(30) Tormey DC, Waalkes TP, Kuo KC, Gehrke CW. Biologic markers in breast carcinoma: Clinical correlations with urinary polyamines. Cancer 1980; 46:741–747.

(31) Snedecor GW, Cochran WG. Statistical methods. 7th ed. Ames, Iowa: Iowa State Univ Press, 1980.

(32) Nie NH, Hull CH, Jenkins JG, Steinbrenner K, Bent DH. SPSS statistical package for the social sciences. 2nd ed. New York: McGraw-Hill, 1975.

(33) Rosen SW, Kaminska J, Calvert IS, Aaronson S. Human fibroblasts produce "pregnancy-specific" beta$_1$-glycoprotein in vitro. Am J Obstet Gynecol 1979; 134:734–738.

(34) Envall E, Hayman EG, Ruoslahti E. Expression of pregnancy specific β_1-glycoprotein, SP$_1$, in cancer sera and in cultured cells. Fed Proc 1980; 39:549.

(35) Heikinheimo M, Paasivuo R, Wahlstrom T. Cells from normal brain and gliomas synthesize pregnancy-specific β_1-glycoprotein-like material in vitro. Br J Cancer 1981; 43:654–658.

blank page

Carcinoembryonic Antigen in Nonhuman Primates [1,2,3]

Darrow E. Haagensen, Jr., [4,5,6] **Richard S. Metzgar,** [7,8] **Brent Swenson,** [8] **William G. Dilley,** [9] **Charles E. Cox,** [9] **Sarah Davis,** [4] **Janet Murdoch,** [9] **Norman Zamcheck,** [4,10] *and* **Samuel A. Wells, Jr.** [9]

ABSTRACT—Blood levels of carcinoembryonic antigen (CEA) have been measured in several nonhuman primate species. Only gorillas and chimpanzees were found to have significant elevations of CEA-like activity in their blood compared to the normal values of less than 2.5 ng/ml in humans. The average CEA level in 134 chimpanzees was 25.2 ng/ml (range, 4.2–95 ng/ml) and in 13 gorillas it was 32 ng/ml (range, 12.4–61.9 ng/ml). These levels were not related to sex. Blood levels repeatedly taken over a 1½-year period remained relatively stable in both species. Analysis of parallelism of immunologic reactivity showed chimpanzee CEA to be similar to but not identical with human CEA. The molecular size of chimpanzee CEA was also similar to that of human CEA.—JNCI 1982; 69:1073–1076.

CEA was identified by Gold and Freedman (*1*) to be a glycoprotein expressed on colon carcinoma cells and by the fetal colon. Subsequent investigations have indicated that CEA is associated with carcinomas derived from both ectodermal and endodermal origins and is present as a luminal secretion from normal colon mucosa cells (*2, 3*). Circulating plasma levels of CEA are less than 2.5 ng/ml in normal individuals (*2*). Elevated plasma levels of CEA are useful in detecting and monitoring disease status of metastases for colon carcinoma and possibly for other major forms of carcinoma [breast, pancreas, lung, stomach, ovary, and cervix (*4*)].

The presence of CEA in species other than humans has not been studied extensively. Engvall et al. (*5*) have examined *Macaca* monkey lung and spleen tissues and have isolated a molecule that is immunochemically cross-reactive with CEA; however, the molecule most closely resembles human normal cross-reactive antigen. We report here our finding of a substance immunologically similar to CEA present in the circulation of certain nonhuman primates.

MATERIALS AND METHODS

Primate blood samples.—Chimpanzee (*Pan*) blood was obtained for CEA analysis from Yerkes Primate Center, Lemsip Primate Center (Tuxedo, N.Y.), and ICES (Holloman Air Force Base, N. Mex.). Blood samples from gorillas (*Gorilla*), black apes (*Cynopithecus*), and orangutans (*Pongo*) were obtained from Yerkes Primate Center. Baboon (*Papio*) and macaque (*Macaca*) blood samples were from Yerkes and Duke University Primate Centers. Blood samples were predominantly collected as serum for analysis; however, K_3 EDTA plasma samples were also collected from some chimpanzees, orangutans, and old-world monkeys. No differences in mean level of CEA were noted between plasma and serum samples of each of the species when both were tested.

CEA assay.—CEA levels were determined by a modification of the Hansen assay procedure (*6*). Aliquots of 0.5 ml of serum or plasma were PCA extracted, and the PCA was separated from the CEA by a buffer exchange column (*7*) to give a final assay sample volume of 6.5 ml. The CEA RIA utilized Roche CEA-kit reagents (Hoffmann-La Roche, Inc.) in an isotope dilution assay in which ^{125}I-labeled CEA and goat anti-CEA were added simultaneously to the assay tubes. The assay tubes were incubated overnight at room temperature and then the assay was terminated by the addition of 1 ml of a 2% suspension of donkey anti-goat antibody attached to a vinylidene fluoride bead (from Dr. Hans Hansen, Hoffmann-La Roche, Inc.). Assay tubes were centrifuged, the supernatant was decanted, and the pellets were counted. The binding of radioactive CEA by antibody in the absence of added cold antigen (Bo) was set at approximately 50% of added counts. A 6-point inhibition curve was generated with 0, 1.25, 3.125, 6.25, 9.375, and 12.5 ng of unlabeled CEA. The binding at 12.5 ng of added cold CEA was approximately 20% of added counts.

When CEA values were above 25 ng/ml, we determined the CEA level by assaying a 1.5-ml aliquot from the initial 6.5-ml PCA extract sample volume. The aliquot volume was brought up to 6.5 ml for analysis by addition of 5 ml of standard curve buffer (⅒ dilution of Roche EDTA stock buffer).

Comparison of chimpanzee CEA activity with human CEA activity in RIA was performed with a pool of 20 different PCA-extracted chimpanzee blood samples, which were concentrated by ultrafiltration on a PM 10 membrane (Amicon Corp., Lexington, Mass.) to approximately 50 ng/ml of CEA activity. This concentrate was tested in RIA

ABBREVIATIONS USED: CEA=carcinoembryonic antigen; ICES=International Center of Environmental Safety; PCA=perchloric acid; RIA=radioimmunoassay.

---

[1] Received October 30, 1981; revised April 20, 1982; accepted May 12, 1982.

[2] Supported in part by Public Health Service (PHS) grant CA-04486 from the National Cancer Institute; by PHS grant AM-08054 from the National Institute of Arthritis, Diabetes, and Digestive and Kidney Diseases; and by PHS grant FR-00165 from the Division of Research Resources, National Institutes of Health. Also supported by a research donation from Hoffmann-La Roche, Inc., Nutley, N.J.

[3] Research procedures were in accord with the ethical standards of the Yerkes Primate Research Center.

[4] Mallory Gastrointestinal Laboratory, Mallory Institute of Pathology, Boston City Hospital, Boston, Mass. 02118.

[5] Department of Surgery, New England Deaconess Hospital, Harvard Medical School, Boston, Mass. 02115.

[6] *Address reprint requests to* Dr. Haagensen, Department of Surgery, New England Deaconess Hospital, Harvard Medical School, 185 Pilgrim Rd., Boston, Mass. 02115.

[7] Department of Microbiology and Immunology, Duke University Medical Center, Durham, N.C. 27710.

[8] Yerkes Primate Research Center, Emory University, Atlanta, Ga. 30322.

[9] Department of Surgery, Duke University Medical Center.

[10] Department of Medicine, Harvard Medical School.

versus a human CEA preparation also at 50 ng/ml for parallelism of inhibition at 25, 50, 75, 100, 150, and 200 µl of sample added to 6.4 ml of ⅒ EDTA buffer. Roche goat and baboon anti-CEA antibodies were used in separate assays to identify the CEA activity in the human versus the chimpanzee CEA antigen preparations. The baboon anti-CEA antibody inhibition assay was performed in a manner identical to that of the assay with goat anti-CEA antibody, except that the baboon anti-CEA antibody inhibition assay was terminated by addition of 1 ml of Roche Z-gel as described previously (*6*).

Chromatography.—Column chromatography was performed with Sephadex G-200 (Pharmacia Fine Chemicals, Piscataway, N.J.) in a 2.5×90-cm column. The column was equilibrated in 0.01 *M* ammonium acetate buffer (pH 7.0) containing 0.001 *M* Na azide. The pooled PCA-extracted chimpanzee blood sample concentrate used above for RIA assay was also used for column chromatography. The concentrate was adjusted to be approximately 250 ng/ml by Amicon ultrafiltration, and then to 1 ml of the concentrate was added 20 mg of crystalline bovine albumin (Miles Laboratories Inc., Kankakee, Ill.) for internal standardization before application to the column. Column fractions of 5.5 ml were collected for analysis.

RESULTS

A total of 134 chimpanzee blood samples were analyzed for CEA content. These samples had been obtained from three separate primate centers that maintained colonies of chimpanzees (text-fig. 1). All chimpanzee blood samples had detectable CEA levels (range, 4.2–95 ng/ml; average, 25.2 ng/ml). The average CEA level in 63 male chimpanzees was 27 versus 23.5 ng/ml in 71 females. Twenty of the blood samples from the ICES colony were obtained from chimpanzees less than 1 year of age. The CEA levels in this group ranged from 12.1 to 35.1 ng/ml, with an average value of 23.4 ng/ml. Two young female chimpanzees from the nursery at the Yerkes primate colony were analyzed for blood CEA level at 4½ months of age. One of the 2 chimpanzees had been taken from the mother on the day of birth (CEA level, 28.1 ng/ml). The other chimpanzee had been kept

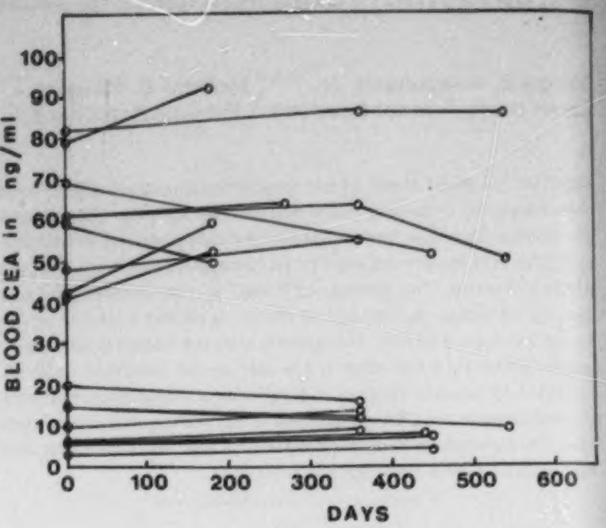

TEXT-FIGURE 2.—Repeated analysis of blood CEA levels for 17 chimpanzees.

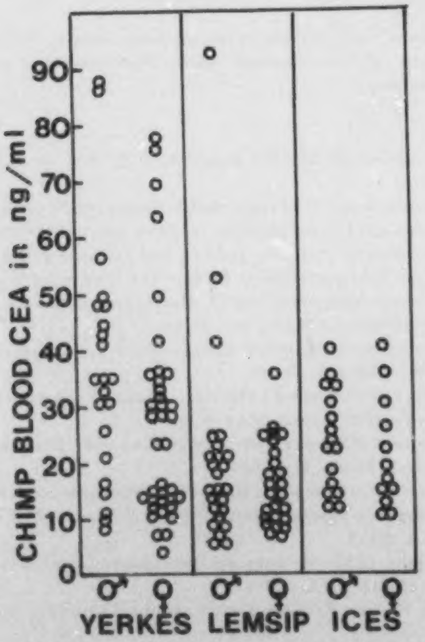

TEXT-FIGURE 1.—Blood CEA levels for 134 chimpanzees maintained at three primate colonies.

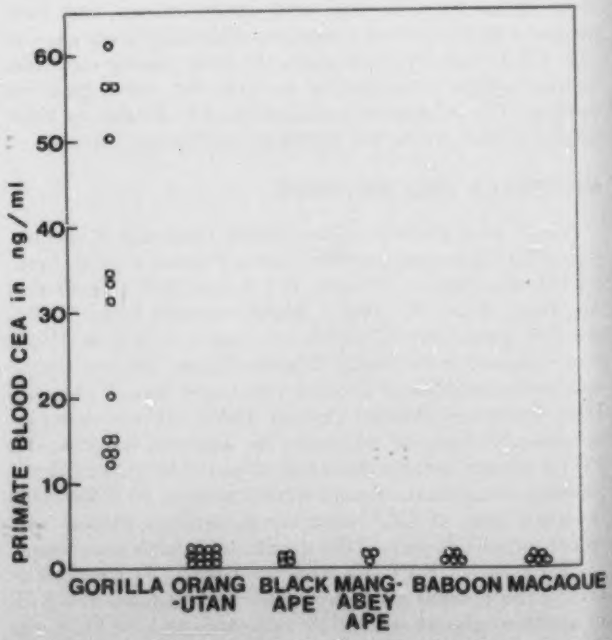

TEXT-FIGURE 3.—Blood CEA levels for several species of primates. Only gorillas had CEA levels above the normal range found in humans.

with the mother for 10 days before being separated (CEA level, 23.4 ng/ml).

Measurement of CEA levels was repeated on 17 of the Yerkes primate colony chimpanzees at approximately 6 months to 1½ years (text-fig. 2). Eight of these chimpanzees had CEA levels below 20 ng/ml, whereas 9 chimpanzees had levels above 40 ng/ml. In both groups some fluctuation of CEA level occurred. However, on repeated analysis, no change in the CEA level greater than ±50% of the initial value was observed, and only 2 of the 17 chimpanzees had CEA level changes greater than ±30% of the initial value.

Six other nonhuman primate species were tested for CEA level and only the gorilla had CEA levels above 2.5 ng/ml (text-fig. 3). The range of CEA levels in the 13 gorillas studied was 12.4–61.9 ng/ml, with an average value of 32 ng/ml. Three of these animals had repeated CEA determinations, which showed less than a ±15% variation in CEA level over a 1-year time span.

For a further definition of the CEA activity in the chimpanzee blood, PCA extracts from 20 blood samples were pooled, concentrated, and then column chromatographed on Sephadex G-200. Depicted in text-figure 4 (A and B) is the molecular size elution pattern of chimpanzee CEA versus human CEA. The chimpanzee CEA eluted from Sephadex G-200 as a single peak of an approximately 200,000-dalton molecular size, which was similar to the CEA peak found in a human plasma sample.

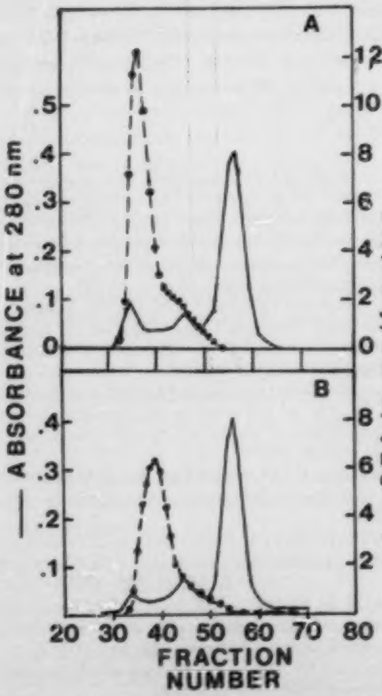

TEXT-FIGURE 4.—Sephadex G-200 elution profile of CEA activity in the PCA extract of serum. A) Twenty 0.5-ml samples of chimpanzee serum were PCA extracted, buffer exchanged, pooled, and concentrated to an activity of ≈250 ng/ml. To 1 ml of this concentrate was added 20 mg of bovine albumin. This sample was applied to the Sephadex G-200 column, and 5.5-ml fractions were collected for analysis. B) Plasma (6 ml) from a patient with 40 ng/ml of CEA activity was processed in a fashion identical to that used for the chimpanzee serum.

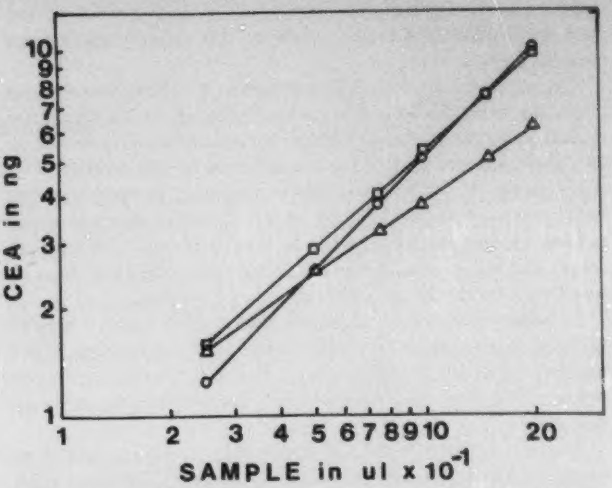

TEXT-FIGURE 5.—Depicted on a log–log scale is a 6-point inhibition assay for 20 PCA-extracted chimpanzee sera that were buffer exchanged, pooled, and concentrated to a CEA activity of ≈50 ng/ml. This concentrate was assayed at 6-sample volumes (25, 50, 75, 100, 150, and 200 µl) for CEA activity in comparison with a human CEA standard at 50 ng/ml activity (○). Chimpanzee CEA activity was detected by Roche goat anti-CEA antibody (□) and by baboon anti-CEA antibody (△). Human CEA activity showed a steeper inhibition line than chimpanzee CEA activity detected by either antiserum.

We compared the immunologic similarity between the chimpanzee CEA and the human CEA by determining the parallelism of antigenic activity in RIA for a 6-point inhibition curve of human CEA versus the pooled chimpanzee blood samples that had been PCA extracted (*see* "Materials and Methods"). Both goat and baboon anti-CEA antibodies were used to detect the CEA activity. The chimpanzee CEA activity more closely paralleled the human CEA activity with goat anti-CEA antibody than with baboon anti-CEA antibody (text-fig. 5). However, human CEA showed a steeper inhibition slope than chimpanzee CEA with both types of anti-CEA antibody.

DISCUSSION

In humans the luminal CEA produced by normal mucosal cells does not appear to cause elevations of CEA (>2.5 ng/ml) in the circulation. It is only in disease states where tight junctions and basement membranes are disrupted that CEA enters the circulatory system in detectable quantities. Various pathologic types of carcinoma of both endodermal and ectodermal origins can produce CEA, and with metastatic disease very high plasma levels of CEA can occur (up to 100,000 ng/ml). Inflammatory disease (ulcerative colitis, pancreatitis, emphysema, and benign liver disease) can also cause modest elevations in blood levels of CEA up to approximately 20 ng/ml.

Two of the great apes (chimpanzees and gorillas) had normal CEA plasma levels, which in humans would be considered significantly abnormal. The mean value in 134 chimpanzees was 25 ng/ml, and in 13 gorillas the mean value was 32 ng/ml. All chimpanzees and gorillas tested had detectable CEA levels; however, the values ranged from 4 to 95 ng/ml.

On repeated analysis, CEA levels in 17 chimpanzees and 3 gorillas were fairly stable over a 6-month to 1½-year time frame. Also the elevated CEA level occurred early in life in the chimpanzees and did not appear to be sex related. The wide range of CEA blood levels observed in chimpanzees and gorillas (4–95 ng/ml), however, indicates that variation occurs between animals in the factors regulating CEA blood level. We were unable to attribute this variation to any health problems in the chimpanzees or gorillas.

In addition to the chimpanzee and gorilla, 5 other species of nonhuman primates were tested for circulating CEA activity (text-fig. 3). All 5 species had CEA levels that were below 2.5 ng/ml and that were at the lower limit of assay detectability.

The chimpanzee CEA on molecular sizing appeared to be quite similar to human CEA (≈200,000 daltons). RIA inhibition analysis for serial dilutions of chimpanzee CEA showed a close similarity to human CEA when assayed against Roche goat anti-CEA antibody. However, less identity of human and chimpanzee CEA activities was shown when baboon anti-CEA antibody was used for CEA identification (text-fig. 5). The differences in chimpanzee CEA activity versus human CEA activity recognized by goat and baboon anti-CEA antibodies indicates that some antigenic determinants on the chimpanzee CEA are quite similar to those on the human CEA, whereas others have undergone some antigenic variation. Baboon anti-CEA antibody has previously been shown to have a narrower range of CEA determinant recognition than does goat anti-CEA antibody (*6*). The baboon anti-CEA antibody does not recognize the "common-site" determinant(s) on CEA, which is one of the two predominant determinants recognized by goat anti-CEA antibody (*6*).

The finding that human CEA and chimpanzee CEA are not absolutely immunologically identical means that measurements of the chimpanzee CEA level with the use of a human CEA standard result in some degree of underestimation of the level of chimpanzee CEA activity in blood samples. This situation is most evident when the baboon anti-CEA antibody is used for detection of chimpanzee CEA activity (text-fig. 5).

The molecular sizing and parallelism of inhibition studies indicate that chimpanzee CEA is similar but not identical to human CEA. This is not an unexpected finding because chimpanzees and humans appear to have evolutionally separated approximately 6 million years ago (*8*).

For the primate species less closely related to humans than the chimpanzee or gorilla, similar CEA-like substances may still exist in the blood. However, due to evolutionary structural diversity these substances may no longer be capable of being recognized antigenically as CEA by either goat or baboon anti-CEA antisera. Also, evolutionary divergence may have occurred in the site and/or amount of CEA production and in the metabolism of CEA.

Elucidation of why elevated blood levels of CEA immunologic activity occur in the chimpanzee and gorilla will require determination of organ and tissue location(s) of the CEA as well as metabolic half-life studies. A predominant route of clearance of human CEA in experimental systems appears to be the liver (*9*). If the clearance mechanism for chimpanzee CEA and gorilla CEA is different from that for human CEA (we have no evidence that it is), this could explain in part the observed elevated CEA levels in these 2 species. However, in the Yerkes chimpanzees and gorillas in which CEA levels were elevated, compared to levels in humans, serial measurements of liver function by enzyme levels and serum chemistry values were normal. Also, the health status of the chimpanzees with CEA levels above 40 ng/ml was in general good and did not differ from that of the chimpanzees with lower CEA levels.

Also important is the potential for immunologic recognition of CEA by various primate species. Ruoslahti et al. (*10*) have immunized the *Macaca iris* monkey with human CEA and observed a predominantly specific site response. The common baboon (*Papio*) anti-human CEA antibody that we have produced is also a high-titer specific site antibody to CEA (*6*). Since the normal chimpanzee has a circulating molecule immunologically similar to human CEA, one might expect the chimpanzee to be immunologically tolerant to CEA. However, we have been able to generate in the chimpanzee an antibody response to human CEA. This antibody is very ineffective in recognizing the chimpanzee's own CEA activity but recognizes human CEA equivalent to baboon or goat anti-CEA antibody. This is further evidence of some genetic diversity between human CEA and chimpanzee CEA and will be the subject of a separate report (Haagensen DE, et al: Manuscript in preparation).

REFERENCES

(*1*) Gold P, Freedman SO. Demonstration of tumor-specific antigens in human colonic carcinomata by immunological tolerance and absorption techniques. J Exp Med 1965; 121:439–467.

(*2*) Hansen HJ, Snyder JJ, Miller E, et al. Carcinoembryonic antigen (CEA) assay. a laboratory adjunct in the diagnosis and management of cancer. Hum Pathol 1974; 5:139–147.

(*3*) Egan ML, Pritchard DG, Todd CW, Go VL. Isolation and immunochemical and chemical characterization of carcinoembryonic antigen-like substances in colon lavages of healthy individuals. Cancer Res 1977; 37:2638–2643.

(*4*) Goldenberg DM, Neville AM, Carter AC, et al. Carcinoembryonic antigen: Its role as a marker in the management of cancer. A National Institutes of Health Consensus Conference. Ann Intern Med 1981; 94:407–409.

(*5*) Engvall E, Vuento M, Ruoslahti E. A monkey antigen cross reactant with carcinoembryonic antigen, CEA. Br J Cancer 1976; 34:341–345.

(*6*) Haagensen DE Jr, Cox CE, Dilley WG, et al. Evaluation of baboon antiserum to carcinoembryonic antigen. Clin Chem 1980; 26:1787–1790.

(*7*) Haagensen DE Jr, Easterday RL, Stolle CA, Wells SA Jr. Buffer-exchange column for rapid separation of carcinoembryonic antigen from perchloric acid. Clin Chem 1978; 24:135–137.

(*8*) Unis JJ, Prakash O. The origin of man: A chromosomal pictorial legacy. Science 1982; 215:1525–1530.

(*9*) Thomas P, Hems DA. The hepatic clearance of circulating native and asialo carcinoembryonic antigen by the rat. Biochem Biophys Res Commun 1975; 67:1205–1209.

(*10*) Ruoslahti E, Engvall E, Vuento M, Wigzell H. Monkey antisera with increased specificity to carcinoembryonic antigen (CEA). Int J Cancer 1976; 17:358–361.

Spontaneous Leukemia Viruses: Lymphomagenic Ecotropic Viruses of AKR Mice[1,2,3]

Esther F. Hays,[4,5] Nadine Margaretten,[4] *and* Stephen K. Swanson[4,6]

ABSTRACT—The spontaneous leukemia (SL) viruses are ecotropic lymphomagenic viruses isolated from AKR spontaneous lymphomas. These viruses are produced stably by continuous cell lines from spontaneous lymphomas and by a cell line derived from the bone marrow stroma of an AKR mouse neonatally inoculated with an SL virus. All cell lines cloned from the parent lymphoma cell lines consistently produce SL viruses. These viruses can be passaged in vivo and maintain their leukemogenic properties. Cloned isolates of SL viruses accelerate lymphoma in AKR mice and induce thymic lymphoma in mice of other strains. Thus their lymphomagenic properties are conclusively shown. In a study with the use of a sensitive host range assay, xenotropic and/or dual-host range viruses are consistently found in spontaneous lymphomas and cell lines derived from them. However, viruses able to replicate in mink lung cells are not expressed in SL virus-induced lymphomas or their derived cell lines.—JNCI 1982; 69:1077-1082.

Previous experiments have determined that viruses found in young AKR mice were not lymphomagenic, whereas viruses found in the spleen and thymus of older animals as well as in spontaneous lymphomas had lymphomagenic properties (*1, 2*). Lymphomagenesis was measured by the acceleration of onset of thymic lymphoma after neonatal inoculation of test virus in newborn AKR mice. In addition, cell lines from spontaneous thymomas of AKR mice were established, and the properties of viruses found in the supernatants of these cell cultures were studied (*3*). Most cell lines produced ecotropic viruses. Six of eight lines produced viruses that accelerated AKR lymphoma. One line produced xenotropic viruses, and one line produced viruses with dual-host range. All viruses produced by these lines were negative with the XC plaque assay, formed foci with the S^+L^- assay, and had the property of "converting" to XC positivity when grown on mouse embryo cells (*4*). We consider these ecotropic viruses to represent a late-appearing class of lymphomagenic viruses of AKR mice. The following report describes further studies with these viruses and documents that they are stable in culture and in cloned lymphoma cell lines, that they can be cloned, and that they are lymphomagenic in other mouse strains.

MATERIALS AND METHODS

Mice.—Mice were of the inbred AKR and SJL strains maintained in this laboratory. The inbred C3H/HeJ mice were obtained from The Jackson Laboratory, Bar Harbor, Maine.

Viruses.—The ecotropic-oncogenic viruses obtained from lymphoma cell lines are referred to as SL viruses and designated by the cell line from which they were derived; e.g., AKR SL3 cell line produced AKR SL3 viruses. Viruses were harvested 24 hours after the cultures were split. Medium and cells were removed and frozen at −70°C and then thawed and filtered prior to use. MCF-247, AKv-1, and AKR xenotropic virus were obtained from Dr. Janet W. Hartley, National Institute of Allergy and Infectious Diseases, Bethesda, Md. Cloned G-MuLV was obtained from Dr. D. Buchhagen, Downstate Medical Center, Brooklyn, N.Y.

Cell lines.—The cell lines described below produce ecotropic viruses that accelerate lymphoma when they are inoculated into newborn AKR mice.

Lymphoma cells: The lymphoma cell lines AKR SL1, AKR SL2, AKR SL3, AKR SL4, AKR SL7, AKR SL10, and AKR SL11 were established in continuous culture as described previously (*3*). They are maintained in RPMI-1640 medium with 10% NCS and split at 3-day intervals. They are comprised of Thy 1.1-positive lymphoblasts that, when inoculated ip, iv, and sc into young AKR mice, produce progressively growing lymphomas. Lines AKR SL3-A and AKR SL3-B were established from the thymuses of 2 AKR mice with thymic lymphomas accelerated by AKR SL3 virus. Line AKR A2 was derived from the thymus of a G-MuLV-accelerated lymphoma.

MAC 12: This line was derived from the adherent stromal layer of a long-term bone marrow culture from a healthy AKR mouse inoculated when newborn with the leukemia-accelerating virus AKR SL3 (*5*). These adherent cells were transferred by trypsin EDTA treatment at weekly intervals. They reached confluence 7 days after inoculation of 10^6 cells in 25-cm^2 flasks. Although these cells have the morphologic appearance of macrophages, they were not phagocytic, did not have Fc receptors, and did not stain for nonspecific esterase. They are considered to be transformed bone mar-

---

ABBREVIATIONS USED: DMEM=Dulbecco's modified Eagle's minimum essential medium; G-MuLV=Gross murine leukemia virus; MLC=mink lung cells; NCS=newborn calf serum; NIH ME=National Institutes of Health mouse embryo cells; PFU=plaque-forming units; PS=physiologic saline; RT=reverse transcriptase; SL=spontaneous leukemia.

---

[1] Received November 9, 1981; revised April 30, 1982; accepted May 27, 1982.

[2] Supported by Department of Energy contract DE-AM03-76-SF00012 and by Public Health Service grant CA-12386 from the National Cancer Institute.

[3] Animals were maintained under the guidelines set forth by the University of California at Los Angeles.

[4] Department of Medicine, School of Medicine, University of Calfiornia at Los Angeles, 405 Hilgard Ave., Los Angeles, Calif. 90024.

[5] *Address reprint requests to* Dr. Hays at the Laboratory of Biomedical and Environmental Sciences, University of California at Los Angeles, 900 Veteran Ave., Los Angeles, Calif. 90024.

[6] We thank Mr. Donald Tenney of Dr. William Haseltine's laboratory at Harvard University of supplying the cloned viruses SL3-1, SL3-2, and SL3-3.

row stromal elements. When inoculated into syngeneic mice, they produced osteosarcomas, chondrosarcomas, and fibrosarcomas.

Cloned cell lines from AKR SL4: We made cell clones by diluting and aliquoting the cells into Falcon microtiter cell culture plates. Wells containing progeny of a single cell were observed daily and transferred to successively larger plates. After a healthy cell population derived from a single cell had been transferred a number of times in 25-cm^2 tissue culture flasks, viruses produced by the cells were studied.

Preparation of cell-free filtrates.—The cell-free filtrates were made by removal of the thymus, spleen, and lymph nodes from mice with lymphoma and preparation of a 20% (wt/vol) homogenate of the tissue in phosphate-buffered saline. The homogenate was centrifuged for 3,000×*g* for 10 minutes, and the supernatant was centrifuged at 7,000×*g* for 15 minutes. The final supernatant was passed through a 0.45-μm filter and stored frozen until animals were available for inoculation. The above procedure was done at 4°C.

Virus cloning.—Cloned viruses were derived from NIH ME cells infected with viruses derived from AKR SL3 cell culture supernatants. The viruses were selected by end-point titration. One milliliter of DMEM containing 10% NCS, 10 μg Polybrene/ml, and 2×10^4 NIH ME cells was added to each of 24 wells in Falcon microtiter cell culture plates. After cell attachment, the medium was aspirated and 0.1 ml of filtered culture fluid from AKR SL3/NIH cultures was added to each well in tenfold serial dilutions ranging from 10^{-2} to 10^{-6}. Six replicate wells were inoculated with each dilution. After 3–4 weeks with cell passage at 3- to 4-day intervals, the wells were analyzed for viral RT activity. Positive supernatants appearing in the highest dilution wells were selected as clones. The isolates derived in this manner were end point titrated two more times. The cloned viruses were designated AKR SL3- SX4, AKR SL3-SX5, and AKR SL3-H55. Cloned viruses AKR SL3-1, AKR SL3-2, and AKR SL3-3 were obtained from Haseltine (*6*).

Virus assays.—RT: The RT assay utilized the method of Roy-Burman et al. (*7*).

S^+L^- assay: This assay was performed with the use of S^+L^- cells obtained from Dr. R. H. Bassin, Laboratory of Tumor Virus Genetics, Division of Cancer Cause and Prevention, National Cancer Institute, Bethesda, Md., by means of the following method: S^+L^- cells were plated at 5×10^4 cells/35-mm tissue culture dishes in 10 μg Polybrene/ml in DMEM, 10% NCS, and 1% PS. Serial dilutions were made 24 hours later for each virus from a 1× concentration to a 1:10^4 dilution. Plates were infected with 0.2 ml of each virus dilution in duplicate. Positive and negative controls were utilized. The plates were incubated for 1 hour, during which time they were shaken several times lightly back and forth to evenly distribute the virus. At the end of 1 hour, the plates were overlaid in 2.0 ml of the above medium containing 0.5% methylcellulose. Three days later, 1 ml of medium was added per plate. When the S^+L^- cells reached confluence, the medium was aspirated, and the cells were fixed with 2.0 ml in 0.25% methylene blue–3.7% Formalin in saline. The plates were rinsed 4 hours later. Plaques were counted with the aid of a dissecting microscope.

XC assay: This assay was performed with a modification of the method described by Rowe et al. (*8*). NIH ME cells were plated at 5×10^4 cells/35-mm tissue culture dishes as above. Plates were infected 24 hours later with virus as above. The plates were overlaid with DMEM, 10% NCS, and 1% PS. When the cells reached confluence (3–4 days later), the plates were irradiated with UV light for 20 seconds at 70 erg/mm^2/second, from 28 cm above the monolayer. XC cells were overlaid with 6×10^5 cells/plate. Two days later, the medium was changed. One-half to 1 day later, the medium was aspirated and the plates were stained as described above. Syncytia formed by fusion of XC cells were counted on the stained plates by means of a dissecting microscope.

Assay for lymphomagenesis: Mice were inoculated ip within 4 days of birth with 0.1 ml of test material. AKR mice were observed for 150 days. Spontaneous thymic lymphoma did not develop in these animals before 180 days of age. SJL mice were observed for 250 days. Spontaneous thymic lymphoma is rarely seen in this strain. Between 240 and 365 days of age, 2–37% of SJL mice in our breeding colony developed the disease. After 365 days, the animals developed a characteristic reticulum cell sarcoma. In several of the SJL tests, uninoculated littermate controls were used to further control for specific oncogenicity of the inoculated materials. C3H/HeJ mice were observed for 1 year. Spontaneous lymphoma did not occur in this strain prior to 1 year and rarely occurred in older mice.

Cocultivation infection for host range determination: Indicator cells, NIH ME, SC-1, or MLC, were plated in multiwells in medium containing 10 μg Polybrene/ml. When the cells reached 25% confluence, the cells to be tested were added at a ratio of 1:1–5:1 over the indicator cells. The indicator cells were then cultured as usual (i.e., passaged twice weekly). We removed the lymphoma cells by washing the adherent fibroblasts with trypsin before subculturing the first two times. No lymphoma cells were evident after two passages. After 3 weeks, the culture medium was tested for the presence of RT.

Assay for phenotypically mixed virus: Virus-infected NIH ME cells or MLC were cocultivated with MLC or SC-1 cells, respectively, for at least four passages. Twenty-four-hour medium from each culture was then filtered (0.45 μm Millex) and added to uninfected MLC and SC-1 cells. These cultures were assayed at two passage levels (starting at passage 3) for the presence of extracellular particles containing RNA-dependent DNA polymerase. In cases in which phenotypically mixed viruses (i.e., xenotropic or dual-host range genomes with ecotropic coats) were detected, the unmasked viruses growing in MLC were assayed for host range with direct infection of MLC, NIH ME, and SC-1 cells.

RESULTS

Stability of Oncogenic Properties of SL Viruses

Continuous cultures of AKR SL3 and MAC 12 cells were monitored at 6-month intervals for 2 years for virus production and oncogenicity. The cells continuously produced viruses that had an ecotropic host range and accelerated lymphoma in AKR mice. The results of two time periods, 1 year apart, are presented in table 1.

To test the stability with in vivo passage, we inoculated filtered AKR SL3 supernatants into newborn AKR mice. A cell-free filtrate was prepared from a mouse that developed lymphoma 70 days after inoculation. This filtrate accelerated lymphoma in all inoculated animals and has done so through eight consecutive animal passages. All of the inoculated animals died of typical thymic lymphoma within 70–85 days after inoculation of the test filtrate.

Lymphoma cell lines were established from the thymomas of 2 mice with lymphoma accelerated by neonatal AKR SL3 virus inoculation. These lines were designated "AKR SL3-A and AKR SL3-B." Filtrates from the AKR SL3-A line had a titer of 4.7×10^2 PFU/ml with the S^+L^- assay and were XC-positive (2.7×10^2 PFU/ml). They produced accelerated lymphoma in 9 of 9 mice within 77–95 days after inoculation. The AKR SL3-B line filtrate had a virus titer of 3.3×10^2 PFU/ml with the S^+L^- assay. It was XC-positive (titer, 20 PFU/ml). This supernatant produced lymphomas in 6 of 6 neonatally inoculated AKR mice at 86–99 days.

Studies With Cloned Cells From the AKR SL4 Line

Four clones were established from single cells from the AKR SL4 lymphoma cell line. These lines produce XC-negative, ecotropic lymphoma-accelerating virus. The results are presented in table 2 and clearly show that production of XC-negative viruses with lymphoma-accelerating properties was a characteristic of individual cells and their progeny when cloned from the parent cell line.

Tests of AKR SL4 Viruses for Leukemia-Inducing Properties in SJL Mice

When the AKR-derived G-MuLV is inoculated into newborn SJL mice, thymic lymphomas develop within 2–4 months (Hays EF: Unpublished observation). We wished to determine if the SL viruses that we had shown to be lymphoma accelerating in AKR mice would, like G-MuLV, be lymphoma inducing (i.e., induce thymic lymphoma), or if they had lymphoma-accelerating properties (i.e., accelerate the onset of the naturally occurring reticulum cell sarcoma in the SJL mice.

TABLE 1.—*Virus studies of cell supernatants from two cell lines*[a]

Cell line	Date	Titer on S^+L^-, PFU/ml	Lymphoma acceleration[b]
AKR SL3	11/79	1.4×10^3	4/4 (93–112)
	11/80	2.2×10^4	7/7 (87–90)
MAC 12	11/79	4.8×10^4	12/13 (71–120)
	11/80	2.2×10^6	7/7 (86–98)

[a] RT of these culture supernatants was strongly positive. Supernatants and cells were removed from the cell lines in growth phase. They were frozen and thawed, then centrifuged at 3,000×*g* for 10 min. The supernatant was then passed through a 0.45-µm filter and stored in aliquots at −70°C prior to inoculation into mice and prior to test in the S^+L^- assay.

[b] Number of thymic lymphomas at <150 days/number of mice inoculated as newborn (AKR). *Numbers in parentheses* are days after inoculation.

TABLE 2.—*Virus assays of filtrates of cells cloned from lymphoma cell line ARK SL4*[a]

AKR SL4 clone No.	RT, cpm/ml$\times10^6$	S^+L^-, PFU/ml	Lymphoma acceleration[b]
1	9.3	3.6×10^3	5/5 (61–80)
2	8.1	2.3×10^3	9/9 (70–81)
3	3.8	3.5×10^2	6/8 (77–91)
4	6.7	1.6×10^3	14/14 (67–88)

[a] The AKR SL4 line is a continuously replicating lymphoma cell line derived from an AKR spontaneous lymphoma. It produces XC^- ecotropic lymphoma-accelerating virus. Clones 1-4 were established from single cells and grown as the parent line with RPMI-1640 medium and 10% NCS. All assays were done on filtered (0.45 µm) supernatants from the cell lines. All cell clones produced XC^- viruses.

[b] Number of thymic lymphomas at 150 days/number of mice inoculated as newborn (ARK). *Numbers in parentheses* are days after inoculation.

A filtered (0.45 µm) supernatant from AKR SL4 cells was studied on two occasions in both neonatal AKR and SJL mice. The results of each study were identical. AKR SL4 cells produced a low-titer virus, which always accelerated thymic lymphoma in AKR mice and induced a morphologically identical disease in SJL mice (table 3). Cell-free filtrates prepared from the SJL-induced thymic lymphomas had lymphomagenic properties for SJL and AKR mice. In a second experiment, the use of littermate controls unambiguously demonstrated the lymphoma-inducing properties of the test filtrates in SJL mice (table 3).

Studies With Cloned Viruses From AKR SL3 Cell Line

Three virus clones were isolated by end-point dilution from NIH mouse embryo cells infected with virus from filtered supernatants of AKR SL3 cells. These viruses were studied for host range on NIH ME cells and MLC, for plaque formation with S^+L^- cells, and for syncytia formation with XC cells, as well as for leukemia acceleration in AKR mice and leukemia induction of SJL mice.

The data are presented in tables 4 and 5. They show that ecotropic viruses that are negative or positive with the XC

TABLE 3.—*Induction of thymic lymphoma in SJL/J mice by filtrates from AKR SL4 cells*[a]

Parameter	Experiment 1		Experiment 2		
Titer S^+L^-, PFU/ml XC assay	1.2×10^2 Negative		4×10^2 Negative		
	AKR	SJL	AKR	SJL	SJL control littermate
Lymphoma acceleration–induction[b]	9/9 (73–110)	8/8 (81/119)	17/17 (68–88)	11/11 (84–103)	0/9

[a] Supernatants prepared from AKR SL4 cells were filtered (0.45 µm) and stored in aliquots at −7°C until used. Experiments 1 and 2 were done 2 yr apart showing the stability of the lymphomagenic properties of the viruses produced by this in vitro cell line.

[b] Lymphoma acceleration–induction is expressed as number of thymic lymphomas at <150 days/number of mice inoculated as newborn. *Numbers in parentheses* are days after inoculation.

TABLE 4.—*Properties of cloned viruses from AKR SL3 cells*[a]

Clone	S^+L^- titer, PFU/ml	XC titer, PFU/ml	AKR lymphoma acceleration[b]	SJL lymphoma induction[b]	
				Injected	Littermate control
AKR SL3-3	5.2×10^4	5.5×10^4	11/11 (69–95)	11/13 (76–97)	0/5
AKR SL3-2	1.75×10^2	0	10/10 (77–145)	7/12 (210–297)	0/7
AKR SL3-1	1×10^2	5×10^2	5/10 (125–135)	3/7 (108, 119, 295)	0/9

[a] All cloned viruses were ecotropic. They were obtained from supernatants of NIH ME cells infected with the cloned isolates. Supernatants were prepared by trypsinizing the NIH ME cells, adding them to the culture fluid, freezing them, thawing them, and centrifuging them at 3,000×*g* for 10 min. The resulting supernatant was passed through a 0.45-μm filter and frozen in aliquots to use in the in vitro and in vivo assays.

[b] Number of thymic lymphomas/number of mice inoculated in the newborn period. *Numbers in parentheses* are days after inoculation.

assay and did not contain phenotypically mixed particles can be cloned from the AKR SL3 virus-infected NIH mouse embryo cells. Lymphoma-accelerating (AKR) and lymphoma-inducing (SJL) properties are found in both XC-positive and XC-negative clones. The longer latent periods and lower incidence of accelerated and induced lymphomas with AKR SL3-1 and SKR SL3-2 probably reflect the low titer of viruses used in these studies. The AKR SL3-3 clone also induced lymphoma in C3H/HeJ mice. Of 9 mice inoculated as newborns, 7 developed thymic lymphoma at 105–176 days.

Three additional virus clones (AKR SL3-SX4, AKR SL3-SX5, and AKR SL3-H55) were isolated from AKR SL3 supernatants. At least two of these stocks were composed of a mixture of XC-positive ecotropic and phenotypically mixed viruses (table 5). All three stocks were lymphoma accelerating and induced thymic lymphoma in SJL mice. Thus six successive isolates of virus from AKR SL3 lymphoma cells done on mouse embryo fibroblasts were oncogenic.

Phenotypically Mixed Viruses

Many of the cloned SL stocks were assayed for the presence of xenotropic (ecotropic)[7] or dual-host range (ecotropic) viruses. Phenotypically mixed virus particles were found in several, but not all, virus stocks. AKR SL3-2, AKR SL3-3, and G-MuLV were all exclusively ecotropic leukemia viruses (table 5). The composition of three of the other virus stocks isolated from AKR SL3 cells was a combination of phenotypically mixed and ecotropic viruses. In the one case studied so far, the unmasked virus found in the AKR SL3-SX5 stock appears to have a dual-host range. However, this virus must be cloned to verify this.

We are in the process of determining what contribution, if any, the phenotypically mixed particles make to lymphomagenesis. As shown in table 6 and discussed below, only ecotropic virus was detected in accelerated AKR lymphomas following AKR SL3-SX4, AKR SL3-SX5, and AKR SL3-H55 virus inoculation. All lymphoma cells and cell lines were assayed by cocultivation with MLC and NIH ME cells.

TABLE 5.—*Assay for phenotypically mixed particles in virus stocks*[a]

Virus	XC	Direct infection	Infection following cocultivation[b]	
			MLC	SC-1
AKv-1	+	Ecotropic	–	++
AKR SL3-2	–	Ecotropic	–	++
AKR SL3-3	+	Ecotropic	–	++
G-MuLV	+	Ecotropic	–	++
AKR SL3-SX5	+	Ecotropic	++	++
AKR SL3-H55	+	Ecotropic	++	+
MCF-247	–	Dual host	++	++
AKR xenotropic	–	Xenotropic[c]	++	±

[a] Method of assay is described in "Materials and Methods."

[b] –=no virus replicates; ±=very low-titer virus (10^1 PFU/ml); +=moderate titer virus (10^2, 10^3 PFU/ml); ++=high-titer virus (10^4, 10^5 PFU/ml).

[c] As reported by Hartley and Rowe (*9*), SC-1 cells are weakly susceptible to AKR xenotropic virus infection. However, this virus can easily be distinguished from dual-host range viruses, which are able to replicate equally well on SC-1 and MLC.

Recovery of Viruses From Cell Lines and Spontaneous and Virus-Accelerated Lymphomas

We had previously reported that most cell lines established from AKR spontaneous lymphoma produced only ecotropic XC-negative viruses (*3*). In the following experiment, cell lines and lymphomas were tested by cocultivation infection with the use of untreated lymphoma cells. The results are presented in table 6. All cell lines that were derived from spontaneous lymphomas and two cell clones from line AKR SL1 produced a mixture of viruses able to replicate in MLC and mouse cells. This was also the case when cells from thymomas of 2 spontaneously occurring AKR lymphomas were tested directly.

In contrast, host range studies of viruses produced from the cell lines established from lymphoma accelerated by SL3 viruses, SL3-A, and SL3-B showed only viruses with ecotropic properties. A cell line established from a thymic lymphoma accelerated by G-MuLV that had been maintained in vitro for 3 years (AKR A2) was also found to produce only ecotropic viruses when tested as indicated above. Similar results were obtained with fresh cells prepared from 5 lymphomas accelerated by the cloned AKR SL3 isolates AKR SL3-3, AKR SL3-SX4, AKR SL3-SX5, and AKR SL3-H55, and 3 C3H lymphomas accelerated by SL3-3. In the one case studied so far, AKR SL3 xenotropic virus was not oncogenic in AKR or SJL mice. Thus the

---

[7] By convention, the first term indicates the viral genotype and the second term, *in parentheses*, indicates the host range as determined by the viral glycoprotein.

TABLE 6.—*Recovery of virus that will grow in NIH mouse embryo cells and MLC from cells of spontaneous and accelerated lymphomas and cell lines established from them*[a]

Spontaneous lymphomas, mice 7–12 mo of age			Accelerated lymphoma, mice 2–3 mo of age		
Cell lines	NIH ME	MLC	Cell lines	NIH ME	MLC
AKR SL1 cell line	+	+	AKR SL3-A cell line (AKR SL3)	+	–
AKR SL1a cell clone	+	+	AKR SL3-B cell line (AKR SL3)	+	–
AKR SL1b cell clone	+	+	AKR A2 cell line (G-MuLV)	+	–
AKR SL2 cell line	+	+	A50-1 (AKR SX4)	+	–
AKR SL3 cell line	+	+	A51-2 (AKR SL3-H55)	+	–
AKR SL7 cell line	+	+	A53-3 (AKR SL3-SX5)	+	–
AKR SL11 cell line	+	+	A53-4 (AKR SL3-SX5)	+	–
AKR SL12 cell line	+	+	A54-4 (AKR SL3-SX5)	+	–
Spontaneous lymphoma 1	+	+	C3H-1 (AKR SL3-3)	+	–
Spontaneous lymphoma 2	+	+	C3H-2 (AKR SL3-3)	+	–
			C3H-3 (AKR SL3-3)	+	–

[a] Cell lines are lymphoma cells originally derived from spontaneous or virus-accelerated lymphomas and maintained as continuous in vitro suspension cultures. Notations *in parentheses* after the accelerated lymphomas are the virus stocks used to accelerate the lymphoma. Cells from spontaneous lymphomas 1 and 2 and accelerated lymphomas A50-1, A51-2, A53-3, A53-4, A54-4, and C3H lymphomas 1, 2, and 3 were obtained from the thymic tumors of animals with generalized lymphoma and cocultivated directly with NIH ME cells or MLC.

spontaneous lymphomas or cell lines established from them produced a mixture of virus able to replicate in both mouse cells and MLC, whereas cells and cell lines from lymphomas accelerated by AKR-derived ecotropic viruses produced only ecotropic viruses.

DISCUSSION

These experiments show that AKR spontaneous lymphomas maintained as continuous lines in vitro produce ecotropic viruses that we have called SL viruses, which not only accelerate thymic lymphomas in AKR mice but also induce thymic lymphomas in SJL/J, C3H/HeJ, and CBA/H mice (Hays EF: Unpublished observation). These findings, as well as the published observations from Pedersen et al. (*6*), which show leukemia induction in C3H$_f$/Bi mice by the cloned AKR SL3 viruses, conclusively prove the oncogenicity of this virus class. The lymphomagenic SL viruses, described in this report, are produced by lymphoma cells from in vitro lines over long periods of time. They are also continuously produced by an in vivo transformed bone marrow stromal cell line from an AKR mouse neonatally inoculated with AKR SL3 virus. We point out that the lymphoma-accelerating properties of the SL viruses persist with in vivo passage and that XC-positive SL viruses are found in lymphoma cells established as in vitro lines from tumors accelerated by SL viruses. We present evidence to show that the ecotropic and lymphomagenic properties are found in cloned isolates of SL viruses. Further evidence for the lymphomagenicity of the AKR SL3 virus genome is provided by the fact that molecularly cloned SL3-3 virus DNA has been found to be leukemogenic for C3H$_f$/Bi mice (Haseltine W: Unpublished observation). We have also shown that the lymphomas accelerated by the cloned SL viruses produce only ecotropic virus, suggesting that these lymphomas produce the virus repsonsible for their development. It is also noteworthy, as we have shown in this report, that SL virus-induced thymic lymphoma of SJL mice contains virus that can again accelerate AKR lymphoma and induce disease in the SJL mice. This is also true for MCF viruses inasmuch as MCF virus was found in an AKR lymphoma accelerated by the dual-host range virus MCF-247 (*10*).

The results of the experiments presented in this report are compatible with the idea that AKR mice develop thymic lymphomas when viruses that appear during aging interact in an as yet unknown way with progenitors of thymic lymphocytes. These viruses are usually ecotropic and always induce thymic lymphomas. The G-MuLV (*11*), which was derived from an AKR spontaneous lymphoma, is ecotropic as determined by cocultivation infection (table 5). It accelerates lymphoma in AKR mice and induces lymphoma in SJL mice as well as in mouse strains with a low incidence of spontaneous lymphoma (*11*).

Viruses with dual-host range, i.e., properties of growth on both mouse cells MLC, can also be isolated from age AKR thymocytes and AKR lymphoma cells when they are cultivated initially on MLC (*12*). Cloned isolates of some of these viruses have been shown to accelerate lymphomas in AKR mice (*3, 13, 14*); they also induce a lymphoma in other strains (*15*). In our laboratory, we have tested two of these polytropic viruses, MCF-247 and MCF-13. Both of these viruses accelerate AKR lymphoma, and MCF-247 induces lymphoma in SJL mice (Hays EF: Unpublished observation).

The inability to form syncytia on XC cells is a characteristic of ecotropic SL virus, G-MuLV (derived from cell lines established from G-MuLV-accelerated lymphomas), and MCF viruses. However, some of the SL viruses "convert" to XC-positive on mouse embryo cells (*4*) and, as noted in the present study, both of the cell lines established from a lymphoma accelerated by AKR SL3 virus (SL3-A and SL3-B) produce XC-positive lymphoma-accelerating virus. The property of leukemia acceleration–induction is therefore associated with three classes of viruses: 1) SL XC$^-$ (AKR SL3, AKR SL4, AKR SL4 cell clones 1–4, G-MuLV from AKR A2 cell line, and cloned virus AKR SL3-2); 2) SL XC$^+$, (AKR SL3-A and -B and cloned viruses AKR SL3-1, AKR SL3-3, and possibly AKR SL3-SX4, AKR SL3-SX5, and AKR SL3-H55; and 3) MCF XC$^-$ (MCF-247 and MCF-13). Thus the phenotypic characteristics of host range and XC syncytia-forming ability are not necessarily related to lymphomagenic properties of these AKR-derived viruses. This fact is corroborated by the finding of SL XC⁻ and MCF XC⁻ viruses that are not associated with leukemogenesis (*3, 13, 15*). Additional recent confirmation of the uniqueness of the SL virus is provided by studies of the viral genome by oligonucleotide mapping. These studies have shown the AKR SL3 viruses (cloned and uncloned) and AKR SL4 virus to be a distinct class with variant 3′ region. Their oligonucleotide map is different from that of the MCF viruses (*16*).

Published studies show that viruses able to induce a T-cell lymphoma in mice are recombinants of two endogenous viruses carried in the germ line plus additional cellular sequences (*6, 17–20*). Although the MCF viruses are the most widely studied of these viruses, this class is clearly not the exclusive domain of lymphomagenic viruses. Undoubtedly, there are specific nucleotide sequences necessary for oncogenic properties, but these are separate from those responsible for host range and XC fusion. In fact, Pedersen et al. (*6*) have evidence that these oncogenic sequences are not present in the *env* gene but are located much closer to the 3′ end of the viral genome.

It is not clear whether phenotypically mixed viruses are merely annoying byproducts of viral interactions, which only confuse the situation, or whether their formation is an important part of lymphomagenesis. The experiments described here would suggest that the first explanation is correct. In cases in which MCF viruses are involved, however, pseudotype formation may be important because MCF viruses do not replicate well in all mouse cells.

The sensitive method of cocultivation-infection with untreated cells was able to detect xenotropic and/or dual-host range viruses in all of the spontaneous lymphoma cells and lines when supernatants from these lines were negative for virus replicating on MLC. However, even with cocultivation, xenotropic virus and/or dual-host range virus was not produced by the accelerated lymphomas. These lymphomas occur in young mice, and xenotropic virus does not appear in the AKR mouse thymus at 8–12 weeks of age (*21, 22*). From these studies, we conclude that thymic lymphomagenesis is not dependent on host xenotropic virus expression after introduction of an ecotropic SL virus.

REFERENCES

(*1*) Nishizuka Y, Nakakuki K. Acceleration of leukemogenesis in AKR mice by grafts, cell suspensions and cell-free centrifugates of thymuses from preleukemic AKR donors. Int J Cancer 1968; 3:203–210.

(*2*) Hays EF, Vredevoe DL. A discrepancy in XC and oncogenicity assays for murine leukemia viruses in AKR mice. Cancer Res 1977; 31:726–730.

(*3*) Nowinski RC, Hays EF. Oncogenicity of AKR endogeneous leukemia viruses. J Virol 1978; 27:13–18.

(*4*) Nowinski RC, Hays EF, Doyle T, Linkhart S, Medeiros E, Pickering R. Oncornaviruses produced by murine leukemia cells in culture. Virology 1977; 81:363–370.

(*5*) Hays EF, Warren J, Hale L, Rodensky D. AKR murine leukemia viruses and long-term bone marrow cultures from AKR and SJL mice. Exp Hematol 1980; 8:134–146.

(*6*) Pedersen FS, Crowther RL, Tenney DY, Reimold AM, Haseltine WA. Novel leukaemogenic retroviruses isolated from cell line derived from spontaneous AKR tumour. Nature 1981; 292:167–170.

(*7*) Roy-Burman P, Dougherty M, Pal BK, Charman HP, Klement V, Gardner MB. Assay for type C virus in mouse sera based on particulate reverse transcriptase activity. J Virol 1976; 19:1107–1110.

(*8*) Rowe WP, Pugh WE, Hartley JW. Plaque assay technics for murine leukemia viruses. Virology 1970; 42:1136–1139.

(*9*) Hartley JW, Rowe WP. Clonal cell lines from a feral mouse embryo which lacks host-range restrictions for murine leukemia viruses. Virology 1975; 65:128–134.

(*10*) Pedersen FS, Buchhagen DL, Chen CY, Hays EF, Haseltine WA. Characterization of virus produced by a lymphoma induced by inoculation of AKR MCF-247 virus. J Virol 1980; 35:211–218.

(*11*) Gross L. High susceptibility of 1–14 days old C3H mice to "passage A" leukemic filtrates. Proc Soc Exp Biol Med 1958; 97:300–304.

(*12*) Hartley JW, Wolford NK, Old LJ, Rowe WP. A new class of murine leukemia viruses associated with the development of spontaneous lymphomas. Proc Natl Acad Sci USA 1977; 74:789–792.

(*13*) O'Donnell PV, Stockert E, Obuta Y, DeLeo AB. Murine-leukemia-virus-related cell surface antigens as serological markers of AKR ecotropic xenotropic and dualtropic viruses. Cold Spring Harbor Symp Quant Biol 1979; 14:1255–1264.

(*14*) Rowe WP, Cloyd MW, Hartley JW. Status of the association of mink cell focus forming viruses and leukemogenesis. Cold Spring Harbor Symp Quant Biol 1979; 14:1265–1268.

(*15*) Cloyd MW, Hartley JW, Rowe WP. Lymphomagenicity of recombinant mink cell focus-inducing murine leukemia viruses. J Exp Med 1980; 151:542–552.

(*16*) Pedersen FS, Crowther RL, Hays EF, Nowinski RC, Haseltine WA. Structure of retroviral RNA's produced in cell lines derived from spontaneous lymphomas of AKR mice. J Virol 1982; 41:18–29.

(*17*) Elder JH, Gantsch JW, Jensen FC, Lerner RA, Hartley JW, Rowe EP. Biochemical evidence that MCF murine leukemia viruses are envelope (*env*) gene recombinants. Proc Natl Acad Sci USA 1977; 74:4676–4680.

(*18*) Rommelaere J, Faller DV, Hopkins N. Characterization and mapping of RNase T_1-resistant oligonucleotides derived from the genomes of Akv and MCF murine leukemia viruses. Proc Natl Acad Sci USA 1978; 75:495–499.

(*19*) Green N, Hiai H, Elder J, et al. Expression of leukemogenic recombinant viruses associated with a recessive gene in HRS/J mice. J Exp Med 1980; 152:249–264.

(*20*) Chattopadhyay SK, Lander MR, Gupta S, Rands E, Lowy DR. Origin of mink cytopathic focus-forming (MCF) viruses: Comparison with ecotropic and xenotropic murine leukemia virus genomes. Virology 1981; 113:465–483.

(*21*) Kawashima K, Ikeda H, Hartley JW, Stockart E, Rowe WP, Old LJ. Changes in expression of murine virus antigens and production of xenotropic virus in the late preleukemic period in AKR mice. Proc Natl Acad Sci USA 1976; 76:4680–4684.

(*22*) Hays EF, Beardsley T. Interactions of thymic epithelial cells, lymphocytes and murine leukemia viruses. In: Proffitt MR, ed. Virus-lymphocyte interactions: Implications for disease. Amsterdam: Elsevier/North-Holland, 1979:157–166.

Prostaglandin-Induced Differentiation or Dimethyl Sulfoxide-Induced Differentiation: Reduction of the Neoplastic Potential of a Rat Mammary Tumor Stem-Cell Line[1, 2]

Philip S. Rudland,[3] Anna Twiston Davies,[3] *and* Michael J. Warburton[3, 4]

ABSTRACT—Differentiation of the rat mammary stem cell line Rama 25 to alveolar-like cells was monitored both by the increased production of domes (hemispherical blisters) in the cell monolayer and by immunoreactive casein in the tissue culture medium. In addition to the synthetic inducer dimethyl sulfoxide (DMSO), prostaglandin (PG)E_1, and to a lesser extent PGE_2 and $PGF_{2\alpha}$ (concentration range, 50–500 ng/ml) in the presence of the hormones prolactin (Pr), hydrocortisone (HC), insulin (I), and 17β-estradiol (E) also accelerated this step. A combination of PGE_1, HC, and I was active in promoting doming even in serum-free medium, whereas PGE_1, all four hormones, and serum were required for maximum production of immunoreactive casein. The DNA synthetic rate was concomitantly reduced during this differentiation step. Rama 25 readily formed tumors in young, female *nu/nu* mice. When Rama 25 cells were treated with PGE_1 or DMSO and the four hormones yielding the droplet and doming cultures, subsequent injection of these cultures into *nu/nu* mice led to a reduced incidence of tumors compared with injections of untreated cultures. Variant cell lines were selected from a subclone of elongated, myoepithelial-like Rama 29 cells that had been derived from Rama 25 and directly from Rama 25 itself. The former were elongated cells and termed "Rama 521," and the latter were cuboidal epithelial cells and termed "Rama 259." Both these variants were resistant to the actions of PGE_1 or DMSO and to the mammotropic hormones in accelerating the rate of formation of domes, producing immunoreactive casein, in substantially reducing the DNA synthetic rate, and in reducing the incidence of tumors when injected into *nu/nu* mice. We have therefore shown that conversion of Rama 25 stem cells to alveolar-like cells in culture is specifically accompanied by a reduction in their neoplastic potential in *nu/nu* mice.—JNCI 1982; 69:1083–1093.

Three main types of epithelial cells are distinguishable in rat mammary glands: those lining the alveoli, those lining the ducts, and the myoepithelial cells (*1*). These three cell types can also be recognized in carcinogen-induced tumors (*2*). Whether these three cell types, and in particular the ductal and alveolar cells, represent discrete cell types or the same cell within different glandular compartments is uncertain [*see* (*3*)]. For clarification of this point, a clonal cuboidal epithelial stem cell line, Rama 25, has been isolated from a DMBA-induced rat mammary adenocarcinoma (*3*). This cell line can differentiate in culture into either droplet and doming (alveolar-like) or elongated (myoepithelial-like) cells (*4, 5*). One such elongated cell line is Rama 29. Differentiation to alveolar-like cells can be followed by the appearance of two markers, the ability of the monolayer cultures to form hemispherical blisters or domes (*6*), and the secretion of immunoreactive casein into the culture medium. This differentiation process is directly accelerated by a combination of DMSO, an agent that induces differentiation in Friend erythroleukemia cells(*7, 8*), together with the mammotropic hormones Pr, HC, and I. This stem cell line, Rama 25, also readily forms tumors in immunodeficient *nu/nu* mice (*3, 9*), and hence this cell line can be used to test whether alveolar-like cells formed from it have an altered tumor-forming ability when injected into *nu/nu* mice.

DMSO and other Friend cell inducers, however, are synthetic compounds that must be used at relatively high concentrations to produce their differentiation-inducing effects. Thus the physiologic relevance of these effects may be open to question. We have therefore sought to replace the artificial inducers by more naturally occurring compounds. One such group, the PG, can exert many diverse hormone-like actions in vivo, including luteinic and renal antihypertensive effects (*10, 11*). However, whether the PG act directly on the target tissue or work by stimulating the production of secondary hormone agents is open to doubt (*10, 11*). The PG also promote erythroid progenitors to differentiate and form erythroid colonies in vitro (*12*), and there is an inverse correlation between the spontaneous differentiation rates in vitro of different Friend murine erythroleukemia cell lines and their ability to form tumors in syngeneic mice (*13*). We have therefore investigated the ability of the PG to replace DMSO in inducing the differentiation of our stem cell line to alveolar-like cells in culture, and we relate this change to the concomitant change in our stem cell line's neoplastic potential when injected into *nu/nu* mice.

MATERIALS AND METHODS

Routine tissue culture.—The isolation of the rat mammary cloned cell lines Rama 25 and Rama 29 has been described previously (*3*). Rama 25 and Rama 29 were routinely grown

---

ABBREVIATIONS USED: CLM=cloning medium; CM=conditioned medium; DMBA=7,12-dimethylbenz[*a*]anthracene; DMEM=Dulbecco's modified Eagle's minimum essential medium; DMSO=dimethylsulfoxide; E=17β-estradiol; FCS=fetal calf serum; HC=hydrocortisone; [^{3}H]dThd=tritiated thymidine; H & E=hematoxylin and eosin; I=insulin; LI=labeling index; PBS=phosphate-buffered saline; PG=prostaglandin(s); Pr=prolactin; Rama 25-25=Rama 25, passage 25; Rama 29-31=Rama 29, passage 31; RM=routine medium.

---

[1] Received November 27, 1981; accepted May 10, 1982.

[2] Animals were maintained under the guidelines of the Ludwig Institute for Cancer Research (London Branch).

[3] Ludwig Institute for Cancer Research (London Branch), Royal Marsden Hospital, Sutton, Surrey SM2 5PX, England.

[4] We thank Mrs. Ruth Thompson, Mrs. Sharon Ferns, Miss Linda Lovell, Mr. Geoffrey Webby, and Miss Christine Hughes for expert technical assistance; Prof. A. J. Davies, Institute of Cancer Research, London, England, for supplying the nude mice; and Dr. J. Pike, The Upjohn Co., Kalamazoo, Mich., for gifts of PGE_1, PGE_2, and $PGF_{2\alpha}$.

in DMEM containing 10% (vol/vol) FCS, 50 ng HC/ml, and 50 ng I/ml (this formulation constituted RM) in 9-cm petri dishes (A/S Nunc, Roskilde, Denmark) at 37°C in an atmosphere of 10% (vol/vol) CO_2. The cell lines were transferred subconfluently at a dilution factor of 1:8 by detachment with trypsin-EDTA, as previously described (*3*). Experiments were done in which initial stocks of Rama 25-25 and Rama 29-31 were used with not more than two and six subsequent transfers, respectively. Rama 25-25 cells contained less than 1% contamination of elongated cells, as determined in a single cell cloning assay. CLM was prepared from 50% CM plus 40% DMEM plus 10% fresh FCS, 50 ng HC/ml, and 50 ng I/ml. CM consisted of Ham's medium F12 that contained 5% FCS and was adjusted to 3.7 mg/ml $NaHCO_3$ and which was then exposed for 1 day to 2×10^6 Rama 29 cells/10 ml medium (*3, 5*). Ham's medium F12 (catalog #176) was purchased from Gibco Europe Ltd. (Paisley, Scotland).

Living cells were photographed by a Zeiss ICM 405 automatic inverted microscope fitted with phase-contrast optics. Photography was done on Ilford Pan F film, and a green filter was used.

Production of doming cultures.—Because the higher concentrations of Ca^{2+} and Mg^{2+} in DMEM could interfere in the casein assay, DMEM was replaced by Ham's medium F12 before the experiment commenced. Thus Rama cell lines were plated at 10^6 cells/5-cm petri dish and grown to confluence in 5 ml of RM. Two protocols were subsequently used. In protocol I, the medium was changed on day 5 to 5 ml of Ham's medium F12, 10% FCS, 50 ng I/ml, 50 ng HC/ml, 500 ng Pr/ml, and an extra 2.1 mg $NaHCO_3$/ml. On day 7, the medium was removed and replaced with 5 ml of fresh Ham's medium F12 containing HC, extra $NaHCO_3$, 500 ng I/ml, 5 μg Pr/ml, 2.7 ng E/ml, and various additives. In protocol II, the medium was changed on day 4 to 5 ml of RM supplemented with 500 ng Pr/ml and 2.7 ng E/ml; then on day 7, the RM was changed to the same medium as that used on day 7 in protocol I, but no additives were used. Finally, on day 9, the medium was again changed to that of day 7, but at this time the various additives were included. For experiments in serum-free medium, the medium of protocol II was removed on day 7 and the monolayer cultures were washed twice with Ca^{2+}- and Mg^{2+}-free PBS; then, Ham's medium F12 containing 2.1 mg $NaHCO_3$/ml was added to each dish. Finally, on day 9, Ham's medium F12 with extra $NaHCO_3$ and the hormones HC, I, Pr, and E were added as before in protocol II together with various additives as indicated. The number of domes per 14-mm^2 field was measured in an Olympus CK inverted microscope (40 ×), usually after 24 or 48 hours. All results are the average of two dishes in which four fields/dish were counted.

Measurement of casein production and DNA synthesis.—The amount of casein released by cell lines into the medium was measured by a radioimmunoassay (*14–16*). Under the conditions of the experiment with Rama cell lines, the cellular protein content of confluent cell monolayers was approximately 0.5 mg for each 5-cm petri dish. Hence the amount of casein secreted is expressed per dish. Casein remaining within the cells was less than 10% of the casein secreted into the medium (*4*). The material being precipitated in the radioimmunoassay was identified as casein as previously reported (*14, 15*).

DNA synthesis measurements were done by radioactively labeling the cultures with 3 μCi $[^3H]$dThd/ml at 1 μM for the stated time and then by processing the cultures for autoradiography as previously described (*17*). The fraction of cells with radioactively labeled nuclei was recorded from two dishes; 4 fields of about 200 cells/dish were counted.

Induction of tumors in nude mice.—Cultured cells were grown as described in protocol II, in which 600-ml flasks (Falcon Plastics, Oxnard, Calif.) containing 50 ml of medium were used. After 48 hours of exposure to Ham's medium F12, 10% FCS, 0.5 μg I/ml, 50 ng HC/ml, 2.1 mg $NaHCO_3$/ml, and various additives, the medium was removed, the cell monolayer was washed twice with PBS, incubated for 30 minutes at 37°C with 0.5 mM EDTA-disodium salt in PBS, and then removed by digestion with trypsin-EDTA solutions at 37°C, as described earlier. Cells were collected in ice-cold PBS supplemented with 10% FCS and were centrifuged at $200\times g$ for 5 minutes. (One flask yielded $\approx1.5\times10^7$ cells.) The cells were then resuspended in ice-cold Ca^{2+}- and Mg^{2+}-free PBS and centrifuged four more times, by which the FCS was removed. More than 95% of the cells excluded trypan blue after this procedure. The cells were finally resuspended at 10^7 cells/ml in the PBS, and 0.2 ml of this suspension (2×10^6 cells) was injected through the skin into the right inguinal mammary gland of 6-week-old female C57BL *nu/nu* mice [(*18*), Institute of Cancer Research, London, England]. Tumors were sized by measurement of two diameters at right angles; this procedure was repeated at about weekly intervals, and the mean diameters were recorded. Animals were usually killed after a further 6 weeks when the tumors were removed, sized, and fixed in Formol-saline for histologic examination. The right inguinal regions of mice without tumors were also dissected, and any small lumps present were subjected to histologic examination. Histologic sections were stained with H & E, mounted, and then photographed on a Reichert Polyvar automatic microscope fitted with Ilford Pan F film and a blue-green filter.

RESULTS

Isolation of DMSO-Resistant Cell Variants

Variant cell lines were isolated either from Rama 29 or from Rama 25 (fig. 1A, text-fig. 1). Isolates from Rama 29 were obtained by passage of Rama 29-32 eight times at high cell densities; then the cultures were plated sparsely and spindly, crisscross cells (frequency <1/1,000) were picked by means of a ring clone (*3, 4*). These variant cells were grown up and were subsequently single-cell cloned (*3*) (cloning efficiency, 75%). One such line was called "Rama 521" (fig. 1B), and cell stocks from it were frozen at passage 43. The variants from Rama 25 were obtained by growing Rama 25-25 for a further six passages in RM containing 1.8% (vol/vol) DMSO. Cultures were then plated sparsely, and a ring clone of cuboidal epithelial cells was picked and grown in CLM containing 1.8% DMSO. This ring clone was single-cell cloned in CLM containing 1.8% DMSO (cloning efficiency, cuboidal cells: 10%; elongated cells: 4%). Thereafter, cultures were initiated in RM without DMSO. All cuboidal epithelial cell lines so produced (Rama 250–Rama 259) were relatively resistant to the effects of DMSO in enhancing the rate of dome formation in confluent cultures, although the cell lines still yielded elongated cells and droplet cells–doming cultures without DMSO in the same frequency range as that of Rama 25 (table 1). The most resistant to DMSO was Rama 259, which was selected for subsequent use, and cell stocks were frozen at passage 37 (fig. 1C). Cuboidal epithelial cell lines which were cloned from Rama 25-25 in the absence of DMSO (Rama 25-Cl.37 and Cl.38) converted to droplet cells (fig. 1d) and domes at higher rates with DMSO (table 1).

PG and Differentiation of Rama Cell Lines in Culture

Confluent 7-day cultures of Rama 25 were initiated according to protocol I ("Materials and Methods"). Increasing concentrations of PGE_1 (50–500 ng/ml), when added to such cultures with fresh 10% FCS and the hormones Pr, HC, E, and I, increased the rate of formation of domes (text-fig. 2). The kinetics showed two distinct phases. Initially, there was a lag phase of 6–8 hours, the duration of which was independent of the concentration of PGE_1 added. Thereafter, there was an abrupt change to a new rate of formation of domes; the new rate was dependent on the concentration of PGE_1 up to a maximum of about 500 ng/ml (text-fig. 2). Above this concentration the rate was relatively independent of the concentration of PGE_1; this observation was true up to 5 μg PGE_1/ml (text-fig. 3). After about 2 days' exposure to the higher concentrations of PGE_1 (≥500 ng/ml), the numbers of domes per field also started to decline (text-fig. 2). By comparison, the maximum effect with the optimum concentrations of DMSO (1.8%) was observed after 24 rather than after 48 hours and was roughly double (30 domes/field) than with the optimum concentration of PGE_1 (15 domes/field).

However, if the cultures were maintained at confluence for a further 2 days with fresh serum and hormones before the inducers were added (protocol II), both the basal and PGE_1-stimulated numbers of domes per microscopic field were increased, but those with DMSO remained unchanged. The effect with 500 ng PGE_1/ml was then close to that observed with 1.8% DMSO after 48 hours (table 2). PGE_2 and $PGF_{2\alpha}$ were both about half as effective as PGE_1 in stimulating doming when they were added to 9-day cultures of Rama 25 (table 2). PGE_1 with the four hormones and FCS caused maximum production of domes and immuno-

TABLE 1.—*Conversion frequencies of DMSO-resistant cuboidal epithelial cells*

Cell line	No. of domes/field ± SEM[a]		Percentage of elongated cell colonies[b] ± SEM
	2 days	5 or 10 days[c]	
Rama 250	0±0	2.2±0.6*	6.1±1.8
Rama 251	0±0	8.2±1.3*	5.2±0.6
Rama 252	0±0	CD	3.0±1.0
Rama 253	0±0	CD	4.5±1.5
Rama 254	0±0	4.2±0.7	5.8±1.0
Rama 255	1.2±0.5	7.9±1.0	11±4
Rama 256	0±0	2.1±0.4	16±4
Rama 257	0.6±0.2	6.2±1.0	12±2
Rama 258	0±0	1.9±0.6	2.4±1.0
Rama 259	0±0	0.5±0.4	1.6±0.6
Rama 25	30±5	24±2*	1.9±0.5
Rama 25-Cl.37	35±1	—	3.3±0.5
Rama 25-Cl.38	14±2	—	16±3

[a] Cultures were plated and grown as described in protocol II ("Materials and Methods"), and the No. of domes per 14-mm^2 microscopic field was estimated.

[b] Cultures were plated at 2,000 cells/9-cm dish, and the fraction as the percent of colonies containing elongated cells was scored after 1 wk.

[c] Those estimations that were recorded at 5 days are marked with an *asterisk*. CD=cell detachment; —=not done.

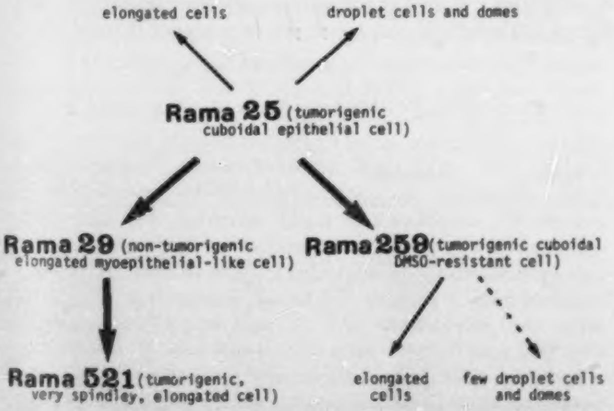
elongated cells
droplet cells and domes
Rama 25 (tumorigenic cuboidal epithelial cell)
Rama 29 (non-tumorigenic elongated myoepithelial-like cell)
Rama 259 (tumorigenic cuboidal DMSO-resistant cell)
Rama 521 (tumorigenic, very spindley, elongated cell)
elongated cells
few droplet cells and domes

TEXT-FIGURE 1.—Summary of the isolation of clonal cell lines and their cellular interconversions. Cell lines isolated from Rama 25 are shown by *thick arrows*; cellular interconversions of the individual cell lines are shown by *thin arrows*. *Hatched arrow* indicates that, although droplet cells and domes can be formed by Rama 259 cells, this process is not accelerated with DMSO, unlike the acceleration in Rama 25.

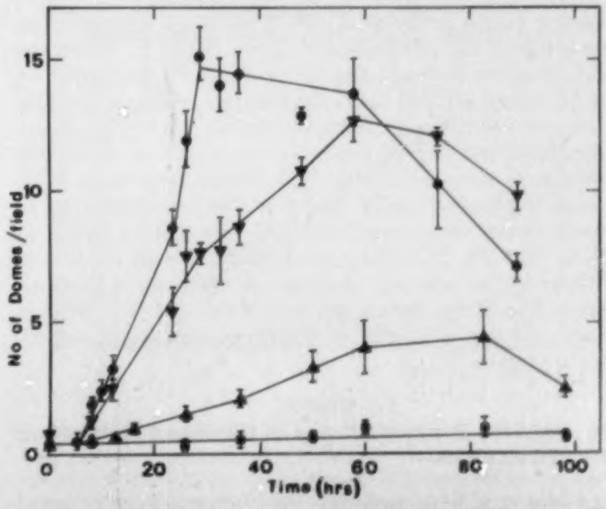

TEXT-FIGURE 2.—Kinetics of doming after additions of PGE_1. Rama 25 cultures were grown to confluence according to protocol I ("Materials and Methods"). On day 7, the medium was replaced with fresh medium containing HC, I, Pr, E, and 500 ng (●), 200 ng (▼), 50 ng (▲) PGE_1/ml. Fresh medium without PGE_1 but with the hormones was also added (■). The number of domes per 14-mm^2 field was observed with time.

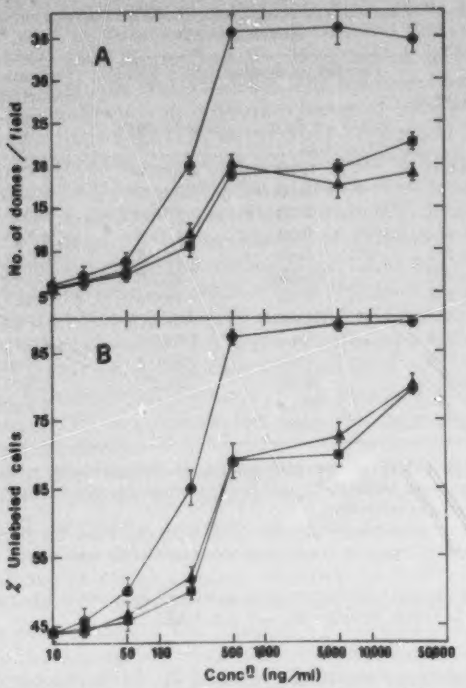

TEXT-FIGURE 3.—Effects of varying concentrations of different PG on Rama 25 cells in culture. Cultures were grown for 9 days according to protocol II ("Materials and Methods"). Varying concentrations (Conc^{n}) (ng/ml) of the PG [PGE_1 (●), PGE_2 (▲), or $PGF_{2\alpha}$ (■)] were added with fresh medium containing HC, I, Pr, and E. In A) the number of domes per 14-mm^2 field formed after 48 hr ± SEM and in B) the percentage of cells remaining unlabeled after a 48-hr exposure to [^3H]dThd (percent unlabeled cells) ± SEM were recorded. Control cultures with no additions and no medium change yielded 89±1% unlabeled cells.

reactive casein, whereas removal of Pr or E resulted in inhibition of the production of casein (table 2). There was little effect on doming when the hormone I was omitted for 24 hours, but after 48 hours the numbers of domes per field were reduced (table 2). PGE_1 or DMSO and the hormones stimulated the rate of formation of domes in serum-free medium at about 50% (table 3) of the rate observed in FCS-containing medium (table 2). There was little production of casein under these conditions. The stimulatory effects of PGE_1 (figs. 2A, 2C), $PGF_{2\alpha}$, or DMSO on both markers of differentiation were not observed in confluent cultures of Rama 29 and the variant cell lines Rama 521 (fig. 2B) and Rama 259 (fig. 2D) (table 4) when they were grown according to protocol II.

PG and DNA Synthetic Rates of Confluent Cultures of Rama Cell Lines

Addition of fresh medium, 10% FCS, and Pr, HC, and I to confluent cultures of Rama 25 caused an acceleration of the rate of DNA synthesis as measured by the incorporation of [^3H]dThd into DNA or by the fraction of [^3H]dThd-labeled cells for fixed periods of 4 hours. The rate remained constant for 6–8 hours and then reached a maximum after 16–18 hours (*5*). When PGE_1 was added with FCS and hormones, the enhanced [^3H]dThd LI due to FCS and hormones alone was reduced after 48 hours (table 2). The optimum concentration (500 ng/ml) required to reduce the 48-hour [^3H]dThd LI was the same as that required for promoting the increase in doming rate as measured in parallel cultures (text-fig. 3). This reduction was about the same as that caused by 1.8% DMSO. PGE_2 and $PGF_{2\alpha}$ at 500 ng/ml were about half as effective as PGE_1 in reducing the [^3H]dThd LI. PGE_1 and DMSO also inhibited the [^3H]dThd LI in confluent cultures of Rama 25 maintained in serum- and hormone-free media. There was little effect for the first 5 hours, but thereafter this LI was greatly reduced (table 3). PGE_1, $PGF_{2\alpha}$, and DMSO failed to reduce the LI in confluent cultures of the variant cell lines Rama 259 and Rama 521 when grown according to protocol II (table 4).

TABLE 2.—*PG or DMSO and Rama 25 cells in serum-supplemented medium*

Additions[a]	No. of domes/field ± SEM[b,c]	Casein secreted, ng ± SEM[b]	Labeled nuclei, % ± SEM[b,d]
None	7±1	0.4±0.5	51±4
PGE_1	32±1	16.4±0.9	13±1
PGE_2	16±2	1.2±0.2	25±6
$PGF_{2\alpha}$	18±1	0.1±0.0	32±5
DMSO	34±1	23.2±0.1	14±5
PGE_1–HC	17±2	0.0±0.4	—
PGE_1–Pr	30±2	0.0±0.4	—
PGE_1–E	31±1	0.0±0.4	—
PGE_1–I	16±1	0.4±0.4	—
PGE_1–HC, I, and Pr	12±1	0.4±0.4	—
PGE_1–FCS	16±1	0.4±0.6	—

[a] Rama 25 cultures were plated and grown as described in protocol II ("Materials and Methods"). On day 9, the medium from the confluent cultures was changed when different agents were omitted and 500 ng PGE_1, PGE_2, or $PGF_{2\alpha}$/ml or 1.8% DMSO was added as indicated.

[b] The number of domes per 14-mm^2 microscopic field, the total immunoreactive casein released into the medium, and the fraction of cells in parallel cultures having [^3H]dThd-labeled nuclei in 48 hr were recorded.

[c] A combination of PGE_1 and DMSO yielded 61±8 domes/field.

[d] —=not done.

TABLE 3.—*PGE_1 or DMSO and Rama 25 cells in serum-free medium*

Time, hr	Additions[a]	No. of domes/ field ± SEM	Labeled nuclei, % ± SEM
5	None	0±0	5±1
	PGE_1	1±0	5±1
	DMSO	0±0	5±1
24	None	1±1	25±2
	PGE_1	12±2	18±4
	DMSO	14±2	10±3
48	None	1±1	44±2
	PGE_1	13±2	16±2
	DMSO	17±1	13±2

[a] Rama 25 cultures were grown as described in protocol II in serum-free medium. On day 9 the medium was replaced when the hormones HC, I, Pr, and E were added back (none) together with either 500 ng PGE_1/ml or 1.8% DMSO. The number of domes per 14-mm^2 field and the percentage of cells with [^3H]dThd-labeled nuclei were recorded after 5, 24, and 48 hr.

TABLE 4.—*PG or DMSO and the variant cell lines*[a]

Cell line[b]	Additions[c]	No. of domes/field ± SEM[d]	Casein secreted, ng ± SEM[d]	Labeled nuclei, % ± SEM[d]
Rama 259	None	0±0	0.0±0.02	53±4
	PGE$_1$	0±0	0.0±0.02	58±6
	PGF$_{2\alpha}$	0±0	0.0±0.01	52±5
	DMSO	0±0	0.0±0.01	44±5
Rama 521	None	0±0	0.0±0.01	33±2
	PGE$_1$	0±0	0.0±0.01	32±4
	PGF$_{2\alpha}$	0±0	0.0±0.04	29±3
	DMSO	0±0	0.0±0.01	20±1

[a] This experiment was done at the same time as that reported in table 2; PGE$_1$ and DMSO were seen to cause increased doming, increased casein secretion, and a reduced [^{3}H]dThd LI in Rama 25 cultures.

[b] Rama 259 and 521 cultures were grown according to protocol II ("Materials and Methods").

[c] On day 9, 500 ng PGE$_1$ or PGF$_{2\alpha}$/ml or 1.8% DMSO was added to the medium that contained FCS and HC, I, Pr, and E.

[d] After 48 hr the number of domes per 14-mm^2 field, the amount of casein secreted per dish, and the percentage of cells with [^{3}H]dThd-labeled nuclei in parallel cultures were recorded.

TABLE 5.—*PG or DMSO and the formation of tumors in* nu/nu *mice*

Cell line injected	Treatment in vitro[a]	No. of survivors	Tumor incidence, % ± SEM[b]
Rama 25	None	20	95±5
	Hormones	20	80±9
	PGE$_1$ − hormones	19	74±10
	PGE$_1$ + hormones	18	17±9
	PGE$_2$ + hormones	19	42±12
	PGF$_{2\alpha}$ + hormones	19	47±12
	DMSO − hormones	20	70±11
	DMSO + hormones	19	11±7
Rama 259	None	20	90±7
	PGE$_1$ + hormones	19	89±7
	DMSO + hormones	21	91±7
Rama 521	None	19	84±9
	PGE$_1$ + hormones	20	90±7
	DMSO + hormones	19	89±7

[a] Cultured cells that had been grown to confluence according to protocol II had their medium changed to that containing I and HC (none) or to that containing I, HC, Pr, and E (hormones) with 0.5 μg PG/ml or 1.8% DMSO as indicated. After 48 hr, cells were inoculated into *nu/nu* mice.

[b] Tumor incidence ± SEM was recorded after 6 wk.

Previous Exposure of Confluent Cultures to PG and DMSO and the Incidence of Cell-Induced Tumors in Nude Mice

Confluent cultures of Rama 25 were incubated with fresh medium, FCS, Pr, HC, I, E, and 500 ng PGE$_1$/ml or 1.8% DMSO (protocol II) and were then tested for neoplastic potential by injecting them into *nu/nu* mice. The number of tumors formed in 6 weeks was only 18% of the tumors obtained when cells were incubated without PGE$_1$ and hormones; this new incidence of tumors was approximately the same as the incidence with DMSO and hormones (table 5). This fractional decrease was maintained for animals kept as long as 3 months; both the fraction of mice bearing a tumor (text-fig. 4A) and the average size of the tumor (text-fig. 4B) showed a similar decrease. Previous treatment of Rama 25 cultures both with hormones and inducer (PGE$_1$ or DMSO) was required for maximum reduction in the yield of tumors (table 5). The optimum concentration of PGE$_1$ for reducing the incidence of tumors was 500 ng/ml (data not shown), and PGE$_2$ and PGF$_{2\alpha}$ were only about 60% as effective at this concentration (table 5). Rama 259 and Rama 521 formed tumors in *nu/nu* mice just as readily as did Rama 25 itself (table 5). Both PGE$_1$ and DMSO failed to reduce the incidence of tumors caused by either variant cell line (table 5). Rama 25 and Rama 259 formed histologically identical tumors in which two structures predominated: circular rings of cells typical of adenocarcinoma and spindle cell regions. Rama 521 formed tumors containing only spindle cells (fig. 3). The few tumors that arose from Rama 25 and those that arose from Rama 259 and Rama 521 that had all been treated with PGE$_1$ were histologically identical to those tumors obtained with untreated cultures. The normal elongated cell converts from Rama 25, including Rama 29, failed to induce tumors in the same period (Rudland PS, Gusterson B, Hughes C, Ormerod EJ, Warburton MJ: Manuscript in preparation).

To exclude the possibility that PGE$_1$ may be selectively

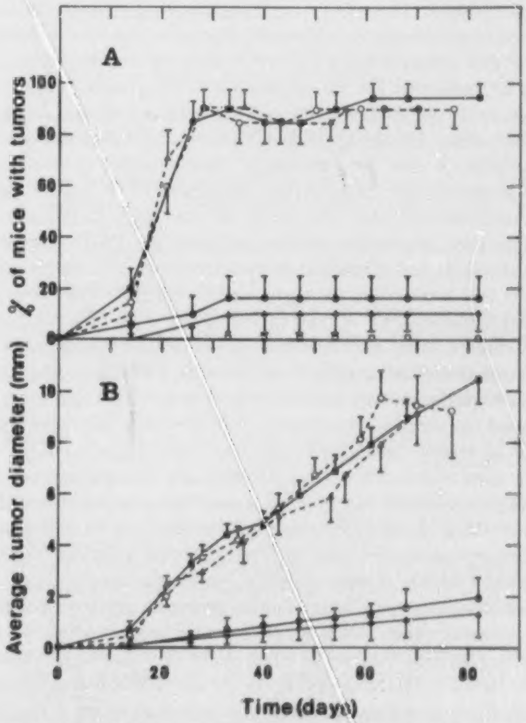

TEXT-FIGURE 4.—Kinetics of tumor formation in *nu/nu* mice. Cultured cells were inoculated into *nu/nu* mice and A) the percentage of mice with a tumor ± SEM and B) the average diameter of the tumor in mm ± SEM were followed with time in days. Cell lines Rama 25 (—, ●, ▲, ■) and Rama 259 (---, ○, △) were grown to confluence according to protocol II; then they were changed to medium containing I, HC, E, or Pr with either 1.8% DMSO (▲, △) or 0.5 μg/ml PGE$_1$ (●, ○) for 2 days before they were inserted into the mice. Rama 25 cultures with hormones but without inducers were also included (■), and injection of PBS alone is also shown (□).

killing Rama 25 but not Rama 259 or Rama 521 cultures, we performed the following controls: 1) The medium containing PGE_1 was removed, and the Rama 25 cell monolayers were washed twice with fresh medium containing serum and hormones; incubation was continued in this medium for a further 2 days until no domes or casein was detectable. When the resultant cells were injected into *nu/nu* mice, 85–95% of the mice developed tumors within 6 weeks. 2) Cell suspensions from PGE_1- and hormone-treated and untreated cultures were analyzed for viable cells by single cell cloning assays in fresh medium. In both treated and untreated cultures removed after extensive (10×) washings, the cloning efficiencies were the same. 3) Time-lapse cinematography of confluent cultures in which individual cells were continuously monitored showed that few cells (<5%) died and detached from the dish during the 48-hour exposure to PGE_1. Upon removal of PGE_1 and its replacement by fresh serum and medium (dedifferentiation), 25–30% of the cells had divided after 48 hours, and most (≥80%) went on to divide over 14 days.

DISCUSSION

The major area in which the effects of the PG on cell proliferation and differentiation have been investigated is in hematopoiesis. However, the PG effects are obscure because the early precursor or stem cells that give rise to the various blood cell lineages have not been isolated and therefore can only be recorded by the appearance of colonies of differentiated cells. In such mixed cell cultures of mouse hematopoietic cells, PG of type E (PGE_1 and PGE_2) are potent inhibitors of the production of neutrophilic granulocytes and mononuclear phagocytes, whereas PG of type F series are stimulatory, and the effect of the type E PG can be reversed by a specific growth factor (*12*). PGE_1, however, also stimulates erythroid colony formation (*12*). With established cell lines of certain precursor cells, the Friend erythroleukemia cells, PGA_1 can induce both their differentiation and reduce their proliferation rates (*19*). Moreover, treatment of these cells with 16,16-dimethyl-PGE_2 methyl ester in vitro before they were injected into DBA/2J mice increased the median survival time of the mice compared with mice in which untreated cells had been injected (*20*). We have now shown that near-physiologic concentrations of a natural hormonal agent, PGE_1, and the mammotropic hormones Pr, E, I, and HC can increase the rate at which a rat mammary stem cell line differentiates to alveolar-like cells in vitro, which makes possible molecular analysis of this differentiation step. There is also a corresponding reduction in the stem cells' DNA synthetic rate and in their tumor-forming abilities in *nu/nu* mice after this differentiation to alveolar-like cells. However, the exact relationship between these three processes is more complicated than if the relationship were simply linear. Tumorigenic cell variants that are resistant to the action of PGE_1 or DMSO in accelerating this differentiation step also show little or no reduction in their DNA synthetic rates or in their incidence of tumors in nude mice. However, the naturally occurring PG are not unique in their ability to stimulate mammary stem cells to differentiate because agents other than the synthetic DMSO behave similarly (*5*).

Whether the PG ever naturally induce differentiation and cause cessation of tumor growth in vivo is unclear. Nevertheless, PG are produced by many diverse cells including those from murine breast (*21*) and human breast (*22, 23*) tumors at concentrations sufficient to elicit the changes reported in our rat mammary system. Thus various PG could possibly influence the progression of a tumor not only by increasing (*24*) or decreasing (*25*) rates of cell replication of the mammary tumor cells themselves (*4*), but the various PG could also promote differentiation of the tumor stem cells to new cell types having an altered neoplastic potential. There is some evidence that PG may be involved in the development of certain animal tumors because the PG synthetase inhibitors aspirin and indomethacin inhibit osteolytic tumor deposits and hypercalcemia in rats with Walker carcinosarcomas (*26*), but in human breast disease there is no evidence that these inhibitors have any anticancer activity (*27*). It is also unlikely that systemic therapy in which more stable analogues of the PG are used would be considered appropriate in the treatment of disseminated breast disease in humans because the wide spectrum of PG activities in various organs and tissues would probably preclude their use. Moreover, our stem cell lines, which can be induced to differentiate, have been obtained from the early carcinogen-induced tumors of the rat, and these tumors pathologically resemble the benign breast lesions in humans rather than the truly malignant ductal adenocarcinomas (*28*). The malignant metastasizing lesions of the human breast usually contain cells with an apparently lower capability to differentiate, as judged from their histologic appearance (Gusterson B, Warburton MJ, Mitchell D, Rudland PS: Manuscript in preparation), and therefore it may be anticipated that the PG would be much less efficient in promoting their differentiation.

The mechanism of action of the PG on Rama 25 stem cells is unclear. Two extremes may be considered. Either the PG behave rather nonspecifically acting as lipophilic agents that are dissolvable to varying degrees in the plasma membrane (*29*) or they act through specific receptors (*30*). Either mechanism may then trigger changes in such phenomena as the plasma membrane enzyme systems, ion fluxes, or cyclic nucleotide concentrations as reported for $PGF_{2\alpha}$ and PGE_1 on cultured Swiss mouse 3T3 cells (*31*). The fact that diverse agents including DMSO in addition to the PG accelerate the rate of differentiation of Rama 25 stem cells without affecting the rate of the DMSO-resistant stem cell line Rama 259 may favor the nonspecific mechanism. However, because the effects of the PG can be achieved with near physiologic concentrations (*11, 32*), the fact that in freshly confluent cultures DMSO and PGE_1 are synergistic in promoting doming (table 2 legend) and the fact that another inducer, retinoic acid, is also synergistic with DMSO (*5*) suggest that the initial interaction of the PG with the cells may be different from the interaction of DMSO and the cells and that the initial reaction is more closely akin to that of the retinoids. Whatever the mechanism, the differentiation of Rama 25 cells is reversible within a few days of the removal of the PG from the culture medium. Thus differentiated Rama 25 cells when injected into nude mice probably fail to establish themselves within this time. If the differentiated Rama 25 cells survive for longer times, then presumably they would revert to the original stem cells and produce tumors at the original frequency.

Although the cause of breast cancer in humans is not known, epidemiologic surveys suggest that the hormone status of the female may influence the likelihood of this disease *(33)*. Among the protective factors are a first full-term pregnancy before 25 years of age and a late menarche. In the rat, the incidence of mammary tumors induced by chemical carcinogens *(34, 35)* can be reduced by previous exposure of the gland to those hormones that induce lobuloalveolar development *(36–38)*. The mammary adenocarcinomas arise predominantly from undifferentiated terminal end buds and terminal ducts of young, virgin rats *(39)*. With the onset of pregnancy and lactation, the terminal end buds and terminal ducts are gradually replaced by more differentiated structures, the alveolar buds and lobules. This developmental change is also accompanied by a reduction in the average proliferation rate of the cells within these structures *(40, 41)*. Of the three ultrastructurally distinct epithelial cell types described by Russo et al. *(42)* in the normal mammary gland, our stem cell line Rama 25 most closely resembles the intermediate type *(3)*. This intermediate type is also the predominant type found in DMBA-induced adenocarcinomas *(43)* and in terminal end buds (Russo J: Personal communication). We have also isolated from normal glands clonal cell lines that are similar to Rama 25 in their capability of converting to droplet and doming cultures with DMSO, PGE$_1$, and the mammotropic hormones *(44)*. Thus the protective effect of the mammotropic hormones and other agents in vivo against carcinogenic attack could be exerted by promoting differentiation of stem cells of the mammary gland into cells with lower proliferation rates. These differentiation-inducing agents could then act either at an early stage, converting normal stem cells to less susceptible differentiated cells, or at a later stage in the carcinogenic process, converting neoplastic stem cells to differentiated cells of lower neoplastic potential. Therefore, it may not be surprising that alterations in the environment of breast tissues that favor differentiation of quickly to slowly proliferating cells also confer a degree of protection against the formation of carcinomas in rats and humans *(33)*.

REFERENCES

(1) Kon SK, Cowie AT. In: Milk: The mammary gland and its secretions, chapt 1. New York: Academic Press, 1961:3–46.

(2) Young S, Hallowes RC. Tumors of the mammary gland. In: Turusov VS, ed. Pathology of tumors in laboratory animals. Vol 1. Tumors of the rat. IARC Sci Publ 1973; 3:31–74.

(3) Bennett DC, Peachey LA, Durbin H, Rudland PS. A possible mammary stem cell line. Cell 1978; 15:283–298.

(4) Rudland PS, Bennett DC, Warburton MJ. Hormonal control of growth and differentiation of cultured mammary gland epithelial cells. In: Sato G, Ross R, eds. Hormones and cell cultures. Cold Spring Harbor conference on cell proliferation. Vol 6. New York: Cold Spring Harbor Laboratory, 1979:677–699.

(5) Rudland PS, Bennett DC, Ritter MA, Newman RA, Warburton MJ. Differentiation of a rat mammary stem cell line in culture. In: Jimenez de Asua L, Levi Montalcini R, Shields R, Iacobelli S, eds. Control mechanisms in animal cells. New York: Raven Press, 1980:341–365.

(6) McGrath CM. Cell organization and responsiveness to hormones in vitro: Genesis of domes on mammary cultures. Am J Zool 1975; 15:231–236.

(7) Friend C, Scher W, Holland JG, Sato T. Hemoglobin synthesis in murine virus-induced leukemic cells in vitro: Stimulation of erythroid differentiation by dimethyl sulfoxide. Proc Natl Acad Sci USA 1971; 68:378–382.

(8) Reuben RC, Wife RL, Breslow R, Rifkind RA, Marks PA. A new group of potent inducers of differentiation in murine erythroleukemic cells. Proc Natl Acad Sci USA 1976; 73:862–866.

(9) Rudland PS, Ormerod EJ, Paterson F. Stem cells in rat mammary development and cancer: A review. J R Soc Med 1980; 73:437–442.

(10) Pharriss BB, Tillson SA, Erickson RR. Prostaglandins and luteal function. Recent Prog Horm Res 1972; 28:51–89.

(11) Lee JB. Prostaglandins and the renal antihypertensive and natriuretic endocrine function. Recent Prog Horm Res 1974; 30:481–532.

(12) Cline MJ, Golde DW. Cellular interactions in haematopoiesis. Nature 1979; 277:177–181.

(13) Axelrod DE, Majumdar SK, Wivell JA, Terry RW. Tumorigenicity of Friend murine erythroleukemia cell lines differing in spontaneous differentiation rates. Int J Cancer 1980; 26:799–804.

(14) Enami J, Nandi S. Hormonal control of milk protein synthesis in cultured mouse mammary explants. Cell Differ 1977; 6:217–227.

(15) Warburton MJ, Head L, Rudland PS. Induction of casein synthesis in a rat mammary tumor epithelial cell line by dimethyl sulfoxide. Biochem Soc Trans 1979; 7:115–116.

(16) Hendrick JC, Franchimont P. Radioimmunoassay of casein in the serum of normal subjects and of patients with various malignancies. Eur J Cancer 1974; 10:725–730.

(17) Rudland PS, Hallowes RC, Durbin H, Lewis D. Mitogenic activity of pituitary hormones on cell cultures of normal and carcinogen-induced tumor epithelium from rat mammary glands. J Cell Biol 1977; 73:561–577.

(18) Davies AJ. Immunodeficient animals. In: Sparrow S, ed. Immunodeficient animals for cancer research. London: Macmillan, 1980:1–4.

(19) Santoro MG, Benedetto A, Jaffe BM. Prostaglandin A$_1$ induces differentiation in Friend erythroleukemic cells. Prostaglandins 1978; 17:719–727.

(20) Santoro MG, Jaffe BM. Inhibition of Friend erythroleukaemia-cell tumours in vivo by a synthetic analogue of prostaglandin E$_2$. Br J Cancer 1979; 39:408–413.

(21) Tan WC, Privett OS, Goldyne ME. Studies of prostaglandins in rat mammary tumors induced by 7,12-dimethylbenz(*a*)anthracene. Cancer Res 1974; 34:3229–3231.

(22) Dowsett M, Easty GC, Powles TJ, Easty DM, Neville AM. Human breast tumor-induced osteolysis and prostaglandins. Prostaglandins 1976; 11:447–460.

(23) Bennett A, Charlier EM, McDonald AM, Simpson JS, Stamford IF. Bone destruction by breast tumors. Prostaglandins 1976; 11:461–463.

(24) Jimenez de Asua L, Clingan D, Rudland PS. Initiation of cell proliferation in cultured mouse fibroblasts by prostaglandin F$_{2\alpha}$. Proc Natl Acad Sci USA 1975; 72:2724–2728.

(25) Otten J, Johnson GS, Pastan I. Regulation of cell growth by cyclic adenosine 3′,5′-monophosphate. J Biol Chem 1972; 247:7082–7087.

(26) Powles TJ, Clark SA, Easty DM, Easty GC, Neville AM. The inhibition by aspirin and indomethacin of osteolytic tumour deposits and hypercalcaemia in rats with Walker tumour and its possible application to human breast cancer. Br J Cancer 1973; 28:316–321.

(27) Powles TJ. PG synthetase inhibitors in patients with cancer. In: Ramwell P, ed. Prostaglandins and related lipids. Vol I. Prostaglandin synthetase inhibitors. New York: Liss, 1980:183–186.

(28) Williams JC, Gusterson B, Humphreys J, et al. *N*-Methyl-*N*-nitrosourea-induced rat mammary tumors. Hormone responsiveness but lack of spontaneous metastasis. JNCI 1981; 66:147–155.

(29) Clark GD, Ryan PJ. Tranquillizers can block mitogenesis in 3T3 cells and induce differentiation in Friend cells. Nature 1980; 287:160–161.

(30) Kuehl FA, Humes JL. Direct evidence for a prostaglandin receptor and its applications to prostaglandin measurements. Proc Natl

Acad Sci USA 1972; 69:480–484.

(*31*) Rudland PS, Jimenez de Asua L. Action of growth factors in the cell cycle. Biochim Biophys Acta 1979; 560:91–133.

(*32*) Samuelson B. Prostaglandins and thromboxanes. Recent Prog Horm Res 1978; 34:239–258.

(*33*) MacMahon B, Cole P, Brown J. Etiology of human breast cancer: A review. J Natl Cancer Inst 1973; 50:21–42.

(*34*) Huggins C, Grand LC, Brillantes FP. Mammary cancer induced by a single feeding of polynuclear hydrocarbons and its suppression. Nature 1961; 189:204–207.

(*35*) Dao TL. Mammary cancer induction by 7,12-dimethylbenz[*a*]anthracene: Relation to age. Science 1969; 165:810–811.

(*36*) Dao TL, Bock FG, Greiner MJ. Mammary carcinogenesis by 3-methylcholanthrene. II. Inhibitory effect of pregnancy and lactation on tumor induction. J Natl Cancer Inst 1960; 25:991–1003.

(*37*) Welsch CW, Clemens JA, Meites J. Effects of multiple pituitary homografts or progesterone on 7,12-dimethylbenz[*a*]anthracene-induced mammary tumors in rats. J Natl Cancer Inst 1968; 41:465–471.

(*38*) Moon RC. Relationship between previous reproductive history and chemically induced mammary cancer in rats. Int J Cancer 1969; 4:312–317.

(*39*) Russo J, Saby J, Isenberg WM, Russo IH. Pathogenesis of mammary carcinomas induced in rats by 7,12-dimethylbenz[*a*]anthracene. J Natl Cancer Inst 1977; 59:435–445.

(*40*) Russo J, Russo IH. Influence of differentiation and cell kinetics on the susceptibility of the rat mammary gland to carcinogenesis. Cancer Res 1980; 40:2677–2687.

(*41*) Sinha DK, Pazik JE. Tumorigenesis of mammary gland by 7,12-dimethylbenz[*a*]anthracene during pregnancy: Relationship with DNA synthesis. Int J Cancer 1981; 27:807–810.

(*42*) Russo IH, Ireland M, Isenberg W, Russo J. Ultrastructural description of three different epithelial cell types in rat mammary gland. Proc Annu Meet Electron Microsc Soc Am 1976; 34:146–147.

(*43*) Russo J, Isenberg W, Ireland M, Russo IH. Ultrastructural changes in the mammary epithelial cell population during neoplastic development induced by chemical carcinogen. Proc Annu Meet Electron Microsc Soc Am 1976; 34:250–251.

(*44*) Rudland PS, Bennett DC, Warburton MJ. Growth and differentiation of cultured rat mammary epithelial cells. In: Iacobelli S, King RJ, Lindler HR, Lippman ME, eds. Hormones and cancer. New York: Raven Press, 1980:255–269.

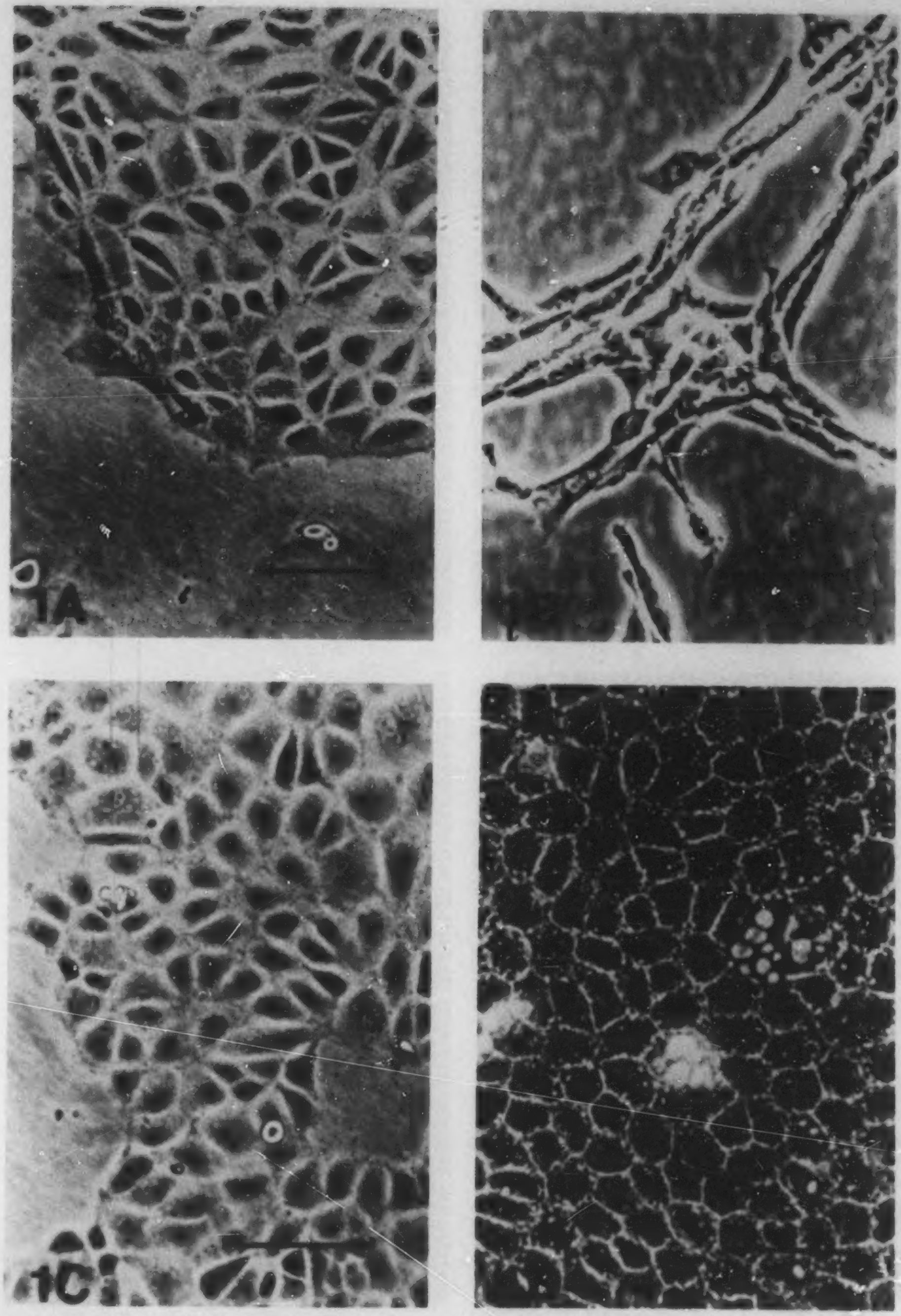

FIGURE 1.—A) Growing colony of Rama 25 cuboidal cells. *Bar*=100 μm. × 165. B) Crisscross elongated cells cloned from Rama 29, Rama 521. *Bar*=50 μm. × 380. C) DMSO-resistant clone of Rama 25, Rama 259. *Bar*=100 μm. × 195. D) Confluent culture of Rama 25-Cl.37 treated for 2 days with DMSO and hormones and showing droplet cells. *Bar*=50 μm. × 380. Living cultures were photographed with phase-contrast optics.

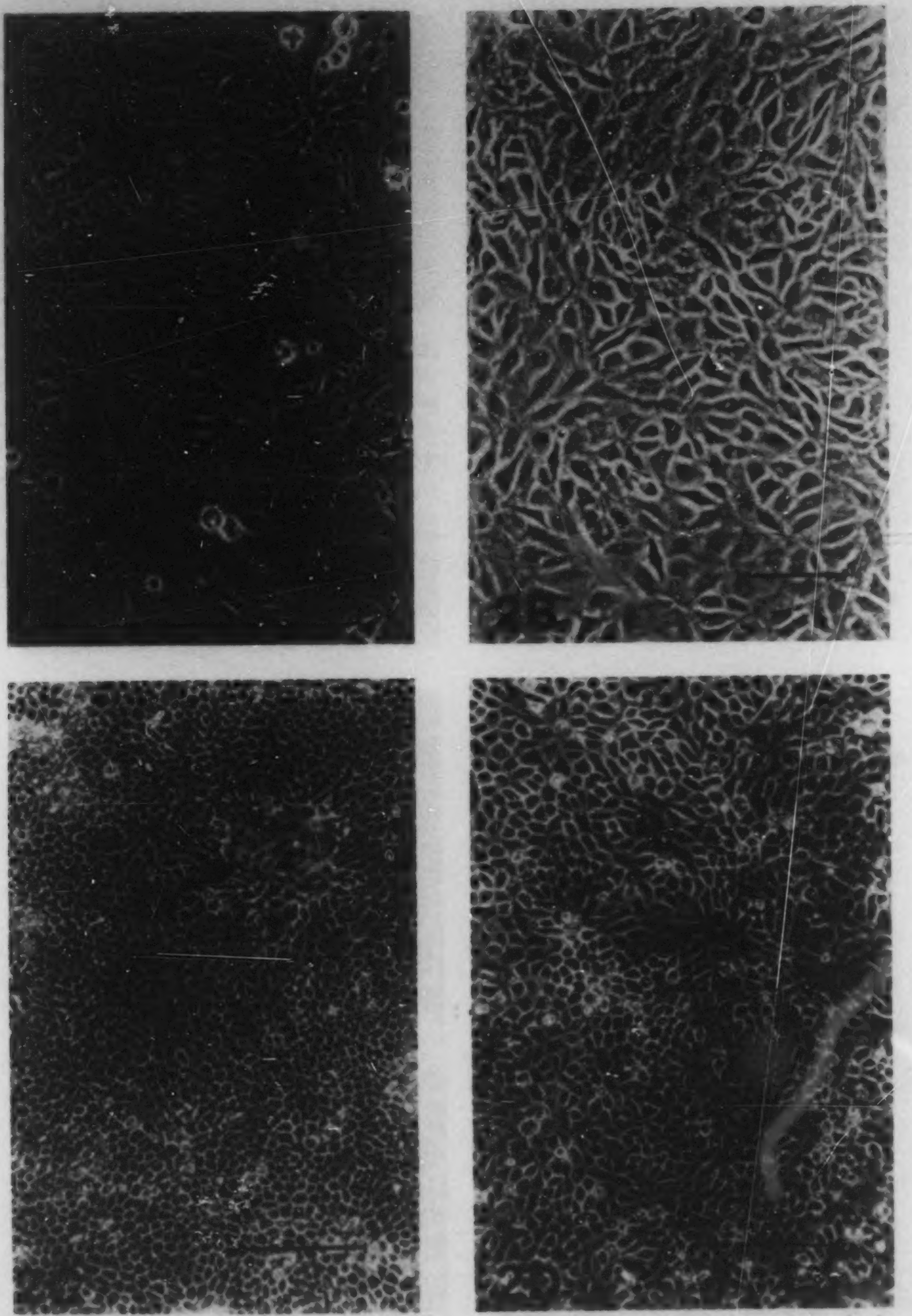

FIGURE 2.--A) Confluent culture of cuboidal Rama 25 cells treated with hormones but not with PGE_1 for 2 days. *Bar*=100 µm. × 140. B) Confluent culture of crisscross elongated Rama 521 cells treated with hormones and 0.5 µg PGE_1/ml for 2 days. *Bar*=100 µm. × 160. C) Confluent culture of Rama 25 cells treated for 2 days with hormones and PGE_1 and showing droplet cells and a dome (D). *Bar*=200 µm. × 95. D) Confluent culture of Rama 259 cells treated for 2 days with hormones and PGE_1. *Bar*=200 µm. × 95. Living cells were photographed with phase-contrast optics.

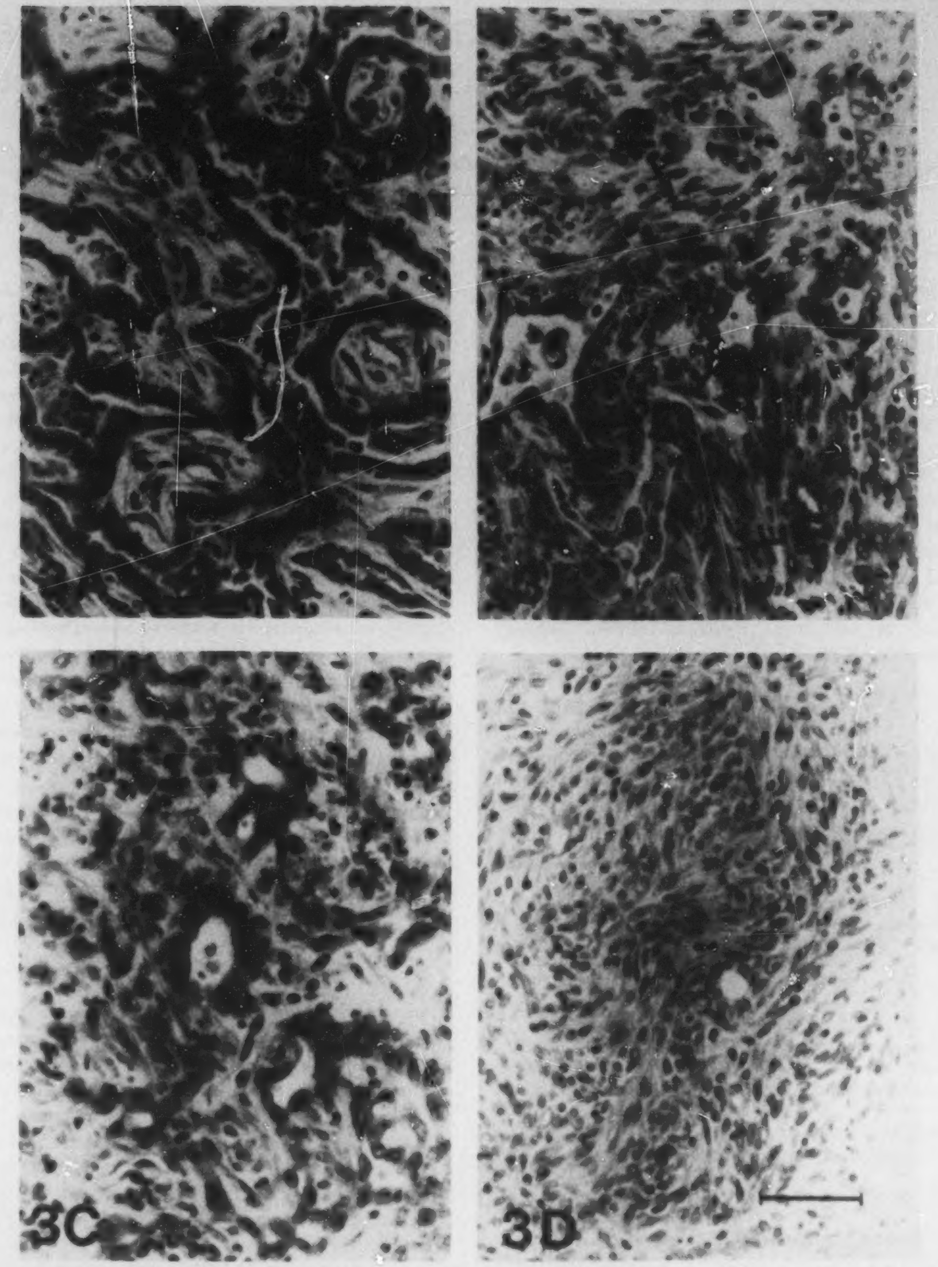

FIGURE 3.—Tumors were caused in 6 wk in *nu/nu* mice by the injection of confluent rat mammary cultures of the following cell lines: A and B, Rama 25; C, Rama 259; and D, Rama 521. Most tumors formed from Rama 25 and Rama 259 were of mixed cell types, as in B), comprising both circular arrays of cuboidal cells (C) and elongated cells (E). H & E. *Bars*=50 μm. × 300.

blank page

Immunotherapy by Intralesional Injection of BCG Cell Walls or Live BCG in Bovine Ocular Squamous Cell Carcinoma: A Preliminary Report[1,2]

Wim R. Klein,[3] **E. Joost Ruitenberg,**[4] **Peter A. Steerenberg,**[4,5] **Wim H. de Jong,**[4,6] **Wim Kruizinga,**[4] **Wim Misdorp,**[7] **Jürgen Bier,**[8] **Rudy H. Tiesjema,**[9] **Johan G. Kreeftenberg,**[10] **Jacob S. Teppema,**[4] *and* **Herbert J. Rapp**[11,12,13]

ABSTRACT—Cows of the Dutch Frisian and Maas-Rijn-IJssel breed with histologically confirmed ocular squamous cell carcinoma showed complete regression of the primary tumor in 70 or 60% of the cases after intralesional injection of a BCG cell wall or live BCG vaccine, respectively. Recurrence of the tumor was observed in 57% of the animals treated with BCG cell walls and in 25% of the animals treated with live BCG vaccine. Spontaneous regression was seen in 20% of the untreated cows. In a second control group, radical surgery, the most successful treatment for primary stage I tumors in humans, resulted in a 90% cure. Influence of immunotherapy on metastases could not yet be fully evaluated. White blood cell counts were not changed after therapy. It was not possible to link a favorable response to BCG therapy with the intensity of the delayed type hypersensitivity (DTH) reaction to purified protein derivative of mycobacteriae (PPD) or the formation of antibodies to BCG as determined by a micro-enzyme-linked immunosorbent assay. However, in animals that showed tumor regression, the DTH reaction to PPD had a tendency to persist for a longer period of time. It was concluded that 1) block resection was the best method of treatment for this tumor, 2) a single intralesional injection of a BCG cell wall vaccine was as effective as live BCG vaccine in the induction of complete regression of the primary tumor, 3) in this preliminary study BCG cell wall vaccine was less effective than live BCG vaccine in the prevention of recurrence, and 4) this naturally occurring tumor model is well suited for the study of the influence of BCG immunotherapy in a primary stage I tumor.—JNCI 1982; 69: 1095–1103.

BCG immunotherapy by intralesional injection has been shown to be successful in various chemically induced tumors in laboratory animals (*1–3*) as well as in naturally occurring tumors, such as canine venereal tumors (*4*), eye carcinomas in cattle (*5–7*), and sarcoids in horses (*8*).

Intralesional immunotherapy with BCG is based mainly on the results of studies in a syngeneic guinea pig model in which a 7-day-old intradermally growing hepatocellular carcinoma can be cured and micrometastases are eliminated (*9*). The regression of the primary tumor is followed by induction of specific immunity (*10*). In this model similar results were obtained with both live BCG (*1, 9*) and a non-living BCG cell wall preparation emulsified in mineral oil (*11*).

In studies with naturally occurring bovine ocular squamous cell carcinoma stage I, intralesional therapy with BCG cell walls also induces tumor regression in significant numbers of animals (*5–7*). Bovine ocular squamous cell carcinoma might be considered a relevant analogue for human carcinoma. The similarities observed for this type of human and bovine tumors are local destructive growth with bone involvement, which is seldom found in experimentally induced tumors, and spread of tumor cells into the draining lymph nodes, which in the advanced stage leads to generalized metastases preferentially in the lungs (*12*). Before the application of intralesional immunotherapy in human patients whose disease has not exceeded clinical stage I, further confirmation of the results with the bovine "cancer eye" could be of great importance.

In the present trial a comparison was made between immunotherapies with BCG cell walls and live BCG. The effect of immunotherapy was compared to an untreated control group and to a group that underwent radical surgery that is similar to the clinical situation in humans. During this trial the WBC counts, DTH reactions to PPD and to *Candida albicans* antigen, and the antibody production against BCG measured with ELISA were studied.

MATERIALS AND METHODS

Animals.—Fifty tumor-bearing cows of the Dutch Frisian and Maas-Rijn-IJssel dairy breed, 4–13 years of age, 400–600 kg body weight, were purchased during 3 years from farmers all over The Netherlands. During the experiment

---

ABBREVIATIONS USED: CP=culturable particle(s); DTH=delayed-type hypersensitivity; ELISA=enzyme-linked immunosorbent assay; PPD=purified protein derivative of mycobacteria; WBC=white blood cell(s).

---

[1] Received December 10, 1981, accepted April 16, 1982.

[2] Animals were maintained under the guidelines set forth by the Faculty of Veterinary Medicine, State University, Utrecht, The Netherlands.

[3] Institute for Veterinary Surgery, State University, Yalelaan 12 3584 CM Utrecht, The Netherlands.

[4] Laboratory of Pathology, National Institute of Public Health (NIPH), P.O. Box 1, 3720 BA Bilthoven, The Netherlands.

[5] *Address reprint requests to* Dr. Steerenberg.

[6] Grant recipient of the Koningin Wilhelmina Fonds (Netherlands Cancer Foundation).

[7] Laboratory of Pathology, Netherlands Cancer Institute, Amsterdam, The Netherlands.

[8] Free University of Berlin, Steglitz Clinic, Berlin, Federal Republic of Germany.

[9] Vaccine Department, NIPH, Bilthoven.

[10] Laboratory for the Control of Bacterial Vaccines, NIPH, Bilthoven.

[11] Laboratory of Immunobiology, Division of Cancer Biology and Diagnosis, National Cancer Institute, National Institutes of Health, Public Health Service, U.S. Department of Health and Human Services, Bethesda, Md. 20505.

[12] Deceased September 25, 1981.

[13] We thank Dr. J. S. M. M. van Dieten for conducting the anesthesia during surgery, Mr. F. A. Blok for photography of the tumors, Ms. M. I. J. A. Polak and Mr. J. Bolhuis for the white blood cell differentiation, and Mr. P. S. Ursem and Mr. H. Ettekoven for their excellent technical assistance.

the pregnant cows calved, lactated 8–10 months, and were not newly inseminated. Food was composed of grass, hay, and fattening fodder. Only animals in good physical health with tumor sizes between 1×1 and 3×4 cm were accepted. Animals with a positive Mantoux reaction to PPD and those suspected of metastases after palpation of the regional lymph nodes were not accepted in the trial.

Tumors.—The biology of the disease in Dutch dairy cattle is described elsewhere (*13*). The incidence of ocular squamous cell carcinoma in Dutch cattle is approximately 0.04% (own observations based on 35,000 examined animals), which is much lower than the incidence reported for the Hereford breed in various geographic areas (*12, 14–17*). For histologic confirmation of the carcinoma diagnosis, biopsy specimens were taken from the base of the tumor, fixed in 10% buffered Formalin, and embedded in Paraplast, and 5-μm sections were stained with hematoxylin and eosin. Biopsies and intralesional injections were performed under local anesthesia with 2% lidocaine. Forty-eight tumors were located on the membrana nictitans and 2 on the bulbus oculi. Not one of the membrane nictitans of the affected eyes of the 50 cows was pigmented.

BCG preparations.—The BCG cell wall preparation (lot #236) was obtained from the National Cancer Institute, Bethesda, Md. The final preparation contained 3 mg BCG cell walls/ml, 3% mineral oil (Drakeol 6VR), and 0.2% Tween-80 in physiologic saline solution and was emulsified by ultrasound. BCG lots #048 and #060 were produced in the National Institute of Public Health, Bilthoven, The Netherlands, as concentrated preparations, especially intended for experimental immunotherapy. The bacteria were grown in homogeneous culture under continuous stirring in Ungar medium with 0.05% Tween-80, harvested by centrifugation, resuspended in a stabilizing medium (containing 83 g Haemaccel/liter, 50 g D-glucose/liter, and 50 mg Tween-80/liter), filled in 2-ml portions, and lyophilized (*18*). One vial of BCG lot #048 contained 160×10^6 CP in 0.2 mg dry weight (800×10^6 CP/mg), and one vial in lot #060 contained 36×10^6 CP in 0.3 mg dry weight (120×10^6 CP/mg). Each vial was resuspended in 2 ml physiologic saline solution shortly before use. Depending on the size of the tumor, 2–8 ml vaccine was injected so the whole tumor would be saturated with vaccine.

Experimental design.—All accepted cows were randomly divided into 5 groups of 10 animals each: group 1, no treatment; group 2, intralesional application of BCG cell walls; group 3, intralesional application of live BCG 048; group 4, intralesional application of live BCG 060; group 5, radical surgery, i.e., extirpation of the primary tumor (enucleatio bulbi et adnexa), the subparotoid lymph node, the parotid gland, and the retropharyngeal lymph node (*19*).

Tumor measurements and photography were done before the animals entered the trial, then 1 week later, then monthly during the first 6 months, and then every 3 months for the next 1.5 years. Tumor size was expressed as the product of two perpendicular measurements.

Blood was collected before treatment, and at 1, 3, 6, 12, 18, and 24 months after treatment for WBC differentiation. Sera for measurement of antibodies to BCG were stored at −20°C.

The presence of DTH reactions was tested before treatment, and at 3, 6, 12, 18, and 24 months after treatment by intradermal injection of 1.0 mg PPD (Centraal Diergeneeskundig Instituut, Rotterdam, The Netherlands) in 0.1 ml phosphate-buffered saline, and 0.9 mg *Candida albicans* antigen in 0.1 ml phosphate-buffered saline. Skin swelling was measured at 20 minutes and at 72 hours.

To determine the production of antibodies to BCG, investigators developed a micro-ELISA (*20, 21*). In this assay, which will be reported in detail elsewhere (Klein WR et al.: Manuscript in preparation), twofold serum dilutions were incubated in microtiter plates coated with PPD antigen. To determine the antigen-antibody complex, we used rabbit antibovine IgG conjugated with horse-radish peroxidase, which was visualized after oxidation of 5-aminosalicylic acid and H_2O_2. We measured the reaction product with a multichannel spectrophotometer at 449 nm; the product was expressed as the extinction value. All serum samples taken at various time intervals were investigated on the same day. An animal was considered to react positively when the extinction value increased during the first 3 months by at least 0.200 in comparison with the pretreatment value at a serum dilution of 1:16.

During the experiment animals were under regular clinical observation. Animals were killed when the tumor showed progressive growth (exceeding ≈7×7 cm) or after 2 years of observation. Besides gross examination, draining lymph nodes, lungs, spleen, and liver were examined microscopically for the presence of metastases.

RESULTS

Effect of Treatment on Tumors

In the untreated group, 2 of 10 animals showed spontaneous regression of the primary tumor 1–6 months after randomization. Autopsies were performed on 9 animals: Four showed metastases in the regional lymph nodes, and 2 of these had metastases in the lungs.

Seven of the 10 cows treated by intralesional injection of BCG cell walls showed complete regression of the primary tumor between 2 and 7 months. In 4 of these animals the tumor recurred 1–13 months after regression. Autopsies on 10 animals revealed that 3 had metastases in the regional lymph nodes, and 2 of these 3 animals also had metastases in the lungs. Thus 30% of the animals treated with BCG cell walls were clinically and histologically tumor-free after the 2-year observation period (text-figs. 1, 2; table 1).

For the evaluation of the results with live BCG, the groups treated with BCG 048 and BCG 060 were pooled. Complete regression of the primary tumor was seen in 11 of 20 animals between 2 and 8 months; regression occurred in 1 at approximately 20 months. In 3 of these 12 animals the tumor recurred 4–16 months after regression. Autopsy was performed on 9 animals: 5 (55%) were clinically and histologically tumor-free. One of the 4 tumor-bearing animals (cow 142) showed metastases in the regional lymph node (text-fig. 1).

After radical surgery in 1 animal a tumor developed at the site of the subparotid lymph node. The animal was

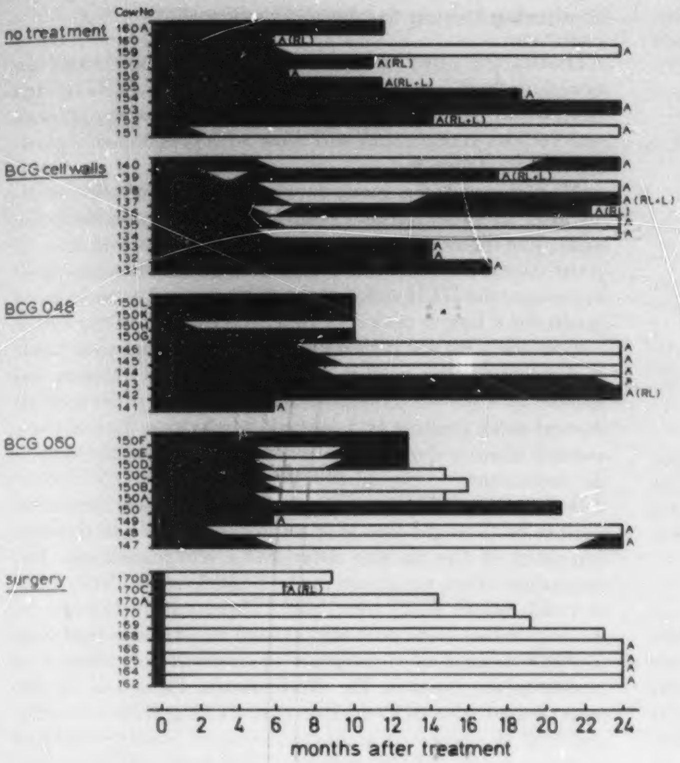

TEXT-FIGURE 1.—Preliminary results of BCG immunotherapy on bovine ocular squamous cell carcinoma compared to radical surgery. ▬, tumor present; A, autopsy; RL, metastases in regional lymph node; L, metastases in lungs.

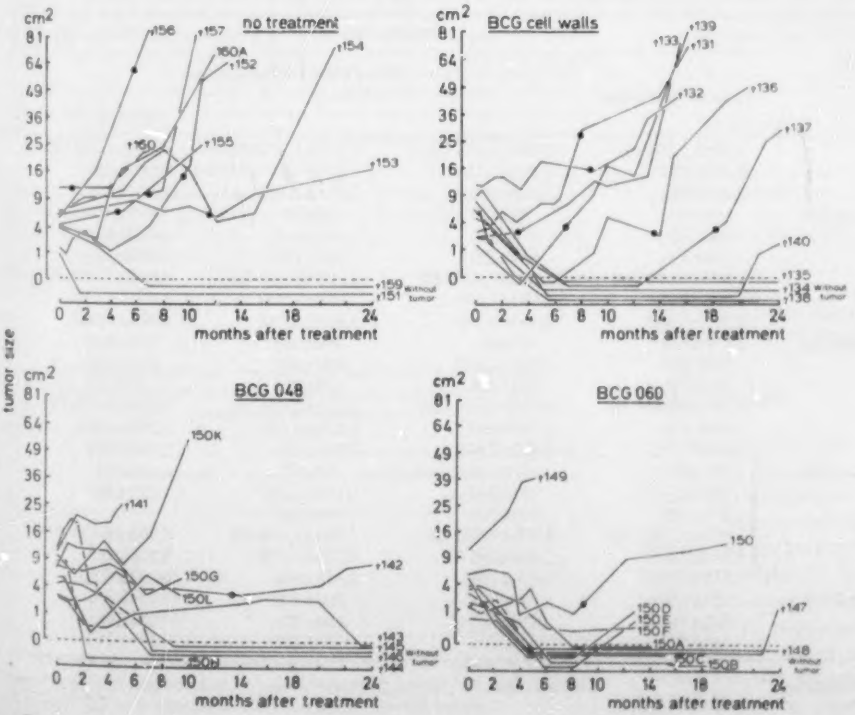

TEXT-FIGURE 2.—Effect of intralesional BCG immunotherapy on growth of bovine ocular squamous cell carcinoma. *Ordinates* represent tumor sizes that are the products of 2 perpendicular measurements. ●, onset of lymph node enlargement; †, autopsy.

TABLE 1.—*Summary of clinical outcome of intralesional BCG immunotherapy in cattle with ocular squamous cell carcinoma*

Treatment	Regression of primary tumor[a]	Recurrence[b]	Intercurrently killed animals[c]	Metastases at autopsy[d]
BCG cell walls	7/10	4/7	5/10	3/10
BCG 048 + BCG 060	12/20	3/12	2/20	1/9
Surgery	—	0/10	1/10	1/5
Control	2/10	0/2	6/10	4/9

[a] No. of animals with tumor regression/No. of animals >3 mo in trial.

[b] No. of animals with tumor recurrence/No. of animals with previous tumor regression.

[c] No. of animals intercurrently killed/No. of animals >3 mo in trial.

[d] No. of animals with histologically confirmed metastases (regional lymph node and/or lungs)/No. of animals killed intercurrently or after 2 yr in trial.

killed at 7 months because of the growing tumor. Four animals killed at 24 months were free of metastases. The other 5 cows that underwent surgery are in good health and are clinically tumor-free.

Reactions After Injection of BCG Vaccines

During the 2–4 days after intralesional injection of BCG cell walls or live BCG, we observed a swelling of the tumor in all the animals. As shown in figure 2, in some animals enlargement of the tumor was observed before regression started. Ulceration was not more severe than it was before injection or in untreated animals. We have not seen clinical signs of discomfort or temperature elevations after injection of the BCG vaccines.

Monitoring During the Experiment

During the observation period no differences were observed in WBC counts between either the BCG-treated groups and the control group (table 2) or between animals with tumors in regression and those with progressively growing tumors (table 3).

All BCG-treated animals developed a palpable skin swelling after tuberculination except 1 animal treated with live BCG. The diameters of the skin reactions measured after 72 hours varied between 1 and 20 mm. In animals with tumor regression, the DTH reactions to PPD showed a tendency to persist for a longer period of time. Recurrence of the tumor had no effect on the persistence of the DTH reaction (table 4). *Candida albicans,* used in humans as a recall antigen, was applied as a non-BCG-related antigen. Seven of 50 animals showed weak positive (<5 mm) skin reactions. Five of these animals already showed positive reactions before the start of the experiment.

Besides the DTH reaction to PPD, antibody formation against BCG might also give an impression of the immune reactivity of the patient after BCG administration. The extinction values measured in the ELISA ranged from 0.200 to 1.000 before BCG treatment. These relatively high extinction values were probably caused by previous injections of PPD as part of a program to monitor the absence of bovine tuberculosis in The Netherlands. Fifteen of 24 animals treated with BCG antigen (live BCG or BCG cell walls) and 2 of 19 untreated animals developed positive reactions as shown by the ELISA (table 5). No correlation was found between tumor regression and the presence of BCG antibodies (table 6).

TABLE 2.—*Differential WBC counts after intralesional BCG immunotherapy in cattle with ocular squamous cell carcinoma*

Treatment	Cell type	Leukocyte count[a,b]			
		Prior to treatment	Time after treatment, mo		
			1	3	6
No treatment	Total leukocytes	6,050±1,850 (9)	6,625±2,425 (9)	7,175±1,300 (8)	6,050±1,475 (6)
	Lymphocytes	2,500±775	3,250±1,150	2,875±800	2,850±525
	Neutrophils	2,450±850	2,250±800	2,975±1,100	1,975±775
	Nonsegmented neutrophils	100±100	70±130	80±90	480±920
	Eosinophils	800±510	870±740	1,000±510	470±250
	Monocytes	150±205	190±220	220±150	270±350
BCG cell walls	Total leukocytes	7,075±1,675 (10)	8,400±2,875 (10)	9,225±4,400 (4)	6,025±2,025 (9)
	Lymphocytes	2,42[illegible]0	3,400±1,100	3,900±1,300	2,775±1,150
	Neutrophils	3,350±1,300	3,050±1,125	3,850±2,725	2,075±1,000
	Nonsegmented neutrophils	170±150	60±80	360±680	210±280
	Eosinophils	820±385	1,485±1,570	930±430	850±585
	Monocytes	330±220	400±330	170±210	110±180
BCG 048	Total leukocytes	5,750±1,450 (10)	6,700±2,925 (10)	7,375±2,625 (8)	8,350±5,575 (2)
	Lymphocytes	2,450±550	2,725±950	3,350±1,700	5,700±4,650
	Neutrophils	2,300±1,025	2,825±2,000	2,350±525	2,025±250
	Nonsegmented neutrophils	60±60	110±140	50±80	70±90
	Eosinophils	750±525	680±630	1,165±1,235	620±690
	Monocytes	260±190	340±210	240±200	0
BCG 060	Total leukocytes	7,900±3,300 (10)	6,900±1,675 (9)	7,300±1,875 (6)	6,450±1,400 (10)
	Lymphocytes	3,550±1,600	2,950±950	3,725±1,275	2,475±725
	Neutrophils	3,175±1,400	2,675±950	2,825±800	2,825±1,225
	Nonsegmented neutrophils	90±120	60±40	220±400	130±190
	Eosinophils	835±740	690±585	580±305	760±485
	Monocytes	440±500	230±280	110±130	170±210

[a] Mean ± SD of No. of animals noted *in parentheses.*

[b] $\times 10^6$/liter.

TABLE 3.—*Differential WBC counts in relation to tumor regression after intralesional BCG immunotherapy in cattle with ocular squamous cell carcinoma*

Treatment	Cell type	Regression of primary tumor	WBC count[a,b]			
			Prior to treatment	Time after treatment, mo		
				1	3	6
BCG cell walls	Total leukocytes	+	6,700±1,200 (6)	7,900±2,300 (6)	6,050±210 (2)	6,200±1,730 (5)
		−	7,800±2,750 (3)	9,450±4,650 (3)	12,400±4,250 (2)	5,900±3,200 (3)
	Lymphocytes	+	2,170±325	3,460±1,180	2,940±150	2,890±760
		−	2,800±1,450	3,150±1,350	4,900±1,150	2,650±2,000
	Neutrophils	+	3,300±1,320	2,780±1,110	1,940±320	2,060±1,100
		−	3,550±1,770	3,650±1,390	5,800±2,700	1,950±1,220
	Nonsegmented neutrophils	+	240±160	80±95	30±40	310±340
		−	35±60	45±80	690±980	110±120
	Eosinophils	+	690±420	1,060±755	880±75	860±510
		−	1,100±220	2,600±2,600	980±740	1,040±790
	Monocytes	+	290±190	540±200	270±290	100±220
		−	310±265	0	70±110	160±140
Live BCG (048+060)	Total leukocytes	+	5,720±1,100 (5)	6,750±510 (4)	7,400±2,425 (4)	6,200±1,800 (5)
		−	8,000±4,500 (5)	6,700±2,300 (5)	7,100±400 (3)	7,200±1,200 (3)
	Lymphocytes	+	2,550±475	3,100±210	3,920±1,600	2,740±990
		−	3,550±1,950	3,100±1,450	2,780±910	2,200±250
	Neutrophils	+	2,300±800	2,650±870	2,730±990	2,500±1,080
		−	3,150±2,000	2,600±1,175	2,625±220	3,550±1,700
	Nonsegmented neutrophils	+	120±150	75±15	80±160	25±60
		−	90±90	55±60	330±575	295±215
	Eosinophils	+	410±320	580±360	530±270	710±350
		−	900±920	760±590	1,180±620	710±550
	Monocytes	+	385±240	400±325	160±130	195±270
		−	320±235	450±140	20±40	130±220

[a] Mean ± SD of No. of animals noted *in parentheses*.
[b] $\times 10^6$/liter.

TABLE 4.—*DTH reactions to tuberculin (PPD) after intralesional BCG immunotherapy in cattle with ocular squamous cell carcinoma*

Response to treatment	No. of animals with positive DTH reactions/No. of animals tested					
	Prior to treatment	Time after treatment, mo				
		3	6	12	18	24
No regression	6/11	8/9	7/7	2/6	2/5	0/1
Regression with subsequent recurrence	0/7	2/2	2/2	4/6	3/3	3/3
Regression	0/12	5/5	7/7	9/10	2/3	7/8

TABLE 5.—*Antibody response (measured in ELISA) after intralesional BCG immunotherapy in cattle with ocular squamous cell carcinoma*

Treatment	No. of animals with anti-BCG antibodies/No. of animals tested[a]
None	0/10
Surgery	2/9
BCG cell walls	5/10
BCG 048	4/6
BCG 060	6/8

[a] An animal was considered to react positively when at a serum dilution of 1:16 the extinction value increased during the first 3 mo by at least 0.200 in comparison with the pretreatment value.

TABLE 6.—*Antibody response in relation to tumor regression after intralesional BCG immunotherapy in cattle with ocular squamous cell carcinoma*

Treatment	Response to treatment	No. of animals tested	No. of animals with BCG antibodies[a]
BCG cell walls	Regression	7	4
	No regression	3	1
BCG 048 + BCG 060	Regression	9	5
	No regression	5	4

[a] An animal was considered to react positively when at a serum dilution of 1:16 the extinction value increased during the first 3 mo by at least 0.200 in comparison with the pretreatment value.

DISCUSSION

The incidence and localization of ocular squamous cell carcinoma (cancer eye) in Dutch cattle differ from those found in Hereford cattle from various geographic areas (*12, 14-17*). We found that the great majority of tumors were located on the membrana nictitans. Furthermore, the membrana nictitans of the affected eyes of all 50 cows in this trial were nonpigmented. Anderson et al. (*22, 23*) found that lack of pigmentation is a contributing factor in the development of eye carcinoma. The validity of this observation for the Dutch cattle will be further explored and included in the final evaluation of our experiment. No evidence was found that cancer eye occurred more frequently in one geographic area of The Netherlands than in another.

It was clearly shown for this tumor that (radical) surgery is the best method of treatment. In veterinary practice surgical treatment of this tumor is limited to the extirpation of the membrana nictitans or to enucleatio bulbi et adnexa. In this study, radical surgery was chosen *a*) to compare immunotherapy with the best possible surgical method of treatment and *b*) because radical surgery is the therapy of choice in humans. At this time it is not yet possible to evaluate the influence of surgery on metastasis.

Tumor sizes, ranging from 1 to 14 cm^2, had no correlation with the response to treatment. This observation was probably due to the dosage of vaccine used in this experiment; i.e., each tumor was saturated with vaccine. Furthermore, complete regression was obtained in 60–70% of the animals after one single intratumoral vaccine injection, regardless which of the vaccines was used. This fact is in keeping with the guinea pig model (*1, 9, 11*) in which similar results were obtained with the use of either vaccine.

With regard to recurrence rate, we found a difference between the animals treated with the live BCG vaccine (3/12) and the BCG cell wall vaccine (4/7). This difference could not be found in the guinea pig model, because in guinea pigs recurrences are prevented by the induction of a specific antitumor immunity. Recurrences in the live BCG-treated animals occurred only in those treated with BCG 060, which could be attributed to the lower number of CP administered. The maximum dose based on the number of CP for BCG 060 was approximately equal to the number of CP in the lowest dose for BCG 048. However, no differences were present between the two batches when dosage was expressed in milligrams. Another explanation for the difference in recurrence rates could be the higher rate of dead versus live bacteria in the BCG 060 batch that might interfere with the BCG adjuvant activity (*24, 25*). Whether this is also true for the induction of tumor immunity is not yet known.

In general, if an animal was responding to the BCG immunotherapy, complete tumor regression occurred during the 2d to 7th month. Thus a time limit might be set for response to treatment, after which repeated injections might be considered as it was reported for sarcoids in horses (*8*). This consideration is also applicable to the animals that show tumor recurrence. In the guinea pig model nonspecific stimulation by intralesional BCG injection induced specific immunity toward the tumor (*10*). Since tumor recurrence is not expected in immune animals, the relatively high recurrence rate in our cow study is probably due to the lack of a sufficient degree of specific immunity after regression of the primary tumor. When complete tumor regression occurs, tumor antigenic material becomes available for immunologic triggering. However, in some cases immunity is not induced as indicated by recurrence of the tumor. Presumably the adjuvant activity of a single intralesional BCG injection was not strong enough to induce specific immunity. Therefore, the effect of repeated BCG injections will be studied in a follow-up trial with regard to the induction of specific immunity.

From the spontaneous regression observed in 2 untreated animals, it seems likely that the bovine cancer eye has immunogenic properties that might be partially responsible for the relatively high response rate of 60–70% after BCG treatment. Also, the observed tumor regression obtained after a single im injection of a saline-phenol tumor extract (*28*) indicates immunogenicity and even the existence of common antigens for the bovine cancer eye (*26–29*).

In nonresponding animals (8/20 treated with live BCG and 3/10 treated with BCG cell walls) no indications were found for tumor growth enhancement; none of the tumors grew more rapidly than those of the control group (text-fig. 2).

Contradictory results were reported with regard to the correlation between Mantoux conversion and tumor regression (*30–32*). In our experiment DTH reactions to PPD could not be used as a prognostic value since all BCG-treated animals, except 1, showed a conversion. However, reactions to PPD showed a tendency to persist for a longer period of time in animals with a favorable response to immunotherapy. This might suggest that these animals were more immunocompetent at the time of therapy. With regard to *C. albicans*, our results clearly show that this antigen cannot be used as "recall" antigen in cows.

With regard to the results obtained in the ELISA, it should be kept in mind that besides a cellular reaction to PPD, the induction of antibodies as a reaction to PPD administration is also possible (*33*).

Block resection was found to be the best method of treatment for this tumor. However, our preliminary data show that the cow model is also suited for the study of the effect of BCG immunotherapy on a primary stage I tumor. Therefore, studies in the cow model might be used as a guide for the application of BCG immunotherapy in primary tumors in humans. We shall examine the effect of repeated BCG applications in a follow-up study.

REFERENCES

(*1*) Zbar B, Tanaka T. Immunotherapy of cancer: Regression of tumors after intralesional injection of living *Mycobacterium bovis*. Science 1971; 172:271–273.

(*2*) Salomon JC, Lynch N. Intralesional injection of immunostimulants in rat and mouse tumors. Cancer Immunol Immunother 1976; 1:145–151.

(*3*) Kreider JW, Bartlett GL, Boyer CM, Purnell DM. Conditions for effective Bacillus Calmette-Guérin immunotherapy of postsurgical metastases of 13762A rat mammary adenocarcinoma. Cancer Res 1979; 39:987–992.

(*4*) Hess AD, Catchatourian R, Zander AR, Epstein RB. Intralesional Bacillus Calmette-Guérin immunotherapy of canine venereal tumors. Cancer Res 1977; 37:3990–3994.

(*5*) Kleinschuster SJ, Rapp HJ, Luerer DC, Kainer RA. Regression of bovine ocular carcinoma by treatment with a mycobacterial vaccine. J Natl Cancer Inst 1977; 58:1807–1814.

(*6*) Waldhalm DG, McLaughlin CA, Hall RF, Ribi E. Use of endotoxin and mycobacterial fractions in treating malignant epithelioma of the bovine eye. Proc Annu Meet US Anim Health Assoc 1977; 81:64–66.

(*7*) Kleinschuster SJ, Rapp HJ, Green SB, Bier J, Van Kampen K. Efficacy of intratumorally administered mycobacterial cell walls in the treatment of cattle with ocular carcinoma. JNCI 1981; 67:1165–1171.

(*8*) Murphy JM, Severin GA, Lavach JD, Hepler DI, Luerer DC.

Immunotherapy in ocular equine sarcoid. JAVMA 1979; 174:269-272.

(9) Zbar B, Berstein ID, Bartlett GL, Hanna MG Jr, Rapp HJ. Immunotherapy of cancer: Regression of intradermal tumors and prevention of growth of lymph node metastases after intralesional injection of living *Mycobacterium bovis*. J Natl Cancer Inst 1972; 49:119-130.

(10) Hanna MG Jr, Snodgrass MJ, Zbar B, Rapp HJ. Histopathology of tumor regression after intralesional injection of *Mycobacterium bovis*. IV. Development of immunity to tumor cells and BCG. J Natl Cancer Inst 1973; 51:1897-1908.

(11) Zbar B, Ribi E, Meyer T, Azuma I, Rapp HJ. Immunotherapy of cancer: Regression of established intradermal tumors after intralesional injection of mycobacterial cell walls attached to oil droplets. J Natl Cancer Inst 1974; 52:1571-1577.

(12) Russel WO, Wynne ES, Loquvam GS, Mehl DA. Studies on bovine ocular squamous carcinoma ("cancer eye"). Cancer 1956; 1:1-52.

(13) Misdorp W. Tumors in slaughter animals in The Netherlands. Tijdschr Diergeneesk 1967; 92:1195-1204.

(14) Blackwell RL, Anderson DE, Knox JH. Age incidence and heritability of cancer eye in Hereford cattle. J Anim Sci 1956; 15:943-951.

(15) Russel WO, Burkes G, Kainer RA. Incidence and heritability of OSCC in Hereford cattle. J Anim Sci 1976; 43:1156-1162.

(16) Hamir AN, Parry OB. An abattoir study of bovine neoplasms with particular reference to ocular squamous cell carcinoma in Canada. Vet Rec 1980; 106:551-553.

(17) French GT. A clinical and genetic study of eye cancer in Hereford cattle. Aust Vet J 1959; 35:474-481.

(18) Van Hemert PA. Vaccine production as a unit process. Ph.D. thesis. Delft: The Netherlands: Technical University, 1973.

(19) Bier J, Kleinschuster SJ, Corbett R. Radical surgery of bovine ocular squamous cell carcinoma (cancer eye): A new procedure. Vet Sci Commun 1979; 3:221-230.

(20) Engvall E, Perlmann P. Enzyme linked immunosorbent assay (ELISA). Quantitative assay of immunoglobulin G. Immunochemistry 1971; 8:871-874.

(21) Ruitenberg EJ, Steerenberg PA, Brosi BJ, Buys J. Evaluation of the reliability of immunoenzymatic techniques for the serodiagnosis in *Trichinella spiralis* infections. In: Feldmann G, Druet P, Bighon J, eds. Proceedings of the first international symposium on immunoenzymatic techniques. INSERM symposium No. 2. Amsterdam: North-Holland, 1976:149-166.

(22) Anderson DE, Lush JL, Chambers D. Studies on bovine ocular squamous cell carcinoma ("cancer eye"). II. Relationship between eyelid pigmentation and occurrence of cancer eye lesions. J Anim Sci 1957; 16:739-746.

(23) Anderson DE. Studies on bovine ocular squamous cell carcinoma ("cancer eye"). V. Genetic aspects. J Hered 1960; 51:51-58.

(24) Mackaness GB, Auclair DJ, Lagrange PH. Immunopotentiation with BCG. I. Immune response to different strains and preparations. J Natl Cancer Inst 1973; 51:1655-1667.

(25) Ruitenberg EJ, De Jong WH, Kreeftenberg JG, Steerenberg PA, Kruizinga W. BCG preparations, cultured homogeneously dispersed or as a surface pellicle, elicit different immunopotentiating effects but have similar antitumor activity in a murine fibrosarcoma. Cancer Immunol Immunother 1981; 11:45-51.

(26) Hoffmann D, Jennings PA, Spradbrow PB. Immunotherapy of bovine ocular squamous cell carcinoma with phenol-saline extracts of allogenic carcinomas. Aust Vet J 1981; 57:159-162.

(27) Van Kampen KR, Crisp WE, De Martini JC, Ellsworth HS. The immunologic therapy of squamous cell carcinoma—a preliminary report. Am J Obstet Gynecol 1973; 116:569-574.

(28) Spradbrow PB, Wilson BE, Hoffmann D, Kelly WR, Francis J. Immunotherapy of bovine ocular squamous cell carcinomas. Vet Rec 1977; 100:376-378.

(29) Fivaz BH. The immunotherapy of bovine ocular squamous cell carcinoma. Rhodesian Vet J 1978; 9:24-27.

(30) Kaplan MH, Amstrong D, Pinsky C. Antibody responses to mycobacterial antigens in patients immunized with BCG for the treatment of neoplastic disease. Cancer 1980; 46:2195-2202.

(31) Hortobagyi GN, Smith TL, Swenerton KD, et al. Prognostic value of prechemotherapy skin tests in patients with metastic breast carcinoma. Cancer 1981; 47:1369-1376.

(32) Jansen HM, Thé TH, Orie NG. Adjuvant immunotherapy with BCG in squamous cell bronchial carcinoma. Thorax 1980; 35:781-787.

(33) Hiroyuki Y, Nozaki C. Serologic diagnosis of bovine tuberculosis. Am J Vet Res 1972; 33:1377-1384.

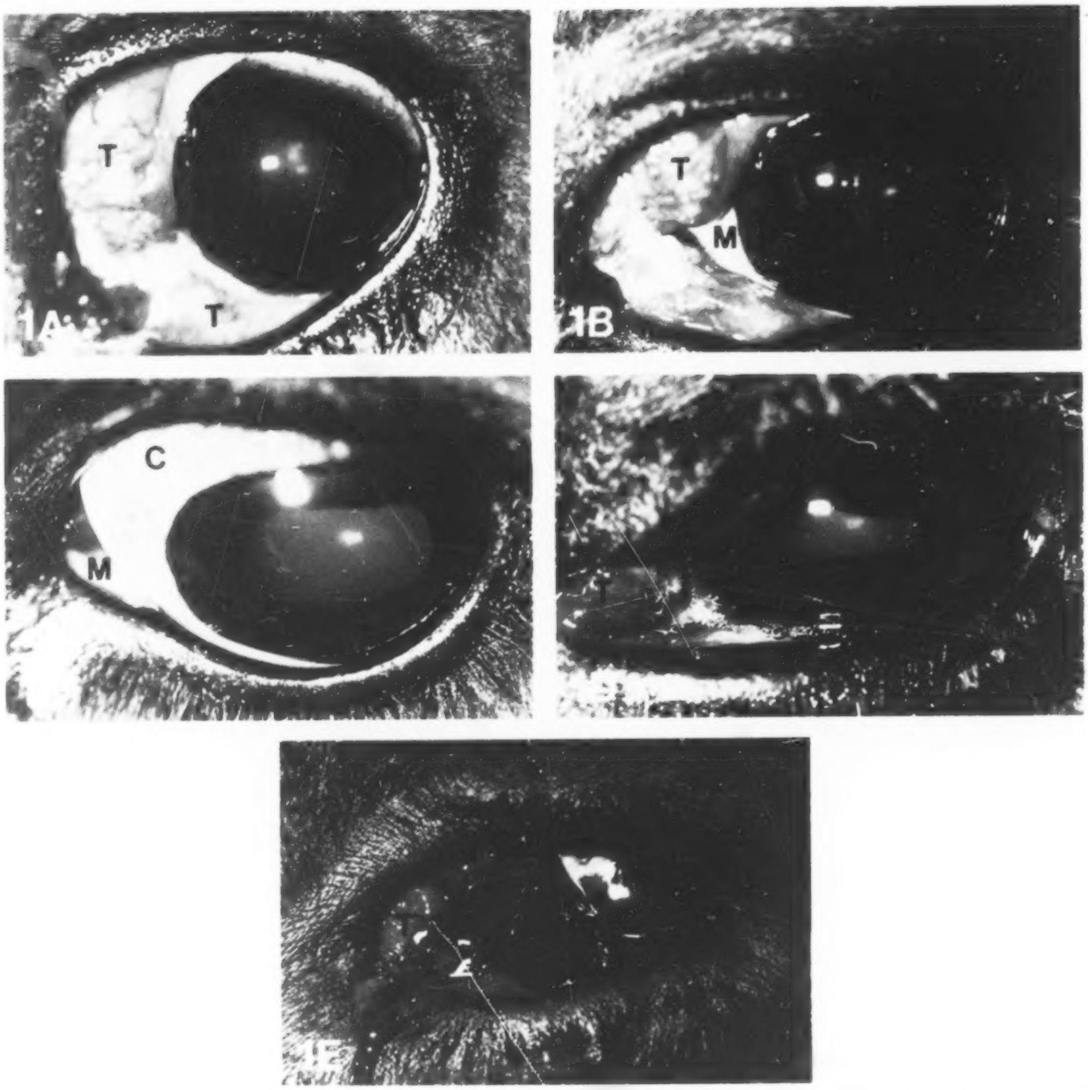

FIGURE 1.—Regression and recurrence of a bovine ocular squamous cell carcinoma of the membrana nictitans after intralesional treatment with BC [illegible] [illegible]. A) Tumor before treatment. B) Reduction of tumor 1 mo after treatment. C) Clinical absence of tumor between 3 and 14 mo [illegible] treatment. D) Recurrence of the tumor of the membrana nictitans at 18 mo; recurrence started at 15 mo. E) Tumor at 20 mo after start of treatm [illegible] T=tumor; M=membrana nictitans; C=conjunctiva bulbi.

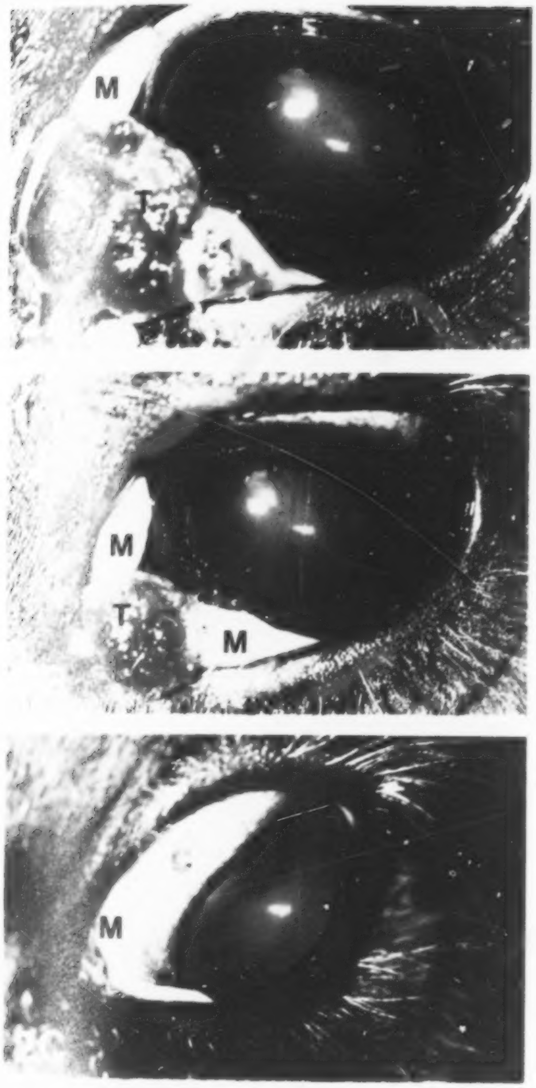

FIGURE 2. Regression of a bovine ocular squamous-cell carcinoma of the membrana nictitans after intralesional treatment with live BCG vaccine (cow 34). A: Tumor before treatment. B: Reduction of tumor 2 mo after treatment. C: Clinical absence of tumor from 7 mo on until end of observation period at 34 mo. T=tumor; M=membrana nictitans; C=conjunctiva bulbi.

blank page

Expression of Fibronectin and Laminin in the Rat Liver After Partial Hepatectomy, During Carcinogenesis, and in Transplantable Hepatocellular Carcinomas[1,2,3]

Stewart Sell[4,5] *and* Erkki Ruoslahti[6,7]

ABSTRACT—The distribution in the F344 rat liver of two extracellular matrix and basement membrane components, fibronectin and laminin, was studied by immunofluorescence. Fibronectin was found diffusely in normal liver lining the sinusoids and in connective tissue surrounding blood vessels and bile ducts; laminin was present predominantly in the basement membranes of blood vessels and bile ducts and was only inconsistently seen lining the sinusoids. After partial hepatectomy (PH), there was a transient decrease of fibronectin in the central and midzone sinusoidal hepatic areas. This decrease was most marked on day 3 after the PH. Carcinogens caused marked changes in the distribution of fibronectin. Large extracellular deposits of fibronectin were seen in areas of oval cell proliferation in livers of rats treated with *N*-2-fluorenylacetamide (2-FAA) while being fed a choline-deficient diet. In contrast, the nodules that developed in these livers were almost completely devoid of fibronectin staining. Neoplastic nodules produced in rats by cyclic feedings of 2-FAA or by injections of diethylnitrosamine also contained little or no fibronectin. Laminin staining did not change markedly during these treatments, but increased staining was seen associated with the newly formed ductlike structures and oval cells in livers of rats treated with carcinogens. Transplantable hepatomas varied in their fibronectin staining from fibronectin-negative hepatomas to ones with fibronectin staining within or around every tumor cell. Laminin was only found around the vascular structures within the tumors. The presence or absence of fibronectin in hepatomas did not show an obvious correlation to growth rate or metastatic potential of the tumors studied.—JNCI 1982; 69:1105–1114.

Fibronectin is a high-molecular-weight glycoprotein present in extracellular matrices, at cell surfaces, and in the blood (*1, 2*). Fibronectin binds to collagen (*3*) and mediates attachment of cells to collagen matrices and other surfaces in vitro (*4–8*). Fibronectin is frequently absent from the surface of malignantly transformed cells (*9–11*), and this absence is thought to play a role in the ability of such cells to grow invasively and to metastasize (*12, 13*).

Laminin is a newly discovered basement membrane glycoprotein (*14–16*) somewhat similar to fibronectin but biochemically and immunochemically distinct from it (*15–17*). Laminin also appears to be involved in cellular adhesion but with a specificity different from that of fibronectin (*18–20*).

Although fibronectin has been studied extensively, the function of this protein is not known. The liver provides a unique model for studies on a number of processes involving carcinogenesis and tissue remodeling inasmuch as this tissue has been extensively studied with regard to cellular events that take place during such processes (*21–24*). We thought that useful information about the role of fibronectin and laminin in normal and malignant tissues might be obtained by studying the distribution of these proteins during liver regeneration and carcinogenesis, and we thought that such information might also be useful for interpreting the cellular changes during these processes. We report here that marked changes take place in the distribution of fibronectin and lesser changes take place in the distribution in laminin during treatment of the liver with carcinogens. We also find that transplantable hepatomas may or may not contain fibronectin, suggesting that no simple relationship exists between the expression of fibronectin and the malignant phenotype.

MATERIALS AND METHODS

Tissue blocks from the livers of F344 rats that had been prepared as components of a number of earlier experiments (*25–32*) were fixed in a cold 95% ethanol–1% acetic acid solution and were dehydrated, cleared, and embedded in low-melting-point paraffin. Before fixation, the livers were perfused with saline via the inferior vena cava, which flushed out serum proteins (*33, 34*).

Rabbit antisera to rat fibronectin (*35*) and rat laminin (*18*) and affinity-purified antibodies from such sera (*35–37*) were used at 1:5–1:20 dilutions as the first antibodies.

Microscopic sections cut from the blocks were deparaffinized at 56°C, flooded with 1:5–1:20 dilutions of the first antiserum for 30 minutes at room temperature, were washed in cold phosphate-buffered saline, and were then labeled by addition of FITC-conjugated polyvalent goat IgG anti-rabbit Ig (*27*). Controls included unlabeled sections, normal serum dilutions as the first antibody, and the FITC-labeled goat IgG anti-rabbit Ig only.

Transplantable hepatocellular carcinomas 7777, 8994, and 9098 were obtained from Harold Morris of Howard University, Washington, D.C.; tumors FB 56, 252, and 311

ABBREVIATIONS USED: AFP=α-fetoprotein; CD=choline-deficient; DDPMN =*p,p'*-diaminodiphenylmethane; DENA=diethylnitrosamine; 2-FAA=*N*-2-fluorenylacetamide; FITC=fluorescein isothiocyanate; PH=partial hepatectomy.

---

[1] Received January 19, 1982; accepted May 20, 1982.

[2] Supported by Public Health Service grants CA-29368 (to S. S.), CA-28896 (to E. R.), and CA-27460 (to E. R.) from the National Cancer Institute.

[3] Animals were maintained under the guidelines of the Office of Animal Resources, UCSD Medical School.

[4] Department of Pathology, School of Medicine, University of California, San Diego, La Jolla, Calif. 92093.

[5] Address reprint requests to Dr. Sell at his present address: Department of Pathology and Laboratory of Medicine, University of Texas Health Science Center at Houston, Houston, Tex. 77025.

[6] La Jolla Cancer Research Foundation, 2945 Science Park Rd., La Jolla, Calif. 92037.

[7] We thank Dr. Frederick Becker for samples from diethylnitrosamine-treated animals.

were obtained from Frederick F. Becker, M. D. Anderson Hospital, Houston, Tex. These tumors were maintained by intramuscular passage in the thigh muscle as described (*32*).

RESULTS

Normal and regenerating liver.—In agreement with earlier results (*17, 18, 38*), the normal liver showed staining for fibronectin in the sinusoidal, blood vessel, and bile duct walls (fig. 1). Liver regeneration induced by PH caused a transient decrease in the fibronectin staining in the sinusoidal areas, particularly in the central and midzones. Livers were studied from animals in three different experiments, and in each experiment, a decrease of fibronectin staining was observed between days 2 and 4 after the PH. A representative series of such staining results is shown in figure 1. Laminin was found prominently surrounding the blood vessel and bile duct walls of the normal liver (fig. 2). Staining of laminin lining hepatic sinusoids was inconsistently seen, but it was faintly visible in some sections (fig. 2A). It was not possible to determine if a decrease or increase in laminin labeling occurred during regeneration.

Carcinogenesis.—Focal increases and decreases in the intensity of fibronectin and laminin labeling occurred after exposure to hepatocarcinogens (figs. 3, 4). A marked increase in fibronectin was associated with "oval cell" proliferation in the portal zone after the rats were fed 2-FAA in a CD diet (*29, 31, 39*). In the same tissue, a decrease in fibronectin labeling was seen in the central zone of the liver. Newly forming, ductlike structures were surrounded by intensive labeling for fibronectin. Labeling for laminin was increased in zones of oval cell proliferation (fig. 3D), resulting in delineation of cords and ductlike structures formed by oval cells. A variable distribution of fibronectin occurred after DENA exposure, with intensively labeled areas alternating with lightly labeled areas (fig. 4). A few liver cells also stained intensely for fibronectin. In hyperplastic (nonnodular) zones seen after cyclic feeding of 2-FAA, fibronectin labeling remained in the sinusoids (fig. 4E). In neoplastic nodules, intensity of labeling was weak (fig. 4F). Laminin was not seen in nodules.

Transplantable hepatocellular carcinomas.—Six transplantable hepatocellular carcinomas were examined for fibronectin and laminin (figs. 5, 6). Laminin was only found around vascular structures (figs. 5C, 5D). The distribution of fibronectin was different with each tumor. Three locations were apparent: around vascular structures and in connective tissue within the tumor, surrounding individual tumor cells, and within individual tumor cells. A summary of the labeling patterns and a comparison with other properties of the tumors are given in table 1. In 2 tumors, 7777 and 8994, abundant fibronectin was found to be associated with the surface of tumor cells. Each cell in these 2 tumors was surrounded by fibronectin (figs. 5, 6). Hepatoma 252 showed a similar staining pattern, but it was weaker (fig. 6). One tumor (311) had intracellular fibronectin fluorescence, but it had no cell surface-associated fibronectin (fig. 6). The distribution of fibronectin did not correlate with growth rate, because the 3 Morris hepatomas (7777, 8994, and 9098) are all fast growing (*30*) and the Becker hepatomas (311, 252, and FB 56) have similar growth rates (Becker F: Personal communication). In addition, no clear correlation with other properties was apparent. Although intense fibronectin labeling was generally seen in the high-AFP-producing tumors, not enough tumors were studied to permit a definite conclusion on the association of serum protein production and fibronectin.

TABLE 1.—*Correlation of properties of transplantable hepatocellular carcinomas*

Hepatoma	Serum AFP, μg/ml	Immunofluorescence labeling intensity[a]				
				Fibronectin		
		AFP	Albumin	Connective tissue	Extracellular	Intracellular
7777	5,000	++++	+++	+++	++	0
8994	3,000	+++	++++	+++	+++	0
FB 56	50	++	ND	++	0	0
311	13	++	+++	+	+	+++
252	<0.05	0	++	++	+	+
9098	<0.05	0	ND	0	0	0

[a] ND=not done; 0 to ++++ are relative degrees of immunofluorescence.

DISCUSSION

The main findings in this work are that the amount of fibronectin is reduced in regenerating liver, that areas of oval cell production show a marked increase in fibronectin in the associated connective tissue, that neoplastic nodules show a decrease of fibronectin, and that hepatomas have different patterns of fibronectin distribution. Under these experimental situations there is less change in laminin distribution, but laminin was increased in zones of oval cell proliferation.

Extracellular matrix degradation and synthesis are thought to be important in tissue remodeling. A decrease of fibronectin in the liver during the peak of the regenerative response is found in central and midzones of the liver. Increased amounts of laminin can be demonstrated in mouse liver during regeneration following carbon tetrachloride poisoning and also to some extent after PH (*18*). In the present work, we did not see an increase in laminin after PH. This may depend on a species difference or technical differences. Frozen sections were used for laminin evaluation in the previous work, and subtle differences in laminin concentration may have been more easily detected in the frozen sections than in the fixed tissues used in this study. In any event, these results show that changes in the extracellular matrix components accompany the regenerative process.

The relationship between the marked differences in tissue distribution of fibronectin and the cellular changes during carcinogenesis is intriguing, but it is not readily interpretable at the present time. The increase in fibronectin associated with oval cell proliferation is marked. In these areas, the degree of connective tissue involvement suggests deposition of collagen associated with oval cells. Early investigators interpreted this as a form of cirrhosis (*40*), but there is no evidence of progressive fibrosis as a result of the rat's being fed 2-FAA. In areas of disorientated liver cells that are not nodular, fibronectin is present in normal intensity, but fibronectin is markedly decreased in well-delineated neoplastic nodules. Thus nodules were found to resemble normal regenerating liver cells in that both of these areas had decreased amounts of fibronectin.

The normal distribution of laminin changed little during carcinogenesis, but the distribution during carcinogenesis did give us further insights. The ductlike structures that arise in association with oval cells as a result of carcinogen exposure (tubuloform degeneration) are faintly delineated by laminin, whereas normal bile ducts and the new ducts induced by feeding the noncarcinogenic agent DDPM, which produces marked bile duct proliferation, are highlighted by a much more visible surrounding layer of laminin (*41*). The ductlike structures that appear during carcinogenesis frequently contain AFP and/or albumin in contrast to normal and DDPM-induced ducts which do not (*27, 31*). These findings may be relevant to conclusions regarding the lineage of cellular changes in the liver. A number of investigators have suggested that oval cells are ductal in origin because the development of these ductlike structures is associated with oval cell proliferation (*22, 42*). However, these newly appearing ducts have properties more consistent with a hepatocyte origin than with a bile duct origin (*24*).

The distribution of fibronectin in transplantable hepatocellular carcinomas is quite variable and does not support a relationship between tumor growth and metastatic potential and contrarily fibronectin content. Although the number of tumors studied is not large enough for definitive conclusions, it appears that the presence of fibronectin shows some relationship to the ability of these tumors to produce other proteins (*43*). However, at this time, the fibronectin seen cannot be concluded to have actually arisen from tumor production. Fibronectin is present in the circulation at a relatively high concentration (300 μg/ml) (*44*). The origin of the circulating fibronectin is not known. It could be that it is made in the liver and that its synthesis is coupled to that of other serum proteins. Because it has been shown that circulating fibronectin can become insolubilized in tissues (*45*), the fibronectin surrounding the hepatoma cells could be of the type that arises from plasma fibronectin.

It is not possible at this time to differentiate plasma fibronectin from other fibronectins. A monoclonal antibody that reacts more strongly with fibronectin from fibroblasts than with fibronectin from plasma has been reported (*46*), but this difference is not large enough to allow distinction by immunofluorescence in tissue (Hynes RO: Personal communication).

Fibronectin is often absent from the surface of malignant cells cultured in vitro (*10*), and a correlation has been found between the amount of cell surface fibronectin expressed in vitro and the tumorigenic (*12*) and metastatic potential (*13*) of such cells. Relatively few studies have explored the expression of fibronectin in tumors in vivo. Labat-Roberts et al. (*47*) and Asch et al. (*48*) found fibronectin expressed at reduced levels compared to normal tissues in human and mouse mammary carcinomas at early stages, whereas Stenman and Vaheri (*49*) could not demonstrate any fibronectin in human epithelial tumors. Because the series of Stenman and Vaheri did not include human liver cancers, we do not know whether hepatomas in humans would also be fibronectin-positive. However, at least one human hepatoma cell line (*50*) has fibronectin in vitro (Ruoslahti E: Unpublished observations).

Because each of the hepatomas we studied is relatively fast growing (*30*) and the fibronectin-distribution is quite different, a correlation between cell surface fibronectin as expressed in vivo and the rate of tumor growth in this system is not apparent. A similar conclusion has recently been reached from studies with rat mammary tumors growing in vivo (*51*) and in a number of in vitro studies (*52–55*).

The metastatic potential for each of the hepatomas used in this study is not known. However, after amputation of the transplant site of hepatoma 7777, pulmonary metastases regularly occur (*32*). Thus the presence of fibronectin surrounding each tumor cell is not associated with a low metastatic potential of at least this tumor. The profound effects of fibronectin on cellular adhesion, including adhesion of hepatocytes (*5, 6, 18*), and on cellular motility (*56*) suggest that cell surface fibronectin is one of the factors that affects tumorigenicity and metastasis, but a simple relationship such as that proposed in earlier studies seems unlikely.

REFERENCES

(*1*) Mosher DF. Fibronectin. Prog Hemost Thromb 1980; 5:111–151.

(*2*) Ruoslahti E, Hayman EG, Engvall E. Fibronectin: Current concepts of its structure and functions. Collagen Res 1981; 1:95–128.

(*3*) Engvall E, Ruoslahti E. Binding of soluble form of fibroblast surface protein, fibronectin, to collagen. Int J Cancer 1977; 20:1–5.

(*4*) Grinnell F. Fibroblast cell-substratum interactions: Role of cold insoluble globulin (plasma fibronectin). Experientia 1980; 36:505–507.

(*5*) Höök M, Rubin K, Oldberg A, Vaheri A. Cold-insoluble globulin mediates the adhesion of rat liver cells to plastic petri dishes. Biochem Biophys Res Commun 1977; 79:726–733.

(*6*) Klebe RJ. Isolation of a collagen-dependent cell attachment factor. Nature 1974; 250:248–251.

(*7*) Pearlstein E. Plasma membrane glycoprotein which mediates adhesion of fibroblasts to collagen. Nature 1976; 262:497–500.

(*8*) Yamada KM, Yamada SS, Pastan I. Quantitation of a transformation-sensitive, adhesive cell surface glycoprotein. J Cell Biol 1977; 74:649–654.

(*9*) Hynes RO. Alteration of cell-surface proteins by viral transformation and by proteolysis. Proc Natl Acad Sci USA 1973; 70:3170–3174.

(*10*) Vaheri A, Mosher DF. High molecular weight, cell surface-associated glycoprotein (fibronectin) lost in malignant transformation. Biochim Biophys Acta 1978; 516:1–25.

(*11*) Vaheri A, Rouslahti E. Disappearance of a major cell-type specific surface glycoprotein antigen (SF) after transformation of fibroblasts by Rous sarcoma virus. Int J Cancer 1974; 13:579–586.

(*12*) Chen LB, Gallimore PH, McDougall JK. Correlation between tumor induction and the large external transformation-sensitive protein on the cell surface. Proc Natl Acad Sci USA 1976; 73:3570–3574.

(*13*) Smith HS, Riggs JL, Mosesson MW. Production of fibronectin by human epithelial cells in culture. Cancer Res 1979; 39:4138–4144.

(*14*) Chung AE, Freeman IL, Braginski JE. A novel extracellular membrane elaborated by a mouse embryonal carcinoma-derived cell line. Biochem Biophys Res Commun 1977; 79:859–868.

(*15*) Chung AE, Jaffe R, Freeman IL, Vergnes J-P, Braginski JE, Carlin B. Properties of a basement membrane-related glycoprotein synthesized in culture by a mouse embryonal carcinoma derived cell line. Cell 1979; 16:227–287.

(*16*) Timpl R, Rohde H, Robey PG, Rennard SI, Foidart J-M, Martin GR. Laminin—a glycoprotein from basement membranes. J Biol

Chem 1979; 254:9933–9937.

(*17*) Sakashita S, Ruoslahti E. Laminin-like glycoproteins in extracellular matrix of endodermal cells. Arch Biochem Biophys 1981; 205:283–290.

(*18*) Carlsson RN, Engvall E, Freeman A, Ruoslahti E. Laminin and fibronectin in cell adhesion: Enhanced adhesion of cells from regenerating liver to laminin. Proc Natl Acad Sci USA 1981; 78:2403–2406.

(*19*) Terranova VP, Rohrbach DH, Martin GR. Role of laminin in the attachment of PAM 212 (epithelial) cells to basement membrane collagen. Cell 1980; 22:719–726.

(*20*) Vlodavsky I, Gospodarowicz D. Respective roles of laminin and fibronectin in adhesion of human carcinoma and sarcoma cells. Nature 1981; 289:304–306.

(*21*) Farber E. Carcinogenesis–cellular evolution as a unifying thread: Presidential address. Cancer Res 1973; 33:2537–2550.

(*22*) Farber E, Cameron R. The sequential analysis of cancer development. Adv Cancer Res 1980; 31:125–226.

(*23*) Lesch R, Reutter W, eds. Liver regeneration after experimental injury. New York: Stratton Intercon, 1975.

(*24*) Sell S, Leffert HL. An evaluation of cellular lineages in the pathogenesis of experimental hepatocellular carcinoma. Hepatology 1982; 2:77–86.

(*25*) Becker F, Sell S. Differences in serum alpha-fetoprotein concentrations during the carcinogenic sequences resulting from exposure to diethylnitrosamine or acetylaminofluorene. Cancer Res 1979; 39:1437–1442.

(*26*) Sell S. Distribution of alpha-fetoprotein and albumin containing cells in the livers of Fischer rats fed four cycles of *N*-2-fluorenylacetamide. Cancer Res 1978; 38:3107–3113.

(*27*) ———. Heterogeneity of alphafetoprotein and albumin containing cells in normal and pathological permissive states for ATP production: AFP containing cells induced in adult rats recapitulate the appearance of AFP containing hepatocytes in fetal rats. Oncodev Biol Med 1980; 1:93–105.

(*28*) Sell S, Becker F, Lombardi B, Shinozuka H, Reddy J. Alpha-fetoprotein production by normal and abnormal liver cells. II. Differences in the sequence of morphologic events and kinetics of elevation of serum AFP during chemical induction of liver cancer. In: Lehman F-G, ed. Carcioembryonic proteins. Vol I. Amsterdam: Elsevier/North-Holland 1979:129–136.

(*29*) Sell S, Leffert HL, Shinozuka H, Lombardi B. Rapid development of large numbers of alphafetoprotein containing "oval cells" in Fischer rats fed *N*-2-fluorenylacetamide in a choline devoid diet. Gan 1981; 72:479–487.

(*30*) Sell S, Morris H. Relationship of rat alpha-fetoprotein to growth rate and chromosome composition of Morris hepatomas. Cancer Res 1974; 34:1413–1417.

(*31*) Sell S, Osborn K, Leffert H. Autoradiography of "oval cells" appearing rapidly in livers of rats fed *N*-2-fluorenylacetamide in a choline devoid diet. Carcinogenesis 1981; 2:7–14.

(*32*) Sell S, Wepsic HT, Nickel R, Nichols M. Rat alpha$_1$ fetoprotein. IV. Effect of growth and surgical removal of Morris hepatoma 7777 on the serum α_1F concentration of Buffalo rats. J Natl Cancer Inst 1974; 52:133–137.

(*33*) LeBouton AV, Masse JP. A random arrangement of albumin-containing hepatocytes seen with histo-immunologic methods. I. Verification of the artifact. Anat Rec 1980; 197:183–194.

(*34*) ———. A random arrangement of albumin-containing hepatocytes seen with histo-immunologic methods. II. Conditions that produce the artifact. Anat Rec 1980; 197:195–203.

(*35*) Ruoslahti E, Vuento M, Engvall E. Interaction of fibronectin with antibodies and collagen in radioimmunoassay. Biochim Biophys Acta 1978; 534:210–218.

(*36*) Albrechtsen R, Nielsen M, Wewer U, Engvall E, Ruoslahti E. Basement membrane changes in breast cancer detected by immunohistochemical staining for laminin. Cancer Res 1981; 41:5076–5081.

(*37*) Wewer U, Albrechtsen R, Ruoslahti E. Laminin, a noncollagenous component of epithelial basement membranes synthesized by a rat yolk sac tumor. Cancer Res 1981; 41:1518–1524.

(*38*) Stenman S, Vaheri A. Distribution of a major connective tissue protein, fibronectin, in normal human tissues. J Exp Med 1978; 147:1054–1064.

(*39*) Shinozuka H, Sells MA, Katyal S, Sell S, Lombardi B. Effects of a choline-devoid diet on the emergence of alpha-glutamyltranspeptidase-positive foci in the liver of carcinogen-treated rats. Cancer Res 1979; 39:2515–2521.

(*40*) Reuber M. Development of preneoplastic and neoplastic lesions of the liver in male rats given 0.025 percent *N*-2-fluorenyldiacetamide. J Natl Cancer Inst 1965; 34:697–724.

(*41*) Sell S. A comparison of carcinogen induced oval cell proliferation and chemically induced bile duct proliferation in rat liver. Fed Proc 1982; 41:378.

(*42*) Farber E. Similarities in the sequence of early histologic changes induced in the liver of the rat by ethionine, 2-acetyl-aminofluorene and 3′-methyldimethylaminobenzene. Cancer Res 1956; 16:142–148.

(*43*) Sell S, Thomas K, Michalson M, Sala-Trepat J, Bonner J. Control of albumin and alpha-fetoprotein expression in rat liver and some transplantable hepatocellular carcinomas. Biochim Biophys Acta 1979; 56 173–178.

(*44*) Mosesson MW, Umfleet RA. The cold-insoluble globulin of human plasma. J Biol Chem 1970; 254:5728–5736.

(*45*) Oh E, Pierschbacher M, Ruoslahti E. Deposition of plasma fibronectin in tissues. Proc Natl Acad Sci USA 1981; 78:3218–3221.

(*46*) Atherton BT, Hynes RO. A difference between plasma and cellular fibronectins located with monoclonal antibodies. Cell 1981; 25:133–141.

(*47*) Labat-Robert J, Birembaut P, Adnet JJ, Mercantini F, Robert L. Loss of fibronectin in human breast cancer. Cell Biol Int Rep 1980; 4:609–616.

(*48*) Asch BB, Kamat BR, Burstein NA. Interactions of normal, dysplastic, and malignant mammary epithelial cells with fibronectin in vivo and in vitro. Cancer Res 1981; 41:2115–2125.

(*49*) Stenman S, Vaheri A. Fibronectin in human solid tumors. Int J Cancer 1981; 27:427–435.

(*50*) Knowles BB, Howe CC, Aden DP. Human hepatocellular carcinoma cell lines secrete the major plasma proteins and hepatitis B surface antigen. Science 1980; 209:497–499.

(*51*) Neri A, Ruoslahti E, Nicholson GL. Distribution of fibronectin on clonal cell lines of a rat mammary adenocarcinoma growing in vitro and in vivo at primary and metastatic sites. Cancer Res 1981; 41:5082–5095.

(*52*) Der CJ, Stanbridge EJ. Lack of correlation between the decreased expression of cell surface LETS protein and tumorigenicity in human cell hybrids. Cell 1978; 15:1241–1251.

(*53*) Jones PA, Laug WE, Gardner A, Nye CA, Fink LM, Benedict WF. In vitro correlates of transformation in C3H/10T½ clone 8 mouse cells. Cancer Res 1976; 36:2863–2867.

(*54*) Kahn P, Shin S. Cellular tumorigenicity in nude mice. J Cell Biol 1979; 82:1–16.

(*55*) Gallimore PH, McDougall JK, Chen LB. In vitro traits of adenovirus-transformed cell lines and their relevance to tumorigenicity in nude mice. Cell 1977; 10:669–678.

(*56*) Ali IU, Hynes RO. Effects of cytochalasin B and colchichine on attachment of a major surface protein of fibroblasts. Biochim Biophys Acta 1977; 471:16–24.

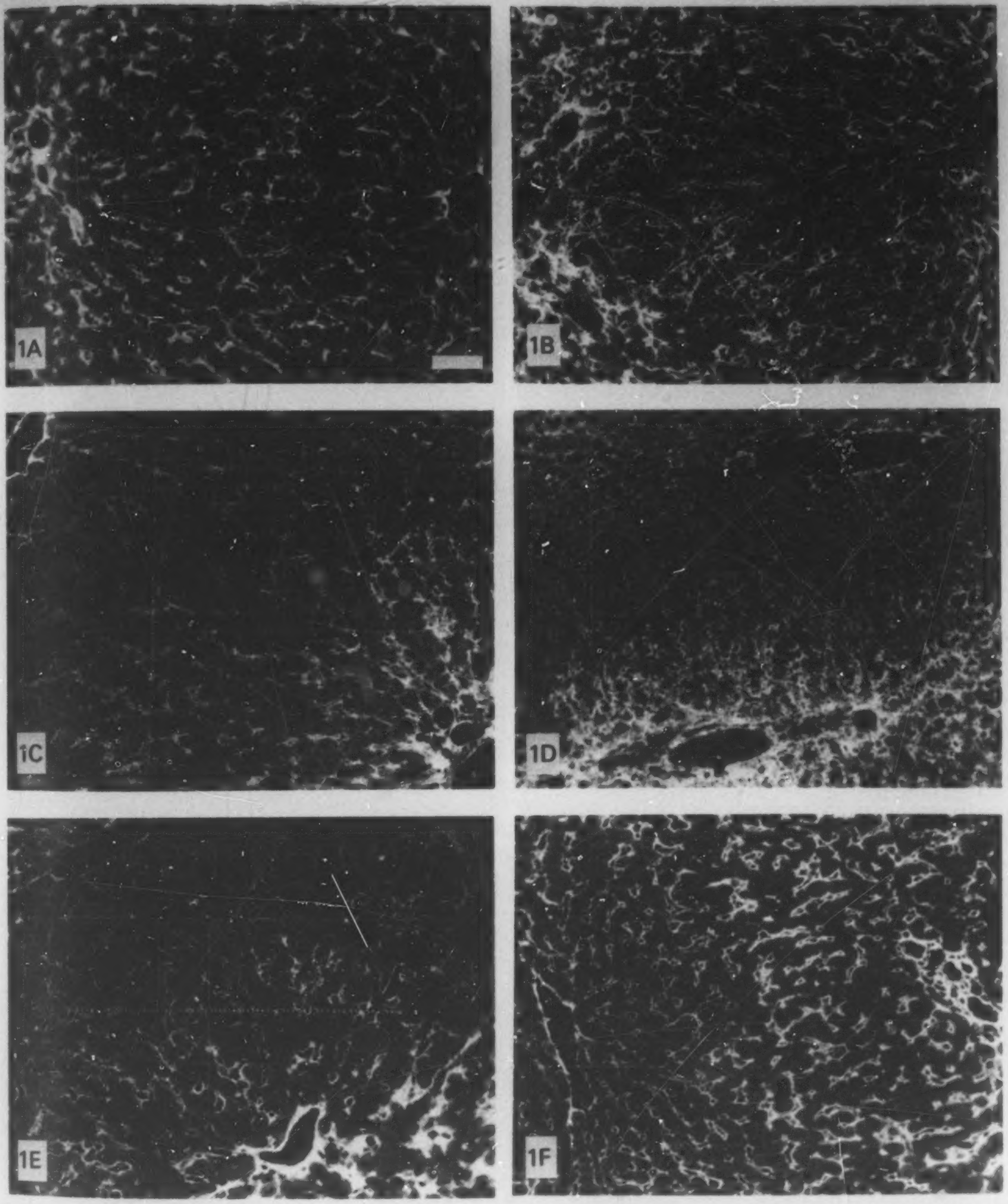

FIGURE 1.—Immunofluorescent localization of fibronectin in A) normal liver and in regenerating livers obtained at B) 1, C) 2, D) 3, E) 5, and F) 7 days after PH. Each picture includes an area of liver containing all three lobular zones (central, midzone, and portal). In normal liver and by 7 days after PH, fibronectin is uniformly distributed in all zones of the liver. At 1 day after PH, staining of fibronectin in the midzone is slightly reduced. This reduced staining is more pronounced on days 2 and 3, when some reduction is also present in the central zone. *Note* decreased staining intensity and loss of linearity in (C) as compared to that in (A) and (F). By 5 days, midzone staining has increased, and by 7 days, normal staining is evident in all three zones. The changing pattern of fibronectin staining was seen in three experiments. *Bar*=50 μm. × 180.

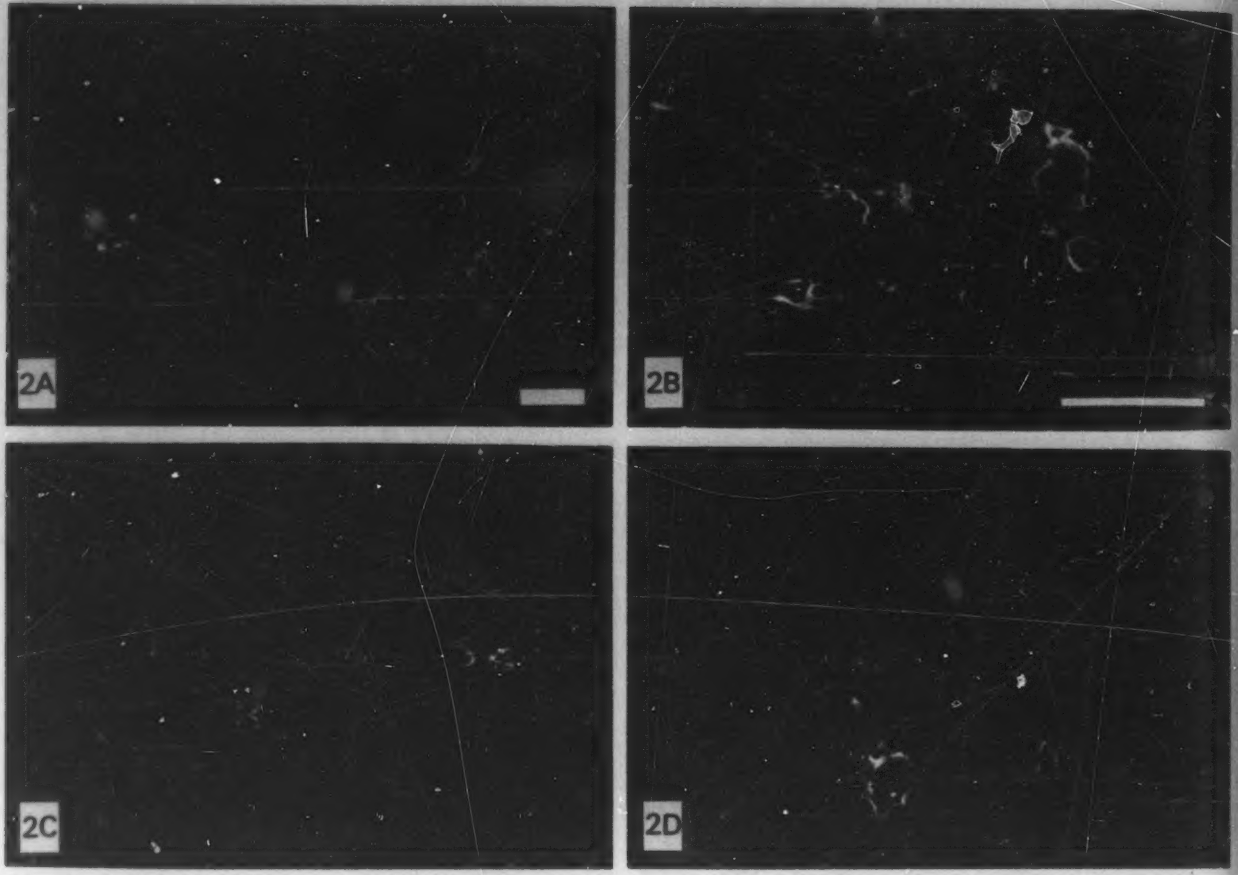

FIGURE 2.—Laminin in normal liver (A, 180 ×; B, 450 ×) and in regenerating rat liver obtained 1 day (C, 180 ×) and 3 days (D, 180 ×) after PH. Laminin is present mainly around bile ducts and hepatic arteries with lesser fluorescence around portal veins. Central veins are not stained, and sinusoids (A) in the liver lobule are very faintly and inconsistently labeled. *Bars* = *50 µm.*

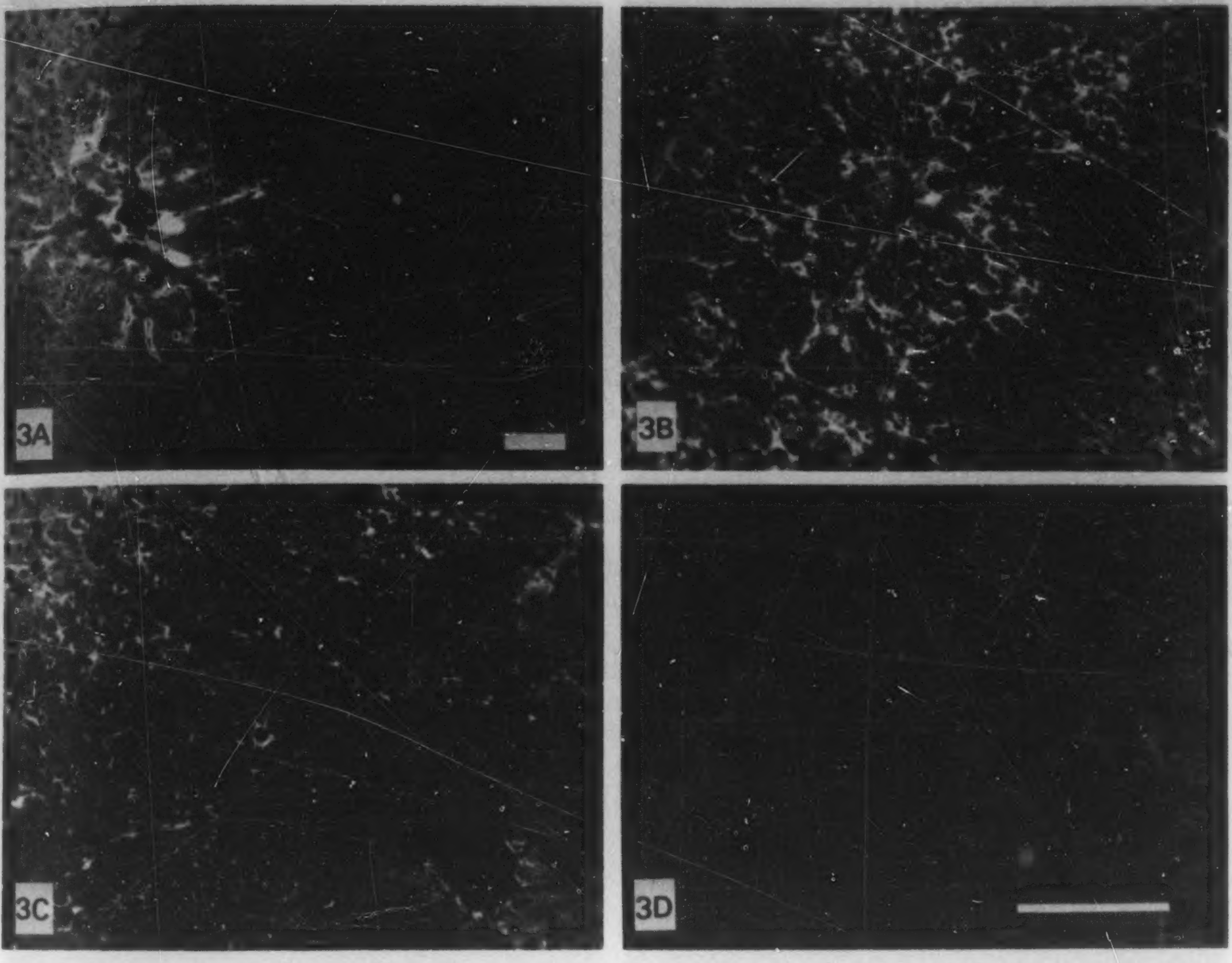

FIGURE 3.—Immunofluorescent localization of fibronectin in livers of rats fed 2-FAA in a CD diet for A) 6, B) 16, and C) 28 days (180 ×), and laminin in a liver of a rat 1 wk after having been fed E) 2-FAA in a CD diet for 13 days (450 ×). After F344 male rats were fed 2FAA in a CD diet, oval cells extending from the portal triad rapidly proliferated. Fibronectin staining increased in the portal zones after 6 days of 2-FAA feeding in a CD diet (A) and later extended from the portal zone through the midzone (B, C) (180 ×). Laminin staining in zones of oval cell proliferation increased, with ductlike structures and cords of oval cells being partially outlined (E). *Bars*=50 µm.

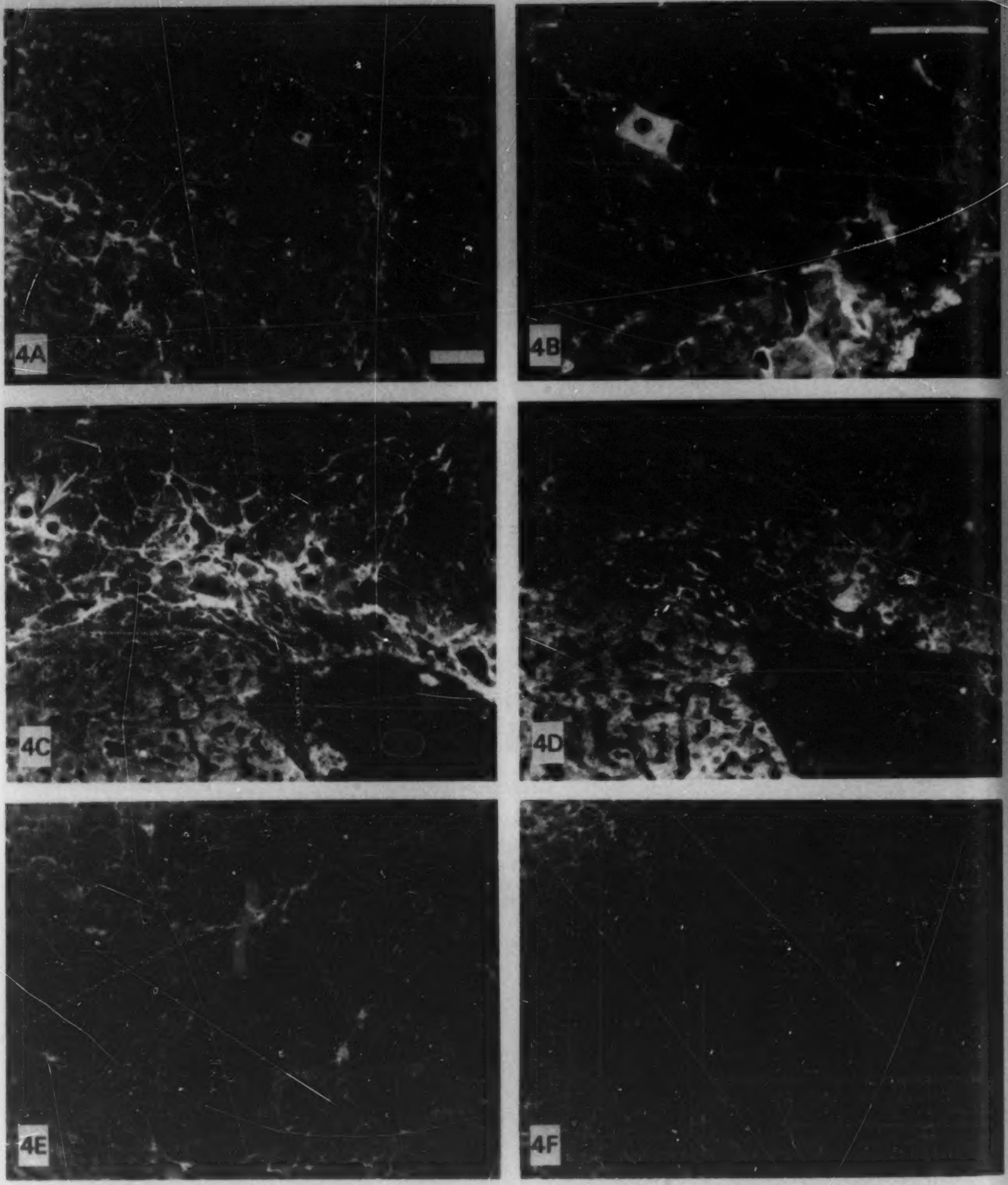

FIGURE 4.—Immunofluorescent localization of fibronectin (A–C, E, F) and laminin (D) in livers of rats treated with DENA (A–D) or fed diets containing 2-FAA for four 2-wk cycles (E, F). A (180 ×) and B (450 ×) illustrate variable distribution of fibronectin in livers after DENA, with the cytoplasm of a large cell staining for fibronectin. Areas of increased and decreased staining for fibronectin are seen. C and D (180 ×) illustrate fibronectin and laminin staining, respectively, of serial sections of a portal area. Staining of extracellular areas for fibronectin is increased irregularly, as are two cells staining for fibronectin (*arrow*). Laminin staining is limited to portal triads, where it is localized around ductules and arteries. E and F (180 ×) illustrate areas of hyperplasia and nodularity, respectively, seen in rats fed four cycles of 2-FAA. Neoplastic nodules consistently and definitely had decreased fibronectin staining. *Bars*=50 µm.

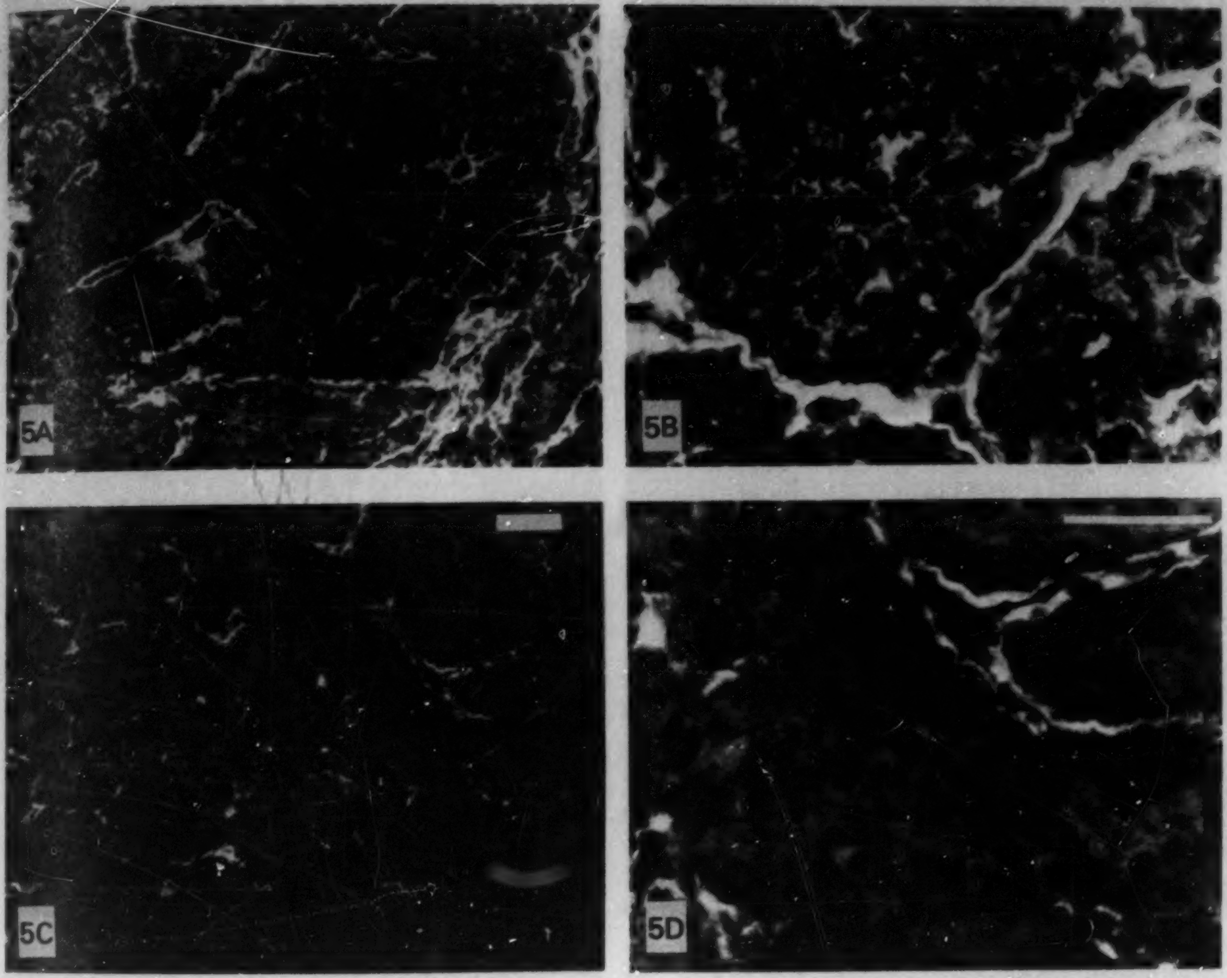

FIGURE 5.—Immunofluorescent localization of fibronectin (A, 180 ×; B, 450 ×) and laminin (C, 180 ×; D, 450 ×) in transplantable Morris hepatoma 7777. Intense fluorescence of fibronectin is seen in vascular areas and in connective tissue stroma as well as around each individual cell. Laminin is also present in stromal tissue but is not seen around individual cells. The appearance of the cells in (D) does not represent specific fluorescence but is due to background yellow fluorescence of the tumor cells. *Bars*=50 µm.

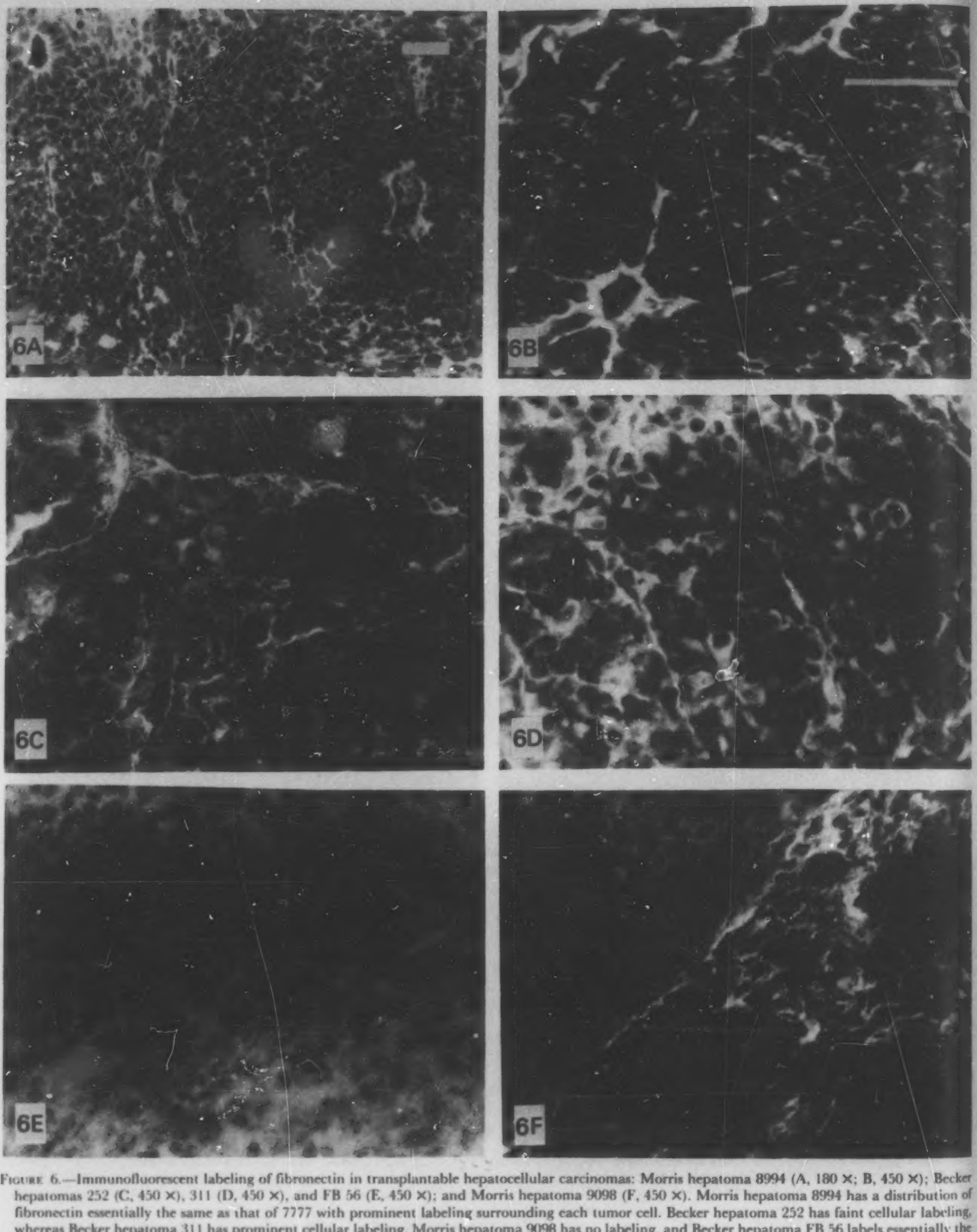

FIGURE 6.—Immunofluorescent labeling of fibronectin in transplantable hepatocellular carcinomas: Morris hepatoma 8994 (A, 180 ×; B, 450 ×); Becker hepatomas 252 (C, 450 ×), 311 (D, 450 ×), and FB 56 (E, 450 ×); and Morris hepatoma 9098 (F, 450 ×). Morris hepatoma 8994 has a distribution of fibronectin essentially the same as that of 7777 with prominent labeling surrounding each tumor cell. Becker hepatoma 252 has faint cellular labeling, whereas Becker hepatoma 311 has prominent cellular labeling. Morris hepatoma 9098 has no labeling, and Becker hepatoma FB 56 labels essentially the same as Morris hepatoma 252. *Bars*=50 μm.

Effects of Isoproterenol on Mammary Gland Tumors Induced by *N*-Nitroso-*N*-Methylurea and Salivary Gland Tumors Induced by 7,12-Dimethylbenz[*a*]anthracene[1,2,3]

Tibor Barka[4,5,6]

ABSTRACT—The effect of isoproterenol (IPR) (20 mg/kg, twice per wk) on mammary gland tumors induced by *N*-nitroso-*N*-methylurea (NMU) (40 or 77 mg/kg, iv) was studied. Within 18 weeks 50–60% of the noninbred female Sprague-Dawley rats that received a single injection of NMU developed carcinomas of the mammary gland. In addition, a malignant lymphoma was observed. There was no change in the incidence of tumors if NMU was administered at the time that DNA synthesis was stimulated in the submandibular glands by two injections of IPR (160 mg/kg, ip) given 24 hours apart. Tumors of unequivocal salivary gland origin were not observed, irrespective of whether NMU was given at the peak of stimulated DNA synthesis or without pretreatment with IPR. However, in 10% of the tumor-bearing rats, tumors were found in the neck region. These tumors could be separated from the salivary glands by dissection and were of mammary gland origin. Chronic treatment with IPR caused marked enlargements of the parotid and submandibular glands with hypertrophy of the acinar cells and degeneration of the duct system. Such a treatment caused a high death rate but no change in the incidence of the tumors. The effect of chronic IPR treatment (10 mg/kg twice per wk or 5 mg/kg three times per wk) on submandibular gland tumors induced by 7,12-dimethylbenz[*a*]anthracene (DMBA) was also studied. With the intraglandular injection of 100 or 200 μg of DMBA, the incidences of squamous cell carcinomas in the glands were 6.8 and 38.6%, respectively. Chronic administration of IPR after the instillation of DMBA caused a high death rate but no statistically significant change in the incidence of salivary gland tumors—JNCI 1982; 69:1115–1120.

DNA synthesis of the acinar cells in the parotid and submandibular glands of rats and mice can be stimulated by the administration of the beta-adrenergic agonist IPR. Repeated administration of this drug leads to hyperplastic and hypertrophic enlargements of the glands (*1–11*). IPR thus provides a means to study the effects of induced cell proliferation and hyperplastic and hypertrophic growth on the induction and development of tumors of the salivary glands. Specifically, this study was concerned with two related problems: 1) the role of cell replication in the induction of salivary gland tumors and 2) the possible promoting effect of IPR in chemical carcinogenesis of the salivary glands.

The rationale of the experiments to analyze the first problem was as follows: The rate of DNA synthesis and cell replication in the parotid and submandibular glands of adult rats is very low (>0.1%). Both DNA synthesis and cell replication can be stimulated greatly by IPR. It was established previously (*3*) that two injections of 160 mg IPR/kg, given 2 hours apart ip to female rats, maximally stimulate DNA synthesis in the parotid and submandibular glands; the peak of DNA synthesis occurs 24 hours after the second injection of the drug. At that time, a significant proportion of acinar cells in the parotid and submandibular glands are in the S-phase of the cell cycle. By selection of an appropriate carcinogen, which acts during the time of induced DNA synthesis, the role of cell replication in the initial step of carcinogenesis in the glands could be studied. I have selected NMU as the carcinogen because it fulfills the following criteria: It is a potent carcinogen capable of producing tumors in a wide variety of organs, even as a single injection given systematically (*12*); it does not require metabolic activation (*13*); and it is quickly metabolized and eliminated (*14*). Hence the initial interactions of NMU with its target molecules are restricted for a short period of time. Of the large number of diverse tumors induced by NMU, Druckrey et al. (*12*) have reported the occurrence of only 1 parotid gland tumor. However, Parkin and Neale (*15*) described a 10% incidence of salivary gland tumors induced by NMU in female Wistar rats pretreated with IPR. Our findings, reported in this communication, are at variance with those of Parkin and Neale. Since the single injection of NMU produced a high incidence of mammary gland tumors, our observations bear also on the possible effect of adrenergic stimulation on the development of mammary gland tumors.

For the study of the possible tumor-promoting effect of IPR, rats were treated chronically with IPR following the instillation of DMBA in doses that produced carcinomas in less than 50% of the animals.

MATERIALS AND METHODS

Six-week old, female Sprague-Dawley rats (Zivic-Miller Laboratories, Allison Park, Pa.), weighing approximately 150 g, were used. The rats were housed in air-conditioned (20–22°C, 50% relative humidity) quarters, 3/cage, and had

---

Abbreviations used: DMBA=7,12-dimethylbenz[*a*]anthracene; IPR=isoproterenol; NMU=*N*-nitroso-*N*-methylurea.

---

[1] Received February 2, 1982; accepted June 3, 1982.

[2] Supported by Public Health Service grant CA-24005 from the National Cancer Institute.

[3] Animals were maintained under the guidelines set forth by the Mount Sinai School of Medicine.

[4] Department of Anatomy and Department of Pathology, Mount Sinai School of Medicine of The City University of New York, New York, N.Y. 10029.

[5] *Address reprint requests to* Dr. Barka at Department of Anatomy, Mount Sinai School of Medicine, One Gustave L. Levy Place, New York, N.Y. 10029.

[6] I am indebted to Dr. M. Kaneko, Department of Pathology, Mount Sinai School of Medicine, for consultation concerning the diagnosis and classification of tumors and to Ms. H. van der Noen and Ms. P. Musikant for their excellent assistance.

free access to rat chow and water. The number of animals in the various experimental groups, the doses of carcinogens, and treatment with IPR are given in table 1.

A 2% solution of NMU (ICN Pharmaceuticals Inc. Plainview, N.Y.) in saline was given iv into the femoral vein of rats under light ether anesthesia. DMBA (Eastman Kodak Co., Rochester, N.Y.) was dissolved in liquid petrolatum (4 or 8 mg/ml) and was injected (25 µl) into the left lobe of the submandibular gland disposed by a midline incision under aseptic conditions. The skin incision was closed with metal clips. Isoproterenol-HCl (Winthrop Laboratories, New York, N.Y.) was dissolved (8 or 1%) in 0.1% sodium metabisulfite and was given ip.

Autopsies, excluding the brain, were performed on all rats that were killed or died. Routinely, the submandibular, sublingual, and parotid glands, the cervical lymph nodes, and the tumors were examined microscopically. Histologic examinations were extended to other organs if pathologic lesions were suspected on the basis of gross examinations. The tissues were fixed in Formalin and embedded in paraffin. The sections were stained with hematoxylin and eosin.

Statistical analyses of tumor rates and death rates were performed according to Peto (*16*).

RESULTS

Table 1 summarizes the experiments and results. Text-figure 1 shows the death rates in all experimental groups.

Experiment I

Experiment I was designed to test two hypotheses: *a*) NMU, a short-lived carcinogen, induces tumors of the parotid and/or submandibular glands in high incidence in rats only if DNA synthesis is stimulated (by IPR) concomitantly in these organs (groups 1, 2, and 3). *b*) The development of salivary gland tumors induced by NMU is promoted by the chronic administration of IPR, which causes marked hyperplastic and hypertrophic enlargements of the parotid and submandibular glands (groups 4 and 5).

To test the first hypothesis, I gave rats two injections of IPR (160 mg/kg) 24 hours apart, followed by MNU (40 or 77 mg/kg) 24 hours after the second injection of IPR. Female animals were used because stimulation of DNA synthesis by IPR is more pronounced in female than in male rats (17).

Of the 46 rats that received 40 mg NMU/kg following the two injections of IPR (group 1), 40 survived 18 weeks when the experiment was terminated. Six rats died shortly after the IPR–NMU injections and were excluded. In this group, 23 (50%) rats developed 36 mammary gland tumors. The tumors were adenocarcinomas, most showing a high degree of differentiation. One rat had a tumor in the neck region, which adhered to and partially surrounded the parotid and submandibular glands but could be separated from them by a careful dissection with the aid of a stereomicroscope. Histologically, this tumor was also an adenocarcinoma (fig. 1).

Of the 40 rats given 77 mg NMU/kg following two injections of IPR (group 2), 24 (60%) had developed tumors within 22 weeks when the experiment was terminated. There was no death within this time period. In 1 rat a diffuse, histiocytic malignant lymphoma, involving lymph nodes, spleen, mesentery, liver, kidney, and salivary glands, was found. All remaining tumors were adenocarcinomas of the mammary glands, 1 invading the skin (fig. 2). Three tumors were located in the neck region, but they did not originate from or involve the salivary glands.

Of the 43 rats that were given 40 mg NMU/kg only (group 3), 23 (53%) had a total of 35 tumors. These tumors were also carcinomas of mammary glands, 4 in the neck region, but not involving the salivary glands.

I concluded from these experiments that: 1) A single iv injection of NMU induced no tumors of the salivary glands, even if it was given at the peak of stimulation of DNA synthesis in the glands by IPR. 2) More than 50% of rats given a single injection iv of NMU in a dose of 40 or 77 mg/kg developed single or multiple mammary gland tumors. These tumors grew large, frequently causing ulceration of the skin, but did not produce distant metastases. 3) Of the

TABLE 1.—*Induction of tumors by MNU and DMBA in control and IPR-treated rats*[a]

Expt No.	Group No.	No. of rats	Carcinogen	Dose	IPR before carcinogen[b]	IPR after carcinogen[b]	Duration of expt, wk	No. of rats alive at end of expt (%)	No. of tumor-bearing rats (%)
I	1	46	MNU	40 mg/kg	+	–	18	40 (87)	23 (50)
	2	40	MNU	77 mg/kg	+	–	22	40 (100)	24 (60)
	3	43	MNU	40 mg/kg	–	–	18	34 (79)	23 (53)
	4	48	MNU	40 mg/kg	+	+	18	5 (83)	4 (8)
	5	43	MNU	40 mg/kg	–	+	18	8 (19)	7 (16)
II	1	44	MNU	40 mg/kg	–	+	18	3 (7)	10 (23)
	2	44	MNU	40 mg/kg	–	–	18	21 (48)	31 (70)
III	1	45	DMBA	100 µg	–	+	17	4 (9)	0 (0)
	2	44	DMBA	100 µg	–	–	22	27 (61)	3 (7)
	3	45	DMBA	200 µg	–	+	16	9 (20)	3 (7)
	4	44	DMBA	200 µg	–	–	16	44 (100)	7 (39)

[a] Details of the experiments are given in "Materials and Methods." NMU (2% in saline) was injected iv as a single dose. DMBA was dissolved in liquid petrolatum and injected intraglandularly. IPR (8 or 1% solution in 0.1% sodium metabisulfite) was given ip. In expt I, group 2, a malignant lymphoma was found. The rest of the NMU-induced tumors were adenocarcinomas. All the DMBA-induced tumors were squamous cell carcinomas.

[b] + = IPR given; – = IPR not given.

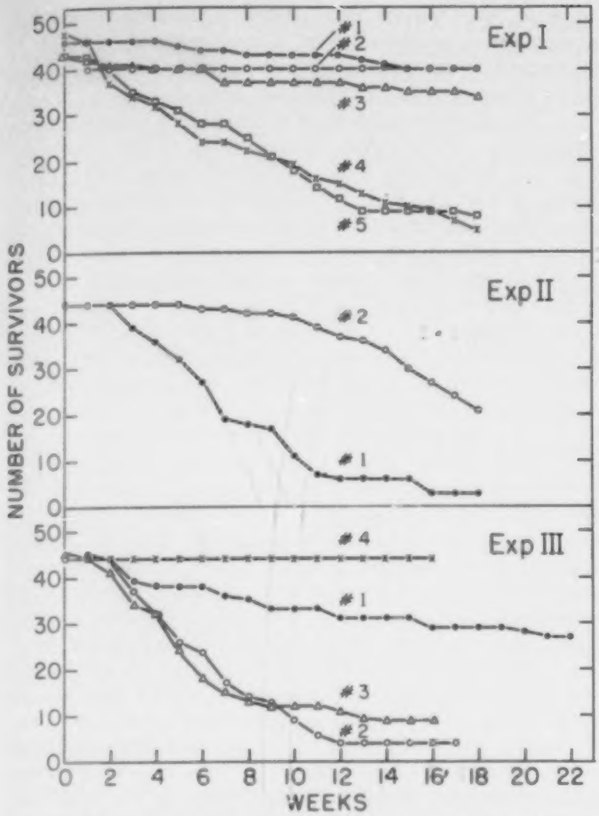

TEXT-FIGURE 1.—Survival of rats in the various experimental groups. Experimental groups and the treatment of rats in each group are given in table 1. The *graphs* show the number of rats alive at the end of each week.

69 rats that developed tumors, 1 (1.4%) had a malignant lymphoma. The rest of the tumors were adenocarcinomas. 4) Eight of the tumors were located in the ventral neck region. Those tumors were also adenocarcinomas and most likely originated in mammary glands. 5) Administration of IPR prior to the injection of NMU had no effect on the incidence of mammary gland tumors.

To test the second hypothesis, I treated rats chronically with IPR; these rats had received NMU, either after 2 injections of high doses of IPR (group 4) or without preceding administration of IPR (group 5) (20 mg/kg, twice per week).

The animals that were treated with IPR chronically had a high rate of death (text-fig. 1). This high death rate was unexpected since in several previous studies this dose of IPR was found to be well tolerated by rats. The cause of the high incidence of death is unknown. Of the 48 rats chronically treated with IPR following IPR and NMU injections (group 4), 4 rats developed mammary gland tumors, detected on 64, 64, 76, and 88 days after the administration of NMU, respectively. Of the 43 rats that received the same dose of NMU (40 mg/kg) followed by the chronic administration of IPR (group 5), 7 developed mammary gland tumors. In 2 rats the tumor was located in the neck region without involving the salivary glands. All tumors were carcinomas showing different degrees of differentiation. No tumor of salivary gland origin was observed.

As described previously (*6–11*), the parotid and submandibular glands of rats chronically treated with IPR were markedly enlarged. In these glands the acinar cells were enlarged and were filled with secretory material. The ratio of ducts to acini was decreased, with frequent degenerative changes of the duct system. In the submandibular glands the granular convoluted duct (or tubule) cells were devoid of secretory granules. The sublingual glands were not affected or only minimally affected by the treatment with IPR.

The incidence of mammary gland tumors induced by NMU appeared to be greatly reduced by the chronic administration of IPR (group 3 vs. group 5 and group 4 vs. group 1). However, the lower incidence of tumors in IPR-treated rats was probably caused by the high death rate; death prevented the development of the tumor in some of the animals. A statistical analysis of these data from the point of view of a possible effect of IPR on the incidence of mammary gland tumors is not feasible, since these experiments were set up to study possible effects of the drug on salivary gland tumors and not on tumorigenesis in the mammary gland. Thus rats in which mammary gland tumors were detected during the life of the animal were not killed to allow for possible tumor development in the salivary glands. Hence the mammary gland tumors were neither "incidental" findings nor diagnosed during the life of the animal (*16*).

Experiment II

Experiment II was set up to study the possible effect of chronic IPR treatment on the development of mammary gland tumors induced by NMU. NMU (40 mg/kg) was given to 88 rats, which then were divided into 2 groups of equal size. Rats in group 1 were given injections twice weekly of 20 mg IPR/kg; rats in group 2 were given the solvent (sodium metabisulfite). Ten rats in group 1 and 31 rats in group 2 bearing mammary gland tumors were found. Morphologically, these neoplasma were similar. Statistical analysis of these data indicated, however, that treatment with IPR had no significant effect on the incidence of mammary gland tumors.

Experiment III

Experiment III was designed to test whether chronic administration of IPR, which produces enlargements of the submandibular and parotid glands, has an effect on the induction of tumors by DMBA. DMBA (groups 1 and 2, 100 μg; groups 3 and 4, 200 μg) was injected into the submandibular glands of rats that were then divided into groups treated with IPR (group 1, 10 mg/kg, twice weekly; group 3, 5 mg/kg, three times a week) or with the solvent (sodium metabisulfite) (groups 2 and 4).

Animals that died or were killed were autopsied, and the parotid glands, the injected and uninjected submandibular glands, and adjacent lymph nodes were examined histologically.

As in previous groups, IPR, even in the lower dose of 5 mg/kg, caused a high incidence of death (text-fig. 1). Of the 44 rats that received injections of 100 μg DMBA (group 2), 3 (6.8%) developed squamous cell carcinomas in the submandibular gland at the site of injection. Two of these tumors were found in rats that died after 16 weeks, and 1 was found in a rat killed at the end of the 22d week, when the experiment was terminated. Of the 45 rats that were treated with 10 mg IPR/kg after the injection of DMBA (group 1), only 4 were alive at the end of the 17th week, when they were killed. In this group no tumors were found.

In view of the low number of tumors found in the control group after the injection of 100 μg DMBA and because of the high rate of mortality in the IPR group, the experiment was repeated with the use of 200 μg DMBA and reduction of the dose of IPR to 5 mg/kg.

Of the 44 rats receiving injections of the higher dose of DMBA (group 4), tumors were observed in the submandibular glands of 17 (38.6%) rats at the end of the 16th week, when all animals were killed. All these tumors were squamous cell carcinomas developed at the injection site. At the end of the 16th week, only 9 of the 45 rats that were treated with IPR (5 mg/kg, three times a week) were alive. In this group (group 3), 3 squamous cell carcinomas were found. The earliest of those was found in the submandibular gland of a rat that died 6 weeks after the instillation of DMBA. The other 2 tumors were detected after the 13th and 16th weeks, respectively. Statistical analysis indicated that treatment with IPR had no significant effect on the induction of tumors by DMBA. The injected glands in which tumors were observed were infiltrated frequently with lymphoid cells. Such glands consisted mostly of ducts with few islands of remaining acini. In the glands of the rats in which no tumors were observed, large cysts lined with squamous epithelium and varying degrees of chronic inflammation were present. The uninjected submandibular gland and the parotid glands of the rats treated with IPR chronically were enlarged and showed hypertrophy, hyperplasia, and degenerative changes of the duct cells, as described above.

DISCUSSION

Neoplasms of rodents' salivary glands are readily induced by intraglandular, but not by systemic, administration of chemical carcinogens (*18–26*). Hence the report of Parkin and Neale (*15*) on the induction of salivary gland tumors in rats by NMU given iv is of considerable interest. These authors described that with a single injection of NMU, salivary gland tumors developed in animals *a*) in which DNA synthesis in the glands was stimulated by IPR (*1*) and *b*) that received the carcinogen at the peak of DNA synthesis. The findings of Parkin and Neale imply that DNA synthesis is a critical factor in NMU-induced carcinogenesis of the salivary glands and, as a corollary, that the low rate of cell replication is, at least in part, responsible for the lack of tumor induction in these organs by systemic carcinogens.

In our series of experiments, a single iv injection of NMU induced mammary gland tumors in about 50% of the rats. Most of these tumors were well-differentiated adenocarcinomas, which in the absence of metastases are difficult to distinguish from polymorphic adenomas. Induction of mammary gland tumors by NMU has been described (*12, 27–29*). The incidence of tumors is dependent on the species, strain, dose, and schedule of application of the carcinogen (*12, 30*). Parkin and Neale (*15*) have found that 17% of female Wistar rats given 77 mg MNU/kg developed mammary gland tumors within 12 weeks and that the percentage of tumor-bearing rats and the average number of tumors were increased if the carcinogen was given at the peak of DNA synthesis induced by IPR.

At variance with the findings of Parkin and Neale (*15*), I have observed no tumors of unequivocal salivary gland origin, irrespective of whether NMU was given at the peak of stimulated DNA synthesis or without pretreatment with IPR. There were, however, 4 of 47 tumor-bearing rats in the IPR–NMU groups (expt. I, groups 1 and 2) and 3 of 23 tumor-bearing rats in the NMU group (expt I, group 4) that developed tumors on the ventral neck region. These tumors could be separated by careful dissections from the parotid and/or submandibular glands. These adenocarcinomas probably originated in mammary glands encountered not infrequently both in rats and mice (*31*) in the subcutaneous tissue adjacent to the parotid gland. Although some mammary gland tumors are difficult to distinguish from sweat gland tumors, sweat glands apparently are not found in the neck region in the rat. The salivary gland tumors described by Parkin and Neale were "pleomorphic adenomas" with the exception of 1 tumor that arose "from keratinized squamous epithelium of salivary duct." One of the 6 salivary gland tumors observed by Parkin and Neale originated from the sublingual gland. This is of interest because DNA synthesis is not stimulated significantly by IPR in the sublingual gland.

Further experiments are required to explain the discrepancy between the findings of Parkin and Neale (*15*) and mine. Strain differences may account for the induction of salivary gland tumors by NMU in Wistar rats and the lack of induction in Sprague-Dawley rats. It is conceivable, however, that the tumors observed by the British authors did not originate in the salivary glands either but that they surrounded or perhaps invaded these glands.

The conspicuous enlargement of the parotid and submandibular glands has been well characterized since its first description by Selye and his co-workers (*6*). Chronic administration of IPR seemed to reduce the incidence of mammary gland tumors induced by NMU, but it also caused an unexpected high rate of death. By taking into account the high death rate, which "prevented" tumor development in some animals, I could detect no statistically significant effect of chronic IPR administration on tumor development of the mammary gland.

DMBA and other polycyclic hydrocarbon carcinogens instilled into the submandibular gland produce tumors in a dose-dependent manner (*23*). With two doses of DMBA (100 and 200 μg) I have observed a 6.8 and 38.6% incidence, respectively, of tumors in the submandibular glands. All these tumors were squamous cell carcinomas. These doses of DMBA were chosen to investigate possible tumor-promoting effects of IPR. Chronic treatment with IPR caused a high mortality rate. In several previously published and in my unpublished experiments, it was found that rats tolerated well much higher doses of IPR than those used in this study. The cause of this unexpected high death rate is not known, but it may be related to an exacerbation of a subclinical (pulmonary) infection. A statistical analysis of the data according to Peto (*16*), which accounts for the death of experimental animals not caused by the tumors, indicated that chronic administration of IPR had no significant effect on the induction of tumors by DMBA. According to Shklar and Cataldo (*24*), chronic administration of IPR, commencing with the implantation of 5 mg DMBA into the submandibular gland, reduced both the size and number of tumors. Since such a high dose of DMBA induces tumors in 100% of the animals, the interpretation of the data of Sklar and Cataldo is difficult. The dose (200 μg) used in this study seems optimal for detection of inhibitory or promoting effects on tumorigenesis. Since IPR can produce marked hyperplastic and hypertrophic enlargements of the salivary glands even in much smaller doses than those used in this study, further experiments with low doses of IPR in combination with DMBA (200 μg) are warranted. Such experiments should provide a definite answer on the effect of IPR on the induction of salivary gland tumors by a polycyclic hydrocarbon carcinogen.

REFERENCES

(*1*) Barka T. Induced cell proliferation: The effect of isoproterenol. Exp Cell Res 1965; 37:662–679.

(*2*) ———. Stimulation of DNA synthesis by isoproterenol in the salivary gland. Exp Cell Res 1965; 39:355–364.

(*3*) Barka T, van der Noen H. Stimulated growth of submandibular gland. Lab Invest 1976: 35:507–514.

(*4*) Baserga R. Heffler S. Stimulation of DNA synthesis by isoproterenol and its inhibition by actinomycin D. Exp Cell Res 1967: 46:571–580.

(*5*) Baserga R. Inhibition of stimulation of DNA synthesis by isoproterenol in submandibular glands of mice. Life Sci 1966; 5:2033–2039.

(*6*) Selye H, Cantin M, Veilleux R. Excessive stimulation of salivary gland growth by isoproterenol. Science 1961; 133:44–45.

(*7*) Brown-Grant K. Enlargement of salivary glands in mice treated with isopropylnoradrenaline. Nature 1961; 191:1076–1078.

(*8*) Novi AM, Baserga R. Association of hypertrophy and DNA synthesis in mouse salivary glands after chronic administration of isoproterenol. Am J Pathol 1971; 62:295–308.

(*9*) Pohto P. Catecholamine-induced salivary gland enlargement in rats. Acta Odontol Scand 1966; 24:1–73.

(*10*) Schneyer CH. Salivary gland changes after isoproterenol-induced enlargement. Am J Physiol 1962; 203:232–236.

(*11*) Wells H. Submandibular salivary gland weight increase by administration of isoproterenol to rats. Am J Physiol 1962; 202:425–428.

(*12*) Druckrey H, Preussmann R, Ivankovic S, et al. Organotrope carcinogene Wirkungen bei 65 verschiedenen *N*-Nitroso-Verbindungen an BD-Ratten. Z Krebsforsch 1967; 69:103–201.

(*13*) Magee PN, Barnes JM. Carcinogenic nitroso compounds. Adv Cancer Res 1967; 10:163–246.

(*14*) Swann PF. The rate of breakdown of methyl methane-sulphonate, dimethylsulphate and *N*-methyl-*N*-nitrosourea in the rat. Biochem J 1968: 110:49–52.

(*15*) Parkin R, Neale S. Effect of isoprenaline on induction of tumours by methyl nitrosourea in salivary and mammary glands of female Wistar rats. Br J Cancer 1976; 34:437–443.

(*16*) Peto R. Guidelines on the analysis of tumour rates and death rates in experimental animals. Br J Cancer 1974; 29:101–105.

(*17*) Barka T. Stimulation of deoxyribonucleic acid synthesis in the salivary gland by isoproterenol. The effect of sex. Exp Cell Res 1967; 48:33–40.

(*18*) Bauer WH, Byrne JJ. Induced tumors of the parotid gland. Cancer Res 1950; 10:755–761.

(*19*) Glucksmann A, Cherry CP. The effect of sex and of sex and thyroid hormones on the induction of cancers in the salivary glands of rats. Br J Cancer 1966; 20:760–777.

(*20*) Franseen CC, Aub JC, Simpson CL. Experimental tumors in lymph nodes and in endocrine and salivary glands. Cancer Res 1941; 1:489–493.

(*21*) Matsumura T. Enzyme histochemistry of experimentally induced tumors in the mouse submaxillary and sublingual glands during carcinogenesis. Gan 1966; 57:251–263.

(*22*) Rusch HP, Baumann CA, Maison GL. Production of internal tumours with chemical carcinogens. Arch Pathol 1940; 29:8–19.

(*23*) Schmutz JA, Chaudhry AP. Incidence of induced tumors in the rat submandibular gland with different doses of 7,12-dimethylbenz-alpha-anthracene. J Dental Res 1969; 48:1316.

(*24*) Shklar G, Cataldo E. Effects of a chemical carcinogen on the submaxillary gland of albino rats treated with isoproterenol. Cancer Res 1966; 26:1319–1323.

(*25*) Steiner PE. Comparative pathology of induced tumors of the salivary glands. Arch Path 1942; 34:613–624.

(*26*) Wigley CB, Carbonell AW. The target cell in the chemical induction of carcinomas in mouse submandibular gland. Eur J Cancer 1976; 12:737–741.

(*27*) Bots GT, Willighagen RG. Tumours in the mammary gland induced in Lewis rats by intravenous methylnitrosourea. Br J Cancer 1975; 31:372–374.

(*28*) Gullino PM, Pettigrew HM, Grantham FH. *N*-Nitrosomethylurea as mammary gland carcinogen in rats. J Natl Cancer Inst 1975; 54:401–414.

(*29*) Turcot-Lemay L, Kelly PA. Characterization of estradiol, progesterone, and prolactin receptors in nitrosomethylurea-induced mammary tumors and effect of antiestrogen treatment on the development and growth of these tumors. Cancer Res 1980; 40:3232–3240.

(*30*) Swenberg JA, Koestner A, Wechsler W, Brunden MN, Abe H. Differential oncogenic effects of methylnitrosourea. J Natl Cancer Inst 1975; 54:89–96.

(*31*) Dawe CJ. Tumors of the salivary and lacrymal glands, nasal fossa and maxillary sinuses. In: Turusov VS, ed. Pathology of tumors in laboratory animals. Vol II. Lyon: IARC, 1979:91–134.

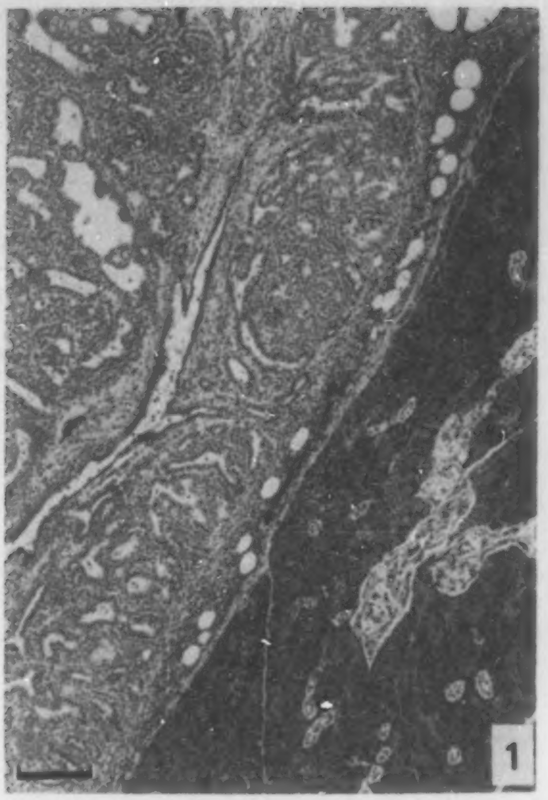

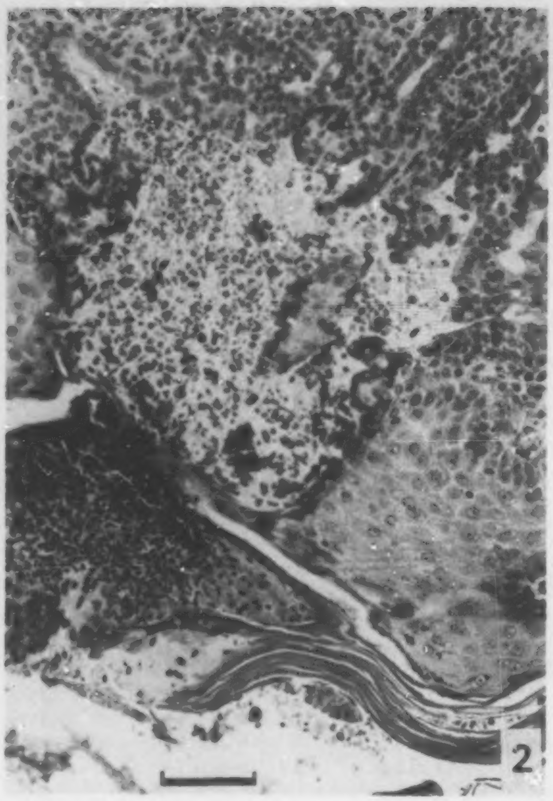

FIGURE 1.—This low-power photomicrograph illustrates an adenocarcinoma adjacent to the parotid gland. The tumor developed in a rat given 40 mg NMU/kg following two injections of IPR (expt I, group 1). The tumor could be separated from the gland by dissection. *Bar*=200 µm.

FIGURE 2.—Partially necrotic adenocarcinoma of the mammary gland invading the skin. The tumor developed in a rat that received 77 mg MNU/kg following two injections of IPR (expt I, group 2). *Bar*=100 µm.

Immunotherapeutic Effects of Partially Purified Tumor-Specific Transplantation Antigens on Pulmonary Metastases of a 3-Methylcholanthrene-Induced Sarcoma in Mice: A Preliminary Report[1,2,3]

Tsuguo Tanaka,[4] Neal R. Pellis,[4] *and* Barry D. Kahan[4,5]

ABSTRACT—Tumor-specific transplantation antigens (TSTA), which were partially purified by preparative isoelectric focusing of 3-*M* KCl extracts of a fibrosarcoma MCA-F induced in inbred female C3H/HeJ mice with 3-methylcholanthrene and previously shown to display immunotherapeutic activity against subcutaneous neoplasms, were effective against pulmonary metastases. Weekly sc injections of 25 μg fraction 15 decreased the number of pulmonary colonies after iv injection of tumor cells into syngeneic, virgin C3H/HeJ mice. The effect was immunologically specific; the immunoprotective fraction from the heterotypic, antigenically distinct MCA-D tumor did not affect the number of pulmonary MCA-F tumor colonies. Because fraction 15 treatment did not alter the number of extrapulmonary tumor colonies, the survival rates of hosts challenged iv with MCA-F cells were unaffected. The variant cell line MCA-F-4 was selected to detect prolonged host survival as a result of a therapeutic effect against pulmonary metastases. This line was selected for its proclivity for lung colonization and low propensity for growth in extrapulmonary sites. Cross-immunoprotection tests demonstrated that MCA-F-4 shares a TSTA with the parent tumor. Therapeutic administration of fraction 15 prolonged the survival of hosts in two settings: 1) after artificial iv injection of MCA-F-4 cells and 2) as treatment for hosts resected of 1-cm subcutaneous MCA-F-4 primary tumors and at high risk for spontaneous pulmonary metastases. Therefore, fraction 15 displayed therapeutic effects on both artificially induced and spontaneous pulmonary metastases.—JNCI 1982; 69:1121–1126.

TSTA have been extracted from MCA-induced guinea pig hepatomas (*1, 2*), virus-induced tumors (*3*), and MCA-induced murine sarcomas (*4–6*) with the use of hypertonic potassium chloride (3*M* KCl). Pretreatment of syngeneic murine hosts with 0.5–1.0 mg protein of crude 3-*M* KCl extracts of MCA-induced fibrosarcomas induces specific resistance against sc challenge with one hundredfold the lethal dose of the homotypic tumor (*4, 7, 8*). Fiftyfold purification of the active principle was obtained by isoelectric focusing (*9*): 10–25 μg fraction 15 (pI 5.8–6.0) specifically protects syngeneic hosts. The focused material evokes delayed-type hypersensitivity in syngeneic hosts immunized with irradiated cells or with purified plasma membranes and does not contain H-2 alloantigenic activity (*10*). Weekly injections of fraction 15 enhance host resistance against subcutaneous primary tumors, supralethal challenges after complete tumor excision, and residual neoplastic cells following partial resection (*11*).

In clinical practice, however, therapeutic failures tend to occur when there has been intravenous, rather than local, dissemination of tumor cells. In many cases, patients succumb to micrometastases that have occurred prior to surgery. The present studies were designed to investigate the therapeutic effects of fraction 15 on neoplastic progression after hematogenous dissemination of tumor cells produced artificially or spontaneously. Weekly administration of fraction 15 decreased the number of pulmonary, but not extrapulmonary, tumor colonies following artificial, iv injection of MCA-F cells into virgin C3H/HeJ mice or into hosts resected of 1-cm MCA-F tumors. Using a cell variant MCA-F-4, which displays selectivity for the lung and spontaneous pulmonary metastases after resection of subcutaneous primary tumors, we demonstrated that fraction 15 therapy prolongs host survival. Thus therapeutic administration of fraction 15 at weekly intervals stimulates host immunity to resist hematogenously disseminated cells capable of forming metastatic deposits in the lung.

MATERIALS AND METHODS

Tumors.—Several antigenically distinct tumors induced in inbred female C3H/HeJ mice (The Jackson Laboratory, Bar Harbor, Maine) by injection of 179 μg MCA have been characterized (*7*). The present studies used 2 fibrosarcomas, MCA-F and MCA-D, which were serially passaged sc in 4- to 6-week-old female syngeneic C3H/HeJ mice. All experiments used cells from the fourth to sixth transplant generation.

Extraction and purification of TSTA.—Freshly excised 1.5-cm tumors were minced with scissors and treated three or four times with 0.25% trypsin in Hanks' solution for 20 minutes at 37°C. The cell suspension was washed three times with EMEM. TSTA was extracted by the 3-*M* KCl method

ABBREVIATIONS USED: EMEM=minimum essential medium; MCA=3-methylcholanthrene; MTD=minimum tumorigenic dose(s); PBS=phosphate-buffered saline; pI=isoelectric point; TSTA=tumor-specific transplantation antigen(s).

---

[1] Received February 2, 1982; accepted June 3, 1982.

[2] Supported by American Cancer Society grant IM-62G.

[3] Animals were maintained under the guidelines set forth by the Division of Immunology and Organ Transplantation, Department of Surgery, The University of Texas Medical School at Houston in accordance with guidelines provided by the National Institutes of Health.

[4] Division of Immunology and Organ Transplantation, Department of Surgery, The University of Texas Medical School at Houston, 6431 Fannin, Houston, Tex. 77030.

[5] *Address reprint requests to* Dr. Kahan.

(*7, 12*): Tumor cells were suspended in a solution of 3 *M* KCl in 0.15 *M* PBS (pH 7.2). After 16 hours at 4°C, the insoluble cell debris was sedimented at 165,000×*g* for 60 minutes. The supernatant was concentrated by dialysis against 50% sucrose in PBS and then dialyzed against 200 volumes of PBS to remove sucrose and KCl. Precipitates formed during dialysis were removed by a second 165,000×*g* ultracentrifugation for 60 minutes. The protein content in the final supernatant, designated "crude" antigen, was measured with the use of the Lowry assay with albumin as a standard (*13*).

The crude extract was fractionated by preparative isoelectric focusing by means of a modification of the method of Radola (*14*), described in detail previously (*9*). The pI-5.9 zone (fraction 15), previously demonstrated to bear immunoprophylactic and immunotherapeutic activities (*9*), was first demonstrated to induce immunoprophylaxis, i.e., to protect syngeneic hosts against challenge 10 days later with 100 MTD of the corresponding MCA-induced tumor (*9*). Fraction 15 was injected sc into the flanks on a weekly schedule at a dose of 25 μg protein, the optimal amount in the immunoprotection test that was assumed to be the best therapeutic dose, beginning 1 day after challenge or resection of a primary tumor.

Experimental intravenous metastasis.—C3H/HeJ mice anesthetized by ether inhalation were given injections via the femoral vein of a variable number of viable tumor cells suspended in 0.2 ml Hanks' solution. The mice were killed 21 days later for enumeration of extrapulmonary and pulmonary tumor colonies. Extrapulmonary tumor colonies, located primarily in subcutaneous tissues, skeletal muscles, kidney, mediastinum, and/or mesentery, were counted macroscopically at autopsy if they were greater than 1 mm in diameter. The intracranial space was not examined. Pulmonary tumor colonies were enumerated with the use of the india ink insufflation method of Wexler (*15*) with the aid of a dissecting microscope. The size of individual metastases was not measured; therefore, one cannot be assured that the observed numerical differences do not reflect a shift to a size below that visible with a dissecting microscope.

Immunologic specificity of fraction 15.—For evaluation of immunologic specificity, groups of 10 mice given injections iv of 10^5 MCA-F cells were treated weekly on three occasions with 25 μg MCA-F fraction 15 or with 20 μg MCA-D fraction 15. At 21 days after injection, the number of pulmonary colonies counted in the 2 therapy groups was compared with the number in an untreated, control group.

Selection of the metastatic variant MCA-F-4.—The variant cell line MCA-F-4 was selected from the parent MCA-F tumor by the method of Fidler (*16*). A single cell suspension of the MCA-F tumor, which had been prepared from a 1.5-cm neoplasm in the sixth in vivo passage with the use of sequential treatments with 0.25% trypsin in Hanks' solution, was inoculated iv at a dose of 10^5 trypan blue-excluding viable cells in 0.2 ml Hanks' solution. Three representative pulmonary tumor colonies were aseptically isolated 21 days later. The cells dissociated from the lung lesions were suspended in EMEM supplemented with 10% fetal calf serum, 100 U penicillin/ml, 100 μg streptomycin/ml, and 2 m*M* L-glutamine and incubated in 5% CO_2 at 37°C (10^6 viable cells). After growth to confluence, these cells denoted "MCA-F-1" were dissociated from tissue culture flasks and injected iv into virgin C3H/HeJ hosts. Three weeks later, the mice were killed and pulmonary tumor colonies were isolated and grown in tissue culture for a second cycle (MCA-F-2 cells). This procedure was repeated four times. The daughter cell line designated "MCA-F-4" was thereafter maintained by in vivo passage. In addition to its propensity to form pulmonary nodules upon iv injection, the MCA-F-4 cell line displays spontaneous lung metastases following excision of 1-cm primary subcutaneous tumors.

*Immunoprotection test with the use of 3-*M *KCl extracts from MCA-F and MCA-F-4 tumors.*—Cross-immunoprotection tests were performed to investigate the antigenic relationship between MCA-F and its variant MCA-F-4. Groups of 10 mice were immunized with 3-*M* KCl extracts prepared from either MCA-F or MCA-F-4. Ten days later, immunized as well as nonimmunized hosts were challenged sc with 10^4 (100 MTD) MCA-F or MCA-F-4 cells. Tumor diameters were serially measured, mean tumor diameters were computed, and the differences between immunized and nonimmunized groups were compared by means of Student's *t*-test.

Protocol design.—Effect of fraction 15 on the formation of pulmonary and extrapulmonary tumor colonies: Five groups of 30 mice received injections iv of 10^2, 10^3, 10^4, 10^5, or 10^6 MCA-F cells. One day later, 15 mice in each group were treated with three weekly sc injections of 25 μg fraction 15. In addition, 15 mice were not treated. At 21 days after iv challenge, all mice were killed; pulmonary tumor colonies were enumerated, and the groups were compared by means of the Wilcoxon two-sample rank sum test.

Effect of fraction 15 on the survival rates of hosts challenged iv with MCA-F or MCA-F-4 cells: Groups of virgin C3H/HeJ mice received injections iv of varying numbers of MCA-F cells—10^3 (10 MTD; No. of mice=30), 10^4 (100 MTD; No. of mice=40), 10^5 (1,000 MTD; No. of mice=30), or 10^6 (10,000 MTD; No. of mice=30). Separate groups of virgin mice received injections of MCA-F-4 cells at a dose of either 10^4 (100 MTD; No.=40) or 10^5 cells (1,000 MTD; No.=40). One day later, half the members of each group were treated with weekly sc injections of 25 μg fraction 15; the other half were not treated. Differences in survival rates among animals in these groups as computed by the 50% survival time were analyzed by means of the chi-square method, previously described (*7*).

Effect of fraction 15 on spontaneous pulmonary metastases: The therapeutic effect of fraction 15 on spontaneous pulmonary metastases was investigated with the use of a metastatic variant MCA-F-4. Two groups of 25 mice were inoculated sc in the flanks with 10^5 MCA-F-4 cells. Mice were resected of 1.0- to 1.5-cm tumors at 14 days after the inoculation. One group of 25 mice was treated with weekly injections of 25 μg fraction 15; the other group of 25 mice was not treated. At 21 days after resection, all mice were killed and pulmonary metastases were enumerated. The incidence of metastases, i.e., the proportion of hosts displaying nodules, in the 2 groups was compared by the chi-square test. The number of metastases per mouse was compared by means of the Wilcoxon two-sample rank sum test.

RESULTS

Effect of immunotherapy on tumor colonies in pulmonary and extrapulmonary tissues.—Pulmonary tumor colonies were enumerated 21 days after iv inoculation of 10^2, 10^3, 10^4, 10^5, or 10^6 MCA-F cells into syngeneic, virgin C3H/HeJ mice. Mice given injections of 10^2, 10^3, or 10^4 MCA-F cells displayed only rare colonies in the lungs, presumably due to the low incidence of cell variants capable of forming pulmonary metastases. As the inoculum dose increased, an effect of therapy was apparent. The average number of pulmonary tumor colonies in mice challenged iv with 10^5 cells was 6.8±1.7 in untreated hosts and 2.5±0.7 in treated animals ($P<0.05$). Untreated mice given injections iv of 10^6 cells showed 21.6±3.0 (mean ± SE) pulmonary colonies, whereas the treated group displayed 11.0±2.2 pulmonary colonies ($P<0.01$) (text-fig. 1). Therefore, three weekly injections of fraction 15 after iv challenge with MCA-F cells significantly decreased the number of pulmonary tumor colonies. A second experiment confirmed the original one: The number of nodules in each afflicted animal was reduced, but the incidence of mice with pulmonary metastases was unaffected (table 1). Furthermore, fraction 15 had no therapeutic effect on metastases in extrapulmonary sites (table 1). Although not statistically significant, there appeared to be an increased incidence and number of extrapulmonary metastases in treated hosts.

Immunologic specificity.—To ascertain immunologic specificity, we treated groups of C3H mice with fraction 15 prepared from either MCA-F or MCA-D tumors following iv challenge with 10^5 MCA-F cells. Whereas MCA-F fraction 15 decreased the number of pulmonary tumor colonies produced by homotypic MCA-F cells, the immunoprotective fraction from the antigenically distinct MCA-D tumor, which was demonstrated to display specific immunoprophylaxis against 100 MTD of MCA-D [data not shown but similar to those in (*7*)], had no effect on the formation of MCA-F pulmonary tumor colonies. Thus the effect of fraction 15 on pulmonary tumor colonies is immunologically specific (table 2).

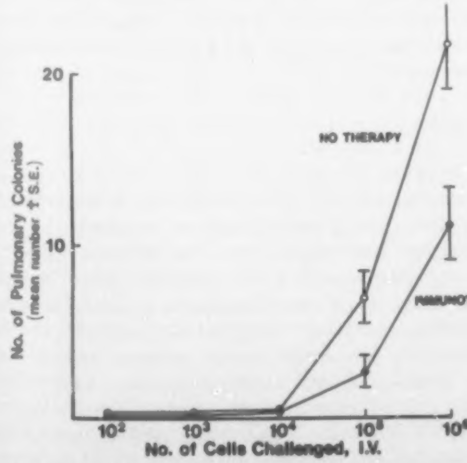

TEXT-FIGURE 1.—Effect of fraction 15 on the formation of pulmonary tumor colonies. A group of 30 mice were given injections iv of 10^6 MCA-F cells. One day later, 15 mice received either three weekly injections of 25 µg fraction 15 (●——●) or were not treated (○——○). At 21 days all mice were killed, and pulmonary tumor colonies were enumerated.

TABLE 1.—*Effect of fraction 15 on the formation of tumor colonies in pulmonary and extrapulmonary tissues after the iv injection of MCA-F cells*[a]

Groups	Pulmonary tumor colonies		Extrapulmonary tumor colonies	
	Incidence, % (No. of mice with colonies/total No. of mice inoculated)	No. of colonies/mouse, mean ± SE	Incidence, % (No. of mice with colonies/total No. of mice inoculated)	No. of colonies/mouse, mean ± SE
No therapy	82 (18/22)	5.8±1.0	64 (14/22)	1.1±0.2
Immunotherapy	67 (14/21)	1.6±0.4[b]	71 (15/21)	2.3±0.5

[a] Groups of C3H/HeJ mice were given injections iv of 10^5 MCA-F cells. One group of mice was treated with weekly injections of 25 µg fraction 15; another group of mice was not treated. At 21 days after iv injection, all mice were killed. Tumor colonies in pulmonary and extrapulmonary tissues were enumerated.

[b] Significant difference ($P<0.05$) by Wilcoxon two-sample rank sum test comparing treated and untreated groups. All other comparisons between control and immunotherapy groups were not statistically significant.

TABLE 2.—*Effects of fraction 15 from MCA-F tumor or MCA-D tumor on the formation of MCA-F pulmonary tumor colonies*[a]

Treatment	Antigen source	No. of pulmonary tumor colonies, mean ± SE	P[b]
None	—	5.0±1.2	—
Fraction 15	MCA-D	5.5±1.3	NS
Fraction 15	MCA-F	1.8±0.6	<0.05

[a] Groups of 10 mice were given injections iv of 10^5 MCA-F cells. One day later, 1 group of mice was treated with three weekly injections of fraction 15 extracted from the MCA-F tumor; a second group was treated with fraction 15 from the heterotypic tumor MCA-D. A third group of mice was not treated. At 21 days after injection, mice were killed, and the pulmonary tumor colonies were enumerated.

[b] *P*-values were determined by the Wilcoxon two-sample rank sum test. NS=not significant.

TABLE 3.—*Effect of fraction 15 on survival of hosts challenged iv with either MCA-F or MCA-F-4*[a]

Dose	Group	MCA-F		MCA-F-4	
		ST_{50}[b]	P[c]	ST_{50}[b]	P[c]
10^4	Untreated	54.4	—	24.2	—
	Immunotherapy	55.2	NS	32.4	<0.01
10^5	Untreated	25.1	—	20.0	—
	Immunotherapy	26.4	NS	18.0	NS

[a] Groups of C3H/HeJ mice were challenged with either 10^4 or 10^5 MCA-F or MCA-F-4 cells iv. One group of mice was treated with weekly injections of 25 µg fraction 15; another group was not treated.

[b] ST_{50} was calculated as 50% survival time of inoculated hosts, in days.

[c] Significance was assessed by chi-square analysis. NS=not significant.

Pulmonary metastases of the metastatic variant MCA-F-4.—The variant cell line MCA-F-4 was selected by four cycles of

TABLE 4.—*Immunotherapeutic effects of fraction 15 on spontaneous pulmonary metastases of MCA-F-4 cell line*[a]

Groups	Total No. of mice with metastases/total No. of mice inoculated (%)	Mice with local recurrences		Mice without local recurrences	
		No. of mice with metastases/total No. of mice inoculated (%)	No. of metastases/mouse	No. of mice with metastases/total No. of mice inoculated (%)	No. of metastases/mouse
No therapy	14/23 (61)	9/11 (82)	0, 0, 1, 1, 2, 2, 2, 2, 4, 16, 21	5/12 (42)[b]	0, 0, 0, 0, 0, 0, 0, 1, 1, 2, 5, 6
Immunotherapy	7/25 (28)[c]	3/13 (23)[d]	0, 0, 0, 0. 0, 0, 0, 0, 0, 0, 4, 5, 5[e]	4/12 (33)	0, 0, 0, 0, 0, 0, 0, 1, 3, 4, 17

[a] Groups of 25 mice were inoculated sc with 10^5 MCA-F-4 cells in the flank. At 14 days after inoculation when the tumor diameters were 1.0-1.5 cm, mice underwent resection. One group of mice was treated with weekly injections of 25 μg fraction 15; another group of mice was not treated. At 21 days after the resection, all mice were killed, and pulmonary metastases were enumerated.

[b] Significant difference in the incidence of metastases between local recurrence-positive and local recurrence-negative groups ($P<0.05$).

[c] Significant difference in the incidence of metastases by chi-square test between therapy and no-therapy groups ($P<0.05$).

[d] Significant difference in the incidence of metastases between therapy and no-therapy groups ($P<0.01$).

[e] Significant difference in the number of metastases/mouse between immunotherapy and no-therapy groups with the use of the Wilcoxon two-sample rank sum test ($P<0.01$).

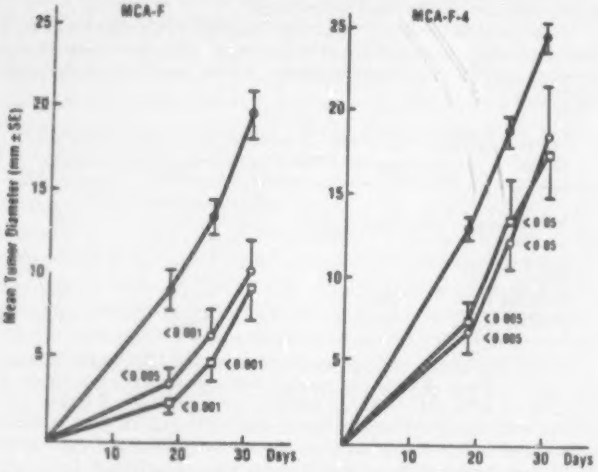

TEXT-FIGURE 2.—Cross-immunoprotection test. Groups of 10 mice were immunized with 3-*M* KCl extracts from MCA-F (○) or MCA-F-4 tumor (□). Ten days later, immunized as well as nonimmunized hosts (●) were challenged sc with 10^4 (100 MTD) MCA-F cells (*left panel*) or MCA-F-4 cells (*right panel*). Tumor diameters were serially measured, and mean tumor diameters were computed.

lung passage in vivo. The variant displays greater avidity for pulmonary, compared to extrapulmonary, tissues. Not only was the number of pulmonary nodules decreased but also the length of host survival was prolonged in hosts treated with fraction 15 after iv injection of 10^4, but not of 10^5, cells (table 3). The slightly prolonged survival of animals inoculated with MCA-F-4 may have been due to the reduced incidence of lethal extrapulmonary metastases, which apparently escape the immunotherapeutic effect of fraction 15 (data not shown).

MCA-F-4 cells implanted sc spontaneously metastasize to the lung during early stages of tumor growth. Treatment with 25 μg fraction 15 reduced the incidence of pulmonary metastases in treated hosts (table 4): 61% of untreated but only 28% of fraction 15-treated mice displayed pulmonary metastases 21 days after resection of 1-cm MCA-F-4 flank tumors. The average number of metastatic foci in afflicted mice was not significantly different between treated and untreated groups (data not shown). The benefit of immunotherapy was most evident in mice bearing local recurrences of the MCA-F-4 tumor; 82% of untreated hosts displaying a local recurrence bore pulmonary metastases. In contrast, three weekly injections of 25 μg fraction 15 significantly decreased the incidence of pulmonary metastases in the recurrence group to 23% ($P<0.01$). The results demonstrate that fraction 15 treatment reduces the incidence of spontaneous hematogenous metastases following resection of a primary tumor, particularly in hosts at high risk for disease recurrence.

Common TSTA between unselected MCA-F and variant MCA-F-4 tumors.—Text-figure 2 shows the outgrowth of MCA-F and MCA-F-4 tumors after immunoprophylaxis with 3-*M* KCl extracts. Mice immunized with crude tumor extracts, either from the original MCA-F tumor or from MCA-F-4, were protected against challenge with either the parent MCA-F or the variant MCA-F-4 tumors. Since the tumors share a cross-reactive TSTA, a major antigenic modulation during the process of selection of the metastatic variant is excluded. These findings are consistent with the suggestion that the therapeutic effects of MCA-F fraction 15 are due to the induction and/or potentiation of host resistance against a TSTA shared with MCA-F-4.

DISCUSSION

Immunotherapeutic application of a tumor extract demands antineoplastic effects not only against local recurrences but also against hematogenous metastases. The investigations described herein extend our previous report (*11*) of therapeutic effects against subcutaneous growths of the MCA-F sarcoma to therapeutic effects against hematogenous pulmonary metastases induced artifically by iv injection or naturally by dissemination from a subcutaneous neoplasm. Weekly administration of fraction 15 decreased the number of pulmonary tumor colonies 3 weeks after iv injection of MCA-F cells. The protection was immunologically specific: MCA-D fraction 15 had no effect on pulmonary nodules following iv inoculation of the heterotypic MCA-F tumor. These findings demonstrate that pulmonary metastases bear at least one common surface antigen present on subcutaneous MCA-F tumors from which fraction 15 was prepared, in addition to any distinctive markers that have been suggested in previous reports (*17–20*).

Fraction 15 treatment did not prolong the survival of hosts challenged iv with MCA-F cells. Although the therapeutic regimen reduced the number of MCA-F lung colonies, it had no effect on extrapulmonary tumor metastases that displayed unimpeded progression leading to death. The differential susceptibility of pulmonary, but not extrapulmonary, metastases to fraction 15 may reflect 1) unique properties of the induced systemic immune response that favor the elimination of cells bearing specific surface properties leading to proclivity for pulmonary colonization, 2) a possible effect of fraction 15 to promote natural killer activity eliminating intravascularly disseminated cells destined to be pulmonary metastases, 3) redirection of cells potentially capable of implanting in the lung to extrapulmonary sites, 4) differential activation of pulmonary host defense mechanisms by fraction 15 therapy, and 5) loss of the TSTA on extrapulmonary metastases. Failure to affect extrapulmonary metastasis is distinctive of fraction 15 therapy, because treatment with crude butanol extracts of MCA-F is equally effective against pulmonary and extrapulmonary metastases (*21*). Therefore, it is most likely that the differential effect of the immunity induced by fraction 15 reflects either a unique susceptibility of variants forming pulmonary metastases or host defenses resisting neoplastic cells destined for, or resident in, the lung.

To demonstrate an effect of fraction 15 immunotherapy on the survival of hosts artificially challenged iv with tumor cells, we used the method described by Fidler for B-16 melanoma in C57BL/6 mice (*16*) to isolate the MCA-F-4 cell variant, which displayed a propensity to form pulmonary, but not extrapulmonary, metastases. Fraction 15 immunotherapy prolonged the survival of hosts inoculated iv with MCA-F-4, presumably due to the aversion of the tumor to grow in subcutaneous sites. Of greater importance as a model for metastatic neoplastic disease was the tendency of MCA-F-4 implanted sc to disseminate hematogenously as spontaneous lung metastases; 61% of mice showed spontaneous pulmonary metastases 21 days after the resection of exponentially growing 1-cm subcutaneous tumors. Conversely, mice bearing 2-cm MCA-F neoplasms display only an 8.7% incidence of pulmonary metastases (data not shown). Furthermore, the 82% incidence of pulmonary metastases in mice with local recurrences of MCA-F-4 after resection of 1-cm tumors was almost twice the incidence in animals free of a local recurrence. The greater immunotherapeutic effect of antigen in hosts at high risk for disease recurrence may be due to the necessity to potentiate their weak resistance (*22–27*), which is otherwise insufficient to overcome residual neoplastic cells, particularly when reactivity is dampened by surgical procedures (*28–32*). These findings are consistent with our recent observations that tumor extract therapy yields superior results in hosts with low concomitant immunity (Inabass S, Pellis NR, Kahan BD: Unpublished observations).

The effect of immunotherapy on the number of lung metastases is critically dependent on the antigen dose and the tumor burden at the time of treatment (*17, 33*). Administration of excess soluble TSTA (*34*) or irradiated tumor cells (*35*) has been shown to impair the expression of concomitant immunity after surgery, to antagonize host resistance, and to increase the number of metastases. These effects may be due at least in part to the presence of antigenic determinants stimulating immune responses that facilitate neoplastic outgrowth (*36*). Contrarily, the results presented herein demonstrate that separation of the immunogenic fraction 15 from antigens facilitating tumor growth provides an effective stimulus to boost host resistance against hematogenous metastases. These effects of fraction 15 compel further evaluation of the potential of tumor extracts as tools for adjuvant immunotherapy of human cancer.

REFERENCES

(*1*) Meltzer MS, Leonard EJ, Hardy AS, Rapp HJ. Protective tumor immunity induced by potassium chloride extracts of guinea pig hepatomas. J Natl Cancer Inst 1975; 54:1349–1354.

(*2*) Leonard EJ, Meltzer MS, Borsos T, Rapp HJ. Properties of tumor-specific antigen solubilized by hypertonic potassium chloride. Natl Cancer Inst Monogr 1972; 35:129–134.

(*3*) Blasekci JA, Tevethia SS. In vitro assay of cellular immunity to tumor-specific antigen(s) of virus-induced tumor by macrophage migration inhibition. J Immunol 1973; 110:590–594.

(*4*) Pellis NR, Tom BH, Kahan BD. Tumor specific and allospecific immunogenicity of soluble extracts from chemically induced murine sarcomas. J Immunol 1974; 113:708–711.

(*5*) Forbes JT, Nakao Y, Smith RT. Tumor-specific immunity to chemically induced tumors: Evidence for immunologic specificity and shared antigenicity in lymphocyte responses to soluble tumor antigens. J Exp Med 1975; 141:1181–1200.

(*6*) Minami A, Mizushima Y, Takeichi N, Hosokawa M, Kobayashi H. Dissociation of anti-tumor immune responses in rats immunized with solubilized tumor-associated antigens from a methylcholanthrene-induced fibrosarcoma. Int J Cancer 1979; 23:358–365.

(*7*) Pellis NR, Kahan BD. Methods to demonstrate the immunogenicity of soluble tumor specific transplantation antigens. I. The immunoprotection assay. Methods Cancer Res 1976; 13:291–330.

(*8*) ———. Specific tumor immunity induced with soluble materials: Restricted range of antigen dose and of challenge tumor load for immunoprotection. J Immunol 1975; 115:1717–1722.

(*9*) Pellis NR, Yamagishi H, Macek CM, Kahan BD. Specificity and biological activity of extracted murine tumor-specific transplantation antigens. Int J Cancer 1980; 26:443–449.

(*10*) Macek CM, Kahan BD, Pellis NR. Delayed hypersensitivity to crude and partially purified murine tumor-specific transplantation antigens and alloantigens utilizing the footpad swelling assay. J Immunol 1980; 125:1639–1643.

(*11*) Kahan BD, Tanaka T, Pellis NR. Immunotherapy of a carcinogen-induced murine sarcoma with soluble tumor-specific transplantation antigens. JNCI 1980; 65:1001–1004.

(*12*) Reisfeld RA, Kahan BD. Biologic and chemical characterization of human histocompatibility antigens. Fed Proc 1970; 29:2034.

(*13*) Lowry OH, Rosebrough MJ, Farr AL, Randall RJ. Protein measurement with Folin phenol reagent. J Biol Chem 1951; 193:265–275.

(*14*) Radola BJ. Isoelectric focusing in layers of granulated gels. II. Preparative isoelectric focusing. Biochim Biophys Acta 1974; 386:181–195.

(*15*) Wexler H. Accurate identification of experimental pulmonary metastases. J Natl Cancer Inst 1966; 36:641–645.

(*16*) Fidler IJ. Selection of successive tumor lines for metastasis. Nature [New Biol] 1974; 242:148–149.

(*17*) Fogel M, Gorelik E, Segal S, Feldman M. Differences in cell surface antigens of tumor metastases and those of the local tumor. JNCI 1979; 62:585–588.

(*18*) Sugarbaker EV, Cohen AM. Altered antigenicity in spontaneous pulmonary metastases from an antigenic murine sarcoma. Surgery 1972; 72:155–161.

(*19*) Pimm MV, Embleton MJ, Baldwin RW. Multiple antigenic specificities with primary 3-methylcholanthrene-induced rat sarcomas and metastases. Int J Cancer 1980; 25:621–629.

(*20*) Faraci RP. In vitro demonstration of altered antigenicity of metastases from a primary methylcholanthrene-induced sarcoma. Surgery 1980; 76:469–473.

(*21*) Kahan BD, Pellis NR, LeGrue SJ, Tanaka T. Immunotherapeutic effects of tumor specific transplantation antigens released by 1-butanol. Cancer 1982; 49:1168–1173.

(*22*) Fisher B, Saffer EA, Fisher ER. Comparison of concomitant and sinecomitant tumor immunity. Proc Soc Exp Biol Med 1970; 135:68–71.

(*23*) Proctor JW, Rudenstam CM, Alexander P. A factor preventing the development of tumour metastases in rats with sarcomas. Nature 1973; 242:29–31.

(*24*) Vaage J. Concomitant immunity and specific depression of immunity by residual or reinjected syngeneic tumor tissue. Cancer Res 1971; 31:1655–1662.

(*25*) Deckers PJ, Davis RC, Parker GA, Mannick JA. The effect of tumor size on concomitant immunity. Cancer Res 1973; 33:33–39.

(*26*) Gershon RK, Carter RL, Kondo K. On concomitant immunity in tumour-bearing hamsters. Nature 1967; 213:674–676.

(*27*) Milas L, Hunter N, Mason K, Withers HR. Immunological resistance to pulmonary metastases in C3Hf/Bu mice bearing syngeneic fibrosarcoma of different sizes. Cancer Res 1974: 34:61–71.

(*28*) Gershon RK, Carter RL, Kondo K. Immunologic defenses against metastases: Impairment by excision of an allotransplanted lymphoma. Science 1968; 159:646–648.

(*29*) Simpson-Herren L, Sanford AH, Holmquist JP. Effects of surgery on the cell kinetics of residual tumor. Cancer Treat Rep 1977; 60:1749–1760.

(*30*) Lundy J, Lovett EJ III, Wolinsky SM, Conran P. Immune impairment and metastatic tumor growth. The need for an immunorestorative drug as an adjunct to surgery. Cancer 1979; 43:945–951.

(*31*) Schatten WE, Kramer WM. An experimental study of postoperative tumor metastases. II. Effects of anesthesia, operation and cortisone administration on growth of pulmonary metastases. Cancer 1958; 11:460–462.

(*32*) Romsdahl MM. Influence of surgical procedures on development of spontaneous lung metastases. J Surg Res 1964; 4:363–370.

(*33*) Vanwijk RR, Godrick EA, Smith HG, Goldweitz J, Wilson RE. Stimulation or suppression of metastases with graded doses of tumor cells. Cancer Res 1971; 31:1559–1563.

(*34*) Thomson DM, Proctor JW, Grosser N, Sutherland M. Impairment of systemic concomitant antitumor immunity by excess soluble tumor antigens. Cancer Immunol Immunother 1980; 8:127–132.

(*35*) Proctor J, Rudenstam CM, Alexander P. Increased incidence of lung metastases following treatment of rats bearing hepatomas with irradiated tumor cells and the beneficial effect of *Corynebacterium parvum* in this system. Biomedicine 1973; 19:248–252.

(*36*) Yamagishi H, Pellis NR, Mokyr MR, Kahan BD. Specific and nonspecific immunologic mechanisms of tumor growth facilitation. Cancer 1980; 45:2929–2933.

Dose-Response Studies With Nitrosoheptamethyleneimine and its α-Deuterium-Labeled Derivative in F344 Rats[1,2,3]

W. Lijinsky,[4] M. D. Reuber,[4] T. S. Davies,[4] *and* C. W. Riggs[4]

ABSTRACT—A dose-response study of the carcinogenicity of nitrosoheptamethyleneimine (N-HEP) in inbred F344 male and female rats was performed by administration of the nitrosamine at several concentrations in drinking water to groups of 20 rats. The concentrations differed by a factor of nearly 2.5 and ranged from 1.0 to 100 mg/liter. The duration of treatment was 13, 25, 50, or 100 weeks, after which the animals were allowed to die naturally of tumors induced. In most treated groups the incidence of tumors of the upper gastrointestinal tract approached 100%. However, at the higher doses there was an inverse relationship between total dose and survival time of the rats. Matched treatment of groups of rats with N-HEP labeled with deuterium in the alpha positions resulted in longer survival. The slower action of the deuterium-labeled compound, as measured by a lower rate of death from tumors, suggests that cleavage of a carbon–hydrogen bond at an alpha position is a rate-limiting step in carcinogenesis by N-HEP in rats.—JNCI 1982; 69:1127–1133.

Experiments in which deuterium-labeled nitrosomorpholine, nitroso-2,6-dimethylmorpholine, and nitrosoazetidine have been used have shown that, in rats, replacement of hydrogen at the α-carbon atoms with deuterium reduces carcinogenic potency (*1–3*). A similar observation was made with deuterium-labeled nitrosodimethylamine (*4*) and suggested that, in both cyclic and open-chain nitrosamines, oxidation at the α-carbon atom was a rate-limiting step in carcinogenesis. Analysis of the effects of deuterium substitution was more difficult for the asymmetric nitrosomethylethylamine (*5*), nitrosomethyl-2-phenylethylamine (*6*), and nitrosomethyl-*n*-butylamine (*7*). All of the foregoing compounds induced tumors either in the liver or esophagus of rats, and some compounds induced tumors in both locations. To expand our understanding of the role of alpha oxidation in carcinogenesis by nitrosamines, we examined the effect of deuterium substitution on the carcinogenic potency of N-HEP in rats. This compound has been reported to induce lung tumors in rats (*8, 9*). Because several dose rates must be used to establish the effect of deuterium substitution with some certainty, a dose-response study of N-HEP was done and is reported here.

MATERIALS AND METHODS

Chemicals.—N-HEP was prepared as described previously (*8, 9*).

N-HEP-d_4 was prepared by exchange of 8 g of N-HEP with 60 ml of deuterium oxide in the presence of 30 g of sodium ethoxide, the reaction mixture being boiled under reflux for 4 hours. After cooling, 100 ml methylene chloride was added to the dark brown reaction mixture, followed by 100 ml water. The mixture was shaken gently, and after the layers were allowed to separate, the lower, pale yellow solution was separated off and the upper layer was discarded. The lower (methylene chloride) layer was washed twice with 30 ml water, after which the methylene chloride was distilled off, leaving a light brown oil. This was then exchanged with deuterium oxide and sodium ethoxide, exactly as described above. The procedure was repeated an additional three times (a total of five exchanges), and the product was distilled under reduced pressure, yielding 4 g of yellow liquid which had a boiling point of 98–99°C at 2 mm Hg. The mass spectrum of the product after each exchange was measured, and the spectrum showed progressive replacement of hydrogen by deuterium, as reflected by increase in the ions of mass 145 and 146 at the expense of ions of mass 142 and 143. The mass spectrum of the product after five exchanges showed that 93% of the hydrogens at the alpha positions had been replaced by deuterium and that ions of mass 146 comprised the overwhelming proportion of the molecular ions, observations consistent with a majority of the molecules being N-HEP-d_4.

Animal treatments.—Groups of 20 male F344 rats of the colony of the NCI-Frederick Cancer Research Facility were used for each treatment; they were 7–8 weeks old at the beginning of the treatment. The animals were housed four to a plastic cage with a wire-mesh bottom. Each cage of rats was given 80 ml of a solution of N-HEP as drinking water on each of 5 days/week; on the other 2 days, tap water was given ad libitum so that the animals could make up any water deficit they had incurred. After the animals became accustomed to the taste of the N-HEP solution, which took a few days, almost all of the solutions were consumed, with little spillage, so that the average dose received by the animals could be estimated reasonably well. Each treatment solution was prepared by dilution of a stock solution of N-HEP in ethanol, prepared once every 3 months, with deionized water at pH 6.8–7.2. The treatment solutions were dispensed to the animals for prescribed numbers of weeks, after which the animals were allowed to die naturally (a few were killed when moribund); each animal was given a complete necropsy and any lesions and all major organs were fixed for histologic examination.

The animals in groups 1–9, 13, and 14 (table 1) and the untreated controls were all from the same lot and were introduced to the experiment simultaneously. To assess the

---

ABBREVIATIONS USED: GI=gastrointestinal; N-HEP=nitrosoheptamethyleneimine; N-HEP-d_4=α-deuterium-labeled N-HEP.

---

[1] Received February 9, 1982; accepted June 3, 1982.

[2] Supported by Public Health Service contract N01CO-75380 from the Office of the Director, National Cancer Institute.

[3] Animals were maintained under the guidelines of the NCI-Frederick Cancer Research Facility.

[4] Chemical Carcinogenesis Program, NCI-Frederick Cancer Research Facility, P.O. Box B, Frederick, Md. 21701.

best copy available

TABLE 1.—*Neoplastic lesions in F344 rats given N-HEP*

Parameter	Treatment group[a]														
	C[b]	1	2	3	4	5	6	7	8	9	10	11	12	13	14
Dose rate, mg/liter		100	40	16	6.4	6.4	2.6	2.6	1.0	1.0	100	40	40	40	100
Duration, wk		13	25	25	25	50	50	100	50	100	13	13	13	25	13
Total dose, mg		130	100	40	16	32	13	26	5	10	130	52	52	100	130
Sex	♂	♂	♂	♂	♂	♂	♂	♂	♂	♂	♀	♀	♀	♂	♂
Deuterium labeled[c]	–	–	–	–	–	–	–	–	–	–	–	–	+	+	+
	Tumor found														
Adrenal gland															
Cortical carcinoma	1														
Hyperplastic nodule							1								
Pheochromocytoma	7				4	1	5	2	2	3					1
Bladder															
Papilloma					1										
Bone															
Osteoma					1					1					
Brain															
Olfactory carcinoma													1		
Bronchus															
Basal cell carcinoma												1			
Basal cell papilloma												1			
Squamous cell carcinoma											1	1			
Squamous cell papilloma												1			
Duodenum															
Adenocarcinoma							1								
Esophagus															
Basal cell carcinoma		4	9	10	3	13	2	7		2	6	9	15	17	13
Basal cell papilloma		8	3	5	2	1		6		1		13	8		5
Papilloma		4	4	1											3
Squamous cell carcinoma		1	1	1							1			2	1
Forestomach															
Basal cell carcinoma			1	1	2	2	3	2		3				1	1
Basal cell papilloma				1	3		3	1	1	2					
Papilloma															1
Squamous cell carcinoma															1
Liver															
Adenoma									1						
Hemangioma	1														
Hepatocellular carcinoma									5	1					
Hyperplastic nodule		1							4	1					
Lymphangioma									1						
Early leukemia													2		
Lung															
Adenocarcinoma			1												
Adenoma				1											1
Basal cell carcinoma								1							
Basal cell tumor						1									
Interstitial cell carcinoma										1					
Papilloma				1											
Squamous cell carcinoma			2			1					1		1		1
Undifferentiated tumor		1													
Lymph node															
Hemangioma						2									
Lymphosarcoma								1							
Metastatic basal cell carcinoma					2										
Metastatic C-cell carcinoma	1														
Mammary gland															
Adenoma	1														
Carcinoma	1									1					
Fibroadenoma	1				1					1					
Fibroadenoma—focal carcinoma	1														
Fibroma	1				1				1	2					
Leiomyoma					1				1						
Multiple organs															
Early leukemia	2				3	1									1
Monocytic leukemia	9				9		8	6	13	14		1		1	2

[a] Groups 10-12 were added later to provide male-female comparisons.
[b] C=control.
[c] –=no (given N-HEP); +=yes (given N-HEP-d_4).

TABLE 1 (continued).—*Neoplastic lesions in F344 rats given N-HEP*

Parameter	Treatment group[a]														
	C[b]	1	2	3	4	5	6	7	8	9	10	11	12	13	14
	Tumor found														
Nasal cavity															
Adenocarcinoma													1		
Carcinoma					1										2
Basal cell carcinoma					3	2	1	1				1	2		1
Basal cell papilloma					1	1							1		
Squamous cell carcinoma					1			1				1		1	1
Notochord															
Chordoma									1						
Oral cavity															
Basal cell papilloma						1									
Oropharynx															
Basal cell carcinoma					4		3	4	1						
Basal cell papilloma								4							
Neurosarcoma									1						
Squamous cell carcinoma					1		2		1						
Pancreas															
Acinar hyperplastic nodule									1						
Islet cell adenoma	2				1		1	1	6	2					
Islet cell carcinoma	1								2	1					
Mixed cell adenoma	1														
Parathyroid gland															
Adenoma								1							
Peritoneum															
Metastatic mesothelioma	3								1						
Pituitary gland															
Adenoma	3				2	1		4					1		
Carcinoma	2						6	1	4	7					
Hemangioma	1														
Preputial gland															
Carcinoma	1														
Skin															
Basal cell carcinoma	1				2	1	2	1	1					1	
Lipoma						1			1						
Neurosarcoma	1				1										
Sebaceous gland carcinoma									1						
Squamous cell carcinoma							1	1							
Spleen															
Eerly leukemia													2		
Hemangioma				1	2										
Hemangiosarcoma		1						1	1	2					
Monocytic leukemia									1						
Stomach															
Basal cell carcinoma													1		
Basal cell papilloma												2			
Squamous cell carcinoma													1		
Testes															
Interstitial cell adenoma	2				4		4	3	2	6					1
Interstitial cell carcinoma	17				4		3	7	10	12					
Mesothelioma	3								1	2					
Thyroid gland															
C-cell adenoma	1						1		1						
C-cell carcinoma	1								4	1					
F-cell carcinoma	1														
Tongue															
Basal cell carcinoma					3	10	4	6	1	6					1
Basal cell papilloma					2		1	4	1	1		2	2		
Papilloma					1	1				1					
Squamous cell carcinoma						1	1						2		
Squamous cell papilloma													1		
Upper GI tract															
Carcinomas	0	4	10	11	12	16	12	13	2	8	7	9	16	18	13
All tumors	0	14	15	17	15	16	13	17	2	10	7	18	18	18	18

[a] Groups 10–12 were added later to provide male-female comparisons.
[b] C=control.

TABLE 1 (continued).—*Neoplastic lesions in F344 rats given N-HEP*

Parameter	Treatment group[a]														
	C[b]	1	2	3	4	5	6	7	8	9	10	11	12	13	14
	Tumor found														
Urethra															
Basal cell carcinoma						1									
Uterus															
Polyp													1		

[a] Groups 10–12 were added later to provide male–female comparisons.
[b] C=control.

differences between male and female F344 rats in response to N-HEP and to assess the effect of deuterium substitution thereon, we began groups 10–12, each containing 20 females, later. Groups 12–14 were given the deuterium-labeled nitrosamine; all other groups received the unlabeled compound.

Statistical methods.—The survival patterns for many of the test groups were compared both graphically and analytically. The graphs of the survival curves were constructed on the basis of the Kaplan-Meier methodology (*10*), which adjusts for censored observations. The censored observations resulted from those relatively few animals that survived until the termination of the study and the several animals that were killed in one of the groups during the course of the study. The individual survival curves were comparable, pairwise, when the method of Mantel and Haenszel (*11*) was used. When the incidence of upper GI tract tumors did not differ significantly between groups of rats receiving different treatments, the only difference in carcinogenic effectiveness that could be measured easily was a difference in survival between the groups, inasmuch as the tumors lead to death of the animals. The analyses were produced with the computer program developed and described by Thomas et al. (*12*). Tumor incidences were compared by the exact test of Fisher (*13*).

RESULTS

In table 1 is listed every tumor found in our F344 rats, according to treatment group. Among the rats given N-HEP, the commonest sites of occurrence of tumors not found in the untreated rats were in the upper GI tract (esophagus, oropharynx, tongue, and forestomach). These tumors were also not seen in a large survey of untreated F344 rats in other laboratories (*14*). A few tumors of the nasal cavity occurred, but these appeared only in certain dosage groups. In marked contrast with a previous study in F334 rats (*15*), in the present study very few tumors in the lungs developed, perhaps because in the former study N-HEP was given in oil solution by gavage.

As measured by the mortality rate from tumors of the upper GI tract in our rats (text-fig. 1), carcinogenic effectiveness of the treatment decreased from group 1 to group 4. Although we originally planned to treat all groups for a minimum of 25 weeks, this was not possible in group 1 because the animals had begun to die with tumors at the 12th week; consequently, treatment was stopped at the 13th week, which formed the rationale for stopping treatment in

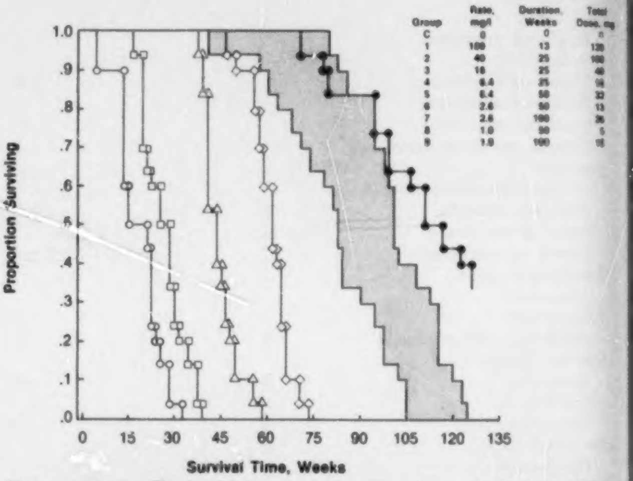

TEXT-FIGURE 1.—Kaplan-Meier survival curves for unlabeled N-HEP-treated groups, individually represented, with respect to death from all causes. Group 1, ○; group 2, □; group 3, △; group 5, ◇; and untreated control (C), ●. Curves for groups 4 and 6–9 all lie within the *shaded area*. *See* table 1 for parameters of treatment for groups C–9.

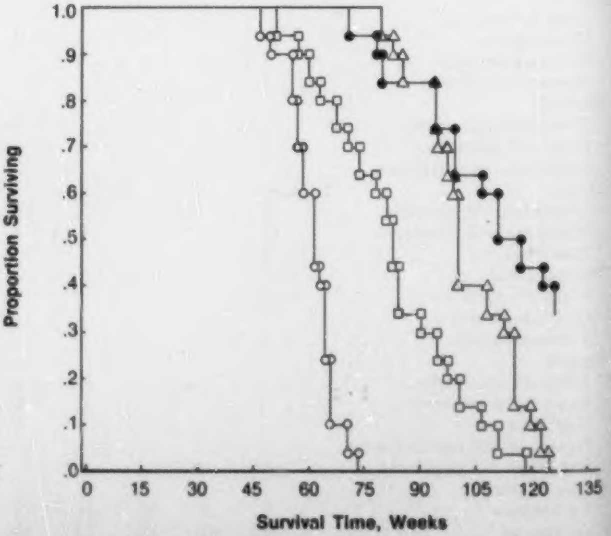

TEXT-FIGURE 2.—Survival curves with respect to death from all causes for groups receiving unlabeled N-HEP for 50 wk. Group 5, ○, received 6.4 mg N-HEP/liter; group 6, □, received 2.6 mg N-HEP/liter; group 8, △, received 1.0 mg N-HEP/liter; and the control, ●, was untreated.

all of the comparable groups at week 13. The rate of mortality in group 5 was considerably greater than that in group 4, corresponding with the longer treatment with 6.4 mg N-HEP/liter. The mortality rates in groups 4, 6, and 7 were greater than the rates in the untreated animals, although the rates were not statistically different from each other. Mortality in groups 8 and 9 was also significantly different from that of the untreated rats, but the difference in mortality between group 8 and group 9 was not significant. The number of animals in group 8 with tumors of the upper GI tract was 2, not a significant incidence if considered alone. For those groups treated for 50 weeks (groups 5, 6, and 8), significant differences in mortality rates were observed; each of the groups also differed from the untreated control (text-fig. 2).

Considering the effect of deuterium labeling on carcinogenicity, we saw no significant difference in numbers of animals with upper GI tract tumors between group 1 and group 14 both of which received 100 mg N-HEP/liter for 13 weeks, although fewer animals had malignant tumors (carcinomas) in group 1 than in group 14, presumably reflecting longer survival of group 14 animals. Examining the mortality of the rats in groups 1 and 14 (text-fig. 3), we found that rats in group 1 died considerably more rapidly than rats in group 14, the group that received the deuterium-labeled compound. At 40 mg N-HEP/liter, the effect of deuterium labeling was similar; as shown in text-figure 4A, the mortality in group 2 (given N-HEP) was much greater than that in group 13 (given N-HEP-d_4). Similarly, in females given the same concentration of N-HEP or N-HEP-d_4 for 13 weeks (text-fig. 4B), group 11 (given N-HEP) showed a higher mortality rate than did group 12 (given N-HEP-d_4). The death rate of the females given 40 mg N-HEP/liter (group 11) appeared higher than that of the males (group 2), even though the former received N-HEP for only 13 weeks (compared with 25 wk for the latter), and the higher death rate of the females was probably due to the higher dose per unit body weight which they received during the first 13 weeks, which perhaps is the crucial period for induction of tumors of the upper GI tract by N-HEP.

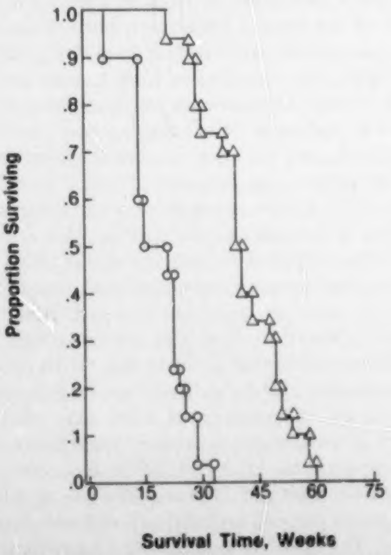

TEXT-FIGURE 3.—Survival curves for selected treatment groups receiving 100 mg N-HEP or 100 mg N-HEP-d_4/liter for 13 wk. Group 1, ○, was from the original, unlabeled set; group 14, △, was deuterium labeled and tested concurrently with group 1.

Table 2 shows the incidence of tumors of the upper GI tract for selected groups. For those groups receiving the lower doses of N-HEP for 50 and 100 weeks, a clear dose-response relationship emerged both for carcinomas alone and for total tumors. However, for those groups receiving the higher doses for 25 weeks, no dose-response relationship emerged for either carcinomas alone or total tumors; this is most likely a result of the highly significant inverse relationship between dose level and survival time.

Table 3 provides a comparison of tumor incidence for the N-HEP and N-HEP-d_4 groups for both males and females. Although the total tumor incidence was essentially unchanged by the addition of the deuterium label, the incidence of carcinomas was significantly greater for the groups receiving the labeled compound; the most likely explanation for this difference is the longer survival of the groups receiving the labeled compound.

TABLE 2.—*Incidence of tumors of the upper GI tract[a] in N-HEP-treated male rats*

Dose rate, mg/liter	Duration, wk	Total dose, mg	Carcinoma[b]		Carcinoma and/or papilloma[c]	
			Incidence	Probability[d]	Incidence	Probability[d]
0	0	0	0/20	—	0/20	—
1	100	10	8/20	0.0016	10/20	0.00022
2.6	100	26	13/20	0.00001	17/20	<0.00001
1	50	5	2/20	0.24	2/20	0.24
2.6	50	13	11/20	0.00007	13/20	0.00001
6.4	50	32	16/20	<0.00001	16/20	<0.00001
6.4	25	16	12/20	0.00002	15/20	<0.00001
16	25	40	11/20	0.00007	17/20	<0.00001
40	25	100	10/20	0.00022	15/20	<0.00001

[a] Includes animals with 1 tumor or more of the esophagus, forestomach, tongue, oropharynx, or oral cavity.

[b] Animals with a carcinoma only or a carcinoma and papilloma.

[c] Animals in "Carcinoma" column plus those with only a papilloma.

[d] Probability level is for the comparison of the control group with a treated group; these one-tailed probabilities were obtained with the Fisher exact test.

TABLE 3.—*Incidence of tumors of the upper GI tract[a] in N-HEP- and N-HEP-d_4-treated rats*

Sex	Dose rate of 40 mg/liter		Deuterium labeled[b]	Carcinoma[c]	Carcinoma and/or papilloma[d]	Group
	Duration, wk	Total dose, mg				
♂	25	100	−	10/20	15/20	2
♂	25	100	+	18/20	18/20	13
♀	13	52	−	9/20	18/20	11
♀	13	52	+	16/20	18/20	12

[a] Includes animals with 1 tumor or more of the esophagus, forestomach, tongue, oropharynx, or oral cavity.

[b] − = no (given N-HEP); + = yes (given N-HEP-d_4).

[c] Animals with a carcinoma only or a carcinoma and papilloma.

[d] Animals in "Carcinoma" column plus those with only a papilloma.

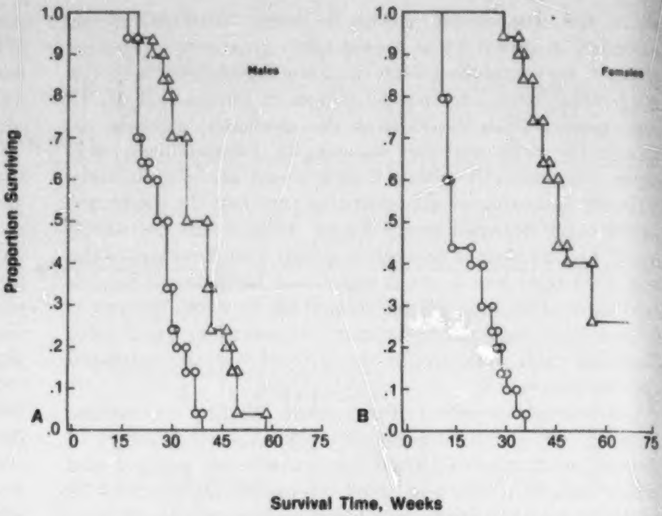

TEXT-FIGURE 4.—Survival curves for groups receiving 40 mg N-HEP or 40 mg N-HEP-d_4/liter for 25 wk (males) and for 13 wk (females). Groups 2 and 11, ○, received N-HEP; and groups 13 and 12, △, received N-HEP-d_4.

DISCUSSION

An examination of the mortality rates in text-figures 1 and 2 shows a clear relationship between the dose rate of N-HEP and the carcinogenic effectiveness of the treatment as measured by higher mortality. This pattern is shown both for the groups treated for 25 weeks and for the groups treated for 50 weeks. The incidence of tumors of the upper GI tract in group 8 was small (2/20), and 1 mg N-HEP/liter for 50 weeks (a total of 5 mg) might represent the smallest effective dose of N-HEP in an animal group of this size. This observation contrasts with the findings with nitrosodiethylamine (*16*) and nitrosomethyl-2-phenylethylamine (*6*), in which total doses of less than 3 mg gave rise to highly significant incidences of tumors of the upper GI tract.

At 100 mg N-HEP/liter, the compound was quite toxic; it led to early death of many rats with pneumonia, and it possibly accelerated death of the remaining tumor-bearing rats. This might explain the small number of carcinomas of the upper GI tract in animals of group 1 as compared with the number in group 14: Not only were the animals in group 1 dying before they developed carcinomas, but also the females in group 10 largely succumbed to the toxic action of N-HEP (of the 20 group 10 animals, 13 were dead by the 12th wk and the remaining 7 animals all developed carcinomas). The fact that the smaller females received a relatively larger dose per unit body weight than the males is probably a factor.

At 40 mg N-HEP/liter, deuterium labeling had a very clear effect in reducing the carcinogenic effectiveness (as measured by increased survival) of N-HEP in both males and females (text-fig. 4). This result lends additional support to the concept that carcinogenesis by nitrosamines (at least in rats) begins with oxidation at the carbon atom alpha to the nitroso function, which is, therefore, a rate-limiting step in carcinogenesis. Hecht and Young (*17*) have recently shown that deuterium labeling at the α-carbons of nitrosomorpholine leads to a lower formation rate for those metabolites that arise from alpha oxidation, which correlates well with the diminished carcinogenicity of nitrosomorpholine when deuterium replaces hydrogen at the alpha positions (*1*). An anomaly is the enhancing effect of deuterium labeling in the alpha position on carcinogenesis by nitroso-2,6-dimethylmorpholine in Syrian golden hamsters (*18*), which suggests that induction of pancreas tumors by this nitrosamine in hamsters might proceed by a mechanism other than alpha oxidation.

One surprising result of this study is the low incidence of lung tumors in our F344 rats treated with N-HEP in their drinking water. Previous experiments in which N-HEP was given to MRC Wistar-derived rats (*8, 9*) and to Sprague-Dawley rats (*19*) in their drinking water or was even given in the form of its precursors, heptamethyleneimine plus nitrite, in the drinking water of Sprague-Dawley rats (*20*) have led to the induction of high incidences of squamous cell tumors of the lung. Likewise, in both Sprague-Dawley and F344 rats treated with N-HEP in oil by gavage or by sc injection, significant numbers of lung tumors were induced (*15*). In all of these experiments, the incidence of tumors of the upper GI tract was also high, as was true for Syrian golden hamsters, but no lung tumors occurred in the hamsters (*21*). In guinea pigs, however, N-HEP failed to induce any tumors (*22*), a rare example of a carcinogenic nitrosamine finding a nonsusceptible species. We must assume, because of these differences, that the metabolism of N-HEP in F344 rats, when given in drinking water (and therefore at relatively low rates per unit time), is such that the lung is insufficiently affected for it to give rise to tumors. Studies of the metabolism of N-HEP in F344 rats (with special attention to metabolism in lung vs. liver) are in progress and will be expanded to comparisons of F344 rats with Sprague-Dawley rats in an attempt to answer this question.

Our conclusions are that N-HEP is a potent carcinogen for the upper GI tract of F344 rats, effective at total doses of a few milligrams per rat, and shows a definite dose-response relationship. The effect of α-deuterium labeling in reducing carcinogenic potency of N-HEP (as measured by reduced time to death from tumors) indicated that oxidation of an α-carbon atom was a rate-limiting step in carcinogenesis.

REFERENCES

(*1*) Lijinsky W, Taylor HW, Keefer LK. Reduction of rat liver carcinogenicity of 4-nitrosomorpholine by α-deuterium substitution. J Natl Cancer Inst 1976; 57:1311–1313.

(*2*) Lijinsky W, Saavedra JE, Reuber MD, Blackwell B-N. The effect of deuterium labeling on the carcinogenicity of nitroso-2,6-dimethylmorpholine in rats. Cancer Lett 1980; 10:325–331.

(*3*) Lijinsky W, Taylor HW. Carcinogenicity of nitrosoazetidine and tetradeuteronitrosoazetidine in Sprague-Dawley rats. Z Krebsforsch 1977; 89:215–219.

(*4*) Keefer LK, Lijinsky W, Garcia H. *Brief communication*: Deuterium isotope effect on the carcinogenicity of dimethylnitrosamine in rat liver. J Natl Cancer Inst 1973; 51:299–302.

(*5*) Lijinsky W, Reuber MD. Carcinogenicity in rats of nitrosomethylethylamines labeled with deuterium in several positions. Cancer Res 1980; 40:19–21.

(*6*) Lijinsky W, Reuber MD, Davies TS, Saavedra JE, Riggs CW. Dose-response studies in carcinogenesis by nitrosomethyl-2-phenylethylamine in rats and the effect of deuterium. Food Cosmet Toxicol. In press.

(*7*) Lijinsky W, Reuber MD, Saavedra JE, Blackwell B-N. Effect of deuterium on the carcinogenicity of nitroso-methyl-*n*-butylamine. Carcinogenesis 1980; 1:157–160.

(*8*) Lijinsky W, Tomatis L, Wenyon CE. Lung tumors in rats treated with *N*-nitrosoheptamethyleneimine and *N*-nitrosooctamethyleneimine. Proc Soc Exp Biol Med 1969; 130:945–949.

(*9*) Garcia H, Lijinsky W. Tumorigenicity of five cyclic nitrosamines in MRC rats. Z Krebsforsch 1972; 77:257–261.

(*10*) Kaplan EL, Meier P. Non-parametric estimation from incomplete observations. J Am Stat Assoc 1958; 53:457–481.

(*11*) Mantel N, Haenszel W. Statistical aspects of the analysis of data from retrospective studies of disease. J Natl Cancer Inst 1959; 22:719–748.

(*12*) Thomas DG, Breslow N, Gart JJ. Trend and homogeneity analysis of proportions and life table data. Comput Biomed Res 1977; 10:373–381.

(*13*) Fisher RA. Statistical methods for research workers. 10th ed. New York: Stechert & Co., 1946:96–97.

(*14*) Goodman DG, Ward JM, Squire RA, Chu KC, Linhart MS. Neoplastic and nonneoplastic lesions in aging F344 rats. Toxicol Appl Pharmacol 1979; 48:237–248.

(*15*) Taylor HW, Nettesheim P. Influence of administration route and dosage schedule on tumor response to nitrosoheptamethyleneimine in rats. Int J Cancer 1975; 15:301–307.

(*16*) Lijinsky W, Reuber MD, Riggs CW. Dose-response studies in rats with nitrosodiethylamine. Cancer Res 1981; 41:4997–5003.

(*17*) Hecht SS, Young R. Metabolic α-hydroxylation of *N*-nitrosomorpholine and 3,3,5,5-tetradeutero-*N*-nitrosomorpholine in the F344 rat. Cancer Res 1981; 41:5039–5043.

(*18*) Rao MS, Scarpelli DG, Lijinsky W. Carcinogenesis in Syrian hamsters by *N*-nitroso-2,6-dimethylmorpholine, its *cis* and *trans* isomers, and the effect of deuterium labeling. Carcinogenesis 1981; 2:731–735.

(*19*) Schreiber H, Nettesheim P, Lijinsky W, Richter CB, Walburg HE Jr. Induction of lung cancer in germfree, specific-pathogen-free, and infected rats by *N*-nitrosoheptamethyleneimine: Enhancement by respiratory infection. J Natl Cancer Inst 1972; 49:1107–1114.

(*20*) Taylor HW, Lijinsky W. Tumor induction in rats by feeding heptamethyleneimine and nitrite in water. Cancer Res 1975; 35:812–815.

(*21*) Lijinsky W, Ferrero A, Montesano R, Wenyon CE. Tumorigenicity of cyclic nitrosamines in Syrian golden hamsters. Z Krebsforsch 1970; 74:185–189.

(*22*) Cardy RH, Lijinsky W. Comparison of the carcinogenic effects of five nitrosamines in guinea pigs. Cancer Res 1980; 40:1879–1884.

blank page

Induction of Mammary Neoplasms in the ACI Rat by 430-keV Neutrons, X-Rays, and Diethylstilbestrol[1,2,3]

Claire J. Shellabarger,[4] **Danielle Chmelevsky,**[5] **Albrecht M. Kellerer,**[5] **J. Patrick Stone,**[4] *and* **Seymour Holtzman**[4,6]

ABSTRACT—Mammary tumorigenesis was studied in female ACI rats after treatment with X-irradiation or neutron-irradiation, with or without diethylstilbestrol (DES) treatment. The mortality-corrected cumulative tumor rate based on all mammary neoplasms and the mortality-corrected incidence based on the first neoplasms only have been derived. In non-DES-treated animals, at the relatively high radiation doses studied, all dose–effect relationships were consistent with relative biological effectiveness (RBE) values slightly in excess of 10. In DES-treated rats definite findings were observed at neutron doses as low as 0.01 Gy (1 rad). The dose–effect relationship in DES-treated rats showed a strong sublinearity (dose exponent <1) at low neutron doses. RBE values in DES-treated rats increased in inverse proportion to the square root of the neutron dose, and exceeded 100 at a neutron dose of 0.01 Gy (1 rad).—JNCI 1982; 69:1135–1146.

In female rats of the ACI strain, both low LET and high LET radiations induce mammary AC and mammary FA (*1, 2*). In this strain of rat, a form of synthetic estrogen, DES, induces mammary AC, but no mammary FA, when given in the form of a 20-mg pellet of 25% DES and 75% cholesterol (*3*). Furthermore, in ACI rats, the effect of DES and ionizing radiations appears to be synergistic for mammary AC formation, as shown in studies with X-rays by Segaloff (*4*) and later by Stone et al. (*2*), and in studies with neutrons by Shellabarger et al. (*5*).

The present work is primarily aimed not at the further elucidation of the synergistic effect but at the comparison of the effects of X-rays and neutrons at low doses. Therefore, graded X-ray and neutron doses were applied and only one dose of DES was utilized. The interest in this investigation is due to the theoretical prediction (*6*) and the experimental observation in various systems (*7–9*) of high-neutron RBE, which may be of considerable impact to radiation protection because they support the suggestion that the quality factor of 10, now used for neutrons, should be reconsidered (*10*). The only source of human data for neutrons, the Japanese atomic bomb survivors, may be lost due to the revision of neutron dosimetry (*11*); thus data from animal studies with low doses of neutrons have gained importance.

In an earlier experiment with Sprague-Dawley rats, very low doses of neutrons were used, and for a neutron dose of 1 mGy an RBE in excess of 100 was found (*12, 13*). However, it remained unclear whether this finding was specific to the Sprague-Dawley rats only, with the high spontaneous incidence and with a considerably larger number of FA than AC characteristic to this strain. Therefore, it appeared desirable to conduct analogous studies with ACI rats that have a very low spontaneous incidence of mammary neoplasms and show predominantly AC when treated with DES.

A second aspect of the earlier findings on Sprague-Dawley rats was of particular importance and has been an additional motivation of the present study. This was the finding of a substantial *sublinearity*, i.e., a negative curvature of the dose-effect relationship, at small neutron doses. Such a sublinearity implies that the effect per unit dose is largest at smallest doses and is therefore of evident concern in radiation protection, for which risk assessments are commonly based on the linear hypothesis. Sublinearity is also of interest because it occurs at doses that are sufficiently small that only few cells are traversed by any neutron recoil, and the probability of several recoils can be disregarded (*14, 15*). In this dose range the tendency is to postulate linear dose dependences for neutrons, because the number of cells that receive any energy deposition is merely proportional to dose. The failure to find a linear relation has therefore been interpreted as evidence of a multicellular reaction or a radiation-induced tissue factor (*15*). Examination of the linearity or nonlinearity of the dose–effect relationship for neutrons was accordingly another main goal in the present investigation.

MATERIALS AND METHODS

Rats and treatment schedules.—Approximately 800 weanling, virgin, female ACI rats were purchased from M.A. Bioproducts, Walkersville, Md. Rats were delivered to this laboratory in eight shipments of at least 50 rats at weekly intervals. From each shipment 3 rats were assigned to each of 14 groups that were to be irradiated, and 4 rats were assigned to each of 2 groups that were reserved as nonirradiated controls. This procedure was repeated with another 400 rats. Thus all 16 groups were matched closely for age both in regard to the average age and the range of ages. Neutron irradiation was given to rats with an average age of 88 days, and X-irradiation was given to rats with an average age of

---

ABBREVIATIONS USED: AC=adenocarcinoma(s); DES=diethylstilbestrol; FA=fibroadenoma(s); Gy (gray)=unit of absorbed dose in the International System of Units (Gy=J/kg or 100 rad); LET=linear energy transfer; RBE=relative biological effectiveness.

---

[1] Received February 17, 1982; accepted July 6, 1982.

[2] Supported by Public Health Service contract X01CP-60219 from the Division of Cancer Cause and Prevention, National Cancer Institute; by contract DE-AC02-76CH00016 from the U.S. Department of Energy; and by Euratom Research contract BIO-286-81 D (B).

[3] Animals were maintained under the guidelines set forth by the Animal Welfare Act in facilities accredited by the American Association for Accreditation of Laboratory Animal Care.

[4] Medical Department, Brookhaven National Laboratory, Associated Universities, Inc., Upton, N.Y. 11973.

[5] Institut für Medizinische Strahlenkunde, Universität Würzburg, Versbacher Str. 5, 8700 Würzburg, Federal Republic of Germany.

[6] We thank Ms. Lindora Boyd, Ms. Elizabeth M. Jellett, Mr. John P. Shanley, Mr. Leon J. Goodman, and Ms. Mary R. Snead for technical assistance.

89 days. All irradiations were done as described previously (*5*). DES (5 mg) was given, in pellet form, 2 days before irradiation, with methods described earlier (*4*). All data were recorded in days after the date of DES administration and, for simplicity, all ages, life-spans, and times quoted in this article refer to the date of DES administration as time 0.

All rats were kept in temperature-controlled (21–23°C) and humidity-controlled (45–65%) animal rooms with 12 hours (8 a.m.–8 p.m.) of fluorescent light. The animals were maintained on commercial rat chow and water ad libitum. Each rat was examined at least weekly for the presence of mammary tumors, and all mammary tumors were studied microscopically and given a pathologic classification of either AC or FA according to criteria consistent with those of Young and Hallowes (*16*).

Tumor methodology.—Each rat was identified by a numbered ear tag. The anatomic location of each mammary tumor was recorded with the nipples as reference points. Because two distinct types of mammary tumor responses were found, individual or multiple, each was recorded separately. Individual mammary tumors were removed under ether anesthesia at a size of about 2 cm. If a second tumor was found at the site of a previously removed tumor, it was not recorded as a second individual tumor unless a 10-week period had elapsed between removal of the first tumor and the detection of the subsequent tumor. In the other type of mammary tumor response, which was confined to mammary AC in DES-treated rats, multiple AC were often detected within a single quadrant of mammary tissue over about 1 week. Because too many tumors existed to be counted by palpation alone, the entire quadrant was removed, fixed, defatted, stained with hematoxylin, cleared, and stored in methyl salicylate. Each quadrant was examined under a dissecting microscope at magnification 10X, and all presumed pathologic areas were removed individually for sectioning. The minimum number of these multiple AC was never less than 4 per quadrant. Even though there were often too many multiple AC per quadrant to be counted accurately, an individual quadrant was assigned a maximum number of 4 AC. Thus an individual rat could then have a maximum number of 16 AC. The multiple AC response within a single quadrant was usually found within a 1–3-week period. However, quadrants were removed not more often than twice per week. Rats were killed when they showed a multiple tumor response in all four quadrants, when they became moribund, or when tumor removal was no longer feasible. All remaining DES-treated rats were killed at days 523–525. Of the non-DES-treated rats still alive, approximately half of each treatment group was killed either on day 712 or on days 726–730. At autopsy, confirmation of DES treatment was made by locating the DES pellet. An abnormal pituitary gland was recorded as a pituitary tumor if the pituitary was hemorrhagic and fragile and exceeded a weight of 50 mg. Pituitary tumors were found in 30% of the untreated control rats, in 39% of the irradiated only rats, in 90% of the DES only rats, and in 79% of the irradiated plus DES-treated rats. The combined incidence of pituitary tumors in all nonirradiated rats was 58% compared to 52% in all irradiated rats, and the combined incidence in all non-DES-treated rats was 38% compared to 81% in all DES-treated rats. These results are in agreement with those of Stone et al. (*3*).

RESULTS

Of a total of 789 rats studied, 348 rats received DES and 441 did not receive DES. Of the rats that received DES, only 6.3% developed FA. Because of the small yield of FA in DES-treated rats (a total of 32 FA vs. 2,474 AC), the FA response in DES-treated animals was not analyzed. Among the non-DES-treated animals, 47% showed mammary neoplasms, 35% developed FA, and 26% developed AC; in view of their limited number, both types of neoplasms were pooled in the analysis.

Summary of Observations

The results of this study will first be presented in elementary form; the more rigorous actuarial analysis will be given

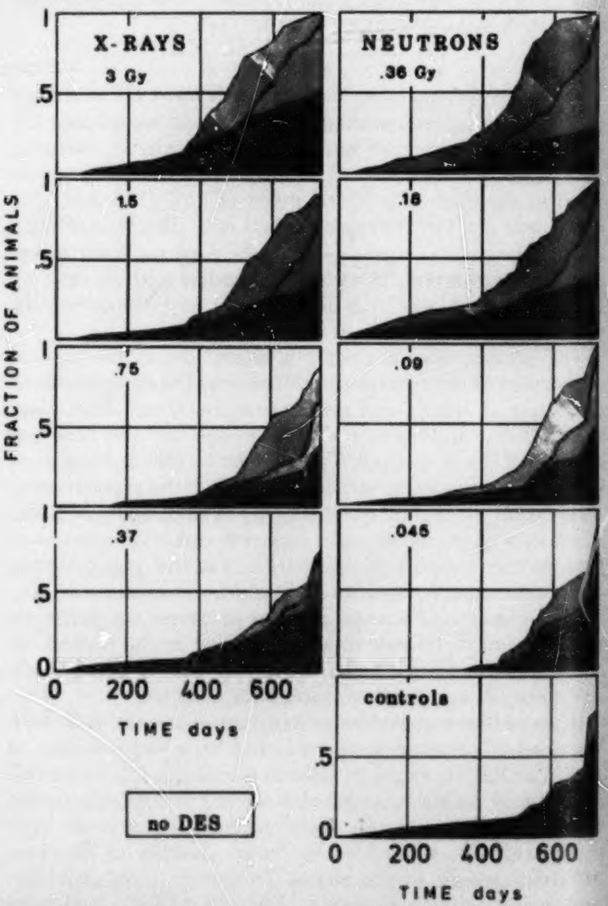

Text-figure 1.—Fraction of the non-DES-treated animals dead or alive with and without FA and/or AC as a function of time after irradiation. Group sizes are given in table 3. ■, Fraction of animals dead without neoplasm; ▩, fraction of animals dead with at least 1 neoplasm; ▨, fraction of animals alive with at least 1 neoplasm; □, fraction of animals alive without a neoplasm.

in a second part. Text-figure 1 represents the time course of tumor incidence and mortality of the animals not treated with DES. The heavy solid lines indicate the fraction of animals dead at the specified times. The lower black areas indicate the fraction of animals dead without neoplasms; the lower shaded areas give the fraction of animals that have died with at least 1 neoplasm. The upper shaded areas give the fraction of animals alive with at least 1 mammary neoplasm. For all doses of X-rays and neutrons, the increased incidence of neoplasms is readily evident. A substantial increase of mortality is apparent only for the highest X-ray and neutron doses. The analysis of radiation-induced life shortening cannot, however, be an objective of the present study, because the surgical procedures and the killing after multiple tumor response enhance mortality.

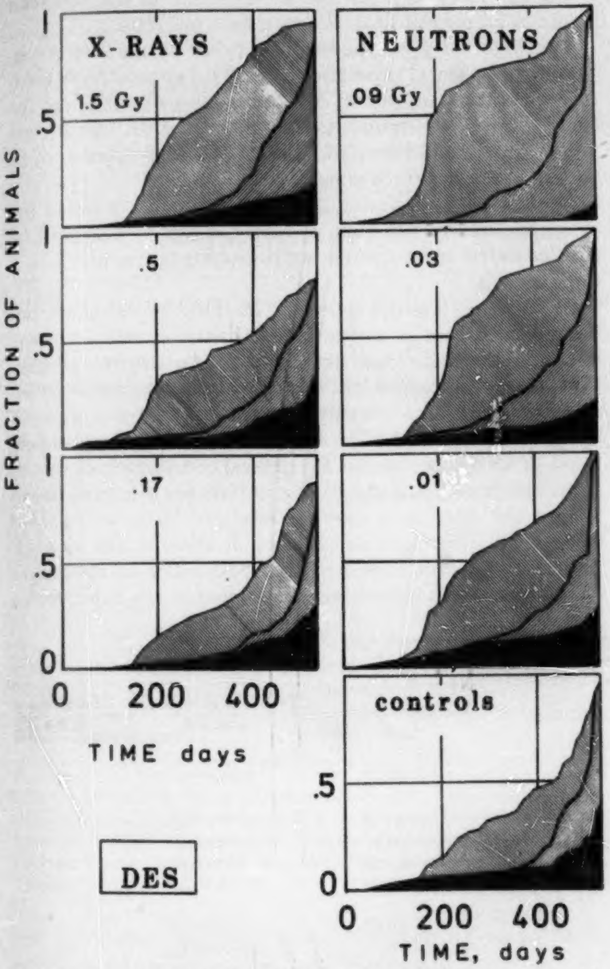

TEXT-FIGURE 2.—Fraction of the DES-treated animals dead or alive with and without AC, as a function of time after irradiation. Group sizes are given in table 1. ■, Fraction of animals dead without AC: ▩, fraction of animals dead with at least 1 AC; ▨, fraction of animals alive with at least 1 AC; □, fraction of animals alive without AC.

Text-figure 2 is the analogous representation for the animals treated with DES. The graphs extend over a shorter period after irradiation, since the DES-treated animals have a significantly reduced life-span. In comparison to the controls in text-figure 1, the high incidence of mammary neoplasms due to DES alone is recognizable. A considerable further increase due to the irradiations is evident for the highest X-ray dose and for all neutron doses. Mortality is not substantially increased due to the irradiations in comparison to that of the control group that is treated only with DES.

Text-figures 1 and 2 are only restricted representations of the neoplastic response. In particular, multiple mammary neoplasms in an animal are not taken into account. Furthermore, no distinction is made between the two types of neoplasms, i.e., FA and AC, that occur in the non-DES-treated animals. The DES-treated animals develop almost exclusively AC.

Table 1 lists the number of animals with specified numbers of mammary AC throughout life for the DES-treated animals. In addition, it gives the mean number of AC per animal, the fraction of animals with AC, and the total number of AC. Mean lifetimes of the animals, mean AC-free lifetimes, and mean times of the first AC and of all AC are given in table 2. The analogous data for the non-DES-treated animals are given separately for FA and AC in tables 3–5.

Different types of dose–effect relationships can be derived from the raw data in the tables. Text-figure 3 gives the conventional raw incidence versus absorbed dose or the fraction of animals that develop at least 1 mammary neoplasm throughout life. The standard errors are derived from the binomial distribution. The dose scales for the X-rays

TABLE 1.—*Mammary AC response in DES-treated ACI rats*

Absorbed radiation dose, Gy	Initial No. of animals	No. of animals with specified No. of AC throughout lifetime												Mean No. of AC/animal throughout lifetime[a]	Fraction of animals with AC	Total No. of AC
		0	1	2	3	4	5	6	7	8	9	10	>10			
Controls	63	15	6	5	5	2	3	3	4	5	4	3	8	4.8±0.5	48/63=0.76	304
Neutrons																
0.01	48	8	2	0	1	1	2	5	3	3	2	2	19	8.1±0.8	40/48=0.83	388
0.03	48	8	2	2	1	1	5	3	3	1	1	4	17	7.9±0.8	40/48=0.83	380
0.09	47	2	1	2	1	1	4	2	1	3	3	3	24	10.0±0.7	45/47=0.95	468
X-rays																
0.17	47	9	5	1	1	3	1	4	4	3	3	1	12	6.1±0.5	38/47=0.81	287
0.5	47	10	4	2	1	3	2	5	4	4	0	2	10	5.9±0.5	37/47=0.79	278
1.5	48	8	4	2	3	2	0	1	1	5	1	2	19	7.7±0.8	40/48=0.83	369

[a] Values are means ± SE.

and the neutrons in this and in the subsequent text-figures differ by a factor of 10. Data for the non-DES-treated animals indicate an RBE of neutrons somewhat larger than 10. For the DES-treated animals, RBE is substantially larger and may apparently exceed 100 at the lowest dose; however, it is difficult to infer accurate values of RBE from this crude analysis.

An RBE-versus-dose relationship for neutrons will be given at the end of this paper. The curves drawn through the data in text-figure 3 correspond to this RBE–dose relationship. The same applies to the dose–effect relationships given in subsequent text-figures. These curves will not always be the best fits to the individual data, but they are always consistent with them, and they are inserted to permit a judgment of the RBE–dose relationship of the last text-figure as an overall fit to the experimental data.

Text-figure 4 gives the mean number of mammary neoplasms per animal throughout life. The approximate coincidence of the two curves for X-rays and neutrons for the non-DES-treated animals indicates again RBE values close to 10. For the DES-treated animals the RBE appears to be well in excess of 100 at small doses.

Similar conclusions can be drawn from the values of the mean tumor-free life-span in tables 2 and 5. This will be substantiated by a competing-risk-corrected analysis in a later section.

Text-figures 3 and 4 show, for the DES experiments, not only RBE values in excess of 100 but also *sublinear* dose-effect relationships (dose exponent <1) for neutron irradiation. Similarly, high RBE values and sublinear dose–effect relations were also obtained in earlier experiments with Sprague-Dawley rats (*12, 13*). In view of the evident importance of such observations for general considerations on the effects of small doses of ionizing radiations, it is essential to submit the data to a rigorous analysis. Such an analysis corrects for differences in life-span. It also permits an evaluation of the time course of the appearance of mammary neoplasms; this is particularly important in the experiments

TABLE 2.—*Temporal mammary AC response in DES-treated ACI rats*[a]

Absorbed radiation dose, Gy	Lifetime	AC-free lifetime	Time of appearance of first AC	Time of appearance of all AC
Controls	456±13	374±18	372±19	434±6
Neutrons				
0.01	446±17	305±20	314±22	396±6
0.03	435±17	268±17	253±16	374±6
0.09	455±12	260±19	251±19	354±6
X-rays				
0.17	471±13	378±19	381±21	448±6
0.5	445±16	341±23	338±26	405±7
1.5	432±16	301±18	292±20	373±6

[a] Values are mean No. of days ± SE.

TABLE 3.—*Mammary FA response in non-DES-treated ACI rats*

Absorbed radiation dose, Gy	Initial No. of animals	No. of animals with specified No. of FA throughout lifetime								No. of FA/animal throughout lifetime[a]	Fraction of animals with FA	Total No. of FA
		0	1	2	3	4	5	6	7			
Controls	61	59	0	2	0					0.07±0.05	2/61=0.03	4
Neutrons												
0.045	46	32	11	1	1	0	1			0.46±0.14	14/46=0.30	21
0.09	48	24	11	7	5	0	1			0.94±0.17	24/48=0.50	45
0.18	48	23	12	7	3	0	1	1	1	1.10±0.23	25/48=0.52	53
0.36	48	19	11	5	6	0	4	2	1	1.63±0.29	29/48=0.60	78
X-rays												
0.37	48	43	4	0	1					0.15±0.07	5/48=0.10	7
0.75	48	29	13	5	1					0.54±0.11	19/48=0.40	26
1.5	46	27	8	4	5	1	0	1		0.89±0.20	19/46=0.41	41
3	48	29	8	9	1	0	1			0.71±0.15	19/48=0.40	34

[a] Values are means ± SE.

TABLE 4.—*Mammary neoplastic response in non-DES-treated rats*

Absorbed radiation dose, Gy	Initial No. of animals	No. of animals with specified No. of AC throughout lifetime										No. of AC/animal throughout lifetime[a]	No. of AF and AC[a]	Fraction of animals with AC	Fraction of animals with AC and/or FA	Total No. of AC
		0	1	2	3	4	5	6	7	8	>8					
Controls	61	56	5	0								0.08±0.04	0.15±0.06	5/61=0.08	6/61=0.10	5
Neutrons																
0.045	46	40	4	0	1	0	0	0	0	1	0	0.33±0.18	0.78±0.26	6/46=0.13	16/46=0.35	15
0.09	48	39	4	2	1	2						0.40±0.14	1.33±0.23	9/48=0.19	27/48=0.56	19
0.18	48	32	8	2	3	3						0.69±0.17	1.79±0.30	16/48=0.33	31/48=0.65	33
0.36	48	26	8	7	1	1	2	1	0	1	1	1.31±0.24	2.94±0.42	22/48=0.46	36/48=0.75	63
X-rays																
0.37	48	42	4	1	0	0	1					0.23±0.11	0.37±0.15	6/48=0.12	10/48=0.21	11
0.75	48	38	5	2	1	1	1					0.44±0.15	0.98±0.20	10/48=0.21	25/48=0.52	21
1.5	46	25	12	6	0	1	1	0	1			0.87±0.21	1.76±0.32	21/46=0.46	29/46=0.63	40
3	48	29	10	6	1	0	0	0	1	0	1	0.90±0.25	1.60±0.32	19/48=0.40	27/48=0.56	43

[a] Values are means ± SE.

TABLE 5.—*Temporal mammary neoplastic response in non-DES-treated ACI rats*[a]

Absorbed radiation dose, Gy	Lifetime	AC-free lifetime	FA-free lifetime	Tumor-free lifetime	Time of appearance of: First AC	Time of appearance of: First FA	Time of appearance of: First tumor	Time of appearance of: All AC	Time of appearance of: All FA	Time of appearance of: All tumors
Controls	630±21	627±21	626±21	624±21	690±11	590±11	658±23	690±11	631±24	663±15
Neutrons										
0.045	655±13	644±14	619±16	614±16	603±35	572±28	566±26	615±19	587±22	599±15
0.09	629±20	617±19	560±21	586±20	574±21	534±22	533±20	602±13	567±15	577±11
0.18	580±26	501±26	533±24	472±28	429±53	572±19	494±32	523±31	616±13	580±15
0.36	590±18	496±26	500±15	444±21	426±43	507±19	437±26	509±25	576±12	546±13
X-rays										
0.37	614±25	603±25	602±25	591±25	542±36	580±60	549±34	585±27	573±43	580±23
0.75	646±20	621±20	603±19	585±19	560±29	595±15	574±15	585±22	616±14	602±12
1.5	617±24	577±23	558±23	535±22	603±18	545±24	555±18	613±12	588±15	600±10
3.	537±24	498±22	487±22	460±20	523±20	505±22	498±18	573±13	529±14	554±10

[a] Values are mean No. of days ± SE.

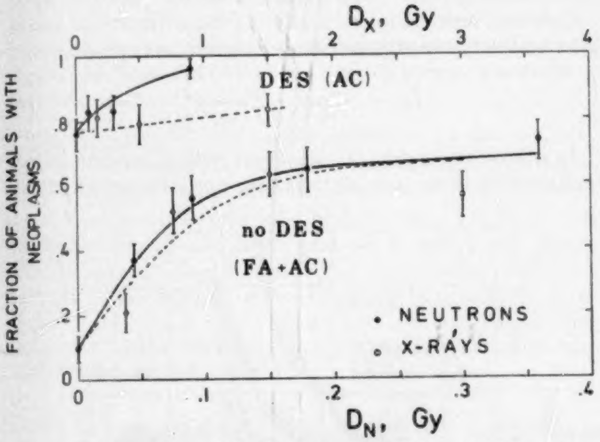

TEXT-FIGURE 3.—Fraction of animals with mammary neoplasms as a function of the neutron or the X-ray dose. Scales for the neutron (D_N) and the X-ray (D_X) doses differ by a factor of 10. Data are given with standard errors. *Solid lines* refer to the neutron irradiations; *dashed lines*, to the X-irradiations.

with DES where the raw incidence is always close to 100% regardless of radiation dose, and where, accordingly, dose-effect curves can be constructed only on the basis of the temporal distribution of neoplasms.

Actuarial Analysis

Estimates of Cumulative Tumor Rate and Cumulative Tumor Incidence

The same basic quantities will be utilized that have been employed in the preceding article on the induction of mammary neoplasms in the Sprague-Dawley rat (*13, 17*). The tumor rate $r(t)$ is the probability per unit time interval for an animal to develop a neoplasm at time t. Because the actual time of origin of a neoplasm is unknown, it is identified with the time of first observation. The cumulative tumor rate $R(t)$ is defined as time integral of the tumor rate:

$$R(t) = \int_0^t r(t')\,dt'. \qquad [1]$$

It is difficult to estimate the tumor rate with sufficient precision, and its integral $R(t)$ is therefore a quantity more suitable to characterize the time course of the incidence of neoplasms. $R(t)$ can be considered as the expected number of neoplasms up to time t for animals that are at risk throughout the whole time period from 0 to t. However, $R(t)$ may differ from the actual mean number of neoplasms in those animals that survive up to time t; the reason is that $R(t)$ is estimated on the basis of the complete information, including tumor incidence in those animals that do not survive up to time t.

As shown in our preceding article (*13*), the cumulative tumor rate can be estimated from the formula:

$$\hat{R}(t) = \sum_i \frac{1}{N(t_i)} \pm \sqrt{\sum_i \frac{1}{N(t_i)^2}}, \qquad [2]$$

where t_i are the times of appearance of the individual neoplasms up to time t, and $N(t_i)$ are the numbers of animals still at risk at these times. The numerical values and the standard errors resulting from equation 2 are given in text-figure 5 for the DES-treated animals.

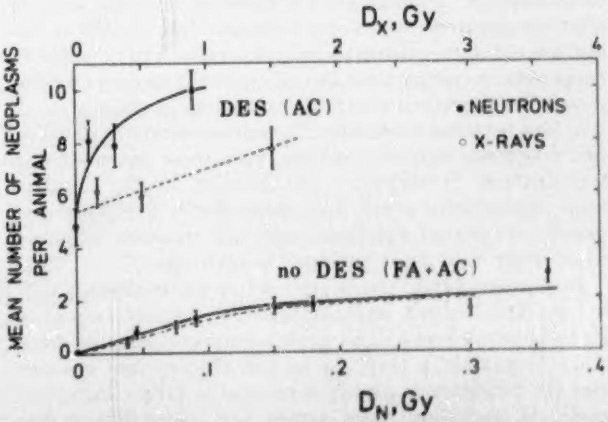

TEXT-FIGURE 4.—Mean number of mammary neoplasms as a function of the neutron or the X-ray dose. Scales for the neutron (D_N) and the X-ray (D_X) doses differ by a factor of 10. Data are given with standard errors. *Solid lines* refer to neutron irradiations; *dashed lines*, to X-irradiations.

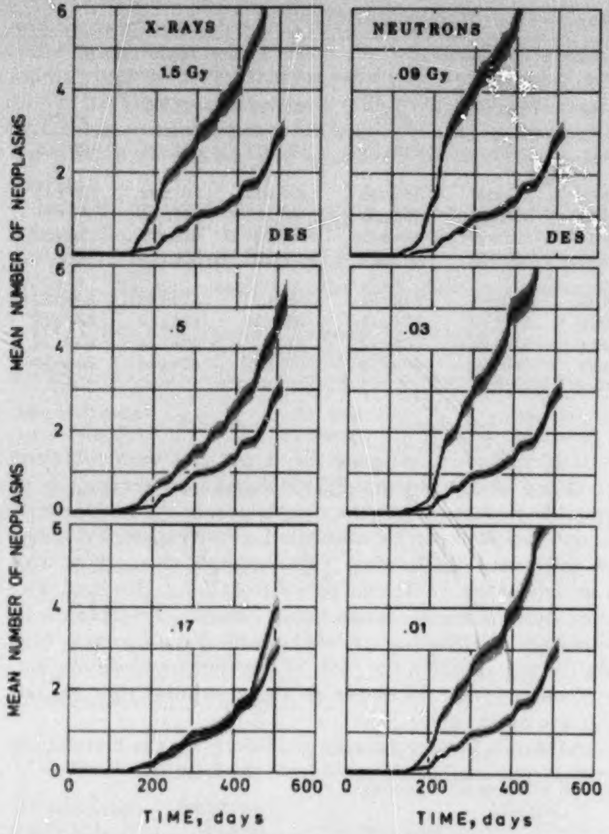

TEXT-FIGURE 5.—Cumulative tumor rates $R(t)$ also designated as mean number of neoplasms, as a function of time after exposure to X-rays *left panels* or to neutrons *right panels* for DES-treated animals. Curves are given with their standard errors. Absorbed doses are noted in the individual *panels*. The *curve* for the unirradiated but DES-treated animals is repeated in *each panel*.

The results in text-figure 5 are obtained on the basis of all neoplasms, i.e., animals are not removed from the analysis after the occurrence of a first neoplasm but remain at risk and are not distinguished from animals that had no previous neoplasms. A comparative analysis in the subsequent section shows that the tumor rate is above average in those animals that had previous neoplasms. Therefore, estimates based on first neoplasms only will be lower than those represented in text-figure 5. Furthermore, the formula for the standard error applies strictly only to independently occurring neoplasms; the actual standard errors will therefore be somewhat larger than those indicated in text-figure 5.

A synopsis of the cumulative tumor rates at all doses both for the DES-treated and the non-DES-treated animals is given in text-figure 6. The spontaneous incidence of mammary neoplasms is very low in non-DES-treated animals, and the incidence is greatly enhanced in DES-treated animals. All radiation doses except the lowest X-ray dose enhance markedly the incidence of mammary neoplasms in DES-treated animals.

The most striking observation is the very substantial enhancement of tumor incidence due to 0.01 Gy (1 rad) of neutrons in DES-treated animals. Even without further detailed analysis, it is evident that the dose dependence for neutron irradiation of DES-treated animals is sublinear; i.e., it corresponds to a dose exponent <1. This will be substantiated in the section dealing with dose–effect relationships.

The cumulative tumor rates are not given separately for the two types of neoplasms in DES-treated animals. The absolute numbers of these neoplasms are too small to permit the identification of possible differences in the time dependence for the two types of neoplasms. Instead of the cumulative tumor rate $R(t)$, one can also derive the cumulative incidence $I(t)$, i.e., the mortality-corrected probability per animal to have at least 1 tumor. This quantity is derived by the Kaplan–Meier product limit estimate (*18*):

$$\hat{I}(t) = 1 - \prod_i \left[1 - \frac{1}{N(t_i)}\right] \pm [1 - \hat{I}(t)] \cdot \sqrt{\sum_i \frac{1}{N(t_i)^2}}. \qquad [3]$$

One may note that very nearly the same numerical values are obtained from the sum limit estimate (*see* equation 2):

$$\hat{I}(t) = 1 - \exp\left[-\sum_i \frac{1}{N(t_i)}\right]. \qquad [4]$$

In equations 3 and 4 the numbers $N(t_i)$ of animals at risk include only those animals that have not incurred an earlier

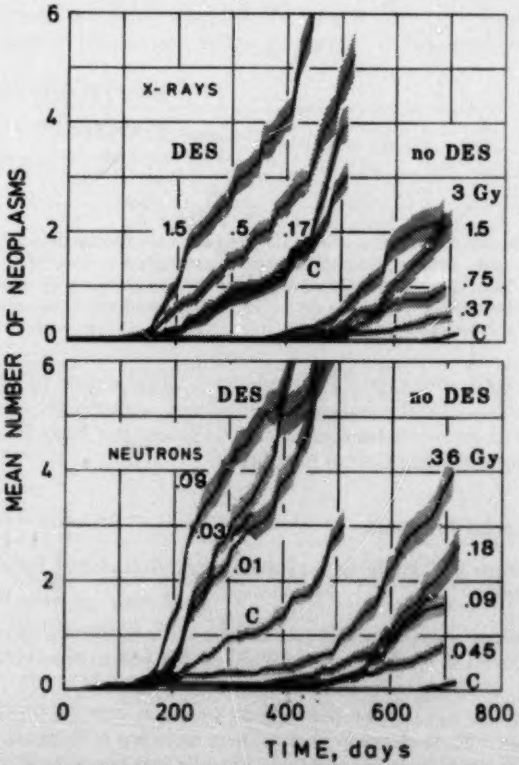

TEXT-FIGURE 6.—Cumulative tumor rates $R(t)$ also designated as mean number of neoplasms, as a function of time after exposure to X-rays *upper panel* or to neutrons *lower panel*. Curves and their standard errors are given both for DES-treated and non-DES-treated animals. Absorbed doses are noted on the *curves*. C designates controls, i.e., unirradiated animals. For non-DES-treated animals, both FA and AC are included; for DES-treated animals, only AC are included.

neoplasm. If all neoplasms were statistically independent, and if one were to deal with an entirely homogeneous population, one could include all animals and would then obtain somewhat better statistical accuracy, and, in particular, one would then have the relation:

$$I(t)=1-\exp[-R(t)]. \qquad [5]$$

However, it will be seen in the subsequent section that these conditions are not fulfilled in the present experiment. $I(t)$ is therefore determined from equation 3 by considering only those animals that had no earlier neoplasms.

Text-figures 7 and 8 represent the time course of the cumulative incidence $I(t)$ for non-DES-treated and for DES-treated animals. In both text-figures the control curve is repeated in each panel.

The difference between the estimates of $R(t)$ from all neoplasms and first neoplasms only will be considered next.

Difference of Cumulative Tumor Rates Obtained From All Neoplasms, From First Neoplasms per Quadrant, and From First Neoplasm per Animal

Text-figure 9 gives the estimates of the cumulative tumor rates for DES-treated animals that are obtained if all mammary neoplasms, if only the first neoplasms per quadrant of the mammary tissue, or if only the first mammary neoplasms per animal are utilized in the analysis. As stated, one should obtain essentially the same estimates if the tumor rate in the animals, or in the quadrants with previous neoplasms, were equal to the tumor rate without previous neoplasms. The difference would merely be that taking all neoplasms into account would result in a somewhat better statistical accuracy. In reality, the estimates are considerably higher if all neoplasms are included, i.e., if the animals with previous neoplasms are retained in the analysis. The estimates are much lower if only the first neoplasm per animal is taken into account, i.e., if an animal is removed from the analysis as soon as a first neoplasm has occurred. If only first neoplasms per quadrant are considered, one obtains intermediate values of the cumulative tumor rate. In this latter type of analysis, an animal is taken to be *partially at risk* according to the fraction of quadrants still unaffected.

The substantial differences in the estimates of $R(t)$ in the DES experiments indicate large differences of the tumor rates between animals with and without previous neoplasms. A similar but less substantial effect has been found in the earlier experiment with the Sprague-Dawley rats (*13*). It has also been pointed out earlier that the effect could either be due to an increase of the tumor rate after the incidence of neoplasms or, and this may be more likely, to inherent differences in sensitivity within the strain.

Text-figure 10 shows that there is also a certain decrease of the cumulative tumor rate in non-DES-treated animals if first neoplasms only are considered. However, the difference is smaller, and, in view of the modest size of the effect, only the curves for all neoplasms and for the first neoplasm per animal are plotted.

Dose-Effect and RBE-Dose Relationships

The results from the actuarial analysis can be used in several ways for the construction of dose-effect relations; it

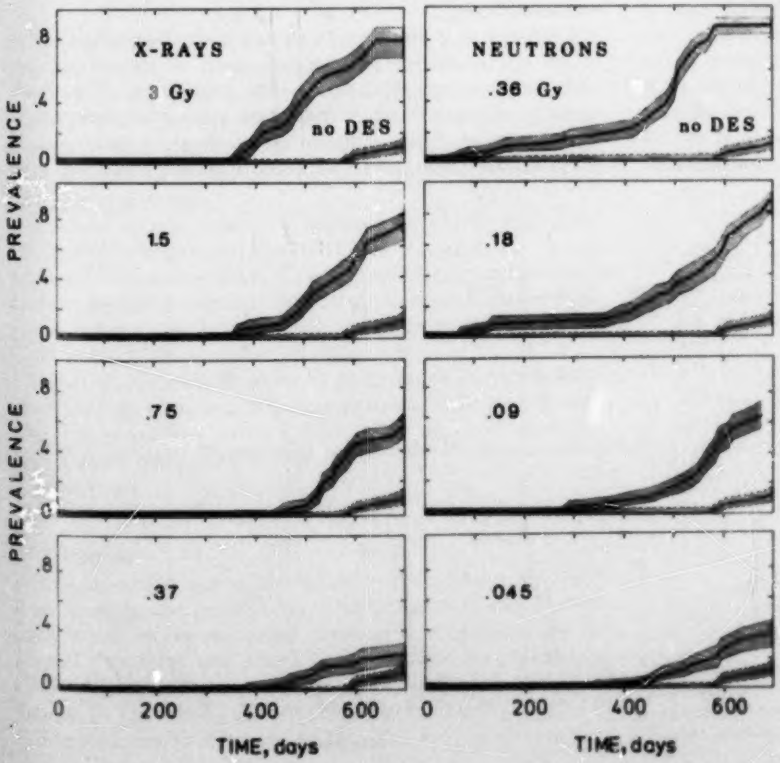

TEXT-FIGURE 7.—Cumulative incidences $I(t)$ and their standard errors as a function of time after exposure to X-rays *left panels* or to neutrons *right panels* for non-DES-treated animals. Results are based both on AC and FA. Absorbed doses are given in the individual *panels*. The *curve* for the controls is repeated in *each panel*.

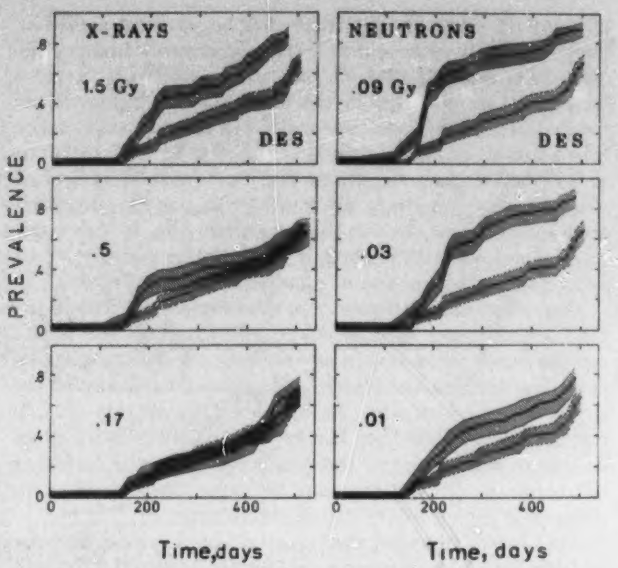

TEXT-FIGURE 8.—Cumulative incidences $I(t)$ and their standard errors as a function of time after exposure to X-rays *left panels* or to neutrons *right panels* for DES-treated animals. Results are based on AC only. Absorbed doses are given in the individual *panels*. The *curve* for the unirradiated, but DES-treated controls is repeated in *each panel*.

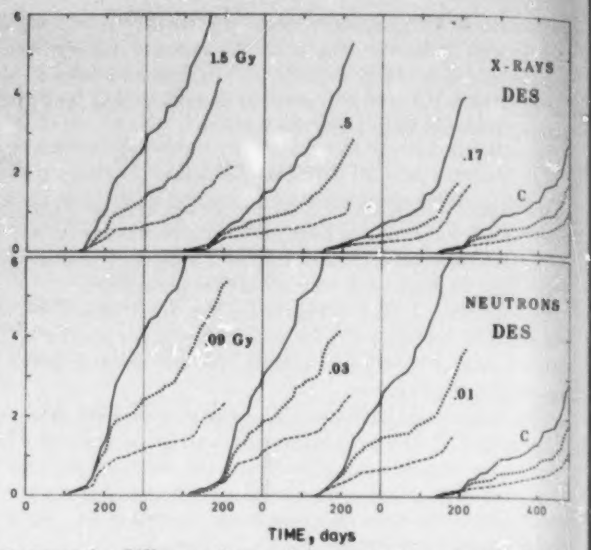

TEXT-FIGURE 9.—Different estimates of the cumulative tumor rate $R(t)$ for DES-treated animals as a function of time after exposure to X-rays *upper panel* and to neutrons *lower panel*. *Solid lines* are obtained on the basis of all AC, *dotted lines* on the basis of first AC in a quadrant, and *dashed lines* on the basis of the first AC in an animal. Absorbed doses are noted on the *curves*; *C* designates unirradiated but DES-treated animals.

is of particular interest to examine these possibilities and to assess the consistency of their conclusions as well as those from text-figures 3 and 4 that had been based on the conventional analysis.

In the earlier experiment with Sprague-Dawley rats, it has been found that the results can adequately be described in terms of a radiation-induced forward shift in time in the occurrence of tumors. In the present experiment no such conclusion can be drawn for the non-DES-treated animals because the spontaneous incidence is too low to permit a comparison to the time course of the radiation-induced incidence. Alternatively, the neoplasms appear so early in the DES-treated animals that there can be only limited further shortening of the latent period and, accordingly, any simple linear relationship appears unlikely. The construction of dose-effect curves must therefore be based on other considerations.

One relatively simple way to construct dose-effect curves is the determination of the increment of the cumulative tumor rate at specified times after irradiation. The disadvantage of the method is that there are no obvious criteria for the proper choice of the reference time. In text-figure 11 the resulting dose-effect relationships are given for non-

TEXT-FIGURE 10.—Different estimates of the cumulative tumor rate $R(t)$ for non-DES-treated animals as a function of time after exposure to X-rays *upper panel* or to neutrons *lower panel*. Both FA and AC are taken into account. *Solid lines* are obtained on the basis of all mammary neoplasms; *dashed lines*, on the basis of first neoplasms in an animal. Absorbed doses are noted on the curves; *C* designates unirradiated animals.

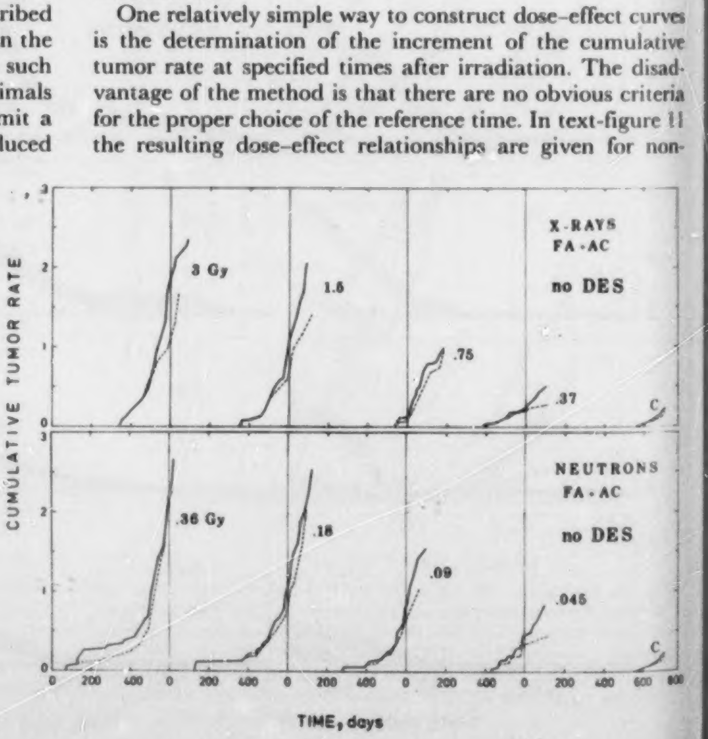

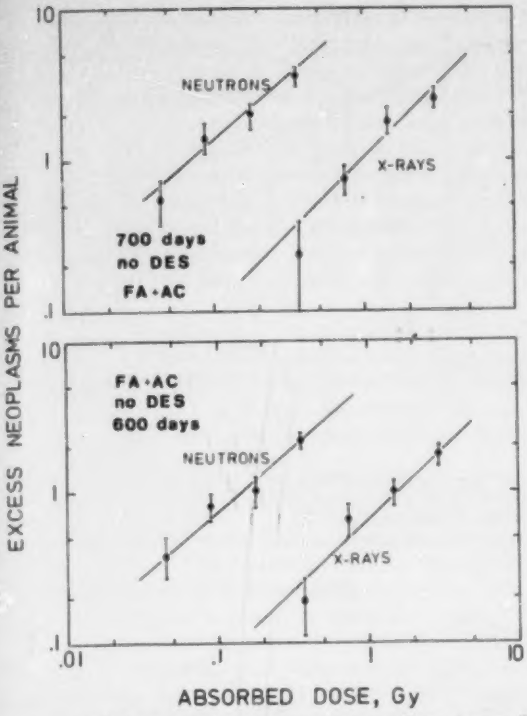

TEXT-FIGURE 11.—Excess number of mammary neoplasms in non-DES-treated animals, i.e., increase of the cumulative tumor rate $R(t)$ over the control level, at 600 *lower panel* and at 700 days *upper panel* after irradiation. Data are given with their standard errors.

DES-treated animals at two different times after irradiation (600 and 700 days). An analogous plot is given in text-figure 12 for DES-treated animals; in keeping with the shorter lifespans, shorter reference times, 300 and 500 days, are chosen. Consistent with the results of the conventional analysis, the RBE appears to exceed 100 at the lowest neutron dose in the DES experiment.

It would be tempting to investigate separately the dose-effect relationships and the RBE for FA and AC in the experiments without DES. Text-figure 13 gives such a separate analysis that appears to indicate somewhat larger RBE values for the FA; however, the absolute numbers are too small to establish a confirmed difference.

Dose-effect curves also can be constructed in a somewhat more general way, and two possibilities will be considered. The first possibility utilizes $R(t)$ and a quantity that has been termed *effect period* Θ (*12, 17*):

$$\Theta=\int_0^{t_{max}} R(t)\,dt. \qquad [6]$$

In this definition t_{max} is the maximum time for which $R(t)$ is obtained in the experiment. The quantity Θ can then be understood as the expected time with neoplasms for an animal that is at risk up to t_{max}; multiple neoplasms are counted with a corresponding factor so that Θ can ultimately, at high doses, exceed the period of observation.

The quantity Θ is estimated by

$$\hat{\Theta}=\sum_i \frac{1}{N(t_i)}(t_{max}-t_i)\pm\sqrt{\sum_i \frac{1}{N(t_i)^2}(t_{max}-t_i)^2}. \qquad [7]$$

The summation extends over all $t_i<t_{max}$, and t_i and $N(t_i)$ have the same meaning as in equation 2. Text-figure 14 gives a plot of $\hat{\Theta}$ as a function of dose. t_{max} has been taken as 500 days in the DES experiment and as 700 days in the experiment without DES.

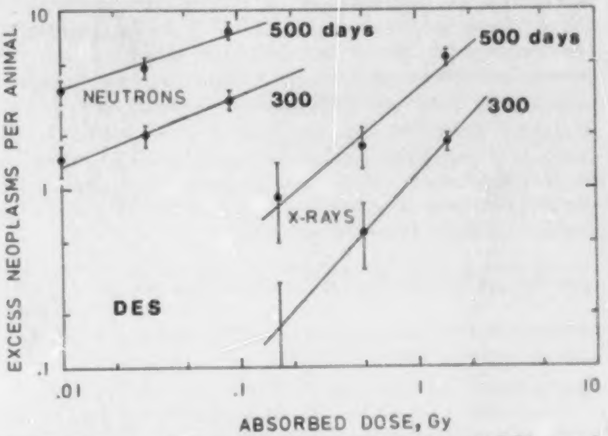

TEXT-FIGURE 12.—Excess number of mammary neoplasms in DES-treated animals, i.e., increase of the cumulative tumor rate $R(t)$ over the control level at 300 and 500 days after irradiation. Data are given with their standard errors.

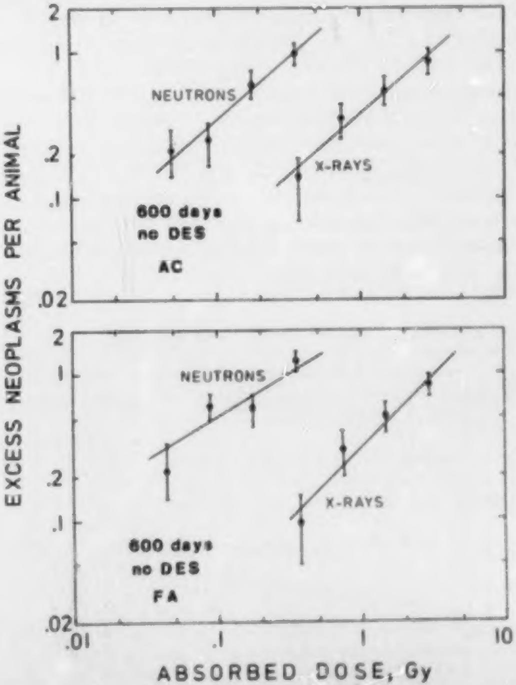

TEXT-FIGURE 13.—Excess number of mammary neoplasms in non-DES-treated animals, i.e., increase of the cumulative tumor rate $R(t)$ over the control level, separately for FA *lower panel* and AC *upper panel* at 600 days after irradiation. Data are given with their standard errors.

An alternative construction of a dose–effect plot is based on a quantity that is similar to Θ but differs from it in depending on first neoplasms only. Hoel and Walburg (*19*) have defined a quantity

$$\mu = \int_0^\infty [1 - I(t)/I(\infty)]dt \qquad [8]$$

that is frequently applied in studies of life shortening, i.e., in the analysis of lethal diseases (*20, 21*). In these studies it is called "mean age at death," and $I(t)$ is either the overall cumulative mortality or the cumulative mortality due to a particular risk. However, it is evident that the quantity proposed by Hoel and Walburg can also be applied in the analysis of nonlethal diseases. In the present case $I(t)$ is the cumulative incidence of mammary neoplasms (*see* equation 5), $I(\infty)$ is set equal to 1 and, as in the determination of Θ, the integration is terminated at t_{max}=500 or 700 days. The formula for the estimation of μ is then:

$$\hat{\mu} = \Sigma[\hat{I}(t_i) - \hat{I}(t_{i-1})]\cdot t_i \pm \sqrt{\{\Sigma t_i^2[-\hat{I}(t_i)]/N(t_i) - \hat{\mu}^2\}/(n-1)} \qquad [9]$$

(summation over all t_i up to t_{max}; n is the number of animals with neoplasm). The standard error in equation 9 corresponds to the formula given by Hoel and Walburg (*19*).

The symbol μ stands for a competing-risk-corrected mean time without mammary neoplasm for the animals. The influence of the correction is substantial, as seen from a comparison of text-figure 15 with the mean tumor-free lifetimes in tables 2 and 5. The dose dependence of μ in text-figure 15 is yet another confirmation of the sublinearity in the DES experiment at small neutron doses; it also confirms the high RBE values in excess of 100 for the DES experiment and close to 10 for the experiment without DES.

Text-figure 16 gives, both for the experiments with and without DES, the RBE of neutron irradiation as a function of dose. These curves have been derived from the mortality-corrected results, i.e., from text-figures 11, 12, 14, and 15. The curves inserted in text-figures 3 and 4 are in agreement with these RBE–dose relationships. The RBE–dose relationship from the earlier experiment with Sprague-Dawley rats (*13*) is inserted for comparison.

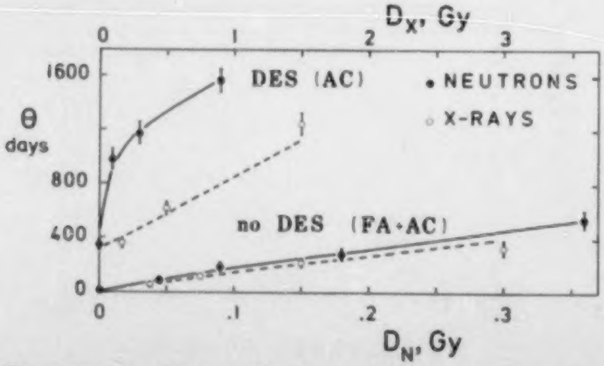

TEXT-FIGURE 14.—*Effect period* Θ and its standard error (*see* equation 7) for DES-treated and non-DES-treated animals. Scales for the neutron (D_N) and the X-ray (D_X) doses differ by a factor of 10. *Solid lines* refer to neutron irradiations; *dashed lines*, to X-irradiations.

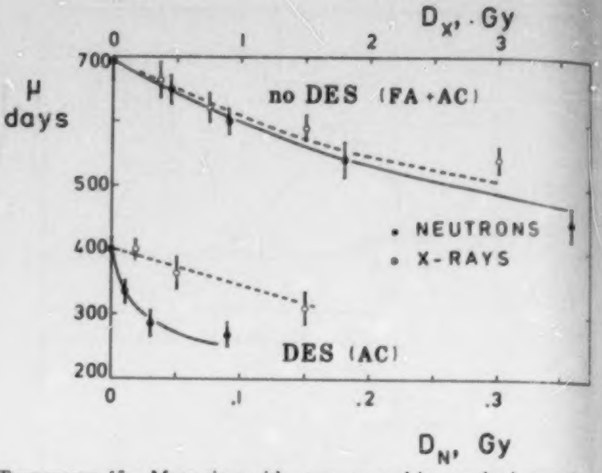

TEXT-FIGURE 15.—Mean time without tumor and its standard error (*see* equation 9) for DES-treated and non-DES-treated animals. Scales for the neutron (D_N) and X-ray (D_X) doses differ by a factor of 10. *Solid lines* refer to neutron irradiations; *dashed lines*, to X-irradiations.

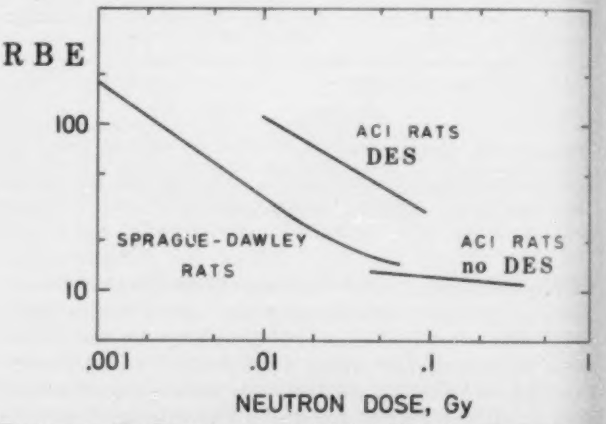

TEXT-FIGURE 16.—Dependence of the RBE of 430-keV neutrons on dose for the induction of mammary neoplasms. Results for the Sprague-Dawley rats are from an earlier study (*13*) (rats were not treated with DES). Results for ACI rats are from the present investigation. Line segments for ACI rats correspond to the curves in text-figs. 3, 4, 11, 12, 14, and 15.

DISCUSSION

Previous experiments (*12, 13*) with female Sprague-Dawley rats had led to the conclusion that the RBE of neutron irradiation for the induction of mammary neoplasms exceeds 100 at an absorbed dose of 1 mGy (0.1 rad). In agreement with earlier microdosimetric considerations (*6*), it had also been found that the RBE of neutron irradiation increases in inverse proportion to the square root of the neutron dose. A further finding was a strong sublinearity (dose exponent ≈0.5) of the dose–effect relationship at small neutron doses. In view of the potential implications of such findings for radiation protection, it seemed desirable to inquire whether similar results are obtained in other strains. The present experiment has been designed for this purpose.

The incidence of mammary neoplasms in control female ACI rats is low. However, the mammary carcinogenic response of non-DES-treated ACI rats to irradiation is relatively small, thus requiring relatively high doses of X-rays and neutrons to produce incidence values large enough to be analyzed statistically. In this part of the experiment, RBE values of neutron irradiation somewhat in excess of 10 are found for the FA and AC, which is in agreement with the values for Sprague-Dawley rats at comparable doses. Experiments with considerably larger numbers of animals would be required to determine the RBE of neutrons at smaller doses.

In ACI rats treated with DES, a large number of early mammary AC is found. With neutron doses as low as 0.01 Gy (1 rad), this incidence is further substantially enhanced. The RBE of neutrons at 0.01 Gy is in excess of 100, and this is even larger than the corresponding value for Sprague-Dawley rats at this neutron dose.

A similar experiment designed with three rat strains (Sprague-Dawley, Wistar WAG/Rij, and Brown Norway) is currently under way at the Toegepast Natuurwetenschappelijk Onderzoek in The Netherlands. Interim results (*22, 23*) of this investigation indicate RBE values from 8 to 25 for neutrons of 0.5 MeV energy at somewhat higher doses than in our study; they also point at considerable differences in susceptibility between the three strains. Quantitative comparisons with the results of the present experiment will have to await completion of the experiment.

The high RBE for mammary tumor carcinogenesis in rats are in line with earlier findings of high neutron RBE in other biological systems. They are also consistent with predictions based on microdosimetric data and support the proposal that the quality factor of 10 presently used for neutrons in radiation protection may need to be reconsidered (*10*).

The observed nonlinear dose–effect relationship for neutrons has an even greater potential impact on radiation protection. At doses below 0.01 Gy of sparsely ionizing radiations, a mammalian cell is traversed by a substantial number of electrons. At comparable doses, the number of cells traversed by any neutron recoil is small. Accordingly, one should expect dose dependence diagrams with positive curvature for sparsely ionizing radiations and linear dose–effect relationships for neutrons; in the dose range where there is a quadratic dependence on X-ray dose and a linear dependence on neutron dose, the neutron RBE has to be inversely proportional to the square root of the neutron dose. In the present experiment, as with the earlier findings on Sprague-Dawley rats, the dose–effect relationships are not of the expected shape; they are not recognizably different from a linear relationship for X-rays and have negative curvature for neutrons. Nevertheless, one obtains the familiar dependence of the RBE of neutrons on the square root of the neutron dose. It appears, therefore, that the characteristic difference between the densely ionizing neutron radiation and the sparsely ionizing X-rays is preserved but that a multicellular reaction or a tissue factor causes a similar distortion for both dose–effect relationships. It must be concluded, that the dose–effect relationships for radiation tumorigenesis are not as yet fully understood, whereas the RBE–dose dependence reflects known biophysical principles.

It is evident that data obtained in animal experiments cannot provide numerical risk estimates for humans. However, the high values of RBE and the negative curvature of the dose–effect relationship at small neutron doses are of sufficient concern to necessitate further radiation carcinogenesis studies with low doses of neutrons.

REFERENCES

(*1*) Shellabarger CJ, Stone JP, Holtzman S. Rat differences in mammary tumor induction with estrogen and neutron radiation. JNCI 1978; 61:1505–1508.

(*2*) Stone JP, Holtzman S, Shellabarger CJ. Synergistic interactions of various doses of diethylstilbestrol and X-irradiation on mammary neoplasia in female ACI rats. Cancer Res 1980; 40:3966–3972.

(*3*) ———. Neoplastic responses and correlated plasma prolactin levels in diethylstilbestrol-treated ACI and Sprague-Dawley rats. Cancer Res 1979; 39:773–778.

(*4*) Segaloff A, Maxfield WS. The synergism between radiation and estrogen in the production of mammary cancer in the rat. Cancer Res 1971; 31:166–168.

(*5*) Shellabarger CJ, Stone JP, Holtzman S. Synergism between neutron radiation and diethylstilbestrol in the production of mammary adenocarcinomas in the rat. Cancer Res 1976; 36:1019–1022.

(*6*) Kellerer AM, Rossi HH. The theory of dual radiation action. Curr Top Radiat Res Q 1972; 8:85–158.

(*7*) Vogel HH. Mammary gland neoplasms after fission neutron irradiation. Nature 1969; 222:1279–1281.

(*8*) Bateman JL, Rossi HH, Kellerer AM, Robinson CV, Bond VP. Dose dependence of fast neutron RBE for lens opacification in mice. Radiat Res 1972; 51:381–390.

(*9*) Sparrow AH, Underbrink AG, Rossi HH. Mutations induced in Tradescantia by small doses of X-rays and neutrons: Analysis of dose–response curves. Science 1972; 176:916–918.

(*10*) Rossi HH. A proposal for revision of the quality factor. Rad Environ Biophys 1977; 14:275–283.

(*11*) Loewe WE, Mendelsohn E. Revised dose estimates at Hiroshima and Nagasaki. Health Physics 1981; 41:663–666.

(*12*) Shellabarger CJ, Brown RD, Rao AR, et al. Rat mammary carcinogenesis following neutron or X-radiation. In: Biological effects of neutron irradiation. Vienna: International Atomic Energy Agency, 1974:391–400.

(*13*) Shellabarger CJ, Chmelevsky D, Kellerer AM. Induction of mammary neoplasms in the Sprague-Dawley rat by 430-keV neutrons and X-rays. JNCI 1980; 64:821–833.

(*14*) Rossi HH, Kellerer AM. Radiation carcinogenesis at low doses. Science 1972; 175:200–202.

(*15*) Kellerer AM, Rossi HH. Biophysical aspects of radiation carcinogenesis. In: Becker FF, ed. Cancer. Vol 1. 1st ed. 1975:405–439; 2nd ed. New York: Plenum, 1982:569–616.

(*16*) Young S, Hallowes RC. Tumors of the mammary gland. In: Turusov VS, ed. Pathology of tumors in laboratory animals. Vol 1. Lyon: IARC, 1973:31–74.

(*17*) United Nations Scientific Committee on the Effects of Atomic Radiation report. Sources and effects of ionizing radiation. United Nations, General Assembly, 32d session, Suppl No. 40 (A/32/40). New York: United Nations, 1977.

(*18*) Kaplan EL, Meier P. Nonparametric estimation from incomplete observations. J Am Stat Assoc 1958; 53:457–481.

(*19*) Hoel DG, Walburg HE Jr. Statistical analysis of survival experiments. J Natl Cancer Inst 1972; 49:361–372.

(*20*) Storer JB, Serrano LJ, Darden EB Jr, Jernigan MC, Ullrich RL. Life shortening in RFM and BALB/c mice as a function of radiation quality, dose and dose rate. Radiat Res 1979; 78:122–161.

(*21*) Thomson JF, Williamson FS, Grahn D, Ainsworth EJ. Life shortening in mice exposed to fission neutrons and γ rays. I. Single and short-term fractionated exposures. Radiat Res 1981; 86:559–572.

(*22*) Broerse JJ, Knaan S, van Bekkum DW, Hollander CF, Noteboom

AL, van Zwieten MJ. Mammary carcinogenesis in rats after X- and neutron irradiation and hormone administration. In: Proceedings of the international symposium on the late biological effects of ionizing radiation. Vol 2. Vienna: International Atomic Energy Agency, 1978:13–27.

(23) Van Bekkum DW, Broerse JJ, van Zwieten MJ, Hollander CF, Blankenstein MA. Radiation-induced mammary cancer in the rat. Okada S, Imamura H, Terashima T, Yamaguchi H, eds. Proceedings of the sixth international congress on radiation research, Tokyo, May 13–19. Tokyo: Toppan, 1979:734–752.

Inhibition by Tumor-Promoting Phorbol Esters of Procollagen Synthesis in Promotable JB6 Mouse Epidermal Cells[1]

L. David Dion,[2] Jenifer Bear,[2] John Bateman,[3,4] Luigi M. De Luca,[5] *and* Nancy H. Colburn[2,6,7]

ABSTRACT—The JB6 mouse epidermal cell line has been developed to study promotion of neoplastic transformation in vitro. Treatment of JB6 cells with 12-*O*-tetradecanoylphorbol 13-acetate (TPA) or other tumor promoters resulted in the irreversible acquisition by JB6 cells of tumorigenicity in nude mice and anchorage-independent growth in soft agar. As previously reported, one of the biochemical responses that occurs during TPA treatment is a greater than 75% reduction in a mannose-labeled glycoprotein with an apparent molecular weight of 180,000. This TPA-sensitive glycoprotein has now been identified on the basis of collagenase and pepsin sensitivity as procollagen pro-α1(I) chain. [^{3}H]proline labeling also demonstrated a parallel decrease in the 150,000 procollagen pro-α2(I) component. Two nonphorbol promoters, mezerein and epidermal growth factor, were also active in decreasing procollagen synthesis. Promotion-sensitive and promotion-resistant clonal derivatives of JB6 showed similar basal levels of collagen synthesis as well as similar degrees of TPA-dependent procollagen loss indicating that the collagen decrease may be necessary but is not sufficient to produce the promotion response. Comparison of chemically transformed mouse epidermal cell lines with paired nontransformants suggests that reduced procollagen synthesis is a stably acquired phenotypic change and may therefore be involved in maintenance of the transformed phenotype as well as in its induction.—JNCI 1982; 69:1147–1154.

Tumor-promoting phorbol esters evoke a wide range of biochemical and cellular responses [reviewed in (*1, 2*)]. Many of these responses are clearly membrane-associated events, such as enhanced 2-deoxyglucose uptake (*3*), phospholipase A_2 stimulation (*4*), ganglioside changes (*5*), glycopeptide changes (*6*), and the loss of the extracellular matrix components fibronectin (*7*) and procollagen (*8*). Because of the pleiotropic nature of the phorbol ester response, it has been difficult to distinguish those elements of the TPA response that contribute directly to the acquisition of the tumor cell phenotype from those elements that are merely coincidental.

We have developed the JB6 mouse epidermal cell line (*9–12*) as a model for studying the mechanism of late-stage promotion of transformation. The JB6 cell line is anchorage-dependent and nontumorigenic in nude mice but, unlike a variety of normal cells, irreversibly acquires anchorage independence and tumorigenicity after exposure in monolayer or in soft agar to tumor-promoting phorbol esters or other promoters (*9–12*). As in many other systems, the anchorage-independent phenotype correlates well with tumorigenicity (*12*). Studies employing the promotable JB6 cell model therefore offer the potential to elucidate the biochemical events directly involved in phorbol ester induction of the neoplastic phenotype.

Retinoids have been demonstrated to be potent inhibitors of in vivo tumor promotion by phorbol esters (*13*). These compounds also block phorbol ester promotion of transformation in vitro as shown by Colburn et al. (*14*) and Bertram et al. (*15*). The retinoids thus appear to be a useful tool to probe the biochemical events that accompany exposure to phorbol esters since at least one biochemical step critical to the promotion pathway should be blocked or antagonized by the retinoids.

Retinoid enhancement of a 180,000-M_r glycoprotein has been reported by several laboratories using various cell culture models (*16–18*). Strickland et al. (*19*) have identified a retinoid-induced glycoprotein in embryonal carcinoma cells as procollagen. These reports along with the report of Delclos and Blumberg (*8*) of a TPA-dependent loss of procollagen from CEF suggested that procollagen might offer a well-defined biochemical entity with which to study retinoid antagonism of TPA-induced promotion.

We have recently reported that TPA reduces and RA enhances the synthesis of a 180,000-M_r glycoprotein by JB6 cells (*20*). We report here the identification of the gp180 from JB6 cells as procollagen. The TPA-dependent procollagen loss occurs rapidly and persists with continued TPA treatment. Reduced procollagen synthesis appears to be a stable, acquired characteristic of malignantly transformed mouse epidermal cells.

MATERIALS AND METHODS

The derivation of the JB6 cell line from mouse primary epidermal cell cultures has been described elsewhere (*12*), as has the derivation by nonselective cloning of promotable and nonpromotable JB6 clonal cell lines (*11*). Nontrans-

---

Abbreviations used: CEF=chick embryo fibroblast(s); DMSO=dimethyl sulfoxide; EGF=epidermal growth factor; M_r=molecular weight (relative); PAGE=polyacrylamide gel electrophoresis; RA=retinoic acid; SDS=sodium dodecyl sulfate; TPA=12-*O*-tetradecanoylphorbol 13-acetate.

---

[1] Received February 19, 1982; accepted June 3, 1982.

[2] Laboratory of Viral Carcinogenesis, Division of Cancer Cause and Prevention, National Cancer Institute, National Institutes of Health, Public Health Service, U.S. Department of Health and Human Services, Frederick, Md. 21701.

[3] Laboratory of Biochemistry, Divison of Cancer Biology and Diagnosis National Cancer Institute, Bethesda, Md. 20205.

[4] *Present address:* Department of Orthopaedics, Royal Childrens Hospital, Parkville, Victoria, Australia 3052.

[5] Laboratory of Cellular Carcinogenesis and Tumor Promotion, Division of Cancer Cause and Prevention, National Cancer Institute, Bethesda, Md. 20205.

[6] *Address reprint requests to* Dr. Colburn, Building 560, Room 12-89, NCI-Frederick Cancer Research Facility, Frederick, Md. 21701.

[7] We thank Dr. Anton Jetten, Dr. Beverly Peterkofsky, and Dr. Thomas Gindhart for fruitful discussions and Dr. Peterkofsky for generously supplying the purified bacterial collagenase.

formed mouse epidermal cell lines were obtained from BALB/c (JB1 and JB6) (*12*) or from Sencar (D1 and 3M12a) (*10*) primary epidermal cultures. Transformed mouse epidermal cells were obtained from JB6 cells (RT101, R24, R681, T^{3}6271, and T^{3}6274) after TPA exposure in agar (*10, 21*) or after exposure to 7,12-dimethylbenz[*a*]anthracene (D11a and DT2) or *N*-methyl-*N*-nitro-*N*-nitrosoguanidine (JB8 and 3M12b) (*10, 12*). JB6 cells were passaged after trypsinization with a 0.06% trypsin solution, and cultures were always maintained below confluence. Minimum essential medium with Earle's salts (GIBCO, Grand Island, N.Y.) was supplemented with 10% fetal bovine serum (Flow Laboratories, Inc., Rockville, Md.) and antibiotics.

Phorbol esters were purchased from Chemical Carcinogenesis, Eden Prairie, Minn. Stock solutions at 0.1 mg/ml in spectral grade DMSO were stored at −20°C in a desiccated container. At the time of use, the stock was diluted 10^4-fold with medium to give a final concentration of 10 ng TPA/ml (1.6×10^{-8} *M*).

RA was from Hoffmann-La Roche Inc., Nutley, N.J. Stocks were maintained as dry crystals in small screw-cap vials stored in desiccators at −20°C. We prepared small stock solutions by dissolving 3 mg RA/ml DMSO. Stock solutions were not used longer than a week, and all operations were conducted under light from General Electric gold fluorescent lamps.

Metabolic labeling.—L-[5-^{3}H]proline (catalog No. NET 573) was purchased from New England Nuclear Corp., Boston, Mass. D-[2-^{3}H]mannose (catalog No. TRK 364) was purchased from Amersham, Corp., Arlington Heights, Ill. Cultures were incubated for 2 hours after radionuclides were added to the serum containing medium at 10 μCi/ml.

When [^{3}H]mannose was used, the medium was aspirated and replaced with low-glucose medium (50 mg/liter). Use of low-glucose medium did not change the pattern of glycoproteins obtained from SDS gels but did give a tenfold increase of incorporation into acid-precipitable material.

The cells were washed twice with phosphate-buffered saline and, when 35-mm dishes were used, dissolved directly into 300 μl of SDS sample buffer, transferred to 1.5 ml Eppendorf tubes, boiled for 3–5 minutes, sonicated, and immediately frozen. The SDS sample buffer consisted of 2.0% SDS, 0.1 *M* dithiothreitol, 0.08 *M* Tris, 10% glycerol, 0.002 *M* phenylmethyl sulfonyl fluoride, and 0.0012% bromophenol blue (pH 6.8).

Gel electrophoresis.—Polyacrylamide gels were prepared by the method of Laemmli (*22*) with the use of a Bio-Rad model 200 gel-casting apparatus. Separatory gels were 7.5% and stacking gels were 3.5%. Gels were loaded with equal trichloroacetic acid-precipitable counts per track to permit detection of changes in relative amounts of synthesis independently of changes in precursor uptake. Typically, 10,000–20,000 cpm was applied on each track for [^{3}H]mannose and 100,000 cpm for [^{3}H]proline, representing extracts from 200,000 to 300,000 cells. Electrophoresis was done for 4.5 hours at 25 mA/gel. Gels were fixed overnight in 7% acetic acid and 5% methanol, saturated with Enhance (New England Nuclear Corp.) for 2 hours, and washed with water for 2 additional hours. The gels were dried on a Bio-Rad gel dryer and autoradiographed on Kodak X-Omat XR-5 film. ^{14}C-labeled marker proteins were purchased from Amersham Corp. Scanning densitometry of the autoradiographs was done with the use of an EC scanning densitometer. When the relative collagen content was determined in this manner, the integrated areas under the 180,000- and 150,000-M_r peaks were added together and divided by the integrated value for the entire autoradiograph.

Collagenase digestion.—The collagen content of the cells was determined by a modification of the method of Peterkofsky and Diegelmann (*23*). Subconfluent monolayers of cells were treated with DMSO, TPA, or RA for 24 hours followed by a 6-hour labeling period with the use of 1 μCi L-[^{14}C]proline/ml. L-[^{14}C]proline was purchased from New England Nuclear Corp. (catalog No. NEC-285) (250 mCi/mmol). The acid-precipitable material was exhaustively digested with purified bacterial collagenase. The solubilized radioactivity represents collagen protein.

Pepsin digestion.—Pepsin-resistant α-chains of collagen were determined by treatment of [^{3}H]proline-labeled cell lysates with 100 μg pepsin/ml in 0.5 *M* acetic acid for 1 hour at room temperature.

RESULTS

Preferential Incorporation of [^{3}H]proline Into TPA-Sensitive 180,000- and 150,000-M_r Glycoproteins

When JB6 cells were treated with TPA (10 ng/ml) for 24 hours and then labeled with [^{3}H]mannose for an additional 8 hours, the synthesis of [^{3}H]mannose-labeled 180,000- and 150,000-M_r cell-associated glycoproteins was inhibited (*20*). When [^{3}H]leucine or [^{35}S]methionine was used as a precursor, TPA-sensitive components at 180,000 and 150,000 were only minimally labeled (data not shown). [^{3}H]proline (fig. 1), however, was preferentially incorporated into a 180,000 and a 150,000 protein [pro-α1(I) and pro-α2(I), respectively]. These two proteins displayed a marked TPA-dependent reduction, and the concentration dependency (fig. 1) of the response of the [^{3}H]proline-labeled 180,000 protein was the same as that of the [^{3}H]mannose-labeled gp180 (*20*). The effect in both cases was fully expressed at 1 ng TPA/ml medium and minimally observable at 0.1 ng TPA/ml. Figure 1 also shows a reduction in a [^{3}H]proline-labeled 220,000 band after TPA exposure. This 220,000 band has been identified as fibronectin by immunoprecipitation (data not shown). As described before (*20*), fibronectin appears to be affected by TPA and RA in a manner parallel to that observed for the 180,000 band, although to a lesser degree.

Identification of gp180 as Procollagen

The preferential labeling of the gp180 with [^{3}H]proline together with the previous report by Delclos and Blumberg (*8*) that TPA markedly reduced procollagen synthesis in CEF cultures suggested the identity of JB6 gp180. Figure 2 presents the results of a digestion of [^{3}H]mannose-labeled JB6 glycoproteins by purified bacterial collagenase. Most of the [^{3}H]mannose incorporated into 180,000- and 150,000-M_r material was collagenase-sensitive, and gp180 and gp150 were the only proteins that were digested under these conditions. The appearance of a [^{3}H]mannose-labeled 35,000-

M_r glycoprotein in collagenase-treated samples (fig. 2) is consistent with the enzymatic release of the COOH terminal peptide (*21*).

Collagen in helical form is resistant to pepsin, whereas most other proteins are not. After pepsin digestion of nonhelical N— and C— terminal regions, collagen is converted to α-chains (*24*). The partial purification of procollagen in the JB6 cells before pepsin (fig. 2) reflects the high solubility of procollagen in 0.5 *M* acetic acid relative to the solubility of other proteins. Pepsin digestion of [^{3}H]proline-labeled JB6 cell extracts demonstrates the formation of two chains in the molecular weight range of 100,000 corresponding to α1 and α2 chains (*24*). This finding therefore confirms the identity of the 180,000 and 150,000 proteins as collagen in JB6 cells.

Quantitation of Collagen Synthesis Responses

JB6 cells were labeled for 6 hours with [^{14}C]proline after 24-48 hours of exposure to TPA. We harvested the cells by scraping them, and we analyzed them for collagen content by the method of Peterkofsky and Dieglemann (*23*), which involves an enzymatic digestion with purified bacterial collagenase and determination of collagenase-sensitive cpm as a percent of total. In response to TPA, JB6 cells showed a 75% inhibition of collagen synthesis at both 24 and 48 hours (table 1). RA enhanced procollagen synthesis and partially antagonized the TPA-dependent decrease at 48 hours. At 24 hours, however, the RA had little effect on procollagen synthesis either alone or in combination with TPA. When the effect of TPA on collagen secretion was examined (not shown), TPA treatment was found to produce a 50–75% decrease. This effect on collagen secretion thus paralleled that on collagen synthesis.

Induction by Complete and Second-Stage Tumor Promoters of a Procollagen Loss by JB6 Cells

Analogues of phorbol esters were found to vary in their effectiveness at inhibiting procollagen synthesis in a manner that correlated with their activity in promotion of transformation (*25*) (table 2). TPA, as expected, was the most active phorbol ester used in this assay. Phorbol 12,13-didecanoate and mezerein, a nonphorbol diterpene, were nearly as active as was TPA.

TABLE 1.—*Collagenase digestion of [^{14}C]proline-labeled proteins showing TPA inhibition and RA enhancement of collagen from JB6 cells*[a]

Duration of treatment, hr	Percent collagen protein			
	DMSO, 0.02%	RA, 10^{-6} *M*	TPA, 10 ng/ml	RA + TPA
24	1.87±0.31	1.70±0.31	0.33±0.15	0.57±0.08
48	2.04±0.16	2.71±0.09	0.43±0.06	1.34±0.12

[a] Values were corrected for the fivefold enhancement of proline in collagen proteins and are expressed as ± one-half the range for duplicate culture dishes. Thus 10% collagenase-soluble radioactivity is expressed as 2% collagen protein. Cells were plated at 20,000/cm^2 and grown for 1 day before initial treatment. Treatment was continued for the duration indicated, followed by a 6-hr labeling period with [^{14}C]proline. Addition of 50 μg ascorbic acid/ml to the medium did not significantly affect precursor incorporation into collagen of JB6 cells.

TABLE 2.—*Induction by complete and second-stage tumor promoters of procollagen loss by JB6 cells*

Promoters[a]	Concentration, ng/ml[b]				
	0.1	1	10	50	100
TPA	−	+	+		+
Mezerein	−	±	+		+
Phorbol didecanoate	−	±	+		+
Phorbol dibenzoete	−	−	±		+
Phorbol dibutyrate	−	−	±		+
4-*O*-Methyl-TPA	−	−	−		+
Phorbol diacetate	−	−	−		−
Phorbol triacetate	−	−			−
EGF		−	+	+	
A23187		−	−	−	−

[a] Saccharin and sodium cyclamate were inactive at 1–500 mg/ml.

[b] Autoradiographs were scored for reduction of the 180,000-M_r band. + indicates ≈50% or greater reduction in optical density; − indicates no observable reduction in optical density; ± indicates <50% reduction in optical density.

Slaga et al. (*26, 27*) have recently demonstrated that tumor promotion is a multistage process and that tumor promoters can be categorized as being complete, early-stage, or late-stage promoters. Within this scheme, TPA is considered to be a complete promoter, since it is capable of promoting transformation of initiated mouse skin. Mezerein is a second-stage promoter in that it is capable of completing promotion only if it follows a TPA exposure but not if used alone. In this context, the strong mezerein effect on collagen synthesis is interesting because this response is consistent with the observation that mezerein is active as a promoter of transformation in JB6 cells (*11, 25*).

Mezerein has been shown to be similar in activity to phorbol didecanoate at releasing arachidonic acid and prostaglandin E_2 from CEF (*4*). 4-*O*-Methyl-TPA, which has been shown to be a weak complete promoter in vivo (*27*) and a weak promoter in the JB6 promotion of anchorage independence assay (not shown), was minimally active in this procollagen decrease assay. Phorbol diacetate and phorbol triacetate were inactive in this assay, as they were in the promotion of anchorage independence assay.

We have tested two other nonphorbol tumor promoters for procollagen-inhibiting activity. The calcium ionophore A23187 has been shown to be a first-stage promoter in mouse skin (*27*). Consistent with the other data showing that JB6 cells are partially promoted, A23187 does not induce anchorage independence in JB6 cells (*25*). A23187 also was inactive as an inhibitor of procollagen synthesis. EGF was active at 10–50 ng/ml in decreasing procollagen synthesis and has been shown to irreversibly promote JB6 cells to anchorage independence (*11, 28*). It appears that agents which are known as second-stage or complete promoters had a pronounced inhibitory effect on procollagen synthesis in JB6 cells, whereas first-stage and nonpromoting analogues were inactive at producing this biochemical response.

TABLE 3.—*Collagenase digestion of [^{14}C]proline-labeled proteins that shows TPA reduction of collagen in promotable and nonpromotable JB6 cell clones*

Cell line (phenotype)	Collagen content as a percent of [^{14}C]proline-labeled protein[a]		Ratio TPA:DMSO
	DMSO	TPA	
JB6 (parent cell line)	1.87±0.31	0.4±0.43	0.21±0.02
Promotable	1.65±0.22	0.33±0.15	0.20±0.12
Cl 41 (promotable)	1.89±0.54	0.32±0.28	0.15±0.10
Cl 21 (promotable)	1.00±0.19	0.23±0.06	0.23±0.03
Cl 30 (nonpromotable)	1.22±0.13	0.42±0.07	0.34±0.03
Cl 25 (nonpromotable)	1.76±0.06	0.64±0.08	0.36±0.04

[a] Values were corrected for the fivefold enhancement of proline in collagen proteins and are expressed as ± one-half the range for duplicate culture dishes. Thus 10% collagenase-soluble counts are expressed as 2% collagen protein. TPA (10 ng/ml) or DMSO (0.02%) was added 24 hr after the cells had been plated. The cultures were treated for 24 hr followed by a 6-hr labeling period.

Demonstration by Both Promotable and Nonpromotable Clones of JB6 of TPA-Dependent Reduction of Collagen

The JB6 cell line has been used to generate cloned populations of cells that vary a hundredfold in their promotion responsiveness to TPA (*10, 11*). We have chosen two TPA promotion-sensitive cell lines (clones 41 and 21) and two TPA-resistant cell lines (clones 25 and 30) to determine whether the TPA-dependent reduction in collagen might correlate with promotion sensitivity. Table 3 demonstrates that when the collagenase digestion technique was used to determine the [^{14}C]proline-labeled collagen content, both promotable and nonpromotable cells demonstrated a similar (≈80%) collagen loss in response to TPA. Hence promotion resistance is not attributable to lack of procollagen response to TPA. Furthermore, the basal levels of collagen were similar, showing that lower (or higher) basal levels of collagen synthesis do not predispose the cells to promotability.

Rapid and Persistent TPA-Mediated Decrease of Procollagen Synthesis

Cultures of parental JB6 cells or clonal lines JB6 Cl 41 or JB6 Cl 30 were treated with TPA (1 ng/ml) for 1–8 days, and the cells were terminally labeled with [^{3}H]proline for 2 hours to determine whether the procollagen loss was a persistent effect of TPA treatment. We found (text-fig. 1) that the TPA caused a decrease in procollagen synthesis in all three cell lines as determined by densitometry of gel autoradiographs to 30–50% of control by 24 hours. Continuous exposure to TPA up to 8 days resulted in persistence of the reduced procollagen levels observed at 24 hours. Thus the JB6 cells do not become refractory to TPA for this phenotypic change but appear to undergo a persistent decrease in procollagen synthesis at least in the presence of TPA.

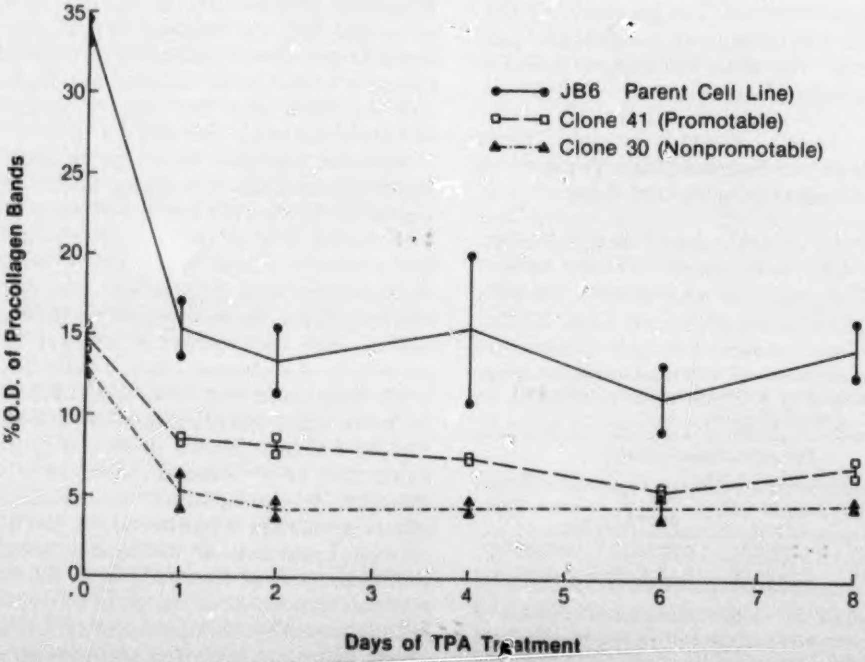

TEXT-FIGURE 1.—TPA-dependent reduction of procollagen is rapid and persistent. Cells were exposed to 1 ng TPA/ml as described in "Materials and Methods." Autoradiographs of SDS–polyacrylamide gels were prepared as described with the use of [^{3}H]proline-labeled proteins [(*20*); *see also* legend to fig. 1]. Scanning densitometer tracings of the autoradiographs were prepared and the integrated area under both the 180,000 and 150,000 regions as a percentage of the total integrated area was compared. Results are expressed as collagen optical density (O.D.) as a percent of total O.D. Values have not been corrected for the fivefold enhancement of proline in collagen protein. Hence 35% O.D. in procollagen is equivalent to ≈7% of total protein.

TABLE 4.—*Reduced procollagen synthesis in transformed mouse epidermal cell lines*[a]

Nontransformants		Paired transformants	
Cell line	[^{3}H]proline in collagen bands, %	Cell line	[^{3}H]proline in collagen bands, %
JB6	17.6±1.6	RT101	6.1±0.9
		R24	7.7±0.5
		R681	8.6±0.0
		T^{3}6271	15.0±0.75
		T^{3}6274	12.8±0.6
D1	16.3±1.8	D11a	11.0±1.4
		DT2	6.9±0.3
JB1	13.3±0.4	JB8	5.7±0.1
3M12a	22.5±0.6	3M12b	14.3±0.0

[a] Cells were plated at 10,000/cm^2; 24 hr after plating, the cultures were labeled with [^{3}H]proline for 2 hr. The labeled proteins were separated by SDS-PAGE. Autoradiographs were analyzed by scanning densitometry and results are expressed as percent of total optical density ± one-half the range for duplicate samples. Cell lines have been scored as transformed because they were demonstrated to be anchorage-independent and/or tumorigenic (*10, 12, 21*). Nontransformed lines were negative by both assays.

Retention by Transformed Mouse Epidermal Cells of Low Procollagen Phenotype

To further investigate the persistence of the TPA-produced procollagen decrease, we compared TPA-promoted, transformed cells with their nontransformed precursor (JB6) or with nontransformants of a different origin and their transformed derivatives (D1, JB1, 3M12a and D11a, DT2, JB8, 3M12b). As shown in table 4 when we labeled with [^{3}H]proline and compared for SDS-PAGE profiles, we found that the transformed cells synthesized less procollagen than did their paired nontransformed counterparts. This change was not dependent on the transforming agent since D11a (transformed) and DT2 (transformed) were transformed by 7,12-dimethylbenz[*a*]anthracene (*10*), whereas (*10*), the RT101, R24, and R681 were obtained after promotion to the transformed state by TPA exposure of JB6 Cl 41 cells (*21*). The magnitude of the change appeared to be similar to that found after TPA exposure of promotable cells shown in text-figure 1 with the use of the same methodology. This method may underestimate the magnitude of the TPA or transformation-sensitive decrease due to the presence of some noncollagen [^{3}H]proline-labeled material in the 180,000 and 150,000 bands. Due to its specificity, the collagenase digestion method used in tables 1 and 3 probably gives a more accurate measure of the decrease.

DISCUSSION

Our studies of glycoprotein changes induced by phorbol esters during promotion of transformation in JB6 cells were initially stimulated by previous reports that TPA inhibited the expression of two glycoproteins, fibronectin and procollagen (*7, 8*). The well-documented reports that retinoids generally enhanced glycoprotein synthesis and that retinoids antagonize TPA-induced preneoplastic progression further suggested that the two molecules may act antagonistically on glycoprotein synthesis. [For review, *see* (*1, 14*).] We have found that TPA and RA produce major and opposite effects on the synthesis in promotable JB6 cells of 180,000- and 150,000-M_r glycoproteins (*20*), which have been identified here as type I procollagen.

The identification of the TPA-sensitive gp180 and gp150 as procollagen is supported by four lines of evidence. The [^{3}H]mannose-labeled gp180 and gp150 glycoproteins were sensitive to hydrolysis by purified bacterial collagenase. Digestion with collagenase generated a 35,000 glycoprotein consistent with its being the carboxy terminal end of the procollagen peptides. The TPA- and RA-responsive 180,000 and 150,000 proteins are preferentially labeled with [^{3}H]-proline. That procollagen determined by collagenase digestion of [^{14}C]proline-labeled proteins shows the same decrease in response to TPA and increase in response to RA as observed for the 180,000 and 150,000 gel electrophoresis bands provides further confirming evidence for the procollagen identity of these two bands.

The presence of two molecular weight components and the failure of either to be precipitated by anti-type IV collagen antibody (Sobel M: Personal communication) have lead to the characterization of JB6 procollagen as type I procollagen. The presence of type I instead of type IV collagen in cultures of cloned cells that are well characterized as being of epidermal origin (*10*) may reflect an altered differentiation associated with growth as a cell line or may be part of the preneoplastic phenotype of the JB6 cells.

Another suggested identity for the TPA-sensitive gp180 was EGF receptor which has been reported to have a molecular weight around 165,000–180,000 (*29*). Antibody to EGF receptor did not isolate a glycoprotein from JB6 cells which could be seen in the 180,000 region of SDS gels (data not shown).

The TPA effect on procollagen synthesis is striking in both the extent to which and speed with which TPA acts. The procollagen [both the 180,000 pro-α1(I) and the 150,000 pro-α2(I) bands] content is depressed by more than 50% within 24 hours. The magnitude of collagen reduction was similar to that obtained with TPA-exposed CEF cultures (*8*), but maximum reduction was attained at a slower rate in CEF. Continued exposure to TPA over 8 days led to persistently reduced procollagen. Preliminary evidence suggests that more than 72 hours of TPA treatment are required to irreversibly reduce procollagen (Dion LD: Unpublished data). The reduced procollagen persists into the tumorigenic state.

We have screened several more promotable clones of JB6 for a loss of the mannose-labeled gp180 after TPA exposure (data not shown). All promotable cell lines tested have shown similar losses of gp180 in response to TPA. A promotable cell that does not give a reduced procollagen response would be needed to exclude this biochemical effect from the set of those effects that are necessary for promotion. Hence the procollagen decrease may be a required event. This response to promoters is, however, not sufficient to set in motion all subsequent events that bring about promotion of transformation in JB6 cells since it occurs in nonpromotable variants. It may be an event that is necessary for promotion and one that is involved in the antipromoting action of retinoids.

That reduced collagen occurs repeatedly in transformed mouse epidermal cells suggests that it may be involved not only in induction of the transformed phenotype but also in its maintenance. Reduced collagen synthesis in cells transformed by DNA viruses (*30*), RNA viruses (*8, 31–33*), and chemical carcinogen (*32*) has been a frequent observation. Recently, Bateman and Peterkofsky (*33*) reported that a shift to nonpermissive temperature of cells transformed by a temperature-sensitive retrovirus resulted in reversal of both collagen reduction and growth in soft agar. This observation also suggests the possible role of reduced collagen in maintenance of the transformed phenotype. Alternatively, both collagen reduction and neoplastic transformation could have a common cause without a causal relationship to each other.

TPA treatment of JB6 cells clearly reduced the synthesis and therefore the secretion of procollagen. Other secreted molecules may also be affected in a parallel manner. The secreted proteins, including collagens, fibronectin, chondronectin, laminin, and glycosaminoglycans, may all share some degree of coordinate regulation as part of the phenotypic state of differentiation. TPA by altering the spectrum of secreted molecules may thus be altering both a cell's program of gene expression and its extracellular microenvironment. The influence of the extracellular matrix on promotion of transformation is possibly of considerable importance but is a subject that has received little investigation.

Our current approach is to identify the biochemical level at which TPA and RA affect procollagen synthesis. Preliminary results suggest that TPA may be specifically inhibiting RNA transcription for procollagen (Sobel M, Dion LD: Unpublished data).

REFERENCES

(*1*) Colburn NH. Tumor promotion and preneoplastic progression. In: Slaga TJ, Sivak A, Boutwell RK, eds. Carcinogenesis, a comprehensive survey. Vol 5. New York: Raven Press, 1980:33–56.

(*2*) Blumberg PM. In vitro studies on the mode of action of the phorbol esters, potent tumor promoters. Part 1. CRC Crit Rev Toxicol 1980; 8:152–197.

(*3*) Dreidger PE, Blumberg PM. The effect of phorbol diesters on chicken embryo fibroblasts. Cancer Res 1977; 37:3257–3265.

(*4*) Mufson RA, De Feo D, Weinstein IP. Effects of phorbol ester promoters on arachidonic acid metabolism in chick embryo fibroblasts. Mol Pharmol 1979; 16:569–578.

(*5*) Huberman E, Heckman C, Langenbach R. Stimulation of differentiated functions in human melanoma cells by tumor-promoting agents and dimethyl sulfoxide. Cancer Res 1979; 39:2618–2624.

(*6*) Weinstein IB, Wigler M, Pietropaolo C. The action of tumor promoting agents in cell culture. In: Origins of human cancer. Cold Spring Harbor, N.Y.: Cold Spring Harbor Press, 1977:751–772.

(*7*) Blumberg PM, Driedger PE, Rossow PW. Effect of a phorbol ester on a transformation-sensitive surface protein of chick fibroblasts. Nature 1976; 254:445–447.

(*8*) Declos KB, Blumberg PM. Decrease in collagen production in normal and Rous sarcoma virus-transformed chick embryo fibroblasts induced by phorbol myristate acetate. Cancer Res 1979; 39:1667–1672.

(*9*) Colburn NH, Former BF, Nelson KA, Yuspa SH. Tumour promoter induces anchorage independence irreversibly. Nature 1979; 282:589–591.

(*10*) Colburn NH. The use of tumor promoter responsive cell lines to study preneoplastic progression. In: Franks LM, Wigley CB, eds. Neoplastic transformation in differentiated epithelial cell systems in vitro. New York: Academic Press, 1979:113–134.

(*11*) Colburn NH, Koehler BA, Nelson KJ. A cell culture assay for tumor-promoter-dependent progression toward neoplastic phenotype: Detection of tumor promoters and promotion inhibitors. Teratogenesis Carcinog Mutagen 1980; 1:87–96.

(*12*) Colburn NH, Vorder Bruegge WF, Bates JR, et al. Correlation of anchorage-independent growth with tumorigenicity of chemically transformed mouse epidermal cells. Cancer Res 1978; 38:624–634.

(*13*) Verma AK, Shapas BG, Rice HM, Boutwell RK. Correlation of the inhibition by retinoids of tumor promoter-induced mouse epidermal ornithine decarboxylase activity of skin tumors. Cancer Res 1979; 39:419–425.

(*14*) Colburn NH, Ozanne S, Lichti U, et al. Retinoids inhibit promoter-dependent pre-neoplastic progression in mouse epidermal cell lines. In: Modulation of cellular interactions by vitamin A and derivatives (retinoids). Ann NY Acad Sci 1981; 359:251–259.

(*15*) Bertram JS, Mordan LJ, Blair SJ, Hui S. Effects of retinoids on neoplastic transformation, cell adhesion, and membrane topography of cultured 10T1/2 cells. In: Modulation of cellular interactions by vitamin A and derivatives (retinoids). Ann NY Acad Sci 1981; 359:218–236.

(*16*) Patt LM, Itaya K, Hakomori S. Retinal induces density-dependent growth inhibition and changes in glycolipids and LETS. Nature 1978; 273:379–381.

(*17*) Sasak W, De Luca LM, Dion LD, Silverman-Jones CS. Effect of retinoic acid on cell surface glycopeptide of cultured spontaneously transformed mouse fibroblasts (BALB/c 3T12-3 cells). Cancer Res 1980; 40:1933–1939.

(*18*) Lotan R, Kramer RH, Neumann G, Lotan D, Nicolson GL. Retinoic acid-induced modifications in growth and cell surface components of a human carcinoma (HeLa) cell line. Exp Cell Res 1980; 130:401–414.

(*19*) Strickland S, Smith KK, Marotti KR. Hormonal induction of differentiation in teratocarcinoma stem cells: Generation of parietal endoderm by retinoic acid and dibutyryl cAMP. Cell 1980; 21:347–355.

(*20*) Dion LD, De Luca LM, Colburn NH. Phorbol ester-induced anchorage independence and its antagonism by retinoic acid correlates with altered expression of specific glycoproteins. Carcinogenesis 1981; 2:951–958.

(*21*) Colburn NH, Wendel EJ, Abruzzo G. Dissociation of mitogenesis and late-stage promotion of tumor cell phenotype by phorbol esters: Mitogen resistant variants are sensitive to promotion. Proc Natl Acad Sci USA 1981; 78:6912–6916.

(*22*) Laemmli UK. Cleavage of structural proteins during the assembly of the head of bacteriophage T4. Nature 1970; 227:680–685.

(*23*) Peterkofsky B, Diegelmann R. Use of a mixture of proteinase-free collagenases for the specific assay of radioactive collagen in the presence of other proteins. Biochemistry 1971; 10:988–994.

(*24*) Bornstein P, Sage H. Structurally distinct collagen types. Ann Rev Biochem 1980; 49:957–1003.

(*25*) Colburn NH, Wendel E, Srinivas L. Responses of preneoplastic epidermal cells to tumor promoters and growth factors: Use of promoter resistant variants for mechanism studies. J Cell Biochem 1982; 18:261–270.

(*26*) Slaga TJ, Fischer SM, Nelson K, Gleason GL. Studies on the mechanism of skin tumor promotion: Evidence for several stages in promotion. Proc Natl Acad Sci USA 1980; 77:3659–3663.

(*27*) Slaga TJ, Fischer SM, Weeks CE, Klein-Szanto AJ, Reiner J. Studies on the mechanisms involved in multistage carcinogenesis in mouse skin. J Cell Biochem 1982; 18:99–119.

(*28*) Colburn NH, Gindhart TD. Specific binding of transforming growth factor correlates with promotion of anchorage independence in EGF receptorless mouse JB-6 cells. Biochem Biophys Res Commun 1981; 102:799–807.

(*29*) Cohen S, Carpenter G, King L. Epidermal growth factor–receptor kinase interactions: Co-purification of receptor and epidermal growth factor-enhanced phosphorylation activity. J Biol Chem 1980; 255:4834–4842.

(*30*) Green H, Todaro GJ, Goldberg B. Collagen synthesis in fibroblast transformed by oncogenic viruses. Nature 1966; 204:916–917.

(*31*) Levinson W, Bhatnagar RS, Liu TZ. Loss of ability to synthesize collagen in fibroblasts transformed by Rous sarcoma virus. J Natl Cancer Inst 1975; 55:807–810.

(32) Hata N-I, Peterkofsky B. Specific changes in the collagen phenotype of BALB 3T3 cells as a result of transformation by sarcoma viruses or a chemical carcinogen. Proc Natl Acad Sci USA 1977; 74:2933-2937.

(33) Bateman JF, Peterkofsky B. Mechanisms of Kirsten murine sarcoma virus transformation-induced changes in the collagen phenotype and synthetic rate of BALB 3T3 cells. Proc Natl Acad Sci USA 1981; 78:6028-6032.

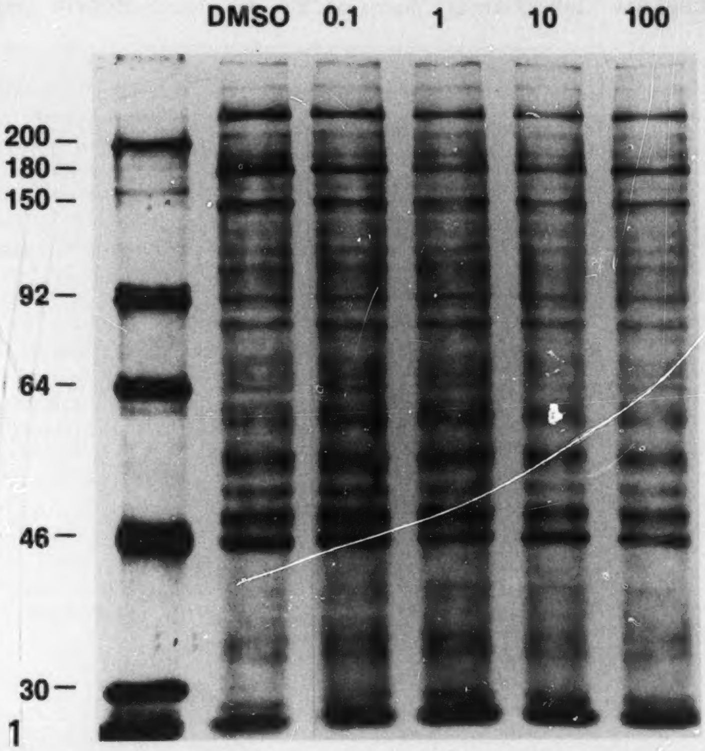

Figure 1.—[^{3}H]proline preferentially labels the 180,000- and 150,000-M_r TPA-inhibited proteins of JB6 cells. JB6 cells were treated with the indicated concentrations of TPA or 0.01% DMSO for 24 hr followed by a 2-hr labeling period with 10 μCi/ml of [^{3}H]proline. Total cellular proteins were separated by SDS-PAGE for autoradiography as described previously (*20*). *Left lane* contains ^{14}C-labeled molecular weight markers purchased from Amersham Corp.

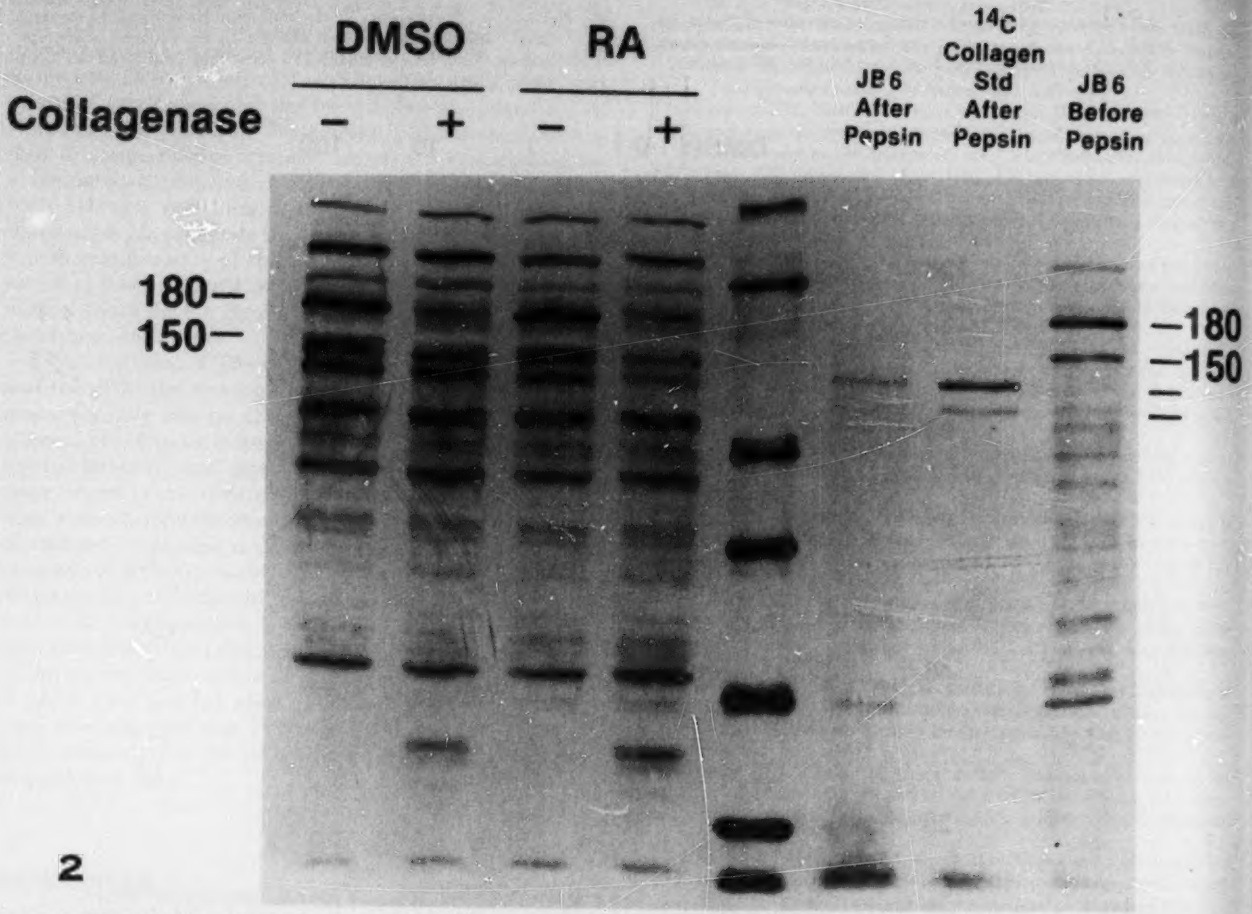

2

FIGURE 2.—The 180,000- and 150,000-M_r glycoproteins are collagenase-sensitive and yield pepsin-resistant glycoproteins characteristic of collagen. Collagenase-sensitive glycoproteins were determined by treatment of JB6 cells with DMSO (0.01%) or RA (10^{-6} *M*) for 24 hr followed by a 6-hr labeling period with [^{3}H]mannose (20 μCi/ml). Cells were harvested by being scraped into Tris-buffered saline (pH 7.4) and sonicated. The sample was split into two 100-μl aliquots, one of which received 10 μl of a Tris buffer containing purified collagenase (100-200 μg/ml) plus calcium chloride. The other aliquot received 10 μl of buffer without collagenase. The digestion proceeded at 37°C for 90 min and was stopped by introduction of an equal volume of a twofold concentration of SDS sample buffer. For the determination of pepsin-resistant proteins, [^{3}H]proline-labeled JB6 cells were harvested in 0.5 *M* acetic acid. Replicate aliquots received one-tenth volume of 0.5 *M* acetic acid ± pepsin to give a final pepsin concentration of 100 μg/ml. Incubation proceeded for 1 hr at room temperature. The acetic acid was removed by lyophilization. The lyophilyzed powder was solubilized in SDS-sample buffer. The positions of the characteristic pepsin-resistant products of collagen digestion are indicated by *horizontal marks*. These pepsin-resistant proteins have been identified as α1 and α2 collagen (*24*). Std=standard.

Effect of Carcinogen Release Rate on the Incidence of Preneoplastic and Neoplastic Lesions of the Respiratory Tract Epithelium in Rats [1,2,3]

Mitsutoshi Shiba,[4] **Andres J. P. Klein-Szanto,**[5] **Ann C. Marchok,**[5] **Bimal C. Pal,**[5] *and* **Paul Nettesheim**[6,7]

ABSTRACT—Inbred F344 rat tracheal transplants were exposed to 7,12-dimethylbenz[*a*]anthracene (DMBA) delivered at different release rates from intraluminal pellets made of various matrices to study the effect of carcinogen dose rate on the induction of lesions in the epithelium. These matrices were beeswax, beeswax–stearyl alcohol, and beeswax–cholesterol. In addition, DMBA adsorbed onto carbon particles was dispersed in beeswax–stearyl alcohol. The fastest release was obtained from beeswax pellets from which 99% of the carcinogen (198 μg) was released in 4 weeks, and the slowest release was from DMBA adsorbed on carbon at a ratio of 1:9 from which only 56% (113 μg) was released in 16 weeks. Morphometry of histologic sections showed marked differences in the percentage of luminal surface covered by dysplastic–neoplastic epithelium (i.e., 7.5% in the tracheas exposed to the fastest releasing pellets and 46.3% in the tracheas exposed to the slowest releasing pellets). An inverse linear correlation was found between the cumulative amount of DMBA released from the different pellet matrices at 2 weeks and the incidence of dysplastic plus neoplastic lesions of tracheal epithelium at 16 weeks. The results indicate that lower doses of carcinogen delivered slowly are more effective in producing dysplastic plus neoplastic lesions than higher doses delivered rapidly.—JNCI 1982; 69:1155–1161.

During the past several years, considerable effort has been put forth to develop animal models of respiratory carcinogenesis in which carcinogen dose and the tumorigenic response could be carefully quantitated (*1*). In this respect, the tracheal transplant model developed in our laboratory has many advantages. In this model a known target, the heterotopically transplanted trachea, is exposed to carcinogen released from an intraluminal rod-shaped pellet from which a known amount of carcinogen can be delivered (*2, 3*). Several studies have been done with the use of this system, including dose-response studies with several polycyclic hydrocarbons and heavy metals on the induction of preneoplastic and neoplastic lesions, and two-step carcinogenesis (*4–10*). Since the establishment of this model (*2*), improved carcinogen delivery systems have been developed that permit slower release of both soluble and insoluble materials. In other in vivo experimental protocols, lipid matrices were often used to slow the release of polycyclic hydrocarbons to the tissue [e.g., (*11–16*)]. Recently, several systems for controlled release of carcinogens to the tracheal transplant have been reported by Pal et al. (*17*) and Klein-Szanto et al. (*18*). Beeswax, stearyl alcohol, cholesterol, or stearyl alcohol plus carbon was used as a vehicle, and more moderate, controlled release of carcinogens and of a tumor promoter was achieved. This report quantitates the effects of delivering the carcinogen DMBA at different dose rates directly on the epithelium of the tracheal transplant. Several matrices, allowing different release rates of DMBA, were used, and a morphometric evaluation of the epithelial changes was performed to measure the effects of dose rate on the induction of preneoplastic and neoplastic lesions.

MATERIALS AND METHODS

Materials.—White (U.S.P. grade) beeswax was obtained from Fisher Scientific Co. (Pittsburgh, Pa.). Before use, the molten beeswax was filtered under vacuum through a steam-heated funnel with a fritted glass disk of medium porosity. DMBA was obtained from Eastman Organic Chemicals (Rochester, N.Y.) and was purified by recrystallization from ethanol as described previously (*17*). Carbon particles (nut shell charcoal; Barnebey-Cheney Co., Columbus, Ohio; catalog #JF) were sequentially passed through sieve #200 and sieve #325, and the particles retained on sieve #325 were used. Cholesterol (primary standard grade, 99.5% by differential scanning colorimetry) was obtained from Eastman Organic Chemicals, and stearyl alcohol was obtained from Sigma Chemical Co. (St. Louis, Mo.).

Preparation of the pellets.—Beeswax, beeswax–cholesterol (1:1 and 1:9), and beeswax–stearyl alcohol (1:1 and 1:9) pellets containing DMBA were prepared with a pellet maker as described previously (*17*) with some modifications. Weighed amounts of DMBA and the matrix medium were heated in a glass scintillation vial placed in a cavity in an aluminum block heated on a thermostatically controlled hot plate. A clear homogeneous melt of beeswax and beeswax-

---

ABBREVIATIONS USED: BP=benzo[*a*]pyrene; DMBA=7,12-dimethylbenz[*a*]-anthracene.

---

[1] Received March 9, 1982; accepted June 3, 1982.

[2] Supported jointly by the National Institute of Environmental Health Sciences, by the Environmental Protection Agency, and by the National Cancer Institute, Division of Cancer Cause and Prevention, under interagency agreements Y01ES-50200, EPA 81-D-X0533, and Y01CP-90207, respectively; and by the Office of Health and Environmental Research, U.S. Department of Energy, under contract W-7405-eng-26 with the Union Carbide Corporation.

[3] Animals were maintained under the guidelines set forth by the National Research Council.

[4] University of Tennessee–Oak Ridge Graduate School of Biomedical Sciences, Oak Ridge, Tenn. 37830.

[5] Biology Division, Oak Ridge National Laboratory, P.O. Box Y, Oak Ridge, Tenn. 37830.

[6] National Institute of Environmental Health Sciences, P.O. Box 12233, Research Triangle Park, N.C. 27709.

[7] The skillful technical assistance of Mr. Donald H. Martin and Mrs. Clarenne M. Howard is gratefully acknowledged. We also thank Dr. Steven A. McGuire for statistical consultation and Mrs. Norma Kwaak for excellent secretarial assistance.

stearyl alcohol was obtained at 80°C; for cholesterol pellets it was necessary to heat to 150°C. An appropriate aliquot of the melt was transferred to the recess in the bottom half of the preheated pellet maker. The top half of the pellet maker was placed on the bottom half, and the melt rose to fill the cylindrical cavities in the top half. The mold was then rapidly cooled by being placed on a cylindrical copper block (3×3 inches in diameter) cooled on ice. When the melt solidified, the two halves were separated and the pellets were removed with a push pin.

Pellets containing carbon could not be prepared in the pellet maker because these particles have a tendency to settle and agglomerate. Therefore, we made these pellets of carbon particles coated by heating and stirring with DMBA in an acetone solution as reported earlier for BP (*17*), except that we heated the final mixture of carbon and DMBA to 160°C for 1 minute. The final product was cooled in a desiccator. Then weighed beeswax–stearyl alcohol (1:9) was melted in a hot mortar and mixed thoroughly with the DMBA-loaded carbon particles by use of mortar and pestle. The complete mixture was allowed to cool until it congealed. It was then scraped out of the mortar and packed in the cell of a Greenerd Arbor Press (Fisher Scientific Co.) fitted with a disk with a hole (1.5 mm in diameter) in the middle. The cell was warmed to a suitable temperature (below the melting point of the mix), and the mixture was extruded rapidly. The extruded material was cut into equal lengths by use of a channeled Teflon block with a design similar to that of a carpenter's miter box. This procedure assures a uniform charcoal particle dispersion in the matrix as determined by spectrophotometric assays of random samples. This is an improvement on the previously reported method in which some difficulty in obtaining stable distribution was reported (*17*).

In this study, seven types of carcinogen-containing pellets were prepared: beeswax; 1:1 and 1:9 stearyl alcohol pellets in which beeswax and stearyl alcohol were mixed at weight ratios of 1:1 and 1:9; and 1:4 and 1:9 carbon pellets in which DMBA was adsorbed to carbon at weight ratios of 1:4 and 1:9 in a 1:9 beeswax–stearyl alcohol matrix. All these pellets contained 200 μg DMBA. Pellets in which beeswax and cholesterol were mixed at ratios of 1:1 and 1:9 contained 250 μg DMBA. On the basis of preliminary studies, we used 250 μg DMBA in the cholesterol-containing pellets to obtain the release of higher amounts of DMBA than the amounts obtained from rapid-releasing beeswax pellets (1:1 cholesterol pellets) and intermediate released amounts (1:9 cholesterol pellets). Four types of blank pellets were prepared: beeswax, beeswax–stearyl alcohol (1:9), beeswax–cholesterol (1:9), and beeswax–stearyl alcohol (1:9) containing 1,800 μg carbon (the amount used in 1:9 DMBA-carbon-coated particles).

Assay of the pellets.—We determined the uniformity of the pellets by assaying DMBA in pellets selected at random. The average weight of beeswax pellets was 24.48±0.62 mg (SD). Pellets containing DMBA were individually weighed, and those that did not fall within ±2% of the mean pellet weight were rejected. We determined the DMBA content of the pellets by extracting them for 2 hours with benzene in a Soxhlet extractor with a double-thickness cellulose thimble (Whatman, Inc., Clifton, N.J.). DMBA was assayed spectrophotometrically with $\epsilon_{301}=79{,}000$. The recovery of DMBA and the UV absorption spectra indicated negligible degradation of DMBA during the pellet-making process. This small variation in the pellet weight values as well as the careful and uniform preparation of the carcinogen matrix mixtures assured the homogeneity of the pellets.

Animals and tissues.—F344 female rats 10 weeks old, bred and maintained in our specific-pathogen-free barrier facility, were used. Tracheas attached to polyethylene tubing were transplanted into subcutaneous pockets on the backs of isogeneic recipients as previously described (*4*). Two tracheas were transplanted per animal. Twenty-eight days after transplantation, pellets were inserted into the tracheal lumina through an incision made at the end of the transplants. The incision was then closed with tantalum hemostatic clips (E. Weck Co., Research Triangle Park, N.C.). The skin wound was closed with metal clips.

A total of 156 tracheal transplants were prepared for this study. Twenty tracheas were used for each experimental group, and four grafts were removed at 1, 2, 4, 8, and 16 weeks after pellet insertion. The pellets removed from the

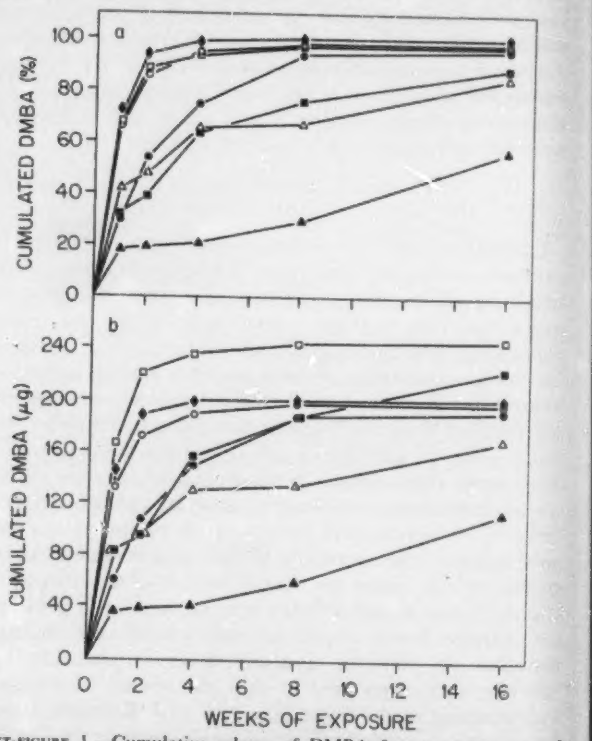

TEXT-FIGURE 1.—Cumulative release of DMBA from various types of pellets in the tracheal lumen during carcinogen exposure. a) *Points* represent mean percentages of DMBA released. b) *Points* represent mean amount of DMBA released. ◆, beeswax pellets containing 200 μg DMBA; □, 1:1 beeswax–cholesterol pellets containing 250 μg DMBA; ○, 1:1 beeswax–stearyl alcohol pellets containing 200 μg DMBA; ●, 1:9 beeswax–stearyl alcohol pellets containing 200 μg DMBA; ■, 1:9 beeswax-cholesterol pellets containing 250 μg DMBA; △, 1:4 carbon pellets containing 200 μg DMBA; ▲, 1:9 carbon pellets containing 200 μg DMBA. All the standard errors of each value were <1.5% (3 μg) for the 200-μg DMBA pellets and 4% (10 μg) for the 250-μg DMBA pellets.

tracheas at these times were assayed for remaining DMBA. For each control group, four tracheal transplants were removed at 16 weeks. After excision, the transplants were fixed in Bouin's fluid. For histologic assessment, each trachea was cross-sectioned into 8–10 pieces and embedded into one block of paraffin. At least four sections 150 μm apart were made from each paraffin block and stained with hematoxylin and eosin. The histopathology of these sections was assessed.

Histopathologic assessment.—The percentage of the tracheal luminal surface covered by different types of epithelium was calculated in all carcinogen-exposed animals with the use of cross sections of each trachea, as previously described (*19*). The following epithelial types were determined as defined in previous publications (*20, 21*): *a*) normal mucociliary epithelium, *b*) columnar hyperplastic epithelium, *c*) atrophic or cuboidal epithelium, *d*) squamous metaplasia with no or mild atypia, *e*) squamous metaplasia with moderate atypia, *f*) squamous metaplasia with severe atypia or carcinoma in situ, and *g*) invasive carcinoma. Each section was directly projected with a Zeiss projecting microscope attached to the screen of a Ladd graphic digitizer interphased with a Monroe 1860 calculator, and the extent of the luminal surface covered by each epithelial type was measured. This procedure is shown in figure 1. Lesions smaller than 100 μm could not be resolved by this method and were not included in this study. This analytic system permitted a precise planimetric determination of each type of epithelium. Percentages of the tracheal surface occupied by each type of epithelium were calculated for each trachea. The mean percentage from four tracheas was calculated to estimate the pathologic status of each group. Since the percentage of luminal surface covered by different lesions does not give an estimate of the number of lesions involved, the number of focal epithelial lesions including lesions less than 100 μm in diameter were counted. The total numbers of these lesions per trachea were averaged to give another estimate of the pathologic status of each group.

RESULTS

Delivery of DMBA In Vivo

The matrices composed of either beeswax, 1:1 beeswax–cholesterol, or 1:1 beeswax–stearyl alcohol exhibited a very fast release of DMBA (i.e., ≈90% of the DMBA was released in 2 wk and almost 100% of the DMBA was released in 4 wk) (text-fig. 1,a). Although these three matrices showed a similar release rate, the beeswax pellets presented a slightly faster release rate (text-fig. 1,a). In addition, since the beeswax–cholesterol pellets contained 250 μg DMBA and all the other pellets had only 200 μg DMBA, the cumulated DMBA released from the former pellets was slightly higher (text-fig. 1,b). When the beeswax-to-stearyl alcohol ratio was increased to 1:9, release of 90% DMBA required 8 weeks. With 1:9 cholesterol or 1:4 carbon pellets, 80–90% release of DMBA was achieved at 16 weeks. Finally, with 1:9 carbon pellets, only 56% of the DMBA was released at 16 weeks.

Histologic Observations

Control Pellets

None of the compounds used to make the pellet matrices (blank pellets) produced marked changes of the tracheal mucosa. Beeswax blanks induced no lesions, whereas 1:9 beeswax–cholesterol pellets caused occasional atrophy and/or hyperplasia of the epithelium. Pellets made of 1:9 beeswax–stearyl alcohol and this matrix with 1,800 μg of carbon

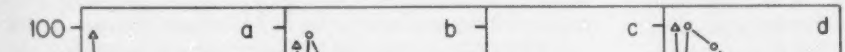

TEXT-FIGURE 2.—Percentages of the epithelial surface exhibiting specific types of nondysplastic epithelium in tracheas at different times after implantation of the following: a) beeswax pellets containing 200 μg DMBA, b) 1:1 beeswax–cholesterol pellets containing 250 μg DMBA, c) 1:1 beeswax–stearyl alcohol pellets containing 200 μg DMBA, d) 1:9 beeswax–stearyl alcohol pellets containing 200 μg DMBA, e) 1:4 carbon pellets containing 200 μg DMBA, f) 1:9 beeswax–cholesterol pellets containing 250 μg DMBA, and g) 1:9 carbon pellets containing 200 μg DMBA. ◆, normal columnar ciliated epithelium; □, hyperplastic epithelium; △, atrophic epithelium; ○, regular squamous metaplastic epithelium or squamous metaplastic epithelium with mild atypia. Standard errors of each value were ≤18.0% of the mean.

caused a somewhat stronger reaction, resulting in a few small foci of flattened or atrophic epithelium (not shown).

DMBA Pellets

Nondysplastic lesions appeared very early after DMBA exposure. The types of lesions and their extent at different time points depended on the release rate of DMBA (text-fig. 2).

Early epithelial atrophy was seen in all groups and occupied a large percentage of the luminal surface at 1 week. The faster the release rate of DMBA, the larger the extent of luminal surface covered by atrophic epithelium at this time point (text-fig. 2,a–f). After the 1st week the percentage of atrophic epithelium covering the luminal surface decreased abruptly, and in most cases the atrophic epithelium was absent at 2 or 4 weeks. After 4 weeks the percentage of atrophic epithelium increased gradually, reaching in most cases a second, although lower, peak at 16 weeks. The extent of atrophic epithelium found in the trachea at this time was directly proportional to the DMBA dose rate. With fast DMBA release (e.g., beeswax, 1:1 beeswax–cholesterol), 40–60% of the luminal surface was occupied by atrophic epithelium. With slow DMBA release (e.g., 1:9 beeswax–cholesterol and 1:9 carbon pellets), atrophic epithelium covered approximately 10% of the luminal surface. The other pellets with moderate release rates showed intermediate values.

For determination of an eventual relationship between the initial toxic events induced by the early release of DMBA and the later appearance of involutional changes in the epithelium (atrophic epithelium), the percentage of luminal surface covered by atrophic epithelium at 16 weeks was plotted against the cumulative amount of DMBA released to the trachea at 1 and 2 weeks (plots not shown). Although no correlation was found at 1 week, a linear correlation (r=0.797, P<0.05) was noted between the relative percentages of the luminal surface covered by atrophic epithelium at 16 weeks and cumulative dosage of DMBA at 2 weeks.

Regular squamous metaplasia, which was practically absent at 1 week in all groups except the low-dose-rate groups (text-fig. 2,f and g), increased markedly between 2 and 4 weeks. This increase coincided with a reduction in the percentage of luminal surface occupied by atrophic epithelium. After this peak the extent of regular squamous metaplasia decreased gradually, and at 16 weeks the percentage of luminal surface occupied by this type of epithelium was 20–60%, being more prominent in the low-dose-rate group.

After 4 weeks of exposure most tracheal transplants began to develop dysplastic lesions (text-fig. 3). Although at 4 weeks the grade of atypia was moderate, some of the rapid-releasing pellets (i.e., beeswax and 1:1 beeswax–stearyl alcohol pellets) induced more extensive dysplastic lesions. At 8 weeks of exposure the total percentage of luminal surface occupied by all types of dysplastic lesions increased markedly in all groups, and severe dysplasia was also evident. Between 8 and 16 weeks the percentage of luminal surface occupied by dysplastic lesions continued to increase. This increase coincided with a reduction in the percentage of luminal surface covered by regular squamous metaplasia. At 16 weeks tracheas in the slow-release group (i.e., exposed to DMBA released from 1:9 stearyl alcohol, 1:4 and 1:9 carbon, 1:9 cholesterol pellets) showed three to six times higher percentages of luminal dysplasias than those in the fast-release group (beeswax, 1:1 cholesterol, 1:1 stearyl alcohol). All DMBA-exposed groups except the 1:1 cholesterol group showed invasive carcinomas.

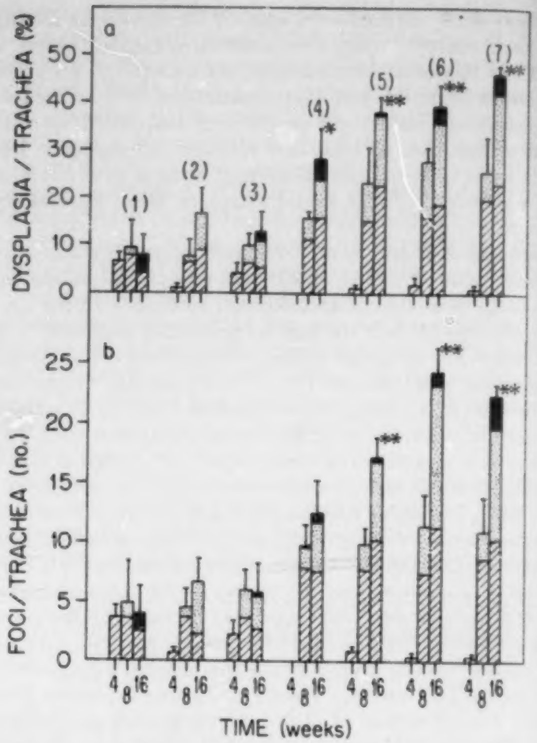

TEXT-FIGURE 3.—Incidence of specific types of dysplastic epithelia in tracheal transplants at different time points after implantation of (1) beeswax pellets containing 200 μg DMBA, (2) 1:1 beeswax–cholesterol pellets containing 250 μg DMBA, (3) 1:1 beeswax–stearyl alcohol pellets containing 200 μg DMBA, (4) 1:9 beeswax–stearyl alcohol pellets containing 200 μg DMBA, (5) 1:4 carbon pellets containing 200 μg DMBA, (6) 1:9 beeswax–cholesterol pellets containing 250 μg DMBA, and (7) 1:9 carbon pellets containing 200 μg DMBA. a) Percentage of tracheal luminal surface occupied by dysplasia per each trachea + SEM. b) Number of dysplastic foci per each trachea + SEM. ▨, metaplasia with moderate atypia; ▩, metaplasia with severe atypia or carcinoma in situ; ■, invasive carcinoma. *, significant at P<0.05, compared with beeswax pellets containing 200 μg DMBA by Student's t-test. **, significant at P<0.01, compared with beeswax pellets containing 200 μg DMBA by Student's t-test.

The alterations in the epithelium of the tracheal mucosa were also quantitated in terms of numbers of foci of different types of dysplastic lesions per trachea (text-fig. 3,b). The dysplastic plus neoplastic foci were counted. In general, these data are similar to those found above (text-fig. 3,a). Tracheas in the slower release groups (i.e., 1:9 stearyl alcohol, the carbon-containing, and 1:9 cholesterol pellets) showed two to five times more dysplastic plus neoplastic foci than were seen with DMBA released from beeswax pellets.

The percentage of lumen covered by metaplasia with severe atypia plus carcinoma at the late time point was related to the cumulative amount of DMBA released to the

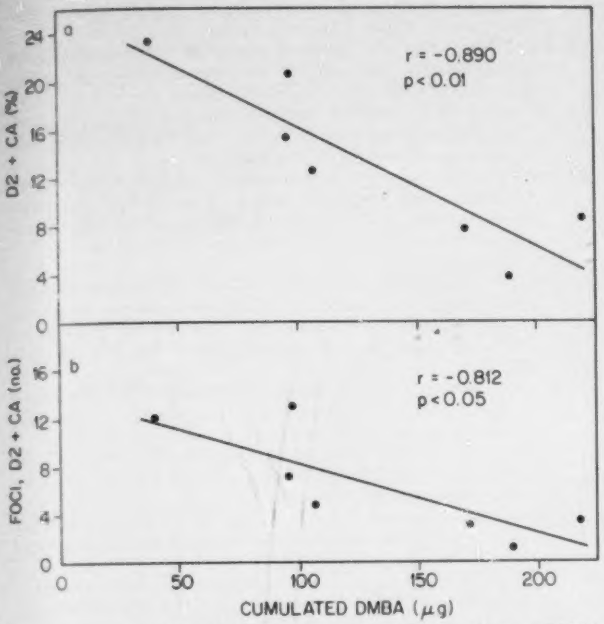

TEXT-FIGURE 4.—a) Correlation between cumulative amount of DMBA released at 2 wk of exposure and percentage of severe atypical metaplasia and carcinoma in situ (D2) plus invasive carcinoma (CA) at 16 wk. b) Correlation between cumulative amount of DMBA released at 2-wk exposure and number of foci of severe atypical metaplasia and carcinoma in situ (D2) plus invasive carcinoma (CA) at 16 wk.

tracheas at early time points. An inverse linear correlation ($P<0.01$) was noted between the relative percentage of these dysplastic and neoplastic epithelia at 16 weeks and the cumulative dosage of DMBA at 2 weeks (text-fig. 4,a). A similar but less significant negative correlation ($P<0.05$) was also observed between the number of dysplastic and neoplastic foci per trachea at 16 weeks and cumulative dosage of DMBA at 2 weeks (text-fig. 4,b).

DISCUSSION

In this study, we demonstrate that higher incidences of dysplastic plus neoplastic lesions are induced in the tracheal mucosa when the rate of release of DMBA to the trachea is lowered. These higher incidences were seen even though the total dose of carcinogen delivered at 16 weeks was also markedly reduced. The different rates of release were obtained by addition of various substances into the beeswax pellet matrix used to deliver carcinogen to tracheal transplants.

In the present experiments, carcinogen exposure was modified by incorporation of varying amounts of cholesterol, stearyl alcohol, and carbon particles into the beeswax matrix. Cholesterol has been previously used as a matrix for controlled release of steroids (*22*). Adding these substances to the beeswax was very effective in altering the release of DMBA when one considers that in 2 weeks 94% of the total DMBA was released from beeswax pellets and 39% was released from the 1:9 beeswax–cholesterol pellets, whereas only 19% was released when the DMBA was first adsorbed to carbon, and these were mixed into a 1:9 beeswax–stearyl alcohol matrix. Several attempts to decrease the release rate of carcinogen at different sites of the respiratory tract have been previously reported (*11–16, 23–27*). Shors et al. (*28*) and Saffiotti et al. (*29*), using BP within a silicon rubber matrix implanted intraluminally in the bronchi of hamsters, suggested that sustained slow exposure was more effective than previous instillation methods in which large doses were delivered in short exposures.

Carcinogen release from cylindrically shaped pellets such as those used by Shors et al. (*28*) and by us follows Fick's first law of diffusion (*30*). The release is controlled by diffusion rate and surface area and follows an exponential function. The detailed mechanism of release of BP from beeswax has been discussed by Pal et al. (*17*). It has been shown that at high concentration, most of the BP is present in the pellet in crystalline form. The crystals of BP gradually dissolve in the beeswax and diffuse into the surrounding medium. As for DMBA, it is conceivable that its release follows a similar mechanism. Since aromatic hydrocarbons are less soluble in cholesterol and/or stearyl alcohol than in beeswax, we selected these substances to obtain a slower release of carcinogen. In addition, DMBA absorbed on carbon particles is released with difficulty to the surrounding matrix. In the initial release phase, cylindrical pellets show an abrupt short-lived rapid-release rate which is called a "burst effect" (*31*). This rapid release probably has a very toxic effect on the surrounding tissues. By introducing cholesterol and stearyl alcohol and by changing the ratio of the pellet matrix components, we attained significant decreases in the release rate. Consequently, this produced a decrease in the initial burst effect, thus reducing the acute toxic effects and enhancing the chronic action of the carcinogen.

Histologic features of tracheal epithelium exposed to varying doses of DMBA with beeswax pellets have been reported earlier (*4, 20, 21*). In these earlier studies, extensive atrophy persisted a long time after the relatively brusque exposure to carcinogen. In our experiment, atrophic epithelium was the predominant type covering all tracheas 1 week after DMBA exposure, irrespective of the release rate. However, lower percentages of atrophic epithelium were noted in tracheas from some of the slow-release groups, compared with tracheas exposed to DMBA released from beeswax pellets. The percentages of atrophic epithelium that reappeared at later stages of exposure had significant positive correlation with higher amounts of DMBA released at early time points. These phenomena might suggest that such atrophic epithelium is a consequence of toxic damage to the epithelial cells as reported previously (*21*), and decreased toxicity is achieved with slow-release exposure.

Regular metaplasia was observed in all experimental groups, and no marked differences were observed between fast- and slow-release groups in the relative percentage of the lumina occupied by regular metaplasia. The percentage of the luminal surface covered by regular metaplasia at early time points was not a good indicator of the degree of dysplasia or neoplasia that appeared in later stages. These observations are coincident with the fact that early regular metaplasia disappeared after cessation of carcinogen exposure (*20*).

In the later stages of exposure, the slow-release pellets induced a higher percentage of dysplastic and neoplastic epithelia, though the total released dose of DMBA was smaller. In other respiratory carcinogenesis models, similar dose relationships have been reported. In hamsters, intratracheal BP-ferric oxide instillations, when administered repeatedly in fractioned small doses, were more effective in inducing respiratory tract tumors than was a large, single dose (*32, 33*). In rats, nitrosoheptamethyleneimine given orally in multiple small doses was more effective than a large equivalent single administration (*34*). Although it is difficult, if not impossible, to evaluate the amount of carcinogen delivered to the respiratory tract epithelium in these models, the observations imply that fractionation of the carcinogen dose is more effective in inducing neoplasia than the same total dose given in a single administration.

The rat tracheal transplant system, which allows a precise carcinogen exposure of a localized portion of the respiratory tract epithelium and at the same time allows a quantitative estimation of the amount of carcinogen released from the carcinogen delivery devices, is the model of choice to study the dose-rate relation of carcinogens. Our data show that the dose rate is an important factor in carcinogenesis, since an inverse correlation between initial cumulated amount of DMBA and final amount of dysplastic epithelium was observed. By the further development of sustained carcinogen-release technology, which is closer to naturally occurring carcinogenesis, more precise analyses of preneoplastic stages of respiratory epithelium should be achieved.

REFERENCES

(*1*) Nettesheim P, Griesemer RA. Experimental models for studies of respiratory tract carcinogenesis. In: Harris C, ed. Pathogenesis and therapy of lung cancer. New York: Marcel Dekker, 1978:75–188.

(*2*) Kendrick J, Nettesheim P, Hammons AS. Tumor induction in tracheal grafts: A new experimental model for respiratory carcinogenesis studies. J Natl Cancer Inst 1974; 52:1317–1325.

(*3*) Griesemer RA, Kendrick J, Nettesheim P. Tracheal grafts. In: Karbe K, Park JF, eds. Experimental lung cancer: Carcinogenesis and bioassays. Berlin: Springer-Verlag, 1974:539–547.

(*4*) Griesemer RA, Nettesheim P, Martin DH, Caton JE Jr. Quantitative exposure of grafted rat tracheas to 7,12-dimethylbenz(*a*)anthracene. Cancer Res 1977; 37:1266–1271.

(*5*) Nettesheim P, Griesemer RA, Martin DH, Caton JE Jr. Induction of preneoplastic and neoplastic lesions in grafted rat tracheas continuously exposed to benzo(*a*)pyrene. Cancer Res 1977; 37:1271–1278.

(*6*) Topping DC, Pal BC, Martin DH, Melson FR, Nettesheim P. Pathologic changes induced in respiratory tract mucosa by polycyclic hydrocarbons of differing carcinogenic activity. Am J Pathol 1978; 93:311–324.

(*7*) Yarita T, Nettesheim P. Carcinogenicity of nickel subsulfide for respiratory tract mucosa. Cancer Res 1978; 38:3140–3145.

(*8*) Topping DC, Nettesheim P. Promotion-like enhancement of tracheal carcinogenesis in rats by TPA (12-*O*-tetradecanoylphorbol-13-acetate). Cancer Res 1980; 40:4352–4355.

(*9*) ———. Two-stage carcinogenesis studies with asbestos in Fischer 344 rats. JNCI 1980; 65:627–630.

(*10*) Topping DC, Nettesheim P, Martin DH. Toxic and tumorigenic effects of asbestos on tracheal mucosa. J Environ Pathol Toxicol 1980; 3:261–275.

(*11*) Bryan GT. Pellet implantation studies of carcinogenic compounds. J Natl Cancer Inst 1969; 43:255–261.

(*12*) Hirano T, Stanton M, Layard M. Measurement of epidermoid carcinoma development induced in the lungs of rats by 3-methylcholanthrene-containing beeswax pellets. J Natl Cancer Inst 1974; 53:1209–1219.

(*13*) Veal JT, Dagle GF. Evaluation of beeswax-tricaprylic vehicle for pulmonary carcinogenesis studies. Toxicol Appl Pharmacol 1976; 35:157–164.

(*14*) Rubin IB, Guerin MR. Chemical evaluation of the beeswax pellet implantation bioassay model for studies of environmental carcinogens. J Natl Cancer Inst 1976; 58:641–644.

(*15*) Dagle GE, McDonald KE, Smith LG, Stevens DL Jr. Pulmonary carcinogenesis in rats given implants of cigarette smoke condensate in beeswax pellets. JNCI 1978; 61:905–910.

(*16*) Whitmire CE, Lopez A. Comparison of the effects of beeswax: Trioctanoin and trioctanoin vehicles on 3-methylcholanthrene, benzo[*a*]pyrene, and 7,12-dimethylbenz[*a*]anthracene subcutaneous carcinogenesis in three strains of mice and one hybrid. JNCI 1978; 61:1107–1111.

(*17*) Pal BC, Topping DC, Griesemer RA, Nelson FR, Nettesheim P. Development of a system for controlled release of benzo(*a*)pyrene, 7,12-dimethylbenz(*a*)anthracene, and phorbol ester for tumor induction in heterotopic tracheal grafts. Cancer Res 1978; 38:1376–1383.

(*18*) Klein-Szanto AJ, Pal BC, Terzaghi M, Marchok AC. Heterotopic tracheal transplants: Techniques and applications. In: Hook GE, ed. Pulmonary toxicology. New York: Raven Press. In press.

(*19*) Klein-Szanto AJ, Clark JN, Martin DH. Sexual difference in the distribution of epithelial alterations in vitamin A-deficient rats. Int J Vitam Nutr Res 1980; 50:61–69.

(*20*) Topping DC, Griesemer RA, Nettesheim P. Development and fate of focal epithelial lesions in tracheal mucosa following carcinogen exposure. Cancer Res 1978; 39:4829–4837.

(*21*) ———. Quantitative assessment of generalized epithelial changes in tracheal mucosa following exposure to 7,12-dimethylbenz(*a*)anthracene. Cancer Res 1979; 39:4823–4828.

(*22*) Kent JS, Vickery BH, McRae GI. The use of a cholesterol matrix pellet implantation for early studies on prolonged release in animals of agonist analogs of luteinizing hormone releasing hormone. In: Proceedings of the seventh international symposium on controlled release of bioactive materials, July 28–30, 1980. Akron, Ohio: The Controlled Release Society, Inc., 1980:67.

(*23*) Roseman TJ, Higuchi WI. Release of medroxyprogesterone acetate from a silicone polymer. J Pharm Sci 1970; 59:353–357.

(*24*) Kennedy AR, Little JB. Localization of polycyclic hydrocarbon carcinogens in the lung following intratracheal instillation in gelatin solution. Cancer Res 1975; 35:1563–1567.

(*25*) Lane BP, Mass MJ. Carcinogenicity and cocarcinogenicity of chromium carbonyl in heterotopic tracheal grafts. Cancer Res 1977; 37:1476–79.

(*26*) Matsumura K, Shors EC, Fu PC, Cohen AH, Benfield JR. Sustained-release implants of chemical carcinogens in the canine tracheobronchial tree. Ann Thorac Surg 1978; 25:112–116.

(*27*) Mossman BT, Craighead JE. Induction of neoplasms in hamster tracheal grafts with 3-methylcholanthrene-coated Lycra fibers. Cancer Res 1978; 38:3717–3722.

(*28*) Shors EC, Fu PC, Matsumura K, Cohen A, Benfield JR. Sustained release of benzo(*a*)pyrene from silicone polymer into the tracheobronchial tree of hamsters and dogs. Cancer Res 1980; 40:2288–2294.

(*29*) Saffiotti U, Montesano R, Sellakumar AR, Kaufman DG. Respiratory tract carcinogenesis induced in hamsters by different dose levels of benzo[*a*]pyrene and ferric oxide. J Natl Cancer Inst 1972; 49:1199–1204.

(*30*) Kinel FA, Rudel HW. Sustained release hormonal preparations. Acta Endocrinol 1971; suppl 151:5–30.

(*31*) Higuchi T. Rate of release of medicaments from ointment bases containing drugs in suspension. J Pharm Sci 1963; 52:1145–1150.

(*32*) Montesano R, Saffiotti U, Shubik P. The role of topical and systemic factors in experimental respiratory carcinogenesis. In: Hanna MG Jr, Nettesheim P, Gilbert JR, eds. Inhalation carcinogenesis. Oak Ridge, Tenn. AEC Symp Ser 18, Division of Technical Information Extension, 1970.

(*33*) Saffiotti U, Montesano R, Sellakumar AR, Cafis F, Kaufman DG. Respiratory tract carcinogenesis in hamsters induced by different numbers of administrations of benzo(*a*)pyrene and ferric oxide. Cancer Res 1972; 32:1073–1081.

(*34*) Taylor HW, Nettesheim P. Influence of administration route and dosage schedule on tumor response to nitrosoheptamethyleneimine in rats. Int J Cancer 1975; 15:301–307.

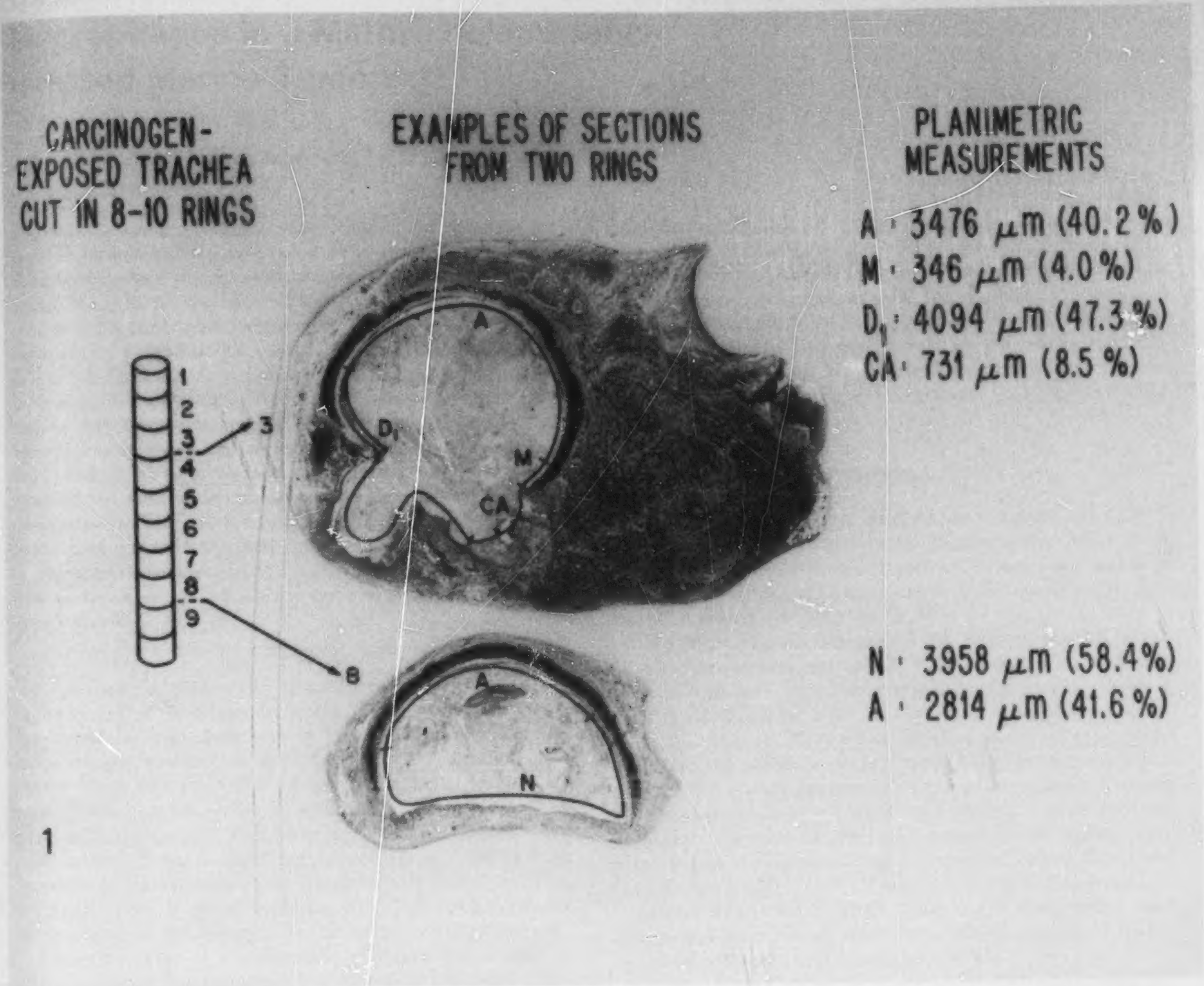
CARCINOGEN-EXPOSED TRACHEA CUT IN 8-10 RINGS
EXAMPLES OF SECTIONS FROM TWO RINGS
PLANIMETRIC MEASUREMENTS
1
2
3
4
5
6
7
8
9
3
8
A
D1
M
CA
A · 3476 µm (40.2 %)
M · 346 µm (4.0 %)
D1 · 4094 µm (47.3 %)
CA · 731 µm (8.5 %)
A
N
N · 3958 µm (58.4%)
A · 2814 µm (41.6 %)
1

FIGURE 1.—Schematic presentation of morphometric method. Carcinogen-exposed tracheal transplants were cut in 8 or 10 rings and processed for routine histologic observation. Hematoxylin and eosin sections were directly projected on the screen of a graphic digitizer interphased with a calculator. Planimetric measurements were performed on these sections. In these two examples, the following epithelial types were detected: N, normal mucociliary epithelium; A, atrophic epithelium; M, regular squamous metaplasia; D_1, squamous metaplasia with moderate atypia; CA, invasive carcinoma. The extent of each epithelial type was determined and expressed in microns. *Numbers in parentheses* are percentages of luminal circumference occupied by each epithelial type. These determinations were performed in all tracheal rings, and average values obtained from all rings were used as a representative figure for each tracheal transplant.

blank page

Exclusive Binding of Immunoglobulin to Fcγ Receptors on Macrophages in 3-Methylcholanthrene-Induced Murine Tumors[1,2,3]

John M. Lindsay,[4] Linda Manning,[4] *and* Gary W. Wood[4]

ABSTRACT—Immunogenic, chemically induced, murine tumors generally are infiltrated with large numbers of Fcγ receptor (FcγR)-positive cells, most of which are mononuclear phagocytes. This study demonstrates in inbred C3H/HeN mice that such immunogenic tumors contain large amounts of cell-bound immunoglobulin (Ig) and that, within the sensitivity limits of indirect immunofluorescence, the tumor-associated Ig is bound exclusively to host-derived FcγR-positive cells. Depletion of FcγR-positive cells from tumor cell suspensions removed all Ig-bearing cells. Specific competitive elution of the endogenous Ig with heterologous nonimmune IgG established that the endogenous Ig was bound through the FcγR. Tumor-associated FcγR-positive, Ig-bearing cells could be detected with soluble antigen–antibody complexes, and mononuclear phagocytes to which the exogenous complexes were bound expressed FcγR at a level significantly above normal. The role of this macrophage-associated Ig in determining the level of interaction between host cells and the tumor remains to be determined.—JNCI 1982; 69:1163–1174.

Experimental chemically induced tumors evoke an immune response in syngeneic hosts. Those tumors also are infiltrated by high numbers of host cells, predominantly macrophages, monocytes, and K-cells (*1–4*). Although it is controversial (*5*), the response appears to be dependent on tumor immunogenicity (*6, 7*) and intact T-lymphocyte-dependent function [(*8*); Gollahon K, Wood G: Unpublished observation]. Even tumors that are infiltrated by very high numbers of macrophages grow progressively to kill the host, although there is some evidence that infiltrating macrophages have an inhibitory effect on tumor metastasis (*3, 6*).

Although there is considerable evidence for a cellular antitumor immune response, less attention has been given to humoral immune responses to tumors. Nevertheless, antibodies to antigens on chemically induced tumors are detected in autochthonous tumor-bearing animals (*9, 10*). Natural antibodies to tumor-associated antigens also have been detected (*11, 12*). The influence of antibodies on tumor behavior is unknown, but the potential is considerable for interaction between the cellular and humoral aspects of the host response to tumors. Cytotoxic cellular antitumor responses are blocked by antibody (antigen–antibody complexes) (*13, 14*). Antibody may either mediate or, if in its complexed form, block antibody-dependent cellular cytotoxicity (*15, 16*).

A few studies of both human and experimental tumors have indicated that tumor-associated Ig may be bound to host cells within tumors (*17–19*). It is not clear whether this bound Ig represents antitumor antibody because antigen–antibody complexes unrelated to the tumor will bind to tumor-associated cells (*18, 20*). The suggestion has been made that some of the antibody could be anti-idiotype (*21*). Finally, it is not clear how much of the tumor-associated Ig is bound to host cells relative to the amount bound to tumor cells. Many of the discrepancies may relate to differences in tumors studied; i.e., cells free in the peritoneum may not have the same properties as solid tumor cells.

The present study was designed to use an extensively studied chemically induced tumor system, murine MCA-induced sarcoma, to investigate the form of interaction between Ig and host cells within primary and passaged solid tumors.

MATERIALS AND METHODS

Tumors.—Tumors were induced in male inbred C3H/HeN mice (M.A. Bioproducts, Walkersville, Md.) with MCA and appeared in 3–5 months. Tumors were removed and tissue was immediately frozen in liquid nitrogen and stored in sealed vials at −70°C.

Two of the tumors, designated MCA-80-36 and MCA-80-42, were passaged to normal C3H/HeN male mice and have been maintained by subcutaneous implantation. These 2 tumors subsequently were also established in tissue culture. To obtain tumors from which single cell suspensions could be produced, we gave normal male C3H/HeN mice injections of 10^6 washed tumor cells from tissue culture. Tumors appeared in 10 days to 2 weeks and generally were removed at about 3 weeks. Single cell suspensions of tumor were prepared by collagenase (type I, 1 mg/ml; Sigma Chemical Co., St. Louis, Mo.) and DNase (0.025 mg/ml) digestion.

Normal tissue.—C3H/HeN male mice were killed and spleen and liver tissues were removed, immediately frozen in liquid nitrogen, and stored at −70°C.

Glucan (beta-1,3-polyglucose)-stimulated liver tissue.—Activation of the mononuclear phagocyte system with glucan was performed as described previously (*22*). Male C3H/HeN mice were given a single iv injection of either 15 or 30 mg glucan/kg body weight (from Dr. Y. Yamamura, Department of Pathology, Loyola University, Chicago, Ill.), or they

---

Abbreviations used: BSA=bovine serum albumin; EA=erythrocyte-antibody; FcγR=receptor for Fc portion of IgG; Ig=immunoglobulin(s); MCA=3-methylcholanthrene; SRBC=sheep red blood cells.

---

[1] Received March 12, 1982; accepted May 27, 1982.

[2] Supported in part by Public Health Service grants CA-19333 and CA-25183 from the National Cancer Institute.

[3] Animals were maintained under the guidelines set forth by The University of Kansas College of Health Sciences and Hospital and by the National Research Council.

[4] Department of Pathology and Oncology, The University of Kansas Medical Center, 39th and Rainbow Blvd., Kansas City, Kans. 66103.

were given injections of an equivalent volume of physiologic saline as a control. After 24 hours, the livers and spleens were removed from mice in each group, frozen in liquid nitrogen, and stored at −70°C.

Antisera.—Rabbit antisera to murine IgG$_1$, IgG$_{2a}$, IgG$_{2b}$, IgG$_3$, IgA, and IgM were purchased from Litton Bionetics, Kensington, Md.

Specific rabbit anti-mouse macrophage serum was prepared as described previously (*23*). Rabbits were immunized with peritoneal exudate cells from C3H/HeN mice, and the immune serum was absorbed exhaustively with murine kidney homogenate and murine thymus homogenate. The antiserum was used routinely at a dilution of 1:40, and at that concentration it demonstrated no reactivity with C3H/-HeN thymocytes in cytotoxicity and immunofluorescence assays, produced positive fluorescence with 75% of C3H/-HeN peritoneal exudate cells, and failed to react with mouse serum by Ouchterlony gel-diffusion analysis.

Monoclonal antibodies to murine Ia^k antigens were obtained in cell culture from a hybridoma cell line (10-2.16), which was received from the Salk Institute Cell Distribution Center, La Jolla, Calif. The antibodies were of the IgG$_{2b}$ class.

Anti-BSA was produced in rabbits by footpad injection of BSA in Freund's adjuvant. The pooled antiserum was diluted and found to give a positive line of precipitation at a dilution of 1:16 in an Ouchterlony gel-diffusion test against 1 mg BSA/ml in Dulbecco's phosphate-buffered saline. The antiserum contained no rheumatoid factor activity as determined by a human IgG-coated latex agglutination test.

A 1.8-*M* ammonium sulfate fraction of rabbit anti-BSA was reduced with 0.1 *M* 2-mercaptoethanol and alkylated with 0.2 *M* iodoacetamide as described previously (*24*). The protein concentration of the reduced and alkylated antiserum was determined by the Lowry method (*25*). The reduced and alkylated anti-BSA produced a detectable precipitation line with 1 mg BSA/ml at a dilution of 1:16. Another portion of the fractioned antiserum was enzymatically cleaved with pepsin by means of standard methods. The $F(ab')_2$ fragments of anti-BSA produced detectable precipitation in gel diffusion at a dilution of 1:2.

Preparation of soluble immune complexes.—Soluble immune complexes were prepared in threefold antigen excess (by weight). A 1:40 dilution of whole rabbit anti-BSA was mixed with an equal volume of 250 µg BSA/ml, incubated 18 hours at 37°C, and centrifuged for removal of precipitates. The supernatant containing soluble complexes was removed and used in indirect immunofluorescence assays on tumor tissue.

Indirect immunofluorescence.—Indirect immunofluorescence was performed as described previously (*23*). All antisera were used at optimal concentrations, predetermined empirically to be the highest dilution at which a strong, positive reaction was produced. The reaction was developed with fluorescein isothiocyanate-conjugated goat anti-rabbit Ig. The anti-rabbit Ig failed to cross-react with mouse IgG in gel-precipitation analysis. The fluorescein-to-protein ratio of the conjugate was 3.8, and the dilution at which it was routinely used was 1:40. All reagents were centrifuged for 60 minutes at 140,000×*g* prior to use for removal of Ig aggregates.

Rosette formation with antibody-coated SRBC.—The percentage of FcγR-positive cells in tumors was determined by EA rosette formation with SRBC coated with rabbit anti-SRBC as described previously (*2*).

To deplete rosette-positive cells from the tumor cell suspension, we devised the following procedure: 2×10^7 tumor cells were mixed with an appropriate amount of EA, and the cells were rosetted. After the rosetted cells were sedimented, the supernatant was removed, and 20 ml of goat anti-rabbit IgG diluted 1:50 was added to the cells, which were resuspended and incubated for 15 minutes at 37°C. This procedure resulted in passive agglutination of the SRBC. The cells then were sedimented. The highly agglutinated rosettes were gently resuspended and allowed to resediment at unit gravity. The supernatant containing tumor cells essentially free of rosetted cells was removed and sedimented, and excess SRBC were lysed with Tris–ammonium chloride.

RESULTS

Association of Ig With Macrophages

Of 29 primary MCA-induced tumors, 27 were infiltrated by significant numbers of mononuclear phagocytes as determined by morphology, EA rosette formation, and nonspecific esterase staining (*23*). Tumor-associated macrophages were identifiable in sections of tumors with the use of anti-mouse macrophage serum (fig. 1), the specificity of which has been documented previously (*23*). The tumors also were stained with antiserum to various murine Ig (IgG$_1$, IgG$_{2a}$, IgG$_{2b}$, IgG$_3$, IgA, and IgM) (fig. 2). All IgG classes were represented in the tumors; IgA and IgM were variably detected. Details of these observations have been reported previously (*19*).

Qualitatively, the distribution of Ig and macrophages was similar when sequential sections of tumor were stained (figs. 1, 2). When double-labeling experiments were performed with rhodamine-tagged anti-mouse IgG and fluorescence-tagged antimacrophage serum on selected tumors, the red- and green-staining patterns were coincident. The distribution of macrophages and cells positive for Ig also was quantitatively similar. The two tumors that contained no identifiable macrophages also contained very small amounts of Ig. Tumors containing few sparsely distributed macrophages had comparable numbers of cells bearing identifiable Ig, and tumors that were heavily infiltrated with macrophages contained very high levels of Ig-bearing cells.

Coincidence of staining for Ig with distribution of FcγR-positive cells allows the possibility of an artifactual explanation. Therefore, it was necessary to exclude nonspecific interaction of reagents with FcγR. Normal rabbit serum at a fivefold higher concentration than that of the specific reagents did not exhibit significant attachment to tumor sections. When we removed tumor-associated Ig from sections by washing them with 0.1 *M* (pH 2.5) glycine–HCl buffer, we observed no FcγR-dependent attachment of anti-Ig reagents.

Observations of tissue sections necessarily are qualitative, demonstrating only that some tumor-associated Ig is associated with the FcγR-positive tumor-associated macrophages. To determine if most or all Ig was macrophage associated, we removed passaged tumors containing 30–50% macrophages from animals, and we tested single cell suspensions for Ig-bearing cells. Two cell populations were tested: the original cell population and a cell population depleted of FcγR-positive cells by unit gravity sedimentation of EA-rosetted cells. The cells then were stained by indirect immunofluorescence with rabbit anti-mouse IgG_1 and IgG_{2a}. Representative data are included in table 1. The percentages of cells with surface-associated Ig were similar to the percentages of EA rosette-positive cells in the suspensions. Thus when FcγR-positive cells were depleted from the tumor suspensions, Ig-positive cells also were removed. These experiments also demonstrated that at least some of the Ig observed in tumor tissue sections was bound to cell membranes.

Association of Ig With FcγR

Essentially, all Ig detectable by indirect immunofluorescence was eluted from each of the tumors when the tumor sections were washed at 22°C for 10 minutes with acetate buffer (pH 5.0). Two types of controls were introduced for this experiment. Two antisera that are reactive with macrophage-associated antigens were used as negative controls: the heterologous rabbit anti-mouse macrophage serum and a monoclonal alloantiserum reactive with Ia^k antigens. When tumor sections were reacted with either antiserum and then washed at 22°C for 30 minutes at pH 5.0, the amount of antibody bound to the tumor-associated macrophages was undiminished (fig. 3), whereas washing the tissue with glycine–HCl buffer (pH 2.5) totally removed the bound antibodies. Whereas in all tumors tested an approximately equal proportion of tumor-associated cells were Ig-positive, FcγR-positive, and reactive with the antimacrophage serum, a lower percentage of the cells was outlined by the anti-Ia^k serum; i.e., a subpopulation of the tumor-associated FcγR-positive cells was Ia antigen-positive. The positive control was provided when tumor sections were exposed to soluble antigen–antibody complexes (BSA and anti-BSA), washed at pH 5.0, and then stained for residual rabbit Ig. The pH-5.0 buffer treatment of sections covered with exogenous complexes resulted in complete removal of the added complexes. Tissue sections pretreated with pH-5.0 or pH-2.5 buffer bound high levels of exogenous complexes, demonstrating that receptors were unaffected.

TABLE 1.—*Association between Ig and cells isolated from progressing MCA-induced tumors*

Tumor[a]	Percent of total cells positive				
	FcγR[b]	Macrophage[c]	IgG_1[d]	IgG_{2a}[d]	IgM[d]
MCA-80-36 original[e]	37	39	32	35	12
MCA-80-36 depleted[e]	<5	<5	<1	<1	<1
MCA-80-42 original	47	43	34	38	20
MCA-80-42 depleted	6	5	<5	<5	<5

[a] Tumors were produced by sc injection of tumor cells from tissue cultures.

[b] Percentage of tumor cell suspension comprised by FcγR-positive cells was determined by EA rosette formation.

[c] Percentage of tumor cell suspension comprised by macrophages was determined by indirect immunofluorescence with antimacrophage serum.

[d] Percentage of tumor cell suspension comprised by cells with membrane-bound Ig determined by indirect immunofluorescence.

[e] The original cell suspension was derived by collagenase–DNase digestion of minced tumor. FcγR-positive cells were depleted from EA-rosetted tumor cell suspensions by agglutination and unit gradient sedimentation.

The second piece of experimental evidence demonstrating that the macrophage-associated Ig was bound to FcγR was obtained through competitive removal of endogenous Ig in the presence of a high concentration of heterologous IgG. Tumor sections were incubated in the presence of 10 mg normal human Ig/ml at 22°C for 60 minutes and then stained for residual murine Ig. This procedure reduced murine Ig to below detectable levels in each of the tumors tested (fig. 4), but tumors then were coated with significant amounts of human Ig. Tumor sections incubated in the presence of equivalent concentrations of albumin as a control were unaffected; i.e., significant amounts of Ig still were detected bound to the macrophages (fig. 5).

Attachment of Soluble Antigen–Antibody Complexes to Tumor-Associated Cells

Previous studies of FcγR-positive cells in tumor tissue used particulate antibody-coated erythrocytes, a method that does not outline individual cells (*1–4*). In the present study, soluble antigen–antibody complexes attached to cells in tissue sections and exhibited a distribution similar to that of macrophage antigen and Ig-positive cells (fig. 6).

All of the above results, including anti-Ig positivity, could be explained if the tumor-associated Ig contained rheumatoid factor. This possibility was excluded because complexes formed with BSA and mildly reduced and alkylated anti-BSA, which bind strongly to rheumatoid factor but not FcγR, failed to attach to tumor tissue, even though the presence of complexes was documented by sucrose density gradient sedimentation and gel-diffusion analysis. Further evidence for the lack of anti-Ig activity in tumor-associated Ig was obtained by elution of Ig from tissue at pH 2.5 and by demonstration that soluble complexes still attached to the tumor.

The fact that soluble antigen–antibody complexes exhibited facile binding to most tumor-associated macrophages in each of the tumors studied suggested that those cells might have altered, e.g., increased, FcγR expression. To test that possibility, we performed parallel experiments wherein exogenous complexes were added to the tumor, liver, and spleen. As in previous experiments, consistent attachment occurred to tumor-associated cells, but complexes failed to attach to cells in normal liver or spleen, suggesting that neither the Kupffer cells nor the splenic FcγR-positive cells expressed FcγR with sufficient density or affinity to bind the soluble complexes. Cells in livers and spleens from tumor-bearing animals were intermediate. Complexes attached weakly to Kupffer cells and splenic FcγR-positive cells from some animals but not others.

To test the possibility that, at the level of sensitivity of the soluble complex assay, there was discrimination between normal resting tissue macrophages and stimulated tumor-associated macrophages with heightened FcγR activity, we exposed normal mice to a reticuloendothelial system stimulant and then tested them for FcγR expression. Three groups of normal male C3H/HeN mice were given injections iv of 0, 15, and 30 mg/glucan kg body weight; glucan is a known stimulator of the mononuclear phagocyte system (*22*). Twenty-four hours later the animals were tested for FcγR expression. No attachment to liver sections from control mice (saline injected) was observed (fig. 7), but complexes attached to most, if not all, macrophages in livers from animals given injections of 30 mg glucan/kg (fig. 8). Animals given injections of 15 mg glucan/kg exhibited some attachment of complexes to liver sections, but this attachment was sparse and of low intensity. This experiment was repeated on several occasions with comparable results.

DISCUSSION

A great deal of confusion exists with respect to the association between host Ig and tumor cells (*9*). This is understandable because most of the early studies were performed without knowledge that very high numbers of host-derived cells could be present within tumors. Moreover, these studies were performed with methodology, such as ^{125}I-antiglobulin labeling, which is incapable of discriminating cell types, and methodology, which was not properly controlled for FcγR reactivity.

The variety of potential roles that antibody can play in an immune response to tumors requires that those problems be solved and the antibody–cell interaction be evaluated. In addition to direct, complement-dependent cytotoxicity on cells, antibody may be involved in mediating or blocking antibody-dependent cellular cytotoxicity (*15, 16*), it may function as a "blocking factor" (*13, 14*), or it could be involved in anti-idiotype regulation (*21*). The present study was designed to answer the following questions. With the use of the extensively studied MCA-induced murine sarcoma system, a prototype for immunogenic, rarely metastasizing tumors, how does Ig interact with tumor cells and/or tumor-associated host cells? Is Ig predominantly associated with one or the other? If Ig is associated with host cells, is it bound to cell antigens or is it bound to FcγR? If it is bound to FcγR, do those receptors have greater than normal avidity for Ig?

The results established several points: 1) In these particular tumors, at the sensitivity level of indirect immunofluorescence, Ig is bound exclusively to FcγR-positive cells. Numerous studies have established that, with the exception of a few granulocytes, the FcγR-positive cells are entirely accounted for as macrophages or monocytes (*1–4*). Therefore, most Ig was macrophage associated. Recently, several studies have indicated the presence of functionally defined "natural killer" and "natural cytotoxic" cells within tumors. Since we have not defined cells in any functional way, it is not clear what relationship there is to those types of cells. 2) Ig was both on the membrane of cells and in cell cytoplasm. This may be interpreted to mean that Ig first interacted with cell membranes and was then endocytosed. 3) Ig was FcγR associated. Many pieces of indirect evidence support this conclusion, but proof is provided by the fact that Ig could be specifically eluted with heterologous normal IgG. This is classic proof of receptor–ligand interaction. 4) The tumor-associated Ig exhibited no anti-Ig activity, but this did not formally prove absence of anti-idiotype. 5) The tumor-associated FcγR exhibited a significantly increased binding of Ig in the form of complexes in comparison with FcγR on normal resting macrophages. Uncomplexed Ig still exhibited minimal binding to the macrophages' FcγR. This finding is consistent with the observation that a variety of stimuli can result in increased expression of FcγR on monocytes and macrophages (*26*).

The results failed to establish several points, two of which are of extreme importance: 1) It is unclear whether the macrophage-associated Ig represented antibody to tumor antigens or was simply FcγR-associated normal Ig or unrelated complexes. 2) It is unclear whether the FcγR-associated Ig was in the form of cytophilic antibody, antigen-antibody complexes, or both. Nevertheless, we believe that the results we have presented in this study provide significant insight into the interaction between the immune system and developing tumors.

REFERENCES

(*1*) Evans R. Macrophages in syngeneic animal tumors. Transplantation 1972; 14:468–473.

(*2*) Wood GW, Gillespie GY. Studies on the role of macrophages in regulation of growth and metastasis of murine chemically induced fibrosarcomas. Int J Cancer 1975; 16:1022–1029.

(*3*) Kerbel RS, Pross HR, Elliott HR. Origin and partial characterization of Fc-receptor bearing cells found within experimental carcinomas and sarcomas. Int J Cancer 1975; 15:918–932.

(*4*) Roubin R, Cesarini JP, Feidman WH, Pavie-Fischer J, Peter HH. Characterization of the mononuclear cell infiltrate in human malignant melanoma. Int J Cancer 1975; 16:61–73.

(*5*) Evans R, Eidlen DM. Macrophage accumulation in transplanted tumors is not dependent on host immune responsiveness or presence of tumor-associated rejection antigens. J Reticuloendothel Soc 1981; 30:425–437.

(*6*) Eccles SA, Alexander P. Macrophage content of tumours in relation to metastatic spread and host immune reaction. Nature 1974; 250:667–669.

(*7*) Moore K, Moore M. Intra-tumour host cells of transplanted rat neoplasms of different immunogenicity. Int J Cancer 1977; 19:803–813.

(*8*) Eccles SA, Styles JM, Hobbs SM, Dean CJ. Metastasis in the nude rat associated with lack of immune response. Br J Cancer 1979; 40:802–809.

(*9*) Witz I. Tumor bound immunoglobulins: In situ expressions of humoral immunity. Adv Cancer Res 1977; 25:95–148.

(*10*) Wood G. Antibody responses to tumors. In: Haskill S, ed. Tumor immunity in prognosis: The role of mononuclear cell infiltration. New York: Marcell Dekker, 1982:333–358.

(*11*) Martin SB, Martin WJ. Anti-tumour antibodies in normal mouse sera. Int J Cancer 1975; 15:658–664.

(*12*) Wolosin LB, Greenberg AH. Murine natural anti-tumour antibodies. I. Rapid in vivo binding of natural antibody by tumour cells in syngeneic mice. Int J Cancer 1979; 23:519–529.

(*13*) Hellström K, Hellström I, Nepom J. Specific blocking factors—are they important? Biochim Biophys Acta 1977; 473:121–248.

(*14*) Baldwin RW, Robins RA. Factors interfering with immunologic rejection of tumours. Br Med Bull 1976; 32:118–130.

(*15*) Murray F, Ruyzrok S, Milton GW, Hersey P. Analysis of serum blocking factors against leukocyte dependent antibody in melanoma patients. Int J Cancer 1978; 21:578-589.

(16) Walker L, Hay FC, Roitt IM. Characteristics of complexes for arming and inhibiting effector cells for antibody dependent cell-mediated cytotoxicity. Clin Exp Immunol 1979; 36:397-407.

(17) Lewis MG, Proctor JW, Thompson DM, Rowden G, Phillips T. Cellular localisation of immunoglobulin within human malignant melanomata. Br J Cancer 1976; 33:260-266.

(18) Braslawsky G, Yaackubowicz M, Frensdorj A, Witz I. Receptors for immune complexes on cells within a non-lymphoid tumor. J Immunol 1976; 116:1571-1578.

(19) Wood GW, Tilzer SA, Gollahon KA, Lindsay JM. Association between immunoglobulin and macrophages in primary methylcholanthrene induced sarcomas. Cancer Res 1979; 39:4588-4593.

(20) Wood GW, Gillespie GY, Barth RF. Recepter sites for antigen antibody complexes on cells derived from solid tumors. J Immunol 1975; 114:950-955.

(21) Hartman D, Lewis MG, Proctor JW, Lyons H. In vitro interactions between anti-tumour antibodies and antiantibodies in malignancy. Lancet 1973; 1:1481-1483.

(22) Benacerraf B, Sebestyen MM. A reticuloendothelial stimulant isolated from the cell wall of *Saccharomyces cerevesiae*. Res Proc 1957; 16:860.

(23) Wood GW, Gollahon KA. T lymphocytes and macrophages in primary murine fibrosarcomas at different stages in their progression. Cancer Res 1978; 38:1857-1865.

(24) Haakenstad AO, Mannik M. The disappearance kinetics of soluble immune complexes prepared with reduced and alkylated antibodies and with intact antibodies in mice. Lab Invest 1976; 35:283-289.

(25) Lowry OH, Rosebrough NJ, Farr AL, Randall RJ. Protein measurement with the Folin phenol reagent. J Biol Chem 1951; 193:265-275.

(26) Rhodes J. Macrophage heterogeneity in receptor activity: The activation of macrophage Fc receptor function in vitro and in vivo. J Immunol 1975; 114:976-982.

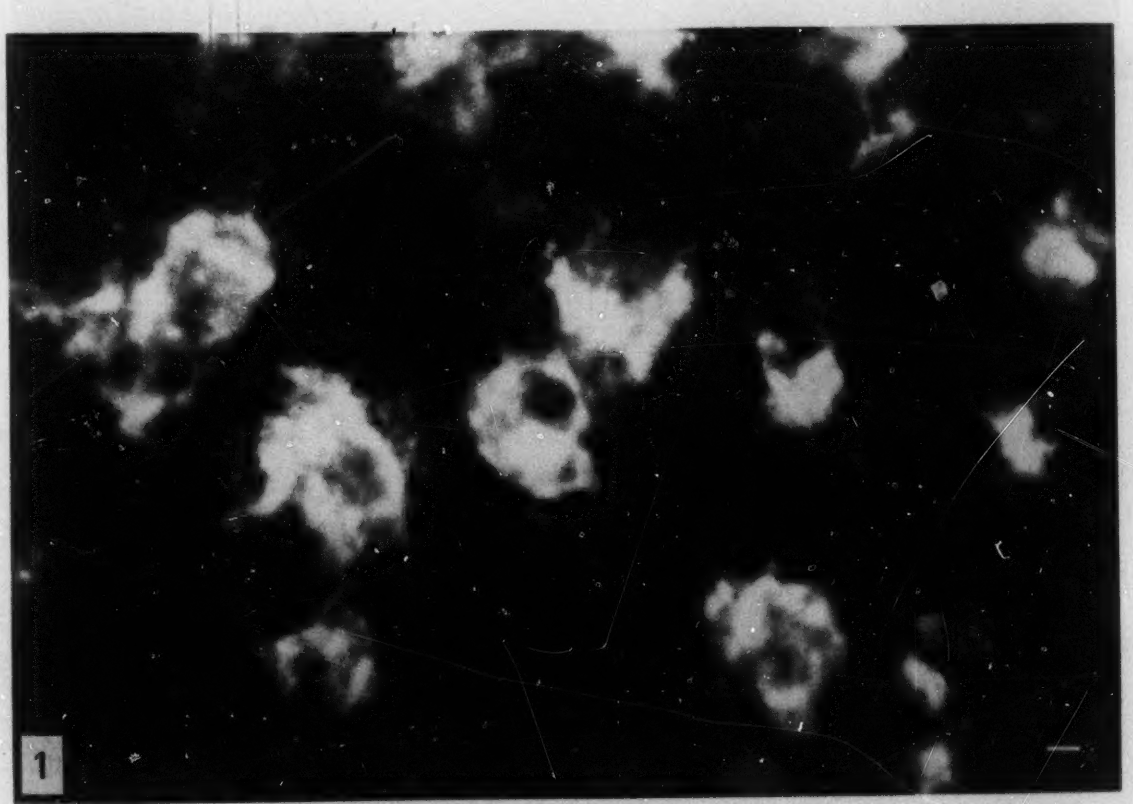

Figure 1.—Primary MCA-induced tumor stained by indirect immunofluorescence with specific rabbit anti-mouse macrophage serum. *Bar*=10 *µm*. × 480

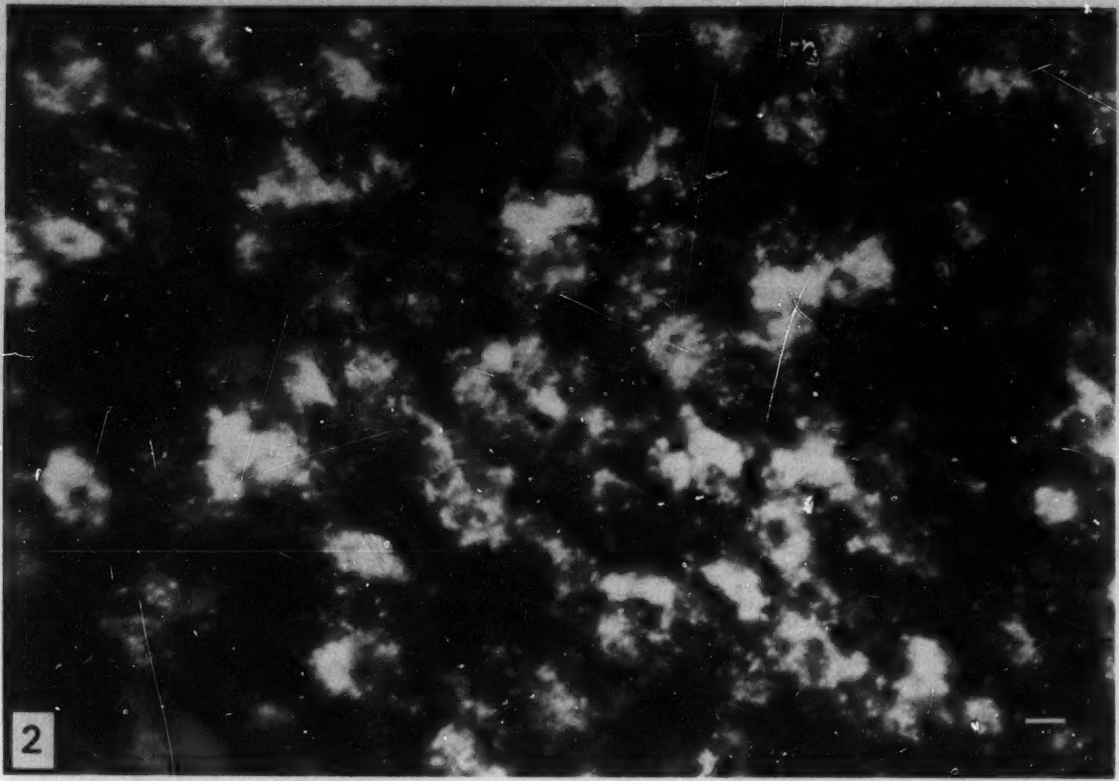

FIGURE 2.—Primary MCA-induced tumor stained by indirect immunofluorescence with rabbit anti-mouse IgG_{2a}. Similar pattern of reactivity seen with anti-IgG_1, IgG_{2b}, IgG_3, and IgA. *Bar*=20 µm. × 290

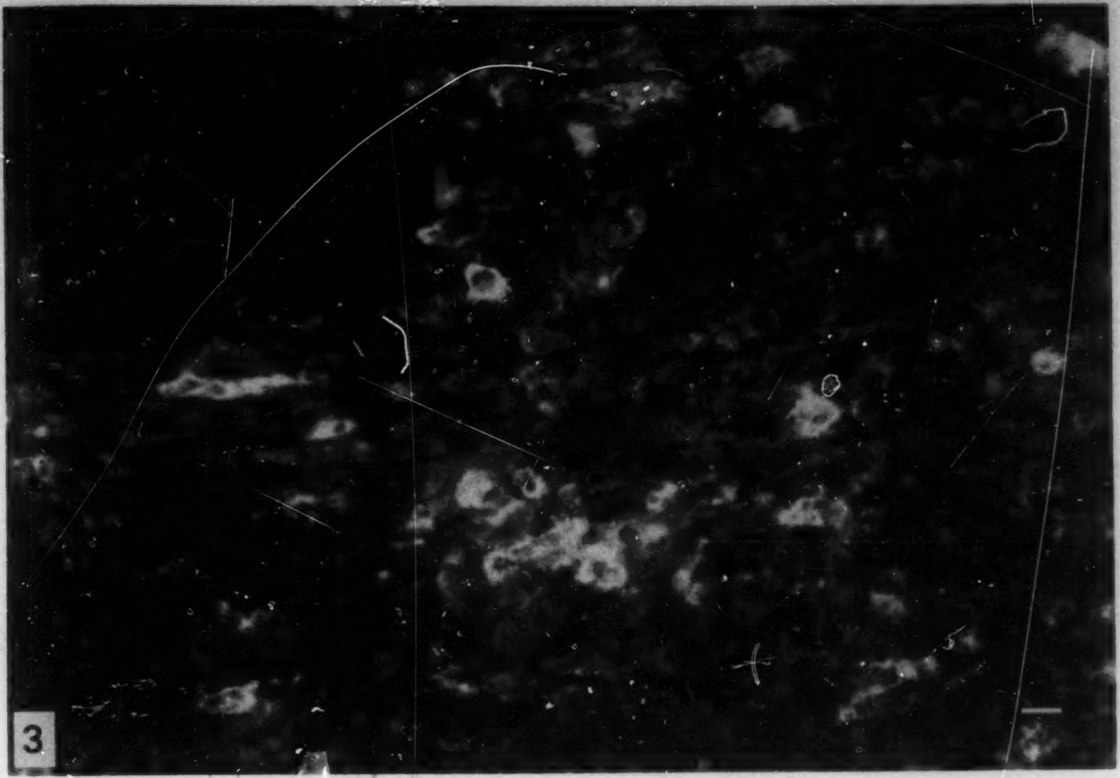

FIGURE 3.—Primary MCA-induced tumor stained by indirect immunofluorescence with monoclonal mouse anti-Ia^k. Sections were prewashed with glycine HCl (pH 2.5) for removal of endogenous Ig, because the antiserum is of mouse origin. After sections were reacted with the antiserum, they were washed with acetate buffer (pH 5.0) and then stained with fluorescence-developing reagent. *Bar* = 20 μm. × 290

FIGURE 4.—Primary MCA-induced tumor section incubated for 60 min at 37°C in human γ-globulin (10 mg/ml) and then stained by indirect immunofluorescence for murine IgG_{2a}. No areas of positive fluorescence remained. *Bar*=20 µm. × 290

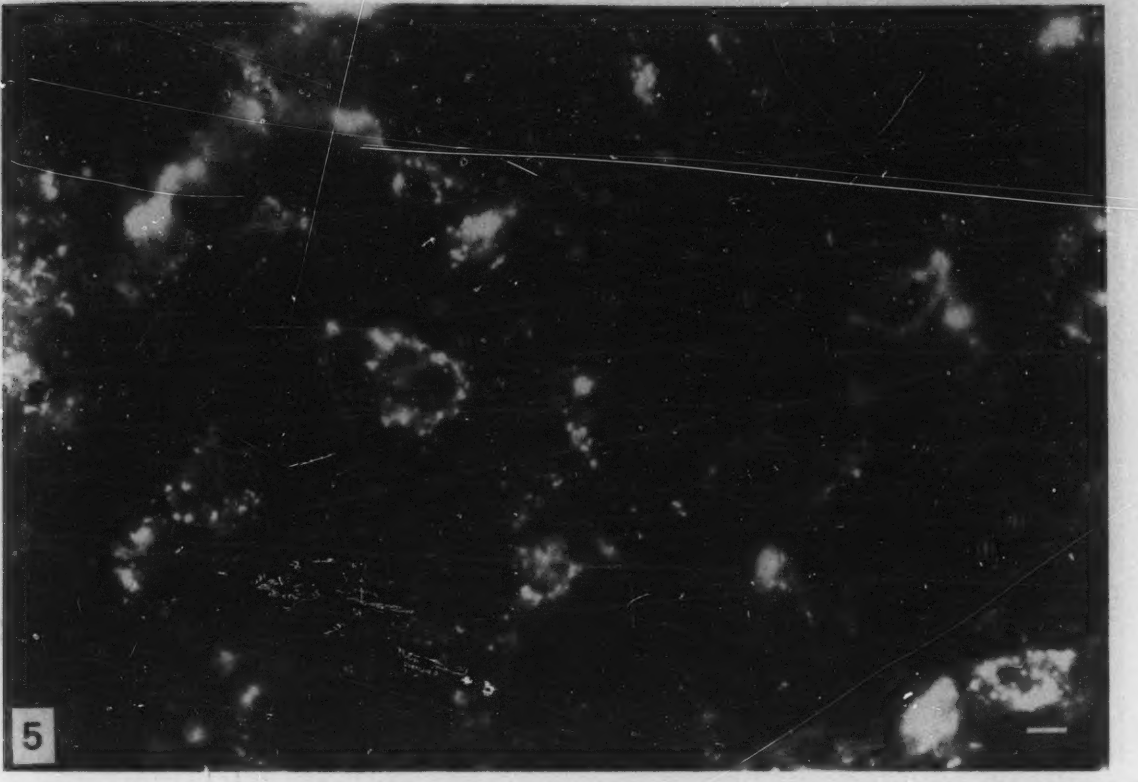

FIGURE 5.—Primary MCA-induced tumor section incubated for 60 min at 37°C in BSA (10 mg/ml) and then stained by indirect immunofluorescence for murine IgG_{2a}. Some cytoplasmic Ig washed out, but significant fluorescence remained. *Bar*=20 μm. × 290

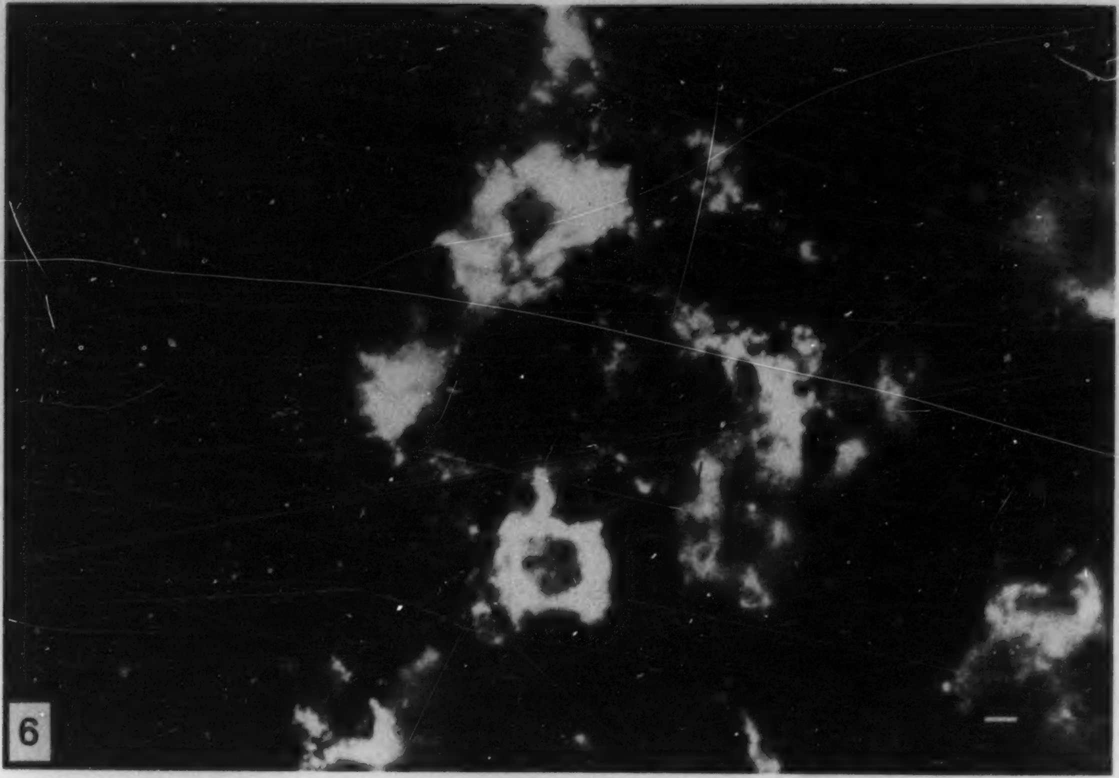

FIGURE 6.—Primary MCA-induced tumor incubated with soluble antigen-antibody complexes (BSA anti-BSA) and then stained by indirect immunofluorescence for localization of bound complexes. *Bar*=10 μm. × 480

7

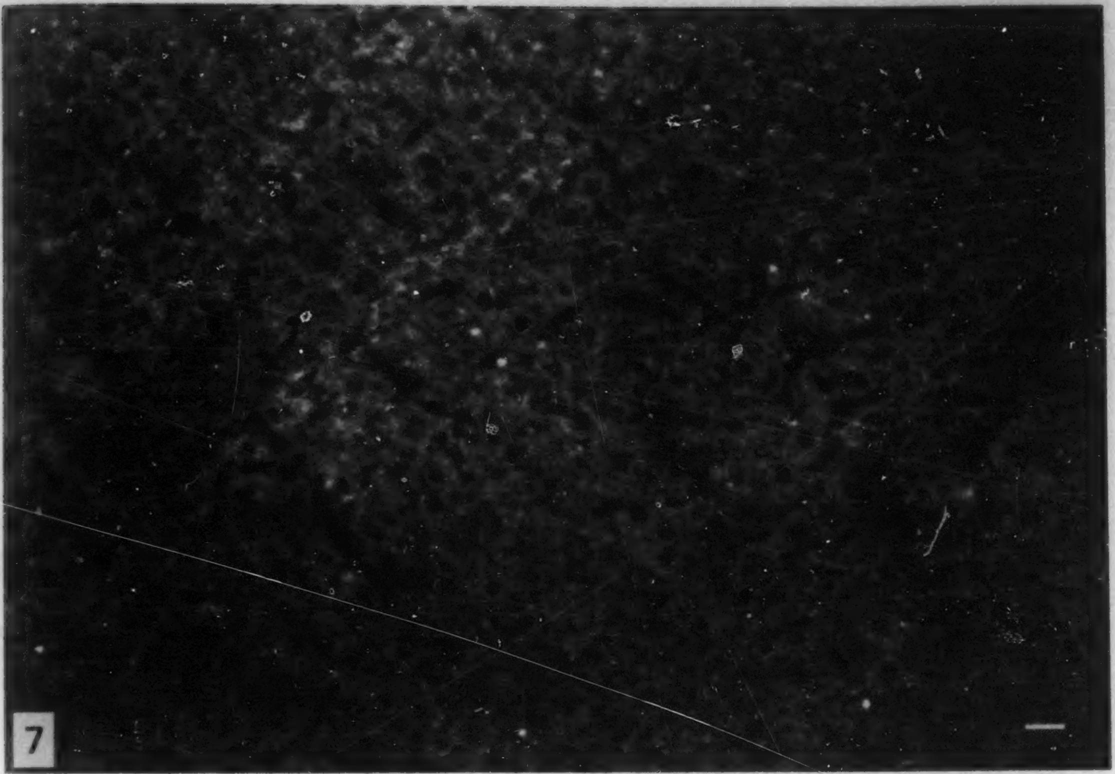

FIGURE 7.—Murine liver incubated with soluble antigen-antibody complexes (BSA anti-BSA) and then stained by indirect immunofluorescence for localization of complexes. No detectable binding was observed. *Bar*=20 μm. × 290

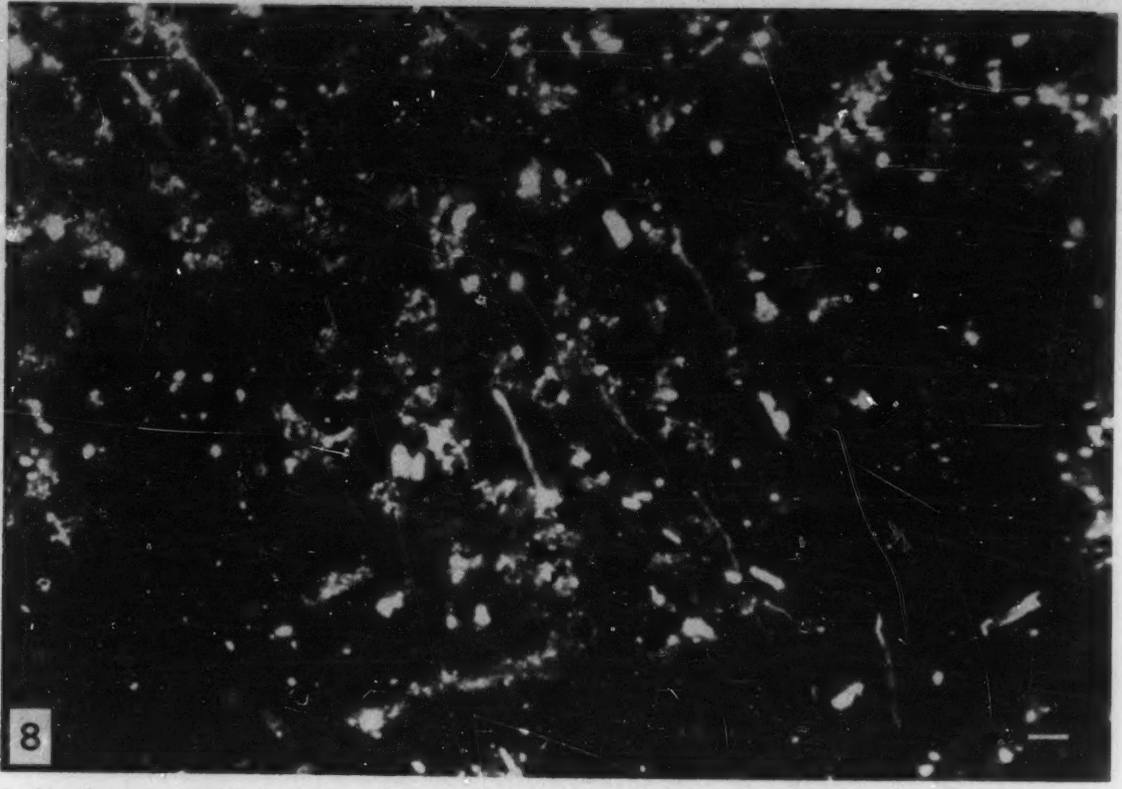

FIGURE 8.—Liver from mice given injections of 30 mg glucan/kg. Sections were incubated with soluble antigen-antibody complexes (BSA anti-BSA) and then stained by indirect immunofluorescence for localization of complexes. *Note* binding of complexes to Kupffer cells. *Bar*=20 µm. × 290

Independent Expression of Chemical Carcinogen-Induced Phenotypic Properties Frequently Associated With the Neoplastic State in a Cultured Guinea Pig Cell Line[1,2]

Charles H. Evans[3,4] *and* **Joseph A. DiPaolo**[3]

ABSTRACT—Relationships among carcinogen-induced morphologic transformation, anchorage independence, susceptibility to growth inhibition by the immunologic hormone lymphotoxin and to natural killer cell and natural lymphoid cell cytotoxicity, natural delayed-type (tuberculin) skin reactivity, and tumorigenicity were investigated with the use of a guinea pig cell culture model of carcinogenesis characterized by sequential, extended developmental stages. Twelve cultures of passage 90 nontumorigenic fibroblast-like line 118 cells derived from a 36-day-old strain 2/N guinea pig fetus were treated with 10 μg benzo[*a*]pyrene or 1 μg *N*-nitroso-*N*-methylnitroguanidine/ml medium for 3 days and maintained in exponential growth. One week later, all cultures exhibited morphologic alteration, and by 8 weeks two-thirds exhibited morphologic transformation. After 4 months, morphologically altered or transformed cells expressed progressive colony growth in semisolid 0.35% agar medium. Susceptibility to lymphotoxin colony inhibitory activity developed subsequent to morphologic transformation but independently of growth in semisolid medium. Susceptibility to natural lymphoid cell destruction was also independent of growth in semisolid medium. All four phenotypic properties were expressed only after carcinogen treatment and 12 months later remained unaccompanied by either natural delayed-type skin reactivity or by the ability of the cells to grow as tumors in syngeneic guinea pigs or *nu/nu* nude mice. Thus while morphologic transformation, colony formation in semisolid medium, and susceptibility to lymphotoxin and to natural lymphoid cell cytotoxicity were frequently associated with neoplasia, they could be expressed independently of one another; individually or collectively in a specific developmental sequence, they were insufficient for expression of either natural delayed-type skin reactivity or tumorigenicity.—JNCI 1982; 69:1175–1182.

Chemical carcinogen and irradiation carcinogenesis in strain 2/N guinea pig fetal fibroblast-like cells in culture develops with a latent period from 4 to 24 or more months between carcinogen treatment and neoplastic transformation (the ability of cells to grow as a tumor) (*1, 2*). This long latent period of carcinogenesis is characterized by discrete, extended, and sequential preneoplastic stages of morphologic alteration, a persistent deviation from the normal growth pattern, and morphologic transformation (a lack of orientation with random crisscrossing and piling up of cells) (*1*). Morphologic transformation, moreover, often develops months before the transformed cells are able to produce tumors. The expressions of carcinogen-induced phenotypic alterations in Syrian golden hamster (*3*) and in mouse (*4, 5*) cells also can develop sequentially, although their expressions frequently are more telescoped into a shorter latent period than those in guinea pig (*1, 2*), human (*6–8*), or rat (*9, 10*) cells. The presence of extended stages during the process of transformation in guinea pig cells derived from syngeneic animals with well-characterized tumor immunology (*11, 12*) facilitates study of the relationships among carcinogen-induced somatic cell alterations in terms of their temporal and sequential expression, interdependence, contribution to neoplastic transformation, and interaction with natural immunobiologic mechanisms possessing the potential to control carcinogenesis (*2, 13, 14*).

Morphologically transformed guinea pig cells with the ability to form progressively growing tumors express a variety of other phenotypic properties, including growth in semisolid agar medium (*1, 2*), susceptibility to the growth inhibitory activity of the immunologic hormone lymphotoxin (*2, 13, 15*), increased susceptibility to natural (spontaneous) lymphoid cell destruction (*11, 14*), and intradermal delayed-type (tuberculin-like) skin reactivity in nonimmune guinea pigs (*12, 15*). These somatic cell alterations appearing after carcinogen treatment of early-passage fetal guinea pig cells frequently develop temporally in close association with expression of tumorigenicity (*1, 2, 13*). This investigation further defines the relationships among these different somatic cell phenotypic properties after chemical carcinogen treatment of a more homogeneous cell population than is present in freshly isolated cells derived from whole fetuses. The temporal acquisition of these phenotypic properties during chemical carcinogen-induced transformation was, therefore, studied with the use of pseudodiploid, morphologically nontransformed and nontumorigenic cells of a strain 2/N guinea pig fibroblast-like permanent cell line, designated 118, that retains its nontumorigenicity and associated nontransformed properties after continuous cultivation for more than 1 year (*1, 16*). Originally, line 118 cells were the acetone-treated control for sister cultures transformed by a chemical carcinogen to the neoplastic state. Characteristics of those tumorigenic cells were an extended minimal latent period of 18 months between carcinogen insult and their ability to form colonies in agar and produce tumors in vivo (*1*). Because sequential preneoplastic stages of morphologic alteration and transformation were expressed during the development of carcinogenesis in those

---

ABBREVIATIONS USED: BP=benzo[*a*]pyrene; dThd=thymidine; FBS=fetal bovine serum; MNNG=*N*-nitroso-*N*-methylnitroguanidine.

---

[1] Received March 24, 1982; accepted June 30, 1982.

[2] Animals were maintained under the guidelines set forth by the National Institutes of Health Policy on Humane Care and Use of Animals and by the Animal Welfare Act.

[3] Laboratory of Biology, Division of Cancer Cause and Prevention, National Cancer Institute, National Institutes of Health, Public Health Service, U.S. Department of Health and Human Services, Bethesda, Md. 20205.

[4] *Address reprint requests to* Dr. Evans, Building 37, Room 2A17, National Institutes of Health, Bethesda, Md. 20205.

cells, we decided to study the temporal expression of a variety of carcinogen-induced phenotypic properties in the more homogeneous line 118 cells derived from the same fetus.

MATERIALS AND METHODS

Derivation and carcinogen treatment of guinea pig line 118 cells.—The fibroblast-like, morphologically nontransformed and nontumorigenic guinea pig continuous cell line 118 was originally derived from a 36-day strain 2/N fetus (*1*). Cells stored in a liquid-nitrogen refrigerator were reintroduced in culture at the 88th 1:10 passage and subcultured in RPMI-1640 medium–10% FBS as previously described (*17*). Twelve 100-mm tissue culture dishes (Falcon Plastics, Oxnard, Calif.) were seeded with 1×10^5 cells at the 90th subculture; 24 hours later, six dishes (BP1–6) were treated with 10 μg BP/ml medium and 6 dishes (MNNG1–6) were treated with 1 μg MNNG/ml medium (*1*). After 3 days, the dishes were refed with medium without carcinogen. Subsequently, cells were detached when confluent with 0.1% trypsin and serially subcultured 1:3 to maintain continuous exponential growth. Development of morphologically altered cells and of morphologic transformation was monitored by examination of Giemsa-stained mass cultures and colonies from sparsely seeded cells (*1*).

Growth of cells in semisolid agar media.—The ability of carcinogen-treated line 118 cells to form progressively growing macroscopic colonies of greater than 50–100 cells in 0.35% agar medium (*1*) was evaluated at monthly intervals. We seeded 10^2, 10^3, 10^4, and 10^5 cells in 4 ml 0.35% agar–RPMI-1640–10% FBS over a 4-ml 0.7% basal agar medium layer in 60-mm tissue culture dishes. Ten or more dishes, collectively containing a minimum of 10^6 seeded cells, were examined microscopically for progressively growing colonies at 7, 14, and 21 days. Macroscopic colonies growing in the agar in dishes seeded with the lowest cell concentration producing colonies were individually isolated at 15 or 22 days by aspiration into a Pasteur pipette and dispersed by repeated pipetting; then the cells were subcultured as described for the parent cultures.

Lymphotoxin susceptibility.—Using a colony inhibition assay with a reproducibility of ±5% (*13*), we analyzed the sensitivity of the carcinogen-treated cells to the growth inhibitory activity of lymphotoxin at monthly intervals. Interferon-free lymphotoxin was obtained from 10^7 mineral oil-induced strain 2/N guinea pig peritoneal leukocytes incubated for 24 hours with 1 mg phytohemagglutinin in 10 ml RPMI-1640 medium–10% FBS. The resulting cell-free lymphokine medium with lymphotoxin activity was frozen and stored at −35°C. The units of lymphotoxin in the lymphokine medium were determined as previously described (*14*). The colony inhibitory activity of the lymphotoxin was assessed with the use of BP-transformed 104C1 syngeneic guinea pig tumorigenic cells (*1*) as a positive control. In the assays for lymphotoxin susceptibility of carcinogen-treated line 118 cell cultures, 100 cells in RPMI-1640 medium–10% FBS were mixed with dilutions of the lymphotoxin and 4 ml of the cell mixture was added to a 60-mm tissue culture dish. We determined colony formation by counting the number of colonies greater than 0.2 mm in diameter present after 7 days' growth. Colony formation was expressed at each lymphotoxin concentration as a percentage of the colonies formed in dishes without lymphotoxin. Inhibition was present when there was a 10% or greater reduction in the number of colonies of cells incubated with lymphotoxin. Frozen aliquots of the same lymphotoxin preparation stored at −35°C were used throughout the investigation.

Susceptibility to natural killer cell- and natural lymphoid cell-mediated destruction.—Whole spleen leukocytes and spleen leukocytes nonadherent to glass and nylon wool were prepared and added to 10^4 $[^3H]$dThd and ^{51}Cr-labeled target cells, respectively, at effector-to-target cell ratios from 1:1 through 200:1; the specific $[^3H]$dThd release and specific ^{51}Cr release were measured at 72 hours for natural lymphoid and 4 hours for natural killer cell cytotoxicity, respectively, with a reproducibility of ±5%, as described elsewhere (*2, 14*).

Natural skin reactivity.—Natural skin reactivity is the ability of cells to produce a persistent or increasing induration in the skin of nonimmune, healthy syngeneic guinea pigs, as evidenced by a zero or positive slope during the 4 days following injection of the cells (*12*). Natural skin reactivity in nonimmunized guinea pigs was measured as is tuberculin delayed-type hypersensitivity skin reactivity in specifically immune animals. The degree of skin induration after intradermal injection of 5×10^6 cells into syngeneic nonimmune 4- to 6-month-old male guinea pigs was measured daily. As previously described (*12*), each animal in groups of 6 received four different cell inocula at separate sites; at one site BP tumorigenic 104C1 cells (*1*) were injected as the positive control. Cultures were initially evaluated 4 months after carcinogen treatment and subsequently once every 2 months if colony formation in agar medium or susceptibility to lymphotoxin had occurred.

Tumorigenicity assessment.—Commencing 4 months after carcinogen treatment, cultures were evaluated once every 2 months for natural skin reactivity and for their ability to grow as progressively enlarging tumors in syngeneic newborn (<24 hr old) male guinea pigs and in 8- to 10-week-old male *nu/nu* NIH Swiss mice as described elsewhere (*17*). Cells were detached from monolayer cultures with the use of 0.1% trypsin, centrifuged at 200×*g*, and resuspended in medium without serum. Guinea pigs and nude mice received sc injections of 10^7 and 5×10^7 cells, respectively, in 0.5 ml medium by means of a 21-gauge needle. Groups of 3 animals were used for each culture evaluated for tumorigenicity. Nude mice were observed for 6 months and guinea pigs for 2 years before being considered as negative for tumor growth. Injections of 104C1 cells with a threshold subcutaneous tumorigenicity of 10^3 cells in guinea pigs and 5×10^5 cells in nude mice served as the positive controls (*17*).

RESULTS

After 1 week, all line 118 BP and MNNG-treated cells displayed morphologic alterations (fig. 1C); by 2 months, morphologic transformation (fig. 1D), i.e., a loss of cell orientation, developed in 67% (8/12) of the cell cultures (table 1). Morphologic transformation persisted with sub-

TABLE 1.—*Temporal appearance of chemical carcinogen-induced somatic cell alterations in guinea pig cells*[a]

Culture[b]	Months of subculture after MNNG treatment	Morphology[c]	Colony formation in agar[d]	Susceptibility to lymphotoxin[e]	Natural skin reactivity and tumorigenicity
HM4	1	A			
	5	A	0	0	
	8	T	0	+	0
	9	T	0	+	0
	11	T	+	+	+
BP1	1	T	0	0	
	4	T	0	0	0
BP2	1	A	0	0	
	4	T	0	0	0
BP3	1	A	0	0	
	4	T	0	0	0
BP4	1	A	0	0	
	4	A	+	0	0
BP4 subline	6	A	+	0	0
	8	A	+	0	0
	12	A	+	0	0
BP5	1	A	0	0	
	4	A	0	0	0
BP6	1	A	0	0	
	4	T	0	0	0
MNNG1	1	T	0	0	0
	4	T	0	0	0
MNNG2	1	T	0	0	
	4	T	0	0	0
	6	T	0	0	0
	8	T	0	+	0
	12	T	0	+	0
MNNG3	1	A	0	0	
	4	T	0	0	0
	6	T	+	0	0
	8	T	+	+	0
	12	T	+	+	0
MNNG3 subline	8	T	+	+	0
	12	T	+	+	0
MNNG4	1	A	0	0	
	4	T	+	0	0
	6	T	+	0	0
	8	T	+	+	0
	12	T	+	+	0
MNNG4 subline	6	T	+	0	0
	8	T	+	+	0
	12	T	+	+	0
MNNG5	1	A	0	0	
	4	A	0	0	0
MNNG6	1	A	0	0	
	4	A	0	0	0
Percent change at 4 mo		A=100, T=62	8	0	0
Percent change at 12 mo		A=100, T=80	80	80	8

[a] 0=absent; +=present.

[b] HM4 cells were derived from a 49-day strain 2/N guinea pig fetus treated in utero with MNNG 48 hr before introduction of cells in culture (*1*). BP and MNNG cultures were derived from a morphologically transformed and nontumorigenic strain 2/N guinea pig continuous cell line treated for 3 days with BP or MNNG 18 mo after establishment in culture from a 36-day fetus. Subline BP4 was derived from a colony in semisolid medium at 4 mo. Sublines MNNG3 and MNNG4 were derived from colonies in semisolid medium at 6 and 4 mo, respectively. Untreated (control) line 118 cells at the time of BP and MNNG treatment of sister cultures (passage 90) and 12 mo later remained morphologically unaltered (fig. 1A, 1B), did not form colonies in semisolid medium, did not exhibit susceptibility to lymphotoxin, and did not produce natural skin reactivity or tumors in nude mice or syngeneic guinea pigs.

[c] A=altered; T=transformed.

[d] Colony formation in 0.35% semisolid medium of BP4 at 4 mo, MNNG3 at 6 mo, and MNNG4 at 4 mo was 1×10^{-5}, 5×10^{-2}, and 5×10^{-4}, respectively; for sublines derived from colonies in semisolid medium, the frequencies when returned to semisolid medium were $1\text{-}9\times10^{-1}$. Frequency for HM4 was 2.5×10^{-1}. Untreated parent line 118 cells never formed colonies in semisolid medium.

[e] Susceptibility was defined as ≥10% colony inhibition (*see* "Materials and Methods").

culturing, and neither altered nor transformed morphology was observed with untreated cells during 12 months of subculturing (figs. 1A, 1B). Morphologic alteration and morphologic transformation were dissociated from each other and the other studied phenotypic alterations. For example, either morphologic alteration (BP4) or morphologic transformation (MNNG4) was accompanied by or unaccompanied by (the remaining 11 cultures) colony formation in semisolid medium 4 months after carcinogen treatment (table 1). Twelve months after carcinogen treatment, morphologic alteration was accompanied by colony formation in semisolid medium (BP4), and morphologic transformation was accompanied by lymphotoxin susceptibility (MMNG2) or by lymphotoxin susceptibility and colony formation in semisolid medium (MNNG3 and MNNG4), further demonstrating the dissociability of morphologic changes from these other carcinogen-induced phenotypic alterations.

Colony formation in semisolid medium assessed at monthly intervals was first observed with a frequency of $>10^{-6}$ at 4 months in both morphologically altered (BP4) and transformed (MNNG4) cell populations. In some instances, the ability to form colonies in semisolid medium was expressed without the subsequent development of (BP4 cells) or prior to (MNNG3 and MNNG4 cells) the cells exhibiting susceptibility to lymphotoxin (table 1; text-fig. 1). Lymphotoxin susceptibility also incurred in morphologically transformed cells without subsequent development of the ability of the cells to form colonies in semisolid medium (MNNG2 in table 1).

The analysis of sublines, each derived from a colony growing in semisolid medium, verified that development of the ability of cells to proliferate in semisolid medium can precede expression of lymphotoxin susceptibility by an extended time. For example, MNNG4 formed colonies in semisolid medium at 4 months. One subline retained the ability to form colonies in semisolid medium, but the cells did not develop susceptibility to the growth inhibitory activity of lymphotoxin until 8 months after carcinogen treatment (table 1). Similarly, 4 sublines derived from 4 different MNNG3 colonies in semisolid medium at 6 months also developed sensitivity to lymphotoxin at the same time as the parent MNNG3 cultured, 8 months after carcinogen treatment.

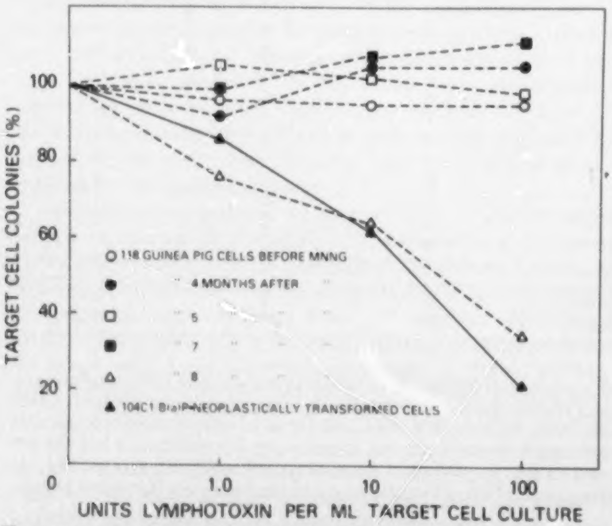

TEXT-FIGURE 1.—Susceptibility of continually subcultured MNNG-treated cells, culture MNNG3, to the growth inhibitory activity of lymphotoxin. Aliquots of lymphotoxin were incubated with 100 target cells in 4 ml medium/60-mm dish. The number of colonies >0.2 mm in diameter present after 7 days' incubation was counted, and the ratio of the number of colonies formed in the presence of lymphotoxin was compared to the number in medium alone expressed as percentage. B(a)P=BP. *Solid line,* 104C1 cells; *dashed lines,* 118 cell series.

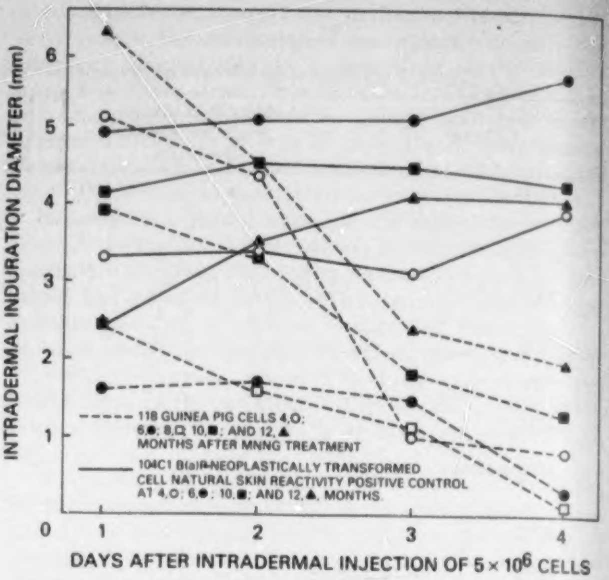

TEXT-FIGURE 2.—Natural skin test reactivity of tumorigenic and continually subcultured MNNG-treated cells, culture MNNG3, in healthy, nonimmunized 14- to 16-wk-old syngeneic male guinea pigs. Values are mean diameters of induration (in mm) for groups of 6 animals. B(a)P=BP.

All 12 carcinogen-treated cell populations were nontumorigenic at 4 months following treatment. Three of these (MNNG2, MNNG3, and MNNG4) as well as sublines derived from colonies of BP4, MNNG3, and MNNG4 cells in semisolid medium were subsequently evaluated once every 2 months for natural delayed-type skin reactivity and tumorigenicity. Neither property was observed as late as 12 months after carcinogen treatment (table 1; text-fig. 2). At that time each line had acquired an increased susceptibility to natural killer cell-mediated cytotoxicity and/or natural lymphoid cell-mediated cytotoxicity (text-fig. 3). Susceptibility to natural lymphoid cell cytotoxicity was independent of expression of proliferation in semisolid medium; e.g., line MNNG2 that remained anchorage-dependent was the most susceptible to natural cytotoxicity. In the traditional 4-hour natural killer cell assay, moreover, several anchorage-independent sublines (MNNG3 and MNNG4) expressed the same susceptibility as the parent nontransformed 118 cells. The expression of carcinogen-induced morphologic alteration or transformation, anchorage-independent growth, and the susceptibility to growth inhibition by lymphotoxin, natural killer cells, or lymphoid cells in line 118 cell populations,

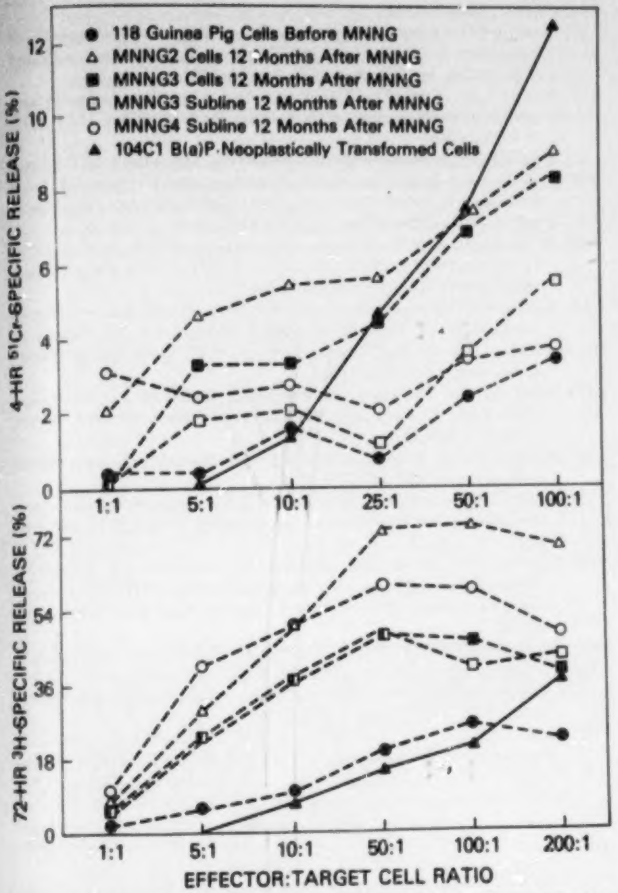

TEXT-FIGURE 3.—Susceptibility of line 118 cells to destruction mediated by syngeneic guinea pig spleen natural killer cells (4-hr ^{51}Cr release) and natural lymphoid cells (72-hr ^{3}H release). B(a)P=BP.

therefore, can develop independently of one another, of natural skin reactivity, and of the ability to grow progressively as tumors in newborn syngeneic guinea pigs or homozygous *nu/nu* nude mice.

DISCUSSION

The following are characteristics of tumorigenic fetal guinea pig fibroblast-like cells descended from carcinogen-treated, early-passage cell cultures (*1, 2, 12*): Morphologic transformation as a measure of diminished density-dependent inhibition of growth, colony formation in semisolid medium as a measure of anchorage-independent growth, and lymphotoxin, natural killer cell, and lymphoid cell susceptibility and natural delayed-type skin reactivity as measures of possible natural immunobiologic cytotoxicity. None of these phenotypic properties develops during culture of cells treated with noncarcinogenic chemicals. Whereas carcinogen-treated cultures of early-passage cells, including cells derived from the same fetus from which line 118 cells were derived, often develop morphologic transformation months before expression of tumorigenicity, the other properties frequently develop in closer temporal relationship with one another and with tumorigenicity (*1, 2, 12, 13*). Similar sequential–temporal (*3, 6–8*) yet dissociable relationships among morphologic transformation (*18*), anchorage independence (*19*), and tumorigenicity have been described for Syrian golden hamster and human cells.

The present investigation demonstrates that, as was observed in freshly isolated diploid cells, chemical carcinogen-induced changes in cells of a long-term continuous guinea pig fibroblast-like cell line develop with an extended and variable latent period between carcinogen treatment and expression of the various phenotypic somatic cell properties. Morphologic transformation, colony formation in a semisolid medium, and susceptibility to the growth inhibitory activity of lymphotoxin and to natural killer cell and lymphoid cell cytotoxicity, moreover, can develop independently of one another. In addition, during 12 months of continuous cultivation, the expression of these properties can be unaccompanied by the development of natural delayed-type skin reactivity or by any demonstrable ability of the cells to grow as a tumor in either newborn syngeneic guinea pigs or immunodeficient homozygous *nu/nu* nude mice with the use of identical conditions previously establishing the nontumorigenic or tumorigenic nature of strain 2/N fibroblasts including line 118 cells in this model of carcinogenesis (*17*). Morphologic transformation and susceptibility to lymphotoxin and to natural killer cell cytotoxicity, furthermore, have also been observed to occur independently of one another and before colony growth in semisolid medium, natural skin reactivity, or tumorigenicity in early-passage MNNG-treated or UV radiation-treated strain 2/N guinea pig fetal cells after treatment with a tumor-promoting compound, 12-*O*-tetradecanoylphorbol-13-acetate (*2*). Thus the independent expression of phenotypic properties during carcinogenesis may be more common than was previously recognized.

In other investigations in which colony formation in semisolid medium has been observed in the absence of tumorigenicity, it has been suggested that the lack of tumorigenicity might reflect residual immunologic rejection activity of the immunodeficient nude mice (*20, 21*) or immunosuppressed syngeneic mice (*22*). In the present investigation, large inocula of 1×10^7 cells for syngeneic guinea pigs and of 5×10^7 cells for nude mice were administered to reduce this possibility. These inoculum sizes greatly exceed those required to demonstrate tumorigenicity in all previously tested guinea pig cells. For example, the observed threshold tumorigenic inoculum of strain 2/N guinea pig fibroblast-like cell lines chemically transformed by carcinogens including BP, 3-methylcholanthrene, MNNG, and aflatoxin B_1 ranges from 10^3 to between 10^4 and 10^5 cells (*17*). This inoculum is one hundredfold or less cells than those inoculated in the current investigation. The MNNG-transformed HM4C1 cells, moreover, are immunogenic (*23*) and 10^3 cells produce tumors in fully immunocompetent, syngeneic guinea pigs (*14, 23*). An additional observation supporting the nontumorigenicity of the carcinogen-treated 118 cells is that all previously tested chemical carcinogen-transformed guinea pig cells in vitro having tumor-producing potential express a natural intradermal delayed-type skin reactivity in nonimmune syngeneic guinea pigs that does not occur with nontumorigenic cells, regardless of their phenotypic properties (*12*). Although carcinogen-treated line 118 cells have acquired many phenotypic alterations associated with tumor-producing cells, the lack of natural delayed-type skin reactivity in every instance is further evidence of their nontumorigenic nature.

Therefore, while independence from density-dependent inhibition of growth, presence of anchorage-independent growth, and susceptibility to the growth inhibitory activity of lymphotoxin and to natural killer cell and natural lymphoid cell cytotoxicity ordinarily are phenotypic properties possessed by tumorigenic guinea pig cells, they can be independent and possibly secondary carcinogen-induced alterations. Furthermore, they may be expressed in a random sequence and are not in themselves responsible for expression of conventionally assessed tumorigenicity. This situation is reminiscent of chemical carcinogen-induced transplantation rejection neoantigens in which the degree of immunogenicity of the tumor cells can increase in proportion to the carcinogen concentration but without neoantigen induction being a prerequisite for neoplasia since carcinogen-induced nonantigenic tumors do occur (*24–27*). Moreover, carcinogen-induced, tumor-specific neoantigen expression can be a preneoplastic event (*28, 29*). Transformation of guinea pig (*16*) and Syrian hamster (*30*) cells by chemical carcinogens can also occur in the absence of detectable chromosome abnormalities, suggesting that some of the many varied marker chromosomes and karyotypic patterns often observed in transformed cells are independent of or secondary alterations accompanying neoplastic transformation. Analysis of chemical carcinogen-treated Chinese hamster primary cell lines (*31*) and spontaneously transformed Syrian golden hamster cells (*18*) also demonstrates that morphologic transformation, karyotypic variation, and growth in semisolid agar medium can develop independently of one another. A similar dissociation of multiple phenotypic properties from each other has been observed in temperature-sensitive mutants of chemically transformed C3H/10T½ mouse cells (*32*) in which type I versus type II and III foci (*4, 5*) may be analogous to morphologic alteration and to morphologic transformation, respectively, in guinea pig cells. The present investigation is the first demonstration that carcinogen-induced phenotypic somatic cell alterations, which may be focal points for natural immunobiologic control of cell growth, can develop in a temporally dissociated manner, independently of one another, and in the absence of neoplastic transformation.

The development of persistent phenotypic alterations during the preneoplastic stages of carcinogenesis warrants further investigation. Why cells expressing such properties remain nontumorigenic is worthy of additional study in the several species where observations of this nature have now been described. Although nonessential for expression of tumorigenicity, such somatic cell alterations may provide selective advantages to the preneoplastic cell as well as be the basis for development of methods to enable the host to control or prevent the development of cancer.

REFERENCES

(*1*) Evans CH, DiPaolo JA. Neoplastic transformation of guinea pig fetal cells in culture induced by chemical carcinogens. Cancer Res 1975; 35:1035–1044.

(*2*) Ransom JH, Evans CH. Lymphotoxin enhances the susceptibility of neoplastic and preneoplastic cells to natural killer cell mediated destruction. Int J Cancer 1982; 29:451–458.

(*3*) Barrett JC, Ts'o PO. Evidence for the progressive nature of neoplastic transformation in vitro. Proc Natl Acad Sci USA 1978; 75:3761–3765.

(*4*) Reznikoff CA, Bertram JS, Brankow DW, Heidelberger C. Quantitative and qualitative studies of chemical transformation of cloned C3H mouse embryo cells sensitive to post confluence inhibition of cell division. Cancer Res 1973; 33:3239–3249.

(*5*) Jones PA, Laug WE, Gardner A, Nye CA, Fink LM, Benedict WF. In vitro correlates of transformation in C3H/10T½ clone 8 mouse cells. Cancer Res 1976; 36:2863–2867.

(*6*) Kakunaga T. The transformation of human diploid cells by chemical carcinogens. In: Hiatt H, Watson J, Weinstein A, eds. Origins in human cancer. Cold Spring Harbor, N.Y.: Cold Spring Harbor Laboratory, 1977:1537–1548.

(*7*) Milo GE Jr, DiPaolo JA. Neoplastic tranformation of human diploid cells in vitro after chemical carcinogen treatment. Nature 1978; 275:130–132.

(*8*) Borek C. X-ray-induced neoplastic transformation of human diploid cells. Nature 1980; 283:776–778.

(*9*) Lasne C, Gentil A, Chouroulinkov I. Two-stage malignant transformation of rat fibroblasts in tissue culture. Nature 1974; 247:490–491.

(*10*) Greiner JW, Evans CH, McCabe RP, DiPaolo JA. Sequential dynamics of 7,12-dimethylbenz[*a*]anthracene (DMBA) induced mammary carcinogenesis in vitro. Proc Am Assoc Cancer Res 1982; 23:76.

(*11*) Zwilling BS, Meltzer MS, Evans CH. Differential cytotoxicity of tumorigenic and nontumorigenic strain-2 guinea pig cells as mediated by syngeneic phytohemagglutinin-stimulated peritoneal exudate cells. J Natl Cancer Inst 1975; 54:743–747.

(*12*) Evans CH, Cooney AM, DiPaolo JA. Colony inhibition mediated by nonimmune leukocytes in vitro and skin reactivity in vivo as indices of tumorigenicity of guinea pig cultures transformed by chemical carcinogens. Cancer Res 1975; 35:1045–1052.

(*13*) Evans CH, Rabin ES, DiPaolo JA. The susceptibility of guinea pig cells to the colony-inhibitory activity of lymphotoxin during carcinogenesis. Cancer Res 1977; 37:898–903.

(*14*) Evans CH. The role of lymphotoxin in natural cell-mediated cytotoxicity. Cell Immunol 1981; 63:1–15.

(*15*) McCabe RP, Evans CH. Plasminogen activator, fibronectin, lymphotoxin sensitivity, and natural skin reactivity relationships to guinea pig cell tumorigenicity. JNCI 1982; 68:329–336.

(*16*) Popescu NC, Evans CH, DiPaolo JA. Chromosome patterns (G and C bands) of in vitro chemical carcinogen-transformed guinea pig cells. Cancer Res 1976; 36:1404–1413.

(*17*) Evans CH, DiPaolo JA. Comparison of nude mice with the host species for evaluation of the tumorigenicity of guinea pig and hamster cells transformed in vitro by chemical carcinogens. Cancer Res 1976; 36:128–131.

(*18*) Barrett JC. A preneoplastic stage in the spontaneous neoplastic transformation of Syrian hamster embryo cells in culture. Cancer Res 1980; 40:91–94.

(*19*) Sutherland BM, Cimino JS, Delihas N, Shih AG, Oliver RP. Ultraviolet light-induced transformation of human cells to anchorage-independent growth. Cancer Res 1980; 40:1934–1939.

(*20*) Freedman VH, Shin S. Use of nude mice for studies on the tumorigenicity of animal cells. In: Fogh J, Giovanella BC, ed. The nude mouse in experimental and clinical research. New York: Academic Press, 1978:353–384.

(*21*) Kahn P, Shin S. Cellular tumorigenicity in nude mice. Test of associations among loss of cell-surface fibronectin, anchorage independence, and tumor-forming ability. J Cell Biol 1979; 82:1–16.

(*22*) Patek PO, Collins JL, Cohn M. Transformed cell lines susceptible or resistant to in vivo surveillance against tumourigenesis. Nature 1978; 276:510–511.

(*23*) Zbar B, Ribi E, Kelly M, Granger D, Evans C, Rapp HJ. Immunologic approaches to the treatment of human cancer based on a guinea pig model. Cancer Immunol Immunother 1964; 1:127–137.

(*24*) Carbone G, Parmiani G. Nonimmunogenic sarcomas induced by 3-

methylcholanthrene treatment of murine fibroblasts in diffusion chambers. J Natl Cancer Inst 1975; 55:1195–1197.

(25) Embleton MJ, Heidelberger C. Neoantigens on chemically transformed cloned C3H mouse embryo cells. Cancer Res 1975; 35:2049–2055.

(26) Prehn RT. Relationship of tumor immunogenicity to concentration of the oncogen. J Natl Cancer Inst 1975; 55:189–190.

(27) Ohanian SH, McCabe RP, Evans CH. Immunogenicity of guinea pig cells transformed in culture by chemical carcinogens. JNCI 1981; 67:1363–1368.

(28) Lin JL, Hiasa Y, Farber E. Preneoplastic antigen as a marker for endoplasmic reticulum of putative premalignant hepatocytes during liver carcinogenesis. Cancer Res 1977; 37:1972–1981.

(29) Embleton MJ, Baldwin RW. Tumor-related antigen specificities associated with 3-methylcholanthrene-treated rat embryo cells. Int J Cancer 1979; 23:840–845.

(30) DiPaolo JA, Popescu NC. Relationship of chromosome changes to neoplastic cell transformation. Am J Pathol 1976; 85:709–738.

(31) Connell JR, Ockey CH. Analysis of karyotype variation following carcinogen treatment of Chinese hamster primary cell lines. Int J Cancer 1977; 20:768–779.

(32) Boreiko C, Heidelberger C. Isolation of mutants temperature-sensitive for expression of the transformed state from chemically transformed C3H/10T½ cells. Carcinogenesis 1980; 1:1059–1073.

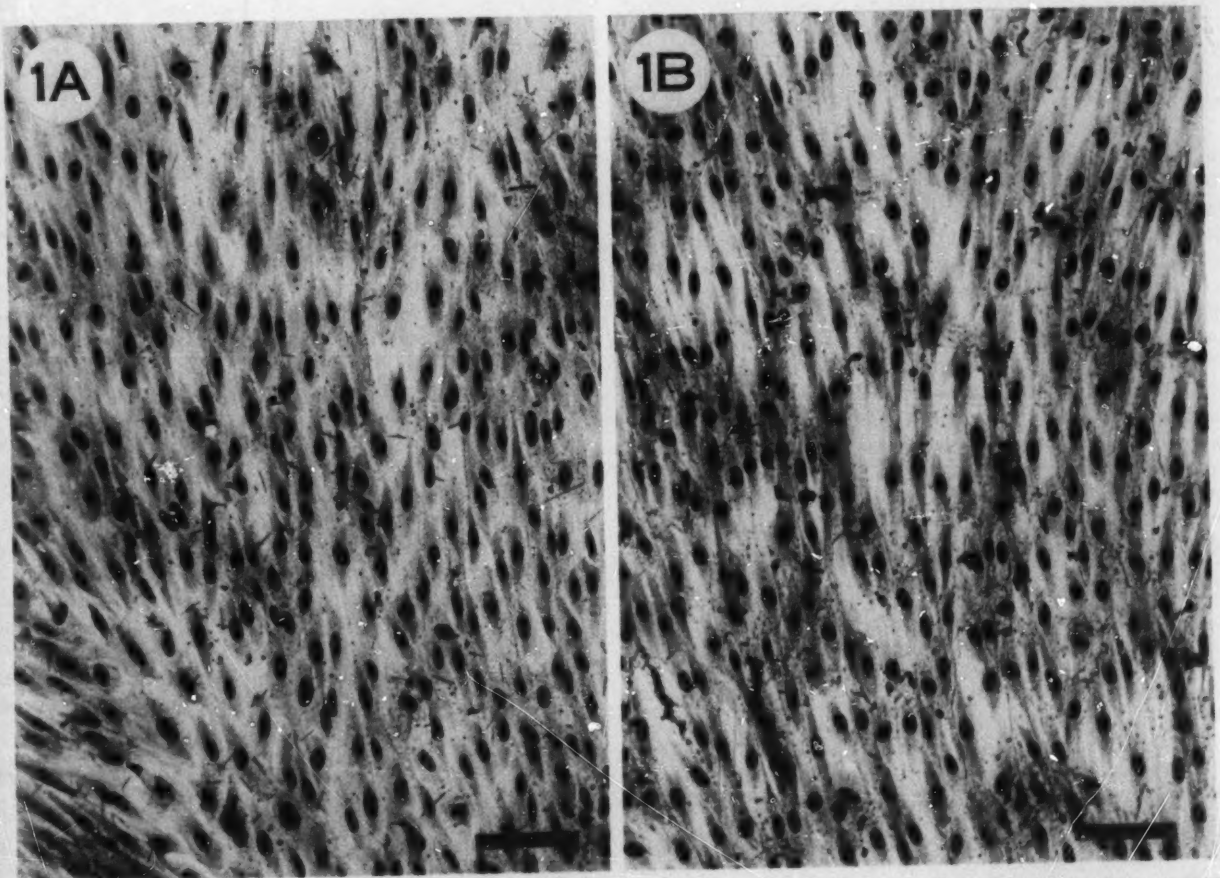

Figure 1.—Morphologic transformation of guinea pig line 118 cells following treatment with MNNG. Untreated cells at time of sister culture carcinogen exposure (A) and 12 mo later (B) compared to morphologically altered cells (culture MNNG3) at 3 wk (C) and morphologically transformed cells at 4 mo (D) following carcinogen exposure. Giemsa. *Bar* = *50 μm*. × 400

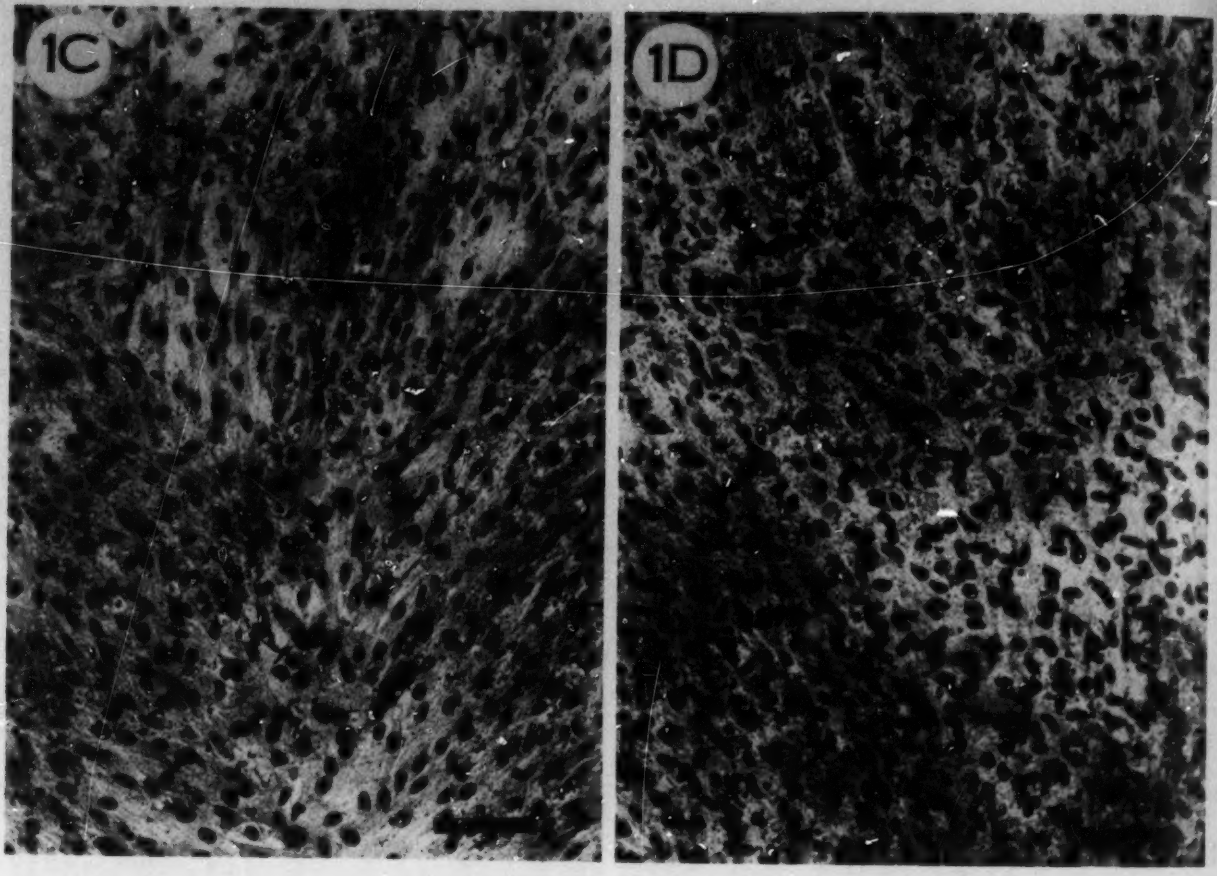
1C
1D

Ceruloplasmin, Copper Ions, and Angiogenesis[1, 2]

Katari S. Raju,[3] Giulio Alessandri,[3] Marina Ziche,[3] *and* Pietro M. Gullino[3, 4]

ABSTRACT—The ability to induce new formation of capillaries in the cornea was tested for ceruloplasmin, the copper carrier of serum, for fragments of the ceruloplasmin molecule with and without copper, for heparin, and for glycyl-L-histidyl-L-lysine, bound or not bound to copper ions. Male or female 2- to 3-kg New Zealand White rabbits were used. These experiments were prompted by the previous observation of copper accumulation in the cornea during angiogenesis and by the inability of copper-deficient rabbits to mount an angiogenic response. The results showed that the three different molecules were all able to induce angiogenesis provided that they were bound to copper. Fragments of the ceruloplasmin molecule also induced angiogenesis but only when copper was bound to the peptides. The data are interpreted to indicate that copper ions are involved in the sequence of events leading to angiogenesis and that the carrier molecules may be of quite a different nature.—JNCI 1982; 69:1183–1188.

The ability of transplanted tissues to elicit vascularization from the host has long been recognized as an essential factor for the survival of a transplant or for the growth of a tumor. However, the conditions that control the formation of a capillary network during growth of primary or metastatic tumors are poorly defined. In previous work undertaken in our laboratory, E-type PG, PGE_1 in particular, were found to be highly angiogenic in the rabbit cornea test at doses insufficient to induce an inflammatory reaction. Moreover, an accumulation of copper ions was detected within the cornea during the angiogenic response induced by PGE_1 (*1*).

Serum ceruloplasmin, the copper-carrier protein, has often been found to be increased in humans and in experimental animals bearing a variety of tumors (*2–4*), and under the same conditions, an elevated production of PG has also been frequently observed (*5–7*). The reciprocal relationship between PG production by the tumors and serum ceruloplasmin levels was particularly striking in the VX_2 carcinoma of the rabbit. Plasma PGE metabolites and ceruloplasmin rose about twentyfold and sixfold, respectively, 3–4 weeks after VX_2 transplantation. Indomethacin, an inhibitor of PG synthesis, substantially reduced the ceruloplasmin levels in serum either when the administration was started at the time of tumor transplantation or later during tumor growth when hyperprostaglandinemia was established (*8*).

The objective of this study was to ascertain whether ceruloplasmin is angiogenic in the corneal assay or whether the transfer of copper is the event controlling angiogenesis.

MATERIALS AND METHODS

Reagents.—Human ceruloplasmin (type III), porcine heparin (intestine), and trypsin (type XI, diphenyl carbamyl chloride-treated) were purchased from Sigma Chemical Co., St. Louis, Mo. Sephadex G-50 and Ultragel AcA 202 gel filtration columns were purchased from Pharmacia, Piscataway, N.J., and LKB Instruments, Inc., Rockville, Md. respectively. DEAE–cellulose (DE.52) was purchased from Whatman, Inc., Clifton, N.J. Reagents for copper determination were purchased from the G. Fredrick Smith Chemical Co., Columbus, Ohio. The tripeptide GHL was purchased from Pierce Chemical Co., Rockford, Ill. All other chemicals were of analytical grade.

Angiogenesis assay.—The angiogenic activities of the samples were evaluated by the rabbit cornea assay as previously reported (*9, 10*). A pocket, about 2×3 mm, was surgically prepared in the cornea of a 2- to 3-kg male or female New Zealand White rabbit. The material to be tested was incorporated into a polymer pellet and introduced into the pocket. The pellet assured slow release of the angiogenic stimuli, an essential condition for angiogenesis to occur (*11*). The pellet consisted of an ethylenevinyl acetate copolymer (Elvax 40; DuPont Co., Wilmington, Del.) prepared from a casting solution of 10% Elvax 40 in methylene chloride. Under sterile conditions the test material was lyophilized and carefully mixed in the appropriately diluted solution of Elvax. Drops of 10–20 µl of the solution were deposited with a glass micropipette on a sterile surface and evaporated under vacuum to produce hard pellets of repolymerized Elvax. Before use the pellets were kept under vacuum at 4°C overnight. All tests were performed under "blind" conditions. On days 4–5 after implantation, capillary buds appeared on the limbal vessels facing the pellet. By the 7th day, a dense network of capillaries had invaded the cornea and was progressing toward the pellet (fig. 1). Since the cornea is avascular and transparent, the new formation of vessels is clearly visible and was followed daily in the unanesthetized rabbit with the use of a Zeiss slit lamp stereomicroscope. Histologic examinations were performed on each cornea at the end of the assay.

Preparation of ceruloplasmins with various copper contents.—The commercial preparation of human ceruloplasmin was purified further by DEAE–cellulose chromatography to obtain a fraction containing 6 copper atoms per molecule (native ceruloplasmin) (table 1; text-fig. 1A). Ceruloplasmin was dialyzed against 0.05 *M* sodium acetate (pH 7.2) and loaded on a DE.52 column (1.5×25 cm) equilibrated with the same

---

ABBREVIATIONS USED: DDC=diethyldithiocarbamate; GHL=glycyl-L-histidyl-L-lysine; M_r=molecular weight (relative); PG=prostaglandin(s).

---

[1] Received March 24, 1982; accepted June 17, 1982.

[2] Animals were maintained under the guidelines set forth by the National Institutes of Health Policy on Humane Care and Use of Animals.

[3] Laboratory of Pathophysiology, Division of Cancer Biology and Diagnosis, National Cancer Institute, National Institutes of Health, Public Health Service, U.S. Department of Health and Human Services, Bethesda, Md. 20205.

[4] *Address reprint requests to* Dr. Gullino, Building 10, Room 5B36, National Institutes of Health, Bethesda, Md. 20205.

buffer. The chromatogram was developed by a constant volume gradient elution in which the higher salt concentration was 0.4 *M* NaCl in 0.05 *M* sodium acetate (pH 7.2).

A colorless ceruloplasmin with 3 copper atoms per molecule (Tris-ceruloplasmin) was prepared by the treatment of ceruloplasmin with Tris-HCl buffer (0.1 *M* ionic strength) at pH 8.0 for 48 hours. This treatment converts only a fraction of the native protein to the more acidic colorless component (*12*). Native and colorless ceruloplasmins were separated by DEAE-cellulose chromatography (text-fig. 1B).

Apo-ceruloplasmin containing 0.44 copper atoms per molecule or less was prepared by the DDC method of Morell and Scheinberg (*13*). Native ceruloplasmin, 200 mg, was taken in 25 ml of 1.2 *M* sodium acetate buffer (pH 5.2), and 125 mg of crystalline ascorbic acid was added, which instantly decolorized the blue solution. During the next 5 hours the solution was stirred and kept at 4°C, while 6.5 ml of 0.4% sodium DDC in water was added dropwise. The final mixture, golden brown and slightly cloudy, was centrifuged for 3 hours at 40,000 rpm at 4°C. The black precipitate was discarded. The slightly yellowish but clear supernatant solution was passed through a column of ion-exchange resins containing 1R-120 and 1RA-400. From this procedure, a flow-through fraction—a clear, colorless solution that contained the apo-protein—was obtained (*13*). The apo-protein still contained small amounts of the colorless component with about 2 copper atoms per molecule. These components were separated by DEAE-cellulose chromatography.

Isolation of copper-rich peptides (11K fragment).—Native ceruloplasmin (100 mg) was digested with trypsin in 5 ml of 0.2 *M* ammonium bicarbonate at an enzyme-to-protein ratio of 1:25 (wt/wt). The trypsin digestion lasted 18 hours at 37°C, and then the products were lyophilized, dissolved in 0.05 *M* ammonium acetate buffer (pH 7.0), and fractionated by gel filtration chromatography on a Sephadex G-50 column (1.5×50 cm) equilibrated with the same buffer. Peptides eluted from the column were detected by absorbance at 280 nm. The copper content of each fraction was estimated by a colorimetric method as described below. The copper-rich fractions were pooled, lyophilized, and further purified by gel filtration on an AcA 202 column (1.5×50 cm) equilibrated with 0.05 *M* ammonium acetate buffer (pH 7.0). The angiogenic activities of the copper-rich fractions eluted from this column were tested.

Apo-ceruloplasmin was subjected to tryptic digestion in the same manner as the native ceruloplasmin. The absorbance profile of the peptides was identical except that copper was not detected in any fraction.

Copper content estimation.—Copper content was determined by the method of Diehl and Smith (*14*) modified to analyze copper concentrations of 0.5–2.5 µg per sample. The sample was digested with 0.1 ml of concentrated H_2SO_4, cooled, and further ashed by the addition of H_2O_2, until the digest (~0.02 ml) was clear and colorless. After cooling, 0.2 ml of 10% hydroxylammonium chloride and 1.5 ml of 5 *M* sodium acetate (pH 7.0) were added and the sample was mixed thoroughly. The orange color of bisbathocuproine was formed by the addition of 0.2 ml of 0.01 *M* bathocuproinedisulfonic acid in water followed by vigorous mixing for about 2 minutes. Absorbance was measured at 479 nm against a cupric sulfate standard in the range of 0.5–2.5 µg per sample.

Protein estimation and molecular weight determination.—Protein was estimated by the method of Lowry et al. (*15*). Molecular weight for the copper-rich peptide was determined by gel filtration chromatography (*16*) on an AcA 202 column in 0.05 *M* ammonium acetate buffer (pH 7.0). RNase a (13,700), cytochrome c (11,500), insulin (6,000), and bacitracin (1,422) were used as molecular weight standards.

Amino acid composition.—The protein samples were hydrolyzed for 22 hours at 110°C in sealed, evacuated tubes containing 400 µl of 5.7 *N* HCl and 1 µl of 1% phenol. Amino acid analyses were done on a Beckman amino acid analyzer (model 121 M) according to the method of Spackman et al. (*17*). The mole percents obtained were corrected for decompositions during acid hydrolysis of threonine (7%), serine (10%), and tyrosine (2%).

Preparation of copper-carrying GHL and heparin.—GHL-copper complexes were obtained by the procedure of Pickart and Thaler (*18*). $CuSO_4$ (0.5 m*M*) and GHL tripeptide (0.5 m*M*) were dissolved together in phosphate-buffered saline at pH 7.4, allowed to stand overnight, and then chromatographed on a Sephadex G-10 column equilibrated in water. GHL-copper complexes elute before GHL and were detected by chromatographic profile and by copper content determination.

Copper was bound to heparin as described by Lages and Stivala (*19*). Heparin (25 mg) and $CuSO_4$ (5 mg) were dissolved in 3 ml of 0.1 *M* Tris-HCl (pH 7.5) buffer, allowed to stand overnight, and chromatographed on a Sephadex G-25 column equilibrated in water. Fractions containing copper-heparin complexes were detected by absorbance at 237 nm or by copper content determination (*14*).

RESULTS

Angiogenesis by Ceruloplasmin

The first group of experiments was designed to assess whether the angiogenic capacity of ceruloplasmin depended on the presence of copper in the molecule. From a commercial source of human ceruloplasmin, three fractions were prepared to contain 6.0, 2.3, and 0.44 copper atoms per molecule, respectively. Text-figure 1A shows the peak of native ceruloplasmin and the fraction (zone A) utilized to test both copper content and angiogenic activity. Text-figure 1B shows the pattern obtained after the native ceruloplasmin was treated with Tris buffer (pH 8). The fractions indicated by zone B were pooled and tested for copper content and angiogenesis. Text-figure 1C illustrates the pattern obtained after DDC treatment of native ceruloplasmin. The fractions indicated by zone C were pooled and tested.

Table 1 reports the copper content and the angiogenic capacity of these fractions. Each sample was lyophilized and incorporated into an Elvax pellet. Each pellet contained the same amount of protein and different amounts of copper. In the first experiment, 10 rabbits received native cerulo-

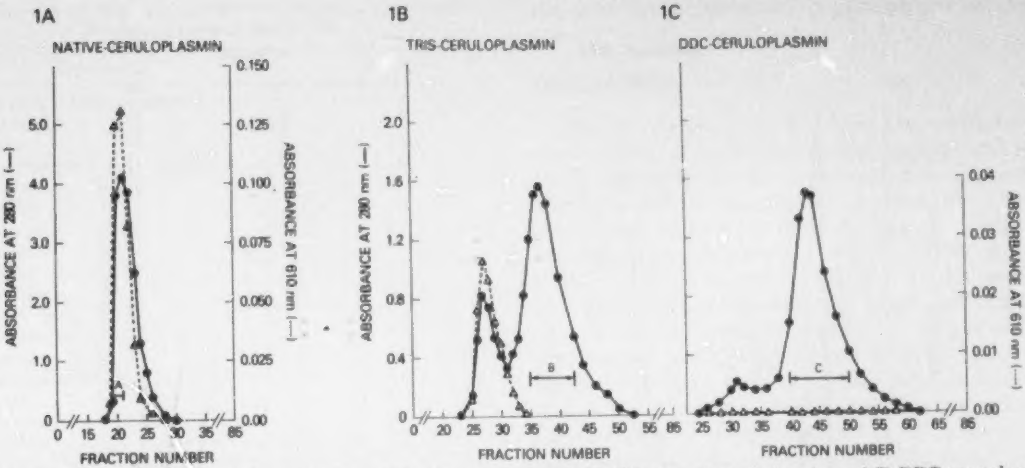

TEXT-FIGURE 1.—DEAE-cellulose column chromatography of A) native ceruloplasmin, B) Tris-treated ceruloplasmin, and C) DDC-treated ceruloplasmin. Ceruloplasmin, native or treated (20-30 mg), was dialyzed against 0.05 *M* sodium acetate buffer (pH 7.2) and loaded on a column equilibrated in the same buffer. The ceruloplasmins, native or treated, did bind to the column. The chromatogram was developed by a linear gradient elution in which the higher salt concentration was 0.4 *M* NaCl in 0.05 *M* sodium acetate (pH 7.2). Marked zones (2.35 ml/tube) were pooled, tested for copper content, lyophilized, and tested for angiogenic activity.

TABLE 1.—*Angiogenic response of ceruloplasmin with various copper contents*

Material tested	Copper/mg protein,[a] µg	Copper atoms/ molecule[b]	Protein/pellet, µg	Copper/pellet, µg	Samples showing positive angiogenic response/total samples
Native ceruloplasmin	2.45	6.0	200	0.5	19/25
Tris-treated ceruloplasmin	0.94	2.3	200	0.2	1/5
Apo-ceruloplasmin	0.18	0.44	200	0.08	0/10
Elvax 40	—	—	—	—	0/10

[a] Copper content was estimated as described in "Materials and Methods." Protein content was determined by the method of Lowry et al. (*15*).

[b] The number of copper atoms per molecule was calculated from the measurement of copper content and by the assumption of a molecular weight of the purified ceruloplasmin to be 132,000.

plasmin in the right cornea and Elvax alone in the opposite cornea. In the second experiment, 10 rabbits were implanted with native ceruloplasmin in one cornea and apo-ceruloplasmin in the contralateral cornea. In the third experiment, 5 rabbits received native ceruloplasmin in one cornea and Tris-ceruloplasmin in the opposite cornea. In table 1 the angiogenic responses to native ceruloplasmin observed with three separate experiments have been added. Table 1 shows that removal of copper from the molecule coincides with the disappearance of the angiogenic capacity.

Angiogenesis by Ceruloplasmin Fractions

In a second group of experiments, we evaluated whether induction of angiogenesis required the whole ceruloplasmin molecule or a smaller "angiogenesis-active site" and, if so, whether the site or sites coincided with molecular fragments rich in copper.

Tryptic digests were prepared from native ceruloplasmin (text-fig. 1A, zone A) and from native ceruloplasmin deprived of copper by DDC treatment (text-fig. 1C, zone C). The digests were fractionated with Sephadex G-50. From the native ceruloplasmin digest, the fractions corresponding to zone 1 of text-figure 2A were the richest in copper. They were pooled, and further concentrations of copper-bearing peptides were obtained in the AcA 202 column. The peptide absorbance pattern of 280 nm comprised a single broad peak with a shoulder; the copper content pattern, however, showed a single sharp peak (text-fig. 2B). The fractions of zone 2 of text-figure 2B, the richest in copper, were pooled, lyophilized, and incorporated into Elvax pellets in the appropriate amounts for testing. The same procedure was followed for the DDC-treated ceruloplasmin.

An aliquot of zone 2 fractions (text-fig. 2B) was taken for the determination of the molecular weight by gel filtration chromatography; a value of 11,000 was estimated (11K fraction).

Angiogenic activity was tested by the implantation in the same rabbit of a pellet containing the 11K fraction from native ceruloplasmin in one cornea and a pellet with the 11K fraction from apo-ceruloplasmin in the contralateral cornea. Each pellet contained 100 µg of protein. For the fraction containing copper, 12 of 15 implants gave positive responses. In contrast, for the fraction devoid of copper, only 3 of 15 implants gave positive responses. The experiment was repeated with each pellet containing 50 µg of protein, and the results were comparable to those of the experiment with the pellet that carried 100 µg protein. Comparison of

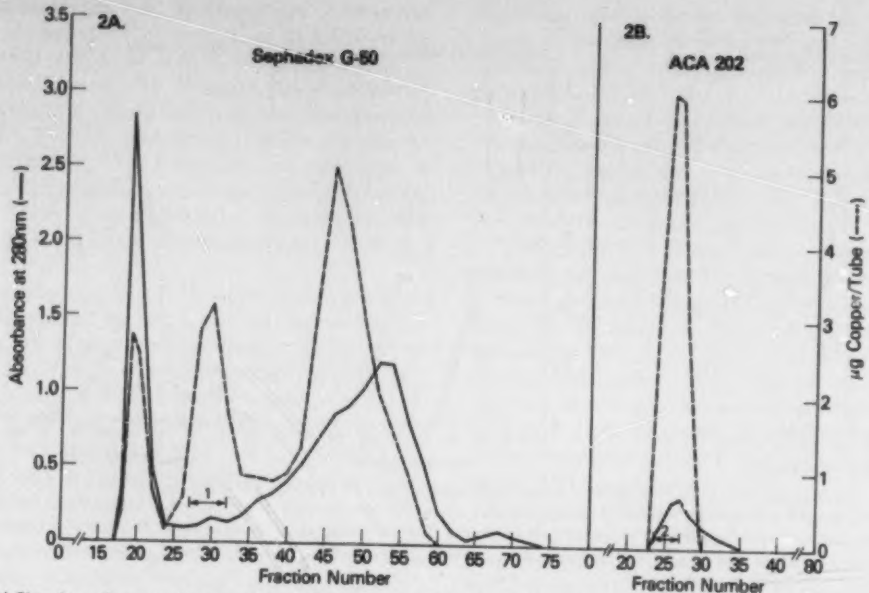

TEXT-FIGURE 2.—A) Gel filtration of tryptic digest products of native ceruloplasmin on a Sephadex G-50 superfine column (1.5×50 cm) equilibrated with 0.05 *M* ammonium acetate buffer (pH 7.0). Flow rate was 10 ml/hr. Fractions (1.5 ml/tube) were collected and monitored by absorption at 280 nm for protein and by reaction with bathocuproinedisulfonic acid for copper determination. Marked zone 1 was pooled and further purified; *see* 2B. B) Gel filtration of zone 1 of 2A on an AcA 202 column (1.5×50 cm) equilibrated with 0.05 *M* ammonium acetate buffer (pH 7.2). Flow rate was 8 ml/hr. Fractions (1.5 ml/tube) were collected and monitored for peptide absorbance and copper determination as described in 2A.

TABLE 2.—*Angiogenic responses to ceruloplasmin fractions*

Material tested	Copper atoms/ molecule[a]	Protein/ pellet, µg	Copper/ pellet,[b] µg	Samples showing positive angiogenic response/total samples
Native ceruloplasmin fraction (11K)	3	100	1.6	12/15
	3	50	0.8	8/10
	3	50	0.8	4/6
	3	30	0.5	9/10
Apo-ceruloplasmin fraction (11K)	0	100	0	3/15
	0	50	0	3/10
Sephadex G-50 fractions 60–65[c]	0	100	0	1/16

[a] The number of copper atoms per molecule was calculated from the copper content of the sample and by the assumption of the molecular weight of the native ceruloplasmin fraction to be 11,000.

[b] The amount of copper released by each pellet was estimated to be ≈1.0 ng/hr. The value was calculated by the preparation of 10 equal pellets and the measurements of the copper content in 5 at the time the remaining 5 were implanted in the corneas. After 7 days, the implanted pellets were removed and the copper content was determined. A reduction of 160±12 ng was found.

[c] The results of two experiments have been added; the contralateral cornea was implanted with 11K fraction of native ceruloplasmin, 50 µg per pellet in the first experiment and 30 µg per pellet in the second experiment.

the 11K fraction from native ceruloplasmin at 50 and 30 µg protein in each pellet with fractions 60–65 of the Sephadex G-50 columns (text-fig. 2A) that were totally deprived of copper again showed that removal of copper from the molecule sharply reduced the angiogenic response. Moreover, the 11K fraction was actively angiogenic at relatively low doses (table 2).

The amino acid composition of the 11K fraction (table 3) was compared with the amino acid sequence of 50,000-M_r and 19,000-M_r fragments of ceruloplasmin, as reported by Dwulet and Putnam (*20*). The high content of acidic amino acids and isoleucine suggested that more than a single peptide constituted the 11K fraction. Indeed, electrophoresis in 7.5% acrylamide gel revealed the presence of three bands indicating that at least three peptides were present within the 11K fraction.

Angiogenesis by Copper Carriers

From the above observations we conjectured that if the angiogenic activity of ceruloplasmin and the 11K ceruloplasmin fraction depended on the presence of copper, other copper carriers could also be angiogenic.

Copper was bound to two quite different molecules—a tripeptide, GHL, and heparin, a sulfated polysaccharide. A dose of 150 µg of heparin in each Elvax pellet was implanted in one cornea and compared with the same dose of heparin bound to copper implanted in the contralateral cornea of the same rabbit. The "control" dose of 150 µg of heparin for each pellet was selected because it was not angiogenic and did not mobilize inflammatory cells during the 6–7 days of the experiment. In a second experiment, the angiogenic activities of smaller doses of heparin bound to copper were evaluated. Pellets with 60 µg heparin and copper were implanted in one cornea and pellets with 30 µg heparin and copper were implanted in the opposite cornea of the same rabbit. The data reported in table 4 indicate that copper

TABLE 3.—*Amino acid composition of 11,000-M_r copper-rich fraction of ceruloplasmin*

Amino acid	Mol %[a]
Aspartic acid or asparagine	13.2
Threonine	6.3
Serine	7.1
Glutamic acid or glutamine	15.9
Proline	4.6
Glycine	7.0
Alanine	6.4
Cysteine	0.4
Valine	3.8
Methionine	0.3
Isoleucine	13.1
Leucine	7.8
Tyrosine	1.3
Phenylalanine	5.6
Lysine	1.7
Histidine	3.9
Arginine	1.8

[a] Averages of three experiments.

TABLE 4.—*Angiogenesis by copper carriers*

Carrier compound	Amount/pellet, μg		Positive angiogenic response/ total samples
	Carrier	Copper[a]	
Heparin	150	0	0/10
	150	2.5	8/10
	60	1.0	8/10
	30	0.5	1/10
GHL	200	0	0/10
	200	3.7	10/14[b]
$CuCl_2$		10.0	8/10
		5.0	2/6
		1.0	0/7
		0.5	0/8

[a] The amount of copper released by each pellet was estimated to be ≈2.0 ng/hr. The computation was done as explained in footnote *b*, table 2.

[b] Results from two experiments were added, the first with 7/10 positive implants and the second with 3/4 positive implants. In the second experiment 1.0 μg $CuCl_2$/pellet was implanted in the contralateral cornea.

attached to heparin transforms the molecule into an effective "angiogenic factor."

The same type of experiment was repeated for the tripeptide GHL. A dose of 200 μg of tripeptide was not sufficient to mobilize inflammatory cells and was not angiogenic. In 10 rabbits, 200 μg GHL bound to copper was implanted in one cornea and the same amount without copper was implanted in the contralateral cornea. The copper-carrying peptide was strongly angiogenic in 7 of 10 implants, whereas none of the 10 implants of the copper-free peptide was angiogenic (table 4).

The angiogenic capacity of copper chloride was also tested. Pellets that contained more than 10 μg of copper chloride elicited rapid migration of inflammatory cells. Pellets with 10 μg of copper chloride at each dose were angiogenic but often mobilized leukocytes. Doses of 5 μg or less were not inflammatory and were only slightly angiogenic. We found it difficult to induce angiogenesis with copper chloride without mobilizing inflammatory cells. We reached the same conclusion when we used copper sulfate (data not shown).

DISCUSSION

The experiments reported here were stimulated by two observations: *a*) In rabbits, during angiogenesis induced by PGE_1, copper ions were concentrated in the cornea immediately before the capillaries invaded the tissue, and *b*) rabbits kept on a copper-deficient diet were unable to mount an angiogenic response to neoplastic cells or to doses of PGE_1 that were strongly angiogenic in the intact host (*1*). Since ceruloplasmin is the natural copper carrier in blood (*21*), it seemed logical to evaluate the roles of ceruloplasmin and copper in the angiogenesis process. The experiments showed that *a*) ceruloplasmin was angiogenic in the rabbit cornea assay provided that copper ions remained bound to the molecule, *b*) small fragments of the ceruloplasmin molecule were still able to induce angiogenesis if they carried copper, *c*) heparin and GHL acquired angiogenic activities when bound to copper, and *d*) copper chloride as well as copper sulfate were angiogenic only at doses that usually induced an inflammatory reaction.

The compound to be tested was incorporated within an Elvax pellet to obtain slow release (*11*), and the initial dose was always chosen so that it would produce a transparent cornea at 48 hours after the pellet implant.

Inflammatory cells are powerful inducers of angiogenesis (*22, 23*); therefore, in experiments that utilize the corneal test, one has to make sure that the response obtained is not due to an inflammatory reaction. The formation of the corneal pocket always induces edema and the mobilization of a few leukocytes, despite sterile conditions. Within 48 hours, however, both the edema and leukocytes disappear and the cornea becomes transparent when observed with the slit lamp microscope. By day 4 or 5, the capillary buds penetrate the cornea and a vascular network is formed. If at this time any leukocytes are found on a histologic section, one cannot be sure whether they are the effectors of angiogenesis or have just escaped from the newly formed capillaries that are notoriously leaky at the time of canalization. To avoid these uncertainties, we always compared the molecules carrying copper with the analogues without copper in the same animal. Under these conditions the mobilization of some leukocytes is equal in both corneas at the time of implant, but at day 6 one cornea shows a positive response, whereas the other cornea of the same rabbit exhibits a negative angiogenesis response. This observation indicates that the few leukocytes mobilized by the initial surgery are not determinant effectors of the angiogenesis process.

The data presented are interpreted to indicate that copper ions are involved in the sequence of events that induces angiogenesis. The role of copper carriers, however, remains obscure. It seems clear that molecules of different nature can act as carriers; however, native ceruloplasmin and 11K fractions were angiogenic at a dose containing copper in amounts smaller than those bound by heparin and GHL. Moreover, copper in the form of chloride or sulfate salt induced angiogenesis only at elevated concentrations and in most cases with mobilization of inflammatory cells. Copper (*24*) and heparin (*25*) have also been shown to enhance the motility of the endothelium. In vitro observations on the chemokinetic and chemotactic effects of copper carriers on capillary endothelium will be reported in a forthcoming paper.

REFERENCES

(1) Ziche M, Jones J, Gullino PM. Role of prostaglandin E_1 and copper in angiogenesis. JNCI 1982; 69:475-482.

(2) Linder MC, Bryant RR, Lim S, Scott LE, Moor JE. Ceruloplasmin elevation and synthesis in rats with transplantable tumors. Enzyme 1979; 24:85-95.

(3) Volm M, Wayss K, Wesch H, Zimmerer J. Korrelation zwischen der Kupfer-und Caeruloplasminkonzentration im Plasma und dem ^{3}H-Thymidin-Einbau des Walker-Karzinosarkoms. Arch Geschwulstforsh 1972; 40:248-258.

(4) Ungar-Waron H, Gluckman A, Spira E, Waron M, Trainin Z. Ceruloplasmin as a marker of neoplastic activity in rabbits bearing the VX-2 carcinoma. Cancer Res 1978; 38:1296-1299.

(5) Goodwin JS, Husby G, Williams RC Jr. Prostaglandin E and cancer growth. Cancer Immunol Immunother 1980; 8:3-7.

(6) Leaper DJ, French BT, Bennett A. Breast cancer and prostaglandins: A new approach to treatment. Br J Surg 1979; 66:683-686.

(7) Lynch NR, Castes M, Astoin M, Salomon JC. Mechanism of inhibition of tumour growth by aspirin and indomethacin. Br J Cancer 1978; 38:503-512.

(8) Voelkel EF, Levine L, Alper CA, Tashjian AH Jr. Acute phase reactants ceruloplasmin and haptoglobin and their relationship to plasma prostaglandins in rabbits bearing the VX_2 carcinoma. J Exp Med 1978; 147:1078-1088.

(9) Gimbrone MA Jr, Cotran RS, Leapman SB, Folkman J. Tumor growth and neovascularization: An experimental model using the rabbit cornea. J Natl Cancer Inst 1974; 52:413-427.

(10) Gullino PM. Angiogenesis factor(s). In: Baserga R, ed. Tissue growth factors. Handbook of experimental pharmacology. Vol 57. New York: Springer-Verlag, 1981:427-449.

(11) Langer R, Folkman J. Polymers for the sustained release of proteins and other macromolecules. Nature 1976; 263:797-800.

(12) Kasper CB, Deutsch HF. Physicochemical studies of human ceruloplasmin. J Biol Chem 1963; 238:2325-2337.

(13) Morell AG, Scheinberg HI. Preparation of an apoprotein from ceruloplasmin by reversible dissociation of copper. Science 1958; 127:588-590.

(14) Diehl HD, Smith FG. In: Schilt AA, McBride L, eds. The copper reagents: Cuproine, neocuproine, bathocuproine. 2d ed. Columbus, Ohio: G. Frederick Smith Chemical Co., 1972:26-35.

(15) Lowry OH, Rosebrough NJ, Farr AL, Randall RJ. Protein measurement with the Folin phenol reagent. J Biol Chem 1951; 193:265-275.

(16) Whitaker JR. Determination of molecular weights of proteins by gel filtration on Sephadex. Anal Chem 1963; 35:1950-1953.

(17) Spackman DH, Stein WH, Moore S. Automatic recording apparatus for use in the chromatography of amino acids. Anal Chem 1958; 30:1190-1206.

(18) Pickart L, Thaler MM. Growth-modulating tripeptide (glycylhistidyllysine) association with copper and iron in plasma, and stimulating adhesiveness and growth of hepatoma cells in culture by tripeptide-metal ion complexes. J Cell Physiol 1980; 102:129-139.

(19) Lages B, Stivala SS. Interaction of the polyelectrolyte heparin with copper (II) and calcium. Biopolymers 1973; 12:127-143.

(20) Dwulet FE, Putnam FW. Internal duplication and evolution of human ceruloplasmin. Proc Natl Acad Sci USA 1981; 78:2805-2809.

(21) Frieden E. Caeruloplasmin: A multi-functional metalloprotein of vertebrate plasma. In: Evered D, Lawrenson G, eds. Biological roles of copper. New York: Excerpta Medica, 1980:93-113.

(22) Pliskin ME, Ginsberg SM, Carp N. Induction of neovascularization by mitogen-activated spleen cells and their supernatants. Transplantation 1980; 29:255-258.

(23) Polverini PJ, Cotran RS, Gimbrone MA Jr, Unanue EF. Activated macrophages induce vascular proliferation. Nature 1977; 269:804-806.

(24) McAuslan BR. A new theory of neovascularization based on identification of an angiogenic factor and its effects on cultured endothelial cells. In: Jemenez de Asua L, Levi-Montalcini R, Shields R, et al., eds. Control mechanisms in animal cells. New York: Raven Press, 1980:285-292.

(25) Azizkhan RG, Azizkhan JC, Zetter BR, Folkman J. Mast cell heparin stimulates migration of capillary endothelial cells in vitro. J Exp Med 1980; 152:931-944.

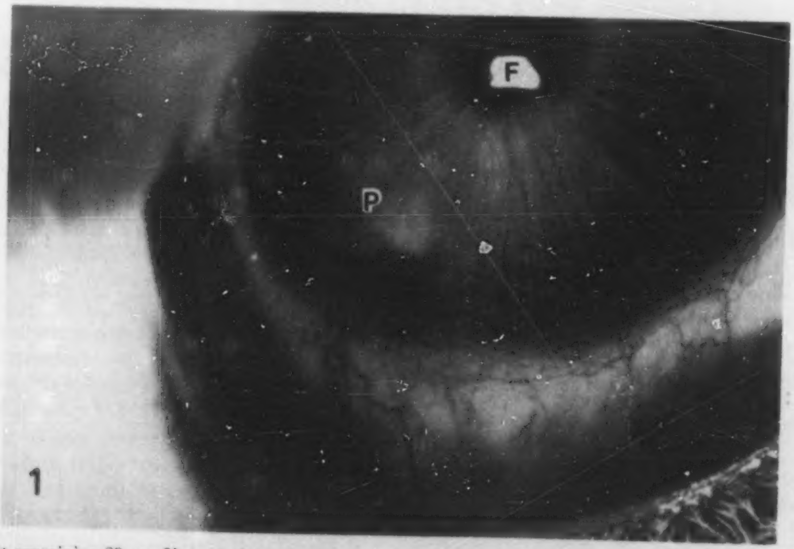

Figure 1.—An Elvax 40 pellet containing 60 μg of heparin bound to copper (1 μg) had been implanted in the rabbit cornea 6 days before the photograph was taken. *Note* the brush of capillaries progressing from the limbus toward the pellet (P). In the *background* the iris vessels, visible through the transparent cornea, have a radial orientation. F=filament of the stereomicroscope lamp. × 6

Isolation of Tumoricidal Macrophages From Lung Melanoma Metastases of Mice Treated Systemically With Liposomes Containing a Lipophilic Derivative of Muramyl Dipeptide[1,2,3,4]

M. E. Key,[5] J. E. Talmadge,[5] W. E. Fogler,[5] C. Bucana,[6] *and* I. J. Fidler[5]

ABSTRACT—The systemic administration of multilamellar liposomes—composed of phosphatidylcholine and phosphatidylserine (7:3 mol ratio), containing the immunomodulator, muramyl tripeptide phosphatidylethanolamine (MTP-PE)—into C57BL/6N mice bearing the syngeneic B16-BL6 melanoma was associated with the eradication of spontaneous lung and lymph node metastases. Immunofluorescence and electron microscopic analyses revealed that 24 hours after the tumor-bearing mice were given iv injections of liposomes, 15% of the alveolar macrophages and 5% of the metastasis-associated macrophages contained phagocytosed liposomes. However, only macrophages isolated from lungs or metastases of mice given injections of liposomes containing MTP-PE (treatment success), but not macrophages from mice treated with empty liposomes (treatment failure), were tumoricidal against the target cells in vitro. These data provide direct evidence that the regression of established metastases, after treatment of tumor-bearing mice with liposomes containing MTP-PE, was associated with tumoricidal macrophages residing within the metastases.—JNCI 1982; 69:1189–1198.

Normal noncytotoxic macrophages can be rendered tumoricidal in vitro or in vivo after interaction with various biological agents such as lymphokines (*1*, *2*), whole microorganisms, or their products (*3*, *4*). MDP, a microbial product initially isolated from *Mycobacterium* and subsequently synthesized, can activate macrophages to the tumoricidal state (*5*). Recent studies in our laboratory have shown that free MDP or MDP entrapped within liposomes activates macrophages to the tumoricidal state both in vitro (*6*) and in vivo (*7*). Furthermore, the repeated injection of liposome-entrapped MDP into tumor-bearing mice resulted in destruction of spontaneous lung and lymph node metastases (*8*). Subsequent studies have provided circumstantial evidence that macrophage activation and regression of metastases are related; e.g., we have shown that when macrophages activated in vitro with liposome-entrapped MDP were adoptively transferred into mice bearing metastases, the growth of the metastases was significantly inhibited. However, pretreatment of mice bearing metastases with macrophage toxins abrogated the therapeutic effectiveness of the treatment with liposome-entrapped MDP (*9*).

Although these data strongly suggested that activated macrophages were involved in the destruction of metastases in this tumor system, their precise role remained unclear. In this report, we provide direct evidence that tumoricidal macrophages are the effector cells responsible for the destruction of established metastases in mice treated systemically with liposome-entrapped MDP. We base this conclusion on morphological and functional analysis of macrophages isolated from pulmonary metastases of mice given iv injections of liposomes containing an MDP derivative, MTP-PE. Specifically, we show that in these mice macrophages containing phagocytosed liposomes infiltrate and localize within pulmonary metastases. Furthermore, once localized, macrophages that have engulfed liposomes containing MTP-PE (treatment success), but not macrophages that have engulfed liposomes containing a placebo (treatment failure), retain their tumoricidal activity against the metastatic tumor cells.

MATERIALS AND METHODS

Animals.—Specific-pathogen-free C57BL/6N mice were obtained from the NCI-Frederick Cancer Research Facility's Animal Production Area. Mice used in each experiment were matched by age (6–8 wk) and sex.

Tumor culture.—B16-BL6, a tumor variant obtained by in vitro selection for invasion (*10*), originated from the spontaneous malignant B16 melanoma, which is syngeneic to the C57BL/6N mouse. The B16-BL6 tumor cells were grown as monolayer cultures and were maintained in Eagle's minimum essential medium supplemented with 5% fetal bovine serum, vitamin solution, sodium pyruvate, L-glutamine, and other nonessential amino acids. The components of this medium were obtained from Flow Laboratories, Inc., Rockville, Md. The medium was endotoxin-free as determined by the *Limulus* amoebocyte lysate assay (Associates of Cape Cod, Woods Hole, Mass.). Cultures were incubated at 37°C in a humidified atmosphere containing 5% CO_2. All cell

---

ABBREVIATIONS USED: HBSS = Hanks' balanced salt solution; $[^{125}I]$IdUrd = 5-iodo-2′-deoxyuridine; MDP = *N*-acetylmuramyl-L-alanyl-D-isoglutamine (muramyl dipeptide); MTP-PE = *N*-acetylmuramyl-L-alanyl-D-isoglutaminyl-L-alanyl-2-(1′,2′-dipalmitoyl-*sn*-glycero-3′-phosphoryl) ethylamide (muramyl tripeptide phosphatidylethanolamine); NBD-PE = *N*-4-nitro-benzo-2-oxa-1,3-diazole phosphatidylethanolamine; PC = phosphatidylcholine; PMN = polymorphonuclear leukocyte(s); PS = phosphatidylserine; SRBC = sheep red blood cells.

---

[1] Received March 30, 1982; accepted June 22, 1982.

[2] Supported by Public Health Service contract N01-CO-75380 from the Office of the Director, National Cancer Institute, with Litton Bionetics, Inc.

[3] Animals were maintained under the guidelines set forth by the National Institutes of Health Policy in Humane Care and Use of Animals and by the Animal Welfare Act in facilities accredited by the American Association for Accreditation of Laboratory Animal Care.

[4] The contents of this report do not necessarily reflect the views or policies of the U.S. Department of Health and Human Services, nor does mention of trade names, commercial products, or organizations imply endorsement by the U.S. Government.

[5] Cancer Metastasis and Treatment Laboratory, NCI-Frederick Cancer Research Facility, P.O. Box B, Frederick, Md. 21701.

[6] Cancer Biology Program, NCI-Frederick Cancer Research Facility.

cultures were free of mycoplasma, reovirus type 3, pneumonia virus of mice, K-virus, Theiler's encephalitis virus, lymphocytic choriomeningitis virus, ectromelia virus, and lactate dehydrogenase virus (assayed by M.A. Bioproducts, Walkersville, Md.).

Metastasis system.—The pulmonary tumor colonies (experimental metastases) used in this study were obtained from syngeneic mice that had been given 1×10^5 tumor cells iv into a lateral tail vein. Cells to be injected were harvested by trypsinization from cultures at mid-log phase, and single cell suspensions of >95% viability were resuspended in Ca^{2+}- and Mg^{2+}-free HBSS. Within 4 weeks of injection, all inoculated mice had macroscopic and/or microscopic pulmonary metastases.

Mice bearing established spontaneous pulmonary and lymph node metastases were used in therapy studies. To initiate spontaneous metastases, we gave an injection of 2.5×10^4 viable tumor cells, suspended in 0.05 ml HBSS, into one hind footpad of each mouse. When the local tumors had reached 10–12 mm in diameter, the tumor-bearing legs, including the popliteal lymph node, were amputated at midfemur. This experimental protocol results in metastases in the lungs and lymph nodes of approximately 90% of the mice (*10*).

Reagents.—Synthetic hydrophilic MDP and a lipophilic derivative, MTP-PE, were the generous gifts of Ciba-Geigy Ltd. (Basel, Switzerland). Neither the MDP nor MTP-PE contained endotoxins as detected by the *Limulus* amoebocyte lysate assay. Chromatographically pure egg PC and beef brain PS were purchased from Avanti Polar Lipids, Inc. (Birmingham, Ala.).

Preparation of liposomes.—Multilamellar lipid vesicles (liposomes) were prepared from a mixture of PC and PS (7:3 mol ratio) and were formed as previously described (*11*). Liposomes containing MTP-PE were prepared by the combining of 5 µg MTP-PE/1 µmol lipid, as described elsewhere (*12*). Fluorescent liposomes were prepared by incorporation of 0.1% of the fluorescent lipid NBD-PE into the liposomes, as described in (*12*). PC-PS liposomes were used because they are not toxic at the doses used in this study and because, when they are injected iv, they are arrested efficiently in the lungs (and in other organs of the reticuloendothelial system) (*13*).

In situ activation of metastasis-associated macrophages.—Mice bearing experimentally induced metastases ranging in size up to 4 mm in diameter (≈4 wk after injection of tumor cells) were given injections on 3 consecutive days of liposomes (2.5 µmol lipid), containing a total of 10 µg MTP-PE, or injections of liposomes containing HBSS and suspended in 10 µg MDP (placebo preparation). Fluorescent liposomes were used in the final injection. Mice were killed 24 hours after the last injection, and the lung metastases were recovered. Single cell suspensions prepared from these tissues by enzymatic dissociation were analyzed by means of fluorescence and electron microscopy.

Treatment of spontaneous metastases by iv injection of liposomes containing MTP-PE.—Three days after surgical removal of the primary footpad tumor, mice bearing spontaneous lung and lymph node metastases were given iv injections of liposomes (2.5 µmol phospholipid) suspended in 0.2 ml HBSS. The liposomes contained either MTP-PE (10 µg/mouse) or HBSS. Liposomes containing HBSS were then resuspended in HBSS containing free MDP (10 µg/mouse). An additional control group included mice that received iv injections of HBSS only. The animals were treated twice a week for 4 weeks and were monitored daily for 180 days. Dead or moribund animals were necropsied to ascertain the presence or absence of secondary tumors. Animals surviving at least 100 days after the last liposome treatment were considered to be disease-free (*14*).

Determination of macrophage content.—Experimentally induced pulmonary metastases, ranging in size up to 4 mm in diameter, were removed en bloc and dissected free of nontumorous tissue. Normal lung parenchyma or tumor fragments of approximately 1 mm^3 were digested with continuous stirring in trypsinization flasks at 37°C, as previously described (*15*). Three 30-minute digestion cycles produced 95–100% digestion of the tumor fragments and 65–85% digestion of the lung fragments to single cell suspensions. The digestion medium consisted of HBSS containing 0.14% collagenase type I and 0.10% deoxyribonuclease type I (Sigma Chemical Co., St. Louis, Mo.). The suspension of single cells was adjusted to contain $1–5\times10^6$ cells/ml serum-free medium. India ink (0.10 ml; 1:40 dilution) was added to the cells. This mixture was placed in a 5-ml polystyrene tube and incubated for 2 hours at 37°C. The cells were then washed twice with serum-free medium and adjusted to 5×10^5 cells/ml in medium containing 10% fetal bovine serum. Cytocentrifuge preparations of all cell suspensions were fixed, stained with Giemsa, and prepared for light microscopy. The percentage of macrophages present in the preparations was determined by identifying the cells morphologically and by observing the phagocytosis of carbon particles. A minimum of 200 cells/slide were examined to determine the percentage of macrophages.

To determine the macrophage content of the dissociated tissues when examined by fluorescence microscopy, we used the method of Korn et al. (*16*) for detecting Fc-receptor-positive cells. SRBC were sensitized with a subagglutinating dilution of murine anti-SRBC antisera. A sensitizing dilution was chosen that allowed most macrophages and monocytes, but not lymphocytes or granulocytes, to bind with the sensitized SRBC. Sensitized SRBC were incubated for 5 minutes on ice with the single cell suspensions from the tissue digests at a ratio of 30 SRBC:1 nucleated cell. After centrifugation the pellet was gently resuspended, and the cells were prepared for fluorescence microscopy. To test the validity of this technique, cytocentrifuge preparations of some of the cell suspensions were stained with Giemsa and examined by light microscopy.

Macrophage-mediated cytotoxicity assay.—Macrophages were isolated from the single cell suspensions by allowing them to adhere to plastic. Two methods of isolating macrophages were used: 1) Tumor or lung digests were seeded into MicroTest II wells (Falcon Plastics, Oxnard, Calif.) and allowed to adhere for 5 minutes. The wells were rinsed, and the process was repeated until the desired density of adhering cells was obtained, as determined by cell counts in an inverted microscope. 2) The adherent cells were removed from a plastic petri dish by means of a rubber policeman.

The recovered cells were counted and replated at the desired density into MicroTest wells. Because viability of the recovered cells was about 60%, plating was based on viable cell counts only. In both procedures, we estimated that macrophages composed about 80% of the cell population, as determined by their ability to form rosettes with sensitized SRBC. Most of the contaminating cells appeared to be tumor cells. We did not observe any differences in the ability to adhere to plastic among the macrophages obtained from the various treatment groups.

Macrophage-mediated cytotoxicity was assessed by a radioactive release assay, as described previously (*17*). Macrophage monolayers were washed with medium, and 5×10^3 [^{125}I]IdUrd-labeled B16-BL6 target cells were added to each well in 0.2 ml medium. Target cells alone were always plated as an additional control. The cultures were washed 24 hours after the addition of target cells and then were refed to remove nonplated cells. Adherent target cells were lysed with 0.1 ml of 0.2 *N* NaOH at 72 hours after plating. The lysate was absorbed on cotton swabs and monitored for radioactivity in a γ-counter. The percentage of specific cytotoxicity in the macrophage assays was computed by the following formula: [(cpm target cells with control macrophages − cpm targets cells with activated macrophages)/cpm target cells with control macrophages]×100. The statistical significance of differences between groups was determined by Student's two-tailed *t*-test.

Analysis with fluorescence microscopy.—Cell suspensions were examined on a hemacytometer with the use of a Zeiss fluorescence microscope (Carl Zeiss, Inc., New York, N.Y.). The number of cells containing fluorescent material was scored in each section of the hemacytometer, and by means of light microscopy the total cell count was estimated by counting all cells contained within a single section. In this way we were able to rapidly evaluate several thousand cells per tissue digest.

Analysis with electron microscopy.—The dissociated cells were centrifuged, and the cell pellet was fixed with 3% glutaraldehyde and 2% paraformaldehyde in 0.1 *M* cacodylate buffer at pH 7.4 for 1 hour. The cells were then rinsed in buffer, fixed for 20 minutes with 1% tannic acid in 2% glutaraldehyde, rinsed in buffer, and fixed for 1 hour with 1% buffered OsO_4. After a brief rinse in distilled water, the cells were stained with 1% aqueous uranyl acetate for 30 minutes and then rinsed again with distilled water. The samples were dehydrated in a graded series of ethanol and embedded in Spurr's low-viscosity medium. Thin sections were cut with a glass knife in a LKB Ultratome III, (LKB Instruments, Inc., Rockville, Md.), counter stained with Reynold's lead citrate, and examined in a Hitachi HU-12A electron microscope (Hitachi Scientific Instruments, Tokyo, Japan) at an accelerating voltage of 75 kV.

RESULTS

Treatment of spontaneous metastases by systemic administration of liposome-entrapped MTP-PE.—The repeated administration of liposomes (PC:PS, 7:3 mol ratio) containing MTP-PE was associated with the regression of established pulmonary and lymph node metastases. Nearly all mice treated with HBSS or with liposomes containing HBSS and suspended in free MDP had died by day 90 (table 1). In contrast, 70% of mice given iv injections of liposomes containing MTP-PE survived for more than 100 days after the last iv treatment. This period exceeds the time (40–50 days) necessary for as few as 10 surviving tumor cells to kill their host (*14*). These mice were killed on day 180 of the experiment and found to be disease-free.

Macrophage content of lung tissue and lung metastases.—The content of macrophages in lung parenchyma (nontumorous) and in pulmonary metastases from untreated or liposome-treated mice was determined from single cell preparations of the dissociated tissues. Tissues from both tumor-bearing and tumor-free mice were analyzed. Treatment with liposomes containing MTP-PE or liposomes containing HBSS and suspended in MDP was given once daily for 3 days prior to determination of macrophage content. As shown in table 2, the percentage of macrophages infiltrating into lung metastases of the B16-BL6 melanoma ranged from 11 to 13% and was independent of treatment with either type of

TABLE 1.—*Eradication of spontaneous metastases by the systemic administration of liposomes containing MTP-PE*

Treatment group[a]	Mice, %, surviving by day:[b]					
	30	60	90	120	150	180
HBSS injections	100	90	35	10	10	10
Liposome–HBSS	100	70	15	10	10	10
Liposome–MTP-PE	100	85	70	70	70	70

[a] Viable B16-BL6 cells (25,000) were implanted in the footpads of syngeneic C57BL/6 mice (20 mice/group). Tumors (10–12 mm in diameter) were amputated 4 wk later. Liposome therapy commenced 3 days after surgery and consisted of iv injections of 2.5 μmol liposomes/mouse twice weekly for 4 wk. Liposomes either contained HBSS and were suspended in 10 μg MDP (liposome–HBSS) or contained 10 μg MTP-PE (liposome–MTP-PE).

[b] Differences in median life-span were highly significant ($P < 0.001$, chi-square test).

TABLE 2.—*Macrophage content of nontumorous lung tissues and lung melanoma metastases*

Treatment group[a]	Macrophages, %, in:[b,c]	
	Melanoma metastases	Nontumorous lung tissue
Controls		
None		21
Liposome–HBSS		29
Liposome–MTP-PE		25
Tumor-bearing mice		
None	11	22
Liposome–HBSS	11	31
Liposome–MTP-PE	13	33

[a] Mice received iv injections of 1×10^5 B16-BL6 tumor cells 4 wk before assay. Control and tumor-bearing mice were treated daily for 3 consecutive days with 2.5 μmol liposomes containing HBSS and suspended in 10 μg MDP (liposome–HBSS) or with liposomes containing 10 μg MTP-PE (liposome–MTP-PE). Macrophages were harvested 24 hr after the third treatment.

[b] Macrophages in single cell suspensions of lung or tumor tissue were identified by phagocytosis of india ink.

[c] Pulmonary metastases or nontumorous lung tissue were harvested and pooled; 3 mice/group.

liposome preparation. The content of lung macrophages in mice bearing metastases increased slightly after treatment with liposomes (31 and 33% vs. 22%). This increase was less apparent in the lungs of liposome-treated, tumor-free mice (29 and 25% vs. 21%). We concluded that treatment of mice with either liposome preparation had little effect on the macrophage content of pulmonary metastases.

Characterization of macrophages containing liposomes.—After we ascertained that 11–13% of the cells in pulmonary metastases of the B16-BL6 melanoma were actually infiltrating macrophages, we determined whether cells of the macrophage type that had engulfed liposomes within the lung microvasculature (*18*) could infiltrate and localize within pulmonary metastases. Liposomes containing NBD-PE (fluorescent lipid) were injected iv into mice, and 24 hours later lungs and pulmonary tumor colonies were removed, dissociated, and prepared for macrophage analysis. To identify the macrophages, we used a technique based on the ability of these cells to form rosettes with sensitized SRBC (*16*). The validity of this procedure was first analyzed by light microscopy in cell preparations stained with Giemsa.

Under the conditions used, most of the macrophages from both tumor tissue and nontumorous lung tissue (92 and 69%, respectively) formed rosettes with sensitized SRBC, whereas only 5% of PMN and 2% of lymphocytes from lungs formed rosettes. Tumor-infiltrating PMN and lymphocytes, which comprised less than 5% of the total cell population, were not observed forming rosettes with sensitized SRBC. Examination of cell suspensions by fluorescence microscopy revealed that all cells exhibiting fluorescent liposomes also formed rosettes with sensitized SRBC. Thus liposome-containing cells recovered from either nontumorous lung tissue or pulmonary metastases were identified as Fc-receptor-positive cells with a macrophage-like morphology. A typical example of cells isolated from a progressing lung metastasis of the B16-BL6 melanoma is shown in figure 1. Fluorescence microscopy revealed that one of the cells exhibited numerous fluorescent bodies; light microscopy revealed that this same cell formed a rosette with sensitized SRBC, thus identifying it as a macrophage. PMN are another type of phagocytic cell that could infiltrate into tumors; however, we did not observe PMN containing liposomes in tissue samples prepared 24 hours after liposomes were administered systemically (fig. 2).

We verified by electron microscopy that the liposome-containing cells residing within metastases were in fact macrophages. Liposomes within cells were readily identified at the ultrastructural level by their characteristic multilamellar configuration (*19*). In some experiments ferritin encapsulated within liposomes was used as a marker for the identification of internalized liposomes. Macrophages seen in dissociated tumor preparations varied in their internal structure. Most macrophages contained membrane-bound aggregates of melanin, large vacuoles with remnants of melanin granules, or lysosomes associated with aggregates of melanin. These macrophages often had an eccentric nucleus and prominent cytoplasmic processes or vellum (fig. 3). A second type of macrophage had the normal complement of cytoplasmic organelles as well as prominent cytoplasmic processes (fig. 4) but no internalized melanin granules. Both types of macrophages, however, contained intracytoplasmic liposomes. The multilamellar structure of the internalized liposomes is clearly visible in figures 3 and 4. In the macrophage shown in figure 3, the liposomes appear to be contained within a single phagosome, whereas the macrophage shown in figure 4 contains liposomes within individual phagocytic vacuoles.

Quantitation of macrophages containing liposomes.—Twenty-four hours after mice were given injections of fluorescent liposomes, the animals' lungs and pulmonary tumor metastases were removed and analyzed for the presence of macrophages containing fluorescent material (table 3). Only macrophages obtained from mice that had been treated with fluorescent liposomes displayed fluorescent material, suggesting that the fluorescent staining was not caused by autofluorescent artifacts. Only minor differences in the percentage of macrophages containing liposomes were observed between mice that received iv injections of liposomes containing MTP-PE and mice that received iv injections of liposomes containing HBSS. This suggested that the uptake of liposomes by macrophages in situ is independent of the MTP-PE component. The percentage of liposome-containing cells within tumors was relatively low compared to the total cell population. However, when these numbers were

TABLE 3.—*Localization of macrophages containing liposomes in nontumorous lung tissue and lung metastases*

Treatment group[a]	No. (%) of fluorescent cells/total No. of cells in:		Fluorescent macrophages, %, in:[b]	
	Lung metastases	Nontumorous lung tissue	Lung metastases	Nontumorous lung tissue
Controls				
None		0		0
Liposome–HBSS		22/500 (4.4)		15.2
Liposome–MTP-PE		15/500 (3.0)		12.0
Mice with metastases				
None	0	0	0	0
Liposome–HBSS	17/3,200 (0.53)	18/500 (3.6)	4.8	11.6
Liposome–MTP-PE	38/6,000 (0.63)	23/500 (4.6)	4.8	13.9

[a] Mice received iv injections of 1×10^5 B16-BL6 cells 4 wk before assay. All mice were treated daily for 3 consecutive days with 2.5 μmol liposomes containing HBSS and suspended in 10 μg MDP (liposome–HBSS) or with liposomes containing 10 μg MTP-PE (liposome–MTP-PE). Final injection was with fluorescent liposomes 24 hr before assay. Pulmonary metastases or nontumorous lung tissues were pooled and enzymatically dissociated to obtain single cell suspensions; 3 mice/group.

[b] Per total No. of macrophages isolated from samples. Duplicate assays showed that all fluorescent cells also formed rosettes when exposed to sensitized SRBC.

TABLE 4.—*Tumoricidal properties of macrophages isolated from nontumorous lung tissue or lung metastases after iv injection of liposomes*

Treatment group[a]	Radioactivity (cpm) in viable tumor cells 72 hr after incubation with macrophages isolated from:[b]			
	Nontumorous lung tissue		Lung metastases	
	Technique 1	Technique 2	Technique 1	Technique 2
None; tumor cells alone	4,933±69		4,933±69	
Tumor-free mice				
Liposome–HBSS	4,619±36	4,725±21		
Liposome–MTP-PE	1,998±60 (57)	2,121±36 (55)		
Tumor-bearing mice				
Liposome–HBSS	4,774±46	4,802±58	4,699±35	4,882±63
Liposome–MTP-PE	2,390±37 (50)	2,117±60 (56)	3,203±16 (32)	2,924±40 (40)

[a] Mice received iv injections of 1×10^5 B16-BL6 cells 4 wk before assay. Mice were treated daily for 3 consecutive days with 2.5 µmol liposomes containing HBSS and suspended in 10 µg MDP (liposome–HBSS) or liposomes containing 10 µg MTP-PE (liposome–MTP-PE).

[b] 1×10^4 B16-BL6 tumor cells prelabeled with [^{125}I]IdUrd were plated onto macrophage monolayers (*see* "Material and Methods"). Cultures were refed 24 hr after tumor cells were added and then incubated for an additional 48 hr. Data are expressed as mean cpm ± SD from triplicate cultures. Pulmonary metastases or nontumorous lung tissues were pooled and enzymatically dissociated to obtain single cell suspensions; 3 mice/group. *Numbers in parentheses* show percent cytotoxicity as compared to control macrophages ($P<0.01$, Student's *t*-test).

converted to reflect the percentage of fluorescent macrophages (as determined from table 2), we found that approximately 5% of the tumor-associated macrophages were labeled within a 24-hour period. This figure was somewhat higher for lung (alveolar) macrophages and ranged from 11.6 to 15.2% (table 3). Again, the tumor-bearing status or treatment of the host had relatively little effect on the uptake of liposomes by macrophages.

Activation of tumor-associated and alveolar macrophages.—We next wished to determine whether the systemic treatment of mice with liposomes containing MTP-PE would lead to activation of the metastasis-associated macrophages. Macrophages were isolated from the cell suspensions by allowing them to briefly (5 min) adhere to the plastic test wells. Because it was difficult to control accurately the precise number of adhering effector cells, we also used a second technique to isolate macrophages. In this technique, macrophages were first allowed to adhere to plastic petri dishes. The adherent cells were then recovered with a rubber policeman and replated at the desired concentration of viable cells per well. Despite the use of different isolation techniques, both methods yielded similar results. The data in table 4 demonstrate that only macrophages derived from animals given injections of liposomes containing MTP-PE were tumoricidal. Alveolar macrophages from both tumor-bearing and tumor-free mice mediated a similar degree of cytotoxicity (50–57%), which was somewhat greater than the cytotoxicity expressed by tumor-associated macrophages (32–40%). However, the lower levels of cytotoxicity mediated by tumor-associated macrophages may have been due to the lower percentage of macrophages containing liposomes (table 3). Macrophages obtained from either nontumorous lung tissue or lung metastases of mice that were not given iv injections or that received injections of liposomes containing HBSS were not tumoricidal in vitro (table 4).

DISCUSSION

In the present studies we investigated the mechanism by which systemic treatment of tumor-bearing mice with liposomes containing MDP or its derivatives leads to eradication of spontaneous lung and lymph node metastases. Because the iv injection of liposome-entrapped MDP can generate tumoricidal macrophages in vivo (*7*) and macrophages have been implicated in the regression of tumors in several systems (*20–22*), we wanted to determine whether liposome-activated macrophages were the effector cells responsible for the destruction of the metastases in the tumor system used in this study. Twenty-four hours after the iv injection of fluorescent liposomes into tumor-bearing mice, 5% of the macrophages isolated from lung metastases contained liposomes. Recent studies demonstrated that free liposomes do not extravasate through capillaries to reach organ parenchyma but, rather, are first engulfed by fixed and circulating phagocytic cells that later extravasate into organ parenchyma (*18*). Those data suggest that the metastasis-associated, liposome-positive macrophages probably originate from the circulating blood monocyte pool. Furthermore, our data would indicate that during a 24-hour period, the influx of macrophages into lung metastases is at least 5% of the total number of infiltrating macrophages. When one considers the rapidity with which macrophages enter the metastases and the relatively long duration of macrophage activation achieved by this treatment (*8*), it seems likely that well-timed multiple liposome treatments could activate a high proportion of metastasis-associated macrophages to the tumoricidal state.

The presence of tumor-associated macrophages containing liposomes was also confirmed by electron microscopic analysis. Two morphologically distinct types of macrophages were observed. In one type, large accumulations of melanin granules were observed, and the intracytoplasmic liposomes were contained within a single phagocytic vacuole. In the other type, the macrophage did not contain melanin granules, and the liposomes remained in individual phagosomes. Melanin deposits in macrophages suggest that these cells have been in contact with tumor material long enough to have phagocytosed some of the tumor cell products, whereas the absence of intracytoplasmic melanin deposits may characterize a newly arrived blood monocyte. Previous in vitro studies had shown that liposomes engulfed by macrophages eventually are concentrated into a common phagocytic vacuole before their fusion (*19*). Presumably, a similar sequence of events also occurs in vivo.

Multiple iv injections of liposomes containing MTP-PE, but not those containing HBSS, led to eradication of metastases in 70% of mice bearing spontaneous lung and lymph node metastases. Furthermore, metastasis-associated macrophages obtained from mice treated with liposomes containing MTP-PE (treatment success) but not from mice treated with liposomes containing HBSS (treatment failure) were able to express tumoricidal activity in vitro. These findings suggest that there is a direct correlation between the activation of macrophages by liposomes containing immunomodulators and the regression of disseminated tumor. However, the protocol for studying activation of metastasis-associated macrophages was not the same as that for studying regression of metastases (therapy). Macroscopic metastases that can be recovered and dissociated (>1 mm in diameter) are already too large to respond to therapy, whereas microscopic metastases, which will respond to treatment, are too small to allow studies of macrophage content. Therefore, this problem required that we study metastases of different sizes and under different conditions. Despite these differences there is no reason to assume that microscopic metastases are not also infiltrated with activated macrophages. Indeed, histologic studies have shown that pulmonary metastases of the B16-BL6 melanoma are infiltrated with macrophages at the earliest stages at which these lesions can be identified (Key et al.: Unpublished observations).

Further evidence that macrophages play a role in the regression of these metastases is provided by the observations that 1) only liposomes that localize in lungs are able to activate alveolar macrophages and eradicate pulmonary metastases (*9*, *13*), 2) agents toxic to macrophages abrogate the therapeutic effectiveness of this treatment (*9*), and 3) macrophages activated in vitro with MDP are effective in eliminating tumors when adoptively transferred into tumor-bearing hosts (*9*). In the present studies, we found that the iv injection of liposomes into mice bearing pulmonary metastases did not lead to an increase in the number of macrophages infiltrating the tumor nodules. Thus the effectiveness of systemic administration of liposomes containing MTP-PE in eradicating metastases could not be related simply to an increase in the number of macrophages infiltrating metastases. These findings agree with previous reports that the regression of tumors in several systems is influenced not only by the presence of macrophages but also by their cytotoxic potential (*20*, *22*). We consider it most significant that only macrophages from mice given injections of liposomes containing MTP-PE were cytotoxic to tumor cell targets in vitro. Thus the only difference we have been able to detect in the macrophage populations among the different treatment groups was a quantitative increase in the tumoricidal activity of macrophages infiltrating the metastases of the mice that responded to therapy.

In summary, we conclude that systemically administered liposomes (PC:PS, 7:3 mol ratio) containing MTP-PE are phagocytosed by macrophages that subsequently infiltrate lung metastases. These metastasis-associated macrophages can be shown to be tumoricidal in vitro. In contrast, metastasis-associated macrophages isolated from mice given injections of liposome preparations that have no therapeutic benefit are not tumoricidal against the target cells. These data provide direct evidence that the regression of metastases that occurs after multiple iv injections of liposomes containing macrophage activators (*8*, *23*) is mediated by tumoricidal macrophages.

REFERENCES

(*1*) Churchill WH, Jr, Piessens WF, Sulis CA, David JR. Macrophages activated as suspension cultures with lymphocyte mediators devoid of antigen become cytotoxic for tumor cells. J Immunol 1975; 115:781–786.

(*2*) Piessens WF, Churchill WH Jr, David JR. Macrophages activated in vitro with lymphocyte mediators kill neoplastic but not normal cells. J Immunol 1975; 114:293–299.

(*3*) Hibbs JB Jr, Lambert LH Jr, Remington JS. Resistance to murine tumors conferred by chronic infection with intracellular protozoa, *Toxoplasma gondii* and *Besnoitia jellisoni*. J Infect Dis 1971; 124:587–592.

(*4*) Hibbs JB Jr. Discrimination between neoplastic and non-neoplastic cells in vitro by activated macrophages. J Natl Cancer Inst 1974; 53:1487–1492.

(*5*) Chedid L, Carelli L, Audibert F. Recent developments concerning muramyl dipeptide, a synthetic immunoregulating molecule. J Reticuloendothel Soc 1974; 26:631–641.

(*6*) Sone S, Fidler IJ. In vitro activation of tumoricidal properties in rat alveolar macrophages by synthetic muramyl dipeptide encapsulated in liposomes. Cell Immunol 1981; 57:42–50.

(*7*) Fidler IJ. In situ induction of tumoridical activity in alveolar macrophages by liposomes containing muramyl dipeptide is a thymus-independent process. J Immunol 1981; 127:1719–1720.

(*8*) Fidler IJ, Sone S, Fogler WE, Barnes ZL. Eradication of spontaneous metastases and activation of alveolar macrophages by intravenous injection of liposomes containing muramyl dipeptide. Proc Natl Acad Sci USA 1981; 78:1680–1684.

(*9*) Fidler IJ, Barnes ZL, Fogler WE, Kirsh R, Bugelski P, Poste G. Involvement of macrophages in the eradication of established metastases following intravenous injection of liposomes containing macrophage activators. Cancer Res 1982; 42:496–501.

(*10*) Hart IR. The selection and characterization of an invasive variant of the B16 melanoma. Am J Pathol 1979; 97:587–600.

(*11*) Poste G, Kirsh R, Fogler WE, Fidler IJ. Activation of tumoricidal properties in mouse macrophages by lymphokines encapsulated in liposomes. Cancer Res 1979; 39:881–892.

(*12*) Schroit AJ, Fidler IJ. Effects of liposome structure and lipid composition on the activation of the tumoricidal properties of macrophages by liposomes containing muramyl dipeptide. Cancer Res. 1982; 42:161–167.

(*13*) Fidler IJ, Raz A, Fogler WE, Kirsh R, Bugelski P, Poste G. Design of liposomes to improve delivery of macrophage-augmenting agents to alveolar macrophages. Cancer Res 1980; 40:4460–4466.

(*14*) Griswold DP Jr. Consideration of the subcutaneously implanted B16 melanoma as a screening model for potential anticancer agents. Cancer Chemother Rep 1972; 3:315–323.

(*15*) Talmadge JE, Key M, Fidler IJ. Macrophage content of metastatic and nonmetastatic rodent neoplasms. J Immunol 1981; 126:2245–2248.

(*16*) Korn JH, Haskill JS, Holden HT, Radov LA, Ritter FL. In situ Fc receptor-bearing cells in two murine tumors. I. Isolation and identification. J Natl Cancer Inst 1978; 60:1387–1390.

(*17*) Raz A, Fogler WE, Fidler IJ. The effects of experimental conditions on the expression of in vitro mediated tumor cytotoxicity mediated by murine macrophages. Cancer Immunol Immunother 1979; 7:157–163.

(*18*) Poste G, Bucana C, Raz A, Bugelski P, Kirsh R, Fidler IJ. Analysis of the fate of systemically administered liposomes and implications for their use in drug delivery. Cancer Res 1982; 42:1412–1422

(*19*) Raz A, Bucana C, Fogler WE, Poste G, Fidler IJ. Biochemical, morphological and ultrastructural studies on the uptake of liposomes by murine macrophages. Cancer Res 1981; 41:487–494.

(*20*) Russell SW, Cochrane CG. The cellular events associated with regression and progression of murine (Moloney) sarcoma. Int J Cancer 1974; 13:54–63.

(*21*) Hanna MG Jr, Bucana C, Hobbs B, Fidler IJ. Morphological aspects of tumor cell cytotoxicity by effector cells of the macrophage-histiocyte compartment: In vitro and in vivo studies in BCG-mediated tumor regression. In: Fink M, ed. The macrophage in neoplasia. New York: Academic Press, 1976:113–133.

(*22*) Key ME, Haskill JS. Immunohistologic evidence for the role of antibody and macrophages in regression of the murine T1699 mammary adenocarcinoma. Int J Cancer 1981; 28:225–236.

(*23*) Fidler IJ. Therapy of spontaneous metastases by intravenous injection of liposomes containing lymphokines. Science 1980; 208:1469–1471.

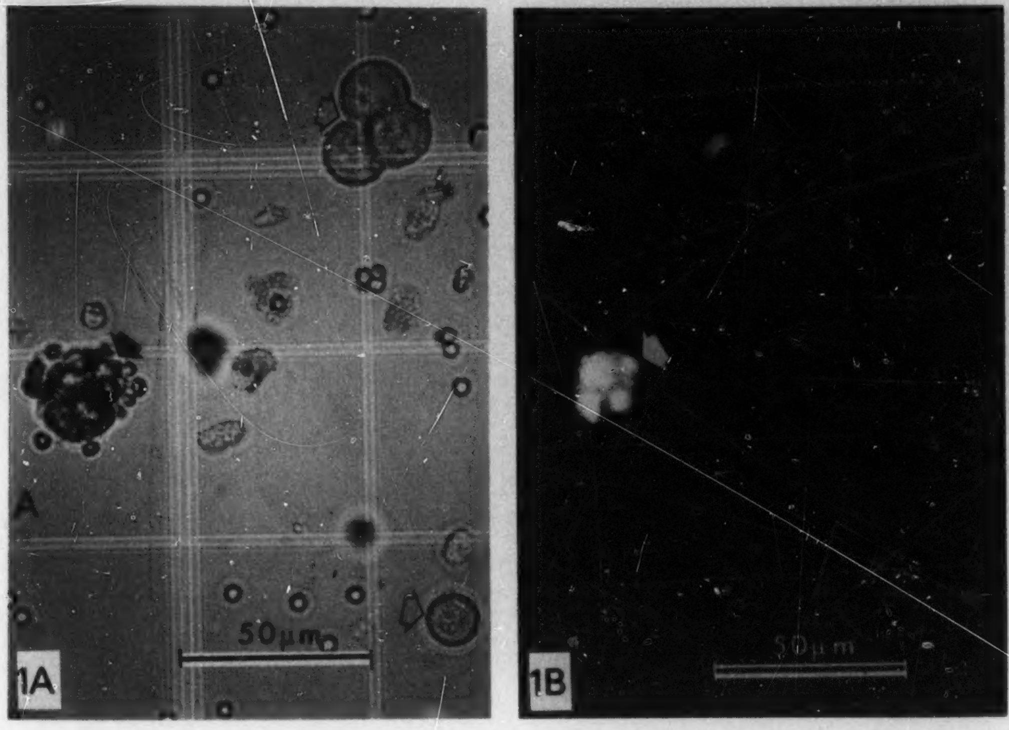

Figure 1.—Cell suspension from an enzymatically dissociated pulmonary metastasis. 1A) As seen by phase microscopy. *Empty arrows* show typical B16-BL6 tumor cells. *Black arrow* shows cell forming rosette with sensitized SRBC, identifying it as a probable macrophage. 1B) As seen by fluorescence microscopy. *White arrow* shows that the only cell containing fluorescent liposomes corresponds to the rosette-positive macrophage. × 400.

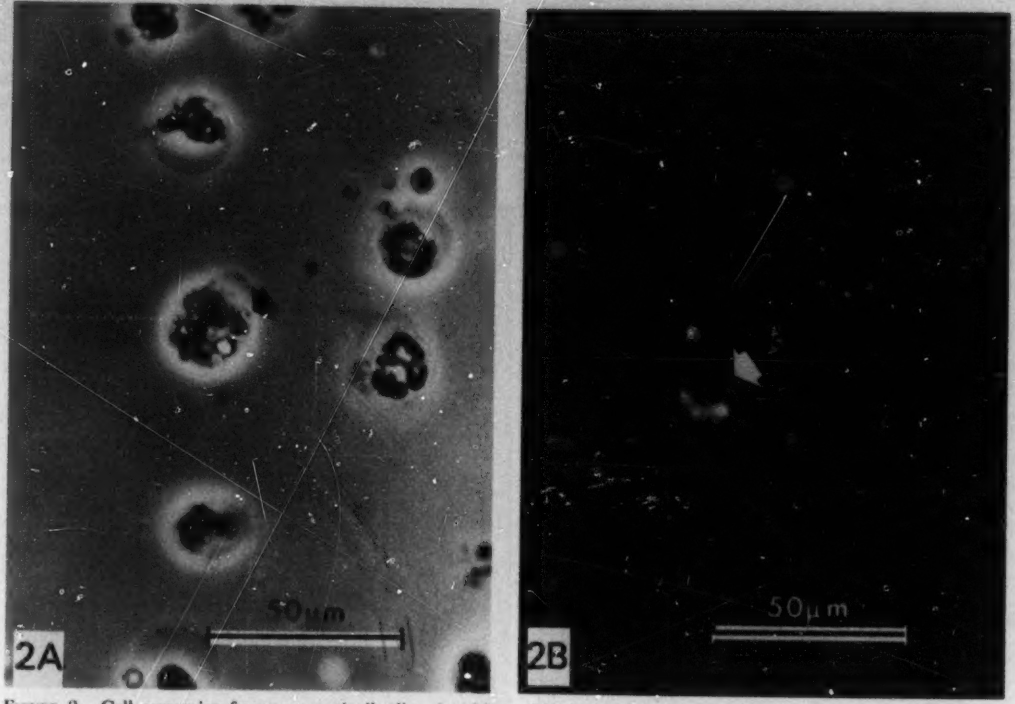

FIGURE 2.—Cell suspension from enzymatically dissociated lung. 2A) As seen by phase microscopy. *Arrow* shows a single cell with macrophage morphology among a group of PMN. 2B) As seen by fluorescence microscopy. *Arrow* shows that the only cell containing fluorescent liposomes corresponds to the macrophage. × 400.

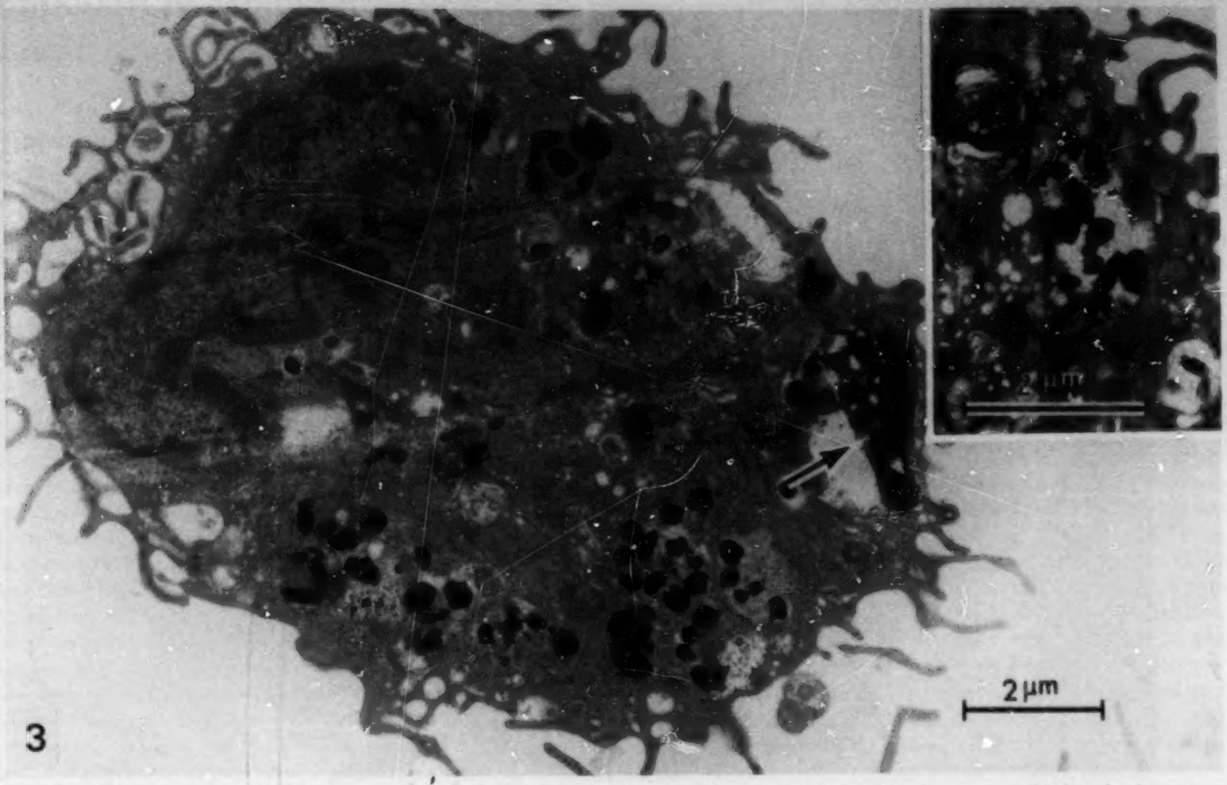

FIGURE 3.—Macrophage isolated from pulmonary metastasis showing internalized melanin granules and myelin structures (*arrow*) believed to be remnants of liposomes that were previously internalized. × 10,000. *Inset* shows a section from another cell containing both internalized melanin granules and a liposome. × 13,200.

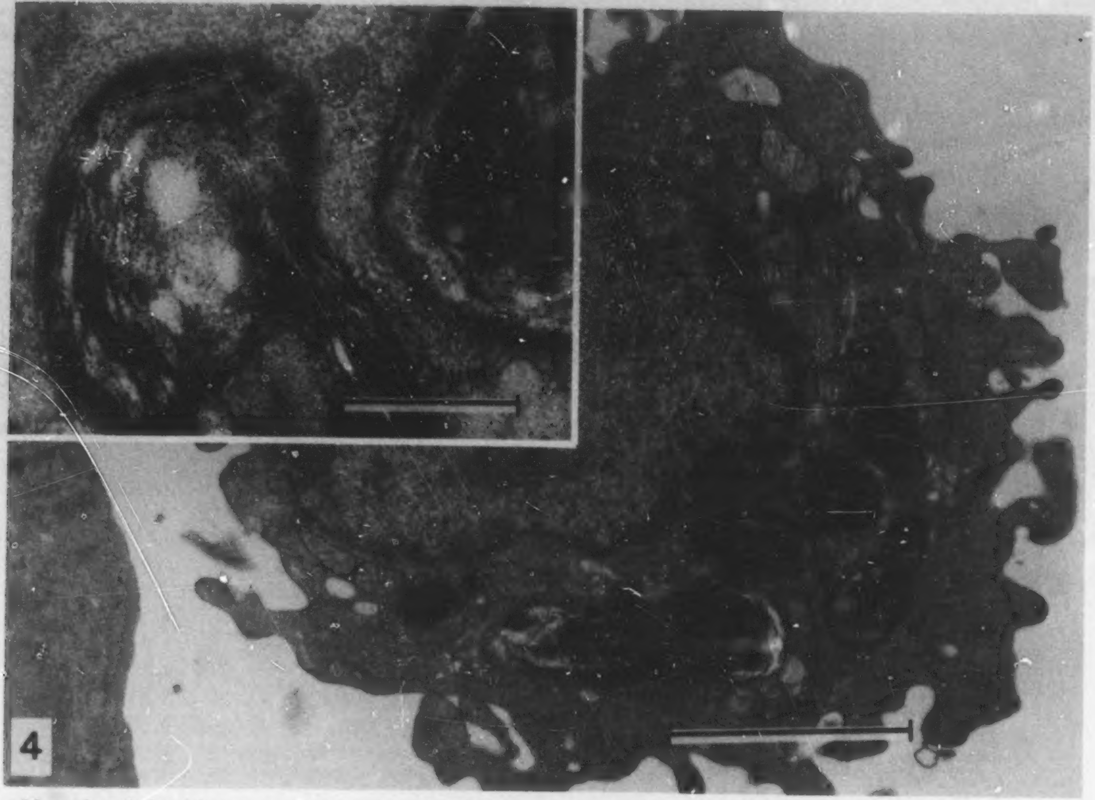

FIGURE 4.—Macrophage isolated from a pulmonary metastasis containing numerous internalized liposomes. Serial sections of this cell showed that some of the large liposomes were >2 μm in diameter. × 17,600. Ferritin was encapsulated in the liposomes used in these experiments, and clusters of ferritin were present inside the liposome, as shown in the *inset*. × 64,000.

Induction of Mammary Tumors in Virgin Female BALB/c Mice by Single Low Doses of 7,12-Dimethylbenz[*a*]anthracene[1,2,3]

Stephen P. Ethier[4] *and* **Robert L. Ullrich**[5,6]

ABSTRACT—The induction of mammary tumors in virgin female inbred BALB/c mice after administration of 7,12-dimethylbenz[a]anthracene (DMBA) over a wide range of doses was studied. Mice were exposed at 12 weeks of age to single or multiple doses of DMBA ranging from 0.0025 to 12.0 mg by gastric intubation and were checked regularly for mammary tumors. The experiment was terminated when the mice were 800 days of age. In the dose range of 0.0025–0.125 mg DMBA, the incidence of mammary tumors was dose-dependent. At higher doses, the mammary tumor incidence became less dose-dependent and was nearly independent of doses above the 0.25-mg level. Analysis of the data for the rate of appearance of mammary tumors with age of the animals and for the age at death of non-mammary tumor-bearing animals indicated that in the low dose range induction of mammary tumors was the predominant effect of DMBA exposure, whereas at moderate to high doses the toxic and carcinogenic effects of DMBA on other tissues significantly influenced the final incidence of mammary tumors. Greater than 90% of the tumors that resulted from administration of low doses of DMBA were adenocarcinomas. In contrast, adenocarcinomas and adenoacanthomas were found in approximately equal proportions following administration of high doses of DMBA. JNCI 1982; 69:1199–1203.

The mouse mammary tumor system has been used for many years for the study of factors that are involved in the development of neoplastic disease. This model system is an attractive one because of the numerous factors that can be studied which influence tumorigenesis in this system. Although it has long been known that chemicals such as 3-methylcholanthrene and DMBA are carcinogenic to mammary tissue (*1–4*), most experiments in which these agents were used have been designed to study the role of the MuMTV (*5*) or the influence of gonadotropic and mammotropic hormones on the pathogenesis of this disease (*6–10*). The few experiments that have been reported in which virgin female MuMTV$^-$ mice were exposed to carcinogenic chemicals alone have involved exposure regimens in which high doses of carcinogen were administered (*11–13*). For example, Butel et al. (*13*) reported that exposure of virgin female BALB/c mice to 2, 4, or 6 mg DMBA, delivered as weekly 1-mg exposures, resulted in mammary tumor frequencies of 25, 39, and 26%, respectively.

The purpose of these experiments was to extend the information concerning the induction of mammary tumors by DMBA, over a wide range of doses, and to thereby determine the dose range over which mammary tumor induction is dose-dependent. These experiments have also been designed to investigate the relative effectiveness of single versus multiple carcinogen exposures in the induction of mammary tumors in virgin female BALB/c mice.

MATERIALS AND METHODS

Animals.—The animals were germfree-derived, specific-pathogen-free virgin female BALB/cAnNBd mice, which were bred and maintained in the Biology Division barrier facility. The mice were housed 8 per cage and were fed Purina Laboratory Chow and water ad libitum.

Carcinogen exposure.—DMBA (Sigma Chemical Co., St. Louis, Mo.) was dissolved in stripped corn oil (Eastman Kodak Co., Rochester, N.Y.) and administered to unanesthetized mice by gastric intubation via a 20-gauge needle ending in a silver-soldered bulb. Control animals were given stripped corn oil only.

Experimental protocol.—DMBA or corn oil was administered to the mice when they were 12 weeks old. When multiple exposures were used, the mice were given their first dose when 12 weeks old and then weekly thereafter. The mice were checked regularly for mammary tumors and were killed either when mammary tumors attained a size of 10 mm or when the mice reached 800 days of age. The experiment was terminated at this time because in previous experiments in this laboratory no further increase in the incidence of mammary tumors in control animals was observed beyond this time (*14*). All mice were necropsied and mammary tumors were processed for histologic examination. The tissues were fixed in Zenker's fixative and embedded in paraffin from which 5-μm sections were prepared. Histologic sections were stained with hematoxylin and eosin.

Correction procedure.—A modification of the age-adjustment procedure was used to compensate for different distributions of ages at death among the various groups. This procedure adjusts the incidence values to those that presumably would have been observed if all the groups had the same distribution of age at death as had the control group. In this procedure we calculate an expected incidence by multiplying the age-specific death rates for the disease in question observed in the experimental group by the number of days at risk in the control population as follows: In the ith interval, $d_i(X)$=number of deaths due to the disease of interest in the group treated at dose X and $N_i(X)$=number of mouse days at risk at dose X.

ABBREVIATIONS USED: DMBA=7,12-dimethylbenz[*a*]anthracene; MuMTV =murine mammary tumor virus.

---

[1] Received April 6, 1982; accepted June 30, 1982.

[2] Supported by the Office of Health and Environmental Research, U.S. Department of Energy, under contract W-7405-eng-26 with the Union Carbide Corporation.

[3] Guidelines for the care and use of laboratory animals were followed as set forth by the Oak Ridge National Laboratory and as approved by the American Association for Accreditation of Animal Care.

[4] University of Tennessee-Oak Ridge Graduate School of Biomedical Science, P.O. Box Y, Oak Ridge, Tenn. 37830.

[5] Biology Division, Oak Ridge National Laboratory, P.O. Box Y, Oak Ridge, Tenn. 37830.

[6] *Address reprint requests to* Dr. Ullrich.

Our model is that $d_i(X)$ has a Poisson distribution with mean $\lambda_i(X)\ ng(X)$, where $\lambda_i(X)$ is the true death rate from the disease of interest in the ith interval at dose X. If the treated group has the same distribution of mouse days at risk as the control group, then the expected number of tumors in the treated group, summed over all intervals, is

$$E(X)=\Sigma_i\lambda_i\quad(X)n_i\text{ (control)}.$$

This expected number can be estimated by

$$\hat{E}(X)=\Sigma_i\frac{d_i(X)}{n_i(X)}n_i\text{ (control)},$$

where n_i (control) is the mouse days at risk in the ith interval in the control group; since we assume that $d_i(X)$ has a Poisson distribution, the estimated variance of $E(X)$ can be obtained by

$$\text{Est var }\hat{E}(X)=\Sigma_i\frac{n_i^2\text{ (control) }d_i(X)}{n_i^2(X)}.$$

We convert the values to percent incidence by dividing by the sample size of the control population. The assumptions and limitations of this procedure have been presented in previous publications (*14, 15*).

RESULTS

Induction of Mammary Tumors by Single or Multiple Doses of DMBA

The dose-response relationships for the induction of mammary tumors following administration of single doses of DMBA are shown in text-figure 1. As can be seen from the text-figure, the dose-response curve rose rapidly and the incidence of mammary tumors increased even at a dose level of 0.0025 mg of DMBA. Further, in the range of 0.0025–0.125 mg DMBA, the incidence of mammary tumors increased steadily with increasing dose. At doses greater than 0.125 mg DMBA, the dose-response curve became progressively more shallow and became nearly flat in the range of 0.25–1.25 mg DMBA.

To examine the effects of higher doses of DMBA on mammary tumor induction, we exposed several groups of mice to doses of DMBA ranging from 1.5 to 12.0 mg. In these groups the DMBA was administered in several weekly fractions to reduce the toxic effect of the treatment. The data obtained from these groups are given in table 1. Administration of 1.5, 3.0, or 6.0 mg DMBA resulted in mammary tumor frequencies not significantly different from those obtained following administration of a single dose of 0.25 mg DMBA. Thus these data agreed with the data obtained from the groups exposed to single doses of DMBA and indicated that the final incidence of mammary tumors was independent of dose at levels greater than 0.25 mg DMBA.

We examined the influence of fractionating the total dose of DMBA on mammary tumor incidence by exposing several groups of animals to low total doses of DMBA (for which single-dose data were available) in either 2 or 10 weekly fractions (table 1). Administration of 0.125 mg DMBA as multiple exposures did not significantly change the incidence of mammary tumors relative to that observed following exposure to DMBA as a single dose. Similar results were obtained when total doses of 0.025 or 0.25 mg were administered as 2 weekly fractions. Inasmuch as it has been demonstrated that sensitivity to mammary carcinogenesis after DMBA exposure in the rat declines with increasing age (*16, 17*), 1 group of animals was exposed when 22 weeks of age to 0.125 mg DMBA as a single dose. This protocol

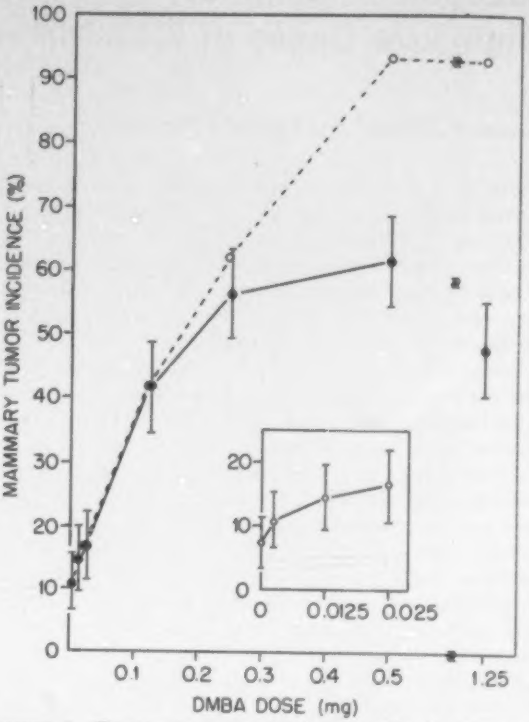

TEXT-FIGURE 1.—Dose-response curve for the cumulative incidence (*solid line*) and age-adjusted incidence (*broken line*) of mammary tumors following single doses of DMBA.

TABLE 1.—*Induction of mammary tumors by single or multiple DMBA exposures*

Dose, mg	Schedule of doses, mg (No. of exposures)	No. of mice with tumors/total No. of mice (%)[a]	Mean age±SE at death of animals without mammary tumors, days
0	—	3/42 (7.1±4.0)	732.3±123
0.025	0.025 (1)	7/40 (17.5±6.0)	761±55.5
0.025	0.0125 (2)	5/48 (10.4±4.4)	695.7±95
0.125	0.125 (1)	20/47 (42.6±7.2)	715.5±109
0.125	0.125 (1)[b]	17/45 (37.8±7.2)	714.8±121
0.125	0.063 (2)	17/47 (36.2±7.0)	731.6±89.5
0.125	0.0125 (10)	19/45 (42.2±7.4)	678.1±182
0.25	0.25 (1)	27/48 (56.3±7.2)	630.3±129
0.25	0.125 (2)	25/47 (53.2±7.3)	678.1±182
0.5	0.5 (1)	29/48 (60.4±7.1)	385.0±200
1.25	1.25 (1)	23/46 (50.0±7.4)	476.5±101
1.5	0.25 (6)	14/23 (60.9±10.2)	379.8±174.1
3.0	0.5 (6)	14/22 (63.6±10.3)	391.6±116
6.0	1.0 (6)	12/21 (57.1±10.8)	328.8±109
12.0	2.0 (6)	7/23 (36.4±9.6)	328.8±93

[a] *Numbers in parentheses* are the percent tumor incidence±SE.
[b] Animals were exposed to DMBA at 22 wk of age.

resulted in a tumor incidence not significantly different from that observed following a similar exposure of animals at 12 weeks of age (table 1). This finding is consistent with previous observations for mammary tumorigenesis in these mice following neutron irradiation over the age span of 12–25 weeks (*14*). These data indicate that the mammary tumor incidences which we observed were not influenced by the mode of carcinogen administration and that age-related changes in susceptibility did not significantly influence our results.

The data for the incidence of mammary tumors as a function of the age of the animals for the various exposure groups are shown graphically in text-figure 2. Mammary tumors first appeared in control animals at approximately 650 days of age. The mammary tumor incidence in control animals then increased with time until a tumor incidence of 7.1% was attained by 800 days of age. In other studies from this laboratory, no further increase in mammary tumor incidence has been observed in control mice that lived through 1,000 days of age (*14*). The incidence versus time curves for the groups exposed to single doses of DMBA indicated that a significant effect of exposure was to shorten the time of appearance of mammary tumors. The data shown in text-figure 2 indicate that the time of appearance of mammary tumors was shortened progressively as the dose of DMBA was increased. Administration of higher doses of DMBA given as multiple exposures served to shorten still further the time of appearance of mammary tumors without, however, increasing the final incidence. Thus while increasing the dose of DMBA above the 0.25-mg level was not effective in increasing the tumor frequency, higher doses of DMBA did result in earlier expression of mammary tumors. These higher doses affected the life-span of non-mammary tumor-bearing animals in a similar manner. Over the dose range of 0.0025–0.125 mg, DMBA had little influence on the survival times of those animals that did not develop mammary tumors, whereas at doses above 0.25 mg, the mean survival times of the non-mammary tumor-bearing animals were clearly reduced.

Deaths from other causes can potentially have a confounding influence on observed tumor incidences (*18*). Since at high doses DMBA influenced both the time of appearance of mammary tumors and the survival times of animals that did not develop mammary tumors, the present data suggested that deaths from other causes may have influenced the incidences of mammary tumors observed at these doses. To examine the influence of competing risks, we also evaluated the data by using a procedure that compensates for competing causes of death. The data analyzed in this fashion are shown in text-figure 1. There were essentially no differences in the observed or age-adjusted incidences in the dose range of 0–0.125 mg. At higher doses the age-adjusted incidences, rather than plateauing like the nonadjusted data, continued to increase to an incidence of greater than 90% at 0.5 mg DMBA.

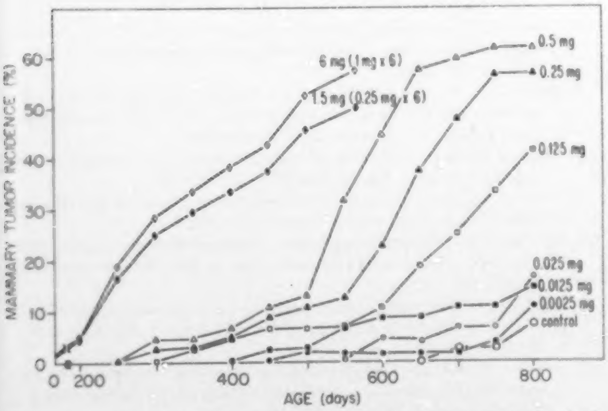

Text-figure 2.—Incidence versus time curves for groups exposed to single and multiple doses of DMBA.

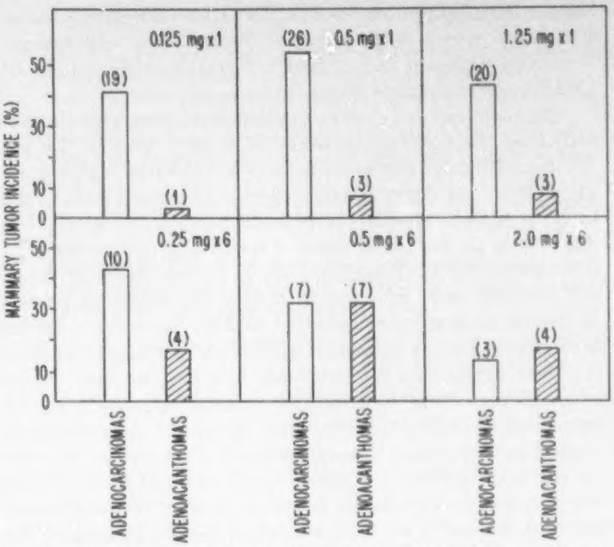

Text-figure 3.—Distribution of adenocarcinomas and adenoacanthomas in groups exposed to low and high doses of DMBA.

Histologic Classification of DMBA-Induced Mammary Tumors

The mammary tumors that we observed in this study were classified either as adenocarcinomas or adenoacanthomas, and the relative abundance of these tumor types is given in text-figure 3. As is shown in the text-figure, adenocarcinomas were by far the predominant tumor type in groups exposed to low to moderate doses of DMBA. The histologic appearance of the adenocarcinomas varied widely. Most tumors were highly variable in appearance and exhibited tightly spaced chords of epithelial cells as well as cysts and papillary structures. A few tumors had areas that appeared fairly well differentiated and exhibited many closely spaced acini; however, even these tumors exhibited significant variability. Thus most tumors would be classified as type B adenocarcinomas according to Dunn's classification. (*19*).

DISCUSSION

The principal aim of the experiments reported here was to examine the relationship between exposure of virgin female BALB/c mice to DMBA and mammary tumor frequency over a wide range of doses. These experiments were also designed to compare the relative effectiveness of DMBA given as single or multiple exposures.

The dose-response curve obtained from these experiments indicated that at doses between 0.0025 and 0.125 mg DMBA, the incidence of mammary tumors was highly dose-dependent. At doses greater than 0.125 mg DMBA, the incidence of mammary tumors became progressively less dependent on dose and became essentially independent of dose above the 0.25-mg level. Thus in the low dose range (<0.125 mg) the induction of mammary tumors appeared to be the predominant effect of DMBA exposure, whereas at higher doses the influence of DMBA was more complex. At doses above 0.25 mg, the toxic and carcinogenic effects of DMBA on other tissues became important, which in turn appeared to influence the final incidence of mammary tumors at these doses. The influence of these competing risks on the final incidence of mammary tumors at doses of 0.25 mg and greater was clearly demonstrated by our analysis of the data in which we used a method that compensated for competing causes of death. The data for the incidence of mammary tumors as a function of age given in text-figure 2 and the data from table 1 showing the survival times for those animals that did not develop mammary tumors also support this view. At doses of 0.25 mg and above, the incidence of mammary tumors rose steadily in animals 600–700 days of age. Since the survival times of non-mammary tumor-bearing animals were reduced by these doses, few animals survived to be at risk for the further development of mammary tumors beyond these times. Thus no further increase in tumor incidence was possible. At the 0.5-mg level, only 3 of 48 animals survived to 700 days of age, whereas at higher doses, no animals survived to this age. At 0.25 mg DMBA, the incidence was probably also affected by these same factors on the basis of the slight increase in incidence seen after the age adjustment and the reduction in the mean survival time of non-mammary tumor-bearing animals (only 8 of 48 animals survived beyond 700 days), although the effect was not as dramatic as at higher doses. Thus these data suggest that at doses above 0.125 mg DMBA, competing risks for other neoplasms as well as the toxic effects of DMBA significantly affect the final incidence of mammary tumors such that at these doses the observed incidence of mammary tumors depends largely on the number of animals that live long enough to develop these neoplasms. At doses below 0.125 mg DMBA, which did not appear to significantly decrease the life-span of the non-mammary tumor-bearing animals, the primary effect of DMBA was on the development of mammary tumors. Over this lower dose range, the incidence of mammary tumors was dose-dependent.

These findings are particularly relevant to studies in which modifying influences of DMBA-induced mammary tumorigenesis have been investigated. Smith et al. (*5*) found that exposure of MuMTV-S^+ C3H/StWi mice to 6.0 mg of DMBA resulted in mammary tumor frequencies not significantly different from those obtained following similar treatment of C3H/StWi mice that were free of MuMTV. Similarly, no interaction was observed in a study reported by Butel et al. (*13*) in which BALB/c mice were exposed to 6.0 mg DMBA in combination with 200 rad X-rays. These authors interpreted these findings to indicate that neither the mammary tumor virus nor X-rays interact with DMBA in the induction of mammary tumors in mice. Our data, however, suggest that 6.0 mg DMBA is more than sufficient to induce the maximum frequency of mammary tumors. Thus if these agents have the potential for interaction, it may not have been detectable given the protocols used in the above experiments. In this regard, it would be of considerable interest and importance to examine the potential for interaction after lower single doses of DMBA.

A final aspect of the data obtained from these experiments concerns the distribution of the histologic types of tumors observed in the DMBA-treated groups. In all dose groups where the DMBA was administered in a single exposure (≤1.25 mg), adenocarcinomas were by far the predominant tumor type and adenoacanthomas were rarely observed. Adenoacanthomas became more prevalent, however, in the groups exposed to higher doses. This finding is consistent with reports of other workers (*9, 10, 20, 21*) of a high proportion of adenoacanthomas in BALB/c mice after administration of relatively high doses of DMBA.

In summary, our experiments provided what is to our knowledge the first data concerning the induction of mammary tumors in virgin mice by DMBA over a wide range of doses. The data obtained from these experiments indicated that the predominant effect of low doses of DMBA is the induction of mammary tumors and that the expression of these tumors is relatively uncomplicated by other effects of DMBA. In contrast, the final incidence of mammary tumors following moderate to high doses of DMBA is strongly influenced by the toxic and carcinogenic effects of this chemical on other tissues.

REFERENCES

(*1*) Englebreth-Holm J. Acceleration of development of mammary carcinomas in mice by methylcholanthrene. Cancer Res 1941; 1:109–112.

(*2*) Kirchbaum A, Williams WL, Bittner JJ. Induction of mammary cancer with methylcholanthrene: Histogenesis of induced neoplasms. Cancer Res 1946; 6:354–362.

(*3*) Andervont HB, Dunn TB. Responses of strain DBA_f/2 mice, without the mammary tumor agent, to oral administration of methylcholanthrene. J Natl Cancer Inst 1953; 14:329–339.

(*4*) Bonser GM. Evolution of mammary cancer in virgin female IF mice with minimal doses of locally acting methylcholanthrene. J Pathol 1954; 68:531–546.

(*5*) Smith GH, Arthur LA, Medina D. Evidence of separate pathways for viral and chemical carcinogenesis in C3H/StWi mouse mammary glands. Int J Cancer 1980; 26:373–379.

(*6*) Haran-Ghera N. The role of mammotropin in mammary tumor induction in mice. Cancer Res 1961; 21:790–795.

(*7*) ———. The mechanism of carcinogenesis in breast tumor development in mice. Acta UICC 1963; 19:765–768.

(*8*) Faulkin LJ Jr. Hyperplastic lesions of mouse mammary glands after treatment with 3-methylcholanthrene. J Natl Cancer Inst 1966; 36:289–298.

(*9*) Medina D. Mammary tumorigenesis in chemical carcinogen-treated mice. I. Incidence in BALB/c and C57BL mice. J Natl Cancer Inst 1974; 53:213–221.

(*10*) ———. Mammary tumorigenesis in chemical carcinogen-treated mice. II. Dependence on hormone stimulation for tumorigenesis. J Natl Cancer Inst 1974; 53:223–226.

(*11*) Smith GH, Pauley RJ, Socher SH, Medina D. Chemical carcinogenesis in C3H/StWi mice, a worthwhile experimental model for breast cancer. Cancer Res 1978; 38:4504–4509.

(*12*) Medina D, Butel JS, Socher SH, Miller FL. Mammary tumorigenesis in 7,12-dimethylbenz(*a*)anthracene-treated C57BL × DBA/2F$_2$ mice. Cancer Res 1980; 40:368–373.

(*13*) Butel JS, Dusing-Swartz S, Socher SH, Medina D. Partial expression of endogenous mouse mammary tumor virus in mammary tumors induced in BALB/c mice by chemical hormonal and physical agents. J Virol 1981; 38:571–580.

(*14*) Ullrich RL, Jernigan MC, Storer JB. Neutron carcinogenesis, dose and dose-rate effects in BALB/c mice. Radiat Res 1977; 72:487–498.

(*15*) Yuhas JM. Recovery from radiation carcinogenic injury to the mouse ovary. Radiat Res 1974; 60:321–332.

(*16*) Huggins C, Briziarelli G, Sutten H. Rapid induction of mammary carcinoma in the rat and the influence of hormones on the tumors. J Exp Med 1959; 109:25–42.

(*17*) Dao TL. Mammary cancer induction by 7,12-dimethylbenz(*a*)anthracene: Relation to age. Science 1969; 165:810–811.

(*18*) Hoel DG, Waldberg HE. Statistical analysis of survival experiments. J Natl Cancer Inst 1972; 49:361–372.

(*19*) Dunn TB. Physiopathology of cancer. In: Homburger F, ed. Morphology of mammary tumors in mice. New York: Hoeber, 1959:38–84.

(*20*) Slemmer G. Interactions of separate types of cells during normal and neoplastic mammary gland growth. J Invest Dermatol 1974; 63:27–47.

(*21*) Deringer MK. Occurrence of mammary tumors, reticular neoplasms, and pulmonary tumors in strain BALB/cAnDe breeding female mice. J Natl Cancer Inst 1965; 35:1047–1052.

blank page

Announcements

The Journal *will publish notices of major meetings dealing with cancer. Submission of notices 6 months in advance is requested to permit timely publication.*

New NIH Biotechnology High Voltage Electron Microscope (HVEM) Resource Available to Biological and Medical Researchers

The Biotechnology Resources Program, Division of Research Resources, National Institutes of Health, is supporting part of the operation of the 1.2-million volt electron microscope at the New York State Department of Health installation at Albany. This installation, under the direction of Dr. Donald Parsons, is operated as a State facility in the Northeast Region, and is now available to users on a national basis. Users must be qualified scientists with appropriate biomedical projects, regardless of institutional affiliation or geographical location.

When applying, please state justification for appropriateness of the Albany installation. Interested scientists should submit a brief proposal of 1-4 pages, which includes the following information:

1) title, name, address, and phone number
2) curriculum vitae of the investigator
3) description of the proposed project demonstating how the HVEM study will be part of this project
4) statement of the biomedical value of the project
5) justification for the use of the HVEM (explanation of its appropriateness to the project proposed)
6) results already obtained by light or conventional electron microscopy at 100 kv, 200 kv, or lower voltages; selected micrographs should be enclosed
7) nature of the specimens, specific methods used in specimen preparation, and suitability for HVEM should be documented
8) a concise bibliography directly relevant to the proposed project should be given
9) microscope time must be estimated in your application; an initial visit for a pilot study will be allowed in relation to your plan for microscope time, with further visits subject to review by the Advisory Committee.

Potential users are encouraged to consult members of the Resource Group and the Advisory Committee for technical advice on specimen preparation; advance study is advisable before a visit. Instructions on HVEM technique, the various modes of operation, and the accessories of the HVEM are available from the Resource Group and should be obtained early. Periodic workshops on the theory and practice of HVEM and associated image processing will be arranged.

Please mail your outline to Dr. Donald F. Parsons, Director, HVEM Laboratory, Center for Laboratories and Research, New York State Department of Health, Empire State Plaza, Albany, New York 12201 (telephone: 518-474-7047/7049).

Harvard Medical School Continuing Education Program

The following course is being offered by the Department of Continuing Education, Harvard Medical School, and the Joint Program in Nuclear Medicine:

Clinical Nuclear Medicine: 1983—Seventh Annual Postgraduate Course; AMA Category I credit 24 hours; William D. Kaplan, M.D., Program Director; course date March 14-18, 1983.

The following course is being offered by the Department of Continuing Education, Harvard Medical School, and the Department of Radiology, Brigham and Women's Hospital:

Orthopedic Radiology; AMA Category I credit 26 hours; Barbara N. Weissman, M.D., Program Director; course date April 25-28, 1983.

For additional information contact Ms. Jo-Anne Latino, Coordinator, Continuing Education Department, Harvard Medical School, 25 Shattuck Street, Boston, Massachusetts 02115 (telephone: 617-732-6265).

The 1983 Oncology Update Symposium

This symposium, sponsored by Northridge Hospital Medical Center, will be held at the Biltmore Hotel, Los Angeles, California, on April 9, 1983. The meeting is designed to update the medical community on advancements in oncology and will feature leading oncology specialists speaking on the latest developments in cancer prevention, early cancer detection, cancer immunology, cancer surgery, and oncology nursing.

Registrants can receive eight hours of Category I credit toward the California Medical Association's Certificate in Continuing Medical Education, the American Medical Association's Physician Recognition Award. This course has been approved for eight hours by the California Board of Registered Nursing.

For reservations or further information contact Ms. Sandra Rozzen, Northridge Hospital Medical Center, 18300 Roscoe Boulevard, Northridge, California 91328 (telephone: 213-885-5311).

Sixty-Fifth Annual Meeting of the American Radium Society

Savannah, Georgia, will be the site of this meeting to be held on April 5-9, 1983 at the Hyatt Regency Hotel. For additional information contact Mrs. Sally Polek, Office of the Secretariat, American Radium Society, 925 Chestnut Street, Philadelphia, Pennsylvania 19107 (telephone: 215-574-3179).

Eighth Summer Program in Methods of Immunologic Research and Diagnosis

The eighth biennial program on current methods of immunologic research and diagnosis will be offered by The Earnest Witebsky Center for Immunology of the State University of New York at Buffalo, New York, in June 1983. The opportunity will be presented for a choice between a three-week program for tyros that comprises elementary and advanced technologies or a two-week program offering only the advanced procedures for persons more familiar with the basic immunologic techniques.

Both programs will consist primarily of combination of core and elective practical laboratory exercises to allow the participant to become acquainted with the techniques by personally carrying them out at the bench. These will be complemented by demonstrations, lectures, and discussions so that the entire program is designed to provide the participant with a survey of presently available methodology together with insight into the underlying immunologic principles. It is open to individuals at the post-doctoral level, supervisory senior technologists, and graduate students beyond the master's level.

Further information may be obtained from Dr. James F. Mohn, M.D., Director, The Ernest Witebsky Center for Immunology, State University of New York at Buffalo, 210 Sherman Hall, Buffalo, New York 14214 (telephone: 716-831-2848). Inquiries should be received by January 15, 1983.

Eighth International Congress of Cytology

This Congress, organized by the International Academy of Cytology, the Canadian Association of Pathologists, and the Canadian Society of Cytology and cosponsored by the Quebec Association of Pathologists and National and Regional Societies of Cytology, will be held on June 19–23, 1983 at the Queen Elizabeth Hotel in Montréal, Canada. The scientific program will comprise the most recent advances in all fields of diagnostic and investigative cytology as of 1983.

There will be invited and guest lectures, lectures by the recipients of the 1981, 1982, and 1983 Goldblatt Cytology Awards, panel discussions, symposia, a slide seminar, and proffered papers.

Please address inquires to Dr. Alexander Meisels, M.D., Secretary-General, Eighth International Congress of Cytology, 1050, Chemin Sainte-Foy, Québec, P.Q., Canada G1S 4L8 (telephone: 418-688-3640).

E.O.R.T.C. Symposium on Treatment of Advanced Gastrointestinal Cancer

Padua, Italy, will be the site of this symposium to be held on June 23–24, 1983. The aim of the symposium is to evaluate the current modalities available for the treatment of advanced tumors of the gastrointestinal tract. The meeting will focus on chemotherapy, radiotherapy, and surgery, either alone or in combination. The program will include invited presentations and free communications. Free communications will be selected on the basis of submitted abstracts.

Abstracts should be received no later than March 31, 1983; address abstracts to Pr. M. Lise, Director, Istituto di Patologia Chirurgica I^a, Universita degli Studi di Padova, 64 via Gattamelata, 35100 Padua, Italy. Seating is limited and preregistration is recommended. For further information and registration contact Ms. D. Eeckhoudt, Executive Secretary, EORTC Data Center, 1 rue Héger-Bordet, 1000 Brussels, Belgium (telephone: (2)539.30.20 - Telex: 22773).

☆ U.S. GOVERNMENT PRINTING OFFICE: 1982-361-145/60

JNCI (NIH Publication No. 82-13)

69/6

JNCI

Journal of the National Cancer Institute

December 1982
Volume 69
Number 6

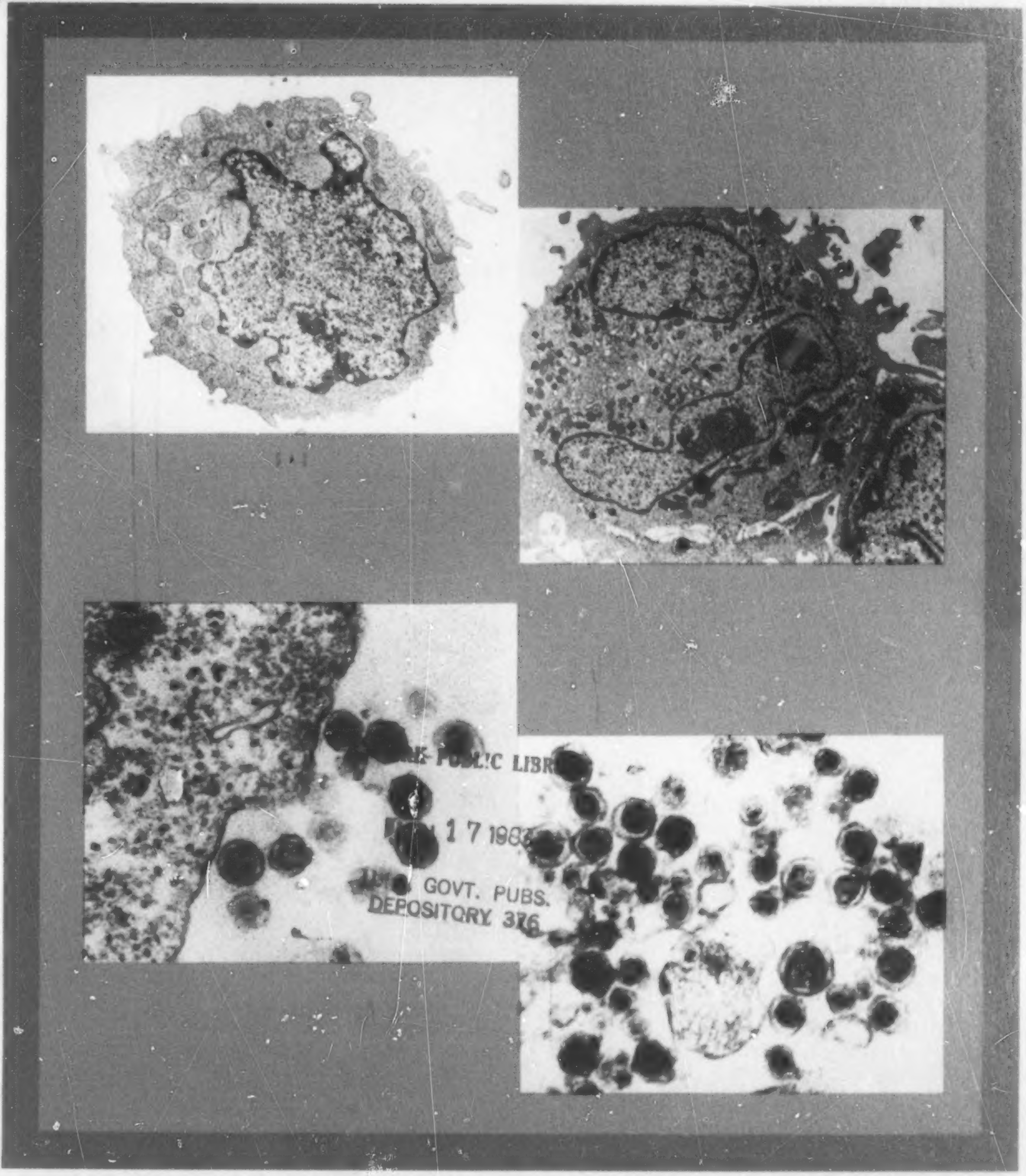

PUBLIC LIBR
17 198
GOVT. PUBS.
DEPOSITORY 376

U.S. DEPARTMENT OF HEALTH AND HUMAN SERVICES Public Health Service National Institutes of Health

HE20.3161:

The electron micrographs on the cover illustrate transformation of human cord blood T-lymphocytes by human T-cell leukemia-lymphoma virus (HTLV). *Top left panel* shows normal human cord blood T-lymphocytes grown with T-cell growth factor. Infection with HTLV (two strains of which are shown in the *bottom panels*; *left* is a strain from a U.S. patient, *right* is from a Japanese patient) results in morphologic changes, as demonstrated with an HTLV-infected cord blood T-lymphocyte (*top right*), and in a reduced dependence on or an independence of T-cell growth factor (*see* guest editorial by Gallo and Reitz on pages 1209–1214). [Electron micrographs courtesy of M. Popovic, P. Sarin, M. Robert-Guroff, et al.]

JNCI

Journal of the National
Cancer Institute

December 1982
Volume 69
Number 6

THE JOURNAL of the National Cancer Institute solicits manuscripts on original observations in laboratory and clinical research from all scientists. A manuscript is considered for publication with the understanding that it has not been published previously and is submitted exclusively to the Journal. Opinions expressed by the authors are not necessarily those of the publisher or its editors.

THE JOURNAL is published monthly (two volumes a year). The Secretary of Health and Human Services has determined that the publication of this periodical is necessary in the transaction of the public business required by law of this Department. Use of funds for printing this periodical has been approved by the Director of the Office of Management and Budget through August 30, 1985.

A MONOGRAPH SERIES covering proceedings of scientific meetings pertaining to cancer is also published. These books may be purchased from the Superintendent of Documents. Series subscriptions are not available and monographs are not included in a subscription to the Journal.

THE JOURNAL is for sale by the Superintendent of Documents, U.S Government Printing Office, Washington, D.C. 20402. Price per copy, $7.00. Subscription price for two volumes per year in the United States, $70.00; foreign, $87.50. Payment is required in advance, and check or money order should be made payable to the Superintendent of Documents.

All inquiries regarding purchase of subscriptions or depository library distribution, including inquiries about missing issues and change of address, should be addressed to the Government Printing Office. The Government Printing Office requires payment in advance on all orders. Inquiries regarding missing issues or change of address for official subscriptions should be addressed to the Editorial Office, Room 850, Westwood Building, 5333 Westbard Avenue, Bethesda, Md. 20816.

VINCENT T. DEVITA, JR., *Director, National Cancer Institute*

BOARD OF EDITORS

PETER GREENWALD, *Editor in Chief*
ELIZABETH K. WEISBURGER, *Assistant Editor in Chief*
STUART A. AARONSON, *Associate Editor*
JOSEPH W. CULLEN, *Associate Editor*
CHARLES H. EVANS, *Associate Editor*
MARY A. FINK, *Associate Editor*
JANET W. HARTLEY, *Associate Editor*
DONALD HENSON, *Associate Editor*
RONALD B. HERBERMAN, *Associate Editor*
GEORGE S. JOHNSON, *Associate Editor*
KURT W. KOHN, *Associate Editor*
ARTHUR S. LEVINE, *Associate Editor*
JOHN J. MULVIHILL, *Associate Editor*
ALAN S. RABSON, *Associate Editor*
RICHARD M. SIMON, *Associate Editor*
JEROME W. YATES, *Associate Editor*

EDITORIAL STAFF

EDWIN A. HAUGH, *Managing Editor*
PAMELA T. ALLEN, *Assistant Managing Editor*
FLORENCE I. GREGORIC, *Monograph Editor*
Editors: DOROTHY D. KATZ, MERCEDES B. LA CHARITY,
I. AGNES REVESZ, JOAN O'BRIEN RODRIGUEZ,
CONSTANCE R. STONESTREET, and ANNA B. WITTIG

JNCI (NIH Publication No. 83-13)

U.S. DEPARTMENT OF HEALTH AND HUMAN SERVICES Public Health Service National Institutes of Health

Instructions to Authors

Text: Send one original and two copies. **Text-figures** (graphs, charts, and line drawings): Send one original and two copies. **Figures** (photomicrographs and photographs): Send three original glossy prints, unmounted. **Tables:** Send tabular material in typewritten form; do not submit tables as glossy prints to be photographed. The entire manuscript including footnotes, legends, and references must be typed double spaced. Single-spaced portions of a manuscript will be returned to the author for retyping. The mailing address is: Journal of the National Cancer Institute, Westwood Building, Room 850, 5333 Westbard Avenue, Bethesda, Maryland 20816.

Manuscripts should be accompanied by a covering letter from the author responsible for correspondence about the manuscript. The covering letter should contain a statement that the manuscript has been seen and approved by all authors and that all persons listed as authors have made significant (not merely administrative, technical, or supervisory) contributions to the content of the paper. The letter should also state that the manuscript or substantial portions thereof have not been previously published nor are they under consideration for publication in another journal.

Data too extensive for inclusion in a manuscript, but which may be of interest to other investigators, may be deposited with the National Auxiliary Publications Service (NAPS), c/o Microfiche Publications, P.O. Box 3513, Grand Central Station, New York, New York 10017. Authors using the NAPS facilities should indicate in a footnote how their additional data may be obtained.

Approximately one-half of all manuscripts submitted to the Journal are accepted for publication. Publication of manuscripts is contingent on transfer of copyright to the Journal. Forms for this purpose will be sent to authors when a manuscript has been approved for publication. All material published in the Journal is in the public domain; therefore, permission to reproduce any portions is not necessary. As a matter of courtesy, communication should be made to the author(s) concerned.

TITLE: Be brief (no more than 14 words, if possible), but for indexing purposes include all key words. The annual subject index is prepared directly from the titles. Titles that form complete sentences are not acceptable. Do not use abbreviations or chemical formulas in titles.

BYLINE: Supply the complete first name, middle initial, and last name of each author. Avoid use of nicknames. Academic degree is optional; however, if a degree is provided for one author, it should be provided for all authors on a manuscript. Include the name of the institution, address, and zip code for each author. Indicate address for reprint requests in a footnote on the byline.

ACKNOWLEDGMENTS: Financial aid in support of research should be recognized in a footnote. Aid in technical fields, animal care, photography, stenography, and other areas may be mentioned in a separate footnote. Indicate the title (Dr., Mr., Mrs., Miss, Ms.) and affiliation of each person acknowledged.

ABSTRACT: Provide an abstract, 150 words or less, on a separate page. The abstract should describe only *results* of the work being reported. Speculation, historical background, or reference to published works will be deleted from abstracts. Any inbred strains, noninbred stocks, cell lines, or other living materials used in the work should be noted in the abstract.

TEXT: Avoid the use of laboratory jargon and abbreviations not in common usage. When possible, refrain from the use of abbreviations that form words (exceptions are PAGE, ALL). Whenever possible, write mathematical equations and chemical formulas on a single line; submit complicated chemical structures as artwork. Avoid repetition of data in the text when it is presented in tables or text-figures.

Use the following style sources: Webster's *Third New International Dictionary* and Dorland's *Illustrated Medical Dictionary* (25th ed) for spelling; *Council of Biology Editors Style Manual* (4th ed) for scientific abbreviations and symbols: *Government Printing Office Style Manual* for other abbreviations and symbols, punctuation, and hyphenation; *Biochemical Nomenclature and Related Documents* (IUB, 1978) for abbreviations of chemical substances; *Enzyme Nomenclature*, recommendations (1978) of the IUB for recommended names of enzymes and information on nomenclature of isozymes; *The Merck Index* (9th ed) for chemical compounds; "Standard Nomenclature for Inbred Strains of Mice: Seventh Listing" by Joan Staats (Cancer Res 1980;40: 2083–2128) for inbred mouse strains; "Standardized Nomenclature for Inbred Strains of Rats: Fourth Listing" by Joan Staats and Michael Festing (Transplantation 1973;16:221–245) for designations of inbred rat strains; *Animals for Research* (9th ed) prepared by the Institute of Laboratory Animal Resources, National Academy of Sciences, for designations of laboratory animal stocks and strains.

TABLES: Submit tabular material typed double spaced on a separate page. Computer print-outs of tables are acceptable only if they are double spaced and with satisfactory title, column headings, legends, and other textual material. Provide headings for all columns of a table and indicate units of measurement where applicable.

TEXT-FIGURES: Refer to graphs, charts, and line drawings as text-figures. Make the abbreviations on text-figures identical to the abbreviations used in the text and legends. Symbols and lettering should be large enough to be legible if reduced. Glossy prints or original drawings in black ink are acceptable; orient vertically instead of horizontally.

FIGURES: Refer to photomicrographs and photographs as figures. Figures and their legends should fit a 7.5- by 9-inch dimension. Calculate that nine typewritten lines of legend will require 1 inch of vertical space. Type figure legends on a separate sheet and identify in the legend any lettering used on the figure. Trim photographs to show only important areas. Do not number face of photographs; use the back or overlay to indicate the top and number of each. Printed indicators may be included on photographs; do not use hand-drawn indicators. *Insert internal scale markers on all photomicrographs*. Color photographs must be grouped as a single plate. For color reproduction, submit both color transparencies and high-quality black and white reproductions. The need for color must be documented before it will be considered.

REFERENCES: Use any recent issue of the Journal as a style guide for reference lists. Number references in order of citation in both text and reference list. For periodicals, provide author(s), title of paper, journal, year, volume, and first and last page numbers. For books, give the author(s), title, name(s) of editor(s), location and name of publisher, year, pertinent chapter or section title, and page numbers. Follow *Index Medicus* for punctuation and abbreviations. Citations of papers in preparation or submitted for publication, unpublished observations, and personal communications should be noted parenthetically in the text. Do *not* include them in the reference list. The accuracy of all references is the responsibility of the authors and not of the editorial staff.

LETTERS TO THE EDITOR should pertain to recent articles in the Journal and should not contain new data unless relevant to the discussion of a particular paper. The authors addressed will be invited to reply to comments before correspondence is published. Letters will be edited by the Staff, subject to contributor approval.

FURTHER DETAILS on the preparation of manuscripts are set forth in the document "Uniform Requirements for Manuscripts Submitted to Biomedical Journals" prepared by the International Steering Committee of medical editors (*see* Am Rev Respir Dis 1979;119:3–10/Ann Intern Med 1979;90:95–99/Br Med J 1979;1:532–535/ or Lancet 1979;1:428–430).

UNITED STATES GOVERNMENT PRINTING OFFICE, WASHINGTON, D.C.: 1982

Table of Contents

Vol. 69, No. 6—December 1982

Letters to the Editor

1207 Noncontraceptive estrogen use and the occurrence of ovarian cancer *Carlo La Vecchia, Alessandro Liberati, Silvia Franceschi*

1208 Immune alterations related to age, sex, and mammary tumor detection in murine mammary tumor virus-infected mice *Hervé Benoist, Jean Dufer, Cécile Bouchet, Andrée Desplaces*

Guest Editorial

1209 Human retroviruses and adult T-cell leukemia-lymphoma *Robert C. Gallo, Marvin S. Reitz, Jr.*

Investigations on Man

1215 Changes in human adenovirus 5 propagated in Burkitt's lymphoma cells *Nicole Faucon, Georges Ogier, Yvette Chardonnet*

1221 Primary liver carcinoma and liver cirrhosis in atomic bomb survivors, Hiroshima and Nagasaki, 1961–75, with special reference to hepatitis B surface antigen *Masahide Asano, Hiroo Kato, Keiko Yoshimoto, Shinichi Seyama, Hideyo Itakura, Tadao Hamada, Soichi Iijima*

1229 Epidemiology of familial predisposition for breast cancer in Japan *Motoi Murata, Keijiro Kuno, Atsuo Fukami, Goi Sakamoto*

1235 Establishment and characterization of a human colony-stimulating factor-producing cell line from a squamous cell carcinoma of the thyroid gland *Tetsuro Okabe, Hitoshi Nomura, Nakaaki Oshawa*

1245 In vitro studies on the cell-mediated immune response to human brain tumors. I. Requirement for third-party stimulator lymphocytes in the induction of cell-mediated cytotoxic responses to allogeneic cultured gliomas *Maurice K. Gately, Moshe Glaser, Steven J. Dick, Ray W. Mettetal, Jr., Paul L. Kornblith*

1255 Isozymes of acid esterase and acid phosphatase in permanent human hematopoietic cell lines *Christer Sundström, Heinz J. Radzun, Mohammad R. Parwaresch*

1261 Subpopulations of human T-lymphocytes. XIX. T-cells and T-cells with receptors for IgMFc (Tμ), IgGFc (Tγ), or IgAFc (Tα) in the peripheral blood and regional lymph nodes of patients with untreated breast cancer *Sudhir Gupta, Susanna Cunningham-Rundles*

1265 Epidemic curve of respiratory cancer due to chloromethyl ethers *William Weiss*

1271 Epithelial line from normal human colon mucosa *B. Shannon Danes, E. Sutanto*

1277 DNA content of liver cell nuclei of *N*-2-fluorenylacetamide-induced altered foci and neoplasms in rats and human hyperplastic foci *Hideki Mori, Takuji Tanaka, Shigeyuki Sugie, Masayoshi Takahashi, Gary M. Williams*

1283 No seasonality in the diagnosis of acute leukemia in the United States *Alexander M. Walker, Paulus A. H. van Noord*

1289 Probable clonal origin of neurofibrosarcoma in a patient with hereditary neurofibromatosis *Jan M. Friedman, Philip J. Fialkow, Claudia L. Greene, Michael N. Weinberg*

Investigations on Nonhuman Systems

1293 Accessory cell function in tumor-bearing mice and effects of *Corynebacterium parvum* *Seiya Okuda, Kazuto Taniguchi, Chiharu Kubo, Kikuo Nomoto*

1299 Induction of γ-glutamyltransferase-positive and nonspecific esterase-positive foci in rat liver by partial hepatectomy following single injection of *N*-nitrosodiethylamine *Norio Hirota, Shinichi Moriyama, Takeshi Yokoyama*

1305 Evidence for involvement of mast cells in tumor suppression in mice *Hiroshi Tanooka, Yukihiko Kitamura, Toshihiko Sado, Kazuhiko Tanaka, Mizue Nagase, Sohei Kondo*

1311 *H-2* expression on a teratocarcinoma-derived cell line, TerC *David B. Searls, Michael Edidin*

1317 Inhibitory effect of fumaric acid on forestomach and lung carcinogenesis by a 5-nitrofuran naphthyridine derivative in mice *Keiko Kuroda, Masayoshi Kanisawa, Mitsutaro Akao*

1321 Characterization of anti-inflammatory factors produced by murine tumor cells in culture *S. J. Normann, J. Cornelius*

1329 Collagenolytic activity of rabbit V_2 carcinoma implanted in the nude mouse *Chitra Biswas, Kurt J. Bloch, Jerome Gross*

1337 Immunoadjuvant effects of *Blastomyces dermatitidis* against EL 4 lymphoma in C57BL/6J mice *L. Scott McDaniel, George C. Cozad*

1343 Suppression of 7,12-dimethylbenz[*a*]anthracene-induced chromosome aberrations in rat bone marrow cells after treatment with Sudan III and related azo dyes *Yoshiaki Ito, Sakan Maeda, Tetsuo Fujihara, Norifumi Ueda, Taketoshi Sugiyama*

1347 Growth of mouse mammary glands after neonatal sex hormone treatment *Yasuhiro Tomooka, Howard A. Bern*

1353 Effects of nicotinamide, isonicotinamide, and bleomycin on DNA synthesis and repair in rat hepatocytes and hepatoma cells *Rosemary Barra, Verrell Randolph, MariaElaina Sumas, Kevin Lanighan, Michael A. Lea*

1359 Tumor-associated antigens produced by mouse mammary tumor cells in artificial capillary culture *Jean C. Hager, S. Spiegelman, M. Ramanarayanan, James Bausch, Pierre M. Galletti, Paul Calabresi*

1367 Glycosylated podophyllotoxin congeners: Loss of microtubule inhibition and permission of invasion in vitro — *Marc M. Mareel, Christian H. Dragonetti, Georges K. De Bruyne, Rita M.-L. Van Cauwenberge*

1375 Detection of aflatoxins and related metabolites by radioimmunoassay — *Philippe Sizaret, Christian Malaveille, Ruggero Montesano, Charles Frayssinet*

1383 Carcinogenic effect of carbazole in the liver of (C57BL/6N × C3H/HeN)F_1 mice — *Hiroyuki Tsuda, Akihiro Hagiwara, Michiko Shibata, Masato Ohshima, Nobuyuki Ito*

1391 Hormone requirements of the pregnancy-dependent mammary tumor of GR/A mice: An in vitro study — *John W. Harbell, Jackie S. Papkoff, Charles W. Daniel*

1403 Analysis of lymphoid cells responding to virus- and tumor-associated antigens in spleens of syngeneic mouse mammary tumor systems with low and high oncogenic potentials — *Diana M. Lopez, Ronald D. Paul*

1411 Genetics of transplacentally induced teratogenic and carcinogenic effects in rabbits treated with *N*-nitroso-*N*-ethylurea — *R. R. Fox, H. Meier, H. G. Bedigian, D. D. Crary*

Meeting Highlights

1419 Job-exposure matrices in occupational epidemiology — *Shelia K. Hoar*

Announcements

1421 Seventeenth Annual Clinical Symposium of St. Jude Children's Research Hospital

1421 Eighteenth Annual San Francisco Cancer Symposium

1421 Second Annual A.A.I. Course in Advanced Immunology

1421 Eleventh International Symposium for Comparative Research on Leukemia and Related Diseases

1421 Eleventh Annual Meeting of the International Society for Oncodevelopmental Biology and Medicine

1421 Seventh Meeting of the European Association for Cancer Research (EACR)

1423 **Acknowledgment**

1429 **Index of Authors**

1435 **Permuted Title Index**

1461 **1982 Table of Contents**

Letters to the Editor

Noncontraceptive Estrogen Use and the Occurrence of Ovarian Cancer[1,2]

SIR: Dr. Weiss and his colleagues[3] reported on an increased risk of endometrioid carcinoma of the ovary related to noncontraceptive estrogen use, even if the overall risk for all types of epithelial ovarian cancers was not significantly increased. For this reason and for other reasons (only a 56% interview rate among users and the lack of increased risk with increased dosage and duration of use), Weiss et al. concluded that "... the observed association between menopausal estrogen use and the occurrence of ovarian endometrioid tumor should be interpreted cautiously until the results of additional studies are available."

We had the opportunity to consider the histology-specific pattern of noncontraceptive estrogen use in a case–control study on ovarian cancer and have reported the general methods and results elsewhere.[4] Cases were 161 patients with epithelial ovarian cancers admitted between May 1979 and February 1980 to the first Obstetrics and Gynecology Clinic of the University of Milan; controls (561) were age-matched patients who had not undergone bilateral oophorectomy and who had been admitted for acute disorders other than malignant, hormonal, or gynecological disorders to six wards of four major university hospitals in Milan. None of the eligible patients and controls refused to be interviewed. All histologic specimens were reviewed by the same pathologist who was unaware of the epidemiologic data, and the interviewers did not know the histologic diagnosis. Only the 135 cases and 437 controls aged 40–69 were considered here (noncontraceptive estrogen use being concentrated in these age groups). The estimated relative risks for the use of estrogen-replacement therapy are given in table 1. Although exposure to noncontraceptive estrogens was not associated with an increased likelihood of developing ovarian cancer [relative risk (RR)=1.0], there was an excess risk of borderline significance [RR=2.3; 95% confidence interval (CI)=1.0–5.3] of endometrioid cancers and a nonsignificant one (RR=1.6; 95% CI=0.3–8.4) of clear cell cancers. (Since adjustment for age in decades by the Mantel-Haenszel procedure did not materially change any of the RR estimates, unadjusted ones are chosen for presentation.) Three patients with endometrioid tumors, but only 2 in the other categories, reported a long-term use (>5 yr), but no clear duration–risk relationship was evident.

A more detailed analysis of the histologic tumor type-specific epidemiologic and clinical characteristics of a part of our study population has been published elsewhere.[5] Ovarian cancer patients showed several characteristics that have been described as risk factors for endometrial cancer, but patients with endometrioid carcinomas seemed to have them to a greater extent, especially late menopause and nulliparity or low parity. It is also of interest that the RR estimate for estrogen use in endometrioid cancers (RR=2.3 is similar to that found in a case–control study of endometrial cancer conducted on the same Italian population.[6] Thus there seems to be a broad agreement between our data and the suggestions made by Weiss et al.,[3] although the following points are worth stressing:

1) Our findings, too, are based on limited numbers and, methodologically, represent a typical example of data dredging. Therefore, they should be taken more as a further suggestion than as a confirmation.

2) The possibility that estrogens may affect the histologic tumor type differentiation of preexisting ovarian neoplasms rather than actually inducing the tumor appears unlikely to be ruled out by a case–control study of this size.

CARLO LA VECCHIA
ALESSANDRO LIBERATI
Mario Negri Institute for Pharmacological Research
Via Eritrea 62
20157 Milan, Italy
SILVIA FRANCESCHI
Cancer Studies Unit
Radcliffe Infirmary
University of Oxford
Oxford OX2 6HE, United Kingdom

TABLE 1.—*Distribution of 135 epithelial ovarian cancers and 437 controls according to estrogen use and histologic type: Milan, Italy, 1979–80.*[a]

Histologic type	Estrogen ever-users		Nonestrogen users		Rate ratio (95% CI)
	No.	Percent	No.	Percent	
Controls	86	20	351	80	(1)[b]
Serous-mucinous-undifferentiated	16	16	87	84	0.8 (0.4–1.3)
Endometrioid	9	36	16	64	2.3 (1.0–5.3)
Clear cell	2	29	5	71	1.6 (0.3–8.4)

[a] Only women 40–69 yr old were included.
[b] Reference category.

---

[1] Supported by a Consiglio Nazionale delle Ricerche (Italian National Research Council) grant on clinical pharmacology and rare diseases.

[2] Dr. Silvestro Carinelli, Laboratorio di Anatomia et Istologia Patologica, Instituti Clinici di Perfezionamento di Milan, reviewed the pathologic material.

[3] WEISS NS, LYON JL, KRISHNAMURTHY S, DIETERT SE, LIFF JM, DALING JR. Noncontraceptive estrogen use and the occurrence of ovarian cancer. JNCI 1982; 68:95–98.

[4] FRANCESCHI S, LA VECCHIA C, HELMRICH SP, MANGIONI C, TOGNONI G. Risk factors for epithelial ovarian cancer in Italy. Am J Epidemiol 1982; 115:714–719.

[5] LA VECCHIA C, FRANCESCHI S, BOERI R, et al. Caratteristiche istologiche, etio-patologiche e cliniche del carcinoma epiteliale dell'ovaio: Analisi di 115 casi. Ann Ostet Ginecol Med Perinat 1981; 102:10–16.

[6] LA VECCHIA C, FRANCESCHI S, GALLUS G, et al. Oestrogens and obesity as risk factors for endometrial cancer in Italy. Int J Epidemiol 1982; 11:120–126.

Immune Alterations Related to Age, Sex, and Mammary Tumor Detection in Murine Mammary Tumor Virus-Infected Mice

SIR: In a recent paper, Specter and Friedman[1] reached the conclusions that in inbred RIII mice, known to be infected neonatally by murine mammary tumor virus (MuMTV), female mice, compared to male mice of the same ages and in spite of a constant increased spleen weight, had a significant depression of the antibody response of their splenocytes against sheep red blood cells (SRBC). This depression was deepened by the presence of a detectable adenocarcinoma. Furthermore, using blastogenic tests with lipopolysaccharide (LPS) or phytohemagglutinin (PHA), the authors reported that old tumor-bearing female mice alone showed a significant decrease of their response to PHA.

Using C3H/Bi mice, also known to be infected by MuMTV, our group has obtained almost identical results.[2] As compared to age-matched males, female mice display constant increased spleen cell numbers. The antibody response to SRBC is significantly decreased in aged (5–6 mo) female mice as compared to young (2–4 mo) female mice or male mice of the same ages. This decrease seems not to be due to a B-cell defect since antibody response to trinitrophenyl-substituted LPS, a T-independent antigen,[3] remains constant throughout the first 8 months of life of female mice. In addition, PHA blastogenic response of spleen cells does not decrease with age in female mice, but a significant depression is observed in old tumor-bearing mice as compared to tumor-free female mice of the same age.

One of the major discrepancies between the results observed in RIII mice[1] or C3H/Bi mice[2] resides in the antibody response against SRBC in old tumor-bearing mice. Whereas in RIII mice tumor presence is associated with a strong depression of the immune response, in C3H/Bi mice the presence of an adenocarcinoma is associated with an increase of the anti-SRBC antibody response in tumor-bearing female mice compared to tumor-free female mice of the same age. Although this unexpected event seems to be related to tumor emergence in C3H/Bi mice, we agree with Specter and Friedman's conclusions on the difficulty of attributing a specific immune phenomenon to tumor appearance, taking into account the complex relationships between sex, age, and immune responsiveness in these two MuMTV-positive mouse strains. The discrepancies observed at the antibody production level between tumor-bearing RIII and C3H/Bi mice could be attributed to many other parameters, such as genetic background, hormonal factors (since we used C3H/Bi breeders whereas Specter and Friedman used RIII virgin mice), or intrinsic viral properties because it has been recently reported[4] that MuMTV displayed different bioactivities in C3H and RIII mice.

HERVÉ BENOIST
Pharmacy Teaching and Research Unit
University of Reims
F-51096 Reims, France

JEAN DUFER
Jean Godinot Cancer Institute
F-51100 Reims, France

CÉCILE BOUCHET
ANDRÉE DESPLACES
Laboratoire d'Immunologie
René Huguenin Cancer Center
35 rue Dailly
F-92211 Saint Cloud, France

---

[1] SPECTER S, FRIEDMAN H. Age- and sex-related differences in antibody formation and blastogenic responsiveness of splenocytes from RIII mice developing virus-induced mammary adenocarcinoma. JNCI 1981; 67:1347–1351.

[2] DUFER J, BENOIST H, BOUCHET C, DESPLACES A, SARACINO RT. Modifications de l'état immunitaire en fonction de l'âge et de l'apparition de tumeur mammaire spontanée chez la souris C3H/Bi. Bull Cancer (Paris) 1982; 69:143–148.

[3] FIDLER JM. In vivo immune response to TNP hapten coupled to thymus-independent carrier lipopolysaccharide. Cell Immunol 1975; 16:223–236.

[4] LOPEZ DM, SIGEL MM, SCHLOM J. Detection of type-specific antigenic determinants of murine mammary tumor viruses with cell-mediated immune assays. Proc Soc Exp Biol Med 1982; 169:144–148.

Guest Editorial

Robert C. Gallo[1,2] *and* **Marvin S. Reitz, Jr.**[1]

Human Retroviruses and Adult T-Cell Leukemia–Lymphoma[3]

The last several years have seen exciting developments concerning the presence of retroviruses in humans and its association with certain types of T-cell leukemia–lymphoma. Retroviruses have long been identified in many species and have been shown to induce leukemias and lymphomas or have been closely implicated in the etiology of these diseases in a number of species. Transmission of leukemia with cell-free filtrates was reported for chickens in 1908 by Ellerman and Bang (*1*). Gross (*2*) later showed the induction of leukemia in inbred strains of mice with murine leukemia virus. Induction of leukemia was demonstrated in cats with FeLV by Jarrett et al. (*3*), and seroepidemiologic studies among outbred cat populations by Cotter et al. (*4*) showed that transmission of FeLV is responsible for most, if not all, naturally occurring leukemias in cats. Retroviruses are primary causes of naturally occurring leukemias in at least several other species, including cattle, turkeys, and gibbon apes [for reviews, *see* (*5, 6*)].

There are two general categories of retroviruses based on their life cycles. Endogenous viruses are contained in the germ line of a species, transmitted genetically, not usually expressed into RNA, protein, or extracellular virus, and do not seem to be pathogenic except in some inbred animals. The retroviruses associated with leukemias and lymphomas, in contrast, are transmitted by infection with exogenous virus. These retroviruses can also be subdivided into 2 general groups based on their biologic activity, a reflection, of course, of differences in their genome. One group is competent for virus replication, causes disease after a long latent period, and does not appear to directly transform cells. BLV and FeLV belong to this group. The other group is generally replication-defective and is comprised of viruses that have undergone recombination with host cell DNA sequences. These host cell sequences, called "*onc*" genes, allow these viruses to directly transform cells in vitro, and disease onset is rapid. Sarcoma viruses and Abelson murine leukemia virus belong to this group. Replication is possible only in the presence of competent "helper" viruses.

Identification and Characterization of a Human Retrovirus

Until recently, retroviruses had never been unequivocally demonstrated in humans, although data suggestive of their presence were frequently reported. For example, definitive evidence was obtained in human leukemias for virus-like reverse transcriptase (*7*), and extra, presumably acquired, DNA sequences were also reported in this disease (*8*). No convincing evidence or demonstration of a human retrovirus, however, was reported. It is now evident that the inability to show the existence of retroviruses was in part due to the uncertainty of where to look (tissue type, cell type, and type of diseases) and in a large part due to the inability to successfully culture the appropriate types of cells in vitro.

Our laboratory had long been interested in learning how to grow different types of hematopoietic cells. In particular, the growth of T-cells seemed of interest since many virally induced leukemias of animals are of T-cell origin (*9*). In 1976, we reported the discovery of a factor from short-term cultures of mitogen-stimulated peripheral blood human lymphocytes. This factor (TCGF) supported the long-term growth of human mature T-cells (*10, 11*). TCGF has been purified to near homogeneity and is a protein whose monomeric molecular weight is 12,000–13,000 (*12*).

With the use of purified or partially purified TCGF, mature T-cells from normal sources could be grown only after mitogen activation, indicating that TCGF is a second signal in T-cell growth (*12*) due to lack of TCGF receptors on unactivated T-cells. It was soon realized, however, that purified TCGF alone was sufficient to grow mature T-cells from the blood of patients with cutaneous T-cell lymphoma–leukemia and certain other T-cell cancers (*13*). Some of the biochemical markers of these cells, as well as the requirement for prior activation of normal T-cells for TCGF-supported growth, suggest that the T-cells grown with purified TCGF consist, at least in part, of the malignant T-cells of these patients. The lack of a requirement for prior activation of these cells appears to be due to their constitutive expression of receptors for TCGF (*14*).

Several such cell lines were studied from an adult black man (CR) with a particularly aggressive cutaneous T-cell lymphoma (mycosis fungoides) (*15*). Typical retrovirus particles were visible by electron microscopy (fig. 1), and particulate reverse transcriptase activity was detected in the media. This enzyme activity had all of the biochemical parameters of retrovirus reverse transcriptase, and both the

---

ABBREVIATIONS USED: ATL=adult T-cell leukemia–lymphoma; BLV=bovine leukemia virus; FeLV=feline leukemia virus; HTLV=human T-cell leukemia–lymphoma virus; TCGF=T-cell growth factor.

---

[1] Laboratory of Tumor Cell Biology, Division of Cancer Treatment, National Cancer Institute, National Institutes of Health, Public Health Service, U.S. Department of Health and Human Services, Bethesda, Md. 20205.

[2] *Address reprint requests to* Dr. Gallo, Building 37, Room 6A09, National Institutes of Health, Bethesda, Md. 20205.

[3] Received July 13, 1982.

Editor's note: Periodically, the Journal publishes solicited guest editorials as a means of transmitting to investigators in cancer research the essence of current work in a special field of study. The Board of Editors welcomes suggestions for future editorials that succinctly summarize current work toward a clearly defined hypothesis regarding the causes or cure of cancer.

particles and the reverse transcriptase activity banded in equilibrium sucrose density gradients at the appropriate density (1.16 g/cm^3). The reverse transcriptase activity was not inhibited by antisera against the reverse transcriptases of several other retroviruses, including primate retroviruses. This virus was provisionally designated HTLV. The genomic RNA of HTLV was shown to be a polyadenylated 70S RNA, in common with other retroviruses. With the use of cDNA transcribed from the viral genomic RNA, it was shown that HTLV was not significantly related to any previously described animal retroviruses and that it was not endogenous to humans [i.e., not a ubiquitously germ line-transmitted human virus (*16*)]. Furthermore, HTLV was not transmitted via the germ line in patient CR but was acquired by postzygotic infection. This conclusion was based on the presence of HTLV provirus in the DNA of some of the T-cells from three independently derived T-cell lines from CR, including one from the laboratories of Dr. S. Broder and Dr. T. Waldmann (National Cancer Institute), and its absence from the DNA of a B-cell line from the same patient, as well as from DNA of other T-cells (*17*). All these lines were positively identified as having originated from patient CR by their HLA haplotype (*17*).

The major HTLV core protein was identified as p24, which was shown to be serologically distinct from the core proteins of all previously described viruses (*18*). A second core protein, p19, was also shown to be novel (*19*). The reverse transcriptase (also serologically distinct) is somewhat larger than that of type C retroviruses (95,000 daltons) and slightly prefers Mg^{2+} over Mn^{2+} as the divalent cation, a property shared by the reverse transcriptase of BLV (20). Consistent with this observation, the amino acid sequence of the p24 core protein has recently been determined by Oroszlan et al. (*21*) to be most closely homologous to that of the major core protein of BLV among all the analogous retroviral proteins tested. On the basis of this finding, HTLV appears to be distantly related specifically to BLV. However, the relationship is not sufficiently close to suggest current interspecies transmission. In fact, by conventional immunologic assays and nucleic acid hybridization assays, the proteins and nucleic acids of BLV and HTLV are not detectably related (*16, 18, 19*). In addition, natural antibodies to BLV in cows do not react with proteins of HTLV, and, conversely, human antibodies to HTLV do not react with BLV (*22, 23*).

A second isolate of HTLV was subsequently obtained from the cultured T-cells of another adult patient (MB) with a highly malignant variant of Sézary T-cell leukemia (*24*). This virus was shown by nucleic acid hybridization and protein serology to be very closely related or identical to HTLV. Moreover, viral proteins and proviral DNA were detected in *uncultured* tissue from the same patient, which virtually ruled out a laboratory contamination.

Presence of HTLV in Japanese ATL

Because of the initial association of HTLV with cutaneous T-cell lymphoma (patient CR) and Sézary T-cell leukemia (patient MB), a number of serum samples were screened from each type of patient. With the use of solid-phase immunocompetition and competition radioimmunoprecipitation assays, antibodies to p24 and p19 were detected in the sera of a few of these patients and shown to be absolutely specific for HTLV (*22, 23*). Antibody to HTLV p24 was also found in the normal spouse of one of the HTLV-infected T-cell lymphoma patients, although all other normal sera were negative. It has become apparent that most cases readily identifiable as positive for HTLV have strikingly common clinical features: adult onset, usually a rapid disease course, often hepatosplenomegaly, lymphadenopathy, large and usually pleomorphic lymphocytes with lobulated nuclei and mature T-cell surface phenotype markers (usually OKT4$^+$), often hypercalcemia, and skin manifestations in over half. In spite of the OKT4$^+$ phenotype, the T-cells from this type of disease often have a suppressor function [*see* CTC-16 in (*25*)]. A typical cell is shown in figure 2. Despite the similarity in most cases of HTLV-positive disease, however, HTLV has also been identified in a few instances in the typical, more benign Sézary syndrome (Popovic M, Sarin P, Robert-Guroff M, et al.: Manuscript in preparation). Moreover, since in most instances we have tested only for serum antibodies to HTLV and since we have identified HTLV antigen in cultured T-cells of a few antibody-negative persons, HTLV may be more prevalent in classical Sézary syndrome and mycosis fungoides than is now evident.

A T-cell cancer, representing a type of leukemia observed in adults and endemic to regions of southern Japan, was first recognized and described by Takatsuki and his colleagues (*26*). This disease, called ATL, has clinical symptoms very similar to those observed with HTLV-positive cases of cutaneous T-cell lymphoma and frequently has cutaneous manifestations (*27, 28*). Like the T-cells from cases in the United States, the T-cells from these patients are generally OKT4$^+$ and function as suppressor cells. These similarities prompted us to make a seroepidemiologic survey of patients with this disease from the endemic region of Japan. It was quickly evident that almost all of these ATL patients had specific antibodies to HTLV p19 and p24, while a few normal persons from this region were also antibody-positive (*29–31*). Consistent with these findings were the subsequent results obtained by investigators in several laboratories in Japan. These investigators have shown the presence by electron microscopy of retrovirus particles in cultured T-lymphocytes from a few ATL patients and have demonstrated serum antibodies directed against determinants on cells producing these particles in almost all Japanese ATL patients (as well as 26% of normal persons from the endemic area of Japan) (*32, 33*). The similarity in the distribution of this antibody and the antibody against HTLV suggested that the two agents are very similar or identical. This relationship has now been confirmed in our laboratory in collaboration with colleagues in Japan by characterizing the virus produced by two of the cell lines, MT-1 and MT-2, used in the studies by Hinuma et al. (*32*) and Miyoshi et al. (*33*). This virus has antigenic determinants identical to those of HTLV p24 and p19, and its mRNA and provirus hybridize virtually completely to cDNA from HTLV (*34*).

Cocultivation of the other cell line in (*33*), i.e., MT-2, with cord blood T-lymphocytes results in the induction of TCGF-independent T-cell lines (*35*). This result suggests that in the MT-2 cell line the virus may have acquired an oncogene, enabling it to directly transform human T-cells. We found that transmission of several of our strains of HTLV to cord blood T-cells usually results in several reproducible biologic effects, including a reduction in their requirement for TCGF, an apparent loss of the so-called "crisis period" which generally prevents these cells from growing indefinitely in vitro, the capacity to form large colonies in agar, and the ability to grow to high cell density (Popovic M, Sarin P, Robert-Guroff M, et al.: Manuscript in preparation). In at least some cases, TCGF independence is induced. Moreover, the virus apparently infects only mature T-cells and, despite repeated efforts, we have been unable to infect human B-cells, fibroblasts of human and animal origins, or human bone marrow cells.

Presence of HTLV in ATL in the Caribbean

In collaboration with Dr. W. Blattner and his colleagues (Environmental Epidemiology Branch, National Cancer Institute), Dr. D. Catovsky and Dr. D. Galton (Medical Research Council Leukemia Unit, Hammersmith Hospital, London), and Dr. M. Greaves (Imperial Cancer Research Fund Laboratories, London), our laboratory has found that the Caribbean basin is a second region in which HTLV is unusually prevalent. A relatively high incidence of a disease clinically similar to ATL was identified among blacks of Caribbean origin in Great Britain. All cases tested to date have antibody to HTLV (*36*) and, when available, the leukemia cells have released infectious HTLV. T-cell leukemia–lymphoma also seems to be of relatively high incidence in the Caribbean itself, and antibody to HTLV is found in those patients with the disease, as well as in some normal persons (*37*). Various types of T-cell leukemia–lymphoma in conjunction with HTLV have now been found in the southeastern United States, the Boston area, the Seattle area, Japan, the Caribbean, Venezuela, Brazil, Guyana, Ecuador, Israel, and Alaska (*38*). It seems likely that, as other populations are tested, HTLV will also be identified in other parts of the world.

How might HTLV induce ATL? One possibility is that insertion of a viral RNA transcriptional promotor switches on cellular genes whose inappropriate expression results in the leukemia phenotype. This phenomenon has been shown to occur in avian bursal lymphomas and has been termed "downstream promotion" (*39, 40*). It has been suggested that infection with HTLV may result in the downstream promotion of the gene for TCGF, causing its constitutive and inappropriate expression, and some but not all of the available evidence favors this model (*41*). Obviously, infection with HTLV is not in itself sufficient to induce ATL, since not only do many nonleukemic persons manifest persistent serum antibodies to HTLV (*23, 29–32, 37*), but also, in at least some cases, they harbor HTLV in some of their peripheral blood T-cells (Robert-Guroff M, Kalyanaraman VS, Blattner WA, et al.: Submitted for publication). Host-specific or environmental factors, age at first infection, repeated infections, route of infection, or even random chance, as for example, the appropriate integration site, may play a role in pathogenesis by HTLV. Estimates of HTLV infection and association with leukemia or lymphoma have been made by Suchi (personal communication) who believes that about 1 in 2,000 infected people develop disease. This incidence is similar to BLV induction of bovine leukemia. Perhaps HTLV is involved in other diseases, including some of a nonneoplastic nature.

Are all isolates identical? The three CR isolates, the MB isolate, and the MT-1 isolate are certainly very closely related (*24, 34*). In addition, five other isolates (from the Caribbean, the United States, Japan, and Israel) are very closely related by serology and molecular hybridization (Popovic M, Sarin P, Robert-Guroff M, et al.: Manuscript in preparation). One isolate, however, from the Mo cell line (*42*) (originating from a patient in the United States described as having a T-cell variant of hairy cell leukemia) appears to differ in the serologic behavior of its p24. Although this virus thus also belongs to the HTLV group, it may represent a second subtype (HTLV-II). It is possible that others of this type, or yet different types, will be identified in the future. Our provisional nomenclature refers to each strain of HTLV in the order of establishment as a separate strain by Roman numeral followed with letters for the patient or cell line [e.g., HTLV-I(CR)]. A detailed comparison of all the HTLV-I isolates and the possible example mentioned above of HTLV-II will be greatly facilitated by the molecular cloning of a portion of the HTLV genome which has recently been achieved (Wong-Staal F, Manzari V, Gallo RC: Manuscript in preparation).

How is HTLV transmitted? If a substantial portion of the population in the endemic area is indeed infected, as judged by serum antibodies to HTLV, there is probably no need for a nonhuman reservoir to maintain the presence of HTLV. It seems that HTLV is not readily infectious and may require prolonged intimate contact for transmission. This transmission might occur within families (e.g., mother's milk and sexual contact) or could result from, for example, blood transfusions or insect vector transmission. Although a large body of data has become available on HTLV, obviously a great deal of work remains. The identification of this virus, however, raises the possibility of eventually being better able to find, treat, and prevent ATL. Moreover, it may also stimulate thoughts about certain other human neoplasias and the possible role of this type of virus.

REFERENCES

(*1*) Ellerman V, Bang O. Experimentelle Leukamie bei Huhnern. Centralbl Bakteriol, Abt 1 (Orig), 1908; 46:595–604.

(*2*) Gross L. "Spontaneous" leukemia developing in C3H mice following inoculation, in infancy, with AK-leukemic extracts, or AK-embryos. Proc Soc Exp Biol Med 1951; 78:27–40.

(*3*) Jarrett WF, Martin WB, Crighton GW, Dalton R, Stewart M. Leukaemia in the cat. Transmission experiments with leukaemia (lymphosarcoma). Nature 1964; 202:566–567.

(*4*) Cotter S, Essex M, Hardy W. Serologic studies of normal and leukemic cats in a multiple-case leukemia cluster. Cancer Res 1974; 34:1061–1068.

(*5*) Gallo RC. Leukemia, environmental factors, and viruses. In: Kurstak E, Maramorosch K, eds. Viruses and environment. New York: Academic Press, 1978:43–78.

(*6*) Wong-Staal F, Gallo RC. Retroviruses and leukemia. In: Gunz F, Henderson E, eds. Leukemia. New York: Grune. In press.

(*7*) Sarngadharan MG, Sarin PS, Reitz MS, Gallo RC. Reverse transcriptase activity of human acute leukaemic cells: Purification of the enzyme response to AMV 70S RNA, and characterization of the DNA product. Nature [New Biol] 1972; 240:67–72.

(*8*) Baxt WG, Spiegelman S. Nuclear DNA sequences present in human leukemic cells and absent in normal leukocytes. Proc Natl Acad Sci USA 1972; 69:3737–3741.

(*9*) Kaplan H. Leukemia and lymphoma in experimental and domestic animals. Ser Hematol 1974; 7:94–163.

(*10*) Morgan DA, Ruscetti FW, Gallo RC. Selective in vitro growth of T-lymphocytes from normal human bone marrows. Science 1976; 193:1007–1008.

(*11*) Ruscetti FW, Morgan DA, Gallo RC. Functional and morphologic characterization of human T-cells continuously grown in vitro. J Immunol 1977; 119:131–138.

(*12*) Mier JW, Gallo RC. Purification and some characteristics of human T-cell growth factor from phytohemagglutinin-stimulated lymphocyte-conditioned media. Proc Natl Acad Sci USA 1980; 77:6815–6819.

(*13*) Poiesz BJ, Ruscetti FW, Mier JW, Woods AM, Gallo RC. T-cell lines established from human T-lymphocytic neoplasias by direct response to T-cell growth factor. Proc Natl Acad Sci USA 1980; 77:6815–6819.

(*14*) Gootenberg JE, Ruscetti FW, Mier JW, Gazdar AF, Gallo RC. Human cutaneous T-cell lymphoma and leukemic cell lines produce and respond to T-cell growth factor. J Exp Med 1981; 154:1403–1418.

(*15*) Poiesz BJ, Ruscetti FW, Gazdar AF, Bunn PA, Minna JD, Gallo RC. Detection and isolation of type C retrovirus particles from fresh and cultured lymphocytes of a patient with cutaneous T-cell lymphoma. Proc Natl Acad Sci USA 1980; 77:7415–7419.

(*16*) Reitz MS, Poiesz BJ, Ruscetti FW, Gallo RC. Characterization and distribution of nucleic acid sequences of a novel type C retrovirus isolated from neoplastic human T lymphocytes. Proc Natl Acad Sci USA 1981; 78:1887–1891.

(*17*) Gallo RC, Mann D, Broder S, et al. Human T-cell leukemia-lymphoma virus (HTLV) is in T- but not B-lymphocytes from a patient with cutaneous T-cell lymphoma. Proc Natl Acad Sci USA. In press.

(*18*) Kalyanaraman VS, Sarngadharan MG, Poiesz BJ, Ruscetti FW, Gallo RC. Immunological properties of a type C retrovirus isolated from cultured human T-lymphoma cells and comparison to other mammalian retroviruses. J Virol 1981; 38:906–915.

(*19*) Robert-Guroff M, Ruscetti FW, Posner LE, Poiesz BJ, Gallo RC. Detection of the human T-cell lymphoma virus p19 in cells of some patients with cutaneous T-cell lymphoma and leukemia using a monoclonal antibody. J Exp Med 1981; 154:1957–1964.

(*20*) Rho HM, Poiesz BJ, Ruscetti FW, Gallo RC. Characterization of the reverse transcriptase from a new retrovirus (HTLV) produced by a human cutaneous T-cell lymphoma cell line. Virology 1981; 112:355–360.

(*21*) Oroszlan S, Sarngadharan MG, Copeland TD, Kalyanaraman VS, Gilden RV, Gallo RC. Primary structure analysis of the major internal protein p24 of human type C T-cell virus. Proc Natl Acad Sci USA 1982; 79:1291–1294.

(*22*) Posner LE, Robert-Guroff M, Kalyanaraman VS, et al. Natural antibodies to the human T-cell lymphoma virus in patients with cutaneous T-cell lymphoma. J Exp Med 1981; 154:333–346.

(*23*) Kalyanaraman VS, Sarngadharan MG, Bunn PA, Minna JD, Gallo RC. Antibodies in human sera reactive against an internal structural protein of human T-cell lymphoma virus. Nature 1981; 294:271–273.

(*24*) Poiesz BJ, Ruscetti FW, Reitz MS, Kalyanaraman VS, Gallo RC. Isolation of a new type C retrovirus (HTLV) in primary uncultured cells of a patient with Sézary T-cell leukaemia. Nature 1981; 294:268–271.

(*25*) Uchiyama T, Broder S, Bonnard G, Waldmann T. Immunoregulatory functions of cultured human T-lymphocytes. Trans Assoc Am Physicians 1980; 93:251–262.

(*26*) Takatsuki K, Uchiyama T, Sagawa K, Yodoi J. Adult T-cell leukemia in Japan. In: Seno S, Takaku F, Irino S, eds. Topics in hematology. Amsterdam and Oxford: Excerpta Medica, 1977:73–77.

(*27*) Takatsuki K, Uchiyama T, Ueshima Y, Hattori T. Adult T-cell leukemia: Further clinical observations and cytogenetic and functional studies of leukemic cells. Jpn J Clin Oncol 1979; 9:317–324.

(*28*) Uchiyama T, Yodoi J, Sagawa K, Takatsuki K, Uchino H. Adult T-cell leukemia: Clinical and hematologic features of 16 cases. Blood 1977; 50:481–492.

(*29*) Gallo RC, Robert-Guroff M, Kalyanaraman VS, et al. Human T-cell retrovirus and adult T-cell lymphoma and leukemia: Possible factors on viral incidence. In: Chandra P, ed. Biochemical and biological markers on neoplastic transformation. New York: Plenum Press. In press.

(*30*) Robert-Guroff M, Nakao Y, Notake K, Ito Y, Sliski A, Gallo RC. Natural antibodies to human retrovirus HTLV in a cluster of Japanese patients with adult T-cell leukemia. Science 1982; 215:975–978.

(*31*) Kalyanaraman VS, Sarngadharan MG, Nakao Y, Ito Y, Aoki T, Gallo RC. Natural antibodies to the structural core protein (p24) of the human T-cell leukemia (lymphoma) retrovirus found in sera of leukemic patients in Japan. Proc Natl Acad Sci USA 1982; 79:1653–1657.

(*32*) Hinuma Y, Nagata K, Misoka M, et al. Adult T-cell leukemia: Antigen in an ATL cell line and detection of antibodies to the antigen in human sera. Proc Natl Acad Sci USA 1981; 78:6476–6480.

(*33*) Miyoshi I, Kubonishi I, Yoshimoto S, et al. Type C virus particles in a cord T-cell line derived by co-cultivating normal human leukocytes and human leukaemic T-cells. Nature 1981; 294:770–771.

(*34*) Popovic M, Reitz MS, Sarngadharan MG, et al. The virus of Japanese adult T-cell leukemia is a virus of the HTLV group. Nature 1982. In press.

(*35*) Miyoshi I, Kubonishi I, Sumida M, et al. Transformation of normal human cord lymphocytes by co-cultivation with a lethally irradiated human T-cell line carrying type-C virus particles. Gan 1981; 71:155–156.

(*36*) Catovsky D, Greaves MF, Rose M, et al. Adult T-cell lymphoma-leukemia in blacks from the West Indies. Lancet 1982; 1:639–643.

(*37*) Blattner WA, Kalyanaraman VS, Robert-Guroff M, et al. The human type C retrovirus, HTLV, in blacks from the Caribbean region, and relationship to adult T-cell leukemia/lymphoma. Int J Cancer. In press.

(*38*) Gallo RC, Kalyanaraman VS, Sarngadharan MG, et al. The human type-C retrovirus: Association with a subset of adult T-cell malignancies. N Engl J Med. In press.

(*39*) Hayward WS, Neel BG, Astrin SM. Activation of a cellular *onc* gene by promotor insertion in ALV-induced lymphoid leukosis. Nature 1981; 290:475–480.

(*40*) Neel BG, Hayward WS, Robinson HL, Fang J, Astrin SM. Avian leukosis virus-induced tumors have common proviral integration sites and synthesize discrete new RNAs: Oncogenesis by promoter insertion. Cell 1981; 23:323–334.

(*41*) Gallo RC. Regulation of human T-cell proliferation: T-cell growth factor, T-cell leukemias and lymphomas, and isolation of a new type-C retrovirus. In: Kaplan HS, Rosenberg SA, eds. Malignant lymphomas: Etiology, immunology, pathology, treatment. New York: Academic Press. In press.

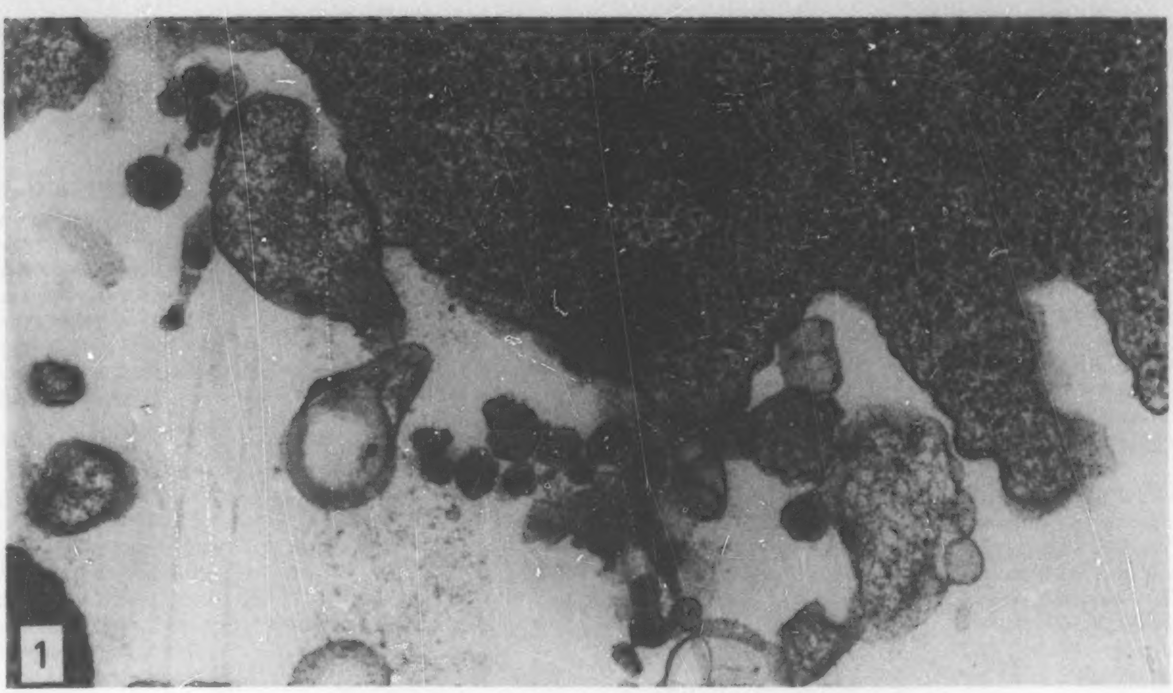

FIGURE 1.—HTLV particles from CR T-cell line HUT-102. × 105,000

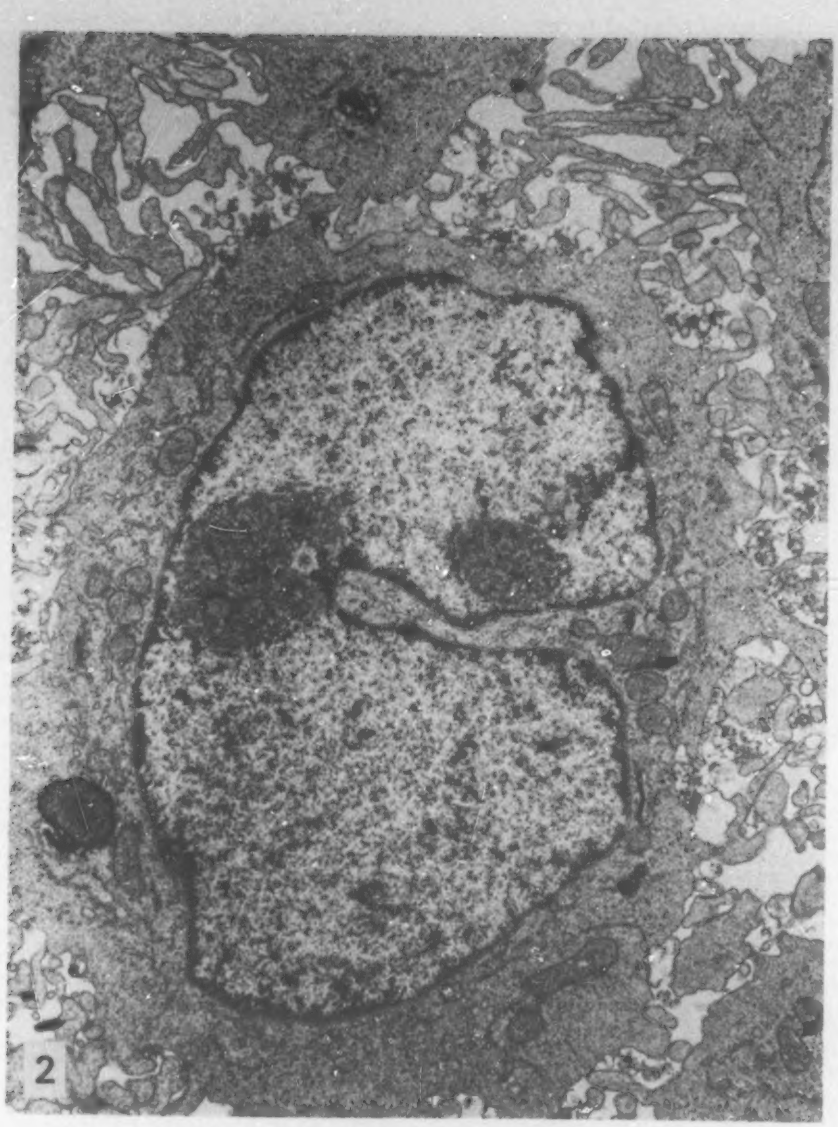

FIGURE 2.—Cells from CR T-cell line CTC-16. × 7,000

Changes in Human Adenovirus 5 Propagated in Burkitt's Lymphoma Cells[1]

Nicole Faucon,[2] Georges Ogier,[2] *and* Yvette Chardonnet[2,3]

ABSTRACT—The effect of host cells on human adenovirus 5 properties was studied with the use of Burkitt's lymphoma cell lines (Raji and Jijoye) that poorly replicate the virus. Only a small fraction of the cell population was producing adenovirus 5. The major virus components were synthesized; however, the purified virus particles differed from those produced in HeLa cells by lower density in CsCl gradient, lower content in DNA, limited changes in DNA restriction enzyme pattern, and polypeptide composition. After one passage in HeLa cells, modifications of polypeptides reversed.—JNCI 1982; 69:1215–1220.

In humans, lymphocytes harbor some viruses, particularly Ad that replicate poorly in these cells. In vivo and in vitro interactions between Ad and lymphocytes have not yet been extensively studied. We previously reported that cultures of human cord blood lymphocytes can produce very low amounts of virus (*1*) and that virus production is enhanced when these lymphocytes are transformed by EBV (*2*). Several established B-cell lines either having tumor origin or transformed in vitro by EBV also support Ad5 replication (*3–5*). However, only a small proportion of the cell population is involved in virus replication. The virus produced is modified in its structure. In this paper, we have studied the infection with human Ad5 of human cells derived from Burkitt's lymphoma and we describe the properties of the modified virus.

MATERIALS AND METHODS

Cells.—The lines Jijoye (EBV-positive) and Raji (EBV-negative) were derived from Burkitt's lymphoma. They were propagated in suspension in medium RPMI-1640 (GIBCO, Grand Island, N.Y.) containing 20% heat-inactivated fetal calf serum. HeLa cells were maintained in minimum essential medium containing 10% heat-inactivated fetal calf serum.

Virus.—Ad5 (Ad75 prototype; from Dr. G. C. Godman, Columbia University, New York, N.Y. was multiplied in HeLa cells and used between passages 16 and 35.

Infection of cell lines with Ad.—Cells were infected with Ad5 at a multiplicity of 50–100 PFU/cell. The viruses were studied either immediately after infection or after three serial passages of infected cells.

Labeling of Ad5 components.—Viral DNA was labeled by the addition of [^{3}H]thymidine (sp act, 35 Ci/mmol; CEA, Saclay, France) to infected cultures. Proteins were labeled by the addition of [^{35}S]methionine (sp act, 700–900 and 1,013 Ci/mmol; CEA and New England Nuclear Corp., respectively) to a medium containing 5% of the normal concentration of methionine and 10% dialyzed fetal calf serum.

Purification of the virus.—Pooled lysates from about 10^8 infected cells (Raji, Jijoye, and HeLa) were used as previously described (*6*). The lysates were frozen and thawed six times. Cellular debris were removed by low-speed centrifugation, the supernatant was treated twice by Freon, and centrifuged on a discontinuous CsCl gradient of densities 1.3–1.6 g/ml for 90 minutes at 45,000 rpm in an SW50-1 rotor. The band of partially purified virus was recovered from the interface and centrifuged on a continuous CsCl gradient (1.2–1.4 g/ml).

In some experiments, to avoid disrupting virus particles, we did the second centrifugation on a 5–20% preformed sucrose density gradient at equilibrium. In both centrifugation procedures, the band of purified virus was dialyzed against 10 m*M* Tris-HCl (pH 7.2) for 24 hours.

Assays of Ad.—Infectivity was titrated either on HeLa cells in plates of 96 wells with dilution step $10^{0.5}$ (three to five wells were used) or by a plaque assay on A 549 cells, a heteroploid non-HeLa cell line established from a human lung tumor by Dr. W. A. Nelson-Rees (University of California, Oakland, Calif.) and given to us by Dr. G. Winberg (Karolinska Institute, Stockholm, Sweden). The titers were expressed either in ID on HeLa cells or in PFU on A 549 cells. Several titrations of the same inoculum in duplicate on HeLa and A 549 cells have established that 1 ID equals 10 PFU. For neutralization tests, the virus was diluted to contain 100–500 PFU/assay.

Hemagglutination was done with a unit volume of 50 µl and a 0.5% suspension of rat (Sprague-Dawley) red blood cells with the addition of Ad6 antiserum at a dilution of 1/200. Under these conditions, the hemagglutination activity was enhanced; both pentons and fibers were detected (*7*).

Indirect immunofluorescence tests were done on cell smears fixed with acetone, with the use of either specific Ad5 rabbit antiserum or immune sera raised to specific virus components.

Immune sera.—Ad5 antisera were prepared in rabbits (*6*) and in Hartley guinea pigs with purified virus replicated in HeLa cells; the antisera were absorbed on uninfected HeLa cells before use.

Two antisera against P-antigen were used: One was prepared in rabbits (*7*) by injection of P-antigen extracted from rabbit kidney cells treated with cytosine arabinoside early after infection; the other was a rabbit antiserum provided by Dr. W. C. Russell (Mill Hill, London). Both sera precip-

---

ABBREVIATIONS USED: Ad=adenovirus(es); CEA=Comissariat à l'Energie Atomique; EBV=Epstein-Barr virus; ID=infective dose; OD=optical density; PFU=plaque-forming unit(s).

---

[1] Received 12, 1981; revised May 7, 1982; accepted May 27, 1982.

[2] Unité de Virologie, Institut National de la Santé et de la Recherche Médicale, Centre National de la Recherche Scientifique, 1, Place du Professeur Joseph Renaut, 69371 Lyon Cedex 2, France.

[3] *Address reprint requests to* Dr. Chardonnet.

best copy available

itated a major polypeptide 58 K but also other polypeptides (72 K and slightly 120 K).

Other antisera were obtained in guinea pigs against the structural components of Ad5 (hexon, penton, and fiber) produced in HeLa cells (6). Reference antisera were guinea pig antihexon (gift from Dr. H. G. Pereira, Mill Hill, London), rabbit antipenton, and rabbit antifiber (gift from Dr. G. Wadell, Karolinska Institute).

DNA analysis.—Labeled viral DNA was studied in infected Raji or Jijoye cells by use of an alkaline sodium iodide sedimentation gradient (*8*). Pooled fractions of each peak of DNA were dialyzed against 10 m*M* Tris and 1 m*M* EDTA buffer (pH 7.9) and hybridized on a filter with cold HeLa Ad5 DNA (*9*). Hirt supernatants were prepared from infected Raji, Jijoye, and HeLa cells. The density of viral DNA was determined by equilibrium sedimentation through CsCl gradient. Cleavage pattern of the DNA was analyzed with restriction enzymes: Kpn I, Bam I, and XBa (New England Biolabs, Beverly, Mass.) and Eco RI (Boehringer Mannheim Biochemicals, Indianapolis, Ind.). For fragment analysis, 1% agarose gels were used (*10*). The electrophoresis buffer contained 0.04 *M* Tris, 0.02 *M* sodium acetate, and 2 m*M* edetate (pH 8). The gels were immersed in buffer containing 0.5 μg of homidium bromide/ml and photographed under UV illumination.

RESULTS

Multiplication of Ad5 in Raji and Jijoye Cells

Raji or Jijoye cells infected with Ad5 yielded low amounts of infectious virus, either at the first passage (table 1, A) or after several serial passages of infected cells (table 1, B). At the first passage, in three independent experiments, the infectivity and hemagglutinating activity reached maximum levels 3-4 days post infection. Cellular growth was not inhibited and 70-100% of the cells remained viable. By indirect immunofluorescence with Ad5 rabbit antiserum only a few cells were found to contain specific Ad antigens (hexons, pentons, and fibers). The positivity to fluorescence began 2-3 days post infection and increased up to 3-4 days. Positive cells varied from 0.5 to 2% for Raji and from 1 to 5% for Jijoye cells in the different experiments. The fluorescent cells appeared to be two- to three-times larger. No fluorescence was detected in uninfected cells.

When infected cells were propagated serially in four independent experiments, the Ad5 production not only was maintained but also was enhanced until it reached a maximum level after 3-4 passages. In a typical experiment (table 1, B), in Raji cells the infectivity increased twofold to threefold, the hemagglutinating activity increased eightfold, and the number of fluorescent cells rose to 4%. For Jijoye cells, the respective values were one hundredfold, thirtyfold, and 12-13%. The rate of cellular growth slowed down, but the cells remained viable.

Reactions of immunofluorescence were positive with antibodies raised to purified hexons, pentons, fibers, and P-antigen. Virus components were unevenly distributed among the infected cells. More cells were positive with immune sera against pentons, fibers, and P-antigen than with immune sera against complete particles. In any case the fluorescence was less bright than in HeLa cells. The double-immunofluorescence reaction, with the use of fluorescein isothiocyanate-labeled EBV antibodies and rhodamine B-labeled Ad antibodies on Raji or Jijoye cells superinfected with Ad5, revealed both antigens in the same cells.

With extracts from infected cells, the Laurell technique (*11*) and immunodiffusion assays (*12*) also showed that viral antigens were present. In thin sections, virus particles were seen in the electron microscope.

The Ad5 produced in Raji and Jijoye cells was neutralized specifically by antisera raised in guinea pigs or in rabbits against purified HeLa Ad5. Hemagglutination of Raji and Jijoye Ad5 was also inhibited by these antisera.

When cells were infected at lower multiplicity (1-10 instead of 50-100 PFU/cell), the Ad5 multiplication decreased significantly. When the virus was serially propagated in Raji or Jijoye cells, the cell growth was not in-

TABLE 1.—*Ad5 production in serial passages of infected Raji and Jijoye cells*[a]

Passage	Day	Raji cells: Cell No., $\times 10^6$	Raji cells: Percent fluorescent	Raji cells: Infectivity, PFU/10^6 cells	Raji cells: Hemagglutination, U/10^6 cells	Jijoye cells: Cell No., $\times 10^6$	Jijoye cells: Percent fluorescent	Jijoye cells: Infectivity, PFU/10^6 cells	Jijoye cells: Hemagglutination, U/10^6 cells
A: First passage[b]	0	2	0	ND	0	2	0	ND	0
	1	ND	ND	ND	ND	7.5	0	0.9×10^3	0
	2	5.6	0	2.9×10^4	320	18	0	ND	ND
	3	6.0	0.5	1.4×10^7	640	18	0.5	4.3×10^5	120
	4	6.4	1.0	2.4×10^7	640	15	1.6	0.9×10^6	60
B: Serial passages[b]									
1	4	4	1.0	0.5×10^8	640	20	1.6	1.0×10^6	80
2	3	3.8	1.0	0.5×10^8	1,280	9.5	3.0	0.5×10^7	640
3	4	3.6	4.0	1.4×10^8	5,120	12.0	8.0	0.8×10^7	2,560
4	3	2.8	3.0	1.1×10^8	5,120	13.0	12.0	0.9×10^8	1,280

[a] Samples of 2×10^6 were infected with 50 PFU Ad5 per cell and incubated at 37°C for 2 hr. Excess virus was removed and 2 ml medium was added to each sample. Uninfected and infected cells were further incubated at 37°C for 4 days at the first passage. They were subsequently propagated every 3-4 days. At each passage, samples were adjusted to 2×10^6 cells in 2 ml medium. Samples were taken at different times. Cells were enumerated; positive fluorescent cells with specific Ad5 rabbit antiserum were counted from ≈20,000 cells/sample; infectivity was expressed in PFU/10^6 cells; hemagglutinating activity was given in U/10^6 cells. ND=not done.

[b] In each part only one typical experiment was reported.

hibited; the percentage of fluorescent cells was in the same range as the percentage in the first passage; the infectivity and the hemagglutinating activity reached maximum levels after two to three passages in Jijoye cells, whereas they decreased at the second passage in Raji cells.

The observed differences in multiplication of Ad5 in Raji and Jijoye cells were not due to variations in adsorption or to inhibitors. Control experiments with Ad5 plus radioactively labeled DNA showed that the rate of adsorption on Raji and Jijoye cells did not differ significantly from that observed with HeLa cells, but the maximum level of adsorbed radioactivity was reached at different times post infection: 2 hours for HeLa, 4 hours for Raji, and 6 hours for Jijoye cells (text-fig. 1). Adsorption on individual cells was confirmed by an immunofluorescence test developed in our previous study with HeLa cells (*6*): At 6 hours most of the cells had virus attached to them. However, when these cells were cloned, only a few cells contained viral antigens in each colony. We concluded that all the cells can adsorb virus but that only a few replicate it.

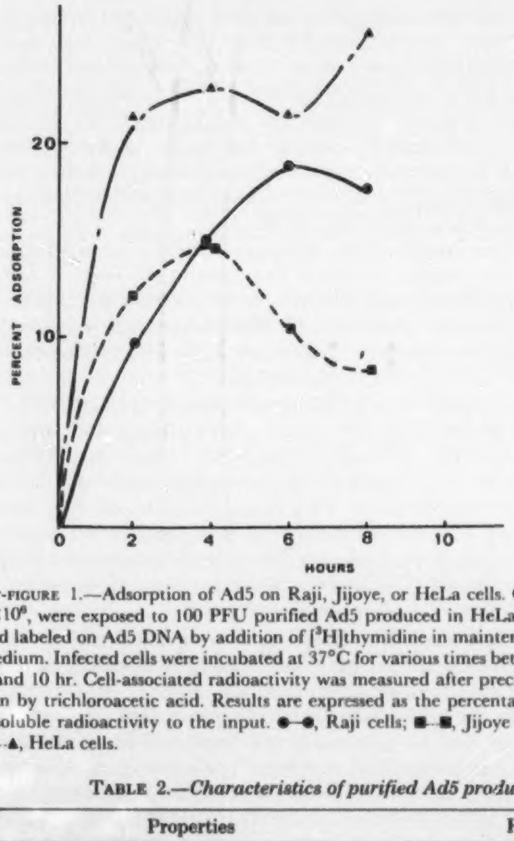

TEXT-FIGURE 1.—Adsorption of Ad5 on Raji, Jijoye, or HeLa cells. Cells, 2×10^6, were exposed to 100 PFU purified Ad5 produced in HeLa cells and labeled on Ad5 DNA by addition of [^{3}H]thymidine in maintenance medium. Infected cells were incubated at 37°C for various times between 2 and 10 hr. Cell-associated radioactivity was measured after precipitation by trichloroacetic acid. Results are expressed as the percentage of insoluble radioactivity to the input. ●—●, Raji cells; ■--■, Jijoye cells; ▲--▲, HeLa cells.

Further experiments were done to eliminate the role of inhibitors. Extracts of uninfected Raji cells did not prevent the Ad5 multiplication in HeLa cells. No interferon was ever detected in uninfected and infected Raji or Jijoye cells.

Properties of Purified Ad5 Produced in Raji and Jijoye Cells

Ad5 was purified through two CsCl gradients from pellets of infected Raji (five expts) and Jijoye cells (six expts) at the third passage. A unique band of virus was found at densities of 1.26–1.29 g/ml in four experiments with Raji cells and in three experiments with Jijoye cells. In other experiments another thin band was also detected at 1.33–1.34 g/ml similar to that obtained with Ad5 purified from HeLa cells. In some experiments, the virus was further purified on a CsCl equilibrium density gradient and no Raji or Jijoye Ad5 was recovered, indicating the virus' fragility. Under the same conditions, HeLa Ad5 was found at 1.34 g/ml. After sucrose centrifugation, Raji or Jijoye Ad5 was recovered.

In the electron microscope, the viruses banding at 1.26–1.29 g/ml were not distinguishable from the virus of HeLa cells and appeared as complete particles of similar sizes. No EBV was seen in these preparations. The usual amount of cellular contaminants was seen. The degree of purity was independent of the number of cells used per pellet or of the high content of serum in the medium. However, Ad5 from lymphoma cells differed from HeLa Ad5 in several properties (table 2). The OD ratio 260:280 nm was lower in Raji and Jijoye Ad5 than in HeLa Ad5, indicating a different ratio of DNA to proteins. The yield of infectious virus per 10^6 cells was reduced 10^5-fold in Raji and four hundredfold in Jijoye cells as compared to that in the HeLa cells. These values varied from one experiment to another as shown by the standard deviation. The infectivities expressed per unit of OD at 260 nm were two thousandfold and twelvefold lower for Raji and Jijoye cells, respectively. Similar results were obtained when expressed per unit OD at 280 nm. With the assumption that only fluorescent cells were producing virus particles, the number of PFU per cell would still be reduced by 7,500-fold and fortyfold.

TABLE 2.—*Characteristics of purified Ad5 produced after three serial passages of infected Raji and Jijoye cells*[a]

Properties	Raji cells	Jijoye cells	HeLa cells
OD ratio 260:280 nm	1.26±0.08 (5)	1.22±0.07 (6)	1.43±0.02 (17)
Production of infectious virus			
PFU/10^6 cells	$7.8\pm3.6\times10^4$ (5)	$3.8\pm2.6\times10^7$ (4)	$1.4\pm0.7\times10^{10}$ (9)
PFU/OD 260 nm	$7.9\pm6.8\times10^8$ (5)	$1.2\pm1.1\times10^{11}$ (11)	$1.5\pm0.8\times10^{12}$ (9)
PFU/10^6 fluorescent cells[b]	2.0×10^6	3.8×10^8	1.5×10^{10}
Hemagglutinating activity, U/OD 260 nm	$6.4\pm5.9\times10^4$ (4)	$5.2\pm4.8\times10^4$ (4)	$1.6\pm0.6\times10^6$ (3)
No. of particles/10^6 cells[c]	$4.3\pm1.0\times10^8$ (5)	$1.5\pm0.4\times10^9$ (5)	$1.0\pm0.1\times10^{10}$ (17)
µg DNA/10^{10} particles	2.34±0.07 (5)	2.13±0.02 (6)	0.447±0.003 (10)
µg Proteins/10^{12} particles	1.93±0.31 (5)	2.00±0.32 (6)	0.26±0.03 (10)

[a] Virus banding at 1.26–1.29 g/ml in CsCl gradient. Means ± SD are accompanied by number of experiments *in parentheses.*

[b] Evaluation with 4% positive fluorescent Raji cells; 10% Jijoye cells, and 90% HeLa cells obtained in indirect immunofluorescence test in the presence of specific Ad5 rabbit antiserum.

[c] The number of particles produced by 10^6 cells was estimated according to the procedures described by Maizel et al. (*13*).

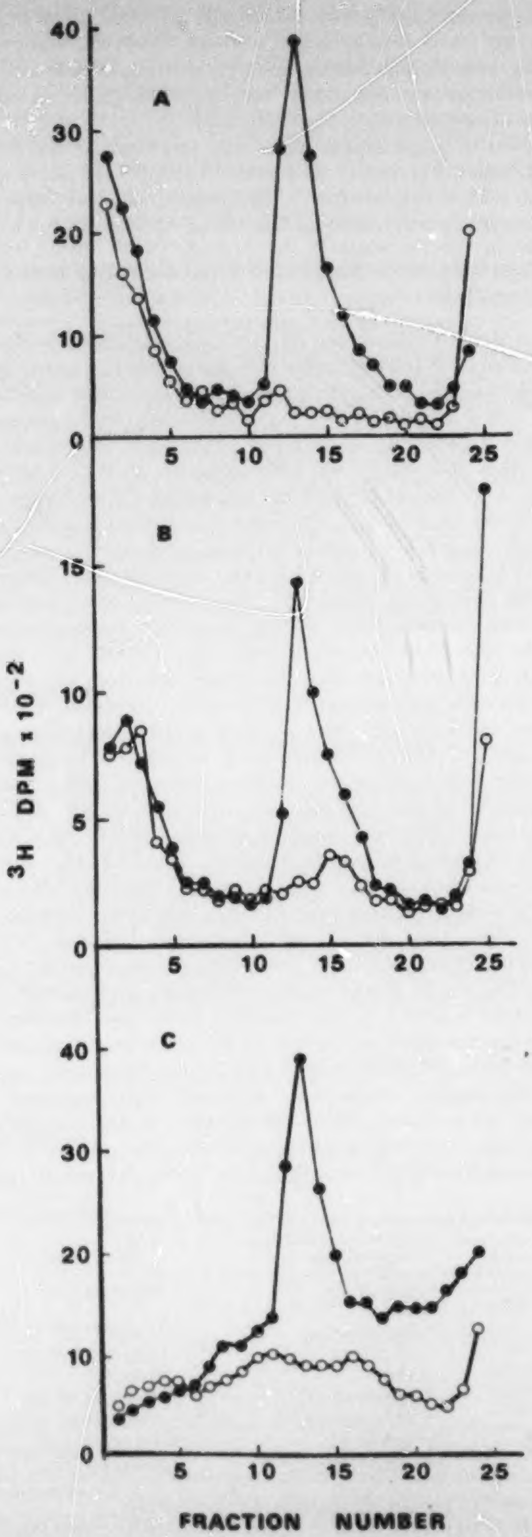

TEXT-FIGURE 2.—Ad5 DNA synthesis in Raji, Jijoye, and HeLa cells. Samples of 5–6×10^6 Raji or Jijoye cells were infected with 100 PFU/cell and incubated at 37°C. On day 3 after infection, 100 μCi [^{3}H]thymidine/ml was added to the medium. After a further incubation for 5 hr at 37°C, the samples were harvested. HeLa cells infected with 100 PFU/cell were used as controls. Uninfected cells were set up in parallel. Pellets of cells were washed twice in phosphate-buffered saline, resuspended at a concentration of 2×10^6 cells/ml (equivalent to 1–2×10^3 positive fluorescent Raji or Jijoye cells), and placed in 0.2 ml lysing solution directly on top of an alkaline sodium iodide density gradient (*8*). After 1 hr at room temperature, the gradients were spun in a Beckman centrifuge (SW41 rotor) at 18,000 rpm for 18 hr at 20°C. Fractions of 400 μl were collected with a Büchler Autodensi-flow RII, and aliquots of 100 μl each were precipitated by 10% trichloroacetic acid. ●—●, DNA from infected cells; ○—○, DNA from control cells. A) Raji cells, 3 days post infection; B) Jijoye cells, 3 days post infection; C) HeLa cells, 17–22 hr post infection. The direction of sedimentation is *from left to right.* DPM=disintegrations/min.

The number of physical particles produced, estimated per 10^6 cells, was similar for Raji and Jijoye cells but one hundredfold lower than that for HeLa cells. Similar amounts of hemagglutinin were found in the three cell lines when estimated per unit OD at 260 nm. From our data of OD at 260 and 280 nm, an estimation suggested that the DNA and protein contents were higher in particles produced in Raji or Jijoye cells than in those produced in HeLa cells—fourfold and sevenfold, respectively.

Virus located in the denser band had a hemagglutinating activity similar to that of the virus in the upper band, but its infectivity remained low. The OD ratio 260:280 nm was close to that of HeLa Ad5. This observation suggested that these virus particles contained more DNA than the light ones but were still not infectious.

Polyacrylamide gel electrophoresis of standard HeLa Ad5 and of the lower and upper bands of Raji and Jijoye Ad5 showed that only upper bands from Raji and Jijoye Ad5 differed by having less hexons and an enlarged 64,000–66,000 band. This finding was similar to a previous description of the virus at the first passage (*5*). The major components were present. The modifications of the polypeptide pattern were also observed after an equilibrium sedimentation sucrose gradient.

When Raji and Jijoye Ad5 were back passed once in HeLa cells, the progeny had polypeptides similar to those of Ad5 serially propagated in HeLa cells.

We did not reduce the infectivity on HeLa cells of Raji or Jijoye Ad5 by increasing one hundredfold to 10^4-fold the number of defective particles. The production of infectious particles was similar when HeLa cells were infected with the same multiplicity of Raji or Jijoye or HeLa Ad5, although the number of particles was significantly different.

The tumor-inducing capacity of Raji and Jijoye Ad5 was tested in newborn and 3-week-old hamsters (10^6 PFU/animal). No tumor was ever observed for 10 months, indicating that the virus did not acquire a higher oncogenicity than did HeLa Ad5. In vitro, these viruses had no higher capacity than did HeLa Ad5 to transform hamster kidney cells or hamster embryo cells and to establish human cord blood lymphocytes as a cell line.

Viral DNA in Infected Raji and Jijoye Cells

DNA synthesized in infected Raji and Jijoye cells was analyzed by alkaline density gradient centrifugation of la-

TABLE 3.—*Ad5 DNA synthesis in Raji, Jijoye, and HeLa cells after three serial passages: Sequential hybridization of Raji, Jijoye, and HeLa Ad5 DNA to HeLa Ad5 DNA*[a]

Unlabeled DNA on filter	^{3}H-labeled DNA	Input, dpm	Hybridized, dpm	Percent hybridization
HeLa Ad5	Raji Ad5			
	Peak 1	15,840	841	5.3
	Peak 2	13,719	770	7.1
	Peak 3	10,332	1,357	13.1
	Peak 4	9,253	2,298	24.8
HeLa Ad5	Jijoye Ad5			
	Peak 1	5,795	1,413	24.4
	Peak 2	5,681	1,468	25.8
	Peak 3	6,420	1,515	23.6
	Peak 4	8,932	2,375	26.6
HeLa Ad5	HeLa Ad5	1,153	830	71.9

[a] Ad5 DNA synthesis was analyzed by alkaline density gradient centrifugation of labeled DNA as described in text-fig. 2. Peak 4 of DNA from Ad5-infected Raji or Jijoye cells was found in the fraction at the same density as the density for HeLa Ad5 DNA. Peaks 1–3 have a low molecular weight. When cellular DNA's were tested with HeLa Ad5 DNA, 1–5% of disintegrations/min (dpm) were hybridized with the use of empty filters that were treated identically to the other filters except that Ad5 HeLa DNA was not adsorbed to them; Raji Ad5 DNA or Jijoye Ad5 DNA hybridized to empty filters to 1–3% of the experimental values.

beled DNA. At the first passage (text-fig. 2), a single peak was observed at the same density for each batch of infected cells. At the third passage, four peaks were found and were tested by hybridization with HeLa Ad5 DNA (table 3). The extent of hybridization was lower for DNA from Ad5-infected Raji and Jijoye cells. For Raji cells only the heavy peak of DNA hybridized with HeLa Ad5 DNA, whereas for Jijoye cells the four peaks of DNA hybridized to the same extent with HeLa Ad5 DNA.

For further studies of the viral DNA, Hirt supernatants of [^{3}H]thymidine-labeled Raji and Jijoye Ad5 were prepared from infected cells at the third passage. The DNA banded at 1.690 instead of 1.715 g/ml for HeLa Ad5 in CsCl gradient centrifugation.

Cleavage by endonucleases of HeLa Ad5 DNA and Jijoye Ad5 DNA, used in equivalent amounts, showed different patterns (fig. 1). Kpn I enzyme gave eight fragments with HeLa Ad5 DNA (fig. 1, col 1) and five fragments with Jijoye Ad5 DNA (fig. 1, col 2). Generally, 10 fragments were detected with Kpn I and HeLa Ad5 DNA, but some fragments that had close molecular weights (1.5×10^6 and 1.4×10^6; 2.3×10^6 and 2.2×10^6) were not separated in our experiment. Moreover, the Jijoye Ad5 DNA was not completely digested as compared to the same amount of HeLa Ad5 DNA, so that much DNA was found at the top of the gel. Bam I endonuclease gave two similarly sized fragments with both DNA's. XBa I and Eco RI each produced four fragments for Jijoye Ad5 DNA versus 3 and 3 fragments, respectively, for HeLa Ad5 DNA.

DISCUSSION

We have shown that human B-lymphocyte lines (Raji and Jijoye), derived from human Burkitt's lymphoma replicated human Ad5, although poorly as compared to the replication by HeLa cells. Virus production was enhanced by serial passages of infected cells. These particles were intermediate between mature and empty particles: They contained less DNA, their polypeptide composition was modified, and they had a low infectivity. The virus genome was also modified. The DNA cleavage pattern by restriction enzymes of Jijoye Ad5 DNA was slightly different from that of HeLa Ad5 DNA, but there was a heterogeneous spread of small fragments throughout in the Jijoye Ad5 DNA sample. Furthermore, Jijoye Ad5 DNA was fragmented at the third passage of infected cells, whereas at the first passage it was not fragmented like the DNA from HeLa Ad5. Factors influencing the production of defective or incomplete particles were not determined.

Only a small proportion of Raji and Jijoye cells was producing Ad5, as shown by immunofluorescence with immune sera and by electron microscopy, although almost every individual cell was infectible as demonstrated by our data on adsorption. Possibly, each cell produced all viral proteins in such low amounts that they were undetectable. Also, some cells might synthesize some components but not others. This hypothesis suggests that some cellular factor(s) active in permissive cells is required for the complete Ad5 cycle and that this factor(s) was present only in a limited number of cells. Furthermore, Ad particles do not always replicate efficiently even in permissive cells that generally produce virus as shown by some enteric Ad (*14*).

It is not known why human B-cell lines were more sensitive to human Ad5 than was the primary culture of lymphocytes. Such a difference could be more general since Ad replication has been reported to be also more efficient in established continuous cultures of oral tumors than in cultures at early passages (*15*).

The yield of defective particles could be influenced by the high multiplicity of infection used. However, at low multiplicity (1 PFU) no infectious virus was detected, and at 10 PFU the virus production was low. In contrast to particles previously described by Daniell (*16*), these particles were not found to interfere with the infectious particles.

In previous experiments, our laboratory (*2*) reported that transformation by EBV of cord blood B-lymphocytes was a necessary step for Ad multiplication. The highest production of Ad5 was obtained in EBV-positive Jijoye cells. However, replication of EBV was not required since phosphonoacetic acid did not prevent replication of Ad5 (*5*). Further experiments with leukemia cell lines also suggest that the EBV genome was not necessary (Faucon N, Ogier G: Unpublished results). The important factor seems to be the state of cell differentiation either induced by EBV or present in some leukemia states or in lymphoma cells or acquired during in vitro cultivation.

The low infectivity of Ad5 produced in Raji and Jijoye cells could be due to changes in viral genome. The fragmentation of viral DNA could be related to its accessibility and its sensitivity to deoxyribonucleases from infected cells. Also, possibly some host cell DNA pieces were encapsidated into the virions. Such DNA structures have been described for Ad2 (*17*) and Ad16 (*18*).

Assuming that in vitro observed modifications of the virus could reflect variations in the expression of the virus in vivo, one may consider the possibility that in humans some pathologic conditions could induce changes in Ad5 during its latency. The modified virus could interact with other factors mainly in cancer.

REFERENCES

(1) Perrinet MC, Chardonnet Y, Sohier R. Etude préliminaire de la multiplication in vitro de l'adénovirus type 5 dans les lymphocytes de sang de cordon ombilical. Ann Microbiol 1974; 125B:575–580.

(2) Faucon N, Desgranges C. Persistence of human adenovirus 5 in human cord blood lymphoblastoid cell lines transformed by Epstein-Barr virus. Infect Immun 1980; 29:1180–1184.

(3) Chardonnet Y, Perrinet MC, Faucon N. Superinfection with adenovirus of lymphoblastoid cell lines. In: de-Thé G, Epstein MA, Zur Hausen H, eds. Oncogenesis and herpesviruses. Vol II. Lyon: IARC, 1975:497–500.

(4) Faucon N, Chardonnet Y, Perrinet MC, Sohier R. Superinfection with adenovirus of Burkitt's lymphoma cell lines. J Natl Cancer Inst 1974; 53:305–308.

(5) Faucon N, Ogier G, Chardonnet Y. Expression of human adenovirus 5 in human and simian lymphoblastoid cell lines after one passage. Microbios Lett 1979; 11:157–162.

(6) Chardonnet Y, Lyon M, Soula A. Identification of the adenovirus components during the penetration in HeLa cells by immunofluorescence technique. Arch Virol 1977; 54:189–199.

(7) Russell WC, Hayashi K, Sanderson PJ, Pereira HG. Adenovirus antigens. A study of their properties and sequential development in infection. J Gen Virol 1967; 1:495–507.

(8) Szafarz D. An improved method for DNA alkaline gradient analysis and its application of the effect of carcinogens on mouse liver DNA. Biochimie 1977; 59:775–778.

(9) Denhardt DT. A membrane filter technique for the detection of complementary DNA. Biochem Biophys Res Commun 1966; 23:641–646.

(10) Aaij C, Borst P. The gel electrophoresis of DNA. Biochim Biophys Acta 1972; 269:192–200.

(11) Laurell CB. Antigen-antibody crossed electrophoresis. Anal Biochem 1965; 10:358–361.

(12) Ouchterlony O. Antigen-antibody reactions in gels. Acta Pathol Microbiol Scand 1949; 26:507–515.

(13) Maizel JV, White DO, Scharff MD. The polypeptides of adenovirus. I. Evidence for multiple protein components in the virion and a comparison of types 2, 7A and 12. Virology 1968; 36:115–125.

(14) Retter M, Middleton PJ, Tam JS, Petric M. Enteric adenoviruses: detection, replication, and significance. J. Clin Microbiol 1979; 10:574–578.

(15) Guest GF, Winters WD. Sensitivity of human oral tumor cells to human adenovirus. J Dent Res 1979; 58:1815–1823.

(16) Daniell E. Genome structure of incomplete particles of adenovirus. J Virol 1976; 19:685–708.

(17) Khittoo G, Weber JM. The nature of the DNA associated with incomplete particles of adenovirus type 2. J Gen Virol 1981; 54:343–355.

(18) Hammarskjold ML, Winberg G, Noorby E, Wadell G. Isolation of incomplete adenovirus 16 particles containing viral and host cell DNA. Virology 1977; 82:449–461.

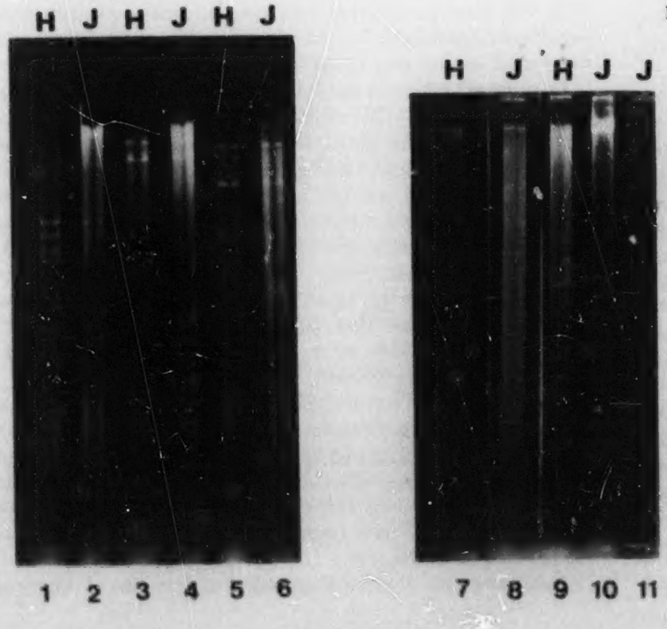

1

Figure 1.—Cleavage by restriction enzymes of HeLa and Jijoye Ad5 DNA Hirt supernatants were prepared from infected HeLa cells (H), fro infected Jijoye cells (J) after three serial passages, and from uninfecte Jijoye cells. Viral DNA was recovered from an equilibrium sedimentati cesium chloride gradient (35,000 rpm for 60 hr). Purified DNA su pressed at 1 mg was mixed with the following restriction enzymes appropriate buffers and incubated for 1 hr at 37°C: 5 U Kpn I (1, 2), U Bam I (3, 4), 5 U XBa (5, 6), and 5 U Eco RI (7, 8). Reaction w stopped by cooling the samples in ice. Whole mixture was layered on 1% agarose gel for analysis. Controls were run simultaneously wi uncleaved HeLa Ad5 DNA, Jijoye Ad5 DNA, and Hirt supernatant Jijoye cell DNA (9, 10, 11).

Primary Liver Carcinoma and Liver Cirrhosis in Atomic Bomb Survivors, Hiroshima and Nagasaki, 1961–75, With Special Reference to Hepatitis B Surface Antigen[1]

Masahide Asano, *M.D.,*[2] **Hiroo Kato,** *M.D.,*[3,4] **Keiko Yoshimoto,** *B.S.,*[3] **Shinichi Seyama,** *M.D.,*[2]
Hideyo Itakura, *M.D.,*[5] **Tadao Hamada,** *M.D.,*[6] *and* **Soichi Iijima,** *M.D.*[7,8]

ABSTRACT—During 1961–75, 128 cases of primary liver carcinoma (PLC) in the Radiation Effects Research Foundation life-span study extended sample and 301 cases of liver cirrhosis in the pathology study sample were observed. The presence of hepatitis B surface antigen (HBsAg) was assessed in all of the cases with the use of orcein and aldehyde fuchsin stains and was confirmed by the immunofluorescence technique. The incidence of PLC was two times higher in Nagasaki than in Hiroshima, which was statistically significant, but little difference was noted in the prevalence of cirrhosis in the two cities. Findings that might possibly explain the higher PLC incidence in Nagasaki were 1) the 2.3 times higher presence in Nagasaki than in Hiroshima of HBsAg in the livers of subjects without liver disease and 2) the two times higher prevalence in Nagasaki than in Hiroshima of cirrhosis with PLC. We believe that the higher incidence of PLC in Nagasaki is attributable to hepatitis B virus infection, although other factors (e.g., immunologic competence affected by radiation) cannot be excluded. In both cities, a suggestive relationship of radiation dose to cirrhosis prevalence, but not to PCL prevalence, was noted. To clarify possible radiation effects on cirrhosis prevalence, further follow-up of the populations of these two cities is necessary.—JNCI 1982; 69:1221–1227.

A relationship between ionizing radiation and solid tumors has been found for cancers of the thyroid gland, breast, and lung from studies on atomic bomb survivors (*1*), but no suggestion has emerged of a relationship between radiation and liver tumors among the survivors (*2, 3*). However, ionizing radiation from other sources (e.g., Thorotrast) has been clinically linked to liver carcinogenesis (*4*), and atomic bomb radiation increased the incidence of liver cell carcinoma in experimental mice, even though no clear relationship between dose and tumor incidence was found (*5*). Recently, Shikata et al. (*6*) reported that orcein and/or aldehyde fuchsin stains, in the form of a surface coat, could be used to demonstrate HBV antigen in Formalin-fixed paraffin tissue sections. Several researchers, including Nayak and Sachdeva (*7*), confirmed by an immunofluorescence technique the identity of the material in liver that stained with orcein and/or aldehyde fuchsin as HBsAg.

In the present study we analyzed the relationship between the effect of ionizing radiation and the incidence of PLC and liver cirrhosis and examined the possible relationship between them and the presence of HBsAg.

MATERIALS AND METHODS

The study of PLC was made from records obtained from the Tumor and Tissue Registry Associations of both Hiroshima and Nagasaki and from surgical pathology and autopsy files at the RERF (formerly the ABCC–Japanese National Institute of Health) for 1961–75. Data for the cirrhosis study were obtained from autopsied cases in the pathology study sample[9] for the same period in both cities. All 128 PLC and 301 cirrhosis cases were histologically confirmed by the investigators upon examination of two or more tissue specimens from each subject. Samples were stained by hematoxylin and eosin, Masson's trichrome, van Gieson's elastic fiber, periodic acid–Schiff, and argyrophilic fiber techniques. Each specimen of PLC included a portion of nontumorous tissue. For assessment of HBsAg in tissue, two slides stained by orcein and aldehyde fuchsin were used. Positive cases were further confirmed by the immunofluorescence technique, in which the sections of tissue were incubated with fluorescein isothiocyanate-conjugated, anti-human HBs serum. The sections then were examined with an Olympus A-REL fluorescence microscope for deposition of HBsAg.

PLC cases were classified by Edmondson's criteria (*9*): liver cell carcinoma (grades I, II, III, and IV), bile duct carcinoma, multiple or combined primary carcinoma (carcinosarcoma, separate liver cell and bile duct carcinomas, and hepatobiliary carcinoma), and squamous cell carcinoma. For analysis, hepatobiliary carcinoma was included in the liver cell carcinoma category, as was done in (*10, 11*).

Liver cirrhosis was classified by Gall's criteria (*12*):

ABBREVIATIONS USED: ABCC = Atomic Bomb Casualty Commission; ATB = at time of bomb; HBsAg = hepatitis B surface antigen; HBV = hepatitis B virus; LSS = life-span study; NIC = not in the city; PLC = primary liver carcinoma; RERF = Radiation Effects Research Foundation; T65 DR = tentative dose, 1965 revised.

---

[1] Received June 23, 1981; revised April 19, 1982; accepted May 12, 1982.

[2] Department of Pathology, Radiation Effects Research Foundation (RERF), 1-2, Sakurababa 1 Chome, Nagasaki 850, Japan.

[3] Department of Epidemiology and Statistics, RERF, 5-2 Hijiyama Park, Minami Ward, Hiroshima City 736, Japan.

[4] *Address reprints requests to* Dr. Kato.

[5] Department of Pathology, Institute for Tropical Medicine, Nagasaki University, Nagasaki, Japan.

[6] Japan Red Cross Atomic Bomb Hospital, Hiroshima, Japan.

[7] Department of Pathology, Nagoya University School of Medicine, Nagoya, Japan.

[8] We sincerely appreciate the diagnostic materials contributed by the member institutions of the Tumor and Tissue Registry Associations of Hiroshima and Nagasaki, which helped to make this study possible.

[9] The pathology study sample, comprised of subjects who had died in the extended LSS, is related to two major programs: the extended LSS and the adult health study sample (*8*).

posthepatitic, postnecrotic, nutritional, congestive, obstructive, pigmentary, and mixed forms of cirrhosis. The few cases of congestive, obstructive, pigmentary, and mixed forms of cirrhosis in the present study were grouped as "other cirrhosis."

Age- and sex-adjusted prevalence rates for PLC and cirrhosis by exposure dose groups were tested for linear increase with dose and for homogeneity (*13*).

RESULTS

Incidence Difference Between Hiroshima and Nagasaki

A total of 128 PLC cases (77 in Hiroshima and 51 in Nagasaki) in the LSS extended sample[10] were examined: 103 (80.5%) liver cell carcinomas (which included hepatobiliary carcinomas), 24 (18.8%) bile duct carcinomas, and 1 (0.78%) squamous cell carcinoma. The sex ratio of males to females was approximately 2.1:1. The average PLC incidence per year was 0.76/10^4 persons in Hiroshima and 1.51/10^4 persons in Nagasaki. The average incidence in Nagasaki was two times higher ($P\leq0.001$) than in Hiroshima (table 1). The average age ATB of patients with PLC was 40.1 years. The age at death among subjects with PLC in Hiroshima ranged from 29 to 83 years (average, 65.3 yr) and from 26 to 83 years (average, 61.7 yr) in Nagasaki.

Of the 128 PLC cases, 43 (55.8%) in Hiroshima and 28 (54.9%) in Nagasaki were associated with liver cirrhosis; no difference in the proportion of cases between cities was noted. Bile duct carcinoma associated with cirrhosis was seen only in two cases (1.5%) (table 2).

TABLE 2.—*Proportion of PLC cases associated with cirrhosis, by city and histologic type, 1961–75*

Histologic type	Incidence, No. (%), in:	
	Hiroshima	Nagasaki
Liver cell carcinoma	62	41
With cirrhosis	42 (67.7)	27 (65.9)
Bile duct carcinoma	14	10
With cirrhosis	1 (7.1)	1 (10.0)
Total, all PLC	77[a]	51
With cirrhosis	43 (55.8)	28 (54.9)

[a] Total includes 1 PLC case classified "other carcinoma" (*see* table 1).

A total of 301 cases of liver cirrhosis (225 in Hiroshima and 76 in Nagasaki) were available in the autopsy series: 225 (74.8%) posthepatitic, 49 (16.3%) postnecrotic, 16 (5.3%) nutritional, and 11 (3.7%) other types of liver cirrhosis. The number of autopsied cases during 1961–75 was 4,920 [3,857 in Hiroshima and 1,063 in Nagasaki (*15*)]. The prevalence rate for cirrhosis was 5.8% in Hiroshima and 7.2% in Nagasaki, with no statistically demonstrable difference between the two cities (table 3). The average age ATB of patients with cirrhosis was 41.4 years in Hiroshima and 37.4 in Nagasaki. The average age at death of patients with cirrhosis was 63.2 years in Hiroshima and 60.5 years in Nagasaki.

Of the 301 cases of cirrhosis, 67 (22.2%) were accompanied by PLC, including 59 (26.7%) posthepatitic, 1 (7.0%) postnecrotic, 4 (25%) nutritional, and 3 (20%) obstructive type. The proportion of cirrhosis associated with PLC was two times higher in Nagasaki than in Hiroshima (table 4).

---

[10] The LSS extended sample, a matched, fixed population of ≈110,000 persons who were living in Hiroshima and Nagasaki at the time of the Atomic Bomb Survivors Survey in 1950 (*14*), is comprised of 2 groups: individuals who had been exposed to the atomic bombs and their controls who were NIC ATB.

TABLE 1.—*Annual incidence rate per 10,000 for PLC, by city, sex, and histologic type, 1961–75*

Histologic type	Hiroshima			Nagasaki			χ^2 test for city difference[a]
	No. of person-years	No. of cases	Incidence rate[b]	No. of person-years	No. of cases	Incidence rate[b]	
			Males				
Liver cell carcinoma		45	1.14		32	2.25	**
Bile duct carcinoma		8	0.20		2	0.14	
Other carcinoma		0	0.00		0	0.00	
Totals	395,370	53	1.34	142,191	34	2.39	**
			Females				
Liver cell carcinoma		17	0.27		9	0.46	*
Bile duct carcinoma		6	0.10		8	0.41	**
Other carcinoma		1	0.02		0	0.00	
Totals	619,027	24	0.39	194,775	17	0.87	**
			Both sexes				
Liver cell carcinoma		62	0.61		41	1.22	**
Bile duct carcinoma		14	0.14		10	0.30	**
Other carcinoma		1	0.01		0	0.00	
Totals	1,014,397	77	0.76	336,966	51	1.51	**

[a] $*=0.01<P\leq0.05$, $**=P\leq0.01$.

[b] Calculated per 10,000 person-years.

TABLE 3.—*Prevalence rate (%) for cirrhosis, by city, sex, and histologic type, 1961–75*

Histologic type	Hiroshima			Nagasaki			χ^2 test for city difference[a]
	No. of autopsies	No. of cases	Prevalence rate[b]	No. of autopsies	No. of cases	Prevalence rate[b]	
Males							
Posthepatitic		112	5.81		42	7.04	
Postnecrotic		20	1.04		8	1.34	
Nutritional		4	0.21		4	0.67	Suggested
Other cirrhosis		3	0.16		4	0.67	
Totals	1,927	139	7.21	597	58	9.72	
Females							
Posthepatitic		62	3.21		9	1.93	Suggested
Postnecrotic		17	0.88		4	0.86	
Nutritional		6	0.31		2	0.43	
Other cirrhosis		1	0.05		3	0.64	
Totals	1,930	86	4.46	466	18	3.86	
Both sexes							
Posthepatitic		174	4.51		51	4.80	
Postnecrotic		37	0.96		12	1.13	
Nutritional		10	0.26		6	0.56	Suggested
Other cirrhosis		4	0.10		7	0.66	
Totals	3,857	225	5.83	1,063	76	7.15	

[a] $0.05<P\leq0.10$.
[b] Calculated per No. of autopsies.

TABLE 4.—*Proportion of cirrhosis cases associated with PLC, by city and histologic type, 1961–75*

Histologic type	Incidence, No. (%), in:	
	Hiroshima	Nagasaki
Posthepatitic cirrhosis	174	51
With PLC	37 (21.3)	22 (43.1)
Postnecrotic cirrhosis	37	12
With PLC	0	1 (8.3)
Nutritional cirrhosis	10	6
With PLC	2 (20.0)	2 (33.3)
Total, all cirrhosis[a]	225	76
With PLC	40 (17.8)	27 (35.5)

[a] Totals for the two cities include 11 cirrhosis cases classified as "other cirrhosis" (*see* table 3).

Incidence Relationship to Radiation

In both cities the air dose estimated for each survivor was based on his or her distance ATB from the hypocenter, as modified by various transmission factors, and was expressed in terms of tissue kerma in the air. The estimated dose system was developed in 1965, was revised in 1980, and now is known as T65 DR.[11] The annual incidence rate was calculated for 5 dose groups: 0, 1–49, 50–99, 100–199, and $\geq$200 rad as shown in table 5. The nonexposed NIC group is included in this table. No relationship between radiation dose and PLC incidence (table 5) and of PLC incidence accompanied by cirrhosis was demonstrated. An association between radiation dose and cirrhosis prevalence was suggested. (Four cases in the unknown dose group were excluded.) A significant association of postnecrotic cirrhosis with radiation dose ($P\leq0.01$) was noted (table 6; text-fig. 1). No relationship was observed between radiation dose and the prevalence of cirrhosis combined with PLC.

The relationship between radiation dose and the incidence of PLC or cirrhosis was further investigated in 4 groups categorized by age ATB. However, although the prevalence of cirrhosis in the $\geq$100-rad group seems higher than that of the controls (NIC + 0-rad group) at ages 0–19 and 35–49 years ATB, the difference was not statistically significant.

HBsAg Detection in Liver Tissue

HBsAg in the livers of persons with PLC and with cirrhosis was determined with the use of orcein and aldehyde fuchsin stain, and the positive cases were confirmed with the immunofluorescence technique. Of 128 PLC cases and 301 cirrhosis cases, 106 and 231, respectively, were available for the HBsAg study. Hepatocytes positive for HBsAg were present mainly in the noncancerous areas of the liver and were unevenly distributed. Cellular deposition of orcein and aldehyde fuchsin stains appeared in the cytoplasm but rarely was found near the cytoplasmic membrane. The HBsAg-positive rate was 20.0% for PLC cases in Hiroshima and 19.6% in Nagasaki (table 7) and was 18.7% for cirrhosis cases in Hiroshima and 18.4% for Nagasaki (table 8). Con-

---

[11] A reevaluation of the atomic bomb dosimetry is in progress (*16*). Preliminary estimates suggest lower neutron and higher γ-ray doses from the Hiroshima bomb than those calculated according to the T65 DR and smaller changes in dose estimates for Nagasaki. However, because the total estimated doses are similar to those calculated according to the T65 DR system, and the dose categories used in the current analysis are broad, the conclusions reached would not be altered were the suggested new dosimetry adopted.

TABLE 5.—*Annual incidence rate per 10,000 for PLC, by dose and histologic type, 1961–65*

Histologic type	Incidence, No. (rate per 10,000)						χ^2 test[a]	
	NIC	T65 DR, rad						
		0	1–49	50–99	100–199	≥200	L[b]	H[c]
Liver cell carcinoma	30 (0.89)	23 (0.60)	36 (0.83)	9 (1.57)	2 (0.40)	3 (0.61)	NS	*
Bile duct carcinoma	6 (0.18)	7 (0.18)	10 (0.21)	0	1 (0.26)	0	NS	NS
Total, all PLC	37[d] (1.09)	30 (0.78)	46 (1.05)	9 (1.58)	3 (0.62)	3 (0.66)	NS	Suggested

[a] NS=not significant ($P>0.10$).

[b] L=linear increase with dose (one tailed).

[c] H=homogeneity of dose groups regardless of pattern; *=$0.01<P\leq0.05$; suggested=$0.05<P\leq0.10$.

[d] Total includes 1 PLC case classified as "other carcinoma" (*see* table 1).

TABLE 6.—*Prevalence of cirrhosis, by radiation dose and histologic type, 1961–75*

Histologic type	Prevalence, No. (%)						χ^2 test	
	NIC	T65 DR, rad						
		0	1–49	50–99	100–199	≥200	L[a]	H[b]
Posthepatitic	71 (6.61)	58 (4.07)	61 (3.54)	16 (6.55)	6 (3.32)	10 (5.26)	*	**
Postnecrotic	9 (0.84)	7 (0.50)	18 (1.05)	7 (2.62)	4 (2.11)	3 (1.57)		
Nutritional	3 (0.28)	4 (0.28)	9 (0.52)	0	0	0		
Total, all cirrhosis[c]	84 (7.81)	72 (5.14)	93 (5.36)	24 (9.77)	11 (5.98)	13 (6.72)	Suggested	

[a] L=linear increase with dose (one-tailed); *=$0.01<P\leq0.05$, Suggested=$0.05<P\leq0.10$.

[b] H=homogeneity of dose regardless of pattern; **=$0.001<P\leq0.01$.

[c] Totals include 3 posthepatitic cases and 1 postnecrotic case classified in "unknown dose group" that were excluded from this analysis and 11 cases classified as "other cirrhosis" (*see* table 3).

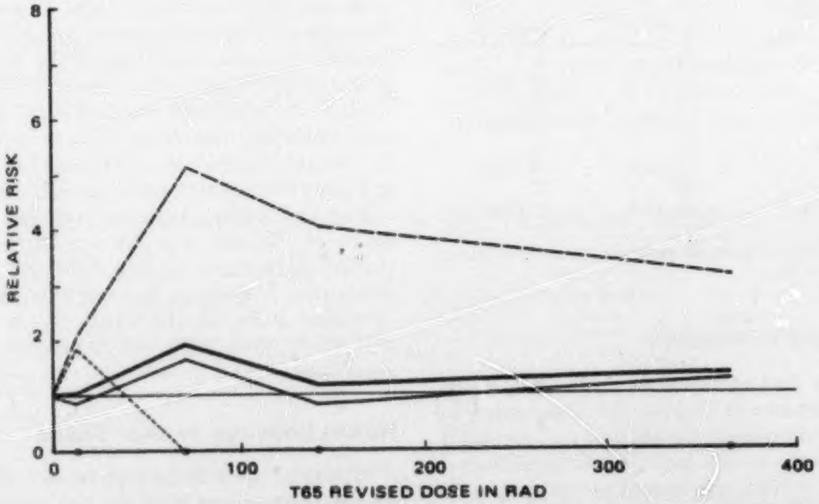

TEXT-FIGURE 1.—Relative risk of liver cirrhosis, by dose and histologic type, for Hiroshima and Nagasaki combined. ▬ = total, ___ = posthepatitic, - - - = postnecrotic, ····· = nutritional.

versely, a higher percentage of positive HBsAg was detected in PLC cases with cirrhosis [35.5% in Hiroshima and 35.7% in Nagasaki (table 7)] and in cirrhosis cases with PLC [39.3% in Hiroshima and 33.3% in Nagasaki (table 8)]. The HBsAg-positive rate seemed unrelated to radiation dose in both PLC and cirrhosis (tables 7, 8).

HBsAg was positive in the cytoplasm of tumor cells in 4 PLC cases, as confirmed by orcein and aldehyde fuchsin staining and also by the immunofluorescence technique. The cytoplasm of some giant cells also was positive. The cytoplasm in most tumor cells was diffusely positive, and in some the positive material was localized as a granular mass like an inclusion body. Nuclei were never positive. The 4 HBsAg-positive cases, 2 in each city, were classified as grade III liver cell carcinoma by Edmondson's criteria (*9*).

When randomly selected livers of subjects without overt liver disease (102 in Hiroshima and 111 in Nagasaki) were examined for HBsAg, positive findings were 5.4% for Hiroshima subjects and 12.5% for Nagasaki subjects. Consequently, HBsAg was 2.3 times more common in Nagasaki than in Hiroshima; the lowest positive rate was for those persons 50 years of age or older (table 9). Positive rates tend to be lower for the older age-ATB group.

TABLE 7.—*Proportion of HbsAg-positive PLC cases, by city and radiation dose, 1961–75*

Histologic type	No. (%) of cases			
	T65 DR, rad			Total
	NIC+0	1–99	≥100	
Hiroshima				
PLC	31	23	1	55
HBsAg-positive PLC	6 (19.4)	4 (17.4)	1 (100.0)	11 (20.0)
PLC with cirrhosis	16	14	1	31
HBsAg-positive PLC with cirrhosis	6 (37.5)	4 (28.6)	1 (100.0)	11 (35.5)
Nagasaki				
PLC	20	26	5	51
HBsAg-positive PLC	6 (30.0)	3 (11.5)	1 (20.0)	10 (19.6)
PLC with cirrhosis	11	14	3	28
HBsAg-positive PLC with cirrhosis	6 (54.5)	3 (21.4)	1 (33.3)	10 (35.7)
Both cities				
PLC	51	49	6	106
HBsAg-postive PLC	12 (23.5)	7 (16.7)	2 (33.3)	21 (19.8)
PLC with cirrhosis	27	28	4	59
HBsAg-positive PLC with cirrhosis	12 (44.4)	7 (25.0)	2 (50.0)	21 (35.6)

TABLE 8.—*Proportion of HbsAg-positive cirrhosis cases, by city and radiation dose, 1961–75*

Histologic type	No. (%) of cases			
	T65 DR, rad			Total
	NIC+0	1–99	≥100	
Hiroshima				
Cirrhosis	82	58	11	155[a]
HBsAg-positive cirrhosis	17 (20.7)	7 (12.1)	5 (45.5)	29 (18.7)
Cirrhosis with PLC	14	13	1	28
HBsAg-positive cirrhosis with PLC	6 (42.9)	4 (30.8)	1 (100.0)	11 (39.3)
Nagasaki				
Cirrhosis	29	37	10	76
HBsAg-positive cirrhosis	8 (27.6)	4 (10.8)	2 (20.0)	14 (18.4)
Cirrhosis with PLC	11	13	3	27
HBsAg-positive cirrhosis with PLC	6 (54.5)	2 (15.4)	1 (33.3)	9 (33.3)
Both cities				
Cirrhosis	111	95	21	231[a]
HBsAg-postive cirrhosis	25 (22.5)	11 (11.6)	7 (33.3)	43 (18.6)
Cirrhosis with PLC	25	26	4	55
HBsAg-positive cirrhosis with PLC	12 (48.0)	6 (23.1)	2 (50.0)	20 (36.4)

[a] Total includes 4 cirrhosis cases classified in "unknown dose groups" that were excluded from analysis.

TABLE 9.—*HBsAg-positive rate for control group, 1961–75*

Age ATB	Hiroshima		Nagasaki	
	No. of controls	No. (%) HBsAg-positive cases	No. of controls	No. (%) HBsAg-positive cases
0–9	13	1 (7.69)	21	3 (14.29)
10–19	23	1 (4.35)	33	7 (21.21)
20–34	21	2 (9.52)	24	4 (16.67)
35–49	27	1 (3.70)	21	1 (4.76)
≥50	18	0 (0.00)	12	0 (0.00)
Totals	102	5 (4.90)	111	15 (13.51)
Age-adjusted rate[a]		(5.37)		(12.51)

[a] Statistical test for difference in age-adjusted rate between Hiroshima and Nagasaki is $0.05<P<0.10$.

DISCUSSION

Schreiber et al. (*2, 3*) reported that the twofold difference between Hiroshima and Nagasaki in PLC prevalence was in part explained by the greater tendency in Nagasaki subjects for cirrhosis to be associated with PLC. Furthermore, no effect of radiation on the PLC prevalence was observed, but a positive association was made between radiation and cirrhosis prevalence in a study of the ABCC 1961–67 autopsy series. In the present study, the number of specimens examined was increased by inclusion of tissues obtained during surgery and the time was extended to 1975. The average PLC incidence per year was two times higher in Nagasaki than in Hiroshima, and a suggestive association existed between cirrhosis prevalence and radiation dose. The higher incidence of PLC in Nagasaki cannot be explained by an increased prevalence of cirrhosis, because no clear difference was found in the number of cirrhosis cases for the two cities (5.8% in Hiroshima and 7.2% in Nagasaki). Conversely, as pointed out by Schreiber et al. (*2, 3*), the fact that 21% of posthepatitic cirrhosis was associated with PLC in Hiroshima and 43% in Nagasaki may be a contributing factor. Lewin and Millis (*17*) reported that atrophy with lobular collapse and portal tract fibrosis occurred in a later stage of liver damage due to radiation, but that the condition was not the same as radiation-induced liver cirrhosis. Inasmuch as a tendency toward a greater incidence of cirrhosis associated with PLC was observed in the NIC and 0-rad group as well as in the 1-rad-or-more groups, some factors other than radiation probably were involved in the genesis of combined PLC and cirrhosis.

Viral hepatitis is generally accepted as being one of the more important antecedent lesions to posthepatitic or postnecrotic cirrhosis. Reports from several countries (*18*) reveal a strong correlation between HBsAg prevalence and PLC mortality. In the present study, the HBsAg-positive rate for both cities combined was about 20% for livers with PLC, 19% for livers with cirrhosis, 35.6% for livers with both PLC and cirrhosis diagnosed as PLC, and 36.4% for livers with both PLC and cirrhosis diagnosed as cirrhosis. Corresponding rates between the two cities were not significantly different. For the livers of Nagasaki subjects with PLC, HBsAg-positive rates of 54.8 and 29% were reported by Kanda (*19*) and Sato et al. (*26*), respectively. In Tokushima Prefecture, where the rate of death from PLC is the highest, HBsAg was positive for 60% of the livers of subjects with PLC (*21*). The relatively lower positive rate for HBsAg in the present study might be explained by sample bias. The sample, composed of relatively older survivors and restricted to those who lived in Hiroshima or Nagasaki, excluded individuals living in places where the positive rate is particularly high. Sakurai (*22*) reported that the HBsAg was more frequent in livers than in sera of patients with PLC and/or cirrhosis. A decrease in HBsAg prevalence was observed in the sera of older people (*23*). Such a trend also was recognized for the livers of the subjects in our study. Despite the failure to detect any difference between the two cities in the prevalence of positive HBsAg in the livers of patients with PLC and/or cirrhosis, the HBsAg-positive rates for the livers of patients without overt disease were 4.9% in Hiroshima and 13.5% in Nagasaki. Belsky et al. (*24*) reported that the occurrence of hepatitis-associated antigen in the sera of Nagasaki subjects was almost 1.4 times that of the Hiroshima subjects. Kato et al. (*25*) recently confirmed that the frequency of positive HBsAg in sera from the same sample as in (*24*) (the adult health study[12] sample) was about 1.5 times higher in Nagasaki (3.3%) than in Hiroshima (2.0%).

Thung et al. (*26*) and several other investigators (*7, 27, 28*) have reported that HBsAg was found in tumor cells. In our study, HBsAg-positive tumor cells were detected in only 4 of 128 PLC cases, and the distribution of cases was similar for the two cities.

In an international workshop on hepatitis B and liver cancer, Ziegler et al. (*29*) concluded that risk factors may include exposure to HBV, age at onset of infection (tolerance), duration of infection, immunologic determinants, nutritional status, and virus strain (virulence). Ziegler and colleagues reported evidence of HBV infection in the early life of some PLC patients, indicating perinatal infection from mothers who were carriers. Macnab et al. (*30*) described a human hepatoma cell line, PLC/PRF/5, that produces HBsAg in vitro. They also reported spherical virions (seen by electron microscope) in the supernatant tissue culture medium of the cell line. Gyorkey et al. (*31*) described multifocal PLC in postnecrotic cirrhotic nodules when juvenile monkeys were given HBV before the administration of diethylnitrosamine. Thus the high incidence of PLC in Nagasaki might be attributed to early HBV infection. The twofold difference in the prevalence of bile duct carcinoma between Hiroshima and Nagasaki subjects has not been explained. Further studies on other factors, such as nutritional status, mycotoxins, tolerance, immunologic competence, and virulence of HBV, are necessary.

REFERENCES

(*1*) Finch SC, Moriyama IM. The delayed effects of radiation exposure among atomic bomb survivors, Hiroshima and Nagasaki, 1945–79. A brief summary. Radiation Effects Research Foundation technical report 16, 1978.

(*2*) Schreiber WM, Kato H, Robertson JD. Primary carcinoma of the liver in Hiroshima and Nagasaki, Japan. Cancer 1970; 26:69–75 (also ABCC TR 15–69).

(*3*) ———. Cirrhosis of the liver, Hiroshima–Nagasaki, 1 October 1961–31 December 1967. Atomic Bomb Casualty Commission technical report 17, 1969.

(*4*) Hutchinson GB. Carcinogenic effects of medical irradiation. In: Hiatt HH, et al., eds. Origins of human cancer. Cold Spring Harbor, N.Y.: Cold Spring Harbor Laboratories, 1977:501–509.

(*5*) Upton AC, Furth WK, Christenberry KW, et al. Some delayed effects of atomic bomb radiations in mice. Cancer Res 1960; 20:1–62.

(*6*) Shikata T, Uzawa T, Yoshiwara N, et al. Staining methods of Australia antigen in paraffin section—detection of cytoplasmic inclusion bodies. Jpn J Exp Med 1974; 44:25–36.

(*7*) Nayak NC, Sachdeva R. Localization of hepatitis B surface antigen in conventional paraffin sections of the liver. Am J Pathol 1975; 81:479–492.

(*8*) Atomic Bomb Casualty Commission–Japanese National Institute of Health. ABCC–JNIH pathology studies, Hiroshima–Nagasaki, research plan. Atomic Bomb Casualty Commission technical report, 12, 1962.

(*9*) Edmondson HA, Steiner PE. Primary carcinoma of the liver. A study of 100 cases among 48,900 necropsies. Cancer 1954; 7:462–503.

(*10*) Patton RB, Horn RC Jr. Primary liver carcinoma. Autopsy study of 60 cases. Cancer 1964; 17:757–768.

(*11*) Gall EA. Primary and metastatic carcinoma of the liver. Relationship to hepatic cirrhosis. Arch Pathol Lab Med 1960; 71:226–232.

(*12*) ———. Posthepatitic, postnecrotic and nutritional cirrhosis. Am J Pathol 1960; 36:241–271.

(*13*) Beebe, GW, Kato H, Land CE. Studies of the mortality of A-bomb survivors. 4. Mortality and radiation dose, 1950–66. Radiat Res 1971; 48:613–649.

(*14*) ———. Studies of the mortality of A-bomb survivors. 6. Mortality and radiation dose, 1950–74. Radiat Res 1978; 75:138–201 (also RERF TR 1–77).

(*15*) Yamamoto T, Moriyama IM, Asano M, Guralnick L. The autopsy program and the Life-Span Study, January 1961–December 1975. Radiation Effects Research Foundation technical report 18, 1978.

(*16*) Reevaluations of dosimetric factors, Hiroshima and Nagasaki. Symposium sponsored by the U.S. Department of Energy. Germantown, Md., Sept. 15–16, 1981.

(*17*) Lewin KL, Millis RR. Human radiation hepatitis. A morphologic study with emphasis on the late changes. Arch Pathol 1973; 96:21–26.

(*18*) Blumberg BS, Larouzé B, London WT, et al. The relation of infection with the hepatitis B agent to primary hepatic carcinoma. Am J Pathol 1975; 81:669–682.

(*19*) Kanda T. Hepatitis B surface antigen in cirrhosis of the liver and primary liver carcinoma in Nagasaki area. A histopathological study. Jpn J Tropic Med Hyg 1977; 5:117–139.

(*20*) Satoh T, Takahara O, Takahashi N, et al. Clinicopathological study on the primary hepatoma of the atomic bomb survivors. Nagasaki Med J 1978; 53:392–397.

(*21*) Nose T, Akagi G, Otsuka H. Studies on autopsy cases of liver cirrhosis in Tokushima, with special reference to HB antigen and liver diseases. Acta Hepatol Jpn 1976; 17:109–115.

(*22*) Sakurai M. A histopathologic study of cirrhosis and hepatitis B antigen in hepatocarcinogenesis. Igaku No Ayumi 1981; 118:520–527.

(*23*) Szmuness W. Recent advances in the study of the epidemiology of hepatitis B. Am J Pathol 1975; 81:629–650.

(*24*) Belsky JL, King RA, Ishimaru T, Hamilton HB, Nakahara Y. Hepatitis-associated antigen in atomic bomb survivors and nonexposed control subjects: Seroepidemiologic survey in a fixed cohort. J Infect Dis 1973; 128:1–6 (also ABCC-JNIH TR 30–71).

(*25*) Kato H, Mayumi M, Nishioka K, Hamilton HB. The relationship

---

[12] The adult health study is a program of systematic medical examinations at RERF outpatient clinics, at 2-yr intervals, of selected subjects in Hiroshima and Nagasaki. The study, a subsample of the LSS extended sample, initially numbered ≈20,000 individuals.

of HBs antigen antibody to radiation in the Adult Health Study sample, 1975–77. Radiation Effects Research Foundation technical report 13-80.

(26) THUNG SN, GERBER MA, SARNO E, POPPER H. Distribution of five antigens in hepatocellular carcinoma. Lab Invest 1979; 41:101–105.

(27) KOSTICH ND, INGHAM CD. Detection of hepatitis B surface antigen by means of orcein staining of liver. Am J Clin Pathol 1977; 67:20–30.

(28) PUI-CHEE WU. Patterns of hepatitis B surface antigen. Localization in cells of hepatocellular carcinoma. Arch Pathol Lab Med 1975; 103:165–168.

(29) ZIEGLER JL, ADAMSON RH, BARKER LF, FRAUMENI JF JR, GERIN J, PURCELL, RH. International workshop on hepatitis B and liver cancer: *Special report.* J Natl Cancer Inst1978; 60:717.

(30) MACNAB GM, ALEXANDER JJ, LECATSAS G, et al. Hepatitis B surface antigen produced by a human hepatoma cell line. Br J Cancer 1976; 34:509–515.

(31) GYORKEY F, MELNICK JL, MIRKOVIC R, CABRAL GA, GYORKEY P, HOLLINGER FB. Experimental carcinoma of liver in macaque monkeys exposed to diethylnitrosamine and hepatitis B virus. J Natl Cancer Inst 1977; 59:1451–1467.

blank page

Epidemiology of Familial Predisposition for Breast Cancer in Japan[1, 2]

Motoi Murata, *Ph.D.*,[3] **Keijiro Kuno**, *M.D.*,[4] **Atsuo Fukami**, *M.D.*,[4] *and* **Goi Sakamoto**, *M.D.*[5,6]

ABSTRACT—The physical and reproductive traits known to be risk factors for breast cancer were correlated with familial predisposition for this disease by the use of hospital records of 3,867 patients with breast cancer, of whom 186 had one or more relatives with breast cancer and were called "familial patients." Various characteristics in the total series of patients were compared with familial patients matched for year of birth. The mean age at menarche was significantly less in familial compared with the total series of patients, especially for premenopausal patients; however, no difference was observed in the mean age at marriage between the two groups. Familial patients were slightly taller as compared to the total series of patients, but no difference was detected in body weight between the two groups. Because age at menarche and the stature are highly correlated, they may be influenced by an underlying common hormone effect that may influence the familial nature of breast cancer.—JNCI 1982; 69:1229–1234.

The familial nature of breast cancer has been well demonstrated by a number of studies (*1–5*). So far, however, our knowledge of the nature of the genetic effect responsible for this familial observation is very poor. Studies on various genetic markers such as blood groups, serum proteins, red cell enzyme polymorphisms, cerumen type, and HLA antigens in breast cancer patients have not been revealing (*6–9*). The glutamic-pyruvic transaminase locus might be chromosomally linked to the possible dominant gene relevant to a specific hereditary type of breast cancer, but it is not necessarily linked to familial nature of breast cancer in general (*10*). Genetic control in the etiologic role of hormone factors has also been suspected. Studies on the familial relationship of breast cancer with various endocrine profiles such as the estrogen quotient (ratio of estriol to estrone plus estradiol) and prolactin level in urine or plasma have until now provided conflicting results (*11–15*).

In the present study, we attempt an epidemiologic approach to this problem by using hospital records of breast cancer patients in Japan. In discriminating a familial predisposition to breast cancer among the total breast cancer patients, we are not aware of any dominant type of hereditary breast cancer, as has been reported by other authors (*16, 17*), because patients having more than one relative with the disease are reported very rarely in this country. It is presently not clear what fraction of hereditary breast cancer is generally composed of those dominant types. Thus in this study, we define familial breast cancer as including all patients with any familial history of the disease, and we examine the association of familial history and other risk factors. Specifically, we attempt to determine whether the familial cases differ from unselected total cases in any one of those physical and reproductive traits that are generally known to be associated with breast cancer etiology (*18, 19*).

MATERIALS AND METHODS

Epidemiologic data.—Hospital records of 3,867 patients with breast cancer who were treated at the Cancer Institute Hospital, Tokyo, during 1946–77 formed the basis of the present study. The hospital records included information on the following epidemiologic properties: birth date; residence (registered domicile); age(s) at surgery, menarche, marriage, and menopause; parity; number of miscarriages; lactation, medical, and family histories; body height and weight at the time of admission; site of tumor; and histologic diagnosis. Because these demographic, reproductive, and physical traits are well known to have been changing for the last several decades in Japan (*20*), all patients were grouped into cohorts of 5-year birth periods (table 1). Among all items, information on body size was available only for patients treated between 1969 and 1977 (1,826 patients). Registered domicile is not necessarily the present address, but it is mostly that at the time of the patient's marriage and sometimes her or her husband's birthplace. Family history of cancer was obtained by a patient being asked if she ever knew about any contraction of cancer in her first- and second-degree relatives. Totally, 186 patients were recorded as having one or more relatives with breast cancer (table 2). These patients who responded affirmatively will hereafter be called "familial patients." Despite the fact that the information of family history had not been medically verified, information of a positive family history is likely to be accurate, whereas information of a negative family history may or may not be correct.

We emphasize that completion of individual items in the hospital record depended solely on the examining clinician at the time of the patient's admission; as such, the quality of some items is not necessarily homogeneous among different years. If any clinicians were not willing to obtain epidemiologic data, the individual items were left unanswered and such "unknown" items are not distinguishable from truly negative ones. Evaluation of such traits as being married or unmarried, parity, and number of miscarriages was rather ambiguous. To eliminate the instances of un-

---

[1] Received July 15, 1981; revised May 27, 1982; accepted June 17, 1982.

[2] Supported in part by a Grant-in-Aid for Cancer Research from the Ministry of Health and Welfare of Japan.

[3] Division of Genetics, National Institute of Radiological Sciences, Chiba 260, Japan.

[4] Department of Surgery, Cancer Institute Hospital, Tokyo 170, Japan.

[5] Department of Pathology, Cancer Institute, Tokyo 170, Japan.

[6] We are indebted to Dr. D. E. Anderson for his careful reading of and comments on the manuscript, and we also thank Mrs. S. H. Tsuji for her technical help in preparing the manuscript.

TABLE 1.—*Number of breast cancer patients and controls by birth cohorts*

Birth years	Breast cancer patients		Controls
	Premenopausal (familial)	Postmenopausal (familial)	
-1884	0	29	0
1885–89	0	38	0
1890–94	1	80 (2)	0
1895–99	6	137 (2)	0
1900–04	46 (1)	235 (13)	0
1905–09	96 (5)	265 (20)	98
1910–14	178 (7)	273 (6)	463
1915–19	281 (18)	219 (4)	1,297
1920–24	434 (20)	163 (12)	3,362
1925–29	554 (20)	91 (8)	5,799
1930–34	410 (28)	25	7,986
1935–39	192 (12)	6 (1)	9,960
1940–44	84 (7)	1	8,393
1945–49	15	1	2,076
1950-	7	0	122
Total	2,304 (118)	1,563 (68)	39,556

known items as much as possible, we tried to use those patients who were recorded as having a positive family history of any cancer (1,401 patients) in place of using total patients. These positive family history patients were representative of the total series with regard to such things as the distribution of birth year, age at surgery, and residence.

Because a control group matched for such characteristics as age and residence was not available, we were obliged to use as the reference population a group of women participating in a cervical cancer screening program. This group will hereafter be called the "control population." It comprises 39,556 women living in Chiba prefecture who attended the screening clinic from April 1977 to March 1978 and who were known to be healthy. Distribution of their birth dates, ages, and residences differ noticeably from those of the patient group. Information on lactation and body size was not available for the control population. In addition, marital status of the control population was dissimilar to that of the general population, single women being very rare among the control population. Data on body height and weight of healthy Japanese women can be obtained from the results of the National Survey on Nutritional Condition conducted by the Ministry of Health and Welfare for 1969–77 (*21*). This survey includes about 14,000 women randomly sampled from all over Japan every year. Accordingly, the data obtained by this survey may be regarded as the national mean value. The expected value of height and weight for breast cancer patients was calculated from the survey results by the year and age at observation being matched. It is, however, generally known that both body measurements vary by districts, especially between urban and rural areas, in Japan (*22*). Because about one-half of the patients were living in the Tokyo metropolitan area, the observed value for body size may be larger than the expected value.

TABLE 2.—*Distribution of positive familial history of breast cancer*[a]

Kinship	Premenopausal	Postmenopausal
Mother	41	11
Sister	37	34
Grandmother		
Paternal	4	2
Maternal	4	2
Aunt		
Paternal	16	7
Maternal	28	8
Daughter	0	9
Paternal uncle	1	0
Total single cases	107	62
Total multiple cases	11	6

[a] Data were derived from hospital records of patients with breast cancer who were treated at the Cancer Institute Hospital, 1946–77.

For individual items the mean values were compared, in different birth cohorts, between the patient and control groups and were further compared within the patient group between the familial and total patients. We did not use the usual method for comparison of familial and nonfamilial patients because we would need to illustrate additional comparisons between the nonfamilial and total patients, even though no differences might be expected between them because of the meagerness of the familial patient series.

Multivariate analysis.—Because the interrelatedness of some of these traits is known, association of a specific one to a familial predisposition for breast cancer should be evaluated after that trait is adjusted for the other variables. For this purpose, multiple regression analysis with a logistic model (*23*) was performed. If Y_i is a binary expression (yes–no) of family history in the ith patient, then the logit of Y_i is given by a linear combination of predictor variables X, $\log[Y_i/(1 - Y_i)] = b_0 + b_1X_{1i} + b_2X_{2i} + \ldots + b_kX_{ki}$, where b_1 to b_k are partial regression coefficients. For the X's, ages at menarche and marriage, body height and weight, residence, and parity were chosen. For postmenopausal patients only, age at menopause was included. Thus $k=6$ and 7, for premenopausal and postmenopausal patients, respectively. Lactation history was not included because of its categorical characteristic. Residence, though it is indeed categorical, was dealt with as a quantitative trait by numbers being assigned as follows: 1 for urban (special wards of Metropolitan Tokyo and large cities), 2 for smaller cities, and 3 for rural areas. Patients married longer than 40 years were counted at 40 years of age at marriage.

It is rather cumbersome to deal quantiatively with unmarried patients, especially when age at surgery was les than 40 years. We would need to introduce a function o probability of being married later than that age. Instead just arbitrarily, 3 years plus age at surgery were given fo the unmarried patients. Incidentally, of those women wh were unmarried at age 30, one-third to one-half will marr by age 40 in Japan (*24*). The concealed discrimination o unmarried and ever married was included when parity wa counted. Because a complete set of information was require for each patient, patients included in the regression analysi were restricted to those treated in 1969 and later, of whic 55 were familial premenopausal and 30 were familial pos menopausal patients, respectively.

We made 10 analyses by using the same set of thes familial patients and different sets of twice as many nonfa milial patients randomly chosen every time by matchin age and birth year. We calculated the maximum likelihoo estimates of the regression coefficients by using the Newton-Raphson iterative technique. Association of a specific variable can be evaluated by a significance test of the *t*-value for the coefficient *b*.

RESULTS

Distribution of age at surgery in the total breast cancer series as well as in the familial series of patients is shown in text-figure 1, according to menopausal status. The mean age in the total series was 48.5±0.2 years and, in the familial series, 47.2±0.7 years, with a nonsignificant difference. The distribution for familial patients appears to be bimodal. A statistical test (*25*) for "bitangentiality" indicated two peaks around the ages of 40 and 46 years, but the bimodality was not statistically significant. Familial cases were slightly more frequent in premenopausal (5.1%) than in postmenopausal patients (4.4%).

Residence of the patients was classified as urban, suburban (small cities), or rural as described in "Materials and Methods." The relative proportions of patients varied among the different residence groups, though the differences were not significant; the proportion of urban patients was highest in the familial postmenopausal patients (62.7%) and was lowest in the familial premenopausal patients (47.8%) whereas it was 54.9% in the total patients

The mean age at menarche in individual birth cohorts is given in text-figure 2. It shows a continuous decline since the early 1900's at a rate of 0.055±0.005 years/chronologic year in the control population. This decline coincides with the secular trend observed in other survey studies (*20, 22*). The leveling off seen around the 1930's probably reflects the inferior nutritional condition during the Second World War. Although not illustrated, the mean age at menarche in urban- and suburban-dwelling women was consistently less than that of rural women, the difference averaging 0.34±0.07 years ($P<0.01$). This finding suggests that the age at menarche is considerably influenced by the women's living environment and/or life-style. The age at menarche in breast cancer patients is consistently less than that of the control population, the difference averaging about 0.26±0.06 years ($P<0.01$), which in turn is smaller than the urban–rural difference. Familial patients exhibit a still younger age at menarche compared with the age at menarche of the total patients, the difference being 0.34±0.10 years ($P<0.01$). After only premenopausal patients are chosen, the disparity appears even more convincing (0.36±0.07, $P<0.01$).

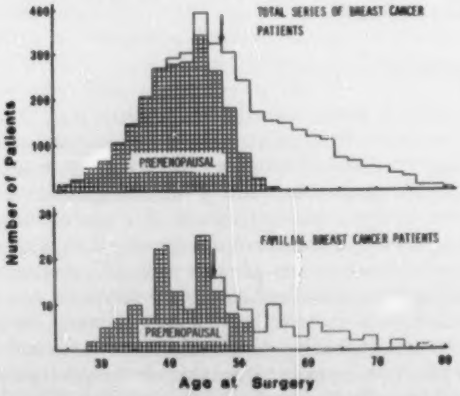

TEXT-FIGURE 1.—Age distribution of breast cancer patients treated at the Cancer Institute Hospital, 1946–77. *Arrow* indicates mean age.

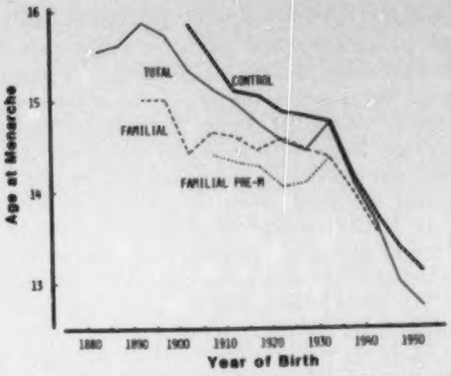

TEXT-FIGURE 2.—Changes in mean age at menarche by year of birth for total and familial series of patients and for familial premenopausal patients (PRE-M) and controls.

With respect to the age at marriage, the control population shows a gradual increase up to the 1930's, after which it declines. A consecutively older age at marriage was observed in urban and suburban residents as compared with rural residents ($P<0.01$). Breast cancer patients tended to marry about 1 year later than control women ($P<0.01$), with no difference between the total and familial series. Information on their first childbearing was not available; however, this may be related to their age at marriage. We discovered, using about 900 cervical cancer patients at the National Institute of Radiological Sciences, that the two ages (i.e., ages at marriage and first childbearing) exhibited a strict linear relationship except for marriage at ages over 32 years. Thus the difference observed above in the age at marriage seems congruent with the difference observed in the age at first childbearing (*26, 27*). The proportion of unmarried women in breast cancer patients was 8.4%, with no difference due to family history of cancer. The corresponding value in the general population was roughly 5% by age 45, though there have been some fluctuations in these decades (*24*).

The proportion of nulliparous among ever-married patients was 21.1%. The corresponding value in the general population was reported at 7–8% by a national census (*24*) or 5–6% by the Survey Study of Reproductive Force (*28*). In familial patients, nulliparous women constitued 16.5%, being not significantly different from 21.1%. The mean number of either live-born children or miscarriages per ever-married patient was 2.2±0.13 and 0.8±0.09, respectively, whereas it was 2.0±0.05 and 0.7±0.03, respectively, among ever-married familial patients. These are all smaller than the corresponding values (2.4±0.04 and 1.1±0.05, respectively) of the control population. Thus the differences observed between the patient and control groups for various reproductive traits compare well to the results reported by other authors (*18, 19*), though any conclusive remarks should not be stated because this is not a case-control study. Regarding lactation history, the proportion of patients who never breast fed as well as the proportion of patients of poor milk secretion were both slightly lower in familial patients than they were in the total series, for which we lack control data. Mean age at menopause was not different between the familial and the total series of patients, either with or without distinguishing cases of artificial menopause.

Body height and weight changes in breast cancer patients by birth cohorts are given with expected values in text-figure 3. For body height, the observed value was consistently larger than the expected in any birth cohorts. The difference was, on the average, 2.2 cm ($P<0.001$) for premenopausal and 3.0 cm ($P<0.001$) for postmenopausal patients, respectively. This taller stature might be attributable to the effect of unmatched residence. Disparity between the total and familial series of patients was also noted and, especially in premenopausal patients, was statistically significant (1.2 cm, $P<0.01$). The correlation coefficient between the stature and the age at menarche was estimated at −0.118, which is, even though very small, statistically significant ($P<0.01$). For body weight, the observed value was larger than expected only in the older cohort groups, which mostly consist of postmenopausal patients. If confined to such patients, the difference was 2.3 kg ($P<0.001$). Familial patients were only slightly heavier but were not thought to be more obese, as measured in terms of the Quetelet Index (weight/height^2) when compared to the total patients.

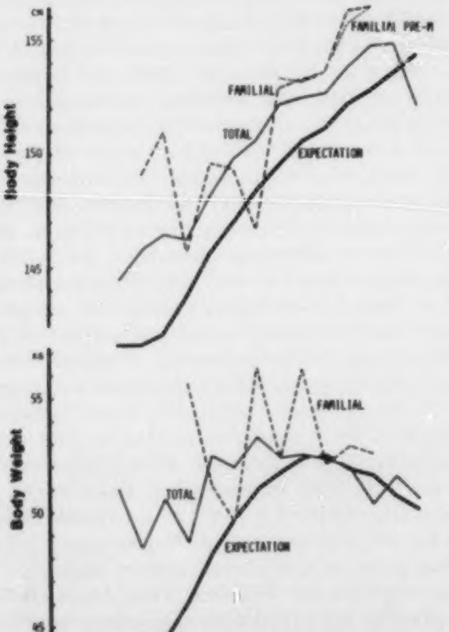

TEXT-FIGURE 3.—Changes in mean body height and weight by year of birth of unselected breast cancer patients in 1969–77. Expected values were calculated from National Survey data. For body weight data, dotted line includes familial patients as well as familial premenopausal patients.

TABLE 3.—*Family history of breast cancer and various risk factors for the disease*

Variable	Partial regression coefficients (*b*) and their *t*-values[a]			
	Premenopausal		Postmenopausal	
	b	*t*	*b*	*t*
Age at menarche	−0.415	2.15	0.286	1.10
Body height	0.160	0.84	0.510	1.93
Body weight	0.132	0.70	0.040	0.16
Residence	0.142	0.81	−0.203	0.75
Age at marriage	−0.143	0.66	0.377	1.40
Parity	0.023	0.12	0.465	1.56
Age of menopause	—	—	0.047	0.18

[a] Mean of 10 repeated analyses.

No disparity was observed between the total and familial series of patients in the distribution of histologic types of tumor, nor was there disparity in the family history of other cancers. Earlier benign breast disease such as mastopathy, mastitis, and benign tumor was reported in about 13% of the patients, with no difference due to the family history of breast cancer.

Results of multiple regression analysis are shown in table 3. Association of each variable with family history of breast cancer can be evaluated with the *t*-value for the regression coefficient. Values given in table 3 represent the mean of 10 estimates obtained recurrently. In premenopausal patients, only the age at menarche is significantly associated with family history; taller stature is not statistically significant in contrast with the feature observed in text-figure 3. In postmenopausal patients, however, the association of body height is very close to the significant level, whereas the age at menarche is not. Furthermore, with respect to such traits as residence, age at marriage, and parity, the association of family history is very different in premenopausal and postmenopausal patients. Although the regression coefficient is not statistically significant for any of these traits, familial postmenopausal patients seem more likely to live in an urban or Western environment in comparison to the other groups of patients.

DISCUSSION

The present results have provided some insight into the nature of the familial predisposition of breast cancer. Familial aggregation of a disease can be caused by *a*) genetic similarity, *b*) common environmental exposure within a family, or *c*) the combined effects of *a* and *b*. One of us (Murata M: Unpublished observations), by analyzing the family history of cancer in the control population, has observed a site-specific intrafamilial correlation not only in blood relatives but also in relatives by marriage for cancers of various sites including the breast. Environmental factors, such as life-style, nutritional intake, and socioeconomic status, should be adjusted so that the true genetic contributions to the etiology are clarified (*29*). Unfortunately, the present analysis lacks such information. Nevertheless, with multivariate analysis, it seems to have elucidated some interesting results regarding this point. The association of various risk factors with the familial nature of breast cancer differs according to whether this cancer occurs in premenopausal or postmenopausal patients: early menarche and/or taller stature are important characteristics of familial premenopausal patients, whereas in postmenopausal patients only body height is strongly correlated with a familial predisposition.

It might be argued that the difference observed between the total and familial series of patients in either the age at menarche (0.36 yr) or body height (1.2 cm) is too small to totally explain the twofold to threefold excess risk of familial predisposition to breast cancer among women (*18, 19*). The evidence is that both of these traits are genetically controlled: The heritability estimate from the parent–child correlation shows a considerably high value (*30–32*), and studies of twins have also revealed a marked hereditary component (*33*). However, it is also true that both traits are strongly influenced by environmental, especially nutritional, conditions. Rapid chronologic changes as well as urban–rural differences observed in the present data confirm it. If considering that such environmental effects would have concealed a possible underlying genetic contribution, the genetic correlation between the disease susceptibility and the relevant trait might become smaller. Because we know nothing about chromosome linkage between the genes controlling breast cancer susceptibility and the aforementioned trait (menarche or stature), we are not sure whether the observed correlation might be attributable to genetic or nongenetic causes. However, the discordant features observed in premenopausal and postmenopausal patients could not be explained satisfactorily by either genetic or nongenetic causes alone.

Consequently, the present results may be interpreted as follows: Familial predisposition of breast cancer in premenopausal patients is primarily attributable to genetic causes, at least a part of which should be related with body growth in infancy and childhood and thus with the age at menarche. Probably, some underlying hormone conditions are controlled by the same genetic factor, which in turn enhances the susceptibility of the mammary tissue to certain environmental carcinogens. Almost nothing is known about genetic heterogeneity among individuals of the general population with respect to various endocrine profiles. Endocrinologic control of puberty is as yet quite obscured (*34*). Thus, even though several interesting studies on the relation of the hormone factors with the family history of breast cancer have been reported recently (*12–15, 35–37*), interpretation of the present finding should wait for further accumulation of data. Familial predisposition in postmenopausal patients, however, seems to be influenced by some different factors, because early menarche does not bear any relation to familial breast cancer. If any genetic determinant of body growth is associated as a risk factor for the late-onset disease, the determinant must be of a kind that is independent of menarche-related effects. Because such nongenetic traits as residence and age at marriage are moderately related to the familial predisposition of this group, it is conceivable that stature also represents some nutritional circumstances rather than its being simply a hereditary characteristic of a family. If so, various nongenetic risk factors could be thought to cause familial predisposition of postmenopausal breast cancer.

The positive association between age at menarche and family history of breast cancer may alternatively be explained by a synergistic effect of both traits: As such, some nonhormone hereditary factor is more likely to be expressed as breast cancer in women with early menarche. Positive (*38*) and negative (*3*) findings on the synergistic effect of both traits have been reported. Such an effect could really not be clarified with the present data and probably could not be clarified by even a more refined analysis with matched controls, when consideration is given to the fact that family history of cancer is by no means independent of nongenetic risk factors as discussed above.

With respect to the age at onset of disease, it has been frequently reported that patients with a positive family history of breast cancer tend to be diagnosed from several to more than 10 years earlier than are nonfamilial patients (*39, 40*). Anderson (*2*) has proposed that the effect of a hereditary factor should be more predominant in premenopausal than postmenopausal breast cancer. Familial cases, as reported here, are also slightly more frequent in premenopausal than postmenopausal patients. Nevertheless, average age at surgery is not significantly different between the total and familial series of patients. This lack of significance may be interpreted by the fact that the relative proportion of postmenopausal breast cancer is as yet not so large in Japan (40%) as it is in the Caucasian populations (70%). Furthermore, a comparative pathology study (*41*) has demonstrated that postmenopausal breast cancer in Japanese women, as contrasted with that in American women, still has predominant characteristics of the premenopausal disease, even though it has been diagnosed after the menopause: Incidence of lobular carcinoma is quite infrequent, whereas that of papillotubular carcinoma is more common in Japanese women. The differential prognosis of premenopausal and postmenopausal patients in the United States is nonexistent in Japan. Hence it is presumed that both types of breast cancer may also resemble each other according to their etiologic aspects in Japan. However, Adami et al. (*42*) found no significant trend toward early occurrence of familial breast cancer in Sweden. In addition, we carefully reexamined Macklin's data (*43*) on the age-specific mortality rate of breast cancer in blood relatives of patients with the disease and noticed that the rate is consistently higher at all ages as compared with that in the U.S. general population, except at the perimenopausal ages, i.e., 55–59 years. Thus even with Caucasian patients, the age reduction due to the familial predisposition is not necessarily a general finding. As the age–incidence relationship could be an eloquent tool for investigating the etiologic role of the possible hereditary susceptibility in carcinogenesis (*44*), more convincing studies would be required.

REFERENCES

(*1*) CLEMMESEN J. Statistical studies in the aetiology of malignant neoplasms. I. Review and results. Acta Pathol Microbiol Scand 1965; suppl 174:1–543.

(2) Anderson DE. A genetic study of human breast cancer. J Natl Cancer Inst 1972; 48:1029–1034.

(3) Brinton LA, Williams RR, Hoover RN, Stegens NL, Feinleib M, Fraumeni JF Jr. Breast cancer risk factors among screening program participants. JNCI 1979; 62:37–44.

(4) Adami HO, Hansen J, Jung B, Rimsten Å. Familiality in breast cancer: A case-control study in a Swedish population. Br J Cancer 1980; 42:71–77.

(5) Holm NV, Hauge M, Harvald B. Etiologic factors of breast cancer elucidated by a study of unselected twins. JNCI 1980; 65:285–298.

(6) Vogel F. ABO blood groups and disease. Am J Hum Genet 1970; 22:464–475.

(7) King MC, Petrakis NL. Genetic markers and cancer. In: Mulvihill JJ, Miller RW, Fraumeni JF Jr, eds. Genetics of human cancer. New York: Raven Press, 1977:281–290.

(8) Petrakis NL. Genetic cerumen type, breast secretory activity, and breast cancer epidemiology. In: Mulvihill JJ, Miller RW, Fraumeni JF Jr, eds. Genetics of human cancer. New York: Raven Press, 1977:297–300.

(9) Anderson DE, Haas C. Genetic marker study in familial breast cancer. In: Severi L, ed. Tumor of early life in man and animals. Perugia: Perugia Quadrennial International Conferences on Cancer, 1978:537–549.

(10) King MC, Go RC, Elston RC, Lynch HT, Petrakis NL. Allele increasing susceptibility to human breast cancer may be linked to the glutamate-pyruvate transaminase locus. Science 1980; 208:406–408.

(11) Lemon HM. Genetic predisposition to carcinoma of the breast: Multiple human genotypes for estrogen 16 alpha hydroxylase activity in Caucasians. J Surg Oncol 1972; 4:255–273.

(12) Henderson BE, Gerkins V, Rosario I, Casagrande J, Pike MC. Elevated serum levels of estrogen and prolactin in daughters of patients with breast cancer. N Engl J Med 1975; 293:790–795.

(13) Morgan RW, Vakil DV, Brown JB, Elinson L. Estrogen profiles in young women: Effect of maternal history of breast cancer. JNCI 1978; 60:965–967.

(14) Fishman J, Fukushima DK, O'Conner J, Lynch HT. Low urinary estrogen glucuronides in women at risk for familial breast cancer. Science 1979; 204:1089–1091.

(15) Boffard K, Clark GM, Irvine JB, et al. Serum prolactin, androgens, oestradiol and progesterone in adolescent girls with or without a family history of breast cancer. Eur J Cancer Clin Oncol 1981; 17:1071–1077.

(16) Lynch HT, Krush AJ, Lemon HM, Kaplan AR, Condit PT, Bottomley RH. Tumor variation in families with breast cancer. JAMA 1972; 222:1631–1635.

(17) Anderson DE. Breast cancer in families. Cancer 1977; 40:1855–1860.

(18) Volherr H, Messer RH. Breast cancer: Potentially predisposed and protecting factors. Am J Obstet Gynecol 1978; 130:335–358.

(19) Thomas DB. Epidemiologic and related studies of breast cancer etiology. In: Lilienfeld AM, ed. Reviews in cancer epidemiology. Vol 1. Amsterdam: Elsevier/North-Holland 1980:153–217.

(20) Takahashi E. Ecologic human biology in Japan. Tokyo: Medical Information Services, 1978:218.

(21) Department of Public Health, Ministry of Health and Welfare. Present status of nutritional condition in Japan. 1974. Tokyo: Daiichi Shuppan, 1977:220.

(22) Kimura K. Growth studies of the Japanese. In: Watanabe S, Kondo S, Matsunaga E, eds. Anthropological and genetic studies on the Japanese. Tokyo: Univ Tokyo Press, 1975:15–32.

(23) Cox DR. The analysis of binary data. London: Chapman, 1970.

(24) Bureau of Statistics, Office of the Prime Minister. Summary of the results of the 1970 population census of Japan. 1975.

(25) Haldane JB. Simple tests for bimodality and bitangentiality. Ann Eugen 1952; 16:359–364.

(26) MacMahon B, Cole P, Lin TM, et al. Age at first birth and breast cancer risk. Bull WHO 1970; 43:209–221.

(27) Tulinius H, Day NE, Johannesson G, Bjarnason Ó, Gonzales M. Reproductive factors and risk for breast cancer in Iceland. Int J Cancer 1980; 21:724–730.

(28) Institute of Population Problems, Ministry of Health and Welfare. Report of the seventh survey of reproductive force of Japanese women, conducted in 1977. 1978.

(29) Tokuhata GK. Morbidity and mortality among offspring of breast cancer mothers. Am J Epidemiol 1969; 89:139–153.

(30) Damon A, Damon ST, Reed RB. Age at menarche of mother and daughters with a note on accuracy of recall. Hum Biol 1969; 41:161–175.

(31) Roberts JA. Multifactorial inheritance in relation to human traits. Br Med Bull 1961; 17:241–246.

(32) Furusho T. Genetic study on stature. Jpn J Hum Genet 1974; 19:1–25.

(33) Cavalli-Sforza LL,Bodmer WF. The Genetics of human populations. San Francisco: Freeman, 1971:965.

(34) Brook CG. Endocrinological control of growth at puberty. Br Med Bull 1981; 37:281–285.

(35) Siiteri PK, Hammond GL, Nisker JA. Increased availability of serum estrogens in breast cancer: A new hypothesis. In: Pike MC, Siiteri PK, Welsch CW, eds. Hormones and breast cancer. Cold Spring Harbor, N.Y.: Cold Spring Harbor Laboratory, 1981:87–106.

(36) Bulbrook RD, Thomas BS, Fantl VE, Hayward JL. A prospective study of the relation between thyroid function and subsequent breast cancer. In: Pike MC, Siiteri PK, Welsch CW, eds. Hormones and breast cancer. Cold Spring Harbor, N.Y.: Cold Spring Harbor Laboratory, 1981:131–141.

(37) Ottman R, Hoffman PG, Siiteri PK. Estrogen receptor assays in familial and nonfamilial breast cancer. In: Pike MC, Siiteri PK, Welsch CW, eds. Hormones and breast cancer. Cold Spring Harbor, N.Y.: Cold Spring Harbor Laboratory, 1981:197–211.

(38) Bain C, Speizer FE, Rosner B, Belanger C, Hennekens CH. Family history of breast cancer as a risk indicator for the disease. Am J Epidemiol 1980; 111:301–308.

(39) Haagensen CD. Disease of the breast. Philadelphia: Saunders, 1970.

(40) Anderson DE. Genetic predisposition to breast cancer. Recent Results Cancer Res 1976; 57:10–20.

(41) Sakamoto G, Sugano H, Hartmann WH. Comparative pathological study of breast carcinoma among American and Japanese women. In: McGuire WL, ed. Breast cancer. Vol 4. New York: Plenum, 1981:211–231.

(42) Adami HO, Hansen J, Jung B, Rimsten Å. Characteristics of familial breast cancer in Sweden: Absence of relation to age and unilateral versus bilateral disease. Cancer 1980; 48:1688–1695.

(43) Macklin MT. Comparison of the number of breast-cancer deaths observed in relatives of breast-cancer patients, and the number expected on the basis of mortality rates. J Natl Cancer Inst 1959; 22:927–951.

(44) Moolgavkar SH, Knudson AG Jr. Mutation and cancer: A model for human carcinogenesis. JNCI 1981; 66:1037–1052.

Establishment and Characterization of a Human Colony-Stimulating Factor-Producing Cell Line From a Squamous Cell Carcinoma of the Thyroid Gland [1,2,3]

Tetsuro Okabe,[4] Hitoshi Nomura,[5] *and* Nakaaki Oshawa[4,5,6]

ABSTRACT—A human colony-stimulating factor (CSF)-producing cell line, T3M-5, has been established in vitro from a squamous cell carcinoma of the thyroid gland transplanted into athymic nude mice [congenitally athymic BALB/c (*nu/nu*) mice; Central Institute for Experimental Animals, Kawasaki, Japan]. Contaminating fibroblasts derived from a host nude mouse were eliminated by treatment with antiserum raised against nude mouse cells. T3M-5 cells have been continuously propagated during 3 years. The cells grew in a monolayered sheet with about 22 hours of population-doubling time and showed about 40% plating efficiency. The cells exhibited an epithelium-like morphology resembling the structure of the original tumor and showed tumor takes when inoculated into nude mice. Chromosome analysis revealed the cell line to be a human aneuploid line with a hypertriploid mode. The cells possessed the characteristic function of human CSF production in vitro and produced marked neutrophilia in tumor-bearing nude mice that were inoculated with the cultured cells. The molecular weight of the CSF was estimated at about 27,000 and was stable over the pH range 1.0–9.0 at 4°C for 21 hours. The CSF activity was destroyed by either trypsin or chymotrypsin, but it resisted neuraminidase, DNase, and RNase. The cells could be well propagated in roller bottles. About 100 liters of the conditioned medium was obtained with the roller bottle culture method, which formed approximately 500,000,000 colonies of human bone marrow cells. The rate of recovery of CSF activity from the gel-filtration column was high (68.9%). This cell line is therefore expected to aid in the large-scale preparation of human CSF.—JNCI 1982; 69:1235–1243.

Studies on thyroid cancer have been hampered by the lack of suitable experimental models. A readily available, relatively inexpensive means of growing such tumors would aid many investigations. The advent of in vitro model systems of human thyroid cancer has increased the demand for tumor cell lines from this cancer. Since the first report in 1967 by Jones et al. (*1*), few such cell lines of undisputed pedigree have been described (*2*). In an attempt to isolate a human tumor cell line, xenotransplantation of tumors seemed at first remarkably convenient for repetition of the primary culture. However, it was rather difficult to remove contaminating host fibroblasts from the cultures.

Recently, we have succeeded in the elimination of host fibroblasts for the cultivation of human tumors transplanted into nude mice (*3*). With the use of this method, a new human thyroid cancer cell line that produces human CSF has been established in vitro. Human CSF-producing cell lines have been isolated from a variety of tumors, such as squamous cell carcinoma of the oral cavity (*4*), large cell carcinoma of the lungs (*5*), carcinoma of the pancreas (*6*), hematologic cancers (*7, 8*), and transformed trophoblasts (*9*). However, until now, no thyroid cancer cell lines have been shown to produce CSF in vitro. Partial purification and characterization of the CSF are also described in this report.

MATERIALS AND METHODS

A 71-year-old Japanese female died of disseminated metastases of thyroid squamous cell carcinoma on February 2, 1978. A moderate granulocytosis and hypercalcemia persisted throughout her hospital course. At autopsy the tumor mass was transplanted into athymic nude mice and has been maintained since then by serial passages (*10*). One tumor of the second transfer generation was removed from the nude mouse on December 7, 1978, in an attempt to establish a squamous cell carcinoma cell line of the thyroid gland.

Culture medium.—The cell line was established and maintained in F-10 synthetic medium (Flow Laboratories Inc., Rockville, Md.) supplemented with 10% FBS (Flow Laboratories Inc.), 100 μg streptomycin/ml, and 100 U penicillin/ml. Cells were harvested with 0.25% trypsin (1:250; Difco Laboratories, Detroit, Mich.) and 0.02% EDTA in calcium- and magnesium-free balanced salt solution.

Elimination of fibroblasts in primary culture.—The tumor tissues were rinsed twice with F-10 medium and minced finely with small surgical scissors. The minced pieces were treated with trypsin solution and then incubated in EDTA as described previously (*3*). The treated pieces were dispersed in F-10 medium with 10% FBS, immediately dispensed into plastic culture vessels (Falcon 3002 and 3013; Falcon Plastics, Oxnard, Calif.), and incubated at 37°C in a humidified atmosphere of 5% CO_2 in air. Sparsely populated colonies of large epithelial cells attached to grow within 1–2 weeks.

ABBREVIATIONS USED: BSA=bovine serum albumin; CSF=colony-stimulating factor; FBS=fetal bovine serum; H & E=hematoxylin and eosin; MW=molecular weight; pI=isoelectric point.

---

[1] Received December 28, 1981; revised May 21, 1982; accepted June 17, 1982.

[2] Supported by cancer research grants from the Japanese Ministry of Health and Welfare and from the Japanese Ministry of Education, Science and Culture, Tokyo, Japan.

[3] Animals were maintained under the guidelines set forth by the Central Institute for Experimental Animals, Kawasaki, Japan.

[4] The Third Department of Internal Medicine, Faculty of Medicine, University of Tokyo, Hongo 7-3-1, Tokyo, 113 Japan.

[5] Central Institute for Experimental Animals, Kawasaki, 211 Japan.

[6] We thank Dr. Y. Ueyama, the Central Institute for Experimental Animals, for provision of human tumors; and Dr. N. Sato, the Third Department of Internal Medicine, Faculty of Medicine, University of Tokyo, for his support.

They were surrounded by considerable numbers of fibroblasts that were derived from stromal tissues of the tumor. To remove the fibroblasts, we treated the cultures with rabbit antiserum raised against nude mouse spleen cells in the presence of complement as described previously (*2*).

Serial subcultures.—During the subsequent 3 weeks of the primary culture, it became apparent that a heterologous population of polygonal cells with large nuclei had propagated and reached confluence. We initiated subcultures at 1:3 dilution with trypsin and EDTA solution. Adaptation to rapid growth on the medium was accomplished during the subsequent 4 months of continuous culture. At the time of the submission of this report, the cells had been subcultured to passage 112. During this period of continuous propagation, cells of different passages were stored in liquid nitrogen. After thawing, the stored cells could be propagated in culture without noticeable change in growth and CSF production.

Transplantation of cells into nude mice.—The cells (5×10^6) of passage 80 were harvested in 0.3 ml of medium and inoculated sc into the tissue on the flank of 3 nude mice. Nodules were detected in all 3 animals 2 weeks after the transplantation. Peripheral granulocyte counts were examined, and the mice were killed and submitted to histologic section.

Growth curve.—The cells of passage 60 were studied to estimate the population doubling time. The initial cell number was 5×10^4 cells per dish for a total of 16 dishes (Falcon 3001; 35×10 mm). The cells were grown in 2 ml of medium as described for serial subcultures. A cell count was taken each day in two dishes, and the growth medium was changed every day.

Histologic examination.—All the extirpated tumors from the nude mice were fixed in isotonic buffered Formalin (10%, vol/vol) stained with H & E, and examined under a light microscope. Cells in the petri dishes were photographed directly without stain with the use of a phase-contrast condenser.

Chromosome analysis.—For chromosome preparations, the cultured cells in exponential growth phase were treated with 0.2 μg Colcemid/ml (Grand Island Biological Co., Grand Island, N.Y.) for 2–3 hours at 37°C and then with hypotonic 0.5% KCl solution for 20 minutes. The cells were then fixed with methanol-acetic acid (3:1). After three changes of the fixative, the cells were dropped onto wet slides, air dried, and stained with conventional Giemsa dye.

Characterization of granulocytic CSF.—The cells were cultivated in 570-mm roller bottles at 0.5 rpm velocity. The confluent culture was incubated in serum-free medium supplemented with 1% BSA fraction V detoxicated by the method of McLeod et al. (*11*). The conditioned medium was harvested, centrifuged at 3,000 rpm for 20 minutes to remove cellular debris and precipitated material, and then stored at −20°C until used. Pooled conditioned medium was concentrated twelvefold to sixteenfold by ultrafiltration, with the use of the thin-channel apparatus with PM-10 membrane. We then transferred a 500-ml sample to a Sephadex G-75 column (35×50 cm; flow rate 700 ml/hr) equilibrated with 0.01 *M* Tris-HCl buffer (pH 7.4), containing 0.15 *M* NaCl and Tween 20. The void volume of this column was 15 liters, determined by blue dextran. The fractions containing CSF activity were pooled and concentrated twentyfold by ultrafiltration with a PM-10 membrane. The pooled fractions with CSF activity on human bone marrow cells (4 mg/ml; sp act, 2,280 U/mg) were incubated with 20 μg trypsin/ml (sp act, 1,000 U/mg), and 20 μg chymotrypsin/ml (sp act, 50 U/mg) in 0.01 *M* Tris-HCl buffer (pH 7.4) for 2 hours at 37°C. In each case the fraction-to-enzyme ratio was 1:1 and 10:1. For neuraminidase treatment, the fraction was incubated with 2 μg neuraminidase/ml (sp act, 29 U/mg) in 0.04 *M* acetate buffer (pH 5.0) for 2 hours at 37°C. For DNase or RNase treatment, the fraction was incubated with 1 mg DNase I/ml (sp act, 3,175 U/mg) or 1 mg RNase A/ml (sp act, 50 U/mg) in 0.01 *M* Tris-HCl buffer (pH 7.4) for 2 hours at 37°C. The reaction was terminated by the addition of 250 μl of FBS, and the mixture was then dialyzed against 0.01 *M* Tris-HCl buffer (pH 7.4) and assayed.

Effect of temperature on CSF activity.—The fraction containing CSF activity on human bone marrow cells (4 mg/ml; sp act, 2,280 U/mg) was heated for 30 minutes in a water bath at various temperatures up to 75°C. It was then cooled, dialyzed against 0.01 *M* Tris-HCl buffer (pH 7.4), and assayed.

Effect of pH on CSF activity.—The fraction with CSF activity on human bone marrow cells was incubated in various buffers at pH 1.0–13.0 by the addition of 1.0 *M* HCl or NaOH for 21 hours at 2°C. For adjustment we used 0.1 *M* KCl-HCl buffer (pH 1.0), citrate-phosphate buffer (pH 3.0, or 5.0, or 7.0), glycin-NaOH (pH 9.0 or 11.0), and KCl-NaOH buffer (pH 13.0). A test sample of 25 μl was incubated with 975 μl of each buffer, 10% FBS was added, and the sample was dialyzed against 0.01 *M* Tris-HCl buffer (pH 7.4) and assayed.

CSF activity.—The procedure of Bradley and Metcalf (*12*) was used with a slight modification. C3H/HeN mouse and human bone marrow cells (from healthy volunteers) were seeded at 100,000 and 200,000 per plate, respectively, after removal of adherent cells by the method of Messner et al. (*13*). The factor was added directly to the plates and always assayed at two levels, usually 0.05 and 0.1 ml per plate. We incubated the culture at 37°C in 7.5% CO_2. We determined the number of colonies (≥50 cells) on day 7 (mouse cells) and day 10 (human marrow cells) with a dissecting microscope at 25× magnification. We aspirated individual aggregates with a micropipette and stained them with 0.6% orcein in 60% acetic acid for morphologic identification. A unit of activity represents one colony formed during the time period of the assay.

Morphologic analysis of colonies—We performed routine morphologic analysis on human colonies after 14 days of culture when eosinophil, macrophage, and neutrophil colonies were enumerated. We also used the following cytochemical methods for the identification of the cells: naphthol ASD chloroacetate esterase, naphthol AS-D acetate with and without addition of sodium fluoride, Biebrich Scarlet, and acid phosphatase. We used any of these methods independently or in combination with another cytochemical method to demonstrate a particular type of cell.

RESULTS

Isolation of the T3M-5 human thyroid carcinoma cell line.—In the primary culture of a human thyroid carcinoma transplanted into nude mice, sparsely populated colonies of large polygonal cells attached to grow slowly in 1 or 2 weeks. The colonies were usually surrounded by a considerable number of fibroblasts. The culture was then treated with a thirtyfold diluted antiserum raised against nude mouse cells in the presence of complement (fig. 1A). Mouse fibroblasts did not reappear in the post-treatment culture after the initial single treatment (fig. 1B). The cells of the original T3M-5 cell line established in this manner were characterized by large epithelial cell-like shapes with prominent nuclei (fig. 2) that were generally found in the center of the cytoplasm and were pleomorphic in shape. The cell membrane was usually rough and irregular, sometimes with one or more extending appendages. The cells formed characteristic colonies that coalesced and formed a monolayer.

CSF production in the T3M-5 cell culture.—We incubated the confluent T3M-5 culture with the complete growth medium. The level of human CSF activity in the cultured medium was 5,000 U/ml. Of the colonies stimulated by the medium, 87.5% were granulocytic. The time course of change in human CSF activity of the medium is shown in text-figure 1. CSF activity in the cultured medium increased daily to a maximum activity on the 7th day of the culture in the roller bottles.

Growth characteristics.—A kinetic study on the in vitro growth of the cultured T3M-5 cells is shown in text-figure 2. The cells used for the study were the 60th transfer generation cells, completely adapted to the in vitro conditions, and were growing vigorously. The experimental cultures were initiated with an inoculum of 5×10⁴ cells and incubated in a 5% CO_2 chamber at 37°C. The growth curve was obtained by the number of cells per dish being counted as a function of time. Population doubling time was estimated as 22 hours from the growth curve.

Xenotransplantation of T3M-5 cells.—We tested the growth of the cultured T3M-5 cells to see whether they were able to grow in nude mice and whether a marked granulocytosis would develop. The retransplantation from tissue culture was successful in all cases; the animals showed perfect tumor takes. A remarkable granulocytosis was observed in all the animals that received xenotransplanted T3M-5 cells (table 1).

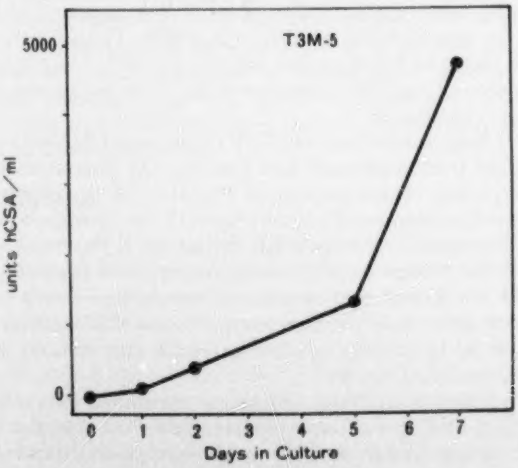

TEXT-FIGURE 1.—Changes in human CSF activities of the conditioned medium of T3M-5 cells in roller bottle culture.

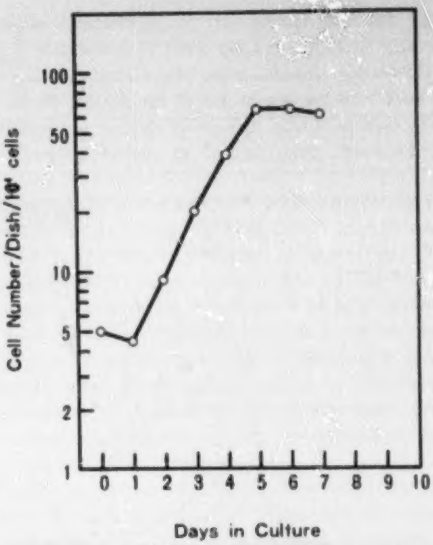

TEXT-FIGURE 2.—Growth curve of cultured cells at the 60th transfer generation of T3M-5 under 5% CO_2 atmosphere. *Each point* represents the mean value from two dishes.

Figure 3 shows typical features of a tumor obtained by the inoculation of the cultured T3M-5 cells into nude mice. The histology of the tumor was similar to that of the original tumor grown in nude mice after direct transplantation from the human tumor. Both tumors were squamous cell carcinomas with occasional pearl formation (figs. 3, 4).

Chromosomal findings—The modal number of the T3M-5 cell line was 80 in the second passage and 72 in the 57th passage, with considerable scattering in the counts (table 2). Not a single normal metaphase was observed.

Characterization of CSF.—The cells propagated well in 570-mm roller bottles at the velocity of 0.5 rpm. When the cultures reached confluence, they were incubated in serum-free medium supplemented with 1% BSA. A concentrated conditioned medium (500 ml) was loaded on a Sephadex G-75 chromatography column after equilibration by dialysis with 0.01 *M* Tris-HCl (pH 7.4). We observed a broad peak of CSF activity with the use of mouse bone marrow cells as targets. The fractions of this peak region (B, C; text-fig. 3) were pooled and repeatedly chromatographed by Ultrogel AcA 54 column. Elution profile by the repeated chromatography was similar to the original one showing a broad peak of activity after the BSA region. Two small peaks were noted

TABLE 1.—*Peripheral blood leukocyte counts in tumor-bearing nude mice*

Mouse	Tumor size, mm	Leukocyte counts/mm³	Neutrophils, %
1	15×12×10	52,000	92.5
2	13×11×11	312,600	98.2
3	12×11×12	135,000	96.3
Control	—	6,150	35.2

TABLE 2.—*Chromosomal pattern of the T3M-5 cell line*

Passage No.	Distribution at chromosome 56	57	58	59	60	61	62	63	64	65	66	67	68	69	70	71	72	73	74	75	76	77	78	79	80	81	82	83	84	85	86	87	Total No. of cells
2	0	0	0	0	0	0	0	1	0	0	0	1	2	0	2	1	1	3	4	2	2	4	7	5	8	7	3	4	1	1	2	1	62
57	1	0	1	2	2	0	1	0	4	0	3	2	2	3	5	4	12	7	3	2	1	0	0	1	0	0	0	0	0	0	0	0	56

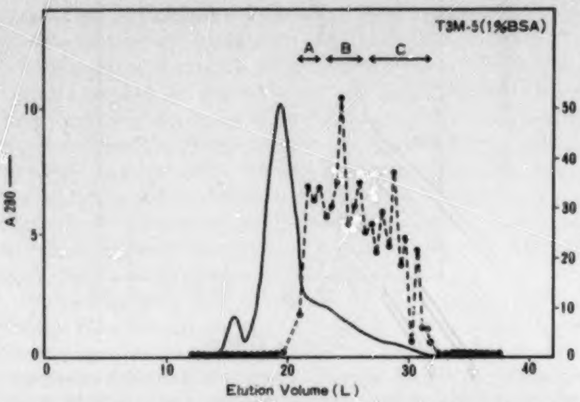

TEXT-FIGURE 3.—Gel-filtration profile of T3M-5-conditioned medium on Sephadex G-75. Activities were assayed on mouse bone marrow cells (mCSA). Different fractions of the A-, B-, and C-regions were pooled, respectively, and assayed against human bone marrow cells.

TABLE 3.—*Recovery of human CSF activity from gel-filtration column*[a]

Substance assayed	Volume, ml	Protein, mg	Activity, ×10⁶ U (yield, %)	Sp act, U/mg
T3M-5 conditioned medium, 1% BSA	6,200	62,000	31.0 (100)	500
Fractions from A-region	88	8,890	6.57 (21.2)	740
Fractions from B-region	73	9,340	21.35 (68.9)	2,280
Fractions from C-region	73	4,090	6.42 (20.7)	1,570

[a] Fractions containing mCSA were pooled respectively in the regions of A, B, and C, concentrated, and assayed against human bone marrow cells. One unit represents one colony formed from 2×10^5 nonadherent human bone marrow cells.

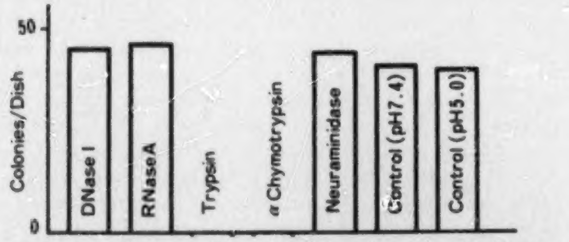

TEXT-FIGURE 4.—Treatment of concentrate from fractions of the B-region in text-fig. 3 with DNase, RNase, trypsin, chymotrypsin, and neuraminidase. *Each column* represents the mean colony No./plate (0.1 ml of stimulant) for three plates.

in the broad peak region. We estimated the MW of the proteins represented by these 2 peaks to be approximately 30,000 and 15,000, respectively, with the use of BSA, cytochrome c, and ovalbumin as protein markers. Only a small amount of protein was associated with the first peak, and the specific activity increased to 2,280 U/mg protein on human bone marrow cells (table 3). The recovery of CSF activity was 68.8% in the first peak region. The second small peak showed a lower specific activity of 1,570 U/mg protein. The recovery of CSF activity was 20.7% in the second peak region (text-fig. 3).

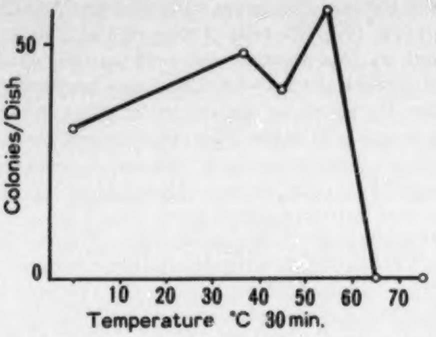

TEXT-FIGURE 5.—Heat inactivation of CSF from fractions of the B-region in text-fig. 3.

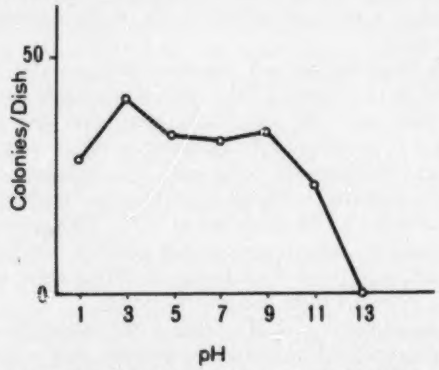

TEXT-FIGURE 6.—Stability during pH change of CSF fractions of the B-region in text-fig. 3.

Partially purified human CSF from pooled fractions from the first peak region (B) was used for the characterization experiments. The resistance of human CSF to RNase and DNase is demonstrated in text-figure 4. No biologic activity was lost when active purified DNase or RNase was incubated for 2 hours at 37°C with concentrated fractions (B), under conditions that caused the enzymes to break down rapidly their respective substrates. Human CSF activity was destroyed by trypsin or chymotrypsin, but resisted neuraminidase (text-fig. 4).

To examine the effects of heat, we incubated the partially purified CSF at various temperatures for 30 minutes. CSF activity was stable at 4°C, at room temperature, and at 45°C, but it was lost completely within 30 minutes at 65°C (text-fig. 5).

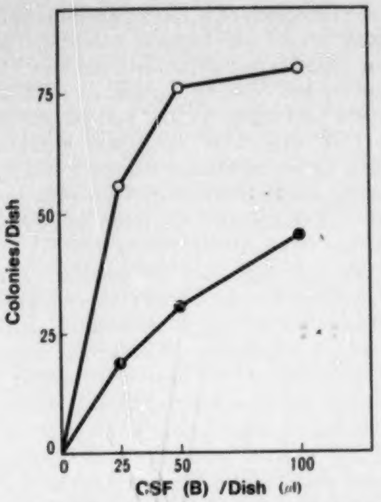

TEXT-FIGURE 7.—Relative stimulation of human and mouse cell colonies by CSF from fractions of the B-region in text-fig. 3.

TABLE 4.—*Morphology of human marrow colonies stimulated by different sources of CSF*[a]

Sources of CSF	Colonies, %			
	Neutrophil	Neutrophil-macrophage	Macrophage	Eosinophil
T3M-5 conditioned medium	41.7	29.2	12.5	16.7
GCT conditioned medium	33.3	35.3	21.6	9.8
Placental conditioned medium	58.0	7.0	22.0	13.0
T3M-5 high-MW CSF	56.3	37.5	3.1	3.1

[a] Colonies were stained after 14 days of culture.

CSF activity was stable over the pH range of 1.0–9.0. At pH 13, however, the activity was completely lost (text-fig. 6).

Cell populations of the colonies.—High-MW T3M-5 CSF from pooled fractions of the first peak region (B) was more active against human bone marrow than against mouse marrow cells and stimulated predominantly neutrophilic colonies (text-fig. 7; table 4). Crude and partially purified CSF stimulated the formation of both neutrophil and eosinophil colonies on day 14.

DISCUSSION

We have described the establishment of a human CSF-producing cell line derived from a squamous cell carcinoma of the thyroid gland, and the characterization of the CSF. The original cell line designated T3M-5 has been propagated continuously by serial passages during the past 34 months, and it has been producing human CSF in vitro.

Squamous cell carcinoma is rare among primary thyroid cancers. It has been shown to account for only 1% of all the neoplasms of this gland. Since there are no squamous cells in intact thyroid glands, the origin of this tumor remains unclear. One theory is that the tumor may originate from the follicular epithelium of the gland through squamous metaplastic alteration. T3M-5 cells produce a squamous cell carcinoma in athymic nude mice, thereby providing a clue to the understanding of the pathogenesis of this thyroid cancer. Prognosis for patients with this tumor is very poor, since the tumor resists radiation and chemotherapeutic agents.

For examination of the sensitivity of this type of tumor to antineoplastic agents, the T3M-5 cell line is expected to serve as a useful in vitro experimental model in culture and in vivo experimental model in nude mice. T3M-5 cells reveal a high colony-forming capacity in vitro and show perfect tumor takes when inoculated into nude mice. Recently, T3M-5 cells have been shown to be extremely sensitive to bleomycin in vitro (text-fig. 8), which is usually effective against a variety of squamous cell carcinomas. Bleomycin may be a potential choice for the treatment of squamous cell carcinoma of the thyroid gland.

A moderate leukocytosis is often observed in patients with squamous cell carcinoma of the thyroid gland (*14–16*). The precise mechanism of this phenomenon, however, remains unexplained in most cases. In 1977, we described a poorly differentiated squamous cell carcinoma of the lung that produced human colony-stimulating factor(s) in nude mice (*17*). Recently, a human CSF-producing cell line was isolated from a squamous cell carcinoma of the oral cavity (*4*). T3M-5 cells possess a characteristic function of human CSF production in vitro; a marked granulocytosis developed in nude mice bearing the tumors produced by inoculation with the cultured cells. Leukocytosis often seen in patients with squamous cell carcinoma of the thyroid gland may be due in part to CSF production by the tumor cells themselves.

In the conditioned medium of T3M-5 cells, gel column chromatography showed a broad peak of CSF activity with two small peaks indicating substances with MW of about

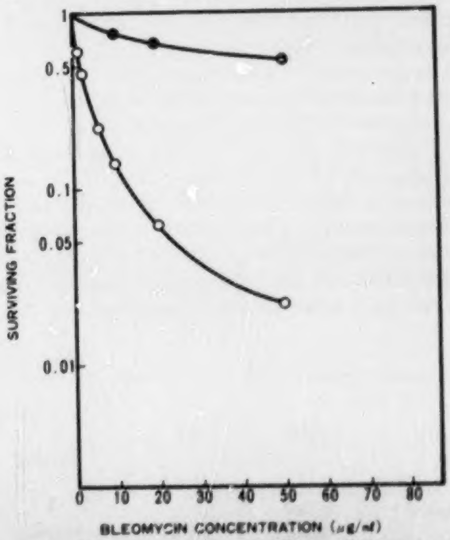

TEXT-FIGURE 8.—Effect of various concentrations of bleomycin on survival of dividing T3M-5 cells. Survival response of L-929 cells treated for 1 hr with bleomycin is shown for reference. *Each point* represents the mean values for 4 dishes from 3 expts. Plating efficiency of T3M-5 cells was 33–48% throughout the experiments.

30,000 and 15,000. To estimate the accurate MW of the high-MW CSF, we pooled the first peak region (B) obtained from the Sephadex G-75 fractionation and chromatographed it again on an AcA 54 column after fractionation under dissociating conditions with the use of phenyl-Sepharose CL-6B and 6 *M* guanidine hydrochloride (*18*). The CSF obtained from the phenyl-Sepharose fractionation eluted from Ultrogel AcA 54 column with an apparent MW of 27,000 (data not shown). The pI of this CSF was 5.5 with a relative narrow half-width or a half a pH unit. Wu and Yunis (*19*) and Wu et al. (*20*) described two common types of CSF in several human sources, one of which was purified and had a MW of about 50,000, stimulating only mouse marrow cells, but not human cells (mouse-active CSF). This type of CSF was polydisperse on isoelectrofocusing and showed multiple peaks with a pI between 3.6 and 4.7 and stimulated the formation of predominantly macrophage colonies in mouse bone marrow culture.

Activities that stimulate mouse macrophage colony formation were not demonstrated in any of the fractions obtained by Sephadex G-75 column chromatography. As described above, further characterization of the high-MW CSF in T3M-5 conditioned medium showed that this form of CSF had an apparent MW of 27,000 and pI of 5.5 with a relative narrow half-width or a half a pH unit, and exhibited higher activity in human bone marrow than in mouse marrow, yielding predominantly granulocytic colonies (text-fig. 7). These observations suggest that the high-MW CSF in T3M-5 conditioned medium was functionally and structurally distinct from the mouse active CSF. The CSF from human sources has been shown to stimulate human granulocytic colony formation (human active CSF). Most of the colonies grown in the presence of this type of CSF were granulocytic. These two types of CSF were demonstrated in the conditioned media from leukocytes, lungs, placenta, and cancer cells.

A previous study demonstrated that in a squamous cell carcinoma cell line, T3M-1, the mouse active factor was not detected in the conditioned medium (*21*). To compare the subtypes of these CSF produced by malignant cell lines, further purification studies are required (*22*).

Table 5 shows a summary of the properties of the CSF from malignant cell lines. Human active CSF from all the cell lines had an approximate MW of 30,000; the activity was destroyed by trypsin but resisted neuraminidase. With the exception of the CSF with 34,000 MW released from a T-lymphoblastoid cell line, all human active CSF, including T3M-5 CSF, have failed to bind concanavilin A–Sepharose (*23*). With the exception of a T-lymphoblastoid cell line, all human sources of CSF also support mouse marrow growth. From human leukocyte-conditioned medium, Price et al. (*24*) separated three types of human active CSF with approximate MW of 14,700, 36,500, and 96,000. Several human active CSF with MW of 25,000–40,000 have been isolated from a variety of human tissues (*25–27*). For studies to determine the similarities and differences between cancer-derived CSF and the other CSF, large quantities of highly purified CSF are required (*21, 23, 28, 29*).

Nicola et al. (*18*) suggested the possible existence of at least three forms of human active CSF in placental conditioned medium, one of which stimulated predominantly neutrophil colony formation. Most of the colonies in the presence of this form of CSF were neutrophilic at all dilutions of stimulus. Another form of human active CSF preferentially stimulated macrophage colony formation. Since this form of CSF was not separable from eosinophil CSF, it also stimulated eosinophil colony formation. Human active CSF obtained from a lymphoblastoid cell line or a monocyte-like cell line also stimulated eosinophil colony formation. In T3M-1 conditioned medium stimulation of eosinophil colony formation or macrophage colony formation was not demonstrated (*21*).

To establish whether T3M-5 conditioned medium contained neutrophil CSF, macrophage CSF, or eosinophil CSF, we performed morphologic subtyping of the colonies with the use of conventional Wright-Giemsa stain and special cytochemical stain (nonspecific esterase, naphthol AS-D chloroacetate esterase, and Biebrich Scarlet). Morphologies of colonies stimulated by conditioned media from T3M-5, GCT, and human placenta, and those by high-MW T3M-5 CSF are summarized in table 4. Eosinophil colonies were demonstrated in all of the conditioned media. Although T3M-5 conditioned medium seems to contain not only neutrophil CSF but also eosinophil CSF, high-MW T3M-5 CSF stimulated a few eosinophil colonies (<5%). Most of the colonies were neutrophilic, and the percentage of macrophage colonies was low (<3%).

Both T3M-1 and T3M-5 CSF were destroyed when kept at 65°C for 30 minutes. CSF from GCT or Mo cells was not destroyed at 65°C but was inactivated at 90°C (table 5). T3M-5 CSF differed from T3M-1 CSF in neuraminidase sensitivity (*21*). In T3M-1 CSF, partial loss of the activity occurred with neuraminidase treatment, whereas T3M-5 CSF activity was not destroyed.

To remove sialic acid from the high-MW CSF, we performed selective acid cleavage (*18*). Recovery of T3M-1

TABLE 5.—*Sources of human active CSF*[a]

Cell line	MW	pI	Effect of:			Inactivation at:		Eosinophil CSA	Presence of neutrophilia in patient
			Trypsin	Neuraminidase	Con A binding	Heat, °C	pH		
MiaPaca-2	27,000	5.7	?	?	?	?	?	?	?
GCT	30,000	5.0	Sensitive	Resistant	−	90	?	+	?
Mo	34,000	4.0–5.2	Sensitive	Resistant	+	90	3–10	+	?
T3M-1	30,000	5.5	Sensitive	Partially sensitive	−	65	1–11	−	+
T3M-5	27,000	5.5	Sensitive	Resistant	−	65	1–9	+	+

[a] ?=not known; +=present; −=absent.

CSF was less than 20% after this procedure, in contrast to the complete recovery of T3M-5 CSF (data not shown). Relationships between the sialic acid content and the functional properties of these tumor-derived CSF remain unclear. Differences and similarities among these CSF will be elucidated by the further purification studies.

At any rate, it is essential to obtain material sources with high biologic activities in extraordinarily large quantities, since multistep purification procedures of human active CSF usually yield low recoveries of active materials. T3M-5 cells can be well propagated in roller bottles and produce large quantities of human active CSF. The cells have the advantage of being able to produce significantly larger quantities of human active CSF than the other cell lines. The conditioned medium obtained from roller bottle cultures exhibited a greater activity (5,000 U/ml) than that from T3M-1 cells (1,440 U/ml) or that from GCT cells (1,300 U/ml). Within 1 month, 45 570-mm bottles yielded about 100 liters of conditioned medium that stimulated approximately 500,000,000 human granulocytic colonies. The recovery of the activity from a gel-filtration column was high (68.9%). This cell line is therefore expected to provide a superior starting material for purification, which facilitates greatly the studies on this granulopoietic factor.

REFERENCES

(*1*) Jones GW, Simkovic D, Biedler JL, Southam CM. Human anaplastic thyroid carcinoma in tissue culture. Proc Soc Exp Biol Med 1967; 126:426–428.

(*2*) Hirose M. Tissue culture of human thyroid cancer. Acta Med Okayama 1968; 22:185–202.

(*3*) Okabe T, Suzuki A, Ohsawa N, Kosaka K, Terasima T. Immune elimination of host fibroblasts for the cultivation of human tumors transplanted into nude mice. Cancer Res 1979; 39:4189–4194.

(*4*) Okabe T, Sato N, Kondo Y, et al. Establishment and characterization of a human cancer cell line that produces human colony-stimulating factor. Cancer Res 1978; 38:3910–3917.

(*5*) Kimura N, Niho Y, Ono J, Miyamoto N, Shibuyd T, Takai R. An established lung cancer cell line producing colony-stimulating activity. Proc Jpn Acad Sci Ser B 1978; 54:548–552.

(*6*) Wu MC, Cini JK, Yunis AA. Purification of a colony-stimulating factor from cultured pancreatic carcinoma cells. J Biol Chem 1979; 245:6226–6228.

(*7*) Di Persio JF, Brennan JK, Lichtman MA, Speiser BL. Human cell lines that elaborate colony-stimulating activity for the marrow cells of man and other species. Blood 1978; 51:507–519.

(*8*) Golde DW, Quan SG, Cline MJ. Human T lymphocyte cell line producing colony-stimulating activity. Blood 1978; 52:1068–1072.

(*9*) Ruscetti FW, Chou JY, Gallo RC. Human trophoblasts: Cellular source of colony-stimulating activity in placental tissue. Blood 1982; 59:86–90.

(*10*) Saito K, Tomotsune Y, Yamamoto K, Saito T, Kuzuya T, Yoshida S. A case of primary squamous cell carcinoma of the thyroid associated with marked neutrophilia and hypercalcemia. Jpn J Soc Intern Med 1980; 68:88–94.

(*11*) McLeod DL, Shreeve MM, Axelrad AA. Improved plasma culture system for production of erythrocytic colonies in vitro: Quantitative assay method for CFU-E. Blood 1974; 44:517–534.

(*12*) Bradley TR, Metcalf D. The growth of mouse bone marrow cells in vitro. Aust J Exp Med Sci 1966; 44:287–300.

(*13*) Messner HA, Till JE, McCulloch EA. Interacting cell populations affecting granulopoietic colony formation by normal and leukemic human bone marrow cells. Blood 1973; 42:701–710.

(*14*) Bahuleyan CK, Ramachandran P. Primary squamous cell carcinoma of thyroid. Ind J Cancer 1972; 9:89–91.

(*15*) Prakash A, Kukreti SC, Sharma MP. Primary squamous cell carcinoma of the thyroid gland. Int Surg 1968; 50:538–541.

(*16*) Wilflingseder P. Mitteilung eines Falles von Plattenepithel Krebs des Schilddrüse. Wien Klin Wochenschr 1947; 59:346–347.

(*17*) Asano S, Urabe A, Okabe T, et al. Demonstration of granulopoietic factor(s) in the plasma of nude mice transplated with a human lung cancer and in the tumor tissue. Blood 1977; 49:845–852.

(*18*) Nicola NA, Metcalf D, Johnson GR, Burgess AW. Separation of functionally distinct human granulocyte-macrophage colony-stimulating factors. Blood 1979; 54:614–627.

(*19*) Wu MC, Yunis AA. Common pattern of two distinct types of colony-stimulating factors in human tissues and cultured cells. J Clin Invest 1980; 65:772–775.

(*20*) Wu MC, Miller AM, Yunis AA. Immunological and functional differences between human type I and II colony-stimulating factors. J Clin Invest 1981; 67:1588–1591.

(*21*) Okabe T, Nomura H, Sato N, Ohsawa N. Large-scale preparation and characterization of human colony-stimulating factor. J Cell Physiol 1982; 110:43–49.

(*22*) Okabe T, Ohsawa N. Human colony-stimulating factor producing cell line. Cell Mol Biol 1981; 27:579–587.

(*23*) Lusis AJ, Quon DH, Golde DW. Purification and characterization of a human T-lymphocyte-derived granulocyte-macrophage colony-stimulating factor. Blood 1981; 57:13–21.

(*24*) Price GB, Senn JS, McCulloch EA, Till JE. The isolation and properties of granulocytic colony-stimulating activities from medium conditioned by human peripheral blood. Biochem J 1975; 148:209–217.

(*25*) Fojo SS, Wu MC, Gross MA, Yunis AA. The isolation and characterization of a colony-stimulating factor from human lung. Biochim Biophys Acta 1977; 492:92–99.

(*26*) Shah RG, Caporale LH, Moore MS. Characterization of colony-stimulating activity produced by human monocytes and phytohemagglutinin-stimulated lymphocytes. Blood 1977; 50:811–821.

(*27*) Burgess AW, Wilson EM, Metcalf D. Stimulation by human placental conditioned medium of hematopoietic colony formation by human marrow cells. Blood 1977; 49:573–583.

(*28*) DiPersio JF, Brennan JK, Lichtman MA, Abboud CN, Kirkpatrik FH. The fractionation, characterization, and subcellular localization of colony-stimulating activities released by the human monocyte-like cell line, GCT. Blood 1980; 56:717–727.

(*29*) Abboud CN, Brennan JK, Barlow GH, Lichtman MA. Hydrophobic adsorption chromatography of colony-stimulating activities and erythroid-enhancing activity from the human monocyte-like cell line, GCT. Blood 1981; 58:1148–1154.

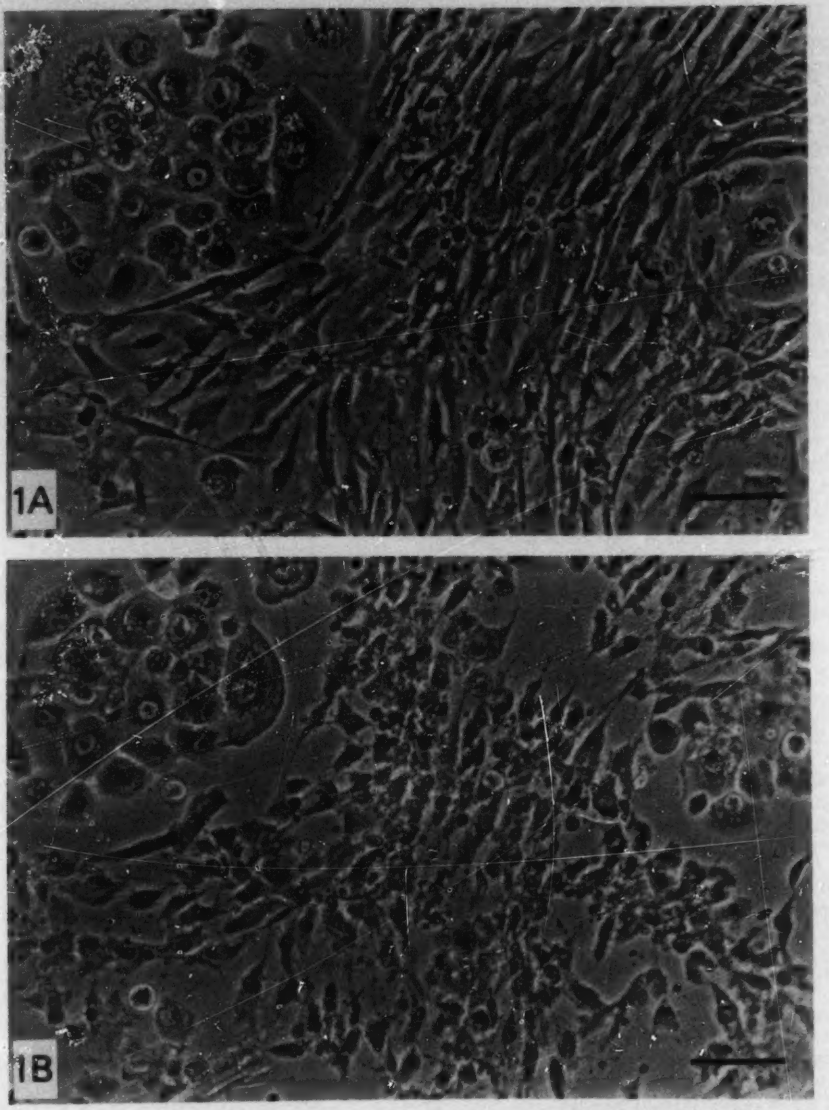

FIGURE 1.—Removal of fibroblasts from the primary culture. A) An epithelial cell colony surrounded by fibroblasts before the addition of the antiserum, diluted 1:30 with complete growth medium and complement. B) The same culture 24 hr after the addition of the antiserum and complement. Phase-contrast microscopy. *Bar*=50 µm. × 280

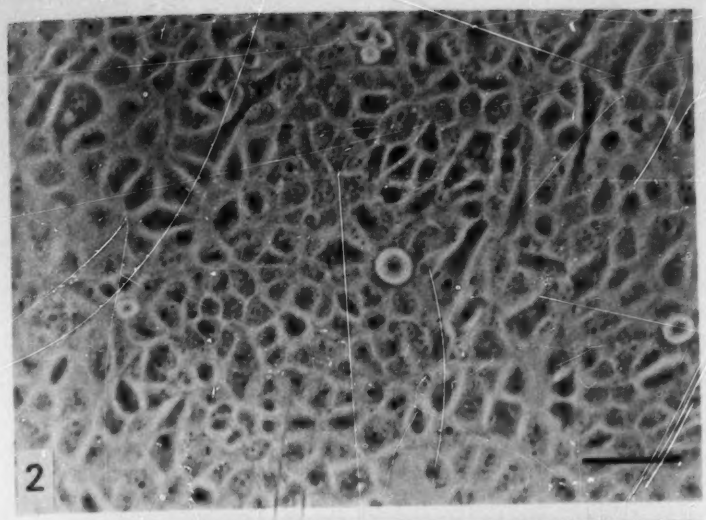

FIGURE 2.—Monolayer-cultured T3M-5 cells were epithelial cell-like in shape (63d transfer generation). Phase-contrast microscopy. *Bar*=50 µm. × 280

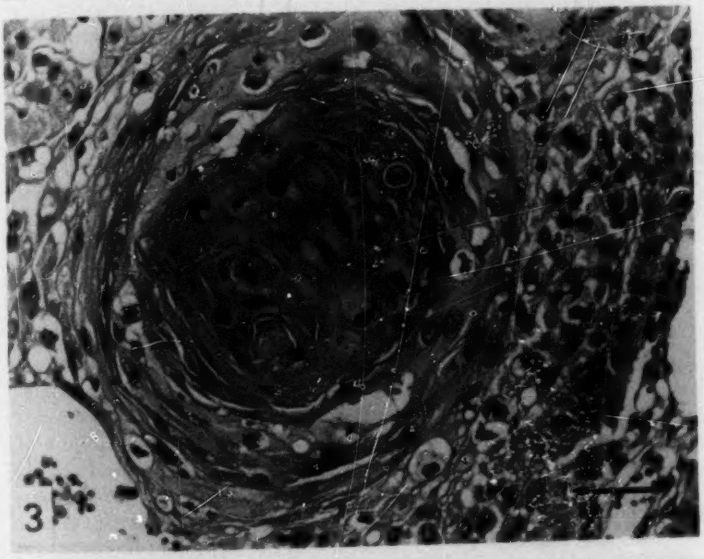

FIGURE 3.—Histology of the tumor obtained by inoculating the 80th transfer generation of T3M-5 cells into nude mice has the appearance of squamous cell carcinoma. *Bar*=100 µm. H & E. × 560

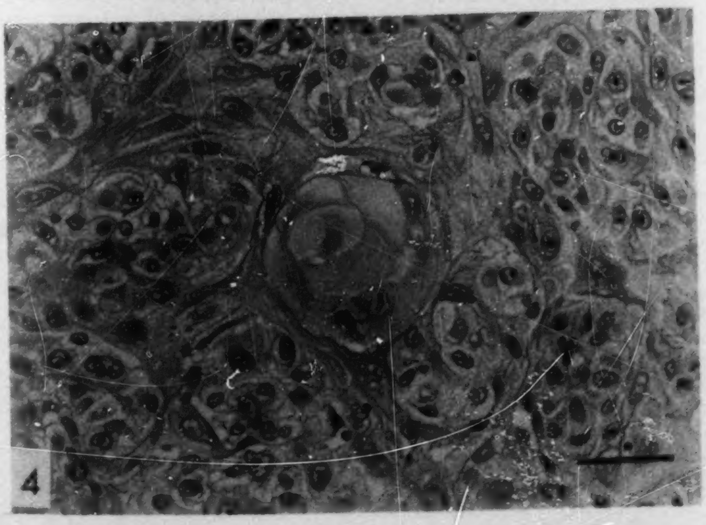

FIGURE 4.—Histology of the original tumor grown in nude mice after direct transplantation from patient at autopsy, showing a differentiated squamous cell carcinoma. *Bar*=100 µm. H & E. × 560

blank page

In Vitro Studies on the Cell-Mediated Immune Response to Human Brain Tumors. I. Requirement for Third-Party Stimulator Lymphocytes in the Induction of Cell-Mediated Cytotoxic Responses to Allogeneic Cultured Gliomas[1,2]

Maurice K. Gately,[3,4] Moshe Glaser,[3] Steven J. Dick,[3] Ray W. Mettetal, Jr.,[3] *and* Paul L. Kornblith[3,5]

ABSTRACT—For study of those properties of human gliomas that might contribute to their ability to escape cell-mediated immune attack, cultured human glioma cells were examined for their ability to elicit allogeneic cytolytic lymphocyte responses in vitro. Of 9 glioma lines, 5 were unable to elicit allogeneic cytolytic lymphocyte responses in mixed lymphocyte–tumor cultures although the concentration of stimulating glioma cells was varied over a fortyfold range. However, lymphocytes specifically cytolytic for 4 of the nonstimulatory lines could be generated if irradiated, third-party stimulator lymphocytes were added to cultures containing responder lymphocytes and glioma cells. The specific cytolytic lymphocytes produced in these cultures were inactivated by treatment with the monoclonal anti-T-cell antibody OKT3 plus complement and were thus identified as T-cells. However, nonspecific, non-T-lytic effectors were also generated. The results of these experiments demonstrated that certain cultured gliomas possessed a defect in immunogenicity that can be overcome by "help" from an allogeneic mixed lymphocyte reaction. The possible nature of this help and the potential implications of these results for the immunotherapy of human gliomas are discussed.—JNCI 1982; 69:1245–1254.

In contrast to the many chemical- or virus-induced tumors that are able to elicit strong immune responses, most spontaneously arising tumors have been found to be only weakly immunogenic or nonimmunogenic (*1–5*). The factors contributing to this lack of immunogenicity are poorly defined. In our current studies we have examined the ability of one class of human neoplasms, the astrocytomas, to elicit cellular immune responses in an attempt to delineate those properties of astrocytoma cells that might contribute to their escaping cell-mediated immune attack. We approached this investigation by examining the ability of cultured glioma cells to induce cytolytic lymphocyte responses in vitro. Such glioma lines were previously shown to possess both common and highly restricted glioma-specific antigens (*6–9*) as well as HLA antigens (*10*) and in some cases Ia-like (*11, 12*) antigens. Nevertheless, initial attempts to elicit autologous tumor-specific CTL responses were unsuccessful. To define properties of glioma cells that might contribute to their failure to stimulate *autologous* responses, we have examined their ability to elicit *allogeneic* CTL responses. Since allogeneic reactions should be substantially stronger than tumor-specific autologous responses, it seems likely that factors impeding allogeneic responses should be at least equally effective in abrogating autologous sensitization to tumor-specific antigens. These experiments have led to the identification of several properties of human glioma cells that interfere with their ability to stimulate CTL responses in vitro. In this report we demonstrate that certain human glioma lines possess a defect in immunogenicity such that they are unable by themselves to elicit an allogeneic CTL response in MLTC but can elicit a response in the presence of "help" from an allogeneic MLR.

MATERIALS AND METHODS

Cell lines.—Portions of tumor samples obtained by biopsy at craniotomy were minced into 1-mm^3 pieces and explanted into 75-cm^2 Falcon flasks (Falcon Plastics, Oxnard, Calif.) in F-10 nutrient medium containing 10% FBS (Grand Island Biological Co., Grand Island, N.Y.). After tumor outgrowth began, the medium was changed regularly, and the cells were subcultured when needed with 0.25% trypsin. The sources and properties of the astrocytoma lines used in this study are summarized in table 1. Histologic diagnosis was made by Dr. Paul McKeever (Surgical Neurology Branch, NINCDS). The Kernohan grading of astrocytomas from grades I to IV denotes an increasing histologic scale of anaplasia (*13*). The malignant and glial properties of these lines were established by ultrastructural (*14, 15*), biochemical (*16*), and biophysical (*17*) techniques. The cell lines were routinely examined for mycoplasma contamination by Dr. Richard Del Guidice (NCI-Frederick Cancer Research Facility, Frederick, Md.) and were negative for mycoplasma at all times.

Fibroblasts were cultured from skin biopsies or from fragments of galea taken at operation. Cells of the erythroleukemia line K562 were donated by Dr. John Ortaldo, the

---

ABBREVIATIONS USED: CTL=cytolytic T-lymphocyte(s); FBS=fetal bovine serum; IL-2=interleukin-2; MLR=mixed lymphocyte reaction(s); MLTC=mixed lymphocyte–tumor culture(s); NINCDS=National Institute of Neurological and Communicative Disorders and Stroke; NK=natural killer; PBS=phosphate-buffered saline; PHA=phytohemagglutinin; TCM=tissue culture medium.

---

[1] Received January 4, 1982; accepted June 3, 1982.

[2] Research procedures were in accord with the ethical standards of the National Institute of Neurological and Communicative Disorders and Stroke Clinical Research Subpanel (No. 79-N-133).

[3] Surgical Neurology Branch, Intramural Research Program, National Institute of Neurological and Communicative Disorders and Stroke, National Institutes of Health, Public Health Service, U.S. Department of Health and Human Services, Bethesda, Md. 20205.

[4] *Address reprint requests to* Dr. Gately, Building 10A, Room 3E68, National Institutes of Health, Bethesda, Md. 20205.

[5] We are grateful to Mrs. Martha Johnson for her excellent technical assistance and to Dr. Henry McFarland for his help in performing the indirect immunofluorescence studies.

National Cancer Institute, Bethesda, Md., and were maintained by passage in RPMI-1640 medium with 5% FBS.

Patients.—Lymphocytes from 9 astrocytoma patients were studied as part of this investigation. One patient's tumor was diagnosed histologically as astrocytoma grade II; all other patients had grade III or IV astrocytomas. Patients' ages ranged from 27 to 64 years (mean: 41 yr). All patients received therapy appropriate for their grade of tumor within the Surgical Neurology Branch, NINCDS. Patient #10, who was unique in the ability of his lymphocytes to lyse allogeneic glioma cells (*see* "Results"), was a 41-year-old male from South America who had a grade IV astrocytoma. He was studied immunologically at regular intervals beginning 5 months after his tumor had been surgically removed.

Sensitization of lymphocytes in MLTC.—Blood from tumor patients and from normal blood bank donors was drawn into syringes containing preservative-free heparin, 5 U/ml. Mononuclear cells were isolated by centrifugation on discontinuous Ficoll-Hypaque gradients (*18*) followed by centrifugation through 20% sucrose in RPMI-1640 with 1% human blood type AB serum for removal of contaminating platelets (*19*). Final cell pellets were resuspended in TCM consisting of a 1:1 mixture of RPMI-1640 and Dulbecco's modified Eagle's minimum essential medium supplemented with 5% human blood type AB serum, 5×10^{-5} *M* 2-mercaptoethanol, nonessential amino acids, 2 m*M* L-glutamine, 100 U penicillin/ml, and 100 μg streptomycin/ml (Grand Island Biological Co.).

Cytolytic lymphocytes were generated by incubation of responder lymphocytes with stimulator lymphocytes and/or glioma cells in 2 ml TCM in the wells of Costar 3524 tissue culture plates (Costar, Cambridge, Mass.). Stimulator lymphocytes received 2,000 R of γ-radiation prior to culture, and glioma cells received 10,000 R of γ-radiation. Responder and stimulator lymphocytes were each cultured at a density of 2×10^6 cells/well. Optimal glioma cell density was found to be $0.5\text{–}2\times10^5$ cells/well (*see* "Results"). Responder lymphocytes were harvested from primary sensitizing cultures after 7–12 days and were assayed for cytolytic activity. Alternatively, responder cells were harvested from primary MLTC after 13–16 days and reexposed to fresh stimulator lymphocytes and/or glioma cells with the use of culture conditions identical to those described above. Cytolytic activity was measured 3–4 days after the initiation of these secondary MLTC. Whereas early experiments involved the use of primary MLTC only, in later experiments both primary and secondary sensitizations were carried out because the ratio of specific to nonspecific effectors (*see* "Results") was increased in secondary cultures. Nevertheless, gliomas, which by themselves were nonstimulatory in primary MLTC, failed to elicit a response in secondary MLTC also (*see* "Results").

Cytolytic assays.—Freshly trypsinized glioma cells or fibroblasts to be used as targets in lytic assays were incubated with 100 μCi sterile [^{51}Cr]sodium chromate (New England Nuclear Corp., Boston, Mass.) in 0.5 ml TCM for 1 hour at 37°C. The cells were then washed three times and resuspended at a concentration of 5×10^4 cells/ml. Aliquots (0.1 ml) of this suspension were added to wells of Costar 3696 "half-area" MicroTest plates. The plates were incubated at 37°C for 18 hours for the cells to adhere and spread on the floors of the wells. The culture medium was then aspirated from each well and replaced with 0.1 ml of lymphocyte suspension. Lymphocytes were incubated with target cells for 18–24 hours at 37°C. At the end of this time, 0.05 ml culture medium was withdrawn from each well, and the amount of ^{51}Cr in each sample was measured in a gamma counter. The total amount of ^{51}Cr in the glioma cells was determined by addition of 1% sodium dodecyl sulfate to control wells. The percent specific ^{51}Cr release was calculated as $[(e-c)/(100-c)]\times100$, where e is the percentage of ^{51}Cr released from glioma cells incubated with lymphocytes and c is the percentage of ^{51}Cr released spontaneously from glioma cells incubated alone. All assays were performed in triplicate, and values given in tables represent the means ± 1 SE of replicate samples. Lytic activity of similar specificity could be observed when assays were terminated after 6 hours rather than 18 hours; however, effector:target ratios approximately fivefold greater were required to yield similar levels of lysis (Gately MK, Glaser M: Unpublished data).

Lymphocytes to be used as targets in cytolytic assays were incubated at a density of 1×10^6 cells/ml in 2 ml TCM containing 1 μg "PHA-L"/ml (E-Y Laboratories, San Mateo, Calif.) at 37°C for 3–4 days. [^{51}Cr]sodium chromate (100 μCi) was added 18 hours prior to the assay. The ^{51}Cr-labeled, PHA-activated cells were washed three times with 0.1 *M N*-acetyl-D-galactosamine (Sigma Chemical Co., St. Louis, Mo.) in TCM and then twice in TCM alone. The final cell pellet was resuspended in TCM at a concentration of 2×10^4 cells/ml. K562 cells to be used as targets were likewise labeled overnight with [^{51}Cr]sodium chromate, washed three times with TCM, and adjusted to 2×10^4 cells/ml. Then 0.1-ml aliquots of ^{51}Cr-labeled PHA blasts or K562 were mixed with 0.1-ml aliquots of effector cells in the wells of Linbro 76-311-05 round-bottom MicroTest plates. The microplates were centrifuged at $500\times g$ for 5 minutes at room temperature and then incubated for 4 hours at 37°C. At the end of this time, the MicroTest plates were again centrifuged, and supernatants containing released ^{51}Cr were harvested with the use of a Titertek supernatant collection system (Flow Laboratories, Inc., McLean, Va.). The percent specific ^{51}Cr release was calculated as above.

Treatment of cells with OKT3 plus complement.—Effector cells were suspended at 5×10^6 cells/ml in a 1:50 dilution of the monoclonal anti-T-cell antibody OKT3 (Ortho Pharmaceutical Corp., Raritan, N.J.) in L-15 medium with 1% FBS. After incubation for 15 minutes at 37°C, the cell suspensions were mixed with an equal volume of rabbit complement, which had been obtained from 6-week-old New Zealand White rabbits and stored at −80°C until use. The mixtures were incubated for 1 hour at 37°C, after which the cells were washed twice in TCM, and the number of viable cells remaining was determined by trypan blue dye exclusion. Treatment of cells with complement alone reduced the number of viable cells by 10% or less.

Indirect immunofluorescence.—The presence of HLA or Ia-like antigens on the glioma lines was examined by indirect immunofluorescence with the use of xenogeneic monoclonal anti-HLA-A, -B, -C and anti-HLA-DR antibodies directed at nonpolymorphic determinants. Glioma cells adherent to glass cover slips were incubated with monoclonal anti-HLA-A, -B, -C (clone 61D2; Bethesda Research Laboratories, Inc., Gaithersburg, Md.) or with monoclonal anti-HLA-DR (clone L243; Becton, Dickinson & Co., Sunnyvale, Calif.) for 45 minutes at room temperature. The cover slips were then rinsed in PBS, and the cells were further exposed for 45 minutes to fluorescein-labeled goat anti-mouse IgG (Cappel Laboratories, Cochranville, Pa.). The cover slips were rinsed again, mounted, and examined for the presence of surface fluorescence on the glioma cells. Controls in which the glioma cells were first incubated with PBS and then with fluorescein-labeled anti-mouse IgG were in all cases negative. These tests were performed and scored by Dr. Henry McFarland of the Neuroimmunology Branch, NINCDS.

RESULTS

Requirement for Third-Party Stimulator Lymphocytes in the Generation of Lymphocytes Specifically Cytotoxic for Certain Glioma Lines

Freshly isolated peripheral blood lymphocytes from 7 glioma patients failed to cause lysis of autologous glioma cells in vitro to an extent significantly greater than that caused by lymphocytes from normal donors (data not shown). These results were obtained in 18-hour ^{51}Cr release assays with the use of an effector-to-target cell ratio of 100:1. Likewise, peripheral blood lymphocytes from 7 of 8 glioma patients failed to cause substantial lysis of allogeneic gliomas when assayed in a similar manner (for the one exception, *see below*). These results led us to initiate a series of experiments to examine those properties of human glioma cells that might contribute to their ability to escape cell-mediated immune attack.

As an approach to this problem, we examined the ability of human glioma cells to elicit cytolytic lymphocyte responses in MLTC. Despite serologic evidence from two separate laboratories (*7, 9*) that human glioma lines possess tumor-specific surface antigens, initial attempts to elicit tumor-specific CTL with the use of autologous combinations of lymphocytes and glioma cells from 5 different patients were unsuccessful. Therefore, to define those properties of human glioma cells that might contribute to their failure to stimulate *autologous* responses, we examined their ability to stimulate *allogeneic* CTL responses, for which sufficient reagents to permit detailed studies were more readily available. Of the 9 glioma lines studied, 5 were unable by themselves to elicit such responses (tables 1–3). However, 4 of the nonstimulatory lines could elicit the generation of lymphocytes specifically cytolytic for the glioma if sensitization was carried out in the presence of third-party stimulator lymphocytes (tables 1, 2). When added to a mixture of responder and stimulator lymphocytes, the 5th nonstimulatory line termed "GB" did not elicit a cytolytic lymphocyte response but rather suppressed the MLR that would otherwise have occurred. This suppression was due to the secretion of a macromolecular, nonspecific immunosuppressive substance (*20*).

Several types of targets were used to examine the specificity of the cytolytic lymphocyte responses induced in these experiments. In addition to being assayed against one or more glioma lines, effectors were also assayed for their ability to lyse K562, an erythroleukemia line that lacks HLA and Ia-like antigens (*21*) but is highly susceptible to lysis by NK and "NK-like" effectors (*22–24*), and for their ability to lyse PHA-activated stimulator lymphocyte blasts. These blast targets were used to monitor the level of cytolytic activity directed against alloantigens on the third-party stimulator lymphocytes; however, the lysis of PHA blasts may, to a lesser extent, reflect the activity of NK-like cells as well (*24*).

Since the various targets differed in their susceptibility to lysis, the specificity of effectors generated in these experiments could not be determined by simple comparisons of absolute levels of lysis of the different targets. Rather, the specificity of effectors was evaluated by examination of the *ratio* of the lytic activity generated in the presence of glioma stimulators to the lytic activity generated in their absence and then comparison of the ratios observed for the different targets. For example, in table 2, experiment 1, incubation of responder lymphocytes in MLTC with NN glioma alone led to little or no generation of cytolytic activity. Culture of responder lymphocytes with stimulator lymphocytes resulted in the generation of cytolytic effectors capable of

TABLE 1.—*Sources and properties of glioma lines*

Source			Glioma line designation	Passage No. at time of study	Reacts with:[a]		Directly stimulates CTL response	Stimulates CTL response with help from allogeneic MLR
Patient's code No.	Age, yr	Histologic diagnosis			Anti-HLA-A, -B, -C	Anti-HLA-DR		
1	38	Astrocytoma IV	JM	15	±	−	Yes	
2	36	Astrocytoma III—oligodendroglioma	AB	30–32	+	−	Yes	
3	68	Astrocytoma II–III	LH	2–4	+	−	Yes	
4	23	Astrocytoma III—ependymoma	NN	13–35	+	−	No	Yes
5	57	Astrocytoma IV	LM	130–150	+	−	No	Yes[b]
6	64	Astrocytoma IV	RB	10–20	+	−	No	Yes
7	55	Astrocytoma IV	GB	4–12	+	+	No	No
8	68	Astrocytoma II	FG	30–35	+	−	Yes	
9	47	Astrocytoma IV	RF	20–25	NT	NT	No	Yes

[a] ±=faintly positive; −=negative; +=positive. NT=not tested.

[b] LM glioma required the presence of both third-party stimulator lymphocytes and the enzyme hyaluronidase for a specific cytolytic response to be generated (*20*).

TABLE 2.—*Requirement for third-party stimulator lymphocytes in the generation of lymphocytes specifically cytotoxic for allogeneic NN, RB, and RF gliomas*

Expt No.	Contents of MLTC[a]			Percent specific ^{51}Cr release from:[b]				
	Responder lymphocytes	Stimulator lymphocytes	Glioma	NN glioma	RB glioma	RF glioma	LM glioma	Stimulator PHA blasts
1[c]	+			−1.9±1.0			2.1±0.3	3.9±3.7
	+		NN	5.1±1.1			1.4±0.9	8.7±4.4
	+	+		16.1±1.0			15.9±1.1	35.2±1.3
	+	+	NN	41.5±1.8			8.5±1.9	29.7±1.4
2[d]	+			18.2±2.5	18.1±2.4			2.7±0.9
	+		RB	6.3±0.9	4.4±1.3			2.1±0.4
	+		NN	10.4±1.4	8.3±0.7			4.1±0.8
	+	+		30.8±1.6	49.3±3.4			18.0±0.3
	+	+	RB	34.1±1.0	68.7±2.1			7.4±0.4
	+	+	NN	61.0±2.5	54.2±0.7			16.0±0.4
3[e]	+			17.5±0.8		3.5±2.6		
	+		RF	8.4±0.4		3.8±1.3		
	+		NN	14.1±2.0		4.6±3.8		
	+	+		22.6±1.3		6.7±1.5		
	+	+	RF	19.8±2.7		27.1±1.3		
	+	+	NN	46.3±0.9		8.9±1.2		

[a] +=present in MLTC.

[b] Values are means ± 1 SE of replicate samples.

[c] In expt 1, glioma cells were added to the MLTC at a concentration of 5×10^4 cells/well. Cytolytic activity was assayed on day 7 of the primary MLTC with the use of effector-to-target cell ratios of 6:1 for glioma targets and 15:1 for PHA blasts. Spontaneous ^{51}Cr release was 26, 22, and 35% from NN glioma, LM glioma, and PHA blasts, respectively.

[d] In expt 2, concentrations of glioma cells in MLTC were 5×10^4 RB cells/well or 1×10^5 NN cells/well. Responders were harvested from primary MLTC on day 13 and reexposed to fresh stimulator lymphocytes and/or glioma cells. Cytolytic activity in the secondary MLTC was assayed after 3 days. Effector-to-target cell ratios in cytolytic assays were 5:1 both for glioma targets and for PHA blasts. Spontaneous ^{51}Cr release was 28% from NN glioma, 34% from RB glioma, and 7% from the PHA blasts.

[e] In expt 3, both NN and RF gliomas were added to MLTC at 5×10^4 cells/well. Effectors were harvested on day 12 of primary MLTC and assayed for lytic activity at effector-to-target cell ratios of 20:1 for NN glioma and 5:1 for RF glioma. Spontaneous ^{51}Cr release was 27 and 21% from the NN and RF gliomas, respectively.

TABLE 3.—*Lack of requirement for third-party stimulator lymphocytes in the generation of lymphocytes specifically cytotoxic for allogeneic AB and LH gliomas*

Expt No.	Contents of MLTC[a]			Percent specific ^{51}Cr release from:[b]				
	Responder lymphocytes	Stimulator lymphocytes	Glioma	AB glioma	LH glioma	K562	LM glioma	Stimulator PHA blasts
1[c]	+			10.7±2.2		19.0±0.3		
	+		AB	56.9±2.1		27.7±0.7		
	+	+		36.0±0.9		45.0±0.3		
	+	+	AB	59.7±0.4		47.0±0.3		
2[d]	+				3.3±1.4	20.1±2.5	3.8±0.7	4.0±1.1
	+		LH		46.8±2.0	20.0±1.6	4.5±0.8	2.6±0.1
	+	+			55.9±1.7	45.4±0.2	12.2±1.1	19.3±2.9
	+	+	LH		77.8±0.4	38.5±3.1	13.5±1.3	22.8±2.5

[a] +=present in MLTC.

[b] Values are means ± 1 SE of replicate samples.

[c] In expt 1, glioma cells were added to MLTC at 5×10^4 cells/well. Cells were harvested on day 15 of the primary MLTC and boosted in secondary MLTC. Cytolytic activity was assayed 4 days later. Effector-to-target cell ratios were 7:1 for both targets, and the spontaneous ^{51}Cr release was 29% for AB glioma and 28% for K562.

[d] In expt 2, concentration of glioma cells in MLTC was 5×10^4 cells/well, and cytolytic activity was assayed on day 12 of the primary MLTC. Effector-to-target cell ratios in the cytolytic assays were 24:1 for glioma targets and 40:1 for PHA blasts and K562. Spontaneous ^{51}Cr release was 15, 28, 29, and 10% from LH glioma, K562, LM glioma, and PHA blasts, respectively.

causing significant lysis not only of the stimulator PHA blasts but also of the glioma targets. The lysis of glioma targets by these effectors might have resulted from the action of specific cytolytic lymphocytes recognizing antigens on the glioma cells that were identical to or cross-reactive with antigens on the stimulator lymphocytes. Alternatively, lysis could have been caused by nonspecific "anomalous" or NK-like effectors that are generated in such cultures (*22–24*). In fact, as shown below, probably the NK-like effector was responsible for most glioma cell lysis produced under these conditions.

In table 2, experiment 1, when MLTC contained NN glioma stimulators as well as responder and stimulator lymphocytes, the resulting lysis of NN glioma targets was increased 2.6-fold over that caused by effectors generated from responder cells incubated with stimulator lymphocytes alone. In contrast, lysis of the LM glioma targets and of stimulator PHA blasts did not increase but rather decreased when NN glioma stimulators were included with responder and stimulator lymphocytes in the MLTC. Likewise, lysis of K562 was not increased when effectors were from such cultures (*see* table 4, expt 1). Thus in MLTC containing responder lymphocytes, stimulator lymphocytes, and NN glioma cells, a mixture of cytolytic effectors was produced. Substantially enhanced lysis of the NN glioma but not of the LM glioma or of stimulator PHA blasts provided clear evidence for the generation of a population of effectors capable of specifically recognizing and lysing the NN glioma cells. However, this lysis was superimposed on the lysis caused by nonspecific effectors that were produced as a result of the interaction between the responder and stimulator lymphocytes, regardless of whether or not NN glioma cells were present in the mixed leukocyte cultures. Further evidence of the phenotypic distinction between these two types of effectors is presented below (*see* table 4). Results similar to those of table 2, experiment 1, are presented for the NN, RB, and RF gliomas in experiments 2 and 3, table 2. In addition, experiments 2 and 3 contain *reciprocal specificity* controls, which clearly established that effectors specific for antigens on the glioma cells were generated when glioma cells were cultured with responder and stimulator lymphocytes in MLTC.

Although the nature of the antigens recognized in these experiments was not rigorously defined, most likely they were alloantigens. In experiments (not shown) in which fibroblasts autologous to the glioma stimulators were included as targets, lysis of the fibroblasts paralleled that of the corresponding glioma targets. However, lysis of fibro-

TABLE 4.—*Identification of specific cytolytic lymphocytes generated against allogeneic NN glioma in the presence of third-party stimulator lymphocytes as T-cells*[a]

Expt	Contents of MLTC	Treatment following MLTC	Viable cells/culture after treatment	Percent specific ^{51}Cr release at viable E:T[b]		Lytic units[c]/culture after treatment	Ratio of lytic units: (R+S+glioma)/(R+S)
				10:1	4:1		
Part A: Target=NN glioma							
Expt 1	R	Medium	6×10^5	13.6±1.7		5	
	R+S	Medium	12×10^5	19.5±0.7	11.5±0.8	15	
	R+S	C	12×10^5	18.8±0.8	6.6±0.9	13	
	R+S	OKT3+C	5×10^5	29.4±3.0	17.9±0.7	11	
	R+S+glioma	Medium	12×10^5	49.6±0.4	31.6±2.1	51	3.4
	R+S+glioma	C	12×10^5	57.8±4.5	27.1±0.4	54	4.1
	R+S+glioma	OKT3+C	5×10^5	35.3±0.9	16.0±0.3	10	0.9
Expt 2	R	Medium	12×10^5	3.6±3.0	0.7±1.8	<1	
	R+glioma	Medium	12×10^5	−0.3±0.6	−0.2±0.3	<1	
	R+S	Medium	18×10^5	10.5±2.5	3.0±2.2	12	
	R+S	C	18×10^5	14.5±1.6	6.3±1.9	15	
	R+S	OKT3+C	6×10^5	25.1±0.7	11.2±0.5	10	
	R+S+glioma	Medium	15×10^5	32.3±2.0	14.7±0.5	33	2.8
	R+S+glioma	C	15×10^5	36.9±0.6	15.6±2.3	39	2.6
	R+S+glioma	OKT3+C	6×10^5	28.1±1.5	14.2±1.6	12	1.2
				20:1	7:1		
Part B: Target-K562							
Expt 1	R	Medium	6×10^5	41.3±0.3	19.0±0.3	23	
	R+S	Medium	12×10^5	51.1±0.4	35.0±0.3	103	
	R+S	C	12×10^5	48.0±1.0	37.5±0.5	109	
	R+S	OKT3+C	5×10^5	60.6±0.3	52.3±0.4	119	
	R+S+glioma	Medium	12×10^5	54.2±0.4	37.9±0.4	113	1.1
	R+S+glioma	C	12×10^5	54.3±0.8	32.7±1.0	103	0.9
	R+S+glioma	OKT3+C	5×10^5	61.8±1.5	50.4±1.0	113	0.9

[a] In both experiments, NN glioma cells were added to MLTC at 1×10^5 cells/well. Cells were harvested from primary MLTC on day 14 and boosted in secondary MLTC. After 4 days, cells were harvested from the secondary MLTC and treated with medium, complement (C) alone, or OKT3 plus C as described in "Materials and Methods." The remaining viable cells were then enumerated and assayed for lytic activity. Spontaneous ^{51}Cr release from the NN glioma was 20% in expt 1 and 28% in expt 2. Spontaneous ^{51}Cr release from K562 in expt 1 was 28%. Results shown for expt 1, parts A and B, represent the results of a single experiment in which various untreated and treated effector populations were assayed for lytic activity on two separate targets. R=responder lymphocytes; S=stimulator lymphocytes.

[b] Values are means ± 1 SE of replicate samples. E:T=effector-to-target cell ratio.

[c] One lytic unit was defined as the number of viable effectors required to cause 30% specific ^{51}Cr release from the targets. Values for specific ^{51}Cr release were graphed on a semi-log plot in which the *ordinate* was 100 minus the percent specific release and the *abscissa* was the effector-to-target cell ratio (25). Such plots were linear for values of percent specific release <50%. In the case of effector populations for which the maximum percent specific release was <30%, the effector-to-target cell ratio required to give 30% specific release was extrapolated, with linearity assumed.

TABLE 5.—*Ability of lymphocytes from a patient with evidence of in vivo sensitization against antigens on the NN glioma to respond to the NN glioma in vitro in the absence of third-party stimulator lymphocytes*[a]

Contents of MLTC[b]			Percent specific ^{51}Cr release from:[c]			
Lymphocytes of patient #10 with NA glioma	Stimulator lymphocytes	Glioma	NN glioma	Autologous NA fibroblasts	K562	Stimulator PHA blasts
+			2.4±5.8	−0.6±0.8	6.3±3.2	1.7±1.9
+		NN	37.6±2.5	7.5±0.9	23.4±0.3	14.6±1.8
+	+		11.8±4.8	30.9±3.1	59.7±1.3	48.6±1.1
+	+	NN	37.8±2.6	25.4±1.4	73.8±4.8	56.5±1.0

[a] Effector cells were harvested from primary MLTC on day 10 and assayed for cytolytic activity. Effector-to-target cell ratios were 20:1 for glioma and fibroblast targets and 10:1 for K562 and PHA blasts. Spontaneous ^{51}Cr release was 36, 29, 17, and 15% from NN glioma, NA fibroblasts, K562, and PHA blasts, respectively.

[b] +=present in MLTC.

[c] Values are means ± 1 SE of replicate samples.

blasts autologous to the responders paralleled the lysis of K562 (table 5).

When the AB or LH gliomas were incubated with responder lymphocytes from normal donors, they directly elicited allogeneic cytolytic lymphocyte responses in the absence of any third-party stimulator lymphocytes (table 3). The cytolytic lymphocyte response elicited by the LH glioma appeared to be highly specific. In contrast, the AB glioma seemed to elicit a mixture of specific and nonspecific (lytic for K562) effectors; however, it is unclear from the data in table 3 to what extent each of these two types of effectors contributed to the lysis of AB targets.

From among the nonstimulatory gliomas, the NN glioma was selected for further studies regarding the nature of its immunogenic deficit. This line was chosen both because its rapid doubling time of 3–4 days permitted the growth of many cells for use in experiments and because it had previously been studied in detail with the use of serologic techniques and had been shown to possess both common and restricted glioma-specific antigens (*9*) as well as HLA antigens (this report). To determine whether the inability of this line to directly elicit a cytolytic lymphocyte response was due simply to an inappropriate choice of the concentration of glioma cells to be added to the MLTC, we performed two experiments in which the concentration of NN glioma cells in the MLTC was varied over a fortyfold range. These experiments yielded similar results, and one of them is summarized in table 6. In this experiment, incubation of responder lymphocytes from a normal donor with NN glioma at concentrations varying from 1.25×10^4 to 4×10^5 glioma cells/well did not lead to the generation of a significant amount of cytolytic activity. When more than 4×10^5 glioma cells were added per well, the glioma monolayers became overly dense and retracted off the floor of the well. Optimal glioma concentration for eliciting a cytolytic lymphocyte response in the presence of help from an allogeneic MLR was 5×10^4 to 2×10^5 cells/well. At higher concentrations suppression of the response was observed. It is unclear whether this resulted from the secretion of some immunosuppressive entity or simply from overcrowding and competition for critical nutrients. Thus the NN glioma was unable to elicit a cytolytic lymphocyte response in the absence of allogeneic help at all cell concentrations tested; however, at high cell concentrations weak immunogenicity could have been masked by an overriding immunosuppressive effect.

T-Cell Nature of Specific Cytolytic Lymphocytes Generated in the Presence of Allogeneic Help

Zarling and Kung (*26*), Zarling et al. (*27*), and Platsoucas and Good (*28*) demonstrated that specific cytolytic T-cells can be distinguished from nonspecific NK-like cells, which are likewise generated in MLR, by treatment of effector cells with the monoclonal anti-T-cell antibody OKT3 plus complement. Such treatment abolishes the activity of CTL but not that of NK-like cells. In the two experiments shown in table 4, this approach was used to determine the identity of the glioma-specific effectors generated in the presence of third-party stimulator lymphocytes.

In both experiments responder lymphocytes from normal donors were incubated with either stimulator lymphocytes or stimulator lymphocytes plus NN glioma. Effectors harvested from MLTC containing stimulator lymphocytes plus NN glioma were threefold- to fourfold-more effective in lysing the NN glioma than were effectors from cultures containing only responder and stimulator lymphocytes. OKT3 and complement treatment of effectors from responder and stimulator lymphocyte cultures caused only a minimal decrease in the lytic units per culture and increased the lytic units per viable cell. In contrast, similar treatment of effectors that had been sensitized against the NN glioma in the presence of allogeneic help reduced the lytic units per culture threefold to fivefold to a value essentially identical to the number of lytic units remaining in cultures of responder plus stimulator lymphocytes after treatment with OKT3 and complement. Thus these results provided phenotypic evidence that in MLTC containing responder lymphocytes with glioma cells and third-party stimulator lymphocytes at least two types of effectors were generated: CTL specific for antigens on the glioma cell and nonspecific, non-T-effectors, presumably NK-like cells. Non-T-effectors were produced to the same extent as in cultures containing responder and stimulator lymphocytes without glioma cells.

As a specificity control, the lysis of K562 by the various untreated and treated cell populations was also examined

TABLE 6.—*Effect of number of glioma cells in MLTC on generation of lymphocytes cytotoxic for allogeneic NN glioma*[a]

Contents of MLTC:[b]			Percent specific ^{51}Cr release from NN glioma[c]	Difference between percent specific release: (R+S+glioma)−(R+S)[d]
Responder lymphocytes	Stimulator lymphocytes	NN glioma/culture		
+		0	−2.8±1.8	
+	+	0	21.8±1.7	
+		4×10^5	5.2±1.9	
+	+	4×10^5	35.0±0.5	13.2
+		2×10^5	−0.9±1.2	
+	+	2×10^5	44.8±2.4	23.0
+		1×10^5	−4.0±0.8	
+	+	1×10^5	42.6±0.9	20.8
+		5×10^4	−2.3±1.1	
+	+	5×10^4	37.9±1.5	16.1
+		2.5×10^4	−4.4±0.9	
+	+	2.5×10^4	34.1±0.8	12.3
+		1.25×10^4	−4.7±1.1	
+	+	1.25×10^4	27.6±3.4	5.8

[a] Effector cells were harvested from primary MLTC after 7 days and assayed for cytolytic activity at an effector-to-glioma ratio of 5:1. The spontaneous ^{51}Cr release from NN glioma was 22%.

[b] +=present in MLTC.

[c] Values are means ± 1 SE of replicate samples.

[d] R=responder lymphocytes; S=stimulator lymphocytes.

in experiment 1, table 4. Consistent with the results in table 2, addition of NN glioma to cultures of responder and stimulator lymphocytes did not lead to any increase in the generation of lytic activity as assayed on K562 (in contrast to the threefold to fourfold enhancement of lytic activity as assayed on the NN glioma). Likewise, in accordance with the results of previous authors (*26–28*), treatment of effectors with OKT3 and complement did not appreciably alter the lytic units per culture as assayed on K562; i.e., lysis due to the action of NK-like cells was unaffected.

Ability of Lymphocytes From a Glioma Patient With Evidence of In Vivo Sensitization Against Antigens on the NN Glioma To Respond to the NN Glioma in MLTC in the Absence of Third-Party Stimulator Lymphocytes

One patient (#10) with NA glioma has been unique among the glioma patients studied to date in that freshly isolated peripheral blood mononuclear cells from this patient caused substantial lysis of all three allogeneic glioma lines tested [NN, LM (table 7), and GB] and of 1 of 2 allogeneic fibroblast lines (NN but not GB fibroblasts were lysed). However, lymphocytes of patient #10 lysed neither autologous cultured glioma nor autologous fibroblasts, and they caused no greater lysis of an allogeneic colon adenocarcinoma than did lymphocytes from normal controls (data not shown). The ability of this patient's lymphocytes to lyse allogeneic glioma cells did not correlate with their NK activity as measured on K562 targets (table 7); in contrast to NK-mediated lysis of K562, lysis of allogeneic gliomas was virtually abolished by treatment of the effectors with OKT3 and complement (table 7). Thus patient #10 with NA glioma had apparently made a CTL response in vivo against some antigen present on the NN and other glioma lines. It is not known whether this was an antigen cross-reactive with some environmental antigen, an alloantigen against which sensitization had occurred as a result of blood transfusion, or some tumor-related antigen that had been lost from the patient's own cultured glioma line. However, this patient's lytic activity against allogeneic glioma cells remained at essentially constant levels during serial assays over a 10-month period, and similar reactivity was not observed for lymphocytes from any of 6 other glioma patients or 34 normal donors.

When lymphocytes from patient #10 with NA glioma were incubated with NN glioma cells in MLTC, an enhanced cytolytic lymphocyte response occurred in the absence of third-party stimulator lymphocytes (table 5). This observation was in contrast to the inability of lymphocytes from four other glioma patients or nine normal donors to make any direct response to the NN glioma in MLTC (cf. tables 2, 4, 6). As in experiment 1, table 3, the cytolytic response appeared to consist of a mixture of specific and nonspecific elements, since exposure of NA lymphocytes to NN glioma in MLTC resulted in enhanced lysis not only of the NN glioma but also of K562. Nevertheless, effectors generated in an allogeneic MLR containing NA lymphocytes as responders and allogeneic stimulator lymphocytes lysed K562 to a substantially greater extent than the NN glioma, whereas effectors generated by the incubation of

TABLE 7.—*Presence of T-cells capable of lysing allogeneic NN and LM gliomas in freshly isolated peripheral blood mononuclear cells from patient #10 with NA glioma*[a]

Expt No.	Lymphocyte donor	Treatment of lymphocytes	Percent specific ^{51}Cr release from:[b]		
			NN glioma	LM glioma	K562
1	Normal #1	Medium	3.8±2.7		13.8±2.2
	Normal #2	Medium	5.2±1.5		4.6±1.1
	Patient #10	Medium	52.0±2.0		25.9±1.7
	Patient #10	C	50.3±1.3		22.7±0.6
	Patient #10	OKT3+C	7.2±2.2		23.2±1.3
2	Normal #3	Medium	15.2±2.2	10.8±1.9	77.8±6.0
	Normal #4	Medium	8.9±0.7	4.4±0.6	61.5±4.4
	Patient #10	Medium	39.6±1.0	41.8±0.3	73.7±0.5
	Patient #10	C		44.5±6.6	
	Patient #10	OKT3+C		7.3±1.6	

[a] Freshly isolated peripheral blood mononuclear cells were treated with medium, complement (C), or OKT3 plus C as described in "Materials and Methods" and then assayed for their ability to lyse NN glioma, LM glioma, and K562. Treatment with OKT3 and C caused a 67% reduction in viable cells in expt 1 and a 74% reduction in expt 2. Treatment with C alone lysed ≤10% of cells in both experiments. Effector-to-target cell ratio was 50:1 in expt 1 and 70:1 in expt 2. The spontaneous ^{51}Cr release was 27% from NN glioma and 29% from K562 in expt 1 and 27, 23, and 13% from NN glioma, LM glioma, and K562, respectively, in expt 2.

[b] Values are means ± 1 SE of replicate samples.

responders with NN glioma were more highly lytic for the NN glioma than for K562. These observations suggested that the increased lysis of the NN glioma caused by the effectors generated by incubation of responders with NN glioma was due to the action of specific cytolytic lymphocytes rather than to an unusually high sensitivity of the NN glioma to lysis by NK-like cells. In a separate experiment it was found that NA lymphocytes, in contrast to lymphocytes from other glioma patients or from normal donors, also could react directly against the LM glioma in MLTC in the absence of allogeneic help (data not shown). Thus it appeared that, if sensitization to antigens on a normally nonstimulatory glioma cell line such as NN had occurred in vivo, such a cell line could elicit an enhanced cytolytic lymphocyte response in vitro in the absence of allogeneic help if responders were from the sensitized individual.

Ability of Glioma Cell Lines To Directly Stimulate an Allogeneic CTL Response; Lack of Correlation With the Presence of Ia-Like Antigens on the Glioma Line

In collaboration with Dr. McFarland, we examined the glioma lines used in these studies for the presence of HLA and Ia-like antigens by means of indirect immunofluorescence employing xenogeneic monoclonal anti-HLA-A, -B, -C and anti-HLA-DR antibodies recognizing nonpolymorphic determinants. As indicated in table 1, only one line, GB, reacted with the anti-HLA-DR antibody. However, that line, because of its production of an immunosuppressive substance, could not elicit cytolytic lymphocyte responses. Rather, GB glioma cells inhibited MLR to which they were added (20). Thus there was no correlation between the presence of Ia-like antigens on these lines, at least as determined by the anti-HLA-DR antibody used in these experiments, and the ability of these lines to elicit a CTL response.

DISCUSSION

The immune response to astrocytomas may be of particular interest to tumor immunologists for several reasons. Since these tumors arise in a location, the brain, which has traditionally been regarded as an "immunologically privileged site" (*29*), one might expect that in the absence of selective pressure from a hostile immune system such tumors would have a higher probability of expressing strong tumor-specific antigens than tumors arising in the periphery. Nevertheless, as these tumors grow, the blood-brain barrier is breached (*30*), so that interactions between the tumor and the host's immune system can occur. Substantial evidence indicates that most astrocytoma patients do make humoral immune responses to their own tumors (*7, 9*). These studies likewise provide evidence for the existence of both common and restricted glioma-specific antigens on these tumors. The evidence that astrocytoma patients make significant cellular immune responses to their own tumors is, however, more tenuous and controversial (*8, 31*). Because conventional therapy, consisting of surgery, irradiation, and chemotherapy, has had only a minor impact in improving the prognosis of patients with high-grade gliomas (*32*), interest in the use of less conventional therapeutic modalities, including immunotherapy, has risen. Although astrocytomas display extensive local growth and infiltration, they rarely metastasize; thus elimination of the tumor at its site of origin should be curative. Current technology permits the successful growth of astrocytomas in culture in over 90% of cases (*33*); hence detailed studies on the properties of glioma cells in vitro and of their potential for use in immunotherapy are readily feasible.

We have examined the ability of human glioma cells to elicit allogeneic CTL responses in vitro so that we could define those properties of glioma cells that may contribute to their ability to escape cellular immune attack. In addition to the defect in immunogenicity described in this paper, two other escape mechanisms have been identified: *a*) the production by certain glioma lines of an immunosuppressive substance and *b*) the secretion by some glioma lines of a protective mucopolysaccharide coat that impedes contact between lymphocytes and glioma cells (*20*). The experiments reported in this paper demonstrate that certain cultured glioma lines possess a defect in immunogenicity such that they are unable by themselves to elicit an allogeneic cytolytic lymphocyte response in MLTC but can elicit a response in the presence of help from an allogeneic MLR. Whether this defect exists in gliomas in vivo or represents a characteristic acquired in vitro is unclear. There was no obvious correlation between the inability to stimulate CTL responses and the length of time the lines had been in culture (table 1). It is unclear what property of a glioma line determines its ability to directly elicit a CTL response. Stimulatory capacity was not correlated with the presence of Ia-like antigens, as determined by the ability of the glioma lines to react with a xenogeneic monoclonal anti-HLA-DR antibody (table 1). However, it is well documented, at least in murine systems, that I-region differences in MLR are not necessarily required for the generation of a CTL response (*34, 35*). Preliminary experiments suggest that the ability of at least some glioma lines to directly stimulate cytolytic responses could relate to the acquisition of fetal calf serum components during culture. The LH line (table 3) was divided into two portions, one of which was cultured in TCM with human blood type AB serum for more than 2 months while the other was cultured in medium containing FBS. LH cells grown in human blood type AB serum lost the ability to directly elicit cytolytic responses, although LH-specific responses could still be generated in the presence of third-party stimulator lymphocytes (Gately MK, Dick SJ: Unpublished results). LH cells grown in FBS retained the ability to directly elicit cytolytic responses as shown in table 3 (the same normal donor was used as the source of responder cells in all experiments).

Third-party stimulator lymphocytes have been used by others to facilitate the induction of CTL responses to autologous human leukemias (*36–38*), to autologous human trinitrophenyl-modified lymphocytes (*39*), and to UV-irradiated murine lymphocytes (*40–42*). Our experiments extend this approach to a class of *human solid* tumors, the gliomas. The ability of NA lymphocytes to respond directly to the NN glioma establishes a further parallel with observations on the CTL response to UV-irradiated lymphocytes. UV-irradiated murine lymphocytes have been observed to stimulate CTL responses in the absence of allogeneic help when responder cells have been previously sensitized to antigens carried by the stimulator lymphocytes (*43–45*). It has been shown that the inability of UV-irradiated murine lymphocytes to elicit primary CTL responses is due to an inability to stimulate helper T-cells and that the mechanism of help provided by allogeneic MLR involves the secretion of a nonspecific helper factor identical to IL-2 (*46–48*). Possibly, the mechanism of allogeneic help in the human glioma system is similar.

Alternatively, the mechanism of allogeneic help in the glioma system could involve the production of lymphoid cells or soluble factors that act directly upon the glioma cells to alter their properties as stimulators. Such alteration could involve either a reduction or counterbalancing of suppressive influences exerted by the glioma cells or changes that directly enhance their immunogenicity. We are currently attempting to circumvent the requirement for third-party stimulator lymphocytes in our experiments by the use of lymphokine-containing supernatants. If successful, we could better define the mechanism of allogeneic help in the human glioma system.

Injection of irradiated autologous glioma cells into patients with high-grade astrocytomas has been reported neither to prolong patient survival nor to elicit cell-mediated antiglioma immunity, as determined by intradermal skin testing (*49*). The results of our experiments provide one possible explanation for the failure of this type of specific immunotherapy in glioma patients. If cultured glioma cells, such as NN glioma cells, are to be used effectively in specific active immunotherapy, they most likely will need to be modified by chemical, enzymatic, or other means for the enhancement of their immunogenicity. Alternatively, patients' lymphocytes might be sensitized in vitro to the autologous tumor and the sensitized cells grown in IL-2 for use in adoptive immunotherapy. Attempts in our laboratory to sensitize patients' lymphocytes to autologous tumor in the presence of allogeneic MLR have, in general, been unsuccessful (Gately MK, Glaser M: Unpublished results). However, since such autologous reactions would be expected to be substantially weaker than the allogeneic reactions described in this paper, the generation of small numbers of specific CTL in the autologous MLTC might have been obscured by the presence of the nonspecific, non-T-effectors, which are likewise produced in such cultures (cf. table 4). The possible generation of such nonspecific effectors, which are only poorly capable of lysing normal lymphocytes (*22–24*), clouds the interpretation of some of the previous reports (*36, 37, 50*) in which cytolytic lymphocytes specific for autologous human tumor cells were thought to have been produced but in which failure of effectors to lyse normal lymphocytes constituted the primary specificity control. To use allogeneic MLR to facilitate the induction of autologous tumor-specific CTL, one will likely need to find ways of inactivating or depleting the nonspecific effectors while leaving specific CTL functionally intact. Studies on these problems are in progress.

REFERENCES

(*1*) Herberman RB. Immunogenicity of tumor antigens. Biochim Biophys Acta 1977; 473:93–119.

(*2*) Prehn RT. Relationship of tumor immunogenicity to concentration of the oncogen. J Natl Cancer Inst 1975; 55:189–190.

(*3*) Hewitt HB, Blake ER, Walder AS. A critique of the evidence for active host defence against cancer, based on personal studies of 27 murine tumours of spontaneous origin. Br J Cancer 1976; 33:241–259.

(*4*) Weiss DW. The questionable immunogenicity of certain neoplasms: What then the prospects for immunological intervention in malignant disease? Cancer Immunol Immunother 1977; 2:11–19.

(*5*) Klein G, Klein E. Rejectability of virus-induced tumors and nonrejectability of spontaneous tumors: A lesson in contrasts. Transplant Proc 1977; 9:1095–1104.

(*6*) Coakham H. Surface antigen(s) common to human astrocytoma cells. Nature 1974; 250:328–330.

(*7*) Pfreundschuh M, Shiku H, Takahashi T, et al. Serological analysis of cell surface antigens of malignant human brain tumors. Proc Natl Acad Sci USA 1978; 75:5122–5126.

(*8*) Levy NL. Specificity of lymphocyte-mediated cytotoxicity in patients with primary intracranial tumors. J Immunol 1978; 121:903–915.

(*9*) Coakham HB, Kornblith PL, Quindlen EA, Pollock LA, Wood WC, Hartnett LC. Autologous humoral response to human gliomas and analysis of certain cell surface antigens: In vitro study with the use of microcytotoxicity and immune adherence assays. JNCI 1980; 64:223–233.

(*10*) Wikstrand CJ, Mahaley MS, Bigner DD. Surface antigenic characteristics of human glial brain tumor cells. Cancer Res 1977; 37:4267–4275.

(*11*) Winchester RJ, Kunkel HG. The human Ia system. Adv Immunol 1979; 28:221–292.

(*12*) Herlyn M, Clark WH Jr, Mastrangelo MJ, et al. Specific immunoreactivity of hybridoma-secreted monoclonal anti-melanoma antibodies to cultured cells and freshly derived human cells. Cancer Res 1980; 40:3602–3609.

(*13*) Kernohan JW, Sayre GP. Tumors of the central nervous system. American Registry of Pathology. Washington, D.C.: Armed Forces Institute of Pathology, 1952.

(*14*) Weinstein RS, Kornblith PL. Ultrastructure of a cloned astrocytoma in tissue culture. Cancer 1971; 27:1174–1181.

(*15*) Pontén J. Neoplastic human glial cells in culture. In: Fogh J, ed. Human tumor cells in vitro. New York: Plenum Press, 1975:175.

(*16*) Dohan FC, Kornblith PL, Wellum GR, Pfeiffer SF, Levine L. S-100 protein and 2′,3′-cyclic nucleotide 3′-phospho-hydrolase in human brain tumors. Acta Neuropathol (Berl) 1977; 40:123–128.

(*17*) Trachtenberg MC, Kornblith PL, Hauptli J. Biophysical properties of cultured human glial cells. Brain Res 1972; 38:279–298.

(*18*) Böyum A. Isolation of mononuclear cells and granulocytes from human blood. Isolation of mononuclear cells by one centrifugation, and of granulocytes by combining centrifugation and sedimentation at 1 g. Scand J Clin Lab Invest 1968; 21 (suppl 97):77–89.

(*19*) Perper RJ, Zee TW, Mickelson MM. Purification of lymphocytes and platelets by gradient centrifugation. J Lab Clin Med 1968; 72:842–848.

(*20*) Gately MK, Glaser M, McCarron RM, et al. Mechanisms by which human gliomas may escape cellular immune attack. Acta Neurochir. In press.

(*21*) Drew SI, Terasaki PI, Billing RJ, Bergh OJ, Minowada J, Klein E. Group-specific human granulocyte antigens on a chronic myelogenous leukemia cell line with a Philadelphia chromosome marker. Blood 1977; 49:715–718.

(*22*) Seeley JK, Masucci G, Poros A, Klein E, Golub SH. Studies on cytotoxicity generated in human mixed lymphocyte cultures. II. Anti-K562 effectors are distinct from allospecific CTL and can be generated from NK-depleted T cells. J Immunol 1979; 123:1303–1311.

(*23*) Masucci MG, Klein E, Argov S. Disappearance of the NK effect after explantation of lymphocytes and generation of similar nonspecific cytotoxicity correlated to the level of blastogenesis in activated cultures. J Immunol 1980; 124:2458–2463.

(*24*) Bolhuis RL, Schellekens H. Induction of natural killer cell activity and allocytotoxicity in human peripheral blood lymphocytes after mixed lymphocyte culture. Scand J Immunol 1981; 13:401–412.

(*25*) Gately MK, Martz E. Comparative studies on the mechanisms of nonspecific, con A-dependent cytolysis and specific T cell-mediated cytolysis. J Immunol 1977; 119:1711–1722.

(*26*) Zarling JM, Kung PC. Monoclonal antibodies which distinguish between human NK cells and cytotoxic T lymphocytes. Nature 1980; 288:394–396.

(*27*) Zarling JM, Bach FH, Kung PC. Sensitization of lymphocytes against pooled allogeneic cells. II. Characterization of effector cells cytotoxic for autologous lymphoblastoid cell lines. J Immunol 1981; 126:375–378.

(*28*) Platsoucas CD, Good RA. Inhibition of specific-cell-mediated cytotoxicity by monoclonal antibodies to human T cell antigens. Proc Natl Acad Sci USA 1981; 78:4500–4504.

(*29*) Neuwelt EA, Clark WK. Unique aspects of central nervous system immunology. Neurosurgery 1978; 3:419–430.

(*30*) Long DM. Capillary ultrastructure and the blood-brain barrier in human malignant brain tumors. J Neurosurg 1970; 32:127–144.

(*31*) Woosley RE, Mahaley MS Jr, Mahaley JL, Miller GM, Brooks WH. Immunobiology of primary intracranial tumors. Part 3: Microcytotoxicity assays of specific immune responses of brain tumor patients. J Neurosurg 1977; 47:871–885.

(*32*) Walker MD, Alexander E Jr, Hunt WE, et al. Evaluation of BCNU and/or radiotherapy in the treatment of anaplastic gliomas. J Neurosurg 1978; 49:333–343.

(*33*) Kornblith PL. Role of tissue culture in prediction of malignancy. Clin Neurosurg 1978; 25:346–376.

(*34*) Forman J, Klein J. Immunogenetic analysis of *H-2* mutations. II. Cellular immunity to the $H\text{-}2^{da}$ mutation. J Immunol 1975; 115:711–715.

(*35*) Hodes RJ, Schmitt-Verhulst A-M, Hathcock KS, Shearer GM. Mixed lymphocyte reactivity and cell-mediated lympholysis to D-end differences of the murine major histocompatibility complex. Comparison of in vitro responses to exclusive D-end or more extensive MHC differences. Scand J Immunol 1976; 5:369–382.

(*36*) Zarling JM, Raich PC, McKeough M, Bach FH. Generation of cytotoxic lymphocytes in vitro against autologous human leukaemia cells. Nature 1976; 262:691–693.

(*37*) Sondel PM, O'Brien C, Porter L, Schlossman SF, Chess L. Cell-mediated destruction of human leukemic cells by MHC identical lymphocytes: Requirement for a proliferative trigger in vitro. J Immunol 1976; 117:2197–2203.

(*38*) Lee SK, Oliver RT. Autologous leukemia-specific T-cell-mediated lymphocytotoxicity in patients with acute myelogenous leukemia. J Exp Med 1978; 147:912–922.

(*39*) Friedman SM, Neyhard N, Chess L. Cell-mediated lympholysis of trinitrophenyl-derivatized autologous human cells: In vitro triggering by nonspecific signals. J Immunol 1978; 120:630–637.

(*40*) Lafferty KJ. Misko IS, Cooley MA. Allogeneic stimulation modulates the in vitro response of T cells to transplantation antigen. Nature 1974; 249:275–276.

(*41*) Röllinghoff M, Wagner H. Effect of *M*-locus dependent T-cell proliferation upon the induction of anti H-2 cytotoxic T effector cells. J Immunogenet 1975; 2:301–308.

(*42*) Bach FH, Bach ML, Sondel PM. Differential function of major histocompatibility complex antigens in T-lymphocyte activation. Nature 1976; 259:273–281.

(*43*) Röllinghoff M, Wagner H. Secondary cytotoxic allograft response in vitro. I. Antigenic requirements. Eur J Immunol 1975; 5:875–879.

(*44*) Grillot-Courvalin C, Alter BJ, Bach FH. Antigenic requirements for the generation of secondary cytotoxicity. J Immunol 1977; 119:1253–1259.

(*45*) Okada M, Henney CS. The differentiation of cytotoxic T cells in vitro. III. The role of helper T cells and their products in the differentiation of cytotoxic cells from "memory" cell populations. J Immunol 1980; 125:850–857.

(*46*) Sopori ML, Alter BJ, Bach FH, Bach ML. Cell-free factor substitute for "signal 2" in generating cytotoxic reactions. Eur J Immunol 1977; 7:823–825.

(*47*) Okada M, Klimpel GR, Kuppers RC, Henney CS. The differentiation of cytotoxic T cells in vitro. I. Amplifying factor(s) in the primary response is Lyt 1^{+} cell dependent. J Immunol 1979; 122:2527–2533.

(*48*) Kern DE, Gillis S, Okada M, Henney CS. The role of interleukin-2 (IL-2) in the differentiation of cytotoxic T cells: The effect of monoclonal anti-IL-2 antibody and absorption with IL-2 dependent T cell lines. J Immunol 1981; 127:1323–1328.

(*49*) Bloom HJ, Peckham MJ, Richardson AE, Alexander PA, Payne PM. Glioblastoma multiforme: A controlled trial to assess the value of specific active immunotherapy in patients treated by radical surgery and radiotherapy. Br J Cancer 1973; 27:253–267.

(*50*) Strausser JL, Mazumder A, Grimm EA, Lotze MT, Rosenberg SA. Lysis of human solid tumors by autologous cells sensitized in vitro to alloantigens. J Immunol 1981; 127:266–271.

Isozymes of Acid Esterase and Acid Phosphatase in Permanent Human Hematopoietic Cell Lines[1,2]

Christer Sundström,[3] **Heinz J. Radzún,**[4] *and* **Mohammad R. Parwaresch**[4,5]

ABSTRACT—Net enzyme activities of normal human blood cells were measured, and isoelectric focusing patterns of acid esterase (AcE) (EC 3.1.1.6) and acid phosphatase (AcP) (EC 3.1.3.2) were compared with corresponding data obtained for two acute T-lymphoblastic leukemia cell lines (JM, Molt-4), one acute B-lymphoblastic leukemia cell line (Ball-1), one acute non-B-non-T-lymphoblastic leukemia cell line (KM 3), and one promyelocytic leukemia cell line (HL-60). The AcE isozymes, found in the individual blood cell types, were regularly expressed by the corresponding cell lines. AcP was regularly expressed by lines HL-60 and KM 3, but lines JM, Molt-4, and Ball-1 showed additional isozymes and/or reduction of the intensity of the typical isozymes found in the presumed normal counterparts. This phenomenon resulted partly in an obscuration of the typical isozyme patterns. Our study documents the applicability of isozyme mapping to the characterization of permanent hematopoietic cell lines. The results suggest that long-term culture conditions can repress phenotypic properties and/or derepress gene activities.—JNCI 1982; 69:1255–1260.

Normal human blood cells are distinguished by cell-specific isozymes of their lysosomal acid phosphatase (EC 3.1.3.2) and acid esterase (EC 3.1.1.6). The isozyme patterns remain detectable during neoplastic and functional transformations. With the use of the isoelectric focusing technique, we have been able to describe distinct AcP and AcE isozyme patterns for different subsets of lymphocytes, myeloid cells, and monocytes, and for different categories of non-Hodgkin's lymphomas (*1–5*).

In the study reported here, we extended our investigation of AcP and AcE heterogeneity to include a panel of permanent human hematopoietic cell lines established from several acute leukemias. These cell lines are ideal for such studies inasmuch as they are monoclonal expansions of tumor cells without the presence of contaminating normal cells (*6*). The study of the isozyme heterogeneity of these cell lines adds further knowledge to that obtained in previous functional studies (*7–10*) and provides clues to the understanding of the biology of the malignant diseases from which these cells were derived.

MATERIALS AND METHODS

Cell lines.—Five hematopoietic cell lines were studied, the origin of which is given in table 1. The cell lines were grown with a cell concentration never exceeding 5×10^5 cells/ml to ensure logarithmic growth. Ham's F-10 tissue culture medium (GIBCO, Grand Island, N.Y.), supplemented with 10% fetal calf serum and antibiotics (100 IU penicillin/ml, 50 µg streptomycin/ml, 1.25 µg amphotericin B/ml), was changed twice a week (*8*). Cells (total, 1×10^9) were harvested at regular intervals from logarithmically growing cultures, washed twice in phosphate-buffered saline (pH 7.4), and kept frozen at −70°C until further analyses.

Separation of normal blood cells.—For comparison, normal human granulocytes and T-lymphocytes were separated from heparinized fresh venous blood, as described elsewhere (*1, 2*). After centrifugation on a one-step Ficoll-Urografin gradient (Pharmacia Fine Chemicals, Uppsala, Sweden; Schering Aktiengesellschaft, Berlin, Federal Republic of Germany), granulocytes were obtained from the bottom fraction (*15*). T-lymphocytes were enriched from the nonadherent fraction of the interphase by passing the lymphocyte fraction over an immunoglobulin-anti-immunoglobulin C3 column (*16*). In addition, B-lymphocytes were separated from minced and sieved specimens of tonsil tissue, and the contaminating T-lymphocytes were excluded by means of rosetting with sheep red blood cells and by sedimentation (*17, 18*). Only highly purified viable cell fractions, as checked by cytochemical and immunological tests and trypan blue exclusion, were used (*1, 2*).

Activity assay and isoelectric focusing of AcE.—For extraction of the lysosomal hydrolases, cell pellets were incubated with 1% (vol/vol) Triton X-100 solution (Serva Feinbiochemica GmbH, Heidelberg, Federal Republic of Germany) for 30 minutes at room temperature and then ultracentrifuged (100,000×*g* for 60 min at 4°C). [In preliminary experiments no substantial differences appeared in the isoelectric focusing patterns, whether whole cells or the separated lysosomal fraction for enzyme extraction was used (*2, 4*).] AcE activity was measured in the clear supernatant, with α-naphthyl acetate (Sigma Chemie GmbH, Munich, Federal Republic of Germany) as substrate and fast blue RR (Sigma Chemie GmbH) as coupler at pH 5.8. The activity was spectrophotometrically evaluated at 500 nm and related to 1×10^7 cells.

On 4.3% polyacrylamide (Canalco, Rockville, Md.) slabs, 60 mU AcE activity in 20 µl sample volume was subjected to isoelectric focusing with the use of the multiphor system 2117 from LKB-Produkter AB (Bromma, Sweden). The gels contained 13.3% (wt/vol) sucrose, 1% (wt/vol) Triton X-100, 0.057% (wt/vol) riboflavin (Canalco), and, for maintenance of the pH gradient, 5% (vol/vol) ampholine, pH 3.5–10.0 (LKB-Produkter AB); 0.036% (vol/vol) ampholine,

---

ABBREVIATIONS USED: AcE=acid esterase; AcP=acid phosphatase; ALL=acute lymphoblastic leukemia; pI=isoelectric point(s).

---

[1] Received February 1, 1982; accepted June 3, 1982.

[2] Supported by grant 55-B75-11XA from the Swedish Cancer Society, by grant SFB 111 (projects CL3 and CN 2) from the Deutsche Forschungsgemeinschaft, and by a grant from the Krebsgesellschaft Schleswig-Holstein.

[3] Department of Pathology, University of Uppsala, S-75122 Uppsala, Sweden.

[4] Institute of Pathology, University of Kiel, Hospitalstrasse 42, 23 Kiel, Federal Republic of Germany.

[5] We thank Miss H. Jacobsen for her excellent technical assistance.

TABLE 1.—*Analyzed hematopoietic cell lines*

Cell line	Original diagnosis	Reference
HL-60	Promyelocytic leukemia	Collins SJ et al. (*11*)
Ball-1	B-ALL	Hiraki S et al. (*12*)
JM	T-ALL	Schneider U, Schwenk HU (*13*)
Molt-4	T-ALL	Minowada J et al. (*14*)
KM 3	0-ALL	Schneider U, Schwenk HU (*13*)

pH 4.0–6.0; and 0.036% (vol/vol) ampholine, pH 5.0–7.0. As anolyte and catholyte, 1 *M* phosphoric acid and 1 *M* sodium hydroxide were used (*19*). After a running time of 4 hours at 4°C, during which the initial voltage of 200 V was raised to a terminal level of 1,200 V, the AcE enzyme bands were visualized with α-naphthyl acetate as substrate and hexazonium pararosanilin as coupler at pH 5.8, according to the histochemical method described by Mueller et al. (*20*). The gels were photographed, scanned at 537 nm (flying spot, TLD-100; Vitatron, Cologne, Federal Republic of Germany), and the pI of the bands were determined by measurement of the pH of aliquots of gel strips.

Activity assay and isoelectric focusing of AcP.—The procedures for enzyme extraction and isoelectric focusing were identical to those described above for AcE. For the AcP assay we used commercial kits (Boehringer Mannheim GmbH, Mannheim, Federal Republic of Germany), with *p*-nitrophenylphosphate as substrate (*21*). A minimum of 8 mU of enzyme activity, which prevented overlooking weak bands and gave optimal resolution, was subjected to isoelectric focusing. For visualization of AcP variants, the histochemical method as described by Barka and Anderson (*22*) was applied, with naphthol-AS-BI phosphate as substrate and hexazonium pararosanilin as coupler at pH 5.0.

In parallel runs all samples were studied after neuraminidase (type V; Sigma Chemie GmbH) treatment (2 hr at 37°C, pH 5.5) as described in (*3*).

RESULTS

AcE and AcP Activities

Table 2 gives a survey of the activities of the analyzed lysosomal hydrolases per 1×10⁷ cells.

The acute lymphoblastic leukemia lines of the B- and T-cell type (Ball-1, JM, Molt-4) revealed similar AcE activities, exceeding the value for the promyelocytic leukemia line (HL-60) by a factor of two. Granulocytes isolated from normal human peripheral blood showed a net enzyme activity of 0.9±0.5 mU/1×10⁷ cells, whereas B- and T-lymphocytes had a sixfold higher AcE activity value (table 3).

TABLE 2.—*Activities of AcE and AcP in the analyzed cell lines*[a]

Cell line	AcE	AcP
HL-60	6.1	25.6
Ball-1	12.9	21.2
JM	11.2	18.6
Molt-4	12.4	15.6
KM 3	6.3	8.6

[a] mU/1×10⁷ cells.

TABLE 3.—*Activities of AcE and AcP in normal blood cells*[a]

Cell population	AcE	AcP
Granulocytes	0.9±0.5 (*n*=5)	5.8±3.4 (*n*=6)
B-lymphocytes	5.5±3.3 (*n*=6)	1.8±1.3 (*n*=6)
T-lymphocytes	5.3±1.8 (*n*=4)	2.8±1.2 (*n*=4)

[a] mU/1×10⁷ cells.

The acute lymphoblastic leukemia lines of the B- and T-cell type displayed AcP values of nearly the same order: 21.2, 18.6, and 15.6 mU/1×10⁷ cells (table 2). The promyelocytic cell line HL-60 showed only slightly higher AcP values. Corresponding values for AcP of normal human blood cells were 5.8±3.4 for granulocytes, 1.8±1.3 for B-lymphocytes, and 2.8±1.2 for T-lymphocytes (table 3). Line KM 3 showed values of 6.3 and 8.6 mU for AcE and AcP, respectively.

AcE Isoelectric Focusing Patterns

The AcE isoelectric focusing patterns for the individual permanent cell lines and for the corresponding normal human blood cell types are shown in figures 1A and 1B. A schematic comparison of the analyzed cell lines and the normal counterparts is shown in text-figure 1.

HL-60 displayed three AcE bands between pH 5.0 and 4.8 and an additional band at pH 5.75. In the cathodal region of the gel, three weak bands with pI values of 7.7, 7.5, and 7.0 could be seen. Ball-1 was characterized by four AcE bands with strong activity between pH 6.4 and 5.9. The AcE activity in JM was localized in two complexes between pH 6.4 and 5.9 and pH 5.0 and 4.5, with five and four bands, respectively. Two additional bands were detectable at pH 5.7 and 5.3. The same isoelectric focusing pattern was observed in Molt-4, but with only four AcE bands between pH 6.4 and 5.9. KM 3 showed three AcE bands, with pI values of 6.4, 6.3, and 6.2, and one band at pH 4.85.

In comparisons with the normal counterparts (text-fig. 1), a good correlation was found between Ball-1 and normal human B-lymphocytes. The five typical bands of normal B-

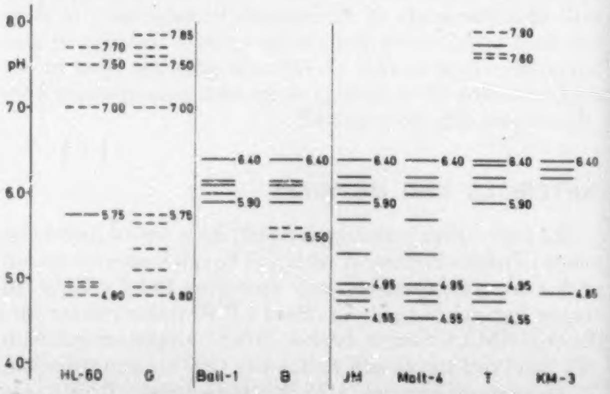

TEXT-FIGURE 1.—Schematic AcE isoelectric focusing patterns in the analyzed hematopoietic cell lines matched with the corresponding patterns of the presumed normal counterparts. G=granulocytes, B=B-lymphocytes, T=T-lymphocytes. *Interrupted lines* stand for bands with weak activity.

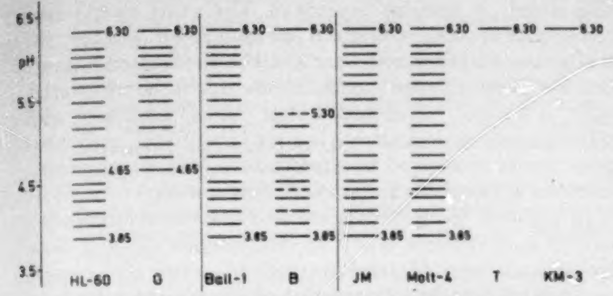

TEXT-FIGURE 2.—Schematic AcP isoelectric focusing patterns in the analyzed hematopoietic cell lines matched with the corresponding patterns of the presumed normal counterparts. G=granulocytes, B=B-lymphocytes, T=T-lymphocytes. *Interrupted lines* stand for bands with weak activity.

lymphocytes were also detectable in the Ball-1 line. In HL-60, some of the AcE bands of normal granulocytes were expressed. JM and Molt-4 clearly showed two of the three AcE complexes found in normal T-lymphocytes between pH 6.4 and 5.9 and between pH 5.0 and 4.5. KM 3 displayed only a few of the AcE bands seen in the middle and anodal AcE complexes of normal T-lymphocytes.

AcP Isoelectric Focusing Patterns

Figures 2A and 2B show the original AcP isoelectric focusing patterns for the permanent cell lines and their normal counterparts, which are matched schematically in text-figure 2.

The AcP isoelectric focusing patterns for normal human blood cells were clearly shared by HL-60 and KM 3. HL-60 expressed the main activity between pH 6.3 and 6.0, with three bands also characteristic for normal granulocytes. The nine bands of normal granulocytes between pH 5.9 and 4.65 showed only weak intensity. An additional six AcP bands could be seen, with pI values extending from 4.5 to 3.8. Like normal T-lymphocytes, KM 3 displayed one band at pH 6.3. The other 3 cultured cell lines (Ball-1, Molt-4, JM) revealed regularly arranged AcP bands between pH 6.3 and 3.8, separated by pH distances of 0.1–0.2 and without any characteristic distribution pattern in the pI values or in the intensity. In Ball-1, the typical AcP pattern of normal B-lymphocytes—1 band at pH 6.3 and 11 bands between pH 5.3 and 3.85—could not be verified.

Samples of cell lines as well as of normal cells treated with neuraminidase showed in some cases a cathodic shift of individual enzyme bands. The distribution pattern and the number and intensity of the bands, however, remained unaltered.

DISCUSSION

The lysosomal hydrolases AcE and AcP have often been studied in investigations of normal and neoplastic blood cells (*23–26*). In recent reports we demonstrated that the different cytochemical patterns of AcE and AcP activity in normal human blood cells are associated with blood cell-specific isozymes, as analyzed by isoelectric focusing (*1, 2*). Using the cell-specific isozyme pattern as a biochemical blood cell marker, we were able to trace the B-cell origin of human malignant lymphomas (*3*) as well as the cellular derivation of different leukemias (*5*). Furthermore, the monocytic origin of resident human peritoneal macrophages could be established by the blood cell-specific AcE isoelectric focusing patterns (*4*). These results demonstrated that the isozyme patterns of AcE and AcP can be regarded as reliable blood cell markers, in terms of physicochemical properties and antigenicity (*27*), and that they resist functional alterations and neoplastic transformations.

Attempts to relate enzyme banding patterns obtained by isoelectric focusing to the isozyme distributions obtained by conventional standard electrophoresis (*28, 29*) failed to demonstrate a clear correlation (*30, 31*). The main difficulty arose in relating certain standard electrophoresis patterns or bands to individual cell types. In contrast, with the use of isoelectric focusing, we were able to establish a clearly defined cell-specific pattern for the individual blood cell types (*1, 2*). This certainly is due to the far better resolution capacity of isoelectric focusing than that of standard electrophoresis. In addition, isoelectric focusing seems to circumvent difficulties expected from the microheterogeneity of the enzyme proteins. Treatment of crude samples with hydrolytic enzymes (e.g., neuraminidase) does not alter number, intensity, and distribution pattern of the individual bands (*3*). For the human system, however, no information is available as to the genetic control of the individual enzyme protein variants that are neither resolved by standard electrophoresis nor by isoelectric focusing. Nevertheless, no significant variations were observed in intensity, number, and location of the bands among normal human donors (*1, 2*).

We thought it of interest to study the expression of isozymes in different blood cell types also under long-term cell culture conditions. Thus we analyzed AcE and AcP in five well-defined permanent cell lines derived from human leukemias.

A direct comparison of the total enzyme values of normal and neoplastic cells is not possible, inasmuch as the exact normal cellular counterparts of the analyzed neoplasias are not available. All 5 cell lines analyzed in this study displayed considerably higher activities for both enzymes (table 2) than did the normal cells (table 3). Enzyme inductions have been shown for a panel of lysosomal hydrolases during different growth phases of lymphoid cell line culture (*32*). A similar phenomenon repeatedly has been reported to occur during cultivation of monocytes and macrophages (*33*). Thus culture conditions seem to stimulate lysosomal enzyme production. Furthermore, neoplastic cell lines have been found to develop a higher synthetic activity for lysosomal enzymes under culture conditions than do cultured normal cell lines. Sippell et al. (*34*) encountered a significantly higher rise in the activities of α-glucosidase, β-glucosidase, β-galactosidase, β-glucuronidase, *N*-acetyl-β-glucosaminidase, and AcP in malignant lymphoid cell lines than in cultured normal lymphocytes. The differences were attributed to the higher general metabolic activity as well as to the growth rate of neoplastic cells in cultures.

The results of isoelectric focusing of AcE in the analyzed cell lines (fig. 1A) showed that the banding patterns of normal cells (fig. 1B) were basically detectable in the corresponding neoplastic cell lines. The two acute T-lymphoblastic leukemia lines (JM, Molt-4) and KM 3 displayed two of the three AcE complexes found in normal T-lymphocytes (text-fig. 1). Whether these cell lines are derived from different T-cell subpopulations, which are known to differ in their Fc receptor for immunoglobulins as well as in their cytochemical AcE and AcP reaction patterns (*35, 36*), remains to be determined. Another possibility as the underlying reason for the observed differences in isozyme patterns could be the immaturity of the cultured cell lines as compared to the mature state of normal T-lymphocytes of peripheral blood. The promyelocytic leukemia line HL-60 expressed only 7 of the 11 AcE isozymes found in normal granulocytes (text-fig. 1). This is probably due to the relative immaturity of HL-60 as compared with normal mature granulocytes of the peripheral blood. In cytochemical terms, typical patterns of activity of lysosomal enzymes have been found for the individual maturation stages of human granulocytes (*37–39*), which might reflect the phenotypic expression of repression or derepression of the corresponding genes.

In contrast to AcE, the classification of the analyzed cell lines by AcP isozymes was only possible for two lines (fig. 2A, 2B; text-fig. 2). For line KM 3, reliable assertion could be made only for lymphocytic origin. This cell line showed the typical intense single AcP band at pH 6.3, as in the B- and T-lymphocytes (*1*). The granulocytic derivation of HL-60 was documented by the occurrence of the 12 typical AcP bands seen in normal granulocytes. A similar conclusion could not be made for lines Ball-1, JM, and Molt-4 because of the uncharacteristic distribution pattern of AcP isozymes.

Several investigators have studied enzyme activity and polymorphism under in vitro conditions, by cytochemical as well as electrophoretic methods, and have found a good correlation between normal cells and malignant cell lines with respect to cytochemical behavior and isozyme patterns. Some results, however, indicated the possibility that in vitro culture might lead to quantitative and qualitative alterations of enzyme expression. This was specifically the case for the cytochemical behavior of AcE in neoplastic T-lymphocytes (*40*) and β-glucuronidase in neoplastic B-lymphocytes (*8*), as compared to the behavior of their normal counterparts. Conversely, Povey et al. (*41*) demonstrated typical electrophoretic patterns of enzyme phenotypes that resisted culture manipulations. In other studies Wright et al. (*42, 43*) reported isozyme stability after malignant transformation of normal cells in vivo and long-term culture of neoplastic cells in vitro. Although the stability of banding patterns in long-established cell lines also was demonstrated by Hunter (*44*), he pointed out that under different culture conditions as well as during long-term culture, changes in cell population composition or cell characteristics were detectable. Furthermore, the isozyme expression of cultured cell lines may be the result of facultative hybridization, as proposed by Heyden et al. (*45*).

Our results mainly confirm that culture conditions leave the basic patterns of isozymes unaltered. Isozyme mapping, therefore, can be applied to problems concerning derivation of a given cell type. In some instances of AcP activity, culture conditions seem to exert stimulatory and/or repressive effects on isozyme expression. The exact mechanisms responsible for such alterations are not known. Not only the malignant transformation but also the accelerated cell replication under culture conditions are apt to be influential. Also, it cannot be excluded that minor subclones with different enzyme expression, not yet identifiable, may overgrow under prolonged in vitro culture (*46*). Furthermore, isozymes might differ in terms of their stability.

In addition to morphological and functional studies (*6*), as well as cytochemical (*8*), surface receptor (*7*) and chromosome analyses (*47*), and the study of surface glycoprotein patterns (*9, 10*), the investigation of enzyme polymorphism seems to be a reliable method for the characterization of cell lines and for the monitoring of their population composition. Whether all or which of these isozymes might represent distinctive cell-specific markers in biochemical (*1, 2, 4*) and immunological terms (*27*) has yet to be determined. Further systematic investigations, are required to extend our thinking on the diversity of cell surface properties (differentiation antigens, cell cycle antigens, tissue antigens, fetal antigens, tumor antigens, etc.) to include the enormous body of intracytoplasmic enzyme proteins and their polymorphic subtypes. We are, therefore, currently studying cell-specific isozymes of AcE as intracytoplasmic targets for corresponding monoclonal antibodies.

REFERENCES

(*1*) Radzun HJ, Parwaresch MR, Kulenkampff C, Stein H. Lysosomal acid phosphatase: Activity and isoenzymes in separated normal human blood cells. Clin Chim Acta 1980; 102:227–235.

(*2*) Radzun HJ, Parwaresch MR, Kulenkampff C, Staudinger M, Stein H. Lysosomal acid esterase: Activity and isoenzymes in separated normal human blood cells. Blood 1980; 55:891–897.

(*3*) Schmidt D, Radzun HJ, Schwarze E-W, Stein H, Parwaresch MR. Activity and isoenzymes of acid phosphatase in human B-cell lymphomas of low-grade malignancy: A novel aid in the classification of malignant lymphoma. Cancer 1980; 46:2676–2681.

(*4*) Parwaresch MR, Radzun, HJ, Dommes M. The homogeneity and monocytic origin of human peritoneal macrophages evidenced by comparison of esterase polymorphism. Am J Pathol 1981; 102:209–218.

(*5*) Radzun HJ, Parwaresch MR, Feller AC. Cell specific polymorphism of acid phosphatase in human blood cells, their functional and leukemic variants. Proc Soc Exp Biol Med 1981; 167:394–401.

(*6*) Nilsson K, Pontén J. Classification and biological nature of established human hematopoietic cell lines. Int J Cancer 1975; 15:321–341.

(*7*) Huber CH, Sundström C, Nilsson K, Wigzell H. Surface receptors on human haematopoietic cell lines. Clin Exp Immunol 1976; 25:367–376.

(*8*) Sundström C, Nilsson K. Cytochemical profile of human haematopoietic biopsy cells and derived cell lines. Br J Haematol 1977; 37:489–501.

(*9*) Andersson LC, Gahmberg CG, Nilsson K, Wigzell H. Surface glycoprotein patterns of normal and malignant human lymphoid cells. I. T cells, T blasts and leukemic T cell lines. Int J Cancer 1977; 20:702–707.

(*10*) Nilsson K, Andersson LC, Gahmberg CG, Wigzell H. Surface glycoprotein patterns of normal and malignant human lymphoid cells. II. B cells, B blasts and Epstein-Barr virus (EBV)-positive and -negative B lymphoid cell lines. Int J Cancer 1977; 20:708–716.

(*11*) Collins SJ, Gallo RC, Gallagher RE. Continuous growth and differentiation of human myeloid leukaemic cells in suspension culture. Nature 1977; 270:347–349.

(*12*) Hiraki S, Miyoshi I, Masuji H, et al. Establishment of an Epstein-

Barr virus-determined nuclear antigen-negative human B-cell line from acute lymphoblastic leukemia: *Brief communication.* J Natl Cancer Inst 1977; 59:93–94.

(13) Schneider U, Schwenk HU. Characterization of "T" and "non-T" cell lines established from children with acute lymphoblastic leukemia and non-Hodgkin lymphoma after leukemic transformation. In: Thierfelder S, Rodt H, Thiel E, eds. Immunological diagnosis of leukemias and lymphomas. Berlin, Heidelberg, and New York: Springer-Verlag, 1977:265–269.

(14) Minowada J, Ohnuma T, Moore GE. *Brief communication:* Rosette-forming human lymphoid cell lines. I. Establishment and evidence for origin of thymus-derived lymphocytes. J Natl Cancer Inst 1972; 49:891–895.

(15) Böyum A. Isolation of mononuclear cells and granulocytes from human blood. Scand J Lab Invest 1968; 21 (Suppl):77–109.

(16) Wigzell H, Andersson B. Cell eparation on antigen-coated columns: Elimination of high rate antibody-forming cells and immunological memory cells. J Exp Med 1969; 129:23–46.

(17) Kaplan ME, Clark C. An improved rosetting assay for detection of human T-lymphocytes. J Immunol Methods 1974; 5:131–135.

(18) Wybran J, Chantler S, Fudenberg, HH. Isolation of normal T cells in chronic lymphatic leukaemia. Lancet 1973; 1:126–129.

(19) Vesterburg O. Isoelectric focusing of proteins in polyacrylamide gels. Biochim Biophys Acta 1972; 257:11–19.

(20) Mueller J, Brun del Re G, Buerki H, Keller HU, Hess MW, Cottier H. Nonspecific acid esterase activity: A criterion for differentiation of T and B lymphocytes in mouse lymph nodes. Eur J Immunol 1975; 5:270–274.

(21) Andersch MA, Szczypinski AJ. Use of *p*-nitrophenyl-phosphate as the substrate in determination of serum acid phosphatase. Am J Clin Pathol 1947; 17:571–574.

(22) Barka T, Anderson PJ. Histochemical methods for acid phosphatase using hexazonium pararosanilin as coupler. J Histochem Cytochem 1962; 10:741–753.

(23) Barr RD, Perry S. Lysosomal acid hydrolases in human lymphocyte subpopulations. Br J Haematol 1976; 32:565–572.

(24) Wehinger H, Möbius W. Cytochemical studies on T and B lymphocytes and lymphoblasts with special references to acid phosphatase. Acta Haematol 1976; 56:129–136.

(25) Higgy KE, Burns GF, Hayhoe FG. Discrimination of B, T, and null lymphocytes by esterase cytochemistry. Scand J Haematol 1977; 18:437–449.

(26) Kulenkampff J, Janossy G, Greaves MF. Acid esterase in human lymphoid cells and leukaemic blasts: A marker for T lymphocytes. Br J Haematol 1977; 36:231–240.

(27) Radzun HJ, Parwaresch MR, Wittke JW. Polymorphism and antigenic specificity of monocytic acid esterase (EC 3.1.1.6). Cell Immunol 1981; 63:400–408.

(28) Li CY, Yam LT, Lam KW. Acid phosphatase isoenzyme in human leukocytes in normal and pathologic conditions. J Histochem Cytochem 1970; 18:473–481.

(29) Li CY, Lam KW, Yam LT. Esterases in human leukocytes. J Histochem Cytochem 1973; 21:1–12.

(30) Kass L, Munster D. Nonspecific esterases in normal human blood cells: Characterization of isoenzymes by isoelectric focusing in polyacrylamide gel. Exp Hematol 1979; 7:535–540.

(31) Gaedicke G, Arndt R, Kabisch H, Landbeck G. Isoenzyme studies on human leukemia. I. Acid phosphatase. Leuk Res 1979; 3:417–423.

(32) Matsuda I, Yamamoto J, Nagata, N, et al. Lysosomal enzyme activities in cultured lymphoid cell lines. Clin Chim Acta 1977; 80:483–486.

(33) Musson RA, Shafran H, Henson PM. Intracellular levels and stimulated release of lysosomal enzymes from human peripheral blood monocytes and monocyte-derived macrophages. J Reticuloendothel Soc 1980; 28:249–264.

(34) Sippel WG, Antonowicz I, Lazarus H, Shwachman H. Lysosomal and mitochondrial enzyme activities in human lymphoid cell lines obtained from children with acute lymphoblastic leukemia and controls. Exp Cell Res 1975; 91:152–158.

(35) Grossi CE, Webb SR, Zicca A, et al. Morphological and histochemical analyses of two human T-cell subpopulations bearing receptors for IgM or IgG. J Exp Med 1978; 147:1405–1417.

(36) Feller AC, Parwaresch MR. Zytochemische Darstellung der Blasten bei akuter T-lymphoblastischer Leukämie mit Hilfe der Glycylprolyl-4-methoxy-beta-naphthylamid-Peptidase (DAP IV). Klin Padiatr 1980; 192:150–153.

(37) Parwaresch MR, Sadighi R. Cytophotometrische Messung der Aktivität von Naphthol-AS-D-Chloracetat-Esterase in den normalen menschlichen basophilen Granulopoiesezellen. Virchows Arch [Cell Pathol] 1970; 6:88–96.

(38) Parwaresch MR, Müller-Hermelink HK, Lennert K. Leukemic anaplasias reflecting physiologic cytogenesis of the myeloid system. In: Neth R, Gallo RC, Mannweiler K, Moloney WC, eds. Modern trends in human leukemia II. Munich: Lehmann, 1976:95–99.

(39) Parwaresch MR. The human blood basophil. Berlin, Heidelberg, and New York: Springer-Verlag, 1976.

(40) Sundström C, Nilsson K, Ranki A, Häyry P. Presence of α-naphthyl acetate esterase activity in human haematopoietic cell lines and in fresh biopsy specimens of lymphoma and myeloma. Scand J Haematol 1978; 21:47–59.

(41) Povey S, Gardinger SE, Watson B, et al. Genetic studies on human lymphoblastoid lines: Isozyme analysis on cell lines from forty-one different individuals and on mutants produced following exposure to a chemical mutagen. Ann Hum Genet 1973; 36:247–267.

(42) Wright WC, Daniels WP, Fogh J. Stability of polymorphic enzyme phenotypes in human tumor cell lines. Proc Soc Exp Biol Med 1979; 162:503–509.

(43) ———.Distinction of seventy-one cultured human tumor cell lines by polymorphic enzyme analysis. JNCI 1981; 66:239–247.

(44) Hunter L. Glucose-6-phosphatase dehydrogenase isoenzyme in cultured human cell lines: Separation by isoelectric focusing. Anal Biochem 1980; 101:78–87.

(45) Heyden HW, Weber R, Stuckstedte H, Saal JG, Fresen KO. Isoenzyme-Muster der sauren Phosphatasen von Epstein-Barr-Virus-DNS enthaltenden, permanent wachsenden Zell-Linien. Blut 1977; 35:395–404.

(46) Adams A, Strander H, Canteli K. Sensitivity of the Epstein-Barr virus transformed human lymphoid cell lines to interferon. J Gen Virol 1975; 28:207–217.

(47) Zech L, Haglund U, Nilsson K, Klein G. Characteristic chromosomal abnormalities in biopsies and lymphoid-cell lines from patients with Burkitt and non-Burkitt lymphomas. Int J Cancer 1976; 17:47–56.

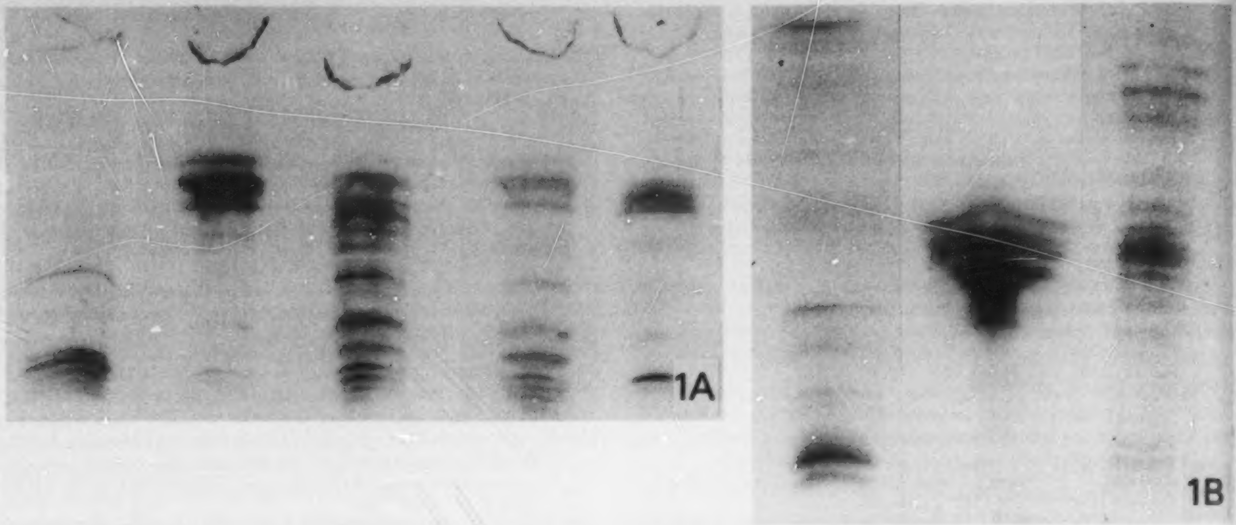

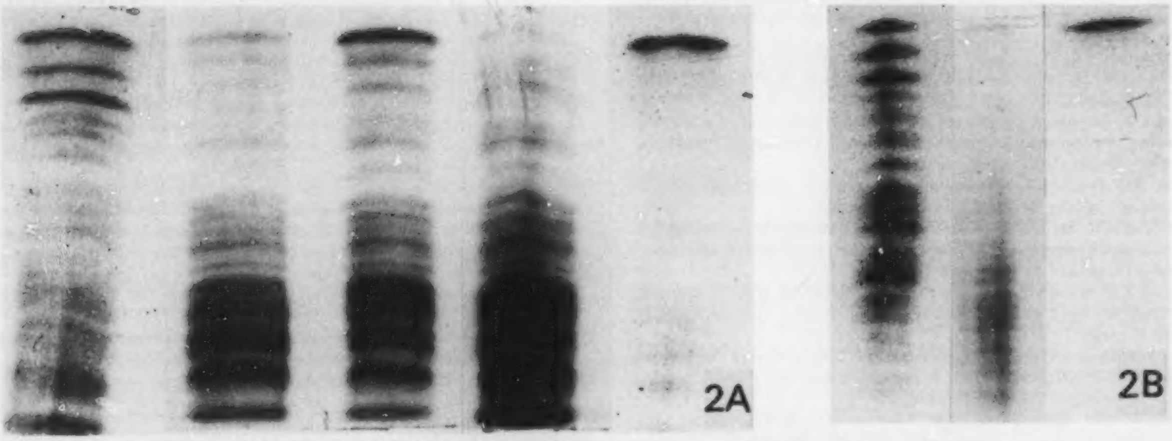

FIGURE 1.—AcE isoelectric focusing patterns: A) in hematopoietic cell lines HL-60, Ball-1, JM, Molt-4, KM 3 (from *left* to *right*); B) in normal human granulocytes, B-lymphocytes, and T-lymphocytes (from *left* to *right*).

FIGURE 2.—AcP isoelectric focusing patterns: A) in hematopoietic cell lines HL-60, Ball-1, JM, Molt-4, KM 3 (from *left* to *right*); B) in normal human granulocytes, B-lymphocytes, and T-lymphocytes (from *left* to *right*).

Subpopulations of Human T-Lymphocytes. XIX. T-Cells and T-Cells With Receptors for IgMFc ($T\mu$), IgGFc ($T\gamma$), or IgAFc ($T\alpha$) in the Peripheral Blood and Regional Lymph Nodes of Patients With Untreated Breast Cancer[1,2,3]

Sudhir Gupta[4,5] *and* **Susanna Cunningham-Rundles**[4]

ABSTRACT—Peripheral blood and regional lymph node mononuclear cells from 43 untreated patients with breast cancer were analyzed for the proportions of total T-cells and T-cells with receptors for the Fc portion of IgM ($T\mu$), IgG ($T\gamma$), or IgA ($T\alpha$). Proportions of total T-cells and $T\mu$ cells both in peripheral blood and lymph nodes from breast cancer patients were comparable to those from health controls. The proportion of $T\gamma$ cells, however, was significantly ($P<0.01$) increased in the peripheral blood and lymph nodes from breast cancer patients as compared to that from controls. The proportion of $T\alpha$ in the peripheral blood was comparable; however, when compared to the number of $T\alpha$ cells in control lymph nodes, $T\alpha$ cells were increased ($P<0.025$) in the regional lymph nodes from patients with breast cancer. When data on the proportions of T-cells and T-cell subsets were analyzed according to the presence or absence of metastatic disease in the regional lymph nodes, the proportion of $T\gamma$ cells was significantly ($P<0.025$) higher in the peripheral blood from patients with metastatic disease than in patients with nonmetastatic disease. This study demonstrates an abnormality of T-cell subsets in the peripheral blood and the regional lymph nodes from patients with breast cancer. The significance of these observations is discussed—JNCI 1982; 69: 1261–1264.

Several studies have reported immunologic abnormalities in patients with breast cancer. These abnormalities include impairment of proliferative response to mitogens, depressed delayed cutaneous hypersensitivity, alterations in NK and antibody-dependent cellular cytotoxicity, and increased levels of circulating immune complexes (*1–10*). Data regarding absolute lymphocyte counts and total T-lymphocytes in breast cancer are, however, conflicting (*10–15*). Furthermore, in most of these reports simultaneous immunologic studies have not been done in the peripheral blood and regional lymph nodes in patients with breast cancer. It is now well recognized that T-lymphocytes are heterogeneous with regard to their effector and immunoregulatory functions (*16*). Therefore, altered immune response in breast cancer could be a consequence of change in the proportions of distinct subsets of T-lymphocytes. Recently, functionally distinct subpopulations have been classified on the basis of the presence of receptors for immunoglobulin isotypes (*16–19*) and differentiation antigens as defined with monoclonal antibodies (*20*). T-cells with receptors for IgMFc ($T\mu$) have been shown to provide help in the differentiation of B-cells to plasma cells in a pokeweed mitogen-driven system, whereas T-cells with receptors for IgGFc ($T\gamma$) suppress the differentiation of B-cells to plasma cells in a similar system (*21*). Reinherz et al. (*22*) using monoclonal antibody analysis demonstrated that the $T\gamma$ cells reacted with the OKM1 antibody that is said to define the antigen present on cells of the monocyte–myeloid lineage. However, Fox et al. (*23*) and others [reviewed in (*16*)] using monoclonal antibodies and other criteria have shown that $T\gamma$ cells belong to the T-cell lineage. Heterogeneity of $T\mu$ cells (*16*) has been demonstrated by the presence of concanavalin A-inducible suppressor cells in $T\mu$ cells. Similar heterogeneity exists in monoclonal antibody-defined T-cells as well. Thomas et al. (*24*) have demonstrated the presence of suppressor cell activity in OKT_4^+ cells. T-cells with receptors for IgAFc ($T\alpha$) have been shown to be distinct from $T\mu$ or $T\gamma$ cells (*25–27*) and appear to contain cells with immunoregulatory activity for an IgA-specific response (*28*). We have shown that $T\gamma$ cells also mediate natural killing and antibody-dependent cytotoxicity (*29*). Natural killing has been suggested to play an important role in immune surveillance against tumors (*30*). Therefore, in this study we examined the proportions of total T-cells and $T\mu$, $T\gamma$, and $T\alpha$ cells in the peripheral blood and regional lymph nodes from patients with untreated breast cancer and correlated them with the presence or absence of metastatic disease. At the time this study was initiated, monoclonal antibodies defining T-cell subsets were commercially unavailable.

MATERIALS AND METHODS

Peripheral venous blood and regional lymph nodes from 43 women with breast cancer were studied. Analysis of peripheral blood and lymph nodes from each patient was done on the same day. The entire section of lymph node (not the fragments) was used. Eighteen patients had metastatic disease, whereas 25 patients had no evidence of metastasis. All lymph nodes from patients with metastatic

---

ABBREVIATIONS USED: FCS=fetal calf serum; FH=Ficoll–Hypaque; HBSS=Hanks' balanced salt solution; NK=natural killer; OXRBC=ox red blood cells; SRBC=sheep red blood cell(s).

---

[1] Received March 9, 1982; accepted June 30, 1982.

[2] Supported by Public Health Service (PHS) grant CA-17404 from the National Cancer Institute (NCI) and by PHS contract CB-84228 from the Division of Cancer Biology and Diagnosis, NCI.

[3] Research procedures were in accord with the ethical standards of the Clinical Investigation Committee, Memorial Sloan-Kettering Cancer Center.

[4] Memorial Sloan-Kettering Cancer Center, 1275 York Ave., New York, N.Y. 10021.

[5] *Address reprint requests to* Dr. Gupta at his *present address:* Department of Medicine, California College of Medicine, University of California, Irvine, Calif. 92717.

disease were tumor bearing. Forty healthy age-matched women served as controls for peripheral blood. Analysis of normal lymph nodes obtained from 15 subjects with nonmalignant disease at the Memorial Hospital was performed at different times. Total peripheral blood lymphocyte counts in patients and controls were similar; therefore, data will be presented for the percentage of lymphocyte subpopulations.

Isolation of mononuclear cells.—Lymph node tissues were gently teased with sterile 18-gauge needles and were washed twice by centrifugation. One-half of each lymph node was retained for histopathologic examination. Mononuclear cells from peripheral venous blood were isolated on an FH density gradient. Blood and lymph node mononuclear cells were washed three times in HBSS. A small sample of mononuclear cells was incubated with latex particles (The Dow Chemical Co., Indianapolis, Ind.) for the identification of contaminating monocytes and was used for the enumeration of total T-cells. For the analysis of T-cell subsets, mononuclear cells were resuspended in medium containing 20% FCS at 4×10^6/ml. To this suspension was added carbonyl iron (Lymphocyte Separator Reagent, Technicon Instruments Corp., Tarrytown, N.Y.) at a ratio of 2:1 (vol/vol), followed by incubation on a rotator at 37°C for 30 minutes. Phagocytic cells were depleted on another FH gradient (*31*). Phagocytic cell-depleted lymphoid cells were washed three times in HBSS and resuspended at a concentration of 4×10^6/ml. This preparation contained less than 2% monocytes. The viability was greater than 98% as tested by the trypan blue dye exclusion test. These cells were used to separate T- and non-T-cells.

Purification of T-cells.—Aliquots (1 ml) of phagocytic cell-depleted lymphoid cell suspensions were mixed with an equal volume of 1% neuraminidase-treated SRBC, incubated at 37°C for 5 minutes, centrifuged at $200\times g$ for 5 minutes, and incubated further on ice for an additional 1 hour. Pellets were gently resuspended, and rosetting T-cells were separated from nonrosetting non-T-cells on an FH gradient (*31*). SRBC attached to T-cells were lysed with Tris buffer containing ammonium chloride (pH 7.2). Cells were washed three times in HBSS, resuspended in medium containing 20% FCS, and incubated overnight at 37°C. Following incubation, T-cells were washed with HBSS, resuspended in HBSS at 3×10^6/ml, and assayed for T-cell subsets. These preparations contained greater than 97% T-cells, as determined by rosette formation with SRBC and lack of cells with readily demonstrable surface immunoglobulins.

Enumeration of total T-cells.—One hundred microliters of latex-ingested mononuclear cell suspension were mixed with an equal volume of 1% SRBC and 25 μl of heat-inactivated SRBC-absorbed human AB serum. The mixture was incubated at 37°C for 5 minutes, centrifuged at $50\times g$ for 5 minutes, and further incubated overnight on ice. The pellet was gently resuspended, a drop of trypan blue was added, and rosette-forming cells were counted in a hemacytometer. The results are expressed as percent of total lymphocytes.

Determination of T-cell substrates.—T-cell subsets were assayed by rosette formation with OXRBC-IgM anti-OXRBC (EA_M), OXRBC-IgG anti-OXRBC (EA_G), or trinitrophenyl-coated OXRBC-MOPC-315 IgA myeloma (EA_A) complexes. Preparation of these complexes is described elsewhere (*31, 32*).

Purified T-cell suspensions (100 μl) were mixed with an equal volume of 1% EA_M (for Tμ), EA_G (for Tγ), or EA_A (for Tα) complexes and centrifuged at $200\times g$ for 5 minutes, followed by incubation on ice for 1 hour. Pellets were resuspended and rosette-forming lymphocytes counted. A lymphocyte with three or more OXRBC attached was considered a rosette. Tμ and Tγ cells were counted with a light microscope. Cytocentrifuge preparations of Tγ cells were stained with nonspecific esterase to exclude any contamination of monocytes. In a Tα cell suspension, a drop of 0.01% euchrysine was added and rosette-forming Tα cells were counted with a Leitz Orthoplan fluorescence microscope equipped with epi-illumination. T-cell subsets were expressed as percent of total T-cells. Statistical analysis was performed by the Student's *t*-test.

RESULTS

Data for T-cells and T-cell subpopulations in the peripheral blood from patients with breast cancer and healthy controls are shown as means plus or minus standard deviations in text-figure 1. The proportions of total T-cells, Tμ cells, and Tα cells were comparable in 2 groups; however, the proportion of Tγ cells in the patient group was significantly ($P<0.01$) increased when compared to that in the controls. The ranges for total T-cells, Tμ cells, Tγ cells, and Tα cells in the patient group were 54–92, 22–87, 6–54, and 0–32%, respectively; in controls, they were 60–93, 25–75, 6–20, and 2–22%, respectively.

Results obtained with T-cells and T-cell subsets in the regional draining lymph nodes from patients with breast cancer and normal lymph nodes are shown in text-figure 2. The proportions of total T-cells and Tμ cells were comparable in the 2 groups; however, the proportions of Tγ cells

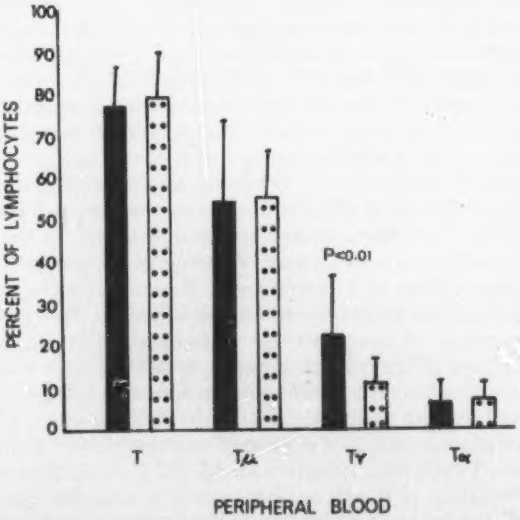

TEXT-FIGURE 1.—T-cells and T-cell subpopulations in the peripheral blood of patients with breast cancer (■) and healthy controls (⊡). Results are means ± SD.

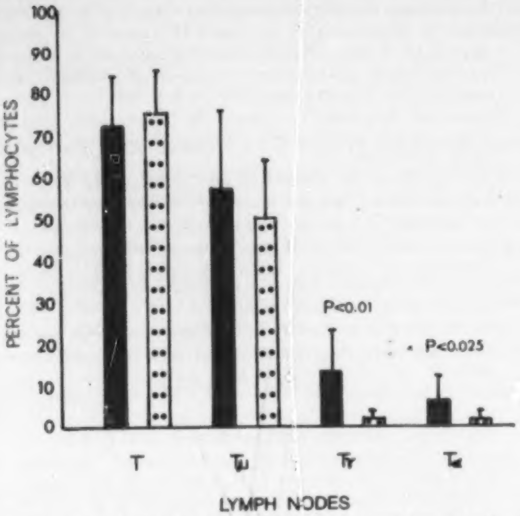

TEXT-FIGURE 2.—T-cells and T-cell subsets in regional lymph nodes from patients with breast cancer (■) and cervical lymph nodes from subjects with nonmalignant disease (▨). Results are means ± SD.

and Tα cells were significantly ($P<0.01$; $P<0.025$) increased in the lymph nodes from cancer patients as compared to the proportions in normal lymph nodes. The ranges for total T-cells, Tμ cells, Tγ cells, and Tα cells in lymph nodes from cancer patients were 50–90, 20–87, 2–43, and 0.5–25%, respectively; in control lymph nodes, ranges were 56–84, 22–79, 0–6, and 1–7%, respectively.

Data on T-cells and T-cell subsets in patients with or without metastatic disease were compared. Results of such an analysis in the peripheral blood are shown in text-figure 3. The proportion of Tγ cells was significantly ($P<0.025$) increased in the blood of patients with metastatic disease (range 6–54%) when compared to that in the blood of patients without metastatic disease (range, 6–34%). The proportions of T-cells, Tμ cells, and Tα cells in the group with metastatic disease (range, 70–92, 22–83, 2–25%, respectively) were comparable to values in the group without metastatic disease (range, 54–90, 21–87, 0–32%).

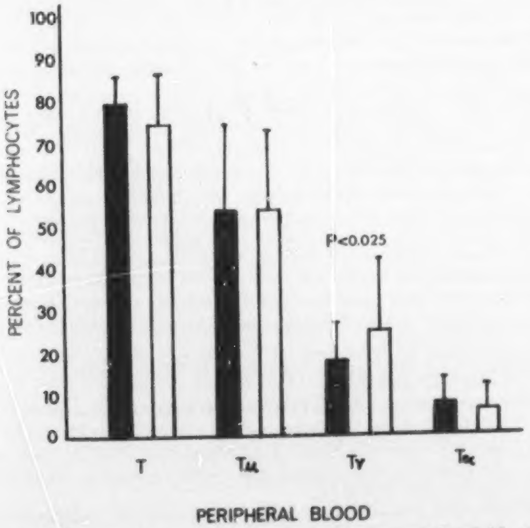

TEXT-FIGURE 3.—T-cells and T-cell subsets in the peripheral blood of patients with (□) or without (■) metastatic breast cancer. Results are means ± SD.

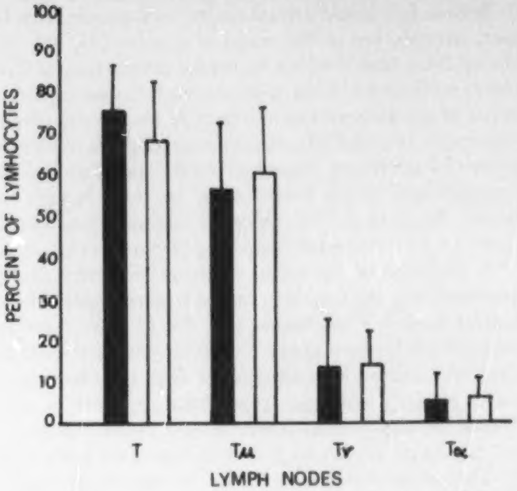

TEXT-FIGURE 4.—T-cells and T-cell subsets in the regional lymph nodes from patients with (□) or without (■) metastatic breast cancer. Results are means ± SD.

Text-figure 4 shows no significant difference in the proportions of T-cells, Tμ cells, Tγ cells, and Tα cells in the lymph nodes from patients with metastatic disease (range, 50–90, 20–84, 2–43, 0.5–25%, respectively) or without metastatic disease (range, 50–86, 20–87, 2–28, and 0–18%, respectively).

DISCUSSION

In this study, we have demonstrated a significant increase in the proportion of Tγ cells in the peripheral blood and regional lymph nodes from patients with breast cancer and a significantly increased proportion of Tα cells in the regional lymph nodes from patients with breast cancer when compared to the values in controls. When data were analyzed according to the presence or absence of metastasis, Tγ cells were increased in the peripheral blood of patients having lymph nodes with metastatic disease. Cunningham-Rundles et al. (*7*) have reported an increase in NK function in lymph nodes from a *subset* of patients with breast cancer. Since Tγ cells have been shown to contain NK function, it remains to be determined whether the increase in Tγ cells in the peripheral blood represents a subpopulation that contains suppressor activity or NK activity. In a few patients in whom both NK activity and T-cell subset analyses were done on the same samples, a correlation between increased Tγ cells and increased NK activity was observed in only 50% of the cases studied (data not shown). Ermin et al. (*8, 10*) reported variable but prominent NK function in patients with breast cancer. Tα cells have been shown to contain immunoregulatory functions for an IgA-specific response

(*28*). Serum IgA levels are increased in patients with breast cancer, irrespective of the stage of disease (*33, 34*). In this study we have observed an increased proportion of $T\alpha$ cells in the lymph nodes from patients with breast cancer, irrespective of the presence or absence of metastatic disease. It is reasonable to speculate that increased levels of serum IgA in patients with breast cancer could be due to an increase in the proportion of $T\alpha$ helper cells in their lymph nodes. Recently, Pucci et al. (*35*) reported increased proportions of $T\alpha$ cells in patients with bronchogenic and colon carcinomas. A number of investigators have reported decreased proportions of total T-cells in breast cancer, especially in the advanced stage of the disease (*11, 13, 14*). We have found normal proportions of total T-cells in patients with breast cancer; this finding is in agreement with the observation of Goust et al. (*15*) who have reported a decrease in a subset of T-cells in patients with metastatic breast cancer. This subset has been shown to inversely correlate with $T\gamma$ cells (*36*). This relationship would be in agreement with our observation of increased $T\gamma$ cells in metastatic breast cancer. Studies are required of lymphocyte subpopulations in the peripheral blood, regional lymph nodes, and primary tumor tissue with the use of monoclonal antibodies to understand the mechanism(s) for immune alterations in patients with breast cancer.

REFERENCES

(*1*) Catalona WJ, Sample WF, Chretien PB. Lymphocyte reactivity in cancer patients: Correlation with tumor histology and clinical stage. Cancer 1973; 31:65–71.

(*2*) Bolton PM, Teasdale C, Mander AM, et al. Immune competence in breast cancer—relationship of pre-treatment immunologic tests of diagnosis and tumor stage. Cancer Immunol Immunother 1976; 1:251–258.

(*3*) Nemoto T, Han T, Minowada J, Angkur V, Chamberlain A, Dao TL. Cell-mediated immune status of breast cancer patients: Evaluation by skin tests, lymphocyte stimulation, and counts of rosette-forming cells. J Natl Cancer Inst 1974; 53:641–645.

(*4*) Menconi E, Barzi A, Greco M., Caprino MC, De Vecchis L, Muggia E. Immunological profile of breast cancer patients in early or advanced disease. Experientia 1979; 35:820–822.

(*5*) Asano S, Mandel TE. Colonies formed in agar from human breast cancer and their identification as T-lymphocytes. JNCI 1981; 67:25–32.

(*6*) Haim N, Rudik L, Samuelly B, Mekori T, Robinson E. Immune status in patients cured of breast and gynaecological cancer. Clin Oncol 1981; 7:141–147.

(*7*) Cunningham-Rundles S, Filippa D, Braun DW Jr, Antonelli P, Ashikari H. Natural cytotoxicity of peripheral blood lymphocytes and regional lymph node cells in breast cancer in women. JNCI 1981; 67:585–590.

(*8*) Eremin O, Coombs RR, Ashby J. Lymphocytes infiltrating human breast cancers lack K-cell activity and show low levels of NK cell activity. Br J Cancer 1981; 44:166–176

(9) Inman RD, Day NK. Immunologic and clinical aspects of immune complex disease. Am J Med 1981; 70:1097–1106.

(*10*) Eremin O, Ashby J, Stephens JP. Human natural cytotoxicity in the blood and lymphoid organs of healthy donors and patients with malignant disease. Int J Cancer 1978; 21:35–41.

(*11*) Whitehead RH, Roberts GP, Thatcher J, Teasdale C, Hughes LE. Masking of receptors for sheep erythrocytes on human T-lymphocytes by sera from breast cancer patients. J Natl Cancer Inst 1977; 58:1573–1576.

(*12*) Heidenreich W, Jagla K, Schussler J, et al. Immunological characterization of mononuclear cells in peripheral blood and regional lymph nodes of breast cancer patients. Cancer 1978; 43:1308–1313.

(*13*) Petrini B, Wasserman J, Blomgren H, Baral E, Strender LE, Wallgren A. Blood lymphocyte subpopulations in breast cancer patients following post-operative adjuvant chemotherapy or radiotherapy. Clin Exp Immunol 1979; 38:361–365.

(*14*) Keller SE, Loachim HL, Pearse T, Siletti DM. Decreased T lymphocytes in patients with mammary cancer. Am J Clin Pathol 1976; 65:445–449.

(*15*) Goust JM, Roof BS, Fudenberg HH, O'Brien PH. T cell markers in breast cancer patients at diagnosis. Clin Immunol Immunopathol 1979; 12:396–403.

(*16*) Gupta S, Good RA. Subpopulations of human T lymphocytes. Laboratory and clinical studies. Immunol Rev 1981; 56:89–114.

(*17*) Gupta S. Functionally distinct subpopulations of human T lymphocytes. A review. Clin Bull 1978; 8:100–107.

(*18*) Gupta S, Good RA. Markers of lymphocytes in primary immunodeficiency and lymphoproliferative disorders. Semin Hematol 1980; 17:1–29.

(*19*) Moretta L, Ferrarini M, Cooper MD. Characterization of human T-cell subpopulations as defined by specific receptors for immunoglobulins. Contemp Top Immunobiol 1978; 8:19–53.

(*20*) Reinherz EL, Schlossman SF. Current concepts in immunology: Regulation of the immune response—inducer and suppressor T-lymphocyte subsets in human beings. N Engl J Med 1980; 303:370–373

(21) Moretta L, Webb SR, Grossi CE, Lydyard PM, Cooper MD. Functional analysis of two human T cell subpopulations. Help and suppression of B cell responses by T cell-bearing receptors for IgM (T_M) and IgG (T_G). J Exp Med 1977; 146:184–200.

(*22*) Reinherz EL, Moretta L, Roper M, et al. Human T lymphocyte subpopulations defined with Fc receptors and monoclonal antibodies. A comparison. J Exp Med 1980; 151:969–974.

(*23*) Fox RI, Thompson LF, Huddlestone JR. $T\gamma$ cell express T lymphocyte-associated antigens. J Immunol 1981; 126:2062–2063.

(*24*) Thomas Y, Rogozinski L, Irigoyen OH, et al. Functional analysis of human T cell subsets defined with monoclonal antibodies. V. Suppressor cells within the activated OKT_4^+ population belong to a distinct subset. J Immunol 1982; 126:1386–1390.

(*25*) Lum LG, Muchmore AV, Keren D, et al. A receptor for IgA on human T lymphocytes. J Immunol 1979; 122:65–69.

(*26*) Gupta S, Good RA. Subpopulations of human T lymphocytes. XV. T-lymphocytes with receptors for IgA ($T\alpha$), a distinct subpopulation of T lymphocytes. Studies in patients with primary immunodeficiency disorders. Clin Exp Immunol 1980; 41:363–371.

(*27*) Gupta S, Platsoucas CD, Schulof RS, Good RA. Receptors for IgA on a subpopulation of human T and B lymphocytes. Cell Immunol 1978; 45:469–470.

(*28*) Endoh M, Sakai H, Nomoto Y, Tomino Y, Kaneshige H. IgA-specific helper activity of $T\alpha$ cells in human peripheral blood. J Immunol 1981; 127:2612–2613.

(*29*) Gupta S, Fernandes G, Nair M, Good RA. Spontaneous and antibody-dependent cytotoxicity by human T lymphocytes. Proc Natl Acad Sci USA 1978; 75:5137–5141.

(*30*) Herberman RB, Ortaldo JR. Natural killer cells: Their role in defenses against disease. Science 1981; 214:24–30.

(*31*) Gupta S, Good RA. Subpopulations of human T lymphocytes. III. Distribution and quantitation in peripheral blood, cord blood, tonsils, bone marrow, thymus, lymph nodes and spleen. Cell Immunol 1978; 36:263–270.

(*32*) Gupta S, Platsoucas CD, Good RA. Receptors for IgA on a subpopulation of human B lymphocytes. Proc Natl Acad Sci USA 1979; 76:4025–4028.

(*33*) Alsabti EA. Serum immunoglobulins in breast cancer. J Surg Oncol 1979; 11:129–133.

(*34*) Roberts MM, Bathgate FM, Stevenson A. Serum immunoglobulin levels in patients with breast cancer. Cancer 1975; 36:221–224.

(*35*) Pucci A, Clancy RL, Doe WF. Increased circulating $T\alpha$ lymphocyte population in bronchogenic and colonic carcinoma. Clin Exp Immunol 1981; 46:130–133.

(*36*) Goust JM, Hoffman PM, Pryjama J, Hogan EL, Fudenberg HH. Defective immunoregulation in multiple sclerosis. Ann Neurol 1980; 8:526–533.

Epidemic Curve of Respiratory Cancer Due to Chloromethyl Ethers[1,2]

William Weiss, M.D.[3]

ABSTRACT—In 1962, suspicion arose that an excess of lung cancers was developing in a chemical plant. A prospective cohort study of 125 male workers was begun, and the group was followed from January 1963 to the end of 1979. A small epidemic of respiratory cancer evolved, including 14 cases of lung cancer (13 were the small cell type) and 2 cases of laryngeal cancer among 91 men exposed to chloromethyl ethers in the 17-year period, as compared to 2 cases of lung cancer among 34 unexposed men. The lung cancer epidemic peaked 15–19 years after onset of exposure and began to subside thereafter.—JNCI 1982; 69:1265–1270.

In parallel with the rising incidence of lung cancer in the U.S. male population, cases of lung cancer began to appear in the work force of approximately 2,000 employees at a large chemical plant in the 1950's. The cumulative number of lung cancer cases (text-fig. 1) rose steadily at a rate of 1–2 per year until 1962 when 7 cases developed. During the next 5 years, the annual number of lung cancers ranged from 1 to 4, averaging 2.2. By use of the scan statistic for detection of clustering over time (*1*), the incidence of 7 cases in 1962 did not prove to be a cluster that was statistically significant at the 0.05 level. Therefore, an ongoing program of annual surveillance might not have uncovered the onset of a microepidemic if statistical evaluation alone had been used as the criterion for significance.

However, among the 7 cases were 3 characterized by their occurrence in men 33–39 years old, all of whom worked in a single building (building B) which housed approximately 45 employees. This cluster of cases attracted the attention of the plant physician and stimulated further investigation in December 1962.

In January 1963, a semiannual screening study of all 45 men who had been working 3 months or more in the building in question and 80 men in other buildings was begun. Four cases of lung cancer, all small cell carcinomas, developed in this cohort during the next 5 years, but only 1 of these occurred in the suspect building. In 1968, animal studies by Van Duuren et al. (*2*) provided information indicating that BCME was carcinogenic for mouse skin and when injected sc in rats. In the suspect building at this plant, CMME was being used as an alkylating agent in the production of various organic chemicals. It was contaminated with small amounts of BCME, but Van Duuren had not found CMME to be carcinogenic in animals. This fact and the observation that only 1 of 4 cases of lung cancer in the cohort had worked in the suspect building where CMME was being made suggested that CMME was not causing cancer in this cohort.

In 1971, a preliminary report by Laskin et al. (*3*) indicated that BCME is a very potent carcinogen when inhaled by rats. Since CMME in the industrial setting was contaminated with small amounts of BCME, the CMME process was promptly eliminated until it could be completely automated, and an epidemiologic investigation of the entire plant was initiated. Hereafter, industrial CMME will be called CME.

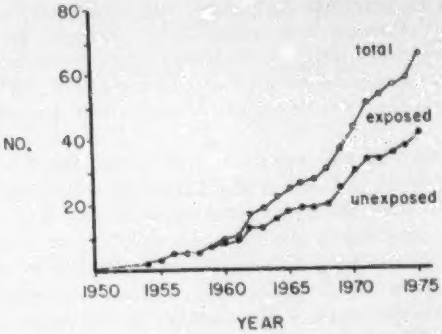

TEXT-FIGURE 1.—Cumulative number of lung cancer cases (1950–75) by exposure to chloromethyl ethers, in a large chemical plant. *Upper curve* is total No. of cases, *lower curve* is No. among unexposed workers, and intercurve area is No. among exposed workers.

CME had first been used in the plant in 1948. It was produced and used in two other buildings, hereafter called buildings A 1 and 2. A retrospective assessment of exposure on a semiquantitative scale in every plant worker over the 24 years from 1948 to 1971 was initiated, and it became clear that the 3 men who developed lung cancer in 1963–68 but were not working in the suspect building, hereafter called building B, had been exposed earlier in buildings A 1 and 2.

In 1973, a preliminary report of the microepidemic in the cohort of 125 men established in 1963 was published (*4*). The further development of exposure data led to publication of a series of papers on various aspects of the cohort study (*5–9*) as well as of reports on a historical prospective study of all workers at the plant (*10, 11*).

The purpose of this paper is to update the results of the cohort study begun in 1963, to report the results of 17 years of follow-up (1963–79), and to document the epidemic curve of respiratory cancer in this group of 125 chemical workers.

METHOD

A group of 125 male production workers was assembled in January–March 1963 and screened with 70-mm chest

---

ABBREVIATIONS USED: BCME=bis-chloromethyl ether; CME=chloromethyl methyl ether contaminated with BCME; CMME=chloromethyl methyl ether; SIR=standardized incidence ratio; SMR=standardized mortality ratio(s).

---

[1] Received March 12, 1982; accepted August 4, 1982.

[2] Supported by the Rohm and Haas Co.

[3] Room 421, Bellet Bldg., The Hahnemann Medical College & Hospital, 230 North Broad St., Philadelphia, Pa. 19102.

photofluorograms and questionnaires regarding age, smoking habits, and respiratory symptoms. These men included 45 who had worked 3 months or more in building B and 80 from other buildings. Among the 80 men were 18 who had worked in building B in previous years and 28 who had worked in buildings A 1 and 2 and had been exposed to CME. Follow-up was maintained through semiannual screening for 5 years and thereafter by periodic tracing. Vital status was determined as of December 31, 1979, for all but 3 members of the cohort. These 3 were assumed to be alive.

For the 116 men who were white and the 9 who were black, 1,869.5 man-years of observation were available for 1963–79. SMR for lung cancer were calculated by comparing the observed to the expected numbers of lung cancer deaths. The expected number was estimated by applying Philadelphia 5-year age-specific and period-specific white male mortality rates to the number of man-years of observation in each 5-year age group in each 5-year period (except for the initial period of 1963–64). White male rates were used because 93% of the cohort was white. These rates were derived from official population estimates and numbers of deaths reported for 1960–64, 1965–69, 1970–74, and 1975–79. Because the Philadelphia population figures for the years 1971–79 have proved to be overestimated in comparison with the overall population count of the 1980 census and because, for 1980, counts by age, race, and sex are not yet available (November 1981), estimates of the age-, race-, and sex-specific population bases for 1971–79 were obtained from the Population Division, U.S. Bureau of the Census. The method for making these estimates is described in (*12*). Population estimates for 1972 were combined with 1970–74 death counts to obtain white male age-specific mortality rates for the 1970–74 period, and population estimates for 1977 were similarly used for the 1975–79 period.

Inasmuch as the chemical plant was located in an area of Philadelphia (Health District No. 7) that had relatively high lung cancer mortality rates in 1968–72 (*13*), the SMR was also calculated from Health District No. 7 data. Although these rates included only part of the follow-up period 1963–79, they dealt with data from approximately the middle 5 years in the 17-year follow-up period. Therefore, despite the changing lung cancer mortality rates, the use of these rates is reasonable.

An SIR was also separately calculated for lung cancer and for laryngeal cancer by use of the average white male cancer registry data reported by Waterhouse et al. (*14*) in the San Francisco Bay, Alameda, and Detroit registries for 1969–73, the middle 5 years of the 17-year observation period. The number of attributable cases was calculated as the difference between the observed and expected numbers of cases.

The development of exposure data was difficult because CME had been manufactured and used in three buildings at different times, changes of employees relative to the chemical processes had been frequent, and employee exposure to CME had diminished as a result of process improvements over time. Because suitable workplace chemical determinations of CMME or BCME concentrations had not been made in the study period before automation of the process, supervisory personnel associated with the manufacture and use of CME during 1948–72 were asked to rank the exposure for all job classifications. This was done retrospectively on an arbitrary scale from 0 to 6. Work histories and exposure ratings for each job at every important stage in the development of the process were used to calculate the time-weighted average exposure ratings and total exposure times for each employee. An exposure index was calculated for each man by cumulation of the total exposure.

In the group of 125 men, 34 had had no exposure to CME whereas 91 had had varying cumulative exposures. The temporal trends in exposure on a population basis were calculated from a mean annual exposure index for a given group of men for each year of exposure, as follows: For each man per group per year, the number of months spent at each exposure rating was multiplied by that rating, and the results were summed. The annual exposure thus calculated was summed over all the men exposed in that year and divided by the number of men in the group living in that year, whether exposed or not in that year. Although the distribution of annual exposures was not Gaussian, this calculation provided an annual per capita exposure which gave a rough estimate of population exposure for any group of ever-exposed men.

The pattern of CME exposure differed in two groups. One group of 28 men was exposed more intensely and for a shorter time in buildings A 1 and 2 during 1948–54 when the process was being developed, whereas the other group of 63 men was exposed to a lesser degree over a more prolonged period in building B during 1954–71. From 1962 on, the latter group received decreasing exposures because control procedures were instituted in the manufacturing process. There was very little overlap between these 2 groups because employees usually did not transfer when a process was moved. In this cohort only 4 of the 91 exposed men were exposed at both plant sites, and these doubly exposed men were allocated arbitrarily to the group for which exposure was limited to building B. None of those 4 developed cancer.

All CME-exposed men were assigned to groups according to the total cumulative exposure index (dose) attained by the time of death or by 1971, whichever came first, for the purpose of calculating crude 17-year respiratory cancer risks on a percentage basis. These groups were delineated by dose as follows: less than 10.0, 10–24.9, and 25 U or more. These doses were based on estimates of exposure to CME. In 1948–50, several batches of BCME were made in building A 1, but no attempt was made to account for this type of exposure when the rating system was developed because the greater potency of BCME compared to CMME as a carcinogen was uncertain at the time the rating system was devised, the exposure to BCME batches was limited, and there are no records as to who was exposed to the batches of BCME; therefore, no correction was feasible retrospectively.

Microscopic sections of all but 1 of the cancers were reviewed by Dr. Oscar Auerbach, Distinguished Physician, East Orange Veterans Administration Hospital, East Orange, N.J. Each tumor was typed according to a modification of the World Health Organization classification of lung cancer (*11*).

RESULTS

Incidence and Mortality

The cohort of 125 men experienced 37 deaths in the 17 years 1963–79. The expected number of deaths from all causes on the basis of Philadelphia white male age- and period-specific rates was 22.02; therefore, the overall SMR was 1.68. Fifteen of the 37 deaths were due to lung cancer, and 13.23 were attributable to exposure to CME. Thus lung cancer accounted for almost all the excess mortality.

The incidence of respiratory cancer in the whole cohort during the 17-year observation period was 18, including 16 lung cancers and 2 laryngeal cancers. Fifteen of the 16 men with lung cancer died during the period, whereas 1 was diagnosed in 1979 but was still alive at the end of the period. Among the 15 lung cancer deaths, all but one were attributed to this disease on the death certificate; the certified cause of death in the single exception was "undifferentiated malignancy" in 1 of the 4 men who died in the most recent 5-year period. The clinical records in this case confirmed the diagnosis of bronchogenic carcinoma.

The SMR for lung cancer was 8.45, from the use of Philadelphia white male lung cancer death rates, and 13.23 cases were attributable to chemical exposure. The figures were almost the same when lung cancer mortality rates for Health District No. 7 (the area surrounding the plant) in 1968–72 were utilized: The SMR was 7.43 with 12.98 attributable cases. Likewise, the SIR of 8.52, as based on male cancer registry rates in 1969–73, was almost identical with the SMR based on Philadelphia mortality rates, although the attributable number was a little higher, 14.12, on the basis of incidence. All of the ratios were elevated statistically to a highly significant degree, as determined by the Poisson distribution ($P<0.001$).

There were 2 cases of laryngeal cancer in 1974 and 1975; both were squamous cell carcinomas. The expected number on the basis of registry rates was 0.28; the resultant SIR of 7.09 was almost as high as that for lung cancer. This elevation, however, was not quite statistically significant ($P=0.08$). Inasmuch as a large proportion of men with laryngeal cancer do not die of their disease, the SMR was not calculated.

Two cases of lung cancer (5.9%) developed among 34 men who had not been exposed to CME, whereas 14 cases of lung cancer and 2 cases of laryngeal cancer (total of 17.6%) occurred among 91 men who were exposed.

Temporal Trends

Text-figure 2 shows the temporal relationship of cancer cases to exposure in the two different plant sites: building B and buildings A 1 and 2. The curves for the mean annual exposure index, on a group basis, show that the population exposure was more intense over a shorter and earlier period for the men who worked in buildings A 1 and 2 than for those who worked in building B. Correspondingly, the cancer cases occurred earlier among the former group, the last case appearing in 1972. There was a large gap between last exposure and the first cancer case in this group. In contrast, there was overlap of exposure and cancer appearance in the group exposed in building B. The frequency of cases in this group was highest in the first half of the decade of the 1970's, and only 1 case occurred in the last 4 years, 1976–79.

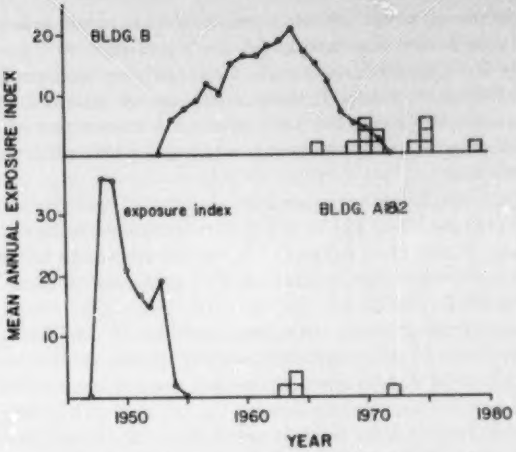

TEXT-FIGURE 2.—Mean annual exposure index among 91 employees exposed to chloromethyl ethers and the occurrence of respiratory (lung and laryngeal) cancer cases, 1948–79. *Each block* represents 1 cancer case. Data are divided by building in which exposure occurred.

The latent period, herein defined as the interval from onset of exposure to time of disease, in the 4 cases of lung cancer among men exposed in buildings A 1 and 2 ranged from 16 to 25 years, with a median of 17 years. Among men exposed in building B, the latent period in the 10 cases of lung cancer ranged from 10 to 23 years, with a median of 15.5 years. The latent periods in the 2 men who developed laryngeal cancer among the men exposed in building B were 16 and 17 years. The potential duration of the latent period which could be observed was constrained by the length of follow-up. Among the 91 exposed men, 93% could have been followed 20 years or more, but only 68% could have been followed 25 years or more. These percentages varied very little in subgroups of differing CME doses.

Among the 34 unexposed men, 2 cases of lung cancer occurred; 0.51 had been expected ($P>0.05$). The facts that both cases occurred in men who were cigarette smokers and that one man had a squamous cell carcinoma and the other had a large cell carcinoma suggest that these cases were not attributable to any undocumented exposure to CME.

All but 1 of the 13 lung cancer deaths in the exposed men were due to small cell carcinomas. The single exception, approximating the expected number of 1.26 cases, was a large cell carcinoma. Of the 13 men who died of lung cancer, 7 were current cigarette smokers in 1963 when observation began, 2 were ex-smokers of cigarettes, 1 smoked an occasional cigar, and 3 had never smoked.

Because all 16 respiratory (14 pulmonary and 2 laryngeal) cancer cases among the 91 exposed men occurred only among the 58 men with moderate-to-heavy CME exposure (cumulative dose index, ≥10 U), the remaining analysis will be limited to this group. Text-figure 2 shows that exposure patterns were quite different according to site of CME exposure. Because the median and the range of latent periods were similar for both groups, the epidemic curve can be examined in all 58 men, provided that other potential risk factors were also similar for the 2 groups.

Age is a potential risk factor. Thirteen men were exposed in buildings A 1 and 2; their mean age at onset of CME exposure was 33.15 (SD=3.85). Forty-five men were exposed in building B; their mean age was almost identical: 33.16 (SD=7.70).

The cumulative exposure index was also very similar for the 2 groups: 22.66 (SD=10.71) for the 13 men in buildings A 1 and 2 and 23.27 (SD=11.21) for the 45 men in building B. This difference is not statistically significant (Student's *t*-test=0.17, $P>0.05$).

The smoking factor was examined by the building in which the men were exposed to CME (table 1). While the proportion of nonsmokers was higher among the 13 men in buildings A 1 and 2 than among the 45 men in building B, the numbers of men were so small that this factor had no discernible effect on the crude respiratory cancer risk in the 2 groups. Table 1 shows that the crude 17-year cancer incidence was about twice as high among the nonsmokers as among the smokers in each group, but the overall crude incidence in each group was about the same.

Table 2 shows that the SMR were almost the same for the 2 groups. Therefore, it seems likely that the difference in dose rate experienced in the 2 groups shown in text-figure 2 had no discernible effect on risk.

TABLE 1.—*Distribution of and respiratory cancer incidence in men occupationally exposed to CME*[a]

Groups by workplace and cigarette habit in 1963	Distribution		Respiratory cancer	
	No. of men	Percent	No. of men	Percent of group
Buildings A 1 and 2	13	100	4	31
Nonsmokers	7	54	3	43
Smokers	6	46	1	17
Building B	45	100	12	27
Nonsmokers	7	16	3	43
Smokers	38	84	9[b]	24
Total	58	100	16[b]	28
Nonsmokers	14[c]	24	6	43
Smokers	44	76	10	23

[a] Crude 17-yr (1963-79) cancer incidence was determined for 58 men with moderate-to-heavy CME exposure.

[b] Includes 2 cases of laryngeal cancer.

[c] The 14 nonsmokers included 9 men who had never smoked any form of tobacco, 3 ex-smokers of cigarettes of >1 yr duration at registration, and 2 cigar smokers.

TABLE 2.—*SMR and attributable numbers of lung cancer deaths by building*[a]

Type of data	Building(s)	
	A 1 and 2	B
Man-years	134	475
Observed No.	4	9
Expected No.[b]	0.1929	0.4732
SMR	20.74	19.02
Attributable No.	3.81	8.53
P[c]	<0.0005	<0.0005

[a] Values were obtained from 1963-79 data for 58 men moderately to heavily CME exposed.

[b] From Philadelphia lung cancer 5-yr age-specific and period-specific mortality rates.

[c] From the Poisson distribution.

TABLE 3.—*Age at onset of CME exposure and man-years of follow-up*[a]

Age at onset	Onset of exposure, No. of men	Follow-up, No. of man-years				
		Total	No. of man-years from onset of exposure			
			10-14	15-19	20-24	25-29
20-24	7					
25-29	11					
30-34	17	13	13			
35-39	10	57.5	45.5	12		
40-44	10	102	44.5	48.5	9	
45-49	3	117	31	58.5	24.5	3
50-54		135	37	49	39	10
55-59		116.5	25	32.5	34	25
60-64		63		22	22	19
65-69		27.5		2	17.5	8
70-74		2				2
Total	58	633.5	196	224.5	146	67

[a] Interval from onset of exposure to follow-up was determined for 58 men moderately to heavily CME exposed, 1963-79.

TABLE 4.—*SMR and attributable numbers of lung cancer deaths by interval from onset of exposure*[a]

Type of data	Total	Years from onset of exposure			
		10-14	15-19	20-24	25-29
Man-years	633.5	196	224.5	146	67
Observed No.	13	3	7	2	1
Expected No.[b]	0.6661	0.1166	0.2179	0.2404	0.1488
SMR	19.52	25.72	32.13	8.32	6.72
Attributable No.	12.33	2.88	6.78	1.76	0.85
P[c]	<0.0005	<0.0005	<0.0005	<0.05	>0.05

[a] Values were obtained from 1963-79 data for 58 men moderately to heavily CME exposed.

[b] From Philadelphia lung cancer 5-yr age-specific and period-specific mortality rates.

[c] From the Poisson distribution.

In view of this lack of differences by age, cumulative CME exposure, or smoking habit between the 2 groups and in view of the failure of dose rate to influence overall risk of respiratory cancer, the 2 groups have been combined for an examination of the epidemic curve from onset of exposure. Table 3 presents a distribution of the 58 men by age at onset of exposure and the distribution of man-years of observation in 1963-79 by years from onset of exposure. Observation for the 13 men exposed in buildings A 1 and 2 began 15 years after the onset of exposure, inasmuch as the earliest exposure occurred in 1948 and observation started in 1963. Observation for the 45 men in building B was possible beginning not more than 9 years after onset of exposure, inasmuch as the earliest exposure occurred in 1954.

Table 4 shows data for the epidemic curve limited to the 13 lung cancer deaths so that SMR could be calculated. The SMR peaked 15-19 years after onset of exposure when 7 cases were observed, 32 times the expected number. The SMR fell markedly in the two later periods. The attributable number of deaths also peaked at 15–19 years and fell to an even greater extent than the SMR. At 25–29 years, there was only one death, and the SMR was no longer statistically significantly elevated; however, the numbers are small.

DISCUSSION

The degree to which this cohort of 125 men was representative of either the entire plant population or the general population is unknown, except for the men's smoking habits. The percentage of current cigarette smokers in the cohort was 77% in 1963. Age-specific prevalence rates in U.S. males reported for 1966 (*15*) were used to calculate the expected number of current cigarette smokers in the cohort, 56%. Thus smoking was considerably more common in the chemical workers. This complicates an interpretation.

Another potential problem in assessing the results of this cohort study concerns the possibility for some selection bias. The cohort included all men working in building B at the end of 1962. Inasmuch as CME was made and used in the building for 8 years before this time, some men who had been exposed earlier might have failed to be registered in the cohort because of transfers or terminations. It may be possible to investigate the degree to which this happened and to determine whether these individuals differed in certain ways from those who were included in the cohort. In addition, the method by which men from other buildings, some of whom had been exposed to CME in buildings A 1 and 2, were selected for the cohort is uncertain.

A final problem in this research has been the lack of data on CME concentrations in the workplace. This problem has necessitated semiquantitative estimates of dose. These estimates are based on assumptions as to the relationship between the estimates and the actual exposures, and this relationship may not be linear. In addition, the degree to which CMME was contaminated by BCME, a much more potent carcinogen than CMME in animals, may have varied. Neither this factor nor the exposure of certain employees to several batches of pure BCME in building A 1 was taken into consideration in the dose estimates.

Because lung cancer is a common disease in males of the general population as a result of the high prevalence of cigarette smoking, the epidemic curve was described not only in terms of the number of cases observed among the exposed workers but also in terms of relative risk and the attributable number of cases. It is heartening to see that the curves in terms of both methods are subsiding 20–24 years after onset of exposure. It is possible that the descending limb of a curve may be skewed into a long tail because *a*) low doses may be associated with longer latent periods (*10*), *b*) a previous study of this plant suggests (*11*) that low doses may be associated with adenocarcinoma of the lung rather than with small cell carcinoma, and *c*) adenocarcinomas tend to grow more slowly than small cell carcinomas (*16*). Further follow-up is indicated.

The results of this investigation are particularly interesting because the epidemic curve of lung cancer has seldom been described. Several examples come to mind. The cohort study of British physicians by Doll and Peto (*17*) contains significant data showing that the risk of lung cancer in ex-smokers drops slowly but dramatically over 10–15 years.

A more clear-cut example of an epidemic curve for this disease is provided by the follow-up of atom bomb survivors in Hiroshima and Nagasaki. Data published by Beebe et al. (*18*) show that the ratio of observed to expected lung cancer deaths was elevated significantly only among those people exposed to 100 rad or more at the time of the bomb. In this group, lung cancer began to occur 9–12 years after the bomb, with an observed-to-expected ratio of 3.3, but the ratio subsided thereafter to 2.2 at 13–16 years and to 1.7 or less at 17–28 years.

Enterline and Marsh (*19*) have likewise found among employees of a copper smelter that "workers who worked 10 years or less showed large relative excesses in respiratory cancer in the decade following termination of employment and these relative excesses all but disappeared in the next 20 years."

In each of these studies, the decline in risk was related to cessation of exposure. In a situation, such as that described in the present report, in which the pattern of exposure varied by intensity and duration, the description of the epidemic curve in relation to only cessation of exposure may be unrewarding.

In a recent analysis of lung cancer mortality results at the same plant in which the present cohort study was done, Pasternack and Shore (*20*) reported no decrease in relative risk as a function of years since last exposure. Their data showed a relative risk of 2.3 at 1–4 years after exposure stopped, 0.7 at 5–9 years, 1.0 at 10–14 years, and 1.5 at 15–25 years. The trend was irregular, but it may have been confounded by the pattern of exposure.

In the present cohort study, examining crude risk by pattern of exposure (*see* text-fig. 2: short, intense exposure vs. prolonged, less intense exposure) suggests that excess risk began to subside more than 20 years after onset of exposure, regardless of exposure pattern. An examination of the crude risk of respiratory cancer by the interval from cessation of exposure confirmed the observation of Pasternack and Shore: There was essentially no change in the percentage of men who developed cancer. Inasmuch as other important risk factors were similar in the 2 groups with different exposure patterns and inasmuch as the overall SMR were also similar, the observations reported herein suggest that earlier exposures to CME were more important in the eventual development of lung cancer than were the later ones. The importance of early exposures to cigarette smoke in determining the eventual risks of lung cancer has been stressed by Doll and Peto (*21*). Further study of this point is needed.

REFERENCES

(*1*) Wallenstein S. A test for detection of clustering over time. Am J Epidemiol 1980; 111:367–372.

(*2*) Van Duuren BL, Goldschmidt BM, Katz C, Langseth L, Mercado G, Sivak A. Alpha-haloethers: A new type of alkylating carcinogen. Arch Environ Health 1968; 16:472–476.

(*3*) Laskin S, Kuschner M, Drew RT, Capiello VP, Nelson N. Tumors of the respiratory tract induced by inhalation of bis(chloromethyl)ethers. Arch Environ Health 1971; 23:135–136.

(*4*) Figueroa WG, Raszkowski R, Weiss W. Lung cancer in chloromethyl methyl ether workers. N Engl J Med 1973; 288:1096–1097.

(*5*) Weiss W, Boucot KR. The respiratory effects of chloromethyl methyl ether. JAMA 1975; 234:1139–1142.

(*6*) Weiss W. Chloromethyl ethers, cigarettes, cough and cancer. J Occup Med 1976; 18:194–199.

(*7*) Weiss W, Figueroa WG. The characteristics of lung cancer due to chloromethyl ethers. J Occup Med 1976; 18:623–627.

(*8*) Weiss W. The forced end-expiratory flow rate in chloromethyl ether workers. J Occup Med 1977; 19:611–614.

(*9*) ———. The cigarette factor in lung cancer due to chloromethyl ethers. J Occup Med 1980; 22:527–529.

(*10*) DeFonso LR, Kelton SC Jr. Lung cancer following exposure to chloromethyl methyl ether. Arch Environ Health 1976; 31:125–130.

(*11*) Weiss W, Moser RL, Auerbach O. Lung cancer in chloromethyl ether workers. Am Rev Respir Dis 1979; 120:1031–1037.

(*12*) U.S. Bureau of the Census. Methodology for experimental estimates of the population of counties, by age and sex. Washington, D.C.: U.S. Govt Print Off, 1975:23 (current population reports, special studies, No. 103).

(*13*) Weiss W. Lung cancer mortality and urban air pollution. Am J Public Health 1978; 68:773–775.

(*14*) Waterhouse JA, Muir CS, Correa P, Powell J, Davis W, eds. Cancer incidence in five continents. Vol III. IARC Sci Publ No. 15. Lyon: IARC, 1976:178, 186, 206.

(*15*) National Center for Health Statistics. Changes in cigarette-smoking habits between 1955 and 1966. Rockville, Md.: National Center for Health Statistics, 1970:7 (Public Health Service Publication No. 1000-Series 10-No. 59, April 1970).

(*16*) Weiss W. Peripheral measurable bronchogenic carcinoma: Growth rate and period of risk after therapy. Am Rev Respir Dis 1971; 103:198–208.

(*17*) Doll R, Peto R. Mortality in relation to smoking: 20 years' observations on male British doctors. Br Med J 1976; 2:1525–1536.

(*18*) Beebe GW, Kato H, Land CE. Studies of the mortality of A-bomb survivors. 6. Mortality and radiation dose, 1950–1974. Radiat Res 1978; 75:138–201.

(*19*) Enterline PE, Marsh GM. Cancer among workers exposed to arsenic and other substances in a copper smelter. Am J Epidemiol. In press.

(*20*) Pasternack BS, Shore RE. Lung cancer following exposure to chloromethyl ethers. In: Chwat M, Dror K, eds. Proceedings of the international conference on critical current issues in environmental health hazards. Tel-Aviv, Israel, March 4–7, 1979, 76–84.

(*21*) Doll R, Peto R. The causes of cancer: Quantitative estimates of avoidable risks of cancer in the United States today. Appendix E. JNCI 1981; 66:1191–1308 (*see* 1292).

Epithelial Line From Normal Human Colon Mucosa[1,2,3,4]

B. Shannon Danes[5] *and* **E. Sutanto**[5,6]

ABSTRACT—An epithelial line was established from an explant culture derived from human colon mucosa exhibiting a normal phenotype by taking advantage of two differences in in vitro cell behavior of mixed cell (epithelial-fibroblast) monolayer [rate of adherence to a plastic surface from a suspension and toxicity to collagenase (25 U/ml medium) in the culture medium]. Cells with an epithelial morphology could be identified at all times throughout the first 5 culture months— first as epithelial sheets migrating from explants, then as small clusters within the fibroblast monolayer, and finally after 5 months of selective culturing as the only cell type present. The line maintained an epithelium-like morphology and growth pattern through 27 continuous culture months (35 subcultures) and was clearly distinguishable from colon fibroblast cultures grown under the same conditions. The ultrastructural features of this line that grew as a continuum included extensive membrane interdigitations with intercellular junctions, tonofilaments, mucus droplets, no Weibel-Palade bodies (characteristic of endothelial cells), and microridges uniformly covering the cell surfaces; all of these features were absent in colon fibroblast cultures. Growth kinetics (generation time, saturation density, and life-span) were distinctly different from those of colon fibroblast cultures grown under the same conditions. During 27 continuous culture months, the cells remained diploid (2-3% hyperdiploidy) and showed no evidence of senescence.—JNCI 1982; 69:1271-1276.

Since human colon pathology is predominantly expressed in the mucosa, normal colon mucosal lines are needed for in vitro studies on pathogenesis. Although short-term cultures have been established from normal colon (*1, 2*) and colon adenocarcinoma tissue (*3, 4*), there have been no epithelial lines derived from normal human colon mucosa.

The purpose of this paper was to describe the establishment of a human colon mucosal line that exhibits a normal phenotype and has grown in continuous culture for 27 months.

MATERIALS AND METHODS

Establishment of primary mixed (epithelial-fibroblast) cultures.—A biopsy (1×1 cm) sample was taken from the mucosal surface of a surgical colon specimen obtained at surgical resection for trauma to the colon from a 37-year-old male (blood group O) who had had no family history of colon cancer. This biopsy sample was placed in chilled culture medium [modified EMEM with 10% (vol) FBS containing 50 μg gentamicin and Fungizone/ml medium (pH 7.4)] to be taken to the laboratory. It was then cut into small pieces (1×1 mm), placed in a culture tube containing the same medium, and kept at 4°C for 12 hours. The mucosal pieces were then cut into smaller fragments and washed in fresh medium.

The culture vessel used was a double petri dish (a 60/15-mm dish in a 100/20-mm dish as isolation against external contamination). Four such fragments were placed in the inner dish containing approximately 1 ml medium [EMEM with 25% (vol) FBS without any antibiotics (pH 7.4)]. Optimal migration of epithelial cells was obtained when a 1-ml/28-cm^2 surface area was used to just cover the fragments and floor of the culture dish. The culture vessel was then placed in an incubator having a humidified atmosphere of 5% CO_2 in air at 37°C and left undisturbed for 10 days. At that time each culture was examined microscopically for epithelial migration. Fragments that showed no epithelial migration were removed. Three milliliters of medium was added to the culture with care being taken not to loosen the fragments. The medium was completely changed twice each week.

After the culture floor was completely covered by cells, the mixed cell population was subcultured. The culture was rinsed twice with a trypsin-Versene solution (0.5% trypsin-0.02% Versene, sodium ethylenediaminetetraacetate, in Hanks' balanced salt solution without calcium and magnesium) and then incubated in 1 ml of the same solution for 3-5 minutes at 39°C. After the cells had rounded up but were still adhered, the solution was removed, medium was added, and the cells were loosened into suspension by gentle pipetting by means of a Pasteur pipette. One-half of the cell suspension was put into each of two new culture dishes, which were then placed in a humidified CO_2 incubator. One hour later the medium was changed to remove any cellular debris and traces of the trypsin-Versene solution.

Selection of epithelial cells from mixed monolayer culture.—At each subculture two differences in cell behavior were utilized: 1) rate of adherence to a plastic surface from a suspension and 2) toxicity to the addition of collagenase to the culture medium (*5*).

There was an observed difference in the rate of readherence of cells to the plastic floor. When the cell suspension was introduced into the new dishes, the subcultures were kept at room temperature for 15 minutes. The medium containing the nonadherent cells was transferred to another

ABBREVIATIONS USED: EMEM=Eagle's minimum essential medium; FBS=fetal bovine serum.

---

[1] Received March 22, 1982; accepted July 22, 1982.

[2] Supported by Public Health Service grant CA-15973 from the National Large Bowel Cancer Project, Division of Cancer Research Resources and Centers, National Cancer Institute.

[3] Research procedures were in accord with the ethical standards of the Committee on Human Rights in Research, Cornell University Medical College.

[4] Available from the American Type Culture Collection catalog No. ATCC-CCL 239.

[5] Laboratory for Cell Biology, Department of Medicine, Cornell University Medical College, 1300 York Ave., New York, N.Y. 10021.

[6] We are indebted to Dr. Martha Spiegelman, Memorial Sloan-Kettering Cancer Center, New York, N.Y., for the guidance given in the preparation and interpretations of the electron micrographs.

dish, and both dishes were incubated. If the predominant cell type in the subcultures containing the cells that adhered in the first 15 minutes were fibroblasts, these dishes were then identified as fibroblasts and used to establish colon fibroblast cultures so that their characteristics could be compared with those of the epithelial line.

Fibroblast growth was suppressed by the incorporation of 25 U collagenase/ml medium (collagenase source— *Clostridium histolyticum*; Grand Island Biological Co.). Collagenase-containing medium was used in cultures for 3 days after subculture followed by 11 days of growth in medium without collagenase and then subcultured into two petri dishes.

These two procedures were repeated at each subculture (every 2 wk) until the morphology of the total cell population was epithelial. From then on the line was grown in double petri dish cultures containing EMEM with 25% (vol) FBS without antibiotics (pH 7.4) in humidified 5% CO_2 in air at 37°C. Every 2–3 weeks the line was subcultured (1:2 split). Cultures were routinely checked for bacteria and mycoplasma and found to be uncontaminated.

Characterization of epithelial line—Morphology was examined under light, phase, transmission (*6*), and scanning electron (*7*) microscopies. Growth kinetics of both the colon epithelial line and colon fibroblasts were compared by methods previously described in detail (*8*). Every month after the establishment of the line (5–35 subcultures), chromosome preparations were made, stained in acetic orcein, and examined for variations from diploidy. Growth of cells in the nude mouse was determined for evidence of tumorigenicity (*8*).

RESULTS

The sheets of epithelium, observed in the migration zone around each explant during the 1st culture week, increased in surface area gradually over the next 2 months. Such sheets occasionally dispersed into small islands or clumps. Migration of fibroblasts from the explant started in the 2d culture week and continued as long as the explant was present. After the first subculture (after 2 culture mo), several islands of cells with epithelial morphology were observed in the predominantly fibroblast monolayer. With the elimination of fibroblasts by selection (differential adherence to plastic surface and incorporation of collagenase in the medium) at each subculturing, there was a gradual shift in the proportion of epithelial cells to fibroblasts. By the 5th culture month, all cells in the monolayer had an epithelial morphology (fig. 1).

At the 10th and 30th subcultures, the cultures were examined for ultramicroscopic epithelial structures. Numerous intercellular junctions were observed (fig. 2A). Some had the characteristics of desmosomes, and others were nonspecific intercellular junctions, perhaps intermediary in type. Cytoplasmic tonofilaments (9.6 nm in diameter) were also observed. Edges of adjoining cells were connected by extensive membrane interdigitations in which intercellular junctions were frequently seen (fig. 2A). Other structures present were mucus droplets and pinocytotic vesicles (fig. 2C). Microridges uniformly covered the cell surfaces exposed to the culture medium (fig. 3). Weibel-Palade bodies (*9, 10*) and bundles of fine filaments (*10*) as seen in human endothelial cells were not observed.

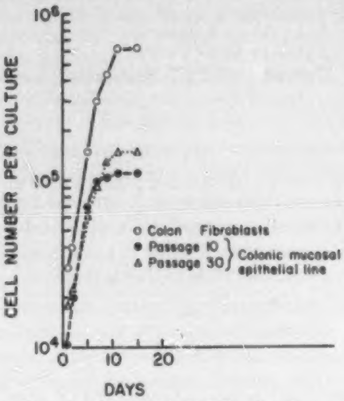

TEXT-FIGURE 1.—Growth of the epithelial line from normal human colon mucosa at passages 10 (5th culture mo) and 30 (23d culture mo) and a colon fibroblast culture at passage 10 (5th culture mo). Cell samples were plated into plastic petri dishes (growth surface, 28 cm^2) containing EMEM with 25% (vol) FBS and grown in a humidified atmosphere of 5% CO_2 in air at 37°C (pH 7.4). Cell counts were done and medium was changed every 3 days for 15 days.

During logarithmic growth (text-fig. 1), the generation time for this cell line was 31 hours at the 10th subculture and 28 hours at the 30th subculture; colon fibroblast cultures had a generation time of 25 hours at the 10th subculture and had ceased to grow and had been discarded by the 25th subculture. Saturation density occurred at 1.1×10^3 cells/cm^2 growth area, which was at a lower cell density than that for colon fibroblasts (2.2×10^4 cells/cm^2 growth area).

The karotype was 46,XY without obvious chromosome aberrations. The chromosome frequency distribution at the 10th subculture was 99% diploid and 1% hyperdiploid. By the 35th subculture (after 27 continuous culture mo), there had been little change in this distribution (97% diploid and 3% hyperdiploid). Metaphases with diplochromosomes indicating endoreduplication were observed occasionally throughout the 27 culture months. Tumorigenicity was not observed because none of the samples from the cell line inoculated sc into athymic nude mice produced tumors in a 6-month period.

DISCUSSION

In the human colon the epithelial cells are arranged as a single layer of columnar cells lining indentations (crypts of Lieberkühn) into the colon wall. Because replicating colon epithelial cells are found only in the lower two-thirds of the crypt (*11*), it was assumed that the epithelial cells constituting the original cells of this line came from this region.

Lasfargues and Moore (*12*) introduced the incorporation of collagenase into the culture medium to discourage fibroblast growth and thus enhance growth of epithelial cells. Webber (*5*) utilized this selective process to establish short-term cultures of normal and benign human prostate epithelia. If this technique was combined with the difference in the rate of adherence of different cell types from a cell suspension from a mixed (epithelial–fibroblast) monolayer, it was possible to select an epithelial cell population from a mixed fibroblast–epithelial monolayer derived from a colon mucosal biopsy specimen. Cells with an epithelial morphology were identifiable at all times throughout the culture period (5 mo) to establish this line. Initially, the epithelial cells were in sheets migrating from explants, then they were present as small clusters within the fibroblast monolayer, and later, by selection, they were the only cell type present (fig. 1). During the establishment of the cell line, there appeared to be some cell-to-cell interaction and cooperation between the fibroblast and epithelial populations which may have been essential to the epithelial cells. Primary cultures that showed only epithelial migration and no subsequent fibroblast growth grew poorly and failed to subculture.

The culture properties of this cell line met the criteria for cultured epithelium. This line maintained an epithelium-like morphology and growth pattern through 35 subcultures and was clearly distinguishable from fibroblast-like cultures derived from the colon and grown under the same conditions. The line grew as a sheet (fig. 1), whereas the monolayer of colon fibroblasts grew as swirls, the usual pattern for cultured fibroblasts.

Intercellular junctions were numerous (fig. 2A, 2B). In vivo colon epithelial cells are coupled by junctions having three components (tight, intermediary, and desmosome) in apical-basal sequence (*13*). Short-term cultures (up to 8 wk in culture) have shown all three components in sequence (*2*). In this line cell junctions appeared to be single and randomly distributed (fig. 2). Some of the junctions had the morphologic features of desmosomes (*13*) (fig. 2B), but others appeared to be nonspecific intercellular junctions, perhaps intermediary. In this line there was no evidence of a basal-apical orientation. In electron micrographs the cell surface did not have a brush border (fig. 2); in scanning electron micrographs the nonadherent cell surface was covered with microridges (fig. 3) and was quite distinct from the smooth surface of the cultured colon fibroblast. Numerous membrane interdigitations between adjoining cells were present (figs. 1B, 1C, 2A).

Culture senescence was not observed throughout 27 months of continuous culture. The extended life-span of this line was not related to the presence of adventitious agents because routine examinations of cultures for the presence of mycoplasma, bacteria, fungi, protozoa, and viruses were negative. Constancy of culture conditions appeared essential for such continuous growth. A constant pH 7.4, complete medium change twice each week, and subculture (1:2 split) every 2–3 weeks were essential for sustained growth.

On the basis of the definitions adopted by the Terminology Committee of the Tissue Culture Association (*14*), this continuous culture was designated a line even though all cell types present at the first subculture of the primary explant culture were not present. The designation of strain was withheld until specific colon mucosal markers, such as colon-specific antigens, have been identified (*15*). Other mucosal lines have been established with the use of the methodology described for this line, and their properties are currently being characterized.

REFERENCES

(*1*) DANES BS. Establishment of human colonic mucosal culture strains from colonoscopy specimens. Birth Defects 1980; 16:275–281.

(*2*) FRIEDMAN EA, HIGGINS PJ, LIPKIN M, SHINYA H, GELB AM. Tissue culture of human epithelial cells from benign colonic tumors. In Vitro 1981; 17:632–644.

(*3*) OWENS RB, SMITH HS, NELSON-REES WA, SPRINGER EL. *Brief communication*: Epithelial cell cultures from normal and cancerous human tissues. J Natl Cancer Inst 1976; 56:843–849.

(*4*) TOM BH, RUTZKY LP, JAKSTYS MM, DYASA R, KAYE CI, KAHAN BD. Human colonic adenocarcinoma cells. I. Establishment and description of a new line. In Vitro 1976; 12:180–191.

(*5*) WEBBER MM. Normal and benign human prostatic epithelium in culture. I. Isolation. In Vitro 1979; 15:967–982.

(*6*) BRIGHTMAN MW, REESE TS. Junctions between intimately apposed cell membranes in the vertebrate brain. J Cell Biol 1969; 40:648–677.

(*7*) ANDREWS PM, PORTER KR. The ultrastructural morphology and possible functional significance of mesothelial microvilli. Anat Rec 1973; 177:409–426.

(*8*) DANES BS, BÜLOW S, SVENDSEN LB. Hereditary colon cancer syndromes: An in vitro study. Clin Genet 1980; 18:128–136.

(*9*) WEIBEL ER, PALADE GE. New cytoplasmic components in arterial endothelia. J Cell Biol 1964; 23:101–112.

(*10*) JAFFE EA, NACHMAN RL, BECKER CG, MINICK CR. Culture of human endothelial cells derived from unbilical veins. Identification by morphologic and immunological criteria. J Clin Invest 1973; 52:2745–2756.

(*11*) LIPKIN M, BELL B, SHERLOCK P. Cell proliferation kinetics in the gastrointestinal tract of man. I. Cell renewal in colon and rectum. J Clin Invest 1963; 42:767–776.

(*12*) LASFARGUES EY, MOORE DH. A method for the continuous cultivation of mammary epithelium. In Vitro 1971; 7:21–25.

(*13*) FARQUHAR MG, PALADE GE. Junctional complexes in various epithelia. J Cell Biol 1963; 17:375–412.

(*14*) SCHAEFFER WI. Proposed usage of animal tissue culture terms, revised 1978. Tissue Culture Assoc Manual 1978; 4:779–792.

(*15*) GOLDENBURG DM, PEGRAM CA, VASQUEZ JJ. Identification of a colon-specific antigen (CSA) in normal and neoplastic tissues. J Immunol 1975; 114:1008–1013.

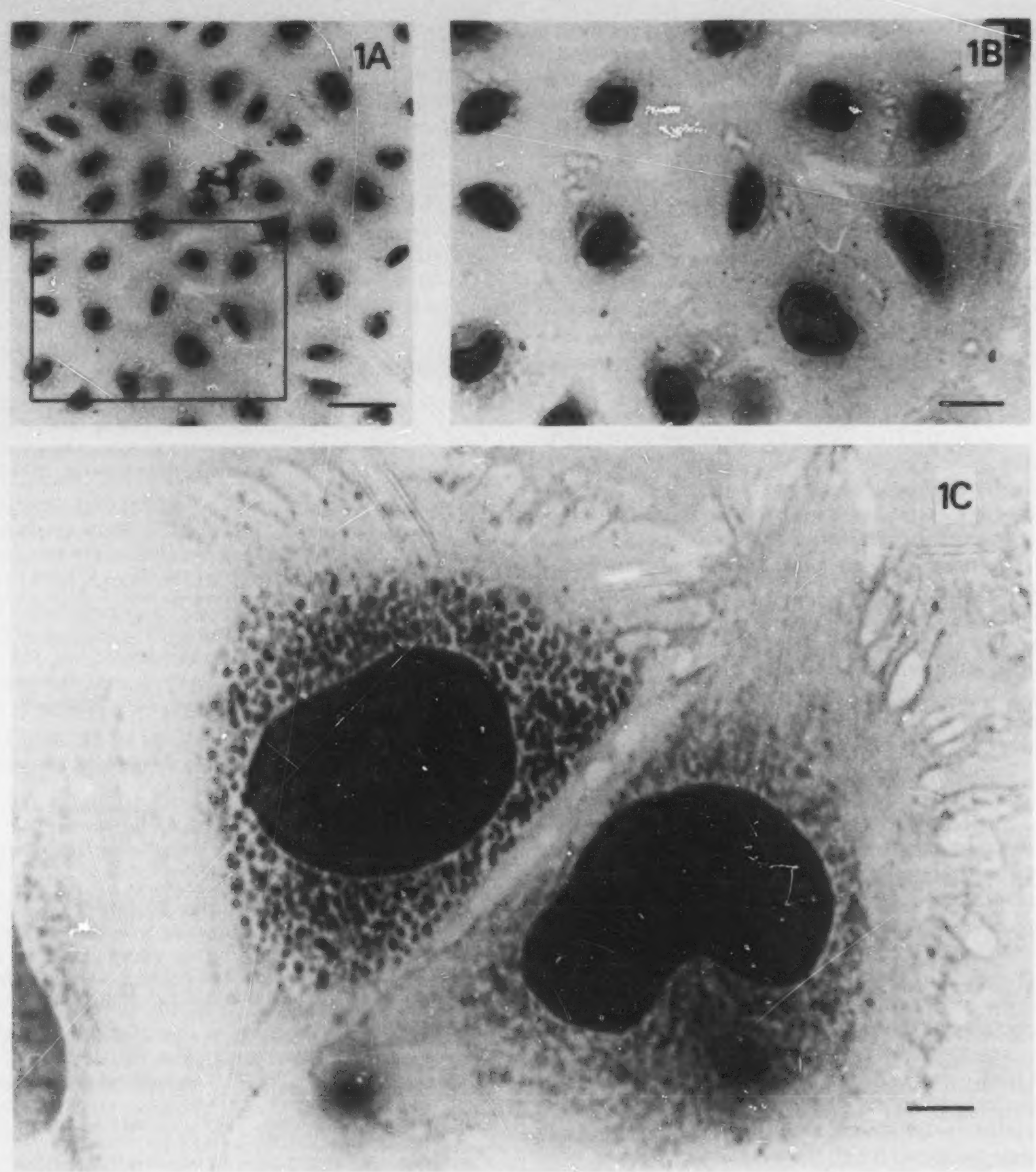

FIGURE 1.—Culture of normal human colon mucosal line grown in continuous culture for 23 mo. Fixed in buffered Formalin and stained with hematoxylin and eosin. A) Field to illustrate uniformity of cell morphology. *Bar*=20 µm. × 500. B) *Inset* in A to show membrane interdigitations. *Bar*=10 µm. × 1,000. C) Cells to show membrane interdigitations. *Bar*=2 µm. × 5,000.

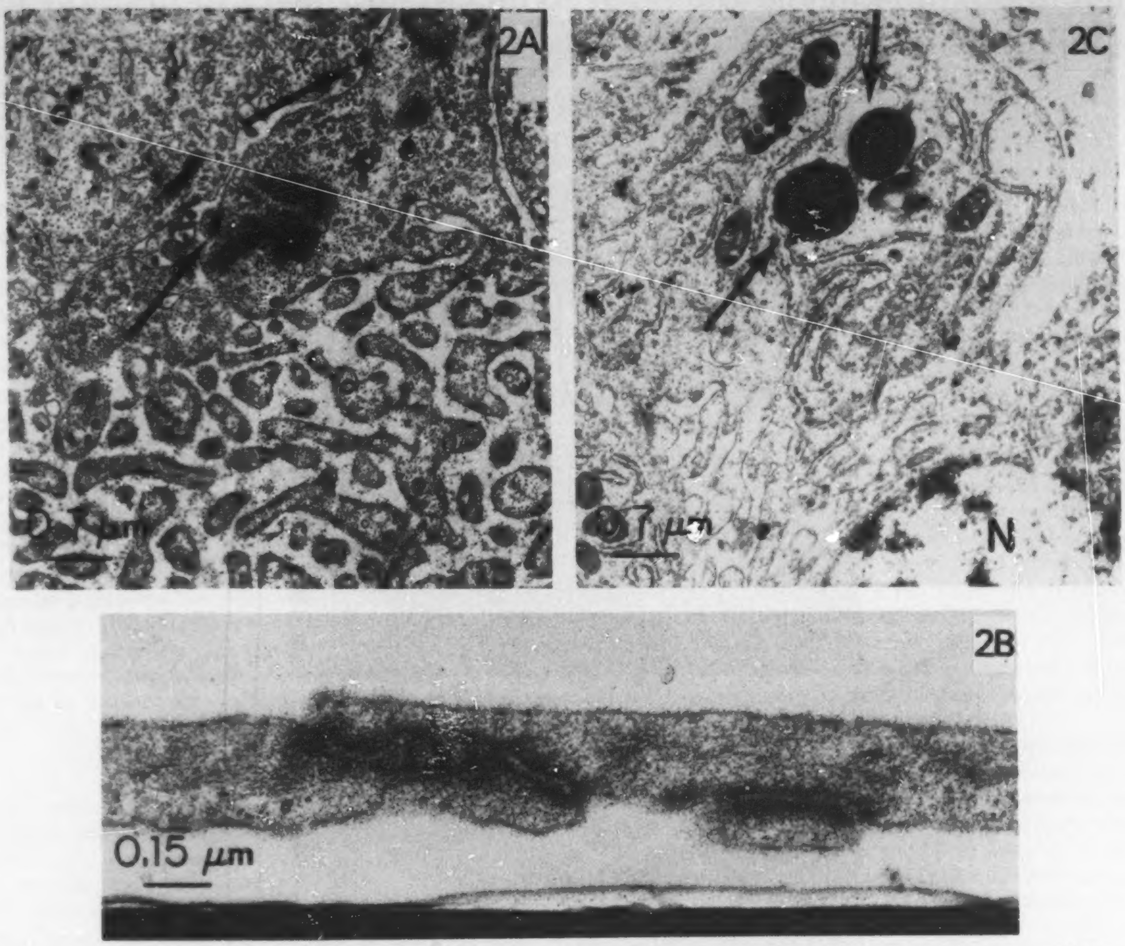

FIGURE 2.—Electron micrographs illustrating epithelial structures in normal human colon mucosal line. A) Membrane interdigitations with intercellular junctions (*arrows*). × 14,000. B) Intercellular junctions (desmosomes). × 67,000. C) Intercellular mucus droplets (*arrows*). N=nucleus. × 14,000.

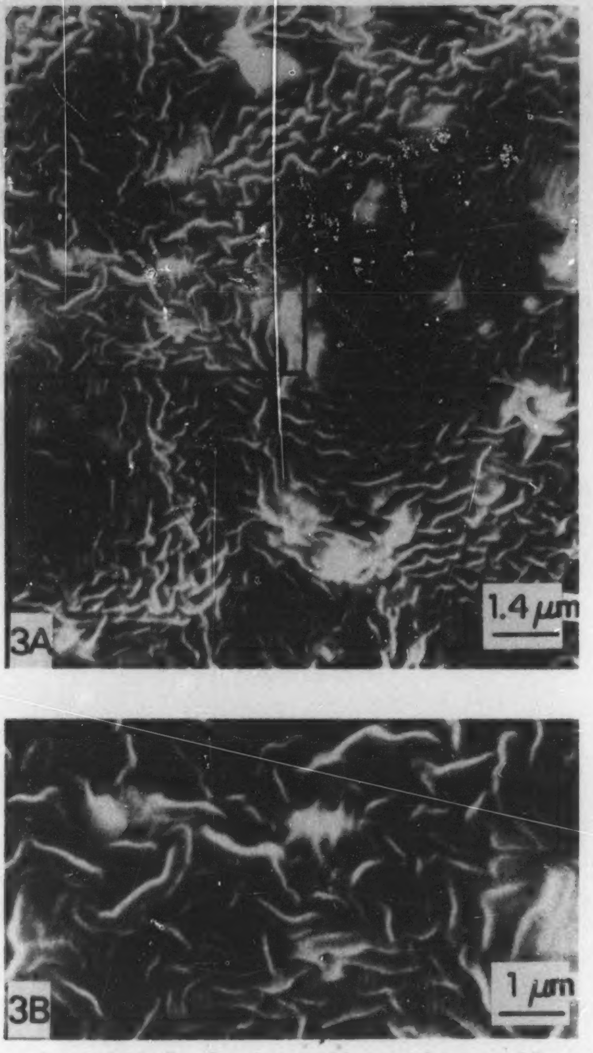

FIGURE 3.—A scanning electron micrograph of cell surfaces in normal human colon mucosal line grown in culture for 23 mo. A) Microridges cover cell surfaces. × 7,000. B) *Inset* in A to show uniformity of distribution of microridges over cell surfaces exposed to culture medium. × 10,000.

DNA Content of Liver Cell Nuclei of *N*-2-Fluorenylacetamide-Induced Altered Foci and Neoplasms in Rats and Human Hyperplastic Foci[1,2]

Hideki Mori,[3] Takuji Tanaka,[3] Shigeyuki Sugie,[3] Masayoshi Takahashi[3] *and* **Gary M. Williams[4]**

ABSTRACT—The DNA content of cell nuclei of liver lesions induced in inbred male ACI rats by administration of 0.02% *N*-2-fluorenylacetamide (2-FAA) diet was measured with a microspectrophotometer in Feulgen-stained specimens. Altered liver foci of the eosinophilic, clear, and simple basophilic (toluidine blue weakly positive or negative) types had modal DNA values with a wider deviation (2C–10C) than the euploid pattern of normal hepatocytes (2C–6C). However, the DNA histograms of cells in hyperbasophilic (intensely toluidine blue-positive) foci were aneuploid (2C–18C) and resembled those of cells in hepatocellular carcinomas (2C–23C). Conversely, the modal DNA values of neoplastic nodules showed a narrower range (2C–12C). These results confirm that the hyperbasophilic foci may be a population similar to carcinoma in situ or may be a direct precursor lesion of hepatocellular carcinoma. In the livers from 4 humans, 3 of whom had a history of long-term use of some drugs, multiple hyperplastic foci resembling eosinophilic or clear cell foci in rats were identified. The modal DNA values of the cell nuclei in these foci showed a wider deviation (2C–10C) than in surrounding hepatocytes (2C–6C). In 2 patients, the lesions contained neoplasms and, therefore, hyperplastic foci in humans may be related to tumor development.—JNCI 1982; 69:1277–1282.

In experimental hepatocarcinogenesis in the rat, the altered focus (enzyme-altered focus), which appears soon after exposure to carcinogens, is a proliferative lesion that has been regarded as a precursor of hepatocellular neoplasms (*1–9*). These altered foci are histologically classified as eosinophilic, basophilic, and clear cell in H & E-stained preparations (*10*). Basophilic foci can be subdivided into two types on the basis of staining with toluidine blue (*4, 11*). Hyperbasophilic foci, which are intensely toluidine blue-positive, have been suggested to be related to cancer development (*4, 11, 12*) or even to be microcarcinomas (*13*). Foci have been found to display a number of abnormal properties (*14–19*) that could reflect genetic aberrations (*9*). Morphologic abnormalities in the nuclei of cells in foci have been described (*20*), but genotypic alterations have not been documented. One means of studying the genotype of cells is by measurement of their DNA content (*21–23*).

The amount of DNA in nuclei of neoplastic cells is higher and more variable than that in nuclei of normal cells (*24–30*). Correlations between DNA content and histologic type of cancer or degree of malignancy of tumors have also been documented (*23, 31, 32*). Inui et al. (*33*) reported differences between the modal DNA values of cell nuclei of liver cell adenomas or hepatocellular carcinomas experimentally induced in mice and those of normal hepatocytes. Therefore, the DNA content of the early-appearing altered foci in rat liver that were induced by a hepatocarcinogen was analyzed to further clarify the basic nature of these foci and to determine their potential as precursors of carcinomas.

In the present study, microspectrophotometric estimations of the nuclear DNA content of foci altered by 2-FAA in rats were performed and compared with those of normal liver, neoplastic nodules, and hepatocellular carcinomas. In addition, the DNA values of human hyperplastic liver foci resembling some of the altered foci in rats were also measured. The possible significance of these human liver lesions is discussed.

MATERIALS AND METHODS

Twenty inbred male ACI rats 1.5 months old were fed a 0.02% 2-FAA diet for 15–19 weeks. Twelve of these rats were killed at the termination of feeding. The remaining 8 rats were then transferred to the basal diet CE-2 (Japan Clea Co., Tokyo, Japan) for 10 weeks after which they were killed. Four rats 5–7 months old were used as controls. At necropsy of the animals, each liver lobe was sliced at 4-mm intervals and fixed in Carnoy's solution. The embedded liver slices were cut as three serial sections and stained with H & E (first section) and toluidine blue (second section) and by the Feulgen reaction (third section).

In the liver sections, 28 altered foci [7 eosinophilic foci, 7 clear cell foci, 7 simple basophilic foci (toluidine-blue-negative or weakly positive), and 7 hyperbasophilic foci (intensely toluidine blue-positive)] were obtained in the rats killed at the termination of the 15- to 19-week 2-FAA diet. Seven neoplastic nodules and 5 hepatocellular carcinomas were found in rats given 2-FAA for the same period and then given basal diet for 10 more weeks.

Among recent autopsies of human patients performed at Gifu University Hospital, we encountered 4 cases in which the liver contained multiple hyperplastic hepatocellular foci resembling the altered foci in rats. The morphology and speculated etiology of the liver foci in 1 case have been reported (*34*). In the present study, 20 hyperplastic liver foci were analyzed.

For the measurement of DNA content in cell nuclei, a microspectrophotometer MMSP (Olympus Co., Tokyo, Japan) was used at 545 nm on interphase nuclei. Random samples of 50 Feulgen-reacted nuclei contained within a

---

ABBREVIATIONS USED: 2-FAA=*N*-2-fluorenylacetamide; H & E=hematoxylin and eosin; HBsAg=hepatitis B surface antigen; PAS=periodic acid-Schiff.

---

[1] Received April 6, 1982; accepted June 30, 1982.

[2] Supported in part by a grant from the Ministry of Education, Science and Culture, Japan.

[3] Department of Pathology, Gifu University School of Medicine, 40 Tsukasa-machi, Gifu 500, Japan.

[4] Division of Pathology and Toxicology, Naylor Dana Institute for Disease Prevention, American Health Foundation, Valhalla, N.Y. 10595.

liver section were counted with the use of small lymphocytes as a diploid (2C) control.

RESULTS

The modal DNA values of hepatocellular nuclei of the normal rats and nonlesional portions of the liver in rats given a 2-FAA diet are shown in text-figure 1. The values of hepatocellular nuclei of the normal liver exhibited a fairly sharp modal peak in the diploid region, whereas a secondary peak appeared in the hypotetraploid region with limited deviations around these two modes. About 97% of the cells in the normal liver had DNA values below 5C (table 1). The DNA histograms of hepatocytes in the nonlesional portions of the livers in rats killed after 15–19 weeks on the 2-FAA diet or killed after being fed the 2-FAA diet followed by the basal diet for 10 weeks differed from those of normal liver (text-fig. 1). The modal DNA values of hepatocytes in these livers were slightly deviated to the multiploid range.

Altered foci displayed an architectural pattern that was different from normal, but the plates of hepatocytes were as a rule in continuity with those of surrounding parenchyma and the foci never compressed the surrounding hepatic plates. The DNA patterns of the cell nuclei of hepatocytes in the altered foci induced by 2-FAA administration are shown in text-figure 2. Generally, the DNA values of foci with the exception of hyperbasophilic foci were alike. The DNA histograms of cells in the altered foci of the three types usually ranged between 2C and 8C with a wider spread than those of control hepatocytes. In some cells, the DNA values reached 10C. About 20–30% of hepatocytes in these foci exhibited DNA values above 5C with major peaks around 3C.

The hyperbasophilic foci had more irregular nuclei and prominent nucleoli than other types of foci. The DNA histograms of cell nuclei of the hyperbasophilic foci were all quite different from those of cell nuclei of other types of altered foci. The values ranged between 2C and 18C and showed an aneuploid pattern without a detectable stem cell line (text-fig. 2). Of the cells in the hyperbasophilic foci, 77% were multiploid (exceeding 5C), whereas only 1% had DNA values below 2.5C (table 1).

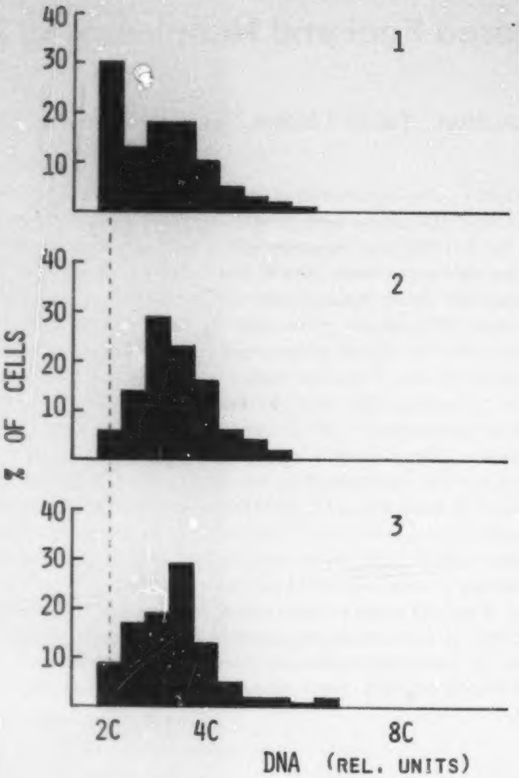

TEXT-FIGURE 1.—Nuclear DNA content of control liver. Each histogram is from averaged values of five sites. 1) Normal liver from control rats. 2) Nonlesional portions of the liver in rats killed after 15–19 wk on the 2-FAA diet. 3) Nonlesional portions of the liver in rats given the 2-FAA diet for 15–19 wk and a normal diet for 10 more wk.

Neoplastic nodules observed in this study were all sharply demarcated from the surrounding parenchyma. They were generally composed of acidophilic cells, and the cell plates of the nodules were discontinuous from those of adjacent liver tissue and compressed the hepatic plates. Modal DNA values of cells in the neoplastic nodules showed a wider deviation than altered foci like the eosinophilic type, but the range was narrower than that of hyperbasophilic foci (text-fig. 2). The DNA histograms of neoplastic nodules revealed basically polyploid patterns; 48% of cells exceeded 5C, and 45% were between 2.5C and 5C (table 1).

TABLE 1.—*DNA content of cells from different populations in rat and human livers*

Type of liver cell	Species	No. of sites	No. of cells measured	Cell DNA content, %		
				<2.5C	2.5C–5C	>5C
Normal liver, control	Rat	5	250	30	67	3
Nonlesional portion in rat given 2-FAA	Rat	5	250	10	85	5
Nonlesional portion in rat given 2-FAA followed by basal diet	Rat	5	250	6	92	2
Eosinophilic cell focus	Rat	7	350	7	71	22
Clear cell focus	Rat	7	350	10	67	23
Simple basophilic cell focus	Rat	7	350	8	62	30
Hyperbasophilic cell focus	Rat	7	350	1	22	77
Neoplastic nodule	Rat	7	350	7	45	48
Hepatocellular carcinoma	Rat	5	250	1	19	80
Nonlesional portion surrounding focal lesion	Human	4	200	40	57	3
Hyperplastic focus	Human	20[a]	1,000	9	67	24

[a] From 4 cases of the liver (each five sites).

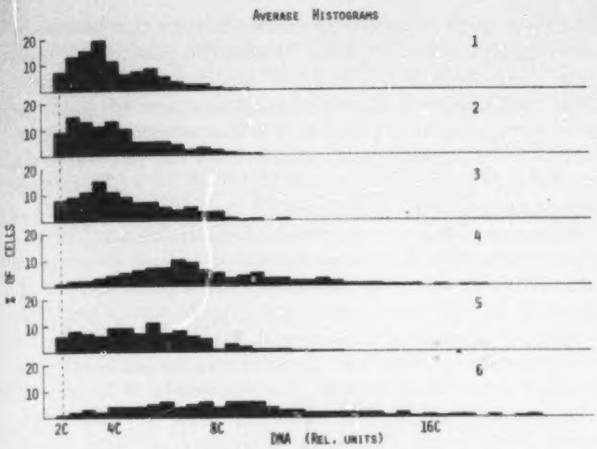

TEXT-FIGURE 2.—Average histograms from different rat liver lesions. 1) Eosinophilic foci. 2) Clear cell foci. 3) Simple basophilic foci. 4) Hyperbasophilic foci. 5) Neoplastic nodules. 6) Hepatocellular carcinomas.

The hepatocellular carcinomas used in this study were of the well-differentiated or moderately differentiated trabecular type. The histograms of cells in hepatocellular carcinomas showed an aneuploid pattern with widespread DNA values. Moreover, the ploidy distribution was different in each carcinoma. Some of the histograms of carcinoma cells were narrower than that of hyperbasophilic foci, and some of were extremely wide with a range between 2C and 23C (text-fig. 2).

Hyperplastic human liver foci were found in the livers from 4 aged people, 3 of whom had a history of long-term drug use for hyperlipidemia or hypertension. The foci were sharply demarcated from the surrounding hepatocytes, and their plates merged imperceptibly with those of adjacent hepatocytes (figs. 1, 2) similar to what was seen in the altered foci in rats. As a rule, these lesions did not compress the surrounding parenchyma. The cells in foci had clear or acidophilic cytoplasms, and the cytoplasms were strongly PAS-positive (fig. 3). The frequency of these foci was approximately 1.0–3.4/cm^2 of the liver. Of the 4 cases, 3 had the focal lesions in the absence of other changes, such as cirrhosis or severe bile duct proliferation. One of the cases also had adenomatous nodular lesions in the liver, and another had cirrhosis and hepatocellular carcinoma (table 2). The modal DNA values of the cell nuclei in the human hyperplastic foci were similar to those in the altered foci of the eosinophilic or clear cell type of rats. They ranged between 2C and 10C with major peaks around 3C (text-fig. 3). Unlike the surrounding normal hepatocytes that scarcely possessed DNA values exceeding 5C, about 23% of these cells fell into the range above 5C.

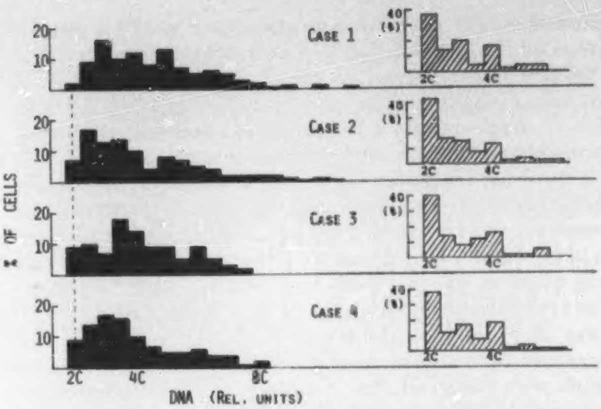

TEXT-FIGURE 3.—Histograms of nuclear DNA content of human hyperplastic foci in the livers of 4 patients. Each histogram is obtained from five sites of foci. *Inserted histograms with oblique lines* are those from the corresponding surrounding hepatocytes.

DISCUSSION

The studies reported here document a number of abnormalities in the DNA contents of carcinogen-induced rat liver lesions and hyperplastic foci occurring in the livers of humans with a history of drug exposure and/or other liver pathology.

The modal DNA values of cell nuclei in eosinophilic, clear cell, and simple basophilic rat liver foci showed a wider deviation than those of normal hepatocytes or hepatocytes outside the foci. Some of the increase could be due to higher rates of cell proliferation, but the results also support the concept that such liver foci are truly an "altered" hepatocellular population. The DNA patterns of the altered foci are in some respects comparable to those of metaplastic or dysplastic tissues and are regarded as "precancerous changes" in uterine cervix (*28, 35*), skin (*26*), or bronchus (*36*). Of particular significance was the finding that the DNA histograms of cells in hyperbasophilic foci showed an aneuploid pattern. This pattern distinguished these foci from the other types and established a possible relationship to hepatocellular carcinomas which were also aneuploid. In tumor development in the human uterine cervix, Böhm and

TABLE 2.—*Human hyperplastic liver foci and the clinical data of patients*

Case No.	Age, yr	Sex	No. of foci per cm^2	Other pathologic liver lesions	Drugs (duration)	Clinical information
1	76	♀	2.8	Adenomatous nodules	Clofibrate (7 yr)	Hyperlipidemia, cerebral bleeding
2	68	♂	3.4		Trichlormethiazide (8 yr), digitalis (8 yr), phenobarbital (6 yr)	Hypertension, lung cancer
3	78	♀	1.0		Reserpine (5 yr), hydrochlorothiazide (5 yr)	Hypertension, lung cancer
4	60	♀	2.2	Hepatocellular carcinoma and liver cirrhosis		Positive HBsAg

Sandritter (*23*) reported that alterations in DNA content preceded the invasive stage of carcinoma and suggested that "the first important step in the direction of malignancy is the transformation of the euploid-polyploid DNA distribution of dysplasia into a heterogenous aneuploid cell population of carcinoma in situ." Several investigators (*4, 11, 37, 38*) have considered basophilic liver lesions to be a transformed or transitional population between hyperplasia and neoplasia. Grundman and Sieburg (*13*) suggested that these lesions might even be microcarcinomas. A similarity of enzymatic or biologic properties between hyperbasophilic foci and hepatocellular carcinomas is also known (*11, 12*). Over 20 years ago, Maini and Stich (*39*) and Stich (*29*) described the presence of a genetically heterogenous population with abnormal chromosomes and different aneuploid amounts of DNA in precancerous livers of rats fed 4-(dimethylamino)azobenzene. The hepatocellular population they observed could correspond to the hepatocytes of the altered hyperbasophilic foci in the current study. The present finding of abnormally increased nuclear DNA content in hyperbasophilic foci thus suggests that hyperbasophilic foci are probably a population comparable to carcinoma in situ or a direct precursor lesion of hepatocellular carcinomas. Furthermore, these results support the hypothesis (*9*) that genetic alteration in hepatocytes renders them capable of forming altered foci and that altered foci may progress to hepatocellular neoplasms.

The DNA mode of neoplastic nodules showed a wider distribution than that of altered foci of the eosinophilic or clear cell type. Evidence indicates that neoplastic nodules arise by progressive growth of altered foci (*3, 10*). In the present study the development of neoplastic nodules after cessation of carcinogen exposure confirms a previous report (*40*) that these lesions are a progressively growing population. Their more deviant DNA content compared to the content of foci supports the concept that these lesions represent a further progression in neoplastic development (*9*). The cumulative evidence on the nature of nodules therefore continues to conform with their original designation by Sasaki and Yoshida (*41*) as adenomas. The present findings of a narrower distribution of modal DNA pattern of the nodules than that of hyperbasophilic foci or hepatocellular carcinomas is further evidence for the benign nature of the nodule.

In this study, compared to the DNA mode of hyperbasophilic foci, the DNA mode of some hepatocellular carcinomas also showed narrower distributions. Well-differentiated carcinomas are known to exhibit a narrower distribution of modal DNA values than do poorly differentiated carcinomas (*23, 31, 32*). Ploidy reduction in carcinomas may relate to the selection during proliferation of a near-diploid stem line (*23, 25*).

Human hyperplastic liver foci observed in this study also showed a wider distribution of their DNA mode than did the surrounding hepatocytes, and the pattern resembled that of some altered foci in rats. In the literature, such focal lesions in the human liver only have been reported infrequently (*42*). In the present study, the livers of 3 patients did not display major pathologic changes such as cirrhosis, and abnormalities in liver function tests were not detected. Therefore, such small liver lesions could be overlooked in many human livers. In these 3 cases, the patients all used some drugs such as clofibrate or antihypertensive agents. Both clofibrate and an analogue, nafenopin, are carcinogenic in experimental animals (*43*). Tumorigenicity or genotoxicity of some antihypertensive drugs has recently been described (*44, 45*). The promoting effect in experimental hepatocarcinogenesis of long-acting barbiturates (*46, 47*) is well known. Thus the ocurrence of multiple small hyperplastic foci in this study may be related to long-term use of some drugs. In one case, the patient had a positive HBsAg. Hir[illegible]a et al. (*42*) have reported a possible role of hepatitis B virus in producing such lesions. Thus advanced age or viral hepatitis could be other possible etiologic factors in the development of these lesions. The occurrence of hepatocellular adenomatous lesions (*34*) or of hepatocellular carcinomas in the livers of 2 patients suggests that these hyperplastic foci may be one of the precursor lesions of hepatocellular adenomas or carcinomas, as in experimental animals.

REFERENCES

(*1*) Kitagawa T. Histochemical analysis of hyperplastic lesions and hepatoma of the liver of rats fed *N*-2-fluorenylacetamide. Gan 1971; 62:207–216.

(*2*) Bannasch P. Cytology and cytogenesis of neoplastic (hyperplastic) hepatic nodules. Cancer Res 1976; 36:2540–2543.

(*3*) Williams GM, Klaiber M, Parker SE, Farber E. Nature of early appearing carcinogen-induced liver lesions resistant to iron accumulation. J Natl Cancer Inst 1976; 57:157–165.

(*4*) Daoust R. Hyperbasophilic foci as sites of neoplastic transformation in hepatic parenchyma. Cancer Res 1971; 31:1290–1296.

(*5*) Schauer A, Kunze E. Enzymhistochemische und autoradiographische Untersuchungen während der Cancerisierung der Rattenleber mit Diäthylnitrosamin. Z Krebsforsch 1968; 70:252–266.

(*6*) Emmelot P, Scherer E. The first relevant cell stage in rat liver carcinogenesis: A quantitative approach. Biochim Biophys Acta 1980; 605:247–304.

(*7*) Farber E. The sequential analysis of liver cancer induction. Biochim Biophys Acta 1980; 605:149–166.

(*8*) Pitot HC, Sirica AE. The stages of initiation and promotion in hepatocarcinogenesis. Biochim Biophys Acta 1980; 605:191–215.

(*9*) Williams GM. The pathogenesis of rat liver cancer caused by chemical carcinogens. Biochim Biophys Acta 1980; 605:167–189.

(*10*) Stewart HL, Williams G, Keysser CH, Lombard LS, Montali RJ. Histologic typing of liver tumors of the rat. JNCI 1980; 64:177–206.

(*11*) Daoust R, Molnar F. Cellular populations and mitotic activity in rat liver parenchyma during azo dye carcinogenesis. Cancer Res 1964; 24:1898–1909.

(*12*) Karasaki S. Ultrastructural and cytochemical studies on hyperbasophilic foci with special reference to the demonstration of cell surface alterations in hepatocarcinogenesis. Cancer Res 1976; 36:2567–2572.

(*13*) Grundman E, Sieburg H. Die Histogenese und Cytogenese des Lebercarcinomas der Ratte durch Diäthylnitrosamin im lichtmikroskopischen Bild. Beitr Pathol 1962; 126:57–90.

(*14*) Kalengayi MM, Ronchi G, Desmet VJ. Histochemistry of gamma-glutamyl transpeptidase in rat liver during aflatoxin B_1-induced carcinogenesis. J Natl Cancer Inst 1975; 55:579–588.

(*15*) Börner P, Gössner W. Enzymhistochemische Untersuchungen der Adenosine-Triphosphatase, der alkalischen und sauren Phosphatase sowie der Succinodehydrogenase im Leberparenchym der Ratte während der Einwirkung des Cancerogens Diäthylnitrosamine. Z Naturforsch [C] 1968; 19:1085–1091.

(*16*) Daoust R. Focal loss of ribonuclease activity. Cancer Res 1971; 32:2502–2509.

(17) Gössner W, Friedrich-Freksa H. Histochemische Untersuchungen über die Glucose-6-phosphatase in der Ratten Leber während der Canzerisierung durch Nitrosamine. Z Naturforsch 1964; 19b:862-863.

(18) Bannasch P. The cytoplasm of hepatocytes during carcinogenesis. Recent Results Cancer Res 1968; 19:18-48.

(19) Williams GM, Yamamoto RS. Absence of stainable iron from preneoplastic and neoplastic lesions in rat liver with 8-hydroxyquinoline-induced siderosis. J Natl Cancer Inst 1972; 49:685-692.

(20) Williams GM, Watanabe K. Quantitative kinetics of development of *N*-2-fluorenylacetamide-induced, altered (hyperplastic) hepatocellular foci resistant to iron accumulation and of their reversion or persistence following removal of carcinogen. JNCI 1978; 61:113-121.

(21) Barlogie B, Hittleman W, Spitzer G, et al. Correlation of DNA distribution abnormalities with cytogenetic findings in human adult leukemia and lymphoma. Cancer Res 1977; 37:4400-4407.

(22) Stöhr M. On the correlation of chromosome number and DNA content in HeLa clones. Acta Cytol 1975; 19:299-305.

(23) Böhm N, Sandritter W. DNA in human tumors: A cytophotometric study. Curr Top Pathol 1975; 60:151-219.

(24) Leuchtenberger C, Leuchtenberger R, Davis A. A microspectrophotometric study of desoxyribonucleic acid (DNA) content in cells of normal and malignant human tissues. Am J Pathol 1954; 30:65-85.

(25) Atkins NB. DNA content of breast lesions. Lancet 1966; 1:1372.

(26) Inui N, Oota K. Measurement of deoxyribonucleic acid by Feulgen-microspectrophotometry on Friend's disease cells. Gan 1965; 56:301-307.

(27) Inui N, Takayama S. Comparative studies on the amount DNA in cell nuclei of mouse skin after administration of carcinogenic and non-carcinogenic substances. Int J Cancer 1968; 3:701-711.

(28) Atkin NB. Nuclear size in carcinoma of cervix; its relation to DNA content and to prognosis. Cancer 1964; 17:1391-1399.

(29) Stich HF. The DNA content of tumor cells. II. Alterations during the formation of hepatomas in rats. J Natl Cancer Inst 1960; 24:1283-1297.

(30) Stich HF, Steele HD. DNA content of tumors cells. III. Mosaic composition of sarcomas and carcinomas in man. J Natl Cancer Inst 1962; 28:1207-1218.

(31) Lederer B, Mikuz G, Gütter W, Nedden G. Zytophotometrische Untersuchungen von Tumoren des Übergangsepithels des Harnblase. Beitr Pathol 1972; 147:379-389.

(32) Kieffer G, Sandritter W. DNA and the cell cycle. Beitr Pathol 1976; 158:332-362.

(33) Inui N, Takayama S, Kuwabara N. DNA measurement on cell nucleus of normal liver, adenoma, and hepatoma in mice: Histologic features. J Natl Cancer Inst 1971; 47:47-58.

(34) Mori H, Tanaka T, Sugie S, Takahashi M. Adenoma with multiple hyperplastic nodules in noncirrhotic liver possibly related to long-term administration of a hypolipidemic drug. Acta Pathol Jap 1982; 32:671-676.

(35) Sandritter W, Fischer R. Der DNS-gehalt des normalen Plattenepithels, des Carcinoma in situ und des invasiven Carcinomas der Portio. In: Proceedings of the first International Congress of Exfoliative Cytology, Vienna, Austria, July 31-Aug. 2, 1961. Philadelphia: Lippincott, 1962:189-195.

(36) Nasiell M, Kato H, Auer G, Zetterburg A, Roger V, Karlen L. Cytomorphologic grading and Feulgen DNA analysis of metaplastic and neoplastic bronchial cells. Cancer 1978; 41:1511-1521.

(37) Opie EL. The pathogenesis of tumors of the liver produced by butter yellow. J Exp Med 1944; 80:231-246.

(38) Newberne PM. Experimental hepatocellular carcinogenesis. Cancer Res 1976; 36:2567-2572.

(39) Maini MM, Stich HF. Chromosomes of tumor cells. II. Effect of various liver carcinogens on mitosis of hepatic cells. J Natl Cancer Inst 1961; 26:1413-1427.

(40) Hirota N, Williams GM. Persistence and growth of rat liver neoplastic nodules following cessation of carcinogen exposure. JNCI 1979; 63:1257-1265.

(41) Sasaki T, Yoshida T. Experimentelle Erzeugung des Lebercarcinoms durch Fütterung mit *o*-Amidoazotoluol. Virchows Arch [Pathol Anat] 1935; 259:175-200.

(42) Hirota N, Hamazaki M, Williams GM. Resistance to iron accumulation and presence of hepatitis B surface antigen in preneoplastic and neoplastic lesions in human hemochromatotic livers. Hepatogastroenterology 1982; 29:49-51.

(43) Reddy JK, Rao MS. Malignant tumors in rats fed nafenopin, a hepatic peroxisome proliferator. J Natl Cancer Inst 1977; 59:1645-1650.

(44) Toth B. Tumorigenic effect of 1-hydrazinophthalazine hydrochloride in mice. JNCI 1978; 61:1363-1365.

(45) Williams GM, Mazue G, Maqueen CA, Shimada T. Genotoxicity of the antihypertensive drugs hydralazine and dihydralazine. Science 1980; 210:329-330.

(46) Peraino C, Fry RJ, Staffedt E. Reduction and enhancement by phenobarbital of hepatocarcinogenesis induced in the rat by 2-acetylaminofluorene. Cancer Res 1971; 31:1506-1512.

(47) Mori H, Tanaka T, Nishikawa A, Takahashi M, Williams GM. Enhancing effect of barbital on *N*-2-fluorenylacetamide-induced rat liver lesions. Gan 1981; 72:798-801.

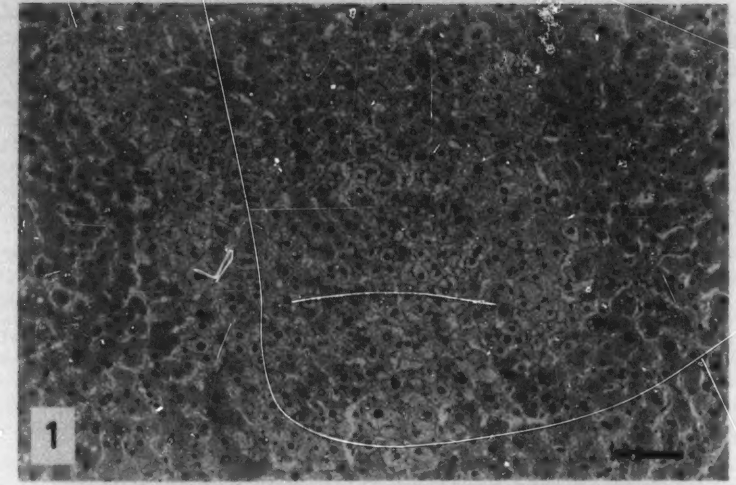

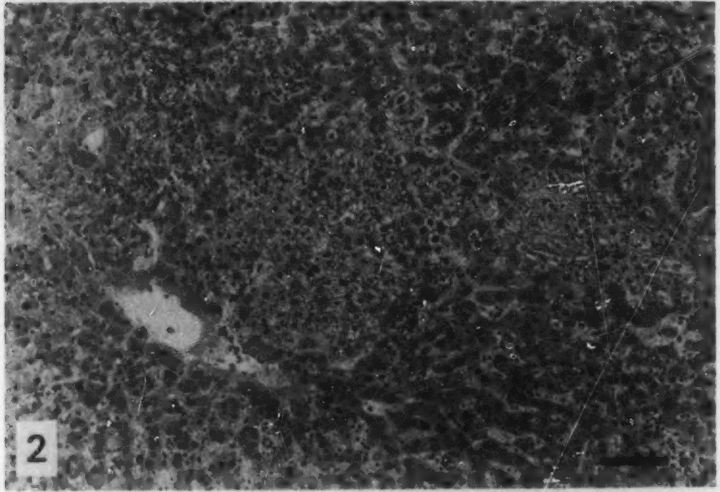

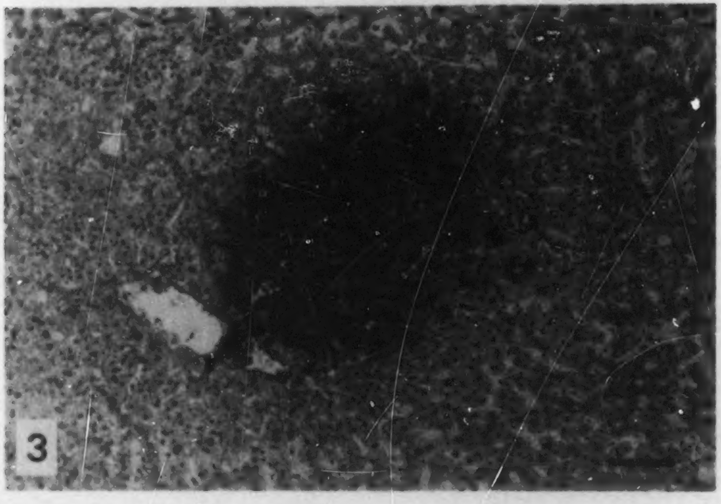

FIGURE 1.—A human hyperplastic liver focus (case 1). H & E. *Bar*=100 µm. × 100

FIGURE 2.—Human hyperplastic liver focus (case 2). H & E. *Bar*=100 µm. × 100

FIGURE 3.—Same lesion illustrated in fig. 2 showing intensely positive reaction for PAS. *Bar*=100 µm. × 100

No Seasonality in the Diagnosis of Acute Leukemia in the United States[1,2]

Alexander M. Walker, *M.D., D.P.H,*[3,4] *and* **Paulus A. H. van Noord**, *M.D., M.Sc.*[3,5]

ABSTRACT—Dates of diagnosis of 7,000 cases of acute leukemia occurring in the United States between 1969 and 1981 were reviewed for detection of seasonal patterns. No strong evidence was found for seasonality in the diagnosis of acute leukemias as a whole or for subgroups based on cell type, age, or geography. Previous indications of seasonal fluctuation may represent the selective reporting of chance events.—JNCI 1982; 69:1283–1287.

Reports of seasonal fluctuations in the occurence of acute leukemia have appeared in the past (*1–10*), but their utility has been limited by lack of standard terminology and frequently by the absence of data on the source populations giving rise to the cases. Ages and seasons of peak occurrence have varied from one series to another, and the literature is, as a whole, a hodgepodge of individually impressive communications, which seem to represent the selective reporting of random quirks of disease incidence.

Seasonal fluctuations in disease occurrence can provide insight into possible pathogenic mechanisms and deserve to be documented, if they exist. To this end we have reviewed data from the TNCS, the SEER Program, and the CCPDS to ascertain the seasonality of the incidence of the acute leukemias.

DATA AND METHODS

The purposes and methods of the TNCS and SEER Program have been described elsewhere (*11, 12*). From the TNCS and the SEER data through 1977 we abstracted the following information on all cases of acute leukemia [codes 204.0, 205.0, 206.0, and 207.0 in International Classification of Disease, Eighth Revision (*13*)]: histology, age in years at diagnosis, date of diagnosis, race or ethnic background, sex, and place of residence at the time of diagnosis (TNCS or SEER reporting area). Although different areas reported for different periods within the total time intervals covered by these data (1969–71, 1973–77), each reporting center did provide data for some series of complete calendar years, so no month was overrepresented or underrepresented in the data by virtue of representing more or fewer reporting center-years.

Patterns of occurrence of cases were examined by visual inspection of cross-tabulations of age by month of diagnosis stratified by place of residence, ethnic background, year of diagnosis, and histologic type. Stratified data were extensively explored through Edwards's technique for seasonal analysis (*14*), through examination of partial autocorrelation functions (*15*), and through graphical techniques. We further evaluated major aggregations of cases by fitting a sine curve to the monthly pattern; we used the technique of Nelson et al. (*16*), with case counts assigned in a block to the middle of each month. This method involves mathematically transforming seasonal data in such a way that ordinary least-squares regression techniques can be utilized to estimate seasonal coefficients, test their statistical significance, and construct confidence intervals. No correction was made for the different lengths of months, but as will be evident from the results, such small corrections could not affect the final interpretation of the data in any important way. The term "amplitude" will be used here to describe the peak-to-trough differences for fitted sine curves. "Relative amplitude" will be used to describe the amplitude divided by the average monthly count.

Hypotheses raised on the basis of the TNCS–SEER data were tested with the use of comparable information from the files of the CCPDS. CCPDS is an association of 21 comprehensive cancer centers in the United States and has been collecting a standardized "minimal patient dataset" on all patients seen for diagnosis and therapy in the cancer centers since July 1, 1977. Items available on all patients give information on demographic characteristics, diagnoses, prior and newly initiated therapies, survival, and (when applicable) cause of death. This information is obtained by local data managers through chart review, hospital-based tumor registries, and direct contact with physicians. Data managers are given extensive initial training, are subjected to periodic quality control checks, and are supported by a central data management staff. Details of the organizational structure and operating procedures for CCPDS have been presented in (*17*). The data required for the present study were, as it turned out, age and month of diagnosis for subjects with acute monocytic leukemia [code 9891/3 in International Classification of Diseases for Oncology (*18*)], admitted to CCPDS centers in the 4-year period beginning July 1, 1977.

ABBREVIATIONS USED: CCPDS=Centralized Cancer Patient Data System; SEER=Surveillance, Epidemiology, and End Results; TNCS=Third National Cancer Survey.

---

[1] Received June 2, 1982; accepted July 16, 1982.

[2] Supported in part by Public Health Service grants CA-24996 and CA-06516 from the National Cancer Institute and by a grant from the Netherlands Cancer Foundation K.W.F.

[3] Department of Epidemiology, Harvard School of Public Health, Boston, Mass. 02115.

[4] *Address reprint requests to* Dr. Walker, Division of Biostatistics and Epidemiology, Sidney Farber Cancer Institute, 44 Binney St., Boston, Mass. 02115.

[5] Sandra Steinhorn, the Biometric Research and Analytic Studies Section, Biometry Branch, National Cancer Institute, and Mark Schmidt and Steven Dahlberg, the Centralized Cancer Patient Data System, provided valuable technical assistance in making the data presented here available for analysis.

Table 1.—*TNCS and SEER acute leukemia cases—month of diagnosis by age at diagnosis*

Leukemia case in month diagnosed	Total	Subject's age at diagnosis, yr					
		0–2	3–9	10–19	20–49	50–69	≥70
All leukemias							
January	621	29	77	66	102	160	187
February	503	33	54	55	90	124	147
March	556	33	72	54	96	133	168
April	575	28	80	49	101	154	163
May	547	21	70	47	84	158	167
June	587	39	79	51	101	155	162
July	566	35	76	51	99	141	164
August	526	20	61	51	84	139	171
September	563	25	58	60	99	165	156
October	551	44	62	47	88	142	168
November	549	28	65	53	90	133	180
December	550	37	61	49	87	152	164
Unknown	54	3	2	4	11	15	19
Acute leukemia, histology not otherwise specified							
January	59	3	9	4	6	14	23
February	54	6	7	4	8	12	17
March	59	6	7	3	5	15	23
April	74	9	14	5	8	15	23
May	55	5	11	2	11	8	18
June	64	6	7	7	6	18	20
July	61	9	12	5	9	14	12
August	36	2	7	4	6	7	10
September	52	2	11	6	9	10	14
October	50	5	6	7	3	14	15
November	57	6	7	7	5	13	19
December	57	6	9	6	4	12	20
Unknown	11	0	0	0	2	2	7
Acute lymphocytic leukemia							
January	170	21	61	34	14	14	26
February	141	22	46	31	19	6	17
March	153	21	52	30	16	12	22
April	143	16	56	29	15	10	17
May	138	14	52	28	15	11	18
June	161	26	64	24	18	12	17
July	165	23	56	31	18	16	21
August	135	11	42	32	15	17	18
September	141	15	38	32	23	22	11
October	152	29	47	26	23	14	13
November	142	17	48	25	17	20	15
December	142	28	45	24	14	18	13
Unknown	9	3	2	1	2	0	1
Acute myeloid leukemia							
January	350	5	7	25	72	118	123
February	276	4	1	19	56	96	100
March	317	6	12	21	70	98	110
April	328	3	9	14	71	116	115
May	330	2	7	16	56	128	121
June	339	7	7	19	74	114	118
July	319	3	7	15	70	104	120
August	335	6	11	13	62	111	132
September	352	6	9	22	62	125	128
October	321	9	9	12	58	104	129
November	333	4	10	20	67	95	137
December	327	3	7	18	64	112	123
Unknown	31	0	0	3	6	13	9
Acute monocytic leukemia							
January	42	0	0	3	10	14	15
February	32	1	0	1	7	10	13
March	27	0	1	0	5	8	13
April	30	0	1	1	7	13	8
May	24	0	0	1	2	11	10
June	23	0	1	1	3	11	7
July	21	0	1	0	2	7	11
August	20	1	1	2	1	4	11
September	18	2	0	0	5	8	3
October	28	1	0	2	4	10	11
November	17	1	0	1	1	5	9
December	24	0	0	1	5	10	8
Unknown	3	0	0	0	1	0	2

RESULTS

Table 1 presents the monthly distribution of cases cross-tabulated by age and histology. In text-figure 1, the relative amplitude and timing of the peak incidence of cases are plotted on polar coordinates for each of the four histologic types: acute lymphocytic, acute myelocytic, acute monocytic, and acute with histology not otherwise specified. The distance of each point from the center of the circle corresponds to the relative amplitude of fluctuation, and the direction from the center to each point indicates the timing of the peak. Of the four histologic types, only acute monocytic leukemia shows any important seasonal variation, with a relative amplitude of fluctuation of 55% and a seasonal peak in February. The 95% confidence region for acute monocytic leukemia (shown speckled) indicates that while the data were (barely) inconsistent with the null hypothesis of zero amplitude, they were quite consistent with underlying patterns of fluctuation of widely varying intensity and timing. In text-figure 2, the counts listed in table 1 for monocytic leukemia are plotted against the fitted sine curve. From table 1, it appears that any seasonality in monocytic leukemia incidence could be common to all age groups; in every group over the age of 9 years, January was the month of peak occurrence. The numbers of cases are too small to permit a statistical test of acceptable power comparing the different age groups with one another.

Further sifting through the data failed to reveal any other consistent seasonal patterns. Text-figure 3 shows the relative amplitude and timing of fitted sine curves for each reporting area. For none of the areas did the 95% confidence region exclude zero amplitude, and taken together, the data were not suggestive of any important overall fluctuation or any geographic correlates. Examination of age, race, and histology-specific patterns within each of the regions brought to light no relations that were obscured in the aggregate data. Further categorization of TNCS-SEER reporting areas according to climate, latitude, coastal versus central location, urbanization, and duration of continuously reported surveillance was similarly not helpful, as were analyses based

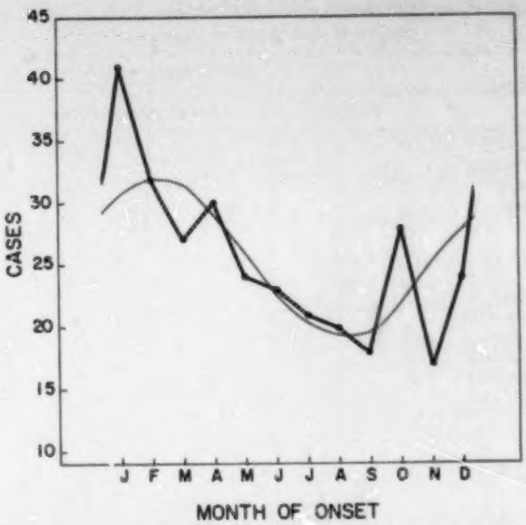

Text-figure 2.—Observed number of cases of acute monocytic leukemia in TNCS-SEER Program by month (J-D=January-December) of diagnosis (*solid line*) and the best-fitting sinusoidal curve (*dotted line*).

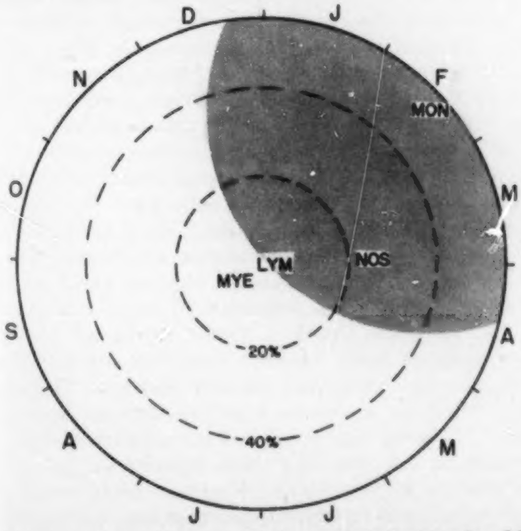

Text-figure 1.—Acute leukemia: Timing and relative intensity of fitted sine curves by histologic type in TNCS-SEER Program. Only acute monocytic leukemia (MON) shows a strong seasonality. *Distance from the center* indicates the relative amplitude of seasonal variation. *Direction from the center* indicates the month (J-D=January-December) of peak amplitude. LYM=acute lymphocytic leukemia, MYE=acute myelocytic leukemia, NOS=acute leukemia, histology not otherwise specified. *Shaded area* is a 95% confidence region for MON leukemia.

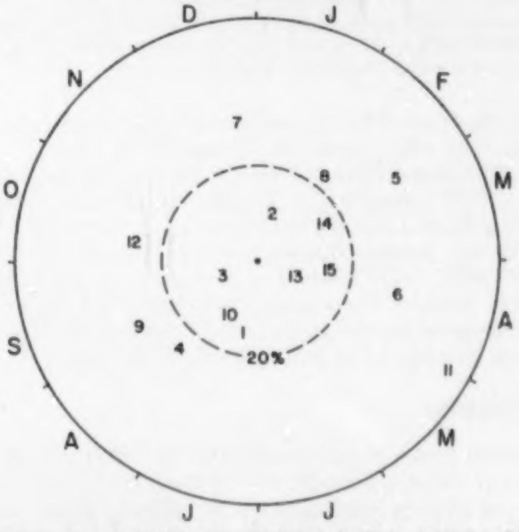

Text-figure 3.—Acute leukemia: Timing and relative intensity of fitted sine curves by U.S. region. SEER-TNCS reporting regions show no pattern of seasonality that has any ready geographic interpretation. *Distance from the center* indicates the relative amplitude of seasonal variation. *Direction from the center* indicates the month (J-D=January-December) of peak amplitude. 1) San Francisco, 2) Detroit, 3) Iowa, 4) Atlanta, 5) Connecticut, 6) Hawaii, 7) New Mexico, 8) New Orleans, 9) Seattle, 10) Utah, 11) Birmingham, 12) Colorado, 13) Dallas, 14) Minneapolis, and 15) Pittsburgh. None of the points has a confidence region that excludes zero relative amplitude.

TABLE 2.—*CCPDS acute monocytic leukemia cases by month of diagnosis and by age at diagnosis*

Month	Total	Age at diagnosis, yr					
		0–2	3–9	10–19	20–49	50–69	≥70
January	9	1	0	1	4	2	1
February	3	1	0	0	0	2	0
March	12	1	0	1	1	6	3
April	6	1	0	1	2	1	1
May	9	0	1	1	3	4	0
June	11	0	0	1	4	5	1
July	6	2	0	1	1	2	0
August	11	2	1	0	3	2	3
September	11	0	1	1	5	1	3
October	8	1	0	0	1	2	4
November	6	1	0	1	2	1	1
December	12	2	0	2	3	5	0

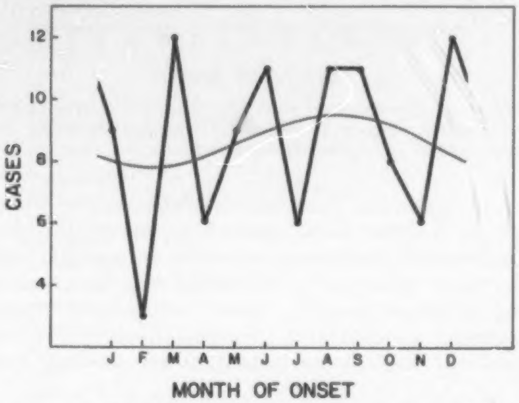

TEXT-FIGURE 4.—Observed number of cases of acute monocytic leukemia in CCPDS by month of diagnosis (*solid line*) and the best-fitting sinusoidal curve (*dotted line*). J–D=January–December.

on methods for detecting seasonality other than those of Nelson et al. (*16*) summarized in text-figures 1 and 2.

CCPDS data on acute monocytic leukemia for the period July 1, 1977, through June 30, 1981, are shown in table 2 and text-figure 4. Counts refer to new patients entering the CCPDS, i.e., patients diagnosed within a month of coming to a CCPDS center where they received their first cancer-directed therapy. There were 104 eligible patients, whose distribution of months of diagnosis showed no trace of the seasonal patterns noted in the TNCS–SEER data.

DISCUSSION

Common acute leukemias noted in the TNCS and SEER reporting systems through 1977 showed no consistent or even suggestive seasonal patterns of incidence. Acute monocytic leukemia, which accounts for about 5% of all acute leukemias, did show a distinct late winter peak of marginal statistical significance. Data from an independent source (CCPDS) failed, however, to corroborate the latter finding.

The availability of independent reporting systems with patient accruals as large as those of the SEER Program and CCPDS provides an important opportunity for cross-checking new and potentially significant findings. CCPDS does not, like the SEER Program, provide population-based data; so disease incidence rates are not calculable. However, CCPDS can generally provide relative frequencies of disease subtypes or, as in the present case, certain details of relative incidence that are unlikely to be distorted by cancer center referral patterns. Four of the 22 CCPDS centers are in SEER reporting regions; therefore, some cases are reported through both systems. In areas in which cases are reported in common, concordance is not complete, however, since catchment areas of the CCPDS centers generally extend far beyond the SEER regions within which the centers are located, and the SEER centers register all regional cases, only some of which come through the local CCPDS center. Because in the present case the overlap in calendar time between cases reported from the SEER Program and CCPDS was only 6 months and because the CCPDS data did not support the hypothesis of seasonality raised in the TNCS–SEER Program, elimination of the overlapping center-months could not substantially affect conclusions based on tables 1 and 2.

Previous reports of seasonal variation in leukemia incidence have emphasized the possibility of an infectious origin of the disease. Observations cited to support this theory have been individually very impressive, but in the aggregate contradictory. Lambin and Gerard (*1*) reported a relative amplitude of variation of more than 100%, with a winter peak in their Belgian clinic. Engelbreth-Holm (*2*) found a similar pattern (but in adults only) in Copenhagen. Several Italian investigators (*3–6*) have addressed the question of seasonality, with findings that seemed to confirm the earlier work, at least in adults. Storti and Brotto (*3*), considering all ages, found acute leukemia to peak in November and December, with a relative amplitude of variation of about 60%. Scanu (*4*) in Naples found an adult winter peak as striking as many other winter peaks previously reported and noted a summer peak in children under 12 years of age. Fantuzzi (*5*) reported the opposite of Scanu's latter finding, i.e., a pediatric winter peak, to which Gerola (*6*) added data supporting a pronounced late spring peak in children. All of these reports were based on the experience of single clinics or small geographic areas and covered periods of less than a decade. Lee (*7, 8*) employed data from the National Cancer Registration Scheme of the United Kingdom covering a period of 15 years to discover a previously unseen pattern—a more shallow summer increase found in both children and adults but restricted to acute lymphocytic leukemia. In North Carolina, Hayes (*9*) found a modest winter excess in acute leukemia cases but was unable to demonstrate any association between leukemia occurrence and the incidence of common infectious diseases. Spiers and Quade (*10*) found that childhood lymphoblastic leukemia occurrence as inferred from three separate surveys in the United States and the United Kingdom could be successfully fit to a model in which occurrence was tied to seasonality through entry into schools.

For seasonality of leukemia onsets to appear in data such as those presented here, there would have to be an agent, itself seasonally distributed, which would lead either to the onset or the diagnosis of cancer. That agent would have to be widespread geographically (covering at least large parts of SEER regions or CCPDS catchment areas), and it would have to lead to a diagnosis within a fairly short time (months rather than years) after exposure; the variability of a long preclinical period would be likely to smear out the effect even of strong seasonality in exposure times. Moreover, if the effect were to be restricted to a few age groups, it would have to result in a large relative amplitude to be detectable with any reliability. The negative results presented here then do not completely rule out an infectious role, for example, in the genesis of leukemia. However, the TNCS-SEER and CCPDS data on acute leukemia onsets are more extensive than any reported so far and probably at least as reliable; so the lack of consistent findings of seasonal fluctuation strengthens the supposition that earlier reports of annual variations in leukemia incidence were specious. These earlier reports may reflect only part of the sociology of science: Positive findings gain prominence from the natural interest of investigators, their colleagues, and the editors of journals; negative results excite less attention.

REFERENCES

(*1*) Lambin P, Gerard MJ. Variations de fréquence saisonnières de la leucémie aiguë. Sang 1934; 8:730–732.

(*2*) Engelbreth-Holm J. An die Jahreszeit gebundene Schwankungen im Vorkommen akuter Leukose. Klin Wochenschr 1935; 14:1677–1679.

(*3*) Storti E, Brotto M. Studio statistico, clinicoanatomopathologico su 157 casi di leucemia. Haematologica (Paris) 1940; 21:37–107.

(*4*) Scanu A. Frequenza stagionale delle emopatie acute e sub-acute di tipo leucemico in Campania e in Sardegna. Riforma Medica 1954; 68:449–452.

(*5*) Fantuzzi B. Sull'incidenza stagionale della leucemia acuta nel bambino. Minerva Pediatr 1955; 7:604–606.

(*6*) Gerola M. Contributo statistico sull'andamento stagionale delle leucemie. Aggiorn Pediatr 1958; 9:187–189.

(*7*) Lee JA. Seasonal variation in the clinical onset of leukaemia in young people. Br Med J 1962; 3:1737–1738.

(*8*) ———. Seasonal variation in leukaemia incidence. Br Med J 1963; 3:623.

(*9*) Hayes DM. The seasonal incidence of acute leukemia. Cancer 1961; 28:1301–1305.

(*10*) Spiers PS, Quade D. On the question of an infectious process in the origin of childhood leukemia. Biometrics 1970; 26:723–736.

(*11*) Cutler SJ, Young JL Jr, eds. Third National Cancer Survey: Incidence data. Natl Cancer Inst Monogr 1975; 41:1–454.

(*12*) Young JL Jr, Percy C, Asire AJ, eds. Surveillance, epidemiology, and end results: Incidence and mortality, 1973–77. Natl Cancer Inst Monogr 1981; 57:1–1082.

(*13*) National Center for Health Statistics. International classification of diseases. Eighth revision. Washington, D.C.: U.S. Govt Print Off, 1967 (PHS publication No. 1693).

(*14*) Edwards JH. The recognition and estimation of cyclic trends. Ann Hum Genet 1961; 25:83–87.

(*15*) McCain LJ, McCleary R. The statistical analysis of the simple interrupted time-series quasi experiment. In: Cook TD, Campbell DT, eds. Quasi-experimentation. Chicago: Rand McNally, 1979.

(*16*) Nelson W, Tong YL, Lee J-K, Halberg F. Methods for cosinor-rhythmometry. Chronobiologia 1979; 6:305–323.

(*17*) Feigl P, Breslow NE, Laszlo J, Priore RL, Taylor WF. U.S. Centralized Cancer Patient Data System for uniform communication among cancer centers. JNCI 1981; 67:1017–1024.

(*18*) World Health Organization. International classification of diseases for oncology. 3d ed. Geneva, Switzerland, 1976.

blank page

Probable Clonal Origin of Neurofibrosarcoma in a Patient With Hereditary Neurofibromatosis[1,2,3]

Jan M. Friedman, *M.D., Ph.D.,*[4] **Philip J. Fialkow,** *M.D.,*[5,6] **Claudia L. Greene,** *M.D.,*[7] *and* **Michael N. Weinberg,** *M.D.*[8,9]

ABSTRACT—A neurofibroma, a fibroma, a primary neurofibrosarcoma, and four neurofibrosarcoma metastases from a woman with hereditary neurofibromatosis who was heterozygous (Gd^{B}/Gd^{A-}) for the X-linked enzyme glucose-6-phosphate dehydrogenase were studied to determine the number of cells from which the tumors developed. Both enzyme types were observed in the benign tumors in proportions similar to those present in seven different normal tissues studied. These findings indicated that the benign tumors arose from many cells. In marked contrast, only type A activity was detected in the primary neurofibrosarcoma and in all of the metastases. Two or more steps probably were involved in the development of neurofibrosarcoma in this patient: the inherited genetic mutation producing neurofibromatosis and a rare event or combination of events that permitted a single cell to undergo malignant proliferation.—JNCI 1982; 69:1289–1292.

Hereditary neurofibromatosis (von Recklinghausen's disease) is one of the most common human autosomal dominant diseases. Patients with this disorder characteristically have many benign soft tissue tumors containing excessive disorganized overgrowths of Schwann's cells associated with perineural and endoneural elements. These neurofibromas, which may be hamartomas rather than true neoplasms, have been shown to arise from many cells in patients with hereditary neurofibromatosis (*1*). This finding contrasts with the apparent clonal development of most studied neoplasms (*2, 3*).

Neurofibrosarcomas arise in at least 2–3% of all patients with hereditary neurofibromatosis (*4, 5*) and may be even more common in older patients (*6*). To investigate carcinogenesis in hereditary neurofibromatosis, we studied benign and malignant tumors from a woman with this disease who was heterozygous at the X-linked G-6-PD locus. Because one X-chromosome in each somatic cell in a female is inactive, a given cell expresses the products of only one of the two X-chromosomes. In women heterozygous for electrophoretic variants of G-6-PD, normal tissues consist of a mixture of cells expressing type A enzyme and cells expressing type B enzyme. With this cell marker system, it is possible to determine if a neoplasm in a heterozygous woman is clonal, i.e., exhibits only type A *or* type B enzyme, or has multicellular origin, in which case it may exhibit *both* enzyme types. Single-cell origin implies that a neoplasm developed as a result of a rare event (e.g., somatic mutation) or a rare series of events. In contrast, multiple-cell origin suggests that a tumor arose by a process involving many cells, e.g., overstimulation by a circulating substance such as nerve growth factor (*7*).

METHODS

Patient report.—A 28-year-old black woman was diagnosed as having hereditary neurofibromatosis after rectal nodules were found on pelvic examination. She had mild scoliosis, many cafe au lait spots, axillary freckling, and several subcutaneous nodules. The patient's mother and brother were known to have the same disorder, and one of her children had several cafe au lait spots noted at birth.

In December 1978, the patient developed paresthesia and hyperesthesia in association with a right forearm mass, which had been enlarging for about a year. On January 22, 1979, the mass was removed along with a small muscular branch of the median nerve from which it apparently arose. The tumor measured 8×5.5 cm and was found on histologic examination to be a neurofibrosarcoma. The contiguous nerve was thickened along several branches into a plexiform neurofibroma.

During the next few months, a large, painful tumor reappeared at the site of previous surgery. On June 13, 1979, amputation of the right arm above the elbow was performed. The tumor, which was 13 cm in diameter, involved all of the flexor muscles of the forearm but not the median nerve. Microscopically, the tumor was a high-grade neurofibrosarcoma (fig. 1) with evidence of invasion of muscle. Portions of this tumor were tested for G-6-PD phenotype.

The patient recovered from surgery uneventfully. About 2 months later she noted that a mass that had been present on her left chest for some time was enlarging rapidly. On August 16, 1979, this mass was removed. The well-encapsulated, 10-cm tumor was a typical neurofibroma with

---

Abbreviation used: G-6-PD=glucose-6-phosphate dehydrogenase.

---

[1] Received June 25, 1982; accepted August 4, 1982.

[2] Supported by The Veterans Administration and by Public Health Service grant CA-16448 from the National Cancer Institute.

[3] Research procedures were in accord with the ethical standards of the Human Research Review Committee, The University of Texas Health Science Center at Dallas.

[4] Division of Clinical Genetics, Department of Obstetrics and Gynecology, and the Cecil H. and Ida Green Center for Reproductive Biology, The University of Texas Health Science Center at Dallas, 5323 Harry Hines Blvd., Dallas, Tex. 75235.

[5] Medical Service, Veterans Administration Medical Center, 4435 Beacon Ave. South, Seattle, Wash. 98108.

[6] Department of Medicine, University of Washington, Seattle, Wash. 98195.

[7] Department of Pathology, Baylor University Medical Center, Dallas, Tex. 75246.

[8] Department of Pathology, Good Samaritan Hospital, Dayton, Ohio 45406.

[9] We are grateful for the technical assistance of Mr. John Maxey, The University of Texas Health Science Center, and Mr. Gabe Herner, University of Washington.

TABLE 1.—*Relative amounts of G-6-PD enzymes types*[a] *in normal tissues and benign and malignant tumors*[b]

Specimen	Relative percent of G-6-PD enzyme types in sample No.:										
	1	2	3	4	5	6	7	8	9	10	11
Normal tissues											
White blood cells	50	50									
Muscle	40	40	50	40							
Skin	50										
Lungs	35	40									
Liver	35	35	35	35	50	50					
Rectum	50	50									
Pancreas	50	50	50								
Benign tumors											
Neurofibroma, left chest wall	60	50	60	50	60	60	60	65			
Fibroma, rectum	35	35									
Malignant tumors											
Neurofibrosarcoma, right forearm	100	100	100	100							
Lung metastasis #1	100	100	100	100	100						
Lung metastasis #2	100	100	100	100	75	100	100	100	100	100	100
Liver metastasis # 1	100	100	100	100							
Liver metastasis # 2	100	100									

[a] Expressed as visually estimated percentage of total G-6-PD activity (A-type + B-type) present in the A-enzyme band.

[b] Typing of red blood cells indicates that this patient is Gd^B/Gd^{A-}.

myxoid degeneration. This tumor was also tested for G-6-PD phenotype.

The patient was subsequently noted to have another rapidly enlarging mass, this time involving the left thigh. Biopsy on February 15, 1980, revealed neurofibrosarcoma. This tumor, which is believed to have been a second primary cancer, was resected on March 27, 1980. The tumor was 6.4 cm in diameter and was found to be a neurofibrosarcoma with patchy lymphocytic infiltration throughout. The neoplasm was associated with several plexiform neurofibromas.

The patient died of metastatic disease involving the lungs, liver, pancreas, intestines, and bones on October 14, 1980. Post mortem, metastatic nodules of typical neurofibrosarcoma removed from the liver and lung were tested for G-6-PD phenotype. A rectal fibroma was also removed and tested.

Specimens.—Tumor specimens were prepared and analyzed for G-6-PD phenotype by starch gel and cellulose acetate electrophoresis as previously described (*8–11*). We estimated the ratio of A:B G-6-PD activity by visually using prepared standards as controls (*11*). Because there was excellent agreement between the methods, only the data from the starch gels were reported. All specimens included in table 1 were free from appreciable gross contamination with blood or microscopic vascular invasion or lymphocytic infiltration. Red cell and buffy coat preparations from peripheral blood, samples of uninvolved muscle and skin from the right forearm and left chest, respectively, and samples of normal lung, liver, rectum, and pancreas were also studied.

RESULTS

The results of the electrophoretic G-6-PD assays are shown in table 1. Both types A and B enzymes were found in all normal tissues studied, indicating that the patient is heterozygous for G-6-PD. Approximately equal amounts of both enzyme types were also observed in the benign tumors. In contrast, only A-type G-6-PD was detected in the primary neurofibrosarcoma from the right forearm and in all the neurofibrosarcoma metastases.

DISCUSSION

The finding of a double-enzyme phenotype in the benign neurofibroma and fibroma from this patient with hereditary neurofibromatosis is consistent with the conclusion that such growths develop from many cells. Other possible explanations for a double-enzyme phenotype are very unlikely (*1*).

In marked contrast to the double-enzyme phenotype found for this hereditary neurofibroma and for all 14 similar tumors previously reported (*1*), the primary neurofibrosarcoma from this patient's right forearm and all four neurofibrosarcoma metastases studied exhibited single-enzyme phenotypes. The finding of a single-enzyme phenotype in these malignant tumors is consistent with clonal origin of neurofibrosarcoma in this patient. However, a single-enzyme phenotype could also occur in a neoplasm of multicellular origin if cells containing one or the other active X-chromosome had a marked selective advantage or if the normal cells from which the tumor arose were arranged in large patches of contiguous cells of a single-enzyme type. Neither of these last two possibilities seems likely because the large, rapidly growing but benign neurofibroma in this same patient exhibited a double-enzyme phenotype similar to that of adjacent normal tissues (capsule and skin; table 1). Thus the malignant neoplasm probably developed from a single transformed cell.

Our demonstration that benign hereditary neurofibroma arises from many cells whereas neurofibrosarcoma is clonal is consistent with the hypothesis that malignant transformation is a multistep process. One possibility, suggested by Knudson and Meadows (*12*), is that hereditary neurofibromas are collections of neural crest-derived cells that form benign tumors because their normal development is altered by the inherited mutation. One or more further events within such premalignant cells might result in transformation into neurofibrosarcoma. The intimate association of the neurofibrosarcomas with neurofibromas in this patient suggests that malignant transformation did indeed occur within preexisting neurofibroma cells.

Several possible mechanisms exist that, acting alone or in combination, might produce a clonal cancer within a neurofibroma. First, one cell might have become transformed because of a rare alteration, e.g., a "spontaneous" somatic mutation or a specific chromosomal rearrangement. Second, malignant transformation might have resulted from a series of events, each of which involved several cells, but which occurred in such a manner that any single cell was very unlikely to undergo the entire requisite set. Finally, all cells of a neurofibroma might be potentially malignant, but escape of a cell from normal tumor surveillance or control mechanisms might be rare. Available data do not permit favoring any one of these pathogenic models over the others. However, the data clearly support the hypothesis that development of neurofibrosarcoma in this patient was a multistep process. The first step was genetic—the inherited autosomal mutation that causes neurofibromatosis. A rare event or combination of events then occurred in a cell, permitting it to undergo malignant neoplastic proliferation.

REFERENCES

(*1*) Fialkow PJ, Sagebiel RW, Gartler SM, Rimoin DL. Multiple cell origin of hereditary neurofibromas. N Engl J Med 1971; 284:298-300.

(*2*) Fialkow PJ. The origin and development of human tumors studied with cell markers. N Engl J Med 1974; 291:26-35.

(*3*) ———. Clonal origin of human tumors. Ann Rev Med 1979; 30:135-143.

(*4*) Crowe FW, Schull WJ, Neel JV. A clinical, pathological and genetic study of multiple neurofibromatosis. Springfield, Ill.: Thomas, 1956.

(*5*) D'Agostino AN, Soule EH, Miller RH. Sarcomas of the peripheral nerves and somatic soft tissues associated with multiple neurofibromatosis (von Recklinghausen's disease). Cancer 1963; 16:1015-1027.

(*6*) Brasfield RD, Das Gupta TK. Von Recklinghausen's disease: A clinicopathological study. Ann Surg 1972; 175:86-104.

(*7*) Schenkein I, Bueker ED, Helson L, Axelrod F, Dancis J. Increased nerve-growth-stimulating activity in disseminated neurofibromatosis. N Engl J Med 1974; 290:613-614.

(*8*) Fildes RA, Parr CW. Human red-cell phosphogluconate dehydrogenases. Nature 1963; 200:890-891.

(*9*) Fialkow PJ, Gartler SM, Yoshida A. Clonal origin of chronic myelocytic leukemia in man. Proc Natl Acad Sci USA 1967; 58:1468-1471.

(*10*) Sparkes RS, Baluda MC, Townsend DE. Cellulose acetate electrophoresis of human glucose-6-phosphate dehydrogenase. J Lab Clin Med 1969; 73:531-534.

(*11*) Fialkow PJ. Primordial cell pool size and lineage relationships of five human cell types. Ann Hum Genet 1973; 37:39-48.

(*12*) Knudson AG, Meadows AT. Regression of neuroblastoma IV-S: A genetic hypothesis. N Engl J Med 1980; 302:1254-1256.

FIGURE 1.—Neurofibrosarcoma from the patient's right forearm. This was an aggressive spindle cell tumor composed of wavy, small cells with pleomorphic, bizarre nuclei and a high mitotic rate. Hematoxylin and eosin. *Bar*=0.10 mm. × 600

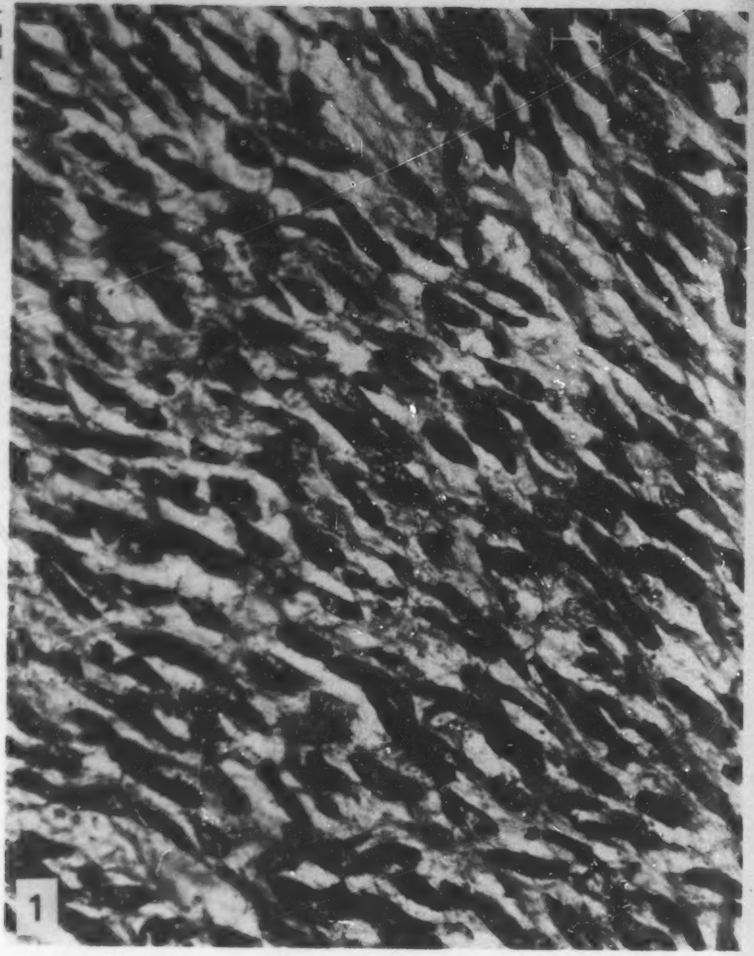

Accessory Cell Function in Tumor-Bearing Mice and Effects of *Corynebacterium parvum* [1,2,3]

Seiya Okuda,[4] **Kazuto Taniguchi,**[4] **Chiharu Kubo,**[5] *and* **Kikuo Nomoto**[4]

ABSTRACT—Primary in vivo production of antibody to sheep red blood cells (SRBC) was consistently suppressed in EL 4 tumor-bearing C57BL/6 mice, but the secondary response was not suppressed. This suppressed primary in vivo production of antibody was partially restored by systemic administration of *Corynebacterium parvum*. For investigation of the mechanism of the immunosuppression in tumor-bearing mice and the effects of *C. parvum*, the accessory cell function of adherent cells from tumor-bearing mice and *C. parvum*-treated tumor-bearing mice in in vitro cultures was studied. Peritoneal and splenic cells from tumor-bearing mice were less efficient in promoting in vitro production of antibody to SRBC by macrophage-depleted normal nonadherent cells than the adherent cells from normal mice. *C. parvum* treatment restored the accessory cell function of splenic adherent cells from tumor-bearing mice but not that of peritoneal cells. Furthermore, adherent cells from tumor-bearing mice did not show suppressive activity against the in vitro plaque-forming cell response.—JNCI 1982; 69:1293–1297.

Many reports are concerned with depressed immune responses in tumor-bearing mice, but the mechanism of immunosuppression in the tumor-bearing state is not completely understood since the immune response requires various types of cells.

Functional abnormalities of macrophages, including defective mobility and chemotaxis (*1–3*), impaired inflammatory response (*4, 5*), and increase and decrease in phagocytic activity (*6, 7*) have been found in tumor-bearing individuals. However, little information exists about the accessory cell function for the induction of immune responses in tumor-bearing mice.

We (*8*) previously reported that depressed immune responses in EL 4 tumor-bearing C57BL/6 mice are restored by treatment with *Corynebacterium parvum* or by in vivo transfer of splenic adherent cells of *C. parvum*-treated normal mice. *C. parvum* has been shown to exert a stimulatory effect on the function of accessory cells (*9, 10*). These results suggest that immunosuppression in tumor-bearing mice may be due to the suppression of the accessory cell function of adherent cells from EL 4 tumor-bearing mice in in vitro culture and from the effects of *C. parvum* treatment on these cells.

MATERIALS AND METHODS

Animals.—Male mice of an inbred C57BL/6 strain were obtained from the Breeding Unit of Kyushu University and used at 8 weeks of age. Each experimental group included 8–10 mice.

Tumor.—EL 4 tumor, a thymus-deprived benzo[*a*]pyrene-induced lymphoma of C57BL/6 origin, has been maintained in the ascites form through syngeneic C57BL/6 mice. After sc inoculation of 10^6 cells into the right flanks of C57BL/6 mice, palpable tumors appeared in a few days, grew progressively, and killed all the hosts within 2 weeks.

Antigen.—SRBC were obtained from the Laboratory of Biotest (Tokyo, Japan).

In vivo immunization.—Mice were inoculated ip with 10^8 SRBC in saline. For primary immunization in the tumor-bearing state, mice received injections of SRBC 4, 8, or 10 days after tumor inoculation. For secondary immunization in the tumor-bearing state, mice were inoculated with tumor cells 20 days after the primary immunization and with SRBC 4, 8, or 10 days later.

C. parvum *injections.*—A suspension of heat- and Formalin-killed *C. parvum* (IM1585; Institute Merieux 17, Lyon, France) containing 2 mg organisms/ml was obtained commercially. Mice were inoculated ip with various doses of this suspension 7 days before in vivo immunization or before cell harvest for in vitro culture. (In our preliminary experiments, *C. parvum* showed a maximal effect for 7–10 days after injection.)

Assay of PFC.—Spleen cells were obtained 5 days after primary immunization or 3 days after secondary immunization. The number of PFC against SRBC in individual mice was determined by the method of Cunningham and Szenberg (*11*). Indirect PFC were developed in rabbit anti-mouse immunoglobulin serum (Institute for Medical Biology, Nagoya, Japan) and enumerated according to the method of Dresser and Greaves (*12*).

Preparation of splenic and peritoneal adherent cells.—We exposed mice to 1,300 rad of whole-body radiation 24 hours before in vitro culture to eliminate lymphocytes and tumor cells. X-rays were delivered with a Shimazu 250-kVp machine operating at 200 kVp with 0.3-mm copper and 1-mm aluminum filters. Spleen cells were suspended at 2×10^7/ml in HBSS and incubated in a glass petri dish at 37°C for 1 hour in a 5% CO_2 atmosphere. Nonadherent cells were removed with a rubber policeman. Peritoneal exudate cells were harvested by irrigation of the peritoneal cavity with HBSS 2 days after an ip injection of 2 ml of 10% sterile

---

ABBREVIATIONS USED: HBSS=Hanks' balanced salt solution; kVp=kV peak; LDV=lactate dehydrogenase virus; 2-ME=2-mercaptoethanol; SRBC=sheep red blood cells.

---

[1] Received June 18, 1981; revised June 29, 1982; accepted July 16, 1982.

[2] Supported by a Grant-In-Aid from the Ministry of Education, Science and Culture, Japan.

[3] Guidelines for the care and use of laboratory animals were followed as set forth by the Breeding Unit of Kyushu University.

[4] Department of Immunology, Cancer Research Institute, School of Medicine, Kyushu University, Maidashi 3-1-1, Higashi-ku, Fukuoka, Japan 812.

[5] Department of Microbiology, School of Medicine, Kyushu University.

TABLE 1.—*Primary and secondary in vitro production of antibody to SRBC in tumor-bearing mice*

Source of spleen cells	Days after tumor inoculation[a]	Primary antibody production, direct PFC/10^6 cells[b]	Secondary antibody production, indirect PFC/10^6 cells[c]
Normal mice	—	3,160±253	5,021±456
Tumor-bearing mice	4	1,781±208	4,887±715
Tumor-bearing mice	8	836±94	5,224±683
Tumor-bearing mice	10	847±92	4,563±875

[a] C57BL/6 mice were primarily or secondarily immunized with SRBC (1×10^8) 4, 8, or 10 days after tumor inoculation.

[b] Spleen cells were obtained 5 days after immunization. Values are means ± SD.

[c] Mice were inoculated with tumor cells 20 days after primary immunization. Spleen cells were obtained 3 days after secondary immunization. Values are means ± SD.

proteose peptone (Difco Laboratories, Detroit, Mich.). Peritoneal adherent cells were prepared in the same manner as splenic adherent cells.

Preparation of nonadherent cells.—Adherent cells were removed from normal or primed spleen cells by passage through an SG-10 column prepared according to the method of Ly and Mishell (*13*) with some modification. Swollen, washed, autoclaved SG-10 (3 g, dry wt; Pharmacia Chemicals AB, Uppsala, Sweden) was loaded into a sterile plastic 10-ml syringe packed with 2 ml of glass wool. The column was washed repeatedly with a total of 30 ml HBSS and loaded with spleen cells suspended in HBSS at $1\text{-}2\times10^7$/ml. The initial cell specimens usually contained 10–15% macrophages as estimated by latex particle injection assay. After one passage through the column, the cell suspensions contained less than 1% macrophages. Spleen cells were used as a nonadherent cell population after three passages.

In vitro culture.—The test for in vitro PFC response to SRBC was conducted according to the method of Mishell and Dutton (*14*). RPMI-1640 (GIBCO, Grand Island, N. Y.) supplemented with 10% heat-inactivated fetal calf serum, 20 m*M* HEPES[6] (Dojin Chemical Laboratory, Kumamoto, Japan), 100 U penicillin/ml, and 100 μg streptomycin/ml and adjusted to pH 7.2 with $NaHCO_3$ was used as culture medium. In some experiments, 2-ME was added to the cultures (5×10^{-5} *M*). The nonadherent cells obtained by SG-10 column separation were used as responder cells. The immunizing SRBC were washed three times and added to the culture. The adherent cells prepared as described above were added in various ratios. For in vitro culture, 1×10^6 nonadherent cells, 2×10^5 SRBC, and $1\text{-}10\times10^4$ adherent cells were suspended together in 0.3 ml of culture medium in a well of a culture plate (A/S Nunc, Roskilde, Denmark) and cultured in a humidified atmosphere containing 5% CO_2 in air for 5 days. We used 40 wells for each experimental group. At the time of harvest, the cells were resuspended by gentle agitation. The cell suspensions from eight wells were pooled, centrifuged at 1,000 rpm for 10 minutes, at 4°C, and incubated with SRBC and complement for 1 hour in a Cunningham chamber. The mean numbers of PFC were calculated from the numbers of PFC in five Cunningham chambers.

Statistical analyses.—The standard Student's *t*-test was used for the determination of statistical significance.

RESULTS

Primary and secondary production of antibody to SRBC in tumor-bearing mice.—Mice were primarily or secondarily immunized as described in "Materials and Methods." Spleens were obtained 5 days after primary immunization or 3 days after secondary immunization (table 1). The primary response assayed by production of direct PFC was consistently depressed in the tumor-bearing mice compared with that in normal control mice ($P<0.001$). The degree of the suppression was marked in the late stages of tumor bearing, 8 or 10 days after tumor inoculation. However, the secondary response, assayed by production of indirect PFC, in the tumor-bearing mice was at almost the same level as that in normal mice. These results were confirmed by two other experiments (data not shown).

Effect of C. parvum *on suppressed primary production of antibody in tumor-bearing mice.*—Mice received various injected doses of *C. parvum* and SRBC 1 and 8 days after tumor inoculation, respectively. The suppressed direct PFC response in tumor-bearing mice was restored to some extent by the injection of 0.5 mg or by more of *C. parvum* ($P<0.005$) (table 2). The results showed that the optimal doses of *C. parvum* were 0.5 or 1.0 mg.

Accessory cell function of tumor-bearing mice in in vitro antibody production.—Accessory cell functions of peritoneal and splenic adherent cells from normal and tumor-bearing mice were investigated in an in vitro culture system. Macrophage-depleted normal spleen cells were cultured, and various numbers of peritoneal or splenic adherent cells from normal and tumor-bearing mice were added to this culture (text-fig. 1). When the ratio of responding nonadherent cells to added adherent cells was 10:1, the direct PFC response was very weak irrespective of the origin of the adherent cells. The effect of peritoneal adherent cells on the restoration of

TABLE 2.—*Restorative effect of* C. parvum *on suppressed in vivo production of antibody to SRBC in tumor-bearing mice*

Source of spleen cells	Dose of *C. parvum*, mg	Direct PFC, 10^6/cells[a]		
		Expt I	Expt II	Expt III
Normal mice	—	3,854±545[c]	5,264±324	4,025±461
C. parvum-treated normal mice	0.5	—	—	4,736±694
Tumor-bearing mice[b]	—	1,035±87	1,216±248	1,120±227
C. parvum-treated tumor-bearing mice[c]	0.1	974±151	1,392±164	—
	0.25	1,369±402	1,325±648	—
	0.5	2,243±648	3,241±1,028	2,667±742
	1.0	3,204±862	2,369±246	—
	2.0	1,501±248	2,249±824	—

[a] Values are means ± SD.

[b] C57BL/6 mice were immunized with SRBC 8 days after tumor inoculation. Number of PFC was determined 5 days after immunization.

[c] *C. parvum* was injected ip 1 day after tumor inoculation.

---

[6] 4-(2-Hydroxyethyl)-1-piperazine ethanesulfonic acid.

the PFC response was stronger than that of splenic adherent cells, when these cells were obtained from normal mice. The ability to restore the PFC response was slightly depressed in peritoneal and splenic adherent cells obtained 4 days after tumor inoculation and markedly depressed in those obtained 8 or 10 days after tumor inoculation ($P<0.005$). The numbers of PFC in the cultures to which 2-ME was added were similar to those in the cultures without 2-ME.

Lack of suppressive effect of adherent cells from tumor-bearing mice on in vitro culture.—To determine whether adherent cells of tumor-bearing mice include suppressor macrophages that actively depress in vitro antibody production, adherent cells were obtained 8 days after tumor inoculation and added to the cultures with the same number of adherent cells from normal mice (table 3). The number of direct PFC in the culture to which both cells were added was similar to that in the culture to which only normal adherent cells were added, suggesting that adherent cells from tumor-bearing mice do not possess suppressive activity in in vitro cultures.

Restorative effect of C. parvum *on depressed accessory cell function.*—To determine the effect of *C. parvum* on the depressed accessory cell function in tumor-bearing mice, peritoneal or splenic adherent cells from *C. parvum*-treated tumor-bearing mice were added to nonadherent responding cells (table 4). The donors of adherent cells were inculated with tumor cells 8 days and with *C. parvum* 7 days before cell harvest. The ability of the peritoneal and splenic adherent cells to restore the in vitro PFC response was partially suppressed in tumor-bearing mice. *C. parvum* treatment of the donors restored the ability of splenic adherent cells of tumor-bearing mice to respond ($P<0.005$) but had no effect on their peritoneal adherent cells. The level of response of splenic adherent cells in *C. parvum*-treated tumor-bearing mice did not reach that of splenic adherent cells in the normal control mice. Other experiments showed that the adherent cells from *C. parvum*-treated normal mice produced a similar number of PFC to that of normal mice when they were added to the cultures (data not shown). These results suggested that *C. parvum* may have restored the accessory cell function of spleen adherent cells from tumor-bearing mice.

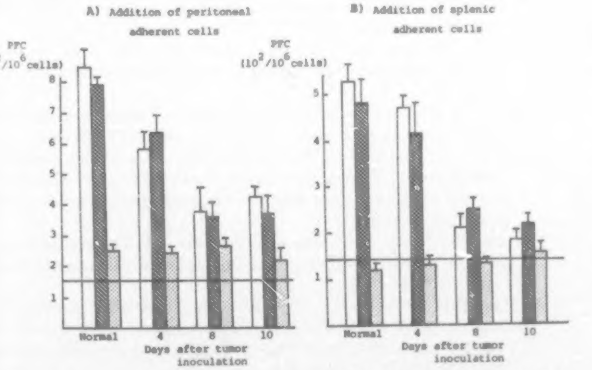

TEXT-FIGURE 1.—Depressed accessory cell function of peritoneal and spleen cells from tumor-bearing mice in in vitro production of antibody to SRBC by macrophage-depleted normal spleen cells. The 1×10^6 nonadherent cells and 2×10^5 SRBC were suspended together in 0.3 ml culture medium in a well and cultured for 5 days. Adherent cells were obtained 4, 8, or 10 days after tumor inoculation and added to the wells at concentrations of 1×10^4 (□), 2×10^4 (▩), and 10×10^4 (▨). *Horizontal line* represents the mean PFC of the culture without adherent cells. *Vertical lines* represent standard deviations.

TABLE 3.—*Lack of suppressive effect of adherent cells from tumor-bearing mice on in vitro culture*[a]

Addition of cells		Direct PFC, 10^6 cells[b]
Cell lot	Cells	
1	10^4 peritoneal adherent cells from normal mice	982±121
2	10^4 peritoneal adherent cells from tumor-bearing mice[c]	409±42
3	Lot 1 + lot 2	1,128±98
4	10^4 splenic adherent cells from normal mice	631±49
5	10^4 splenic adherent cells from tumor-bearing mice[c]	121±44
6	Lot 4 + lot 5	682±35
7	None	75±10

[a] The 1×10^6 nonadherent cells and 2×10^5 SRBC were suspended together in 0.3 ml culture medium in a well and cultured for 5 days.

[b] Values are means ± SD.

[c] Peritoneal and splenic cells were obtained from tumor-bearing mice 8 days after tumor inoculation.

TABLE 4.—*Restorative effect of* C. parvum *on depressed accessory cell function of splenic adherent cells from tumor-bearing mice in in vitro antibody production*[a]

Added cells, 10^4/well	Direct PFC, 10^6 cells[b]	
	Expt I	Expt II
Peritoneal adherent cells from normal mice	769±64	1,017±60
Peritoneal adherent cells from tumor bearing mice[c]	427±42	428±50
Peritoneal adherent cells form *C. parvum*-treated tumor-bearing mice[d]	397±32	448±31
Splenic adherent cells from normal mice	498±20	698±65
Splenic adherent cells from tumor-bearing mice[c]	228±18	267±19
Splenic adherent cells from *C. parvum*-treated tumor-bearing mice[d]	366±47	512±26
None	93±27	149±30

[a] The 1×10^6 nonadherent cells and 2×10^5 SRBC were suspended together in 0.3 ml of culture medium in a well.

[b] Values are means ± SD.

[c] Peritoneal and splenic cells were obtained from tumor-bearing mice 8 days after tumor inoculation.

[d] *C. parvum* was injected ip 7 days before in vitro culture.

DISCUSSION

Primary in vivo production of antibody to SRBC was suppressed in tumor-bearing mice (table 1). The immunosuppresssion was restored to some extent by systemic administration of *C. parvum*. In in vitro culture, adherent cells from the peritoneal cavity and spleen of tumor-bearing mice did not restore the ability of nonadherent cells to produce antibody against SRBC (text-fig. 1).

Administration of *C. parvum* restored the accessory cell function of such splenic adherent cells but not of peritoneal adherent cells (table 4). These results suggest that immunosuppression in tumor-bearing mice may be related to the depression of the function of macrophages as accessory cells and that the restoration of the depressed immune reaction by *C. parvum* treatment may be due to an adjuvant effect of *C. parvum* on the accessory cell function of splenic adherent cells.

The results in our previous (*8*) and present studies and those of Joshua et al. (*15*) suggest that depression of immune responses in tumor-bearing mice may be due at least in part to the depressed function of accessory cells. However, the mechanisms of such a depression are not clearly understood. There are several possible explanations for the phenomenon. Macrophages capable of functioning as accessory cells may accumulate primarily around the tumor and become scarce in the splenic or peritoneal cavity. Alternatively, binding of the complex of antibodies against tumors and tumor antigens on the surface of accessory cells may block antigen-binding sites of the cells. We have no evidence to support any explanation strongly; many other mechanisms can be suggested.

Multiply passed tumors such as EL 4 are reported to be contaminated with LDV (*16*). Some investigators (*17, 18*) have shown that macrophage function is severely depressed in LDV-infected mice. To examine mice bearing EL 4 tumors for the presence of LDV, we measured lactate dehydrogenase activity in their sera and found that it was less than twice that in normal mice. Therefore, we do not think that the EL 4 tumor was contaminated with LDV.

Some investigators emphasize the role of suppressor macrophages in immunosuppression in tumor-bearing mice (*19, 20*). To determine whether adherent cells from tumor-bearing mice included suppressor macrophages in our in vitro experiments, we studied the effects of adherent cells from tumor-bearing mice on in vitro antibody production by nonadherent spleen cells supplemented with normal adherent cells. The number of PFC in this culture was similar to that in the culture to which only normal adherent cells were added. These results suggest that suppressor macrophages are not involved in the depressed PFC response, at least in our system.

In the secondary response, the PFC response was not affected by the tumor-bearing state. This finding is in agreement with reports by Zolla (*21*) and Kamo and Friedman (*22*). Pierce (*23*) reported that macrophage dependency is lower in the secondary response than in the primary response. The difference in the suppressive effect between the primary and secondary response in our study may be explained by a difference in the requirement for macrophages to process and present antigen.

C. parvum is able to stimulate phagocytosis, increase resistance to infection, stimulate antibody response, and augment antitumor activity. Many of these phenomena have been shown to be due to macrophage functions activated by *C. parvum*. Wiener (*9*) showed that macrophages of *C. parvum*-treated mice are more effective than normal macrophages in promoting in vitro response to SRBC by macrophage-depleted spleen cells. Furthermore, Wiener and Bandieri (*10*) reported that *C. parvum*-activated macrophages retained much antigen on their surfaces, which intensified the presentation of antigen to lymphocytes. Such a mechanism may contribute to the restorative effect of *C. parvum* in our study. Although *C. parvum* restored the accessory function of splenic adherent cells of tumor-bearing mice in vitro, it did not restore that of peritoneal adherent cells, which may show a difference in susceptibility to *C. parvum* of splenic and peritoneal adherent cells in tumor-bearing mice. In further experiments, we are studying surface markers and morphologic changes in peritoneal and splenic adherent cells in tumor-bearing mice and *C. parvum*-treated tumor-bearing mice.

REFERENCES

(*1*) Boetcher DA, Leonard EJ. Abnormal monocyte chemotactic response in cancer patients. J Natl Cancer Inst 1974; 52:1091–1099.

(*2*) Eccles SA, Alexander P. Sequestration of macrophage in growing tumours and its effect on the immunological capacity of the host. Br J Cancer 1974; 30:42–49.

(*3*) Normann SJ, Sorkin EJ. Cell-specific defect in monocyte function during tumor growth. J Natl Cancer Inst 1976; 57:135–140.

(*4*) Bernstein ID, Zbar B, Rapp HJ. Impaired inflammatory response in tumor-bearing guinea pig. J Natl Cancer Inst 1972; 49:1641–1647.

(*5*) Snyderman R, Pike MC, Blaylock BL, Weinstein P. Effects of neoplasmas on inflammation: Depression of macrophage accumulation after tumor implantation. J Immunol 1976; 116:585–589.

(*6*) Franchi G, Innoceti IR, Standen S, Grattini S. The inhibitory effect of cancer cell dissemination on the phagocytic activity of the reticuloendothelial system in tumor-bearing mice. J Reticuloendothel Soc 1972; 12:618–628.

(*7*) Donovan AJ. Reticuloendothelial function in patients with cancer. Am J Surg 1967; 114:230–238.

(*8*) Okuda S, Taniguchi K, Kubo C, Nomoto K. Effects of *Corynebacterium parvum* on depressed immunological reactions in EL-4-tumor-bearing mice. Cancer Immunol Immunother 1981; 11:17–22.

(*9*) Wiener E. The role of macrophages in the amplified in vitro response to sheep red blood cells by spleen cells from *Corynebacterium parvum* treated mice. Cell Immunol 1975; 19:1–7.

(*10*) Wiener E, Bandieri A. Modification in the handling in vitro of ^{125}I-labeled keyhole limpet haemocyanin by peritoneal macrophages from mice pretreated with the adjuvant *Corynebacterium parvum*. Immunology 1975; 29:265–274.

(*11*) Cunningham AJ, Szenberg A. Further improvements in the plaque technique for detecting single antibody-forming cells. Immunology 1968; 14:559-600.

(*12*) Dresser DW, Greaves MF. Assay for antibody-producing cells. In: Weir DM, ed. Handbook of experimental immunology. 2d ed. Oxford: Blackwell, 1973:27.1–27.29.

(*13*) Ly IA, Mishell RI. Separation of mouse spleen cells by passage through columns of Sephadex G-10. J Immunol Methods 1974; 5:239–247.

(*14*) Mishell RI, Dutton RW. Immunization of dissociated spleen cell culture from normal mice. J Exp Med 1967; 126:423–442.

(*15*) Joshua DE, Brown G, MacLannan IC. Immune suppression in BALB/c mice bearing the plasmacytoma TEPC-183: Evidence for normal lymphocyte but defective macrophage function. Int J Cancer 1979; 23:663–672.

(*16*) Riley V, Lilly F, Huerto E, Bardell D. Transmissible agent associated with 26 types of experimental mouse neoplasms. Science 1960; 132:545–547.

(*17*) Mahy BW, Rowson KE, Parr CW, Salaman MH. Studies on the mechanism of action of Riley virus. I. Action of substances affecting the reticuloendothelial system on plasma enzyme levels in mice. J Exp Med 1965; 122:967–981.

(*18*) Rowson KE, Mahy BW, Salaman MH. Studies on the mechanism of action of Riley virus. II. Action of substances affecting the reticuloendothelial system on the level of viraemia. J Exp Med 1965; 122:983–992.

(*19*) Kolb J-P, Arrian S, Zolla-Pazner S. Suppression of the humoral immune response by plasmacytomas: Mediation by adherent mononuclear cells. J Immunol 1977; 118:702–709.

(*20*) Krakauer RS, Strober W, Waldmann TA. Hypogammaglobulinemia in experimental myeloma: The role of suppressor factors from mononuclear phagocytes. J Immunol 1977; 118:1385–1390.

(*21*) Zolla SJ. The effect of plasmacytomas on the immune response of mice. J Immunol 1972; 108:1039–1048.

(*22*) Kamo I, Friedman H. Differential immunosuppressive effects of ascites fluid from mastocytoma-bearing mice on primary vs. secondary immunocyte responses. J Immunol 1978; 120:558–562.

(*23*) Pierce CW. Immune response in vitro. I. Cellular requirements for the immune response by non-primed and primed spleen cells in vitro. J Exp Med 1969; 130:345–364.

blank page

Induction of γ-Glutamyltransferase-Positive and Nonspecific Esterase-Positive Foci in Rat Liver by Partial Hepatectomy Following Single Injection of *N*-Nitrosodiethylamine[1]

Norio Hirota,[2] Shinichi Moriyama,[2] *and* Takeshi Yokoyama[2,3]

ABSTRACT—The effect of partial hepatectomy (PH) on alteration of liver foci induced by *N*-nitrosodiethylamine (DENA) was studied in inbred F344 male rats. As early as 2 weeks after PH was performed 6 hours after an injection of 100 mg DENA/kg, γ-glutamyltransferase-positive hepatocellular foci were induced, whereas DENA alone induced no foci until 12 weeks after PH. The focus counts of the group with PH performed 6 hours after an injection of 100 mg DENA/kg were consistently greater than those of a group with PH performed at 24 hours following DENA injection. At 3 and 6 weeks after PH was done at 12 weeks following treatment with 100 or 200 mg DENA/kg, the focus count was significantly increased compared with that in nonhepatectomized groups. The results indicate that increased liver cell proliferation resulting from PH enhances the conversion of persisting DNA damage to a permanent alteration in DNA. The effect at 12 weeks after exposure supports the concept that DNA damage in hepatocytes is highly persistent.—JNCI 1982; 69:1299–1304.

In experimental hepatocarcinogenesis, initiated cells or focally altered islands of hepatocytes are recognized by varied histochemical phenotypes including *a*) positivity for GGT, deficiency for ATP or glucose-6-phosphatase and *b*) resistance to iron accumulation (*1–10*). Hirota and Williams (*11*) recently reported that most of the iron-resistant hepatocellular altered foci were persistent in nature even to the point that nodules or carcinomas developed multicentrically, and Hirota et al. (*12*) observed similar foci in hemochromatotic human livers in association with hepatocellular carcinomas. Thus such persistently altered foci might be the precursors of neoplastic nodules or carcinomas (*4, 7, 11, 13–15*).

Scherer et al. (*16*) reported that the number of altered foci detected by ATP deficiency was significantly increased by PH performed before the administration of carcinogen. Liver cancer has rarely been reported to be produced by a single administration of carcinogen to rats. This phenomenon seems to be related to the possibility that DNA damage of hepatocytes induced by a single exposure to a hepatocarcinogen is generally repaired in time. Craddock (*17, 18*), however, documented a high incidence of liver cell cancers in rats after a single treatment with a hepatocarcinogen given during the period of semisynchronized increased DNA synthesis following PH. Recently, Ishikawa et al. (*19*) reported a correlation between the time of PH after treatment with DENA followed by phenobarbital and the appearance of ATP-deficient islands in rat livers. The functionally altered foci identified by histochemical abnormalities may be composed of phenotypic hepatocytes with defective DNA or with an inappropriate form of DNA repair (misrepair) following initial DNA damage by carcinogen exposure to the liver. We hypothesize that DNA damage initiated by a limited injection of DENA may persist indefinitely to some extent and that increased DNA synthesis induced by PH may contribute to the effect of induced proliferation in converting persisting DNA damage to a permanent alteration in DNA leading to the formation of histochemically altered foci.

In the present study, we investigate the effect of PH on the formation of histochemically altered foci following the exposure to hepatocarcinogen. PH without any other subsequent treatment such as administration of phenobarbital was done at various times after DENA treatment of rats. For histochemical analysis not only GGT but also NSE was used. The data indicate that the focus formation in terms of the number and size of foci is closely related to the interval between DENA injection and PH.

MATERIALS AND METHODS

Animals and chemicals.—Inbred F344 male rats (Charles River Japan Inc., Kanagawa, Japan), weighing 180–200 g, were maintained on a high-protein (23.0%) basal diet (CRF-1; Oriental Yeast Co., Ltd., Tokyo, Japan) for at least 1 week before the experiments were begun. The animals were housed in metal cages in an air-conditioned room at 24°C with food and water available ad libitum. DENA was obtained from Tokyo Chemical Industry Co., Ltd., Tokyo. It was dissolved in a 0.9% NaCl solution and injected ip.

Experimental design.—The experimental design is shown in text-figure 1. Experiment 1 (groups 1–4) was designed to investigate the effect of PH on the evolution of initiated cells recognized by the formation of GGT-positive or NSE-positive foci. Groups 1 and 2 were given an injection of 100 mg DENA/kg body weight followed by PH with the use of the technique of Higgins and Anderson (*20*). PH was performed in group 1 at 6 hours after DENA injection and in group 2 at 24 hours after DENA injection. Group 3 received 100 mg DENA/kg but was not subjected to PH. Animals in group 4 were subjected to PH at approximately 10 weeks, the same age as that of groups 1–3, but were not treated with DENA.

ABBREVIATIONS USED: DENA=*N*-nitrosodiethylamine; 2-FAA=*N*-2-fluorenylacetamide; GGT=γ-glutamyltransferase; NSE=nonspecific esterase; PH=partial hepatectomy.

---

[1] Received July 21, 1981; revised May 23, 1982; accepted June 3, 1982.

[2] Department of Pathology, Jichi Medical School, Minamikawachi-machi, Kawachi-gun Tochigi, Japan 329-04.

[3] We thank Ms. Keiko Ohtomo for excellent assistance with the animal handling and histochemical procedures; the technical staffs of the Department of Pathology for the preparation of histological slides; and Dr. Gary M. Williams, Associate Director of Naylor Dana Institute for Disease Prevention, for reviewing the manuscript.

Five animals in group 1 were killed at weeks 2, 6, 12, and 18 after the commencement of the experiment. The same number of animals in group 2 were killed at weeks 2, 6, and 12 and in group 3 at weeks 2, 6, 12, 15, and 18. In group 4, 3 animals were killed at the same times as in group 2.

On the basis of our preliminary results that the earliest GGT-positive foci were induced at 12 weeks after a single injection of 100 mg DENA/kg (Hirota N, Moriyama S, Yokoyama T: Unpublished data), PH in experiment 2 (groups 5-7) was done 12 weeks following an injection of DENA at a dose of 100 mg/kg for group 5 and at a dose of 200 mg/kg for group 6 to test the effect of PH when some altered foci were already present. PH was not performed on group 7, which received a single injection of 200 mg DENA/kg. Animals in experiments 1 and 2 were fed a basal diet during the experiments. Five animals in groups 5 and 6 were killed at weeks 15 and 18 and 5 animals in group 7 were killed at weeks 2, 6, 12, 15, and 18 after DENA treatments.

Histochemistry of and quantitative analysis for induced altered foci.—Liver sections (3–5 mm thick) were obtained from the right anterior, right posterior, and caudate lobes of both hepatectomized and nonhepatectomized animals. They were fixed in cold acetone (4°C). The NSE reaction was used as an additional histochemical marker for altered foci because we have found that neoplastic nodules induced by 2-FAA in rat liver showed, on occasion, more evenly strong positivity for NSE than for GGT (Hirota N, Moriyama S, Yokoyama T: Unpublished data). Staining for both GGT and NSE was done on paraffin-embedded serial sections (4–5 μm). For GGT staining, the sections were incubated in a freshly prepared medium containing 6-glutamyl-4-methoxy-2-naphthylamine as substrate and fast blue BBN as the coupling agent (*21*). Following the method of Burstone (*22*) for NSE staining, we used naphthol AS-D (3-hydroxy-2-naphthol-*o*-toluidide) acetate as substrate and garnet GBC as the coupling agent. Counterstaining for GGT was done with hematoxylin, but no counterstaining for NSE was done. We quantitatively analyzed induced altered foci by calculating their numbers and measuring the area—by use of the method previously employed (*11, 23*)—of the foci identified by histochemically positive reactions for GGT and NSE.

RESULTS

Effects of PH Before Appearance of Altered Foci in Liver Exposed to a Single Injection of DENA (Expt 1)

A small number of GGT-positive hepatocytes occasionally scattered loosely in the periportal area was not counted as foci, but the foci were limited to discrete hepatocellular lesions forming GGT-positive islands (fig. 1). A strong positive reaction for NSE was frequently evident in the foci in contrast to a weak positive reaction for NSE found primarily in the central zone of the hepatic lobule from any liver examined (fig. 2). The results, summarized in table 1 and in text-figure 2, show that PH after a single injection of DENA induced hepatocellular altered foci much earlier than did DENA alone and that the number of foci was closely related to the interval between DENA treatment and PH.

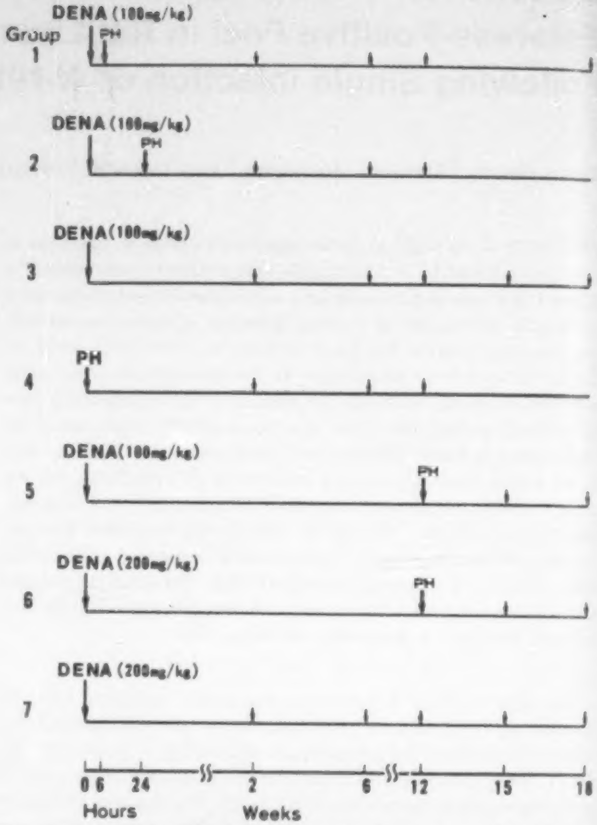

TEXT-FIGURE 1.—Diagramatic representation of experimental designs for the study of the effect of PH on the formation of histochemically altered foci after DENA injection. *Small arrows*=time periods when animals were killed.

In the group of animals subjected to PH at 6 hours after an injection of 100 mg DENA/kg (group 1), GGT-positive foci were observed as early as 2 weeks after PH (average number of foci, ≈11/cm^2), whereas no foci were found in group 3 until 12 weeks after DENA (100 mg/kg) treatment without PH. The number of foci decreased slightly by the 6th week but was maintained at almost the same level until the 18th week. As compared with the number of foci in the group that received DENA alone, the number of foci in group 1 was about four times greater at the 18th week. In some instances, large areas of foci almost exceeding those of the hepatic lobule were observed at the 12th or 18th week.

In the group of animals subjected to PH 24 hours after the DENA treatment (group 2), the number of foci also increased but the number at each time point after PH was less than half that in group 1. The number of foci at any time point, however, was still greater than that in group 3. No foci were found in the group treated with PH alone (group 4) for the duration of the experiment.

Effect of PH After Appearance of Altered Foci in Liver Exposed to a Single Injection of DENA (Expt 2)

A small number of GGT-positive foci (0.6/cm^2) and of NSE-positive foci (0.2/cm^2) was present at 12 weeks after

TABLE 1.—*Number[a] of histochemically altered foci, with a comparison of positivity for GGT and NSE*

Group	Treatment	Histochemistry	Weeks after treatment[b]				
			2	6	12	15	18
1	DENA (100 mg/kg) + PH (6)[c]	GGT	11.2 (5)	8.5 (5)	7.4 (5)	ND	7.3 (5)
		NSE	0.2	1.5	1.7	ND	2.0
2	DENA (100 mg/kg) + PH (24)[c]	GGT	4.9 (5)	3.4 (5)	2.6 (5)	ND	ND
		NSE	0.1	0.5	0.7	ND	ND
3	DENA (100 mg/kg)	GGT	0 (5)	0 (5)	0.6 (5)	1.2 (5)	1.9 (5)
		NSE	0	0	0.2	0.2	0.3
4	PH alone	GGT	0 (3)	0 (3)	0 (3)	ND	ND
		NSE	0	0	0	ND	ND
5	DENA (100 mg/kg) + PH (12)[d]	GGT	—	—	—	3.0 (5)	6.0 (5)
		NSE	—	—	—	1.1	2.9
6	DENA (200 mg/kg) + PH (12)[d]	GGT	—	—	—	4.9 (5)	10.3 (5)
		NSE	—	—	—	2.0	3.9
7	DENA (200 mg/kg)	GGT	0 (5)	1.2 (5)	3.2 (5)	3.4 (5)	3.5 (5)
		NSE	0	0.1	1.0	0.7	0.7

[a] Average value per cm^2 obtained as described in "Materials and Methods" from sections from three hepatic lobes.
[b] *Numbers in parentheses*=No. of animals. ND=not done.
[c] Number of hours at partial hepatectomy after DENA injection *in parentheses*.
[d] Number of weeks at partial hepatectomy after DENA injection *in parentheses*.

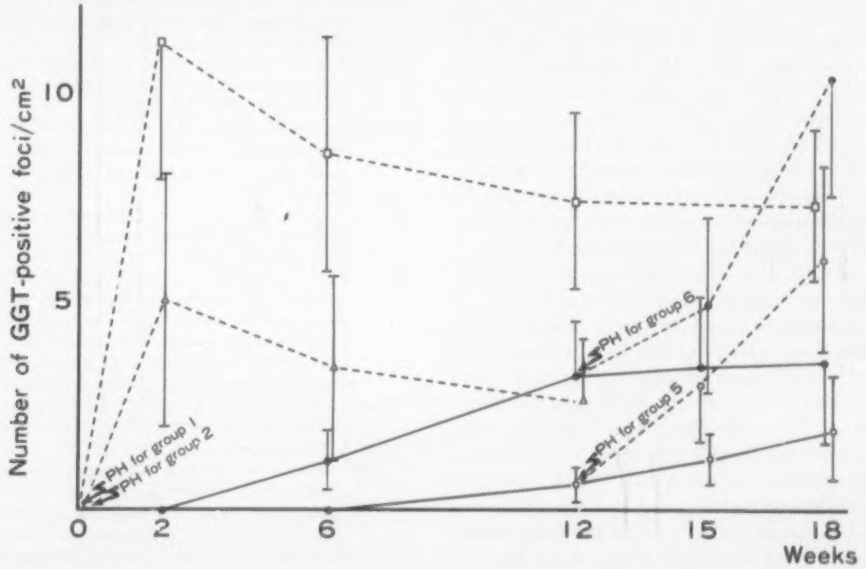

TEXT-FIGURE 2.—Effect of PH after DENA injection on the induction of GGT-positive foci as measured by the number of foci/cm^2. Graphs for group 4 (PH alone). which gave no foci at any point examined, is eliminated in this text-fig. □----□, group 1; △-----△, group 2; ○——○, group 3; ○----○, group 5; ●----●; group 6; ●——● group 7; *bars*, SEM.

an injection of 100 mg DENA/kg (group 3). At the same number of weeks after treatment with 200 mg DENA/kg (group 7), the number of both foci was about five times as high as that in group 3. As shown in table 1 and text-figure 2, at 3 or 6 weeks after PH, the number of foci in both groups 5 and 6 significantly increased in contrast to the focus counts in groups 3 and 7, which slightly increased or remained almost constant. The number of GGT-positive foci in both groups 5 and 6 reached approximately three times greater levels at 6 weeks following PH as compared to the levels seen in the nonhepatectomized groups 3 and 7, respectively.

GGT-positive foci were more frequently detected than NSE-positive foci at any point in experiment 2 as well as experiment 1 (table 1). The former foci on occasion did not necessarily correspond to the latter foci (figs. 3, 4) but not vice versa.

DISCUSSION

The present studies document that PH performed even up to 12 weeks after a single exposure to DENA enhances the formation of altered foci. Foci are believed to be the progeny of liver cells in which the carcinogen damage to genetic material has been converted into a permanently altered genome (*24–27*). Since DENA alkylates DNA (*28–*

30), the effect of PH is interpreted to represent the enhanced conversion of DNA damage to permanent mutations during the cell replication induced by PH. This interpretation is consistent with the finding that increased replication of liver cells in culture enhances the mutagenic effects of alkylating agents (*31, 32*).

With time, damage to DNA will be repaired (*28, 30, 33, 34*). The difference between groups 1 and 2 in the increasing number of foci following PH further supports the concept that DNA damage will be repaired over time, if not to the point of absolute elimination. The present data agree with a recent hypothesis of Ishikawa et al. (*19*) that the extent of repair of carcinogen-induced DNA damage is proportionally related to the length of the resting phase of the cell cycle. Although DNA repair in the target cells appears to occur with time following DNA damage by carcinogen exposure, the significant increase in foci effected by PH, which was observed in groups 5 and 6, conceivably indicates that some minor fraction of liver cells continues to have DNA damage even as long as 12 weeks after a single treatment with DENA.

The present approach in which PH is used to enhance the appearance of foci provides a means in vivo to distinguish genotoxic carcinogens from epigenetic carcinogens, since the former induce DNA damage but the latter do not, according to the concepts proposed by Williams (*35, 36*). A single injection of DENA into rats provided an excellent system for in vivo study of the mechanism of DNA damage and repair because there was no need to resort to techniques for acceleration, such as repeated exposure to carcinogen or other chemicals. PH has been applied extensively by Ito et al. (*37*) and Tsuda et al. (*38*) to the short-term in vivo assay in rat liver for the assessment of the carcinogenicity of various chemical compounds. However, Ito et al. and Tsuda et al. used some complex modalities. The former group (*37*) used 2-FAA or DENA as initiator followed by PH performed in the middle of administration of test chemicals; the latter group (*38*) performed PH prior to or after the treatment with the test compounds followed by an injection of carbon tetrachloride in the midst of 2-FAA feeding (*38*). The possibility exists that the length of time required for the assessment of the genotoxic carcinogenicity of other chemicals to various target organs other than the liver could also be shortened in vivo by use of techniques that stimulate cell proliferation.

In regard to histoenzymic markers employed, we found that phenotypic heterogeneity occurred between foci for the two markers GGT and NSE and that NSE was relatively less sensitive for the detection of foci than GGT and yet an increase of GGT-positive and NSE-positive foci was induced by PH. Considerable phenotypic heterogeneity among foci, possibly reflecting multiple genotypic changes in the cells of foci, was also described previously by Hirota and Williams (*9*) who studied the sensitivity and heterogeneity of various histochemical markers for 2-FAA-induced altered foci; these authors found that, compared to any of the other histochemical properties in the siderotic liver, which was sufficiently loaded with iron, resistance to iron accumulation was the property that identified the greatest number of foci, with GGT positivity being the next most sensitive property.

REFERENCES

(*1*) Gössner W, Friedrich-Freksa H. Histochemische Untersuchungen über die Glucose-6-phosphatase in der Rattenleber während der Kanzerisierung durch Nitrosamine. Z Naturforsch 1964; 19:852–862.

(*2*) Bannasch P. The cytoplasm of hepatocytes during carcinogenesis. Recent Results Cancer Res 1968; 19:18–48.

(*3*) Börner P, Gössner W. Enzymhistochemische Untersuchungen der Adenosin-triphosphatase, der alkalischen und sauren Phosphatase sowie der Succinatdehydrogenase im Leberparenchym der Ratte während der Einwirkung des kanzerogens Diäthylnitrosamin. Z Naturforsch [C] 1968; 19:1085–1091.

(*4*) Kitagawa T. Histochemical analysis of hyperplastic lesions and hepatomas of the liver of rats fed 2-fluorenylacetamide. Gan 1971; 62:207–216.

(*5*) Williams GM, Yamamoto RS. Absence of stainable iron from preneoplastic lesions in rat liver with 8-hydroxyquinoline-induced siderosis. J Natl Cancer Inst 1972; 49:685–692.

(*6*) Kalengayi MM, Ronchi G, Desmet VJ. Histochemistry of gamma-glutamyl transpeptidase in rat liver during aflatoxin B_1-induced carcinogenesis. J Natl Cancer Inst 1975; 55:579–588.

(*7*) Scherer E, Emmelot P. Kinetics of induction and growth of enzyme-deficient islands involved in hepatocarcinogenesis. Cancer Res 1976; 36:2544–2554.

(*8*) Pitot HC, Barsness L, Goldsworthy T, Kitagawa T. Biochemical characterisation of stages of hepatocarcinogenesis after a single dose of diethylnitrosamine. Nature 1978; 271:456–458.

(*9*) Hirota N, Williams GM. The sensitivity and heterogeneity of histochemical markers for altered foci involved in liver carcinogenesis. Am J Pathol 1979; 95:317–324.

(*10*) Lipsky MM, Hinton DE, Goldblatt PJ, Klaunig JE, Trump BF. Iron negative foci and nodules in safrole-exposed mouse liver made siderotic by iron-dextran injection. Pathol Res Pract 1979; 164:178–185.

(*11*) Hirota N, Williams GM. Persistence and growth of rat liver neoplastic nodules following cessation of carcinogen exposure. JNCI 1979; 63:1257–1265.

(*12*) Hirota N, Hamazaki M, Williams GM. Resistance to iron accumulation and presence of hepatitis B surface antigen in preneoplastic and neoplastic lesions in human hemochromatotic livers. Hepatogastroenterology 1982; 29:49–51.

(*13*) Williams GM. Functional markers and growth behavior of preneoplastic hepatocytes. Cancer Res 1976; 36:2540–2543.

(*14*) Reuber MD. Development of preneoplastic and neoplastic lesions of the liver in male rats given 0.025 percent *N*-2-fluorenyldiacetamide. J Natl Cancer Inst 1965; 34:697–724.

(*15*) Newberne PM, Wogan GN. Sequential morphologic changes in aflatoxin B_1 carcinogenesis in the rat. Cancer Res 1968; 28:770–781.

(*16*) Scherer E, Hoffmann M, Emmelot P, Friedrich-Freksa M. Quantitative study on foci of altered liver cells induced in the rat by a single dose of diethylnitrosamine and partial hepatectomy. J Natl Cancer Inst 1972; 49:93–106.

(*17*) Craddock VM. Liver carcinomas induced in rat by single administration of diethylnitrosamine after partial hepatectomy. J Natl Cancer Inst 1971; 47:899–907.

(*18*) ———. Induction of liver tumours in rats by a single treatment with nitroso compounds given after partial hepatectomy. Nature 1973; 245:386–388.

(*19*) Ishikawa T, Takayama S, Kitagawa T. Correlation between time of partial hepatectomy after a single treatment with diethylnitrosamine and induction of adenosinetriphosphatase-deficient islands in rat liver. Cancer Res 1980; 40:4261–4264.

(*20*) Higgins GM, Anderson RM. Experimental pathology of the liver. I. Restoration of the liver of the white rat following partial surgical removal. Arch Pathol 1931; 12:186–202.

(*21*) Rutenburg AM, Kim H, Fischbein JW, Hanker JS, Wasserkrug HL, Seligman AM. Histochemical and ultrastructural demonstration of γ-glutamyl transpeptidase activity. J Histochem Cytochem 1969; 17:517–526.

(*22*) Burstone MS. Esterase in neoplasm. In: Enzyme histochemistry and its application in the study of neoplasms. New York: Academic Press, 1962:324–325.

(*23*) Williams GM, Watanabe K. Quantitative kinetics of development of *N*-2-fluorenylacetamide-induced, altered (hyperplastic) hepatocellular foci resistant to iron accumulation and of their reversion or persistence following removal of carcinogen. JNCI 1978; 61: 113–121.

(*24*) Stich HF. The DNA content of tumor cells. II. Alterations during the formation of hepatomas in rats. J Natl Cancer Inst 1960; 24:1283–1297.

(*25*) Scherer E, Hoffmann M. Probable clonal genesis of cellular islands induced in rat liver by diethylnitrosamine. Eur J Cancer 1971; 7:369–371.

(*26*) Farber E. Studies on the molecular mechanisms of carcinogenesis. In: Whelan WJ, Schultz J, eds. Homologies in enzymes and metabolic pathways and metabolic alterations in cancer. Amsterdam and London: Elsevier/North-Holland, 1970:314–334.

(*27*) Williams GM. The pathogenesis of rat liver cancer caused by chemical carcinogens. Biochim Biophys Acta 1980; 605:167–189.

(*28*) Scherer E, Steward AP, Emmelot P. Kinetics of formation of O^6-ethylguanine in, and its removal from, liver DNA of rats receiving diethylnitrosamine. Chem Biol Interact 1977; 19:1–11.

(*29*) Pegg AE. Formation and metabolism of alkylated nucleosides: Possible role of carcinogenesis by nitroso compounds and alkylating agents. Adv Cancer Res 1977; 25:195–269.

(*30*) Margison GP, Curtin NJ, Snell K, Craig AW. Effect of chronic *N,N*-diethylnitrosamine on the excision of O^6-ethylguanine from rat liver DNA. Br J Cancer 1979; 40:809–813.

(*31*) Berman JJ, Tong C, Williams GM. Enhancement of mutagenesis during cell replication of cultured liver epithelial cells. Cancer Lett 1978; 4:277–283.

(*32*) Tong C, Fazio M, Williams GM. Cell cycle-specific mutagenesis at the hypoxanthine phosphoribosyltransferase locus in adult rat liver epithelial cells. Proc Natl Acad Sci USA 1980; 77:7377–7379.

(*33*) Nicoll JW, Swann PF, Pegg AE. Effect of dimethylnitrosamine on persistence of methylated guanines in rat liver and kidney DNA. Nature 1975; 254:261–262.

(*34*) Montesano R, Bresil H, Planche-Mortel G, Margison GP, Pegg AE. Effect of chronic treatment of rats with dimethylnitrosamine on the removal of O^6-methylguanine from DNA. Cancer Res 1980; 40:452–458.

(*35*) Williams GM. Review of in vitro test system using DNA damage and repair for screening of chemical carcinogens. J Assoc Off Anal Chem 1979; 62:857–863.

(*36*) ———. Classification of genotoxic and epigenetic hepatocarcinogens using liver culture assays. Ann NY Acad Sci 1980; 349:273–282.

(*37*) Ito N, Tatematsu M, Nakanishi K, et al. The effect of various chemicals on the development of hyperplastic liver nodules in hepatectomized rats treated with *N*-nitrosodiethylamine or *N*-2-fluorenylacetamide. Gan 1980; 71:832–842.

(*38*) Tsuda H, Lee G, Farber E. Induction of resistant hepatocytes as a new principle for a possible short-term in vivo test for carcinogens. Cancer Res 1980; 40:1157–1164.

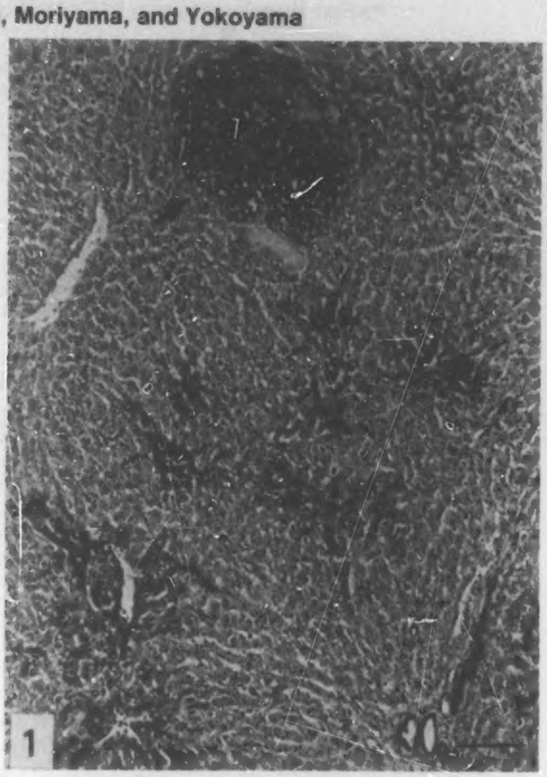

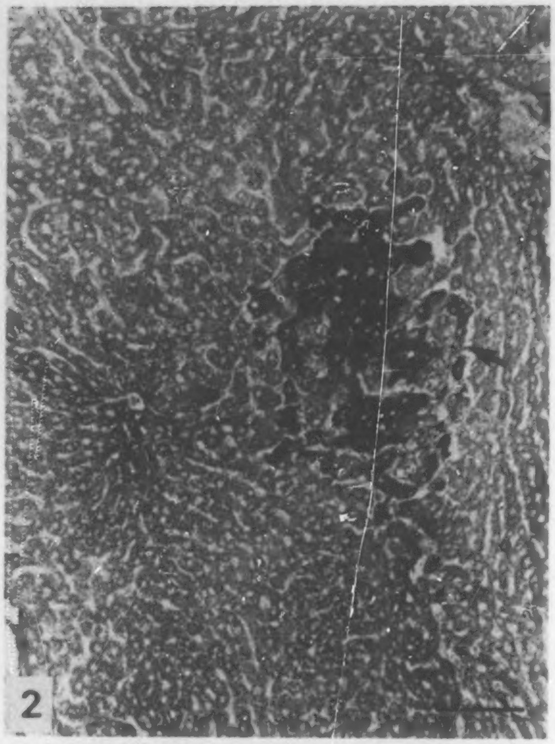

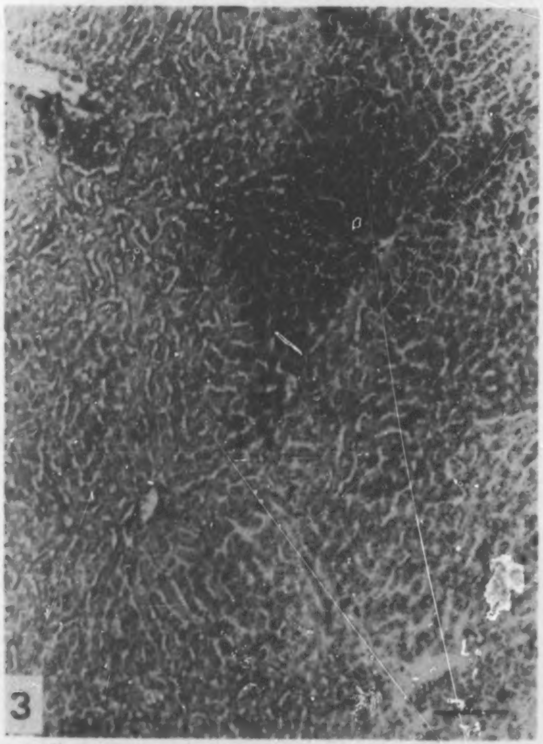

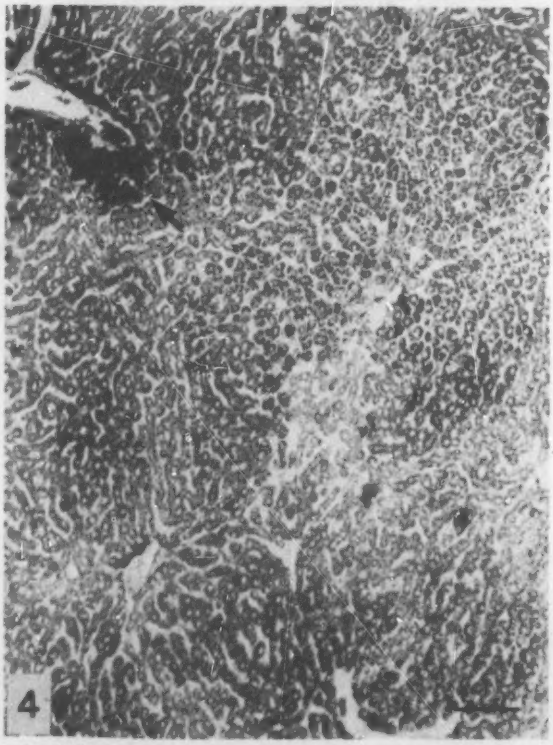

FIGURE 1.—GGT-positive focus forming a discrete island (*large arrow*) at 6 wk after PH in group 1. GGT-positive hepatocytes also are loosely scattered primarily in the periportal area (*small arrows*). GGT reaction, counterstained with hematoxylin. *Bar*=100 µm. × 95.

FIGURE 2.—NSE-positive focus (*large arrow*) at 12 wk after PH in group 1 in contrast to weak positive hepatocytes in the central zone of a hepatic lobule (*small arrows*). NSE reaction, not counterstained. *Bar*=100 µm. × 130.

FIGURE 3.—Two GGT-positive foci at 6 wk after PH in group 6. GGT reaction, counterstained with hematoxylin. *Bar*=100 µm. × 110.

FIGURE 4.—Same as fig. 3. One focus (*arrow*) is positive for NSE, but larger focus in fig. 3 is negative. NSE reaction, not counterstained (serial section to that of fig. 3). *Bar*=100 µm. × 110.

Evidence for Involvement of Mast Cells in Tumor Suppression in Mice[1,2,3]

Hiroshi Tanooka,[4] Yukihiko Kitamura,[5] Toshihiko Sado,[6] Kazuhiko Tanaka,[4] Mizue Nagase,[4] *and* Sohei Kondo[5,7]

ABSTRACT—Mast cell-deficient W/W^v mice had an increased tumor incidence after subcutaneous treatment with 3-methylcholanthrene, compared with that in normal congenic mice treated in the same way. This increased tumor incidence was suppressed to the normal level when the carcinogen was given after the mast cell deficiency had been overcome by transplantation of bone marrow cells from normal congenic mice. The W/W^v mice, however, were not defective in natural killer and T-cell-mediated cytotoxic activities. These results support the hypothesis that mast cells are involved in tumor suppression.—JNCI 1982; 69:1305–1309.

A role of immunosurveillance for tumor suppression has been suggested (*1*). However, no clear evidence exists that the candidates for this role, such as T-cells or NK cells, have this function, inasmuch as mutant mice deficient in these cells, i.e., beige and nude mice, do not show a higher incidence of autochthonous tumors after treatment with carcinogen than their normal counterparts (*2, 3*). Nevertheless, earlier studies (*4–6*) have suggested involvement of mast cells in tumor suppression, and a recent review (*7*) indicated the possible importance of an allergic type reaction in host resistance to solid tumors and hence the possible involvement of mast cells. More directly, isolated mast cells were shown to inactivate tumor cells selectively in vitro (*8, 9*).

To test the hypothesis that mast cells are involved in tumor suppression, we used mice with a mutant genotype, W/W^v (*10*); these mice lack hair pigmentation and are anemic and sterile. W/W^v mice were recently found to be deficient in mast cells, and this characteristic has been extensively studied (*11, 12*). Spontaneous development of leukemia (*13, 14*) and forestomach papillomas (*15*) have been reported in the W/W^v mice. In the experiments reported herein, we observed an increased tumor incidence in the W/W^v mice, over that in normal congenic +/+ mice, after sc injection of MCA.

Furthermore, mast cell deficiency in these mice can be overcome by transplantation of bone marrow cells from normal congenic mice (*11*). We, therefore, tested tumor induction in W/W^v mice after bone marrow transplantation to demonstrate more directly the effect of mast cells. The results were consistent with the hypothesis that mast cells are involved in tumor suppression.

MATERIALS AND METHODS

Mice.—Mice with a W or W^v mutation (*10*) were originally obtained from The Jackson Laboratory, Bar Harbor, Maine. A cross between WB-$W/+$ ($H\text{-}2^w$) and C57BL/6-$W^v/+$ ($H\text{-}2^b$) mice yielded WBB6F$_1$ offspring of the genotypes W/W^v, $W/+$, $W^v/+$, and $+/+$. W/W^v and $+/+$ mice, which were easily distinguishable by their hair color, were used in this experiment. The mice were given free access to a mouse diet (CE-1; Clea Japan Inc., Tokyo, Japan) and water and kept in cages in an isolation rack supplied with filtered air. Both males and females were 2–3 months old when used in the experiments.

Bone marrow transplantation.—Bone marrow was obtained from the femurs of +/+ mice, and a homogeneous suspension of cells in Eagle's minimum essential medium was prepared. About 3×10^7 bone marrow cells of +/+ mice were transplanted intravenously into W/W^v mice 2 months before the experiments commenced (*11*).

Tumor induction and analysis of data.—MCA (Fluka AG, Buchs, Switzerland) was dissolved in olive oil at 5 or 0.5 mg/ml, and 0.1 ml of the mixture was injected sc into the right groin of the mice, as described in (*16*). Tumor formation was examined by palpation at intervals after the carcinogen injection, and the day of tumor appearance and the day of death of animals without tumors were recorded. Data from two independent experiments were combined, and cumulative tumor incidence rates were calculated by the Kaplan-Meier method (*17*). Statistical significances of differences in tumor incidences between the two groups were evaluated by the log-rank test (*18*). Tumor size was measured with a caliper, and the volume-doubling time was determined from the slope of the initial portion of the tumor growth curve, as described previously (*16*). The tumors produced were examined histologically after being stained with H & E and with toluidine blue (pH 3.0) to confirm the presence of mast cells (*11*).

ABBREVIATIONS USED: Con A=concanavalin A; H & E=hematoxylin and eosin; LPS=lipopolysaccharide; MCA=3-methylcholanthrene; NK=natural killer; PHA=phytohemagglutinin.

---

[1] Received October 20, 1981; revised June 30, 1982; accepted July 22, 1982.

[2] Supported by Grants-in-Aid for Cancer Research from the Ministry of Health and Welfare and the Ministry of Education, Science and Culture of Japan, and by a grant from the Adult Disease Clinic Memorial Foundation, Tokyo, Japan.

[3] Animals were maintained under the guidelines of the National Cancer Center Research Institute, Japan.

[4] Radiobiology Division, National Cancer Center Research Institute, Tsukiji 5-1-1, Chuo-ku, Tokyo 104, Japan.

[5] Medical School, Osaka University, Nakanoshima 4-3-57, Kita-ku, Osaka 530, Japan.

[6] Division of Physiology and Pathology, National Institute of Radiological Sciences, Anagawa 4-9-1, Chiba 260, Japan.

[7] We thank Dr. H. Hoshino and Dr. S. Watanabe for help in histologic examinations, Mr. M. Shiraishi and Mrs. H. Arimoto for help in computer analysis of experimental data, and Mrs. T. Kawasaki and Mrs. M. Ebinuma for animal care.

NK activity.—NK activity was assessed by a direct ^{51}Cr release assay in vitro (*19*). A fixed number of spleen cells from a single test mouse was incubated for 6 hours with 2×10^4 YAC-1 target cells labeled with ^{51}Cr ($Na_2{}^{51}CrO_4$; sp act, 568 mCi/mg; New England Nuclear Corp., Boston, Mass.) at two effector-to-target cell ratios, 50:1 and 100:1. Cytotoxicity was expressed as the percentage release of ^{51}Cr.

Cytotoxic T-cells.—Cytotoxic T-cell activity was assayed, as described previously (*20*), with a 6-day mixed lymphocyte culture of test spleen cells and 1,500-rad-irradiated allogeneic (B10.D2, *H-2^d*) spleen cells; ^{51}Cr release was assayed with DBA/2 (*h-2^d*)-derived L5178Y target cells. Results, expressed as lytic units per culture and per spleen, were calculated by the method of Cerottini et al. (*21*). One lytic unit is defined as the number of effector cells that kills 50% of 4×10^4 target cells.

Mitogen responsiveness.—The method for assessing the proliferative response of spleen lymphocytes to mitogens has been described in detail elsewhere (*22*). The mitogens used were PHA (Wellcome Reagents Limited, London, U.K.), LPS (Difco Laboratories, Detroit, Mich.), and Con A (Sigma Chemical Co., St. Louis, Mo.).

RESULTS

Tumor induction.—Text-figure 1A shows the cumulative tumor incidences in *W/W^v* mice and congenic +/+ mice after injection of 0.5 mg MCA/animal. The tumor incidence in *W/W^v* mice was significantly higher than that in +/+ mice. Incidence reached 100% in *W/W^v* mice on day 163, when it was still 65% in +/+ mice. The higher tumor incidence in *W/W^v* mice was more significant with a lower MCA dose of 0.05 mg/animal (text-fig. 1B). No significant difference was apparent in each group between the incidence in males and the incidence in females.

To demonstrate the effect of mast cells on tumor induction

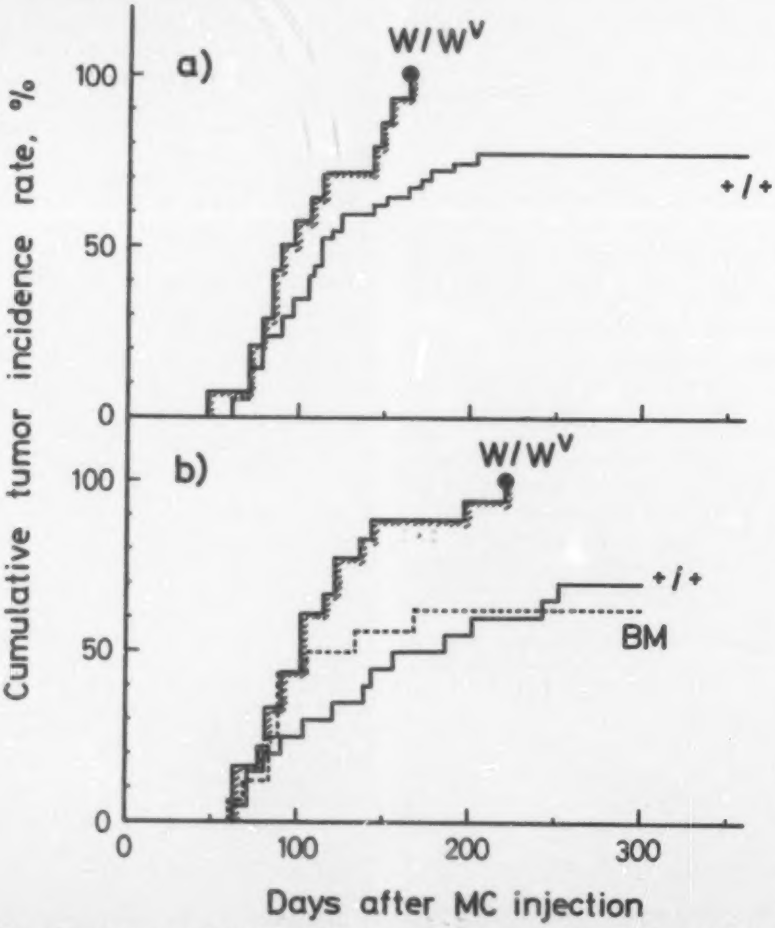

TEXT-FIGURE 1.—Tumor incidence after sc injection of MCA into *W/W^v* and +/+ mice, and effect of transplantation of bone marrow from +/+ mice into *W/W^v* mice on the incidence. a) Tumor induction with 0.5 mg MCA. Final tumor incidence: *W/W^v*, 14/14; +/+, 30/39. Death without tumors: 1 +/+ mouse. Significance of difference in tumor incidence between *W/W^v* and +/+ mice evaluated by the log-rank test (*18*): $P<0.05$. b) Tumor induction with 0.05 mg MCA. Final tumor incidence: *W/W^v*, 18/18; +/+, 14/20; and bone-marrow-transplanted *W/W^v* mice (BM), 10/16. Death without tumors: 0. Significance of difference between tumor incidence in *W/W^v* and +/+, and in *W/W^v* and bone marrow-transplanted mice: $P<0.005$ and $P<0.05$, respectively.

more directly, we gave iv injections of bone marrow cells from normal +/+ mice to *W/W^v* mice. The shift in size of the red blood cells in the peripheral blood of *W/W^v* mice (62 μm^3) to normal size (47 μm^3)—an indicator of the effectiveness of bone marrow transplantation that is substantiated by the appearance of mast cells in various organs (*11*)—was monitored with a Coulter counter. Two months after this transplantation, normal blood cells proliferated fully in all the *W/W^v* mice. The mice were then given sc injections of 0.05 mg MCA. The time course of tumor formation is shown in text-figure 1B. Data show that bone marrow transplantation suppressed the higher tumor incidence in *W/W^v* mice to the level in normal +/+ mice.

Except for 1 squamous cell carcinoma and 1 adenocarcinoma in +/+ mice treated with 0.5 mg MCA, all the tumors produced in the present experiments were sarcomas [fibrosarcomas, 77%; malignant fibrous histiocytomas, 16%; other sarcomas (pleiomorphic, myogenic, and liposarcomas, 7%)]. No mast cells were detectable around the tumors that developed in the *W/W^v* mice. In contrast, many mast cells were observed surrounding the tumors that developed either in the +/+ mice or in the *W/W^v* mice that had been given injections of bone marrow cells from the +/+ donors (fig. 1). Even in such cases, mast cells were scarcely detected within the tumors.

Tumor volume-doubling times were determined from the sarcoma growth curves. The average values after treatment with 0.5 mg MCA were 2.8±1.0 days for *W/W^v* mice and 3.1±1.1 days for +/+ mice; after treatment with 0.05 mg MCA the values were 2.9±0.7 days for *W/W^v* mice and 2.9±0.5 days for +/+ mice. The volume-doubling time was independent of the time of tumor appearance, and the results show that tumors grew at the same speed in *W/W^v* and +/+ mice.

Immunologic parameters of splenic lymphocytes of W/W^v *and +/+ mice.*—Several immunologic parameters of spleen lymphocytes from *W/W^v* and +/+ mice were assessed, including NK and cytotoxic T-cell activity and the proliferative response to mitogens. The results summarized in table 1 indicate the following: 1) The total number of viable cells per spleen was higher in *W/W^v* than in +/+ mice. The difference was highly significant. 2) NK activity, assessed with a fixed number of spleen cells, was slightly lower in *W/W^v* mice, but the difference was not significant. Correction of NK activity for total spleen cells resulted in much closer values for the 2 groups (data not shown). 3) Cytotoxic T-cell activity in total spleen was higher in *W/W^v* than in +/+ mice. However, this difference was not significant when the activity was normalized for the cell number. 4) The proliferative responses to PHA and Con A were significantly lower, and the response to LPS was considerably lower, in *W/W^v* than in +/+ spleens when compared on the basis of ^{3}H-labeled thymidine uptake by 5×10^5 cells.

TABLE 1.—*Immunologic parameters of splenic lymphocytes of +/+ and* W/W^v *mice*[a]

Parameter	+/+	*W/W^v*	Statistical significance[b]
Total No. of viable cells per spleen ($\times10^6$)	127.7±13.1	248.6±24.4	$P<0.001$
NK cell[c]	24.3±2.3	18.3±7.6	$0.5>P>0.4$
Cytotoxic T-cell[d]	62.4±16.8	235.5±39.1	$0.01>P>0.001$
Mitogen response[e]			
PHA	4.385±0.017	4.121±0.085	$0.02>P>0.01$
LPS	4.124±0.054	3.56±0.29	$0.1>P>0.05$
Con A	4.330±0.054	3.82±0.11	$0.01>P>0.001$

[a] Sample size, 7 mice per group; 3-mo-old females.
[b] Student's *t*-test.
[c] Percent specific cytotoxicity at effector-to-target cell ratio of 100:1.
[d] Lytic units per spleen.
[e] Log Δ cpm/5×10^5 cells.

DISCUSSION

The present work shows that tumor incidence after MCA treatment is higher in *W/W^v* mice than in normal congenic mice. In addition to being deficient in mast cells, *W/W^v* mice also differ from +/+ mice in showing marked symptoms of anemia. However, we know of no report of an increased incidence of solid tumors in anemic mice after treatment with a carcinogen. Moreover, our results indicate that *W/W^v* mice show no significant defects in NK, T-cell-mediated cytotoxic activity or in the proliferative responses of their spleen lymphocytes to mitogens. Mekori and Phillips (*23*) reported that the antibody-forming ability of B-cells and the helper function of T-cells were normal in the *W/W^v* mice, and Bennett (*24*) stated that alloantigen-sensitive cells of the *W/W^v* mice had normal function. The conclusions of these authors are consistent with the results we obtained. Thus we regard the findings of our study as evidence for the hypothesis that mast cells are involved in tumor suppression.

The growth rates of tumors in *W/W^v* and +/+ mice, however, were equal, which suggests that the tumor-suppressing action of mast cells becomes inefficient after the tumors have grown to a certain size. Mast cells were found around the periphery of tumor masses in histologic sections, but not many were seen inside the masses. Such histologic features are similar to those described by Cramer and Simpson (*6*) who investigated the reaction of mast cells to epithelial tumors induced by skin painting with MCA. Furthermore, increased ornithine decarboxylase activity, an indicator of tumor promotion, did not differ in *W/W^v* and +/+ mice after treatment of the skin with 12-*O*-tetradecanoyl phorbol 13-acetate (Fujiki H, Tanooka H: Unpublished observation). The action of mast cells, therefore, seems to be exerted at an early stage of tumorigenesis.

REFERENCES

(*1*) BURNET FM. Immunological surveillance. Sydney, Australia: Pergamon Press, 1970.

(*2*) STUTMAN O. Tumor development after 3-methylcholanthrene in immunologically deficient athymic-nude mice. Science 1974; 183:534–536.

(*3*) SALMON JC, CREAU-GOLDBERG N, LYNCH NR. Cancer induction by methylcholanthrene and metastatic spread of transplantable tumor in Chediak Higashi (beige) mice. Cancer Immunol Immunother 1980; 8:67–70.

(*4*) EHRLICH P. Beiträge zur Kenntnis der granulirten Bindegewebezellen und der eosinophilen Leukocythen. Arch Anat Physiol 1879; 3:166–169.

(*5*) Selye H. The mast cells. Washington, D.C.: Butterworth, 1965:247–300.

(*6*) Cramer W, Simpson WL. Mast cells in experimental skin carcinogenesis. Cancer Res 1944; 4:601–616.

(*7*) Lynch NR, Salomon JC, Turner KJ. Evolutionary development of IgE and the role of anaphylactic-type reactions in resistance to solid tumors. Cancer Immunol Immunother 1978; 4:223–228.

(*8*) Farram E, Nelson DS. Mouse mast cells as anti-tumor effector cells. Cell Immunol 1980; 55:294–301.

(*9*) Henderson WR, Chi EY, Jong EC, Klebanoff SJ. Mast cell-mediated tumor-cell cytotoxicity: Role of the peroxidase system. J Exp Med 1981; 153:520–533.

(*10*) Russell ES. Blood and blood formation. In: Green EL, ed. Biology of the laboratory animals. 2d ed. New York: McGraw-Hill, 1966:351–377.

(*11*) Kitamura Y, Go S, Hatanaka K. Decrease of mast cells in W/W^v mice and their increase by bone marrow transplantation. Blood 1978; 52:447–452.

(*12*) Go S, Kitamura Y, Nishimura M. Effect of W and W^v alleles on production of tissue mast cells in mice. J Heredity 1980; 71:41–44.

(*13*) Russell ES, Murphy ED, Roths JB. Life shortening effect of single genes. In: Bailey DW, ed. Forty-fifth annual report, 1973–74, The Jackson Laboratory, Bar Harbor, Maine. Bar Harbor: The Jackson Laboratory, 1974:71.

(*14*) Murphy ED. Effects of mutant steel alleles on leukemogenesis and life-span in the mouse. J Natl Cancer Inst 1977; 58:107–110.

(*15*) Kitamura Y, Yokoyama M, Matsuda H, Shimada M. Coincidental development of forestomach papilloma and prepyloric ulcer in nontreated mutant mice of W/W^v and Sl/Sl^d genotypes. Cancer Res 1980; 40:3392–3397.

(*16*) Tanooka H, Hoshino H, Tanaka K, Nagase M. Experimental radiation therapy and apparent radioresistance of autochthonous tumors subcutaneously induced with 3-methylcholanthrene in mice. Cancer Res 1980; 40:2547–2551.

(*17*) Hoel DG, Walburg HR Jr. Statistical analysis of survival experiments. J Natl Cancer Inst 1972; 49:361–372.

(*18*) Peto R, Pike MC, Armitage R, et al. Design and analysis of randomised clinical trials requiring prolonged observation of each patient. II. Analysis and examples. Br J Cancer 1977; 35:1–39.

(*19*) Hochman PS, Cudkowicz G, Dausset J. Decline of natural killer cell activity in sublethally irradiated mice. JNCI 1978; 61:265–268.

(*20*) Muto M, Sado T, Aizawa S, Kamisaku H, Kubo E. Bone marrow transplantation across the major histocompatibility barrier in specific-pathogen-free mice: Effects of intact versus T-cell depleted bone marrow on the expression of anti-host reaction in the recipient spleens. J Immunol 1981; 127:2421–2425.

(*21*) Cerottini JC, Engers HD, Robson H, MacDonald HR, Brunner KT. Generation of cytotoxic T-lymphocytes in vitro. I. Response of normal and immune mouse spleen cells in mixed leucocyte cultures. J Exp Med 1974; 140:703–717.

(*22*) Sado T, Kamisaku H, Aizawa S. Nature of T-cells resident in spleens of thymectomized, lethally irradiated, bone marrow-reconstituted mice. Cell Immunol 1980; 49:51–63.

(*23*) Mekori T, Phillips RA. The immune response in mice of genotypes W/W^v and Sl/Sl^d. Proc Soc Exp Biol Med 1969; 132:115–119.

(*24*) Bennett M. Graft-versus-host reaction in mice. I. Kinetic and immunogenetic studies on alloantigen-sensitive units of lymphoid tissue. Transplantation 1971; 11:158–169.

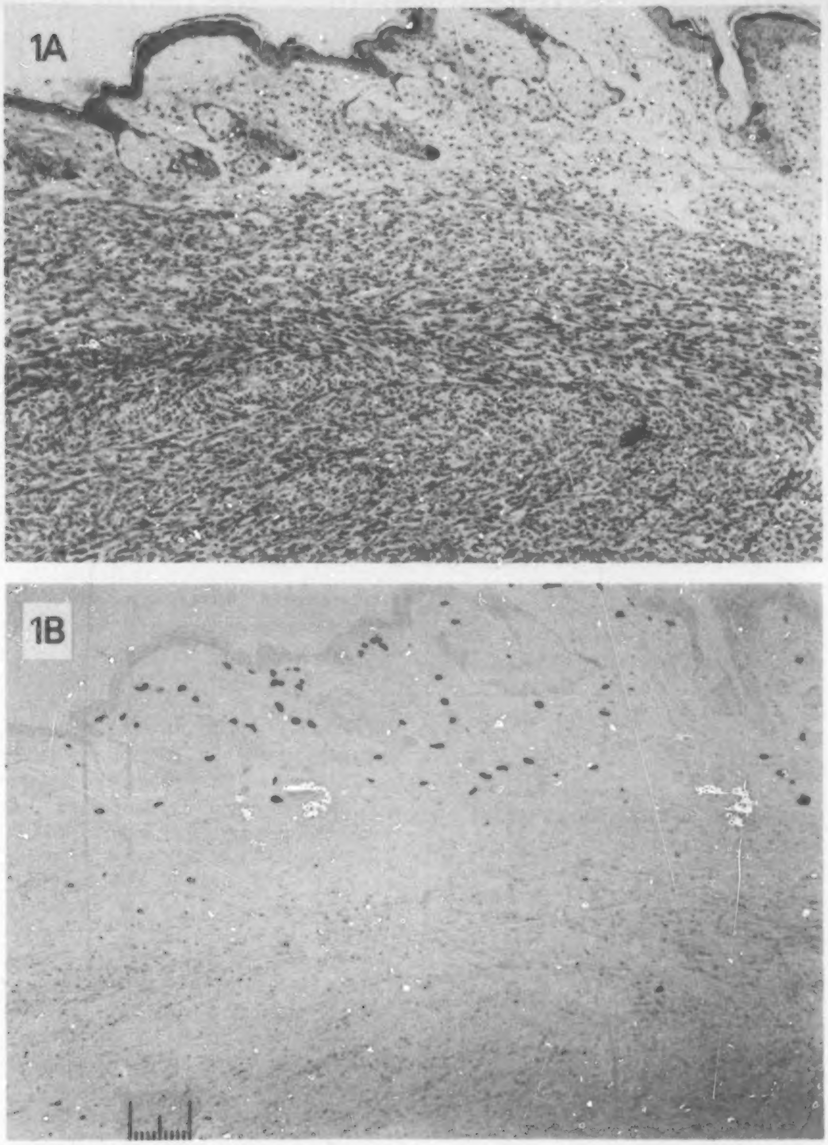

FIGURE 1.—Histologic sections of the boundary of a subcutaneous tumor (fibrosarcoma) induced with 0.05 mg MCA in a W/W^v mouse that had been given an injection of bone marrow cells from a +/+ donor. A) Section stained with H & E. B) Section stained with toluidine blue. *Scale*=0.1 mm.

blank page

H-2 Expression on a Teratocarcinoma-Derived Cell Line, TerC[1,2,3]

David B. Searls[4,5] *and* **Michael Edidin**[4]

ABSTRACT—The murine teratocarcinoma-derived cell line TerC, previously thought to lack products of the major histocompatibility locus *H-2*, was shown to express low levels of *K*- and *D*-end H-2 specificities with the use of a sensitive cytotoxic assay. The assay, based on the ability of antibody and complement to inhibit uptake of the thymidine analogue $[^{125}\text{I}]$5-iodo-2′-deoxyuridine, detected appropriate public and private specificities, as demonstrated with the use of oligospecific antisera and by absorption analyses. A series of clones of TerC varied only slightly in *H-2* expression, and there was no tendency for expression to increase with time in culture; thus the low levels of H-2 were not the result of a differentiating subpopulation.—JNCI 1982; 69: 1311–1315.

Because of their embryonic character, teratocarcinoma-derived cell lines have been used as immunogens in the study of embryonic and oncofetal antigens [*see* (*1*) for review]. The primary stem cell lines of these tumors, termed "embryonal carcinomas," have proved particularly useful for the production and characterization of antisera and monoclonal antibodies that cross-react with various stages and cell types of the early mouse embryo (*2, 3*). Embryonal carcinomas appear to be devoid of products of the mouse major histocompatibility complex *H-2* (*4*), a unique trait that not only makes these cells intrinsically interesting but also has proved useful in the study of H-2 restriction phenomena (*5*). Using cell hybridization techniques (*6*) and by following differentiation in vitro (*7*), other investigators have used teratocarcinoma-derived cell lines to study the regulation of *H-2* expression.

One of the first cell lines to be used in the study of oncofetal antigens was the 402AX teratocarcinoma-derived cell line TerC. Gooding and Edidin (*8*) characterized a xenoantiserum against this cell. This xenoantiserum contained multiple specificities defining embryonic and tumor antigens. Subsequent work has elucidated the chemical nature of some TerC-defined antigens (*9, 10*), and cellular immune reactions against these antigens have been investigated (*11*). Early studies reported that a small percentage of TerC was H-2-positive as judged by immunofluorescence and that large inocula of TerC slightly accelerated *H-2*^{b} skin graft rejection on congenic *H-2*^{k} mice (*12*). However, the cells are resistant to lysis by anti-H-2 antibody and complement and TerC can produce tumors in various allogeneic mice (*13*).

Further study of *H-2* expression on TerC cells would seem to be warranted to resolve the discrepancies in the published data. Also, TerC appears to resemble primitive endoderm, rather than embryonal carcinoma (*14*). Differentiation to endoderm is among the first events seen in embryogenesis (where endoderm arises from the inner cell mass) (*15*), as well as in the differentiation of embryonal carcinoma cells, both in vivo (in the formation of endoderm-coated embryoid bodies in ascites) (*16*) and in vitro (*17*). Thus the low levels of *H-2* expression on TerC might effectively model the earliest appearance of H-2 in both these systems, an unresolved aspect of early mouse development (*18*) that bears on the suggestion that H-2 antigens may be important in cell associations during early development (*19, 20*) and on the problem of maternal tolerance of the fetal allograft. Though another group did not detect H-2 antigens on endodermal derivatives of a pluripotent embryonal carcinoma (*7*), we find that low levels of H-2K and H-2D molecules are indeed present on teratocarcinoma-derived primitive endodermal cell lines.

MATERIALS AND METHODS

Cells.—TerC and cl1D (LM-TK^{-}) have been described previously (*16*). LM cells were donated by Dr. Richard Pagano, Carnegie Institution of Washington, Department of Embryology, Baltimore, Md., and EL 4 G-cells were donated by Dr. R. B. Herberman, National Cancer Institute, Bethesda, Md., (*21*). Embryonal carcinoma F9 (*22*) and the parietal endoderm cells PYS-2 (*23*) derived from teratocarcinoma OTT6050 were the gifts of Dr. Karen Artz, Memorial Sloan-Kettering Cancer Center, New York, N.Y. All cells were grown in Eagle's minimum essential medium (GIBCO, Grand Island, N.Y.) supplemented with 5% (vol/vol) fetal bovine serum (Reheis Chemical Co., Phoenix, Ariz.) and 1% antibiotic–antimycotic (GIBCO). Adherent cell lines were harvested with a mixture of 0.2% (wt/vol) trypsin, 0.002% (wt/vol) collagenase, and 2.5% (vol/vol) chick serum in Ca–Mg-free Hanks' balanced salt solution. They were then passaged every 3 days.

Cell cloning.—Cells were diluted to approximately 2×10^{2} cells/ml in growth medium, and 10-μl droplets of this suspension were placed in the center of each well of a 24-well plate (Linbro, subsidiary of Flow Laboratories, Inc., McLean, Va.). Each droplet was examined visually with an inverted phase-contrast microscope, and wells containing a single cell were filled with growth medium consisting of approximately 10^{3} irradiated primary embryonic fibroblasts. Cloning efficiency for the TerC cell line was about 90%.

ABBREVIATION USED: $[^{125}\text{I}]$IdUrd=$[^{125}\text{I}]$5-iodo-2′-deoxyuridine.

---

[1] Received December 11, 1981; revised May 19, 1982; accepted July 16, 1982.

[2] Supported by Public Health Service grant AI-14584 from the National Institute of Allergy and Infectious Diseases (to M. E.) and by a training grant from the National Institute of Health to the Department of Biology, The Johns Hopkins University.

[3] Contribution #1157 from the Department of Biology, The Johns Hopkins University.

[4] Department of Biology, The Johns Hopkins University, 34th and North Charles Sts., Baltimore, Md. 21218.

[5] *Address reprint requests to* Dr. Searls at his *present address*: The Wistar Institute, 36th St. at Spruce, Philadelphia, Pa. 19104.

Antisera.—High-titered anti-H-2 antisera were raised in mice in the congenic combination C3H anti-C3H.SW (anti-$H\text{-}2^b$) and its reciprocal, C3H.SW anti-C3H (anti-$H\text{-}2^k$) by use of the following protocol: day 0, inject ip spleen and mesenteric lymph node cells in a donor:recipient ratio of 1:4; day 14, follow the same procedure as used on day 0; day 35, inject sc spleen and lymph node, sonicated with complete Freund's adjuvant, at 1:4; day 45, bleed from the retro-orbital sinus; day 50, inject ip spleen and lymph node at 1:5; days 52 and 59, bleed; day 63, inject ip spleen and lymph node at 1:5 with 10^6 Ehrlich ascites tumor cells; day 72, bleed and remove ascites; day 78, bleed terminally and remove ascites. High titers of polyspecific antibodies were found in both serum and ascitic fluid. For this study, only serum from the final bleed was used; reactions with lymphocytes of different *H-2* haplotypes are shown in table 1. Low levels of reactivity against L-cells were found in the anti-$H\text{-}2^b$ serum but were removed by absorption without affecting reactivity against TerC or EL 4. Age-matched and sex-matched C3H normal mouse serum was used as a control. All sera were heated for 30 minutes at 56°C, a procedure that removed some nonspecific reactions without affecting titers.

Putatively monospecific anti-H-2 sera were obtained from the Genetics and Transplantation Biology Branch, National Institute of Allergy and Infectious Diseases, Bethesda, Md.

Sera were titered against mouse lymphocytes by a two-step microcytoxicity assay (*24*).

Assay for cell damage by [^{125}I]IdUrd uptake.—This assay is an adaptation of the [^{14}C]uridine method of Garrido et al. (*25*). Freshly harvested cells were brought to a concentration of 5×10^6 cells/ml growth medium, and 30 µl of this suspension was dispensed into each well of a 96-well microtiter plate (Costar, Data Packaging Corp., Cambridge, Mass.). Between steps of the procedure, plates were returned to a humidified, 5% CO_2, 37°C incubator; 10 µl of appropriately diluted antiserum (or, in control wells, growth medium) was added, for a final dilution of 1:4 of the initial dilution. After 10 minutes, 10 µl of diluted rabbit serum used as a source of complement (Pel-Freez Bio-Animals, Inc., Rogers, Ariz.) was added, for a final dilution 1:5 of the initial dilution. Growth medium was added to some wells instead of complement to gauge the nonspecific effects of complement alone. After 10 minutes, 100 µl of growth medium with a total of 2% antibiotic–antimycotic was added, and the plates were incubated for 2–4 hours. At the end of this time, 10 µl of [^{125}I]IdUrd (New England Nuclear Corp., Boston, Mass.) at 0.1 µCi/ml in growth medium was added to each well for a final dilution of 1 µCi/well. (Addition of the label immediately after the other steps resulted in an appreciable reduction in uptake.) Cells were allowed to take up label overnight (16–18 hr) and were then collected in a cell harvester (Otto Hiller Co., Madison, Wis.) with the use of 934 AH glass fiber filter paper (Whatman Inc., Clifton, N.J.). Filters were counted in a Beckman gamma counter.

Percent inhibition of [^{125}I]IdUrd uptake was calculated as follows, where *C* is the mean uptake (in cpm) in control wells, *E* is the uptake in those containing antiserum, and *B* is the counter background:

$$\text{Percent inhibition} = \frac{C-E}{C-B} \times 100.$$

The standard deviation of the percent inhibition is given as

$$\frac{E}{C} \times \sqrt{\frac{e^2}{E^2} + \frac{c^2}{C^2}},$$

where lowercase letters represent the standard deviations of their respective (uppercase letters) means.

A large number of lots of rabbit serum were tested in this assay, and about one lot in seven was selected and pooled on the basis of relatively high specific and low nonspecific activities. Complement was generally used at a final dilution of 1:20, a concentration that nonspecifically inhibited [^{125}I]IdUrd uptake by approximately 20% while maintaining maximal specific reactions.

All additions to the wells were sterile except for antisera and complement. The concentration of antibiotic–antimycotic was raised to 2% as a precaution; visual inspection revealed no evidence of contamination attributable to the nonsterilized additions, and test wells containing label but no cells gave no counts above background.

Absorption assay.—Varying numbers of cells were used to absorb 50 µl of anti-H-2 sera for 2 hours on ice. Antisera were diluted to give approximately 90% lysis of target cells (mesenteric node lymphocytes), as judged by nigrosin dye exclusion. Cell diameters were determined with a Zeiss micrometer eyepiece.

RESULTS

Characterization of *H-2* Expression on TerC

The titers of our antisera in a conventional complement-dependent cytoxicity assay on lymphocytes are given in

TABLE 1.—*Titers of anti-*H-2 *sera by conventional microcytotoxicity against a standard panel of lymphocytes*

Strain	Haplotype	Anti-$H\text{-}2^b$	Anti-$H\text{-}2^k$	D-2	D-5AF	D-28(2)	D-29	D-33	D-35
C3H.SW	*b*	2,560	—	80	40	160	40	1,280	40
B10.D2	*d*	160	640	—	—	80	40	—	40
B10.M	*f*	80	—	—	—	—	—	—	—
C3H.JK	*j*	1,280	640	5	—	20	10	—	40
C3H/He	*k*	—	1,280	—	160	—	—	—	10
DBA/1	*q*	2,560	640	10	80	40	10	—	—
RIII/2J	*r*	80	1,280	—	20	—	—	—	—
SJL/J	*s*	1,280	80	—	40	1,280	—	—	—
B10.PL	*u*	1,280	—	—	40	40	40	10	20
B10.SM	*v*	80	—	—	160	20	80	80	—
B10.A	*a*	640	640	—	80	80	20	—	20

table 1. These antisera are described fully in table 2, which also indicates their activity in the [^{125}I]dUrd-uptake inhibition assay against TerC and two control cell lines, EL 4 (*H-2^b*) and LM (*H-2^k*). Antisera detecting both *K*- and *D*-end private specificities (after absorptions that rendered them monospecific) reacted with TerC to some degree, as did at least two antisera against public specificities. Two other antisera with weak titers against *H-2^b* public antigens did not show appreciable reactions with TerC. High-titered oligospecific antisera against *H-2^k* public and private specificities were also tested (data not shown) and did not react with TerC. The polyspecific anti-*H-2^b* antiserum also reacted at high concentrations, whereas the reciprocal anti-*H-2^k* did not. All antisera reacted as expected with the H-2-positive control cell lines.

The anti-*H-2^b* antiserum was absorbed with the control cell lines and with a series of B10-congenic lymphocytes as shown in table 3. EL 4 cells were able to completely absorb the activity of this antiserum with TerC, whereas LM cells failed to do so. An appropriate number of *H-2^b* lymphocytes also ablated the reactivity; *H-2^k* lymphocytes were ineffective. Recombinant haplotypes absorbed only part of the serum's activity, which confirmed that products at both ends of the *H-2* complex were being detected by the polyspecific anti-*H-2^b* serum.

Clonal Variation in *H-2* Expression

Even at high concentrations of anti-*H-2^b*, specific inhibition of TerC seldom exceeded 50%. This observation raised the possibility that a subpopulation of cells was expressing relatively higher levels of the antigen. To test this possibility, we cloned the line and tested several of the resulting clonal lines along with a series of control cell lines as shown in table 4. Some variation was found; two clones, TerCb and TerCe, consistently demonstrated the highest and lowest reactivities, respectively. Nevertheless, growth even of TerCb was never completely inhibited, and all of the clones reacted to some degree. The F9 embryonal carcinoma cells, though derived from the same mouse strain as TerC, were not damaged by anti-*H-2^b*. The PYS-2 parietal endoderm cells from the same strain were somewhat more sensitive to the antiserum than were any of the TerC clones. Like the parent cell line, these clones were completely negative by immunofluorescence when the same antisera were used at a 1:2 dilution (data not shown).

Reactivity of the TerC clones tended to level off at the higher antiserum concentrations (table 4). Inasmuch as antibody is probably in excess at this point, it may be that antigens are saturated with antibody but that they are too few in number to effect efficient complement-mediated killing by IgG antibodies; it is also possible that TerC is intrinsically resistant to complement-dependent lysis. However, since teratocarcinoma-derived cell lines tend to differ-

TABLE 3.—*Effect of absorption of anti-H-2^b with tumor cells and lymphocytes on inhibition of [^{125}I]IdUrd uptake by TerC*[a]

Absorbing cell	*H-2* haplotype	No. of cells, $\times 10^{-6}$	Residual inhibition, %
EL 4	*b*	1	12±6
LM	*k*	1	100±24
B10	*b*	1	95±3
B10	*b*	2	73±3
B10	*b*	4	16±6
B10	*b*	8	22±4
B10	*b*	16	−13±5
B10.Br	*k*	16	100±3
B10.A(2R)	*k/b*	16	51±5
B10.A(4R)	*k/b*	16	61±3
B10.A(5R)	*b/d*	16	60±19

[a] 100 µl of anti-*H-2^b* at a 1:10 dilution was absorbed as indicated and then tested against TerC by [^{125}I]IdUrd uptake inhibition at a final dilution of 1:40. Residual inhibition is shown as a percent of inhibition by unabsorbed antiserum.

TABLE 2.—*Reactivities of anti-H-2 sera by inhibition of [^{125}I]IdUrd uptake*

Antiserum	Immunization	Preparative absorptions[a]	Specificity No. (description)	Percent inhibition of [^{125}I]IdUrd uptake		
				EL 4	LM	TerC
Anti-*H-2^b*	C3H anti-C3H.SW	—	Polyspecific	99±0	−5±14	47±5
Anti-*H-2^k*	C3H.SW anti-C3H	—	Polyspecific	−10±9	97±2	6±12
D-2	[B10.A(5R) × LP.RIII] anti-B10	q[b]	2 (*D*-end private)	77±8	1±11	33±8
D-5AF	(B10.M × DBA/2) anti-B10.PL	—	5 (public)	65±7	55±24	27±4
D-28(2)	(B10.Br × LP.RIII) anti-B10.A(2R)	—	28, 36 (publics)	99±0	−2±12	64±2
D-29	(SJL × AKR) anti-AKR.M	d[c]	56 (public)	Not done	Not done	16±9
D-33	(B10.D2 × A) anti-B10.A(5R)	q,[d] u,[e] v[f]	33 (*K*-end private)	99±0	9±13	49±15
D-35	[B10.A(2R) × A.CA] anti-B10.Y	—	35 (public)	26±3	−16±23	21±15

[a] These absorptions remove undesired reactions observed in the panel test above and also noted in the National Institutes of Health Catalog of Mouse Alloantisera. Generally, 2–3 volumes of appropriately diluted antisera were absorbed for 2 hr on ice with 1 volume of packed lymphocytes teased from spleens and lymph nodes of mice noted below.

[b] Absorption with DBA/1 removes a weak reaction against *H-2.56*.

[c] Precautionary absorption with B10.D2 removes a potential reaction against *H-2.29* (not present, according to the National Institutes of Health catalog).

[d] Precautionary absorption with DBA/1 removes a potential reaction against *H-2.54* (weak, according to the National Institutes of Health catalog, and not detected in the panel test above).

[e] Absorption with B10.PL removes a weak reaction against *H-2.53*.

[f] Absorption with B10.SM removes a nonspecific reaction, also noted in the National Institutes of Health catalog. All antisera were tested against control cell lines EL 4 and LM at dilutions of 1:500 and against TerC at a dilution of 1:20.

best copy available

TABLE 4.—*Inhibition of [^{125}I]IdUrd uptake of TerC clones and control cell lines by anti-*H-2 *sera and complement*

Antiserum	Dilution	EL 4	LM	TerCa	TerCb	TerCe	TerCf	TerCg	F9	PYS-2
C3H anti-C3H.SW (anti-$H\text{-}2^b$)	40	100±1	−19±15	32±10	64±17	19±8	25±3	26±8	9±16	80±10
	200	100±1	1±14	32±11	67±15	16±10	19±5	19±10	13±14	49±7
	1,000	100±1	—	5±16	35±8	11±7	15±8	−5±8	7±13	22±18
	5,000	100±3	—	8±10	23±8	−1±11	2±8	−2±14	−3±20	20±8
	25,000	77±3	—	—	—	—	—	—	0±17	15±35
C3H.SW anti-C3H (anti-$H\text{-}2^k$)	40	−19±14	100±1	−14±10	2±29	−12±12	−4±4	−18±18	−13±20	−5±30
	200	—	100±1	—	—	—	—	—	—	—
	1,000	—	100±1	—	—	—	—	—	—	—
	5,000	—	72±9	—	—	—	—	—	—	—
	25,000	—	28±12	—	—	—	—	—	—	—
C3H normal mouse serum	40	18±12	18±11	5±12	−5±21	−6±7	—[a]	—[a]	3±13	9±10

[a] Not done.

TABLE 5.—*Effects of time in culture on inhibition of [^{125}I]IdUrd uptake by anti-*H-2^b *and complement*[a]

Expt No.	Time in culture	TerCb	TerCe
1	3 days since subculturing	64±17	29±1
	12 days since subculturing	43±13	10±9
2	1 mo since cloning	56±8	30±2
	4 mo since cloning	36±11	35±5
	8 mo since cloning	28±13	13±4

[a] Data are expressed as percent inhibition relative to that of normal mouse serum. Anti-$H\text{-}2^b$ was used at a final dilution of 1:40. Percent inhibition with anti-$H\text{-}2^k$ at 1:40 never exceeded 10%.

TABLE 6.—*Quantitative absorption of anti-*H-2 *sera*[a]

Antiserum (immunization)	Absorbing cell (haplotype)	No. of absorbing cells, × 10^{-6}	Percent cytotoxicity
Anti-$H\text{-}2^b$ (C3H anti-C3H.SW)	129/SvSl ($H\text{-}2^{bc}$)	1/64	90
		1/16	75
		1/4	40
		1	20
	TerCb ($H\text{-}2^{bc}$)	1/8	95
		1/2	85
		2	45
		8	15
	TerCe ($H\text{-}2^{bc}$)	1/8	95
		1/2	90
		2	50
		8	25
Anti-$H\text{-}2^k$ (C3H.SW anti-C3H)	C3H/He ($H\text{-}2^k$)	1/64	90
		1/16	75
		1/4	25
		1	10
	TerCb	8	80
	TerCe	8	85

[a] Antisera were diluted and absorbed as described in "Materials and Methods." Anti-$H\text{-}2^b$ was tested against 129/SvSl lymphocytes, and anti-$H\text{-}2^k$ was tested against C3H/He lymphocytes by standard microcytotoxicity.

entiate spontaneously, even their clones may produce heterogeneous cell populations despite clonal origins.

If TerC were exhibiting a tendency to differentiate to an H-2-positive cell type, it might be expected that the proportion of such cells would increase with time in culture or [by analogy with the differentiation of pluripotent embryonal carcinoma cells in culture (*7*)] with time after subculturing. As can be seen in table 5, this is not the case; the reactivity of TerC clones with anti-H-2^b, in fact, decreased somewhat under both circumstances.

Quantitation of H-2 Antigens

To quantitate relative levels of *H-2* expression on these lines, we used TerCb and TerCe to absorb anti-*H-2* sera, which were then retested on the appropriate target lymphocytes by standard microcytotoxicity. Table 6 shows the results of these absorptions in comparison with absorptions by the target lymphocytes. The TerC clones were five to ten times less effective than lymphocytes in absorbing anti-$H\text{-}2^b$ reactivity. Inasmuch as the cell diameters of the TerC lines are about three times greater than those of lymphocytes, the ratio of their surface areas is approximately 9:1 [neglecting microvilli, which are found on both cell types (Ostrand-Rosenberg S: Personal communication)]. Thus the density of H-2 antigens on the TerC lines appears to be fiftyfold to a hundredfold less than that on lymphocytes.

DISCUSSION

An assay for antibody plus complement-mediated cell damage, measured by inhibition of [^{125}I]IdUrd uptake, has been used to detect low levels of *K*- and *D*-end gene products of the *H-2* complex on the teratocarcinoma-derived cell line TerC. This conclusion is supported by the cell line's reaction with a wide variety of anti-$H\text{-}2^b$ sera, including operationally monospecific reagents detecting both private specificities, and by the absorption of the activity against TerC with lymphocytes of the appropriate haplotypes. The partial absorptions observed with recombinant haplotypes also suggest that the reactions are not due solely to closely linked loci on one side or the other of the *H-2* complex, such as the *Qa*, the *Tla*, or the *T*-locus. It is also unlikely that the reactions with TerC are attributable to Ia antigens, since absorption with the Ia-negative, $H\text{-}2^b$-positive cell line EL 4 (*26*) completely removed the activity. Although it is possible that the assay is detecting fetal or tumor antigens with determinants cross-reactive with H-2 specificities, this alternative explanation is highly unlikely since many specificities of the $H\text{-}2^b$ haplotype are expressed while no specificities of the $H\text{-}2^k$ haplotype appear to be present.

Using a highly sensitive [^{14}C]uridine-uptake inhibition assay (from which the present assay was adapted), Garrido et al. (*25*) detected numerous "inappropriate" H-2 specificities in virally transformed cell lines. The failure of a high-titered, polyspecific anti-*H-2*^{k} serum (in which only H-2^{b} specificities are "covered") to react with TerC suggests that no such unexpected specificities are being detected. Using cell lines derived from mouse blastocysts in quantitative absorption studies, Ostrand-Rosenberg et al. (*24*) found that individual H-2 specificities were present in widely varying proportions relative to each other on embryo-derived cell lines when compared to adult lymphocytes. In the absence of such quantitative absorptions with monospecific sera, such a phenomenon cannot be ruled out with the TerC line, but the reactivities of the antisera employed in this study against lymphocytes, the EL 4 cell line, and TerC were of roughly the same degree relative to each other; i.e., relative to those antisera with weak titers, antisera with high titers against *H-2*^{b} lymphocytes in standard microcytotoxicity reacted strongly in [^{125}I]IdUrd uptake inhibition with EL 4 and TerC. Thus neither unexpected specificities nor unusual proportions of appropriate specificities relative to each other have been detected in the data presented.

The nullipotent embryonal carcinoma line F9 showed no specific anti-*H-2*^{b} reactivity when our [^{125}I]IdUrd assay was used (table 4). However PYS-2, a parietal yolk-sac carcinoma derived from the same tumor, reacted somewhat more strongly than did TerC. Thus endodermal derivatives of the teratocarcinoma model system appear to demonstrate *H-2* expression quantitatively lower than but qualitatively similar to adult patterns of *H-2* expression.

REFERENCES

(*1*) Wiley LM. Early embryonic cell surface antigens as developmental probes. Curr Top Dev Biol 1979; 13:167.

(*2*) Gachelin G. The cell surface antigens of mouse embryonal carcinoma cells. Biochim Biophys Acta 1978; 516:27–60.

(*3*) Solter D, Knowles BB. Monoclonal antibody defining a stage-specific mouse embryonic antigen (SSEA-1). Proc Natl Acad Sci USA 1978; 75:5565–5569.

(*4*) Artzt K, Jacob F. Absence of a serologically detectable H-2 on primitive teratocarcinoma cells in culture. Transplantation 1974; 17:632–634.

(*5*) Doherty PC, Solter D, Knowles BB. *H-2* gene expression is required for T cell-mediated lysis of virus-infected target cells. Nature 1977; 266:361.

(*6*) Gmur R, Solter D, Knowles BB. Independent regulation of *H-2K* and *H-2D* gene expression in murine teratocarcinoma somatic cell hybrids. J Exp Med 1980; 151:1349–1359.

(*7*) Stern PL, Martin GR, Evans MJ. Cell surface antigens of clonal teratocarcinoma cells at various stages of differentiation. Cell 1975; 6:455–465.

(*8*) Gooding LR, Edidin M. Cell surface antigens of a mouse testicular teratoma. Identification of an antigen physically associated with H-2 antigens on tumor cells. J Exp Med 1974; 140:61–78.

(*9*) Gooding LR. Expression of early fetal antigens on transformed mouse cells. Cancer Res 1976; 36:3499–3502.

(*10*) Larraga V, Edidin M. Immunochemical characterization of surface antigens of TerC, a teratocarcinoma-derived cell line. Proc Natl Acad Sci USA 1979; 76:2912–2916.

(*11*) Bartlett PF, Fenderson BA, Edidin M. Inhibition of tumor growth mediated by lymphocytes sensitized in vitro to a syngeneic murine teratocarcinoma 402AX. J Immunol 1978; 120:1211–1217.

(*12*) Edidin M, Gooding LR, Johnson MH. Surface antigens of normal early embryos and a tumour model system useful for their further study. In: Diczfalusy E, ed. Immunological approaches to fertility control. Stockholm: Karolinska Institute, 1974:336–356.

(*13*) Ostrand-Rosenberg S, Rider TM, Twarowski A. Susceptibility of allogeneic mice to teratocarcinoma 402AX. Immunogenetics 1980; 10:607–612.

(*14*) Searls DB. Studies with teratocarcinoma-derived cell lines. Ph.D. thesis. Baltimore: The Johns Hopkins University, 1980.

(*15*) Snell GD, Stevens LC. Early embryology. In: Green EL, ed. Biology of the laboratory mouse. New York: McGraw-Hill, 1966:205–246.

(*16*) Pierce GB, Dixon FJ, Verney E. Testicular teratoma. I. Demonstration of teratogenesis by metamorphosis of multipotential cells. Cancer 1959; 12:573–583.

(*17*) Martin GR, Evans MJ. Differentiation of clonal lines of teratocarcinoma cells: Formation of embryoid bodies in vitro. Proc Natl Acad Sci USA 1975; 72:1441–1445.

(*18*) Solter D, Knowles BB. Developmental stage-specific antigens during mouse embryogenesis. Curr Top Dev Biol 1979; 13:139–165.

(*19*) Bennett D, Boyse EA, Old LJ. Cell surface immunogenetics in the study of morphogenesis. In: Silvestri LG, ed. Cell interactions. Amsterdam: Elsevier/North-Holland, 1971:247–263.

(*20*) Edelman GM. Perspective. In: Kahan B, Reisfeld R, eds. The cell surface: Immunological and chemical approaches. New York: Plenum Press, 1975:260–266.

(*21*) Herberman RB, Kirchner H, Holden HT, Glaser M, Haskill S, Bonnard GD. Cell mediated immunity in murine virus tumor systems. In: Crowell R, Friedman H, Prier J, eds. Tumor virus infections and immunity. Baltimore: Univ Park Press, 1976: 147–164.

(*22*) Artzt K, Dubois P, Bennett D, Condamine H, Babinet C, Jacob F. Surface antigens common to mouse cleavage embryos and primitive teratocarcinoma cells in culture. Proc Natl Acad Sci USA 1973; 70:2988–2992.

(*23*) Lehman JM, Speers WC, Swartzendruber DE, Pierce GB. Neoplastic differentiation: Characteristics of cell lines derived from a murine teratocarcinoma. J Cell Physiol 1974; 84:13–28.

(*24*) Ostrand-Rosenberg S, Hammerberg C, Edidin M, Sherman MI. Expression of histocompatibility-2 antigens on cultured cell lines derived from mouse blastocysts. Immunogenetics 1977; 4:127–136.

(*25*) Garrido R, Schirrmacher V, Festenstein H. *H-2*-like specificities of foreign haplotypes on a mouse sarcoma after vaccinia virus infection. Nature 1976; 259:228–229.

(*26*) Sachs DH, Cone JL. Ir-associated murine alloantigens: Demonstration of multiple Ia specificities in *H-2* alloantisera after selective absorptions. J Immunol 1975; 114:165–169.

blank page

Inhibitory Effect of Fumaric Acid on Forestomach and Lung Carcinogenesis by a 5-Nitrofuran Naphthyridine Derivative in Mice[1]

Keiko Kuroda,[2] Masayoshi Kanisawa,[3] *and* Mitsutaro Akao[2]

ABSTRACT—The inhibitory effect of fumaric acid (FA) on carcinogenesis by potassium 1-methyl-7-[2-(5-nitro-2-furyl)vinyl]-4-oxo-1,4-dihydro-1,8-naphthyridine-3-carboxylate (*trans*, NFN) was examined histologically with male ICR/JCL mice. NFN was fed to mice at a dose level of 0.012% in the diet for 14 weeks. These mice were then divided into 2 groups. One group was given a basal diet, and the other group was given a diet containing 1% FA in the subsequent 39 weeks. In the group of 30 mice fed NFN alone, squamous cell carcinomas were found in the stomachs of 7 mice, multiple papillomas in the stomachs of 13 mice, and multiple and large papillary adenocarcinomas in the lungs of 27 animals. The administration of FA suppressed the NFN-induced stomach and lung carcinogenesis. In the group of 32 mice fed NFN and FA, no stomach tumors developed except 1 early-stage of squamous cell carcinoma. In the lungs, only a small focus of mild atypical hyperplasia and a few early-stage adenocarcinomas were noted in 7 and 11 animals, respectively.—JNCI 1982; 69:1317–1320.

Previously, we indicated that the extract of *Capsella bursa-pastoris* (Cruciferae) herb has various kinds of pharmacologic activities such as diuretic, oxytocic, anti-inflammatory, antiulcerative, and anticarcinogenic (*1–4*). Later we isolated and identified FA as the component of the herb responsible for inhibiting the growth of subcutaneously transplanted Ehrlich tumors in mice (*5*) or gastric ulcers in rats (*6*).

NFN (*trans*) was synthesized by Nishigaki et al. (*7*) as a therapeutic agent for *Pseudomonas* infection but later was found by Kanisawa et al. (*8*) to be carcinogenic to the stomach and lung in mice fed the 5-nitrofuran with their diets and to the oral mucosa, esophagus, forestomach, lung, and mammary gland in animals given NFN with their drinking water (Kanisawa M: Unpublished data).

Recently, we (*9, 10*) found that FA reduced toxicity in mice exposed to mitomycin C and aided in the recovery of cultured cells that had been exposed to mitomycin C, NFN, and other carcinogens. In the present study, we examined the effect of FA on the carcinogenic processes in the stomach and lung tissues of mice fed the 5-nitrofuran carcinogen.

MATERIALS AND METHODS

Chemicals.—NFN (*trans*) was prepared by Daiichi Pharmaceutical Co., Tokyo, Japan, and FA was purchased from Nakarai Chemicals Ltd., Kyoto, Japan.

Animals and feed.—A total of 81 male ICR/JCL mice (CLEA Japan Inc., Tokyo), 5 weeks old, were used. Commercial diet CE-2 (CLEA Japan Inc.) was used as the basal diet, and an experimental diet containing either 0.012% of NFN or 1% of FA was also prepared by the same manufacturer. The animals were housed in an air-conditioned room kept at 23°C and 60% relative humidity with 12-hour light and 12-hour dark cycles.

Experimental procedure.—The feeding schedule is shown in text-figure 1. The animals were divided into 3 groups. Sixty-six mice weighing about 25 g were given the diet containing 0.012% of NFN for 14 weeks, and then the mice were divided into groups 1 and 2. Thirty-three mice of group 1 were given the basal diet for 39 weeks, while the same number of mice of group 2 were given the diet containing 1% FA for the same period. Fifteen mice of the control group were given the basal diet for 53 weeks. All animals were killed at the end of 53 weeks, and all organs except brain and bone marrow were fixed in a 10% Formalin solution. The stomach and lung were particularly fixed with instillation of 10% Formalin solution into the gastric or bronchial lumen. Animals that died during the feeding experiment were also necropsied. Five animals of group 1 and 1 animal of group 2, all of whom died after 7 months of the experiment, were counted as effective animals, inasmuch as the 5 animals of group 1 were found to have developed lung carcinomas. After macroscopic observation, all the tissues and tumors found in the gastric mucosa and the pleural surface of the lung were sliced, embedded in paraffin, sectioned, stained with hematoxylin and eosin, and examined histologically.

RESULTS

Untreated control mice showed no neoplastic changes in the stomach and lung. The administration of NFN to mice resulted in widespread growth of 7 squamous cell carcinomas (23% in incidence with regard to the effective number of animals; figs. 1–3), 3 keratinized and 4 nonkeratinized, and 13 multiple squamous cell papillomas (43%), which sometimes showed focal atypia (figs. 4, 5) in the stomachs. Leiomyosarcoma was found in the forestomach wall of 1 animal. NFN administration also produced large and multiple papillotubular adenocarcinomas (figs. 7–9) in the lungs of most animals (90%). In the mice given FA after the administration of NFN, the development of neoplastic changes was almost completely inhibited (fig. 6). Squamous epithelium of the forestomach as well as the glandular stomach mucosa showed no pathologic alterations, except

---

ABBREVIATIONS USED: FA=fumaric acid; NFN=potassium 1-methyl-7-[2-(5-nitro-2-furyl)vinyl]-4-oxo-1,4-dihydro-1,8-naphthyridine-3-carboxylate.

---

[1] Received January 4, 1982; revised July 10, 1982; accepted August 4, 1982.

[2] Department of Toxicology and Experimental Pathology, Research Institute for Chemobiodynamics, Chiba University, Inohana, Chiba 280, Japan.

[3] Department of Pathology, Yokohama City University, School of Medicine, Urafune-cho, Minami-ku, Yokohama 232, Japan.

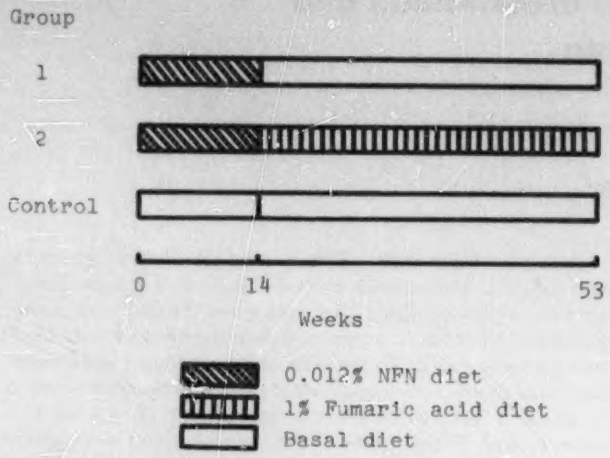

TEXT-FIGURE 1.—Experimental methods.

TABLE 1.—*Inhibitory effect of FA on induction of tumors and associated lesions in mice fed NFN*

Site of tumor	Tumor type	Group[a]		
		Control (15)	NFN (30)	NFN+FA (32)
Forestomach	Keratinized squamous cell carcinomas	0	3	0[b]
	Nonkeratinized squamous cell carcinomas	0	4	0[b]
	Early stage of squamous cell carcinoma	0	0	1
	Multiple papillomas	0	13	0
	Leiomyosarcoma	0	1	0
Lung	Papillotubular adenocarcinomas	0	27	0[c]
	Early stage of adenocarcinomas	0	2	11
	Mild atypical hyperplasia	0	1	7

[a] *Numbers in parentheses* are the effective No. of animals.

[b] Significant at $P<0.05$ by Fisher's exact probability test as compared with the induction of squamous cell carcinomas in NFN group.

[c] Significant at $P<0.01$ as compared with NFN group.

for the presence of an early-stage squamous cell carcinoma that showed minimal invasive growth of atypical squamous cells into the submucosa. Macroscopic observation of the lungs failed to indicate obvious tumor development, but histologic examination revealed early stages of adenocarcinoma in 11 mice (34%; fig. 10) and a small focus of hyperplasia of atypical bronchiolar cells in 7 mice (22%; fig. 11). Results obtained are summarized in table 1. In other organs no tumor development was observed except leukemia; 1 leukemia was seen in the group fed NFN alone and 2 leukemias were found in the group fed NFN and FA. Microscopic examination also indicated that no pathologic change was induced by NFN or FA at the dose levels used in this experiment.

DISCUSSION

In our previous experiment (*4*) we used the extract of *C. bursa-pastoris*, which completely inhibited hepatocarcinogenesis in the rats fed the 0.06% 3-methyl-4′-(dimethylamino)azobenzene-containing diet for 50 days and then given drinking water containing the herb extract at a concentration of 0.2% for 285 days. In the present study, a possible inhibitory effect of FA (an active component of the herb extract) on the carcinogenic process by a different carcinogen, NFN, was examined histologically. As a result, induction of forestomach cancer as well as neoplastic papillomatous growth in the mice fed a carcinogenic amount of NFN was almost completely inhibited by the subsequent administration of FA. This anticarcinogenic activity was also noted in the lung, although it was not as complete as in the stomach. The reason for this difference in the anticarcinogenic activity of FA is so far unknown. There may be certain differences in the susceptibility or affinity of the target cells of the gastric and respiratory epithelia to NFN. This hypothesis is supported by the fact that the feeding of a higher dose (0.1% in the diet) of NFN for 1 week produced multiple pulmonary tumors (7.6 nodules/mouse) in more than 90% of ICR mice, whereas in the stomach only benign papillomas (60% in incidence) developed. Also, the induction time of pulmonary tumors was earlier (*8*). These results indicating the vulnerability of respiratory epithelium to NFN might be related to the fact that NFN produces its carcinogenic effect quite selectively and quickly on the bronchiolar nonciliated Clara cells without causing any obvious morphologic changes in the forestomach epithelium (*11*). Another possible explanation for the above-mentioned results is that FA affects nonspecifically tissues of the whole body. FA has various kinds of activities supposedly related to the present finding; i.e., FA inhibits gastric ulceration in rats (*6*), inhibits the solid growth of Ehrlich tumors in mice (*5*), and reduces the toxicity of mitomycin C and some carcinogens including NFN (*9*, *10*). Either of these activities or a combination of these activities of FA might be associated with the inhibitory effect on carcinogenesis. The increase of the concentration of FA in the diet or the simultaneous administration of FA with NFN would be expected to bring about a complete inhibition of cancerous changes in the lung.

REFERENCES

(*1*) KURODA K, TAKAGI K. Physiologically active substance in *Capsella bursa-pastoris*. Nature 1968; 220:707–708.

(*2*) ———. Studies on *Capsella bursa-pastoris*. I. General pharmacology of ethanol extract of the herb. Arch Int Pharmacodyn Ther 1969; 178:382–391.

(*3*) ———. Studies on *Capsella bursa-pastoris*. II. Diuretic, anti-inflammatory and anti-ulcer action of ethanol extract of the herb. Arch Int Pharmacodyn Ther 1969; 178:392–399.

(*4*) KURODA K, AKAO M, KANISAWA M, MIYAKI K. Inhibitory effect of *Capsella bursa-pastoris* on hepatocarcinogenesis induced by 3′-methyl-4-(dimethylamino)azobenzene in rats. Gan 1974; 65:317–321.

(*5*) ———. Inhibitory effect of *Capsella bursa-pastoris* extract on growth of Ehrlich solid tumor in mice. Cancer Res 1976; 36:1900–1903.

(*6*) KURODA K, AKAO M. Inhibitory effect of fumaric acid and dicarboxylic acids on gastric ulceration in rats. Arch Int Pharmacodyn Ther 1977; 226:324–330.

(*7*) NISHIGAKI S, YONEDA F, OGIWARA K, et al. Synthesis of 1-substituted-1,4-dihydro-7-[2-(5-nitro-2-furyl)vinyl]-4-oxo-1,8-naphthyridine derivatives. I. Chem Pharm Bull (Tokyo) 1969; 17:1827–1831.

(*8*) KANISAWA M, KATOH H, AISO K. Carcinogenicity of potassium 1-methyl-7-[2-(5-nitro-2-furyl)vinyl]-4-oxo-1,4-dihydro1,8-naphthyridine-3-carboxylate in ICR mice. Gan 1974; 65:1–11.

(*9*) KURODA K, AKAO M. Reduction by fumaric acid of side effects of mitomycin C. Biochem Pharmacol 1980; 29:2839–2844.

(*10*) ———. Antitumor and anti-intoxication activities of fumaric acid in cultured cells. Gan 1981; 72:777–782.

(*11*) KANISAWA M. Experimental studies on peripheral pulmonary tumors in mice—its histogenesis and modes of action of carcinogens administered to remote tissues. Lung Cancer 1980; 20:35–51 (in Japanese).

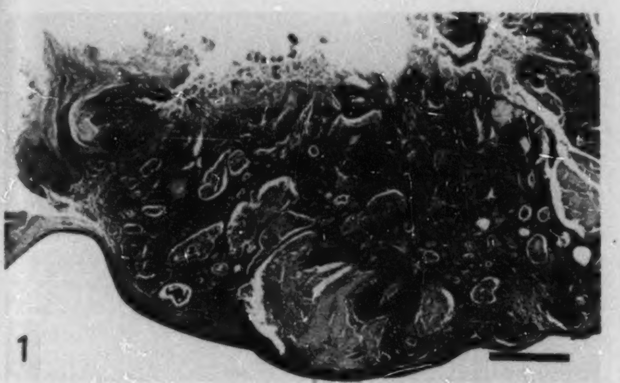

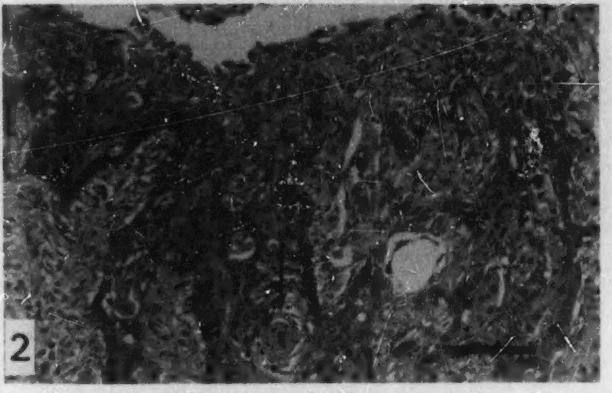

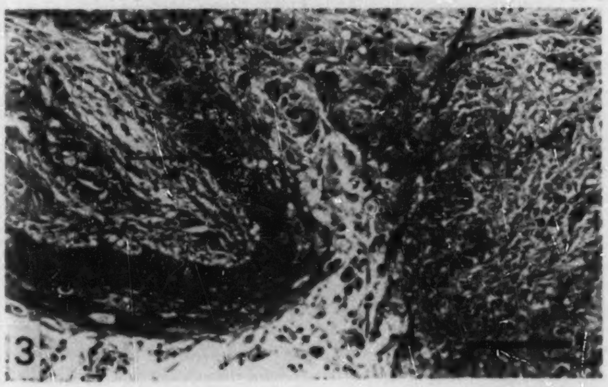

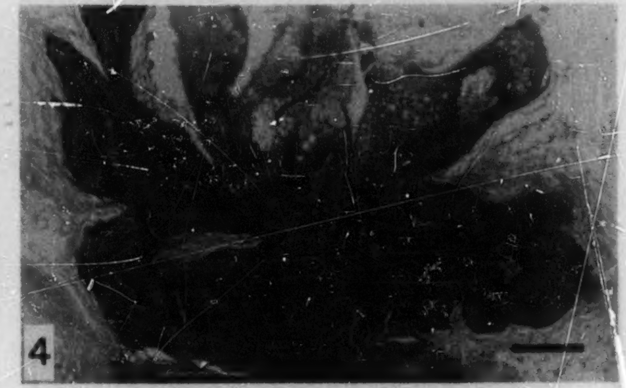

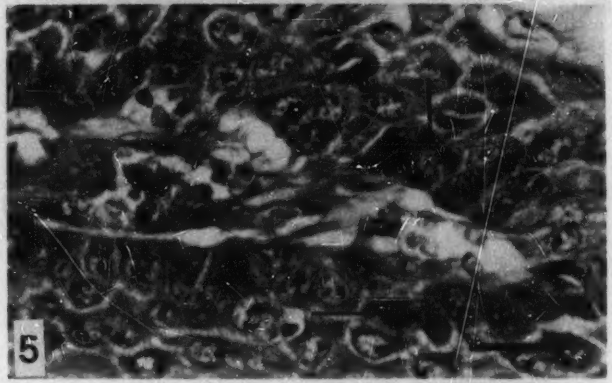

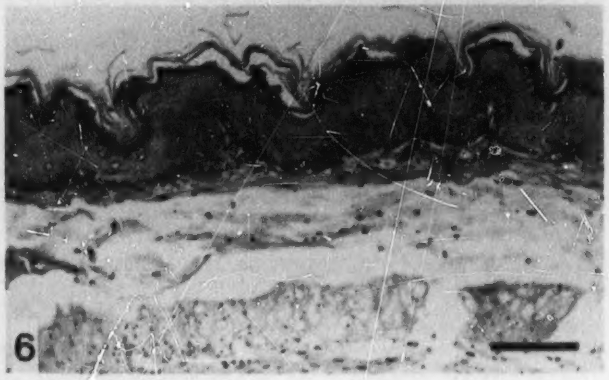

FIGURE 1.—Low power microphotograph of longitudinally sliced stomach with keratinized squamous cell carcinoma in a mouse given 0.012% NFN diet for 14 wk. Nearly whole stomach wall is involved with carcinoma tissue. *Bar* = 1 mm. × 12

FIGURE 2.—Keratinized squamous cell carcinoma in the forestomach of a mouse given NFN diet. Invasive growth of moderately differentiated squamous cell carcinoma with keratinization is demonstrated. *Arrow* indicates a keratin pearl. *Bar* = 100 μm. × 130

FIGURE 3.—Border of normal epithelium and squamous cell carcinoma in the forestomach of a mouse given NFN diet. *Arrow* indicates border. Some individual cell keratinization is also seen. *Bar* = 155 μm. × 100

FIGURE 4.—Multibranched papilloma of squamous epithelium of forestomach of a mouse given NFN diet. A part of papilloma shows marked atypia (*arrow* and fig. 5). *Bar* = 200 μm. × 52

FIGURE 5.—Higher magnification of atypical area of fig. 4. *Arrows* indicate mitotic figures. *Bar* = 25 μm. × 620

FIGURE 6.—Squamous epithelium of the forestomach of a mouse given 1% FA diet for 39 wk after being fed 0.012% NFN diet for 14 wk. Neither pathology of the epithelium nor neoplastic change is observed. *Bar* = 100 μm. × 130

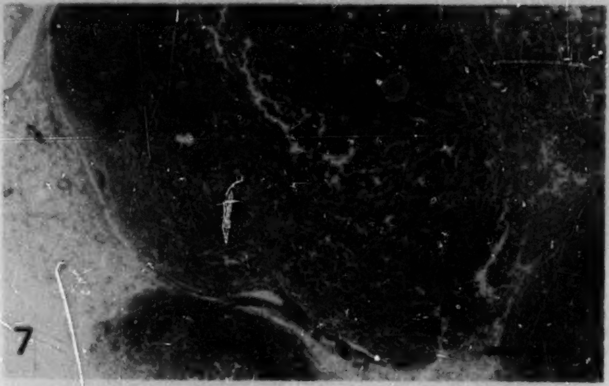

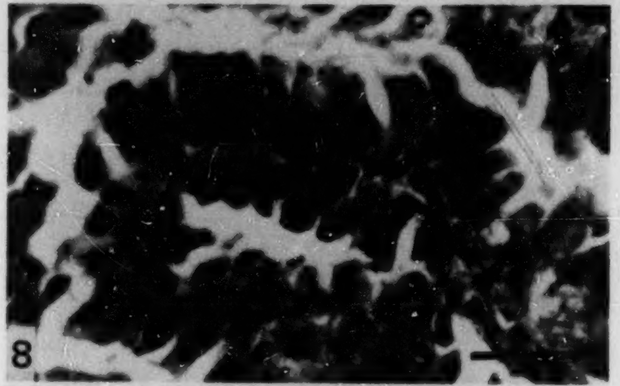

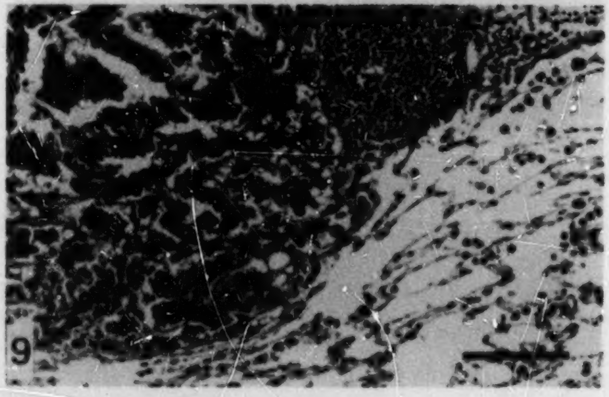

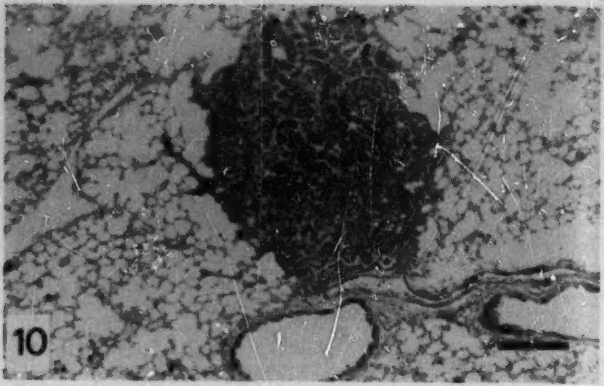

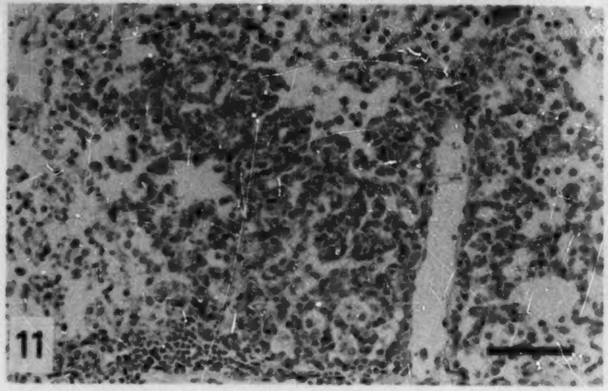

FIGURE 7.—Multiple and large, conglomerated growths of pulmonary carcinoma in a mouse given NFN diet. *Bar* = 1 mm. × 13

FIGURE 8.—Higher magnification of fig. 7. Single-layered high columnar cells contain somewhat irregularly contoured nuclei located at fairly higher position in the cytoplasm and show domelike protrusion of the apical cytoplasm. Such features suggest that these cells may have been derived from Clara cells (*11*). *Bar* = 25 µm. × 620

FIGURE 9.—Border of pulmonary tumor and compressed normal lung tissue in a mouse given NFN diet. Invasive growths of the tumor cells are partly observed. *Bar* = 100 µm. × 52

FIGURE 10.—Solitary papillary adenoma of the lung found by microscopic examination in a mouse given 1% FA diet after being fed NFN diet. Tumor is rather small and is observed only by microscopic examination. *Bar* = 200 µm. × 52

FIGURE 11.—Very mild, atypical cell growth on the alveolar wall of a mouse given 1% FA diet after being fed NFN diet. *Bar* = 100 µm. × 130

Characterization of Anti-Inflammatory Factors Produced by Murine Tumor Cells in Culture[1,2,3]

S. J. Normann[4,5,6] *and* J. Cornelius[4]

ABSTRACT—P-815 mastocytoma cells from DBA/2 mice and a 3-methylcholanthrene-induced fibrosarcoma from C57BL/6 mice produced in culture at least two soluble anti-inflammatory factors that inhibited macrophage accumulation in vivo when the factors were injected sc into syngeneic recipients. One factor was a low-molecular-weight peptide (<1,000), as judged by ultrafiltration, failure of extraction by lipid solvents, nonsusceptibility to DNase or RNase, partial inactivation by trypsin, and complete inactivation by carboxypeptidase B. The second anti-inflammatory factor had a molecular weight between 30,000 and 100,000 and was also not extractable with lipid solvents. Production of anti-inflammatory factors by P-815 mastocytoma cells was inhibited by cycloheximide and cell irradiation but not by colchicine pretreatment of the cells, suggesting a relationship to protein synthesis rather than cell growth. Soluble anti-inflammatory factors depressed granulocyte as well as macrophage responses. Anti-inflammatory factors were not found in supernatants from cultures of splenocytes, peritoneal exudate cells, or murine lung fibroblasts.—JNCI 1982; 69:1321–1327.

Tumor bearing in experimental animals usually inhibits macrophage accumulation at inflammatory sites (*1–5*), and this phenomenon may be related to soluble anti-inflammatory factors (*6–10*). Such anti-inflammation has been observed during growth of both spontaneously arising (*11–13*) and transplanted tumors (*1–4*). Cell-free homogenates of transplanted tumors (*6, 7, 9*) and tumor ascitic fluid (*14*) contain factors that inhibit macrophage inflammatory responses when the factors are injected into normal animals. These factors are dialyzable (*6, 7*), unrelated to LDH viral infection (*15*), stimulatory to macrophage phagocytosis, but inhibitory to adherence and chemotaxis (*9, 10*), and have been associated with tumor virulence in a mouse lymphoma cell line (*8*).

Appropriately activated macrophages can alter the growth kinetics of tumor cells both in vitro (*16, 17*) and in vivo (*18–20*). Therefore, what inhibits macrophage accumulation at inflammatory sites in the tumor-bearing host is a critical issue. We previously reported that culture supernatants from rapidly proliferating cells inhibit macrophage chemotaxis in vitro and diminish macrophage accumulation in vivo in response to peritoneal stimuli (*21*). We now extend these studies using cell culture techniques to examine the types of cells that produce anti-inflammatory factors, the requirements for cell growth or protein synthesis in their production, and the nature of the factors themselves. We obtained evidence that multiple factors may be involved and that one of these is a very low-molecular-weight peptide.

MATERIALS AND METHODS

Mouse tumors.—Cryopreserved P-815 mastocytoma cells were obtained from the Mason Research Institute, Worchester, Mass., and passaged in syngeneic DBA/2 mice. These tumor cells had been tested and found to be free of mycoplasma as well as a variety of viruses including LDH virus. A 3-methylcholanthrene-induced fibrosarcoma designated PC-8 was obtained from the Tumor Biology Unit, University of Florida, and passaged in syngeneic C57BL/6 mice. Tumor cells were periodically tested and remained free of LDH virus as measured by normal serum LDH levels after tumor transplantation into syngeneic mice (*22*). All DBA/2 and C57BL/6 mice (20–25 g) were obtained from The Jackson Laboratory, Bar Harbor, Maine.

Cell culture.—First-generation cultures of tumor cells were used throughout. P-815 cells were obtained 6–7 days after the ip transplantation of 1×10^6 tumor cells into syngeneic DBA/2 mice. Cells were obtained by ip injection of 1.0 ml sterile RPMI-1640 medium containing 10 U heparin, by gentle massage of the belly, and by aspiration of 2 ml fluid by syringe containing about 10^8 cells, of which more than 95% were mastocytoma cells. The cell suspension was washed twice and adjusted to 5×10^6 cells/ml. For culturing, 0.5×10^6 cells were added to 10 ml medium in a 25-cm T-flask (Falcon Plastics, Oxnard, Calif.). PC-8 tumors were obtained 17 days after sc transplantation of 2×10^6 tumor cells into syngeneic C57BL/6 mice. The tumors were finely minced, digested with trypsin (0.25%) and DNase for 60 minutes at room temperature with stirring, passed through a sterile gauze, and collected by centrifugation. After being washed three times, 2.5×10^6 viable tumor cells were seeded into 25-cm^2 tissue culture flasks containing 10 ml culture medium. Culture medium for both tumors consisted of bicarbonate-buffered RPMI-1640 medium supplemented with L-glutamine, 10% fetal bovine serum, and 1% antibiotic–antimycotic solution (GIBCO, Grand Island, N.Y.). The cells were cultured at 37°C in a 95% humidified atmosphere containing 5% CO_2. Culture supernatants were harvested (usually, after 2 or 4 days) by decantation into a 50-ml conical centrifuge tube and centrifugation at 750×*g* for 10 minutes to remove cells and then at 25,000×*g* for 30

ABBREVIATIONS USED: FCS=fetal calf serum; LDH=lactate dehydrogenase; PHA=phytohemagglutinin; PMN=polymorphonuclear leukocyte(s); V_0=void volume.

---

[1] Received January 15, 1982; accepted July 27, 1982.

[2] Supported by Public Health Service grant CA-22517-04 from the National Cancer Institute and by grant 3-603-80 from the Swiss National Science Foundation and the Swiss Cancer League.

[3] Animals were maintained under the guidelines set forth in the "Guide for the Care and Use of Laboratory Animals" by the Institute of Laboratory Animal Resources, National Research Council.

[4] College of Medicine, Department of Pathology, Box J-275, University of Florida, Gainesville, Fla. 32610.

[5] Swiss Institute for Medical Research, Davos, Switzerland.

[6] *Address reprint requests to* Dr. Normann at the University of Florida.

minutes to remove cellular debris. The clear supernatant was stored at −20°C in sterile plastic tubes. No decay of anti-inflammatory activity was noted up to 2 months of storage, but longer storage appeared detrimental.

Control cultures consisted of splenocytes and peritoneal exudate cells from non-tumor-bearing DBA/2 mice and of splenocytes and lung fibroblasts from normal C57BL/6 mice. We obtained splenocytes by cutting the spleen into fine fragments and passing the fragments first through a 40-mesh screen and then in succession through 19-, 21-, and 23-gauge needles to ensure a single cell suspension. The cells were washed twice and seeded as 1.5×10^6 cells/2.0 ml culture medium in 12×75-mm Falcon polypropylene tubes. Peritoneal exudate cells were obtained 3 days after ip injection of proteose peptone and contained 30% lymphocytes, 48% macrophages, and 19% polymorphonuclear leukocytes. The cells were washed twice and seeded as 5×10^5 cells/10 ml culture medium in 25-cm Falcon T-flasks. We obtained fibroblasts from the lungs of normal adult C57BL/6 mice by removing the lung, mincing the tissue, and digesting the tissue for 90 minutes in a solution containing trypsin, EDTA, and collagenase. The fibroblasts were passaged for 19 generations and then seeded as 5×10^5 fibroblasts/10 ml culture medium in a 25-cm^2 tissue culture flask.

Assay for anti-inflammatory activity.—Biologic testing was performed with the use of syngeneic male mice of at least 16 weeks of age. For each test, a control test was performed simultaneously consisting of culture medium processed identically. Each mouse received sc 0.5 ml test solution in each hind leg. Twenty-four hours later the mouse was given an ip injection of 1.3 ml 8% proteose peptone, and 3 days later the peritoneal cells were harvested with 10 ml RPMI-1640 medium containing 10 U heparin/ml in a total of five washings. The cells were pooled, collected by centrifugation, washed once, and enumerated by means of a Coulter counter. Differential cell counts were made on cytocentrifuge-prepared slides stained with Wright's Giemsa. In addition to being recognized by their morphology, macrophages were recognized by their capacity for carbon phagocytosis (*14*) and/or their content of nonspecific esterase (*23*). We have observed seasonal variation in macrophage responses with higher responses in winter than in summer. Accordingly, each reported experiment includes its own control.

Anti-inflammatory activity directed against PMN was evaluated by ip injection of 1.3 ml sterile sodium caseinate in place of proteose peptone. The exudates were harvested 18 hours later and evaluated for total and differential cell counts.

Irradiation.—Mastocytoma cells were added to 25-cm^2 T-flasks (8×10^6 cells/10 ml culture medium) and irradiated with 6,000 rad from a cesium source (model M gammator; Radiation Machinery Corp., Parsippany, N.J.).

Ultrafiltrations.—Culture medium or 2-day cell culture supernatants were ultrafiltered in an Amicon (Lexington, Mass.) microultrafiltration unit 8MC with the use of nitrogen gas (5 atm/cm^2) as a pressure source. A UM-2 membrane (mol wt cutoff, 1,000) was used to prepare the low-molecular-weight anti-inflammatory factor. Ultrafiltrates were collected and stored frozen (−20°C) until used. In some instances, ultrafiltrates were prepared with the use of a PM-30 membrane (mol wt cutoff, 30,000) or an XM-100 membrane (mol wt cutoff, 100,000).

Molecular sieving.—G-25 Sephadex (Pharmacia Fine Chemicals, Piscataway, N.J.) was swollen overnight in 0.02 *M* phosphate buffer (pH 7.4) without stirring. A 2.5×24-cm column of G-25 Sephadex was used in downward flow. Since the sample fraction that appeared in the V_0 was diluted about fourfold, it was lyophilized and reconstituted with the use of water in a volume equivalent to that of the sample applied.

Lipid extraction.—Culture medium and supernatants were extracted with ethyl acetate (1:2 vol/vol) after being acidified to pH 4.0 with 0.1 *N* HCl as described by Hensby (*24*) for extraction of prostaglandins. They were extracted also with chloroform only (2:1 vol/vol) as described by Cheung et al. (*9*) after acidification to pH 1.6 with 0.5 *N* HCl. Chloroform–methanol solution (2:1 vol/vol) was used as 3.5:1 volumes of aqueous culture medium or supernatant. All extractions were repeated three times, and the fractions were pooled, evaporated to near dryness, and redissolved in phosphate-buffered saline.

Enzymatic degradation.—Insoluble trypsin, DNase I (DN-25), and RNase A (type III) were obtained from Sigma Chemical Co., St. Louis, Mo., and carboxypeptidase B was obtained from Worthington Biochemical Co., Freehold, N.J. Insoluble trypsin was used at a concentration of 1 mg/ml (pH 7.6), DNase at 1 mg/ml in the presence of 0.1 *M* magnesium sulfate (pH 7.0), RNase at 1 mg/ml (pH 7.3), and carboxypeptidase B at 100 µg/ml (pH 7.6). All enzymatic reactions were performed at room temperature for 1 hour with stirring. Biologic testing was performed both before and after removal of the enzyme by centrifugation or refiltration through a UM-2 membrane. Since results were essentially identical, they have been combined in reporting biologic activity.

Statistics.—Differences between two means were analyzed by Student's *t*-test. Data are reported as means ± 1 standard error.

RESULTS

Anti-Inflammatory Factors From Cultured Cells

Growth of P-815 mastocytoma cells in vitro was associated with the rapid appearance in the culture supernatant of a factor or factors inhibitory to macrophage inflammatory responses (text-fig. 1). Anti-inflammatory activity preceded and rose concurrently with cell growth. Maximum anti-inflammatory activity was consistently observed in 2-day culture supernatants at 100% concentration, which decreased in proportion to dilution. Accordingly, such supernatants were used in all subsequent work with this tumor. Similar to the growth of the P-815 mastocytoma, growth of the PC-8 fibrosarcoma was associated with rapid appearance of anti-inflammatory activity in the culture supernatant (text-fig. 2). The fibrosarcoma grew more slowly than the mastocytoma, and maximum activity did not appear until day 4.

Not all cells in culture elaborated anti-inflammatory factors (table 1). Spleen cells from normal mice or peritoneal

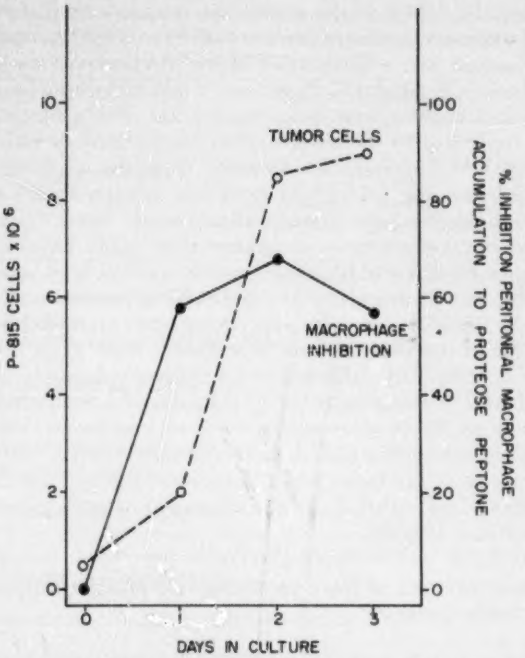

TEXT-FIGURE 1.—Appearance of anti-inflammatory activity in culture supernatants of P-815 mastocytoma cells.

exudate cells from mice given injections of proteose peptone produced no detectable anti-inflammatory activity in culture. Cultures of splenocytes were examined unstimulated or after stimulation with PHA either for 48 hours (DBA/2) or for 96 hours (C57BL/6). Normal lung fibroblasts grew rapidly in culture, and supernatants were examined either during rapid cell growth (2 days in culture) or after the cells had reached confluence and were in a stationary growth phase (days 3 and 4). No significant anti-inflammatory activity was observed in any of these supernatants obtained from splenocytes, peritoneal exudate cells, or murine lung fibroblasts.

We next examined certain requirements for producing anti-inflammatory activity by P-815 mastocytoma cells. One objective was to explore further the relationship between production of anti-inflammatory activity and tumor cell growth. In the first experiment, cell growth was arrested by irradiation with 6,000 rad. Supernatants from irradiated cells grown 2 days in culture were compared to those from nonirradiated cells (table 2). In contrast to nonirradiated cells, irradiated cells elaborated no detectable anti-inflammatory activity. In a second experiment, 0.2 mg colchicine/ml was used to inhibit mitotic division. When supernatants from such colchicine-pretreated cells were examined, they were found to contain anti-inflammatory activity. In a third experiment, tumor cells were cultured in the presence of 100 μg cycloheximide/ml, which interferes with protein synthesis. Cycloheximide markedly decreased anti-inflammatory activity such that the marginal residual activity in supernatants from treated cells was not statistically different from that in supernatants from nontreated cells. These data suggested that production of anti-inflammatory activity was related more to protein synthesis than to actual cell proliferation. A second objective was to examine the requirement for serum proteins in the culture medium. For this experiment, 1×10^6 P-815 cells were seeded into 10 ml medium without FCS, and after 2 days in culture 3×10^6 cells were recovered. While the cells grew in the absence of FCS, they did not do so as readily as in the presence of FCS. Nonethe-

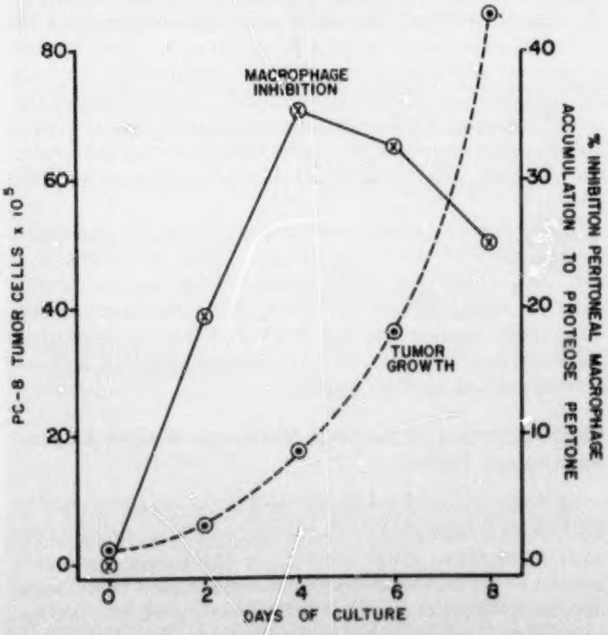

TEXT-FIGURE 2.—Appearance of anti-inflammatory activity in culture supernatants of PC-8 fibrosarcoma cells.

TABLE 1.—*Presence of anti-inflammatory activity in culture supernatants from tumor but not normal cells*

Materials tested	No. of trials	Yield of macrophages, $\times10^{5a}$	Degree of inhibition, %[b]
DBA/2 mice			
Culture medium only	8	52±6	
Culture supernatants[c]			
P-815 mastocytoma	6	22±3	58
Peritoneal exudate from normal mice	6	50±4	NS
Splenocytes from normal mice	7	46±5	NS
Splenocytes + PHA	5	47±4	NS
C57BL/6 mice			
Culture medium only	9	37±3	
Culture supernatants[d]			
PC-8 fibrosarcoma	12	23±4	38
Normal fibroblasts			
Proliferating	6	49±6	None
Confluent	7	41±5	None
Splenocytes + PHA	6	33±3	NS

[a] Data are means ± SE.
[b] NS = not significant.
[c] Supernatants were obtained after 2 days in culture.
[d] Supernatants were obtained after 4 days in culture except syngeneic lung fibroblasts, which were obtained after 2 days (proliferating) or 3 days (confluent).

Table 2.—*Effect of inhibitors of cell growth and protein synthesis on production of anti-inflammatory activity by P-815 mastocytoma cell cultures*[a]

Materials tested	No. of trials	Yield of macrophages, $\times 10^{5}$[b]	Degree of inhibition, %
Culture medium alone	16	43±3	
Medium + cycloheximide	7	45±5	None
Culture supernatants from			
P-815 cells	7	16±2[c]	63
X-irradiated P-815 cells	10	40±3	7
Cycloheximide-treated P-815 cells	10	36±4	16
Colchicine-pretreated P-815 cells	8	17±3[c]	60
P-815 cells grown in absence of FCS	11	15±3[c]	65

[a] All supernatants were obtained after 2 days in culture of P-815 mastocytoma cells from DBA/2 mice. Irradiated cells received 6,000 rad. Cycloheximide was used at 100 μg/ml. Colchicine pretreatment consisted of incubation of 6.9×10^{6} cells in 5 ml of RPMI-1640 containing 0.2 mg colchicine/ml for 90 min. Subsequently, the cells were collected by centrifugation, resuspended in 0.5 ml RPMI-1640, and added to 10 ml culture medium.

[b] Data are means ± SE.

[c] Significant difference from culture medium alone.

less, P-815 cells in the absence of FCS produced anti-inflammatory activity.

The molecular size of the anti-inflammatory factor(s) was examined in a series of experiments summarized in table 3. During these experiments, it emerged that more than one anti-inflammatory factor existed. Using 2-day P-815 mastocytoma culture supernatants, we demonstrated that one factor was a low-molecular-weight entity capable of crossing a dialysis membrane (Union Carbide Corp., Chicago, Ill.). However, exhaustive dialysis did not eliminate anti-inflammatory activity from the retained fraction. The impression of at least two anti-inflammatory factors was confirmed by the following experiment. An ultrafiltrate was obtained by means of a UM-2 Diaflo membrane (mol wt cutoff, 1,000) that contained anti-inflammatory activity. This low-molecular-weight anti-inflammatory factor was removed by passage over a Sephadex G-25 column, which retards molecules with molecular weights of less than 5,000. This assumption was confirmed by the absence of anti-inflammatory activity in the UM-2 ultrafiltrate obtained from the V_0 fraction. Nonetheless, the V_0 fraction itself was strongly inhibitory. Accordingly, a second anti-inflammatory factor existed whose molecular weight was greater than 5,000. This factor did not cross a PM-30 Diaflo membrane (mol wt cutoff, 30,000) but did cross an XM-100 Diaflo membrane (mol wt cutoff, 100,000). A similar experiment was conducted with the use of the 4-day culture supernatant from PC-8 fibrosarcoma cells. Anti-inflammatory activity was found in both the UM-2 filtrate and in the V_0 fractions of a Sephadex G-25 column. From these experiments, we concluded that at least two anti-inflammatory factors existed in tumor culture supernatants, one factor having a molecular weight less than 1,000 and the other having a molecular weight between 30,000 and 100,000.

Table 3.—*Evidence for two anti-inflammatory factors in culture supernatants of tumor cells, one of which is a low-molecular-weight entity*

Materials tested	No. of trials	Yield of macrophages, $\times 10^{5}$[a]	Degree of inhibition, %
DBA/2 mice			
Culture medium alone	5	39±4	
Culture supernatant			
Dialysate	7	23±4[b]	41
Retained fraction	5	11±2[b]	72
UM-2 filtrate[c]	7	15±2[b]	62
V_0 fraction G-25 Sephadex column	10	17±2[b]	56
UM-2 filtrate	6	37±4	5
PM-30 filtrate	5	41±4	None
XM-100 filtrate	5	26±4[b]	33
C57BL/6 mice			
Culture medium alone	8	43±2	
PC-8 fibrosarcoma culture supernatant	12	29±2[b]	33
UM-2 filtrate[c]	10	32±3[b]	26
G-25 V_0 fraction	10	28±3[b]	35

[a] Data are means ± SE.

[b] Significant difference from culture medium alone.

[c] The UM-2 Diaflow membrane has a mol wt cutoff of 1,000.

Characteristics of the Low-Molecular-Weight Anti-Inflammatory Factor

Our attempts to extract the anti-inflammatory factor by use of organic solvents were unsuccessful (table 4). First, we tried to extract the factor with chloroform at pH 1.6 as recommended by Cheung et al. (*9*) for extracting factors from tumor homogenates with antimacrophage activities. However, such extracts of UM-2 filtrates did not contain anti-inflammatory activity. Next we attempted to extract the UM-2 filtrate with ethyl acetate at pH 4.0 following the procedure described by Hensby (*24*) for extraction of prostaglandins. This extraction also failed to contain anti-inflammatory activity. The addition of methanol to the UM-2 filtrate either at 22 or at 4°C resulted in a fine, whitish precipitate and inactivation of the anti-inflammatory factor. As expected, a chloroform–methanol (2:1) extraction resulted in no anti-inflammatory activity. In each instance, an oily substance could be extracted into the organic phase, but this substance actually enhanced macrophage accumulation.

Table 5 summarizes results obtained on the enzymatic susceptibility of the low-molecular-weight anti-inflammatory factor. The anti-inflammatory factor was not inactivated by either RNase or DNase, although these enzymes were active against purified RNA or DNA. In contrast, it was completely inactivated by carboxypeptidase B and was partially inactivated by trypsin.

Characteristics of the High-Molecular-Weight Anti-Inflammatory Factor

The high-molecular-weight factor contained in the V_0 fraction of a Sephadex G-25 column could not be extracted with chloroform, ethyl acetate, or chloroform–methanol. Similar to the findings with the low-molecular-weight factor, methanol addition (50% vol/vol) formed a whitish precipitate upon addition to the G-25 V_0 fraction. After removal of the precipitate, the remaining fluid possessed no inhibitory

TABLE 4.—*Failure to extract the low-molecular-weight anti-inflammatory factor with lipid solvents from culture supernatants of P-815 mastocytoma cells*[a]

Materials tested	Yield of macrophages, ×10⁵: Mice given injections of:[b]		Change, %
	Culture medium	Culture supernatant, UM-2 filtrate	
No extraction	38±4	19±4[c]	−50
Chloroform extract[d] (pH 1.6), organic phase	38±1	46±9	+21
Ethyl acetate extract[d] (pH 4.0), organic phase	35±6	46±2[c]	+31
Methanol addition, (2:1 vol/vol)			
22°C	41±5	54±4	+32
4°C		49±5	+20
Chloroform–methanol extract[e] (pH 7.0), organic phase	35±2	46±3	+31

[a] Experiments were performed with the use of a UM-2 ultrafiltrate of a 2-day culture supernatant from P-815 mastocytoma cells. Acidification to desired pH was performed by addition of 0.1 *N* HCl. Data are for 5–8 trials per determination.

[b] Data are means ± SE.

[c] Significant reduction from culture medium alone.

[d] Extraction was performed by (2:1 vol/vol) addition of either chloroform or ethyl acetate to medium or supernatant. All solutions were readjusted to pH 7.0 prior to injection into mice.

[e] Chloroform–methanol (1:1 vol/vol) extraction was performed with the use of 3.5:1.0 vol/vol medium or supernatant.

activity. The high-molecular-weight factor was not inactivated by DNase or RNase.

Inhibition of PMN by Tumor Culture Supernatants

Anti-inflammatory activity associated with tumor bearing has been reported by some to be specific for macrophages (*1*, *2*), whereas others describe activity against PMN (*25*, *26*). Therefore, we tested culture supernatants of P-815 tumor cells for their effect on PMN (table 6). Whole supernatants strongly inhibited peritoneal PMN accumulation to sodium caseinate as an irritant and this activity was present as both a low- and a high-molecular-weight inhibitor. In contrast to macrophages, however, the low-molecular-weight inhibitor was less potent than the high one.

TABLE 5.—*Inactivation of low-molecular-weight anti-inflammatory factor in culture supernatants of P-815 tumor cells by trypsin and carboxypeptidase B but not by RNase or DNase*[a]

Materials tested	Yield of macrophages, ×10⁵: Mice given injections of:[b]		Degree of inhibition, %
	Culture medium	Culture supernatant, UM-2 filtrate	
No enzyme	35±2	17±1[c]	51
After enzyme treatment[d]			
RNase	46±3	27±4[c]	41
DNase	34±6	19±4[c]	44
Trypsin	39±8	31±2	21
Carboxypeptidase B	35±3	32±3	9

[a] Experiments were performed with the use of a UM-2 ultrafiltrate of a 2-day culture supernatant from P-815 mastocytoma cells. Data are for 5–8 trials per determination.

[b] Data are means ± SE.

[c] Significant difference from culture medium alone.

[d] Conditions were 1 mg RNase/ml (pH 7.3), 1 mg DNase/ml (pH 7.0) with magnesium, 1 mg trypsin/ml (pH 7.6), and 100 μg carboxypeptidase B/ml (pH 7.6). In each instance, the culture medium contained the corresponding enzyme at an equivalent concentration.

TABLE 6.—*Inhibition of PMN accumulation by anti-inflammatory factors in 2-day supernatants of P-815 tumor cultures*

Materials tested	No. of trials	Yield of PMN, ×10⁵[a]	Degree of inhibition, %
Culture medium only	10	63±6	
Whole supernatant	11	20±5[b]	68
UM-2 filtrate	9	43±3[b]	32
Sephadex G-25 V_0 fraction	9	30±7[b]	52

[a] Data are means ± SE.

[b] Significant difference from culture medium alone. Data are for 5–8 trials per determination.

DISCUSSION

Tumor bearing alters macrophage function as indicated in experimental animals by decreased accumulation at inflammatory foci in vivo and in humans by decreased chemotactic migration in vitro. It has been reported that the mechanism of inhibition may involve soluble anti-inflammatory factors (*6–10*). Our studies support this hypothesis but indicate that more than one factor may be involved.

The following evidence suggests that one factor affecting macrophage is an anti-inflammatory peptide. *a*) An anti-inflammatory factor was identified in culture supernatants of P-815 mastocytoma cells; this factor was dialyzable, retarded on a Sephadex G-25 column, and had a molecular weight of less than 1,000 by ultrafiltration. *b*) This anti-inflammatory factor could not be extracted by organic solvents used to extract lipids and prostaglandins. However, the failure to extract activity with organic solvents does not necessarily preclude some lipid content in the active factor. *c*) This factor was resistant to both DNase and RNase but was completely inactivated by carboxypeptidase and partially inactivated by trypsin. A second anti-inflammatory factor was identified that was not dialyzable, not extractable with lipid solvents, appeared in the V_0 of a Sephadex G-25 column, and by ultrafiltration had a molecular weight between 30,000 and 100,000. It is not clear whether this second factor is a distinct entity or is due to aggregation or adsorption of the low-molecular-weight factor to some substance in the culture medium.

Anti-inflammatory factors have been obtained from tumor homogenates, from urine, plasma, and ascitic fluid of tumor-bearing animals, and from supernatants of cultured tumor cells. The nature and specificity of these factors are under investigation. Pike and Snyderman (*7*) first described a dialyzable anti-inflammatory factor in homogenates prepared by sonication of cancerous tissues that had a molecular weight of less than 25,000 by ultrafiltration but eluted from a Sephadex G-50 column in the region of 6,000–10,000

(*10*). The chemical nature of this factor was not defined, although it occurred in spontaneously arising cancers (*13*). Cheung et al. (*9*) described a lipid-like inhibitor of less than 3,500 in tumor homogenates that altered macrophage spreading and migration. While we concur that one anti-inflammatory factor has a molecular weight less than that reported by Snyderman's group, we believe this factor to be a peptide rather than a lipid since it is inactivated by carboxypeptidase and not extractable by methanol, chloroform, or ethyl acetate. Factors obtained from homogenized tissue may differ from those obtained from culture supernatants, and different functions may be affected by different factors. We tested macrophage inflammatory responses in vivo, whereas Cheung et al. (*9*) used an in vitro assay of macrophage spreading. Nelson and Nelson (*27*) reported isolating a low-molecular-weight factor from tumor culture supernatants; this factor inhibited the early phase of a prolonged delayed-type hypersensitivity reaction in vivo as well as macrophage migration and motility in vitro. While most workers describe antimacrophage activity, Stahl et al. (*26*) reported a carboxypeptidase B- and trypsin-sensitive factor that affected granulocytes in 48-hour tumor culture supernatants whose molecular weight was 500–2,000. This factor has many similarities to our low-molecular-weight factor. Since the factor described by Stahl et al. (*26*) was considered to be toxic to macrophages, it may be identical to the low-molecular-weight anti-inflammatory factor described here.

P-815 cells growing intraperitoneally produce tumorous ascitic fluid that contains anti-inflammatory activity (*14*). The use of culture supernatants rather than whole tumors allowed us to examine certain conditions essential for the production of these factors. Appearance of the factors in the culture supernatant preceded rapid cell proliferation and suggested a relationship between factor production and tumor growth. This hypothesis seemed to be supported by the observation that cell irradiation sufficient to inhibit proliferation blocked production of the anti-inflammatory factor. However, prior treatment of the cells with colchicine did not inhibit factor production, although it arrested mitotic division. Such data suggest that factor production did not depend on actual cell division but required intact DNA and probably DNA transcription which was inhibited by cell irradiation. Cycloheximide inhibits protein synthesis by blocking transfer of activated amino acids from tRNA to growing polypeptide chains without inhibiting DNA synthesis. Thus the fact that cycloheximide prevented appearance of anti-inflammatory activity supports the contention that factor production was related to protein synthesis. Further, anti-inflammatory activity did not require serum proteins in the culture medium, and this observation supports the contention that the factors were produced by the cells.

In conclusion, multiple anti-inflammatory factors appear to be produced by primary tumor cells in culture but not by normal fibroblasts, splenocytes, or peritoneal exudate cells. Additional work is necessary to determine if the various factors are related or are distinct entities. We have identified one factor as a very low-molecular-weight peptide. The capacity to produce such factors in vitro may help clarify their nature, source, and mode of action in the tumor-bearing host.

REFERENCES

(*1*) Normann SJ, Sorkin E. Cell-specific defect in monocyte function during tumor growth. J Natl Cancer Inst 1976; 57:135–140.

(*2*) Snyderman RM, Pike MC, Blaylock BL, Weinstein P. Effects of neoplasms on inflammation: Depression of macrophage accumulation after tumor implantation. J Immunol 1976; 116:585–589.

(*3*) Normann SJ, Cornelius J. Concurrent depression of tumor macrophage infiltration and systemic inflammation by progressive cancer growth. Cancer Res 1978; 38:3453–3459.

(*4*) Normann SJ, Schardt M, Sorkin E. Cancer progression and monocyte inflammatory dysfunction: Relationship to tumour excision and metastasis. Int J Cancer 1979; 23:110–113.

(*5*) Nolibe D, Masse R, Giroud JP. Effect of tumor growth on inflammatory macrophages. In: Willoughby DA, Giroud GP, Velo GP, eds. Future trends in inflammation. Vol IV. Lancaster, England: MTP Press, 1980:675–682.

(*6*) Snyderman R, Pike MC. An inhibitor of macrophage chemotaxis produced by neoplasms. Science 1976; 192:370–372.

(*7*) Pike MC, Snyderman R. Depression of macrophage function by a factor produced by neoplasms: A mechanism for abrogation of immune surveillance. J Immunol 1976; 117:1243–1249.

(*8*) Pasternack GR, Snyderman R, Pike MC, Johnson RJ, Shin HS. Resistance of neoplasms to immunological destruction: Role of a macrophage chemotaxis inhibitor. J Exp Med 1978; 148:93–102.

(*9*) Cheung HT, Cantarow WD, Sundharadas G. Characteristics of a low-molecular-weight factor extracted from mouse tumors that affects in vitro properties of macrophages. Int J Cancer 1979; 23:344–352.

(*10*) Snyderman R, Pike MC. Biological activities of a macrophage chemotaxis inhibitor (MCI) produced by neoplasms. In: Quastel MR, ed. Cell biology and immunology of leukocyte functions. New York: Academic Press, 1979:535–546.

(*11*) Normann SJ, Schardt M, Sorkin E. Anti-inflammatory effect of spontaneous lymphoma in SJL/J mice. JNCI 1979; 63:825–833.

(*12*) ———. Alteration of macrophage function in AKR leukemia. JNCI 1981; 66:157–162.

(*13*) Cianciolo GJ, Herberman RB, Snyderman R. Depression of murine macrophage accumulation by low-molecular-weight factors derived from spontaneous mammary carcinoma. JNCI 1980; 65:829–834.

(*14*) Normann SJ. Tumor cell threshold required for suppression of macrophage inflammation. J Natl Cancer Institute 1978; 60:1091–1096.

(*15*) Snyderman R, Cianciolo GJ. Further studies of a macrophage chemotaxis inhibitor (MCI) produced by neoplasms: Murine tumors free of lactic dehydrogenase virus produce MCI. J Reticuloendothel Soc 1979; 26:453–458.

(*16*) Hibbs JB Jr, Taintor RR, Chapman HA Jr, Weinberg JB. Macrophage tumor killing: Influence of the local environment. Science 1977; 197:279–282.

(*17*) Hibbs JB Jr, Chapman HA Jr, Weinberg JB. The macrophage as an antineoplastic surveillance cell: Biological perspectives. J Reticuloendothel Soc 1978; 24:549–570.

(*18*) Fidler IJ. Inhibition of pulmonary metastasis by intravenous injection of specifically activated macrophages. Cancer Res 1974; 34:1074–1078.

(*19*) Wood GW, Gillespie GY. Studies on the role of macrophages in regulation of growth and metastasis of murine chemically induced fibrosarcomas. Int J Cancer 1975; 16:1022–1029.

(*20*) Keller R. Promotion of tumor growth in vivo by antimacrophage agents. J Natl Cancer Inst 1976; 57:1355–1361.

(*21*) Normann SJ, Sorkin E. Inhibition of macrophage chemotaxis by neoplastic and other rapidly proliferating cells in vitro. Cancer Res 1977; 37:705–711.

(*22*) Riley V. Lactate dehydrogenase in the normal and malignant state in mice and the influence of a benign enzyme-elevating virus. Methods Cancer Res 1968; 4:493–618.

(*23*) Knowles DM, Hoffman T, Ferrarini M, Kunkel HG. The demonstration of acid alpha-naphthyl acetate esterase activity in human lymphocytes: Usefulness as a T-cell marker. Cell Immunol

1978; 35:112–123.

(*24*) HENSBY C. Physical methods in prostaglandin research. In: Crabbe P, ed. Prostaglandin research. New York: Academic Press, 1977:89–120.

(*25*) FAUVE RM, HEVIN B, JAKOB H, GAILLARD JA, JACOB F. Anti-inflammatory effects of murine malignant cells. Proc Natl Acad Sci USA 1974; 71:4052–4056.

(*26*) STAHL KW, HEVIN B, FAUVE RM. Purification and gel filtration chromatography (GFC) of an anti-inflammatory and macrophagotoxic peptide from murine malignant cells. In: James K, McBride B, Stuart A, eds. The macrophage and cancer. Edinburgh: Econopress, 1977:271–280.

(*27*) NELSON M, NELSON DS. Macrophages and resistance to tumors. IV. Influence of age on susceptibility of mice to anti-inflammatory and antimacrophage effects of tumor cell products. JNCI 1980; 65:781–789.

blank page

Collagenolytic Activity of Rabbit V_2 Carcinoma Implanted in the Nude Mouse[1,2,3,4]

Chitra Biswas,[5,6] **Kurt J. Bloch,**[5] *and* **Jerome Gross**[5,7]

ABSTRACT—The relative contribution of host cells and tumor cells to the production of collagenase and its regulation during tumorigenesis were studied with the use of a heterologous rabbit tumor–nude mouse host system. The V_2 carcinoma, a malignant neoplasm of the New Zealand White rabbit, behaved as a nonmetastasizing, noninvasive tumor when implanted and grown in the inbred Swiss albino nude mouse. The extracts from both tumors contained similar levels of collagenase. Tumor explants also released enzyme into culture medium in both cases, but the rabbit tumor produced approximately 10 times more collagenase than the nude mouse. Freeze-thawing of the explants or treatment with cycloheximide markedly inhibited the appearance of enzyme in the medium from the rabbit tumor but not from the nude mouse tumor. The relative proportions of mouse- and rabbit-derived collagenase in the nude mouse tumor extracts and culture medium were determined with the use of antibodies specific for rabbit V_2 tumor and mouse bone collagenases. Approximately 70% of the nude mouse tumor enzyme was derived from the rabbit tumor, and approximately 30% was derived from the mouse host. These findings indicate that the former might represent stored enzyme carried over during tumor transplantation into the nude mouse, whereas the latter might have originated from stimulation of host cells during tumorigenesis.—JNCI 1982; 69:1329–1336.

Increased collagenase activity and degradation of connective tissue matrix in the host have been found to be associated with several neoplasms (*1–8*). However, the cellular source and the regulation of collagenase activity during tumorigenesis are still not well understood. We have approached this problem by implanting rabbit V_2 carcinoma in the nude mouse. This heterologous host–tumor model system has permitted us to identify the source of tumor enzyme on the basis of differences in immunologic characteristics of the collagenase from the two species. In addition, we have been able to compare the levels of collagenase present in invasive and noninvasive tumors derived from the same tumor cell origin since the V_2 carcinoma is invasive in the rabbit but noninvasive in the nude mouse.

The V_2 carcinoma is an epithelially derived tumor originally obtained from Shope virus-induced papillocarcinoma (*9*). The tumor grows rapidly in muscle and in subcutaneous tissue of the rabbit and is lethal to the host. McCroskery et al. (*5*) extracted relatively large amounts of active collagenase from this tumor implanted in muscle. We observed that the subcutaneously implanted V_2 carcinoma contained extractable collagenase in latent form requiring activation by trypsin, whereas muscle tumor extracts rarely contained significant amounts of active or latent collagenase (*8*). Upon implantation of tumor in intramuscular and subcutaneous sites in the same rabbit, extractable latent enzyme was obtained from both sites (*8*).

In this paper, we have compared some biochemical properties of the collagenase obtained by extraction and culture of V_2 carcinoma implanted subcutaneously in both the rabbit and nude mouse hosts and determined the contribution of host and tumor cells to the collagenase present in the nude mouse tumor with the use of antibodies raised against rabbit tumor enzyme and normal mouse bone enzyme.

MATERIALS AND METHODS

Reagents and their sources included: TPCK-trypsin and SBTI from Worthington Biochemical Corp., Freehold, N.J.; pancreatic trypsin (type I) from Sigma Chemical Co., St. Louis, Mo; [^{14}C]acetic anhydride and ^{14}C-labeled amino acid mixture from New England Nuclear Corp., Boston, Mass.; DMEM from Grand Island Biological Co., Grand Island, N.Y.; Diaflo PM-10 membranes from Amicon Corp., Lexington, Mass.; and Sephacryl S-200 and DEAE-Sephadex A-50 from Pharmacia Chemicals AB, Uppsala, Sweden. Ultrogel ACA-54 was obtained from LKB Producter AB, Stockholm, Sweden; *Staphylococcus aureus*-Cowan I strain (IgG-Sorb) from The Enzyme Center, Boston, Mass.; and Whatman DEAE-cellulose (DE-52) from Metropolitan Supply Corp., Cambridge, Mass.

Maintenance and implantation of V_2 carcinoma.—Rabbit V_2 carcinoma was maintained by serial im passage in New Zealand White rabbits as described previously (*8*). The tumor was provided by Dr. Judah Folkman, Children's Hospital, Boston, Mass. Six-week-old male and female Swiss albino nude mice of *nu/nu* genotype were obtained from Life Sciences, Inc., St. Petersburg, Fla. Suspensions of rabbit

---

ABBREVIATIONS USED: CFA=complete Freund's adjuvant; DMEM=Dulbecco's modified Eagle's minimum essential medium; IFA=incomplete Freund's adjuvant; SBTI=soybean trypsin inhibitor; TCA=trichloroacetic acid; TPCK=chloromethyl L-(2-phenyl-1-*p*-toluenesulfonamido)ethyl ketone.

---

[1] Received January 22, 1982; accepted July 16, 1982.

[2] Supported by Public Health Service grants CA-19158 from the National Cancer Institute and AM-03564 from the National Institute of Arthritis, Diabetes, and Digestive and Kidney Diseases; and by a grant from the Arthritis Foundation.

[3] Animals were maintained under the guidelines set forth by the Massachusetts General Hospital.

[4] This is publication No. 897 of the Robert W. Lovett Memorial Group for the Study of Diseases Causing Deformities.

[5] Developmental Biology Laboratory and the Clinical Immunology and Allergy Unit of the Medical Services, Massachusetts General Hospital, and the Department of Medicine, Harvard Medical School, Boston, Mass. 02114.

[6] *Address reprint requests to* Dr. Biswas at her *present address*: Department of Anatomy and Cellular Biology, Tufts University School of Medicine, Boston, Mass. 02111.

[7] We thank Mr. Richard W. Nichols and Ms. Michelle S. Finck for their excellent technical assistance and Dr. R. B. Colvin for reviewing the histologic sections.

tumor prepared as described previously (*8*) were centrifuged at 240×*g*, and the cell pellet was washed twice with sterile mammalian Ringer solution and suspended in the same medium. About 1 g tumor in 0.5 ml Ringer solution was injected sc in the scapular region of both the rabbit and the mouse. After 3–4 weeks, the animals were killed and the tumors were removed for histologic examination, tissue culture, and extraction of enzyme. The yield of tumor was approximately 10–20 g from each rabbit and 1–1.5 g from each nude mouse.

Preparation of enzymes.—Rabbit tumor collagenase: Approximately 30 g of tumor tissue was homogenized in a buffer containing 50 m*M* Tris-HCl, 1 *M* NaCl, and 5 m*M* $CaCl_2$ (pH 7.4). The homogenate was clarified by centrifugation, and the enzyme precipitated with $(NH_4)_2SO_4$ between 20 and 50% saturation as described previously (*8*). The resulting fraction was dialyzed against 50 m*M* Tris-HCl, 0.2 *M* NaCl, and 1 m*M* $CaCl_2$ (pH 7.4) (buffer A) and activated with trypsin as described below. The active enzyme was fractionated on a Sephacryl S-200 column (4×100 cm) equilibrated with buffer A. The fractions containing collagenase activity were combined, and the pooled fractions were concentrated to one-third of the starting volume by ultrafiltration on a Diaflo PM-10 membrane. The concentrated fraction was dialyzed against buffer A free of NaCl and applied to a column of DEAE-Sephadex (2×10 cm) equilibrated with this buffer. Collagenase activity was eluted with the same buffer. Eluted fractions were adjusted to 0.2 *M* NaCl, the enzyme activity was determined, and the active fractions were pooled, concentrated, and used as antigen for injection into goats. The specific activity of the preparation was 10 U collagenase/mg protein (*see* below for definition of units); the purification achieved was fiftyfold to seventyfold.

Mouse collagenase: Calvarias from 150- to 200-g Swiss-Webster mice 4–5 days old were cultured in serum-free Tyrode's solution in the presence of heparin as described by Shimizu et al. (*10*). The media were harvested after 4 days, replaced with fresh media, and collected again after a 4-day period. The media were pooled, buffered with 1 *M* Tris-HCl (pH 7.5) to a final molarity of 50 m*M*, and concentrated five times on a PM-10 membrane. The concentrated culture media were fractionated by $(NH_4)_2SO_4$ at 70% saturation, and the precipitate was suspended in buffer A and dialyzed against the same buffer. The dialyzed enzyme preparation containing latent collagenase activity was fractionated on an Ultrogel ACA 54 (1.8×90 cm) column equilibrated with the same buffer. The column fractions were assayed for both active and latent collagenase. The eluted column fractions showed only active collagenase, suggesting that the latent enzyme was autoactivated during the column fractionation. The enzymatically active fractions were pooled, concentrated five times on a PM-10 membrane, and used as antigen for injection into rabbits. The specific activity of the final preparation was 10 U/mg protein; the purification achieved was fiftyfold.

Nude mouse tumor collagenase: Tumor tissue was homogenized and fractionated by $(NH_4)_2SO_4$ as described for the rabbit tumor enzyme. Since only 1–1.5 g of tumor tissue was obtained from each nude mouse, tumors from several animals were pooled. The latent collagenase present in the $(NH_4)_2SO_4$ fractionated (20–50%) preparation was further fractionated on a Sephacryl S-200 column, and the fractionated concentrated enzyme was used for all experiments.

All buffers used for enzyme preparation contained 0.02% sodium azide, and the procedures were conducted at 4°C.

Preparation of anticollagenase antisera.—Goats were immunized with rabbit tumor collagenase. Two goats were each given an im injection of 1.5 mg partially purified enzyme preparation emulsified in CFA, followed by two additional injections of 0.7 mg enzyme emulsified in IFA, at 10-day intervals. The animals were bled on the 14th day after the second booster injection. The antisera were fractionated and tested as described below.

Rabbits were immunized with partially purified mouse bone enzyme. Two rabbits were each given an injection of 300 µg collagenase preparation emulsified in CFA, followed by two additional injections of 150 µg in IFA. The animals were bled on day 14 after the second injection.

The IgG fraction was obtained from the goat and rabbit antisera by precipitation with $(NH_4)_2SO_4$ brought to 50% saturation. The precipitate was suspended and dialyzed against 0.01 *M* phosphate buffer (pH 7.4) and applied to a DEAE-cellulose column equilibrated with the same buffer (*11*). The proteins eluted with this buffer were dialyzed against water and lyophilized. The lyophilized powders were reconstituted at a concentration of 15–20 mg/ml in buffer A, and the purity of the preparation was tested by agarose gel electrophoresis in sodium barbital buffer (pH 9.0) (*12*). Preparations containing a single protein band migrating in the "slow" IgG region were used in the assays (*see* below). Nonimmune goat and rabbit sera were similarly treated to obtain the IgG fractions.

Interaction of enzyme with antibodies.—Increasing amounts of immune or nonimmune IgG fractions were added to a fixed amount of enzyme solution in a total volume of 0.45 ml, and the mixtures were incubated for 16 hours at 4°C. Two procedures were then used to measure the reaction of enzyme samples with different IgG preparations. In the first case, 200 µl of each enzyme-IgG mixture was tested directly for enzyme activity. In the second case, 50-µl suspension of IgG-Sorb (an amount previously determined by titration to remove 100% of the IgG) was added to each mixture as an absorbent for antigen-antibody complexes (*13*), the mixture was further incubated at 25°C for 1 hour and centrifuged at 900×*g* in a Beckman microcentrifuge for 15 minutes at 4°C, and 200 µl of each supernatant was tested for collagenase activity. Addition of IgG-Sorb alone to enzyme samples did not affect collagenase activity. For both procedures the interaction of enzyme with IgG is expressed as percentage of inhibition of collagenase activity in the mixtures of enzyme and IgG. The term "inhibition" is used here to denote removal of the enzyme from solution by interaction with IgG only or by subsequent treatment with IgG-Sorb.

Enzyme assays.—Type I collagenase: Collagenase activity was determined by measurement of soluble radioactive peptides released from ^{14}C-labeled, reconstituted collagen fibrils. ^{14}C-acetylated rat tail tendon collagen was prepared according to the method of Gisslow and McBride (*14*) as modified by Johnson-Wint (*15*). Enzyme samples (100–200 µl) were added to the fibrillar substrate and incubated at 37°C in a total volume of 200 μl for 4 hours. Each assay included a trypsin blank (0.01%) and a buffer blank as controls. At the end of the incubation, the unreacted substrate was sedimented in a Beckman microcentrifuge, and the radioactivity present in 200 μl of the supernatant was measured. Collagenase activity was also determined by a fibril film lysis assay (*15*) in which the Microwells of 96-well plates (Linbro Scientific Inc., Hamden, Conn.) were coated with radioactive collagen solution and the collagen was polymerized to fibrils at 37°C for 1 hour. Enzyme samples were added and incubated as described above. The radioactivity released into the supernatant served as an indicator of enzyme activity. The amount of radioactive collagen used in either assay corresponded to approximately 5,000 cpm. One unit of collagenase activity is defined as the amount of enzyme required to degrade 1 μg collagen/minute.

Both active and trypsin-activable (latent) collagenolytic activities were assayed. Samples were incubated with TPCK-trypsin for 5 minutes at 37°C, followed by the addition of a fivefold excess of SBTI. The concentration of TPCK-trypsin required for maximal activation of latent collagenase was 90 μg/ml sample for rabbit and nude mouse tumor extracts and 18 μg/ml for mouse calvaria culture medium. The optimal concentrations of TPCK-trypsin required for activation of collagenase were determined in a separate experiment.

Collagen degradation products were identified by polyacrylamide disk gel electrophoresis at pH 4.0 as described by Nagai et al. (*16*).

Type IV collagenase: Radioactively labeled type IV collagen from two sources was used for the assay. A purified preparation of type IV collagen extracted with acetic acid from bovine anterior lens capsule was supplied by Dr. Carlo Mainardi, Veterans Administration Hospital, Memphis, Tenn. The other preparation was from murine EHS fibrosarcoma and was provided by Dr. Lance Liotta, National Cancer Institute, Bethesda, Md. Enzyme assays, with the use of either substrate, were performed according to the procedure described by Garbisa et al. (*17*). The total amount of radioactivity used in each assay was 3,000 cpm. The total volume of the incubation mixture was 270 μl, and incubation time was 4 hours at 37°C. Type IV collagenase was assayed before and after trypsin activation.

Type V collagenase: Radioactively labeled type V collagen from human placenta was obtained from Dr. Liotta. Enzyme assay was performed according to the procedure of Liotta et al. (*18*) before and after trypsin activation. The total volume of the incubation mixture was 270 μl, and the incubation period was 4 hours at 37°C. The total amount of radioactivity used in the assays was 1,600 cpm.

Culture of tumor tissue.—Fragments of tumor approximately 1–2 mm^3 were washed three to four times in serum-free DMEM containing 100 U penicillin/ml and 100 μg streptomycin/ml. The fragments were distributed in plastic tissue culture dishes (0.6 g tissue/6-cm dish) with 2 ml DMEM and incubated at 37°C in a moist atmosphere with 5% CO_2 and 95% air. Portions of the subcutaneous tumor from rabbits were dissected free of the surrounding normal tissue and necrotic tumor tissue and placed in culture. The entire tumor from the nude mouse, free of normal tissue, was sliced and used for culture. The culture medium was harvested and replaced daily. The media from three to four dishes were pooled and centrifuged at 20,000×*g* for 30 minutes; the unconcentrated supernatants were assayed for collagenase activity before and after trypsin activation.

To investigate whether protein synthesis is required for the presence of collagenase in culture media of tumor explants, we cultured the explants in the presence of cycloheximide. Furthermore, to ensure that the cycloheximide was effectively inhibiting protein synthesis, we determined incorporation of ^3H-labeled amino acid into TCA-precipitable proteins of cultured explants. The tumor fragments were preincubated at 37°C for 30 minutes in DMEM. The medium was then replaced with 1 ml fresh medium with or without cycloheximide (10 or 50 μg/ml) containing 10 μCi of a mixture of ^3H-labeled amino acids (sp act, 1 mCi/ml; New England Nuclear Corp.). After 24 or 48 hours of incubation at 37°C, the tumor explants were removed, washed extensively with Hanks' balanced salt solution, suspended in 5 volumes of 10% TCA, and homogenized. The TCA precipitate was collected by centrifugation, washed two times with absolute ethanol, and dissolved in NCS tissue solubilizer (Amersham Corp., Arlington Height's, Ill.); the radioactivity in 0.25-ml samples was measured in a scintillation spectrometer.

RESULTS

Morphologic Characteristics of V_2 Carcinoma in Rabbits and Nude Mice

Two weeks after subcutaneous implantation of V_2 carcinoma in rabbits or in nude mice, large palpable tumors developed at the site of injection. In rabbits, the neoplasm was firmly attached to the subcutaneous and surrounding tissue, whereas in the mouse it was loosely attached to the subcutaneous tissue and was readily removable. The central, pink tumor mass was surrounded by a thicker and more diffuse connective tissue layer in the rabbit than in the mouse. During later stages of growth (usually, 5 wk), central necrosis was observed in both hosts. In rabbits, tumor metastases were observed in lymph nodes and, occasionally, in liver and lung, but none was found in nude mice.

Histologic examination of the tumor from both species revealed certain characteristic features. In the 10 rabbits studied, fibrosis was extensive, and clusters of tumor cells extended from the central mass deep into the surrounding connective tissue in all cases. In contrast, tumor implants in nude mice were well circumscribed, and the interface of the thin fibrous layer with the tumor mass was sharply defined. Infiltration of this connective tissue layer by tumor cells was observed in only 1 of 10 animals.

Collagenase Activity in Rabbit and Nude Mouse Tumor Extracts

Extracts prepared from subcutaneously implanted V_2 carcinoma in rabbits or in nude mice were assayed for both latent and active forms of collagenase (*19*). Only trypsin-activable enzyme activity was detected in extracts, and approximately the same amount of enzyme per gram of tumor tissue was obtained from the two hosts, viz., 2.68±0.40 U/g for 56 of 70 rabbits and 2.76±0.93 U/g for 100 nude mice. Extracts prepared from tumors for the other 14 rabbits were inactive before or after treatment with trypsin.

Collagenase Activity in Rabbit and Nude Mouse Tumor Explant Cultures

Tumor explants from both hosts released collagenase into the culture medium. In the rabbit, enzyme activity appeared in the medium of three of seven cultures (each from an individual animal) after an initial lag period of 1–2 days. Two cycles of collagenase production were observed: The first occurred during days 2 and 3, and the second occurred during days 7 and 8 (text-fig. 1); no activity was detected thereafter. In the other four cultures, enzyme activity appeared on the 1st day; then after a quiescent period of 1–4 days, a peak of enzyme release occurred lasting 1–3 days. Thus trypsin-activable collagenase was obtained from all seven cultures. Furthermore, explants of tumor from 2 rabbits also released spontaneously active enzyme in addition to trypsin-activable enzyme. The total amount of latent enzyme released into the culture medium from day 1 to day 9 ranged from 15 to 23 U/g of tumor tissue. Cultures of necrotic tumor tissue released lesser amounts of enzyme. Repeated freeze-thawing of the tumor tissue before culture prevented the appearance of enzyme in the medium. Addition of cycloheximide (10 or 50 μg/ml) to the rabbit tumor explants in culture blocked the appearance of 90% of collagenase activity in the medium after day 1 (text-fig. 1). Cycloheximide, in concentrations of 10 and 50 μg/ml, inhibited incorporation of ^{3}H-labeled amino acids into total protein 37 and 75%, respectively.

The pattern of appearance of enzyme activity in the culture medium of the nude mouse tumor differed significantly from that of the rabbit. In all cultures from 6 groups of animals, the maximum amount of enzyme activity appeared on the 1st day of culture (text-fig. 2). The enzyme activity decreased sharply by the 2d day and was not detectable subsequently. All cultures released trypsin-activable enzyme, although three of the six cultures also had spontaneously active enzyme. The amount of enzyme activity obtained in different experiments during the culture period of day 1–day 9 ranged from 0.7 to 2 U/g. In the presence of cycloheximide (10 or 50 μg/ml), the level of collagenase activity decreased by 20–50% of that of controls in four experiments; there was no change in the pattern of release (text-fig. 2). Cycloheximide at the same concentrations blocked 75% of the incorporation of ^{3}H-labeled amino acids into total protein. Although repeated freeze-thawing of the rabbit tumor explants inhibited the appearance of enzyme in the media, it did not have any effect on the nude mouse tumor explants.

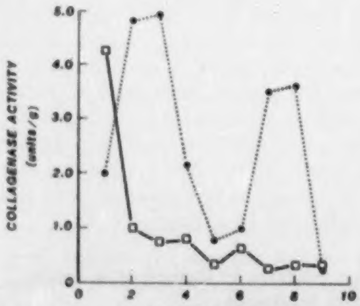

TEXT-FIGURE 1.—Release of collagenase into serum-free medium from explants of V_2 carcinoma obtained from rabbits. Explants were cultured in the absence (●) and presence (□) of cycloheximide (10 μg/ml culture medium). Results shown represent levels of trypsin-activable collagenase activity.

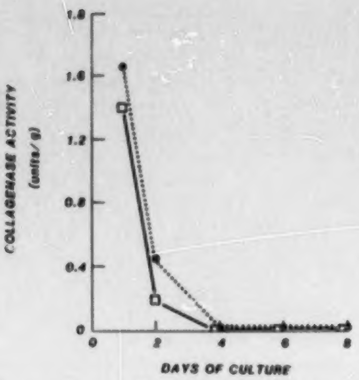

TEXT-FIGURE 2.—Release of collagenase into serum-free medium by explants of V_2 carcinoma obtained from nude mouse. Explants were cultured in the absence (●) and presence (□) of cycloheximide. Results shown represent levels of trypsin-activable collagenase activity.

These results indicate that explants from the invasive V_2 carcinoma have the capacity to produce relatively large amounts of collagenase over a considerable period of culture, whereas explants from the noninvasive nude mouse tumor mainly release stored enzyme into the medium and have a low capacity for continued collagenase production.

Activity of Collagenase Preparations Toward Type IV and V Collagen

Enzyme preparations from rabbit V_2 carcinoma, nude mouse tumor, and mouse calvaria were tested for their ability to cleave type IV and type V collagen. With all three enzymes, the activity against type I collagen was greater than that toward type IV and type V. In each case, with the use of the same assay conditions, 90% of the type I substrate was cleaved, whereas with type IV or V only 20–30% was degraded.

Some Properties of Collagenase Preparations

The collagenase activity of extracts of V_2 carcinoma from the rabbit and the nude mouse was completely inhibited by 10 m*M* EDTA or 3 m*M* dithiothreitol. Acid gel electrophoresis of collagenase cleavage products produced by enzyme from extracts or culture media of both hosts showed the TC^A and TC^B fragments, characteristic of animal collagenase reaction products (*16*). The enzyme from mouse calvaria had similar properties.

Gel filtration on Sephacryl S-200 of extracts prepared from rabbit tumor revealed a single major peak of latent collagenase with an apparent molecular weight of approximately 40,000, which was reduced to 20,000 after trypsin activation. A major peak of collagenase activity with a similar molecular weight was obtained upon fractionation of the nude mouse tumor extract. However, the chromatographic profile of the nude mouse tumor extract was somewhat heterogeneous, suggesting the presence of large molecular weight forms of enzyme. Trypsin activation of the nude mouse enzyme gave rise to increased heterogeneity with peaks of activity ranging from 12,000 to 20,000 and from 34,000 to 50,000. About 20% of the amount of trypsin required for activation of unfractionated samples was optimal for activation of the eluted column fractions in each case; higher concentrations of trypsin diminished the collagenase activity.

Concentrated culture medium containing mouse bone enzyme was applied to a Sephacryl S-200 column; a single peak of active collagenase with an apparent molecular weight of 90,000 was eluted.

In each of the above experiments, approximately 70% of applied enzyme activity was recovered.

Effect of Antibodies on Rabbit Tumor Collagenase and Normal Mouse Bone Collagenase

The specificity of the antibodies directed against rabbit tumor and normal mouse bone collagenases was tested prior to reaction with the enzyme from the nude mouse tumor.

Inhibition of rabbit tumor collagenase by the isologous antibody was concentration-dependent, reaching a maximum of 92% of control values (text-fig. 3). Goat anti-rabbit tumor collagenase IgG also inhibited the enzyme prepared from normal rabbit synovial cells and skin fibroblasts (not shown). This antibody was ineffective against mouse bone collagenase. Addition of the IgG fraction of normal goat serum to rabbit tumor collagenase did not affect enzyme activity. Similarly, rabbit anti-mouse bone collagenase IgG selectively blocked the mouse enzyme to a maximum level of 80% (text-fig. 3) and had no blocking action on rabbit tumor collagenase. The IgG fraction from nonimmune rabbit serum did not affect the mouse enzyme. Similar results were obtained by the two procedures for measurement of interaction of enzyme with antibodies (*see* "Materials and Methods").

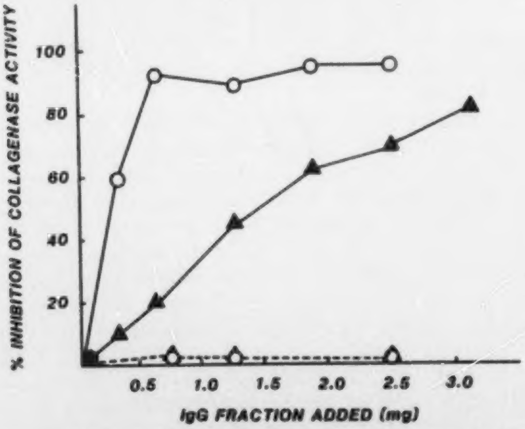

TEXT-FIGURE 3.—Specificity of antibodies against rabbit tumor and normal mouse bone collagenases. Amounts of 0.05 U normal mouse bone enzyme (▲——▲) and 0.08 U rabbit tumor enzyme (○——○) were incubated for 16 hr at 4°C with their corresponding IgG fractionated from rabbit antisera and goat antisera, respectively, and the supernatants were assayed for collagenase activity. Control incubations were performed with collagenase from mouse and rabbit mixed with the γ-globulin fractions from nonimmune rabbit (▲- - -▲) and goat serum (○- - -○), respectively.

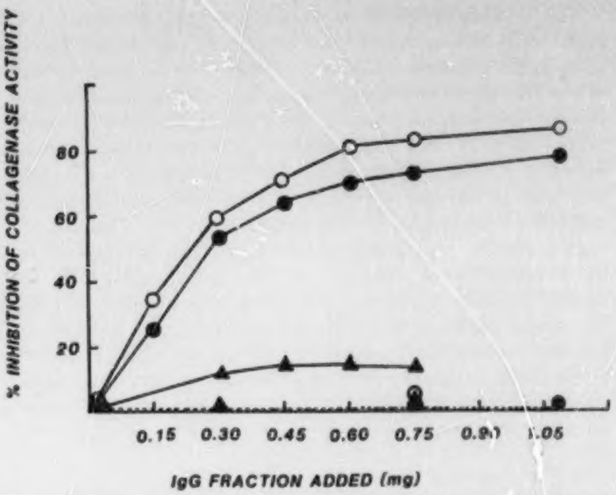

TEXT-FIGURE 4.—Interaction of antibody against rabbit tumor collagenase with different enzyme preparations. Amounts of 0.1 U enzyme from rabbit tumor (○——○) and nude mouse tumor (●——●) and 0.07 U enzyme from mouse bone (▲——▲) were each incubated for 16 hr at 4°C with the indicated amounts of IgG. After incubation, 50 µl reconstituted IgG-Sorb was added to each incubation mixture, and these mixtures were incubated further for 45 min at 25°C. Mixtures were centrifuged to remove the precipitated immune complexes, and the supernatants were assayed for collagenase activity. Control incubations were performed with each enzyme with the γ-globulin fraction from nonimmune goat serum (○- - -○, ●- - -●, ▲- - -▲).

Effect of Antibodies on Nude Mouse Tumor Collagenase

Antibodies to rabbit V_2 carcinoma collagenase resulted in 67–80% inhibition of nude mouse tumor enzyme in six experiments (text-fig. 4). The IgG fraction of nonimmune goat serum had no effect on nude mouse tumor enzyme.

Antibodies to normal mouse bone collagenase also partially inhibited nude mouse tumor enzyme; the degree of inhibition varied from 30 to 40% in six experiments, and no further inhibition was observed with additional increments of γ-globulin (text-fig. 5). Nonimmune rabbit γ-globulin had no effect on nude mouse tumor collagenase (text-fig 5). Similar results were obtained by the two procedures used to measure interaction of enzyme with antibodies (*see* "Materials and Methods"). The inhibitory effect of the antibodies against rabbit tumor and mouse bone collagenase on the enzyme activity present in nude mouse tumor culture medium was also examined. The antibody against rabbit collagenase inhibited this activity by approximately 65% and that against mouse enzyme by 34% (data not shown).

The combined effect of antibodies against rabbit and mouse enzymes on nude mouse tumor collagenase was found to be approximately additive (table 1). The combined effect of the two antibodies on artificial mixtures of rabbit tumor enzyme and normal mouse bone collagenase was also measured (table 2). For these experiments the enzymes were mixed in a ratio of 70:30 to mimic the proportions of rabbit and mouse enzyme detected in the nude mouse tumor collagenase as shown in text-figures 4 and 5. The dose of each antibody was chosen so as to inhibit the corresponding individual enzyme to an extent of approximately 50% (as shown in table 2–52% for the rabbit enzyme and 55% for the mouse enzyme). Thus the anti-rabbit tumor collagenase antibody would be expected to inhibit the mixture of enzyme preparations by 35% and the anti-mouse bone collagenase antibody by 16%. The actual results obtained were 48 and 20%, respectively. When both IgG fractions were added together to the enzyme mixture, 67% inhibition of the enzyme activity was observed, a value that closely corresponds to the sum of the inhibitory effects of the inidividual antibodies.

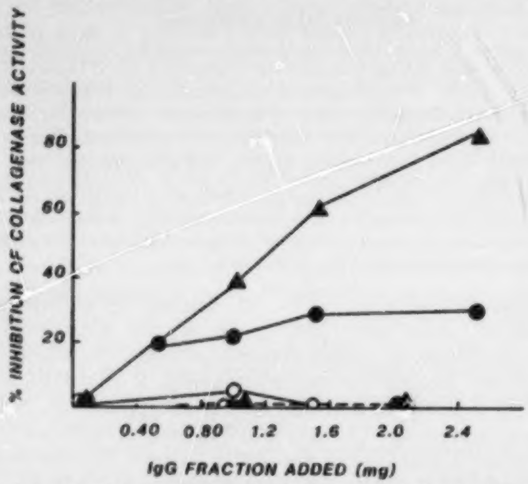

TEXT-FIGURE 5.—Interaction of antibody against mouse bone collagenase with different enzyme preparations. A total of 0.04 U enzyme from normal mouse bone (▲——▲), nude mouse tumor (●——●), and rabbit tumor (○——○) was incubated for 16 hr at 4°C with the indicated amounts of IgG. After incubation, 50 µl IgG-Sorb was added to each incubation mixture, and the mixtures were further incubated for 45 min at 25°C and assayed for collagenase activity. Control incubations were performed with the γ-globulin fraction from nonimmune rabbit serum (●- - -●, ○- - -○, ▲- - -▲).

TABLE 1.—*Effect of simultaneous addition of antibodies to nude mouse tumor collagenase*[a]

Expt No.[b]	Percent inhibition of collagenase activity		
	Goat anti-rabbit collagenase IgG	Rabbit anti-mouse bone collagenase IgG	Combined goat and rabbit IgG
1	49	18	57
2	71	26	87

[a] A total of 0.06 U of nude mouse tumor enzyme was incubated with the IgG fraction of the antisera added either separately or in combination. Residual enzyme activity in the supernatant was measured after removal of immune complexes (*see* "Materials and Methods").

[b] Expt 1—0.12 mg anti-rabbit IgG and 0.7 mg anti-mouse IgG; expt 2—0.62 mg anti-rabbit IgG and 2.0 mg anti-mouse IgG.

TABLE 2.—*Effect of addition of antibodies to a mixture of rabbit tumor and normal mouse bone collagenase*[a]

Source of enzyme	Percent inhibition of collagenase activity		
	Goat anti-rabbit collagenase IgG	Rabbit anti-mouse bone collagenase IgG	Combined goat and rabbit IgG[b]
Rabbit V_2 carcinoma	52	0	ND
Mouse calvaria	0	55	ND
Rabbit V_2 carcinoma and mouse calvaria mixture, 70 and 30%	48	20	67

[a] A total of 0.07 U rabbit V_2 carcinoma enzyme and 0.03 U normal mouse bone enzyme was mixed and incubated with the IgG fraction of the antisera either alone or in combination. The residual enzyme activity in the supernatant was measured after removal of immune complexes (*see* "Materials and Methods"), and 0.12 mg of goat IgG and 0.17 mg rabbit IgG were used in the experiment.

[b] ND=not determined.

DISCUSSION

Two major conclusions can be drawn from these studies. First, extracts of invasive and noninvasive V_2 carcinomas, grown in the rabbit and nude mouse, respectively, contain similar amounts of collagenase, whereas cultured explants of invasive tumors from the rabbit produce approximately 10 times more collagenase than explants of noninvasive tumors from the nude mouse. Second, it was shown, with the use of antibodies directed against rabbit and mouse collagenases, that both the nude mouse tumor extracts and culture medium contain a mixture of host mouse and rabbit tumor enzymes.

Implantation of the rabbit V_2 carcinoma into the nude mouse gave rise to a noninvasive tumor in which no infiltration of tumor cells into neighboring host tissue and no metastases were noted. Most other malignant tumors are known to behave similarly in the nude mouse (*20, 21*). The ability of the nude mouse to retard the malignant behavior of tumors has been attributed to an active natural killer cell system present in these hosts (*22*). Despite the difference in malignancy of the V_2 carcinoma implanted in the rabbit and the nude mouse, no significant difference in level of collagenase activity was observed in extracts from the two types of tumor. The major difference between the two neoplasms with respect to collagenase was in the pattern of release of enzyme from the cultured explants. In the rabbit, maximum activity often appeared after an initial lag period, and collagenase was produced by the explants over several days, resulting in accumulation of approximately tenfold more enzyme than that obtained in extracts of the tumor. Similar patterns of enzyme production have been observed in nearly all tissue culture systems producing collagenase

(*23, 24*). In the nude mouse, in contrast, the maximum amount of enzyme was obtained on the 1st day of culture followed by a rapid decrease to a base-line level within 2–3 days. The total amount of enzyme released per gram of tissue was very similar to that present in tumor extracts. Further, there was a marked difference in susceptibility of the explants to inhibition of collagenase production by cycloheximide and freeze-thawing. These procedures had much less effect on the appearance of enzyme in culture media of nude mouse tumor explants than in rabbit tumor explant cultures. These results suggest that in the nude mouse tumor explants, much of the enzyme was released from storage and was not newly synthesized, whereas in the rabbit explants de novo synthesis continued for a considerable period. Thus it appears that regulation of collagenase production in the invasive V_2 tumor is clearly different from that in the noninvasive V_2 tumor. Both types of tumor differ from normal tissue where little or no extractable enzyme accumulates but de novo synthesis in explant culture usually occurs (*25*).

Collagenase has been detected in several neoplasms (*1–7*), and the enzyme has been localized in the connective tissue stroma surrounding some tumors by immunofluorescence (*26*), leading to suggestions that collagen degradation is involved in tumor infiltration. Our recent morphologic studies on V_2 carcinoma implanted in rabbit cornea revealed disruption of the compact laminated collagenous structure associated with collagenase production (*27*). Both collagenolysis and tumor growth were inhibited by the presence of medroxyprogesterone or dexamethasone (*27*). However, the presence of detectable collagenase in tumors, for example, in the noninvasive V_2 carcinoma of the nude mouse, is not sufficient for the migration or penetration of tumor cells through connective tissue barriers; additional conditions are obviously necessary. Among other factors, the production of hyaluronate may be involved, since the invasive rabbit V_2 carcinoma growing in the rabbit contains larger amounts of this polysaccharide, which is often associated with cell migration (*28*), than does the tumor grown in the nude mouse (*29*). Failure of the V_2 carcinoma to metastasize in the nude mouse cannot be attributed to a lack of type IV or type V collagenase because both enzyme activities were detected at similar low levels in extracts of both the nude mouse and the rabbit V_2 carcinomas. It is not known whether the type I, IV, and V collagen-degrading activities of the V_2 carcinoma represent a single enzyme or a mixture of enzymes.

In the present studies, we sought to determine whether or not host–tumor cell interactions lead to production of collagenase by host cells associated with the tumor. Antibodies were induced to the rabbit tumor and mouse bone enzyme. Mouse bone was selected as a source of mouse collagenase because this tissue has been reported to yield larger amounts of enzyme in culture than do other mouse tissues (*30, 31*). These antibodies reacted only with autologous antigen and thus could be used to determine whether the collagenase present in nude mouse tumor originated in host or tumor cells. The results indicated that, in the V_2 carcinoma implanted into nude mice, the major portion of collagenase activity (≈70%) is contributed by rabbit cells, but a significant amount (≈30%) is produced by mouse cells. The source of rabbit enzyme in the nude mouse tumor is probably tumor cells, rather than fibroblasts, since implantation of normal rabbit muscle or synovial cells into the nude mouse did not result in any growth. However, the possibility that normal rabbit fibroblasts do survive and multiply in nude mice in the presence of tumor cells and that these cells might be a source of rabbit collagenase cannot be excluded. In support of our observation that host–tumor cell interaction might lead to production of collagenase by host cells are the studies reported by Harris et al. (*32*). They showed that the central tumor tissue from rabbit V_2 carcinoma does not synthesize enzyme in culture, whereas the surrounding connective tissue does. Possibly, in their tumor system, collagenase production occurred in the connective tissue layer because of the presence of both host and tumor cells in that region, whereas in the central tumor mass only tumor cells predominate.

Since macrophage infiltration of tumors (*33*) and collagenase production by stimulated macrophages in culture are known to occur (*34, 35*), these may be the host cell source of enzyme. Werb and Gordon (*34*) reported that these cells secrete small amounts of collagenase for prolonged periods in culture and that secretion is inhibited by cycloheximide, thus suggesting de novo synthesis of the enzyme in culture. However, our data on the profile of enzyme production by nude mouse tumor explants in culture and enzyme production's relative insensitivity to the presence of cycloheximide suggest that most of the measurable enzyme is stored within cells or bound to collagen fibrils rather than being newly synthesized.

Although, immunologically, the nude mouse tumor extracts were shown to contain a mixture of rabbit and mouse collagenases, it was difficult to ascertain biochemically whether both enzymes were present. The rabbit tumor enzyme was shown to have a molecular weight of 40,000, whereas the mouse bone enzyme was of molecular weight 90,000. In the case of the nude mouse, the enzyme was somewhat heterogeneous, with the major component of molecular weight 40,000 and a minor component of higher molecular weight. However, it cannot be concluded with certainty that the minor component was of molecular weight 90,000, which would be expected if the mixture contained mouse enzyme.

Cell–cell interactions regulating collagenase production have been documented in normal systems in which factors secreted by blood-derived mononuclear cells (*36, 37*), epithelial cells (*38, 39*), or macrophages (*40*) enhance production of this enzyme by connective tissue cells. Preliminary in vitro experiments have shown that co-culture of mouse B-16 melanoma or A-10 adenocarcinoma cells with normal rabbit fibroblasts results in stimulation of collagenase production (*41*). The tumor cells have been found to secrete factor(s) that stimulate the fibroblasts to produce elevated levels of the enzyme. Thus it is possible that in vivo tumor cells may interact with host cells to stimulate collagenase production.

REFERENCES

(*1*) DRESDEN MH, HEILMAN SA, SCHMIDT JD. Collagenolytic enzymes in human neoplasm. Cancer Res 1972; 32:993–996.

(2) Hashimato K, Yamanishi Y, Dabbous MK. Electron microscopic observations of collagenolytic activity of basal cell epithelioma of the skin in vivo and in vitro. Cancer Res 1972; 32:2561-2567.

(3) Hashimato K, Yaminishi Y, Maeyens E, Dabbous MK, Kanzaki T. Collagenolytic activities of squamous cell carcinoma of the skin. Cancer Res 1973; 33:2790-2801.

(4) Abramson MA, Shilinc RW, Huang C, Salome GR. Collagenase activity in epidermoid carcinoma of the oral cavity and larynx. Ann Otol 1975; 84:158-163.

(5) McCroskery PA, Richards JF, Harris ED Jr. Purification and characterization of a collagenase extracted from rabbit tumors. Biochem J 1975; 152:131-142.

(6) Bauer EA, Gordon JM, Reddick ME, Eisen AZ. Quantitation and immunocytochemical localization of human skin collagenase in basal cell carcinoma. J Invest Dermatol 1977; 69:363-367.

(7) Dabbous MR, Robert AN, Brinkley B. Collagenase and neutral protease activity in culture of rabbit V_2-carcinoma. Cancer Res 1977; 37:3587-3594.

(8) Biswas C, Moran WM, Block KJ, Gross J. Collagenolytic activity of rabbit V_2-carcinoma growing at multiple sites. Biochem Biophys Res Commun 1978; 80:33-38.

(9) Kidd JG, Rous Rj. A transplantable rabbit carcinoma originating in a virus-induced papilloma and containing the virus in masked or altered form. J Exp Med 1940; 71:813-837.

(10) Shimizu M, Glimcher MJ, Travis D, Goldhaber P. Mouse bone collagenase: Isolation, partial purification and mechanism of action. Proc Soc Exp Biol Med 1969; 130:1175-1180.

(11) Fahey JL, Terry EW. Ion exchange chromatography and gel filtration. I. In: Weir DM, ed. Handbook of experimental immunology. Philadelphia: Blackwell, 1980:81-816.

(12) Laurell CB. Electrophoresis, specific protein assays or both in measurement of plasma proteins. Clin Chem 1973; 19:99-102.

(13) Kessler SW. Rapid isolation of antigens from cells with a Staphylococcal protein A-antibody absorbent: Parameters of the interaction of antibody-antigen complexes with protein A. J Immunol 1975; 115:1617-1624.

(14) Gisslow MT, McBride BC. A rapid sensitive collagenase assay. Anal Biochem 1975; 68:70-78.

(15) Johnson-Wint B. A quantitative collagenase film assay for large numbers of samples. Anal Biochem 1980; 104:175-181.

(16) Nagai Y, Gross J, Piez KA. Disc electrophoresis of collagenase components. Ann NY Acad Sci 1964; 121:494-500.

(17) Garbisa S, Tryggvason K, Foidart JM, Liotta LA. Assay for radiolabeled Type IV collagen in the presence of other proteins using a specific collagenase. Anal Biochem 1980; 107:187-192.

(18) Liotta LA, Lanzer WL, Garbisa S. Identification of a Type V collagenolytic enzyme. Biochem Biophys Res Commun 1981; 98:184-190.

(19) Steven FS, Itzhaki S. Evidence for a latent form of collagenase extracted from rabbit tumor cells. Biochim Biophys Acta 1977; 496:241-246.

(20) Shimosato Y, Kameya T, Nagai K, et al. Transplantation of human tumors in nude mice. J. Natl Cancer Inst 1976; 56:1251-1260.

(21) Giovanella BC, Fogh J. The nude mouse as a recipient of human tumor transplants. In: Fogh J, Giovanella BC, eds. The nude mouse in experimental and clinical research. New York: Academic Press, 1978:281-312.

(22) Hanna N, Fidler I. Role of natural killer cells in the destruction of circulating tumor emboli. JNCI 1980; 65:801-809.

(23) Nagai Y, Lapiere CM, Gross J. Tadpole collagenase. Preparation and purification. Biochemistry 1966; 5:3123-3160.

(24) Evanson JM, Jeffrey JJ, Krane SM. The studies on collagenase from rheumatoid synovium in tissue culture. J Clin Invest 1968; 47:639-651.

(25) Gross J. Aspects of animal collagenases. In: Ramachandran GN, Reddi AH, eds. New York: Plenum Press, 1980:275-317.

(26) Woolley DE, Tetlow LC, Evanson JH. Collagenase immunolocalization. Studies in normal and pathological connective tissues. In: Woolley DE, Evanson JM, eds. Collagenase in normal and pathological connective tissues. New York: Wiley, 1980:105-125.

(27) Gross J, Azizkhan RG, Biswas C, Bruns RR, Hsieh DS, Folkman J. Inhibition of tumor growth, vascularization and collagenolysis in the rabbit cornea by medroxyprogesterone. Proc Natl Acad Sci USA 1981; 78:1176-1180.

(28) Toole BP. Glycosaminoglycans in morphogenesis. In: Hay E, ed. Cell biology of extracellular matrix. New York: Plenum Press, 1982:259-294.

(29) Toole BP, Biswas C, Gross J. Hyaluronate and invasiveness of the rabbit V2 carcinoma. Proc Natl Acad Sci USA 1979; 76:6299-6303.

(30) Vaes G. The release of collagenase as an inactive proenzyme by bone explants in culture. Biochem J 1975; 126:275-289.

(31) Sakamoto S, Sakamoto M, Goldhaber P, Glimcher MJ. Mouse bone collagenase. Arch Biochem Biophys 1978, 188:438-449.

(32) Harris ED Jr, Faulkner CS, Wood S. Collagenase in carcinoma cells. Biochem Biophys Res Commun 1972; 48:1247-1253.

(33) Thornthwaite JT, Sugarbaker EV. An examination of the macrophage response after challenge with murine, syngenic sarcoma cells. Exp Mol Pathol 1980; 33:185-202.

(34) Werb Z, Gordon S. Secretion of a specific collagenase by stimulated macrophages. J Exp Med 1975; 142:346-360.

(35) Boner PA, Leibovich SJ. Production of collagenase by mouse peritoneal macrophages in vitro. Characterization of sites of cleavage of tropocollagen. Biochim Biophys Acta 1976; 444:626-632.

(36) Dayer JM, Breard L, Chess L, Krane SM. Participation of monocyte-macrophages and lymphocytes in the production of a factor that stimulates collagenase and prostaglandin release by rheumatoid synovial cells. J Clin Invest 1979; 64:1386-1392.

(37) Newsome DA, Gross J. Regulation of corneal collagenase production: Stimulation of serially passaged stromal cells by blood mononuclear cells. Cell 1979; 16:895-900.

(38) Johnson-Wint B. Regulation of stromal cell collagenase production in adult rabbit cornea: In vitro stimulation and inhibition by epithelial cell products. Proc Natl Acad Sci USA 1980; 77:5331-5335.

(39) Johnson-Wint B, Gross J. Regulators or connective tissue collagenase production derived from epithelial cells of multiple sources. J Cell Biol 1981; 91:158a.

(40) Huybrechts-Godin G, Hauser P, Vaes G. Macrophage-fibroblast interactions in collagenase production and cartilage degradation. Biochem J 1979; 184:643-650.

(41) Biswas C, Gross J. Fibroblast-tumor cell interaction in collagenase production. J Cell Biol 1981; 91-163a.

Immunoadjuvant Effects of *Blastomyces dermatitidis* Against EL 4 Lymphoma in C57BL/6J Mice [1,2,3]

L. Scott McDaniel [4,5] *and* George C. Cozad [4,6]

ABSTRACT—The ability of thimerosal-killed *Blastomyces dermatitidis* yeast cells, which greatly enhance the cell-mediated immune response in C57BL/6J mice, to act as an immunopotentiator against EL 4 lymphoma was investigated. Mice treated with yeast cells were protected from as many as 10^4 tumor cells. Complete suppression of tumor growth was observed in treated animals that received ip injections of 10^2 or 10^3 tumor cells. The mice, however, were not immune to further EL 4 lymphoma cell challenge. The lack of tumor-specific immunity indicated nonspecific suppression of tumor growth probably by macrophages. Ten days after treatment, the peritoneal macrophages from mice that showed complete tumor suppression were tested for their ability to prevent in vitro tumor cell proliferation. These macrophages demonstrated 90% inhibition of [^{3}H]thymidine incorporation by EL 4 tumor cells at a 100:1 effector-to-target cell ratio. Macrophages from *B. dermatitidis*-treated animals exhibited a twofold increase in specific lysis of EL 4 at 10 and 15 days compared to resident macrophages. Spleen and lymph node cells from protected animals showed no cytotoxic activity against EL 4 in a ^{51}Cr release assay. Treatment of tumor-bearing mice with a single dose of *B. dermatitidis* was effective only if administered within 24 hours of tumor establishment. These results demonstrated that nonviable *B. dermatitidis* prohibits the growth of EL 4 under conditions where *Corynebacterium parvum* fails to do so.—JNCI 1982; 69;1337–1342.

It is a generally accepted theory that macrophages play a major role in resistance against growth of tumor cells within the host tissue. The in vitro cytolytic capacity of activated macrophages is well substantiated (*1, 2*). Also, macrophages activated by bacterial or protozoal infections are able to inhibit the growth of tumor cells in vivo (*3, 4*). Microorganisms such as BCG (*2*), *Toxoplasma gondii* (*3*), or *Corynebacterium parvum* (*4*) are capable of inducing macrophages that have the capacity to distinguish tumor cells from normal cells. There is a great interest in agents that enhance the ability of macrophages to nonspecifically kill tumor cells. Various agents are also able to activate cultured resident macrophages to a tumoricidal state. These include lymphokines (*2*), LPS (*5*), and poly I:C (*6*). Evidence continues to mount for the importance of macrophages as primary targets of such immunomodulating agents.

Past studies in our laboratory with yeast cells of the dimorphic fungus *Blastomyces dermatitidis* indicated that this organism elicits a strong cell-mediated immune response (*7, 8*). We report here results of experiments on the protective effects of *B. dermatitidis*-induced resistance in C57BL/6J mice against the syngeneic lymphoma EL 4.

MATERIALS AND METHODS

Culture.—The thimerosal-killed whole yeast cell Ag was prepared by the method of Restrepo-Moreno and Schneidau (*9*) as modified by Spencer and Cozad (*7*). In all experiments the *B. dermatitidis* was washed three times in 10 volumes of a sterile PSS to remove the thimerosal. The yeast phase culture of *B. dermatitidis* 242 was originally isolated from a fatal human case of blastomycosis. The culture was maintained on BHI agar slants at 37°C.

Test animals.—Inbred C57BL/6J mice of both sexes, 2–3 months old were used in this study. The strain was originally obtained from The Jackson Laboratory, Bar Harbor, Maine, and bred in our animal facilities. The mice were separated by sex and given water and Purina Mouse Chow (Ralston Purina Co., St. Louis, Mo.) ad libitum.

Cell line.—The thymus-derived benzo[*a*]pyrene-induced lymphoma EL 4 of C57BL mice was used in this study. The cells were maintained as ascites tumors in 8–12-week-old C57BL/6J mice. Transfers were made at 10–12 days by ip injection of 10^6 cells in 0.2 ml HBSS (GIBCO, Grand Island, N.Y.). In vitro cultures of the EL 4 lymphoma were maintained as suspensions in RPMI-1640 medium (GIBCO) supplemented with 10% heat-inactivated FCS (M.A. Bioproducts, Walkersville, Md.). The medium also included 2 m*M* L-glutamine, 100 U penicillin/ml, and 100 µg streptomycin/ml (GIBCO). Cells were carried in logarithmic growth (12- to 14-hr doubling time) within a cell density of 1×10^5–2×10^6 cells/ml. EL 4 tumor cell viability under these growth conditions was between 97 and 100% as determined by the trypan blue exclusion test.

Preparation of immunizing inoculum and assessment of delayed hypersensitivity.—An Ag emulsion of thimerosal-killed *B. der-*

ABBREVIATIONS USED: Ag=antigen; BHI=brain–heart infusion; E:T=effector-to-target cell ratio(s); FCS=fetal calf serum; HBSS=Hanks' balanced salt solution; [^{3}H]dThd=tritiated thymidine; [^{125}I]IdUrd=[^{125}I]-5-iodo-2′-deoxyuridine; LPS=lipopolysaccharide; PBS=Dulbecco's phosphate-buffered saline; PSS=physiologic salt solution; SEM=scanning electron microscopy.

---

[1] Received February 1, 1982; revised May 28, 1982; accepted August 4, 1982.

[2] Supported by Public Health Service grant 2-S07-RR07078 from the Division of Research Resources, National Institutes of Health.

[3] Animals were maintained under the guidelines set forth by the University of Oklahoma.

[4] Department of Botany and Microbiology, University of Oklahoma, Norman, Okla. 73019.

[5] *Address reprint requests to* Dr. McDaniel at his *present address*: Comprehensive Cancer Center, School of Medicine, The University of Alabama in Birmingham, University Station, Birmingham, Ala. 35294.

[6] We thank Dr. John J. Skvarla, University of Oklahoma, for the use of the electron microscopy facilities and Mr. William Chissoe for technical assistance. We also thank Dr. Dalikeh Olga McDaniel, The University of Alabama in Birmingham, for advice and assistance; Dr. David Briles, The University of Alabama, for criticism of the manuscript; and Ms. Ann Brookshire for typing the manuscript. Special thanks is given to Dr. G. M. Kollmorgan, Oklahoma Medical Research Foundation, for providing cell lines.

matitidis yeast cells was prepared by the mixing of equal volumes of the yeast suspension and Freund's incomplete adjuvant (Difco Laboratories, Detroit, Mich.). A control suspension was prepared by substitution of PSS for the yeast suspension.

The mice were sensitized according to the method of Cozad and Chang (*8*). On days 0 and 7, mice were inoculated sc in the inguinal area with 0.1 ml Ag emulsion (containing 2 mg dry wt equivalent of killed *B. dematitidis* yeast cells). A control group was inoculated in the same manner with the PSS emulsion. Some animals were given ip 0.1 or 1.0 mg killed *B. dermatitidis* in 0.2 ml PBS 5 days before tumor challenge.

To determine the delayed hypersensitivity pattern, we gave 3 mice from each group footpad tests on days 3, 15, and 30 after the initial injection with a killed whole yeast cell suspension. We performed the footpad tests by the procedure of Youmans and Youmans (*10*), as described by Cozad and Chang (*8*).

Tumor inoculations.—We conducted preliminary experiments to determine the median survival time of mice that received 10^2–10^7 tumor cells without treatment. To test the effect of preimmunization with the Ag emulsion, we challenged groups of 10 mice with a range of 10^2–10^6 ip tumor cell injections on days 0, 3, and 15 after the initial Ag emulsion injection. We performed all experiments at least twice.

We also evaluated the protective effects by mixing the yeast cells with tumor cells prior to injection. The mice were given 0.2 ml ip injections of 10^2–10^6 EL 4 cells mixed with 0.1 or 1.0 mg killed *B. dermatitidis* yeast cells. Survival of the animals was checked daily for 2 months.

To test the therapeutic potential of *B. dermatitidis*, we gave mice ip inoculations of 10^2–10^6 EL 4 cells and treated them with ip injections of 1.0 mg *B. dermatitidis* in 0.2 ml PBS at various times after tumor challenge. A control group of tumor-bearing mice received ip injections of PBS alone. Treatment times were at 2 hours and at 1, 2, 3, 5, 8, and 11 days.

Collection of peritoneal cells.—We collected peritoneal cells without the use of an exudate-inducing agent by a modification of the method described by Tolnai (*11*). Five milliliters cold RPMI-1640 medium containing 10 U sodium heparin/ml (Fellows Medical Manufacturing Co., Inc., Anaheim, Calif.) and 1% FCS was injected into the peritoneal cavity. The fluid was withdrawn after a short massage.

We pooled the cells from 3 animals and assessed their viability by the trypan blue exclusion test. After centrifugation, we resuspended the cells at the concentration of 5×10^6 cells/ml in cold RPMI-1640 medium with 1% FCS and placed 0.1 ml of the suspension into wells of a Falcon MicroTest II plate (style 3040; Falcon Plastics, Oxnard, Calif.). After adherence for 60 minutes at 37°C in 5% CO_2, we removed nonadherent cells by washing twice with warm PBS and by suction through a Pasteur pipette. Then we added 0.1 ml fresh warm medium containing 10% FCS to the chambers and incubated the plates for 18–24 hours at 37°C in 5% CO_2.

Cytostasis assay.—We used a modified version of the procedure described by Goldman and Bar-Shavit (*12*). After the 24-hour incubation, we added to the wells 0.1 ml RPMI-1640 with 10% FCS containing the desired concentration of EL 4 cells. We set up controls of 0.2 ml RPMI-1640 medium with tumor cells alone, reincubated the plates for 7 hours, and added 0.5 μCi [^{3}H]dThd (20 Ci/mmol; New England Nuclear Corp., Boston, Mass.). Controls containing macrophages alone with [^{3}H]dThd were included. We incubated the plates at 37°C and 5% CO_2 for an additional 24 hours and then harvested the samples with a MASH unit (M.A. Bioproducts). We dried the filter strips, placed the disks in toluene scintillation fluid, and counted them in a Beckman LS 100C liquid scintillation counter.

Cytotoxicity assay.—We labeled the EL 4 cells by incubating 5×10^6 cells for 3 hours in 1.0 ml RPMI-1640 medium with 10% FCS containing 10 μCi [^{125}I]IdUrd (5 Ci/mg; Amersham Corp., Arlington Heights, Ill.) (*13*). After incubation we washed the cells three times with medium and resuspended them at 5×10^6 cells/ml.

We added the desired concentration of labeled EL 4 cells in 0.1 ml medium to wells containing 5×10^5 macrophages that had been incubated for 24 hours. Wells were set up for spontaneous and maximum release for each tumor cell concentration used. We ran all samples in triplicate. We incubated the plates for an additional 27–30 hours at 37°C and 5% CO_2, added 0.1 ml of a 2 *N* HCl solution to the maximum-release wells to obtain total counts, and centrifuged the plates for 15 minutes at 200× *g*. We then removed 0.1-ml samples and counted the radioactive label in a Packard Tri-Carb gamma counter. The percentage of specific lysis was obtained with the use of the formula: Percent specific lysis = [(cpm test sample − cpm spontaneous release)/maximum cpm of target cells]×100.

SEM of EL 4 lymphoma cells and macrophages.—After the harvest of the peritoneal cells, a 5.0-ml suspension of 1×10^6 cells/ml was plated in petri dishes that contained three glass cover slips. After 60 minutes at 37°C and 5% CO_2, all nonadhering cells were washed away with warm PBS. We added fresh warm medium containing 10% FCS and incubated the culture for 18–24 hours at 37°C in 5% CO_2.

After 24 hours, we replaced the medium with fresh medium containing 5×10^3 EL 4 cells/ml and incubated it for various time intervals up to 48 hours at 37°C and 5% CO_2. The medium was then aspirated, and the cover slips were fixed with 0.5% glutaraldehyde in PBS at room temperature for 18–24 hours.

We further prepared the samples for SEM by submitting them to a series of ethyl alcohol dehydrations. The cover slips were critical point dried in a Pelco Critical Point Dryer (No. 99 model H; Ted Pella Co., Trustin, Calif.) with the use of liquid CO_2 at a critical pressure of 1,072 pounds per square inch. The samples were then gold coated in a Technics Hummer sputter coater and examined in an International Scientific Instruments Super II scanning electron microscope at the noted magnifications with an accelerating voltage of 25 kV.

Chromium release assay.—We evaluated the cytotoxic activity of lymphocytes with the use of an established procedure (*14*). EL 4 cells, 1×10^7 in 1.0 ml, were incubated in serum-free RPMI-1640 medium containing 100 μCi ^{51}Cr–sodium chromate (500 mCi/mg; Amersham Corp.) for 1 hour at

37°C in 5% CO_2. After incubation, the cells were washed twice and adjusted to 2×10^5 cells/ml (target cells) in RPMI-1640 with 10% FCS. Spleen or lymph node cells (effector cells) from mice showing tumor suppression at 10 or 15 days were adjusted to 1×10^7 cells/ml. Then 0.1 ml of the target cells were placed in a round-bottomed microtiter plate (Linbro Scientific Co., Inc., Hamden, Conn.). The plate was incubated at 37°C in 5% CO_2 for 4 hours. At the end of this time, we centrifuged the plate at 200×*g* for 15–20 minutes, removed carefully 0.1 ml supernatant, transferred it to a 7.5×100-mm disposable glass tube, and counted the radioactivity for 10 minutes in a Packard Tri-Carb gamma counter. The percent cytotoxicity was obtained by the formula: Percent specific lysis = [(counts of test group − spontaneous release)/maximum cpm of target cells]×100.

RESULTS

Preimmunization effects on survival of mice.—We then preimmunized the mice with *B. dermatitidis* in Freund's incomplete adjuvant. Footpad tests with representative mice demonstrated a delayed hypersensitivity pattern that is consistent for *B. dermatitidis* (*8*), with a peak response at 15–18 days post primary injection. We then challenged the remaining mice with various tumor inocula at different times post primary immunizing dose. The results are presented in text-figure 1. Mice challenged 3 days after the initial *B. dermatitidis* injection showed a significant increase in mean survival time. The lower the initial tumor inoculum, the more significant was the increase in mean survival time compared to that of controls.

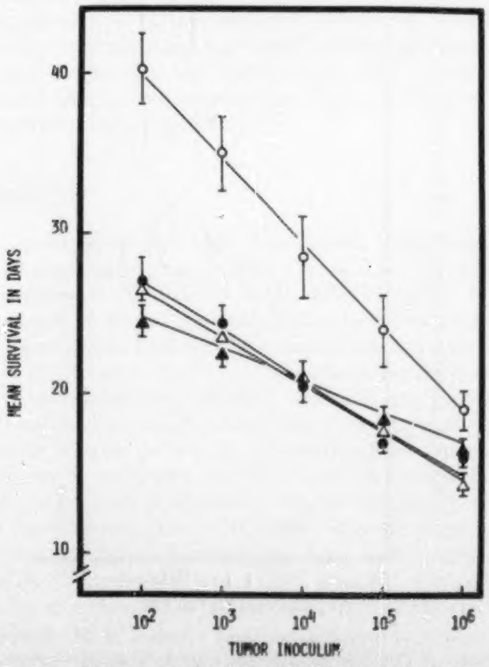

TEXT-FIGURE 1.—Preimmunization of C57BL/6J mice with *B. dermatitidis* in Freund's incomplete adjuvant. Survival at: ○——○, 3 days post primary infection; △——△, at day 0; ▲——▲, at 15 days post primary infection; ●——●, controls (received no treatment prior to the EL 4 challenge). Results are mean survival times ± SE.

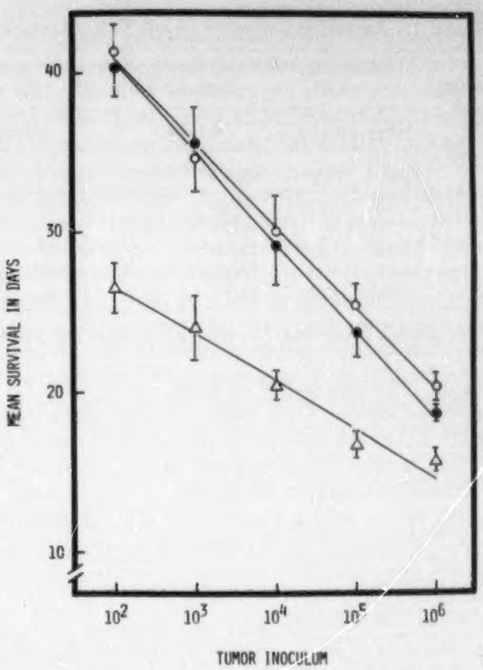

TEXT-FIGURE 2.—Preimmunization of C57BL/6J mice with 1.0 mg (○——○) and 0.1 mg (●——●) *B. dermatitidis* by ip injection 5 days prior to challenge with EL 4. ▲——▲, controls. Results are mean survival times ± SE.

In some experiments, mice were given ip injections of 0.1 or 1.0 mg killed *B. dermatitidis* in PBS without adjuvant 5 days prior to tumor challenge. Both doses of yeast cells caused significant (and similar) increases in mean time of survival of treated mice compared to that of control mice (text-fig. 2). The increase in survival was very similar to that seen in mice immunized 3 days before tumor challenge with *B. dermatitidis* in Freund's incomplete adjuvant (text-fig. 1).

Mixing of EL 4 cells with B. dermatitidis.—We mixed a dry equivalent weight of 0.1 or 1.0 mg killed *B. dermatitidis* with 10^2–10^6 EL 4 cells and immediately injected the mixture ip into mice to determine if *B. dermatitidis* could induce a host response capable of suppressing tumor growth. EL 4 cells in these mixtures showed no significant decrease in viability even after 4 hours as determined by trypan blue exclusion test. Within several days, all mice that had received the mixture developed an inflammatory response at the site of injection. Mice that received EL 4 alone showed no such response. At 30 days, the inflammation had receded in a majority of the animals that received *B. dermatitidis*. By 60 days, all mice in the control groups were dead as the result of tumor growth, but a significant number of animals that received the mixture were alive and free of tumors (table 1). At 65 days, the living mice were challenged with 1×10^4 EL 4 cells given by ip injection. The mice all died as a result of tumor development.

Treatment of EL 4 cells with B. dermatitidis.—To determine if *B. dermatitidis* could cause regression of established tumors,

TABLE 1.—*Suppression of tumor growth by* B. dermatitidis

No. of EL 4 tumor cells injected	Tumor suppression 60 days post treatment with *B. dermatitidis*[a]					
	None, control		0.1 mg		1.0 mg	
	Expt 1	Expt 2	Expt 1	Expt 2	Expt 1	Expt 2
10^6	0/10	0/10	0/10	0/10	0/10	0/10
10^5	0/10	0/10	1/10	0/10	2/10	1/10
10^4	0/10	0/10	10/10	6/10	10/10	8/10
10^3	0/10	0/10	10/10	10/10	10/10	10/10
10^2	0/10	0/10	10/10	10/10	10/10	10/10

[a] No. of animals tumor-free/No. given EL 4 tumor cell injections.

we treated mice inoculated with EL 4 cells with 1.0 mg *B. dermatitidis* at various times (table 2). Animals that received 10^5 or 10^6 EL 4 cells showed no regression of tumor growth. There was no significant increase in the mean survival of these animals compared with that of the controls. Mice given 10^2, 10^3, or 10^4 EL 4 cells showed a significantly high survival if treated with *B. dermatitidis* within 2 hours of tumor cell injection. The amount of survival decreased at least threefold if the treatment was given 1 day after tumor cell injection. No animal treated between 3 and 11 days with a single dose of *B. dermatitidis* showed significant increase in survival (text-fig. 2).

Effect of macrophages on tumor proliferation.—To determine if peritoneal macrophages could halt the growth of EL 4 cells in vitro, we examined [^{3}H]dThd incorporation by EL 4 cells in the presence of various macrophage preparations (text-fig. 3). At a 100:1 E:T, resident macrophages reduced [^{3}H]dThd incorporation into EL 4 by 44%. A significant difference in the amount of incorporation was not seen in the presence of macrophages from mice given 0.1 or 1.0 mg *B. dermatitidis* 5 days before harvesting. The results obtained with the use of macrophages derived from animals given sc injections of *B. dermatitidis* 3 days before harvesting were almost identical to those seen with animals given ip injections 5 days prior to harvesting (data not shown). Macrophages from mice that received a mixture of 10^4 EL 4 and *B. dermatitidis* 10 days earlier caused 90% inhibition of [^{3}H]dThd incorporation at a 100:1 E:T. This was greater than a 45% difference when compared to resident macrophages at the same concentration. The difference between these 2 groups was even greater at 1:1 and 10:1 E:T.

TABLE 2.—*Regression of established tumors after treatment with* B. dermatitidis

No. of EL 4 tumor cells injected	Treatment time	Tumor regression 60 days post treatment with:[a]		*P*-value[b]
		1.0 mg *B. dermatitidis*	0.2 ml PBS	
10^4	2 hr	6/10	0/10	<0.02
	1 day	2/10	0/10	NS
	2 days	0/10	0/10	
10^3	2 hr	9/10	0/10	<0.001
	1 day	2/10	0/10	NS
	2 days	0/10	0/10	
10^2	2 hr	10/10	0/10	<0.001
	1 day	6/10	0/10	<0.02
	2 days	4/10	0/10	<0.08

[a] No. of animals tumor-free/No. given injections of tumor.

[b] Chi-square test with Yates' correction. NS=not significant; $P \geq 0.10$.

In vitro cytotoxicity of peritoneal macrophages.—We tested peritoneal macrophages taken from mice 10–15 days after receiving 0.1 or 1.0 mg *B. dermatitidis* mixed with 10^4 EL 4 cells for their ability to release [^{125}I]IdUrd-prelabeled EL 4 cells. The data in text-figure 4 show that there was at least a twofold difference in the amount of lysis caused by macrophages from treated mice compared to the amount from normal resident macrophages. There was a consistent drop in the amount of lysis when the E:T was increased from 10:1 to 100:1.

Interaction between activated macrophages and target cells.—The EL 4 lymphoma cells were readily identifiable in the SEM. When EL 4 cells were seen in the presence of resident macrophages, there was no evidence of macrophage aggression toward the lymphoma cells. Macrophages collected from mice 10 days after receiving 1.0 mg *B. dermatitidis* mixed with 10^4 EL 4 cells (test macrophages) were examined for their ability to interact in vitro with EL 4. Test macrophages showed strong evidence of interaction with tumor cells as early as at 4 hours. However, there were no apparent morphologic alterations in the EL 4 cells at this point. By 30 hours, there was visible evidence of lysis of EL 4 cells by test macrophages.

Lymphocyte cytotoxicity.—We performed tests to investigate whether cytotoxic lymphocytes were present in the spleen and lymph nodes of mice that received ip injections of 0.1

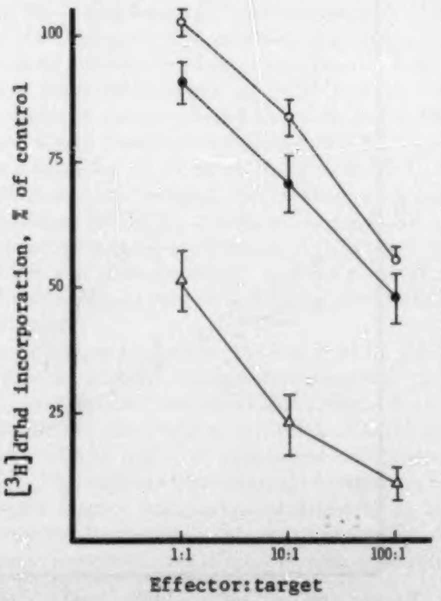

TEXT-FIGURE 3.—Macrophage-mediated cytostasis of EL 4 assessed by inhibition of [^{3}H]dThd incorporation. ○——○, Resident macrophages or macrophages collected from normal mice; ●——●, macrophages from mice that had received 1.0 mg *B. dermatitidis* 5 days earlier; △——△, macrophages from mice showing complete suppression of tumor growth at 10 days after having received 10^4 EL 4 + 1.0 mg *B. dermatitidis*. Data are means ± SE.

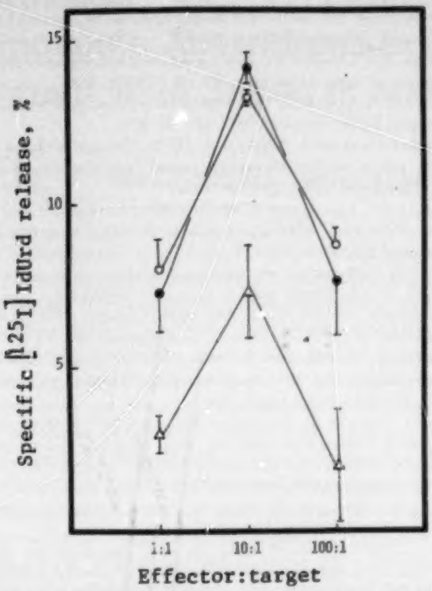

TEXT-FIGURE 4.—Release of ^{125}I from EL 4 target cells after 30 hr in culture. The target cells were cultured with effector macrophages: △——△, resident macrophages collected from normal mice; or macrophages from mice showing complete suppression of tumor growth at 10 days (○——○) or 15 days (●——●) after receiving 10^4 EL 4 + 1.0 mg *B. dermatitidis*. Data are means ± SE.

or 1.0 mg *B. dermatitidis* mixed with 10^4 EL 4 cells. The tests were done at 10 and 15 days after injection of the mixture. In one experiment, lymph node and spleen cells were taken at 10 days from mice that had received the mixture on days 0, 3, and 5. No cytotoxic lymphocytes were detected in spleen and lymph node preparations from mice that showed suppression of tumor growth.

DISCUSSION

The results presented here demonstrate that thimerosal-killed *B. dermatitidis* yeast cells can cause suppression of EL 4 lymphoma in C57BL/6J mice. Other studies on the mechanisms of tumor regression by immunopotentiating agents have shown that macrophages are important effector cells (*1, 3*). Previous studies in this laboratory have shown that *B. dermatitidis* can activate macrophages to become fungicidal (McDaniel LS, Cozad GC: Submitted for publication). It is possible that *B. dermatitidis*-dependent tumor suppression is mediated by activated macrophages. Although the possible involvement of other mechanisms in the tumor suppression cannot be ruled out, our experiments show that peritoneal macrophages from mice treated with nonviable *B. dermatitidis* yeast cells plus EL 4 lymphoma cells have an enhanced potential for in vitro tumor cell stasis and killing.

Nonviable *B. dermatitidis* yeast cells appear to be more effective than *C. parvum* at stopping the growth of EL 4 tumor in vivo. As evidence, O'Neill and Stebbing (*15*) recently reported that preimmunization of mice with *C. parvum* failed to inhibit the growth of EL 4 in C57BL/6J mice. Conversely, preimmunization with *B. dermatitidis* significantly increased the mean survival time of mice challenged with EL 4. This protective effect was seen at 3–6 days after sc or ip injection of *B. dermatitidis*. It is curious that the route of injection had little effect on the time sequence of protective effects.

It was originally thought that the highest degree of enhanced survival would coincide with the peak in phagocytic activity of peritoneal macrophages (i.e., 15–18 days post primary *B. dermatitidis* injection). However, our experiments showed that this was not the case. The protective effects dropped off, and the mean survival time returned to that of the controls by day 15, even though peritoneal macrophages remained activated. An interpretation of these results may include the possible involvement of natural killer cells. Alternatively, the lack of correlation between antitumor and phagocytic activities could be the result of induction of functionally different macrophage populations as has been reported in other systems (*16*).

B. dermatitidis produces a granulomatous reaction in tissue (*17*). Such reactions have been reported for other agents currently used in immunotherapy (*18*). *B. dermatitidis* yeast cells are known to contain cell wall-associated toxin (*19*). Although the *B. dermatitidis* endotoxin has not been extensively characterized, it is doubtful that this toxin is identical to bacterial endotoxin that is capable of activating macrophages in vitro to a tumoricidal state (*5*). As evidence, it has been reported that *C. albicans* possesses an endotoxin that shares some of the properties of bacterial LPS but is not exactly comparable to it (*20*). Nevertheless, such a substance could mediate the protective effects we observed.

We have considered the possibility of direct interaction between nonviable *B. dermatitidis* and EL 4 tumor cells. Our data suggest that some interaction may be important since the highest degree of protection was obtained by the mixing of yeast cells with tumor cells prior to injection. However, we do not believe that the protective effects result solely from an adverse action of yeast cells against tumor cells. For example, significant protection was obtained by preimmunization of mice with *B. dermatitidis* alone. There were no adverse effects on EL 4 observed by the light microscope. Also, at a 10:1 ratio of nonviable yeast cells to tumor cells in vitro, the EL 4 cells continued to incorporate [^{3}H]dThd at near normal levels (data not shown). In addition, the protective effects were not limited to mixing yeast cells with tumor cells in vitro; the same results could be obtained by the injection of yeast cells and tumor cells separately on opposite sides of the peritoneum.

The preliminary results we obtained on the therapeutic potential of *B. dermatitidis* indicate that the yeast cells had a therapeutic effect only if administered within 24 hours after tumor transplantation. It has been reported that immunoadjuvants can generate cells that are capable of suppressing cell-mediated immune responses (*21*). Possibly, *B. dermatitidis* suppresses cellular immunity in tumor-bearing mice, thereby enhancing tumor growth. However, no conclusion can be drawn until further data have been gathered on the effects of *B. dermatitidis* on tumor-bearing mice. A regimen that involves several doses of *B. dermatitidis* over a period of time probably would be more therapeutically effective than a single dose.

The SEM revealed that there was strong interaction between macrophages from mice that showed complete suppression of tumor growth and EL 4 cells in vitro. A lack of such interaction between EL 4 and resident macrophages was also noted. Also, it has been reported that intimate contact between target cells and macrophages is required for tumor cell lysis in vitro (*22, 23*). Our observations of EL 4 with the SEM agree with these findings.

We were unable to detect cytotoxic lymphocytes in the spleen or lymph nodes of mice that showed suppression of tumor cell growth. Local immunity could have generated cytotoxic lymphocytes within the peritoneum, but we did not test for such cells. However, the fact that mice showing tumor suppression were not resistant to further EL 4 challenge indicates a lack of specific immunity. This observation supports the idea of nonspecific suppression of tumor growth by macrophages.

Our experiments indicate that nonviable *B. dermatitidis* yeast cells can significantly effect the outcome of tumor growth in the mouse system. This preparation may offer a significant advantage over other agents because it is not viable, and when applied in human beings, the possibility of infection in relatively immunodeficient cancer patients would be eliminated.

REFERENCES

(*1*) Hibbs JB, Lambert LH, Remington JS. Macrophage-mediated nonspecific cytotoxicity. Possible role in tumour resistance. Nature 1972; 235:48–50.

(*2*) Piessens WF, Churchill WH, David JR. Macrophages activated in vitro with lymphocyte mediators kill neoplastic but not normal cells. J Immunol 1975; 114:293–299.

(*3*) Hibbs JB, Lambert LH, Remington JS. Resistance to murine tumors conferred by chronic infection with intracellular protozoa, *Toxoplasma gondii* and *Besnoitia jellisoni*. J Infect Dis 1971; 124:587–592.

(*4*) Kaplan AM, Morahan PS. Macrophage-mediated tumor cell cytotoxicity. Ann NY Acad Sci 1976; 276:134–145.

(*5*) Cheung HT, Cantarow WD, Sundharadas G. Tumoricidal activity of macrophages induced by lipopolysaccharide and its inhibition by a low molecular weight factor extracted from tumors. J Reticuloendothel Soc 1979; 26:21–30.

(*6*) Taniyama T, Holden HT. Cytolytic activity against tumor cells by macrophage cell lines and augmentation by macrophage stimulants. Int J Cancer 1980; 26:61–69.

(*7*) Spencer HD, Cozad GC. Role of delayed hypersensitivity in blastomycosis of mice. Infect Immun 1973; 7:329–334.

(*8*) Cozad GC, Chang CT. Cell-mediated immunoprotection in blastomycosis. Infect Immun 1980; 28:398–403.

(*9*) Restrepo-Moreno A, Schneidau JD Jr. Nature of the skin reactive principle in culture filtrates prepared from *Paracoccidioides brasiliensis*. J Bacteriol 1967; 93:1741–1748.

(*10*) Youmans GP, Youmans AS. Allergenicity of mycobacterial ribosomal and ribonucleic acid preparations in mice and guinea pigs. J Bacteriol 1969; 97:134–139.

(*11*) Tolnai S. Cultivation of peritoneal mononuclear phagocytes. In: Evans V, ed. Tissue culture manual: Techniques, methods, and procedures for cell, tissue and organ culture. Procedure #41722. Rockville, Md.: Tissue Culture Association, 1975:17–19.

(*12*) Goldman R, Bar-Shavit Z. Dual effect of normal and stimulated macrophages and their conditioned media on target cell proliferation. JNCI 1979; 63:1009–1016.

(*13*) Lang H, Domzig W, Lohmann-Matthes ML. Cooperative effects between lymphokine-induced and antibody-dependent macrophage-mediated cytotoxicity in C57BL/10 and C3H/HeJ mice. Immunobiology 1980; 157:109–121.

(*14*) Sharma B, Terasaki PI. In vitro immunization to cultured cells. Cancer Res 1974; 34:115–118.

(*15*) O'Neill GJ, Stebbing N. Influence of *C. parvum* on the effectiveness of passive serotherapy in the control of the EL4 lymphoma in C57BL/6 mice. Br J Cancer 1980; 41:243–249.

(*16*) Rice SG, Fishman M. Functional and morphological heterogeneity among rabbit peritoneal macrophages. Cell Immunol 1974; 11:130–145.

(*17*) Rippon JW. Blastomycosis. In: Medical mycology. The pathogenic fungi and the pathogenic actiomycetes. Philadelphia: Saunders, 1974:297–320.

(*18*) Granger DL, Brehmer W, Yamamoto K, Ribi E. Cutaneous granulomatous response to BCG cell walls with reference to cancer immunotherapy. Infect Immun 1976; 13:543–553.

(*19*) Cox RA, Mills LR, Best GK, Denton JF. Histologic reactions to cell walls of an avirulent and a virulent strain of *Blastomyces dermatitidis*. J Infect Dis 1974; 129:179–186

(*20*) Cutler JE, Friedman L, Milner KC. Biological and chemical characterization of toxic substances from *Candida albicans*. Infect Immun 1972; 6:616–627.

(*21*) Lichtenstein A, Murahata R, Sugasawara R, Zighelboim J. Suppressor T cells and suppressor macrophages induced by *Corynebacterium parvum*. Cell Immunol 1981; 58:257–268.

(*22*) Marino PA, Adams DO. Interaction of Bacillus Calmette-Guerin-activated macrophages and neoplastic cells in vitro. 1. Conditions of binding and its selectivity. Cell Immunol 1980; 54:1–25.

(*23*) Nabarra B, Cavelier JF, Dy M, Dimitriu A. Scanning electron microscopic studies of activated macrophages in the mouse. J Reticuloendothel Soc 1978; 24:489–498.

Suppression of 7,12-Dimethylbenz[*a*]anthracene-Induced Chromosome Aberrations in Rat Bone Marrow Cells After Treatment With Sudan III and Related Azo Dyes[1,2]

Yoshiaki Ito,[3,4,5] Sakan Maeda,[3] Tetsuo Fujihara,[3] Norifumi Ueda,[3] *and* Taketoshi Sugiyama[3]

ABSTRACT—Noninbred Long-Evans rats fed Sudan III at 24 hours before they were given an injection of 7,12-dimethylbenz[a]anthracene (DMBA) displayed prominently suppressed DMBA-induced chromosome aberrations (CA) in their bone marrow cells. Rats fed Sudan III simultaneously with the DMBA injection showed no suppressed CA effect. The suppressive effect of Sudan III on DMBA-induced CA paralleled the dose rate of Sudan III when given in the range between 1 and 10 mg Sudan III/kg body weight; higher doses produced no additional suppression. The capacity of various Sudan III-related chemicals to prevent DMBA-induced CA paralleled their capacity to prevent DMBA-induced adrenal apoplexy and mammary cancer. Among the azo dyes investigated, Sudan III was most efficient in protecting against DMBA-induced CA. Polychlorinated biphenyl and phenobarbital, inducers of drug-metabolizing enzymes, also suppressed DMBA-induced CA.—JNCI 1982; 69:1343–1346.

The powerful hydrocarbon carcinogens DMBA and TMBA induce not only cancers in various animals (*1–4*) but also massive adrenal necrosis in the rat (*5, 6*). Since 1965, Huggins and Pataki (*7*) and Huggins et al. (*8*) have reported that pretreatment of rats with Sudan III [1-(*p*-phenylazophenylazo)-2-naphthol] and the related azo dyes prevents mammary cancer (*7*), leukemia (*8*), adrenal apoplexy (*7*), and fatal toxicity (*8*) induced by these chemical carcinogens and that the protection from PAH-induced adrenal apoplexy in these rats provides a useful preliminary screen for compounds that suppress PAH-induced cancer (*7*). This phenomenon is explained by inactivation of PAH with drug-metabolizing enzymes induced by Sudan dyes (*8*). Evidence of DMBA-induced chromosome damage in the rat bone marrow cells as the earliest host reaction to DMBA (*9*) stimulated us to study the effect of Sudan III and the related azo dyes on DMBA-induced CA.

MATERIALS AND METHODS

Animals.—Noninbred Long-Evans male rats at 28–35 days of age and weighing 50–80 g were used. They were kept in an air-conditioned room and fed NMF (Oriental Ferment Co., Tokyo) and permitted water ad libitum.

Chemicals.—DMBA and NBU were purchased from Eastman Organic Chemicals, Rochester, N.Y., and Izumi Chemical Research Laboratory, Tokyo, Japan, respectively. A 15% lipid emulsion containing 0.5% (wt/wt) of recrystallized DMBA was produced by a Manton-Gaulin submicron homogenizing system in our laboratory by the method of Schurr (*10*). NBU was dissolved at 20 mg/ml of sesame oil before use. Sudan III and Sudan IV [1-(*o*-tolylazo-*o*-tolylazo)-2-naphthol] (Chroma, Stuttgart, Federal Republic of Germany) and Sudan I (1-phenylazo-2-naphthol), yellow AB (1-phenylazo-2-naphthylamine), α-naphthyl red (4-phenylazo-1-naphthylamine), *p*-aminoazobenzene, and azobenzene (Tokyo Chemical Synthetic Industry Co., Ltd., Tokyo, Japan) were recrystallized from appropriate solvents and dissolved in sesame oil by gentle heat. These azo compounds were selected from the list of chemicals tested for protection of DMBA-induced adrenal apoplexy (*7*). They were administered by gastric instillation to lightly ether-anesthetized rats. Control animals were given sesame oil only. PCB (Kanechlor-400; Kanegafuchi Kagaku Kogyo Co., Osaka, Japan) was dissolved at 2.0 mg/ml of sesame oil, and PB (Yoneyama Yakuhin Kogyo Co., Osaka, Japan) was dissolved at 2.0 mg/ml of physiologic saline. PCB and PB were given to the rat for comparative inhibition studies of the DMBA effects.

A lipid emulsion of 50 mg DMBA/kg was injected into the caudal vein. NBU was dissolved in sesame oil and fed by gastric instillation at 200 mg/kg. CA were analyzed at various times after the DMBA and NBU treatments. Sudan III was also given at various times before the carcinogen treatment, and the effects of these administrations on carcinogen-induced CA were studied. Each experimental group consisted of 6 animals.

Chromosome analysis.—Colchicine (0.3 mg/rat), dissolved in physiologic saline, was injected ip 1 hour before the rats were killed. Chromosome specimens were prepared from the femoral bone marrow by the conventional method and were stained in 2% Giemsa solution. Metaphase cells having one CA or more were scored from 50 well-spread metaphases/rat or 300 metaphases/each group, and the frequency of CA was expressed by the percent of aberrant metaphase cells. CA consisted of gaps, breaks, and chromosome exchanges. Gaps were defined by an achromatic lesion with chromatid continuity, and breaks were defined by discontinuity shown by chromatid dislocation. Multiple CA were defined by uncountable (numerous, >5) CA per cell.

ABBREVIATIONS USED: CA=chromosome aberration(s); DMBA=7,12-dimethylbenz[*a*]anthracene; NBU=*N*-nitroso-*N*-butylurea; PAH=polycyclic aromatic hydrocarbon(s); PB=phenobarbital; PCB=polychlorinated biphenyl; TMBA=7,8,12-trimethylbenz[*a*]anthracene.

---

[1] Received February 17, 1982; accepted July 2, 1982.

[2] Supported by grants for cancer research from the Ministry of Education, Science and Culture, Japan.

[3] Department of Pathology, Kobe University School of Medicine, Kusunoki-cho, Chuo-ku, Kobe, Japan 650.

[4] Public Health Research Institute of Kobe City, Minatojima-Nakamachi, Chuo-ku, Kobe, Japan 650.

[5] *Address reprint requests to* Dr. Ito at the Department of Pathology, Kobe University School of Medicine.

RESULTS

Suppression of DMBA-induced CA by Sudan III pretreatment.—A single iv injection of DMBA, 50 mg/kg body weight, induced an increase in the percentage of aberrant metaphase cells in the bone marrow at a maximum level of 70.0±9.7% at 18 hours after the DMBA treatment. Rats fed 1 mg of Sudan III at 24 hours before they were given an injection of DMBA displayed a considerably suppressed incidence of DMBA-induced CA in their bone marrow cells, with a peak percentage of aberrant metaphases of 15.3±6.2% (text-fig. 1). The number of gaps, breaks, exchanges, and multiple CA per 100 cells was 46.7±6.8, 6.8±3.5, 0.8±1.2, and 27.7±10.1, respectively, at 18 hours in the DMBA (50 mg/kg)-injected group, and it was 14.2±5.1, 1.2±1.7, 0.1±0.5, and 0.7±1.3, respectively, in the Sudan III-fed–DMBA-injected group. Rats fed Sudan III simultaneously with the DMBA injection showed no suppressed CA effect, and the maximum suppression was obtained in rats fed Sudan III 24 hours before they received the DMBA treatment (text-fig. 2). The suppressive effect of Sudan III on DMBA-induced CA paralleled the dose rate of Sudan III when given between 1 and 10 mg/kg body weight; higher doses produced no additional suppression (text-fig. 3).

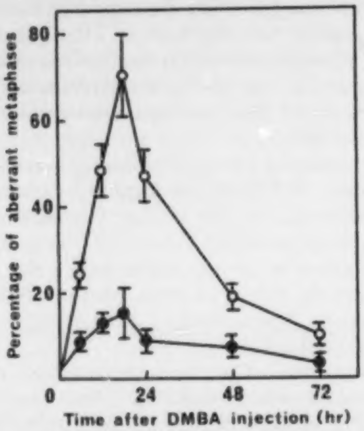

TEXT-FIGURE 1.—Effect of Sudan III on DMBA (50 mg/kg)-induced CA. In group 1 (●), rats were fed 1 mg of Sudan III 24 hr before DMBA injection. In group 2 (○), rats were fed sesame oil without Sudan III 24 hr before DMBA injection. *Each point* represents the mean ± SD for 6 rats.

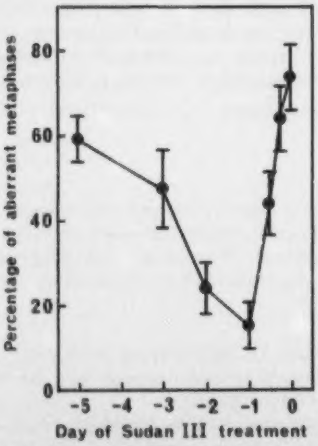

TEXT-FIGURE 2.—Suppression of DMBA (50 mg/kg)-induced CA by Sudan III administered various times before DMBA injection. Sudan III was given orally at 1 mg/rat on the day designated (*abscissa*) before DMBA treatment. Chromosome specimens were prepared 18 hr after DMBA injection. *Each point* represents the mean ± SD for 6 rats.

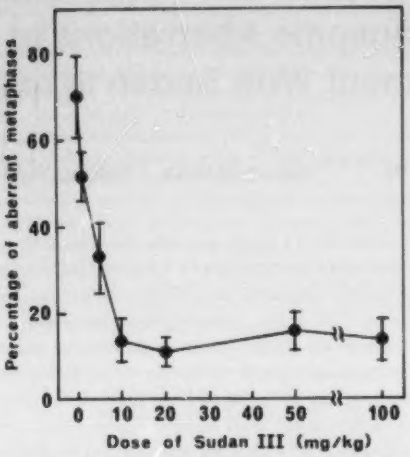

TEXT-FIGURE 3.—Suppression of DMBA (50 mg/kg)-induced CA by various doses of Sudan III. Sudan III was administered orally 24 hr before DMBA injection. Chromosome specimens were prepared 18 hr after DMBA injection. *Each point* represents the mean ± SD for 6 rats.

TABLE 1.—*Suppression of DMBA-induced CA by azo dyes, PCB, and PB*

Compounds[a]	CA, %[b]	Suppression, %[c]	P[d]
None	70.0±9.7	—	
Sudan III	10.7±3.5	85	<0.01
Sudan IV	39.3±4.1	44	<0.01
Sudan I	55.7±6.3	20	<0.05
α-Naphthyl red	63.7±4.1	9	
p-Aminoazobenzene	66.8±3.4	5	
Yellow AB	67.0±6.0	4	
Azobenzene	68.0±9.3	3	
PCB			
Expt 1	27.3±6.2	61	<0.01
Expt 2	10.3±3.9	85	<0.01
PB			
Expt 1	62.3±2.0	11	
Expt 2	35.3±5.0	50	<0.01

[a] For azo dyes and PCB or PB in expt 1, 56.8 μM/kg body wt was administered by gastric instillation 24 hr before DMBA injection. For PCB or PB in expt 2, administration was that usually used for drug-metabolizing enzymes: For 5 days before DMBA injections, 500 mg PCB/kg body wt was administered ip, and for 1 wk before DMBA injections, 0.1% PB was administered in the animal's drinking water.

[b] Chromosome specimens were prepared and analyzed 18 hr after 50 mg DMBA/kg body wt was injected iv. Values are means ± SD for 6 rats.

[c] Each value represents mean suppression expressed as maximum incidence of DMBA-induced CA at 18 hr for 6 rats. —=not applicable.

[d] Statistical significance was determined by Student's *t*-test.

Protective action of various azo dyes and enzyme inducers.—The protective action of various azo dyes was tested by percent aberrant metaphases 18 hours after DMBA administration.

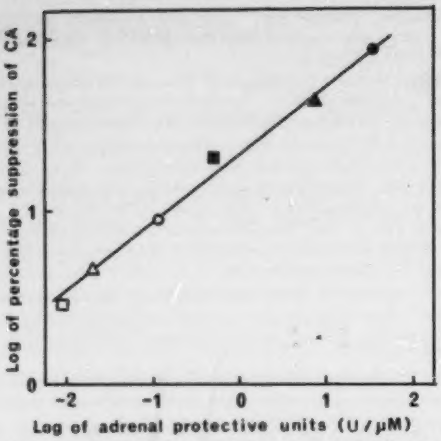

TEXT-FIGURE 4.—Relationship between the capacity of various azo dyes to protect DMBA-induced CA and the capacity to prevent DMBA-induced adrenal apoplexy. Data for adrenal apoplexy were cited from the report of Huggins and Pataki (*7*). ●=Sudan III; ▲=Sudan IV; ■=Sudan I; ○=naphthyl red; △=*p*-aminoazobenzene; □=azobenzene.

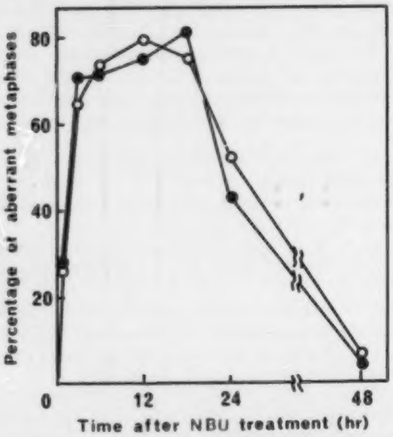

TEXT-FIGURE 5.—Effect of Sudan III on NBU (200 mg/kg)-induced CA. In group 1 (●), rats were fed 20 mg of Sudan III/kg body wt 24 hr before oral NBU administration. In group 2 (○), rats were fed sesame oil without Sudan III 24 hr before NBU administration. *Each point* represents the mean for 6 rats.

Protection was shown with all compounds tested, although it was statistically significant only with Sudan I, Sudan IV, and Sudan III (table 1). These results paralleled those of Huggins and Pataki (*7*) and showed a clear positive relationship between protection against CA and protection against adrenal apoplexy (text-fig. 4). Two azo dyes, Sudan IV and yellow AB, induced CA in 5% of the metaphase cells at the oral doses used without DMBA, although the percent aberrant cells remained within the normal level (<2%) with other compounds.

PCB and PB given similarly suppressed the incidence of DMBA-induced aberrant metaphase cells by 61 and 11%, respectively. PCB and PB suppressed aberrant metaphase cells by 85 and 50%, respectively, when they were given in a manner usually used for induction of hepatic microsome enzymes (*11*, *12*).

Effect of Sudan III on NBU-induced CA.—NBU also induced elevations of CA which lasted for 3–24 hours. However, Sudan III pretreatment did not suppress the incidence of NBU-induced CA (text-fig. 5).

DISCUSSION

The present studies indicated that rats fed 1 mg of Sudan III as a single dose before they were DMBA treated showed manifestly suppressed DMBA-induced CA in their bone marrow cells. DMBA-induced CA consisted mainly of gaps and breaks. Exchanges were observed infrequently (<1%). Gaps, breaks, exchanges, and multiple CA were suppressed as well by Sudan III pretreatment.The most efficient inhibitory effect of Sudan III was shown when it was given at 24 hours before DMBA treatment. The maximum inhibition was obtained above the dose of 10 mg Sudan III/kg body weight. Huggins and Pataki (*7*) and Huggins et al. (*8*) have shown inhibition of PAH-induced mammary cancer [10/10=100% inhibited to 4/10=40% (*7*)] and leukemia [13/14=93% inhibited to 3/15=20% (*8*)] by Sudan III pretreatment. Therefore, the present results are consistent with these results reported by Huggins and his co-workers.

CA are generally considered to be lethal to cells. Therefore, the present results essentially indicate that Sudan III pretreatment suppresses the fatal toxicity of DMBA to cells. However, the positive correlations among CA, mutagenicity, and carcinogenicity as well as between DNA repair and CA have been widely recognized. Therefore, we consider that the number of viable cells with subtle genetic changes might be increased in proportion to the increase of aberrant cells induced by chemical carcinogens.

Among the azo dyes investigated, Sudan III was the most efficient in protecting cells against DMBA-induced CA. The capacity of various Sudan III-related dyes to protect against DMBA-induced CA paralleled the capacity of the azo dyes to prevent DMBA-induced adrenal apoplexy. In protecting the cells against the effects of DMBA, the size, geometry, and solubility of the Sudan dyes are important (*7*). Adrenal apoplexy is a phenomenon specific to DMBA, TMBA, and the related PAH (*7*). Therefore, the present system provides another useful screen for the identification of compounds that suppress carcinogenesis.

PAH carcinogens such as DMBA and TMBA require metabolic activation by mixed function oxidases contained in microsomes of mammalian cells (*13–15*). PAH carcinogens are metabolized into compounds such as phenols, dihydrodiols, quinones, and epoxides (*16–18*). Recent studies (*19*) indicate that a major ultimate form of DMBA is a bay region diol-epoxide (DMBA-*trans*-3,4-diol-1,2-epoxide). Metabolic formation of the diol-epoxide is believed to proceed by a sequence involving epoxidation with mixed function oxidases, hydration with epoxide hydrase, and further epoxidation. Moschel et al. (*20*) also reported that reaction with DNA occurred through formation of diol-oxide in the 1,2,3,4-ring of DMBA. Another possibility of metabolic activation of DMBA may be that the methyl group on the benzene ring is hydroxylated by mixed function oxidases and that an active carbonium ion which is formed alkylates DNA or other biopolymers (*18*, *21*). Analogous to *N*-nitroso-

N-methylurea metabolism (*22–24*), however, NBU is converted into nitrosobutylamine nonenzymatically, and the product is converted rapidly through butyldiazohydroxide to the butylcarbonium ion. This reaction proceeds chemically and does not require drug-metabolizing enzymes.

Huggins and Pataki (*7*), Huggins et al. (*8*), and Huggins and Fukunishi (*25*) have shown induction of NAD(P)H dehydrogenase (quinone) after Sudan III pretreatment. PCB and PB are used to induce drug-metabolizing enzymes (*26–28*). Our results also showed suppression of DMBA-induced CA after the PCB and PB treatment. Inasmuch as NBU-induced CA were not influenced by Sudan III, the present results are consistent with the view that Sudan III pretreatment induces drug-metabolizing enzymes which detoxify carcinogens subsequently introduced.

REFERENCES

(*1*) Gelboin HV, Wiebel F, Diamond L. Dimethylbenzanthracene tumorigenesis and aryl hydrocarbon hydroxylase in mouse skin: Inhibition by 7,8-benzoflavone. Science 1970; 170:169–171.

(*2*) Huggins C, Grand LC, Brillantes FP. Mammary cancer induced by a single feeding of polynuclear hydrocarbons, and its suppression. Nature 1961; 189:204–207.

(*3*) Huggins C, Sugiyama T. Induction of leukemia in rat by pulse doses of 7,12-dimethylbenz[*a*]anthracene. Proc Natl Acad Sci USA 1966; 55:74–81.

(*4*) Huggins C, Grand LC, Oka H. Hundred day leukemia: Preferential induction in rat by pulse doses of 7,8,12-trimethylbenz[*a*]anthracene. J Exp Med 1970; 131:321–330.

(*5*) Huggins C, Morii S. Selective adrenal necrosis and apoplexy induced by 7,12-dimethylbenz[*a*]anthracene. J Exp Med 1961; 114:741–760.

(*6*) Huggins C, Morii S, Pataki J. Selective destruction of adrenal cortex by pulse doses of derivatives of 12-methylbenz[*a*]anthracene. Proc Natl Acad Sci USA 1969; 62:704–707.

(*7*) Huggins C, Pataki J. Aromatic azo derivatives preventing mammary cancer and adrenal injury from 7,12-dimethylbenz[*a*]anthracene. Proc Natl Acad Sci USA 1965; 53:791–796.

(*8*) Huggins C, Ueda N, Russo A. Azo dyes prevent hydrocarbon-induced leukemia in the rat. Proc Natl Acad Sci USA 1978; 75:4524–4527.

(*9*) Sugiyama T. Specific vulnerability of the largest telocentric chromosome of rat bone marrow cells to 7,12-dimethylbenz[*a*]anthracene. J Natl Cancer Inst 1971; 47:1267–1275.

(*10*) Schurr PE. Composition and preparation of experimental intravenous fat emulsions. Cancer Res 1969; 29:258–260.

(*11*) Ames BN, Durston WE, Yamasaki E, Lee FD. Carcinogens are mutagens: A simple test system combining liver homogenates for activation and bacteria for detection. Proc Natl Acad Sci USA 1973; 70:2281–2285.

(*12*) Ames BN, McCann J, Yamasaki E. Methods for detecting carcinogens and mutagens with the *Salmonella*/mammalian-microsome mutagenicity test. Mutat Res 1975; 31:347–364.

(*13*) Huberman E, Sachs L. Cell-mediated mutagenesis of mammalian cells with chemical carcinogens. Int J Cancer 1974; 13:326–333.

(*14*) Miller JA. Carcinogenesis by chemicals: An overview—G. H. A. Clowes memorial lecture. Cancer Res 1970; 30:559–576.

(*15*) Gelboin HV, Wiebel F. Mechanism of aryl hydrocarbon hydroxylase induction and its role in cytotoxicity and tumorigenicity. Ann NY Acad Sci 1971; 179:529–547.

(*16*) Sims P, Grover PL. Quantitative aspects of the metabolism of 7,12-dimethylbenz[*a*]anthracene by liver homogenates from animals of different age, sex and species. Biochem Pharmacol 1968; 17:1751–1758.

(*17*) Sims P. Qualitative and quantitative studies on the metabolism of a series of aromatic hydrocarbons by rat-liver preparations. Biochem Pharmacol 1970; 19:795–818.

(*18*) Yang SK, Dower WV. Metabolic pathways of 7,12-dimethylbenz[*a*]anthracene in hepatic microsomes. Proc Natl Acad Sci USA 1975; 72:2601–2605.

(*19*) Huberman E, Chou MW, Yang SK. Identification of 7,12-dimethylbenz[*a*]anthracene metabolites that lead to mutagenesis in mammalian cells. Proc Natl Acad Sci USA 1979; 76:862–866.

(*20*) Moschel RC, Baird WM, Dipple A. Metabolic activation of the carcinogen 7,12-dimethylbenz[*a*]anthracene for DNA binding. Biochem Biophys Res Commun 1977; 76:1092–1098.

(*21*) Pataki J, Huggins C. Molecular site of substituents of benz[*a*]anthracene related to carcinogenicity. Cancer Res 1969; 29:506–509.

(*22*) Kirmse W, Schütte H. Deamination reactions III: Cyclopropyldiazonium ions and cyclopropyl cations. Chem Ber 1968; 101:1674–1688.

(*23*) Magee PN, Montesano R, Preussmann R. N-nitroso compounds and related carcinogens. In: Searle CE, ed. Chemical carcinogens. American Chemical Society monograph 173. Washington, D. C.: Am Chem Soc, 1976:491–625.

(*24*) Montesano R, Bartsch H. Mutagenic and carcinogenic N-nitroso compounds: Possible environmental hazards. Mutat Res 1976; 32:179–227.

(*25*) Huggins C, Fukunishi R. Induced protection of adrenal cortex against 7,12-dimethylbenz[*a*]anthracene. J Exp Med 1964; 119:923–942.

(*26*) Conney AH. Pharmacological implications of microsomal enzyme induction. Pharmacol Rev 1967; 19:317–366.

(*27*) Orrenius S, Ernster L. Phenobarbital-induced synthesis of oxidative demethylating enzymes of rat liver microsomes. Biochem Biophys Res Commun 1964; 16:60–65.

(*28*) Alvares AP, Bickers DR, Kappas A. Polychlorinated biphenyls: A new type of inducer of cytochrome P-448 in the liver. Proc Natl Acad Sci USA 1973; 70:1321–1325.

Growth of Mouse Mammary Glands After Neonatal Sex Hormone Treatment [1,2,3]

Yasuhiro Tomooka [4] *and* **Howard A. Bern** [4,5,6]

ABSTRACT—Mammary gland growth was examined in female mice immediately and during 1 month after neonatal treatment with sex hormones. BALB/c mice were given daily injections of hormones for the first 5 days after birth. As a criterion of growth, the number of ductal branchings was counted in stained wholemounts of the fourth (inguinal) pair of glands. At day 6, the growth of the glands was significantly inhibited in animals treated with 17β-estradiol (E) or diethylstilbestrol (DES); after treatment with progesterone (P) or androgens no immediate effect was evident. At day 33, neonatal treatment with E stimulated growth, as did neonatal treatment with testosterone (T) or 5α-dihydrotestosterone (5α-DHT); treatment with a high dose of DES inhibited growth. Treatment with P or 5β-dihydrotestosterone had no effect. In conclusion, neonatal treatment with sex hormones has two distinct effects on the growth of mouse mammary gland: 1) inhibition by estrogens, observed immediately after treatment, and 2) stimulation by E, T, and 5α-DHT, observed 4 weeks after treatment.—JNCI 1982; 69:1347–1352.

Neonatal injections of sex hormones are known to cause a permanent functional change in the hypothalamus of female rats and mice resulting in an "anovulatory syndrome." Ovaries of these animals produce continuously low levels of estrogen, which induce persistent vaginal cornification. The vaginal and cervical epithelia of these animals develop hyperplastic areas and downgrowths into the stroma (*1*). The persistent vaginal cornification is abolished by ovariectomy of mice given low doses of sex hormones neonatally. If large amounts of hormones are injected into neonatal mice, irreversible changes may occur in the cervicovaginal epithelium, which persistently cornifies even after ovariectomy. The cervicovaginal epithelium of these ovariectomized animals also shows hyperplastic areas and downgrowths into the stroma and occasionally develops tumors (*2*).

Mori (*3, 4*) first reported a higher incidence of mammary tumors among mice neonatally exposed to estrogens. Subsequent studies in our laboratory show that neonatal exposure to various sex hormones enhanced tumorigenesis in the mammary glands of mice with expressed MTV and enhanced lobuloalveolar development generally, whether MTV was expressed or not (*5*).

Little information is available regarding immediate mammary gland responses to neonatal sex hormone exposure. Warner (*6*) found that mammary growth was stimulated at 5 weeks of age in mice given high doses of estrogen neonatally. In the present report, growth responses of mammary glands are followed quantitatively during the 1st month after neonatal exposure to various sex hormones.

MATERIALS AND METHODS

BALB/cCrgl female mice were used. From the day of birth (day 1), litter size was kept between 4 and 6 pups per mother by addition, if needed, of male pups born on the same day. Animals were given sc injections of hormones (text-fig. 1; tables 1, 2) dissolved in sesame oil for 5 consecutive days, starting within 24 hours after birth. Control animals were either given injections of oil vehicle or left untreated. In series I, groups of animals were autopsied weekly for 4 weeks beginning on day 6. In series II, animals were autopsied on day 6 and day 33. In series III, animals were autopsied on day 33. The mammary glands were fixed in 10% Formalin and stained as wholemounts with iron-hematoxylin. The numbers of mammary ductal branchings in the fourth inguinal pair of mammary glands were counted under a dissecting microscope (*6, 7*). Statistical analysis was performed with the use of Dunnett's two-sided multiple comparisons test.

RESULTS

Series I.—In this experiment the effect of the major natural sex steroids was examined. On day 1, mammary glands showed a rudimentary ductal system, and a mean of 42.8±6.7 (8 animals) ductal branchings was counted. In the control group the number of ductal branchings almost doubled by day 6 but remained constant for the following 3 weeks. The number of ductal branchings then doubled again between day 26 and day 33 (text-fig. 1).

Administration of 5 μg E for 5 days significantly inhibited the increase of ductal branchings from day 1 to day 6. This inhibitory effect was more prominent in animals treated with 20 μg E (figs. 1, 2). The number of ductal branchings in the group given 5 μg E remained constant for the following 3 weeks. In the group given 20 μg E, the number of ductal branchings increased slightly, but not significantly, on day 19 and day 26. However, the number of ductal branchings almost tripled by day 33 in the group given 5

ABBREVIATIONS USED: DES=diethylstilbestrol; 5α-DHT=5α-dihydrotestosterone; 5β-DHT=5β-dihydrotestosterone; E=17β-estradiol; MTV=mammary tumor virus; P=progesterone; T=testosterone.

---

[1] Received February 17, 1982; accepted July 16, 1982.

[2] Supported by Public Health Service grant CA-05388 from the National Cancer Institute.

[3] Animals were maintained under the guidelines set forth in the "Guide for the Care and Use of Laboratory Animals" by the Institute of Laboratory Animal Resources, National Research Council; and by the University of California at Berkeley.

[4] Department of Zoology and Cancer Research Laboratory, University of California at Berkeley, 230 Warren Hall, Berkeley, Calif. 94720.

[5] *Address reprint requests to* Dr. Bern.

[6] We are grateful to Ms. Karen Tanada Mills for technical assistance, to Mr. John Underhill for the photography, to Mr. William Young for animal care, and to Ms. Susie Castillo for typing the manuscript.

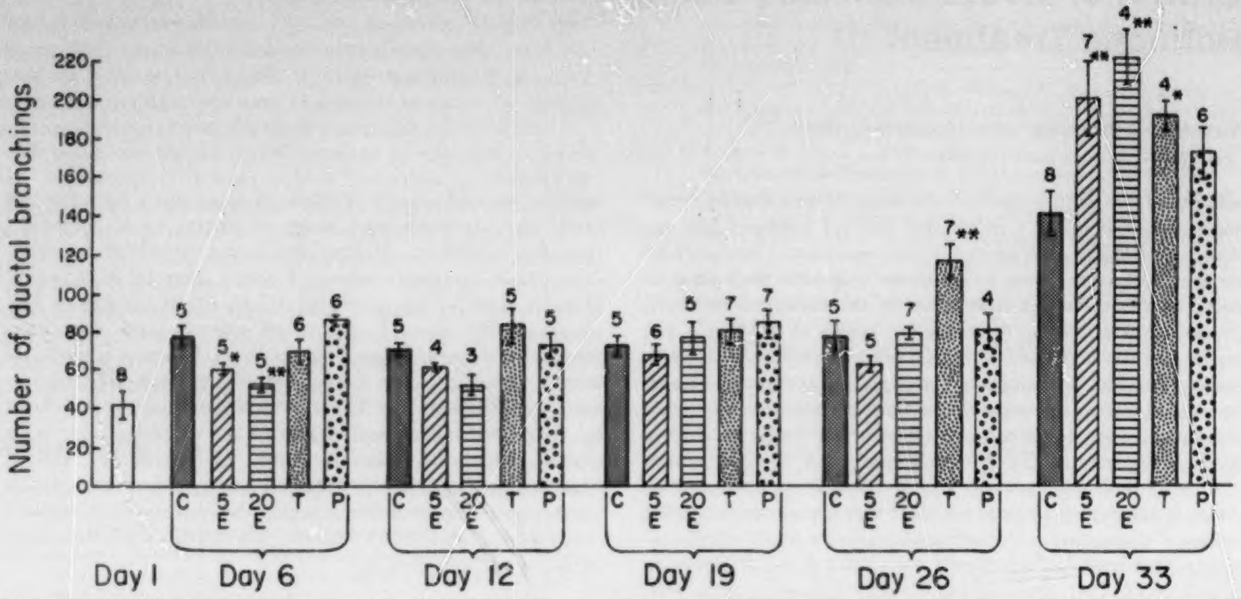

TEXT-FIGURE 1.—Mammary gland responses of female BALB/c mice to neonatal sex hormone exposure—series I. Animals were treated with 5 μg E (5E), 20 μg E (20E), 20 μg T, 100 μg P, or oil vehicle as control (C) for 5 consecutive days, starting within 24 hr after birth. Eight animals were autopsied without treatment on day 1 (the day of birth). Number of ductal branchings was counted as described in "Materials and Methods." *Vertical bar* indicates SEM. *Figure above the bar* is the number of animals in each group. * $P<0.05$ and ** $P<0.01$ (different from oil-treated control by Dunnett's two-sided multiple comparisons test).

μg E and in the group given 20 μg E (text-fig. 1; figs. 3, 4). In contrast to both treatments with E, treatment with 20 μg T did not affect branching when glands were examined on day 6; however, this treatment induced a precocious increase in branching by day 26, which on day 33 was also significantly higher than that seen in the control group. The group treated with 100 μg P did not differ significantly from controls from day 6 to day 33.

Series II.—In this experiment the effects of additional sex hormones and doses were examined on the two critical days for inhibition (day 6) and stimulation (day 33) (table 1).

TABLE 1.—*Mammary gland response of female BALB/c mice to neonatal sex hormone exposure—series II*

Treatment[a]	No. of ductal branchings in right and left #4 mammary glands at:[b]	
	6 days of age	33 days of age
Oil-treated control	85.0±4.9 (8)	138.9±7.4 (7)
Untreated control	94.8±2.8 (8)	147.4±10.1 (10)
5 μg E	66.4±4.3* (9)	155.1±7.2 (7)
20 μg E	58.9±1.8** (7)	208.1±19.7 (9)
5 μg T	76.9±4.5 (8)	192.0±27.3 (8)
20 μg T	77.7±4.4 (7)	266.8±21.6** (9)
10^{-1} μg DES	64.3±3.9* (7)	189.9±9.2 (8)
2 μg DES	57.9±2.8** (7)	95.5±14.1 (6)
100 μg P	98.3±8.7 (6)	98.0±13.8 (5)
20 μg 5α-DHT	85.5±3.4 (8)	246.6±24.5** (7)
20 μg 5β-DHT	80.3±4.4 (7)	133.8±31.8 (6)

[a] Treatment with sex hormones or oil daily for 5 days after birth.

[b] Results are expressed as means ± SE. Number of mice is shown *in parentheses*. * $P<0.05$ and ** $P<0.01$ (different from oil-treated control by Dunnett's two-sided multiple comparisons test).

TABLE 2.—*Mammary gland response of female BALB/c mice to neonatal sex hormone exposure—series III*

Treatment[a]	No. of ductal branchings in right and left #4 mammary glands at 33 days of age[b]
Oil-treated control	136.5±7.3 (27)
5 μg E	194.5±16.3** (15)
5 μg T	218.6±10.4** (14)
2 μg DES	90.3±7.0** (19)
100 μg P	120.4±8.2 (17)

[a] Treatment with sex hormones or oil daily for 5 days after birth.

[b] Results are expressed as means ± SE. Number of mice is shown *in parentheses*. ** $P<0.01$ (different from oil-treated control by Dunnett's two-sided multiple comparisons test).

Again, an inhibitory effect with both doses of E by day 6 was observed. Both doses of DES also had an inhibitory effect. Neither the androgens nor P significantly affected the number of ductal branchings at this age. The stimulatory effect observed on day 33 in series I was also observed in animals treated with 20 μg T and 20 μg 5α-DHT; the increased branching in groups treated with 5 and 20 μg E, 5 μg T, and 10^{-1} μg DES was not statistically significant from that seen in controls. The number of ductal branchings in the groups treated with 2 μg DES and 100 μg P was not significantly lower than that in the controls. 5β-DHT at 20 μg had no effect on the number of ductal branchings on either day 6 or day 33.

Series III.—This experiment was done to reexamine the effects of hormones giving differing results at day 33 in series I and II. Table 2 shows the stimulatory effect of T and E on the number of ductal branchings. DES at 2 μg significantly lowered the number of ductal branchings, indicating a sustained inhibitory effect. P at 100 μg had no effect.

DISCUSSION

During the first 3 weeks of postnatal life, there is little change in the gross morphology of the mammary glands in the mouse; the glands normally begin to increase in size by the beginning of the 4th week (*8*). The number of branchings in the ductal system remains almost constant from day 7 to day 21, and then there is a rapid increase in area and ductal junctions of the glands around day 24 (*7*). Text-figure 1 indicates that the pattern of growth in our control animals is similar to that reported earlier.

E and DES consistently inhibited growth of the mammary glands immediately after the completion of the 5-day neonatal treatment. Androgens (T, 5α-DHT, and 5β-DHT) and P had no immediate inhibitory effect on the glands, indicating that this effect seems to be specific to estrogenic hormones. Higher doses of E and DES resulted in more prominent inhibition. This immediate inhibitory effect of neonatal estrogenic hormone treatment has not been previously reported, although high doses of estrogen administered to pregnant mice inhibited mammary growth when offspring were examined on day 35 (*9*). The glands recovered by day 80. In the present study, treatment of newborn mice with 2 μg DES daily resulted in significantly less ductal branching at day 33 than seen in control animals (table 2); however, mammary glands treated with 20 μg E recovered from the initial inhibition and showed more ductal branching at day 33 (text-fig. 1).

The mechanism involved in the immediate inhibitory effect of estrogenic hormones on mammary growth is unknown. Prenatal exposure of rats to DES during midpregnancy inhibits DNA and RNA syntheses by mammary ductal epithelium at 5 days of age (*10*). Direct responses to neonatal sex hormone treatment occur in mouse cervicovaginal epithelium (*2, 11*), resulting in irreversible and permanent changes. The growth of neonatally steroid-exposed mammary glands was indistinguishable from that of host glands after their transplantation into cleared host fat pads immediately after completion of treatment (*12*). This observation and that of Jean (*9*), in addition to findings from our studies, indicate that the glands may recover from the immediate inhibitory effect of estrogens in later life. However, if the treatment is intense enough, recovery may not occur. In series III the number of ductal branchings in the group given 2 μg DES was significantly less than that in controls. Neonatal treatments with higher doses of DES (5 or 20 μg) for 5 days after birth resulted in atrophic mammary glands in mice when examined at 7 and 15 months of age (Bern HA, Kohrman AF, Mills KT, Louie JK: Unpublished observations). The inhibitory effect of DES may arise from its estrogenic potency (toxicity?) owing to absence of binding to α-fetoprotein, which is known to bind E specifically (*13*); it is not known whether DES or its metabolites influence mammary growth by an effect other than that consequent to their estrogenicity.

Neonatal estrogen and androgen exposure resulted in another effect on the mammary glands, evident when they were examined at around day 30. At this time ductal branching increased sharply in animals neonatally treated with E, T, and 5α-DHT. This delayed response does not seem to be a long-lasting effect of neonatally administered hormones because the number of ductal branchings remained almost constant for the preceding 3 weeks. Rather, the changes appear to be mediated by the hypothalamo–hypophysio–ovarian axis. This neuroendocrine pathway is known to be permanently altered by neonatal treatment of mice with E (*14–16*), T (*14, 16*), P (*15*), and presumably the nonaromatizable androgen 5α-DHT (*17*). Precocious activation of the hypothalamo–hypophysio–ovarian axis by neonatal sex hormone exposure would accelerate and enhance the growth of mammary glands. Neonatally sex hormone-exposed mice (*18*) and rats (*19–22*) show precocious vaginal opening, indicating that ovaries functionally secrete estrogen which might stimulate the secretion of prolactin from the pituitary gland. In the mouse prolactin levels in plasma increase toward the time of puberty (*23, 24*). The number of prolactin cells significantly increases in mice treated neonatally with steroids (*25*), and blood prolactin levels may be higher than those in control mice (*16, 26*), at least at some stages in some strains.

Warner (*6*) reported that only doses over 25 μg E stimulated growth of mammary glands in BALB/c mice examined at 5 weeks of age. In the same mouse strain under the same experimental conditions, we found that 20 μg E consistently showed a stimulatory effect; even 5 μg E resulted in significant stimulation in two of three sets of our experimental series.

P (*15*) and 5β-DHT (*27*) reportedly alter the development of the hypothalamus, resulting in a higher incidence of mouse mammary tumors in MTV-expressed strains of mice. In our experiments, neither P nor 5β-DHT had an effect on ductal branching from day 6 to day 33. Possibly, the altered hypothalamus exerts its influence in mice only at later ages after these steroid treatments.

Because of variation in some of the results obtained on day 33 from the three series of experiments, statistical analysis (multiple comparison test of Duncan) was performed on combined results in the following groups: 5 μg E (series I–III), 20 μg E (series I, II), 5 μg T (series II, III), 100 μg P (series I–III), 2 μg DES (series II, III), and control (series I–III). The number of ductal branchings was significantly higher ($P<0.01$) in the groups treated with 5 μg E, 20 μg E, and 5 μg T than in the controls, but significantly lower ($P<0.01$) in the group treated with 2 μg DES. There was no significant difference in the number of ductal branchings in the groups given 100 μg P from that in the control groups.

Our experiments have demonstrated that mammary growth is inhibited after E or DES exposure immediately after cessation of neonatal treatment and that mammary growth accelerates around 30 days of age in animals treated neonatally with E, T, and 5α-DHT. Warner and associates (*28–30*) have shown increases in growth, hormone responsiveness, and casein mRNA levels in mammary explants from mice 34–39 days old that had been neonatally treated with estrogen and primed in vivo with steroids at 4 weeks of age. A relationship between these early stimulatory effects mediated by the hypothalamo–hypophysio–ovarian axis and later mammary tumorigenesis has yet to be established. However, if, as it appears, the hypothalamic change involves increased mammary gland exposure to endogenous prolactin (increased levels and/or continuous secretion), the increased tumorigenesis that occurs in MTV-expressed mice as a consequence of neonatal sex hormone exposure (*14*) becomes explicable.

REFERENCES

(*1*) Bern HA, Talamantes FJ. Neonatal mouse models and their relation to disease in the human female. In: Herbst AL, Bern HA, eds. Development effects of diethylstilbestrol (DES) in pregnancy. New York: Thieme-Stratton, 1981:129-147.

(*2*) Takasugi N. Cytological basis for permanent vaginal changes in mice treated neonatally with steroid hormones. Int Rev Cytol 1976; 44:193-224.

(*3*) Mori T. Changes in reproductive organs and some other glands in old C3H/MS mice treated neonatally with low doses of estrogen. Annot Zool Jpn 1968; 41:43-52.

(*4*) ———. Changes in the reproductive and some other organs in old C3H/MS mice given high dose estrogen injections during neonatal life. Annot Zool Jpn 1968; 41:85-94.

(*5*) Mori T, Nagasawa H, Bern HA. Long-term effects of perinatal exposure to hormones on normal and neoplastic mammary growth in rodents: A review. J Environ Path Toxicol 1979; 3:191-205.

(*6*) Warner MR. Effect of various doses of estrogen to BALB/cCrgl neonatal female mice on mammary growth and branching at 5 weeks of age. Cell Tissue Kinet 1976; 9:429-438.

(*7*) Flux DS. Growth of the mammary duct system in intact and ovariectomized mice of the CHI strain. J Endocrinol 1954; 11:223-237.

(*8*) Nandi S. Hormonal control of mammogenesis and lactogenesis in the C3H/HeCrgl mouse. Univ Calif Publ Zool 1959; 65:1-128.

(*9*) Jean C. Developpement mammaire post-natal de la souris issue de mère traitée par l'oestradiol pendant la gestation. Arch Sci Physiol 1971; 25:145-185.

(*10*) Bergman RS, Boylan ES. Autoradiographic analysis of DNA and RNA synthesis in neonatal rat mammary gland after prenatal exposure to diethylstilbestrol (DES). Proc Endocrine Soc 64th Annual Mtg 1982; abstract No. 1404.

(*11*) Forsberg JG, Kalland T. Neonatal estrogen treatment and epithelial abnormalities in the cervicovaginal epithelium of adult mice. Cancer Res 1981; 41:721-734.

(*12*) Mori T, Mills KT, Bern HA. Lack of evidence for a direct permanent effect of neonatal sex steroid exposure on mouse mammary gland. IRCS Med Sci 1979; 7:201.

(*13*) Plapinger L, McEwen BS. Gonadal steroid-brain interactions in sexual differentiation. In: Hutchinson JB, ed. Biological determination of sexual behavior. New York: Wiley, 1978:153-218.

(*14*) Mori T, Bern HA, Mills KT, Young PN. Long-term effects of neonatal steroid exposure on mammary gland development and tumorigenesis in mice. J Natl Cancer Inst 1976; 57:1057-1062.

(*15*) Jones LA, Bern HA. Long-term effects of neonatal treatment with progesterone, alone and in combination with estrogen, on the mammary gland and reproductive tract of female BALB/cfC3H mice. Cancer Res 1977; 37:67-75.

(*16*) Nagasawa H, Mori T, Yanai R, Bern HA, Mills KT. Long-term effects of neonatal hormonal treatments on plasma prolactin levels in female BALB/cfC3H and BALB/c mice. Cancer Res 1978; 38:942-945.

(*17*) Iguchi T, Takasugi N. Occurrence of permanent anovulation in mouse ovaries and permanent changes in the vaginal and uterine epithelia following neonatal treatment with large doses of 5α-dihydrotestosterone. Endocrinol Jpn 1981; 28:207-213.

(*18*) Talamantes F, Browning HC. Effect of neonatal administration of norethynodrel-mestranol on the reproductive system of female mice. Tex Rep Biol Med 1972; 39:361-369.

(*19*) Jacobsohn D. Development of female rats injected shortly after birth with testosterone or "anabolic steroids." Acta Endocrinol (Copenh) 1964; 45:402-414.

(*20*) Kind FA, Folch AP, Maqueo M, Lasso LH, Oriol A, Dorfman RI. Inhibition of sexual development in male and female rats treated with various steroids at the age of five days. Acta Endocrinol (Copenh) 1965; 49:193-206.

(*21*) Kind FA, Maqueo M. Prevention by progesterone of steroid-induced sterility in neonatal male and female rats. Endocrinology 1965; 77:859-862.

(*22*) Mallampati RS, Johnson DC. Gonadotropins in female rats androgenized by various treatments: Prolactin as an index to hypothalamic damage. Neuroendocrinology 1974; 15:255-266.

(*23*) Michael SD, Kaplan SB, Macmillan BT. Peripheral plasma concentrations of LH, FSH, prolactin and GH from birth to puberty in male and female mice. J Reprod Fertil 1980; 59:217-222.

(*24*) Michael SD, Taguchi O, Nishizuka Y. Effect of neonatal thymectomy on ovarian development and plasma LH, FSH, GH and PRL in the mouse. Biol Reprod 1980; 22:343-350.

(*25*) Kawashima S, Bern HA, Jones LA, Mills KT. Histometric study of the pituitary in mice treated neonatally with steroids and the relationship between prolactin cells and mammary tumorigenesis. Endocrinol Jpn 1978; 25:341-348.

(*26*) Nagasawa H, Yanai R, Jones LA, Bern HA, Mills KT. Ovarian dependence of the stimulatory effect of neonatal hormone treatment on plasma levels of prolactin in female mice. J Endocrinol 1978; 79:391-392.

(*27*) Yanai R, Mori T, Nagasawa H. Long-term effects of prenatal and neonatal administration of 5β-dihydrotestosterone on normal and neoplastic mammary development in mice. Cancer Res 1977; 37:4456-4459.

(*28*) Warner MR, Warner RL. Effects of perinatal estrogen on mouse mammary response to corticoids in vitro. In Vitro 1977; 13:477-483.

(*29*) Warner MR. Effect of perinatal oestrogen on the pretreatment required for mouse mammary lobular formation in vitro. J Endocrinol 1978; 77:1-10.

(*30*) Warner MR, Yau L, Rosen JM. Long term effects of perinatal injection of estrogen and progesterone on the morphological and biochemical development of the mammary gland. Endocrinology 1980; 106:823-832.

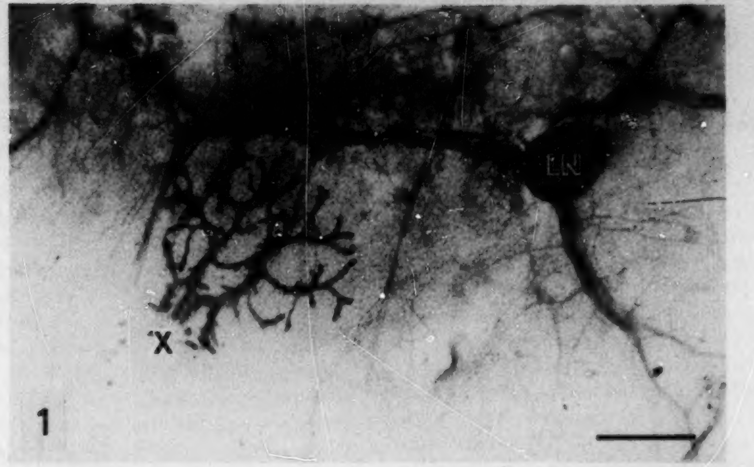

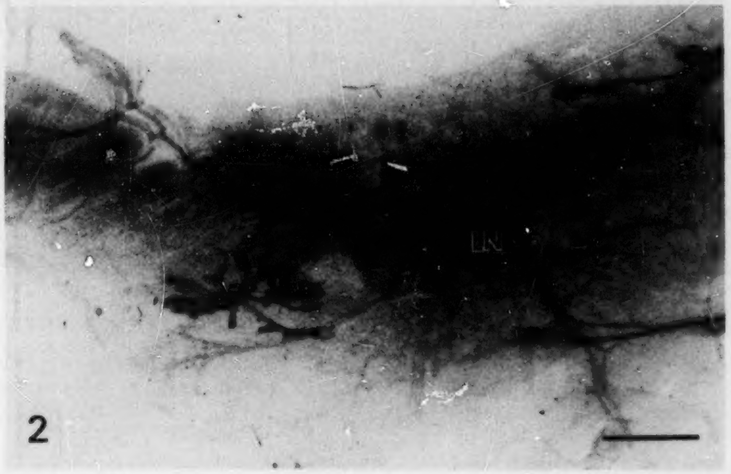

FIGURE 1.—Fourth (inguinal) mammary gland from an oil-treated mouse on day 6. LN, lymph node. Nipple broken off at X. *Bar*=1 mm. × 15

FIGURE 2.—Fourth (inguinal) mammary gland from a 20-μg E-treated mouse on day 6. Note inhibited growth of the gland. LN, lymph node. *Bar*=1 mm. × 15

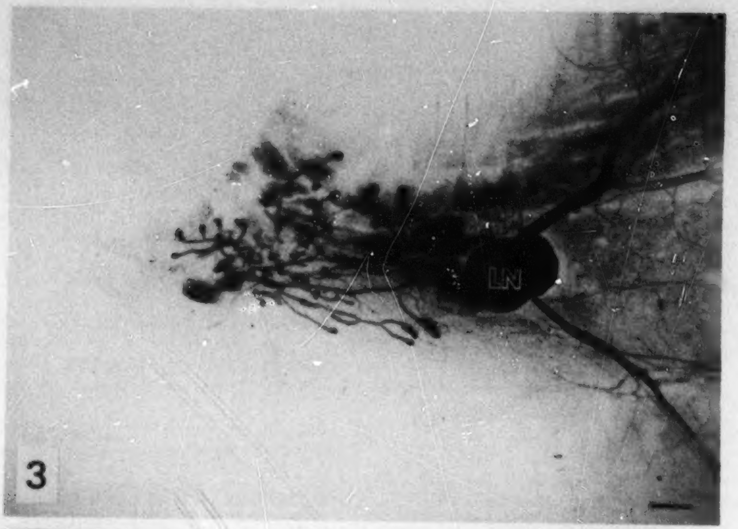

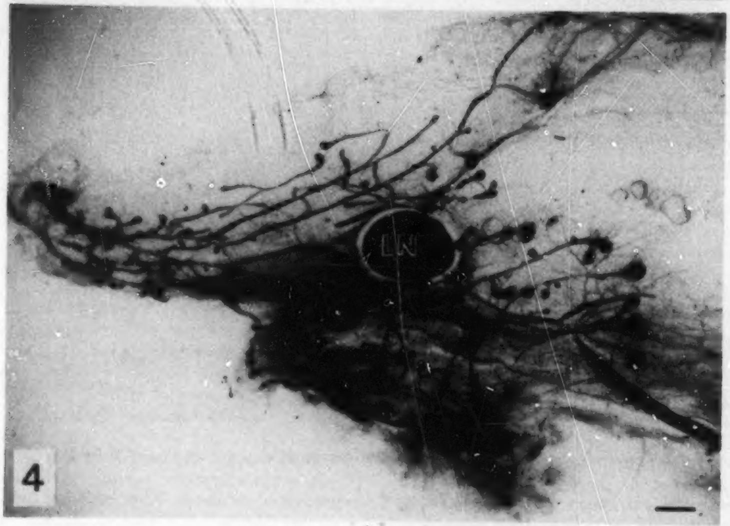

FIGURE 3.—Fourth (inguinal) mammary gland from an oil-treated mouse on day 33. The gland shows prominent end buds but does not grow beyond lymph node (LN). *Bar*=1 mm. × 6

FIGURE 4.—Fourth (inguinal) mammary gland from a 20-μg E-treated mouse on day 33. Gland shows numerous end buds growing beyond lymph node (LN). *Bar*=1 mm. × 6

Effects of Nicotinamide, Isonicotinamide, and Bleomycin on DNA Synthesis and Repair in Rat Hepatocytes and Hepatoma Cells[1,2,3]

Rosemary Barra,[4,5] **Verrell Randolph,**[6] **MariaElaina Sumas,**[4] **Kevin Lanighan,**[4] *and* **Michael A. Lea**[6]

ABSTRACT—Because inhibitors of poly (ADP-ribose) synthetase have been found to influence DNA synthesis in some systems, the possibility that nicotinamide or isonicotinamide might potentiate the effect of bleomycin on DNA replication and repair was examined. After a 30-minute incubation with bleomycin (200 μg/ml), tritiated thymidine ([^{3}H]dThd) incorporation into DNA was stimulated during a subsequent 30-minute incubation with hepatocytes of inbred BUF rats but was decreased in HTC cells of BUF rats. When unscheduled DNA synthesis was measured in the presence of 10 m*M* hydroxyurea, bleomycin (200 μg/ml) increased [^{3}H]dThd incorporation in both cell types. A dose of 20 m*M* nicotinamide and isonicotinamide caused an approximately 50% inhibition of total [^{3}H]dThd incorporation in HTC cells. Significant inhibitory effects of 20 m*M* nicotinamide and isonicotinamide on unscheduled DNA synthesis were observed after preincubation of hepatocytes and HTC cells with bleomycin. When the effects of bleomycin on DNA structure were assessed fluorometrically with ethidium bromide after mild alkaline incubation, nicotinamide and isonicotinamide did not significantly affect the damage revealed with bleomycin alone. When HTC cells were incubated for 48 hours with bleomycin (20 μg/ml), the increase in cell numbers was about 50% of that in control cultures. Nicotinamide and isonicotinamide also inhibited the proliferation of HTC cells, but the effects were not additive with the effect of bleomycin.—JNCI 1982; 69:1353–1357.

The poly (ADP-ribosylation) of nuclear proteins has been correlated with diverse aspects of the regulation of macromolecular synthesis (*1*, *2*). In some systems poly (ADP-ribose) synthetase activity appears related to changes in the rate of DNA replication (*3–5*) or repair (*6–9*). Although there are many conflicting observations on the relationship between poly (ADP-ribose) synthetase and DNA synthesis (*2*, *10*, *11*), there have been several reports that the activity of poly (ADP-ribose) synthetase can be increased by agents that damage DNA (*6*, *12*, *13*). There is evidence that the magnitude and regulation of poly (ADP-ribose) synthetase activity differ in rat liver and hepatomas (*14–18*). While semiconservative DNA replication is generally enhanced in hepatomas relative to that in normal livers, the capacity for DNA repair may be diminished (*17*, *19*). Nduka and coworkers (*20*) observed enhanced cytotoxicity for L1210 cells with DNA-damaging agents in the presence of inhibitors of poly (ADP-ribose) synthetase. In the present work we have examined the influence of nicotinamide and isonicotinamide, two inhibitors of poly (ADP-ribose) synthetase, on DNA synthesis in hepatocytes and hepatoma cells. The response of cells to DNA damage was determined after exposure to bleomycin and was followed by measurement of cellular proliferation, the incorporation of [^{3}H]dThd into DNA, and the integrity of DNA as judged by fluorescent dye binding. The objective of this study was to determine if the effects of bleomycin on DNA could be enhanced by nicotinamide or isonicotinamide. A preliminary communication of the work has been presented (*21*).

MATERIALS AND METHODS

Cells.—Hepatomas were maintained as subcutaneous transplants in BUF strain rats. Hepatocytes were isolated from the livers of control rats of the same strain. The hepatocytes and hepatoma cells were isolated by collagenese digestion as previously described (*22*).

Chemicals and isotopes.—Bleomycin was donated by Bristol Laboratories Inc., Syracuse, N.Y. Materials for tissue culture media were obtained from Grand Island Biological Co., Grand Island, N.Y. ICN Pharmaceuticals Inc., Irvine, Calif., was the source of [*methyl*-^{3}H]dThd (70 Ci mmol^{-1}).

Assay conditions for [^{3}H]dThd incorporation.—Incubations for [^{3}H]dThd incorporation into DNA were performed in a volume of 0.8 ml EMEM at 37°C. The incubation was terminated by the addition of 1.2 ml 16.7% TCA and 8.35% sodium pyrophosphate. Following centrifugation at 800×*g* for 10 minutes, the pellet was washed three times with 4 ml 10% TCA and 5% sodium pyrophosphate. The pellet was dissolved in 1 ml 0.33 *N* KOH and incubated at 37°C for 45 minutes. The tubes were cooled, and additions were made of 0.3 ml 1 *N* HCl and 1.3 ml 20% TCA and 10% sodium pyrophosphate. After centrifugation at 800×*g* for 10 minutes, the pellet was washed with 4 ml 10% TCA and 5% sodium pyrophosphate. DNA was extracted from the pellet in 1.5 ml 5% TCA at 90°C for 20 minutes. Radioactivity was measured by liquid scintillation counting in a system with a counting efficiency of 30–32% for ^{3}H.

Fluorometric analysis of DNA unwinding.—The procedure for fluorometric analysis of DNA unwinding was essentially as described by Birnboim and Jevcak (*23*) using the fluorescence given by ethidium bromide in the presence of double-stranded DNA. The conditions for alkaline incubation of cell lysates were such that there was minimal unwinding of DNA from control cells but there was a readily measurable increase of unwinding in DNA with strand breaks. Preceding

---

ABBREVIATIONS USED: EMEM=Eagle's minimum essential medium containing 50 m*M* *N*-2-hydroxyethylpiperazine-*N*-2-ethanesulfonate (pH 7.4); [^{3}H]dThd=tritiated thymidine; TCA=trichloroacetic acid.

---

[1] Received March 5, 1982; accepted August 10, 1982.

[2] Supported in part by Public Health Service grant CA-16274 from the National Cancer Institute and by a 1981 grant from the Undergraduate Research Program–National Science Foundation.

[3] Animals were maintained under the guidelines set forth by the New Jersey Medical School.

[4] Department of Chemistry and Chemical Engineering, Stevens Institute of Technology, Hoboken, N.J. 07030.

[5] *Address reprint requests to* Dr. Barra, 1404 Franklin St., Fredericksburg, Va. 22401.

[6] Department of Biochemistry, New Jersey Medical School, Newark, N.J. 07103.

this assay, 6.5×10^6 cells were incubated at 37°C for 30 minutes in 3 ml EMEM or EMEM containing the drugs under study. The cells were centrifuged at $50\times g$ for 3 minutes. The supernatant was discarded, and the cells were suspended in 5 ml 0.87% NH_4Cl and 10 m*M* Tris-HCl (pH 7.2). After being held on ice for 20 minutes the cells were centrifuged at $50\times g$ for 3 minutes and washed with 5 ml 0.87% NH_4Cl and 10 m*M* Tris-HCl (pH 7.2). The pellet was suspended in 1.3 ml 0.25 *M meso*-inositol, 10 m*M* sodium phosphate, and 1 m*M* $MgCl_2$ (pH 7.2). Aliquots of this suspension (0.2 ml) were distributed to six disposable glass tubes designated in duplicate as T, P, or B. The remaining procedures were exactly as described by Birnboim and Jevcak (*23*) except that the P- and B-tubes were not subjected to incubation at 15°C because the effects of bleomycin were of sufficient magnitude to be detected during alkaline incubation on ice. In this procedure the DNA in the T-tubes is not exposed to a sufficiently high pH to cause unwinding as is the case in the P- and B-tubes. In addition to a pH of 12.8 in the P- and B-tubes, the DNA in the B-tubes is subject to sonication to ensure complete denaturation. We have used the relationship of fluorescence readings $(P-B) \div (T-B) \times 100$ to describe the percent double-stranded DNA remaining after alkaline incubation as suggested by Birnboim and Jevcak (*23*). In addition, we have found that treatment of cells with bleomycin could significantly decrease fluorescence in the T-tubes. In "Results" we have presented the relationship of fluorescence readings $(T-B)$ experimental $\div$ $(T-B)$ control $\times$ 100 as the apparent double-stranded DNA expressed as a percent of control incubations.

Effects on cell proliferation.—HTC cells grown in monolayer cultures in Swim's 67 medium containing 10% calf serum were harvested and resuspended in 5.0 ml medium. Triplicate flasks were prepared for each experimental condition containing 1×10^5 cells in a total volume of 10 ml Swim's 67 medium. The flasks were incubated at 37°C for 48 hours. After washing the monolayer with a 0.9% NaCl solution, we harvested the cells and determined the total cell number by using a Royco cell counter.

Expression and evaluation of results.—Data are presented as means ± SE. The results were subjected to statistical evaluation by the *t*-test, which was a paired test where appropriate. Differences between means giving $P<0.05$ were considered to be significant.

RESULTS

In a preliminary experiment in which the incorporation of [^{3}H]dThd into DNA of HTC cells was determined in a 60-minute incubation, it was found that the incorporation was decreased in the presence of 10 m*M* nicotinamide or 10 m*M* benzamide to 55 and 50%, respectively, of control values. When the concentration of these two inhibitors of poly (ADP-ribose) synthetase was increased to 20 m*M*, the incorporation was 42% of control values in the presence of nicotinamide and 38% of control values with benzamide (data not shown). To determine if compounds of this type have effects on DNA replication and repair synthesis in normal and neoplastic hepatic cells, we also examined the incorporation of [^{3}H]dThd into DNA in hepatocytes and HTC cells which had been preincubated with bleomycin and then washed and suspended in fresh medium (table 1). The incorporations for control hepatocytes and HTC cells were 669±133 and 22,624±6,091 cpm per 2×10^5 cells, respectively. Incubation with bleomycin (200 mg/ml) stimu-

TABLE 1.—*Effects of nicotinamide and isonicotinamide on incorporation of [^{3}H]dThd into DNA of hepatocytes and HTC cells after preincubation with bleomycin*[a]

Preincubation with bleomycin[b]	Concentration of added drugs, m*M*			Incorporation into DNA[c]	
	Hydroxyurea	Nicotinamide	Isonicotinamide	Hepatocytes	HTC cells
−	0	0	0	100	100
+		0	0	255±21	73±10
−		2	0	85±7	79±5
−		20	0	58±12	46±9
−		0	2	88±4	87±11
−		0	20	59±8	53±15
+		20	0	172±31	40±11
+		0	20	150±23	51±16
−	10	0	0	58±6	14±3
+		0	0	242±26	19±4
−		20	0	40±7	6±1
−		0	20	40±7	8±1
+		2	0	212±30	22±5
+		20	0	167±17	10±1
+		0	2	217±18	24±4
+		0	20	148±31	11±2

[a] Cells were incubated with bleomycin (200 μg/ml) for 30 min at 37°C, centrifuged at $50\times g$ for 3 min, and washed with EMEM. The cells were suspended in EMEM, and 2×10^5 cells were incubated in 0.8 ml EMEM containing 4 μCi [^{3}H]dThd for 30 min at 37°C. Drugs, when added, were present for the second incubation only.

[b] − = absence of bleomycin; + = presence of bleomycin.

[c] Data are expressed as percentages of control values in the absence of added drugs. Means ± SE for five hepatocyte preparations and seven HTC cell preparations are given. Triplicate incubations were performed for each cell preparation for each incubation medium.

TABLE 2.—*Fluorometric analysis of double-stranded DNA after incubation of cells with bleomycin and nicotinamide*

Cells[a]	Concentration in the incubation medium		No. of cell preparations	Apparent double-stranded DNA as percent of control incubations[b]	Percent double-stranded DNA remaining after alkaline incubation[b]
	Nicotinamide, m*M*	Bleomycin, μg/ml			
Hepatocytes	0	0	14	100	79±3
	20	0		109±9	71±4
	0	200		68±6[c]	56±5[c]
	20	200		62±6[c]	61±4[c]
HTC cells	0	0	5	100	88±2
	20	0		102±5	81±6
	0	200		67±4[c]	51±6[c]
	20	200		66±2[c]	41±6[c]

[a] Cells (6.5×10^6/3 ml) were incubated at 37°C for 30 min.

[b] Means ± SE.

[c] $P<0.001$.

TABLE 3.—*Fluorometric analysis of double-stranded DNA after incubation of HTC cells with bleomycin, nicotinamide, and isonicotinamide*[a]

Procedure No.	Concentration in the incubation medium: Nicotinamide, m*M*	Concentration in the incubation medium: Isonicotinamide, m*M*	Concentration in the incubation medium: Bleomycin, μg/ml	No. of cell preparations	Apparent double-stranded DNA as percent of control incubations[b,c]	Percent double-stranded DNA remaining after alkaline incubation[c]
1	0	0	0	7	100	87±3
	20	0	0		94±3	84±3
	0	0	200		56±5[d]	22±4[d]
	20	0	200		63±7[d]	32±6[d]
	0	0	0	5	100	92±1
	0	20	0		93±6[e]	84±1[d]
	0	0	200		68±6	40±8[d]
	0	20	200		66±11[f]	48±9[e]
2	0	0	0	7	100	82±3
	20	0	0		109±6	73±4
	0	0	200		88±5[f]	48±4[d]
	20	0	200		88±7	48±5[d]
	0	0	0	5	100	82±4
	0	20	0		104±4	77±8
	0	0	200		87±7	57±8[f]
	0	20	200		91±4	53±8[f]

[a] Cells (6.5×10^6/3 ml) were incubated at 37°C for 30 min (procedure 1). In procedure 2 the cells were then centrifuged at 50×*g* for 3 min, washed with 5 ml EMEM, suspended in 3 ml EMEM, and incubated for a further 30 min. When nicotinamide or isonicotinamide was added, each was present in both incubations, whereas bleomycin was present in the first incubation only.

[b] Experiments with nicotinamide and isonicotinamide were performed with different cell preparations. Each group is presented relative to its own control cells.

[c] Means ± SE.

[d] $P>0.001$.

[e] $P>0.01$.

[f] $P>0.05$.

lated the incorporation in HTC cells. The data in table 1 revealed a statistically significant inhibition of [^{3}H]dThd incorporation in hepatocytes when incubated with 20 m*M* nicotinamide or 2 and 20 m*M* isonicotinamide. In HTC cells the incorporation of [^{3}H]dThd was significantly inhibited by 2 m*M* nicotinamide and 20 m*M* isonicotinamide. When cells were incubated with 10 m*M* hydroxyurea to inhibit preferentially the replicative synthesis of DNA, it was found that bleomycin caused a greater response in DNA repair synthesis in hepatocytes than in the hepatoma cells. A paired analysis of cells preincubated with bleomycin and incubated with 10 m*M* hydroxyurea indicated that 20 m*M* nicotinamide and 20 m*M* isonicotinamide inhibited [^{3}H]-dThd incorporation into DNA of both hepatocytes and HTC cells.

Incubations similar to those described in table 1 were performed in which bleomycin was retained with the cells during the incubation with [^{3}H]dThd. Under these conditions, in the presence of 10 m*M* hydroxyurea, incubation with bleomycin (200 μg/ml) stimulated the mean incorporation of [^{3}H]dThd in hepatocytes and HTC cells to 427 and 257%, respectively, of values obtained with hydroxyurea alone (data not shown). With this experimental protocol, nicotinamide and isonicotinamide at 2 and 20 m*M* did not have a statistically significant effect on the stimulation of incorporation caused by bleomycin in the two cell types. There was also no significant effect in an additional experimental protocol which differed from that described in table 1 in that [^{3}H]dThd was not added until the end of the second 30-minute incubation and incorporation was measured in HTC cells over a subsequent 4-hour period (data not shown).

Evidence for damage of DNA by incubation of cells with bleomycin was obtained by the change of fluorescence with ethidium bromide which is dependent on the double-stranded character of the DNA (table 2). This could be seen for hepatocytes and hepatoma cells both in the initial fluorescence and in the more rapid decrease in fluorescence after an alkaline incubation, where the unwinding of strands would be facilitated by strand breaks. Incubation with 20 m*M* nicotinamide did not have a significant effect on fluorescence and, when present together with bleomycin, had little or no effect beyond that seen with bleomycin alone. In another series of experiments presented in table 3, these conclusions were further supported by additional HTC cell preparations, and it was found that 20 m*M* isonicotinamide did not significantly affect DNA structure as judged by the fluorometric analysis. When HTC cells were examined 30 minutes after a preincubation with bleomycin (procedure 2 in table 3), there was an indication of a limited degree of recovery from the effects of the bleomycin but very little, if any, effect of incubation with 20 m*M* nicotinamide or 20 m*M* isonicotinamide.

Longer term studies on the effects of bleomycin were performed with a concentration of 20 μg/ml, which caused an approximately 50% inhibition of the proliferation of HTC cells over a 48-hour period (table 4). In the studies with nicotinamide, the number of cells in control cultures increased from 1×10^5 to $4.05\pm0.09\times10^5$ after 48 hours. The proliferation of HTC cells was significantly inhibited in the presence of 20 m*M* nicotinamide and at all isonicotinamide concentrations examined (2–20 m*M*). Neither nicotinamide nor isonicotinamide caused a significant inhibition of cell proliferation beyond that seen with bleomycin alone.

TABLE 4.—*Effects of bleomycin, nicotinamide, and isonicotinamide on proliferation of HTC cells*[a]

Nicotinamide or isonicotinamide concentration	Bleomycin concentration	
	0[b]	20 μg/ml[b]
Control	100	52±4
Nicotinamide, m*M*:		
2	89±6	55±3
5	94±9	46±2
10	83±8	43±5
20	46±4	42±6
Control	100	41±3
Isonicotinamide, m*M*:		
2	96	44±3
5	81±2	41±2
10	79±2	40±4
20	68±3	37±3

[a] The increase in cell number after a 48-hr incubation was determined as described in "Materials and Methods." Data represent the means of three experiments with triplicate incubations for each experiment and are presented as percentages of the increase in numbers in control cultures. Experiments with nicotinamide and isonicotinamide were done at different times with their own control incubations in the absence and presence of bleomycin.

[b] Means ± SE.

DISCUSSION

Subcellular distribution studies of mono and poly (ADP-ribosyl) proteins in rat liver indicate that the latter are mainly confined to the nucleus (*24*). The activity of poly (ADP-ribose) synthetase is inhibited by nicotinamide, but nicotinamide is also a precursor for the substrate of this enzyme, NAD. Diminished concentrations of NAD have long been recognized as a frequent finding in neoplastic tissues (*25*). Isonicotinamide does not serve as a precursor for NAD synthesis, and the interpretation of its action may be simpler than for nicotinamide. However, it is probable that there is no inhibitor of poly (ADP-ribose) synthetase with absolute specificity (*26*).

In the present work nicotinamide and isonicotinamide inhibited cell proliferation and the incorporation of [^{3}H]-dThd into DNA of hepatoma cells. This inhibition was also seen for the action of nicotinamide on mouse L-cells in the work of Colyer et al. (*3*). However, another inhibitor of poly (ADP-ribose) synthetase, i.e., 5-methylnicotinamide, was shown to be capable of inhibiting division in HeLa cells under conditions in which DNA synthesis was not affected (*27*). Some of the effects of nicotinamide may be remote from nucleic acid synthesis. For example, nicotinamide was found to cause a large stimulation of glycolysis in homogenates of rat liver but not in homogenates of Morris hepatoma 7777 (*28*).

Bleomycin is believed to influence DNA synthesis primarily by strand scission of the DNA template, but there may be some direct inhibition of DNA polymerase α (*29*). Differences in cell sensitivity to bleomycin may arise not only from differences in the activity of repair enzymes but also from differences in cell membrane permeability and the rate of inactivation of bleomycin (*30*). Because there is little semiconservative DNA replication in hepatocytes, the action of bleomycin in stimulating unscheduled DNA synthesis was more apparent than in hepatoma cells. It was necessary to inhibit DNA replication with hydroxyurea before a stimulation of unscheduled DNA synthesis could be detected in the hepatoma cells. The incorporation of [^{3}H]dThd into DNA in the presence of hydroxyurea may give an estimate of unscheduled DNA which is influenced by the hydroxyurea itself (*31*). One must, therefore, interpret with some caution the relative rates in the hepatocytes and hepatoma cells.

Much evidence suggests a role for poly (ADP-ribosylation) of nuclear proteins in DNA repair with a possible involvement in the activity of an endonuclease (*32, 33*) or in changing chromatin structure (*2, 34*). This hypothesis must be reconciled with observations that nicotinamide can, under some circumstances, stimulate unscheduled DNA synthesis (*17, 35–37*). Miwa et al. (*37*) thought it conceivable that when poly (ADP-ribose) synthesis is inhibited, unscheduled DNA synthesis does not stop at the correct point but continues, resulting in a longer chain of DNA displacing the parental strand. Durkacz et al. (*38*) have suggested that poly (ADP-ribose) may covalently modify protein(s) involved in the process leading to re-ligation. An action on DNA ligation would be expected to influence DNA replication and repair. It appears that other sites must also be involved because inhibitors of poly (ADP-ribose) synthetase have caused greater inhibition of DNA repair after DNA damage by alkylation than after strand scission resulting from ionizing radiation (*38*). In addition, Nolan and Kidwell (*34*) have concluded from their studies on *Drosophila* that repair of DNA strand breaks caused by ionizing radiation is independent of poly (ADP-ribose) synthesis. In our work we have seen some small inhibitory effects on unscheduled DNA synthesis caused by nicotinamide and isonicotinamide but have obtained no evidence for an inhibitory effect on strand rejoining after incubation of hepatocytes and hepatoma cells with bleomycin. It appears, therefore, that the effects on DNA repair of inhibitors of poly (ADP-ribose) synthetase after DNA damage by bleomycin were small or insignificant. This finding is similar to results obtained from previous studies using ionizing radiation (*4, 34, 38*) and may be a common feature of agents that act directly to cause DNA strand breaks.

Inhibitors of poly (ADP-ribose) synthetase activity have been reported to enhance the cytotoxicity of alkylating agents (*20*), and Smulson et al. (*39*) observed that nicotinamide increased the enhancement of survival times of mice bearing L1210 cells that were treated with *N*-methy-*N*-nitrosourea. There was only a small enhancement of the toxicity to L1210 cells of γ-radiation by inhibitors of poly (ADP-ribose) synthetase (*20*). Our studies have revealed no enhancement of the toxicity of bleomycin as judged by its effects on the proliferation of HTC cells. It is possible that inhibitors of poly (ADP-ribose) synthetase will be more effective in increasing toxicity of DNA alkylating agents than of agents that cause DNA strand scission. The present results revealed that nicotinamide and isonicotinamide can inhibit DNA synthesis in normal and neoplastic liver cells, but these compounds appeared to have limited potential for affecting the action of bleomycin.

REFERENCES

(*1*) Hayaishi O, Ueda K. Poly (ADP-ribose) and ADP-ribosylation of proteins. Ann Rev Biochem 1977; 46:95–116.

(*2*) Purnell MR, Stone PR, Whish WJ. ADP-ribosylation of nuclear proteins. Biochem Soc Trans 1980; 8:215–227.

(*3*) Colyer RA, Burdette KE, Kidwell WR. Poly ADP-ribose synthesis and DNA replication in synchronized mouse L-cells. Biochem Biophys Res Commun 1973; 53:960–966.

(*4*) Perrella FW. Poly (ADP-ribose) synthetase activity in mitogen stimulated bovine lymphocytes: Effects of polyamines and endogenous nuclease activity. In: Hayaishi O, Ueda K, eds. ADP-ribosylation reactions. New York: Academic Press, 1982:451–464.

(*5*) Rochette-Egly C, Ittel ME, Bilen J, Mandel P. Effect of nicotinamide on RNA and DNA synthesis and on poly (ADP-ribose) polymerase activity in normal and phytohemagglutinin stimulated human lymphocytes. FEBS Lett 1980; 120:7–11.

(*6*) Benjamin RC, Gill DM. Poly (ADP-ribose) synthesis in vitro programed by damaged DNA. J Biol Chem 1980; 255:10502–10508.

(*7*) Berger NA, Sikorski GW. Poly (adenosine diphosphoribose) synthesis in ultraviolet-irradiated xeroderma pigmentosum cells reconstituted with *Micrococcus luteus* UV endonuclease. Biochemistry 1981; 20:3610–3614.

(*8*) Durkacz BW, Omidiji O, Gray DA, Shall S. (ADP-ribose)$_n$ participates in DNA excision repair. Nature 1980; 283:593–596.

(*9*) Gray DA, Durkacz BW, Shall S. Inhibitors of nuclear ADP-ribosyl transferase retard DNA repair after *N*-methyl-*N*-nitrosourea. FEBS Lett 1981; 131:173–177.

(*10*) Jackowski G, Kun E. Age-dependent variation of rates of polyadenosine-diphosphoribose synthesis by cardiocyte nuclei and the lack of correlation of enzymatic activity with macromolecular size distribution of DNA. J Biol Chem 1981; 256:3667–3670.

(*11*) Savard P, Poirier GG, Sheinin R. Poly (ADP-ribose) polymerase activity in mouse cells which exhibit temperature-sensitive DNA synthesis. Biochim Biophys Acta 1981; 653:271–275.

(*12*) Berger NA, Petzold SJ, Berger SJ. Association of poly (ADP-ribose) synthesis with cessation of DNA synthesis and DNA fragmentation. Biochim Biophys Acta 1979; 564:90–104.

(*13*) Juarez-Salinas H, Sims JL, Jacobson MK. Poly (ADP-ribose) levels in carcinogen-treated cells. Nature 1979; 282:740–741.

(*14*) Burzio L, Koide SS. In vitro effects of NAD on DNA synthesis in isolated nuclei from regenerating rat liver and Novikoff hepatoma. FEBS Lett 1972; 20:29–32.

(*15*) Hilz H, Kittler M. Lack of correlation between poly ADP-ribose formation and DNA synthesis. Hoppe Seylers Z Physiol Chem 1971; 352:1693–1704.

(*16*) Perrella FW, Lea MA. Spermine-induced variations in the adenosine 5′-diphosphate ribosylation patterns of nuclear proteins from rat liver and hepatoma. Cancer Res 1979; 39:1382–1389.

(*17*) ———. Adenosine 5′-diphosphate ribosylation of nuclear proteins from rat liver and hepatomas: Effects of polyamines and implications in DNA repair. In: Smulson ME, Sugimura T, eds. Novel ADP-ribosylation of regulatory enzymes and proteins. New York: Elsevier/North-Holland, 1980:99–109.

(*18*) Suhadolnik RJ, Baur R, Lichtenwalner DM, et al. ADP-ribosylation of isolated nuclei from HeLa cells, rat liver, fetal rat liver and Novikoff hepatoma. Effect of nicotinamide adenine dinucleotide analogs on template activity for DNA synthesis, incorporation into nuclear proteins, and a new $1'' \rightarrow 3'$ osidic linkage. J Biol Chem 1977; 252:4134–4144.

(*19*) Spangler M, Sartiano GP, Coetzee ML, Ove P. Effect of bleomycin on [^{3}H]thymidine 5′-triphosphate incorporation into host liver and hepatoma nuclei. Cancer Res 1976; 36:1339–1346.

(*20*) Nduka N, Skidmore CJ, Shall S. The enhancement of cytotoxicity of *N*-methyl-*N*-nitrosourea and of γ-radiation by inhibitors of poly (ADP-ribose) polymerase. Eur J Biochem 1980; 105:525–530.

(*21*) Barra R, Randolph V, Sumas M, Lanighan KW, Lea MA. Effects of bleomycin, nicotinamide, and isonicotinamide on DNA replication and repair in hepatoma cells and hepatocytes. J Cell Biol 1981; 91:131a.

(*22*) Barra R, Collin GR, Parson J, Lea MA. Differences in cytosol factors in liver and hepatomas revealed by real or apparent effects on the incorporation of [^{3}H]thymidine. Int J Biochem 1981; 13:1233–1240.

(*23*) Birnboim HC, Jevcak JJ. Fluorometric method for rapid detection of DNA strand breaks in human white blood cells produced by low doses of radiation. Cancer Res 1981; 41:1889–1892.

(*24*) Adamietz P, Wielckens K, Bredehorst R, Lengyel H, Hilz H. Subcellular distribution of mono (ADP-ribose) protein conjugates in rat liver. Biochem Biophys Res Commun 1981; 101:96–103.

(*25*) Morton RK. Enzymatic synthesis of coenzyme 1 in relation to chemical control of cell growth. Nature 1958; 181:540–542.

(*26*) Johnson GS. Benzamide and its derivatives inhibit nicotinamide methylation as well as ADP-ribosylation. Biochem Int 1981; 2:611–617.

(*27*) Kidwell WR, Burdette KE. Poly (ADP-ribose) synthesis and cell division. Biochem Biophys Res Commun 1974; 61:766–773.

(*28*) Lea MA, Sasovetz D, Morris HP. Some factors affecting carbohydrate metabolism in hepatic tissues of different growth rates. Int J Cancer 1969; 4:487–494.

(*29*) Fitzgerald G, Wick MM. Inhibition of DNA polymerase α by bleomycin. Biochem Biophys Res Commun 1981; 101:734–739.

(*30*) Miyaki M, Morohashi S, Ono T. Single strand scission and repair of DNA in bleomycin-sensitive and resistant rat ascites hepatoma cells. J Antibiot (Tokyo) 1973; 26:369–373.

(*31*) Cleaver JE. DNA repair and its coupling to DNA replication in eukaryotic cells. Biochim Biophys Acta 1978; 516:489–516.

(*32*) Miller EG. Stimulation of nuclear poly (adenosine diphosphate ribose) polymerase activity from HeLa cells by endonucleases. Biochim Biophys Acta 1975; 395:191–200.

(*33*) Nomura H, Tanigawa Y, Kitamura A, Kawakami K, Shimoyama M. "Poly (ADP-ribose)-sensitive endonuclease" and the repair of DNA damaged by *N*-methyl-*N*-nitrosourea. Biochem Biophys Res Commun 1981; 98:806–814.

(*34*) Nolan NL, Kidwell WR. Effect of heat shock on poly (ADP-ribose) synthetase and DNA repair in *Drosophila* cultured cells. Radiat Res 1982; 90:187–203.

(*35*) Althaus FR, Lawrence SD, Sattler GL, Pitot HC. The effect of nicotinamide on unscheduled DNA synthesis in cultured hepatocytes. Biochem Biophys Res Comun 1980; 95:1068–1070.

(*36*) Berger NA, Sikorski G. Nicotinamide stimulates repair of DNA damage in human lymphocytes. Biochem Biophys Res Commun 1980; 95:67–72.

(*37*) Miwa M, Kanai M, Kondo T, Hoshino H, Ishihara K, Sugimura T. Inhibitors of poly (ADP-ribose) polymerase enhance unscheduled DNA synthesis in human peripheral lymphocytes. Biochem Biophys Res Commun 1981; 100:463–470.

(*38*) Durkacz BW, Irwin J, Shall S. Inhibition of (ADP ribose)$_n$ biosynthesis retards DNA repair but does not inhibit DNA repair synthesis. Biochem Biophys Res Commun 1981; 101:1433–1441.

(*39*) Smulson ME, Schein P, Mullins DW, Sudhakar S. A putative role for nicotinamide adenine dinucleotide-promoted nuclear protein modification in the antitumor activity of *N*-methyl-*N*-nitrosourea. Cancer Res 1977; 37:3006–3012.

blank page

Tumor-Associated Antigens Produced by Mouse Mammary Tumor Cells in Artificial Capillary Culture [1,2,3]

Jean C. Hager,[4] S. Spiegelman,[5] M. Ramanarayanan,[5] James Bausch,[5] Pierre M. Galletti,[6] *and* Paul Calabresi[7,8]

ABSTRACT—Mouse mammary tumor cells were cultured on a three-dimensional bundle of semipermeable hollow fibers as a prototype system for large-scale in vitro production of mammary tumor-associated antigens. Cells were seeded onto the surface of the hollow fibers that served as an artificial capillary network. The cells grew to tissue-like densities within 3 weeks, achieving the high density and three-dimensional intercellular relationships known to potentiate expression of murine mammary tumor virus (MuMTV) antigens. Significant levels of a 52,000-relative-molecular-weight (M_r) glycoprotein antigen of MuMTV (gp52) were detected on the cell side of the semipermeable membrane of the hollow fibers in a yield at least fiftyfold greater than that produced by monolayer cultures. Antigen could be collected from capillary cultures for 6–12 weeks, rather than days from monolayer cultures. Further, gp52 was collected in an undegraded state. Perfusates contained lesser amounts of cross-reactive antigenic species that were predominantly smaller than 50,000 M_r, which suggests that the fibers may be used to separate antigens from their degradation products. The production of nonviral, mammary tumor-associated antigens by cells on artificial capillaries was also demonstrated. Artificial capillary cell culture systems provide a means to obtain significant quantities of tumor-relevant antigens in a semipurified natural state.—JNCI 1982; 69:1359–1366.

The wide variation in reproducibility reported for many cancer-associated immunologic tests (*1*) may well be due to lack of standardization of the immunologic reagents with respect to both potency and specificity. A major deterrent to overcoming these obstacles has been the difficulty in preparing large quantities of standardized reagents in an unaltered state.

The development of the artificial capillary cell culture technique (*2–6*) may provide a solution to this problem. This technique permits in vitro culture of cells on bundles of parallel hollow fibers (artificial capillaries) resulting in growth of the cells in a dense, tissue-like, three-dimensional configuration. The cells are maintained in a physiologic microenvironment (*2–6*). Studies on tumor-associated antigens such as those of MuMTV indicate that antigen production is strongly favored in three-dimensional relative to monolayer culture (*7–9*). It has also been shown that antigen production is enhanced in high-cell-density cultures (*10–12*). We report here an evaluation of the growth of mammary tumor cells on artificial capillaries for the purpose of producing tumor-related antigens in large quantities and in an undegraded form.

MATERIALS AND METHODS

Cells and monolayer culture.—Cell lines 66, 67, 168, and 68H were isolated from a single spontaneous BALB/cfC3H mouse mammary tumor (*13*) and have been maintained in our laboratories for over 3 years. More than 95% of line 68H cells express MuMTV cell surface antigens detectable by immunofluorescence with the use of a rabbit anti-C3H MuMTV, whereas lines 66, 67, and 168 do not (*13*). Lines 66, 67, and 168 can be induced by 5-iodo-2′-deoxyuridine or 10^{-5} *M* dexamethasone to express viral antigens (*14, 15*). We used as specificity controls in transplantation resistance assays a Moloney sarcoma cell line obtained from Dr. Sylvia Pollack, Fred Hutchinson Cancer Research Center, Seattle, Wash.

Cells were routinely grown in Falcon tissue culture dishes (Falcon Plastics, Oxnard, Calif.) in Waymouth's medium supplemented with 15% heat-inactivated FCS, 2 m*M* L-glutamine, and 20 μg gentamicin/ml (Schering Diagnostics, Port Reading, N.J.) or 100 U penicillin/ml and 100 μg streptomycin/ml and buffered with $NaHCO_3$. Unless otherwise stated, all culture reagents were purchased from

---

ABBREVIATIONS USED: BSA=bovine serum albumin; CTX=Cytoxan (cyclophosphamide); ECS=extracapillary space; ELISA=enzyme-linked immunosorbent assay; FCS=fetal calf serum; gp52=52,000-M_r glycoprotein antigen of murine mammary tumor virus; M_r=relative molecular weight; MuMTV=murine mammary tumor virus; p28=28,000-M_r protein antigen of MuMTV; PBS=phosphate-buffered saline (0.1 *M* at pH 7.6); RIA=radioimmunoassay.

---

[1] Received March 23, 1982; accepted July 22, 1982.

[2] Supported by Public Health Service grants CA-13943 and CA-22453 from the National Cancer Institute and HL-11945 from the National Heart, Lung, and Blood Institute; by an Institutional Grant to the Michigan Cancer Foundation from the United Foundation of Greater Detroit; and by the E. Walter Albachten bequest.

[3] Animals were maintained under the guidelines set forth by Roger Williams General Hospital and Brown University.

[4] Department of Cell Biology, AMC Cancer Research Center and Hospital, 6401 West Colfax Ave., Lakewood, Colo. 80214.

[5] Institute of Cancer Research, College of Physicians and Surgeons, Columbia University, New York, N.Y. 10032.

[6] Artificial Organ Laboratory, Division of Biology and Medicine, Brown University, Providence, R.I. 02912.

[7] Department of Medicine, Roger Williams General Hospital, and Division of Biology and Medicine, Brown University, Providence, R.I. 02908.

[8] We thank Dr. Roger Hu and Dr. K. Prasad for some of the radioimmunoassays, Dr. I. Keydar and Dr. R. Mesa-Tejada for the immunoperoxidase immunohistochemical staining, Dr. Lowell Kopp for lactate dehydrogenase assays, Dr. L. Roi for statistical analyses, Dr. Barry Solomon for providing Amicon hollow fibers and encouragement, Mr. George Panol for fabrication of the capillary devices, Mr. S. Chester for assistance with the immunogenicity studies, and Dr. I. Diamond for making available the facilities of the Department of Pathology, Roger Williams General Hospital. Excellent technical assistance was provided by Ms. Kim Amoruso McCarthy, Ms. Betsy Vokac, and Ms. Irene Fong. We are grateful to Dr. Gloria Heppner and Dr. Philip Furmanski for their encouragement and many helpful discussions.

GIBCO, Grand Island, N.Y. For routine subculture, cells from monolayers were harvested with 0.125% trypsin and 0.05% EDTA in 0.9% NaCl solution, centrifuged for 5 minutes at $400\times g$, resuspended in Waymouth's medium, and plated in Falcon culture dishes. All cultures were kept at 37°C in a humidified atmosphere of 5% CO_2 in air.

Artificial capillary cell culture.—Artificial capillary cell culture systems were based on those originally described by Knazek et al. (*2–6*) and are schematically presented in text-figure 1. Capillary culture units either were vitafiber units (Amicon Corp., Lexington, Mass.) or were manufactured in the Artificial Organ Laboratory, Brown University. The capillary units consisted of a bundle of 100 microporous hollow fibers (Amicon Corp.), 11 cm long, potted in epoxy at each end, and encased in a polycarbonate shell equipped with shell ports. Vitafiber units (Amicon Corp.) were 11 cm long. Unless otherwise specified, we used XM50-type fibers composed of polyacrylate, with a tight semipermeable membrane on the luminal side that prevents cell passage but allows solute exchange with the culture medium. The XM50 type of fiber has a nominal exclusion of 50,000 M_r. In some experiments, we used P30-type fibers that are composed of polysulfone and have a nominal exclusion of 30,000 M_r. The artificial capillary system, a closed circuit, was perfused with culture medium with the use of a Holter model 911 roller pump (pump and fittings; Extracorporeal Medical Specialties, King of Prussia, Pa.). The culture media were either Waymouth's medium supplemented with 15% FCS or Iemzo medium supplemented with 1% FCS and 0.1 IU insulin/ml; both media were further supplemented with 100 U penicillin/ml, 100 µg streptomycin/ml, and 50 U Trasylol/ml (Mobay, New York, N.Y.) and were buffered with 0.075% $NaHCO_3$. Media for culture of line 68H cells were further supplemented with 10^{-6} *M* dexamethasone.

Capillary culture systems were sterilized by ethylene oxide and the fibers wetted by circulation of sterile Hanks' balanced salt solution (GIBCO). For culture studies, 5×10^6 cells in suspension were injected through the shell ports and seeded onto the surface of the hollow fibers. Systems were placed in the incubator, and cells were allowed to attach for 2 hours at 37°C without perfusion of the culture medium. Medium was perfused at 5–10 ml/minute.

Growth of cells on artificial capillaries was monitored by glucose consumption. The glucose concentration in the medium was evaluated by the glucose oxidase test. When the glucose level dropped to less than 50 mg/ml, the medium was changed by replacement of the reservoir with another containing 125 ml fresh medium. Medium was changed approximately three times during the 1st week of culture and daily during the 3d and 4th weeks.

Histologic evaluation of cell growth on artificial capillaries.—Cells were fixed by perfusion with Bouin's fluid for 2 hours. After fixation, the lumina of the hollow fibers and the ECS were filled with 1.5% Noble agar in medium at 45°C. The agar was solidified at 4°C and the encased fiber bundle extracted. Segments of the bundle were tied off with sutures. Sections were cut between sutures and processed for routine paraffin embedding and histologic examination as if the bundle segment were a piece of tissue.

Immunohistochemical detection of MuMTV antigens.—An indirect immunoperoxidase immunohistochemical stain was used to localize the presence of MuMTV antigens in cells grown on artificial capillaries. The staining technique was applied to 5-µm serial sections of Bouin's fluid-fixed, paraffin-embedded segments of fiber bundles. Details of the procedure have been described previously (*16*). The primary antibody was rabbit IgG from animals immunized against whole disrupted RIII MuMTV (*16*). The second antibody was peroxidase-conjugated goat anti-rabbit IgG (*16*). Stained sections were counterstained in dilute methylene blue. Sections were examined by light microscopy, and a positive reaction was indicated by a brownish precipitate.

Sample collection from artificial capillary cultures.—Samples (1 ml) of ECS fluids, from the cell side of the membrane, were collected daily through the ports in the shell surrounding the hollow fiber. An iv injection set was inserted into the

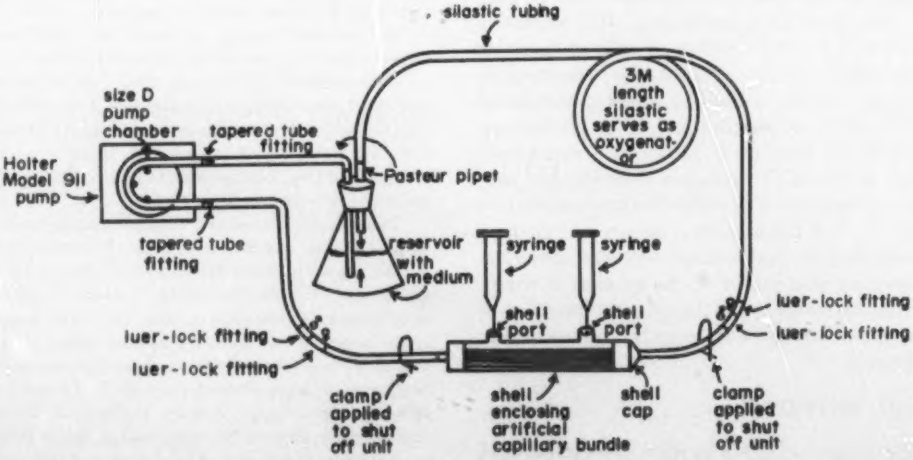

TEXT-FIGURE 1.—The artificial capillary cell culture system. Cells are introduced through the shell ports and grow on the external surface of the capillaries. Medium is perfused through the lumina of the hollow fibers or artificial capillaries and is recirculated by the roller pump. Antigens are collected from the ECS through the shell ports and from the perfusate by sampling medium in the reservoir. The entire system is placed in a 37°C incubator with a 5% CO_2 atmosphere, and the pH of the medium is maintained by gas exchange through the silastic tubing.

shell port, and sample fluids were collected by positive ultrafiltration forces. Samples of the perfusate were also collected daily and stored at −80°C until tested.

RIA detection of MuMTV antigens in culture fluids.—The presence of gp52 and p28 in the ECS and perfusate was determined by blocking RIA in which delayed addition of labeled antigen was used to maximize sensitivity. The gp52 was purified by the method of Ritzi et al. (*17*) and iodinated with ^{125}I-labeled Bolton-Hunter reagent as previously described (*17*). The ^{125}I-labeled gp52 was more than 90% precipitable with 10% trichloroacetic acid.

ELISA detection of gp52 in culture fluids.—The ELISA was applied to culture fluids for detection and quantitation of gp52. Antibody against highly purified gp52 was prepared as previously described (*18*) and conjugated with horseradish peroxidase (*16*). To each well of a microTest plate (Dynatech Laboratories, Inc., Alexandria, Va.) was added 200 µl of anti-gp52 IgG diluted in 50 m*M* carbonate–bicarbonate buffer (pH 9.6) to a final concentration of 10 µg/ml, and the plate was sealed and incubated overnight at 4°C. After incubation, unbound antibody was washed off by PBS with 0.1% Tween 20. The plate was sealed and stored at −20°C until used.

To the antibody-coated wells was added a 200-µl aliquot of either the test sample or standard gp52 or disrupted MuMTV proteins as appropriate. For each test, six different concentrations of sample were made in the range of 0.1–10 µl and diluted to a final volume of 200 µl in PBS containing 5% chicken serum, 5% Trasylol, and 0.1 m*M* Merthiolate. The plate was sealed and incubated overnight at 4°C, and unbound antigen was washed off with PBS–Tween 20 as above. Then 200 µl of conjugate at 10 µg/ml in PBS–chicken serum was added, and the plate was sealed and incubated at room temperature for 4 hours. To each well was added 250 µl of the peroxidase substrate [0.5 mg *o*-phenylenediamine dihydrochloride/ml in McIlvaine's citrate–phosphate buffer (pH 6.0) containing 0.006% H_2O_2]. The plate was incubated at room temperature for 1 hour after which 25 µl of the reaction mixture was diluted to 250 µl with 0.5 *N* H_2SO_4 to stop the reaction. The orange color of the reaction product in 0.5 *N* H_2SO_4 (max, 492 nm) was measured in a spectrophotometer against an appropriate reagent blank. The ELISA gave a linear response to gp52 of 1–30 ng. The gp52 content of test samples was calculated from the linear portions of the standard curve for gp52 generated in the same assay.

Characterization of particulate and soluble gp52.—A 650-µl portion of pooled ECS fluid was centrifuged in a microtube at $189{,}000\times g$ for 45 minutes, and the supernatant was removed and designated "soluble fraction." The pellet was resuspended in 65 µl of disruption buffer (0.2 *M* sodium phosphate at pH 6.8, 0.01 *M* EDTA, 0.2% 2-mercaptoethanol, and 1% Nonidet P40) and incubated at 4°C for 30 minutes and then at 37°C for 30 minutes after which it was made up to 650 µl (original vol of starting sample) with 0.02 *M* Tris-HCl (pH 7.2) and 0.2% 2-mercaptoethanol and designated "particulate fraction." These fractions were evaluated by the ELISA for gp52 content.

Protein determination.—The total protein content of samples was determined by the method of Lowry et al. (*19*). BSA was used as the standard.

Ouchterlony double-diffusion analysis.—The Ouchterlony method of double diffusion in gels (*20*) was used to detect the presence of BSA in samples. The reaction was done with prepared immunodiffusion plates containing agar gel (Hyland Diagnostics, Deerfield, Ill.). Antibody to BSA was obtained from Cappel Laboratories, Cochranville, Pa.

Molecular sizing.—Capillary fluids were applied to a gel filtration column (Ultrogel AcA 54; LKB Instruments, Inc., Rockville, Md.), and the fractions collected were assayed by RIA for the presence of material reactive with antiserum to gp52 in the ELISA. The following standards were used to estimate the molecular weights of the antigenic material: lysozyme, M_r 14,300; trypsinogen, M_r 24,800; ovalbumin, M_r 45,000; BSA, M_r 68,000.

Mice.—BALB/c and BALB/cfC3H mice were used. They were descendants of breeding pairs obtained from the Cancer Research Laboratory, University of California at Berkeley. These mice were maintained by brother × sister mating. The BALB/cfC3H mice carry the standard MuMTV (*21*).

Immunization and challenge.—Fluids were collected daily from ECS of appropriate capillary cultures and pooled, and the total protein and gp52 levels were determined. Mice were immunized by ip injection with varying concentrations of the ECS pool diluted in PBS. The immunized mice were challenged on day 21 with 5×10^5 tumor cells of the appropriate syngeneic cell line. Animals were examined three times per week. Tumor appearance was recorded when a palpable mass was detected.

Immunomodulation.—CTX (Mead Johnson & Co., Evansville, Ill.), 300 mg/kg, was given ip to immunized mice.

Statistical methods.—Data in the immunogenicity tests were analyzed by the chi-square test.

RESULTS

Evaluation of Cell Growth on Artificial Capillaries

All cell lines examined in this study were able to grow on artificial capillary matrices composed of either polyacrylate or polysulfone. Growth of cells on artificial capillaries cannot be visualized as in monolayer culture vessels. In the capillary cultures, growth was monitored by glucose consumption. A typical glucose consumption curve for a capillary culture is illustrated in text-figure 2. The overall pattern was an initial slow rate of glucose consumption, 40–50 mg/100 ml/day, for the first 10 days of culture, followed by an exponential phase, 70–250 mg/100 ml/day, and finally a plateau and eventual decline. Glucose consumption also increased sharply for the 24 hours immediately following each medium change. This glucose consumption pattern was consistent for all cultures tested, although the phases were of variable lengths and amplitude depending on the fiber material, cell type, and number of cells inoculated.

Using other types of perfusion cultures, Kruse (*22*) estimated that 0.9 mg/100 ml glucose is consumed per day for every 10^6 cells (*22*). With the use of this relationship, the number of cells present in a capillary culture was estimated to be 300×10^6 cells on the 25th day of the culture illustrated in text-figure 2. In other cultures, a total of nearly 10^9 cells was obtained.

Cells seeded onto the hollow fibers grew on the surface of

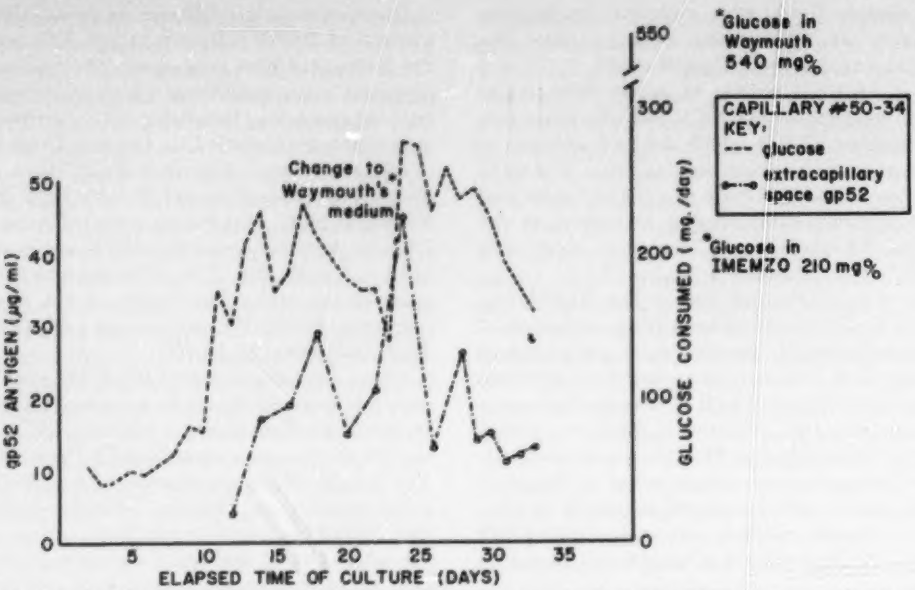

TEXT-FIGURE 2.—Production of gp52 antigen (ELISA) and growth curve (glucose consumption) of cell line 68H grown on artificial capillaries of 50,000-M_r nominal exclusion. mg%=mg/100 ml.

each fiber, extended into the pores of the polymeric substrate, and filled the spaces between the fibers. Tissue-like densities of cells (fig. 1) were achieved within 3 weeks when 5×10^6 cells were seeded onto the capillaries and could be maintained for as long as 3 months.

Immunohistochemical Detection of MuMTV Antigens

To determine whether viral antigens were expressed by cells in capillary culture, we grew line 68H cells on 50,000-M_r exclusion artificial capillaries. After 35 days in culture, the cells on the artificial capillaries were fixed in Bouin's fluid, processed for histologic examination, and stained by the immunoperoxidase procedure. All line 68H cells gave a strong positive reaction for the viral antigens similar to the reaction observed in mouse mammary tumors (*16*). The reaction could be prevented by preadsorption of the antiserum with whole MuMTV.

Sample Collection From Capillary Cultures

One aim of this study was to evaluate the production of soluble antigens by cells grown on artificial capillaries. We therefore had to develop a method of reproducibly sampling the ECS fluids in a way that would minimize disturbance of cellular architecture and would result in minimal antigen dilution. To develop an optimal method, we performed a series of pilot experiments using the enzyme lactate dehydrogenase which could be readily quantitated.

The optimal collection procedure was one using the ultrafiltration forces (created by the fluid passage through the capillary device) in which the sample is pumped into a collection tube at approximately 1–5 ml/minute. Using this technique, we could collect 75% of the lactate dehydrogenase enzymatic activity injected into the ECS in the first 1-ml sample. Similar efficiency of collection was obtained with a Harvard pump withdrawing fluid at the rate of 1 ml/10 minutes. However, the injection set method was more convenient to use routinely. Use of hand-held syringes and evacuation resulted in highly variable collections with perturbation of cellular architecture at the port of withdrawal.

Detection of MuMTV Antigens in Capillary Fluids

To determine whether antigens were shed from cells and could be harvested from capillary fluids, we evaluated the presence of MuMTV-associated antigens in fluids of line 68H cells grown in artificial capillaries. The XM50 (50,000-M_r exclusion)-type hollow fibers were chosen in an effort to retain and concentrate gp52 in the ECS and at the same time exclude the large proteins such as albumin on the luminal side of the membrane.

The fluids in the ECS and the perfusate were sampled daily from two parallel capillary cultures and assayed by RIA and the ELISA for the presence of gp52. The levels of gp52 detected in one culture are illustrated in text-figure 2. The content of gp52 in the ECS fluids in the culture illustrated ranged from 5 to 45 µg/ml in daily 1-ml samples. The ECS fluids also contained 0.2–0.6 µg p28/ml. The perfusates contained 200–300 ng/ml of material that reacted with anti-gp52.

Characterization of MuMTV Antigens From Capillary Cultures

Molecular sieve gel filtration of the capillary fluids was used to characterize the gp52-competitive species. The antigenic material in the ECS fluid ranged in size from 50,000 to 68,000 M_r. The perfusate contained material that ranged from 35,000 to 55,000 with a peak at 46,000 M_r.

ECS fluids from 2 weeks of culture of line 68H cells on two capillary units (not illustrated) were pooled. The pooled fluid was analyzed by the ELISA and contained 14.2 μg gp52/ml. A sample was centrifuged and the particulate and soluble fractions were evaluated. The particulate fraction contained 9,800 ng gp52/ml, whereas the soluble fraction contained 4,500 ng gp52/ml, a ratio of 2 parts particulate: 1 part soluble.

Comparison of Production of MuMTV Antigens in Capillary and Monolayer Cultures

The culture fluids overlaying monolayer cultures of 68H cells were tested for content of gp52 and their content of gp52 was compared with the content of gp52 in capillary cultures. Monolayers produced from 400 to 1,245 ng gp52/ml/day for 4–7 days, which was equivalent to 60–100 ng/ml/10^6 cells/day, depending on the culture and the type of medium used. By comparison, in our overall experience, capillary cultures produced 1,200–51,000 ng gp52/ml/day, which was equivalent to 150–200 ng/ml/10^6 cells/day estimated by the glucose consumption of the cell culture. Generally, capillary cultures produced these quantities of antigens daily for 3–12 weeks.

Contaminating Antigens

The ECS fluids were tested by Ouchterlony analysis for the presence of BSA. Both XM50 (50,000-M_r nominal exclusion) and P30 (30,000-M_r nominal exclusion) hollow fibers were found to allow the BSA to cross from the perfusate to appear in the ECS.

To determine if the albumin was intact or fragmented, a 2-ml sample of ECS fluid from one of the line 68H cultures was reduced tenfold by lyophilization and subjected to gel filtration in a 1×50-cm column of ultrogel AcA 54. Most protein appeared as a sharp peak immediately after the void volume. These protein fractions were found by Ouchterlony analysis to contain BSA, whereas the later fractions did not, which suggests that the albumin in the ECS is intact with an M_r of 68,000.

Antigens Produced by Other Mammary Tumor Cell Lines

Cell lines 66, 67, and 168 do not express MuMTV cell surface antigens in monolayer culture, although lines 66 and 168 appear to express viral antigens as determined by transplantation resistance (*23*) and can be induced to express these antigens in monolayer culture by 5-iodo-2′-deoxyuridine or dexamethasone (*14, 15*). These lines were grown in capillary culture, and the ECS fluid was examined for the presence of gp52. Pooled ECS fluids from a 2-week culture of line 66 contained 674 ng/ml. A pool of ECS fluids from a 2-week culture of line 67 contained 380 ng particulate gp52/ml and 480 ng soluble gp52/ml. Daily samples of a culture of line 168 contained 70–299 ng gp52/ml.

Mammary Tumor-Associated Antigens Produced in Capillary Culture

Mice were immunized with ECS fluids from line 67, since this line had been previously shown to express tumor-associated nonviral antigens (*23*). Both BALB/c and BALB/cfC3H mice were immunized because BALB/c mice can respond to both MuMTV-associated and unique tumor-specific antigens, whereas the BALB/cfC3H mice develop transplantation immunity primarily to the unique antigen (*24, 25*). By using both types of mice, we were able to test for immunity to nonviral tumor antigens. The results of subsequent challenge with the same and syngeneic tumor cells are presented in table 1.

Immunization of BALB/c mice with 100 μg of the line 67 capillary-derived antigen resulted in inhibition of the growth of line 67 tumor cells. In contrast, immunization of BALB/cfC3H mice with 100 μg of the same antigen resulted in specific enhancement of line 67 tumor growth. That this enhancement was due to immunologic mechanisms was indicated by its abrogation by an immunosuppressive regimen of CTX given 2 days prior to immunization (*26*). The specificity of the response for the unique antigen was shown by the failure of immunization with line 67 ECS to enhance line 68H tumor growth. Line 68H tumors do not induce transplantation immunity to the unique antigen (*23*). Further evidence of the specificity of immunization with line 67-derived capillary fluids was shown by the lack of any effect of immunization with these fluids on the growth of Moloney sarcoma cells in either strain of mice.

The immunizing pool of 67 capillary fluids contained a small amount of MuMTV gp52 antigen (690 ng/ml). Only picogram amounts of gp52 are present in 10 μg total capillary fluid. Such low concentrations are not likely to be sufficient for immunization, although they possibly could cause low-dose tolerance.

TABLE 1.—*Immunogenicity of capillary-derived antigens from cell line 67*

Mouse strain	Treatment	Tumor incidence at day 53/No. challenged with line 67 cells (%)[a]
BALB/c[b]	100 μg line 67, day 0	1/10 (10)[c]
	10 μg line 67, day 0	5/10 (50)
	1 μg line 67, day 0	6/10 (60)
	0 μg line 67, day 0	7/10 (70)
BALB/cfC3H[d]	100 μg line 67, day 0	11/20 (55)[e]
	100 μg line 67, days 0 and 7	14/20 (70)[f]
	10 μg line 67, day 0	2/10 (20)
	1 μg line 67, day 0	1/10 (10)
	0 μg line 67, day 0	3/30 (10)
	100 μg line 67, day 0, plus 30 mg CTX/kg given 2 days before immunization	1/10 (10)[g]

[a] Challenged on day 21 with 5×10^5 tumor cells [*see* (*23*)].

[b] The dose responses in BALB/c mice are independent ($\chi^2=8.32$; $P<0.04$).

[c] Significant reduction in tumorigenicity ($\chi^2=7.5$; $P<0.01$).

[d] The dose responses in BALB/cfC3H mice are independent ($\chi^2=26.45$; $P<0.01$).

[e] Significant enhancement of tumorigenicity ($\chi^2=12.05$; $P<0.0001$).

[f] Significant enhancement of tumorigenicity ($\chi^2=19.25$; $P<0.0001$).

[g] Enhancement of tumorigenicity eliminated, identical to control.

DISCUSSION

We have applied the artificial capillary cell culture technique to the production of antigens by mammary tumor cells. The purpose was to use the unique features of the capillary cell culture system to optimize antigen production. The tridimensional capillary matrix supports cell growth under conditions in which fresh nutrients are continuously supplied while waste products are removed (*2–6*). All the mammary tumor cell lines tested were capable of luxuriant growth on hollow fibers composed of either polyacrylate or polysulfone. Tissue-like densities of cells were achieved within a few weeks, and cultures remained metabolically active for 6–12 weeks.

We have previously demonstrated that normal hepatocytes can similarly be maintained for 6–8 weeks and retain the capabilities of production of plasma proteins, metabolism of drugs, and production of urea (*27*). Using capillary cell culture technology, other investigators have established long-term cultures of choriocarcinoma cells that produce human chorionic gonadotropin (*4*), human pituitary cells that secrete prolactin and growth hormone (*5*), pancreatic beta cells that produce insulin (*28, 29*), and minimally changed hepatoma cells that can conjugate bilirubin (*30*).

Artificial capillary cell culture systems proved to be efficient means for production of MuMTV antigens. It is not possible to accurately determine at this time if the antigen production is increased in capillary cultures on a per-cell basis compared to monolayer cultures or whether the increase is due to the much larger number of cells in the capillary cultures. From the glucose consumption data, we have estimated that the capillary cultures produced at least double the amount of antigen per 10^6 cells and produced antigen for an extended period of time. This suggests an increase in antigen production per cell over and above the increased number of cells in the capillary cultures.

The hollow fibers are constructed with a semipermeable membrane on their luminal surfaces. In initial studies, XM50-type fibers were used with a nominal exclusion of 50,000 M_r. This exclusion was selected to retain and concentrate antigens with an M_r greater than 50,000, like that of gp52, on the cell side of the membrane. The gp52 competitive species in the perfusate were smaller than 52,000, which suggests that these were breakdown products of the gp52. In contrast, the gp52 present on the cell side was in its 52,000-M_r form. It appeared as both particulate and soluble gp52. The particulate gp52 most likely represents virions and membrane-bound antigens. Disruption of the particulate gp52 prior to analysis resulted in a tenfold increase in detectable antigen, which suggested that gp52 is present both in virions and in lipid-bound and lipoprotein-bound complexes, since disruption of virions alone generally gives only twofold to threefold increases in detection.

The p28 in the ECS is most likely present primarily in the form of virions. Free species of 28,000 M_r would be expected to readily cross the membrane barrier.

Another expectation of the membrane barrier had been that large proteins of FCS used in culture media would be retained in the perfusate. This expectation was not fully realized. The XM50 and P30 membranes are sufficiently leaky to consistently permit intact BSA (M_r 68,000) to cross the barrier into the ECS. Thus the capillary culture system failed to fulfill the initial expectation that it would provide antigen completely free from contamination with FCS proteins.

This is the first demonstration that viral antigens can be harvested in large quantities from capillary cultures and that such culture systems are feasible for large-scale production of tumor virus products. Previously, Johnson et al. (*31*) have shown that several cell types could be infected with Venezuelan equine encephalitis virus in capillary culture with the production of a high titer of infectious virus.

Interestingly, cell lines 66 and 67, which do not express MuMTV antigens under conventional monolayer conditions (*13*), did so under capillary culture conditions. These lines do express these antigens in monolayer when treated with various inducers (*14, 15*) and appear to do so in vivo (*23*). This finding provides further evidence that capillary conditions potentiate the expression of antigens. The mechanism for this antigen-induction effect remains to be explored.

The MuMTV antigen studies were initiated to use well-characterized antigens as a model for the development of a means to produce tumor-relevant nonviral antigens. The next step in this development was to generate tumor-associated non-MuMTV antigens. For these experiments, we used line 67 cells that had been shown to immunize against only the unique, tumor-specific antigens of mouse mammary tumors (*23*). The results of pilot studies indicate that it is, in fact, possible to harvest tumor-associated antigens in a useful form from capillary cultures of tumor cells. The antigens produced were immunogenic in syngeneic animals, and the response to these antigens was modulated with an agent known to influence the immune response (*29*).

Preliminary results have indicated that the mouse mammary tumor cells described here also shed the mouse mammary epithelial antigens described by Ceriani et al. (*32*) when these cells were grown either in monolayer or on artificial capillaries (Hager JC, Ceriani RL: Unpublished observations). Experiments are under way to determine if capillary culture enhances the production of these antigens as well.

In summary, artificial capillary cell culture systems provide a means for long-term culture and production of mammary tumor-associated antigens by tumor cells. We are currently determining whether human breast cancer antigens can similarly be produced by human breast cancer cells in artificial capillary cell culture.

REFERENCES

(*1*) Hager JC, Heppner GH. Evaluation of specific immune reactivity in human patients with solid cancers. In: Waters H, ed. The handbook of cancer immunology. Vol 4. New York: Garland, 1978:196–218.

(*2*) Knazek RA, Gullino PM, Kohler PO, Dedrick RL. Cell culture on artificial capillaries: An approach to tissue growth in vitro. Science 1972; 178:65–67.

(*3*) Knazek RA. Solid tissue masses formed in vitro from cells cultured on artificial capillaries. Fed Proc 1974; 33:1978–1981.

(*4*) Knazek RA, Kohler PO, Gullino PM. Hormone production by cells grown in vitro on artificial capillaries. Exp Cell Res 1974; 84:251–254.

(*5*) Knazek RA, Skyler JS. Secretion of human prolactin in vitro. Proc Soc Exp Biol Med 1976; 151:551–564.

(*6*) Knazek RA, Lippman ME, Chopra HC. *Brief communication*: Formation of solid human mammary carcinoma in vitro. J Natl Cancer Inst 1977; 58:419–422.

(*7*) McGrath CM, Nandi S, Young L. Relationship between organization of mammary tumors and the ability of tumor cells to replicate mammary tumor virus and to recognize growth-inhibitory contact signals in vitro. J Virol 1972; 9:367–376.

(*8*) McGrath CM. Replication of mammary tumor virus in tumor cell cultures: Dependence on hormone-induced cellular organization. J Natl Cancer Inst 1971; 47:455–467.

(*9*) Yagi MJ. Cultivation and characterization of BALB/cfC3H mammary tumor cell lines. J Natl Cancer Inst 1973; 51:1849–1860.

(*10*) Dickson C, Haslam S, Nandi S. Conditions for optimal MTV synthesis in vitro and the effect of steroid hormones on virus production. Virology 1974; 62:242–252.

(*11*) Young LJ, Cardiff RD, Ashley RL. Long-term primary culture of mouse mammary tumor cells: Production of virus. J Natl Cancer Inst 1975; 54:1215–1221.

(*12*) Cardiff RD, Blair PB, DeOme KB. In vitro cultivation of the mouse mammary tumor virus: Replication of MTV in tissue culture. Virology 1968; 36:313–317.

(*13*) Dexter DL, Kowalski HM, Blazar B, Fligiel Z, Vogel R, Heppner GH. Heterogeneity of tumor cells from a single mouse mammary tumor. Cancer Res 1978; 38:3174–3181.

(*14*) Hager JC, Dexter DL, Calabresi P, Heppner GH. Heterogeneity of MuMTV antigen expression and induction in mouse mammary tumor cells. Proc Am Assoc Cancer Res 1979; 20:246.

(*15*) Avyagari LR, Soule HD, McGrath CM. Mouse mammary carcinoma cell subpopulations are variable in MuMTV provirus sequence complexity and glucocorticoid inducibility. Proc Am Assoc Cancer Res 1979; 20:269.

(*16*) Keydar I, Mesa-Tejada R, Ramanarayanan M, et al. The detection of viral proteins in mouse mammary tumors by immunoperoxidase staining of paraffin sections. Proc Natl Acad Sci USA 1978; 75:1524–1528.

(*17*) Ritzi E, Baldi A, Spiegelman S. The purification of a gs antigen of the murine mammary tumor virus and its quantitation by radioimmunoassay. Virology 1976; 75:188–197.

(*18*) Mesa-Tejada R, Keydar I, Ramanarayanan M, Ohno T, Fenoglio C, Spiegelman S. The detection in human breast cancer of an antigen immunologically related to a group specific antigen of the mouse mammary tumor virus. Proc Natl Acad Sci USA 1978; 75:1529–1533.

(*19*) Lowry OH, Rosebrough NJ, Farr AL, Randall RJ. Protein measurement with the Folin phenol reagent. J Biol Chem 1951; 193:265–275.

(*20*) Ouchterlony O. Antigen–antibody reactions in gels. Acta Pathol Microbiol Scand 1953; 32:231–240.

(*21*) Bentvelzen P, Daams JH, Hageman P, Calafat J. Genetic transmission of viruses that incite mammary tumor in mice. Proc Natl Acad Sci USA 1970; 67:377–384.

(*22*) Kruse PF Jr. Use of perfusion systems for growth of cell and tissue cultures. In: Rothblat GH, Cristofalo VJ, eds. Growth, nutrition and metabolism of cells in culture. Vol 2. New York: Academic Press, 1972:11–66.

(*23*) Miller FR, Heppner GH. Immunologic heterogeneity of tumor cell subpopulations from a single mouse mammary tumor. JNCI 1979; 63:1457–1463.

(*24*) Vaage J. Nonvirus-associated antigens in virus-induced mouse mammary tumors. Cancer Res 1968; 28:2477–2483.

(*25*) Blair PB, Lane MA, Yagi MJ. In vitro detection of immune responses to MTV-induced mammary tumors: Activity of spleen cell preparations from both MTV-free and MTV-infected mice. J Immunol 1974; 112:693–705.

(*26*) Heppner GH, Calabresi P. Selective suppression of humoral immunity by antineoplastic drugs. Ann Rev Pharmacol Toxicol 1976; 16:367–379.

(*27*) Hager JC, Carman R, Stoller R, et al. A prototype for a hybrid artificial liver. Trans Am Soc Artif Intern Organs 1978; 24:250–253.

(*28*) Chick WL, Like AA, Lauris V. Beta cell culture on synthetic capillaries. Science 1975; 187:847–849.

(*29*) Chick WL, Like AA, Lauris V, et al. A hybrid artificial pancreas. Trans Am Soc Artif Intern Organs 1975; 21:8–15.

(*30*) Wolf CF, Munkelt BE. Bilirubin conjugation by an artificial liver composed of cultured cells and synthetic capillaries. Trans Am Soc Artif Intern Organs 1975; 21:16–25.

(*31*) Johnson AD, Eddy GA, Gangemi JD, Ramsburg HH, Metzger JF. Production of Venezuelan equine encephalitis virus on cells grown on artificial capillaries. Appl Environ Microbiol 1978; 35:431–434.

(*32*) Ceriani RL, Peterson JA, Abraham S. Immunologic methods for the identification of cell types. II. Expression of normal mouse mammary epithelial cell antigens in mammary neoplasia. JNCI 1978; 61:747–751.

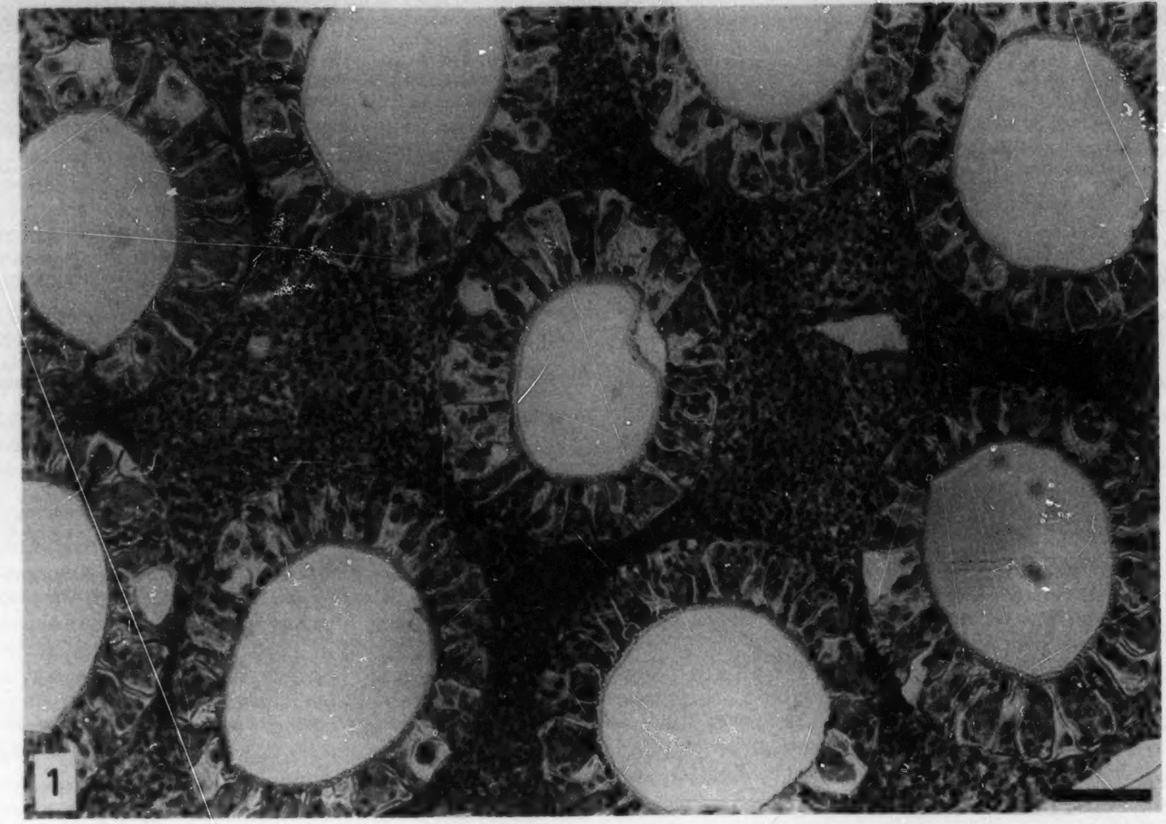

FIGURE 1.—Mouse mammary tumor cells (line 67) grown for 11 wk on a bundle of artificial capillaries have achieved tissue-like density. Artificial capillaries are cut in cross section and appear as thick-walled tubular structures. The semipermeable membrane on the luminal surface of the hollow fibers can be observed in the central lumen where the microtome knife has separated the membrane from the fiber wall matrix. The cells grow in the pores of the matrix of the hollow fibers and on their surface, filling the intercapillary spaces. *Bar*=100 µm. × 630

Glycosylated Podophyllotoxin Congeners: Loss of Microtubule Inhibition and Permission of Invasion In Vitro[1,2]

Marc M. Mareel,[3] Christian H. Dragonetti,[3] Georges K. De Bruyne,[3] *and* Rita M.-L. Van Cauwenberge[3,4]

ABSTRACT—Podophyllotoxin (PPT) and its glycosylated congeners, 4′-demethylepipodophyllotoxin 9-[4,6-*O*-(R)-ethylidene-*β*-D-glucopyranoside] (VP-16-213) and 4′-demethylepipodophyllotoxin 9-[4,6-*O*-(R)-thenylidene-*β*-D-glucopyranoside] (VM-26), were studied for their effects on the following activities of MO$_4$ mouse fibrosarcoma cells in vitro: growth as an aggregate in culture on a gyrotory shaker, directional migration from an aggregate explanted on glass, organization of the cytoplasmic microtubule complex as inferred from immunostaining with an antiserum against tubulin, and invasion into fragments of 9-day-old embryonic chick cardiac muscle. At concentrations that inhibited growth (≥0.03 μg/ml), PPT arrested directional migration, abolished the cytoplasmic microtubule complex, and interfered with invasion. VM-26 (0.1–1.0 μg/ml) and VP-16-213 (1–30 μg/ml) interfered with growth but permitted directional migration, organization of the cytoplasmic microtubule complex, and invasion. These observations imply that microtubule inhibitors are anti-invasive because they interfere with the assembly of the cytoplasmic microtubule complex and not because they inhibit growth.—JNCI 1982; 69:1367–1374.

Previously, we reported that microtubule inhibitors prevent the invasion of MO$_4$ mouse fibrosarcoma cells in organ culture. In contrast, antiproliferative agents that do not affect microtubules permit invasion. The anti-invasive activity of microtubule inhibitors was ascribed to abolishment of the cytoplasmic microtubule complex. This complex is necessary for directional migration presumed to be a vital, but not the only, activity of invading cells (*1–3*).

PPT was shown to prevent microtubule assembly (*4*) and, therefore, could be expected to interfere with invasion. The semisynthetic derivatives of PPT, VP-16-213 and VM-26, no longer affected microtubules but retained the antiproliferative activity of the native PPT (*5, 6*). Obviously, a comparative study of the effect of PPT and its glycosylated congeners on invasion might provide direct evidence of a correlation between anti-invasive activity and microtubule inhibition.

We describe here the effect of PPT, VP-16-213, and VM-26 on the following in vitro activities of MO$_4$ cells: growth as an aggregate in culture on a gyrotory shaker, directional migration from an aggregate explanted on glass, assembly of the cytoplasmic microtubule complex, and invasion into fragments of cardiac muscle in organ culture.

MATERIALS AND METHODS

MO$_4$ cells.—MO$_4$ cells are virally transformed C3H mouse cells (*7*). MO$_4$ cell monolayers have been maintained in our laboratory since 1975, with several periods of storage in liquid nitrogen. They were regularly tested for their malignant status and produced invasive and metastasizing sarcomas in syngeneic animals (*8, 9*). In all experiments with MO$_4$ cells the culture medium consisted of Eagle's minimum essential medium (N.V. GIBCO Europe S.A., Gent, Belgium) plus 10% fetal bovine serum (N.V. GIBCO Europe S.A.) and 0.05% L-glutamine. Aggregates of MO$_4$ cells were prepared from cell suspensions incubated on a gyrotory shaker (New Brunswick Scientific Co., New Brunswick, N.J.) as described previously (*10*). Aggregates with a diameter of 0.2 or 0.4 mm were selected under a stereomicroscope (× 25) and washed in an excess of culture medium before use in the present assays.

Drugs.—PPT (Aldrich-Europe Division, Janssen Pharmaceutica, Beerse, Belgium) was dissolved at 5 mg/ml in 0.2% *N,N*-dimethylformamide, and control cultures were incubated with the solvent only. Dissolved VM-26 and VP-16-213 were from commercial stock. The solvent of VM-26 and VP-16-213 was not investigated. Other authors (*11*) have seen no effect on cells incubated with the solvent alone. Therefore, the culture medium was used as a control in experiments with VP-16-213 or VM-26. Stock solutions were further diluted in culture medium before use to obtain concentrations between 10 and 0.001 μg/ml (PPT and VM-26) and between 100 and 0.01 μg/ml (VP-16-213).

Assay for growth.—Growth of MO$_4$ cell populations was evaluated from daily measurements of the diameters of aggregates incubated individually on a gyrotory shaker. In spheroidal aggregates in vitro and in solid tumors in vivo, growth results from cell proliferation and cell loss; the volume of individual cells and the intercellular space are additional factors, as discussed previously (*12*). In this assay, aggregates with a diameter of 0.2 mm were used. Drugs were added at the beginning of the culture. To determine whether growth arrest resulted mainly from inhibition of proliferation or from the balance between proliferation and

---

ABBREVIATIONS USED: H & E=hematoxylin and eosin; PPT=podophyllotoxin; VM-26=4′-demethylepipodophyllotoxin 9-[4,6-*O*-(R)-thenylidene-*β*-D-glucopyranoside]; VP-16-213=4′-demethylepipodophyllotoxin 9-[4,6-*O*-(R)-ethylidene-*β*-D-glucopyranoside].

---

[1] Received March 26, 1982; accepted July 16, 1982.

[2] Supported by grants from the Nationaal Fonds voor Wetenschappelijk Onderzoek, Belgium (20093), and from the Kankerfonds van de Algemene Spaar- en Lijfrentekas, Brussels, Belgium.

[3] Laboratory of Experimental Cancerology, Department of Radiotherapy and Nuclear Medicine, University Hospital, De Pintelaan 185, B-9000 Ghent, Belgium.

[4] We thank Miss L. Baeke, Miss B. Buysse, Miss O. Claeys, and Miss M. Nijs for technical assistance, Mr. J. Roels van Kerckvoorde for preparing the illustrations, and Mrs. G. Matthys-De Smet for typing the manuscript. We also thank Bristol Benelux N.V., Brussels, Belgium, for kindly providing the VP-16-213 and VM-26; and Dr. M. De Brabander and Dr. J. De Mey, Janssen Pharmaceutica, Beerse, Belgium, for their generous gift of antiserum against tubulin.

cell loss, the presence of mitotic figures was examined on histologic sections from selected aggregates fixed in Zenker's solution. Reversibility of growth inhibition was studied after removal of drugs and daily refreshment of the culture medium, as reported previously (*3*).

Assay for directional migration.—MO_4 cell aggregates with 0.2-mm diameter were explanted on a cover slip in a Leighton tube (VEL, N.V., Leuven, Belgium) as described earlier (*12*). The circular area covered by MO_4 cells that had migrated radially from the aggregate was calculated from daily measurements of the mean diameter (microscope, × 40) and used as an index of directional migration (for discussion, *see 13, 14*). Drugs were added to the culture medium 2 days after explanation of the aggregate. At the end of the assay (7 days after addition of drug), cultures were fixed either in a solution of alcohol:Formalin:acetic acid (75:20:5) for staining with H & E or in glutaraldehyde (1% in cacodylate buffer, 0.1 *M*, pH=7.4) for staining with an antiserum against tubulin (dilution, 1/200 in Tris-buffered saline), according to the method described by De Mey et al. (*15*).

Assay for invasiveness in vitro.—MO_4 cell aggregates with 0.2-mm diameter were confronted with precultured fragments of 9-day-old embryonic chick cardiac muscle (diameter, 0.4 mm) in individual cultures on a gyrotory shaker (*10*). The relevance and the specificity of this method were recently reviewed (*16*). At growth inhibitory concentrations of the drugs, MO_4 cell aggregates with 0.4-mm diameter were also used to compensate for the lower number of cells. Drugs were added at the onset of the culture on the gyrotory shaker. Confronting pairs were fixed in Bouin Hollande's solution (*17*) for embedding in paraffin and complete sectioning into 8-µm-thick sections, or in glutaraldehyde for embedding in Araldite and sectioning into 2-µm-thick sections. Selected areas on these sections were processed for transmission electron microscopy. Details of the histologic and ultrastructure techniques were provided in a previous paper (*3*). Consecutive 8-µm-thick sections were stained with H & E and with an antiserum against embryonic chick heart (*17*). In all experiments triplicate cultures were used, and each experiment with active concentrations of drugs was repeated at least once. Control cultures without drug were included in each series of assays.

RESULTS

Growth

The effects of PPT, VP-16-213, and VM-26 at selected concentrations on the growth of MO_4 cell aggregates in culture on the gyrotory shaker are shown in text-figure 1. Mitoses were absent in the aggregates, the growth of which was completely inhibited. This indicates that inhibition of proliferation was responsible for growth arrest. However, individual cells were larger than in control cultures, suggesting that cellular hypertrophy might compensate to some extent for cell loss. Disintegration of aggregates was observed only with VM-26 at concentrations of 10 µg/ml.

Reversibility of growth inhibition was observed in most aggregates treated with 0.1 µg PPT/ml for 2 or 4 days. Reversibility was also observed in some aggregates treated with 1 µg VM-26/ml or with 10 µg VP-16-213/ml for 2 or 4 days, so that these drugs could not be considered as fully irreversible inhibitors of the growth of MO_4 cell aggregates.

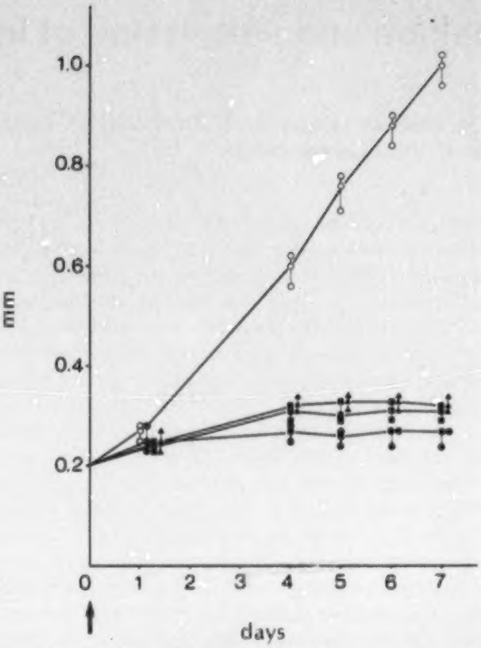

TEXT-FIGURE 1.—Growth of MO_4 cell aggregates: untreated (○), with 0.1 µg PPT/ml (●), with 1 µg VM-26/ml (■), and with 10 µg VP-16-213/ml (▲). *Ordinate*: mean diameter of aggregates (median and extreme values from 5 cultures). *Abscissa*: time of incubation. *Arrow* indicates addition of drug.

Directional Migration

The effects on directional migration of PPT, VP-16-213, and VM-26 at concentrations that fully inhibited growth (text-fig. 1) are shown in text-figure 2. Obviously, VP-16-213 and VM-26, in contrast to PPT, hardly affected directional migration during the first 4 days after addition of the drugs. Dose-response curves are shown in text-figure 3. Inhibition of directional migration and inhibition of growth occurred at approximately the same concentration of PPT. VM-26 or VP-16-213 concentrations that inhibited growth were two orders of magnitude lower than concentrations that produced an effect in the assay of directional migration.

Cultures treated with PPT (fig. 1B) at concentrations of 0.03 µg/ml or higher, and fixed 7 days after addition of the drug, showed the following histologic alterations: appearance of abnormal metaphases, as described by Levan (*18*), and of multimicronucleated cells, as defined by De Brabander et al. (*19*); absence of postmetaphase figures; alteration of cell shape from bipolar to polygonal or round; and loss of radial orientation of cells in the corona. Cultures treated with VM-26 (fig. 1C) at concentrations between 0.1 and 1 µg/ml or with VP-16-213 (fig. 1D) at concentrations between 1 and 10 µg/ml showed hypertrophic cells with large nuclei (diameter, 25–50 µm as compared to 10–20 µm in controls). Most cells were mononucleated, but some were polynucleated (2–6 nuclei of approximately normal size); mitotic figures were absent. Large variations in the shape of cells (bipolar, stellate, and polygonal) occurred, but radial orientation of cells in the corona was still obvious. Treatment with higher doses (10 μg VM-26/ml, 100 μg VP-16-213/ml) had little effect on the size of the cells (nuclei diameters, 10–25 μm). Some of them were vacuolated; the appearance of round cells and an obvious decrease in the total amount of cells suggested extensive cell loss at these higher doses.

Organization of the cytoplasmic microtubule complex was evaluated as follows in cultures fixed, permeabilized, and stained with antiserum against tubulin: normal—when long tracks of microtubules irradiated from the perinuclear area and were oriented toward the cell periphery; disturbed—when short tracks were scattered over the cytoplasm without distinct orientation; absent—when the cytoplasm was diffusely stained. A normal cytoplasmic microtubule complex was found in most (≥80%) interphase cells of controls and of cultures treated with VP-16-123 or VM-26. In large cells produced by VM-26 (1 μg/ml) or by VP-16-213 (10 μg/ml), the cytoplasmic microtubule complex was normally organized but hypertrophic (fig. 1C, 1D). After treatment with 0.1 μg PPT/ml, the cytoplasmic microtubule complex was absent in most cells (≈80%) and disturbed in the others. At 1 μg/ml, all cells were diffusely stained (fig. 1B).

Invasion Into Chick Cardiac Muscle

In all control cultures, MO$_4$ cells invaded the cardiac muscle, as described previously (*10*). When such cultures (original diameters of MO$_4$ cell aggregate and heart fragment were 0.2 and 0.4 mm, respectively) were fixed after 4 days, small remnants of cardiac muscle were found mostly in the center of the majority of MO$_4$ cells (fig. 2). At concentrations of 0.03 μg PPT/ml or higher, invasion was inhibited in all cultures when aggregates of both 0.2 or 0.4 mm were used (fig. 3) in a way similar to that described for the vinca alkaloids (*3*). In contrast, treatment with VM-26 (0.1–1.0 μg/ml) or VP-16-213 (1–30 μg/ml) permitted invasion of MO$_4$ cells into the cardiac muscle in all cultures (figs. 4, 5). Quantitation of invasion was not possible. Nevertheless, differences between cultures treated with PPT and with VP-16-213 or VM-26 were distinct with regard to both the occupation of the cardiac muscle by MO$_4$ cells and the amount of immunoreactive tissue that remained at the end of the assay (cf. fig. 3 with figs. 4, 5). With VP-16-213 and VM-26 the amount of cardiac tissue that remained after 4 days was larger when aggregates of 0.2 mm instead of 0.4 mm were used, but occupation of the cardiac muscle by MO$_4$ cells occurred with both types of aggregates.

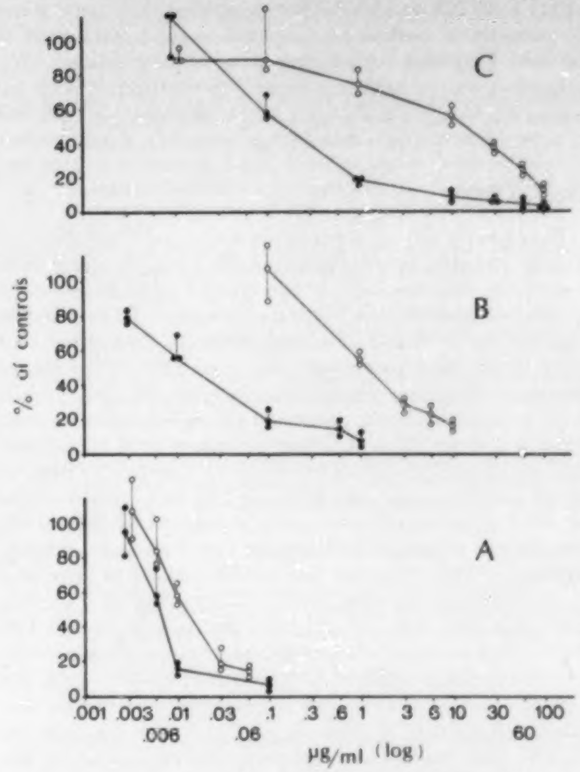

TEXT-FIGURE 3.—Inhibition of growth (●) and inhibition of directional migration (○) by PPT (A), VM-26 (B), and VP-16-213 (C). *Ordinate*: volume of aggregates (●) and surface of circular area covered by cells (○) as percent of controls 4 days after addition of drug. *Abscissa*: concentration of drug.

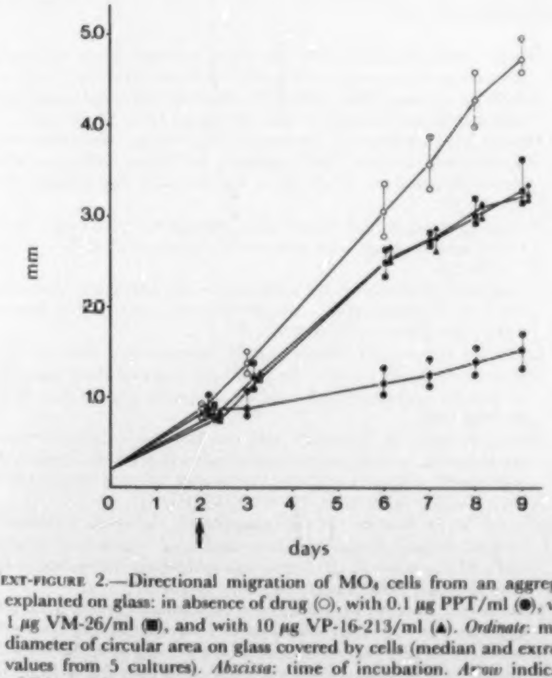

TEXT-FIGURE 2.—Directional migration of MO$_4$ cells from an aggregate explanted on glass: in absence of drug (○), with 0.1 μg PPT/ml (●), with 1 μg VM-26/ml (■), and with 10 μg VP-16-213/ml (▲). *Ordinate*: mean diameter of circular area on glass covered by cells (median and extreme values from 5 cultures). *Abscissa*: time of incubation. *Arrow* indicates addition of drug.

Transmission electron micrographs of selected areas showed that PPT produced ultrastructure alterations typical of microtubule inhibitors, as described previously in (*20*, *3*): scarceness or absence of microtubules, accumulation of 10-nm filaments, scattering of Golgi complexes, and appearance of annulate lamellae. The ultrastructure of MO$_4$ cells treated with VP-16-213 or with VM-26 suggested that most, if not all, subcellular systems participated in the hypertrophy of the cells. Degenerative alterations, as reported earlier (*21*), were observed in cardiac muscle cells confronted with invading MO$_4$ cells (fig. 6). Such alterations were not observed in areas of the cardiac muscle that were free of MO$_4$ cells.

DISCUSSION

The present experiments provided a new argument in favor of the opinion that microtubule inhibitors were anti-invasive in vitro because they interfered with the assembly of the cytoplasmic microtubule complex (*1, 3*). Recent experiments by Atassi and co-workers (*22*) suggested that microtubule inhibitors might also exert their anti-invasive activity in vivo. The present observations with PPT, known to prevent microtubule assembly (*4*), confirmed the anti-invasive activity of microtubule inhibitors. Structural modification of PPT resulting in loss of its capacity to bind to tubulin (*6*) was accompanied by loss of anti-invasive activity. PPT at antiproliferative concentrations abolished the cytoplasmic microtubule complex (fig. 1B) and inhibited invasion of MO$_4$ cells into the cardiac muscle in vitro (fig. 3), in contrast to the effects with VM-26 (figs. 1C, 4A, 4B) and VP-16-213 (figs. 1D, 5A, 5B). In the VM-26 and VP-16-213 cultures, even when larger aggregates (0.4 mm) were used to correct the number of potentially invasive cells, the disposition of MO$_4$ cells and remnant cardiac muscle was different from that in controls (cf. fig. 2 with figs. 4A, 4B, 5A, 5B). One factor contributing to this difference was the absence of proliferation of cells that had already occupied the cardiac muscle.

Alteration of the capacity to bind to tubulin was, however, not the only consequence of the modification of the PPT molecule. VP-16-213 and VM-26 prevented entry of cells in mitosis (M-phase) by arresting them in the G$_2$ phase (*23–25*). PPT permitted transition of cells from G$_2$ phase to M-phase. Since PPT was considered to arrest cells in metaphase by interference with the mitotic spindle (*26*), one might argue that differences in the anti-invasive activity of PPT and its glycosylated congeners were due to the arrest of cells in different phases of the mitotic cycle. In our opinion this was unlikely for the following reasons: 1) The effect of PPT or other microtubule inhibitors (*27*) on cycling MO$_4$ cells could not be considered as metaphase arrest. PPT produced multimicronucleated cells that respread after M-phase and developed undulating membrane activity all around their periphery. Such cells were unable to invade. 2) We have been able to demonstrate the anti-invasive effect of microtubule inhibitors on MO$_4$ cells arrested before M-phase with 5-fluorouracil (*1*). Obviously, our present results could not rule out that both abolishment of the cytoplasmic microtubule complex and arrest of growth in any phase of the cycle were necessary to inhibit invasion.

The differential effects on directional migration of PPT and its glycosylated congeners at antiproliferative concentrations confirmed that directional migration was a more important activity of invading cell populations in vitro than was growth. We wish to emphasize that this statement does not imply that directional migration was the only vital activity of invading cells or that growth was without influence on invasion. Our data further confirmed that the simple and rapid assay for directional migration may predict the anti-invasiveness of PPT—in contrast to VP-16-213 and VM-26 which permit invasion—illustrating the value of this assay for screening potentially anti-invasive drugs (*28*).

Comparison of the effect of PPT and of its glycosylated congeners also stressed the role of the cytoplasmic microtubule complex in directional migration as reported earlier (*19, 29, 30*). Cells arrested in G$_2$ phase by VP-16-213 or VM-26 displayed a well-elaborated cytoplasmic microtubule complex and were able to perform directional migration. The hypertrophy of the cytoplasmic microtubule complex was most probably one aspect of the continuation of macromolecular synthesis in G$_2$-arrested cells (*23*). It is known that cells stop locomoting during the mitotic cycle. The activities of G$_2$-arrested cells observed in our study indicated that MO$_4$ cells stopped migration only when they reached the M-phase.

Extrapolation of our in vitro findings to the mechanism of action of VP-16-213 or VM-26 in vivo necessitates that consideration be given to the following possibilities: 1) Aglycone metabolites of VP-16-213 or VM-26, which are tenfold more active than the parent drugs, might be produced in vivo (*31*), and 2) inasmuch as the glycoside moiety of the drugs sterically interfered with binding to tubulin (*6*), the aglycone metabolites of VP-16-213 or VM-26 might act as microtubule inhibitors in vivo.

Our data on the reversibility of growth inhibition do not support the opinion that G$_2$ arrest by VP-16-213 or VM-26 is totally irreversible (*5, 11, 24*). Continuation of invasion by these G$_2$-arrested cells, therefore, cannot be considered to be completely harmless.

REFERENCES

(*1*) Mareel MM, De Brabander MJ. Effect of microtubule inhibitors on malignant invasion in vitro. JNCI 1978; 61:787–792.

(*2*) Storme G, Mareel MM. Effect of anticancer agents on invasion of mouse fibrosarcoma cells in vitro. Oncology 1981; 38:182–186.

(*3*) Mareel MM, Storme GA, De Bruyne GK, Van Cauwenberge RM. Vinblastine, vincristine and vindesine: Antiinvasive effect on MO$_4$ mouse fibrosarcoma cells in vitro. Eur J Cancer Clin Oncol 1982; 18:199–210.

(*4*) Wilson L, Bamburg JR, Mizel SB, Grisham LM, Creswell KM. Interaction of drugs with microtubule proteins. Fed Proc 1974; 33:158–166.

(*5*) Stähelin H. 4′-Demethyl-epipodophyllotoxin thenylidene glucoside (VM-26), a podophyllum compound with a new mechanism of action. Eur J Cancer 1970; 6:303–311.

(*6*) Loike JD, Brewer CF, Sternlicht H, Gensler WJ, Horwitz SB. Structure–activity study of the inhibition of microtubule assembly in vitro by podophyllotoxin and its congeners. Cancer Res 1978; 38:2688–2693.

(*7*) Billiau A, Sobis H, Eyssen H, Van den Berghe H. Non-infectious intracisternal A-type particles in a sarcoma-positive, leukemia-negative mouse cell line transformed by murine sarcoma virus (MSV). Arch Gesamte Virusforsch 1973; 43:345–351.

(*8*) Mareel M, De Ridder L, De Brabander M, Vakaet L. Characterization of spontaneous, chemical, and viral transformants of a C3H/3T3-type mouse cell line by transplantation into young chick blastoderms. J Natl Cancer Inst 1975; 54:923–929.

(*9*) Meyvisch C, Mareel M. Influence of implantation site of MO$_4$ cell aggregates on formation of metastases. Invas Metast 1982. In press.

(*10*) Mareel M, Kint J, Meyvisch C. Methods of study of the invasion of malignant C3H-mouse fibroblasts into embryonic chick heart in vitro. Virchows Arch [Cell Pathol] 1979; 30:95–111.

(*11*) Huang CC, Hou Y, Wang JJ. Effects of a new antitumor agent, epipodophyllotoxin, on growth and chromosomes in human hematopoietic cell lines. Cancer Res 1973; 33:3123–3129.

(*12*) Storme G, Mareel MM. Effect of anticancer agents on directional migration of malignant C3H mouse fibroblastic cells in vitro. Cancer Res 1980; 40:943–948.

(*13*) Storme G, Mareel M, De Bruyne G. Influence of cell number on directional migration of MO$_4$ cells in vitro. Arch Geschwulstforsch 1981; 51:45–50.

(*14*) Mareel M, Kieler J, Van Cauwenberge R. Loss of directional migration after round-cell transformation of malignant ST/A mouse lung cells. Cell Biol Int Rep 1981; 5:921–928.

(*15*) De Mey J, Hoebeke J, De Brabander M, Geuens G, Joniau M. Immunoperoxidase visualisation of microtubules and microtubular proteins. Nature 1976; 264:273–275.

(*16*) Mareel MM. The use of embryo organ cultures to study invasion in vitro. In: Liotta L, Hart I, eds. Tumor invasion and metastasis. The Hague: Nijhoff, 1982:207–230.

(*17*) Mareel MM, De Bruyne GK, Vandesande F, Dragonetti C. Immunohistochemical study of embryonic chick heart invaded by malignant cells in three-dimensional culture. Invas Metast 1981; 1:195–204.

(*18*) Levan A. Colchicine-induced C-mitosis in two mouse ascites tumours. Hereditas 1954; 40:1–64.

(*19*) De Brabander MJ, Van de Veire RM, Aerts FE, Borgers M, Janssen PA. The effects of methyl [5-(2-thienylcarbonyl)-1*H*-benzimidazol-2-yl]carbamate, (R 17934; NSC 238159), a new synthetic antitumoral drug interfering with microtubules, on mammalian cells cultured in vitro. Cancer Res 1976; 36:905–916.

(*20*) De Brabander M, Borgers M. The formation of annulated lamellae induced by the disintegration of microtubules. J Cell Sci 1975; 19:331–340.

(*21*) Mareel MM, Kieler JV, Bruyneel E, Van Cauwenberge R, Dragonetti C. Invasiveness of malignant ST/A mouse lung cells in vitro. Virchows Arch [Cell Pathol] 1981; 38:101–116.

(*22*) Atassi G, Dumont P, Vandendris M. Effect of desacetyl vinblastine amide sulphate or vindesine (VDS) against the in-vivo invasion and formation of tumor metastasis. In: Davis W, Tanneberger S, eds. The control of tumor growth and its biological basis. Berlin: Akademic-Verlag. In press.

(*23*) Grieder A, Maurer R, Stähelin H. Effect of an epipodophyllotoxin derivate (VP-16-213) on macromolecular synthesis and mitosis in mastocytoma cells in vitro. Cancer Res 1974; 34:1788–1793.

(*24*) Krishan A, Paika K, Frei E. Cytofluorometric studies on the action of podophyllotoxin and epipodophyllotoxins (VM-26, VP-16-213) on the cell cycle traverse of human lymphoblasts. J Cell Biol 1975; 66:521–530.

(*25*) Rao AP, Rao PN. The cause of G_2-arrest in Chinese hamster ovary cells treated with anticancer drugs. J Natl Cancer Inst 1976; 57:1139–1143.

(*26*) Kelly MG, Hartwell JL. The biological effects and the chemical composition of podophyllin: A review. J Natl Cancer Inst 1954; 14:967–1010.

(*27*) De Brabander M, Geuens G, De Mey J, Joniau M. Light microscopic and ultrastructural distribution of immunoreactive tubulin in mitotic mammalian cells. Biol Cellul 1979; 34:213–226.

(*28*) Mareel MM, Storme G, Dragonetti C, De Bruyne G, Van Cauwenberge R. Anti-invasiveness and inhibition of directional migration by vinca alkaloids and their congeners. In: Proceedings of the symposium on vinca alkaloids, London, England, Oct. 25, 1981. In press.

(*29*) Vasiliev JM, Gelfand IM, Domnina LV, Ivanova OY, Komm SG, Olshevskaja LV. Effect of colcemid on the locomotory behaviour of fibroblasts. J Embryol Exp Morphol 1970; 24:625–640.

(*30*) Spiro TP, Mundy GR. In vitro migration of Walker 256 carcinosarcoma cells: Dependence on microtubule and microfilament function. JNCI 1980; 65:463–467.

(*31*) Evans WE, Sinkule JA, Crom WR, Dow L, Look T, Rivera G. Pharmacokinetics of VM-26 and VP-16 in children with cancer. In: Proceedings of the first international symposium on the podophyllotoxins in cancer therapy, Southampton, England, July 8–9, 1981. In press.

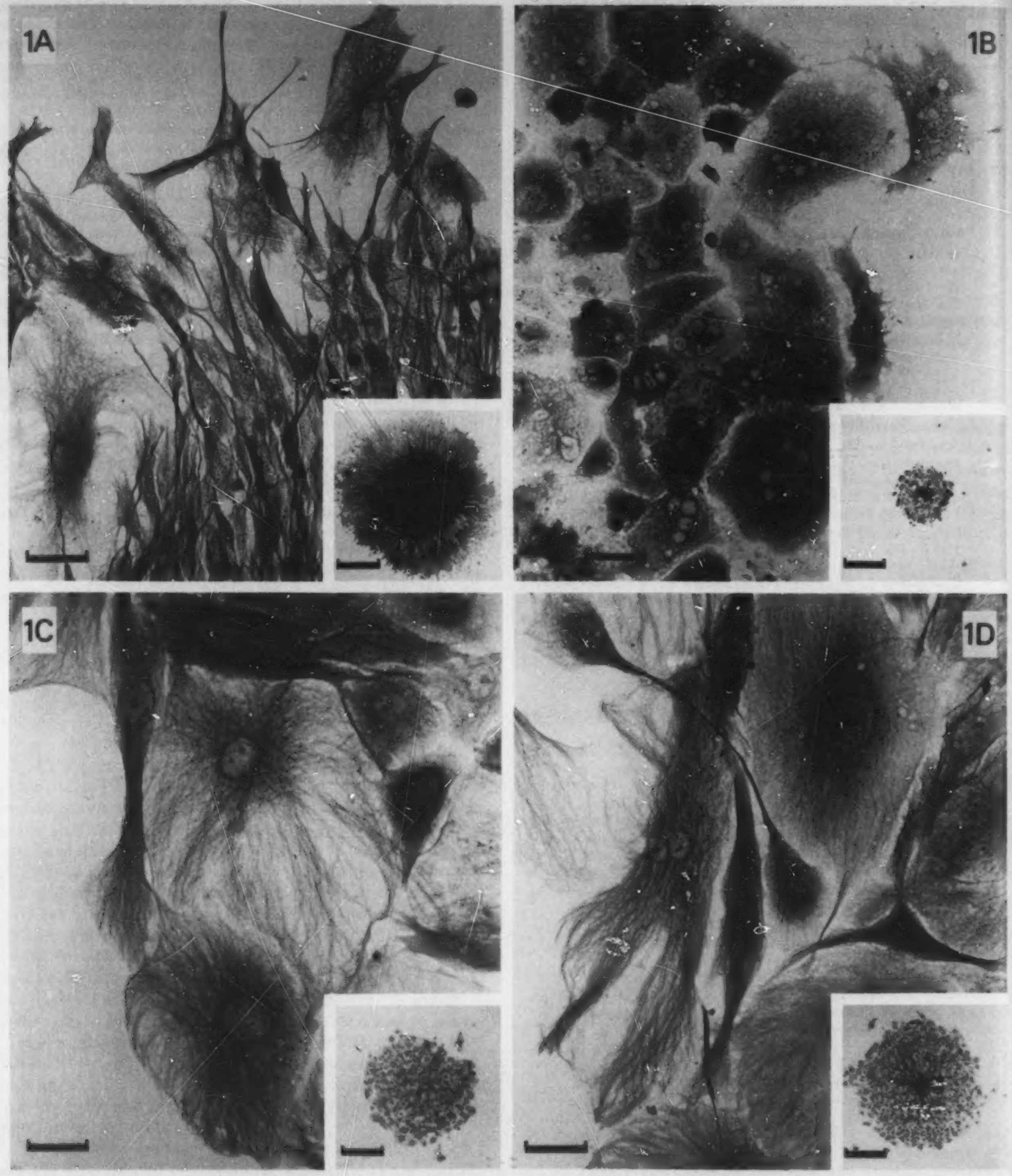

FIGURE 1.—Light micrographs of aggregates of MO_4 cells explanted on glass without drug (A), with 1 μg PPT/ml (B), with 1 μg VM-26/ml (C), and with 10 μg VP-16-213/ml (D). Fixation 7 days after addition of drug and staining with an antiserum against tubulin. *Bar*=50 μm. *Insets* show whole cultures from which details were made. *Bar*=1 mm.

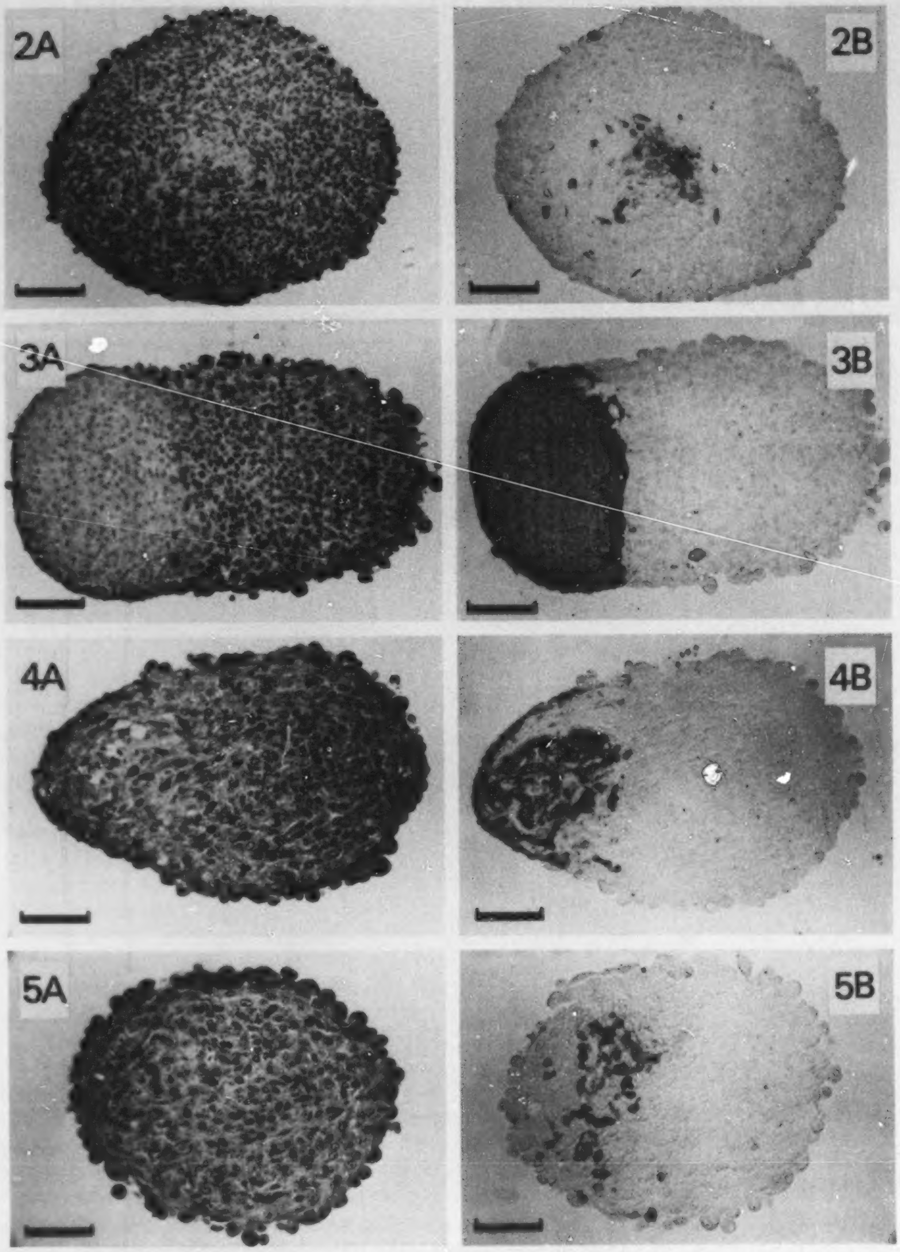

FIGURES 2–5.—Light micrographs of 8-μm-thick sections from aggregates of MO_4 cells, with original diameter of 0.2 mm (fig. 2) and of 0.4 mm (figs. 3–5), confronted with fragments of cardiac muscle without drug (fig. 2), with 0.3 μg PPT/ml (fig. 3), with 1 μg VM-26/ml (fig. 4), and with 10 μg VP-16-213/ml (fig. 5). Fixation after 4 days. All A and B figures are consecutive sections from the same culture stained with H & E (A) or with an antiserum against chick heart (B). Remaining heart, with smaller nuclei (A), stains dark (B). *Bar*=100 μm.

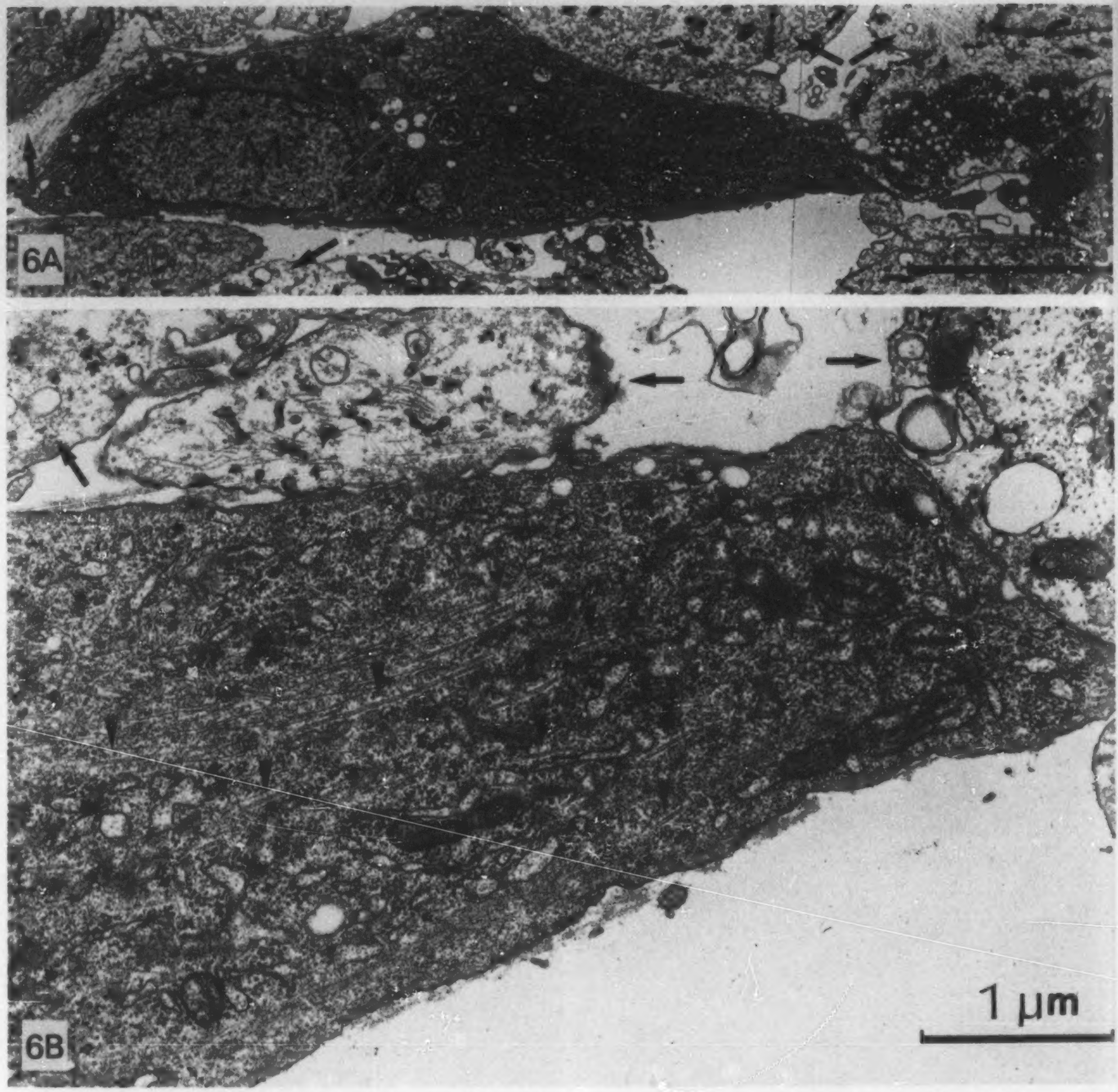

FIGURE 6.—A) Transmission electron micrographs of a MO_4 cell (M) inside the cardiac muscle, from a confrontation of a MO_4 cell aggregate with a fragment of cardiac muscle in the presence of 1 µg VM-26/ml. Fixation after 4 days. *Arrows* indicate cardiac muscle cells. B) Enlarged detail from A. *Arrowheads* show cytoplasmic microtubules.

Detection of Aflatoxins and Related Metabolites by Radioimmunoassay[1,2,3]

Philippe Sizaret,[4] Christian Malaveille,[4] Ruggero Montesano,[4] *and* Charles Frayssinet[5,6]

ABSTRACT—Rabbit (outbred albino New Zealand White) antisera have been raised against aflatoxin B_1 (AFB_1) using as immunogen conjugates in which the hapten was coupled to bovine serum albumin (BSA) either through C1 or C8 with the oxime and the dichloride derivatives of AFB_1 as intermediates. Radioimmunoassay (RIA), with [^{3}H]AFB_1 as tracer, showed that the antiserum prepared with the conjugate in which BSA was coupled to the AFB_1 oxime derivative was highly specific to AFB_1, whereas the antiserum raised against the conjugate in which BSA was coupled to AFB_1 through the AFB_1Cl_2 derivative (C-antiserum) cross-reacted to a large extent with other aflatoxins, including aflatoxin M_1, an important urinary metabolite of AFB_1 in several species including humans. AFB_1-related metabolites in the urine of inbred BD IV adult male rats given AFB_1 orally at doses from 600 pmol to 385 nmol can easily be followed over 9 days by RIA in which the "cross-reactive" C-antiserum is used. This suggests that similar methodologies could be used for the monitoring of human exposure to AFB_1.—JNCI 1982; 69:1375–1381.

Epidemiologic studies indicated associations between various risk factors and specific types of cancer (*1*). The causality of many of these associations, however, is not direct, since they are based on linkages between cancer cases and exposures to risk factors that were either estimated from questionnaires or derived from environmental data. This limitation may be overcome by the development of methodologies that would permit the monitoring of exposure to a suspected or known carcinogenic agent at an individual level. The recent development of immunologic techniques (*2-5*) that use antibodies with a high degree of sensitivity and specificity against certain carcinogens, or against DNA adducts resulting from exposure to various carcinogens including AFB_1 (*6*), opens the possibility to determine individual exposure in a relatively large human population.

It has been shown that chronic infection by hepatitis B virus (*7, 8*), as well as high levels of AFB_1 in food (*9, 10*), is associated with high incidences of primary liver cancer among Africans and Asians. The hepatocarcinogenicity of AFB_1 in various experimental animals (*11*) indicates that exposures to AFB_1 and hepatocellular carcinoma in humans are causally related. The test of this hypothesis requires a technique that can monitor exposure at an individual level.

This paper describes the characterization of antibodies against AFB_1 and the development of an RIA technique aiming at the detection of AFB_1 and/or AFB_1 metabolites in body fluids of individuals potentially exposed to this carcinogen.

MATERIALS AND METHODS

Chemicals.—The following products were used: Cl_2 gas from Compagnie Française des Produits Oxygénés (Vénissieux, Rhône, France); carboxy methoxylamine hemichloride, 94% pure, from EGA-Chemie, Steinheim, Federal Republic of Germany; 1-ethyl-3,3-dimethylamino-propylcarbodiimide and fatty acid-free BSA from Sigma Chemical Co., St. Louis, Mo.; [^{3}H]AFB_1 (30 Ci/mmol) from Moravek, Brea, Calif.; AFM_1, AFP_1, AFB_1-N^7-guanine, and AFB_1-FAPY. The other mycotoxins were purchased from Makor Chemicals, Jerusalem, Israel. All other chemicals were of the purest available grades. Traces of water that may have been present in the methylene chloride and DMSO used for the preparation of AFB_1Cl_2 were removed with molecular sieve beads (3 Å, 2 mm; E. Merck A. G., Darmstadt, Federal Republic of Germany).

Preparation of conjugates.—For the measurement of optical densities (Beckman spectrophotometer), AFB_1 was dissolved in methanol, and BSA and AFB_1 conjugates were dissolved in saline. The protein content of conjugates was determined

---

ABBREVIATIONS USED: AF=aflatoxin(s); AFB_1Cl_2=AFB_1-8,9-dichloride; AFB_1-FAPY=8,9-dihydro-8-(N^7-formyl-2′,5′,6′-triamino-4′-oxo-N^5-pyrimidyl)-9-hydroxy-AFB_1; AFB_1-N^7-guanine=8,9-dihydro-8-(N^7-guanyl)-9-hydroxy-AFB_1; BSA=bovine serum albumin; C-antiserum=antiserum prepared with the C-conjugate as immunogen; C-conjugate=conjugate in which BSA was coupled to AFB_1 through the AFB_1Cl_2 derivative; DMSO=dimethyl sulfoxide; O-antiserum=antiserum prepared with the O-conjugate as immunogen; O-conjugate=conjugate in which BSA was coupled to the AFB_1 oxime derivative; R_f=retardation factor; RIA=radioimmunoassay.

---

[1] Received March 29, 1982; accepted July 16, 1982.

[2] This work was partly supported by the International Programme on Chemical Safety, World Health Organization, Geneva, Switzerland.

[3] Part of this article was presented at the meeting of a working group on the "Development and possible use of immunological techniques to detect individual exposure to carcinogens," Nov. 30–Dec. 1, 1981, Essen, Federal Republic of Germany; and at an international workshop on "Immune assays of nuclear antigens relevant to carcinogens and to chemotherapy," April 26–27, 1982, Manchester, England.

[4] International Agency for Research on Cancer (IARC), 150 cours Albert Thomas, 69372 Lyon cedex 08, France.

[5] Institut de Recherches Scientifiques sur le Cancer, B.P. No. 8, F-94800 Villejuif, France.

[6] We thank Ms. A. M. Aguelon and Mr. G. Toussaint for the preparation of the AFB_1 oxime conjugate; Dr. G. E. Neal of Medical Research Council Laboratories, Carshalton, Surrey, England, and Dr. P. Schuller, Rijksinstituut voorde Volksgezondheid, Bilthoven, The Netherlands, for supplying the AFP_1 and AFM_1; Dr. G. Wogan and Dr. P. R. Donahue of the Department of Nutrition and Food Science, Massachusetts Institute of Technology, Cambridge, Mass., for their gift of AFB_1-N^7 guanine and AFB_1-FAPY; Dr. M. Friesen of IARC for the mass spectrometry analysis; Dr. J. Cabral, Ms. D. Galendo, Ms. M. Collard, Mr. R. Dray, and Mr. J. Garcia for assistance with animal experiments; Mr. J. Déchaux and Mr. G. Mollon for drawing and photographing the charts; Ms. C. Fuchez and Ms. J. Mitchell for secretarial assistance; and Ms. E. Heseltine for editorial help.

according to the method of Lowry et al. (*12*). Radioactivities were counted by liquid scintillation spectrometry with the use of Picofluor 30 as scintillation liquid. Counting efficiency was 40%.

Two types of AFB_1 conjugates were prepared. The first one was an AFB_1 oxime, prepared according to Langone and Van Vunakis (*13*) and coupled to BSA (text-fig. 1) according to Chu and Ueno (*14*). The number of AFB_1 molecules that bound to BSA was determined by spectrophotometry at 362 nm, according to Chu et al. (*15*). We prepared the other conjugate (text-fig. 1) by first synthesizing AFB_1Cl_2 according to a protocol derived from that of Swenson et al. (*16*). We dissolved 6.5 mg AFB_1 and 1.9 ng $[^3H]AFB_1$ in 3 ml methylene chloride; chlorine gas was bubbled through the solution until a yellow color appeared. For determinations of R_f, AFB_1Cl_2 was dissolved in methylene chloride; thin-layer chromatography plates (DC Alufolien Kieselgel 60; E. Merck A. G.) were developed with methylene chloride-acetone (19:1 vol/vol), dried, and developed a second time with the same eluent (*16*). In a parallel experiment, the R_f of the major chlorinated product was determined by thin-layer chromatography to be 0.58. After drying the AFB_1Cl_2 solution in vacuum, we quickly added 4.5 ml 0.01 *M* sodium phosphate buffer (pH 7.4) that contained 9.3 mg BSA; immediately thereafter, we added 0.5 ml DMSO drop by drop under magnetic stirring. We kept the mixture for 30 minutes at 37°C in a water bath under shaking. We removed the insoluble material by centrifugation for 15 minutes at 3,500×*g*. We then precipitated the conjugate by sequential addition of 43 mg NaCl, 6 ml ethyl acetate, and 12 ml acetone under magnetic stirring. We kept the mixture on ice for 15 minutes, then centrifuged it for 15 minutes at 3,500×*g*. We washed the precipitate twice with 22 ml ethanol and once with the same volume of ether. After removal of the ether, we dissolved the conjugate in 8 ml of 0.14 *M* NaCl and sterilized it by filtration through a 0.22-μm Millipore membrane (Millipore Corp., Bedford, Mass.). We then divided the solution into aliquots and stored it at −30°C. The number of molecules of AFB_1 bound to 1 molecule of BSA was determined by measurement of the specific radioactivity of the conjugate.

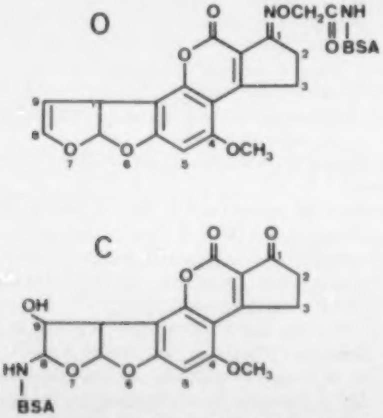

TEXT-FIGURE 1.—Structure of AFB_1 oxime-BSA conjugate (O) and presumed structure of AFB_1Cl_2–BSA conjugate (C) used for the preparation of anti-AFB_1 antisera [adapted from Chu and Ueno (*14*) and Swenson et al. (*16*)].

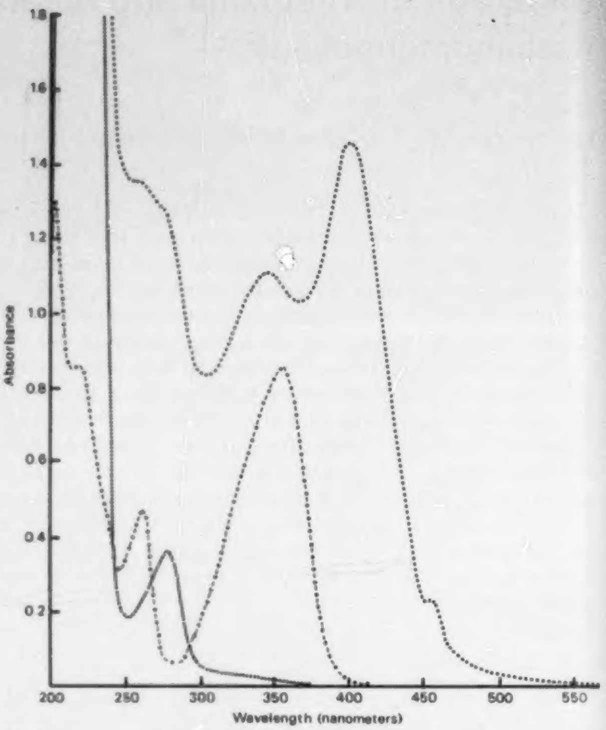

TEXT-FIGURE 2.—Absorption spectra of BSA (····), AFB_1 (·-·-·-), and AFB_1Cl_2–BSA conjugate (—).

Antisera.—Pairs of outbred albino New Zealand White rabbits were immunized with each of the two conjugates by injections into multiple sites of 250 μg immunogen 6 weeks apart according to Chu and Ueno (*14*); after the second injection, 1 rabbit of each pair with the best antiserum titer was kept for further immunization. Altogether, three courses of injections with O-conjugate and five courses of injection with C-conjugate were given to each of the 2 rabbits.

Gel diffusion.—For the study of C-antiserum, we performed double-gel diffusion in 1% agarose A45 (Industrie Biologique Française, Gennevilliers, France) in 0.02 *M* barbital buffer (pH 8.6). After the gel was washed thoroughly, the plates were dried and precipitin lines stained with Coomassie brilliant blue R250 (*17*).

RIA.—We performed RIA with the use of $[^3H]AFB_1$, diluted to introduce about 10^4 cpm (≈0.37 pmol) into each tube (milliR 6PE; Luman, Basel, Switzerland). AF were first dissolved in DMSO and then serially diluted in 0.05 *M* sodium borate buffer containing 1/1,500 thiomerosal and 10% (vol/vol) normal chicken serum; the highest concentration of DMSO in mycotoxin solution was 5% (vol/vol). Rat urine, antisera, and the tracer were also diluted in the borate chicken serum buffer. We assayed in duplicate all dilutions of specimens to be titrated; reagents were introduced in the order of 1) 250 μl mycotoxins or rat urines, 2) 25 μl antiserum, and 3) 25 μl $[^3H]AFB_1$.

After 30 minutes of incubation at 4°C, we precipitated the $[^3H]AFB_1$ bound to the antibodies with half-saturated

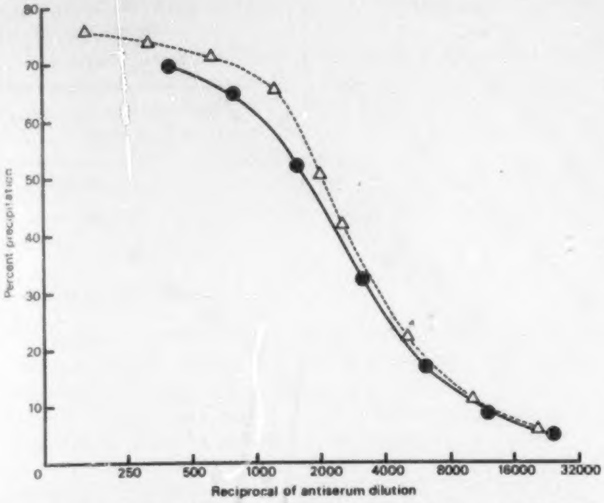

TEXT-FIGURE 3.—Titration curve with RIA of two rabbit anti-AFB_1 antisera with $[^3H]AFB_1$ as tracer. △--△, anti-AFB_1 oxime–BSA conjugate antiserum; ●—●, anti-AFB_1Cl_2–BSA conjugate antiserum.

ammonium sulfate (4.3 ml/tube). The tubes were then centrifuged at 1,000×*g* at 0°C for 1 hour and emptied. Precipitates were dissolved in 250 µl distilled water; we filled the tubes with 4 ml Picofluor 30 (Packard Instruments, Paris-Rungis, France) and agitated them thoroughly. We determined the net percentage of precipitation (antisera) or of inhibition (mycotoxins) as described previously (*18*), affinity constants of antisera according to Müller (*19*), and AFB_1 potencies of rat urines by an RIA with the use of C-antiserum. The percentage of inhibition by the urines was converted into AFB_1 equivalent quantities by reference to a standard curve obtained with known amounts of AFB_1.

Experiments on rats.—We used adult inbred BD IV male rats with about 300 g body weight, bred at the International Agency for Research on Cancer for studies on AFB_1 urinary metabolite excretion. Individual doses of mycotoxins (3.1 µmol sterigmatocystin and doses of AFB_1 ranging from 600 pmol to 385 nmol) were dissolved in 100-µl aliquots of DMSO that were thoroughly mixed with 400 µl olive oil and administered through gastric tubes. We then kept the rats in metabolic cages throughout the experiment and fed them a Charles River CRF diet; we collected urines each day in graduated cylinders and stored them at −20°C until the assay. After the urines thawed, we agitated them thoroughly at room temperature and centrifuged them for 10 minutes at 1,000×*g* to remove insoluble materials.

RESULTS

Preparation of Conjugates

As shown in text-figure 2, the major peak of absorption of the C-conjugate was 405 nm, identical to that found by Swenson et al. (*16*). The amount of AFB_1Cl_2 coupled to BSA was 10.5%. The number of AFB_1 molecules per BSA molecule was 23 for the O- and 14 for the C-conjugate.

Antisera

In double-gel diffusion, C-antiserum precipitated both the corresponding conjugate and BSA (fig. 1). After addition of BSA to the C-antiserum, no more precipitation against the carrier protein was observed, whereas there was still a precipitin line against the conjugate. O-antiserum did not precipitate BSA or O- or C-conjugates. In RIA, dilutions of 1:2,000 O-antiserum and 1:1,800 C-antiserum were capable of precipitating 50% of the tracer (text-fig. 3). We selected these dilutions for inhibition assays. The coefficients of affinity were 2.5×10^9 for the O-antiserum and 2×10^9 for the C-antiserum. Since the presence of anti-BSA antibodies in C-antiserum did not modify the titration curves (data not shown), all assays in which C-antiserum was used were performed with the crude antiserum.

Mycotoxin Assays

The amounts of AFB_1 that inhibited the $[^3H]AFB_1$ precipitation by 50% were 0.72 pmol for the O-antiserum and 0.8 pmol for the C-antiserum (text-figs. 4, 5). As expected, other mycotoxins cross-reacted to various degrees with both

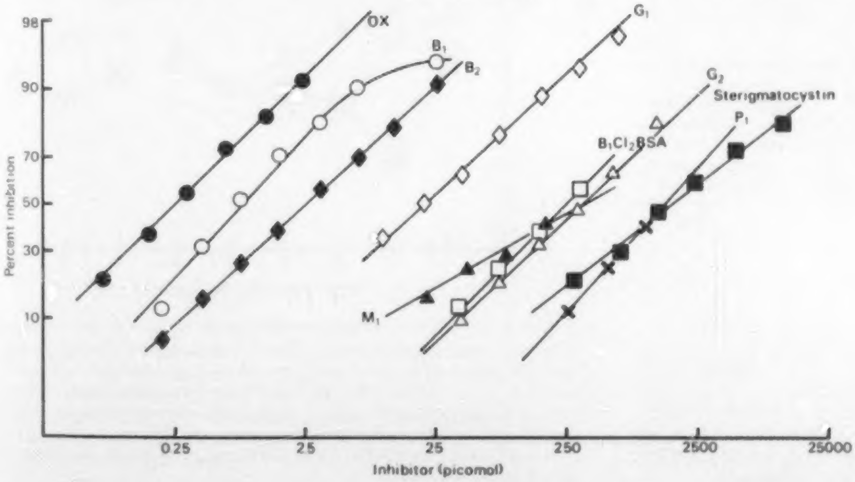

TEXT-FIGURE 4.—Dose-response curves of various AF and sterigmatocystin obtained by RIA with $[^3H]AFB_1$ as tracer; the O-antiserum was raised in a rabbit with the use of AFB_1 oxime–BSA derivative as immunogen. OX=AFB_1 oxime; B_2=AFB_2; G_1=AFG_1; M_1=AFM_1; B_1Cl_2BSA=AFB_1-8,9-dichloride-BSA conjugate; G_2=AFG_2; P_1=AFP_1.

TEXT-FIGURE 5.—Dose-response curves of various AFB$_1$ derivatives and sterigmatocystin obtained by RIA with [^{3}H]AFB$_1$ as tracer. The C-antiserum was raised in a rabbit with the use of AFB$_1$Cl$_2$-BSA derivative as the immunogen. Abbreviations are the same as in the legend to text-fig. 4.

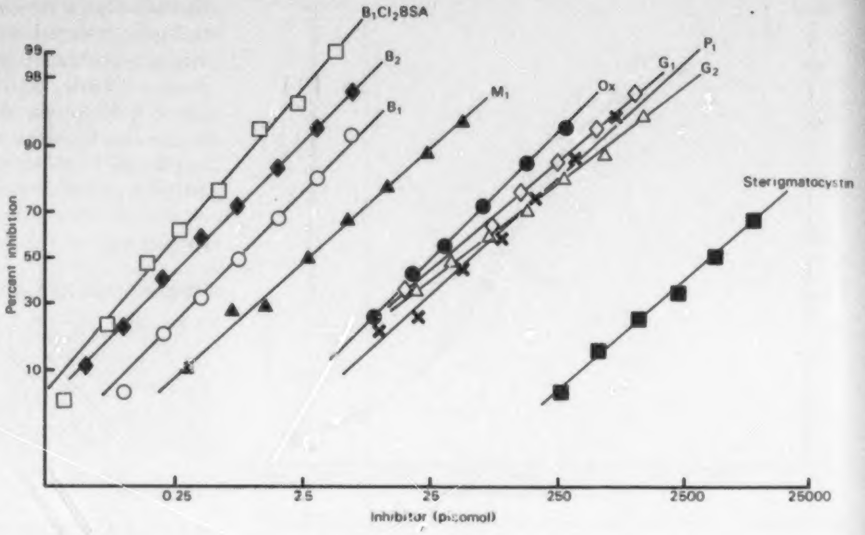

antisera (text-figs. 4, 5; table 1); with O-antiserum about 3.6 times more AFB$_2$ than AFB$_1$ was required to inhibit [^{3}H]AFB$_1$ immune precipitation by 50%, whereas with C-antiserum a smaller amount of AFB$_2$ was necessary. This reduction was not due to the use of higher (AFB$_2$) or lower (AFB$_1$) concentrations of mycotoxin than those stated by the producer, as checked by spectrophotometry. AFG$_1$ cross-reacted with each of the antisera in a rather similar way; however, the lack of a double bond between C8 and C9 considerably diminished the cross-reactivity of AFG$_2$ with O-antiserum, whereas only a slight decrease was observed with C-antiserum compared to AFG$_1$. AFM$_1$ cross-reacted to a large extent with the C-antiserum, which is in keeping with results of Lawellin et al. (*20*) who used AFB$_{2a}$ oxime-BSA conjugate as immunogen. However, the presence of the hydroxyl group at C10 decreased the immune precipitation of [^{3}H]AFB$_1$ by O-antiserum proportionally more. Similarly, AFP$_1$ cross-reacted more with C-antiserum than with O-antiserum. In general, the doses of AFM$_1$ and AFP$_1$ required to inhibit the immune precipitation of [^{3}H]AFB$_1$ by 50%

TABLE 1.—*Inhibition of [^{3}H]AFB$_1$ immune precipitation in RIA*[a]

Inhibitor	Amount of inhibitor required to inhibit tracer–antibody binding by 50%	
	O-antiserum	C-antiserum
AFB$_2$	3.6	0.42
AFG$_1$	29	34
AFG$_2$	520	49
AFM$_1$	210	3.7
AFP$_1$	2,100	60
AFB$_1$ oxime–BSA conjugate	0.35	36
AFB$_1$Cl$_2$–BSA conjugate	370	0.24
Sterigmatocystin	2,400	4,300

[a] The degrees of inhibition are expressed as multiples of AFB$_1$ quantities corresponding to the molar ratio of inhibitor:AFB$_1$. The amounts of AFB$_1$ required to inhibit tracer–antibody binding by 50% were 0.72 pmol for O-antiserum and 0.8 pmol for C-antiserum.

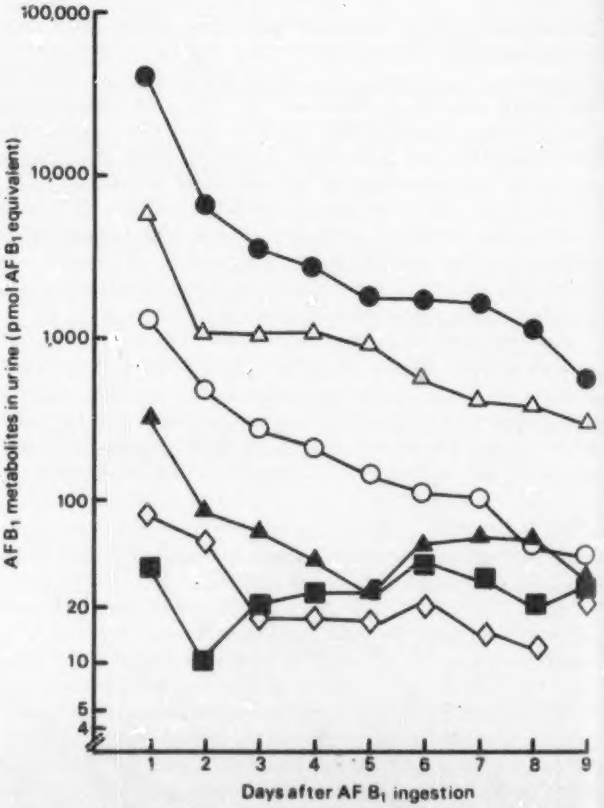

TEXT-FIGURE 6.—Daily urinary excretion of C-antiserum-cross-reacting substances in mycotoxin-treated BD IV adult male rats. On day 0, rats were given oral AFB$_1$ doses, nmol: ●—●, 385; △—△, 77; ○—○, 15.4; ▲—▲, 3.1; ◇—◇, 0.6; or ■—■, 3.1×10^3 nmol sterigmatocystin. Quantities of substances cross-reacting with AFB$_1$ excreted each day were determined by RIA and expressed as pmol of AFB$_1$ equivalent, with reference to a standard AFB$_1$ curve. Other technical details are the same as in legend to text-fig. 5.

were about fiftyfold smaller for the C-antiserum than for the O-antiserum.

The respective AFB_1 conjugates reacted primarily with the corresponding antisera and, on a molecular basis, were even more potent than AFB_1. BSA produced no inhibition at a 500-fold higher molar concentration than that where AFB_1 caused 50% inhibition of the tracer by C-antiserum. This observation confirms that anti-BSA antibodies present in C-antiserum do not interfere with the toxin–antitoxin reaction.

Assays of Rat Urines

Amounts of AFB_1 cross-reacting substances excreted in the urine of rats treated with AFB_1 (600 pmol–385 nmol) and with 3.1 µmol sterigmatocystin are indicated in text-figure 6. Since the inhibition of immune precipitation of $[^3H]AFB_1$ is likely to be due to AFB_1 urinary metabolites, results are expressed as AFB_1 *equivalent*, i.e., amounts of AFB_1 giving equivalent degrees of inhibition. In rats treated with AFB_1, there was an obvious relationship between the dose administered and the "AFB_1 potency" of urines, which decreased with time. Urines of the rats treated with sterigmatocystin also exerted some inhibition on the immune binding of $[^3H]AFB_1$. However, this inhibition was weaker than that of the rats having received the four highest doses of AFB_1 and was relatively stable with time. Text-figure 7 shows the excretion of AFB_1-like substances in the urine of those 4 rats, expressed as the mean value ± standard deviation of doses administered. Amounts less than 1% of the dose could still be detected 9 days after AFB_1 administration.

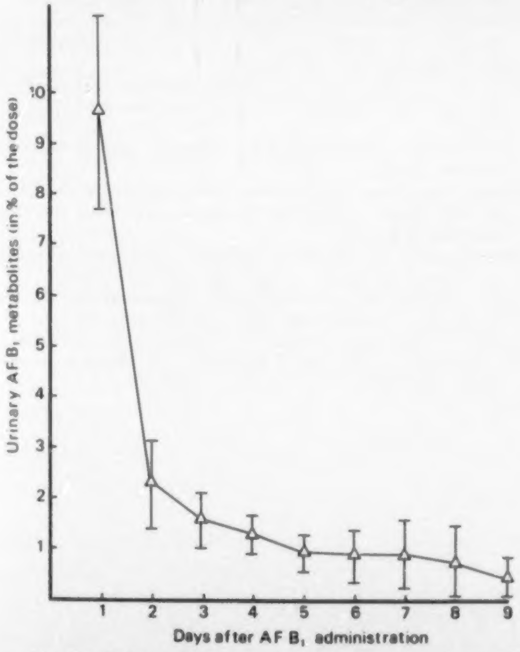

TEXT-FIGURE 7.—Daily urinary excretion in AFB_1-treated rats of substances cross-reacting with C-antiserum. Quantities excreted by the 4 rats treated with AFB_1 doses ranging from 3.1 to 385 nmol (*see* text-fig. 6) were used for the calculation of daily urinary excretion ± SD as percentage of administered doses. RIA was performed as indicated in legends to text-figs. 5 and 6.

DISCUSSION

The stronger reactivity of AFB_1 conjugates with their respective antisera, as compared with AFB_1, is probably due to the presence of several hapten epitopes on each molecule of the carrier protein. We think that the slight cross-reactivity observed with the sterigmatocystin can be explained by the polyclonality of both antisera: It is likely that those parts of the sterigmatocystin molecule that are similar to AFB_1 structures can compete with $[^3H]AFB_1$ for antibody binding.

Landsteiner (*21*) has shown that changes in the structure of haptens that take place near the site of attachment to carrier proteins have little effect on their capacity to react with antibodies directed against the unmodified structure. Swenson et al. (*16*) have shown that AFB_1 reacts with proteins and/or DNA through AFB_1-8,9-oxide primarily at C8. To obtain antibodies that react with various AFB_1 metabolites, it is therefore logical to use conjugates as immunogen in which AFB_1 is bound to the carrier through C8. Such compounds should be able to elicit antibodies that react with parts of the AFB_1 molecule that are located opposite to the site of attachment and which are slightly or not at all modified by metabolism. The greater reactivity of most AF tested with C-antiserum, compared with O-antiserum, is likely to be due to that explanation.

In addition to free AF in the urine of rats treated with AFB_1, possible products cross-reacting with C-antiserum include conjugated AFB_1 metabolites and AFB_1-N^7-guanine (*22*). In the RIA in which we used C-antiserum, AFB_1-N^7-guanine and AFB_1-FAPY formed by hydrolysis of the imidazole ring inhibited the immune precipitation of $[^3H]$-AFB_1, giving dose-response curves parallel to the dose-response curve of AFB_1 (data not shown). For quantitation of individual urinary metabolites, it would be necessary to use specific antisera raised with corresponding immunogens in which haptens are coupled to the carrier protein in the appropriate position.

Dilutions of urines from AFB_1-treated rats that gave 50% inhibition ranged from 1:11 to 1:1,330. At 1:11 dilution, some urine samples from rats that did not receive AFB_1 were also weakly inhibitory (data not shown), corresponding to a maximum theoretical excretion of about 40 pmol AFB_1 equivalent/day. We therefore considered this level to be the "background" level. The level was not increased by administration of the DMSO–olive oil mixture we used as the AFB_1 vehicle. Under the conditions of our experiment, daily urinary excretion of amounts below the background level probably does not indicate exposure of rats to AFB_1. Similar levels were found in the urine of rats that received 600 pmol AFB_1 1 or 2 days previously, which gives an indication of the sensitivity limit of the method.

Why the urine from "normal" rats inhibited slightly the binding of $[^3H]AFB_1$ to antibodies is not known; since the diet was not checked, it is impossible to rule out the presence of small amounts of AFB_1 in the regimen. A more probable explanation is the presence of non-AFB_1-derived but somewhat structurally related compounds in the urine.

If allowance is made for a nonspecific inhibition, it is apparent from text-figure 6 that substances, capable of "specific" inhibition of [^{3}H]AFB$_1$ binding to C-anti-AFB$_1$ antibodies, are released into the urine in increasing quantities with increasing doses of AFB$_1$.

For various reasons, few attempts have been made to isolate AF metabolites in the urine of humans. Campbell et al. (*23*) isolated AFM$_1$ by chloroform extraction and thin-layer chromatography from the urine of individuals who had eaten peanut butter contaminated with AFB$_1$. The results were positive only when more than 48 nmol AFB$_1$ was ingested per day, and no more than 1-4% of AFB$_1$ was excreted in the urine as AFM$_1$. With an assumption of similar yields and a daily excretion of 1,100 ml of urine per person, and depending on the amounts ingested ($\leq$610 nmol), the samples analyzed would have been expected to contain from 0.1 to about 5 pmol of AFM$_1$/250 μl urine. By comparison, with experimental models, it can be anticipated that urines from exposed individuals contain not only chloroform but also water-soluble AFB$_1$ metabolites—both of them theoretically capable of reacting with antibodies present in C-antiserum. However, it is not yet clear whether the technique we used would be suitable for screening purposes.

Our preliminary results were obtained with a technique that has the advantages of not requiring prior clean up or volume reduction of the urine, and its sensitivity can be increased by various refinements, such as solid-phase methods (*24, 25*). We consider these sufficient justifications for further efforts in this direction.

REFERENCES

(*1*) Doll R, Peto R. The causes of cancer: Quantitative estimates of avoidable risks of cancer in the United States today. JNCI 1981; 66:1191-1308.

(*2*) Müller R, Rajewsky MF. Antibodies specific for DNA components structurally modified by chemical carcinogens. J Cancer Res Clin Oncol 1981; 102:99-113.

(*3*) Poirier MC. Antibodies to carcinogen-DNA adducts. JNCI 1981; 67:515-519.

(*4*) Perera FP, Weinstein IB. Molecular epidemiology and carcinogen-DNA adduct detection: New approaches to studies of human cancer causation. J Chron Dis. In press.

(*5*) International Agency for Research on Cancer Working Group. Development and possible use of immunological techniques to detect individual exposure to carcinogens (IARC technical report No. 82/001). Lyon: IARC, 1982.

(*6*) Haugen A, Groopman JD, Hsu IC, Goodrich GR, Wogan GN, Harris CC. Monoclonal antibody to aflatoxin B$_1$ modified DNA detected by enzyme immunoassay. Proc Natl Acad Sci USA 1981; 78:4124-4127.

(*7*) Szmuness W. Hepatocellular carcinoma and the hepatitis B virus: Evidence for a causal association. Progr Med Virol 1978; 24:40-69.

(*8*) Blumberg BS, London WT. Hepatitis B virus and the prevention of primary hepatocellular carcinoma. N Engl J Med 1981; 304:782-784.

(*9*) Peers FG, Linsell CA. Dietary aflatoxins and liver cancer—a population based study in Kenya. Br J Cancer 1973; 27:473-484.

(*10*) Peers FG, Gilman GA, Linsell CA. Dietary aflatoxins and human liver cancer—a study in Swaziland. Int J Cancer 1976; 17:167-176.

(*11*) International Agency for Research on Cancer. Inorganic substances, chlorinated hydrocarbons, aromatic amines, N-nitroso compounds, natural products, miscellaneous. IARC Monogr Eval Carcinog Risk Chem Man 1972; 1:1-184.

(*12*) Lowry OH, Rosebrough NJ, Farr AL, Randall LJ. Protein measurement with the Folin phenol reagent. J Biol Chem 1951; 193:265-275.

(*13*) Langone JJ, Van Vunakis H. Aflatoxin B$_1$: Specific antibodies and their use in radioimmunoassay. J Natl Cancer Inst 1976; 56:591-595.

(*14*) Chu FS, Ueno I. Production of antibody against aflatoxin B$_1$. Appl Environ Microbiol 1977; 33:1125-1128.

(*15*) Chu FS, Hsia MT, Sun PS. Preparation and characterization of aflatoxin B$_1$-1-(*o*-carboxymethyl) oxime. J Assoc Off Anal Chem 1977; 60:791-794.

(*16*) Swenson DH, Miller JA, Miller EC. The reactivity and carcinogenicity of aflatoxin B$_1$-2,3-dichloride, a model for the putative 2,3-oxide metabolite of aflatoxin B$_1$. Cancer Res 1975; 35:3811-3823.

(*17*) Weeke B. General remarks on principles, equipment, reagents and procedures. Quantitative immuno-electrophoresis. Scand J Immunol 1973; 2 (suppl 1):15-35.

(*18*) Sizaret P, Tuyns A, Martel N, et al. Alpha-fetoprotein levels in normal males from seven ethnic groups with different hepatocellular carcinoma risks. Ann NY Acad Sci 1975; 259:136-155.

(*19*) Müller R. Calculation of average antibody affinity in anti-hapten sera from data obtained by competitive radioimmunoassay. J Immunol Methods 1980; 34:345-352.

(*20*) Lawellin DW, Grant DW, Joyce BK. Enzyme-linked immunosorbent analysis for aflatoxin B$_1$. Appl Environ Microbiol 1977; 34:94-96.

(*21*) Landsteiner K. The specificity of serological reaction. Cambridge: Harvard Univ Press, 1945.

(*22*) Bennett RA, Essigmann JM, Wogan GN. Excretion of an aflatoxin-guanine adduct in the urine of aflatoxin B$_1$-treated rats. Cancer Res 1981; 41:650-654.

(*23*) Campbell TC, Caedo JP, Bulatao-Jayme J, Salamat L, Engel RW. Aflatoxin M$_1$ in human urine. Nature 1970; 227:403-404.

(*24*) Pestka JJ, Li Y, Harder WO, Chu FS. Comparison of radioimmunoassay and enzyme-linked immunosorbent assay for determining aflatoxin M$_1$ in milk. J Assoc Off Anal Chem 1981; 64:294-301.

(*25*) Von Bierman A, Terplan G. Nachweis von Aflatoxin B$_1$ mittels ELISA. Arch Lebensmittelhyg 1980; 31:51-57.

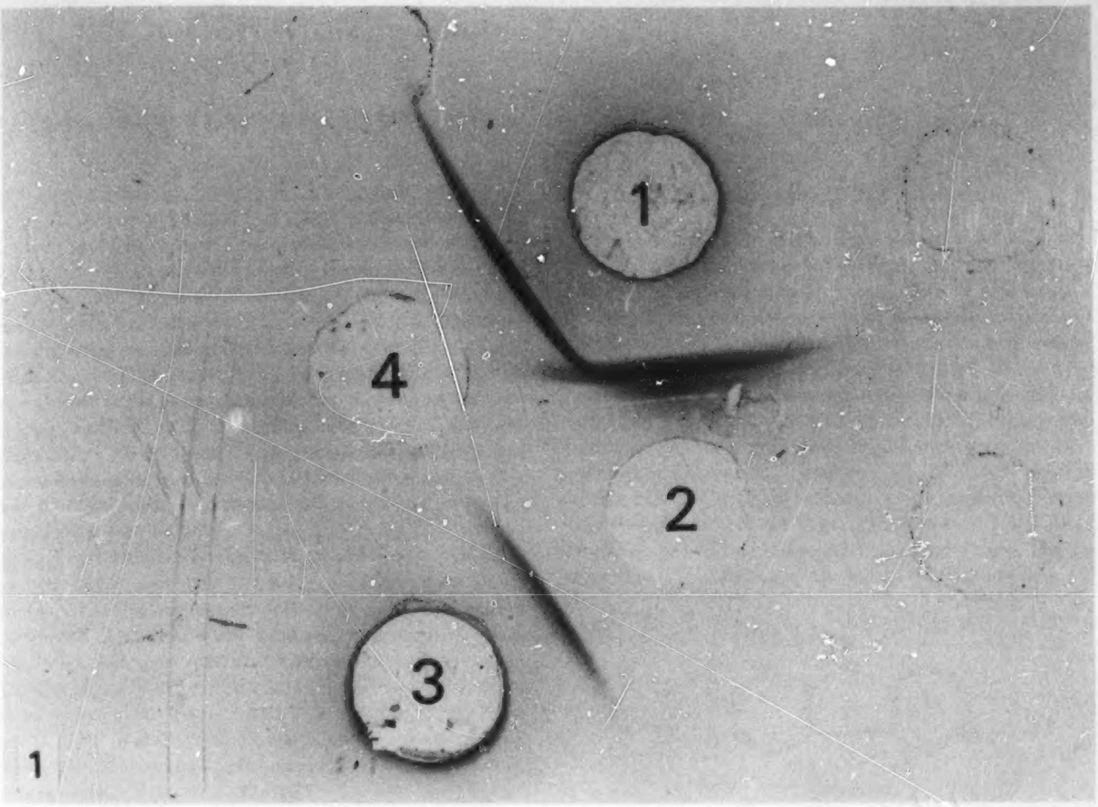

FIGURE 1.—Double-gel diffusion in 1% agarose in 0.02 *M* barbital buffer (pH 8.6). 1=rabbit anti-AFB_1Cl_2–BSA conjugate; 2=160 μg AFB_1Cl_2–BSA conjugate/ml; 3=rabbit anti-AFB_1Cl_2–BSA conjugate after removal of the anti-BSA antibodies; 4=160 μg BSA/ml. Diameter of wells=3.5 mm.

blank page

Carcinogenic Effect of Carbazole in the Liver of (C57BL/6N × C3H/HeN)F_1 Mice[1,2,3]

Hiroyuki Tsuda,[4] Akihiro Hagiwara,[4] Michiko Shibata,[4] Masato Ohshima,[4] *and* Nobuyuki Ito[4]

ABSTRACT—The carcinogenic effect of carbazole (9*H*-carbazole) in (C57BL/6N × C3H/HeN)F_1 (B6C3F_1) mice was examined. Groups of 50 mice of both sexes were given a basal diet containing 0.6, 0.3, or 0.15% carbazole for 96 weeks and were then placed on an unsupplemented basal diet until they were killed at week 104. Mice surviving longer than 52 weeks were included in effective numbers. Significant increases in the induction of neoplastic lesions were found in the livers and forestomachs of mice given carbazole as compared to the control groups. The lesions in the livers were classified into two types, neoplastic nodules or hepatocellular carcinomas. The incidences of both types of lesions were almost 100% in mice treated with carbazole, and both types of lesions were significantly increased in all mice except the males given 0.6% carbazole in their diet. The incidences of hepatocellular carcinomas were in general higher than those of neoplastic nodules. Though not statistically significant, increased incidences of pulmonary metastases were found in the groups given carbazole. Significantly increased incidences of neoplastic lesions and papillomas in the forestomach in all groups of female and male mice were also noted in the mice fed 0.6% carbazole. Squamous cell carcinoma induction was significantly different in male mice given 0.6% carbazole as compared to controls. These results indicate that carbazole is carcinogenic to the liver and forestomach in B6C3F_1 mice and suggest that carbazole may be an environmental carcinogen relevant to cancer risk in humans.—JNCI 1982; 69:1383–1389.

Carbazole (9*H*-carbazole) is widely used industrially as a dye intermediate and is also used in making photographic plates sensitive to UV light. A detectable amount of carbazole was found in air emissions from factories and automobiles and was mixed with many carcinogenic polycyclic aromatic hydrocarbons (*1*). 7*H*-Dibenzo[*c,g*]carbazole, a derivative of carbazole, was found to be present in cigarette smoke (*2*). Since the carcinogenicity of 7*H*-dibenzo[*c,g*]carbazole was first demonstrated by Boyland and Brues (*3*) in mouse skin, evidence for its carcinogenicity has been increasing. The carcinogenicities of several derivatives of carbazole have also been examined, and nitrogen derivatives have been shown to be carcinogenic in mice (*4*). Sellakumar et al. (*5*) also have reported that 7*H*-dibenzo[*c,g*]carbazole when instilled intratracheally induced squamous cell carcinoma in the trachea and bronchi of Syrian golden hamsters of both sexes.

Extensive experimental and clinical studies have been done on the pharmacologic effects of a wide variety of carbazole derivatives. Results showed that these compounds have anti-inflammatory, antiasthmatic, and antiviral effects (*6–8*). They also have antidepressant activity associated with norepinephrine reuptake and amine oxidase (flavin containing) inhibition (*9*). The practical use of carbazole in the chemical industry and the therapeutic use of carbazole-related compounds prompted us to investigate its carcinogenicity in mice fed this compound in a long-term test.

MATERIALS AND METHODS

Animals and diet.—Five-week-old (C57BL/6N × C3H/HeN)F_1 (B6C3F_1) mice of both sexes were obtained from Charles River Japan Inc., Atsugi, Japan. The animals were housed 5 to a plastic cage with wood chips for bedding in an air-conditioned room at controlled temperature (23±1°C) and humidity (55±2%) with a 12-hour light–12-hour dark cycle. Animals were given commercial diet (Oriental M; Oriental Yeast Co., Ltd., Tokyo, Japan) for 1 week before the experiments were begun and tap water ad libitum throughout the experiment.

Chemical.—Carbazole, technical grade at 96% purity, was purchased from Nihon Jyoryu Kogyo Inc., Ichikawa, Japan. It was mixed with Oriental M powdered diet. The chemical structure of carbazole is shown in text-figure 1.

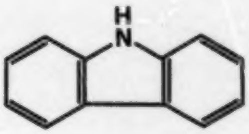

Carbazole

TEXT-FIGURE 1.—Chemical structure of carbazole.

Treatment.—From the age of 6 weeks, groups of 50 mice of each sex were given a diet containing 0.6, 0.3, or 0.15% carbazole. An additional 50 age-matched animals of each sex were fed basal diet without carbazole. Body weight and food consumption were measured weekly throughout the experiment. Animals were fed a carbazole-containing diet for 96 weeks and unsupplemented basal diet for the next 8 weeks and were killed when ether anesthetized (in experimental wk 104). All organs were removed, fixed in 10% buffered Formalin, and routinely stained with H & E for histologic examination. Animals that died or became moribund during the experiment were also autopsied, and mice surviving longer than 52 weeks (the time at which the first liver tumor was found in an animal that subsequently died) were included in effective numbers.

ABBREVIATION USED: H & E=hematoxylin and eosin.

---

[1] Received March 30, 1982; accepted July 16, 1982.

[2] Supported by a Grant-in-Aid for Cancer Research from the Ministry of Health and Welfare, Japan.

[3] Animals were maintained under the guidelines of the Nagoya City University Medical School.

[4] First Department of Pathology, Nagoya City University Medical School, 1 Kawasumi, Mizuho-cho, Mizuho-ku, Nagoya 467, Japan.

RESULTS

Annual Maintenance Data

Food consumption.—There were no consistent differences in the food consumption of either sex in any group during the experiment. The mean food consumption and cumulative carbazole intake are shown in table 1. The total intake of carbazole was approximately proportional to its concentration in the diet (table 1).

Body weight.—The mean body weights of female mice given carbazole were lower for mice fed the higher carbazole concentrations; the dose-dependent effect was clear after week 72. However, from weeks 40 to 72, the body weights of the animals given 0.15% carbazole were higher than those of the controls. Males showed a proportional decrease in body weight as the concentrations of carbazole were increased.

Survival time.—Survival rates for both sexes decreased significantly with increasing concentrations of carbazole during the later stages of the experiment. The main cause of death was massive intraperitoneal hemorrhage due to rupture of liver tumors. All mice given 0.6% carbazole died before the end of the experiment (text-figs. 2, 3).

Histopathologic Findings

Neoplastic lesions in the liver.—Classification of lesions: The neoplastic lesions in the liver observed in the present experiment were tentatively classified histologically into two types: neoplastic nodules and hepatocellular carcinomas.

Neoplastic nodules, occurring either as a single lesion or as multiple lesions, consisted of a proliferation of hepatocytes. They varied in size from small, microscopic lesions to those so massive as to involve a complete liver lobe. The cellular arrangement of the lesions varied from closely packed single liver cell plates that differed little from normal liver structure (fig. 1) to more atypical cells in multicell layers that were devoid of an obvious central vein (terminal hepatic vein) or portal triad (fig. 2). The latter more atypical cells showed expansive growth and compressed the surrounding areas as compared to the former closely packed single liver cell plates.

Hepatocellular carcinomas had a trabecular or papillary structure with cellular or nuclear atypism (fig. 3). Some of these lesions directly invaded the surrounding liver tissue or metastasized to the lung (fig. 4) or adrenal gland.

Incidence of lesions: The results in table 2 show that the incidence of neoplastic nodules was significantly higher in mice of both sexes when treated with any of the carbazole doses used here except in males treated with the highest dose of carbazole (0.6%). Carbazole had a clear dose-dependent effect on the induction of neoplastic nodules in females.

The incidence of hepatocellular carcinomas was also significantly different from that in controls of both sexes. It was highest (77.1%) in males given 0.6% carbazole, whereas it was 4.4% in female controls and 19.6% in male controls. Though no clear dose-dependent effect of carbazole was found in females, the incidence of hepatocellular carcinomas was very high in all test groups, irrespective of the dose.

TABLE 1.—*Food consumption and carbazole intake*

Sex	Carbazole dose, %	Mean food consumption, g/mouse/day					Average food consumption of all wk, g/mouse/day	Average cumulative dose, g/kg body wt
		Wk 1	Wk 40	Wk 80	Wk 96	Wk 104		
Female	0.6	4.3	4.3	5.8	8.7	—[a]	5.8	747.1
	0.3	4.5	4.9	5.7	8.6	6.1	5.9	366.4
	0.15	4.5	4.4	5.4	7.6	5.9	5.7	153.0
	0	3.9	3.7	4.2	4.7	5.3	4.8	0
Male	0.6	4.3	4.4	5.5	7.7	5.4	5.4	628.3
	0.3	4.6	5.0	5.4	6.5	6.0	5.6	290.0
	0.15	4.5	4.9	5.2	6.6	5.7	5.6	139.8
	0	4.1	5.3	5.2	5.7	5.7	5.5	0

[a] All mice died before wk 104.

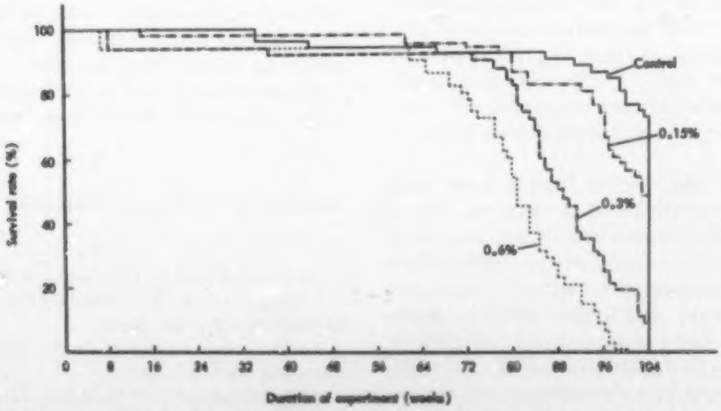

TEXT-FIGURE 2.—Survival times for females. Percentages of carbazole in the diet are indicated.

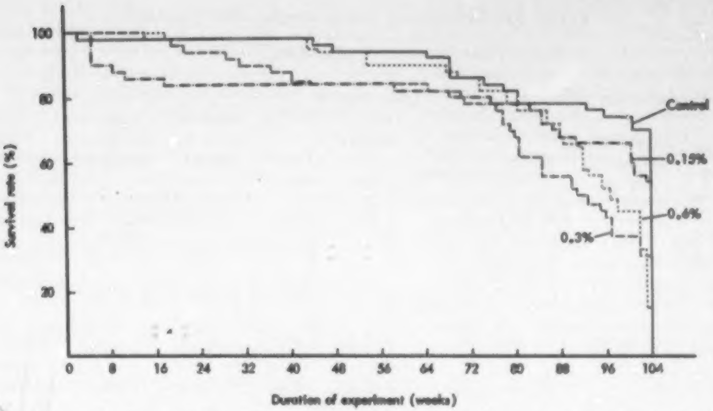

TEXT-FIGURE 3.—Survival times for males. Percentages of carbazole in the diet are indicated.

Many mice with hepatocellular carcinomas had metastases to other organs, especially to the lung, and the incidence of metastasis was significantly higher in males given 0.3% carbazole and in females at all carbazole doses tested. Neoplastic nodules and hepatocellular carcinomas did not differ morphologically between experimental and control groups.

Neoplastic lesions in organs other than the liver.—Table 3 shows the incidences of neoplastic lesions in organs other than the liver. The incidence of papillomas of the forestomach was significantly higher in all groups of females given carbazole and for the group of males given 0.6% carbazole than it was in controls. Squamous cell carcinoma of the forestomach showing invasion to the submucosal layer was also significantly increased in males given 0.6% carbazole (fig. 5). The incidence of lymphoma-leukemia was significantly lower in females given 0.6% carbazole. The incidences of tumors in organs other than the liver and forestomach (e.g., lung adenomas or adenocarcinomas, fibrosarcoma-like lesions, uterine fibromas, thyroid adenomas, harderian gland tumors, and adrenal cortical adenomas) were not significantly different from those of controls of either sex in any of the 4 groups.

DISCUSSION

This study clearly showed that carbazole is carcinogenic to mice of both sexes. Several reports have revealed that some carbazole derivatives are carcinogenic under certain conditions (*2–5*). Therefore, the carcinogenic action of carbazole is not unexpected. However, because carbazole is used as an intermediate in the synthesis of dyes, drugs, and photosensitive materials and because it is also present in automobile emissions as an air pollutant (*1, 2, 10*), it may be hazardous to humans as an environmental carcinogen.

The neoplastic lesions seen in this study were classified as neoplastic nodules and hepatocellular carcinomas. This classification warrants some comment. Walker et al. (*11*) classified mouse hepatic neoplasias into two types, A and B, depending on their histologic characteristics. This classification has been generally accepted (*12, 13*), and both types of nodules are transplantable, with a greater percentage of "takes" of the type B nodules, suggesting their more malignant nature (*14*). It was also noted that type A lesions could be differentiated further into two additional types depending on whether the liver cells were arranged as a single layer (type 1) or as multiple layers (type 2) in plates (*15*). The

TABLE 2.—*Incidence of neoplastic lesions in the liver*

Sex	Carbazole dose, %	No. of mice	Mean survival time ± SD, wk[a]	No. of mice (percent of mice) with:			
				Neoplastic nodules	Hepatocellular carcinoma	Metastasis to:[b]	
						Lungs	Adrenal glands
Female	0.6	46	83±9[b]	16[b] (34.8)	30[b] (65.2)	3 (10.0)	0
	0.3	43	90±12[b]	21[b] (48.8)	24[b] (55.8)	3 (12.5)	1 (4.2)
	0.15	49	98±11[c]	13[c] (26.5)	35[b] (71.4)	5 (14.3)	0
	0	45	103±7	2 (4.4)	2 (4.4)	0	0
Male	0.6	48	95±10[d]	10 (20.9)	37[b] (77.1)	11 (29.7)	0
	0.3	42	93±12	22[d] (52.4)	20[c] (47.4)	7 (35.0)	1 (5.0)
	0.15	42	100±9	30[b] (71.4)	12 (28.6)	2 (16.7)	0
	0	46	100±12	13 (28.2)	9 (19.6)	2 (22.2)	0

[a] Animals surviving <51 wk were excluded from effective numbers.
[b] $P < 0.001$.
[c] $P < 0.01$.
[d] $P < 0.05$.

TABLE 3.—*Incidence of tumors in sites other than liver*

Sex	Carbazole dose, %	No. of mice	No. of mice (percent of mice) with: Forestomach tumors			Lung tumors			Fibrosarcoma-like lesions[a]	Lymphoma-leukemia	Other tumors present[a]	
			Papilloma	Squamous cell carcinoma	Total	Adenoma	Adenocarcinoma	Total			Tissue[b]	Histology
Female	0.6	46	4[c] (8.7)	2 (4.3)	6[c] (13.0)	0	1 (2.2)	1 (2.2)	1 (2.2)	2[c] (4.3)	—	
	0.3	43	7[d] (16.3)	1 (2.3)	8[d] (18.6)	0	0	0	0	4 (9.3)	—	
	0.15	49	5[c] (10.2)	0	5[c] (10.2)	0	0	0	1 (2.2)	7 (14.3)	Uterus Thyroid gland	Fibroma Follicular adenoma
	0	45	0	0	0	2 (4.4)	0	2 (4.4)	2 (4.4)	8 (17.8)	Eye	Harderian gland tumor
Male	0.6	48	4[c] (8.3)	7[d] (14.6)	11[e] (22.9)	0	3 (6.3)	3 (6.3)	1 (2.1)	0	Adrenal gland Pancreas	Cortical adenoma Fibrosarcoma
	0.3	42	1 (2.4)	0	1 (2.4)	0	1 (2.4)	1 (2.4)	8 (19.0)	1 (2.4)	Spleen Heart Thymus	Hemangioma Fibrosarcoma Thymoma
	0.15	42	0	0	0	0	0	0	2 (4.8)	1 (2.4)	Testis Pancreas Kidney	Hemangioma Islet cell adenoma Adenocarcinoma
	0	46	0	0	0	1 (2.2)	3 (6.5)	4 (8.7)	4 (8.7)	2 (4.3)	Adrenal gland Pancreas Subcutaneous	Pheochromocytoma Islet cell adenoma Fibroma

[a] Lesions were found in the subcutaneous tissue.

[b] —=group in which no animal was affected. For every other tissue specified, 1 mouse was affected.

[c] $P < 0.05$, χ^2 test.

[d] $P < 0.01$, χ^2 test.

[e] $P < 0.001$, χ^2 test.

lesions diagnosed as neoplastic nodules in this study include both type 1 and type 2 hyperplastic nodules because in some sections these two types were seen together, making it difficult to distinguish one from the other. Lesions showing well-defined trabecular patterns were classified as hepatocellular carcinomas, inasmuch as they invaded surrounding liver tissue or metastases with high incidence. These lesions correspond to the type B nodules of Walker et al. (*11*). According to Ward's recent investigation (*16*) on the classification of liver tumors in B6C3F$_1$ mice, the tumors were grouped into two main types, hepatocellular adenomas and hepatocellular carcinomas, with further subgroups, tumors with basophilic or eosinophilic cytoplasm. Neoplastic nodules and hepatocellular carcinomas seem to correspond to hepatocellular adenomas and hepatocellular carcinomas, respectively, by their histologic characteristics (*16, 17*).

Incidences of spontaneous tumors in the liver and other organs are not very different from those reported in another study (*18*). Ward (*16*) and Ward et al. (*17*) also reported that neoplastic lesions in the stomach were very low, close to zero.

When specimens had both neoplastic nodules and hepatocellular carcinomas, the more advanced lesion, hepatocellular carcinoma, was used for scoring purposes. Thus in the specimens with hepatocellular carcinomas, the effect of carbazole on the induction of neoplastic nodules was quantitatively assessed conservatively. The total incidence of neoplastic nodules was similar to that of neoplastic nodules plus hepatocellular carcinomas, i.e., almost 100%, in both sexes of mice given carbazole. Therefore, it could be concluded that carbazole is carcinogenic to mouse liver. Inasmuch as the induction of liver tumors in mice is considered as valid evidence of carcinogenicity, as is the induction in rats and/or hamsters of tumors at any site (*16*), carbazole could have carcinogenic effects in other animals including humans. This might also be applicable to the induction of papillomas and squamous cell carcinomas of the stomach because no such lesions were found in the control animals.

ADDENDUM

While this manuscript was in preparation, carbazole was shown at the National Institute of Hygienic Sciences to cause chromosome aberrations in the Chinese hamster fibroblast cell line CHF (Ishidate M: Personal communication).

REFERENCES

(*1*) SELLAKUMAR A, SHUBIK P. Carcinogenicity of different polycyclic hydrocarbons in the respiratory tract of hamsters. J Natl Cancer Inst 1974; 53:1713–1719.

(*2*) VAN DUUREN BL, BILBAO JA, JOSEPH CA. The carcinogenic nitrogen heterocyclics in cigarette-smoke condensate. J Natl Cancer Inst 1960; 25:53–61.

(*3*) BOYLAND E, BRUES AM. Carcinogenic action of dibenzcarbazoles. Proc R Soc Lond [Biol] 1937; 122:429–441.

(*4*) LACASSAGNE A, BUU-HOI NP, ZAJDELA F, PERIN F, JACQUIGNON P. Nature of potent carcinogens: Benzopyridocarbazoles. Nature 1961; 191:1005–1006.

(*5*) SELLAKUMAR A, STENBÄCK F, ROWLAND J, SHUBIK P. Tumor induction by 7*H*-dibenzo(*c,g*)carbazole in the respiratory tract of Syrian hamsters. J Toxicol Environ Health 1977; 3:935–939.

(*6*) ALBRECHT WL, FLEMING RW, HORGAN SW, MAYER GD. Bis-basic-substituted polycyclic aromatic compounds. A new class of antiviral agents. 8. Bis-basic derivatives of carbazole, dibenzofuran, and dibenzothiophene. J Med Chem 1977; 20:364–371.

(*7*) YÜ TF, PEREL J. Pharmacokinetic and clinical studies of carprofen in gout. J Clin Pharmacol 1980; 20:347-351.

(*8*) Mielens Z. The effects of antiasthmatic drugs against immune complex-induced bronchoconstriction in anesthetized dogs. Pharmacology 1979; 18:311-318.

(*9*) Martorana PA, Nitz RE. The new antidepressant pirlindole. A comparison with imipramine and tranylcypromine. Arzneim Forsch 1979; 29:946-949.

(*10*) International Agency for Research on Cancer. Certain polycyclic aromatic hydrocarbons and heterocyclic compounds. IARC Monogr Eval Carcinog Risk Chem Man 1973; 3:260-268.

(*11*) Walker AI, Thorpe E, Stevenson DE. The toxicology of dieldrin (HEOD). I. Long-term oral toxicity studies in mice. Food Cosmet Toxicol 1972; 11:415-432.

(*12*) Butler WH, Newberne PM. Mouse hepatic neoplasia. Amsterdam: Elsevier, 1975.

(*13*) Frith CH, Dooley K. *Brief communication:* Hepatic cytologic and neoplastic changes in mice given benzidine dihydrochloride. J Natl Cancer Inst 1976; 56:679-682.

(*14*) Williams GM, Hirota N, Rice JT. The resistance of spontaneous mouse hepatocellular neoplasms to iron accumulation during rapid iron loading by parenteral administration and their transplantability. Am J Pathol 1979; 94:65-74.

(*15*) Tsuda H, Sarma DS, Rajalakshmi S, et al. Induction of hepatic neoplastic lesions in mice with a single dose of hycanthone methanesulfonate after partial hepatectomy. Cancer Res 1979; 39:4491-4496.

(*16*) Ward JM. Morphology of hepatocellular neoplasms in B6C3F$_1$ mice. Cancer Lett 1980; 9:319-325.

(*17*) Ward JM, Goodman DG, Squire RA, Chu KC, Linhart MS. Neoplastic and nonneoplastic lesions in aging (C57BL/6N × C3H/HeN)F$_1$ (B6C3F$_1$) mice. JNCI 1979; 63:849-854.

(*18*) Tomatis L, Partensky C, Montesano R. The predictive value of mouse liver tumor induction in carcinogenicity testing—a literature survey. Int J Cancer 1973; 12:1-20.

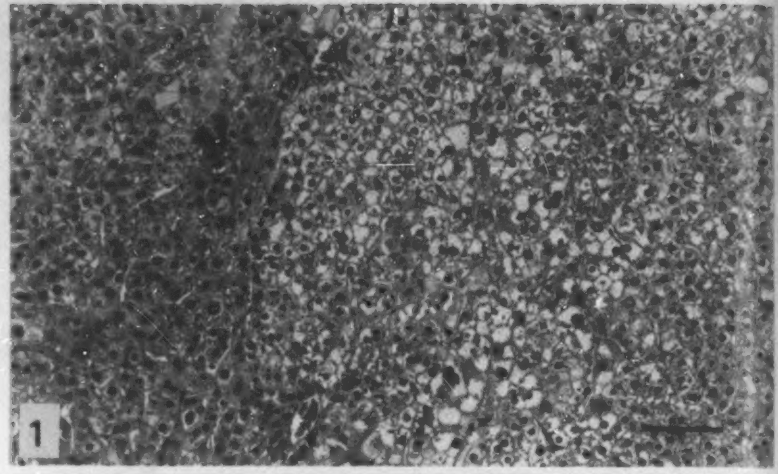

FIGURE 1.—Neoplastic nodule in a female given 0.3% carbazole. Dense proliferation of hepatocytes with an indistinct liver cell plate slightly compresses surrounding normal hepatocytes. H & E. *Bar*=0.1 mm. × 100

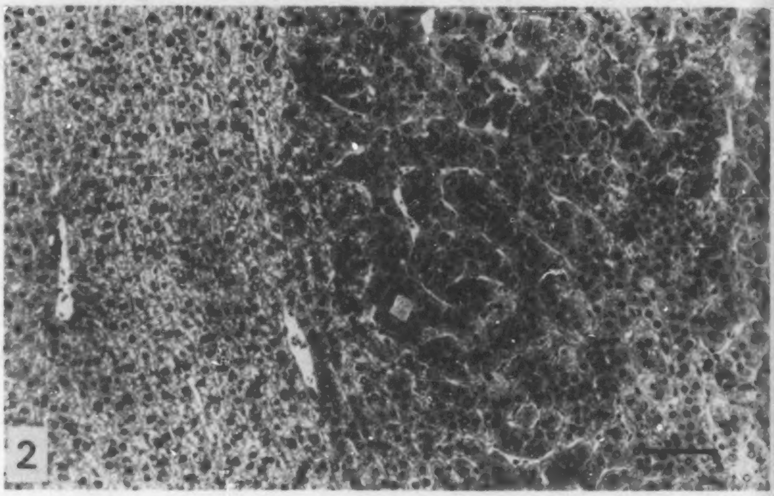

FIGURE 2.—Neoplastic nodule in a male given 0.6% carbazole. Liver cell plates are several cells thick and show expansive growth. H & E. *Bar*= 0.1 mm. × 100

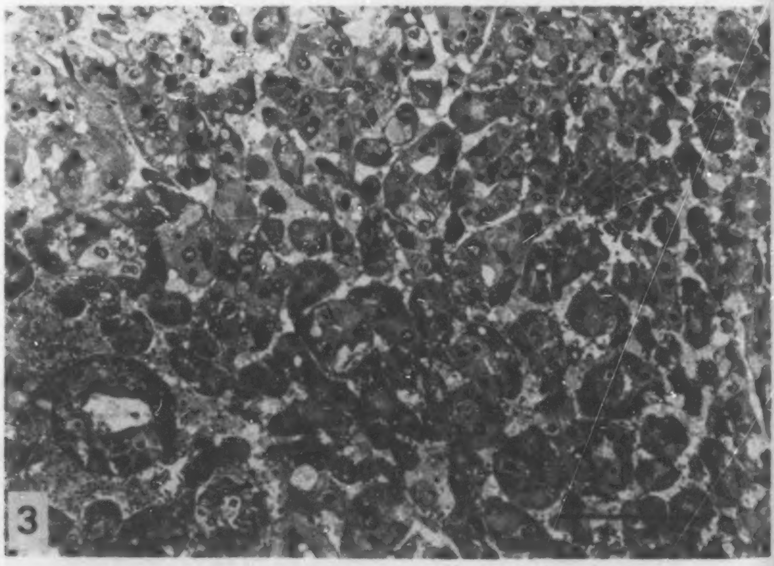

FIGURE 3.—Hepatocellular carcinoma in a male given 0.6% carbazole. Tumor cells are irregular in size and shape and have a trabecular or glandular arrangement. H & E. *Bar*=0.1 mm. × 200

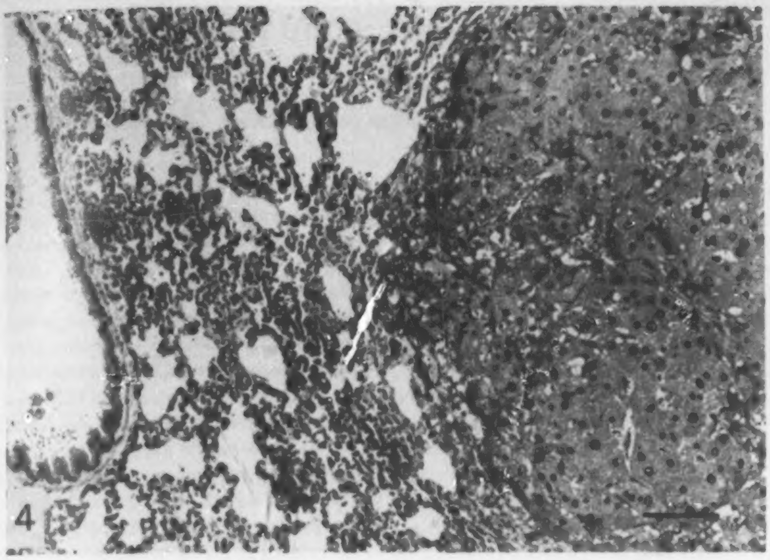

FIGURE 4.—Pulmonary metastasis of a hepatocellular carcinoma in a male given 0.6% carbazole. H & E. *Bar*=0.1 mm. × 100

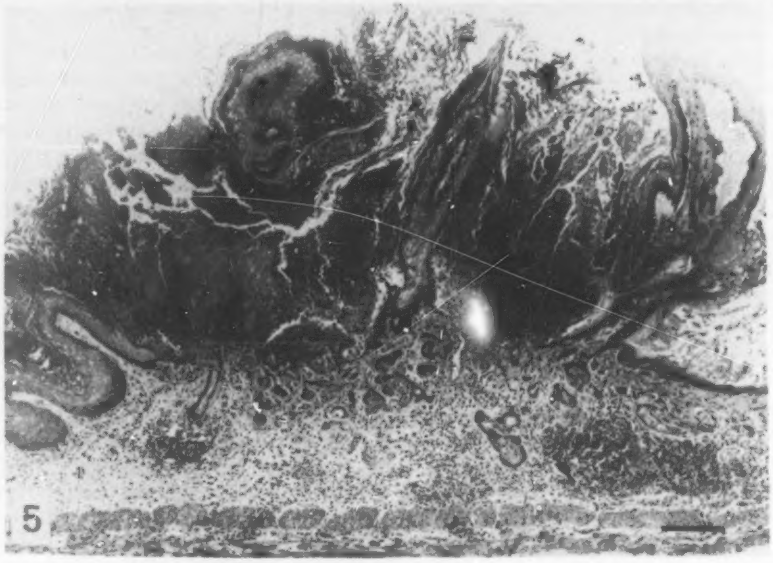

FIGURE 5.—Squamous cell carcinoma of the forestomach in a male given 0.6% carbazole. Invasions to the submucosal layer are evident. H & E. *Bar*= 0.2 mm. × 40

blank page

Hormone Requirements of the Pregnancy-Dependent Mammary Tumor of GR/A Mice: An In Vitro Study[1,2,3,4]

John W. Harbell,[5,6] Jackie S. Papkoff,[5,7] *and* Charles W. Daniel[5,8]

ABSTRACT—The hormones required for cell replication and structural integrity of the inbred GR/A mouse strain-derived, pregnancy-dependent mammary tumor (PDT) were studied with the use of explant organ culture. Through 6 days of culture, a combination of insulin (I), progesterone (P), and prolactin was sufficient to maintain continued cell replication, tissue architecture, and cell integrity. In contrast, the GR/A pregnancy-independent mammary tumors (PIT) required only I to sustain cell replication. Syngeneic transplants of PDT explants after culture yielded predominantly ductal outgrowths with no PIT. These findings are consistent with data obtained in vivo and suggest that the extreme dependence of this tumor on the hormones of pregnancy is best accounted for by considering P to be the pivotal control hormone which, in turn, acts with constitutively present I and pregnancy-stimulated pituitary and placental prolactin activities to promote tumor growth.—JNCI 1982; 69:1391–1402.

The PDT of inbred RIII (*1*), DD (*2*), and GR/A (*3*) mice constitute a unique class of tumors with respect to their extreme hormone dependence. During pregnancy these tumors grow rapidly within the mammary fat pad until parturition, when growth abruptly ceases. The tumors then spontaneously regress, leaving a residue of ductal growth that is similar in appearance to the normal mammary gland of nonpregnant mice. By comparison, mammary adenomas and carcinomas may arise sooner or with increased frequency under the influence of certain hormones, but once induced they show little or no dependence on these hormones for their continued growth (*4*, *5*).

The demonstration by van Nie and Thung (*6*) that exogenous steroid hormones could promote the reappearance of regressed GR/A PDT in nonpregnant hosts strongly suggested that the hormone milieu of pregnancy was the primary promoting agent for their growth. Since this initial study, other workers have attempted to further define the hormone requirements for PDT growth, especially the possible involvement of pituitary and placental hormones (*7–9*).

The present study was done in vitro, with the use of explant organ culture, to obtain a more precise definition of the hormonal milieu and to allow multiple explants from a single primary tumor to be studied under many conditions simultaneously. Explant organ culture rather than monolayer culture was chosen to maintain normal tissue structure and cell interactions. The effects of various hormone concentrations were compared by measurement of the $[^3H]$-thymidine LI and by use of light microscopy and electron microscopy to study structural changes.

MATERIALS AND METHODS

Inbred GR/A mice for breeding were obtained from the Cancer Research Laboratory, University of California, Berkeley. Pregnant females 4–8 months old bearing a spontaneous PDT, usually measuring less than 1 cm across, were anesthetized with Metofane (Pitman-Moore, Inc.) or Nembutal (Abbott Laboratories). Most of the tumor was removed and placed in warm culture medium, while the remaining portion was left in the donor to verify regression after parturition. Following recovery and later delivery of her pups, the donor was monitored by palpation to verify complete regression of the PDT.

The portion of the tumor removed for culture was sliced with a razor blade first into slabs and then into 2-mm explants. All explants were placed in a petri dish partially filled with warm medium. The PDT pieces remained on the dish bottom, whereas any explants of normal tissue that may have been inadvertently taken floated because of their high fat content. Explants of PIT were prepared in the same way from tumors taken from nonpregnant donors 4–8 months old.

Explants were cultured by means of a roller tube culture method previously described (*10*). Each explant was cultured individually in a 16 × 125-mm screw-capped culture tube (Corning Glass Works) containing 5 ml of medium 199 (M.A. Bioproducts) buffered with 20 m*M* HEPES (Sigma Chemical Co.)-5 m*M* bicarbonate and containing 50 IU penicillin/ml and 50 μg streptomycin/ml. A mixture of 95% O_2–5% CO_2 was bubbled through the medium in each tube for 10 seconds, and the tube was sealed. Every 2 days the medium was replaced and the gas saturation renewed.

Hormones were prepared according to standard methods.

ABBREVIATIONS USED: BGH=bovine growth hormone; C=corticosterone; E=17β-estradiol; H=hydrocortisone; HCS=human chorionic somatomammotropin; HEPES=4-(2-hydroxyethyl)-1-piperazine ethanesulfonic acid; I=insulin; LI=labeling index (indices); MCS=mouse chorionic somatomammotropin; oPrl=ovine prolactin; P=progesterone; PDT=pregnancy-dependent mammary tumor(s); PIT=pregnancy-independent mammary tumor(s).

---

[1] Received March 30, 1982; accepted August 4, 1982.

[2] Supported by Public Health Service grant CA-18464 from the National Cancer Institute.

[3] Animals were maintained under the guidelines set forth by the University of California at Santa Cruz and by the National Institutes of Health.

[4] The opinions and assertions contained herein are the private views of the authors and are not to be construed as official or as reflecting the views of the U.S. Department of the Army or the U.S. Department of Defense.

[5] Department of Biology, University of California, Santa Cruz, Calif. 95064.

[6] *Address reprint requests to* Dr. Harbell at his *present address*: Department of Clinical Investigation, Fitzsimmons Army Medical Center, Aurora, Colo. 80045.

[7] *Present address:* Department of Biology, University of California, San Diego, Calif. 92037.

[8] We thank Mrs. Phyllis Strickland and Mrs. Patsy Bolt for technical assistance and Dr. Edith Markoff for advice and encouragement.

The Lente preparation of bovine–porcine I (Eli Lilly & Co.) was used as supplied. C, H, P and E (all from Sigma Chemical Co.) were dissolved in 95% ethanol. BGH (NIH-GH-B17) was dissolved in 0.001 *N* sodium hydroxide, whereas oPrl (NIH-PS-10) and HCS (ICN Pharmaceuticals Inc.) were dissolved in HEPES-buffered water.

Tissue for autoradiography was pulsed with 1 μCi/ml of 60 Ci/mmol [^{3}H]thymidine (New England Nuclear Corp.) for 3 hours just before fixation in Tellyesniczky's fluid. After extensive rinsing, the explants were embedded, sectioned, and processed for autoradiography.

In determining the LI, we found it necessary to take into account variations in cell density that developed with time in culture, particularly in those hormone combinations that favored cell replications (*see* figs. 1–5 and tables 1–3). Areas where the cell density was greatest frequently showed less overall labeling, with more localization of the label into the peripheral layers (≈8 cells deep). Less dense areas frequently showed a more uniform pattern of labeling, presumably due to increased diffusion of precursor nutrients. When determining the LI for different treatment groups, therefore, we always selected for counting areas of similar morphology.

We determined the LI after counting 3,000 cells, consisting of either 1,000 cells from each of three explants or 1,000 cells from each of three widely separated sections of the same explant. Whereas the former method was more desirable, the usual PDT was often too small to permit more than one explant for each time point of a given hormone combination.

Pilot studies using five separately cultured replicate explants to a group yielded a standard deviation of the LI mean of 13% when the LI mean was less than 10% and 10% for LI means above 10%. In addition, the relative proportions of mitotic figures paralleled changes in the LI.

To compare the mean LI (derived from the three 1,000-cell counts) promoted by the different hormone combinations at a given time point, we used the new Duncan-Kramer multiple-range test. This test was chosen so that the large number of treatment groups could be accommodated and because no group could be designated as the base line or control to which the others could be compared. We used the 95% confidence limit throughout the study.

For ultrastructural analysis, explants were fixed in cold 2% glutaraldehyde in 0.074 *M* (314 mosmol) cacodylate buffer at pH 7.4 overnight, followed by postfixation in cold 1% osmium tetroxide in 0.01 *M* cacodylate buffer for 2 hours. After washes and dehydration, each explant was embedded in Epon–Araldite (*11*). Silver sections were stained in uranyl acetate and lead citrate for 10 minutes each.

In some experiments, samples of PDT were transplanted after 6 days in culture into the cleared mammary fat pads of syngeneic female hosts by means of the technique of DeOme et al. (*12*) to detect in vitro selection for the PIT state.

RESULTS

Effects of Pharmacologic Concentrations of Hormones on DNA Synthesis

In the initial series of experiments, PDT explants were subjected to a wide range of hormone combinations, and the data from a representative experiment are given in table 1. With the exception of P and estrogen, these hormones were used at pharmacologic concentrations (*13, 14*).

I and glucocorticoids.—I alone could not sustain a high LI; after 2 days in culture, the LI had dropped precipitously, and by days 4 and 6 it had fallen below 3%. I+C was somewhat more effective through day 2 but allowed a similar LI decline by days 4 and 6. Rather than sustaining even limited PDT maintenance, I+H induced a rapid and consistent depression in the LI and marked degeneration of the tumor epithelium.

TABLE 1.—*PDT responses to a wide range of hormone combinations*[a]

Hormones[b]	LI[c] day 2 (SD)	Morphology[d]	LI day 4 (SD)	Morphology[d]	LI day 6 (SD)	Morphology[d]
LI in I						
Alone	6.5 (1.7)	HP	2.8 (0.3)	MP	1.5 (0.1)	MP
+C	10.3 (1.8)	HP	4.6 (1.0)	HP	1.7 (0.2)	HP
+H	1.0 (0.1)	HP	1.0 (0.1)	Degenerated		
+oPrl	5.1 (0.2)	Ductal	5.6 (0.7)	MP	2.8 (0.1)	MP
+BGH	5.4 (0.4)	HP	5.4 (0.6)	HP	3.0 (0.2)	MP
+E+oPrl	7.2 (1.0)	HP, SD	6.8 (0.9)	D	0.7 (0.3)	MP, HP
+E+BGH	3.1 (2.1)	Ductal	3.3 (0.2)	MD	8.2 (1.3)	MP
LI in P+I						
Alone	15.5 (3.3)	HP, D	10.0 (0.8)	D	6.6 (2.7)	D
+oPrl	*16.7 (1.0)	HP	*15.4 (3.0)	HP, MD	7.8 (0.4)	D
+C+oPrl	7.4 (1.4)	MP, HP	4.6 (1.5)	MP	10.0 (1.8)	D
+E+oPrl	11.5 (4.5)	HP	6.5 (0.1)	MP	*13.9 (1.5)	D
+BGH	*16.6 (1.0)	HP	9.2 (0.8)	HP	5.3 (2.5)	HP
+C+BGH	14.4 (2.2)	HP, MD	5.6 (3.0)	HP, MD	5.0 (1.2)	D
+E+BGH	15.1 (1.2)	HP, SD	13.5 (0.8)	HP, SD	5.0 (0.5)	HP
+C+E+BGH	12.1 (1.1)	HP	5.4 (1.0)	HP, MD	4.6 (1.4)	HP, MD
+E+HCS	16.1 (2.9)	HP, MD	*16.4 (3.3)	HP, MD	*12.7 (1.8)	D
+E	12.3 (0.2)	MP	4.2 (0.2)	HP	1.3 (0.3)	HP

[a] *Asterisks* indicate significantly greater values at 0.05% level compared to the other LI means at that time point.

[b] Hormone concentrations: I=0.14 IU/ml; C and H=1 μg/ml; P=31 ng/ml; E=27 pg/ml; and oPrl, BGH, and HCS=5 μg/ml.

[c] Donor LI=28%.

[d] HP=highly papillomatous, MP=moderately papillomatous, D=dense, SD=slightly dense, and MD=moderately dense.

Ovarian steroids.—In combination with I, P was the most effective hormone in maintaining a high LI. Not only did I+P promote an LI higher than that obtained with any other two hormones, but also the epithelium within the explant became very dense by the 4th day in culture. In the absence of P, no hormone combination was able to sustain a high LI.

Estrogen did not act alone or in combination with other hormones to produce a significant stimulatory or inhibitory effect on the PDT LI.

Prolactin, growth hormone, and HCS.—While ineffective in the absence of P, oPrl, BGH, and HCS, in combination with I+P, characteristically promoted the highest sustained LI throughout the culture period. At 5 μg/ml, all showed rather similar stimulatory activities. There were, however, a minority of PDT that were maintained as well by I+P as by I+P + the protein hormones.

Effects of Physiologic Concentrations of C and Pituitary Hormones on DNA Synthesis

The second series of PDT maintenance experiments shown in tables 2–4 was undertaken to examine certain specific aspects of hormone-promoted maintenance. Among these were trials to determine the requirement for I and the effects of oPrl, BGH, and C at physiologic concentrations.

Pituitary hormones.—The data in table 2 show the clear difference in PDT LI maintenance between oPrl and BGH, in combination with I and P, when the concentration of each was reduced to 250 ng/ml. In contrast, to the relative parity in stimulation at 5 μg/ml (table 1), at this lower concentration only oPrl showed synergism with I+P. In addition, the inability of C to substitute for P was clearly demonstrated.

C.—In subsequent cultures (table 3), a concentration of 35 ng/ml was used, which was approximately equal to the physiologic concentration of free hormone reported by Barlow et al. (*15*).

I.—Both active and inactive hormone combinations were tested with and without I (table 4). After only 2 days in culture, the differences in LI and structural maintenance of the PDT epithelium were dramatic. By the 4th culture day, explants of medium without I were largely degenerated. The I synergism with P (or P + prolactin) was observed with I concentrations as low as 14 μIU (data not shown).

Morphologic Changes and Cell Selection in Culture

The third series of PDT maintenance experiments centered on structural changes during culture and characteristics of outgrowths of cultured tumor explants after transplantation into cleared fat pads of syngeneic female hosts.

In situ, PDT were characterized by hyperplastic ducts several to many cells thick, which grew through a connective tissue matrix (fig. 1). With time in culture, morphologic changes occurred to yield areas of dense, unstructured epithelium as well as papillomatous and hyperplastic ducts (fig. 2), sometimes within a single explant. Variations in cell density markedly affected cell labeling, with dense areas commonly showing less overall labeling, with more localization of the label into the peripheral layers (figs. 3–5). Morphologic observation at each time point for a given hormone combination given in tables 1–3.

In two separate experiments, ultrastructural features of PDT explants were examined after culture in I, I+P, I+P+E, I+P+oPrl, and I+P+E+oPrl up to 6 days (hormone concentrations as in table 3). Thick sections were prepared and areas of similar morphology selected for thin sectioning from each treatment group.

Figure 6 shows cell clusters from a PDT explant fixed directly from the donor in the 14th day of pregnancy. The tumor epithelium could be divided into two cell classes on the basis of cytoplasmic staining properties. Dark cells were characterized by uniformly electron-dense cytoplasm which resulted from a high density of particles about the size of free ribosomes. The second and largest class, light cells, showed a more sparse distribution of these particles. Both cell types contained rough endoplasmic reticulum and Golgi complexes as well as occasional A-particles. B-particles were often observed budding into lumina.

TABLE 2.—*Comparison of P with C and oPrl with BGH in maintaining PDT explants*[a]

Hormones[b]	LI[c] day 2 (SD)	Morphology[d]	LI day 4 (SD)	Morphology[d]	LI day 6 (SD)	Morphology[d]
LI in P+I						
Alone	8.9 (1.3)	MD	5.0 (0.3)	HP, MD	3.2 (0.3)	HP, D
+E	6.3 (1.3)	MP	5.3 (0.1)	D	1.9 (0.6)	D
+oPrl	*16.3 (0.5)	MP	*14.0 (0.4)	D	*10.9 (2.8)	HP, D
+BGH	7.7 (0.5)	MP, HP	5.2 (1.4)	MP, D	3.3 (0.8)	D
+oPrl+E	*12.3 (0.3)	MP	*9.9 (1.9)	D	8.1 (1.1)	HP, D
+BGH+E	10.3 (2.7)	HP, MD	4.4 (1.3)	MP, D	5.3 (1.3)	HP, D
LI in C+I						
Alone	4.1 (1.4)	MP, HP	2.6 (0.7)	HP, D	2.9 (0.9)	D
E	2.8 (0.7)	HP, MD	2.0 (1.0)	HP	4.3 (0.3)	HP, D
oPrl	3.1 (1.1)	Ductal	5.2 (0.5)	MP, D	4.0 (0.1)	HP, D
BGH	3.6 (0.5)	MP	3.6 (1.1)	MP	3.4 (0.1)	HP
oPrl+E	2.1 (0.5)	MP	3.4 (0.5)	HP	6.9 (1.6)	MP, HP
BGH+E	5.6 (0.8)	MP	3.5 (0.2)	HP	4.7 (1.7)	MP
I alone	3.6 (1.3)	MP, HP	1.9 (0.3)	MP	3.9 (0.9)	HP

[a] *Asterisks* indicate significantly greater values at the 0.05% level compared to the other LI means after the same time in culture.

[b] Hormone concentrations: I=0.14 IU/ml, C=35 ng/ml, P=31 ng/ml, E=27 pg/ml, BGH= 250 ng/ml, and oPrl=250 ng/ml.

[c] Donor LI=20.4%.

[d] HP=highly papillomatous, MP=moderately papillomatous, D=dense, and MD=moderately dense.

TABLE 3.—*Action of C with supportive hormone combinations on PDT explants*[a]

Hormones[b]	LI[c] day 2 (SD)	Morphology[d]	LI day 4 (SD)	Morphology[d]	LI day 6 (SD)	Morphology[d]
LI in I						
Alone	5.1 (0.4)	HP, MD	2.1 (0.6)	HP	1.5 (0.1)	HP
+P+E	17.9 (2.8)	HP, MD	4.3 (0.3)	D	7.5 (0.4)	MD
+P+oPrl	*21.0 (1.1)	SD	8.8 (0.6)	D	4.4 (0.2)	D
+P+E+oPrl	16.6 (0.9)	HP, D	11.0 (1.1)	SD, D	7.2 (2.8)	HP
LI in C+I						
Alone	5.6 (0.3)	HP, SD	3.5 (1.2)	HP, MD	1.5 (0.1)	D
+P+E	13.7 (1.2)	HP, MD	8.2 (0.1)	D	5.2 (1.6)	D
+P+oPrl	14.2 (1.1)	MD	*15.1 (1.7)	HP, MD	8.1 (1.4)	D
+P+E+oPrl	*18.7 (1.3)	HP, SD	10.4 (0.7)	MD	6.2 (2.3)	D

[a] *Asterisks* indicate significantly greater values at the 0.05% level compared to the other LI means after the same time in culture.

[b] Hormone concentrations: I=0.14 IU/ml, C=35 ng/ml, P=31 ng/ml, E=27 pg/ml, and oPrl= 250 ng/ml.

[c] Donor LI=25%.

[d] HP=highly papillomatous, D=dense, SD=slightly dense, and MD=moderately dense.

After culture in I alone or I+H, considerable degeneration was manifest. As seen in figure 7, extensive autolysis was present in many cells. The mitochondria were swollen and had lost much of their internal structure. Large masses of degenerating cytoplasmic debris as well as lamellar inclusions were found in several cells in each field. Nuclear degeneration was not readily apparent by days 4 and 6.

Explants cultured in I+P+oPrl, I+P+E+oPrl, and I+P+E+HCS (fig. 8) stood in sharp contrast to those cultured in I or I+H. Gross degeneration was absent, and very few cells showed any signs of autolysis. Some cells did contain vacuoles, though for the most part other cytoplasmic components were very much intact. Both A- and B-particles were prevalent. Tumor explants in I+P or I+E+P were not as well maintained as those also receiving oPrl or HCS. Overall, a close correlation was observed between maintenance of a high LI by a hormone combination and the absence of ultrastructural degeneration.

Outgrowths of cultured PDT.—As previously described, PDT explants underwent certain morphologic changes during their period in culture. Those cultured in hormone combinations that did not support continued tumor cell replication often remained only moderately papillomatous or even regressed to a simple ductal morphology, whereas those in which active cell replication continued became very dense. The dense areas of PDT epithelium were often quite anaplastic, and it was not clear from their morphology whether or not these cells had progressed to a more neoplastic state. It was also of interest to determine whether cultures in nonsupportive conditions contained surviving tumor cells that were less hormone-dependent (e.g., PIT cells).

TABLE 4.—*I synergism with other hormones required for PDT maintenance*[a]

Hormones[b]	LI[c] day 2 (SD), with I	LI day 2 (SD), without I
LI in		
Medium 199 alone	1.1 (0.4)	*6.0 (1.2)
oPrl	1.1 (0.5)	*7.0 (0.3)
C+oPrl	2.8 (1.0)	4.0 (0.6)
E+oPrl	4.5 (1.3)	5.0 (0.1)
P	2.6 (0.8)	*22.0 (1.8)
P+oPrl	6.3 (1.0)	*21.0 (2.0)
E+P+oPrl	6.0 (0.9)	*19.3 (1.3)

[a] *Asterisks* indicate significantly greater values at the 0.05 level compared to the same combination without I.

[b] Hormone concentrations: I=0.14 IU/ml, C=35 ng/ml, P=31 ng/ml, E=27 pg/ml, and oPrl=250 ng/ml.

[c] Donor LI=28%.

The cleared fat-pad transplantation technique of DeOme et al. (*12*) provided a means to examine cultured PDT explants for changes in growth potential. Using this technique, we transplanted representative explants from several experiments after 6 days in culture. Explants maintained in the full range of hormone combinations were used: highly active (I+P+oPrl, I+P+E+oPrl, and I+P+E+HCS), moderately active (I+P, I+P+E, I+P+BGH), and nonsupportive (I, I+H, I+oPrl, I+BGH, I+E+oPrl, and I+E).

No PIT growth was observed in any of the outgrowths of cultured PDT tissue, and after 4 months the hosts were bred and the glands removed between days 10 and 15 of gestation. After fixation and staining, the outgrowths were examined as wholemounts.

Most outgrowths were predominantly PDT or PDT with some tissue that resembled normal gland (fig. 9). A few outgrowths were entirely normal, though no consistent pattern between in vitro maintenance and these normal outgrowths was observed. Even PDT explants taken directly from a pregnant donor sometimes gave rise to normal outgrowth (Harbell JW: Unpublished observation), so the absence of PDT growth in these transplants did not necessarily indicate the loss of tumor burden as a function of the culture conditions.

PIT culture.—Unlike the PDT, the PIT was not expected to require the hormones of pregnancy and perhaps not even the mammotropic hormones of the nonpregnant female. The requirement for only constitutive hormones to sustain the PIT would stand in clear contrast to those hormones required by the PDT. Hormone combinations were selected to include those that would maintain the PDT and those that clearly would not.

The data from one such experiment are shown in table 5. In contrast to the results of a similar PDT culture (table 4), the PIT was about equally sustained by all hormone combinations that contained I. The requirement for I appeared to be absolute, irrespective of which other hormones were added.

TABLE 5.—*I-mediated maintenance of the PIT*[a]

Hormones,[b] LI in:	LI[c] day 2 (SD)		LI day 4 (SD)	
	Without I	With I	Without I	With I
Medium 199 alone	1.0 (0.1)	*15.1 (0.4)	1.0 (0.2)	*12.3 (0.6)
oPrl	4.2 (0.6)	*15.6 (0.8)	5.2 (0.8)	*13.5 (1.0)
C+oPrl	2.5 (0.2)	*14.0 (0.6)	1.4 (0.1)	*16.0 (0.8)
P	1.4 (0.6)	*15.0 (0.8)	1.5 (0.2)	*11.0 (0.7)
P+oPrl	1.0 (0.4)	*16.6 (0.9)	1.1 (0.4)	*19.8 (1.4)
E+P+oPrl	3.4 (0.9)	*18.0 (1.1)	3.1 (0.5)	*15.7 (0.9)

[a] *Asterisks* indicate significantly greater values at the 0.05 level compared to the same combination without I.

[b] Hormone concentrations: I=0.14 IU/ml, C=35 ng/ml, P=31 ng/ml, E=27 pg/ml, and oPrl=250 ng/ml.

[c] Donor LI=11.7%.

DISCUSSION

The organ culture technique has proved to be a reliable method for investigations of hormonal requirements of endocrine target tissues (*16*). In the present studies it was consistently found that even the most supportive hormone combinations permitted some reduction in LI over the very high rate found in some tumors in vivo. This appears to be a constraint of the organ culture system, which may be due to the fact that proliferating epithelium in explant cultures does not have unoccupied stroma available into which it can expand. As a result, proliferation is reflected in increased epithelial density in cultured explants, whereas in vivo the same proliferation would result in increased tumor size. In isolated instances (table 1; P+I+C+oPrl, P+I+C+E+oPrl, P+I+E+oPrl), the LI declined at 4 days in culture but increased at 6 days to a value equaling or surpassing that observed at 2 days. We cannot determine at present whether this rebound phenomenon represents a delayed response to pharmacologic doses of pituitary or adrenal hormones or is a result of sampling error associated with the explants at those time points.

The cumulative data from the maintenance experiments indicated that a combination of three hormones, I, P, and prolactin, permitted the PDT epithelial cells to continue replication in vitro. Of these three, P and prolactin have been previously implicated from in vivo studies (*3, 9, 17*), whereas the role of I has only recently been suggested (*18*).

I.—I has been shown to induce limited epithelial cell replication and to act in concert with glucocorticoids and prolactin (or placental lactogen) to promote differentiation in organ culture of normal mouse mammary gland (*19, 20*), including that from the GR/A mouse (*21*). In this study, I also provided sufficient stimulus to allow PIT cell replication to continue in a way similar to results reported for other murine mammary carcinomas (*22*). In contrast to the PIT, I alone did not sustain a high LI in PDT explants but was essential to the action of other hormones. The decline in the LI observed in PDT explants cultured in I alone was paralleled by ultrastructural degeneration, indicative of tumor regression rather than just the cessation of DNA synthesis. Thus while the transition from pregnancy dependence to pregnancy independence reduced or eliminated the need for ovarian and pituitary (placental) hormones, the I requirement was retained. I appeared to be a ubiquitous requirement of normal, PDT, and PIT GR/A mammary epithelium. Such has also been the case for most mammary tumors studied (*22*), though certain lines of the 7,12-dimethylbenz[*a*]anthracene-induced rat mammary tumor (R3230AC) showed decreased growth when exposed to I (*23*).

P and prolactin.—The requirements for P and prolactin in the promotion of PDT growth have been the subject of numerous studies (*3, 7-9, 17*). Most of these reports were concerned with the induction of regrowth from regressed PDT or steroid-induced tumors, and the determination of an effective response was based on the production of palpable or microscopically visible tumors. van Nie and Thung (*6*) were the first to show that exogenous P alone was insufficient to promote regrowth, but a combination of P and estrone was effective.

The data presented from this study demonstrated the direct action of P on PDT epithelial cells and, as suggested by the data of Yanai and Nagazawa (*8*) the data further demonstrated that P was the pivotal hormone required for growth promotion. In the absence of P no hormone combination promoted more than minimal cell replication, though with the exception of a small minority of the PDT examined, significantly more cells continued to cycle when prolactin (or HCS) was combined with I and P. Surprisingly, estrogen, which was required as an exogenous addition with P for tumor regrowth in vivo, could not be shown to exert a consistent, direct, positive influence on PDT maintenance in vitro.

If I, P, and prolactin are the hormones required for PDT growth in vivo, then one or more of them must exert its PDT growth-promoting influence predominantly during pregnancy. Since tumor growth occurs only during pregnancy (*7*), the presence of the promoting agents above the threshold level must be limited to that period. If all three hormones together are the promoting agent, then the lack of only one should be sufficient to prevent promotion or to terminate growth. Of the three, the omnipresent nature of I makes it unlikely to be the factor missing for promotion in the nonpregnant state. Changes in P and/or prolactin concentration are more likely the difference.

Serum prolactin levels have been determined for several mouse strains, in virgin females as well as throughout pregnancy (*24*). Basal serum prolactin levels vary greatly between the strains tested (27–180 ng/ml). The GR/A strain was not among the strains tested. Measurements taken during pregnancy of the C3H strain indicated elevated prolactin levels during the first 10 days, a return to almost preconception levels from days 10 to 15, and a rapid rise from day 15 to parturition (*24*). This pattern was also reported by Murr et al. (*25*) using the outbred C-stock mouse, though the absolute levels detected were over twice those reported by Sinha et al. (*24*) for the C3H strain. After parturition, the highest levels of prolactin were observed. Therefore, while the rise in serum prolactin that began during early pregnancy coincides with early induction of PDT growth, the equally high prolactin levels at parturition would not be expected to bring a cessation of tumor growth.

In contrast to the serum levels of prolactin, the serum levels of P rise and fall concurrently with the beginning of PDT growth and regression. In an unpublished study (Aidells BD) serum P levels during pregnancy of the GR/A mice followed a pattern similar to that reported by Murr et al. (*25*) for the outbred C-stock. Murr et al. found that total (bound and unbound) serum P rose from 10 ng/ml on day 0 to over 40 ng/ml on day 2. The level remained at between 45 and 55 ng/ml through day 9 and dropped to 35 ng/ml on day 10. Following this temporary decline, the level rose progressively to a maximum of 110 ng/ml on day 15. While the level declined rapidly to less than 10 ng/ml on day 19 (parturition), it was still 40 ng/ml on day 18. Thus if the threshold for P activation of PDT growth is below 30 ng/ml, the P available in the virgin would be insufficient to synergize with I and prolactin. Similarly, the reduction in the level of progesterone after day 18 of gestation would account for the cessation of PDT growth. In serum 30 ng corticosterone/ml is not comparable to 30 ng/ml in culture medium because the former is largely protein-bound while the latter is unbound.

The serum concentrations of three other hormones (C, growth hormone, and chorionic somatomammotropin) also undergo substantial increases during pregnancy. Barlow et al. (*15*) reported a dramatic rise in C levels from 0.20 μg/ml on day 10 of gestation to a maximum of 1.4 μg/ml on day 16. The level then rapidly decreased to 0.20 μg/ml on day 20. These were measurements of total serum C, of which less than 2% was unbound. Therefore, the maximum free (active) level was less than 28 ng/ml.

MCS is produced after day 6 of gestation, and its level rises rapidly while the placenta is intact (*26*). Because HCS was effective in promoting PDT growth in consort with I and P, the murine counterpart may possess similar activity. However, Aidells (*27*) has shown that early PDT growth occurred before the placenta was functional. Thus while MCS may be active in supporting PDT growth in vivo, this stimulation may result from its prolactin-like activity (*28*) rather than some unique property of this hormone.

We propose the following model for the promotion of PDT growth in the GR/A mouse during pregnancy. After conception, the elevated circulating level of P acts in association with I and elevated prolactin to promote replication of mammary epithelial cells whose transformation was previously initiated by the murine mammary tumor virus-plaque. P and MCS from the functioning placenta supplement the maternal factors and account for the rapid growth observed during the second half of pregnancy. Not surprisingly, at least some of these hormones are also responsible for the growth of the normal mammary gland during pregnancy (*21*). The cessation of active growth and subsequent regression result from the precipitous decline in circulating P just before parturition. This model is consistent with our data on the maintenance of PDT cell replication in vitro and with known changes in hormone concentrations throughout pregnancy. This model does not, however, account for the failure of exogenous P + estrogen to maintain PDT growth post partum, though regression was much slower in these supplemented hosts.

Sluyser et al. (*29*) have proposed that the hormone-dependent (steroid-induced) mammary tumor in GR mice contains both hormone-dependent and hormone-independent cells. With successive growth cycles, the percentage of hormone-independent cells increases until finally they predominate yielding a hormone-independent tumor. The PDT might also contain PIT cells, though the lack of PIT growth after regression of most PDT suggests that progression to the independent state is a subsequent rather than concurrent event to PDT induction. In addition, the failure of any hormone combination, even those combinations that would clearly not support the PDT cells, to select for appreciable numbers of PIT cells was revealed by the ductal phase outgrowths of cultured PDT explants in syngeneic hosts.

The possibility that small numbers of PIT cells may have been present cannot be ruled out, however. Transplants containing both normal and nodule cells (*30*) and normal and tumor cells (DeOme KB: Personal communication) have been shown to give rise to normal outgrowths if the percentage of normal cells was sufficiently high. Therefore, the outgrowth study might not have revealed a minority population of independent cells if their numbers were sufficiently small.

REFERENCES

(*1*) Foulds L. The histologic analysis of mammary tumors of mice. II. The histology of responsiveness and progression. The origins of tumors. J Natl Cancer Inst 1956; 17:713–753.

(*2*) Matsuzawa A, Yamamoto T. Response of a pregnancy-dependent mouse mammary tumor to hormones. J Natl Cancer Inst 1975; 55:447–453.

(*3*) van Nie R, Dux A. Biological and morphological characteristics of mammary tumors in GR mice. J Natl Cancer Inst 1971; 46:885–897.

(*4*) Welsh CW. Interaction of estrogen and prolactin in spontaneous mammary tumorigenesis of the mouse. J Toxicol Environ Health [Suppl] 1976; 1:161–175.

(*5*) Nandi S, McGrath CM. Mammary neoplasia in mice. Adv Cancer Res 1973; 17:353–414.

(*6*) van Nie R, Thung PJ. Responsiveness of mouse mammary tumors to pregnancy. Eur J Cancer 1965; 1:41–50.

(*7*) Aidells BD, Daniel CW. Hormone-dependent mammary tumors in strain GR/A mice. III. Effectiveness of supplementary hormone treatments in inducing tumorous phase growth. J Natl Cancer Inst 1976; 57:527–537.

(*8*) Yanai R, Nagasawa H. Importance of progesterone in DNA synthesis of pregnancy-dependent mammary tumors in mice. Int J Cancer 1976; 18:317–321.

(*9*) Briand P, Thorpe SM, Daehnfeldt JL. Effect of prolactin and bromocriptine on growth of transplanted hormone-dependent mouse mammary tumours. Br J Cancer 1977; 35:816–821.

(*10*) Harbell JW, Bowman PD, Shannon JM, Daniel CW. Long-term organ culture of mouse mammary gland. In Vitro 1977; 13:490–496.

(*11*) Bojax A. Plastic embedding mixtures for use in electron microscopy. J Stain Tech 1963; 39:111–114.

(*12*) DeOme KB, Faulkin LJ, Bern HA, Blair PB. Development of mammary tumors from hyperplastic alveolar nodules transplanted into gland-free mammary fat pads of female C3H mice. Cancer Res 1959; 19:515–520.

(*13*) Murr SM, Stabenfeldt JL, Bradford GE, Geschwind II. Plasma progesterone during pregnancy in the mouse. Endocrinology 1974; 94:1209–1211.

(*14*) McCormack JT, Greenwald GS. Progesterone and oestradiol-17β concentrations in the peripheral plasma during pregnancy in the mouse. J Endocrinol 1974; 62:101–107.

(*15*) Barlow SM, Morrison PJ, Sullivan FM. Plasma corticosterone levels during pregnancy in the mouse: The relative contributions of the adrenal glands and foeto-placental units. J Endocrinol 1974; 60:473–483.

(16) Forsyth IA, Jones EA. Organ culture of mammary and placenta in the study of hormone action and placental lactogen secretion. In: Balls M, Mommickendam M, eds. Organ culture in biomedical research (Br Soc for Cell Biol Symp 1). Cambridge: Cambridge Univ Press, 1976:201–221.

(17) Yanai R, Nagasawa H. Effect of progesterone and estrogen of DNA synthesis of pregnancy-dependent mammary tumors in GR/A mice. Eur J Cancer 1977; 13:813–816.

(18) Aidells BD. Effect of hormones on primary cell cultures from pregnancy-dependent mouse mammary tumors. Cell Biol Int Rep 1979; 3:359–371.

(19) Rivera EM, Bern HA. Influence of insulin on maintenance and secretory stimulation of mouse mammary tissues by hormones in organ-culture. Endocrinology 1961; 69:340–353.

(20) Hsueh HW, Stockdale FE. Serum and insulin initiation of DNA synthesis in mammary gland epithelium in vitro. J Cell Physiol 1974; 83:297–308.

(21) Harbell JW. Hormone requirements of the pregnancy-dependent mammary tumor from GR mice: An in vitro study. Ph.D. dissertation. Santa Cruz: University of California, 1978.

(22) Welsch CW, De Iturri GC, Brennan MJ. DNA synthesis of human, mouse and rat mammary carcinomas in vitro. Cancer 1976; 38:1272–1281.

(23) Hilf R, Hissin PJ, Shafle SM. Regulatory interrelationships for insulin and estrogen action in mammary tumors. Cancer Res 1978; 38:4076–4085.

(24) Sinha YN, Salocks CB, Vanderlaan WP. Prolactin and growth hormone levels in different inbred strains of mice: Patterns in association with estrous cycle, time of day and perphenazine stimulation. Endocrinology 1975; 97:1112–1122.

(25) Murr SM, Bradford GE, Geschwind II. Plasma leuteinizing hormone, follicle-stimulating hormone and prolactin during pregnancy in the mouse. Endocrinology 1974; 94:112–116.

(26) Markoff E, Talamantes F. Serum placental lactogen in mice in relation to day of gestation, time of day and number of conceptuses. Biol Reprod 1981; 24:846–851.

(27) Aidells BD, Daniel CW. Hormone-dependent mammary tumors in strain GR/A mice. I. Alternation between ductal and tumorous phases of growth during serial transplantation. J Natl Cancer Inst 1974; 52:1855–1863.

(28) Markoff E, Talamantes F. Characterization of mouse placental lactogen. Endocrinology. In press.

(29) Sluyser M, Evers SG, De Goeij CC. Sex hormone receptors in mammary tumours of GR mice. Nature 1976; 263:386–389.

(30) DeOme KB, Miyamoto MJ, Osborn RC, Guzman RC, Lum K. Detection of inapparent nodule-transformed cells in the mammary gland tissue of virgin female BALB/cfC3H mice. Cancer Res 1978; 38:2103–2111.

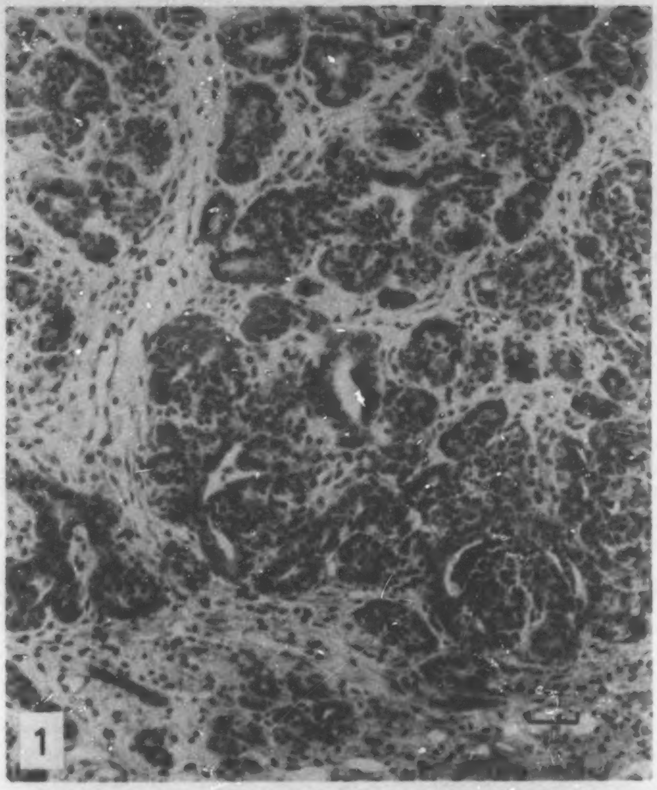

FIGURE 1.—In vivo, the PDT is characterized by hyperplastic ducts growing through a connective tissue matrix. This example was taken on day 16 of gestation and shows the absence of fat cells through which the normal gland grows. *Bar*=50 μm. × 150

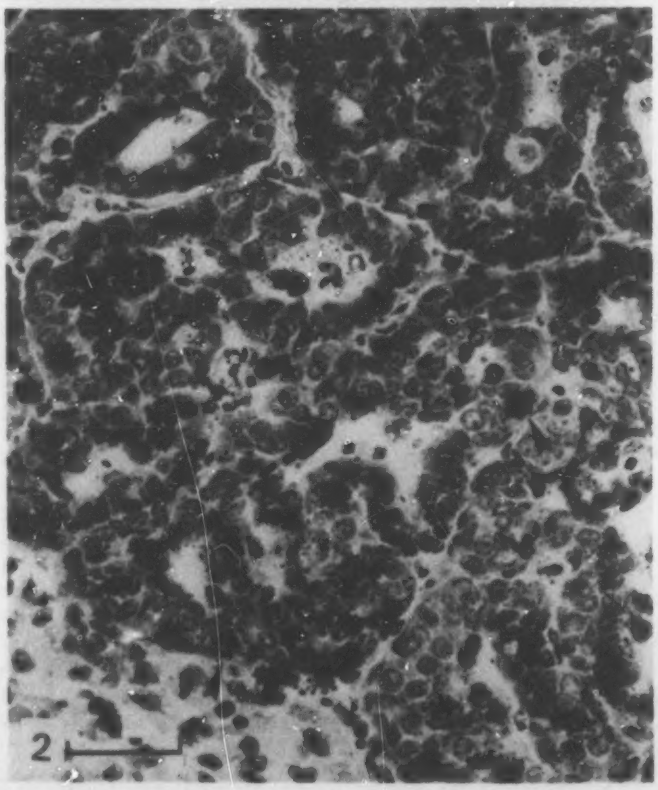

FIGURE 2.—This highly papillomatous morphology was observed by day 2 of culture in explants showing active cell proliferation. Labeled nuclei (*arrowheads*) are seen in this autoradiographic preparation. *Bar*=50 μm. × 350

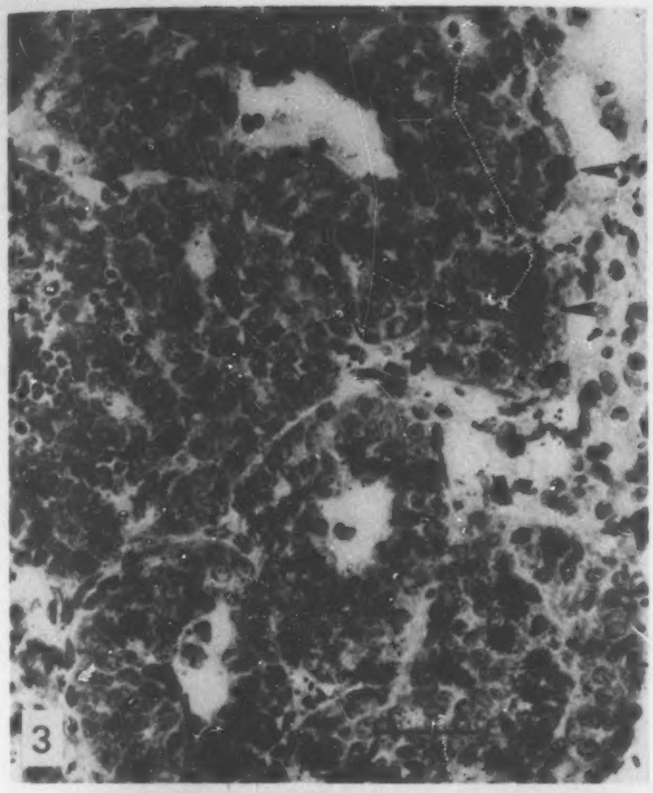

FIGURE 3.—Moderately dense morphology was characterized by increased cell density and partial to complete occlusion of the ductal lumina. Numerous labeled nuclei (*arrowheads*) are also seen. *Bar*=50 µm. × 350

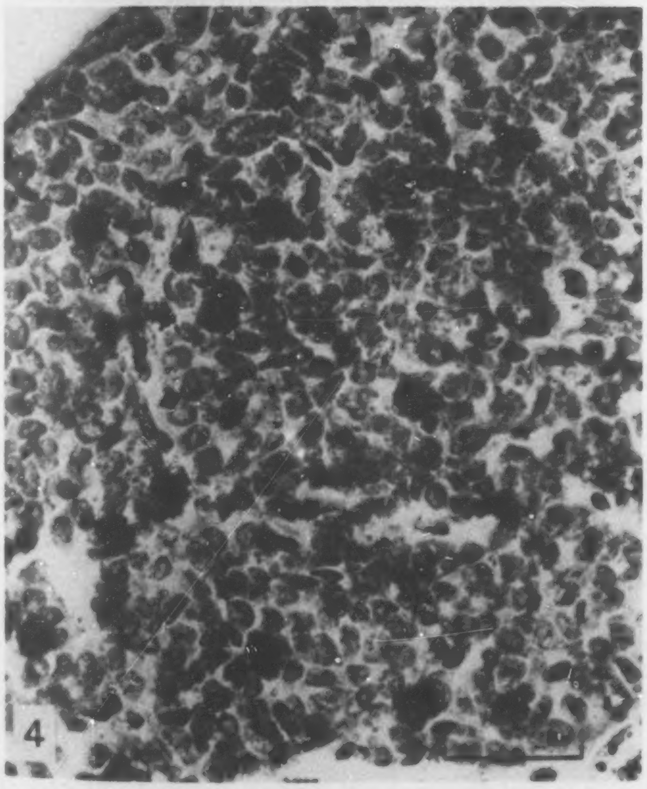

FIGURE 4.—Large, densely cellular areas observed by days 4–6 of culture of actively proliferating explants were often very anaplastic. Autoradiograph. *Bar*=50 µm. × 390

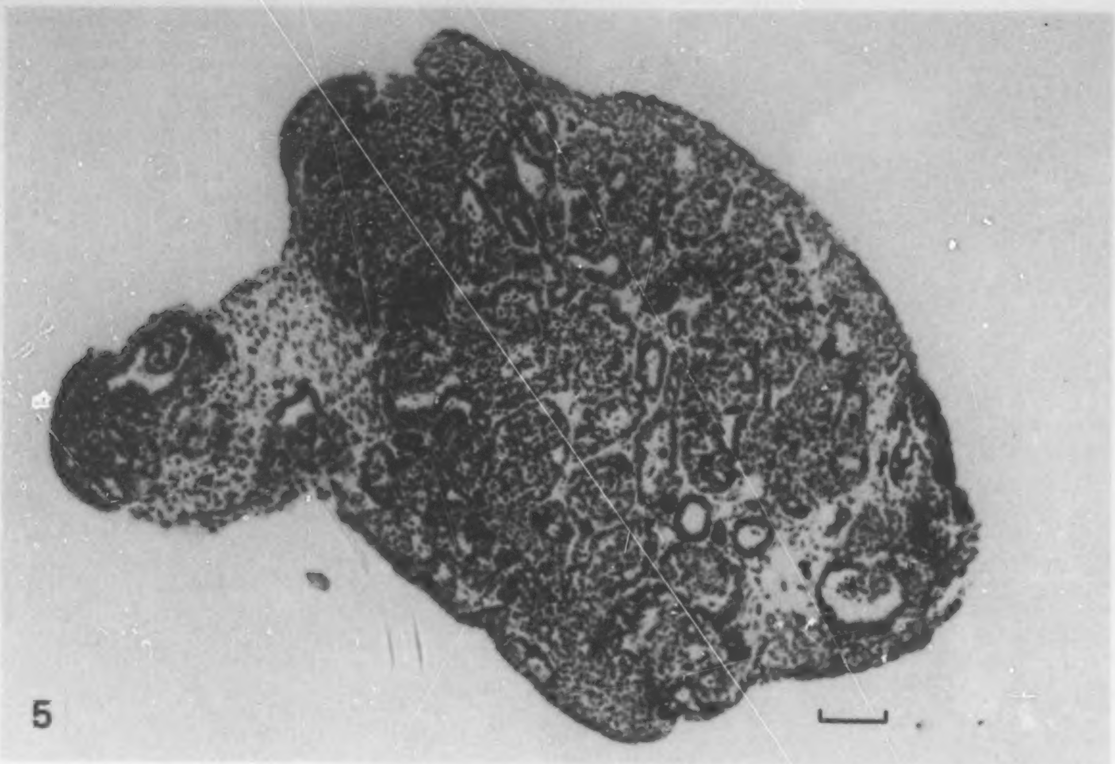

FIGURE 5.—After 6 days in supportive hormone combinations, dense anaplastic structures predominated in the explants. This explant was cultured with I+P+oPrl+C (*see* table 3). *Bar*=100 µm. × 98

FIGURE 6.—Taken directly from the donor, this PDT was composed largely of hyperplastic ducts. Hyperplastic duct shown in this micrograph contains mostly light cells and several small lumina (L) and a portion of one dark cell. Duct was surrounded by a well-formed basal lamina (BL). No virus particles are seen in this micrograph, though they were observed in other areas of this section. *Bar*=1 µm. × 5,610

FIGURE 7.—Extensive ultrastructural degeneration was observed in explants cultured in hormone combinations that did not sustain high LI. This example was cultured in I+H for 4 days. Extensive cytoplasmic vacuolization and autolysis were evident. *Bar*=1 µm. × 5,600

FIGURE 8.—After 4 days in I+P+oPrl, this explant was very well maintained. Virus particles (V) were observed budding into the lumen and from the cells on the explant surface. *Bar*=1 µm. × 5,610

FIGURE 9.—These outgrowths of contralaterally transplanted cultured PDT explants were removed from the host on day 11 of gestation. Dense areas of PDT growth are evident (*arrowhead*) as well as areas of apparent normal morphology (N). *Bar*=1 mm. × 11

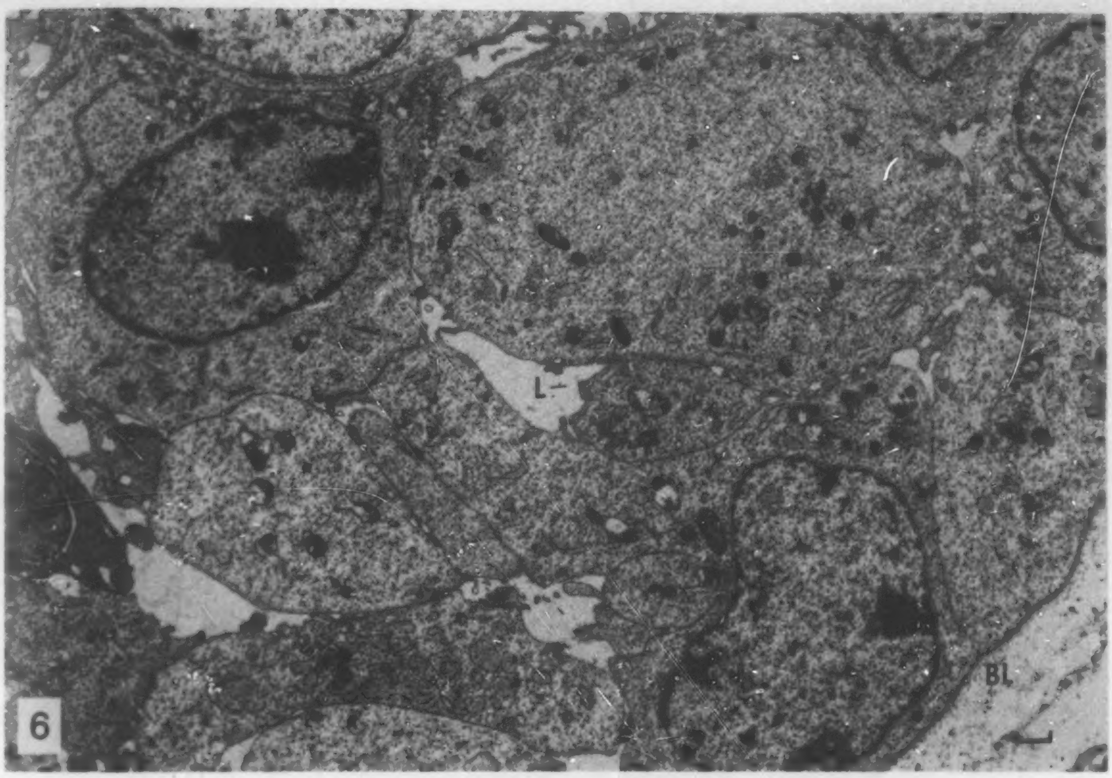
6
L
BL

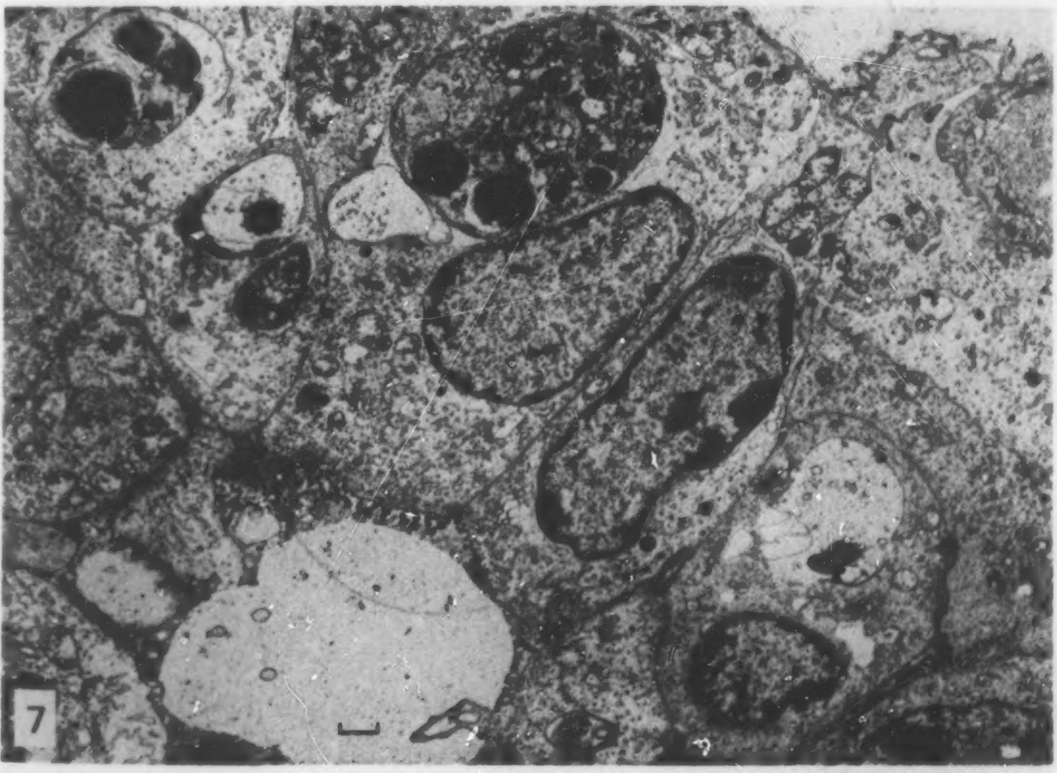
7

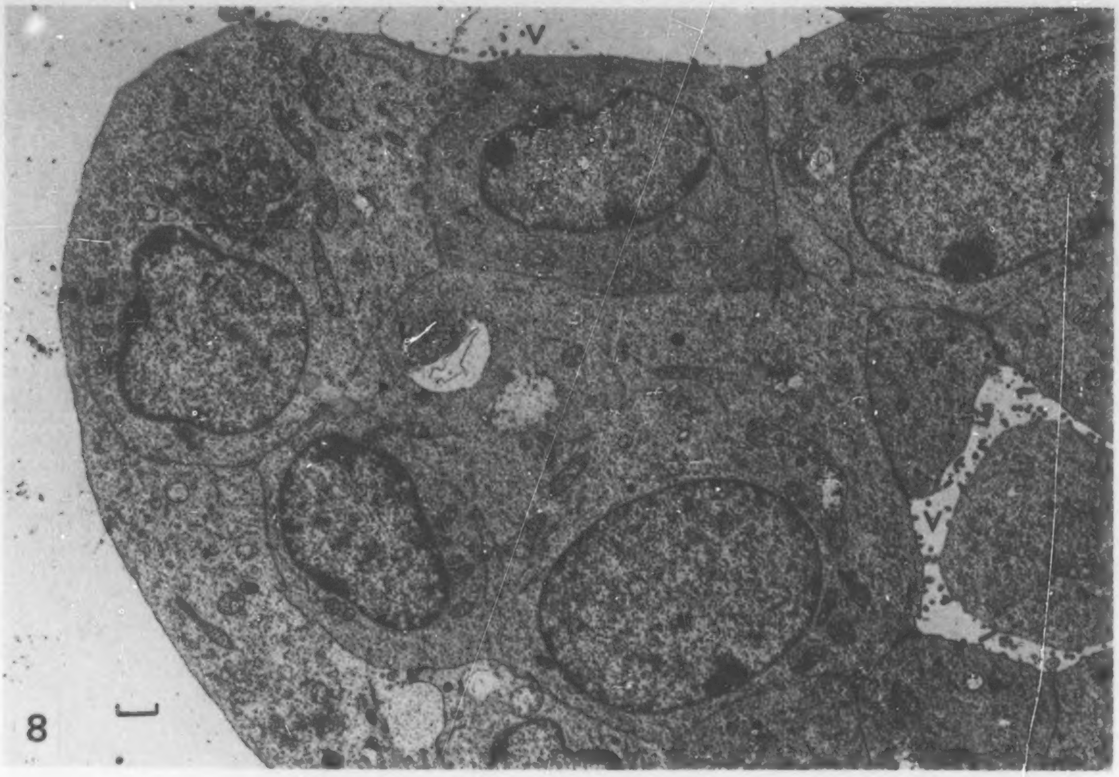
8

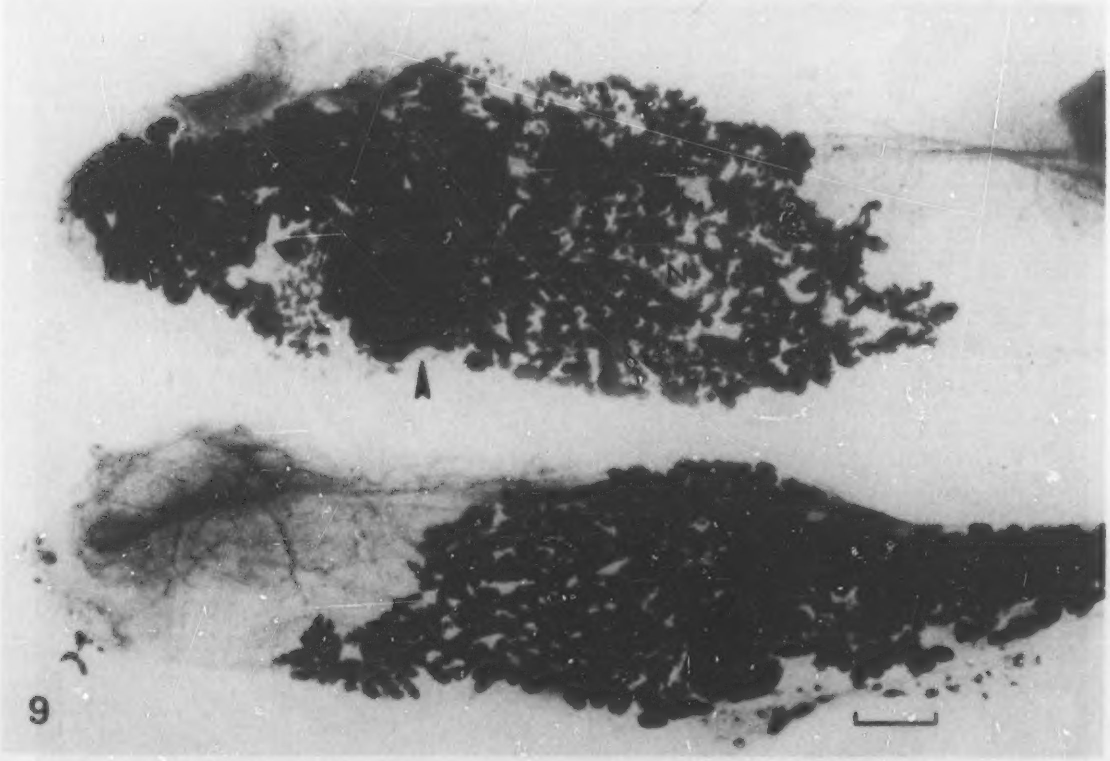
9

Analysis of Lymphoid Cells Responding to Virus- and Tumor-Associated Antigens in Spleens of Syngeneic Mouse Mammary Tumor Systems With Low and High Oncogenic Potentials[1,2,3]

Diana M. Lopez[4,5] *and* **Ronald D. Paul**[4,5,6]

ABSTRACT—Nylon-nonadherent cells obtained from the spleens of tumor bearers of two BALB/c mouse colonies with different oncogenic potentials were found to be the lymphocyte subclass responsive in blastogenesis to their tumor-associated antigens (TAA). Thus Thy 1-positive spleen cells from BALB/cCrgl mice that received implants of a syngeneic, chemically induced mammary tumor and BALB/cfC3H mice bearing spontaneous mammary tumors (SMT) incorporated high levels of $[^3H]$thymidine after in vitro exposure to homologous TAA preparations. These responses were evident in animals at the early stages of tumorigenesis but could not be detected in the T-cells of animals with large tumor burdens. Responses to murine mammary tumor virus (MuMTV) antigens were observed likewise in the nylon-nonadherent spleen cell population of the MuMTV-positive BALB/cfC3H mice bearing small SMT. The responsiveness to viral antigens also decreased with progression of the disease. In BALB/cCrgl mice, which have a low incidence of SMT and are devoid of intact mouse mammary tumor virions, T-lymphocytes appeared to be nonresponsive to MuMTV antigens, but nylon-adherent spleen lymphocytes were capable of being stimulated by MuMTV. The blastogenic response of these B-lymphocytes was not altered by tumor initiation or progression. Depletion studies with the use of either anti-Thy 1 or antisurface immunoglobulin sera plus complement confirmed the validity of the results observed in the nylon wool column separation studies. Flow cytometric analyses of the spleen cells of tumor-bearing mice from both colonies revealed a depression of the levels of T-lymphocytes with increasing tumor burden while there was no decrease in the percentage of B-cells. These results provided a possible explanation for the loss of blastogenic response to tumor antigens and to MuMTV observed in spleen cells of BALB/cfC3H mice with increasing tumor burden and for the unalterable responses to MuMTV that appeared in splenocytes of BALB/cCrgl mice at all stages of tumorigenesis.—JNCI 1982; 69:1403–1409.

Neoplasms induced by a single viral agent appear to have a common tumor antigen (*1–3*). In contrast, tumors induced by chemical or physical agents have been shown to possess antigens specific for each tumor (*4–6*).

Studies in several laboratories including our own laboratory (*7–11*) have indicated that in mammary tumors there may be at least three types of antigens relevant to the host defenses: virion-associated, virus-induced, and nonviral TAA. In our investigations we have used two syngeneic BALB/c colonies, BALB/cCrgl and BALB/cfC3H, in an attempt to elucidate the individual contributions of the various antigenic moieties to the development of resistance to mammary tumors. BALB/cCrgl mice and their splenocytes react to purified MuMTV in cell-mediated immune reactions (*12*). These reactivities correlated with a very low incidence of SMT. In contrast, syngeneic BALB/cfC3H mice obtained by foster nursing BALB/cCrgl mice on C3H mothers contain MuMTV particles and have a high incidence of SMT in which MuMTV can be detected. Splenocytes of these mice have low levels of responsiveness to MuMTV except after development or transplantation with SMT (*13*). Both lines of mice have similar patterns in cell-mediated immune assays to their respective TAA. Thus they show no responses before transplantation, have peaked reactivities 2–3 weeks after implantation of tumors, and fail to respond when their tumors reach maximum size (*14*). A similar pattern is also observed when spleen cells of BALB/cfC3H mice are exposed to MuMTV antigen(s) in vitro, indicating a de novo sensitization, while in BALB/cCrgl mice there appears to be a dissociation of responses to TAA and viral antigens.

The relevance of the responsiveness of lymphoid cells from BALB/cCrgl mice to MuMTV antigens has been explored in in vivo studies (*14*). Inoculation of MuMTV-positive SMT cells in MuMTV-negative BALB/cCrgl mice and in MuMTV-positive BALB/cfC3H mice resulted in a lower incidence of tumors in the MuMTV-negative BALB/cCrgl mice. Moreover, the time of appearance and the progression of the tumors were delayed in the MuMTV-negative mice.

In the present work, we have analyzed the lymphoid cells responding to TAA and to MuMTV in our model systems. Flow cytometric determinations of lymphocyte membrane markers were performed with the use of splenocytes of normal and, at different stages of tumor development, mammary tumor-bearing BALB/cCrgl and BALB/cfC3H mice.

ABBREVIATIONS USED: Con A=concanavalin A; FITC=fluorescein isothiocyanate; HBSS=Hanks' balanced salt solution; LPS Ec=lipopolysaccharide of *Escherichia coli*; MuMTV=murine mammary tumor virus; PHA=phytohemagglutin; sIg=surface immunoglobulin; SMT=spontaneous mammary tumor(s); TAA=tumor-associated antigen(s).

---

[1] Received April 6, 1982; accepted July 22, 1982.

[2] Supported by Public Health Service grant R01CA-25583 from the National Cancer Institute.

[3] Guidelines for the care and use of laboratory animals were followed as set forth by the University of Miami.

[4] Department of Microbiology D4-4, University of Miami School of Medicine, P.O. Box 016960, Miami, Fla. 33101. *Address reprint requests to* Dr. Lopez at this address.

[5] The Comprehensive Cancer Center for the State of Florida, R-71, P.O. Box 016960, Miami, Fla. 33101.

[6] We gratefully appreciate the excellent technical assistance of Mrs. Lynn Herbert and Mr. Mantley Dorsey, Jr. We thank Mrs. Frances Susi for typing the manuscript.

These studies, which reveal significant changes in the relative representations of spleen cell populations in animals with large mammary tumors, may provide an explanation for the results observed.

MATERIALS AND METHODS

Animals and tumors.—Geographically separated colonies of BALB/cfC3H and BALB/cCrgl mice, initially obtained from the Cancer Research Genetics Laboratory of the University of California, Berkeley, Calif., have been maintained by brother × sister mating in our laboratory for the past 8 years. The SMT line arose in a BALB/cfC3H female breeder and expresses MuMTV antigens. The syngeneic transplantable mammary tumor designated as D1-DMBA-3 originated from a hormonally stimulated preneoplastic nodule transplanted to a mouse treated with 7,12-dimethylbenz[*a*]anthracene (*15*) and has been consistently found to be devoid of complete MuMTV particles by means of immunofluorescence studies and in radioimmunoassays. Both lines of tumors are routinely transplanted in the subline of origin by sc injections of minced tumor preparations. All mice were 12–16 weeks of age.

Viral antigen and TAA preparations.—MuMTV purified by a combination of rate zonal and isopyknic centrifugations from RIII milk was provided by the Biological Carcinogenesis Branch, National Cancer Institute, Bethesda, Md., from stocks supplied by the Meloy Laboratories Inc., Springfield, Va. In our studies we used a stock containing 1 mg virus/ml. Tumor antigen extracts were prepared as previously described (*14*).

Preparation of cells.—Cells from aseptically removed spleens from normal and tumor-bearing mice were passed through a stainless steel mesh with siliconized rubber stoppers and washed through with 10 ml HBSS. Clumps were removed by filtration through loosely packed nylon fibers; the resulting suspension was centrifuged and the cell pellet subjected to a hypotonic shock for elimination of contaminating red blood cells. The cells were washed in HBSS and incubated on glass surfaces for 2 hours at room temperature for removal of adherent cells. With this procedure, the final cell population contained mainly T- and B-lymphocytes. Macrophages were reduced to less than 1% as indicated by a lipase staining (*16*, *17*) and by phagocytic studies. No remaining granulocytes could be detected with Wright-Giemsa staining.

Nylon wool column purification.—The method described by Julius et al. (*18*) was used with the modification described by Epstein et al. (*19*). The resulting nylon-nonadherent and nylon-adherent populations were characterized, respectively, as T- and B-lymphocytes by means of cell surface markers, i.e., presence of Thy 1 antigen or sIg, and by functional tests. As previously described (*19*, *20*), the nylon-nonadherent population we routinely obtain possesses 91±3 Thy 1-positive lymphocytes and 4±3 sIg-positive cells. This population responds vigorously to the T-cell mitogens PHA and Con A but not to the B-cell mitogen LPS Ec. The nylon-adherent population possesses 2±2 Thy 1-positive lymphocytes and 89±4 sIg-positive splenocytes and has high levels of responses to LPS Ec but not to PHA and Con A.

Cell-depletion studies.—The spleen cells prepared as described above were incubated for 1 hour at 4°C with a final dilution of 1:10 of goat anti-sIg (provided by the Virus Cancer Program, National Cancer Institute, from stocks supplied by the NCI-Frederick Cancer Research Facility, Frederick, Md.) and with a final dilution of 1:20 of anti-Thy 1 (Accurate Chemicals and Scientific Corporation, Hicksville, N.Y.). The cells were washed twice in RPMI-1640, and 1:10 final dilutions of Low-tox guinea pig complement (Cedarlane Laboratories, Hicksville, N.Y.) were added. The mixtures were incubated at 37°C for 1 hour. Several controls were included in all experiments, i.e., cultures with complement alone and anti-sIg or anti-Thy 1 in the absence of complement. None of the control treatments were toxic to the lymphocytes. B-lymphocytes were significantly depleted (down to 7% sIg-positive) after treatment with anti-sIg and complement, whereas these cells were enriched (up to 74% positive) after anti-Thy 1 and complement treatment. The cells subjected to the various treatments were washed extensively and resuspended to the concentrations appropriate for the blastogenic assays.

Lymphocyte transformation assay.—Various lymphocyte fractions were centrifuged and adjusted to a concentration of 1×10^6 cells/ml in the growth medium described by Click et al. (*21*). MuMTV and TAA were added in 25-µl volumes at final concentrations of 4 and 50 µg, respectively. Cultures were maintained for 3 days in MicroTest culture plates (Linbro; Flow Laboratories, Inc., Rockville, Md.) with 2×10^5 cells/well and were given an 18-hour pulse of [^{3}H]thymidine (0.5 µCi/well; Amersham/Searle Corp., Arlington Heights, Ill.). The cells were collected on glass fiber filter paper with distilled water in a Skatron multiple automated sample harvester. The filters were counted for radioactivity in a Packard scintillation spectrometer, and results were expressed as cpm of stimulated cultures minus the background cpm of cultures containing no stimulus. Unstimulated spleen lymphocyte cultures from normal BALB/cCrgl mice incorporated 649±113 cpm of [^{3}H]thymidine, whereas those from normal BALB/cfC3H mice incorporated 679±181 cpm. Unstimulated lymphocyte cultures from small-tumor-bearing and large-tumor-bearing BALB/cCrgl mice had, respectively, 729±187 and 998±201 cpm. Background cultures of spleen lymphocytes of small- and large-tumor-bearing BALB/cfC3H mice incorporated, respectively, 698±158 and 1,017±227 cpm.

Flow cytometric determinations.—Levels of T- and B-lymphocytes were determined by flow cytometric analysis of fluorescence by use of a fluorescence-activated cell sorter (FACS III; Becton Dickinson Monoclonal Antibody Center, Mountain View, Calif.). FITC-conjugated monoclonal anti-Thy 1.2 was purchased from Beckton Dickinson Monoclonal Antibody Center. FITC-conjugated rabbit anti-mouse immunoglobulin was donated by the Biological Carcinogenesis Branch, National Cancer Institute, from stocks supplied by the NCI-Frederick Cancer Research Facility. Spleen single cell suspensions were stained as described by Rabellino et al. (*22*) with either the anti-Thy 1.2 or the anti-mouse immunoglobulin reagents. One hundred thousand cells were analyzed for each preparation. Fluorescent histograms of stained lymphocytes from normal mice and tumor-bearing mice are presented. Autofluorescence of unstained cells is shown as background. The percentages of fluorescent lymphocytes as determined per 10^5 cells are given in "Results."

RESULTS

Nylon Wool Separation Studies

The blastogenic responses of unseparated or nylon wool-fractionated spleen cells from normal and SMT-bearing BALB/cfC3H mice were assessed in cultures containing tumor antigen extracts or MuMTV. The results of such studies, presented in text-figure 1, are expressed as the mean cpm plus or minus the standard error of four separate experiments. Animals with tumors of 1–2 g were defined as small-tumor bearers, whereas animals with tumors of 4–5 g were defined as large-tumor bearers. Unseparated or nylon wool-adherent separated spleen cells from normal BALB/cfC3H mice exhibited no reactivity when they were exposed to either MuMTV or to TAA from MuMTV-expressing tumors of spontaneous origin in the BALB/cfC3H colony. BALB/cfC3H mice bearing small SMT had vigorous responses both to extracts of their mammary tumors and to MuMTV, and these responses were restricted to the nylon-nonadherent population. Spleen cells from large-tumor-bearing BALB/cfC3H mice were incapable of being stimulated in the blastogenic assay either to MuMTV or to TAA. This unresponsiveness extended to the nylon wool-separated populations.

A similar study of the responses to TAA and viral antigens was performed with the use of spleen cells of normal and mammary tumor-bearing BALB/cCrgl mice (text-fig. 2). Spleen lymphocytes from normal BALB/cCrgl mice did not respond to TAA from the D1-DMBA-3 tumors but had vigorous responses to MuMTV antigens. Upon separation on nylon wool, these responses were confined to the nylon-adherent population. Mice bearing small D1-DMBA-3 mammary tumors (1–2 g) possessed lymphocytes capable of responding to D1-DMBA-3 TAA, and the cells responding to the TAA were nylon-nonadherent lymphocytes. The responses to TAA were not evident in either the T- or B-cell fractions of spleens from animals bearing large mammary tumors (4–5 g). In contrast, the responses of splenocytes from both small- and large-tumor bearers to MuMTV antigens remained constant during tumor growth and, as was the case in the normal BALB/cCrgl mice, were solely a function of the nylon-adherent cells.

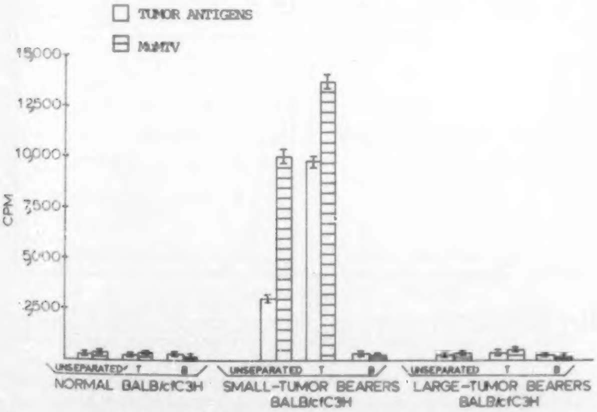

TEXT-FIGURE 1.—[^{3}H]thymidine incorporation of unseparated and nylon wool column-separated splenocytes from normal, small-tumor-bearing, and large-tumor-bearing BALB/cfC3H mice after exposure to TAA and MuMTV. Results are cpm of stimulated cultures minus background cpm and represent the means ± SE of four separate experiments.

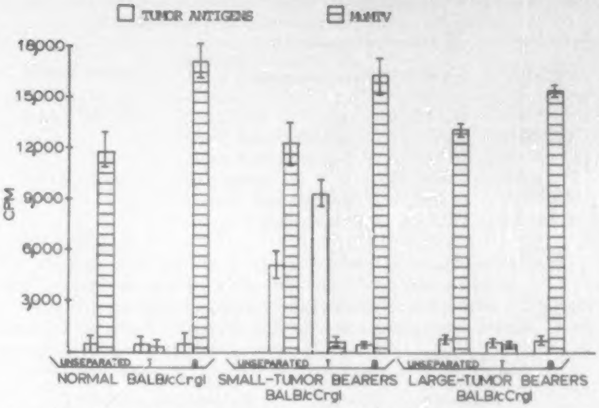

TEXT-FIGURE 2.—Blastogenic responses to TAA and MuMTV of unseparated and nylon wool column-fractionated spleen cells from normal, small-tumor-bearing, and large-tumor-bearing BALB/cCrgl mice. Results are cpm of stimulated cultures minus cpm of unstimulated cultures and represent the mean cpm ± SE of four separate experiments.

Depletion Studies With Anti-Thy 1 or Anti-sIg Sera and Complement

Depletion studies were performed to ascertain the validity of the results obtained with the nylon wool separation technique. Since BALB/cfC3H and BALB/cCrgl animals bearing mammary tumors of 4–5 g were unresponsive to TAA in the blastogenic assay, only animals bearing small tumors were used in these depletion experiments. Treatment of unseparated spleen cells from SMT-bearing BALB/cfC3H mice with anti-sIg and guinea pig complement resulted in a significant increase of responses to the TAA in comparison to the responses obtained in nondepleted cultures, which are represented by the complement control (text-fig. 3). When these spleen cells were treated with anti-Thy 1 serum and complement, the blastogenic responses totally disappeared, thus indicating the T-cell nature of the responding population. The responses to MuMTV were assessed in B- and T-cell-depleted spleen cells from normal and small-tumor-bearing BALB/cfC3H mice. The low responses to MuMTV antigens observed in the complement control cultures of normal BALB/cfC3H mice were reduced in the cultures treated with anti-Thy 1 and complement and essentially unaffected in the cultures treated with anti-sIg and complement. This pattern was repeated in the cultures of spleen cells from small-tumor-bearing BALB/cfC3H mice stimulated with MuMTV but with a much more pronounced diminishing effect in the levels of incorporation of [^{3}H]thymidine in the cultures treated with anti-Thy 1 and complement.

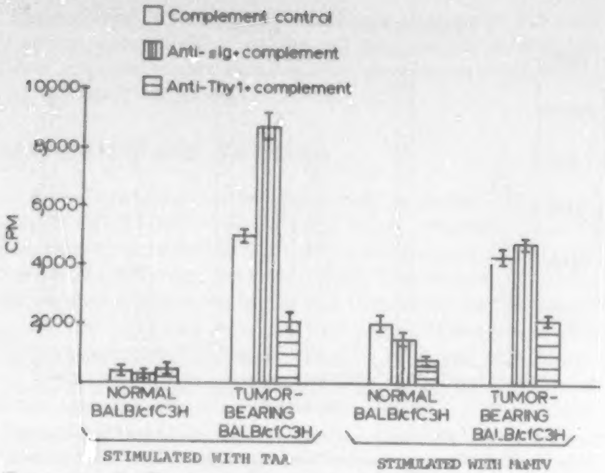

TEXT-FIGURE 3.—Blastogenic responses to TAA and to MuMTV of spleen cells of normal and small-tumor-bearing BALB/cfC3H mice after various cytotoxic treatments. Anti-sIg and complement were used to deplete B-lymphocytes, and anti-Thy 1 and complement were used to eliminate T-cells. Results are cpm of stimulated cultures minus background cpm and are the means ± SE of four separate experiments.

Similar depletion studies performed in the BALB/cCrgl colony (text-fig. 4) confirmed the results obtained in the nylon wool experiments and demonstrated that the responses to TAA were a function of the T-lymphocytes, whereas the MuMTV responses were due to the sIg-positive lymphocytes.

In all these depletion studies, the total cpm incorporated in the cultures that had positive responses were substantially lower than those observed in the nylon wool experiments, a probable reflection of some toxic activity of the complement used in the control and treated cultures.

Flow Cytometric Analysis

The effect of mammary tumor development on the percentages of B- and T-lymphocytes present in the spleens of BALB/cfC3H and BALB/cCrgl mice was analyzed by flow cytometry with the use of a fluorescence-activated cell sorter (FACS III). Text-figure 5 shows the fluorescent histograms of the spleen cells from BALB/cfC3H mice bearing small or large SMT. In every histogram is included the pattern given for unstained cells as a reference point, and the fluorescent histograms of normal mice are presented for comparison. No significant differences were seen in the patterns obtained with spleen cells from normal BALB/cfC3H or tumor-bearing mice of this animal colony when the cells were stained for sIg (text-fig. 5, A and B). Analysis of the spleen cells stained with monoclonal antibodies against Thy 1.2 (text-fig. 5C, 5D) revealed that whereas no major differences were seen between the percentages of T-lymphocytes present in the spleens of normal mice and BALB/cfC3H mice bearing small mammary tumors, a decrease was seen in the percentages of lymphocytes with the Thy 1.2 marker in animals bearing large mammary tumors.

We performed similar experiments using spleen cells from normal or tumor-bearing BALB/cCrgl mice. In text-figure 6 (A, B) no significant differences are seen among the percentages of sIg-positive lymphocytes derived from the spleens of the 3 groups of mice tested, i.e., normal mice, small-tumor bearers, or large-tumor bearers. In a previous

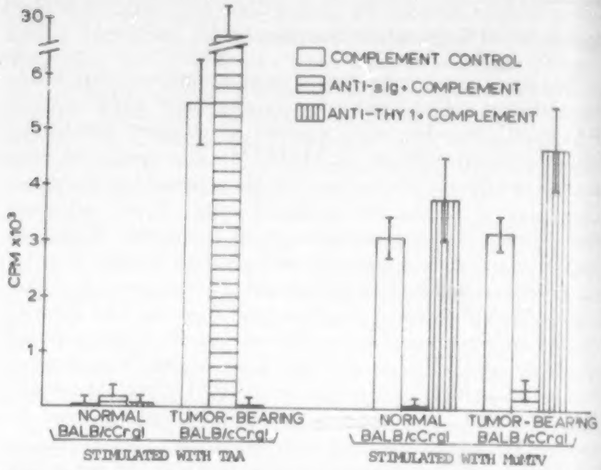

TEXT-FIGURE 4.—Effect of treatment with anti-sIg and complement and of anti-Thy 1 and complement on the blastogenic responses to TAA and MuMTV of normal and small-tumor-bearing BALB/cCrgl mice. Results are cpm of stimulated cultures minus cpm of cultures with no added stimulus. *Each bar* represents the mean ± SE of four separate experiments.

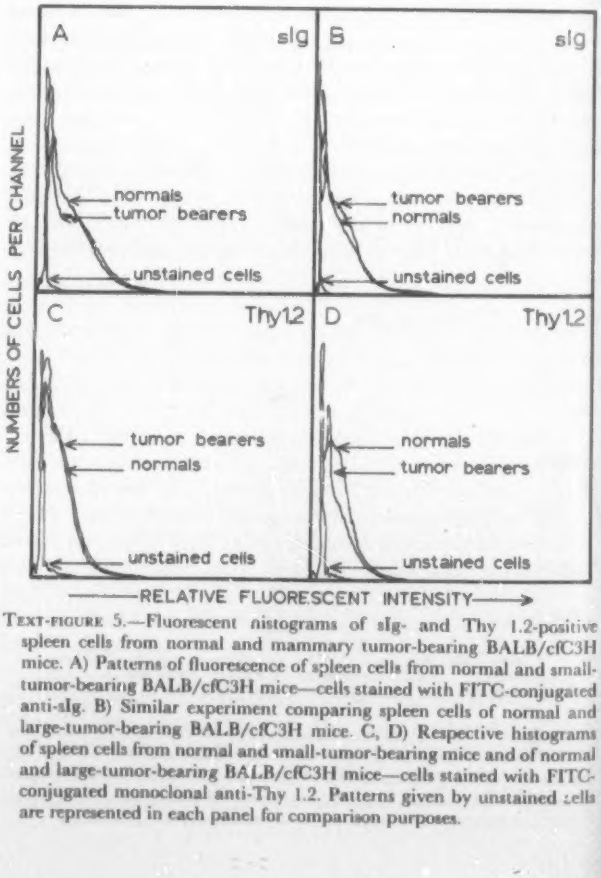

TEXT-FIGURE 5.—Fluorescent histograms of sIg- and Thy 1.2-positive spleen cells from normal and mammary tumor-bearing BALB/cfC3H mice. A) Patterns of fluorescence of spleen cells from normal and small-tumor-bearing BALB/cfC3H mice—cells stained with FITC-conjugated anti-sIg. B) Similar experiment comparing spleen cells of normal and large-tumor-bearing BALB/cfC3H mice. C, D) Respective histograms of spleen cells from normal and small-tumor-bearing mice and of normal and large-tumor-bearing BALB/cfC3H mice—cells stained with FITC-conjugated monoclonal anti-Thy 1.2. Patterns given by unstained cells are represented in each panel for comparison purposes.

study (*23*) with FITC-conjugated F(ab')$_2$ rabbit anti-mouse IgG, no differences were detected by immunofluorescence in the percentages of sIg-positive splenocytes from BALB/cCrgl mice that were normal or that bore large mammary tumors. While the percentages of Thy 1.2-positive splenocytes in small-tumor bearers were very similar to those in normal mice, there was a profound depression in the percentages of the T-lymphocytes in the spleens of BALB/cCrgl mice bearing large mammary tumors as compared with their normal counterparts.

Table 1 gives the percentages of sIg-positive and Thy 1.2-positive spleen lymphocytes of normal and mammary tumor-bearing mice from the BALB/cfC3H and BALB/cCrgl colonies. The values obtained represent the mean percent of sIg or Thy 1-positive cells plus or minus the standard error of 3-8 animals/group. One hundred thousand cells were counted per experimental animal. The data clearly demonstrate that the percentages of B-lymphocytes were not altered by the development of mammary tumors in either BALB/cfC3H or BALB/cCrgl mice. Similarly, no changes in the percentages of Thy 1.2-positive cells were observed in either animal colony for mice that had small mammary tumors. However, a 30-40% reduction in the levels of T-lymphocytes was detected in the spleens of animals with mammary tumors of 4-5 g, when compared to normal controls in both the BALB/cfC3H and BALB/cCrgl colonies.

Our laboratory (*24*) has previously shown that mice bearing large tumor burdens have splenomegaly and a concomitant spleen hypercellularity. Thus the absolute numbers of Thy 1-positive cells per spleen of large-tumor-bearing mice (46.0×10^6 in BALB/cCrgl and 47.5×10^6 in BALB/cfC3H) were only slightly reduced or unchanged when compared to those of normal mice (51.6×10^6 in BALB/cCrgl and 48.1×10^6 in BALB/cfC3H) or those of small-tumor bearers (55.2×10^6 in BALB/cCrgl and 48.1×10^6 in BALB/cfC3H). With the same criterion, the absolute numbers of sIg-positive lymphocytes per spleen were significantly increased in animals bearing large tumors (76.0×10^6 in the BALB/cCrgl and 83.6×10^6 in the BALB/cfC3H) as compared to those of normal mice (46.8×10^6 in BALB/cCrgl and 53.3×10^6 in BALB/cfC3H) or those of small-tumor bearers (50.4×10^6 in BALB/cCrgl and 54.6×10^6 in BALB/cfC3H).

TABLE 1.—*Effect of increasing tumor burden on the levels of B- and T-spleen cells as determined by flow cytometry*

Mouse colony	Clinical condition of animals[a]	sIg^{+b}	Thy 1.2^{+b}
BALB/cfC3H	No tumors	41.0±1.94	37.0±0.84
	Small-tumor bearers	42.0±1.91	37.0±1.06
	Large-tumor bearers	44.0±1.60	25.0±4.1
BALB/cCrgl	No tumors	39.0±1.15	43.0±2.11
	Small-tumor bearers	42.0±1.91	46.0±3.78
	Large-tumor bearers	38.0±0.71	23.0±3.00

[a] Animals with tumors 1-2 g are defined as small-tumor bearers. Animals with tumors 4-5 g are defined as large-tumor bearers.

[b] Results are mean percents of fluorescent-positive cells ± SE. One hundred thousand cells were counted per experimental animal. There were 3-8 animals tested per group.

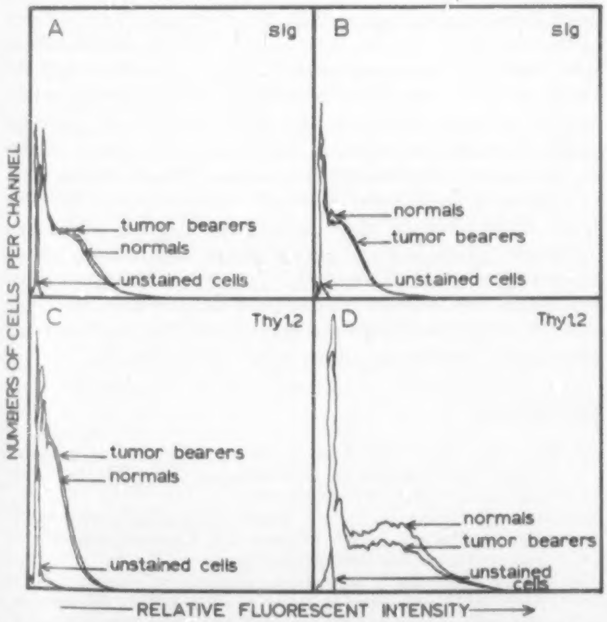

TEXT-FIGURE 6.—Fluorescent histograms of sIg- and Thy 1.2-positive spleen cells from normal and mammary tumor-bearing BALB/cCrgl mice. A, B) sIg-positive cells of normal and small-tumor bearers and of normal and large-tumor-bearing BALB/cCrgl mice, respectively. C, D) Respective histograms of Thy 1.2-positive spleen cells from normal and small-tumor-bearing mice and of normal and large-tumor-bearing BALB/cCrgl mice. Unstained cells are included as reference controls.

DISCUSSION

Resistance against development of mammary tumors is a result of complex interactions between host and tumor factors. It is possible to demonstrate TAA in experimentally induced mammary tumors as well as in mammary tumors of spontaneous origin (*9-11*). Since most mammary tumors that arise spontaneously occur in mouse strains in which MuMTV is readily demonstrable, viral antigens may play an important role in the host-tumor interactions of these systems, regardless of whether the MuMTV is the etiologic agent of these tumors. Common antigens have been described in MuMTV-expressing mammary tumors (*3, 7*) but appear to be lacking in MuMTV-negative tumors originated by the carcinogenic action of 7,12-dimethylbenz[*a*]anthracene (*13, 25*).

Humoral and cellular immune responses to viral antigens and TAA of mouse mammary tumors have been described by several investigators (*26-28*); however, the roles of these responses in providing protection against the appearance of SMT or the development of such tumors are not completely understood. In our studies we have observed a correlation with positive responses to TAA and a good prognosis. BALB/cfC3H and BALB/cCrgl animals with small mammary tumors respond in migration inhibition and lymphocyte transformation assays to extracts of their tumors and these responses are severely diminished by large tumor burdens (*11*). When the tumors are surgically removed, the responses are restored; however, they become depressed if the tumor reappears. Thus a correlation seems to exist between immunologic status and postsurgical fate of the animals (*29*). In our flow cytometric studies a depression in the percentages of T-lymphocytes is apparent in large-tumor bearers of the BALB/cfC3H and BALB/cCrgl colonies. Since T-lymphocytes have been shown to be responder cells to TAA in these animals, these data may explain the decreased responsiveness observed with increasing tumor size. An equally tenable hypothesis is to postulate the appearance of suppressor cells and/or factors in the animals bearing large tumors that could be responsible for the lack of reactivity of their spleen cells to TAA. We have described the emergence in our mammary tumor system of new subsets of T-lymphocytes (*19, 30*) that could be causing such regulatory activities. Since the absolute numbers of Thy 1-positive cells per spleen of large-tumor bearers are equal to or slightly less than those of their normal counterparts, it is conceivable that a shift in T-cell subpopulations might have occurred that could account for the observed results.

In contrast with the above results, the responses to the MuMTV antigen(s) in BALB/cCrgl mice have been shown to be present in both normal mice and tumor bearers and, in addition, to be unaltered by the course of tumor growth. We have speculated about the origin of the sensitivity of spleen cells from MuMTV-negative normal mice to MuMTV antigen(s) (*23*). After considering several hypotheses, we favor the interpretation that this sensitivity represents a recognition of a product resulting from expression of an endogenous MuMTV viral gene(s). Analysis of the cells responding to MuMTV antigen(s) in this colony has revealed that B-lymphocytes are the cells responding in lymphocyte transformation assay to MuMTV antigen(s). In addition, we have observed that B-lymphocytes when stimulated in vitro with MuMTV will differentiate into blast and plasma cells as detected in morphologic studies with Wright-Giemsa stains (Charyulu V, Lopez DM: Unpublished observations).

In our studies, nylon-nonadherent lymphocytes were not stimulated by MuMTV antigens. One could argue that the lack of responses of the T-lymphocytes to viral antigens may be due to the absence of the small percentages of macrophages (<1%) that can be detected by lipase staining in our nylon-adherent population. These cells might be necessary for eliciting positive blastogenic responses in the T-cell population (*31*). In recent experiments (*23*) in which parallel cultures of the various lymphocyte subpopulations were supplemented with macrophage-rich peritoneal exudate cells, addition of these cells exerted no significant enhancement on the rsponses of either B- or T-cells to MuMTV-associated antigen(s). Since in our flow cytometric determinations we observed no changes in the percentages of sIg-positive spleen lymphocyte populations in mice with small or large mammary tumors, one could hypothesize that in the BALB/cCrgl colony the blastogenic responses to MuMTV remain unalterable due to the intactness of the responding cell population.

In the BALB/cfC3H colony, the MuMTV responses appear to reside in the nylon-nonadherent spleen cell population. Blastogenic responses to viral antigens in the T-cell fraction of normal and tumor-bearing MuMTV-positive mice have been demonstrated by Creemers and Bentvelzen (*32*). At the present time, however, we cannot exclude the possibility that only virus-associated antigens are being detected in this assay. In this connection, Westenbrink and Koornstra (*33*) could find no evidence of nonvirion cell surface antigens on virally induced murine mammary tumor cells. The finding that the T-lymphocytes are the responders in the lymphocyte transformation assay in the BALB/cfC3H colony is similar to the situation in human breast cancer, since in recent studies we have reported that the erythrocyte-rosetting lymphocytes of breast cancer patients are the peripheral blood cells capable of being stimulated by antigens of the MuMTV (*34*).

One important question arises: Why do the normal BALB/cfC3H mice lack the high levels of responsiveness to MuMTV that are observed in the syngeneic BALB/cCrgl mice? Several possibilities could account for this apparent paradox: *a*) Since antibodies to MuMTV can be detected in MuMTV-expressing mouse strains (*35*) such as BALB/cfC3H mice, they may form immune complexes with the viral particles, the immune complexes having the ability to suppress the blastogenic reactions. Inhibition of cellular immune responses has been reported to be mediated by immune complexes (*36*), and there is some evidence to this effect in an MuMTV model system (*37*). *b*) A genetic drift may occur between the BALB/cfC3H and BALB/cCrgl colonies, which could account for the differences in responses to MuMTV; however, this is an unlikely explanation, inasmuch as the two colonies are syngeneic as shown by in vivo and in vitro methods (*11, 14*). *c*) In normal BALB/cfC3H mice a deficiency is induced by the presence of the virus in either the levels or the functionality of the B-cell subset involved in the responses to viral antigen in normal BALB/cCrgl mice. *d*) There is a generation of specific suppressor cells in animals actively producing viruses, which could be modulating the immune reactivities of these animals. These suppressor cells could be induced either directly by the virus or indirectly by antigen-antibody complexes (*32, 36, 38*). Such an occurrence may explain the lack of protection afforded by high levels of anti-MuMTV antibody to mammary tumor development (*39, 40*) and could explain why transplanted mammary tumors grow faster in mice in which anti-MuMTV antibodies are present than in mice with no detectable humoral immunity to the virus (*26, 35*).

REFERENCES

(*1*) Klein G, Sjögren HO, Klein E. Demonstration of host resistance against isotransplantation of lymphomas induced by the Gross agent. Cancer Res 1962; 22:955-962.

(*2*) Glynn JP, McCoy JL, Fefer A. Cross-resistance to the transplantation of syngeneic Friend, Moloney and Rauscher virus-induced tumors. Cancer Res 1968; 28:434-439.

(*3*) Muller M, Zotter S. Spontaneous immunity to mammary tumor virus (MTV)-associated antigens in mice and its influence on syngeneic mammary tumor growth. Eur J Cancer 1972; 8:495-500.

(*4*) Baldwin RW, Moore M. Isolation of membrane-associated tumor specific antigen from an aminoazo dye-induced rat hepatoma. Int J Cancer 1969; 4:753-759.

(*5*) Basombrio MA, Prehn RT. Antigenic diversity of tumors chemically induced within the progeny of a single cell. Int J Cancer 1972; 10:1-9.

(*6*) Hellström KE, Hellström I, Brown JP. Unique and common tumor-specific transplantation antigens of chemically induced mouse sarcomas. Int J Cancer 1978; 21:317-322.

(*7*) Lavrin DH, Blair PB, Weiss DW. Immunology of spontaneous mammary carcinomas in mice. IV. Association of the mammary tumor virus with the immunogenicity of C3H nodules and tumors. Cancer Res 1966; 26:929-934.

(*8*) Vaage J. Non-virus-associated antigens in virus-induced mouse mammary tumors. Cancer Res 1968; 28:2477-2483.

(*9*) Morton DL, Miller GF, Wood DA. Demonstration of tumor-specific immunity against antigens unrelated to the mammary tumor virus in spontaneous mammary adenocarcinomas. J Natl Cancer Inst 1969; 42:289-301.

(*10*) Heppner GH, Pierce G. In vitro demonstration of tumor specific antigens in spontaneous mammary tumors of mice. Int J Cancer 1969; 4:212-218.

(*11*) Sigel MM, Lopez DM, Ortiz-Muniz G. In vitro immune responses to viral and tumor antigens in murine breast cancer. Cancer Res 1976; 36:748-752.

(*12*) Lopez DM, Ortiz-Muniz G, Sigel MM. Macrophage migration inhibition and lymphocyte stimulation with mammary tumor virus associated antigens in BALB/c mice. Proc Soc Exp Biol Med 1976; 151:225-230.

(*13*) Sigel MM, Lopez DM, Ortiz-Muniz G. Migration inhibition and blastogenic reactions with viral and tumor antigens in transplantable mammary tumor systems. Ann NY Acad Sci 1976; 276:358-368.

(*14*) Lopez DM, Sigel MM, Charyulu VL. Kinetics of responses to tumor antigens and mouse mammary tumor virus in BALB/cCrgl mice. JNCI 1981; 66:191-196.

(*15*) Medina D, DeOme KB. Response of hyperplastic alveolar nodule outgrowth-line D1 to mammary tumor virus, nodule-inducing virus, and prolonged hormonal stimulation acting singly and in combination. J Natl Cancer Inst 1969; 42:303-310.

(*16*) Orinstein L. Automated white blood cell analysis. Tarrytown, N.Y.: Technicon Technical Publication, 1969.

(*17*) Lief RC, Easter HN Jr, Warters RL, Thomas RA, Dunlop LA, Austin MF. Centrifugal cytology. I. A quantitative technique for the light and scanning electron microscope. J Histochem Cytochem 1971; 19:203-215.

(*18*) Julius MM, Simon E, Herzenberg LA. A rapid method for the isolation of functional thymus derived murine lymphocytes. Eur J Immunol 1973; 3:645-649.

(*19*) Epstein RS, Lopez DM, Ortiz-Muniz G, Sigel MM. Emergence of a subpopulation of lymphocytes bearing θ antigen and complement receptor during tumor growth. Int J Cancer 1976; 28:458-461.

(*20*) Charyulu V, Sigel MM, Durden DL, Lopez DM. Mouse mammary tumor virus (MMTV) antigen(s) are present in B lymphocytes of BALB/c mice. Int J Cancer 1979; 24:813-818.

(*21*) Click RE, Benck L, Alter BJ. Immune responses in vitro. I. Culture conditions for antibody synthesis. Cell Immunol 1972; 3:264-276.

(*22*) Rabellino R, Colon S, Grey HM, Unanue ER. Immunoglobulins on the surface of lymphocytes. I. Distribution and qualifications. J Exp Med 1971; 133:156-167.

(*23*) Lopez DM, Charyulu V, Sigel MM. Subset of spleen lymphocytes from BALB/cCrgl mice stimulated by mouse mammary tumor virus. Cancer Res 1981; 41:813-818.

(*24*) Dorizzi M, Ortiz-Muniz G, Lopez DM, Sigel MM, Epstein RS. Increase in the proportion of cells with the C'3 receptor in BALB/c mice bearing mammary tumors. Int J Cancer 1975; 16:1015-1021.

(*25*) Halpin ZT, Vaage J, Blair PB. Lack of antigenicity of mammary tumors induced by carcinogens in a non-antigenic preneoplastic lesion. Cancer Res 1972; 32:2197-2200.

(*26*) Bowen JM, Dmochowoski L, Miller MF, et al. Implications of humoral antibody in mice and humans to breast tumor and mouse mammary tumor virus-associated antigens. Cancer Res 1976; 36:759-764.

(*27*) Stutman O. Correlation of in vitro and in vivo studies of antigens relevant to the control of murine breast cancer. Cancer Res 1976; 36:739-747.

(*28*) Tagliabue A, Herberman RB, Arthur LO, McCoy JL. Cellular immunity to tumor-associated antigens of transplantable mammary tumors of C3H/HeN mice. Cancer Res 1979; 39:35-41.

(*29*) Lopez DM, Sigel MM. Correlation of tumor growth and cell-mediated immune responses to mice bearing mammary tumors following surgical procedures. J Reticuloendothel Soc 1975; 18:305-312.

(*30*) Epstein RS, Lopez DM, Sigel MM. Divergent appearance of complement receptors and Fc receptors on T cells in a murine mammary tumor system. Cell Immunol 1978; 40:154-163.

(*31*) Rosenstreich DL, Farrar JJ, Dougherty S. Absolute macrophage dependency of T lymphocyte activation by mitogens. J Immunol 1976; 116:131-137.

(*32*) Creemers P, Bentvelzen P. The role of T and suppressor cells in MTV-directed cellular immunity. Eur J Cancer 1977; 13:261-267.

(*33*) Westenbrink F, Koornstra W. Lack of evidence for non-virion cell surface antigens on virally-induced murine mammary tumor cells. Eur J Cancer 1980; 16:763-773.

(*34*) Lopez DM, Parks WP, Silverman MA, Distasio JA. Lymphoproliferative responses to mouse mammary tumor virus in lymphocyte subsets of breast cancer patients. JNCI 1981; 67:353-358.

(*35*) Ihle JN, Arthur LO, Fine DL. Autogenous immunity to mouse mammary tumor virus in mouse strains of high and low mammary incidence. Cancer Res 1976; 36:2840-2844.

(*36*) Gorczynski RM, Kilburn DG, Knight RA, Norby C, Parker DC, Smith JB. Nonspecific and specific immunosuppression in tumour-bearing mice by soluble immune complexes. Nature 1975; 254:141-143.

(*37*) Creemers P, Brinkhof J. Factors interfering with cellular immunological responses to the murine mammary tumor virus in tumor-bearing mice. Int J Cancer 1977; 20:441-447.

(*38*) Myburgh JA, Mitchinson NA. Suppressor mechanism in neonatally acquired tolerance to a Gross virus-induced lymphoma in rats. Transplantation 1976; 22:236-241.

(*39*) Creemers P, Ouwehand J, Bentvelzen P. Murine mammary tumor virus protein vaccine: Induction of antivirus immunity and inhibition or acceleration of growth of transplanted mammary tumors. J Natl Cancer Inst 1977; 59:895-903.

(*40*) Arthur LO, Fine DL. Naturally occurring humoral immunity to murine mammary tumor virus (MuMTV) and MuMTV gp52 in mice with low mammary tumor incidence. Int J Cancer 1978; 22:734-740.

blank page

Genetics of Transplacentally Induced Teratogenic and Carcinogenic Effects in Rabbits Treated With *N*-Nitroso-*N*-ethylurea[1,2,3]

R. R. Fox,[4] **H. Meier,**[5] **H. G. Bedigian,**[4] *and* **D. D. Crary**[4,6]

ABSTRACT—Pregnant rabbits of three partially inbred strains, WH/J, IIIVO/J, and X/J, mated to either IIIVO/J or WH/J males were given ip injections of 60 mg of *N*-nitroso-*N*-ethylurea dissolved in trioctanoin on day 18 of gestation. Genetic differences in tumor susceptibility between strains WH/J (low-tumor-incidence strain) and IIIVO/J (high-tumor-incidence strain) have previously been demonstrated. Of 22 WH/J × IIIVO/J hybrid progeny weaned, 17 developed primary renal tumors at 5.0±0.5 (mean ± SE) months of age. Of 17 IIIVO/J × WH/J hybrid progeny weaned, 16 developed primary renal tumors at 4.0±0.7 months of age. Of 5 X/J × IIIVO/J hybrid progeny weaned, all developed primary renal tumors at 4.2±0.5 months of age. In addition, 8 metastatic nephroblastomas were observed, with the lung being the primary site of metastasis. Neurofibromas were observed in 12 per 22, 12 per 17, and 3 per 5 rabbits, respectively, from the various hybrid groups, many of which also had neurilemmal cysts. In addition, 1 hepatoma and 2 hemangiomas were observed. Also, teratogenic effects of disproportionate miniaturization including a left–right reduction in ear length were observed. Epidermoid cysts also formed and then regressed during the development of these treated animals. The following conclusions can be drawn from the data: The susceptibility to renal tumor and to neurofibroma induction appears to be inherited as a dominant characteristic. The disproportionate miniaturization is greatly dependent on the maternal genotype of the particular hybrid. The presence of this disproportionate miniaturization appears to be related to renal tumor induction. The epidermoid cysts, the renal tumor, and the neurofibromas all appear to be of independent etiologies.—JNCI 1982; 69:1411–1416.

The transplacental induction of primary renal tumors in rabbits by either acute or chronic administration of NEU or its precursors has been demonstrated (*1–6*). Neurogenic tumors can also be induced by the transplacental administration of NEU at certain stages of organogenesis (*6–8*). The pregnant rabbit provides an excellent mammalian model system for the investigation of placental transfer of teratogenic and carcinogenic agents because both rabbits and humans have the same type of placentation (hemochorial), allowing the closest contact between maternal and fetal circulation (*9*).

The spectrum of tumors induced transplacentally by the administration of NEU appears to depend on a number of factors including species, genetic differences within a species, stage of organogenesis, and dosage of NEU. The tumor latency ranged from 3 months to about 2 years of age, probably depending on genetic differences in the breed or strain of rabbit used (*1–6*) and whether the treatment was given in an acute (*3, 4*) or chronic (*6*) regimen. The frequency of renal tumor induction was also dependent on the strain of rabbit used but not on whether the treatment regimen was NEU or its precursors or whether NEU was given in an acute or chronic dosage (*3, 4, 6*). The sex of the progeny did not influence the susceptibility to tumor induction in the rabbit (*3, 4, 6*), as has been demonstrated with the hamster (*10*). The genetic differences in susceptibility to primary renal tumor induction between two of the partially inbred strains of rabbits at The Jackson Laboratory were 35% for strain WH/J and 86% for strain IIIVO/J (*6, 11*). Because of this genotype-dependent susceptibility, we decided to try to determine the genetic basis for these differences by making reciprocal crosses between strains with high and low susceptibilities and to test their progeny for their susceptibility to the transplacental induction of tumors by NEU.

We now report that susceptibility to the oncogenic effects of NEU appears to have a dominant mode of inheritance, whereas the teratogenic effects of NEU are influenced greatly by the maternal genotype.

MATERIALS AND METHODS

Rabbits of three partially inbred strains, IIIVO/J, WH/J, and X/J (*11*), were used. The females were mated to males of either the WH/J or the IIIVO/J strain, and the date and time of day were recorded. Pregnancy was determined by palpation approximately 14 days after mating. Purified crystalline NEU (K & K #22890, lot #1373^{1AP}; K & K Laboratories, New York, N.Y.) was freshly prepared in trioctanoin (Eastman Kodak Co., Rochester, N.Y.) at a concentration of 30 mg NEU/ml immediately before injection. The NEU was preground as described previously (*6*). Pregnant rabbits were given a single ip injection of 60 mg NEU/kg body weight on day 18 of gestation. The progeny were routinely palpated for gross evidence of tumor development, and packed cell volumes were determined from marginal ear vein blood samples. We looked for evidence of hemoconcentration, a feature often associated with renal function failure (*3*). Latency time was recorded as the time from the day of birth to the day tumors were either observed at necropsy or first palpable, whichever occurred first. The treated pregnant females were killed when their litters were

---

ABBREVIATION USED: NEU=*N*-nitroso-*N*-ethylurea.

---

[1] Received April 22, 1982; accepted July 16, 1982.

[2] Supported in part by a grant from the Council for Tobacco Research, USA, Inc.; by Public Health Service (PHS) research contract N01CP-33255 from the Special Virus Cancer Program, Division of Cancer Cause and Prevention, National Cancer Institute; by grant 80-05503 from the National Science Foundation; and by PHS research grant RR-00251 from the Division of Research Resources, National Institutes of Health.

[3] The Jackson Laboratory is fully accredited by the American Association for Accreditation of Laboratory Animal Care.

[4] The Jackson Laboratory, Bar Harbor, Maine 04609.

[5] Deceased, formerly of The Jackson Laboratory.

[6] We acknowledge the assistance of Mr. Robert F. Norberg and Mr. Eugene E. Farrin.

weaned, because they were shown to be only slightly susceptible, if at all, to tumor induction by NEU (*5, 6*).

Rabbits were killed by cervical dislocation or exsanguination, and tissues were obtained for gross morphologic and histologic evaluations. Tissues were fixed in Tellyesniczky's fluid as modified by Fekete (*12*) and processed for histologic examination according to standard procedures; sections were cut at 8 μm and stained with hematoxylin and eosin.

RESULTS AND DISCUSSION

The number of does treated and the progeny born and weaned are illustrated in table 1. Also given are summary data on both teratogenic and carcinogenic effects. Elevated erythrocyte counts (≅1.25 times the normal count) were observed associated with tumor development and probable renal function failure as previously observed (*3, 4, 6*). In past experiments (*3*), because a large volume (3.4 ml) of trioctanoin was required to dissolve 60 mg NEU, the trioctanoin was shown to be extremely toxic. In the present experiment and in accord with our previous work (*6*), we were able to greatly decrease this toxic effect of trioctanoin by pregrinding the NEU so that only 2 ml of trioctanoin was needed to dissolve 60 mg NEU. This toxic effect can be seen in the induction of abortions, resorptions, or death of the doe. The frequency of disproportionate miniaturization was reduced in these hybrid progeny when compared with the effects observed with low chronic administration of NEU to their parental strains (*6*). The maternal strain, however, was important in determining whether we observed such miniaturization or not, indicating a definitely maternal influence on the induction of teratogenic effects in these animals. This maternal effect supports our previous work (*6*) in which the WH/J strain had 28% with disproportionate miniaturization and 52% with holes in the parietal bones in contrast to the IIIVO/J strain where the frequencies were 6 and 2%, respectively. An example of the left–right disproportionate miniaturization is illustrated in figure 1. The disproportionate miniaturization observed only at birth and the holes of the parietal bones have been previously described in detail (*6*). Epidermoid cysts (fig. 2) were observed to appear and regress, usually within the first 8 weeks of life. We have seen as many as three of these cysts at the same time in a given individual hybrid but have not observed these cysts in any of the parental strains similarly treated (*3, 4, 6*). These cysts attained a maximum size of 3 mm^3. The frequencies of renal tumors in the three hybrid populations are not significantly different from each other. Their overall tumor frequency of 86% is in excellent accord with the frequency of 86% reported for the IIIVO/J strain (*6*). However, this frequency is in contrast to that for the WH/J strain where it is only 35% (*6*). Therefore, we conclude that the susceptibility to primary renal tumor induction is associated with a dominant mode of inheritance. Similarly, the presence of neurofibromas at frequencies of greater than 50% in these three hybrid populations is more in accord with the 50% frequency reported for the IIIVO/J rabbits than it is for the 0% frequency observed in the WH/J progeny (*6*). Here if we assume that the chronic treatment of NEU (*6*) elevated the threshold response sufficiently to observe neurofibromas in the parental strains, then we can also conclude that the susceptibility to neurofibroma induction is also associated with a dominant mode of inheritance.

The lack of any sex effect on renal tumor frequency observed in our data is in accord with our previous NEU experiments (*3, 4, 6*) but does not agree with data on the hamster where females were observed to be fivefold more susceptible than males to tumor development when NEU precursors were administered (*10*).

The presence of 2 lymphosarcomas in these WH/J × IIIVO/J hybrid progeny is extremely interesting, particularly because previously we observed 4 lymphosarcomas (*3, 6*) in the WH/J progeny of rabbits treated with NEU, which we attributed to the presence of the inherited condition for lymphosarcoma (*ha/ha*) known to be present in that strain (*6, 13, 14*). In these experiments the presence of the *ha* gene in a homozygous condition is impossible unless the IIIVO/J male used in the cross also carries this gene undetected. To test this hypothesis, we examined other matings that this male had made within the IIIVO/J strain and

TABLE 1.—*Transplacental effect of acute administration of NEU to pregnant rabbits*

Strain of progeny[a]	No. of does treated	No. of does D, AB, or R[b]	No. of progeny born[c]	No. with disproportionate miniaturization[d]/total No. examined	No. with holes in parietal bones[e]/total No. examined	No. with epidermoid cysts/total No. examined	No. weaned	No. of renal tumors	Latent period for renal tumors[f]	No. of metastases	No. of neurofibromas	No. and types of other tumors
WH/J × IIIVO/J	10	2	46 (8)	10/45	0/10	9/26	22	17	5.0±0.5	4	12	2 lymphosarcomas, 1 hepatoma
IIIVO/J × WH/J	6	0	30 (3)	0/29	0/12	9/18	17	16	4.0±0.7	2	12	1 hemangioma (liver)
X/J × IIIVO/J	4	1	16 (5)	2/16	0/11	3/5	5	5	4.2±0.5	2	3	1 hemangioma (spleen)

[a] First strain listed denotes female parent.

[b] D=died; AB=aborted; R=resorbed.

[c] *Numbers in parentheses* are numbers of stillborn progeny.

[d] Marked disproportionate miniaturization at birth or a 20% reduction in ear or tail length measured at 4 wk.

[e] Data were based on rabbits necropsied ≤1 mo of age.

[f] Data are means ± SE. Epidermoid cysts appeared and then regressed usually during the first 8 wk of life. They reached a maximum size of 3 mm^3.

found no evidence for lymphosarcoma in any of the progeny or in any animal of that strain in the past 10 years. The male also was bred to 8 of his IIIVO/J daughters, producing 46 progeny for which we have data. The probability of this male being of the +/*ha* genotype and producing 46 normal progeny when bred back to his daughters is $(7/8)^{46}$ or 0.002. The WH/J strain rabbits with lymphosarcoma have a mean age at death of about 8 months, and the 2 hybrids we observed with lymphosarcoma in these data were about 7 months of age. The necropsy information on the 46 progeny of this IIIVO/J male bred back to his daughters was all based on animals over 9 months of age with a mean age of 17.5±1.2 months. We are confident, therefore, that this IIIVO/J male does not carry the *ha* gene. Thus we conclude that either lymphosarcoma is another effect of the NEU treatment or NEU, in conjunction with one dose of the *ha* gene, can work synergistically to produce this pathology.

Table 2 gives detailed information on the tumors observed. From this table, one can make some inferences about the interrelationships of the types of tumors and the possible relationship of teratogenic to carcinogenic effects. If one looks first at the metastases that were observed, the lung was clearly the primary site for metastatic nephroblastomas because the lung was involved in 7 of the 8 cases of metastases. In addition, three other sites were observed. The omentum by itself and two sites, the maxilla and the sacrum, were observed in the same animals where lung metastases were also found. These hybrid progeny appear to be more susceptible to metastases (21% overall) than were their parental strains in which only one case (3% overall) was observed (*3, 4, 6*). For this comparison of the frequency of metastases, the data from the three regimens used to induce renal tumors in the parental strains were combined, since the frequency of induced primary renal tumors depended on the strain of rabbit but not on whether the regimen was either the acute or chronic administration of NEU or its precursors (*3, 4, 6*). That single case of metastatic nephroblastoma in the parental strains, however, did involve the lungs as well as the jaw and liver. The effect of the disproportionate miniaturization on renal tumor development can be inferred, but on the basis of the number of cases we observed, it is hard to state with certainty. However, in all 7 cases in which we observed disproportionate miniaturization in animals that survived, nephroblastomas were observed subsequently. This observation certainly suggests a relationship and is in contrast to any association between the presence of epidermoid cysts, renal tumors, metastases, and neurofibromas, which all appeared independently, except for the obvious relationship of the metastases to the renal tumors.

TABLE 2.—*Teratogenic and carcinogenic effects of acute administration of NEU to pregnant rabbits*

Strain of progeny[a]	Disproportionate miniaturization[b]	Epidermoid cysts[c]	Sex and animal, No.	Initial renal tumor observation		Death of animal		Histopathologic findings
				Method[d]	Age, mo	Mode[e]	Age, mo	
WH/J × IIIVO/J			♂782884			K	7	Lymphosarcoma
		Yes	♀782891	P	2.5	K	3.50	Nephroblastoma on left kidney and vascular bloom and cysts on right kidney (kidney wt: 80.1 g left; 7.8 g right). Metastasis to omentum.
			♂782892	A	8.25	D	8.25	Small nephroblastoma on right kidney, vascular bloom on both kidneys, and cysts on left kidney. Subcutaneous neurofibromatosis on right side at base of rib cage (3×2×0.5 cm).
			♀782893	P	5.25	K	8.75	Nephroblastoma on left kidney and vascular bloom on both kidneys (kidney wt: 242 g left; 5.0 g right). Neurofibromatosis (2.5×2×1 cm) on right scapula.
		Yes	♀782894			K	6.75	Lymphosarcoma
		Yes	♀782895			K	12.75	Vascular bloom on both kidneys. Two neurofibromas [one (2×1.5×1.5 cm) on left posterior midcervical and the other (3.5×3×1 cm) on the posterior hip at junction of femur and pelvis].
			♂783174	P	3.25	K	5.25	Bilateral Wilms'-like renal tumors, nephroblastomas, vascular bloom, and cysts on both kidneys (kidney wt: 28.6 g left; 13.7 g right)
			♀783176	P	11.75	D	15.50	Nephroblastoma on left kidney and vascular bloom and cysts on both kidneys (kidney wt: 129.7 g left; 9.9 g right)
			♂783177	P	5.25	K	12.50	Nephroblastoma on right kidney and vascular bloom on left kidney (kidney wt: 6.7 g left; 458.2 g right). Two neurofibromas [one (6.5×6.5×2 cm) on ventral surface near sternum and the other (1.5×0.5×0.5 cm) in neck muscle at level of sixth nerve].

[a] First strain denotes female parent—only weaned progeny are included in table.
[b] Marked disproportionate miniaturization at birth or a 20% reduction in ear or tail length measured at 4 wk.
[c] Epidermoid cysts appeared and then regressed usually during the first 8 wk of life. They reached a maximum size of 3 mm^3.
[d] P=palpation or elevated packed cell volume. A=autopsy.
[e] D=natural death. K=killed.

TABLE 2 (continued).—*Teratogenic and carcinogenic effects of acute administration of NEU to pregnant rabbits*

Strain of progeny[a]	Disproportionate miniaturization[b]	Epidermoid cysts[c]	Sex and animal No.	Initial renal tumor observation		Death of animal		Histopathologic findings
				Method[d]	Age, mo	Mode[e]	Age, mo	
WH/J × IIIVO/J			♂783179	P	4.5	K	12.50	Nephroblastoma on left kidney and vascular bloom on right kidney (kidney wt: 404.5 g left; 9.2 g right). Neurofibromatosis (1.5×1×0.3 cm) below right scapula near spine.
			♀783180			K	12.50	Vascular bloom and cysts on both kidneys. Neurofibromatosis (2×1.5×1 cm) near right eye.
			♀793685	A	3.25	D	3.25	Nephroblastoma (0.8×0.8×0.5 cm) on right kidney and vascular bloom and cysts on both kidneys
			♂793686	P	4.25	K	8.00	Nephroblastoma on left kidney and vascular bloom and cysts on both kidneys (kidney wt: 161 g left; 9.3 g right)
		Yes	♂800405			K	15.0	Vascular bloom and cysts on both kidneys
	Yes	Yes	♂800406	P	4.25	K	15.0	Nephroblastoma on left kidney and vascular bloom and cysts on both kidneys (kidney wt: 205 g left; right kidney was inadvertently not weighed but appeared normal in size, i.e., ≈7 g). Metastases to lungs. Two neurofibromas with neurilemmal cysts [one (7×5×1.5 cm) on left flank and the other (2.5×1.5×0.5 cm) near right kidney].
	Yes	Yes	♂800408	P	4.25	K	9.0	Nephroblastoma on left kidney and vascular bloom on right kidney (kidney wt: 326.4 g left, 6.5 g right). Neurofibromatosis with neurilemmal cyst on midline in upper lumbar area.
	Yes		♀800409	A	2.75	D	2.75	Nephroblastoma (2×1.5×1.3 cm) on left kidney, vascular bloom on both kidneys, and cysts on right kidney. Two neurofibromas (one on right upper lip and the other on cervical nerve).
			♂800473	P	5.25	K	14.75	Nephroblastoma (1 cm^3) on right kidney and vascular bloom and cysts on both kidneys (kidney wt: 7.9 g left; 8.2 g right)
		Yes	♀800474	P	7.50	K	15.0	Nephroblastoma on right kidney and vascular bloom and cysts on both kidneys (kidney wt: 7.5 g left; 20.2 g right). Three small neurofibromas (1×1×0.2 cm) located subcutaneously and 1 neurofibroma with neurilemmal cyst (3×2.5×1.5 cm) on stomach.
			♂800475	P	4.0	K	10.75	Bilateral nephroblastomas and vascular bloom on both kidneys and cysts on left kidney (kidney wt: 288.5 g left; 722.6 g right). Metastases to lung. Neurofibroma with neurilemmal cysts (1.5×0.5×0.5 cm). Hepatoma beginning.
	Yes		♂800476	P	4.0	K	10.75	Bilateral nephroblastomas (kidney wt: 147.0 g left; 351.7 g right). Metastases to right maxilla and to lungs.
	Yes	Yes	♂800477	P	4.0	K	6.25	Bilateral nephroblastomas and vascular bloom on both kidneys and cysts on right kidney (kidney wt: 118.1 g left; 72.2 g right). Neurofibroma on second cervical nerve.
IIIVO/J × WH/J		Yes	♀800700	P	6.5	K	15.75	Nephroblastoma on right kidney and vascular bloom and cysts on both kidneys (kidney wt: 8.4 g left; 40.0 g right). Neurofibroma with neurilemmal cyst (2×3×1 cm) located subcutaneously between right ear and eye.
			♂800702	P	3.0	K	8.75	Nephroblastoma on left kidney and vascular bloom and cysts on both kidneys (kidney wt: 185.6 g left; 10.7 g right). Two neurofibromas (1.5×1×0.4 cm and 1×0.5×0.3 cm) on ventral internal abdominal wall.
			♀800703			K	16.5	Vascular bloom and cysts on both kidneys
		Yes	♂801078	P	3.25	K	5.5	Bilateral nephroblastomas, vascular bloom, and cysts on both kidneys (kidney wt: 130.7 g left; 74.3 g right)

[a] First strain denotes female parent—only weaned progeny are included in table.

[b] Marked disproportionate miniaturization at birth or a 20% reduction in ear or tail length measured at 4 wk.

[c] Epidermoid cysts appeared and then regressed usually during the first 8 wk of life. They reached a maximum size of 3 mm^3.

[d] P=palpation or elevated packed cell volume. A=autopsy.

[e] D=natural death. K=killed.

TABLE 2 (continued).—*Teratogenic and carcinogenic effects of acute administration of NEU to pregnant rabbits*

Strain of progeny[a]	Disproportionate miniaturization[b]	Epidermoid cysts[c]	Sex and animal No.	Initial renal tumor observation		Death of animal		Histopathologic findings
				Method[d]	Age, mo	Mode[e]	Age, mo	
IIIVO/J × WH/J		Yes	♀801079	P	1.75	D	4.0	Bilateral nephroblastomas, vascular bloom, and cysts on left kidney (kidney wt: 16.8 g left; 213.9 g right). Neurofibromas with neurilemmal cysts on second and sixth cervical nerves.
		Yes	♂801080	P	2.5	K	3.5	Bilateral nephroblastomas, vascular bloom, and cysts on both kidneys (kidney wt: 195.5 g left; 106 g right). Neurofibroma with neurilemmal cyst (1×1×2.5 cm) located subcutaneously in thoracic lymph node on left side.
		Yes	♂801081	P	3.25	K	8.75	Nephroblastoma on right kidney and vascular bloom and cysts on both kidneys (kidney wt: 17.7 g left; 1,123.5 g right). Metastases to lung. Three neurofibromas with neurilemmal cysts [two (6×3×3 cm and 5×3×3 cm) in muscle of left femur and a small one on the stomach].
			♀801787	P	3.75	K	12.0	Nephroblastoma with Wilms'-like features on right kidney and vascular bloom on both kidneys (kidney wt: 6.2 g left; 1,097.5 g right). Neurofibroma with neurilemmal cysts below stomach. Liver hemangioma.
		Yes	♀801788	P	3.75	K	8.25	Bilateral nephroblastomas, vascular bloom, and cysts on left kidney (kidney wt: 215 g left; 332 g right). Neurofibroma mixed in with the nephroblastoma.
		Yes	♂801789	P	3.75	K	6.5	Bilateral nephroblastomas and cysts on both kidneys (kidney wt: 32.6 g left; 231.9 g right). Neurofibroma (0.8×0.8×0.2 cm) on right side ventral to linea alba of abdominal wall.
		Yes	♀801790	P	3.75	K	12.0	Bilateral nephroblastomas with Wilms'-like features, vascular bloom, and cysts on left kidney (kidney wt: 309.9 g left; 711.5 g right). Metastases to lung. Two neurofibromas [one (3.5×2×0.5 cm) on right mandible and a small sublingual one].
			♂801792	A	13.75	K	13.75	Nephroblastoma on left kidney, vascular bloom on both kidneys, and cysts on left kidney (kidney wt: 9.6 g left; 7.1 g right). Two neurofibromas with neurilemmal cysts [one (0.5×0.5×0.1 cm) on left flank and the other (1×1×0.3 cm) on left shoulder].
			♀801794	P	3.0	K	11.0	Bilateral nephroblastomas and vascular bloom on both kidneys and cysts on right kidney (kidney wt: 600.7 g left; 338.4 g right). Neurofibroma with neurilemmal cyst on left hip.
			♀801973	P	3.25	K	3.50	Nephroblastoma on left kidney and vascular bloom and cysts on both kidneys (kidney wt: 22 g left; 7 g right)
			♂801974	P	3.25	K	11.75	Bilateral nephroblastomas and vascular bloom and cysts on both kidneys (kidney wt: 212.5 g left; 95.9 g right). Four neurofibromas with neurilemmal cysts [two (1.5×1.5×0.5 cm and 3.5×2×0.5 cm) in left lower peritoneum, one (2.5×1.5×1 cm) in neck region, and the other (3×2×0.5 cm) in left mandible area].
		Yes	♂801975	A	2.75	D	2.75	Nephroblastoma (1 cm^3) on left kidney and vascular bloom and cysts on both kidneys
			♂801976	P	2.50	K	5.50	Bilateral nephroblastomas and vascular bloom on both kidneys and cysts on right kidney (kidney wt: 247 g left; 55.3 g right)
X/J × IIIVO/J	Yes	Yes	♀801137	A	3.75	D	3.75	Bilateral nephroblastomas (1×1×1 cm on left and 1.5×2.5×1 cm on right)
			♂801138	P	5.0	K	6.50	Nephroblastoma on left kidney and vascular bloom and cysts on both kidneys (kidney wt: 30.4 g left; 7.8 g right)

---

[a] First strain denotes female parent—only weaned progeny are included in table.

[b] Marked disproportionate miniaturization at birth or a 20% reduction in ear or tail length measured at 4 wk.

[c] Epidermoid cysts appeared and then regressed usually during the first 8 wk of life. They reached a maximum size of 3 mm^3.

[d] P=palpation or elevated packed cell volume. A=autopsy.

[e] D=natural death. K=killed.

TABLE 2 (continued) *—Teratogenic and carcinogenic effects of acute administration of NEU to pregnant rabbits*

Strain of progeny[a]	Disproportionate miniaturization[b]	Epidermoid cysts[c]	Sex and animal No.	Initial renal tumor observation		Death of animal		Histopathologic findings
				Method[d]	Age, mo	Mode[e]	Age, mo	
X/J × IIIVO/J		Yes	♀801450	P	2.5	D	12.0	Bilateral nephroblastomas and vascular bloom on both kidneys (kidney wt: 440.4 g left; 285.3 g right). Metastases to lungs. Neurofibroma (5×4×3 cm) on right nephroblastoma. Spleen hemangioma.
			♀801451	P	5.25	K	14.5	Nephroblastoma on left kidney and vascular bloom on both kidneys (kidney wt: 633 g left; 9.3 g right). Metastases to lungs and sacral neurofibroma area. Two neurofibromas [one (2×1×1 cm) inside left lower lip and the other (2×1×1 cm) in right sacral area].
	Yes	Yes	♂801798	P	4.25	K	10.75	Bilateral nephroblastomas and vascular bloom on right kidney (kidney wt: 92.8 g left; 71.6 g right). Neurofibroma with neurilemmal cyst (5×4×4 cm) in right flank area under kidney.

[a] First strain denotes female parent—only weaned progeny are included in table.
[b] Marked disproportionate miniaturization at birth or a 20% reduction in ear or tail length measured at 4 wk.
[c] Epidermoid cysts appeared and then regressed usually during the first 8 wk of life. They reached a maximum size of 3 mm^3.
[d] P=palpation or elevated packed cell volume. A=autopsy.
[e] D=natural death. K=killed.

REFERENCES

(*1*) Güthert H, Jackel EM, Warzok R. Zur Karzinogenen Wirkung von *N*-Äthyl-*N*-Nitrosoharnstoff (ÄNH) bei Kaninchen. Zentrabl Allg Pathol 1973; 117:461–471.

(*2*) Stavrou D, Hänichen T, Wriedt-Lübbe I. Oncogene Wirkung von Äthylnitrosoharnstoff beim Kaninchen während der pränatalen Periode. Z Krebsforsch 1975; 84:207–215.

(*3*) Fox RR, Diwan BA, Meier H. Transplacental induction of primary renal tumors in rabbits treated with 1-ethyl-1-nitrosourea. J Natl Cancer Inst 1975; 54:1439–1448.

(*4*) ———. Transplacental carcinogenic effects of combined treatment of ethylurea and sodium nitrite in rabbits. J Natl Cancer Inst 1977; 59:427–429.

(*5*) Dimant IN, Beniashvili DS. The significance of some modifying factors during transplacental blastomogenesis by ethylnitrosourea in rabbits. Neoplasma 1978; 25:453–460.

(*6*) Fox RR, Meier H, Pottathil R, Bedigian HG. Transplacental teratogenic and carcinogenic effects in rabbits chronically treated with *N*-ethyl-*N*-nitrosourea. JNCI 1980; 65:607–614.

(*7*) Stavrou D, Dahme E, Schröder B. Transplacentare neuroonkogene Wirkung von Äthylnitrosoharnstoff beim Kaninchen während der frühen Graviditätsphase. Z Krebsforsch 1977; 89:331–339.

(*8*) ———. On the question of transplacental induction of neurogenic tumors in rabbits. In: Severi L, ed. Tumours of early life in man and animals. Sixth Perugia quadrennial international conference on cancer. Monteluce, Italy: Perugia Quadrennial Int Conf Cancer, 1978:445–453.

(*9*) Kozma C, Macklin W, Cummins LM, Mauer R. Anatomy, physiology and biochemistry of the rabbit, chapt 3. In: Weisbroth SH, Flatt RE, Kraus AL, eds. The biology of the laboratory rabbit. New York: Academic Press, 1974:49–72.

(*10*) Rustia M, Shubik P. *Brief communication:* Prenatal induction of neurogenic tumors in hamsters by precursors ethylurea and sodium nitrite. J Natl Cancer Inst 1974; 52:605–608.

(*11*) Fox RR. Handbook on genetically standardized JAX rabbits. 1st ed. Bar Harbor, Maine: The Jackson Laboratory, 1975.

(*12*) Fekete E. A morphological study of the ovaries of virgin inbred mice of eight inbred strains showing quantitative differences in their hormone producing components. Anat Rec 1953; 117:93–113.

(*13*) Fox RR, Meier H, Crary DD, Myers DD, Norberg RF, Laird CW. Lymphosarcoma in the rabbit: Genetics and pathology. J Natl Cancer Inst 1970; 45:719–729.

(*14*) Fox RR, Meier H. Identical genetic basis for lymphosarcoma and hemolytic anemia in the rabbit. J Hered 1976; 67:99–102.

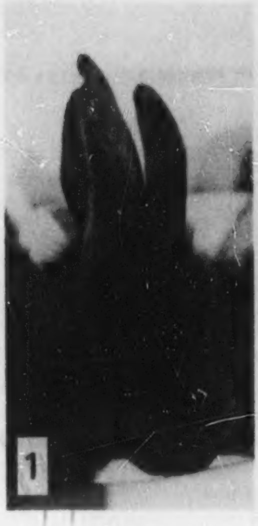

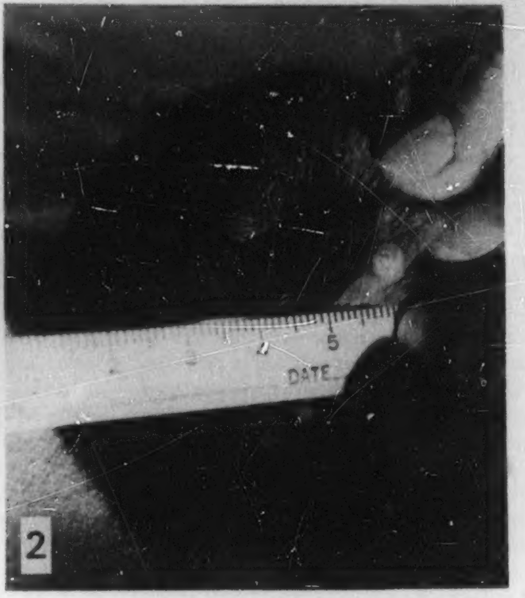

Figure 1.—Male WH/J × IIIVO/J hybrid rabbit (4 wk old) illustrating the left-right disproportionate miniaturization induced transplacentally by NEU.

Figure 2.—Epidermoid cyst observed at base of ear in a 4-wk-old male WH/J × IIIVO/J hybrid rabbit. Such cysts would attain a maximum size of 3 mm^3 and then regress usually during the first 8 wk of life.

blank page

Meeting Highlights

Job-Exposure Matrices in Occupational Epidemiology

Analyses of occupational hazards are most powerful when subjects are grouped by exposure. However, epidemiologic studies have traditionally been based on job title and industry, which are often poor surrogates for exposure; e.g., persons with the same job title in different industries can have vastly different exposures. Misclassification of exposure status reduces the power of an analysis and dilutes risk estimates. In response to this problem, several researchers developed job-exposure matrices (JEM), which are cross-classifications of industry-specific job titles with agents to which persons in the jobs are exposed. Thus the JEM allow the researchers to translate job and industry data into exposure data. On April 19–21, 1982, the University of Southampton, England, and its Medical Research Council (MRC) Environmental Epidemiology Unit sponsored a meeting of approximately 60 scientists to discuss approaches for developing JEM and and related issues.

Matrices developed before collection of any study data ("a priori") enhance evaluation of routinely collected records such as cancer registry data and death certificates. Researchers from the United States, Italy, and England described their a priori JEM, and persons from Scandinavia and Canada presented some possible applications of JEM to census, pension, employment, morbidity, and mortality files. JEM can be used for both hypothesis generating and testing.

A priori JEM have some limitations. They are based on exposures inferred from job title and industry, not actual exposure histories for individual study subjects. Ambiguous job titles which vary over time and place can result in inaccurate exposure assignment. JEM do not usually contain dose measurements. Often, entire classes of chemicals are indicted when only a few chemicals in the class are hazardous. Also, most of the JEM currently contain only known or suspect chemical carcinogens. Finally, associations observed through the use of JEM may be confounded by nonoccupational factors and other hazardous occupational exposures.

Despite these limitations, JEM are a valuable adjunct to occupational epidemiology. Although JEM do not eliminate misclassification of exposure status, they certainly reduce it. Many of the deficiencies of a priori JEM are due to the pilot nature of the JEM developed thus far and can be corrected by further research. Even restricted to known or suspected carcinogens, JEM can address whether occupational exposure to these chemicals can induce cancer in people.

A different technique for translating occupational histories into exposure profiles involves determining exposures on a case-by-case basis. Canadian investigators proposed that inasmuch as each person's job title, industry, and exposure history are idiosyncratic, the data should be treated as such. Subjects in the Canadian project complete short questionnaires, which are reviewed by chemist-engineers who determine the pertinent detailed questions to be asked in a second interview. Theoretically, the resulting matrix should contain more accurate qualitative and quantitative exposure information for the individual for use in case-control studies. When completed, the results of the Canadian project will need to be evaluated in terms of the extra expenditure of time and money involved. This approach is not feasible for analyzing numerous routinely collected records, such as cancer registry data.

All conference attendees agreed that better characterization of exposure and dose is needed. Industrial hygienists should have a major role in constructing JEM. The variation of exposure by place and time needs to be taken into consideration. The sensitivity and specificity of a job-exposure matrix should be compared to actual exposures as recorded or reported by the study subject.

A discussion developed concerning the advisability of creating internationally standardized occupational and exposure codes comparable to the International Classification of Diseases. The general consensus was that variation in the meaning of job titles makes it impossible to create an international occupational code. The observation also was made that there is no need for such a code because analysis should ultimately be based on chemical and physical exposures, instead of job title. Therefore, the greater need is for a standardized exposure code. Chemical abstract (CAS) numbers are assigned uniquely and recognized internationally but do not facilitate the grouping of chemicals by class. A recommendation was made to use the CAS numbers in conjunction with another system that allowed easy grouping. Route of contact, calendar year, and geographic location at time of use of the agents could be added to JEM in the future.

An interesting proposal was made to use JEM to identify work areas and populations for environmental air and blood and urine sampling. The materials could be collected every 5 years from a large population-based sample and, in conjunction with morbidity and mortality rates, could be used to calculate dose-response data. Technical, political, and ethical considerations and a pilot project were discussed. Arguments against the "biological sample" bank included the need for information on confounding factors, the questionable ability to assay suspected carcinogens in samples collected years earlier, and the possibility that the persons most heavily exposed to a potential carcinogen may refuse to participate in the voluntary sampling program. The suggestion also was made that a national registry of industrial hygiene data and occupational histories should be created before complicated biologic monitoring is attempted.

The conference, like most meetings on occupational hazards, voiced support for legislation requiring employers to retain a minimum data set of employees' demographic characteristics and occupational histories.

Dr. E. Donald Acheson[1], the conference organizer, is preparing the proceedings for publication in approximately 1 year.

---

[1] MRC Environmental Epidemiology Unit, University of Southampton, South Academic Block, Southampton General Hospital, Southampton, S09 4XY, England.

Shelia K. Hoar, *Sc.D.*
Environmental Epidemiology Branch
National Cancer Institute
National Institutes of Health
Public Health Service
U. S. Department of Health and Human Services
Landow Building, Room 3C06
Bethesda, Maryland 20205

Announcements

The Journal will publish notices of major meetings dealing with cancer. Submission of notices 6 months in advance is requested to permit timely publication.

Seventeenth Annual Clinical Symposium of St. Jude Children's Research Hospital

St. Jude Children's Hospital, Memphis, Tennessee, will be the site of this symposium to be held on February 25-26, 1983. The symposium will focus on current results in the treatment of children with cancer and leukemia. Emphasis will be on diagnosis and treatment programs for primary disease as well as the care of complications. There will be discussions of various aspects of supportive care as an essential adjunct to chemotherapy regimens.

The symposium will be open to all physicians who wish to attend. Approximately 200 physicians will be accepted for participation on a first-come basis; there are no registration or other fees.

Physicians may register by writing to the Associate Director for Clinical Research, St. Jude Children's Research Hospital, Box 318, Memphis, Tennessee 38101.

Eighteenth Annual San Francisco Cancer Symposium

"Hyperthermia and Radiation Therapy in the Treatment of Cancer" is the title of this symposium to be held at the Sheraton Palace Hotel, San Francisco, California, on March 5-6, 1983. The symposium is being presented by the West Coast Cancer Foundation in association with the American Cancer Society, California Division, and St. Mary's Hospital and Medical Center, and is open to members of the medical and health communities.

Twelve hours of Category I CMA/AMA credit will be offered to physicians and physicists. Nurses will be offered twelve hours of credit by the California Board of Registered Nursing. There will be a reduction in cost if registration is made before February 1, 1983.

For further information contact the West Coast Cancer Foundation, 50 Francisco Street, Suite 200, San Francisco, California 94133 (telephone: 415-981-4590).

Second Annual A.A.I. Course in Advanced Immunology

The American Association of Immunologists will sponsor this course in advanced immunology entitled "Regulatory Elements of the Immune System" to be held at the Duke Marine Laboratory, Beaufort, North Carolina, on June 5-12, 1983. The course will focus on recent advances in immunobiology, immunogenetics, and molecular and clinical immunology as they relate to immune regulation. Topics will include: MHC gene organization and control, MHC restriction and Ir gene control, regulation by interleukins, T-suppressor cell clones and hybrids, B-cell growth and differentiation, immunoglobulin gene organization and isotype switching, effector mechanisms and immunologic analysis and manipulation in human disease.

This course is intended primarily for advanced graduate students and post-doctoral and clinical fellows who wish to expand their knowledge of modern immunology.

Since space is limited, early application is recommended. To apply for the course, please submit a letter documenting your background in immunology and stating your reasons for wishing to attend, as well as current research/teaching activities and a brief c.v., no later than March 1, 1983 to: Dr. David W. Scott, AAI Course, Box 3010, Division of Immunology, Duke University Medical Center, Durham, North Carolina 27710.

Eleventh International Symposium for Comparative Research on Leukemia and Related Diseases

Cambridge, England, will be the site of this meeting to be held on July 3-8, 1983 at Cambridge University. For additional information, complete program, and registration materials please contact Dr. David S. Yohn, Secretary General, International Association for Comparative Research on Leukemia and Related Diseases, Suite 302, 410 West Twelfth Avenue, Columbus, Ohio 43210.

Eleventh Annual Meeting of the International Society for Oncodevelopmental Biology and Medicine

The Karolinska Institute, Stockholm University, Umeå University, and National Bacteriological Laboratory will sponsor this meeting to be held in Stockholm, Sweden, on September 11-15, 1983. The purpose of this interdisciplinary meeting is to provide a forum for communication of recent advances in basic research on oncofetal proteins and their clinical application as tumor and fetal diagnostic markers. As such, this conference will be of interest to both clinicians and scientists working in areas of oncology, tumor immunobiology, developmental biology, and areas of reproductive medicine related to fetal development and the prenatal detection of birth defects.

Deadline for abstract submissions is April 30, 1983. For additional information contact the Congress Secretariat, ISOBM Congress, % RESO Congress Service, S-10524 Stockholm, Sweden (telephone: +468144910; telex: 17639; telegram: FOLKRESO).

Seventh Meeting of the European Association for Cancer Research (EACR)

The Danish Cancer Society will sponsor this meeting to be held in Copenhagen, Denmark, on September 19-21, 1983. The major theme of this meeting will be "Chemical Carcinogenesis." Plenary sessions will include presentations by invited speakers and selected papers submitted by the participants. Other communications may be presented in parallel sessions or as posters. The topics of these presentations may be related to any field in cancer research although papers closely related to the main subject will be considered for inclusion in plenary sessions. The second Otto Mühlbock Memorial Lecture will be presented.

The meeting is open to members and non-members of the EACR. Papers may be submitted for presentation by non-members only if sponsored by a member. The deadline for submission of abstracts is May 1, 1983.

A satellite meeting on modifiers of carcinogenesis, organized by Dr. E. Thorling, will follow the main meeting on September 22–23, 1983. For further information concerning the meeting please apply to Dr. J. Kieler, The Danish Cancer Society, Laboratory of Environmental Carcinogenesis, Ndr Frihavnsgade 70, DK-2100 Copenhagen Ø, Denmark.

Acknowledgment

The Board of Editors acknowledges with gratitude the generous assistance of the following reviewers who, between August 1, 1981, and August 1, 1982, helped in the evaluation of manuscripts submitted for publication. The Board is especially grateful to the first 41 reviewers, who reviewed five or more papers during the past year.

M. R. Banerjee
M. A. Chirigos
P. Cole
C. J. Dawe
I. J. Fidler
D. G. Gilmour
A. Goldin
E. Gorelik
P. M. Gullino
A. J. Hackett
C. C. Harris
S. Haskill
W. Henle
G. Heppner
R. B. Herberman
J. N. Ihle
B. A. Laishes
L. A. Liotta
R. P. McCabe
K. R. McIntire
D. Medina
M. S. Meltzer
A. S. Morrison
S. D. Morrison
R. K. Oldham
R. T. Prehn
J. H. Ransom
R. A. Reisfeld
C. W. Reynolds
M. J. Rogers
B. Sass
J. Schlom
S. Sell
J. Silver
W. G. Taylor
C. W. Todd
J. M. Ward
J. B. Weinberg
S. H. Yuspa
J. M. Zarling
B. Zbar

* * *

C. N. Abboud
K. M. Abdo
C. W. Abell
D. V. Ablashi
A. M. Acierto
S. A. Adam
D. O. Adams
G. E. Adams
R. A. Adams
K. C. Agarwal
R. P. Agarwal
J. Aggeler
D. L. Ahmann
A. C. Aisenberg
J. Albores-Saavedra
N. W. Alcock
P. Alexander
J. C. Allegra
D. W. Alling
B. W. Altrock
H. Amos
L. M. Anderson
W. B. Anderson
A. W. Andrews
J. F. Annegers
F. R. Appelbaum
E. Appella
D. L. Aronson
B. B. Asch
H. Auchincloss, Jr.
L. Aurelian
S. D. Aust
H. N. Autrup
A. A. Axelrad
C. Aylsworth
G. F. Babcock
F. H. Bach
J. L. Bader
C. B. Bagwell
S. M. Baird
L. H. Baker
D. Balinsky
D. Banas
P. Bannasch
S. Bansal
T. Barka
S. Baron
S. H. Barondes
R. Barth
S. W. Barthold
G. L. Bartlett
A. A. Bartolucci
R. H. Bassin
R. C. Bast, Jr.
M. A. Bean
P. Becci
G. W. Beebe
Z. Beg
F. A. Beland
C. E. Bell, Jr.
S. H. Benedict
W. F. Benedict
K. Benirschke
R. Benjamin
D. Bennett
M. Bennett
N. A. Berger
E. Bergstrahl
M. I. Bernhard
A. Bernstein
I. D. Bernstein
J. R. Bertino
J. S. Bertram
N. E. Bharucha
J. Biedler
R. J. Biggar
C. A. H. Bigger
R. J. Billing
A. E. Blair
W. A. Blattner
W. A. Bleyer
J. B. Block
W. J. Blot
P. M. Blumberg
G. P. Bodey
A. E. Bogden
D. R. Boggs
J. D. Boice, Jr.
F. J. Bollum
D. P. Bolognesi
B. Bonavida
P. K. Bondy
V. H. Bono
M. B. Bornstein
T. Borsos
R. K. Boutwell
G. T. Bowden
J. Bowen
E. A. Boylan
E. A. Boyse
J. A. Braatz
M. O. Bradley
H. L. Bradlow
K. G. Brand
M. G. Brattain
R. C. Braylan
T. R. Breitman
E. J. Breyere
L. Brinton
M. W. Brockhaus

L. Broder
S. Broder
G. M. Brodeur
A. M. H. Brodie
J. D. Broome
I. D. J. Bross
C. C. Brown
H. E. Broxmeyer
H. W. Bruckner
M. J. Brunda
G. T. Bryan
J. D. Buckley
P. J. Buckley
R. Buick
C. R. Buncher
J. H. Burchenal
S. Burstein
P. Burtin
W. B. Butler
D. P. Byar
J. E. Byfield
V. J. Cairoli
R. Callahan
B. W. Calnek
G. P. Canellos
G. B. Cannon
K. P. Cantor
R. A. Carchman
R. D. Cardiff
D. N. Carney
G. Carpenter
B. Carr
A. V. Carrano
K. L. Carraway
K. Carroll
R. A. Cartwright
J. Casagrande
W. Ceglowski
G. J. Chader
K. K. Chan
W. W. L. Chang
R. K. Chawla
M. A. Cheever
B. Chesebro
Y. S. Cho-Chung
G. W. Chodak
W. H. Churchill, Jr.
F. Chytil
G. J. Cianciolo
E. A. Clark
R. A. Clasen
J. E. Cleaver
J. Clement
P. H. Cleveland
K. H. Clifton
J. F. Codington
J. H. Coggin, Jr.
C. Cohen
S. M. Cohen
N. H. Colburn
T. Colton
P. S. Coogan
H. G. Coon
D. A. Cooney
A. G. Cooper
M. D. Cooper
T. H. Corbett
D. K. Corle
M. Cornforth
P. Correa
J. Costa
A. H. Coulson
L. S. Covey
J. Cradock
D. A. Creasia
C. M. Croce
D. F. Cruess
G. Cudkowicz
S. J. Cutler
J. Cuzick
J. E. Dahlberg
I. Damjanov
P. S. Dannies
T. L. Dao
J. M. Davie
S. Davis
G. Dawson
P. J. Dawson
J. Delarco
A. DeLeo
L. DeLuca
D. DeMarini
W. R. deMonsabert
R. DePue
M. K. Deringer
F. R. DeRubertis
E. E. Deschner
E. R. DeSombre
L. A. Dethlefsen
S. S. Devesa
W. D. DeWys
L. Diamond
A. K. Diehl
G. Dinse
L. D. Dion
J. A. DiPaolo
A. Dipple
B. A. Diwan
I. Djerassi
R. Doll
A. Dorfman
L. Dow
E. L. Dowell
J. R. Drago
G. J. Draper
S. Dray
G. R. Dreesman
B. Drewinko
M. Drolette
J. M. Ducore
J. P. Dudley
E. A. Duell
V. C. Dunkel
H. F. Dvorak
W. E. Eckhart
S. Economou
M. L. Egan
C. Eil
H. N. Eisen
R. Eisenstein
H. Elias
S. S. Ellenberg
A. Y. Elliott
R. R. Ellison
S. W. Ely
E. Engvall
P. E. Enterline
J. Epstein
L. B. Epstein
R. B. Epstein
L. Erickson
I. Ernberg
V. Ernster
M. Essex
C. H. Evans
R. Evans
R. P. Evarts
G. Eyssen
A. Faras
E. Farber
J. L. Farber
W. L. Farrar
J. G. Farrelly
P. E. Fast
E. Fernandez-Cruz
J. F. Ferrer
S. Ferrone
E. S. Fiala
S. E. Fiala
H. Firminger
P. J. Fischinger
A. Fisher
E. R.Fisher
R. I. Fisher
J. Fishman
F. W. Fitch
A. Fjelde
E. Fleissner
J. W. Flesher
J. E. Fogh
J. Folkman
K. Foon
P. D. Forbes
A. J. Fornace
C. H. Fox
J. F. Fraumeni, Jr.
T. N. Fredrickson
I. Fridovich
G. H. Friedell
G. D. Friedman
Herman Friedman
Howard Friedman
M. A. Friedman
R. M. Friedman
S. J. Friedman
C. Frith
R. J. M. Fry
H. H. Fudenberg
R. A. Fugmann
L. T. Furcht
R. E. Gallagher
S. J. Galli
R. C. Gallo
R. Ganapathy
J. D. Gardner
M. B. Gardner
L. Garfinkel
D. W. Gaylor

A. F. Gazdar
C. W. Gehrke
H. V. Gelboin
R. Gelman
S. George
M. Gerber
H. Gershman
G. E. Gifford
R. V. Gilden
R. W. Gillette
S. Gillis
M. E. Ginevan
B. C. Giovanella
B. M. Glaser
D. Glaubiger
E. Gold
N. D. Goldberg
D. M. Goldenberg
R. H. Goldfarb
S. Goldfarb
A. Goldfeder
B. M. Goldschmidt
E. G. Golub
S. H. Golub
R. A. Good
D. G. Goodman
M. H. Gottesman
A. A. Gottlieb
M. S. Gottlieb
J.-M. Goust
T. Graf
S. Graham
T. E. Gram
C. H. Granatek
G. A. Granger
J. D. Gray
M. R. Green
W. Green
A. Greenberg
P. Greenberg
M. H. Greene
M. I. Greene
O. Greengard
J. W. Greiner
R. A. Griesemer
A. C. Griffin
P. M. Grimley
E. A. Grimm
G. B. Grindey
D. P. Griswold
J. D. Groopman
S. Grufferman
H. L. Gurtoo
M. Haas
J. W. Hadden
W. M. Haenszel
S. Hakomori
N. E. L. Hall
P. F. Hall
R. E. Hall
A. W. Hamburger
B. Hampar
H. Hanafusa
P. H. Hand
B. F. Hankey
W. D. Hankins
M. G. Hanna, Jr.
D. Hansburg
H. Hansen
H. C. Harder
W. D. Hardy, Jr.
J. B. Harley
J. M. Harmon
J. E. Harris
J. Harshbarger
I. R. Hart
P. Hartman
V. C. Hascall, Jr.
J. K. Haseman
J. N. Hatgi
G. Haughton
C. W. Heath
S. S. Hecht
I. Hellström
K. E. Hellström
B. E. Henderson
J. F. Henderson
C. H. Hennekens
C. S. Henney
H. Hennings
K. M. Herrold
F. Herz
J. B. Hibbs, Jr.
J. Higginson
R. Hilf
G. H. Hinkle
S. K. Hoar
J. Hochman
P. Hochman
M. E. Hodes
M. B. Hoff
T. Hoffman
D. Hoffmann
G. L. Hoffmann
M. Hogan
J. Holland
J. F. Holland
P. Holland
R. W. Holley
E. C. Holmes
K. V. Holmes
J. H. Hoofnagle
E. B. Hook
K. L. Hoover
R. N. Hoover
N. Hopkins
J. W. Horm
J. Horton
K. Horwitz
D. Houchens
D. R. Howard
G. R. Howe
M. K. Howett
P. M. Howley
B. Hulka
R. V. P. Hutter
D. C. Ihde
C. Ip
Z. M. Iqbal
R. F. Irie
H. J. Isard
M. Jacobs
E. S. Jaffe
M. Jain
D. Janevich
N. Javadpour
D. W. Jayme
A. M. Jeffrey
A. G. Johnson
D. Johnson
G. S. Johnson
M. F. Johnson
R. K. Johnson
R. J. Jones
R. T. Jones
R. A. Jungmann
A. Kagan
T. Kakunaga
E. Kaminskas
J. B. Kampert
A. E. Kaplan
L. Karavodin
R. C. Karn
M. J. Karnovsky
B. S. Katzenellenbogen
J. Kelsey
M. I. Kelsey
R. L. Kempson
K. A. Kennedy
D. E. Kennell
R. S. Kerbel
D. Kessel
I. I. Kessler
M. E. Key
G. Khoury
K. A. Kicke
W. R. Kidwell
E. Kieff
J. Y. Killen
J. H. Kim
E. S. Kimball
I. Kimber
G. A. King
H. King
M.-C. King
L. J. Kinlen
T. Kinsella
R. L. Kisliuk
E. S. Kleinerman
A. Klein-Szanto
A. Kligerman
R. A. Knazek
D. M. Knowles
A. G. Knudson
R. J. Kociba
A. Koestner
H. S. Koren
S. G. Korenman
D. Korn
P. Kornblith
R. E. Kouri
C. Kozak
K. H. Kraemer
M. Krailow
I. H. Krakoff
R. Kramer
J. W. Kreider
M. Kripke

D. Kritchevsky
H. S. Kruth
D. Kufe
C. H. Kuhn III
F. C. Kull, Jr.
L. T. Kurland
C. E. Land
J. R. Landolph
J. M. Landry
B. P. Lane
R. Langenbach
W. R. Laster, Jr.
J. Laszlo
E. C. Lattim
L. W. Law
J. S. Lazo
C. P. Leblond
J. F. Lechner
J. A. H. Lee
Y. J. Lee
L. J. Lerner
D. Le Roith
M. Lesser
R. Lev
R. Levenson
B. G. Leventhal
D. L. Levin
V. Levin
H. B. Levy
J. A. Levy
J. J. Li
A. Lichter
W. Lijinsky
F. Lilly
M. C. Linder
T. J. Linna
M. Lippman
M. M. Lipsky
R. B. Livingston
K. O. Lloyd
R. R. Lobb
A. F. LoBuglio
G. H. Loew
W. T. London
C. Longcope
D. S. Longnecker
D. L. Longo
T. L. Loo
D. L. Loriaux
P. D. Lotlikar
W. L. Lourie, Jr.
M. C. Lowe
D. R. Lowy
J. H. Lubin
D. Lucas
J. K. Luce
F. C. Luft
J. L. Lyon
K. Macarty
T. M. Mack
I. T. Magrath
E. O. Mahboubi
P. K. Majumder
R. W. Makuch
L. Malan-Shibley
D. Malejka-Giganti
A. Malkin
A. Maluish
T. I. Mandybur
B. M. Mankaverich
J. A. Mannick
L. A. Manson
N. Mantel
R. K. Margolis
L. D. Marrett
E. W. Martin, Jr.
G. R. Martin
P. Martin
R. G. Martin
L. J. Marton
T. J. Mason
M. Mastrangelo
J. Mattes
J. Mattsson
C. W. Mays
R. F. McCallum
J. McCann
K. S. McCarty
E. McConnell
D. L. McCormick
J. L. McCoy
E. A. McCulloch
R. W. McDivitt
E. McDowell
D. L. McGee
C. M. McGrath
K. L. McIvor
P. McKeever
A. J. McMichael
A. T. Meadows
R. G. Mehta
A. Meister
J. Meites
M. R. Melamed
H. R. Menck
M. L. Mendelsohn
T. C. Merigan, Jr.
G. Merlino
D. Meruelo
M. F. Mescher
G. L. Messerschmidt
A. B. Miller
F. R. Miller
H. C. Miller
J. M. Miller
M. D. Miller
O. J. Miller
R. A. Miller
R. W. Miller
G. E. Milo
P. Minden
J. D. Minna
S. Mirvish
M. S. Mitchell
S. Mondal
J. A. Montgomery
S. H. Moolgavkar
F. L. Moolten
L. Moore
W. E. C. Moore
P. S. Morahan
A. C. Morgan, Jr.
D. J. Morré
H. C. Morse III
D. F. Mosher
G. H. Moyer
L. R. Muenz
C. Muir
M. T. Muller
D. E. Mullins
J. Mulshine
J. J. Mulvihill
M. N. Mulvihill
A. S. K. Murthy
M. H. Myers
W. E. Nance
S. Nandi
V. L. Narayanan
P. Nasca
C. F. Nathan
K. Nazerian
D. L. Nelson
J. S. Nelson
N. Nelson
P. Nettesheim
P. M. Newberne
G. R. Newell
G. L. Nicolson
N. D. Nigro
S. P. Nissley
R. L. Noble
A. Norman
H. Norris
P. C. Nowell
S. J. O'Brien
P. V. O'Donnell
H. F. Oettgen
S. H. Ohanian
L. J. Old
S. J. Opella
S. F. Order
J. R. Ortaldo
A. A. Ovejera
R. F. Ozols
A. Paganini-Hill
J. S. Pagano
D. L. Page
V. M. Pain
W. B. Panko
B. W. Papermaster
R. E. Paque
A. B. Pardee
W. P. Parks
R. T. Parmley
B. S. Pasternack
J. Pawelek
L. N. Payne
G. Pearson
O. H. Pearson
J. C. Peckham
P. L. Pedersen
T. C. Pederson
A. Pegg
L. Pelus
T. W. Pendergrass
C. Peraino
C. Percy
F. W. Perrella

B. Peterkofsky
H. Peters
R. L. Peters
W. H. Peters
N. L. Petrakis
H. M. Pettigrew
G. B. Pierce
J. H. Pierce
J. Pierce-Hoeltzer
Malcolm C. Pike
Marilyn C. Pike
T. Pincus
D. A. Pistenma
H. C. Pitot
J. A. Poiley
L. A. Poirier
M. Poirier
R. Pollack
M. Pollard
N. C. Popescu
G. Poste
M. Potter
P. M. Pour
M. D. Prager
G. Prantera
R. Prentice
A. Prestayko
T. G. Pretlow
P. C. Prorok
H. Pross
T. T. Puck
R. H. Purcell
J. F. Quast
J. R. Quesada
H. Rabin
M. Rabinovitz
R. Ranken
M. S. Rao
P. N. Rao
R. E. Rasmussen
V. Raso
G. Reaman
B. S. Reddy
J. K. Reddy
T. Reddy
D. J. Reed
N. D. Reed
E. Reich
A. E. Reif
A. R. Rein
H. M. Reznik-Schüller
J. S. Rhim
E. Ribi
J. M. Rice
A. A. Rimm
G. Ringold
R. Risser
M. A. Ritter
J. Ritz
A. Rivenson
E. Roberts
H. Robinson
W. R. Robinson
H. E. Rockette
R. G. Roeder
A. E. Rogers
B. Roizman
P. P. Roller
M. M. Romsdahl
L. Ronstrom
D. Roopenian
P. P. Rosen
S. W. Rosen
S. A. Rosenberg
M. H. Ross
R. Ross
R. D. Rossen
J. Roth
S. I. Roth
K. J. Rothman
I. D. Rotkin
J. Rotter
G. Rovera
W. P. Rowe
J. D. Rowley
F. H. Ruddle
P. S. Rudland
J. Rundo
E. Ruoslahti
S. W. Russell
A. B. Russfield
A. Russo
I. H. Russo
J. Russo
G. Sachdev
P. Sairn
S. E. Salmon
D. Salomon
J. Sampugna
A. A. Sandberg
H. H. Sandstead
K. K. Sanford
A. Santoni
D. S. R. Sarma
S. B. Sasson
H. N. Sather
D. G. Scarpelli
K. A. Schat
B. Schaumann
G. P. Schechter
C. D. Scher
L. M. Schiffer
S. I. Schlager
R. Schmidt
M. A. Schneiderman
D. Schottenfeld
H. Schumacher
R. S. Schwartz
J. Scotto
J. D. Scribner
R. E. Scully
A. Segaloff
F. Seigal
I. J. Selikoff
A. R. Sellakumar
R. Seltzer
S. Serrate
I. F. Sevin
R. C. Shank
H. S. Shannon
W. R. Shapiro
B. S. Sharma
G. M. Shearer
B. Sherman
S. Sherwin
E. M. Shevach
M. B. Shimkin
H. Shinozuka
R. E. Shore
H. Sidransky
S. M. Sieber
R. Silber
R. E. Silverman
L. Siminovitch
R. L. Simmons
R. M. Simon
M. F. Singer
S. Singer
B. Singir
D. Sinha
J. E. Sinsheimer
H. K. Slocum
B. Smith
G. H. Smith
H. S. Smith
I. C. P. Smith
J. Bruce Smith
J. Bryan Smith
P. G. Smith
M. Smulson
M. E. Sobel
S. Sorof
M. Spector
T. Spector
J. Spira
M. B. Sporn
B. Sredni
L. Srinivas
E. J. Stanbridge
G. M. Stancel
J. Stanton
G. Steele
R. E. Steele
V. Steele
R. A. Steeves
D. L. Steffen
K. S. Stenn
J. R. Stephenson
Z. Steplewski
H. C. Stevenson
H. L. Stewart
S. F. Stinson
G. D. Stoner
T. C. Storch
F. K. Storm
R. Storm
J. D. Strandberg
L. C. Strong
G. P. Studzinski
R. M. Sutherland
J. A. Swenberg
P. W. Sylvester
M. Szklo
C. W. Tabor
E. Tabor
K. K. Takemoto
J. F. Tallman, Jr.
J. E. Talmadge

S. R. Tannenbaum
R. Tarone
H. W. Taylor
S. I. Taylor
J. H. M. Temmink
S. S. Tevethia
G. A. Theis
A. N. Theofilopoulos
C. B. Thomas
C. G. Thomas, Jr.
D. B. Thomas
D. G. Thomassen
D. Thompson
D. J. Thompson
J. Thompson
W. D. Thompson
D. E. Thor
S. S. Thorgeirsson
C.-C. Ting
R. C. Ting
J. Tobacman
G. J. Todaro
R. F. Todd III
Q. Tonelli
G. Tosato
E. Trapido
E. L. Travis
J. M. Trent
J. J. Trentin
B. Tribukait
D. Trichopoulos
J. Trosko
B. F. Trump
A. S. Tu
M. A. Tucker
B. Turnbull
R. L. Tuttle
J. J. Twomey
B. Ulland
F. Urbach
J. Vaage
B. Vallee
B. L. Van Duuren
D. L. Van Dyke
J. Varani
L. Varesio
A. Varki
J. M. Venditti
J. Vilcek
C. A. Villee
H. H. Vogel, Jr.
B. K. Vonderhaar
D. D. Von Hoff
B. M. Vose
T. P. Waalkes
D. G. Waldhalm
T. A. Waldmann
D. L. Walker
S. Wall
N. L. Warner
L. Warren
E. Watson
L. Wattenberg
R. J. Waxweiler
E. T. Wei
S. Weinhouse
I. B. Weinstein
R. S. Weinstein
E. K. Weisburger
O. S. Weislow
K. M. Weiss
N. Weiss
W. Weiss
H. Wekerle
S. R. Wellings
C. W. Welsch
R. M. Welsh, Jr
F. Wendling
Z. Werb
W. Wertelecki
J. Whang-Peng
G. P. Wheeler
L. L. Wheeless, Jr.
J. K. Whisnant
H. Whitten
P. H. Wiernik
J. R. Wilkins III
L. J. Wilkoff
G. M. Williams
J. Williams
R. D. Williams
R. M. Williams
J. L. Wilmer
D. B. Wilson
M. J. Wilson
S. H. Wilson
R. Wiltrout
S. J. Winawer
P. J. Wirth
J. S. Wishnok
H. R. Withers
H. P. Witschi
G. N. Wogan
G. Wolberg
S. Wolff
H. H. Wotiz
W. C. Wright
J. R. Wunderlich
D. H. Wurster-Hill
E. L. Wynder
K. Yamada
Y. Yamamura
M. B. Yatvin
S. Yen
D. M. Young
J. L. Young, Jr.
J. S. Youngner
J. M. Yuhas
A. A. Yunis
D. S. Zaharko
N. Zamcheck
M. Zatz
M. S. Zedeck
J. L. Ziegler
R. G. Ziegler
J. Zighelboim
S. Zolla-Pazner
K. C. Zoon
D. A. Zopf
M. Zweig
L. A. Zwelling
D. Zwerner
B. S. Zwilling

Index of Authors

Volumes 68–69
January–December 1982

Page numbers in italics indicate senior authorship.

Abbott BJ, 68:249
Ablashi D, 69:585
Abou-Issa H, 69:443
Adler A, 68:*963*
Akamatsu N, 68:563
Akao M, 69:1317
Akatsuka A, 68:449
Akiyoshi T, 69:*345*
Albanese EA, 68:*407*
Albert RE, 68:*597*
Albrecht S, 69:997
Alessandri G, 69:1183
Alexander NJ, 69:551
Alford TC, 68:935
Allavena P, 68:*555*
Alousi MA, 69:103
Altbaum I, 68:963
Altrock BW, 68:*1037*
Andersen FA, 69:*151*, 155
Andersen P, 69:585
Anderson DJ, 69:*551*
Anuszewska EL, 69:9
Aoki K, 68:91
Armstrong G, 69:585
Armstrong RB, 69:237
Asano M, 69:*1221*
Ashley RL, 69:*639*
Ashwood-Smith MJ, 69:*189*
Asire AJ, 69:833
Atchison M, 69:*503*
Auerbach R, 69:699
August CS, 69:393
Awad AB, 69:*320*
Ayres KN, 68:*919*

Bach FH, 68:15
Bagne C, 68:743
Bain C, 68:*537*
Banerjee MR, 69:453
Barclay THC, 68:445
Barka T, 69:*1115*
Barra R, 69:*1353*
Barsky SH, 68:935
Bateman J, 69:1147
Bausch J, 69:1359
Bawol RD, 68:885
Bear J, 69:1147
Beckwith JB, 68:429
Bedigian HG, 69:1411
Belanger C, 68:537
Bender TR, 69:1005
Bennett JM, 68:43
Benoist H, 69:*1208*
Ber R, 68:179, 197, 841
Beral V, 69:387
Beran M, 68:35
Berard CW, 68:43
Berkelhammer J, 68:*461*
Berkowitz R, 69:23
Bern HA, 69:1347
Bernard C, 68:*951*
Bianchi R, 68:817
Bier J, 69:1095
Biggar RJ, 69:787
Bigotti A, 68:761
Bisballe S, 68:179
Biswas C, 69:*1329*
Black JJ, 69:*915*
Black MM, 68:*445*
Blair AH, 69:823
Blatt J, 68:*391*
Bloch KJ, 69:1329
Block NL, 69:79
Blog FB, 69:245
Blot WJ, 68:211; 69:1063
Bluestone JA, 69:*953*
Bockstahler LE, 69:*183*
Bogliolo G, 68:971
Bohnert A, 68:415
Boice JD Jr, 69:1027
Bojko C, 68:325
Bolanča M, 68:891
Bolognesi DP, 69:509
Bonmassar E, 68:817
Bonnard GD, 69:339
Boone CW, 68:115
Borsos T, 68:*177*
Bosmann HB, 68:259
Boss LP, 69:*1005*
Bouchet C, 69:1208
Boukamp P, 68:*415*
Boyd NF, 68:*357*
Brattain DE, 69:767
Brattain MG, 69:*767*
Braun DG, 68:203
Braun DP, 68:549
Breitkreutz D, 68:415
Brenes MM, 68:219
Breslow NE, 68:*429*
Brinton LA, 69:*817*
Brown CA, 68:293
Bucana C, 69:1189
Budd HS, 69:647
Budker VG, 69:67
Buhler DR, 69:725
Bull AW, 69:103
Burger DR, 69:551
Buring JE, 68:91
Burk MW, 68:703
Burmeister LF, 68:915
Burns PE, 68:211
Butler JJ, 68:43
Byers T, 69:*1059*
Byrne GE Jr, 68:43

Calabresi P, 68:1011; 69:1359
Calarco PG, 68:643
Calnek BW, 69:*709*, 715
Cameron AM, 69:659
Campbell EW, 69:415
Cannon GB, 68:*935*
Cantrell J, 69:495
Cantwell JM, 69:183
Cardiff RD, 68:613, 1037; 69:639
Cariile T, 68:357
Carney JA, 68:573
Carraway CAC, 69:33
Carraway KL, 69:33
Castro JA, 69:687
Cave WT Jr, 68:*319*
Chabner BA, 68:227
Chang RL, 69:725
Chardonnet Y, 69:1215
Chen C-LH, 69:709, 715
Chen DJ, 69:199
Cheresh DA, 68:69, *779*
Chiasson MA, 68:997
Chmelevsky D, 69:1135
Chopra DP, 69:*895*
Chu C, 69:503
Chu CY-T, 68:*75*
Chu TM, 68:99
Chuang C, 69:647
Claflin AJ, 69:*79*
Clemmesen J, 69:*549*
Clincea R, 68:325
Codington JF, 68:981; 69:371
Cohen LF, 68:391
Cohen N, 68:133
Colburn NH, 68:469; 69:1147
Colton T, 68:743
Comstock GW, 68:3
Conley FK, 69:*465*
Conney AH, 69:725
Coohill TP, 69:183
Coombs RRA, 69:1
Cornelius J, 69:1321
Cowell JK, 69:*425*
Cox CE, 69:1073
Cozad GC, 69:1337
Crabtree GW, 68:1011
Cramer D, 69:1035
Crary DD, 69:1411
Cravioto H, 68:501
Creel RJ, 69:1055
Creighton AM, 68:977
Cunningham-Rundles S, 69:1261
Cupissol D, 69:*27*
Curtis RE, 69:1027
Cuthbertson AM, 68:579
Cuzick J, 69:387

Dahlmann N, 69:*569*
Dalbey WE, 69:117
Daling JR, 68:95
D'Amore F, 68:971
D'Amore P, 68:711
Danes BS, 69:*1271*
Daniel CW, 69:1391
Davies AT, 69:1083
Davies RE, 69:229
Davies TS, 69:1127
Davis S, 69:1073
Dean JH, 68:935
de Both NJ, 69:945
de Britton RC, 68:219

De Bruyne GK, **69:**1367
De Clercq E, **69:***653*
de Fenos OM, **69:**687
de Ferreyra EC, **69:**687
de Jong WH, **69:**1095
DeLong ER, **68:**107
DeLor DKD, **68:**993
De Luca LM, **69:**1147
Delzeil ES, **68:**107
DeMarinis AJ, **69:**737
DeMartino JA, **69:**799
Deneke SM, **69:**205
Dent PB, **68:**19
Desplaces A, **69:**1208
Dexter DL, **68:**1011
Diamond I, **68:**1011
Díaz Gómez MI, **69:**687
Dick SJ, **69:**1245
Dicke KA, **68:**35
Dietert SE, **68:**95
Dilley WG, **69:**1073
Dion LD, **69:***1147*
DiPaolo JA, **68:**127; **69:***531*, 737, 741, 1175
Distasio JA, **68:***59*, 779
Djiane J, **69:**447
Dobrjansky A, **68:**997
Dohan PH, **69:**1005
Doll R, **69:***550*
Donehower RC, **68:**227
Doniger J, **69:**531
Dorey F, **68:**703
Dorfman RF, **68:**43
Dourson ML, **69:***851*, 859
Dragonetti CH, **69:**1367
Dufer J, **69:**1208
Dulmadge EA, **68:**1023
Dzarlieva RT, **68:**415

Ebbesen P, **68:***691*
Eberlein TJ, **69:***109*
Edgar DH, **68:***977*
Edidin M, **69:**1311
Egan ML, **68:***338*
Eisenstark A, **69:***177*
El-Gerzawi S, **69:***577*
Emerit I, **68:**951
Endo H, **68:**823
Endrich B, **68:***475*
Ensign BM, **68:**461
Enterline PE, **68:***925*
Epstein JH, **69:***265*
Eremin O, **69:***1*
Erickson-Lucas MJ, **68:**319
Erlichman C, **68:***227*
Ernberg I, **68:**197
Ernster VL, **68:**9, **69:***773*
Escobales N, **68:**651
Essex M, **69:***981*
Ethier SP, **69:***1199*
Evans CH, **68:***127*, 329; **69:***737*, 741, *1175*
Evans DL, **69:**53
Evans ED, **69:**915
Evans VJ, **68:**895
Evans WH, **69:**591
Evarts RP, **68:***293*
Eyre DR, **69:**1009

Fagg B, **68:***457*
Falletta JM, **68:**107
Fang WD, **68:**279
Farmer JH, **69:**659
Faucon N, **69:***1215*
Faulkin LJ, **68:***613*; **69:**639
Fears TR, **69:***365*
Feinleib M, **69:**989
Ferioli ME, **68:**751
Ferrarini M, **68:**233
Ferri HA, **68:**357
Ferrone S, **68:**761; **69:**823
Fiala E, **68:**867
Fialkow PJ, **69:**1289
Fidler IJ, **69:**137, 975, 1189
Fine WD, **69:**767
Fioretti MC, **68:**817
Fishell E, **68:**357
Flannery JT, **69:**1027
Foecking MK, **69:***443*
Fogler WE, **69:**1189
Fonseca LS, **68:**673
Forbes PD, **69:**229
Forrest APM, **69:**1055
Fox MA, **68:**43
Fox RR, **69:***1411*
Franceschi S, **69:**1207
Fraumeni JF Jr, **68:**211; **69:**817, 1027, 1063
Frayssinet C, **69:**1375
Friedl HP, **68:**729
Friedman GD, **68:**885
Friedman JM, **69:***1289*
Fritz E, **68:**729
Frizzera G, **68:**15
Fujihara T, **69:**1343
Fujita T, **69:**963
Fukami A, **69:**1229
Fukui H, **68:**449
Fukushima S, **68:**497
Fulgham DL, **69:**551
Fuller TC, **69:**371
Furukawa K, **69:**683
Fusenig NE, **68:**415

Gabriai GN, **68:***785*
Gaedke H, **69:**813
Gail MH, **69:**1067
Galletti PM, **69:**1359
Gallo RC, **69:**435, *1209*
Galton JE, **69:***535*
Ganapathi R, **68:***1027*
Gandilhon P, **69:***447*
Gangji D, **68:**391
Ganguly N, **69:***453*
Ganguly R, **69:**453
Gantt R, **69:**409
Gately MK, **69:***1245*
Gaugas JM, **69:***329*
Gaylor DW, **69:**659
Gerber P, **69:***585*
Gerner EW, **68:**487
Ghio R, **68:**233, 971
Ghose T, **69:***823*
Giovanella BC, **68:***249*
Glaser M, **69:**1245
Glazer RI, **68:**391
Godoy HM, **69:***687*
Goguel A-F, **68:***657*
Gold DV, **69:**381
Goldapfel M, **68:**841
Goldman M, **68:**613
Goldstein AL, **69:**27
Goldstein DP, **69:**23
Golemboski KA, **68:***993*
Golub SH, **68:***703*, *711*
Gorelik E, **69:***89*
Götz A, **68:**475
Govers F, **69:**945
Graham S, **69:**1059
Granger GA, **69:**879, 889
Grantham FH, **68:**519
Green S, **68:***997*
Greenberg ER, **68:***743*
Greenberger JS, **68:**305
Greene CL, **69:**1289
Gregoire A, **68:**357
Griffin TW, **69:***799*
Gross J, **69:**1329
Grufferman S, **68:***107*, 573
Gruntenko YV, **69:**67
Gryschek G, **69:**997
Gullino PM, **68:***519*; **69:**475, 483, 1183
Gupta S, **69:***1261*

Haag D, **68:**415
Haagensen DE Jr, **69:***1073*
Habeeb AFSA, **68:***651*
Habu S, **68:**449
Hagemeijer A, **69:***945*
Hager JC, **69:***1359*
Hagiwara A, **68:**497; **69:**1383
Halliday WJ, **69:***939*
Hamada T, **69:**1221
Hamburger AW, **68:***945*
Hammersen F, **68:**475
Hamuro J, **69:**807
Hankey BF, **68:**445
Hankin JH, **68:**401
Hann H-WL, **69:***393*
Hanna N, **69:**665
Hara D, **68:**703
Haraguchi S, **69:**527
Harbell JW, **69:***1391*
Harber LC, **69:***237*
Hardy WD Jr, **69:**333
Hargrove ME, **69:**873
Harkrader RJ, **68:**665
Harris JE, **68:**549
Harshbarger JC, **69:**915
Harte PJ, **69:**23
Hartsock RJ, **68:**43
Hatanaka M, **68:**115
Hawkins JG, **69:**767
Haynes LR, **69:**799
Hays EF, **69:***1077*
Head KW, **68:**239
Heatfield BM, **69:**577, 751, *757*
Hecker CJ, **68:**461
Heckman CA, **69:***117*
Heilbrun LK, **68:**401
Heinbaugh JA, **69:**737
Helleberg A, **68:**351
Hellman S, **68:**639
Hendler FJ, **68:**719
Henle KJ, **68:***1033*
Hennekens CH, **68:**537
Henning MM, **69:**619
Henshaw EC, **69:**647
Henson DE, **68:**338
Herberman RB, **69:**89, 339
Herman TS, **68:***487*
Hersh EM, **68:**139
Hiai H, **69:**627
Hiasa Y, **69:***963*

Hiatt RA, 68:*885*
Himeno K, 68:823
Hinds MW, 68:*395*
Hint E, 69:1035
Hirohashi S, 69:*565*
Hirohata T, 68:823
Hirota N, 69:*1299*
Hisano G, 69:*665*
Hoar SK, 69:*1419*
Hochwald GM, 68:501; 69:535
Hocking GR, 68:*579*
Hod I, 69:747
Hogarth PM, 69:*619*
Holland LM, 69:415
Hollander V, 68:325
Hollingsworth MA, 69:*53*
Holly EA, 69:773
Holtzman S, 69:1135
Hook RR Jr, 68:461
Hoover R, 69:817
Horan PK, 69:647
Horm JW, 69:*833*
Hoshi A, 68:287
Houghton JA, 68:*437*
Houghton PJ, 68:437
Howard SC, 69:*33*
Huang TTF Jr, 68:*643*
Huggins JW, 69:33
Hughes ESR, 68:579
Hull SR, 69:33
Hunter JE, 69:*319*
Hunter JT, 68:673
Hunter N, 68:139
Hurwitz E, 69:*47*
Hutchinson WB, 69:1017
Huygen K, 69:653

Ichikawa H, 69:237
Ichiki S, 69:401
Ichimaru M, 69:*323*
Ide F, 69:*557*
Iglehart JD, 69:509
Iijima S, 69:1221
Ikawa Y, 69:544
Imai K, 68:*761*; 69:823
Imlah P, 68:239
Inaji H, 68:99
Ino Y, 69:565
Introna M, 68:555
Ip C, 69:729
Ip MM, 69:*673*
Irons G, 68:771
Irvin GL, 69:79
Ishidate T, 68:401
Ishii DN, 68:*299*
Ishikawa T, 69:557
Ishimaru T, 69:323
Itakura H, 69:1221
Ito N, 68:497; 69:1383
Ito Y, 69:*1343*
Ivie GW, 69:*259*
Iwasawa H, 69:95

Jackson RC, 68:665
Jahnke MR, 69:371
Jain RK, 68:519
Jeanloz RW, 69:371
Jerina DM, 69:725
Jerome LF, 68:935
Jirtle RL, 68:771
Johnson AE, 69:*253*
Johnson WR, 68:579
Jones GM, 69:409
Jones J, 69:475
Jones RD, 69:573
Jones RS, 68:771
Joplin CFB, 68:219

Kahan BD, 69:131, 1121
Kahn SJ, 69:839
Kaidbey KH, 69:269
Kakunaga T, 69:503
Kalebic T, 69:1049
Kaledin VI, 69:*67*
Kamiya K, 69:595
Kamiyama S, 68:401
Kanisawa M, 69:1317
Kanzawa F, 68:*287*
Karas M, 69:15
Karlin DA, 69:*573*
Kasahara T, 69:807
Kashi R, 69:47
Katayama S, 68:*867*
Kato H, 69:1221
Kawaguchi M, 69:345
Kawaguchi T, 68:507
Kellerer AM, 69:1135
Kelly PA, 68:381; 69:447
Kelly RW, 69:1055
Key ME, 69:*1189*
Khosravi M, 68:19
Kibbey WE, 69:443
Kidwell WR, 68:267
Kieran MW, 69:357
Kiernan M, 68:357
Killian CS, 68:99
Kim H, 68:*43*
Kim U, 69:673, 729
Kimm SYS, 68:107
King EB, 68:9
Kinsella TJ, 68:*697*
Kishi K, 69:565
Kitahori Y, 69:963
Kitamura Y, 69:1305
Klecker R, 68:227
Klein G, 68:179, *197*, 981
Klein WR, 69:*1095*
Kleinerman RA, 69:*1027*
Klein-Szanto AJP, 69:1155
Kligman AM, 69:*269*
Klostergaard J, 69:879, 889
Knudson AG, 69:543
Koba F, 69:345
Koch M, 69:*813*
Koch P, 69:393
Kodama Y, 69:*595*
Kodell RL, 69:*659*
Kohn PH, 68:267
Kolb R, 68:735
Kolonel LN, 68:395
Komitowski D, 68:*147*
Kondo S, 69:1305
Konishi N, 69:963
Konishi Y, 68:*859*
Koppi TA, 69:939
Kornblith PL, 69:1245
Kornhauser A, 69:245
Koss LG, 69:15
Kovacs S, 69:177
Koziorowska JH, 69:9
Kraemer KH, 69:*219*
Kraemer PM, 69:415
Kreeftenberg JG, 69:1095
Krinsky NI, 69:*205*
Kripke ML, 68:*685*, 691; 69:*171*
Krishan A, 68:1027
Krishnamurthy S, 68:95
Kruizinga W, 69:1095
Kubai L, 69:699
Kubo C, 69:1293
Kuno K, 69:1229
Kuretani K, 68:287
Kuriyama M, 68:*99*
Kuroda K, 69:*1317*
Kuroki Masahide, 69:*401*
Kuroki Motomu, 69:401
Kuschner M, 68:597
Kuzumaki N, 69:*527*
Kwong PC, 68:19

Lai LT-Y, 68:75
Landry RJ, 69:*155*
Lang NP, 69:*339*
Lanier AP, 69:1005
Lanighan K, 69:1353
Laskin S, 68:597
Laub W, 68:147
Lauriola L, 69:827
La Vecchia C, 69:*1207*
Lea MA, 69:1353
Leck I, 68:91
Lee CL, 68:99
Lee D, 69:*381*
Lee J, 68:395
Lee KP, 68:*157*
Lees AW, 68:211
LeGrue SJ, 69:*131*
Leitmeyer JE, 69:393
Lepp KA, 68:541
Lerman S, 69:*287*
Lespinats G, 68:657
Leuthauser SWC, 68:*123*
Levenson SM, 68:835; 69:73
Levin W, 69:725
Levine PH, 69:787
Levy WE III, 69:879
Lewis JL Jr, 69:1039
Leyten R, 69:653
Li FP, 68:573, 697; 69:1063
Li JJ, 69:41
Li J-Y, 69:1063
Li SA, 69:*41*
Liao S-K, 68:*19*
Liberati A, 69:1207
Lichtenstein A, 69:*495*
Liff JM, 68:95
Lijinsky W, 68:*681*, *989*, *1127*
Lin MF, 68:99
Lindsay JM, 69:*1163*
Liotta LA, 69:1049
Lippman ME, 68:267
Little JB, 68:697
Lohrmann H-P, 68:*541*
Longenecker BM, 69:357
Longley JD, 68:357
Loor RM, 68:99
Lopez C, 69:953
Lopez DM, 68:69, 779; 69:*1403*
Lovett EJ, 68:957
Lubin JH, 68:*211*
Luccarelli G, 68:751

Ludwig H, **68**:*729*
Lui MS, **68**:*665*
Lukasewycz OA, **69**:*489*
Lukes RJ, **68**:43
Lund JK, **68**:1037
Lundgren B, **68**:*351*
Luner SJ, **69**:823
Lyon JL, **68**:95
Lytle CD, **69**:183

Macek CM, **69**:131
MacInnes JI, **69**:933
MacLean GD, **69**:*357*
MacMahon B, **69**:*1035*
Maeda M, **68**:287
Maeda S, **69**:1343
Mage MG, **69**:591
Maggiano N, **69**:827
Magrath I, **69**:585
Malaveille C, **69**:1375
Malejka-Giganti D, **69**:41
Malinin T, **69**:79
Mangioni C, **68**:555
Mann RB, **68**:43
Manning L, **69**:1163
Mantovani A, **68**:555
Marchetto DJ, **68**:*691*
Marchok AC, **69**:1155
Marel MM, **69**:*1367*
Margaretten N, **69**:1077
Margulies IM, **69**:1049
Markham PD, **69**:435
Markovich RP, **69**:333
Marotti T, **68**:891
Marsh GM, **68**:925
Martin RH, **69**:823
Maruyama H, **68**:859
Marzi A, **69**:687
Maslow DE, **68**:*721*
Massa G, **68**:*971*
Mastromarino AJ, **69**:573
Masucci G, **68**:179
Masuda H, **68**:401
Masuhara K, **68**:859
Matanoski GM, **68**:3
Mathews-Roth MM, **69**:*279*
Matienko NA, **69**:67
Matsunaga M, **69**:323
Matsuo T, **69**:527
Matsuoka Y, **69**:401
Matthews RH, **69**:443
May C, **68**:211
Mayhew EG, **69**:721
McCabe RP, **68**:*329*
McCoy JL, **68**:935
McCredie KB, **68**:35
McCune CS, **69**:*647*
McDaniel LS, **69**:*1337*
McGregor JF, **68**:*605*
McKenzie IFC, **69**:619, 939
McLain JR, **68**:771
McPherson TA, **69**:813
McRae LJ, **69**:767
McTaggart HS, **68**:*239*
Mehta NM, **69**:453
Meier H, **69**:1411
Melancon R, **69**:447
Merrill DW, **69**:773
Messmer K, **68**:475
Mettetal RW Jr, **69**:1245
Metzgar RS, **69**:1073
Meyer RJ, **68**:697
Michalopoulos G, **68**:771
Mickache M, **68**:735
Mii Y, **68**:859
Mikami M, **69**:323
Milas L, **68**:*139*
Milholland RJ, **69**:673
Miller AB, **68**:357
Miller EC, **68**:271
Miller JA, **68**:271
Miller RW, **69**:1063
Miller SB, **68**:*851*
Miller SC, **68**:*981*
Miller WR, **69**:*1055*
Minakawa H, **69**:527
Minale P, **68**:233
Minato N, **69**:807
Minowada J, **69**:393
Minton JP, **69**:443
Mirvish SS, **69**:*961*
Misdorp W, **69**:1095
Miska D, **68**:*259*
Mitchell DJ, **68**:613
Mitchell MS, **69**:607, 613
Mitsuma T, **68**:385
Miyaki M, **68**:*563*
Miyata M, **69**:807
Miyauchi Y, **68**:859
Miyazaki S, **69**:345
Miyazaki T, **69**:527
Modena D, **68**:751
Monaco ME, **68**:*267*
Monaghan P, **68**:799
Monroe MT, **69**:839
Montesano R, **69**:1375
Moore DE, **69**:*591*
Moore GE, **68**:365
Moore MR, **68**:*271*
Moore SP, **69**:183
Morantz RA, **68**:27
Morgan RT, **68**:365
Mori H, **69**:*1277*
Morikawa S, **69**:*95*
Morioka Y, **69**:807
Morison WL, **68**:685
Moriyama S, **69**:1299
Morris LE, **68**:211
Morris VL, **69**:933
Morrison AS, **68**:*91*
Morrow GR, **68**:*585*
Morton DL, **68**:703
Moskowitz M, **68**:357
Mostafa MH, **68**:293
Mulvey JJ, **68**:755
Mulvihill JJ, **68**:*173*
Munroe AE, **69**:23
Murahata RI, **69**:*607*, *613*
Murata M, **69**:*1229*
Murdoch J, **69**:1073
Murphy GP, **68**:99
Musiani P, **69**:*827*
Muthukkaruppan VR, **69**:*699*
Muzzulini C, **68**:971
Myers DK, **68**:605

Nagase M, **69**:1305
Nahrwold DL, **68**:619
Nairn RC, **68**:579
Naitoh M, **69**:95
Nakamura T, **69**:777
Nakanishi K, **68**:*497*
Nardelli B, **68**:817
Natale RB, **69**:1039
Natali PG, **68**:761
Natarajan AT, **69**:189
Nauciel C, **68**:657
Neequaye J, **69**:787
Neiman RS, **68**:43
Nelson N, **68**:597
Neri A, **68**:*507*
Nesnow S, **68**:*829*
Nettesheim P, **69**:1155
Newberne PM, **68**:785
Newman MS, **69**:725
Nichols WW, **69**:*543*
Nicolson GL, **68**:507
Nielsen A, **69**:549
Nigro ND, **69**:*103*
Nikolin VP, **69**:67
Nishi Y, **69**:*627*
Nishiura T, **68**:99
Nishizuka Y, **69**:627
Nixon JE, **68**:623
Nkrumah FK, **69**:787
Nocera A, **68**:233
Noguchi T, **69**:*907*
Nomoto K, **68**:823; **69**:1293
Nomura A, **68**:*401*
Nomura H, **69**:1235
Normann SJ, **69**:*1321*
Norvell ST Jr, **69**:823
Notake K, **69**:627
Nove J, **68**:697
Novicki DL, **68**:771
Novotny A, **68**:771
Nowell PC, **69**:593
Nylander G, **68**:813

Obata K, **68**:91
Obbagy JE, **68**:639
Oberley LW, **68**:123
Oberley TD, **68**:123
Odaka T, **68**:1005
O'Donnell RW, **69**:647
O'Flaherty EJ, **69**:851, *859*
Ogier G., **69**:1215
Ohno Y, **68**:91
Ohshima M, **69**:963, 1383
Okabe T, **69**:*1235*
Okinaka RT, **69**:199
Okuda S, **69**:*1293*
Okumura K, **68**:449
O'Malley RF, **69**:725
Ono T, **68**:563
Ortaldo JR, **69**:339
Oshawa N, **69**:1235
Ostertag W, **68**:457
Oxenhandler RW, **68**:461
Ozols RF, **68**:115

Padawer J, **68**:835
Pal BC, **69**:1155
Pannacciulli I, **68**:971
Papkoff JS, **69**:1391
Papsidero LD, **68**:99
Parrish JA, **68**:685; **69**:*273*
Parry DM, **68**:*573*
Parshad R, **69**:*409*
Parwaresch MR, **69**:1255
Pastan I, **69**:*544*

Pasternak G, **69:***997*
Pathak MA, **69:***163*
Patterson WB, **68:**697
Paul RD, **69:**1403
Pavelić J, **68:**891
Pavelić K, **68:***891*
Pellis NR, **69:**1121
Percy DH, **69:***933*
Perk K, **69:***747*
Persing JP, **69:**1017
Petitclerc M, **68:**357
Peto R, **69:**550
Petrakis NL, **68:***9*
Pfreundschuh M, **68:***501*
Piantelli M, **69:**827
Pihl E, **68:**579
Pine MJ, **69:***729*
Pistoia V, **68:***233*
Pitot HC, **68:**271
Platica M, **68:***325*
Plumb D, **69:**1
Pokala HP, **68:**75
Pollack A, **69:**79
Pollack VA, **69:***137*
Pollard M, **68:***884*
Pomrehn PR, **68:**915
Pooler JP, **69:***211*
Poplack DG, **68:**391
Potter GD, **69:**573
Poulton GA, **69:**189
Povey S, **68:**179
Pratt TS, **69:**639
Presta M, **68:**669
Preston AM, **68:**651
Pretlow TG II, **68:**851
Pretlow TP, **68:**851
Prohaska JR, **69:**489
Prospero TD, **69:**1
Puerari M, **68:**751
Puma JP, **68:**1037
Purde M, **69:**1035

Quinn LA, **68:**365

Radzun HJ, **69:**1255
Ragnotti G, **68:***669*
Rainey M, **68:**711
Raju KS, **69:***1183*
Ralph P, **68:**179
Ramanarayanan M, **69:**1359
Ramonas LM, **68:**875
Ranchalis J, **69:**793
Randolph V, **69:**1353
Ransohoff J, **68:**501
Ransom JH, **69:***741*
Rapp HJ, **68:**673; **69:**1095
Rappaport H, **68:**43
Rayner AA, **69:***23*
Raz A, **68:***629*
Rebuck JW, **68:**43
Reddy BS, **68:**867
Reeves WC, **68:***219*
Reidarson TH, **69:***879*, *889*
Reimer RR, **68:**573
Reinhöfer J, **69:**997
Reiter W, **68:**1027
Reitz MS Jr, **69:**1209
Rettura G, **68:**835; **69:***73*
Reuber MD, **68:**681, 989; **69:**1127
Rey A, **69:**27
Reznik-Schüller HM, **69:***927*
Riboni L, **68:**669
Riccardi R, **68:**391
Richards TC, **69:***693*
Riehl RK, **68:**415
Riggs CW, **69:**1127
Rios-Candelore M, **69:**1049
Ritter MA, **68:**799
Rivenson A, **68:**867
Rivera EM, **69:***517*
Roberts MM, **69:**1055
Rodrick ML, **69:**23
Rodrigues D, **69:**867
Roeser R, **69:**349
Rolland JM, **68:**579
Rollins-Smith LA, **68:***133*
Romani L, **68:***817*
Rose RC, **68:***619*
Rosen F, **69:**673
Rosen SW, **69:***1067*
Rosenberg MR, **68:**771
Rosenberg SA, **69:**109
Rosenfelder G, **68:***203*
Rosenstein M, **69:**109
Rosner B, **68:**537
Rost C, **68:**915
Rothschild H, **68:***755*
Rubin H, **68:***883*
Rubio CA, **68:***813*
Rudland PS, **68:***799*; **69:***1083*
Ruitenberg EJ, **69:**1095
Runge RG, **69:**961
Ruoslahti E, **69:**1105
Russo RG, **69:**1049
Rutzky LP, **68:***81*

Saavedra JE, **68:**681
Sacks ST, **68:**9; **69:**773
Sado T, **69:**1305
Saffold PC, **68:**549
Sakakeeny MA, **68:***305*
Sakamoto G, **69:**1229
Salahuddin Z, **69:**435
Salmasi S, **69:**961
Salner AL, **68:***639*
Sanabria P, **68:**651
Sandler DP, **68:***3*
Sanefuji H, **69:***751*, 757
Sanford KK, **68:***895*; **69:**409
Sarrif AM, **69:**767
Sasaki T, **68:**287
Sass B, **68:**147
Sato E, **69:**777
Sawada N, **69:***683*
Scalabrino G, **68:***751*
Schat KA, **69:**709, *715*
Schilder RJ, **68:**69
Schlott B, **68:**997
Schmidt BJ, **69:**183
Schmidt-Ullrich R, **69:***839*
Schottenfeld D, **68:**573
Schrager TF, **68:**785
Schreiber K, **69:**15
Schreml W, **68:**541
Schur PH, **69:**23
Scott JA, **68:**851
Scotto J, **69:**365
Searls DB, **69:***1311*
Seehafer J, **69:**357
Seifter E, **68:***835*; **69:**73
Sekiya S, **69:**95
Sell S, **69:***1105*
Sellakumar AR, **68:**597
Selvin S, **69:**773
Semple TU, **68:***365*
Serrou B, **69:**27
Sessa C, **68:**555
Seyama S, **69:**1221
Seyama T, **69:**595
Shapiro FD, **69:***1009*
Shapiro S, **69:***349*
Shaw ARE, **69:**357
Sheehan WW, **68:**43
Shek WR, **69:**709, 715
Shellabarger CJ, **69:***1135*
Shepard RC, **68:**249
Sherman A, **69:**15
Sherwin SA, **69:**793
Shiba M, **69:***1155*
Shibata M, **69:**1383
Shimamura K, **68:***449*
Shimosato Y, **69:**565
Shisa H, **69:**627
Shklar G, **68:***791*
Shochat D, **69:**381
Shu S, **68:***673*
Siciliano MJ, **68:**81
Sidell N, **68:***589*
Silverman J, **68:**867
Silverman MA, **68:**69
Siminovitch L, **69:**543
Simor IS, **68:**357
Singer GM, **68:**989
Singer SS, **68:**681, 989
Sinnhuber RO, **68:**623
Sizaret P, **69:***1375*
Slack NH, **68:**99
Slaga TJ, **68:**829; **69:**725
Smit EME, **69:**945
Smith GD, **68:**461
Snyder CA, **68:**597
Sonnenfeld G, **68:**993
Sordillo PP, **69:***333*
Sorlie PD, **69:***989*
Soullier BK, **69:**103
Sparnins VL, **68:***493*
Speizer FE, **68:**537
Spennacchio JL, **69:**647
Speyer JL, **68:**227
Spiegelman S, **69:**1359
Spiess PJ, **69:**109
Spitzer G, **68:***35*
Spremulli E, **68:***1011*
Srinivas L, **68:***469*
Steele G Jr, **69:**23
Steerenberg PA, **69:**1095
Stehlin JS, **68:**249
Stemmermann GN, **68:**395, 401
Steuer AF, **69:***435*
Stevens LC, **69:**907
Stone JP, **69:**1135
Stratford F, **69:**73
Strax P, **69:**349
Streips UN, **68:**993
Stringfellow DA, **68:**139
Strniste GF, **69:***199*
Strobl JS, **68:**267
Stroehlein JR, **69:**573
Strom SC, **68:***771*
Strong LC, **68:**573
Studzinski GP, **68:**407
Sugie S, **69:**1277

Sugiyama T, **69:**1343
Sumas ME, **69:**1353
Sundström C, **69:***1255*
Sutanto E, **69:**1271
Swanson M, **69:**1059
Swanson SK, **69:**1077
Swartzendruber DE, **69:**415
Sweets CC, **68:**487
Swenson B, **69:**1073
Szabo G, **69:***245*

Tacha DE, **69:**693
Takagi M, **69:**557
Takahashi M, **69:**1277
Takamizawa H, **69:**95
Takayama S, **69:**557
Takeda B, **69:**95
Talmadge JE, **69:***975*, 1189
Tamano S, **68:**497
Tamaoki N, **68:**449
Tamura H, **69:**59
Tanaka K, **69:**1305
Tanaka S, **69:**777
Tanaka Takuji, **69:**1277
Tanaka Tsuguo, **69:***1121*
Taniguchi H, **69:**59
Taniguchi K, **69:**1293
Tanooka H, **69:***1305*
Tarone RE, **69:**409
Tatsuta M, **69:***59*
Tautt JW, **69:***9*
Taylor SG IV, **68:***549*
Telang NT, **68:***1015*
Tencer K, **68:**945
Teppema JS, **69:**1095
Terasaki P, **68:**179
Terry J, **69:**177
Thomas DB, **69:***1017*
Thomas K, **69:**1049
Thompson WS, **69:**839
Thorbecke GJ, **69:**535
Thorgeirsson UP, **69:***1049*
Tiesjema RH, **69:**1095
Tilgen W, **68:**415
Ting C-C, **69:***867*, *873*
Ting RC, **69:**435
Tinley V, **68:**935
Todaro GJ, **69:**793
Tomita Y, **68:***823*
Tomooka Y, **69:***1347*
Tonali P, **69:**827
Tonomura A, **68:**563
Tormey DC, **69:**1067
Trach L, **69:**585
Triplett LL, **68:**829
Trochimowicz HJ, **68:**157
Trump BF, **69:**577, 751, 757
Tsuda H, **69:***1383*
Tsuji H, **69:**345
Tsukada H, **69:**683
Turcot-Lemay L, **68:***381*
Tuttle R, **69:**495
Twardzik DR, **69:***793*

Uchida A, **68:***735*
Ueda N, **69:**1343
Ullrich RL, **69:**1199
Umemura S, **69:**557
Urbach F, **69:***229*
Ury HK, **68:**885
Utsunomiya J, **68:**563

Vakhrusheva TE, **69:**67
Valdés PF, **68:**219
Valenzeno DP, **69:**211
Van Cauwenberge RM-L, **69:**1367
Vandenbark AA, **69:**551
Van Duuren BL, **69:**503
van Noord PAH, **69:**1283
Varani J, **68:***957*
Variakojis D, **68:**43
Veček N, **68:**891
Velez R, **69:***387*
Venditti JM, **68:**249
Venegas PL, **68:**493
Venet L, **69:**349
Venet W, **69:**349
Venner PM, **68:**391
Verhoek WG, **68:**91
Verma DS, **68:**35
Vijayaraghavan S, **69:**517
Vitetta ES, **68:**719
Vogel CL, **68:**69, 779
Vogt A, **68:**385
von Broen B, **69:**997
Vuk-Pavlović S, **68:**891

Wakasugi H, **69:***807*
Walker AM, **69:***1283*
Walker-Nasir E, **69:***371*
Wallace RB, **68:***915*
Wallach DFH, **69:**839
Wallen WC, **69:***787*
Wang HH, **68:**107
Wang MC, **68:**99
Warburton MJ, **68:**799; **69:**1083
Ward EC, **69:***509*
Warren JR, **69:***969*
Warrington RC, **68:***279*
Washer G, **69:**813
Wattenberg LW, **68:**493
Webber BL, **68:**437
Weber G, **68:**665
Weichselbaum RR, **68:**697
Weinberg MN, **69:**1289
Weinhold KJ, **69:**509
Weinhouse S, **68:***343*
Weisburger JH, **68:**867
Weiss NS, **68:***95*
Weiss W, **69:***1265*
Welander CE, **69:***1039*
Welch D, **68:**507
Wells RS, **69:***415*
Wells SA Jr, **69:**1073
Wenner CE, **69:**721
Wernet P, **68:**203
White CP, **68:**945
White DM, **68:**487
Whitham M, **68:***623*
Wigley CB, **69:**425
Wilchek M, **69:**47
Wilkoff LJ, **68:***1023*
Willett W, **68:**537
Williams GM, **68:**867, 1015; **69:**1277
Wilson BS, **68:**761
Wilson JF, **68:**43
Wilson PS, **69:**103
Wilson RE, **69:**23
Wolfson C, **68:**357
Wolley RC, **69:***15*
Wood AW, **69:***725*
Wood GW, **68:***27*; **69:**1163
Woods LK, **68:**365
Wu P-C, **68:***115*

Xue B, **69:**535

Yamakawa H, **68:**401
Yamamoto N, **68:***385*
Yamamura H, **69:**59
Yang H-Y, **68:**395
Yap PL, **69:**1055
Yefenof E, **68:***841*
Yokoro K, **69:**595
Yokose Y, **68:**859
Yokoyama T, **69:**1299
Yonezawa S, **69:***777*
Yoshida TO, **69:**527
Yoshikawa K, **69:**627
Yoshikura H, **68:***1005*
Yoshimoto K, **69:**1221
Young JD Jr, **69:**751
Yuan D, **68:***719*
Yuasa T, **69:**963

Zaharko DS, **68:***875*
Zamcheck N, **69:**23, 1073
Zander AR, **68:**35
Zavanella T, **68:**669
Zeigel RF, **69:**915
Zelman RJ, **68:**43
Zervos C, **69:***305*
Zeuthen J, **68:***179*, 197
Zhang Z-X, **69:**653
Ziche M, **69:***475*, *483*, 1183
Ziegler A, **68:**203
Ziegler HW, **68:***15*
Ziegler JL, **68:***337*
Zighelboim J, **69:**495

Permuted Title Index

Volumes 68 and 69
January–December 1982

acetoxime in MRC-Wistar rats /Carcinogenicity test of 69:961
A-chain-anticarcinoembryonic antigen antibody conjugate for human colon adenocarcinoma cell line /Selective cytotoxicity of a ricin 69:799
acid esterase and acid phosphatase in permanent human hematopoietic cell lines /Isozymes of 69:1255
α-1-acid glycoprotein assay in the detection of human colorectal cancer: Comparison with carcinoembryonic antigen /Value of plasma 68:75
(α_1-acid glycoprotein) levels /Mitogen-induced blastogenesis and receptor mobility inhibition by breast cancer serum with elevated 68:779
acid phosphatase in permanent human hematopoietic cell lines /Isozymes of acid esterase and 69:1255
acinar carcinoma /Secretagogue response in rat pancreatic 69:969
ACI rat by 430-keV neutrons, X-rays, and diethylstilbestrol /Induction of mammary neoplasms in the 69:1135
acute leukemia in the United States /No seasonality in the diagnosis of 69:1283
acute leukemia: Possible subsets in childhood leukemia /Changes in clonal expression during the course of 69:393
acute urethan dose and target cell number /Relationship of lung adenoma prevalence and growth rate to 69:851
adenocarcinoma cell lines and tissues /Various isozyme gene expression patterns among human colorectal 68:81
adenocarcinoma cell line /Selective cytotoxicity of a ricin A-chain-anticarcinoembryonic antigen antibody conjugate for human colon 69:799
adenocarcinoma cells: Lack of therapeutic action of supplemental ascorbic acid /Prophylactic and therapeutic actions of supplement- 69:73
adenocarcinoma /Development and biologic properties of malignant cell sublines and clones of a spontaneously metastasizing rat mam- 68:507
adenocarcinoma /Gastrin protection against chemically induced gastric adenocarcinomas in Wistar rats: Histopathology of the gland- 69:59
adenocarcinoma grown in vivo and in vitro /Flow cytometric analysis of R3327 rat prostate 69:79
adenocarcinoma induced by *N*-hydroxy-*N*-2-fluorenylacetamide /Steroid hormone receptors in the rat mammary 69:41
adenocarcinoma in rats: Induction by 3,2′-dimethyl-4-aminobiphenyl /Prostate 68:867
adenocarcinoma of the uterus in androgen-sterilized SD rats /Spontaneous occurrence of atypical hyperplasia and 69:95
adenocarcinoma /Relationship between xenotransplantability and cell surface properties of ascites sublines of a rat mammary 69:33
adenocarcinomas in virus-infected leopard frog tadpoles /Effect of thymectomy on development of Lucké renal 68:133
adenocarcinomas in Wistar rats: Histopathology of the glandular stomach and incidence of gastric adenocarcinoma /Gastrin pro- 69:59
adenocarcinomas xenotransplanted into nude mice /α_1-Protease inhibitor production by human 69:381
adenoma, and carcinoma of the human large bowel /Glycoconjugate with *Ulex europaeus* agglutinin-I-binding sites in normal mucosa, 69:777
adenoma latency: Relevance of tumor growth rate and target cell number /Relationship between urethan dose rate and 69:859
adenoma prevalence and growth rate to acute urethan dose and target cell number /Relationship of lung 69:851
adenomatosis coli /Morphologic transformation and chromosomal changes induced by chemical carcinogens in skin fibroblasts from pa- 68:563
adenosylmethionine decarboxylase levels /Degrees of malignancy in human primary central nervous system tumors: Ornithine decar- 68:751
adherent cell contact-mediated modulation of normal myeloid colony formation /Human 68:35
adjuvant chemotherapy of breast cancer /Intrastage prognostic heterogeneity: Implications for 68:445
adriamycin levels and cytotoxicity in adriamycin-sensitive and adriamycin-resistant P388 mouse leukemia cells /Intracellular 68:1027
aflatoxin B_1 as a measure of hepatocarcinoma initiation in rainbow trout /Liver DNA bound in vivo with 68:623
aflatoxin B_1 in large doses /Cholangiocellular carcinomas induced in Syrian golden hamsters administered 68:271
aflatoxins and related metabolites by radioimmunoassay /Detection of 69:1375
African Burkitt's lymphoma with central nervous system involvement /Cerebrospinal fluid markers in 69:787
agar /Effect of enzymatic disaggregation on proliferation of human tumor cells in soft 68:945
agarose without feeder layers /High cloning efficiency of human lymphoid cells in 68:919
age and anatomical site on ultraviolet carcinogenesis in BALB/c mice /Influences of 68:691
age at diagnosis /Risk factors for breast cancer in women in northern Alberta, Canada, as related to 68:211
age at first and subsequent births: A study in the population of the Estonian Republic /Association of breast cancer risk with 69:1035
age-dependent data on multiple myeloma in Austria /Epidemiologic and 68:729
age, sex, and mammary tumor detection in murine mammary tumor virus-infected mice /Letter to the Editor: Immune alterations re- 69:1208
agglutinin-I-binding sites in normal mucosa, adenoma, and carcinoma of the human large bowel /Glycoconjugate with *Ulex europaeus* 69:777
AKR mice /Spontaneous leukemia viruses: Lymphomagenic ecotropic viruses of 69:1077
Alaskan Natives: 1070–79 /Cancers of the gallbladder and biliary tract in 69:1005
Alberta, Canada, as related to age at diagnosis /Risk factors for breast cancer in women in northern 68:211
albumin /Methylazoxymethanol: Effect on the immune response of rats to human serum 68:651
alcohol, and a retinoid: Association with esophageal cancer in rats /Zinc deficiency, 68:785
allergic, and carcinogenic aspects with emphasis on predicting effects in humans—an introduction /Photochemical toxicity: Toxic, 69:151
Alloantigenic phenotype of radiation-induced thymomas in the mouse 69:619
alloantigen /Modulation of cell-mediated alloimmunity by BCG. II. Induction of specific, nonadherent, non-T-killer cells by BCG and 69:613
alloantigens in mice /Effects of different fractions of *Corynebacterium parvum* on the cytotoxic T-cell response to 69:495
alloimmunity by BCG. I. Antagonism and potentiation of immunosuppression caused by cytarabine /Modulation of cell-mediated 69:607
alloimmunity by BCG. II. Induction of specific, nonadherent, non-T-killer cells by BCG and alloantigen /Modulation of cell-mediated 69:613
allotransplantability and the presence of the cell surface glycoprotein epiglycanin in the TA3-MM mouse mammary carcinoma ascites cell 68:981

Americans: 1969–78 /Changes in lung cancer incidence and mortality rates among ... 69:833
amino acid pools of rodent mammary tumors /Free ... 69:729
aminonucleoside on normal and transformed human fibroblasts /Basis for the differential action of ... 68:407
aminophosphorothioate drug activity with polyamine oxidase susceptibility /Possible association of radioprotective and chemoprotective ... 69:329
anatomical site on ultraviolet carcinogenesis in BALB/c mice /Influences of age and ... 68:691
anchorage in the expression of tumorigenicity of untransformed mouse cell lines /Role of ... 69:415
Andervont, *D.Sc.*—A Tribute /Howard Bancroft. ... 68:1
Androgen conjugates in human breast cyst fluids ... 69:1055
Androgen control of cytosol progesterone receptor levels in the MT-W9B transplantable mammary tumor in the rat ... 69:673
androgen-sterilized SD rats /Spontaneous occurrence of atypical hyperplasia and adenocarcinoma of the uterus in ... 69:95
Angiogenesis and neoplastic progression in vitro ... 69:483
angiogenesis /Ceruloplasmin, copper ions, and ... 69:1183
angiogenesis /Role of prostaglandin E_1 and copper in ... 69:475
anthracycline antibiotics /B16 melanoma cell variants: Irreversible inhibition of growth and induction of morphologic differentiation by ... 68:629
antibiotics /B16 melanoma cell variants: Irreversible inhibition of growth and induction of morphologic differentiation by anthracycline ... 68:629
antibodies and breast cancer /Meeting Highlights: Monoclonal ... 68:338
antibodies. I. Heterogeneous expression of Ia-like and HLA-like antigenic determinants /Antigenic heterogeneity of human colorectal ... 69:357
antibodies /Immunotherapy of a murine leukemia virus-infected, chemically induced murine sarcoma with antiviral ... 69:509
antibody conjugate for human colon adenocarcinoma cell line /Selective cytotoxicity of a ricin A-chain–anticarcinoembryonic antigen ... 69:799
antibody /Imaging of human melanoma xenografts in nude mice with a radiolabeled monoclonal ... 69:823
antibody on a Rous sarcoma virus-induced mouse tumor /Individually distinct tumor-specific cell surface antigen identified by mono- ... 69:527
antibody reactive with a subset of human breast tumors /Characterization of a monoclonal ... 68:719
Anticancer drugs: Effect on the cloning of Raji lymphoma cells in soft agar ... 68:115
anticarcinoembryonic antigen antibody conjugate for human colon adenocarcinoma cell line /Selective cytotoxicity of a ricin A-chain– ... 69:799
antigen and nonspecific cross-reacting antigen by a continuous cell line from a human pancreatic tumor /Coproduction of carcinoem- ... 69:401
antigen antibody conjugate for human colon adenocarcinoma cell line /Selective cytotoxicity of a ricin A-chain–anticarcinoembryonic ... 69:799
antigen by a continuous cell line from a human pancreatic tumor /Coproduction of carcinoembryonic antigen and nonspecific cross-re- ... 69:401
antigen during differentiation of cultured stem cells /Thy-1 antigen on normal and neoplastic rat mammary tissues: Changes in loca- ... 68:799
antigen expressed in hematopoietic cells derived from $Fv\text{-}4^r$ mouse strains /Surface ... 68:1005
antigenic determinants /Antigenic heterogeneity of human colorectal cancer cell lines analyzed by a panel of monoclonal antibod- ... 69:357
antigen identified by monoclonal antibody on a Rous sarcoma virus-induced mouse tumor /Individually distinct tumor-specific cell sur- ... 69:527
antigen in hamsters /Simian virus 40 (SV40)-specific isoelectric point-4.7–94,000-M_r membrane glycoprotein: Major peptide ho- ... 69:839
antigen in nonhuman primates /Carcinoembryonic ... 69:1073
antigen /Primary liver carcinoma and liver cirrhosis in atomic bomb survivors, Hiroshima and Nagasaki, 1961–75, with special re- ... 69:1221
antigens and β_2-microglobulin on cultured human melanoma cells by interferon /Enhanced expression of melanoma-associated ... 68:19
antigens by patients with hyperplastic benign breast disease /Cell-mediated immunity to mouse mammary tumor virus ... 68:935
antigens. I. Characterization of the cell components for induction of suppression /Tumor cell-triggered macrophage-mediated suppres- ... 69:867
antigens. II. Mechanisms for induction of suppression /Tumor cell-triggered macrophage-mediated suppression of the T-cell cytotoxic ... 69:873
antigens in human liver cell carcinoma and surrounding nontumorous liver /Distribution of hepatitis B surface and core ... 69:565
antigens in spleens of syngeneic mouse mammary tumor systems with low and high oncogenic potentials /Analysis of lymphoid cells re- ... 69:1403
antigens in vasectomized men /Immunity to tumor-associated ... 69:551
antigens /Multiple marker evaluation in human prostate cancer with the use of tissue-specific ... 68:99
antigens on Marek's disease lymphoblastoid tumor cell lines /Surface ... 69:715
antigens on pulmonary metastases of a 3-methylcholanthrene-induced sarcoma in mice: A preliminary report /Immunotherapeutic ef- ... 69:1121
antigens produced by mouse mammary tumor cells in artificial capillary culture /Tumor-associated ... 69:1359
antigens with the nonionic detergent octyl-β-D-glucopyranoside /Noncytolytic extraction of murine tumor-specific transplantation ... 69:131
antigen: Usefulness as a postsurgical method in the detection of recurrence in Dukes stage B_2 and C colorectal cancers /Carcinoembry- ... 69:813
antigen /Value of plasma α-1-acid glycoprotein assay in the detection of human colorectal cancer: Comparison with carcinoembryonic ... 68:75
anti-inflammatory factors produced by murine tumor cells in culture /Characterization of ... 69:1321
antitumor activities of pyrimidinone-interferon inducers. I. Effect against artificial and spontaneous lung metastases of murine tumors ... 68:139
antitumor activity according to peptide structure and route of injection /Peptidoglycans extracted from gram-positive bacteria: Expres- ... 68:657
Antitumor activity of picolinic acid in CBA/J mice ... 68:123
antitumor agent ICRF 159 in somatic cell hybrids /Inheritance of cellular resistance to the ... 68:977
Antitumor immunity induced by hybrid murine tumor cells: Requirements for optimal immunization ... 69:647
antitumor immunoglobulins that specifically inhibit DNA synthesis of mouse tumor cells /Platinum-complexed ... 69:47
antitumor resistance of B57BL/6 mice by leukemogenic doses of radiation and restoration of resistance by transfer of bone marrow or spleen ... 69:89
antiviral antibodies /Immunotherapy of a murine leukemia virus-infected, chemically induced murine sarcoma with ... 69:509
A-particles in mouse embryos and neoplastic cell lines /Immunologic relatedness of intracisternal ... 68:643
ascites cell /Further studies on the relationship between allotransplantability and the presence of the cell surface glycoprotein epigly- ... 68:981
ascites sublines of a rat mammary adenocarcinoma /Relationship between xenotransplantability and cell surface properties of ... 69:33

ascorbic acid /Prophylactic and therapeutic actions of supplemental β-carotene in mice inoculated with C3HBA adenocarcinoma cells: 69:73
atomic bomb survivors, Hiroshima and Nagasaki, 1961–75, with special reference to hepatitis B surface antigen /Primary liver carci- 69:1221
atomic bomb survivors in Hirishima and Nagasaki, 1950–76: Relationship to radiation dose absorbed by marrow /Multiple myeloma 69:323
Austria /Epidemiologic and age-dependent data on multiple myelona in 68:729
autoradiography of the trachea in fetal Syrian golden hamsters treated transplacentally with *N*-nitrosodiethylamine /Electron micro- 69:927
azo dyes /Suppression of 7,12-dimethylbenz[*a*]anthracene-induced chromosome aberrations in rat bone marrow cells after treatment 69:1343
azoxymethane-induced intestinal cancer in rats /Combined inhibitors of carcinogenesis: Effect on 69:103

B16 melanoma cell variants: Irreversible inhibition of growth and induction of morphologic differentiation by anthracycline antibiotics 68:629
bacteria: Expression of antitumor activity according to peptide structure and route of injection /Peptidoglycans extracted from gram- 68:657
BALB/c mice by single low doses of 7,12-dimethylbenz[*a*]anthracene /Induction of mammary tumors in virgin female 69:1199
BALB/c mice. I. Enhancement of in vivo rejection responses by combined chemotherapy-immunotherapy /Development of resist- 68:963
BALB/c mice /Influences of age and anatomical site on ultraviolet carcinogenesis in 68:691
Balb/3T3 cells with catechol as cocarcinogen /Chemical cocarcinogenesis with the use of a subclone derived from 69:503
B-cell markers /Human lymphoma–lymphoma hybrids and lymphoma–leukemia hybrids. I. Isolation, characterization, cell surface 68:179
BCG. I. Antagonism and potentiation of immunosuppression caused by cytarabine /Modulation of cell-mediated alloimmunity by 69:607
BCG. II. Induction of specific, nonadherent, non-T-killer cells by BCG and alloantigen /Modulation of cell-mediated alloimmunity by 69:613
BCG cell walls or live BCG in bovine ocular squamous cell carcinoma: A preliminary report /Immunotherapy by intralesional injection 69:1095
behavior and histology of transplanted mammary tumors in GR mice /Comparison of biologic 69:933
beta-adrenoreceptor blocking agent in female rats /Liver tumors induced by a new 68:669
Bile acids: Effects on absorption of 1,2-dimethylhydrazine and 7,12-dimethylbenz[*a*]anthracene in the colon of the rat and guinea pig 68:619
biliary tract in Alaskan Natives: 1970–79 /Cancers of the gallbladder and 69:1005
biochemical aspects of photosensitization in livestock and poultry /Chemical and 69:259
biochemical markers for human hematopoietic cell lines /Ganglioside patterns: New 68:203
Biokinetics of activation and release in vitro /Inducible macrophage cytotoxins. I. 69:879
biologic behavior and histology of transplanted mammary tumors in GR mice /Comparison of 69:933
biologic properties of malignant cell sublines and clones of a spontaneously metastasizing rat mammary adenocarcinoma /Development 68:507
births: A study in the population of the Estonian Republic /Association of breast cancer risk with age at first and subsequent 69:1035
1,3-bis(2-chloroethyl)-1-nitrosourea, and 1-(2-chloroethyl)-3-(4-methylcyclohexyl)-1-nitrosourea: Effect on the human granulopoietic system 68:541
bis(*N*-ethylidene vindesine) disulfide, disulfate /Cross-resistance of cultured murine leukemia vincristine-resistant P388 cells to vin- 68:1023
bladder in vitro /*N*-Methyl-*N*-nitrosourea and saccharin: Effects on epithelium of normal human urinary 69:577
bladder tumors in male F344 rats /Organ-specific promoting effects of phenobarbital sodium and sodium saccharin in the induction of 68:497
blastic activation /Functional properties of human thymoma lyphocytes: Role of subcellular factors in 69:827
blastogenesis and receptor mobility inhibition by breast cancer serum with elevated orosomucoid (α_1-acid glycoprotein) levels /Mi- 68:779
blastogenic responses of lymphocytes from breast cancer patients and controls by the use of α-methyl-D-mannoside /Maximizing differ- 68:69
Blastomyces dermatitidis against EL 4 lymphoma in C57BL/6J mice /Immunoadjuvant effects of 69:1337
bleomycin on DNA synthesis and repair in rat hepatocytes and hepatoma cells /Effects of nicotinamide, isonicotinamide, and 69:1353
blocking agent in female rats /Liver tumors induced by a new beta-adrenoreceptor 68:669
blood and regional lymph nodes of patients with untreated breast cancer /Subpopulations of human T-lymphocytes. XIX. T-cells and 69:1261
blood and tumor-associated lymphocytes against human ovarian carcinoma cells /Interferon effect on cytotoxicity of peripheral 68:555
blood flow, capillary morphology, and local oxygen pressure of the hamster amelanotic melanoma A-Mel-3 /Microcirculatory 68:475
blood levels of substance(s) immunologically cross-reactive with insulin /Carcinomas of the cervix and corpus uteri in humans: Stage- 68:891
blood of brain tumor patients /In vitro reversal of depressed T-lymphocyte function in the peripheral 68:27
B-lymphoblast tumorigenicity in nude mice /Effect of type C viral expression and cellular karotype on human 69:435
B-lymphocyte subpopulations infiltrating human mammary carcinomas /T-Lymphocyte and 69:1
bone marrow cell injection /Decrease of tumor growth in mice after intravenous thymosin-treated 69:27
bone marrow cells after treatment with Sudan III and related azo dyes /Suppression of 7,12-dimethylbenz[*a*]anthracene-induced 69:1343
bone marrow cultures and factor-dependent cell line generation: Significant variation among 28 inbred mouse strains and outbred stocks 68:305
bone marrow fractions /Differing stem cell self-renewal of lectin-separated murine 68:639
bone marrow or spleen cells from normal, but not beige, syngeneic mice /Depression of natural antitumor resistance of C57BL/6 69:89
bovine ocular squamous cell carcinoma: A preliminary report /Immunotherapy by intralesional injection of BCG cell walls or live 69:1095
bowel /Glycoconjugate with *Ulex europaeus* agglutinin-I-binding sites in normal mucosa, adenoma, and carcinoma of the human large 69:777
brain tumor patients /In vitro reversal of depressed T-lymphocyte function in the peripheral blood of 68:27
brain tumors. I. Requirement for third-party stimulator lymphocytes in the induction of cell-mediated cytotoxic responses to allogeneic cul- 69:1245
Breast cancer and serum cholesterol 68:885
breast cancer in Japan /Epidemiology of familial predisposition for 69:1229
breast cancer /Interaction of familial and hormonal risk factors for 69:817
breast cancer /Intrastage prognostic heterogeneity: Implications for adjuvant chemotherapy of 68:445
breast cancer in women in northern Alberta, Canada, as related to age at diagnosis /Risk factors for 68:211

breast cancer in women /Single oblique-view mammography for periodic screening for ... 68:351
breast cancer in women with benign breast diseases /Exogenous estrogens and other risk factors for ... 69:1017
breast cancer /Meeting Highlights: Monoclonal antibodies and ... 68:338
breast cancer mortality /Ten- to fourteen-year effect of screening on ... 69:349
breast cancer patients and controls by the use of α-methyl-D-mannoside /Maximizing differences in the concanavalin A-induced blasto- ... 68:69
breast cancer risk factors /Epithelial dysplasia in nipple aspirates of breast fluid: Association with family history and other ... 68:9
breast cancer risk with age at first and subsequent births: A study in the population of the Estonian Republic /Association of ... 69:1035
breast cancer serum with elevated orosomucoid (α_1-acid glycoprotein) levels /Mitogen-induced blastogenesis and receptor mobility in- ... 68:779
breast cancer /Subpopulations of human T-lymphocytes. XIX. T-cells and T-cells with receptors for IgMFc (Tμ), IgGFc (Tγ), or IgAFc ... 69:1261
breast carcinoma /Isolation and partial characterization of surface components of cell line MDA-MB-231 derived from a human metas- ... 69:371
breast cyst fluids /Androgen conjugates in human ... 69:1055
breast disease /Cell-mediated immunity to mouse mammary tumor virus antigens by patients with hyperplastic benign ... 68:935
breast diseases /Exogenous estrogens and other risk factors for breast cancer in women with benign ... 69:1017
breast fluid: Association with family history and other breast cancer risk factors /Epithelial dysplasia in nipple aspirates of ... 68:9
breast in women /Use of circulating pregnancy-specific β_1 glycoprotein as a marker in carcinoma of the ... 69:1067
breast tumors /Characterization of a monoclonal antibody reactive with a subset of human ... 68:719
breast tumors /Prolactin receptors in human ... 68:381
Breath methane excretion in patients with unresected colorectal cancer ... 69:573
breeding lines that differ in chromosome breakage /Diverse xenotropic virus expressions in two NZB mouse ... 68:951
Burkitt's lymphoma cells /Changes in human adenovirus 5 propagated in ... 69:1215
Burkitt's lymphoma with central nervous system involvement /Cerebrospinal fluid markers in African ... 69:787

C3HBA adenocarcinoma cells: Lack of therapeutic action of supplemental ascorbic acid /Prophylactic and therapeutic actions of sup- ... 69:73
C3H/10T½ cells /Resting state depth and saturation density as modulated by tumor promoters and culture conditions: Relation- ... 68:259
C57BL/6 mice by leukemogenic doses of radiation and restoration of resistance by transfer of bone marrow or spleen cells from normal, ... 69:89
C57BL/6J mice /Immunoadjuvant effects of *Blastomyces dermatitidis* against EL 4 lymphoma in ... 69:1337
(C57BL/6N × C3H/HeN)F_1 mice /Carcinogenic effect of carbazole in the liver in ... 69:1383
Calorie restriction: Effect on growth of human tumors heterotransplanted in nude mice ... 68:249
Canada, as related to age at diagnosis /Risk factors for breast cancer in women in northern Alberta, ... 68:211
Cancer incidence in the Republic of Panama, 1974–78 ... 68:219
cancer incidence in the United States: Sources and uses of data /Measurement of ... 68:743
cancer mortality /Ten- to fourteen-year effect of screening on breast ... 69:349
capillary culture /Tumor-associated antigens produced by mouse mammary tumor cells in artificial ... 69:1359
capillary morphology, and local oxygen pressure of the hamster amelanotic melanoma A-Mel-3 /Microcirculatory blood flow, ... 68:475
carbazole in the liver of (C57BL/6N × C3H/HeN)F_1 mice /Carcinogenic effect of ... 69:1383
carcinoembryonic antigen and nonspecific cross-reacting antigen by a continuous cell line from a human pancreatic tumor /Coproduc- ... 69:401
Carcinoembryonic antigen in nonhuman primates ... 69:1073
Carcinoembryonic antigen: Usefulness as a postsurgical method in the detection of recurrence in Dukes stage B_2 and C colorectal cancer ... 69:813
carcinoembryonic antigen /Value of plasma α-1-acid glycoprotein assay in the detection of human colorectal cancer: Comparison with ... 68:75
carcinogenesis and by dietary constituents /Glutathione *S*-transferase activity: Enhancement by compounds inhibiting chemical ... 68:493
carcinogenesis, and in transplantable hepatocellular carcinomas /Expression of fibronectin and laminin in the rat liver after par- ... 69:1105
carcinogenesis by a 5-nitrofuran naphthyridine derivative in mice /Inhibitory effect of fumaric acid on forestomach and lung ... 69:1317
carcinogenesis by 1,2-dimethylhydrazine /Surgical resection of the rat colon: Effects on ... 68:813
Carcinogenesis by isomers of *N*-nitroso-3,5-dimethylpiperidine ... 68:989
carcinogenesis: Effect on azoxymethane-induced intestinal cancer in rats /Combined inhibitors of ... 69:103
carcinogenesis in BALB/c mice /Influences of age and anatomical site on ultraviolet ... 68:691
carcinogenesis in F344 rats by nitrosomethylethylamines substituted in the ethyl group /Esophageal ... 68:681
carcinogenesis in hamsters: Inhibition by vitamin E /Oral mucosal ... 68:791
carcinogenesis in vivo /Lymphotoxin prevention of diethylnitrosamine ... 69:741
carcinogenesis: Mechanisms of natural immunity /Immunomodulation of the lymphoresponsive phases of ... 69:737
carcinogenesis /Meeting Highlights: Host factors in human ... 68:173
carcinogenesis of human prostate. II. Long-term explant culture of normal prostate and benign prostatic hyperplasia: Light microscopy ... 69:751
carcinogenesis of human prostate. III. Long-term explant culture of normal prostate and benign prostatic hyperplasia: Transmission ... 69:757
carcinogenesis studies /Influence of cause-of-death assignment on time-to-tumor analyses in animal ... 69:659
carcinogenic aspects with emphasis on predicting effects in humans—an introduction /Photochemical toxicity: Toxic, allergic, and ... 69:151
Carcinogenic effect of carbazole in the liver of (C57BL/6N × C3H/HeN)F_1 mice ... 69:1383
carcinogenic effects in rabbits treated with *N*-nitroso-*N*-ethylurea /Genetics of transplacentally induced teratogenic and ... 69:1411
Carcinogenicity test of acetoxime in MRC-Wistar rats ... 69:961
Carcinogen-induced DNA damage and cellular alterations in F344 rat colon organ cultures ... 68:1015

carcinogen-induced morphologic transformation of Syrian hamster embryo cells /Equivalency of endothelial cell growth supple- 68:127
carcinogen-induced phenotypic properties frequently associated with the neoplastic state in a cultured guinea pig cell line /Inde- 69:115
carcinogen-induced preneoplastic hepatocytes of rats /In vitro measurement of resistance to phalloidin and γ-glutamyltransferase of 69:683
carcinogen-induced rat mammary tumors in gland-free mammary fat pads /Proliferation of ductal outgrowths by 69:517
carcinogen release rate on the incidence of preneoplastic and neoplastic lesions of the respiratory tract epithelium in rats /Effect of 69:1155
carcinogens /A high-tumor-incidence subline of the D1 mouse mammary hyperplastic outgrowth line: Effect of 69:639
carcinogens in short-term organ culture /Unscheduled DNA synthesis in human oral mucosa treated with chemical 69:557
carcinogens in skin fibroblasts from patients with familial adenomatosis coli /Morphologic transformation and chromosomal changes 68:563
carcinogen-treated rats /Purification and transplantation of hepatocytes from livers of 68:851
carcinoma and liver cirrhosis in atomic bomb survivors, Hiroshima and Nagasaki, 1961–75, with special reference to hepatitis B 69:1221
carcinoma and surrounding nontumorous liver /Distribution of hepatitis B surface and core antigens in human liver cell 69:565
carcinoma: An endemic analogue of a sporadic human neoplasm /Guest Editorial: Sheep lung 69:747
carcinoma: A preliminary report /Immunotherapy by intralesional injection of BCG cell walls or live BCG in bovine ocular squamous 69:1095
carcinoma ascites cell /Further studies on the relationship between allotransplantability and the presence of the cell surface glyco- 68:981
carcinoma cells /A 94,000-dalton glycoprotein expressed by human melanoma and 68:761
carcinoma cells /Interferon effect on cytotoxicity of peripheral blood and tumor-associated lymphocytes against human ovarian 68:555
carcinoma implanted in the nude mouse /Collagenolytic activity of rabbit V_2 .... 69:1329
carcinoma /Indirect macrophage migration inhibition response to 3-*M* KCI extract of gastric 69:345
carcinoma /Isolation and partial characterization of surface components of cell line MDA-MB-231 derived from a human meta- 69:371
carcinoma /Lymphocyte fluorescence polarization changes after phytohemagglutinin stimulation in the diagnosis of colorectal 68:579
carcinoma of human skin /Phenotypic and genotypic characteristics of a cell line from a squamous cell 68:415
carcinoma of the breast in women /Use of circulating pregnancy-specific β_1 glycoprotein as a marker in 69:1067
carcinoma of the human large bowel /Glycoconjugate with *Ulex europaeus* agglutinin-I-binding sites in normal mucosa, adenoma, and 69:777
carcinoma of the thyroid gland /Establishment and characterization of a human colony-stimulating factor-producing cell line 69:1235
carcinomas and its relationship to clinical behavior /DNA distribution in human colon 69:15
carcinoma /Secretagogue response in rat pancreatic acinar 69:969
carcinomas /Expression of fibronectin and laminin in the rat liver after partial hepatectomy, during carcinogenesis, and in transplant- 69:1105
carcinomas induced in Syrian golden hamsters administered aflatoxin B_1 in large doses /Cholangiocellular 68:271
Carcinomas of the cervix and corpus uteri in humans: Stage-dependent blood levels of substance(s) immunologically cross-reactive with in- 68:891
carcinomas /T-Lymphocyte and B-lymphocyte subpopulations infiltrating human mammary 69:1
carcinoma /Temperature gradients and local perfusion in a mammary 68:519
β-carotene in mice inoculated with C3HBA adenocarcinoma cells: Lack of therapeutic action of supplemental ascorbic acid /Prophy- 69:73
β-carotene /Moloney murine sarcoma virus tumors in CBA/J mice: Chemopreventive and chemotherapeutic actions of supplemental 68:835
carotenoids /Interaction of oxygen and oxy-radicals with 69:205
carotenoids /Photosensitization by porphyrins and prevention of photosensitization by 69:279
Carotid body tumors in humans: Genetics and epidemiology 68:573
Cartesian reductionism and cancer /Letter to the Editor 68:883
catechol as cocarcinogen /Chemical cocarcinogenesis with the use of a subclone derived from Balb/3T3 cells with 69:503
CBA/J mice /Antitumor activity of picolinic acid in 68:123
CBA/J mice: Chemopreventive and chemotherapeutic actions of supplemental β-carotene /Moloney murine sarcoma virus tumors in 68:835
Cell damage by near ultraviolet radiation: Role of DNA–protein cross-links 69:177
cell hybrid /Nonimmunogenic radiation-induced lymphoma: Immunity induction by a somatic 68:841
cell interactions and cancer /Meeting Highlights: Brief summary of the third joint meeting of the United States–Japan Cooperative 69:544
cell interactions in vitro /Some effects of the tumor promoter 12-*O*-tetradecanoylphorbol 13-acetate on 69:721
cell-mediated alloimmunity by BCG. I. Antagonism and potentiation of immunosuppression caused by cytarabine /Modulation of 69:607
cell-mediated alloimmunity by BCG. II. Induction of specific, nonadherent, non-T-killer cells by BCG and alloantigen /Modulation of 69:613
cell-mediated cytotoxic responses to allogeneic cultured gliomas /In vitro studies on the cell-mediated immune response to human 69:1245
cell-mediated immune response to human brain tumors. I. Requirement for third-party stimulator lymphocytes in the induction of cell-me- 69:1245
Cell-mediated immunity to mouse mammary tumor virus antigens by patients with hyperplastic benign breast disease 68:935
cell-mediated immunologic reactivity to Moloney murine sarcoma virus-induced tumors. III. Further characterization of tumor-specific 69:939
cell membranes /A method to quantify the potency of photosensitizers that modify 69:211
cell surface antigen identified by monoclonal antibody on a Rous sarcoma virus-induced mouse tumor /Individually distinct tumor- 69:527
cell surface glycoprotein epiglycanin in the TA3-MM mouse mammary carcinoma ascites cell /Further studies on the relationship be- 68:981
cell surface markers, and B-cell markers /Human lymphoma–lymphoma hybrids and lymphoma–leukemia hybrids. I. Isolation, char- 68:179
cell surface properties of ascites sublines of a rat mammary adenocarcinoma /Relationship between xenotransplantability and 69:33
cellular alterations in F344 rat colon organ cultures /Carcinogen-induced DNA damage and 68:1015
Cellular events associated with changes in natural killer cytotoxicity /Systemic administration of human leukocyte interferon to mel- 68:711
cellular karyotype on human B-lymphoblast tumorigenicity in nude mice /Effect of type C viral expression and 69:435
cellular resistance to the antitumor agent ICRF 159 in somatic cells hybrids /Inheritance of 68:977
central nervous system and systemic organs of mice. Distribution of $[^{125}I]$5-iodo-2′-deoxyuridine-labeled KHT tumor cells after left intra- 69:465

central nervous system involvement /Cerebrospinal fluid markers in African Burkitt's lymphoma with 69:787
central nervous system tumors: Ornithine decarboxylase levels as better indicators than adenosylmethionine decarboxylase levels /De- 68:751
Cerebrospinal fluid levels of 2'-deoxycoformycin after systemic administration in monkeys 68:391
Cerebrospinal fluid markers in African Burkitt's lymphoma with central nervous system involvement 69:787
Ceruloplasmin, copper ions, and angiogenesis 69:1183
cervical cancer /Second cancers following radiotherapy for 69:1027
cervix and corpus uteri in humans: Stage-dependent blood levels of substance(s) immunologically cross-reactive with insulin /Carcino- 68:891
cervix and penis in China /Correlation between cancers of the uterine 69:1063
chemical agents /Modification of photocarcinogenesis by 69:229
Chemical and biochemical aspects of photosensitization in livestock and poultry 69:259
chemical carcinogenesis and by dietary constituents /Glutathione *S*-transferase activity: Enhancement by compounds inhibiting 68:493
chemical carcinogen-induced phenotypic properties frequently associated with the neoplastic state in a cultured guinea pig cell line 69:1175
chemical carcinogens in short-term organ culture /Unscheduled DNA synthesis in human oral mucosa treated with 69:557
chemical carcinogens in skin fibroblasts from patients with familial adenomatosis coli /Morphologic transformation and chromosmal 68:563
Chemical cocarcinogenesis with the use of a subclone derived from Balb/3T3 cells with catechol as cocarcinogen 69:503
chemically induced gastric adenocarcinomas in Wistar rats: Histopathology of the glandular stomach and incidence of gastric adeno- 69:59
chemically induced murine sarcoma with antiviral antibodies /Immunotherapy of a murine leukemia virus-infected, ... 69:509
Chemical phototoxicity in humans 69:265
chemicals /Human models for identification of photosensitizing 69:269
chemicals /Tumor virus induction and host cell capacity inactivation: Possible in vitro tests for photosensitizing 69:183
chemical transformation in C3H/10T½ cells /Resting state depth and saturation density as modulated by tumor promoters and cul- 68:259
Chemopreventive and chemotherapeutic actions of supplemental β-carotene /Moloney murine sarcoma virus tumors in CBA/J mice 68:835
chemoprotective aminophosphorothioate drug activity with polyamine oxidase susceptibility /Possible association of radioprotective and 69:329
chemotherapeutic actions of supplemental β-carotene /Moloney murine sarcoma virus tumors in CBA/J mice: Chemopreventive and 68:835
chemotherapeutic drugs /Effect of rate of heating on lethality due to hyperthermia and selected 8:487
chemotherapy-immunotherapy /Development of resistance to MOPC-315 plasmacytoma after intralesional and intraperitoneal mel- 68:963
chemotherapy of breast cancer /Intrastage prognostic heterogeneity: Implications for adjuvant 68:445
chemotherapy patients /Prevalence and correlates of anticipatory nausea and vomiting in 68:585
Chemotherapy with Lycurim and Pyrazofurin /Rat hepatomas: 68:665
chicken fibrosarcoma lines: Differences in metastasizing properties and organ specificity /Derivation of transplantable 7,12-dimethyl- 69:535
Chicken resistance to dimethylnitrosamine acute effects on the liver: A comparative study with other species 69:687
childhood /Environmental factors in the etiology of rhabdomyosarcoma in 68:107
childhood leukemia /Changes in clonal expression during the course of acute leukemia: Possible subsets in 69:393
childhood radium irradiation of the nasopharynx /Neoplasms following 68:3
childhood rhabdomyosarcomas as xenografts /Growth and characterization of 68:437
China /Correlation between cancers of the uterine cervix and penis in 69:1063
chloralkenes /Neoplastic transformation of Syrian hamster cells by putative epoxide metabolites of commercially utilized 69:531
1-(2-chloroethyl)-3-(4-methylcyclohexyl)-1-nitrosourea: Effect on the human granulopoietic system /5-Fluorouracil, 1,3-bis(2-chloroeth- 68:541
chloromethyl ethers /Epidemic curve of respiratory cancer due to 69:1265
Cholangiocellular carcinomas induced in Syrian golden hamsters administered aflatoxin B_1 in large doses 68:271
cholesterol /Breast cancer and serum 68:885
cholesterol-cancer relationship: An analysis of time trends in the Framingham Study /The serum 69:989
chromosomal changes induced by chemical carcinogens in skin fibroblasts from patients with familial adenomatosis coli /Morpholog- 68:563
chromosome aberrations in rat bone marrow cells after treatment with Sudan III and related azo dyes /Suppression of 7,12-dimethyl- 69:1343
chromosome breakage /Diverse xenotropic virus expressions in two NZB mouse breeding lines that differ in 68:951
Chromosome changes associated with the progression of cell liness from preneoplastic to tumorigenic phenotype during transformation of 69:425
chromosome changes in Rauscher murine leukemia virus-induced leukemia cell lines /Trisomy 15 and other nonrandom 69:945
chromosome damage induced by X-irradiation during G_2 phase in a line of normal human fibroblasts and its malignant derivative 69:409
chromosome 1 in cells of a transplantable granulocytic leukemia (GL-13) in guinea pigs /A deletion in 69:591
chronic lymphocytic leukemia /Phytohemagglutinin or pokeweed mitogen induction of in vitro colony formation by T-cells from pa- 68:233
chronic tobacco smoke inhalation /Pathogenesis of lesions induced in rat lung by 69:117
cigarette smoke condensate following β-irradiation in rats /Enhancement of skin tumorigenesis by 68:605
cirrhosis in atomic bomb survivors, Hiroshima and Nagasaki, 1961-75, with special reference to hepatitis B surface antigen /Primary 69:1221
clonal expression during the course of acute leukemia: Possible subsets in childhood leukemia /Changes in 69:393
clonal origin of neurofibrosarcoma in a patient with hereditary neurofibromatosis /Probable 69:1289
clones of a spontaneously metastasizing rat mammary adenocarcinoma /Development and biologic properties of malignant cell sublines 68:507
cloning efficiency of human lymphoid cells in agarose without feeder layers /High 68:919
cloning of Raji lymphoma cells in soft agar /Anticancer drugs: Effect on the 68:115
cocarcinogen /Chemical cocarcinogenesis with the use of a subclone derived from Balb/3T3 cells with catechol 69:503
cocarcinogenesis with the use of a subclone derived from Balb/3T3 cells with catechol as cocarcinogen /Chemical 69:503

Coffee drinking and cancer of the lower urinary tract ... 68:91
Collagenolytic activity of rabbit V_2 carcinoma implanted in the nude mouse ... 69:1329
Collagen polymorphism in extracellular matrix of human osteosarcoma ... 69:1009
colon adenocarcinoma cell line /Selective cytotoxicity of a ricin A-chain–anticarcinoembryonic antigen antibody conjugate for human ... 69:799
colon carcinomas and its relationship to clinical behavior /DNA distribution in human ... 69:15
colon during treatment with 1,2-dimethylhydrazine /Effects of sublethal irradiation on changes in crypts of the mouse ... 69:693
colon: Effects on carcinogenesis by 1,2-dimethylhydrazine /Surgical resection of the rat ... 68:813
colon mucosa /Epithelial line from normal human ... 69:1271
colon of the rat and guinea pig /Bile acids: Effects on absorption of 1,2-dimethylhydrazine and 7,12-dimethylbenz[*a*]anthracene in the ... 68:619
colon organ cultures /Carcinogen-induced DNA damage and cellular alterations in F344 rat ... 68:1015
colony formation /Human adherent cell contact-mediated modulation of normal myeloid ... 68:35
colony-stimulating factor-producing cell line from a squamous cell carcinoma of the thyroid gland /Establishment and characterization ... 69:1235
colorectal adenocarcinoma cell lines and tissues /Various isozyme gene expression patterns among human ... 68:81
colorectal cancer /Breath methane excretion in patients with unresected ... 69:573
colorectal cancer cell lines analyzed by a panel of monoclonal antibodies. I. Heterogeneous expression of Ia-like and HLA-like antigenic de- ... 69:357
colorectal cancer: Comparison with carcinoembryonic antigen /Value of plasma α-1-acid glycoprotein assay in the detection of human ... 68:75
colorectal cancer risk in women /Parity and ... 69:1059
colorectal cancers /Carcinoembryonic antigen: Usefulness as a postsurgical method in the detection of recurrence in Duke stage B_2 and ... 69:813
colorectal carcinoma /Lymphocyte fluorescence polarization changes after phytohemagglutinin stimulation in the diagnosis of ... 68:579
complement and Epstein-Barr virus receptors in human lymphoblastoid cell lines /Tumor promoter 12-*O*-tetradecanoylphorbol 13- ... 68:385
concanavalin A-induced blastogenic responses of lymphocytes from breast cancer patients and controls by the use of α-methyl-D-mannoside ... 68:69
congenital testicular teratomas /Primordial germ cell proliferation in fetal testes in mouse strains with high and low incidences of ... 69:907
contraceptive use and malignant melanoma /Oral ... 68:537
copper-deficient mice /Immunization against transplantable leukemia impaired in ... 69:489
copper in angiogenesis /Role of prostaglandin E_1 and ... 69:475
copper ions, and angiogenesis /Ceruloplasmin, ... 69:1183
copper mining wastes /Epizootic neoplasms in fishes from a lake polluted by ... 69:915
core antigens in human liver cell carcinoma and surrounding nontumorous liver /Distribution of hepatitis B surface and ... 69:565
corpus uteri in humans: Stage-dependent blood levels of substance(s) immunologically cross-reactive with insulin /Carcinomas of the ... 68:891
Corynebacterium parvum /Accessory cell function in tumor-bearing mice and effects of ... 69:1293
C. parvum on the cytotoxic T-cell response to alloantigens in mice /Effects of different fractions of ... 69:495
crypts of the mouse colon during treatment with 1,2-dimethylhydrazine /Effects of sublethal irradiation on changes in ... 69:693
cyclamate /Inhibition of iodinated nerve growth factor binding by the suspected tumor promoters saccharin and ... 68:299
β-Cyclodextrin: Promoting effect on the development of renal tubular cell tumors in rats treated with *N*-ethyl-*N*-hydroxyethylnitrosamine ... 69:963
cyst fluids /Androgen conjugates in human breast ... 69:1055
cytarabine /Modulation of cell-mediated alloimmunity by BCG. I. Antagonism and potentiation of immunosuppression caused by ... 69:607
Cytokinetic and ultrastructural alterations /Squamous metaplasia in organ cultures of vitamin A-deficient hamster trachea: ... 69:895
cytometric analysis of R3327 rat prostate adenocarcinoma grown in vivo and in vitro /Flow ... 69:79
cytosine arabinoside and 5-fluorouracil in cultured mouse spleen cells /L-Histidinol protection against cytotoxic action of ... 68:279
cytosol progesterone receptor levels in the MT-W9B transplantable mammary tumor in the rat /Androgen control of ... 69:673
cytotoxic action of cytosine arabinoside and 5-fluorouracil in cultured mouse spleen cells /L-Histidinol protection against ... 68:279
cytotoxicity in adriamycin-sensitive and adriamycin-resistant P388 mouse leukemia cells /Intracellular adriamycin levels and ... 68:1027
cytotoxicity /Interferon and prostaglandins: Effects on human natural and lectin-induced ... 69:339
cytotoxicity of a ricin A-chain–anticarcinoembryonic antigen antibody conjugate for human colon adenocarcinoma cell line /Selective ... 69:799
cytotoxicity of peripheral blood and tumor-associated lymphocytes against human ovarian carcinoma cells /Interferon effect on ... 68:555
cytotoxicity /Systemic administration of human leukocyte interferon to melanoma patients. II. Cellular events associated with changes ... 68:711
cytotoxic reactivity for a syngeneic murine lymphoma /Generation of long-term T-lymphoid cell lines with specific ... 69:109
cytotoxic responses to allogeneic cultured gliomas /In vitro studies on the cell-mediated immune response to human brain tumors. ... 69:1245
cytotoxic response to tumor-associated antigens. I. Characterization of the cell components for induction of suppression /Tumor cell- ... 69:867
cytotoxic response to tumor-associated antigens. II. Mechanisms for induction of suppression /Tumor cell-triggered macrophage-medi- ... 69:873
cytotoxic T-cell response to alloantigens in mice /Effects of different fractions of *Corynebacterium parvum* on the ... 69:495
cytotoxins. I. Biokinetics of activation and release in vitro /Inducible macrophage ... 69:879
cytotoxins. II. Tumor lysis mechanism involving target cell-binding proteases /Inducible macrophage ... 69:889

D1 mouse mammary hyperplastic outgrowth line: Effect of carcinogens /A high-tumor-incidence subline of the ... 69:639
4-demethoxydaunorubicin and doxorubicin /Hematopoietic precursor cells in mice treated with ... 68:971
2′-deoxycoformycin after systemic administration in monkeys /Cerebrospinal fluid levels of ... 68:391
2′-Deoxycoformycin-induced hemolysis in the mouse ... 68:1011

detergent octyl-β-D-glucopyranoside /Noncytolytic extraction of murine tumor-specific transplantation antigens with the nonionic 69:131
α-deuterium-labeled derivative in F344 rats /Dose-response studies with nitrosoheptamethyleneimine and its 69:1127
dietary constituents /Glutathione *S*-transferase activity: Enhancement by compounds inhibiting chemical carcinogenesis and by 68:493
dietary lipids on lactogenic hormone receptor binding in rat mammary tumors /Effects of 68:319
diethylnitrosamine carcinogenesis in vivo /Lymphotoxin prevention of 69:741
diethylstilbestrol /Induction of mammary neoplasms in the ACI rat by 430-keV neutrons, X-rays, and 69:1135
diet /Intestinal metaplasia in Japan: Association with 68:401
3,2′-dimethyl-4-aminobiphenyl /Prostate adenocarcinoma in rats: Induction by 68:867
7,12-dimethylbenz[*a*]anthracene /Effects of isoproterenol on mammary gland tumors induced by *N*-nitroso-*N*-methylurea and salivary 69:1115
7,12-dimethylbenz[*a*]anthracene-induced chicken fibrosarcoma lines: Differences in metastasizing properties and organ specificity /Der- 69:535
7,12-dimethylbenz[*a*]anthracene-induced chromosome aberrations in rat bone marrow cells after treatment with Sudan III and related 69:1343
7,12-dimethylbenz[*a*]anthracene-induced mammary tumor growth: Correlation with prostaglandin E_2 content /Hormone dependence 69:443
7,12-dimethylbenz[*a*]anthracene-induced mammary tumors in the rat /Comparison of ovariectomy and retinyl acetate on the growth 69:447
7,12-dimethylbenz[*a*]anthracene /Induction of mammary tumors in virgin female BALB/c mice by single low doses of 69:1199
7,12-dimethylbenz[*a*]anthracene in the colon of the rat and guinea pig /Bile acids: Effects on absorption of 1,2-dimethylhydrazine and 68:619
7,12-dimethylbenz[*a*]anthracene on production and action of gamma interferon /Effect of 68:993
1,2-dimethylhydrazine and 7,12-dimethylbenz[α]anthracene in the colon of the rat and guinea pig /Bile acids: Effects on absorption of 68:619
1,2-dimethylhydrazine /Effects of sublethal irradiation on changes in crypts of the mouse colon during treatment with 69:693
1,2-dimethylhydrazine /Surgical resection of the rat colon: Effects on carcinogenesis by 68:813
dimethylnitrosamine acute effects on the liver: A comparative study with other species /Chicken resistance to 69:687
dimethylnitrosamine after partial hepatectomy /Production of kidney tumors in rats with low dose of 68:293
dimethyl sulfoxide-induced differentiation: Reduction of the neoplastic potential of a rat mammary tumor stem-cell line /Prostaglandin 69:1063
DNA bound in vivo with aflatoxin B_1 as a measure of hepatocarcinoma initiation in rainbow trout /Liver 68:623
DNA content of liver cell nuclei of *N*-2-fluorenylacetamide-induced altered foci and neoplasms in rats and human hyperplastic foci 69:1277
DNA damage and cellular alterations in F344 rat colon organ cultures /Carcinogen-induced 68:1015
DNA distribution in human colon carcinomas and its relationship to clinical behavior 69:15
DNA-protein cross-links /Cell damage by near ultraviolet radiation: Role of 69:177
DNA synthesis and repair in rat hepatocytes and hepatoma cells /Effects of nicotinamide, isonicotinamide, and bleomycin on 69:1353
DNA synthesis in human oral mucosa treated with chemical carcinogens in short-term organ culture /Unscheduled 69:557
DNA synthesis of mouse tumor cells /Platinum-complexed antitumor immunoglobulins that specifically inhibit 69:47
Dose-response studies with nitrosoheptamethyleneimine and its α-deuterium-labeled derivative in F344 rats 69:1127
doxorubicin /Hematopoietic precursor cells in mice treated with 4-demethoxydaunorubicin and 68:971
drug photoallergy and their correlation with drug photoallergy in humans /Current status of predictive animal models for 69:237
drug photosensitivity with special emphasis on psoralen photosensitization reaction /Molecular aspects of 69:163
drugs /Effect of rate of heating on lethality due to hyperthermia and selected chemotherapeutic 68:487
drugs: Effect on the cloning of Raji lymphoma cells in soft agar /Anticancer 68:115
drug treatment in vivo /Intracerebral adoptive immunotherapy of a murine lymphoma antigenically altered by 68:817
dTTPase activities in sera of patients with advanced cancer /Elevated 69:569
ductal outgrowths by carcinogen-induced rat mammary tumors in gland-free mammary fat pad /Proliferation of 69:517
Dukes stages B_2 and C colorectal cancers /Carcinoembryonic antigen: Usefulness as a postsurgical method in the detection of recur- 69:813
dysplasia in nipple aspirates of breast fluid: Association with family history and other breast cancer risk factors /Epithelial 68:9

EL 4 lymphoma in C57BL/6J mice /Immunoadjuvant effects of *Blastomyces dermatitidis* against 69:1337
embryo cells /Equivalency of endothelial cell growth supplement to irradiated feeder cells in carcinogen-induced morphologic trans- 68:127
embryos and neoplastic cell lines /Immunologic relatedness of intracisternal A-particles in mouse 68:643
endothelial cell growth supplement to irradiated feeder cells in carcinogen-induced morphologic transformation of Syrian hamster em- 68:127
England and Wales; 1950–79: Are the changes real? /Increasing trends of multiple myeloma mortality in 69:387
Environmental factors in the etiology of rhabdomyosarcoma in childhood 68:107
environmental particulate emissions on SENCAR mouse skin /Comparative tumor-initiating activity of complex mixtures from 68:829
enzymatic disaggregation on proliferation of human tumor cells in soft agar /Effect of 68:945
Epidemic curve of respiratory cancer due to chloromethyl ethers 69:1265
Epidemiological features of Wilms' tumor: Results of the National Wilms' Tumor Study 68:429
Epidemiologic and age-dependent data on multiple myeloma in Austria 68:729
epidemiology /Carotid body tumors in humans: Genetics and 68:573
epidemiology /Meeting Highlights: Job-exposure matrices in occupational 69:1419
epidermal cells: Antagonism by an antipromoter /Ganglioside changes induced by tumor promoters in promotable JB6 mouse 68:469
epidermal cells /Inhibition by tumor-promoting phorbol esters of procollagen synthesis in promotable JB6 mouse 69:1147
epiglycanin in the TA3-MM mouse mammary carcinoma ascites cell /Further studies on the relationship between allotransplantabil- 68:981

epithelial cells transformed in organ culture /Growth and differentiation of hyperplastic outgrowths derived from mouse mammary 69:453
Epithelial dysplasia in nipple aspirates of breast fluid: Association with family history and other breast cancer risk factors 68:9
Epithelial line from normal human colon mucosa 69:1271
epithelial reticular cells /Formation of symbiotic complex by microenvironment-dependent mouse leukemias and thymic 69:627
epithelium in rats /Effect of carcinogen release rate on the incidence of preneoplastic and neoplastic lesions of the respiratory tract 69:1155
epithelium in vitro /Chromosome changes associated with the progression of cell lines from preneoplastic to tumorigenic phenotype 69:425
epithelium of normal human urinary bladder in vitro /*N*-Methyl-*N*-nitrosourea and saccharin: Effects on 69:577
epoxide metabolites of commercially utilized chloroalkenes /Neoplastic transformation of Syrian hamster cells by putative 69:531
Epstein-Barr virus induction patterns /Human lymphoma-lymphoma hybrids and lymphoma-leukemia hybrids. II 68:197
Epstein-Barr virus in high passages of P3HR-1 cell lines /Persistence of transforming and nontransforming 69:585
Epstein-Barr virus receptors in human lymphoblastoid cell lines /Tumor promoter 12-*O*-tetradecanoylphorbol 13-acetate: Effect on 69:385
erythroid differentiation in mice /Friend erythroleukemia virus complex: Role of viral components in modifying 68:457
erythroleukemia virus complex: Role of viral components in modifying erythroid differentiation in mice /Friend 68:457
esophageal cancer in rats /Zinc deficiency, alcohol, and a retinoid: Association with 68:785
Esophageal carcinogenesis in F344 rats by nitrosomethylethylamines substituted in the ethyl group 68:681
esophagus, larynx, and lung by sex and by income level /Major histologic types of cancers of the gum and mouth, 69:773
esterase-positive foci in rat liver by partial hepatectomy following single injection of *N*-nitrosodiethylamine /Induction of γ-glutamyl- 69:1299
Estonian Republic /Association of breast cancer risk with age at first and subsequent births: A study in the population of the 69:1035
estrogens and other risk factors for breast cancer in women with benign breast diseases /Exogenous 69:1017
estrogen use and the occurrence of ovarian cancer /Letter to the Editor: Noncontraceptive 69:1207
estrogen use and the occurrence of ovarian cancer /Noncontraceptive 68:95
N-ethyl-*N*-hydroxyethylnitrosamine /β-Cyclodextrin: Promoting effect on the development of renal tubular cell tumors in rats treated 69:963
eye /Tumor-induced neovascularization in the mouse 69:699

F344 rat colon organ cultures /Carcinogen-induced DNA damage and cellular alterations in 68:1015
F344 rats by nitrosomethylethylamines substituted in the ethyl group /Esophageal carcinogenesis in 68:681
F344 rats /Dose-response studies with nitrosoheptamethyleneimine and its α-deuterium-labeled derivative in 69:1127
F344 rats /Organ-specific promoting effects of phenobarbital sodium and sodium saccharin in the induction of liver and urinary 68:497
familial adenomatosis coli /Morphologic transformation and chromosomal changes induced by chemical carcinogens in skin fibroblasts 68:563
familial and hormonal risk factors for breast cancer /Interaction of 69:817
familial predisposition for breast cancer in Japan /Epidemiology of 69:1229
farming /An increased risk for lung cancer mortality associated with sugarcane 68:755
fat pads /Proliferation of ductal outgrowths by carcinogen-induced rat mammary tumors in gland-free mammary 69:517
fatty acids in tumor development /Letter to the Editor: *Trans* 69:319
Fcγ receptors on macrophages in 3-methylcholanthrene-induced murine tumors /Exclusive binding of immunoglobulin to 69:1163
feline leukemia virus infection in humans with leukemias, lymphomas, or soft tissue sarcomas /Search for evidence of 69:333
fetal extracts: Cross-reactions between man and mouse /Reactivity in neoplasia, preneoplasia, and pregnancy of lymphocytes against 69:997
fetal Syrian golden hamsters treated transplacentally with *N*-nitrosodiethylamine /Electron microscopic autoradiography of the trachea 69:927
fetal tests in mouse strains with high and low incidences of congenital testicular teratomas /Primordial germ cell proliferation in 69:907
fibroblasts and its malignant derivative /Repair of chromosome damage induced by X-irradiation during G_2 phase in a line of normal 69:409
fibroblasts /Basis for the differential action of aminonucleoside on normal and transformed human 68:407
fibroblasts /Enhancement of growth of human colon tumor cell lines by feeder layers of murine 69:767
fibroblasts from patients with familial adenomatosis coli /Morphologic transformation and chromosomal changes induced by chem- 68:563
fibroblasts in two families with Gardner's syndrome /Heterogeneous response to X-ray and ultraviolet light irradiations of cultured skin 68:697
fibronectin and laminin in the rat liver after partial hepatectomy, during carcinogenesis, and in transplantable hepatocellular carcinomas 69:1105
fibronectin, lymphotoxin sensitivity, and natural skin reactivity relationships to guinea pig cell tumorigenicity /Plasminogen activator, 68:329
fibrosarcoma lines: Differences in metastasizing properties and organ specificity /Derivation of transplantable 7,12-dimethylbenz[*a*]- 69:535
fishes from a lake polluted by copper mining wastes /Epizootic neoplasms in 69:915
fluorescence polarization changes after phytohemagglutinin stimulation in the diagnosis of colorectal carcinoma /Lymphocyte 68:579
fluorine-substituted benz[*a*]anthracenes /Mouse skin tumor-initiating activity of 5-, 7-, and 12-methyl- and 69:725
N-2-fluoroenylacetamide-induced altered foci and neoplasms in rats and human hyperplastic foci /DNA content of liver cell nuclei of 69:1277
5-fluorouracil and the growth of allotransplantable and syngeneic tumors in mice /Combined treatments with vitamin A and 68:823
5-Fluorouracil, 1,3-bis(2-chloroethyl)-1-nitrosourea, and 1(2-chloroethyl)-3-(4-methylcyclohexyl)-1-nitrosurea: Effect on the human granulo- 68:541
5-fluorouracil given by bolus injection /Phase I-Phase II trial of *N*-phosphonacetyl-L-aspartic acid given by intravenous infusion and 68:227
5-fluorouracil in cultured mouse spleen cells /L-Histidinol protection against cytotoxic action of cytosine arabinoside and 68:279
Food and Drug Administration science symposia /Photochemical toxicity—proceedings of the seventh 69:147
forestomach and lung carcinogenesis by a 5-nitrofuran naphthyridine derivative in mice /Inhibitory effect of fumaric acid on 69:1317
formaldehyde and hydrogen chloride induction of nasal cancer in the rat /Gaseous 68:597

Framingham Study /The serum cholesterol-cancer relationship: An analysis of time trends in the 69:989
Friend erythroleukemia virus complex: Role of viral components in modifying erythroid differentiation in mice 68:457
frog tadpoles /Effect of thymectomy on developement of Lucké renal adenocarcinomas in virus-infected leopard 68:133
fumaric acid on forestomach and lung carcinogenesis by a 5-nitrofuran naphthyridine derivative in mice /Inhibitory effect of 69:1317
Fv-4^r mouse strains /Surface antigen expressed in hematopoietic cells derived from 68:1005

G_2 phase in a line of normal human fibroblasts and its malignant derivative /Repair of chromosome damage induced by X-irradiation 69:409
gallbladder and biliary tract in Alaskan Natives: 1970-79 /Cancers of the 69:1005
gamma interferon /Effect of 7,12-dimethylbenz[*a*]anthracene on production and action of 68:993
Ganglioside changes induced by tumor promoters in promotable JB6 mouse epidermal cells: Antagonism by an antipromoter 68:469
Ganglioside patterns: New biochemical markers for human hematopoietic cell lines 68:203
ganglio-*N*-tetraosylceramide-positive lymphocyte mediators of natural killer activity /Morphology and function of 68:449
Gardner's syndrome /Heterogeneous response to X-ray and ultraviolet light irradiations of cultured skin fibroblasts in two families with 68:697
gastric adenocarcinomas in Wistar rats: Histopathology of the glandular stomach and incidence of gastric adenocarcinoma /Gastrin 69:59
gastric carcinoma /Indirect macrophage migration inhibition response to 3-*M* KCl extract of 69:345
Gastrin protection against chemically induced gastric adenocarcinomas in Wistar rats: Histopathology of the glandular stomach and 69:59
gene expression patterns among human colorectal adenocarcinoma cell lines and tissues /Various isozyme 68:81
gene regulation in cancer? /Guest Editorial: What are isozymes telling us about 68:343
Genetics and epidemiology /Carotid body tumors in humans: 68:573
genetics of malignancy workshop /Meeting Highlights: Cytogenetics and somatic cell 69:543
Genetics of transplacentally induced teratogenic and carcinogenic effects in rabbits treated with *N*-nitroso-*N*-ethylurea 69:1411
Genotoxic effects of sunlight-activated waste water in cultured mammalian cells 69:199
genotypic characteristics of a cell line from a squamous cell carcinoma of human skin /Phenotypic and 68:415
germ cell proliferation in fetal testes in mouse strains with high and low incidences of congenital testicular teratomas /Primordial 69:907
gestational trophoblastic neoplasia /Circulating immune complex levels in patients with 69:23
(GL-13) in guinea pigs /A deletion in chromosome 1 in cells of a transplantable granulocytic leukemia 69:591
gliomas /In vitro studies on the cell-mediated immune response to human brain tumors. I. Requirement for third-party stimulator 69:1245
gliomas /Serologic analysis of nitrosurea-induced rat 68:501
γ-glutamyltransferase of carcinogen-induced preneoplastic hepatocytes of rats /In vitro measurement of resistance to phalloidin and 69:683
γ-glutamyltransferase-positive and nonspecific esterase-positive foci in rat liver by partial hepatectomy following single injection of *N*- 69:1299
Glutathione *S*-transferase activity: Enhancement by compounds inhibiting chemical carcinogenesis and by dietary constituents 68:493
β_1 glycoprotein as a marker in carcinoma of the breast in women /Use of circulating pregnancy-specific 69:1067
glycoprotein assay in the detection of human colorectal cancer: Comparison with carcinoembryonic antigen /Value of plasma α-1-acid 68:75
glycoprotein epiglycanin in the TA3-MM mouse mammary carcinoma ascites cell /Further studies on the relationship between allo- 68:981
glycoprotein expressed by human melanoma and carcinoma cells /A 94,000-dalton 68:761
glycoprotein) levels /Mitogen-induced blastogenesis and receptor mobility inhibition by breast cancer serum with elevated oroso- 68:779
glycoprotein: Major peptide homology exhibited with the nuclear and membrane-associated 94,000-M_r SV40 T-antigen in hamsters 69:839
golden hamsters administrated aflatoxin B_1 in large doses /Cholangiocellular carcinomas induced in Syrian 68:271
golden hamsters treated transplacentally with *N*-nitrosodiethylamine /Electron microscopic autoradiography of the trachea in fetal 69:927
gp70-specific suppressor T-cells in mice inoculated with virus-producing tumor cells /Induction of 69:953
graft acceptance /Successful transplantation of a human leukemia cell into nude mice: Conditions optimizing 68:15
gram-positive bacteria: Expression of antitumor activity according to peptide structure and route of injection /Peptidoglycans extracted 68:657
granulocytic leukemia (GL-13) in guinea pigs /A deletion in chromosome 1 in cells of a transplantable 69:591
Granulopoiesis longevity in continuous bone marrow cultures and factor-dependent cell line generation: Significant variation among 28 68:305
granulopoietic system /5-Fluorouracil, 1,3-bis(2-chloroethyl)-1-nitrosourea, and 1-(2-chloroethyl)-3-(4-methylcyclohexyl)-1-nitrosourea: 68:541
GR mice /Comparison of biologic behavior and histology of transplanted mammary tumors in 69:933
GR/A mice: An in vitro study /Hormone requirements of the pregnancy-dependent mammary tumor of 69:1391
Guest Editorial: Human retroviruses and adult T-cell leukemia-lymphoma 69:1209
Guest Editorial: Sheep lung carcinoma: An endemic analogue of a sporadic human neoplasm 69:747
Guest Editorial: What are isozymes telling us about gene regulation in cancer? 68:343
guinea pig /Bile acids: Effects on absorption of 1,2-dimethylhydrazine and 7,12-dimethylbenz[*a*]anthracene in the colon of the rat and 68:619
guinea pig cell line /Independent expression of chemical carcinogen-induced phenotypic properties frequently associated with the neo- 69:1175
guinea pig cell tumorigenicity /Plasminogen activator, fibronectin, lymphotoxin sensitivity, and natural skin reactivity relationships to 68:329
guinea pigs /A deletion in chromosome 1 in cells of a transplantable granulocytic leukemia (GL-13) in 69:591
guinea pig tumor. I. Quantitative analysis of adoptive immunity /Mechanisms of immunologic eradication of a syngeneic 68:673; 69:987
gum and mouth, esophagus, larynx, and lung by sex and by income level /Major histologic types of cancers of the 69:773

H-2 expression on a teratocarcinoma-derived cell line, TerC 69:1311

hamster amelanotic melanoma A-Mel-3 /Microcirculatory blood flow, capillary morphology, and local oxygen pressure of the 68:475

hamster cells by putative epoxide metabolites of commercially utilized chloroalkenes /Neoplastic transformation of Syrian 69:531

hamster embryo cells /Equivalency of endothelial cell growth supplement to irradiated feeder cells in carcinogen-induced morpho- 68:127

hamsters administered aflatoxin B_1 in large doses /Cholangiocellular carcinomas induced in Syrian golden 68:271

hamsters: Inhibition by vitamin E /Oral mucosal carcinogenesis in 68:791

hamsters /Simian virus 40 (SV40)-specific isoelectric point-4.7-94,000-M_r membrane glycoprotein: Major peptide homology exhibited 69:839

hamsters treated transplacentally with *N*-nitrosodiethylamine /Electron microscopic autoradiography of the trachea in fetal Syrian 69:927

hamster trachea: Cytokinetic and ultrastructural alterations /Squamous metaplasia in organ cultures of vitamin A-deficient 69:895

heating on lethality due to hyperthermia and selected chemotherapeutic drugs /Effect of rate of 68:487

hematopoietic cell lines /Ganglioside patterns: New biochemical markers for human 68:203

hematopoietic cell lines /Isozymes of acid esterase and acid phosphatase in permanent human 69:1255

hematopoietic cells derived from *Fc-4*^{r} mouse strains[a] /Surface antigen expressed in 68:1005

Hematopoietic precursor cells in mice treated with 4-demethoxydaunorubicin and doxorubicin 68:971

hemolysis in the mouse /2′-Deoxycoformycin-induced 68:1011

hepatectomy, during carcinogenesis, and in transplantable hepatocellular carcinomas /Expression of fibronectin and laminin in the rat 69:1105

hepatectomy following single injection of *N*-nitrosodiethylamine /Induction of γ-glutamyltransferase-positive and nonspecific esterase- 69:1299

hepatectomy /Production of kidney tumors in rats with low dose of dimethylnitrosamine after partial 68:293

hepatitis B surface and core antigens in human liver cell carcinoma and surrounding nontumorous liver /Distribution of 69:565

hepatitis B surface antigen /Primary liver carcinoma and liver cirrhosis in atomic bomb survivors, Hiroshima and Nagasaki, 1961–75, 69:1221

hepatocarcinoma initiation in rainbow trout /Liver DNA bound in vivo with aflatoxin B_1 as a measure of 68:623

hepatocellular carcinomas /Expression of fibronectin and laminin in the rat liver after partial hepatectomy, during carcinogenesis, 69:1105

hepatocytes and hepatoma cells /Effects of nicotinamide, isonicotinamide, and bleomycin on DNA synthesis and repair in rat 69:1353

hepatocytes from livers of carcinogen-treated rats /Purification and transplantation of 68:851

hepatocytes /Isolation, culture, and transplantation of human 68:771

hepatocytes of rats /In vitro measurement of resistance of phalloidin and γ-glutamyltransferase of carcinogen-induced preneoplastic 69:683

hepatoma cells /Effects of nicotinamide, isonicotinamide, and bleomycin on DNA synthesis and repair in rat hepatocytes and 69:1353

hepatomas: Chemotherapy with Lycurim and Pyrazofurin /Rat 68:665

hereditary lymphosarcoma (leukemia) /Causes of death and sex differences in survival times of pigs with untreated 68:239

hereditary neurofibromatosis /Probable clonal origin of neurofibrosarcoma in a patient with 69:1289

heterogeneity of human colorectal cancer cell lines analyzed by a panel of monoclonal antibodies. I. Heterogeneous expression of Ia-like 69:357

hexamethylphosphoramide by inhalation /Induction of nasal tumors in rats exposed to 68:157

Hiroshima and Nagasaki, 1950–76: Relationship to radiation dose absorbed by marrow /Multiple myeloma among atomic bomb 69:323

Hiroshima and Nagasaki, 1961–75, with special reference to hepatitis B surface antigen /Primary liver carcinoma and liver cirrhosis in 69:1221

L-Histidinol protection against cytotoxic action of cytosine arabinoside and 5-fluorouracil in cultured mouse spleen cells 68:279

histiocytomas induced by 4-(hydroxyamino)quinoline 1-oxide in rats /Malignant fibrous 68:859

HLA-like antigenic determinants /Antigenic heterogeneity of human colorectal cancer cell lines analyzed by a panel of monoclonal 69:357

homosexual men /Meeting Highlights: Kaposi's sarcoma in 68:337

hormonal risk factors for breast cancer /Interaction of familial and 69:817

Hormone dependence of 7,12-dimethylbenz[*a*]anthracene-induced mammary tumor growth: Correlation with prostaglandin E_2 content 69:443

hormone receptor binding in rat mammary tumors /Effects of dietary lipids on lactogenic 68:319

hormone receptors in the rat mammary adenocarcinoma induced by *N*-hydroxy-*N*-2-fluorenylacetamide /Steroid 69:41

Hormone requirements of the pregnancy-dependent mammary tumor of GR/A mice: An in vitro study 69:1391

hormone treatment /Growth of mouse mammary glands after neonatal sex 69:1347

human adenocarcinomas xenotransplanted into nude mice /α_1-Protease inhibitor production by 69:381

human adenovirus 5 propagated in Burkitt's lymphoma cells /Changes in 69:1215

Human adherent cell contact-mediated modulation of normal myeloid colony formation 68:35

human B-lymphoblast tumorigenicity in nude mice /Effect of type C viral expression and cellular karyotype on 69:435

human brain tumors. I. Requirement for third-party stimulator lymphocytes in the induction of cell-mediated cytotoxic responses to al- 69:1245

human breast cyst fluids /Androgen conjugates in 69:1055

human breast tumors /Characterization of a monoclonal antibody reactive with a subset of 68:719

human breast tumors /Prolactin receptors in 68:381

human carcinogenesis /Meeting Highlights: Host factors in 68:173

human colon adenocarcinoma cell line /Selective cytotoxity of a ricin A-chain–anticarcinoembryonic antigen antibody conjugate for 69:799

human colon carcinomas and its relationship to clinical behavior /DNA distribution in 69:15

human colon mucosa /Epithelial line from normal 69:1271

human colon tumor cell lines by feeder layers of murine fibroblasts /Enhancement of growth of 69:767

human colony-stimulating factor-producing cell line from a squamous cell carcinoma of the thyroid gland /Establishment and charac- 69:1235

human colorectal adenocarcinoma cell lines and tissues /Various isozyme gene expression patterns among 68:81

human colorectal cancer cell lines analyzed by a panel of monoclonal antibodies. I. Heterogeneous expression of Ia-like and HLA-like 69:357

human colorectal cancer: Comparison with carcinoembryonic antigen /Value of plasma α-1-acid glycoprotein assay in the detection 68:75

human fibroblasts and its malignant derivative /Repair of chromosome damage induced by X-irradiation during G_2 phase in a line of 69:409

human fibroblasts /Basis for the differential action of aminonucleoside on normal and transformed 68:407

human granulopoietic system /5-Fluorouracil, 1,3-bis(2-chloroethyl)-1-nitrosourea, and 1-(2-chloroethyl)-3-(4-methylcyclohexyl)-1-nitro- 68:541

human hematopoietic cell lines /Ganglioside patterns: New biochemical markers for 68:203

human hematopoietic cell lines /Isozymes of acid esterase and acid phosphatase in permanent 69:1255

human hepatocytes /Isolation, culture, and transplantation of 68:771

human hyperplastic foci /DNA content of liver cell nuclei of *N*-2-fluorenylacetamide-induced altered foci and neoplasms in rats and 69:1277

human large bowel /Glycoconjugate with *Ulex europaeus* agglutinin-I-binding sites in normal mucosa, adenoma, and carcinoma of the 69:777

human leukemia cell into nude mice: Conditions optimizing graft acceptance /Successful transplantation of a 68:15

human leukocyte interferon to melanoma patients. I. Effects on natural killer function and cell populations /Systemic administration of 68:703

human leukocyte interferon to melanoma patients. II. Cellular events associated with changes in natural killer cytotoxicity /Sys- 68:711

human liver cell carcinoma and surrounding nontumorous liver /Distribution of hepatitis B surface and core antigens in 69:565

Human lymphoblastoid cell lines /Tumor promoter 12-*O*-tetradecanoylphorbol 13-acetate: Effect on complement and Epstein-Barr 68:385

human lymphoid cells in agarose without feeder layers /High cloning efficiency of 68:919

human lymphoid cells /In vitro assay of the effects of psoralens plus ultraviolet radiation on 69:219

Human lymphoma-lymphoma hybrids and lymphoma-leukemia hybrids. I. Isolation, characterization, cell surface markers, and B-cell 68:179

Human lymphoma-lymphoma hybrids and lymphoma-leukemia hybrids. II. Epstein-Barr virus induction patterns 68:197

human mammary carcinomas /T-Lymphocyte and B-lymphocyte subpopulations infiltrating 69:1

human melanoma and carcinoma cells /A 94,000-dalton glycoprotein expressed by 68:761

human melanoma cells by interferon /Enhanced expression of melanoma-associated antigens and β_2-microglobulin on cultured 68:19

human melanoma xenografts in nude mice with a radiolabeled monoclonal antibody /Imaging of 69:823

human metastatic breast carcinoma /Isolation and partial characterization of surface components of cell line MDA-MB-231 derived 69:371

Human models for identification of photosensitizing chemicals 69:269

human natural and lectin-induced cytotoxicity /Interferon and prostaglandins: Effects on 69:339

human natural killer cell activity by a streptococcal preparation, OK-432: Interferon and interleukin-2 participation in the stimulation with 69:807

human neoplasm /Guest Editorial: Sheep lung carcinoma: An endemic analogue of a sporadic 69:747

human neuroblastoma cells in vitro /Retinoic acid-induced growth inhibition and morphologic differentiation of 68:589

human oral mucosa treated with chemical carcinogens in short-term organ culture /Unscheduled DNA synthesis in 69:557

human osteosarcoma /Collagen polymorphism in extracellular matrix of 69:1009

human ovarian cancer cells by xenogeneic peritoneal macrophages /In vitro growth stimulation of 69:1039

human ovarian carcinoma cells /Interferon effect on cytotoxicity of peripheral blood and tumor-associated lymphocytes against 68:555

human pancreatic tumor /Coproduction of carcinoembryonic antigen and nonspecific cross-reacting antigen by a continuous cell line 69:401

human primary central nervous system tumors: Ornithine decarboxylase levels as better indicators than adenosylmethionine decarbox- 68:757

human prostate cancer with the use of tissue-specific antigens /Multiple marker evaluation in 68:99

human prostate. II. Long-term explant culture of normal prostate and benign prostatic hyperplasia: Light microscopy /Studies on 69:751

human prostate. III. Long-term explant culture of normal prostate and benign prostatic hyperplasia: Transmission and scanning elec- 69:757

Human retroviruses and adult T-cell leukemia-lymphoma /Guest Editorial: 69:1209

human retrovirus /Meeting Highlights: Adult T-cell leukemia-lymphoma: Role of a 69:981

humans—an introduction /Photochemical toxicity: Toxic, allergic, and carcinogenic aspects with emphasis on predicting effects in 69:151

humans /Chemical phototoxicity in 69:265

humans /Current status of predictive animal models for drug photoallergy and their correlation with drug photoallergy in 69:237

human serum albumin /Methylazoxymethanol: Effect on the immune response of rats to 68:651

humans: Genetics and epidemiology /Carotid body tumors in 68:573

human skin /Phenotypic and genotypic characteristics of a cell line from a squamous cell carcinoma of 68:415

humans: Relationship to plasma lipids and relative weight /Cancer incidence in 68:915

humans: Stage-dependent blood levels of substance(s) immunologically cross-reactive with insulin /Carcinomas of the cervix and corpus 68:891

humans /Therapeutic in vivo photochemistry: Photochemical toxicity studies in 69:273

humans /Transforming growth factors in the urine of normal, pregnant, and tumor-bearing 69:793

humans with leukemias, lymphomas, or soft tissue sarcomas /Search for evidence of feline leukemia virus infection in 69:333

human thymoma lymphocytes: Role of subcellular factors in blastic activation /Functional properties of 69:827

human T-lymphocytes. XIX. T-cells and T-cells with receptors for IgMFc (Tμ), IgGFc (Tγ), or IgAFc (Tα) in the peripheral blood and re- 69:1261

human tumor cells in soft agar /Effect of enzymatic disaggregation on proliferation of 68:945

human tumors heterotransplanted in nude mice /Calorie restriction: Effect on growth of 68:249

human urinary bladder in vitro /*N*-Methyl-*N*-nitrosourea and saccharin: Effects on epithelium of normal 69:577

hybrid murine tumor cells: Requirements for optimal immunization /Antitumor immunity induced by 69:647

hybrid /Nonimmunogenic radiation-induced lymphoma: Immunity induction by a somatic cell 68:841

hybrids. I. Isolation, characterization, cell surface markers, and B-cell markers /Human lymphoma-lymphoma hybrids and lympho- 68:179

hybrids. II. Epstein-Barr virus induction patterns /Human lymphoma-lymphoma hybrids and lymphoma-leukemia 68:197

hybrids /Inheritance of cellular reistance to the antitumor agent ICRF 159 in somatic cell 68:977

hydrogen chloride induction of nasal cancer in the rat /Gaseous formaldehyde and 68:597
4-(hydroxyamino)quinoline 1-oxide in rats /Malignant fibrous histiocytomas induced by 68:859
N-hydroxy-*N*-2-fluorenylacetamide /Steroid hormone receptors in the rat mammary adenocarcinoma induced by 69:41
hyperthermia and selected chemotherapeutic drugs /Effect of rate of heating on lethality due to 68:487

Ia-like and HLA-like antigenic determinants /Antigenic heterogeneity of human colorectal cancer cell lines analyzed by a panel of 69:357
ICRF 159 in somatic cell hybrids /Inheritance of cellular resistance to the antitumor agent 68:977
IgMFc (Tμ), IgGFc (Tγ), or IgAFc (Tα) in the peripheral blood and regional lymph nodes of patients with untreated breast cancer 69:1261
Immune alterations related to age, sex, and mammary tumor detection in murine mammary tumor virus-infected mice /Letter to the 69:1208
immune complex levels in patients with gestational trophoblastic neoplasia /Circulating 69:23
immune response of rats to human serum albumin /Methylazoxymethanol: Effect on the 68:651
immune response to human brain tumors. I. Requirement for third-party stimulator lymphocytes in the induction of cell-mediated cyto- 69:1245
immunity /Immunomodulation of the lymphoresponsive phases of carcinogenesis: Mechanisms of natural 69:737
immunity induced by hybrid murine tumor cells: Requirements for optimal immunization /Antitumor 69:647
Immunity induction by a somatic cell hybrid /Nonimmunogenic radiation-induced lymphoma: 68:841
immunity to mouse mammary tumor virus antigens by patients with hyperplastic benign breast disease /Cell-mediated 68:935
Immunity to tumor-associated antigens in vasectomized men 69:551
Immunization against transplantable leukemia impaired in copper-deficient mice 69:489
immunization /Anterior immunity induced by hybrid murine tumor cells: Requirements for optimal 69:647
Immunoadjuvant effects of *Blastomyces dermatitidis* against EL 4 lymphoma in C57BL/6J mice 69:1337
immunoglobulins that specifically inhibit DNA synthesis of mouse tumor cells /Platinum-complexed antitumor 69:47
immunoglobulin to Fcγ receptors on macrophages in 3-methylcholanthrene-induced murine tumors /Exclusive binding of 69:1163
immunologic characterization of 3-methylcholanthrene-induced sarcoma cell lines metastasizing widely in mice and exhibiting distinct 69:595
immunologic eradication of a syngeneic guinea pig tumor. I. Quantitative analysis of adoptive immunity /Mechanisms of 68:673; 69:987
immunologic reactivity to Moloney murine sarcoma virus-induced tumors. III. Further characterization of tumor-specific serum block- 69:939
Immunologic relatedness of intracisternal A-particles in mouse embryos and neoplastic cell lines 68:643
Immunomodulation of the lymphoresponsive phases of carcinogenesis: Mechanisms of natural immunity 69:737
immunomodulation on the fate of tumor cells in the central nervous system and systemic organs of mice. Distribution of [^{125}I]5-iodo- 69:465
immunosuppression caused by cytarabine /Modulation of cell-mediated alloimmunity by BCG. I. Antagonism and potentiation of 69:607
Immunosuppressive effects of ultraviolet (280–320 nm) radiation and psoralen plus ultraviolet (320–400 nm) radiation in mice 69:171
Immunotherapeutic effects of partially purified tumor-specific transplantation antigens on pulmonary metastases of a 3-methylcholan- 69:1121
Immunotherapy by intralesional injection of BCG cell walls or live BCG in bovine ocular squamous cell carcinoma: A prelimary report 69:1095
immunotherapy /Development of resistance to MOPC-315 plasmacytoma after intralesional and intraperitoneal melphalan therapy of 68:963
Immunotherapy of a murine leukemia virus-infected, chemically induced murine sarcoma with antiviral antibodies 69:509
immunotherapy of a murine lymphoma antigenically alteraed by drug treatment in vivo /Intracerebral adoptive 68:817
income level /Major histologic types of cancers of the gum and mouth, esophagus, larynx, and lung by sex and by 69:773
inhalation /Induction of nasal tumors in rats exposed to hexamethylphosphoramide by 68:157
inhibitors of carcinogenesis: Effect on azoxymethane-induced intestinal cancer in rats /Combined 69:103
insulin /Carcinomas of the cervix and corpus uteri in humans: Stage-dependent blood levels of substance(s) immunologically cross- 68:891
Interferon and interleukin-2 participation in the stimulation with OK-432 /In vitro potentiation of human natural killer cell activity 69:807
Interferon and prostaglandins: Effects on human natural and lectin-induced cytotoxicity 69:339
interferon /Effect of 7,12-dimethylbenz[*a*]anthracene on production and action of gamma 68:993
Interferon effect on cytotoxicity of peripheral blood and tumor-associated lymphocytes against human ovarian carcinoma cells 68:555
interferon /Enhanced expression of melanoma-associated antigens and β_2-microglobulin on cultured human melanoma cells by 68:19
interferon inducers. I. Effect against artificial and spontaneous lung metastases of murine tumors /Studies on the antitumor activi- 68:139
interferon on the growth of spontaneous mammary tumors in mice /Inhibitory effect of 69:653
interferon to melanoma patients. I. Effects on natural killer function and cell populations /Systemic administration of human leukocyte 68:703
interferon to melanoma patients. II. Cellular events associated with changes in natural killer cytotoxicity /Systemic administration of 68:711
interleukin-2 participation in the stimulation with OK-432 /In vitro potentiation of human natural killer cell activity by a strepto- 69:807
intestinal cancer in rats /Combined inhibitors of carcinogenesis: Effect on azoxymethane-induced 69:103
Intestinal metaplasia in Japan: Association with diet 68:401
intracardial injection /Effect of immunomodulation on the fate of tumor cells in the central nervous system and systemic organs of 69:465
Intracerebral adoptive immunotherapy of a murine lymphoma antigenically altered by drug treatment in vivo 68:817
intracisternal A-particles in mouse embryos and neoplastic cell lines /Immunologic relatedness of 68:643
iodinated nerve growth factor binding by the suspected tumor promoters saccharin and cyclamate /Inhibition of 68:299
[^{125}I]5-iodo-2′-deoxyuridine-labeled KHT tumor cells after left intracardial injection /Effect on immunomodulation on the fate of tumor 69:465
irradiated feeder cells in carcinogen-induced morphologic transformation of Syrian hamster embryo cells /Equivalency of endothelial 68:127

irradiation during G_2 phase in a line of normal human fibroblasts and its malignant derivative /Repair of chromosome damage in- 69:409
β-irradiation in rats /Enhancement of skin tumorigenesis by cigarette smoke condensate following 68:605
irradiation of the nasopharynx /Neoplasms following childhood radium 68:3
irradiation on changes in crypts of the mouse colon during treatment with 1,2-dimethylhydrazine /Effects of sublethal 69:693
irradiations of cultured skin fibroblasts in two families with Gardner's syndrome /Heterogeneous response to X-ray and ultraviolet light ... 68:697
isoelectric point-4.7–94,000-M_r membrane glycoprotein: Major peptide homology exhibited with the nuclear and membrane-associated 69:839
isonicotinamide, and bleomycin on DNA synthesis and repair in rat hepatocytes and hepatoma cells /Effects of nicotinamide, ... 69:1353
isoproterenol on mammary gland tumor induced by *N*-nitroso-*N*-methylurea and salivary gland tumors induced by 7,12-dimethylbenz- 69:1115
isozyme gene expression patterns among human colorectal adenocarcinoma cell lines and tissues /Various 68:81
Isozymes of acid esterase and acid phosphatase in permanent human hematopoietic cell lines 69:1255
isozymes telling us about gene regulation in cancer? /Guest Editorial: What are 68:343

Japan: Association with diet /Intestinal metaplasia in 68:401
Japan Cooperative Cancer Research Program on cell interactions and cancer /Meeting Highlights: Brief summary of the third joint 69:544
Japan /Epidemiology of familial predisposition for breast cancer in 69:1229
JB6 mouse epidermal cells: Antagonism by an antipromoter /Ganglioside changes induced by tumor promoters in promotable 68:469
JB6 mouse epidermal cells /Inhibition by tumor-promoting phorbol esters of procollagen synthesis in promotable 69:1147
jejunum /Thermotolerance in the murine 68:1033
Job-exposure matrices in occupational epidemiology /Meeting Highlights: 69:1419

Kaposi's sarcoma in homosexual men /Meeting Highlights: 68:337
karyology, and biochemical analysis /Multiple cell lines from patients with malignant melanoma: Morphology, ... 68:365
karotype on human B-lymphoblast tumorigenicity in nude mice /Effect of type C viral expression and cellular 69:435
KCl extract of gastric carcinoma /Indirect macrophage migration inhibition responses to 3-*M* 69:345
KHT tumor cells after left intracardial injection /Effect of immunomodulation on the fate of tumor cells in the central nervous system ... 69:465
kidney tumors in rats with low dose of dimethylnitrosamine after partial hepatectomy /Production of 68:293
killer activity in cancer patients after surgery /Generation of suppressor cells for natural 68:735
killer activity /Morphology and function of ganglio-*N*-tetraosylceramide-positive lymphocyte mediators of natural 68:449
killer cell activity by a streptococcal preparation, OK-432: Interferon and interleukin-2 participation in the stimulation with OK-432 .... 69:807
killer cells: Regulatory mechanisms of activation or suppression /Murine lymph node natural 69:665
killer cytotoxicity /Systemic administration of human leukocyte interferon to melanoma patients. II. Cellular events associated with 68:711
killer function and cell populations /Systemic administration of human leukocyte interferon to melanoma patients. I. Effects on natural .. 68:703

L1210 leukemia in mice /Comparison of in vitro and in vivo effects of thymidine on 68:875;
69:547
L5178Y cells resistant to purine antagonists: Differences in cross-resistance to thioguanine–platinum(II) and selenoguanine–platinum(II) 68:287
lactogenic hormone receptor binding in rat mammary tumors /Effects of dietary lipids on 68:319
laminin in the rat liver after partial hepatectomy, during carcinogenesis, and in transplantable hepatocellular carcinomas /Expres- 69:1105
large bowel /Glycoconjugate with *Ulex europaeus* agglutinin-I-binding sites in normal mucosa, adenoma, and carcinoma of the human 69:777
larynx, and lung by sex and by income level /Major histologic types of cancers of the gum and mouth, esophagus, ... 69:773
lectin-induced cytotoxicity /Interferon and prostaglandins: Effects on human natural and 69:339
lectin-separated murine bone marrow fractions /Differing stem cell self-renewal of 68:639
leopard frog tadpoles /Effect of thymectomy on development of Lucké renal adenocarcinomas in virus-infected 68:133
lethality due to hyperthermia and selected chemotherapeutic drugs /Effect of rate of heating on 68:487
Letter to the Editor: Cartesian reductionism and cancer 68:883
Letter to the Editor: Immune alterations related to age, sex, and mammary tumor detection in murine mammary tumor virus-infected mice ... 69:1208
Letter to the Editor: Morbidity versus mortality 69:549
Letter to the Editor: Noncontraceptive estrogen use and the occurrence of ovarian cancer 69:1207
Letter to the Editor: Spontaneous liver tumors in laboratory rats 68:884
Letter to the Editor: *Trans* fatty acids in tumor development 69:319
(leukemia) /Causes of death and sex differences in survival times of pigs with untreated hereditary lymphosarcoma 68:239
leukemia cell into nude mice: Conditions optimizing graft acceptance /Successful transplantation of a human 68:15
leukemia cell lines /Trisomy 15 and other nonrandom chromosome changes in Rauscher murine leukemia virus-induced 69:945

leukemia cells /Intracellular adriamycin levels and cytotoxicity in adriamycin-sensitive and adriamycin-resistant P388 mouse ... 68:1027
leukemia cells /Murine tumor necrosis-inducing factor: Purification and effects on myelomonocytic ... 68:997
leukemia /Changes in clonal expression during the course of acute leukemia: Possible subsets in childhood ... 69:393
leukemia (GL-13) in guinea pigs /A deletion in chromosome 1 in cells of a transplantable granulocytic ... 69:591
leukemia hybrids. I. Isolation, characterization, cell surface markers, and B-cell markers /Human lymphoma–lymphoma hybrids and ... 68:179
leukemia hybrids. II. Epstein-Barr virus induction patterns /Human lymphoma–lymphoma hybrids and lymphoma– ... 68:197
leukemia impaired in copper-deficient mice /Immunization against transplantable ... 69:489
leukemia in mice /Comparison of in vitro and in vivo effects of thymidine on L1210 ... 68:875; 69:547
leukemia in the United States /No seasonality in the diagnosis of acute ... 69:1283
leukemia–lymphoma /Guest Editorial: Human retroviruses and adult T-cell ... 69:1209
leukemia–lymphoma: Role of a human retrovirus /Adult T-cell ... 69:981
leukemia /Phytohemagglutinin or pokeweed mitogen induction of in vitro colony formation by T-cells from patients with chronic lym- ... 68:233
leukemias and thymic epithelial reticular cells /Formation of symbiotic complex by microenvironment-dependent mouse ... 69:627
leukemias, lymphomas, or soft tissue sarcomas /Search for evidence of feline leukemia virus infection in humans with ... 69:333
leukemia vincristine-resistant P388 cells to vinblastine, vindesine, and bis(*N*-ethylidene vindesine) disulfide, disulfate /Cross-resist- ... 68:1023
leukemia viruses: Lymphomagenic ecotropic viruses of AKR mice /Spontaneous ... 69:1077
leukemia virus-induced leukemia cell lines /Trisomy 15 and other nonrandom chromosome changes in Rauscher murine ... 69:945
leukemia virus-infected, chemically induced murine sarcoma with antiviral antibodies /Immunotherapy of a murine ... 69:509
leukemia virus infection in humans with leukemias, lymphomas, or soft tissue sarcomas /Search for evidence of feline ... 69:333
leukemogenic doses of radiation and restoration of resistance by transfer of bone marrow or spleen cells from normal, but not beige, syn- ... 69:89
leukocyte adherence inhibition phenomenon /T_G cell involvement in the ... 68:549
leukocyte interferon to melanoma patients. I. Effects on natural killer function and cell populations /Systemic administration of human ... 68:703
leukocyte interferon to melanoma patients. II. Cellular events associated with changes in natural killer cytotoxicity /Systemic adminis- ... 68:711
leukocyte reactivity /Growth and spontaneous regression of swine melanoma: Relationship of in vitro ... 68:461
lipids and relative weight /Cancer incidence in humans: Relationship to plasma ... 68:915
lipids on lactogenic hormone receptor binding in rat mammary tumors /Effects of dietary ... 68:319
lipophilic derivative of muramyl dipeptide /Isolation of tumoricidal macrophages from lung melanoma metastases of mice treated sys- ... 69:1189
Lipopolysaccharide and pristane-induced peritoneal exudate requirements for plasma tumor cell colony formation ... 68:325
liposomes containing a lipophilic derivative of muramyl dipeptide /Isolation of tumoricidal macrophages from lung melanoma metasta- ... 69:1189
liposomes: Transport to the lymph nodes in mice /Subcutaneously injected radiolabeled ... 69:67
liver: A comparative study with other species /Chicken resistance to dimethylnitrosamine acute effects on the ... 69:687
liver after partial hepatectomy, during carcinogenesis, and in transplantable hepatocellular carcinomas /Expression of fibronectin and ... 69:1105
liver and urinary bladder tumors in male F344 rats /Organ-specific promoting effects of phenobarbital sodium and sodium saccharin ... 68:497
liver by partial hepatectomy following single injection of *N*-nitrosodiethylamine /Induction of γ-glutamyltransferase-positive and non- ... 69:1299
liver carcinoma and liver cirrhosis in atomic bomb survivors, Hiroshima and Nagasaki, 1961–75, with special reference to hepatitis B sur- ... 69:1221
liver cell carcinoma and surrounding nontumorous liver /Distribution of hepatitis B surface and core antigens in human ... 69:565
liver cell nuclei of *N*-2-fluorenylacetamide-induced altered foci and neoplasms in rats and human hyperplastic foci /DNA content of ... 69:1277
liver cirrhosis in atomic bomb survivors, Hiroshima and Nagasaki, 1961–75, with special reference to hepatitis B surface antigen /Pri- ... 69:1221
liver /Distribution of hepatitis B surface and core antigens in human liver cell carcinoma and surrounding nontumorous ... 69:565
Liver DNA bound in vivo with aflatoxin B_1 as a measure of hepatocarcinoma initiation in rainbow trout ... 68:623
liver of $(C57BL/6N \times C3H/HeN)F_1$ mice /Carcinogenic effect of carbazole in the ... 69:1383
livers of carcinogen-treated rats /Purification and transplantation of hepatocytes from ... 68:851
Liver tumors induced by a new beta-adrenoreceptor blocking agent in female rats ... 68:669
liver tumors in laboratory rats /Letter to the Editor: Spontaneous ... 68:884
livestock and poultry /Chemical and biochemical aspects of photosensitization in ... 69:259
livestock /Toxicologic aspects of photosensitization in ... 69:253
longevity in continuous bone marrow cultures and factor-dependent cell line generation: Significant variation among 28 inbred mouse ... 68:305
Lucké renal adenocarcinomas in virus-infected leopard frog tadpoles /Effect of thymectomy on development of ... 68:133
lung adenoma prevalence and growth rate to acute urethan dose and target cell number /Relationship of ... 69:851
lung by chronic tobacco smoke inhalation /Pathogenesis of lesions induced in rat ... 69:117
lung by sex and by income level /Major histologic types of cancers of the gum and mouth, esophagus, larynx, and ... 69:773
lung cancer incidence and mortality rates among Americans: 1969–78 /Changes in ... 69:833
lung cancer mortality associated with sugarcane farming /An increased risk for ... 68:755
lung cancer survival in women /Smoking history and ... 68:395
lung carcinogenesis by a 5-nitrofuran naphthyridine derivative in mice /Inhibitory effect of fumaric acid on forestomach and ... 69:1317
lung carcinoma: An endemic analogue of a sporadic human neoplasm /Guest Editorial: Sheep ... 69:747
lung melanoma metastases of mice treated systemically with liposomes containing a lipophilic derivative of muramyl dipeptide /Isola- ... 69:1189
lung metastases of murine tumors /Studies on the antitumor activities of pyrimidinone-interferon inducers. I. Effect against artificial ... 68:139
Lycurim and Pyrazofurin /Rat hepatomas: Chemotherapy with ... 68:665

lymph node natural killer cells: Regulatory mechanisms of activation or suppression /Murine 69:665
lymph nodes in mice /Subcutaneously injected radiolabeled liposomes: Transport to the 69:67
lymph nodes of patients with untreated breast cancer /Subpopulations of human T-lymphocytes. XIX. T-cells and T-cells with recep- 69:1261
lymphoblastoid cell lines /Tumor promoter 12-*O*-tetradecanoylphorbol 13-acetate: Effect on complement and Epstein-Barr virus recep- 68:385
lymphoblastoid tumor cell lines /Surface antigens on Marek's disease 69:715
lymphoblast tumorigenicity in nude mice /Effect of type C viral expression and cellular karyotype on human B- 69:435
Lymphocyte fluorescence polarization changes after phytohemagglutinin stimulation in the diagnosis of colorectal carcinoma 68:579
lymphocyte function in the peripheral blood of brain tumor patients /In vitro reversal of depressed T- 68:27
lymphocyte mediators of natural killer activity /Morphology and function of ganglio-*N*-tetraosylceramide-positive 68:449
lymphocytes against fetal extracts: Cross-reactions between man and mouse /Reactivity in neoplasia, preneoplasia, and pregnancy of 69:997
lymphocytes against human ovarian carcinoma cells /Interferon effect on cytotoxicity of peripheral blood and tumor-asociated 68:555
lymphocytes from breast cancer patients and controls by the use of α-methyl-D-mannoside /Maximizing differences in the concanava- 68:69
lymphocytes in the induction of cell-mediated cytotoxic responses to allogeneic cultured gliomas /In vitro studies on the cell-mediated 69:1245
lymphocytes: Role of subcellular factors in blastic activation /Functional properties of human thymoma 69:827
lymphocyte subpopulations infiltrating human mammary carcinomas /T-Lymphocyte and B- 69:1
lymphocytes with Marek's disease virus /In vitro infection of 69:709
lymphocytic leukemia /Phytohemagglutinin or pokeweed mitogen induction of in vitro colony formation by T-cells from patients with 68:233
lymphoid cell lines with specific cytotoxic reactivity for a syngeneic murine lymphoma /Generation of long-term T- 69:109
lymphoid cells in agarose without feeder layers /High cloning efficiency of human 68:919
lymphoid cells /In vitro assay of the effects of psoralens plus ultraviolet radiation on human 69:219
lymphoid cells responding to virus- and tumor-associated antigens in spleens of syngeneic mouse mammary tumor systems with low and 69:1403
lymphoma antigenically altered by drug treatment in vivo /Intracerebral adoptive immunotherapy of a murine 68:817
lymphoma cells /Changes in human adenovirus 5 propagated in Burkitt's 69:1215
lymphoma cells in soft agar /Anticancer drugs: Effect on the cloning of Raji 68:115
lymphoma clinical studies: A comprehensive analysis of cases accumulated since its inception /Pathology panel for 68:43
lymphoma /Generation of long-term T-lymphoid cell lines with specific cytotoxic reactivity for a syngeneic murine 69:109
Lymphomagenic ecotropic viruses of AKR mice /Spontaneous leukemia viruses: 69:1077
lymphoma /Guest Editorial: Human retroviruses and adult T-cell leukemia- 69:1209
lymphoma hybrids and lymphoma-leukemia hybrids. I. Isolation, characterization, cell surface markers, and B-cell markers /Hu- 68:179
lymphoma hybrids and lymphoma-leukemia hybrids. II. Epstein-Barr virus induction patterns /Human lymphoma- 68:197
lymphoma: Immunity induction by a somatic cell hybrid /Nonimmunogenic radiation-induced 68:841
lymphoma in C57BL/6J mice /Immunoadjuvant effects of *Blastomyces dermatitidis* against EL 4 ..... 69:1337
lymphoma L5178Y cells resistant to purine antagonists: Differences in cross-resistance to thioguanine-platinum(II) and selenoguanine- 68:287
lymphoma-leukemia hybrids. I. Isolation, characterization, cell surface markers, and B-cell markers /Human lymphoma-lymphoma 68:179
lymphoma-leukemia hybrids. II. Epstein-Barr virus induction patterns /Human lymphoma-lymphoma hybrids and 68:197
lymphoma: Role of a human retrovirus /Meeting Highlights: Adult T-cell leukemia- 69:981
lymphomas, or soft tissue sarcomas /Search for evidence of feline leukemia virus infection in humans with leukemias, ... 69:333
lymphoma with central nervous system involvement /Cerebrospinal fluid markers in African Burkitt's 69:787
lymphoresponsive phases of carcinogenesis: Mechanisms of natural immunity /Immunomodulation of the 69:737
lymphosarcoma (leukemia) /Causes of death and sex differences in survival times of pigs with untreated hereditary 68:239
Lymphotoxin prevention of diethylnitrosamine carcinogenesis in vivo 69:741
lymphotoxin sensitivity, and natural skin reactivity relationships to guinea pig cell tumorigenicity /Plasminogen activator, fibronectin, ... 68:329
lysis mechanism involving target cell-binding proteases /Inducible macrophage cytotoxins. II. Tumor 69:889

macrophage cytotoxins. I. Biokinetics of activation and release in vitro /Inducible 69:879
macrophage cytotoxins. II. Tumor lysis mechanism involving target cell-binding proteases /Inducible 69:889
macrophage-mediated suppression of the T-cell cytotoxic response to tumor-associated antigens. I. Characterization of the cell components 69:867
macrophage-mediated suppression of the T-cell cytotoxic response to tumor-associated antigens. II. Mechanisms for induction of suppression 69:873
macrophage migration inhibition response to 3-*M* KCl extract of gastric carcinoma /Indirect 69:345
macrophages from lung melanoma metastases of mice treated systemically with liposomes containing a lipophilic derivative of mu- 69:1189
macrophages in 3-methylcholanthrene-induced murine tumors /Exclusive binding of immunoglobulin to FCγ receptors on 69:1163
macrophages /In vitro growth stimulation of human ovarian cancer cells by xenogeneic peritoneal 69:1039
mammalian cells /Genotoxic effects of sunlight-activated waste water in cultured 69:199
mammary adenocarcinoma /Development and biologic properties of malignant cell sublines and clones of a spontaneously metastasiz- 68:507
mammary adenocarcinoma induced by *N*-hydroxy-*N*-2-fluorenylacetamide /Steroid hormone receptors in the rat 69:41
mammary adenocarcinoma /Relationship between xenotransplantability and cell surface properties of ascites sublines of a rat 69:33
mammary carcinoma ascites cell /Further studies on the relationship between allotransplantability and the presence of the cell sur- 68:981
mammary carcinomas /T-Lymphocyte and B-lymphocyte subpopulations infiltrating human 69:1

mammary carcinoma /Temperature gradients and local perfusion in a ... 68:519
mammary epithelial cells transformed in organ culture /Growth and differentiation of hyperplastic outgrowths derived from mouse ... 69:453
mammary fat pads /Proliferation of ductal outgrowths by carcinogen-induced rat mammary tumors in gland-free ... 69:517
mammary glands after neonatal sex hormone treatment /Growth of mouse ... 69:1347
mammary gland transplants of normal, hyperplastic, and tumor tissues exposed to X-rays /Survival of mouse ... 68:613
mammary gland tumors induced by *N*-nitroso-*N*-methylurea and salivary gland tumors induced by 7,12-dimethylbenz[*a*]anthracene ... 69:1115
mammary hyperplastic outgrowth line: Effect of carcinogens /A high-tumor-incidence subline of the D1 mouse ... 69:639
mammary neoplasms in the ACI rat by 430-keV neutrons, X-rays, and diethylstilbestrol /Induction of ... 69:1135
mammary tissues: Changes in location and amount of antigen during differentiation of cultured stem cells /Thy-1 antigen on normal ... 68:799
mammary tumor cells in artificial capillary culture /Tumor-associated antigens produced by mouse ... 69:1359
mammary tumor cells /Vasopressin: Action in WRK-1 rat ... 68:267
mammary tumor classification: Notes on comparative aspects /Rat ... 68:147
mammary tumor detection in murine mammary tumor virus-infected mice /Letter to the Editor: Immune alterations related to age, ... 69:1208
mammary tumor growth: Correlation with prostaglandin E_2 content /Hormone dependence of 7,12-dimethylbenz[*a*]anthracene-in- ... 69:443
mammary tumor in the rat /Androgen control of cytosol progesterone receptor levels in the MT-W9B transplantable ... 69:673
mammary tumor of GR/A mice: An in vitro study /Hormone requirements of the pregnancy-dependent ... 69:1391
mammary tumors /Effects of dietary lipids on lactogenic hormone receptor binding in rat ... 68:319
mammary tumors /Free amino acid pools of rodent ... 69:729
mammary tumors from low-expressor, low-risk mice /Detection of acquired provirus sequences in ... 68:1037
mammary tumors in gland-free mammary fat pads /Proliferation of ductal outgrowths by carcinogen-induced rat ... 69:517
mammary tumors in GR mice /Comparison of biologic behavior and histology of transplanted ... 69:933
mammary tumors in mice /Inhibitory effect of interferon on the growth of spontaneous ... 69:653
mammary tumors in the rat /Comparison of ovariectomy and retinyl acetate on the growth of established 7,12-dimethylbenz[*a*]anthra- ... 69:447
mammary tumors in virgin female BALB/c mice by single low doses of 7,12-dimethylbenz[*a*]anthracene /Induction of ... 69:1199
mammary tumor stem-cell line /Prostaglandin-induced differentiation or dimethyl sulfoxide-induced differentiation: Reduction of ... 69:1083
mammary tumor systems with low and high oncogenic potentials /Analysis of lymphoid cells responding to virus- and tumor-asso- ... 69:1403
mammary tumor virus antigens by patients with hyperplastic benign breast disease /Cell-mediated immunity to mouse ... 68:935
mammary tumor virus-infected mice /Letter to the Editor: Immune alterations related to age, sex, and mammary tumor detection in ... 69:1208
mammography for periodic screening for breast cancer in women /Single oblique-view ... 68:351
man and mouse /Reactivity in neoplasia, preneoplasia, and pregnancy of lymphocytes against fetal extracts: Cross-reactions between ... 69:997
Marek's disease lymphoblastoid tumor cell lines /Surface antigens on ... 69:715
Marek's disease virus /In vitro infection of lymphocytes with ... 69:709
marker evaluation in human prostate cancer with the use of tissue-specific antigens /Multiple ... 68:99
marker in carcinoma of the breast in women /Use of circulating pregnancy-specific β_1 glycoprotein as a ... 69:1067
markers for human hematopoietic cell lines /Ganglioside patterns: New biochemical ... 68:203
markers /Human lymphoma-lymphoma hybrids and lymphoma-leukemia hybrids. I. Isolation, characterization, cell surface markers, ... 68:179
markers in African Burkitt's lymphoma with central nervous system involvement /Cerebrospinal fluid ... 69:787
marrow /Multiple myeloma among atomic bomb survivors in Hiroshima and Nagasaki, 1950–76: Relationship to radiation dose ab- ... 69:323
mast cells in tumor suppression in mice /Evidence for involvement of ... 69:1305
MDA-MB-231 derived from a human metastatic breast carcinoma /Isolation and partial characterization of surface components of cell ... 69:371
Meeting Highlights: Adult T-cell leukemia–lymphoma: Role of a human retrovirus ... 69:981
Meeting Highlights: Brief summary of the third joint meeting of the United States–Japan Cooperative Cancer Research Program on ... 69:544
Meeting Highlights: Cytogenetics and somatic cell genetics of malignancy workshop ... 69:543
Meeting Highlights: Host factors in human carcinogenesis ... 68:173
Meeting Highlights: Job-exposure matrices in occupational epidemiology ... 69:1419
Meeting Highlights: Kaposi's sarcoma in homosexual men ... 68:337
Meeting Highlights: Monoclonal antibodies and breast cancer ... 68:338
melanocytes: Use of animal models in pigment research /Toxic effect of ultraviolet light on ... 69:245
melanoma A-Mel-3 /Microcirculatory blood flow, capillary morphology, and local oxygen pressure of the hamster amelanotic ... 68:475
melanoma and carcinoma cells /A 94,000-dalton glycoprotein expressed by human ... 68:761
melanoma-associated antigens and β_2-microglobulin on cultured human melanoma cells by interferon /Enhanced expression of ... 68:19
melanoma cell variants: Irreversible inhibition of growth and induction of morphologic differentiation by anthracycline antibiotics /B16 ... 68:629
melanoma metastases of mice treated systemically with liposomes containing a lipophilic derivative of muramyl dipeptide /Isola- ... 69:1189
melanoma: Morphology, karyology, and biochemical analysis /Multiple cell lines from patients with malignant ... 68:365
melanoma /Oral contraceptive use and malignant ... 68:537
melanoma patients. I. Effects on natural killer function and cell populations /Systemic administration of human leukocyte interferon to ... 68:703
melanoma patients. II. Cellular events associated with changes in natural killer cytotoxicity /Systemic administration of human leuko- ... 68:711
melanoma: Relationship of in vitro leukocyte reactivity /Growth and spontaneous regression of swine ... 68:461
melanoma xenografts in nude mice with a radiolabeled monoclonal antibody /Imaging of human ... 69:823
melphalan therapy of tumor-bearing BALB/c mice. I. Enhancement of in vivo rejection responses by combined chemotherapy- ... 68:963

membrane-associated 94,000-M_r SV40 T-antigen in hamsters /Simian virus 40 (SV40)-specific isoelectric point-4.7-94,000-M_r mem- 69:839
membrane glycoprotein: Major peptide homology exhibited with the nuclear and membrane-associated 94,000-M_r SV40 T-antigen 69:839
membranes /A method to quantify the potency of photosensitizers that modify cell 69:211
men /Immunity to tumor-associated antigens in vasectomized 69:551
men /Meeting Highlights: Kaposi's sarcoma in homosexual 68:337
metabolites by radioimmunoassay /Detection of aflatoxins and related 69:1375
metabolites of commercially utilized chloroalkenes /Neoplastic transformation of Syrian hamster cells by putative epoxide 69:531
metaplasia in Japan: Association with diet /Intestinal 68:401
metaplasia in organ cultures of vitamin A-deficient hamster trachea: Cytokinetic and ultrastructural alterations /Squamous 69:895
metastases of a 3-methylcholanthrene-induced sarcoma in mice: A preliminary report /Immunotherapeutic effects of partially purified 69:1121
metastases of heterogeneous murine tumors /Enhanced metastatic potential of tumor cells harvested from spontaneous 69:975
metastases of mice treated systemically with liposomes containing a lipophilic derivative of muramyl dipeptide /Isolation of tumori- 69:1189
metastases of murine tumors /Studies on the antitumor activities of pyrimidinone-interferon inducers. I. Effect against artificial 68:139
metastasis /Establishment and immunologic characterization of 3-methylcholanthrene-induced sarcoma cell lines metastasizing widely 69:595
metastasizing properties and organ specificity /Derivation of transplantable 7,12-dimethylbenz[*a*]anthracene-induced chicken fibrosar- 69:535
metastasizing rat mammary adenocarcinoma /Development and biologic properties of malignant cell sublines and clones of a sponta- 68:507
metastatic breast carcinoma /Isolation and partial characterization of surface components of cell line MDA-MB-231 derived from a 69:371
metastatic potential from nonsyngeneic neoplasma /Use of young nude mice for selection of subpopulations of cells with increased 69:137
metastatic potential of tumor cells harvested from spontaneous metastases of heterogeneous murine tumors /Enhanced 69:975
methane excretion in patients with unresected colorectal cancer /Breath 69:573
Methionine regulation of *N*-5-methyltetrahydrofolate:homocysteine methyltransferase and its influence on the growth and protein syn- 69:9
methoxsalen plus ultraviolet (320–400 nm) radiation /Induction and transplantation of murine skin cancers induced by 68:685
5-, 7-, and 12-methyl- and fluorine-substituted benz[*a*]anthracenes /Mouse skin tumor-initiating activity of 69:725
Methylazoxymethanol: Effect on the immune response of rats to human serum albumin 68:651
3-methylcholanthrene-induced murine tumors /Exclusive binding of immunoglobulin to Fcγ receptors on macrophages in 69:1163
3-methylcholanthrene-induced sarcoma cell lines metastasizing widely in mice and exhibiting distinct and selective propensities for the 69:595
3-methylcholanthrene-induced sarcoma in mice: A preliminary report /Immunotherapeutic effects of partially purified tumor- 69:1121
α-methyl-D-mannoside /Maximizing differences in the concanavalin A-induced blastogenic responses of lymphocytes from breast 68:69
N-Methyl-*N*-nitrosourea and saccharin: Effects on epithelium of normal human urinary bladder in vitro 69:577
N-5-methyltetrahydrofolate:homocysteine methyltransferase and its influence on the growth and protein synthesis in normal, neoplastic, 69:9
Microcirculatory blood flow, capillary morphology, and local oxygen pressure of the hamster amelanotic melanoma A-Mel-3 68:475
microenvironment-dependent mouse leukemias and thymic epithelial reticular cells /Formation of symbiotic compex by 69:627
β_2-microglobulin on cultured human melanoma cells by interferon /Enhanced expression of melanoma-associated antigens and 68:19
microtubule inhibition and permission of invasion in vitro /Glycosylated podophyllotoxin congeners: Loss of 69:1367
mining wastes /Epizootic neoplasms in fishes from a lake polluted by copper 69:915
Mitogen-induced blastogenesis and receptor mobility inhibition by breast cancer serum with elevated orosomucoid (α_1-acid glycoprotein) 68:779
mitogen induction of in vitro colony formation by T-cells from patients with chronic lymphocytic leukemia /Phytohemagglutinin or 68:233
Molecular aspects of drug photosensitivity with special emphasis on psoralen photosensitization reaction 69:163
Moloney murine sarcoma virus-induced tumors. III. Further characterization of tumor-specific serum blocking factors /Regulation of 69:939
Moloney murine sarcoma virus tumors in CBA/J mice: Chemopreventive and chemotherapeutic actions of supplemental β-carotene 68:835
monkeys /Cerebrospinal fluid levels of 2'-deoxycoformycin after systemic administration in 68:391
Monoclonal antibodies and breast cancer /Meeting Highlights 68:338
monoclonal antibodies. I. Heterogeneous expression of Ia-like and HLA-like antigenic determinants /Antigenic heterogeneity of 69:357
monoclonal antibody /Imaging of human melanoma xenografts in nude mice with a radiolabeled 69:823
monoclonal antibody on a Rous sarcoma virus-induced mouse tumor /Individually distinct tumor-specific cell surface antigen identified 69:527
monoclonal antibody reactive with a subset of human breast tumors /Characterization of a 68:719
MOPC-315 plasmacytoma after intralesional and intraperitoneal melphalan therapy of tumor-bearing BALB/c mice. I. Enhancement of in 68:963
morbidity between 1971–72 and 1977–78 /Changes in skin cancer 69:365
Morbidity versus mortality /Letter to the Editor: 69:549
Mortality among workers in a nickel refinery and alloy manufacturing plant in West Virginia 68:925
mortality associated with surgarcane farming /An increased risk for lung cancer 68:755
mortality in England and Wales; 1950–79: Are the changes real? /Increasing trends of multiple myeloma 69:387
mortality /Letter to the Editor: Morbidity versus 69:549
mortality rates among Americans: 1969–78 /Changes in lung cancer incidence and 69:833
mortality /Ten- to fourteen-year effect of screening on breast cancer 69:349
mouth, esophagus, larynx, and lung by sex and by income level /Major histologic types of cancers of the gum and 69:773
MRC-Wistar rats /Carcinogenicity test of acetoxime in 69:961
MT-W9B transplantable mammary tumor in the rat /Androgen control of cytosol progesterone receptor levels in the 69:673
mucosa, adenoma, and carcinoma of the human large bowel /Glycoconjugate with *Ulex europaeus* agglutinin-I-binding sites in normal 69:777
mucosa /Epithelial line from normal human colon 69:1271

mucosal carcinogenesis in hamsters: Inhibition by vitamin E /Oral 68:791
mucosa treated with chemical carcinogens in short-term organ culture /Unscheduled DNA synthesis in human oral 69:557
Multiple myeloma among atomic bomb survivors in Hiroshima and Nagasaki, 1950–76: Relationship to radiation dose absorbed by marrow 69:323
multiple myeloma mortality in England and Wales; 1950–79: Are the changes real? /Increasing trends of 69:387
muramyl dipeptide /Isolation of tumoricidal macrophages from lung melanoma metastases of mice treated systemically with lipo- 69:1189
murine fibroblasts /Enhancement of growth of human colon tumor cell lines by feeder layers of 69:767
murine jejunum /Thermotolerance in the 68:1033
murine leukemia vincristine-resistant P388 cells to vinblastine, vindesine, and bis(*N*-ethylidene vindesine) disulfide, disulfate /Cross-re- 68:1023
murine leukemia virus-induced leukemia cell lines /Trisomy 15 and other nonrandom chromosome changes in Rauscher 69:945
murine leukemia virus-infected, chemically induced murine sarcoma with antiviral antibodies /Immunotherapy of a 69:509
Murine lymph node natural killer cells: Regulatory mechanisms of activation or suppression 69:665
murine lymphoma antigenically altered by drug treatment in vivo /Intracerebral adoptive immunotherapy of a 68:817
murine lymphoma /Generation of long-term T-lymphoid cell lines with specific cytotoxic reactivity for a syngeneic 69:109
Murine lymphoma L5178Y cells resistant to purine antagonists: Differences in cross-resistance to thioguanine–platinum(II) and selenogua- 68:287
murine mammary tumor virus-infected mice /Letter to the Editor: Immune alterations related to age, sex, and mammary tumor detec- 69:1208
murine sarcoma virus-induced tumors. III. Further characterization of tumor-specific serum blocking factors /Regulation of cell-me- 69:939
murine sarcoma virus tumors in CBA/J mice: Chemopreventive and chemotherapeutic actions of supplemental β-carotene /Moloney 68:835
murine sarcoma with antiviral antibodies /Immunotherapy of a murine leukemia virus-infected, chemically induced 69:509
murine tumor cells in culture /Characterization of anti-inflammatory factors produced by 69:1321
murine tumor cells in vitro and in vivo /Phenotypic stability of 68:957
murine tumor cells: Requirements for optimal immunization /Antitumor immunity induced by hybrid 69:647
Murine tumor necrosis-inducing factor: Purification and effects on myelomonocytic leukemia cells 68:997
murine tumors /Enhanced metastatic potential of tumor cells harvested from spontaneous metastases of heterogeneous 69:975
murine tumors /Exclusive binding of immunoglobulin to Fcγ receptors on macrophages in 3-methylcholanthrene-induced 69:1163
murine tumor-specific transplantation antigens with the nonionic detergent octyl-β-D-glucopyranoside /Noncytolytic extraction of 69:131
murine tumors /Studies on the antitumor activities of pyrimidinone-interferon inducers. I. Effect against artificial and spontaneous 68:139
myeloid colony formation /Human adherent cell contact-mediated modulation of normal 68:35
myeloma among atomic bomb survivors in Hiroshima and Nagasaki, 1950–76: Relationship to radiation dose absorbed by marrow 69:323
myeloma in Austria /Epidemiologic and age-dependent data on multiple 68:729
myeloma mortality in England and Wales; 1950–79; Are the changes real? /Increasing trends of multiple 69:387
myelomonocytic leukemia cells /Murine tumor necrosis-inducing factor: Purification and effects on 68:997

Nagasaki, 1950–76: Relationship to radiation dose absorbed by marrow /Multiple myeloma among atomic bomb survivors in Hiroshi- 69:323
Nagasaki, 1961–75, with special reference to hepatitis B surface antigen /Primary liver carcinoma and liver cirrhosis in atomic bomb 69:1221
nasal cancer in the rat /Gaseous formaldehyde and hydrogen chloride induction of 68:597
nasal tumors in rats exposed to hexamethylphosphoramide by inhalation /Induction of 68:157
nasopharynx /Neoplasms following childhood radium irradiation of the 68:3
natural killer activity in cancer patients after surgery /Generation of suppressor cells for 68:735
natural killer activity /Morphology and function of ganglio-*N*-tetraosylceramide-positive lymphocyte mediators of 68:449
natural killer cell activity by a streptococcal preparation, OK-432: Interferon and interleukin-2 participation in the stimulation with OK- 69:807
natural killer cytotoxicity /Systemic administration of human leukocyte interferon to melanoma patients. II. Cellular events associated 68:711
natural killer function and cell populations /Systemic administration of human leukocyte interferon to melanoma patients. I. Effects on 68:703
nausea and vomiting in chemotherapy patients /Prevalence and correlates of anticipatory 68:585
necrosis-inducing factor: Purification and effects on myelomonocytic leukemia cells /Murine tumor 68:997
nerve growth factor binding by the suspected tumor promoters saccharin and cyclamate /Inhibition of iodinated 68:299
neuroblastoma cells in vitro /Retinoic acid-induced growth inhibition and morphologic differentiation of human 68:589
neurofibromatosis /Probable clonal origin of neurofibrosarcoma in a patient with hereditary 69:1289
neurofibrosarcoma in a patient with hereditary neurofibromatosis /Probable clonal origin of 69:1289
neutrons, X-rays, and diethylstilbestrol /Induction of mammary neoplasms in the ACI rat by 430-keV 69:1135
nickel refinery and alloy manufacturing plant in West Virginia /Mortality among workers in a 68:925
nicotinamide, isonicotinamide, and bleomycin on DNA synthesis and repair in rat hepatocytes and hepatoma cells /Effects of 69:1353
nipple aspirates of breast fluid: Association with family history and other breast cancer risk factors /Epithelial dysplasia in 68:9
5-nitrofuran naphthyridine derivative in mice /Inhibitory effect of fumaric acid on forestomach and lung carcinogenesis by a 69:1317
N-nitrosodiethylamine /Electron microscopic autoradiography of the trachea in fetal Syrian golden hamsters treated transplacentally 69:927
N-nitrosodiethylamine /Induction of γ-glutamyltransferase-positive and nonspecific esterase-positive foci in rat liver by partial hepatec- 69:1299
N-nitroso-3,5-dimethylpiperidine /Carcinogenesis by isomers of 68:989
N-nitroso-*N*-ethylurea /Genetics of transplacentally induced teratogenic and carcinogenic effects in rabbits treated with 69:1411
nitrosoheptamethyleneimine and its α-deuterium-labeled derivative in F344 rats /Dose-response studies with 69:1127

nitrosomethylethylamines substituted in the ethyl group /Esophageal carcinogenesis in F344 rats by ... 68:681
N-nitroso-*N*-methylurea and salivary gland tumors induced by 7,12-dimethylbenz[*a*]anthracene /Effects of isoproterenol on mammary ... 69:1115
nitrosourea-induced rat gliomas /Serologic analysis of ... 68:501
Noncontraceptive estrogen use and the occurrence of ovarian cancer ... 68:95
Noncontraceptive estrogen use and the occurrence of ovarian cancer /Letter to the Editor ... 69:1207
non-T-killer cells by BCG and alloantigen /Modulation of cell-mediated alloimmunity by BCG. II. Induction of specific, nonadherent, ... 69:613
nuclear and membrane-associated 94,000-M_r SV40 T-antigen in hamsters /Simian virus 40 (SV40)-specific isoelectric point-4.7– ... 69:839
nuclei of *N*-2-fluorenylacetamide-induced altered foci and neoplasms in rats and human hyperplastic foci /DNA content of liver cell ... 69:1277
nude mice /Calorie restriction: Effect on growth of human tumors heterotransplanted in ... 68:249
nude mouse /Collagenolytic activity of rabbit V_2 carcinoma implanted in the ... 69:1329
nude mice: Conditions optimizing graft acceptance /Successful transplantation of a human leukemia cell into ... 68:15
nude mice /Effect of type C viral expression and cellular karyotype on human B-lymphoblast tumorigenicity in ... 69:435
nude mice for selection of subpopulations of cells with increased metastatic potential from nonsyngeneic neoplasms /Use of young ... 69:137
nude mice /α_1-Protease inhibitor production by human adenocarcinomas xenotransplanted into ... 69:381
nude mice with a radiolabeled monoclonal antibody /Imaging of human melanoma xenografts in ... 69:823
NZB mouse breeding lines that differ in chromosome breakage /Diverse xenotropic virus expressions in two ... 68:951

Obituary—Herbert Joseph Rapp ... 68:177
occupational epidemiology /Meeting Highlights. Job-exposure matrices in ... 69:1419
octyl-*β*-D-glucopyranoside /Noncytolytic extraction of murine tumor-specific transplantation antigens with the nonionic detergent ... 69:151
Ocular phototoxicity and psoralen plus ultraviolet radiation (320–400 nm) therapy: An experimental and clinical evaluation ... 69:287
ocular squamous cell carcinoma: A preliminary report /Immunotherapy by intralesional injection of BCG cell walls or live BCG in bo- ... 69:1095
OK-432: Interferon and interleukin-2 participation in the stimulation with OK-432 /In vitro potentiation of human natural killer cell ... 69:807
oncogenic potentials /Analysis of lymphoid cells responding to virus- and tumor-associated antigens in spleens of syngeneic mouse ... 69:1403
Optical radiation measurement: Instrumentation and sources of error ... 69:155
Oral contraceptive use and malignant melanoma ... 68:537
Oral mucosal carcinogenesis in hamsters: Inhibition by vitamin E ... 68:791
oral mucosa treated with chemical carcinogens in short-term organ culture /Unscheduled DNA synthesis in human ... 69:557
organ culture /Growth and differentiation of hyperplastic outgrowths derived from mouse mammary epithelial cells transformed in ... 69:453
organ cultures /Carcinogen-induced DNA damage and cellular alterations in F344 rat colon ... 68:1015
organ cultures of vitamin A-deficient hamster trachea: Cytokinetic and ultrastructural alterations /Squamous metaplasia in ... 69:895
organ culture /Unscheduled DNA synthesis in human oral mucosa treated with chemical carcinogens in short-term ... 69:557
organs of mice. Distribution of [^{125}I]5-iodo-2′-deoxyuridine-labeled KHT tumor cells after left intracardial injection /Effect of immuno- ... 69:465
organ specificity /Derivation of transplantable 7,12-dimethylbenz[*a*]anthracene-induced chicken fibrosarcoma lines: Differences in me- ... 69:535
Organ-specific promoting effects of phenobarbital sodium and sodium saccharin in the induction of liver and urinary bladder tumors in ... 68:497
Ornithine decarboxylase levels as better indicators than adenosylmethionine decarboxylase levels /Degrees of malignancy in human pri- ... 68:751
orosomucoid (α_1-acid glycoprotein) levels /Mitogen-induced blastogenesis and receptor mobility inhibition by breast cancer serum with ... 68:779
osteosarcoma /Collagen polymorphism in extracellular matrix of human ... 69:1009
ovarian cancer cells by xenogeneic peritoneal macrophages /In vitro growth stimulation of human ... 69:1039
ovarian cancer /Letter to the Editor: Noncontraceptive estrogen use and the occurrence of ... 69:1207
ovarian cancer /Noncontraceptive estrogen use and the occurrence of ... 68:95
ovarian carcinoma cells /Interferon effect on cytotoxicity of peripheral blood and tumor-associated lymphocytes against human ... 68:555
ovariectomy and retinyl acetate on the growth of established 7,12-dimethylbenz[*a*]anthracene-induced mammary tumors in the rat ... 69:447
oxygen and oxy-radicals with carotenoids /Interaction of ... 69:205
oxygen pressure of the hamster amelanotic melanoma A-Mel-3 /Microcirculatory blood flow, capillary morphology, and local ... 68:475
oxy-radicals with carotenoids /Interaction of oxygen and ... 69:205

P388 cells to vinblastine, vindesine, and bis(*N*-ethylidene vindesine) disulfide, disulfate /Cross-resistance of cultured murine leu- ... 68:1023
P388 mouse leukemia cells /Intracellular adriamycin levels and cytotoxicity in adriamycin-sensitive and adriamycin-resistant ... 68:1027
P3HR-1 cell lines /Persistence of transforming and nontransforming Epstein-Barr virus in high passages of ... 69:585
Panama, 1974–78 /Cancer incidence in the Republic of ... 68:219
pancreatic acinar carcinoma /Secretagogue response in rat ... 69:969
pancreatic tumor /Coproduction of carcinoembryonic antigen and nonspecific cross-reacting antigen by a continuous cell line from a ... 69:401
Parity and colorectal cancer risk in women ... 69:1059
Pathogenesis of lesions induced in rat lung by chronic tobacco smoke inhalation ... 69:117
Pathology panel for lymphoma clinical studies: A comprehensive analysis of cases accumulated since its inception ... 68:43

penis in China /Correlation between cancers of the uterine cervix and 69:1063
peptide homology exhibited with the nuclear and membrane-associated 94,000-M_r SV40 T-antigen in hamsters /Simian virus 40 69:839
peptide structure and route of injection /Peptidoglycans extracted from gram-positive bacteria: Expression of antitumor activity accord- 68:657
Peptidoglycans extracted from gram-positive bacteria: Expression of antitumor activity according to peptide structure and route of injection 68:657
peripheral blood and regional lymph nodes of patients with untreated breast cancer /Subpopulations of human T-lymphocytes. XIX. 69:1261
peripheral blood and tumor-associated lymphocytes against human ovarian carcinoma cells /Interferon effect of cytotoxicity of 68:555
peripheral blood of brain tumor patients /In vitro reversal of depressed T-lymphocyte function in the 68:27
peritoneal exudate requirements for plasma tumor cell colony formation /Lipopolysaccharide and pristane-induced 68:325
peritoneal macrophages /In vitro growth stimulation of human ovarian cancer cells by xenogeneic 69:1039
phalloidin and γ-glutamyltransferase of carcinogen-induced preneoplastic hepatocytes of rats /In vitro measurement of resistance to 69:683
phenobarbital sodium and sodium saccharin in the induction of liver and urinary bladder tumors in male F344 rats /Organ-specific 68:497
phenotype during transformation of mouse salivary gland epithelium in vitro /Chromosome changes associated with the progression of 69:425
phenotype of radiation-induced thymomas in the mouse /Alloantigenic 69:619
Phenotypic and genotypic characteristics of a cell line from a squamous cell carcinoma of human skin 68:415
phenotypic properties frequently associated with the neoplastic state in a cultured guinea pig cell line /Independent expression of 69:1175
Phenotypic stability of murine tumor cells in vitro and in vivo 68:957
phorbol esters of procollagen synthesis in promotable JB6 mouse epidermal cells /Inhibition by tumor-promoting 69:1147
N-phosphonacetyl-L-aspartic acid given by intravenous infusion and 5-fluorouracil given by bolus injection /Phase I-Phase II trial of 68:227
photoallergy and their correlation with drug photoallergy in humans /Current status of predictive animal models for drug 69:237
photobiology of psoralens /Comparative 69:189
photocarcinogenesis by chemical agents /Modification of 69:229
Photochemical toxicity studies in humans /Therapeutic in vivo photochemistry: 69:273
Photochemical toxicity: Toxic, allergic, and carcinogenic aspects with emphasis on predicting effects in humans—an introduction 69:151
photosensitivity with special emphasis on psoralen photosensitization reaction /Molecular aspects of drug 69:163
photosensitization by carotenoids /Photosensitization by porphyrins and prevention of 69:279
Photosensitization by porphyrins and prevention of photosensitization by carotenoids 69:279
photosensitization in livestock and poultry /Chemical and biochemical aspects of 69:259
photosensitization in livestock /Toxicologic aspects of 69:253
photosensitization reaction /Molecular aspects of drug photosensitivity with special emphasis on psoralen 69:163
photosensitizers that modify cell membranes /A method to quantify the potency of 69:211
photosensitizing chemicals /Human models for identification of 69:269
photosensitizing chemicals /Tumor virus induction and host cell capacity inactivation: Possible in vitro tests for 69:183
phototoxicity and psoralen plus ultraviolet radiation (320–400 nm) therapy: An experimental and clinical evaluation /Ocular 69:287
phototoxicity in humans /Chemical 69:265
Phytohemagglutinin or pokeweed mitogen induction of in vitro colony formation by T-cells from patients with chronic lymphocytic leuke- 68:233
phytohemagglutinin stimulation in the diagnosis of colorectal carcinoma /Lymphocyte fluorescence polarization changes after 68:579
picolinic acid in CBA/J mice /Antitumor activity of 68:123
pigment research /Toxic effect of ultraviolet light on melanocytes: Use of animal models in 69:245
pigs with untreated hereditary lymphosarcoma (leukemia) /Causes of death and sex differences in survival times of 68:239
plasma α-1-acid glycoprotein assay in the detection of human colorectal cancer: Comparison with carcinoembryonic antigen /Value of 68:75
plasmacytoma after intralesional and intraperitoneal melphalan therapy of tumor-bearing BALB/c mice. I. Enhancement of in vivo re- 68:963
plasma lipids and relative weight /Cancer incidence in humans: Relationship to 68:915
plasma tumor cell colony formation /Lipopolysaccharide and pristane-induced peritoneal exudate requirements for 68:325
Plasminogen activator, fibronectin, lymphotoxin sensitivity, and natural skin reactivity relationships to guinea pig cell tumorigenicity 68:329
Platinum-complexed antitumor immunoglobulins that specifically inhibit DNA synthesis of mouse tumor cells 69:47
podophyllotoxin congeners: Loss of microtubule inhibition and permission of invasion in vitro /Glycosylated 69:1367
pokeweed mitogen induction of in vitro colony formation by T-cells from patients with chronic lymphocytic leukemia /Phytohemagglu- 68:233
polyamine oxidase susceptibility /Possible association of radioprotective and chemoprotective aminophosphorothioate drug activity with 69:329
porphyrins and prevention of photosensitization by carotenoids /Photosensitization by 69:279
poultry /Chemical and biochemical aspects of photosensitization in livestock and 69:259
pregnancy-dependent mammary tumor of GR/A mice: An in vitro study /Hormone requirements of the 69:1391
pregnancy of lymphocytes against fetal extracts: Cross-reactions between man and mouse /Reactivity in neoplasia, preneoplasia, and 69:997
pregnancy-specific β_1 glycoprotein as a marker in carcinoma of the breast in women /Use of circulating 69:1067
pregnant, and tumor-bearing humans /Transforming growth factors in the urine of normal, 69:793
primates /Carcinoembryonic antigen in nonhuman 69:1073
Primordial germ cell proliferation in fetal testes in mouse strains with high and low incidences of congenital testicular teratomas 69:907
pristane-induced peritoneal exudate requirements for plasma tumor cell colony formation /Lipopolysaccharide and 68:325
procollagen synthesis in promotable JB6 mouse epidermal cells /Inhibition by tumor-promoting phorbol esters of 69:1147
progesterone receptor levels in the MT-W9B transplantable mammary tumor in the rat /Androgen control of cytosol 69:673
prognostic heterogeneity: Implications for adjuvant chemotherapy of breast cancer /Intrastage 68:445

Prolactin receptors in human breast tumors 68:381
prostaglandin E_1 and copper in angiogenesis /Role of 69:475
prostaglandin E_2 content /Hormone dependence of 7,12-dimethylbenz[*a*]anthracene-induced mammary tumor growth: Correlation with 69:443
Prostaglandin-induced differentiation or dimethyl sulfoxide-induced differentiation: Reduction of the neoplastic potential of a rat mam- 69:1083
prostaglandins: Effects on human natural and lectin-induced cytotoxicity /Interferon and 69:339
prostate adenocarcinoma grown in vivo and in vitro /Flow cytometric analysis of R3327 rat 69:79
Prostate adenocarcinoma in rats: Induction by 3,2′-dimethyl-4-aminobiphenyl 68:867
prostate cancer with the use of tissue-specific antigens /Multiple marker evaluation in human 68:99
prostate. II. Long-term explant culture of normal prostate and benign prostatic hyperplasia: Light microscopy /Studies on carcinogene- 69:751
prostate. III. Long-term explant culture of normal prostate and benign prostatic hyperplasia: Transmission and scanning electron microscopy 69:757
α_1-Protease inhibitor production by human adenocarcinomas xenotransplanted into nude mice 69:381
protease inhibitors and a chemoattractant on tumor cell invasion in vitro /Effect of natural 69:1049
proteases /Inducible macrophage cytotoxins. II. Tumor lysis mechanism involving target cell-binding 69:889
protein cross-links /Cell damage by near ultraviolet radiation: Role of DNA– 69:177
protein synthesis in normal, neoplastic, and transformed cells in culture /Methionine regulation of *N*-5-methyltetrahydrofolate:homo- 69:9
provirus sequences in mammary tumors from low-expressor, low-risk mice /Detection of acquired 68:1037
psoralen photosensitization reaction /Molecular aspects of drug photosensitivity with special emphasis on 69:163
psoralen plus ultraviolet (320–400 nm) radiation in mice /Immunosuppressive effects of ultraviolet (280–320 nm) radiation and 69:171
psoralen plus ultraviolet radiation (320–400 nm) therapy: An experimental and clinical evaluation /Ocular phototoxicity and 69:287
psoralens /Comparative photobiology of 69:189
psoralens plus ultraviolet radiation on human lymphoid cells /In vitro assay of the effects of 69:219
pulmonary metastases of a 3-methylcholanthrene-induced sarcoma in mice: A preliminary report /Immunotherapeutic effects of par- 69:1121
purine antagonists: Differences in cross-resistance to thioguanine-platinum(II) and selenoguanine-platinum(II) /Murine lymphoma 68:287
Pyrazofurin /Rat hepatomas: Chemotherapy with Lycurim and 68:665
pyrimidinone-interferon inducers. I. Effect against artificial and spontaneous lung metastases of murine tumors /Studies on the anti- 68:139

R3327 rat prostate adenocarcinoma grown in vivo and in vitro /Flow cytometric analysis of 69:79
rabbit V_2 carcinoma implanted in the nude mouse /Collagenolytic activity of 69:1329
radiation and psoralen plus ultraviolet (320–400 nm) radiation in mice /Immunosuppressive effects of ultraviolet (280–320 nm) 69:171
radiation and restoration of resistance by transfer of bone marrow or spleen cells from normal, but not beige, syngeneic mice /Depres- 69:89
radiation dose absorbed by marrow /Multiple myeloma among atomic bomb survivors in Hiroshima and Nagasaki, 1950–76: Relation- 69:323
radiation-induced lymphoma: Immunity induction by a somatic cell hybrid /Nonimmunogenic 68:841
radiation-induced thymomas in the mouse /Alloantigenic phenotype of 68:619
radiation /Induction and transplantation of murine skin cancers induced by methoxsalen plus ultraviolet (320–400 nm) 68:685
radiation measurements: Instrumentation and sources of error /Optical 69:155
radiation on human lymphoid cells /In vitro assay of the effects of psoralens plus ultraviolet 69:219
radiation: Role of DNA–protein cross-links /Cell damage by near ultraviolet 69:177
radiation (320–400 nm) therapy: An experimental and clinical evaluation /Ocular phototoxicity and psoralen plus ultraviolet 69:287
radioimmunoassay /Detection of aflatoxins and related metabolites by 69:1375
radiolabeled monoclonal antibody /Imaging of human melanoma xenografts in nude mice with a 69:823
radioprotective and chemoprotective aminophosphorothioate drug activity with polyamine oxidase susceptibility /Possible association 69:329
radiotherapy for cervical cancer /Second cancers following 69:1027
radium irradiation of the nasopharynx /Neoplasms following childhood 68:3
rainbow trout /Liver DNA bound in vivo with aflatoxin B_1 as a measure of hepatocarcinoma initiation in 68:623
Raji lymphoma cells in soft agar /Anticancer drugs: Effect on the cloning of 68:115
Rapp /Obituary—Herbert Joseph 68:177
Rauscher murine leukemia virus-induced leukemia cell lines /Trisomy 15 and other nonrandom chromosome changes in 69:945
renal adenocarcinomas in virus-infected leopard frog tadpoles /Effect of thymectomy on development of Lucké 68:133
renal tubular cell tumors in rats treated with *N*-ethyl-*N*-hydroxyethylnitrosamine /*β*-Cyclodextrin: Promoting effect on the develop- 69:963
Republic of Panama, 1974–78 /Cancer incidence in the 68:219
respiratory cancer due to chloromethyl ethers /Epidemic curve of 69:1265
respiratory tract epithelium in rats /Effect of carcinogen release rate on the incidence of preneoplastic and neoplastic lesions of the 69:1155
reticular cells /Formation of symbiotic complex by microenvironment-dependent mouse leukemias and thymic epithelial 69:627
Retinoic acid-induced growth inhibition and morphologic differentiation of human neuroblastoma cells in vitro 68:589
retinoid: Association with esophageal cancer in rats /Zinc deficiency, alcohol, and a 68:785
retinyl acetate on the growth of established 7,12-dimethylbenz[*a*]anthracene-induced mammary tumors in the rat /Comparison of 69:447
retroviruses and adult T-cell leukemia–lymphoma /Guest Editorial: Human 69:1209
retrovirus /Meeting Highlights: Adult T-cell leukemia–lymphoma: Role of a human 69:981

rhabdomyosarcoma in childhood /Environmental factors in the etiology of 68:107
rhabdomyosarcomas as xenografts /Growth and characterization of childhood 68:437
ricin A-chain–anticarcinoembryonic antigen antibody conjugate for human colon adenocarcinoma cell line /Selective cytotoxicity of a 69:799
rodent mammary tumors /Free amino acid pools of 69:729
Rous sarcoma virus-induced mouse tumor /Individually distinct tumor-specific cell surface antigen identified by monoclonal antibody 69:527

saccharin and cyclamate /Inhibition of iodinated nerve growth factor binding by the suspected tumor promoters 68:299
saccharin: Effects on epithelium of normal human urinary bladder in vitro /*N*-Methyl-*N*-nitrosourea and 69:577
saccharin in the induction of liver and urinary bladder tumors in male F344 rats /Organ-specific promoting effects of phenobarbital so- 68:497
salivary gland epithelium in vitro /Chromosome changes associated with the progression of cell lines from preneoplastic to tumori- 69:425
salivary gland tumors induced by 7,12-dimethylbenz[*a*]anthracene /Effects of isoproterenol on mammary gland tumors induced by *N*- 69:1115
sarcoma cell lines metastasizing widely in mice and exhibiting distinct and selective propensities for the mode of metastasis /Establish- 69:595
sarcoma in homosexual men /Meeting Highlights: Kaposi's 68:337
sarcoma in mice: A preliminary report /Immunotherapeutic effects of partially purified tumor-specific transplantation antigens on pul- 69:1121
sarcomas /Search for evidence of feline leukemia virus infection in humans with leukemias, lymphomas, or soft tissue 69:333
sarcoma virus-induced mouse tumor /Individually distinct tumor-specific cell surface antigen identified by monoclonal antibody on a 69:527
sarcoma virus-induced tumors. III. Further characterization of tumor-specific serum blocking factors /Regulation of cell-mediated im- 69:939
sarcoma virus tumors in CBA/J mice: Chemopreventive and chemotherapeutic actions of supplemental β-carotene /Moloney murine 68:835
sarcoma with antiviral antibodies /Immunotherapy of a murine leukemia virus-infected, chemically induced murine 69:509
screening on breast cancer mortality /Ten- to fourteen-year effect of 69:349
SD rats /Spontaneous occurrence of atypical hyperplasia and adenocarcinoma of the uterus in androgen-sterilized 69:95
Secretagogue response in rat pancreatic acinar carcinoma 69:969
selenoguanine-plantinum(II) /Murine lymphoma L5178Y cells resistant to purine antagonists: Differences in cross-resistance to thio- 68:287
SENCAR mouse skin /Comparative tumor-initiating activity of complex mixtures from environmental particulate emissions on 68:829
sera of patients with advanced cancer /Elevated dTTPase activities in 69:569
Serologic analysis of nitrosourea-induced rat gliomas 68:501
serum albumin /Methylazoxymethanol: Effect on the immune response of rats to human 68:651
serum blocking factors /Regulation of cell-mediated immunologic reactivity to Moloney murine sarcoma virus-induced tumors. III. 69:939
serum cholesterol /Breast cancer and 68:885
serum cholesterol–cancer relationship: An analysis of time trends in the Framingham Study /The 69:989
serum with elevated orosomucoid (α_1-acid glycoprotein) levels /Mitogen-induced blastogenesis and receptor mobility inhibition by 68:779
sex and by income level /Major histologic types of cancers of the gum and mouth, esophagus, larynx, and lung by 69:773
sex, and mammary tumor detection in murine mammary tumor virus-infected mice /Letter to the Editor: Immune alterations related 69:1208
sex differences in survival times of pigs with untreated hereditary lymphocarcoma (leukemia) /Causes of death and 68:239
sex hormone treatment /Growth of mouse mammary glands after neonatal 69:1347
Sheep lung carcinoma: An endemic analogue of a sporadic human neoplasm /Guest Editorial: 69:747
Simian virus 40 (SV40)-specific isoelectric point-4.7-94,000-M_r membrane glycoprotein: Major peptide homology exhibited with the nuclear 69:839
Skin cancer morbidity between 1971–72 and 1977–78 /Changes in 69:365
skin cancers induced by methoxsalen plus ultraviolet (320–400 nm) radiation /Induction and transplantation of murine 68:685
skin /Comparative tumor-initiating activity of complex mixtures from environmental particulate emissions on SENCAR mouse 68:829
skin fibroblasts from patients with familial adenomatosis coli /Morphologic transformation and chromosomal changes induced by 68:563
skin fibroblasts in two families with Gardner's syndrome /Heterogeneous response to X-ray and ultraviolet light irradiations of cultured 68:697
skin /Phenotypic and genotypic characteristics of a cell line from a squamous cell carcinoma of human 68:415
skin reactivity relationships to guinea pig cell tumorigenicity /Plasminogen activator, fibronectin, lymphotoxin sensitivity, and natural 68:329
skin tumorigenesis by cigarette smoke condensate following β-irradiation in rats /Enhancement of 68:605
skin tumor-initiating activity of 5-, 7-, and 12-methyl- and fluorine-substituted benz[*a*]anthracenes /Mouse 69:725
smoke condensate following β-irradiation in rats /Enhancement of skin tumorigenesis by cigarette 68:605
smoke inhalation /Pathogenesis of lesions induced in rat lung by chronic tobacco 69:117
Smoking history and lung cancer survival in women 68:395
sodium saccharin in the induction of liver and urinary bladder tumors in male F344 rats /Organ-specific promoting effects of phenobar- 68:497
soft tissue sarcomas /Search for evidence of feline leukemia virus infection in humans with leukemias, lymphomas, or 69:333
somatic cell genetics of malignancy workshop /Meeting Highlights: Cytogenetics and 69:543
somatic cell hybrid /Nonimmunogenic radiation-induced lymphoma: Immunity induction by a 68:841
somatic cell hybrids /Inheritance of cellular resistance to the antitumor agent ICFR 159 in 68:977
spleen cells from normal, but not beige, syngeneic mice /Depression of natural antitumor resistance of C57BL/6 mice by leukemogenic 69:39
spleen cells /L-Histidinol protection against cytotoxic action of cytosine arabinoside and 5-fluorouracil in cultured mouse 68:279
spleens of syngeneic mouse mammary tumor systems with low and high oncogenic potentials /Analysis of lymphoid cells responding to 69:1403
spleen suppressor cell content in rats with progressing and regressing tumors /Differences in 69:53

Spontaneous leukemia viruses: Lymphemagenic ecotropic viruses of AKR mice ... 69:1077
Spontaneous liver tumors in laboratory rats /Letter to the Editor: ... 68:884
spontaneous lung metastases of murine tumors /Studies on the antitumor activities of pyrimidinone-interferon inducers. I. Effect ... 68:139
spontaneously metastasizing rat mammary adenocarcinoma /Development and biologic properties of malignant cell sublines and clones ... 68:507
"spontaneous" malignant transformation in culture with associated advances in culture technology /A quest for mechanism of ... 68:895
spontaneous mammary tumors in mice /Inhibitory effect of interferon on the growth of ... 69:653
spontaneous metastases of heterogeneous murine tumors /Enhanced metastatic potential of tumor cells harvested from ... 69:975
Spontaneous occurrence of atypical hyperplasia and adenocarcinoma of the uterus in androgen-sterilized SD rats ... 69:95
spontaneous regression of swine melanoma: Relationship of in vitro leukocyte reactivity /Growth and ... 68:461
squamous cell carcinoma: A preliminary report /Immunotherapy by intralesional injection of BCG cell walls or live BCG in bovine ... 69:1095
squamous cell carcinoma of human skin /Phenotypic and genotypic characteristics of a cell line from a ... 68:415
squamous cell carcinoma of the thyroid gland /Establishment and characterization of a human colony-stimulating factor-producing cell ... 69:1235
Squamous metaplasia in organ cultures of vitamin A-deficient hamster trachea: Cytokinetic and ultrastructural alterations ... 69:895
stem-cell line /Prostaglandin-induced differentiation or dimethyl sulfoxide-induced differentiation: Reduction of the neoplastic poten- ... 69:1083
stem cell self-renewal of lectin-separated murine bone marrow fractions /Differing ... 68:639
stem cells /Thy-1 antigen on normal and neoplastic rat mammary tissues: Changes in location and amount of antigen during differenti- ... 68:799
Steroid hormone receptors in the rat mammary adenocarcinoma induced by *N*-hydroxy-*N*-2-fluorenylacetamide ... 69:41
stomach and incidence of gastric adenocarcinoma /Gastrin protection against chemically induced gastric adenocarcinomas in Wistar ... 69:59
streptococcal preparation, OK-432: Interferon and interleukin-2 participation in the stimulation with OK-432 /In vitro potentiation of ... 69:807
Sudan III and related azo dyes /Suppression of 7,12-dimethylbenz[*a*]anthracene-induced chromosome aberrations in rat bone marrow ... 69:1343
sugarcane farming /An increased risk for lung cancer mortality associated with ... 68:755
sunlight-activated waste water in cultured mammalian cells /Genotoxic effects of ... 68:199
suppressor cells for natural killer activity in cancer patients after surgery /Generation of ... 68:735
suppressor T-cells in mice inoculated with virus-producing tumor cells /Induction of gp70-specific ... 69:953
surface and core antigens in human liver cell carcinoma and surrounding nontumorous liver /Distribution of hepatitis B ... 69:565
Surface antigen expressed in hematopoietic cells derived from *Fv-4*^{r} mouse strains ... 68:1005
surface antigen /Primary liver carcinoma and liver cirrhosis in atomic bomb survivors, Hiroshima and Nagasaki, 1961–75, with ... 69:1221
Surface antigens on Marek's disease lymphoblastoid tumor cell lines ... 69:715
surgery /Generation of suppressor cells for natural killer activity in cancer patients after ... 68:735
Surgical resection of the rat colon: Effects on carcinogenesis by 1,2-dimethylhydrazine ... 68:813
SV40 T-antigen in hamsters /Simian virus 40 (SV40)-specific isoelectric point-4.7–94,000-M_r membrane glycoprotein: Major peptide ... 69:839
swine melanoma: Relationship of in vitro leukocyte reactivity /Growth and spontaneous regression of ... 68:461
symbiotic complex by microenvironment-dependent mouse leukemias and thymic epithelial reticular cells /Formation of ... 69:627
Syrian golden hamsters administered aflatoxin B_1 in large doses /Cholangiocellular carcinomas induced in ... 68:271
Syrian golden hamsters treated transplacentally with *N*-nitrosodiethylamine /Electron microscopic autoradiography of the trachea in ... 69:927
Syrian hamster cells by putative epoxide metabolites of commercially utilized chloroalkenes /Neoplastic transformation of ... 69:531
Syrian hamster embryo cells /Equivalency of endothelial cell growth supplement to irradiated feeder cells in carcinogen-induced mor- ... 68:127

TA3-MM mouse mammary carcinoma ascites cell /Further studies on the relationship between allotransplantability and the presence ... 68:981
tadpoles /Effect of thymectomy on development of Lucké renal adenocarcinomas in virus-infected leopard frog ... 68:133
T-antigen in hamsters /Simian virus 40 (SV40)-specific isoelectric point-4.7–94,000-M_r membrane glycoprotein: Major peptide ho- ... 69:839
T-cell cytotoxic response to tumor-associated antigens. I. Characterization of the cell components for induction of suppression /Tumor ... 69:867
T-cell cytotoxic response to tumor-associated antigens. II. Mechanisms for induction of suppression /Tumor cell-triggered macro- ... 69:873
T-cell leukemia–lymphoma /Guest Editorial: Human retroviruses and adult ... 69:1209
T-cell leukemia–lymphoma: Role of a human retrovirus /Meeting Highlights: Adult ... 69:981
T-cell response to alloantigens in mice /Effects of different fractions of *Corynebacterium parvum* on the cytotoxic ... 69:495
T-cells and T-cells with receptors for IgMFc (Tμ), IgGFc (Tγ), or IgAFc (Tα) in the peripheral blood and regional lymph nodes of patients ... 69:1261
T-cells from patients with chronic lymphocytic leukemia /Phytohemagglutinin or pokeweed mitogen induction of in vitro colony for- ... 68:233
T-cells in mice inoculated with virus-producing tumor cells /Induction of gp70-specific suppressor ... 69:953
Temperature gradients and local perfusion in a mammary carcinoma ... 68:519
teratocarcinoma-derived cell line, TerC /*H-2* expression on a ... 69:1311
teratogenic and carcinogenic effects in rabbits treated with *N*-nitroso-*N*-ethylurea /Genetics of transplacentally induced ... 69:1411
teratomas /Primordial germ cell proliferation in fetal testes in mouse strains with high and low incidences of congenital testicular ... 69:907
TerC /*H-2* expression on a teratocarcinoma-derived cell line, ... 69:1311
testicular teratomas /Primordial germ cell proliferation in fetal testes in mouse strains with high and low incidences of congenital ... 69:907
12-*O*-tetradecanoylphorbol 13-acetate: Effect of complement and Epstein-Barr virus receptors in human lymphoblastoid cell lines ... 68:385
12-*O*-tetradecanoylphorbol 13-acetate on cell interactions in vitro /Some effects of the tumor promoter ... 69:721
T_G cell involvement in the leukocyte adherence inhibition phenomenon ... 68:549

Thermotolerance in the murine jejunum 68:1033
thioguanine-platinum(II) and selenoguanine-platinum(II) /Murine lymphoma L5178Y cells resistant to purine antagonists: Differ- 68:287
Thy-1 antigen on normal and neoplastic rat mammary tissues: Changes in location and amount of antigen during differentiation of cul- 68:799
thymectomy on development of Lucké renal adenocarcinomas in virus-infected leopard frog tadpoles /Effect of 68:133
thymic epithelial reticular cells /Formation of symbiotic complex by microenvironment-dependent mouse leukemias and 69:627
thymidine on L1210 leukemia in mice /Comparison of in vitro and in vivo effects of 68:875; 69:547
thymoma lymphocytes: Role of subcellular factors in blastic activation /Functional properties of human 69:827
thymomas in the mouse /Alloantigenic phenotype of radiation-induced 69:619
thymosin-treated bone marrow cell injection /Decrease of tumor growth in mice after intravenous 69:27
thyroid gland /Establishment and characterization of a human colony-stimulating factor-producing cell line from a squamous cell carci- 69:1235
T-Lymphocyte and B-lymphocyte subpopulations infiltrating human mammary carcinomas 69:1
T-lymphocyte function in the peripheral blood of brain tumor patients /In vitro reversal of depressed 68:27
T-lymphocytes. XIX. T-cells and T-cells with receptors for IgMFc (Tμ), IgGFc (Tγ), or IgAFc (Tα) in the peripheral blood and regional 69:1261
T-lymphoid cell lines with specific cytotoxic reactivity for a syngeneic murine lymphoma /Generation of long-term 69:109
tobacco smoke inhalation /Pathogenesis of lesions induced in rat lung by chronic 69:117
trachea: Cytokinetic and ultrastructural alterations /Squamous metaplasia in organ cultures of vitamin A-deficient hamster 69:895
trachea in fetal Syrian golden hamsters treated transplacentally with *N*-nitrosodiethylamine /Electron microscopic autoradiography of 69:927
transformation and chromosomal changes induced by chemical carcinogens in skin fibroblasts from patients with familial adenomatosis coli 68:563
transformation in C3H/10T½ cells /Resting state depth and saturation density as modulated by tumor promoters and culture condi- 68:259
transformation in culture with associated advances in culture technology /A quest for the mechanism of "spontaneous" malignant 68:895
transformation of mouse salivary gland epithelium in vitro /Chromosome changes associated with the progression of cell lines 69:425
transformation of Syrian hamster cells by putative epoxide metabolites of commercially utilized chloroalkenes /Neoplastic 69:531
transformation of Syrian hamster embryo cells /Equivalency of endothelial cell growth supplement to irradiated feeder cells in car- 68:127
transformed cells in culture /Methionine regulation of *N*-5-methyltetrahydrofolate:homocysteine methyltransferase and its influence on 69:9
transformed human fibroblasts /Basis for the differential action of aminonucleoside on normal and 68:407
transforming and nontransforming Epstein-Barr virus in high passages of P3HR-1 cell lines /Persistence of 69:585
transplacentally induced teratogenic and carcinogenic effects in rabbits treated with *N*-nitroso-*N*-ethylurea /Genetics of 69:1411
transplantable 7,12-dimethylbenz[*a*]anthracene-induced chicken fibrosarcoma lines: Differences in metastatizing properties and organ 69:535
transplantable granulocytic leukemia (GL-13) in guinea pigs /A deletion in chromosome 1 in cells of a 69:591
transplantable hepatocellular carcinomas /Expression of fibronectin and laminin in the rat liver after partial hepatectomy, during car- 69:1105
transplantable leukemia impaired in copper-deficient mice /Immunization against 69:489
transplantable mammary tumor in the rat /Androgen control of cytosol progesterone receptor levels in the MT-W9B 69:673
transplantation antigens on pulmonary metastases of a 3-methylcholanthrene-induced sarcoma in mice: A preliminary report /Immu- 69:1121
transplantation antigens with the nonionic detergent octyl-β-D-glucopyranoside /Noncytolytic extraction of murine tumor-specific 69:131
transplantation of a human leukemia cell into nude mice: Conditions optimizing graft acceptance /Successful 68:15
transplantation of hepatocytes from livers of carcinogen-treated rats /Purification and 68:851
transplantation of human hepatocytes /Isolation, culture, and 68:771
transplantation of murine skin cancers induced by methoxsalen plus ultraviolet (320-400 nm) radiation /Induction and 68:685
transplanted mammary tumors in GR mice /Comparison of biologic behavior and histology of 69:933
transplants of normal, hyperplastic, and tumor tissues exposed to X-rays /Survival of mouse mammary gland 68:613
Trisomy 15 and other nonrandom chromosome changes in Rauscher murine leukemia virus-induced leukemia cell lines 69:945
trophoblastic neoplasia /Circulating immune complex levels in patients with gestational 69:23
tubular cell tumors in rats treated with *N*-ethyl-*N*-hydroxyethylnitrosamine /β-Cyclodextrin: Promoting effect on the development of 69:963
tumor-associated antigens. I. Characterization of the cell components for induction of suppression /Tumor cell-triggered macrophage- 69:867
tumor-associated antigens. II. Mechanisms for induction of suppression /Tumor cell-triggered macrophage-mediated suppression of the 69:873
tumor-associated antigens in spleens of syngeneic mouse mammary tumor systems with low and high oncogenic potentials /Anal- 69:1403
tumor-associated antigens in vasectomized men /Immunity to 69:551
Tumor-associated antigens produced by mouse mammary tumor cells in artificial capillary culture 69:1359
tumor-associated lymphocytes against human ovarian carcinoma cells /Interferon effect on cytotoxicity of peripheral blood and 68:555
tumor-bearing BALB/c mice. I. Enhancement of in vivo rejection responses by combined chemotherapy-immunotherapy /Develop- 68:963
tumor-bearing humans /Transforming growth factors in the urine of normal, pregnant, and 69:793
tumor-bearing mice and effects of *Corynebacterium parvum* /Accessory of cell function in 69:1293
tumor cell invasion in vitro /Effect of natural protease inhibitors and a chemoattractant on 69:1049
Tumor cell-triggered macrophage-mediated suppression of the T-cell cytotoxic response to tumor-associated antigens. I. Characterization 69:867
Tumor cell-triggered macrophage-mediated suppression of the T-cell cytotoxic response to tumor-associated antigens. II. Mechanisms for in- 69:873
tumor development /Letter to the Editor: *Trans* fatty acids in 69:319
tumor growth in mice after intravenous thymosin-treated bone marrow cell injection /Decrease of 69:27
tumor growth rate and target cell number /Relationship between urethan dose rate and adenoma latency: Relevance of 69:859
tumoricidal macrophages from lung melanoma metastases of mice treated systemically with liposomes containing a lipophilic deriva- 69:1189

tumorigenesis by cigarette smoke condensate following β-irradiation in rats /Enhancement of skin 68:605

tumorigenicity in nude mice /Effect of type C viral expression and cellular karyotype on human B-lymphoblast 69:435

tumorigenicity of untransformed mouse cell lines /Role of anchorage in the expression of 69:415

tumorigenicity /Plasminogen activator, fibronectin, lymphotoxin sensitivity, and natural skin reactivity relationships to guinea pig cell 68:329

tumorigenic phenotype during transformation of mouse salivary gland epithelium in vitro /Chromosome changes associated with 69:425

Tumor-induced neovascularization in the mouse eye 69:699

tumor-initiating activity of complex mixtures from environmental particulate emissions on SENCAR mouse skin /Comparative 68:829

Tumor lysis mechanism involving target cell-binding proteases /Inducible macrophage cytotoxins. II. 69:889

tumor necrosis-inducing factor: Purification and effects on myelomonocytic leukemia cells /Murine 68:997

tumor promoters and culture conditions: Relationship to chemical transformation in C3H/10T½ cells /Resting state depth and satu- 68:259

tumor promoters in promotable JB6 mouse epidermal cells: Antagonism by an antipromoter /Ganglioside changes induced by 68:469

tumor promoters saccharin and cyclamate /Inhibition of iodinated nerve growth factor binding by the suspected 68:299

Tumor promoter 12-*O*-tetradecanoylphorbol 13-acetate: Effect on complement and Epstein-Barr virus receptors in human lymphoblas- 68:385

tumor promoter 12-*O*-tetradecanoylphorbol 13-acetate on cell interactions in vitro /Some effects of the 69:721

tumor-promoting phorbol esters of procollagen synthesis in promotable JB6 mouse epidermal cells /Inhibition by 69:1147

tumor-specific cell surface antigen identified by monoclonal antibody on a Rous sarcoma virus-induced mouse tumor /Individually dis- 69:527

tumor-specific serum blocking factors /Regulation of cell-mediated immunologic reactivity to Moloney murine sarcoma virus-induced 69:939

tumor-specific transplantation antigens on pulmonary metastases of a 3-methylcholanthrene-induced sarcoma in mice: A preliminary report 69:1121

tumor-specific transplantation antigens with the nonionic detergent octyl-β-D-glucopyranoside /Noncytolytic extraction of murine 69:131

tumor stem-cell line /Prostaglandin-induced differentiation or dimethyl sulfoxide-induced differentiation: Reduction of the neoplastic 69:1083

tumor suppression in mice /Evidence for involvement of mast cells in 69:1305

tumor virus antigens by patients with hyperplastic benign breast disease /Cell-mediated immunity to mouse mammary 68:935

Tumor virus induction and host cell capacity inactivation: Possible in vitro tests for photosensitizing chemicals 69:183

type C viral expression and cellular karyotype on human B-lymphoblast tumorigenicity in nude mice /Effect of 69:435

Ulex europaeus agglutinin-I-binding sites in normal mucosa, adenoma, and carcinoma of the human large bowel /Glycoconjugate with 69:777

ultraviolet carcinogenesis in BALB/c mice /Influences of age and anatomical site on 68:691

ultraviolet light irradiations of cultured skin fibroblasts in two families with Gardner's syndrome /Heterogeneous response to X-ray and 68:697

ultraviolet light on melanocytes: Use of animal models in pigment research /Toxic effect of 69:245

ultraviolet (280–320 nm) radiation and psoralen plus ultraviolet (320–400 nm) radiation in mice /Immunosuppressive effects of 69:171

ultraviolet (320–400 nm) radiation /Induction and transplantation of murine skin cancers induced by methoxsalen plus 68:685

ultraviolet radiation on human lymphoid cells /In vitro assay of the effects of psoralens plus 69:219

ultraviolet radiation: Role of DNA–protein cross-links /Cell damage by near 69:177

ultraviolet radiation (320–400 nm) therapy: An experimental and clinical evaluation /Ocular phototoxicity and psoralen plus 69:287

United States–Japan Cooperative Cancer Research Program on cell interactions and cancer /Meeting Highlights: Brief summary of the 69:544

United States /No seasonality in the diagnosis of acute leukemia in the 69:1283

United States: Sources and uses of data /Measurement of cancer incidence in the 68:743

urethan dose and target cell number /Relationship of lung adenoma prevalence and growth rate to acute 69:851

urethan dose rate and adenoma latency: Relevance of tumor growth rate and target cell number /Relationship between 69:859

urinary bladder in vitro /*N*-Methyl-*N*-nitrosourea and saccharin: Effects on epithelium of normal human 69:577

urinary bladder tumors in male F344 rats /Organ-specific promoting effects of phenobarbital sodium and sodium saccharin in the in- 68:497

urinary tract /Coffee drinking and cancer of the lower 68:91

urine of normal, pregnant, and tumor-bearing humans /Transforming growth factors in the 69:793

uterine cervix and penis in China /Correlation between cancers of the 69:1063

uterus in androgen-sterilized SD rats /Spontaneous occurrence of atypical hyperplasia and adenocarcinoma of the 69:95

V_2 carcinoma implanted in the nude mouse /Collagenolytic activity of rabbit 69:1329

vasectomized men /Immunity to tumor-associated antigens in 69:551

Vasopressin: Action in WRK-1 rat mammary tumor cells 68:267

vinblastine, vindesine, and bis(*N*-ethylidene vindesine) disulfide, disulfate /Cross-resistance of cultured murine leukemia vincristine-re- 68:1023

vincristine-resistant P388 cells to vinblastine, vindesine, and bis(*N*-ethylidene vindesine) disulfide, disulfate /Cross-resistance of cul- 68:1023

vindesine, and bis(*N*-ethylidene vindesine) disulfide, disulfate /Cross-resistance of cultured murine leukemia vincristine-resistant P388 68:1023

viral components in modifying erythroid differentiation in mice /Friend erythroleukemia virus complex: Role of 68:457

virus- and tumor-associated antigens in spleens of syngeneic mouse mammary tumor systems with low and high oncogenic potentials 69:1402

virus antigens by patients with hyperplastic benign breast disease /Cell-mediated immunity to mouse mammary tumor 68:935

virus complex: Role of viral components in modifying erythroid differentiation in mice /Friend erythroleukemia 68:457
viruses of AKR mice /Spontaneous leukemia viruses: Lymphomagenic ecotropic 69:1077
virus expressions in two NZB mouse breeding lines that differ in chromosome breakage /Diverse xenotropic 68:951
virus-induced leukemia cell lines /Trisomy 15 and other nonrandom chromosome changes in Rauscher murine leukemia 69:945
virus-induced mouse tumor /Individually distinct tumor-specific cell surface antigen identified by monoclonal antibody on a Rous sar- 69:527
virus-induced tumors. III. Further characterization of tumor-specific serum blocking factors /Regulation of cell-mediated immuno- 69:939
virus induction and host cell capacity inactivation: Possible in vitro tests for photosensitizing chemicals /Tumor 69:183
virus induction patterns /Human lymphoma-lymphoma hybrids and lymphoma-leukemia hybrids. II. Epstein-Barr 68:197
virus-infected, chemically induced murine sarcoma with antiviral antibodies /Immunotherapy of a murine leukemia 69:509
virus-infected leopard frog tadpoles /Effect of thymectomy on development of Lucké renal adenocarcinomas in 68:133
virus-infected mice /Letter to the Editor: Immune alterations related to age, sex, and mammary tumor detection in murine mammary 69:1208
virus infection in humans with leukemias, lymphomas, or soft tissue sarcomas /Search for evidence of feline leukemia 69:333
virus in high passages of P3HR-1 cell lines /Persistence of transforming and nontransforming Epstein-Barr 69:585
virus /In vitro infection of lymphocytes with Marek's disease 69:709
virus-producing tumor cells /Induction of gp70-specific suppressor T-cells in mice inoculated with 69:953
virus receptors in human lymphoblastoid cell lines /Tumor promoter 12-*O*-tetradecanoylphorbol 13-acetate: Effect on complement 68:385
virus tumors in CBA/J mice: Chemopreventive and chemotherapeutic actions of supplemental β-carotene /Moloney murine sarcoma 68:835
vitamin A and 5-fluorouracil and the growth of allotransplantable and syngeneic tumors in mice /Combined treatments with 68:823
vitamin A-deficient hamster trachea: Cytokinetic and ultrastructural alterations /Squamous metaplasia in organ cultures of 69:895
vitamin E /Oral mucosal carcinogenesis in hamsters: Inhibition by 68:791
vomiting in chemotherapy patients /Prevalence and correlates of anticipatory nausea and 68:585

Wales; 1950–79: Are the changes real? /Increasing trends of multiple myeloma mortality in England and 69:387
water in cultured mammalian cells /Genotoxic effects of sunlight-activated waste 69:199
weight /Cancer incidence in humans: Relationship to plasma lipids and relative 68:915
West Virginia /Mortality among workers in a nickel refinery and alloy manufacturing plant in 68:925
Wilms' tumor: Results of the National Wilms' Tumor Study /Epidemiological features of 68:429
Wistar rats: Histopathology of the glandular stomach and incidence of gastric adenocarcinoma /Gastrin protection against chemically 69:59
women in northern Alberta, Canada, as related to age at diagnosis /Risk factors for breast cancer in 68:211
women /Parity and colorectal cancer risk in 69:1059
women /Single oblique-view mammography for periodic screening for breast cancer in 68:351
women /Smoking history and lung cancer survival in 68:395
women /Use of circulating pregnancy-specific β_1 glycoprotein as a marker in carcinoma of the breast in 69:1067
women with benign breast diseases /Exogenous estrogens and other risk factors for breast cancer in 69:1017
WRK-1 rat mammary tumor cells /Vasopressin: Action in 68:267

xenografts /Growth and characterization of childhood rhabdomyosarcomas as 68:437
xenografts in nude mice with a radiolabeled monoclonal antibody /Imaging of human melanoma 69:823
xenotransplantability and cell surface properties of ascites sublines of a rat mammary adenocarcinoma /Relationship between 69:33
xeromammograms /Observer variation in the interpretation of 68:357
X-irradiation during G_2 phase in a line of normal human fibroblasts and its malignant derivative /Repair of chromosome damage in- 69:409
X-ray and ultraviolet light irradiations of cultured skin fibroblasts in two families with Gardner's syndrome /Heterogeneous response to 68:697
X-rays, and diethylstilbestrol /Induction of mammary neoplasms in the ACI rat by 430-keV neutrons, 69:1135
X-rays /Survival of mouse mammary gland transplants of normal, hyperplastic, and tumor tissues exposed to 68:613

Zinc deficiency, alcohol, and a retinoid: Association with esophageal cancer in rats 68:785

blank page

Table of Contents

Volumes 68–69
January–December 1982

Vol 68, No.1—JANUARY 1982

1 Howard Bancroft Andervont, *D.Sc*—A Tribute

Investigations on Man

3	Neoplasms following childhood radium irradiation of the nasopharynx	*Dale P. Sandler, George W. Comstock, Genevieve M. Matanoski*
9	Epithelial dysplasia in nipple aspirates of breast fluid: Association with family history and other breast cancer risk factors	*Nicholas L. Petrakis, Virginia L. Ernster, Eileen B. King, Susan T. Sacks*
15	Successful transplantation of a human leukemia cell into nude mice: Conditions optimizing graft acceptance	*H. W. (Löms) Ziegler, Glauco Frizzera, Fritz H. Bach*
19	Enhanced expression of melanoma-associated antigens and β_2-microglobulin on cultured human melanoma cells by interferon	*Shuen-Kuei Liao, Pak C. Kwong, Mohammed Khosravi, Peter B. Dent*
27	In vitro reversal of depressed T-lymphocyte function in the peripheral blood of brain tumor patients	*Gary W. Wood, Robert A Morantz*
35	Human adherent cell contact-mediated modulation of normal myeloid colony formation	*Gary Spitzer, Dharmvir S. Verma, Miloslav Beran, Axel R. Zander, Kenneth B. McCredie, Karel A. Dicke*
43	Pathology panel for lymphoma clinical studies: A comprehensive analysis of cases accumulated since its inception	*Hun Kim, Ronald J. Zelman, Michael A. Fox, John M. Bennett, Costan W. Berard, James J. Butler, Gerald E. Byrne, Jr., Ronald F. Dorfman, Robert J. Hartsock, Robert J. Lukes, Risa B. Mann, Richard S. Neiman, John W. Rebuck, William W. Sheehan, Daina Variakojis, John F. Wilson, Henry Rappaport*
69	Maximizing differences in the concanavalin A-induced blastogenic responses of lymphocytes from breast cancer patients and controls by the use of α-methyl-D-mannoside	*John A. Distasio, David A. Cheresh, Russel J. Schilder, Charles L. Vogel, Michael A. Silverman, Diana M. Lopez*
75	Value of plasma α-1-acid glycoprotein assay in the detection of human colorectal cancer: Comparison with carcinoembryonic antigen	*Clement Y-T. Chu, Lilian T-Y. Lai, Hari P. Pokala*
81	Various isozyme gene expression patterns among human colorectal adenocarcinoma cell lines and tissues	*Lynne P. Rutzky, Michael J. Siciliano*
91	Coffee drinking and cancer of the lower urinary tract	*Alan S. Morrison, Julie E. Buring, Wendy G. Verhoek, Kunio Aoki, Ian Leck, Yoshiyuki Ohno, Koji Obata*
95	Noncontraceptive estrogen use and the occurrence of ovarian cancer	*Noel S. Weiss, J. Lynn Lyon, Sarala Krishnamurthy, Scott E. Dietert, Jonathan M. Liff, Janel R. Daling*
99	Multiple marker evaluation in human prostate cancer with the use of tissue-specific antigens	*M. Kuriyama, M. C. Wang, C. L. Lee, C. S. Killian, L. D. Papsidero, H. Inaji, R. M. Loor, M. F. Lin, T. Nishiura, N. H. Slack, G. P. Murphy, T. M. Chu*
107	Environmental factors in the etiology of rhabdomyosarcoma in childhood	*Seymour Grufferman, Helen H. Wang, Elizabeth R. DeLong, Sue Y. S. Kimm, Elizabeth S. Delzell, John M. Falletta*
115	Anticancer drugs: Effect on the cloning of Raji lymphoma cells in soft agar	*Pao-Chen Wu, Robert F. Ozols, Masakazu Hatanaka, Charles W. Boone*

Investigations on Nonhuman Systems

123	Antitumor activity of picolinic acid in CBA/J mice	*Susan W. C. Leuthauser, Larry W. Oberley, Terry D. Oberley*

127 Equivalency of endothelial cell growth supplement to irradiated feeder cells in carcinogen-induced morphologic transformation of Syrian hamster embryo cells — *Charles H. Evans, Joseph A. DiPaolo*

133 Effect of thymectomy on development of Lucké renal adenocarcinomas in virus-infected leopard frog tadpoles — *Louise A. Rollins-Smith, Nicholas Cohen*

139 Studies on the antitumor activities of pyrimidinone-interferon inducers. I. Effect against artificial and spontaneous lung metastases of murine tumors — *Luka Milas, Evan M. Hersh, Dale A. Stringfellow, Nancy Hunter*

147 Rat mammary tumor classification: Notes on comparative aspects — *Dymitr Komitowski, Bernard Sass, Walter Laub*

157 Induction of nasal tumors in rats exposed to hexamethylphosphoramide by inhalation — *Ki P. Lee, Henry J. Trochimowicz*

Meeting Highlights

173 Host factors in human carcinogenesis — *John J. Mulvihill*

Announcements

175 Sixteenth Annual Clinical Symposium

175 Thirty-Second Annual Conference of The National Council on the Aging, Inc.

175 Oncology Update 1982

175 North American Society for Cardiac Radiology—1982 Postgraduate Course

175 Second Annual Washington Imaging Conference

175 Fourth Annual Course in Flow Cytometry

175 Educational Video Cassettes

Vol 68, No. 2—FEBRUARY 1982

177 Obituary—Herbert Joseph Rapp — *Tibor Borsos*

Investigations on Man

179 Human lymphoma-lymphoma hybrids and lymphoma-leukemia hybrids. I. Isolation, characterization, cell surface markers, and B-cell markers — *Jesper Zeuthen, George Klein, Rosalie Ber, Giuseppe Masucci, Susanne Bisballe, Susan Povey, Paul Terasaki, Peter Ralph*

197 Human lymphoma-lymphoma hybrids and lymphoma-leukemia hybrids. II. Epstein-Barr virus induction patterns — *George Klein, Jesper Zeuthen, Rosalie Ber, Ingemar Ernberg*

203 Ganglioside patterns: New biochemical markers for human hematopoietic cell lines — *Günter Rosenfelder, Andreas Ziegler, Peter Wernet, Dietmar G. Braun*

211 Risk factors for breast cancer in women in northern Alberta, Canada, as related to age at diagnosis — *Jay H. Lubin, Patricia E. Burns, William J. Blot, Alan W. Lees, Carol May, Linda E. Morris, Joseph F. Fraumeni, Jr.*

219 Cancer incidence in the Republic of Panama, 1974-78 — *William C. Reeves, Plinio F. Valdés, María M. Brenes, Rosa C. de Britton, Claire F. B. Joplin*

227 Phase I–Phase II trial of *N*-phosphonacetyl-L-aspartic acid given by intravenous infusion and 5-fluorouracil given by bolus injection — *Charles Erlichman, Ross C. Donehower, James L. Speyer, Ray Klecker, Bruce A. Chabner*

233 Phytohemagglutinin or pokeweed mitogen induction of in vitro colony formation by T-cells from patients with chronic lymphocytic leukemia — *Vito Pistoia, Arcangelo Nocera, Riccardo Ghio, Paola Minale, Manlio Ferrarini*

Investigations on Nonhuman Systems

239 Causes of death and sex differences in survival times of pigs with untreated hereditary lymphosarcoma (leukemia) — *H. S. McTaggart, P. Imlah, K. W. Head*

249 Calorie restriction: Effect on growth of human tumors heterotransplanted in nude mice — *Beppino C. Giovanella, Randall C. Shepard, John S. Stehlin, John M. Venditti, Betty J. Abbott*

259 Resting state depth and saturation density as modulated by tumor promoters and culture conditions: Relationship to chemical transformation in C3H/10T½ cells — *David Miska, H. Bruce Bosmann*

267 Vasopressin: Action in WRK-1 rat mammary tumor cells — *M. E. Monaco, P. H. Kohn, W. R. Kidwell, J. S. Strobl, M. E. Lippman*

271 Cholangiocellular carcinomas induced in Syrian golden hamsters administered aflatoxin B_1 in large doses — *Michael R. Moore, Henry C. Pitot, Elizabeth C. Miller, James A. Miller*

279 L-Histidinol protection against cytotoxic action of cytosine arabinoside and 5-fluorouracil in cultured mouse spleen cells — *Robert C. Warrington, Wei D. Fang*

287 Murine lymphoma L5178Y cells resistant to purine antagonists: Differences in cross-resistance to thioguanine–platinum(II) and selenoguanine–platinum(II) — *Fumihiko Kanzawa, Mitsuaki Maeda, Takuma Sasaki, Akio Hoshi, Kazuo Kuretani*

293 Production of kidney tumors in rats with low dose of dimethylnitrosamine after partial hepatectomy — *Ritva P. Evarts, Carolyn A. Brown, Mostafa Hassan Mostafa*

299 Inhibition of iodinated nerve growth factor binding by the suspected tumor promoters saccharin and cyclamate — *Douglas N. Ishii*

305 Granulopoiesis longevity in continuous bone marrow cultures and factor-dependent cell line generation: Significant variation among 28 inbred mouse strains and outbred stocks — *Mary Ann Sakakeeny, Joel S. Greenberger*

319 Effects of dietary lipids on lactogenic hormone receptor binding in rat mammary tumors — *William T. Cave, Jr., Marsha J. Erickson-Lucas*

325 Lipopolysaccharide and pristane-induced peritoneal exudate requirements for plasma tumor cell colony formation — *Micsunica Platica, Catherine Bojko, Radu Clincea, Vincent Hollander*

329 Plasminogen activator, fibronectin, lymphotoxin sensitivity, and natural skin reactivity relationships to guinea pig cell tumorigenicity — *Richard P. McCabe, Charles H. Evans*

Meeting Highlights

337 Kaposi's sarcoma in homosexual men — *John L. Ziegler*

338 Monoclonal antibodies and breast cancer — *Marianne L. Egan, Donald E. Henson*

Announcements

341 National Toxicology Program Conference

341	Latest NCI Monographs Published	
341	Other Monographs Available	

Vol 68, No. 3—MARCH 1982

Guest Editorial

343	What are isozymes telling us about gene regulation in cancer?	*Sidney Weinhouse*

Investigations on Man

351	Single oblique-view mammography for periodic screening for breast cancer in women	*Bengt Lundgren, Anders Helleberg*
357	Observer variation in the interpretation of xeromammograms	*Norman F. Boyd, Christina Wolfson, Myron Moskowitz, Thomas Carlile, Michel Petitclerc, Helen A. Ferri, Eve Fishell, Andre Gregoire, Matthew Kiernan, J. Donald Longley, Imre S. Simor, Anthony B. Miller*
365	Multiple cell lines from patients with malignant melanoma: Morphology, karyology, and biochemical analysis	*Toni U. Semple, George E. Moore, Robert T. Morgan, Linda K. Woods, Laurie A. Quinn*
381	Prolactin receptors in human breast tumors	*Lucile Turcot-Lemay, Paul A. Kelly*
385	Tumor promoter 12-*O*-tetradecanoylphorbol 13-acetate: Effect on complement and Epstein-Barr virus receptors in human lymphoblastoid cell lines	*Naoki Yamamoto, Takashi Mitsuma, Arnold Vogt*
391	Cerebrospinal fluid levels of 2′-deoxycoformycin after systemic administration in monkeys	*Julie Blatt, Peter M. Venner, Riccardo Riccardi, Lawrence F. Cohen, Daimon Gangji, Robert I. Glazer, David G. Poplack*
395	Smoking history and lung cancer survival in women	*M. Ward Hinds, Hong-Yi Yang, Grant Stemmermann, James Lee, Laurence N. Kolonel*
401	Intestinal metaplasia in Japan: Association with diet	*Abraham Nomura, Hiroshi Yamakawa, Takuzo Ishidate, Sigetosi Kamiyama, Hisayuki Masuda, Grant N. Stemmermann, Lance K. Heilbrun, Jean H. Hankin*
407	Basis for the differential action of aminonucleoside on normal and transformed human fibroblasts	*Ernest A. Albanese, George P. Studzinski*
415	Phenotypic and genotypic characteristics of a cell line from a squamous cell carcinoma of human skin	*Petra Boukamp, Wolfgang Tilgen, Rule T. Dzarlieva, Dirk Breitkreutz, Dietrich Haag, Rüdiger K. Riehl, Axel Bohnert, Norbert E. Fusenig*
429	Epidemiological features of Wilms' tumor: Results of the National Wilms' Tumor Study	*Norman E. Breslow, J. Bruce Beckwith*
437	Growth and characterization of childhood rhabdomyosarcomas as xenografts	*J. A. Houghton, P. J. Houghton, B. L. Webber*
445	Intrastage prognostic heterogeneity: Implications for adjuvant chemotherapy of breast cancer	*Maurice M. Black, Benjamin F. Hankey, Thomas H. C. Barclay*

Investigations on Nonhuman Systems

449	Morphology and function of ganglio-*N*-tetraosylceramide-positive lymphocyte mediators of natural killer activity	*Kazuo Shimamura, Sonoko Habu, Hiroyasu Fukui, Akira Akatsuka, Ko Okumura, Norikazu Tamaoki*
457	Friend erythroleukemia virus complex: Role of viral components in modifying erythroid differentiation in mice	*Barbara Fagg, Wolfram Ostertag*
461	Growth and spontaneous regression of swine melanoma: Relationship of in vitro leukocyte reactivity	*Jane Berkelhammer, Bonnie M. Ensign, Reuel R. Hook, Jr., Cynthia J. Hecker, Gerald D. Smith, Ronald W. Oxenhandler*

469	Ganglioside changes induced by tumor promoters in promotable JB6 mouse epidermal cells: Antagonism by an antipromoter	*Leela Srinivas, Nancy H. Colburn*
475	Microcirculatory blood flow, capillary morphology, and local oxygen pressure of the hamster amelanotic melanoma A-Mel-3	*Bernhard Endrich, Frithjof Hammersen, Alwin Götz, Konrad Messmer*
487	Effect of rate of heating on lethality due to hyperthermia and selected chemotherapeutic drugs	*Terence S. Herman, Cynthia C. Sweets, David M. White, Eugene W. Gerner*
493	Glutathione *S*-transferase activity: Enhancement by compounds inhibiting chemical carcinogenesis and by dietary constituents	*Velta L. Sparnins, Plarida L. Venegas, Lee W. Wattenberg*
497	Organ-specific promoting effects of phenobarbital sodium and sodium saccharin in the induction of liver and urinary bladder tumors in male F344 rats	*Keisuke Nakanishi, Shoji Fukushima, Akihiro Hagiwara, Seiko Tamano, Nobuyuki Ito*
501	Serologic analysis of nitrosourea-induced rat gliomas	*Michael Pfreundschuh, Humberto Cravioto, Gerald Hochwald, Joseph Ransohoff*
507	Development and biologic properties of malignant cell sublines and clones of a spontaneously metastasizing rat mammary adenocarcinoma	*Anthny Neri, Dan Welch, Takanori Kawaguchi, Garth L. Nicolson*
519	Temperature gradients and local perfusion in a mammary carcinoma	*Pietro M. Gullino, Rakesh K. Jain, Flora H. Grantham*

Correction

535	November 1981, Vol 67, No. 5, page 991: "Letters to the Editor, BCG and Cancer" (reply)	*George W. Comstock*

Announcements

535 Harvard Medical School Continuing Education Program

535 Aspirin Foundation of America

535 Cancer Management 1982

535 World Symposium on Asbestos

535 Fist International Symposium on the Endocrine Lung in Health and Disease

535 World Congress of Gastroenterology, Digestive Endoscopy, and Colo-Proctology

536 Annual Course in Advanced Immunology

536 First Conference on Radioprotectors and Anticarcinogens

536 Design and Analysis of Scientific Experiments

536 Veterinary Cancer Society

Vol 68, No. 4—APRIL 1982

Investigations on Man

537	Oral contraceptive use and malignant melanoma	*Christopher Bain, Charles H. Hennekens, Frank E. Speizer, Bernard Rosner, Walter Willett, Charlene Belanger*

541	5-Fluorouracil, 1,3-bis(2-chloroethyl)-1-nitrosourea, and 1-(2-chloroethyl)-3-(4-methylcyclohexyl)-1-nitrosourea: Effect on the human granulopoietic system	*Hans-Peter Lohrmann, Karin A. Lepp, Wolfgang Schreml*
549	T_G cell involvement in the leukocyte adherence inhibition phenomenon	*S. G. Taylor IV, Patricia C. Saffold, Donald P. Braun, Jules E. Harris*
555	Interferon effect on cytotoxicity of peripheral blood and tumor-associated lymphocytes against human ovarian carcinoma cells	*Paola Allavena, Martino Introna, Cristiana Sessa, Costantino Mangioni, Alberto Mantovani*
563	Morphologic transformation and chromosomal changes induced by chemical carcinogens in skin fibroblasts from patients with familial adenomatosis coli	*Michiko Miyaki, Noriko Akamatsu, Tetsuo Ono, Akira Tonomura, Joji Utsunomiya*
573	Carotid body tumors in humans: Genetics and epidemiology	*Dilys M. Parry, Frederick P. Li, Louise C. Strong, J. Aidan Carney, David Schottenfeld, Ronald R. Reimer, Seymour Grufferman*
579	Lymphocyte fluorescence polarization changes after phytohemagglutinin stimulation in the diagnosis of colorectal carcinoma	*Glenn R. Hocking, Jennifer M. Roland, Richard C. Nairn, Eric Pihl, Alan M. Cuthbertson, Edward S. R. Hughes, William R. Johnson*
585	Prevalence and correlates of anticipatory nausea and vomiting in chemotherapy patients	*Gary R. Morrow*
589	Retinoic acid-induced growth inhibition and morphologic differentiation of human neuroblastoma cells in vitro	*Neil Sidell*

Investigations on Nonhuman Systems

597	Gaseous formaldehyde and hydrogen chloride induction of nasal cancer in the rat	*Roy E. Albert, Arthur R. Sellakumar, Sidney Laskin, Marvin Kuschner, Norton Nelson, Carroll A. Snyder*
605	Enhancement of skin tumorigenesis by cigarette smoke condensate following β-irradiation in rats	*John F. McGregor (with revisions by D. K. Myers)*
613	Survival of mouse mammary gland transplants of normal, hyperplastic, and tumor tissues exposed to X-rays	*Leslie J. Faulkin, Dan J. Mitchell, Robert D. Cardiff, Marvin Goldman*
619	Bile acids: Effects on absorption of 1,2-dimethylhydrazine and 7,12-dimethylbenz[*a*]anthracene in the colon of the rat and guinea pig	*Richard C. Rose, David L. Nahrwold*
623	Liver DNA bound in vivo with aflatoxin B_1 as a measure of hepatocarcinoma initiation in rainbow trout	*Mark Whitham, Joseph E. Nixon, R. O. Sinnhuber*
629	B16 melanoma cell variants: Irreversible inhibition of growth and induction of morphologic differentiation by anthracycline antibiotics	*Avraham Raz*
639	Differing stem cell self-renewal of lectin-separated murine bone marrow fractions	*Andrew L. Salner, Jane E. Obbagy, Samuel Hellman*
643	Immunologic relatedness of intracisternal A-particles in mouse embryos and neoplastic cell lines	*Thomas T. F. Huang, Jr., Patricia G. Calarco*
651	Methylazoxymethanol: Effect on the immune response of rats to human serum albumin	*Ahmed F. S. A. Habeeb, Alan M. Preston, Priscila Sanabria, Nelson Escobales*
657	Peptidoglycans extracted from gram-positive bacteria: Expression of antitumor activity according to peptide structure and route of injection	*Anne-François Goguel, Geneviève Lespinats, Charles Nauciel*
665	Rat hepatomas: Chemotherapy with Lycurim and Pyrazofurin	*May S. Lui, Robert C. Jackson, Ronald J. Harkrader, George Weber*
669	Liver tumors induced by a new beta-adrenoreceptor blocking agent in female rats	*Giovanni Ragnotti, Marco Presta, Laura Riboni, Teresa Zavanella*

673 Mechanisms of immunologic eradication of a syngeneic guinea pig tumor. I. Quantitative analysis of adoptive immunity *Suyu Shu, James T. Hunter, Herbert J. Rapp, Leila S. Fonseca*

681 Esophageal carcinogenesis in F344 rats by nitrosomethylethylamines substituted in the ethyl group *William Lijinsky, Joseph E. Saavedra, Melvin D. Reuber, Sandra S. Singer*

685 Induction and transplantation of murine skin cancers induced by methoxsalen plus ultraviolet (320-400 nm) radiation *M. L. Kripke, W. L. Morison, J.A. Parrish*

691 Influences of age and anatomical site on ultraviolet carcinogenesis in BALB/c mice *Peter Ebbesen, Margaret L. Kripke*

Announcements

---

695 American Cancer Society National Conference—The Primary Care Physician and Cancer

695 Eleventh Annual Meeting of the International Society for Experimental Hematology

695 Workshop on "Coagulation, Cancer, and Inflammation"

695 Approaches to the Management of Pain

695 Eighth Biannual Morris Hepatoma Symposium

695 Fourteenth Meeting of the International Society for Pediatric Oncology (SIOP)

695 Second International Congress of the T. and L. de Beaumont Bonelli Foundation for Cancer Research

695 Large Bowel Cancer: Biology and Control

Vol 68, No. 5—MAY 1982

Investigations on Man

---

697 Heterogeneous response to X-ray and ultraviolet light irradiations of cultured skin fibroblasts in two families with Gardner's syndrome *Timothy J. Kinsella, John B. Little, John Nove, Ralph R. Weichselbaum, Frederick P. Li, Robert J. Meyer, David J. Marchetto, W. Bradford Patterson*

703 Systemic administration of human leukocyte interferon to melanoma patients. I. Effects on natural killer function and cell populations *Sidney H. Golub, Fred Dorey, Dean Hara, Donald L. Morton, Martyn W. Burk*

711 Systemic administration of human leukocyte interferon to melanoma patients. II. Cellular events associated with changes in natural killer cytotoxicity *Sidney H. Golub, Paula D'Amore, Marcia Rainey*

719 Characterization of a monoclonal antibody reactive with a subset of human breast tumors *Dorothy Yuan, Fred J. Hendler, Ellen S. Vitetta*

729 Epidemiologic and age-dependent data on multiple myeloma in Austria *Heinz Ludwig, Elke Fritz, Hans P. Friedl*

735 Generation of suppressor cells for natural killer activity in cancer patients after surgery *Atsushi Uchida, Roland Kolb, Michael Micksche*

743 Measurement of cancer incidence in the United States: Sources and uses of data *E. Robert Greenberg, Theodore Colton, Curtis Bagne*

751 Degrees of malignancy in human primary central nervous system tumors: Ornithine decarboxylase levels as better indicators than adenosylmethionine decarboxylase levels *Giuseppe Scalabrino, Daniela Modena, Maria Elena Ferioli, Mirella Puerari, Giovanni Luccarelli*

755	An increased risk for lung cancer mortality associated with sugarcane farming	*Henry Rothschild, James J. Mulvey*
761	A 94,000-dalton glycoprotein expressed by human melanoma and carcinoma cells	*Kohzoh Imai, Barry S. Wilson, Aldo Bigotti, Pier G. Natali, Soldano Ferrone*
771	Isolation, culture, and transplantation of human hepatocytes	*S. C. Strom, R. L. Jirtle, R. S. Jones, D. L. Novicki, M. R. Rosenberg, A. Novotny, G. Irons, J. R. McLain, G. Michalopoulos*
779	Mitogen-induced blastogenesis and receptor mobility inhibition by breast cancer serum with elevated orosomucoid (α_1-acid glycoprotein) levels	*David A. Cheresh, John A. Distasio, Charles L. Vogel, Diana M. Lopez*

Investigations on Nonhuman Systems

785	Zinc deficiency, alcohol, and a retinoid: Association with esophageal cancer in rats	*Gamal N. Gabrial, Thomas F. Schrager, Paul M. Newberne*
791	Oral mucosal carcinogenesis in hamsters: Inhibition by vitamin E	*Gerald Shklar*
799	Thy-1 antigen on normal and neoplastic rat mammary tissues: Changes in location and amount of antigen during differentiation of cultured stem cells	*Philip S. Rudland, Michael J. Warburton, Paul Monaghan, Mary A. Ritter*
813	Surgical resection of the rat colon: Effects on carcinogenesis by 1,2-dimethylhydrazine	*C. A. Rubio, G. Nylander*
817	Intracerebral adoptive immunotherapy of a murine lymphoma antigenically altered by drug treatment in vivo	*L. Romani, M. C. Fioretti, R. Bianchi, B. Nardelli, E. Bonmassar*
823	Combined treatments with vitamin A and 5-fluorouracil and the growth of allotransplantable and syngeneic tumors in mice	*Yoshifumi Tomita, Kunisuke Himeno, Kikuo Nomoto, Hideya Endo, Tomio Hirohata*
829	Comparative tumor-initiating activity of complex mixtures from environmental particulate emissions on SENCAR mouse skin	*Stephen Nesnow, Larry L. Triplett, Thomas J. Slaga*
835	Moloney murine sarcoma virus tumors in CBA/J mice: Chemopreventive and chemotherapeutic actions of supplemental β-carotene	*Eli Seifter, Giuseppe Rettura, Jacques Padawer, Stanley M. Levenson*
841	Nonimmunogenic radiation-induced lymphoma: Immunity induction by a somatic cell hybrid	*Eitan Yefenof, Mira Goldapfel, Rosalie Ber*
851	Purification and transplantation of hepatocytes from livers of carcinogen-treated rats	*Steven B. Miller, Theresa P. Pretlow, Joe A. Scott, Thomas G. Pretlow II*
859	Malignant fibrous histiocytomas induced by 4-(hydroxyamino)quinoline 1-oxide in rats	*Yoichi Konishi, Hiroshi Maruyama, Yoshio Mii, Yoshizumi Miyauchi, Yoshihiko Yokose, Kenji Masuhara*
867	Prostate adenocarcinoma in rats: Induction by 3,2′-dimethyl-4-aminobiphenyl	*Shoichi Katayama, Emerich Fiala, Bandaru S. Reddy, Abraham Rivenson, Jerald Silverman, Gary M. Williams, John H. Weisburger*
875	Comparison of in vitro and in vivo effects of thymidine on L1210 leukemia in mice	*Daniel S. Zaharko, Lori M. Ramonas*

Announcements

881 Gordon Research Conference
881 Seventh European Symposium on Hormones and Cell Regulation
881 Southeastern Cancer Research Association Meeting
881 Seventh International Symposium of the World Association of Veterinary Microbiologists, Immunologists, and Specialists in Infectious Diseases

881 Chemotherapy Foundation Symposium V

881 Harvard Medical School Continuing Education Program

881 NIH Consensus Development Panel Statement Available

882 Availability of Serum Panels

882 Scientists Center for Animal Welfare Invites New Applications

882 Disposal of Laboratory Wastes Project

Vol 68, No. 6—JUNE 1982

Letters to the Editor

883	Cartesian reductionism and cancer	*Harry Rubin*
884	Spontaneous liver tumors in laboratory rats	*Morris Pollard*

Investigations on Man

885	Breast cancer and serum cholesterol	*Robert A. Hiatt, Gary D. Friedman, Richard D. Bawol, Hans K. Ury*
891	Carcinomas of the cervix and corpus uteri in humans: Stage-dependent blood levels of substance(s) immunologically cross-reactive with insulin	*K. Pavelić, M. Bolanča, N. Veček, J. Pavelić, T. Marotti, S. Vuk-Pavlović*
895	A quest for the mechanism of "spontaneous" malignant transformation in culture with associated advances in culture technology	*Katherine K. Sanford, Virginia J. Evans*
915	Cancer incidence in humans: Relationship to plasma lipids and relative weight	*R. B. Wallace, C. Rost, L. F. Burmeister, P. R. Pomrehn*
919	High cloning efficiency of human lymphoid cells in agarose without feeder layers	*Kathleen N. Ayres*
925	Mortality among workers in a nickel refinery and alloy manufacturing plant in West Virginia	*Philip E. Enterline, Gary M. Marsh*
935	Cell-mediated immunity to mouse mammary tumor virus antigens by patients with hyperplastic benign breast disease	*G. B. Cannon, S. H. Barsky, T. C. Alford, L. F. Jerome, V. Tinley, J. L. McCoy, J. H. Dean*
945	Effect of enzymatic disaggregation on proliferation of human tumor cells in soft agar	*Anne W. Hamburger, Christine P. White, Kathleen Tencer*

Investigations on Nonhuman Systems

951	Diverse xenotropic virus expressions in two NZB mouse breeding lines that differ in chromosome breakage	*Carmen Bernard, Ingrid Emerit*
957	Phenotypic stability of murine tumor cells in vitro and in vivo	*James Varani, Edmund J. Lovett*
963	Development of resistance to MOPC-315 plasmacytoma after intralesional and intraperitoneal melphalan therapy of tumor-bearing BALB/c mice. I. Enhancement of in vivo rejection responses by combined chemotherapy-immunotherapy	*Aliza Adler, Irit Altbaum*
971	Hematopoietic precursor cells in mice treated with 4-demethoxydaunorubicin and doxorubicin	*Giulio Massa, Giuseppe Bogliolo, Francesco D'Amore, Carlo Muzzulini, Riccardo Ghio, Ivo Pannacciulli*

977	Inheritance of cellular resistance to the antitumor agent ICRF 159 in somatic cell hybrids	*David H. Edgar, Andrew M. Creighton*
981	Further studies on the relationship between allotransplantability and the presence of the cell surface glycoprotein epiglycanin in the TA3-MM mouse mammary carcinoma ascites cell	*Scott C. Miller, John F. Codington, George Klein*
989	Carcinogenesis by isomers of *N*-nitroso-3,5-dimethylpiperidine	*W. Lijinsky, M. D. Reuber, Sandra S. Singer, George M. Singer*
993	Effect of 7,12-dimethylbenz[*a*]anthracene on production and action of gamma interferon	*Karen A. Golemboski, Debra K. D. DeLor, Uldis N. Streips, Gerald Sonnenfeld*
997	Murine tumor necrosis-inducing factor: Purification and effects on myelomonocytic leukemia cells	*Saul Green, Areta Dobrjansky, Mary Ann Chiasson*
1005	Surface antigen expressed in hematopoietic cells derived from $Fv\text{-}4^r$ mouse strains	*Hiroshi Yoshikura, Takeshi Odaka*
1011	2′-Deoxycoformycin-induced hemolysis in the mouse	*Ellen Spremulli, Gerald W. Crabtree, Daniel L. Dexter, Israel Diamond, Paul Calabresi*
1015	Carcinogen-induced DNA damage and cellular alterations in F344 rat colon organ cultures	*Nitin T. Telang, Gary M. Williams*
1023	Cross-resistance of cultured murine leukemia vincristine-resistant P388 cells to vinblastine, vindesine, and bis(*N*-ethylidene vindesine) disulfide, disulfate	*Lee J. Wilkoff, Elizabeth A. Dulmadge*
1027	Intracellular adriamycin levels and cytotoxicity in adriamycin-sensitive and adriamycin-resistant P388 mouse leukemia cells	*Ram Ganapathi, William Reiter, Awtar Krishan*
1033	Thermotolerance in the murine jejunum	*Kurt J. Henle*
1037	Detection of acquired provirus sequences in mammary tumors from low-expressor, low-risk mice	*Bruce W. Altrock, Robert D. Cardiff, John P. Puma, Judi K. Lund*

Announcements

1043 Ions, Cell Proliferation, and Cancer Symposium

1043 Laser, Microwaves, Ultraviolet, and Ultrasound: Biophysical and Biological Basis, Applications, and Hazards in Medicine in Industry Program

1043 Fourth Annual Pharmacy Symposium on Cancer Chemotherapy

1043 A New Organization—American College of Epidemiology

1043 Annual Meeting of the American College of Epidemiology

1043 International Cancer Symposium

1043 Symposium on Application of Biological Markers to Carcinogen Testing

1044 A New Journal—Survey of Immunologic Research

1044 Eighth FDA Science Symposium

Vol 69, No. 1—JULY 1982

Investigations on Man

1	T-Lymphocyte and B-lymphocyte subpopulations infiltrating human mammary carcinomas	*Oleg Eremin, Robin R. A. Coombs, Terence D. Prospero, David Plumb*

9	Methionine regulation of *N*-5-methyltetrahydrofolate:homocysteine methyltransferase and its influence on the growth and protein synthesis in normal, neoplastic, and transformed cells in culture	*Jadwiga W. Tautt, Elżbieta L. Anuszewska, Jadwiga H. Koziorowska*
15	DNA distribution in human colon carcinomas and its relationship to clinical behavior	*R. C. Wolley, K. Schreiber, L. G. Koss, M. Karas, A. Sherman*
23	Circulating immune complex levels in patients with gestational trophoblastic neoplasia	*Anthony A. Rayner, Ross Berkowitz, Glenn Steele, Jr., Peter H. Schur, Mary L. Rodrick, Donald P. Goldstein, Paul J. Harte, Richard E. Wilson, Norman Zamcheck, Alelia E. Munroe*

Investigations on Nonhuman Systems

27	Decrease of tumor growth in mice after intravenous thymosin-treated bone marrow cell injection	*Didier Cupissol, Augustin Rey, Allan L. Goldstein, Bernard Serrou*
33	Relationship between xenotransplantability and cell surface properties of ascites sublines of a rat mammary adenocarcinoma	*Susan C. Howard, Steven R. Hull, John W. Huggins, Coralie A. Carothers Carraway, Kermit L. Carraway*
41	Steroid hormone receptors in the rat mammary adenocarcinoma induced by *N*-hydroxy-*N*-2-fluorenylacetamide	*Sara Antonia Li, Danuta Malejka-Giganti, Jonathan J. Li*
47	Platinum-complexed antitumor immunoglobulins that specifically inhibit DNA synthesis of mouse tumor cells	*Esther Hurwitz, Rina Kashi, Meir Wilchek*
53	Differences in spleen suppressor cell content in rats with progressing and regressing tumors	*Michael A. Hollingsworth, Donald L. Evans*
59	Gastrin protection against chemically induced gastric adenocarcinomas in Wistar rats: Histopathology of the glandular stomach and incidence of gastric adenocarcinoma	*Massaharu Tatsuta, Hisako Yamamura, Haruo Taniguchi, Hiroshi Tamura*
67	Subcutaneously injected radiolabeled liposomes: Transport to the lymph nodes in mice	*Vasily I. Kaledin, Nellie A. Matienko, Valery P. Nikolin, Yevgeny V. Gruntenko, Vladimir G. Budker, Tamara E. Vakhrusheva*
73	Prophylactic and therapeutic actions of supplemental β-carotene in mice inoculated with C3HBA adenocarcinoma cells: Lack of therapeutic action of supplemental ascorbic acid	*Giuseppe Rettura, Francis Stratford, Stanley M. Levenson, Eli Seifter*
79	Flow cytometric analysis of R3327 rat prostate adenocarcinoma grown in vivo and in vitro	*Alice J. Claflin, Alan Pollack, Theodore Malinin, Norman L. Block, George L. Irvin*
89	Depression of natural antitumor resistance of C57BL/6 mice by leukemogenic doses of radiation and restoration of resistance by transfer of bone marrow or spleen cells from normal, but not beige, syngeneic mice	*E. Gorelik, R. B. Herberman*
95	Spontaneous occurrence of atypical hyperplasia and adenocarcinoma of the uterus in androgen-sterilized SD rats	*Shinichi Morikawa, Souei Sekiya, Masabumi Naitoh, Hiroshi Iwasawa, Bin Takeda, Hiroyoshi Takamizawa*
103	Combined inhibitors of carcinogenesis: Effect on azoxymethane-induced intestinal cancer in rats	*Norman D. Nigro, Arthur W. Bull, Paulette S. Wilson, Barbara K. Soullier, Majid A. Alousi*
109	Generation of long-term T-lymphoid cell lines with specific cytotoxic reactivity for a syngeneic murine lymphoma	*Timothy J. Eberlein, Maury Rosenstein, Paul J. Spiess, Steven A. Rosenberg*
117	Pathogenesis of lesions induced in rat lung by chronic tobacco smoke inhalation	*Carol A. Heckman, Walden E. Dalbey*
131	Noncytolytic extraction of murine tumor-specific transplantation antigens with the nonionic detergent octyl-β-D-glucopyranoside	*Stephen J. LeGrue, Catherine M. Macek, Barry D. Kahan*
137	Use of young nude mice for selection of subpopulations of cells with increased metastatic potential from nonsyngeneic neoplasms	*Vincent A. Pollack, Isaiah J. Fidler*

Photochemical Toxicity—Proceedings of the seventh in the series of Food and Drug Administration Science Symposia

Introduction

151 Photochemical toxicity: Toxic, allergic, and carcinogenic aspects with emphasis on predicting effects in humans—an introduction *F. Alan Andersen*

Basic Chemistry, Physics, and Biology Relating to Photosensitization

155 Optical radiation measurements: Instrumentation and sources of error *Robert J. Landry, F. Alan Andersen*
163 Molecular aspects of drug photosensitivity with special emphasis on psoralen photosensitization reaction *Madhu A. Pathak*
171 Immunosuppressive effects of ultraviolet (280–320 nm) radiation and psoralen plus ultraviolet (320–400 nm) radiation in mice *Margaret L. Kripke*

Cellular Assay Systems

177 Cell damage by near ultraviolet radiation: Role of DNA–protein cross-links *A. Eisenstark, S. Kovacs, J. Terry*
183 Tumor virus induction and host cell capacity inactivation: Possible in vitro tests for photosensitizing chemicals *L. E. Bockstahler, T. P. Coohill, C. D. Lytle, S. P. Moore, J. M. Cantwell, B. J. Schmidt*
189 Comparative photobiology of psoralens *M. J. Ashwood-Smith, A. T. Natarajan, G. A. Poulton*
199 Genotoxic effects of sunlight-activated waste water in cultured mammalian cells *Gary F. Strniste, David J. Chen, Richard T. Okinaka*
205 Interaction of oxygen and oxy-radicals with carotenoids *Norman I. Krinsky, Susan M. Deneke*
211 A method to quantify the potency of photosensitizers that modify cell membranes *John P. Pooler, Dennis P. Valenzeno*

Experimental Animal Systems

219 In vitro assay of the effects of psoralens plus ultraviolet radiation on human lymphoid cells *Kenneth H. Kraemer*
229 Modification of photocarcinogenesis by chemical agents *Frederick Urbach, P. Donald Forbes, Ronald E. Davies*
237 Current status of predictive animal models for drug photoallergy and their correlation with drug photoallergy in humans *Leonard C. Harber, Robert B. Armstrong, Hideyuki Ichikawa*
245 Toxic effect of ultraviolet light on melanocytes: Use of animal models in pigment research *George Szabo, Frederick B. Blog, Andrija Kornhauser*

Animal Photochemical Toxicity Effects

253 Toxicologic aspects of photosensitization in livestock *A. Earl Johnson*
259 Chemical and biochemical aspects of photosensitization in livestock and poultry *G. Wayne Ivie*

Human Photochemical Toxicity Effects

265 Chemical phototoxicity in humans *John H. Epstein*

269 Human models for identification of photosensitizing chemicals *Albert M. Kligman, Kays H. Kaidbey*

273 Therapeutic in vivo photochemistry: Photochemical toxicity studies in humans *John A. Parrish*

279 Photosensitization by porphyrins and prevention of photosensitization by carotenoids *Micheline M. Mathews-Roth*

287 Ocular phototoxicity and psoralen plus ultraviolet radiation (320–400 nm) therapy: An experimental and clinical evaluation *Sidney Lerman*

Summary and Conclusions

303 Concluding remarks *Constantine Zervos*

307 Registrants

Correction

317 June 1981, Vol 66, No. 6, pages 1203 and 1233: "The Causes of Cancer: Quantitative Estimates of Avoidable Risks of Cancer in the United States Today" *Richard Doll, Richard Peto*

Announcements

317 Second International Congress on Hormones and Cancer

317 Workshop Conference on Diet and Cancer

317 Annual Symposium on Diagnostic Imaging

317 Fourth International Symposium on Nasopharyngeal Carcinoma

317 Fifth Annual Bristol-Myers Symposium on Cancer Research

317 Twenty-Sixth Annual Clinical Conference

318 European Organization for Research on Treatment of Cancer Symposium

318 Thirtieth Annual Scientific Meeting of the American Society of Cytology

318 Sixteenth Midyear Topical Symposium of the Health Physics Society

318 Urological Cancer Symposium

Vol 69, No. 2—AUGUST 1982

Letters to the Editor

319 *Trans* fatty acids in tumor development *J. Edward Hunter*

320 Reply *Atif B. Awad*

Investigations on Man

323	Multiple myeloma among atomic bomb survivors in Hiroshima and Nagasaki, 1950–76: Relationship to radiation dose absorbed by marrow	*Michito Ichimaru, Toranosuke Ishimaru, Motoko Mikami, Masako Matsunaga*
329	Possible association of radioprotective and chemoprotective aminophosphorothioate drug activity with polyamine oxidase susceptibility	*Joseph M. Gaugas*
333	Search for evidence of feline leukemia virus infection in humans with leukemias, lymphomas, or soft tissue sarcomas	*Peter P. Sordillo, R. Pincow Markovich, William D. Hardy, Jr.*
339	Interferon and prostaglandins: Effects on human natural and lectin-induced cytotoxicity	*Nicholas P. Lang, John R. Ortaldo, Guy D. Bennard, Ronald B. Herberman*
345	Indirect macrophage migration inhibition response to 3-*M* KCl extract of gastric carcinoma	*Tsuyoshi Akiyoshi, Fumio Koba, Michihiro Kawaguchi, Soichiro Miyazaki, Hideo Tsuji*
349	Ten- to fourteen-year effect of screening on breast cancer mortality	*Sam Shapiro, Wanda Venet, Philip Strax, Louis Venet, Ruth Roeser*
357	Antigenic heterogeneity of human colorectal cancer cell lines analyzed by a panel of monoclonal antibodies. I. Heterogeneous expression of Ia-like and HLA-like antigenic determinants	*Grant D. MacLean, Jutta Seehafer, Andrew R. E. Shaw, Mark W. Kieran, B. Michael Longenecker*
365	Changes in skin cancer morbidity between 1971–72 and 1977–78	*Thomas R. Fears, Joseph Scotto*
371	Isolation and partial characterization of surface components of cell line MDA-MB-231 derived from a human metastatic breast carcinoma	*Evelyne Walker-Nasir, John F. Codington, Marianne R. Jahnke, Thomas C. Fuller, Roger W. Jeanloz*
381	α_1-Protease inhibitor production by human adenocarcinomas xenotransplanted into nude mice	*Dorothy Lee, Dan Shochat, David V. Gold*
387	Increasing trends of multiple myeloma mortality in England and Wales; 1950–79: Are the changes real?	*Ramon Velez, Valerie Beral, Jack Cuzick*
393	Changes in clonal expression during the course of acute leukemia: Possible subsets in childhood leukemia	*Hie-Won L. Hann, Peter C. Nowell, Penelope Koch, Jun Minowada, John E. Leitmeyer, Charles S. August*
401	Coproduction of carcinoembryonic antigen and nonspecific cross-reacting antigen by a continuous cell line from a human pancreatic tumor	*Masahide Kuroki, Sadanori Ichiki, Motomu Kuroki, Yuji Matsuoka*
409	Repair of chromosome damage induced by X-irradiation during G_2 phase in a line of normal human fibroblasts and its malignant derivative	*Ram Parshad, Raymond Gantt, Katherine K. Sanford, Gary M. Jones, Robert E. Tarone*

Investigations on Nonhuman Systems

415	Role of anchorage in the expression of tumorigenicity of untransformed mouse cell lines	*Robert S. Wells, Evelyn W. Campbell, Douglas E. Swartzendruber, Lawrence M. Holland, Paul M. Kraemer*
425	Chromosome changes associated with the progression of cell lines from preneoplastic to tumorigenic phenotype during transformation of mouse salivary gland epithelium in vitro	*John K. Cowell, Caroline B. Wigley*
435	Effect of type C viral expression and cellular karyotype on human B-lymphoblast tumorigenicity in nude mice	*Anton F. Steuer, Robert C. Ting, Phillip D. Markham, Zaki Salahuddin, Robert C. Gallo*
443	Hormone dependence of 7,12-dimethylbenz[*a*]anthracene-induced mammary tumor growth: Correlation with prostaglandin E_2 content	*M. Katherine Foecking, William E. Kibbey, Hussein Abou-Issa, Richard H. Matthews, John P. Minton*
447	Comparison of ovariectomy and retinyl acetate on the growth of established 7,12-dimethylbenz[*a*]anthracene-induced mammary tumors in the rat	*Philippe Gandilhon, Réjean Melancon, Jean Djiane, Paul A. Kelly*

453	Growth and differentiation of hyperplastic outgrowths derived from mouse mammary epithelial cells transformed in organ culture	*Nivedita Ganguly, Ranjan Ganguly, Nozer M. Mehta, Mihir R. Banerjee*
465	Effect of immunomodulation on the fate of tumor cells in the central nervous system and systemic organs of mice. Distribution of $[^{125}\text{I}]$5-iodo-2′-deoxyuridine-labeled KHT tumor cells after left intracardial injection	*Frances K. Conley*
475	Role of prostaglandin E_1 and copper in angiogenesis	*Marina Ziche, John Jones, Pietro M. Gullino*
483	Angiogenesis and neoplastic progression in vitro	*Marina Ziche, Pietro M. Gullino*
489	Immunization against transplantable leukemia impaired in copper-deficient mice	*Omelan A. Lukasewycz, Joseph R. Prohaska*
495	Effects of different fractions of *Corynebacterium parvum* on the cytotoxic T-cell response to alloantigens in mice	*Alan Lichtenstein, Richard Tuttle, John Cantrell, Jacob Zighelboim*
503	Chemical cocarcinogenesis with the use of a subclone derived from Balb/3T3 cells with catechol as cocarcinogen	*Mahalakshmi Atchison, Ching-shan Chu, Takeo Kakunaga, Benjamin L. Van Duuren*
509	Immunotherapy of a murine leukemia virus-infected, chemically induced murine sarcoma with antiviral antibodies	*Edward C. Ward, J. Dirk Iglehart, Kent J. Weinhold, Dani P. Bolognesi*
517	Proliferation of ductal outgrowths by carcinogen-induced rat mammary tumors in gland-free mammary fat pads	*Evelyn M. Rivera, Srinivasan Vijayaraghavan*
527	Individually distinct tumor-specific cell surface antigen identified by monoclonal antibody on a Rous sarcoma virus-induced mouse tumor	*Noboru Kuzumaki, Hidetaka Minakawa, Takashige Miyazaki, Soichi Haraguchi, Tetsumichi Matsuo, Takato O. Yoshida*
531	Neoplastic transformation of Syrian hamster cells by putative epoxide metabolites of commercially utilized chloroalkenes	*Joseph A. DiPaolo, Jay Doniger*
535	Derivation of transplantable 7,12-dimethylbenz[*a*]anthracene-induced chicken fibrosarcoma lines: Differences in metastasizing properties and organ specficity	*J. E. Galton, B. Xue, G. M. Hochwald, G. J. Thorbecke*

Meeting Highlights

543	Cytogenetics and somatic cell genetics of malignancy workshop	*Warren W. Nichols, Alfred G. Knudson, Louis Siminovitch*
544	Brief summary of the third joint meeting of the United States–Japan Cooperative Cancer Research Program on cell interactions and cancer	*Ira Pastan, Yoji Ikawa*

Corrections

547	May 1982, Vol 68, No. 5, page 878: "Comparison of In Vitro and In Vivo Effects of Thymidine on L1210 Leukemia in Mice"	*Daniel S. Zaharko, Lori M. Ramonas*
	NCI Monograph No. 58, page 47: "Carcinogenic and Mutagenic N-Substituted Aryl Compounds"	

Announcements

547	Temporomandibular Joint—Pain and Dysfunction Course
547	Second Annual International Symposium on the Clinical Applications of Cardiopulmonary Imaging

547 Fifteenth Annual Malignant Disease Symposium

547 Pediatric Radiology Course

547 New Monographs Available

548 Public Health Controversies—Food Safety Laws: Delaney and Other Dilemmas

Vol 69, No. 3—SEPTEMBER 1982

Letters to the Editor

549 Morbidity versus mortality *Johannes Clemmesen, Arne Nielsen*

550 Reply *Richard Doll, Richard Peto*

Investigations on Man

551 Immunity to tumor-associated antigens in vasectomized men *Deborah J. Anderson, Nancy J. Alexander, David L. Fulgham, Arthur A. Vandenbark, Denis R. Burger*

557 Unscheduled DNA synthesis in human oral mucosa treated with chemical carcinogens in short-term organ culture *Fumio Ide, Takatoshi Ishikawa, Minoru Takagi, Shinichiro Umemura, Shozo Takayama*

565 Distribution of hepatitis B surface and core antigens in human liver cell carcinoma and surrounding nontumorous liver *Setsuo Hirohashi, Yukio Shimosato, Yoshinori Ino, Kiyozo Kishi*

569 Elevated dTTPase activities in sera of patients with advanced cancer *Nicolaus Dahlmann*

573 Breath methane excretion in patients with unresected colorectal cancer *David A. Karlin, R. D. Jones, John R. Stroehlein, Anthony J. Mastromarino, Gregory D. Potter*

577 *N*-Methyl-*N*-nitrosourea and saccharin: Effects on epithelium of normal human urinary bladder in vitro *Shadia El-Gerzawi, Barry M. Heatfield, Benjamin F. Trump*

585 Persistence of transforming and nontransforming Epstein-Barr virus in high passages of P3HR-1 cell lines *Paul Gerber, Dharam Ablashi, Ian Magrath, Gary Armstrong, Philip Andersen, Luba Trach*

Investigations on Nonhuman Systems

591 A deletion in chromosome 1 in cells of a transplantable granulocytic leukemia (GL-13) in guinea pigs *Dorothy E. Moore, Warren H. Evans, Michael G. Mage*

595 Establishment and immunologic characterization of 3-methylcholanthrene-induced sarcoma cell lines metastasizing widely in mice and exhibiting distinct and selective propensities for the mode of metastasis *Yuso Kodama, Toshio Seyama, Kenji Kamiya, Kenjiro Yokoro*

607 Modulation of cell-mediated alloimmunity by BCG. I. Antagonism and potentiation of immunosuppression caused by cytarabine *Richard I. Murahata, Malcolm S. Mitchell*

613 Modulation of cell-mediated alloimmunity by BCG. II. Induction of specific, nonadherent, non-T-killer cells by BCG and alloantigen *Richard I. Murahata, Malacolm S. Mitchell*

619 Alloantigenic phenotype of radiation-induced thymomas in the mouse *P. Mark Hogarth, Margaret M. Henning, Ian F. C. McKenzie*

627 Formation of symbiotic complex by microenvironment-dependent mouse leukemias and thymic epithelial reticular cells *Yoshimi Nishi, Kazuhiro Yoshikawa, Hiroshi Hiai, Kunihiro Notake, Hayase Shisa, Yasuaki Nishizuka*

639	A high-tumor-incidence subline of the D1 mouse mammary hyperplastic outgrowth line: Effect of carcinogens	*Rhoda L. Ashley, Robert D. Cardiff, Terry S. Pratt, Leslie J. Faulkin*
647	Antitumor immunity induced by hybrid murine tumor cells: Requirement for optimal immunization	*Craig S. McCune, Robert W. O'Donnell, Paul K. Horan, Hollis S. Budd, Janice L. Spennacchio, Christy Chuang, Edgard C. Henshaw*
653	Inhibitory effect of interferon on the growth of spontaneous mammary tumors in mice	*Erik De Clercq, Zhen-Xi Zhang, Kris Huygen, Roger Leyten*
659	Influence of cause-of-death assignment on time-to-tumor analyses in animal carcinogenesis studies	*Ralph L. Kodell, John H. Farmer, David W. Gaylor, Alexander M. Cameron*
665	Murine lymph node natural killer cells: Regulatory mechanisms of activation or suppression	*Goro Hisano, Nabil Hanna*
673	Androgen control of cytosol progesterone receptor levels in the MT-W9B transplantable mammary tumor in the rat	*Margot M. Ip, Richrad J. Milholland, Untae Kim, Fred Rosen*
683	In vitro measurement of resistance to phalloidin and γ-glutamyltransferase of carcinogen-induced preneoplastic hepatocytes of rats	*Norimasa Sawada, Kazunori Furukawa, Hideyuki Tsukada*
687	Chicken resistance to dimethylnitrosamine acute effects on the liver: A comparative study with other species	*H. M. Godoy, M. I. Díaz Gómez, A. Marzi, E. C. de Ferreyra, O. M. de Fenos, J. A. Castro*
693	Effects of sublethal irradiation on changes in crypts of the mouse colon during treatment with 1,2-dimethylhydrazine	*Thomas C. Richards, David E. Tacha*
699	Tumor-induced neovascularization in the mouse eye	*V. R. Muthukkaruppan, L. Kubai, R. Auerbach*
709	In vitro infection of lymphocytes with Marek's disease virus	*Bruce W. Calnek, Karel A. Schat, William R. Shek, Chen-Lo H. Chen*
715	Surface antigens on Marek's disease lymphoblastoid tumor cell lines	*Karel A. Schat, Chen-Lo H. Chen, William R. Shek, Bruce W. Calnek*
721	Some effects of the tumor promoter 12-*O*-tetradecanoylphorbol 13-acetate on cell interactions in vitro	*David E. Maslow, Eric G. Mayhew, Charles E. Wenner*
725	Mouse skin tumor-initiating activity of 5-, 7-, and 12-methyl- and fluorine-substituted benz[α]anthracenes	*Alexander W. Wood, Wayne Levin, Richard L. Chang, Allan H. Conney, Thomas J. Slaga, Robert F. O'Malley, Melvin S. Newman, Donald R. Buhler, Donald M. Jerina*
729	Free amino acid pools of rodent mammary tumors	*Martin J. Pine, Untae Kim, Clement Ip*
737	Immunomodulation of the lymphoresponsive phases of carcinogenesis: Mechanisms of natural immunity	*Charles H. Evans, Joseph A. DiPaolo, Jeffrey A. Heinbaugh, Anthony J. DeMarinis*
741	Lymphotoxin prevention of diethylnitrosamine carcinogenesis in vivo	*Janet H. Ransom, Charles H. Evans, Joseph A. DiPaolo*

Announcements

745	Advances in Pediatric Oncology Seminar
745	Thirty-Sixth Annual Symposium on Fundamental Cancer Research
745	Twenty-Fourth Postgraduate Institute for Pathologists in Clinical Cytopathology
745	Accredited Visiting Faculty Program on Colorectal Cancer

Vol 69, No. 4—OCTOBER 1982

Guest Editorial

747	Sheep lung carcinoma: An endemic analogue of a sporadic human neoplasm	*K. Perk, I. Hod*

Investigations on Man

751	Studies on carcinogenesis of human prostate. II. Long-term explant culture of normal prostate and benign prostatic hyperplasia: Light microscopy	*Hayato Sanefuji, Barry M. Heatfield, Benjamin F. Trump, John D. Young, Jr.*
757	Studies on carcinogenesis of human prostate. III. Long-term explant culture of normal prostate and benign prostatic hyperplasia: Transmission and scanning electron microscopy	*Barry M. Heatfield, Hayato Sanefuji, Benjamin F. Trump*
767	Enhancement of growth of human colon tumor cell lines by feeder layers of murine fibroblasts	*M. G. Brattain, D. E. Brattain, A. M. Sarrif, L. J. McRae, W. D. Fine, J. G. Hawkins*
773	Major histologic types of cancers of the gum and mouth, esophagus, larynx, and lung by sex and by income level	*V. L. Ernster, S. Selvin, S. T. Sacks, D. W. Merrill, E. A. Holly*
777	Glycoconjugate with *Ulex europaeus* agglutinin-I-binding sites in normal mucosa, adenoma, and carcinoma of the human large bowel	*Suguru Yonezawa, Takao Nakamura, Sadao Tanaka, Eiichi Sato*
787	Cerebrospinal fluid markers in African Burkitt's lymphoma with central nervous system involvement	*William C Wallen, Robert J. Biggar, Paul H. Levine, Janet Neequaye, Francis K. Nkrumah*
793	Transforming growth factors in the urine of normal, pregnant, and tumor-bearing humans	*Daniel R. Twardzik, Stephen A. Sherwin, Jane Ranchalis, George J. Todaro*
799	Selective cytotoxicity of a ricin A-chain–anticarcinoembryonic antigen antibody conjugate for human colon adenocarcinoma cell line	*Thomas W. Griffin, Linda R. Haynes, Julie A. DeMartino*
807	In vitro potentiation of human natural killer cell activity by a streptococcal preparation, OK-432: Interferon and interleukin-2 participation in the stimulation with OK-432	*Hiro Wakasugi, Tadashi Kasahara, Nagahiro Minato, Junji Hamuro, Michio Miyata, Yasuhiko Morioka*
813	Carcinoembryonic antigen: Usefulness as a postsurgical method in the detection of recurrence in Dukes stage B_2 and C colorectal cancers	*Maria Koch, Graeme Washer, Herta Gaedke, Thomas A. McPherson*
817	Interaction of familial and hormonal risk factors for breast cancer	*Louis A. Brinton, Robert Hoover, Joseph F. Fraumeni, Jr.*
823	Imaging of human melanoma xenografts in nude mice with a radiolabeled monoclonal antibody	*Tarun Ghose, Soldano Ferrone, Kohzoh Imai, Stevens T. Norvell, Jr., Steven J. Luner, Robert H. Martin, A. Huntley Blair*
827	Functional properties of human thymoma lymphocytes: Role of subcellular factors in blastic activation	*Piero Musiani, Libero Lauriola, Nicola Maggiano, Pietro Tonali, Mauro Piantelli*
833	Changes in lung cancer incidence and mortality rates among Americans: 1969–78	*John W. Horm, Ardyce J. Asire*

Investigations on Nonhuman Systems

839	Simian virus 40 (SV40)-specific isoelectric point-4.7–94,000-M_r membrane glycoprotein: Major peptide homology exhibited with the nuclear and membrane-associated 94,000-M_r SV 40 T-antigen in hamsters	*Rupert Schmidt-Ullrich, W. Scott Thompson, Stuart J. Kahn, Maureen T. Monroe, Donald F. H. Wallach*
851	Relationship of lung adenoma prevalence and growth rate to acute urethan dose and target cell number	*Michael L. Dourson, Ellen J. O'Flaherty*
859	Relationship between urethan dose rate and adenoma latency: Relevance of tumor growth rate and target cell number	*Ellen J. O'Flaherty, Michael L. Dourson*
867	Tumor cell-triggered macrophage-mediated suppression of the T-cell cytotoxic response to tumor-associated antigens. I. Characterization of the cell components for induction of suppression	*Chou-Chik Ting, Dennis Rodrigues*

873 Tumor cell-triggered macrophage-mediated suppression of the T-cell cytotoxic response to tumor-associated antigens. II. Mechanisms for induction of suppression — *Chou-Chik Ting, Myrthel E. Hargrove*

879 Inducible macrophage cytotoxins. I. Biokinetics of activation and release in vitro — *Thomas H. Reidarson, Walter E. Levy III, Jim Klostergaard, Gale A. Granger*

889 Inducible macrophage cytotoxins. II. Tumor lysis mechanism involving target cell-binding proteases — *Thomas H. Reidarson, Gale A. Granger, Jim Klostergaard*

895 Squamous metaplasia in organ cultures of vitamin A-deficient hamster trachea: Cytokinetic and ultrastructural alterations — *Dharam P. Chopra*

907 Primordial germ cell proliferation in fetal testes in mouse strains with high and low incidences of congenital testicular teratomas — *Takehiko Noguchi, Leroy C. Stevens*

915 Epizootic neoplasms in fishes from a lake polluted by copper mining wastes — *John J. Black, Elwin D. Evans, John C. Harshbarger, Robert F. Zeigel*

927 Electron microscopic autoradiography of the trachea in fetal Syrian golden hamsters treated transplacentally with *N*-nitrosodiethylamine — *Hildegard M. Reznik-Schüller*

933 Comparison of biologic behavior and histology of transplanted mammary tumors in GR mice — *Dean H. Percy, Vincent L. Morris, Janet I. MacInnes*

939 Regulation of cell-mediated immunologic reactivity to Moloney murine sarcoma virus-induced tumors. III. Further characterization of tumor-specific serum blocking factors — *William J. Halliday, Thelma A. Koppi, Ian F. C. McKenzie*

945 Trisomy 15 and other nonrandom chromosome changes in Rauscher murine leukemia virus-induced leukemia cell lines — *Anne Hagemeijer, Elisabeth M. E. Smit, Francine Govers, Nico J. de Both*

953 Induction of gp70-specific suppressor T-cells in mice inoculated with virus-producing tumor cells — *Jeffrey A. Bluestone, Carlos Lopez*

961 Carcinogenicity test of acetoxime in MRC-Wistar rats — *Sidney S. Mirvish, Shahrokh Salmasi, Richard G. Runge*

963 *β*-Cyclodextrin: Promoting effect on the development of renal tubular cell tumors in rats treated with *N*-ethyl-*N*-hydroxyethylnitrosamine — *Yoshio Hiasa, Masato Ohshima, Yoshiteru Kitahori, Noboru Konishi, Toyohisa Fujita, Takashi Yuasa*

969 Secretagogue response in rat pancreatic acinar carcinoma — *John R. Warren*

975 Enhanced metastatic potential of tumor cells harvested from spontaneous metastases of heterogeneous murine tumors — *James E. Talmadge, Isaiah J. Fidler*

Meeting Highlights

981 Adult T-cell leukemia-lymphoma: Role of a human retrovirus — *Max Essex*

Corrections

987 December 1981, Vol 67, No. 6 page 1328: "Enhancement of Experimental Pancreatic Cancer in Syrian Golden Hamsters by Dietary Fat" — *Diane F. Birt, Sharokh Salmasi, Parviz M Pour*

987 April 1982, Vol 68, No. 4, page 678: "Mechanisms of Immunologic Eradication of a Syngeneic Guinea Pig Tumor" — *Suyu Shu, James T. Hunter, Herbert J. Rapp, Leila S. Fonesca*

Announcements

987 Formaldehyde Toxicology Meeting

987	Symposium on Application of Biological Markers to Carcinogen Testing	
987	Eighth Annual Postgraduate Course	
987	Seventh Annual Meeting of the Cell Kinetics Society	
987	First International Meeting on Cell Biochemistry and Function	
988	The Fourth Annual Meeting of the Society for Clinical Trials	
988	Thirteenth International Congress of Chemotherapy	

Vol 69, No. 5—NOVEMBER 1982

Investigations on Man

989	The serum cholesterol–cancer relationship: An analysis of time trends in the Framingham Study	*Paul D. Sorlie, Manning Feinleib*
997	Reactivity in neoplasia, preneoplasia, and pregnancy of lymphocytes against fetal extracts: Cross-reactions between man and mouse	*Günter Pasternak, Bernhard Schlott, Jürgen Reinhöfer, Günter Gryschek, Bodo von Broen, Sybille Albrecht*
1005	Cancers of the gallbladder and biliary tract in Alaskan Natives: 1970–79	*Leslie P. Boss, Anne P. Lanier, Peter H. Dohan, Thomas R. Bender*
1009	Collagen polymorphism in extracellular matrix of human osteosarcoma	*Frederic D. Shapiro, David R. Eyre*
1017	Exogenous estrogens and other risk factors for breast cancer in women with benign breast diseases	*David B. Thomas, Joyce P. Persing, William B. Hutchinson*
1027	Second cancers following radiotherapy for cervical cancer	*Ruth A. Kleinerman, Rochelle E. Curtis, John D. Boice, Jr., John T. Flannery, Joseph F. Fraumeni, Jr.*
1035	Association of breast cancer risk with age at first and subsequent births: A study in the population of the Estonian Republic	*Brian MacMahon, Maret Purde, Daniel Cramer, Evi Hint*
1039	In vitro growth stimulation of human ovarian cancer cells by xenogeneic peritoneal macrophages	*Charles E. Welander, Ronald B. Natale, John L. Lewis, Jr.*
1049	Effect of natural protease inhibitors and a chemoattractant on tumor cell invasion in vitro	*U. P. Thorgeirsson, L. A. Liotta, T. Kalebic, I. M. Margulies, K. Thomas, M. Rios-Candelore, R. G. Russo*
1055	Androgen conjugates in human breast cyst fluids	*W. R. Miller, M. M. Roberts, R. J. Creel, P. L. Yap, R. W. Kelly, A. P. M. Forrest*
1059	Parity and colorectal cancer risk in women	*Tim Byers, Saxon Graham, Mya Swanson*
1063	Correlation between cancers of the uterine cervix and penis in China	*Jun-Yao Li, Frederick P. Li, William J. Blot, Robert W. Miller, Joseph F. Fraumeni, Jr.*
1067	Use of circulating pregnancy-specific β_1 glycoprotein as a marker in carcinoma of the breast in women	*Saul W. Rosen, Mitchell H. Gail, Douglass C. Tormey*

Investigations on Nonhuman Systems

1073	Carcinoembryonic antigen in nonhuman primates	*Darrow E. Haagensen, Jr., Richard S. Metzgar, Brent Swenson, William G. Dilley, Charles E. Cox, Sarah Davis, Janet Murdoch, Norman Zamcheck, Samuel A. Wells, Jr.*
1077	Spontaneous leukemia viruses: Lymphomagenic ecotropic viruses of AKR mice	*Esther F. Hays, Nadine Margaretten, Stephen K. Swanson*

1083	Prostaglandin-induced differentiation or dimethyl sulfoxide-induced differentiation: Reduction of the neoplastic potential of a rat mammary tumor stem-cell line	*Philip S. Rudland, Anna Twiston Davies, Michael J. Warburton*
1095	Immunotherapy by intralesional injection of BCG cell walls or live BCG in bovine ocular squamous cell carcinoma: A preliminary report	*Wim R. Klein, E. Joost Ruitenberg, Peter A. Steerenberg, Wim H. de Jong, Wim Kruizinga, Wim Misdorp, Jürgen Bier, Rudy H. Tiesjema, Johan G. Kreeftenberg, Jacob S. Teppema, Herbert J. Rapp*
1105	Expression of fibronectin and laminin in the rat liver after partial hepatectomy, during carcinogenesis, and in transplantable hepatocellular carcinomas	*Stewart Sell, Erkki Ruoslahti*
1115	Effects of isoproterenol on mammary gland tumors induced by *N*-nitroso-*N*-methylurea and salivary gland tumors induced by 7,12-dimethylbenz[*a*]anthracene	*Tibor Barka*
1121	Immunotherapeutic effects of partially purified tumor-specific transplantation antigens on pulmonary metastases of a 3-methylcholanthrene-induced sarcoma in mice: A preliminary report	*Tsuguo Tanaka, Neal R. Pellis, Barry D. Kahan*
1127	Dose-response studies with nitrosoheptamethyleneimine and its α-deuterium-labeled derivative in F344 rats	*W. Lijinsky, M. D. Reuber, T. S. Davies, C. W. Riggs*
1135	Induction of mammary neoplasm in the ACI rat by 430-keV neutrons, X-rays, and diethylstilbestrol	*Claire J. Shellabarger, Danielle Chmelevsky, Albrecht M. Kellerer, J. Patrick Stone, Seymour Holtzman*
1147	Inhibition by tumor-promoting phorbol esters of procollagen synthesis in promotable JB6 mouse epidermal cells	*L. David Dion, Jenifer Bear, John Bateman, Luigi M. De Luca, Nancy H. Colburn*
1155	Effect of carcinogen release rate on the incidence of preneoplastic and neoplastic lesions of the respiratory tract epithelium in rats	*Mitsutoshi Shiba, Andres J. P. Klein-Szanto, Ann C. Marchok, Bimal C. Pal, Paul Nettesheim*
1163	Exclusive binding of immunoglobulin to Fcγ receptors on macrophages in 3-methylcholanthrene-induced murine tumors	*John M. Lindsay, Linda Manning, Gary W. Wood*
1175	Independent expression of chemical carcinogen-induced phenotypic properties frequently associated with the neoplastic state in a cultured guinea pig cell line	*Charles H. Evans, Joseph A. DiPaolo*
1183	Ceruloplasmin, copper ions, and angiogenesis	*Katari S. Raju, Giulio Alessandri, Marina Ziche, Pietro M. Gullino*
1189	Isolation of tumoricidal macrophages from lung melanoma metastases of mice treated systemically with liposomes containing a lipophilic derivative of muramyl dipeptide	*M. E. Key, J. E. Talmadge, W. E. Fogler, C. Bucana, I. J. Fidler*
1199	Induction of mammary tumors in virgin female BALB/c mice by single low doses of 7,12-dimethylbenz[*a*]anthracene	*Stephen P. Ethier, Robert L. Ullrich*

Announcements

1205	New NIH Biotechnology High Voltage Electron Microscope (HVEM) Resource Available to Biological and Medical Researchers
1205	Harvard Medical School Continuing Education Program
1205	The 1983 Oncology Update Symposium
1205	Sixty-Fifth Annual Meeting of the American Radium Society
1205	Eighth Summer Program in Methods of Immunologic Research and Diagnosis
1206	Eighth International Congress of Cytology
1206	E.O.R.T.C. Symposium on Treatment of Advanced Gastrointestinal Cancer

Vol 69, No. 6—DECEMBER 1982

Letters to the Editor

1207 Noncontraceptive estrogen use and the occurrence of ovarian cancer — *Carlos La Vecchia, Allesandro Liberati, Silvia Franceschi*

1208 Immune alterations related to age, sex, and mammary tumor detection in murine mammary tumor virus-infected mice — *Hervé Benoist, Jean Dufer, Cécile Bouchet, Andrée Desplaces*

Guest Editorial

1209 Human retroviruses and adult T-cell leukemia–lymphoma — *Robert C. Gallo, Marvin S. Reitz, Jr.*

Investigations on Man

1215 Changes in human adenovirus 5 propagated in Burkitt's lymphoma cells — *Nicole Faucon, Georges Ogier, Yvette Chardonnet*

1221 Primary liver carcinoma and liver cirrhosis in atomic bomb survivors, Hiroshima and Nagasaki, 1961–75, with special reference to hepatitis B surface antigen — *Masahide Asano, Hiroo Kato, Keiko Yoshimoto, Shinichi Seyama, Hideyo Itakura, Tadao Hamada, Soichi Iijima*

1229 Epidemiology of familial predisposition for breast cancer in Japan — *Motoi Murata, Keijiro Kuno, Atsuo Fukami, Goi Sakamoto*

1235 Establishment and characterization of a human colony-stimulating factor-producing cell line from a squamous cell carcinoma of the thyroid gland — *Tetsuro Okabe, Hitoshi Nomura, Nakaaki Oshawa*

1245 In vitro studies on the cell-mediated immune response to human brain tumors. I. Requirement for third-party stimulator lymphocytes in the induction of cell-mediated cytotoxic responses to allogeneic cultured gliomas — *Maurice K. Gately, Moshe Glaser, Steven J. Dick, Ray W. Mettetal, Jr., Paul L. Kornblith*

1255 Isozymes of acid esterase and acid phosphatase in permanent human hematopoietic cell lines — *Christer Sundström, Heinz J. Radzun, Mohammad R. Parwaresch*

1261 Subpopulations of human T-lymphocytes. XIX. T-cells and T-cells with receptors for IgMFc (Tμ), IgGFc (Tγ), or IgAFc (Tα) in the peripheral blood and regional lymph nodes of patients with untreated breast cancer — *Sudhir Gupta, Susanna Cunningham-Rundles*

1265 Epidemic curve of respiratory cancer due to chloromethyl ethers — *William Weiss*

1271 Epithelial line from normal human colon mucosa — *B. Shannon Danes, E. Sutanto*

1277 DNA content of liver cell nuclei of *N*-2-fluorenylacetamide-induced altered foci and neoplasms in rats and human hyperplastic foci — *Hideki Mori, Takuji Tanaka, Shigeyuki Sugie, Masayoshi Takahashi, Gary M. Williams*

1283 No seasonality in the diagnosis of acute leukemia in the United States — *Alexander M. Walker, Paulus A. H. van Noord*

1289 Probable clonal origin of neurofibrosarcoma in a patient with hereditary neurofibromatosis — *Jan M. Friedman, Philip J. Fialkow, Claudia L. Greene, Michael N. Weinberg*

Investigations on Nonhuman Systems

1293 Accessory cell function in tumor-bearing mice and effects of *Corynebacterium parvum* — *Seiya Okuda, Kazuto Taniguchi, Chiharu Kubo, Kikuo Nomoto*

1299	Induction of γ-glutamyltransferase-positive and nonspecific esterase-positive foci in rat liver by partial hepatectomy following single injection of *N*-nitrosodiethylamine	*Norio Hirota, Shinichi Moriyama, Takeshi Yokoyama*
1305	Evidence for involvement of mast cells in tumor suppression in mice	*Hiroshi Tanooka, Yukihiko Kitamura, Toshihiko Sado, Kazuhiko Tanaka, Mizue Nagase, Sohei Kondo*
1311	*H-2* expression on a teratocarcinoma-derived cell line, TerC	*David B. Searls, Michael Edidin*
1317	Inhibitory effect of fumaric acid on forestomach and lung carcinogenesis by a 5-nitrofuran naphthyridine derivative in mice	*Keiko Kuroda, Masayoshi Kanisawa, Mitsutaro Akao*
1321	Characterization of anti-inflammatory factors produced by murine tumor cells in culture	*S. J. Normann, J. Cornelius*
1329	Collagenolytic activity of rabbit V_2 carcinoma implanted in the nude mouse	*Chitra Biswas, Kurt J. Bloch, Jerome Gross*
1337	Immunoadjuvant effects of *Blastomyces dermatitidis* against EL 4 lymphoma in C57BL/6J mice	*L. Scott McDaniel, George C. Cozad*
1343	Suppression of 7,12-dimethylbenz[*a*]anthracene-induced chromosome aberrations in rat bone marrow cells after treatment with Sudan III and related azo dyes	*Yoshiaki Ito, Sakan Maeda, Tetsuo Fujihara, Norifumi Ueda, Taketoshi Sugiyama*
1347	Growth of mouse mammary glands after neonatal sex hormone treatment	*Yasuhiro Tomooka, Howard A. Bern*
1353	Effects of nicotinamide, isonicotinamide, and bleomycin on DNA synthesis and repair in rat hepatocytes and hepatoma cells	*Rosemary Barra, Verrell Randolph, MariaElaina Sumas, Kevin Lanighan, Michael A. Lea*
1359	Tumor-associated antigens produced by mouse mammary tumor cells in artificial capillary culture	*Jean C. Hager, S. Spiegelman, M. Ramanarayanan, James Bausch, Pierre M. Galletti, Paul Calabresi*
1367	Glycosylated podophyllotoxin congeners: Loss of microtubule inhibition and permission of invasion in vitro	*Marc M. Mareel, Christian H. Dragonetti, Georges K. De Bruyne, Rita M.-L. Van Cauwenberge*
1375	Detection of aflatoxins and related metabolites by radioimmunoassay	*Philippe Sizaret, Christian Malaveille, Ruggero Montesano, Charles Frayssinet*
1383	Carcinogenic effect of carbazole in the liver of (C57BL/6N × C3H/HeN)F_1 mice	*Hiroyuki Tsuda, Akihiro Hagiwara, Michiko Shibata, Masato Ohshima, Nobuyuki Ito*
1391	Hormone requirements of the pregnancy-dependent mammary tumor of GR/A mice: An in vitro study	*John W. Harbell, Jackie S. Papkoff, Charles W. Daniel*
1403	Analysis of lymphoid cells responding to virus- and tumor-associated antigens in spleens of syngeneic mouse mammary tumor systems with low and high oncogenic potentials	*Diana M. Lopez, Ronald D. Paul*
1411	Genetics of transplacentally induced teratogenic and carcinogenic effects in rabbits treated with *N*-nitroso-*N*-ethylurea	*R. R. Fox, H. Meier, H. G. Bedigian, D. D. Crary*

Meeting Highlights

1419	Job-exposure matrices in occupational epidemiology	*Shelia K. Hoar*

Announcements

1421 Seventeenth Annual Clinical Symposium of St. Jude Children's Research Hospital

1421 Eighteenth Annual San Francisco Cancer Symposium

1421 Second Annual A.A.I. Course in Advanced Immunology

1421 Eleventh International Symposium for Comparative Research on Leukemia and Related Diseases

1421 Eleventh Annual Meeting of the International Society for Oncodevelopmental Biology and Medicine

1421 Seventh Meeting of the European Association for Cancer Research (EACR)

1423 **Acknowledgement**

1429 **Index of Authors**

1435 **Permuted Title Index**

1463 **1982 Table of Contents**

★U.S. GOVERNMENT PRINTING OFFICE: 1982-381-145/61

best copy available

JNCI (NIH Publication No. 83-13)